



## Abstract Archives of the RSNA, 2022

M2-SPBR

### Breast Monday Poster Discussions

Monday, Nov. 28 9:00AM - 9:30AM Room: Learning Center - BR DPS

#### Participants

Ellen Mendelson, MD, Chicago, IL (*Moderator*) Medical Advisory Board, Seno Medical Instruments, Inc; Medical Advisory Board, Delphinus Medical Technologies, Inc

#### Sub-Events

### M2-SPBR-1 Post-market Real-world Data Demonstrates that an AI System Can Detect Cancers Missed by Human Readers in Breast Cancer Screening Without Unnecessary Recalls: A Stepping Stone Towards Implementation

#### Participants

Jonathan Nash, San Francisco, CA (*Presenter*) Medical Director, Kheiron Medical Technologies Ltd; Stockholder, Kheiron Medical Technologies Ltd

#### PURPOSE

To demonstrate real-world post-market benefit of artificial intelligence (AI) as an extra reader in breast cancer screening (BCS).

#### METHODS AND MATERIALS

A commercially available AI system was employed as an extra reader (XR) in addition to standard human double reading (HDR) at a breast cancer screening center from Apr-Sept 2021. The XR workflow involved flagging cases the AI suggested to recall which HDR did not recall, i.e. positive discordant cases, for arbitration by an experienced radiologist. The deep learning model and the thresholds for the operating points of the AI were predefined and validated in previous studies. Primary outcome was cancer detection rate. All detected cancers were pathology-confirmed.

#### RESULTS

Standard HDR for 3746 patients had an arbitration rate of 3.0% (114 patients), a recall rate of 6.7% (250 patients), and a cancer detection rate (CDR) of 12.5/1000 (47 cancer cases). Of the cases that were not recalled by HDR, the AI flagged 396 cases to recommend recall (positive discordance rate 10.6%). Extra arbitration resulted in recalling 6 patients, all of whom were diagnosed with breast cancer. This equated to a total arbitration rate of 13.6% and 1.6/1000 increase in CDR (sum 14.1/1000). An exact simulation with a less sensitive AI operating point yielded a total arbitration rate of 5.3%, while still detecting 5 of 6 extra cancer cases.

#### CONCLUSION

This real-world deployment of AI increased cancer detection rates without recalling extra false positives, indicating the effectiveness of AI as an extra reader. Combining the XR workflow with workflows focused on workload savings will mitigate the increased arbitration rate and optimise clinical and operational benefits. The results provide important, real-world evidence showing the benefit of using an AI reader in breast cancer screening, paving the way for innovative workflows where synergy of humans and AI achieve optimal performance for patients.

#### CLINICAL RELEVANCE/APPLICATION

One of the first prospectively collected data sets where AI is actually being employed in real-world breast cancer screening shows increased cancer detection rate for AI as an extra reader.

### M2-SPBR-2 Artificial-Intelligence-Driven Volumetric Breast Density Estimation as a Predictor of Individualized Breast Cancer Risk

#### Participants

Vinayak Ahluwalia, BS, Philadelphia, PA (*Presenter*) Nothing to Disclose

#### PURPOSE

Breast density is a well-established risk factor for breast cancer. We present an artificial intelligence (AI) algorithm to estimate volumetric breast density (VBD) solely from 3D-reconstructed digital breast tomosynthesis (DBT) images, rather than raw images rarely kept by clinical centers, and analyze its ability to perform individualized breast cancer risk assessment.

#### METHODS AND MATERIALS

We retrospectively analyzed 1,080 negative DBT screening exams obtained between 2011 and 2016 from the Hospital of the University of Pennsylvania (41.2% White, 54.2% Black, 4.6% Other; mean age  $\pm$  SD, 57  $\pm$  11 years; mean BMI  $\pm$  SD, 28.7  $\pm$  7.1 kg/m<sup>2</sup>), for which both 2D raw and 3D reconstructed DBT images (Selenia Dimensions, Hologic Inc) were available. Corresponding 3D reference-standard tissue segmentations were generated from previously validated software that uses both 3D reconstructed slices and raw 2D DBT data. We based our deep learning algorithm on the U-Net architecture within the open-source Generally

Nuanced Deep Learning Framework (GaNDLF) and created a 3-label image segmentation task (background, dense tissue, and fatty tissue). Our dataset was randomly split into training (70%), validation (15%) and test (15%) sets. Our evaluation measure was the weighted Dice score (DSC), with 0 signifying no overlap and 1 signifying perfect overlap, overall and separately for each label. Subsequently, we created a conditional logistic regression model using an independent case-control set of 907 subjects from the same hospital system to evaluate if the VBD estimated from the AI algorithm and BMI is associated with breast cancer risk.

## RESULTS

On an independent testing set, our AI algorithm achieved unweighted and weighted DSC of 0.78 (STD=0.09) and 0.56 (STD=0.19), respectively. It accurately segmented the three labels of background, fatty tissue, and dense tissue, with Dice scores of 0.94, 0.89, and 0.49, respectively. In conditional logistic regression, VBD (Odds ratio 1.27, 95% confidence interval [1.03, 1.55],  $p=0.022$ ) and BMI (Odds ratio 1.37, 95% confidence interval [1.12, 1.68],  $p=0.002$ ) were shown to be statistically significant factors in individualized breast cancer prediction.

## CONCLUSION

This AI method demonstrates promise in the estimation of VBD from 3D-reconstructed DBT images. Moreover, this estimation, along with BMI, has been shown to be associated with breast cancer risk. Such a tool can enable large retrospective epidemiological and personalized risk assessments of breast density with DBT.

## CLINICAL RELEVANCE/APPLICATION

We have created an AI algorithm for estimating VBD from 3D-reconstructed DBT images that does not require the use of raw image data and could aid in predicting an individual's risk of breast cancer.

### M2-SPBR-3 Clinical Implications of Changes in Artificial Intelligence Software Case Scores from Prior to Current Digital Breast Tomosynthesis Screening Exam

#### Participants

Emily F. Conant, MD, Philadelphia, PA (*Presenter*) Research Grant, Hologic, Inc; Advisory Panel, Hologic, Inc; Research Grant, OM1, Inc; Research Grant, iCad, Inc; Advisory Panel, iCad, Inc; Speaker, WebMD LLC

#### PURPOSE

To evaluate the degree of change in digital breast tomosynthesis (DBT) artificial intelligence software (AI-CAD) case scores over sequential screens relative to outcomes.

#### METHODS AND MATERIALS

In an IRB-approved, HIPAA-compliant observational study at a single site from 2/3/20-3/16/22, a total of 25220 DBT screens were performed on 18251 women of which 22927 were scored at the exam-level with a DBT-derived, AI algorithm (Profound AI v2, iCAD, Inc.). Study outcome groups were compared using EMR/tumor registry data. For true negatives (TN) and false positives (FP) screens, 1 year follow-up was required. Biopsy-proven, cancer cases were deemed either true positive (TP) or false negative (FN) based on mode of detection. The differences in AI-derived case score between second screen ( $time2 = t2$ , "current screen") and first screen ( $time1 = t1$ , "prior screen") were compared across outcome groups based on outcome of the current screen. For each outcome group, the mean and median change in case scores was calculated.

## RESULTS

Of 22927 screens with case scores, outcomes were: 159 TP and 18 FN cancer cases and 20777 negative or 1973 benign. For non-cancer cases with 1 year follow-up, there were 9527 TN and 765 FP. Average age was TP: 62.6, FP: 55.5, TN: 58.5, FN: 58.5; 5467 of the women were Black, 4299 White, 325 Asian, 378 "Other". The average (range) of case scores was: TP-75 (7-100), FP-42 (0-100), TN-34 (0-100), FN-37 (0-88). The 10469 screens were in 10219 women with TP, FP, TN or FN; 9969 had a single screen and 250 had 2 screens. Of women with only one screen, there were: TP=132, FP=743, TN=9079, FN=15. Of 250 women with 2 screens (and 1 year follow-up for TN and FPs), there were: TP=27, FP=13, TN=207, FN=3 on current screens and FP=9, TN=241 on prior screens. DBT AI-CAD case score change from prior to current screen in the 250 women based on outcomes demonstrated median and mean differences in case score for  $t2 - t1$  were: TP: 15 and 22.8; FP: 3 and 2.4; TN: 0 and -1.6; FN: -10 and -6.

## CONCLUSION

DBT AI-CAD case scores from sequential screens allow assessment of score changes, with larger increases in mean score difference from prior to current for women with screen-detected cancers compared to other outcomes

## CLINICAL RELEVANCE/APPLICATION

Changes in DBT AI-derived case scores over sequential screens should be considered; the degree of AI-derived score change may be indicative of increased likelihood of screen-detected cancer.

### M2-SPBR-4 Assessment of Breast Positioning in Digital Mammography: Performance of Artificial Intelligent Quality Control System and Agreement Between AI and Radiographers

#### Participants

Huizhi Cao, PhD, (*Presenter*) Nothing to Disclose

#### PURPOSE

To evaluate the performance of breast positioning in digital mammography using an artificial intelligent quality control system (AIQCS) and determine the agreement between AI system and radiographers.

#### METHODS AND MATERIALS

Assessment of breast positioning was performed by AI system (Edison, GE Healthcare) and by four radiographers on 1223 examinations of women. Nine image quality criteria were used for craniocaudal and mediolateral-oblique views. The criteria evaluated the appearance of the nipple, breast rotation, pectoral muscle, inframammary fold, pectoral nipple line, shoulder overlap shadow, abdominal skin, contralateral breast and foreign body. The area under the receiver operating characteristic curve (AUC) of poor imaging quality prediction by AI system according to incomplete gland, incomplete pectoralis muscle, over or insufficient exposure were calculated and overall accuracy were evaluated. Intraclass correlation and Cohen's kappa coefficient (?) were used

to investigate the correlation and agreement between the radiographer's assessments and AI.

## RESULTS

The AUC of poor imaging quality prediction by AI system according to incomplete gland, incomplete pectoralis muscle, over or insufficient exposure was (0.903 vs 0.937 vs 0.982). Overall accuracy of AI system were 0.958. The intraclass correlation for the pectoral nipple line between the radiographers and AI was >0.80. A substantial to almost perfect agreement ( $\kappa > 0.85$ ) was observed between the radiographers and AI on the nipple in profile criterion. We observed a slight to moderate agreement for the other criteria ( $\kappa = 0.40-0.65$ ) and generally a higher agreement between the two pairs of radiographers (mean  $\kappa = 0.70$ ) than between the radiographers and AI (mean  $\kappa = 0.61$ ).

## CONCLUSION

s AI has great potential in evaluating breast position criteria in mammography by reducing subjectivity. However, varying agreement between radiographers and AI was observed.

## CLINICAL RELEVANCE/APPLICATION

Breast position with AI system has great importance for quality control of mammography and are great value to reach optimal image quality in mammography.

## M2-SPBR-5 Initial Experience with Contrast-Enhanced Mammography Guided Biopsy: A Single Institution Case Series

### Participants

Abeer Mousa, MD, Phoenix, AZ (*Presenter*) Nothing to Disclose

## PURPOSE

CEM (contrast-enhanced mammography) utilizes iodinated contrast to highlight areas of neovascularity in the breast tissues with sensitivity comparable to that of breast MR imaging. Review of our data has shown that 4% of our CEM cases have suspicious areas of CEM enhancement, which are mammographically and sonographically-occult. In these instances, we have previously performed MRI-guided biopsies given the lack of CEM-guided biopsy capability. In 2020, the FDA cleared a device to support CEM biopsy. As a pilot site testing the Hologic Affirm contrast biopsy device, we present a preliminary overview of our experience with this new technology.

## METHODS AND MATERIALS

IRB approved, HIPAA compliant post-market, prospective case review of 28 patients who underwent a CEM-guided biopsy for suspicious CEM only findings. Six biopsies were canceled due to lack of lesion enhancement at the time of biopsy (n=5) or benign skin lesion (n=1). Hologic Selenia Dimensions mammography system with updated I-View software for CEM localization and biopsy was used. After intravenous injection of iodinated contrast, enhancing lesions were localized using 2D stereotactic image acquisition followed by stereotactic biopsy.

## RESULTS

28 patients underwent CEM guided biopsy, mean patient age 57.2 years (34-78y). Mean size of biopsied lesion was 12 mm (5-29 mm). Pathology demonstrated malignancy in 5/28 (18%) (3 invasive lobular carcinoma, 2 ductal carcinoma in situ), high risk lesions in 6/28 (21%), and benign findings in 17/28 (61%). When available, average length of procedure was 11 min (5-20 min). One patient with a benign biopsy was categorized as clinically discordant and had subsequent MRI-guided biopsy, which demonstrated invasive ductal carcinoma, resulting in one false negative.

## CONCLUSION

s Our study demonstrates that CEM-guided biopsies are technically feasible, with average length of time relatively shorter than that of MR biopsy. Pathology concordance remains of utmost importance using a newer biopsy technique.

## CLINICAL RELEVANCE/APPLICATION

As future work evolves, CEM and CEM-guided biopsies could provide for a more cost-effective and relatively quick breast tissue biopsy mechanism. Future work will need to be performed to compare costs, patient wait times, procedure times and patient experience of CEM to MRI biopsy.

## M2-SPBR-6 Explorative Multicenter Study to Assess Patient Comfort: Radiographers Usability and Image Quality of Spiral Breast CT

### Participants

Matthias Wetzl, MD, Erlangen, Germany (*Presenter*) Nothing to Disclose

## PURPOSE

Dedicated spiral breast CT is a promising method in breast imaging and is increasingly used in radiology departments. This explorative, multicenter study aimed to assess image quality of dedicated spiral breast CT and its acceptability among patients and radiographers in different radiology sites.

## METHODS AND MATERIALS

The prospective study was approved by the local ethics committee and conducted in three centers from August 2021 to March 2022. On a 5-point Likert Scale, patient comfort (1 = very good comfort; 5 = severe injury) and usability by radiographers (1 = very good usability; 5 = examination not possible) were assessed. Radiologists rated overall image quality (1 = very good; 5 = diagnosis not possible), depiction of calcifications (1 = very good; 5 = diagnosis not possible), and coverage of breast tissue (1 = glandular tissue complete and parts of pectoralis muscle; 2 = almost complete glandular tissue and part of pectoralis muscle; 3 = major parts of glandular tissue and no pectoralis muscle; 4 = major parts of glandular tissue missing).

## RESULTS

393 women (age: 59 years old, range 35 - 89) participated in the study. Both breasts were examined in 92 % and intravenous

contrast media was applied in 39 % of patients. Patient comfort (n = 313) was very good in 71 % (CI 67 - 76 %) and good in 28 % (CI 22 - 32 %), while 1 % had minor problems. One woman needed physiotherapy due to pain in cervical spine, which exaggerated after the procedure. Usability by radiographers (n = 298) was very good in 61 % (CI 55 - 66 %) and good in 26 % (CI 22 - 31 %), while examination was not possible in one women, since the breasts were too large for the scanner. Image quality (n = 224) was rated very good in 57 % (CI 51 - 64 %) and good in 34 % (CI 29 - 40 %). Detectability of calcifications (n = 116) was very good in 75 % (CI 67 - 83 %), while 8 % (CI 3 - 13 %) of calcifications presented insufficiently (Likert Scale 3 - 5). Breast coverage (n = 224) was complete in 38 % (CI 32 - 45 %), almost complete in 29 % (CI 23 - 34 %), major parts of glandular tissue were covered in 30 % (CI 23 - 35 %), and coverage was insufficient in 3 % (CI 1 - 6 %).

## CONCLUSION

s Dedicated spiral breast CT has a high acceptance among patients and radiographers. Image quality is high in dedicated breast CT and breast coverage adequate.

## CLINICAL RELEVANCE/APPLICATION

Dedicated spiral breast CT delivers a high image quality and is well accepted by radiographers and patients in a prospective multicenter study.

## M2-SPBR-7 Preoperative MRI Characteristics of Invasive Breast Cancer: Association with Lympho Vascular Invasion and Disease-free Survival

Participants

Zeyan Xu, (*Presenter*) Nothing to Disclose

## PURPOSE

As an adverse prognostic factor in patients with invasive breast cancer, lymphovascular invasion (LVI) is closely associated with axillary lymph node (ALN) involvement, disease recurrence, and distant metastasis. This study aims to investigate the relationship of preoperative MRI characteristics with LVI and disease-free survival (DFS).

## METHODS AND MATERIALS

This retrospective study included patients with available LVI status who underwent preoperative MRI examination at two hospitals from January 2013 to August 2020. Univariable and multivariable logistic regression analyses were performed to evaluate the independent predictors of LVI. A prediction model was established and a scoring system was carried out according to the odds ratio of multivariable analysis in the primary set, and the results were further verified in the validation set. The Kaplan-Meier method and log-rank test were applied to analyze the association of the risk score with DFS.

## RESULTS

A total of 575 women (median age, 50 years; range, 24-79 years) were included. LVI-positive status was confirmed in 26.9% (104 of 386) and 27.5% (52 of 189) of the primary and validation set. At the primary set, Ki-67 index, MRI-ALN status, breast edema score, multicentricity or multifocality showed significantly independent values in predicting LVI status (P It; 0.05). The area under the receiver operating characteristic curve of the model using these predictors in the primary and validation set was 0.75 (95% confidence interval [CI]: 0.69, 0.81) and 0.75 (95% CI: 0.67, 0.83), respectively. Across the entire study population, higher grades of simplified scores tended to have a higher proportion of positive LVI status. Furthermore, patients with high-score were significantly associated with a worse DFS (HR for high vs. low, 3.08; 95% CI: 1.32-7.18, P = 0.006).

## CONCLUSION

s The prediction model incorporating Ki-67 index, MRI-ALN status, breast edema score, multicentricity or multifocality shows good predictive performance for LVI status and is associated with DFS in patients with invasive breast cancer.

## CLINICAL RELEVANCE/APPLICATION

A feasible predictive model combining preoperative breast MRI characteristics and clinicopathological factors can help identify the presence of lymphovascular invasion in patients with invasive breast cancer. Furthermore, the variables used in our model are readily available in routine clinical practice and could help optimize clinical workflows.

Printed on: 02/07/23



## Abstract Archives of the RSNA, 2022

M2-SPBR-1

### Post-market Real-world Data Demonstrates that an AI System Can Detect Cancers Missed by Human Readers in Breast Cancer Screening Without Unnecessary Recalls: A Stepping Stone Towards Implementation

Monday, Nov. 28 9:00AM - 9:30AM Room: Learning Center - BR DPS

#### Participants

Jonathan Nash, San Francisco, CA (*Presenter*) Medical Director, Kheiron Medical Technologies Ltd; Stockholder, Kheiron Medical Technologies Ltd

#### PURPOSE

To demonstrate real-world post-market benefit of artificial intelligence (AI) as an extra reader in breast cancer screening (BCS).

#### METHODS AND MATERIALS

A commercially available AI system was employed as an extra reader (XR) in addition to standard human double reading (HDR) at a breast cancer screening center from Apr-Sept 2021. The XR workflow involved flagging cases the AI suggested to recall which HDR did not recall, i.e. positive discordant cases, for arbitration by an experienced radiologist. The deep learning model and the thresholds for the operating points of the AI were predefined and validated in previous studies. Primary outcome was cancer detection rate. All detected cancers were pathology-confirmed.

#### RESULTS

Standard HDR for 3746 patients had an arbitration rate of 3.0% (114 patients), a recall rate of 6.7% (250 patients), and a cancer detection rate (CDR) of 12.5/1000 (47 cancer cases). Of the cases that were not recalled by HDR, the AI flagged 396 cases to recommend recall (positive discordance rate 10.6%). Extra arbitration resulted in recalling 6 patients, all of whom were diagnosed with breast cancer. This equated to a total arbitration rate of 13.6% and 1.6/1000 increase in CDR (sum 14.1/1000). An exact simulation with a less sensitive AI operating point yielded a total arbitration rate of 5.3%, while still detecting 5 of 6 extra cancer cases.

#### CONCLUSION

This real-world deployment of AI increased cancer detection rates without recalling extra false positives, indicating the effectiveness of AI as an extra reader. Combining the XR workflow with workflows focused on workload savings will mitigate the increased arbitration rate and optimise clinical and operational benefits. The results provide important, real-world evidence showing the benefit of using an AI reader in breast cancer screening, paving the way for innovative workflows where synergy of humans and AI achieve optimal performance for patients.

#### CLINICAL RELEVANCE/APPLICATION

One of the first prospectively collected data sets where AI is actually being employed in real-world breast cancer screening shows increased cancer detection rate for AI as an extra reader.

Printed on: 02/07/23



## Abstract Archives of the RSNA, 2022

M2-SPBR-2

### Artificial-Intelligence-Driven Volumetric Breast Density Estimation as a Predictor of Individualized Breast Cancer Risk

Monday, Nov. 28 9:00AM - 9:30AM Room: Learning Center - BR DPS

#### Participants

Vinayak Ahluwalia, BS, Philadelphia, PA (*Presenter*) Nothing to Disclose

#### PURPOSE

Breast density is a well-established risk factor for breast cancer. We present an artificial intelligence (AI) algorithm to estimate volumetric breast density (VBD) solely from 3D-reconstructed digital breast tomosynthesis (DBT) images, rather than raw images rarely kept by clinical centers, and analyze its ability to perform individualized breast cancer risk assessment.

#### METHODS AND MATERIALS

We retrospectively analyzed 1,080 negative DBT screening exams obtained between 2011 and 2016 from the Hospital of the University of Pennsylvania (41.2% White, 54.2% Black, 4.6% Other; mean age  $\pm$  SD, 57  $\pm$  11 years; mean BMI  $\pm$  SD, 28.7  $\pm$  7.1 kg/m<sup>2</sup>), for which both 2D raw and 3D reconstructed DBT images (Selenia Dimensions, Hologic Inc) were available. Corresponding 3D reference-standard tissue segmentations were generated from previously validated software that uses both 3D reconstructed slices and raw 2D DBT data. We based our deep learning algorithm on the U-Net architecture within the open-source Generally Nuanced Deep Learning Framework (GaNDLF) and created a 3-label image segmentation task (background, dense tissue, and fatty tissue). Our dataset was randomly split into training (70%), validation (15%) and test (15%) sets. Our evaluation measure was the weighted Dice score (DSC), with 0 signifying no overlap and 1 signifying perfect overlap, overall and separately for each label. Subsequently, we created a conditional logistic regression model using an independent case-control set of 907 subjects from the same hospital system to evaluate if the VBD estimated from the AI algorithm and BMI is associated with breast cancer risk.

#### RESULTS

On an independent testing set, our AI algorithm achieved unweighted and weighted DSC of 0.78 (STD=0.09) and 0.56 (STD=0.19), respectively. It accurately segmented the three labels of background, fatty tissue, and dense tissue, with Dice scores of 0.94, 0.89, and 0.49, respectively. In conditional logistic regression, VBD (Odds ratio 1.27, 95% confidence interval [1.03, 1.55],  $p=0.022$ ) and BMI (Odds ratio 1.37, 95% confidence interval [1.12, 1.68],  $p=0.002$ ) were shown to be statistically significant factors in individualized breast cancer prediction.

#### CONCLUSION

This AI method demonstrates promise in the estimation of VBD from 3D-reconstructed DBT images. Moreover, this estimation, along with BMI, has been shown to be associated with breast cancer risk. Such a tool can enable large retrospective epidemiological and personalized risk assessments of breast density with DBT.

#### CLINICAL RELEVANCE/APPLICATION

We have created an AI algorithm for estimating VBD from 3D-reconstructed DBT images that does not require the use of raw image data and could aid in predicting an individual's risk of breast cancer.

Printed on: 02/07/23



## Abstract Archives of the RSNA, 2022

M2-SPBR-3

### Clinical Implications of Changes in Artificial Intelligence Software Case Scores from Prior to Current Digital Breast Tomosynthesis Screening Exam

Monday, Nov. 28 9:00AM - 9:30AM Room: Learning Center - BR DPS

#### Participants

Emily F. Conant, MD, Philadelphia, PA (*Presenter*) Research Grant, Hologic, Inc; Advisory Panel, Hologic, Inc; Research Grant, OM1, Inc; Research Grant, iCad, Inc; Advisory Panel, iCad, Inc; Speaker, WebMD LLC

#### PURPOSE

To evaluate the degree of change in digital breast tomosynthesis (DBT) artificial intelligence software (AI-CAD) case scores over sequential screens relative to outcomes.

#### METHODS AND MATERIALS

In an IRB-approved, HIPAA-compliant observational study at a single site from 2/3/20-3/16/22, a total of 25220 DBT screens were performed on 18251 women of which 22927 were scored at the exam-level with a DBT-derived, AI algorithm (Profound AI v2, iCAD, Inc.). Study outcome groups were compared using EMR/tumor registry data. For true negatives (TN) and false positives (FP) screens, 1 year follow-up was required. Biopsy-proven, cancer cases were deemed either true positive (TP) or false negative (FN) based on mode of detection. The differences in AI-derived case score between second screen (time2 = t2, "current screen") and first screen (time1 = t1, "prior screen") were compared across outcome groups based on outcome of the current screen. For each outcome group, the mean and median change in case scores was calculated.

#### RESULTS

Of 22927 screens with case scores, outcomes were: 159 TP and 18 FN cancer cases and 20777 negative or 1973 benign. For non-cancer cases with 1 year follow-up, there were 9527 TN and 765 FP. Average age was TP: 62.6, FP: 55.5, TN: 58.5, FN: 58.5; 5467 of the women were Black, 4299 White, 325 Asian, 378 "Other". The average (range) of case scores was: TP-75 (7-100), FP-42 (0-100), TN-34 (0-100), FN-37 (0-88). The 10469 screens were in 10219 women with TP, FP, TN or FN; 9969 had a single screen and 250 had 2 screens. Of women with only one screen, there were: TP=132, FP=743, TN=9079, FN=15. Of 250 women with 2 screens (and 1 year follow-up for TN and FPs), there were: TP=27, FP=13, TN=207, FN=3 on current screens and FP=9, TN=241 on prior screens. DBT AI-CAD case score change from prior to current screen in the 250 women based on outcomes demonstrated median and mean differences in case score for t2 - t1 were: TP: 15 and 22.8; FP: 3 and 2.4; TN: 0 and -1.6; FN: -10 and -6.

#### CONCLUSION

s DBT AI-CAD case scores from sequential screens allow assessment of score changes, with larger increases in mean score difference from prior to current for women with screen-detected cancers compared to other outcomes

#### CLINICAL RELEVANCE/APPLICATION

Changes in DBT AI-derived case scores over sequential screens should be considered; the degree of AI-derived score change may be indicative of increased likelihood of screen-detected cancer.

Printed on: 02/07/23

## Abstract Archives of the RSNA, 2022

M2-SPBR-4

### Assessment of Breast Positioning in Digital Mammography: Performance of Artificial Intelligent Quality Control System and Agreement Between AI and Radiographers

Monday, Nov. 28 9:00AM - 9:30AM Room: Learning Center - BR DPS

#### Participants

Huizhi Cao, PhD, (Presenter) Nothing to Disclose

#### PURPOSE

To evaluate the performance of breast positioning in digital mammography using an artificial intelligent quality control system(AIQCS) and determine the agreement between AI system and radiographers.

#### METHODS AND MATERIALS

Assessment of breast positioning was performed by AI system ( Edison, GE Healthcare)and by four radiographers on 1223 examinations of women. Nine image quality criteria were used for craniocaudal and mediolateral-oblique views. The criteria evaluated the appearance of the nipple, breast rotation, pectoral muscle, inframammary fold, pectoral nipple line, shoulder overlap shadow, abdominal skin, contralateral breast and foreign body. The area under the receiver operating characteristic curve (AUC) of poor imaging quality prediction by AI system according to incomplete gland, incomplete pectoralis muscle, over or insufficient exposure were calculated and overall accuracy were evaluated. Intraclass correlation and Cohen's kappa coefficient (?) were used to investigate the correlation and agreement between the radiographer's assessments and AI.

#### RESULTS

The AUC of poor imaging quality prediction by AI system according to incomplete gland, incomplete pectoralis muscle, over or insufficient exposure was (0.903 vs 0.937 vs 0.982). Overall accuracy of AI system were 0.958. The intraclass correlation for the pectoral nipple line between the radiographers and AI was >0.80. A substantial to almost perfect agreement (? > 0.85) was observed between the radiographers and AI on the nipple in profile criterion. We observed a slight to moderate agreement for the other criteria (? = 0.40-0.65) and generally a higher agreement between the two pairs of radiographers (mean ? = 0.70) than between the radiographers and AI (mean ? = 0.61).

#### CONCLUSION

AI has great potential in evaluating breast position criteria in mammography by reducing subjectivity. However, varying agreement between radiographers and AI was observed.

#### CLINICAL RELEVANCE/APPLICATION

Breast position with AI system has great importance for quality control of mammography and are great value to reach optimal image quality in mammography.

Printed on: 02/07/23

## Abstract Archives of the RSNA, 2022

M2-SPBR-5

### Initial Experience with Contrast-Enhanced Mammography Guided Biopsy: A Single Institution Case Series

Monday, Nov. 28 9:00AM - 9:30AM Room: Learning Center - BR DPS

#### Participants

Abeer Mousa, MD, Phoenix, AZ (*Presenter*) Nothing to Disclose

#### PURPOSE

CEM (contrast-enhanced mammography) utilizes iodinated contrast to highlight areas of neovascularity in the breast tissues with sensitivity comparable to that of breast MR imaging. Review of our data has shown that 4% of our CEM cases have suspicious areas of CEM enhancement, which are mammographically and sonographically-occult. In these instances, we have previously performed MRI-guided biopsies given the lack of CEM-guided biopsy capability. In 2020, the FDA cleared a device to support CEM biopsy. As a pilot site testing the Hologic Affirm contrast biopsy device, we present a preliminary overview of our experience with this new technology.

#### METHODS AND MATERIALS

IRB approved, HIPAA compliant post-market, prospective case review of 28 patients who underwent a CEM-guided biopsy for suspicious CEM only findings. Six biopsies were canceled due to lack of lesion enhancement at the time of biopsy (n=5) or benign skin lesion (n=1). Hologic Selenia Dimensions mammography system with updated I-View software for CEM localization and biopsy was used. After intravenous injection of iodinated contrast, enhancing lesions were localized using 2D stereotactic image acquisition followed by stereotactic biopsy.

#### RESULTS

28 patients underwent CEM guided biopsy, mean patient age 57.2 years (34-78y). Mean size of biopsied lesion was 12 mm (5-29 mm). Pathology demonstrated malignancy in 5/28 (18%) (3 invasive lobular carcinoma, 2 ductal carcinoma in situ), high risk lesions in 6/28 (21%), and benign findings in 17/28 (61%). When available, average length of procedure was 11 min (5-20 min). One patient with a benign biopsy was categorized as clinically discordant and had subsequent MRI-guided biopsy, which demonstrated invasive ductal carcinoma, resulting in one false negative.

#### CONCLUSION

Our study demonstrates that CEM-guided biopsies are technically feasible, with average length of time relatively shorter than that of MR biopsy. Pathology concordance remains of utmost importance using a newer biopsy technique.

#### CLINICAL RELEVANCE/APPLICATION

As future work evolves, CEM and CEM-guided biopsies could provide for a more cost-effective and relatively quick breast tissue biopsy mechanism. Future work will need to be performed to compare costs, patient wait times, procedure times and patient experience of CEM to MRI biopsy.

Printed on: 02/07/23

## Abstract Archives of the RSNA, 2022

M2-SPBR-6

### Explorative Multicenter Study to Assess Patient Comfort: Radiographers Usability and Image Quality of Spiral Breast CT

Monday, Nov. 28 9:00AM - 9:30AM Room: Learning Center - BR DPS

#### Participants

Matthias Wetzl, MD, Erlangen, Germany (*Presenter*) Nothing to Disclose

#### PURPOSE

Dedicated spiral breast CT is a promising method in breast imaging and is increasingly used in radiology departments. This explorative, multicenter study aimed to assess image quality of dedicated spiral breast CT and its acceptability among patients and radiographers in different radiology sites.

#### METHODS AND MATERIALS

The prospective study was approved by the local ethics committee and conducted in three centers from August 2021 to March 2022. On a 5-point Likert Scale, patient comfort (1 = very good comfort; 5 = severe injury) and usability by radiographers (1 = very good usability; 5 = examination not possible) were assessed. Radiologists rated overall image quality (1 = very good; 5 = diagnosis not possible), depiction of calcifications (1 = very good; 5 = diagnosis not possible), and coverage of breast tissue (1 = glandular tissue complete and parts of pectoralis muscle; 2 = almost complete glandular tissue and part of pectoralis muscle; 3 = major parts of glandular tissue and no pectoralis muscle; 4 = major parts of glandular tissue missing).

#### RESULTS

393 women (age: 59 years old, range 35 - 89) participated in the study. Both breasts were examined in 92 % and intravenous contrast media was applied in 39 % of patients. Patient comfort (n = 313) was very good in 71 % (CI 67 - 76 %) and good in 28 % (CI 22 - 32 %), while 1 % had minor problems. One woman needed physiotherapy due to pain in cervical spine, which exaggerated after the procedure. Usability by radiographers (n = 298) was very good in 61 % (CI 55 - 66 %) and good in 26 % (CI 22 - 31 %), while examination was not possible in one women, since the breasts were too large for the scanner. Image quality (n = 224) was rated very good in 57 % (CI 51 - 64 %) and good in 34 % (CI 29 - 40 %). Detectability of calcifications (n = 116) was very good in 75 % (CI 67 - 83 %), while 8 % (CI 3 - 13 %) of calcifications presented insufficiently (Likert Scale 3 - 5). Breast coverage (n = 224) was complete in 38 % (CI 32 - 45 %), almost complete in 29 % (CI 23 - 34 %), major parts of glandular tissue were covered in 30 % (CI 23 - 35 %), and coverage was insufficient in 3 % (CI 1 - 6 %).

#### CONCLUSION

Dedicated spiral breast CT has a high acceptance among patients and radiographers. Image quality is high in dedicated breast CT and breast coverage adequate.

#### CLINICAL RELEVANCE/APPLICATION

Dedicated spiral breast CT delivers a high image quality and is well accepted by radiographers and patients in a prospective multicenter study.

Printed on: 02/07/23

## Abstract Archives of the RSNA, 2022

M2-SPBR-7

### Preoperative MRI Characteristics of Invasive Breast Cancer: Association with Lympho Vascular Invasion and Disease-free Survival

Monday, Nov. 28 9:00AM - 9:30AM Room: Learning Center - BR DPS

#### Participants

Zeyan Xu, (*Presenter*) Nothing to Disclose

#### PURPOSE

As an adverse prognostic factor in patients with invasive breast cancer, lymphovascular invasion (LVI) is closely associated with axillary lymph node (ALN) involvement, disease recurrence, and distant metastasis. This study aims to investigate the relationship of preoperative MRI characteristics with LVI and disease-free survival (DFS).

#### METHODS AND MATERIALS

This retrospective study included patients with available LVI status who underwent preoperative MRI examination at two hospitals from January 2013 to August 2020. Univariable and multivariable logistic regression analyses were performed to evaluate the independent predictors of LVI. A prediction model was established and a scoring system was carried out according to the odds ratio of multivariable analysis in the primary set, and the results were further verified in the validation set. The Kaplan-Meier method and log-rank test were applied to analyze the association of the risk score with DFS.

#### RESULTS

A total of 575 women (median age, 50 years; range, 24-79 years) were included. LVI-positive status was confirmed in 26.9% (104 of 386) and 27.5% (52 of 189) of the primary and validation set. At the primary set, Ki-67 index, MRI-ALN status, breast edema score, multicentricity or multifocality showed significantly independent values in predicting LVI status ( $P < 0.05$ ). The area under the receiver operating characteristic curve of the model using these predictors in the primary and validation set was 0.75 (95% confidence interval [CI]: 0.69, 0.81) and 0.75 (95% CI: 0.67, 0.83), respectively. Across the entire study population, higher grades of simplified scores tended to have a higher proportion of positive LVI status. Furthermore, patients with high-score were significantly associated with a worse DFS (HR for high vs. low, 3.08; 95% CI: 1.32-7.18,  $P = 0.006$ ).

#### CONCLUSION

The prediction model incorporating Ki-67 index, MRI-ALN status, breast edema score, multicentricity or multifocality shows good predictive performance for LVI status and is associated with DFS in patients with invasive breast cancer.

#### CLINICAL RELEVANCE/APPLICATION

A feasible predictive model combining preoperative breast MRI characteristics and clinicopathological factors can help identify the presence of lymphovascular invasion in patients with invasive breast cancer. Furthermore, the variables used in our model are readily available in routine clinical practice and could help optimize clinical workflows.

Printed on: 02/07/23

## Abstract Archives of the RSNA, 2022

M2-SPCA

### Cardiac Monday Poster Discussions

Monday, Nov. 28 9:00AM - 9:30AM Room: Learning Center - CA DPS

#### Sub-Events

#### M2-SPCA-1 Photon-Counting CT Coronary Stent Imaging with Dedicated Ultra-Sharp Convolution Kernels: A Phantom Study

##### Participants

Bernhard Petritsch, MD, Wuerzburg, Germany (*Presenter*) Research Consultant, Siemens AG

##### PURPOSE

To assess the impact of different dedicated (ultra-) sharp vascular convolution kernels on quantitative and subjective image characteristics using a clinical photon-counting detector (PCD) CT system in comparison to a conventional energy-integrating detector (EID) CT system.

##### METHODS AND MATERIALS

In this phantom study, 10 different coronary stents (3.0 mm diameter) were expanded into plastic vessel phantoms filled with contrast agent. Stent-containing vessel phantoms were positioned in an anthropomorphic phantom (QRM) simulating a medium-sized patient. CT scans were acquired parallel to the scanners z-axis using a 1st generation PCD CT system (NAEOTOM Alpha, Siemens). Examinations were performed with two different scan-modes (standard-resolution [SR mode - 2x2 binning] and ultra-high-resolution [UHR mode- subpixels readout separately]). A state of the art EID CT system from the same vendor served as reference standard (SOMATOM Force, Siemens). CT DIvol matched images were reconstructed with identical reconstruction parameters using different convolution kernels (Bv59 [EID]; Bv60 [SR-PCD], Bv68 [SR + UHR-PCD], Bv84 [UHR-PCD]). In-stent lumen visibility (%), image noise (HU), and subjective image quality (IQ) (Likert scale 1-4) were assessed.

##### RESULTS

PCD-UHR mode in Bv84 achieved highest in-stent lumen visibility and best subjective IQ [=1] while PCD-SR mode in Bv60 provided lowest noise levels and comparable IQ [=3] to the EID CT. In-stent lumen visibility was significantly higher ( $p < 0.001$ ) with PCD UHR in Bv68 (73.3%) [IQ=2], and PCD UHR in Bv84 (83.3%) when compared to conventional EID (60.0%). Image noise of PCD CT was significantly lower ( $p < 0.001$ ) for Bv60 SR (24 HU), and Bv68 UHR (27 HU) mode compared to conventional EID images (66 HU). The ultra sharp Bv84 kernel provided similar ( $p = 1.000$ ) noise levels (68 HU) as conventional Bv59 EID images.

##### CONCLUSION

In an in vitro setting, the combination of PCD CT and ultra-sharp convolution kernels provides superior in-stent lumen visibility and subjective image quality at identical (Bv84) or even lower (Bv68) noise levels when compared to conventional EID CT technology.

##### CLINICAL RELEVANCE/APPLICATION

PCD CT allows for improved assessment of coronary artery stents and potentially in-stent restenosis in particular, respectively.

#### M2-SPCA-2 Dual Energy versus Single Energy Coronary CT Angiography for The Evaluation of Coronary Artery Disease

##### Participants

Carlos Capunay, MD, Vicente Lopez, Argentina (*Presenter*) Nothing to Disclose

##### PURPOSE

To explore the diagnostic performance of dual energy CT coronary angiography (DE-CTCA) in comparison with single energy CTCA (SE-CTCA) in patients with intermediate to high likelihood of coronary artery disease (CAD) referred to invasive coronary angiography (ICA).

##### METHODS AND MATERIALS

Study protocol include consecutive symptomatic patients with suspected CAD referred for ICA who underwent DE-CTCA and a coronary artery calcium scoring (CACS) within the month before the ICA. DE-CTCA was analyzed in a polychromatic fashion to resemble a SE-CTCA and using monochromatic images at 85 keV to reduce blooming artifact. Two blinded experienced observers (O) analyzed the images. O1 analyzed DE-CTCA and O2 analyzed the equivalent SE-CTCA group of images. Stenosis over 50% were considered a positive finding. The 95% confidence interval for the proportions were calculated by the exact binomial method. ROC curve analyses were performed using specific software for ROC analysis. Pairwise comparison of ROC curves were performed using the method of DeLong et al. for detection of differences between two AUC, and calculated the binomial exact confidence interval for the AUC. A two-sided p value of less than 0.05 indicated statistical significance.

##### RESULTS

Fifty patients were included, mean age 63 years-old; 70% male. The mean effective radiation dose of DE-CTCA was 4 mSv. The

ifty patients were included, mean age 65 years-old, 70% male. The mean effective radiation dose of DE-CTCA was 4 mSv. The median CAC scoring of the patients was 589 (interquartile range 183-1085). The sensitivity, specificity, PPV, NPV, LR +, LR - and AUC for the detection of stenosis = 50% (per segment analysis; 711 segments) for SE-CTA were 93.8%, 90.7%, 71.7%, 98.3%, 10.1, 0.07 and 0.92; for DE-CTA 94.4%, 96.2%, 84.3%, 98.7%, 24.7, 0.05 and 0.95. Improvement of PPV, LR+ and in diagnostic performance was observed between techniques,  $p=0.006$ .

## CONCLUSION

s In symptomatic patients with intermediate to high likelihood of CAD, DE-CTCA showed a good diagnostic performance to identify obstructive disease with better diagnostic performance than SE-CTCA.

## CLINICAL RELEVANCE/APPLICATION

Dual Energy computed tomography coronary angiography emerged as a novel promising CT technology to attenuate some of the limitations related to the polychromatic nature of the x-rays (such as blooming artifact).

## M2-SPCA-3 Coronary Stent Image Quality with A Spectral Photon Counting CT: Initial Results in Humans

Participants

Sara Boccalini, MD, PhD, Lyon, France (*Presenter*) Nothing to Disclose

## PURPOSE

The aim of this study is to compare the image quality (IQ) of in-vivo coronary stents between a dual-energy dual-source CT (DECT) and a clinical prototype of Spectral Photon Counting CT (SPCCT).

## METHODS AND MATERIALS

In January-April 2021 patients with coronary stents were prospectively enrolled to undergo a coronary CT with a DECT (IQon, Philips) and a SPCCT (Philips). The study was approved by the local ethical committee and patients signed an informed consent. An acquisition with retrospective ECG gating was performed with optimized matching parameters on the two scanners (DECT: collimation=64x0.625, kV=120, mAs=255, dose modulation, rotation time=0.27; SPCCT: collimation=64x0.275, kV=120, mAs=255, rotation time=0.33). The injection protocol was the same on the two scanners: 65-75mL of Iomeron (Bracco) at 5mL/sec. Images were reconstructed with slice thickness of 0.67mm, 512 matrix, XCD kernel, iDose 3 for DECT and 0.25mm slice thickness, 1024 matrix and sharp kernel, iDose 6 for SPCCT. ROIs were drawn in the lumen of the stent and of the upstream coronary artery and the difference (?HU) between the respective values was calculated. Measures of the proximal and distal outer and inner diameter of the stents were used to quantify blooming artefacts. For subjective IQ, 2 experienced observers graded with a 4-point scale the image quality of different parameters: coronary wall before the stent, stent lumen, stent structure, calcifications surrounding the stent, beam hardening artefacts.

## RESULTS

7 patients (age: 69±5; all males; BMI: 25.9±2.1) with 14 stents were scanned. Two stents were not evaluable due to motion artifacts. Of the remaining, 7 were active stents of Platinum-Chromium (5 Synergy; 1 Promus) and Cobalt-Chromium (Ultimaster); for the others no information could be retrieved. Whereas HU values within the coronary arteries on the two scanners were similar ( $p=0.56$ ), the ?HU was higher for the DECT (median(IQ)=201(278) vs 112(59);  $p<0.01$ ). The mean external diameter of the stents was 4.5 vs 4mm and the internal 1.5 vs 2.2mm (without the 1 stent the internal diameter of which was not assessable on the DECT). Blooming artefacts were more pronounced on the DECT (69%(16) vs 48%(10);  $p<0.001$ ). SPCCT IQ had higher subjective scores for stent lumen, stent structure, surrounding calcifications and beam hardening (all  $p=0.001$ ). The IQ of the coronary wall scored higher as well, but not significantly (3 vs 2;  $p=0.19$ ).

## CONCLUSION

s SPCCT demonstrated improved objective and subjective image quality as compared to DECT for the evaluation of coronary stents.

## CLINICAL RELEVANCE/APPLICATION

Stent assessment remains a challenge of coronary CT. With its proven higher spatial resolution and artefacts reduction capabilities, SPCCT might overcome these limitations.

Printed on: 02/07/23

## Abstract Archives of the RSNA, 2022

M2-SPCA-1

### Photon-Counting CT Coronary Stent Imaging with Dedicated Ultra-Sharp Convolution Kernels: A Phantom Study

Monday, Nov. 28 9:00AM - 9:30AM Room: Learning Center - CA DPS

#### Participants

Bernhard Petritsch, MD, Wuerzburg, Germany (*Presenter*) Research Consultant, Siemens AG

#### PURPOSE

To assess the impact of different dedicated (ultra-) sharp vascular convolution kernels on quantitative and subjective image characteristics using a clinical photon-counting detector (PCD) CT system in comparison to a conventional energy-integrating detector (EID) CT system.

#### METHODS AND MATERIALS

In this phantom study, 10 different coronary stents (3.0 mm diameter) were expanded into plastic vessel phantoms filled with contrast agent. Stent-containing vessel phantoms were positioned in an anthropomorphic phantom (QRM) simulating a medium-sized patient. CT scans were acquired parallel to the scanners z-axis using a 1st generation PCD CT system (NAEOTOM Alpha, Siemens). Examinations were performed with two different scan-modes (standard-resolution [SR mode - 2x2 binning] and ultra-high-resolution [UHR mode- subpixels readout separately]). A state of the art EID CT system from the same vendor served as reference standard (SOMATOM Force, Siemens). CTDIvol matched images were reconstructed with identical reconstruction parameters using different convolution kernels (Bv59 [EID]; Bv60 [SR-PCD], Bv68 [SR + UHR-PCD], Bv84 [UHR-PCD]). In-stent lumen visibility (%), image noise (HU), and subjective image quality (IQ) (Likert scale 1-4) were assessed.

#### RESULTS

PCD-UHR mode in Bv84 achieved highest in-stent lumen visibility and best subjective IQ [=1] while PCD-SR mode in Bv60 provided lowest noise levels and comparable IQ [=3] to the EID CT. In-stent lumen visibility was significantly higher ( $p<0.001$ ) with PCD UHR in Bv68 (73.3%) [IQ=2], and PCD UHR in Bv84 (83.3%) when compared to conventional EID (60.0%). Image noise of PCD CT was significantly lower ( $p<0.001$ ) for Bv60 SR (24 HU), and Bv68 UHR (27 HU) mode compared to conventional EID images (66 HU). The ultra sharp Bv84 kernel provided similar ( $p=1.000$ ) noise levels (68 HU) as conventional Bv59 EID images.

#### CONCLUSION

In an in vitro setting, the combination of PCD CT and ultra-sharp convolution kernels provides superior in-stent lumen visibility and subjective image quality at identical (Bv84) or even lower (Bv68) noise levels when compared to conventional EID CT technology.

#### CLINICAL RELEVANCE/APPLICATION

PCD CT allows for improved assessment of coronary artery stents and potentially in-stent restenosis in particular, respectively.

Printed on: 02/07/23

## Abstract Archives of the RSNA, 2022

M2-SPCA-2

### Dual Energy versus Single Energy Coronary CT Angiography for The Evaluation of Coronary Artery Disease

Monday, Nov. 28 9:00AM - 9:30AM Room: Learning Center - CA DPS

#### Participants

Carlos Capunay, MD, Vicente Lopez, Argentina (*Presenter*) Nothing to Disclose

#### PURPOSE

To explore the diagnostic performance of dual energy CT coronary angiography (DE-CTCA) in comparison with single energy CTCA (SE-CTCA) in patients with intermediate to high likelihood of coronary artery disease (CAD) referred to invasive coronary angiography (ICA).

#### METHODS AND MATERIALS

Study protocol include consecutive symptomatic patients with suspected CAD referred for ICA who underwent DE-CTCA and a coronary artery calcium scoring (CACS) within the month before the ICA. DE-CTCA was analyzed in a polychromatic fashion to resemble a SE-CTCA and using monochromatic images at 85 keV to reduce blooming artifact. Two blinded experienced observers (O) analyzed the images. O1 analyzed DE-CTCA and O2 analyzed the equivalent SE-CTCA group of images. Stenosis over 50% were considered a positive finding. The 95% confidence interval for the proportions were calculated by the exact binomial method. ROC curve analyses were performed using specific software for ROC analysis. Pairwise comparison of ROC curves were performed using the method of DeLong et al. for detection of differences between two AUC, and calculated the binomial exact confidence interval for the AUC. A two-sided p value of less than 0.05 indicated statistical significance.

#### RESULTS

Fifty patients were included, mean age 63 years-old; 70% male. The mean effective radiation dose of DE-CTCA was 4 mSv. The median CAC scoring of the patients was 589 (interquartile range 183-1085). The sensitivity, specificity, PPV, NPV, LR +, LR - and AUC for the detection of stenosis = 50% (per segment analysis; 711 segments) for SE-CTA were 93.8%, 90.7%, 71.7%, 98.3%, 10.1, 0.07 and 0.92; for DE-CTA 94.4%, 96.2%, 84.3%, 98.7%, 24.7, 0.05 and 0.95. Improvement of PPV, LR+ and in diagnostic performance was observed between techniques, p=0.006.

#### CONCLUSION

In symptomatic patients with intermediate to high likelihood of CAD, DE-CTCA showed a good diagnostic performance to identify obstructive disease with better diagnostic performance than SE-CTCA.

#### CLINICAL RELEVANCE/APPLICATION

Dual Energy computed tomography coronary angiography emerged as a novel promising CT technology to attenuate some of the limitations related to the polychromatic nature of the x-rays (such as blooming artifact).

Printed on: 02/07/23

## Abstract Archives of the RSNA, 2022

M2-SPCA-3

### Coronary Stent Image Quality with A Spectral Photon Counting CT: Initial Results in Humans

Monday, Nov. 28 9:00AM - 9:30AM Room: Learning Center - CA DPS

#### Participants

Sara Boccalini, MD, PhD, Lyon, France (*Presenter*) Nothing to Disclose

#### PURPOSE

The aim of this study is to compare the image quality (IQ) of in-vivo coronary stents between a dual-energy dual-source CT (DECT) and a clinical prototype of Spectral Photon Counting CT (SPCCT).

#### METHODS AND MATERIALS

In January-April 2021 patients with coronary stents were prospectively enrolled to undergo a coronary CT with a DECT (IQon, Philips) and a SPCCT (Philips). The study was approved by the local ethical committee and patients signed an informed consent. An acquisition with retrospective ECG gating was performed with optimized matching parameters on the two scanners (DECT: collimation=64x0.625, kV=120, mAs=255, dose modulation, rotation time=0.27; SPCCT: collimation=64x0.275, kV=120, mAs=255, rotation time=0.33). The injection protocol was the same on the two scanners: 65-75mL of Iomeron (Bracco) at 5mL/sec. Images were reconstructed with slice thickness of 0.67mm, 512 matrix, XCD kernel, iDose 3 for DECT and 0.25mm slice thickness, 1024 matrix and sharp kernel, iDose 6 for SPCCT. ROIs were drawn in the lumen of the stent and of the upstream coronary artery and the difference (?HU) between the respective values was calculated. Measures of the proximal and distal outer and inner diameter of the stents were used to quantify blooming artefacts. For subjective IQ, 2 experienced observers graded with a 4-point scale the image quality of different parameters: coronary wall before the stent, stent lumen, stent structure, calcifications surrounding the stent, beam hardening artefacts.

#### RESULTS

7 patients (age: 69±5; all males; BMI: 25.9±2.1) with 14 stents were scanned. Two stents were not evaluable due to motion artifacts. Of the remaining, 7 were active stents of Platinum-Chromium (5 Synergy; 1 Promus) and Cobalt-Chromium (Ultimaster); for the others no information could be retrieved. Whereas HU values within the coronary arteries on the two scanners were similar (p=0.56), the ?HU was higher for the DECT (median(IQ)=201(278) vs 112(59); p<0.01). The mean external diameter of the stents was 4.5 vs 4mm and the internal 1.5 vs 2.2mm (without the 1 stent the internal diameter of which was not assessable on the DECT). Blooming artefacts were more pronounced on the DECT (69%(16) vs 48%(10); p<0.001). SPCCT IQ had higher subjective scores for stent lumen, stent structure, surrounding calcifications and beam hardening (all p=0.001). The IQ of the coronary wall scored higher as well, but not significantly (3 vs 2; p=0.19).

#### CONCLUSION

s SPCCT demonstrated improved objective and subjective image quality as compared to DECT for the evaluation of coronary stents.

#### CLINICAL RELEVANCE/APPLICATION

Stent assessment remains a challenge of coronary CT. With its proven higher spatial resolution and artefacts reduction capabilities, SPCCT might overcome these limitations.

Printed on: 02/07/23

## Abstract Archives of the RSNA, 2022

M2-SPCH

### Chest Monday Poster Discussions

Monday, Nov. 28 9:00AM - 9:30AM Room: Learning Center - CH DPS

#### Sub-Events

#### M2-SPCH-1 CT Findings of Systemic Sclerosis: Precise Radiologic-pathologic Correlation in 29 Patients

##### Participants

Taiki Fukuda, MD, PhD, Tokyo, Japan (*Presenter*) Nothing to Disclose

##### PURPOSE

There has been no report of a precise radiologic-pathologic correlation of systemic sclerosis-related interstitial lung disease (SSc-ILD). Moreover, despite the early therapeutic intervention is desirable, early CT findings of SSc-ILD has been still unclear. The purposes of this study were two-fold; (1) To decide pathological backgrounds of CT findings of SSc-ILD and (2) To clarify the early CT findings and their pathological features.

##### METHODS AND MATERIALS

Twenty-nine patients with SSc-ILD diagnosed by surgical lung biopsy (SLB) were enrolled. A total of 82 specimens were obtained. The histological findings of each specimen were correlated with the corresponding CT side by side by two radiologists and two pathologists. Whole lung CT was evaluated by the other two radiologists, independently. Early CT findings were extracted from the whole lung CT according to the rationale that diseases with lower lobe predominance show their early findings in more upper zones. Their pathological findings were examined from the area of SLB which corresponded to early CT findings.

##### RESULTS

Pathologically, non-specific interstitial pneumonia was diagnosed in 18 cases, while usual interstitial pneumonia and fibrosing organizing pneumonia were diagnosed in 9 and 2 cases respectively. Emphysematous change was pathologically observed in 19 cases and identified on CT in 11 cases. Four of those were non-smokers. Pathologically, vascular wall thickening was observed in 14 cases. Small faint nodules superimposed on amorphous ground-glass opacity within 1 cm from the pleura, which we term faint amorphous opacity (FAC), were present in 18 cases, particularly in the anterolateral upper lobes. FAC pathologically corresponded to either peribronchial metaplasia, centriacinar mucostasis or periacinar alveolar septal fibrosis.

##### CONCLUSION

Pathological detectability of the emphysematous changes was superior to CT. Vasculopathy might be another cause of emphysema other than smoking. FAC could be an early CT finding of SSc-ILD, representing either peribronchial metaplasia, centriacinar mucostasis, or periacinar alveolar septal fibrosis pathologically.

##### CLINICAL RELEVANCE/APPLICATION

Understanding the pathological features of SSc-ILD will help to analyze the pathogenesis and determine the disease progression on CT. The aforementioned early CT finding may allow a more accurate diagnosis of SSc-ILD and prompt therapeutic intervention.

#### M2-SPCH-2 Radiologic Predictors of Pulmonary Hypertension in Patients with Fibrosing Interstitial Lung Disease

##### Participants

Lubna Siddiqi, MD, (*Presenter*) Nothing to Disclose

##### PURPOSE

The development of pulmonary hypertension (PH) in fibrosing ILD is associated with significantly shorter survival. Currently, risk stratification for PH is exclusively based on clinical and echocardiographic findings. We sought to use objective values from CT imaging to predict the presence of associated pulmonary hypertension in patients with fibrosing interstitial lung disease (ILD).

##### METHODS AND MATERIALS

An initial 128 patients with fibrosing ILD followed at the London Health Sciences Centre underwent right heart catheterization (RHC). Of these, 94 patients (66 male, 28 female, with average age of 66.2) with CT thorax within 6 months of RHC were assessed for main pulmonary artery to aorta ratio (MPA:AO), right to left ventricular ratio (RV:LV), caliber of the right and left pulmonary arteries, interventricular septal thickness, and right ventricular wall thickness, as well as the presence of pulmonary thromboembolic disease and degree of mosaic attenuation. PH was defined as a mean pulmonary arterial pressure (mPAP)  $\geq$  25 mmHg on RHC. Radiologic data were then analyzed using stepwise regression analysis to determine the best predictors of associated PH. Results were adjusted for sex, BMI, and age.

##### RESULTS

Thirty-eight patients (40%) underwent RHC electively and 56 (60%) as part of a lung transplant (LTx) assessment. Average mPAP was 25 $\pm$ 6 mmHg, wedge pressure 9 $\pm$ 4 mmHg, cardiac output 5.0 $\pm$ 1.0 L/min and pulmonary vascular resistance 3.3 $\pm$ 1.4 Wood units.

Sixty-six patients (70%) had PH. Among patients with PH, average mPAP was  $38\pm 11$  mmHg and PVR was  $5.7\pm 2.6$  Wood Units. On stepwise multiple regression analysis, MPA and RV diameter were independent and significant predictors of PVR (F ratio 6.64 and 6.32, p-values 0.0137 and 0.0159 respectively). Importantly, the correlation between MPA and RV was weak (Spearman's rank 0.17, not significant), with no collinearity observed. MPA was also a significant predictor of mPAP (F ratio 11.5, p-value 0.0015).

## CONCLUSION

The presence of associated PH has a significant impact on the appearance of CT thorax in fibrosing ILD. Both MPA and RV diameter are predictors of PH. A combination of radiologic parameters obtained from CT thorax may be used to reliably risk stratify patients with fibrosing ILD for the presence and severity of associated PH. We will seek validation of these data in a separate cohort of patients.

## CLINICAL RELEVANCE/APPLICATION

In patients with fibrosing ILD, a combination of radiologic parameters may be used to predict the presence and severity of PH and to guide clinical decisions on RHC, LTx assessment and prognosis. These parameters could be especially helpful in populations for whom RHC is not readily available, or is a contraindication.

### M2-SPCH-3 Deep Learning-based Fibrosis Quantification on Chest CT as a Prognostic Predictor in Patient with Idiopathic Pulmonary Fibrosis

Participants

Ju Gang Nam, MD, Seoul, Korea, Republic Of (*Presenter*) Research Grant, VUNO Inc

## PURPOSE

Radiology plays a crucial role in the diagnosis and management of patients with idiopathic pulmonary fibrosis (IPF), however, degree of fibrosis on CT is not easy to be quantified and thus seldom used as an objective prognostic factor. We aimed to explore prognostic value of the CT-quantified degree of lung fibrosis using a commercial deep learning software.

## METHODS AND MATERIALS

Patients diagnosed with IPF and underwent nonenhanced chest CT and spirometry within 3 months in between 2005-2009 were retrospectively collected from a single institution, and their overall survival information were documented. Proportions of normal lung volume (CT-Norm%) and fibrotic lung volume (CT-Fib%), including reticular opacities and honeycombing, were calculated on chest CT using a commercial deep learning software. Correlation of CT-Norm% and CT-fib% with spirometry results including forced vital capacity (FVC) and diffusion capacity of carbon monoxide (DLCO) were calculated. The multivariable-adjusted hazard ratios (aHRs) of CT-Norm% and CT-Fib% were evaluated with clinical prognostic factors using the Cox regression. Survival prediction performances of modified GAP indices utilizing CT-norm% (CTNorm%-GAP) or CT-fib% (CTFib%-GAP) instead of DLCO were evaluated using Harrell C index at 5-year and compared with that of original GAP index.

## RESULTS

A total of 170 patients (median age [interquartile range], 68 years [62-73]; 104 men) were evaluated. CT-Norm% and CT-Fib% showed significant correlation with FVC (Pearson coefficient, 0.40 [95% CI; 0.25, 0.52;  $P<.001$ ] for CT-Norm% and -0.37 [-0.47, -0.24;  $P<.001$ ] for CT-Fib%) and DLCO (0.52 [0.43, 0.60;  $P<.001$ ] for CT-Norm% and -0.46 [-0.56, -0.33;  $P<.001$ ] for CT-Fib%). On multivariable Cox regression, both CT-Norm% and CT-Fib% worked as independent survival predictors when adjusted to age, sex, smoking status, comorbidities of chronic diseases, FVC, and DLCO (aHRs per 1% increment, 0.98 [0.97, 0.99;  $P=.002$ ] for CT-Norm% and 1.03 [1.01, 1.05;  $P=.01$ ] for CT-Fib%). Modified GAP indices showed comparable C indices compared with the original GAP index without information of DLCO (CTNorm%-GAP vs. GAP, 0.76 vs. 0.75;  $P=.89$  and CTFib%-GAP vs. GAP, 0.77 vs. 0.75;  $P=.27$ ).

## CONCLUSION

Normal lung and fibrotic lung proportions calculated from chest CT-based deep learning algorithm worked as independent predictors of the patients' overall survival. Modified GAP indices showed comparable survival prediction performance to the original GAP index.

## CLINICAL RELEVANCE/APPLICATION

Predicting prognosis is important in determining treatment options and follow-up intervals in patients with IPF. Automatic CT quantification using deep learning may provide additional prognostic information in routine practice.

### M2-SPCH-4 Generalized Lymphatic Anomaly of The Chest: Pathological Subtypes and Imaging Manifestations

Participants

Qi Hao, Beijing, China (*Presenter*) Nothing to Disclose

## PURPOSE

Generalized lymphatic Abnormal(GLA) is a complex type of lymphatic malformation or lymphangiomas characterized by diffuse or multiple organ involvement. This study is to analyze retrospectively the imaging manifestations of three subtypes of GLA in the chest.

## METHODS AND MATERIALS

From June 2006 to March 2020, 86 patients with GLA in our hospital were collected, including 37 males and 49 females, aged from 1 month to 58 years (median age 15.8). All patients underwent X-ray film, CT scan and ultrasound examination, 76 MRI or MRL in 76, 62 direct lymphangiography and MSCT lymphangiography in 62, and Nuclide lymphoscintigraphy in 57. Follow up for two years, 5 cases died 32 cases (37.2%) died and 54 cases (62.8%) had poor prognosis.

## RESULTS

According to the clinical and imaging features, 86 GLAs were divided into three subtypes: kaposiform lymphangiomas(KIA, n=32), multifocal Lymphangiomas (ML,n=36), giant complex Lymphangiomas (GCL, n=18). The imaging features included: (1) 80 cases (93%) with abnormal mediastinum, including thickening and turbidity of mediastinum (n=39, 32/KIA,5/ML,2/GCL); thin-walled cystic cavity (n=24, 24/ML) and huge mixed cystic lesions(n=17, 16/GCL, 1/ML); (2) pulmonary lesions (n=49, 32/KIA, 9/ML, 8/GCL),

including thickening of bronchovascular bundle and interlobular septum (n=46, 32/KIA, 11/ML, 3/GCL, P<0.05), GGO (n=42, 32/KIA, 7/ML, 3/GCL, P<0.05), consolidation shadow (n=17, 13/KIA, 1/ML, 3/GCL, P<0.05), and cystic nodules or masses (n=12, 5/KIA, 7/ML); (3) pleural or extrapleural and chest wall lesions (n=72, 30/KIA, 31/ML, 11/GCL); (4) osteo-lesions (n=31, 9/KIA, 18/ML, 4/GCL, P<0.05).

## CONCLUSION

The three subtypes of GLA have different clinical manifestations, imaging types and histopathological features. Multimodality image are important methods for accurate diagnosis, staging and grading evaluation of lymphatic diseases.

## CLINICAL RELEVANCE/APPLICATION

Multimodality image are important methods for accurate diagnosis of the three subtypes of GLA.

## M2-SPCH-5 What Happens when Artificial Intelligence (AI) Feedback Is Wrong? A Multi-reader Pilot Study Examining the Human Factors of AI Implementation

Participants

Grayson Baird, PhD, Providence, RI (*Presenter*) Nothing to Disclose

## PURPOSE

To examine whether incorrect AI feedback impacts radiologist performance, and if so, whether human factors can be optimized to reduce error.

## METHODS AND MATERIALS

A prospective multi-reader design was used, where 6 radiologists interpreted 90 identical chest radiographs (follow-up CT needed: yes/no) on four occasions from 09/20 to 01/22. Sessions were separated by a minimum of 1 month, and the order of chest radiographs was identical in each session. In session 1, the radiologist interpreted images without AI. Sham AI feedback was provided for sessions 2-4, and 12 cases were manipulated to be incorrect (8 False Positives [FP], 4 False Negatives [FN]) (.87 ROCAUC). Radiologists anticipated a performance evaluation. In the Delete AI (No Box) condition, radiologists were told AI results would not be saved for the evaluation. In Keep AI (No Box) and Keep AI (Box), radiologists were told results would be saved. Radiologists were told these instructions were analogous to keeping or deleting AI feedback in the patient's record. In Keep AI (Box), the ostensible AI program visually outlined the region of suspicion. AI feedback was constant between conditions. FP and FN rates for the 12 erroneous cases were examined between conditions using generalized linear mixed modeling (GLMM) assuming a binary distribution.

## RESULTS

Relative to the No AI condition (FN=2.7%, FP=51.4%), FN and FP rates were higher in the Keep AI (No Box) (FN=33.0%, FP=86.0%), Delete AI (No Box) (FN=26.7%, FP=80.5%), and Keep AI (Box) conditions (FN= 20.7%, FP=80.5%), all  $p < .05$ . FN rates were higher in the Keep AI (No Box) condition (33.0%) than the Keep AI (Box) condition (20.7%),  $p = .04$ . FP rates were higher in the Keep AI (No Box) (86.0%) condition than the Delete AI (No Box) condition (80.5%),  $p = .03$ .

## CONCLUSION

Incorrect AI causes radiologists to make incorrect follow-up decisions when they were correct without AI. This effect is mitigated when a box is provided around the region of interest and when AI feedback is deleted from the patient's record. Human factors for AI implementation are important.

## CLINICAL RELEVANCE/APPLICATION

AI is often right but sometimes wrong. To maximize patient outcomes, we must consider how to prevent radiologists from being influenced by incorrect feedback.

## M2-SPCH-6 Prevalence and Long-term Outcome of Interstitial Lung Abnormality in the Asian Health-screening Population: A Multicenter Study

Participants

Seolbin Park, MD, Gwangju, Korea, Republic Of (*Presenter*) Nothing to Disclose

## PURPOSE

To investigate interstitial lung abnormality (ILA) prevalence in the Asian health-screening population and determine rates and risks for disease progression, lung cancer development, and 10-year mortality.

## METHODS AND MATERIALS

This observational, retrospective, multicenter study included subjects = 50 years old who underwent chest computed tomography (CT) at three health screening centers over a 4-year period (2007 - 2010). ILA status was classified as none, equivocal ILA, and ILA, and ILA was further subcategorized into non-fibrotic or fibrotic ILA. Progression was evaluated between baseline and last follow-up CT. Kaplan-Meier analysis with the log-rank test was performed to estimate mortality according to ILA status. Cox proportional hazards models were used to assess factors associated with ILA progression, lung cancer development, and mortality.

## RESULTS

In total, 2,765 subjects who underwent health screening chest CT were identified (mean age, 59±7 years; 2,068 men). Of the 2,765 subjects, 94 (3%) had a finding of ILA (35 non-fibrotic and 59 fibrotic ILA), and 119 (4%) had a finding of equivocal ILA. The mean follow-up period was approximately 12 years, and ILA progression was observed in 85% (34/40) of fibrotic ILA patients and 70% (14/20) of non-fibrotic ILA patients. Kaplan-Meier analysis showed subjects with ILA had a significantly higher mortality rate than those without ILA ( $P < .05$ ). Multivariate Cox proportional hazards analysis revealed that fibrotic ILA was significantly associated with ILA progression (hazard ratio [HR], 10.3; 95% confidence interval [CI], 6.4-16.4;  $P < .001$ ) and lung cancer development (HR, 4.4, 95% CI, 2.1-9.1;  $P < .001$ ). Furthermore, subjects with fibrotic ILA had a significantly higher risk of disease-specific mortality (HR, 6.7; 95% CI, 3.6-12.2;  $P < .001$ ) and all-cause mortality (HR, 2.5; 95% CI, 1.6 - 3.8;  $P < .001$ ) than those without ILA.

## CONCLUSION

s The prevalence of ILA in the Asian health-screening population was approximately 3%, and fibrotic ILA was an independent risk factor for disease progression, lung cancer development, and mortality over a 10-year follow-up period.

## CLINICAL RELEVANCE/APPLICATION

Our study reveals ILA prevalence in the Asian health-screening population and demonstrates the association between ILAs and long-term outcomes.

### **M2-SPCH-7 Survival Impact of Incidental Abnormalities on Screening Thoracic Computed Tomography: Long-term Follow-up Analysis**

Participants

Jaehyun Park, MD, Gwangju, Korea, Republic Of (*Presenter*) Nothing to Disclose

## PURPOSE

The present study aimed to assess the association between long-term mortality and incidental abnormalities on thoracic computed tomography (CT) among the general screening population.

## METHODS AND MATERIALS

We retrospectively collected the medical records and CT images of subjects who visited a single health promotion center between 2007 and 2010. Two thoracic radiologists independently reviewed all CT images and evaluated incidental abnormalities by visual assessment, which is interstitial lung abnormality (ILA), emphysema, and coronary artery calcification (CAC). Kaplan-Meier analysis was performed using a log-rank test to evaluate the association between incidental CT abnormalities and mortality. A Cox proportional hazards model was used to analyze the association factors between incidental CT abnormalities and mortality.

## RESULTS

A total of 859 subjects were identified ( $59 \pm 6.7$  years of age, 582 men). The median follow-up time was approximately 10.9 years. Of the 859 subjects, 57 (6.6%), 318 (37%), and 178 (21%) had findings of ILA, CAC, and emphysema, respectively. Subjects with fibrotic ILA, CAC of any degree, and emphysema of any degree exhibited significantly higher mortality during Kaplan-Meier analysis with the log-rank test ( $p < 0.05$ ). A multivariate Cox proportional hazards model revealed that fibrotic ILAs were independently associated with higher mortality (hazard ratio, 2.59, [95% confidence interval, 1.07-6.27],  $p = 0.035$ ) among the incidental CT abnormalities and clinically relevant factors.

## CONCLUSION

s Incidental abnormalities on screening thoracic CT were associated with an increased hazard of mortality in the general screening population. Fibrotic ILAs in particular were independently associated with increased hazard of mortality compared to other incidental CT abnormalities.

## CLINICAL RELEVANCE/APPLICATION

Our study reveals the relationship between incidental abnormalities found in screening thoracic CT and long-term mortality.

### **M2-SPCH-8 Post-COVID-19 Interstitial Lung Disease (PC-ILD): The Role of Lung Imaging and Pulmonary Function Testing in The Long-term Follow-up of Patients with COVID-19 Pneumonia**

Participants

Emanuele Messina, MD, Roma, Italy (*Presenter*) Nothing to Disclose

## PURPOSE

Post COVID-19 Interstitial Lung Disease (PC-ILD) is characterized by fibrotic-like signs at High Resolution Computed Tomography (HRCT) and Pulmonary Function Tests (PFTs) abnormalities after SARS-CoV-2 infection. It is still not clear how frequent these tests should be performed to rule out long-term consequences of COVID-19 pneumonia. The aims of our study are to evaluate the incidence and risk factors of PC-ILD and possibly to propose a long-term follow-up program.

## METHODS AND MATERIALS

In this prospective single-center study, 100 patients, hospitalized in our ward for moderate to critical COVID-19, underwent two follow-up visits at 3 and 15 months, performing HRCT and PFTs.

## RESULTS

At 3-month follow up, HRCTs showed that lung parenchymal abnormalities were still present in 22% of patients, mainly consisting in ground glass opacities (GGO) and fibrotic-like alterations (63% and 78%, respectively); 37% showed PFTs abnormalities consistent with PC-ILD. 48 patients underwent the 15-month follow up: at HRCT, residual fibrotic-like abnormalities were found in 40% of patients with almost complete reduction of GGO and consolidation; at PFTs, 33.3% showed residual respiratory functional impairment (PC-ILD); 8% of patients showed residual radiological and functional signs consistent with PC-ILD. All but one of these patients had already demonstrated PFTs and HRCT alterations at first follow-up visit, the last one patient showed worsening of lung function during follow up.

## CONCLUSION

s These findings highlight the negative predictive value of HRCT and PFTs at three months follow-up for the development of PC-ILD. Ageing, severity of COVID-19 and degree of pulmonary involvement during acute infection proved to be significant risk factors for developing PC-ILD. Our study highlights the importance of PFTs in the long-term follow-up of patients affected by moderate to critical COVID-19 pneumonia. HRCT should be obtained in those patients still presenting PFTs abnormalities at 15 months.

## CLINICAL RELEVANCE/APPLICATION

This is the first study investigating such a long-term follow up with HRCT and PFTs, at fifteen months.



## Abstract Archives of the RSNA, 2022

M2-SPCH-1

### CT Findings of Systemic Sclerosis: Precise Radiologic-pathologic Correlation in 29 Patients

Monday, Nov. 28 9:00AM - 9:30AM Room: Learning Center - CH DPS

#### Participants

Taiki Fukuda, MD, PhD, Tokyo, Japan (*Presenter*) Nothing to Disclose

#### PURPOSE

There has been no report of a precise radiologic-pathologic correlation of systemic sclerosis-related interstitial lung disease (SSc-ILD). Moreover, despite the early therapeutic intervention is desirable, early CT findings of SSc-ILD has been still unclear. The purposes of this study were two-fold; (1) To decide pathological backgrounds of CT findings of SSc-ILD and (2) To clarify the early CT findings and their pathological features.

#### METHODS AND MATERIALS

Twenty-nine patients with SSc-ILD diagnosed by surgical lung biopsy (SLB) were enrolled. A total of 82 specimens were obtained. The histological findings of each specimen were correlated with the corresponding CT side by side by two radiologists and two pathologists. Whole lung CT was evaluated by the other two radiologists, independently. Early CT findings were extracted from the whole lung CT according to the rationale that diseases with lower lobe predominance show their early findings in more upper zones. Their pathological findings were examined from the area of SLB which corresponded to early CT findings.

#### RESULTS

Pathologically, non-specific interstitial pneumonia was diagnosed in 18 cases, while usual interstitial pneumonia and fibrosing organizing pneumonia were diagnosed in 9 and 2 cases respectively. Emphysematous change was pathologically observed in 19 cases and identified on CT in 11 cases. Four of those were non-smokers. Pathologically, vascular wall thickening was observed in 14 cases. Small faint nodules superimposed on amorphous ground-glass opacity within 1 cm from the pleura, which we term faint amorphous opacity (FAC), were present in 18 cases, particularly in the anterolateral upper lobes. FAC pathologically corresponded to either peribronchial metaplasia, centriacinar mucostasis or periacinar alveolar septal fibrosis.

#### CONCLUSION

s Pathological detectability of the emphysematous changes was superior to CT. Vasculopathy might be another cause of emphysema other than smoking. FAC could be an early CT finding of SSc-ILD, representing either peribronchial metaplasia, centriacinar mucostasis, or periacinar alveolar septal fibrosis pathologically.

#### CLINICAL RELEVANCE/APPLICATION

Understanding the pathological features of SSc-ILD will help to analyze the pathogenesis and determine the disease progression on CT. The aforementioned early CT finding may allow a more accurate diagnosis of SSc-ILD and prompt therapeutic intervention.

Printed on: 02/07/23

## Abstract Archives of the RSNA, 2022

M2-SPCH-2

### Radiologic Predictors of Pulmonary Hypertension in Patients with Fibrosing Interstitial Lung Disease

Monday, Nov. 28 9:00AM - 9:30AM Room: Learning Center - CH DPS

#### Participants

Lubna Siddiqi, MD, (*Presenter*) Nothing to Disclose

#### PURPOSE

The development of pulmonary hypertension (PH) in fibrosing ILD is associated with significantly shorter survival. Currently, risk stratification for PH is exclusively based on clinical and echocardiographic findings. We sought to use objective values from CT imaging to predict the presence of associated pulmonary hypertension in patients with fibrosing interstitial lung disease (ILD).

#### METHODS AND MATERIALS

An initial 128 patients with fibrosing ILD followed at the London Health Sciences Centre underwent right heart catheterization (RHC). Of these, 94 patients (66 male, 28 female, with average age of 66.2) with CT thorax within 6 months of RHC were assessed for main pulmonary artery to aorta ratio (MPA:Ao), right to left ventricular ratio (RV:LV), caliber of the right and left pulmonary arteries, interventricular septal thickness, and right ventricular wall thickness, as well as the presence of pulmonary thromboembolic disease and degree of mosaic attenuation. PH was defined as a mean pulmonary arterial pressure (mPAP)  $\geq$ 25 mmHg on RHC. Radiologic data were then analyzed using stepwise regression analysis to determine the best predictors of associated PH. Results were adjusted for sex, BMI, and age.

#### RESULTS

Thirty-eight patients (40%) underwent RHC electively and 56 (60%) as part of a lung transplant (LTx) assessment. Average mPAP was  $25 \pm 6$  mmHg, wedge pressure  $9 \pm 4$  mmHg, cardiac output  $5.0 \pm 1.0$  L/min and pulmonary vascular resistance  $3.3 \pm 1.4$  Wood units. Sixty-six patients (70%) had PH. Among patients with PH, average mPAP was  $38 \pm 11$  mmHg and PVR was  $5.7 \pm 2.6$  Wood Units. On stepwise multiple regression analysis, MPA and RV diameter were independent and significant predictors of PVR (F ratio 6.64 and 6.32, p-values 0.0137 and 0.0159 respectively). Importantly, the correlation between MPA and RV was weak (Spearman's rank 0.17, not significant), with no collinearity observed. MPA was also a significant predictor of mPAP (F ratio 11.5, p-value 0.0015).

#### CONCLUSION

The presence of associated PH has a significant impact on the appearance of CT thorax in fibrosing ILD. Both MPA and RV diameter are predictors of PH. A combination of radiologic parameters obtained from CT thorax may be used to reliably risk stratify patients with fibrosing ILD for the presence and severity of associated PH. We will seek validation of these data in a separate cohort of patients.

#### CLINICAL RELEVANCE/APPLICATION

In patients with fibrosing ILD, a combination of radiologic parameters may be used to predict the presence and severity of PH and to guide clinical decisions on RHC, LTx assessment and prognosis. These parameters could be especially helpful in populations for whom RHC is not readily available, or is a contraindication.

Printed on: 02/07/23

## Abstract Archives of the RSNA, 2022

M2-SPCH-3

### Deep Learning-based Fibrosis Quantification on Chest CT as a Prognostic Predictor in Patient with Idiopathic Pulmonary Fibrosis

Monday, Nov. 28 9:00AM - 9:30AM Room: Learning Center - CH DPS

#### Participants

Ju Gang Nam, MD, Seoul, Korea, Republic Of (*Presenter*) Research Grant, VUNO Inc

#### PURPOSE

Radiology plays a crucial role in the diagnosis and management of patients with idiopathic pulmonary fibrosis (IPF), however, degree of fibrosis on CT is not easy to be quantified and thus seldom used as an objective prognostic factor. We aimed to explore prognostic value of the CT-quantified degree of lung fibrosis using a commercial deep learning software.

#### METHODS AND MATERIALS

Patients diagnosed with IPF and underwent nonenhanced chest CT and spirometry within 3 months in between 2005-2009 were retrospectively collected from a single institution, and their overall survival information were documented. Proportions of normal lung volume (CT-Norm%) and fibrotic lung volume (CT-Fib%), including reticular opacities and honeycombing, were calculated on chest CT using a commercial deep learning software. Correlation of CT-Norm% and CT-fib% with spirometry results including forced vital capacity (FVC) and diffusion capacity of carbon monoxide (DLCO) were calculated. The multivariable-adjusted hazard ratios (aHRs) of CT-Norm% and CT-Fib% were evaluated with clinical prognostic factors using the Cox regression. Survival prediction performances of modified GAP indices utilizing CT-norm% (CTNorm%-GAP) or CT-fib% (CTFib%-GAP) instead of DLCO were evaluated using Harrell C index at 5-year and compared with that of original GAP index.

#### RESULTS

A total of 170 patients (median age [interquartile range], 68 years [62-73]; 104 men) were evaluated. CT-Norm% and CT-Fib% showed significant correlation with FVC (Pearson coefficient, 0.40 [95% CI; 0.25, 0.52; P<.001] for CT-Norm% and -0.37 [-0.47, -0.24; P<.001] for CT-Fib%) and DLCO (0.52 [0.43, 0.60; P<.001] for CT-Norm% and -0.46 [-0.56, -0.33; P<.001] for CT-Fib%). On multivariable Cox regression, both CT-Norm% and CT-Fib% worked as independent survival predictors when adjusted to age, sex, smoking status, comorbidities of chronic diseases, FVC, and DLCO (aHRs per 1% increment, 0.98 [0.97, 0.99; P=.002] for CT-Norm% and 1.03 [1.01, 1.05; P=.01] for CT-Fib%). Modified GAP indices showed comparable C indices compared with the original GAP index without information of DLCO (CTNorm%-GAP vs. GAP, 0.76 vs. 0.75; P=.89 and CTFib%-GAP vs. GAP, 0.77 vs. 0.75; P=.27).

#### CONCLUSION

s Normal lung and fibrotic lung proportions calculated from chest CT-based deep learning algorithm worked as independent predictors of the patients' overall survival. Modified GAP indices showed comparable survival prediction performance to the original GAP index.

#### CLINICAL RELEVANCE/APPLICATION

Predicting prognosis is important in determining treatment options and follow-up intervals in patients with IPF. Automatic CT quantification using deep learning may provide additional prognostic information in routine practice.

Printed on: 02/07/23

## Abstract Archives of the RSNA, 2022

M2-SPCH-4

### Generalized Lymphatic Anomaly of The Chest: Pathological Subtypes and Imaging Manifestations

Monday, Nov. 28 9:00AM - 9:30AM Room: Learning Center - CH DPS

#### Participants

Qi Hao, Beijing, China (*Presenter*) Nothing to Disclose

#### PURPOSE

Generalized lymphatic Abnormal(GLA) is a complex type of lymphatic malformation or lymphangiomatosis characterized by diffuse or multiple organ involvement. This study is to annlysis retrospectively the imaging manifestations of three subtypes of GLA in the chest.

#### METHODS AND MATERIALS

From June 2006 to March 2020, 86 patients with GLA in our hospital were collected, including 37 males and 49 females, aged from 1 month to 58 years (median age 15.8). All patients underwent X-ray film, CT scan and ultrasound examination, 76 MRI or MRL in 76, 62 direct lymphangiography and MSCT lymphangiography in 62, and Nuclide lymphoscintigraphy in 57. Follow up for two years, 5 cases died 32 cases (37.2%) died and 54 cases (62.8%) had poor prognosis.

#### RESULTS

According to the clinical and imaging features, 86 GLAs were divided into three subtypes: kaposiform lymphangiomatosis(KIA, n=32), multifocal Lymphangiomas (ML,n=36), giant complex Lymphangiomas (GCL, n=18). The imaging features included: (1) 80 cases (93%) with abnormal mediastinum, including thickening and turbidity of mediastinum (n=39, 32/KIA,5/ML,2/GCL); thin-walled cystic cavity (n=24, 24/ML) and huge mixed cystic lesions(n=17, 16/GCL, 1/ML); (2) pulmonary lesions (n=49, 32/KIA, 9/ML, 8/GCL), including thickening of bronchovascular bundle and interlobular septum (n=46, 32/KIA, 11/ML, 3/GCL, P<0.05), GGO (n=42, 32/KIA, 7/ML, 3/GCL, P<0.05), consolidation shadow(n=17, 13/KIA, 1/ML, 3/GCL, P<0.05), and cystic nodules or masses(n=12, 5/KIA, 7/ML); (3) pleural or extrapleural and chest wall lesions(n=72, 30/KIA, 31/ML, 11/GCL); (4)osteo-lesions(n=31, 9/KIA, 18/ML, 4/GCL, P<0.05).

#### CONCLUSION

s The three subtypes of GLA have different clinical manifestations, imaging types and histopathological features. Multimodality image are important methods for accurate diagnosis, staging and grading evaluation of lymphatic diseases.

#### CLINICAL RELEVANCE/APPLICATION

Multimodality image are important methods for accurate diagnosis of the three subtypes of GLA.

Printed on: 02/07/23

## Abstract Archives of the RSNA, 2022

M2-SPCH-5

### What Happens when Artificial Intelligence (AI) Feedback Is Wrong? A Multi-reader Pilot Study Examining the Human Factors of AI Implementation

Monday, Nov. 28 9:00AM - 9:30AM Room: Learning Center - CH DPS

#### Participants

Grayson Baird, PhD, Providence, RI (*Presenter*) Nothing to Disclose

#### PURPOSE

To examine whether incorrect AI feedback impacts radiologist performance, and if so, whether human factors can be optimized to reduce error.

#### METHODS AND MATERIALS

A prospective multi-reader design was used, where 6 radiologists interpreted 90 identical chest radiographs (follow-up CT needed: yes/no) on four occasions from 09/20 to 01/22. Sessions were separated by a minimum of 1 month, and the order of chest radiographs was identical in each session. In session 1, the radiologist interpreted images without AI. Sham AI feedback was provided for sessions 2-4, and 12 cases were manipulated to be incorrect (8 False Positives [FP], 4 False Negatives [FN]) (.87 ROCAUC). Radiologists anticipated a performance evaluation. In the Delete AI (No Box) condition, radiologists were told AI results would not be saved for the evaluation. In Keep AI (No Box) and Keep AI (Box), radiologists were told results would be saved. Radiologists were told these instructions were analogous to keeping or deleting AI feedback in the patient's record. In Keep AI (Box), the ostensible AI program visually outlined the region of suspicion. AI feedback was constant between conditions. FP and FN rates for the 12 erroneous cases were examined between conditions using generalized linear mixed modeling (GLMM) assuming a binary distribution.

#### RESULTS

Relative to the No AI condition (FN=2.7%, FP=51.4%), FN and FP rates were higher in the Keep AI (No Box) (FN=33.0%, FP=86.0%), Delete AI (No Box) (FN=26.7%, FP=80.5%), and Keep AI (Box) conditions (FN= 20.7%, FP=80.5%), all  $p < .05$ . FN rates were higher in the Keep AI (No Box) condition (33.0%) than the Keep AI (Box) condition (20.7%),  $p = .04$ . FP rates were higher in the Keep AI (No Box) (86.0%) condition than the Delete AI (No Box) condition (80.5%),  $p = .03$ .

#### CONCLUSION

s Incorrect AI causes radiologists to make incorrect follow-up decisions when they were correct without AI. This effect is mitigated when a box is provided around the region of interest and when AI feedback is deleted from the patient's record. Human factors for AI implementation are important.

#### CLINICAL RELEVANCE/APPLICATION

AI is often right but sometimes wrong. To maximize patient outcomes, we must consider how to prevent radiologists from being influenced by incorrect feedback.

Printed on: 02/07/23

## Abstract Archives of the RSNA, 2022

M2-SPCH-6

### Prevalence and Long-term Outcome of Interstitial Lung Abnormality in the Asian Health-screening Population: A Multicenter Study

Monday, Nov. 28 9:00AM - 9:30AM Room: Learning Center - CH DPS

#### Participants

Seolbin Park, MD, Gwangju, Korea, Republic Of (*Presenter*) Nothing to Disclose

#### PURPOSE

To investigate interstitial lung abnormality (ILA) prevalence in the Asian health-screening population and determine rates and risks for disease progression, lung cancer development, and 10-year mortality.

#### METHODS AND MATERIALS

This observational, retrospective, multicenter study included subjects = 50 years old who underwent chest computed tomography (CT) at three health screening centers over a 4-year period (2007 - 2010). ILA status was classified as none, equivocal ILA, and ILA, and ILA was further subcategorized into non-fibrotic or fibrotic ILA. Progression was evaluated between baseline and last follow-up CT. Kaplan-Meier analysis with the log-rank test was performed to estimate mortality according to ILA status. Cox proportional hazards models were used to assess factors associated with ILA progression, lung cancer development, and mortality.

#### RESULTS

In total, 2,765 subjects who underwent health screening chest CT were identified (mean age, 59±7 years; 2,068 men). Of the 2,765 subjects, 94 (3%) had a finding of ILA (35 non-fibrotic and 59 fibrotic ILA), and 119 (4%) had a finding of equivocal ILA. The mean follow-up period was approximately 12 years, and ILA progression was observed in 85% (34/40) of fibrotic ILA patients and 70% (14/20) of non-fibrotic ILA patients. Kaplan-Meier analysis showed subjects with ILA had a significantly higher mortality rate than those without ILA ( $P<.05$ ). Multivariate Cox proportional hazards analysis revealed that fibrotic ILA was significantly associated with ILA progression (hazard ratio [HR], 10.3; 95% confidence interval [CI], 6.4-16.4;  $P<.001$ ) and lung cancer development (HR, 4.4, 95% CI, 2.1-9.1;  $P<.001$ ). Furthermore, subjects with fibrotic ILA had a significantly higher risk of disease-specific mortality (HR, 6.7; 95% CI, 3.6-12.2;  $P<.001$ ) and all-cause mortality (HR, 2.5; 95% CI, 1.6 - 3.8;  $P<.001$ ) than those without ILA.

#### CONCLUSION

The prevalence of ILA in the Asian health-screening population was approximately 3%, and fibrotic ILA was an independent risk factor for disease progression, lung cancer development, and mortality over a 10-year follow-up period.

#### CLINICAL RELEVANCE/APPLICATION

Our study reveals ILA prevalence in the Asian health-screening population and demonstrates the association between ILAs and long-term outcomes.

Printed on: 02/07/23

## Abstract Archives of the RSNA, 2022

M2-SPCH-7

### Survival Impact of Incidental Abnormalities on Screening Thoracic Computed Tomography: Long-term Follow-up Analysis

Monday, Nov. 28 9:00AM - 9:30AM Room: Learning Center - CH DPS

#### Participants

Jaehyun Park, MD, Gwangju, Korea, Republic Of (*Presenter*) Nothing to Disclose

#### PURPOSE

The present study aimed to assess the association between long-term mortality and incidental abnormalities on thoracic computed tomography (CT) among the general screening population.

#### METHODS AND MATERIALS

We retrospectively collected the medical records and CT images of subjects who visited a single health promotion center between 2007 and 2010. Two thoracic radiologists independently reviewed all CT images and evaluated incidental abnormalities by visual assessment, which is interstitial lung abnormality (ILA), emphysema, and coronary artery calcification (CAC). Kaplan-Meier analysis was performed using a log-rank test to evaluate the association between incidental CT abnormalities and mortality. A Cox proportional hazards model was used to analyze the association factors between incidental CT abnormalities and mortality.

#### RESULTS

A total of 859 subjects were identified ( $59 \pm 6.7$  years of age, 582 men). The median follow-up time was approximately 10.9 years. Of the 859 subjects, 57 (6.6%), 318 (37%), and 178 (21%) had findings of ILA, CAC, and emphysema, respectively. Subjects with fibrotic ILA, CAC of any degree, and emphysema of any degree exhibited significantly higher mortality during Kaplan-Meier analysis with the log-rank test ( $p < 0.05$ ). A multivariate Cox proportional hazards model revealed that fibrotic ILAs were independently associated with higher mortality (hazard ratio, 2.59, [95% confidence interval, 1.07-6.27],  $p = 0.035$ ) among the incidental CT abnormalities and clinically relevant factors.

#### CONCLUSION

Incidental abnormalities on screening thoracic CT were associated with an increased hazard of mortality in the general screening population. Fibrotic ILAs in particular were independently associated with increased hazard of mortality compared to other incidental CT abnormalities.

#### CLINICAL RELEVANCE/APPLICATION

Our study reveals the relationship between incidental abnormalities found in screening thoracic CT and long-term mortality.

Printed on: 02/07/23

## Abstract Archives of the RSNA, 2022

M2-SPCH-8

### **Post-COVID-19 Interstitial Lung Disease (PC-ILD): The Role of Lung Imaging Andpulmonary Function Testing in The Long-term Follow-up of Patients with COVID-19 Pneumonia**

Monday, Nov. 28 9:00AM - 9:30AM Room: Learning Center - CH DPS

#### **Participants**

Emanuele Messina, MD, Roma, Italy (*Presenter*) Nothing to Disclose

#### **PURPOSE**

Post COVID-19 Interstitial Lung Disease (PC-ILD) is characterized by fibrotic-like signs at High Resolution Computed Tomography (HRCT) and Pulmonary Function Tests (PFTs) abnormalities after SARS-CoV-2 infection. It is still not clear how frequent these tests should be performed to rule out long-term consequences of COVID-19 pneumonia. The aims of our study are to evaluate the incidence and risk factors of PC-ILD and possibly to propose a long-term follow-up program.

#### **METHODS AND MATERIALS**

In this prospective single-center study, 100 patients, hospitalized in our ward for moderate to critical COVID-19, underwent two follow-up visits at 3 and 15 months, performing HRCT and PFTs.

#### **RESULTS**

At 3-month follow up, HRCTs showed that lung parenchymal abnormalities were still present in 22% of patients, mainly consisting in ground glass opacities (GGO) and fibrotic-like alterations (63% and 78%, respectively); 37% showed PFTs abnormalities consistent with PC-ILD. 48 patients underwent the 15-month follow up: at HRCT, residual fibrotic-like abnormalities were found in 40% of patients with almost complete reduction of GGO and consolidation; at PFTs, 33.3% showed residual respiratory functional impairment (PC-ILD); 8% of patients showed residual radiological and functional signs consistent with PC-ILD. All but one of these patients had already demonstrated PFTs and HRCT alterations at first follow-up visit, the last one patient showed worsening of lung function during follow up.

#### **CONCLUSION**

These findings highlight the negative predictive value of HRCT and PFTs at three months follow-up for the development of PC-ILD. Ageing, severity of COVID-19 and degree of pulmonary involvement during acute infection proved to be significant risk factors for developing PC-ILD. Our study highlights the importance of PFTs in the long-term follow-up of patients affected by moderate to critical COVID-19 pneumonia. HRCT should be obtained in those patients still presenting PFTs abnormalities at 15 months.

#### **CLINICAL RELEVANCE/APPLICATION**

This is the first study investigating such a long-term follow up with HRCT and PFTs, at fifteen months.

Printed on: 02/07/23

## Abstract Archives of the RSNA, 2022

M2-SPGI

### Gastrointestinal Monday Poster Discussions

Monday, Nov. 28 9:00AM - 9:30AM Room: Learning Center - GI DPS

#### Participants

Mark Sugi, MD, San Francisco, CA (*Moderator*) Consultant, Nextrast, Inc; Author with royalties, RELX

#### Sub-Events

### M2-SPGI-1 Automated multi-organ segmentation tool for both non-contrast and post-contrast abdominal CT: a deep learning algorithm developed using dual-energy CT images

#### Participants

Sun Kyung Jeon, MD, Seoul, Korea, Republic Of (*Presenter*) Nothing to Disclose

#### PURPOSE

To develop and validate a deep learning-based fully-automated abdominal multi-organ segmentation algorithm, robust to both non-contrast and post-contrast CT images, using dual-energy CT (DECT) images.

#### METHODS AND MATERIALS

For development, 75 abdominal DECT scans (portal venous phase (PVP) images and the spatiotemporally matched virtual non-contrast (VNC) images; 18174 slices in each) were used as the input. A single three-dimensional (3D) nnU-Net-based algorithm for multi-organ segmentation (liver, spleen, right kidney, left kidney, and pancreas, respectively) was trained. On an external validation set of 30 single-energy CT scans with both PVP and true non-contrast (TNC) images, the performance of the developed algorithm for each organ was evaluated using the dice similarity score (DSS) for segmentation; and linear regression analysis and Bland-Altman analysis for measurement of the volumetric indices, in comparison to the ground truth manual segmentation.

#### RESULTS

For 3D segmentation of the liver, spleen, right kidney, left kidney, and pancreas, the fully-automated segmentation algorithm achieved a mean DSS of 0.982, 0.972, 0.972, 0.970, 0.847 in PVP image; and 0.968, 0.956, 0.940, 0.955, and 0.807 in TNC images, respectively. For the measurement of volumetric indices of those organs, manual and automated organ segmentation strongly correlated both in PVP and TNC ( $R^2 = 0.99, 0.99, 0.99, 0.98, \text{ and } 0.80$  in PVP; and  $0.98, 0.99, 0.95, 0.98, 0.72$  in TNC, all  $P < 0.001$ ), and the mean differences (95 % limits of agreement) were  $-1.0\%$  ( $-3.2, 1.1$ ),  $0.3\%$  ( $-5.2, 5.8$ ),  $-0.9\%$  ( $-5.5, 3.8$ ),  $-2.3\%$  ( $-7.2, 2.5$ ),  $5.8\%$  ( $-20.1, 31.8$ ) in PVP images; and  $-1.9\%$  ( $-3.7, 7.5$ ),  $-3.1\%$  ( $-10.9, 4.6$ ),  $2.2\%$  ( $-7.0, 11.3$ ),  $3.4\%$  ( $-1.0, 7.9$ ),  $-0.3\%$  ( $-25.8, 25.2$ ) in TNC images, respectively.

#### CONCLUSION

The deep learning-based fully-automated segmentation algorithm developed using virtual non-contrast and post-contrast CT images from DECT provided accurate segmentation of abdominal solid organs at both CT scans with and without contrast.

#### CLINICAL RELEVANCE/APPLICATION

By using paired DECT images, a fully-automated multi-organ segmentation algorithm that is robust to both non-contrast and post-contrast CT can be developed with a relatively small number of datasets, which can be applied to volumetric analysis of abdominal organs of large cohort studies.

### M2-SPGI-10 A review of the use of Computed Tomography (CT) Colonography in acute diverticulitis follow up

#### Participants

Amy Verrinder, MBBS, (*Presenter*) Nothing to Disclose

#### PURPOSE

Direct visualisation of the bowel lumen is recommended as follow up for all acute diverticulitis cases. This includes CT Colonography (CTC). In Newcastle Upon Tyne Hospitals (NUTH), surgical practice is that all patients admitted with diverticulitis have a follow up CTC approximately 3 months from discharge.

#### METHODS AND MATERIALS

A Radiology Information system (RIS) search of CTCs performed in NUTH trust between 1/1/2019-31/12/2019. Reports were excluded if the indication was not acute diverticulitis follow-up. Remaining reports were assessed for compliance with standards. Joint guidance from the BSGAR and RCR: Standards of practice for CTC (2021); and Royal College of Surgeons commissioning guide into Colonic Diverticular disease (2014). Percentage of CTC reports following acute diverticulitis accordant with standards of practice. 1. CTC should be completed within 3 months of acute episode 2. Local target of 100% sensitivity for colonic malignancy. 3. Polyp identification rate of >13% of patients 4. Indeterminate CTC report (leading to further investigation) in <25% References: Royal College of Radiologists. (2021). Joint guidance from the BSGAR and RCR: Standards of practice for CTC. Royal College of Surgeons. (2014). Colonic Diverticular disease - Commissioning Guide.

## RESULTS

Of the 1282 CTC reports identified, 1207 (94%) were excluded. Of the remaining 75 reports, no cases had a colonic malignancy later identified which was not reported at the time of CTC (100% sensitivity). There was a wide range in the time interval to CTC, from 3 to 69 weeks. 15 cases (20%) had polyps identified. 6 reports (8%) were indeterminate (C score of 3c) and required further investigation.

## CONCLUSION

s CTC in acute diverticulitis follow-up achieved targets in malignancy and polyp sensitivity, and indeterminate rates. However, the time interval was very variable and could be standardised to produce a more robust pathway for patients requiring acute diverticulitis follow-up. Results have been presents regionally.

## CLINICAL RELEVANCE/APPLICATION

CTC in acute diverticulitis follow up has superseded the Colonoscopy at NUTH. This has been a success story for the Radiology teams with increased trust in CTC reports from the General Surgical teams. This audit shows this trust is well placed with national standards met using this less invasive, more accessible and better tolerated test. Going forward this pathway could be standardised to set up a routine follow up time interval for CTC following acute diverticulitis which would stream line patient management and improve efficiency.

## M2-SPGI-2 Phenotypic and Biomarker Associations with Lean Steatosis using Image-derived Phenotypes from Abdominal CT Scans

Participants  
Hersh Sagreiya, MD, Philadelphia, PA (*Presenter*) Nothing to Disclose

## PURPOSE

Although non-alcoholic fatty liver disease (NAFLD) is associated with obesity, a significant subgroup of NAFLD patients have normal body mass index (BMI) or "lean steatosis." We investigated characteristics associated with lean steatosis using biobank data by aggregating ICD codes and CT scans to perform a phenome-wide association study (PheWAS) and biomarker analysis.

## METHODS AND MATERIALS

We collected chest and abdominal CTs, blood biomarkers, and ICD-9 codes from 11,559 biobank participants, excluding patients with alcohol use disorder, alcohol-related liver disease, and end-stage liver disease (ESLD). CT scans were segmented using deep learning. Hepatic fat (HF) was estimated by computing liver attenuation - spleen attenuation (in Hounsfield units); a lower value indicated more HF. Lean patients were defined as those with BMI 18.5- 25. PheWAS was conducted for HF, and logistic regression determined the interaction between the variables 'lean' and 'HF,' controlling for age, gender, and race. Livers were categorized as steatotic or non-steatotic according to an attenuation threshold determined by receiver operating characteristic analysis of biopsy-obtained HF measurement. Biomarkers included AST, ALT, ALP, HDL, LDL, triglycerides, total cholesterol, and hemoglobin A1c.

## RESULTS

4650 NAFLD and 879 lean steatotic patients were identified. PheWAS yielded 35 significant associations, with links to several renal pathologies. Lean steatosis patients had higher ALP and HDL and lower ALT, triglycerides, and hemoglobin A1c compared to overweight steatosis patients. AST, LDL, and total cholesterol were not significantly different.

## CONCLUSION

s Our study is the first to link CKD and other renal pathologies to lean steatosis using a high-throughput imaging-guided pipeline. We report several metabolic biomarker differences between lean and overweight steatotic patients. These associations remained significant when removing ESLD patients and controlling for age, race, and gender. We plan further study to characterize the risk factors and pathophysiologic mechanisms contributing to the metabolic and renal associations with lean steatosis.

## CLINICAL RELEVANCE/APPLICATION

Applying deep learning, PheWAS, and biomarker analysis to CT scans can provide new clinical insights, differentiating overweight steatosis from the less well-understood lean steatosis phenotype.

## M2-SPGI-4 Evaluation of Respiratory-Related Predictors for Image Quality of Respiratory-gating and Breath-hold 3D Magnetic Resonance Cholangiopancreatography (MRCP): A Single-Center Prospective Study

Participants  
Ke Wang, MD, (*Presenter*) Nothing to Disclose

## PURPOSE

The study aimed to compare the image quality of single breath-hold 3D GRASE MRCP (BH-MRCP) and respiratory-gating 3D FSE MRCP (RG-MRCP), and to explore the respiratory factors based on the breathing curve that may affect the image quality of BH- and RG- MRCP sequences.

## METHODS AND MATERIALS

A total of 126 study participants were enrolled from May to December 2021 and underwent RG-MRCP and BH-MRCP at a 3-T MR scanner (uMR790, United Imaging Healthcare, Shanghai, China). The imaging was evaluated by three radiologists based on a 5-point Likert scale. Respiratory parameters were extracted from the breathing curve (Fig.1). Wilcoxon test was used to compare the image quality between two MRCPs. Multivariable linear regression and logistic regression analyses were performed to identify breathing predictor variables of a higher image quality score and better image quality.

## RESULTS

The overall image quality scores were  $4.45 \pm 0.73$  for RG-MRCP and  $4.69 \pm 0.6$  for BH-MRCP ( $p < 0.05$ ). Multivariable predictors of a higher RG-MRCP image quality score ( $\beta = -0.455$  to  $-0.307$ ) included lower Standard deviation of respiratory amplitude on minimum-peak (SDamp-minimum-peak) ( $p < 0.001$ ) and lower standard deviation of time interval between the two trigger points (SDbreath-time) ( $p < 0.001$ ) (Fig. 2). A higher BH-MRCP image quality score was predicted by lower standard deviation of respiratory amplitude

(SDamp) ( $\beta = -0.630$ ,  $p < 0.001$ ) (Fig. 3). The results of multivariable logistic regression showed that lower SDamp-minimum-peak (OR=0.147, 95% CI=0.058-0.370,  $p < 0.001$ ) was the only predictor of relatively good RG-MRCP image quality. For BH-MRCP, the factor predicting relatively good image quality was SDamp (OR=0.665, 95% CI= 0.572-0.773,  $p < 0.001$ ) (Table 1).

## CONCLUSION

In conclusion, both RG-MRCP and BH-MRCP demonstrated satisfied image quality. The overall image quality of BH-GRASE-MRCP was significantly better than RG-MRCP on group level, but not for every individual. Respiratory conditions exerted significant impact on the image quality of MRCP, and parameters derived from respiratory curve could help predict image quality of both sequences.

## CLINICAL RELEVANCE/APPLICATION

The evaluation of the breathing curve could benefit for the individualized scanning plan. In addition, during breathing training, patients could be guided in a more targeted manner. The evaluation of the breathing curve was not limited to the application of MRCP, and could also be applied in the whole process of MRI scanning of the upper abdomen.

## M2-SPGI-5 Preoperative CT Staging of Intrahepatic Cholangiocarcinoma: Impact of Up-staging of Tumor Multiplicity on Survival Outcomes

Participants

June Park, MD, Seoul, Korea, Republic Of (*Presenter*) Nothing to Disclose

## PURPOSE

To develop a preoperative CT staging system for intrahepatic cholangiocarcinoma (iCCA) using American Joint Committee on Cancer (AJCC) staging parameters and focusing on tumor multiplicity.

## METHODS AND MATERIALS

Patients who underwent preoperative multiphase CT and curative-intent resection for mass-forming iCCA were retrospectively recruited from multiple institutions from January 2009 to December 2015. Based on Cox proportional hazards regression analysis of the AJCC staging parameters, preoperative CT staging system was modified from the AJCC system with subdivision of tumor multiplicity (satellitosis vs. intrahepatic metastasis). Kaplan-Meier method was used to estimate overall survival (OS). Harrell's concordance indices (C-indices) of AJCC and modified systems were compared with bootstrap methods.

## RESULTS

This study included 319 patients (median age, 64 years; 208 men). In the modified staging system, multiple tumors (adjusted hazard ratio [HR]; satellitosis, 3.03,  $P < 0.001$ ; intrahepatic metastasis, 3.92,  $P < 0.001$ ) were up-staged from T2 to T3 (T3a, satellitosis; T3b, intrahepatic metastasis); solitary tumor with intrahepatic vascular invasion (adjusted HR, 1.98,  $P = 0.003$ ) or solitary tumor perforating the visceral peritoneum (adjusted HR, 2.00,  $P = 0.001$ ) were designated as T2. Preoperative T2 and T3 stages according to the AJCC system failed to discriminate the survival curves (log-rank  $P$  value for T2 vs. T3 = 0.812; 5-year OS, 23.4% vs. 26.8%), but modified T2 stage showed better OS outcomes than modified T3 stage (log-rank  $P$  value for T2 vs. T3a vs. T3b = 0.003; 5-year OS, 33.8% vs. 8.4% vs. 4.8%). The C-indices of modified staging system were higher than those of AJCC staging system for predicting OS, marginally approaching the statistical significance (T staging, 0.647 vs. 0.626,  $P = 0.061$ ; tumor-node-metastasis staging, 0.636 vs. 0.614,  $P = 0.069$ ).

## CONCLUSION

The modified staging system which upstages tumor multiplicity provides better prognostic stratification for OS than AJCC staging system when applied to preoperative CT in patients with iCCA.

## CLINICAL RELEVANCE/APPLICATION

The presence of tumor multiplicity on preoperative CT indicates worse prognosis than current AJCC T2 or T3 staging parameters, and may need subdivision into satellitosis and intrahepatic metastasis.

## M2-SPGI-7 A Diagnostic Value of MR Radiomics for Predicting Lateral Pelvic Lymph Node Metastasis in Patients with Locally Advanced Rectal Cancer: A Multicenter Retrospective Study

Participants

Jeongin Yoo, Seoul, Korea, Republic Of (*Presenter*) Nothing to Disclose

## PURPOSE

To develop a MRI radiomics-based prediction model for lateral pelvic lymph node (LPLN) metastasis in rectal cancer patients who underwent LPLN dissection as well as to validate model performance using an external validation dataset.

## METHODS AND MATERIALS

A total of 344 patients (198 in the development cohort and 146 in the validation cohort) who underwent rectal cancer surgery and LPLN dissection were enrolled. Patients' clinical and laboratory features were recorded. Radiomics features of LPLN were extracted from pre- post-chemoradiation therapy high-resolution T2-weighted axial or coronal MR images. The least absolute shrinkage and selection operator regression analysis was conducted to select predictive radiomics features in the development cohort, and a radiomics score for predicting LPLN metastasis was calculated based on the selected features. Model performance was assessed by receiver operating characteristics curve, calibration curves, and decision curve analysis (DCA). The prediction model was externally validated in the validation cohort.

## RESULTS

In the development cohort, 70 (35.4%) of 198 patients had metastatic LPLN. Of clinical features, neoadjuvant radiotherapy is the sole significant feature. Of 116 radiomics features, histogram-based energy and histogram-based total energy were selected as significant features. Radiomics score can be calculated as a following formula: radiomics score =  $-0.58618 + 1.7252902E-9 \times$  histogram-based energy +  $1.1056922E-9 \times$  histogram-based total energy. A combined model using clinical features and radiomics score showed better prediction performance compared to the clinical feature only (area under the curve [AUC] value: 0.73 vs 0.61) in the development cohort ( $P < 0.0001$ ). DCA demonstrated that the combined model has the highest net benefit in threshold probability of 25% - 75%. In the validation cohort, a combined model using clinical features and radiomics score showed better

prediction performance compared to the clinical feature only (AUC value: 0.61 vs 0.51) (P=0.0318) and had the highest net benefit in threshold probability of 30%-75%.

## CONCLUSION

s An application of radiomics on rectal MRI showed the best prediction performance of a combined model using clinical features and radiomics score to predict LPLN metastasis.

## CLINICAL RELEVANCE/APPLICATION

An application of radiomics on rectal MRI can be useful for accurately predicting LPLN metastasis in patients with rectal cancer

### M2-SPGI-8 Diagnostic performance of Apparent Diffusion Coefficient to assess the therapeutic response to biological therapy in Crohn's disease

#### Participants

Jordi Rimola, MD, PhD, (*Presenter*) Consultant, Alimentiv Health Trust; Speaker, Takeda Pharmaceutical Company Limited; Consultant, Johnson & Johnson; Consultant, Boehringer Ingelheim GmbH; Research Grant, AbbVie Inc

#### PURPOSE

to determine prospectively the performance of the Apparent Diffusion Coefficient (ADC) to assess response to biological therapy in Crohn's disease (CD) using MR enterography (MRE) and ileocolonoscopy as reference standards.

#### METHODS AND MATERIALS

Seventy four CD & 9;patients underwent MRE with ADC calculation before and at 46-week after treatment with biological therapy. MRE images were analyzed including measurement of ADC. Segmental MaRIA was considered the reference standard to identify presence and severity of inflammation. Similar analysis was done in the 41 subjects who underwent ileocolonoscopy at both time points.

#### RESULTS

MRE identified 125 intestinal segments with severe inflammation (MaRIA  $\geq$  11) at baseline. Of them, 54% achieved healing of severe inflammation (MaRIA  $<$ 11) at week 46. & 9;Using a receiver operating characteristic (ROC) curve, we determined at baseline an ADC threshold of  $1.301 \times 10^{-3} \text{mm}^2/\text{s}$  to predict severity, yielding a sensitivity of 0.78 and specificity of 0.94 to identify segments with MaRIA  $\geq$  11 (AUROC=0.92). Using the same threshold, ADC has a sensitivity and specificity of 0.90 and 0.75 respectively to identify healing of severe inflammation (MaRIA $<$ 11) at week 46. Using ileocolonoscopy as reference, the ADC threshold to predict endoscopic severity (ulcers) was very similar ( $1.382 \times 10^{-3} \text{mm}^2/\text{s}$ ) yielding a sensitivity and specificity of 0.76 and 0.89, and 0.95 and 0.71 to identify endoscopic ulcer healing. The MaRIA score was superior to ADC to predict endoscopic ulcer healing (AUROC 0.94 vs. 0.83 p=0.01).

## CONCLUSION

s ADC showed robust thresholds to predict severe inflammation in CD using either MaRIA or ileocolonoscopy, and could be used as an alternative to the MaRIA index to assess therapeutic response in CD.

## CLINICAL RELEVANCE/APPLICATION

ADC is a potential imaging biomarker alternative to MaRIA score or ileocolonoscopy to assess the treatment response to biological therapy in Crohn's disease

### M2-SPGI-9 MRI Defecography: A Useful Tool to Guide Surgical Management in Patients With Pelvic Floor Dysfunction

#### Participants

John Gao, MD, Kansas City, KS (*Presenter*) Nothing to Disclose

#### PURPOSE

To retrospectively evaluate magnetic resonance (MR) defecography findings in patients with pelvic floor dysfunction to assess which findings on MR defecography influence decisions to perform subsequent pelvic floor surgery.

#### METHODS AND MATERIALS

This retrospective cohort study included women 18 and older who had an MRI defecography exam from 1/1/2017 - 6/30/2021. Patients were excluded if they were male, under 18, unable to comply with the exam, or had insufficient imaging. Demographic, clinical, and imaging information were obtained from the electronic medical record and Picture Archiving and Communications Systems (PACS). Imaging reports were retrospectively reviewed using the original interpretations.

#### RESULTS

One hundred sixty-eight patients with 171 MR defecography exams were included. Twenty out of 168 total patients (11.9%) patients had subsequent pelvic floor surgery in the year following their exam. Multiple measurements on MRI demonstrated a statistically significant odds ratio for subsequent pelvic floor surgery, including M line at maximal strain (OR=1.5, p=0.070) and the presence of sigmoidocele (OR=27.7, p=0.011) and enterocele (OR=6.8, p=0.015). Patients in the surgical group had higher M-lines at maximal strain (5.7 cm) than in the non-surgical group (4.7 cm).

## CONCLUSION

s MRI defecography is an important tool to evaluate anatomical and functional abnormalities in patients with pelvic floor dysfunction. Certain measurements and findings may help guide decisions to pursue surgical treatment. The presence of sigmoidoceles and enteroceles is a significant finding that may direct patients and clinicians to pursue surgical management, which should be highlighted in the radiology report.

## CLINICAL RELEVANCE/APPLICATION

Radiologists should highlight key measurements and findings on MRI defecography exams as well as recommend surgical consultation

in certain patients.

Printed on: 02/07/23

## Abstract Archives of the RSNA, 2022

M2-SPGI-1

### Automated multi-organ segmentation tool for both non-contrast and post-contrast abdominal CT: a deep learning algorithm developed using dual-energy CT images

Monday, Nov. 28 9:00AM - 9:30AM Room: Learning Center - GI DPS

#### Participants

Sun Kyung Jeon, MD, Seoul, Korea, Republic Of (*Presenter*) Nothing to Disclose

#### PURPOSE

To develop and validate a deep learning-based fully-automated abdominal multi-organ segmentation algorithm, robust to both non-contrast and post-contrast CT images, using dual-energy CT (DECT) images.

#### METHODS AND MATERIALS

For development, 75 abdominal DECT scans (portal venous phase (PVP) images and the spatiotemporally matched virtual non-contrast (VNC) images; 18174 slices in each) were used as the input. A single three-dimensional (3D) nnU-Net-based algorithm for multi-organ segmentation (liver, spleen, right kidney, left kidney, and pancreas, respectively) was trained. On an external validation set of 30 single-energy CT scans with both PVP and true non-contrast (TNC) images, the performance of the developed algorithm for each organ was evaluated using the dice similarity score (DSS) for segmentation; and linear regression analysis and Bland-Altman analysis for measurement of the volumetric indices, in comparison to the ground truth manual segmentation.

#### RESULTS

For 3D segmentation of the liver, spleen, right kidney, left kidney, and pancreas, the fully-automated segmentation algorithm achieved a mean DSS of 0.982, 0.972, 0.972, 0.970, 0.847 in PVP image; and 0.968, 0.956, 0.940, 0.955, and 0.807 in TNC images, respectively. For the measurement of volumetric indices of those organs, manual and automated organ segmentation strongly correlated both in PVP and TNC ( $R^2 = 0.99, 0.99, 0.99, 0.98, \text{ and } 0.80$  in PVP; and  $0.98, 0.99, 0.95, 0.98, 0.72$  in TNC, all  $P_s < 0.001$ ), and the mean differences (95 % limits of agreement) were  $-1.0\%$  ( $-3.2, 1.1$ ),  $0.3\%$  ( $-5.2, 5.8$ ),  $-0.9\%$  ( $-5.5, 3.8$ ),  $-2.3\%$  ( $-7.2, 2.5$ ),  $5.8\%$  ( $-20.1, 31.8$ ) in PVP images; and  $-1.9\%$  ( $-3.7, 7.5$ ),  $-3.1\%$  ( $-10.9, 4.6$ ),  $2.2\%$  ( $-7.0, 11.3$ ),  $3.4\%$  ( $-1.0, 7.9$ ),  $-0.3\%$  ( $-25.8, 25.2$ ) in TNC images, respectively.

#### CONCLUSION

The deep learning-based fully-automated segmentation algorithm developed using virtual non-contrast and post-contrast CT images from DECT provided accurate segmentation of abdominal solid organs at both CT scans with and without contrast.

#### CLINICAL RELEVANCE/APPLICATION

By using paired DECT images, a fully-automated multi-organ segmentation algorithm that is robust to both non-contrast and post-contrast CT can be developed with a relatively small number of datasets, which can be applied to volumetric analysis of abdominal organs of large cohort studies.

Printed on: 02/07/23

## Abstract Archives of the RSNA, 2022

M2-SPGI-10

### A review of the use of Computed Tomography (CT) Colonography in acute diverticulitis follow up

Monday, Nov. 28 9:00AM - 9:30AM Room: Learning Center - GI DPS

#### Participants

Amy Verrinder, MBBS, (Presenter) Nothing to Disclose

#### PURPOSE

Direct visualisation of the bowel lumen is recommended as follow up for all acute diverticulitis cases. This includes CT Colonography (CTC). In Newcastle Upon Tyne Hospitals (NUTH), surgical practice is that all patients admitted with diverticulitis have a follow up CTC approximately 3 months from discharge.

#### METHODS AND MATERIALS

A Radiology Information system (RIS) search of CTCs performed in NUTH trust between 1/1/2019-31/12/2019. Reports were excluded if the indication was not acute diverticulitis follow-up. Remaining reports were assessed for compliance with standards. Joint guidance from the BSGAR and RCR: Standards of practice for CTC (2021); and Royal College of Surgeons commissioning guide into Colonic Diverticular disease (2014). Percentage of CTC reports following acute diverticulitis accordant with standards of practice. 1. CTC should be completed within 3 months of acute episode 2. Local target of 100% sensitivity for colonic malignancy. 3. Polyp identification rate of >13% of patients 4. Indeterminate CTC report (leading to further investigation) in <25% References: Royal College of Radiologists. (2021). Joint guidance from the BSGAR and RCR: Standards of practice for CTC. Royal College of Surgeons. (2014). Colonic Diverticular disease - Commissioning Guide.

#### RESULTS

Of the 1282 CTC reports identified, 1207 (94%) were excluded. Of the remaining 75 reports, no cases had a colonic malignancy later identified which was not reported at the time of CTC (100% sensitivity). There was a wide range in the time interval to CTC, from 3 to 69 weeks. 15 cases (20%) had polyps identified. 6 reports (8%) were indeterminate (C score of 3c) and required further investigation.

#### CONCLUSION

s CTC in acute diverticulitis follow-up achieved targets in malignancy and polyp sensitivity, and indeterminate rates. However, the time interval was very variable and could be standardised to produce a more robust pathway for patients requiring acute diverticulitis follow-up. Results have been presents regionally.

#### CLINICAL RELEVANCE/APPLICATION

CTC in acute diverticulitis follow up has superseded the Colonoscopy at NUTH. This has been a success story for the Radiology teams with increased trust in CTC reports from the General Surgical teams. This audit shows this trust is well placed with national standards met using this less invasive, more accessible and better tolerated test. Going forward this pathway could be standardised to set up a routine follow up time interval for CTC following acute diverticulitis which would stream line patient management and improve efficiency.

Printed on: 02/07/23

## Abstract Archives of the RSNA, 2022

M2-SPGI-2

### Phenotypic and Biomarker Associations with Lean Steatosis using Image-derived Phenotypes from Abdominal CT Scans

Monday, Nov. 28 9:00AM - 9:30AM Room: Learning Center - GI DPS

#### Participants

Hersh Sagreiya, MD, Philadelphia, PA (*Presenter*) Nothing to Disclose

#### PURPOSE

Although non-alcoholic fatty liver disease (NAFLD) is associated with obesity, a significant subgroup of NAFLD patients have normal body mass index (BMI) or "lean steatosis." We investigated characteristics associated with lean steatosis using biobank data by aggregating ICD codes and CT scans to perform a phenome-wide association study (PheWAS) and biomarker analysis.

#### METHODS AND MATERIALS

We collected chest and abdominal CTs, blood biomarkers, and ICD-9 codes from 11,559 biobank participants, excluding patients with alcohol use disorder, alcohol-related liver disease, and end-stage liver disease (ESLD). CT scans were segmented using deep learning. Hepatic fat (HF) was estimated by computing liver attenuation - spleen attenuation (in Hounsfield units); a lower value indicated more HF. Lean patients were defined as those with BMI 18.5- 25. PheWAS was conducted for HF, and logistic regression determined the interaction between the variables 'lean' and 'HF,' controlling for age, gender, and race. Livers were categorized as steatotic or non-steatotic according to an attenuation threshold determined by receiver operating characteristic analysis of biopsy-obtained HF measurement. Biomarkers included AST, ALT, ALP, HDL, LDL, triglycerides, total cholesterol, and hemoglobin A1c.

#### RESULTS

4650 NAFLD and 879 lean steatotic patients were identified. PheWAS yielded 35 significant associations, with links to several renal pathologies. Lean steatosis patients had higher ALP and HDL and lower ALT, triglycerides, and hemoglobin A1c compared to overweight steatosis patients. AST, LDL, and total cholesterol were not significantly different.

#### CONCLUSION

Our study is the first to link CKD and other renal pathologies to lean steatosis using a high-throughput imaging-guided pipeline. We report several metabolic biomarker differences between lean and overweight steatotic patients. These associations remained significant when removing ESLD patients and controlling for age, race, and gender. We plan further study to characterize the risk factors and pathophysiologic mechanisms contributing to the metabolic and renal associations with lean steatosis.

#### CLINICAL RELEVANCE/APPLICATION

Applying deep learning, PheWAS, and biomarker analysis to CT scans can provide new clinical insights, differentiating overweight steatosis from the less well-understood lean steatosis phenotype.

Printed on: 02/07/23

## Abstract Archives of the RSNA, 2022

M2-SPGI-4

### Evaluation of Respiratory-Related Predictors for Image Quality of Respiratory-gating and Breath-hold 3D Magnetic Resonance Cholangiopancreatography (MRCP): A Single-Center Prospective Study

Monday, Nov. 28 9:00AM - 9:30AM Room: Learning Center - GI DPS

#### Participants

Ke Wang, MD, (Presenter) Nothing to Disclose

#### PURPOSE

The study aimed to compare the image quality of single breath-hold 3D GRASE MRCP (BH-MRCP) and respiratory-gating 3D FSE MRCP (RG-MRCP), and to explore the respiratory factors based on the breathing curve that may affect the image quality of BH- and RG- MRCP sequences.

#### METHODS AND MATERIALS

A total of 126 study participants were enrolled from May to December 2021 and underwent RG-MRCP and BH-MRCP at a 3-T MR scanner (uMR790, United Imaging Healthcare, Shanghai, China). The imaging was evaluated by three radiologists based on a 5-point Likert scale. Respiratory parameters were extracted from the breathing curve (Fig.1). Wilcoxon test was used to compare the image quality between two MRCPs. Multivariable linear regression and logistic regression analyses were performed to identify breathing predictor variables of a higher image quality score and better image quality.

#### RESULTS

The overall image quality scores were  $4.45 \pm 0.73$  for RG-MRCP and  $4.69 \pm 0.6$  for BH-MRCP ( $p < 0.05$ ). Multivariable predictors of a higher RG-MRCP image quality score ( $\beta = -0.455$  to  $-0.307$ ) included lower Standard deviation of respiratory amplitude on minimum-peak (SDamp-minimum-peak) ( $p < 0.001$ ) and lower standard deviation of time interval between the two trigger points (SDbreath-time) ( $p < 0.001$ ) (Fig. 2). A higher BH-MRCP image quality score was predicted by lower standard deviation of respiratory amplitude (SDamp) ( $\beta = -0.630$ ,  $p < 0.001$ ) (Fig. 3). The results of multivariable logistic regression showed that lower SDamp-minimum-peak (OR=0.147, 95% CI=0.058-0.370,  $p < 0.001$ ) was the only predictor of relatively good RG-MRCP image quality. For BH-MRCP, the factor predicting relatively good image quality was SDamp (OR=0.665, 95% CI= 0.572-0.773,  $p < 0.001$ ) (Table 1).

#### CONCLUSION

In conclusion, both RG-MRCP and BH-MRCP demonstrated satisfied image quality. The overall image quality of BH-GRASE-MRCP was significantly better than RG-MRCP on group level, but not for every individual. Respiratory conditions exerted significant impact on the image quality of MRCP, and parameters derived from respiratory curve could help predict image quality of both sequences.

#### CLINICAL RELEVANCE/APPLICATION

The evaluation of the breathing curve could benefit for the individualized scanning plan. In addition, during breathing training, patients could be guided in a more targeted manner. The evaluation of the breathing curve was not limited to the application of MRCP, and could also be applied in the whole process of MRI scanning of the upper abdomen.

Printed on: 02/07/23

## Abstract Archives of the RSNA, 2022

M2-SPGI-5

### Preoperative CT Staging of Intrahepatic Cholangiocarcinoma: Impact of Up-staging of Tumor Multiplicity on Survival Outcomes

Monday, Nov. 28 9:00AM - 9:30AM Room: Learning Center - GI DPS

#### Participants

June Park, MD, Seoul, Korea, Republic Of (*Presenter*) Nothing to Disclose

#### PURPOSE

To develop a preoperative CT staging system for intrahepatic cholangiocarcinoma (iCCA) using American Joint Committee on Cancer (AJCC) staging parameters and focusing on tumor multiplicity.

#### METHODS AND MATERIALS

Patients who underwent preoperative multiphase CT and curative-intent resection for mass-forming iCCA were retrospectively recruited from multiple institutions from January 2009 to December 2015. Based on Cox proportional hazards regression analysis of the AJCC staging parameters, preoperative CT staging system was modified from the AJCC system with subdivision of tumor multiplicity (satellitosis vs. intrahepatic metastasis). Kaplan-Meier method was used to estimate overall survival (OS). Harrell's concordance indices (C-indices) of AJCC and modified systems were compared with bootstrap methods.

#### RESULTS

This study included 319 patients (median age, 64 years; 208 men). In the modified staging system, multiple tumors (adjusted hazard ratio [HR]; satellitosis, 3.03,  $P < 0.001$ ; intrahepatic metastasis, 3.92,  $P < 0.001$ ) were up-staged from T2 to T3 (T3a, satellitosis; T3b, intrahepatic metastasis); solitary tumor with intrahepatic vascular invasion (adjusted HR, 1.98,  $P = 0.003$ ) or solitary tumor perforating the visceral peritoneum (adjusted HR, 2.00,  $P = 0.001$ ) were designated as T2. Preoperative T2 and T3 stages according to the AJCC system failed to discriminate the survival curves (log-rank  $P$  value for T2 vs. T3 = 0.812; 5-year OS, 23.4% vs. 26.8%), but modified T2 stage showed better OS outcomes than modified T3 stage (log-rank  $P$  value for T2 vs. T3a vs. T3b = 0.003; 5-year OS, 33.8% vs. 8.4% vs. 4.8%). The C-indices of modified staging system were higher than those of AJCC staging system for predicting OS, marginally approaching the statistical significance (T staging, 0.647 vs. 0.626,  $P = 0.061$ ; tumor-node-metastasis staging, 0.636 vs. 0.614,  $P = 0.069$ ).

#### CONCLUSION

The modified staging system which upstages tumor multiplicity provides better prognostic stratification for OS than AJCC staging system when applied to preoperative CT in patients with iCCA.

#### CLINICAL RELEVANCE/APPLICATION

The presence of tumor multiplicity on preoperative CT indicates worse prognosis than current AJCC T2 or T3 staging parameters, and may need subdivision into satellitosis and intrahepatic metastasis.

Printed on: 02/07/23

## Abstract Archives of the RSNA, 2022

M2-SPGI-7

### **A Diagnostic Value of MR Radiomics for Predicting Lateral Pelvic Lymph Node Metastasis in Patients with Locally Advanced Rectal Cancer: A Multicenter Retrospective Study**

Monday, Nov. 28 9:00AM - 9:30AM Room: Learning Center - GI DPS

#### **Participants**

Jeongin Yoo, Seoul, Korea, Republic Of (*Presenter*) Nothing to Disclose

#### **PURPOSE**

To develop a MRI radiomics-based prediction model for lateral pelvic lymph node (LPLN) metastasis in rectal cancer patients who underwent LPLN dissection as well as to validate model performance using an external validation dataset.

#### **METHODS AND MATERIALS**

A total of 344 patients (198 in the development cohort and 146 in the validation cohort) who underwent rectal cancer surgery and LPLN dissection were enrolled. Patients' clinical and laboratory features were recorded. Radiomics features of LPLN were extracted from pre- post-chemoradiation therapy high-resolution T2-weighted axial or coronal MR images. The least absolute shrinkage and selection operator regression analysis was conducted to select predictive radiomics features in the development cohort, and a radiomics score for predicting LPLN metastasis was calculated based on the selected features. Model performance was assessed by receiver operating characteristics curve, calibration curves, and decision curve analysis (DCA). The prediction model was externally validated in the validation cohort.

#### **RESULTS**

In the development cohort, 70 (35.4%) of 198 patients had metastatic LPLN. Of clinical features, neoadjuvant radiotherapy is the sole significant feature. Of 116 radiomics features, histogram-based energy and histogram-based total energy were selected as significant features. Radiomics score can be calculated as a following formula: radiomics score =  $-0.58618 + 1.7252902E-9 \times$  histogram-based energy +  $1.1056922E-9 \times$  histogram-based total energy. A combined model using clinical features and radiomics score showed better prediction performance compared to the clinical feature only (area under the curve [AUC] value: 0.73 vs 0.61) in the development cohort ( $P < 0.0001$ ). DCA demonstrated that the combined model has the highest net benefit in threshold probability of 25% - 75%. In the validation cohort, a combined model using clinical features and radiomics score showed better prediction performance compared to the clinical feature only (AUC value: 0.61 vs 0.51) ( $P = 0.0318$ ) and had the highest net benefit in threshold probability of 30%-75%.

#### **CONCLUSION**

An application of radiomics on rectal MRI showed the best prediction performance of a combined model using clinical features and radiomics score to predict LPLN metastasis.

#### **CLINICAL RELEVANCE/APPLICATION**

An application of radiomics on rectal MRI can be useful for accurately predicting LPLN metastasis in patients with rectal cancer

Printed on: 02/07/23

## Abstract Archives of the RSNA, 2022

M2-SPGI-8

### Diagnostic performance of Apparent Diffusion Coefficient to assess the therapeutic response to biological therapy in Crohn's disease

Monday, Nov. 28 9:00AM - 9:30AM Room: Learning Center - GI DPS

#### Participants

Jordi Rimola, MD, PhD, (*Presenter*) Consultant, Alimentiv Health Trust; Speaker, Takeda Pharmaceutical Company Limited; Consultant, Johnson & Johnson; Consultant, Boehringer Ingelheim GmbH; Research Grant, AbbVie Inc

#### PURPOSE

to determine prospectively the performance of the Apparent Diffusion Coefficient (ADC) to assess response to biological therapy in Crohn's disease (CD) using MR enterography (MRE) and ileocolonoscopy as reference standards.

#### METHODS AND MATERIALS

Seventy four CD & patients underwent MRE with ADC calculation before and at 46-week after treatment with biological therapy. MRE images were analyzed including measurement of ADC. Segmental MaRIA was considered the reference standard to identify presence and severity of inflammation. Similar analysis was done in the 41 subjects who underwent ileocolonoscopy at both time points.

#### RESULTS

MRE identified 125 intestinal segments with severe inflammation (MaRIA  $\geq 11$ ) at baseline. Of them, 54% achieved healing of severe inflammation (MaRIA  $< 11$ ) at week 46. Using a receiver operating characteristic (ROC) curve, we determined at baseline an ADC threshold of  $1.301 \times 10^{-3} \text{mm}^2/\text{s}$  to predict severity, yielding a sensitivity of 0.78 and specificity of 0.94 to identify segments with MaRIA  $\geq 11$  (AUROC=0.92). Using the same threshold, ADC has a sensitivity and specificity of 0.90 and 0.75 respectively to identify healing of severe inflammation (MaRIA  $< 11$ ) at week 46. Using ileocolonoscopy as reference, the ADC threshold to predict endoscopic severity (ulcers) was very similar ( $1.382 \times 10^{-3} \text{mm}^2/\text{s}$ ) yielding a sensitivity and specificity of 0.76 and 0.89, and 0.95 and 0.71 to identify endoscopic ulcer healing. The MaRIA score was superior to ADC to predict endoscopic ulcer healing (AUROC 0.94 vs. 0.83  $p=0.01$ ).

#### CONCLUSION

s ADC showed robust thresholds to predict severe inflammation in CD using either MaRIA or ileocolonoscopy, and could be used as an alternative to the MaRIA index to assess therapeutic response in CD.

#### CLINICAL RELEVANCE/APPLICATION

ADC is a potential imaging biomarker alternative to MaRIA score or ileocolonoscopy to assess the treatment response to biological therapy in Crohn's disease

Printed on: 02/07/23



## Abstract Archives of the RSNA, 2022

M2-SPGI-9

### MRI Defecography: A Useful Tool to Guide Surgical Management in Patients With Pelvic Floor Dysfunction

Monday, Nov. 28 9:00AM - 9:30AM Room: Learning Center - GI DPS

#### Participants

John Gao, MD, Kansas City, KS (*Presenter*) Nothing to Disclose

#### PURPOSE

To retrospectively evaluate magnetic resonance (MR) defecography findings in patients with pelvic floor dysfunction to assess which findings on MR defecography influence decisions to perform subsequent pelvic floor surgery.

#### METHODS AND MATERIALS

This retrospective cohort study included women 18 and older who had an MRI defecography exam from 1/1/2017 - 6/30/2021. Patients were excluded if they were male, under 18, unable to comply with the exam, or had insufficient imaging. Demographic, clinical, and imaging information were obtained from the electronic medical record and Picture Archiving and Communications Systems (PACS). Imaging reports were retrospectively reviewed using the original interpretations.

#### RESULTS

One hundred sixty-eight patients with 171 MR defecography exams were included. Twenty out of 168 total patients (11.9%) patients had subsequent pelvic floor surgery in the year following their exam. Multiple measurements on MRI demonstrated a statistically significant odds ratio for subsequent pelvic floor surgery, including M line at maximal strain (OR=1.5,  $p=0.070$ ) and the presence of sigmoidocele (OR=27.7,  $p=0.011$ ) and enterocele (OR=6.8,  $p=0.015$ ). Patients in the surgical group had higher M-lines at maximal strain (5.7 cm) than in the non-surgical group (4.7 cm).

#### CONCLUSION

s MRI defecography is an important tool to evaluate anatomical and functional abnormalities in patients with pelvic floor dysfunction. Certain measurements and findings may help guide decisions to pursue surgical treatment. The presence of sigmoidoceles and enteroceles is a significant finding that may direct patients and clinicians to pursue surgical management, which should be highlighted in the radiology report.

#### CLINICAL RELEVANCE/APPLICATION

Radiologists should highlight key measurements and findings on MRI defecography exams as well as recommend surgical consultation in certain patients.

Printed on: 02/07/23

## Abstract Archives of the RSNA, 2022

M2-SPGU

### Genitourinary Monday Poster Discussions

Monday, Nov. 28 9:00AM - 9:30AM Room: Learning Center - GU DPS

#### Sub-Events

#### **M2-SPGU-1 Comparison of diagnostic accuracy between an artificial-intelligence-based prostate MRI protocol, mpMRI and bpMRI in dependence on the radiologist experience**

##### Participants

Daniel Nissler, MD, (*Presenter*) Grant, Zentrales Innovations; Speaker, Bayer AG; Travel support, Bayer AG

##### PURPOSE

Evaluation of the diagnostic accuracy of three rating radiologists with different degree of experience in prostate MRI assessment for an artificial intelligence supported biparametric MRI protocol (ai) in comparison to a multiparametric MRI (mp) as well as a biparametric MRI (bp) protocol.

##### METHODS AND MATERIALS

In this retrospective study, the diagnostic accuracy of prostate cancer detection between ai, mp and bp was compared. The software used T2-weighted and diffusion sequences from a 3.0 T MRI system to run an automatic segmentation of suspicious prostate lesions using an Aniso-3D-U-Net and a VGG-Net for lesion classification. Three radiologist with different degree of experience in prostate MRI (1- high, 2- intermedium, 3- low) evaluated the PI-RADS score for the patients in three different branches of the study: ai, mp, bp. Ground truth was the histology from the combined systematic and targeted transrectal US fusion biopsy.

##### RESULTS

PI-RADS scores from 105 men (median age, 66 years; range, 46-85 years/ median PSA, 9.4 [ng/ml]; range, 1-56 [ng/ml]) were matched with the Gleason score (GS) to determine the AUC for each branch (ai, mp, bp) and reader (1-3). The AUC to detect prostate cancer (GS = 3 + 3) for reader 1 was 0.850 for ai, 0.849 for mp, and 0.829 for bp. The corresponding values for reader 2 were 0.847 (ai), 0.781 (mp), 0.762 (bp) and for reader 3 0.819 (ai), 0.775 (mp), 0.712 (bp). There were no statically significant differences for reader 1 between ai, mp and bp. The difference between ai and bp for reader 2 ( $p = 0,006$ ) and 3 ( $p = 0.008$ ) was statically significant. For all readers the diagnostic accuracy for bp was lower than mp, but not statically significant.

##### CONCLUSION

s Radiologist with low or intermedium degree of experience in prostate MRI assessment benefit from ai and reach higher accuracy than mp and bp, whereas radiologist with high experience reached equal AUC for ai and mp. For all readers ai can compensate the decreased accuracy in bp.

##### CLINICAL RELEVANCE/APPLICATION

The results reveal first signs, that the ai protocol shows similarly good values as the mp protocol, so that an ai supported bp protocol could possibly detach a contrast agent assisted protocol.

#### **M2-SPGU-2 Image quality of virtual monochromatic imaging of half-iodine-load contrast-enhanced abdomen-pelvis CT by Gemstone Spectral Imaging with deep learning reconstruction**

##### Participants

Shingo Harashima, Tokyo, Japan (*Presenter*) Nothing to Disclose

##### PURPOSE

Image quality (IQ) of Gemstone Spectral Imaging (GSI) has been improving with recent introduction of deep learning reconstruction (DLR). We prospectively assessed IQ of virtual monochromatic imaging (VMI) of half-iodine-load contrast-enhanced abdomen-pelvis CT (CE-APCT) with the minimal slice thickness by GSI with DLR.

##### METHODS AND MATERIALS

In 28 patients with moderate-severe renal impairment who underwent half-iodine-load (300 mgI/kg) CE-APCT during the nephrographic phase using a 256-detector GSI scanner (Revolution CT, GE), we reconstructed VMI at 40-140 keV (1-keV interval) of the minimal slice thickness of 0.625 mm with filtered back projection (FBP), iterative reconstruction (IR), and DLR (TrueFidelity, GE); placed regions of interest in the liver, spleen, aorta, portal vein, paraspinal muscle, and subcutaneous fat in the abdomen and in the prostate/uterus, gluteal muscle, and subcutaneous fat in the pelvis to measure each organ's CT value and contrast-noise ratio (CNR) as (CT value of each organ - that of the muscle)/standard deviation of CT value of the fat in the abdomen and pelvis; determined the optimal keV to achieve the maximal CNR. Two independent radiologists subjectively assessed image noise, contrast, and sharpness, delineation of small structures, and overall IQ using a 4-point scale (1, poor; 4, excellent; 2-4, acceptable). We used Kruskal-Wallis test with Bonferroni correction to compare each organ's CT value and CNR and subjective IQ scores among FBP, IR, and DLR and weighted  $\chi^2$  test to quantify inter-reader agreement.

## RESULTS

Each organ's CT value and CNR continuously increased from 140 to 40 keV with FBP, IR, and DLR. At the optimal keV (i.e., 40 keV), CNR of the prostate/uterus was significantly greater with DLR than with FBP ( $P < 0.05$ ) but comparable between FBP and IR and between IR and DLR ( $P > 0.05$ ) and CNR of any other organs significantly increased from FBP to IR to DLR ( $P < 0.05$ ), whereas each organ's CT value was comparable among the 3 reconstructions ( $P > 0.05$ ). All the IQ scores significantly improved from FBP to IR to DLR ( $P < 0.05$ ) and were acceptable in all the patients only with DLR. Inter-reader agreement was substantial ( $\kappa = 0.65$ ).

## CONCLUSION

s Combined use of 40 keV and DLR offers the maximal CNR and subjectively acceptable IQ in VMI of half-iodine-load CE-APCT with the minimal slice thickness.

## CLINICAL RELEVANCE/APPLICATION

VMI at 40 keV by GSI can preserve image contrast and improve delineation of fine anatomies and lesions in half-iodine-load CE-APCT with the minimal slice thickness by achieving acceptable IQ by DLR.

Printed on: 02/07/23

## Abstract Archives of the RSNA, 2022

M2-SPGU-1

### Comparison of diagnostic accuracy between an artificial-intelligence-based prostate MRI protocol, mpMRI and bpMRI in dependence on the radiologist experience

Monday, Nov. 28 9:00AM - 9:30AM Room: Learning Center - GU DPS

#### Participants

Daniel Nissler, MD, (*Presenter*) Grant, Zentrales Innovations;Speaker, Bayer AG;Travel support, Bayer AG

#### PURPOSE

Evaluation of the diagnostic accuracy of three rating radiologists with different degree of experience in prostate MRI assessment for an artificial intelligence supported biparametric MRI protocol (ai) in comparison to a multiparametric MRI (mp) as well as a biparametric MRI (bp) protocol.

#### METHODS AND MATERIALS

In this retrospective study, the diagnostic accuracy of prostate cancer detection between ai, mp and bp was compared. The software used T2-weighted und diffusion sequences from a 3.0 T MRI system to run an automatic segmentation of suspicious prostate lesions using an Aniso-3D-U-Net and a VGG-Net for lesion classification. Three radiologist with different degree of experience in prostate MRI (1- high, 2- intermedium, 3- low) evaluated the PI-RADS score for the patients in three different branches of the study: ai, mp, bp. Ground truth was the histology from the combined systematic and targeted transrectal US fusion biopsy.

#### RESULTS

PI-RADS scores from 105 men (median age, 66 years; range, 46-85 years/ median PSA, 9.4 [ng/ml]; range, 1-56 [ng/ml]) were matched with the Gleason score (GS) to determine the AUC for each branch (ai, mp, bp) and reader (1-3). The AUC to detect prostate cancer (GS = 3 + 3) for reader 1 was 0.850 for ai, 0.849 for mp, and 0.829 for bp. The corresponding values for reader 2 were 0.847 (ai), 0.781 (mp), 0.762 (bp) and for reader 3 0.819 (ai), 0.775 (mp), 0.712 (bp). There were no statically significant differences for reader 1 between ai, mp and bp. The difference between ai and bp for reader 2 ( $p = 0,006$ ) and 3 ( $p = 0.008$ ) was statically significant. For all readers the diagnostic accuracy for bp was lower than mp, but not statically significant.

#### CONCLUSION

s Radiologist with low or intermedium degree of experience in prostate MRI assessment benefit from ai and reach higher accuracy then mp and bp, whereas radiologist with high experience reached equal AUC for ai and mp. For all readers ai can compensate the decreased accuracy in bp.

#### CLINICAL RELEVANCE/APPLICATION

The results reveal first signs, that the ai protocol shows similarly good values as the mp protocol, so that an ai supported bp protocol could possibly detach a contrast agent assisted protocol.

Printed on: 02/07/23

## Abstract Archives of the RSNA, 2022

M2-SPGU-2

### Image quality of virtual monochromatic imaging of half-iodine-load contrast-enhanced abdomen-pelvis CT by Gemstone Spectral Imaging with deep learning reconstruction

Monday, Nov. 28 9:00AM - 9:30AM Room: Learning Center - GU DPS

#### Participants

Shingo Harashima, Tokyo, Japan (*Presenter*) Nothing to Disclose

#### PURPOSE

Image quality (IQ) of Gemstone Spectral Imaging (GSI) has been improving with recent introduction of deep learning reconstruction (DLR). We prospectively assessed IQ of virtual monochromatic imaging (VMI) of half-iodine-load contrast-enhanced abdomen-pelvis CT (CE-APCT) with the minimal slice thickness by GSI with DLR.

#### METHODS AND MATERIALS

In 28 patients with moderate-severe renal impairment who underwent half-iodine-load (300 mgI/kg) CE-APCT during the nephrographic phase using a 256-detector GSI scanner (Revolution CT, GE), we reconstructed VMI at 40-140 keV (1-keV interval) of the minimal slice thickness of 0.625 mm with filtered back projection (FBP), iterative reconstruction (IR), and DLR (TrueFidelity, GE); placed regions of interest in the liver, spleen, aorta, portal vein, paraspinal muscle, and subcutaneous fat in the abdomen and in the prostate/uterus, gluteal muscle, and subcutaneous fat in the pelvis to measure each organ's CT value and contrast-noise ratio (CNR) as (CT value of each organ - that of the muscle)/standard deviation of CT value of the fat in the abdomen and pelvis; determined the optimal keV to achieve the maximal CNR. Two independent radiologists subjectively assessed image noise, contrast, and sharpness, delineation of small structures, and overall IQ using a 4-point scale (1, poor; 4, excellent; 2-4, acceptable). We used Kruskal-Wallis test with Bonferroni correction to compare each organ's CT value and CNR and subjective IQ scores among FBP, IR, and DLR and weighted  $\chi^2$  test to quantify inter-reader agreement.

#### RESULTS

Each organ's CT value and CNR continuously increased from 140 to 40 keV with FBP, IR, and DLR. At the optimal keV (i.e., 40 keV), CNR of the prostate/uterus was significantly greater with DLR than with FBP ( $P < 0.05$ ) but comparable between FBP and IR and between IR and DLR ( $P > 0.05$ ) and CNR of any other organs significantly increased from FBP to IR to DLR ( $P < 0.05$ ), whereas each organ's CT value was comparable among the 3 reconstructions ( $P > 0.05$ ). All the IQ scores significantly improved from FBP to IR to DLR ( $P < 0.05$ ) and were acceptable in all the patients only with DLR. Inter-reader agreement was substantial ( $\kappa = 0.65$ ).

#### CONCLUSION

Combined use of 40 keV and DLR offers the maximal CNR and subjectively acceptable IQ in VMI of half-iodine-load CE-APCT with the minimal slice thickness.

#### CLINICAL RELEVANCE/APPLICATION

VMI at 40 keV by GSI can preserve image contrast and improve delineation of fine anatomies and lesions in half-iodine-load CE-APCT with the minimal slice thickness by achieving acceptable IQ by DLR.

Printed on: 02/07/23

## Abstract Archives of the RSNA, 2022

M2-SPHN

### Head and Neck Monday Poster Discussions

Monday, Nov. 28 9:00AM - 9:30AM Room: Learning Center - HN DPS

#### Sub-Events

#### M2-SPHN-1 How Reliably can MRI Visualize the Endolymphatic Duct in Patients With and Without Vestibular Aqueduct Enlargement?

##### Awards

Trainee Research Prize - Fellow

##### Participants

Olutayo Olubiyi, MBChB, MPH, (*Presenter*) Nothing to Disclose

##### PURPOSE

To determine 1) whether normal-sized endolymphatic ducts (ELD) are routinely visible on high-resolution temporal bone MRI and 2) how reliably MRI detects vestibular aqueduct (VA) enlargement.

##### METHODS AND MATERIALS

The study was approved by our center's IRB. 100 pediatric patients who underwent temporal bone CT and MRI between January 2017 and December 2020 were included for this study. VA width was measured at the midpoint and operculum on axial CT and at the midpoint on Poschl reconstructions. Enlargement of the VA (eVA) was determined using the Cincinnati criteria. Corresponding heavily T2-weighted high-resolution MRI images were reviewed, with visibility of each ELD categorized as: type 1=not visible; type 2=indistinct; or type 3=easily visible (Figure). Mixed-effect logistic regression analyses were used to evaluate 1) whether MRI visibility was associated with eVA and 2) whether mean vestibular aqueduct diameters differ based on MRI visibility. A p-value <0.05 was used as the level of statistical significance in all analyses.

##### RESULTS

eVA was identified in 21% of the analyzed ears. There was a significant association between the presence of eVA on CT and ELD visibility on MRI ( $p=0.0001$ ). In eVA- ears, ELD visibility on MRI was type 1 in 87%, type 2 in 13%, and type 3 in 0%. In eVA+ ears, the ELDs were type 1 in 21%, type 2 in 21%, and type 3 in 57%. There were significant differences in predicted mean VA widths based on MRI visibility ( $p<0.0001$ ) regardless of the method of VA measurement. E.g., the mean predicted axial mid-VA widths were: 0.63 mm for type 1, 0.97 mm for type 2, and 2.1 mm for type 3 ELDs (Tukey-adjusted p-value <0.0001 for all comparisons).

##### CONCLUSION

s ELDs were never easily visible and were usually invisible on high-resolution MRI in eVA- ears on CT. Easy visibility of the ELD was only noted in eVA+ ears, in whom, the majority of cases were type 3; however, in 21% of eVA+ ears, the ELD was not visible on MRI, suggesting that MRI should not be used as a substitute for CT in ruling out eVA.

##### CLINICAL RELEVANCE/APPLICATION

Our data suggested that MRI cannot be substituted for temporal bone CT to rule out eVA in pediatric patients. Furthermore, in the vast majority of ears without eVA, the ELD is not visible on MRI.

#### M2-SPHN-3 CT-guided Core Needle Biopsy in Head and Neck Masses: Evaluation of Accuracy and Safety

##### Participants

Thomas J. Vogl, MD, PhD, Frankfurt, Germany (*Presenter*) Nothing to Disclose

##### PURPOSE

To evaluate the procedure of CT-guided core needle biopsy of head and neck masses focusing on accuracy and safety.

##### METHODS AND MATERIALS

In this retrospective single-center study the accuracy and safety of CT-guided core needle biopsies in head and neck masses was evaluated from April 2007 to December 2021. A total of 154 patients (mean: 55.9y; 61% males, 39% females) with biopsies were evaluated. 57.1% of all patients had a history of malignoma, 56.7% of the lesions were located cranial to the os hyoideum. The most common needle approach of suprahyoid lesions (33%) was the subzygomatic approach. The average diameters of all lesions were 36x23mm. The location of the lesions was divided in cranial and caudal to the os hyoideum. To ensure the diagnostic accuracy, the initial histological results were compared with the final medical diagnosis and an additional follow-up of at least six months.

##### RESULTS

10 of 154 biopsies showed insufficient and inconclusive samples and were excluded from the evaluation. The remaining 144 biopsies

showed a sensitivity of 94.1%, a specificity of 100% and an accuracy of 97.3%. There were four false negative and no false positive biopsies, resulting in a positive predictive value of 100% and a negative predictive value of 95.1%. Eight cases presented minor complications such as postpunctate hematomas, without requiring any intervention. The average dosis-length-product was 276,4 mGy x cm.

#### **CONCLUSION**

s CT-guided core needle biopsy of head and neck masses is a safe and effective procedure, which shows a low rate of complications with a high diagnostic accuracy.

#### **CLINICAL RELEVANCE/APPLICATION**

CT-guided biopsy of head and neck masses is of high clinical relevance

Printed on: 02/07/23

## Abstract Archives of the RSNA, 2022

M2-SPHN-1

### How Reliably can MRI Visualize the Endolymphatic Duct in Patients With and Without Vestibular Aqueduct Enlargement?

Monday, Nov. 28 9:00AM - 9:30AM Room: Learning Center - HN DPS

#### Awards

Trainee Research Prize - Fellow

#### Participants

Olutayo Olubiyi, MBChB, MPH, (*Presenter*) Nothing to Disclose

#### PURPOSE

To determine 1) whether normal-sized endolymphatic ducts (ELD) are routinely visible on high-resolution temporal bone MRI and 2) how reliably MRI detects vestibular aqueduct (VA) enlargement.

#### METHODS AND MATERIALS

The study was approved by our center's IRB. 100 pediatric patients who underwent temporal bone CT and MRI between January 2017 and December 2020 were included for this study. VA width was measured at the midpoint and operculum on axial CT and at the midpoint on Poschl reconstructions. Enlargement of the VA (eVA) was determined using the Cincinnati criteria. Corresponding heavily T2-weighted high-resolution MRI images were reviewed, with visibility of each ELD categorized as: type 1=not visible; type 2=indistinct; or type 3=easily visible (Figure). Mixed-effect logistic regression analyses were used to evaluate 1) whether MRI visibility was associated with eVA and 2) whether mean vestibular aqueduct diameters differ based on MRI visibility. A p-value <0.05 was used as the level of statistical significance in all analyses.

#### RESULTS

eVA was identified in 21% of the analyzed ears. There was a significant association between the presence of eVA on CT and ELD visibility on MRI ( $p=0.0001$ ). In eVA- ears, ELD visibility on MRI was type 1 in 87%, type 2 in 13%, and type 3 in 0%. In eVA+ ears, the ELDs were type 1 in 21%, type 2 in 21%, and type 3 in 57%. There were significant differences in predicted mean VA widths based on MRI visibility ( $p<0.0001$ ) regardless of the method of VA measurement. E.g., the mean predicted axial mid-VA widths were: 0.63 mm for type 1, 0.97 mm for type 2, and 2.1 mm for type 3 ELDs (Tukey-adjusted p-value <0.0001 for all comparisons).

#### CONCLUSION

s ELDs were never easily visible and were usually invisible on high-resolution MRI in eVA- ears on CT. Easy visibility of the ELD was only noted in eVA+ ears, in whom, the majority of cases were type 3; however, in 21% of eVA+ ears, the ELD was not visible on MRI, suggesting that MRI should not be used as a substitute for CT in ruling out eVA.

#### CLINICAL RELEVANCE/APPLICATION

Our data suggested that MRI cannot be substituted for temporal bone CT to rule out eVA in pediatric patients. Furthermore, in the vast majority of ears without eVA, the ELD is not visible on MRI.

Printed on: 02/07/23

## Abstract Archives of the RSNA, 2022

M2-SPHN-3

### CT-guided Core Needle Biopsy in Head and Neck Masses: Evaluation of Accuracy and Safety

Monday, Nov. 28 9:00AM - 9:30AM Room: Learning Center - HN DPS

#### Participants

Thomas J. Vogl, MD, PhD, Frankfurt, Germany (*Presenter*) Nothing to Disclose

#### PURPOSE

To evaluate the procedure of CT-guided core needle biopsy of head and neck masses focusing on accuracy and safety.

#### METHODS AND MATERIALS

In this retrospective single-center study the accuracy and safety of CT-guided core needle biopsies in head and neck masses was evaluated from April 2007 to December 2021. A total of 154 patients (mean: 55.9y; 61% males, 39% females) with biopsies were evaluated. 57.1% of all patients had a history of malignoma, 56.7% of the lesions were located cranial to the os hyoideum. The most common needle approach of suprahyoid lesions (33%) was the subzygomatic approach. The average diameters of all lesions were 36x23mm. The location of the lesions was divided in cranial and caudal to the os hyoideum. To ensure the diagnostic accuracy, the initial histological results were compared with the final medical diagnosis and an additional follow-up of at least six months.

#### RESULTS

10 of 154 biopsies showed insufficient and inconclusive samples and were excluded from the evaluation. The remaining 144 biopsies showed a sensitivity of 94.1%, a specificity of 100% and an accuracy of 97.3%. There were four false negative and no false positive biopsies, resulting in a positive predictive value of 100% and a negative predictive value of 95.1%. Eight cases presented minor complications such as postpunctate hematomas, without requiring any intervention. The average dosis-length-product was 276,4 mGy x cm.

#### CONCLUSION

s CT-guided core needle biopsy of head and neck masses is a safe and effective procedure, which shows a low rate of complications with a high diagnostic accuracy.

#### CLINICAL RELEVANCE/APPLICATION

CT-guided biopsy of head and neck masses is of high clinical relevance

Printed on: 02/07/23



## Abstract Archives of the RSNA, 2022

M2-SPIN

### Informatics Monday Poster Discussions

Monday, Nov. 28 9:00AM - 9:30AM Room: Learning Center - IN DPS

#### Sub-Events

#### M2-SPIN-1 Mask Interpolation, Autocorrection, and Fast Annotation for Medical Imaging Labels

Participants

Kuan Zhang, PhD, , MN (*Presenter*) Nothing to Disclose

#### PURPOSE

Training a segmentation model requires human annotations, which are tedious. Since the annotation is performed among slices, the out-of-plane signals can be noisy with heterogeneous artifacts. There is a growing demand for efficient mask interpolation to alleviate annotation efforts and help with data preprocessing and augmentation. Here, we developed new interpolation and autocorrection algorithms for mask data. Based on them, a simple fast-annotation scheme was proposed.

#### METHODS AND MATERIALS

Tri-cubic interpolation (TCI) is often used to normalize imaging data as it provides more smooth transitions than nearest-neighbor interpolation (NNI). However, both methods fail for mask data due to the piecewise distribution. In addition to the zig-zag artifacts in the lateral planes, TCI can result in in-plane discontinuity artifacts. We created a distance field (dist-field) evaluating the nearest distance to the label boundary before TCI. It helps convert the piecewise mask data into continuous functions and corrects artifacts. Given the noisy signals in the lateral planes, we developed a label autocorrection (LAC) algorithm by optimizing the signals with a total-variation (TV) regularization term. We applied the TV on the dist-field rather than the original mask. Besides, the regularization rate is tuned pixel-wisely given the size and smoothness of the object obtained from the connected component analysis. We evaluated methods applied on our annotations of LITZ data and compared with the official mask data as the ground truth. Besides, we trained and evaluated 3D U-Net models on the original body-decomposition labels and the labels with LAC.

#### RESULTS

Full annotation achieves a Dice Score (DS) as 0.966 (0.964 - 0.967) for liver and 0.862 (0.802 - 0.895) for tumor. Applying LAC on the full annotation, the DS increased to 0.974 (0.972 - 0.976) for liver and 0.890 (0.834 - 0.918) for tumor. Performing the fast-annotation scheme can achieve DS 0.970 (0.965 - 0.974) for liver and 0.873 (0.806 - 0.920) for tumor. Besides, if we label every five slices and do TCI, the DS decreased to 0.963 (0.959 - 0.966) for liver and 0.857 (0.793 - 0.898) for tumor. The time spent on fast annotation is one-fifth of the full annotation. Trained on body-decomposition datasets, the validation DS increased among 23 organs and decreased among five. The medium difference with and without LAC is +0.018.

#### CONCLUSION

s We developed new algorithms to interpolate, autocorrect and fast annotate imaging labels.

#### CLINICAL RELEVANCE/APPLICATION

DL segmentation is widely performed in clinical practice and research. Human annotations limit its development in terms of efficiency and accuracy. The proposed methods can be smoothly embedded into the routine pipeline and improve performance.

#### M2-SPIN-2 Transformation of Multiphasic Intraprocedural Angiograms into Physiologic Models for Identification of Tumor Bed Saturation in Y-90 Radioembolization Planning

Participants

John Mayfield, MD, MS, Lithia, FL (*Presenter*) Nothing to Disclose

#### PURPOSE

Since the first appearance of CT angiography in Radiology in 1992, this technology has found a growing use in Interventional Radiology. A large volume of literature has evolved describing how to best provide intraprocedural and as well as predictive surrogates of pathophysiological processes. Past attempts of translating images into realistic models ranged from two-dimensional flow diagrams to three-dimensional rigid wall synthetic structures. We propose a unique method of using multiphase intra-arterial CT angiogram in a population of patients with Neuroendocrine tumor liver metastases (NETLMs).

#### METHODS AND MATERIALS

We retrospectively reviewed three patients with NETLMs who were candidates for Y-90 radioembolization. Pre-embolization mapping was carried out in the angiography suite of two target hepatic arteries with injection of Isovue-250® (iopamidol, Bracco diagnostics Inc, Monroe Township, NJ) during intra-arterial CT angiography (CTA) on a Canon 4D Scanner (Canon Medical Systems, Tustin, CA) captured at 6 and 14 seconds to provide multiphase images. Subsequent CTAs were deidentified and exported as DICOM images to Mimics and 3Matic software packages (Materialise, Plymouth, MI) where the artery distal to the tip of microcatheter placement was segmented and exported to COMSOL Multiphysics (COMSOL, Stockholm, Sweden). From the intraprocedural nursing records, the patient's specific vital signs and physiologic parameters were parameterized in the model with

Monte Carlo simulation until a solution converged.

## RESULTS

In all three patients, late-phase (14s) intraprocedural angiograms demonstrated significantly improved visualization of the tumor vascular beds in comparison to the early arterial phase (6s). The tumor vascular bed and feeding arteries were effectively segmented and represented in the resultant geometry in the modeling software. Variant flow patterns were mapped in the distal feeding vessels as well as tumor vascular beds. Four maximum velocity thresholds helped identify potential areas of low perfusion or “blind spots” where the Y-90 radioembolization microspheres would not deposit adequately based upon blood flow distribution.

## CONCLUSION

s We demonstrate that utilization of multiphase intra-arterial CT angiography provides high-quality images that include tumor vascular beds, which in turn allow effective, patient-specific computational modeling of these systems from an off-the-shelf software suite that can be utilized in mapping hepatic tumors.

## CLINICAL RELEVANCE/APPLICATION

Visualization of the three-dimensional blood flow behavior can help to identify potential regions of decreased radioembolization based upon bead distribution and alter treatment delivery mechanisms and dose.

## M2-SPIN-4 FDA's list of Artificial Intelligence and Machine Learning Enabled Medical Devices- Radiology Leads the Way

Participants

Larisa Gorenstein, MD, (*Presenter*) Nothing to Disclose

## PURPOSE

The US food and drug administration (FDA) ensures the safety and efficacy of healthcare-related products and promotes public health through innovation. Artificial intelligence (AI) has become an area of extreme interest in healthcare in the past decade. Understanding FDA-approved application trends in different medical fields can direct future industry and research resource allocations and regulatory efforts. Our objective was to assess the role of radiology in the FDA's list of AI-enabled medical devices.

## METHODS AND MATERIALS

We accessed the list of Artificial Intelligence and Machine Learning Enabled Medical Devices-publicly available on the FDA website (<https://www.fda.gov/medical-devices/software-medical-device-samd/artificial-intelligence-and-machine-learning-aiml-enabled-medical-devices>). The site was Accessed on 1/4/2022, and the data is current to 09/22/2021. Entries' medical field and registration dates were analyzed.

## RESULTS

A total of 343 entries were listed. 241 (70%) of the entries are from Radiology. 41 (12%) cardiovascular devices. 13 (4%) hematological entries, and 12 (3.5%) from the field of Neurology. Gastroenterology-Urology, General and Plastic Surgery, Anesthesiology, Microbiology, Pathology, Orthopedics, Obstetrics and gynecology and Dental had less than ten entries each. 38 (11%) were listed in 2021, only partially included. 29 (76%) of those were from Radiology. In 2020 out of 100 entries 54 were in Radiology. The largest number of entries by a single conglomerate was 22 (6%), all from the field of Radiology. All devices except one were submitted via 510(k) clearance or De Novo request.

## CONCLUSION

s Radiology led the FDA's list by a wide margin with a rise in recent years. AI in medical imaging is in the front line of the entire healthcare innovation. In light of our findings, prioritization of the regulatory resources for radiological medical devices should be considered. The substantial number of devices approved in radiology and the nuances of this field require specialists in radiology to be an integral part of the regulatory process.

## CLINICAL RELEVANCE/APPLICATION

The allocation of regulatory resources towards radiology should be considered.

## M2-SPIN-5 Long-Tailed Classification of Thorax Diseases on Chest X-Ray

Participants

Yifan Peng, New York, NY (*Presenter*) Nothing to Disclose

## PURPOSE

Medical imaging exams, such as CXR, will yield a small set of common findings and a much larger set of uncommon findings. While a trained radiologist can learn uncommon findings by studying a few representative examples, it is more difficult to train a machine learning model from such a “long-tailed” distribution. In this work, we present a comprehensive benchmark study of the long-tailed learning problem in the specific domain of thorax diseases on CXR.

## METHODS AND MATERIALS

We introduced a new challenging CXR benchmark to facilitate research on developing long-tailed learning methods. The benchmark consists of two datasets, NIH-CXR-LT and MIMIC-CXR-LT, for 19- and 20-way thorax disease classification, respectively (Figure 1). We compared 15 different long-tail learning methods (Figure 2), which could be grouped into three categories: re-balancing, augmentation, and others. We present results on both the balanced test set and the imbalanced test set for each model and dataset.

## RESULTS

For the NIH-CXR-LT, the baseline of softmax cross-entropy loss achieves a group-wise average accuracy of 0.168, but improves to 0.260 and 0.264 when using class-balanced and sklearn weights, respectively (Figure 2). Furthermore, re-weighting constantly improves performance, and class-balanced methods achieve the highest group-wise average accuracy on the balanced test set. On the MIMIC-CXR-LT, re-weighting is always beneficial; for example, class-balanced re-weighting and sklearn re-weighting improve

focal loss performance from 0.181 to 0.278 and 0.299, respectively. However, unlike the NIH-CXR-LT results, DRW brings more gains to a re-weighted LDAM loss, improving group-wise accuracy by an absolute margin of at least 0.05. Interestingly, classifier re-training achieves both the highest group-wise average accuracy on the balanced test set and the highest balanced accuracy on the test set by a considerable margin.

## CONCLUSION

We conducted the first comprehensive study of long-tailed learning methods for disease classification on CXR. We will publicly release all code, models, and data to encourage the development of long-tailed learning methods for medical image classification.

## CLINICAL RELEVANCE/APPLICATION

Medical imaging exams often yield a small set of common but a much larger set of uncommon findings. We present a benchmark study of long-tailed learning on chest X-rays to facilitate future research.

## M2-SPIN-6 Development and Validation of A Deep Learning Model for Prediction of The 30-day Mortality of Patients With Community-acquired pneumonia from Chest X-ray

### Participants

Changi Kim, BS, Seoul, Korea, Republic Of (*Presenter*) Nothing to Disclose

## PURPOSE

To develop and validate a deep learning (DL) model to predict the 30-day mortality of patients with community-acquired pneumonia (CAP) using the chest X-ray (CXR) of patients.

## METHODS AND MATERIALS

For model development, initial CXRs of patients diagnosed with CAP at a single institution (Institution A) between 2013 and 2019 were included (Developmental dataset). A convolutional neural network-based DL model was trained to predict the hazard of death within 30 days from the diagnosis of CAP. [B1] For validation of model performance, patients who visited the emergency departments of three institutions (Institutions A [temporally separated with developmental dataset], B, and C) due to CAP were included (External validation datasets). The predictive performance for the 30-day mortality was evaluated using the area under the receiver operating characteristic curves (AUCs). The AUC of the DL model was compared with that of CURB-65 score, a widely used tool for risk evaluation in CAP. Finally, the results from the DL model were categorized into three risk groups, and simply added to the CURB-65 scores (combined scores), and the AUC of the combined score was compared with that of the CURB-65 score.

## RESULTS

Developmental dataset comprised 7,105 patients (62% men; mean age, 68 years; 30-day mortality rate, 11.4%), while external validation datasets from institution A, B, and C comprised 947 (63% men; mean age, 71 years; 30-day mortality rate, 17.6%), 467 (63% men; mean age, 73 years; 30-day mortality rate, 8.4%), and 381 (63.8% men; mean age, 71 years; 30-day mortality rate, 10.8%) patients, respectively. The DL model exhibited significantly higher AUC than CURB-65 score in external validation dataset from institution A (0.77 vs. 0.67,  $P < .001$ ); while the difference did not reach statistical significance in datasets from institutions B (0.80 vs. 0.73,  $P = .194$ ) and C (0.80 vs. 0.72,  $P = .081$ ). Finally, combined scores exhibited significantly higher AUCs than CURB-65 scores in all three external validation datasets (Institution A, 0.74,  $P < .001$ ; Institution B, 0.80,  $P = .002$ ; Institution C, 0.79,  $P < .001$ ).

## CONCLUSION

A DL model could predict the 30-day mortality of patients with CAP using CXRs, with higher performance than the CURB-65 score. Adding risk scores from the DL model to the CURB-65 score could improve the prediction performance.

## CLINICAL RELEVANCE/APPLICATION

Evaluation of CXRs of patients with CAP using the DL model for mortality prediction may help improve risk stratification and clinical decision-making for hospitalization or intensive care.

Printed on: 02/07/23



## Abstract Archives of the RSNA, 2022

M2-SPIN-1

### Mask Interpolation, Autocorrection, and Fast Annotation for Medical Imaging Labels

Monday, Nov. 28 9:00AM - 9:30AM Room: Learning Center - IN DPS

#### Participants

Kuan Zhang, PhD, , MN (*Presenter*) Nothing to Disclose

#### PURPOSE

Training a segmentation model requires human annotations, which are tedious. Since the annotation is performed among slices, the out-of-plane signals can be noisy with heterogeneous artifacts. There is a growing demand for efficient mask interpolation to alleviate annotation efforts and help with data preprocessing and augmentation. Here, we developed new interpolation and autocorrection algorithms for mask data. Based on them, a simple fast-annotation scheme was proposed.

#### METHODS AND MATERIALS

Tri-cubic interpolation (TCI) is often used to normalize imaging data as it provides more smooth transitions than nearest-neighbor interpolation (NNI). However, both methods fail for mask data due to the piecewise distribution. In addition to the zig-zag artifacts in the lateral planes, TCI can result in in-plane discontinuity artifacts. We created a distance field (dist-field) evaluating the nearest distance to the label boundary before TCI. It helps convert the piecewise mask data into continuous functions and corrects artifacts. Given the noisy signals in the lateral planes, we developed a label autocorrection (LAC) algorithm by optimizing the signals with a total-variation (TV) regularization term. We applied the TV on the dist-field rather than the original mask. Besides, the regularization rate is tuned pixel-wisely given the size and smoothness of the object obtained from the connected component analysis. We evaluated methods applied on our annotations of LITZ data and compared with the official mask data as the ground truth. Besides, we trained and evaluated 3D U-Net models on the original body-decomposition labels and the labels with LAC.

#### RESULTS

Full annotation achieves a Dice Score (DS) as 0.966 (0.964 - 0.967) for liver and 0.862 (0.802 - 0.895) for tumor. Applying LAC on the full annotation, the DS increased to 0.974 (0.972 - 0.976) for liver and 0.890 (0.834 - 0.918) for tumor. Performing the fast-annotation scheme can achieve DS 0.970 (0.965 - 0.974) for liver and 0.873 (0.806 - 0.920) for tumor. Besides, if we label every five slices and do TCI, the DS decreased to 0.963 (0.959 - 0.966) for liver and 0.857 (0.793 - 0.898) for tumor. The time spent on fast annotation is one-fifth of the full annotation. Trained on body-decomposition datasets, the validation DS increased among 23 organs and decreased among five. The medium difference with and without LAC is +0.018.

#### CONCLUSION

s We developed new algorithms to interpolate, autocorrect and fast annotate imaging labels.

#### CLINICAL RELEVANCE/APPLICATION

DL segmentation is widely performed in clinical practice and research. Human annotations limit its development in terms of efficiency and accuracy. The proposed methods can be smoothly embedded into the routine pipeline and improve performance.

Printed on: 02/07/23

## Abstract Archives of the RSNA, 2022

M2-SPIN-2

### Transformation of Multiphase Intra-procedural Angiograms into Physiologic Models for Identification of Tumor Bed Saturation in Y-90 Radioembolization Planning

Monday, Nov. 28 9:00AM - 9:30AM Room: Learning Center - IN DPS

#### Participants

John Mayfield, MD, MS, Lithia, FL (*Presenter*) Nothing to Disclose

#### PURPOSE

Since the first appearance of CT angiography in Radiology in 1992, this technology has found a growing use in Interventional Radiology. A large volume of literature has evolved describing how to best provide intra-procedural and as well as predictive surrogates of pathophysiological processes. Past attempts of translating images into realistic models ranged from two-dimensional flow diagrams to three-dimensional rigid wall synthetic structures. We propose a unique method of using multiphase intra-arterial CT angiogram in a population of patients with Neuroendocrine tumor liver metastases (NETLMs).

#### METHODS AND MATERIALS

We retrospectively reviewed three patients with NETLMs who were candidates for Y-90 radioembolization. Pre-embolization mapping was carried out in the angiography suite of two target hepatic arteries with injection of Isovue-250® (iopamidol, Bracco diagnostics Inc, Monroe Township, NJ) during intra-arterial CT angiography (CTA) on a Canon 4D Scanner (Canon Medical Systems, Tustin, CA) captured at 6 and 14 seconds to provide multiphase images. Subsequent CTAs were deidentified and exported as DICOM images to Mimics and 3Matic software packages (Materialise, Plymouth, MI) where the artery distal to the tip of microcatheter placement was segmented and exported to COMSOL Multiphysics (COMSOL, Stockholm, Sweden). From the intra-procedural nursing records, the patient's specific vital signs and physiologic parameters were parameterized in the model with Monte Carlo simulation until a solution converged.

#### RESULTS

In all three patients, late-phase (14s) intra-procedural angiograms demonstrated significantly improved visualization of the tumor vascular beds in comparison to the early arterial phase (6s). The tumor vascular bed and feeding arteries were effectively segmented and represented in the resultant geometry in the modeling software. Variant flow patterns were mapped in the distal feeding vessels as well as tumor vascular beds. Four maximum velocity thresholds helped identify potential areas of low perfusion or "blind spots" where the Y-90 radioembolization microspheres would not deposit adequately based upon blood flow distribution.

#### CONCLUSION

s We demonstrate that utilization of multiphase intra-arterial CT angiography provides high-quality images that include tumor vascular beds, which in turn allow effective, patient-specific computational modeling of these systems from an off-the-shelf software suite that can be utilized in mapping hepatic tumors.

#### CLINICAL RELEVANCE/APPLICATION

Visualization of the three-dimensional blood flow behavior can help to identify potential regions of decreased radioembolization based upon bead distribution and alter treatment delivery mechanisms and dose.

Printed on: 02/07/23



## Abstract Archives of the RSNA, 2022

M2-SPIN-4

### FDA's list of Artificial Intelligence and Machine Learning Enabled Medical Devices- Radiology Leads the Way

Monday, Nov. 28 9:00AM - 9:30AM Room: Learning Center - IN DPS

#### Participants

Larisa Gorenstein, MD, (*Presenter*) Nothing to Disclose

#### PURPOSE

The US food and drug administration (FDA) ensures the safety and efficacy of healthcare-related products and promotes public health through innovation. Artificial intelligence (AI) has become an area of extreme interest in healthcare in the past decade. Understanding FDA-approved application trends in different medical fields can direct future industry and research resource allocations and regulatory efforts. Our objective was to assess the role of radiology in the FDA's list of AI-enabled medical devices.

#### METHODS AND MATERIALS

We accessed the list of Artificial Intelligence and Machine Learning Enabled Medical Devices-publicly available on the FDA website (<https://www.fda.gov/medical-devices/software-medical-device-samd/artificial-intelligence-and-machine-learning-aiml-enabled-medical-devices>). The site was Accessed on 1/4/2022, and the data is current to 09/22/2021. Entries' medical field and registration dates were analyzed.

#### RESULTS

A total of 343 entries were listed. 241 (70%) of the entries are from Radiology. 41 (12%) cardiovascular devices. 13 (4%) hematological entries, and 12 (3.5%) from the field of Neurology. Gastroenterology-Urology, General and Plastic Surgery, Anesthesiology, Microbiology, Pathology, Orthopedics, Obstetrics and gynecology and Dental had less than ten entries each. 38 (11%) were listed in 2021, only partially included. 29 (76%) of those were from Radiology. In 2020 out of 100 entries 54 were in Radiology. The largest number of entries by a single conglomerate was 22 (6%), all from the field of Radiology. All devices except one were submitted via 510(k) clearance or De Novo request.

#### CONCLUSION

Radiology led the FDA's list by a wide margin with a rise in recent years. AI in medical imaging is in the front line of the entire healthcare innovation. In light of our findings, prioritization of the regulatory resources for radiological medical devices should be considered. The substantial number of devices approved in radiology and the nuances of this field require specialists in radiology to be an integral part of the regulatory process.

#### CLINICAL RELEVANCE/APPLICATION

The allocation of regulatory resources towards radiology should be considered.

Printed on: 02/07/23



## Abstract Archives of the RSNA, 2022

M2-SPIN-5

### Long-Tailed Classification of Thorax Diseases on Chest X-Ray

Monday, Nov. 28 9:00AM - 9:30AM Room: Learning Center - IN DPS

#### Participants

Yifan Peng, New York, NY (*Presenter*) Nothing to Disclose

#### PURPOSE

Medical imaging exams, such as CXR, will yield a small set of common findings and a much larger set of uncommon findings. While a trained radiologist can learn uncommon findings by studying a few representative examples, it is more difficult to train a machine learning model from such a "long-tailed" distribution. In this work, we present a comprehensive benchmark study of the long-tailed learning problem in the specific domain of thorax diseases on CXR.

#### METHODS AND MATERIALS

We introduced a new challenging CXR benchmark to facilitate research on developing long-tailed learning methods. The benchmark consists of two datasets, NIH-CXR-LT and MIMIC-CXR-LT, for 19- and 20-way thorax disease classification, respectively (Figure 1). We compared 15 different long-tail learning methods (Figure 2), which could be grouped into three categories: re-balancing, augmentation, and others. We present results on both the balanced test set and the imbalanced test set for each model and dataset.

#### RESULTS

For the NIH-CXR-LT, the baseline of softmax cross-entropy loss achieves a group-wise average accuracy of 0.168, but improves to 0.260 and 0.264 when using class-balanced and sklearn weights, respectively (Figure 2). Furthermore, re-weighting constantly improves performance, and class-balanced methods achieve the highest group-wise average accuracy on the balanced test set. On the MIMIC-CXR-LT, re-weighting is always beneficial; for example, class-balanced re-weighting and sklearn re-weighting improve focal loss performance from 0.181 to 0.278 and 0.299, respectively. However, unlike the NIH-CXR-LT results, DRW brings more gains to a re-weighted LDAM loss, improving group-wise accuracy by an absolute margin of at least 0.05. Interestingly, classifier re-training achieves both the highest group-wise average accuracy on the balanced test set and the highest balanced accuracy on the test set by a considerable margin.

#### CONCLUSION

s We conducted the first comprehensive study of long-tailed learning methods for disease classification on CXR. We will publicly release all code, models, and data to encourage the development of long-tailed learning methods for medical image classification.

#### CLINICAL RELEVANCE/APPLICATION

Medical imaging exams often yield a small set of common but a much larger set of uncommon findings. We present a benchmark study of long-tailed learning on chest X-rays to facilitate future research.

Printed on: 02/07/23

## Abstract Archives of the RSNA, 2022

M2-SPIN-6

### Development and Validation of A Deep Learning Model for Prediction of The 30-day Mortality of Patients With Community-acquired pneumonia from Chest X-ray

Monday, Nov. 28 9:00AM - 9:30AM Room: Learning Center - IN DPS

#### Participants

Changi Kim, BS, Seoul, Korea, Republic Of (*Presenter*) Nothing to Disclose

#### PURPOSE

To develop and validate a deep learning (DL) model to predict the 30-day mortality of patients with community-acquired pneumonia (CAP) using the chest X-ray (CXR) of patients.

#### METHODS AND MATERIALS

For model development, initial CXRs of patients diagnosed with CAP at a single institution (Institution A) between 2013 and 2019 were included (Developmental dataset). A convolutional neural network-based DL model was trained to predict the hazard of death within 30 days from the diagnosis of CAP. [B1] For validation of model performance, patients who visited the emergency departments of three institutions (Institutions A [temporally separated with developmental dataset], B, and C) due to CAP were included (External validation datasets). The predictive performance for the 30-day mortality was evaluated using the area under the receiver operating characteristic curves (AUCs). The AUC of the DL model was compared with that of CURB-65 score, a widely used tool for risk evaluation in CAP. Finally, the results from the DL model were categorized into three risk groups, and simply added to the CURB-65 scores (combined scores), and the AUC of the combined score was compared with that of the CURB-65 score.

#### RESULTS

Developmental dataset comprised 7,105 patients (62% men; mean age, 68 years; 30-day mortality rate, 11.4%), while external validation datasets from institution A, B, and C comprised 947 (63% men; mean age, 71 years; 30-day mortality rate, 17.6%), 467 (63% men; mean age, 73 years; 30-day mortality rate, 8.4%), and 381 (63.8% men; mean age, 71 years; 30-day mortality rate, 10.8%) patients, respectively. The DL model exhibited significantly higher AUC than CURB-65 score in external validation dataset from institution A (0.77 vs. 0.67,  $P < .001$ ); while the difference did not reach statistical significance in datasets from institutions B (0.80 vs. 0.73,  $P = .194$ ) and C (0.80 vs. 0.72,  $P = .081$ ). Finally, combined scores exhibited significantly higher AUCs than CURB-65 scores in all three external validation datasets (Institution A, 0.74,  $P < .001$ ; Institution B, 0.80,  $P = .002$ ; Institution C, 0.79,  $P < .001$ ).

#### CONCLUSION

s A DL model could predict the 30-day mortality of patients with CAP using CXRs, with higher performance than the CURB-65 score. Adding risk scores from the DL model to the CURB-65 score could improve the prediction performance.

#### CLINICAL RELEVANCE/APPLICATION

Evaluation of CXRs of patients with CAP using the DL model for mortality prediction may help improve risk stratification and clinical decision-making for hospitalization or intensive care.

Printed on: 02/07/23

## Abstract Archives of the RSNA, 2022

M2-SPIR

### Interventional Monday Poster Discussions

Monday, Nov. 28 9:00AM - 9:30AM Room: Learning Center - IR DPS

#### Sub-Events

#### **M2-SPIR-1 Strategy of Target Biopsy and Number of Target Cores for a PI-RADS 3-5 Index Lesion to Reduce Gleason Score Underestimation: A Propensity Score Matching Analysis**

##### Participants

Byung Kwan Park, MD, PhD, (*Presenter*) Nothing to Disclose

##### PURPOSE

To determine the number of target cores and targeting strategy to reduce GS underestimation.

##### METHODS AND MATERIALS

Between May 2017 and April 2020, a total of 385 patients undergoing target cognitive or image fusion biopsy of PI-RADS 3-5 index lesions and radical prostatectomies (RP) were 2:1 matched with propensity score using multiple variables and divided into the 1-4 core (n = 242) and 5-6 core (n = 143) groups, which were obtained with multiple logistic regression with restricted cubic spline curve. Target cores of 1-3 and 4-6 were sampled from central and peripheral areas, respectively. Pathologic outcomes and target cores were retrospectively assessed to analyze the GS difference or changes between biopsy and RP with Wilcoxon signed-rank test.

##### RESULTS

The median of target cores was 3 and 6 in the 1-4 core and 5-6 core groups, respectively (p < 0.001). Restricted cubic spline curve showed that GS upgrade was significantly reduced from the 5th core and there was no difference between 5th and 6th cores. Among the matched patients, 35.4% (136/385; 95% confidence interval, 0.305-0.403) had a GS upgrade after RP. The GS upgrades in the 1-4 core and 5-6 core groups were observed in 40.6% (98/242, 0.343-0.470) and 26.6% (38/143, 0.195-0.346), respectively (p = 0.023). Although there was no statistical difference between the matched groups in terms of RP GS (p = 0.092), the 5-6 core group had significantly higher biopsy GS (p = 0.006) and lower GS change from biopsy to RP (p = 0.027).

##### CONCLUSION

Five or more target cores sampling from both periphery and center of an index tumor contribute to reduce GS upgrade.

##### CLINICAL RELEVANCE/APPLICATION

1. Five or more cores reduces underestimation of Gleason score compared to four or less in targeting an index lesion of PI-RADS 3-5. [D1]
2. Sampling the periphery as well as the center of an index lesion may reduce underestimation of Gleason grade. [D2]

#### **M2-SPIR-2 Renal Mass Biopsy: Evaluating Post-Biopsy Complications to Determine Optimal Observation Time**

##### Participants

Sebastien Robert, MD, (*Presenter*) Nothing to Disclose

##### PURPOSE

This study evaluates post renal mass biopsy (RMB) complications to determine the minimum recovery time for safe discharge.

##### METHODS AND MATERIALS

An approved multi-site retrospective study of 571 patients who underwent percutaneous US or CT guided RMB between January 1, 2008 and June 1, 2020 was performed. Post-RMB clinical course was evaluated for all patients to identify the frequency and timing of all bleeding and non-bleeding related acute (<24 hours) or delayed (<30 days) complications. The timing of bleeding complications was established by first clinical deviation from standard recovery, defined as unplanned imaging, bloodwork, or analgesia. Complications were graded using the SIR Adverse Event Classification system.

##### RESULTS

613 RMB procedures were performed by 22 different radiologists (mean tumor diameter 4.3±3.2 cm, RENAL nephrometry 7.6±2.0). Diagnostic yield was 88% (65% renal cell carcinoma). Acute post-RMB complications occurred in 3.4% (21/613) of cases of which 76% (16/21) were bleeding related. Delayed bleeding complications were reported in 0.5% (3/613) of cases. Of all reported complications, two (0.3%) were deemed severe or life-threatening. Post-RMB interventions included: 3 embolization, 2 patients receiving blood transfusion, and 11 admissions to hospital (median 1 night). No patient deaths were reported. The mean time to clinical deviation from the expected post-RMB course was 59 minutes (range 13-135 minutes) in the acute bleeding complication cohort. Initial deviation occurred within 3 hours in all acute bleeding cases. The remaining delayed post-RMB bleeding cases all presented multiple days following discharge. Pre-RMB platelet counts and endophytic tumor location were independent predictors of bleeding complication (p<0.05). No recorded patient characteristics including age, gender, or prior anticoagulation use were

associated with a significant increase in post-RMB bleeding complications. Kidney characteristics, tumor morphology, and radiologist experience also did not show any association.

## CONCLUSION

s Post-RMB complications are uncommon and usually present acutely. All acute bleeding complications occurred within a 3-hour post-procedure window, suggesting that this time frame may be sufficient for safe patient discharge.

## CLINICAL RELEVANCE/APPLICATION

Short recovery times (2-3 hours) following renal mass biopsy (RMB) might allow for procedural cost efficiency by using a single recovery bed for two sequential RMB procedures.

## M2-SPIR-3 American Society of Anesthesiologists Physical Status Classification as a Predictor of Random Native Kidney Biopsy Complications in Hospitalized Patients

Participants

Anisha Mittal, BA, (*Presenter*) Nothing to Disclose

## PURPOSE

The American Society of Anesthesiology (ASA) physical status classification system is designed to assess a patient's pre-anesthesia physiological status which can be helpful in predicting perioperative risk. We compared the complication rates and types of complications of random native renal biopsies among hospitalized patients with a low ASA classification (best physiological status) vs. a high ASA classification (worse physiological status) to predict perioperative risk of a radiological procedure for which the ASA classification is not commonly used.

## METHODS AND MATERIALS

We conducted a retrospective chart review of 105 consecutive inpatient random native kidney biopsies performed by radiologists between 2006 and 2020 at an academic medical center. Variables included the number and types of perioperative complications per patient. Patients' ASA physical status classification levels were calculated according to the guidelines provided by the ASA based on clinical factors and comorbidities. Hospitalized patients with a low ASA classification (class 1-2) were compared to those with a high ASA classification (class 3-4) for complication rate and types of complications using the Society of Interventional Radiology's Adverse Event Classification system.

## RESULTS

105 hospitalized adult patients (58 females and 47 males; average age 53 years) underwent random native kidney biopsy during the study period. 53 (50.5%) were in ASA class 1-2 and 52 (49.5%) in ASA class 3-4. No patients in our study were in ASA class 5 or 6. Overall complication rates between ASA class 1-2 patients and ASA class 3-4 patients were 10/53 (19%) vs. 23/52 (44%), respectively ( $p = .006$ ). ASA class 1-2 patients had 4 major and 6 minor complications, and ASA class 3-4 patients had 17 major and 6 minor complications.

## CONCLUSION

s High ASA physical status classifications were associated with a higher overall complication rate for random native kidney biopsies as compared to low ASA classifications. While the ASA classification is not commonly used for radiological procedures such as a random native kidney biopsy, this study provides evidence that the ASA classification may be used in conjunction with other clinical factors to help predict the perioperative complication risk of random native kidney biopsy in hospitalized patients.

## CLINICAL RELEVANCE/APPLICATION

A greater utilization of the ASA classification by radiologists may help reduce the perioperative risk of random native kidney biopsy in hospitalized patients.

## M2-SPIR-4 Catheter Tract Seeding in Indwelling Pleural Catheter Placement for the Drainage of Malignant Pleural Effusions: Incidence and Related Clinical and Imaging Factors

Participants

Yoojin Nam, MD, Changwon, Korea, Republic Of (*Presenter*) Nothing to Disclose

## PURPOSE

To evaluate the incidence of IPC-related cancer tract seeding and seek for related demographic, clinical or imaging factors to the tract seeding.

## METHODS AND MATERIALS

This was a retrospective study regarding 124 consecutive patients seen between January 2011 and December 2021 who underwent IPC placement for the drainage of malignant pleural effusion. Chest radiographs before IPC placement and serial chest CT studies were obtained in all patients. The incidence of IPC-related cancer tract seeding, and related factors were assessed by reviewing medical records.

## RESULTS

The incidence of IPC tract seeding was 21.7% (27 of 124 malignant effusions). Of 27 patients with seeding, 15 had primary lung cancer and remaining 12 had extra-thoracic malignancy. Adenocarcinoma (19 of 27, 70.3%) either from the lung ( $n = 12$ ) or extra-thoracic malignancy ( $n = 7$ ) was the most common cell type. Mean time elapsed until tract seeding occurrence after IPC placement was 94 days (ranges; 26-300 days). The survival in seeding group after IPC placement was 123 days (ranges, 16-457 days). On odd ratio analysis, the presence of mediastinal pleural thickening (OR [95% CI]; 9.79 (2.67-35.84),  $P = 0.001$ ) was significantly related to the presence of tract seeding. Neither, tumor volume in pleural space ( $P = 0.168$ ), duration of IPC indwelling ( $P = 0.142$ ), days of survival after IPC placement ( $P = 0.699$ ), nor pleural effusion amount ( $P = 0.481$ ) was related to the cancer tract seeding.

## CONCLUSION

s IPC tract seeding is seen in 27 (21.7%) of 124 malignant pleural effusion patients, particularly with adenocarcinoma cytology. CT

features of mediastinal pleural thickening prior to IPC insertion are related to the occurrence of tract seeding.

#### **CLINICAL RELEVANCE/APPLICATION**

Detailed analysis of CT findings of malignant pleural effusion may help predict oncoming tract seeding after IPC placement for malignant pleural effusion evacuation. When tract seeding is expected with the analyses of CT findings, prophylactic radiation therapy immediately after the placement of the catheter or thoracentesis (reducing intrapleural pressure) before IPC placement may be considered as the way of reducing tract seeding occurrence.

#### **M2-SPIR-5 Multiparametric Bone MRI Targeting Improves CT-guided Sclerotic Bone Biopsy Success in Metastatic Castrate Resistant Prostate Cancer: A Prospective Evaluation**

Participants

Ricardo Donners, MD, (*Presenter*) Nothing to Disclose

#### **PURPOSE**

The purpose of this study was to prospectively validate a multiparametric bone MRI (mpBMRI) target lesion selection algorithm to improve CT-guided sclerotic bone biopsy success in metastatic castrate-resistant prostate cancer (mCRPC) patients with sclerotic bone disease mCRPC.

#### **METHODS AND MATERIALS**

20 CT-guided bone biopsies were performed by interventional radiologists in 17 mCRPC patients with only sclerotic bone disease. Biopsy targets were selected based on mpBMRI, including diffusion-weighted (DWI) and diagnostic, T1-weighted gradient-echo Dixon images, allowing for calculation of apparent diffusion coefficient (ADC) and relative fat-fraction percentages (rFF%), respectively. Bone marrow with high DWI signal, ADC <1100  $\mu\text{m}^2/\text{s}$  and rFF <20% was the preferred biopsy target. Biopsy tumour content and next-generation genomic sequencing (NGS)-feasibility was assessed by a pathologist. Prognostic values of routine laboratory blood parameters, tumour marker levels, target lesion size, biopsy tract length, visual CT density (mild or dense sclerosis), means of HU, ADC and rFF% to distinguish between successful and unsuccessful biopsies were tested for statistical significance ( $p < 0.05 = \text{significant}$ ).

#### **RESULTS**

17/20 (85%) biopsies were tumour-positive and NGS was feasible in 13/18 (72%). Neither laboratory parameters, target diameter, tract length nor visual CT density grading showed significant differences between a positive versus negative or NGS feasible versus non-feasible biopsy result (each  $p > 0.137$ ). Lesion mean HU was  $387 \pm 187$  HU in NGS feasible and  $493 \pm 218$  HU in non-feasible biopsies ( $p = 0.521$ ). 13/14 (93%) biopsies in targets fulfilling mpBMRI selection algorithm criteria were tumour-positive and 10/12 (83%) provided sufficient material for NGS. In six biopsies mean rFF% was >20% (range 21 - 25%). 4/6 (60%) biopsies were tumour-positive and NGS was feasible in 3/6 (50%).

#### **CONCLUSION**

s MpBMRI can facilitate CT-guided bone biopsy target selection in mCRPC patients with sclerotic metastases and improves diagnostic yield and NGS feasibility.

#### **CLINICAL RELEVANCE/APPLICATION**

Obtaining high quality tumour tissue samples for NGS can be challenging in mCRPC patients with sclerotic bone disease. Improving bone biopsy success rates by using multiparametric bone MRI to identify active bone metastases allows this patient cohort to benefit from personalised oncology therapy based on individual tumor genomics.

#### **M2-SPIR-6 Risk Reduction Protocol for Mitigating Bleeding Complications after an Image-Guided Kidney Biopsy**

Participants

Ali Kord, MD, MPH, Cincinnati, OH (*Presenter*) Nothing to Disclose

#### **PURPOSE**

There are Society of Interventional Radiology (SIR) guidelines to correct peri-procedural variables that can affect bleeding complications after kidney biopsy, yet bleedings are seen after kidney biopsies. This study is designed to assess the variables affecting bleeding complications in patients who underwent an image-guided kidney biopsy with controlled peri-procedural clinical variables.

#### **METHODS AND MATERIALS**

A total of 200 consecutive patients (100 native, 100 transplant, Mean age:  $52 \pm 17$  years) underwent an image-guided kidney biopsy. All biopsies were performed using a 17-gauge coaxial access needle and an 18-gauge biopsy needle. Hemoglobin (HGB), Platelet (PLT), international normalized ratio (INR), and systolic and diastolic blood pressure (SBP, DBP) were checked and corrected based on the SIR guidelines, if needed (Table.1). Gelfoam was used in some cases to embolize the biopsy path. Post-procedure bleeding complications were categorized using SIR adverse event classification. The peri-procedural variables were compared between patients without and with bleeding after kidney biopsy using univariate and multivariate analysis. Statistical significance was considered at 0.05.

#### **RESULTS**

Technical success was 99%. Minor and major bleedings were observed in 4.5% and 3.0% of the patients, respectively. As expected, bleeding complications were seen more often after native kidney biopsies compared to the transplant kidneys ( $p < 0.001$ ). Patients with bleeding were more likely to need CT for kidney biopsy ( $p = 0.02$ ). Gelfoam embolization of the biopsy path was not associated with reduced bleeding after kidney biopsy ( $p = 0.8$ ). The mean SBPs and DBPs were higher in patients with bleeding than in patients without bleeding ( $p < 0.05$ , Table.1). In multi-variate analysis, pre- and post-biopsy SBP and DBP remained significantly different between native kidneys with and without bleeding (Fig.1,  $p < 0.04$ ).

#### **CONCLUSION**

s Higher peri-procedural blood pressures are associated with increased bleeding after an image-guided kidney biopsy. A stricter blood pressure control should be considered both before and after kidney biopsy as part of the procedural protocol.

## CLINICAL RELEVANCE/APPLICATION

A stricter blood pressure control should be part of the procedural protocol for native kidney biopsy.

### **M2-SPIR-7 Air Embolism in CT-Guided Transthoracic Needle Biopsy and Localization: Emphasis on Pulmonary Vein Injury**

Participants

Yura Ahn, MD, Seoul, Korea, Republic Of (*Presenter*) Nothing to Disclose

#### **PURPOSE**

To assess whether pulmonary vein injury is detectable on CT and associated with air embolism after percutaneous transthoracic needle biopsy (PTNB) and wire localization in a tertiary referral hospital.

#### **METHODS AND MATERIALS**

Between January 2012 and November 2021, 11905 consecutive CT-guided PTNBs and 1553 wire localizations in 12042 patients were retrospectively evaluated. Air embolism was identified by reviewing radiologic reports. Pulmonary vein injury was defined as the presence of the pulmonary vein in the needle pathway or shooting range of the cutting needle with presence of parenchymal hemorrhage. The association between pulmonary vein injury and air embolism was assessed using logistic regression analysis in matched patients with and without air embolism with a ratio of 1:4.

#### **RESULTS**

A total of 30 cases of air embolism (median age, 67 years; range, 48-80 years; 25 men) was found with an incidence of 0.22% (30/13458). Pulmonary vein injury during the procedures was identifiable on CT in 26 of 30 patients (86.7%) whereas it was 1.7% (2/120) for matched patients without air embolism. The veins beyond the target lesion (65.3% [17/26]) were injured more frequently than the veins in the needle pathway before the target lesion (34.6% [9/26]). In univariable and multivariable analyses, pulmonary vein injury was associated with air embolism (odds ratio, 86.92; 95% confidence interval, 21.71- >999.99,  $p < .001$ ).

#### **CONCLUSION**

Pulmonary vein injury was actually detected on CT and was associated with air embolism.

## CLINICAL RELEVANCE/APPLICATION

Avoiding pulmonary vein injury with careful planning of the needle pathway on CT may reduce air embolism risk.

### **M2-SPIR-8 The Effect of Music on Patients Anxiety in CT-guided Percutaneous Interventions: A Prospective Randomized Controlled Trial**

Participants

Florian Fleckenstein, MS, (*Presenter*) Nothing to Disclose

#### **PURPOSE**

CT-guided percutaneous interventions oftentimes cause patients to experience a high level of stress and anxiety before the operation. As a proven medium to lessen anxiety and pain in the peri-operational setting, music could potentially serve as relief. The aim of this study is to contribute to further understanding the effect of music on anxiety and pain compared to basic operational procedures.

#### **METHODS AND MATERIALS**

A total of 178 patients were included in this randomized controlled trial. The participants were randomized in a music group (MG) and a control group (CG). Items of anxiety were analysed by using the STAI-6 pre- and post-intervention, while a numeric rating scale with faces served to rate the level of pain after the procedure. Post-interventional state anxiety levels and the reduction of anxiety were set as primary outcomes, whereas the level of pain experienced during the procedure was chosen as a secondary outcome.

#### **RESULTS**

176 patients were eligible for statistical analysis. N=91 patients underwent the procedure in the MG, compared to n=85 participants in the CG. Median post-interventional item values in the MG ranked more towards lower levels of anxiety than the same item values of the CG ( $p < 0.001$ ). The reduction of anxiety between pre- and post-procedural states was stronger in the MG, but also detectable in the CG ( $p < 0.001$ ). Of note, the level of experienced post-procedural pain was significantly lower in the MG ( $p < 0.001$ ).

#### **CONCLUSION**

This study could show, that exposure to music during CT-guided percutaneous procedures can aid in lowering peri-interventional anxiety and pain thus improves patient care without any negative side-effects.

## CLINICAL RELEVANCE/APPLICATION

Music can act as a safe, easily applicable, free of charge and non-invasive aid to reduce anxiety in the peri-interventional setting to improve quality of care. Apart from statistical significances, we believe our findings are of high clinical relevance beyond the field of IR.

### **M2-SPIR-9 Safety of Image-guided Splenic Biopsy: Retrospective Outcomes Analysis From Eight Academic Institutions**

Participants

Hadiseh Kavandi, MD, Boston, MA (*Presenter*) Nothing to Disclose

#### **PURPOSE**

To evaluate the safety of image-guided targeted and non-targeted splenic biopsy as performed in eight US academic institutions.

## **METHODS AND MATERIALS**

This retrospective IRB-approved, HIPAA-compliant, multi-institutional study included consecutive patients that underwent ultrasound or CT-guided splenic biopsy between 3/1/2001 and 3/31/2022. Significant bleeding after the procedure was defined by the presence of bleeding on CT performed within 30 days or angiography and/or surgery performed to manage the bleeding.

## **RESULTS**

384 splenic biopsies, ultrasound (97/384, 25%) and CT-guided (287, 75%), on 372 patients from 8 academic institutions were included (age 59±17 years, 183 (48%) female, 337 (88%) targeted, 184 (48%) co-axial, 312 (81%) core biopsy, median of 3 samples). Bleeding occurred following 31/384 (8%) biopsies, treated angiographically in 4/384 (1%) cases and surgically in 3/384 (1%) cases; one of the surgical cases had IR intervention before surgery. 8/384 (2%) patients received RBC transfusion. 4/384 (1%) patients readmitted (3 (1%) for bleeding, 1 (0.5%) for sepsis) and 8/384 (2%) had ED visits for pain management. There were no deaths related to the biopsy. Bleeding risk was inversely associated with lesion size, with a median size of 2.1 cm in patients who bled vs. 3.6 cm in patients who did not,  $p=0.03$ . In patients with a history of lymphoma or leukemia, there was a lower incidence of bleeding 3/92 (3%) vs. 28/292 (10%),  $p=0.05$ . There was no association of bleeding with patient's gender, age, history of anticoagulation, modality of guidance, targeted vs. non-targeted, coaxial vs non-coaxial technique, number of samples, the gauge of core biopsy, or core vs. FNA; lesion location, CT attenuation, US echogenicity, vascularity, all  $p>0.05$ . Incidence of bleeding was higher in patients with tract embolization (10/59, 17% vs. 18/301, 6%), as tract embolization was likely performed to treat the bleeding.

## **CONCLUSION**

s Bleeding after splenic biopsy occurred after 8% of procedures, with 2% requiring medical, 1% angiographic, and 1% surgical management. Smaller lesions and patients with no hematological history had a higher incidence of bleeding.

## **CLINICAL RELEVANCE/APPLICATION**

The image-guided splenic biopsy is safe with a small number of patients requiring treatment for clinically significant post-procedure bleeding.

Printed on: 02/07/23

## Abstract Archives of the RSNA, 2022

M2-SP1R-1

### Strategy of Target Biopsy and Number of Target Cores for a PI-RADS 3-5 Index Lesion to Reduce Gleason Score Underestimation: A Propensity Score Matching Analysis

Monday, Nov. 28 9:00AM - 9:30AM Room: Learning Center - IR DPS

#### Participants

Byung Kwan Park, MD, PhD, (Presenter) Nothing to Disclose

#### PURPOSE

To determine the number of target cores and targeting strategy to reduce GS underestimation.

#### METHODS AND MATERIALS

Between May 2017 and April 2020, a total of 385 patients undergoing target cognitive or image fusion biopsy of PI-RADS 3-5 index lesions and radical prostatectomies (RP) were 2:1 matched with propensity score using multiple variables and divided into the 1-4 core (n = 242) and 5-6 core (n = 143) groups, which were obtained with multiple logistic regression with restricted cubic spline curve. Target cores of 1-3 and 4-6 were sampled from central and peripheral areas, respectively. Pathologic outcomes and target cores were retrospectively assessed to analyze the GS difference or changes between biopsy and RP with Wilcoxon signed-rank test.

#### RESULTS

The median of target cores was 3 and 6 in the 1-4 core and 5-6 core groups, respectively ( $p < 0.001$ ). Restricted cubic spline curve showed that GS upgrade was significantly reduced from the 5th core and there was no difference between 5th and 6th cores. Among the matched patients, 35.4% (136/385; 95% confidence interval, 0.305-0.403) had a GS upgrade after RP. The GS upgrades in the 1-4 core and 5-6 core groups were observed in 40.6% (98/242, 0.343-0.470) and 26.6% (38/143, 0.195-0.346), respectively ( $p = 0.023$ ). Although there was no statistical difference between the matched groups in terms of RP GS ( $p = 0.092$ ), the 5-6 core group had significantly higher biopsy GS ( $p = 0.006$ ) and lower GS change from biopsy to RP ( $p = 0.027$ ).

#### CONCLUSION

s Five or more target cores sampling from both periphery and center of an index tumor contribute to reduce GS upgrade.

#### CLINICAL RELEVANCE/APPLICATION

1. Five or more cores reduces underestimation of Gleason score compared to four or less in targeting an index lesion of PI-RADS 3-5. [D1]
2. Sampling the periphery as well as the center of an index lesion may reduce underestimation of Gleason grade.[D2]

Printed on: 02/07/23

## Abstract Archives of the RSNA, 2022

M2-SP1R-2

### Renal Mass Biopsy: Evaluating Post-Biopsy Complications to Determine Optimal Observation Time

Monday, Nov. 28 9:00AM - 9:30AM Room: Learning Center - IR DPS

#### Participants

Sebastien Robert, MD, (*Presenter*) Nothing to Disclose

#### PURPOSE

This study evaluates post renal mass biopsy (RMB) complications to determine the minimum recovery time for safe discharge.

#### METHODS AND MATERIALS

An approved multi-site retrospective study of 571 patients who underwent percutaneous US or CT guided RMB between January 1, 2008 and June 1, 2020 was performed. Post-RMB clinical course was evaluated for all patients to identify the frequency and timing of all bleeding and non-bleeding related acute (<24 hours) or delayed (<30 days) complications. The timing of bleeding complications was established by first clinical deviation from standard recovery, defined as unplanned imaging, bloodwork, or analgesia. Complications were graded using the SIR Adverse Event Classification system.

#### RESULTS

613 RMB procedures were performed by 22 different radiologists (mean tumor diameter 4.3±3.2 cm, RENAL nephrometry 7.6±2.0). Diagnostic yield was 88% (65% renal cell carcinoma). Acute post-RMB complications occurred in 3.4% (21/613) of cases of which 76% (16/21) were bleeding related. Delayed bleeding complications were reported in 0.5% (3/613) of cases. Of all reported complications, two (0.3%) were deemed severe or life-threatening. Post-RMB interventions included: 3 embolization, 2 patients receiving blood transfusion, and 11 admissions to hospital (median 1 night). No patient deaths were reported. The mean time to clinical deviation from the expected post-RMB course was 59 minutes (range 13-135 minutes) in the acute bleeding complication cohort. Initial deviation occurred within 3 hours in all acute bleeding cases. The remaining delayed post-RMB bleeding cases all presented multiple days following discharge. Pre-RMB platelet counts and endophytic tumor location were independent predictors of bleeding complication ( $p < 0.05$ ). No recorded patient characteristics including age, gender, or prior anticoagulation use were associated with a significant increase in post-RMB bleeding complications. Kidney characteristics, tumor morphology, and radiologist experience also did not show any association.

#### CONCLUSION

Post-RMB complications are uncommon and usually present acutely. All acute bleeding complications occurred within a 3-hour post-procedure window, suggesting that this time frame may be sufficient for safe patient discharge.

#### CLINICAL RELEVANCE/APPLICATION

Short recovery times (2-3 hours) following renal mass biopsy (RMB) might allow for procedural cost efficiency by using a single recovery bed for two sequential RMB procedures.

Printed on: 02/07/23



## Abstract Archives of the RSNA, 2022

M2-SP1R-3

### American Society of Anesthesiologists Physical Status Classification as a Predictor of Random Native Kidney Biopsy Complications in Hospitalized Patients

Monday, Nov. 28 9:00AM - 9:30AM Room: Learning Center - IR DPS

#### Participants

Anisha Mittal, BA, (Presenter) Nothing to Disclose

#### PURPOSE

The American Society of Anesthesiology (ASA) physical status classification system is designed to assess a patient's pre-anesthesia physiological status which can be helpful in predicting perioperative risk. We compared the complication rates and types of complications of random native renal biopsies among hospitalized patients with a low ASA classification (best physiological status) vs. a high ASA classification (worse physiological status) to predict perioperative risk of a radiological procedure for which the ASA classification is not commonly used.

#### METHODS AND MATERIALS

We conducted a retrospective chart review of 105 consecutive inpatient random native kidney biopsies performed by radiologists between 2006 and 2020 at an academic medical center. Variables included the number and types of perioperative complications per patient. Patients' ASA physical status classification levels were calculated according to the guidelines provided by the ASA based on clinical factors and comorbidities. Hospitalized patients with a low ASA classification (class 1-2) were compared to those with a high ASA classification (class 3-4) for complication rate and types of complications using the Society of Interventional Radiology's Adverse Event Classification system.

#### RESULTS

105 hospitalized adult patients (58 females and 47 males; average age 53 years) underwent random native kidney biopsy during the study period. 53 (50.5%) were in ASA class 1-2 and 52 (49.5%) in ASA class 3-4. No patients in our study were in ASA class 5 or 6. Overall complication rates between ASA class 1-2 patients and ASA class 3-4 patients were 10/53 (19%) vs. 23/52 (44%), respectively ( $p = .006$ ). ASA class 1-2 patients had 4 major and 6 minor complications, and ASA class 3-4 patients had 17 major and 6 minor complications.

#### CONCLUSION

High ASA physical status classifications were associated with a higher overall complication rate for random native kidney biopsies as compared to low ASA classifications. While the ASA classification is not commonly used for radiological procedures such as a random native kidney biopsy, this study provides evidence that the ASA classification may be used in conjunction with other clinical factors to help predict the perioperative complication risk of random native kidney biopsy in hospitalized patients.

#### CLINICAL RELEVANCE/APPLICATION

A greater utilization of the ASA classification by radiologists may help reduce the perioperative risk of random native kidney biopsy in hospitalized patients.

Printed on: 02/07/23

## Abstract Archives of the RSNA, 2022

M2-SP1R-4

### **Catheter Tract Seeding in Indwelling Pleural Catheter Placement for the Drainage of Malignant Pleural Effusions: Incidence and Related Clinical and Imaging Factors**

Monday, Nov. 28 9:00AM - 9:30AM Room: Learning Center - IR DPS

#### **Participants**

Yoojin Nam, MD, Changwon, Korea, Republic Of (*Presenter*) Nothing to Disclose

#### **PURPOSE**

To evaluate the incidence of IPC-related cancer tract seeding and seek for related demographic, clinical or imaging factors to the tract seeding.

#### **METHODS AND MATERIALS**

This was a retrospective study regarding 124 consecutive patients seen between January 2011 and December 2021 who underwent IPC placement for the drainage of malignant pleural effusion. Chest radiographs before IPC placement and serial chest CT studies were obtained in all patients. The incidence of IPC-related cancer tract seeding, and related factors were assessed by reviewing medical records.

#### **RESULTS**

The incidence of IPC tract seeding was 21.7% (27 of 124 malignant effusions). Of 27 patients with seeding, 15 had primary lung cancer and remaining 12 had extra-thoracic malignancy. Adenocarcinoma (19 of 27, 70.3%) either from the lung (n = 12) or extra-thoracic malignancy (n = 7) was the most common cell type. Mean time elapsed until tract seeding occurrence after IPC placement was 94 days (ranges; 26-300 days). The survival in seeding group after IPC placement was 123 days (ranges, 16-457 days). On odd ratio analysis, the presence of mediastinal pleural thickening (OR [95% CI]; 9.79 (2.67-35.84), P = 0.001) was significantly related to the presence of tract seeding. Neither, tumor volume in pleural space (P = 0.168), duration of IPC indwelling (P = 0.142), days of survival after IPC placement (P = 0.699), nor pleural effusion amount (P = 0.481) was related to the cancer tract seeding.

#### **CONCLUSION**

s IPC tract seeding is seen in 27 (21.7%) of 124 malignant pleural effusion patients, particularly with adenocarcinoma cytology. CT features of mediastinal pleural thickening prior to IPC insertion are related to the occurrence of tract seeding.

#### **CLINICAL RELEVANCE/APPLICATION**

Detailed analysis of CT findings of malignant pleural effusion may help predict oncoming tract seeding after IPC placement for malignant pleural effusion evacuation. When tract seeding is expected with the analyses of CT findings, prophylactic radiation therapy immediately after the placement of the catheter or thoracentesis (reducing intrapleural pressure) before IPC placement may be considered as the way of reducing tract seeding occurrence.

Printed on: 02/07/23

## Abstract Archives of the RSNA, 2022

M2-SP1R-5

### **Multiparametric Bone MRI Targeting Improves CT-guided Sclerotic Bone Biopsy Success in Metastatic Castrate Resistant Prostate Cancer: A Prospective Evaluation**

Monday, Nov. 28 9:00AM - 9:30AM Room: Learning Center - IR DPS

#### **Participants**

Ricardo Donners, MD, (*Presenter*) Nothing to Disclose

#### **PURPOSE**

The purpose of this study was to prospectively validate a multiparametric bone MRI (mpBMRI) target lesion selection algorithm to improve CT-guided sclerotic bone biopsy success in metastatic castrate-resistant prostate cancer (mCRPC) patients with sclerotic bone disease mCRPC.

#### **METHODS AND MATERIALS**

20 CT-guided bone biopsies were performed by interventional radiologists in 17 mCRPC patients with only sclerotic bone disease. Biopsy targets were selected based on mpBMRI, including diffusion-weighted (DWI) and diagnostic, T1-weighted gradient-echo Dixon images, allowing for calculation of apparent diffusion coefficient (ADC) and relative fat-fraction percentages (rFF%), respectively. Bone marrow with high DWI signal, ADC <1100  $\mu\text{m}^2/\text{s}$  and rFF <20% was the preferred biopsy target. Biopsy tumour content and next-generation genomic sequencing (NGS)-feasibility was assessed by a pathologist. Prognostic values of routine laboratory blood parameters, tumour marker levels, target lesion size, biopsy tract length, visual CT density (mild or dense sclerosis), means of HU, ADC and rFF% to distinguish between successful and unsuccessful biopsies were tested for statistical significance ( $p < 0.05 = \text{significant}$ ).

#### **RESULTS**

17/20 (85%) biopsies were tumour-positive and NGS was feasible in 13/18 (72%). Neither laboratory parameters, target diameter, tract length nor visual CT density grading showed significant differences between a positive versus negative or NGS feasible versus non-feasible biopsy result (each  $p > 0.137$ ). Lesion mean HU was  $387 \pm 187$  HU in NGS feasible and  $493 \pm 218$  HU in non-feasible biopsies ( $p = 0.521$ ). 13/14 (93%) biopsies in targets fulfilling mpBMRI selection algorithm criteria were tumour-positive and 10/12 (83%) provided sufficient material for NGS. In six biopsies mean rFF% was >20% (range 21 - 25%). 4/6 (60%) biopsies were tumour-positive and NGS was feasible in 3/6 (50%).

#### **CONCLUSION**

s MpBMRI can facilitate CT-guided bone biopsy target selection in mCRPC patients with sclerotic metastases and improves diagnostic yield and NGS feasibility.

#### **CLINICAL RELEVANCE/APPLICATION**

Obtaining high quality tumour tissue samples for NGS can be challenging in mCRPC patients with sclerotic bone disease. Improving bone biopsy success rates by using multiparametric bone MRI to identify active bone metastases allows this patient cohort to benefit from personalised oncology therapy based on individual tumor genomics.

Printed on: 02/07/23

## Abstract Archives of the RSNA, 2022

M2-SPIR-6

### Risk Reduction Protocol for Mitigating Bleeding Complications after an Image—Guided Kidney Biopsy

Monday, Nov. 28 9:00AM - 9:30AM Room: Learning Center - IR DPS

#### Participants

Ali Kord, MD, MPH, Cincinnati, OH (*Presenter*) Nothing to Disclose

#### PURPOSE

There are Society of Interventional Radiology (SIR) guidelines to correct peri-procedural variables that can affect bleeding complications after kidney biopsy, yet bleedings are seen after kidney biopsies. This study is designed to assess the variables affecting bleeding complications in patients who underwent an image-guided kidney biopsy with controlled peri-procedural clinical variables.

#### METHODS AND MATERIALS

A total of 200 consecutive patients (100 native, 100 transplant, Mean age:  $52 \pm 17$  years) underwent an image-guided kidney biopsy. All biopsies were performed using a 17-gauge coaxial access needle and an 18-gauge biopsy needle. Hemoglobin (HGB), Platelet (PLT), international normalized ratio (INR), and systolic and diastolic blood pressure (SBP, DBP) were checked and corrected based on the SIR guidelines, if needed (Table.1). Gelfoam was used in some cases to embolize the biopsy path. Post-procedure bleeding complications were categorized using SIR adverse event classification. The peri-procedural variables were compared between patients without and with bleeding after kidney biopsy using univariate and multivariate analysis. Statistical significance was considered at 0.05.

#### RESULTS

Technical success was 99%. Minor and major bleedings were observed in 4.5% and 3.0% of the patients, respectively. As expected, bleeding complications were seen more often after native kidney biopsies compared to the transplant kidneys ( $p < 0.001$ ). Patients with bleeding were more likely to need CT for kidney biopsy ( $p = 0.02$ ). Gelfoam embolization of the biopsy path was not associated with reduced bleeding after kidney biopsy ( $p = 0.8$ ). The mean SBPs and DBPs were higher in patients with bleeding than in patients without bleeding ( $p < 0.05$ , Table.1). In multi-variate analysis, pre- and post-biopsy SBP and DBP remained significantly different between native kidneys with and without bleeding (Fig.1,  $p < 0.04$ ).

#### CONCLUSION

Higher peri-procedural blood pressures are associated with increased bleeding after an image-guided kidney biopsy. A stricter blood pressure control should be considered both before and after kidney biopsy as part of the procedural protocol.

#### CLINICAL RELEVANCE/APPLICATION

A stricter blood pressure control should be part of the procedural protocol for native kidney biopsy.

Printed on: 02/07/23

## Abstract Archives of the RSNA, 2022

M2-SP1R-7

### Air Embolism in CT-Guided Transthoracic Needle Biopsy and Localization: Emphasis on Pulmonary Vein Injury

Monday, Nov. 28 9:00AM - 9:30AM Room: Learning Center - IR DPS

#### Participants

Yura Ahn, MD, Seoul, Korea, Republic Of (*Presenter*) Nothing to Disclose

#### PURPOSE

To assess whether pulmonary vein injury is detectable on CT and associated with air embolism after percutaneous transthoracic needle biopsy (PTNB) and wire localization in a tertiary referral hospital.

#### METHODS AND MATERIALS

Between January 2012 and November 2021, 11905 consecutive CT-guided PTNBs and 1553 wire localizations in 12042 patients were retrospectively evaluated. Air embolism was identified by reviewing radiologic reports. Pulmonary vein injury was defined as the presence of the pulmonary vein in the needle pathway or shooting range of the cutting needle with presence of parenchymal hemorrhage. The association between pulmonary vein injury and air embolism was assessed using logistic regression analysis in matched patients with and without air embolism with a ratio of 1:4.

#### RESULTS

A total of 30 cases of air embolism (median age, 67 years; range, 48-80 years; 25 men) was found with an incidence of 0.22% (30/13458). Pulmonary vein injury during the procedures was identifiable on CT in 26 of 30 patients (86.7%) whereas it was 1.7% (2/120) for matched patients without air embolism. The veins beyond the target lesion (65.3% [17/26]) were injured more frequently than the veins in the needle pathway before the target lesion (34.6% [9/26]). In univariable and multivariable analyses, pulmonary vein injury was associated with air embolism (odds ratio, 86.92; 95% confidence interval, 21.71- >999.99,  $p < .001$ ).

#### CONCLUSION

Pulmonary vein injury was actually detected on CT and was associated with air embolism.

#### CLINICAL RELEVANCE/APPLICATION

Avoiding pulmonary vein injury with careful planning of the needle pathway on CT may reduce air embolism risk.

Printed on: 02/07/23

## Abstract Archives of the RSNA, 2022

M2-SP1R-8

### The Effect of Music on Patients Anxiety in CT-guided Percutaneous Interventions: A Prospective Randomized Controlled Trial

Monday, Nov. 28 9:00AM - 9:30AM Room: Learning Center - IR DPS

#### Participants

Florian Fleckenstein, MS, (*Presenter*) Nothing to Disclose

#### PURPOSE

CT-guided percutaneous interventions oftentimes cause patients to experience a high level of stress and anxiety before the operation. As a proven medium to lessen anxiety and pain in the peri-operational setting, music could potentially serve as relief. The aim of this study is to contribute to further understanding the effect of music on anxiety and pain compared to basic operational procedures.

#### METHODS AND MATERIALS

A total of 178 patients were included in this randomized controlled trial. The participants were randomized in a music group (MG) and a control group (CG). Items of anxiety were analysed by using the STAI-6 pre- and post-intervention, while a numeric rating scale with faces served to rate the level of pain after the procedure. Post-interventional state anxiety levels and the reduction of anxiety were set as primary outcomes, whereas the level of pain experienced during the procedure was chosen as a secondary outcome.

#### RESULTS

176 patients were eligible for statistical analysis. N=91 patients underwent the procedure in the MG, compared to n=85 participants in the CG. Median post-interventional item values in the MG ranked more towards lower levels of anxiety than the same item values of the CG ( $p<0.001$ ). The reduction of anxiety between pre- and post-procedural states was stronger in the MG, but also detectable in the CG ( $p<0.001$ ). Of note, the level of experienced post-procedural pain was significantly lower in the MG ( $p<0.001$ ).

#### CONCLUSION

This study could show, that exposure to music during CT-guided percutaneous procedures can aid in lowering peri-interventional anxiety and pain thus improves patient care without any negative side-effects.

#### CLINICAL RELEVANCE/APPLICATION

Music can act as a safe, easily applicable, free of charge and non-invasive aid to reduce anxiety in the peri-interventional setting to improve quality of care. Apart from statistical significances, we believe our findings are of high clinical relevance beyond the field of IR.

Printed on: 02/07/23

## Abstract Archives of the RSNA, 2022

M2-SPIR-9

### Safety of Image-guided Splenic Biopsy: Retrospective Outcomes Analysis From Eight Academic Institutions

Monday, Nov. 28 9:00AM - 9:30AM Room: Learning Center - IR DPS

#### Participants

Hadiseh Kavandi, MD, Boston, MA (*Presenter*) Nothing to Disclose

#### PURPOSE

To evaluate the safety of image-guided targeted and non-targeted splenic biopsy as performed in eight US academic institutions.

#### METHODS AND MATERIALS

This retrospective IRB-approved, HIPAA-compliant, multi-institutional study included consecutive patients that underwent ultrasound or CT-guided splenic biopsy between 3/1/2001 and 3/31/2022. Significant bleeding after the procedure was defined by the presence of bleeding on CT performed within 30 days or angiography and/or surgery performed to manage the bleeding.

#### RESULTS

384 splenic biopsies, ultrasound (97/384, 25%) and CT-guided (287, 75%), on 372 patients from 8 academic institutions were included (age 59±17 years, 183 (48%) female, 337 (88%) targeted, 184 (48%) co-axial, 312 (81%) core biopsy, median of 3 samples). Bleeding occurred following 31/384 (8%) biopsies, treated angiographically in 4/384 (1%) cases and surgically in 3/384 (1%) cases; one of the surgical cases had IR intervention before surgery. 8/384 (2%) patients received RBC transfusion. 4/384 (1%) patients readmitted (3 (1%) for bleeding, 1 (0.5%) for sepsis) and 8/384 (2%) had ED visits for pain management. There were no deaths related to the biopsy. Bleeding risk was inversely associated with lesion size, with a median size of 2.1 cm in patients who bled vs. 3.6 cm in patients who did not,  $p=0.03$ . In patients with a history of lymphoma or leukemia, there was a lower incidence of bleeding 3/92 (3%) vs. 28/292 (10%),  $p=0.05$ . There was no association of bleeding with patient's gender, age, history of anticoagulation, modality of guidance, targeted vs. non-targeted, coaxial vs non-coaxial technique, number of samples, the gauge of core biopsy, or core vs. FNA; lesion location, CT attenuation, US echogenicity, vascularity, all  $p>0.05$ . Incidence of bleeding was higher in patients with tract embolization (10/59, 17% vs. 18/301, 6%), as tract embolization was likely performed to treat the bleeding.

#### CONCLUSION

Bleeding after splenic biopsy occurred after 8% of procedures, with 2% requiring medical, 1% angiographic, and 1% surgical management. Smaller lesions and patients with no hematological history had a higher incidence of bleeding.

#### CLINICAL RELEVANCE/APPLICATION

The image-guided splenic biopsy is safe with a small number of patients requiring treatment for clinically significant post-procedure bleeding.

Printed on: 02/07/23

## Abstract Archives of the RSNA, 2022

M2-SPMK

### Musculoskeletal Monday Poster Discussions

Monday, Nov. 28 9:00AM - 9:30AM Room: Learning Center - MK DPS

#### Participants

Barry Hansford, MD, Lake Oswego, OR (*Moderator*) Nothing to Disclose

#### Sub-Events

#### M2-SPMK-1 Diagnosis of Foot and Ankle Injuries with Multiple-view Radiographic Studies by HAMIL-Net

#### Participants

Amilcare Gentili, MD, MBA, San Diego, CA (*Presenter*) Institutional Grant, VoxelCloud

#### PURPOSE

Automated diagnosis of orthopaedic injuries can save time by providing a preliminary interpretation on the presence of orthopaedic trauma. AI deep learning has been shown to be promising but many challenges need to be overcome. For orthopaedic injuries, one of the key challenges is that a radiographic study usually consists of multiple image views of different angles of different body parts, but the available data might not pinpoint specific views where abnormalities are observable. For example, MURA, a widely used dataset in the public domain, provides a single label of normal or abnormal for each study. While providing view-level labels is expensive.

#### METHODS AND MATERIALS

We considered "HAMIL-Net," a deep neural net architecture with hierarchical attention (HA) mechanism and multiple instance learning (MIL) to discriminate body parts and selectively attend to different views and regions. Previously, 0.91 AUC for MURA was reported. The study team used a dataset of 580K musculoskeletal imaging studies for 138K patients with 17 body parts. 148K were foot and ankle. We designed an ontology that consists of 26 orthopaedic pathologies with 8 levels of classification of positive/negative, high/low certainty, and acute/chronic and leveraged PyContextNLP, a rule-based natural language processing (NLP) tool to semi-automatically label each study based on the ontology. To compare with MURA, we focused on 8 pathologies (i.e., fracture, hardware, arthritis, subluxations etc.) with high certainty. 24K abnormal and 47K normal studies were included. Image views per study were 3.16 (2.72 in MURA). Data were randomly split at 8:2 for training/test.

#### RESULTS

HAMIL-Net achieved 0.84 AUC (95% CI 0.8475, 0.8325), compared to 0.82(95% CI 0.8244, 0.8155) by ResNet34 and 0.83(95% CI 0.8343, 0.8257) by DenseNet169 as baselines. The baselines, however, classified each view instead of the whole study. When considering fracture only, HAMIL-Net achieved 0.86 AUC (95% CI 0.8687, 0.8513). Pretraining HAMIL-Net with MURA did not improve or degrade the performance.

#### CONCLUSION

Foot and ankle studies contain more views per study than upper extremity studies in MURA and may be more challenging. HAMIL-Net outperformed baselines by considering multiple views and performed even better when considering fracture only. Our HAMIL-Net implementation considered four views for all studies. Our future work is to relax this limitation.

#### CLINICAL RELEVANCE/APPLICATION

Automated initial interpretation of orthopaedic injury studies by shortening the communication gap between the point of injury and patient care, which could lead to earlier treatment and better outcomes.

#### M2-SPMK-2 Will Novel Deep Learning Architectures 'Transform' MSK Radiograph Diagnosis? A Comparison of Vision Transformers and Convolutional Neural Networks for Abnormality Detection in Extremity Radiographs

#### Participants

Paul Yi, MD, Baltimore, MD (*Presenter*) Consultant, FH Orthopedics SAS; Consultant, BunkerHill Health

#### PURPOSE

Visual transformers (VTs) are a new type of deep learning algorithm that has shown advantage in classification tasks for general imaging datasets compared to traditional convolutional neural networks (CNNs). However, it is unclear if these advantages translate to radiology-specific tasks. We compared performance, sample efficiency, and hidden stratification of multiple ViT and CNN architectures for diagnosis of abnormalities on extremity radiographs using transfer learning.

#### METHODS AND MATERIALS

We used Stanford's MURA dataset of 40,005 upper extremity radiographs from five anatomic regions labeled as normal or abnormal; these images were divided into 70/20/10% train/validation/testing splits. We finetuned Data-efficient Image Transformer (DeiT) ViT and CNN classification models pretrained on ImageNet using these images to identify abnormal images. Performance was assessed

using weighted AUROC across anatomical regions (wAUC). Our primary comparison was DeiT-B ViT vs. DenseNet121 CNN with secondary comparisons including DeiT-Ti, ResNet152, and EfficientNetB7. We evaluated sample efficiency by training models on varying dataset sizes ranging from 1% to 100% of total data. We evaluated hidden stratification by comparing prevalence of arthritis, fracture, and hardware in false positive (FP) and false negative (FN) predictions. Finally, we visually compared the localization ability of ViT attention and CNN grad-CAM heatmaps.

## RESULTS

DeiT-B wAUC was significantly lower than DenseNet121 (0.887 vs. 0.893,  $p < 0.001$ ). DeiT-B and DeiT-Ti both performed worse than all CNNs evaluated ( $p < 0.001$ , all comparisons). ViTs and CNNs showed similar sample efficiency. There was no significant difference in hidden stratification between ViTs and CNNs with arthritis being more prevalent in FP and FN predictions than fracture or hardware. ViT attention heatmaps qualitatively were more accurate and tightly bounded to radiographic abnormalities compared to CNN heatmaps.

## CONCLUSION

Although DeiT ViT models had lower wAUCs than CNNs for extremity abnormality diagnosis, the absolute differences were small. Additionally, ViT models had similar sample efficiency with more reassuring heatmaps that may prove more useful for disease localization than CNN heatmaps. As ViT architectures are in their infancy, there will almost assuredly continue to be improvements in performance and we optimistically recommend continued evaluation of ViTs for MSK imaging as they mature in the coming years.

## CLINICAL RELEVANCE/APPLICATION

Even in their early stages, visual transformers provide similar performance to convolutional neural networks while outputting more reassuring heatmaps, which may prove useful for disease localization in MSK radiograph diagnosis.

### M2-SPMK-3 Patient-Specific Hip Arthroplasty Dislocation Risk Calculator: An Explainable Multimodal Machine Learning Based Approach

Participants

Bardia Khosravi, MD, MPH, Rochester, MN (*Presenter*) Nothing to Disclose

## PURPOSE

Total hip arthroplasty (THA) is among the most common elective surgeries in the United States. While typically THA is quite successful, complications can occur. Implant dislocation is the most common complication of THA that might require revision surgery. However, there are also well-described intraoperative choices within a surgeon's control that can be used to mitigate the risk of dislocation. This study develops a multimodal machine learning-based pipeline to predict the patient-specific risk of dislocation following primary THA that can help surgeons with preoperative planning.

## METHODS AND MATERIALS

This study retrospectively evaluates 17,073 patients who underwent primary THA between 1998-2018. A test set of 1,733 patients was held out. A hybrid network of EfficientNet-B4 and Swin-B vision transformer was developed to classify patients based on 5-year dislocation outcomes from preoperative anteroposterior (AP) pelvis radiographs and clinical (demographics, comorbidities, and surgical) characteristics. The most informative imaging features, that the mentioned model extracted were selected and concatenated with clinical features. A collection of these features was then used to train a multimodal survival XGBoost model to predict the individualized risk of dislocation. A clinical-only survival XGBoost was trained as a benchmark to compare addition of imaging features. C-index was used to evaluate the multimodal survival model on the test set and compare it with the clinical-only model. Integrated gradient maps and Shapley additive explanation (SHAP) values were used for the classifier and survival model explanation, respectively.

## RESULTS

On the holdout test set, the clinical-only model achieved a C-index of 63.8% (95% CI: 59.5%-68.1%); adding imaging features boosted multimodal model performance to a C-index of 73.6% (95% CI: 69.2%-78.0%). Imaging features represented 4 of the top 5 and 10 of the top 13 most influential variables in the multimodal model. The imaging feature showed focus of the model on the area of maximum load in the hip joint articulation, the lesser trochanter, and the acetabular teardrop.

## CONCLUSION

A multimodal calculator for predicting dislocation was introduced by combining preoperative characteristics and radiographic features of patients undergoing primary THA. This study highlights the superiority of imaging features compared to clinical variables and the synergy between these modes of patient evaluation.

## CLINICAL RELEVANCE/APPLICATION

The developed tool enables patient-specific dislocation risk prediction with an acceptable C-index, and more importantly, shows the degree to which this risk is modified by decisions within a surgeon's control.

### M2-SPMK-4 Deep-Learning-Based Evaluation and Quantification of Real-Time MRI for the Assessment of Active Wrist Motion in Health and Disease

Participants

Lena Wilms, Dusseldorf, Germany (*Presenter*) Nothing to Disclose

## PURPOSE

For wrist imaging, clinical MRI sequences focus on the morphologic appearance of a structure to assess its condition. Yet, such MRI sequences are acquired in a static condition, thereby potentially missing complex dynamic instability patterns. Based on real-time MRI during active wrist motion and deep-learning based image post-processing using convolutional neural networks (CNN), this study aimed to develop and validate an automated wrist motion quantification method.

## METHODS AND MATERIALS

After systematic Fast Low Angle Shot (FLASH) sequence variation, 56 bilateral wrists (28 healthy volunteers) were imaged during continuous active radioulnar abduction at a temporal resolution of 95 ms/image. After CNN based segmentations of carpal bone

contours, scapholunate (SL) and lunotriquetral (LT) gap widths were determined as a function of wrist position across the entire range-of-motion. Manual segmentations and quantification of gap widths served as reference standard. Clinical applicability of the framework was assessed in two ligament-injured patients (partial and complete SL injuries). Mean SL and LT gap widths were evaluated using a linear mixed model based on multivariable statistics. Bland-Altman plots were used comparatively evaluate automatically and manually determined SL and LT gap widths and wrist angles.

## **RESULTS**

Automatic segmentations agreed excellently with manual reference segmentations, performed independently by two radiologists, as shown by the Dice similarity coefficients of  $0.96 \pm 0.02$  and the consistent and unskewed Bland-Altman plots. Clinical applicability of the framework was demonstrated in two patients with diagnosed SL injuries indicating significantly greater SL gap widths over the entire range-of-motion in patients than in controls (SL gap widths:  $3.4 \pm 1.2$ mm [patients],  $1.6 \pm 0.4$ mm [controls],  $p < 0.001$ ), particularly at maximum radial abduction, and displaying distinctly different motion patterns and trajectories.

## **CONCLUSION**

s The combination of advanced image acquisition and post-processing techniques permits dynamic wrist assessment over the entire range of active radioulnar motion, both in healthy volunteers and ligament-injured patients. Merging real-time wrist MRT and the introduced technical framework, thus, provides a powerful diagnostic tool for dynamic quantification of wrist function and, if confirmed in clinical trials, dynamic carpal instability that may elude static assessment using clinical-standard morphologic MRI.

## **CLINICAL RELEVANCE/APPLICATION**

If confirmed in clinical trials, the combination of advanced image acquisition using real-time wrist MRI and post-processing techniques may serve as a contrast agent-free surrogate of carpus integrity and dynamic wrist function.

Printed on: 02/07/23

## Abstract Archives of the RSNA, 2022

M2-SPMK-1

### Diagnosis of Foot and Ankle Injuries with Multiple-view Radiographic Studies by HAMIL-Net

Monday, Nov. 28 9:00AM - 9:30AM Room: Learning Center - MK DPS

#### Participants

Amicare Gentili, MD, MBA, San Diego, CA (*Presenter*) Institutional Grant, VoxelCloud

#### PURPOSE

Automated diagnosis of orthopaedic injuries can save time by providing a preliminary interpretation on the presence of orthopaedic trauma. AI deep learning has been shown to be promising but many challenges need to be overcome. For orthopaedic injuries, one of the key challenges is that a radiographic study usually consists of multiple image views of different angles of different body parts, but the available data might not pinpoint specific views where abnormalities are observable. For example, MURA, a widely used dataset in the public domain, provides a single label of normal or abnormal for each study. While providing view-level labels is expensive.

#### METHODS AND MATERIALS

We considered "HAMIL-Net," a deep neural net architecture with hierarchical attention (HA) mechanism and multiple instance learning (MIL) to discriminate body parts and selectively attend to different views and regions. Previously, 0.91 AUC for MURA was reported. The study team used a dataset of 580K musculoskeletal imaging studies for 138K patients with 17 body parts. 148K were foot and ankle. We designed an ontology that consists of 26 orthopaedic pathologies with 8 levels of classification of positive/negative, high/low certainty, and acute/chronic and leveraged PyContextNLP, a rule-based natural language processing (NLP) tool to semi-automatically label each study based on the ontology. To compare with MURA, we focused on 8 pathologies (i.e., fracture, hardware, arthritis, subluxations etc.) with high certainty. 24K abnormal and 47K normal studies were included. Image views per study were 3.16 (2.72 in MURA). Data were randomly split at 8:2 for training/test.

#### RESULTS

HAMIL-Net achieved 0.84 AUC (95% CI 0.8475, 0.8325), compared to 0.82(95% CI 0.8244, 0.8155) by ResNet34 and 0.83(95% CI 0.8343, 0.8257) by DenseNet169 as baselines. The baselines, however, classified each view instead of the whole study. When considering fracture only, HAMIL-Net achieved 0.86 AUC (95% CI 0.8687, 0.8513). Pretraining HAMIL-Net with MURA did not improve or degrade the performance.

#### CONCLUSION

Foot and ankle studies contain more views per study than upper extremity studies in MURA and may be more challenging. HAMIL-Net outperformed baselines by considering multiple views and performed even better when considering fracture only. Our HAMIL-Net implementation considered four views for all studies. Our future work is to relax this limitation.

#### CLINICAL RELEVANCE/APPLICATION

Automated initial interpretation of orthopaedic injury studies by shortening the communication gap between the point of injury and patient care, which could lead to earlier treatment and better outcomes.

Printed on: 02/07/23



## Abstract Archives of the RSNA, 2022

M2-SPMK-2

### Will Novel Deep Learning Architectures 'Transform' MSK Radiograph Diagnosis? A Comparison of Vision Transformers and Convolutional Neural Networks for Abnormality Detection in Extremity Radiographs

Monday, Nov. 28 9:00AM - 9:30AM Room: Learning Center - MK DPS

#### Participants

Paul Yi, MD, Baltimore, MD (*Presenter*) Consultant, FH Orthopedics SAS; Consultant, BunkerHill Health

#### PURPOSE

Visual transformers (VTs) are a new type of deep learning algorithm that has shown advantage in classification tasks for general imaging datasets compared to traditional convolutional neural networks (CNNs). However, it is unclear if these advantages translate to radiology-specific tasks. We compared performance, sample efficiency, and hidden stratification of multiple ViT and CNN architectures for diagnosis of abnormalities on extremity radiographs using transfer learning.

#### METHODS AND MATERIALS

We used Stanford's MURA dataset of 40,005 upper extremity radiographs from five anatomic regions labeled as normal or abnormal; these images were divided into 70/20/10% train/validation/testing splits. We finetuned Data-efficient Image Transformer (DeiT) ViT and CNN classification models pretrained on ImageNet using these images to identify abnormal images. Performance was assessed using weighted AUROC across anatomical regions (wAUC). Our primary comparison was DeiT-B ViT vs. DenseNet121 CNN with secondary comparisons including DeiT-Ti, ResNet152, and EfficientNetB7. We evaluated sample efficiency by training models on varying dataset sizes ranging from 1% to 100% of total data. We evaluated hidden stratification by comparing prevalence of arthritis, fracture, and hardware in false positive (FP) and false negative (FN) predictions. Finally, we visually compared the localization ability of ViT attention and CNN grad-CAM heatmaps.

#### RESULTS

DeiT-B wAUC was significantly lower than DenseNet121 (0.887 vs. 0.893,  $p < 0.001$ ). DeiT-B and DeiT-Ti both performed worse than all CNNs evaluated ( $p < 0.001$ , all comparisons). ViTs and CNNs showed similar sample efficiency. There was no significant difference in hidden stratification between ViTs and CNNs with arthritis being more prevalent in FP and FN predictions than fracture or hardware. ViT attention heatmaps qualitatively were more accurate and tightly bounded to radiographic abnormalities compared to CNN heatmaps.

#### CONCLUSION

Although DeiT ViT models had lower wAUCs than CNNs for extremity abnormality diagnosis, the absolute differences were small. Additionally, ViT models had similar sample efficiency with more reassuring heatmaps that may prove more useful for disease localization than CNN heatmaps. As ViT architectures are in their infancy, there will almost assuredly continue to be improvements in performance and we optimistically recommend continued evaluation of ViTs for MSK imaging as they mature in the coming years.

#### CLINICAL RELEVANCE/APPLICATION

Even in their early stages, visual transformers provide similar performance to convolutional neural networks while outputting more reassuring heatmaps, which may prove useful for disease localization in MSK radiograph diagnosis.

Printed on: 02/07/23

## Abstract Archives of the RSNA, 2022

M2-SPMK-3

### Patient-Specific Hip Arthroplasty Dislocation Risk Calculator: An Explainable Multimodal Machine Learning Based Approach

Monday, Nov. 28 9:00AM - 9:30AM Room: Learning Center - MK DPS

#### Participants

Bardia Khosravi, MD, MPH, Rochester, MN (*Presenter*) Nothing to Disclose

#### PURPOSE

Total hip arthroplasty (THA) is among the most common elective surgeries in the United States. While typically THA is quite successful, complications can occur. Implant dislocation is the most common complication of THA that might require revision surgery. However, there are also well-described intraoperative choices within a surgeon's control that can be used to mitigate the risk of dislocation. This study develops a multimodal machine learning-based pipeline to predict the patient-specific risk of dislocation following primary THA that can help surgeons with preoperative planning.

#### METHODS AND MATERIALS

This study retrospectively evaluates 17,073 patients who underwent primary THA between 1998-2018. A test set of 1,733 patients was held out. A hybrid network of EfficientNet-B4 and Swin-B vision transformer was developed to classify patients based on 5-year dislocation outcomes from preoperative anteroposterior (AP) pelvis radiographs and clinical (demographics, comorbidities, and surgical) characteristics. The most informative imaging features, that the mentioned model extracted were selected and concatenated with clinical features. A collection of these features was then used to train a multimodal survival XGBoost model to predict the individualized risk of dislocation. A clinical-only survival XGBoost was trained as a benchmark to compare addition of imaging features. C-index was used to evaluate the multimodal survival model on the test set and compare it with the clinical-only model. Integrated gradient maps and Shapley additive explanation (SHAP) values were used for the classifier and survival model explanation, respectively.

#### RESULTS

On the holdout test set, the clinical-only model achieved a C-index of 63.8% (95% CI: 59.5%-68.1%); adding imaging features boosted multimodal model performance to a C-index of 73.6% (95% CI: 69.2%-78.0%). Imaging features represented 4 of the top 5 and 10 of the top 13 most influential variables in the multimodal model. The imaging feature showed focus of the model on the area of maximum load in the hip joint articulation, the lesser trochanter, and the acetabular teardrop.

#### CONCLUSION

A multimodal calculator for predicting dislocation was introduced by combining preoperative characteristics and radiographic features of patients undergoing primary THA. This study highlights the superiority of imaging features compared to clinical variables and the synergy between these modes of patient evaluation.

#### CLINICAL RELEVANCE/APPLICATION

The developed tool enables patient-specific dislocation risk prediction with an acceptable C-index, and more importantly, shows the degree to which this risk is modified by decisions within a surgeon's control.

Printed on: 02/07/23

## Abstract Archives of the RSNA, 2022

M2-SPMK-4

### Deep-Learning-Based Evaluation and Quantification of Real-Time MRI for the Assessment of Active Wrist Motion in Health and Disease

Monday, Nov. 28 9:00AM - 9:30AM Room: Learning Center - MK DPS

#### Participants

Lena Wilms, Dusseldorf, Germany (*Presenter*) Nothing to Disclose

#### PURPOSE

For wrist imaging, clinical MRI sequences focus on the morphologic appearance of a structure to assess its condition. Yet, such MRI sequences are acquired in a static condition, thereby potentially missing complex dynamic instability patterns. Based on real-time MRI during active wrist motion and deep-learning based image post-processing using convolutional neural networks (CNN), this study aimed to develop and validate an automated wrist motion quantification method.

#### METHODS AND MATERIALS

After systematic Fast Low Angle Shot (FLASH) sequence variation, 56 bilateral wrists (28 healthy volunteers) were imaged during continuous active radioulnar abduction at a temporal resolution of 95 ms/image. After CNN based segmentations of carpal bone contours, scapholunate (SL) and lunotriquetral (LT) gap widths were determined as a function of wrist position across the entire range-of-motion. Manual segmentations and quantification of gap widths served as reference standard. Clinical applicability of the framework was assessed in two ligament-injured patients (partial and complete SL injuries). Mean SL and LT gap widths were evaluated using a linear mixed model based on multivariable statistics. Bland-Altman plots were used comparatively evaluate automatically and manually determined SL and LT gap widths and wrist angles.

#### RESULTS

Automatic segmentations agreed excellently with manual reference segmentations, performed independently by two radiologists, as shown by the Dice similarity coefficients of  $0.96 \pm 0.02$  and the consistent and unskewed Bland-Altman plots. Clinical applicability of the framework was demonstrated in two patients with diagnosed SL injuries indicating significantly greater SL gap widths over the entire range-of-motion in patients than in controls (SL gap widths:  $3.4 \pm 1.2$ mm [patients],  $1.6 \pm 0.4$ mm [controls],  $p < 0.001$ ), particularly at maximum radial abduction, and displaying distinctly different motion patterns and trajectories.

#### CONCLUSION

The combination of advanced image acquisition and post-processing techniques permits dynamic wrist assessment over the entire range of active radioulnar motion, both in healthy volunteers and ligament-injured patients. Merging real-time wrist MRI and the introduced technical framework, thus, provides a powerful diagnostic tool for dynamic quantification of wrist function and, if confirmed in clinical trials, dynamic carpal instability that may elude static assessment using clinical-standard morphologic MRI.

#### CLINICAL RELEVANCE/APPLICATION

If confirmed in clinical trials, the combination of advanced image acquisition using real-time wrist MRI and post-processing techniques may serve as a contrast agent-free surrogate of carpus integrity and dynamic wrist function.

Printed on: 02/07/23

## Abstract Archives of the RSNA, 2022

M2-SPMS

### Multisystem Monday Poster Discussions

Monday, Nov. 28 9:00AM - 9:30AM Room: Learning Center - MS DPS

#### Sub-Events

#### M2-SPMS-1 Functional Imaging with Dual-energy Computed Tomography for Supplementary Non-invasive Assessment of Mast Cell Burden in Systemic Mastocytosis

##### Participants

Julia Riffel, MD, (*Presenter*) Nothing to Disclose

##### PURPOSE

Systemic mastocytosis (SM) is characterized by multifocal accumulation of neoplastic mast cells (MCs), predominately affecting the bone marrow (BM). Imaging with computed tomography (CT) is routinely used for assessment of bone mineral density and bone structure. However, the value of functional imaging with dual-energy CT (DECT) and the assessment of virtual-non-calcium attenuation values (VNCA-AV) for visualization of BM disease burden in SM has not yet been assessed.

##### METHODS AND MATERIALS

DECT of the axial skeleton was performed in 18 patients with SM (indolent SM [ISM], n=6; smoldering SM [SSM]/advanced SM [AdvSM], n=12) and 18 control subjects. VNCA-AV were obtained in 5 representative vertebrae per patient and correlated with laboratory, morphologic and molecular parameters. Visual evaluation of osteosclerosis was performed on morphologic CT images.

##### RESULTS

VNCA-AV strongly correlated with quantitative bone marrow mast infiltration ( $r=0.7$ ,  $R^2=0.49$ ,  $P=0.001$ ) and serum tryptase levels ( $r=0.7$ ,  $R^2=0.54$ ,  $P<0.001$ ). Mean VNCA-AV were significantly higher in patients with SSM/AdvSM as compared to ISM (-9HU vs. -54HU,  $P<0.005$ ) and controls (38HU,  $P<0.005$ ). Nine of 10 (90%) patients with a VNCA-AV  $> -30$ HU and 7/7 (100%) patients with a VNCA-AV  $> -10$ HU had SSM or AdvSM.

##### CONCLUSION

s Bone marrow VNCA-AV provide information about the mast cell burden of SM patients and correlate with SM subtypes. Since conventional CT is used to assess for organomegaly, pathological bone mineral density, osteolyses and fractures, functional imaging with DECT may serve as supplementary tool for diagnosis, subclassification and monitoring of SM disease in a one-stop-shop session.

##### CLINICAL RELEVANCE/APPLICATION

Dual-energy CT allows non-invasive assessment of the mast cell burden in systemic mastocytosis and may serve as supplementary tool for diagnosis, subclassification and monitoring of systemic mastocytosis in a one-stop-shop session.

Printed on: 02/07/23

## Abstract Archives of the RSNA, 2022

M2-SPMS-1

### Functional Imaging with Dual-energy Computed Tomography for Supplementary Non-invasive Assessment of Mast Cell Burden in Systemic Mastocytosis

Monday, Nov. 28 9:00AM - 9:30AM Room: Learning Center - MS DPS

#### Participants

Julia Riffel, MD, (*Presenter*) Nothing to Disclose

#### PURPOSE

Systemic mastocytosis (SM) is characterized by multifocal accumulation of neoplastic mast cells (MCs), predominately affecting the bone marrow (BM). Imaging with computed tomography (CT) is routinely used for assessment of bone mineral density and bone structure. However, the value of functional imaging with dual-energy CT (DECT) and the assessment of virtual-non-calcium attenuation values (VNCa-AV) for visualization of BM disease burden in SM has not yet been assessed.

#### METHODS AND MATERIALS

DECT of the axial skeleton was performed in 18 patients with SM (indolent SM [ISM], n=6; smoldering SM [SSM]/advanced SM [AdvSM], n=12) and 18 control subjects. VNCa-AV were obtained in 5 representative vertebrae per patient and correlated with laboratory, morphologic and molecular parameters. Visual evaluation of osteosclerosis was performed on morphologic CT images.

#### RESULTS

VNCa-AV strongly correlated with quantitative bone marrow mast infiltration ( $r=0.7$ ,  $R^2=0.49$ ,  $P=0.001$ ) and serum tryptase levels ( $r=0.7$ ,  $R^2=0.54$ ,  $P<0.001$ ). Mean VNCa-AV were significantly higher in patients with SSM/AdvSM as compared to ISM (-9HU vs. -54HU,  $P<0.005$ ) and controls (38HU,  $P<0.005$ ). Nine of 10 (90%) patients with a VNCa-AV  $> -30$ HU and 7/7 (100%) patients with a VNCa-AV  $> -10$ HU had SSM or AdvSM.

#### CONCLUSION

s Bone marrow VNCa-AV provide information about the mast cell burden of SM patients and correlate with SM subtypes. Since conventional CT is used to assess for organomegaly, pathological bone mineral density, osteolyses and fractures, functional imaging with DECT may serve as supplementary tool for diagnosis, subclassification and monitoring of SM disease in a one-stop-shop session.

#### CLINICAL RELEVANCE/APPLICATION

Dual-energy CT allows non-invasive assessment of the mast cell burden in systemic mastocytosis and may serve as supplementary tool for diagnosis, subclassification and monitoring of systemic mastocytosis in a one-stop-shop session.

Printed on: 02/07/23

## Abstract Archives of the RSNA, 2022

M2-SPNMMI

### Nuclear Medicine/Molecular Imaging Monday Poster Discussion

Monday, Nov. 28 9:00AM - 9:30AM Room: Learning Center - NMMI DPS

#### Participants

Lilja Solnes, MD, Owings Mills, MD (*Moderator*) Consultant, Lantheus Holdings; Research funded, Novartis AG; Research funded, Precision Molecular Inc; Research funded, Cellectar Biosciences, Inc; Royalties, RELX

Lilja Solnes, MD, Owings Mills, MD (*Moderator*) Consultant, Lantheus Holdings; Research funded, Novartis AG; Research funded, Precision Molecular Inc; Research funded, Cellectar Biosciences, Inc; Royalties, RELX

Frederick Grant, MD, Philadelphia, PA (*Moderator*) Nothing to Disclose

Frederick Grant, MD, Philadelphia, PA (*Moderator*) Nothing to Disclose

#### Sub-Events

### M2-SPNMMI-PET Respiratory Motion Correction Improves Metabolic Tumor Volume Accuracy for Lung Base Lesions on Oncologic PET/CT<sup>1</sup>

#### Participants

Genevieve Munoz, (*Presenter*) Nothing to Disclose

#### PURPOSE

Respiratory motion can distort lung base tumors on PET imaging, potentially altering metabolic tumor volume (MTV) and impacting radiotherapy planning. This study assessed the impact of several respiratory motion mitigation strategies on lung base tumor MTVs, utilizing CT-based segmentation volumes as the reference standard.

#### METHODS AND MATERIALS

To date, this IRB-approved, HIPAA-compliant prospective study has enrolled 10 patients with tracer-avid lung base tumors. All subjects provided written informed consent. Imaging occurred on a Biograph Vision PET/CT (Siemens Healthineers). A weight-based radiotracer dose was given ~60 min before imaging. Four PET reconstructions were performed: 1) without motion correction (uncorrected); 2) using end-expiratory counts (EE-gate); 3) using elastic motion correction with deblurring (EMCD) to correct counts to a reference gate, as informed by the Anzai system (Anz-EMCD); and 4) using EMCD to correct counts to a reference gate via a purely data-driven approach (OncoFreeze AI). For each reconstruction, metabolic tumor volume (MTV) was calculated in MIM software using an adaptive segmentation strategy. Each lesion was manually segmented on CT. Differences between MTVs and reference CT volumes (MTV-CT) were compared across reconstructions. Statistical comparisons were based on the Wilcoxon signed-rank test ( $\alpha = 0.05$ ).

#### RESULTS

All data reported are median MTV-CTs [interquartile ranges] for the 10 subjects. The MTV-CT was significantly higher for uncorrected (0.96 ml [3.57]) images than for EE-gate (0.55 ml [0.72];  $p < 0.05$ ), Anz-EMCD (0.35 ml [0.38];  $p = 0.005$ ), or OncoFreeze AI (0.37 ml [0.39];  $p = 0.012$ ) images. MTV-CT was not significantly different for EE-gate versus Anz-EMCD ( $p = 0.646$ ) or Anz-EMCD versus OncoFreeze AI ( $p > 0.05$ ) images. Visually, image noise was lower and overall image quality was higher for Anz-EMCD and OncoFreeze AI images relative to EE-gate images.

#### CONCLUSION

For lung base tumors, PET reconstructions without motion correction exhibit greater bias toward higher MTVs than EE-gate, Anz-EMCD, or OncoFreeze AI reconstructions. Anz-EMCD and OncoFreeze AI reconstructions, which utilize all counts, result in better image quality than end-expiratory gated reconstructions.

#### CLINICAL RELEVANCE/APPLICATION

EMCD using the Anzai system or OncoFreeze AI improves PET volume quantification without sacrificing image quality, potentially resulting in more accurate tumor response assessments and more precise radiotherapy plans.

### M2-SPNMMI-Does the Finding of Two Areas of Tc-99m Sestamibi Retention on Parathyroid Scintigraphy Always Indicate Double Parathyroid Adenomas? Results of a 10-Year Analysis<sup>3</sup>

#### Participants

Charles M. Intenzo, MD, Philadelphia, PA (*Presenter*) Nothing to Disclose

#### PURPOSE

Tc-99m sestamibi (MIBI) scintigraphy is commonly utilized for the preoperative localization of parathyroid adenomas. A focal area of tracer retention that persists on delayed images is fairly specific for a parathyroid adenoma. Occasionally, there are 2 foci of MIBI retention on delayed imaging, which theoretically suggests a double parathyroid adenoma. However, on follow-up review of pathology reports, many of these were signed out as "asymmetric parathyroid hyperplasia" by the cytopathologist. Our aim was to determine just how often this finding was shown to represent a double parathyroid adenoma.

## **METHODS AND MATERIALS**

Over a 10-yea interval, both retrospectively and prospectively, all parathyroid scans with the finding of 2 areas of MIBI concentration in initial images of the neck, that retained the tracer on 3-hour delayed images were collected and corresponding histopathological results were reviewed.

## **RESULTS**

A total of 49 patients demonstrated the above finding. Of these, 41 underwent neck exploration; 33 were diagnosed as having asymmetric parathyroid gland hyperplasia, while only 8 were diagnosed with double parathyroid adenoma.

## **CONCLUSION**

s Of the group of 41 patients whose parathyroid scintigraphy showed 2 areas of MIBI retention on 3-hour delayed images of neck, 33 (80.5%) had asymmetric parathyroid gland hyperplasia, whereas only 8 patients with this finding had true double adenoma. In parathyroid scintigraphy, 2 foci of tracer retention more than likely indicate parathyroid gland hyperplasia, as opposed to double parathyroid adenoma.

## **CLINICAL RELEVANCE/APPLICATION**

For the finding of 2 focal areas of sestamibi retention on sestamibi scintigraphy, both parathyroid gland hyperplasia and double parathyroid adenoma should be given as a differential diagnosis in the scan report summary.

Printed on: 02/07/23

## Abstract Archives of the RSNA, 2022

M2-SPNMMI-1

### **PET Respiratory Motion Correction Improves Metabolic Tumor Volume Accuracy for Lung Base Lesions on Oncologic PET/CT**

Monday, Nov. 28 9:00AM - 9:30AM Room: Learning Center - NMMI DPS

#### **Participants**

Genevieve Munoz, (Presenter) Nothing to Disclose

#### **PURPOSE**

Respiratory motion can distort lung base tumors on PET imaging, potentially altering metabolic tumor volume (MTV) and impacting radiotherapy planning. This study assessed the impact of several respiratory motion mitigation strategies on lung base tumor MTVs, utilizing CT-based segmentation volumes as the reference standard.

#### **METHODS AND MATERIALS**

To date, this IRB-approved, HIPAA-compliant prospective study has enrolled 10 patients with tracer-avid lung base tumors. All subjects provided written informed consent. Imaging occurred on a Biograph Vision PET/CT (Siemens Healthineers). A weight-based radiotracer dose was given ~60 min before imaging. Four PET reconstructions were performed: 1) without motion correction (uncorrected); 2) using end-expiratory counts (EE-gate); 3) using elastic motion correction with deblurring (EMCD) to correct counts to a reference gate, as informed by the Anzai system (Anz-EMCD); and 4) using EMCD to correct counts to a reference gate via a purely data-driven approach (OncoFreeze AI). For each reconstruction, metabolic tumor volume (MTV) was calculated in MIM software using an adaptive segmentation strategy. Each lesion was manually segmented on CT. Differences between MTVs and reference CT volumes (MTV-CT) were compared across reconstructions. Statistical comparisons were based on the Wilcoxon signed-rank test ( $\alpha = 0.05$ ).

#### **RESULTS**

All data reported are median MTV-CTs [interquartile ranges] for the 10 subjects. The MTV-CT was significantly higher for uncorrected (0.96 ml [3.57]) images than for EE-gate (0.55 ml [0.72];  $p < 0.05$ ), Anz-EMCD (0.35 ml [0.38];  $p = 0.005$ ), or OncoFreeze AI (0.37 ml [0.39];  $p = 0.012$ ) images. MTV-CT was not significantly different for EE-gate versus Anz-EMCD ( $p = 0.646$ ) or Anz-EMCD versus OncoFreeze AI ( $p > 0.05$ ) images. Visually, image noise was lower and overall image quality was higher for Anz-EMCD and OncoFreeze AI images relative to EE-gate images.

#### **CONCLUSION**

For lung base tumors, PET reconstructions without motion correction exhibit greater bias toward higher MTVs than EE-gate, Anz-EMCD, or OncoFreeze AI reconstructions. Anz-EMCD and OncoFreeze AI reconstructions, which utilize all counts, result in better image quality than end-expiratory gated reconstructions.

#### **CLINICAL RELEVANCE/APPLICATION**

EMCD using the Anzai system or OncoFreeze AI improves PET volume quantification without sacrificing image quality, potentially resulting in more accurate tumor response assessments and more precise radiotherapy plans.

Printed on: 02/07/23

## Abstract Archives of the RSNA, 2022

M2-SPNMMI-3

### Does the Finding of Two Areas of TC-99M Sestamibi Retention on Parathyroid Scintigraphy Always Indicate Double Parathyroid Adenomas? Results of a 10-Year Analysis

Monday, Nov. 28 9:00AM - 9:30AM Room: Learning Center - NMMI DPS

#### Participants

Charles M. Intenzo, MD, Philadelphia, PA (*Presenter*) Nothing to Disclose

#### PURPOSE

Tc-99m sestamibi (MIBI) scintigraphy is commonly utilized for the preoperative localization of parathyroid adenomas. A focal area of tracer retention that persists on delayed images is fairly specific for a parathyroid adenoma. Occasionally, there are 2 foci of MIBI retention on delayed imaging, which theoretically suggests a double parathyroid adenoma. However, on follow-up review of pathology reports, many of these were signed out as "asymmetric parathyroid hyperplasia" by the cytopathologist. Our aim was to determine just how often this finding was shown to represent a double parathyroid adenoma.

#### METHODS AND MATERIALS

Over a 10-year interval, both retrospectively and prospectively, all parathyroid scans with the finding of 2 areas of MIBI concentration in initial images of the neck, that retained the tracer on 3-hour delayed images were collected and corresponding histopathological results were reviewed.

#### RESULTS

A total of 49 patients demonstrated the above finding. Of these, 41 underwent neck exploration; 33 were diagnosed as having asymmetric parathyroid gland hyperplasia, while only 8 were diagnosed with double parathyroid adenoma.

#### CONCLUSION

Of the group of 41 patients whose parathyroid scintigraphy showed 2 areas of MIBI retention on 3-hour delayed images of neck, 33 (80.5%) had asymmetric parathyroid gland hyperplasia, whereas only 8 patients with this finding had true double adenoma. In parathyroid scintigraphy, 2 foci of tracer retention more than likely indicate parathyroid gland hyperplasia, as opposed to double parathyroid adenoma.

#### CLINICAL RELEVANCE/APPLICATION

For the finding of 2 focal areas of sestamibi retention on sestamibi scintigraphy, both parathyroid gland hyperplasia and double parathyroid adenoma should be given as a differential diagnosis in the scan report summary.

Printed on: 02/07/23

## Abstract Archives of the RSNA, 2022

M2-SPNPM

### Noninterpretive Skills/Quality Improvement/Practice Management Monday Poster Discussions

Monday, Nov. 28 9:00AM - 9:30AM Room: Learning Center - NPM DPS

#### Participants

Matthew Bucknor, MD, San Francisco, CA (*Moderator*) Nothing to Disclose

#### Sub-Events

#### M2-SPNPM- Reliability of 3D Image Analysis and Comparison of Diagnostic Accuracy of 2D and 3D Measurements to Determine Opportunistic Screening of Osteoporosis Using the Proximal Femur on Abdomen-Pelvic CT

#### Participants

Minsu Park, MD, (*Presenter*) Nothing to Disclose

#### PURPOSE

To evaluate the reliability of 3D image analysis and compare the osteoporosis-predicting ability of computed tomography (CT) indexes in abdomen-pelvic CT (APCT) using the proximal femur and the reliability of measurements in two and three-dimensional analyses.

#### METHODS AND MATERIALS

430 female patients who underwent dual-energy X-ray absorptiometry (DXA) and APCT within 1 month were retrospectively selected. The volumes of interest (VOIs) from the femoral head to the lesser trochanter and the femoral neck were expressed as 3DFemur. Total volume, mean-HU, and HU histogram analysis (HUHA) values of the extracted femur were calculated. Also, round regions of interest (ROIs) of image plane drawn over the femoral neck touching the outer cortex were determined as 2Dcoronal. In HUHA, the percentages of HU histogram ranges related to the ROI or VOI were classified as HUHAfat (<0HU) and HUHAbone (126HU=). Reliability of 3D image analysis was assessed by calculating intra- and interobserver correlation coefficients (ICCs). In addition, diagnostic performance, correlation analysis and measurement reliability were analyzed by receiver operating characteristic curves, correlation coefficient and ICC, respectively. Furthermore, the effect of contrast medium administration was evaluated by the paired t-test.

#### RESULTS

All ICCs of 3D volume measurements showed excellent reproducibility (all ICCs>0.90). AUCs of each HUHA and mean-HU measurement on 2D-ROI and 3D-VOI were 0.94 or higher ( $P<0.001$ ). Both 3DFemur-mean-HU and 3DFemur-HUHAbone showed the highest AUC (0.96). The cut-off value of 3DFemur-mean-HU was 231HU or less ( $P<0.001$ ) for diagnosis of osteoporosis. There was no superiority between AUCs in 2D-ROI and 3D-VOI measurements ( $P>0.05$ ). Reliability of the 3D-VOI measurement showed perfect agreement (ICC=0.94), and 2D-ROI showed moderate to good agreement (ICC range: 0.63~0.84). The mean difference in HU after contrast agent administration (-2.2HU) was not significant ( $P=0.27$ ).

#### CONCLUSION

s Image analysis based on 3D volume measurement of the proximal femur showed excellent reliability with the contrast agent administration showing negligible influence on the mean-HU, and CT indexes on 3D-VOI for predicting femoral osteoporosis showed similar diagnostic accuracy with better reproducibility of measurement, compared with 2D-ROI.

#### CLINICAL RELEVANCE/APPLICATION

Since DXA is a 2D technique, clinically relevant diagnostic errors can be made. Using APCT, BMD can be assessed in femur by measuring HU without additional imaging, radiation exposure, or patient time. Also, measurements performed with a VOI in the 3D image plane may not be substantially affected by structural complexity of femur and cross-section selection as well as the ROI location.

#### M2-SPNPM- Observer Recall Bias in Diagnostic Test Accuracy Comparative Studies: Much Room for Improvement

#### Participants

Bharadwaj Pindiprolu, MD, (*Presenter*) Nothing to Disclose

#### PURPOSE

Diagnostic test accuracy (DTA) studies often compare two or more imaging modalities, yet little is known on the impact of reading-order effects. Observer recall bias occurs when a subsequently performed test seems more accurate than an earlier test due to retention of information from the earlier test, rather than a true difference in test performance. The purpose of this study was to perform a methodological review of DTA comparative studies to assess strategies employed to limit observer recall bias.

#### METHODS AND MATERIALS

MEDLINE was used to identify DTA systematic reviews published in imaging journals from 2000 to 2021. Two reviewers

independently conducted title, abstract and full-text review to identify all systematic reviews comparing two or more index tests including at least one diagnostic imaging modality. Each reviewer extracted data from the primary studies within each systematic review. Disagreements were resolved by consensus or using a third reviewer where needed.

## **RESULTS**

87 radiologic comparative DTA studies were included, of which 38 (44%) had the same radiologist interpret both modalities, 24 (28%) used separate radiologists, and 25 (29%) provided no details. A minimum time delay between interpretations was only reported in 25 studies. Most studies (24%) required a minimum of 1 week between reads, followed by 2 weeks (16%) and 3 weeks (12%). Two readers were most frequently used (44/87; 50.6%) to interpret index tests and most commonly, reading sessions were conducted independently (40/87; 46.0%) rather than by consensus (14/87; 16.1%). Reader order was randomized in 20/87 (23%) studies. 54/87 (62.1%) studies utilized some form of blinding to minimize clinical review bias.

## **CONCLUSION**

s Strategies for addressing observer recall bias vary considerably in DTA comparative studies and are often suboptimal. Increased awareness of this potential source of bias is needed.

## **CLINICAL RELEVANCE/APPLICATION**

Reading-order effects are a potential source of bias in many diagnostic test accuracy comparative studies; increased recognition of this pitfall could improve study quality and reporting consistency.

Printed on: 02/07/23

## Abstract Archives of the RSNA, 2022

M2-SPNPM-1

### Reliability of 3D Image Analysis and Comparison of Diagnostic Accuracy of 2D and 3D Measurements to Determine Opportunistic Screening of Osteoporosis Using the Proximal Femur on Abdomen-Pelvic CT

Monday, Nov. 28 9:00AM - 9:30AM Room: Learning Center - NPM DPS

#### Participants

Minsu Park, MD, (*Presenter*) Nothing to Disclose

#### PURPOSE

To evaluate the reliability of 3D image analysis and compare the osteoporosis-predicting ability of computed tomography (CT) indexes in abdomen-pelvic CT (APCT) using the proximal femur and the reliability of measurements in two and three-dimensional analyses.

#### METHODS AND MATERIALS

430 female patients who underwent dual-energy X-ray absorptiometry (DXA) and APCT within 1 month were retrospectively selected. The volumes of interest (VOIs) from the femoral head to the lesser trochanter and the femoral neck were expressed as 3DFemur. Total volume, mean-HU, and HU histogram analysis (HUHA) values of the extracted femur were calculated. Also, round regions of interest (ROIs) of image plane drawn over the femoral neck touching the outer cortex were determined as 2Dcoronal. In HUHA, the percentages of HU histogram ranges related to the ROI or VOI were classified as HUHAfat (<0HU) and HUHAbone (126HU=). Reliability of 3D image analysis was assessed by calculating intra- and interobserver correlation coefficients (ICCs). In addition, diagnostic performance, correlation analysis and measurement reliability were analyzed by receiver operating characteristic curves, correlation coefficient and ICC, respectively. Furthermore, the effect of contrast medium administration was evaluated by the paired t-test.

#### RESULTS

All ICCs of 3D volume measurements showed excellent reproducibility (all ICCs>0.90). AUCs of each HUHA and mean-HU measurement on 2D-ROI and 3D-VOI were 0.94 or higher ( $P<0.001$ ). Both 3DFemur-mean-HU and 3DFemur-HUHAbone showed the highest AUC (0.96). The cut-off value of 3DFemur-mean-HU was 231HU or less ( $P<0.001$ ) for diagnosis of osteoporosis. There was no superiority between AUCs in 2D-ROI and 3D-VOI measurements ( $P>0.05$ ). Reliability of the 3D-VOI measurement showed perfect agreement (ICC=0.94), and 2D-ROI showed moderate to good agreement (ICC range: 0.63~0.84). The mean difference in HU after contrast agent administration (-2.2HU) was not significant ( $P=0.27$ ).

#### CONCLUSION

s Image analysis based on 3D volume measurement of the proximal femur showed excellent reliability with the contrast agent administration showing negligible influence on the mean-HU, and CT indexes on 3D-VOI for predicting femoral osteoporosis showed similar diagnostic accuracy with better reproducibility of measurement, compared with 2D-ROI.

#### CLINICAL RELEVANCE/APPLICATION

Since DXA is a 2D technique, clinically relevant diagnostic errors can be made. Using APCT, BMD can be assessed in femur by measuring HU without additional imaging, radiation exposure, or patient time. Also, measurements performed with a VOI in the 3D image plane may not be substantially affected by structural complexity of femur and cross-section selection as well as the ROI location.

Printed on: 02/07/23



## Abstract Archives of the RSNA, 2022

M2-SPNPM-2

### Observer Recall Bias in Diagnostic Test Accuracy Comparative Studies: Much Room for Improvement

Monday, Nov. 28 9:00AM - 9:30AM Room: Learning Center - NPM DPS

#### Participants

Bharadwaj Pindiprolu, MD, (*Presenter*) Nothing to Disclose

#### PURPOSE

Diagnostic test accuracy (DTA) studies often compare two or more imaging modalities, yet little is known on the impact of reading-order effects. Observer recall bias occurs when a subsequently performed test seems more accurate than an earlier test due to retention of information from the earlier test, rather than a true difference in test performance. The purpose of this study was to perform a methodological review of DTA comparative studies to assess strategies employed to limit observer recall bias.

#### METHODS AND MATERIALS

MEDLINE was used to identify DTA systematic reviews published in imaging journals from 2000 to 2021. Two reviewers independently conducted title, abstract and full-text review to identify all systematic reviews comparing two or more index tests including at least one diagnostic imaging modality. Each reviewer extracted data from the primary studies within each systematic review. Disagreements were resolved by consensus or using a third reviewer where needed.

#### RESULTS

87 radiologic comparative DTA studies were included, of which 38 (44%) had the same radiologist interpret both modalities, 24 (28%) used separate radiologists, and 25 (29%) provided no details. A minimum time delay between interpretations was only reported in 25 studies. Most studies (24%) required a minimum of 1 week between reads, followed by 2 weeks (16%) and 3 weeks (12%). Two readers were most frequently used (44/87; 50.6%) to interpret index tests and most commonly, reading sessions were conducted independently (40/87; 46.0%) rather than by consensus (14/87; 16.1%). Reader order was randomized in 20/87 (23%) studies. 54/87 (62.1%) studies utilized some form of blinding to minimize clinical review bias.

#### CONCLUSION

Strategies for addressing observer recall bias vary considerably in DTA comparative studies and are often suboptimal. Increased awareness of this potential source of bias is needed.

#### CLINICAL RELEVANCE/APPLICATION

Reading-order effects are a potential source of bias in many diagnostic test accuracy comparative studies; increased recognition of this pitfall could improve study quality and reporting consistency.

Printed on: 02/07/23



## Abstract Archives of the RSNA, 2022

M2-SPNR

### Neuroradiology Monday Poster Discussions

Monday, Nov. 28 9:00AM - 9:30AM Room: Learning Center - NR DPS

#### Participants

Noah N. Chasen, MD, Houston, TX (*Moderator*) Nothing to Disclose  
Noah N. Chasen, MD, Houston, TX (*Moderator*) Nothing to Disclose  
Noah N. Chasen, MD, Houston, TX (*Moderator*) Nothing to Disclose  
Celso Hygino, MD, PhD, Rio de Janeiro, RJ (*Moderator*) Nothing to Disclose  
Celso Hygino, MD, PhD, Rio de Janeiro, RJ (*Moderator*) Nothing to Disclose  
Celso Hygino, MD, PhD, Rio de Janeiro, RJ (*Moderator*) Nothing to Disclose  
Ajay Malhotra, MD, New Canaan, CT (*Moderator*) Nothing to Disclose  
Ajay Malhotra, MD, New Canaan, CT (*Moderator*) Nothing to Disclose  
Ajay Malhotra, MD, New Canaan, CT (*Moderator*) Nothing to Disclose

#### Sub-Events

### M2-SPNR-1 How Are We Handling All Those Fluoroscopic Guided Lumbar Puncture Requests? A Nationwide Survey of Practice Trends

#### Participants

Tyler Richards, MD, Salt Lake City, UT (*Presenter*) Nothing to Disclose

#### PURPOSE

Our study's purpose was to determine how radiologists in different practice settings manage fluoroscopy guided lumbar puncture (FGLP) referrals.

#### METHODS AND MATERIALS

An online questionnaire was sent to radiologists and trainees to survey their methodology of handling FGLP requests, pre-procedural work-up including lab value and head imaging requirements, utilization of physician extenders (PEs)/trainees to perform FGLPs, among others. Odds ratio (OR) was used to compare the categories.

#### RESULTS

Of 131 responses, 93.9% were from the U.S. and 81.7% were from an academic practice (AP) and 18.3% from a private practice (PP). Regarding FGLP referrals, 27.5% of respondents stated it was not standard practice in their department that a bedside lumbar puncture is attempted by a clinician prior to FGLP referral, a practice 4 x more common among PP respondents (OR 4.19 (95% CI: 1.86,9.65)). Morbid obesity (80.2%), congenitally altered anatomy (71.0%), and prior lumbar surgery with hardware (61.1%) were some of the most frequent reasons respondents did not require a bedside LP attempt prior to referral for FGLP. 95.8% of PP and 84.1% of AP respondents were asked often to perform an FGLP by clinicians because the clinician does not feel competent performing LPs. Of those, 74.3% stated they will always or sometimes agree to the request; a 4.7 higher likelihood that a PP radiologist would oblige and always agree to perform the FGLP compared to an academic radiologist (OR 4.7 (95% CI: 1.3-20.5)). 42.0% of respondents stated that they would always comply if a patient specifically requests an FGLP without a bedside LP attempt, 2.5 x higher likelihood for PP respondents (OR 2.5 (95%CI: 1.15-5.56)). Regarding FGLP operators, AP respondents were less likely to have PEs perform FGLPs compared to PP respondents (31.8% vs. 45.8%; (OR 0.65 (95% CI: 0.3,1.42)). In academic practices, 72.9% reported trainees perform >50% of their FGLPs. Regarding pre-procedural work up, 42.0% of respondents stated that they check coagulation labs on all patients prior to FGLP and 84.0% of respondents stated that patients should get a head CT prior to an FLGP only if there is high suspicion for increased intracranial pressure, similar between PP and AP respondents.

#### CONCLUSION

This survey demonstrates that many academic and private practice radiology practitioners are relatively lenient in obliging to perform FGLPs in patients. There were many differences and some similarities in management of FGLP referrals and pre-procedural workup between academic and private practice groups.

#### CLINICAL RELEVANCE/APPLICATION

Our findings demonstrate the current methods of how private practice and academic radiologists handle FGLPs referrals and can be potentially used to develop guidelines of best FGLP practices.

### M2-SPNR-11 Leptomeningeal Metastases in Glioma Revisited: High Incidence and Their Molecular Predictors based on Recent Imaging and Molecular Diagnostics

#### Participants

Sung Soo Ahn, MD, Seoul, Korea, Republic Of (*Presenter*) Nothing to Disclose

#### PURPOSE

Leptomeningeal metastases (LM) in glioma has been underestimated due to low incidence and lack of reliable imaging. This study

Leptomeningeal metastases (LM) in glioma has been underestimated due to low incidence and lack of reliable imaging. This study aimed to investigate a real-world incidence of LM using a CSF-sensitive MR imaging technique and analyze molecular predictors for LM in the molecular era.

## **METHODS AND MATERIALS**

Total 1,405 adult glioma patients underwent post-contrast fluid attenuated inversion recovery (FLAIR) imaging at initial diagnosis and during treatment monitoring between March 2001 and October 2021. Molecular data included isocitrate dehydrogenase (IDH) mutation, 1p/19q co-deletion, H3 K27M alteration, and O6-methylguanine-methyltransferase (MGMT) promoter methylation status. Multivariable logistic regression analysis for LM development was performed in molecular data, clinical data, and imaging characteristics. Median overall survival (OS) was compared between patients with and without LM using Kaplan-Meier survival curves and log-rank test.

## **RESULTS**

LM was identified in 16.2% of glioma (228 of 1405), with 7.8% (110 of 1405) at initial diagnosis, and 8.4% (118 of 1405) at recurrence. Among molecular diagnostics, IDH-wildtype (odds ratio [OR] 3.14, P = .001) and MGMT promoter unmethylation (OR 1.43, P = .034) were independent predictors of LM. WHO grade 4 (OR 10.52, P <.001) and nonlobar location (OR 1.54, P=.048) were associated with LM at initial diagnosis, whereas IDH-wildtype (OR 5.04, P <.001) and H3 K27M alteration (OR 3.39, P =.003) were significantly associated with LM at recurrence. Patients with LM had a worse median OS than those without LM (16.7 vs. 32.0 months, log-rank test; P <.001). N

## **CONCLUSION**

s CSF-sensitive MR imaging diagnostics aid diagnosis of LM and reduced an underdiagnosed condition in adult gliomas. Molecular markers affect LM at initial diagnosis and at recurrence, and patients with aggressive molecular markers warrant imaging surveillance of LM.

## **CLINICAL RELEVANCE/APPLICATION**

The incidence of LM in glioma is underestimated due to lack of sensitive imaging protocol. Here, we utilized CSF-sensitive MRI with post-contrast FLAIR and discovered a high frequency of 228 (16.2%) patients diagnosed with LM in 1,405 diffuse glioma patients. Our findings emphasize the role of molecular markers in the development of LM in glioma patients. Patients with aggressive molecular markers such as IDH-wildtype and H3 K27M alteration warrant imaging surveillance of LM.

## **M2-SPNR-12 Use of VASARI Features for The Systematic Identification of Typical and Atypical Primary Central Nervous System Lymphomas**

Participants

Irene Dixe de Oliveira Santo, MD, New Haven, CT (*Presenter*) Nothing to Disclose

## **PURPOSE**

The imaging appearance of PCNSL is highly variable with a significant proportion of cases demonstrating atypical features, frequently leading to a significant delay in diagnosis. Standardized classification of features has the potential to improve recognition of atypical variants, which is especially important given the drastically different treatment approach from the similar-appearing gliomas.

## **METHODS AND MATERIALS**

Presurgical MR images of 71 patients with histologically-proven PCNSL were scored independently according to the VASARI (Visually Accessible Rembrandt Images) features by two different neuroradiologists. Classification into typical versus atypical PCNSL was based on enhancement pattern, presence or absence of necrosis, hemorrhage, and calcification. Age at diagnosis, gender, presenting symptoms, immune status, biochemical and molecular profile of the neoplasms, treatment, and overall survival were also recorded. The influence of visual appearance (atypical versus typical) on overall survival was analyzed using the Kaplan-Meier method and tested for significance using log-rank test (alpha=0.05).

## **RESULTS**

Appearance of PCNSL was highly variable ranging from multiple infiltrative solid masses to ring-enhancing lesions. Periventricular and ependymal involvement were among the most common locations. Systematic scoring classified 44 (62%) patients into typical and 27 (38%) patients into atypical PCNSL. Presence of hemorrhage on SWI was often responsible for classification into atypical. Regarding survival, median OS was significantly lower for atypical (203 days) compared to typical (767 days) PCNSL (p = 0.012).

## **CONCLUSION**

s Up to a third of our PCNSL patients demonstrated atypical MRI features, which may complicate diagnosis.

## **CLINICAL RELEVANCE/APPLICATION**

Awareness of varying imaging presentations of PCNSL may alert the interpreting radiologist to consider lymphoma early and expedite diagnosis and treatment.

## **M2-SPNR-13 Usefulness of the Wave-CAIPI for the Post-contrast 3D T1-SPACE in The Evaluation of Brain Metastases**

Participants

Youngjin Heo, MD, (*Presenter*) Nothing to Disclose

## **PURPOSE**

High-resolution post-contrast 3D T1WI is a widely used sequence for evaluating brain metastasis, despite the long scan time. This study aimed to compare highly accelerated post-contrast 3D T1-weighted sampling perfection with application-optimized contrasts by using different flip angle evolution using Wave-controlled aliasing in parallel imaging (Wave-T1-SPACE) with the commonly used standard high-resolution post-contrast 3D T1-SPACE for the evaluation of brain metastases.

## **METHODS AND MATERIALS**

Among the 387 patients who underwent post-contrast wave-T1-SPACE and standard SPACE, 56 patients with suspected brain metastases were retrospectively included. Two neuroradiologists assessed the number of enhancing lesions according to lesion size, contrast-to-noise ratio (CNR) lesion/parenchyma, CNR white matter/gray matter, contrast ratio (CR) lesion/parenchyma, and overall image quality for the two different sequences.

## RESULTS

Although there was no significant difference in the evaluation of larger enhancing lesions (>5 mm) between the two different sequences ( $P=0.66$  for observer 1,  $P=0.26$  for observer 2), wave-T1-SPACE showed significantly lower number of smaller enhancing lesions (<5 mm) than standard SPACE ( $1.61\pm 0.29$  vs  $2.84\pm 0.47$  for observer 1,  $1.41\pm 0.19$  vs  $2.68\pm 0.43$  for observer 2). Furthermore, mean CNR<sub>lesion/parenchyma</sub> and overall image quality of wave-T1-SPACE were significantly lower than standard SPACE.

## CONCLUSION

Post-contrast wave-T1-SPACE showed comparable diagnostic performance for larger enhancing lesions (>5 mm) and marked scan time reduction as compared with standard SPACE. However, post-contrast wave-T1-SPACE showed underestimation of smaller enhancing lesions (<5 mm) and lower image quality than standard SPACE. Therefore, post-contrast wave-T1-SPACE should be interpreted carefully in the evaluation of brain metastasis.

## CLINICAL RELEVANCE/APPLICATION

Recently, accelerated 3D acquisition techniques have been developed to reduce the scan time of high-resolution 3D T1WI sequences while preserving image quality. Wave-controlled aliasing in parallel imaging (Wave-CAIPI; Siemens Healthineers) is an advanced parallel imaging technique that combines a corkscrew gradient trajectory with CAIPI shifts in the ky and kz directions to efficiently encode k-space and evenly spread the voxel aliasing in all dimensions. This allows to take better advantage of the 3D coil sensitivity information to provide highly accelerated parallel imaging with negligible artifacts and signal-to-noise ratio penalties. Therefore, we evaluated the diagnostic performance according to the lesion size and overall image quality of post-contrast wave-T1-SPACE for the evaluation of brain metastases.

## M2-SPNR-14 White Matter Hyperintensities in Younger Mild Traumatic Brain Injured Patients

Participants

Priya Santhanam, PhD, (*Presenter*) Nothing to Disclose

## PURPOSE

This study aims to identify associations between white matter hyperintensities (WMH) and the presentation and progression of post-concussive symptoms in patients 40 years and younger with mild traumatic brain injury (mTBI).

## METHODS AND MATERIALS

mTBI patients ( $n=152$ ; mean age=30 yrs) without preexisting head pathology were included in this study. Axial T2-weighted and T2-FLAIR sequences were performed on a 3.0 Tesla MR Signa HDxt system. Hyperintensities were regionally classified by lobe (frontal, parietal, temporal, or occipital) or cerebellum. Clinical data, including presence of several post-concussive symptoms, was obtained via retrospective chart review. Patient groups were compared by the presence or absence of WMH on imaging as well as by whether the patient had loss-of-consciousness (LOC) during injury. Interval-censored data analyses were performed to test the time to recovery between the comparison groups as recovery is only known to be between two examinations.

## RESULTS

At least one WMH was present in 44% of male and 52% of female patients. Single WMH were predominantly located in the frontal lobe (84%) and more commonly in the left hemisphere (65%). LOC was more prevalent ( $p=0.018$ ) in those with WMH as compared to those without WMH. While symptoms improved or resolved in both groups, a larger percentage of patients without WMH showed improvement as compared to patients with WMH. Patients with WMH also took significantly longer to recover from cognitive deficits than those without WMH ( $p=0.0177$ ). Patients with LOC had a higher incidence of balance deficits as compared to patients without LOC ( $p=0.0391$ ), while a larger percentage of those without LOC showed improvement or resolution of symptoms, specifically headache ( $p=0.0406$ ), balance deficits ( $p=0.0173$ ), and cognitive deficit ( $p=0.0341$ ).

## CONCLUSION

This study revealed several significant associations between quantitative WMH findings, loss of consciousness, and clinical outcomes following mTBI. Taken together, findings suggest the presence of WMH in younger TBI patients may influence patient symptomatology, while co-morbid LOC may lead to poor outcomes and recovery for affected individuals.

## CLINICAL RELEVANCE/APPLICATION

The presence of white matter hyperintensities in younger patients with mild traumatic brain injury and loss of consciousness could be related to symptom prevalence, long-term outcomes, and recovery.

## M2-SPNR-15 IDH and 1p19q Diagnosis in Diffuse Glioma from Preoperative MRI Using Artificial Intelligence

Participants

Hugh McHugh, BMBCh, Auckland, New Zealand (*Presenter*) Clinical AI Registrar, Harrison AI Research Grant, RANZCR

## PURPOSE

Isocitrate dehydrogenase (IDH) mutation and 1p19q codeletion are key molecular markers in glioma which both confer a more favorable prognosis. In the 2021 WHO classification of CNS tumours IDH and 1p19q status determine the glioma sub-categories of glioblastoma, astrocytoma and oligodendroglioma. IDH and 1p19q status is unknown until after surgery unless there is a biopsy which is uncommon. Reliable preoperative molecular characterization may facilitate tailored treatment approaches, for example if molecular status affects the optimal extent of tumor resection. Emerging research supports the potential of MRI-based IDH and 1p19q diagnosis. A limitation is the relative lack of generalization and external validation outside the widely used The Cancer Imaging Archive (TCIA) dataset. We present a combined IDH and 1p19q classification algorithm and assess performance on a local retrospective cohort and a fully independent cohort from the Erasmus Glioma Database (EGD).

## METHODS AND MATERIALS

2D convolutional neural networks were trained to provide IDH and 1p19q classification. Inputs are T1 post-contrast, T2, and FLAIR sequences. Training data consists of preoperative imaging from the TCIA dataset (n=184) and images from a locally obtained cohort that were obtained prior to 1/1/2018 (n=349). Evaluation data consists of the most recent cases from the local cohort obtained between 1/1/2018 and 31/8/2021 (n=205) and the EGD (n=420).

## RESULTS

Subject-wise IDH classification accuracy was 93.3% and 91.5% on the local cohort and EGD, with AUC of 95.4% and 95.8%, respectively. 1p19q accuracy was 94.5% and 87.5% with AUC of 92.5% and 85.4% on the local cohort and EGD. Combined subject-wise IDH and 1p19q accuracy was 90.4% and 84.3% on the local cohort and EGD, with AUC of 92.4% and 91.2%.

## CONCLUSION

High IDH and 1p19q classification performance was achieved on the local retrospective cohort. Generalization to the EGD was robust, demonstrating the potential for clinical translation. This method is able to non-invasively predict tumor subtypes according to the WHO 2021 classification with high accuracy using readily available imaging without the need for MR spectroscopy. This may better inform patients and clinicians prior to surgery and demonstrates the high potential impact in glioma diagnostics.

## CLINICAL RELEVANCE/APPLICATION

This research externally validates non-invasive IDH and 1p19q diagnosis in glioma from preoperative MRI using artificial intelligence techniques allowing tumor classification by WHO 2021 criteria.

## M2-SPNR-16 Compare the Performance of MRI-based 2.5D and 3D Convolutional Neural Networks in Differential Diagnosis of High-grade Gliomas and Single Brain Metastases

Participants

Bin Zhang, (*Presenter*) Nothing to Disclose

## PURPOSE

The 2.5D convolutional neural network models have unique advantages for studies with moderate sample sizes, while the 3D model can completely extract tumor and peritumoral features. To explore and compare the value of preoperative differential diagnosis of high-grade gliomas (HGG) and single brain metastases (BM) under 2.5D and 3D convolutional neural network models.

## METHODS AND MATERIALS

T2WI and contrast-enhanced T1WI(CE T1WI) images of 230 patients with HGG and 111 patients with BM confirmed by surgery and pathology were retrospectively collected. The radiologist delineated the regions of interests (ROIs) of the input images of the 2.5D networks and 3D networks on the T2WI and CE T1WI axial images of the registered MRI. The slice nth with the largest tumor parenchyma area on the MRI image was determined, and then the tumor area (including tumor parenchyma and peritumoral edema area) of the slice of (n-2)th, nth and (n+2)th was delineated respectively. Define a minimum rectangular box as the ROIs of the 2.5D models that can cover all tumor areas at the three slices. Define the smallest 3D rectangular box that can completely contain the tumor area at all slices as the ROIs of the 3D models. Finally, based on DenseNet convolutional neural networks respectively build prediction models for T2WI and CE T1WI sequences under 2.5D and 3D model. The predictive performance of each model was evaluated by the receiver operating characteristic(ROC) curve, and the differences in the ROC curves of the models built by different convolutional neural networks were compared in pairs by Delong's test.

## RESULTS

The best AUC values of the 3D model on CE T1WI and T2WI were 0.852 and 0.802, respectively. And the best AUC values of the 2.5D model on CE T1WI and T2WI were 0.831 and 0.784, respectively. The performance of the 3D models were better than that of the 2.5D models. Delong's test showed that the differences between the models were statistically significant ( $P < 0.05$ ).

## CONCLUSION

The MRI-based 2.5D and 3D convolutional neural network models have better diagnostic performance in differentiating HGG and single BM, and the 3D models have better diagnostic performance than 2.5D models. The deep learning model can be used to identify HGGs and BMs and assist in clinical formulation of precise treatment plans potential tool.

## CLINICAL RELEVANCE/APPLICATION

The 2.5D model has better advantages in the deep learning model with a medium sample size, which can make up for the problem of the large data demand of the 3D model. While the 3D convolutional neural network structure analyzes the lesion information more completely, so it is easier to apply to clinical practice. The establishment of the prediction model will be able to differential diagnose HGG and single BM through non-invasive imaging examination.

## M2-SPNR-17 Predicting the Isocitrate Dehydrogenase Wildtype in Non-enhancing or Poorly Enhancing Glioma by Conventional MRI Features and Apparent Diffusion Coefficient

Participants

Jiyoung Song, MD, Seoul, Korea, Republic Of (*Presenter*) Nothing to Disclose

## PURPOSE

To develop predictive models using clinically available MRI parameters for predicting isocitrate dehydrogenase (IDH) status of gliomas with no or poor enhancement, which is considered as a radiologically low-grade feature.

## METHODS AND MATERIALS

This retrospective study included 241 patients with surgically resected and pathologically confirmed gliomas that showed no or poor enhancement (less than 5% of the entire tumor volume) in the preoperative MRI. Visual rating of imaging features (T1-weighted, T2-weighted, FLAIR, contrast-enhanced T1-weighted images, and cerebral blood volume map) was performed. Regions of interest were drawn to acquire the apparent diffusion coefficient (ADC) mean (ADCmean) and minimum (ADCmin) in tumor and ADCnawm in normal-appearing white matter. Univariable and multivariable logistic regression analyses were performed for each imaging feature

and ADC value. Then, receiver operating characteristic curve analysis was done with probability index calculated from the multivariable logistic regression model. A subgroup analysis was performed to predict IDH status in the non-enhancing gliomas.

## RESULTS

In 241 non-enhancing or poorly enhancing gliomas, T2/FLAIR mismatch sign showed 100% specificity (42 of 42) to predict IDH-mutant gliomas. Among 199 gliomas with negative T2/FLAIR mismatch signs, 78 were IDH-wildtype. A predictive model incorporating age, calcification, multifocality, FLAIR homogeneity, ADCmin-to-ADCmax ratio, and cortical involvement showed area under the curve (AUC) of 0.909 (95% CI: 0.858-0.946) with 90.8% sensitivity and 81.2% specificity. In the subgroup analysis for 116 non-enhancing tumors (46 IDH-wildtypes and 70 IDH-mutants) a predictive model that consisted of the same variables showed AUC of 0.883 (95% CI: 0.808-0.935), 82.6% sensitivity, and 88.1% specificity.

## CONCLUSION

Algorithms incorporating T2/FLAIR mismatch sign, age, calcification, multifocality, FLAIR homogeneity, ADCmin-to-ADCmax ratio, and cortical involvement predicted IDH wild-type gliomas with radiologically low-grade feature.

## CLINICAL RELEVANCE/APPLICATION

According to 2021 WHO classification for adult-type diffuse gliomas, even if a tumor seems low-grade, being IDH-wildtype satisfies a necessary condition to be diagnosed as glioblastoma. This study developed models using clinically available MRI parameters for predicting IDH status of gliomas with no or poor enhancement, which is considered as a radiologically low-grade feature.

## M2-SPNR-18 High-resolution Clinical Functional MRI at 7T in Patients with Brain Tumors: Initial Assessment

Participants

Kinsey Lano, BS, Houston, TX (*Presenter*) Nothing to Disclose

## PURPOSE

This study aimed to evaluate spatial localization accuracy of a high-resolution (1.4 mm isotropic) 7T fMRI protocol and compare with a clinical 3T protocol with typical resolution (1.9 x 1.9 x 4 mm<sup>3</sup>).

## METHODS AND MATERIALS

Hand motor fMRI studies of 24 patients (n=12 on 7T and 12 on 3T) were evaluated. The 7T patients included 1 with brain mets, 3 with low-grade, and 8 with high-grade gliomas. The 3T patients included 4 with low-grade and 8 with high-grade gliomas. The fMRI paradigm consisted of 6 cycles of resting and bilateral hand-motor task blocks. T2\*-weighted EPI sequences were used for the fMRI at 7T (TR/TE=2000 ms/24 ms, PI=3, SMS=2, 1.4 x 1.4 x 1.4 mm<sup>3</sup>) and at 3T (TR/TE=3000 ms/25 ms, PI=2, 1.9 x 1.9 x 4.0 mm<sup>3</sup>). The fMRI pre-processing included motion correction and co-registration with 3D T1-weighted images. Functional t-value maps were then generated by the standard GLM method. The t-value maps were thresholded at two statistical levels: (1) FWE-corrected p < 0.05 (t > 5.5 and 6.1 for 7T and 3T, respectively), and (2) t > 4.0. For each patient, the most relevant motor-activation cluster on the lesion side was visually determined. The smallest distance between the center of the cluster and the central sulcus was measured and categorized: (1) < 2 mm, (2) 2-4 mm, and (3) 5-10 mm.

## RESULTS

At 7T, activation clusters at expected hand motor areas were detected in 7 (58%) and 9 (75%) out of the 12 patients at the statistical level of p < 0.05, FWE corrected, and t > 4.0, respectively. The spatial localization accuracy was within 2 mm for all the 9 patients with detected activation clusters. At 3T, hand motor activations were detected in 11 (92%) and 12 (100%) out of the 12 patients at the two statistical levels. The spatial localization accuracy assessment found 4 (33%), 6 (50%), and 2 (17%) patients having the detected activation cluster centered at < 2mm, 2-4 mm, and 5-10 mm, respectively, from the central sulcus.

## CONCLUSION

We demonstrated that high-resolution fMRI at 7T is feasible for mapping primary motor areas in clinical routine. More accurate functional localization was achieved using the high-resolution 7T protocol compared to our routine protocol at 3T.

## CLINICAL RELEVANCE/APPLICATION

The higher fMRI sensitivity at 7T allows imaging at higher spatial resolution, which leads to improved localization accuracy for presurgical functional mapping.

## M2-SPNR-19 Nomogram for Predicting Early Recurrence in Patients with High Grade Glioma

Participants

Qing Zhou, Lanzhou, China (*Presenter*) Nothing to Disclose

## PURPOSE

To develop a nomogram to predict early recurrence of high-grade glioma (HGG) based on clinical factors, genetic factors, and MRI parameters.

## METHODS AND MATERIALS

154 HGG patients were classified into recurrence and non-recurrence groups based on pathological diagnosis and RANO criteria. Clinical information included age, sex, and preoperative Karnofsky Performance Status (KPS) scores. Gene information included P53, IDH1, MGMT, and TERT status. All patients had baseline MRIs before treatment, including T1WI, T2WI, T1C, Flair and DWI examinations. The tumor location, single/multiple tumors, tumor diameter, peritumoral edema, necrotic cyst, hemorrhage, average apparent diffusion coefficient(ADC) value and minimum ADC values were evaluated. Univariate and multivariate logistic regression were used to determine the predictors of early recurrence and to build the nomogram.

## RESULTS

Univariate analysis showed that the number of tumors (OR, 0.258; 95% CI: 0.104, 0.639; P = 0.003) and peritumoral edema (OR, 0.965; 95% CI 0.942, 0.988; P = 0.003; mean in the recurrence group 22.04±17.21 mm; mean in the non-recurrence group 14.22±12.84 mm) were statistically significantly different in patients with early recurrence. Genetic factors included IDH1 (OR,

4.405; 95% CI 1.874, 10.353;  $P = 0.001$ ), and MGMT (OR, 2.389; 95% CI 1.234, 4.628;  $P = 0.010$ ). Multivariate logistic regression analysis revealed that the number of tumors (OR, 0.227; 95% CI 0.084, 0.616;  $P = 0.004$ ), peritumoral edema (OR, 0.969; 95% CI 0.945, 0.993;  $P = 0.013$ ) and IDH1 (OR, 4.200; 95% CI 1.602, 10.013;  $P = 0.004$ ) were independent risk factors for early recurrence. The nomogram showed the highest net benefit when the threshold probability was less than 63%.

## CONCLUSION

A nomogram prediction model based on results that are easily available before surgery can effectively aid clinical treatment decisions for newly diagnosed HGG patients.

## CLINICAL RELEVANCE/APPLICATION

A nomogram prediction model can effectively aid treatment decisions in newly diagnosed HGG patients. Neurosurgeons may adjust the surgical decision on the scope of tumor resection based on the prediction model. For tumor tissues with a high risk of recurrence and high infiltration, the radiation oncologist can also upgrade the radiation dose to high-risk areas.

## M2-SPNR-20 Peritumoral MR Imaging Radiomic Features Improves Identification of Circumscribed Astrocytic Gliomas and High-grade Gliomas

Participants

Shuang Li, (*Presenter*) Nothing to Disclose

## PURPOSE

In the 2021 WHO classification of tumors of the central Nervous System, the terms of "diffuse" and "circumscribed" were applied to the classification of gliomas, diffuse gliomas are characterized by extensive infiltration, while circumscribed astrocytic gliomas show a solid growth pattern. The most common circumscribed astrocytic gliomas are pilocytic astrocytoma (PA) and pleomorphic xanthoastrocytoma (PXA). MR imaging findings of them can resemble high grade gliomas (HGGs). We aimed to develop an MRI-based radiomics model to distinguish circumscribed glioma from HGGs.

## METHODS AND MATERIALS

Preoperative T2 fluid-attenuated inversion recovery (T2 FLAIR) and contrast-enhanced T1-weighted imaging (CE-T1WI) data were obtained from 160 patients (91 circumscribed astrocytic gliomas and 69 glioblastoma) between 2016 and 2020. 1288 features were obtained in tumor region and the 5 mm thickness peritumoral region, respectively. We up-sampled features by repeating random cases to make samples balance. Then, we applied the normalization on the feature matrix. Feature pairs with PCC values larger than 0.990 will be removed. Before build the model, we used recursive feature elimination (RFE) to select features. Support vector machine (SVM) was used as a classifier. To determine the hyper-parameter of model, we applied cross validation with 10-fold on the training data set. The hyper-parameters were set according to the model performance on the validation data set. The performance of the model was evaluated using receiver operating characteristic (ROC) curve analysis. The area under the ROC curve (AUC) was calculated for quantification. We also estimated the 95% confidence interval by bootstrap with 1000 samples.

## RESULTS

Intratumor radiomic features achieved AUCs of 0.820(CE-T1WI) and 0.787(T2 FLAIR). The integrated model, incorporating intra- and peritumoral features extracted from T2 FLAIR and CE-T1WI images, improved the AUCs to 0.889 on the same test set.

## CONCLUSION

An imaging-based model combining tumor and peritumor radiomics can help to distinguish between circumscribed astrocytic gliomas and high-grade gliomas.

## CLINICAL RELEVANCE/APPLICATION

Circumscribed astrocytic gliomas had better prognosis than HGGs. Correct differential diagnosis is vital for preoperative decision-making and prognostic evaluation. Radiomic features extracted from intra- and peritumoral region may help the identification.

## M2-SPNR-4 Discriminative Power of Macro- And Microstructural MRI in the Differential Diagnosis of Neurodegenerative Parkinsonian Syndromes

Participants

Alexander Rau, MD, Freiburg, Germany (*Presenter*) Nothing to Disclose

## PURPOSE

To investigate the discriminative performance of macro- and microstructural MRI in the differential diagnosis of neurodegenerative parkinsonian syndromes (NPS).

## METHODS AND MATERIALS

We included patients with NPS according to current consensus diagnostic criteria, i.e. 136 patients with Parkinson's disease (PD), 32 patients with progressive supranuclear palsy (PSP), 41 patients with multiple system atrophy (MSA) as well as 37 healthy controls (HC) in this monocentric retrospective cross-sectional study. Tissue probability values for gray matter, white matter and CSF were automatically obtained by CAT12. In addition, the microstructure of the patients was analyzed using a mesoscopic approach by diffusion tensor imaging (DTI) and diffusion microstructure imaging (DMI). Respective parameters were extracted using the AAL3-atlas and ROIs with great relevance for PSP. Based on this, a linear support vector machine (SVM) was trained and optimized in respect of ROC-AUC in a one-vs-rest (OVR) classifier. The diagnostic performance of SVM was compared with respect to different inputs, i.e. TPV, DTI and DMI individually.

## RESULTS

Diffusion MRI outperformed the T1w derived TPV with a correct classification in 80% for DTI, 79% for DMI and 52% for TPV. The corresponding OVR-ROC-AUC of DTI was 0.92 for HC, 0.89 for PD, 0.95 for MSA and 0.93 for PSP and for DMI 0.91 (HC), 0.90 (PD), 0.96 (MSA) and 0.93 (PSP).

## CONCLUSION

Microstructural parameters as obtained in a mesoscopic approach using diffusion MRI data outperformed structural data derived

s microstructural parameters as obtained in an mesoscopic approach using diffusion MRI data outperformed structural data derived by conventional imaging in the diagnosis of NPS. The particularly good performance of microstructural approaches in the diagnosis of PD, as a weak point in conventional MRI, underlines the potential of this approach. The introduced automatic approach might facilitate the MRI diagnosis of patients with suspected NPS.

#### CLINICAL RELEVANCE/APPLICATION

The developed approach might facilitate the differential diagnosis of neurodegenerative parkinsonian syndromes in an objective manner and is therefore of high clinical relevance.

#### M2-SPNR-6 Usefulness of 3D FIESTA in Differentiating Parkinson's Disease From Parkinson Syndrome: Volumetric Alternation of Olfactory Bulb

Participants

Ide Ide, MD, (*Presenter*) Nothing to Disclose

#### PURPOSE

Parkinson's disease (PD) is a neurodegenerative disease, related with deposition of Lewy body. Braak stage of Lewy pathology shows the initiation sites are in the olfactory bulb (OB), hence, olfactory dysfunction is among the earliest nonmotor features of PD. It's sometimes difficult to differentiate PD from parkinson syndrome (PS), such as multiple system atrophy (MSA), corticobasal syndrome (CBS), and progressive supranuclear palsy (PSP) using conventional MRI and clinical symptom. It's known that olfactory loss occurs to a lesser extent or is absent in PS. Therefore, we hypothesized OB change may be useful in differential diagnosis. 3D fast imaging employing steady-state acquisition (FIESTA) results in good delineation of cranial nerves, however, no study demonstrated OB volume change between PD and PS using 3D-FIESTA. Our purpose is to determine whether OB measurement on 3D-FIESTA is useful for differentiating PD from PS.

#### METHODS AND MATERIALS

Sixty-four PD (mean age  $\pm$  SD: 71.5  $\pm$  9.4), 8 MSA (68.9  $\pm$  8.9), 10 PSP (75.9  $\pm$  8.3), and 8 CBS (73.8  $\pm$  8.9) patients were recruited. Thirty-three healthy subjects (HS) (63.8  $\pm$  18.6) were also recruited as normal controls. The diagnoses were made according to the diagnostic criteria by an experienced neurologist. The parameter of 3D-FIESTA is following: 3T SIGNA Premier (GE), FA 45deg, TR 4ms, TE 2ms, matrix 512 $\times$ 512, slice thickness 1.0mm, scan time 2:27, spatial resolution: 0.6 $\times$ 0.6 $\times$ 0.8 mm. The cross-sectional area of the OB was measured using manual ROI method, and we used maximum area of OB in coronal plane. The average of bilateral OB was calculated for each subject. We performed group comparison and diagnostic accuracy test using Welch's t test and ROC analysis, respectively. All statistics were performed with BellCurve for Excel (Social Survey Research Information Co., Ltd.).

#### RESULTS

The mean area of OB was significantly smaller for PD patients (mean area  $\pm$  SD mm<sup>2</sup>: 4.1  $\pm$  1.0) than for HSs (6.6  $\pm$  1.4,  $p$ <0.01). Moreover, that of PD were also significantly smaller than that of MSA (6.0  $\pm$  1.4,  $p$ =.007), PSP (4.8  $\pm$  0.9,  $p$ =.03), and CBS (5.3  $\pm$  1.2,  $p$ =.03), respectively (Figure 1 and 2). The ROC analyses showed that good diagnostic performance, especially in analysis of PD vs MSA (AUC: 0.874, optimal cut off points: 5.6 mm<sup>2</sup>, sensitivity: 93.8%, specificity: 87.5%).

#### CONCLUSION

s Our results suggest the OB volume loss in PD, which may reflect degeneration due to deposition of Lewy body. OB volumetry using 3D-FIESTA can be useful to differentiate PD from PS, especially for MSA.

#### CLINICAL RELEVANCE/APPLICATION

OB volumetry with 3D-FIESTA may contribute precise diagnoses in PD and PS showing atypical MR findings. 3D-FIESTA is a common and widespread MR technique, which can work as clinical routine MR application in patients with Parkinsonism.

#### M2-SPNR-7 Altered Cerebral Blood Flow in Spinocerebellar Degeneration Patients

Participants

Bing Liu, Beijing, China (*Presenter*) Nothing to Disclose

#### PURPOSE

Spinocerebellar degeneration (SCD) comprises a multitude of disorders with sporadic and hereditary forms, including spinocerebellar ataxia (SCA), cerebellum-type of multiple system atrophy (MSA) and more complex phenotypes. Except for progressive cerebellar ataxia and structural atrophy, hemodynamic changes have also been demonstrated in SCD. This study aimed to clarify the whole-brain altered patterns of cerebral blood flow (CBF) and its correlations with disease severity and emotional abnormalities in SCD via arterial spin labeling (ASL).

#### METHODS AND MATERIALS

Thirty SCD patients and 30 age- and sex-matched healthy controls (HC) were prospectively recruited to undergo ASL examinations in a 3.0T MR scanner. The Scale for Assessment and Rating of Ataxia (SARA) and the International Cooperative Ataxia Rating Scale (ICARS) scores were used to reflect the disease severity in SCD patients. Additionally, the status of anxiety and depression among all patients were evaluated by the Self-Rating Anxiety Scale (SAS) and the Self-Rating Depression Scale (SDS). We compared the whole-brain CBF between SCD group and HC group at voxel level. And the ROI-based correlation analyses between CBF and disease severity as well as emotional abnormalities were performed for SCD group.

#### RESULTS

Compared with HC, SCD patients exhibited decreased CBF in two clusters (FWE corrected  $P$ <0.05), covering bilateral dentate and fastigii nuclei, lobule VIX, lobule VX, bilateral lobule HI-IV and lobule HIX, left lobule HVI and right lobule HVIIb as Cluster1 and the dorsal part of raphe nucleus in midbrain as Cluster2. The CBF of Cluster 1 was negatively correlated with SARA scores (Spearman's  $\rho$ =-0.374,  $P$ =0.042) and SDS standard scores (Spearman's  $\rho$ =-0.388,  $P$ =0.034), respectively. While the CBF of Cluster2 also had negative correlations with SARA scores (Spearman's  $\rho$ =-0.370,  $P$ =0.044) and ICARS scores (Pearson  $r$ =-0.464,  $P$ =0.010).

#### CONCLUSION

s The SCD-related whole-brain CBF changes were mainly involved in cerebellum and midbrain, partially overlapped with hand, foot

s The SCD-related whole-brain CBF changes were mainly involved in cerebellum and midbrain, partially overlapped with hand, foot and tongue movement activations areas. Decreased CBF was related to disease severity and depression status in SCD. Therefore, CBF may be a promising neuroimaging biomarker to reflect the severity of neurodegeneration and to provide warnings for emotional changes.

#### CLINICAL RELEVANCE/APPLICATION

Decreased CBF in cerebellum and midbrain were associated with disease severity and depression level in SCD, which may help reflect the degree of neurodegeneration in vivo, and give early warnings for SCD-related depression.

#### M2-SPNR-8 Diagnostic Performance of Susceptibility Map-weighted MRI According to Acquisition Plane for Differentiating Neurodegenerative Parkinsonism

Participants

Suiji Lee, MD, Seoul, Korea, Republic Of (*Presenter*) Nothing to Disclose

#### PURPOSE

To evaluate the diagnostic performance of SMwI according to the acquisition plane for differentiating neurodegenerative parkinsonism.

#### METHODS AND MATERIALS

This retrospective, observational, single-institution study included patients who were consecutively enrolled from those who visited movement disorder clinics and underwent both brain MRI and 18F-FP-CIT with clinical symptoms of suspected parkinsonism between September 2021 and December 2021. Both oblique coronal plane (vertical to the midbrain) and anterior commissure-posterior commissure (AC-PC) plane of SMwI were acquired. Abnormality was determined when there was any hypointense area that obliterated the differentiation of the three layers and classified into 3 categories (0: normal, 1: intermediate, 2: abnormal) by two neuroradiologists. 18F-FP-CIT PET served as the reference standard. The diagnostic performance of the oblique plane and AC-PC plane of SMwI were assessed per substantia nigra and per participant. Inter-rater agreement was assessed using Cohen's kappa coefficient. McNemar's test was used to test the diagnostic performance of oblique coronal plane and AC-PC plane of SMwI.

#### RESULTS

Total 194 patients (mean age  $\pm$  SD, 67  $\pm$ 10 years, 91 men) were included. Among them, 84 patients were diagnosed with IPD, 26 with MSA, 3 with PSP, 10 with CBS, 35 with ET, 10 with DIP, 4 with NPH and 22 with others. The overall inter-rater agreement for both oblique and AC-PC plane was good ( $\kappa = 0.747$  and 758 for each,  $P < .001$ ). In per participant analysis, the overall inter-rater agreement for both oblique and AC-PC plane was good ( $\kappa = 0.747$  and 758 for each,  $P < .001$ ). For reader 1, the overall sensitivity of the oblique plane was 89.9% and that of the AC-PC plane was 91.7% ( $P = .727$ ). The overall specificity of the oblique plane was 87.1% and that of AC-PC plane was 88.2% ( $P = .727$ ). The overall accuracy of the oblique plane was 88.7% and that of AC-PC plane was 90.2%, with p-value of 0.607. Reader 2 demonstrated similar results. For both readers, there was no significant difference of sensitivity, specificity and accuracy between the oblique plane and the AC-PC plane.

#### CONCLUSION

s There was no significant difference of diagnostic performance between the oblique plane and the AC-PC plane of SMwI in differentiating parkinsonism.

#### CLINICAL RELEVANCE/APPLICATION

This study assures clinics can choose any one of MRI acquisition planes of SMwI between oblique plane and AC-PC plane according to their clinical settings in the diagnosis of parkinsonism.

#### M2-SPNR-9 Brain Connectivity Changes in Resting-State Functional MRI in Patients with HIV-Associated Neurocognitive Disorder (HAND): A Multi-voxel Pattern Analysis (MVPA) Approach Using Mutual Connectivity Analysis (MCA)

Participants

Ali Vosoughi, Rochester, NY (*Presenter*) Nothing to Disclose

#### PURPOSE

To develop and evaluate a novel machine learning framework for identifying subjects with HIV-Associated Neurocognitive Disorder (HAND) using Mutual Connectivity Analysis (MCA) by capturing connectivity differences in resting-state functional MRI (rsfMRI).

#### METHODS AND MATERIALS

Resting-state fMRI scans (3T, EPI sequence, TR=1.65s, 250 acquisitions) were acquired in a cohort of 45 age-matched subjects (20 healthy, 25 HIV+, 16 of whom had HAND symptoms (HAND+)). After pre-processing, data was parcellated into 90 regions using the Automated Anatomical Labeling atlas. Regions were represented by their average time-series. A nonlinear machine learning connectivity analysis method (MCA [Citation blinded for review]), was used to quantify interdependence of region-specific time-series producing a 8100-element connectivity matrix. Generalized matrix learning vector quantization feature selection revealed regional connections that were most different between the groups. These were used for subsequent identification of HAND+ subjects using an adaptive boosting classifier in a Multi-Voxel Pattern Analysis (MVPA) framework. For both feature selection and classification, strict data separation (90% train/10% test) was carried out in a 100-iteration cross-validation scheme. For comparison, MCA was evaluated against the clinical standard technique of functional connectivity analysis using cross-correlating (CC) low-pass filtered fMRI time-series. Area Under the Curve (AUC) for Receiver Operator Characteristics (ROC) analysis was used to quantitatively evaluate diagnostic quality of HAND+ subject classification.

#### RESULTS

The MCA rsfMRI connectivity analysis method clearly outperformed the clinical standard CC technique in identifying HAND+ subjects with AUC of  $0.85 \pm 0.27$  for MCA, and  $0.71 \pm 0.31$  for CC, respectively. Diagnostic quality differences between both methods were statistically significant ( $p < 0.05$ , Wilcoxon signed-rank test).

#### CONCLUSION

s Our results suggest that MCA significantly improves the diagnostic accuracy of identification of patients with HAND based on

s Our results suggest that MCA significantly improves the diagnostic accuracy of identification of patients with HAND based on rsfMRI neuroimaging. We conclude that, when compared to conventional CC analysis, our MVPA framework is better suited to capture disease-related brain network connectivity changes in HAND.

#### **CLINICAL RELEVANCE/APPLICATION**

The MCA method classifies HAND+ subjects and controls by identifying relevant changes in fMRI connectivity. Such changes can be useful diagnostic imaging biomarkers for HIV-related neurologic disease.

Printed on: 02/07/23



## Abstract Archives of the RSNA, 2022

M2-SPNR-1

### How Are We Handling All Those Fluoroscopic Guided Lumbar Puncture Requests? A Nationwide Survey of Practice Trends

Monday, Nov. 28 9:00AM - 9:30AM Room: Learning Center - NR DPS

#### Participants

Tyler Richards, MD, Salt Lake City, UT (*Presenter*) Nothing to Disclose

#### PURPOSE

Our study's purpose was to determine how radiologists in different practice settings manage fluoroscopy guided lumbar puncture (FGLP) referrals.

#### METHODS AND MATERIALS

An online questionnaire was sent to radiologists and trainees to survey their methodology of handling FGLP requests, pre-procedural work-up including lab value and head imaging requirements, utilization of physician extenders (PEs)/trainees to perform FGLPs, among others. Odds ratio (OR) was used to compare the categories.

#### RESULTS

Of 131 responses, 93.9% were from the U.S. and 81.7% were from an academic practice (AP) and 18.3% from a private practice (PP). Regarding FGLP referrals, 27.5% of respondents stated it was not standard practice in their department that a bedside lumbar puncture is attempted by a clinician prior to FGLP referral, a practice 4 x more common among PP respondents (OR 4.19 (95% CI: 1.86,9.65)). Morbid obesity (80.2%), congenitally altered anatomy (71.0%), and prior lumbar surgery with hardware (61.1%) were some of the most frequent reasons respondents did not require a bedside LP attempt prior to referral for FGLP. 95.8% of PP and 84.1% of AP respondents were asked often to perform an FGLP by clinicians because the clinician does not feel competent performing LPs. Of those, 74.3% stated they will always or sometimes agree to the request; a 4.7 higher likelihood that a PP radiologist would oblige and always agree to perform the FGLP compared to an academic radiologist (OR 4.7 (95% CI: 1.3-20.5)). 42.0% of respondents stated that they would always comply if a patient specifically requests an FGLP without a bedside LP attempt, 2.5 x higher likelihood for PP respondents (OR 2.5 (95%CI: 1.15-5.56)). Regarding FGLP operators, AP respondents were less likely to have PEs perform FGLPs compared to PP respondents (31.8% vs. 45.8%; (OR 0.65 (95% CI: 0.3,1.42)). In academic practices, 72.9% reported trainees perform >50% of their FGLPs. Regarding pre-procedural work up, 42.0% of respondents stated that they check coagulation labs on all patients prior to FGLP and 84.0% of respondents stated that patients should get a head CT prior to an FLGP only if there is high suspicion for increased intracranial pressure, similar between PP and AP respondents.

#### CONCLUSION

s This survey demonstrates that many academic and private practice radiology practitioners are relatively lenient in obliging to perform FGLPs in patients. There were many differences and some similarities in management of FGLP referrals and pre-procedural workup between academic and private practice groups.

#### CLINICAL RELEVANCE/APPLICATION

Our findings demonstrate the current methods of how private practice and academic radiologists handle FGLPs referrals and can be potentially used to develop guidelines of best FGLP practices.

Printed on: 02/07/23

## Abstract Archives of the RSNA, 2022

M2-SPNR-11

### Leptomeningeal Metastases in Glioma Revisited: High Incidence and Their Molecular Predictors based on Recent Imaging and Molecular Diagnostics

Monday, Nov. 28 9:00AM - 9:30AM Room: Learning Center - NR DPS

#### Participants

Sung Soo Ahn, MD, Seoul, Korea, Republic Of (*Presenter*) Nothing to Disclose

#### PURPOSE

Leptomeningeal metastases (LM) in glioma has been underestimated due to low incidence and lack of reliable imaging. This study aimed to investigate a real-world incidence of LM using a CSF-sensitive MR imaging technique and analyze molecular predictors for LM in the molecular era.

#### METHODS AND MATERIALS

Total 1,405 adult glioma patients underwent post-contrast fluid attenuated inversion recovery (FLAIR) imaging at initial diagnosis and during treatment monitoring between March 2001 and October 2021. Molecular data included isocitrate dehydrogenase (IDH) mutation, 1p/19q co-deletion, H3 K27M alteration, and O6-methylguanine-methyltransferase (MGMT) promoter methylation status. Multivariable logistic regression analysis for LM development was performed in molecular data, clinical data, and imaging characteristics. Median overall survival (OS) was compared between patients with and without LM using Kaplan-Meier survival curves and log-rank test.

#### RESULTS

LM was identified in 16.2% of glioma (228 of 1405), with 7.8% (110 of 1405) at initial diagnosis, and 8.4% (118 of 1405) at recurrence. Among molecular diagnostics, IDH-wildtype (odds ratio [OR] 3.14,  $P = .001$ ) and MGMT promoter unmethylation (OR 1.43,  $P = .034$ ) were independent predictors of LM. WHO grade 4 (OR 10.52,  $P < .001$ ) and nonlobar location (OR 1.54,  $P = .048$ ) were associated with LM at initial diagnosis, whereas IDH-wildtype (OR 5.04,  $P < .001$ ) and H3 K27M alteration (OR 3.39,  $P = .003$ ) were significantly associated with LM at recurrence. Patients with LM had a worse median OS than those without LM (16.7 vs. 32.0 months, log-rank test;  $P < .001$ ). N

#### CONCLUSION

CSF-sensitive MR imaging diagnostics aid diagnosis of LM and reduced an underdiagnosed condition in adult gliomas. Molecular markers affect LM at initial diagnosis and at recurrence, and patients with aggressive molecular markers warrant imaging surveillance of LM.

#### CLINICAL RELEVANCE/APPLICATION

The incidence of LM in glioma is underestimated due to lack of sensitive imaging protocol. Here, we utilized CSF-sensitive MRI with post-contrast FLAIR and discovered a high frequency of 228 (16.2%) patients diagnosed with LM in 1,405 diffuse glioma patients. Our findings emphasize the role of molecular markers in the development of LM in glioma patients. Patients with aggressive molecular markers such as IDH-wildtype and H3 K27M alteration warrant imaging surveillance of LM.

Printed on: 02/07/23

## Abstract Archives of the RSNA, 2022

M2-SPNR-12

### Use of VASARI Features for The Systematic Identification of Typical and Atypical Primary Central Nervous System Lymphomas

Monday, Nov. 28 9:00AM - 9:30AM Room: Learning Center - NR DPS

#### Participants

Irene Dixe de Oliveira Santo, MD, New Haven, CT (*Presenter*) Nothing to Disclose

#### PURPOSE

The imaging appearance of PCNSL is highly variable with a significant proportion of cases demonstrating atypical features, frequently leading to a significant delay in diagnosis. Standardized classification of features has the potential to improve recognition of atypical variants, which is especially important given the drastically different treatment approach from the similar-appearing gliomas.

#### METHODS AND MATERIALS

Presurgical MR images of 71 patients with histologically-proven PCNSL were scored independently according to the VASARI (Visually Accessible Rembrandt Images) features by two different neuroradiologists. Classification into typical versus atypical PCNSL was based on enhancement pattern, presence or absence of necrosis, hemorrhage, and calcification. Age at diagnosis, gender, presenting symptoms, immune status, biochemical and molecular profile of the neoplasms, treatment, and overall survival were also recorded. The influence of visual appearance (atypical versus typical) on overall survival was analyzed using the Kaplan-Meier method and tested for significance using log-rank test ( $\alpha=0.05$ ).

#### RESULTS

Appearance of PCNSL was highly variable ranging from multiple infiltrative solid masses to ring-enhancing lesions. Periventricular and ependymal involvement were among the most common locations. Systematic scoring classified 44 (62%) patients into typical and 27 (38%) patients into atypical PCNSL. Presence of hemorrhage on SWI was often responsible for classification into atypical. Regarding survival, median OS was significantly lower for atypical (203 days) compared to typical (767 days) PCNSL ( $p = 0.012$ ).

#### CONCLUSION

Up to a third of our PCNSL patients demonstrated atypical MRI features, which may complicate diagnosis.

#### CLINICAL RELEVANCE/APPLICATION

Awareness of varying imaging presentations of PCNSL may alert the interpreting radiologist to consider lymphoma early and expedite diagnosis and treatment.

Printed on: 02/07/23

## Abstract Archives of the RSNA, 2022

M2-SPNR-13

### Usefulness of the Wave-CAIPI for the Post-contrast 3D T1-SPACE in The Evaluation of Brain Metastases

Monday, Nov. 28 9:00AM - 9:30AM Room: Learning Center - NR DPS

#### Participants

Youngjin Heo, MD, (Presenter) Nothing to Disclose

#### PURPOSE

High-resolution post-contrast 3D T1WI is a widely used sequence for evaluating brain metastasis, despite the long scan time. This study aimed to compare highly accelerated post-contrast 3D T1-weighted sampling perfection with application-optimized contrasts by using different flip angle evolution using Wave-controlled aliasing in parallel imaging (Wave-T1-SPACE) with the commonly used standard high-resolution post-contrast 3D T1-SPACE for the evaluation of brain metastases.

#### METHODS AND MATERIALS

Among the 387 patients who underwent post-contrast wave-T1-SPACE and standard SPACE, 56 patients with suspected brain metastases were retrospectively included. Two neuroradiologists assessed the number of enhancing lesions according to lesion size, contrast-to-noise ratio (CNR) lesion/parenchyma, CNR white matter/gray matter, contrast ratio (CR) lesion/parenchyma, and overall image quality for the two different sequences.

#### RESULTS

Although there was no significant difference in the evaluation of larger enhancing lesions (>5 mm) between the two different sequences ( $P=0.66$  for observer 1,  $P=0.26$  for observer 2), wave-T1-SPACE showed significantly lower number of smaller enhancing lesions (<5 mm) than standard SPACE ( $1.61\pm 0.29$  vs  $2.84\pm 0.47$  for observer 1,  $1.41\pm 0.19$  vs  $2.68\pm 0.43$  for observer 2). Furthermore, mean CNR<sub>lesion/parenchyma</sub> and overall image quality of wave-T1-SPACE were significantly lower than standard SPACE.

#### CONCLUSION

Post-contrast wave-T1-SPACE showed comparable diagnostic performance for larger enhancing lesions (>5 mm) and marked scan time reduction as compared with standard SPACE. However, post-contrast wave-T1-SPACE showed underestimation of smaller enhancing lesions (<5 mm) and lower image quality than standard SPACE. Therefore, post-contrast wave-T1-SPACE should be interpreted carefully in the evaluation of brain metastasis.

#### CLINICAL RELEVANCE/APPLICATION

Recently, accelerated 3D acquisition techniques have been developed to reduce the scan time of high-resolution 3D T1WI sequences while preserving image quality. Wave-controlled aliasing in parallel imaging (Wave-CAIPI; Siemens Healthineers) is advanced parallel imaging technique that combines a corkscrew gradient trajectory with CAIPI shifts in the ky and kz directions to efficiently encode k-space and evenly spread the voxel aliasing in all dimensions. This allow to take better advantage of the 3D coil sensitivity information to provide highly accelerated parallel imaging with negligible artifacts and signal-to-noise ratio penalties. Therefore, we evaluated the diagnostic performance according to the lesion size and overall image quality of post-contrast wave-T1-SPACE for the evaluation of brain metastases.

Printed on: 02/07/23

## Abstract Archives of the RSNA, 2022

M2-SPNR-14

### White Matter Hyperintensities in Younger Mild Traumatic Brain Injured Patients

Monday, Nov. 28 9:00AM - 9:30AM Room: Learning Center - NR DPS

#### Participants

Priya Santhanam, PhD, (*Presenter*) Nothing to Disclose

#### PURPOSE

This study aims to identify associations between white matter hyperintensities (WMH) and the presentation and progression of post-concussive symptoms in patients 40 years and younger with mild traumatic brain injury (mTBI).

#### METHODS AND MATERIALS

MTBI patients (n=152; mean age=30 yrs) without preexisting head pathology were included in this study. Axial T2-weighted and T2-FLAIR sequences were performed on a 3.0 Tesla MR Signa HDxt system. Hyperintensities were regionally classified by lobe (frontal, parietal, temporal, or occipital) or cerebellum. Clinical data, including presence of several post-concussive symptoms, was obtained via retrospective chart review. Patient groups were compared by the presence or absence of WMH on imaging as well as by whether the patient had loss-of-consciousness (LOC) during injury. Interval-censored data analyses were performed to test the time to recovery between the comparison groups as recovery is only known to be between two examinations.

#### RESULTS

At least one WMH was present in 44% of male and 52% of female patients. Single WMH were predominantly located in the frontal lobe (84%) and more commonly in the left hemisphere (65%). LOC was more prevalent ( $p=0.018$ ) in those with WMH as compared to those without WMH. While symptoms improved or resolved in both groups, a larger percentage of patients without WMH showed improvement as compared to patients with WMH. Patients with WMH also took significantly longer to recover from cognitive deficits than those without WMH ( $p=0.0177$ ). Patients with LOC had a higher incidence of balance deficits as compared to patients without LOC ( $p=0.0391$ ), while a larger percentage of those without LOC showed improvement or resolution of symptoms, specifically headache ( $p=0.0406$ ), balance deficits ( $p=0.0173$ ), and cognitive deficit ( $p=0.0341$ ).

#### CONCLUSION

s This study revealed several significant associations between quantitative WMH findings, loss of consciousness, and clinical outcomes following mTBI. Taken together, findings suggest the presence of WMH in younger TBI patients may influence patient symptomatology, while co-morbid LOC may lead to poor outcomes and recovery for affected individuals.

#### CLINICAL RELEVANCE/APPLICATION

The presence of white matter hyperintensities in younger patients with mild traumatic brain injury and loss of consciousness could be related to symptom prevalence, long-term outcomes, and recovery.

Printed on: 02/07/23



## Abstract Archives of the RSNA, 2022

M2-SPNR-15

### IDH and 1p19q Diagnosis in Diffuse Glioma from Preoperative MRI Using Artificial Intelligence

Monday, Nov. 28 9:00AM - 9:30AM Room: Learning Center - NR DPS

#### Participants

Hugh McHugh, BMBCh, Auckland, New Zealand (*Presenter*) Clinical AI Registrar, Harrison AI Research Grant, RANZCR

#### PURPOSE

Isocitrate dehydrogenase (IDH) mutation and 1p19q codeletion are key molecular markers in glioma which both confer a more favorable prognosis. In the 2021 WHO classification of CNS tumours IDH and 1p19q status determine the glioma sub-categories of glioblastoma, astrocytoma and oligodendroglioma. IDH and 1p19q status is unknown until after surgery unless there is a biopsy which is uncommon. Reliable preoperative molecular characterization may facilitate tailored treatment approaches, for example if molecular status affects the optimal extent of tumor resection. Emerging research supports the potential of MRI-based IDH and 1p19q diagnosis. A limitation is the relative lack of generalization and external validation outside the widely used The Cancer Imaging Archive (TCIA) dataset. We present a combined IDH and 1p19q classification algorithm and assess performance on a local retrospective cohort and a fully independent cohort from the Erasmus Glioma Database (EGD).

#### METHODS AND MATERIALS

2D convolutional neural networks were trained to provide IDH and 1p19q classification. Inputs are T1 post-contrast, T2, and FLAIR sequences. Training data consists of preoperative imaging from the TCIA dataset (n=184) and images from a locally obtained cohort that were obtained prior to 1/1/2018 (n=349). Evaluation data consists of the most recent cases from the local cohort obtained between 1/1/2018 and 31/8/2021 (n=205) and the EGD (n=420).

#### RESULTS

Subject-wise IDH classification accuracy was 93.3% and 91.5% on the local cohort and EGD, with AUC of 95.4% and 95.8%, respectively. 1p19q accuracy was 94.5% and 87.5% with AUC of 92.5% and 85.4% on the local cohort and EGD. Combined subject-wise IDH and 1p19q accuracy was 90.4% and 84.3% on the local cohort and EGD, with AUC of 92.4% and 91.2%.

#### CONCLUSION

High IDH and 1p19q classification performance was achieved on the local retrospective cohort. Generalization to the EGD was robust, demonstrating the potential for clinical translation. This method is able to non-invasively predict tumor subtypes according to the WHO 2021 classification with high accuracy using readily available imaging without the need for MR spectroscopy. This may better inform patients and clinicians prior to surgery and demonstrates the high potential impact in glioma diagnostics.

#### CLINICAL RELEVANCE/APPLICATION

This research externally validates non-invasive IDH and 1p19q diagnosis in glioma from preoperative MRI using artificial intelligence techniques allowing tumor classification by WHO 2021 criteria.

Printed on: 02/07/23

## Abstract Archives of the RSNA, 2022

M2-SPNR-16

### Compare the Performance of MRI-based 2.5D and 3D Convolutional Neural Networks in Differential Diagnosis of High-grade Gliomas and Single Brain Metastases

Monday, Nov. 28 9:00AM - 9:30AM Room: Learning Center - NR DPS

#### Participants

Bin Zhang, (*Presenter*) Nothing to Disclose

#### PURPOSE

The 2.5D convolutional neural network models have unique advantages for studies with moderate sample sizes, while the 3D model can completely extract tumor and peritumoral features. To explore and compare the value of preoperative differential diagnosis of high-grade gliomas (HGG) and single brain metastases (BM) under 2.5D and 3D convolutional neural network models.

#### METHODS AND MATERIALS

T2WI and contrast-enhanced T1WI(CE T1WI) images of 230 patients with HGG and 111 patients with BM confirmed by surgery and pathology were retrospectively collected. The radiologist delineated the regions of interests (ROIs) of the input images of the 2.5D networks and 3D networks on the T2WI and CE T1WI axial images of the registered MRI. The slice  $n$ th with the largest tumor parenchyma area on the MRI image was determined, and then the tumor area (including tumor parenchyma and peritumoral edema area) of the slice of  $(n-2)$ th,  $n$ th and  $(n+2)$ th was delineated respectively. Define a minimum rectangular box as the ROIs of the 2.5D models that can cover all tumor areas at the three slices. Define the smallest 3D rectangular box that can completely contain the tumor area at all slices as the ROIs of the 3D models. Finally, based on DenseNet convolutional neural networks respectively build prediction models for T2WI and CE T1WI sequences under 2.5D and 3D model. The predictive performance of each model was evaluated by the receiver operating characteristic(ROC) curve, and the differences in the ROC curves of the models built by different convolutional neural networks were compared in pairs by Delong's test.

#### RESULTS

The best AUC values of the 3D model on CE T1WI and T2WI were 0.852 and 0.802, respectively. And the best AUC values of the 2.5D model on CE T1WI and T2WI were 0.831 and 0.784, respectively. The performance of the 3D models were better than that of the 2.5D models. Delong's test showed that the differences between the models were statistically significant ( $P < 0.05$ ).

#### CONCLUSION

The MRI-based 2.5D and 3D convolutional neural network models have better diagnostic performance in differentiating HGG and single BM, and the 3D models have better diagnostic performance than 2.5D models. The deep learning model can be used to identify HGGs and BMs and assist in clinical formulation of precise treatment plans potential tool.

#### CLINICAL RELEVANCE/APPLICATION

The 2.5D model has better advantages in the deep learning model with a medium sample size, which can make up for the problem of the large data demand of the 3D model. While the 3D convolutional neural network structure analyzes the lesion information more completely, so it is easier to apply to clinical practice. The establishment of the prediction model will be able to differential diagnose HGG and single BM through non-invasive imaging examination.

Printed on: 02/07/23

## Abstract Archives of the RSNA, 2022

M2-SPNR-17

### **Predicting the Isocitrate Dehydrogenase Wildtype in Non-enhancing or Poorly Enhancing Glioma by Conventional MRI Features and Apparent Diffusion Coefficient**

Monday, Nov. 28 9:00AM - 9:30AM Room: Learning Center - NR DPS

#### **Participants**

Jiyoung Song, MD, Seoul, Korea, Republic Of (*Presenter*) Nothing to Disclose

#### **PURPOSE**

To develop predictive models using clinically available MRI parameters for predicting isocitrate dehydrogenase (IDH) status of gliomas with no or poor enhancement, which is considered as a radiologically low-grade feature.

#### **METHODS AND MATERIALS**

This retrospective study included 241 patients with surgically resected and pathologically confirmed gliomas that showed no or poor enhancement (less than 5% of the entire tumor volume) in the preoperative MRI. Visual rating of imaging features (T1-weighted, T2-weighted, FLAIR, contrast-enhanced T1-weighted images, and cerebral blood volume map) was performed. Regions of interest were drawn to acquire the apparent diffusion coefficient (ADC) mean (ADC<sub>mean</sub>) and minimum (ADC<sub>min</sub>) in tumor and ADC<sub>nawm</sub> in normal-appearing white matter. Univariable and multivariable logistic regression analyses were performed for each imaging feature and ADC value. Then, receiver operating characteristic curve analysis was done with probability index calculated from the multivariable logistic regression model. A subgroup analysis was performed to predict IDH status in the non-enhancing gliomas.

#### **RESULTS**

In 241 non-enhancing or poorly enhancing gliomas, T2/FLAIR mismatch sign showed 100% specificity (42 of 42) to predict IDH-mutant gliomas. Among 199 gliomas with negative T2/FLAIR mismatch signs, 78 were IDH-wildtype. A predictive model incorporating age, calcification, multifocality, FLAIR homogeneity, ADC<sub>min</sub>-to-ADC<sub>nawm</sub> ratio, and cortical involvement showed area under the curve (AUC) of 0.909 (95% CI: 0.858-0.946) with 90.8% sensitivity and 81.2% specificity. In the subgroup analysis for 116 non-enhancing tumors (46 IDH-wildtypes and 70 IDH-mutants) a predictive model that consisted of the same variables showed AUC of 0.883 (95% CI: 0.808-0.935), 82.6% sensitivity, and 88.1% specificity.

#### **CONCLUSION**

s Algorithms incorporating T2/FLAIR mismatch sign, age, calcification, multifocality, FLAIR homogeneity, ADC<sub>min</sub>-to-ADC<sub>nawm</sub> ratio, and cortical involvement predicted IDH wild-type gliomas with radiologically low-grade feature.

#### **CLINICAL RELEVANCE/APPLICATION**

According to 2021 WHO classification for adult-type diffuse gliomas, even if a tumor seems low-grade, being IDH-wildtype satisfies a necessary condition to be diagnosed as glioblastoma. This study developed models using clinically available MRI parameters for predicting IDH status of gliomas with no or poor enhancement, which is considered as a radiologically low-grade feature.

Printed on: 02/07/23

## Abstract Archives of the RSNA, 2022

M2-SPNR-18

### High-resolution Clinical Functional MRI at 7T in Patients with Brain Tumors: Initial Assessment

Monday, Nov. 28 9:00AM - 9:30AM Room: Learning Center - NR DPS

#### Participants

Kinsey Lano, BS, Houston, TX (*Presenter*) Nothing to Disclose

#### PURPOSE

This study aimed to evaluate spatial localization accuracy of a high-resolution (1.4 mm isotropic) 7T fMRI protocol and compare with a clinical 3T protocol with typical resolution (1.9 x 1.9 x 4 mm<sup>3</sup>).

#### METHODS AND MATERIALS

Hand motor fMRI studies of 24 patients (n=12 on 7T and 12 on 3T) were evaluated. The 7T patients included 1 with brain mets, 3 with low-grade, and 8 with high-grade gliomas. The 3T patients included 4 with low-grade and 8 with high-grade gliomas. The fMRI paradigm consisted of 6 cycles of resting and bilateral hand-motor task blocks. T2\*-weighted EPI sequences were used for the fMRI at 7T (TR/TE=2000 ms/24 ms, PI=3, SMS=2, 1.4 x 1.4 x 1.4 mm<sup>3</sup>) and at 3T (TR/TE=3000 ms/25 ms, PI=2, 1.9 x 1.9 x 4.0 mm<sup>3</sup>). The fMRI pre-processing included motion correction and co-registration with 3D T1-weighted images. Functional t-value maps were then generated by the standard GLM method. The t-value maps were thresholded at two statistical levels: (1) FWE-corrected p lt 0.05 (t gt 5.5 and 6.1 for 7T and 3T, respectively), and (2) t gt 4.0. For each patient, the most relevant motor-activation cluster on the lesion side was visually determined. The smallest distance between the center of the cluster and the central sulcus was measured and categorized: (1) gt 2 mm, (2) 2-4 mm, and (3) 5-10 mm.

#### RESULTS

At 7T, activation clusters at expected hand motor areas were detected in 7 (58%) and 9 (75%) out of the 12 patients at the statistical level of p lt 0.05, FWE corrected, and t gt 4.0, respectively. The spatial localization accuracy was within 2 mm for all the 9 patients with detected activation clusters. At 3T, hand motor activations were detected in 11 (92%) and 12 (100%) out of the 12 patients at the two statistical levels. The spatial localization accuracy assessment found 4 (33%), 6 (50%), and 2 (17%) patients having the detected activation cluster centered at gt 2mm, 2-4 mm, and 5-10 mm, respectively, from the central sulcus.

#### CONCLUSION

s We demonstrated that high-resolution fMRI at 7T is feasible for mapping primary motor areas in clinical routine. More accurate functional localization was achieved using the high-resolution 7T protocol compared to our routine protocol at 3T.

#### CLINICAL RELEVANCE/APPLICATION

The higher fMRI sensitivity at 7T allows imaging at higher spatial resolution, which leads to improved localization accuracy for presurgical functional mapping.

Printed on: 02/07/23

## Abstract Archives of the RSNA, 2022

M2-SPNR-19

### Nomogram for Predicting Early Recurrence in Patients with High Grade Glioma

Monday, Nov. 28 9:00AM - 9:30AM Room: Learning Center - NR DPS

#### Participants

Qing Zhou, Lanzhou, China (*Presenter*) Nothing to Disclose

#### PURPOSE

To develop a nomogram to predict early recurrence of high-grade glioma (HGG) based on clinical factors, genetic factors, and MRI parameters.

#### METHODS AND MATERIALS

154 HGG patients were classified into recurrence and non-recurrence groups based on pathological diagnosis and RANO criteria. Clinical information included age, sex, and preoperative Karnofsky Performance Status (KPS) scores. Gene information included P53, IDH1, MGMT, and TERT status. All patients had baseline MRIs before treatment, including T1WI, T2WI, T1C, Flair and DWI examinations. The tumor location, single/multiple tumors, tumor diameter, peritumoral edema, necrotic cyst, hemorrhage, average apparent diffusion coefficient (ADC) value and minimum ADC values were evaluated. Univariate and multivariate logistic regression were used to determine the predictors of early recurrence and to build the nomogram.

#### RESULTS

Univariate analysis showed that the number of tumors (OR, 0.258; 95% CI: 0.104, 0.639; P = 0.003) and peritumoral edema (OR, 0.965; 95% CI 0.942, 0.988; P = 0.003; mean in the recurrence group 22.04±17.21 mm; mean in the non-recurrence group 14.22±12.84 mm) were statistically significantly different in patients with early recurrence. Genetic factors included IDH1 (OR, 4.405; 95% CI 1.874, 10.353; P= 0.001), and MGMT (OR, 2.389; 95% CI 1.234, 4.628; P= 0.010). Multivariate logistic regression analysis revealed that the number of tumors (OR, 0.227; 95% CI 0.084, 0.616; P = 0.004), peritumoral edema (OR, 0.969; 95% CI 0.945, 0.993; P = 0.013) and IDH1 (OR, 4.200; 95% CI 1.602, 10.013; P= 0.004) were independent risk factors for early recurrence. The nomogram showed the highest net benefit when the threshold probability was less than 63%.

#### CONCLUSION

A nomogram prediction model based on results that are easily available before surgery can effectively aid clinical treatment decisions for newly diagnosed HGG patients.

#### CLINICAL RELEVANCE/APPLICATION

A nomogram prediction model can effectively aid treatment decisions in newly diagnosed HGG patients. Neurosurgeons may adjust the surgical decision on the scope of tumor resection based on the prediction model. For tumor tissues with a high risk of recurrence and high infiltration, the radiation oncologist can also upgrade the radiation dose to high-risk areas.

Printed on: 02/07/23

## Abstract Archives of the RSNA, 2022

M2-SPNR-20

### Peritumoral MR Imaging Radiomic Features Improves Identification of Circumscribed Astrocytic Gliomas and High-grade Gliomas

Monday, Nov. 28 9:00AM - 9:30AM Room: Learning Center - NR DPS

#### Participants

Shuang Li, (*Presenter*) Nothing to Disclose

#### PURPOSE

In the 2021 WHO classification of tumors of the central Nervous System, the terms of "diffuse" and "circumscribed" were applied to the classification of gliomas, diffuse gliomas are characterized by extensive infiltration, while circumscribed astrocytic gliomas show a solid growth pattern. The most common circumscribed astrocytic gliomas are pilocytic astrocytoma (PA) and pleomorphic xanthoastrocytoma (PXA). MR imaging findings of them can resemble high grade gliomas (HGGs). We aimed to develop an MRI-based radiomics model to distinguish circumscribed glioma from HGGs.

#### METHODS AND MATERIALS

Preoperative T2 fluid-attenuated inversion recovery (T2 FLAIR) and contrast-enhanced T1-weighted imaging (CE-T1WI) data were obtained from 160 patients (91 circumscribed astrocytic gliomas and 69 glioblastoma) between 2016 and 2020. 1288 features were obtained in tumor region and the 5 mm thickness peritumoral region, respectively. We up-sampled features by repeating random cases to make samples balance. Then, we applied the normalization on the feature matrix. Feature pairs with PCC values larger than 0.990 will be removed. Before build the model, we used recursive feature elimination (RFE) to select features. Support vector machine (SVM) was used as a classifier. To determine the hyper-parameter of model, we applied cross validation with 10-fold on the training data set. The hyper-parameters were set according to the model performance on the validation data set. The performance of the model was evaluated using receiver operating characteristic (ROC) curve analysis. The area under the ROC curve (AUC) was calculated for quantification. We also estimated the 95% confidence interval by bootstrap with 1000 samples.

#### RESULTS

Intratumor radiomic features achieved AUCs of 0.820(CE-T1WI) and 0.787(T2 FLAIR). The integrated model, incorporating intra- and peritumoral features extracted from T2 FLAIR and CE-T1WI images, improved the AUCs to 0.889 on the same test set.

#### CONCLUSION

An imaging-based model combining tumor and peritumor radiomics can help to distinguish between circumscribed astrocytic gliomas and high-grade gliomas.

#### CLINICAL RELEVANCE/APPLICATION

Circumscribed astrocytic gliomas had better prognosis than HGGs. Correct differential diagnosis is vital for preoperative decision-making and prognostic evaluation. Radiomic features extracted from intra- and peritumoral region may help the identification.

Printed on: 02/07/23

## Abstract Archives of the RSNA, 2022

M2-SPNR-4

### Discriminative Power of Macro- And Microstructural MRI in the Differential Diagnosis of Neurodegenerative Parkinsonian Syndromes

Monday, Nov. 28 9:00AM - 9:30AM Room: Learning Center - NR DPS

#### Participants

Alexander Rau, MD, Freiburg, Germany (*Presenter*) Nothing to Disclose

#### PURPOSE

To investigate the discriminative performance of macro- and microstructural MRI in the differential diagnosis of neurodegenerative parkinsonian syndromes (NPS).

#### METHODS AND MATERIALS

We included patients with NPS according to current consensus diagnostic criteria, i.e. 136 patients with Parkinson's disease (PD), 32 patients with progressive supranuclear palsy (PSP), 41 patients with multiple system atrophy (MSA) as well as 37 healthy controls (HC) in this monocentric retrospective cross-sectional study. Tissue probability values for gray matter, white matter and CSF were automatically obtained by CAT12. In addition, the microstructure of the patients was analyzed using a mesoscopic approach by diffusion tensor imaging (DTI) and diffusion microstructure imaging (DMI). Respective parameters were extracted using the AAL3-atlas and ROIs with great relevance for PSP. Based on this, a linear support vector machine (SVM) was trained and optimized in respect of ROC-AUC in a one-vs-rest (OVR) classifier. The diagnostic performance of SVM was compared with respect to different inputs, i.e. TPV, DTI and DMI individually.

#### RESULTS

Diffusion MRI outperformed the T1w derived TPV with a correct classification in 80% for DTI, 79% for DMI and 52% for TPV. The corresponding OVR-ROC-AUC of DTI was 0.92 for HC, 0.89 for PD, 0.95 for MSA and 0.93 for PSP and for DMI 0.91 (HC), 0.90 (PD), 0.96 (MSA) and 0.93 (PSP).

#### CONCLUSION

s Microstructural parameters as obtained in an mesoscopic approach using diffusion MRI data outperformed structural data derived by conventional imaging in the diagnosis of NPS. The particularly good performance of microstructural approaches in the diagnosis of PD, as a weak point in conventional MRI, underlines the potential of this approach. The introduced automatic approach might facilitate the MRI diagnosis of patients with suspected NPS.

#### CLINICAL RELEVANCE/APPLICATION

The developed approach might facilitate the differential diagnosis of neurodegenerative parkinsonian syndromes in an objective manner and is therefore of high clinical relevance.

Printed on: 02/07/23

## Abstract Archives of the RSNA, 2022

M2-SPNR-6

### Usefulness of 3D FIESTA in Differentiating Parkinson's Disease From Parkinson Syndrome: Volumetric Alternation of Olfactory Bulb

Monday, Nov. 28 9:00AM - 9:30AM Room: Learning Center - NR DPS

#### Participants

Ide Ide, MD, (*Presenter*) Nothing to Disclose

#### PURPOSE

Parkinson's disease (PD) is a neurodegenerative disease, related with deposition of Lewy body. Braak stage of Lewy pathology shows the initiation sites are in the olfactory bulb (OB), hence, olfactory dysfunction is among the earliest nonmotor features of PD. It's sometimes difficult to differentiate PD from parkinson syndrome (PS), such as multiple system atrophy (MSA), corticobasal syndrome (CBS), and progressive supranuclear palsy (PSP) using conventional MRI and clinical symptom. It's known that olfactory loss occurs to a lesser extent or is absent in PS. Therefore, we hypothesized OB change may be useful in differential diagnosis. 3D fast imaging employing steady-state acquisition (FIESTA) results in good delineation of cranial nerves, however, no study demonstrated OB volume change between PD and PS using 3D-FIESTA. Our purpose is to determine whether OB measurement on 3D-FIESTA is useful for differentiating PD from PS.

#### METHODS AND MATERIALS

Sixty-four PD (mean age  $\pm$  SD: 71.5  $\pm$  9.4), 8 MSA (68.9  $\pm$  8.9), 10 PSP (75.9  $\pm$  8.3), and 8 CBS (73.8  $\pm$  8.9) patients were recruited. Thirty-three healthy subjects (HS) (63.8  $\pm$  18.6) were also recruited as normal controls. The diagnoses were made according to the diagnostic criteria by an experienced neurologist. The parameter of 3D-FIESTA is following: 3T SIGMA Premier (GE), FA 45deg, TR 4ms, TE 2ms, matrix 512 $\times$ 512, slice thickness 1.0mm, scan time 2:27, spatial resolution: 0.6 $\times$ 0.6 $\times$ 0.8 mm. The cross-sectional area of the OB was measured using manual ROI method, and we used maximum area of OB in coronal plane. The average of bilateral OB was calculated for each subject. We performed group comparison and diagnostic accuracy test using Welch's t test and ROC analysis, respectively. All statistics were performed with BellCurve for Excel (Social Survey Research Information Co., Ltd.).

#### RESULTS

The mean area of OB was significantly smaller for PD patients (mean area  $\pm$  SD mm<sup>2</sup>: 4.1  $\pm$  1.0) than for HSs (6.6  $\pm$  1.4,  $p$ <0.01). Moreover, that of PD were also significantly smaller than that of MSA (6.0  $\pm$  1.4,  $p$ =.007), PSP (4.8  $\pm$  0.9,  $p$ =.03), and CBS (5.3  $\pm$  1.2,  $p$ =.03), respectively (Figure 1 and 2). The ROC analyses showed that good diagnostic performance, especially in analysis of PD vs MSA (AUC: 0.874, optimal cut off points: 5.6 mm<sup>2</sup>, sensitivity: 93.8%, specificity: 87.5%).

#### CONCLUSION

Our results suggest the OB volume loss in PD, which may reflect degeneration due to deposition of Lewy body. OB volumetry using 3D-FIESTA can be useful to differentiate PD from PS, especially for MSA.

#### CLINICAL RELEVANCE/APPLICATION

OB volumetry with 3D-FIESTA may contribute precise diagnoses in PD and PS showing atypical MR findings. 3D-FIESTA is a common and widespread MR technique, which can work as clinical routine MR application in patients with Parkinsonism.

Printed on: 02/07/23

## Abstract Archives of the RSNA, 2022

M2-SPNR-7

### Altered Cerebral Blood Flow in Spinocerebellar Degeneration Patients

Monday, Nov. 28 9:00AM - 9:30AM Room: Learning Center - NR DPS

#### Participants

Bing Liu, Beijing, China (*Presenter*) Nothing to Disclose

#### PURPOSE

Spinocerebellar degeneration (SCD) comprises a multitude of disorders with sporadic and hereditary forms, including spinocerebellar ataxia (SCA), cerebellum-type of multiple system atrophy (MSA) and more complex phenotypes. Except for progressive cerebellar ataxia and structural atrophy, hemodynamic changes have also been demonstrated in SCD. This study aimed to clarify the whole-brain altered patterns of cerebral blood flow (CBF) and its correlations with disease severity and emotional abnormalities in SCD via arterial spin labeling (ASL).

#### METHODS AND MATERIALS

Thirty SCD patients and 30 age- and sex-matched healthy controls (HC) were prospectively recruited to undergo ASL examinations in a 3.0T MR scanner. The Scale for Assessment and Rating of Ataxia (SARA) and the International Cooperative Ataxia Rating Scale (ICARS) scores were used to reflect the disease severity in SCD patients. Additionally, the status of anxiety and depression among all patients were evaluated by the Self-Rating Anxiety Scale (SAS) and the Self-Rating Depression Scale (SDS). We compared the whole-brain CBF between SCD group and HC group at voxel level. And the ROI-based correlation analyses between CBF and disease severity as well as emotional abnormalities were performed for SCD group.

#### RESULTS

Compared with HC, SCD patients exhibited decreased CBF in two clusters (FWE corrected  $P < 0.05$ ), covering bilateral dentate and fastigii nuclei, lobule VIX, lobule VX, bilateral lobule HI-IV and lobule HIX, left lobule HVI and right lobule HVIIIb as Cluster1 and the dorsal part of raphe nucleus in midbrain as Cluster2. The CBF of Cluster 1 was negatively correlated with SARA scores (Spearman's  $\rho = -0.374$ ,  $P = 0.042$ ) and SDS standard scores (Spearman's  $\rho = -0.388$ ,  $P = 0.034$ ), respectively. While the CBF of Cluster2 also had negative correlations with SARA scores (Spearman's  $\rho = -0.370$ ,  $P = 0.044$ ) and ICARS scores (Pearson  $r = -0.464$ ,  $P = 0.010$ ).

#### CONCLUSION

s The SCD-related whole-brain CBF changes were mainly involved in cerebellum and midbrain, partially overlapped with hand, foot and tongue movement activations areas. Decreased CBF was related to disease severity and depression status in SCD. Therefore, CBF may be a promising neuroimaging biomarker to reflect the severity of neurodegeneration and to provide warnings for emotional changes.

#### CLINICAL RELEVANCE/APPLICATION

Decreased CBF in cerebellum and midbrain were associated with disease severity and depression level in SCD, which may help reflect the degree of neurodegeneration in vivo, and give early warnings for SCD-related depression.

Printed on: 02/07/23

## Abstract Archives of the RSNA, 2022

M2-SPNR-8

### Diagnostic Performance of Susceptibility Map-weighted MRI According to Acquisition Plane for Differentiating Neurodegenerative Parkinsonism

Monday, Nov. 28 9:00AM - 9:30AM Room: Learning Center - NR DPS

#### Participants

Suiji Lee, MD, Seoul, Korea, Republic Of (*Presenter*) Nothing to Disclose

#### PURPOSE

To evaluate the diagnostic performance of SMwI according to the acquisition plane for differentiating neurodegenerative parkinsonism.

#### METHODS AND MATERIALS

This retrospective, observational, single-institution study included patients who were consecutively enrolled from those who visited movement disorder clinics and underwent both brain MRI and 18F-FP-CIT with clinical symptoms of suspected parkinsonism between September 2021 and December 2021. Both oblique coronal plane (vertical to the midbrain) and anterior commissure-posterior commissure (AC-PC) plane of SMwI were acquired. Abnormality was determined when there was any hypointense area that obliterated the differentiation of the three layers and classified into 3 categories (0: normal, 1: intermediate, 2: abnormal) by two neuroradiologists. 18F-FP-CIT PET served as the reference standard. The diagnostic performance of the oblique plane and AC-PC plane of SMwI were assessed per substantia nigra and per participant. Inter-rater agreement was assessed using Cohen's kappa coefficient. McNemar's test was used to test the diagnostic performance of oblique coronal plane and AC-PC plane of SMwI.

#### RESULTS

Total 194 patients (mean age  $\pm$  SD, 67  $\pm$ 10 years, 91 men) were included. Among them, 84 patients were diagnosed with IPD, 26 with MSA, 3 with PSP, 10 with CBS, 35 with ET, 10 with DIP, 4 with NPH and 22 with others. The overall inter-rater agreement for both oblique and AC-PC plane was good ( $\kappa = 0.747$  and  $0.758$  for each,  $P < .001$ ). In per participant analysis, the overall inter-rater agreement for both oblique and AC-PC plane was good ( $\kappa = 0.747$  and  $0.758$  for each,  $P < .001$ ). For reader 1, the overall sensitivity of the oblique plane was 89.9% and that of the AC-PC plane was 91.7% ( $P = .727$ ). The overall specificity of the oblique plane was 87.1% and that of AC-PC plane was 88.2% ( $P = .727$ ). The overall accuracy of the oblique plane was 88.7% and that of AC-PC plane was 90.2%, with p-value of 0.607. Reader 2 demonstrated similar results. For both readers, there was no significant difference of sensitivity, specificity and accuracy between the oblique plane and the AC-PC plane.

#### CONCLUSION

There was no significant difference of diagnostic performance between the oblique plane and the AC-PC plane of SMwI in differentiating parkinsonism.

#### CLINICAL RELEVANCE/APPLICATION

This study assures clinics can choose any one of MRI acquisition planes of SMwI between oblique plane and AC-PC plane according to their clinical settings in the diagnosis of parkinsonism.

Printed on: 02/07/23

## Abstract Archives of the RSNA, 2022

M2-SPNR-9

### **Brain Connectivity Changes in Resting-State Functional MRI in Patients with HIV-Associated Neurocognitive Disorder (HAND): A Multi-voxel Pattern Analysis (MVPA) Approach Using Mutual Connectivity Analysis (MCA)**

Monday, Nov. 28 9:00AM - 9:30AM Room: Learning Center - NR DPS

#### **Participants**

Ali Vosoughi, Rochester, NY (*Presenter*) Nothing to Disclose

#### **PURPOSE**

To develop and evaluate a novel machine learning framework for identifying subjects with HIV-Associated Neurocognitive Disorder (HAND) using Mutual Connectivity Analysis (MCA) by capturing connectivity differences in resting-state functional MRI (rsfMRI).

#### **METHODS AND MATERIALS**

Resting-state fMRI scans (3T, EPI sequence, TR=1.65s, 250 acquisitions) were acquired in a cohort of 45 age-matched subjects (20 healthy, 25 HIV+, 16 of whom had HAND symptoms (HAND+)). After pre-processing, data was parcellated into 90 regions using the Automated Anatomical Labeling atlas. Regions were represented by their average time-series. A nonlinear machine learning connectivity analysis method (MCA [Citation blinded for review]), was used to quantify interdependence of region-specific time-series producing a 8100-element connectivity matrix. Generalized matrix learning vector quantization feature selection revealed regional connections that were most different between the groups. These were used for subsequent identification of HAND+ subjects using an adaptive boosting classifier in a Multi-Voxel Pattern Analysis (MVPA) framework. For both feature selection and classification, strict data separation (90% train/10% test) was carried out in a 100-iteration cross-validation scheme. For comparison, MCA was evaluated against the clinical standard technique of functional connectivity analysis using cross-correlating (CC) low-pass filtered fMRI time-series. Area Under the Curve (AUC) for Receiver Operator Characteristics (ROC) analysis was used to quantitatively evaluate diagnostic quality of HAND+ subject classification.

#### **RESULTS**

The MCA rsfMRI connectivity analysis method clearly outperformed the clinical standard CC technique in identifying HAND+ subjects with AUC of  $0.85 \pm 0.27$  for MCA, and  $0.71 \pm 0.31$  for CC, respectively. Diagnostic quality differences between both methods were statistically significant ( $p < 0.05$ , Wilcoxon signed-rank test).

#### **CONCLUSION**

Our results suggest that MCA significantly improves the diagnostic accuracy of identification of patients with HAND based on rsfMRI neuroimaging. We conclude that, when compared to conventional CC analysis, our MVPA framework is better suited to capture disease-related brain network connectivity changes in HAND.

#### **CLINICAL RELEVANCE/APPLICATION**

The MCA method classifies HAND+ subjects and controls by identifying relevant changes in fMRI connectivity. Such changes can be useful diagnostic imaging biomarkers for HIV-related neurologic disease.

Printed on: 02/07/23

## Abstract Archives of the RSNA, 2022

M2-SPOB

### OB/Gynecology Monday Poster Discussions

Monday, Nov. 28 9:00AM - 9:30AM Room: Learning Center - OB DPS

#### Participants

Dorothy Shum, MD, San Francisco, CA (*Moderator*) Nothing to Disclose

#### Sub-Events

#### M2-SPOB-1 Assessment of Fetoplacental Unit by Intravoxel Incoherent Motion MRI: Diffusion and Perfusion Properties of Fetal Lungs and Placenta in Intrauterine Growth Restriction

#### Participants

Roberta Ninkova, MD, Rome, Italy (*Presenter*) Nothing to Disclose

#### PURPOSE

To investigate the potential use of Intravoxel Incoherent Motion (IVIM) imaging in the study of microperfusion and microstructural characteristics of fetal lungs and placenta in IUGR fetuses, comparing IVIM parameters with those of a healthy control group.

#### METHODS AND MATERIALS

Eighty-eight pregnancies (26 IUGR; 62 normal) will be enrolled. MR examinations will be performed at 1.5 T, using a DWI sequence with 10 different b-values (0,10,30,50,75,100,200,400,700,1000 s/mm<sup>2</sup>). For each fetus, two bilateral ROIs will be manually placed in lung parenchyma; six ROIs will be placed on both fetal and maternal sides of each placenta. Differences of mean values of perfusion fraction f, diffusion coefficient D, and pseudo-diffusion coefficient D\* and their correlation with Gestational Age (GA) and Birth Weight (BW) will be investigated in both IUGR and control group.

#### RESULTS

- In fetal lungs, we found a significant difference in f mean values between IUGR fetuses and the healthy control group ( $p=0.0000004$ ). No statistically significant difference was observed for D and D\* values. In normal fetuses we found a positive correlation between f and GA ( $p<001$ ); no correlation with GA was found in pathological fetuses.- Concerning the placenta, in the fetal side of placenta f and D\* allowed to discriminate SGA (Small for Gestational Age) from real FGR (Fetal Growth Restriction) ( $p=0.021$ ;  $p=0.036$ , respectively), with FGR showing lower values. SGA showed intermediate impaired perfusion pattern in terms of f and D\* compared to FGR and healthy controls. A significant positive correlation was found between f and BW in IUGR fetuses. A significant negative correlation was found between D and GA in IUGR fetuses.

#### CONCLUSION

s Complex interactions between placental and fetal environments ensure normal fetal growth. Impairment of the fetoplacental unit may lead to Intrauterine Growth Restriction (IUGR), which is associated with perinatal morbidity and mortality, neonatal complications such as ARDS, and long-term complications, like cardiovascular disease and neurodevelopmental delay. Preliminary results show that IVIM parameters, with special regard to perfusion fraction f, may be potential in vivo biomarkers to discriminate between IUGR and healthy fetuses, and correlate with GA and BW.

#### CLINICAL RELEVANCE/APPLICATION

The development of new non-invasive techniques for prompt and accurate prenatal diagnosis is critical to improve the prenatal and postnatal outcomes of IUGR fetuses. The clinical significance of IVIM-MRI may lie in providing in vivo imaging biomarkers of IUGR severity useful in predicting perinatal outcome and guiding treatment decisions.

Printed on: 02/07/23

## Abstract Archives of the RSNA, 2022

M2-SPOB-1

### Assessment of Fetoplacental Unit by Intravoxel Incoherent Motion MRI: Diffusion and Perfusion Properties of Fetal Lungs and Placenta in Intrauterine Growth Restriction

Monday, Nov. 28 9:00AM - 9:30AM Room: Learning Center - OB DPS

#### Participants

Roberta Ninkova, MD, Rome, Italy (*Presenter*) Nothing to Disclose

#### PURPOSE

To investigate the potential use of Intravoxel Incoherent Motion (IVIM) imaging in the study of microperfusion and microstructural characteristics of fetal lungs and placenta in IUGR fetuses, comparing IVIM parameters with those of a healthy control group.

#### METHODS AND MATERIALS

Eighty-eight pregnancies (26 IUGR; 62 normal) will be enrolled. MR examinations will be performed at 1.5 T, using a DWI sequence with 10 different b-values (0,10,30,50,75,100,200,400,700,1000 s/mm<sup>2</sup>). For each fetus, two bilateral ROIs will be manually placed in lung parenchyma; six ROIs will be placed on both fetal and maternal sides of each placenta. Differences of mean values of perfusion fraction f, diffusion coefficient D, and pseudo-diffusion coefficient D\* and their correlation with Gestational Age (GA) and Birth Weight (BW) will be investigated in both IUGR and control group.

#### RESULTS

- In fetal lungs, we found a significant difference in f mean values between IUGR fetuses and the healthy control group ( $p=0.0000004$ ). No statistically significant difference was observed for D and D\* values. In normal fetuses we found a positive correlation between f and GA ( $p<0.001$ ); no correlation with GA was found in pathological fetuses.- Concerning the placenta, in the fetal side of placenta f and D\* allowed to discriminate SGA (Small for Gestational Age) from real FGR (Fetal Growth Restriction) ( $p=0.021$ ;  $p=0.036$ , respectively), with FGR showing lower values. SGA showed intermediate impaired perfusion pattern in terms of f and D\* compared to FGR and healthy controls. A significant positive correlation was found between f and BW in IUGR fetuses. A significant negative correlation was found between D and GA in IUGR fetuses.

#### CONCLUSION

s Complex interactions between placental and fetal environments ensure normal fetal growth. Impairment of the fetoplacental unit may lead to Intrauterine Growth Restriction (IUGR), which is associated with perinatal morbidity and mortality, neonatal complications such as ARDS, and long-term complications, like cardiovascular disease and neurodevelopmental delay. Preliminary results show that IVIM parameters, with special regard to perfusion fraction f, may be potential in vivo biomarkers to discriminate between IUGR and healthy fetuses, and correlate with GA and BW.

#### CLINICAL RELEVANCE/APPLICATION

The development of new non-invasive techniques for prompt and accurate prenatal diagnosis is critical to improve the prenatal and postnatal outcomes of IUGR fetuses. The clinical significance of IVIM-MRI may lie in providing in vivo imaging biomarkers of IUGR severity useful in predicting perinatal outcome and guiding treatment decisions.

Printed on: 02/07/23

## Abstract Archives of the RSNA, 2022

M2-SPPD

### Pediatric Monday Poster Discussions

Monday, Nov. 28 9:00AM - 9:30AM Room: Learning Center - PD DPS

#### Participants

Usha D. Nagaraj, MD, Cincinnati, OH (*Moderator*) Author with royalties, Reed Elsevier;

#### Sub-Events

### M2-SPPD-2 Radiogenomics in Pediatric Neuroblastoma: Radiomics Signature With Imaging Features Based on Computed Tomography in Predicting Segmental Chromosomal Aberrations at 1p36 and 11q23

#### Participants

Haoru Wang, (*Presenter*) Nothing to Disclose

#### PURPOSE

To build and evaluate a CT-based radiomics signature with imaging features in predicting SCAs status at 1p36 and 11q23 in pediatric neuroblastoma.

#### METHODS AND MATERIALS

Eighty-seven neuroblastoma patients with detection of SCAs at 1p36 and 11q23 were retrospectively enrolled and randomly stratified into training set (n=60) and test set (n=27). Clinical factors were analyzed and then selected using univariate and multivariate logistic regression analysis. Lesion regions of interest were manually delineated on three-phase CT images, and radiomics features were extracted automatically and selected. Clinical model, radiomics signature and clinical radiomics nomogram were established respectively on the basis of selected clinical factors and radiomics features. The receiver operating characteristic curve analysis and decision curve analysis were used to evaluate the predictive performance of each model.

#### RESULTS

The constructed radiomics signature was composed of eight radiomics features, with area under the curve (AUC) of 0.869 (95% confidence interval [CI]: 0.786, 0.941) and 0.883 (95%CI: 0.761, 0.983) in the training and test sets respectively. The nomogram incorporated of shape, ratio of mean CT values between tumor parenchyma and paraspinal muscle ( $T_{\text{mean}}/\text{muscle}$ ) at venous phase and radiomics signature had better diagnostic efficacy in predicting SCAs compared to the clinical model for training (AUC, 0.893 vs. 0.791) and test (AUC, 0.861 vs. 0.750) sets. Decision curve analysis showed that the nomogram had better clinical practicability than the clinical model alone.

#### CONCLUSION

There are certain relevance between CT imaging features and SCAs status in pediatric neuroblastoma. The CT-based radiomics signature could be helpful for predicting SCAs in neuroblastoma. The nomogram incorporated of shape,  $T_{\text{mean}}/\text{muscle}$  at venous phase and radiomics signature performs better than clinical model in predicting SCAs in neuroblastoma.

#### CLINICAL RELEVANCE/APPLICATION

We used radiomics to predict segmental chromosomal aberrations at 1p36 and 11q23 in pediatric neuroblastoma, and found that radiomics is able to predict segmental chromosomal aberrations at 1p36 and 11q23, which could provide a non-invasive method to predict genomic profiles in neuroblastoma. Meanwhile, we found imaging features based on computed tomography correlate with segmental chromosomal aberrations at 1p36 and 11q23 in neuroblastoma, and this finding is useful to direct clinical decisions and management.

Printed on: 02/07/23

## Abstract Archives of the RSNA, 2022

M2-SPPD-2

### **Radiogenomics in Pediatric Neuroblastoma: Radiomics Signature With Imaging Features Based on Computed Tomography in Predicting Segmental Chromosomal Aberrations at 1p36 and 11q23**

Monday, Nov. 28 9:00AM - 9:30AM Room: Learning Center - PD DPS

#### **Participants**

Haoru Wang, (*Presenter*) Nothing to Disclose

#### **PURPOSE**

To build and evaluate a CT-based radiomics signature with imaging features in predicting SCAs status at 1p36 and 11q23 in pediatric neuroblastoma.

#### **METHODS AND MATERIALS**

Eighty-seven neuroblastoma patients with detection of SCAs at 1p36 and 11q23 were retrospectively enrolled and randomly stratified into training set (n=60) and test set (n=27). Clinical factors were analyzed and then selected using univariate and multivariate logistic regression analysis. Lesion regions of interest were manually delineated on three-phase CT images, and radiomics features were extracted automatically and selected. Clinical model, radiomics signature and clinical radiomics nomogram were established respectively on the basis of selected clinical factors and radiomics features. The receiver operating characteristic curve analysis and decision curve analysis were used to evaluate the predictive performance of each model.

#### **RESULTS**

The constructed radiomics signature was composed of eight radiomics features, with area under the curve (AUC) of 0.869 (95% confidence interval [CI]: 0.786, 0.941) and 0.883 (95%CI: 0.761, 0.983) in the training and test sets respectively. The nomogram incorporated of shape, ratio of mean CT values between tumor parenchyma and paraspinal muscle (Tmean/muscle) at venous phase and radiomics signature had better diagnostic efficacy in predicting SCAs compared to the clinical model for training (AUC, 0.893 vs. 0.791) and test (AUC, 0.861 vs. 0.750) sets. Decision curve analysis showed that the nomogram had better clinical practicability than the clinical model alone.

#### **CONCLUSION**

There are certain relevance between CT imaging features and SCAs status in pediatric neuroblastoma. The CT-based radiomics signature could be helpful for predicting SCAs in neuroblastoma. The nomogram incorporated of shape, Tmean/muscle at venous phase and radiomics signature performs better than clinical model in predicting SCAs in neuroblastoma.

#### **CLINICAL RELEVANCE/APPLICATION**

We used radiomics to predict segmental chromosomal aberrations at 1p36 and 11q23 in pediatric neuroblastoma, and found that radiomics is able to predict segmental chromosomal aberrations at 1p36 and 11q23, which could provide a non-invasive method to predict genomic profiles in neuroblastoma. Meanwhile, we found imaging features based on computed tomography correlate with segmental chromosomal aberrations at 1p36 and 11q23 in neuroblastoma, and this finding is useful to direct clinical decisions and management.

Printed on: 02/07/23

## Abstract Archives of the RSNA, 2022

M2-SPPH

### Physics Monday Poster Discussions

Monday, Nov. 28 9:00AM - 9:30AM Room: Learning Center - PH DPS

#### Participants

Ingrid Reiser, PhD, Chicago, IL (*Moderator*) Family member, Employee, Clarix Imaging

#### Sub-Events

### M2-SPPH-1 Differentiating Patients With Diabetes Mellitus With Pancreatic Extracellular Volume Fraction and Normalized Iodine Concentration Acquired by Dual Energy CT

#### Participants

Xiaoyi Cai, MBBS, (*Presenter*) Nothing to Disclose

#### PURPOSE

To investigate the feasibility of extracellular volume (ECV) fraction and normalized iodine concentration (nIC) using dual energy CT (DECT) to evaluate diabetic patients.

#### METHODS AND MATERIALS

106 patients with known or suspected abdominal disease underwent abdominal precontrast CT scan (120kV) and DECT enhanced scan. Patients were divided into three groups according to the American Diabetes Association criteria: non-diabetes group (HbA1c < 5.7%, 31 patients), pre-diabetes group (5.7% = HbA1c < 6.5%, 36 patients) and diabetes group (HbA1c = 6.5%, 39 patients). Two ECV fractions (ECV-HU = (HUpancreas - equilibrium phase - HUpancreas - precontrast) / (HUabdominal aorta - equilibrium phase - HUabdominal aorta - precontrast) × (100-Hct), ECV-ID = (IDpancrease - equilibrium phase / IDabdominal aorta - equilibrium phase) × (100-Hct)) and the nIC (nIC = ICpancrease - equilibrium phase / ICabdominal aorta - equilibrium phase) of the pancreas were calculated. The correlations of pancreatic ECV-HU, ECV-ID, and nIC with HbA1c value were analyzed by Spearman rank correlation. Pancreatic ECV-HU, ECV-ID and nIC among groups were compared by one-way ANOVA. The diagnostic performance of pancreatic ECV-HU, ECV-ID, and nIC was evaluated by receiver operating characteristic (ROC) curve analysis.

#### RESULTS

In the whole patients, HbA1c was moderately positively correlated with ECV-HU, ECV-ID and nIC ( $r_s = 0.447$ ,  $r_s = 0.541$ ,  $r_s = 0.533$ , respectively; all  $P < 0.001$ ). The pancreatic ECV-HU, ECV-ID and nIC in diabetes group were significantly higher than those in non-diabetes group and pre-diabetes group (all  $P < 0.001$ ). The combination of ECV-ID and nIC has the highest area under the curve (AUC), sensitivity and specificity in differentiating non-diabetic or pre-diabetes from diabetic patients (0.876, 76.9% and 83.9%; 0.820, 71.8% and 88.9%, respectively). Furthermore, in differentiating non-diabetes or pre-diabetes from diabetes group, the AUC was superior in ECV-ID vs. ECV-HU (0.851 vs. 0.799 and 0.787 vs. 0.741, respectively).

#### CONCLUSION

Combined application of pancreatic ECV-ID and nIC is a potential imaging index to evaluate diabetic patients.

#### CLINICAL RELEVANCE/APPLICATION

The diagnosis of diabetes mellitus was associated with pancreatic imaging biomarkers, such as ECV and nIC, which may provide new insights into clinical practice.

### M2-SPPH-2 Impact of Patient Habitus and Energy-Bin Weighting on Monochromatic Image Quality for Photon-Counting CT

#### Participants

Paul E. Kinahan, PhD, Seattle, WA (*Presenter*) Co-founder, PET/X LLC

#### PURPOSE

Photon-counting x-ray computed tomography (PCCT) is a new technology that has the potential to improve clinically relevant image properties such as bias and noise. However, the image reconstruction algorithm must account for energy-dependent physical effects, including Compton scattering in the detectors for the case of silicon-based scanners. We investigated the effects of combining post-log projection data from different edge-on silicon-based PCCT energy bins to form virtual mono-energetic images by minimizing the root-mean-squared error (RMSE).

#### METHODS AND MATERIALS

PCCT and monochromatic images were simulated using the Catsim software package. The XCAT phantom served as a vector-based input to the simulations. Optimization of the projection data weighting and image analysis was done in MATLAB. The patient habitus was varied by modifying the XCAT fields to generate three patient sizes defined as "small", "medium", and "large". For each phantom size, two Catsim simulations were performed: one having a monochromatic x-ray spectrum with standard detection, and one having a full bremsstrahlung spectrum and edge-on silicon-based PCCT detectors that included a model for Compton scatter.

Using a least-squares cost function, PCCT sinograms corresponding to different photon energies were combined to match the monochromatic sinograms at each of the three sizes. These "synthetic monochromatic sinograms" were then reconstructed. The RMSE was computed using the monochromatic images as ground truth.

## RESULTS

The optimal weights for recombining multiple PCCT energy bin sinograms were object dependent. When size-specific weights were used, the RMSEs over all phantom pixels were 22, 41 and 53 HU for the three respective phantom sizes. However, if the coefficients were fixed to those optimal for the medium phantom, the RMSEs for the smaller and larger increased to 28 and 60 HU respectively. For some imaging techniques, photon starvation artifacts would appear for sub-optimal weights.

## CONCLUSION

For PCCT reconstruction algorithms that aim to estimate monochromatic CT data by simple weighting of energy bin sinograms, the use of fixed coefficients will lead to increased noise and artifacts for varying patient sizes.

## CLINICAL RELEVANCE/APPLICATION

Photon-counting CT scanners have a dramatic increase in the amount of spectral (energy) information generated compared to standard energy-integrating CT scanners, even those operated in dual-kVp mode. With this rich source of energy data, there are many new parameters to be evaluated and ideally optimized. This study evaluates one such set of

## M2-SPPH-3 Reporting on Methodology in Dual Energy CT Studies: A Systematic Literature Review

### Participants

Nils Grosse Hokamp, MD, MBA, Koln, Germany (*Presenter*) Research Grant, Koninklijke Philips NV; Speakers Bureau, Koninklijke Philips NV; Consultant, Bristol-Myers Squibb Company

### PURPOSE

The objective of this study was to perform a structured literature review to assess how image acquisition parameters and technical details are reported in clinical dual-energy CT (DECT) studies.

### METHODS AND MATERIALS

A structured query of the PubMed meta-database was performed that covered all studies between the years 2016 and 2020 with a potential utilization of a dual-energy system. After inclusion, the described dual-energy CT methodology was recorded in a structured approach for each study with particular attention to scanning and reconstruction parameters.

### RESULTS

A total of 864 out of 2742 studies were eligible for inclusion. The DECT approach that was used was reported in 87% of all studies, while in 98% of all studies at least the vendor of the DECT system was specified. In most studies, a dual-source system was used (44%), followed by kVp switching (34%) and dual-layer systems (15%), with the remainder using multiple systems or twinbeam technology. The average number of patients included was  $83 \pm 213$ . Data on mAS was reported in 70%, data on tube voltage in 78%, data on gantry rotation time in 60%, data on collimation in 57%, and data on pitch in 60% of the studies.

### CONCLUSION

In dual-energy CT studies between 2016 and 2020, the technical parameters of image acquisition as well as reconstruction parameters are frequently only partially specified, which may significantly limit reproducibility.

### CLINICAL RELEVANCE/APPLICATION

With the increasing complexity of technological concepts to Dual-Energy CT imaging, more caution has to be taken when describing methodology of scientific studies. Only complete details on image acquisition and image reconstruction will allow for transferability of findings among sites and from research into clinics, eventually.

## M2-SPPH-5 Prior-Information-Inspired Deep Learning Noise Reduction for Coronary CT Angiography Acquired with a Photon Counting Detector CT

### Participants

Shaojie Chang, PhD, ROCHESTER, MN (*Presenter*) Nothing to Disclose

### PURPOSE

To develop a deep learning technique that utilizes prior information to reduce noise in high-resolution, photon-counting-detector (PCD) CT coronary CT angiography (CTA).

### METHODS AND MATERIALS

Clinical coronary CTA exams acquired on a PCD-CT (NAEOTOM Alpha, Siemens Healthcare) were considered in this study. Virtual monoenergetic images (VMIs) at different energies (50, 70, 100 keV) were reconstructed using both filtered back projection (FBP) and iterative reconstruction (IR) algorithms, 0.6 mm slice thickness, and a sharp kernel (Bv68). The FBP and IR images were subtracted to generate images composed predominately of noise. The lower noise 70 keV VMI images served as the prior images. To obtain a relatively low-noise signal reference, adjacent IR images and prior images were averaged to simulate thicker slice images (1.5 mm). A convolutional neural network (CNN) was constructed based on a U-Net architecture with mean square error loss. CNN inputs consisted of (1) noise-only images superimposed onto the signal reference images and (2) the prior images. Spatial decoupling between the noise-only image and signal reference was used to avoid overfitting and reduce propagation of IR deficiencies into the CNN model. Image patches of 128x128 pixels were extracted from all available training data and standard data augmentation techniques were applied. Training targets consisted of the signal reference without added noise. Denoising strength was controlled by a weighting factor of the noise patch. The resulting CNN was applied to the original thin slice and sharp kernel FBP images.

### RESULTS

FBP images showed very high noise at all VMI energies given the sharp kernel. While IR images substantially reduced image noise

compared to FBP, noise texture was altered and a patchy appearance was observed. The proposed CNN framework provided strong noise reduction, by  $95 \pm 1$  % relative to FBP and by  $60 \pm 3$  % relative to IR, while maintaining a natural noise texture without a patchy appearance. Additionally, image properties unique to each VMI energy were retained, with increased contrast signal at 50 keV, and decreased calcium blooming at 100 keV.

## CONCLUSION

This prior information inspired CNN framework fully utilized the PCD-CT data along the energy axis to achieve substantial noise reduction while preserving the VMI's properties.

## CLINICAL RELEVANCE/APPLICATION

Improved PCD-CT coronary CTA image quality at different energies is beneficial for improving visualization of non-calcific plaques using low keV VMI and reduction of calcium/stent blooming using high keV VMI.

### M2-SPPH-6 Development of a Dose- And Size- Independent Deep Learning Based Material Decomposition Algorithm Using Photon-Counting CT Images

Participants

Jayasai Rajagopal, BA, Durham, NC (*Presenter*) Nothing to Disclose

## PURPOSE

To develop a material decomposition technique that can accurately characterize k-edge materials in the presence of variable dose conditions

## METHODS AND MATERIALS

Image data was generated using a validated simulation platform (DukeSim, Duke University) to emulate a clinical photon-counting CT system (NAEOTOM Alpha, Siemens Healthineers) with standardized acquisition parameters (120 kV, 20-65 keV detector thresholds). 4200 cases were acquired consisting of cylindrical phantoms at variable sizes (16, 24, 32, 40 cm diameter) containing inserts of iodine and gadolinium (0.25-20 mg/mL) in various configurations including vials with single materials and mixtures and simulated at several dose levels (3.9, 5.9, 11.7 mGy CTD<sub>Ivol</sub>). Dose and size parameters were selected to create variable image quality across the dataset. A convolutional neural network with a U-net architecture was trained using a subset of the cases to learn the relationship between the simulated images and the concentrations of iodine and gadolinium. The model used patch-wise training with a squared-error regression loss function. None of the material concentrations in the testing dataset were present in the training data. Model accuracy was measured by estimating bias and limits of agreement (LoA) in a Bland-Altman analysis and root-mean-square error (RMSE) of concentration estimates from the ground truth values.

## RESULTS

Image noise within vial regions-of-interest increased as dose decreased (32%). Testing results showed a good performance for estimating iodine (bias: -0.1, LoA: -0.6 - 0.4 mg/mL I) and gadolinium (bias: -0.02, LoA: -0.3 - 0.3 mg/mL Gd). RMSE showed an excellent overall performance for iodine (0.1 mg/mL) and gadolinium (0.1 mg/mL).

## CONCLUSION

A deep learning based material decomposition algorithm was able to accurately characterize iodine and gadolinium as single materials and mixtures. The algorithm maintained a desirable performance under low dose conditions.

## CLINICAL RELEVANCE/APPLICATION

A material decomposition technique that can reliably function at different dose levels can increase the clinical viability of material characterization for diagnostic purposes

### M2-SPPH-7 Performance Evaluation of Deep Learning Image Reconstruction for Dual Energy CT - Quantitative Accuracy and Noise Characteristics of Iodine Map

Participants

Benjamin Maloney, PhD, Detroit, MI (*Presenter*) Nothing to Disclose

## PURPOSE

To evaluate the performance of DLIR-GSI, a novel deep learning image reconstruction algorithm for dual energy CT, with a focus on quantitative accuracy and noise characteristics of its generated iodine maps at reduced radiation dose levels.

## METHODS AND MATERIALS

An anthropomorphic lung phantom (CTP698, The Phantom Laboratory) with an inserted syringe filled with iodine solution (ISOVUE 300 and saline mix) was scanned under GSI mode on a Revolution CT scanner (GE Healthcare). Six concentrations of iodine solution (range [1.7, 12.0] mgI/ml), and five CTD<sub>Ivol</sub> levels of CT scan (range [4.2, 19.0] mGy) were used in the experiment. For each scan, the iodine images were reconstructed using five different reconstruction algorithm settings, including FBP (standard), ASIR-V (40%), and DLIR (high, medium, and low strength settings). For each set of iodine images, the iodine concentration within the syringe was measured and its percentage difference relative to the reference value calculated. Also, repeated scans of the phantom without iodine inserts were performed, from which the noise power spectra (NPS) were measured from homogeneous background and the peak frequencies of their radial profiles determined.

## RESULTS

For all reconstruction settings, the largest percentage difference between the measured iodine concentration and the reference value occurred at both the lowest iodine concentration and the lowest CTD<sub>Ivol</sub>; the percentage differences from DLIR-GSI reconstructed images are  $3.6\% \pm 0.3\%$  (DLIR high),  $3.7\% \pm 0.5\%$  (DLIR medium),  $3.9\% \pm 0.6\%$  (DLIR low), compared to  $4.3\% \pm 1.0\%$  (FBP) and  $4.3\% \pm 0.8\%$  (ASIR-V). At the lowest CTD<sub>Ivol</sub>, the peak frequencies of NPS radial profiles from DLIR-GSI reconstructed iodine images are  $0.34 \pm 0.01$  mm<sup>-1</sup> (DLIR high),  $0.33 \pm 0.01$  mm<sup>-1</sup> (DLIR medium),  $0.34 \pm 0.01$  mm<sup>-1</sup> (DLIR low), compared to  $0.34 \pm 0.01$  mm<sup>-1</sup> (FBP) and  $0.30 \pm 0.01$  mm<sup>-1</sup> (ASIR-V).

## CONCLUSION

s The DLIR-GSI algorithm is capable of accurate quantification of iodine at both low iodine concentration and low radiation dose while maintaining the same noise texture as the traditional analytical reconstruction algorithm.

#### **CLINICAL RELEVANCE/APPLICATION**

It provides guidance for dual energy CT protocol optimization for accurate and reliable iodine quantification in clinical applications such as perfusion defect identification and lesion characterization in lung imaging.

#### **M2-SPPH-9 Feasibility of Small Pulmonary Nodule Detection and Characterization Using Edge-On-Irradiated Silicon Detector Photon-Counting CT**

Participants

Zhye Yin, Niskayuna, NY (*Presenter*) Employee, General Electric Company

#### **PURPOSE**

Advanced high-resolution CT is effective at assessing small pulmonary nodules down to 3–5mm in size during screening and oncology exams. However, the clinical value of such findings may be unclear without further tissue characterization. Photon-counting CT (PCCT) with edge-on-irradiated silicon detectors can simultaneously offer improved spectral capability (to enable characterization) and spatial resolution (to measure size). In this study, we demonstrate the feasibility of detecting and providing quantitative spectral characterization of small peripheral pulmonary lung nodules (<5mm) in a phantom study.

#### **METHODS AND MATERIALS**

An anthropomorphic phantom (Lungman, Kyoto Kagaku) with two sets of iodine rods (diameter 2–7mm), placed longitudinally at the peripheral regions of lung, were scanned using a prototype PCCT (GE Healthcare) at 120kVp and CTDIvol of 8.72mGy. Iodine rod concentrations were 1.7mg/ml and 3.0mg/ml. Material images were generated on a 1024×1024 image grid with standard and high-resolution kernels. Quantification accuracy for various nodule sizes was obtained for regions of interest (ROI) on iodine images. Nodule sizes were measured at monochromatic images at 70 keV.

#### **RESULTS**

In the iodine images, the ROI means and standard deviations for 5mm, 4mm, 3mm, and 2mm diameter rods with 3mg/ml concentration were 3.18mg/ml[0.51mg/ml], 3.12mg/ml[0.40mg/ml], 3.21mg/ml[1.32mg/ml], and 2.56mg/ml[1.25mg/ml], respectively. The respective nodule size measurements were 5.08mm, 3.87mm, 3.05mm and 1.94mm.

#### **CONCLUSION**

s Our results indicate that this PCCT prototype can provide, from a single scan, both nodule size and iodine quantification for small lung nodule detection and characterization. Edge-on-irradiated Si-based PCCT thus has the potential to provide additional information on small pulmonary nodules and could have a role in differentiating benign and malignant nodules, obviating the need for follow up imaging or biopsy.

#### **CLINICAL RELEVANCE/APPLICATION**

PCCT with simultaneous high spatial and spectral resolution can provide supplementary information on lung nodules smaller than 3–5mm and simplify the clinical decision process.

Printed on: 02/07/23

## Abstract Archives of the RSNA, 2022

M2-SPPH-1

### Differentiating Patients With Diabetes Mellitus With Pancreatic Extracellular Volume Fraction and Normalized Iodine Concentration Acquired by Dual Energy CT

Monday, Nov. 28 9:00AM - 9:30AM Room: Learning Center - PH DPS

#### Participants

Xiaoyi Cai, MBBS, (Presenter) Nothing to Disclose

#### PURPOSE

To investigate the feasibility of extracellular volume (ECV) fraction and normalized iodine concentration (nIC) using dual energy CT (DECT) to evaluate diabetic patients.

#### METHODS AND MATERIALS

106 patients with known or suspected abdominal disease underwent abdominal precontrast CT scan (120kV) and DECT enhanced scan. Patients were divided into three groups according to the American Diabetes Association criteria: non-diabetes group (HbA1c < 5.7%, 31 patients), pre-diabetes group (5.7% = HbA1c < 6.5%, 36 patients) and diabetes group (HbA1c = 6.5%, 39 patients). Two ECV fractions (ECV-HU = (HUpancreas -equilibrium phase - HUpancreas -precontrast) / (HUabdominal aorta -equilibrium phase - HUabdominal aorta -precontrast) × (100-Hct), ECV-ID = (IDpancrease -equilibrium phase / IDabdominal aorta -equilibrium phase) × (100-Hct)) and the nIC (nIC = ICpancrease-equilibrium phase / ICabdominal aorta-equilibrium phase) of the pancreas were calculated. The correlations of pancreatic ECV-HU, ECV-ID, and nIC with HbA1c value were analyzed by Spearman rank correlation. Pancreatic ECV-HU, ECV-ID and nIC among groups were compared by one-way ANOVA. The diagnostic performance of pancreatic ECV-HU, ECV-ID, and nIC was evaluated by receiver operating characteristic (ROC) curve analysis.

#### RESULTS

In the whole patients, HbA1c was moderately positively correlated with ECV-HU, ECV-ID and nIC (rs =0.447, rs =0.541, rs =0.533, respectively; all P < 0.001). The pancreatic ECV-HU, ECV-ID and nIC in diabetes group were significantly higher than those in non-diabetes group and pre-diabetes group (all P < 0.001). The combination of ECV-ID and nIC has the highest area under the curve (AUC), sensitivity and specificity in differentiating non-diabetic or pre-diabetes from diabetic patients (0.876, 76.9% and 83.9%; 0.820, 71.8% and 88.9%, respectively). Furthermore, in differentiating non-diabetes or pre-diabetes from diabetes group, the AUC was superior in ECV-ID vs. ECV-HU (0.851 vs. 0.799 and 0.787 vs. 0.741, respectively).

#### CONCLUSION

s Combined application of pancreatic ECV-ID and nIC is a potential imaging index to evaluate diabetic patients.

#### CLINICAL RELEVANCE/APPLICATION

The diagnosis of diabetes mellitus was associated with pancreatic imaging biomarkers, such as ECV and nIC, which may provide new insights into clinical practice.

Printed on: 02/07/23

## Abstract Archives of the RSNA, 2022

M2-SPPH-2

### Impact of Patient Habitus and Energy-Bin Weighting on Monochromatic Image Quality for Photon-Counting CT

Monday, Nov. 28 9:00AM - 9:30AM Room: Learning Center - PH DPS

#### Participants

Paul E. Kinahan, PhD, Seattle, WA (*Presenter*) Co-founder, PET/X LLC

#### PURPOSE

Photon-counting x-ray computed tomography (PCCT) is a new technology that has the potential to improve clinically relevant image properties such as bias and noise. However, the image reconstruction algorithm must account for energy-dependent physical effects, including Compton scattering in the detectors for the case of silicon-based scanners. We investigated the effects of combining post-log projection data from different edge-on silicon-based PCCT energy bins to form virtual mono-energetic images by minimizing the root-mean-squared error (RMSE).

#### METHODS AND MATERIALS

PCCT and monochromatic images were simulated using the Catsim software package. The XCAT phantom served as a vector-based input to the simulations. Optimization of the projection data weighting and image analysis was done in MATLAB. The patient habitus was varied by modifying the XCAT fields to generate three patient sizes defined as "small", "medium", and "large". For each phantom size, two Catsim simulations were performed: one having a monochromatic x-ray spectrum with standard detection, and one having a full bremsstrahlung spectrum and edge-on silicon-based PCCT detectors that included a model for Compton scatter. Using a least-squares cost function, PCCT sinograms corresponding to different photon energies were combined to match the monochromatic sinograms at each of the three sizes. These "synthetic monochromatic sinograms" were then reconstructed. The RMSE was computed using the monochromatic images as ground truth.

#### RESULTS

The optimal weights for recombining multiple PCCT energy bin sinograms were object dependent. When size-specific weights were used, the RMSEs over all phantom pixels were 22, 41 and 53 HU for the three respective phantom sizes. However, if the coefficients were fixed to those optimal for the medium phantom, the RMSEs for the smaller and larger increased to 28 and 60 HU respectively. For some imaging techniques, photon starvation artifacts would appear for sub-optimal weights.

#### CONCLUSION

For PCCT reconstruction algorithms that aim to estimate monochromatic CT data by simple weighting of energy bin sinograms, the use of fixed coefficients will lead to increased noise and artifacts for varying patient sizes.

#### CLINICAL RELEVANCE/APPLICATION

Photon-counting CT scanners have a dramatic increase in the amount of spectral (energy) information generated compared to standard energy-integrating CT scanners, even those operated in dual-kVp mode. With this rich source of energy data, there are many new parameters to be evaluated and ideally optimized. This study evaluates one such set of

Printed on: 02/07/23



## Abstract Archives of the RSNA, 2022

M2-SPPH-3

### Reporting on Methodology in Dual Energy CT Studies: A Systematic Literature Review

Monday, Nov. 28 9:00AM - 9:30AM Room: Learning Center - PH DPS

#### Participants

Nils Grosse Hokamp, MD, MBA, Koln, Germany (*Presenter*) Research Grant, Koninklijke Philips NV; Speakers Bureau, Koninklijke Philips NV; Consultant, Bristol-Myers Squibb Company

#### PURPOSE

The objective of this study was to perform a structured literature review to assess how image acquisition parameters and technical details are reported in clinical dual-energy CT (DECT) studies.

#### METHODS AND MATERIALS

A structured query of the PubMed meta-database was performed that covered all studies between the years 2016 and 2020 with a potential utilization of a dual-energy system. After inclusion, the described dual-energy CT methodology was recorded in a structured approach for each study with particular attention to scanning and reconstruction parameters.

#### RESULTS

A total of 864 out of 2742 studies were eligible for inclusion. The DECT approach that was used was reported in 87% of all studies, while in 98% of all studies at least the vendor of the DECT system was specified. In most studies, a dual-source system was used (44%), followed by kVp switching (34%) and dual-layer systems (15%), with the remainder using multiple systems or twinbeam technology. The average number of patients included was  $83 \pm 213$ . Data on mAS was reported in 70%, data on tube voltage in 78%, data on gantry rotation time in 60%, data on collimation in 57%, and data on pitch in 60% of the studies.

#### CONCLUSION

In dual-energy CT studies between 2016 and 2020, the technical parameters of image acquisition as well as reconstruction parameters are frequently only partially specified, which may significantly limit reproducibility.

#### CLINICAL RELEVANCE/APPLICATION

With the increasing complexity of technological concepts to Dual-Energy CT imaging, more caution has to be taken when describing methodology of scientific studies. Only complete details on image acquisition and image reconstruction will allow for transferability of findings among sites and from research into clinics, eventually.

Printed on: 02/07/23

## Abstract Archives of the RSNA, 2022

M2-SPPH-5

### Prior-Information-Inspired Deep Learning Noise Reduction for Coronary CT Angiography Acquired with a Photon Counting Detector CT

Monday, Nov. 28 9:00AM - 9:30AM Room: Learning Center - PH DPS

#### Participants

Shaojie Chang, PhD, ROCHESTER, MN (*Presenter*) Nothing to Disclose

#### PURPOSE

To develop a deep learning technique that utilizes prior information to reduce noise in high-resolution, photon-counting-detector (PCD) CT coronary CT angiography (CTA).

#### METHODS AND MATERIALS

Clinical coronary CTA exams acquired on a PCD-CT (NAEOTOM Alpha, Siemens Healthcare) were considered in this study. Virtual monoenergetic images (VMIs) at different energies (50, 70, 100 keV) were reconstructed using both filtered back projection (FBP) and iterative reconstruction (IR) algorithms, 0.6 mm slice thickness, and a sharp kernel (Bv68). The FBP and IR images were subtracted to generate images composed predominately of noise. The lower noise 70 keV VMI images served as the prior images. To obtain a relatively low-noise signal reference, adjacent IR images and prior images were averaged to simulate thicker slice images (1.5 mm). A convolutional neural network (CNN) was constructed based on a U-Net architecture with mean square error loss. CNN inputs consisted of (1) noise-only images superimposed onto the signal reference images and (2) the prior images. Spatial decoupling between the noise-only image and signal reference was used to avoid overfitting and reduce propagation of IR deficiencies into the CNN model. Image patches of 128x128 pixels were extracted from all available training data and standard data augmentation techniques were applied. Training targets consisted of the signal reference without added noise. Denoising strength was controlled by a weighting factor of the noise patch. The resulting CNN was applied to the original thin slice and sharp kernel FBP images.

#### RESULTS

FBP images showed very high noise at all VMI energies given the sharp kernel. While IR images substantially reduced image noise compared to FBP, noise texture was altered and a patchy appearance was observed. The proposed CNN framework provided strong noise reduction, by  $95 \pm 1\%$  relative to FBP and by  $60 \pm 3\%$  relative to IR, while maintaining a natural noise texture without a patchy appearance. Additionally, image properties unique to each VMI energy were retained, with increased contrast signal at 50 keV, and decreased calcium blooming at 100 keV.

#### CONCLUSION

This prior information inspired CNN framework fully utilized the PCD-CT data along the energy axis to achieve substantial noise reduction while preserving the VMI's properties.

#### CLINICAL RELEVANCE/APPLICATION

Improved PCD-CT coronary CTA image quality at different energies is beneficial for improving visualization of non-calcific plaques using low keV VMI and reduction of calcium/stent blooming using high keV VMI.

Printed on: 02/07/23

## Abstract Archives of the RSNA, 2022

M2-SPPH-6

### Development of a Dose- And Size- Independent Deep Learning Based Material Decomposition Algorithm Using Photon-Counting CT Images

Monday, Nov. 28 9:00AM - 9:30AM Room: Learning Center - PH DPS

#### Participants

Jayasai Rajagopal, BA, Durham, NC (*Presenter*) Nothing to Disclose

#### PURPOSE

To develop a material decomposition technique that can accurately characterize k-edge materials in the presence of variable dose conditions

#### METHODS AND MATERIALS

Image data was generated using a validated simulation platform (DukeSim, Duke University) to emulate a clinical photon-counting CT system (NAEOTOM Alpha, Siemens Healthineers) with standardized acquisition parameters (120 kV, 20-65 keV detector thresholds). 4200 cases were acquired consisting of cylindrical phantoms at variable sizes (16, 24, 32, 40 cm diameter) containing inserts of iodine and gadolinium (0.25-20 mg/mL) in various configurations including vials with single materials and mixtures and simulated at several dose levels (3.9, 5.9, 11.7 mGy CTDIvol). Dose and size parameters were selected to create variable image quality across the dataset. A convolutional neural network with a U-net architecture was trained using a subset of the cases to learn the relationship between the simulated images and the concentrations of iodine and gadolinium. The model used patch-wise training with a squared-error regression loss function. None of the material concentrations in the testing dataset were present in the training data. Model accuracy was measured by estimating bias and limits of agreement (LoA) in a Bland-Altman analysis and root-mean-square error (RMSE) of concentration estimates from the ground truth values.

#### RESULTS

Image noise within vial regions-of-interest increased as dose decreased (32%). Testing results showed a good performance for estimating iodine (bias: -0.1, LoA: -0.6 - 0.4 mg/mL I) and gadolinium (bias: -0.02, LoA: -0.3 - 0.3 mg/mL Gd). RMSE showed an excellent overall performance for iodine (0.1 mg/mL) and gadolinium (0.1 mg/mL).

#### CONCLUSION

A deep learning based material decomposition algorithm was able to accurately characterize iodine and gadolinium as single materials and mixtures. The algorithm maintained a desirable performance under low dose conditions.

#### CLINICAL RELEVANCE/APPLICATION

A material decomposition technique that can reliably function at different dose levels can increase the clinical viability of material characterization for diagnostic purposes

Printed on: 02/07/23

## Abstract Archives of the RSNA, 2022

M2-SPPH-7

### Performance Evaluation of Deep Learning Image Reconstruction for Dual Energy CT - Quantitative Accuracy and Noise Characteristics of Iodine Map

Monday, Nov. 28 9:00AM - 9:30AM Room: Learning Center - PH DPS

#### Participants

Benjamin Maloney, PhD, Detroit, MI (*Presenter*) Nothing to Disclose

#### PURPOSE

To evaluate the performance of DLIR-GSI, a novel deep learning image reconstruction algorithm for dual energy CT, with a focus on quantitative accuracy and noise characteristics of its generated iodine maps at reduced radiation dose levels.

#### METHODS AND MATERIALS

An anthropomorphic lung phantom (CTP698, The Phantom Laboratory) with an inserted syringe filled with iodine solution (ISOVUE 300 and saline mix) was scanned under GSI mode on a Revolution CT scanner (GE Healthcare). Six concentrations of iodine solution (range [1.7, 12.0] mgI/ml), and five CTDIvol levels of CT scan (range [4.2, 19.0] mGy) were used in the experiment. For each scan, the iodine images were reconstructed using five different reconstruction algorithm settings, including FBP (standard), ASIR-V (40%), and DLIR (high, medium, and low strength settings). For each set of iodine images, the iodine concentration within the syringe was measured and its percentage difference relative to the reference value calculated. Also, repeated scans of the phantom without iodine inserts were performed, from which the noise power spectra (NPS) were measured from homogeneous background and the peak frequencies of their radial profiles determined.

#### RESULTS

For all reconstruction settings, the largest percentage difference between the measured iodine concentration and the reference value occurred at both the lowest iodine concentration and the lowest CTDIvol; the percentage differences from DLIR-GSI reconstructed images are 3.6%±0.3% (DLIR high), 3.7%±0.5% (DLIR medium), 3.9%±0.6% (DLIR low), compared to 4.3%±1.0% (FBP) and 4.3%±0.8% (ASIR-V). At the lowest CTDIvol, the peak frequencies of NPS radial profiles from DLIR-GSI reconstructed iodine images are 0.34±0.01 mm<sup>-1</sup> (DLIR high), 0.33±0.01 mm<sup>-1</sup> (DLIR medium), 0.34±0.01 mm<sup>-1</sup> (DLIR low), compared to 0.34±0.01 mm<sup>-1</sup> (FBP) and 0.30±0.01 mm<sup>-1</sup> (ASIR-V).

#### CONCLUSION

The DLIR-GSI algorithm is capable of accurate quantification of iodine at both low iodine concentration and low radiation dose while maintaining the same noise texture as the traditional analytical reconstruction algorithm.

#### CLINICAL RELEVANCE/APPLICATION

It provides guidance for dual energy CT protocol optimization for accurate and reliable iodine quantification in clinical applications such as perfusion defect identification and lesion characterization in lung imaging.

Printed on: 02/07/23

## Abstract Archives of the RSNA, 2022

M2-SPPH-9

### Feasibility of Small Pulmonary Nodule Detection and Characterization Using Edge-On-Irradiated Silicon Detector Photon-Counting CT

Monday, Nov. 28 9:00AM - 9:30AM Room: Learning Center - PH DPS

#### Participants

Zhye Yin, Niskayuna, NY (*Presenter*) Employee, General Electric Company

#### PURPOSE

Advanced high-resolution CT is effective at assessing small pulmonary nodules down to 3–5mm in size during screening and oncology exams. However, the clinical value of such findings may be unclear without further tissue characterization. Photon-counting CT (PCCT) with edge-on-irradiated silicon detectors can simultaneously offer improved spectral capability (to enable characterization) and spatial resolution (to measure size). In this study, we demonstrate the feasibility of detecting and providing quantitative spectral characterization of small peripheral pulmonary lung nodules (<5mm) in a phantom study.

#### METHODS AND MATERIALS

An anthropomorphic phantom (Lungman, Kyoto Kagaku) with two sets of iodine rods (diameter 2–7mm), placed longitudinally at the peripheral regions of lung, were scanned using a prototype PCCT (GE Healthcare) at 120kVp and CT DIvol of 8.72mGy. Iodine rod concentrations were 1.7mg/ml and 3.0mg/ml. Material images were generated on a 1024×1024 image grid with standard and high-resolution kernels. Quantification accuracy for various nodule sizes was obtained for regions of interest (ROI) on iodine images. Nodule sizes were measured at monochromatic images at 70 keV.

#### RESULTS

In the iodine images, the ROI means and standard deviations for 5mm, 4mm, 3mm, and 2mm diameter rods with 3mg/ml concentration were 3.18mg/ml[0.51mg/ml], 3.12mg/ml[0.40mg/ml], 3.21mg/ml[1.32mg/ml], and 2.56mg/ml[1.25mg/ml], respectively. The respective nodule size measurements were 5.08mm, 3.87mm, 3.05mm and 1.94mm.

#### CONCLUSION

Our results indicate that this PCCT prototype can provide, from a single scan, both nodule size and iodine quantification for small lung nodule detection and characterization. Edge-on-irradiated Si-based PCCT thus has the potential to provide additional information on small pulmonary nodules and could have a role in differentiating benign and malignant nodules, obviating the need for follow up imaging or biopsy.

#### CLINICAL RELEVANCE/APPLICATION

PCCT with simultaneous high spatial and spectral resolution can provide supplementary information on lung nodules smaller than 3–5mm and simplify the clinical decision process.

Printed on: 02/07/23



## Abstract Archives of the RSNA, 2022

M2-SPRO

### Radiation Oncology Monday Poster Discussions

Monday, Nov. 28 9:00AM - 9:30AM Room: Learning Center - RO DPS

#### Participants

Anna Shapiro, MD, Syracuse, NY (*Moderator*) Nothing to Disclose

Printed on: 02/07/23

## Abstract Archives of the RSNA, 2022

M5A-SPBR

### Breast Monday Poster Discussions - A

Monday, Nov. 28 12:15PM - 12:45PM Room: Learning Center - BR DPS

#### Participants

Fabiola Kestelman, MD, Iowa City, IA (*Moderator*) Nothing to Disclose

#### Sub-Events

### M5A-SPBR-1 Application of Whole-Image Pixel Analysis to Contrast-Enhanced Mammography: A Potential Supplementary Tool for Evaluating Mammograms

#### Participants

Michael Borten, MD, (*Presenter*) Nothing to Disclose

#### PURPOSE

Contrast-enhanced mammography (CEM) is an emerging breast imaging modality that has been shown to be more sensitive for detecting breast cancer than traditional mammography. This study is a pilot demonstration of whole-image pixel analysis over multiple time points and creation of a color-coded image representing contrast enhancement kinetics.

#### METHODS AND MATERIALS

We first identified retrospectively CEM exams that contained multiple imaging acquisitions of the same position (e.g., CC or MLO), which provided serial imaging of the same breast over several time points. After aligning these serial images using MATLAB, three techniques for overlaying the contrast distribution onto the low energy (LE) traditional mammogram were utilized: 1) direct overlay of the recombined (RC) image onto the LE image, 2) overlaying a color-coded map of change in "early phase" pixel intensity between the first and second time points, and 3) overlaying a color-coded map of "delayed phase" change in pixel intensity between the second and third time points.

#### RESULTS

From 2124 retrospective images of 139 patients, we identified 40 patients with 53 views for which two or more images were acquired (two or more time points). Two patients had three images acquired of the same view. Color maps were successfully created from one time point (single RC image), two time points ("early phase"), and three time points ("delayed phase"). Our imaging data demonstrate better results as the number of time points increases (Figure 1A-C). For one patient with three time points, our technique demonstrated an area of rapid uptake (Figure 1B) and mixed washout/plateau (Figure 1C) which corresponded with the area of biopsy-proven atypical ductal hyperplasia, albeit with noise from inter-acquisition movement. We also found that the mean pixel intensity across the whole breast tended to decrease around two minutes after first image acquisition (Figure 1D-E).

#### CONCLUSION

Our pilot data have demonstrated the feasibility of using serial CEM acquisitions to create a kinetic color map analogous to those routinely utilized with breast MR imaging, which can demonstrate areas of washout that might correlate with suspicious breast findings. Future studies will focus on prospectively acquiring images at systematic time points to allow for more robust and conclusive data analysis.

#### CLINICAL RELEVANCE/APPLICATION

We apply whole-image pixel analysis to contrast-enhanced mammography (CEM) to create color-coded enhancement kinetic maps that could aid clinicians in evaluating findings suspicious for malignancy.

### M5A-SPBR-2 Diagnostic Performance and Image Quality of Contrast Enhanced Spectral Mammography with Low-Dose Contrast Agents in Detecting Breast Lesions

#### Participants

Huizhi Cao, PhD, (*Presenter*) Nothing to Disclose

#### PURPOSE

To explore the clinical value of contrast enhanced spectral mammography with low-dose contrast agents in assessing breast lesions.

#### METHODS AND MATERIALS

In this IRB-approved retrospective study, 223 patients undergoing CESM were randomly assigned into two protocols: 113 patients were carried out exam with conventional dose (Iohexol at 1.5ml/kg; 350 mg/ml), and other 110 patients underwent exam with low dose (Iohexol at 1 ml/kg; 300-350 mg/ml). All the patients accepted MRI examination within one week. The image of CESM, MRI and the histopathological data were analyzed. The clinical value of CESM and MRI were evaluated according to the histopathological results, respectively. The ROC curve was applied to analyze clinical efficiency. The tumor size was measured from CESM, MRI modalities and pathological data. By using the Bland-Altman analysis, the consistency of the maximum tumor size

was assessed.

## RESULTS

Histopathologic result revealed 33 benign and 67 malignant lesions in low dose group, and 35 benign and 78 malignant lesions in conventional group. CESM obtained from conventional group had similar AUC area, sensitivity, specificity, PPV, NPV to MRI imaging (0.928, 0.962, 0.846, 0.783, 0.821 vs. 0.903, 0.974, 0.809, 0.805, 0.856). Importantly, CESM from low dose group showed a comparison of clinical performance to MRI as well. (AUC area: 0.944 vs. 0.925; sensitivity: 0.990 vs. 0.941; specificity: 0.825 vs. 0.831; PPV: 0.802 vs. 0.825; NPV: 0.855 vs. 0.895). For tumor size measurement, mean tumor size was 3.51 cm for CESM (conventional group) and 3.61 cm for MRI, compared with 3.38 cm on histopathological results, the average difference of diameters between CESM (conventional group), MRI and Histopathologic size was -0.02, -0.10cm, respectively. Additionally, average sizes were measured as 4.02 cm, 3.76 cm, 3.96 cm for CESM (low dose group), MRI and Histopathologic result, and the difference diameters compared to Pathologic data were -0.05, -0.08cm. Bland-Altman analysis showed best consistency on tumor size between CESM (low dose group), MRI and pathological results.

## CONCLUSION

Low doses of contrast agents used for CESM show a comparison both in diagnostic performance and tumor size assessment, compared to CESM obtained with conventional dose.

## CLINICAL RELEVANCE/APPLICATION

Contrast enhanced spectral mammography performed at low dose of contrast agents can meet the clinical and imaging requirements without sacrificing diagnostic performance.

### M5A-SPBR-3 Diagnostic Accuracy of Automated ACR BI-RADS Breast Density Classification using Deep Convolutional Neural Networks

Participants

Raphael Sexauer, MD, (*Presenter*) Nothing to Disclose

## PURPOSE

High breast density is a well-known risk factor for breast cancer. This study aimed to develop and adapt two deep convolutional neural networks (DCNN) for the automatic classification of breast density based on the mammographic appearance of the tissue on synthetic 2D tomosynthesis craniocaudal (CC) and mediolateral oblique (MLO) projections.

## METHODS AND MATERIALS

In this study, 4605 mammography tomosynthesis-based synthetic images from 1267 different patients ( $57 \pm 37$  years) were labeled according to the ACR (American College of Radiology) density (A-D) by a radiologist with 2 years of experience in breast imaging. Two DCNN with 11 convolutional layers and 3 fully connected layers were trained with 70% of the data, whereas 20% was used for validation. The remaining 10% were used as a separate test dataset with 460 images (380 patients). All mammograms in the test dataset were read blinded by two radiologists (reader 1 with two and reader 2 with 11 years of dedicated mammographic experience in mammographic imaging), and the consensus was formed as the reference standard. The inter- and intra-reader reliabilities of the density classifications were assessed by calculating Cohen's kappa coefficients, and diagnostic accuracy measures of automated classification were evaluated.

## RESULTS

Two separate models for MLO and CC projections were successfully trained and implemented in the "b-box" artificial intelligence (AI) platform (Medical device type IIa, CE 0297). Mean sensitivity of 80.4 (95%-CI 72.2-86.9) and a specificity of 89.3 (95%-CI 85.4-92.3) in the differentiation between ACR A/B and ACR C/D. DCNN versus human and interhuman agreement was both "substantial" (Cohen's kappa: 0.61 versus 0.63).

## CONCLUSION

The DCNN allows for accurate, standardized, and observer-independent classification of breast density based on the ACR BI-RADS system. The proposed technique is suited for tomosynthesis-based synthetic images.

## CLINICAL RELEVANCE/APPLICATION

DCNNs can be used to accurately mimic human decision-making in breast density assessment for synthetic 2D tomosynthesis.

### M5A-SPBR-4 Screen-detected and Interval Breast Cancer Rates are Significantly Higher in Women with Dense Breasts Across all Age Groups in a Large DBT Dataset

Participants

Giorgia Grisot, PhD, CAMBRIDGE, United Kingdom (*Presenter*) Employee, RadNet, Inc

## PURPOSE

High breast density is associated with both increased breast cancer risk and decreased sensitivity of screening mammography, contributing to higher overall breast cancer rates and interval breast cancer rates. The Breast Cancer Surveillance Consortium (BCSC) previously showed that interval cancer rates are higher in women with dense breasts undergoing screening with full-field digital mammography, but little data is available for digital breast tomosynthesis (DBT). We sought to compare cancer rates by breast density on women undergoing screening with DBT using a dataset comparable to BCSC.

## METHODS AND MATERIALS

Retrospective data was collected including one DBT screening mammogram from each of 559,791 women undergoing screening between 2017-2021 at over 150 clinical locations, excluding first screens, and with at least one year of follow-up. Screen-detected cancer rate and interval cancer rate were calculated per 1000 women. Analyses are separated by women with nondense (fatty or scattered fibroglandular) and dense (heterogeneously dense or very dense) breast tissue, following BI-RADS 5th Edition guidelines.

## RESULTS

Across all age groups, women with dense breasts had a 1.8x higher recall rate, 1.4x higher CDR, and 2.0x higher interval cancer

ACROSS all age groups, women with dense breasts had a 1.6x higher recall rate, 1.4x higher CDR, and 2.9x higher interval cancer rate compared to women with nondense breasts. CDR is higher in women with dense breasts in all age brackets (dense/nondense CDR: age 40-49: 2.0; 50-59: 1.8; 60-69: 1.4; 70-74: 1.4, chi-square  $p < 0.001$  for all differences). Interval cancer rate was higher in women with dense breasts in all age brackets (dense/nondense interval cancer rate: age 40-49: 2.5; 50-59: 3.2; 60-69: 2.8; 70-74: 3.7, chi-square  $p < 0.01$  for all differences). While the positive predictive value of recalls (PPV1) was similar for women with dense breasts compared to nondense breasts in age groups above 50, women ages 40-49 with dense breasts who were recalled were more likely to have cancer detected than women with nondense breasts (dense/nondense PPV1: 1.17).

## CONCLUSION

s In a group of more than half a million women, women with dense breasts undergoing screening mammography with DBT show increased rates of cancer detection and interval cancer rates compared to women without dense breasts, across all age groups. Women aged 40-49 with dense breasts had a higher recall rate but also a higher likelihood of a cancer diagnosis than women without dense breasts. Mammographic breast density, even with DBT, remains associated with higher rates of cancer.

## CLINICAL RELEVANCE/APPLICATION

Mammographic breast density is a strong risk factor for breast cancer and for interval breast cancers, even when DBT is used. Our results suggest women aged 40-49 with dense breasts particularly benefit from screening mammography.

## M5A-SPBR-5 Density Awareness: Do Patients Know About Breast Density? What Are Factors That May Influence Breast Density Awareness?

### Participants

Mary W. Yamashita, MD, South Pasadena, CA (*Presenter*) Research Grant, Delphinus Medical Technologies, Inc; Consultant, Delphinus Medical Technologies, Inc

## PURPOSE

While prior studies have investigated primary or referring physician awareness of breast density and its association with breast cancer, to our knowledge, patient knowledge of breast density has not been assessed. We would like to investigate patients' awareness of breast density, specifically those patients who were previously notified of their dense breasts in the mammography result letter.

## METHODS AND MATERIALS

We conducted a retrospective review of 8317 women who enrolled in the SoftVue™ Prospective Case Collection registry between December 2016 and October 2019 who had heterogeneously or extremely dense breasts. After undergoing mammography (MG) and SoftVue™ automated whole breast ultrasound tomography (SV), all participants completed a history and demographics questionnaire and an experience survey which also measured awareness of their own breast density, anxiety about breast density, and level of worry about breast cancer. We reviewed this data and determined the awareness of dense breasts in this population and its influence on self-reported anxiety about breast cancer and looked at other factors that may influence density awareness.

## RESULTS

A large percentage of women are not aware of the significance of dense breasts, despite many of them having received breast density notification letters prior to participation. Patients who are aware of their breast density report higher anxiety about their breast density compared to those who are not. Non-Hispanic women are more aware of breast density than Hispanic women. Patients who underwent imaging in States where Breast Density Notification Laws were active are more likely to be aware of their breast density, however the wording of the density information letter may impact patient awareness and concern surrounding it.

## CONCLUSION

s Breast density is not well understood by women who are heterogeneously dense or extremely dense. More work needs to be done to educate women with dense breasts about the increased risk of breast cancer and the need for supplementary imaging to mammography.

## CLINICAL RELEVANCE/APPLICATION

Increasing breast density awareness in women with dense breasts will likely empower them to self-advocate for additional imaging for early detection of breast cancer.

## M5A-SPBR-6 SOLUS - Smart Optical and Ultrasound Diagnostics of Breast Cancer: US / DOT Hybrid System for the Characterization of Breast Lesions

### Participants

Elena Venturini, MD, (*Presenter*) Speaker, Bayer AG

## PURPOSE

Presentation of the technology and the first clinical results of a project funded by a Grant Horizon 2020 for the development of a hybrid ultrasound and optical tomography device, created by the SOLUS consortium that unites 9 European partners experts in optical imaging, ultrasound and image processing. The purpose of the clinical study, still ongoing, is to evaluate the feasibility of the SOLUS device in the differentiation of the malignant breast nodules from the benign ones.

## METHODS AND MATERIALS

The SOLUS device is a US/optical hybrid prototype that consists of a commercial Hologic Aixplorer Mach 30 US system combined with an innovative diffuse optical tomography (DOT) system. The SOLUS device includes, in a single exam, B mode ultrasound, color Doppler, shear wave elastography and DOT through a probe that has a normal US transducer in the center, flanked by 8 optodes that emit and receive light in the red and infrared spectrum. The optical study allows one to measure the concentrations of water, lipids, collagen, oxygenated and deoxygenated hemoglobin, as well as to provide information on cell membranes and subcellular organelles. In the clinical study we enroll women with breast nodules = 1 cm, detectable at US, suspicious for malignancy (BI-RADS 4 or 5) or benign (BI-RADS 2 or 3) before breast biopsy, if it is clinically needed. The aim of the clinical study is to compare, in vivo, the parameters obtained from the evaluation of 20 benign and 20 malignant lesions to test the possibility of differentiating them.

## RESULTS

From 10/2021 to 04/2022 we enrolled 17 women with breast nodules; overall 18 breast nodules were evaluated (5 malignant, 13 benign). The preliminary analysis performed have confirmed that the SOLUS device may depict the composition of breast tissue, differentiating breast nodules from the surrounding tissue and distinguishing malignant from benign lesions.

## **CONCLUSION**

s The initial data collected, based mainly on DOT findings guided by US, suggest that a multiparametric analysis, adding also information from US based techniques, may have a role in the characterization of breast lesions.

## **CLINICAL RELEVANCE/APPLICATION**

A multiparametric analysis, based mainly on DOT findings guided by US, may have a role in the characterization of breast lesions.

## **M5A-SPBR-7 Do as We Say, Not as We Do? Our Initial Experience with the Lateral-Arm Needle Approach for Prone Tomosynthesis Breast Biopsy.**

### **Participants**

Ethan O. Cohen, MD, Houston, TX (*Presenter*) Spouse, Consultant, Boehringer Ingelheim GmbH; Spouse, Consultant, Novo Nordisk AS; Spouse, Consultant, Eli Lilly and Company

## **PURPOSE**

Compare conventional and lateral-arm needle approaches for prone tomosynthesis breast biopsy.

## **METHODS AND MATERIALS**

Conventional or lateral-arm needle approach for tomosynthesis biopsy was selected based on radiologist preference during 2016-2019, and these biopsies were retrospectively reviewed after IRB approval. Procedure details and biopsy outcomes were compared with the two-sample t-test and two proportion z-tests.

## **RESULTS**

165 patients (median age, 56 years; interquartile range 48-64) underwent 177 biopsies with a conventional needle approach, and 140 patients (median age 56 years; interquartile range 48-65) underwent 147 biopsies with a lateral-arm needle approach. All were successful. Fewer images were necessary with the lateral-arm needle approach (mean 8 versus 6,  $P < 0.001$ ). There were no differences between needle approaches for the remaining procedure details: total procedure time, lesion targeting time, tissue sampling time, number of samples acquired, biopsy target lesion (calcifications, distortion, asymmetry, or mass), clip migration, and complications ( $P = 0.06-0.96$ ). Outcomes for conventional-needle-approach biopsies were 99 benign (56%), 28 high-risk (16%), and 40 malignant (23%); one discordant benign lesion and two high-risk lesions were upgraded at excision. Outcomes for lateral-arm-approach biopsies were 80 benign (54%), 39 high-risk (27%), and 28 malignant (19%); one high-risk lesion was upgraded at excision. Benign and malignant outcomes were equally common with either needle approach ( $P = 0.44-0.79$ ), but high-risk outcomes were more common with the lateral-arm needle approach (believed to be due to radiologist preference based on lesion type,  $P = 0.02$ ). Positive predictive values were similar between approaches ( $P = 0.33$ ).

## **CONCLUSION**

s The lateral-arm needle approach for prone tomosynthesis breast biopsy is an acceptable alternative to conventional needle approach based on radiologist preference. Fewer images were required for the lateral-arm approach, and other procedure details were similar to the conventional needle approach.

## **CLINICAL RELEVANCE/APPLICATION**

The lateral-arm needle approach for tomosynthesis breast biopsy is a new addition to percutaneous biopsy options, and radiologists should familiarize themselves with its benefits.

Printed on: 02/07/23

## Abstract Archives of the RSNA, 2022

M5A-SPBR-1

### Application of Whole-Image Pixel Analysis to Contrast-Enhanced Mammography: A Potential Supplementary Tool for Evaluating Mammograms

Monday, Nov. 28 12:15PM - 12:45PM Room: Learning Center - BR DPS

#### Participants

Michael Borten, MD, (*Presenter*) Nothing to Disclose

#### PURPOSE

Contrast-enhanced mammography (CEM) is an emerging breast imaging modality that has been shown to be more sensitive for detecting breast cancer than traditional mammography. This study is a pilot demonstration of whole-image pixel analysis over multiple time points and creation of a color-coded image representing contrast enhancement kinetics.

#### METHODS AND MATERIALS

We first identified retrospectively CEM exams that contained multiple imaging acquisitions of the same position (e.g., CC or MLO), which provided serial imaging of the same breast over several time points. After aligning these serial images using MATLAB, three techniques for overlaying the contrast distribution onto the low energy (LE) traditional mammogram were utilized: 1) direct overlay of the recombined (RC) image onto the LE image, 2) overlaying a color-coded map of change in "early phase" pixel intensity between the first and second time points, and 3) overlaying a color-coded map of "delayed phase" change in pixel intensity between the second and third time points.

#### RESULTS

From 2124 retrospective images of 139 patients, we identified 40 patients with 53 views for which two or more images were acquired (two or more time points). Two patients had three images acquired of the same view. Color maps were successfully created from one time point (single RC image), two time points ("early phase"), and three time points ("delayed phase"). Our imaging data demonstrate better results as the number of time points increases (Figure 1A-C). For one patient with three time points, our technique demonstrated an area of rapid uptake (Figure 1B) and mixed washout/plateau (Figure 1C) which corresponded with the area of biopsy-proven atypical ductal hyperplasia, albeit with noise from inter-acquisition movement. We also found that the mean pixel intensity across the whole breast tended to decrease around two minutes after first image acquisition (Figure 1D-E).

#### CONCLUSION

Our pilot data have demonstrated the feasibility of using serial CEM acquisitions to create a kinetic color map analogous to those routinely utilized with breast MR imaging, which can demonstrate areas of washout that might correlate with suspicious breast findings. Future studies will focus on prospectively acquiring images at systematic time points to allow for more robust and conclusive data analysis.

#### CLINICAL RELEVANCE/APPLICATION

We apply whole-image pixel analysis to contrast-enhanced mammography (CEM) to create color-coded enhancement kinetic maps that could aid clinicians in evaluating findings suspicious for malignancy.

Printed on: 02/07/23

## Abstract Archives of the RSNA, 2022

M5A-SPBR-2

### Diagnostic Performance and Image Quality of Contrast Enhanced Spectral Mammography with Low-Dose Contrast Agents in Detecting Breast Lesions

Monday, Nov. 28 12:15PM - 12:45PM Room: Learning Center - BR DPS

#### Participants

Huizhi Cao, PhD, (Presenter) Nothing to Disclose

#### PURPOSE

To explore the clinical value of contrast enhanced spectral mammography with low-dose contrast agents in assessing breast lesions.

#### METHODS AND MATERIALS

In this IRB-approved retrospective study, 223 patients undergoing CESM were randomly assigned into two protocols: 113 patients were carried out exam with conventional dose (Iohexol at 1.5ml/kg;350 mg/ml), and other 110 patients underwent exam with low dose (Iohexol at 1 ml/kg; 300-350 mg/ml). All the patients accepted MRI examination within one week. The image of CESM, MRI and the histopathological data were analyzed. The clinical value of CESM and MRI were evaluated according to the histopathological results, respectively. The ROC curve was to be applied to analyzed clinical efficiency. The tumor size was measured from CESM, MRI modalities and pathological data. By using the Bland-Altman analysis, the consistency of the maximum tumor size was assessed.

#### RESULTS

Histopathologic result revealed 33 benign and 67 malignant lesions in low dose group, and 35 benign and 78 malignant lesions in conventional group. CESM obtained from conventional group had similar AUC area, sensitivity, specificity, PPV, NPV to MRI imaging (0.928, 0.962, 0.846,0.783,0.821 vs. 0.903,0.974,0.809,0.805,0.856). Importantly, CESM from low dose group showed a comparison of clinical performance to MRI as well. (AUC area: 0.944 vs. 0.925; sensitivity:0.990 vs.0.941; specificity:0.825vs.0.831; PPV:0.802 vs. 0.825; NPV:0.855 vs. 0.895). For tumor size measurement, mean tumor size was 3.51 cm for CESM (conventional group) and 3.61 cm for MRI, compared with 3.38 cm on histopathological results, the average difference of diameters between CESM (conventional group), MRI and Histopathologic size was -0.02, -0.10cm, respectively. Additionally, average sizes were measured as 4.02 cm, 3.76 cm, 3.96 cm for CESM (low dose group), MRI and Histopathologic result, and the difference diameters compared to Pathologic data were -0.05, -0.08cm. Bland-Altman analysis showed best consistency on tumor size between CESM (low dose group), MRI and pathological results.

#### CONCLUSION

Low doses of contrast agents used for CESM show a comparison both in diagnostic performance and tumor size assessment, compared to CESM obtained with conventional dose.

#### CLINICAL RELEVANCE/APPLICATION

Contrast enhanced spectral mammography performed at low dose of contrast agents can meet the clinical and imaging requirements without sacrificing diagnostic performance.

Printed on: 02/07/23

## Abstract Archives of the RSNA, 2022

M5A-SPBR-3

### Diagnostic Accuracy of Automated ACR BI-RADS Breast Density Classification using Deep Convolutional Neural Networks

Monday, Nov. 28 12:15PM - 12:45PM Room: Learning Center - BR DPS

#### Participants

Raphael Sexauer, MD, (*Presenter*) Nothing to Disclose

#### PURPOSE

High breast density is a well-known risk factor for breast cancer. This study aimed to develop and adapt two deep convolutional neural networks (DCNN) for the automatic classification of breast density based on the mammographic appearance of the tissue on synthetic 2D tomosynthesis craniocaudal (CC) and mediolateral oblique (MLO) projections.

#### METHODS AND MATERIALS

In this study, 4605 mammography tomosynthesis-based synthetic images from 1267 different patients ( $57 \pm 37$  years) were labeled according to the ACR (American College of Radiology) density (A-D) by a radiologist with 2 years of experience in breast imaging. Two DCNN with 11 convolutional layers and 3 fully connected layers were trained with 70% of the data, whereas 20% was used for validation. The remaining 10% were used as a separate test dataset with 460 images (380 patients). All mammograms in the test dataset were read blinded by two radiologists (reader 1 with two and reader 2 with 11 years of dedicated mammographic experience in mammographic imaging), and the consensus was formed as the reference standard. The inter- and intra-reader reliabilities of the density classifications were assessed by calculating Cohen's kappa coefficients, and diagnostic accuracy measures of automated classification were evaluated.

#### RESULTS

Two separate models for MLO and CC projections were successfully trained and implemented in the "b-box" artificial intelligence (AI) platform (Medical device type IIa, CE 0297). Mean sensitivity of 80.4 (95%-CI 72.2-86.9) and a specificity of 89.3 (95%-CI 85.4-92.3) in the differentiation between ACR A/B and ACR C/D. DCNN versus human and interhuman agreement was both "substantial" (Cohen's kappa: 0.61 versus 0.63).

#### CONCLUSION

The DCNN allows for accurate, standardized, and observer-independent classification of breast density based on the ACR BI-RADS system. The proposed technique is suited for tomosynthesis-based synthetic images.

#### CLINICAL RELEVANCE/APPLICATION

DCNNs can be used to accurately mimic human decision-making in breast density assessment for synthetic 2D tomosynthesis.

Printed on: 02/07/23

## Abstract Archives of the RSNA, 2022

M5A-SPBR-4

### Screen-detected and Interval Breast Cancer Rates are Significantly Higher in Women with Dense Breasts Across all Age Groups in a Large DBT Dataset

Monday, Nov. 28 12:15PM - 12:45PM Room: Learning Center - BR DPS

#### Participants

Giorgia Grisot, PhD, CAMBRIDGE, United Kingdom (*Presenter*) Employee, RadNet, Inc

#### PURPOSE

High breast density is associated with both increased breast cancer risk and decreased sensitivity of screening mammography, contributing to higher overall breast cancer rates and interval breast cancer rates. The Breast Cancer Surveillance Consortium (BCSC) previously showed that interval cancer rates are higher in women with dense breasts undergoing screening with full-field digital mammography, but little data is available for digital breast tomosynthesis (DBT). We sought to compare cancer rates by breast density on women undergoing screening with DBT using a dataset comparable to BCSC.

#### METHODS AND MATERIALS

Retrospective data was collected including one DBT screening mammogram from each of 559,791 women undergoing screening between 2017-2021 at over 150 clinical locations, excluding first screens, and with at least one year of follow-up. Screen-detected cancer rate and interval cancer rate were calculated per 1000 women. Analyses are separated by women with nondense (fatty or scattered fibroglandular) and dense (heterogeneously dense or very dense) breast tissue, following BI-RADS 5th Edition guidelines.

#### RESULTS

Across all age groups, women with dense breasts had a 1.8x higher recall rate, 1.4x higher CDR, and 2.9x higher interval cancer rate compared to women with nondense breasts. CDR is higher in women with dense breasts in all age brackets (dense/nondense CDR: age 40-49: 2.0; 50-59: 1.8; 60-69: 1.4; 70-74: 1.4, chi-square  $p < 0.001$  for all differences). Interval cancer rate was higher in women with dense breasts in all age brackets (dense/nondense interval cancer rate: age 40-49: 2.5; 50-59: 3.2; 60-69: 2.8; 70-74: 3.7, chi-square  $p < 0.01$  for all differences). While the positive predictive value of recalls (PPV1) was similar for women with dense breasts compared to nondense breasts in age groups above 50, women ages 40-49 with dense breasts who were recalled were more likely to have cancer detected than women with nondense breasts (dense/nondense PPV1: 1.17).

#### CONCLUSION

In a group of more than half a million women, women with dense breasts undergoing screening mammography with DBT show increased rates of cancer detection and interval cancer rates compared to women without dense breasts, across all age groups. Women aged 40-49 with dense breasts had a higher recall rate but also a higher likelihood of a cancer diagnosis than women without dense breasts. Mammographic breast density, even with DBT, remains associated with higher rates of cancer.

#### CLINICAL RELEVANCE/APPLICATION

Mammographic breast density is a strong risk factor for breast cancer and for interval breast cancers, even when DBT is used. Our results suggest women aged 40-49 with dense breasts particularly benefit from screening mammography.

Printed on: 02/07/23



## Abstract Archives of the RSNA, 2022

M5A-SPBR-5

### Density Awareness: Do Patients Know About Breast Density? What Are Factors That May Influence Breast Density Awareness?

Monday, Nov. 28 12:15PM - 12:45PM Room: Learning Center - BR DPS

#### Participants

Mary W. Yamashita, MD, South Pasadena, CA (*Presenter*) Research Grant, Delphinus Medical Technologies, Inc; Consultant, Delphinus Medical Technologies, Inc

#### PURPOSE

While prior studies have investigated primary or referring physician awareness of breast density and its association with breast cancer, to our knowledge, patient knowledge of breast density has not been assessed. We would like to investigate patients' awareness of breast density, specifically those patients who were previously notified of their dense breasts in the mammography result letter.

#### METHODS AND MATERIALS

We conducted a retrospective review of 8317 women who enrolled in the SoftVue™ Prospective Case Collection registry between December 2016 and October 2019 who had heterogeneously or extremely dense breasts. After undergoing mammography (MG) and SoftVue™ automated whole breast ultrasound tomography (SV), all participants completed a history and demographics questionnaire and an experience survey which also measured awareness of their own breast density, anxiety about breast density, and level of worry about breast cancer. We reviewed this data and determined the awareness of dense breasts in this population and its influence on self-reported anxiety about breast cancer and looked at other factors that may influence density awareness.

#### RESULTS

A large percentage of women are not aware of the significance of dense breasts, despite many of them having received breast density notification letters prior to participation. Patients who are aware of their breast density report higher anxiety about their breast density compared to those who are not. Non-Hispanic women are more aware of breast density than Hispanic women. Patients who underwent imaging in States where Breast Density Notification Laws were active are more likely to be aware of their breast density, however the wording of the density information letter may impact patient awareness and concern surrounding it.

#### CONCLUSION

Breast density is not well understood by women who are heterogeneously dense or extremely dense. More work needs to be done to educate women with dense breasts about the increased risk of breast cancer and the need for supplementary imaging to mammography.

#### CLINICAL RELEVANCE/APPLICATION

Increasing breast density awareness in women with dense breasts will likely empower them to self-advocate for additional imaging for early detection of breast cancer.

Printed on: 02/07/23



## Abstract Archives of the RSNA, 2022

M5A-SPBR-6

### **SOLUS - Smart Optical and Ultrasound Diagnostics of Breast Cancer: US / DOT Hybrid System for the Characterization of Breast Lesions**

Monday, Nov. 28 12:15PM - 12:45PM Room: Learning Center - BR DPS

#### **Participants**

Elena Venturini, MD, (*Presenter*) Speaker, Bayer AG

#### **PURPOSE**

Presentation of the technology and the first clinical results of a project funded by a Grant Horizon 2020 for the development of a hybrid ultrasound and optical tomography device, created by the SOLUS consortium that unites 9 European partners experts in optical imaging, ultrasound and image processing. The purpose of the clinical study, still ongoing, is to evaluate the feasibility of the SOLUS device in the differentiation of the malignant breast nodules from the benign ones.

#### **METHODS AND MATERIALS**

The SOLUS device is a US/optical hybrid prototype that consists of a commercial Hologic Aixplorer Mach 30 US system combined with an innovative diffuse optical tomography (DOT) system. The SOLUS device includes, in a single exam, B mode ultrasound, color Doppler, shear wave elastography and DOT through a probe that has a normal US transducer in the center, flanked by 8 optodes that emit and receive light in the red and infrared spectrum. The optical study allows one to measure the concentrations of water, lipids, collagen, oxygenated and deoxygenated hemoglobin, as well as to provide information on cell membranes and subcellular organelles. In the clinical study we enroll women with breast nodules = 1 cm, detectable at US, suspicious for malignancy (BI-RADS 4 or 5) or benign (BI-RADS 2 or 3) before breast biopsy, if it is clinically needed. The aim of the clinical study is to compare, in vivo, the parameters obtained from the evaluation of 20 benign and 20 malignant lesions to test the possibility of differentiating them.

#### **RESULTS**

From 10/2021 to 04/2022 we enrolled 17 women with breast nodules; overall 18 breast nodules were evaluated (5 malignant, 13 benign). The preliminary analysis performed have confirmed that the SOLUS device may depict the composition of breast tissue, differentiating breast nodules from the surrounding tissue and distinguishing malignant from benign lesions.

#### **CONCLUSION**

s The initial data collected, based mainly on DOT findings guided by US, suggest that a multiparametric analysis, adding also information from US based techniques, may have a role in the characterization of breast lesions.

#### **CLINICAL RELEVANCE/APPLICATION**

A multiparametric analysis, based mainly on DOT findings guided by US, may have a role in the characterization of breast lesions.

Printed on: 02/07/23

## Abstract Archives of the RSNA, 2022

M5A-SPBR-7

### Do as We Say, Not as We Do? Our Initial Experience with the Lateral-Arm Needle Approach for Prone Tomosynthesis Breast Biopsy.

Monday, Nov. 28 12:15PM - 12:45PM Room: Learning Center - BR DPS

#### Participants

Ethan O. Cohen, MD, Houston, TX (*Presenter*) Spouse, Consultant, Boehringer Ingelheim GmbH; Spouse, Consultant, Novo Nordisk AS; Spouse, Consultant, Eli Lilly and Company

#### PURPOSE

Compare conventional and lateral-arm needle approaches for prone tomosynthesis breast biopsy.

#### METHODS AND MATERIALS

Conventional or lateral-arm needle approach for tomosynthesis biopsy was selected based on radiologist preference during 2016-2019, and these biopsies were retrospectively reviewed after IRB approval. Procedure details and biopsy outcomes were compared with the two-sample t-test and two proportion z-tests.

#### RESULTS

165 patients (median age, 56 years; interquartile range 48-64) underwent 177 biopsies with a conventional needle approach, and 140 patients (median age 56 years; interquartile range 48-65) underwent 147 biopsies with a lateral-arm needle approach. All were successful. Fewer images were necessary with the lateral-arm needle approach (mean 8 versus 6,  $P < 0.001$ ). There were no differences between needle approaches for the remaining procedure details: total procedure time, lesion targeting time, tissue sampling time, number of samples acquired, biopsy target lesion (calcifications, distortion, asymmetry, or mass), clip migration, and complications ( $P = 0.06-0.96$ ). Outcomes for conventional-needle-approach biopsies were 99 benign (56%), 28 high-risk (16%), and 40 malignant (23%); one discordant benign lesion and two high-risk lesions were upgraded at excision. Outcomes for lateral-arm-approach biopsies were 80 benign (54%), 39 high-risk (27%), and 28 malignant (19%); one high-risk lesion was upgraded at excision. Benign and malignant outcomes were equally common with either needle approach ( $P = 0.44-0.79$ ), but high-risk outcomes were more common with the lateral-arm needle approach (believed to be due to radiologist preference based on lesion type,  $P = 0.02$ ). Positive predictive values were similar between approaches ( $P = 0.33$ ).

#### CONCLUSION

The lateral-arm needle approach for prone tomosynthesis breast biopsy is an acceptable alternative to conventional needle approach based on radiologist preference. Fewer images were required for the lateral-arm approach, and other procedure details were similar to the conventional needle approach.

#### CLINICAL RELEVANCE/APPLICATION

The lateral-arm needle approach for tomosynthesis breast biopsy is a new addition to percutaneous biopsy options, and radiologists should familiarize themselves with its benefits.

Printed on: 02/07/23

## Abstract Archives of the RSNA, 2022

M5A-SPCA

### Cardiac Monday Poster Discussions - A

Monday, Nov. 28 12:15PM - 12:45PM Room: Learning Center - CA DPS

#### Sub-Events

#### M5A-SPCA-1 Left ventricular diastolic filling pattern in competitive triathletes with and without myocardial fibrosis compared to sedentary controls by CMR imaging

##### Participants

Hang Chen, MD, Hamburg, Germany (*Presenter*) Nothing to Disclose

##### PURPOSE

Endurance athletes have a higher incidence of myocardial fibrosis than the general population. However, it remains unclear whether myocardial fibrosis leads to any alterations of left ventricular (LV) diastolic function. The aim of this study was to investigate the diastolic LV filling pattern in triathletes, and the influence of myocardial fibrosis by cardiac magnetic resonance (CMR) imaging.

##### METHODS AND MATERIALS

101 male triathletes (age: 43±11 years) and 28 male controls (age: 41±10 years) were recruited through advertisement in local triathlon clubs. All participants underwent CMR including cine SSFP series, late gadolinium enhancement (LGE) imaging and T1 mapping. Functional and morphological ventricular parameters were obtained, including LV mass and ejection fraction (EF). Diastolic LV filling was determined by a time-volume analysis using cine series (25 phases of the cardiac cycle). Early peak-filling rates (EPFR) and atrial peak-filling rates (APFR) as well as peak-filling rate ratios (PFRR=EPFR/APFR) were determined.

##### RESULTS

Focal myocardial fibrosis (LGE+) was detected in 20 triathletes (20%) and in none of the controls. LVEF was similar in both triathletes and controls (61±6 vs. 62±7%; P=0.36). LGE+ triathletes had a higher LV mass (88±10 vs. 80±12 g/m<sup>2</sup>; P<0.01) and extracellular volume (ECV) (26±3 vs. 24±2%; P<0.001) compared to LGE- triathletes. EPFR was similar in LGE- triathletes and controls (216±58 vs. 224±69 ml/s/m<sup>2</sup>; P=0.52). LGE- triathletes had lower APFR (120±46 vs. 147±55 ml/s/m<sup>2</sup>; P<0.05) and higher PFRR (2.1±1 vs. 1.6±0.5; P<0.05) compared to controls. LGE+ triathletes had similar EPFR (212±73 ml/s/m<sup>2</sup>; P=0.80), higher APFR (149±50 ml/s/m<sup>2</sup>; P<0.05) and decreased PFRR (1.6±0.7, P<0.05) compared to LGE- triathletes. EPFR (P=0.52), APFR (P=0.91) and PFRR (P=0.67) were similar in LGE+ triathletes compared to controls.

##### CONCLUSION

While adaptations in diastolic LV filling in LGE- triathletes are characterized by decreased APFR and increased PFRR compared to sedentary controls, LGE+ triathletes demonstrate a pseudo-normalization of APFR and PFRR.

##### CLINICAL RELEVANCE/APPLICATION

LGE+ triathletes show a diastolic LV filling at rest with a compensatory increase of atrial contraction rates compared to LGE- triathletes. This might suggest that diffuse myocardial fibrosis is associated with reduced passive elasticity of the hypertrophied left ventricle.

#### M5A-SPCA-3 Free-breathing pseudo-golden-angle bSSFP cine cardiac MRI for evaluation of biventricular function in patients with congenital heart disease

##### Participants

Dmitrij Kravchenko, MD, Bonn, Germany (*Presenter*) Nothing to Disclose

##### PURPOSE

To compare free-breathing (FB) multi-slice respiratory-triggered pseudo-golden-angle balanced steady state free precession (bSSFP) cine cardiac MRI (CMR) to standard breath hold (BH) sequences in congenital heart disease (CHD) patients who have trouble suspending respiration.

##### METHODS AND MATERIALS

Twenty-five CHD patients (mean age 24±9 years, 17 males) underwent routine CMR including breath-hold (BH) 4-chamber (4C) and short axis (SA) cine imaging. FB pseudo-golden-angle bSSFP cine 4C and SA were acquired using ECG-gating and respiratory belt-triggering (at the expiratory phase with 150 ms duration for start-up excitation to drive the magnetization to steady state). Sequences were quantitatively analyzed for biventricular volumes, function, signal to noise ratio (SNR), and estimated contrast to noise ratio (CNR). Qualitative image comparison was evaluated for contrast, endocardial edge definition, and artefacts, on a 5-point numeric rating scale. Statistical analysis was carried out using a two-tailed paired t-Test and Bland-Altman analysis for direct comparisons.

##### RESULTS

No statistical differences were found between the BH and FB sequences regarding intraventricular septum thickness in diastole

no statistical differences were found between the BH and FB sequences regarding intraventricular septum thickness in diastole (IVSD,  $7.4 \pm 2.0$  mm vs  $7.4 \pm 1.8$  mm,  $p=.71$ ), biventricular ejection fraction (left:  $56.4 \pm 10.3$  % vs  $55.7 \pm 8.5$  %,  $p=.57$ ; right:  $49.3 \pm 9.1$  % vs  $49.3 \pm 10.8$  %,  $p=.93$ ), or biventricular end diastolic volume (left:  $176.3 \pm 65.8$  ml vs  $173.9 \pm 66.6$  ml,  $p=.47$ ; right:  $186.6 \pm 75.8$  ml vs  $184.0 \pm 56.3$  ml,  $p=.81$ ). Average acquisition times for FB SA sequences was 9.22 min. compared to 4.26 min. for BH. Subjective image quality was comparable, yet slightly in favour of the BH sequences (BH 4C  $13.9 \pm 1.8$  and SA  $14.7 \pm 1.0$  vs FB 4C  $13.4 \pm 1.8$  and SA  $13.6 \pm 1.6$ ). SNR and CNR values were higher for the BH sequences compared to FB (SNR SA  $1.0 \pm 0.7$  and CNR SA  $124.1 \pm 35.5$  vs SNR SA  $0.4 \pm 0.3$  and CNR SA  $91.7 \pm 45.7$ , respectively).

## **CONCLUSION**

s FB sequences performed nearly identical to currently available BH sequences regarding ventricular volumetry and function, producing images subjectively slightly inferior to normal BH sequences while remaining diagnostic, providing sufficient data when BH could not be or were insufficiently performed.

## **CLINICAL RELEVANCE/APPLICATION**

Free-breathing respiratory-triggered pseudo-golden-angle bSSFP imaging provides comparable diagnostic quality images to standard BH sequences in CHD patients, offering an alternative when breath-holding capacities are limited.

Printed on: 02/07/23

## Abstract Archives of the RSNA, 2022

M5A-SPCA-1

### Left ventricular diastolic filling pattern in competitive triathletes with and without myocardial fibrosis compared to sedentary controls by CMR imaging

Monday, Nov. 28 12:15PM - 12:45PM Room: Learning Center - CA DPS

#### Participants

Hang Chen, MD, Hamburg, Germany (*Presenter*) Nothing to Disclose

#### PURPOSE

Endurance athletes have a higher incidence of myocardial fibrosis than the general population. However, it remains unclear whether myocardial fibrosis leads to any alterations of left ventricular (LV) diastolic function. The aim of this study was to investigate the diastolic LV filling pattern in triathletes, and the influence of myocardial fibrosis by cardiac magnetic resonance (CMR) imaging.

#### METHODS AND MATERIALS

101 male triathletes (age:  $43 \pm 11$  years) and 28 male controls (age:  $41 \pm 10$  years) were recruited through advertisement in local triathlon clubs. All participants underwent CMR including cine SSFP series, late gadolinium enhancement (LGE) imaging and T1 mapping. Functional and morphological ventricular parameters were obtained, including LV mass and ejection fraction (EF). Diastolic LV filling was determined by a time-volume analysis using cine series (25 phases of the cardiac cycle). Early peak-filling rates (EPFR) and atrial peak-filling rates (APFR) as well as peak-filling rate ratios (PFRR=EPFR/APFR) were determined.

#### RESULTS

Focal myocardial fibrosis (LGE+) was detected in 20 triathletes (20%) and in none of the controls. LVEF was similar in both triathletes and controls ( $61 \pm 6$  vs.  $62 \pm 7\%$ ;  $P=0.36$ ). LGE+ triathletes had a higher LV mass ( $88 \pm 10$  vs.  $80 \pm 12$  g/m<sup>2</sup>;  $P<0.01$ ) and extracellular volume (ECV) ( $26 \pm 3$  vs.  $24 \pm 2\%$ ;  $P<0.001$ ) compared to LGE- triathletes. EPFR was similar in LGE- triathletes and controls ( $216 \pm 58$  vs.  $224 \pm 69$  ml/s/m<sup>2</sup>;  $P=0.52$ ). LGE- triathletes had lower APFR ( $120 \pm 46$  vs.  $147 \pm 55$  ml/s/m<sup>2</sup>;  $P<0.05$ ) and higher PFRR ( $2.1 \pm 1$  vs.  $1.6 \pm 0.5$ ;  $P<0.05$ ) compared to controls. LGE+ triathletes had similar EPFR ( $212 \pm 73$  ml/s/m<sup>2</sup>;  $P=0.80$ ), higher APFR ( $149 \pm 50$  ml/s/m<sup>2</sup>;  $P<0.05$ ) and decreased PFRR ( $1.6 \pm 0.7$ ,  $P<0.05$ ) compared to LGE- triathletes. EPFR ( $P=0.52$ ), APFR ( $P=0.91$ ) and PFRR ( $P=0.67$ ) were similar in LGE+ triathletes compared to controls.

#### CONCLUSION

While adaptations in diastolic LV filling in LGE- triathletes are characterized by decreased APFR and increased PFRR compared to sedentary controls, LGE+ triathletes demonstrate a pseudo-normalization of APFR and PFRR.

#### CLINICAL RELEVANCE/APPLICATION

LGE+ triathletes show a diastolic LV filling at rest with a compensatory increase of atrial contraction rates compared to LGE- triathletes. This might suggest that diffuse myocardial fibrosis is associated with reduced passive elasticity of the hypertrophied left ventricle.

Printed on: 02/07/23

## Abstract Archives of the RSNA, 2022

M5A-SPCA-3

### Free-breathing pseudo-golden-angle bSSFP cine cardiac MRI for evaluation of biventricular function in patients with congenital heart disease

Monday, Nov. 28 12:15PM - 12:45PM Room: Learning Center - CA DPS

#### Participants

Dmitrij Kravchenko, MD, Bonn, Germany (*Presenter*) Nothing to Disclose

#### PURPOSE

To compare free-breathing (FB) multi-slice respiratory-triggered pseudo-golden-angle balanced steady state free precession (bSSFP) cine cardiac MRI (CMR) to standard breath hold (BH) sequences in congenital heart disease (CHD) patients who have trouble suspending respiration.

#### METHODS AND MATERIALS

Twenty-five CHD patients (mean age 24±9 years, 17 males) underwent routine CMR including breath-hold (BH) 4-chamber (4C) and short axis (SA) cine imaging. FB pseudo-golden-angle bSSFP cine 4C and SA were acquired using ECG-gating and respiratory belt-triggering (at the expiratory phase with 150 ms duration for start-up excitation to drive the magnetization to steady state). Sequences were quantitatively analyzed for biventricular volumes, function, signal to noise ratio (SNR), and estimated contrast to noise ratio (CNR). Qualitative image comparison was evaluated for contrast, endocardial edge definition, and artefacts, on a 5-point numeric rating scale. Statistical analysis was carried out using a two tailed paired t-Test and Bland-Altman analysis for direct comparisons.

#### RESULTS

No statistical differences were found between the BH and FB sequences regarding intraventricular septum thickness in diastole (IVSD, 7.4±2.0 mm vs 7.4±1.8 mm, p=.71), biventricular ejection fraction (left: 56.4±10.3 % vs 55.7±8.5 %, p=.57; right: 49.3±9.1 % vs 49.3±10.8 %, p=.93), or biventricular end diastolic volume (left: 176.3±65.8 ml vs 173.9±66.6 ml, p=.47; right: 186.6±75.8 ml vs 184.0±56.3 ml, p=.81). Average acquisition times for FB SA sequences was 9.22 min. compared to 4.26 min. for BH. Subjective image quality was comparable, yet slightly in favour of the BH sequences (BH 4C 13.9±1.8 and SA 14.7±1.0 vs FB 4C 13.4±1.8 and SA 13.6±1.6). SNR and CNR values were higher for the BH sequences compared to FB (SNR SA 1.0±0.7 and CNR SA 124.1±35.5 vs SNR SA 0.4±0.3 and CNR SA 91.7±45.7, respectively).

#### CONCLUSION

s FB sequences performed nearly identical to currently available BH sequences regarding ventricular volumetry and function, producing images subjectively slightly inferior to normal BH sequences while remaining diagnostic, providing sufficient data when BH could not be or were insufficiently performed.

#### CLINICAL RELEVANCE/APPLICATION

Free-breathing respiratory-triggered pseudo-golden-angle bSSFP imaging provides comparable diagnostic quality images to standard BH sequences in CHD patients, offering an alternative when breath-holding capacities are limited.

Printed on: 02/07/23

## Abstract Archives of the RSNA, 2022

M5A-SPCH

### Chest Monday Poster Discussions - A

Monday, Nov. 28 12:15PM - 12:45PM Room: Learning Center - CH DPS

#### Participants

Stephen Hobbs, MD, Lexington, KY (*Moderator*) Author with royalties, Wolters Kluwer nv; Author with royalties, RELX

#### Sub-Events

### M5A-SPCH-2 Quantitative CT and Machine Learning Classification of Fibrotic Interstitial Lung Diseases

#### Participants

Grace Liu, MD, (*Presenter*) Nothing to Disclose

#### PURPOSE

To evaluate quantitative computed tomography (QCT) features and QCT feature-based machine learning (ML) models in classifying interstitial lung diseases (ILDs). To compare QCT-ML and deep learning (DL) models' performance.

#### METHODS AND MATERIALS

We retrospectively identified 1085 patients with pathologically proven usual interstitial pneumonitis (UIP), nonspecific interstitial pneumonitis (NSIP) and chronic hypersensitivity pneumonitis (CHP) who underwent peri-biopsy chest CT. Kruskal-Wallis test evaluated QCT feature associations with each ILD. QCT features, patient demographics and pulmonary function test (PFT) results trained eXtreme Gradient Boosting (training/validation set n=911) yielding 3 models: M1=QCT features only; M2=M1 plus age and sex; M3=M2 plus PFT results. A DL model was also developed. ML and DL model areas under the receiver operating characteristic curve (AUC) and 95% confidence intervals (CIs) were compared for multiclass (UIP vs. NSIP vs. CHP) and binary (UIP vs. non-UIP) classification performances.

#### RESULTS

The majority (69/78 [88%]) of QCT features successfully differentiated the 3 ILDs (adjusted p=0.05). All QCT-ML models achieved higher AUC than the DL model (multiclass AUC micro-averages: 0.910, 0.910, 0.925, 0.798 and macro-averages: 0.895, 0.893, 0.925, 0.779 for M1, M2, M3 and DL respectively; binary AUC: 0.880, 0.899, 0.898, 0.869 for M1, M2, M3 and DL respectively). M3 demonstrated statistically significant better performance compared to M2 (?AUC:0.015, CI:[0.002,0.029]) for multiclass prediction.

#### CONCLUSION

s QCT features successfully differentiated pathologically proven UIP, NSIP and CHP. While QCT-based ML models outperformed a DL model for classifying ILDs, further investigations are warranted to determine if QCT-ML, DL, or a combination will be superior in ILD classification.

#### CLINICAL RELEVANCE/APPLICATION

CALIPER-based ML model demonstrated high performance in classifying UIP, NSIP and CHP using pathology as reference, outperforming a DL model. While further validation is needed, a CALIPER-based ML model may mitigate the need for invasive wedge biopsies and may be useful in multidisciplinary diagnosis.

### M5A-SPCH-3 Deep Learning-Based Survival Prediction in Patients with Idiopathic Pulmonary Fibrosis Using Chest Radiographs

#### Participants

Taehee Lee, MD, Seoul, Korea, Republic Of (*Presenter*) Nothing to Disclose

#### PURPOSE

Predicting prognosis in patients with idiopathic pulmonary fibrosis (IPF) is important in determining management plans and follow-up intervals. Various clinical indices including GAP index had been devised, however, chest radiographs (CXR) were seldom utilized. We aimed to develop and validate a deep learning-based survival prediction algorithm for patients with IPF using CXRs.

#### METHODS AND MATERIALS

Patients diagnosed with IPF and underwent spirometry and CXR within 1 month in a single institution during 2011-2021 were retrospectively collected and split into training (n=911), validation (n=112), and internal test (n=187) datasets. A deep-learning algorithm predicting survival from CXR was trained (DLSP). For external testing, two cohorts were collected from two different institutions (EXT-A and B; n=178 [mean age 66.6 ± 10.3; 116 men] and n=101 [mean age 70.9 ± 7.5; 87 men], each). The discrimination performance of DLSP was evaluated and compared with that of forced vital capacity (FVC) using time-dependent area-under-the-receiver-operating-characteristic curves (TD-AUCs) for 1-year and 3-year survivals. Cox regression was performed to see if DLSP was independent prognostic factor adjusted to FVC. Goodness-of-fit was assessed using the Hosmer-Lemeshow test for model calibration. We proposed modified GAP index (GAP-CXR) which utilizes DLSP instead of DLCO: DLSP results were categorized by quartiles calculated from internal test dataset. TD-AUCs of GAP index and GAP-CXR index were compared.

## RESULTS

DLSP showed 1-yr and 3-yr TD-AUCs of 0.832 and 0.753 in EXT-A cohort and 0.838 and 0.785 in EXT-B cohort, while FVC exhibited 1-yr and 3-yr TD-AUCs of 0.769 and 0.679 in EXT-A cohort and 0.568 and 0.634 in EXT-B cohort. DLSP showed significantly higher performance in predicting 1-yr ( $P=.03$ ) and 3-yr survival ( $P=.02$ ) in EXT-B cohort. In both external test cohorts, DLSP worked as an independent predictor when adjusted to FVC ( $P_s<.001$ ) and showed good calibration ( $P_s>.05$ ). When GAP index was modified to use DLSP instead of DLCO results, GAP-CXR showed comparable performance to original GAP index in EXT-A cohort (1yr TD-AUC, 0.884 vs. 0.893,  $P=.68$ ; 3yr TD-AUC, 0.822 vs. 0.820,  $P=.95$ ) and higher performance in EXT-B cohort (1yr TD-AUC, 0.845 vs. 0.705,  $P=.003$ ; 3yr TD-AUC, 0.718 vs. 0.621,  $P=.03$ ).

## CONCLUSION

s DLSP using chest radiographs worked as a significant survival predictor for patients with IPF, surpassing and independent of FVC. Modified GAP index replacing DLCO by DLSP results showed comparable-to-superior performance than original GAP index.

## CLINICAL RELEVANCE/APPLICATION

By predicting life expectancy of patients with IPF using easily accessible chest radiographs, personalized management could be achieved.

## M5A-SPCH-5 Volumetric and Movement CT Analysis of Lung Parenchyma in Prone Positioning using Deep Neural Networks

Participants

Hyungin Park, MD, Seoul, Korea, Republic Of (*Presenter*) Nothing to Disclose

## PURPOSE

To conduct a volumetric and movement analysis of lung parenchyma in prone positioning using deep neural networks (DNNs).

## METHODS AND MATERIALS

We included patients suspected of interstitial lung abnormalities or disease undergoing full-inspiratory supine and prone chest CT scans in a single institution between June 2021 and March 2022. A thoracic radiologist visually assessed the fibrosis extent in units of 10% of a total lung on supine CT images. Lobar volumes and the extent of overall fibrosis in each lobe were quantified on supine and prone CT images with the help of a previously developed 3DnnUNET. A publicly-available DNN-based deformable image registration, LungReg, was used to register supine and prone CT images: sequential affine and deformable registration. Affine registration matched patient centers and locations between supine and prone CT images. Then, we calculated pixel movement during deformable registration to calculate the x, y, z-axis, and 3-dimensional (3D) lung pixel movement of prone positioning. After registration, the radiologist visually evaluated subtraction images to check whether the registration succeeded.

## RESULTS

A total of 122 CT pairs in patients (mean age, 68.1 years; 65 men) had successful CT image registration. Prone positioning significantly increased left lower ( $90.2\pm 69.5$  mL) and right lower lobar volumes ( $52.5\pm 74.2$  mL), whereas right upper ( $-15.5\pm 54.4$  mL) and middle lobar volumes ( $-33.9\pm 44.8$  mL) decreased (all  $p=.003$ ). During the deformable registration, averaged maximum whole-lung pixel movements between prone and supine positions were 1.5, 1.9, 1.6, and 2.9 cm in x, y, z-axis, and 3D planes, each. Compared to patients having fibrosis <30%, those with fibrosis =30% had a smaller volume change ( $p<.001$ ) and smaller maximum pixel movements in all axes between the positions ( $p=.000$  to  $.007$ ). FVC was correlated with left lower lobar volume increases (Spearman coefficient, .238) and the maximum whole-lung pixel movements in all axes (coefficients, .311 to .357).

## CONCLUSION

s Prone positioning led to the expansion of lower lobes correlated with FVC, and lung fibrosis limited the lung expansion of prone positioning.

## CLINICAL RELEVANCE/APPLICATION

Lower lobe recruitment in prone positioning is quantifiable on CT images and can be a new imaging biomarker for assessing lung function in interstitial lung disease.

## M5A-SPCH-8 Machine Learning Based Computer-Aided Simple Triage (CAST): Capabilities for COVID-19 Pneumonia Triage based on RSNA Expert Consensus Statement and Radiological Finding Evaluations in Multi-Center Study

Participants

Yoshiharu Ohno, MD, PhD, Toyooka, Japan (*Presenter*) Research Grant, Canon Medical Systems Corporation; Research Grant, Daiichi Sankyo Co, Ltd; Research Grant, Ministry of Education, Culture, Sports, Science and Technology

## PURPOSE

To determine the capability of machine learning (ML) based computer-aided simple triage (CAST) software based on RSNA expert consensus statement for diagnosis of COVID-19 pneumonia in multicenter study.

## METHODS AND MATERIALS

174 cases underwent CT and polymerase chain reaction (PCR) test for COVID-19 (87 PCR positive and 87 PCR negative cases) were retrospectively included in this multicenter study. Then, CT data were assessed by CAST and consensus from three independent board-certified chest radiologists, and all cases were divided into three groups as follows: positive cases (i.e. typical and indeterminate appearances), atypical appearance and negative for pneumonia (i.e. latter two groups were assessed as negative cases). To determine radiological finding evaluation capability with CAST, three other board-certified chest radiologists also assessed CAST results of radiological finding including pulmonary emphysema, nodular lesion, consolidation, ground-glass opacity, reticulation and honeycombing within 156 slices selected by central reading team and classified into five criteria as follows: agree, acceptable, disagree, true negative and false positive, respectively. To determine capability of CAST, agreements between CAST and consensus were evaluated by kappa statistics with  $\chi^2$  test. Then, sensitivity (SE), specificity (SP) and accuracy (AC) between CAST and PCR were compared with those between consensus and PCR by McNemar's test. To determine overall radiological finding

evaluation capability, each radiological finding accuracy of CAST (i.e. percentage of agree, acceptable and true negative lesions/ all evaluated lesions) were assessed in all readers. Moreover, overall interobserver agreements between each two readers were determined by kappa statistics with  $\chi^2$  test.

## **RESULTS**

Agreement between CAST and consensus evaluations were determined as moderate ( $\kappa=0.55$ ,  $p<0.0001$ ). No significant difference of SE (88.5%) was observed between CAST and consensus, although SP (47.1%) and AC (67.8%) of CAST were significantly lower than those of consensus (SP: 79.3%,  $p<0.0001$ ; AC: 83.9%,  $p<0.0001$ ). Accuracies for radiological finding evaluation by CAST were determined as follows: reader A, 91.7-99.4%; reader B, 99.4-100%, reader C, 99.4-100%. Overall interobserver agreements between each two readers were assessed as substantial or almost perfect ( $0.65<\kappa<0.96$ ,  $p<0.0001$ ).

## **CONCLUSION**

s This multicenter study shows CAST is considered at least as valuable as radiologists for COVID-19 pneumonia triage with accurate radiological finding evaluations.

## **CLINICAL RELEVANCE/APPLICATION**

CAST is considered at least as valuable as radiologists for COVID-19 pneumonia triage with accurate radiological finding evaluations.

Printed on: 02/07/23

## Abstract Archives of the RSNA, 2022

M5A-SPCH-2

### Quantitative CT and Machine Learning Classification of Fibrotic Interstitial Lung Diseases

Monday, Nov. 28 12:15PM - 12:45PM Room: Learning Center - CH DPS

#### Participants

Grace Liu, MD, (*Presenter*) Nothing to Disclose

#### PURPOSE

To evaluate quantitative computed tomography (QCT) features and QCT feature-based machine learning (ML) models in classifying interstitial lung diseases (ILDs). To compare QCT-ML and deep learning (DL) models' performance.

#### METHODS AND MATERIALS

We retrospectively identified 1085 patients with pathologically proven usual interstitial pneumonitis (UIP), nonspecific interstitial pneumonitis (NSIP) and chronic hypersensitivity pneumonitis (CHP) who underwent peri-biopsy chest CT. Kruskal-Wallis test evaluated QCT feature associations with each ILD. QCT features, patient demographics and pulmonary function test (PFT) results trained eXtreme Gradient Boosting (training/validation set n=911) yielding 3 models: M1=QCT features only; M2=M1 plus age and sex; M3=M2 plus PFT results. A DL model was also developed. ML and DL model areas under the receiver operating characteristic curve (AUC) and 95% confidence intervals (CIs) were compared for multiclass (UIP vs. NSIP vs. CHP) and binary (UIP vs. non-UIP) classification performances.

#### RESULTS

The majority (69/78 [88%]) of QCT features successfully differentiated the 3 ILDs (adjusted p=0.05). All QCT-ML models achieved higher AUC than the DL model (multiclass AUC micro-averages: 0.910, 0.910, 0.925, 0.798 and macro-averages: 0.895, 0.893, 0.925, 0.779 for M1, M2, M3 and DL respectively; binary AUC: 0.880, 0.899, 0.898, 0.869 for M1, M2, M3 and DL respectively). M3 demonstrated statistically significant better performance compared to M2 (?AUC:0.015, CI:[0.002,0.029]) for multiclass prediction.

#### CONCLUSION

s QCT features successfully differentiated pathologically proven UIP, NSIP and CHP. While QCT-based ML models outperformed a DL model for classifying ILDs, further investigations are warranted to determine if QCT-ML, DL, or a combination will be superior in ILD classification.

#### CLINICAL RELEVANCE/APPLICATION

CALIPER-based ML model demonstrated high performance in classifying UIP, NSIP and CHP using pathology as reference, outperforming a DL model. While further validation is needed, a CALIPER-based ML model may mitigate the need for invasive wedge biopsies and may be useful in multidisciplinary diagnosis.

Printed on: 02/07/23

## Abstract Archives of the RSNA, 2022

M5A-SPCH-3

### Deep Learning-Based Survival Prediction in Patients with Idiopathic Pulmonary Fibrosis Using Chest Radiographs

Monday, Nov. 28 12:15PM - 12:45PM Room: Learning Center - CH DPS

#### Participants

Taehee Lee, MD, Seoul, Korea, Republic Of (*Presenter*) Nothing to Disclose

#### PURPOSE

Predicting prognosis in patients with idiopathic pulmonary fibrosis (IPF) is important in determining management plans and follow-up intervals. Various clinical indices including GAP index had been devised, however, chest radiographs (CXR) were seldom utilized. We aimed to develop and validate a deep learning-based survival prediction algorithm for patients with IPF using CXRs.

#### METHODS AND MATERIALS

Patients diagnosed with IPF and underwent spirometry and CXR within 1 month in a single institution during 2011-2021 were retrospectively collected and split into training (n=911), validation (n=112), and internal test (n=187) datasets. A deep-learning algorithm predicting survival from CXR was trained (DLSP). For external testing, two cohorts were collected from two different institutions (EXT-A and B; n=178 [mean age 66.6 ± 10.3; 116 men] and n=101 [mean age 70.9 ± 7.5; 87 men], each). The discrimination performance of DLSP was evaluated and compared with that of forced vital capacity (FVC) using time-dependent area-under-the receiver-operating characteristic curves (TD-AUCs) for 1-year and 3-year survivals. Cox regression was performed to see if DLSP was independent prognostic factor adjusted to FVC. Goodness-of-fit was assessed using the Hosmer-Lemeshow test for model calibration. We proposed modified GAP index (GAP-CXR) which utilizes DLSP instead of DLCO: DLSP results were categorized by quartiles calculated from internal test dataset. TD-AUCs of GAP index and GAP-CXR index were compared.

#### RESULTS

DLSP showed 1-yr and 3-yr TD-AUCs of 0.832 and 0.753 in EXT-A cohort and 0.838 and 0.785 in EXT-B cohort, while FVC exhibited 1-yr and 3-yr TD-AUCs of 0.769 and 0.679 in EXT-A cohort and 0.568 and 0.634 in EXT-B cohort. DLSP showed significantly higher performance in predicting 1-yr (P=.03) and 3-yr survival (P=.02) in EXT-B cohort. In both external test cohorts, DLSP worked as an independent predictor when adjusted to FVC (Ps<.001) and showed good calibration (Ps>.05). When GAP index was modified to use DLSP instead of DLCO results, GAP-CXR showed comparable performance to original GAP index in EXT-A cohort (1yr TD-AUC, 0.884 vs. 0.893, P=.68; 3yr TD-AUC, 0.822 vs. 0.820, P=.95) and higher performance in EXT-B cohort (1yr TD-AUC, 0.845 vs. 0.705, P=.003; 3yr TD-AUC, 0.718 vs. 0.621, P=.03).

#### CONCLUSION

s DLSP using chest radiographs worked as a significant survival predictor for patients with IPF, surpassing and independent of FVC. Modified GAP index replacing DLCO by DLSP results showed comparable-to-superior performance than original GAP index.

#### CLINICAL RELEVANCE/APPLICATION

By predicting life expectancy of patients with IPF using easily accessible chest radiographs, personalized management could be achieved.

Printed on: 02/07/23

## Abstract Archives of the RSNA, 2022

MSA-SPCH-5

### Volumetric and Movement CT Analysis of Lung Parenchyma in Prone Positioning using Deep Neural Networks

Monday, Nov. 28 12:15PM - 12:45PM Room: Learning Center - CH DPS

#### Participants

Hyungin Park, MD, Seoul, Korea, Republic Of (*Presenter*) Nothing to Disclose

#### PURPOSE

To conduct a volumetric and movement analysis of lung parenchyma in prone positioning using deep neural networks (DNNs).

#### METHODS AND MATERIALS

We included patients suspected of interstitial lung abnormalities or disease undergoing full-inspiratory supine and prone chest CT scans in a single institution between June 2021 and March 2022. A thoracic radiologist visually assessed the fibrosis extent in units of 10% of a total lung on supine CT images. Lobar volumes and the extent of overall fibrosis in each lobe were quantified on supine and prone CT images with the help of a previously developed 3DnnUNET. A publicly-available DNN-based deformable image registration, LungReg, was used to register supine and prone CT images: sequential affine and deformable registration. Affine registration matched patient centers and locations between supine and prone CT images. Then, we calculated pixel movement during deformable registration to calculate the x, y, z-axis, and 3-dimensional (3D) lung pixel movement of prone positioning. After registration, the radiologist visually evaluated subtraction images to check whether the registration succeeded.

#### RESULTS

A total of 122 CT pairs in patients (mean age, 68.1 years; 65 men) had successful CT image registration. Prone positioning significantly increased left lower (90.2±69.5 mL) and right lower lobar volumes (52.5±74.2 mL), whereas right upper (-15.5±54.4 mL) and middle lobar volumes (-33.9±44.8 mL) decreased (all p=.003). During the deformable registration, averaged maximum whole-lung pixel movements between prone and supine positions were 1.5, 1.9, 1.6, and 2.9 cm in x, y, z-axis, and 3D planes, each. Compared to patients having fibrosis <30%, those with fibrosis =30% had a smaller volume change (p<.001) and smaller maximum pixel movements in all axes between the positions (p=.000 to .007). FVC was correlated with left lower lobar volume increases (Spearman coefficient, .238) and the maximum whole-lung pixel movements in all axes (coefficients, .311 to .357).

#### CONCLUSION

Prone positioning led to the expansion of lower lobes correlated with FVC, and lung fibrosis limited the lung expansion of prone positioning.

#### CLINICAL RELEVANCE/APPLICATION

Lower lobe recruitment in prone positioning is quantifiable on CT images and can be a new imaging biomarker for assessing lung function in interstitial lung disease.

Printed on: 02/07/23

## Abstract Archives of the RSNA, 2022

M5A-SPCH-8

### Machine Learning Based Computer-Aided Simple Triage (CAST): Capabilities for COVID-19 Pneumonia Triage based on RSNA Expert Consensus Statement and Radiological Finding Evaluations in Multi-Center Study

Monday, Nov. 28 12:15PM - 12:45PM Room: Learning Center - CH DPS

#### Participants

Yoshiharu Ohno, MD, PhD, Toyooka, Japan (*Presenter*) Research Grant, Canon Medical Systems Corporation; Research Grant, Daiichi Sankyo Co, Ltd; Research Grant, Ministry of Education, Culture, Sports, Science and Technology

#### PURPOSE

To determine the capability of machine learning (ML) based computer-aided simple triage (CAST) software based on RSNA expert consensus statement for diagnosis of COVID-19 pneumonia in multicenter study.

#### METHODS AND MATERIALS

174 cases underwent CT and polymerase chain reaction (PCR) test for COVID-19 (87 PCR positive and 87 PCR negative cases) were retrospectively included in this multicenter study. Then, CT data were assessed by CAST and consensus from three independent board-certified chest radiologists, and all cases were divided into three groups as follows: positive cases (i.e. typical and indeterminate appearances), atypical appearance and negative for pneumonia (i.e. latter two groups were assessed as negative cases). To determine radiological finding evaluation capability with CAST, three other board-certified chest radiologists also assessed CAST results of radiological finding including pulmonary emphysema, nodular lesion, consolidation, ground-glass opacity, reticulation and honeycombing within 156 slices selected by central reading team and classified into five criteria as follows: agree, acceptable, disagree, true negative and false positive, respectively. To determine capability of CAST, agreements between CAST and consensus were evaluated by kappa statistics with  $\chi^2$  test. Then, sensitivity (SE), specificity (SP) and accuracy (AC) between CAST and PCR were compared with those between consensus and PCR by McNemar's test. To determine overall radiological finding evaluation capability, each radiological finding accuracy of CAST (i.e. percentage of agree, acceptable and true negative lesions/all evaluated lesions) were assessed in all readers. Moreover, overall interobserver agreements between each two readers were determined by kappa statistics with  $\chi^2$  test.

#### RESULTS

Agreement between CAST and consensus evaluations were determined as moderate ( $\kappa=0.55$ ,  $p<0.0001$ ). No significant difference of SE (88.5%) was observed between CAST and consensus, although SP (47.1%) and AC (67.8%) of CAST were significantly lower than those of consensus (SP: 79.3%,  $p<0.0001$ ; AC: 83.9%,  $p<0.0001$ ). Accuracies for radiological finding evaluation by CAST were determined as follows: reader A, 91.7-99.4%; reader B, 99.4-100%, reader C, 99.4-100%. Overall interobserver agreements between each two readers were assessed as substantial or almost perfect ( $0.65<\kappa<0.96$ ,  $p<0.0001$ ).

#### CONCLUSION

This multicenter study shows CAST is considered at least as valuable as radiologists for COVID-19 pneumonia triage with accurate radiological finding evaluations.

#### CLINICAL RELEVANCE/APPLICATION

CAST is considered at least as valuable as radiologists for COVID-19 pneumonia triage with accurate radiological finding evaluations.

Printed on: 02/07/23

## Abstract Archives of the RSNA, 2022

M5A-SPER

### Emergency Monday Poster Discussions - A

Monday, Nov. 28 12:15PM - 12:45PM Room: Learning Center - ER DPS

#### Participants

Karen S. Lee, MD, Newton, MA (*Moderator*) Nothing to Disclose

#### Sub-Events

### M5A-SPER-1 Blunt Splenic Trauma: Accuracy of Automated Active Bleed and Contained Vascular Injury Detection on CT with Faster R-CNN

#### Participants

Alexander Upegui, Baltimore, MD (*Presenter*) Nothing to Disclose

#### PURPOSE

Contained vascular injury (CVI) and active bleeding (AB) are indications for intervention after blunt splenic trauma. Automated tools in this high-stakes setting require a high level of transparency and interpretability. AB and CVI are components of AAST grading and future interpretable human-centered AAST-based CAD tools will require accurate multi-feature detection. We evaluate performance of a 2D Faster-RCNN deep learning object detection framework for AB and CVI.

#### METHODS AND MATERIALS

An existing single institution dataset was used which included abdominal CT scans from 174 consecutively selected BSI patients archived at 1.5 mm section thickness and with voxelwise labeling of CVI on arterial images and AB on PVP images. 2D Faster-RCNN was employed given its well-known high performance for cross-sectional imaging object detection. Training and validation were performed in 5 folds with 80/20 split of the data using the most appropriate imaging phase for each task (arterial phase- CVI; PVP-active bleed). Since the 2018-AAST scoring system approaches CVI and AB in a binary fashion (intervention is typically warranted if either are present), accuracy metrics were determined at the patient level based on the highest probability box detection for each feature.

#### RESULTS

Of the 174 patients, 28.1% had CVI, and 14.9% had AB. The overall accuracy of Faster R-CNN for AB detection on PVP images was 86% with sens, spec, NPV PPV of 85, 85, 92, and 74%. The accuracy for CVI detection on arterial images was 84%, with sens, spec, NPV PPV of 91, 73, 94, and 61%. In patients with detected vascular lesions, intervention (either embolization or splenectomy) was performed in 88.9%.

#### CONCLUSION

s In this initial proof of concept study with single institution data, Faster R-CNN was useful for confident exclusion of AB or PSA (NPV 92 and 94%). As with lung nodule detection where Faster R-CNN is frequently employed, low PPV remained a challenge owing to false positives. Given the wide variability in appearances of CVI and AB, improved results are expected with large multi-institutional datasets. Further improvements could also be achieved with modifications in pre-processing (e.g., MIPs), and modifications in network architecture (e.g., residual networks) for false positive reduction.

#### CLINICAL RELEVANCE/APPLICATION

To our knowledge, we present the first implementation of object detection for splenic vascular lesions on CT. The method denotes lesions with box proposals and could be incorporated into interpretable automated AAST CAD grading systems in the future.

Printed on: 02/07/23

## Abstract Archives of the RSNA, 2022

M5A-SPER-1

### Blunt Splenic Trauma: Accuracy of Automated Active Bleed and Contained Vascular Injury Detection on CT with Faster R-CNN

Monday, Nov. 28 12:15PM - 12:45PM Room: Learning Center - ER DPS

#### Participants

Alexander Upegui, Baltimore, MD (*Presenter*) Nothing to Disclose

#### PURPOSE

Contained vascular injury (CVI) and active bleeding (AB) are indications for intervention after blunt splenic trauma. Automated tools in this high-stakes setting require a high level of transparency and interpretability. AB and CVI are components of AAST grading and future interpretable human-centered AAST-based CAD tools will require accurate multi-feature detection. We evaluate performance of a 2D Faster-RCNN deep learning object detection framework for AB and CVI.

#### METHODS AND MATERIALS

An existing single institution dataset was used which included abdominal CT scans from 174 consecutively selected BSI patients archived at 1.5 mm section thickness and with voxelwise labeling of CVI on arterial images and AB on PVP images. 2D Faster-RCNN was employed given its well-known high performance for cross-sectional imaging object detection. Training and validation were performed in 5 folds with 80/20 split of the data using the most appropriate imaging phase for each task (arterial phase- CVI; PVP-active bleed). Since the 2018-AAST scoring system approaches CVI and AB in a binary fashion (intervention is typically warranted if either are present), accuracy metrics were determined at the patient level based on the highest probability box detection for each feature.

#### RESULTS

Of the 174 patients, 28.1% had CVI, and 14.9% had AB. The overall accuracy of Faster R-CNN for AB detection on PVP images was 86% with sens, spec, NPV PPV of 85, 85, 92, and 74%. The accuracy for CVI detection on arterial images was 84%, with sens, spec, NPV PPV of 91, 73, 94, and 61%. In patients with detected vascular lesions, intervention (either embolization or splenectomy) was performed in 88.9%.

#### CONCLUSION

In this initial proof of concept study with single institution data, Faster R-CNN was useful for confident exclusion of AB or PSA (NPV 92 and 94%). As with lung nodule detection where Faster R-CNN is frequently employed, low PPV remained a challenge owing to false positives. Given the wide variability in appearances of CVI and AB, improved results are expected with large multi-institutional datasets. Further improvements could also be achieved with modifications in pre-processing (e.g., MIPs), and modifications in network architecture (e.g., residual networks) for false positive reduction.

#### CLINICAL RELEVANCE/APPLICATION

To our knowledge, we present the first implementation of object detection for splenic vascular lesions on CT. The method denotes lesions with box proposals and could be incorporated into interpretable automated AAST CAD grading systems in the future.

Printed on: 02/07/23

## Abstract Archives of the RSNA, 2022

M5A-SPGI

### Gastrointestinal Monday Poster Discussions - A

Monday, Nov. 28 12:15PM - 12:45PM Room: Learning Center - GI DPS

#### Participants

Parag P. Tolat, MD, Milwaukee, WI (*Moderator*) Nothing to Disclose

#### Sub-Events

### M5A-SPGI-1 Prediction of Postoperative Anastomotic Recurrence in Crohn's Disease Using Preoperative CTE Radiomic Data

#### Participants

Xiao Di Shen, (*Presenter*) Nothing to Disclose

#### PURPOSE

More than half of patients with Crohn's disease (CD) need at least one surgery in their life, however, most patients will experience postoperative anastomotic recurrence (PAR). Stratifying them according to the risk of PAR and tailoring therapy are the most cost-effective way to manage these patients. This study aimed to develop and validate a novel preoperative clinical-radiological-radiomic model to predict the risk of PAR.

#### METHODS AND MATERIALS

This retrospective study included 186 CD patients (training cohort: n=103; test cohort 1: n=31; test cohort 2: n=52) who underwent CD-related surgery in one of the three centers. The presence of endoscopic, radiological, or surgical anastomotic recurrence was termed PAR. In training cohort, 106 radiomic features were extracted respectively from bowel lesions and perienteric mesenteric adipose tissues on preoperative venous-phase computed tomography enterography (CTE) images and ranked by SelectKBest to select the key features. Univariate and multivariate analyses with Cox proportional hazards regression were performed to determine the risk factors of PAR and construct the prediction model (so-call clinical-radiological-radiomic model) from various clinical-radiological and radiomic features. The prediction efficacy of clinical-radiological-radiomic model was validated in two external test cohorts.

#### RESULTS

Three mesenteric radiomic features were selected to develop radiomic-mesentery model and four bowel features were selected to construct radiomic-bowel model. In training cohort, radiomic-mesentery model (AUC=0.690; P<0.05) showed higher predicting efficacy than radiomic-bowel model (AUC=0.654; P<0.05) and was thus chose to integrate into the clinical-radiological-radiomic model. In training cohort and test cohorts 1 and 2, the clinical-radiological-radiomic model showed an increase in predicting performance (AUCs: 0.833, 0.778, and 0.742, respectively; all P<0.05) than clinical-radiological model (AUCs: 0.679, 0.674, and 0.687, respectively; all P<0.05). Decision curve analysis demonstrated the clinical usefulness of the clinical-radiological-radiomic model.

#### CONCLUSION

The preoperative clinical-radiological-radiomic model could be a promising tool to accurately identify CD patients at high risk of PAR.

#### CLINICAL RELEVANCE/APPLICATION

To develop and validate a preoperative CTE-based radiomics signature to early predict postoperative anastomotic recurrence in CD.

### M5A-SPGI-10 Hepatobiliary Phase Imaging in cirrhotic patients using Compressed Sensing: Comparison of Image Quality and focal Lesion Detection with the T1-Weighted Sequence using Controlled Aliasing in Parallel Imaging Results in Higher Acceleration

#### Participants

So Hyun Park, MD, (*Presenter*) Nothing to Disclose

#### PURPOSE

We aimed to compare VIBE using compressed sensing (CS) and controlled aliasing in parallel imaging results in higher acceleration (CAIPIRINHA) in subjective and objective image quality in patients with cirrhotic liver for acquisition of single breath-hold on hepatobiliary phase images.

#### METHODS AND MATERIALS

We retrospectively included 244 gadoteric acid-enhanced liver MRI in 244 patients with cirrhosis from July 2020 to December 2020. All patients underwent two hepatobiliary phases (HBP) using CS and CAIPIRINHA. Optimized resolution and scan time for CS-HBP were  $0.9 \times 0.9 \times 1.5$  mm<sup>3</sup> and 15 s, while those for CAIPIRINHA-HBP were  $1.3 \times 1.8 \times 3$  mm<sup>3</sup> and 15 s. Two abdominal radiologists assessed the two MRI data sets for image quality in consensus. We compared subjective and objective image quality in

two sequences.

## RESULTS

CS-HBP showed significantly superior liver edge sharpness and overall image quality, and lesser respiratory motion artifact (all  $P < 0.001$ ), but higher non-respiratory artifact ( $P = 0.014$ ) compared to CAIPIRINHA-HBP. Intraclass correlation coefficients of subjective image quality in CS-HBP was 0.550-0.827 and that in CAIPIRINHA-HBP was 0.530-0.809. CS-HBP showed superior SNR in the liver to CAIPIRINHA-HBP ( $20.8 \pm 9.1$  vs.  $18.8 \pm 7.2$ ;  $P < 0.001$ ) and liver-spleen contrast in two were similar ( $2.0 \pm 1.1$  vs.  $2.1 \pm 1.2$ ,  $P = 0.071$ ), respectively.

## CONCLUSION

CS-HBP identified superior overall image quality, liver edge sharpness, and liver SNR and lesser respiratory motion artifact, but higher non-respiratory artifact and noise and comparable liver-spleen contrast compared to CAIPIRINHA-HBP, with same acquisition time.

## CLINICAL RELEVANCE/APPLICATION

In patient with decreased liver function, HBP image showed non-clean or decreased enhancement of liver. Identification of adequate image quality on HBP applied CS in patients with cirrhosis can help to select protocol. To our knowledge, however, there have been no studies comparing image quality of HBP between CS and CAIPIRINHA in patients with liver cirrhosis.

## M5A-SPGI-2 Comparison of diagnostic performance of Ultrasonography and Magnetic Resonance Enterography in assessment of active bowel lesions in patients with Crohn's disease

Participants

Dain Lee, Seoul, Korea, Republic Of (*Presenter*) Nothing to Disclose

## PURPOSE

We aimed to evaluate and compare the diagnostic performance of ultrasonography (US) and magnetic resonance enterography (MRE) in assessing active bowel lesions in patients with Crohn's disease (CD) through meta-analysis

## METHODS AND MATERIALS

We searched PubMed and EMBASE for studies in which US and MRE were evaluated to assess active bowel lesions in CD patients. Bivariate random effect meta-analytic methods were used to estimate pooled sensitivity, specificity, and hierarchical summary receiver operating characteristic (HSROC) curves. We performed meta-regression analysis according to the characteristics of the study design, study population, reference standards, and US technique.

## RESULTS

Eleven studies involving a total of 752 patients were included. US exhibited a pooled sensitivity of 87.5% (95% confidence interval 73.7-94.6), a pooled specificity of 87.1% (95% CI 72.4-94.6), and HSROC of 0.9 in 10 studies. MRE exhibited a pooled sensitivity of 88.5% (95% CI 76.1-94.9), a pooled specificity of 87.5% (95% CI 73.1-94.8), and HSROC of 0.93 in 8 studies. In 7 studies comparing the diagnostic performance of US and MRE, summary sensitivity of US and MR were 88% (95% CI 65.3-96.6,  $I^2=92.1$ ) and 86% (95% CI 72.4-93.6,  $I^2=92.3$ ) ( $p=0.841$ ) and summary specificity of US and MR were 88% (95% CI 79.7-93.1,  $I^2=64.2\%$ ) and 84% (72.5-90.7,  $I^2=48.9\%$ ) ( $p=0.431$ ), which showed no significant differences. On meta-regression analysis, studies from Europe ( $p=0.002$ ) and studies that used one kind of US probe ( $p=0.012$ ) reported higher US sensitivity than those from other region and used two kind of US probe, and studies with pediatrics reported higher MR specificity than those with adult population ( $p=0.001$ ).

## CONCLUSION

Both US and MRE can diagnose active bowel lesions with comparable diagnostic accuracy in CD patients, although there was significant heterogeneity in the included studies. Study region, number of used US probe for US sensitivity and study population for MR specificity were the potential source of heterogeneity.

## CLINICAL RELEVANCE/APPLICATION

Ultrasonography can be the reliable alternative to MRE in assessing active bowel lesion with free of radiation and easier accessibility in CD patients

## M5A-SPGI-3 Utility of dual-layer spectral-detector CT imaging for assessing pathological tumor stages and histologic grades of colorectal adenocarcinoma

Participants

Weicui Chen, Guangzhou, China (*Presenter*) Nothing to Disclose

## PURPOSE

Pathological tumor (pT) stage and histologic differentiation are the most critical factors for colorectal adenocarcinoma (CRAC) prognosis. This study aims at assessing the utility of Dual-layer spectral-detector CT (DLCT) in predicting the pT stage and histologic grade for CRAC.

## METHODS AND MATERIALS

A total of 131 patients with pathologically confirmed CRAC (82 colon cancers and 49 rectal cancers; 35 pT1-2, 61 pT3, and 35 pT4; 32 high grade and 99 low grade) between May 2021 and March 2022, who received dual-phase DLCT were enrolled in this retrospective study. Normalized iodine concentration (NIC), slope of the spectral HU curve (?HU), and effective atomic number (Eff-Z) were measured for each lesion by two radiologists independently. Intraobserver reliability and interobserver agreement were assessed. The Student's t-test, one-way analysis of variance (ANOVA), Mann-Whitney U test, or Kruskal-Wallis ANOVA test was used to compare the above quantitative parameters between two groups by histologic grades (high and low) and three groups by pT stages (pT1-2, pT3, and pT4). The correlation between the pT stages and above values were assessed by Spearman correlation analysis. ROC analyses were calculated to evaluate the diagnostic efficacy of each parameter for differentiating advanced- (pT3/4) from early-stage (pT1/2) and high- from low-grade CRAC.

## RESULTS

The range of 95% confidence interval (CI) for intraobserver reliability were 0.88 to 0.99. The range of 95% CI for interobserver agreement were 0.74 to 0.98. Eff-Z [7.21(0.09) vs 7.31 (0.10) vs 7.35 (0.19)], NICAP [0.11 (0.05) vs 0.15 (0.08) vs 0.15 (0.08)], NICVP [0.27 (0.06) vs 0.34 (0.11) vs 0.35 (0.12)], ?HUAP [1.20 (0.45) vs 1.93 (1.18) vs 2.37 (0.91)], and ?HUVF [2.07 (0.68) vs 2.35 (0.62) vs 3.09 (1.07)] were significantly different among pT stage groups (all  $p < 0.001$ ) and exhibited a positive correlation with pT stages ( $r = 0.503, 0.455, 0.394, 0.512, 0.376$ , respectively, all  $p < 0.001$ ). Eff-Z [7.37 (0.10) vs 7.28 (0.08)], NICAP [0.20 (0.10) vs 0.13 (0.08)], NICVP [0.35 (0.07) vs 0.31 (0.11)], and ?HUAP [2.59 (1.11) vs 1.63 (0.75)] in the high-grade group were markedly higher than those in the low-grade group (all  $p < 0.05$ ). For discriminating the advanced- from early-stage CRAC, the AUCs of Eff-Z, NICAP, NICVP, ?HUAP, and ?HUVF were 0.83, 0.80, 0.79, 0.86, and 0.68, respectively. For discriminating the high- from low-grade CRAC, the AUCs of Eff-Z, NICAP, NICVP, and ?HUAP were 0.81, 0.81, 0.64, and 0.81, respectively.

## CONCLUSION

s The quantitative parameters derived from DLCT could successfully predict pT stages and histologic differentiation in CRAC.

## CLINICAL RELEVANCE/APPLICATION

DLCT parameters may help characterize the aggressive CRAC.

## M5A-SPGI-4 Prediction of KRAS mutations in colorectal cancer based on dual-energy and perfusion CT parameters

### Participants

Xiaoqiang Lin, Lanzhou, China (*Presenter*) Nothing to Disclose

## PURPOSE

To investigate the predictive value of dual-energy spectral CT (DEsCT) and perfusion CT quantitative parameters for KRAS mutation in colorectal cancer, a diagnostic model was constructed and visualized as a nomogram to assist clinical preoperative treatment decisions.

## METHODS AND MATERIALS

67 patients with colorectal cancer underwent "one-step" abdominal spectral and perfusion CT before surgery and were divided into two groups: group A (wild-type) and group B (mutation). Clinical baseline characteristics included age, gender, tumor location, serum tumor markers, bowel wall thickening pattern and superior rectal vein (SRV) width. A radiologist delineated the regions of interest (ROIs) on the layer of maximum tumor diameter and the nearest upper and lower layers in axial enhanced images and calculated the average value. Monoenergetic CT value, effective atomic number (Eff-Z), iodine concentration (IC) of tumor and artery were acquired to calculate normalized iodine concentration (NIC,  $NIC = IC_{tumor} / IC_{artery}$ ). Perfusion parameters include blood flow (BF), blood volume (BV), mean slope of increase (MSI), mean transit time (MTT), positive enhancement integral (PEI), capillary permeability surface area product (PS) and time to peak (TTP). ?2 test, t-test and U test were used for calculated differences between groups. Then, least absolute shrinkage and selection operator (LASSO) regression and multivariate logistic regression were used to select the most discriminating features, build a predictive model and visualize the model as a nomogram. Concordance index (C-index), calibration curves and decision curves analysis (DCA) were used to evaluate prediction performance and clinical utility.

## RESULTS

30 patients had KRAS mutations in 67 patients. After feature selection, the four variables included BF, BV, 130keVAP and NICAP\*10 were screened by LASSO regression and multivariate logistic regression to construct the nomogram. The C-index and bootstrap C-index of the model were 0.886 (95%CI: 0.808~0.963) and 0.857, respectively. The sensitivity and specificity were 70.0% and 85.7%, respectively. The model showed good calibration, and the DCA demonstrated that the model has a higher net benefit than the best single variable.

## CONCLUSION

s There were differences in LTL, CT perfusion parameters and multiple arteriovenous phases spectral CT parameters in KRAS mutation status. The nomogram based on BF, BV, 130KeVAP and NICAP\*10 is helpful for the preoperative determination of KRAS mutation status in colorectal cancer.

## CLINICAL RELEVANCE/APPLICATION

The nomogram is helpful for the preoperative determination of KRAS mutation status in colorectal cancer, which can assist in clinical preoperative decision-making and patient risk stratification.

## M5A-SPGI-5 Noise power spectrum properties of deep learning-based reconstruction and iterative reconstruction algorithms: Phantom and clinical study

### Participants

Yoshinori Funama, PhD, Kumamoto, Japan (*Presenter*) Nothing to Disclose

## PURPOSE

Recent reconstructions of computed tomography (CT) images are nonlinear in nature. Therefore, the noise power spectrum (NPS) properties of reconstructed images are likely to be clinically more relevant when measured in uniform organs of the human body, such as the bladder, with noise-level matching than the use of phantom images. This study aimed to compare the NPS properties and perform qualitative analysis of hybrid iterative reconstruction (hybrid-IR), model-based IR (MBIR), and deep learning-based IR (DLR) at a similar noise level in a clinical study based on the outcomes of a phantom study.

## METHODS AND MATERIALS

A Catphan phantom with an external body ring was used in the phantom study. In the clinical study, CT examination data of 35 patients were retrospectively reviewed. NPS was calculated from DLR, hybrid IR, and MBIR images using a uniform portion of the phantom and bladder portions of the patients. The noise magnitude ratio (NMR) and central frequency ratio (CFR) were calculated from DLR, hybrid IR, and MBIR images relative to filtered back-projection (FBP) images using NPS. CFR represents the degree of lower frequency shift for NPS. Clinical CT images were independently reviewed by two board-certified general radiologists.

## RESULTS

In the phantom study, DLR achieved substantial noise reduction compared to hybrid IR and MBIR with increasing strength levels. The mean NMR for DLR with a mild level was 0.49, and the noise level was similar to those of hybrid IR at 0.53 and MBIR at 0.65 with strong levels. The CFRs were 0.83, 0.60, and 0.66 for DLR, hybrid IR, and MBIR, respectively; the lower frequency shift for NPS was small level on DLR. Based on the outcomes of the phantom study, the clinical study applied DLR with mild and hybrid IR and MBIR with strong-level images. In the clinical study, the NMR and CFR were 0.39 and 0.35, 0.46 and 0.76, and 0.51 and 0.62 for DLR, hybrid IR, and MBIR, respectively. The visual inspection for DLR with mild-level images was superior to those for hybrid IR and MBIR with strong levels .

## CONCLUSION

s DLR images achieved substantial noise reduction while maintaining image noise texture in the phantom and clinical studies.

## CLINICAL RELEVANCE/APPLICATION

DLR images provide better clinical visibility without the lack of image texture appearance in CT.

## M5A-SPGI-6 Ultra-high resolution computed tomography with deep-learning-reconstruction: Diagnostic ability in the assessment of gastric cancer and the depth of invasion

Participants

Masaya Tanabe, MD, Ube, Japan (*Presenter*) Nothing to Disclose

## PURPOSE

To assess the image quality of ultra-high-resolution CT (U-HRCT) reconstructed with improved deep-learning-reconstruction (DLR) method, the utility in the delineation of the gastric wall structure, and visibility of gastric cancer and its depth invasion.

## METHODS AND MATERIALS

This study included 46 patients with resected gastric cancers who underwent preoperative contrast-enhanced U-HRCT. Image quality of U-HRCT (0.5mm, 1024x1024) reconstructed with three different methods; standard DLR (Advanced intelligent Clear-IQ Engine [AiCE]), improved DLR (AiCE-Body Sharp [BS]) and hybrid-IR (Adaptive Interactive Dose Reduction 3Dimensional [AIDR3D]) was compared for the visualization of the gastric wall. Then, the conspicuity for the three-layered structure of the gastric wall at four regions (fornix, body, angle and antrum) and the visibility of gastric cancers were compared between conventional HRCT (C-HRCT; 2mm, 512x512) and U-HRCT. Finally, the diagnostic ability of U-HRCT with improved AiCE-BS for the depth invasion of gastric cancers was assessed in comparison with actual postoperative pathology specimens.

## RESULTS

The mean noise of U-HRCT with improved AiCE-BS was significantly lower than that with AIDR3D although there was no significant difference between improved AiCE-BS and standard AiCE. The mean overall image quality scores with improved AiCE-BS images were significantly higher than those with the other two methods ( $p < 0.001$ ). Regarding the comparison between C-HRCT and U-HRCT, the mean conspicuity scores for the three-layered structure of the gastric wall on U-HRCT were significantly better than those on C-HRCT in the fornix ( $p < 0.001$ ), body ( $p < 0.001$ ), angle ( $p = 0.007$ ), antrum ( $p = 0.007$ ). In addition, visibility of gastric cancer with U-HRCT was better than that with C-HRCT ( $p < 0.001$ ). Correct diagnosis rate for depth invasion of gastric cancer using U-HRCT was 72%.

## CONCLUSION

s U-HRCT with improved AiCE-BS is capable of depicting the three-layered structure of the gastric wall more clearly than the other two reconstruction methods, and is useful for the visualization of gastric cancers as well as for the assessment of depth invasion.

## CLINICAL RELEVANCE/APPLICATION

U-HRCT using new DLR method will improve overall image quality, delineation of the three-layered structure of gastric wall, visibility of gastric cancer, and diagnostic ability for depth invasion.

## M5A-SPGI-7 Low-Tube-Voltage Whole-Body CT Angiography with Extremely-Low-Iodine Dose: Comparison between Deep Learning-based and Adaptive Statistical Iterative Reconstructions

Participants

Nobuyuki Kawai, MD, Gifu, Japan (*Presenter*) Nothing to Disclose

## PURPOSE

To prospectively compare the arterial enhancement, its depiction and image quality in whole-body CT angiography (CTA) at 80 kVp with equivalent contrast material (CM) of 192 mgI/mL between deep learning image reconstruction (DLIR) and adaptive statistical iterative reconstruction Veo of 40% (ASiR-V).

## METHODS AND MATERIALS

Thirty-four consecutive participants (27 men and 7 women; mean age, 74.2 years) who underwent dual phase whole-body CTA, with images obtained at 80 kVp, for evaluation of aortic diseases between January and July 2020. We used 240-mgI/mL of CM with concurrent administration of its quarter volume of saline, which is corresponding iodine concentration of 192 mgI/mL, and they were intravenously injected at 4 mL/s (iodine mass administered per unit of time; 768 mgI/s) using a commercially available power injector. Three image sets were reconstructed using the ASiR-V, DLIR with middle performance (DLIR-M), and DLIR with high performance (DLIR-H), respectively. A radiologist measured CT values of aortas, iliac arteries, and endoleaks after endovascular aortic repair (EVAR), and one standard deviation (SD) of CT value of subcutaneous fat. Signal-to-noise ratios (SNR) were calculated as CT value/ SD. Two radiologists evaluated the depiction of 25 arteries and image quality on axial, multiplanar-reformatted, and volume-rendered images.

## RESULTS

Mean CM volume and iodine weight were 64.1 mL and 15.4 g, respectively. SNRs of aortas, iliac arteries, and endoleaks after EVAR were significantly higher in the order corresponding to DLIR-H, DLIR-M, and ASiR-V ( $P = 0.001$ , respectively). Depiction of intercostal, dorsal pancreatic, inferior phrenic, lumbar, internal pudendal, and inferior epigastric arteries were significantly better in

DLIR-M and ASiR-V than those in DLIR-H ( $P = 0.001-0.002$ ), however, no significant difference was found in the other arteries ( $P = 0.13-1.00$ ). Image sharpness, noise, and diagnostic acceptability were significantly better in DLIR-M and DLIR-H than in ASiR-V ( $P = 0.001-0.005$ ).

## CONCLUSION

s DLIR significantly improved SNR and image quality compared with ASiR-V in whole-body CTA at 80 kVp with equivalent CM of 192 mgI/mL. DLIR-M seemed well-balanced algorithm compared with ASiR-V and DLIR-H.

## CLINICAL RELEVANCE/APPLICATION

Deep learning image reconstruction was alternative method to adaptive statistical iterative reconstruction Veo on whole-body CT angiography at 80 kVp with equivalent contrast material of 192 mgI/mL.

## M5A-SPGI-8 Is it safe to give iodine- or gadolinium-based contrast agents repeatedly on the same day?: An animal study

Participants

Heejin Bae, (*Presenter*) Nothing to Disclose

## PURPOSE

To investigate molecular and functional consequences of repeated exposures to iodine- or gadolinium-based contrast agents within 24 hours through an animal study.

## METHODS AND MATERIALS

Fifty-six Sprague-Dawley male rats were equally divided into 8 groups: negative control group, positive control group with single dose administration of iodine-based CT contrast agent, and repeated administration of either CT or MRI contrast agents after 2, 4, and 24 hours from the single dose injection of CT contrast agent. Concentrations of BUN, creatinine (SCr), cystatin C (Cys C), and malondialdehyde (MDA) were measured in serum samples and mRNA of kidney injury markers including kidney injury molecule-1 (KIM-1) and neutrophil gelatinase-associated lipocalin (NGAL) were evaluated from kidney tissues. Serum KIM-1 and NGAL proteins were detected by immunoassay and quantified by ELISA.

## RESULTS

Repeated exposure to CT contrast agents significantly increased SCr (0.344 - 0.411 mg/dL,  $P = <0.001$ ) than negative and positive control groups (0.160; 0.207 mg/dL, respectively). SCr concentrations were not significantly different depending on various time intervals ( $P = >0.999$ ). For average levels of Cys C and MDA, statistically significant differences were not observed between the positive control group (0.427 mg/L; 1.802  $\mu$ M) and repeated injection groups (0.549 - 0.550,  $P = 0.256 - 0.362$ ; 1.283 0 2.254,  $P = >0.999$ , respectively). Likewise, additional dose of MRI contrast agent after single dose of CT contrast agent did not affect SCr, Cys C, and MDA (0.171 - 0.230,  $P = >0.999$ ; 0.4,  $P = 0.262$ ; 0.770 - 1.079,  $P = 0.139 - 0.771$ , respectively). mRNA and protein levels of KIM-1 and NGAL were not significantly different among various time intervals of the additional injection of either CT or MRI contrast agents.

## CONCLUSION

s More than 24 hours of interval between the repeated contrast-enhanced CT examinations may be necessary to avoid deterioration in renal function, whereas conducting contrast-enhanced MRI on the same day as contrast-enhanced CT examination may not induce clinically significant kidney injury.

## CLINICAL RELEVANCE/APPLICATION

Repeated exposure to the contrast agents in a short time period is known to be a risk factor for development of contrast-induced nephropathy. However, according to ACR manual on contrast media, the evidence to avoid a repeated contrast agent injection until more than 24 hours is yet insufficient.

## M5A-SPGI-9 Cross-Sectional Comparison of Serum Fib-4 and MRI-Derived Liver T1 as Noninvasive Markers of Liver Fibrosis: An Interim Analysis of the Dallas Heart Study Cohort

Participants

Sujoy Mukherjee, (*Presenter*) Nothing to Disclose

## PURPOSE

Noninvasive serum (e.g. FIB-4)<sup>1</sup> and imaging (e.g. elastography, T1 mapping)<sup>2-4</sup> biomarkers of liver fibrosis have been validated against liver biopsy. Whether these biomarkers are correlative or complementary remains unknown. The purpose of this study is to compare serum FIB-4 and MRI-derived liver T1 in the general adult population in the US.

## METHODS AND MATERIALS

This is an interim analysis of the ongoing Dallas Hearts Study (DHS) third examination, a large multiethnic sampling of adults in Dallas County, Texas. The study collects demographic data, serum laboratory tests needed to calculate FIB-4, and multiparametric liver MRI using LiverMultiScan® 3T protocol (Perspectum, Oxford, UK) to calculate mean hepatic iron-corrected T1 (cT1)<sup>5</sup>. The correlation between FIB-4 and cT1 values was assessed by scatter plots as well as Spearman and Pearson correlation coefficients. The association between FIB-4 = 1.3 and cT1 = 763 msec was assessed by odds ratio, where these thresholds were drawn from the upper limits of the low risk group<sup>6 7</sup>. This study was approved by IRB and was compliant with HIPAA.

## RESULTS

279 adult participants from DHS completed liver cT1 analysis and included 107 males and 172 females, median age [interquartile range] 61 [55-67] years. The median FIB-4 and cT1 were 1.06 [0.84-1.43] and 745 [697-802] msec, with n=93 (33.3%) and n=111 (39.8%) with above-normal FIB-4 and cT1, respectively. No significant correlation was found between FIB-4 and cT1 (Figure 2) by Pearson nor Spearman methods. No significant association was found between above-normal FIB-4 and cT1, with odds ratio [95% confidence interval] of 1.14 [0.69 - 1.90].

## CONCLUSION

s Serum FIB-4 and cT1 were not significantly correlated with each other in the general population. Our finding is consistent with other studies where FIB-4 had a low correlation with viscoelastic transient elastography<sup>8</sup>. Our early data suggest that FIB-4 and cT1 are not correlative, but may be complementary, in evaluating liver disease. Further research is necessary how serum and imaging biomarkers may be used in combination.

#### **CLINICAL RELEVANCE/APPLICATION**

FIB-4 was developed for viral hepatitis. Iron-corrected T1 MRI was developed for nonalcoholic fatty liver disease. While both biomarkers were validated against liver biopsies, they may generate discrepant results when applied to the general population for liver disease screening.

Printed on: 02/07/23

## Abstract Archives of the RSNA, 2022

M5A-SPGI-1

### Prediction of Postoperative Anastomotic Recurrence in Crohn's Disease Using Preoperative CTE Radiomic Data

Monday, Nov. 28 12:15PM - 12:45PM Room: Learning Center - GI DPS

#### Participants

Xiao Di Shen, (*Presenter*) Nothing to Disclose

#### PURPOSE

More than half of patients with Crohn's disease (CD) need at least one surgery in their life, however, most patients will experience postoperative anastomotic recurrence (PAR). Stratifying them according to the risk of PAR and tailoring therapy are the most cost-effective way to manage these patients. This study aimed to develop and validate a novel preoperative clinical-radiological-radiomic model to predict the risk of PAR.

#### METHODS AND MATERIALS

This retrospective study included 186 CD patients (training cohort: n=103; test cohort 1: n=31; test cohort 2: n=52) who underwent CD-related surgery in one of the three centers. The presence of endoscopic, radiological, or surgical anastomotic recurrence was termed PAR. In training cohort, 106 radiomic features were extracted respectively from bowel lesions and perienteric mesenteric adipose tissues on preoperative venous-phase computed tomography enterography (CTE) images and ranked by SelectKBest to select the key features. Univariate and multivariate analyses with Cox proportional hazards regression were performed to determine the risk factors of PAR and construct the prediction model (so-call clinical-radiological-radiomic model) from various clinical-radiological and radiomic features. The prediction efficacy of clinical-radiological-radiomic model was validated in two external test cohorts.

#### RESULTS

Three mesenteric radiomic features were selected to develop radiomic-mesentery model and four bowel features were selected to construct radiomic-bowel model. In training cohort, radiomic-mesentery model (AUC=0.690;  $P<0.05$ ) showed higher predicting efficacy than radiomic-bowel model (AUC=0.654;  $P<0.05$ ) and was thus chose to integrate into the clinical-radiological-radiomic model. In training cohort and test cohorts 1 and 2, the clinical-radiological-radiomic model showed an increase in predicting performance (AUCs: 0.833, 0.778, and 0.742, respectively; all  $P<0.05$ ) than clinical-radiological model (AUCs: 0.679, 0.674, and 0.687, respectively; all  $P<0.05$ ). Decision curve analysis demonstrated the clinical usefulness of the clinical-radiological-radiomic model.

#### CONCLUSION

s The preoperative clinical-radiological-radiomic model could be a promising tool to accurately identify CD patients at high risk of PAR.

#### CLINICAL RELEVANCE/APPLICATION

To develop and validate a preoperative CTE-based radiomics signature to early predict postoperative anastomotic recurrence in CD.

Printed on: 02/07/23

## Abstract Archives of the RSNA, 2022

M5A-SPGI-10

### Hepatobiliary Phase Imaging in cirrhotic patients using Compressed Sensing: Comparison of Image Quality and focal Lesion Detection with the T1-Weighted Sequence using Controlled Aliasing in Parallel Imaging Results in Higher Acceleration

Monday, Nov. 28 12:15PM - 12:45PM Room: Learning Center - GI DPS

#### Participants

So Hyun Park, MD, (Presenter) Nothing to Disclose

#### PURPOSE

We aimed to compare VIBE using compressed sensing (CS) and controlled aliasing in parallel imaging results in higher acceleration (CAIPIRINHA) in subjective and objective image quality in patients with cirrhotic liver for acquisition of single breath-hold on hepatobiliary phase images.

#### METHODS AND MATERIALS

We retrospectively included 244 gadoteric acid-enhanced liver MRI in 244 patients with cirrhosis from July 2020 to December 2020. All patients underwent two hepatobiliary phases (HBP) using CS and CAIPIRINHA. Optimized resolution and scan time for CS-HBP were  $0.9 \times 0.9 \times 1.5$  mm<sup>3</sup> and 15 s, while those for CAIPIRINHA-HBP were  $1.3 \times 1.8 \times 3$  mm<sup>3</sup> and 15 s. Two abdominal radiologists assessed the two MRI data sets for image quality in consensus. We compared subjective and objective image quality in two sequences.

#### RESULTS

CS-HBP showed significantly superior liver edge sharpness and overall image quality, and lesser respiratory motion artifact (all  $P < 0.001$ ), but higher non-respiratory artifact ( $P = 0.014$ ) compared to CAIPIRINHA-HBP. Intraclass correlation coefficients of subjective image quality in CS-HBP was 0.550-0.827 and that in CAIPIRINHA-HBP was 0.530-0.809. CS-HBP showed superior SNR in the liver to CAIPIRINHA-HBP ( $20.8 \pm 9.1$  vs.  $18.8 \pm 7.2$ ;  $P < 0.001$ ) and liver-spleen contrast in two were similar ( $2.0 \pm 1.1$  vs.  $2.1 \pm 1.2$ ,  $P = 0.071$ ), respectively.

#### CONCLUSION

CS-HBP identified superior overall image quality, liver edge sharpness, and liver SNR and lesser respiratory motion artifact, but higher non-respiratory artifact and noise and comparable liver-spleen contrast compared to CAIPIRINHA-HBP, with same acquisition time.

#### CLINICAL RELEVANCE/APPLICATION

In patient with decreased liver function, HBP image showed non-clean or decreased enhancement of liver. Identification of adequate image quality on HBP applied CS in patients with cirrhosis can help to select protocol. To our knowledge, however, there have been no studies comparing image quality of HBP between CS and CAIPIRINHA in patients with liver cirrhosis.

Printed on: 02/07/23

## Abstract Archives of the RSNA, 2022

M5A-SPGI-2

### Comparison of diagnostic performance of Ultrasonography and Magnetic Resonance Enterography in assessment of active bowel lesions in patients with Crohn's disease

Monday, Nov. 28 12:15PM - 12:45PM Room: Learning Center - GI DPS

#### Participants

Dain Lee, Seoul, Korea, Republic Of (*Presenter*) Nothing to Disclose

#### PURPOSE

We aimed to evaluate and compare the diagnostic performance of ultrasonography (US) and magnetic resonance enterography (MRE) in assessing active bowel lesions in patients with Crohn's disease (CD) through meta-analysis

#### METHODS AND MATERIALS

We searched PubMed and EMBASE for studies in which US and MRE were evaluated to assess active bowel lesions in CD patients. Bivariate random effect meta-analytic methods were used to estimate pooled sensitivity, specificity, and hierarchical summary receiver operating characteristic (HSROC) curves. We performed meta-regression analysis according to the characteristics of the study design, study population, reference standards, and US technique.

#### RESULTS

Eleven studies involving a total of 752 patients were included. US exhibited a pooled sensitivity of 87.5 % (95% confidence interval 73.7-94.6), a pooled specificity of 87.1% (95% CI 72.4-94.6), and HSROC of 0.9 in 10 studies. MRE exhibited a pooled sensitivity of 88.5% (95% CI 76.1-94.9), a pooled specificity of 87.5% (95% CI 73.1-94.8), and HSROC of 0.93 in 8 studies. In 7 studies comparing the diagnostic performance of US and MRE, summary sensitivity of US and MR were 88% (95% CI 65.3-96.6, I<sup>2</sup>=92.1) and 86% (95% CI 72.4-93.6, I<sup>2</sup>=92.3) (p=0.841) and summary specificity of US and MR were 88% (95% CI 79.7-93.1, I<sup>2</sup>=64.2%) and 84% (72.5-90.7, I<sup>2</sup>=48.9%) (p=0.431), which showed no significant differences. On meta-regression analysis, studies from Europe (p=0.002) and studies that used one kind of US probe (p=0.012) reported higher US sensitivity than those from other region and used two kind of US probe, and studies with pediatrics reported higher MR specificity than those with adult population (p=0.001>).

#### CONCLUSION

s Both US and MRE can diagnose active bowel lesions with comparable diagnostic accuracy in CD patients, although there was significant heterogeneity in the included studies. Study region, number of used US probe for US sensitivity and study population for MR specificity were the potential source of heterogeneity.

#### CLINICAL RELEVANCE/APPLICATION

Ultrasonography can be the reliable alternative to MRE in assessing active bowel lesion with free of radiation and easier accessibility in CD patients

Printed on: 02/07/23

## Abstract Archives of the RSNA, 2022

M5A-SPGI-3

### Utility of dual-layer spectral-detector CT imaging for assessing pathological tumor stages and histologic grades of colorectal adenocarcinoma

Monday, Nov. 28 12:15PM - 12:45PM Room: Learning Center - GI DPS

#### Participants

Weicui Chen, Guangzhou, China (*Presenter*) Nothing to Disclose

#### PURPOSE

Pathological tumor (pT) stage and histologic differentiation are the most critical factors for colorectal adenocarcinoma (CRAC) prognosis. This study aims at assessing the utility of Dual-layer spectral-detector CT (DLCT) in predicting the pT stage and histologic grade for CRAC.

#### METHODS AND MATERIALS

A total of 131 patients with pathologically confirmed CRAC (82 colon cancers and 49 rectal cancers; 35 pT1-2, 61 pT3, and 35 pT4; 32 high grade and 99 low grade) between May 2021 and March 2022, who received dual-phase DLCT were enrolled in this retrospective study. Normalized iodine concentration (NIC), slope of the spectral HU curve (?HU), and effective atomic number (Eff-Z) were measured for each lesion by two radiologists independently. Intraobserver reliability and interobserver agreement were assessed. The Student's t-test, one-way analysis of variance (ANOVA), Mann-Whitney U test, or Kruskal-Wallis ANOVA test was used to compare the above quantitative parameters between two groups by histologic grades (high and low) and three groups by pT stages (pT1-2, pT3, and pT4). The correlation between the pT stages and above values were assessed by Spearman correlation analysis. ROC analyses were calculated to evaluate the diagnostic efficacy of each parameter for differentiating advanced- (pT3/4) from early-stage (pT1/2) and high- from low-grade CRAC.

#### RESULTS

The range of 95% confidence interval (CI) for intraobserver reliability were 0.88 to 0.99. The range of 95% CI for interobserver agreement were 0.74 to 0.98. Eff-Z [7.21(0.09) vs 7.31 (0.10) vs 7.35 (0.19)], NICAP [0.11 (0.05) vs 0.15 (0.08) vs 0.15 (0.08)], NICVP [0.27 (0.06) vs 0.34 (0.11) vs 0.35 (0.12)], ?HUAP [1.20 (0.45) vs 1.93 (1.18) vs 2.37 (0.91)], and ?HUVP [2.07 (0.68) vs 2.35 (0.62) vs 3.09 (1.07)] were significantly different among pT stage groups (all  $p < 0.001$ ) and exhibited a positive correlation with pT stages ( $r = 0.503, 0.455, 0.394, 0.512, 0.376$ , respectively, all  $p < 0.001$ ). Eff-Z [7.37 (0.10) vs 7.28 (0.08)], NICAP [0.20 (0.10) vs 0.13 (0.08)], NICVP [0.35 (0.07) vs 0.31 (0.11)], and ?HUAP [2.59 (1.11) vs 1.63 (0.75)] in the high-grade group were markedly higher than those in the low-grade group (all  $p < 0.05$ ). For discriminating the advanced- from early-stage CRAC, the AUCs of Eff-Z, NICAP, NICVP, ?HUAP, and ?HUVP were 0.83, 0.80, 0.79, 0.86, and 0.68, respectively. For discriminating the high- from low-grade CRAC, the AUCs of Eff-Z, NICAP, NICVP, and ?HUAP were 0.81, 0.81, 0.64, and 0.81, respectively.

#### CONCLUSION

The quantitative parameters derived from DLCT could successfully predict pT stages and histologic differentiation in CRAC.

#### CLINICAL RELEVANCE/APPLICATION

DLCT parameters may help characterize the aggressive CRAC.

Printed on: 02/07/23

## Abstract Archives of the RSNA, 2022

M5A-SPGI-4

### Prediction of KRAS mutations in colorectal cancer based on dual-energy and perfusion CT parameters

Monday, Nov. 28 12:15PM - 12:45PM Room: Learning Center - GI DPS

#### Participants

Xiaoqiang Lin, Lanzhou, China (*Presenter*) Nothing to Disclose

#### PURPOSE

To investigate the predictive value of dual-energy spectral CT (DECT) and perfusion CT quantitative parameters for KRAS mutation in colorectal cancer, a diagnostic model was constructed and visualized as a nomogram to assist clinical preoperative treatment decisions.

#### METHODS AND MATERIALS

67 patients with colorectal cancer underwent "one-step" abdominal spectral and perfusion CT before surgery and were divided into two groups: group A (wild-type) and group B (mutation). Clinical baseline characteristics included age, gender, tumor location, serum tumor markers, bowel wall thickening pattern and superior rectal vein (SRV) width. A radiologist delineated the regions of interest (ROIs) on the layer of maximum tumor diameter and the nearest upper and lower layers in axial enhanced images and calculated the average value. Monoenergetic CT value, effective atomic number (Eff-Z), iodine concentration (IC) of tumor and artery were acquired to calculate normalized iodine concentration (NIC,  $NIC = IC_{tumor} / IC_{artery}$ ). Perfusion parameters include blood flow (BF), blood volume (BV), mean slope of increase (MSI), mean transit time (MTT), positive enhancement integral (PEI), capillary permeability surface area product (PS) and time to peak (TTP).  $\chi^2$  test, t-test and U test were used for calculated differences between groups. Then, least absolute shrinkage and selection operator (LASSO) regression and multivariate logistic regression were used to select the most discriminating features, build a predictive model and visualize the model as a nomogram. Concordance index (C-index), calibration curves and decision curves analysis (DCA) were used to evaluate prediction performance and clinical utility.

#### RESULTS

30 patients had KRAS mutations in 67 patients. After feature selection, the four variables included BF, BV, 130keVAP and NICAP\*10 were screened by LASSO regression and multivariate logistic regression to construct the nomogram. The C-index and bootstrap C-index of the model were 0.886 (95%CI: 0.808~0.963) and 0.857, respectively. The sensitivity and specificity were 70.0% and 85.7%, respectively. The model showed good calibration, and the DCA demonstrated that the model has a higher net benefit than the best single variable.

#### CONCLUSION

There were differences in LTL, CT perfusion parameters and multiple arteriovenous phases spectral CT parameters in KRAS mutation status. The nomogram based on BF, BV, 130KeVAP and NICAP\*10 is helpful for the preoperative determination of KRAS mutation status in colorectal cancer.

#### CLINICAL RELEVANCE/APPLICATION

The nomogram is helpful for the preoperative determination of KRAS mutation status in colorectal cancer, which can assist in clinical preoperative decision-making and patient risk stratification.

Printed on: 02/07/23



## Abstract Archives of the RSNA, 2022

M5A-SPGI-5

### Noise power spectrum properties of deep learning-based reconstruction and iterative reconstruction algorithms: Phantom and clinical study

Monday, Nov. 28 12:15PM - 12:45PM Room: Learning Center - GI DPS

#### Participants

Yoshinori Funama, PhD, Kumamoto, Japan (*Presenter*) Nothing to Disclose

#### PURPOSE

Recent reconstructions of computed tomography (CT) images are nonlinear in nature. Therefore, the noise power spectrum (NPS) properties of reconstructed images are likely to be clinically more relevant when measured in uniform organs of the human body, such as the bladder, with noise-level matching than the use of phantom images. This study aimed to compare the NPS properties and perform qualitative analysis of hybrid iterative reconstruction (hybrid-IR), model-based IR (MBIR), and deep learning-based IR (DLR) at a similar noise level in a clinical study based on the outcomes of a phantom study.

#### METHODS AND MATERIALS

A Catphan phantom with an external body ring was used in the phantom study. In the clinical study, CT examination data of 35 patients were retrospectively reviewed. NPS was calculated from DLR, hybrid IR, and MBIR images using a uniform portion of the phantom and bladder portions of the patients. The noise magnitude ratio (NMR) and central frequency ratio (CFR) were calculated from DLR, hybrid IR, and MBIR images relative to filtered back-projection (FBP) images using NPS. CFR represents the degree of lower frequency shift for NPS. Clinical CT images were independently reviewed by two board-certified general radiologists.

#### RESULTS

In the phantom study, DLR achieved substantial noise reduction compared to hybrid IR and MBIR with increasing strength levels. The mean NMR for DLR with a mild level was 0.49, and the noise level was similar to those of hybrid IR at 0.53 and MBIR at 0.65 with strong levels. The CFRs were 0.83, 0.60, and 0.66 for DLR, hybrid IR, and MBIR, respectively; the lower frequency shift for NPS was small level on DLR. Based on the outcomes of the phantom study, the clinical study applied DLR with mild and hybrid IR and MBIR with strong-level images. In the clinical study, the NMR and CFR were 0.39 and 0.35, 0.46 and 0.76, and 0.51 and 0.62 for DLR, hybrid IR, and MBIR, respectively. The visual inspection for DLR with mild-level images was superior to those for hybrid IR and MBIR with strong levels.

#### CONCLUSION

s DLR images achieved substantial noise reduction while maintaining image noise texture in the phantom and clinical studies.

#### CLINICAL RELEVANCE/APPLICATION

DLR images provide better clinical visibility without the lack of image texture appearance in CT.

Printed on: 02/07/23

## Abstract Archives of the RSNA, 2022

M5A-SPGI-6

### Ultra-high resolution computed tomography with deep-learning-reconstruction: Diagnostic ability in the assessment of gastric cancer and the depth of invasion

Monday, Nov. 28 12:15PM - 12:45PM Room: Learning Center - GI DPS

#### Participants

Masaya Tanabe, MD, Ube, Japan (*Presenter*) Nothing to Disclose

#### PURPOSE

To assess the image quality of ultra-high-resolution CT (U-HRCT) reconstructed with improved deep-learning-reconstruction (DLR) method, the utility in the delineation of the gastric wall structure, and visibility of gastric cancer and its depth invasion.

#### METHODS AND MATERIALS

This study included 46 patients with resected gastric cancers who underwent preoperative contrast-enhanced U-HRCT. Image quality of U-HRCT (0.5mm, 1024x1024) reconstructed with three different methods; standard DLR (Advanced intelligent Clear-IQ Engine [AiCE]), improved DLR (AiCE-Body Sharp [BS]) and hybrid-IR (Adaptive Interactive Dose Reduction 3Dimensional [AIDR3D]) was compared for the visualization of the gastric wall. Then, the conspicuity for the three-layered structure of the gastric wall at four regions (fornix, body, angle and antrum) and the visibility of gastric cancers were compared between conventional HRCT (C-HRCT; 2mm, 512x512) and U-HRCT. Finally, the diagnostic ability of U-HRCT with improved AiCE-BS for the depth invasion of gastric cancers was assessed in comparison with actual postoperative pathology specimens.

#### RESULTS

The mean noise of U-HRCT with improved AiCE-BS was significantly lower than that with AIDR3D although there was no significant difference between improved AiCE-BS and standard AiCE. The mean overall image quality scores with improved AiCE-BS images were significantly higher than those with the other two methods ( $p < 0.001$ ). Regarding the comparison between C-HRCT and U-HRCT, the mean conspicuity scores for the three-layered structure of the gastric wall on U-HRCT were significantly better than those on C-HRCT in the fornix ( $p < 0.001$ ), body ( $p < 0.001$ ), angle ( $p = 0.007$ ), antrum ( $p = 0.007$ ). In addition, visibility of gastric cancer with U-HRCT was better than that with C-HRCT ( $p < 0.001$ ). Correct diagnosis rate for depth invasion of gastric cancer using U-HRCT was 72%.

#### CONCLUSION

U-HRCT with improved AiCE-BS is capable of depicting the three-layered structure of the gastric wall more clearly than the other two reconstruction methods, and is useful for the visualization of gastric cancers as well as for the assessment of depth invasion.

#### CLINICAL RELEVANCE/APPLICATION

U-HRCT using new DLR method will improve overall image quality, delineation of the three-layered structure of gastric wall, visibility of gastric cancer, and diagnostic ability for depth invasion.

Printed on: 02/07/23

## Abstract Archives of the RSNA, 2022

M5A-SPGI-7

### Low-Tube-Voltage Whole-Body CT Angiography with Extremely-Low-Iodine Dose: Comparison between Deep Learning-based and Adaptive Statistical Iterative Reconstructions

Monday, Nov. 28 12:15PM - 12:45PM Room: Learning Center - GI DPS

#### Participants

Nobuyuki Kawai, MD, Gifu, Japan (*Presenter*) Nothing to Disclose

#### PURPOSE

To prospectively compare the arterial enhancement, its depiction and image quality in whole-body CT angiography (CTA) at 80 kVp with equivalent contrast material (CM) of 192 mgI/mL between deep learning image reconstruction (DLIR) and adaptive statistical iterative reconstruction Veo of 40% (ASiR-V).

#### METHODS AND MATERIALS

Thirty-four consecutive participants (27 men and 7 women; mean age, 74.2 years) who underwent dual phase whole-body CTA, with images obtained at 80 kVp, for evaluation of aortic diseases between January and July 2020. We used 240-mgI/mL of CM with concurrent administration of its quarter volume of saline, which is corresponding iodine concentration of 192 mgI/mL, and they were intravenously injected at 4 mL/s (iodine mass administered per unit of time; 768 mgI/s) using a commercially available power injector. Three image sets were reconstructed using the ASiR-V, DLIR with middle performance (DLIR-M), and DLIR with high performance (DLIR-H), respectively. A radiologist measured CT values of aortas, iliac arteries, and endoleaks after endovascular aortic repair (EVAR), and one standard deviation (SD) of CT value of subcutaneous fat. Signal-to-noise ratios (SNR) were calculated as CT value/ SD. Two radiologists evaluated the depiction of 25 arteries and image quality on axial, multiplanar-reformatted, and volume-rendered images.

#### RESULTS

Mean CM volume and iodine weight were 64.1 mL and 15.4 g, respectively. SNRs of aortas, iliac arteries, and endoleaks after EVAR were significantly higher in the order corresponding to DLIR-H, DLIR-M, and ASiR-V ( $P = 0.001$ , respectively). Depiction of intercostal, dorsal pancreatic, inferior phrenic, lumbar, internal pudendal, and inferior epigastric arteries were significantly better in DLIR-M and ASiR-V than those in DLIR-H ( $P = 0.001-0.002$ ), however, no significant difference was found in the other arteries ( $P = 0.13-1.00$ ). Image sharpness, noise, and diagnostic acceptability were significantly better in DLIR-M and DLIR-H than in ASiR-V ( $P = 0.001-0.005$ ).

#### CONCLUSION

s DLIR significantly improved SNR and image quality compared with ASiR-V in whole-body CTA at 80 kVp with equivalent CM of 192 mgI/mL. DLIR-M seemed well-balanced algorithm compared with ASiR-V and DLIR-H.

#### CLINICAL RELEVANCE/APPLICATION

Deep learning image reconstruction was alternative method to adaptive statistical iterative reconstruction Veo on whole-body CT angiography at 80 kVp with equivalent contrast material of 192 mgI/mL.

Printed on: 02/07/23

## Abstract Archives of the RSNA, 2022

M5A-SPGI-8

### Is it safe to give iodine- or gadolinium-based contrast agents repeatedly on the same day?: An animal study

Monday, Nov. 28 12:15PM - 12:45PM Room: Learning Center - GI DPS

#### Participants

Heejin Bae, (*Presenter*) Nothing to Disclose

#### PURPOSE

To investigate molecular and functional consequences of repeated exposures to iodine- or gadolinium-based contrast agents within 24 hours through an animal study.

#### METHODS AND MATERIALS

Fifty-six Sprague-Dawley male rats were equally divided into 8 groups: negative control group, positive control group with single dose administration of iodine-based CT contrast agent, and repeated administration of either CT or MRI contrast agents after 2, 4, and 24 hours from the single dose injection of CT contrast agent. Concentrations of BUN, creatinine (SCr), cystatin C (Cys C), and malondialdehyde (MDA) were measured in serum samples and mRNA of kidney injury markers including kidney injury molecule-1 (KIM-1) and neutrophil gelatinase-associated lipocalin (NGAL) were evaluated from kidney tissues. Serum KIM-1 and NGAL proteins were detected by immunoassay and quantified by ELISA.

#### RESULTS

Repeated exposure to CT contrast agents significantly increased SCr (0.344 - 0.411 mg/dL,  $P = <0.001$ ) than negative and positive control groups (0.160; 0.207 mg/dL, respectively). SCr concentrations were not significantly different depending on various time intervals ( $P = >0.999$ ). For average levels of Cys C and MDA, statistically significant differences were not observed between the positive control group (0.427 mg/L; 1.802  $\mu$ M) and repeated injection groups (0.549 - 0.550,  $P = 0.256 - 0.362$ ; 1.283 - 2.254,  $P = >0.999$ , respectively). Likewise, additional dose of MRI contrast agent after single dose of CT contrast agent did not affect SCr, Cys C, and MDA (0.171 - 0.230,  $P = >0.999$ ; 0.4,  $P = 0.262$ ; 0.770 - 1.079,  $P = 0.139 - 0.771$ , respectively). mRNA and protein levels of KIM-1 and NGAL were not significantly different among various time intervals of the additional injection of either CT or MRI contrast agents.

#### CONCLUSION

More than 24 hours of interval between the repeated contrast-enhanced CT examinations may be necessary to avoid deterioration in renal function, whereas conducting contrast-enhanced MRI on the same day as contrast-enhanced CT examination may not induce clinically significant kidney injury.

#### CLINICAL RELEVANCE/APPLICATION

Repeated exposure to the contrast agents in a short time period is known to be a risk factor for development of contrast-induced nephropathy. However, according to ACR manual on contrast media, the evidence to avoid a repeated contrast agent injection until more than 24 hours is yet insufficient.

Printed on: 02/07/23

## Abstract Archives of the RSNA, 2022

M5A-SPGI-9

### Cross-Sectional Comparison of Serum Fib-4 and MRI-Derived Liver T1 as Noninvasive Markers of Liver Fibrosis: An Interim Analysis of the Dallas Heart Study Cohort

Monday, Nov. 28 12:15PM - 12:45PM Room: Learning Center - GI DPS

#### Participants

Sujoy Mukherjee, (*Presenter*) Nothing to Disclose

#### PURPOSE

Noninvasive serum (e.g. FIB-4)<sup>1</sup> and imaging (e.g. elastography, T1 mapping)<sup>2-4</sup> biomarkers of liver fibrosis have been validated against liver biopsy. Whether these biomarkers are correlative or complementary remains unknown. The purpose of this study is to compare serum FIB-4 and MRI-derived liver T1 in the general adult population in the US.

#### METHODS AND MATERIALS

This is an interim analysis of the ongoing Dallas Hearts Study (DHS) third examination, a large multiethnic sampling of adults in Dallas County, Texas. The study collects demographic data, serum laboratory tests needed to calculate FIB-4, and multiparametric liver MRI using LiverMultiScan® 3T protocol (Perspectum, Oxford, UK) to calculate mean hepatic iron-corrected T1 (cT1)<sup>5</sup>. The correlation between FIB-4 and cT1 values was assessed by scatter plots as well as Spearman and Pearson correlation coefficients. The association between FIB-4 = 1.3 and cT1 = 763 msec was assessed by odds ratio, where these thresholds were drawn from the upper limits of the low risk group<sup>6 7</sup>. This study was approved by IRB and was compliant with HIPAA.

#### RESULTS

279 adult participants from DHS completed liver cT1 analysis and included 107 males and 172 females, median age [interquartile range] 61 [55-67] years. The median FIB-4 and cT1 were 1.06 [0.84-1.43] and 745 [697-802] msec, with n=93 (33.3%) and n=111 (39.8%) with above-normal FIB-4 and cT1, respectively. No significant correlation was found between FIB-4 and cT1 (Figure 2) by Pearson nor Spearman methods. No significant association was found between above-normal FIB-4 and cT1, with odds ratio [95% confidence interval] of 1.14 [0.69 - 1.90].

#### CONCLUSION

s Serum FIB-4 and cT1 were not significantly correlated with each other in the general population. Our finding is consistent with other studies where FIB-4 had a low correlation with viscoelastic transient elastography<sup>8</sup>. Our early data suggest that FIB-4 and cT1 are not correlative, but may be complementary, in evaluating liver disease. Further research is necessary how serum and imaging biomarkers may be used in combination.

#### CLINICAL RELEVANCE/APPLICATION

FIB-4 was developed for viral hepatitis. Iron-corrected T1 MRI was developed for nonalcoholic fatty liver disease. While both biomarkers were validated against liver biopsies, they may generate discrepant results when applied to the general population for liver disease screening.

Printed on: 02/07/23

## Abstract Archives of the RSNA, 2022

M5A-SPGU

### Genitourinary Monday Poster Discussions - A

Monday, Nov. 28 12:15PM - 12:45PM Room: Learning Center - GU DPS

#### Sub-Events

#### M5A-SPGU-1 External validation of an AI model for prostate mpMRI: a multicenter study

Participants

Kexin Wang, (*Presenter*) Nothing to Disclose

#### PURPOSE

To evaluate the prediction efficacy of an AI model for prostate cancer using external data.

#### METHODS AND MATERIALS

480 cases of mpMRI were retrospectively collected from four hospitals. The pathology diagnosis was clinically significant cancer (csPCa) in 180 cases, and non-csPCa in 300 cases, with a PSA level of 17.79 [0.15,100.00]. A prior trained AI model was used to predict the existence of prostate cancer on DWI and ADC maps. 16 radiologists were asked to interpret the image without knowledge of the clinical information. Each radiologist was assigned 30 cases and interpreted the cases twice in between 1 month, with and without the aid of AI. The cases were randomly separated into 2 groups. For group 1, the case was read firstly without AI and secondly with AI. For group 2, the cases were firstly read with AI and secondly without AI. The radiologist made their diagnosis following PI-RADS v2.1. When the PI-RADS category was 3-5, the case was considered to be diagnosed as positive. On the contrary, when the PI-RADS category was 1 and 2, the case was considered to be diagnosed as negative. The reading time and diagnosis confidence were also recorded during the image interpretation.

#### RESULTS

The AUC for the all the radiologists were 0.791 (95%CI: 0.687-0.956) and 0.699 (95%CI: 0.565-0.773) with and without the aided of AI ( $p < 0.05$ ). The reading time shortened from 350 [27-1140]s (Median [Min, Max]) to 148 [19-948]s. The diagnosis confidence increased in 10 radiologists with the help of AI.

#### CONCLUSION

This multicenter study proved that the AI model for the prediction of prostate cancer on mpMRI could be generalized, and the diagnostic accuracy of csPCa was increased.

#### CLINICAL RELEVANCE/APPLICATION

Validation of AI models requires large samples of external data. This study provides evidence for future practical clinical applications of the AI model for the diagnosis of prostate cancer on mpMRI.

#### M5A-SPGU-2 Multiparametric MR imaging for evaluating early diabetic nephropathy: Changes related to glomerular hypertension

Participants

Akira Yamamoto, MD, PhD, Kurashiki, Japan (*Presenter*) Nothing to Disclose

#### PURPOSE

The purpose of this study was to identify the changes related to glomerular hypertension in multiparametric magnetic resonance imaging (MRI) findings for evaluating early diabetic nephropathy.

#### METHODS AND MATERIALS

The study subjects (N=58) included 35 patients with early diabetic nephropathy (hyperfiltration stage) and 23 healthy volunteers. All subjects underwent non-contrast MRI using a 3-Tesla MRI machine. Measurements were made of the renal cortex and renal medulla T1 values, T2 values, blood oxygenation level dependent (BOLD) imaging (T2\* values and R2\* values), intravoxel incoherent motion (IVIM) imaging (ADC, f, D\* and D values), arterial spin labeling (ASL) as well as optimal inversion time (TI) (= TI of maximum corticomedullary contrast ratio (CMR = signal intensity (SI) of cortex / SI of medulla)) and inverted TI value (value of TI that inverts the renal cortex and renal medulla SI) on steady-state free precession (SSFP) with inversion recovery (IR) pulse with multi TI (TI = 1000, 1100, 1200, 1300, 1400, 1500, 1600, 1700, 1800 msec). A total 21 parameters were compared between healthy groups and early DN group.

#### RESULTS

A significant difference between healthy groups and early diabetic nephropathy group was seen in T2 values of cortex (mean  $\pm$  SD: 101.28 $\pm$ 9.59 msec vs. 107.76.0 $\pm$ 11.39 msec;  $p=0.041$ ) and parameters derived from SSFP with IR pulse with multi TI, inverted TI (mean  $\pm$  SD: 1240.9 $\pm$ 66.6 msec vs. 1278.6 $\pm$ 62.2 msec;  $p=0.029$ ) and optimal TI (mean  $\pm$  SD: 1395.5 $\pm$ 72.2 msec vs. 1437.1 $\pm$ 70.0 msec;  $p=0.019$ ). No other 18 parameters showed significant differences between healthy groups and early DN group. There was no

significant difference in renal cortical thickness, but it showed a large value in the hyperfiltration stage.

## **CONCLUSION**

s T2 value of cortex and parameters derived from SSFP with an ssIR pulse, inverted TI and optimal TI might sensitively capture the changes in glomerular hypertension related changes of the renal cortex in early diabetic nephropathy, can be used to evaluate early diabetic nephropathy non-invasively and in a short period of time.

## **CLINICAL RELEVANCE/APPLICATION**

MR imaging using the T2 value of cortex and parameters derived from SSFP with an ssIR pulse, inverted TI and optimal TI might be useful to evaluate glomerular hypertension in early stage of diabetic nephropathy with non-invasively and in a short period of time.

## **M5A-SPGU-3Application of dual energy spectral CT in Vascular ErectileDysfunction**

Participants

Xiaohu Li, MD, PhD, (*Presenter*) Nothing to Disclose

## **PURPOSE**

To study the value of CT angiography and CT perfusion imaging in guiding the diagnosis of vascular erectile dysfunction and indicating the clinical grading of vascular erectile dysfunction.

## **METHODS AND MATERIALS**

60 patients with erectile dysfunction in our hospital were divided into vascular erectile dysfunction group and non-vascular erectile dysfunction group. The vascular erectile dysfunction group was divided into severe erectile dysfunction group and mild-to-moderate erectile dysfunction group according to IIEF-5. After CT scanning of hypogastrium, we completed the reconstruction of penile blood vessels and the collection of perfusion data of corpus cavernosum and penis root by using post-processing software. Then both the perfusion data and penile vascular status, including Internal pudendal artery, dorsal penile artery and cavernous artery, were analyzed statistically.

## **RESULTS**

vascular abnormalities were found in all cases in vascular erectile dysfunction group, especially in cavernous artery; in non vascular erectile dysfunction group, there were 2 cases of dorsal penile artery and 2 cases of cavernous artery abnormalities, but no internal pudendal artery abnormalities. There were significant differences in the abnormalities of internal pudendal artery, dorsal penile artery and cavernous artery between vascular group and non vascular group ( $p < 0.05$ ), and there was significant correlation between mild to moderate vascular erectile dysfunction group and severe group in vascular subjective score ( $p < 0.05$ ). The BF, BV and T<sub>max</sub> parameters of the penile root and corpus cavernosum in the vascular erectile dysfunction group were statistically significant compared with those in the non vascular erectile dysfunction group ( $p < 0.05$ ), but the PS parameters were not statistically significant ( $p = 0.70$ ,  $p < 0.05$ ).

## **CONCLUSION**

s CT angiography can show the penile blood vessel status of patients with vascular erectile dysfunction, prompt the diseased blood vessels, assist the clinical diagnosis and treatment, and assist the clinical grading of patients with erectile dysfunction through the perfusion data obtained by post-processing software and the analysis of the degree of vascular lesions.

## **CLINICAL RELEVANCE/APPLICATION**

The imaging data of vascular ED patients were analyzed by vascular reconstruction and perfusion parameters, and it was found that CTA can better display the penile blood vessels of patients with vascular erectile dysfunction, indicating the diseased blood vessels and their severity, which has a certain value for clinical diagnosis.

Printed on: 02/07/23

## Abstract Archives of the RSNA, 2022

M5A-SPGU-1

### External validation of an AI model for prostate mpMRI: a multicenter study

Monday, Nov. 28 12:15PM - 12:45PM Room: Learning Center - GU DPS

#### Participants

Kexin Wang, (*Presenter*) Nothing to Disclose

#### PURPOSE

To evaluate the prediction efficacy of an AI model for prostate cancer using external data.

#### METHODS AND MATERIALS

480 cases of mpMRI were retrospectively collected from four hospitals. The pathology diagnosis was clinically significant cancer (csPCa) in 180 cases, and non-csPCa in 300 cases, with a PSA level of 17.79 [0.15,100.00]. A prior trained AI model was used to predict the existence of prostate cancer on DWI and ADC maps. 16 radiologists were asked to interpret the image without knowledge of the clinical information. Each radiologist was assigned 30 cases and interpreted the cases twice in between 1 month, with and without the aid of AI. The cases were randomly separated into 2 groups. For group 1, the case was read firstly without AI and secondly with AI. For group 2, the cases were firstly read with AI and secondly without AI. The radiologist made their diagnosis following PI-RADS v2.1. When the PI-RADS category was 3-5, the case was considered to be diagnosed as positive. On the contrary, when the PI-RADS category was 1 and 2, the case was considered to be diagnosed as negative. The reading time and diagnosis confidence were also recorded during the image interpretation.

#### RESULTS

The AUC for the all the radiologists were 0.791 (95%CI: 0.687-0.956) and 0.699 (95%CI: 0.565-0.773) with and without the aided of AI ( $p < 0.05$ ). The reading time shortened from 350 [27-1140]s (Median [Min, Max]) to 148 [19-948]s. The diagnosis confidence increased in 10 radiologists with the help of AI.

#### CONCLUSION

s This multicenter study proved that the AI model for the prediction of prostate cancer on mpMRI could be generalized, and the diagnostic accuracy of csPCa was increased.

#### CLINICAL RELEVANCE/APPLICATION

Validation of AI models requires large samples of external data. This study provides evidence for future practical clinical applications of the AI model for the diagnosis of prostate cancer on mpMRI.

Printed on: 02/07/23

## Abstract Archives of the RSNA, 2022

M5A-SPGU-2

### Multiparametric MR imaging for evaluating early diabetic nephropathy: Changes related to glomerular hypertension

Monday, Nov. 28 12:15PM - 12:45PM Room: Learning Center - GU DPS

#### Participants

Akira Yamamoto, MD, PhD, Kurashiki, Japan (*Presenter*) Nothing to Disclose

#### PURPOSE

The purpose of this study was to identify the changes related to glomerular hypertension in multiparametric magnetic resonance imaging (MRI) findings for evaluating early diabetic nephropathy.

#### METHODS AND MATERIALS

The study subjects (N=58) included 35 patients with early diabetic nephropathy (hyperfiltration stage) and 23 healthy volunteers. All subjects underwent non-contrast MRI using a 3-Tesla MRI machine. Measurements were made of the renal cortex and renal medulla T1 values, T2 values, blood oxygenation level dependent (BOLD) imaging (T2\* values and R2\* values), intravoxel incoherent motion (IVIM) imaging (ADC, f, D\* and D values), arterial spin labeling (ASL) as well as optimal inversion time (TI) (= TI of maximum corticomedullary contrast ratio (CMR = signal intensity (SI) of cortex / SI of medulla)) and inverted TI value (value of TI that inverts the renal cortex and renal medulla SI) on steady-state free precession (SSFP) with inversion recovery (IR) pulse with multi TI (TI = 1000, 1100, 1200, 1300, 1400, 1500, 1600, 1700, 1800 msec). A total 21 parameters were compared between healthy groups and early DN group.

#### RESULTS

A significant difference between healthy groups and early diabetic nephropathy group was seen in T2 values of cortex (mean  $\pm$  SD: 101.28 $\pm$ 9.59 msec vs. 107.76.0 $\pm$ 11.39 msec; p=0.041) and parameters derived from SSFP with IR pulse with multi TI, inverted TI (mean  $\pm$  SD: 1240.9 $\pm$ 66.6 msec vs. 1278.6 $\pm$ 62.2 msec; p=0.029) and optimal TI (mean  $\pm$  SD: 1395.5 $\pm$ 72.2 msec vs. 1437.1 $\pm$ 70.0 msec; p=0.019). No other 18 parameters showed significant differences between healthy groups and early DN group. There was no significant difference in renal cortical thickness, but it showed a large value in the hyperfiltration stage.

#### CONCLUSION

s T2 value of cortex and parameters derived from SSFP with an ssIR pulse, inverted TI and optimal TI might sensitively capture the changes in glomerular hypertension related changes of the renal cortex in early diabetic nephropathy, can be used to evaluate early diabetic nephropathy non-invasively and in a short period of time.

#### CLINICAL RELEVANCE/APPLICATION

MR imaging using the T2 value of cortex and parameters derived from SSFP with an ssIR pulse, inverted TI and optimal TI might be useful to evaluate glomerular hypertension in early stage of diabetic nephropathy with non-invasively and in a short period of time.

Printed on: 02/07/23

## Abstract Archives of the RSNA, 2022

M5A-SPGU-3

### Application of dual energy spectral CT in Vascular Erectile Dysfunction

Monday, Nov. 28 12:15PM - 12:45PM Room: Learning Center - GU DPS

#### Participants

Xiaohu Li, MD, PhD, (Presenter) Nothing to Disclose

#### PURPOSE

To study the value of CT angiography and CT perfusion imaging in guiding the diagnosis of vascular erectile dysfunction and indicating the clinical grading of vascular erectile dysfunction.

#### METHODS AND MATERIALS

60 patients with erectile dysfunction in our hospital were divided into vascular erectile dysfunction group and non-vascular erectile dysfunction group. The vascular erectile dysfunction group was divided into severe erectile dysfunction group and mild-to-moderate erectile dysfunction group according to IIEF-5. After CT scanning of hypogastrium, we completed the reconstruction of penile blood vessels and the collection of perfusion data of corpus cavernosum and penis root by using post-processing software. Then both the perfusion data and penile vascular status, including Internal pudendal artery, dorsal penile artery and cavernous artery, were analyzed statistically.

#### RESULTS

vascular abnormalities were found in all cases in vascular erectile dysfunction group, especially in cavernous artery; in non vascular erectile dysfunction group, there were 2 cases of dorsal penile artery and 2 cases of cavernous artery abnormalities, but no internal pudendal artery abnormalities. There were significant differences in the abnormalities of internal pudendal artery, dorsal penile artery and cavernous artery between vascular group and non vascular group ( $p < 0.05$ ), and there was significant correlation between mild to moderate vascular erectile dysfunction group and severe group in vascular subjective score ( $p < 0.05$ ). The BF, BV and Tmax parameters of the penile root and corpus cavernosum in the vascular erectile dysfunction group were statistically significant compared with those in the non vascular erectile dysfunction group ( $p < 0.05$ ), but the PS parameters were not statistically significant ( $p = 0.70$ ,  $p < 0.05$ ).

#### CONCLUSION

s CT angiography can show the penile blood vessel status of patients with vascular erectile dysfunction, prompt the diseased blood vessels, assist the clinical diagnosis and treatment, and assist the clinical grading of patients with erectile dysfunction through the perfusion data obtained by post-processing software and the analysis of the degree of vascular lesions.

#### CLINICAL RELEVANCE/APPLICATION

The imaging data of vascular ED patients were analyzed by vascular reconstruction and perfusion parameters, and it was found that CTA can better display the penile blood vessels of patients with vascular erectile dysfunction, indicating the diseased blood vessels and their severity, which has a certain value for clinical diagnosis.

Printed on: 02/07/23

## Abstract Archives of the RSNA, 2022

M5A-SPHN

### Head and Neck Monday Poster Discussions - A

Monday, Nov. 28 12:15PM - 12:45PM Room: Learning Center - HN DPS

#### Sub-Events

#### **M5A-SPHN-1 The Clinical Feasibility of T1-based Dynamic Susceptibility Contrast Perfusion MRI in Head and Neck Cancer Patients**

Participants

Ji Young Lee, MD, PhD, Seoul, Korea, Republic Of (*Presenter*) Nothing to Disclose

#### **PURPOSE**

The T2\*-based dynamic susceptibility contrast (DSC) perfusion MRI has been limited for clinical application in the head and neck MRI due to susceptibility or motion artifact. High temporal resolution enabled the T1-based DSC (T1-DSC) perfusion MRI which provides reliable CBV value. The purpose of this study was to assess the technical and clinical feasibility of T1-DSC perfusion MRI in patients with head and neck cancer.

#### **METHODS AND MATERIALS**

This retrospective study included twelve patients with head and neck cancer who performed the dynamic T1 gradient echo enhancement scans. The CBV maps were obtained from the T1-DSC perfusion MRI and Vp maps were obtained with the T1-DCE perfusion MRI using a commercial software. The statistical analysis was performed to evaluate the relationship between two methods. Spearman correlation and intraclass correlation coefficients (ICC) were obtained.

#### **RESULTS**

The perfusion maps were acquired for the preoperative tumor staging (n=9) and tumor treatment response (n=3). The CBV maps and Vp maps were obtained in the following locations: oral cavity (n=5), sinus cancer (n=2), hypopharynx (n=1), supraglottis (n=1), soft palate (n=1), and lymph node (n=2). The statistical analysis showed the moderate linear correlation between T1-CBV and the Vp (r= 0.67, p=0.01) The ICC was 0.80 (p=0.002).

#### **CONCLUSION**

The relationship between T1-CBV and Vp showed moderate correlation and good reliability. T1-based DSC perfusion MRI can be feasible in head and neck oncology and it could be expected to be useful for the tumor characterization and treatment response assessment in the head and neck cancer patient.

#### **CLINICAL RELEVANCE/APPLICATION**

T1-based DSC perfusion MRI can be feasible in head and neck oncology and it could be expected to be useful for the tumor characterization and treatment response assessment in the head and neck cancer patient.

#### **M5A-SPHN-2 Submental High Frequency Ultrasound to Evaluate the Efficacy of Acupuncture Combined with Electrical Stimulation in PD Dysphagia**

Participants

Huang Meng, (*Presenter*) Nothing to Disclose

#### **PURPOSE**

To observe the effect of acupuncture combined with electrical stimulation on dysphagia in Parkinson Disease (PD) by submental high frequency ultrasound.

#### **METHODS AND MATERIALS**

A total of 64 patients with PD who were hospitalized in our hospital from April 2020 to June 2021 were enrolled in the study group and the control group after they were confirmed to have swallowing dysfunction by videofluoroscopic study of swallowing (VFSS). There were 32 cases in each group. Both groups were treated with basic therapy (i.e., medopa therapy + electrical stimulation therapy). The drinking water test score and VFSS score were used to evaluate the changes of the two groups before and after treatment, and the clinical efficacy of the two groups was compared.

#### **RESULTS**

1. After treatment, the total effective rate of the research group was 90.62%, and the total effective rate of the control group was 71.87% (p<0.05); 2. There was no statistical difference in the overall mean of MHLA between the two groups after treatment (p>0.05); the research group NHLA was greater than that of the control group, and there was a difference in the overall mean of NHLA between the two groups (p < 0.05). 3. There was no significant correlation between MHLA and VFSS score (p>0.05); there was a negative correlation between NHLA and VFSS score (p<0.05), and a positive correlation between HLAS and ASR and VFSS score respectively (p<0.05) . 4. The AUCs of NHLA, HLAS and ASR for the diagnosis of dysphagia in PD were 0.893, 0.831 and

0.968, respectively. The optimal cut-off value of ASR for the diagnosis of dysphagia in PD was 41.09%, and the sensitivity and specificity were 83.65% and 100.00%, respectively.

#### **CONCLUSION**

s 1. Acupuncture combined with electrical stimulation therapy has a better effect on PD swallowing dysfunction, which can significantly improve the quality of life of patients; 2. The measurement indexes of NHLA, HLAS and ASR of submental high-frequency ultrasound can be used to evaluate the therapeutic effect of PD patients with dysphagia. ASR has high sensitivity and specificity in the diagnosis of dysphagia, and it is a reliable index to evaluate the dysphagia of PD patients.

#### **CLINICAL RELEVANCE/APPLICATION**

Acupuncture combined with electrical stimulation therapy is an effective method for the treatment of dysphagia in PD, which can significantly improve the swallowing function of patients with dysphagia in PD. Using submental high-frequency ultrasound to measure HLA can evaluate the efficacy of acupuncture combined with electrical stimulation therapy on PD dysphagia. ASR has high sensitivity and specificity in diagnosing PD dysphagia. Because of its advantages of simplicity, high repeatability, no radiation, safety and non-invasiveness, it is worthy of clinical application.

Printed on: 02/07/23

## Abstract Archives of the RSNA, 2022

M5A-SPHN-1

### The Clinical Feasibility of T1-based Dynamic Susceptibility Contrast Perfusion MRI in Head and Neck Cancer Patients

Monday, Nov. 28 12:15PM - 12:45PM Room: Learning Center - HN DPS

#### Participants

Ji Young Lee, MD, PhD, Seoul, Korea, Republic Of (*Presenter*) Nothing to Disclose

#### PURPOSE

The T2\*-based dynamic susceptibility contrast (DSC) perfusion MRI has been limited for clinical application in the head and neck MRI due to susceptibility or motion artifact. High temporal resolution enabled the T1-based DSC (T1-DSC) perfusion MRI which provides reliable CBV value. The purpose of this study was to assess the technical and clinical feasibility of T1-DSC perfusion MRI in patients with head and neck cancer.

#### METHODS AND MATERIALS

This retrospective study included twelve patients with head and neck cancer who performed the dynamic T1 gradient echo enhancement scans. The CBV maps were obtained from the T1-DSC perfusion MRI and Vp maps were obtained with the T1-DCE perfusion MRI using a commercial software. The statistical analysis was performed to evaluate the relationship between two methods. Spearman correlation and intraclass correlation coefficients (ICC) were obtained.

#### RESULTS

The perfusion maps were acquired for the preoperative tumor staging (n=9) and tumor treatment response (n=3). The CBV maps and Vp maps were obtained in the following locations: oral cavity (n=5), sinus cancer (n=2), hypopharynx (n=1), supraglottis (n=1), soft palate (n=1), and lymph node (n=2). The statistical analysis showed the moderate linear correlation between T1-CBV and the Vp ( $r = 0.67$ ,  $p = 0.01$ ) The ICC was 0.80 ( $p = 0.002$ ).

#### CONCLUSION

The relationship between T1-CBV and Vp showed moderate correlation and good reliability. T1-based DSC perfusion MRI can be feasible in head and neck oncology and it could be expected to be useful for the tumor characterization and treatment response assessment in the head and neck cancer patient.

#### CLINICAL RELEVANCE/APPLICATION

T1-based DSC perfusion MRI can be feasible in head and neck oncology and it could be expected to be useful for the tumor characterization and treatment response assessment in the head and neck cancer patient.

Printed on: 02/07/23

## Abstract Archives of the RSNA, 2022

M5A-SPHN-2

### Submental High Frequency Ultrasound to Evaluate the Efficacy of Acupuncture Combined with Electrical Stimulation in PD Dysphagia

Monday, Nov. 28 12:15PM - 12:45PM Room: Learning Center - HN DPS

#### Participants

Huang Meng, (*Presenter*) Nothing to Disclose

#### PURPOSE

To observe the effect of acupuncture combined with electrical stimulation on dysphagia in Parkinson Disease (PD) by submental high frequency ultrasound.

#### METHODS AND MATERIALS

A total of 64 patients with PD who were hospitalized in our hospital from April 2020 to June 2021 were enrolled in the study group and the control group after they were confirmed to have swallowing dysfunction by videofluoroscopic study of swallowing (VFSS). There were 32 cases in each group. Both groups were treated with basic therapy (i.e., medopa therapy + electrical stimulation therapy). The drinking water test score and VFSS score were used to evaluate the changes of the two groups before and after treatment, and the clinical efficacy of the two groups was compared.

#### RESULTS

1. After treatment, the total effective rate of the research group was 90.62%, and the total effective rate of the control group was 71.87% ( $p < 0.05$ ); 2. There was no statistical difference in the overall mean of MHLA between the two groups after treatment ( $p > 0.05$ ); the research group NHLA was greater than that of the control group, and there was a difference in the overall mean of NHLA between the two groups ( $p < 0.05$ ). 3. There was no significant correlation between MHLA and VFSS score ( $p > 0.05$ ); there was a negative correlation between NHLA and VFSS score ( $p < 0.05$ ), and a positive correlation between HLAS and ASR and VFSS score respectively ( $p < 0.05$ ). 4. The AUCs of NHLA, HLAS and ASR for the diagnosis of dysphagia in PD were 0.893, 0.831 and 0.968, respectively. The optimal cut-off value of ASR for the diagnosis of dysphagia in PD was 41.09%, and the sensitivity and specificity were 83.65% and 100.00%, respectively.

#### CONCLUSION

1. Acupuncture combined with electrical stimulation therapy has a better effect on PD swallowing dysfunction, which can significantly improve the quality of life of patients; 2. The measurement indexes of NHLA, HLAS and ASR of submental high-frequency ultrasound can be used to evaluate the therapeutic effect of PD patients with dysphagia. ASR has high sensitivity and specificity in the diagnosis of dysphagia, and it is a reliable index to evaluate the dysphagia of PD patients.

#### CLINICAL RELEVANCE/APPLICATION

Acupuncture combined with electrical stimulation therapy is an effective method for the treatment of dysphagia in PD, which can significantly improve the swallowing function of patients with dysphagia in PD. Using submental high-frequency ultrasound to measure HLA can evaluate the efficacy of acupuncture combined with electrical stimulation therapy on PD dysphagia. ASR has high sensitivity and specificity in diagnosing PD dysphagia. Because of its advantages of simplicity, high repeatability, no radiation, safety and non-invasiveness, it is worthy of clinical application.

Printed on: 02/07/23

## Abstract Archives of the RSNA, 2022

M5A-SPIN

### Informatics Monday Poster Discussions - A

Monday, Nov. 28 12:15PM - 12:45PM Room: Learning Center - IN DPS

#### Sub-Events

#### **M5A-SPIN-1 Using a Single Artificial Intelligence Solution in Detecting Anatomy, View, and Orientation of X-ray Exams of Adult and Pediatric Population**

##### Participants

Ravi Soni, (*Presenter*) Nothing to Disclose

##### PURPOSE

To use deep learning model in determining if an acquired X-ray image is one of many prevalent anatomies such as chest, abdomen, pelvis, hand, knee, foot, and wrist. Additionally, using the same model to identify a view and an orientation of an x-ray image. Up to 30% of Chest X-rays obtained on fixed systems have been reported as being acquired with the incorrect protocol view. This results in incorrect exposure parameters, incorrect DICOM tags being recorded, and incorrect processing algorithms. Also, radiographers must correct incorrectly orientated acquired images to a reference orientation before sending them to PACS. Across the fixed and mobile systems, we find 53% and 42% of upper and lower extremity exams respectively require manual rotation correction. We propose an AI algorithm to identify the anatomy, view, and detect the orientation of the x-rays. This model helps reduce human operating errors related to protocol mismatches and incorrect orientation.

##### METHODS AND MATERIALS

A convolutional neural network composed of Inception blocks for feature extraction is used to train over a large set of x-ray exams of adult and pediatric population. The size of the convolutional neural network is 5.1 million parameters. The network has multiple outputs: (1) anatomy, (2) view, (3) quadrant, (4) precise orientation. The quadrant branch outputs the coarse orientation of the x-ray image in the step of 90 degrees. While the precise orientation branch outputs the precise orientation degrees of the image. The out-of-scope or low prevalent x-ray exams are excluded and trained as the "others" class.

##### RESULTS

The results showed that the AI model detected the anatomy, view, and quadrant orientation with well above 90% accuracy on a large test set comprised of 13,207 images. Each image was randomly rotated multiple times to find out robustness. The quadrant orientation performance is above 99% while the performance of anatomy and view is around mid-90s%. The Matthew's Correlation Coefficient is higher than 90% for all in-scope anatomies and views.

##### CONCLUSION

s We demonstrated the feasibility and efficacy of artificial convolutional neural network in detecting the multiple anatomies, views, and orientations of x-rays from a large international data set. We believe this is the first time a single deep neural network is used in identifying multiple anatomies of thoracic and MSK radiographic images.

##### CLINICAL RELEVANCE/APPLICATION

A wide variety of x-ray exams are performed to help diagnose a variety of injuries and illnesses in most body parts. To avoid human operating errors related to protocol mismatch and to reduce time for orientation correction, an AI solution is needed to include all high prevalent anatomies and views. The proposed model offers a single solution to address this.

#### **M5A-SPIN-2 A Novel Collaborative Self-Supervised Transformer Neural Network for Radiomic Data Classification**

##### Participants

Zhiyuan Li, BS,MS, (*Presenter*) Nothing to Disclose

##### PURPOSE

To develop a novel collaborative self-supervised transformer neural network for radiomic data classification without large-scale annotated images.

##### METHODS AND MATERIALS

Data acquisition and pre-processing: The proposed approach was developed and validated on a prospective cohort of 392 very preterm infants, enrolled soon after birth. We used each infant's T2-weighted MRI data acquired at term-equivalent age to identify imaging prognostic features of cognitive deficits. We classified infants into one of the two groups - high-risk (Cognitive score  $\leq 85$ ) or low-risk (Cognitive score  $>85$ ) for cognitive deficits based on the standardized Bayley-III Cognitive subscale at 2 years corrected age.. We segmented each T2-weighted brain image into 87 regions of interest (ROIs) and extracted 100 radiomics features from each ROI using the PyRadiomics pipeline, therefore resulting in a 87-by-100 feature map for each subject. Collaborative Self-Supervised Learning: It remains challenging to train robust deep learning models due to the lack of sufficient labeled data. As shown in Figure 1, we developed a collaborative self-supervised learning (SSL) model to solve the challenges posed by the over-dependence of labeled data, particularly for radiomic data classification. We first augmented multiple samples from each subject by

randomly masking/hiding radiomic features from several ROIs, and then we trained a transformer to learn latent features from augmented samples without human labeling by solving two collaborative pretext tasks, including 1) Reconstruction - to reconstruct the hidden radiomic features using the observable ones, and 2) Discrimination - to find similarity and dissimilarity from augmented samples, and to classify all augmented samples from the same subject into one group. Model performance was assessed using 5-fold cross-validation. This process was repeated 100 times.

## RESULTS

Of the original cohort of 392 infants, 318 (81%) had Bayley III cognitive scores assessed at 2 years corrected age. Our model achieved an AUC of 0.78, outperforming the supervised Transformer (AUC=0.61) as well as several peer self-supervised models that were developed for text and/or image data, including Rotation (AUC=0.64), Moco v1 (AUC=0.69), and SimCLR (AUC=0.71). Our method achieved a balanced accuracy of 76.3%, sensitivity of 75.8%, and specificity of 76.7%.

## CONCLUSION

We showed that the proposed model outperformed peer self-supervised models for radiomic data classification in the application of the early prediction of cognitive deficit in very preterm infants.

## CLINICAL RELEVANCE/APPLICATION

The proposed model is able to facilitate the deep learning-based applications in Radiomics without large-scale annotated datasets.

## M5A-SPIN-3 Radiology Trainees Attitudes Towards Artificial Intelligence in Clinical Radiology and Its Implementation in Training and the Curriculum in The United Kingdom

Participants

Obaid Hashmi, MBBS, FRCR, (*Presenter*) Nothing to Disclose

## PURPOSE

Artificial Intelligence (AI) and Machine learning (ML) have garnered significant interest in radiology. AI and ML have been introduced to the 2021 Royal College of Radiologists (RCR) curriculum highlighting its importance to radiology trainees in the United Kingdom (UK). The attitudes of trainees towards AI in Radiology has been reviewed in several countries, however there was no documented survey assessing the attitudes of UK radiology trainees towards AI. A national trainee led survey was created to understand the attitudes of UK radiology trainees, in particular assessing the demand for AI education. This could help guide implementation of AI teaching in radiology training programmes.

## METHODS AND MATERIALS

The survey was created in the Google Forms platform and nationally distributed via email. The survey ran over a period of 2 months. All 37 training programmes in the United Kingdom were targeted. Participants were asked 4 demographic questions and 14 questions relating to the topic of AI in radiology. They were surveyed on their views relating to previous experience with AI, teaching of AI and its future within the career of a radiologist.

## RESULTS

The survey was completed by 149 trainee radiologists with at least 1 response from each of the 37 UK training programmes. 83.7% said they were interested in AI use in Radiology but 71.4% had no experience of working with AI. Most, 79.9%, would like to be involved in AI based projects. Almost all respondents (98.7%) felt that AI should be taught during their training, in particular in the 1st 3 years of training, yet, only 1 respondent stated that their training programme had implemented AI teaching. Respondents indicated that basic understanding, implementation and critical appraisal of AI software should be prioritized in AI teaching. Most trainees preferred teaching to be delivered at a deamery or training programme level. Only 12.8% of respondents said that AI would make them less likely to apply for radiology specialty training. Most responded that AI would be used in regular radiology practice in the next 5 to 10 years with 74.2% of trainees agreeing that AI will improve and enhance the job of radiologists in the next 20 years. The main concerns raised about AI in Radiology were IT/implementation and ethical/regulatory issues.

## CONCLUSION

The attitudes of UK trainees towards AI are mostly positive with many interested in being involved in AI based projects and activities. There is also clear interest and demand for AI teaching within training. However, current discussion, availability of AI based activities and AI teaching within UK training programmes is very limited.

## CLINICAL RELEVANCE/APPLICATION

To help guide the RCR and UK training programmes in their implementation of AI into radiology training.

## M5A-SPIN-4 A Cost-effective Multi-modality Machine Learning Framework for Prediction of Alzheimer' Disease

Participants

Jing Li, (*Presenter*) Nothing to Disclose

## PURPOSE

Machine learning (ML) models integrating multi-modality datasets have shown great promise for disease diagnosis/prognosis. The acquisition costs of different data modalities vary significantly. It is not cost-effective to require all patients acquiring all data modalities. We propose a cost-effective ML framework, called the Uncertainty-driven Modality Selection (UMoS) framework, to sequentially add modalities for each patient on an as-needed basis while at the same time ensuring high diagnostic/prognostic accuracy.

## METHODS AND MATERIALS

We demonstrate UMoS in an application of predicting the risk of progressing to Alzheimer's Disease (AD) for individuals with Mild Cognitive Impairment (MCI). ML models integrating MRI and PET have shown high accuracy in predicting MCI progression to AD. While MRI is used in the standard of care, PET is more costly and has less accessibility to patients. Under UMoS, a patient will be first predicted based on MRI; if the predictive uncertainty is lower than a threshold, the patient will not need PET; otherwise, the patient will need PET and be predicted by an MRI+PET model. To develop UMoS, we need to establish three building blocks: a trained MRI model, an uncertainty quantification approach for the MRI model, and a trained MRI+PET model. We establish these

building blocks and demonstrate UMoS using a dataset from ADNI, which includes 1319 T1-MRI scans from MCI patients with 612 of these MRI scans having accompanying amyloid-PET scans. We extracted regional volumetric and thickness features from MRI using FreeSurfer v7.1 and regional SUVR features from amyloid-PET using our in-house pipeline. To establish the building blocks of UMoS, we first train an MRI+PET model based on the subset of samples with both MRI and PET. Using the MRI+PET model as the teacher model, we further train an MRI model based on all samples using knowledge distillation. Predictive entropy was computed to quantify both the aleatoric and epistemic uncertainties of the MRI model.

## RESULTS

Under 10-fold cross validation, UMoS achieves 0.851 AUC (0.782/0.809 sensitivity/specificity using 0.5 probability cutoff), with 46.7% of patients predicted by the MRI model and 53.3% by the MRI+PET model. If all patients are predicted by the MRI +PET model, the performances are 0.873 AUC (0.776/0.811 sensitivity/specificity).

## CONCLUSION

s Under the UMoS framework, we achieve prediction performance at a similar level to the model that needs both MRI and PET for predicting MRI progression to AD, but UMoS saves 46.7% patients from needing PET.

## CLINICAL RELEVANCE/APPLICATION

This study provides an ML framework that ensures high accuracy in disease diagnosis/prognosis, but saves patients from needing unnecessary data modalities thus saving diagnostic/prognostic costs.

## M5A-SPIN-5 AI-based Bronchial Segmentation and Quantitation Prototype for Chest CT: Can it Help Assess Severity of Obstructive Lung Disease by Pulmonary Function Test?

Participants

Parisa Kaviani, MD, Boston, MA (*Presenter*) Nothing to Disclose

## PURPOSE

The aim of this study was to assess if an artificial intelligence-based bronchial segmentation and quantitation prototype for assessing severity of obstructive lung disease.

## METHODS AND MATERIALS

Our retrospective IRB-approved, HIPAA-compliant study comprised 222 adults (mean age 57±16 years; M:F 116: 106). A total of 107 patients with COPD had both PFT and non-contrast chest CT. The remaining 115 patients had no CT or clinical abnormality suggestive of lung disease (COPD or otherwise). The COPD severity was defined as mild, moderate, and severe based on the forced expiratory volume in 1 second (FEV1). We processed thin-section (1-1.25mm) CT images with the bronchial segmentation and quantitation prototype (Siemens Healthineers) to obtain following metrics: bronchial lumen volume, lumen diameter, lumen area, wall thickness, wall area, wall area ratio, and wall tapering) for total lung volumes and separately for each lung and lung lobe. Data were analyzed with area under the receiver operating characteristics curve (AUC) for distinguishing between mild, moderate, and severe COPD.

## RESULTS

AI algorithm had an AUC of up to 0.79 (95% CI: 0.728-0.852) for differentiating mild, moderate and severe emphysema based on FEV1. The AI algorithm was able to differentiate mild COPD with AUC of 0.86 (95% CI: 0.728-0.852) for the combination of generation 2 wall thickness, generation 0 lumen volume and RUL wall thickness, moderate COPD with AUC of 0.72 (95% CI: 0.728-0.852) for the combination of generation 1 wall thickness and LLL wall area, and severe COPD with 0.79 (95% CI: 0.728-0.852) for the combination of LUL wall thickness, generation 0 lumen volume, and global volume ratio airways vs lung as the best features.

## CONCLUSION

s Fully automated AI-based bronchial tree segmentation and quantitation prototype can differentiate different severity of COPD assessed with pulmonary function tests.

## CLINICAL RELEVANCE/APPLICATION

The quantitative information pertaining to bronchial wall and luminal dimensions estimated from an AI-based prototype can help in diagnosis and treatment of patients with bronchial involvement in COPD.

## M5A-SPIN-6 Semantic Retrieval of Similar Radiological Images using Vision Transformers: CXR and CT study

Participants

Anjali Thakrar, BS, Goleta, CA (*Presenter*) Nothing to Disclose

## PURPOSE

Identifying visually and semantically similar radiological images in a database can facilitate the creation of decision support tools, teaching files, and research cohorts. Existing content based image retrieval tools are often limited to searching by pixel-wise difference or vector distance of model predictions. Vision transformers (ViT) use attention to simultaneously take into account radiological diagnosis as well as visual appearance. Here, we develop a ViT-based image retrieval framework and evaluate the algorithm on the NIH Chest Radiographs (NIH-CXR) and NLST Chest CTs.

## METHODS AND MATERIALS

All 112,120 images from the NIH-CXR and 3246 randomly sampled cases from the NLST CT dataset were used. For CXR, a ViT binary classifier was trained on 4 ground truth labels (Cardiomegaly, Opacity, Emphysema, No Finding) and ensembled to produce multilabel classifications for each CXR. For CT, a regression model was trained to minimize L1 loss on the continuous ground truth labels of patient weight. The ViT image embedding layer was treated as a global image descriptor, using the L2 distance between descriptors as a similarity measure. Normalized discounted cumulative gain (nDCG) and mean average precision (mAP) were calculated from the ground truth labels. Five radiologists performed a reader performance study with random query images (25 CT and 25 CXR) and chose the 5 most similar images to the query from a set of 10 images (consisting of 5 closest to the query and 5 furthest from the query in model space). Inter-radiologist agreement and radiologist-model agreement statistics (Fleiss' and Cohen's kappa) were calculated. A t-SNE of the CT model latent space was generated to confirm clustering of similar images.

## **RESULTS**

The CXR model achieved nDCG@5 of 0.73 ( $p < 0.001$ ) and Cardiomegaly mAP@5 of 0.76 ( $p < 0.001$ ) among other results for CXR. The CT model achieved nDCG of 16.85 ( $p < 0.001$ ). The model prediction agreed with radiologist consensus on 86% of CXR samples and 79.2% of CT samples. Inter-radiologist Fleiss Kappa of 0.51 and radiologist consensus to model Cohen's Kappa of 0.65 were observed. Full code will be made available at the time of presentation.

## **CONCLUSION**

s We have developed and evaluated a vision transformer architecture that can retrieve visually and semantically similar radiological images.

## **CLINICAL RELEVANCE/APPLICATION**

Our vision transformer model can identify radiological images with visual and diagnostic similarities, which may be applied to decision support, teaching file creation, and research cohort creation.

Printed on: 02/07/23



## Abstract Archives of the RSNA, 2022

M5A-SPIN-1

### Using a Single Artificial Intelligence Solution in Detecting Anatomy, View, and Orientation of X-ray Exams of Adult and Pediatric Population

Monday, Nov. 28 12:15PM - 12:45PM Room: Learning Center - IN DPS

#### Participants

Ravi Soni, (*Presenter*) Nothing to Disclose

#### PURPOSE

To use deep learning model in determining if an acquired X-ray image is one of many prevalent anatomies such as chest, abdomen, pelvis, hand, knee, foot, and wrist. Additionally, using the same model to identify a view and an orientation of an x-ray image. Up to 30% of Chest X-rays obtained on fixed systems have been reported as being acquired with the incorrect protocol view. This results in incorrect exposure parameters, incorrect DICOM tags being recorded, and incorrect processing algorithms. Also, radiographers must correct incorrectly orientated acquired images to a reference orientation before sending them to PACS. Across the fixed and mobile systems, we find 53% and 42% of upper and lower extremity exams respectively require manual rotation correction. We propose an AI algorithm to identify the anatomy, view, and detect the orientation of the x-rays. This model helps reduce human operating errors related to protocol mismatches and incorrect orientation.

#### METHODS AND MATERIALS

A convolutional neural network composed of Inception blocks for feature extraction is used to train over a large set of x-ray exams of adult and pediatric population. The size of the convolutional neural network is 5.1 million parameters. The network has multiple outputs: (1) anatomy, (2) view, (3) quadrant, (4) precise orientation. The quadrant branch outputs the coarse orientation of the x-ray image in the step of 90 degrees. While the precise orientation branch outputs the precise orientation degrees of the image. The out-of-scope or low prevalent x-ray exams are excluded and trained as the "others" class.

#### RESULTS

The results showed that the AI model detected the anatomy, view, and quadrant orientation with well above 90% accuracy on a large test set comprised of 13,207 images. Each image was randomly rotated multiple times to find out robustness. The quadrant orientation performance is above 99% while the performance of anatomy and view is around mid-90s%. The Matthew's Correlation Coefficient is higher than 90% for all in-scope anatomies and views.

#### CONCLUSION

s We demonstrated the feasibility and efficacy of artificial convolutional neural network in detecting the multiple anatomies, views, and orientations of x-rays from a large international data set. We believe this is the first time a single deep neural network is used in identifying multiple anatomies of thoracic and MSK radiographic images.

#### CLINICAL RELEVANCE/APPLICATION

A wide variety of x-ray exams are performed to help diagnose a variety of injuries and illnesses in most body parts. To avoid human operating errors related to protocol mismatch and to reduce time for orientation correction, an AI solution is needed to include all high prevalent anatomies and views. The proposed model offers a single solution to address this.

Printed on: 02/07/23

## Abstract Archives of the RSNA, 2022

M5A-SPIN-2

### A Novel Collaborative Self-Supervised Transformer Neural Network for Radiomic Data Classification

Monday, Nov. 28 12:15PM - 12:45PM Room: Learning Center - IN DPS

#### Participants

Zhiyuan Li, BS,MS, (*Presenter*) Nothing to Disclose

#### PURPOSE

To develop a novel collaborative self-supervised transformer neural network for radiomic data classification without large-scale annotated images.

#### METHODS AND MATERIALS

Data acquisition and pre-processing: The proposed approach was developed and validated on a prospective cohort of 392 very preterm infants, enrolled soon after birth. We used each infant's T2-weighted MRI data acquired at term-equivalent age to identify imaging prognostic features of cognitive deficits. We classified infants into one of the two groups - high-risk (Cognitive score  $\leq 85$ ) or low-risk (Cognitive score  $>85$ ) for cognitive deficits based on the standardized Bayley-III Cognitive subscale at 2 years corrected age.. We segmented each T2-weighted brain image into 87 regions of interest (ROIs) and extracted 100 radiomics features from each ROI using the PyRadiomics pipeline, therefore resulting in a 87-by-100 feature map for each subject. Collaborative Self-Supervised Learning: It remains challenging to train robust deep learning models due to the lack of sufficient labeled data. As shown in Figure 1, we developed a collaborative self-supervised learning (SSL) model to solve the challenges posed by the over-dependence of labeled data, particularly for radiomic data classification. We first augmented multiple samples from each subject by randomly masking/hiding radiomic features from several ROIs, and then we trained a transformer to learn latent features from augmented samples without human labeling by solving two collaborative pretext tasks, including 1) Reconstruction - to reconstruct the hidden radiomic features using the observable ones, and 2) Discrimination - to find similarity and dissimilarity from augmented samples, and to classify all augmented samples from the same subject into one group. Model performance was assessed using 5-fold cross-validation. This process was repeated 100 times.

#### RESULTS

Of the original cohort of 392 infants, 318 (81%) had Bayley III cognitive scores assessed at 2 years corrected age. Our model achieved an AUC of 0.78, outperforming the supervised Transformer (AUC=0.61) as well as several peer self-supervised models that were developed for text and/or image data, including Rotation (AUC=0.64), Moco v1 (AUC=0.69), and SimCLR (AUC=0.71). Our method achieved a balanced accuracy of 76.3%, sensitivity of 75.8%, and specificity of 76.7%.

#### CONCLUSION

s We showed that the proposed model outperformed peer self-supervised models for radiomic data classification in the application of the early prediction of cognitive deficit in very preterm infants.

#### CLINICAL RELEVANCE/APPLICATION

The proposed model is able to facilitate the deep learning-based applications in Radiomics without large-scale annotated datasets.

Printed on: 02/07/23

## Abstract Archives of the RSNA, 2022

M5A-SPIN-3

### **Radiology Trainees Attitudes Towards Artificial Intelligence in Clinical Radiology and Its Implementation in Training and the Curriculum in The United Kingdom**

Monday, Nov. 28 12:15PM - 12:45PM Room: Learning Center - IN DPS

#### **Participants**

Obaid Hashmi, MBBS, FRCR, (*Presenter*) Nothing to Disclose

#### **PURPOSE**

Artificial Intelligence (AI) and Machine learning (ML) have garnered significant interest in radiology. AI and ML have been introduced to the 2021 Royal College of Radiologists (RCR) curriculum highlighting its importance to radiology trainees in the United Kingdom (UK). The attitudes of trainees towards AI in Radiology has been reviewed in several countries, however there was no documented survey assessing the attitudes of UK radiology trainees towards AI. A national trainee led survey was created to understand the attitudes of UK radiology trainees, in particular assessing the demand for AI education. This could help guide implementation of AI teaching in radiology training programmes.

#### **METHODS AND MATERIALS**

The survey was created in the Google Forms platform and nationally distributed via email. The survey ran over a period of 2 months. All 37 training programmes in the United Kingdom were targeted. Participants were asked 4 demographic questions and 14 questions relating to the topic of AI in radiology. They were surveyed on their views relating to previous experience with AI, teaching of AI and its future within the career of a radiologist.

#### **RESULTS**

The survey was completed by 149 trainee radiologists with at least 1 response from each of the 37 UK training programmes. 83.7% said they were interested in AI use in Radiology but 71.4% had no experience of working with AI. Most, 79.9%, would like to be involved in AI based projects. Almost all respondents (98.7%) felt that AI should be taught during their training, in particular in the 1st 3 years of training, yet, only 1 respondent stated that their training programme had implemented AI teaching. Respondents indicated that basic understanding, implementation and critical appraisal of AI software should be prioritized in AI teaching. Most trainees preferred teaching to be delivered at a deamery or training programme level. Only 12.8% of respondents said that AI would make them less likely to apply for radiology specialty training. Most responded that AI would be used in regular radiology practice in the next 5 to 10 years with 74.2% of trainees agreeing that AI will improve and enhance the job of radiologists in the next 20 years. The main concerns raised about AI in Radiology were IT/implementation and ethical/regulatory issues.

#### **CONCLUSION**

s The attitudes of UK trainees towards AI are mostly positive with many interested in being involved in AI based projects and activities. There is also clear interest and demand for AI teaching within training. However, current discussion, availability of AI based activities and AI teaching within UK training programmes is very limited.

#### **CLINICAL RELEVANCE/APPLICATION**

To help guide the RCR and UK training programmes in their implementation of AI into radiology training.

Printed on: 02/07/23

## Abstract Archives of the RSNA, 2022

M5A-SPIN-4

### A Cost-effective Multi-modality Machine Learning Framework for Prediction of Alzheimer' Disease

Monday, Nov. 28 12:15PM - 12:45PM Room: Learning Center - IN DPS

#### Participants

Jing Li, (*Presenter*) Nothing to Disclose

#### PURPOSE

Machine learning (ML) models integrating multi-modality datasets have shown great promise for disease diagnosis/prognosis. The acquisition costs of different data modalities vary significantly. It is not cost-effective to require all patients acquiring all data modalities. We propose a cost-effective ML framework, called the Uncertainty-driven Modality Selection (UMoS) framework, to sequentially add modalities for each patient on an as-needed basis while at the same time ensuring high diagnostic/prognostic accuracy.

#### METHODS AND MATERIALS

We demonstrate UMoS in an application of predicting the risk of progressing to Alzheimer's Disease (AD) for individuals with Mild Cognitive Impairment (MCI). ML models integrating MRI and PET have shown high accuracy in predicting MCI progression to AD. While MRI is used in the standard of care, PET is more costly and has less accessibility to patients. Under UMoS, a patient will be first predicted based on MRI; if the predictive uncertainty is lower than a threshold, the patient will not need PET; otherwise, the patient will need PET and be predicted by an MRI+PET model. To develop UMoS, we need to establish three building blocks: a trained MRI model, an uncertainty quantification approach for the MRI model, and a trained MRI+PET model. We establish these building blocks and demonstrate UMoS using a dataset from ADNI, which includes 1319 T1-MRI scans from MCI patients with 612 of these MRI scans having accompanying amyloid-PET scans. We extracted regional volumetric and thickness features from MRI using FreeSurfer v7.1 and regional SUVR features from amyloid-PET using our in-house pipeline. To establish the building blocks of UMoS, we first train an MRI+PET model based on the subset of samples with both MRI and PET. Using the MRI+PET model as the teacher model, we further train an MRI model based on all samples using knowledge distillation. Predictive entropy was computed to quantify both the aleatoric and epistemic uncertainties of the MRI model.

#### RESULTS

Under 10-fold cross validation, UMoS achieves 0.851 AUC (0.782/0.809 sensitivity/specificity using 0.5 probability cutoff), with 46.7% of patients predicted by the MRI model and 53.3% by the MRI+PET model. If all patients are predicted by the MRI +PET model, the performances are 0.873 AUC (0.776/0.811 sensitivity/specificity).

#### CONCLUSION

Under the UMoS framework, we achieve prediction performance at a similar level to the model that needs both MRI and PET for predicting MRI progression to AD, but UMoS saves 46.7% patients from needing PET.

#### CLINICAL RELEVANCE/APPLICATION

This study provides an ML framework that ensures high accuracy in disease diagnosis/prognosis, but saves patients from needing unnecessary data modalities thus saving diagnostic/prognostic costs.

Printed on: 02/07/23

## Abstract Archives of the RSNA, 2022

M5A-SPIN-5

### AI-based Bronchial Segmentation and Quantitation Prototype for Chest CT: Can it Help Assess Severity of Obstructive Lung Disease by Pulmonary Function Test?

Monday, Nov. 28 12:15PM - 12:45PM Room: Learning Center - IN DPS

#### Participants

Parisa Kaviani, MD, Boston, MA (*Presenter*) Nothing to Disclose

#### PURPOSE

The aim of this study was to assess if an artificial intelligence-based bronchial segmentation and quantitation prototype for assessing severity of obstructive lung disease.

#### METHODS AND MATERIALS

Our retrospective IRB-approved, HIPAA-compliant study comprised 222 adults (mean age 57±16 years; M:F 116: 106). A total of 107 patients with COPD had both PFT and non-contrast chest CT. The remaining 115 patients had no CT or clinical abnormality suggestive of lung disease (COPD or otherwise). The COPD severity was defined as mild, moderate, and severe based on the forced expiratory volume in 1 second (FEV1). We processed thin-section (1-1.25mm) CT images with the bronchial segmentation and quantitation prototype (Siemens Healthineers) to obtain following metrics: bronchial lumen volume, lumen diameter, lumen area, wall thickness, wall area, wall area ratio, and wall tapering) for total lung volumes and separately for each lung and lung lobe. Data were analyzed with area under the receiver operating characteristics curve (AUC) for distinguishing between mild, moderate, and severe COPD.

#### RESULTS

AI algorithm had an AUC of up to 0.79 (95% CI: 0.728-0.852) for differentiating mild, moderate and severe emphysema based on FEV1. The AI algorithm was able to differentiate mild COPD with AUC of 0.86 (95% CI: 0.728-0.852) for the combination of generation 2 wall thickness, generation 0 lumen volume and RUL wall thickness, moderate COPD with AUC of 0.72 (95% CI: 0.728-0.852) for the combination of generation 1 wall thickness and LLL wall area, and severe COPD with 0.79 (95% CI: 0.728-0.852) for the combination of LUL wall thickness, generation 0 lumen volume, and global volume ratio airways vs lung as the best features.

#### CONCLUSION

s Fully automated AI-based bronchial tree segmentation and quantitation prototype can differentiate different severity of COPD assessed with pulmonary function tests.

#### CLINICAL RELEVANCE/APPLICATION

The quantitative information pertaining to bronchial wall and luminal dimensions estimated from an AI-based prototype can help in diagnosis and treatment of patients with bronchial involvement in COPD.

Printed on: 02/07/23

## Abstract Archives of the RSNA, 2022

M5A-SPIN-6

### Semantic Retrieval of Similar Radiological Images using Vision Transformers: CXR and CT study

Monday, Nov. 28 12:15PM - 12:45PM Room: Learning Center - IN DPS

#### Participants

Anjali Thakrar, BS, Goleta, CA (*Presenter*) Nothing to Disclose

#### PURPOSE

Identifying visually and semantically similar radiological images in a database can facilitate the creation of decision support tools, teaching files, and research cohorts. Existing content based image retrieval tools are often limited to searching by pixel-wise difference or vector distance of model predictions. Vision transformers (ViT) use attention to simultaneously take into account radiological diagnosis as well as visual appearance. Here, we develop a ViT-based image retrieval framework and evaluate the algorithm on the NIH Chest Radiographs (NIH-CXR) and NLST Chest CTs.

#### METHODS AND MATERIALS

All 112,120 images from the NIH-CXR and 3246 randomly sampled cases from the NLST CT dataset were used. For CXR, a ViT binary classifier was trained on 4 ground truth labels (Cardiomegaly, Opacity, Emphysema, No Finding) and ensemble to produce multilabel classifications for each CXR. For CT, a regression model was trained to minimize L1 loss on the continuous ground truth labels of patient weight. The ViT image embedding layer was treated as a global image descriptor, using the L2 distance between descriptors as a similarity measure. Normalized discounted cumulative gain (nDCG) and mean average precision (mAP) were calculated from the ground truth labels. Five radiologists performed a reader performance study with random query images (25 CT and 25 CXR) and chose the 5 most similar images to the query from a set of 10 images (consisting of 5 closest to the query and 5 furthest from the query in model space). Inter-radiologist agreement and radiologist-model agreement statistics (Fleiss' and Cohen's kappa) were calculated. A t-SNE of the CT model latent space was generated to confirm clustering of similar images.

#### RESULTS

The CXR model achieved nDCG@5 of 0.73 ( $p < 0.001$ ) and Cardiomegaly mAP@5 of 0.76 ( $p < 0.001$ ) among other results for CXR. The CT model achieved nDCG of 16.85 ( $p < 0.001$ ). The model prediction agreed with radiologist consensus on 86% of CXR samples and 79.2% of CT samples. Inter-radiologist Fleiss Kappa of 0.51 and radiologist consensus to model Cohen's Kappa of 0.65 were observed. Full code will be made available at the time of presentation.

#### CONCLUSION

s We have developed and evaluated a vision transformer architecture that can retrieve visually and semantically similar radiological images.

#### CLINICAL RELEVANCE/APPLICATION

Our vision transformer model can identify radiological images with visual and diagnostic similarities, which may be applied to decision support, teaching file creation, and research cohort creation.

Printed on: 02/07/23

## Abstract Archives of the RSNA, 2022

M5A-SPIR

### Interventional Monday Poster Discussions - A

Monday, Nov. 28 12:15PM - 12:45PM Room: Learning Center - IR DPS

#### Sub-Events

#### **M5A-SPIR-1 Percutaneous Transthoracic Lung Biopsy in Patients with Usual Interstitial Pneumonia Pattern in CT: Its Implication on Procedure-related Complications**

Participants

Jongsoo Park, MD, PhD, Seoul, Korea, Republic Of (*Presenter*) Nothing to Disclose

#### **PURPOSE**

We aimed to investigate the incidence and risk factors of major complications (pneumothorax and hemoptysis) after percutaneous transthoracic lung biopsy (PTLB) in patients with usual interstitial pneumonia (UIP) pattern on CT.

#### **METHODS AND MATERIALS**

Patients who underwent PTLB between January 2010 and December 2015 in a tertiary referral hospital were retrospectively included. UIP pattern was determined based on the pre-PTLB chest CT according to the guideline of the American Thoracic Society/European Respiratory Society/Japanese Respiratory Society/Latin American Thoracic Society by consensus reading of two thoracic radiologists. To analyze whether the UIP pattern and its traversal by the needle are the risk factors of PTLB-complications (e.i., pneumothorax, hemoptysis) or not, multivariate logistic regression analyses were performed with other pre-established risk factors.

#### **RESULTS**

A total of 4,187 patients (UIP group: 148 patients [131 men; median age, 70.1 years], non-UIP group: 4,039 patients [2,382 men; median age, 63.6 years]) were assessed in this study. UIP group had higher incidence of pneumothorax (35.1% versus 17.9%,  $P<0.001$ ) and requirements of percutaneous catheter drainage (PCD) (6.1% versus 1.5%) than those of non-UIP group while hemoptysis was frequently occurred in non-UIP group (2% versus 6.1%,  $P=0.034$ ). Adjusted with other pre-established risk factors including emphysema, UIP pattern is associated with pneumothorax occurrence (hazard ratio [HR]: 2.147, 95% confidence interval [CI]: 1.480 - 3.116,  $P<0.001$ ) and event of PCD insertion for pneumothorax (HR: 3.549, 95% CI: 1.602 - 7.861,  $P=0.002$ ), but not for hemoptysis after PTLB. Traversal of UIP pattern had consistent result as a risk factor for complication after PTLB (pneumothorax: HR: 5.198, 95% CI: 2.913 - 9.274,  $P<0.001$ ; PCD insertion for pneumothorax: HR 9.549, 95% CI: 3.741 - 24.377,  $P<0.001$ ). The duration of the PCD placement between UIP- and non-UIP groups was not different (median 3 days [range, 2 - 11 days] versus median 2 days [range, 1 - 12 days],  $P=0.941$ ).

#### **CONCLUSION**

s UIP pattern on CT and traversal of this pattern by the needle are the risk factors for pneumothorax and requirements of PCD insertion after PTLB.

#### **CLINICAL RELEVANCE/APPLICATION**

When performing PTLB, the radiologists should be alert about pneumothorax occurrence in patients with UIP on CT. They avoid traversal of biopsy needle through the UIP pattern as much as possible.

#### **M5A-SPIR-2 Feasibility of EKG gated CT-Fluoroscopy to Guide Percutaneous Biopsy of Cardiac and Pericardial Masses**

Participants

Patrik Rogalla, MD, MBA, Toronto, ON (*Presenter*) Institutional Research Grant, Canon Medical Systems Corporation; Institutional Research Grant, KA Imaging

#### **PURPOSE**

Percutaneous biopsy of the heart and pericardium poses a significant challenge due to the target's continuous motion and potentially life-threatening complications. The purpose of this study was to evaluate the feasibility of an EKG gated CT-fluoroscopy approach along with various methods to minimize the risks and complications, and the clinical outcome of cardiac and pericardial mass biopsies.

#### **METHODS AND MATERIALS**

Between 2018 and 2022, 18 cardiac and pericardial mass biopsies were performed in a quaternary care referral centre after clinical consultation with the cardiac surgical team. With REB approval, the patients' charts were reviewed to extract the history, pathology, and clinical outcomes. All biopsies were performed under conscious sedation using CT-fluoroscopy guidance on a 320-slice cardiac scanner (Canon Medical Systems). The EKG was monitored and used for gated image acquisition during the intervention. Mediastinal widening and iatrogenic capnothorax techniques were applied to gain access when appropriate. Full-size 18G core samples were taken using a BioPince needle, and all samples were evaluated by a specialized cardiac pathologist. The

radiation dose and time to complete the intervention were recorded.

## RESULTS

All 18 biopsies in 17 patients (F:M, 9:8; mean age, 45.8) resulted in definitive pathological diagnoses. The size of the targets ranged from 1 cm to 12 cm. Final histology reported 10 malignant (eg. synovial, spindle cell and angiosarcoma, lymphoma, thymoma) and eight benign diagnoses (eg. IgG4, hibernoma, fibroma, TB, haemangioma, fibromyxoid stroma, lipid hyperplasia). One patient developed a small hemothorax, and another patient developed a small pneumomediastinum immediately post-procedure, both of which were successfully treated conservatively. Specific cardiac-related complications, such as hemopericardium, tamponade, arrhythmia or arrest did not occur in any of the patients. The median DLP for the fluoroscopy guidance was 22.5 mGy\*cm (SD, 22.3), the mean total procedure time 32 minutes. All patients left the hospital following a two-hour recovery in a medical imaging day unit.

## CONCLUSION

s Percutaneous cardiac and pericardial mass biopsies can be safely performed with an acceptable clinical risk and radiation dose profile. CT-fluoroscopy with real-time non-gated and gated image visualization, a well-trained interventional care team, and the backup availability of cardiac surgery may be prerequisites to ensure the best possible patient care.

## CLINICAL RELEVANCE/APPLICATION

Percutaneous cardiac and pericardial biopsies represent a minimally invasive alternative to mediastinoscopy and open cardiac surgery in a specific patient population.

## M5A-SPIR-3 Histotripsy Treatment of Veins as A Mechanism of Endothelial Damage

### Participants

Amanda Smolock, MD, PhD, Milwaukee, WI (*Presenter*) Consultant, HistoSonics, Inc;Shareholder, HistoSonics, Inc;Employee, NeuWave Medical, Inc;Grant, NeuWave Medical, Inc;Consultant, NeuWave Medical, Inc;;

### PURPOSE

Venous insufficiency affects up to a third of the population and can cause significant complications like ulcers which are painful and costly to manage. Histotripsy is a non-invasive, non-thermal focused ultrasound method that mechanically destroys tissue through acoustic cavitation. The aim of this project was to demonstrate the feasibility of using histotripsy to cause controlled mechanical damage to the venous endothelium as a step in inducing venous occlusion for the treatment of venous insufficiency.

### METHODS AND MATERIALS

Excised porcine femoral veins (n=13) were suspended in a mold of degassed 2% agarose gel and treated within 72 hours post-mortem. The mold was degassed in a vacuum overnight. Histotripsy was applied using 3-cycle pulses at 44MPa predicted peak negative pressure by a 1MHz focused ultrasound transducer along 1 cm length of vein with 4 parameter groups: 1) 1Hz pulse repetition frequency (PRF) and 200 pulses per location (ppl) (n=2), 2) 100Hz PRF and 200 ppl (n=3), 3) 100Hz PRF and 500 ppl (n=3), and 4) 100 Hz PRF and 1000 ppl (n=3). Following treatment, veins were removed from the gel mold and placed in 10% formalin. Tissue was sectioned and stained with hematoxylin and eosin. Histology was reviewed for damage to vein wall layers using a standardized scale (0 least - 4 most endothelial attenuation).

### RESULTS

Histology demonstrated intact venous walls with dose-dependent damage to the venous endothelium. Frequency and severity of endothelial loss increased with increasing ppl tested at 100Hz PRF. Endothelial damage was most significant though in veins treated at a lower PRF of 1Hz with 200 ppl.

### CONCLUSION

s Histotripsy causes dose-dependent damage to the endothelium of veins. Endothelial denudation is an initial step in venous thrombosis and ultimately occlusion. Additional in vivo experiments of blood-containing vein are needed to fully test dose parameters for vein histotripsy followed by longitudinal studies to assess for treatment efficacy.

### CLINICAL RELEVANCE/APPLICATION

Histotripsy has the potential to provide a non-invasive and non-thermal outpatient treatment for venous insufficiency.

## M5A-SPIR-4 Using a Quantitative Digital Subtraction Angiography Technique to Determine Treatment Endpoints in Partial Splenic Artery Embolization: Feasibility in an In Vivo Porcine Model

### Participants

Sarvesh Periyasamy, PhD, Madison, WI (*Presenter*) Consultant, Johnson & Johnson;Consultant, HEPTA Medical;Consultant, Vector Surgical LLC

### PURPOSE

Partial splenic artery embolization (PSE) is a method for treating cirrhosis-induced splenomegaly/hypersplenism and complications of portal hypertension. However, there is a direct relationship between the extent of embolization and the severity of post-procedural complications. Using quantitative metrics to determine PSE endpoints may improve procedural outcomes and decrease post-procedural complications. The objective of this study was to determine the feasibility of using a quantitative digital subtraction angiography (qDSA) technique to quantify blood velocity reduction during PSE.

### METHODS AND MATERIALS

Four swine (~50 kg) underwent embolization of the proximal splenic artery using embolic particles of different sizes (100-300, 300-500, or 500-700  $\mu$ m diluted in 10 mL of iohexol 300 mg I/mL). qDSAs were acquired at baseline, and after delivery of 1 mL aliquots of particles until a complete stasis angiographic endpoint was achieved. A retrospective image analysis was performed to calculate blood velocity reduction in the splenic artery using qDSA, which was correlated with time-to-peak signal in the portal vein.

### RESULTS

qDSA demonstrated linear decreases in relative blood velocities from baseline (100-300  $\mu$ m: 11.8%, 34.8%, 300-500  $\mu$ m: 29.3%,

qDSA demonstrated linear decreases in relative blood velocities from baseline (100-300  $\mu\text{m}$ : 11.6%, 34.6%, 300-500  $\mu\text{m}$ : 23.3%, 500-700  $\mu\text{m}$ : 24.4% reduction per mL of particles) and a strong correlation with the volume of embolic particles delivered (mean  $R = -0.96 \pm 0.02$ ,  $R^2 = 0.93 \pm 0.04$ ). There was a strong correlation between the percent reduction in blood velocity calculated by qDSA and the increased time-to-peak signal in the portal vein (mean  $R = -0.94 \pm 0.03$ ,  $R^2 = 0.89 \pm 0.86$ ). Embolizations performed with larger particles had larger overall post-embolization blood velocity reductions (300-500  $\mu\text{m}$ : 88%, 500-700  $\mu\text{m}$ : 90%) compared to embolizations performed with smaller particles (100-300  $\mu\text{m}$ : 71%, 70%)

## CONCLUSION

qDSA was able to quantify intra-procedural reductions in splenic arterial blood velocity during embolization in a porcine model. Blood velocity reductions correlated with an imaging marker of reduced portal venous flow. Further investigation is warranted to evaluate qDSA use in clinical PSE procedures.

## CLINICAL RELEVANCE/APPLICATION

Quantitative digital subtraction angiography may permit the determination of objective treatment endpoints for PSE, improving the safety and efficacy of the procedure.

## M5A-SPiR-5 Preliminary Results from A Prospective Clinical Trial on The Immunological Effects of Locoregional Therapies in Patients with Hepatocellular Carcinoma

Participants

Robin Schmidt, (Presenter) Nothing to Disclose

## PURPOSE

To evaluate the prognostic value of periinterventional peripheral blood immune cell counts on tumor response in patients with hepatocellular carcinoma (HCC) after locoregional therapies (LRT).

## METHODS AND MATERIALS

This interim report of a single-site prospective clinical trial included 76 consecutive patients with unresectable HCC between 08/2020-11/2021, who underwent LRT including high dose-rate brachytherapy alone (BT, n=59) or with prior transarterial chemoembolization (TACE/BT, n=35). Institutional review board approval and informed consent were obtained. Peripheral blood was sampled before, 24h and 8 weeks (wk) after LRT for spectral fluorescence-activated cell sorting (FACS) analysis. A 24-color multiplex staining panel was applied to quantify lymphoid and myeloid cells. Absolute cell counts were obtained by adding precision count beads. FACS data was processed using a robust gating strategy including CD45/CD66/CD16/CD14/CD3/CD4/CD8. Tumor response at 8wk was assessed on multiparametric MRI according to RECIST 1.1 and patients were grouped into responders (R) and non-responders (NR). A nonparametric ANOVA type test statistic was used.

## RESULTS

FACS data at baseline, 24h, and 8wk post-TACE were available for n=84, n=84, and n=72 patients, respectively. As for BT, higher counts of T cells (TC), CD4+TC, and CD8+TC count as well as a lower CD4-to-CD8 TC ratio ( $p = 0.093$ ,  $p = 0.232$ ,  $p = 0.095$  and  $p = 0.152$ , respectively) were found in R compared to NR at all timepoints. However, the opposite trend was observed in patients receiving TACE/BT, who demonstrated lower cell counts for TC, CD4+TC, CD8+TC as well as a higher CD4-to-CD8 ratio ( $p = 0.003$ ,  $p = 0.003$ ,  $p = 0.074$  and  $p = 0.801$ , respectively) for R compared to NR at all timepoints (Figure 1). Neutrophil-to-lymphocyte (NLR) and monocyte-to-lymphocyte (MLR) ratio were similar in R and NR after BT. However, NR after TACE/BT tended to have a lower NLR and higher MLR than R (Figure 2).

## CONCLUSION

The preliminary results of this prospective study state that different types of locoregional therapies may induce different immunological responses in HCC patients and establish the prognostic value of such quantitative inflammatory biomarkers associated with tumor response prior to LRT. Moreover, patient and tumor characteristics at baseline, that determine the assignment to the respective LRT, may potentially reflect the immunological phenotype in these patients.

## CLINICAL RELEVANCE/APPLICATION

If confirmed in the complete cohort, these results may help exploit LRT-induced immune-activation and guide improved personalized monitoring and combinations with immunooncological therapies.

## M5A-SPiR-6 A Phantom for Assessing Histotripsy Treatment Zones on Both Ultrasound and X-ray Imaging

Participants

Ayca Kutlu, MD, Madison, WI (Presenter) Nothing to Disclose

## PURPOSE

Histotripsy is an emerging non-invasive, non-ionizing, and non-thermal focal tumor therapy. While targeting during histotripsy is currently based on ultrasound (US), X-ray-based fusion and targeting techniques are being developed for tumors not visible by US. The objective of this study was to validate a multi-modal phantom that enables assessment of histotripsy treatment zones on both US and X-ray imaging.

## METHODS AND MATERIALS

Six cube-shaped phantoms were created by suspending sheep red blood cells (RBC) in agarose. To provide x-ray contrast, alternating layers with (~1 mm thick) and without barium sulfate (~4 mm thick) were poured in a 2 x 2 x 2 in silicone mold. During histotripsy, adjacent layers in the treatment volume mix and create a homogeneous mixture visible on US and cone beam CT (CBCT). Spherical (2.5 cm diameter) treatments were performed in each phantom and resulting treatment zones measured on US and CBCT. Treatment zone size and location (distance from phantom center) were measured in three orthogonal planes separately. In addition, signal-difference-to-noise ratio (SDNR) was calculated on CBCT images between ablation zones and untreated RBC layers.

## RESULTS

In all cases, histotripsy resulted in homogeneous treatment zones with distinct x-ray attenuation and acoustic impedance, which

made segmentation of the treatment zone on both CBCT and US possible. On US, treatment zone diameters (mean±SD) were 25.5 ± 0.3, 25.0 ± 0.3 and 24.5 ± 0.4 mm on X, Y and Z planes, respectively. Similarly, on CBCT, diameters were 25.8 ± 1.1, 25.3 ± 0.4 and 24.4 ± 0.2 mm. Treatment zone center point location differed by 1.6 ± 0.9, 1.5 ± 1.1 and 2.6 ± 1.2 mm on X, Y and Z planes, respectively between CBCT and US measurements. The average SDNR between ablation zone and RBC layer was 23.1 ± 7.3.

## CONCLUSION

s The proposed multimodal RBC phantom allowed visualization of histotripsy treatment zones on both US and x-ray imaging. Treatment zone diameters and center locations were similar between the two modalities. These phantoms can help validate newly developed fusion and targeting techniques for histotripsy, expanding the scope of treatable lesions.

## CLINICAL RELEVANCE/APPLICATION

A multimodal RBC phantom may be used to develop and validate X-ray-based fusion and targeting techniques for histotripsy, which will facilitate treatment of tumors not visible on US.

## M5A-SPiR-7 Safety and Efficacy of Serial Doxycycline Exchange Sclerotherapy for Lymphatic Malformations

### Participants

Anna Gong, Baltimore, MD (*Presenter*) Nothing to Disclose

### PURPOSE

To assess the efficacy of serial doxycycline exchanges (SDE) for the treatment of lymphatic malformations (LM).

### METHODS AND MATERIALS

We reviewed all patients from 9/2004 to 02/2022 who received SDE after a percutaneous drain placement for an LM at our institution. After initial image-guided drainage catheter placement and sclerotherapy into the LM, the patient was admitted for SDE. Standard procedure involved bedside drainage, and infusion of doxycycline (10mg/mL) 1/3 to 1/2 of the drained volume, which was left to dwell for 4 hours before draining. This was performed twice a day, until the drained volume was sufficiently decreased as per the physician's direction, after which the patient was discharged. Charts were reviewed to assess clinical response, size changes, and complications. Symptom response was classified as resolved, improved, and stable/worsened. LM size change was calculated using difference of pre- and post- procedure MRI of the largest lesion diameter in one plane: complete response (CR, 100% reduction), partial response (PR, 30% reduction), stable disease (SD, =30% reduction or =20% enlargement), progressive disease (PD, =20% size increase). SIR classification criteria were used to classify adverse events. Fisher's Exact Tests were used for statistical analysis.

### RESULTS

43 patients (58.1% M) underwent 82 image-guided sclerotherapy procedures with subsequent SDE (technical success 80/82; 97.6%). An average of 3.87 SDE sessions/admission was reported for an average extended inpatient stay of 92 hours/admission (Total: 201 exchanges). This resulted in 201/283 (71.0%) sclerotherapy sessions that were performed at the bedside. The mean patient follow-up period was 902.15 days (median: 328 days). Most common presenting symptoms were swelling/mass (25, 58.1%), pain (8, 18.6%) and trouble breathing (3, 7.0%). Sclerotherapy significantly improved symptoms with 6.1% (5/82) resolved, 47.6% (39/82) improved, and 46.3% (38/82) stable or worsened ( $p < 0.0001$ ). Embolization also significantly decreased LM size on imaging ( $p = 0.0011$ ). Of the 47 image-guided procedures (47/82, 57.3%) with both pre- and post- MRI imaging, zero patients saw CR, 10 patients (21.3%) experienced PR, 35 patients (74.5%) experienced SD and 2 patients (4.3%) saw PD. Early (30-day) post-procedural complications occurred after 9 of 82 procedures (10.9%), the most common of which were sensory or motor nerve injury (44.4%; 4/9) and mild in severity (44.4%; 4/9).

## CONCLUSION

s SDE significantly decreases lesion size and improves clinical symptoms in LMs.

## CLINICAL RELEVANCE/APPLICATION

SDE is a safe and effective treatment option for LMs that allows for multiple sclerotherapy sessions with a single fluoroscopic procedure.

## M5A-SPiR-8 Silver Nanoparticles-coated Stent for Suppressing Bacterial Growth and Tissue Hyperplasia after Radiofrequency Ablation in the Rabbit Common Bile Duct

### Participants

Yubeen Park, Seoul, Korea, Republic Of (*Presenter*) Nothing to Disclose

### PURPOSE

To investigate the efficacy of silver nanoparticles (AgNPs)-coated self-expandable metal stent (SEMS) placement immediately after radiofrequency (RF) ablation in suppressing thermal damage as well as SEMS-induced bacterial growth and tissue hyperplasia in the common bile duct of rabbits.

### METHODS AND MATERIALS

The release behavior and antibacterial effects of AgNPs-coated SEMSs were evaluated. A total of 12 male New Zealand White rabbits were randomly divided into two groups for verification of the efficacy of AgNPs-coated SEMS placement immediately after RF ablation: the control group received an uncoated SEMS, and the AgNPs group received an AgNPs-coated SEMS. Cholangiography was performed immediately before sacrifice in all rabbits to check the stent patency. Venous blood samples were collected before sacrifice and AST, ALT, ALP, GGT, and total bilirubin levels were analyzed to evaluate hepatobiliary functions. Histological examination was performed about the degree of inflammatory cell infiltration, thickness of submucosal fibrosis, percentage of granulation tissue area, and degree of collagen deposition. Immunohistochemistry analysis was performed about the degree of TUNEL-, HSP 70-, and a-SMA-positive areas.

### RESULTS

Ag ions were rapidly released at the beginning and then showed a gradual release behavior. The AgNPs-coated SEMS significantly inhibited bacterial activity compared to the uncoated SEMS ( $p < 0.05$ ). Stent placement immediately after RF ablation was

successfully performed without procedure-related complications in all rabbits. Jaundice was observed in 3 out of 6 (50%) rabbits in the control group. The luminal diameter in the AgNPs group was greater than that in the control group ( $p < 0.05$ ). AST, ALT, ALP, GGT, and total bilirubin levels were all lower in the AgNPs group than in the control group. Histological examination confirmed that all evaluation results were significantly lower in the AgNPs group than in the control group (all  $p < 0.05$ ). Immunohistochemistry analyses revealed that TUNEL-, HSP 70-, and  $\alpha$ -SMA-positive areas were significantly lower in the AgNPs group than in the control group (all  $p < 0.05$ ).

## CONCLUSION

The AgNPs-coated SEMS significantly inhibited tissue hyperplasia and biofilm induced by heat and mechanical damage in the rabbit common bile duct. The developed method of RF ablation with AgNPs-coated SEMS should be a promising therapeutic strategy for the prevention of RF ablation- and stent-related complications.

## CLINICAL RELEVANCE/APPLICATION

AgNPs-coated SEMS placement immediately after RF ablation might be effective in preventing RF ablation and stent-related complications in patients with unresectable malignant biliary obstruction.

## M5A-SPiR-9 Intra-gastric Satiety-Inducing Device combined with Photodynamic Therapy to Treat Obesity

### Participants

Ji Won Kim, Seoul, Korea, Republic Of (*Presenter*) Nothing to Disclose

## PURPOSE

To evaluate the efficacy and safety of the Chlorin e6-embedded intra-gastric satiety-inducing device (Ce6-embedded ISD) placement with photodynamic therapy (PDT) in suppressing appetite in porcine stomach.

## METHODS AND MATERIALS

The ISD consisted of the lower esophageal part and disk part for the fundus of the stomach. The once dip coating technique was used for the fabrication of Ce6-embedded ISD. A total of 12 minipigs were divided into four groups. PDT group ( $n = 3$ ) received single PDT using Ce6-embedded ISD. ISD group ( $n = 3$ ) received ISD placement. ISD with PDT group ( $n = 3$ ) received single PDT with Ce6-embedded ISD placement. The remaining three weight and age-matched healthy pigs were used as a control group. All pigs were sacrificed 4 weeks after the procedures. The outcomes were assessed by histological examinations and immunohistochemistry analysis. Body weight was monitored weekly, and the percentage of total body weight gain (%TBWG) was calculated.

## RESULTS

A total of 12 minipigs were divided into four groups. PDT group ( $n = 3$ ) received single PDT using Ce6-embedded ISD. ISD group ( $n = 3$ ) received ISD placement. ISD with PDT group ( $n = 3$ ) received single PDT with Ce6-embedded ISD placement. The remaining three weight and age-matched healthy pigs were used as a control group. Anti-ghrelin and TUNEL-positive deposition were significantly increased in PDT, ISD, and ISD with PDT groups compared to the control group (all  $p < 0.001$ ). The weight gain was observed to decrease in the order of PDT, ISD, and ISD with PDT groups compared to the control group, and the ISD with PDT proved to be the most effective for weight loss.

## CONCLUSION

Ce6-embedded ISD was effectively decreases weight gain rate and ghrelin-producing cells in the porcine model. The simple and unique operation extends the point of view in PDT and is expected to be a novel obesity therapy.

## CLINICAL RELEVANCE/APPLICATION

Ce6-embedded ISD, weight loss and stimulation of ghrelin-producing cells, will become strategy for obesity treatment.

Printed on: 02/07/23

## Abstract Archives of the RSNA, 2022

M5A-SPIR-1

### **Percutaneous Transthoracic Lung Biopsy in Patients with Usual Interstitial Pneumonia Pattern in CT: Its Implication on Procedure-related Complications**

Monday, Nov. 28 12:15PM - 12:45PM Room: Learning Center - IR DPS

#### **Participants**

Jongsoo Park, MD, PhD, Seoul, Korea, Republic Of (*Presenter*) Nothing to Disclose

#### **PURPOSE**

We aimed to investigate the incidence and risk factors of major complications (pneumothorax and hemoptysis) after percutaneous transthoracic lung biopsy (PTLB) in patients with usual interstitial pneumonia (UIP) pattern on CT.

#### **METHODS AND MATERIALS**

Patients who underwent PTLB between January 2010 and December 2015 in a tertiary referral hospital were retrospectively included. UIP pattern was determined based on the pre-PTLB chest CT according to the guideline of the American Thoracic Society/European Respiratory Society/Japanese Respiratory Society/Latin American Thoracic Society by consensus reading of two thoracic radiologists. To analyze whether the UIP pattern and its traversal by the needle are the risk factors of PTLB-complications (e.i., pneumothorax, hemoptysis) or not, multivariate logistic regression analyses were performed with other pre-established risk factors.

#### **RESULTS**

A total of 4,187 patients (UIP group: 148 patients [131 men; median age, 70.1 years], non-UIP group: 4,039 patients [2,382 men; median age, 63.6 years]) were assessed in this study. UIP group had higher incidence of pneumothorax (35.1% versus 17.9%,  $P<0.001$ ) and requirements of percutaneous catheter drainage (PCD) (6.1% versus 1.5%) than those of non-UIP group while hemoptysis was frequently occurred in non-UIP group (2% versus 6.1%,  $P=0.034$ ). Adjusted with other pre-established risk factors including emphysema, UIP pattern is associated with pneumothorax occurrence (hazard ratio [HR]: 2.147, 95% confidence interval [CI]: 1.480 - 3.116,  $P<0.001$ ) and event of PCD insertion for pneumothorax (HR: 3.549, 95% CI: 1.602 - 7.861,  $P=0.002$ ), but not for hemoptysis after PTLB. Traversal of UIP pattern had consistent result as a risk factor for complication after PTLB (pneumothorax: HR: 5.198, 95% CI: 2.913 - 9.274,  $P<0.001$ ; PCD insertion for pneumothorax: HR 9.549, 95% CI: 3.741 - 24.377,  $P<0.001$ ). The duration of the PCD placement between UIP- and non-UIP groups was not different (median 3 days [range, 2 - 11 days] versus median 2 days [range, 1 - 12 days],  $P=0.941$ ).

#### **CONCLUSION**

s UIP pattern on CT and traversal of this pattern by the needle are the risk factors for pneumothorax and requirements of PCD insertion after PTLB.

#### **CLINICAL RELEVANCE/APPLICATION**

When performing PTLB, the radiologists should be alert about pneumothorax occurrence in patients with UIP on CT. They avoid traversal of biopsy needle through the UIP pattern as much as possible.

Printed on: 02/07/23

## Abstract Archives of the RSNA, 2022

M5A-SP1R-2

### Feasibility of EKG gated CT-Fluoroscopy to Guide Percutaneous Biopsy of Cardiac and Pericardial Masses

Monday, Nov. 28 12:15PM - 12:45PM Room: Learning Center - IR DPS

#### Participants

Patrik Rogalla, MD, MBA, Toronto, ON (*Presenter*) Institutional Research Grant, Canon Medical Systems Corporation; Institutional Research Grant, KA Imaging

#### PURPOSE

Percutaneous biopsy of the heart and pericardium poses a significant challenge due to the target's continuous motion and potentially life-threatening complications. The purpose of this study was to evaluate the feasibility of an EKG gated CT-fluoroscopy approach along with various methods to minimize the risks and complications, and the clinical outcome of cardiac and pericardial mass biopsies.

#### METHODS AND MATERIALS

Between 2018 and 2022, 18 cardiac and pericardial mass biopsies were performed in a quaternary care referral centre after clinical consultation with the cardiac surgical team. With REB approval, the patients' charts were reviewed to extract the history, pathology, and clinical outcomes. All biopsies were performed under conscious sedation using CT-fluoroscopy guidance on a 320-slice cardiac scanner (Canon Medical Systems). The EKG was monitored and used for gated image acquisition during the intervention. Mediastinal widening and iatrogenic capnothorax techniques were applied to gain access when appropriate. Full-size 18G core samples were taken using a BioPince needle, and all samples were evaluated by a specialized cardiac pathologist. The radiation dose and time to complete the intervention were recorded.

#### RESULTS

All 18 biopsies in 17 patients (F:M, 9:8; mean age, 45.8) resulted in definitive pathological diagnoses. The size of the targets ranged from 1 cm to 12 cm. Final histology reported 10 malignant (eg. synovial, spindle cell and angiosarcoma, lymphoma, thymoma) and eight benign diagnoses (eg. IgG4, hibernoma, fibroma, TB, haemangioma, fibromyxoid stroma, lipid hyperplasia). One patient developed a small hemothorax, and another patient developed a small pneumomediastinum immediately post-procedure, both of which were successfully treated conservatively. Specific cardiac-related complications, such as hemopericardium, tamponade, arrhythmia or arrest did not occur in any of the patients. The median DLP for the fluoroscopy guidance was 22.5 mGy\*cm (SD, 22.3), the mean total procedure time 32 minutes. All patients left the hospital following a two-hour recovery in a medical imaging day unit.

#### CONCLUSION

s Percutaneous cardiac and pericardial mass biopsies can be safely performed with an acceptable clinical risk and radiation dose profile. CT-fluoroscopy with real-time non-gated and gated image visualization, a well-trained interventional care team, and the backup availability of cardiac surgery may be prerequisites to ensure the best possible patient care.

#### CLINICAL RELEVANCE/APPLICATION

Percutaneous cardiac and pericardial biopsies represent a minimally invasive alternative to mediastinoscopy and open cardiac surgery in a specific patient population.

Printed on: 02/07/23

## Abstract Archives of the RSNA, 2022

M5A-SPIR-3

### Histotripsy Treatment of Veins as A Mechanism of Endothelial Damage

Monday, Nov. 28 12:15PM - 12:45PM Room: Learning Center - IR DPS

#### Participants

Amanda Smolock, MD, PhD, Milwaukee, WI (*Presenter*) Consultant, HistoSonics, Inc; Shareholder, HistoSonics, Inc; Employee, NeuWave Medical, Inc; Grant, NeuWave Medical, Inc; Consultant, NeuWave Medical, Inc;;

#### PURPOSE

Venous insufficiency affects up to a third of the population and can cause significant complications like ulcers which are painful and costly to manage. Histotripsy is a non-invasive, non-thermal focused ultrasound method that mechanically destroys tissue through acoustic cavitation. The aim of this project was to demonstrate the feasibility of using histotripsy to cause controlled mechanical damage to the venous endothelium as a step in inducing venous occlusion for the treatment of venous insufficiency.

#### METHODS AND MATERIALS

Excised porcine femoral veins (n=13) were suspended in a mold of degassed 2% agarose gel and treated within 72 hours post-mortem. The mold was degassed in a vacuum overnight. Histotripsy was applied using 3-cycle pulses at 44MPa predicted peak negative pressure by a 1MHz focused ultrasound transducer along 1 cm length of vein with 4 parameter groups: 1) 1Hz pulse repetition frequency (PRF) and 200 pulses per location (ppl) (n=2), 2) 100Hz PRF and 200 ppl (n=3), 3) 100Hz PRF and 500 ppl (n=3), and 4) 100 Hz PRF and 1000 ppl (n=3). Following treatment, veins were removed from the gel mold and placed in 10% formalin. Tissue was sectioned and stained with hematoxylin and eosin. Histology was reviewed for damage to vein wall layers using a standardized scale (0 least - 4 most endothelial attenuation).

#### RESULTS

Histology demonstrated intact venous walls with dose-dependent damage to the venous endothelium. Frequency and severity of endothelial loss increased with increasing ppl tested at 100Hz PRF. Endothelial damage was most significant though in veins treated at a lower PRF of 1Hz with 200 ppl.

#### CONCLUSION

s Histotripsy causes dose-dependent damage to the endothelium of veins. Endothelial denudation is an initial step in venous thrombosis and ultimately occlusion. Additional in vivo experiments of blood-containing vein are needed to fully test dose parameters for vein histotripsy followed by longitudinal studies to assess for treatment efficacy.

#### CLINICAL RELEVANCE/APPLICATION

Histotripsy has the potential to provide a non-invasive and non-thermal outpatient treatment for venous insufficiency.

Printed on: 02/07/23

## Abstract Archives of the RSNA, 2022

M5A-SP1R-4

### Using a Quantitative Digital Subtraction Angiography Technique to Determine Treatment Endpoints in Partial Splenic Artery Embolization: Feasibility in an In Vivo Porcine Model

Monday, Nov. 28 12:15PM - 12:45PM Room: Learning Center - IR DPS

#### Participants

Sarvesh Periyasamy, PhD, Madison, WI (*Presenter*) Consultant, Johnson & Johnson; Consultant, HEPTA Medical; Consultant, Vector Surgical LLC

#### PURPOSE

Partial splenic artery embolization (PSE) is a method for treating cirrhosis-induced splenomegaly/hypersplenism and complications of portal hypertension. However, there is a direct relationship between the extent of embolization and the severity of post-procedural complications. Using quantitative metrics to determine PSE endpoints may improve procedural outcomes and decrease post-procedural complications. The objective of this study was to determine the feasibility of using a quantitative digital subtraction angiography (qDSA) technique to quantify blood velocity reduction during PSE.

#### METHODS AND MATERIALS

Four swine (~50 kg) underwent embolization of the proximal splenic artery using embolic particles of different sizes (100-300, 300-500, or 500-700  $\mu\text{m}$  diluted in 10 mL of iohexol 300 mg I/mL). qDSAs were acquired at baseline, and after delivery of 1 mL aliquots of particles until a complete stasis angiographic endpoint was achieved. A retrospective image analysis was performed to calculate blood velocity reduction in the splenic artery using qDSA, which was correlated with time-to-peak signal in the portal vein.

#### RESULTS

qDSA demonstrated linear decreases in relative blood velocities from baseline (100-300  $\mu\text{m}$ : 11.8%, 34.8%, 300-500  $\mu\text{m}$ : 29.3%, 500-700  $\mu\text{m}$ : 24.4% reduction per mL of particles) and a strong correlation with the volume of embolic particles delivered (mean  $R = -0.96 \pm 0.02$ ,  $R^2 = 0.93 \pm 0.04$ ). There was a strong correlation between the percent reduction in blood velocity calculated by qDSA and the increased time-to-peak signal in the portal vein (mean  $R = -0.94 \pm 0.03$ ,  $R^2 = 0.89 \pm 0.86$ ). Embolizations performed with larger particles had larger overall post-embolization blood velocity reductions (300-500  $\mu\text{m}$ : 88%, 500-700  $\mu\text{m}$ : 90%) compared to embolizations performed with smaller particles (100-300  $\mu\text{m}$ : 71%, 70%)

#### CONCLUSION

qDSA was able to quantify intra-procedural reductions in splenic arterial blood velocity during embolization in a porcine model. Blood velocity reductions correlated with an imaging marker of reduced portal venous flow. Further investigation is warranted to evaluate qDSA use in clinical PSE procedures.

#### CLINICAL RELEVANCE/APPLICATION

Quantitative digital subtraction angiography may permit the determination of objective treatment endpoints for PSE, improving the safety and efficacy of the procedure.

Printed on: 02/07/23

## Abstract Archives of the RSNA, 2022

M5A-SP1R-5

### Preliminary Results from A Prospective Clinical Trial on The Immunological Effects of Locoregional Therapies in Patients with Hepatocellular Carcinoma

Monday, Nov. 28 12:15PM - 12:45PM Room: Learning Center - IR DPS

#### Participants

Robin Schmidt, (*Presenter*) Nothing to Disclose

#### PURPOSE

To evaluate the prognostic value of periinterventional peripheral blood immune cell counts on tumor response in patients with hepatocellular carcinoma (HCC) after locoregional therapies (LRT).

#### METHODS AND MATERIALS

This interim report of a single-site prospective clinical trial included 76 consecutive patients with unresectable HCC between 08/2020-11/2021, who underwent LRT including high dose-rate brachytherapy alone (BT, n=59) or with prior transarterial chemoembolization (TACE/BT, n=35). Institutional review board approval and informed consent were obtained. Peripheral blood was sampled before, 24h and 8 weeks (wk) after LRT for spectral fluorescence-activated cell sorting (FACS) analysis. A 24-color multiplex staining panel was applied to quantify lymphoid and myeloid cells. Absolute cell counts were obtained by adding precision count beads. FACS data was processed using a robust gating strategy including CD45/CD66/CD16/CD14/CD3/CD4/CD8. Tumor response at 8wk was assessed on multiparametric MRI according to RECIST 1.1 and patients were grouped into responders (R) and non-responders (NR). A nonparametric ANOVA type test statistic was used.

#### RESULTS

FACS data at baseline, 24h, and 8wk post-TACE were available for n=84, n=84, and n=72 patients, respectively. As for BT, higher counts of T cells (TC), CD4+TC, and CD8+TC count as well as a lower CD4-to-CD8 TC ratio ( $p=0.093$ ,  $p=0.232$ ,  $p=0.095$  and  $p=0.152$ , respectively) were found in R compared to NR at all timepoints. However, the opposite trend was observed in patients receiving TACE/BT, who demonstrated lower cell counts for TC, CD4+TC, CD8+TC as well as a higher CD4-to-CD8 ratio ( $p=0.003$ ,  $p=0.003$ ,  $0.074$  and  $p=0.801$ , respectively) for R compared to NR at all timepoints (Figure 1). Neutrophil-to-lymphocyte (NLR) and monocyte-to-lymphocyte (MLR) ratio were similar in R and NR after BT. However, NR after TACE/BT tended to have a lower NLR and higher MLR than R (Figure 2).

#### CONCLUSION

The preliminary results of this prospective study state that different types of locoregional therapies may induce different immunological responses in HCC patients and establish the prognostic value of such quantitative inflammatory biomarkers associated with tumor response prior to LRT. Moreover, patient and tumor characteristics at baseline, that determine the assignment to the respective LRT, may potentially reflect the immunological phenotype in these patients.

#### CLINICAL RELEVANCE/APPLICATION

If confirmed in the complete cohort, these results may help exploit LRT-induced immune-activation and guide improved personalized monitoring and combinations with immunooncological therapies.

Printed on: 02/07/23

## Abstract Archives of the RSNA, 2022

M5A-SP1R-6

### A Phantom for Assessing Histotripsy Treatment Zones on Both Ultrasound and X-ray Imaging

Monday, Nov. 28 12:15PM - 12:45PM Room: Learning Center - IR DPS

#### Participants

Ayca Kutlu, MD, Madison, WI (*Presenter*) Nothing to Disclose

#### PURPOSE

Histotripsy is an emerging non-invasive, non-ionizing, and non-thermal focal tumor therapy. While targeting during histotripsy is currently based on ultrasound (US), X-ray-based fusion and targeting techniques are being developed for tumors not visible by US. The objective of this study was to validate a multi-modal phantom that enables assessment of histotripsy treatment zones on both US and X-ray imaging.

#### METHODS AND MATERIALS

Six cube-shaped phantoms were created by suspending sheep red blood cells (RBC) in agarose. To provide x-ray contrast, alternating layers with (~1 mm thick) and without barium sulfate (~4 mm thick) were poured in a 2 x 2 x 2 in silicone mold. During histotripsy, adjacent layers in the treatment volume mix and create a homogeneous mixture visible on US and cone beam CT (CBCT). Spherical (2.5 cm diameter) treatments were performed in each phantom and resulting treatment zones measured on US and CBCT. Treatment zone size and location (distance from phantom center) were measured in three orthogonal planes separately. In addition, signal-difference-to-noise ratio (SDNR) was calculated on CBCT images between ablation zones and untreated RBC layers.

#### RESULTS

In all cases, histotripsy resulted in homogeneous treatment zones with distinct x-ray attenuation and acoustic impedance, which made segmentation of the treatment zone on both CBCT and US possible. On US, treatment zone diameters (mean±SD) were 25.5 ± 0.3, 25.0 ± 0.3 and 24.5 ± 0.4 mm on X, Y and Z planes, respectively. Similarly, on CBCT, diameters were 25.8 ± 1.1, 25.3 ± 0.4 and 24.4 ± 0.2 mm. Treatment zone center point location differed by 1.6 ± 0.9, 1.5 ± 1.1 and 2.6 ± 1.2 mm on X, Y and Z planes, respectively between CBCT and US measurements. The average SDNR between ablation zone and RBC layer was 23.1 ± 7.3.

#### CONCLUSION

The proposed multimodal RBC phantom allowed visualization of histotripsy treatment zones on both US and x-ray imaging. Treatment zone diameters and center locations were similar between the two modalities. These phantoms can help validate newly developed fusion and targeting techniques for histotripsy, expanding the scope of treatable lesions.

#### CLINICAL RELEVANCE/APPLICATION

A multimodal RBC phantom may be used to develop and validate X-ray-based fusion and targeting techniques for histotripsy, which will facilitate treatment of tumors not visible on US.

Printed on: 02/07/23

## Abstract Archives of the RSNA, 2022

M5A-SP1R-7

### Safety and Efficacy of Serial Doxycycline Exchange Sclerotherapy for Lymphatic Malformations

Monday, Nov. 28 12:15PM - 12:45PM Room: Learning Center - IR DPS

#### Participants

Anna Gong, Baltimore, MD (*Presenter*) Nothing to Disclose

#### PURPOSE

To assess the efficacy of serial doxycycline exchanges (SDE) for the treatment of lymphatic malformations (LM).

#### METHODS AND MATERIALS

We reviewed all patients from 9/2004 to 02/2022 who received SDE after a percutaneous drain placement for an LM at our institution. After initial image-guided drainage catheter placement and sclerotherapy into the LM, the patient was admitted for SDE. Standard procedure involved bedside drainage, and infusion of doxycycline (10mg/mL) 1/3 to 1/2 of the drained volume, which was left to dwell for 4 hours before draining. This was performed twice a day, until the drained volume was sufficiently decreased as per the physician's direction, after which the patient was discharged. Charts were reviewed to assess clinical response, size changes, and complications. Symptom response was classified as resolved, improved, and stable/worsened. LM size change was calculated using difference of pre- and post- procedure MRI of the largest lesion diameter in one plane: complete response (CR, 100% reduction), partial response (PR, 30% reduction), stable disease (SD, =30% reduction or =20% enlargement), progressive disease (PD, =20% size increase). SIR classification criteria were used to classify adverse events. Fisher's Exact Tests were used for statistical analysis.

#### RESULTS

43 patients (58.1% M) underwent 82 image-guided sclerotherapy procedures with subsequent SDE (technical success 80/82; 97.6%). An average of 3.87 SDE sessions/admission was reported for an average extended inpatient stay of 92 hours/admission (Total: 201 exchanges). This resulted in 201/283 (71.0%) sclerotherapy sessions that were performed at the bedside. The mean patient follow-up period was 902.15 days (median: 328 days). Most common presenting symptoms were swelling/mass (25, 58.1%), pain (8, 18.6%) and trouble breathing (3, 7.0%). Sclerotherapy significantly improved symptoms with 6.1% (5/82) resolved, 47.6% (39/82) improved, and 46.3% (38/82) stable or worsened ( $p < 0.0001$ ). Embolization also significantly decreased LM size on imaging ( $p = 0.0011$ ). Of the 47 image-guided procedures (47/82, 57.3%) with both pre- and post- MRI imaging, zero patients saw CR, 10 patients (21.3%) experienced PR, 35 patients (74.5%) experienced SD and 2 patients (4.3%) saw PD. Early (30-day) post-procedural complications occurred after 9 of 82 procedures (10.9%), the most common of which were sensory or motor nerve injury (44.4%; 4/9) and mild in severity (44.4%; 4/9).

#### CONCLUSION

SDE significantly decreases lesion size and improves clinical symptoms in LMs.

#### CLINICAL RELEVANCE/APPLICATION

SDE is a safe and effective treatment option for LMs that allows for multiple sclerotherapy sessions with a single fluoroscopic procedure.

Printed on: 02/07/23

## Abstract Archives of the RSNA, 2022

MSA-SPIR-8

### Silver Nanoparticles-coated Stent for Suppressing Bacterial Growth and Tissue Hyperplasia after Radiofrequency Ablation in the Rabbit Common Bile Duct

Monday, Nov. 28 12:15PM - 12:45PM Room: Learning Center - IR DPS

#### Participants

Yubeen Park, Seoul, Korea, Republic Of (*Presenter*) Nothing to Disclose

#### PURPOSE

To investigate the efficacy of silver nanoparticles (AgNPs)-coated self-expandable metal stent (SEMS) placement immediately after radiofrequency (RF) ablation in suppressing thermal damage as well as SEMS-induced bacterial growth and tissue hyperplasia in the common bile duct of rabbits.

#### METHODS AND MATERIALS

The release behavior and antibacterial effects of AgNPs-coated SEMSs were evaluated. A total of 12 male New Zealand White rabbits were randomly divided into two groups for verification of the efficacy of AgNPs-coated SEMS placement immediately after RF ablation: the control group received an uncoated SEMS, and the AgNPs group received an AgNPs-coated SEMS. Cholangiography was performed immediately before sacrifice in all rabbits to check the stent patency. Venous blood samples were collected before sacrifice and AST, ALT, ALP, GGT, and total bilirubin levels were analyzed to evaluate hepatobiliary functions. Histological examination was performed about the degree of inflammatory cell infiltration, thickness of submucosal fibrosis, percentage of granulation tissue area, and degree of collagen deposition. Immunohistochemistry analysis was performed about the degree of TUNEL-, HSP 70-, and  $\alpha$ -SMA-positive areas.

#### RESULTS

Ag ions were rapidly released at the beginning and then showed a gradual release behavior. The AgNPs-coated SEMS significantly inhibited bacterial activity compared to the uncoated SEMS ( $p < 0.05$ ). Stent placement immediately after RF ablation was successfully performed without procedure-related complications in all rabbits. Jaundice was observed in 3 out of 6 (50%) rabbits in the control group. The luminal diameter in the AgNPs group was greater than that in the control group ( $p < 0.05$ ). AST, ALT, ALP, GGT, and total bilirubin levels were all lower in the AgNPs group than in the control group. Histological examination confirmed that all evaluation results were significantly lower in the AgNPs group than in the control group (all  $p < 0.05$ ). Immunohistochemistry analyses revealed that TUNEL-, HSP 70-, and  $\alpha$ -SMA-positive areas were significantly lower in the AgNPs group than in the control group (all  $p < 0.05$ ).

#### CONCLUSION

The AgNPs-coated SEMS significantly inhibited tissue hyperplasia and biofilm induced by heat and mechanical damage in the rabbit common bile duct. The developed method of RF ablation with AgNPs-coated SEMS should be a promising therapeutic strategy for the prevention of RF ablation- and stent-related complications.

#### CLINICAL RELEVANCE/APPLICATION

AgNPs-coated SEMS placement immediately after RF ablation might be effective in preventing RF ablation and stent-related complications in patients with unresectable malignant biliary obstruction.

Printed on: 02/07/23

## Abstract Archives of the RSNA, 2022

M5A-SP1R-9

### Intragastric Satiety-Inducing Device combined with Photodynamic Therapy to Treat Obesity

Monday, Nov. 28 12:15PM - 12:45PM Room: Learning Center - IR DPS

#### Participants

Ji Won Kim, Seoul, Korea, Republic Of (*Presenter*) Nothing to Disclose

#### PURPOSE

To evaluate the efficacy and safety of the Chlorin e6-embedded intragastric satiety-inducing device (Ce6-embedded ISD) placement with photodynamic therapy (PDT) in suppressing appetite in porcine stomach.

#### METHODS AND MATERIALS

The ISD consisted of the lower esophageal part and disk part for the fundus of the stomach. The once dip coating technique was used for the fabrication of Ce6-embedded ISD. A total of 12 minipigs were divided into four groups. PDT group (n = 3) received single PDT using Ce6-embedded ISD. ISD group (n = 3) received ISD placement. ISD with PDT group (n = 3) received single PDT with Ce6-embedded ISD placement. The remaining three weight and age-matched healthy pigs were used as a control group. All pigs were sacrificed 4 weeks after the procedures. The outcomes were assessed by histological examinations and immunohistochemistry analysis. Body weight was monitored weekly, and the percentage of total body weight gain (%TBWG) was calculated.

#### RESULTS

A total of 12 minipigs were divided into four groups. PDT group (n = 3) received single PDT using Ce6-embedded ISD. ISD group (n = 3) received ISD placement. ISD with PDT group (n = 3) received single PDT with Ce6-embedded ISD placement. The remaining three weight and age-matched healthy pigs were used as a control group. Anti-ghrelin and TUNEL-positive deposition were significantly increased in PDT, ISD, and ISD with PDT groups compared to the control group (all p < 0.001). The weight gain was observed to decrease in the order of PDT, ISD, and ISD with PDT groups compared to the control group, and the ISD with PDT proved to be the most effective for weight loss.

#### CONCLUSION

Ce6-embedded ISD was effectively decreases weight gain rate and ghrelin-producing cells in the porcine model. The simple and unique operation extends the point of view in PDT and is expected to be a novel obesity therapy.

#### CLINICAL RELEVANCE/APPLICATION

Ce6-embedded ISD, weight loss and stimulation of ghrelin-producing cells, will become strategy for obesity treatment.

Printed on: 02/07/23



## Abstract Archives of the RSNA, 2022

M5A-SPMK

### Musculoskeletal Monday Poster Discussions - A

Monday, Nov. 28 12:15PM - 12:45PM Room: Learning Center - MK DPS

#### Sub-Events

#### M5A-SPMK-1 Fully Automated CT Imaging Biomarkers for Opportunistic Prediction of Future Hip Fractures

##### Awards

##### Trainee Research Prize - Medical Student

##### Participants

Daniel Liu, (*Presenter*) Nothing to Disclose

##### PURPOSE

Body CT scans are frequently acquired for many targeted indications, but potentially valuable additional biometric information often remains untapped. AI-based algorithms can automate CT-based body composition measures, which can be utilized for opportunistic screening. The purpose of this study was to assess automated CT imaging biomarkers in patients who went on to hip fracture, compared with controls.

##### METHODS AND MATERIALS

In this retrospective case-control study, 6926 total patients underwent initial abdominal CT over a 20-year interval at one institution, including 1308 patients (mean age at initial CT, 70.5±12.0 years; 64.4% female) who went on to hip fracture (mean time to fracture, 4.5 years) and 5618 controls (mean age, 70.25±12.0 years; 61.2% female; mean follow-up interval, 5.2 years). Validated and fully automated quantitative CT algorithms for trabecular bone attenuation (at L1), muscle attenuation (at L3), and abdominal fat area (at L1) were applied to all scans. Univariate and multivariate hazard ratios (HRs) comparing worst quartile to the other three and area under the receiver operating characteristic (AUROC) curve analyses were performed.

##### RESULTS

Hip fracture HRs (with 95% CI) for low trabecular bone HU, low muscle HU, and low subcutaneous adipose tissue (SAT) area were 2.09 (1.86-2.35), 1.36 (1.20-1.54), and 1.68 (1.50-1.89), respectively. Similarly, 10-year AUROC values for predicting hip fracture were 0.702, 0.603, and 0.594, respectively. Multivariate combinations of these CT biomarkers further improved the predictive value. Notably, the 10-year AUROC from combining bone, muscle, and SAT was 0.729, while combining just muscle attenuation and SAT area was 0.679.

##### CONCLUSION

s Automated abdominal CT-based measures of bone, muscle, and subcutaneous fat provide useful risk stratification for future hip fractures. Opportunistic use of these automated CT-based measures can identify patients at higher risk, regardless of the indication for CT imaging.

##### CLINICAL RELEVANCE/APPLICATION

There is growing interest in leveraging opportunistic CT data for patient benefit, and automated AI-based algorithms provide a feasible pathway for this.

#### M5A-SPMK-2 Can Radiomics Diagnose Cancer-associated Cachexia At An Early Stage?

##### Participants

Yufei Zhao, PhD, (*Presenter*) Nothing to Disclose

##### PURPOSE

As one of the most common complications of non-small-cell lung cancer (NSCLC), cancer-associated cachexia (CAC) frequently present with progressive skeletal muscle and adipose tissue wasting. However, as obesity, edema, pleural and ascites fluid, tumor weight and other factors can mask the diagnosis of CAC. Radiomics is expected to be an important research and clinical tool to accurate diagnosis CAC in early stage.

##### METHODS AND MATERIALS

A total of 93 NSCLC patients were enrolled, abdominal and pelvic CT (Siemens SOMATOM Sensation Scanner 64 Computed Tomography) scans were collected from all patients at first diagnosis and 6 months after treatment. The complete psoas major on both sides is automatically segmented by the FCN network. Taking the starting and ending plane of the psoas major as a reference, Extraction of the subcutaneous fat (-190 HU — -30 HU) and visceral fat (-150 HU — -50HU) by threshold. The difference in the volume of the psoas muscle between the two scans was calculated, if the volume decreased by more than 3%, it was classified as a cachexia group, otherwise as non-cachexia group. All above processes were implemented with FeAture Explorer Pro (FAEPro, V 0.4.2) on Python (3.7.6), extracting features of all volume of interest separately included first order statistics, shape-based, wavelet transform, squaregray-level co-occurrence matrix and selecting 65 cases as the training data set, another 28 cases as the

independent testing data set. we used analysis of variance (ANOVA) to select features and the support vector machine (SVM) as the classifier.

## RESULTS

A total of 434 features were extracted for each case and 6 features were screened out finally. There was no difference in the psoas muscle between the cachexia and non-cachexia groups at the baseline of treatment [AUC: 0.62 (95% CI: 0.36, 0.85)], but the difference between the two groups began to appear after 6 months treatment [AUC: 0.73 (95% CI: 0.51, 0.93)]. Differences in subcutaneous adipose tissue and visceral adipose tissue between cachexia [AUC: 0.83 (95% CI: 0.63, 0.97) and 0.72 (95% CI: 0.51, 0.91)] and non-cachexia groups [AUC: 0.69 (95% CI: 0.45, 0.88) and 0.70 (95% CI: 0.49, 0.88)] were present at the start of treatment and persisted 6 months later.

## CONCLUSION

s For the NSCLC patients with CAC, adipose tissue changes earlier than muscle tissue, the radiomics is expected to be an effective means for early diagnosis of CAC.

## CLINICAL RELEVANCE/APPLICATION

Immediate diagnosis of occult CAC by radiomics enables early intervention to slow cancer progression.

## M5A-SPMK-3AI-Detection and Auto-Reporting of Trochlear Groove Anatomic Landmarks

Participants

Justine Lee, (*Presenter*) Nothing to Disclose

## PURPOSE

Total knee arthroplasty is a widely implemented, effective means applied towards the treatment of advanced osteoarthritis. One of the most frequent complications, however, lies in relation to the patellofemoral compartment which remains poorly characterized with marked variability in alignment<sup>1</sup>. With current implant designs falling short of fully restoring normal patellofemoral anatomy<sup>2</sup>, and some even exhibiting characteristics of trochlear dysplasia<sup>3</sup>, our study aimed to utilize artificial intelligence auto-detection in computed tomography (CT) imaging to identify trochlear groove anatomy, a key determinant of patellar biomechanics.

## METHODS AND MATERIALS

This IRB-approved retrospective study is a collaboration between two medical institutions. A database of 219 CT scans of the knee was constructed with healthy subjects 18-40 years, excluding significant pathology such as trauma, infection, or arthroplasty. Axial CT images with bony reconstructions of the trochlear trough were reviewed by radiology and orthopedic residents, in which seven key anatomic points of the distal femur were defined (three points along the anterior femoral trochlea at the medial, central trough, and lateral aspects; two points along the most peripheral medial and lateral epicondyles; and two points at the most posterior medial and lateral condyles), in accordance with prior morphometric studies of the distal femur<sup>4</sup>. These points were subsequently labeled on a web-based viewer, with annotated images used in the creation, training, and validation of our deep learning (DL) model—a ResNet50 model pre-trained on RadImageNet5, a large multimodality radiologic dataset. These seven anatomic landmarks were auto-detected by our DL model, with mean absolute error (MAE) reported in the assessment of model performance.

## RESULTS

Our RadImageNet pre-trained ResNet50 model utilized annotated CT axial images and modified the top layers to output a (14x1) vector containing predicted x and y coordinates of the seven anatomic landmarks. Within the testing dataset, the DL model achieved a MAE of 1.5 mm, successfully identifying the seven key points of the distal femur and trochlear groove as demarcated by the residents.

## CONCLUSION

s Our ResNet50 model successfully achieved our primary aim of identifying seven key landmarks of the femur and trochlear groove, derived morphometric parameters of clinical interest, and auto-generated radiologic measurements targeted for clinical orthopedic use.

## CLINICAL RELEVANCE/APPLICATION

This AI-based tool demonstrates value in characterizing patellofemoral anatomy, streamlining preoperative imaging measurements, and optimizing orthopedic planning of patient-specific implant selection, implant positioning, and surgical approach.

## M5A-SPMK-4 Automated Machine Learning (AutoML) for MSK Radiograph Abnormality Detection: Feasibility Study of Six Codeless Platforms

Participants

Paul Yi, MD, Baltimore, MD (*Presenter*) Consultant, FH Orthopedics SAS; Consultant, BunkerHill Health

## PURPOSE

Coding expertise can be a barrier for radiologists who want to apply deep learning (DL) to musculoskeletal imaging. Automated machine learning (AutoML) platforms that allow for the codeless development of DL models could bridge this gap. We evaluated the feasibility of six AutoML platforms for the development of DL models to identify radiographic abnormalities on musculoskeletal radiographs.

## METHODS AND MATERIALS

We used 40,561 upper extremity radiographs from Stanford's MURA dataset labeled as abnormal or normal by board-certified radiologists. These images were split into 80/20% train/validation datasets. We evaluated 6 AutoML platforms (Amazon, Apple, Clarifai, Google, Microsoft, MedicMind) for 1) feasibility of training a functioning DL model without the need for writing code and with a cost per model <\$100, and 2) performance of the DL model for identification of radiographic abnormalities as measured by F1 scores (the only metric common to all 6 platforms).

## RESULTS

(1) Feasibility: All successfully trained DL models were developed using free tiers of the platforms (i.e., no cost) but only 2 of 6

(I) Feasibility: All successfully trained DL models were developed using free tiers of the platforms (i.e., no cost) but only 2 of 6 platforms allowed for truly codeless DL model development and testing (Apple and MedicMind). Three platforms required some form of coding to train and test the models (Amazon, Google, and Microsoft). One platform (Clarifai) did not successfully train a functioning model - this platform consistently crashed during model development despite numerous attempts. (II) Performance: Diagnostic performance varied between AutoML platforms and the upper extremity region analyzed, ranging from F1 0.25 to 0.99. Stratified by anatomic region, AutoML models performed best analyzing the humerus and worst in the elbow. Google and Microsoft achieved F1 scores >0.90 and >0.85, respectively, in every extremity region. The two truly codeless DL models (Apple and MedicMind) had the lowest F1 scores of the group.

## **CONCLUSION**

s Although advertised as codeless methods to easily develop DL models, only 2 of 6 AutoML platforms allowed for truly codeless development of DL models for extremity radiograph abnormality detection. Nevertheless, some of these platforms did result in high-performing models with F1 scores as high as 0.99. Altogether, these findings suggest that AutoML platforms have promise to democratize DL for radiologists who do not have coding expertise, though there are areas for improving their useability and performance.

## **CLINICAL RELEVANCE/APPLICATION**

AutoML has promise to democratize deep learning for radiologists who do not have coding expertise, albeit with areas for improvement.

Printed on: 02/07/23



## Abstract Archives of the RSNA, 2022

M5A-SPMK-1

### Fully Automated CT Imaging Biomarkers for Opportunistic Prediction of Future Hip Fractures

Monday, Nov. 28 12:15PM - 12:45PM Room: Learning Center - MK DPS

#### Awards

Trainee Research Prize - Medical Student

#### Participants

Daniel Liu, (*Presenter*) Nothing to Disclose

#### PURPOSE

Body CT scans are frequently acquired for many targeted indications, but potentially valuable additional biometric information often remains untapped. AI-based algorithms can automate CT-based body composition measures, which can be utilized for opportunistic screening. The purpose of this study was to assess automated CT imaging biomarkers in patients who went on to hip fracture, compared with controls.

#### METHODS AND MATERIALS

In this retrospective case-control study, 6926 total patients underwent initial abdominal CT over a 20-year interval at one institution, including 1308 patients (mean age at initial CT, 70.5±12.0 years; 64.4% female) who went on to hip fracture (mean time to fracture, 4.5 years) and 5618 controls (mean age, 70.25±12.0 years; 61.2% female; mean follow-up interval, 5.2 years). Validated and fully automated quantitative CT algorithms for trabecular bone attenuation (at L1), muscle attenuation (at L3), and abdominal fat area (at L1) were applied to all scans. Univariate and multivariate hazard ratios (HRs) comparing worst quartile to the other three and area under the receiver operating characteristic (AUROC) curve analyses were performed.

#### RESULTS

Hip fracture HRs (with 95% CI) for low trabecular bone HU, low muscle HU, and low subcutaneous adipose tissue (SAT) area were 2.09 (1.86-2.35), 1.36 (1.20-1.54), and 1.68 (1.50-1.89), respectively. Similarly, 10-year AUROC values for predicting hip fracture were 0.702, 0.603, and 0.594, respectively. Multivariate combinations of these CT biomarkers further improved the predictive value. Notably, the 10-year AUROC from combining bone, muscle, and SAT was 0.729, while combining just muscle attenuation and SAT area was 0.679.

#### CONCLUSION

s Automated abdominal CT-based measures of bone, muscle, and subcutaneous fat provide useful risk stratification for future hip fractures. Opportunistic use of these automated CT-based measures can identify patients at higher risk, regardless of the indication for CT imaging.

#### CLINICAL RELEVANCE/APPLICATION

There is growing interest in leveraging opportunistic CT data for patient benefit, and automated AI-based algorithms provide a feasible pathway for this.

Printed on: 02/07/23

## Abstract Archives of the RSNA, 2022

MSA-SPMK-2

### Can Radiomics Diagnose Cancer-associated Cachexia At An Early Stage?

Monday, Nov. 28 12:15PM - 12:45PM Room: Learning Center - MK DPS

#### Participants

Yufei Zhao, PhD, (Presenter) Nothing to Disclose

#### PURPOSE

As one of the most common complications of non-small-cell lung cancer (NSCLC), cancer-associated cachexia (CAC) frequently present with progressive skeletal muscle and adipose tissue wasting. However, as obesity, edema, pleural and ascites fluid, tumor weight and other factors can mask the diagnosis of CAC. Radiomics is expected to be an important research and clinical tool to accurate diagnosis CAC in early stage.

#### METHODS AND MATERIALS

A total of 93 NSCLC patients were enrolled, abdominal and pelvic CT (Siemens SOMATOM Sensation Scanner 64 Computed Tomography) scans were collected from all patients at first diagnosis and 6 months after treatment. The complete psoas major on both sides is automatically segmented by the FCN network. Taking the starting and ending plane of the psoas major as a reference, Extraction of the subcutaneous fat (-190 HU — -30 HU) and visceral fat (-150 HU — -50HU) by threshold. The difference in the volume of the psoas muscle between the two scans was calculated, if the volume decreased by more than 3%, it was classified as a cachexia group, otherwise as non-cachexia group. All above processes were implemented with FeAture Explorer Pro (FAEPro, V 0.4.2) on Python (3.7.6), extracting features of all volume of interest separately included first order statistics, shape-based, wavelet transform, squaregray-level co-occurrence matrix and selecting 65 cases as the training data set, another 28 cases as the independent testing data set. we used analysis of variance (ANOVA) to select features and the support vector machine (SVM) as the classifier.

#### RESULTS

A total of 434 features were extracted for each case and 6 features were screened out finally. There was no difference in the psoas muscle between the cachexia and non-cachexia groups at the baseline of treatment [AUC: 0.62 (95% CI: 0.36, 0.85)], but the difference between the two groups began to appear after 6 months treatment [AUC: 0.73 (95% CI: 0.51, 0.93)]. Differences in subcutaneous adipose tissue and visceral adipose tissue between cachexia [AUC: 0.83 (95% CI: 0.63, 0.97) and 0.72 (95% CI: 0.51, 0.91)] and non-cachexia groups [AUC: 0.69 (95% CI: 0.45, 0.88) and 0.70 (95% CI: 0.49, 0.88)] were present at the start of treatment and persisted 6 months later.

#### CONCLUSION

s For the NSCLC patients with CAC, adipose tissue changes earlier than muscle tissue, the radiomics is expected to be an effective means for early diagnosis of CAC.

#### CLINICAL RELEVANCE/APPLICATION

Immediate diagnosis of occult CAC by radiomics enables early intervention to slow cancer progression.

Printed on: 02/07/23

## Abstract Archives of the RSNA, 2022

M5A-SPMK-3

### AI-Detection and Auto-Reporting of Trochlear Groove Anatomic Landmarks

Monday, Nov. 28 12:15PM - 12:45PM Room: Learning Center - MK DPS

#### Participants

Justine Lee, (*Presenter*) Nothing to Disclose

#### PURPOSE

Total knee arthroplasty is a widely implemented, effective means applied towards the treatment of advanced osteoarthritis. One of the most frequent complications, however, lies in relation to the patellofemoral compartment which remains poorly characterized with marked variability in alignment<sup>1</sup>. With current implant designs falling short of fully restoring normal patellofemoral anatomy<sup>2</sup>, and some even exhibiting characteristics of trochlear dysplasia<sup>3</sup>, our study aimed to utilize artificial intelligence auto-detection in computed tomography (CT) imaging to identify trochlear groove anatomy, a key determinant of patellar biomechanics.

#### METHODS AND MATERIALS

This IRB-approved retrospective study is a collaboration between two medical institutions. A database of 219 CT scans of the knee was constructed with healthy subjects 18-40 years, excluding significant pathology such as trauma, infection, or arthroplasty. Axial CT images with bony reconstructions of the trochlear trough were reviewed by radiology and orthopedic residents, in which seven key anatomic points of the distal femur were defined (three points along the anterior femoral trochlea at the medial, central trough, and lateral aspects; two points along the most peripheral medial and lateral epicondyles; and two points at the most posterior medial and lateral condyles), in accordance with prior morphometric studies of the distal femur<sup>4</sup>. These points were subsequently labeled on a web-based viewer, with annotated images used in the creation, training, and validation of our deep learning (DL) model—a ResNet50 model pre-trained on RadImageNet5, a large multimodality radiologic dataset. These seven anatomic landmarks were auto-detected by our DL model, with mean absolute error (MAE) reported in the assessment of model performance.

#### RESULTS

Our RadImageNet pre-trained ResNet50 model utilized annotated CT axial images and modified the top layers to output a (14x1) vector containing predicted x and y coordinates of the seven anatomic landmarks. Within the testing dataset, the DL model achieved a MAE of 1.5 mm, successfully identifying the seven key points of the distal femur and trochlear groove as demarcated by the residents.

#### CONCLUSION

Our ResNet50 model successfully achieved our primary aim of identifying seven key landmarks of the femur and trochlear groove, derived morphometric parameters of clinical interest, and auto-generated radiologic measurements targeted for clinical orthopedic use.

#### CLINICAL RELEVANCE/APPLICATION

This AI-based tool demonstrates value in characterizing patellofemoral anatomy, streamlining preoperative imaging measurements, and optimizing orthopedic planning of patient-specific implant selection, implant positioning, and surgical approach.

Printed on: 02/07/23



## Abstract Archives of the RSNA, 2022

M5A-SPMK-4

### Automated Machine Learning (AutoML) for MSK Radiograph Abnormality Detection: Feasibility Study of Six Codeless Platforms

Monday, Nov. 28 12:15PM - 12:45PM Room: Learning Center - MK DPS

#### Participants

Paul Yi, MD, Baltimore, MD (*Presenter*) Consultant, FH Orthopedics SAS; Consultant, BunkerHill Health

#### PURPOSE

Coding expertise can be a barrier for radiologists who want to apply deep learning (DL) to musculoskeletal imaging. Automated machine learning (AutoML) platforms that allow for the codeless development of DL models could bridge this gap. We evaluated the feasibility of six AutoML platforms for the development of DL models to identify radiographic abnormalities on musculoskeletal radiographs.

#### METHODS AND MATERIALS

We used 40,561 upper extremity radiographs from Stanford's MURA dataset labeled as abnormal or normal by board-certified radiologists. These images were split into 80/20% train/validation datasets. We evaluated 6 AutoML platforms (Amazon, Apple, Clarifai, Google, Microsoft, MedicMind) for 1) feasibility of training a functioning DL model without the need for writing code and with a cost per model <\$100, and 2) performance of the DL model for identification of radiographic abnormalities as measured by F1 scores (the only metric common to all 6 platforms).

#### RESULTS

(I) Feasibility: All successfully trained DL models were developed using free tiers of the platforms (i.e., no cost) but only 2 of 6 platforms allowed for truly codeless DL model development and testing (Apple and MedicMind). Three platforms required some form of coding to train and test the models (Amazon, Google, and Microsoft). One platform (Clarifai) did not successfully train a functioning model - this platform consistently crashed during model development despite numerous attempts. (II) Performance: Diagnostic performance varied between AutoML platforms and the upper extremity region analyzed, ranging from F1 0.25 to 0.99. Stratified by anatomic region, AutoML models performed best analyzing the humerus and worst in the elbow. Google and Microsoft achieved F1 scores >0.90 and >0.85, respectively, in every extremity region. The two truly codeless DL models (Apple and MedicMind) had the lowest F1 scores of the group.

#### CONCLUSION

Although advertised as codeless methods to easily develop DL models, only 2 of 6 AutoML platforms allowed for truly codeless development of DL models for extremity radiograph abnormality detection. Nevertheless, some of these platforms did result in high-performing models with F1 scores as high as 0.99. Altogether, these findings suggest that AutoML platforms have promise to democratize DL for radiologists who do not have coding expertise, though there are areas for improving their useability and performance.

#### CLINICAL RELEVANCE/APPLICATION

AutoML has promise to democratize deep learning for radiologists who do not have coding expertise, albeit with areas for improvement.

Printed on: 02/07/23

## Abstract Archives of the RSNA, 2022

M5A-SPNMMI

### Nuclear Medicine/Molecular Imaging Monday Poster Discussion - A

Monday, Nov. 28 12:15PM - 12:45PM Room: Learning Center - NMMI DPS

#### Participants

Lilja Solnes, MD, Owings Mills, MD (*Moderator*) Consultant, Lantheus Holdings; Research funded, Novartis AG; Research funded, Precision Molecular Inc; Research funded, Celectar Biosciences, Inc; Royalties, RELX  
Lilja Solnes, MD, Owings Mills, MD (*Moderator*) Consultant, Lantheus Holdings; Research funded, Novartis AG; Research funded, Precision Molecular Inc; Research funded, Celectar Biosciences, Inc; Royalties, RELX  
Frederick Grant, MD, Philadelphia, PA (*Moderator*) Nothing to Disclose  
Frederick Grant, MD, Philadelphia, PA (*Moderator*) Nothing to Disclose

#### Sub-Events

#### M5A-SPNMMI-1 Role of 68Ga-DOTATOC PET for Pre-operative Prediction of DAXX/ATRX Loss of Expression and Histopathological Characteristics of Pancreatic Neuroendocrine Tumors

#### Participants

Paola Mapelli, Milan, Italy (*Presenter*) Nothing to Disclose

#### PURPOSE

To evaluate the role of 68Ga-DOTATOC PET parameters in predicting PanNET characteristics of aggressiveness before surgery.

#### METHODS AND MATERIALS

Retrospective study including 42 patients with well-differentiated PanNET (15 females, 27 males, median age: 60 years, range: 32-80) who underwent to 68Ga-DOTATOC PET for staging purpose. SUVmax, SUV mean, somatostatin receptor density (SRD) and total lesion somatostatin receptor density (TLSRD) were extracted from primary PanNET and radiological diameter (RD) was measured for each primary PanNET. Appropriate statistical analysis (see results) investigated the ability of imaging parameters predicting DAXX/ATRX loss of expression (LoE), infiltrative growth, microvascular invasion, perineural invasion, lymph node (LN) involvement, grade and presence of liver metastases.

#### RESULTS

Fourteen/42 PanNET patients had DAXX/ATRX LoE and 28/42 maintained the expression. Mann-Whitney U test: SUVmean predicted perineural invasion ( $p=0.049$ ) and grade ( $p=0.048$ ) and RD infiltrative growth ( $p=0.007$ ), DAXX/ATRX LoE ( $p=0.014$ ) and presence of liver metastases ( $p=0.005$ ). SRD and TLSD correlated with Ki67 ( $p=0.047$  and  $0.028$ , respectively). Univariate logistic regression: SUVmax predicted LN involvement ( $p=0.045$ ), SRD and TLSD predicted DAXX/ATRX LoE ( $p=0.044$  and  $0.0497$ , respectively) and presence of liver metastases ( $p=0.0314$  and  $p=0.0299$ , respectively); RD predicted DAXX/ATRX LoE ( $p=0.00614$ ), infiltrative growth ( $p=0.033$ ) and presence of liver metastases ( $p=0.0049$ ). ROC curve analysis: SUVmax and SUVmean predicted perineural invasion (AUC 0.672, 95%CI 0.50-0.82 and AUC 0.686, 95%CI 0.50-0.86, respectively). SUVmax was predictive of LN metastases (AUC 0.689, 95%CI: 0.52-0.84) and SUVmean of grade (AUC 0.682, 95%CI: 0.50-0.84). RD showed a role in predicting DAXX/ATRX LoE, infiltrative growth and liver metastases, with AUC of 0.735 (95%CI 0.54-0.89), 0.789 (95% CI 0.63-0.92) and 0.789 (95% CI 0.61-0.95), respectively.

#### CONCLUSION

s 68Ga-DOTATOC PET parameters showed predictive value in assessing DAXX/ATRX LoE and clinicopathological features of PanNET aggressiveness, thus providing additional information on PanNET behaviour in the preoperative setting.

#### CLINICAL RELEVANCE/APPLICATION

68Ga-DOTATOC PET parameters provide additional information on PanNET behaviour in the preoperative setting, thus improving tumour characterization.

#### M5A-SPNMMI-2 Prognostic Value of 18F-FDG-PET/CT Radiomics Combined with Sarcopenia Status among Patients with Advanced Gastroesophageal Cancer

#### Participants

Ricarda Hinzpeter, MD, Zurich, Switzerland (*Presenter*) Nothing to Disclose

#### PURPOSE

To investigate, whether 18F-FDG-PET/CT- derived radiomics combined with sarcopenia measurements improves survival prognostication among patients with advanced, metastatic gastroesophageal cancer.

#### METHODS AND MATERIALS

In this IRB-approved retrospective study, we included 128 consecutive patients with advanced, metastatic gastroesophageal cancer ( $n=128$ ; 26 females; 102 males; mean age  $63.5\pm 11.7$  years; age range: 29-91 years) undergoing 18F-FDG-PET/CT for

staging between November 2008 and December 2019. Segmentation of the primary tumor and radiomics analysis derived from PET and CT images was performed semi-automatically with a commonly used open-source software platform (LIFEX, Version 6.30, lifexsoft.org). Patients' nutritional status was determined by measuring the skeletal muscle index (SMI) at the level of L3 on the CT component. Univariable and multivariable analyses were performed to establish a survival prediction model including radiomics, clinical data, and SMI score.

## RESULTS

In a univariable Cox proportional hazards model, ECOG ( $p < 0.001$ ) and distant metastasis to the bone ( $p = 0.028$ ) were significant clinical parameters for overall survival (OS) and progression free survival (PFS). Age ( $p = 0.017$ ) was an additional prognostic factor for OS. The multivariable analysis revealed improved overall survival prognostication when adding sarcopenic status, PET and CT radiomics to the model with clinical parameter only over a clinical course of 6 to 36 months (AUC 0.67 vs. 0.82 at 15 months). Similarly, adding sarcopenia measurements, PET and CT radiomics improved the model fit for PFS (AUC 0.65 vs. 0.82 at 12 months).

## CONCLUSION

s PET and CT radiomics derived from 18F-FDG-PET/CT combined with sarcopenia measurements and clinical parameters may improve survival prediction among patients with advanced, metastatic gastroesophageal cancer.

## CLINICAL RELEVANCE/APPLICATION

Increasing knowledge of outcome prognostication, derived from quantitative radiomics features, has the potential for pretreatment risk stratification, allowing clinicians to deliver more patient specific treatment tailored to individual risk.

## M5A-SPNMMI-3 Feasibility of in Vivo MRI Imaging of Human Placental Mesenchymal Stem Cells Labeled With Ultramicro And < Superparamagnetic Iron Oxide Nanoparticles for Targeting Colorectal Cancer

Participants

Hua He, MMedSc, MMedSc, Yinchuan, China (*Presenter*) Nothing to Disclose

## PURPOSE

To transplant human placenta-zoned mesenchymal stem cells (PMSCs) labeled with USPIO-PLL protein complex into nude mice model of implanted tumor, and to explore the feasibility of in vivo MRI imaging of PMSCs.

## METHODS AND MATERIALS

Nude mice were inoculated with human colon cancer cells (HT-29), and then transplanted and passaged between mice to establish a human colon cancer transplanted tumor model in nude mice. The PLL-USPIO-labeled hPMSCs at a concentration of 10  $\mu\text{g/ml}$  were prepared and transplanted into the experimental group colorectal cancer animal model through the tail vein of the rat; T2WI, T2mapping and T2\*mapping sequences were used to perform 3.0T magnetic resonance imaging before the injection of hPMSCs, 1, 3, 7, 10, 14 days after the injection of PMSCs, the MRI signal and tumor image changes of labeled hPMSCs in transplanted mice were dynamically observed, and the SNR, CNR and contrast (C value) of tumor tissues in each sequence were analyzed. Tumor specimens were stained with Prussian blue.

## RESULTS

The morphological and functional properties of the transplanted tumor are basically similar to the primary tumor, and the transplant success rate of the transplanted tumor is 100%, the USPIO labeled hPMSCs showed low signal in all 10 nude mouse models, the image contrast of tumor T2\*mapping sequence is greater than that of T2WI and T2 mapping sequence, and the display of USPIO-labeled cells is more obvious. Prussian blue staining was performed on the specimens of the experimental group: blue iron particles could be seen in the red tumor tissue.

## CONCLUSION

s It is confirmed that the nude mouse model of human colon cancer can be used for MRI in vivo imaging and the T2\*mapping value of the tissue can be used as a quantitative index for analysis.

## CLINICAL RELEVANCE/APPLICATION

Provide basic research data for the targeted therapy of placental mesenchymal stem cells in colorectal cancer.

Printed on: 02/07/23

## Abstract Archives of the RSNA, 2022

M5A-SPNMMI-1

### Role of 68Ga-DOTATOC PET for Pre-operative Prediction of DAXX/ATRX Loss of Expression and Histopathological Characteristics of Pancreatic Neuroendocrine Tumors

Monday, Nov. 28 12:15PM - 12:45PM Room: Learning Center - NMMI DPS

#### Participants

Paola Mapelli, Milan, Italy (*Presenter*) Nothing to Disclose

#### PURPOSE

To evaluate the role of 68Ga-DOTATOC PET parameters in predicting PanNET characteristics of aggressiveness before surgery.

#### METHODS AND MATERIALS

Retrospective study including 42 patients with well-differentiated PanNET (15 females, 27 males, median age: 60 years, range: 32-80) who underwent to 68Ga-DOTATOC PET for staging purpose. SUVmax, SUV mean, somatostatin receptor density (SRD) and total lesion somatostatin receptor density (TLSRD) were extracted from primary PanNET and radiological diameter (RD) was measured for each primary PanNET. Appropriate statistical analysis (see results) investigated the ability of imaging parameters predicting DAXX/ATRX loss of expression (LoE), infiltrative growth, microvascular invasion, perineural invasion, lymph node (LN) involvement, grade and presence of liver metastases.

#### RESULTS

Fourteen/42 PanNET patients had DAXX/ATRX LoE and 28/42 maintained the expression. Mann-Whitney U test: SUVmean predicted perineural invasion ( $p=0.049$ ) and grade ( $p=0.048$ ) and RD infiltrative growth ( $p=0.007$ ), DAXX/ATRX LoE ( $p=0.014$ ) and presence of liver metastases ( $p=0.005$ ). SRD and TLSRD correlated with Ki67 ( $p=0.047$  and  $0.028$ , respectively). Univariate logistic regression: SUVmax predicted LN involvement ( $p=0.045$ ), SRD and TLSRD predicted DAXX/ATRX LoE ( $p=0.044$  and  $0.0497$ , respectively) and presence of liver metastases ( $p=0.0314$  and  $p=0.0299$ , respectively); RD predicted DAXX/ATRX LoE ( $p=0.00614$ ), infiltrative growth ( $p=0.033$ ) and presence of liver metastases ( $p=0.0049$ ). ROC curve analysis: SUVmax and SUVmean predicted perineural invasion (AUC 0.672, 95%CI 0.50-0.82 and AUC 0.686, 95%CI 0.50-0.86, respectively). SUVmax was predictive of LN metastases (AUC 0.689, 95%CI: 0.52-0.84) and SUVmean of grade (AUC 0.682, 95%CI: 0.50-0.84). RD showed a role in predicting DAXX/ATRX LoE, infiltrative growth and liver metastases, with AUC of 0.735 (95%CI 0.54-0.89), 0.789 (95% CI 0.63-0.92) and 0.789 (95% CI 0.61-0.95), respectively.

#### CONCLUSION

s 68Ga-DOTATOC PET parameters showed predictive value in assessing DAXX/ATRX LoE and clinicopathological features of PanNET aggressiveness, thus providing additional information on PanNET behaviour in the preoperative setting.

#### CLINICAL RELEVANCE/APPLICATION

68Ga-DOTATOC PET parameters provide additional information on PanNET behaviour in the preoperative setting, thus improving tumour characterization.

Printed on: 02/07/23

## Abstract Archives of the RSNA, 2022

M5A-SPNMMI-2

### Prognostic Value of 18F-FDG-PET/CT Radiomics Combined with Sarcopenia Status among Patients with Advanced Gastroesophageal Cancer

Monday, Nov. 28 12:15PM - 12:45PM Room: Learning Center - NMMI DPS

#### Participants

Ricarda Hinzpeter, MD, Zurich, Switzerland (*Presenter*) Nothing to Disclose

#### PURPOSE

To investigate, whether 18F-FDG-PET/CT- derived radiomics combined with sarcopenia measurements improves survival prognostication among patients with advanced, metastatic gastroesophageal cancer.

#### METHODS AND MATERIALS

In this IRB-approved retrospective study, we included 128 consecutive patients with advanced, metastatic gastroesophageal cancer (n=128; 26 females; 102 males; mean age 63.5±11.7 years; age range: 29-91 years) undergoing 18F-FDG-PET/CT for staging between November 2008 and December 2019. Segmentation of the primary tumor and radiomics analysis derived from PET and CT images was performed semi-automatically with a commonly used open-source software platform (LIFEX, Version 6.30, lifexsoft.org). Patients' nutritional status was determined by measuring the skeletal muscle index (SMI) at the level of L3 on the CT component. Univariable and multivariable analyses were performed to establish a survival prediction model including radiomics, clinical data, and SMI score.

#### RESULTS

In a univariable Cox proportional hazards model, ECOG (<0.001) and distant metastasis to the bone (p=0,028) were significant clinical parameters for overall survival (OS) and progression free survival (PFS). Age (p=0.017) was an additional prognostic factor for OS. The multivariable analysis revealed improved overall survival prognostication when adding sarcopenic status, PET and CT radiomics to the model with clinical parameter only over a clinical course of 6 to 36 months (AUC 0.67 vs. 0.82 at 15 months). Similarly, adding sarcopenia measurements, PET and CT radiomics improved the model fit for PFS (AUC 0.65 vs. 0.82 at 12 months).

#### CONCLUSION

s PET and CT radiomics derived from 18F-FDG-PET/CT combined with sarcopenia measurements and clinical parameters may improve survival prediction among patients with advanced, metastatic gastroesophageal cancer.

#### CLINICAL RELEVANCE/APPLICATION

Increasing knowledge of outcome prognostication, derived from quantitative radiomics features, has the potential for pretreatment risk stratification, allowing clinicians to deliver more patient specific treatment tailored to individual risk.

Printed on: 02/07/23

## Abstract Archives of the RSNA, 2022

M5A-SPNMMI-3

### Feasibility of in Vivo MRI Imaging of Human Placental Mesenchymal Stem Cells Labeled With Ultramicro And < Superparamagnetic Iron Oxide Nanoparticles for Targeting Colorectal Cancer

Monday, Nov. 28 12:15PM - 12:45PM Room: Learning Center - NMMI DPS

#### Participants

Hua He, MMedSc, MMedSc, Yinchuan, China (*Presenter*) Nothing to Disclose

#### PURPOSE

To transplant human placenta-zoned mesenchymal stem cells (PMSCs) labeled with USPIO-PLL protein complex into nude mice model of implanted tumor, and to explore the feasibility of in vivo MRI imaging of PMSCs.

#### METHODS AND MATERIALS

Nude mice were inoculated with human colon cancer cells (HT-29), and then transplanted and passaged between mice to establish a human colon cancer transplanted tumor model in nude mice. The PLL-USPIO-labeled hPMSCs at a concentration of 10 µg/ml were prepared and transplanted into the experimental group colorectal cancer animal model through the tail vein of the rat; T2WI, T2mapping and T2\*mapping sequences were used to perform 3.0T magnetic resonance imaging before the injection of hPMSCs, 1, 3, 7, 10, 14 days after the injection of PMSCs, the MRI signal and tumor image changes of labeled hPMSCs in transplanted mice were dynamically observed, and the SNR, CNR and contrast (C value) of tumor tissues in each sequence were analyzed. Tumor specimens were stained with Prussian blue.

#### RESULTS

The morphological and functional properties of the transplanted tumor are basically similar to the primary tumor, and the transplant success rate of the transplanted tumor is 100%, the USPIO labeled hPMSCs showed low signal in all 10 nude mouse models, the image contrast of tumor T2\*mapping sequence is greater than that of T2WI and T2 mapping sequence, and the display of USPIO-labeled cells is more obvious. Prussian blue staining was performed on the specimens of the experimental group: blue iron particles could be seen in the red tumor tissue.

#### CONCLUSION

s It is confirmed that the nude mouse model of human colon cancer can be used for MRI in vivo imaging and the T2\*mapping value of the tissue can be used as a quantitative index for analysis.

#### CLINICAL RELEVANCE/APPLICATION

Provide basic research data for the targeted therapy of placental mesenchymal stem cells in colorectal cancer.

Printed on: 02/07/23



## Abstract Archives of the RSNA, 2022

M5A-SPNPM

### Noninterpretive Skills/Quality Improvement/Practice Management Monday Poster Discussions - A

Monday, Nov. 28 12:15PM - 12:45PM Room: Learning Center - NPM DPS

#### Participants

Peter D. Poulos, MD, Stanford, CA (*Moderator*) Nothing to Disclose  
Peter D. Poulos, MD, Stanford, CA (*Moderator*) Nothing to Disclose  
Madelene C. Lewis, MD, Mt Pleasant, SC (*Moderator*) Nothing to Disclose  
Madelene C. Lewis, MD, Mt Pleasant, SC (*Moderator*) Nothing to Disclose

#### Sub-Events

#### M5A-SPNPM-1 Diagnostic Accuracy of an Artificial Intelligence Software in Detecting Incidental Pulmonary Embolism

##### Participants

Madison Adams, MPH, Avon, CT (*Presenter*) Nothing to Disclose

#### PURPOSE

The aim of this study was to assess the diagnostic accuracy of an artificial intelligence-based decision support software in identifying incidental pulmonary emboli (IPE) on CT examinations of the chest and abdomen.

#### METHODS AND MATERIALS

This retrospective study reviewed all consecutive CT chest and CT abdomen and pelvis examinations ordered without a dedicated CT pulmonary angiogram (CTPA) protocol at one institution between September 20, 2021 and March 31, 2022. Triage and notification screening results of the IPE Module by Aidoc Medical were obtained for these non-angiographic CT examinations, indicating the presence or absence of IPE. The subsequent attending radiologists' interpretations for each of these studies were reviewed for the presence or absence of IPE, IPE laterality and location, and study indication. Sensitivity and specificity of the AI software were calculated, and descriptive statistics were used to further characterize the dataset.

#### RESULTS

2,651 CT examinations were analyzed within the study period, including 378 (14%) CTs of the chest and 2,273 (86%) CT scans of the abdomen and pelvis. There were 20 total IPEs (0.7%) identified by the AI software, 40% of which had concordant radiologist interpretations. There were 4 scans (0.1%) with IPEs identified by radiologists that were not detected by the AI software, including 2 scans with multiple, bilateral emboli. The software had a specificity of 0.9954 (95%CI 0.9953-0.9955) and sensitivity of 0.66 (95%CI 0.65-0.67). The 4 false-negative readings reported by the AI module were examinations ordered emergently for specific indications, including suspected aortic dissection, mesenteric ischemia, and intra-abdominal abscess.

#### CONCLUSION

Preliminary data from this institution demonstrate the AI screening software had a high specificity but low sensitivity when detecting IPEs. Higher sensitivity would be ideal when detecting incidental findings, especially when the AI-undetected IPEs in this study were identified on examinations ordered for specific clinical indications, and the radiologist may be less likely to anticipate PE in these scenarios. These results support AI modules currently serve as a reinforcement rather than a replacement for radiologists, improving quality control, and peer-review initiatives.

#### CLINICAL RELEVANCE/APPLICATION

Our data demonstrated increasing the sensitivity of the current IPE AI module would enhance the reliability of this product in triaging patients, notifying physicians, and initiating treatment.

#### M5A-SPNPM-2 Reporting of Participant Demographics in Articles Published in General Radiology Journals from 2013 to 2021

##### Participants

Marlee Parsons, MSc, MD, Montreal, QC (*Presenter*) Nothing to Disclose

#### PURPOSE

Reporting research participant demographics provides insight into representativeness. No previous study has assessed how demographics are reported in radiology research. We sought (1) to determine how frequently participant age, sex and/or gender, race and/or ethnicity, and socio-economic status (SES) are reported and analyzed in randomized clinical trials (RCT) or secondary analyses of RCT published in radiology journals and (2) to evaluate associations between demographics reporting and study characteristics.

#### METHODS AND MATERIALS

Articles presenting RCT and secondary analyses of RCT in human subjects published in the journals Academic Radiology, American Journal of Roentgenology, British Journal of Radiology, European Journal of Radiology, European Radiology, and Radiology between

2013 and 2021 identified on PubMed were included. The continent of the first and senior author, publication year, study design (RCT/secondary analysis, prospective/retrospective), funding status, subspecialty, topic, reporting of age, sex/gender, race/ethnicity, and SES, and analysis of results according to demographics were extracted. Journal impact factors were obtained from the Journal Citation Reports. Associations between the reporting of demographics and study characteristics were analyzed using chi-squared and Mann-Whitney U test for categorical and continuous variables, respectively.

## RESULTS

401 articles were included. Of those, 89% (355) reported age, 89% (358) sex/gender, 6% (23) race/ethnicity, and 3% (12) SES. Amongst articles that reported these demographics and were not specific to a population subgroup, results were analyzed by age in 14% (14/355), sex/gender in 18% (57/313), race/ethnicity in 9% (2/22), and SES in 33% (4/12). Age and sex/gender reporting was associated with first and last author continent, journal, impact factor, study design, and topic. Race/ethnicity and SES reporting was associated with first and last author continent, journal, impact factor, and funding status.

## CONCLUSION

s Participant age and sex/gender are frequently reported whereas race/ethnicity and SES are rarely reported in radiology research. It remains uncertain whether the current reporting practices are optimal.

## CLINICAL RELEVANCE/APPLICATION

Participant race/ethnicity and SES are rarely reported in radiology research, yet they can help inform generalizability. A consensus amongst our research community on when and how to report these demographics is needed.

## M5A-SPNPM-3 Pathway to the C-Suite: A Tristate Analysis of Radiology Representation in Academic Hospital Administration

Participants

Zachary Chung, BS, Elmont, NY (*Presenter*) Nothing to Disclose

## PURPOSE

To investigate the representation of radiologists within academic hospital leadership in New York, New Jersey, and Connecticut Tristate area compared to other subspecialties. Long-term, we hope this will lead to comparisons of graduate medical education (GME) to identify areas that can be modified or augmented in radiology training to encourage further representation in hospital leadership.

## METHODS AND MATERIALS

New York, New Jersey, and Connecticut Hospitals were selected from the DOH Health Profiles website. Teaching hospitals (medical school and resident education). Physician credentials including medical school training, residency training, specialty, as well as healthcare leadership roles were determined utilizing various publicly available databases and analyzed and categorized as demonstrated. Leadership designations/titles included CEO, CMO, CQO, CFO Physician-in-Chief, Chief-of-Staff. Given the arbitrary, non-standardized designation of leadership roles, a qualitative and limited quantitative approach was used to determine the factors associated with physician representation in institutional leadership.

## RESULTS

Of the 196 hospitals sampled, 282 physicians were identified as leaders in academic medical institutions or their respective healthcare systems. Median years experience post-residency was 29.5 yrs. Most common additional degree was MBA, followed by MPH, MHC. Primary Care: Total in Tristate workforce: 38.21%; Total in Academic Leadership: 37.94% Surgery/Surgical Sub-specialties: Total in Tristate workforce: 15.57%; Total in Academic Leadership: 16.31% Additional medical subspecialties: Total in Tristate workforce: 42.49%; Total in Academic Leadership: 43.61% Radiology: Total in Tristate workforce: 3.71%; Total in Academic Leadership: 2.13 %

## CONCLUSION

s In the NY/NJ/CT tristate area, radiologists represent a small fraction of the physician workforce (3.71%) and a significantly smaller portion of academic hospital leadership (2.13%) as opposed to their primary care, surgical, and other subspecialist counterparts. When juxtaposed to primary care, surgical, and other subspecialty counterparts, there is a clear deficit in representation.

## CLINICAL RELEVANCE/APPLICATION

These findings suggest that there is a significant opportunity for the field of radiology to focus on developing and training radiologists who can ascend to executive leadership positions within institutions. This is important because imaging is at the core of patient care and without adequate radiology hospital leadership representation, it may be more difficult to effectively advocate for high-quality imaging or adequate access to imaging modalities that could significantly impact patient outcomes.

Printed on: 02/07/23



## Abstract Archives of the RSNA, 2022

M5A-SPNPM-1

### Diagnostic Accuracy of an Artificial Intelligence Software in Detecting Incidental Pulmonary Embolism

Monday, Nov. 28 12:15PM - 12:45PM Room: Learning Center - NPM DPS

#### Participants

Madison Adams, MPH, Avon, CT (*Presenter*) Nothing to Disclose

#### PURPOSE

The aim of this study was to assess the diagnostic accuracy of an artificial intelligence-based decision support software in identifying incidental pulmonary emboli (IPE) on CT examinations of the chest and abdomen.

#### METHODS AND MATERIALS

This retrospective study reviewed all consecutive CT chest and CT abdomen and pelvis examinations ordered without a dedicated CT pulmonary angiogram (CTPA) protocol at one institution between September 20, 2021 and March 31, 2022. Triage and notification screening results of the IPE Module by Aidoc Medical were obtained for these non-angiographic CT examinations, indicating the presence or absence of IPE. The subsequent attending radiologists' interpretations for each of these studies were reviewed for the presence or absence of IPE, IPE laterality and location, and study indication. Sensitivity and specificity of the AI software were calculated, and descriptive statistics were used to further characterize the dataset.

#### RESULTS

2,651 CT examinations were analyzed within the study period, including 378 (14%) CTs of the chest and 2,273 (86%) CT scans of the abdomen and pelvis. There were 20 total IPEs (0.7%) identified by the AI software, 40% of which had concordant radiologist interpretations. There were 4 scans (0.1%) with IPEs identified by radiologists that were not detected by the AI software, including 2 scans with multiple, bilateral emboli. The software had a specificity of 0.9954 (95%CI 0.9953-0.9955) and sensitivity of 0.66 (95%CI 0.65-0.67). The 4 false-negative readings reported by the AI module were examinations ordered emergently for specific indications, including suspected aortic dissection, mesenteric ischemia, and intra-abdominal abscess.

#### CONCLUSION

Preliminary data from this institution demonstrate the AI screening software had a high specificity but low sensitivity when detecting IPEs. Higher sensitivity would be ideal when detecting incidental findings, especially when the AI-undetected IPEs in this study were identified on examinations ordered for specific clinical indications, and the radiologist may be less likely to anticipate PE in these scenarios. These results support AI modules currently serve as a reinforcement rather than a replacement for radiologists, improving quality control, and peer-review initiatives.

#### CLINICAL RELEVANCE/APPLICATION

Our data demonstrated increasing the sensitivity of the current IPE AI module would enhance the reliability of this product in triaging patients, notifying physicians, and initiating treatment.

Printed on: 02/07/23



## Abstract Archives of the RSNA, 2022

M5A-SPNPM-2

### Reporting of Participant Demographics in Articles Published in General Radiology Journals from 2013 to 2021

Monday, Nov. 28 12:15PM - 12:45PM Room: Learning Center - NPM DPS

#### Participants

Marlee Parsons, MSc, MD, Montreal, QC (*Presenter*) Nothing to Disclose

#### PURPOSE

Reporting research participant demographics provides insight into representativeness. No previous study has assessed how demographics are reported in radiology research. We sought (1) to determine how frequently participant age, sex and/or gender, race and/or ethnicity, and socio-economic status (SES) are reported and analyzed in randomized clinical trials (RCT) or secondary analyses of RCT published in radiology journals and (2) to evaluate associations between demographics reporting and study characteristics.

#### METHODS AND MATERIALS

Articles presenting RCT and secondary analyses of RCT in human subjects published in the journals Academic Radiology, American Journal of Roentgenology, British Journal of Radiology, European Journal of Radiology, European Radiology, and Radiology between 2013 and 2021 identified on PubMed were included. The continent of the first and senior author, publication year, study design (RCT/secondary analysis, prospective/retrospective), funding status, subspecialty, topic, reporting of age, sex/gender, race/ethnicity, and SES, and analysis of results according to demographics were extracted. Journal impact factors were obtained from the Journal Citation Reports. Associations between the reporting of demographics and study characteristics were analyzed using chi-squared and Mann-Whitney U test for categorical and continuous variables, respectively.

#### RESULTS

401 articles were included. Of those, 89% (355) reported age, 89% (358) sex/gender, 6% (23) race/ethnicity, and 3% (12) SES. Amongst articles that reported these demographics and were not specific to a population subgroup, results were analyzed by age in 14% (14/355), sex/gender in 18% (57/313), race/ethnicity in 9% (2/22), and SES in 33% (4/12). Age and sex/gender reporting was associated with first and last author continent, journal, impact factor, study design, and topic. Race/ethnicity and SES reporting was associated with first and last author continent, journal, impact factor, and funding status.

#### CONCLUSION

s Participant age and sex/gender are frequently reported whereas race/ethnicity and SES are rarely reported in radiology research. It remains uncertain whether the current reporting practices are optimal.

#### CLINICAL RELEVANCE/APPLICATION

Participant race/ethnicity and SES are rarely reported in radiology research, yet they can help inform generalizability. A consensus amongst our research community on when and how to report these demographics is needed.

Printed on: 02/07/23



## Abstract Archives of the RSNA, 2022

MSA-SPNPM-3

### Pathway to the C-Suite: A Tristate Analysis of Radiology Representation in Academic Hospital Administration

Monday, Nov. 28 12:15PM - 12:45PM Room: Learning Center - NPM DPS

#### Participants

Zachary Chung, BS, Elmont, NY (*Presenter*) Nothing to Disclose

#### PURPOSE

To investigate the representation of radiologists within academic hospital leadership in New York, New Jersey, and Connecticut Tristate area compared to other subspecialties. Long-term, we hope this will lead to comparisons of graduate medical education (GME) to identify areas that can be modified or augmented in radiology training to encourage further representation in hospital leadership.

#### METHODS AND MATERIALS

New York, New Jersey, and Connecticut Hospitals were selected from the DOH Health Profiles website. Teaching hospitals (medical school and resident education). Physician credentials including medical school training, residency training, specialty, as well as healthcare leadership roles were determined utilizing various publicly available databases and analyzed and categorized as demonstrated. Leadership designations/titles included CEO, CMO, CQO, CFO Physician-in-Chief, Chief-of-Staff. Given the arbitrary, non-standardized designation of leadership roles, a qualitative and limited quantitative approach was used to determine the factors associated with physician representation in institutional leadership.

#### RESULTS

Of the 196 hospitals sampled, 282 physicians were identified as leaders in academic medical institutions or their respective healthcare systems. Median years experience post-residency was 29.5 yrs. Most common additional degree was MBA, followed by MPH, MHCM. Primary Care: Total in Tristate workforce: 38.21%; Total in Academic Leadership: 37.94% Surgery/Surgical Sub-specialties: Total in Tristate workforce: 15.57%; Total in Academic Leadership: 16.31% Additional medical subspecialties: Total in Tristate workforce: 42.49%; Total in Academic Leadership: 43.61% Radiology: Total in Tristate workforce: 3.71%; Total in Academic Leadership: 2.13 %

#### CONCLUSION

In the NY/NJ/CT tristate area, radiologists represent a small fraction of the physician workforce (3.71%) and a significantly smaller portion of academic hospital leadership (2.13%) as opposed to their primary care, surgical, and other subspecialist counterparts. When juxtaposed to primary care, surgical, and other subspecialty counterparts, there is a clear deficit in representation.

#### CLINICAL RELEVANCE/APPLICATION

These findings suggest that there is a significant opportunity for the field of radiology to focus on developing and training radiologists who can ascend to executive leadership positions within institutions. This is important because imaging is at the core of patient care and without adequate radiology hospital leadership representation, it may be more difficult to effectively advocate for high-quality imaging or adequate access to imaging modalities that could significantly impact patient outcomes.

Printed on: 02/07/23

## Abstract Archives of the RSNA, 2022

M5A-SPNR

### Neuroradiology Monday Poster Discussions - A

Monday, Nov. 28 12:15PM - 12:45PM Room: Learning Center - NR DPS

#### Sub-Events

#### M5A-SPNR-1 Non-invasive Prediction of IDH Mutation Status in Gliomas Using Pre-operative Multi-parametric MRI Radiomics Nomogram: A Multi-center Study

Participants

Jun Lu, (*Presenter*) Nothing to Disclose

#### PURPOSE

Accurate identification of IDH mutation status has revolutionized our understanding of the potential for targeted therapeutics using small molecule IDH mutation inhibitors with the update of 2021 WHO classification criterion of gliomas, which might be clinically meaningful for treatment strategy and prognosis stratification of gliomas. This study aimed to establish and validate a radiomics nomogram for predicting IDH mutation status in gliomas using preoperative multiparametric MRI in a multicenter setting.

#### METHODS AND MATERIALS

306 gliomas patients in local institution were enrolled and randomly assigned into a training (n=214) and a test dataset (n=92). 108 patients were collected from TCGA as an independent external validation dataset. The volume of interest (VOI) was delineated manually on the map of contrast-enhanced T1-weighted (CE-T1W) and fluid attenuated inversion recovery (FLAIR). 851 radiomics features were extracted on each VOI. The features were firstly selected using Mann-Whitney U-test, followed by refining using least absolute shrinkage and selection operator (LASSO) regression combining 10-fold cross-validation. The optimal radiomics features with age and sex were processed by multivariate logistic regression to construct a prediction model, which was developed in the training dataset and assessed in the test and external validation datasets. Receiver operating characteristic (ROC), calibration curve and decision curve analysis were applied in the test and external validation datasets to evaluate the discrimination, calibration and clinical utility of prediction model.

#### RESULTS

Ten robust radiomics features were selected from the 1702 features (four CE-T1W and six FLAIR features). A nomogram was plotted to represent the prediction model. The accuracy and AUC of the radiomics nomogram achieved 86.96% and 0.891(0.809-0.947) and 84.26% and 0.881(0.805-0.936) in the test and external validation dataset (all  $p < 0.05$ ). The positive predictive value (PPV) and negative predictive value (NPV) were 83.72%, 87.75% and 87.81%, 82.09% in the test and external validation dataset. The Hosmer-Lemeshow test concluded that the radiomics nomogram showed goodness of fit (all  $p > 0.05$ ). Decision curve analysis demonstrated the clinical value of the radiomics nomogram.

#### CONCLUSION

IDH genotypes of gliomas can be identified by preoperative multiparametric MRI radiomics nomogram and might be clinically meaningful for treatment strategy and prognosis stratification of gliomas.

#### CLINICAL RELEVANCE/APPLICATION

This study aimed to find imaging biomarkers for noninvasively predicting the IDH mutation status for a tailored treatment plan and prognosis stratification in glioma patients from the initial stage of the tumor diagnosis.

#### M5A-SPNR-10 Extent of Resection of Contrast-enhancing and Non-enhancing Tumor - Different Impacts on Survival According to Types of Adult-type Diffuse Gliomas in 2021 WHO Classification

Participants

Sung Soo Ahn, MD, Seoul, Korea, Republic Of (*Presenter*) Nothing to Disclose

#### PURPOSE

To evaluate the impact of extent of resection (EOR) of contrast-enhancing (CE) and nonenhancing (NE) tumors in the types of adult-type diffuse gliomas according to the 2021 WHO classification.

#### METHODS AND MATERIALS

Total 1,196 patients with adult-type diffuse gliomas diagnosed between 2001 and 2021 from a single institution were enrolled (183 patients with IDH-mutant and 1p/19q codeleted oligodendroglioma [herein oligodendroglioma], 211 patients with IDH-mutant astrocytoma, and 802 patients with IDH-wildtype glioblastoma). Multivariable Cox analyses were performed within each type to assess predictors of overall survival, including clinical, imaging data, histological grade, MGMT promoter methylation status, treatment, and EOR of CE and NE tumors. Subgroup analyses were performed in patients with CE tumor. N

#### RESULTS

Among 1,196 patients, 926 (77.4%) patients had CE tumors. In oligodendrogliomas, EOR of NE was not associated with survival (HR

Among 1,120 patients, 520 (46.4%) patients had CE tumors. In oligodendrogliomas, GTR of NE was not associated with survival (HR = 0.41, 95% CI 0.14-1.15, P = 0.088). In 81 (43.3%) oligodendroglioma patients with CE tumor, GTR of CE tumors was the only independent predictor of survival (HR = 0.20, 95% CI 0.05-0.85, P = 0.029) in multivariable analysis. GTR of NE and CE tumors was independently associated with better survival in IDH-mutant astrocytoma and IDH-wildtype glioblastoma (all Ps <0.05) in multivariable analyses.

## CONCLUSION

s GTR of both CE and NE tumors may significantly improve survival within all types of adult-type diffuse gliomas except oligodendrogliomas. In oligodendrogliomas, the EOR of CE tumor may be crucial in survival; aggressive GTR of NE tumor may be unnecessary, whereas GTR of the CE tumor is recommended.

## CLINICAL RELEVANCE/APPLICATION

This study is the first, to our knowledge, to examine the independent role of EOR in both CE and NE tumors across types in adult-type diffuse gliomas according to the 2021 WHO classification. Well-known predictors for survival such as clinical, radiological, and MGMT promoter methylation status were included in the Cox analysis, to demonstrate the independent role of EOR. Our results pave the way for rethinking surgical strategies according to types of adult-type diffuse gliomas.

## M5A-SPNR-11 Application of Brain Tumour Reporting and Data System (BT-RADS) in A Large Population with High-grade Gliomas (HGG) Exhibiting Progression (PD) and Pseudo progression (PSPD) and Correlation with Survival Analysis

Participants  
Ankush Jajodia, MD, MBBS, New Delhi, India (*Presenter*) Nothing to Disclose

## PURPOSE

HGG accounts for approximately 60% of all primary brain tumors. BT-RADS assigns each MRI to study a score or category based on imaging findings. PsPD is an effect usually occurring in the first six months after chemoradiation (CRT), with reported incidence ranging from 2-50%. We investigated the utility of BT-RADS applications in a large population of patients with HGG with PD and PsPD.

## METHODS AND MATERIALS

After institutional review board approval, a retrospective analysis was performed on 437 patients with HGG who underwent Gadolinium-enhanced MRI between 2013-and 2021. Patients were labeled as having PD or PsPD after multidisciplinary team evaluation. Typically we called pseudoprogression as progression on early scans, that stabilizes without further anti cancer therapy vs progression as continual progression. The clinical outcome (dichotomized as stable or worse) was collected from medical records. An experienced neuroradiologist did the BT-RADS category assignment. Kaplan Meier survival analysis and Chi-square test between different groups were done using MedCalc software.

## RESULTS

Two hundred and thirteen patients with HGG after exclusion (Figure1) were included. PsPD (n=109) and PD (n=104) were determined in a multidisciplinary care team after evaluation of clinical information and follow-up imaging. BT-RADS category assignment between the PD and PsPD group and the final clinical outcome dichotomized group (worse and stable) was statistically significant (table). KS survival analysis of BT-RADS assignment during follow-up with the final clinical result is shown in figure 2.

## CONCLUSION

s BT-RADS has a significant correlation with survival and can be an imperative tool for response assessment, especially in resource-constrained setup.

## CLINICAL RELEVANCE/APPLICATION

BT-RADS implementation has the potential to increase the completeness, consistency, and comprehensibility of radiology reports in patients with glioma. This preliminary work summarizes the initial experience and emphasizes its effectiveness in a large subset of patients with HGG.

## M5A-SPNR-12 Analyzing Treatment Response of Recurrent Pediatric Low-Grade Gliomas in Clinical Trials: Comparison of Volumetric and Two-Dimensional Tumor Assessment

Participants  
Ryan C. Bahar, BSc, Yale School of Medicine, New Haven, CT (*Presenter*) Nothing to Disclose

## PURPOSE

The Response Assessment in Neuro-Oncology (RANO) criteria were designed to radiologically evaluate tumor response and endpoints in clinical trials of novel treatments. These criteria estimate tumor size using the two-dimensional (2D) product of maximal perpendicular diameters on axial slices of MR images. Pediatric low-grade gliomas (pLGGs), however, are intratumorally heterogeneous with solid and cystic components. 2D measurements may therefore misevaluate pLGG tumor volume and tumor response, and ultimately affect trial outcome. This study aims to assess tumor response using volumetric assessment of recurrent and progressive pLGGs treated with everolimus. We seek to identify clinically relevant criteria that provide added value to response assessment beyond 2D measurements.

## METHODS AND MATERIALS

Using multiparametric MR imaging from 44 patients in the Pediatric Neuro-Oncology Consortium (PNO) 001 clinical trial, we performed 3D-segmentation of solid, cystic, and whole pLGGs within our PACS-framework to assess tumor response. We compared our results to those from a prior independent central imaging review which had yielded 15 (34%) patients showing progressive disease (PD), 27 (61%) stable disease (SD), 2 (5%) partial response (PR), and 0 (0%) complete response (CR).

## RESULTS

8 (18%) of the 44 tumors were solid-only and 36 (82%) had a mixed solid-cystic appearance. Comparing 2D central imaging review to our volumetric tumor evaluation using the same RANO cutoff criteria, 7 (16%) cases changed from PD to SD, 3 (7%) from SD to

PD, 1 (2%) from SD to PR, and 1 (2%) from PR to SD, constituting an overall discordance in 12 (27%) cases.

## CONCLUSION

s Integration of volumetrics into tumor response assessments provides additional and potentially more accurate information than strictly 2D RANO-based measurements. It is crucial to note that the above-reported changes in assessed tumor response represent numerical discrepancies as opposed to true-to-reality changes in clinical outcome. Determining representative thresholds for the deployment of volumetric measures in clinical trials will be critical. Future work will include data from the PNOC-002 clinical trial and evaluate inter-reader agreement and reader discordance.

## CLINICAL RELEVANCE/APPLICATION

With the availability of PACS-based 3D tools in neuroradiology practice, well-defined volumetric criteria could be incorporated prospectively to enhance tumor response analysis in clinical trials.

### M5A-SPNR-13 SMART Syndrome and Variants: From Clinical Presentation to Imaging: How to Arrive At the Diagnosis

Participants  
Denver Pinto, MD, Miami, FL (*Presenter*) Nothing to Disclose

## PURPOSE

SMART (Stroke-like migraine attacks after radiation therapy) syndrome is a rare clinical-radiological entity characterized by complex neurologic symptoms which may occur years following radiation therapy. The imaging features resemble a subacute infarct, hence, an incorrect diagnosis may lead to unnecessary imaging and treatment. This presentation will help the audience to identify SMART syndrome and to avoid misdiagnosis. We describe and illustrate a small series of SMART cases with the purpose of identifying the varied clinical and imaging features.

## METHODS AND MATERIALS

We conducted a database search involving 3 health systems for cases of SMART syndrome and for "subacute infarcts" in patients status post radiation. We found 7 patients who could be classified as having SMART syndrome or a variant of it based on history, clinical symptoms, clinical follow-up and comparison with prior/follow-up imaging.

## RESULTS

There were 5 patients with features typical of the SMART syndrome and 2 patients with atypical presentations consistent with peri-ictal pseudo-progression (PIPG). All patients had radiation therapy 1.5 years to 25 years before presentation. The most common clinical symptoms were headache (6/7) and seizures (5/7). Cranial nerve involvement (5/7), motor deficits/extremity weakness (3/7) and sensory deficits (2/7) were identified on examination. MRI findings included cortical and subcortical edema, as well as sub-arachnoid, gyriform, parenchymal and punctate contrast enhancement with elevated rCBV. Diffusion restriction in a focal or gyriform pattern was identified both in the typical presentation and in PIPG. Patients with PIPG showed more avid cortical and meningeal enhancement [RQ1] even the absence of headache (1/2). rCBV was reduced in one of our patients with PIPG. In one of our patients, the imaging changes occurred in the radiation field on the side opposite the surgery and another patient had bilateral findings. This symptom-imaging complex occurred following treatment of a wide range of benign and malignant tumors.

## CONCLUSION

s SMART syndrome is a diagnostic confounder that can have undesirable downstream effects if misdiagnosed. MRI findings such as gyriform diffusion restriction, cortical and vasogenic edema as well as cortical or meningeal enhancement in a non-vascular distribution in concert with the clinical information such as the location and time since radiation delivery helps suggest the proper diagnosis.

## CLINICAL RELEVANCE/APPLICATION

Decisions relative to continuing or withholding anti-neoplastic therapy may depend on recognizing this entity. Also a confident diagnosis will prevent extensive and unnecessary stroke or seizure work up because the imaging features may resemble either of these conditions.

### M5A-SPNR-14 Vascular Habitats analysis Based on Preoperative Dynamic Susceptibility-weighted Contrast Perfusion MRI Predicts Recurrence Pattern in High-grade Gliomas

Participants  
Hanwei Wang, (*Presenter*) Nothing to Disclose

## PURPOSE

To evaluate if vascular habitats analysis based on preoperative dynamic susceptibility-weighted contrast perfusion MRI predicts recurrence pattern in high-grade gliomas (WHO grade 3-4, HGG).

## METHODS AND MATERIALS

In this single-center, retrospective study, we included adults with HGG, who received chemoradiotherapy and were diagnosed with recurrence based on RANO criteria or resurgical pathology. A neurosurgeon and a neuroradiologist based on preoperative and follow-up MRI images of patients, classified recurrence patterns into local recurrence (LR) and non-local recurrence (NLR). The LR was further divided into intra-surgical cavity recurrence (ICR) and extra-surgical cavity recurrence (ECR). Kaplan-meier curves were used to analyze the PFS and OS of patients with LR and NLR, ICR recurrence and ECR. And log-rank test was used to compare the differences in patient survival. Based on ONCOhabitats platform (<https://www.oncohabitats.upv.es>) hemodynamic tissue signature (HTS) method automatic segmentation of vascular habitats, evaluate each vascular habitats in the 95th percentile rCBV, rCBF value. Univariate and multivariate logistic regression analysis were used to evaluate the correlation between vascular habitats parameters and recurrence patterns, and to determine the predictors. The prediction efficiency of relevant factors were computed by receiver operating characteristics curve (ROC) and the area under curve (AUC).

## RESULTS

77 HGG were included in this study, of which 60 (77.92%) with LR and 17 (22.08%) with NLR. The LR was divided into ICR (30,

38.96%) and ECR (30, 38.96%). PFS and OS were longer in the LR than in the NLR ( $p < 0.05$ ). There was no significant difference in PFS and OS between ICR and ECR ( $p > 0.05$ ). In univariate logistic regression analysis, rCBVp95 at LAT (OR=2.084 ,95%CI=1.198-3.626), rCBVp95 at IPE (OR=2.840 ,95%CI=1.213-6.648), rCBVp95 at VPE (OR=3.598 ,95%CI=1.256-10.308) and rCBFp95 at VPE (OR=3.793 ,95%CI=1.172-12.270) correlated with ECR. Multivariate logistic regression analysis revealed rCBVp95 at LAT could be used as a predictor of ECR (OR=2.317,95%CI:1.264-4.246, $p=0.007$ ). ROC curve showed that the prediction efficiency is good (AUC=0.743,95%CI=0.614-0.847).

## CONCLUSION

s Preoperative vascular habitats parameters can be used as noninvasive imaging markers to predict ECR, and provide reference for the management and treatment of HGG.

## CLINICAL RELEVANCE/APPLICATION

Preoperative vascular habitats parameters can be used as noninvasive imaging markers to predict extra-surgical cavity recurrence, and provide reference for the management and treatment of high-grade gliomas.

## M5A-SPNR-15 Neuroimaging Findings in Patients with Immune Effector Cell-associated Neurotoxicity Syndrome after CAR-T-cell Therapy

Participants  
Burak Akkurt, MD, Muenster, Germany (*Presenter*) Nothing to Disclose

## PURPOSE

Chimeric antigen receptor T-cell therapy (CART) is a new immunomodulating therapy of relapsed/refractory hematological malignancies, capable of inducing an immune response against tumor cells. CART often comes with relevant organ toxicities, one of which is referred to as immune effector cell-associated neurotoxicity syndrome (ICANS). Symptoms of ICANS are heterogenous and include headache, confusion and encephalopathy. In this study we evaluated ICANS associated neuroimaging findings in cerebral magnetic resonance imaging (cMRI).

## METHODS AND MATERIALS

We reviewed all patients, who received CART infusion at our university hospital between 12/2018 and 09/2021. From the initial 32 patients, 11 received cerebral imaging due to suspected or diagnosed ICANS within a follow-up time of up to 30 days after infusion. Of these 11 patients, 2 presented with ICANS grade I, 5 with ICANS grade 2, and 4 with ICANS grade 3. The routine cMRI images of patients were reviewed by two neuroradiologists with an experience of 3 and 9 years. We correlated the imaging findings with the clinical grading according to ICANS.

## RESULTS

We observed FLAIR hyperintense signal alterations in most cases with pericallosal involvement (5/11, 45 %). Furthermore, we noticed FLAIR hyperintense signal changes in the forceps minor in 5 out of 11 patients (45 %). Other locations of FLAIR alterations were noticed in the capsula interna, foliae cerebelli, thalami, as well as temporal and subsular regions (each in 1 case). We correlated the imaging findings with the clinical grading of the ICANS. According to literature, only ICANS grade =3 shows changes on MRI. However, in our cohort we observed white matter changes in all of our patients with ICANS grades =2 .

## CONCLUSION

s ICANS may show subtle changes on cMRI, with FLAIR hyperintense white matter changes being the most prevalent ones. In our cohort, we found signal alterations in all patients graded ICANS =2. Our findings suggest FLAIR hyperintense signal changes in the forceps minor as a possible specific sign of neurotoxicity after CART, but further prospective evaluation with a larger cohort should be aimed at for confirmation.

## CLINICAL RELEVANCE/APPLICATION

ICANS is one of the major toxicities associated with CAR-T-cell therapy and neuroimaging can help identifying ICANS and should be evaluated in suspected cases.

## M5A-SPNR-16 Magnetic Resonance Imaging and Amino Acid Positron Emission Tomography in Differentiating Tumor Recurrence from Radiation Necrosis in High Grade Gliomas.

Participants  
Antariksh Vijan, MBBS, Mumbai, India (*Presenter*) Nothing to Disclose

## PURPOSE

Differentiating tumor recurrence (TR) from radiation necrosis (RN) in high-grade glioma (HGG) following radiotherapy can be challenging. The ability of conventional magnetic resonance imaging (MRI) to differentiate TR from post-therapeutic effects is often limited. Multiparametric advanced MRI (perfusion) and positron emission tomography (PET) with amino acid tracers, specifically 18F-Fluoroethyl-Tyrosine (FET) can provide relevant additional information on tumor metabolism, which allows for a more accurate diagnosis to differentiate tumor recurrence from radiation necrosis in HGG.

## METHODS AND MATERIALS

Retrospective analysis of 69 lesions in 69 patients with HGG who underwent both MRI and FET-PET imaging within three weeks intervals was done independently by a neuroradiologist and nuclear medicine physician. The study was conducted in the department of radiodiagnosis in a tertiary care oncology center between July 2018 and August 2021. Manually segmented regions of interest were placed over the areas of maximum enhancement/suspicion on MRI and FET uptake, which were used to calculate the rCBV and tumor to white-matter ratios, respectively. Definitive diagnosis (TR versus RN) was made on clinico-radiological follow-up or histopathological report (wherever available).

## RESULTS

Out of the 69 lesions that were studied, 52 and 13 had TR and RN, respectively. 4 cases were excluded from the study as they were lost to follow-up. The rCBV<sub>mean</sub> (mean relative CBV) and mean target-to-background ratios showed an accuracy of 94% and 80% for MRI and FET-PET respectively in the detection of recurrent lesions. The sensitivity and specificity for determination of TR

in HGG with conventional MRI were 98% and 77% respectively, while with FET-PET it was 79% and 85% respectively. A combination of MRI and PET parameters (mean target-to-background ratio), demonstrated an increase in diagnostic accuracy to 98%. A rCBVmax cutoff > 1.48 had a positive predictive value for recurrence of 97.92%. The sensitivity and specificity of rCBV values for determination of TR in treated cases of HGG were 90.38% and 87.50% respectively.

## CONCLUSION

s Cumulative imaging with MRI and FET-PET offers a multiparametric assessment of glioma recurrence that is correlative and complimentary, with higher accuracy and clinical value.

## CLINICAL RELEVANCE/APPLICATION

This study analyses the individual and combined diagnostic performance of MR and amino acid PET to distinguish recurrence from radiation necrosis in treated cases of gliomas.

## M5A-SPNR-17 Critical Information Provided by PACS Based Peritumoral Edema Volumetrics in Assessment of Lung Cancer Brain Metastases after Gamma Knife Therapy

Participants  
Manpreet Kaur, BSc, New Haven, CT (*Presenter*) Nothing to Disclose

## PURPOSE

Gamma Knife (GK) has become standard of care to locally treat BM, however there is insufficient understanding of the natural posttreatment volumetric changes of peritumoral edema of BM due to paucity of tools for volumetric segmentation in neuroradiology practice. Recently PACS-integrated tools have become available in select clinical practices therefore we aimed to compare volumetric response curves of peritumoral edema to response curves of RANO-BM based measurements.

## METHODS AND MATERIALS

Patients with NSCLC BM with longest diameter greater or equal to 10mm on CE-T1WI that were treated with GK were included. Volumetric measurements were performed for up to 7 follow-up studies using a PACS-integrated tool that segments the FLAIR hyperintense volume surrounding the CE lesion. The 2D and volumetric measurements were analyzed using Prism9 and clinical information including steroid timing were incorporated in the assessment.

## RESULTS

41 NSCLC BM were included (59±10 years, 20 pts). The median pretreatment metastasis volume was 8.52cm<sup>3</sup> (IQR 1.01-47.03cm<sup>3</sup>). A significant decrease was measured at 0-90 days post-GK (median 1.16cm<sup>3</sup>, IQR 0.51-6.12cm<sup>3</sup>). The time of peak median peritumoral volume increase was after 365 days post-GK (median 1.42cm<sup>3</sup>, IQR 0.37-8.12cm<sup>3</sup>). There was a significant positive correlation between longest diameter and peritumoral edema volume (r=.75). At 181-270 days post-GK 50% of BM showed an incongruent course of response curves for longest diameter and peritumoral volume. 60% of these lesions could be classified as partial response. The congruence to incongruence ratio of edema to enhancing portion of BM changed over follow-up time.

## CONCLUSION

s Volumetric edema assessment of BM post-GK provides critical additional information as compared to RANO-BM based response curves.

## CLINICAL RELEVANCE/APPLICATION

In the follow-up assessment of BM after GK we recommend including both volumetric response curves of peritumoral edema and CE portion of BM.

## M5A-SPNR-19 Application of Electrical Properties Tomography to Ischemic Stroke: Comparison of Conductivity between Infarct and Contralateral Brain

Participants  
Seong Woo Cho, Hwasun, Korea, Republic Of (*Presenter*) Nothing to Disclose

## PURPOSE

Ischemic stroke is one of the most important causes of neurological morbidity and mortality in the world and remains to be the leading cause of death and disability [1]. Electrical Properties Tomography (EPT) is a new MRI technique that delivers information on tissue electrical properties [2,3]. The aim of this study was to explore the feasibility of using EPT on ischemic stroke and compared the conductivity between infarct and contralateral brain.

## METHODS AND MATERIALS

Twenty-seven patients who presented with acute stroke at a tertiary stroke centre were included in this study. The patients consisted of 19 males and 8 females (mean age=73.75, range=54~90). The EPT data were acquired using a balanced-Fast Field Echo (b-FFE) sequence (TR/TE = 3/1.62 ms, flip angle=30°, pixel size=1.15×1.15×2 mm) from a clinical 3T scanner (Philips, Amsterdam). The EPT data were reconstructed using the previously described method [4]. The conductivity (s) map was quantified and compared between 4 different regions: basal ganglia thalamus (n=10), cerebral hemisphere (n=11), pons (n=5), and cerebellum (n=2).

## RESULTS

The ischemic lesions demonstrated a significantly higher mean conductivity value (0.93 ± 0.097 S/m) than the contralateral brain tissue (0.83 ± 0.095 S/m, p=0.00004). Both basal ganglia thalamus and cerebral hemisphere demonstrated significantly higher levels of conductivity (0.88 ± 0.1 S/m and 0.97 ± 0.097 S/m, respectively) than their contralateral normal brain tissues (0.78 ± 0.093 S/m, p=0.00009 for basal ganglia thalamus and 0.83 ± 0.046 S/m, p=0.0008 for cerebral hemisphere, respectively). The mean lesion basal ganglia thalamus (0.88 ± 0.1 S/m) conductivity value were significantly lower (p < 0.05) than the cerebral hemisphere (0.97 ± 0.09 S/m). The mean contralateral conductivity value in both basal ganglia thalamus (0.78 ± 0.09 S/m, p=0.009) and cerebral hemisphere (0.83 ± 0.05 S/m, p=0.04) were significantly lower than the combined pons and cerebellum (0.92 ± 0.1 S/m).

## CONCLUSION

s The ischemic lesion exhibited significantly higher conductivity values than the contralateral brain tissue in the cerebral brain, while the pons and cerebellum showed similar levels of conductivity values between the lesion and contralateral brain. Interestingly, the levels of conductivity were significantly different between the contralateral normal tissue of supra- and infra-tentorial brains. The results from this study warrant further investigation of this method with a broader range of patients with stroke.

#### CLINICAL RELEVANCE/APPLICATION

This preliminary study demonstrated the feasibility of acquiring EPT from stroke patients and evaluating conductivities in lesion and normal brain. This new imaging contrast may provide an extra value on ischemic stroke.

#### M5A-SPNR-20 IDH-wild type Glioblastoma: Imaging Independent Predictors of Gross Total Resection (GTR) Using the VASARI Feature Set and Tumoral Volumetric Measurements

Participants

Luis Nunez, MD, Houston, TX (*Presenter*) Nothing to Disclose

#### PURPOSE

The aim of this study is to assess the impact of preoperative imaging phenotypes to determine predictors of gross total resection (GTR) using the Visually Accessible Rembrandt Images lexicon (VASARI) and tumoral volumetry measurements

#### METHODS AND MATERIALS

A single center, retrospective study of a prospectively maintained database of 167 patients with GBMs was performed. Fourteen patients (8%) with IDH mutation and 2 subjects (1.1%) with incomplete data were excluded. Among the 146 patients, 85 (59%) were male with a mean age of 59 years (SD +/- 13.6 years). MRI findings were assessed using the VASARI feature set and semi-automated tumoral segmentation. Univariate analysis was performed using X<sup>2</sup>/Fisher's exact test with Monte Carlo simulation for categorical variables and non-parametric analysis with the Mann-Whitney U test for continuous variables. Multivariate analysis was performed using the Logistic regression analysis test and receiver operating characteristic curve (ROC)

#### RESULTS

In total, 79 patients (55%) underwent GTR, 15 (10%) near-total resection (NTR) and 50 (35%) subtotal resection (STR). Out of the 25 VASARI criteria, 4 characteristics were found to be associated with GTR, as follows: 39 GBMs (49%) were in non-eloquent areas ( $p=0.04$ ), 59 (75%) had thick enhancing margins ( $p=0.04$ ), 64 (81%) had no ependymal invasion ( $p=0.02$ ) and 48 (61%) had no deep white matter invasion ( $p=0.03$ ). Additionally, GBMs with GTR were found to have lower tumoral volumes (121 ml [IQR, 51.7-174 ml] versus 163.9 ml [IQR, 121.9-215.3 ml] ( $p<0.01$ ), lower FLAIR volumes (98 ml [IQR, 40.2-134 ml] versus 127 ml [IQR, 87-167 ml] ( $p<0.01$ ), and lower enhancing volumes (14.5 ml [IQR, 8.3-24.7 ml] versus 28.6 ml [IQR, 14.2-42 ml] ( $p<0.01$ ). Logistic regression model demonstrated that thickness of enhancing margins is the only independent predictor of non-gross total resection (odds ratio: 1.57 [95% CI, 1.1-2.2]) ( $p=0.01$ ). ROC analysis of our multivariate model demonstrated an AUC estimate of 0.75 with a sensitivity of 60% and a specificity of 91%

#### CONCLUSION

s Imaging characteristics on standard-of-care (SOC) MR scans may predict gross total resection of GBMs wild-type. Furthermore, thickness of enhancing margins was the only significant predictor of GTR after multivariate analysis. Additionally, a diagnostic model that includes a combination of the discriminating depicted features on SOC MR scans and volumetric measurements, demonstrated to have an acceptable diagnostic performance with a specificity greater than 90%

#### CLINICAL RELEVANCE/APPLICATION

Higher survival rates are seen among glioblastoma patients that undergo gross-total resection (GTR). Our study provides information that m will help to determine prognosis of patients with wild type glioblastomas.

#### M5A-SPNR-3 Study on Cranial Bone Marrow Conversion of High Altitude Polycythemia

Participants

Hai Hua Bao, Xining, China (*Presenter*) Nothing to Disclose

#### PURPOSE

High altitude polycythemia (HAPC) is a chronic disease caused by excessive compensatory proliferation of erythrocytes in the hypoxia environment at high altitude. The disease commonly affects multiple systems throughout the body, leading to an abnormal increase in hemoglobin concentration and red blood cell count. This study aimed to investigate the characteristics of cranial bone marrow conversion in patients with high altitude polycythemia based on conventional magnetic resonance imaging (MRI) and diffusion-weighted imaging (DWI).

#### METHODS AND MATERIALS

30 patients with high altitude polycythemia were included in the experimental group, aged (47.96 ±9.65) years, living at an altitude of (3155 ±736.98) m, with hemoglobin (216.57 ±11.10m) g/mL. 30 healthy subjects matched with the HAPC group in age and living altitude were included as the control group, aged (48.17±8.28) years, living altitude (3124.41±567.36) m, HGB(155.53±18.19) g/mL. The ADC values of the frontal bone, parietal bone, occipital bone and temporal bone were measured at Philips post-processing workstation, and the characteristics of cranial bone marrow conversion in patients with high altitude polycythemia were statistically analyzed.

#### RESULTS

There was no significant difference in age and living altitude between the two groups. Compared with the control group, the hemoglobin (HGB), red blood cell count (RBC) and hematocrit (HCT) in the HAPC group were significantly higher than those in the control group, as shown in Table 1. The ADC values of parietal bone and occipital bone in THE HAPC group were (0.88±0.30) ×10<sup>-3</sup>mm<sup>2</sup>/s and (1.37±0.27) ×10<sup>-3</sup>mm<sup>2</sup>/s, both higher than those in the control group ( $P<0.05$ ), with statistical differences. The ADC values of the frontal bone and temporal bone in THE HAPC group were (1.09±0.24) ×10<sup>-3</sup>mm<sup>2</sup>/s and (1.36±0.27) ×10<sup>-3</sup>mm<sup>2</sup>/s, respectively, which were higher than those in the control group ( $P>0.05$ ). The differences were not statistically significant, as shown in Table 2.

## CONCLUSION

s Under the condition of long-term hypoxia in HAPC, the bone marrow of parietal bone and occipital bone was erythromedularized. This suggests that long-term chronic hypoxia may induce bone marrow erythromyelization, resulting in HAPC.

## CLINICAL RELEVANCE/APPLICATION

Hypoxia is the main cause of altitude sickness. High altitude polycythemia (HAPC) is a common disease threatening people's health in the plateau, which can cause damage to multiple organs. We believe that imaging to explore cranial bone marrow conversion of HAPC patients compared with normal controls may provide an essential basis for understanding bone marrow erythromyelization induced by chronic hypoxia.

## M5A-SPNR-4 Intravoxel Incoherent Motion (IVIM) May Help Distinguishing Gliomas and Solitary Brain Metastasis: A Multi-parameter Magnetic Resonance Imaging Study

Participants

Yifei Su, MS, (*Presenter*) Nothing to Disclose

## PURPOSE

The aim of this study is to investigate the value of diffusion, perfusion and chemical exchange saturation transfer MR imaging in differentiating the gliomas and metastases.

## METHODS AND MATERIALS

65 patients pathologically newly diagnosed gliomas or metastases were enrolled and all were conducted the diffusion weighted imaging, intravoxel incoherent motion (IVIM), and amide proton transfer-weighted (APT) imaging as well as the T1W, T2W, T2FLAIR and enhanced T1W imaging in a 3.0T MR scanner (Discovery MR 750w; GE, Milwaukee, USA). The images were imported to the iQuant software (GE Healthcare, Beijing, China) to calculate parametric maps including the apparent diffusion coefficient from DWI (ADC), diffusion coefficient (D), perfusion fraction (f), pseudo-diffusion coefficient (D\*) from IVIM and the MTRasym (3.5 ppm) from APT imaging. The tumor parenchyma was delineated wherever possible in 3dslicer (<https://www.slicer.org/>, version 4.10). Quantitative values of 10 percentile, 90 percentile, entropy, kurtosis, mean and skewness in parametric maps for region of interest (ROI) were extracted with the pyradiomics plugin and compared. Logistics regression and receiver operator curves (ROC) analysis were performed to explore the independent factors and optimal model. R packages were used for all the statistics (version 4.0.0).

## RESULTS

44 patients were diagnosed as glioma (males:25, females:10, age range: 20-79y), and 21 cases were diagnosed as metastasis (males:10, females:11, age range: 34-80y) from the pathological analysis. No significant difference was observed in clinical manifestations (Table 1). There were significant differences for ADC kurtosis ( $6.43\pm 5.63$  vs.  $4.54\pm 3.23$ ,  $p=0.02$ ), MTRasym (3.5ppm) 10 percentile ( $0.53\pm 0.97$  vs.  $1.00\pm 0.75$ ,  $p=0.05$ ), f 90 percentile ( $23.07\pm 5.14$  vs.  $28.67\pm 5.51$ ,  $p<0.01$ ), f entropy ( $56.00\pm 33.08$  vs.  $85.20\pm 33.08$ ,  $p<0.01$ ), f kurtosis ( $67.56\pm 40.75$  vs.  $39.08\pm 142.84$ ,  $p<0.01$ ), and f mean ( $13.92\pm 2.50$  vs.  $17.38\pm 3.84$ ,  $p<0.01$ ) between gliomas and metastases groups (Table 2). The f kurtosis (OR = 0.66, 95% CI 0.48-0.92,  $p=0.02$ ), and f mean (OR = 1.44, 95% CI 1.16-1.18,  $p<0.01$ ) were found the independent factors for metastases differentiation in logistic regression analysis (Table 3). The AUC of model combined with age, IVIM-f kurtosis and IVIM-f mean was 0.83 while the AUC of model combined with IVIM-f kurtosis and IVIM-f mean with improved sensitivity was 0.81 with no significant difference under Delong test ( $p=0.58$ ). (Table 4, Figure 1).

## CONCLUSION

s The IVIM-f kurtosis and IVIM-f mean demonstrated the differences in perfusion characteristics of gliomas and metastases.

## CLINICAL RELEVANCE/APPLICATION

Accurate identification of these two kinds of tumors will largely benefit the therapy.

## M5A-SPNR-5 Evaluation of RANO Criteria for Assessment of Tumor Progression for Lower-grade Gliomas

Participants

Fabio Raman, MD, PhD, (*Presenter*) Nothing to Disclose

## PURPOSE

The Response Assessment in Neuro-Oncology (RANO) criteria for lower-grade gliomas (LGGs) defines tumor progression as  $\geq 25\%$  change in T2/FLAIR signal based on an operator's discretion of the perpendicular diameter of the largest tumor cross-section. Potential sources of error include limitation of 2D quantification, operator selection of both tumor cross-section and perpendicular parameters, and inability to quantify satellite tumor components. Our goal was to assess accuracy and reproducibility of RANO.

## METHODS AND MATERIALS

651 FLAIR MRIs from 63 participants with LGGs at the University of Alabama at Birmingham were retrospectively analyzed by 3 blinded attending physicians and 3 blinded resident trainees using RANO, 2D visual, and 3D computer-assisted volumetric assessment. Inter- and intra-operator reproducibility was assessed using Pearson correlation, Bland Altman, and Cohen's kappa. Accuracy assessment was performed by comparing RANO to either visual or volumetric assessment, where 2/3 consensus agreement across operators was required to meet RANO and visual growth criteria for a particular tumor measurement. Volumetric assessment was performed by statistical change-of-point method. RANO assessment was performed compared to both previous and baseline scan.

## RESULTS

RANO product measurements had moderate inter-operator reproducibility [ $r_2 = 0.71 - 0.82$ , coefficient of variance (CV) = 81 - 110%), mean percent difference (diff) = 0.4 - 46.8%] and intra-operator reproducibility ( $r_2 = 0.71 - 0.88$ , CV = 31 - 58%, diff = 0.3 - 23.9%, Figure A-B). When comparing to 2D visual gold standard, accuracy of RANO compared to previous and baseline scans were 66.7% and 65.1% with AUC of 0.67 and 0.66, respectively (Figure C). When comparing to volumetric gold standard, accuracy of RANO compared to previous and baseline scans were 21.0% and 48.4% with AUC of 0.39 and 0.55, respectively (Figure D). Median time delay at diagnosis was greater for false negative cases (RANO detected growth after volumetric) than for false positive

cases (RANO growth detected earlier) for RANO assessment compared to previous scan (2.05 > 0.50 years,  $p = 0.003$ ) and baseline scan (1.08 > 0.50 years,  $p = 0.02$ , Figure E).

#### **CONCLUSION**

s RANO has moderate reproducibility and poor accuracy when comparing to either visual or volumetric gold standards.

#### **CLINICAL RELEVANCE/APPLICATION**

Limitations of the RANO criteria for LGGs suggest novel approaches, such as computer-assisted diagnostic tools, are necessary to reduce human variability and accurately assess 3D tumor progression.

Printed on: 02/07/23

## Abstract Archives of the RSNA, 2022

M5A-SPNR-1

### Non-invasive Prediction of IDH Mutation Status in Gliomas Using Pre-operative Multi-parametric MRI Radiomics Nomogram: A Multi-center Study

Monday, Nov. 28 12:15PM - 12:45PM Room: Learning Center - NR DPS

#### Participants

Jun Lu, (*Presenter*) Nothing to Disclose

#### PURPOSE

Accurate identification of IDH mutation status has revolutionized our understanding of the potential for targeted therapeutics using small molecule IDH mutation inhibitors with the update of 2021 WHO classification criterion of gliomas, which might be clinically meaningful for treatment strategy and prognosis stratification of gliomas. This study aimed to establish and validate a radiomics nomogram for predicting IDH mutation status in gliomas using preoperative multiparametric MRI in a multicenter setting.

#### METHODS AND MATERIALS

306 gliomas patients in local institution were enrolled and randomly assigned into a training (n=214) and a test dataset (n=92). 108 patients were collected from TCGA as an independent external validation dataset. The volume of interest (VOI) was delineated manually on the map of contrast-enhanced T1-weighted (CE-T1W) and fluid attenuated inversion recovery (FLAIR). 851 radiomics features were extracted on each VOI. The features were firstly selected using Mann-Whitney U-test, followed by refining using least absolute shrinkage and selection operator (LASSO) regression combining 10-fold cross-validation. The optimal radiomics features with age and sex were processed by multivariate logistic regression to construct a prediction model, which was developed in the training dataset and assessed in the test and external validation datasets. Receiver operating characteristic (ROC), calibration curve and decision curve analysis were applied in the test and external validation datasets to evaluate the discrimination, calibration and clinical utility of prediction model.

#### RESULTS

Ten robust radiomics features were selected from the 1702 features (four CE-T1W and six FLAIR features). A nomogram was plotted to represent the prediction model. The accuracy and AUC of the radiomics nomogram achieved 86.96% and 0.891 (0.809-0.947) and 84.26% and 0.881 (0.805-0.936) in the test and external validation dataset (all  $p < 0.05$ ). The positive predictive value (PPV) and negative predictive value (NPV) were 83.72%, 87.75% and 87.81%, 82.09% in the test and external validation dataset. The Hosmer-Lemeshow test concluded that the radiomics nomogram showed goodness of fit (all  $p > 0.05$ ). Decision curve analysis demonstrated the clinical value of the radiomics nomogram.

#### CONCLUSION

s IDH genotypes of gliomas can be identified by preoperative multiparametric MRI radiomics nomogram and might be clinically meaningful for treatment strategy and prognosis stratification of gliomas .

#### CLINICAL RELEVANCE/APPLICATION

This study aimed to find imaging biomarkers for noninvasively predicting the IDH mutation status for a tailored treatment plan and prognosis stratification in glioma patients from the initial stage of the tumor diagnosis.

Printed on: 02/07/23

## Abstract Archives of the RSNA, 2022

MSA-SPNR-10

### Extent of Resection of Contrast-enhancing and Non-enhancing Tumor - Different Impacts on Survival According to Types of Adult-type Diffuse Gliomas in 2021 WHO Classification

Monday, Nov. 28 12:15PM - 12:45PM Room: Learning Center - NR DPS

#### Participants

Sung Soo Ahn, MD, Seoul, Korea, Republic Of (*Presenter*) Nothing to Disclose

#### PURPOSE

To evaluate the impact of extent of resection (EOR) of contrast-enhancing (CE) and nonenhancing (NE) tumors in the types of adult-type diffuse gliomas according to the 2021 WHO classification.

#### METHODS AND MATERIALS

Total 1,196 patients with adult-type diffuse gliomas diagnosed between 2001 and 2021 from a single institution were enrolled (183 patients with IDH-mutant and 1p/19q codeleted oligodendroglioma [herein oligodendroglioma], 211 patients with IDH-mutant astrocytoma, and 802 patients with IDH-wildtype glioblastoma). Multivariable Cox analyses were performed within each type to assess predictors of overall survival, including clinical, imaging data, histological grade, MGMT promoter methylation status, treatment, and EOR of CE and NE tumors. Subgroup analyses were performed in patients with CE tumor. N

#### RESULTS

Among 1,196 patients, 926 (77.4%) patients had CE tumors. In oligodendrogliomas, GTR of NE was not associated with survival (HR = 0.41, 95% CI 0.14-1.15, P = 0.088). In 81 (43.3%) oligodendroglioma patients with CE tumor, GTR of CE tumors was the only independent predictor of survival (HR = 0.20, 95% CI 0.05-0.85, P = 0.029) in multivariable analysis. GTR of NE and CE tumors was independently associated with better survival in IDH-mutant astrocytoma and IDH-wildtype glioblastoma (all Ps <0.05) in multivariable analyses.

#### CONCLUSION

s GTR of both CE and NE tumors may significantly improve survival within all types of adult-type diffuse gliomas except oligodendrogliomas. In oligodendrogliomas, the EOR of CE tumor may be crucial in survival; aggressive GTR of NE tumor may be unnecessary, whereas GTR of the CE tumor is recommended.

#### CLINICAL RELEVANCE/APPLICATION

This study is the first, to our knowledge, to examine the independent role of EOR in both CE and NE tumors across types in adult-type diffuse gliomas according to the 2021 WHO classification. Well-known predictors for survival such as clinical, radiological, and MGMT promoter methylation status were included in the Cox analysis, to demonstrate the independent role of EOR. Our results pave the way for rethinking surgical strategies according to types of adult-type diffuse gliomas.

Printed on: 02/07/23

## Abstract Archives of the RSNA, 2022

M5A-SPNR-11

### Application of Brain Tumour Reporting and Data System (BT-RADS) in A Large Population with High-grade Gliomas (HGG) Exhibiting Progression (PD) and Pseudo progression (PSPD) and Correlation with Survival Analysis

Monday, Nov. 28 12:15PM - 12:45PM Room: Learning Center - NR DPS

#### Participants

Ankush Jajodia, MD, MBBS, New Delhi, India (*Presenter*) Nothing to Disclose

#### PURPOSE

HGG accounts for approximately 60% of all primary brain tumors. BT-RADS assigns each MRI to study a score or category based on imaging findings. PsPD is an effect usually occurring in the first six months after chemoradiation (CRT), with reported incidence ranging from 2-50%. We investigated the utility of BT-RADS applications in a large population of patients with HGG with PD and PsPD.

#### METHODS AND MATERIALS

After institutional review board approval, a retrospective analysis was performed on 437 patients with HGG who underwent Gadolinium-enhanced MRI between 2013-and 2021. Patients were labeled as having PD or PsPD after multidisciplinary team evaluation. Typically we called pseudoprogession as progression on early scans, that stabilizes without further anti cancer therapy vs progression as continual progression. The clinical outcome (dichotomized as stable or worse) was collected from medical records. An experienced neuroradiologist did the BT-RADS category assignment. Kaplan Meier survival analysis and Chi-square test between different groups were done using MedCalc software.

#### RESULTS

Two hundred and thirteen patients with HGG after exclusion (Figure1) were included. PsPD (n=109) and PD (n=104) were determined in a multidisciplinary care team after evaluation of clinical information and follow-up imaging. BT-RADS category assignment between the PD and PsPD group and the final clinical outcome dichotomized group (worse and stable) was statistically significant (table). KS survival analysis of BT-RADS assignment during follow-up with the final clinical result is shown in figure 2.

#### CONCLUSION

s BT-RADS has a significant correlation with survival and can be an imperative tool for response assessment, especially in resource-constrained setup.

#### CLINICAL RELEVANCE/APPLICATION

BT-RADS implementation has the potential to increase the completeness, consistency, and comprehensibility of radiology reports in patients with glioma. This preliminary work summarizes the initial experience and emphasizes its effectiveness in a large subset of patients with HGG.

Printed on: 02/07/23

## Abstract Archives of the RSNA, 2022

M5A-SPNR-12

### Analyzing Treatment Response of Recurrent Pediatric Low-Grade Gliomas in Clinical Trials: Comparison of Volumetric and Two-Dimensional Tumor Assessment

Monday, Nov. 28 12:15PM - 12:45PM Room: Learning Center - NR DPS

#### Participants

Ryan C. Bahar, BSc, Yale School of Medicine, New Haven, CT (*Presenter*) Nothing to Disclose

#### PURPOSE

The Response Assessment in Neuro-Oncology (RANO) criteria were designed to radiologically evaluate tumor response and endpoints in clinical trials of novel treatments. These criteria estimate tumor size using the two-dimensional (2D) product of maximal perpendicular diameters on axial slices of MR images. Pediatric low-grade gliomas (pLGGs), however, are intratumorally heterogeneous with solid and cystic components. 2D measurements may therefore miscalculate pLGG tumor volume and tumor response, and ultimately affect trial outcome. This study aims to assess tumor response using volumetric assessment of recurrent and progressive pLGGs treated with everolimus. We seek to identify clinically relevant criteria that provide added value to response assessment beyond 2D measurements.

#### METHODS AND MATERIALS

Using multiparametric MR imaging from 44 patients in the Pediatric Neuro-Oncology Consortium (PNOC) 001 clinical trial, we performed 3D-segmentation of solid, cystic, and whole pLGGs within our PACS-framework to assess tumor response. We compared our results to those from a prior independent central imaging review which had yielded 15 (34%) patients showing progressive disease (PD), 27 (61%) stable disease (SD), 2 (5%) partial response (PR), and 0 (0%) complete response (CR).

#### RESULTS

8 (18%) of the 44 tumors were solid-only and 36 (82%) had a mixed solid-cystic appearance. Comparing 2D central imaging review to our volumetric tumor evaluation using the same RANO cutoff criteria, 7 (16%) cases changed from PD to SD, 3 (7%) from SD to PD, 1 (2%) from SD to PR, and 1 (2%) from PR to SD, constituting an overall discordance in 12 (27%) cases.

#### CONCLUSION

Integration of volumetrics into tumor response assessments provides additional and potentially more accurate information than strictly 2D RANO-based measurements. It is crucial to note that the above-reported changes in assessed tumor response represent numerical discrepancies as opposed to true-to-reality changes in clinical outcome. Determining representative thresholds for the deployment of volumetric measures in clinical trials will be critical. Future work will include data from the PNOC-002 clinical trial and evaluate inter-reader agreement and reader discordance.

#### CLINICAL RELEVANCE/APPLICATION

With the availability of PACS-based 3D tools in neuroradiology practice, well-defined volumetric criteria could be incorporated prospectively to enhance tumor response analysis in clinical trials.

Printed on: 02/07/23

## Abstract Archives of the RSNA, 2022

M5A-SPNR-13

### SMART Syndrome and Variants: From Clinical Presentation to Imaging: How to Arrive At the Diagnosis

Monday, Nov. 28 12:15PM - 12:45PM Room: Learning Center - NR DPS

#### Participants

Denver Pinto, MD, Miami, FL (*Presenter*) Nothing to Disclose

#### PURPOSE

SMART (Stroke-like migraine attacks after radiation therapy) syndrome is a rare clinical-radiological entity characterized by complex neurologic symptoms which may occur years following radiation therapy. The imaging features resemble a subacute infarct, hence, an incorrect diagnosis may lead to unnecessary imaging and treatment. This presentation will help the audience to identify SMART syndrome and to avoid misdiagnosis. We describe and illustrate a small series of SMART cases with the purpose of identifying the varied clinical and imaging features.

#### METHODS AND MATERIALS

We conducted a database search involving 3 health systems for cases of SMART syndrome and for "subacute infarcts" in patients status post radiation. We found 7 patients who could be classified as having SMART syndrome or a variant of it based on history, clinical symptoms, clinical follow-up and comparison with prior/follow-up imaging.

#### RESULTS

There were 5 patients with features typical of the SMART syndrome and 2 patients with atypical presentations consistent with peri-ictal pseudo-progression (PIPG). All patients had radiation therapy 1.5 years to 25 years before presentation. The most common clinical symptoms were headache (6/7) and seizures (5/7). Cranial nerve involvement (5/7), motor deficits/extremity weakness (3/7) and sensory deficits (2/7) were identified on examination. MRI findings included cortical and subcortical edema, as well as sub-arachnoid, gyriform, parenchymal and punctate contrast enhancement with elevated rCBV. Diffusion restriction in a focal or gyriform pattern was identified both in the typical presentation and in PIPG. Patients with PIPG showed more avid cortical and meningeal enhancement [RQ1] even the absence of headache (1/2). rCBV was reduced in one of our patients with PIPG. In one of our patients, the imaging changes occurred in the radiation field on the side opposite the surgery and another patient had bilateral findings. This symptom-imaging complex occurred following treatment of a wide range of benign and malignant tumors.

#### CONCLUSION

s SMART syndrome is a diagnostic confounder that can have undesirable downstream effects if misdiagnosed. MRI findings such as gyriform diffusion restriction, cortical and vasogenic edema as well as cortical or meningeal enhancement in a non-vascular distribution in concert with the clinical information such as the location and time since radiation delivery helps suggest the proper diagnosis.

#### CLINICAL RELEVANCE/APPLICATION

Decisions relative to continuing or withholding anti-neoplastic therapy may depend on recognizing this entity. Also a confident diagnosis will prevent extensive and unnecessary stroke or seizure work up because the imaging features may resemble either of these conditions.

Printed on: 02/07/23

## Abstract Archives of the RSNA, 2022

M5A-SPNR-14

### Vascular Habitats analysis Based on Preoperative Dynamic Susceptibility-weighted Contrast Perfusion MRI Predicts Recurrence Pattern in High-grade Gliomas

Monday, Nov. 28 12:15PM - 12:45PM Room: Learning Center - NR DPS

#### Participants

Hanwei Wang, (*Presenter*) Nothing to Disclose

#### PURPOSE

To evaluate if vascular habitats analysis based on preoperative dynamic susceptibility-weighted contrast perfusion MRI predicts recurrence pattern in high-grade gliomas (WHO grade 3-4, HGG).

#### METHODS AND MATERIALS

In this single-center, retrospective study, we included adults with HGG, who received chemoradiotherapy and were diagnosed with recurrence based on RANO criteria or resurgical pathology. A neurosurgeon and a neuroradiologist based on preoperative and follow-up MRI images of patients, classified recurrence patterns into local recurrence (LR) and non-local recurrence (NLR). The LR was further divided into intra-surgical cavity recurrence (ICR) and extra-surgical cavity recurrence (ECR). Kaplan-meier curves were used to analyze the PFS and OS of patients with LR and NLR, ICR recurrence and ECR. And log-rank test was used to compare the differences in patient survival. Based on ONCOhabitats platform (<https://www.oncohabitats.upv.es>) hemodynamic tissue signature (HTS) method automatic segmentation of vascular habitats, evaluate each vascular habitats in the 95th percentile rCBV, rCBF value. Univariate and multivariate logistic regression analysis were used to evaluate the correlation between vascular habitats parameters and recurrence patterns, and to determine the predictors. The prediction efficiency of relevant factors were computed by receiver operating characteristics curve (ROC) and the area under curve (AUC).

#### RESULTS

77 HGG were included in this study, of which 60 (77.92%) with LR and 17 (22.08%) with NLR. The LR was divided into ICR (30, 38.96%) and ECR (30, 38.96%). PFS and OS were longer in the LR than in the NLR ( $p < 0.05$ ). There was no significant difference in PFS and OS between ICR and ECR ( $p > 0.05$ ). In univariate logistic regression analysis, rCBVp95 at LAT (OR=2.084, 95%CI=1.198-3.626), rCBVp95 at IPE (OR=2.840, 95%CI=1.213-6.648), rCBVp95 at VPE (OR=3.598, 95%CI=1.256-10.308) and rCBFp95 at VPE (OR=3.793, 95%CI=1.172-12.270) correlated with ECR. Multivariate logistic regression analysis revealed rCBVp95 at LAT could be used as a predictor of ECR (OR=2.317, 95%CI: 1.264-4.246,  $p = 0.007$ ). ROC curve showed that the prediction efficiency is good (AUC=0.743, 95%CI=0.614-0.847).

#### CONCLUSION

s Preoperative vascular habitats parameters can be used as noninvasive imaging markers to predict ECR, and provide reference for the management and treatment of HGG.

#### CLINICAL RELEVANCE/APPLICATION

Preoperative vascular habitats parameters can be used as noninvasive imaging markers to predict extra-surgical cavity recurrence, and provide reference for the management and treatment of high-grade gliomas.

Printed on: 02/07/23

## Abstract Archives of the RSNA, 2022

M5A-SPNR-15

### Neuroimaging Findings in Patients with Immune Effector Cell-associated Neurotoxicity Syndrome after CAR-T-cell Therapy

Monday, Nov. 28 12:15PM - 12:45PM Room: Learning Center - NR DPS

#### Participants

Burak Akkurt, MD, Muenster, Germany (*Presenter*) Nothing to Disclose

#### PURPOSE

Chimeric antigen receptor T-cell therapy (CART) is a new immunomodulating therapy of relapsed/refractory hematological malignancies, capable of inducing an immune response against tumor cells. CART often comes with relevant organ toxicities, one of which is referred to as immune effector cell-associated neurotoxicity syndrome (ICANS). Symptoms of ICANS are heterogenous and include headache, confusion and encephalopathy. In this study we evaluated ICANS associated neuroimaging findings in cerebral magnetic resonance imaging (cMRI).

#### METHODS AND MATERIALS

We reviewed all patients, who received CART infusion at our university hospital between 12/2018 and 09/2021. From the initial 32 patients, 11 received cerebral imaging due to suspected or diagnosed ICANS within a follow-up time of up to 30 days after infusion. Of these 11 patients, 2 presented with ICANS grade 1, 5 with ICANS grade 2, and 4 with ICANS grade 3. The routine cMRI images of patients were reviewed by two neuroradiologists with an experience of 3 and 9 years. We correlated the imaging findings with the clinical grading according to ICANS.

#### RESULTS

We observed FLAIR hyperintense signal alterations in most cases with pericallosal involvement (5/11, 45 %). Furthermore, we noticed FLAIR hyperintense signal changes in the forceps minor in 5 out of 11 patients (45 %). Other locations of FLAIR alterations were noticed in the capsula interna, foliae cerebelli, thalami, as well as temporal and subinsular regions (each in 1 case). We correlated the imaging findings with the clinical grading of the ICANS. According to literature, only ICANS grade =3 shows changes on MRI. However, in our cohort we observed white matter changes in all of our patients with ICANS grades =2 .

#### CONCLUSION

s ICANS may show subtle changes on cMRI, with FLAIR hyperintense white matter changes being the most prevalent ones. In our cohort, we found signal alterations in all patients graded ICANS =2. Our findings suggest FLAIR hyperintense signal changes in the forceps minor as a possible specific sign of neurotoxicity after CART, but further prospective evaluation with a larger cohort should be aimed at for confirmation.

#### CLINICAL RELEVANCE/APPLICATION

ICANS is one of the major toxicities associated with CAR-T-cell therapy and neuroimaging can help identifying ICANS and should be evaluated in suspected cases.

Printed on: 02/07/23

## Abstract Archives of the RSNA, 2022

M5A-SPNR-16

### **Magnetic Resonance Imaging and Amino Acid Positron Emission Tomography in Differentiating Tumor Recurrence from Radiation Necrosis in High Grade Gliomas.**

Monday, Nov. 28 12:15PM - 12:45PM Room: Learning Center - NR DPS

#### **Participants**

Antariksh Vijan, MBBS, Mumbai, India (*Presenter*) Nothing to Disclose

#### **PURPOSE**

Differentiating tumor recurrence (TR) from radiation necrosis (RN) in high-grade glioma (HGG) following radiotherapy can be challenging. The ability of conventional magnetic resonance imaging (MRI) to differentiate TR from post-therapeutic effects is often limited. Multiparametric advanced MRI (perfusion) and positron emission tomography (PET) with amino acid tracers, specifically 18F-Fluoroethyl-Tyrosine (FET) can provide relevant additional information on tumor metabolism, which allows for a more accurate diagnosis to differentiate tumor recurrence from radiation necrosis in HGG.

#### **METHODS AND MATERIALS**

Retrospective analysis of 69 lesions in 69 patients with HGG who underwent both MRI and FET-PET imaging within three weeks intervals was done independently by a neuroradiologist and nuclear medicine physician. The study was conducted in the department of radiodiagnosis in a tertiary care oncology center between July 2018 and August 2021. Manually segmented regions of interest were placed over the areas of maximum enhancement/suspicion on MRI and FET uptake, which were used to calculate the rCBV and tumor to white-matter ratios, respectively. Definitive diagnosis (TR versus RN) was made on clinico-radiological follow-up or histopathological report (wherever available).

#### **RESULTS**

Out of the 69 lesions that were studied, 52 and 13 had TR and RN, respectively. 4 cases were excluded from the study as they were lost to follow-up. The rCBV<sub>mean</sub> (mean relative CBV) and mean target-to-background ratios showed an accuracy of 94% and 80% for MRI and FET-PET respectively in the detection of recurrent lesions. The sensitivity and specificity for determination of TR in HGG with conventional MRI were 98% and 77% respectively, while with FET-PET it was 79% and 85% respectively. A combination of MRI and PET parameters (mean target-to-background ratio), demonstrated an increase in diagnostic accuracy to 98%. A rCBV<sub>max</sub> cutoff > 1.48 had a positive predictive value for recurrence of 97.92%. The sensitivity and specificity of rCBV values for determination of TR in treated cases of HGG were 90.38% and 87.50% respectively.

#### **CONCLUSION**

s Cumulative imaging with MRI and FET-PET offers a multiparametric assessment of glioma recurrence that is correlative and complimentary, with higher accuracy and clinical value.

#### **CLINICAL RELEVANCE/APPLICATION**

This study analyses the individual and combined diagnostic performance of MR and amino acid PET to distinguish recurrence from radiation necrosis in treated cases of gliomas.

Printed on: 02/07/23

## Abstract Archives of the RSNA, 2022

M5A-SPNR-17

### Critical Information Provided by PACS Based Peritumoral Edema Volumetrics in Assessment of Lung Cancer Brain Metastases after Gamma Knife Therapy

Monday, Nov. 28 12:15PM - 12:45PM Room: Learning Center - NR DPS

#### Participants

Manpreet Kaur, BSc, New Haven, CT (*Presenter*) Nothing to Disclose

#### PURPOSE

Gamma Knife (GK) has become standard of care to locally treat BM, however there is insufficient understanding of the natural posttreatment volumetric changes of peritumoral edema of BM due to paucity of tools for volumetric segmentation in neuroradiology practice. Recently PACS-integrated tools have become available in select clinical practices therefore we aimed to compare volumetric response curves of peritumoral edema to response curves of RANO-BM based measurements.

#### METHODS AND MATERIALS

Patients with NSCLC BM with longest diameter greater or equal to 10mm on CE-T1WI that were treated with GK were included. Volumetric measurements were performed for up to 7 follow-up studies using a PACS-integrated tool that segments the FLAIR hyperintense volume surrounding the CE lesion. The 2D and volumetric measurements were analyzed using Prism9 and clinical information including steroid timing were incorporated in the assessment.

#### RESULTS

41 NSCLC BM were included (59±10 years, 20 pts). The median pretreatment metastasis volume was 8.52cm<sup>3</sup> (IQR 1.01-47.03cm<sup>3</sup>). A significant decrease was measured at 0-90 days post-GK (median 1.16cm<sup>3</sup>, IQR 0.51-6.12cm<sup>3</sup>). The time of peak median peritumoral volume increase was after 365 days post-GK (median 1.42cm<sup>3</sup>, IQR 0.37-8.12cm<sup>3</sup>). There was a significant positive correlation between longest diameter and peritumoral edema volume ( $r=.75$ ). At 181-270 days post-GK 50% of BM showed an incongruent course of response curves for longest diameter and peritumoral volume. 60% of these lesions could be classified as partial response. The congruence to incongruence ratio of edema to enhancing portion of BM changed over follow-up time.

#### CONCLUSION

s Volumetric edema assessment of BM post-GK provides critical additional information as compared to RANO-BM based response curves.

#### CLINICAL RELEVANCE/APPLICATION

In the follow-up assessment of BM after GK we recommend including both volumetric response curves of peritumoral edema and CE portion of BM.

Printed on: 02/07/23

## Abstract Archives of the RSNA, 2022

M5A-SPNR-19

### Application of Electrical Properties Tomography to Ischemic Stroke: Comparison of Conductivity between Infarct and Contralateral Brain

Monday, Nov. 28 12:15PM - 12:45PM Room: Learning Center - NR DPS

#### Participants

Seong Woo Cho, Hwasun, Korea, Republic Of (*Presenter*) Nothing to Disclose

#### PURPOSE

Ischemic stroke is one of the most important causes of neurological morbidity and mortality in the world and remains to be the leading cause of death and disability [1]. Electrical Properties Tomography (EPT) is a new MRI technique that delivers information on tissue electrical properties [2,3]. The aim of this study was to explore the feasibility of using EPT on ischemic stroke and compared the conductivity between infarct and contralateral brain.

#### METHODS AND MATERIALS

Twenty-seven patients who presented with acute stroke at a tertiary stroke centre were included in this study. The patients consisted of 19 males and 8 females (mean age=73.75, range=54~90). The EPT data were acquired using a balanced-Fast Field Echo (b-FFE) sequence (TR/TE = 3/1.62 ms, flip angle=30°, pixel size=1.15×1.15×2 mm) from a clinical 3T scanner (Philips, Amsterdam). The EPT data were reconstructed using the previously described method [4]. The conductivity (s) map was quantified and compared between 4 different regions: basal ganglia thalamus (n=10), cerebral hemisphere (n=11), pons (n=5), and cerebellum (n=2).

#### RESULTS

The ischemic lesions demonstrated a significantly higher mean conductivity value ( $0.93 \pm 0.097$  S/m) than the contralateral brain tissue ( $0.83 \pm 0.095$  S/m,  $p=0.00004$ ). Both basal ganglia thalamus and cerebral hemisphere demonstrated significantly higher levels of conductivity ( $0.88 \pm 0.1$  S/m and  $0.97 \pm 0.097$  S/m, respectively) than their contralateral normal brain tissues ( $0.78 \pm 0.093$  S/m,  $p=0.00009$  for basal ganglia thalamus and  $0.83 \pm 0.046$  S/m,  $p=0.0008$  for cerebral hemisphere, respectively). The mean lesion basal ganglia thalamus ( $0.88 \pm 0.1$  S/m) conductivity value were significantly lower ( $p < 0.05$ ) than the cerebral hemisphere ( $0.97 \pm 0.09$  S/m). The mean contralateral conductivity value in both basal ganglia thalamus ( $0.78 \pm 0.09$  S/m,  $p=0.009$ ) and cerebral hemisphere ( $0.83 \pm 0.05$  S/m,  $p=0.04$ ) were significantly lower than the combined pons and cerebellum ( $0.92 \pm 0.1$  S/m).

#### CONCLUSION

s The ischemic lesion exhibited significantly higher conductivity values than the contralateral brain tissue in the cerebral brain, while the pons and cerebellum showed similar levels of conductivity values between the lesion and contralateral brain. Interestingly, the levels of conductivity were significantly different between the contralateral normal tissue of supra- and infra-tentorial brains. The results from this study warrant further investigation of this method with a broader range of patients with stroke.

#### CLINICAL RELEVANCE/APPLICATION

This preliminary study demonstrated the feasibility of acquiring EPT from stroke patients and evaluating conductivities in lesion and normal brain. This new imaging contrast may provide an extra value on ischemic stroke.

Printed on: 02/07/23

## Abstract Archives of the RSNA, 2022

M5A-SPNR-20

### **IDH-wild type Glioblastoma: Imaging Independent Predictors of Gross Total Resection (GTR) Using the VASARI Feature Set and Tumoral Volumetric Measurements**

Monday, Nov. 28 12:15PM - 12:45PM Room: Learning Center - NR DPS

#### **Participants**

Luis Nunez, MD, Houston, TX (*Presenter*) Nothing to Disclose

#### **PURPOSE**

The aim of this study is to assess the impact of preoperative imaging phenotypes to determine predictors of gross total resection (GTR) using the Visually Accessible Rembrandt Images lexicon (VASARI) and tumoral volumetry measurements

#### **METHODS AND MATERIALS**

A single center, retrospective study of a prospectively maintained database of 167 patients with GBMs was performed. Fourteen patients (8%) with IDH mutation and 2 subjects (1.1%) with incomplete data were excluded. Among the 146 patients, 85 (59%) were male with a mean age of 59 years (SD +/- 13.6 years). MRI findings were assessed using the VASARI feature set and semi-automated tumoral segmentation. Univariate analysis was performed using X<sup>2</sup>/Fisher's exact test with Monte Carlo simulation for categorical variables and non-parametric analysis with the Mann-Whitney U test for continuous variables. Multivariate analysis was performed using the Logistic regression analysis test and receiver operating characteristic curve (ROC)

#### **RESULTS**

In total, 79 patients (55%) underwent GTR, 15 (10%) near-total resection (NTR) and 50 (35%) subtotal resection (STR). Out of the 25 VASARI criteria, 4 characteristics were found to be associated with GTR, as follows: 39 GBMs (49%) were in non-eloquent areas ( $p=0.04$ ), 59 (75%) had thick enhancing margins ( $p=0.04$ ), 64 (81%) had no ependymal invasion ( $p=0.02$ ) and 48 (61%) had no deep white matter invasion ( $p=0.03$ ). Additionally, GBMs with GTR were found to have lower tumoral volumes (121 ml [IQR, 51.7-174 ml] versus 163.9 ml [IQR, 121.9-215.3 ml] ( $p<0.01$ ), lower FLAIR volumes (98 ml [IQR, 40.2-134 ml] versus 127 ml [IQR, 87-167 ml] ( $p<0.01$ ), and lower enhancing volumes (14.5 ml [IQR, 8.3-24.7 ml] versus 28.6 ml [IQR, 14.2-42 ml] ( $p<0.01$ ). Logistic regression model demonstrated that thickness of enhancing margins is the only independent predictor of non-gross total resection (odds ratio: 1.57 [95% CI, 1.1-2.2]) ( $p=0.01$ ). ROC analysis of our multivariate model demonstrated an AUC estimate of 0.75 with a sensitivity of 60% and a specificity of 91%

#### **CONCLUSION**

s Imaging characteristics on standard-of-care (SOC) MR scans may predict gross total resection of GBMs wild-type. Furthermore, thickness of enhancing margins was the only significant predictor of GTR after multivariate analysis. Additionally, a diagnostic model that includes a combination of the discriminating depicted features on SOC MR scans and volumetric measurements, demonstrated to have an acceptable diagnostic performance with a specificity greater than 90%

#### **CLINICAL RELEVANCE/APPLICATION**

Higher survival rates are seen among glioblastoma patients that undergo gross-total resection (GTR). Our study provides information that will help to determine prognosis of patients with wild type glioblastomas.

Printed on: 02/07/23

## Abstract Archives of the RSNA, 2022

M5A-SPNR-3

### Study on Cranial Bone Marrow Conversion of High Altitude Polycythemia

Monday, Nov. 28 12:15PM - 12:45PM Room: Learning Center - NR DPS

#### Participants

Hai Hua Bao, Xining, China (*Presenter*) Nothing to Disclose

#### PURPOSE

High altitude polycythemia (HAPC) is a chronic disease caused by excessive compensatory proliferation of erythrocytes in the hypoxia environment at high altitude. The disease commonly affects multiple systems throughout the body, leading to an abnormal increase in hemoglobin concentration and red blood cell count. This study aimed to investigate the characteristics of cranial bone marrow conversion in patients with high altitude polycythemia based on conventional magnetic resonance imaging (MRI) and diffusion-weighted imaging (DWI).

#### METHODS AND MATERIALS

30 patients with high altitude polycythemia were included in the experimental group, aged (47.96 ±9.65) years, living at an altitude of (3155 ±736.98) m, with hemoglobin (216.57 ±11.10m) g/mL. 30 healthy subjects matched with the HAPC group in age and living altitude were included as the control group, aged (48.17±8.28) years, living altitude (3124.41±567.36) m, HGB(155.53±18.19) g/mL. The ADC values of the frontal bone, parietal bone, occipital bone and temporal bone were measured at Philips post-processing workstation, and the characteristics of cranial bone marrow conversion in patients with high altitude polycythemia were statistically analyzed.

#### RESULTS

There was no significant difference in age and living altitude between the two groups. Compared with the control group, the hemoglobin (HGB), red blood cell count (RBC) and hematocrit (HCT) in the HAPC group were significantly higher than those in the control group, as shown in Table 1. The ADC values of parietal bone and occipital bone in THE HAPC group were (0.88±0.30) ×10-3mm<sup>2</sup>/s and (1.37±0.27) ×10-3mm<sup>2</sup>/s, both higher than those in the control group (P<0.05), with statistical differences. The ADC values of the frontal bone and temporal bone in THE HAPC group were (1.09±0.24) ×10-3mm<sup>2</sup>/s and (1.36±0.27) ×10-3mm<sup>2</sup>/s, respectively, which were higher than those in the control group (P>0.05). The differences were not statistically significant, as shown in Table 2.

#### CONCLUSION

s Under the condition of long-term hypoxia in HAPC, the bone marrow of parietal bone and occipital bone was erythromedularized. This suggests that long-term chronic hypoxia may induce bone marrow erythromyelization, resulting in HAPC.

#### CLINICAL RELEVANCE/APPLICATION

Hypoxia is the main cause of altitude sickness. High altitude polycythemia (HAPC) is a common disease threatening people's health in the plateau, which can cause damage to multiple organs. We believe that imaging to explore cranial bone marrow conversion of HAPC patients compared with normal controls may provide an essential basis for understanding bone marrow erythromyelization induced by chronic hypoxia.

Printed on: 02/07/23

## Abstract Archives of the RSNA, 2022

M5A-SPNR-4

### Intravoxel Incoherent Motion (IVIM) May Help Distinguishing Gliomas and Solitary Brain Metastasis: A Multi-parameter Magnetic Resonance Imaging Study

Monday, Nov. 28 12:15PM - 12:45PM Room: Learning Center - NR DPS

#### Participants

Yifei Su, MS, (Presenter) Nothing to Disclose

#### PURPOSE

The aim of this study is to investigate the value of diffusion, perfusion and chemical exchange saturation transfer MR imaging in differentiating the gliomas and metastases.

#### METHODS AND MATERIALS

65 patients pathologically newly diagnosed gliomas or metastases were enrolled and all were conducted the diffusion weighted imaging, intravoxel incoherent motion (IVIM), and amide proton transfer-weighted (APT) imaging as well as the T1W, T2W, T2FLAIR and enhanced T1W imaging in a 3.0T MR scanner (Discovery MR 750w; GE, Milwaukee, USA). The images were imported to the iQuant software (GE Healthcare, Beijing, China) to calculate parametric maps including the apparent diffusion coefficient from DWI (ADC), diffusion coefficient (D), perfusion fraction (f), pseudo-diffusion coefficient (D\*) from IVIM and the MTRasym (3.5 ppm) from APT imaging. The tumor parenchyma was delineated wherever possible in 3dslicer (<https://www.slicer.org/>, version 4.10). Quantitative values of 10 percentile, 90 percentile, entropy, kurtosis, mean and skewness in parametric maps for region of interest (ROI) were extracted with the pyradiomics plugin and compared. Logistics regression and receiver operator curves (ROC) analysis were performed to explore the independent factors and optimal model. R packages were used for all the statistics (version 4.0.0).

#### RESULTS

44 patients were diagnosed as glioma (males:25, females:10, age range: 20-79y), and 21 cases were diagnosed as metastasis (males:10, females:11, age range: 34-80y) from the pathological analysis. No significant difference was observed in clinical manifestations (Table 1). There were significant differences for ADC kurtosis ( $6.43 \pm 5.63$  vs.  $4.54 \pm 3.23$ ,  $p = 0.02$ ), MTRasym (3.5ppm) 10 percentile ( $0.53 \pm 0.97$  vs.  $1.00 \pm 0.75$ ,  $p = 0.05$ ), f 90 percentile ( $23.07 \pm 5.14$  vs.  $28.67 \pm 5.51$ ,  $p < 0.01$ ), f entropy ( $56.00 \pm 33.08$  vs.  $85.20 \pm 33.08$ ,  $p < 0.01$ ), f kurtosis ( $67.56 \pm 40.75$  vs.  $39.08 \pm 142.84$ ,  $p < 0.01$ ), and f mean ( $13.92 \pm 2.50$  vs.  $17.38 \pm 3.84$ ,  $p < 0.01$ ) between gliomas and metastases groups (Table 2). The f kurtosis (OR = 0.66, 95% CI 0.48-0.92,  $p = 0.02$ ), and f mean (OR = 1.44, 95% CI 1.16-1.18,  $p < 0.01$ ) were found the independent factors for metastases differentiation in logistic regression analysis (Table 3). The AUC of model combined with age, IVIM-f kurtosis and IVIM-f mean was 0.83 while the AUC of model combined with IVIM-f kurtosis and IVIM-f mean with improved sensitivity was 0.81 with no significant difference under Delong test ( $p = 0.58$ ). (Table 4, Figure 1).

#### CONCLUSION

The IVIM-f kurtosis and IVIM-f mean demonstrated the differences in perfusion characteristics of gliomas and metastases.

#### CLINICAL RELEVANCE/APPLICATION

Accurate identification of these two kinds of tumors will largely benefit the therapy.

Printed on: 02/07/23

## Abstract Archives of the RSNA, 2022

M5A-SPNR-5

### Evaluation of RANO Criteria for Assessment of Tumor Progression for Lower-grade Gliomas

Monday, Nov. 28 12:15PM - 12:45PM Room: Learning Center - NR DPS

#### Participants

Fabio Raman, MD, PhD, (*Presenter*) Nothing to Disclose

#### PURPOSE

The Response Assessment in Neuro-Oncology (RANO) criteria for lower-grade gliomas (LGGs) defines tumor progression as  $\geq 25\%$  change in T2/FLAIR signal based on an operator's discretion of the perpendicular diameter of the largest tumor cross-section. Potential sources of error include limitation of 2D quantification, operator selection of both tumor cross-section and perpendicular parameters, and inability to quantify satellite tumor components. Our goal was to assess accuracy and reproducibility of RANO.

#### METHODS AND MATERIALS

651 FLAIR MRIs from 63 participants with LGGs at the University of Alabama at Birmingham were retrospectively analyzed by 3 blinded attending physicians and 3 blinded resident trainees using RANO, 2D visual, and 3D computer-assisted volumetric assessment. Inter- and intra-operator reproducibility was assessed using Pearson correlation, Bland Altman, and Cohen's kappa. Accuracy assessment was performed by comparing RANO to either visual or volumetric assessment, where 2/3 consensus agreement across operators was required to meet RANO and visual growth criteria for a particular tumor measurement. Volumetric assessment was performed by statistical change-of-point method. RANO assessment was performed compared to both previous and baseline scan.

#### RESULTS

RANO product measurements had moderate inter-operator reproducibility [ $r_2 = 0.71 - 0.82$ , coefficient of variance (CV) = 81 - 110%], mean percent difference (diff) = 0.4 - 46.8%] and intra-operator reproducibility ( $r_2 = 0.71 - 0.88$ , CV = 31 - 58%, diff = 0.3 - 23.9%, Figure A-B). When comparing to 2D visual gold standard, accuracy of RANO compared to previous and baseline scans were 66.7% and 65.1% with AUC of 0.67 and 0.66, respectively (Figure C). When comparing to volumetric gold standard, accuracy of RANO compared to previous and baseline scans were 21.0% and 48.4% with AUC of 0.39 and 0.55, respectively (Figure D). Median time delay at diagnosis was greater for false negative cases (RANO detected growth after volumetric) than for false positive cases (RANO growth detected earlier) for RANO assessment compared to previous scan (2.05 > 0.50 years,  $p = 0.003$ ) and baseline scan (1.08 > 0.50 years,  $p = 0.02$ , Figure E).

#### CONCLUSION

s RANO has moderate reproducibility and poor accuracy when comparing to either visual or volumetric gold standards.

#### CLINICAL RELEVANCE/APPLICATION

Limitations of the RANO criteria for LGGs suggest novel approaches, such as computer-assisted diagnostic tools, are necessary to reduce human variability and accurately assess 3D tumor progression.

Printed on: 02/07/23

## Abstract Archives of the RSNA, 2022

M5A-SPOB

### OB/Gynecology Monday Poster Discussions - A

Monday, Nov. 28 12:15PM - 12:45PM Room: Learning Center - OB DPS

#### Participants

Cinthia Cruz, MD, Newton, MA (*Moderator*) Nothing to Disclose

#### Sub-Events

### M5A-SPOB-1 Neoadjuvant Chemotherapy Induces an Elevation of Tumor Apparent Diffusion Coefficient Values in Patients With Ovarian Cancer

#### Participants

Milja Reijonen, MD, (*Presenter*) Nothing to Disclose

#### PURPOSE

Multiparametric magnetic resonance imaging (mMRI) is the modality of choice in the imaging of ovarian cancer (OC). We aimed to investigate the feasibility of different types of regions of interest (ROIs) in the measurement of apparent diffusion coefficient (ADC) values of diffusion-weighted imaging in OC patients treated with neoadjuvant chemotherapy (NACT).

#### METHODS AND MATERIALS

We retrospectively enrolled 23 consecutive patients with advanced OC who had undergone NACT and mMRI. Seventeen of them had been imaged before and after NACT. Two observers independently measured the ADC values in both ovaries and in the metastatic mass by drawing on a single slice of 1) freehand large ROIs (L-ROIs) covering the solid parts of the whole tumour and 2) three small round ROIs (S-ROIs). The side of the primary ovarian tumour was defined. We evaluated the interobserver reproducibility and statistical significance of the change in tumoural pre- and post-NACT ADC values. Each patient's disease was defined as platinum-sensitive, semi-sensitive, or resistant. The patients were deemed either responders or non-responders.

#### RESULTS

The interobserver reproducibility of the L-ROI and S-ROI measurements ranged from good to excellent (ICC range: 0.80-0.99). The mean ADC values were significantly higher after NACT in the primary tumour (L-ROI  $p$  lt; 0.001, S-ROIs  $p$  lt; 0.01) and the increase after NACT was associated with sensitivity to platinum-based chemotherapy. The changes in the ADC values of the omental mass were associated with a response to NACT.

#### CONCLUSION

s The mean ADC values in the primary tumour increased significantly after NACT in the OC patients and the amount of increase in omental mass predicted a response to platinum-based NACT. Our study indicates that quantitative analysis of ADC values with a single slice and a whole tumour ROI placement is a reproducible method that has a potential role in the evaluation of NACT response in patients with OC.

#### CLINICAL RELEVANCE/APPLICATION

Quantitative analysis of ADC values potentially has a role in evaluating the NACT response in patients with OC.

Printed on: 02/07/23

## Abstract Archives of the RSNA, 2022

M5A-SPOB-1

### Neoadjuvant Chemotherapy Induces an Elevation of Tumor Apparent Diffusion Coefficient Values in Patients With Ovarian Cancer

Monday, Nov. 28 12:15PM - 12:45PM Room: Learning Center - OB DPS

#### Participants

Milja Reijonen, MD, (*Presenter*) Nothing to Disclose

#### PURPOSE

Multiparametric magnetic resonance imaging (mMRI) is the modality of choice in the imaging of ovarian cancer (OC). We aimed to investigate the feasibility of different types of regions of interest (ROIs) in the measurement of apparent diffusion coefficient (ADC) values of diffusion-weighted imaging in OC patients treated with neoadjuvant chemotherapy (NACT).

#### METHODS AND MATERIALS

We retrospectively enrolled 23 consecutive patients with advanced OC who had undergone NACT and mMRI. Seventeen of them had been imaged before and after NACT. Two observers independently measured the ADC values in both ovaries and in the metastatic mass by drawing on a single slice of 1) freehand large ROIs (L-ROIs) covering the solid parts of the whole tumour and 2) three small round ROIs (S-ROIs). The side of the primary ovarian tumour was defined. We evaluated the interobserver reproducibility and statistical significance of the change in tumoural pre- and post-NACT ADC values. Each patient's disease was defined as platinum-sensitive, semi-sensitive, or resistant. The patients were deemed either responders or non-responders.

#### RESULTS

The interobserver reproducibility of the L-ROI and S-ROI measurements ranged from good to excellent (ICC range: 0.80-0.99). The mean ADC values were significantly higher after NACT in the primary tumour (L-ROI  $p$  lt; 0.001, S-ROIs  $p$  lt; 0.01) and the increase after NACT was associated with sensitivity to platinum-based chemotherapy. The changes in the ADC values of the omental mass were associated with a response to NACT.

#### CONCLUSION

s The mean ADC values in the primary tumour increased significantly after NACT in the OC patients and the amount of increase in omental mass predicted a response to platinum-based NACT. Our study indicates that quantitative analysis of ADC values with a single slice and a whole tumour ROI placement is a reproducible method that has a potential role in the evaluation of NACT response in patients with OC.

#### CLINICAL RELEVANCE/APPLICATION

Quantitative analysis of ADC values potentially has a role in evaluating the NACT response in patients with OC.

Printed on: 02/07/23

## Abstract Archives of the RSNA, 2022

M5A-SPPD

### Pediatric Monday Poster Discussions - A

Monday, Nov. 28 12:15PM - 12:45PM Room: Learning Center - PD DPS

#### Participants

Shailee Lala, MD, New York, NY (*Moderator*) Editor, RELX

#### Sub-Events

### M5A-SPPD-1 Changes to Image-Defined Risk Factors Based on Computed Tomography With Neoadjuvant Chemotherapy in Pediatric Abdominal Neuroblastoma

#### Participants

Haoru Wang, (*Presenter*) Nothing to Disclose

#### PURPOSE

To observe the changes to CT-based image-defined risk factors (IDRFs) with neoadjuvant chemotherapy in pediatric abdominal neuroblastoma, and to investigate the correlation between residual IDRFs after neoadjuvant chemotherapy and surgery-related events.

#### METHODS AND MATERIALS

A total of forty-three patients were enrolled. Surgical and pathological data, as well as CT images at initial diagnosis and after neoadjuvant chemotherapy of all patients were retrospectively collected and analyzed.

#### RESULTS

The number of IDRFs at first visit was 245, and was significantly reduced to 156 after neoadjuvant chemotherapy ( $p < 0.001$ ). The presence of most IDRFs was significantly improved after neoadjuvant chemotherapy ( $p < 0.05$ ), while the tumor invasion of renal pedicles ( $p > 0.05$ ) and adjacent structures other than kidney ( $p > 0.05$ ) was the least sensitive IDRFs. The loss of IDRFs correlated with the percentage reduction of tumor volume ( $p < 0.001$ ). IDRFs in different neuroblastoma decreased significantly after neoadjuvant chemotherapy ( $p < 0.05$ ), while not significant in neuroblastoma with low and intermediate mitosis-karyorrhexis index ( $p > 0.05$ ). The residual IDRFs correlated with the volume of intraoperative blood loss ( $r = 0.399$ ,  $p = 0.008$ ), while not with the presence of surgical complications ( $r = 0.111$ ,  $p = 0.478$ ).

#### CONCLUSION

Neoadjuvant chemotherapy can effectively improve the majority of IDRFs in pediatric abdominal neuroblastoma. The presence of residual IDRFs after neoadjuvant chemotherapy is helpful for preoperative surgical planning, but not correlate with the occurrence of surgical complications in abdominal neuroblastoma.

#### CLINICAL RELEVANCE/APPLICATION

The present study focused on the changes of CT-based IDRFs with neoadjuvant chemotherapy in pediatric abdominal neuroblastoma. In general, the presence of most IDRFs in abdominal neuroblastoma could be effectively improved by neoadjuvant chemotherapy, while tumor invasion of renal pedicles and adjacent structures other than kidney was least sensitive to neoadjuvant chemotherapy. Meanwhile, we also found that IDRFs of neuroblastoma with low and intermediate MKI do not change significantly after neoadjuvant chemotherapy, and that the residual IDRFs before surgery is helpful for preoperative surgical planning but not correlate with the presence of surgical complications in abdominal neuroblastoma.

Printed on: 02/07/23

## Abstract Archives of the RSNA, 2022

M5A-SPPD-1

### Changes to Image-Defined Risk Factors Based on Computed Tomography With Neoadjuvant Chemotherapy in Pediatric Abdominal Neuroblastoma

Monday, Nov. 28 12:15PM - 12:45PM Room: Learning Center - PD DPS

#### Participants

Haoru Wang, (*Presenter*) Nothing to Disclose

#### PURPOSE

To observe the changes to CT-based image-defined risk factors (IDRFs) with neoadjuvant chemotherapy in pediatric abdominal neuroblastoma, and to investigate the correlation between residual IDRFs after neoadjuvant chemotherapy and surgery-related events.

#### METHODS AND MATERIALS

A total of forty-three patients were enrolled. Surgical and pathological data, as well as CT images at initial diagnosis and after neoadjuvant chemotherapy of all patients were retrospectively collected and analyzed.

#### RESULTS

The number of IDRFs at first visit was 245, and was significantly reduced to 156 after neoadjuvant chemotherapy ( $p < 0.001$ ). The presence of most IDRFs was significantly improved after neoadjuvant chemotherapy ( $p < 0.05$ ), while the tumor invasion of renal pedicles ( $p > 0.05$ ) and adjacent structures other than kidney ( $p > 0.05$ ) was the least sensitive IDRFs. The loss of IDRFs correlated with the percentage reduction of tumor volume ( $p < 0.001$ ). IDRFs in different neuroblastoma decreased significantly after neoadjuvant chemotherapy ( $p < 0.05$ ), while not significant in neuroblastoma with low and intermediate mitosis-karyorrhexis index ( $p > 0.05$ ). The residual IDRFs correlated with the volume of intraoperative blood loss ( $r = 0.399$ ,  $p = 0.008$ ), while not with the presence of surgical complications ( $r = 0.111$ ,  $p = 0.478$ ).

#### CONCLUSION

s Neoadjuvant chemotherapy can effectively improve the majority of IDRFs in pediatric abdominal neuroblastoma. The presence of residual IDRFs after neoadjuvant chemotherapy is helpful for preoperative surgical planning, but not correlate with the occurrence of surgical complications in abdominal neuroblastoma.

#### CLINICAL RELEVANCE/APPLICATION

The present study focused on the changes of CT-based IDRFs with neoadjuvant chemotherapy in pediatric abdominal neuroblastoma. In general, the presence of most IDRFs in abdominal neuroblastoma could be effectively improved by neoadjuvant chemotherapy, while tumor invasion of renal pedicles and adjacent structures other than kidney was least sensitive to neoadjuvant chemotherapy. Meanwhile, we also found that IDRFs of neuroblastoma with low and intermediate MKI do not change significantly after neoadjuvant chemotherapy, and that the residual IDRFs before surgery is helpful for preoperative surgical planning but not correlate with the presence of surgical complications in abdominal neuroblastoma.

Printed on: 02/07/23

## Abstract Archives of the RSNA, 2022

M5A-SPPH

### Physics Monday Poster Discussions - A

Monday, Nov. 28 12:15PM - 12:45PM Room: Learning Center - PH DPS

#### Participants

Kishore Rajendran, PhD, Rochester, MN (*Moderator*) Nothing to Disclose  
Kishore Rajendran, PhD, Rochester, MN (*Moderator*) Nothing to Disclose  
Andrea Ferrero, PhD, Rochester, MN (*Moderator*) Nothing to Disclose  
Andrea Ferrero, PhD, Rochester, MN (*Moderator*) Nothing to Disclose

#### Sub-Events

### M5A-SPPH-1 Feasibility of Simultaneous Iodine and Gadolinium Imaging Using Edge-On-Irradiated Silicon Detector Photon-Counting CT

#### Participants

Zhye Yin, Niskayuna, NY (*Presenter*) Employee, General Electric Company

#### PURPOSE

Photon-counting CT (PCCT) enables novel clinical applications such as dual contrast imaging using I and Gd. PCCTs with edge-on-irradiated Si detectors may offer improved spectral capabilities due to desirable detector characteristics such as a narrow photoelectric peak, low charge-sharing and no relevant K-fluorescence. This study aims to demonstrate, in a phantom, the potential of Si-based PCCT to simultaneously image two contrast agents.

#### METHODS AND MATERIALS

An 20cm cylindrical phantom (Gammex, Sun Nuclear) with two configurations of I and Gd solid inserts was scanned at 120kVp using a prototype PCCT (GE Healthcare) equipped with Si sensors. First, three Gd rods (2.5, 5 and 10mg/ml concentration), and three I rods (2, 5 and 10mg/ml) were scanned in order to demonstrate the separation of I and Gd. Six Gd rods with concentrations ranging from 0.3-10mg/ml were then imaged to determine the lower limit of Gd detection. Circular regions of interest (ROI) were extracted from water and I material basis images to generate a material scatter plot. Gd images were generated by linear combination of water and I material images, and the transform weights estimated based on the scatter plot of known Gd concentrations.

#### RESULTS

Gd rods with concentrations ranging from 2.5-10mg/ml were consistently separated from the I rods with concentrations of 2-10mg/ml in the material scatter plot. Also, we found that Gd at as low a concentration as 1.25mg/ml can be differentiated in the material scatter plot. Literature suggests that in-vivo Gd concentrations for 1.5T MRI acquisitions range from 0-3mg/ml.

#### CONCLUSION

A PCCT system using edge-on-irradiated Si detectors demonstrated separation of I and Gd. Since in vivo Gd concentration in MR acquisitions ranges from 0 to 3mg/ml, our results also suggest that this prototype edge-on-irradiated Si-based CT system can enable Gd detection at contrast dose levels typical of MR. This may enable imaging of multiple contrast agents in the same study and thus the monitoring of multiple phases of contrast enhancement.

#### CLINICAL RELEVANCE/APPLICATION

PCCT with high spectral capability and a high number of energy bins has the potential to support innovative cardiac and oncology applications using multiple contrast agents simultaneously.

### M5A-SPPH-2 Edge-on-irradiated Si-PCCT: Spectral Imaging Performance in a Virtual Imaging Trial

#### Participants

Raj Kumar Panta, (*Presenter*) Nothing to Disclose

#### PURPOSE

To evaluate the spectral imaging performance of an edge-on-irradiated Si photon-counting CT (Si-PCCT) using a virtual imaging trial platform.

#### METHODS AND MATERIALS

An ACR accredited CT phantom and a computational human model with liver lesions were virtually scanned with Si-PCCT under identical imaging conditions. A newly-developed projection-based maximum-likelihood material decomposition (MD) was applied on spectral sinogram domain. Accuracy of material images and virtual mono-chromatic images (VMI) of the ACR phantom were evaluated against reference values. Similarly, virtual non-contrast CT (VNC) images were generated by imaging a computational human model with iodinated contrast. The accuracy of the VNC images were compared against the true non-contrast CT (TNC) images of the computational human model without contrast-enhancement. The spectral imaging performance of Si-PCCT was further evaluated under various imaging conditions (e.g., radiation dose levels, slice thickness and reconstruction kernels).

## RESULTS

Evaluation of material decomposed images revealed that estimated density of calcium and iodine highly correlated ( $R^2 > 0.99$ ) with ground-truth concentrations under various imaging conditions. Similarly, there was a good agreement (> 99%) between virtual monochromatic x-ray attenuation profiles and reference attenuation profiles for various materials. In addition, assessment of the in-plane and cross-plane attenuation profiles showed that mono-chromatic images had less beam-hardening artifacts compared to polychromatic grayscale images. Minor attenuation differences (few HU) were observed between VNC and TNC.

## CONCLUSION

s Edge-on-irradiated Si-PCCT with projection-based MD enables quantitative material density images, and accurate VMI and VNC images under various imaging conditions of radiation dose levels, slice thickness and reconstruction kernels.

## CLINICAL RELEVANCE/APPLICATION

Our virtual imaging trial demonstrates the quantitative spectral imaging performance of an edge-on-irradiated Si-PCCT under various imaging conditions and it demonstrates the promising utility in quality patient care once prototyped.

### **M5A-SPPH-3 Synthesizing 100 kV and 120 kV CT Images From Dual-Energy CT Data Using a Novel Ray-By-Ray Effective Energies**

Participants

Xin Tie, MS, Madison, WI (*Presenter*) Nothing to Disclose

## PURPOSE

Fast-kV switching-based dual-energy CT (DECT) imaging acquires data at 80 kV and 140 kV. Meanwhile, the vast majority of the clinical contrast-enhanced chest and abdominal CTs are performed at 100 or 120 kV. Reference standards for the CT numbers of cystic renal masses, adrenal masses, liver fat fractions, and other quantitative measurements were generally established based on 100 kV and 120 kV CT images. The purpose of this work was to leverage ray-specific effective energies extracted from DECT projection data along with material basis images to accurately synthesize 100 kV and 120 kV CT images desired by radiologists

## METHODS AND MATERIALS

For each image object, the effective energies of each ray in the 80 kV and 140 kV acquisitions were first determined based on the line integrals of water and iodine basis images. Then, they were combined using weighting factors to estimate the effective energies of 100 kV and 120 kV acquisitions. With the estimated effective energies and DECT material basis images, 100 kV and 120 kV sinograms were synthesized. The weighting factors were learned from phantoms with known true 100 kV and 120 kV images. Once learned, the factors were fixed to synthesize 100 kV and 120 kV images from DECT data using the effective energy of each measured projection datum. Rigorous evaluations have been performed on physical phantoms (Gammex and anthropomorphic chest phantoms with various inserts) and human subjects. The quantitative accuracy was benchmarked by true 100 kV and 120 kV images of phantoms using relative root mean squared error (rRMSE) and of humans using box-whisker analysis.

## RESULTS

The median ([25th, 75th percentiles]) of rRMSE were 0.38% [0.30%, 0.67%] and 0.34% [0.22%, 0.62%] for the synthesized 100 kV and 120 kV images, respectively. For the Gammex and chest phantoms, CT numbers of all inserts were accurately depicted in the synthesized images with CT number errors less than 10 HU. 20 ROIs were randomly selected on adipose tissues of human subjects and the box-whisker plot showed a zero bias between our results and true images (median [25th 75th percentile]: 0.0 [-1.0, 1.0] HU for 100 kV; 0.0 [-2.0, 1.0] HU for 120 kV images).

## CONCLUSION

s Using ray-specific effective energies extracted from DECT data, virtual 100 kV and 120 kV CT images can be accurately synthesized without knowing the polychromatic spectra of each scanner.

## CLINICAL RELEVANCE/APPLICATION

Even for DECT, 100 kV and 120 kV CT images are still desired by radiologists due to their training and the existing clinical standards organ CT numbers previously established based on 100 kV and 120 kV CT images. This work enables the accurate synthesis of those polychromatic images without additional data acquisitions.

### **M5A-SPPH-4 Performance Evaluation of Low-contrast Lesion Detectability and Potential Radiation Dose Reduction on Photon-Counting-Detector CT Compared to Energy-integrating-detector CT**

Participants

Liqiang Ren, PhD, Rochester, MN (*Presenter*) Nothing to Disclose

## PURPOSE

To evaluate the performance of low-contrast lesion detectability on a clinical photon-counting-detector CT (PCD-CT) and the potential of radiation dose reduction compared to a single-energy (SE) CT using an energy-integrating-detector (EID).

## METHODS AND MATERIALS

Two holes with a diameter of 4 mm and 8 mm in a water-equivalent cylinder were filled with iodine solutions at a concentration of 0.5 mg/cc to mimic different sizes of lesions, and the cylinder was inserted into one of 3 abdomen phantoms (QRM, lateral widths of 30, 35 and 40 cm). The whole phantom was scanned on a clinical PCD-CT system (NAEOTOM Alpha, Siemens) at 120 kV and a 3rd generation dual-source CT (SOMATOM Force, Siemens) in a single-energy mode at the same tube potential (120 kV). The effective mAs was adjusted on PCD-CT and EID-CT to match the CTDIvol values (7.2, 12.0, and 18.4 mGy for 30, 35, and 40 cm phantom, respectively). Scans were repeated six times for each of the 6 unique conditions: 3 phantom sizes and two dose levels (100% and 75% of the routine dose). Threshold-low (T3D) images from PCD-CT and SECT images on EID-CT were reconstructed with an iterative reconstruction algorithm (Kernel/strength: Br40/3), and slice thickness/increment of 3/3.5 mm. Contrast to noise ratio (CNR) and area under the receiver operating characteristic (ROC) curve (AUC) from a calibrated channelized Hotelling observer (CHO) model observer were calculated as figures of merit for quantifying iodine detection on PCD-CT and EID-CT.

## RESULTS

PCD-CT showed consistently higher iodine CNR and AUC than EID-SECT for all phantom sizes and radiation levels. Compared to EID-CT, the CNR was improved by 30-70% with PCD-CT for the 8 mm lesion. The AUC values derived for 8 mm lesion detection with all phantoms and that for 4 mm lesion with 30 cm phantom on PCD-CT were only slightly better than EID-CT as they were close to saturation. For 4 mm lesion, the AUC values were ranged in 0.96-0.98 (PCD) and 0.90-0.97 (EID) for 35 cm phantom, and 0.88-0.95 (PCD) and 0.87-0.89 (EID) for 40 cm phantom.

## CONCLUSION

s For the identical low-contrast lesion detection task, PCD-CT performs better than EID-CT at all phantom sizes and radiation dose levels, which may allow up to 25% radiation dose reduction depending on lesion and patient sizes while maintaining the same lesion detectability as EID-CT.

## CLINICAL RELEVANCE/APPLICATION

Low-contrast lesion detectability can be improved with PCD-CT over EID-CT or maintained as EID-CT but with a potential of up to 25% dose reduction.

## M5A-SPPH-5 Evaluation of Small Coronary Stents using High-Resolution Mode Imaging with Deep Learning Imaging Reconstruction

### Participants

Kazuki Ishikawa, (*Presenter*) General Electric Company

## PURPOSE

Although the frequency of coronary stent restenosis has decreased with the advent of drug-eluting stents, the diagnostic accuracy of restenosis by conventional coronary CT angiography is not high. Although the high-resolution (HR) imaging seems promising for restenosis evaluation because it improves spatial resolution, increased image noise due to dedicated kernel and tube current limitations is a problem. The purpose of this study was to clarify the usefulness of noise reduction by deep learning imaging reconstruction (DLIR) in the evaluation of coronary stents using HR imaging.

## METHODS AND MATERIALS

We analyzed the images of coronary stents with inner diameters of 3 mm and 2.5 mm in HR and normal (NR) modes. The images were scanned with an ECG-synchronized axial scan on a commercially available 256 MDCT scanner: tube voltage, 120 kV; current, automatic exposure control; and noise index, 26. Images were reconstructed using hybrid iterative reconstruction (HIR, strength 80%), DLIR-Low (L), -Medium (M) and -High (H), respectively. The kernels used were HD-Standard in HR mode and Standard in NR mode. The values of full width at half maximum (FWHM), standard deviation (SD) of the stent profile, and noise power spectrum (NPS) were measured to evaluate image quality.

## RESULTS

The CT dose index volume for HR and NR were both 8.9 mGy. The FWHM of the stent profile in HIR, DLIR-L, DLIR-M, and DLIR-H was 1.00, 1.06, 1.05, and 1.06, respectively for HR at 2.5 mm. For NR at 2.5 mm: 1.42, 1.49, 1.49, and 1.49, respectively. For HR at 3 mm, 0.97, 1.01, 1.01, and 1.01, respectively. For NR at 2.5 mm, 1.28, 1.30, 1.30, and 1.29, respectively. The FWHM between HR and NR differed significantly ( $p < 0.01$ ). The SD difference between HR and NR was 7.74, 9.61, 6.20 and 3.48, respectively. There was a significant difference among the reconstruction methods ( $p < 0.01$ ). The peak frequency of the NPS in HR mode was 0.23, 0.34, 0.28, and 0.22 cycles/mm for HIR, DLIR-L, DLIR-M, and DLIR-H, respectively, and the average frequency was 0.35, 0.42, 0.40, and 0.39 cycles/mm, respectively. Compared to the peak and average frequencies of the filtered back projection (0.54 and 0.48 cycles/mm), these results showed a noise texture change of HIR.

## CONCLUSION

s The use of DLIR in combination with the HR mode improved the visibility of small-diameter coronary stents by minimizing the image noise and maintaining the image texture.

## CLINICAL RELEVANCE/APPLICATION

DLIR minimizes the effects of tube current limitation and noise increase in HR mode. It enables HR mode imaging for larger patients, and can improve the imaging of smaller coronary stents.

## M5A-SPPH-6 Signal-To-Noise Ratio Measurement in CT With Conventional and Textured Phantoms: Comparison of Two Deep-Learning Image Reconstruction Techniques

### Participants

Hiroki Kawashima, PhD, RT, Kanazawa, Japan (*Presenter*) Nothing to Disclose

## PURPOSE

To evaluate signal-to-noise ratio (SNR) improvement by deep-learning image reconstruction (DLIR) techniques, with a conventional method using rod and water phantoms and a new approach using a textured phantom.

## METHODS AND MATERIALS

A water-bath phantom with a diameter of 300 mm was used as a base phantom. A textured phantom with a diameter of 128 mm, made by mixing water and 12 mg/mL diluted iodine equivalent materials (IEM), was placed in the base phantom (non-uniform region). In addition, a simple rod made by IEM was placed. Thirty repeated phantom scans were performed using two CT scanners (GE, Revolution CT Apex Edition; Canon, Aquilion One PRISM Edition) at 5 and 15 mGy. Images were reconstructed with filtered back projection (FBP) and DLIR [GE, TrueFidelity (TF); Canon, Advanced intelligent Clear-IQ (AC)] for three process strengths. The task transfer function (TTF) was measured with the rod image; the noise power spectrum (NPS) was measured in the water-only region. The conventional SNR (SNRC(u)) was calculated as a square root of  $TTF(u)^2/NPS(u)$ . A signal spectrum (S(u)) was measured in an averaged image of the non-uniform region using a Fourier analysis, and a noise spectrum (N(u)) was estimated as an average of 30 spectra (S(u)+N(u)) minus the S(u). An SNR for the non-uniform region (SNRNU(u)) was calculated by  $S(u)/N(u)$ . The SNR improvement factor (SIF) was calculated by SNR of DLIR divided by SNR of FBP.

## RESULTS

The average SIFs of SNRC with TF were 1.88 at 0.1 mm<sup>-1</sup>, 2.92 at 0.5 mm<sup>-1</sup>; those with AC were 2.52 at 0.1 mm<sup>-1</sup>, 6.20 at 0.5 mm<sup>-1</sup>. On the other hand, the SIFs of SNRNU with TF were 1.41 at 0.1 mm<sup>-1</sup>, 1.10 at 0.5 mm<sup>-1</sup>; those with AC were 1.47 at 0.1 mm<sup>-1</sup>, 1.25 at 0.5 mm<sup>-1</sup>, which were notably lower than the SIF of SNRC.

## CONCLUSION

s Both DLIR techniques sufficiently improved the conventional SNR measured with the rod and water images (88-500%). However, the improvements of SNRNU were low (10-47%), which revealed limited performances for the complex structures included in the textured phantom.

## CLINICAL RELEVANCE/APPLICATION

The SIFs measured using the non-uniform region are possibly more clinically relevant compared to the conventional method using simple rods and a uniform water region.

## M5A-SPPH-7 Importance of Larger Reconstruction Matrix Sizes for Super-Resolution Deep Learning Reconstruction

Participants  
Toru Higaki, PhD, Minami-ku, Hiroshima, Japan (*Presenter*) Nothing to Disclose

## PURPOSE

Recently clinically introduced super-resolution deep learning reconstruction (SR-DLR) can convert conventional- to high-resolution CT images. The matrix size of the output images can be selected as either 512×512 as conventional or 1024×1024. In this study, we investigated the effect of the output image matrix size (the pixel size in the output image) on spatial resolution.

## METHODS AND MATERIALS

The SR-DLR was implemented using a super-resolution DCNN (SR-DCNN). It was trained with pairs of high-resolution- and conventional resolution images. The high-resolution images for the training target were acquired using an actual high-resolution CT scanner (Aquilion Precision, Canon Medical Systems Corp.: CMSC) which has a twice larger matrix size. We made a CCTA phantom (Fig. left-bottom) using a 3D printer (Agilista-3200, Keyence). The outer diameter of the phantom was 350×250 mm. Iodine contrast medium diluted with 20 mgI/ml was filled to the simulated left ventricle and coronary arteries. We scanned the CCTA phantom using a conventional CT scanner (Aquilion ONE GENESIS, CMSC) with standard CCTA protocol (tube voltage: 120 kV, tube current: automatic exposure control with SD 23 HU, rotation speed: 0.275 s/rot, ECG-gated volume scan). Images were reconstructed with conventional hybrid iterative reconstruction (IR) (Adaptive Iterative Dose Reduction 3D with FC14 kernel, CMSC) with 512 matrix, SR-DLR with 512 matrix, and SR-DLR with 1024 matrix. The reconstruction FoV was 200 mm, and the pixel sizes of the 512- and 1024-matrix images were 0.39 and 0.195 mm, respectively. We measured profile curves and modulation transfer functions (MTFs) using the edge of a simulated left ventricle and compared their spatial resolution.

## RESULTS

The three reconstructed images shown on the left side of the figure indicate that the 1024 matrix SR-DLR image provides the sharpest edges. The edge profile curves and MTF on the right side of the figure also showed a similar trend. The actual MTF of SR-DLR exceeded the Nyquist frequency of 512 matrix images, and 1024 matrix images were required to fully utilize SR-DLR's performance.

## CONCLUSION

s To fully utilize the spatial resolution of SR-DLR, it is suitable to reconstruct images with 1024 matrices.

## CLINICAL RELEVANCE/APPLICATION

The SR-DLR of 1024 matrix images provides higher spatial resolution, which is useful for the visualization of fine structures such as demonstration of plaques in the coronary artery, and fine lesions in diffuse lung disease.

## M5A-SPPH-8 Ranking the Relative Importance of Image Quality Features in CT by Consensus Survey

Participants  
Dustin Gress, MS, (*Presenter*) Nothing to Disclose

## PURPOSE

To assess consensus opinions from subspecialty radiologists and imaging physicists on the relative importance of image quality features in CT, in order to set subspecialty-informed development priorities for quantitating such features, preferably using automated methods.

## METHODS AND MATERIALS

A web-based pictorial survey was created by subject matter expert radiologists and imaging physicists, requesting respondents to rank the relative importance of ten distinct imaging features in their clinical practice, using a 1 (lowest) to 10 (highest) scale. The survey was first sent to subspecialty radiologists and physicists in volunteer leadership roles in the ACR and RSNA, with such roles assumed as reasonable proxy for expertise. The survey then relied on snowball sampling, where respondents could recommend up to 3 suitable experts for invitation to complete the survey.

## RESULTS

There were 66 total respondents. Median years of respondent experience for all subspecialties ranged 10-16.5 years. Overall mean rankings for features ranged 5.48-8.74; motion and streaking artifact had the highest average across all subspecialties, scored 8.74 and 8.32, respectively. Lowest overall mean score was for blooming artifact (5.48). Musculoskeletal means were highest for noise texture (9.0) and metal artifact (9.4). Emergency, neuro, pediatric, and abdominal radiologists scored motion artifact highest, with means of 9.89, 9.38, 8.5, and 9.0, respectively. Low contrast axial sharpness was second highest for abdominal radiologists (8.94), with streaking third (8.72). Imaging physicist scored low contrast axial sharpness highest and noise magnitude second highest, with means of 8.94 and 8.78, respectively.

## CONCLUSION

s Specific image quality features ranked by expert subspecialty radiologists have relatively higher importance for their routine clinical practice compared to other features, and the importance of identical features also vary between subspecialties. These metrics afford an opportunity to develop targeted image quality measurement tools, especially those that are automated, which can be configurable depending on the practice domain. Limitations include those with expert opinions; responses from thoracic and cardiac radiologists are being collected.

## CLINICAL RELEVANCE/APPLICATION

Automated quantification and reporting of relevant medical image quality metrics is an essential step toward enhancing the value of clinical care in medical imaging. This performance paradigm accounts for both radiation dose index management as well as objective image quality management.

## M5A-SPPH-9 Detectability Index Analysis of Enterprise CT AP Protocols

Participants

Brian Hurley, MS, (*Presenter*) Nothing to Disclose

## PURPOSE

With trends to move toward enterprise-wide radiology management there should be image quality standardization across a hospital system. The purpose is to develop a methodology to assess image quality uniformity for the adult abdomen and pelvis protocol across a hospital enterprise which includes a CT scanner fleet with multiple manufacturers and models.

## METHODS AND MATERIALS

A dose tracking software (Radimetrics) was used to gather data on abdomen and pelvis with contrast scans across a health enterprise for the 2nd Quarter of 2021. (3,603 scans). From this dataset, the 5th, 25th, 50th, 75th, and 95th percentiles of the CTDIVol were extracted for each facility in the hospital enterprise. The ACR CT accreditation phantom was scanned at each of the facility specific CTDIVol values and these scans were assessed using the ImQuest software by Duke CIPG to obtain the detectability index ( $d'$ ). To normalize the dose dependence of the image quality, the  $d'^2$ /CTDIVol for the 25th, 50th and 75th percentiles were calculated and compared to evaluate the protocol performance.

## RESULTS

The range of the  $d'^2$ /CTDIVol for the 25th, 50th and 75th percentiles was 124 to 263, 112 to 267, and 105 to 269 respectively. The absolute differences for the 25th, 50th, and 75th were 139, 155, and 164 which corresponds to a percent difference of 72%, 82% and 88%. When comparing a single institution, the largest percent difference within the scanners at a given institution for the protocol 50th percentile of dose was found to be 29%.

## CONCLUSION

s There is substantial variation in the image quality for the abdomen pelvis protocols across the hospital enterprise examined. Additionally, there is a significant variation within hospitals when multiple makes/models were utilized. Currently much effort is placed on protocol optimization in terms of dose (CTDI, DLP or Effective Dose). Though dose is a loose surrogate for image quality, with advanced applications on modern scanners and the growing push towards enterprise healthcare more focus should be placed on providing uniform image quality for a given protocol across different scanner types at a hospital enterprise. This analysis was done with a 5 mm lesion based on acrylic TTF and contrast, in the future this should be expanded to other lesion sizes and contrast levels with the potential to select the target (lesion size, contrast, etc.) based on clinical indication.

## CLINICAL RELEVANCE/APPLICATION

The findings of this study can be used to help improve image quality uniformity across a large hospital system. This methodology can be applied to other adult and pediatric protocols to assess image quality uniformity across multiple CT scanners independent of make and model.

Printed on: 02/07/23

## Abstract Archives of the RSNA, 2022

M5A-SPPH-1

### Feasibility of Simultaneous Iodine and Gadolinium Imaging Using Edge-On-Irradiated Silicon Detector Photon-Counting CT

Monday, Nov. 28 12:15PM - 12:45PM Room: Learning Center - PH DPS

#### Participants

Zhye Yin, Niskayuna, NY (*Presenter*) Employee, General Electric Company

#### PURPOSE

Photon-counting CT (PCCT) enables novel clinical applications such as dual contrast imaging using I and Gd. PCCTs with edge-on-irradiated Si detectors may offer improved spectral capabilities due to desirable detector characteristics such as a narrow photoelectric peak, low charge-sharing and no relevant K-fluorescence. This study aims to demonstrate, in a phantom, the potential of Si-based PCCT to simultaneously image two contrast agents.

#### METHODS AND MATERIALS

An 20cm cylindrical phantom (Gammex, Sun Nuclear) with two configurations of I and Gd solid inserts was scanned at 120kVp using a prototype PCCT (GE Healthcare) equipped with Si sensors. First, three Gd rods (2.5, 5 and 10mg/ml concentration), and three I rods (2, 5 and 10mg/ml) were scanned in order to demonstrate the separation of I and Gd. Six Gd rods with concentrations ranging from 0.3-10mg/ml were then imaged to determine the lower limit of Gd detection. Circular regions of interest (ROI) were extracted from water and I material basis images to generate a material scatter plot. Gd images were generated by linear combination of water and I material images, and the transform weights estimated based on the scatter plot of known Gd concentrations.

#### RESULTS

Gd rods with concentrations ranging from 2.5-10mg/ml were consistently separated from the I rods with concentrations of 2-10mg/ml in the material scatter plot. Also, we found that Gd at as low a concentration as 1.25mg/ml can be differentiated in the material scatter plot. Literature suggests that in-vivo Gd concentrations for 1.5T MRI acquisitions range from 0-3mg/ml.

#### CONCLUSION

A PCCT system using edge-on-irradiated Si detectors demonstrated separation of I and Gd. Since in vivo Gd concentration in MR acquisitions ranges from 0 to 3mg/ml, our results also suggest that this prototype edge-on-irradiated Si-based CT system can enable Gd detection at contrast dose levels typical of MR. This may enable imaging of multiple contrast agents in the same study and thus the monitoring of multiple phases of contrast enhancement.

#### CLINICAL RELEVANCE/APPLICATION

PCCT with high spectral capability and a high number of energy bins has the potential to support innovative cardiac and oncology applications using multiple contrast agents simultaneously.

Printed on: 02/07/23



## Abstract Archives of the RSNA, 2022

MSA-SPPH-2

### Edge-on-irradiated Si-PCCT: Spectral Imaging Performance in a Virtual Imaging Trial

Monday, Nov. 28 12:15PM - 12:45PM Room: Learning Center - PH DPS

#### Participants

Raj Kumar Panta, (*Presenter*) Nothing to Disclose

#### PURPOSE

To evaluate the spectral imaging performance of an edge-on-irradiated Si photon-counting CT (Si-PCCT) using a virtual imaging trial platform.

#### METHODS AND MATERIALS

An ACR accredited CT phantom and a computational human model with liver lesions were virtually scanned with Si-PCCT under identical imaging conditions. A newly-developed projection-based maximum-likelihood material decomposition (MD) was applied on spectral sinogram domain. Accuracy of material images and virtual mono-chromatic images (VMI) of the ACR phantom were evaluated against reference values. Similarly, virtual non-contrast CT (VNC) images were generated by imaging a computational human model with iodinated contrast. The accuracy of the VNC images were compared against the true non-contrast CT (TNC) images of the computational human model without contrast-enhancement. The spectral imaging performance of Si-PCCT was further evaluated under various imaging conditions (e.g., radiation dose levels, slice thickness and reconstruction kernels).

#### RESULTS

Evaluation of material decomposed images revealed that estimated density of calcium and iodine highly correlated ( $R^2 > 0.99$ ) with ground-truth concentrations under various imaging conditions. Similarly, there was a good agreement ( $> 99\%$ ) between virtual monochromatic x-ray attenuation profiles and reference attenuation profiles for various materials. In addition, assessment of the in-plane and cross-plane attenuation profiles showed that mono-chromatic images had less beam-hardening artifacts compared to polychromatic grayscale images. Minor attenuation differences (few HU) were observed between VNC and TNC.

#### CONCLUSION

s Edge-on-irradiated Si-PCCT with projection-based MD enables quantitative material density images, and accurate VMI and VNC images under various imaging conditions of radiation dose levels, slice thickness and reconstruction kernels.

#### CLINICAL RELEVANCE/APPLICATION

Our virtual imaging trial demonstrates the quantitative spectral imaging performance of an edge-on-irradiated Si-PCCT under various imaging conditions and it demonstrates the promising utility in quality patient care once prototyped.

Printed on: 02/07/23

## Abstract Archives of the RSNA, 2022

M5A-SPPH-3

### Synthesizing 100 kV and 120 kV CT Images From Dual-Energy CT Data Using a Novel Ray-By-Ray Effective Energies

Monday, Nov. 28 12:15PM - 12:45PM Room: Learning Center - PH DPS

#### Participants

Xin Tie, MS, Madison, WI (*Presenter*) Nothing to Disclose

#### PURPOSE

Fast-kV switching-based dual-energy CT (DECT) imaging acquires data at 80 kV and 140 kV. Meanwhile, the vast majority of the clinical contrast-enhanced chest and abdominal CTs are performed at 100 or 120 kV. Reference standards for the CT numbers of cystic renal masses, adrenal masses, liver fat fractions, and other quantitative measurements were generally established based on 100 kV and 120 kV CT images. The purpose of this work was to leverage ray-specific effective energies extracted from DECT projection data along with material basis images to accurately synthesize 100 kV and 120 kV CT images desired by radiologists

#### METHODS AND MATERIALS

For each image object, the effective energies of each ray in the 80 kV and 140 kV acquisitions were first determined based on the line integrals of water and iodine basis images. Then, they were combined using weighting factors to estimate the effective energies of 100 kV and 120 kV acquisitions. With the estimated effective energies and DECT material basis images, 100 kV and 120 kV sinograms were synthesized. The weighting factors were learned from phantoms with known true 100 kV and 120 kV images. Once learned, the factors were fixed to synthesize 100 kV and 120 kV images from DECT data using the effective energy of each measured projection datum. Rigorous evaluations have been performed on physical phantoms (Gammex and anthropomorphic chest phantoms with various inserts) and human subjects. The quantitative accuracy was benchmarked by true 100 kV and 120 kV images of phantoms using relative root mean squared error (rRMSE) and of humans using box-whisker analysis.

#### RESULTS

The median ([25th, 75th percentiles]) of rRMSE were 0.38% [0.30%, 0.67%] and 0.34% [0.22%, 0.62%] for the synthesized 100 kV and 120 kV images, respectively. For the Gammex and chest phantoms, CT numbers of all inserts were accurately depicted in the synthesized images with CT number errors less than 10 HU. 20 ROIs were randomly selected on adipose tissues of human subjects and the box-whisker plot showed a zero bias between our results and true images (median [25th 75th percentile]: 0.0 [-1.0, 1.0] HU for 100 kV; 0.0 [-2.0, 1.0] HU for 120 kV images).

#### CONCLUSION

s Using ray-specific effective energies extracted from DECT data, virtual 100 kV and 120 kV CT images can be accurately synthesized without knowing the polychromatic spectra of each scanner.

#### CLINICAL RELEVANCE/APPLICATION

Even for DECT, 100 kV and 120 kV CT images are still desired by radiologists due to their training and the existing clinical standards organ CT numbers previously established based on 100 kV and 120 kV CT images. This work enables the accurate synthesis of those polychromatic images without additional data acquisitions.

Printed on: 02/07/23

## Abstract Archives of the RSNA, 2022

M5A-SPPH-4

### Performance Evaluation of Low-contrast Lesion Detectability and Potential Radiation Dose Reduction on Photon-Counting-Detector CT Compared to Energy-integrating-detector CT

Monday, Nov. 28 12:15PM - 12:45PM Room: Learning Center - PH DPS

#### Participants

Liqiang Ren, PhD, Rochester, MN (*Presenter*) Nothing to Disclose

#### PURPOSE

To evaluate the performance of low-contrast lesion detectability on a clinical photon-counting-detector CT (PCD-CT) and the potential of radiation dose reduction compared to a single-energy (SE) CT using an energy-integrating-detector (EID).

#### METHODS AND MATERIALS

Two holes with a diameter of 4 mm and 8 mm in a water-equivalent cylinder were filled with iodine solutions at a concentration of 0.5 mg/cc to mimic different sizes of lesions, and the cylinder was inserted into one of 3 abdomen phantoms (QRM, lateral widths of 30, 35 and 40 cm). The whole phantom was scanned on a clinical PCD-CT system (NAEOTOM Alpha, Siemens) at 120 kV and a 3rd generation dual-source CT (SOMATOM Force, Siemens) in a single-energy mode at the same tube potential (120 kV). The effective mAs was adjusted on PCD-CT and EID-CT to match the CTDI<sub>vol</sub> values (7.2, 12.0, and 18.4 mGy for 30, 35, and 40 cm phantom, respectively). Scans were repeated six times for each of the 6 unique conditions: 3 phantom sizes and two dose levels (100% and 75% of the routine dose). Threshold-low (T3D) images from PCD-CT and SECT images on EID-CT were reconstructed with an iterative reconstruction algorithm (Kernel/strength: Br40/3), and slice thickness/increment of 3/3.5 mm. Contrast to noise ratio (CNR) and area under the receiver operating characteristic (ROC) curve (AUC) from a calibrated channelized Hotelling observer (CHO) model observer were calculated as figures of merit for quantifying iodine detection on PCD-CT and EID-CT.

#### RESULTS

PCD-CT showed consistently higher iodine CNR and AUC than EID-SECT for all phantom sizes and radiation levels. Compared to EID-CT, the CNR was improved by 30-70% with PCD-CT for the 8 mm lesion. The AUC values derived for 8 mm lesion detection with all phantoms and that for 4 mm lesion with 30 cm phantom on PCD-CT were only slightly better than EID-CT as they were close to saturation. For 4 mm lesion, the AUC values were ranged in 0.96-0.98 (PCD) and 0.90-0.97 (EID) for 35 cm phantom, and 0.88-0.95 (PCD) and 0.87-0.89 (EID) for 40 cm phantom.

#### CONCLUSION

For the identical low-contrast lesion detection task, PCD-CT performs better than EID-CT at all phantom sizes and radiation dose levels, which may allow up to 25% radiation dose reduction depending on lesion and patient sizes while maintaining the same lesion detectability as EID-CT.

#### CLINICAL RELEVANCE/APPLICATION

Low-contrast lesion detectability can be improved with PCD-CT over EID-CT or maintained as EID-CT but with a potential of up to 25% dose reduction.

Printed on: 02/07/23

## Abstract Archives of the RSNA, 2022

M5A-SPPH-5

### Evaluation of Small Coronary Stents using High-Resolution Mode Imaging with Deep Learning Imaging Reconstruction

Monday, Nov. 28 12:15PM - 12:45PM Room: Learning Center - PH DPS

#### Participants

Kazuki Ishikawa, (*Presenter*) General Electric Company

#### PURPOSE

Although the frequency of coronary stent restenosis has decreased with the advent of drug-eluting stents, the diagnostic accuracy of restenosis by conventional coronary CT angiography is not high. Although the high-resolution (HR) imaging seems promising for restenosis evaluation because it improves spatial resolution, increased image noise due to dedicated kernel and tube current limitations is a problem. The purpose of this study was to clarify the usefulness of noise reduction by deep learning imaging reconstruction (DLIR) in the evaluation of coronary stents using HR imaging.

#### METHODS AND MATERIALS

We analyzed the images of coronary stents with inner diameters of 3 mm and 2.5 mm in HR and normal (NR) modes. The images were scanned with an ECG-synchronized axial scan on a commercially available 256 MDCT scanner: tube voltage, 120 kV; current, automatic exposure control; and noise index, 26. Images were reconstructed using hybrid iterative reconstruction (HIR, strength 80%), DLIR-Low (L), -Medium (M) and -High (H), respectively. The kernels used were HD-Standard in HR mode and Standard in NR mode. The values of full width at half maximum (FWHM), standard deviation (SD) of the stent profile, and noise power spectrum (NPS) were measured to evaluate image quality.

#### RESULTS

The CT dose index volume for HR and NR were both 8.9 mGy. The FWHM of the stent profile in HIR, DLIR-L, DLIR-M, and DLIR-H was 1.00, 1.06, 1.05, and 1.06, respectively for HR at 2.5 mm. For NR at 2.5 mm: 1.42, 1.49, 1.49, and 1.49, respectively. For HR at 3 mm, 0.97, 1.01, 1.01, and 1.01, respectively. For NR at 2.5 mm, 1.28, 1.30, 1.30, and 1.29, respectively. The FWHM between HR and NR differed significantly ( $p < 0.01$ ). The SD difference between HR and NR was 7.74, 9.61, 6.20 and 3.48, respectively. There was a significant difference among the reconstruction methods ( $p < 0.01$ ). The peak frequency of the NPS in HR mode was 0.23, 0.34, 0.28, and 0.22 cycles/mm for HIR, DLIR-L, DLIR-M, and DLIR-H, respectively, and the average frequency was 0.35, 0.42, 0.40, and 0.39 cycles/mm, respectively. Compared to the peak and average frequencies of the filtered back projection (0.54 and 0.48 cycles/mm), these results showed a noise texture change of HIR.

#### CONCLUSION

The use of DLIR in combination with the HR mode improved the visibility of small-diameter coronary stents by minimizing the image noise and maintaining the image texture.

#### CLINICAL RELEVANCE/APPLICATION

DLIR minimizes the effects of tube current limitation and noise increase in HR mode. It enables HR mode imaging for larger patients, and can improve the imaging of smaller coronary stents.

Printed on: 02/07/23

## Abstract Archives of the RSNA, 2022

M5A-SPPH-6

### Signal-To-Noise Ratio Measurement in CT With Conventional and Textured Phantoms: Comparison of Two Deep-Learning Image Reconstruction Techniques

Monday, Nov. 28 12:15PM - 12:45PM Room: Learning Center - PH DPS

#### Participants

Hiroki Kawashima, PhD, RT, Kanazawa, Japan (*Presenter*) Nothing to Disclose

#### PURPOSE

To evaluate signal-to-noise ratio (SNR) improvement by deep-learning image reconstruction (DLIR) techniques, with a conventional method using rod and water phantoms and a new approach using a textured phantom.

#### METHODS AND MATERIALS

A water-bath phantom with a diameter of 300 mm was used as a base phantom. A textured phantom with a diameter of 128 mm, made by mixing water and 12 mg/mL diluted iodine equivalent materials (IEM), was placed in the base phantom (non-uniform region). In addition, a simple rod made by IEM was placed. Thirty repeated phantom scans were performed using two CT scanners (GE, Revolution CT Apex Edition; Canon, Aquilion One PRISM Edition) at 5 and 15 mGy. Images were reconstructed with filtered back projection (FBP) and DLIR [GE, TrueFidelity (TF); Canon, Advanced intelligent Clear-IQ (AC)] for three process strengths. The task transfer function (TTF) was measured with the rod image; the noise power spectrum (NPS) was measured in the water-only region. The conventional SNR (SNRC(u)) was calculated as a square root of  $TTF(u)^2/NPS(u)$ . A signal spectrum (S(u)) was measured in an averaged image of the non-uniform region using a Fourier analysis, and a noise spectrum (N(u)) was estimated as an average of 30 spectra (S(u)+N(u)) minus the S(u). An SNR for the non-uniform region (SNRNU(u)) was calculated by  $S(u)/N(u)$ . The SNR improvement factor (SIF) was calculated by SNR of DLIR divided by SNR of FBP.

#### RESULTS

The average SIFs of SNRC with TF were 1.88 at 0.1 mm<sup>-1</sup>, 2.92 at 0.5 mm<sup>-1</sup>; those with AC were 2.52 at 0.1 mm<sup>-1</sup>, 6.20 at 0.5 mm<sup>-1</sup>. On the other hand, the SIFs of SNRNU with TF were 1.41 at 0.1 mm<sup>-1</sup>, 1.10 at 0.5 mm<sup>-1</sup>; those with AC were 1.47 at 0.1 mm<sup>-1</sup>, 1.25 at 0.5 mm<sup>-1</sup>, which were notably lower than the SIF of SNRC.

#### CONCLUSION

Both DLIR techniques sufficiently improved the conventional SNR measured with the rod and water images (88-500%). However, the improvements of SNRNU were low (10-47%), which revealed limited performances for the complex structures included in the textured phantom.

#### CLINICAL RELEVANCE/APPLICATION

The SIFs measured using the non-uniform region are possibly more clinically relevant compared to the conventional method using simple rods and a uniform water region.

Printed on: 02/07/23

## Abstract Archives of the RSNA, 2022

M5A-SPPH-7

### Importance of Larger Reconstruction Matrix Sizes for Super-Resolution Deep Learning Reconstruction

Monday, Nov. 28 12:15PM - 12:45PM Room: Learning Center - PH DPS

#### Participants

Toru Higaki, PhD, Minami-ku, Hiroshima, Japan (*Presenter*) Nothing to Disclose

#### PURPOSE

Recently clinically introduced super-resolution deep learning reconstruction (SR-DLR) can convert conventional- to high-resolution CT images. The matrix size of the output images can be selected as either 512×512 as conventional or 1024×1024. In this study, we investigated the effect of the output image matrix size (the pixel size in the output image) on spatial resolution.

#### METHODS AND MATERIALS

The SR-DLR was implemented using a super-resolution DCNN (SR-DCNN). It was trained with pairs of high-resolution- and conventional resolution images. The high-resolution images for the training target were acquired using an actual high-resolution CT scanner (Aquilion Precision, Canon Medical Systems Corp.: CMSC) which has a twice larger matrix size. We made a CCTA phantom (Fig. left-bottom) using a 3D printer (Agilista-3200, Keyence). The outer diameter of the phantom was 350×250 mm. Iodine contrast medium diluted with 20 mgI/ml was filled to the simulated left ventricle and coronary arteries. We scanned the CCTA phantom using a conventional CT scanner (Aquilion ONE GENESIS, CMSC) with standard CCTA protocol (tube voltage: 120 kV, tube current: automatic exposure control with SD 23 HU, rotation speed: 0.275 s/rot, ECG-gated volume scan). Images were reconstructed with conventional hybrid iterative reconstruction (IR) (Adaptive Iterative Dose Reduction 3D with FC14 kernel, CMSC) with 512 matrix, SR-DLR with 512 matrix, and SR-DLR with 1024 matrix. The reconstruction FoV was 200 mm, and the pixel sizes of the 512- and 1024-matrix images were 0.39 and 0.195 mm, respectively. We measured profile curves and modulation transfer functions (MTFs) using the edge of a simulated left ventricle and compared their spatial resolution.

#### RESULTS

The three reconstructed images shown on the left side of the figure indicate that the 1024 matrix SR-DLR image provides the sharpest edges. The edge profile curves and MTF on the right side of the figure also showed a similar trend. The actual MTF of SR-DLR exceeded the Nyquist frequency of 512 matrix images, and 1024 matrix images were required to fully utilize SR-DLR's performance.

#### CONCLUSION

s To fully utilize the spatial resolution of SR-DLR, it is suitable to reconstruct images with 1024 matrices.

#### CLINICAL RELEVANCE/APPLICATION

The SR-DLR of 1024 matrix images provides higher spatial resolution, which is useful for the visualization of fine structures such as demonstration of plaques in the coronary artery, and fine lesions in diffuse lung disease.

Printed on: 02/07/23



## Abstract Archives of the RSNA, 2022

MSA-SPPH-8

### Ranking the Relative Importance of Image Quality Features in CT by Consensus Survey

Monday, Nov. 28 12:15PM - 12:45PM Room: Learning Center - PH DPS

#### Participants

Dustin Gress, MS, (*Presenter*) Nothing to Disclose

#### PURPOSE

To assess consensus opinions from subspecialty radiologists and imaging physicists on the relative importance of image quality features in CT, in order to set subspecialty-informed development priorities for quantitating such features, preferably using automated methods.

#### METHODS AND MATERIALS

A web-based pictorial survey was created by subject matter expert radiologists and imaging physicists, requesting respondents to rank the relative importance of ten distinct imaging features in their clinical practice, using a 1 (lowest) to 10 (highest) scale. The survey was first sent to subspecialty radiologists and physicists in volunteer leadership roles in the ACR and RSNA, with such roles assumed as reasonable proxy for expertise. The survey then relied on snowball sampling, where respondents could recommend up to 3 suitable experts for invitation to complete the survey.

#### RESULTS

There were 66 total respondents. Median years of respondent experience for all subspecialties ranged 10-16.5 years. Overall mean rankings for features ranged 5.48-8.74; motion and streaking artifact had the highest average across all subspecialties, scored 8.74 and 8.32, respectively. Lowest overall mean score was for blooming artifact (5.48). Musculoskeletal means were highest for noise texture (9.0) and metal artifact (9.4). Emergency, neuro, pediatric, and abdominal radiologists scored motion artifact highest, with means of 9.89, 9.38, 8.5, and 9.0, respectively. Low contrast axial sharpness was second highest for abdominal radiologists (8.94), with streaking third (8.72). Imaging physicist scored low contrast axial sharpness highest and noise magnitude second highest, with means of 8.94 and 8.78, respectively.

#### CONCLUSION

Specific image quality features ranked by expert subspecialty radiologists have relatively higher importance for their routine clinical practice compared to other features, and the importance of identical features also vary between subspecialties. These metrics afford an opportunity to develop targeted image quality measurement tools, especially those that are automated, which can be configurable depending on the practice domain. Limitations include those with expert opinions; responses from thoracic and cardiac radiologists are being collected.

#### CLINICAL RELEVANCE/APPLICATION

Automated quantification and reporting of relevant medical image quality metrics is an essential step toward enhancing the value of clinical care in medical imaging. This performance paradigm accounts for both radiation dose index management as well as objective image quality management.

Printed on: 02/07/23



## Abstract Archives of the RSNA, 2022

M5A-SPPH-9

### Detectability Index Analysis of Enterprise CT AP Protocols

Monday, Nov. 28 12:15PM - 12:45PM Room: Learning Center - PH DPS

#### Participants

Brian Hurley, MS, (*Presenter*) Nothing to Disclose

#### PURPOSE

With trends to move toward enterprise-wide radiology management there should be image quality standardization across a hospital system. The purpose is to develop a methodology to assess image quality uniformity for the adult abdomen and pelvis protocol across a hospital enterprise which includes a CT scanner fleet with multiple manufacturers and models.

#### METHODS AND MATERIALS

A dose tracking software (Radimetrics) was used to gather data on abdomen and pelvis with contrast scans across a health enterprise for the 2nd Quarter of 2021. (3,603 scans). From this dataset, the 5th, 25th, 50th, 75th, and 95th percentiles of the CTDIVol were extracted for each facility in the hospital enterprise. The ACR CT accreditation phantom was scanned at each of the facility specific CTDIVol values and these scans were assessed using the ImQuest software by Duke CIPG to obtain the detectability index ( $d'$ ). To normalize the dose dependence of the image quality, the  $d'^2$ /CTDIVol for the 25th, 50th and 75th percentiles were calculated and compared to evaluate the protocol performance.

#### RESULTS

The range of the  $d'^2$ /CTDIVol for the 25th, 50th and 75th percentiles was 124 to 263, 112 to 267, and 105 to 269 respectively. The absolute differences for the 25th, 50th, and 75th were 139, 155, and 164 which corresponds to a percent difference of 72%, 82% and 88%. When comparing a single institution, the largest percent difference within the scanners at a given institution for the protocol 50th percentile of dose was found to be 29%.

#### CONCLUSION

There is substantial variation in the image quality for the abdomen pelvis protocols across the hospital enterprise examined. Additionally, there is a significant variation within hospitals when multiple makes/models were utilized. Currently much effort is placed on protocol optimization in terms of dose (CTDI, DLP or Effective Dose). Though dose is a loose surrogate for image quality, with advanced applications on modern scanners and the growing push towards enterprise healthcare more focus should be placed on providing uniform image quality for a given protocol across different scanner types at a hospital enterprise. This analysis was done with a 5 mm lesion based on acrylic TTF and contrast, in the future this should be expanded to other lesion sizes and contrast levels with the potential to select the target (lesion size, contrast, etc.) based on clinical indication.

#### CLINICAL RELEVANCE/APPLICATION

The findings of this study can be used to help improve image quality uniformity across a large hospital system. This methodology can be applied to other adult and pediatric protocols to assess image quality uniformity across multiple CT scanners independent of make and model.

Printed on: 02/07/23

## Abstract Archives of the RSNA, 2022

M5A-SPRO

### Radiation Oncology Monday Poster Discussions - A

Monday, Nov. 28 12:15PM - 12:45PM Room: Learning Center - RO DPS

#### Participants

Tarita Thomas, MD, PhD, Chicago, IL (*Moderator*) Nothing to Disclose

#### Sub-Events

### M5A-SPRO-1 Comparison of Bladder Wall Only- and Whole Bladder Volume- Doses in Neoadjuvant Radiotherapy of Rectal Cancer

#### Participants

Ayşe Dagli, Istanbul, Turkey (*Presenter*) Nothing to Disclose

#### PURPOSE

To dosimetrically compare the bladder doses obtained from whole bladder volume and bladder wall only in neoadjuvant radiotherapy of locally advanced rectal cancer (LARC).

#### METHODS AND MATERIALS

Treatment planning CT images of 65 LARC patients (M/F: 41/24) treated with neoadjuvant radiotherapy were used. Median patient age was 60 (33-82). CT simulation images were taken in supine position with full bladder using iv contrast, with 3.75 mm slice thickness in all patients. Tumor location was proximal rectum in 2 patients, mid-rectum in 27 and distal rectum in 36. Primary tumor was contoured as GTV. CTV-tumor was covering GTV plus 2 cm proximally and distally, and mesorectum radially. Pelvic great vessels, starting from aortic bifurcation, were contoured with a 0.8 cm margin and pre-sacral and obturator regions were included to create CTV-LNs. Whole bladder (WB) and bladder wall only (BW) were separately contoured for study purpose. Prescribed dose was 50.4 Gy in 1.8 Gy/fx for PTV-LNs and PTV-tumor. All plans were done with VMAT using two full arcs. Maximum dose (Dmax), volumes (%) receiving 40 Gy (V40), 45 Gy (V45) and 50 Gy (V50) for WB and BW were recorded and compared. Paired t-test was used for statistical analysis.  $P < 0.05$  was accepted statistically significant.

#### RESULTS

Median GTV length was 8 (5-14) cm. Median GTV and total PTV volumes were 78.4 (30.5-330) and 1133 (784-11451.2) ml, respectively. Median WB and BW volumes were 522.5 (157.7-989.6) and 129.9 (33.2-211.3) ml, respectively. Median Dmax was 53.3 (49.5-54.6) Gy in both WB and BW ( $p=0.5$ ). V40, V45 and V50 were significantly higher for BW than WB ( $p < 0.0001$ ) (Table). Median BW/WB ratios of V40, V45 and V50 were 1.6 (1.1-2.5), 2 (1.2-3.1) and 2.6 (1.6-3.8), respectively. Table. Median (min-max) whole bladder (WB) and bladder wall only (BW) volumes (ml) and volumes receiving 40 Gy (V40), 45 Gy (V45) and 50 Gy (V50) (%).

#### CONCLUSION

Except maximum bladder dose, bladder doses obtained from whole bladder volume does not represent bladder wall doses in LARC patients treated with neoadjuvant radiotherapy. Further studies are needed to evaluate clinical impact of these results.

#### CLINICAL RELEVANCE/APPLICATION

Whole bladder volume doses are being used for bladder dose constraints in neoadjuvant radiotherapy of locally advanced rectal cancer. However, they do not represent bladder wall doses. This may explain higher than expected bladder side effects in some patients. Bladder wall doses may be used to better predict treatment related side effects in rectal cancer patients treated with neoadjuvant radiotherapy.

Printed on: 02/07/23

## Abstract Archives of the RSNA, 2022

M5A-SPRO-1

### Comparison of Bladder Wall Only- and Whole Bladder Volume- Doses in Neoadjuvant Radiotherapy of Rectal Cancer

Monday, Nov. 28 12:15PM - 12:45PM Room: Learning Center - RO DPS

#### Participants

Ayşe Dagli, Istanbul, Turkey (*Presenter*) Nothing to Disclose

#### PURPOSE

To dosimetrically compare the bladder doses obtained from whole bladder volume and bladder wall only in neoadjuvant radiotherapy of locally advanced rectal cancer (LARC).

#### METHODS AND MATERIALS

Treatment planning CT images of 65 LARC patients (M/F: 41/24) treated with neoadjuvant radiotherapy were used. Median patient age was 60 (33-82). CT simulation images were taken in supine position with full bladder using iv contrast, with 3.75 mm slice thickness in all patients. Tumor location was proximal rectum in 2 patients, mid-rectum in 27 and distal rectum in 36. Primary tumor was contoured as GTV. CTV-tumor was covering GTV plus 2 cm proximally and distally, and mezorectum radially. Pelvic great vessels, starting from aortic bifurcation, were contoured with a 0.8 cm margin and pre-sacral and obturator regions were included to create CTV-LNs. Whole bladder (WB) and bladder wall only (BW) were separately contoured for study purpose. Prescribed dose was 50.4 Gy in 1.8 Gy/fx for PTV-LNs and PTV-tumor. All plans were done with VMAT using two full arcs. Maximum dose (Dmax), volumes (%) receiving 40 Gy (V40), 45 Gy (V45) and 50 Gy (V50) for WB and BW were recorded and compared. Paired t-test was used for statistical analysis.  $P < 0.05$  was accepted statistically significant.

#### RESULTS

Median GTV length was 8 (5-14) cm. Median GTV and total PTV volumes were 78.4 (30.5-330) and 1133 (784-11451.2) ml, respectively. Median WB and BW volumes were 522.5 (157.7-989.6) and 129.9 (33.2-211.3) ml, respectively. Median Dmax was 53.3 (49.5-54.6) Gy in both WB and BW ( $p=0.5$ ). V40, V45 and V50 were significantly higher for BW than WB ( $p < 0.0001$ ) (Table). Median BW/WB ratios of V40, V45 and V50 were 1.6 (1.1-2.5), 2 (1.2-3.1) and 2.6 (1.6-3.8), respectively. Table. Median (min-max) whole bladder (WB) and bladder wall only (BW) volumes (ml) and volumes receiving 40 Gy (V40), 45 Gy (V45) and 50 Gy (V50) (%).

#### CONCLUSION

Except maximum bladder dose, bladder doses obtained from whole bladder volume does not represent bladder wall doses in LARC patients treated with neoadjuvant radiotherapy. Further studies are needed to evaluate clinical impact of these results.

#### CLINICAL RELEVANCE/APPLICATION

Whole bladder volume doses are being used for bladder dose constraints in neoadjuvant radiotherapy of locally advanced rectal cancer. However, they do not represent bladder wall doses. This may explain higher than expected bladder side effects in some patients. Bladder wall doses may be used to better predict treatment related side effects in rectal cancer patients treated with neoadjuvant radiotherapy.

Printed on: 02/07/23

## Abstract Archives of the RSNA, 2022

M5A-SPVA

### Vascular Monday Poster Discussions - A

Monday, Nov. 28 12:15PM - 12:45PM Room: Learning Center - VA DPS

#### Sub-Events

#### M5A-SPVA-1 A Comparison of Emergency ECG-gated CT and Surgical Findings in Acute Aortic Syndrome

Participants

Makoto Orii, (*Presenter*) Nothing to Disclose

#### PURPOSE

The accuracy of ECG-gated CT findings in acute aortic syndrome (AAS), compared to surgical confirmation as the reference standard, remains unknown. The purpose of study is to compare the detection accuracies of ECG-gated CT for intimal tear (IT) in aortic dissection (AD) and ulcer-like projection (ULP) in intramural hematoma (IMH).

#### METHODS AND MATERIALS

This retrospective study was conducted from September 2005 to November 2021. The accuracies of detecting IT and ULP were compared among both diastolic- and systolic-phase, only diastolic-phase, and only systolic-phase modalities of ECG-gated CT using the Cochran's Q test.

#### RESULTS

Data from 81 patients (mean age±SD, 67.6 years±11.8; 41 men) who underwent emergency ECG-gated CT and subsequent open surgery or thoracic endovascular aortic repair (TEVAR) for AD (n=52) or IMH (n=29) were included. The detection accuracy for IT and ULP using both diastolic- and systolic-phase, only diastolic-phase, and only systolic-phase modalities of ECG-gated CT was 95% [95% CI: 90-97], 93% [95% CI: 87-97], and 94% [95% CI: 88-97], respectively. There were no significant differences in detection accuracy among the three modalities tested (P=0.55). There were no significant differences among both diastolic- and systolic-phase (96% [95% CI: 96-96]), only diastolic-phase (92% [95% CI: 92-97]), and only systolic-phase ECG-gated CT (94% [91% CI: 91-97], P=0.55) for the detection of IT in AD. Similarly, there were no significant differences in the accuracy of detecting ULP in IMH among both diastolic- and systolic-phase (93% [95% CI: 80-98]), only diastolic-phase (93% [95% CI: 80-98]), and only systolic-phase ECG-gated CT (93% [95% CI: 80-98], P>0.99).

#### CONCLUSION

s ECG-gated CT of the thorax for AAS yields highly accurate findings; however, no significant differences in the accuracy of detecting IT in AD and ULP in IMH were seen among the three modalities of ECG-gated CT.

#### CLINICAL RELEVANCE/APPLICATION

Recently, the detection of IT in AD and ULP in IMH has been recognized as an important factor that affects treatment selection, i.e., open surgery versus TEVAR. This is the first study to investigate the accuracy of both diastolic and systolic-phase ECG-gated CT for detecting IT and ULP with surgical confirmation as the reference standard. Emergency ECG-gated CT provides high diagnostic accuracy for detecting IT in AD and ULP in IMH. The findings of this study will shed light on how surgeons can provide the best care for AAD patients in clinical practice.

Printed on: 02/07/23

## Abstract Archives of the RSNA, 2022

M5A-SPVA-1

### A Comparison of Emergency ECG-gated CT and Surgical Findings in Acute Aortic Syndrome

Monday, Nov. 28 12:15PM - 12:45PM Room: Learning Center - VA DPS

#### Participants

Makoto Orii, (*Presenter*) Nothing to Disclose

#### PURPOSE

The accuracy of ECG-gated CT findings in acute aortic syndrome (AAS), compared to surgical confirmation as the reference standard, remains unknown. The purpose of study is to compare the detection accuracies of ECG-gated CT for intimal tear (IT) in aortic dissection (AD) and ulcer-like projection (ULP) in intramural hematoma (IMH).

#### METHODS AND MATERIALS

This retrospective study was conducted from September 2005 to November 2021. The accuracies of detecting IT and ULP were compared among both diastolic- and systolic-phase, only diastolic-phase, and only systolic-phase modalities of ECG-gated CT using the Cochran's Q test.

#### RESULTS

Data from 81 patients (mean age±SD, 67.6 years±11.8; 41 men) who underwent emergency ECG-gated CT and subsequent open surgery or thoracic endovascular aortic repair (TEVAR) for AD (n=52) or IMH (n=29) were included. The detection accuracy for IT and ULP using both diastolic- and systolic-phase, only diastolic-phase, and only systolic-phase modalities of ECG-gated CT was 95% [95% CI: 90-97], 93% [95% CI: 87-97], and 94% [95% CI: 88-97], respectively. There were no significant differences in detection accuracy among the three modalities tested (P=0.55). There were no significant differences among both diastolic- and systolic-phase (96% [95% CI: 96-96]), only diastolic-phase (92% [95% CI: 92-97]), and only systolic-phase ECG-gated CT (94% [91% CI: 91-97], P=0.55) for the detection of IT in AD. Similarly, there were no significant differences in the accuracy of detecting ULP in IMH among both diastolic- and systolic-phase (93% [95% CI: 80-98]), only diastolic-phase (93% [95% CI: 80-98]), and only systolic-phase ECG-gated CT (93% [95% CI: 80-98], P>0.99).

#### CONCLUSION

s ECG-gated CT of the thorax for AAS yields highly accurate findings; however, no significant differences in the accuracy of detecting IT in AD and ULP in IMH were seen among the three modalities of ECG-gated CT.

#### CLINICAL RELEVANCE/APPLICATION

Recently, the detection of IT in AD and ULP in IMH has been recognized as an important factor that affects treatment selection, i.e., open surgery versus TEVAR. This is the first study to investigate the accuracy of both diastolic and systolic-phase ECG-gated CT for detecting IT and ULP with surgical confirmation as the reference standard. Emergency ECG-gated CT provides high diagnostic accuracy for detecting IT in AD and ULP in IMH. The findings of this study will shed light on how surgeons can provide the best care for AAD patients in clinical practice.

Printed on: 02/07/23

## Abstract Archives of the RSNA, 2022

M5B-SPBR

### Breast Monday Poster Discussions - B

Monday, Nov. 28 12:45PM - 1:15PM Room: Learning Center - BR DPS

#### Participants

Jean Seely, MD, Ottawa, ON (*Moderator*) Nothing to Disclose

#### Sub-Events

### M5B-SPBR-1 Investigating Conducive Conditions for Detecting Breast Biopsy Markers by Ultrasound Color Doppler Twinkling

#### Participants

Christine U. Lee, MD, PhD, Rochester, MN (*Presenter*) Nothing to Disclose

#### PURPOSE

Identifying breast biopsy clips or markers, particularly in patients with breast cancer after neoadjuvant systemic therapy, is necessary for surgical management, but ultrasound detection of these markers can be challenging, if not prohibitive. This study aims to determine what optimizes color Doppler twinkling of breast biopsy markers, when present, and whether marker surface roughness is associated with their twinkling signatures.

#### METHODS AND MATERIALS

Thirty-five biopsy markers were evaluated using three different transducers (ML6-15, 9L, C1-6 on a Logiq E9 scanner, General Electric (GE) Healthcare, Wauwatosa, WI) in three different media (solid gel phantom, ultrasound coupling gel, and ex vivo cadaveric breasts). The twinkling signature was rated on an ordinal scale from 0 (none) to 4 (marked). Actionable ultrasound detection was defined to mean sufficiently confident detection of a target to act on it (e.g., radioactive seed localization) independent of its B-mode conspicuity. Surface roughness measurements and micro-CT images were obtained for each marker. A mixed-effects proportional odds regression model was used to examine the associations of embedding material and transducers with the twinkling scores, and a two-sided Wilcoxon rank sum test was used to compare the surface roughness measurements by twinkling rating actionability.

#### RESULTS

Embedding materials were associated with significantly higher twinkling ratings in both solid gel phantom ( $P < 0.001$ ) and coupling gel media ( $P = 0.002$ ), and there were significant pairwise differences among transducers across all media, with  $C1-6 > 9L > ML6-15$  in solid gel phantom (all  $P < 0.05$ ). Higher surface roughness was associated with actionable twinkling scores in cadaveric breast for both C1-6 ( $P = 0.022$ ) and 9L transducers ( $P = 0.002$ ).

#### CONCLUSION

Color Doppler twinkling signatures of some breast biopsy markers can improve their ultrasound conspicuity. Actionable twinkling is associated with lower transducer frequencies and higher surface roughness of the markers.

#### CLINICAL RELEVANCE/APPLICATION

Breast ultrasound does not conventionally invoke color Doppler twinkling for marker detection, but the added twinkling information can be valuable.

### M5B-SPBR-2 Localizing the Clipped Node in Patients with Node-Positive Breast Cancer Treated with Neoadjuvant Chemotherapy

#### Participants

Veli Süha Ozturk, MD, (*Presenter*) Nothing to Disclose

#### PURPOSE

Clipping of positive axillary lymph nodes before treatment allows conservative surgery in patients with breast cancer down-staged by neoadjuvant chemotherapy (NAC). This study aimed at evaluating the feasibility and identifiability of different clips in the axilla, as well as the performance of preoperative imaging-guided localization of the clipped axillary lymph node.

#### METHODS AND MATERIALS

Institutional ethical committee approval was obtained. Between March 2017 and January 2022, all breast cancer patients with biopsy-confirmed breast tumor and axillary lymph node which clipped at the time of diagnosis who underwent NAC were retrospectively evaluated. Cases with 3 or more pathological lymph nodes were excluded. SenoMarc™ (Bard, Inc.) and Biomarc® (Vigeo, Inc.) were used as 2D rectangular - ribbon shaped metallic tissue markers and Twirl™ (Bard, Inc.) was used as 3D coil like round shaped metallic tissue marker. After primary systemic therapy, clipped lymph nodes were localized by a wire and then operated.

## RESULTS

The study included one hundred thirty eight female breast cancer patients with clipped lymph node. There were 2D tissue markers in one hundred thirteen (81.9%) nodes. Of the clipped nodes, one hundred twenty two (88.4%) were localized under US guidance successfully (Figure 1-2). In sixteen patients, clipped nodes were not visualized by sonography, which all had 2D tissue markers. All 3D markers were detected by ultrasonography (Figure 3). The success rate of the marker placement procedure was 100%. Removals of clipped nodes were confirmed with specimen radiography.

## CONCLUSION

s Ultrasound-guided wire localization of the clipped node is a feasible and useful method in clinical practice, especially with the increased detectability with 3D marker clips.

## CLINICAL RELEVANCE/APPLICATION

Determination of clipped lymph nodes is the crucial part for removal with targeted axillary dissection. Despite being the primary imaging method, ultrasound fails to detect clipped node in some cases. Shape and size play an important role in sonographic visualization of the marker. Appropriate marker selection appears to increase the sensitivity of ultrasound.

## M5B-SPBR-4 Whole-body [18F]FDG PET/MRI Including an Integrated Breast MRI Protocol in Breast Cancer Patients

### Participants

Thiemo Van Nijnatten, Maastricht, Netherlands (*Presenter*) Nothing to Disclose

## PURPOSE

To investigate the feasibility of whole-body 18F-FDG PET/MRI including an integrated breast MRI protocol in breast cancer patients for locoregional and distant staging.

## METHODS AND MATERIALS

Patients diagnosed with histopathologically confirmed breast cancer according to conventional imaging modalities (i.e. mammography and ultrasound) were prospectively included. All patients were considered for further examination with regard to locoregional and distant staging and underwent whole-body 18F-FDG PET/MRI including an integrated breast MRI protocol. The protocol consisted of dedicated breast MRI (prone position) and whole-body PET/MRI (supine position; including T2W, T1W post-contrast, DWI sequences and PET reconstructions) approximately 60 minutes after injection of 18F-FDG. In addition, unenhanced chest CT was performed for pulmonary lesion detection. Results of 18F-FDG PET/MRI, including integrated breast MRI, were compared to conventional imaging modalities in terms of clinical tumour (cT), nodal (cN) and distant (cM) status, according to 8th edition of TNM classification.

## RESULTS

From April 2021 until April 2022, 26 breast cancer patients were included and underwent whole-body 18F-FDG PET/MRI including an integrated breast MRI protocol. According to conventional imaging, cT1-2 breast cancer was present in 22 out of 26 patients, 3 patients had cT3 and one patient cT4 breast cancer. With regard to cN status, 9 patients were considered cN0, 15 cN1 (1-3 suspicious lymph nodes) and 2 patients cN2-3 (four or more suspicious lymph nodes). Whole-body 18F-FDG PET/MRI, including an integrated breast MRI protocol, upstaged cT status in ten patients and cN status in nine patients. In addition, distant metastases were detected in three patients and a fourth patient was diagnosed with a synchronous primary tumour (lung cancer).

## CONCLUSION

s Whole-body 18F-FDG PET/MRI amended by an integrated breast MRI protocol is feasible and upstages locoregional and distant status in a considerable amount of recently diagnosed breast cancer patients with an indication for whole body staging.

## CLINICAL RELEVANCE/APPLICATION

Whole-body 18F-FDG PET/MRI amended by an integrated breast MRI protocol provides a promising new approach in breast cancer patients with regard to locoregional and distant staging.

## M5B-SPBR-5 A Multimodal Nomogram: An Adjunct Tool for Reducing Unnecessary Biopsies of Breast Lesions with Inconsistent BI-RADS Assessments by Ultrasound and Mammography

### Participants

Ziting Xu, Guangdong, China (*Presenter*) Nothing to Disclose

## PURPOSE

To develop and validate a multi-modal nomogram for the differential diagnosis of breast lesions with inconsistent assessments and to explore the practical value of the proposed model in reducing unnecessary breast lesion biopsies.

## METHODS AND MATERIALS

In this retrospective study, patients with a discordant BI-RADS assessment (defined as a difference in BI-RADS classification by US and MG, where one assessed as BI-RADS 4 or 5 and the other assessed the same lesion as BI-RADS 0, 2 or 3) were eligible. Total 604 patients with discordant assessments from Center 1 were included as the training (n = 439) and internal validation (n = 175) cohorts in a ratio of 7:3 between June 2019 and June 2021. An independent cohort of 92 patients from Center 2 were allocated as the external testing (n = 92) cohort between January 2021 and June 2021. Univariate and multivariate logistic regression analyses were used to develop the nomogram. The performances of the model were assessed based on its discrimination and calibration. Receiver operating characteristic (ROC) curves analysis were performed to evaluate the diagnostic performance. The area under the curves (AUCs) were calculated and compared by using the DeLong's test. The differences in sensitivities and specificities were determined by the McNemar's test.

## RESULTS

Multivariate analyses indicated that age, MG features (margin, shape, density, suspicious calcifications and architectural distortion) and US features (margin, shape, and calcifications) were independent risk factors associated with breast cancer. The AUCs of the

nomogram were 0.87 (95% confidence interval [CI], 0.83-0.91) in the training, 0.91 (95% CI, 0.87-0.96) in the internal validation, and 0.92 (95% CI, 0.86 to 0.98) in the external testing cohorts. Calibration curves verified good consistency between the actual and nomogram-predicted malignancy probability. The nomogram had a significant effect improvement in diagnostic efficacy compared to MG or US alone (AUC: 0.889 vs 0.448 vs 0.597,  $P < 0.001$ ), and the potential reduction of unnecessary biopsies was 87.1%.

## CONCLUSION

The multimodal nomogram incorporating clinical information, MG and US imaging features may improve the prediction of breast lesion with inconsistent assessments and is an adjunct reliable tool to make optimal clinical decision and avoid unnecessary biopsies.

## CLINICAL RELEVANCE/APPLICATION

The multimodal nomogram can potentially serve a role in a clinical context as a decision support system to avoid unnecessary biopsies.

## M5B-SPBR-6 Outcomes at Biopsy of Mammographic Architectural Distortions without Definite Ultrasound Findings

### Participants

Ethan O. Cohen, MD, Houston, TX (*Presenter*) Spouse, Consultant, Boehringer Ingelheim GmbH; Spouse, Consultant, Novo Nordisk AS; Spouse, Consultant, Eli Lilly and Company

### PURPOSE

To stratify outcomes for mammographic architectural distortions without definite ultrasound findings.

### METHODS AND MATERIALS

Mammographically guided biopsies performed during 2016-2019 for architectural distortions without definite ultrasound correlates were retrospectively reviewed after IRB approval.

### RESULTS

145 biopsies in 140 patients (median age, 54 years; interquartile range, 47-66 years) yielded the following histologies: 71 benign (49.0%), 47 high-risk (32.4%), and 27 malignant (18.6%). Eleven benign results were discordant. Stromal fibrosis (26 of 71, 36.6%) and fibrocystic changes (25 of 71, 35.2%) were the most common benign concordant lesions. Radial sclerosing lesion without atypia was the most common high-risk lesion (34 of 47, 72.3%). Malignant results were 4 ductal carcinoma in situ, 16 invasive ductal carcinoma, and 7 invasive lobular carcinoma. One benign discordant lesion, one atypical ductal hyperplasia, and one radial sclerosing lesion were upgraded to invasive carcinoma at excision, resulting in a malignancy rate of 20.7% (30 of 145). Positive predictive value for malignancy or high-risk lesion was 51.7% (75 of 145).

## CONCLUSION

In the absence of a characteristically benign etiology, architectural distortion without an ultrasound correlate warrants tissue diagnosis given the malignancy rate of 20.7%.

## CLINICAL RELEVANCE/APPLICATION

Architectural distortion is an increasingly common imaging finding in the era of tomosynthesis screening. Appropriate management recommendations are necessary to ensure timely diagnosis.

## M5B-SPBR-7 Assessing the Diagnostic Yield of Ultrasound, MRI, Sentinel Lymph Node Biopsy (SLNB) in the Axilla in Breast Cancer Patients: A Single Institution Experience

### Participants

Alaa Alhazmi, MD, (*Presenter*) Nothing to Disclose

### PURPOSE

To investigate the diagnostic accuracy of ultrasonography (US) compared to magnetic resonance imaging (MRI) in the pre-operative assessment of metastatic disease to the axilla in breast cancer patients. This will be compared to sentinel lymph node biopsy (SLNB) results.

### METHODS AND MATERIALS

Research ethics board-approved retrospective study was conducted at a single tertiary care institution. Patients who underwent a pre-operative US, MRI, and SLNB between January 2019-September 2021 were included. The US and MRI reports of these patients were reviewed. The results were then compared to the histopathology results based on the SLNB results.

### RESULTS

A total of 104 female patients with primary breast cancer were included in this study. The average age was 58 (range 28-91). Of the 104 patients, 99 (95%) had unilateral breast cancer, and 5 (5%) had bilateral breast cancer. Fifty-two (50%) of patients had Invasive Ductal Carcinoma (IDC), 31 (30%) had Invasive Lobular Carcinoma (ILC), while 21 (20%) had other subtypes. The pre-operative sonographic assessment of the axillary nodes demonstrated an average long axis of 16.3 mm, a short axis of 5.7 mm, and an average cortical thickness of 2.3 mm. The pre-operative MRI assessment of the axillary nodes demonstrated an average long axis of 13.3 mm and a short axis of 7.5 mm. Correlation between the pre-operative sonographic assessment and SLNB results showed a sensitivity of 29.6%, specificity of 85.7%, positive predictive value (PPV) of 42.1%, and a negative predictive value (NPV) of 77.6%. Correlation between the MRI assessment and SLNB biopsy results showed a sensitivity of 37%, specificity of 89.6%, PPV of 55.6%, and NPV of 80.2%. There was an agreement between US and MRI in 91 cases (87.5%).

## CONCLUSION

In patients with primary breast cancer, the pre-operative evaluation of the axilla to assess for nodal metastasis utilizing US and MRI demonstrated comparable results. Both techniques demonstrated high specificity and NPV, while both had poor sensitivity and PPV. These findings should be confirmed in a larger sample of patients, as it can lead to a change in the current work-up of

patients with primary breast cancer.

#### **CLINICAL RELEVANCE/APPLICATION**

In this small sample, US and MRI were comparable in detecting axillary nodal metastasis in patients with primary breast cancer. If confirmed, this can have significant implications on patients, care providers, and the healthcare system.

#### **M5B-SPBR-8 Semiannual Breast US and MRI for Breast Cancer Screening in Patients with Personal History of Breast Cancer**

Participants

Su Min Ha, MD, PhD, Seoul, Korea, Republic Of (*Presenter*) Nothing to Disclose

#### **PURPOSE**

Wide variability of screening imaging patterns in patients with personal history of breast cancer (PHBC) warrants investigation of comparative clinical effectiveness. While more intensive screening with MRI or US at intervals <1 year to supplement annual mammography would increase early stage second breast cancer detection, its benefit has not yet been established. This study investigated outcomes of semiannual multimodality screening in patients with PHBC.

#### **METHODS AND MATERIALS**

We retrospectively searched our academic medical center database for patients who underwent incidence screening with MRI or US from July-December 2019 and three subsequent semiannual screening rounds over a 2-year study period. Routine clinical care included annual screening mammography; MRI or US was performed at the discretion of referring surgeons or radiologists interpreting the prior screening examination (Figure 1). The primary outcome was second breast cancer status identified by malignant pathology by the next screening event. Examination level cancer detection and interval cancer rates were calculated.

#### **RESULTS**

Our final cohort included 3,041 asymptomatic patients (median age 53 years; interquartile range, 46-60 years) (Figure 2). Among 2,031 semiannual MRI and 6,533 semiannual US examinations, the cancer detection rate was 3.9 per 1,000 examinations (8 of 2,031; 95% CI: 2.0, 7.8) and 1.5 per 1,000 examinations (10 of 6,533; 95% CI: 0.8, 2.8), respectively. Interval cancer rates were 0 per 1,000 examinations for both MRI and US. Further, no second breast cancers were identified after negative prior semiannual MRI screening.

#### **CONCLUSION**

Semiannual MRI or US with annual mammography eliminated interval cancers in patients with PHBC, suggesting that either modality may be used for more effective post-treatment screening.

#### **CLINICAL RELEVANCE/APPLICATION**

Semiannual MRI had higher second breast cancer detection rate than semiannual US. Further investigation is needed to establish longer term benefit such as overall survival.

Printed on: 02/07/23

## Abstract Archives of the RSNA, 2022

M5B-SPBR-1

### Investigating Conducive Conditions for Detecting Breast Biopsy Markers by Ultrasound Color Doppler Twinkling

Monday, Nov. 28 12:45PM - 1:15PM Room: Learning Center - BR DPS

#### Participants

Christine U. Lee, MD, PhD, Rochester, MN (*Presenter*) Nothing to Disclose

#### PURPOSE

Identifying breast biopsy clips or markers, particularly in patients with breast cancer after neoadjuvant systemic therapy, is necessary for surgical management, but ultrasound detection of these markers can be challenging, if not prohibitive. This study aims to determine what optimizes color Doppler twinkling of breast biopsy markers, when present, and whether marker surface roughness is associated with their twinkling signatures.

#### METHODS AND MATERIALS

Thirty-five biopsy markers were evaluated using three different transducers (ML6-15, 9L, C1-6 on a Logiq E9 scanner, General Electric (GE) Healthcare, Wauwatosa, WI) in three different media (solid gel phantom, ultrasound coupling gel, and ex vivo cadaveric breasts). The twinkling signature was rated on an ordinal scale from 0 (none) to 4 (marked). Actionable ultrasound detection was defined to mean sufficiently confident detection of a target to act on it (e.g., radioactive seed localization) independent of its B-mode conspicuity. Surface roughness measurements and micro-CT images were obtained for each marker. A mixed-effects proportional odds regression model was used to examine the associations of embedding material and transducers with the twinkling scores, and a two-sided Wilcoxon rank sum test was used to compare the surface roughness measurements by twinkling rating actionability.

#### RESULTS

Embedding materials were associated with significantly higher twinkling ratings in both solid gel phantom ( $P < 0.001$ ) and coupling gel media ( $P = 0.002$ ), and there were significant pairwise differences among transducers across all media, with C1-6 > 9L > ML6-15 in solid gel phantom (all  $P < 0.05$ ). Higher surface roughness was associated with actionable twinkling scores in cadaveric breast for both C1-6 ( $P = 0.022$ ) and 9L transducers ( $P = 0.002$ ).

#### CONCLUSION

s Color Doppler twinkling signatures of some breast biopsy markers can improve their ultrasound conspicuity. Actionable twinkling is associated with lower transducer frequencies and higher surface roughness of the markers.

#### CLINICAL RELEVANCE/APPLICATION

Breast ultrasound does not conventionally invoke color Doppler twinkling for marker detection, but the added twinkling information can be valuable.

Printed on: 02/07/23

## Abstract Archives of the RSNA, 2022

M5B-SPBR-2

### Localizing the Clipped Node in Patients with Node-Positive Breast Cancer Treated with Neoadjuvant Chemotherapy

Monday, Nov. 28 12:45PM - 1:15PM Room: Learning Center - BR DPS

#### Participants

Veli Süha Ozturk, MD, (*Presenter*) Nothing to Disclose

#### PURPOSE

Clipping of positive axillary lymph nodes before treatment allows conservative surgery in patients with breast cancer down-staged by neoadjuvant chemotherapy (NAC). This study aimed at evaluating the feasibility and identifiability of different clips in the axilla, as well as the performance of preoperative imaging-guided localization of the clipped axillary lymph node.

#### METHODS AND MATERIALS

Institutional ethical committee approval was obtained. Between March 2017 and January 2022, all breast cancer patients with biopsy-confirmed breast tumor and axillary lymph node which clipped at the time of diagnosis who underwent NAC were retrospectively evaluated. Cases with 3 or more pathological lymph nodes were excluded. SenoMarc™ (Bard, Inc.) and BiomarC® (Vigeo, Inc.) were used as 2D rectangular - ribbon shaped metallic tissue markers and Twirl™ (Bard, Inc.) was used as 3D coil like round shaped metallic tissue marker. After primary systemic therapy, clipped lymph nodes were localized by a wire and then operated.

#### RESULTS

The study included one hundred thirty eight female breast cancer patients with clipped lymph node. There were 2D tissue markers in one hundred thirteen (81.9%) nodes. Of the clipped nodes, one hundred twenty two (88.4%) were localized under US guidance successfully (Figure 1-2). In sixteen patients, clipped nodes were not visualized by sonography, which all had 2D tissue markers. All 3D markers were detected by ultrasonography (Figure 3). The success rate of the marker placement procedure was 100%. Removals of clipped nodes were confirmed with specimen radiography.

#### CONCLUSION

Ultrasound-guided wire localization of the clipped node is a feasible and useful method in clinical practice, especially with the increased detectability with 3D marker clips.

#### CLINICAL RELEVANCE/APPLICATION

Determination of clipped lymph nodes is the crucial part for removal with targeted axillary dissection. Despite being the primary imaging method, ultrasound fails to detect clipped node in some cases. Shape and size play an important role in sonographic visualization of the marker. Appropriate marker selection appears to increase the sensitivity of ultrasound.

Printed on: 02/07/23

## Abstract Archives of the RSNA, 2022

M5B-SPBR-4

### Whole-body [18F]FDG PET/MRI Including an Integrated Breast MRI Protocol in Breast Cancer Patients

Monday, Nov. 28 12:45PM - 1:15PM Room: Learning Center - BR DPS

#### Participants

Thiemo Van Nijnatten, Maastricht, Netherlands (*Presenter*) Nothing to Disclose

#### PURPOSE

To investigate the feasibility of whole-body 18F-FDG PET/MRI including an integrated breast MRI protocol in breast cancer patients for locoregional and distant staging.

#### METHODS AND MATERIALS

Patients diagnosed with histopathologically confirmed breast cancer according to conventional imaging modalities (i.e. mammography and ultrasound) were prospectively included. All patients were considered for further examination with regard to locoregional and distant staging and underwent whole-body 18F-FDG PET/MRI including an integrated breast MRI protocol. The protocol consisted of dedicated breast MRI (prone position) and whole-body PET/MRI (supine position; including T2W, T1W post-contrast, DWI sequences and PET reconstructions) approximately 60 minutes after injection of 18F-FDG. In addition, unenhanced chest CT was performed for pulmonary lesion detection. Results of 18F-FDG PET/MRI, including integrated breast MRI, were compared to conventional imaging modalities in terms of clinical tumour (cT), nodal (cN) and distant (cM) status, according to 8th edition of TNM classification.

#### RESULTS

From April 2021 until April 2022, 26 breast cancer patients were included and underwent whole-body 18F-FDG PET/MRI including an integrated breast MRI protocol. According to conventional imaging, cT1-2 breast cancer was present in 22 out of 26 patients, 3 patients had cT3 and one patient cT4 breast cancer. With regard to cN status, 9 patients were considered cN0, 15 cN1 (1-3 suspicious lymph nodes) and 2 patients cN2-3 (four or more suspicious lymph nodes). Whole-body 18F-FDG PET/MRI, including an integrated breast MRI protocol, upstaged cT status in ten patients and cN status in nine patients. In addition, distant metastases were detected in three patients and a fourth patient was diagnosed with a synchronous primary tumour (lung cancer).

#### CONCLUSION

s Whole-body 18F-FDG PET/MRI amended by an integrated breast MRI protocol is feasible and upstages locoregional and distant status in a considerable amount of recently diagnosed breast cancer patients with an indication for whole body staging.

#### CLINICAL RELEVANCE/APPLICATION

Whole-body 18F-FDG PET/MRI amended by an integrated breast MRI protocol provides a promising new approach in breast cancer patients with regard to locoregional and distant staging.

Printed on: 02/07/23

## Abstract Archives of the RSNA, 2022

M5B-SPBR-5

### **A Multimodal Nomogram: An Adjunct Tool for Reducing Unnecessary Biopsies of Breast Lesions with Inconsistent BI-RADS Assessments by Ultrasound and Mammography**

Monday, Nov. 28 12:45PM - 1:15PM Room: Learning Center - BR DPS

#### **Participants**

Ziting Xu, Guangdong, China (*Presenter*) Nothing to Disclose

#### **PURPOSE**

To develop and validate a multi-modal nomogram for the differential diagnosis of breast lesions with inconsistent assessments and to explore the practical value of the proposed model in reducing unnecessary breast lesion biopsies.

#### **METHODS AND MATERIALS**

In this retrospective study, patients with a discordant BI-RADS assessment (defined as a difference in BI-RADS classification by US and MG, where one assessed as BI-RADS 4 or 5 and the other assessed the same lesion as BI-RADS 0, 2 or 3) were eligible. Total 604 patients with discordant assessments from Center 1 were included as the training (n = 439) and internal validation (n = 175) cohorts in a ratio of 7:3 between June 2019 and June 2021. An independent cohort of 92 patients from Center 2 were allocated as the external testing (n = 92) cohort between January 2021 and June 2021. Univariate and multivariate logistic regression analyses were used to develop the nomogram. The performances of the model were assessed based on its discrimination and calibration. Receiver operating characteristic (ROC) curves analysis were performed to evaluate the diagnostic performance. The area under the curves (AUCs) were calculated and compared by using the Delong's test. The differences in sensitivities and specificities were determined by the McNemar's test.

#### **RESULTS**

Multivariate analyses indicated that age, MG features (margin, shape, density, suspicious calcifications and architectural distortion) and US features (margin, shape, and calcifications) were independent risk factors associated with breast cancer. The AUCs of the nomogram were 0.87 (95% confidence interval [CI], 0.83-0.91) in the training, 0.91 (95% CI, 0.87-0.96) in the internal validation, and 0.92 (95% CI, 0.86 to 0.98) in the external testing cohorts. Calibration curves verified good consistency between the actual and nomogram-predicted malignancy probability. The nomogram had a significant effect improvement in diagnostic efficacy compared to MG or US alone (AUC: 0.889 vs 0.448 vs 0.597,  $P < 0.001$ ), and the potential reduction of unnecessary biopsies was 87.1%.

#### **CONCLUSION**

The multimodal nomogram incorporating clinical information, MG and US imaging features may improve the prediction of breast lesion with inconsistent assessments and is an adjunct reliable tool to make optimal clinical decision and avoid unnecessary biopsies.

#### **CLINICAL RELEVANCE/APPLICATION**

The multimodal nomogram can potentially serve a role in a clinical context as a decision support system to avoid unnecessary biopsies.

Printed on: 02/07/23



## Abstract Archives of the RSNA, 2022

M5B-SPBR-6

### Outcomes at Biopsy of Mammographic Architectural Distortions without Definite Ultrasound Findings

Monday, Nov. 28 12:45PM - 1:15PM Room: Learning Center - BR DPS

#### Participants

Ethan O. Cohen, MD, Houston, TX (*Presenter*) Spouse, Consultant, Boehringer Ingelheim GmbH; Spouse, Consultant, Novo Nordisk AS; Spouse, Consultant, Eli Lilly and Company

#### PURPOSE

To stratify outcomes for mammographic architectural distortions without definite ultrasound findings.

#### METHODS AND MATERIALS

Mammographically guided biopsies performed during 2016-2019 for architectural distortions without definite ultrasound correlates were retrospectively reviewed after IRB approval.

#### RESULTS

145 biopsies in 140 patients (median age, 54 years; interquartile range, 47-66 years) yielded the following histologies: 71 benign (49.0%), 47 high-risk (32.4%), and 27 malignant (18.6%). Eleven benign results were discordant. Stromal fibrosis (26 of 71, 36.6%) and fibrocystic changes (25 of 71, 35.2%) were the most common benign concordant lesions. Radial sclerosing lesion without atypia was the most common high-risk lesion (34 of 47, 72.3%). Malignant results were 4 ductal carcinoma in situ, 16 invasive ductal carcinoma, and 7 invasive lobular carcinoma. One benign discordant lesion, one atypical ductal hyperplasia, and one radial sclerosing lesion were upgraded to invasive carcinoma at excision, resulting in a malignancy rate of 20.7% (30 of 145). Positive predictive value for malignancy or high-risk lesion was 51.7% (75 of 145).

#### CONCLUSION

In the absence of a characteristically benign etiology, architectural distortion without an ultrasound correlate warrants tissue diagnosis given the malignancy rate of 20.7%.

#### CLINICAL RELEVANCE/APPLICATION

Architectural distortion is an increasingly common imaging finding in the era of tomosynthesis screening. Appropriate management recommendations are necessary to ensure timely diagnosis.

Printed on: 02/07/23

## Abstract Archives of the RSNA, 2022

M5B-SPBR-7

### Assessing the Diagnostic Yield of Ultrasound, MRI, Sentinel Lymph Node Biopsy (SLNB) in the Axilla in Breast Cancer Patients: A Single Institution Experience

Monday, Nov. 28 12:45PM - 1:15PM Room: Learning Center - BR DPS

#### Participants

Alaa Alhazmi, MD, (*Presenter*) Nothing to Disclose

#### PURPOSE

To investigate the diagnostic accuracy of ultrasonography (US) compared to magnetic resonance imaging (MRI) in the pre-operative assessment of metastatic disease to the axilla in breast cancer patients. This will be compared to sentinel lymph node biopsy (SLNB) results.

#### METHODS AND MATERIALS

Research ethics board-approved retrospective study was conducted at a single tertiary care institution. Patients who underwent a pre-operative US, MRI, and SLNB between January 2019-September 2021 were included. The US and MRI reports of these patients were reviewed. The results were then compared to the histopathology results based on the SLNB results.

#### RESULTS

A total of 104 female patients with primary breast cancer were included in this study. The average age was 58 (range 28-91). Of the 104 patients, 99 (95%) had unilateral breast cancer, and 5 (5%) had bilateral breast cancer. Fifty-two (50%) of patients had Invasive Ductal Carcinoma (IDC), 31 (30%) had Invasive Lobular Carcinoma (ILC), while 21 (20%) had other subtypes. The pre-operative sonographic assessment of the axillary nodes demonstrated an average long axis of 16.3 mm, a short axis of 5.7 mm, and an average cortical thickness of 2.3 mm. The pre-operative MRI assessment of the axillary nodes demonstrated an average long axis of 13.3 mm and a short axis of 7.5 mm. Correlation between the pre-operative sonographic assessment and SLNB results showed a sensitivity of 29.6%, specificity of 85.7%, positive predictive value (PPV) of 42.1%, and a negative predictive value (NPV) of 77.6%. Correlation between the MRI assessment and SLNB biopsy results showed a sensitivity of 37%, specificity of 89.6%, PPV of 55.6%, and NPV of 80.2%. There was an agreement between US and MRI in 91 cases (87.5%).

#### CONCLUSION

In patients with primary breast cancer, the pre-operative evaluation of the axilla to assess for nodal metastasis utilizing US and MRI demonstrated comparable results. Both techniques demonstrated high specificity and NPV, while both had poor sensitivity and PPV. These findings should be confirmed in a larger sample of patients, as it can lead to a change in the current work-up of patients with primary breast cancer.

#### CLINICAL RELEVANCE/APPLICATION

In this small sample, US and MRI were comparable in detecting axillary nodal metastasis in patients with primary breast cancer. If confirmed, this can have significant implications on patients, care providers, and the healthcare system.

Printed on: 02/07/23



## Abstract Archives of the RSNA, 2022

M5B-SPBR-8

### Semiannual Breast US and MRI for Breast Cancer Screening in Patients with Personal History of Breast Cancer

Monday, Nov. 28 12:45PM - 1:15PM Room: Learning Center - BR DPS

#### Participants

Su Min Ha, MD, PhD, Seoul, Korea, Republic Of (*Presenter*) Nothing to Disclose

#### PURPOSE

Wide variability of screening imaging patterns in patients with personal history of breast cancer (PHBC) warrants investigation of comparative clinical effectiveness. While more intensive screening with MRI or US at intervals <1 year to supplement annual mammography would increase early stage second breast cancer detection, its benefit has not yet been established. This study investigated outcomes of semiannual multimodality screening in patients with PHBC.

#### METHODS AND MATERIALS

We retrospectively searched our academic medical center database for patients who underwent incidence screening with MRI or US from July-December 2019 and three subsequent semiannual screening rounds over a 2-year study period. Routine clinical care included annual screening mammography; MRI or US was performed at the discretion of referring surgeons or radiologists interpreting the prior screening examination (Figure 1). The primary outcome was second breast cancer status identified by malignant pathology by the next screening event. Examination level cancer detection and interval cancer rates were calculated.

#### RESULTS

Our final cohort included 3,041 asymptomatic patients (median age 53 years; interquartile range, 46-60 years) (Figure 2). Among 2,031 semiannual MRI and 6,533 semiannual US examinations, the cancer detection rate was 3.9 per 1,000 examinations (8 of 2,031; 95% CI: 2.0, 7.8) and 1.5 per 1,000 examinations (10 of 6,533; 95% CI: 0.8, 2.8), respectively. Interval cancer rates were 0 per 1,000 examinations for both MRI and US. Further, no second breast cancers were identified after negative prior semiannual MRI screening.

#### CONCLUSION

s Semiannual MRI or US with annual mammography eliminated interval cancers in patients with PHBC, suggesting that either modality may be used for more effective post-treatment screening.

#### CLINICAL RELEVANCE/APPLICATION

Semiannual MRI had higher second breast cancer detection rate than semiannual US. Further investigation is needed to establish longer term benefit such as overall survival.

Printed on: 02/07/23

## Abstract Archives of the RSNA, 2022

M5B-SPCA

### Cardiac Monday Poster Discussion - B

Monday, Nov. 28 12:45PM - 1:15PM Room: Learning Center - CA DPS

#### Sub-Events

#### **M5B-SPCA-1 Myocardial radiomics texture features associated with increased coronary calcium score - First Results on a Photon-Counting-CT**

##### Participants

Isabelle Ayx, MD, 68167 Mannheim, Germany (*Presenter*) Research Consultant, AstraZeneca PLC

##### PURPOSE

Coronary artery calcium score is an independent risk factor for the development of adverse cardiac events. Other cardiovascular risk factors such as tobacco use are known to influence the texture of the left ventricular myocardium in cardiac magnetic resonance imaging. The severity of coronary artery calcification may influence the myocardial texture. Due to better spatial resolution and signal-to-noise ratio, new CT technologies such as photon-counting computed tomography (PCCT) may improve the detection of texture alterations depending on the severity of coronary artery calcification.

##### METHODS AND MATERIALS

In this retrospective, single-center, IRB-approved study, left ventricular myocardium was segmented on axial slices semiautomatically and radiomics features were extracted using pyradiomics. Statistical analysis was performed in R statistics calculating mean and standard deviation with Pearson correlation coefficient for correlation of features. Visualization as boxplots and heatmaps was performed. For feature selection Random Forest classification was performed.

##### RESULTS

A total of 30 patients (26.7 % female, median age 58) were enrolled in this study. Patients were divided into two subgroups depending on the severity of coronary artery calcification (Agatston score 0 and Agatston score = 100). Random Forest feature selection was performed and a set of four higher-order features could be defined to discriminate myocardial texture between those two groups. Estimation of these radiomics features in the remaining patients (Agatston score 1-99) for validation and visualization as boxplots, confirmed an association between Agatston score severity and feature intensities.

##### CONCLUSION

A subset of radiomics features texture alterations of the left ventricular myocardium was associated with the severity of coronary artery calcification estimated by Agatston score.

##### CLINICAL RELEVANCE/APPLICATION

Due to the implementation of PCCT with better spatial resolution and contrast-to-noise ratio, cardiac CT imaging may possibly open up new options for radiomics feature texture analysis of myocardium depending on cardiovascular risk factors.

#### **M5B-SPCA-2 Prediction of coronary plaque progression via traditional parameters alongside radiomics based on coronary CT angiography**

##### Participants

Yinsu Zhu, (*Presenter*) Nothing to Disclose

##### PURPOSE

To investigate the value of traditional plaque parameters combined with radiomics based on coronary CT angiography (CCTA) in predicting coronary plaque progression.

##### METHODS AND MATERIALS

The clinical data and CCTA images of 400 patients who underwent more than twice CCTA examinations between January 2009 and August 2020 were retrospectively analyzed. Traditional plaque parameters including diameter stenosis, lesion length, vessel volume, total plaque volume and burden, calcified plaque volume and burden, non-calcified plaque volume and burden (NCPB), and pericoronary fat attenuation index (FAI) were measured. Then, the 400 patients were allocated to a training cohort (n = 280) and a validation cohort (n = 120), with a proportion of 7 : 3 via a stratified random splitting method. The two cohorts were divided into plaque progression group and plaque non-progression group according to the median annual change in plaque burden (PB) (?PB/y). A random forest (RF) algorithm was used to tune the optimal radiomics model and calculate the radiomics signature. The area under the receiver operating characteristics curve (AUC) was used to evaluate the diagnostic performance of traditional parameters (model 1), radiomics (model 2), and the combination of the two (model 3).

##### RESULTS

For the training set, FAI and NCPB were independent risk factors for plaque progression. The RF screened out 10 important features

and the most important associated with coronary plaque progression is wavelet-HLH\_first\_order\_Kurtosis. Likewise, the RF provided the radiomics signature, and AUC comparison revealed that model 2 showed better diagnostic performance in predicting plaque progression than model 1 (training set AUC 0.814 vs. 0.646,  $P < 0.001$ ; validation set AUC 0.729 vs. 0.654,  $P = 0.288$ ). Model 3 also showed better diagnostic performance than model 1 (training set AUC 0.824 vs. 0.646,  $P < 0.001$ ; validation set AUC 0.758 vs. 0.654,  $P = 0.042$ ).

## CONCLUSION

s CCTA-based plaque radiomics signature is superior to traditional parameters in predicting coronary plaque progression, but the combination of the radiomics signature and traditional parameters is even better.

## CLINICAL RELEVANCE/APPLICATION

CCTA-based radiomics signature was superior to traditional parameters in terms of predictive value of coronary plaque progression. The combined radiomics signature and traditional plaque parameters further improved its predictive power.

## M5B-SPCA-3 Accelerated-whole-heart mDIXON coronary MRA using deep learning constrained compressed sensing

Participants

Xi Wu, MS, Chengdu, China (*Presenter*) Nothing to Disclose

## PURPOSE

To explore the feasibility of using accelerated-whole-heart modified DIXON (mDIXON) coronary magnetic resonance angiography (MRA) with deep learning (DL) constrained compressed sensing (CS) and evaluate its performance against that of CS and conventional mDIXON approaches at 3 Tesla.

## METHODS AND MATERIALS

Thirty healthy volunteers (15 females and 15 males; mean age of  $28 \pm 10$  years; age range of 20-65 years) were recruited who underwent three mDIXON-based coronary MRA sequences including DL-CS, CS, and conventional sequences in a coronal orientation without contrast material. Image quality and visible coronary artery segments were evaluated for nine segments according to American Heart Association (AHA) guidelines on a four-point scale (1 = poor, 2 = fair, 3 = good, 4 = excellent). The signal-to-noise ratio (SNR) and contrast-to-noise ratio (CNR) of proximal coronary arteries were quantitatively measured.

## RESULTS

The scan time of the DL-CS and CS methods was shorter than that of the conventional method ( $9.6 \pm 3.1$  min vs.  $10.0 \pm 3.4$  min vs.  $13.0 \pm 4.9$  min;  $p < 0.001$ ). The DL-CS sequence obtained highest overall image quality ( $3.83 \pm 0.38$  vs.  $3.10 \pm 0.31$  vs.  $2.90 \pm 0.48$ ), SNR ( $76.06 \pm 15.93$  vs.  $59.24 \pm 14.71$  vs.  $58.88 \pm 16.98$ ) and CNR ( $29.70 \pm 8.67$  vs.  $19.00 \pm 7.87$  vs.  $17.61 \pm 7.71$ ) (all  $p < 0.001$ ) compared to CS and conventional methods. Moreover, 270 coronary artery segments in thirty subjects were assessed and more segments were visualized in the DL-CS and CS methods than in the conventional method (269 [99.6%], 267 [98.9%], and 263 [97.4%],  $p < 0.05$ ).

## CONCLUSION

s The mDIXON-based coronary MRA with the DL constrained CS technique yielded significantly shortened acquisition time compared with the conventional 3D approach and improved image quality compared with the CS and conventional approach.

## CLINICAL RELEVANCE/APPLICATION

The proposed methods could provide additional fat information, and accelerate imaging of coronary arteries while preserving good image quality, which could be a viable alternative to enhance the clinical workflow of coronary MRA.

Printed on: 02/07/23

## Abstract Archives of the RSNA, 2022

M5B-SPCA-1

### Myocardial radiomics texture features associated with increased coronary calcium score - First Results on a Photon-Counting-CT

Monday, Nov. 28 12:45PM - 1:15PM Room: Learning Center - CA DPS

#### Participants

Isabelle Ayx, MD, 68167 Mannheim, Germany (*Presenter*) Research Consultant, AstraZeneca PLC

#### PURPOSE

Coronary artery calcium score is an independent risk factor for the development of adverse cardiac events. Other cardiovascular risk factors such as tobacco use are known to influence the texture of the left ventricular myocardium in cardiac magnetic resonance imaging. The severity of coronary artery calcification may influence the myocardial texture. Due to better spatial resolution and signal-to-noise ratio, new CT technologies such as photon-counting computed tomography (PCCT) may improve the detection of texture alterations depending on the severity of coronary artery calcification.

#### METHODS AND MATERIALS

In this retrospective, single-center, IRB-approved study, left ventricular myocardium was segmented on axial slices semiautomatically and radiomics features were extracted using pyradiomics. Statistical analysis was performed in R statistics calculating mean and standard deviation with Pearson correlation coefficient for correlation of features. Visualization as boxplots and heatmaps was performed. For feature selection Random Forest classification was performed.

#### RESULTS

A total of 30 patients (26.7 % female, median age 58) were enrolled in this study. Patients were divided into two subgroups depending on the severity of coronary artery calcification (Agatston score 0 and Agatston score = 100). Random Forest feature selection was performed and a set of four higher-order features could be defined to discriminate myocardial texture between those two groups. Estimation of these radiomics features in the remaining patients (Agatston score 1-99) for validation and visualization as boxplots, confirmed an association between Agatston score severity and feature intensities.

#### CONCLUSION

A subset of radiomics features texture alterations of the left ventricular myocardium was associated with the severity of coronary artery calcification estimated by Agatston score.

#### CLINICAL RELEVANCE/APPLICATION

Due to the implementation of PCCT with better spatial resolution and contrast-to-noise ratio, cardiac CT imaging may possibly open up new options for radiomics feature texture analysis of myocardium depending on cardiovascular risk factors.

Printed on: 02/07/23

## Abstract Archives of the RSNA, 2022

M5B-SPCA-2

### Prediction of coronary plaque progression via traditional parameters alongside radiomics based on coronary CT angiography

Monday, Nov. 28 12:45PM - 1:15PM Room: Learning Center - CA DPS

#### Participants

Yinsu Zhu, (*Presenter*) Nothing to Disclose

#### PURPOSE

To investigate the value of traditional plaque parameters combined with radiomics based on coronary CT angiography (CCTA) in predicting coronary plaque progression.

#### METHODS AND MATERIALS

The clinical data and CCTA images of 400 patients who underwent more than twice CCTA examinations between January 2009 and August 2020 were retrospectively analyzed. Traditional plaque parameters including diameter stenosis, lesion length, vessel volume, total plaque volume and burden, calcified plaque volume and burden, non-calcified plaque volume and burden (NCPB), and pericoronary fat attenuation index (FAI) were measured. Then, the 400 patients were allocated to a training cohort (n = 280) and a validation cohort (n = 120), with a proportion of 7 : 3 via a stratified random splitting method. The two cohorts were divided into plaque progression group and plaque non-progression group according to the median annual change in plaque burden (PB) (?PB/y). A random forest (RF) algorithm was used to tune the optimal radiomics model and calculate the radiomics signature. The area under the receiver operating characteristics curve (AUC) was used to evaluate the diagnostic performance of traditional parameters (model 1), radiomics (model 2), and the combination of the two (model 3).

#### RESULTS

For the training set, FAI and NCPB were independent risk factors for plaque progression. The RF screened out 10 important features and the most important associated with coronary plaque progression is wavelet-HLH\_first\_order\_Kurtosis. Likewise, the RF provided the radiomics signature, and AUC comparison revealed that model 2 showed better diagnostic performance in predicting plaque progression than model 1 (training set AUC 0.814 vs. 0.646, P < 0.001; validation set AUC 0.729 vs. 0.654, P = 0.288). Model 3 also showed better diagnostic performance than model 1 (training set AUC 0.824 vs. 0.646, P < 0.001; validation set AUC 0.758 vs. 0.654, P = 0.042).

#### CONCLUSION

s CCTA-based plaque radiomics signature is superior to traditional parameters in predicting coronary plaque progression, but the combination of the radiomics signature and traditional parameters is even better.

#### CLINICAL RELEVANCE/APPLICATION

CCTA-based radiomics signature was superior to traditional parameters in terms of predictive value of coronary plaque progression. The combined radiomics signature and traditional plaque parameters further improved its predictive power.

Printed on: 02/07/23

## Abstract Archives of the RSNA, 2022

M5B-SPCA-3

### Accelerated-whole-heart mDIXON coronary MRA using deep learning constrained compressed sensing

Monday, Nov. 28 12:45PM - 1:15PM Room: Learning Center - CA DPS

#### Participants

Xi Wu, MS, Chengdu, China (*Presenter*) Nothing to Disclose

#### PURPOSE

To explore the feasibility of using accelerated-whole-heart modified DIXON (mDIXON) coronary magnetic resonance angiography (MRA) with deep learning (DL) constrained compressed sensing (CS) and evaluate its performance against that of CS and conventional mDIXON approaches at 3 Tesla.

#### METHODS AND MATERIALS

Thirty healthy volunteers (15 females and 15 males; mean age of  $28 \pm 10$  years; age range of 20-65 years) were recruited who underwent three mDIXON-based coronary MRA sequences including DL-CS, CS, and conventional sequences in a coronal orientation without contrast material. Image quality and visible coronary artery segments were evaluated for nine segments according to American Heart Association (AHA) guidelines on a four-point scale (1 = poor, 2 = fair, 3 = good, 4 = excellent). The signal-to-noise ratio (SNR) and contrast-to-noise ratio (CNR) of proximal coronary arteries were quantitatively measured.

#### RESULTS

The scan time of the DL-CS and CS methods was shorter than that of the conventional method ( $9.6 \pm 3.1$  min vs.  $10.0 \pm 3.4$  min vs.  $13.0 \pm 4.9$  min;  $p < 0.001$ ). The DL-CS sequence obtained highest overall image quality ( $3.83 \pm 0.38$  vs.  $3.10 \pm 0.31$  vs.  $2.90 \pm 0.48$ ), SNR ( $76.06 \pm 15.93$  vs.  $59.24 \pm 14.71$  vs.  $58.88 \pm 16.98$ ) and CNR ( $29.70 \pm 8.67$  vs.  $19.00 \pm 7.87$  vs.  $17.61 \pm 7.71$ ) (all  $p < 0.001$ ) compared to CS and conventional methods. Moreover, 270 coronary artery segments in thirty subjects were assessed and more segments were visualized in the DL-CS and CS methods than in the conventional method (269 [99.6%], 267 [98.9%], and 263 [97.4%],  $p < 0.05$ ).

#### CONCLUSION

The mDIXON-based coronary MRA with the DL constrained CS technique yielded significantly shortened acquisition time compared with the conventional 3D approach and improved image quality compared with the CS and conventional approach.

#### CLINICAL RELEVANCE/APPLICATION

The proposed methods could provide additional fat information, and accelerate imaging of coronary arteries while preserving good image quality, which could be a viable alternative to enhance the clinical workflow of coronary MRA.

Printed on: 02/07/23

## Abstract Archives of the RSNA, 2022

M5B-SPCH

### Chest Monday Poster Discussions - B

Monday, Nov. 28 12:45PM - 1:15PM Room: Learning Center - CH DPS

#### Participants

Stephen Hobbs, MD, Lexington, KY (*Moderator*) Author with royalties, Wolters Kluwer nv; Author with royalties, RELX

#### Sub-Events

#### M5B-SPCH-1 Chest CT Findings of COVID-19 in Lung Transplant Recipients

#### Participants

Stephan Altmayer, MD, PhD, Framingham, MA (*Presenter*) Nothing to Disclose

#### PURPOSE

Our goal was to compare the chest computed tomography (CT) findings of COVID-19 in lung transplant recipients (LTR) and a group of controls.

#### METHODS AND MATERIALS

This was a retrospective study including 51 consecutive adults with a history of lung transplantation hospitalized with COVID-19 from two centers. A total of 75 consecutive controls with no history of immunosuppression were also included for the comparison. Images were classified in consensus by two chest radiologists regarding the standardized RSNA category, main pattern of attenuation, longitudinal and axial distribution. Quantitative CT analysis of the areas of high attenuation (-250 to -700 HU) was also performed using the extension Chest Imaging Platform of the open-source 3D Slicer software. Analysis was performed using chi-square tests for categorical variables and unpaired t-tests for continuous variables. The level of significance was set at 0.05. Bonferroni correction was performed when performing multiple tests.

#### RESULTS

There was no significant difference in mean age, gender, or days of symptoms until imaging between groups. A total of 2/51 LTR and 3/75 controls had a negative chest CT on admission. The imaging findings of COVID-19 in LTR were significantly different from controls regarding the RSNA chest CT classification ( $p=0.007$ ) and the main pattern of lung attenuation ( $p=0.001$ ). While a typical pattern was the most common classification in LTR and controls (0.47 vs. 0.74, adjusted- $p=0.006$ ), LTR had a significantly higher proportion of patients with an indeterminate pattern on CT (0.31 vs. 0.11, adjusted- $p=0.014$ ). The most frequent pattern of attenuation in LTR was predominantly consolidations (0.39 vs. 0.22 of controls, adjusted- $p=0.144$ ) followed by a mixed pattern of GGO and consolidation (0.37 vs. 0.20 of controls, adjusted- $p=0.102$ ). On the other hand, the most common pattern seen in controls was GGO predominant (0.58 vs. 0.24 of LTR, adjusted- $p=0.001$ ). No differences were found in the longitudinal ( $p=0.99$ ) and axial distribution ( $p=0.717$ ) of lesions. Both LTR and controls presented either a lower lobe predominant (0.43 vs. 0.43, respectively) or diffuse longitudinal distribution (0.57 vs. 0.56), and predominantly peripheral (0.55 vs. 0.62) or diffuse axial distribution (0.35 vs. 0.29). The percentage of lung areas with high attenuation by QCT was significantly higher in the population of LTR ( $0.372 \pm 0.08$  vs.  $0.148 \pm 0.06$ ,  $p<0.001$ ).

#### CONCLUSION

The most frequent finding of COVID-19 in LTR was a predominant pattern of consolidation followed by a mixed pattern of GGO and consolidation.

#### CLINICAL RELEVANCE/APPLICATION

The radiologist should be aware that the presenting chest CT imaging pattern of COVID-19 in LTR is often different compared to the usual population.

#### M5B-SPCH-10 COV-RADS As a Classification System For the Diagnosis of COVID-19 Pneumonia in Chest Computed Tomography (CT): A Ferman Nationwide Multicenter Validation Study and Pilot Implementation of the Radiological Cooperative Network (RACOON)

#### Participants

Marwin Jonathan Sahn, Aachen, Germany (*Presenter*) Nothing to Disclose

#### PURPOSE

COV-RADS is a classification system which predicts the likelihood of the presence of COVID-19 pneumonia in chest CT and has proven high diagnostic value in a locoregional analysis. Within the German-wide Radiological Cooperative Network (RACOON) capabilities for large multicenter studies were instated. We validated COV-RADS within this nationwide consortium.

#### METHODS AND MATERIALS

A total of 6355 CTs were included in the analysis: Patients with confirmed SARS-CoV 2 (RT-PCR within 7 days before CT;  $n=1286$ ) and CT datasets of representative pulmonary pathologies ( $n=4805$ ) and a control cohort of healthy individuals ( $n=264$ ). All CTs

were assessed in a blinded fashion applying the COV-RADS classification system. Test quality criteria, Clopper-Pearson confidence intervals and ROC with AUC were calculated a) for a high sensitivity setting: Patients with positive RT-PCR and COV-RADS score = 3 were considered true positive, patients with negative RT-PCR and COV-RADS score = 2 were considered true negative; b) for a high specificity setting: patients with positive RT-PCR and COV-RADS score = 4 were considered true positive, patients with negative RT-PCR and COV-RADS score = 2 were considered true negative.

## RESULTS

Test quality criteria for the high sensitivity setting were: Sensitivity 86.6% [84.6-88.4%], specificity 76.0% [74.8-77.1%], PPV 47.7% [45.7-49.8%], NPV 95.7% [95.1-96.3%]. For the high specificity setting) sensitivity was 62.1% [59.4-64.8%], specificity 94.1% [93.4-94.8%], PPV 72.8% [70.1-75.4%], NPV 90.7% [89.9-91.5%]. AUC was 0.859 [0.844-0.874].

## CONCLUSION

s The COV-RADS classification system provides reliable results in the diagnosis of COVID-19 pneumonia using chest CT. Overall tests criteria were acceptable. While sensitivity was high, specificity does not meet the expectations when compared to RT-PCR, even when the cutoff was shifted to aim for high specificity. Therefore, COV-RADS 3 was determined as the most reasonable cutoff in our current setting.

## CLINICAL RELEVANCE/APPLICATION

In the context of lifting COVID restrictions, pandemic preparedness gains importance. Many patients undergo chest CT during routine practice, with a bias towards older patients and patients with comorbidities. Also, these patients are most vulnerable to COVID-19. Therefore, wide deployment of COV-RADS ratings can both serve as an indicator of local prevalence, bolstering pandemic preparedness, while improving patient and staff security. Future viral mutations (variants of concern) could void the effectiveness of rapid antigen tests. Wide deployment of COV-RADS could possibly overcome such a capability gap.

## M5B-SPCH-2 The Impact of Vaccination on the Incidence and Severity of COVID-19 Pneumonia: Effectiveness of mRNA and Adenovirus Vector Vaccines

Participants

Simone Vicini, MD, Latina, Italy (*Presenter*) Nothing to Disclose

## PURPOSE

To evaluate and compare the incidence rate and severity of COVID-19 pneumonia on chest CT imaging in unvaccinated and fully vaccinated individuals positive for SARS-CoV-2, along with the different impact of mRNA and adenovirus vector vaccines in this context

## METHODS AND MATERIALS

Retrospective single-center study. A cohort of consecutive patients positive for SARS-CoV-2 infection who underwent chest CT was evaluated and grouped by vaccination status and type. COVID-19 pneumonia severity was assessed using a semi-quantitative CT Severity Score (CT-SS) system. Morphological CT patterns were evaluated. Sex-stratified and age-stratified differences were assessed between groups. Logistic regression models were built to evaluate the effect of vaccination on the likelihood of presenting severe CT-SS.

## RESULTS

Of the 467 patients with COVID-19 meeting inclusion criteria, 216 were not vaccinated, whereas 251 were fully vaccinated, with either BNT162b2 mRNA Vaccine (167) or ChAdOx1-S Adenovirus Vector Vaccine (84). Overall, 141 (30%) patients showed no signs of COVID-19 pneumonia on chest CT images (CTSS=0). The proportion of patients without pneumonia was higher in BNT162b2 patients (85/167, 51%) than in unvaccinated (32/216, 15%) and ChAdOx1-S (24/84, 29%) patients ( $p < .001$ ). Fully vaccinated patients demonstrated a lower mean CT-SS ( $5.49 \pm 6.06$ ) than unvaccinated patients ( $9.72 \pm 6.14$ ), also considering BNT162b2 ( $5.15 \pm 6.13$ ) and ChAdOx1-S ( $6.17 \pm 5.88$ ) patients separately ( $p < .001$ ). No differences were observed between BNT162b2 and ChAdOx1-S ( $p = 0.240$ ). Pairwise comparisons by sex and age revealed lower mean CT-SS in fully vaccinated patients. Full vaccination resulted to be associated with significantly lower risk of presenting a CT-SS predictive of ICU admission (OR=0.33).

## CONCLUSION

s Fully vaccinated patients, getting either mRNA or adenovirus vector vaccines, experiencing COVID-19 breakthrough infections tend to show a lower incidence rate of COVID-19 pneumonia and less severe lung parenchymal alterations than unvaccinated patients. At the same time, vaccination status is a significant predictor associated with the need for ICU admission in patients with COVID-19.

## CLINICAL RELEVANCE/APPLICATION

COVID-19 pneumonia represents the most common indication for admission to ICU and the leading risk factor of fatal outcome from COVID-19. Full vaccination against SARS-CoV-2 reduce the incidence rate and severity of COVID-19 pneumonia, having the potential to reduce lung complications caused by COVID-19, thus preventing or at least mitigating long-COVID.

## M5B-SPCH-3 Invasive Pulmonary Aspergillosis in Non-onco-hematological Patients: Differential Radiological Features

Participants

Miguel Angel Gomez Bermejo, MD, Madrid, Spain (*Presenter*) Nothing to Disclose

## PURPOSE

To study the radiological manifestations of the different forms of invasive pulmonary aspergillosis (IPA) in non-oncohematological patients according to the underlying type of immunosuppression.

## METHODS AND MATERIALS

A multicenter retrospective study was performed. Data were collected from non-oncohematological patients admitted to four tertiary hospitals (3 in Spain and 1 in Italy) from 1998 to 2021. Three blinded radiologists performed a consensus interpretation of the imaging findings (chest CT scans). The following IPA criteria were used according to the baseline conditions of the patients:

EORTC/MSG criteria for immunocompromised patients, Vandewoude and Blot et al criteria for critically ill patients, Bulpa et al criteria for COPD patients, and Verweij et al criteria for critically ill patients with a viral infection. Patients were divided into three immunosuppression groups: neutropenic group, severe non-neutropenic group (mostly solid organ transplant recipients), and intermediate non-neutropenic group.

## RESULTS

A total of 146 patients were included: 9 (6.16%) neutropenic, 105 (71.9%) severe non-neutropenic, and 32 (21.9%) intermediate non-neutropenic. Bronchoinvasive infection signs were more frequent than angioinvasive infection signs (94.5% vs. 45.2%,  $p=0.023$ ) in all patients. Bronchoinvasive infection signs were evenly distributed among all groups (neutropenic [88.9%] vs severe non-neutropenic [94.3%] vs intermediate non-neutropenic [96.9%],  $p=0.524$ ). Ground glass opacities (64.5%) and bronchial wall thickening (58%) were the most frequent findings. A pure bronchoinvasive pattern was observed more frequently in less immunosuppressed patients (0% vs 41.9% vs 68.8%,  $p<0.0001$ ). Classic CT angioinvasive signs (such as the halo sign) were less commonly observed in less immunosuppressed subjects (88.9% vs 45.7% vs 31.3%,  $p=0.008$ ).

## CONCLUSION

Our data suggest that CT findings in less immunosuppressed patients with IPA more commonly follow a bronchoinvasive pattern. Neutropenic patients are more likely to present radiological findings of angioinvasive IPA.

## CLINICAL RELEVANCE/APPLICATION

The current IPA diagnostic criteria were initially developed in oncohematological patients and do not necessarily apply to other populations. We believe that, by recognizing signs of airway invasion in less neutropenic patients (such as non-oncohematological patients), an earlier IPA diagnosis may be achieved, allowing prompt treatment.

## M5B-SPCH-4 Automatically Generated CT Severity Scores for COVID-19 Predict Death or Intubation at 1-Month Follow-Up

Participants  
Luuk Boulogne, MSc, (Presenter) Institutional Grant, Thirona Bio, Inc

## PURPOSE

To evaluate the ability of CORADS-AI, an automatic system that was originally developed for scoring the presence and current extent of a COVID-19 infection from chest Computed Tomography (CT), to predict death or intubation after one month for positive COVID-19 patients.

## METHODS AND MATERIALS

CORADS-AI was developed in a previous study using CT scans from COVID-19 patients in the Netherlands. From a CT scan, CORADS-AI automatically segments each pulmonary lobe and produces a CT Severity Score (CTSS) at the lobe and patient level. This score is based on the percentage of affected tissue and has been used in routine clinical practice. We applied CORADS-AI to all 1205 patients that were involved in the STOIC study, had a positive COVID-19 RT-PCR result, and for which a CT scan was publicly available. 301 of them had died or had to be intubated at 1-month follow-up. We applied logistic regression with 5-fold cross validation on patient sex, age, and the patient level CTSS output of CORADS-AI to predict death or intubation after one month. We compared our method with the logistic regression model from the original STOIC study. This model received age, sex, several clinical variables, and manual CT annotations for lung disease extent as input. It was developed with all 4238 patients from the STOIC study that were positive for COVID-19 both according to RT-PCR testing and CT reading.

## RESULTS

Our model obtained an AUC of  $0.72\pm 0.02$  (mean $\pm$ std. dev.) for predicting death or intubation after one month. When using solely the patient level CTSS output, we obtained an AUC of  $0.68\pm 0.03$ . In comparison, the original STOIC study reported an AUC of their model of 0.69 (95% CI: 0.67, 0.71).

## CONCLUSION

We showed that CORADS-AI can predict death or intubation after one month for positive COVID-19 patients. Adding age and sex information to the model improved its results. The performance was comparable to that of the model developed in the original STOIC study, which used additional clinical variables and manual CT annotations. This comparison should be interpreted carefully, since that model was evaluated on a different subset of the STOIC cohort.

## CLINICAL RELEVANCE/APPLICATION

We showed the potential of CORADS-AI, of which the output format is already used in clinical practice, for aiding radiologists in predicting the course of a COVID-19 infection.

## M5B-SPCH-5 Chest CT Findings of COVID-19 in Hospitalized Patients: A Comparison between the Delta and Omicron Variants

Participants  
Jong Hyuk Lee, MD, PhD, Seoul, Korea, Republic Of (Presenter) Nothing to Disclose

## PURPOSE

It remains underexplored whether CT manifestations of coronavirus 2019 (COVID-19) differ among variants. This study compared the chest CT findings of COVID-19 between the Delta and Omicron variants.

## METHODS AND MATERIALS

The institutional review board approved this retrospective study and waived informed consent. Baseline CT images of hospitalized patients with COVID-19 were consecutively collected from a secondary referral hospital in November 2021 and February 2022, when the Delta and Omicron variants predominated, respectively. Two radiologists categorized CT images into four patterns based on the Radiological Society of North America classification system for COVID-19 and visually graded pneumonia extent. Pneumonia, pleural effusion, and intrapulmonary vessels were segmented and quantified on CT images using a priori developed neural networks, followed by reader confirmation. Multivariate logistic and linear regression analyses were performed to examine the associations

between the variants and CT category, severity, and peripheral vascularity.

## RESULTS

In total, 176 patients with the Delta (n=88; 67±15 years; 46 men) and Omicron (n=88; 62±19 years; 51 men) variants were included. The Omicron variant was associated with a smaller proportion of patients with a typical CT appearance (32% versus 57%; P=.001), a lower visual pneumonia extent (5.4±6.0 versus 7.7±6.6; P=.017), similar pneumonia volume (5±10% versus 7±11%; P=.143), and a higher proportion of vessels with a cross-sectional area smaller than 5 mm<sup>2</sup> relative to the total pulmonary blood volume (BV5%; 48±11% versus 44±8%; P=.004). When adjusted for confounders including age, comorbidities, vaccination, and infection duration, the Omicron variant was significantly associated with a non-typical appearance (P=.009) and higher BV5 (P=.010), but not with visual pneumonia extent (P=.168) or pneumonia volume (P=.666).

## CONCLUSION

s The Omicron variant showed more frequent non-typical CT appearances of COVID-19 and less pulmonary vascular involvement than the Delta variant in hospitalized patients with comparable CT severity.

## CLINICAL RELEVANCE/APPLICATION

The CT characteristics of Omicron may hamper radiologists from promptly recognizing COVID-19 on CT images when incidentally encountered, and this finding raises an alarm regarding the need to evaluate whether radiologic findings remain consistent or change when new variants appear.

## M5B-SPCH-64 and 12 Months After COVID-19 Pneumonia: Clinical-Functional and Chest CT Findings

Participants

Paula Rodriguez, MD, (*Presenter*) Nothing to Disclose

## PURPOSE

Analyze whether the persistence of radiological lesions 4 and 12 months after COVID-19 pneumonia is related to the presence of residual symptoms and/or whether it has repercussions on respiratory function tests.

## METHODS AND MATERIALS

Prospective study that included patients with COVID-19 pneumonia who underwent chest computed tomography (CT) 16±2 weeks and 52±2 weeks after hospital discharge. The chest CT were evaluated by 2 experienced cardiothoracic radiologists who assessed the presence of ground glass, reticulation and bronchiectasias, their distribution and the percentage of involvement of each of these findings was quantified by lobes. Clinical, analytical and functional variables were recorded, as well as sociodemographic variables, comorbidities and data on the severity of the pneumonic process. One of the parameter to which special attention was paid was membrane diffusing capacity (DMCO) and pulmonary capillary blood volume (Vc)

## RESULTS

93 patients were included, of whom 72% had lesions on chest CT. Male sex and older age are related to these lesions, but we have not found any association with the severity of the pneumonic process. At 4 months, no correlation was demonstrated between the persistence of ground glass and the sensation of dyspnea. Patients who required ICU admission had a higher prevalence of persistent ground glass, although no significant differences were obtained with respect to less severe patients. At 12 months, a decrease in the extension of the lesions was detected due to the decrease in size and/or density of the ground-glass opacities, although this was not observed in the reticulation or in the bronchiectasis. The parameter that best related with the presence of ground glass on CT was a higher DMCO/Vc

## CONCLUSION

s We have observed a high prevalence of ground-glass lesions on chest CT 4 months after COVID pneumonia. The percentage of ground glass was quantified as mild and we don't find a clear correlation with clinical, laboratory or 6-minute walk test variables. At 12 months, the improvement in respiratory function tests is related to the increase in parameters related to the vascular component of diffusion. The functional parameter that best correlates with the finding of ground glass on CT is DMCO/Vc, which is higher in patients with this radiological finding.

## CLINICAL RELEVANCE/APPLICATION

d

## M5B-SPCH-7 AI Denoising Improves Image Quality and Radiological Workflows In Pediatric Ultra-Low-Dose Thorax Computed Tomography Scans

Participants

Andreas Brendlin, Tuebingen, Germany (*Presenter*) Nothing to Disclose

## PURPOSE

To evaluate the impact of an AI denoising algorithm on image quality, diagnostic accuracy, and radiological workflows in the context of pediatric thorax ultra-low-dose CT (ULDCT).

## METHODS AND MATERIALS

100 consecutive pediatric thorax ULDCT were included and reconstructed using weighted filtered back projection (wFBP), iterative reconstruction (ADMIRE 2), and AI denoising (PixelShine). Place-consistent noise measurements were used to compare objective image quality. Eight blinded readers independently rated subjective image quality on a Likert scale (1=worst to 5=best). Each reader wrote a semiquantitative report to evaluate disease severity using a score with six common pathologies. The time to diagnosis was measured for each reader to compare possible workflow benefits. Properly corrected mixed-effects analysis with posthoc subgroup tests were used. Spearman's correlation coefficient measured inter-reader agreement for the subjective image quality analysis and the severity score sheets.

## RESULTS

The highest noise was measured for wFBP, followed by ADMIRE 2, and PixelShine (76.9±9.62 vs. 43.4±4.45 vs. 34.8±3.27 HU; each

The highest noise was measured for wFBP, followed by ADMIRE 2, and PixelShine (7.07±5.02 vs. 43.4±4.43 vs. 34.0±3.27 HU, each p<0.001). The highest subjective image quality was measured for PixelShine, followed by ADMIRE 2, and wFBP (4 [4-5] vs. 3 [4-5] vs. 3 [2-4], each p<0.001) with good inter-rater agreement (r=0.790; p=0.001). In diagnostic accuracy analysis, there was a good inter-rater agreement between the severity scores (r=0.764; p<0.001) without significant differences between severity score items per reconstruction mode (F (5.71;566)=0,792; p=0.570). The shortest time to diagnosis was measured for the PixelShine datasets, followed by ADMIRE 2, and wFBP (2.28±1.56 vs. 2.66±2.31 vs. 2.45±1.90minutes; F(1.000;99.00)=268.1; p<0.001).

## CONCLUSION

s AI denoising significantly improves image quality in pediatric thorax ULDCT without compromising diagnostic confidence and reduces time to diagnosis substantially.

## CLINICAL RELEVANCE/APPLICATION

A promising technique to minimize potentially harmful radiation exposure in pediatric thorax ultra-low-dose CT protocols is to improve the dose-effectiveness by shaping the X-ray spectrum in favor of higher energy photons. However, the typical trade-off of such approaches is lower image quality than standard protocols due to higher image noise.

## M5B-SPCH-8 Chest CT Findings and Pulmonary Function Tests in the Postrecovery Phase of Mild to Severe Cases of COVID-19

### Participants

Patricia Yokoo, MD, Sao Paulo, Brazil (*Presenter*) Nothing to Disclose

### PURPOSE

To correlate follow-up chest computed tomography (CT) and pulmonary function test (PFT) findings of mild to severe COVID-19 survivors.

### METHODS AND MATERIALS

This retrospective study was performed in two medical centers in Sao Paulo, Brazil. Data were collected from consecutive patients who underwent PFT and chest CT (within a maximum interval of 14 days) after recovery from COVID-19 between May and October 2021. Clinical data, spirometric parameters, diffusing capacity for carbon monoxide (DLCO), lung CT abnormalities, distribution and CT extent score were recorded. Clinical and tomographic differences between the patients with normal or abnormal PFTs were assessed by Chi-Square, Mann-Whitney or Fisher tests.

### RESULTS

101 COVID-19 survivors were included (mild disease 48, moderate 40, severe 13), at a median 95 days from initial symptom onset. 33% (33/101) had persistent symptoms. Reduction of DLCO% predicted was the most common abnormality in lung function (19% of the patients). Persistence of symptoms was not associated with abnormal lung function. The presence of reticular opacities (p=0.003), bronchial dilatation (p=0.005) and architectural distortion (p<0.001) in chest CT and a CT extent score > 5 (p=0.006) were significantly more prevalent in patients with impairment of DLCO. The optimal CT score for identifying patients with reduced DLCO% predicted was 5.5 (area under curve = 0.7), with 78.9% sensitivity and 56.1% specificity.

## CONCLUSION

s The presence of reticular opacities, bronchial dilatation and architectural distortion in chest CT and the extent of lung abnormalities was associated with lung function impairment in the postrecovery phase of mild to severe cases of COVID-19.

## CLINICAL RELEVANCE/APPLICATION

The anatomical and functional pulmonary sequelae of SARS-CoV-2 infection are not yet fully understood. The evaluation of late chest CT findings associated with lung function impairment can help to establish the role of imaging in the postrecovery phase of COVID-19 patients.

## M5B-SPCH-9 Comparison of Chest CT Characteristics of COVID-19 Interstitial Pneumonia Between Patients with Different Vaccination Status

### Participants

Francesco Rizzetto, MD, Milan, Italy (*Presenter*) Travel support, Bracco Group

### PURPOSE

To compare the CT imaging characteristics of patients with symptomatic COVID-19 infection according to their SARS-CoV-2 vaccination status (non-vaccinated, incompletely vaccinated and fully vaccinated).

### METHODS AND MATERIALS

The CT examinations performed in the Emergency Department between May and November 2021 for suspicion of COVID-19 pneumonia in patients with positive swab for SARS-CoV-2 were retrospectively included. Three readers (one 13-year experienced radiologist and two 4th-year radiology residents) independently evaluated each chest CT according to CO-RADS and ACR COVID classification and the results were compared for vaccination status. In possible COVID-19 pneumonia cases, defined as CO-RADS 3 to 5 (ACR indeterminate and typical) by each reader, high extent of pulmonary involvement (≥25%) and CT patterns (presence of ground glass opacities, consolidations, crazy paving areas) were compared for vaccination status.

### RESULTS

A total of 184 patients were included, 111 non-vaccinated (60%) for SARS-CoV-2 infection, 21 (11%) with an incomplete vaccination cycle, and 52 (28%) with a complete vaccination cycle (6 different vaccine types). At bivariate logistic regression, the only factor predicting the absence of pneumonia (CO-RADS 1 and ACR negative cases) for the three readers was a complete vaccination cycle (OR=12.8-13.1 compared to non-vaccinated patients, p=0.032). Both CT score and CT patterns of possible COVID-19 pneumonia showed no statistically significant correlation with vaccination status for the three readers.

## CONCLUSION

s Patients with symptomatic SARS-CoV-2 infection and a complete vaccination cycle had 13-times higher odds to present with a

negative chest CT examination in ED compared to non-vaccinated patients. CT involvement and CT patterns of interstitial pneumonia showed no difference between different vaccination status.

**CLINICAL RELEVANCE/APPLICATION**

Symptomatic COVID-19 patient with a complete vaccination cycle may undergo a less aggressive imaging workup.

Printed on: 02/07/23

## Abstract Archives of the RSNA, 2022

M5B-SPCH-1

### Chest CT Findings of COVID-19 in Lung Transplant Recipients

Monday, Nov. 28 12:45PM - 1:15PM Room: Learning Center - CH DPS

#### Participants

Stephan Altmayer, MD, PhD, Framingham, MA (*Presenter*) Nothing to Disclose

#### PURPOSE

Our goal was to compare the chest computed tomography (CT) findings of COVID-19 in lung transplant recipients (LTR) and a group of controls.

#### METHODS AND MATERIALS

This was a retrospective study including 51 consecutive adults with a history of lung transplantation hospitalized with COVID-19 from two centers. A total of 75 consecutive controls with no history of immunosuppression were also included for the comparison. Images were classified in consensus by two chest radiologists regarding the standardized RSNA category, main pattern of attenuation, longitudinal and axial distribution. Quantitative CT analysis of the areas of high attenuation (-250 to -700 HU) was also performed using the extension Chest Imaging Platform of the open-source 3D Slicer software. Analysis was performed using chi-square tests for categorical variables and unpaired t-tests for continuous variables. The level of significance was set at 0.05. Bonferroni correction was performed when performing multiple tests.

#### RESULTS

There was no significant difference in mean age, gender, or days of symptoms until imaging between groups. A total of 2/51 LTR and 3/75 controls had a negative chest CT on admission. The imaging findings of COVID-19 in LTR were significantly different from controls regarding the RSNA chest CT classification ( $p=0.007$ ) and the main pattern of lung attenuation ( $p=0.001$ ). While a typical pattern was the most common classification in LTR and controls (0.47 vs. 0.74, adjusted- $p=0.006$ ), LTR had a significantly higher proportion of patients with an indeterminate pattern on CT (0.31 vs. 0.11, adjusted- $p=0.014$ ). The most frequent pattern of attenuation in LTR was predominantly consolidations (0.39 vs. 0.22 of controls, adjusted- $p=0.144$ ) followed by a mixed pattern of GGO and consolidation (0.37 vs. 0.20 of controls, adjusted- $p=0.102$ ). On the other hand, the most common pattern seen in controls was GGO predominant (0.58 vs. 0.24 of LTR, adjusted- $p=0.001$ ). No differences were found in the longitudinal ( $p=0.99$ ) and axial distribution ( $p=0.717$ ) of lesions. Both LTR and controls presented either a lower lobe predominant (0.43 vs. 0.43, respectively) or diffuse longitudinal distribution (0.57 vs. 0.56), and predominantly peripheral (0.55 vs. 0.62) or diffuse axial distribution (0.35 vs. 0.29). The percentage of lung areas with high attenuation by QCT was significantly higher in the population of LTR ( $0.372 \pm 0.08$  vs.  $0.148 \pm 0.06$ ,  $p < 0.001$ ).

#### CONCLUSION

The most frequent finding of COVID-19 in LTR was a predominant pattern of consolidation followed by a mixed pattern of GGO and consolidation.

#### CLINICAL RELEVANCE/APPLICATION

The radiologist should be aware that the presenting chest CT imaging pattern of COVID-19 in LTR is often different compared to the usual population.

Printed on: 02/07/23

## Abstract Archives of the RSNA, 2022

M5B-SPCH-10

### **COV-RADS As a Classification System For the Diagnosis of COVID-19 Pneumonia in Chest Computed Tomography (CT): A Ferman Nationwide Multicenter Validation Study and Pilot Implementation of the Radiological COoperative Network (RACOON)**

Monday, Nov. 28 12:45PM - 1:15PM Room: Learning Center - CH DPS

#### **Participants**

Marwin Jonathan Sahn, Aachen, Germany (*Presenter*) Nothing to Disclose

#### **PURPOSE**

COV-RADS is a classification system which predicts the likelihood of the presence of COVID-19 pneumonia in chest CT and has proven high diagnostic value in a locoregional analysis. Within the German-wide Radiological Cooperative Network (RACOON) capabilities for large multicenter studies were instated. We validated COV-RADS within this nationwide consortium.

#### **METHODS AND MATERIALS**

A total of 6355 CTs were included in the analysis: Patients with confirmed SARS-CoV 2 (RT-PCR within 7 days before CT; n=1286) and CT datasets of representative pulmonary pathologies (n=4805) and a control cohort of healthy individuals (n=264). All CTs were assessed in a blinded fashion applying the COV-RADS classification system. Test quality criteria, Clopper-Pearson confidence intervals and ROC with AUC were calculated a) for a high sensitivity setting: Patients with positive RT-PCR and COV-RADS score = 3 were considered true positive, patients with negative RT-PCR and COV-RADS score = 2 were considered true negative; b) for a high specificity setting: patients with positive RT-PCR and COV-RADS score = 4 were considered true positive, patients with negative RT-PCR and COV-RADS score = 2 were considered true negative.

#### **RESULTS**

Test quality criteria for the high sensitivity setting were: Sensitivity 86.6% [84.6-88.4%], specificity 76.0% [74.8-77.1%], PPV 47.7% [45.7-49.8%], NPV 95.7% [95.1-96.3%]. For the high specificity setting) sensitivity was 62.1% [59.4-64.8%], specificity 94.1% [93.4-94.8%], PPV 72.8% [70.1-75.4%], NPV 90.7% [89.9-91.5%]. AUC was 0.859 [0.844-0.874].

#### **CONCLUSION**

s The COV-RADS classification system provides reliable results in the diagnosis of COVID-19 pneumonia using chest CT. Overall tests criteria were acceptable. While sensitivity was high, specificity does not meet the expectations when compared to RT-PCR, even when the cutoff was shifted to aim for high specificity. Therefore, COV-RADS 3 was determined as the most reasonable cutoff in our current setting.

#### **CLINICAL RELEVANCE/APPLICATION**

In the context of lifting COVID restrictions, pandemic preparedness gains importance. Many patients undergo chest CT during routine practice, with a bias towards older patients and patients with comorbidities. Also, these patients are most vulnerable to COVID-19. Therefore, wide deployment of COV-RADS ratings can both serve as an indicator of local prevalence, bolstering pandemic preparedness, while improving patient and staff security. Future viral mutations (variants of concern) could void the effectiveness of rapid antigen tests. Wide deployment of COV-RADS could possibly overcome such a capability gap.

Printed on: 02/07/23

## Abstract Archives of the RSNA, 2022

M5B-SPCH-2

### The Impact of Vaccination on the Incidence and Severity of COVID-19 Pneumonia: Effectiveness of mRNA and Adenovirus Vector Vaccines

Monday, Nov. 28 12:45PM - 1:15PM Room: Learning Center - CH DPS

#### Participants

Simone Vicini, MD, Latina, Italy (*Presenter*) Nothing to Disclose

#### PURPOSE

To evaluate and compare the incidence rate and severity of COVID-19 pneumonia on chest CT imaging in unvaccinated and fully vaccinated individuals positive for SARS-CoV-2, along with the different impact of mRNA and adenovirus vector vaccines in this context

#### METHODS AND MATERIALS

Retrospective single-center study. A cohort of consecutive patients positive for SARS-CoV-2 infection who underwent chest CT was evaluated and grouped by vaccination status and type. COVID-19 pneumonia severity was assessed using a semi-quantitative CT Severity Score (CT-SS) system. Morphological CT patterns were evaluated. Sex-stratified and age-stratified differences were assessed between groups. Logistic regression models were built to evaluate the effect of vaccination on the likelihood of presenting severe CT-SS.

#### RESULTS

Of the 467 patients with COVID-19 meeting inclusion criteria, 216 were not vaccinated, whereas 251 were fully vaccinated, with either BNT162b2 mRNA Vaccine (167) or ChAdOx1-S Adenovirus Vector Vaccine (84). Overall, 141 (30%) patients showed no signs of COVID-19 pneumonia on chest CT images (CTSS=0). The proportion of patients without pneumonia was higher in BNT162b2 patients (85/167, 51%) than in unvaccinated (32/216, 15%) and ChAdOx1-S (24/84, 29%) patients ( $p<.001$ ). Fully vaccinated patients demonstrated a lower mean CT-SS ( $5.49 \pm 6.06$ ) than unvaccinated patients ( $9.72 \pm 6.14$ ), also considering BNT162b2 ( $5.15 \pm 6.13$ ) and ChAdOx1-S ( $6.17 \pm 5.88$ ) patients separately ( $p<.001$ ). No differences were observed between BNT162b2 and ChAdOx1-S ( $p=0.240$ ). Pairwise comparisons by sex and age revealed lower mean CT-SS in fully vaccinated patients. Full vaccination resulted to be associated with significantly lower risk of presenting a CT-SS predictive of ICU admission (OR=0.33).

#### CONCLUSION

s Fully vaccinated patients, getting either mRNA or adenovirus vector vaccines, experiencing COVID-19 breakthrough infections tend to show a lower incidence rate of COVID-19 pneumonia and less severe lung parenchymal alterations than unvaccinated patients. At the same time, vaccination status is a significant predictor associated with the need for ICU admission in patients with COVID-19.

#### CLINICAL RELEVANCE/APPLICATION

COVID-19 pneumonia represents the most common indication for admission to ICU and the leading risk factor of fatal outcome from COVID-19. Full vaccination against SARS-CoV-2 reduce the incidence rate and severity of COVID-19 pneumonia, having the potential to reduce lung complications caused by COVID-19, thus preventing or at least mitigating long-COVID.

Printed on: 02/07/23

## Abstract Archives of the RSNA, 2022

M5B-SPCH-3

### Invasive Pulmonary Aspergillosis in Non-onco-hematological Patients: Differential Radiological Features

Monday, Nov. 28 12:45PM - 1:15PM Room: Learning Center - CH DPS

#### Participants

Miguel Angel Gomez Bermejo, MD, Madrid, Spain (*Presenter*) Nothing to Disclose

#### PURPOSE

To study the radiological manifestations of the different forms of invasive pulmonary aspergillosis (IPA) in non-oncohematological patients according to the underlying type of immunosuppression.

#### METHODS AND MATERIALS

A multicenter retrospective study was performed. Data were collected from non-oncohematological patients admitted to four tertiary hospitals (3 in Spain and 1 in Italy) from 1998 to 2021. Three blinded radiologists performed a consensus interpretation of the imaging findings (chest CT scans). The following IPA criteria were used according to the baseline conditions of the patients: EORTC/MSG criteria for immunocompromised patients, Vandewoude and Blot et al criteria for critically ill patients, Bulpa et al criteria for COPD patients, and Verweij et al criteria for critically ill patients with a viral infection. Patients were divided into three immunosuppression groups: neutropenic group, severe non-neutropenic group (mostly solid organ transplant recipients), and intermediate non-neutropenic group.

#### RESULTS

A total of 146 patients were included: 9 (6.16%) neutropenic, 105 (71.9%) severe non-neutropenic, and 32 (21.9%) intermediate non-neutropenic. Bronchoinvasive infection signs were more frequent than angioinvasive infection signs (94.5% vs. 45.2%,  $p=0.023$ ) in all patients. Bronchoinvasive infection signs were evenly distributed among all groups (neutropenic [88.9%] vs severe non-neutropenic [94.3%] vs intermediate non-neutropenic [96.9%],  $p=0.524$ ). Ground glass opacities (64.5%) and bronchial wall thickening (58%) were the most frequent findings. A pure bronchoinvasive pattern was observed more frequently in less immunosuppressed patients (0% vs 41.9% vs 68.8%,  $p<0.0001$ ). Classic CT angioinvasive signs (such as the halo sign) were less commonly observed in less immunosuppressed subjects (88.9% vs 45.7% vs 31.3%,  $p=0.008$ ).

#### CONCLUSION

Our data suggest that CT findings in less immunosuppressed patients with IPA more commonly follow a bronchoinvasive pattern. Neutropenic patients are more likely to present radiological findings of angioinvasive IPA.

#### CLINICAL RELEVANCE/APPLICATION

The current IPA diagnostic criteria were initially developed in oncohematological patients and do not necessarily apply to other populations. We believe that, by recognizing signs of airway invasion in less neutropenic patients (such as non-oncohematological patients), an earlier IPA diagnosis may be achieved, allowing prompt treatment.

Printed on: 02/07/23

## Abstract Archives of the RSNA, 2022

M5B-SPCH-4

### Automatically Generated CT Severity Scores for COVID-19 Predict Death or Intubation at 1-Month Follow-Up

Monday, Nov. 28 12:45PM - 1:15PM Room: Learning Center - CH DPS

#### Participants

Luuk Boulogne, MSc, (*Presenter*) Institutional Grant, Thirona Bio, Inc

#### PURPOSE

To evaluate the ability of CORADS-AI, an automatic system that was originally developed for scoring the presence and current extent of a COVID-19 infection from chest Computed Tomography (CT), to predict death or intubation after one month for positive COVID-19 patients.

#### METHODS AND MATERIALS

CORADS-AI was developed in a previous study using CT scans from COVID-19 patients in the Netherlands. From a CT scan, CORADS-AI automatically segments each pulmonary lobe and produces a CT Severity Score (CTSS) at the lobe and patient level. This score is based on the percentage of affected tissue and has been used in routine clinical practice. We applied CORADS-AI to all 1205 patients that were involved in the STOIC study, had a positive COVID-19 RT-PCR result, and for which a CT scan was publicly available. 301 of them had died or had to be intubated at 1-month follow-up. We applied logistic regression with 5-fold cross validation on patient sex, age, and the patient level CTSS output of CORADS-AI to predict death or intubation after one month. We compared our method with the logistic regression model from the original STOIC study. This model received age, sex, several clinical variables, and manual CT annotations for lung disease extent as input. It was developed with all 4238 patients from the STOIC study that were positive for COVID-19 both according to RT-PCR testing and CT reading.

#### RESULTS

Our model obtained an AUC of  $0.72 \pm 0.02$  (mean  $\pm$  std. dev.) for predicting death or intubation after one month. When using solely the patient level CTSS output, we obtained an AUC of  $0.68 \pm 0.03$ . In comparison, the original STOIC study reported an AUC of their model of 0.69 (95% CI: 0.67, 0.71).

#### CONCLUSION

s We showed that CORADS-AI can predict death or intubation after one month for positive COVID-19 patients. Adding age and sex information to the model improved its results. The performance was comparable to that of the model developed in the original STOIC study, which used additional clinical variables and manual CT annotations. This comparison should be interpreted carefully, since that model was evaluated on a different subset of the STOIC cohort.

#### CLINICAL RELEVANCE/APPLICATION

We showed the potential of CORADS-AI, of which the output format is already used in clinical practice, for aiding radiologists in predicting the course of a COVID-19 infection.

Printed on: 02/07/23

## Abstract Archives of the RSNA, 2022

M5B-SPCH-5

### Chest CT Findings of COVID-19 in Hospitalized Patients: A Comparison between the Delta and Omicron Variants

Monday, Nov. 28 12:45PM - 1:15PM Room: Learning Center - CH DPS

#### Participants

Jong Hyuk Lee, MD, PhD, Seoul, Korea, Republic Of (*Presenter*) Nothing to Disclose

#### PURPOSE

It remains underexplored whether CT manifestations of coronavirus 2019 (COVID-19) differ among variants. This study compared the chest CT findings of COVID-19 between the Delta and Omicron variants.

#### METHODS AND MATERIALS

The institutional review board approved this retrospective study and waived informed consent. Baseline CT images of hospitalized patients with COVID-19 were consecutively collected from a secondary referral hospital in November 2021 and February 2022, when the Delta and Omicron variants predominated, respectively. Two radiologists categorized CT images into four patterns based on the Radiological Society of North America classification system for COVID-19 and visually graded pneumonia extent. Pneumonia, pleural effusion, and intrapulmonary vessels were segmented and quantified on CT images using a priori developed neural networks, followed by reader confirmation. Multivariate logistic and linear regression analyses were performed to examine the associations between the variants and CT category, severity, and peripheral vascularity.

#### RESULTS

In total, 176 patients with the Delta (n=88; 67±15 years; 46 men) and Omicron (n=88; 62±19 years; 51 men) variants were included. The Omicron variant was associated with a smaller proportion of patients with a typical CT appearance (32% versus 57%; P=.001), a lower visual pneumonia extent (5.4±6.0 versus 7.7±6.6; P=.017), similar pneumonia volume (5±10% versus 7±11%; P=.143), and a higher proportion of vessels with a cross-sectional area smaller than 5 mm<sup>2</sup> relative to the total pulmonary blood volume (BV5%; 48±11% versus 44±8%; P=.004). When adjusted for confounders including age, comorbidities, vaccination, and infection duration, the Omicron variant was significantly associated with a non-typical appearance (P=.009) and higher BV5 (P=.010), but not with visual pneumonia extent (P=.168) or pneumonia volume (P=.666).

#### CONCLUSION

The Omicron variant showed more frequent non-typical CT appearances of COVID-19 and less pulmonary vascular involvement than the Delta variant in hospitalized patients with comparable CT severity.

#### CLINICAL RELEVANCE/APPLICATION

The CT characteristics of Omicron may hamper radiologists from promptly recognizing COVID-19 on CT images when incidentally encountered, and this finding raises an alarm regarding the need to evaluate whether radiologic findings remain consistent or change when new variants appear.

Printed on: 02/07/23

## Abstract Archives of the RSNA, 2022

M5B-SPCH-6

### 4 and 12 Months After COVID-19 Pneumonia: Clinical-Functional and Chest CT Findings

Monday, Nov. 28 12:45PM - 1:15PM Room: Learning Center - CH DPS

#### Participants

Paula Rodriguez, MD, (*Presenter*) Nothing to Disclose

#### PURPOSE

Analyze whether the persistence of radiological lesions 4 and 12 months after COVID-19 pneumonia is related to the presence of residual symptoms and/or whether it has repercussions on respiratory function tests.

#### METHODS AND MATERIALS

Prospective study that included patients with COVID-19 pneumonia who underwent chest computed tomography (CT) 16±2 weeks and 52±2 weeks after hospital discharge. The chest CT were evaluated by 2 experienced radiologists who assessed the presence of ground glass, reticulation and bronchiectasias, their distribution and the percentage of involvement of each of these findings was quantified by lobes. Clinical, analytical and functional variables were recorded, as well as sociodemographic variables, comorbidities and data on the severity of the pneumonic process. One of the parameters to which special attention was paid was membrane diffusing capacity (DMCO) and pulmonary capillary blood volume (Vc)

#### RESULTS

93 patients were included, of whom 72% had lesions on chest CT. Male sex and older age are related to these lesions, but we have not found any association with the severity of the pneumonic process. At 4 months, no correlation was demonstrated between the persistence of ground glass and the sensation of dyspnea. Patients who required ICU admission had a higher prevalence of persistent ground glass, although no significant differences were obtained with respect to less severe patients. At 12 months, a decrease in the extension of the lesions was detected due to the decrease in size and/or density of the ground-glass opacities, although this was not observed in the reticulation or in the bronchiectasis. The parameter that best related with the presence of ground glass on CT was a higher DMCO/Vc

#### CONCLUSION

We have observed a high prevalence of ground-glass lesions on chest CT 4 months after COVID pneumonia. The percentage of ground glass was quantified as mild and we don't find a clear correlation with clinical, laboratory or 6-minute walk test variables. At 12 months, the improvement in respiratory function tests is related to the increase in parameters related to the vascular component of diffusion. The functional parameter that best correlates with the finding of ground glass on CT is DMCO/Vc, which is higher in patients with this radiological finding.

#### CLINICAL RELEVANCE/APPLICATION

d

Printed on: 02/07/23

## Abstract Archives of the RSNA, 2022

M5B-SPCH-7

### AI Denoising Improves Image Quality and Radiological Workflows In Pediatric Ultra-Low-Dose Thorax Computed Tomography Scans

Monday, Nov. 28 12:45PM - 1:15PM Room: Learning Center - CH DPS

#### Participants

Andreas Brendlin, Tuebingen, Germany (*Presenter*) Nothing to Disclose

#### PURPOSE

To evaluate the impact of an AI denoising algorithm on image quality, diagnostic accuracy, and radiological workflows in the context of pediatric thorax ultra-low-dose CT (ULDCT).

#### METHODS AND MATERIALS

100 consecutive pediatric thorax ULDCT were included and reconstructed using weighted filtered back projection (wFBP), iterative reconstruction (ADMIRE 2), and AI denoising (PixelShine). Place-consistent noise measurements were used to compare objective image quality. Eight blinded readers independently rated subjective image quality on a Likert scale (1=worst to 5=best). Each reader wrote a semiquantitative report to evaluate disease severity using a score with six common pathologies. The time to diagnosis was measured for each reader to compare possible workflow benefits. Properly corrected mixed-effects analysis with posthoc subgroup tests were used. Spearman's correlation coefficient measured inter-reader agreement for the subjective image quality analysis and the severity score sheets.

#### RESULTS

The highest noise was measured for wFBP, followed by ADMIRE 2, and PixelShine ( $76.9 \pm 9.62$  vs.  $43.4 \pm 4.45$  vs.  $34.8 \pm 3.27$  HU; each  $p < 0.001$ ). The highest subjective image quality was measured for PixelShine, followed by ADMIRE 2, and wFBP (4 [4-5] vs. 3 [4-5] vs. 3 [2-4], each  $p < 0.001$ ) with good inter-rater agreement ( $r = 0.790$ ;  $p = 0.001$ ). In diagnostic accuracy analysis, there was a good inter-rater agreement between the severity scores ( $r = 0.764$ ;  $p < 0.001$ ) without significant differences between severity score items per reconstruction mode ( $F(5.71;566) = 0.792$ ;  $p = 0.570$ ). The shortest time to diagnosis was measured for the PixelShine datasets, followed by ADMIRE 2, and wFBP ( $2.28 \pm 1.56$  vs.  $2.66 \pm 2.31$  vs.  $2.45 \pm 1.90$  minutes;  $F(1.000;99.00) = 268.1$ ;  $p < 0.001$ ).

#### CONCLUSION

AI denoising significantly improves image quality in pediatric thorax ULDCT without compromising diagnostic confidence and reduces time to diagnosis substantially.

#### CLINICAL RELEVANCE/APPLICATION

A promising technique to minimize potentially harmful radiation exposure in pediatric thorax ultra-low-dose CT protocols is to improve the dose-effectiveness by shaping the X-ray spectrum in favor of higher energy photons. However, the typical trade-off of such approaches is lower image quality than standard protocols due to higher image noise.

Printed on: 02/07/23

## Abstract Archives of the RSNA, 2022

M5B-SPCH-8

### Chest CT Findings and Pulmonary Function Tests in the Postrecovery Phase of Mild to Severe Cases of COVID-19

Monday, Nov. 28 12:45PM - 1:15PM Room: Learning Center - CH DPS

#### Participants

Patricia Yokoo, MD, Sao Paulo, Brazil (*Presenter*) Nothing to Disclose

#### PURPOSE

To correlate follow-up chest computed tomography (CT) and pulmonary function test (PFT) findings of mild to severe COVID-19 survivors.

#### METHODS AND MATERIALS

This retrospective study was performed in two medical centers in Sao Paulo, Brazil. Data were collected from consecutive patients who underwent PFT and chest CT (within a maximum interval of 14 days) after recovery from COVID-19 between May and October 2021. Clinical data, spirometric parameters, diffusing capacity for carbon monoxide (DLCO), lung CT abnormalities, distribution and CT extent score were recorded. Clinical and tomographic differences between the patients with normal or abnormal PFTs were assessed by Chi-Square, Mann-Whitney or Fisher tests.

#### RESULTS

101 COVID-19 survivors were included (mild disease 48, moderate 40, severe 13), at a median 95 days from initial symptom onset. 33% (33/101) had persistent symptoms. Reduction of DLCO% predicted was the most common abnormality in lung function (19% of the patients). Persistence of symptoms was not associated with abnormal lung function. The presence of reticular opacities ( $p=0.003$ ), bronchial dilatation ( $p=0.005$ ) and architectural distortion ( $p<0.001$ ) in chest CT and a CT extent score  $> 5$  ( $p=0.006$ ) were significantly more prevalent in patients with impairment of DLCO. The optimal CT score for identifying patients with reduced DLCO% predicted was 5.5 (area under curve = 0.7), with 78.9% sensitivity and 56.1% specificity.

#### CONCLUSION

The presence of reticular opacities, bronchial dilatation and architectural distortion in chest CT and the extent of lung abnormalities was associated with lung function impairment in the postrecovery phase of mild to severe cases of COVID-19.

#### CLINICAL RELEVANCE/APPLICATION

The anatomical and functional pulmonary sequelae of SARS-CoV-2 infection are not yet fully understood. The evaluation of late chest CT findings associated with lung function impairment can help to establish the role of imaging in the postrecovery phase of COVID-19 patients.

Printed on: 02/07/23

## Abstract Archives of the RSNA, 2022

M5B-SPCH-9

### Comparison of Chest CT Characteristics of COVID-19 Interstitial Pneumonia Between Patients with Different Vaccination Status

Monday, Nov. 28 12:45PM - 1:15PM Room: Learning Center - CH DPS

#### Participants

Francesco Rizzetto, MD, Milan, Italy (*Presenter*) Travel support, Bracco Group

#### PURPOSE

To compare the CT imaging characteristics of patients with symptomatic COVID-19 infection according to their SARS-CoV-2 vaccination status (non-vaccinated, incompletely vaccinated and fully vaccinated).

#### METHODS AND MATERIALS

The CT examinations performed in the Emergency Department between May and November 2021 for suspicion of COVID-19 pneumonia in patients with positive swab for SARS-CoV-2 were retrospectively included. Three reader (one 13-year experienced radiologist and two 4th-year radiology residents) independently evaluated each chest CT according to CO-RADS and ACR COVID classification and the results were compared for vaccination status. In possible COVID-19 pneumonia cases, defined as CO-RADS 3 to 5 (ACR indeterminate and typical) by each reader, high extent of pulmonary involvement ( $\geq 25\%$ ) and CT patterns (presence of ground glass opacities, consolidations, crazy paving areas) were compared for vaccination status.

#### RESULTS

A total of 184 patients were included, 111 non-vaccinated (60%) for SARS-CoV-2 infection, 21 (11%) with an incomplete vaccination cycle, and 52 (28%) with a complete vaccination cycle (6 different vaccine types). At bivariate logistic regression, the only factor predicting the absence of pneumonia (CO-RADS 1 and ACR negative cases) for the three readers was a complete vaccination cycle (OR=12.8-13.1 compared to non-vaccinated patients,  $p=0.032$ ). Both CT score and CT patterns of possible COVID-19 pneumonia showed no statistically significant correlation with vaccination status for the three readers.

#### CONCLUSION

Patients with symptomatic SARS-CoV-2 infection and a complete vaccination cycle had 13-times higher odds to present with a negative chest CT examination in ED compared to non-vaccinated patients. CT involvement and CT patterns of interstitial pneumonia showed no difference between different vaccination status.

#### CLINICAL RELEVANCE/APPLICATION

Symptomatic COVID-19 patient with a complete vaccination cycle may undergo a less aggressive imaging workup.

Printed on: 02/07/23



## Abstract Archives of the RSNA, 2022

M5B-SPER

### Emergency Monday Poster Discussions - B

Monday, Nov. 28 12:45PM - 1:15PM Room: Learning Center - ER DPS

#### Participants

Koenraad Nieboer, MD, Brussels, (*Moderator*) Speakers Bureau, General Electric Company

Printed on: 02/07/23

## Abstract Archives of the RSNA, 2022

M5B-SPGI

### Gastrointestinal Monday Poster Discussions - B

Monday, Nov. 28 12:45PM - 1:15PM Room: Learning Center - GI DPS

#### Participants

Jeanne M. Horowitz, MD, Chicago, IL (*Moderator*) Nothing to Disclose

#### Sub-Events

### M5B-SPGI-1 Laterality of Extracellular Volume Fraction of Liver in the Patients of the Pulmonary Hypertension

#### Participants

Tatsuya Nishii, MD, PhD, Suita, Japan (*Presenter*) Speakers Bureau, Guerbet SA; Speakers Bureau, General Electric Company; Speakers Bureau, Siemens AG; Research Grant, Canon Medical Systems Corporation

#### PURPOSE

The liver's extracellular volume fraction (ECV) has attracted attention as an imaging biomarker to measure the degree of liver parenchymal damage, and we hypothesized that it could be used for liver damage associated with pulmonary hypertension (PH). However, the left-right difference in liver ECV in PH patients has not been evaluated. This study evaluated liver ECV and right heart cath (RHC) results in first-time patients referred to a specialized PH hospital.

#### METHODS AND MATERIALS

We retrospectively reviewed consecutive 46 cases (35 women, median 64 years) with suspected chronic thromboembolic PH (CTEPH) who underwent dual-energy CT (DECT) of four minutes delayed phase using 192-row dual-source CT and RHC from January 2021 to March 2022. We calculated the ECV of the right and left lobe of the liver estimated from the iodine map generated via three-material decomposition using DECT images. We evaluated the correlation coefficient between the ECV of the liver (ECV<sub>total</sub>), obtained by averaging those of both lobes, and the results of RHC. Furthermore, patient background and RHC results were evaluated in cases in which the ECV of the left lobe was more than 5% higher than the ECV of the right lobe.

#### RESULTS

In 46 cases (39 CTEPH and seven others), the median (IQR) of ECV<sub>total</sub>, mean pulmonary artery pressure, cardiac index (CI), and pulmonary vascular resistance index was 24.2 (20.4-27.1)%, 36.5 (29-44) mmHg, 2.1 (1.8-2.5) L/min/m<sup>2</sup> and 994 (708-1515) dynes/cm<sup>5</sup>, respectively. ECV<sub>total</sub> moderately correlated with those results of RHC (R=0.42, -0.31, and 0.47, respectively). The median (IQR) of the ECV in left lobe were 26.9 (22.0-31.2) %, significantly higher (mean difference 2.1 [95% CI, 0.8-3.3] %, P=.001) than that of right lobe (25.3 [21.3-28.9] %). The median (IQR) CI were significantly lower (1.8 [1.6-2.1] vs. 2.2 [1.9-2.6] L/min/m<sup>2</sup>, P=.003) in cases whose ECV of left lobe were 5% higher than ECV of the right lobe.

#### CONCLUSION

s ECV of the liver, derived from DECT, significantly correlates with RHC measurements in PH patients. However, in cases with reduced CI, the ECV of the left lobe is measured higher than the right lobe.

#### CLINICAL RELEVANCE/APPLICATION

When using ECVs of the liver clinically or in research studies, radiologists need to consider that a reduction in CI can cause a significant difference in ECV measurements between the left and right lobes.

### M5B-SPGI-2 Radiomics Analysis of Magnetic Resonance-Proton Density Fat Fraction for the Diagnosis of Hepatic Steatosis in Patients with Nonalcoholic Fatty Liver Disease

#### Participants

Hyun Jin Kim, MD, Seoul, Korea, Republic Of (*Presenter*) Nothing to Disclose

#### PURPOSE

To assess the diagnostic feasibility of radiomics analysis based on magnetic resonance (MR)-proton density fat fraction (PDFF) for grading of hepatic steatosis in patients with nonalcoholic fatty liver disease (NAFLD).

#### METHODS AND MATERIALS

One hundred-six patients with suspected NAFLD were retrospectively enrolled. All patients underwent a liver parenchymal biopsy. MR-PDFF and MR spectroscopy (MRS) were performed using a 3.0-T scanner. Following whole volume segmentation of MR-PDFF images, 834 radiomic features were analyzed using a commercial program. Radiologic features were analyzed, such as median and mean values of the volume of interest (VOIs) and variable clinical features. A random forest regressor was employed to extract important radiomic, radiological, and clinical features. It was trained using 20 repeated 10-fold cross-validation to classify the steatosis grade of NAFLD. The area under the receiver operating characteristic curve (AUROC) was evaluated using a classifier for diagnosing the steatosis stage.

## RESULTS

The pathological hepatic steatosis grades were classified as low-grade steatosis (grade 0-1, n=82) and high-grade steatosis (grade 2-3, n=24). Fifteen important features were extracted from radiomics analysis, with the three most important being wavelet-LLL Neighbouring Gray Tone Difference Matrix Coarseness, original First Order Mean and 90th percentile. MRS Mean value was extracted as a more important feature than MR-PDFF Mean or Median in radiologic measures. Alanine aminotransferase has been identified as the most important clinical feature. The AUROC of the classifier using radiomics was comparable to that of radiologic measures (0.94±0.09 and 0.96±0.08, respectively).

## CONCLUSION

s MR-PDFF-derived radiomics may provide a comparable alternative for the grading of hepatic steatosis in patients with NAFLD.

## CLINICAL RELEVANCE/APPLICATION

Non-invasive measurement using MR-PDFF in NAFLD patients with severe steatosis is expected to be accurate and reduce unnecessary biopsies through MR-PDFF. Radiomic analysis based on MR-PDFF may provide similar diagnostic performance for hepatic steatosis and may be an alternative tool.

## M5B-SPGI-3 Volume-assisted estimation of remnant liver function based on Gd-EOB-DTPA enhanced MR relaxometry: a prospective observing trial.

### Participants

Niklas Verloh, MD, Freiburg, Germany (*Presenter*) Speaker, Bayer AG; Research Funded, Bayer AG

## PURPOSE

This study aimed to evaluate an MR image-based liver function analysis that visualizes regional and global liver function and predicts postoperative remaining liver function.

## METHODS AND MATERIALS

The study included patients (n=70) in whom MRI of the liver with Gd-EOB-DTPA was indicated as preoperative preparation before liver resection. These patients received an additional liver function test (indocyanine green clearance test) before and after liver resection. All imaging was performed on a clinical 3T system. T1 maps were obtained before and 20 minutes after contrast injection using a prototypical T1 mapping sequence. The T1 reduction rate of the segmented liver parenchyma between the two sequences was calculated and, using a previously determined formula, converted to a liver function value. Liver resection was simulated with visceral surgery, and the residual function was determined. The ICG test performed postoperatively showed liver dysfunction in 35 patients.

## RESULTS

Assessment of remaining postoperative liver function by MRI was able to predict the occurrence of postoperative liver dysfunction with a sensitivity of 0.86 and a specificity of 0.74 (PPV: 0.77; NPV: 0.84; AUC: 0.80).

## CONCLUSION

s In conclusion, virtual surgical planning using MRI, in addition to revealing the spatial relationships of tumors and vessels, has the potential to reduce the occurrence of small for size syndrome by calculating the postoperative liver function.

## CLINICAL RELEVANCE/APPLICATION

Liver insufficiency after liver resection is often the result of an insufficient remaining functional organ ("small for size syndrome"). Currently, liver function is assessed using preoperative liver volumetry and is based on clinical and biochemical parameters. However, these conventional liver function tests are not sufficient to confidently predict postoperative liver failure. Here, modern techniques can help in surgical planning and positively impact patient care.

## M5B-SPGI-4 Quantitative parameters on contrast-enhanced CT for non-invasive assessment of clinically significant portal hypertension

### Participants

Jinkui Li, MD, (*Presenter*) Nothing to Disclose

## PURPOSE

Hepatic venous pressure gradient (HVPG) is critical for diagnose portal hypertension. However, HVPG measurement is invasive. Non-invasive and accurate assessment of portal hypertension is unmet need in clinics. This study aimed to determine whether the extracellular volume fraction (ECV) of liver and spleen, and the iodine washout rate (IWR) of liver, could provide an estimate of clinically significant portal hypertension (CSPH, HVPG =10 mmHg ) in patients with cirrhosis.

## METHODS AND MATERIALS

101 participants (51 patients with cirrhosis who underwent HVPG measurement and 50 healthy controls who were defined to have normal portal pressure without HVPG measurement) underwent contrast-enhanced CT between January 2018 and December 2020 were retrospectively included. Absolute contrast enhancement of the liver/spleen and the abdominal aorta (subtracting unenhanced from contrast-enhanced attenuation during portal-venous phase [PVP] or delay phase [DP], ?HU) were measured. ECV<sub>liver</sub> and ECV<sub>spleen</sub> were calculated using the following equation:  $ECV_{liver/spleen} = \frac{?HU_{liver/spleen} - DP}{?HU_{aorta} - DP} \times (100 - \text{Hematocrit} [\%])$ . IWR of liver was calculated using the following equation:  $IWR = (1 - ?HU_{liver} - DP / ?HU_{liver} - PVP) \times 100$ . The correlation of non-invasive parameters with HVPG was evaluated. ROC analysis was performed and the areas under the curves (AUCs) were calculated for diagnostic performance.

## RESULTS

The mean of HVPG was 16.55 ± 0.67 mmHg. There were significant differences in CT parameters between cirrhotic patients and healthy controls: ECV<sub>liver</sub> (P < 0.001), ECV<sub>spleen</sub> (P < 0.001), and IWR (P < 0.001). Both ECV<sub>liver</sub> and ECV<sub>spleen</sub> correlated with HVPG (P = 0.007 and 0.001, respectively). ECV<sub>spleen</sub> and IWR were identified to be independently correlated with HVPG (P = 0.001 and 0.022, respectively). ECV<sub>spleen</sub> and IWR revealed perfect diagnostic performance for the identification of CSPH with AUCs of

0.984 and 0.956, respectively, and outperformed ECVliver (AUC, 0.718) ( $P < 0.001$ ). The best cut-off value, ECVliver, ECVspleen, and IWR for identifying CSPH, were = 24.6%, = 38.29%, and =40.06%, respectively.

## CONCLUSION

s ECVspleen and IWR were valuable non-invasive parameters for the assessment of CSPH in cirrhotic patients and outperformed ECVliver. It should be explored further across a broader range of pressure values.

## CLINICAL RELEVANCE/APPLICATION

Such valuable non-invasive parameters including ECV and IWR to assess portal pressure is clinically meaningful for cirrhotic patients. ECV and IWR are easy to obtain and can be retrospectively derived from CT, since CT is routinely used to evaluate the complications of cirrhosis. Such a dual-screening strategy would further improve the cost-effectiveness of CT.

## M5B-SPGI-5 Can CT Spectral Imaging Based on Multi-material Decomposition Algorithm Have Better Ability to Diagnose Chemotherapy Related Fatty Liver Disease than Liver-to-fat ratio?

Participants

Xi Huaze, (*Presenter*) Nothing to Disclose

## PURPOSE

To determine whether CT multi-material decomposition (MMD) spectral examination may improve clinical diagnosis efficiency of chemotherapy related fatty liver disease (CRFLD).

## METHODS AND MATERIALS

Eighty-one patients undergoing CT exams of abdomen (traditional unenhanced imaging enhanced spectral imaging) after chemotherapeutic treatment were retrospectively recruited. All these patients have no history of fatty liver, liver disease, liver tumors and large alcohol intake before chemotherapy. According to the results of ultrasonic or magnetic resonance examination after chemotherapy, patients were divided into clinical CRFLD group and non-CRFLD groups. On liver fat images in venous phase generated by MMD algorithm, three physicians measured liver fat fractions (LFFs) of the whole liver, left lobe and right lobe. When the average values calculated from these three doctors' measurement of the whole liver LFF or either lobe LFF exceeded 5%, the patients were considered as spectrum-CRFLD. On unenhanced CT images, the same three doctors measured CT values of spleen and liver, and calculated average values to acquire the Liver-to-spleen ratio (LSR,  $LSR = \text{CT value}_{\text{liver}} / \text{CT value}_{\text{spleen}}$ ). When it was less than 1, the patients would be regarded as CT-CRFLD. Diagnostic efficiency of spectrum-CRFLD and CT-CRFLD was compared by using McNemar's test.

## RESULTS

Thirty-four of 81 patients (mean age, 57.8 years $\pm$ 11.5; 23 women) were diagnosed as clinical CRFLD. The whole liver LFF showed significantly highest sensitivity, specificity, positive predictive value, negative predictive value, accuracy of diagnosing clinical CRFLD (82.4%, 95.7%, 93.3%, 88.2% and 90.1%, respectively). The diagnostic accuracy of whole liver LFF was significantly higher than both either liver lobe LFF and LSR (both  $p < 0.001$ ).

## CONCLUSION

s The whole liver LFF obtained by CT MMD spectral imaging is a reliable indicator to diagnose CRFLD with more accuracy and sensitivity, compared with the traditional CT liver-to-fat ratio.

## CLINICAL RELEVANCE/APPLICATION

Quantitative measurement of fat fraction in the whole liver through CT spectral imaging can help detect fatty liver caused by chemotherapeutics.

## M5B-SPGI-6 The value of hepatic extracellular volume fraction obtained from iodine map in evaluating liver function of patients with liver cirrhosis

Participants

Yao Wang, (*Presenter*) Nothing to Disclose

## PURPOSE

To explore the correlation between hepatic extracellular volume fraction (fECV) based on iodine density and liver function in cirrhosis patients, and further investigate the diagnostic value of fECV in liver cirrhosis.

## METHODS AND MATERIALS

The patients undergoing enhanced abdominal CT scan with spectral mode were categorized as group F (patients with liver cirrhosis), group F0 (patients without liver cirrhosis). According to the child-Pugh classification, group F was further divided into three subgroups: group FA (child A), group FB (child B) and group FC (child C). The latter two groups represented decompensated cirrhosis. The iodine density of liver and abdominal aorta were measured in iodine map of equilibrium phase to calculate the fECV. The formula for fECV is the iodine density of the liver multiplied by 100 minus Hct and then divided by the iodine density of the abdominal aorta. The fECV values among groups were compared by One-Way ANOVA, LSD method was used for further comparison. Pearson correlation analysis was performed to analyze the correlation between fECV and child-Pugh classification. The diagnostic performance of fECV for the differentiation of liver cirrhosis was assessed using receiver operation characteristic (ROC) curve analysis.

## RESULTS

A total of 157 patients (51 in group F0, 46 in group FA, 38 in group FB, 22 in group FC) were included. The fECV fractions in from F0 to FC showed an upward trend (31.62 $\pm$ 2.00, 37.08 $\pm$ 3.64, 43.39 $\pm$ 6.00). There was significant difference in fECV among groups and between any two groups (all  $P < 0.001$ ). Strong positive correlation of fECV with child-Pugh classification was found ( $r = 0.841$ ). For differentiating liver cirrhosis, the sensitivity and specificity of fECV were 88.68% and 86.27%, respectively, with area under the curve (AUC) of 0.922, when the cut-off value was set at 30.26%. For differentiating decompensated cirrhosis by fECV, a cut-off value of 33.96% resulted in an AUC of 0.938, sensitivity of 90.00% and specificity of 89.13%.

## CONCLUSION

s fECV from iodine map is strongly positively correlated with the Child-Pugh liver function classification, and has a high potential value in the differentiation of liver cirrhosis with different liver function grades.

## CLINICAL RELEVANCE/APPLICATION

ECV measured using Hounsfield units needs precontrast phase, which has the problem of registration and increases the radiation dose. fECV obtained by dual energy spectral examination is a simple and convenient biomarker to identify different degrees of liver cirrhosis without dose compromise, which is suitable for follow-up.

## M5B-SPGI-7 To Characterize Liver Fibrosis using a Four-Compartments Restriction Spectrum Imaging Model

Participants

Cai Yeyu, MD, Changsha, China (*Presenter*) Nothing to Disclose

## PURPOSE

Previous studies have shown that liver fibrosis, caused by chronic liver disease, is closely associated with the progression of various types of liver disease and is a key risk factor for cirrhosis and hepatocellular carcinoma. In this study, we evaluated the feasibility of the 4-compartment RSI model to identify carbon tetrachloride (CCl<sub>4</sub>)-induced liver fibrosis in mouse model.

## METHODS AND MATERIALS

A total of 38 mice in the experiment were divided into CCL<sub>4</sub>-induced liver fibrosis (LF) and control groups, respectively. MRI examinations were performed on a 3T scanner (uMR790, United Imaging Healthcare, Shanghai, China), based on the echo planar imaging sequence (EPI) with a total of 11 b-values ranging from 0-2000 s/mm<sup>2</sup>. Conventional ADC and D values for each compartment in multicompartmental RSI models were calculated on voxel wise basis. The performance of different RSI models was evaluated using the Bayesian Information Criterion. Traditional ADC values and D<sub>i</sub> values of different compartments were further compared between the LF and control groups using Mann-Whitney test, and finally, the receiver operating characteristic (ROC) curve for different parameters were performed.

## RESULTS

All mice in LF group were histologically diagnosed as liver fibrosis (100%). The results showed that the best model to describe the data was the 4-compartment RSI model with the lowest  $\Delta$ BIC value among all RSI models. Significant differences of ADC value and D values of the different compartments in the 4-compartment RSI model were found between LF group and control group. RSI4-C3 was the best single diffusion parameter for the discrimination of liver fibrosis, with the largest AUC value. Furthermore, the AUC value was further increased when ADC and C3 were combined.

## CONCLUSION

s The 4-compartment RSI model can further distinguish the alterations in the LF group from the control group during different diffusion processes. Compared with the conventional ADC values, RSI4-C3 has a better ability to discriminate liver fibrosis. The combined parameter of ADC value and RSI4-C3 can further improve the discrimination performance of liver fibrosis.

## CLINICAL RELEVANCE/APPLICATION

This study demonstrates that the four-compartment RSI model can provide a better identification of liver fibrosis than conventional ADC.

## M5B-SPGI-8 Non-invasive prediction of NASH by PDFF in Patients with Obesity without known Liver Disease

Participants

Nikolaos Panagiotopoulos, MD, Madison, WI (*Presenter*) Institutional Research Grant, Pfizer Inc

## PURPOSE

To assess the value of PDFF, R<sub>2</sub><sup>\*</sup>, T<sub>2</sub><sup>\*</sup>, and T<sub>1</sub> for the detection of NASH in a cohort of subject with obesity without previously known liver disease.

## METHODS AND MATERIALS

This analysis is part of an ongoing study of patients with obesity undergoing weight loss surgery (WLS). Study participants underwent imaging within 1 week prior to WLS and intraoperative wedge biopsy of the liver. Imaging at 3.0T included IDEAL IQ (GE, USA) to quantify PDFF and R<sub>2</sub><sup>\*</sup> and LiverMultiscan (LMS, Perspectum, UK) for PDFF, T<sub>2</sub><sup>\*</sup>, and T<sub>1</sub>. Images were analyzed by placing ROIs in all liver segments. LMS data were analyzed by Perspectum. Liver biopsy samples were classified as normal, non-alcoholic fatty liver (NAFL, ie: steatosis only), or non-alcoholic steatohepatitis (NASH, based on a NASH activity score >5). Receiver operator characteristic (ROC) curve analysis was performed to assess the diagnostic accuracy of PDFF, R<sub>2</sub><sup>\*</sup>, T<sub>2</sub><sup>\*</sup> and T<sub>1</sub> to differentiate NASH from non-NASH (normal or NAFL).

## RESULTS

50 patients (44 female, 45±11 years, BMI: 44±6) were examined and analyzed. 24 subjects had no liver disease, 17 had NAFL and 9 had NASH. IDEAL IQ PDFF achieved separation between NASH and no NASH with an area under the curve of 0.91 (95%CI: 0.79-1). LMS PDFF achieved similarly separation between the groups with AUC=0.98 (95%CI: 0.94-1). At the same PDFF threshold of 11% for IDEAL IQ and LMS, sensitivity was 75% (95%CI: 35-97) and 83% (95%CI: 36-100), respectively, and specificity 98% (95%CI: 87-100) and 100% (95%CI: 89-100). LMS T<sub>1</sub> achieved separation between the groups with an area under the curve of 0.83 (95%CI: 0.68-0.97). For the T<sub>1</sub> threshold of 870ms, sensitivity was 83% (95%CI: 36-100) and specificity was 73% (95%CI: 55-87). Neither R<sub>2</sub><sup>\*</sup> nor T<sub>2</sub><sup>\*</sup> could distinguish between NASH and non-NASH.

## CONCLUSION

s We observed promising performance of PDFF for the detection of NASH in a cohort of patients with obesity without previously known liver disease, in stark contrast to current knowledge. The results support our hypothesis that PDFF can differentiate NASH from NAFL in a cohort of patients with early-stage NASH where the severity of liver fat deposition is still present and relevant. A major limitation of this work is the limited number of patients with NASH to date.

## CLINICAL RELEVANCE/APPLICATION

If confirmed, these results would constitute a paradigm change in the early detection of NASH.

## M5B-SPGI-9 a fully automated hybrid approach to assessing liver fibrosis and necroinflammation on conventional MRI: a multi-center study

Participants

Junhao Zha, MD, (*Presenter*) Nothing to Disclose

## PURPOSE

To develop and validate a combined radiomics-clinic model by a fully automated hybrid approach to diagnosing clinically significant liver fibrosis (=F2) and necroinflammatory activity (=G2), respectively

## METHODS AND MATERIALS

In this retrospective multi-center study, a total of 537 patients were included. From May 2015 to December 2018, 394 patients were randomly distributed in a training (n=276) or internal test (n=118) set at a ratio of 7:3 at center 1. From January 2019 to August 2020, 96 patients considered eligible at center 1 were placed in a temporal test set. An independent external test set from center 2 was used to validate the proposed models. All patients underwent abdominal MRI with pathologically proven liver fibrosis and necroinflammation. An interactive deep learning approach was developed to achieve better automated whole liver segmentation performance of ResUnet. 2880 radiomics features extracted from VOIT2FS, VOIT1delay were analyzed separately to form the radiomics scores (R-scores). The optimal R-scores and clinical biomarkers were integrated into the combined radiomics-clinic model (CRC model) for assessing =F2 or =G2, respectively. The performance of the models was assessed and compared with FIB-4 and APRI

## RESULTS

For staging =F2, AUCs of CRC model are 0.83, 0.79, 0.82, 0.83 in the training, internal test, temporal test, and external test set respectively. CRC model (AUC 0.79) significantly outperformed radiomics model (AUC 0.75;  $P < .05$ ) in the internal test set, and significantly outperformed FIB-4 (AUC 0.69, 0.67, 0.63;  $P < .05$ ), and APRI (AUC 0.69, 0.68, 0.62;  $P < .05$ ) in the internal test, temporal test, and external test set. By using the cutoffs, the CRC model had sensitivities and specificities as follows: 72.4% / 82.1%, 73.1% / 62.5%, 82.4% / 71.1%, 91.4% / 75.0% in the training, internal test, temporal test, and external test set for diagnosing =F2. For classifying =G2, the training, internal test, temporal test, and external test set results of the CRC model were AUC 0.88, 0.86, 0.79, and 0.89, sensitivity 74.6%, 71.4%, 61.5%, and 80.0%, and specificity 85.6%, 90.3%, 82.5%, and 87.1%, respectively. CRC model (AUC 0.86, 0.79, 0.89) significantly outperformed radiomics model (AUC 0.67, 0.69, 0.67;  $P < .05$ ), FIB-4 (AUC 0.67, 0.69, 0.73;  $P < .05$ ), and APRI (AUC 0.74, 0.70, 0.63;  $P < .05$ ) in the internal test, temporal test, and external test set for staging =G2

## CONCLUSION

s The CRC models provide a promising approach for diagnosing liver fibrosis (=F2) and necroinflammatory activity (=G2)

## CLINICAL RELEVANCE/APPLICATION

Traditional MR tissue texture, and routine clinical biomarkers, should be taken into consideration to develop the CRC model, and this mimics the diagnosis in real clinical scenarios.

Printed on: 02/07/23

## Abstract Archives of the RSNA, 2022

M5B-SPGI-1

### Laterality of Extracellular Volume Fraction of Liver in the Patients of the Pulmonary Hypertension

Monday, Nov. 28 12:45PM - 1:15PM Room: Learning Center - GI DPS

#### Participants

Tatsuya Nishii, MD, PhD, Suita, Japan (*Presenter*) Speakers Bureau, Guerbet SA; Speakers Bureau, General Electric Company; Speakers Bureau, Siemens AG; Research Grant, Canon Medical Systems Corporation

#### PURPOSE

The liver's extracellular volume fraction (ECV) has attracted attention as an imaging biomarker to measure the degree of liver parenchymal damage, and we hypothesized that it could be used for liver damage associated with pulmonary hypertension (PH). However, the left-right difference in liver ECV in PH patients has not been evaluated. This study evaluated liver ECV and right heart cath (RHC) results in first-time patients referred to a specialized PH hospital.

#### METHODS AND MATERIALS

We retrospectively reviewed consecutive 46 cases (35 women, median 64 years) with suspected chronic thromboembolic PH (CTEPH) who underwent dual-energy CT (DECT) of four minutes delayed phase using 192-row dual-source CT and RHC from January 2021 to March 2022. We calculated the ECV of the right and left lobe of the liver estimated from the iodine map generated via three-material decomposition using DECT images. We evaluated the correlation coefficient between the ECV of the liver (ECV<sub>total</sub>), obtained by averaging those of both lobes, and the results of RHC. Furthermore, patient background and RHC results were evaluated in cases in which the ECV of the left lobe was more than 5% higher than the ECV of the right lobe.

#### RESULTS

In 46 cases (39 CTEPH and seven others), the median (IQR) of ECV<sub>total</sub>, mean pulmonary artery pressure, cardiac index (CI), and pulmonary vascular resistance index was 24.2 (20.4-27.1)%, 36.5 (29-44) mmHg, 2.1 (1.8-2.5) L/min/m<sup>2</sup> and 994 (708-1515) dynes/cm<sup>5</sup>, respectively. ECV<sub>total</sub> moderately correlated with those results of RHC (R=0.42, -0.31, and 0.47, respectively). The median (IQR) of the ECV in left lobe were 26.9 (22.0-31.2) %, significantly higher (mean difference 2.1 [95% CI, 0.8-3.3] %, P=.001) than that of right lobe (25.3 [21.3-28.9] %). The median (IQR) CI were significantly lower (1.8 [1.6-2.1] vs. 2.2 [1.9-2.6] L/min/m<sup>2</sup>, P=.003) in cases whose ECV of left lobe were 5% higher than ECV of the right lobe.

#### CONCLUSION

s ECV of the liver, derived from DECT, significantly correlates with RHC measurements in PH patients. However, in cases with reduced CI, the ECV of the left lobe is measured higher than the right lobe.

#### CLINICAL RELEVANCE/APPLICATION

When using ECVs of the liver clinically or in research studies, radiologists need to consider that a reduction in CI can cause a significant difference in ECV measurements between the left and right lobes.

Printed on: 02/07/23

## Abstract Archives of the RSNA, 2022

M5B-SPGI-2

### **Radiomics Analysis of Magnetic Resonance-Proton Density Fat Fraction for the Diagnosis of Hepatic Steatosis in Patients with Nonalcoholic Fatty Liver Disease**

Monday, Nov. 28 12:45PM - 1:15PM Room: Learning Center - GI DPS

#### **Participants**

Hyun Jin Kim, MD, Seoul, Korea, Republic Of (*Presenter*) Nothing to Disclose

#### **PURPOSE**

To assess the diagnostic feasibility of radiomics analysis based on magnetic resonance (MR)-proton density fat fraction (PDFF) for grading of hepatic steatosis in patients with nonalcoholic fatty liver disease (NAFLD).

#### **METHODS AND MATERIALS**

One hundred-six patients with suspected NAFLD were retrospectively enrolled. All patients underwent a liver parenchymal biopsy. MR-PDFF and MR spectroscopy (MRS) were performed using a 3.0-T scanner. Following whole volume segmentation of MR-PDFF images, 834 radiomic features were analyzed using a commercial program. Radiologic features were analyzed, such as median and mean values of the volume of interest (VOIs) and variable clinical features. A random forest regressor was employed to extract important radiomic, radiological, and clinical features. It was trained using 20 repeated 10-fold cross-validation to classify the steatosis grade of NAFLD. The area under the receiver operating characteristic curve (AUROC) was evaluated using a classifier for diagnosing the steatosis stage.

#### **RESULTS**

The pathological hepatic steatosis grades were classified as low-grade steatosis (grade 0-1, n=82) and high-grade steatosis (grade 2-3, n=24). Fifteen important features were extracted from radiomics analysis, with the three most important being wavelet-LLL Neighbouring Gray Tone Difference Matrix Coarseness, original First Order Mean and 90th percentile. MRS Mean value was extracted as a more important feature than MR-PDFF Mean or Median in radiologic measures. Alanine aminotransferase has been identified as the most important clinical feature. The AUROC of the classifier using radiomics was comparable to that of radiologic measures (0.94±0.09 and 0.96±0.08, respectively).

#### **CONCLUSION**

s MR-PDFF-derived radiomics may provide a comparable alternative for the grading of hepatic steatosis in patients with NAFLD.

#### **CLINICAL RELEVANCE/APPLICATION**

Non-invasive measurement using MR-PDFF in NAFLD patients with severe steatosis is expected to be accurate and reduce unnecessary biopsies through MR-PDFF. Radiomic analysis based on MR-PDFF may provide similar diagnostic performance for hepatic steatosis and may be an alternative tool.

Printed on: 02/07/23

## Abstract Archives of the RSNA, 2022

M5B-SPGI-3

### **Volume-assisted estimation of remnant liver function based on Gd-EOB-DTPA enhanced MR relaxometry: a prospective observing trial.**

Monday, Nov. 28 12:45PM - 1:15PM Room: Learning Center - GI DPS

#### **Participants**

Niklas Verloh, MD, Freiburg, Germany (*Presenter*) Speaker, Bayer AG; Research Funded, Bayer AG

#### **PURPOSE**

This study aimed to evaluate an MR image-based liver function analysis that visualizes regional and global liver function and predicts postoperative remaining liver function.

#### **METHODS AND MATERIALS**

The study included patients (n=70) in whom MRI of the liver with Gd-EOB-DTPA was indicated as preoperative preparation before liver resection. These patients received an additional liver function test (indocyanine green clearance test) before and after liver resection. All imaging was performed on a clinical 3T system. T1 maps were obtained before and 20 minutes after contrast injection using a prototypical T1 mapping sequence. The T1 reduction rate of the segmented liver parenchyma between the two sequences was calculated and, using a previously determined formula, converted to a liver function value. Liver resection was simulated with visceral surgery, and the residual function was determined. The ICG test performed postoperatively showed liver dysfunction in 35 patients.

#### **RESULTS**

Assessment of remaining postoperative liver function by MRI was able to predict the occurrence of postoperative liver dysfunction with a sensitivity of 0.86 and a specificity of 0.74 (PPV: 0.77; NPV: 0.84; AUC: 0.80).

#### **CONCLUSION**

In conclusion, virtual surgical planning using MRI, in addition to revealing the spatial relationships of tumors and vessels, has the potential to reduce the occurrence of small for size syndrome by calculating the postoperative liver function.

#### **CLINICAL RELEVANCE/APPLICATION**

Liver insufficiency after liver resection is often the result of an insufficient remaining functional organ ("small for size syndrome"). Currently, liver function is assessed using preoperative liver volumetry and is based on clinical and biochemical parameters. However, these conventional liver function tests are not sufficient to confidently predict postoperative liver failure. Here, modern techniques can help in surgical planning and positively impact patient care.

Printed on: 02/07/23

## Abstract Archives of the RSNA, 2022

M5B-SPGI-4

### Quantitative parameters on contrast-enhanced CT for non-invasive assessment of clinically significant portal hypertension

Monday, Nov. 28 12:45PM - 1:15PM Room: Learning Center - GI DPS

#### Participants

Jinkui Li, MD, (Presenter) Nothing to Disclose

#### PURPOSE

Hepatic venous pressure gradient (HVPG) is critical for diagnose portal hypertension. However, HVPG measurement is invasive. Non-invasive and accurate assessment of portal hypertension is unmet need in clinics. This study aimed to determine whether the extracellular volume fraction (ECV) of liver and spleen, and the iodine washout rate (IWR) of liver, could provide an estimate of clinically significant portal hypertension (CSPH, HVPG  $\geq$ 10 mmHg) in patients with cirrhosis.

#### METHODS AND MATERIALS

101 participants (51 patients with cirrhosis who underwent HVPG measurement and 50 healthy controls who were defined to have normal portal pressure without HVPG measurement) underwent contrast-enhanced CT between January 2018 and December 2020 were retrospectively included. Absolute contrast enhancement of the liver/spleen and the abdominal aorta (subtracting unenhanced from contrast-enhanced attenuation during portal-venous phase [PVP] or delay phase [DP], ?HU) were measured. ECVliver and ECVspleen were calculated using the following equation:  $ECV_{liver/spleen} = \frac{HU_{liver/spleen} - DP}{HU_{aorta} - DP} \times (100 - \text{Hematocrit} [\%])$ . IWR of liver was calculated using the following equation:  $IWR = (1 - \frac{HU_{liver} - DP}{HU_{liver} - PVP}) \times 100$ . The correlation of non-invasive parameters with HVPG was evaluated. ROC analysis was performed and the areas under the curves (AUCs) were calculated for diagnostic performance.

#### RESULTS

The mean of HVPG was  $16.55 \pm 0.67$  mmHg. There were significant differences in CT parameters between cirrhotic patients and healthy controls: ECVliver ( $P < 0.001$ ), ECVspleen ( $P < 0.001$ ), and IWR ( $P < 0.001$ ). Both ECVliver and ECVspleen correlated with HVPG ( $P = 0.007$  and  $0.001$ , respectively). ECVspleen and IWR were identified to be independently correlated with HVPG ( $P = 0.001$  and  $0.022$ , respectively). ECVspleen and IWR revealed perfect diagnostic performance for the identification of CSPH with AUCs of 0.984 and 0.956, respectively, and outperformed ECVliver (AUC, 0.718) ( $P < 0.001$ ). The best cut-off value, ECVliver, ECVspleen, and IWR for identifying CSPH, were  $= 24.6\%$ ,  $= 38.29\%$ , and  $= 40.06\%$ , respectively.

#### CONCLUSION

s ECVspleen and IWR were valuable non-invasive parameters for the assessment of CSPH in cirrhotic patients and outperformed ECVliver. It should be explored further across a broader range of pressure values.

#### CLINICAL RELEVANCE/APPLICATION

Such valuable non-invasive parameters including ECV and IWR to assess portal pressure is clinically meaningful for cirrhotic patients. ECV and IWR are easy to obtain and can be retrospectively derived from CT, since CT is routinely used to evaluate the complications of cirrhosis. Such a dual-screening strategy would further improve the cost-effectiveness of CT.

Printed on: 02/07/23

## Abstract Archives of the RSNA, 2022

M5B-SPGI-5

### Can CT Spectral Imaging Based on Multi-material Decomposition Algorithm Have Better Ability to Diagnose Chemotherapy Related Fatty Liver Disease than Liver-to-fat ratio?

Monday, Nov. 28 12:45PM - 1:15PM Room: Learning Center - GI DPS

#### Participants

Xi Huaze, (*Presenter*) Nothing to Disclose

#### PURPOSE

To determine whether CT multi-material decomposition (MMD) spectral examination may improve clinical diagnosis efficiency of chemotherapy related fatty liver disease (CRFLD).

#### METHODS AND MATERIALS

Eighty-one patients undergoing CT exams of abdomen (traditional unenhanced imaging enhanced spectral imaging) after chemotherapeutic treatment were retrospectively recruited. All these patients have no history of fatty liver, liver disease, liver tumors and large alcohol intake before chemotherapy. According to the results of ultrasonic or magnetic resonance examination after chemotherapy, patients were divided into clinical CRFLD group and non-CRFLD groups. On liver fat images in venous phase generated by MMD algorithm, three physicians measured liver fat fractions (LFFs) of the whole liver, left lobe and right lobe. When the average values calculated from these three doctors' measurement of the whole liver LFF or either lobe LFF exceeded 5%, the patients were considered as spectrum-CRFLD. On unenhanced CT images, the same three doctors measured CT values of spleen and liver, and calculated average values to acquire the Liver-to-spleen ratio (LSR,  $LSR = \text{CT value}_{\text{liver}} / \text{CT value}_{\text{spleen}}$ ). When it was less than 1, the patients would be regarded as CT-CRFLD. Diagnostic efficiency of spectrum-CRFLD and CT-CRFLD was compared by using McNemar's test.

#### RESULTS

Thirty-four of 81 patients (mean age, 57.8 years  $\pm$  11.5; 23 women) were diagnosed as clinical CRFLD. The whole liver LFF showed significantly highest sensitivity, specificity, positive predictive value, negative predictive value, accuracy of diagnosing clinical CRFLD (82.4%, 95.7%, 93.3%, 88.2% and 90.1%, respectively). The diagnostic accuracy of whole liver LFF was significantly higher than both either liver lobe LFF and LSR (both  $p < 0.001$ ).

#### CONCLUSION

The whole liver LFF obtained by CT MMD spectral imaging is a reliable indicator to diagnose CRFLD with more accuracy and sensitivity, compared with the traditional CT liver-to-fat ratio.

#### CLINICAL RELEVANCE/APPLICATION

Quantitative measurement of fat fraction in the whole liver through CT spectral imaging can help detect fatty liver caused by chemotherapeutics.

Printed on: 02/07/23

## Abstract Archives of the RSNA, 2022

M5B-SPGI-6

### The value of hepatic extracellular volume fraction obtained from iodine map in evaluating liver function of patients with liver cirrhosis

Monday, Nov. 28 12:45PM - 1:15PM Room: Learning Center - GI DPS

#### Participants

Yao Wang, (*Presenter*) Nothing to Disclose

#### PURPOSE

To explore the correlation between hepatic extracellular volume fraction (fECV) based on iodine density and liver function in cirrhosis patients, and further investigate the diagnostic value of fECV in liver cirrhosis.

#### METHODS AND MATERIALS

The patients undergoing enhanced abdominal CT scan with spectral mode were categorized as group F (patients with liver cirrhosis), group F0 (patients without liver cirrhosis). According to the child-Pugh classification, group F was further divided into three subgroups: group FA (child A), group FB (child B) and group FC (child C). The latter two groups represented decompensated cirrhosis. The iodine density of liver and abdominal aorta were measured in iodine map of equilibrium phase to calculate the fECV. The formula for fecv is the iodine density of the liver multiplied by 100 minus Hct and then divided by the iodine density of the abdominal aorta. The fECV values among groups were compared by One-Way ANOVA, LSD method was used for further comparison. Pearson correlation analysis was performed to analyze the correlation between fECV and child-Pugh classification. The diagnostic performance of fECV for the differentiation of liver cirrhosis was assessed using receiver operation characteristic (ROC) curve analysis.

#### RESULTS

A total of 157 patients (51 in group F0, 46 in group FA, 38 in group FB, 22 in group FC) were included. The fECV fractions in from F0 to FC showed an upward trend ( $31.62 \pm 2.00, 37.08 \pm 3.64, 43.39 \pm 6.00$ ). There was significant difference in fECV among groups and between any two groups (all  $P < 0.001$ ). Strong positive correlation of fECV with child-Pugh classification was found ( $r = 0.841$ ). For differentiating liver cirrhosis, the sensitivity and specificity of fECV were 88.68% and 86.27%, respectively, with area under the curve (AUC) of 0.922, when the cut-off value was set at 30.26%. For differentiating decompensated cirrhosis by fECV, a cut-off value of 33.96% resulted in an AUC of 0.938, sensitivity of 90.00% and specificity of 89.13%.

#### CONCLUSION

s fECV from iodine map is strongly positively correlated with the Child-Pugh liver function classification, and has a high potential value in the differentiation of liver cirrhosis with different liver function grades.

#### CLINICAL RELEVANCE/APPLICATION

ECV measured using Hounsfield units needs precontrast phase, which has the problem of registration and increases the radiation dose. fECV obtained by dual energy spectral examination is a simple and convenient biomarker to identify different degrees of liver cirrhosis without dose compromise, which is suitable for follow-up.

Printed on: 02/07/23

## Abstract Archives of the RSNA, 2022

M5B-SPGI-7

### To Characterize Liver Fibrosis using a Four-Compartments Restriction Spectrum Imaging Model

Monday, Nov. 28 12:45PM - 1:15PM Room: Learning Center - GI DPS

#### Participants

Cai Yeyu, MD, Changsha, China (*Presenter*) Nothing to Disclose

#### PURPOSE

Previous studies have shown that liver fibrosis, caused by chronic liver disease, is closely associated with the progression of various types of liver disease and is a key risk factor for cirrhosis and hepatocellular carcinoma. In this study, we evaluated the feasibility of the 4-compartment RSI model to identify carbon tetrachloride (CCl<sub>4</sub>)-induced liver fibrosis in mouse model.

#### METHODS AND MATERIALS

A total of 38 mice in the experiment were divided into CCL<sub>4</sub>-induced liver fibrosis (LF) and control groups, respectively. MRI examinations were performed on a 3T scanner (uMR790, United Imaging Healthcare, Shanghai, China), based on the echo planar imaging sequence (EPI) with a total of 11 b-values ranging from 0-2000 s/mm<sup>2</sup>. Conventional ADC and D values for each compartment in multicompartamental RSI models were calculated on voxel wise basis. The performance of different RSI models was evaluated using the Bayesian Information Criterion. Traditional ADC values and D<sub>i</sub> values of different compartments were further compared between the LF and control groups using Mann-Whitney test, and finally, the receiver operating characteristic (ROC) curve for different parameters were performed.

#### RESULTS

All mice in LF group were histologically diagnosed as liver fibrosis (100%). The results showed that the best model to describe the data was the 4-compartment RSI model with the lowest  $\Delta$ BIC value among all RSI models. Significant differences of ADC value and D values of the different compartments in the 4-compartment RSI model were found between LF group and control group. RSI4-C3 was the best single diffusion parameter for the discrimination of liver fibrosis, with the largest AUC value. Furthermore, the AUC value was further increased when ADC and C3 were combined.

#### CONCLUSION

The 4-compartment RSI model can further distinguish the alterations in the LF group from the control group during different diffusion processes. Compared with the conventional ADC values, RSI4-C3 has a better ability to discriminate liver fibrosis. The combined parameter of ADC value and RSI4-C3 can further improve the discrimination performance of liver fibrosis.

#### CLINICAL RELEVANCE/APPLICATION

This study demonstrates that the four-compartment RSI model can provide a better identification of liver fibrosis than conventional ADC.

Printed on: 02/07/23

## Abstract Archives of the RSNA, 2022

M5B-SPGI-8

### Non-invasive prediction of NASH by PDFF in Patients with Obesity without known Liver Disease

Monday, Nov. 28 12:45PM - 1:15PM Room: Learning Center - GI DPS

#### Participants

Nikolaos Panagiotopoulos, MD, Madison, WI (*Presenter*) Institutional Research Grant, Pfizer Inc

#### PURPOSE

To assess the value of PDFF, R2\*, T2\*, and T1 for the detection of NASH in a cohort of subject with obesity without previously known liver disease.

#### METHODS AND MATERIALS

This analysis is part of an ongoing study of patients with obesity undergoing weight loss surgery (WLS). Study participants underwent imaging within 1 week prior to WLS and intraoperative wedge biopsy of the liver. Imaging at 3.0T included IDEAL IQ (GE, USA) to quantify PDFF and R2\* and LiverMultiscan (LMS, Perspectum, UK) for PDFF, T2\*, and T1. Images were analyzed by placing ROIs in all liver segments. LMS data were analyzed by Perspectum. Liver biopsy samples were classified as normal, non-alcoholic fatty liver (NAFL, ie: steatosis only), or non-alcoholic steatohepatitis (NASH, based on a NASH activity score >5). Receiver operator characteristic (ROC) curve analysis was performed to assess the diagnostic accuracy of PDFF, R2\*, T2\* and T1 to differentiate NASH from non-NASH (normal or NAFL).

#### RESULTS

50 patients (44 female, 45±11 years, BMI: 44±6) were examined and analyzed. 24 subjects had no liver disease, 17 had NAFL and 9 had NASH. IDEAL IQ PDFF achieved separation between NASH and no NASH with an area under the curve of 0.91 (95%CI: 0.79-1). LMS PDFF achieved similarly separation between the groups with AUC=0.98 (95%CI: 0.94-1). At the same PDFF threshold of 11% for IDEAL IQ and LMS, sensitivity was 75% (95%CI: 35-97) and 83% (95%CI: 36-100), respectively, and specificity 98% (95%CI: 87-100) and 100% (95%CI: 89-100). LMS T1 achieved separation between the groups with an area under the curve of 0.83 (95%CI: 0.68-0.97). For the T1 threshold of 870ms, sensitivity was 83% (95%CI: 36-100) and specificity was 73% (95%CI: 55-87). Neither R2\* nor T2\* could distinguish between NASH and non-NASH.

#### CONCLUSION

s We observed promising performance of PDFF for the detection of NASH in a cohort of patients with obesity without previously known liver disease, in stark contrast to current knowledge. The results support our hypothesis that PDFF can differentiate NASH from NAFL in a cohort of patients with early-stage NASH where the severity of liver fat deposition is still present and relevant. A major limitation of this work is the limited number of patients with NASH to date.

#### CLINICAL RELEVANCE/APPLICATION

If confirmed, these results would constitute a paradigm change in the early detection of NASH.

Printed on: 02/07/23

## Abstract Archives of the RSNA, 2022

M5B-SPGI-9

### **a fully automated hybrid approach to assessing liver fibrosis and necroinflammation on conventional MRI: a multi-center study**

Monday, Nov. 28 12:45PM - 1:15PM Room: Learning Center - GI DPS

#### **Participants**

Junhao Zha, MD, (*Presenter*) Nothing to Disclose

#### **PURPOSE**

To develop and validate a combined radiomics-clinic model by a fully automated hybrid approach to diagnosing clinically significant liver fibrosis (=F2) and necroinflammatory activity (=G2), respectively

#### **METHODS AND MATERIALS**

In this retrospective multi-center study, a total of 537 patients were included. From May 2015 to December 2018, 394 patients were randomly distributed in a training (n=276) or internal test (n=118) set at a ratio of 7:3 at center 1. From January 2019 to August 2020, 96 patients considered eligible at center 1 were placed in a temporal test set. An independent external test set from center 2 was used to validate the proposed models. All patients underwent abdominal MRI with pathologically proven liver fibrosis and necroinflammation. An interactive deep learning approach was developed to achieve better automated whole liver segmentation performance of ResUnet. 2880 radiomics features extracted from VOIT2FS, VOIT1delay were analyzed separately to form the radiomics scores (R-scores). The optimal R-scores and clinical biomarkers were integrated into the combined radiomics-clinic model (CRC model) for assessing =F2 or =G2, respectively. The performance of the models was assessed and compared with FIB-4 and APRI

#### **RESULTS**

For staging =F2, AUCs of CRC model are 0.83, 0.79, 0.82, 0.83 in the training, internal test, temporal test, and external test set respectively. CRC model (AUC 0.79) significantly outperformed radiomics model (AUC 0.75;  $P < .05$ ) in the internal test set, and significantly outperformed FIB-4 (AUC 0.69, 0.67, 0.63;  $P < .05$ ), and APRI (AUC 0.69, 0.68, 0.62;  $P < .05$ ) in the internal test, temporal test, and external test set. By using the cutoffs, the CRC model had sensitivities and specificities as follows: 72.4% / 82.1%, 73.1% / 62.5%, 82.4% / 71.1%, 91.4% / 75.0% in the training, internal test, temporal test, and external test set for diagnosing =F2. For classifying =G2, the training, internal test, temporal test, and external test set results of the CRC model were AUC 0.88, 0.86, 0.79, and 0.89, sensitivity 74.6%, 71.4%, 61.5%, and 80.0%, and specificity 85.6%, 90.3%, 82.5%, and 87.1%, respectively. CRC model (AUC 0.86, 0.79, 0.89) significantly outperformed radiomics model (AUC 0.67, 0.69, 0.67;  $P < .05$ ), FIB-4 (AUC 0.67, 0.69, 0.73;  $P < .05$ ), and APRI (AUC 0.74, 0.70, 0.63;  $P < .05$ ) in the internal test, temporal test, and external test set for staging =G2

#### **CONCLUSION**

s The CRC models provide a promising approach for diagnosing liver fibrosis (=F2) and necroinflammatory activity (=G2)

#### **CLINICAL RELEVANCE/APPLICATION**

Traditional MR tissue texture, and routine clinical biomarkers, should be taken into consideration to develop the CRC model, and this mimics the diagnosis in real clinical scenarios.

Printed on: 02/07/23

## Abstract Archives of the RSNA, 2022

M5B-SPGU

### Genitourinary Monday Poster Discussions - B

Monday, Nov. 28 12:45PM - 1:15PM Room: Learning Center - GU DPS

#### Sub-Events

#### **M5B-SPGU-2 Diffusion Weighted Imaging as a Dominant Sequence for Evaluating Transitional Zone Prostate Cancer: Comparison with Current Prostate Imaging-Reporting Data System (PI-RADS) version 2.1.**

##### Participants

Myoung Seok Lee, MD, Seoul, Korea, Republic Of (*Presenter*) Nothing to Disclose

##### PURPOSE

To explore the performance of Diffusion-weighted imaging (DWI) as a dominant sequence for detecting Transitional-zone Prostate Cancer (TZPCa) compared to current PI-RADS, which designate T2-weighted imaging (T2WI) as a dominant sequence for TZPCa.

##### METHODS AND MATERIALS

Forty patients confirmed as TZPCa and forty age-matched patients confirmed as BPH without TZPCa by radical prostatectomy. Two radiologists recorded every significant prostate cancer (Gleason score(GS)=6, maximal diameter=1cm) on pathologic mapping sheet, and per lesion-base, one-to-one correlation between mapping sheet and corresponding MRI was conducted by consensus of a pathologist and aforementioned radiologist. Another three radiologists independently reviewed MRIs of the patients, and recorded the PI-RADS scores for the case where the DWI was the dominant sequence and the case where the T2WI was the dominant score, with 4 weeks of time interval. The sensitivity, specificity, PPV, NPV and interobserver agreement for the two cases were statistically compared.

##### RESULTS

When the PI-RADS score of 3 or higher is considered to be lesion-positive, the overall specificity, PPV and NPV were significantly higher when DWI was a dominant sequence than when T2WI was a dominant sequence (0.896 vs 0.542, 0.764 vs 0.439, 0.853 vs 0.759, respectively). The sensitivity was similar in the two cases (0.687 vs 0.676). When the PI-RADS score of 4 and 5 were considered as cancer-positive, the specificity and PPV were also higher when regarding DWI as a dominant score (0.986 vs 0.944, 0.943 and 0.810, respectively), however the sensitivity and NPV showed no statistical difference (0.468 vs 0.468, 0.785 vs 0.776, respectively). The interobserver agreement was significantly higher when DWI was a dominant sequence, regardless of the cutoff value of PI-RADS score.

##### CONCLUSION

Regarding DWI as a dominant score for TZPCa improves specificity, PPV and importantly, interobserver agreement without impairment of test sensitivity, compared to current PI-RADS which is using T2WI as a dominant score for TZPCa.

##### CLINICAL RELEVANCE/APPLICATION

Using DWI as a dominant sequence for evaluating transitional zone is supposed to improve specificity and PPV of current PI-RADS. Importantly, the interobserver agreement, one of the problems of PI-RADS, may be improved when using DWI as a dominant sequence. It is thought to be a consideration when revising PI-RADS.

#### **M5B-SPGU-4 Automated Kidney Segmentation in contrast-enhanced Computed Tomography with patch-based 3D UNets on different anatomical planes**

##### Participants

Konstantinos Koukoutegos, (*Presenter*) Nothing to Disclose

##### PURPOSE

Renal volumetric measurements are a critical radiological task, as Total Kidney Volume is a biomarker for assessing the risk of renal insufficiency. This study attempts to develop and validate a CNN-based method for measuring the volume of kidney parenchyma, excluding the collecting system, in contrast-enhanced CT.

##### METHODS AND MATERIALS

A cohort of 89 pre-transplant abdomen CT sequences and their corresponding segmentation masks were used in this retrospective study and split in 62, 14 and 13 for training, validation and testing respectively. A 3D residual UNet variant was used to train 3 separate patch-based models in the coronal, axial and sagittal anatomical views and their results were mutually compared and then combined. Extensive data augmentation techniques (such as intensity shift, Gaussian noise, image dropout) were implemented to increase the training population and offer additional regularization to the neural networks. The network training was performed using PyTorch 1.10 and MONAI 0.80.

##### RESULTS

Each model was trained for 400 epochs in 2 NVIDIA GeForce 1080Ti GPUs for 6 hours. The best-performing coronal, axial and

Each model was trained for 400 epochs in 2 NVIDIA GeForce 1080Ti GPUs for 6 hours. The best-performing coronal, axial and sagittal models achieved an average Dice coefficient of 0.929, 0.926 and 0.925 for the left kidney and 0.924, 0.925 and 0.921 for the right kidney respectively. Their ensemble prediction achieved a Dice of 0.934 for left and 0.936 for right kidney, making the latter the most robust amongst all methods, with paired t-test p values of 0.001, 0.0007 and 0.02 for the coronal, axial and sagittal models versus the combined method. A Volumetric Similarity of  $0.981 \pm 0.014$  and  $0.985 \pm 0.013$  (left and right) as compared with the ground truth data was achieved. The difference in volumetric agreement between manual delineation and predicted volumes is within the 95% confidence intervals for the whole test set with a mean of  $4.53\text{cm}^3$ . The average prediction time measured for a whole abdomen CT is  $19.91 \pm 2.77$  secs.

## **CONCLUSION**

s Combination of models trained in different anatomical planes can better capture the information of the 3D contrast-enhanced CT sequences and was shown to provide accurate measurements of kidney parenchyma.

## **CLINICAL RELEVANCE/APPLICATION**

Robust AI models that perform with near-human accuracy can help as decision support system to achieve faster and more accurate disease diagnosis and treatment planning. We obtained promising results to facilitate the quantification of changes in kidney volume during a specified timeline, upon transplantation or at partial nephrectomy.

Printed on: 02/07/23

## Abstract Archives of the RSNA, 2022

M5B-SPGU-2

### **Diffusion Weighted Imaging as a Dominant Sequence for Evaluating Transitional Zone Prostate Cancer: Comparison with Current Prostate Imaging-Reporting Data System (PI-RADS) version 2.1.**

Monday, Nov. 28 12:45PM - 1:15PM Room: Learning Center - GU DPS

#### **Participants**

Myoung Seok Lee, MD, Seoul, Korea, Republic Of (*Presenter*) Nothing to Disclose

#### **PURPOSE**

To explore the performance of Diffusion-weighted imaging (DWI) as a dominant sequence for detecting Transitional-zone Prostate Cancer (TZPCa) compared to current PI-RADS, which designate T2-weighted imaging (T2WI) as a dominant sequence for TZPCa.

#### **METHODS AND MATERIALS**

Forty patients confirmed as TZPCa and forty age-matched patients confirmed as BPH without TZPCa by radical prostatectomy. Two radiologists recorded every significant prostate cancer (Gleason score(GS)=6, maximal diameter=1cm) on pathologic mapping sheet, and per lesion-base, one-to-one correlation between mapping sheet and corresponding MRI was conducted by consensus of a pathologist and aforementioned radiologist. Another three radiologists independently reviewed MRIs of the patients, and recorded the PI-RADS scores for the case where the DWI was the dominant sequence and the case where the T2WI was the dominant score, with 4 weeks of time interval. The sensitivity, specificity, PPV, NPV and interobserver agreement for the two cases were statistically compared.

#### **RESULTS**

When the PI-RADS score of 3 or higher is considered to be lesion-positive, the overall specificity, PPV and NPV were significantly higher when DWI was a dominant sequence than when T2WI was a dominant sequence (0.896 vs 0.542, 0.764 vs 0.439, 0.853 vs 0.759, respectively). The sensitivity was similar in the two cases (0.687 vs 0.676). When the PI-RADS score of 4 and 5 were considered as cancer-positive, the specificity and PPV were also higher when regarding DWI as a dominant score (0.986 vs 0.944, 0.943 and 0.810, respectively), however the sensitivity and NPV showed no statistical difference (0.468 vs 0.468, 0.785 vs 0.776, respectively). The interobserver agreement was significantly higher when DWI was a dominant sequence, regardless of the cutoff value of PI-RADS score.

#### **CONCLUSION**

s Regarding DWI as a dominant score for TZPCa improves specificity, PPV and importantly, interobserver agreement without impairment of test sensitivity, compared to current PI-RADS which is using T2WI as a dominant score for TZPCa.

#### **CLINICAL RELEVANCE/APPLICATION**

Using DWI as a dominant sequence for evaluating transitional zone is supposed to improve specificity and PPV of current PI-RADS. Importantly, the interobserver agreement, one of the problems of PI-RADS, may be improved when using DWI as a dominant sequence. It is thought to be a consideration when revising PI-RADS.

Printed on: 02/07/23

## Abstract Archives of the RSNA, 2022

M5B-SPGU-4

### Automated Kidney Segmentation in contrast-enhanced Computed Tomography with patch-based 3D UNets on different anatomical planes

Monday, Nov. 28 12:45PM - 1:15PM Room: Learning Center - GU DPS

#### Participants

Konstantinos Koukoutegos, (*Presenter*) Nothing to Disclose

#### PURPOSE

Renal volumetric measurements are a critical radiological task, as Total Kidney Volume is a biomarker for assessing the risk of renal insufficiency. This study attempts to develop and validate a CNN-based method for measuring the volume of kidney parenchyma, excluding the collecting system, in contrast-enhanced CT.

#### METHODS AND MATERIALS

A cohort of 89 pre-transplant abdomen CT sequences and their corresponding segmentation masks were used in this retrospective study and split in 62, 14 and 13 for training, validation and testing respectively. A 3D residual UNet variant was used to train 3 separate patch-based models in the coronal, axial and sagittal anatomical views and their results were mutually compared and then combined. Extensive data augmentation techniques (such as intensity shift, Gaussian noise, image dropout) were implemented to increase the training population and offer additional regularization to the neural networks. The network training was performed using PyTorch 1.10 and MONAI 0.80.

#### RESULTS

Each model was trained for 400 epochs in 2 NVIDIA GeForce 1080Ti GPUs for 6 hours. The best-performing coronal, axial and sagittal models achieved an average Dice coefficient of 0.929, 0.926 and 0.925 for the left kidney and 0.924, 0.925 and 0.921 for the right kidney respectively. Their ensemble prediction achieved a Dice of 0.934 for left and 0.936 for right kidney, making the latter the most robust amongst all methods, with paired t-test p values of 0.001, 0.0007 and 0.02 for the coronal, axial and sagittal models versus the combined method. A Volumetric Similarity of  $0.981 \pm 0.014$  and  $0.985 \pm 0.013$  (left and right) as compared with the ground truth data was achieved. The difference in volumetric agreement between manual delineation and predicted volumes is within the 95% confidence intervals for the whole test set with a mean of 4.53cm<sup>3</sup>. The average prediction time measured for a whole abdomen CT is  $19.91 \pm 2.77$  secs.

#### CONCLUSION

s Combination of models trained in different anatomical planes can better capture the information of the 3D contrast-enhanced CT sequences and was shown to provide accurate measurements of kidney parenchyma.

#### CLINICAL RELEVANCE/APPLICATION

Robust AI models that perform with near-human accuracy can help as decision support system to achieve faster and more accurate disease diagnosis and treatment planning. We obtained promising results to facilitate the quantification of changes in kidney volume during a specified timeline, upon transplantation or at partial nephrectomy.

Printed on: 02/07/23

## Abstract Archives of the RSNA, 2022

M5B-SPHN

### Head and Neck Monday Poster Discussions - B

Monday, Nov. 28 12:45PM - 1:15PM Room: Learning Center - HN DPS

#### Sub-Events

#### M5B-SPHN-1 Lateral Rectus Muscle Displacement in Sagging Eye Syndrome

##### Participants

Rouzbeh Mashayekhi, MD, (*Presenter*) Nothing to Disclose

##### PURPOSE

Sagging Eye Syndrome (SES) is strabismus caused by degeneration of orbital connective tissue predominantly among the elderly. There has been ongoing research to find objective measurements to evaluate SES on Magnetic Resonance Imaging (MRI). Our study examines the vertical displacement angle between the midpoint of the lateral and medial rectus muscles to find an objective tool for SES evaluation.

##### METHODS AND MATERIALS

This is a retrospective study of 11 subjects who had radiologic and clinical confirmation of SES. 11 subjects who had undergone MRI orbital study for multiple sclerosis (MS) were selected as control subjects. Coronal oblique reconstructions were done of the axial 3D gradient echo sequence with the plane parallel to the insertion of the optic nerve and crossing the lacrimal crest to zygomatic arch. The vertical angle difference between the midpoint of the lateral and medial rectus muscles was measured. The Mann Whitney U test was performed to compare the angle measurements between the subjects with SES and the subjects with MS.

##### RESULTS

The 11 subjects with SES had an average age of 69 and 73% were female. The 11 MS subjects had an average age of 60 and 64% were female. The lateral rectus muscle midpoint was on average 3.4 degrees vertically lower relative to the medial rectus muscle midpoint among the SES subjects and 0.3 degrees among the MS subjects. The results showed statistically significant vertical inferior displacement of the lateral rectus muscle relative to the medial rectus muscle ( $P < 0.01$ ).

##### CONCLUSION

This study demonstrates that vertical displacement angle between the midpoint of the lateral and medial rectus muscles may be a useful tool for objectively evaluating for SES on MRI.

##### CLINICAL RELEVANCE/APPLICATION

Strabismus occurs from a variety of conditions including Sagging Eye Syndrome. We examined an ocular muscle angle measurement to provide radiologists with a tool to better evaluate for SES on MRI.

#### M5B-SPHN-2 Multi-Parametric Diffusion Tensor Imaging of The Optic Nerve for Detection of Dysthyroid Optic Neuropathy in Patients with Thyroid-Associated Ophthalmopathy

##### Awards

##### Trainee Research Prize - Medical Student

##### Participants

Ping Liu, MS, (*Presenter*) Nothing to Disclose

##### PURPOSE

To evaluate the microstructural changes of the orbital optic nerve in thyroid-associated ophthalmopathy (TAO) patients with or without dysthyroid optic neuropathy (DON) using diffusion tensor imaging (DTI) and investigate whether DTI can be used to detect DON.

##### METHODS AND MATERIALS

59 bilateral TAO patients with ( $n=23$ ) and without DON (non-DON,  $n=36$ ) who underwent pretreatment DTI were included and 118 orbits were analyzed. The clinical features of all patients were collected. DTI parameters, including mean, axial, and radial diffusivity (MD, AD, and RD, respectively) and fractional anisotropy (FA) of the intra-orbital optic nerve for each orbit were calculated and compared between the DON and non-DON groups. ROC curves were generated to evaluate the diagnostic performance of single or combined DTI parameters. Correlations between DTI parameters and ophthalmological characteristics were analyzed using correlation analysis.

##### RESULTS

Compared with non-DON, the DON group showed decreased FA and increased MD, RD, and AD ( $P < 0.01$ ). In the differentiation of

DON from non-DON, the MD was optimal individually, and the combination of the four parameters had the best diagnostic performance. There were significant correlations between the optic nerve's four DTI metrics and the visual acuity and clinical active score ( $P < 0.05$ ). In addition, optic nerve FA was significantly associated with the amplitude of visual evoked potentials ( $P = 0.022$ ).

## CONCLUSION

s DTI is a promising technique in assessing microstructural changes of optic nerve in patients with DON, and it facilitates differentiation of DON from non-DON eyes in patients with TAO.

## CLINICAL RELEVANCE/APPLICATION

We recommend DTI as a convenient and noninvasive tool for early detection of DON, and as a conventional examination in the clinical pipeline of TAO. Thus, facilitating timely diagnosis and initiation of medical treatment and enabling a better management of DON.

## M5B-SPHN-3 Evaluation of The Efficacy of Postoperative Treatment in Obstructive Sleep Apnea Hypoventilation Syndrome

### Participants

Wenwen Wang, Xian, China (*Presenter*) Nothing to Disclose

### PURPOSE

This study aims to compare the role of CT and MR in assessing the stability of the upper respiratory tract in patients with obstructive sleep apnea syndrome (OSAHS), and to provide evidence for the evaluation of the postoperative treatment effect.

### METHODS AND MATERIALS

A total of 61 patients (mean age:  $36.62 \pm 7.99$  years, range 22-51 years) were diagnosed as OSAHS through the Polysomnography (PSG). All the patients were treated with modified uvulopalatopharyngoplasty. The upper airway anatomy in all patients was evaluated by CT and MRI pre-operation, and 33 patients were followed-up post-operation. The upper airway parameters such as the thickness of lateral pharyngeal wall, the length of the tongue, the length and thickness of the soft palate and the cross-sectional areas of the soft palate on midsagittal planes were measured and compared, and a two-tailed p-value of less than 0.05 was considered statistically significant.

### RESULTS

The minimum area of cross section of the upper airway ( $77.50 \pm 41.92 \text{mm}^2$ ) on CT was significantly higher than the MR image ( $34.64 \pm 19.93 \text{mm}^2$ ) ( $p < 0.05$ ). In 31 patients with self-control, the soft palate thickness measured on nuclear magnetic images before and after surgery were ( $9.67 \pm 2.34$  vs  $11.24 \pm 2.41$ ,  $P < 0.05$ ). The soft palate length, soft palate thickness, and minimum area of upper airway cross section measured on CT images were ( $37.38 \pm 7.86$  vs  $33.62 \pm 5.92$ ,  $10.01 \pm 2.11$  vs  $11.34 \pm 2.43$ ,  $78.40 \pm 40.93$  vs  $145.55 \pm 78.49$ ) (all  $P$  value  $< 0.05$ ).

### CONCLUSION

s Imageological examination may objectively evaluate the improvement of postoperative airway stenosis. In the evaluation of upper respiratory tract stenosis in OSAHS patients, MR and CT imaging findings were differently significant. Compared with preoperative, MR and CT showed increased thickness of the soft palate and decreased soft palate thickness on post-operative; the cross-sectional areas of the soft palate was not changed. with.

### CLINICAL RELEVANCE/APPLICATION

CT and MR examination can effectively evaluate the upper airway status of patients, providing more basis for the diagnosis of OSAHS, the severity of the disease and the treatment effect evaluation.

Printed on: 02/07/23

## Abstract Archives of the RSNA, 2022

M5B-SPHN-1

### Lateral Rectus Muscle Displacement in Sagging Eye Syndrome

Monday, Nov. 28 12:45PM - 1:15PM Room: Learning Center - HN DPS

#### Participants

Rouzbeh Mashayekhi, MD, (*Presenter*) Nothing to Disclose

#### PURPOSE

Sagging Eye Syndrome (SES) is strabismus caused by degeneration of orbital connective tissue predominantly among the elderly. There has been ongoing research to find objective measurements to evaluate SES on Magnetic Resonance Imaging (MRI). Our study examines the vertical displacement angle between the midpoint of the lateral and medial rectus muscles to find an objective tool for SES evaluation.

#### METHODS AND MATERIALS

This is a retrospective study of 11 subjects who had radiologic and clinical confirmation of SES. 11 subjects who had undergone MRI orbital study for multiple sclerosis (MS) were selected as control subjects. Coronal oblique reconstructions were done of the axial 3D gradient echo sequence with the plane parallel to the insertion of the optic nerve and crossing the lacrimal crest to zygomatic arch. The vertical angle difference between the midpoint of the lateral and medial rectus muscles was measured. The Mann Whitney U test was performed to compare the angle measurements between the subjects with SES and the subjects with MS.

#### RESULTS

The 11 subjects with SES had an average age of 69 and 73% were female. The 11 MS subjects had an average age of 60 and 64% were female. The lateral rectus muscle midpoint was on average 3.4 degrees vertically lower relative to the medial rectus muscle midpoint among the SES subjects and 0.3 degrees among the MS subjects. The results showed statistically significant vertical inferior displacement of the lateral rectus muscle relative to the medial rectus muscle ( $P < 0.01$ ).

#### CONCLUSION

s This study demonstrates that vertical displacement angle between the midpoint of the lateral and medial rectus muscles may be a useful tool for objectively evaluating for SES on MRI.

#### CLINICAL RELEVANCE/APPLICATION

Strabismus occurs from a variety of conditions including Sagging Eye Syndrome. We examined an ocular muscle angle measurement to provide radiologists with a tool to better evaluate for SES on MRI.

Printed on: 02/07/23

## Abstract Archives of the RSNA, 2022

M5B-SPHN-2

### Multi-Parametric Diffusion Tensor Imaging of The Optic Nerve for Detection of Dysthyroid Optic Neuropathy in Patients with Thyroid-Associated Ophthalmopathy

Monday, Nov. 28 12:45PM - 1:15PM Room: Learning Center - HN DPS

#### Awards

**Trainee Research Prize - Medical Student**

#### Participants

Ping Liu, MS, (*Presenter*) Nothing to Disclose

#### PURPOSE

To evaluate the microstructural changes of the orbital optic nerve in thyroid-associated ophthalmopathy (TAO) patients with or without dysthyroid optic neuropathy (DON) using diffusion tensor imaging (DTI) and investigate whether DTI can be used to detect DON.

#### METHODS AND MATERIALS

59 bilateral TAO patients with (n= 23) and without DON (non-DON, n= 36) who underwent pretreatment DTI were included and 118 orbits were analyzed. The clinical features of all patients were collected. DTI parameters, including mean, axial, and radial diffusivity (MD, AD, and RD, respectively) and fractional anisotropy (FA) of the intra-orbital optic nerve for each orbit were calculated and compared between the DON and non-DON groups. ROC curves were generated to evaluate the diagnostic performance of single or combined DTI parameters. Correlations between DTI parameters and ophthalmological characteristics were analyzed using correlation analysis.

#### RESULTS

Compared with non-DON, the DON group showed decreased FA and increased MD, RD, and AD ( $P < 0.01$ ). In the differentiation of DON from non-DON, the MD was optimal individually, and the combination of the four parameters had the best diagnostic performance. There were significant correlations between the optic nerve's four DTI metrics and the visual acuity and clinical active score ( $P < 0.05$ ). In addition, optic nerve FA was significantly associated with the amplitude of visual evoked potentials ( $P = 0.022$ ).

#### CONCLUSION

s DTI is a promising technique in assessing microstructural changes of optic nerve in patients with DON, and it facilitates differentiation of DON from non-DON eyes in patients with TAO.

#### CLINICAL RELEVANCE/APPLICATION

We recommend DTI as a convenient and noninvasive tool for early detection of DON, and as a conventional examination in the clinical pipeline of TAO. Thus, facilitating timely diagnosis and initiation of medical treatment and enabling a better management of DON.

Printed on: 02/07/23

## Abstract Archives of the RSNA, 2022

M5B-SPHN-3

### Evaluation of The Efficacy of Postoperative Treatment in Obstructive Sleep Apnea Hypoventilation Syndrome

Monday, Nov. 28 12:45PM - 1:15PM Room: Learning Center - HN DPS

#### Participants

Wenwen Wang, Xian, China (*Presenter*) Nothing to Disclose

#### PURPOSE

This study aims to compare the role of CT and MR in assessing the stability of the upper respiratory tract in patients with obstructive sleep apnea syndrome (OSAHS), and to provide evidence for the evaluation of the postoperative treatment effect.

#### METHODS AND MATERIALS

A total of 61 patients (mean age: 36.62±7.99 years, range 22-51 years) were diagnosed as OSAHS through the Polysomnography(PSG).All the patients were treated with modified uvulopalatopharyngoplasty. The upper airway anatomy in all patients was evaluated by CT and MRI pre-operation, and 33 patients were followed-up post-operation. The upper airway parameters such as the thickness of lateral pharyngeal wall, the length of the tongue, the length and thickness of the soft palate and the cross-sectional areas of the soft palate on midsagittal planes were measured and compared, and a two-tailed p-value of less than 0.05 was considered statistically significant.

#### RESULTS

The minimum area of cross section of the upper airway (77.50±41.92mm<sup>2</sup>) on CT was significantly higher than the MR image (34.64±19.93mm<sup>2</sup>) (p <0.05).In 31 patients with self-control, the soft palate thickness measured on nuclear magnetic images before and after surgery were(9.67±2.34vs11.24±2.41,P<0.05).The soft palate length, soft palate thickness, and minimum area of upper airway cross section measured on CT images were (37.38±7.86vs33.62±5.92,10.01±2.11vs11.34±2.43,78.40±40.93vs145.55±78.49)(all P value <0.05).

#### CONCLUSION

s Imageological examination may objectively evaluate the improvement of postoperative airway stenosis.In the evaluation of upper respiratory tract stenosis in OSAHS patients, MR and CT imaging findings were differently significant.Compared with preoperative, MR and CT showed increased thickness of the soft palate and decreased soft palate thickness on post-operative; the cross-sectional areas of the soft palate was not changed. with.

#### CLINICAL RELEVANCE/APPLICATION

CT and MR examination can effectively evaluate the upper airway status of patients, providing more basis for the diagnosis of OSAHS, the severity of the disease and the treatment effect evaluation.

Printed on: 02/07/23



## Abstract Archives of the RSNA, 2022

M5B-SPIN

### Informatics Monday Poster Discussions - B

Monday, Nov. 28 12:45PM - 1:15PM Room: Learning Center - IN DPS

#### Sub-Events

#### M5B-SPIN-2 A Combined Risk Model Using Imaging and Clinical Parameters in COVID-19 Patients From a Nationwide German Cohort to Predict Disease Progression

##### Participants

Rebecca Armbruster, Bad Rippoldsau-Schapbach, Germany (*Presenter*) Nothing to Disclose

##### PURPOSE

COVID-19 infections are on a steep rise in early 2022 and new mutations are spreading rapidly. Machine learning models predicting severe courses of disease remain of interest to efficiently allocate limited medical resources. Our analysis is based on the large scale network infrastructure of the RACOON project spanning across all University Radiology Departments in Germany.

##### METHODS AND MATERIALS

In RACOON a representative dataset consisting of image-based and complementary non-image based standardized structured reports of COVID patients and COVID-mimics was created in 2021 and 2022 containing more than 6 million datapoints. In this analysis, we included 551 PCR-confirmed COVID-cases from 10 university hospitals out of a nationwide collection of 3065 COVID-cases across all 36 German university hospitals (age:  $60.62 \pm 14.87$ , female/male: 172/372, known comorbidities:  $1.68 \pm 1.47$  [min-max: 0-7]). We combined outcome variables in a binary disease severity-score and trained predictors for severe disease progression. Our cohort included 129 severe (ICU admission and invasive ventilation) and 422 non-severe cases. We leveraged 31 structured CT reporting items per patient. Complementary clinical parameters included 18 additional features as input variables (9 anamnestic parameters, 4 vital parameters, oxygen therapy type, IL-6, lymphocyte-count, CRP and d-dimers). We generated classifiers (RandomForest, GradientBoosting) to estimate likelihood of severe outcomes for hospitalized patients and additionally for all location-specific folds to test generalizability.

##### RESULTS

Predicting the highest treatment status, we achieve an accuracy of 73.19% and increase this by 15pp when predicting the highest ventilatory needs (88.41%). By combining these two metrics, we achieve an accuracy of 94.93%. Compared to models trained on image-derived parameters only, we improve by 8pp. Location-specific train/test-folds achieve an averaged accuracy of  $94.64 \pm 0.03\%$  and show that our model generalizes among clinical settings.

##### CONCLUSION

Our model accurately predicts patients COVID-19 progression at the time of the first CT scan after hospital admission by using baseline parameters complementary to image analysis. Our tool will be made available for public use. This analysis can be expanded to include datasets of further centers of the nationwide RACOON network.

##### CLINICAL RELEVANCE/APPLICATION

Predictive models can be used in clinical setting to predict necessity of intensive care treatment. Our novel large scale national research infrastructure project could create a representative dataset promptly within the pandemic and can be leveraged to continuously address pandemic preparedness and public health research questions.

#### M5B-SPIN-3 Autonomous Machine Learning: Validating the Approach on Use-case for Classifying Clavicle Fractures

##### Participants

Giridhar Dasegowda, MBBS, Boston, MA (*Presenter*) Nothing to Disclose

##### PURPOSE

We created an infrastructure for autonomous machine learning (AML) platform for the non-programming physicians to create AML algorithms for different clinical applications. We tested the autonomous platform by creating an AML for classifying radiographs for presence and absence of clavicle fractures.

##### METHODS AND MATERIALS

Our IRB approved retrospective study included 972 clavicle radiographs from 486 patients (mean age  $53 \pm 19$  years, M:F 249:237) from 5 hospitals (three community and two quaternary care hospitals). Most patient had two-view radiographs with axial and anterior-posterior projections. The positive radiographs had either displaced or non-displaced clavicle fractures. Radiographs with incomplete coverage of clavicles were excluded. The AML platform automatically retrieves imaging exams using series UID from the hospital VNA via WADO. The platform then autonomously trains a model until the validation loss plateaus. For training, the images are resized to 512 x 512 matrix. A DenseNet201 model (pretrained on ImageNet) is used for training with the following types of data augmentation - random rotation, random zoom, and random elastic deformation using splines. Once the testing is complete, the

platform provides the receiver operating characteristics curve and confusion matrix for estimating sensitivity, specificity, and accuracy.

## RESULTS

The AML infrastructure was successful in retrieving radiographs from 5 of 7 sites. The retrieved datasets were successfully parsed for creating an ML classifier with 871 radiographs for the training dataset, 40 radiographs for cross-validation, and 100 radiographs for testing (46 with clavicle fracture, 54 without clavicle fracture). The algorithm identified clavicle fracture with 91% sensitivity, 72% specificity, and 81% accuracy with an AUC of 0.88.

## CONCLUSION

s A fully autonomous ML platform can help physicians create and test successful machine learning models from multicenter imaging datasets such as the one in our study for classifying radiographs based on presence of clavicle fracture.

## CLINICAL RELEVANCE/APPLICATION

A fully autonomous ML platform can help create self-learning ML algorithm with local datasets and high model performance for some tasks such as in classification of imaging tests for presence of specific findings.

## M5B-SPIN-4 Artificial Intelligence-generated Auto-impression from 9.8-Million Radiology Reports as Training Datasets from Multiple Sites and Imaging Modalities

### Awards

#### Trainee Research Prize - Fellow

#### Participants

Parisa Kaviani, MD, Boston, MA (*Presenter*) Nothing to Disclose

## PURPOSE

We developed an artificial intelligence-generated auto-impression from a training dataset of 9.8-million radiology reports for multiple imaging modalities, radiology subspecialties, and sites. We evaluated the relationship, content, and accuracy of an AI-generated auto-impression (AAI) against the radiologists' reported findings and impression (RI).

## METHODS AND MATERIALS

We developed and trained an AAI algorithm (Nuance Communications, Inc.) with 9.8 million radiology reports from multiple sites to generate AAI based on information including protocol name and the radiologists-dictated findings section of radiology reports. In an ongoing evaluation of a separate dataset of 10,000 radiology reports of multiple imaging modalities and from multiple US imaging sites, we assessed if AAI can accurately reproduce the RI in terms of number of clinically significant findings and radiologists' style of reporting, while avoiding potential mismatch (with the findings section in terms of size, location, or side). Separately we recorded the word count for AAI and RI. Data were analyzed with Pearson correlation and paired t-tests.

## RESULTS

AAI reports were deemed either perfect (82.5%) or acceptable (17.5%) for stylistic concurrence with RI. Both AAI (mismatched Haller's Index) and RI (mismatched nodule size) had one mismatch each. There was no difference between the word counts of AAI (mean  $43 \pm 25$  words/impression) and RI (mean  $41 \pm 24$  words/impression) ( $p > 0.1$ ). Overall, there was an excellent correlation ( $r = 0.96$ ) between AAI and RI for the trajectory of findings (negative vs. stable vs. new or increasing vs. resolved or decreasing findings). The AAI output (<4%) requiring major changes pertained to reports with multiple impression items, and those where differential diagnosis or disease trajectories were not described in radiologists' findings section.

## CONCLUSION

s Our AI-generated auto-impression has strong content and stylistic correlation with the radiologists-dictated impression of radiology reports from multiple sites and multiple imaging modalities.

## CLINICAL RELEVANCE/APPLICATION

In clinical settings of radiology exam interpretation, the AI generated auto-impression assessed in our study can save interpretation time; a comprehensive findings section results in best AAI output.

## M5B-SPIN-5 Enhancing Generalizability of a Non-Linear Deep Learning Model by Adjusting Linear Confounding Variables for Bone Age Estimation in Pediatric Hand X-rays

#### Participants

Sunggu Kyung, MS, Seoul, Korea, Republic Of (*Presenter*) Nothing to Disclose

## PURPOSE

To present the differences in performance and generalizability of non-linear deep learning models according to the method of adjusting linear confounding variables.

## METHODS AND MATERIALS

RSNA Pediatric Bone Age Challenge (2017) dataset was used for training deep learning models. Test dataset of RSNA dataset and 227 pediatric hand X-ray images of a tertiary hospital from South Korea were used for the evaluation. Three different deep learning models were developed. Baseline model was simple CNN which takes input values of image and sex for estimating bone age. A double-task model with U-Net based encoder-decoder architecture has been developed, which takes input values of image, sex for estimating bone age and adjusts image related confounding variables by reconstructing the input image. Finally, a U-Net based triple-task model has been developed, which only takes input of image for estimating bone age and adjusts biological confounding variables by predicting sex and adjusts image related confounding variables by reconstructing the input image. The mean average error (MAE) and Pearson's correlation coefficient ( $r$ ) between radiologist-labeled bone age and model prediction was evaluated and compared. In addition, attention map which highlights the region for bone age estimation was averaged and compared according to pubertal stage and sex. Paired t-test was used for statistical comparison

## RESULTS

In test dataset of RSNA dataset, MAEs were 6.77, 5.43, and 7.61, respectively for the baseline, double-task, and triple-task models. The r values were 0.976, 0.988, and 0.972, respectively. There were statistical differences between baseline and double-task model ( $P<0.001$ ) but not between double-task model and triple task model ( $P=0.222$ ). In the tertiary hospital dataset, MAEs were 9.41, 9.10, and 8.35 respectively for the baseline, double-task, and triple-task models. The r values were 0.978, 0.978, and 0.983 respectively. There were statistical differences between triple-task and the other models (baseline,  $P<0.001$ ; double-task,  $P=0.037$ ). The averaged attention maps highlighted proper regions in all models.

## CONCLUSION

s Adjusting linear confounding variables by additional input value can enhance internal performance of deep learning model but may deteriorate generalizability. Adjusting linear confounding variable by predicting it can enhance the generalizability of the deep learning model.

## CLINICAL RELEVANCE/APPLICATION

For developing the model with better performance and multi-ethnic generalizability, the differences in adjustment strategies were used, which could be applicable to real world computer-aided diagnosis practice.

Printed on: 02/07/23



## Abstract Archives of the RSNA, 2022

M5B-SPIN-2

### A Combined Risk Model Using Imaging and Clinical Parameters in COVID-19 Patients From a Nationwide German Cohort to Predict Disease Progression

Monday, Nov. 28 12:45PM - 1:15PM Room: Learning Center - IN DPS

#### Participants

Rebecca Armbruster, Bad Rippoldsau-Schapbach, Germany (*Presenter*) Nothing to Disclose

#### PURPOSE

COVID-19 infections are on a steep rise in early 2022 and new mutations are spreading rapidly. Machine learning models predicting severe courses of disease remain of interest to efficiently allocate limited medical resources. Our analysis is based on the large scale network infrastructure of the RACOON project spanning across all University Radiology Departments in Germany.

#### METHODS AND MATERIALS

In RACOON a representative dataset consisting of image-based and complementary non-image based standardized structured reports of COVID patients and COVID-mimics was created in 2021 and 2022 containing more than 6 million datapoints. In this analysis, we included 551 PCR-confirmed COVID-cases from 10 university hospitals out of a nationwide collection of 3065 COVID-cases across all 36 German university hospitals (age:  $60.62 \pm 14.87$ , female/male: 172/372, known comorbidities:  $1.68 \pm 1.47$  [min-max: 0-7]). We combined outcome variables in a binary disease severity-score and trained predictors for severe disease progression. Our cohort included 129 severe (ICU admission and invasive ventilation) and 422 non-severe cases. We leveraged 31 structured CT reporting items per patient. Complementary clinical parameters included 18 additional features as input variables (9 anamnestic parameters, 4 vital parameters, oxygen therapy type, IL-6, lymphocyte-count, CRP and d-dimers). We generated classifiers (RandomForest, GradientBoosting) to estimate likelihood of severe outcomes for hospitalized patients and additionally for all location-specific folds to test generalizability.

#### RESULTS

Predicting the highest treatment status, we achieve an accuracy of 73.19% and increase this by 15pp when predicting the highest ventilatory needs (88.41%). By combining these two metrics, we achieve an accuracy of 94.93%. Compared to models trained on image-derived parameters only, we improve by 8pp. Location-specific train/test-folds achieve an averaged accuracy of  $94.64 \pm 0.03\%$  and show that our model generalizes among clinical settings.

#### CONCLUSION

Our model accurately predicts patients COVID-19 progression at the time of the first CT scan after hospital admission by using baseline parameters complementary to image analysis. Our tool will be made available for public use. This analysis can be expanded to include datasets of further centers of the nationwide RACOON network.

#### CLINICAL RELEVANCE/APPLICATION

Predictive models can be used in clinical setting to predict necessity of intensive care treatment. Our novel large scale national research infrastructure project could create a representative dataset promptly within the pandemic and can be leveraged to continuously address pandemic preparedness and public health research questions.

Printed on: 02/07/23



## Abstract Archives of the RSNA, 2022

M5B-SPIN-3

### Autonomous Machine Learning: Validating the Approach on Use-case for Classifying Clavicle Fractures

Monday, Nov. 28 12:45PM - 1:15PM Room: Learning Center - IN DPS

#### Participants

Giridhar Dasegowda, MBBS, Boston, MA (*Presenter*) Nothing to Disclose

#### PURPOSE

We created an infrastructure for autonomous machine learning (AML) platform for the non-programming physicians to create AML algorithms for different clinical applications. We tested the autonomous platform by creating an AML for classifying radiographs for presence and absence of clavicle fractures.

#### METHODS AND MATERIALS

Our IRB approved retrospective study included 972 clavicle radiographs from 486 patients (mean age  $53 \pm 19$  years, M:F 249:237) from 5 hospitals (three community and two quaternary care hospitals). Most patient had two-view radiographs with axial and anterior-posterior projections. The positive radiographs had either displaced or non-displaced clavicle fractures. Radiographs with incomplete coverage of clavicles were excluded. The AML platform automatically retrieves imaging exams using series UID from the hospital VNA via WADO. The platform then autonomously trains a model until the validation loss plateaus. For training, the images are resized to 512 x 512 matrix. A DenseNet201 model (pretrained on ImageNet) is used for training with the following types of data augmentation - random rotation, random zoom, and random elastic deformation using splines. Once the testing is complete, the platform provides the receiver operating characteristics curve and confusion matrix for estimating sensitivity, specificity, and accuracy.

#### RESULTS

The AML infrastructure was successful in retrieving radiographs from 5 of 7 sites. The retrieved datasets were successfully parsed for creating an ML classifier with 871 radiographs for the training dataset, 40 radiographs for cross-validation, and 100 radiographs for testing (46 with clavicle fracture, 54 without clavicle fracture). The algorithm identified clavicle fracture with 91% sensitivity, 72% specificity, and 81% accuracy with an AUC of 0.88.

#### CONCLUSION

s A fully autonomous ML platform can help physicians create and test successful machine learning models from multicenter imaging datasets such as the one in our study for classifying radiographs based on presence of clavicle fracture.

#### CLINICAL RELEVANCE/APPLICATION

A fully autonomous ML platform can help create self-learning ML algorithm with local datasets and high model performance for some tasks such as in classification of imaging tests for presence of specific findings.

Printed on: 02/07/23



## Abstract Archives of the RSNA, 2022

M5B-SPIN-4

### Artificial Intelligence-generated Auto-impression from 9.8-Million Radiology Reports as Training Datasets from Multiple Sites and Imaging Modalities

Monday, Nov. 28 12:45PM - 1:15PM Room: Learning Center - IN DPS

#### Awards

Trainee Research Prize - Fellow

#### Participants

Parisa Kaviani, MD, Boston, MA (*Presenter*) Nothing to Disclose

#### PURPOSE

We developed an artificial intelligence-generated auto-impression from a training dataset of 9.8-million radiology reports for multiple imaging modalities, radiology subspecialties, and sites. We evaluated the relationship, content, and accuracy of an AI-generated auto-impression (AAI) against the radiologists' reported findings and impression (RI).

#### METHODS AND MATERIALS

We developed and trained an AAI algorithm (Nuance Communications, Inc.) with 9.8 million radiology reports from multiple sites to generate AAI based on information including protocol name and the radiologists-dictated findings section of radiology reports. In an ongoing evaluation of a separate dataset of 10,000 radiology reports of multiple imaging modalities and from multiple US imaging sites, we assessed if AAI can accurately reproduce the RI in terms of number of clinically significant findings and radiologists' style of reporting, while avoiding potential mismatch (with the findings section in terms of size, location, or side). Separately we recorded the word count for AAI and RI. Data were analyzed with Pearson correlation and paired t-tests.

#### RESULTS

AAI reports were deemed either perfect (82.5%) or acceptable (17.5%) for stylistic concurrence with RI. Both AAI (mismatched Haller's Index) and RI (mismatched nodule size) had one mismatch each. There was no difference between the word counts of AAI (mean  $43 \pm 25$  words/impression) and RI (mean  $41 \pm 24$  words/impression) ( $p > 0.1$ ). Overall, there was an excellent correlation ( $r = 0.96$ ) between AAI and RI for the trajectory of findings (negative vs. stable vs. new or increasing vs. resolved or decreasing findings). The AAI output (<4%) requiring major changes pertained to reports with multiple impression items, and those where differential diagnosis or disease trajectories were not described in radiologists' findings section.

#### CONCLUSION

Our AI-generated auto-impression has strong content and stylistic correlation with the radiologists-dictated impression of radiology reports from multiple sites and multiple imaging modalities.

#### CLINICAL RELEVANCE/APPLICATION

In clinical settings of radiology exam interpretation, the AI generated auto-impression assessed in our study can save interpretation time; a comprehensive findings section results in best AAI output.

Printed on: 02/07/23

## Abstract Archives of the RSNA, 2022

M5B-SPIN-5

### Enhancing Generalizability of a Non-Linear Deep Learning Model by Adjusting Linear Confounding Variables for Bone Age Estimation in Pediatric Hand X-rays

Monday, Nov. 28 12:45PM - 1:15PM Room: Learning Center - IN DPS

#### Participants

Sunggu Kyung, MS, Seoul, Korea, Republic Of (*Presenter*) Nothing to Disclose

#### PURPOSE

To present the differences in performance and generalizability of non-linear deep learning models according to the method of adjusting linear confounding variables.

#### METHODS AND MATERIALS

RSNA Pediatric Bone Age Challenge (2017) dataset was used for training deep learning models. Test dataset of RSNA dataset and 227 pediatric hand X-ray images of a tertiary hospital from South Korea were used for the evaluation. Three different deep learning models were developed. Baseline model was simple CNN which takes input values of image and sex for estimating bone age. A double-task model with U-Net based encoder-decoder architecture has been developed, which takes input values of image, sex for estimating bone age and adjusts image related confounding variables by reconstructing the input image. Finally, a U-Net based triple-task model has been developed, which only takes input of image for estimating bone age and adjusts biological confounding variables by predicting sex and adjusts image related confounding variables by reconstructing the input image. The mean average error (MAE) and Pearson's correlation coefficient (r) between radiologist-labeled bone age and model prediction was evaluated and compared. In addition, attention map which highlights the region for bone age estimation was averaged and compared according to pubertal stage and sex. Paired t-test was used for statistical comparison

#### RESULTS

In test dataset of RSNA dataset, MAEs were 6.77, 5.43, and 7.61, respectively for the baseline, double-task, and triple-task models. The r values were 0.976, 0.988, and 0.972, respectively. There were statistical differences between baseline and double-task model ( $P < 0.001$ ) but not between double-task model and triple task model ( $P = 0.222$ ). In the tertiary hospital dataset, MAEs were 9.41, 9.10, and 8.35 respectively for the baseline, double-task, and triple-task models. The r values were 0.978, 0.978, and 0.983 respectively. There were statistical differences between triple-task and the other models (baseline,  $P < 0.001$ ; double-task,  $P = 0.037$ ). The averaged attention maps highlighted proper regions in all models.

#### CONCLUSION

s Adjusting linear confounding variables by additional input value can enhance internal performance of deep learning model but may deteriorate generalizability. Adjusting linear confounding variable by predicting it can enhance the generalizability of the deep learning model.

#### CLINICAL RELEVANCE/APPLICATION

For developing the model with better performance and multi-ethnic generalizability, the differences in adjustment strategies were used, which could be applicable to real world computer-aided diagnosis practice.

Printed on: 02/07/23

## Abstract Archives of the RSNA, 2022

M5B-SPIR

### Interventional Monday Poster Discussions - B

Monday, Nov. 28 12:45PM - 1:15PM Room: Learning Center - IR DPS

#### Sub-Events

#### M5B-SPIR-1 Novel Stent-based Electrode for Radiofrequency Ablation in the Rat Esophagus: A Preliminary Study

##### Participants

Dong-Sung Won, BS, Seoul, Korea, Republic Of (*Presenter*) Nothing to Disclose

##### PURPOSE

Endoluminal radiofrequency (RF) electrodes have been developed for the management of inoperable biliopancreatic ductal cancers and Barrett's esophagus but, the formation of a uniform ablation zone is still challenging. The purpose of this study was to investigate technical feasibility and efficacy of RF ablation with use of a novel monopolar stent-based electrode (SE) in the rat esophagus.

##### METHODS AND MATERIALS

RF protocol was determined to the exposed rat esophagus reached at 70 °C at 30, 40, and 50 W, respectively. Eighteen of 21 male Sprague-Dawley rats were divided into three groups and received stent-based RF ablation at 40 W, and the remaining three rats received a sham procedure. Histological changes including the thickness of the submucosal fibrosis, thickness of the epithelial layer, degree of inflammatory cell infiltration, and degree of collagen deposition were analyzed and compared with sham control at immediately (n = 6), 1 week (n = 6), and 2 weeks (n = 6). Additionally, TUNEL and HSP70-positive deposition were investigated.

##### RESULTS

The optimal RF protocol was at 40 W and 480 kHz for 60 sec. The stent-based RF ablation was successful in 16 (88.8%) of the 18 rats. Two rats died of dyspnea due to thicker delivery system and were excluded in this study. The degrees of RF-induced fibrotic changes and inflammatory cell infiltration in the RF-ablated rat esophagus were significantly and gradually increased compared with the sham control at 1 and 2 weeks (all p < 0.05). The thickness of epithelial layer was significantly lower at immediately (p < 0.05) but, gradually increased at 1 and 2 weeks (all p < 0.001) compared with the sham control. TUNEL-positive deposition was significantly increased immediately after RF ablation (p < 0.001) and gradually decreased. The HSP70-positive deposition was significantly increased compared with sham control at immediately, 1 and 2 weeks (all p < 0.001).

##### CONCLUSION

The SE can maximize the RF ablation-induced therapeutic effects by fully contacting the inner wall of the rat esophagus. The stent-based RF ablation is technically feasible and effective to evenly induce thermal damages in the rat esophagus.

##### CLINICAL RELEVANCE/APPLICATION

The stent-based RF system might represent a promising new approach for the treatment of endoluminal malignancies in non-vascular luminal organs.

#### M5B-SPIR-2 Efficacy of Thermoplastic Polyurethane and Gelatin blended Nanofibers-coated Stent-graft in the Porcine Iliac Artery

##### Participants

Dae Sung Ryu, BS, Seoul, Korea, Republic Of (*Presenter*) Nothing to Disclose

##### PURPOSE

Stent-grafts composed of expanded polytetrafluoroethylene, polyethylene terephthalate and polyurethane are characterized by poor endothelialization, high modulus, and low compliance, leading to thrombosis and intimal hyperplasia. A composite synthetic/natural matrix is thought to be a promising alternative to conventional synthetic stent-grafts. The purpose of this study was investigated the efficacy of thermoplastic polyurethane (TPU) and gelatin (GL) blended nanofibers (NFs) coated stent-graft in the porcine iliac artery.

##### METHODS AND MATERIALS

The TPU and GL blended NFs membrane was constructed using ES techniques on surface of the stent with 6 mm in diameter and 30 mm in length. A total of twelve Yorkshire domestic pigs were randomly sacrificed 7 days (n = 6) and 28 days (n = 6) after stent-graft placement in the left iliac artery. The efficacy of the TPU and GL blended NFs-coated stent-graft was assessed by comparing the results of follow-up angiography, the degree of thrombosis, and histological examinations.

##### RESULTS

TPU and GL blended NFs-coated stent-grafts were successfully placed in all pigs without procedure-related complications. The mean ( $\pm$  SD) luminal diameters at 28 days follow-up angiography ( $2.8 \pm 0.34$  mm) were significantly lower than those at 7 days

follow-up ( $4.6 \pm 0.39$  mm,  $p < 0.001$ ) and post-procedure ( $5.1 \pm 0.24$  mm,  $p < 0.001$ ) angiographies. The mean ( $\pm$  SD) thrombogenicity score was significantly increased at 28 days than at 7 days ( $2.67 \pm 0.51$  vs.  $1.33 \pm 0.51$ ,  $p < 0.001$ ). The mean ( $\pm$  SD) thickness of neointimal hyperplasia, degree of inflammatory cell infiltration, and degree of collagen deposition were all significantly higher at 28 days than at 7 days ( $847.8 \pm 162.6$   $\mu\text{m}$  vs.  $373.7 \pm 53.25$   $\mu\text{m}$ ,  $3.66 \pm 0.51$  vs.  $1.83 \pm 0.40$ ,  $3.50 \pm 0.83$  vs.  $1.33 \pm 0.51$ , respectively; all  $p < 0.001$ ).

## CONCLUSION

The TPU and GL blended NFs-coated stent-grafts successfully maintained the patency for 28 days in the porcine iliac artery. Although thrombosis with neointimal tissue were observed, there were no subsequent occlusion of the stent-graft until the end of the study. Further preclinical studies are needed to investigate its efficacy and safety.

## CLINICAL RELEVANCE/APPLICATION

A composite synthetic/natural matrix-coated stent-graft using electrospinning may be promising for prolonged stent-graft patency.

## M5B-SPiR-3 A New Paradigm in Procedure Simulation Using 3D Printing and CT Scans

Participants

Eugene Moon, MD, MS, (Presenter) Nothing to Disclose

## PURPOSE

Our purpose is to determine the cost-effectiveness of 3D printing vasculature models for procedure simulation and training. We aim to delineate the process of converting an abdominal computed tomography angiogram (CTA) into a 3D printed model for simulations like splenic artery embolization.

## METHODS AND MATERIALS

CTA image was converted into a 3D digital model and saved as a .stl file using GE Healthcare AW Volumeshare 7. A free automated computer-aided design software, Autodesk MeshMixer, was used to hollow out the arterial model and erase artifacts created during the conversion. The final digital version was then printed on Formlabs Form3 3D printer using Elastic 50A resin. The 3D printed models were further processed by manually removing support structures, washing residual resin off with 100% isopropanol, and treating in UV light at 60°C for 20 min.

## RESULTS

A segment of descending aorta with its celiac vessels was 3D printed using an abdominal CTA image. The 3D printed model was hollow, elastic, and transparent with varying vessel sizes. We found that the minimum limit of the vascular wall thickness and the lumen diameter was approximately 1 mm and 2 mm, respectively. The Form3 printer at the price of \$3,499 printed our model at a resolution of 100  $\mu\text{m}$  layer thickness using a total resin volume of 52 mL. With the current price of resin at \$0.15/mL, our single print costed about \$7.80 of resin.

## CONCLUSION

We were able to 3D print a high-fidelity model of descending aorta and its celiac vessels at a significantly less cost than many models sold for simulation training. Our hollowed and transparent model provides both haptic and visual feedback for catheter and wire advancement simulation. We specifically aimed to 3D print a model for splenic artery embolization simulation because it demonstrates its ability to accurately create both large and small vessels (i.e., aorta and splenic artery).

## CLINICAL RELEVANCE/APPLICATION

Procedure practice provides increased retention, proficiency, and confidence in the trainees that ultimately improves patient outcome. Despite the overwhelming benefits, training opportunities are limited by the cost and availability. However, 3D printed models for simulation overcome those hurdles. Additionally, diverse models of patient-specific anatomy can be made using different CT images, and a finished 3D printable computer file can be reprinted or shared with different institutions.

## M5B-SPiR-4 Sirolimus-loaded Stent Coated with Flexible 3D Nanonetworked Silica Film for Suppressing Tissue Hyperplasia in Rat Esophagus

Participants

Chu Hui Zeng, MEd, Seoul, Korea, Republic Of (Presenter) Nothing to Disclose

## PURPOSE

To investigate the safety and efficacy of a newly developed flexible three-dimensional sirolimus-loaded nano-networked silica film (NSF)-covered stent for suppressing stent-induced tissue hyperplasia in rat esophagus.

## METHODS AND MATERIALS

A total of 30 Sprague-Dawley rats (300-350 g; 9 weeks old) were randomly allocated to three groups with 10 rats in each: Group A received control self-expandable metallic stent (SEMS), Group B received NSF-covered SEMS, and Group C received sirolimus-loaded NSF-covered SEMS. Hematoxylin and eosin staining was performed to determine the degree of submucosal inflammatory cell infiltration, number of epithelial layers, thickness of submucosal fibrosis, and percentage of tissue-hyperplasia area. Masson's trichrome staining was used for the degrees of inflammatory cell infiltration and collagen deposition. The degrees of  $\alpha$ -SMA-, Ki-67-, and TUNEL-positive deposition were subjectively determined by immunohistochemistry.

## RESULTS

Stent placement was successful in all rats. Four of the 30 rats experienced procedure-related death ( $n = 3$ ; 10%) or stent migration ( $n = 1$ ; 3.3%), while the remaining 26 (86.7%) rats survived until the end of study without stent-related complications. Compared with Groups A and B, the mean percentage of tissue-hyperplasia area, mean number of epithelial layers, mean thickness of submucosal fibrosis, and mean degrees of collagen,  $\alpha$ -SMA-, and Ki-67-positive deposition were all significantly lower in Group C (all  $P < 0.05$ ), but no difference was detected in TUNEL-stained tissues among the groups.

## CONCLUSION

This newly developed flexible three-dimensional sirolimus-loaded NSF-covered stent effectively suppressed stent-induced tissue

s This newly developed flexible three-dimensional silicium-loaded NSF-covered stent effectively suppressed stent-induced tissue hyperplasia in rat esophagus. Thus, the developed NSF is a promising polymer-free drug delivery platform to effectively treat esophageal stricture.

#### **CLINICAL RELEVANCE/APPLICATION**

This new flexible 3D nanonetworked silica film may serve as a promising polymer-free drug delivery platform for suppressing stent-induced tissue hyperplasia in the esophagus and other luminal organs.

#### **M5B-SPiR-5 Differentiation Between Arterial and Venous Lines on Virtual Chest Radiographs: Deep Learning vs. Radiologists**

Participants

Akihiro Inoue, BA, Kawadacho Shinjuku-Ku, Japan (*Presenter*) Nothing to Disclose

#### **PURPOSE**

Arterial misinsertion of central venous catheter can cause lethal complications, while it is rare. The purpose of this study is to compare the performances of differentiating between arterial and venous lines on virtual chest radiographs simulating right internal jugular venous (IJV) catheter placement between radiologists and deep learning (DL).

#### **METHODS AND MATERIALS**

Virtual chest radiographs of seven directions at 5° intervals were developed from contrast-enhanced CT images using raysum reconstruction on a 3D workstation in 130 patients. Virtual venous and arterial lines were drawn from the right IJV to the superior vena cava or aorta at the tracheal bifurcation level using curved planar reconstruction function, respectively. Two DL models, object detection and image classification, were developed using IBM Maximo Visual Inspection in 100 cases. The performances of the DL models and three radiologists in differentiating arterial and venous lines were evaluated using 60 virtual chest radiographs in 30 patients and compared using the area under the receiver operating characteristic curve (AUC).

#### **RESULTS**

The sensitivity, specificity, and AUC using confidence scores in the DL model with image classification were 96.7%, 100%, and 1.000, respectively. Those in the DL model with object detection were 100%, 96.7%, and 1.000, respectively. Those of the radiologists were 93.3-100%, 100%, and 0.964-1.000, respectively. Limited to the frontal images, the DL model showed higher or equivalent AUCs (1.000) compared to the radiologists (0.964-1.000,  $P = 0.139-1.000$ ).

#### **CONCLUSION**

s The diagnostic performances of the DL models are equivalent to or greater than those of radiologists in differentiating between arterial and venous lines from the right IJV on virtual chest radiographs. The DL models can contribute to patient safety by detecting arterial misinsertion which can cause serious complications.

#### **CLINICAL RELEVANCE/APPLICATION**

The deep learning models can contribute to patient safety by detecting arterial misinsertion from the right internal jugular vein, which can cause serious complications, on chest radiographs.

#### **M5B-SPiR-6 Radiomics-based Prediction Model for Outcomes of Radioembolization in Metastatic Colorectal Cancer**

Participants

Philipp Schindler, MD, Muenster, Germany (*Presenter*) Nothing to Disclose

#### **PURPOSE**

To evaluate the benefit of a radiomics-based model for predicting response and survival of patients with colorectal liver metastases treated with Yttrium-90 transarterial radioembolization (TARE).

#### **METHODS AND MATERIALS**

In this single center retrospective study fifty-one patients undergoing TARE were included. Treatment response was assessed by the Response Evaluation Criteria in Solid Tumors (RECIST) at follow-up after 3 months. Patients were stratified into responder (complete/partial response and disease control,  $n=24$ ) and non-responder (progressive disease,  $n=27$ ). Radiomic features (RF) were extracted from baseline CT after segmenting liver tumor volume. A radiomics-based model was built based on a radiomics signature consisting of reliable RFs that allow classification of response using multivariate logistic regression. Decision curve analysis was performed to evaluate the clinical benefit of the prediction model. According to a cutoff determined in the model, patients were assigned to either high- or low-risk groups for disease progression. Kaplan-Meier analysis was performed to analyze survival between high- and low-risk groups.

#### **RESULTS**

Two independent radiomic features differentiated well between responders and non-responders. For predicting treatment response, the area under the receiver operating characteristic curve of the radiomics-based model was 0.75 (95% CI, 0.48-1), providing larger net benefit than without radiomics-based model as determined by decision curve analysis. The high-risk group revealed shorter overall survival than the low-risk group (3.4 vs. 6.4 months,  $p<0.001$ ).

#### **CONCLUSION**

s The radiomics-based model may predict the response and survival outcome in patients treated with TARE for colorectal liver metastases.

#### **CLINICAL RELEVANCE/APPLICATION**

This radiomics-based approach may provide an important decision tool for planning TARE and hereby optimize patient selection.

## **M5B-SPIR-7 Defining a Radiomics Feature Selection Method for Predicting Response to Transarterial Chemoembolization in Hepatocellular Carcinoma Patients**

Participants

Amanda Laguna, BS, Laguna Niguel, CA (*Presenter*) Nothing to Disclose

### **PURPOSE**

Defining reliable machine learning methods to predict treatment success in hepatocellular carcinoma (HCC) represents a key step in the management of this disease. In this work, we compared 18 existing radiomics feature selection methods to assess utility in predicting response to transarterial chemoembolization (TACE) when applied to a non-linear support vector machine (SVM) with a Gaussian kernel.

### **METHODS AND MATERIALS**

136 paired MR T1-weighted contrast-enhanced abdominal images with liver tumor masks before and after TACE formed our dataset. Tumors were manually segmented by an experienced radiologist with seven years of experience. Using RECIST and mRECIST criteria, a combined manual label of either CR/PR or SD/PD was applied to each image pair to classify it as demonstrating a TACE-based reduction in tumor size or not, respectively. 100D feature vectors respected to first-order, shape and textual features were generated for the paired tumor areas before and after TACE. Subtracted feature vectors for each pre/post-TACE image pair were obtained. 18 existing methods of feature selection were employed to select the top-k features to train and test a non-linear SVM with a Gaussian kernel. A five-cross validation was performed to identify the highest performing feature selection method.

### **RESULTS**

For images classified with mRECIST criteria that were analyzed with the highest performing feature selection method, the ACC, AUC, and F1-score were 74.29%±11.34%, 71.50%±15.67%, and 81.00%±7.74%, respectively. For images classified with RECIST criteria that were analyzed with the highest performing feature selection method, the ACC, AUC, and F1-score were 75.03%±6.46%, 75.04%±8.66%, and 80.46%±5.08%, respectively.

### **CONCLUSION**

s An L0-based method that selects the top-5 most important features predicted TACE response in HCC patients with the highest accuracy under both RECIST and mRECIST criteria.

### **CLINICAL RELEVANCE/APPLICATION**

TACE is the first-line treatment option for patients with intermediate-stage HCC. However, difficulty arises when managing these patients. Differences in patient characteristics, liver function, tumor burden, and other disease specificities result in only a subset of these patients benefiting from TACE. Therefore, developing a clinical decision making tool for selecting TACE candidates is critical in improving care of HCC patients. The present study suggests that an L0-based machine learning method that selects the top-5 most important radiomic features to predict TACE response may aid in TACE candidate selection.

## **M5B-SPIR-8 A Machine Learning Approach to Procedure-Related Mortality Prediction in Patients Undergoing Lower Extremity Endovascular Interventions**

Participants

Meredith Cox, Durham, NC (*Presenter*) Nothing to Disclose

### **PURPOSE**

A risk assessment for procedure-related mortality following lower extremity endovascular procedures can help clinicians identify optimal treatment plans and set realistic patient expectations. We develop a machine learning model using multi-hospital data to predict risk of death in patients with peripheral artery disease (PAD) undergoing lower extremity endovascular interventions and interpret the model to identify predictive factors for procedure-related mortality.

### **METHODS AND MATERIALS**

Our study included 14,444 patients who underwent lower extremity endovascular procedures for PAD between 2011 and 2018 extracted from the American College of Surgeons National Surgical Quality Improvement Program (ACS NSQIP) database. Missing values were imputed using Optimal Imputation, and we selected an optimal feature set using Minimum Redundancy Maximum Relevance (mRMR). We trained a random forest model to predict 30-day mortality using 9,407 cases from 2011-2016 balanced with random oversampling of the minority class, and the model was tested using 5,037 independent cases from 2017-2018. We used Gini Importance and SHapley Additive exPlanations (SHAP) to understand the features that most significantly influenced model output. We tested for algorithmic fairness by calculating performance metrics across different races, sexes, and age groups.

### **RESULTS**

The 20 predictive variables selected using mRMR were physiologic high-risk factors, elective surgery, functional status, creatinine, INR, BUN, diabetes, claudication, HCT, renal failure, albumin, dyspnea, pulmonary comorbidities, WBC, asymptomatic status, alkaline phosphatase, platelet count, SGOT, PTT, and bilirubin. Using these features, the random forest model achieved an AUC of 0.75 and an accuracy of 0.87 on the testing set. The model performed equally well on white and nonwhite patients (DeLong p-value = 0.295), male and female patients (DeLong p-value = 0.960), and patients under age 65 and patients age 65 and older (DeLong p-value = 0.650).

### **CONCLUSION**

s We present a machine learning model that predicts 30-day mortality outcomes in PAD patients undergoing lower extremity endovascular procedures that is both interpretable and fair. This model may aid in clinical decision-making to reduce procedure-related mortality in patients with PAD.

### **CLINICAL RELEVANCE/APPLICATION**

Our machine learning model performs well for risk stratification in patients undergoing lower-extremity endovascular interventions, which may aid in optimizing patient outcomes.



## Abstract Archives of the RSNA, 2022

M5B-SP1R-1

### Novel Stent-based Electrode for Radiofrequency Ablation in the Rat Esophagus: A Preliminary Study

Monday, Nov. 28 12:45PM - 1:15PM Room: Learning Center - IR DPS

#### Participants

Dong-Sung Won, BS, Seoul, Korea, Republic Of (*Presenter*) Nothing to Disclose

#### PURPOSE

Endoluminal radiofrequency (RF) electrodes have been developed for the management of inoperable biliopancreatic ductal cancers and Barrett's esophagus but, the formation of a uniform ablation zone is still challenging. The purpose of this study was to investigate technical feasibility and efficacy of RF ablation with use of a novel monopolar stent-based electrode (SE) in the rat esophagus.

#### METHODS AND MATERIALS

RF protocol was determined to the exposed rat esophagus reached at 70 °C at 30, 40, and 50 W, respectively. Eighteen of 21 male Sprague-Dawley rats were divided into three groups and received stent-based RF ablation at 40 W, and the remaining three rats received a sham procedure. Histological changes including the thickness of the submucosal fibrosis, thickness of the epithelial layer, degree of inflammatory cell infiltration, and degree of collagen deposition were analyzed and compared with sham control at immediately (n = 6), 1 week (n = 6), and 2 weeks (n = 6). Additionally, TUNEL and HSP70-positive deposition were investigated.

#### RESULTS

The optimal RF protocol was at 40 W and 480 kHz for 60 sec. The stent-based RF ablation was successful in 16 (88.8%) of the 18 rats. Two rats died of dyspnea due to thicker delivery system and were excluded in this study. The degrees of RF-induced fibrotic changes and inflammatory cell infiltration in the RF-ablated rat esophagus were significantly and gradually increased compared with the sham control at 1 and 2 weeks (all p < 0.05). The thickness of epithelial layer was significantly lower at immediately (p < 0.05) but, gradually increased at 1 and 2 weeks (all p < 0.001) compared with the sham control. TUNEL-positive deposition was significantly increased immediately after RF ablation (p < 0.001) and gradually decreased. The HSP70-positive deposition was significantly increased compared with sham control at immediately, 1 and 2 weeks (all p < 0.001)

#### CONCLUSION

s The SE can maximize the RF ablation-induced therapeutic effects by fully contacting the inner wall of the rat esophagus. The stent-based RF ablation is technically feasible and effective to evenly induce thermal damages in the rat esophagus.

#### CLINICAL RELEVANCE/APPLICATION

The stent-based RF system might represent a promising new approach for the treatment of endoluminal malignancies in non-vascular luminal organs.

Printed on: 02/07/23

## Abstract Archives of the RSNA, 2022

M5B-SP1R-2

### Efficacy of Thermoplastic Polyurethane and Gelatin blended Nanofibers-coated Stent-graft in the Porcine Iliac Artery

Monday, Nov. 28 12:45PM - 1:15PM Room: Learning Center - IR DPS

#### Participants

Dae Sung Ryu, BS, Seoul, Korea, Republic Of (*Presenter*) Nothing to Disclose

#### PURPOSE

Stent-grafts composed of expanded polytetrafluoroethylene, polyethylene terephthalate and polyurethane are characterized by poor endothelialization, high modulus, and low compliance, leading to thrombosis and intimal hyperplasia. A composite synthetic/natural matrix is thought to be a promising alternative to conventional synthetic stent-grafts. The purpose of this study was investigated the efficacy of thermoplastic polyurethane (TPU) and gelatin (GL) blended nanofibers (NFs) coated stent-graft in the porcine iliac artery.

#### METHODS AND MATERIALS

The TPU and GL blended NFs membrane was constructed using ES techniques on surface of the stent with 6 mm in diameter and 30 mm in length. A total of twelve Yorkshire domestic pigs were randomly sacrificed 7 days (n = 6) and 28 days (n = 6) after stent-graft placement in the left iliac artery. The efficacy of the TPU and GL blended NFs-coated stent-graft was assessed by comparing the results of follow-up angiography, the degree of thrombosis, and histological examinations.

#### RESULTS

TPU and GL blended NFs-coated stent-grafts were successfully placed in all pigs without procedure-related complications. The mean ( $\pm$  SD) luminal diameters at 28 days follow-up angiography ( $2.8 \pm 0.34$  mm) were significantly lower than those at 7 days follow-up ( $4.6 \pm 0.39$  mm,  $p < 0.001$ ) and post-procedure ( $5.1 \pm 0.24$  mm,  $p < 0.001$ ) angiographies. The mean ( $\pm$  SD) thrombogenicity score was significantly increased at 28 days than at 7 days ( $2.67 \pm 0.51$  vs.  $1.33 \pm 0.51$ ,  $p < 0.001$ ). The mean ( $\pm$  SD) thickness of neointimal hyperplasia, degree of inflammatory cell infiltration, and degree of collagen deposition were all significantly higher at 28 days than at 7 days ( $847.8 \pm 162.6$   $\mu$ m vs.  $373.7 \pm 53.25$   $\mu$ m,  $3.66 \pm 0.51$  vs.  $1.83 \pm 0.40$ ,  $3.50 \pm 0.83$  vs.  $1.33 \pm 0.51$ , respectively; all  $p < 0.001$ ).

#### CONCLUSION

s The TPU and GL blended NFs -coated stent-grafts successfully maintained the patency for 28 days in the porcine iliac artery. Although thrombosis with neointimal tissue were observed, there were no subsequent occlusion of the stent- graft until the end of the study. Further preclinical studies are needed to investigate the its efficacy and safety.

#### CLINICAL RELEVANCE/APPLICATION

A composite synthetic/natural matrix-coated stent-graft using electrospinning may be promising for prolonged stent-graft patency.

Printed on: 02/07/23



## Abstract Archives of the RSNA, 2022

M5B-SP1R-3

### A New Paradigm in Procedure Simulation Using 3D Printing and CT Scans

Monday, Nov. 28 12:45PM - 1:15PM Room: Learning Center - IR DPS

#### Participants

Eugene Moon, MD, MS, (*Presenter*) Nothing to Disclose

#### PURPOSE

Our purpose is to determine the cost-effectiveness of 3D printing vasculature models for procedure simulation and training. We aim to delineate the process of converting an abdominal computed tomography angiogram (CTA) into a 3D printed model for simulations like splenic artery embolization.

#### METHODS AND MATERIALS

CTA image was converted into a 3D digital model and saved as a .stl file using GE Healthcare AW Volumeshare 7. A free automated computer-aided design software, Autodesk MeshMixer, was used to hollow out the arterial model and erase artifacts created during the conversion. The final digital version was then printed on Formlabs Form3 3D printer using Elastic 50A resin. The 3D printed models were further processed by manually removing support structures, washing residual resin off with 100% isopropanol, and treating in UV light at 60°C for 20 min.

#### RESULTS

A segment of descending aorta with its celiac vessels was 3D printed using an abdominal CTA image. The 3D printed model was hollow, elastic, and transparent with varying vessel sizes. We found that the minimum limit of the vascular wall thickness and the lumen diameter was approximately 1 mm and 2 mm, respectively. The Form3 printer at the price of \$3,499 printed our model at a resolution of 100 um layer thickness using a total resin volume of 52 mL. With the current price of resin at \$0.15/mL, our single print costed about \$7.80 of resin.

#### CONCLUSION

s We were able to 3D print a high-fidelity model of descending aorta and its celiac vessels at a significantly less cost than many models sold for simulation training. Our hollowed and transparent model provides both haptic and visual feedback for catheter and wire advancement simulation. We specifically aimed to 3D print a model for splenic artery embolization simulation because it demonstrates its ability to accurately create both large and small vessels (i.e., aorta and splenic artery).

#### CLINICAL RELEVANCE/APPLICATION

Procedure practice provides increased retention, proficiency, and confidence in the trainees that ultimately improves patient outcome. Despite the overwhelming benefits, training opportunities are limited by the cost and availability. However, 3D printed models for simulation overcomes those hurdles. Additionally, diverse models of patient-specific anatomy can be made using different CT images, and a finished 3D printable computer file can be reprinted or shared with different institutions.

Printed on: 02/07/23

## Abstract Archives of the RSNA, 2022

M5B-SP1R-4

### **Sirolimus-loaded Stent Coated with Flexible 3D Nanonetworked Silica Film for Suppressing Tissue Hyperplasia in Rat Esophagus**

Monday, Nov. 28 12:45PM - 1:15PM Room: Learning Center - IR DPS

#### **Participants**

Chu Hui Zeng, MMed, Seoul, Korea, Republic Of (*Presenter*) Nothing to Disclose

#### **PURPOSE**

To investigate the safety and efficacy of a newly developed flexible three-dimensional sirolimus-loaded nano-networked silica film (NSF)-covered stent for suppressing stent-induced tissue hyperplasia in rat esophagus.

#### **METHODS AND MATERIALS**

A total of 30 Sprague-Dawley rats (300-350 g; 9 weeks old) were randomly allocated to three groups with 10 rats in each: Group A received control self-expandable metallic stent (SEMS), Group B received NSF-covered SEMS, and Group C received sirolimus-loaded NSF-covered SEMS. Hematoxylin and eosin staining was performed to determine the degree of submucosal inflammatory cell infiltration, number of epithelial layers, thickness of submucosal fibrosis, and percentage of tissue-hyperplasia area. Masson's trichrome staining was used for the degrees of inflammatory cell infiltration and collagen deposition. The degrees of  $\alpha$ -SMA-, Ki-67-, and TUNEL-positive deposition were subjectively determined by immunohistochemistry.

#### **RESULTS**

Stent placement was successful in all rats. Four of the 30 rats experienced procedure-related death ( $n = 3$ ; 10%) or stent migration ( $n = 1$ ; 3.3%), while the remaining 26 (86.7%) rats survived until the end of study without stent-related complications. Compared with Groups A and B, the mean percentage of tissue-hyperplasia area, mean number of epithelial layers, mean thickness of submucosal fibrosis, and mean degrees of collagen,  $\alpha$ -SMA-, and Ki-67-positive deposition were all significantly lower in Group C (all  $P < 0.05$ ), but no difference was detected in TUNEL-stained tissues among the groups.

#### **CONCLUSION**

s This newly developed flexible three-dimensional sirolimus-loaded NSF-covered stent effectively suppressed stent-induced tissue hyperplasia in rat esophagus. Thus, the developed NSF is a promising polymer-free drug delivery platform to effectively treat esophageal stricture.

#### **CLINICAL RELEVANCE/APPLICATION**

This new flexible 3D nanonetworked silica film may serve as a promising polymer-free drug delivery platform for suppressing stent-induced tissue hyperplasia in the esophagus and other luminal organs.

Printed on: 02/07/23

## Abstract Archives of the RSNA, 2022

M5B-SP1R-5

### Differentiation Between Arterial and Venous Lines on Virtual Chest Radiographs: Deep Learning vs. Radiologists

Monday, Nov. 28 12:45PM - 1:15PM Room: Learning Center - IR DPS

#### Participants

Akihiro Inoue, BA, Kawadacho Shinjuku-Ku, Japan (*Presenter*) Nothing to Disclose

#### PURPOSE

Arterial misinsertion of central venous catheter can cause lethal complications, while it is rare. The purpose of this study is to compare the performances of differentiating between arterial and venous lines on virtual chest radiographs simulating right internal jugular venous (IJV) catheter placement between radiologists and deep learning (DL).

#### METHODS AND MATERIALS

Virtual chest radiographs of seven directions at 5° intervals were developed from contrast-enhanced CT images using raysum reconstruction on a 3D workstation in 130 patients. Virtual venous and arterial lines were drawn from the right IJV to the superior vena cava or aorta at the tracheal bifurcation level using curved planar reconstruction function, respectively. Two DL models, object detection and image classification, were developed using IBM Maximo Visual Inspection in 100 cases. The performances of the DL models and three radiologists in differentiating arterial and venous lines were evaluated using 60 virtual chest radiographs in 30 patients and compared using the area under the receiver operating characteristic curve (AUC).

#### RESULTS

The sensitivity, specificity, and AUC using confidence scores in the DL model with image classification were 96.7%, 100%, and 1.000, respectively. Those in the DL model with object detection were 100%, 96.7%, and 1.000, respectively. Those of the radiologists were 93.3-100%, 100%, and 0.964-1.000, respectively. Limited to the frontal images, the DL model showed higher or equivalent AUCs (1.000) compared to the radiologists (0.964-1.000,  $P = 0.139-1.000$ ).

#### CONCLUSION

The diagnostic performances of the DL models are equivalent to or greater than those of radiologists in differentiating between arterial and venous lines from the right IJV on virtual chest radiographs. The DL models can contribute to patient safety by detecting arterial misinsertion which can cause serious complications.

#### CLINICAL RELEVANCE/APPLICATION

The deep learning models can contribute to patient safety by detecting arterial misinsertion from the right internal jugular vein, which can cause serious complications, on chest radiographs.

Printed on: 02/07/23

## Abstract Archives of the RSNA, 2022

M5B-SP1R-6

### Radiomics-based Prediction Model for Outcomes of Radioembolization in Metastatic Colorectal Cancer

Monday, Nov. 28 12:45PM - 1:15PM Room: Learning Center - IR DPS

#### Participants

Philipp Schindler, MD, Muenster, Germany (*Presenter*) Nothing to Disclose

#### PURPOSE

To evaluate the benefit of a radiomics-based model for predicting response and survival of patients with colorectal liver metastases treated with Yttrium-90 transarterial radioembolization (TARE).

#### METHODS AND MATERIALS

In this single center retrospective study fifty-one patients undergoing TARE were included. Treatment response was assessed by the Response Evaluation Criteria in Solid Tumors (RECIST) at follow-up after 3 months. Patients were stratified into responder (complete/partial response and disease control, n=24) and non-responder (progressive disease, n=27). Radiomic features (RF) were extracted from baseline CT after segmenting liver tumor volume. A radiomics-based model was built based on a radiomics signature consisting of reliable RFs that allow classification of response using multivariate logistic regression. Decision curve analysis was performed to evaluate the clinical benefit of the prediction model. According to a cutoff determined in the model, patients were assigned to either high- or low-risk groups for disease progression. Kaplan-Meier analysis was performed to analyze survival between high- and low-risk groups.

#### RESULTS

Two independent radiomic features differentiated well between responders and non-responders. For predicting treatment response, the area under the receiver operating characteristic curve of the radiomics-based model was 0.75 (95% CI, 0.48-1), providing larger net benefit than without radiomics-based model as determined by decision curve analysis. The high-risk group revealed shorter overall survival than the low-risk group (3.4 vs. 6.4 months,  $p < 0.001$ ).

#### CONCLUSION

The radiomics-based model may predict the response and survival outcome in patients treated with TARE for colorectal liver metastases.

#### CLINICAL RELEVANCE/APPLICATION

This radiomics-based approach may provide an important decision tool for planning TARE and hereby optimize patient selection.

Printed on: 02/07/23

## Abstract Archives of the RSNA, 2022

M5B-SP1R-7

### Defining a Radiomics Feature Selection Method for Predicting Response to Transarterial Chemoembolization in Hepatocellular Carcinoma Patients

Monday, Nov. 28 12:45PM - 1:15PM Room: Learning Center - IR DPS

#### Participants

Amanda Laguna, BS, Laguna Niguel, CA (*Presenter*) Nothing to Disclose

#### PURPOSE

Defining reliable machine learning methods to predict treatment success in hepatocellular carcinoma (HCC) represents a key step in the management of this disease. In this work, we compared 18 existing radiomics feature selection methods to assess utility in predicting response to transarterial chemoembolization (TACE) when applied to a non-linear support vector machine (SVM) with a Gaussian kernel.

#### METHODS AND MATERIALS

136 paired MR T1-weighted contrast-enhanced abdominal images with liver tumor masks before and after TACE formed our dataset. Tumors were manually segmented by an experienced radiologist with seven years of experience. Using RECIST and mRECIST criteria, a combined manual label of either CR/PR or SD/PD was applied to each image pair to classify it as demonstrating a TACE-based reduction in tumor size or not, respectively. 100D feature vectors respected to first-order, shape and textual features were generated for the paired tumor areas before and after TACE. Subtracted feature vectors for each pre/post-TACE image pair were obtained. 18 existing methods of feature selection were employed to select the top-k features to train and test a non-linear SVM with a Gaussian kernel. A five-cross validation was performed to identify the highest performing feature selection method.

#### RESULTS

For images classified with mRECIST criteria that were analyzed with the highest performing feature selection method, the ACC, AUC, and F1-score were 74.29%±11.34%, 71.50%±15.67%, and 81.00%±7.74%, respectively. For images classified with RECIST criteria that were analyzed with the highest performing feature selection method, the ACC, AUC, and F1-score were 75.03%±6.46%, 75.04%±8.66%, and 80.46%±5.08%, respectively.

#### CONCLUSION

s An L0-based method that selects the top-5 most important features predicted TACE response in HCC patients with the highest accuracy under both RECIST and mRECIST criteria.

#### CLINICAL RELEVANCE/APPLICATION

TACE is the first-line treatment option for patients with intermediate-stage HCC. However, difficulty arises when managing these patients. Differences in patient characteristics, liver function, tumor burden, and other disease specificities result in only a subset of these patients benefiting from TACE. Therefore, developing a clinical decision making tool for selecting TACE candidates is critical in improving care of HCC patients. The present study suggests that an L0-based machine learning method that selects the top-5 most important radiomic features to predict TACE response may aid in TACE candidate selection.

Printed on: 02/07/23



## Abstract Archives of the RSNA, 2022

M5B-SP1R-8

### A Machine Learning Approach to Procedure-Related Mortality Prediction in Patients Undergoing Lower Extremity Endovascular Interventions

Monday, Nov. 28 12:45PM - 1:15PM Room: Learning Center - IR DPS

#### Participants

Meredith Cox, Durham, NC (*Presenter*) Nothing to Disclose

#### PURPOSE

A risk assessment for procedure-related mortality following lower extremity endovascular procedures can help clinicians identify optimal treatment plans and set realistic patient expectations. We develop a machine learning model using multi-hospital data to predict risk of death in patients with peripheral artery disease (PAD) undergoing lower extremity endovascular interventions and interpret the model to identify predictive factors for procedure-related mortality.

#### METHODS AND MATERIALS

Our study included 14,444 patients who underwent lower extremity endovascular procedures for PAD between 2011 and 2018 extracted from the American College of Surgeons National Surgical Quality Improvement Program (ACS NSQIP) database. Missing values were imputed using Optimal Imputation, and we selected an optimal feature set using Minimum Redundancy Maximum Relevance (mRMR). We trained a random forest model to predict 30-day mortality using 9,407 cases from 2011-2016 balanced with random oversampling of the minority class, and the model was tested using 5,037 independent cases from 2017-2018. We used Gini Importance and SHapley Additive exPlanations (SHAP) to understand the features that most significantly influenced model output. We tested for algorithmic fairness by calculating performance metrics across different races, sexes, and age groups.

#### RESULTS

The 20 predictive variables selected using mRMR were physiologic high-risk factors, elective surgery, functional status, creatinine, INR, BUN, diabetes, claudication, HCT, renal failure, albumin, dyspnea, pulmonary comorbidities, WBC, asymptomatic status, alkaline phosphatase, platelet count, SGOT, PTT, and bilirubin. Using these features, the random forest model achieved an AUC of 0.75 and an accuracy of 0.87 on the testing set. The model performed equally well on white and nonwhite patients (DeLong p-value = 0.295), male and female patients (DeLong p-value = 0.960), and patients under age 65 and patients age 65 and older (DeLong p-value = 0.650).

#### CONCLUSION

s We present a machine learning model that predicts 30-day mortality outcomes in PAD patients undergoing lower extremity endovascular procedures that is both interpretable and fair. This model may aid in clinical decision-making to reduce procedure-related mortality in patients with PAD.

#### CLINICAL RELEVANCE/APPLICATION

Our machine learning model performs well for risk stratification in patients undergoing lower-extremity endovascular interventions, which may aid in optimizing patient outcomes.

Printed on: 02/07/23

## Abstract Archives of the RSNA, 2022

M5B-SPMK

### Musculoskeletal Monday Poster Discussions - B

Monday, Nov. 28 12:45PM - 1:15PM Room: Learning Center - MK DPS

#### Sub-Events

#### M5B-SPMK-1 Machine-Learning Automated Hip Measurements for Hip Dysplasia Patients Correlate with Patient Reported Outcome Measures

##### Participants

Holden Archer, Dallas, TX (*Presenter*) Nothing to Disclose

##### PURPOSE

Hip dysplasia (HD) with under-coverage of the acetabulum can lead to hip osteoarthritis. There are several radiographic measurements used for the diagnosis of HD, the most common being the Lateral Center Edge Angle (LCEA) followed by the Tönnis angle and the extrusion index. Artificial intelligence (AI)-based software (HIPPO) using a deep learning algorithm produces such radiographic measurements consistently and reproducibly. Importantly, patient reported outcome measures (PROMs) inform treating physicians regarding the patient's subjective perceptions about their health. The aim of this study was to correlate AI-derived and manual measurements to PROMs with the hypothesis that less worse HD measurements linearly correlate with better PROMs.

##### METHODS AND MATERIALS

Using an electronic database of patients from institutional hip preservation clinic, 256 hips from 130 patients with a diagnosis of HD, AI output and PROMs were included. PROMS obtained at initial office visit included HHS, iHOT-12, SF-12, and Eq-VAS scores. Spearman's rank-order correlation was used. Three manual readers'(M) and their correlations were used as a control for AI.

##### RESULTS

With M-derived measurements, ipsilateral HHS weakly correlated with an increasing LCEA at 0.18, decreasing extrusion index at -0.14 ( $p=0.183$ ) and decreasing Tönnis angle at -0.24, respectively. Similarly, AI-derived measurements also weakly correlated with HHS, e.g. Tönnis Angle at -0.20 ( $p=0.509$ ), LCEA at 0.13, extrusion index at -0.15, and Tönnis angle with Eq Vas at -0.11, respectively. Statistical significance was only reached with respect to AI-derived measurement correlations between iHOT12 and SF12 with CCD ( $p=0.042$  and  $0.048$ ).

##### CONCLUSION

s AI-derived radiographic measurements showed weak and fewer than expected correlations with PROM parameters in the setting of HD and while most being non-significant, they suggest a possible future role of AI to predict patient reported clinical outcome measures. Key Points: AI- and manually-derived measurements of LCEA, extrusion index and Tönnis angles showed weak correlations with PROMs. Significant correlations were seen with CCD and PROMs assessing patient's perceptions of own health and quality of life ( $p<0.05$ ). The strength of AI predictability of PROMs is likely limited likely due to the complex disease process of HD.

##### CLINICAL RELEVANCE/APPLICATION

This study suggests a possible future role for AI-determined radiographic measurements for prediction of PROMs.

#### M5B-SPMK-2 How Does an AI Software for Detection of Bone Fractures Influence Radiologists in the Emergency Department?

##### Participants

Gianluca Folco, MD, Milano, Italy (*Presenter*) Nothing to Disclose

##### PURPOSE

To assess the influence of an AI software for bone fracture diagnosis on an Emergency Department (ED) workload.

##### METHODS AND MATERIALS

An AI software for bone fracture diagnosis (BoneView, Gleamer, France) was added to our PACS on January 11; it processes bone X-rays of upper and lower limbs, lumbosacral spine, ribs, pelvis, hips and displays its diagnostic outcome: "fracture", "doubt fracture", or "no fracture". Furthermore, it adds regions of interest to X-ray images, indicating the AI software-detected fractures. Radiologists performed a prospective evaluation, both before and after the display of the AI software outcome, recording the diagnosis of "fracture", "doubt fracture", or "no fracture" and the number of fracture sites. The software's influence on the total X-ray workload of radiologists was also calculated, factoring in the AI outcome "not available" displayed due to incompatible anatomical districts. Concordance between radiological diagnosis without and with the aid of the AI software was compared using Wilcoxon signed-rank test, with significant  $P<0.05$ .

##### RESULTS

A total of 195 exams were evaluated by radiologists, with a diagnosis rate of no fracture, doubt fracture, and fracture of 121 (62%,

95%CI 55-69%), 8 (4%, 95%CI 2-8%), and 66 (34%, 95%CI 27-41%), respectively; AI software evaluation led to a change in diagnosis in 4 cases (2%, 95%CI 1-5%,  $P=0.256$ ), involving 2 "fracture", 1 "doubt fracture" (initially deemed "no fracture"), and 1 "no fracture" (initially deemed "fracture"). The AI software was applicable in 34% of the ED examinations and could perform a diagnostic evaluation for 28% of them, having a decisive impact on 0.7% of the total X-rays.

## CONCLUSION

s In our Emergency Department, the AI software influenced 2% of diagnoses (not statistically significant), with less than 1% impact on the radiological workload.

## CLINICAL RELEVANCE/APPLICATION

We evaluated the impact of an AI software for the detection of bone fractures in our Emergency Department to assess whether its impact on the radiological workload would prove statistically significant. Results showed that the AI software has a relatively small impact on the total ED X-ray workload, making it not particularly cost-effective. However, further studies may show that AI-based detection of fractures improves the overall diagnostic accuracy in the ED, and that it provides a significant impact when only musculoskeletal radiological exams are taken into account.

## M5B-SPMK-3 Noise Reduction and Image Quality Improvement in Ultra-low-dose Whole-body CT Scans Using Deep Learning-based CT Reconstruction Program in Patients with Multiple Myeloma

Participants

Jiseon Oh, MD, Seoul, Korea, Republic Of (*Presenter*) Nothing to Disclose

## PURPOSE

The purpose of our study was to evaluate the effect of a commercial deep learning-based CT reconstruction program (ClariCT.AI; ClariPI) on the image quality of ultra-low-dose whole-body CT scans.

## METHODS AND MATERIALS

Sixteen patients with multiple myeloma who underwent low-dose whole-body CT using dual-source CT scanners (Somatom Force; Siemens Healthineers) were enrolled. All CT scans were taken with a dual tube system, and the radiation dose ratio of A and B tubes was set to be 3 to 1. As a result, three image sets were collected: ultra-low-dose CT using B tube data with iterative reconstruction (ULD-IR), low-dose CT using merged data from A and B tubes with iterative reconstruction (LD-IR), and ultra-low-dose CT using B tube data with deep learning algorithm (ULD-DL). Afterwards, image noise, the signal-to-noise ratio (SNR), and the contrast-to-noise ratio (CNR) were measured for each scan. For subjective evaluation, subjective noise, spatial resolution for bone and soft tissue, and overall image quality were assessed.

## RESULTS

The mean effective dose for the sixteen CT scans was  $6.03 \pm 1.69$  mSv (range, 4.18-9.53 mSv) and estimated mean effective dose of B tube was  $1.56 \pm 0.44$  mSv (range, 1.03-2.49 mSv). The average measured noise for ULD-IR, LD-IR, and ULD-DL was  $27.26 \pm 30.99$ ,  $15.98 \pm 14.13$ , and  $13.72 \pm 13.40$ , respectively ( $p < .05$ ). Deep learning-based image reconstruction significantly improved the SNR and CNR of ULD whole-body CT ( $p = .001$ ), and there was no significant difference in the SNR and CNR between LD-IR and ULD-DL ( $p = .10$ ). In the subjective analysis, LD-IR showed less subjective noise and better overall image quality than ULD-DL ( $p < .05$ ), but there was no significant difference in the spatial resolution for bone and soft tissue between LD-IR and ULD-DL ( $p = .07$ ).

## CONCLUSION

s With 25% of the radiation dose, ULD whole-body CT with deep learning-based algorithm showed comparable image quality to that of LD whole-body CT.

## CLINICAL RELEVANCE/APPLICATION

Deep learning-based algorithm can effectively reduce radiation dose with acceptable image quality, hence enabling the use of ULD whole body CT as an initial examination in multiple myeloma patients.

## M5B-SPMK-4 Value-added Opportunistic Screening: Prediction Model of Osteoporosis Based on Attenuation Value of Thoracic Vertebrae and Clinical Risk Factors

Participants

Jinrong Yang, (*Presenter*) Nothing to Disclose

## PURPOSE

This study is to establish and verify a nomogram model based on attenuation value of thoracic vertebrae and clinical risk factors for predicting the risk of osteoporosis.

## METHODS AND MATERIALS

This is a cross-sectional study. A total of 1046 patients were enrolled and the baseline clinical data, biochemical indicators, concomitant diseases were collected. The volume attenuation values of thoracic vertebrae were automatically measured by artificial intelligence. The whole patients were randomly divided into the training set of 732 cases (70%) and the validation set of 314 cases (30%). Both two sets, the diagnostic criteria established by the World Health Organization (WHO) in 1994 based on dual-energy X-ray absorptiometry (DXA) were adopted for the diagnosis of osteoporosis. In the training set, variance, t-test (for normal distribution) /Mann-Whitney U-test (for non-normal distribution), least absolute shrinkage and selection operator (LASSO) were used for selecting the thoracic vertebrae CT values to construct AI measurement score and multivariate logistic backward stepwise regression were used to analyze the influencing factors of osteoporosis. According to the clinical application for different data conditions, five nomogram prediction models were constructed, named AIMeasure model, BasicClinical model, TotalClinical model, AIBasicClinical model, AITotalClinical model. Moreover, receiver operating characteristic (ROC) curve, calibration curve and decision curve analyses (DCA) were used to test the distinction, accuracy and clinical applicability of the model both in training set and validation set.

## RESULTS

The results showed age, sex, weight, BMI, smoking, high density lipoprotein cholesterol (HDL\_C), low density lipoprotein cholesterol

(LDL\_C), serum calcium and low CT attenuation value were all related to the occurrence of osteoporosis. The area under the ROC curve of the above five models was 0.878, 0.712, 0.738, 0.897, 0.898 in the training set and was 0.887, 0.773, 0.777, 0.900, 0.902 in the verification set, respectively. Moreover, the calibration curves and DCAs of the models containing attenuation values performed well on accuracy and clinical practicality both two sets.

#### **CONCLUSION**

s The risk prediction nomogram models containing attenuation values have good predictive ability and clinical value, which could be used as an effective tool for the risk prediction of osteoporosis. Furthermore, they would facilitate earlier intervention to prevent the future development of osteoporosis and occurrence of osteoporotic fractures.

#### **CLINICAL RELEVANCE/APPLICATION**

This study showed the attenuation values of thoracic vertebrae on chest CT could be used for opportunistic screening of osteoporosis.

Printed on: 02/07/23

## Abstract Archives of the RSNA, 2022

M5B-SPMK-1

### Machine-Learning Automated Hip Measurements for Hip Dysplasia Patients Correlate with Patient Reported Outcome Measures

Monday, Nov. 28 12:45PM - 1:15PM Room: Learning Center - MK DPS

#### Participants

Holden Archer, Dallas, TX (*Presenter*) Nothing to Disclose

#### PURPOSE

Hip dysplasia (HD) with under-coverage of the acetabulum can lead to hip osteoarthritis. There are several radiographic measurements used for the diagnosis of HD, the most common being the Lateral Center Edge Angle (LCEA) followed by the Tönnis angle and the extrusion index. Artificial intelligence (AI)-based software (HIPPO) using a deep learning algorithm produces such radiographic measurements consistently and reproducibly. Importantly, patient reported outcome measures (PROMs) inform treating physicians regarding the patient's subjective perceptions about their health. The aim of this study was to correlate AI-derived and manual measurements to PROMs with the hypothesis that less worse HD measurements linearly correlate with better PROMs.

#### METHODS AND MATERIALS

Using an electronic database of patients from institutional hip preservation clinic, 256 hips from 130 patients with a diagnosis of HD, AI output and PROMs were included. PROMS obtained at initial office visit included HHS, iHOT-12, SF-12, and Eq-VAS scores. Spearman's rank-order correlation was used. Three manual readers'(M) and their correlations were used as a control for AI.

#### RESULTS

With M-derived measurements, ipsilateral HHS weakly correlated with an increasing LCEA at 0.18, decreasing extrusion index at -0.14 ( $p=0.183$ ) and decreasing Tönnis angle at -0.24, respectively. Similarly, AI-derived measurements also weakly correlated with HHS, e.g. Tönnis Angle at -0.20 ( $p=0.509$ ), LCEA at 0.13, extrusion index at -0.15, and Tönnis angle with Eq Vas at -0.11, respectively. Statistical significance was only reached with respect to AI-derived measurement correlations between iHOT12 and SF12 with CCD ( $p=0.042$  and  $0.048$ ).

#### CONCLUSION

s AI-derived radiographic measurements showed weak and fewer than expected correlations with PROM parameters in the setting of HD and while most being non-significant, they suggest a possible future role of AI to predict patient reported clinical outcome measures. Key Points: AI- and manually-derived measurements of LCEA, extrusion index and Tönnis angles showed weak correlations with PROMs. Significant correlations were seen with CCD and PROMs assessing patient's perceptions of own health and quality of life ( $p<0.05$ ). The strength of AI predictability of PROMs is likely limited likely due to the complex disease process of HD.

#### CLINICAL RELEVANCE/APPLICATION

This study suggests a possible future role for AI-determined radiographic measurements for prediction of PROMs.

Printed on: 02/07/23

## Abstract Archives of the RSNA, 2022

M5B-SPMK-2

### How Does an AI Software for Detection of Bone Fractures Influence Radiologists in the Emergency Department?

Monday, Nov. 28 12:45PM - 1:15PM Room: Learning Center - MK DPS

#### Participants

Gianluca Folco, MD, Milano, Italy (*Presenter*) Nothing to Disclose

#### PURPOSE

To assess the influence of an AI software for bone fracture diagnosis on an Emergency Department (ED) workload.

#### METHODS AND MATERIALS

An AI software for bone fracture diagnosis (BoneView, Gleamer, France) was added to our PACS on January 11; it processes bone X-rays of upper and lower limbs, lumbosacral spine, ribs, pelvis, hips and displays its diagnostic outcome: "fracture", "doubt fracture", or "no fracture". Furthermore, it adds regions of interest to X-ray images, indicating the AI software-detected fractures. Radiologists performed a prospective evaluation, both before and after the display of the AI software outcome, recording the diagnosis of "fracture", "doubt fracture", or "no fracture" and the number of fracture sites. The software's influence on the total X-ray workload of radiologists was also calculated, factoring in the AI outcome "not available" displayed due to incompatible anatomical districts. Concordance between radiological diagnosis without and with the aid of the AI software was compared using Wilcoxon signed-rank test, with significant  $P < 0.05$ .

#### RESULTS

A total of 195 exams were evaluated by radiologists, with a diagnosis rate of no fracture, doubt fracture, and fracture of 121 (62%, 95%CI 55-69%), 8 (4%, 95%CI 2-8%), and 66 (34%, 95%CI 27-41%), respectively; AI software evaluation led to a change in diagnosis in 4 cases (2%, 95%CI 1-5%,  $P = 0.256$ ), involving 2 "fracture", 1 "doubt fracture" (initially deemed "no fracture"), and 1 "no fracture" (initially deemed "fracture"). The AI software was applicable in 34% of the ED examinations and could perform a diagnostic evaluation for 28% of them, having a decisive impact on 0.7% of the total X-rays.

#### CONCLUSION

In our Emergency Department, the AI software influenced 2% of diagnoses (not statistically significant), with less than 1% impact on the radiological workload.

#### CLINICAL RELEVANCE/APPLICATION

We evaluated the impact of an AI software for the detection of bone fractures in our Emergency Department to assess whether its impact on the radiological workload would prove statistically significant. Results showed that the AI software has a relatively small impact on the total ED X-ray workload, making it not particularly cost-effective. However, further studies may show that AI-based detection of fractures improves the overall diagnostic accuracy in the ED, and that it provides a significant impact when only musculoskeletal radiological exams are taken into account.

Printed on: 02/07/23

## Abstract Archives of the RSNA, 2022

M5B-SPMK-3

### Noise Reduction and Image Quality Improvement in Ultra-low-dose Whole-body CT Scans Using Deep Learning-based CT Reconstruction Program in Patients with Multiple Myeloma

Monday, Nov. 28 12:45PM - 1:15PM Room: Learning Center - MK DPS

#### Participants

Jiseon Oh, MD, Seoul, Korea, Republic Of (*Presenter*) Nothing to Disclose

#### PURPOSE

The purpose of our study was to evaluate the effect of a commercial deep learning-based CT reconstruction program (ClariCT.AI; ClariPI) on the image quality of ultra-low-dose whole-body CT scans.

#### METHODS AND MATERIALS

Sixteen patients with multiple myeloma who underwent low-dose whole-body CT using dual-source CT scanners (Somatom Force; Siemens Healthineers) were enrolled. All CT scans were taken with a dual tube system, and the radiation dose ratio of A and B tubes was set to be 3 to 1. As a result, three image sets were collected: ultra-low-dose CT using B tube data with iterative reconstruction (ULD-IR), low-dose CT using merged data from A and B tubes with iterative reconstruction (LD-IR), and ultra-low-dose CT using B tube data with deep learning algorithm (ULD-DL). Afterwards, image noise, the signal-to-noise ratio (SNR), and the contrast-to-noise ratio (CNR) were measured for each scan. For subjective evaluation, subjective noise, spatial resolution for bone and soft tissue, and overall image quality were assessed.

#### RESULTS

The mean effective dose for the sixteen CT scans was  $6.03 \pm 1.69$  mSv (range, 4.18-9.53 mSv) and estimated mean effective dose of B tube was  $1.56 \pm 0.44$  mSv (range, 1.03-2.49 mSv). The average measured noise for ULD-IR, LD-IR, and ULD-DL was  $27.26 \pm 30.99$ ,  $15.98 \pm 14.13$ , and  $13.72 \pm 13.40$ , respectively ( $p < .05$ ). Deep learning-based image reconstruction significantly improved the SNR and CNR of ULD whole-body CT ( $p = .001$ ), and there was no significant difference in the SNR and CNR between LD-IR and ULD-DL ( $p = .10$ ). In the subjective analysis, LD-IR showed less subjective noise and better overall image quality than ULD-DL ( $p < .05$ ), but there was no significant difference in the spatial resolution for bone and soft tissue between LD-IR and ULD-DL ( $p = .07$ ).

#### CONCLUSION

s With 25% of the radiation dose, ULD whole-body CT with deep learning-based algorithm showed comparable image quality to that of LD whole-body CT.

#### CLINICAL RELEVANCE/APPLICATION

Deep learning-based algorithm can effectively reduce radiation dose with acceptable image quality, hence enabling the use of ULD whole body CT as an initial examination in multiple myeloma patients.

Printed on: 02/07/23

## Abstract Archives of the RSNA, 2022

M5B-SPMK-4

### Value-added Opportunistic Screening: Prediction Model of Osteoporosis Based on Attenuation Value of Thoracic Vertebrae and Clinical Risk Factors

Monday, Nov. 28 12:45PM - 1:15PM Room: Learning Center - MK DPS

#### Participants

Jinrong Yang, (*Presenter*) Nothing to Disclose

#### PURPOSE

This study is to establish and verify a nomogram model based on attenuation value of thoracic vertebrae and clinical risk factors for predicting the risk of osteoporosis.

#### METHODS AND MATERIALS

This is a cross-sectional study. A total of 1046 patients were enrolled and the baseline clinical data, biochemical indicators, concomitant diseases were collected. The volume attenuation values of thoracic vertebrae were automatically measured by artificial intelligence. The whole patients were randomly divided into the training set of 732 cases (70%) and the validation set of 314 cases (30%). Both two sets, the diagnostic criteria established by the World Health Organization (WHO) in 1994 based on dual-energy X-ray absorptiometry (DXA) were adopted for the diagnosis of osteoporosis. In the training set, variance, t-test (for normal distribution) /Mann-Whitney U-test (for non-normal distribution), least absolute shrinkage and selection operator (LASSO) were used for selecting the thoracic vertebrae CT values to construct AI measurement score and multivariate logistic backward stepwise regression were used to analyze the influencing factors of osteoporosis. According to the clinical application for different data conditions, five nomogram prediction models were constructed, named AIMeasure model, BasicClinical model, TotalClinical model, AIBasicClinical model, AITotalClinical model. Moreover, receiver operating characteristic (ROC) curve, calibration curve and decision curve analyses (DCA) were used to test the distinction, accuracy and clinical applicability of the model both in training set and validation set.

#### RESULTS

The results showed age, sex, weight, BMI, smoking, high density lipoprotein cholesterol (HDL\_C), low density lipoprotein cholesterol (LDL\_C), serum calcium and low CT attenuation value were all related to the occurrence of osteoporosis. The area under the ROC curve of the above five models was 0.878, 0.712, 0.738, 0.897, 0.898 in the training set and was 0.887, 0.773, 0.777, 0.900, 0.902 in the verification set, respectively. Moreover, the calibration curves and DCAs of the models containing attenuation values performed well on accuracy and clinical practicality both two sets.

#### CONCLUSION

The risk prediction nomogram models containing attenuation values have good predictive ability and clinical value, which could be used as an effective tool for the risk prediction of osteoporosis. Furthermore, they would facilitate earlier intervention to prevent the future development of osteoporosis and occurrence of osteoporotic fractures.

#### CLINICAL RELEVANCE/APPLICATION

This study showed the attenuation values of thoracic vertebrae on chest CT could be used for opportunistic screening of osteoporosis.

Printed on: 02/07/23

## Abstract Archives of the RSNA, 2022

M5B-SPMS

### Multisystem Monday Poster Discussions - B

Monday, Nov. 28 12:45PM - 1:15PM Room: Learning Center - MS DPS

#### Sub-Events

#### M5B-SPMS-1 Deep Learning Automation of Kidney, Liver and Spleen Segmentation for Organ Volume Measurements in Autosomal Dominant Polycystic Kidney Disease

#### Awards

##### Trainee Research Prize - Medical Student

#### Participants

Arman Sharbatdaran, MD, (*Presenter*) Nothing to Disclose

#### PURPOSE

Autosomal dominant polycystic kidney disease (ADPKD) is the most common inherited renal disease and it affects other organs including liver, spleen, pancreas, seminal vesicles, arachnoid, lymphatics and the cardiovascular system. Organ volume measurements are a critical clinical metric in managing ADPKD patients. But manually contouring each organ on every image slice is tedious and prone to error/bias. Here we expand a deep learning model optimized for kidney segmentations to also segment liver and spleen in ADPKD.

#### METHODS AND MATERIALS

A 2D U-net deep learning approach to segment kidneys was optimized to also segment liver and spleen volume. This required optimization of image cropping for each organ and an effective algorithm to determine the identity of overlap voxels, which are labeled as more than one organ. Radiologists manually labeled T2-weighted images from 213 ADPKD subjects as ground truth to train the model, which was then validated by 30 additional prospective and 30 external subjects for a total of 319 ADPKD subjects. The mean time and interobserver variability for manual organ segmentation and model-assisted segmentation for the 1st 10 prospective cases were evaluated by 3 trained observers to assess the efficiency of the model.

#### RESULTS

Kidney, liver, and spleen volumes had average percent error of 5%, 4%, and 7%, respectively, on external validation and 9%, 3%, and 5%, respectively on prospective validation. The Dice score associated with left kidney, right kidney, liver, and spleen were 0.96, 0.99, 0.97, 0.96, respectively on external validation and 0.96, 0.96, 0.97, 0.95, respectively on prospective validation. Time required for manual correction of deep learning segmentation errors was only 12:41 minutes compared to 19:19 minutes for completely manual segmentation, a 39% time saving ( $p=0.001$ ). Interobserver variability of model segmentations was reduced 3-fold compared to manual segmentation.

#### CONCLUSION

Deep learning reduces radiologists' time required to perform multi-organ segmentation in ADPKD and reduces measurement variability.

#### CLINICAL RELEVANCE/APPLICATION

Automating organ volume measurements and improving reproducibility will allow for more accurate assessment of disease progressing and response to treatments as well as potentially titration of treatments for improving ADPKD patient care.

Printed on: 02/07/23

## Abstract Archives of the RSNA, 2022

M5B-SPMS-1

### Deep Learning Automation of Kidney, Liver and Spleen Segmentation for Organ Volume Measurements in Autosomal Dominant Polycystic Kidney Disease

Monday, Nov. 28 12:45PM - 1:15PM Room: Learning Center - MS DPS

#### Awards

**Trainee Research Prize - Medical Student**

#### Participants

Arman Sharbatdaran, MD, (*Presenter*) Nothing to Disclose

#### PURPOSE

Autosomal dominant polycystic kidney disease (ADPKD) is the most common inherited renal disease and it affects other organs including liver, spleen, pancreas, seminal vesicles, arachnoid, lymphatics and the cardiovascular system. Organ volume measurements are a critical clinical metric in managing ADPKD patients. But manually contouring each organ on every image slice is tedious and prone to error/bias. Here we expand a deep learning model optimized for kidney segmentations to also segment liver and spleen in ADPKD.

#### METHODS AND MATERIALS

A 2D U-net deep learning approach to segment kidneys was optimized to also segment liver and spleen volume. This required optimization of image cropping for each organ and an effective algorithm to determine the identity of overlap voxels, which are labeled as more than one organ. Radiologists manually labeled T2-weighted images from 213 ADPKD subjects as ground truth to train the model, which was then validated by 30 additional prospective and 30 external subjects for a total of 319 ADPKD subjects. The mean time and interobserver variability for manual organ segmentation and model-assisted segmentation for the 1st 10 prospective cases were evaluated by 3 trained observers to assess the efficiency of the model.

#### RESULTS

Kidney, liver, and spleen volumes had average percent error of 5%, 4%, and 7%, respectively, on external validation and 9%, 3%, and 5%, respectively on prospective validation. The Dice score associated with left kidney, right kidney, liver, and spleen were 0.96, 0.99, 0.97, 0.96, respectively on external validation and 0.96, 0.96, 0.97, 0.95, respectively on prospective validation. Time required for manual correction of deep learning segmentation errors was only 12:41 minutes compared to 19:19 minutes for completely manual segmentation, a 39% time saving ( $p=0.001$ ). Interobserver variability of model segmentations was reduced 3-fold compared to manual segmentation.

#### CONCLUSION

Deep learning reduces radiologists' time required to perform multi-organ segmentation in ADPKD and reduces measurement variability.

#### CLINICAL RELEVANCE/APPLICATION

Automating organ volume measurements and improving reproducibility will allow for more accurate assessment of disease progressing and response to treatments as well as potentially titration of treatments for improving ADPKD patient care.

Printed on: 02/07/23

## Abstract Archives of the RSNA, 2022

M5B-SPNMMI

### Nuclear Medicine/Molecular Imaging Monday Poster Discussion - B

Monday, Nov. 28 12:45PM - 1:15PM Room: Learning Center - NMMI DPS

#### Participants

Mary Ellen Koran, MD, PhD, Nashville, TN (*Moderator*) Nothing to Disclose

Mary Ellen Koran, MD, PhD, Nashville, TN (*Moderator*) Nothing to Disclose

Lilja Solnes, MD, Owings Mills, MD (*Moderator*) Consultant, Lantheus Holdings; Research funded, Novartis AG; Research funded, Precision Molecular Inc; Research funded, Celectar Biosciences, Inc; Royalties, RELX

Lilja Solnes, MD, Owings Mills, MD (*Moderator*) Consultant, Lantheus Holdings; Research funded, Novartis AG; Research funded, Precision Molecular Inc; Research funded, Celectar Biosciences, Inc; Royalties, RELX

#### Sub-Events

#### M5B-SPNMMI-1 MRI Dynamic Tracing Study of the Effect of PLL-USPIONS-PMSCc Molecular Probe on Colorectal Cancer Xenografts in Nude Mice

#### Participants

Hua He, MMedSc, MMedSc, Yinchuan, China (*Presenter*) Nothing to Disclose

#### PURPOSE

Human placental mesenchymal stem cells (PMSCs) labeled with polylysine-ultramicro and superparamagnetic oxide nano-iron particle protein complexes and transplanted into colorectal cancer (CRC) animal models, to explore the feasibility of molecular imaging of PLL-USPIONS-PMSCc targeting CRC tumor-bearing mice and the effect of PMSCs on CRC.

#### METHODS AND MATERIALS

PMSCs were cultured, transfected with polylysine (PLL), and PMSCs-PLL were magnetically labeled with USPIO, the PLL-USPIONS-PMSCc molecular probe was transplanted into the experimental group colorectal cancer animal model through the tail vein of the rat, in the same way, 200  $\mu$ l of PBS without cells was injected into the tumor of the tumor-bearing mice as a blank control, T2WI, T2 mapping, T2\* mapping sequences were used to observe the signal distribution and change characteristics of transplanted tumor and PMSCc, observation of the signal distribution and change characteristics in the two groups of transplanted tumors measured the size, T2, T2\* value of tumor, calculated inhibition rate.

#### RESULTS

? In the experimental group, the low signal of PMSCc could be detected in the transplanted tumor, and the signal and parameter values of PMSCc and tumor changed dynamically over time, Labeling of human placental mesenchymal stem cells with ultra-micro and superparamagnetic iron oxide nanoparticles, the T2 and T2\* values of the transplanted tumors in the experimental group and the control group were  $73.004 \pm 1.529$ ,  $80.357 \pm 4.347$  ( $P < 0.05$ ). ? The growth curves of transplanted tumors in the two groups are similar and there were statistical differences in volume change ( $P < 0.05$ ), inhibitory rate is positive.

#### CONCLUSION

s 3.0T MRI can safely and effectively track PMSCs in vivo. PMSCs have directional chemotaxis to CRC, can accumulate into tumors, and finally inhibit tumor growth through the interaction of promotion and inhibition of tumor growth at different stages.

#### CLINICAL RELEVANCE/APPLICATION

Provide basic research data for the targeted therapy of placental mesenchymal stem cells in colorectal cancer.

#### M5B-SPNMMI-2 Reliability of Deauville Scale for Lymphoma PET Assessment in FIL, IELSG and SAKK Multi-center Clinical Trials

#### Participants

Fabrizio Bergesio, (*Presenter*) Nothing to Disclose

#### PURPOSE

Deauville scale (DS) is the recommended scoring system for reporting Positron Emission Tomography (PET/CT) in FDG-avid lymphoma. In this work we evaluated the reliability of the DS used in multi-center trials of Italian Foundation Lymphoma (FIL), International Extranodal Lymphoma Study Group (IELSG) and Swiss Group for Clinical Cancer Research (SAKK).

#### METHODS AND MATERIALS

Six trials were included in this analysis: FOLL12 (Follicular Lymphoma, ePET), DLCL10 (Diffuse Large B-Cell Lymphoma, ePET), ROUGE (Advanced-stage classical Hodgkin Lymphoma, iPET and ePET), ELDDL (Classical Hodgkin Lymphoma, iPET), IELSG37 (Primary Mediastinal Large B-Cell Lymphoma, ePET), SAKK3819 (Diffuse Large B-Cell Lymphoma, training dataset (tPET) of 40pts). PET/CT images were independently reviewed by a group of nuclear medicine physicians blinded to patient history, clinical data and treatment outcome. The reference lesion was visually scored according to DS. For each study we evaluated the reliability among all

reviewers using: the Krippendorff Alpha (KA) calculated on the discrete (d) 5-point scale and the Cohen Kappa (CK) calculated on the binary PET positive/negative scale using different trial-related threshold of positivity and the percentage overall agreement (OA), the positive agreement (PA), the negative agreement (NA) as the ratio of number of concordant cases plus half of the number of discordant cases respect to the number of cases.

## RESULTS

729ePET (641PET-/88PET+) included in the FIL-FOLL12 trial were reviewed by 6 expertise; the KA, CK,OA, PA, NA values were 0.30, 0.62, 0.92, 0.77, 0.94 respectively. 108ePET (86PET-/22PET+) included in the FIL-DLCL10 trial were reviewed by 5 expertise; the KA, CK, OA, PA, NA values were 0.37, 0.65, 0.88, 0.75, 0.91 respectively.455ePET (239PET-/216PET+) included in the IELSG37 trial were reviewed by 6 expertise; the KA, CK, OA, PA, NA values were 0.49, 0.75, 0.86, 0.86, 0.87 respectively.465 iPET (391PET-/74PET+) and 428ePET (374PET-/54PET+) included in the FIL-ROUGE trial were reviewed by 5 expertise. For iPET the KA, CK, OA, PA, NA values were 0.36, 0.75, 0.94, 0.95, 0.93 respectively. For ePET the KA, CK, OA, PA, NA values were 0.30, 0.75, 0.95, 0.95, 0.94 respectively. 69iPET (50PET-/19PET+) included in the FIL-ELDHL trial were reviewed by 3 expertise; the KA, CK, OA, PA, NA values were 0.40, 0.65, 0.95, 0.95, 0.94 respectively.40 tPET (22PET-/18PET+) included in the training set of SAKK3819 trial were reviewed by 5 expertise; the KA, CK, OA, PA, NA values were 0.48, 0.85, 0.93, 0.94, 0.91 respectively.

## CONCLUSION

s The results show that the Deauville Score is a reproducible technique in clinical trials using FDG-PET/CT for response assessment in several lymphomas diseases

## CLINICAL RELEVANCE/APPLICATION

Clinical Trial

### **M5B-SPNMMI-3 68Ga-DOTATATE PET/MRI for Detection of Liver Metastases from Gastro-entero-pancreatic (GEP) Neuroendocrine Tumors (NETs): A Multi-reader Study**

Participants

Apama Singh, MBBS, Rochester, MN (*Presenter*) Nothing to Disclose

## PURPOSE

To determine if additional list-mode liver PET during 68Ga-DOTATATE PET/MRI increases the diagnostic performance for liver metastases detection vis-à-vis whole-body (WB) PET/MR and liver MR in patients with GEP NETs.

## METHODS AND MATERIALS

In this IRB-approved, HIPAA-compliant retrospective study, 50 patients with GEP NETs underwent a 68Ga-DOTATATE PET/MRI, which included WB PET/MRI followed by focused list-mode respiratory-compensated liver PET and simultaneous co-acquisition of gadoxetate-enhanced liver MR sequences. Liver lesions on WB PET, focused PET, and MR image-sets were independently evaluated by three blinded fellowship-trained radiologists in separate sessions spaced at least 2-weeks apart for number, localization, etiology (benign, metastases, indeterminate), and conspicuity (definitely present, equivocal, definitely absent). Reference standard was histopathology or clinico-radiological follow-up.

## RESULTS

There were 127 liver metastases (98 DOTATATE-avid, 29 non-DOTATATE-avid) in 34 patients whereas 16 patients had benign lesions or no metastases. Lesion-based analyses showed highest sensitivity (95% CI) for focused PET [76.6% (72.1-80.8%)] followed by MRI [74.8% (70.1-79.1%)] and WB PET [70.1% (65.2-74.6%)]. Accuracy was also highest for focused PET [73.3% (68.9-77.2%)] followed by WB PET [68.4% (63.9-72.6%)] and MRI [64.8% (60.7-68.7%)]. Interrater agreement was good for all three image-sets but was highest for focused PET (Fleiss' kappa 0.82) followed by WB PET (0.78) and MRI (0.61),  $p=0.03$ .

## CONCLUSION

s List-mode liver PET during 68Ga-DOTATATE PET/MRI increases the diagnostic performance for liver metastases vis-à-vis WB PET/MR and gadoxetate-enhanced liver MR in patients with GEP NETs.

## CLINICAL RELEVANCE/APPLICATION

A 68Ga-DOTATATE PET/MRI protocol, which includes list-mode respiratory-compensated liver PET with co-acquisition of gadoxetate-enhanced liver MR, can be a one-stop-shop staging exam for patients with GEP NETs.

Printed on: 02/07/23

## Abstract Archives of the RSNA, 2022

M5B-SPNMMI-1

### **MRI Dynamic Tracing Study of the Effect of PLL-USPIONS-PMSCc Molecular Probe on Colorectal Cancer Xenografts in Nude Mice**

Monday, Nov. 28 12:45PM - 1:15PM Room: Learning Center - NMMI DPS

#### **Participants**

Hua He, MMedSc, MMedSc, Yinchuan, China (*Presenter*) Nothing to Disclose

#### **PURPOSE**

Human placental mesenchymal stem cells (PMSCs) labeled with polylysine-ultramicro and superparamagnetic oxide nano-iron particle protein complexes and transplanted into colorectal cancer (CRC) animal models, to explore the feasibility of molecular imaging of PLL-USPIONS-PMSCc targeting CRC tumor-bearing mice and the effect of PMSCs on CRC.

#### **METHODS AND MATERIALS**

PMSCs were cultured, transfected with polylysine (PLL), and PMSCs-PLL were magnetically labeled with USPIO, the PLL-USPIONS-PMSCc molecular probe was transplanted into the experimental group colorectal cancer animal model through the tail vein of the rat, in the same way, 200  $\mu$ l of PBS without cells was injected into the tumor of the tumor-bearing mice as a blank control, T2WI, T2 mapping, T2\* mapping sequences were used to observe the signal distribution and change characteristics of transplanted tumor and PMSCc, observation of the signal distribution and change characteristics in the two groups of transplanted tumors measured the size, T2, T2\* value of tumor, calculated inhibition rate.

#### **RESULTS**

? In the experimental group, the low signal of PMSCc could be detected in the transplanted tumor, and the signal and parameter values of PMSCc and tumor changed dynamically over time, Labeling of human placental mesenchymal stem cells with ultra-micro and superparamagnetic iron oxide nanoparticles, the T2 and T2\* values of the transplanted tumors in the experimental group and the control group were  $73.004 \pm 1.529$ ,  $80.357 \pm 4.347$  ( $P < 0.05$ ). ? The growth curves of transplanted tumors in the two groups are similar and there were statistical differences in volume change ( $P < 0.05$ ), inhibitory rate is positive.

#### **CONCLUSION**

s 3.0T MRI can safely and effectively track PMSCs in vivo. PMSCs have directional chemotaxis to CRC, can accumulate into tumors, and finally inhibit tumor growth through the interaction of promotion and inhibition of tumor growth at different stages.

#### **CLINICAL RELEVANCE/APPLICATION**

Provide basic research data for the targeted therapy of placental mesenchymal stem cells in colorectal cancer.

Printed on: 02/07/23

## Abstract Archives of the RSNA, 2022

M5B-SPNMMI-2

### Reliability of Deauville Scale for Lymphoma PET Assessment in FIL, IELSG and SAKK Multi-center Clinical Trials

Monday, Nov. 28 12:45PM - 1:15PM Room: Learning Center - NMMI DPS

#### Participants

Fabrizio Bergesio, (*Presenter*) Nothing to Disclose

#### PURPOSE

Deauville scale (DS) is the recommended scoring system for reporting Positron Emission Tomography (PET/CT) in FDG-avid lymphoma. In this work we evaluated the reliability of the DS used in multi-center trials of Italian Foundation Lymphoma (FIL), International Extranodal Lymphoma Study Group (IELSG) and Swiss Group for Clinical Cancer Research (SAKK).

#### METHODS AND MATERIALS

Six trials were included in this analysis: FOLL12 (Follicular Lymphoma, ePET), DLCL10 (Diffuse Large B-Cell Lymphoma, ePET), ROUGE (Advanced-stage classical Hodgkin Lymphoma, iPET and ePET), ELDHL (Classical Hodgkin Lymphoma, iPET) IELSG37 (Primary Mediastinal Large B-Cell Lymphoma, ePET). SAKK3819 (Diffuse Large B-Cell Lymphoma, training dataset (tPET) of 40pts). PET/CT images were independently reviewed by a group of nuclear medicine physicians blinded to patient history, clinical data and treatment outcome. The reference lesion was visually scored according to DS. For each study we evaluated the reliability among all reviewers using: the Krippendorff Alpha (KA) calculated on the discrete (d) 5-point scale and the Cohen Kappa (CK) calculated on the binary PET positive/negative scale using different trial-related threshold of positivity and the percentage overall agreement (OA), the positive agreement (PA), the negative agreement (NA) as the ratio of number of concordant cases plus half of the number of discordant cases respect to the number of cases.

#### RESULTS

729ePET (641PET-/88PET+) included in the FIL-FOLL12 trial were reviewed by 6 expertise; the KA, CK, OA, PA, NA values were 0.30, 0.62, 0.92, 0.77, 0.94 respectively. 108ePET (86PET-/22PET+) included in the FIL-DLCL10 trial were reviewed by 5 expertise; the KA, CK, OA, PA, NA values were 0.37, 0.65, 0.88, 0.75, 0.91 respectively. 455ePET (239PET-/216PET+) included in the IELSG37 trial were reviewed by 6 expertise; the KA, CK, OA, PA, NA values were 0.49, 0.75, 0.86, 0.86, 0.87 respectively. 465 iPET (391PET-/74PET+) and 428ePET (374PET-/54PET+) included in the FIL-ROUGE trial were reviewed by 5 expertise. For iPET the KA, CK, OA, PA, NA values were 0.36, 0.75, 0.94, 0.95, 0.93 respectively. For ePET the KA, CK, OA, PA, NA values were 0.30, 0.75, 0.95, 0.95, 0.94 respectively. 69iPET (50PET-/19PET+) included in the FIL-ELDHL trial were reviewed by 3 expertise; the KA, CK, OA, PA, NA values were 0.40, 0.65, 0.95, 0.95, 0.94 respectively. 40 tPET (22PET-/18PET+) included in the training set of SAKK3819 trial were reviewed by 5 expertise; the KA, CK, OA, PA, NA values were 0.48, 0.85, 0.93, 0.94, 0.91 respectively.

#### CONCLUSION

The results show that the Deauville Score is a reproducible technique in clinical trials using FDG-PET/CT for response assessment in several lymphomas diseases

#### CLINICAL RELEVANCE/APPLICATION

Clinical Trial

Printed on: 02/07/23

## Abstract Archives of the RSNA, 2022

M5B-SPNMMI-3

### **68Ga-DOTATATE PET/MRI for Detection of Liver Metastases from Gastro-entero-pancreatic (GEP) Neuroendocrine Tumors (NETs): A Multi-reader Study**

Monday, Nov. 28 12:45PM - 1:15PM Room: Learning Center - NMMI DPS

#### **Participants**

Aparna Singh, MBBS, Rochester, MN (*Presenter*) Nothing to Disclose

#### **PURPOSE**

To determine if additional list-mode liver PET during 68Ga-DOTATATE PET/MRI increases the diagnostic performance for liver metastases detection vis-à-vis whole-body (WB) PET/MR and liver MR in patients with GEP NETs.

#### **METHODS AND MATERIALS**

In this IRB-approved, HIPAA-compliant retrospective study, 50 patients with GEP NETs underwent a 68Ga-DOTATATE PET/MRI, which included WB PET/MRI followed by focused list-mode respiratory-compensated liver PET and simultaneous co-acquisition of gadoxetate-enhanced liver MR sequences. Liver lesions on WB PET, focused PET, and MR image-sets were independently evaluated by three blinded fellowship-trained radiologists in separate sessions spaced at least 2-weeks apart for number, localization, etiology (benign, metastases, indeterminate), and conspicuity (definitely present, equivocal, definitely absent). Reference standard was histopathology or clinico-radiological follow-up.

#### **RESULTS**

There were 127 liver metastases (98 DOTATATE-avid, 29 non-DOTATATE-avid) in 34 patients whereas 16 patients had benign lesions or no metastases. Lesion-based analyses showed highest sensitivity (95% CI) for focused PET [76.6% (72.1-80.8%)] followed by MRI [74.8% (70.1-79.1%)] and WB PET [70.1% (65.2-74.6%)]. Accuracy was also highest for focused PET [73.3% (68.9-77.2%)] followed by WB PET [68.4% (63.9-72.6%)] and MRI [64.8% (60.7-68.7%)]. Interrater agreement was good for all three image-sets but was highest for focused PET (Fleiss' kappa 0.82) followed by WB PET (0.78) and MRI (0.61),  $p=0.03$ .

#### **CONCLUSION**

s List-mode liver PET during 68Ga-DOTATATE PET/MRI increases the diagnostic performance for liver metastases vis-à-vis WB PET/MR and gadoxetate-enhanced liver MR in patients with GEP NETs.

#### **CLINICAL RELEVANCE/APPLICATION**

A 68Ga-DOTATATE PET/MRI protocol, which includes list-mode respiratory-compensated liver PET with co-acquisition of gadoxetate-enhanced liver MR, can be a one-stop-shop staging exam for patients with GEP NETs.

Printed on: 02/07/23



## Abstract Archives of the RSNA, 2022

M5B-SPNPM

### Noninterpretive Skills/Quality Improvement/Practice Management Monday Poster Discussions - B

Monday, Nov. 28 12:45PM - 1:15PM Room: Learning Center - NPM DPS

#### Participants

Madelene C. Lewis, MD, Mt Pleasant, SC (*Moderator*) Nothing to Disclose

#### Sub-Events

#### M5B-SPNPM-1 Current Status and Trends in Diversity by Race, Ethnicity, and Sex among US Diagnostic Radiology Trainees

#### Participants

Kamil Abu-Shaban, BEng, (*Presenter*) Nothing to Disclose

#### PURPOSE

To assess the current status and trends in the diversity of the U.S. diagnostic radiology resident workforce by race, ethnicity, and sex from 2011 to 2020.

#### METHODS AND MATERIALS

Publicly available data was obtained from the Accreditation Council for Graduate Medical Education (ACGME) website regarding US radiology trainees between 2011 and 2020. The most recent demographic data for US medical students was derived from the American Association of Medical Colleges (AAMC) in 2019. Chi-square was used to compare 2011 vs. 2020 URM data, 2020 URM vs. 2020 US Census data, and 2020 URM data vs. 2019 AAMC data. Least-squares linear regression was used to quantify trends in URM representation from 2011-2020.

#### RESULTS

In 2011, 53.7% of trainees were White, 16.7% Asian or Pacific Islander, 2.4% Hispanic, 2.2% Black or African American, 0.28% Native American/Alaskan and 24.78% Other/Unknown. In 2020, 51.27% of trainees were White, 22.7% Asian or Pacific Islander, 4.8% Hispanic, 3.8% Black or African American, 0.30% Native American/Alaskan and 17.1% Other/Unknown. Comparing overall URM percentage from 2011-2020, racial and ethnic URM representation increased for all radiology trainees (4.9% to 9.2%,  $p < .001$ ). Analysis of all other ACGME specialties on average did not show a significant increase in URM percentage (9.6% to 11.5%,  $p = .06$ ). URM percentage in radiology is still less than that of all other ACGME specialties on average in 2020 (9.2% vs. 11.5%,  $p < .001$ ) and 2019 AAMC medical student URM data (9.2% vs 11.1%,  $p < .001$ ). In 2020, the percentage of female radiology trainees was 25.8% compared to 26.7% in 2011, a statistically significant decrease on Chi-square analysis ( $p < .05$ ). Female percentage in radiology trainees was also less than all other specialties in 2020 (25.8% vs. 45.1%,  $p < .001$ ). Comparing the 2020 US census to our results, we found that radiology trainees have less URM in terms of race/ethnicity (31.5% vs. 9.2%,  $p < .001$ ) and female representation (50.8% vs. 25.8%,  $p < .001$ ).

#### CONCLUSION

Though there have been significant increases in URM representation in radiology since 2011, URM trainees remain underrepresented in diagnostic radiology programs. Finally, females remain under-represented, a figure that has statistically worsened since 2011.

#### CLINICAL RELEVANCE/APPLICATION

To recruit the best and brightest, program directors should increase efforts to increase the diversity of radiology programs.

#### M5B-SPNPM-2 Demographics and Life Experiences of International Medical Graduates: Survey Results from IMG Applicants for Radiology Residency

#### Participants

Fernando Rivera-Melendez, Catano, PR (*Presenter*) Nothing to Disclose

#### PURPOSE

International Medical Graduates (IMGs) comprise approximately 25% of the US physician workforce and bring a plethora of diverse life experiences to residency programs. Our purpose was to characterize the demographic characteristics and life experiences of IMG applicants to radiology residency programs using survey data.

#### METHODS AND MATERIALS

Survey questions were modified from the validated AAMC Matriculating Student Questionnaire. Survey participants were derived from a virtual multi-institution Radiology Bootcamp session focused on pathways for success for IMGs interested in Radiology. The survey was emailed in advance to participants. IRB deemed that this anonymous voluntary survey met criteria for exemption.

#### RESULTS

84 respondents met criteria for study inclusion among 92 participants (response rate 91%). Of eligible respondents, 80% were Non-US IMGs and 20% were US IMGs. 19% were Black/African American, 41% were Asian, and 22% were Hispanic/Latinx, a statistically significantly higher proportion of URM trainees compared with US radiology residents ( $p < 0.001$ ). 42% were women; a statistically significantly higher proportion of female trainees compared with US radiology residents ( $p = 0.03$ ). 2% of participants reported a disability. 39% stated that English was their primary language and were fluent in an average of 2.2 languages (range 1-5). 62% of participants reported that they have used an Electronic Health Records system. Before applying to radiology residency, 37% reported practicing independently as physicians, 56% published peer-reviewed papers, 49% presented research findings at conferences/meetings, and 44% participated in leadership positions at local or national societies. Regarding practice plans, 43% plan to practice in underserved areas, 80% were interested in participating in patient care, 79% expressed interest in participating in research, and 75% expressed interested in teaching.

## CONCLUSION

In comparison with the demographics of current radiology residents, international medical graduate applicants to radiology residency programs represent a more diverse applicant pool with an array of professional skills and life experiences.

## CLINICAL RELEVANCE/APPLICATION

Radiology residency programs should consider applications from international medical graduates as a vehicle to enrich training programs with diverse trainees with rich life experiences.

## M5B-SPNPM-3 Finding the Bamboo Ceiling: AAPI Faculty Composition in Academic Radiology

Participants

Dylan Sadowsky, Lakeland, FL (*Presenter*) Nothing to Disclose

## PURPOSE

The purpose of this study is to examine the current distribution of Asian American and Pacific Islander (AAPI) Radiology faculty in medical schools with respect to rank in relation to other demographics.

## METHODS AND MATERIALS

A cross sectional study was performed using the AAMC's 2020 U.S. Medical School Faculty website via Table 19: U.S. Medical School Faculty by Sex, Race/Ethnicity, Rank, and Department, 2020.1 The total number of full-time faculty at all US medical school's radiology departments in each rank (Professor, Associate Professor, Assistant Professor, and Instructor) and the total number of Asian and Native Hawaiian or other Pacific Islander in each of these ranks in 2020 were identified and included. Chi-square analysis was performed to compare the groups at each rank.

## RESULTS

4,395 Radiologists were included in the data with 997 (22.7%) reported to be of AAPI origin. Chi-square analysis of AAPI vs non-AAPI faculty at the Full Professor (12.6% vs 19%), Associate Professor (16.8% vs 20.0%), Assistant Professor (58.1% vs 52.3%), and instructor (12.5% vs 8.8%) ranks were performed demonstrating statistically significant differences in observed versus expected composition ( $p < 0.00001$ ). Of the Asian or Pacific Islanders included, 126 (12.6%), 167 (16.8%), 579 (58.1%), and 125 (12.5%) held the title of professor, associate professor, assistant professor, or instructor, respectively. As opposed to all other races who had 646 (19%), 678 (20.0%), 1776 (52.3%), and 298 (8.8%) professors, associate professors, assistant professors, or instructors, respectively. The chi squared statistic was found to be 39.65 and  $p < 0.01$ . Faculty rank composition when normalized (% at Rank/% AAPI) was 0.72, 0.87, 1.08, 1.30 for Full professor, Associate professor, Assistant professor and instructor levels, respectively.

## CONCLUSION

This study suggests that there are relatively fewer upper level AAPI faculty and more junior AAPI faculty within academic radiology. Nationally, organizations in multidisciplinary fields such as medicine and law have strengthened their commitment to fighting racism and racial inequity.

## CLINICAL RELEVANCE/APPLICATION

Further studies and interventions to address this disparity are warranted to investigate potential racial imbalances in medicine.

Printed on: 02/07/23



## Abstract Archives of the RSNA, 2022

M5B-SPNPM-1

### Current Status and Trends in Diversity by Race, Ethnicity, and Sex among US Diagnostic Radiology Trainees

Monday, Nov. 28 12:45PM - 1:15PM Room: Learning Center - NPM DPS

#### Participants

Kamil Abu-Shaban, BEng, (Presenter) Nothing to Disclose

#### PURPOSE

To assess the current status and trends in the diversity of the U.S. diagnostic radiology resident workforce by race, ethnicity, and sex from 2011 to 2020.

#### METHODS AND MATERIALS

Publicly available data was obtained from the Accreditation Council for Graduate Medical Education (ACGME) website regarding US radiology trainees between 2011 and 2020. The most recent demographic data for US medical students was derived from the American Association of Medical Colleges (AAMC) in 2019. Chi-square was used to compare 2011 vs. 2020 URM data, 2020 URM vs. 2020 US Census data, and 2020 URM data vs. 2019 AAMC data. Least-squares linear regression was used to quantify trends in URM representation from 2011-2020.

#### RESULTS

In 2011, 53.7% of trainees were White, 16.7% Asian or Pacific Islander, 2.4% Hispanic, 2.2% Black or African American, 0.28% Native American/Alaskan and 24.78% Other/Unknown. In 2020, 51.27% of trainees were White, 22.7% Asian or Pacific Islander, 4.8% Hispanic, 3.8% Black or African American, 0.30% Native American/Alaskan and 17.1% Other/Unknown. Comparing overall URM percentage from 2011-2020, racial and ethnic URM representation increased for all radiology trainees (4.9% to 9.2%,  $p < .001$ ). Analysis of all other ACGME specialties on average did not show a significant increase in URM percentage (9.6% to 11.5%,  $p = .06$ ). URM percentage in radiology is still less than that of all other ACGME specialties on average in 2020 (9.2% vs. 11.5%,  $p < .001$ ) and 2019 AAMC medical student URM data (9.2% vs 11.1%,  $p < .001$ ). In 2020, the percentage of female radiology trainees was 25.8% compared to 26.7% in 2011, a statistically significant decrease on Chi-square analysis ( $p < .05$ ). Female percentage in radiology trainees was also less than all other specialties in 2020 (25.8% vs. 45.1%,  $p < .001$ ). Comparing the 2020 US census to our results, we found that radiology trainees have less URM in terms of race/ethnicity (31.5% vs. 9.2%,  $p < .001$ ) and female representation (50.8% vs. 25.8%,  $p < .001$ ).

#### CONCLUSION

Though there have been significant increases in URM representation in radiology since 2011, URM trainees remain underrepresented in diagnostic radiology programs. Finally, females remain under-represented, a figure that has statistically worsened since 2011.

#### CLINICAL RELEVANCE/APPLICATION

To recruit the best and brightest, program directors should increase efforts to increase the diversity of radiology programs.

Printed on: 02/07/23



## Abstract Archives of the RSNA, 2022

M5B-SPNPM-2

### Demographics and Life Experiences of International Medical Graduates: Survey Results from IMG Applicants for Radiology Residency

Monday, Nov. 28 12:45PM - 1:15PM Room: Learning Center - NPM DPS

#### Participants

Fernando Rivera-Melendez, Catano, PR (*Presenter*) Nothing to Disclose

#### PURPOSE

International Medical Graduates (IMGs) comprise approximately 25% of the US physician workforce and bring a plethora of diverse life experiences to residency programs. Our purpose was to characterize the demographic characteristics and life experiences of IMG applicants to radiology residency programs using survey data.

#### METHODS AND MATERIALS

Survey questions were modified from the validated AAMC Matriculating Student Questionnaire. Survey participants were derived from a virtual multi-institution Radiology Bootcamp session focused on pathways for success for IMGs interested in Radiology. The survey was emailed in advance to participants. IRB deemed that this anonymous voluntary survey met criteria for exemption.

#### RESULTS

84 respondents met criteria for study inclusion among 92 participants (response rate 91%). Of eligible respondents, 80% were Non-US IMGs and 20% were US IMGs. 19% were Black/African American, 41% were Asian, and 22% were Hispanic/Latinx, a statistically significantly higher proportion of URM trainees compared with US radiology residents ( $p < 0.001$ ). 42% were women; a statistically significantly higher proportion of female trainees compared with US radiology residents ( $p = 0.03$ ). 2% of participants reported a disability. 39% stated that English was their primary language and were fluent in an average of 2.2 languages (range 1-5). 62% of participants reported that they have used an Electronic Health Records system. Before applying to radiology residency, 37% reported practicing independently as physicians, 56% published peer-reviewed papers, 49% presented research findings at conferences/meetings, and 44% participated in leadership positions at local or national societies. Regarding practice plans, 43% plan to practice in underserved areas, 80% were interested in participating in patient care, 79% expressed interest in participating in research, and 75% expressed interested in teaching.

#### CONCLUSION

In comparison with the demographics of current radiology residents, international medical graduate applicants to radiology residency programs represent a more diverse applicant pool with an array of professional skills and life experiences.

#### CLINICAL RELEVANCE/APPLICATION

Radiology residency programs should consider applications from international medical graduates as a vehicle to enrich training programs with diverse trainees with rich life experiences.

Printed on: 02/07/23



## Abstract Archives of the RSNA, 2022

M5B-SPNPM-3

### Finding the Bamboo Ceiling: AAPI Faculty Composition in Academic Radiology

Monday, Nov. 28 12:45PM - 1:15PM Room: Learning Center - NPM DPS

#### Participants

Dylan Sadowsky, Lakeland, FL (*Presenter*) Nothing to Disclose

#### PURPOSE

The purpose of this study is to examine the current distribution of Asian American and Pacific Islander (AAPI) Radiology faculty in medical schools with respect to rank in relation to other demographics.

#### METHODS AND MATERIALS

A cross sectional study was performed using the AAMC's 2020 U.S. Medical School Faculty website via Table 19: U.S. Medical School Faculty by Sex, Race/Ethnicity, Rank, and Department, 2020.1 The total number of full-time faculty at all US medical school's radiology departments in each rank (Professor, Associate Professor, Assistant Professor, and Instructor) and the total number of Asian and Native Hawaiian or other Pacific Islander in each of these ranks in 2020 were identified and included. Chi-square analysis was performed to compare the groups at each rank.

#### RESULTS

4,395 Radiologists were included in the data with 997 (22.7%) reported to be of AAPI origin. Chi-square analysis of AAPI vs non-AAPI faculty at the Full Professor (12.6% vs 19%), Associate Professor (16.8% vs 20.0%), Assistant Professor (58.1% vs 52.3%), and instructor (12.5% vs 8.8%) ranks were performed demonstrating statistically significant differences in observed versus expected composition ( $p < 0.00001$ ). Of the Asian or Pacific Islanders included, 126 (12.6%), 167 (16.8%), 579 (58.1%), and 125 (12.5%) held the title of professor, associate professor, assistant professor, or instructor, respectively. As opposed to all other races who had 646 (19%), 678 (20.0%), 1776 (52.3%), and 298 (8.8%) professors, associate professors, assistant professors, or instructors, respectively. The chi squared statistic was found to be 39.65 and  $p < 0.01$ . Faculty rank composition when normalized (% at Rank/% AAPI) was 0.72, 0.87, 1.08, 1.30 for Full professor, Associate professor, Assistant professor and instructor levels, respectively.

#### CONCLUSION

s This study suggests that there are relatively fewer upper level AAPI faculty and more junior AAPI faculty within academic radiology. Nationally, organizations in multidisciplinary fields such as medicine and law have strengthened their commitment to fighting racism and racial inequity.

#### CLINICAL RELEVANCE/APPLICATION

Further studies and interventions to address this disparity are warranted to investigate potential racial imbalances in medicine.

Printed on: 02/07/23

## Abstract Archives of the RSNA, 2022

M5B-SPNR

### Neuroradiology Monday Poster Discussions - B

Monday, Nov. 28 12:45PM - 1:15PM Room: Learning Center - NR DPS

#### Participants

Alexander Khalaf, MD, Stanford, CA (*Moderator*) Nothing to Disclose

#### Sub-Events

### M5B-SPNR-1 Occlusion Type, Number of Recanalization Passages and Dose Program Determine Radiation Dose in Endovascular Stroke Thrombectomy

#### Participants

Gregor Peter, (*Presenter*) Nothing to Disclose

#### PURPOSE

Identification of independent treatment factors associated with high radiation exposure during endovascular mechanical thrombectomy (EMT) in acute ischemic stroke.

#### METHODS AND MATERIALS

This retrospective analysis included all patients treated by means of EMT during the 2-year-period 2017-2018 in a comprehensive stroke center. EMT were performed by four internal and three external certified neuroradiologists in a clinic overlapping on call system. Radiation exposure as the dependent variable (dose area product DAP, Gy x cm<sup>2</sup>) was dichotomized in <100 Gy x cm<sup>2</sup> and ≥100 Gy x cm<sup>2</sup>. Independent variables were age (<75 vs. ≥75 y), time of intervention (during vs. beyond workday), treating neuroradiologist (internal vs. external), occlusion type (mono vs. tandem), reperfusion success (TICI 0-2A vs. TICI 2B/3), recanalization attempts (=2 vs. >2) and dose protocol (normal dose in 2017 vs. low dose (LD) in 2018).

#### RESULTS

EMT treatments of 208 patients (111 female, 97 male, mean age 71.6 y) were analyzed. Median DAP was 86.6 Gy x cm<sup>2</sup> and could be reduced from 104.8 Gy x cm<sup>2</sup> (N=105 in 2017) to 73.3 Gy x cm<sup>2</sup> (N=103 in 2018) with LD program. Multivariable binary logistic regression analysis revealed a significantly increased radiation exposure (= 100 Gy x cm<sup>2</sup>) in tandem occlusion type (P<.001), >2 recanalization attempts (P<.001) and normal dose protocol (P=.002).

#### CONCLUSION

Tandem occlusion type and number of recanalization attempts are the dominant treatment factors for the amount of radiation exposure in stroke EMT. Modern dose reduction programs can significantly reduce the radiation exposure in EMT for patients and for the medical staff and should be implemented routinely.

#### CLINICAL RELEVANCE/APPLICATION

Future reference discussion or extensive radiation doses in specific patients should consider the aspects of this study.

### M5B-SPNR-11 Optimization For the Contrast Enhancement at Head Computed Tomography Angiography by Using the Patient Body Size Indexes

#### Participants

Hiroyasu Sanai, RT, Kurashiki, Japan (*Presenter*) Nothing to Disclose

#### PURPOSE

Head computed tomography angiography (CTA) is noninvasive, easy to acquire, and offers excellent detail in identifying site and nature of the lesion. Even if head CTA is performed with the same protocol, the contrast enhancement (CE) differs depending on the patient body size. The purpose of this study was to investigate whether body size indexes (BSI) such as the height, body weight, body mass index, body surface area, lean body weight, and blood volume that calculated by height and body weight estimated middle cerebral artery CE on head CTA scans.

#### METHODS AND MATERIALS

This retrospective study was approved by our institutional review board; informed patient consent was waived. Between April 2020 and October 2021, 99 patients with vascular disease underwent head CTA. The CT number (in Hounsfield units, HU) of the middle cerebral artery at proximal (M1) on unenhanced scans and arterial phase scans was recorded. We calculated changes in the contrast enhancement per iodine dose (HU / gI) (CEID) to evaluate the correlation with BSI. We performed linear regression analyses between CEID and BSI.

#### RESULTS

The CEID of the middle cerebral artery during arterial phase was 15.8 ± 4.1 HU / gI. CEID and BSA showed the strongest inverse

correlation ( $r = 0.779$ ). Among the BSI used in our study, BSA was the most important estimated factor the CEDI of the middle cerebral artery on head CTA acquired during the arterial phase.

## CONCLUSION

s The BSA exhibited the strongest correlation with middle cerebral artery contrast enhancement during the arterial phase.

## CLINICAL RELEVANCE/APPLICATION

BSA tailor contrast injection methods was superior other BSI parameters during the head CTA.

### M5B-SPNR-12 Precise Assessment of Penumbra in Patients with Acute Anterior Circulation Ischemic Stroke by the Multiphase MR Angiography Collateral Map

Participants

Hyun Jeong Kim, MD, PhD, (*Presenter*) Nothing to Disclose

## PURPOSE

Precise collateral and penumbra assessment can identify individual diversity of infarct progression and assist appropriate treatment decision making in patient with acute ischemic stroke. This study is to verify the ability of the multiphase MR angiography collateral map (Cmap) to estimate penumbra in patients with acute ischemic stroke due to large vessel steno-occlusion in the anterior circulation.

## METHODS AND MATERIALS

The secondary analysis of an ongoing prospective observational study included data from participants with acute ischemic stroke due to occlusion or stenosis of the internal carotid artery and/or the middle cerebral artery (M1 or M2 segment) within 8 hours of onset to MR acquisition time and without change in baseline steno-occlusive lesion on follow-up angiography. We measured the volume ratios of follow-up and baseline DWI lesions (lesion growth ratio),  $T_{max} > 6$  seconds lesion and baseline DWI lesion ( $T_{max}/DWI$  mismatch ratio), and, of the Cmap at admission, hypoperfused lesions on immediately preceded phase of the baseline DWI lesion phase and on baseline DWI lesion phase which has the coincided hypoperfused area with the baseline DWI lesion (Cmap mismatch ratio). We compared sensitivity, specificity, accuracy, and AUC of Cmap mismatch ratio and  $T_{max}/DWI$  mismatch ratio in lesion growth and evaluated concordance correlation of  $T_{max}/DWI$  mismatch ratio and Cmap mismatch ratio with lesion growth ratio.

## RESULTS

From March 2016 to March 2021, among 566 participants, 48 participants (27 males, mean age 75) were included. The sensitivities of Cmap and  $T_{max}$  in lesion growth were 97% and 93.9% ( $P=0.56$ ), the specificities were 100% and 80.0% ( $P=0.08$ ), the accuracies were 97.9% and 89.6% ( $P=0.10$ ), and the AUC were 1.0 and 0.84 ( $P=0.04$ ), respectively. The concordance correlation coefficients of Cmap mismatch ratio and  $T_{max}/DWI$  mismatch ratio with lesion growth ratio were 0.95 (95% CI, 0.92-0.97) and 0.28 (95% CI 0.17-0.39), respectively. The difference of concordance correlation coefficients of Cmap mismatch ratio and  $T_{max}/DWI$  mismatch ratio with lesion growth ratio was 0.66 (95% CI 0.34-0.96). Cmap was superior to  $T_{max}$  in prediction of lesion growth and Cmap mismatch ratio was better correlated with infarct growth ratio than  $T_{max}/DWI$  mismatch ratio, significantly.

## CONCLUSION

s Individual-based assessment of penumbra of patients with acute ischemic stroke due to large vessel steno-occlusion in anterior circulation is possible with Cmap.

## CLINICAL RELEVANCE/APPLICATION

Cmap was derived from dynamic contrast-enhanced MR angiography (DCE-MRA). Therefore, within 3 minutes of imaging time for DWI and DCE-MRA, we can estimate baseline infarct volume, causative vessel location, collateral-perfusion status, and penumbra precisely.

### M5B-SPNR-13 Cortical Venous Blood Velocity Changes and Its Value in Predicting Prognosis in Acute Ischemic Stroke Patients with Large Vessel Occlusion

Participants

Jingjie Wang, (*Presenter*) Nothing to Disclose

## PURPOSE

We aimed to explore the cortical venous blood velocity changes in acute ischemic stroke patients with large vessel occlusion (LVO-AIS) and to explore its value in predicting prognosis.

## METHODS AND MATERIALS

The whole-brain 4D-CTA/CTP data and clinical data of LVO-AIS were collected from June 2020 to October 2021. A group of normal 4D-CTA/CTP data was gathered as a control group. The venous inflow time (VIT), the venous peak time (VPT), and the venous outflow time (VOT) of the cerebral cortex on both sides of the patients and the healthy control group were recorded and analyzed. Statistical description and comparison among VIT/VPT/VOT of both sides of patients and the healthy control groups were performed. Then, VIT, VPT, and VOT of patients with different prognoses were then statistically described and compared between groups. Third, logistic regression analysis was used to explore the relationship between the three venous times and prognosis. Finally, ROC curves were drawn to assess the value of the altered cortical vein imaging in predicting prognosis.

## RESULTS

149 LVO-AIS patients and 73 healthy controls were collected. VIT, VPT, and VOT on the patients' both sides showed a significant delay ( $p < 0.05$ ). There were significant differences in VIT and VPT on both sides between the patients with good and poor prognoses ( $p < 0.05$ ). Logistic regression for all the patients showed that VPT on the affected side, arterial collateral score, and NIHSS were independent predictors of poor prognosis, with a correct percentage of 79.6%, AUC of NIHSS was larger (0.786), the AUC of VPT (0.697) on the affected side were smaller. Logistic regression for patients onset within 24 hours showed that VPT on the affected side and NIHSS were independent predictors of poor prognosis, with a correct percentage of 91.5%. the AUC of the NIHSS remains larger (0.753) but declined, while the AUC of VPT (0.711) on the affected side rose.

## CONCLUSION

s Cortical venous blood velocity significantly altered on both the affected and healthy side of LVO-AIS patients. The delayed ipsilateral VPT in LVO-AIS patients can be used as a new imaging indicator to predict poor prognosis.

## CLINICAL RELEVANCE/APPLICATION

The slow venous flow may provide marked information about collateral circulation. The 4D-CTA imaging offers specific blood velocity information to assess the relationship between poor cortical venous visualization and clinical outcomes of LVO-AIS in the early stage. Therefore, we propose quantifying the speed of cortical vein development on the affected side of LVO-AIS using a whole-brain 4D-CTA/CTP technique and exploring the time markers and values of cortical vein development.

## M5B-SPNR- Sex Differences in Intracranial Atherosclerotic Plaques Among Patients with Ischemic Stroke 14

Participants

Xuejiao Yan, (*Presenter*) Nothing to Disclose

## PURPOSE

High-risk intracranial arterial plaques are the most common cause of ischemic stroke and their characteristics vary between male and female patients. However, sex differences in intracranial plaques among symptomatic patients have rarely been discussed. This study aimed to evaluate sex differences in intracranial atherosclerotic plaques among Chinese patients with cerebral ischemia.

## METHODS AND MATERIALS

One hundred and ten patients who experienced ischemic events underwent 3T cardiovascular magnetic resonance vessel wall scanning for the evaluation of intracranial atherosclerotic disease. Each plaque was classified according to its likelihood of causing a stroke (as culprit, uncertain, or non-culprit). The outer wall area (OWA) and lumen area of the lesion and reference sites were measured, and the wall and plaque areas, remodeling ratio, and plaque burden (characterized by a normalized wall index) were further calculated. The composition (T1 hyperintensity, enhancement) and morphology (surface irregularity) of each plaque were analyzed. Sex differences in intracranial plaque characteristics were compared between male and female patient groups.

## RESULTS

Overall, 311 plaques were detected in 110 patients with ischemic stroke (81 and 29 male and female patients, respectively). The OWA ( $P < 0.001$ ) and wall area ( $P < 0.001$ ) of intracranial arterial lesions were significantly larger in male patients. Regarding culprit plaques, the plaque burden in male patients was similar to that in female patients ( $P = 0.178$ , odds ratio [OR]: 0.168, 95% confidence interval [CI]: -0.020 to 0.107). However, the prevalence of plaque T1 hyperintensity was significantly higher than that in female patients ( $P = 0.005$ , OR: 15.362, 95% CI: 2.280 to 103.49). In the overall ischemic stroke sample, intracranial T1 hyperintensity was associated with male sex (OR: 13.480, 95% CI: 2.444-74.354,  $P = 0.003$ ), systolic blood pressure (OR: 1.019, 95% CI: 1.002-1.036,  $P = 0.031$ ), and current smoker (OR: 3.245, 95% CI: 1.097-9.598,  $P = 0.033$ ).

## CONCLUSION

s For patients with ischemic stroke, the intracranial plaque burden in male patients was similar to that in female patients; however, the plaque characteristics in male patients are associated with higher risk, especially in culprit plaques.

## CLINICAL RELEVANCE/APPLICATION

Our findings highlight the sex-specific characteristics of intracranial atherosclerotic plaques. The results suggest that men with ischemic stroke, while having a similar intracranial plaque burden to women, have a higher plaque risk profile, especially for culprit plaques. multi-contrast CMR vessel wall imaging can help stroke patients of different sexes better understand their atherosclerosis risk and further optimize their clinical management.

## M5B-SPNR- Assessing Management of Acute Ischemic Stroke Using DICOM-Timestamps 15

Participants

Alexander Rau, MD, Freiburg, Germany (*Presenter*) Nothing to Disclose

## PURPOSE

Since the management of acute stroke is time crucial, time data are relevant for both research and quality management. In routine clinical practice, these time data are often not reliably captured and documented. We investigated the value of image-based time data as captured automatically in the DICOM format.

## METHODS AND MATERIALS

We enrolled data from two independent stroke centres ( $n=3.151$  and  $n=2.092$ ). Data from the first centre was assessed whether cases with large-vessel-occlusion (LVO,  $n=1.095$ ), small-vessel-occlusions (SVO,  $n=422$ ) and no occlusion ( $n=1634$ ) show different arrival times at the hospital. The DICOM-tag StudyTime was used to analyse the distribution of scan times throughout the day. A convolutional probabilistic model for the distribution was generated with the following assumptions: (A) probability of stroke is uniform throughout the day, (B) people go to sleep at 21:00+/-3h and wake up at 7:00+/-3h, (C) ambulance transport follows combined gaussian and exponential distribution (Fig. 1).

## RESULTS

The temporal distribution at both centres was exceptionally consistent with a peak around 10:00 AM. No relevant difference was found between vascular occlusion groups (large, small, and no occlusions) regarding their arrival time at the hospital. The real-world data and the simulation using a probabilistic model showed very good agreement.

## CONCLUSION

s DICOM-timestamps can be used to assess the time course of management of acute ischemic stroke. Using this data we observed a peak of scans at 10.00 AM which can be explained with a probabilistic model describing a patient waking up, realising new symptoms, calling an ambulance and being transported to hospital. Furthermore, patients with large vessel occlusion do not seem to wake up earlier due to their stroke.

## CLINICAL RELEVANCE/APPLICATION

DICOM-timestamp analysis has the potential to serve as a tool for quality control, optimised resource management, and stroke research in general since they are always automatically captured by the imaging devices as opposed to manual data collection in routine clinical practice.

### M5B-SPNR- 16 **Assessment of Intracranial Atherosclerotic Disease Using PETRA-MRA: Comparison of 3D-TOF and CTA with DSA**

Participants

Junxia Niu, MD, (*Presenter*) Nothing to Disclose

#### PURPOSE

Noninvasive assessment of intracranial atherosclerotic disease is important to manage ischemic stroke patients. 3D pointwise encoding time reduction magnetic resonance angiography (PETRA-MRA) is a promising non-contrast magnetic resonance angiography (MRA) technique for intracranial stenosis assessment. However, few previous studies have compared the diagnostic performance of PETRA-MRA with digital subtraction angiography (DSA) for intracranial atherosclerotic assessment relative to 3D time-of-flight (TOF), magnetic resonance angiography (MRA) and computed tomography angiography (CTA). The study's aim was to evaluate the diagnostic performance of PETRA-MRA, TOF-MRA and CTA, using DSA as a reference standard in patients with intracranial arterial stenosis.

#### METHODS AND MATERIALS

Thirty-eight patients with 66 intracranial arterial plaques (age  $56 \pm 10$  years, 25males) underwent PETRA-MRA, TOF-MRA, CTA and DSA within 1 month. The image quality of MRAs and CTA were graded on a 1-4 scale (1= poor, 4 = excellent) independently by three radiologists. The degree of stenosis and lesion length were measured by two radiologists independently on all imaging modalities.

#### RESULTS

There was an excellent interreader agreement for the stenosis and lesion length assessment on PETRA-MRA, TOF-MRA, CTA and DSA (ICCs > 0.95). PETRA-MRA, TOF-MRA and CTA had excellent image quality ( $3.98 \pm 0.12$ ,  $3.95 \pm 0.21$ ,  $3.94 \pm 0.24$ ,  $P=0.249$ ). PETRA-MRA had better agreement with DSA for stenosis measurements comparing with TOF-MRA and CTA (ICC = 0.92 vs. 0.88, 0.81). PETRA-MRA had higher sensitivity and specificity for detecting stenosis >50% than TOF-MRA and CTA; TOF-MRA had higher sensitivity and specificity for detecting stenosis >75% than PETRA-MRA and CTA, using DSA as the standard. CTA overestimated the degree of stenosis compared to DSA ( $64.3 \pm 20.0$  vs.  $53.3 \pm 18.9\%$ ,  $p = 0.001$ ), while PETRA-MRA and TOF-MRA didn't ( $54.9 \pm 18.1$  vs.  $53.3 \pm 18.9\%$ ,  $p = 0.41$ ;  $55.9 \pm 17.7$  vs.  $53.3 \pm 18.9\%$ ,  $p = 0.68$ ). PETRA-MRA and TOF-MRA had better agreement with DSA for lesion length measurements compared with CTA (ICC = 0.98, 0.97 vs. 0.74).

#### CONCLUSION

PETRA-MRA is accurate for quantifying intracranial arterial stenosis compared with DSA and performs better than TOF-MRA and CTA in stenosis >50%. TOF-MRA performs better than PETRA-MRA and CTA in stenosis >70%. CTA overestimated the degree of stenosis compared to DSA. In lesion length, all 3 images perform well with DSA.

## CLINICAL RELEVANCE/APPLICATION

Comparing with TOF-MRA and CTA, PETRA-MRA is less sensitive to motion effects, can improve flow dephasing to better demonstrate the artery lumina and has the acoustic noise attenuation which is beneficial to the child, the pregnant and the manic patient vulnerable to the noise.

### M5B-SPNR- 17 **Optimal Scan Number of Whole-brain CT Perfusion in Patients with Acute Ischemic Stroke**

Participants

Sentaro Takada, MD, Kumamoto, Japan (*Presenter*) Nothing to Disclose

#### PURPOSE

Computed tomographic perfusion (CTP) imaging is useful for determining the treatment strategy of acute ischemic stroke. The optimal scanning protocol of CTP to obtain reliable lesion volumes with CTP has not been fully established. We aimed to investigate the optimal scanning protocol of CTP in patients with acute ischemic stroke.

#### METHODS AND MATERIALS

This study included 29 consecutive patients with acute ischemic stroke (13 men, 26 women; mean age 77.5 years) who underwent whole-brain CTP on a 320-slice multidetector CT scanner. The data acquisition parameters for dynamic volume scanning were  $320 \times 0.5$ -mm detector collimation, 1.0-s tube rotation time, 100-mA tube current, and 80-kVp tube voltage. Twenty-three sampling scans were performed at the following varied intervals: 2 passes every 3 seconds intended for the prearrival baseline, 16 passes every 1.5 seconds targeting the rise and fall of enhancement, and 5 passes at 5-second intervals to complete and extend the temporal sampling window for 70.5 seconds. The penumbra and core volumes obtained from full imaging data were compared to those obtained from 3/4 and 1/2 imaging data. RAPID was used for penumbra and core quantification; their thresholds were 6-second increase in T<sub>max</sub> compared to healthy side for penumbra and 30% reduction in cerebral blood flow compared to healthy side for core. Spearman correlation coefficient and Bland-Altman analysis were used for the statistical analysis.

#### RESULTS

The penumbra and core volumes obtained from the full, the 3/4, and 1/2 data were  $103.9 \pm 69.7$  ml and  $13.3 \pm 24.0$  ml,  $102.2 \pm 72.0$  ml and  $13.7 \pm 24.2$  ml, and  $102.3 \pm 69.9$  ml and  $13.3 \pm 24.9$  ml, respectively. There was no significant difference between the three groups in penumbra and core volume (penumbra,  $P = 0.99$  and core,  $P = 0.097$ ). Spearman correlation coefficient showed a good agreement between the penumbra and core volumes generated from full and 1/2 data (penumbra,  $R = 0.991$  and core,  $R = 0.999$ ). Bland-Altman analysis showed the mean difference ( $\pm 2SD$ ) for 1/2 data of penumbra and ischemic core volume against full data was 1.6 ml ( $\pm 18.7$ ) and 0.1 ml ( $\pm 2.6$ ).

#### CONCLUSION

In patients with acute ischemic stroke, whole-brain CTP images with half scan data may provide equivalent diagnostic value

compared with full scan data.

#### **CLINICAL RELEVANCE/APPLICATION**

Whole-brain CTP can reduce scan data by half and may reduce radiation exposure.

#### **M5B-SPNR-18 Anterior Ischemic Stroke: Analysis of the Multivariable CT-Based Models for Prediction of Clinical Outcome**

Participants

Aleksandr Drozdov, MD, El Paso, TX (*Presenter*) Nothing to Disclose

#### **PURPOSE**

To determine the predictive value of multiple CT- based measurements, individually and collectively, including arterial collateral filling (AC), tissue perfusion parameters, as well as cortical (CV) and medullary venous (MV) outflow, in patients with acute ischemic stroke (AIS).

#### **METHODS AND MATERIALS**

We retrospectively reviewed a database of patients with AIS in the middle cerebral artery distribution, who were evaluated by multiphase CT-angiography and perfusion. AC pial filling was evaluated using a scoring system described by Menon et al. The CV system was scored by the adopted PRECISE system as described by Parthasarathy et al. The MV status was evaluated using a method described by Drozdov et al. The perfusion parameters were calculated using the FDA-approved automated software. A good clinical outcome was defined as a Modified Rankin Scale of 0-2 at 90 days.

#### **RESULTS**

A total of 64 patients were included. Each of the CT-based measurements were able to predict clinical outcome independently ( $P < 0.05$ ). AC pial filling model did slightly better compared to other measurement models (AUC = 0.659, OR 4.11 (1.35-12.54)) vs CV (AUC=0.644, OR 3.29 (1.16 - 9.3)) vs MV (AUC=0.609 OR 6.17 (1.76 - 21.64)). Among perfusion parameters, the best prediction model was core size  $<30$  ml vs  $\geq 30$  ml (AUC=0.629 OR 4.64 (1.13 - 17.7)). In multivariable modeling with two variables, AC combined with MV had the highest predictive value (AUC=0.721) followed by MV and CV (AUC=0.711). For other combinations, the AUC ranged from 0.684 to 0.698. Multivariable modeling with all 4 variables resulted in the highest predictive value AUC=0.763.

#### **CONCLUSION**

A model using the combination of multiple CT- based measurements is highly predictive of clinical outcomes in acute ischemic stroke and does better compared to the individual measurements alone

#### **CLINICAL RELEVANCE/APPLICATION**

The combination of arterial collateral flow, tissue perfusion, and venous outflow provides a more accurate prediction of clinical outcomes in AIS and performs better than each variable on its own. This additive effect of these techniques suggests that the information collected by each of these methods is only partially overlapping.

#### **M5B-SPNR-19 Recurrent IDH-wild-type Glioblastoma: Association of Baseline Restricted Diffusion Pattern and Tumor Enhancement Volume with Repeat Resection Free Survival**

Participants

David Timaran Montenegro, MD, Houston, TX (*Presenter*) Nothing to Disclose

#### **PURPOSE**

Despite advances in therapeutical options for glioblastoma, the overall prognosis remains poor with only 5.1% of patients surviving 5 years. Standard regimens include surgery and chemoradiation therapy. Repeat resection is a potential treatment option for recurrence aimed to control neurological symptoms and extend overall survival (OS). Recent studies, however, have reported that repeat resection may increase complications and may not benefit OS. Therefore, we aim to evaluate if baseline MRI may predict repeat resection free survival among patients with recurrent IDH-wild-type glioblastoma

#### **METHODS AND MATERIALS**

A single center, retrospective study of a prospectively maintained database of 161 patients with glioblastomas was performed. Fifteen (9.3%) subjects with IDH mutant glioblastomas were excluded. Overall, 146 patients, 86 men (59%) and 60 women (41%), with a median age of 61 years (interquartile range [IQR], 52-68 years) treated with surgical resection were enrolled. Baseline brain MRIs were assessed using the VASARI criteria and semiautomated tumoral segmentation. Linear regression analysis was used to assess associations between tumor volumes and time to repeat resection. Kaplan Meir curve and Long Rank test were used for survival analysis

#### **RESULTS**

In total, 37 patients (25%) required repeat resection at a median time of 6.4 months (IQR, 3.9-10.9 months) due to tumor recurrence. Out of the 25 VASARI criteria, only restricted diffusion was found to affect repeat resection free survival. At 3, 6, 12 and 24 months, overall repeat resection free survival for patients with restricted diffusion was 94%, 29%, 0% and 0% versus 86%, 42%, 28% and 14% for patients with mixed restricted/facilitated diffusion and 92%, 77%, 38% and 7% in patients with facilitated diffusion, respectively (Log-rank/Mantel-Cox estimate, 9.09) ( $p=0.01$ ). In addition, regression analysis revealed that tumor enhancement volumes were associated with repeat resection free survival ( $p=0.04$ ). Patients with tumor enhancement volumes equal or greater than 32 ml had resection free survival rates of 100%, 75%, 50% and 37% at 3, 6, 12 and 24 months, respectively, versus patients with lower tumor enhancement volumes with survival rates of 93%, 44%, 10% and 0%

#### **CONCLUSION**

Patients with IDH-wild-type glioblastomas that had intralesional restricted diffusion and lower enhancing volumes were associated with lower repeat resection rates at 3, 6, 12 and 24 months compared to patients with tumoral facilitated diffusion and larger tumor enhancement volumes

#### **CLINICAL RELEVANCE/APPLICATION**

Our results provide information that will help to determine prognosis of patients with wild type glioblastomas.

## **M5B-SPNR-20 The Statin Medication Efficacy on Intracranial Atherosclerotic Plaque and Its Influencing Factors: A Magnetic Resonance Vessel Wall Imaging Study**

Participants

Cong Liu, (*Presenter*) Nothing to Disclose

### **PURPOSE**

To investigate the value of magnetic resonance vessel wall imaging (VWI) in evaluating the efficacy of statins on intracranial atherosclerotic plaque, and analyze the clinical and plaque characteristics that may be related with the treatment efficacy.

### **METHODS AND MATERIALS**

A total of 53 patients with intracranial atherosclerotic disease and treated with statins were enrolled in this study. All patients underwent VWI scans during the baseline and follow-up period. The plaque characteristics, including plaque length, plaque thickness, plaque burden, the degree of vascular stenosis, the degree of plaque enhancement, vascular remodeling and plaque location were measured. The patient's clinical information at baseline was also collected. The patients were divided into two groups according to the tri-sectional quantiles of rate change of every plaque characteristic (good responder and poor responder). The difference of patient's clinical and plaque characteristics at baseline between the two groups was analyzed with t test, rank sum test or Chi-square test, and the relationship between patient's clinical and plaque characteristics and medication efficacy was assessed with multiple linear regression.

### **RESULTS**

Compared with the baseline, the plaque thickness (1.30[1.05-1.50]mm vs. 1.30[1.20-1.50]mm,  $p=0.016$ ), plaque burden (51.42[33.47-76.98]% vs. 61.39[38.81-83.74]%,  $p=0.001$ ), vessel stenosis (30.00[18.00-54.50]% vs. 39.39[21.00-63.04]%,  $p=0.001$ ) and plaque enhancement (122.3 $\pm$ 49.7% vs. 148.8 $\pm$ 43.1%,  $p<0.001$ ) were significantly reduced in patients after treated with statins, especially in patients treated with statins for more than 6 months. The history of hypertension ( $B=0.188$ ,  $SE=0.086$ ,  $P=0.034$ ) and baseline BMI (kg/m<sup>2</sup>,  $B=0.043$ ,  $SE=0.013$ ,  $P=0.002$ ) were negatively correlated with the reduction of plaque enhancement, while the medication period (month,  $B=-0.03$ ,  $SE=0.011$ ,  $P=0.008$ ) and baseline plaque enhancement ( $B=-0.215$ ,  $SE=0.103$ ,  $P=0.043$ ) were positively correlated with the reduction of plaque enhancement.

### **CONCLUSION**

In this study, we confirmed with VWI that statins can stabilize intracranial atherosclerotic plaques, and the therapeutic effects of statins on intracranial atherosclerotic plaques may have relationship with some of the patient's clinical and plaque characteristics at baseline.

### **CLINICAL RELEVANCE/APPLICATION**

Compared with conventional luminal imaging techniques, VWI can directly provide more detailed plaque morphological information and help assess the statin medication efficacy on intracranial atherosclerotic plaque.

## **M5B-SPNR-4 Comparison of High-Resolution Vessel Wall Magnetic Resonance Imaging with Time of Flight Angiography to Detect Luminal Stenosis in Ischemic Stroke**

Participants

Joel Samuel, MBBS, MD, (*Presenter*) Nothing to Disclose

### **PURPOSE**

Ischemic stroke inflicts a major disease burden worldwide. Assessment of the lumen of intracranial vasculature using magnetic resonance angiography or CT angiography is the conventional method for evaluating pathology in the culprit vessel. High-resolution vessel wall magnetic resonance imaging is an emerging method which allows direct visualization of the vessel wall pathology. In addition, vessel wall imaging sequences can also be used to detect the extent of luminal stenosis. We compare the diagnostic performance of time-of-flight magnetic resonance angiography against vessel wall imaging sequences for detecting luminal stenosis in patients presenting with ischemic stroke. Vessel wall imaging was taken as the reference test. We further determine the correlation between the degree of stenosis in time-of-flight MR angiography and vessel wall imaging sequences.

### **METHODS AND MATERIALS**

A prospective observational study conducted from 2019 - 2020, with a sample size of 150. The study group was patients with a clinical diagnosis of stroke, without hemorrhage on computed tomography, within the age of 18 - 70. Time of flight magnetic resonance angiography and vessel wall images were obtained using a 1.5T MRI system. The images were analyzed by a single observer. The presence of stenosis in the vascular territory of the infarcted region was determined, and the most stenotic lesion was taken as the culprit plaque. The percentage of stenosis was calculated by WASID criteria.

### **RESULTS**

Time of flight magnetic resonance angiography had acceptable performance (AUC 0.896, sensitivity 85.9% and specificity 93.3%) but poor negative predictive value (42.1%) for detection of stenosis with vessel wall imaging as the reference standard. Spearman rank order correlation between degree of stenosis on vessel wall imaging and time-of-flight angiography showed statistically significant but moderate correlation ( $r = 0.715$ ).

### **CONCLUSION**

Vessel wall imaging has superior diagnostic power to detect and quantify luminal stenosis compared to time-of-flight magnetic resonance angiography. Vessel wall imaging has a unique ability to detect non stenotic vulnerable plaques.

### **CLINICAL RELEVANCE/APPLICATION**

The conventional time-of-flight angiography sequence in MR stroke protocols can be replaced by a vessel wall imaging sequence, yielding greater diagnostic information without significant increase in acquisition times.

## **M5B-SPNR-5 The Clinical Significance of the Hyperintense Acute Reperfusion Marker Sign in Subacute Stroke**

Participants  
Ji Young Lee, MD, Seoul, Korea, Republic Of (*Presenter*) Nothing to Disclose

#### **PURPOSE**

The hyperintense acute reperfusion marker (HARM) is characterized by the delayed enhancement of the subarachnoid or subpial space observed on postcontrast fluid-attenuated inversion recovery (FLAIR) images, and is considered a cerebral reperfusion marker for various brain disorders, including infarction. In this study, we evaluated the cerebral distribution patterns of HARM for discriminating between an enhancing subacute infarction and an enhancing mass located in the cortex and subcortical white matter.

#### **METHODS AND MATERIALS**

We analyzed consecutive patients who experienced a subacute ischemic stroke, were hospitalized, and underwent conventional brain magnetic resonance imaging including postcontrast FLAIR within 14 days from symptom onset, as well as those who had lesions corresponding to a clinical sign detected by diffusion-weighted imaging and postcontrast T1-weighted imaging between May 2019 and May 2021. A total of 199 patients were included in the study. Of them, 94 were finally included in the subacute infarction group. During the same period, 76 enhancing masses located in the cortex or subcortical white matter, which were subcategorized as metastasis, malignant glioma, and lymphoma, were analyzed. We analyzed the overall incidence of HARM in subacute ischemic stroke cases, and compared the enhancement patterns between cortical infarctions and cortical masses.

#### **RESULTS**

Among 94 patients with subacute stroke, 78 patients (83%) presented HARM, and among 76 patients with subcortical masses, 48 patients (63%) presented peripheral rim enhancement. Of 170 subcortical enhancing lesions, 88 (51.8%) showed HARM, and 78 (88.6%) were determined to be subacute infarction. Among 94 patients with subacute stroke, 48 patients (51%) had diffusion restrictions, and HARM was found in 39 patients (81.2%). Of the 46 patients (49%) without diffusion restriction, 39 patients (84.8%) showed HARM.

#### **CONCLUSION**

The presence of HARM was significantly associated with subacute infarctions. For the masses, a peripheral rim enhancement pattern was observed around the mass rather than the cerebral sulci on postcontrast FLAIR.

#### **CLINICAL RELEVANCE/APPLICATION**

We found that HARM with enhancing subcortical nodules was highly suggestive of subacute infarctions, and recommended a postcontrast FLAIR sequence for differentiating the ischemic subcortical infarctions from malignant lesions such as small metastasis.

### **M5B-SPNR-7 Towards Personalized Radiotherapy: Tumor Growth Modeling May Supplement Traditional Radiotherapy Planning in Glioblastoma**

Participants  
Marie-Christin Metz, MD, (*Presenter*) Nothing to Disclose

#### **PURPOSE**

One of the main challenges in the treatment of glioblastoma is the prediction of their individual growth behavior to guide more accurate radiotherapy after resection. Here, we introduce a new, deep learning - based tumor growth model which partially exceeds standard radiotherapy plans in covering the recurrence area.

#### **METHODS AND MATERIALS**

Our recently developed tumor growth model is based on a novel deep learning solver of the inverse problem in a Fisher-Kolmogorov growth model. We applied it to 30 cases of our prospective glioma cohort by utilizing FLAIR-, T2-, T1-, and T1-CE-data and compared volume and recurrence coverage with standard radiotherapy plans that were registered to the recurrence image. Statistical analysis was performed by applying Wilcoxon Signed Rank Test.

#### **RESULTS**

Depending on the chosen cut-off value of the predicted tumor cell density we saw a comparable target volume ( $p = 0.769$ ) with slight improvement of the covered recurrence area (mean improvement was 0.8% for a cut-off value of 50% for predicted tumor cell density with no significant difference due to the small sample size,  $p = 0.797$ ). The growth maps especially performed better in tumors with a highly diffuse growth pattern which exceed the traditional radiotherapy margins but are well captured in the estimated tumor spread from the growth model.

#### **CONCLUSION**

Here, we showed that utilizing a novel, deep learning - based tumor growth model for glioblastoma performed at least equally well to traditional radiotherapy plans in terms of recurrence coverage in our cohort, showing promise to improve in particular the planning of radiotherapy for highly infiltrative tumors. In a next step, we aim to correlate the calculated values with biological markers of proliferation and infiltration and validate our assumptions on larger data sets.

#### **CLINICAL RELEVANCE/APPLICATION**

Deep learning- based tumor growth modeling in glioblastoma carries potential to inform more personalized radiotherapy plans by predicting individual tumor spread. This may improve patient outcome in the future.

### **M5B-SPNR-9 Evaluation of A Deep Learning Model For The Detection Of Ischemic Acute Stroke Lesions And Assessment Of ASPECTS On Non-contrast CT Scans: A Multicenter Study**

Participants  
Weidao Chen, Beijing, China (*Presenter*) Nothing to Disclose

#### **PURPOSE**

Early detection of ischemia and assessing Alberta Stroke Project Early CT Score (ASPECTS) on non-contrast computed tomography

Early detection of ischemia and assessing Alberta Stroke Project Early CT Score (ASPECTS) on non-contrast computed tomography (NCCT) plays a crucial role in the treatment of acute ischemic stroke (AIS). We aim to develop a robust deep learning (DL) model for automated detection of AIS lesions and assessment of ASPECTS based on NCCT images

## **METHODS AND MATERIALS**

From January 2013 to December 2017, NCCT images of 1391 AIS patients (<6h from symptom onset to CT) from 5 hospitals were retrospectively collected and divided into the training dataset (n=1179) and internal validation dataset (n=212). Another 85 AIS patients from other three stroke centers were used as external validation dataset. All patients underwent follow-up diffusion-weighted (DW) MRI (within 24h after AIS), and the infarction regions on NCCT were manually contoured on DW MRI scans. A DL model was proposed for assessing ASPECTS, and model performance was evaluated with receiver operating characteristic (ROC) curve. The diagnostic performance of DL model was also compared with that of four experienced radiologists in the external validation dataset

## **RESULTS**

In total 4240 (212 patients × 20 regions) and 1700 (85 patients × 20 regions) ASPECT regions in the internal and external validation datasets were scored. The AUC of the DL model was 0.876 (95% CI, 0.846-0.907) in the internal validation dataset. The DL model exhibited good performance in the external dataset with AUC achieving 0.729 (95% CI, 0.679-0.779), and the performance was non-inferior to that of four experienced radiologists (all p values > 0.05). The diagnostic accuracy of four radiologists was improved after DL model assistance with average sensitivity and specificity increased from 25.4% and 89.6%, to 33.3% and 91.5%, while the average diagnostic time per-case was reduced from 219.0 sec to 175.7 sec (p < 0.01), respectively

## **CONCLUSION**

The NCCT-based DL model shows favorable performance and good robustness in multi-center validation datasets and can assist radiologists to achieve better performance for the early diagnosis of AIS

## **CLINICAL RELEVANCE/APPLICATION**

This multicenter study demonstrated the deep learning model for detection of infarction and assessment of ASPECTS score on non-contrast CT had good feasibility and reliability for AIS patients

Printed on: 02/07/23

## Abstract Archives of the RSNA, 2022

M5B-SPNR-1

### Occlusion Type, Number of Recanalization Passages and Dose Program Determine Radiation Dose in Endovascular Stroke Thrombectomy

Monday, Nov. 28 12:45PM - 1:15PM Room: Learning Center - NR DPS

#### Participants

Gregor Peter, (*Presenter*) Nothing to Disclose

#### PURPOSE

Identification of independent treatment factors associated with high radiation exposure during endovascular mechanical thrombectomy (EMT) in acute ischemic stroke.

#### METHODS AND MATERIALS

This retrospective analysis included all patients treated by means of EMT during the 2-year-period 2017-2018 in a comprehensive stroke center. EMT were performed by four internal and three external certified neuroradiologists in a clinic overlapping on call system. Radiation exposure as the dependent variable (dose area product DAP, Gy x cm<sup>2</sup>) was dichotomized in <100 Gy x cm<sup>2</sup> and ≥100 Gy x cm<sup>2</sup>. Independent variables were age (<75 vs. ≥75 y), time of intervention (during vs. beyond workday), treating neuroradiologist (internal vs. external), occlusion type (mono vs. tandem), reperfusion success (TICI 0-2A vs. TICI 2B/3), recanalization attempts (=2 vs. >2) and dose protocol (normal dose in 2017 vs. low dose (LD) in 2018).

#### RESULTS

EMT treatments of 208 patients (111 female, 97 male, mean age 71.6 y) were analyzed. Median DAP was 86.6 Gy x cm<sup>2</sup> and could be reduced from 104.8 Gy x cm<sup>2</sup> (N=105 in 2017) to 73.3 Gy x cm<sup>2</sup> (N=103 in 2018) with LD program. Multivariable binary logistic regression analysis revealed a significantly increased radiation exposure (= 100 Gy x cm<sup>2</sup>) in tandem occlusion type (P<.001), >2 recanalization attempts (P<.001) and normal dose protocol (P=.002).

#### CONCLUSION

Tandem occlusion type and number of recanalization attempts are the dominant treatment factors for the amount of radiation exposure in stroke EMT. Modern dose reduction programs can significantly reduce the radiation exposure in EMT for patients and for the medical staff and should be implemented routinely.

#### CLINICAL RELEVANCE/APPLICATION

Future reference discussion or extensive radiation doses in specific patients should consider the aspects of this study.

Printed on: 02/07/23



## Abstract Archives of the RSNA, 2022

M5B-SPNR-11

### Optimization For the Contrast Enhancement at Head Computed Tomography Angiography by Using the Patient Body Size Indexes

Monday, Nov. 28 12:45PM - 1:15PM Room: Learning Center - NR DPS

#### Participants

Hiroyasu Sanai, RT, Kurashiki, Japan (*Presenter*) Nothing to Disclose

#### PURPOSE

Head computed tomography angiography (CTA) is noninvasive, easy to acquire, and offers excellent detail in identifying site and nature of the lesion. Even if head CTA is performed with the same protocol, the contrast enhancement (CE) differs depending on the patient body size. The purpose of this study was to investigate whether body size indexes (BSI) such as the height, body weight, body mass index, body surface area, lean body weight, and blood volume that calculated by height and body weight estimated middle cerebral artery CE on head CTA scans.

#### METHODS AND MATERIALS

This retrospective study was approved by our institutional review board; informed patient consent was waived. Between April 2020 and October 2021, 99 patients with vascular disease underwent head CTA. The CT number (in Hounsfield units, HU) of the middle cerebral artery at proximal (M1) on unenhanced scans and arterial phase scans was recorded. We calculated changes in the contrast enhancement per iodine dose (HU / gI) (CEID) to evaluate the correlation with BSI. We performed linear regression analyses between CEID and BSI.

#### RESULTS

The CEID of the middle cerebral artery during arterial phase was  $15.8 \pm 4.1$  HU / gI. CEID and BSA showed the strongest inverse correlation ( $r = 0.779$ ). Among the BSI used in our study, BSA was the most important estimated factor the CEID of the middle cerebral artery on head CTA acquired during the arterial phase.

#### CONCLUSION

s The BSA exhibited the strongest correlation with middle cerebral artery contrast enhancement during the arterial phase.

#### CLINICAL RELEVANCE/APPLICATION

BSA tailor contrast injection methods was superior other BSI parameters during the head CTA.

Printed on: 02/07/23

## Abstract Archives of the RSNA, 2022

M5B-SPNR-12

### Precise Assessment of Penumbra in Patients with Acute Anterior Circulation Ischemic Stroke by the Multiphase MR Angiography Collateral Map

Monday, Nov. 28 12:45PM - 1:15PM Room: Learning Center - NR DPS

#### Participants

Hyun Jeong Kim, MD, PhD, (*Presenter*) Nothing to Disclose

#### PURPOSE

Precise collateral and penumbra assessment can identify individual diversity of infarct progression and assist appropriate treatment decision making in patient with acute ischemic stroke. This study is to verify the ability of the multiphase MR angiography collateral map (Cmap) to estimate penumbra in patients with acute ischemic stroke due to large vessel steno-occlusion in the anterior circulation.

#### METHODS AND MATERIALS

The secondary analysis of an ongoing prospective observational study included data from participants with acute ischemic stroke due to occlusion or stenosis of the internal carotid artery and/or the middle cerebral artery (M1 or M2 segment) within 8 hours of onset to MR acquisition time and without change in baseline steno-occlusive lesion on follow-up angiography. We measured the volume ratios of follow-up and baseline DWI lesions (lesion growth ratio), Tmax > 6 seconds lesion and baseline DWI lesion (Tmax/DWI mismatch ratio), and, of the Cmap at admission, hypoperfused lesions on immediately preceded phase of the baseline DWI lesion phase and on baseline DWI lesion phase which has the coincided hypoperfused area with the baseline DWI lesion (Cmap mismatch ratio). We compared sensitivity, specificity, accuracy, and AUC of Cmap mismatch ratio and Tmax/DWI mismatch ratio in lesion growth and evaluated concordance correlation of Tmax/DWI mismatch ratio and Cmap mismatch ratio with lesion growth ratio.

#### RESULTS

From March 2016 to March 2021, among 566 participants, 48 participants (27 males, mean age 75) were included. The sensitivities of Cmap and Tmax in lesion growth were 97% and 93.9% (P=0.56), the specificities were 100% and 80.0% (P=0.08), the accuracies were 97.9% and 89.6% (P=0.10), and the AUC were 1.0 and 0.84 (P=0.04), respectively. The concordance correlation coefficients of Cmap mismatch ratio and Tmax/DWI mismatch ratio with lesion growth ratio were 0.95 (95% CI, 0.92-0.97) and 0.28 (95% CI 0.17-0.39), respectively. The difference of concordance correlation coefficients of Cmap mismatch ratio and Tmax/DWI mismatch ratio with lesion growth ratio was 0.66 (95% CI 0.34-0.96). Cmap was superior to Tmax in prediction of lesion growth and Cmap mismatch ratio was better correlated with infarct growth ratio than Tmax/DWI mismatch ratio, significantly.

#### CONCLUSION

Individual-based assessment of penumbra of patients with acute ischemic stroke due to large vessel steno-occlusion in anterior circulation is possible with Cmap.

#### CLINICAL RELEVANCE/APPLICATION

Cmap was derived from dynamic contrast-enhanced MR angiography (DCE-MRA). Therefore, within 3 minutes of imaging time for DWI and DCE-MRA, we can estimate baseline infarct volume, causative vessel location, collateral-perfusion status, and penumbra precisely.

Printed on: 02/07/23

## Abstract Archives of the RSNA, 2022

M5B-SPNR-13

### Cortical Venous Blood Velocity Changes and Its Value in Predicting Prognosis in Acute Ischemic Stroke Patients with Large Vessel Occlusion

Monday, Nov. 28 12:45PM - 1:15PM Room: Learning Center - NR DPS

#### Participants

Jingjie Wang, (*Presenter*) Nothing to Disclose

#### PURPOSE

We aimed to explore the cortical venous blood velocity changes in acute ischemic stroke patients with large vessel occlusion (LVO-AIS) and to explore its value in predicting prognosis.

#### METHODS AND MATERIALS

The whole-brain 4D-CTA/CTP data and clinical data of LVO-AIS were collected from June 2020 to October 2021. A group of normal 4D-CTA/CTP data was gathered as a control group. The venous inflow time (VIT), the venous peak time (VPT), and the venous outflow time (VOT) of the cerebral cortex on both sides of the patients and the healthy control group were recorded and analyzed. Statistical description and comparison among VIT/VPT/VOT of both sides of patients and the healthy control groups were performed. Then, VIT, VPT, and VOT of patients with different prognoses were then statistically described and compared between groups. Third, logistic regression analysis was used to explore the relationship between the three venous times and prognosis. Finally, ROC curves were drawn to assess the value of the altered cortical vein imaging in predicting prognosis.

#### RESULTS

149 LVO-AIS patients and 73 healthy controls were collected. VIT, VPT, and VOT on the patients' both sides showed a significant delay ( $p < 0.05$ ). There were significant differences in VIT and VPT on both sides between the patients with good and poor prognoses ( $p < 0.05$ ). Logistic regression for all the patients showed that VPT on the affected side, arterial collateral score, and NIHSS were independent predictors of poor prognosis, with a correct percentage of 79.6%, AUC of NIHSS was larger (0.786), the AUC of VPT (0.697) on the affected side were smaller. Logistic regression for patients onset within 24 hours showed that VPT on the affected side and NIHSS were independent predictors of poor prognosis, with a correct percentage of 91.5%. the AUC of the NIHSS remains larger (0.753) but declined, while the AUC of VPT (0.711) on the affected side rose.

#### CONCLUSION

s Cortical venous blood velocity significantly altered on both the affected and healthy side of LVO-AIS patients. The delayed ipsilateral VPT in LVO-AIS patients can be used as a new imaging indicator to predict poor prognosis.

#### CLINICAL RELEVANCE/APPLICATION

The slow venous flow may provide marked information about collateral circulation. The 4D-CTA imaging offers specific blood velocity information to assess the relationship between poor cortical venous visualization and clinical outcomes of LVO-AIS in the early stage. Therefore, we propose quantifying the speed of cortical vein development on the affected side of LVO-AIS using a whole-brain 4D-CTA/CTP technique and exploring the time markers and values of cortical vein development.

Printed on: 02/07/23

## Abstract Archives of the RSNA, 2022

M5B-SPNR-14

### Sex Differences in Intracranial Atherosclerotic Plaques Among Patients with Ischemic Stroke

Monday, Nov. 28 12:45PM - 1:15PM Room: Learning Center - NR DPS

#### Participants

Xuejiao Yan, (*Presenter*) Nothing to Disclose

#### PURPOSE

High-risk intracranial arterial plaques are the most common cause of ischemic stroke and their characteristics vary between male and female patients. However, sex differences in intracranial plaques among symptomatic patients have rarely been discussed. This study aimed to evaluate sex differences in intracranial atherosclerotic plaques among Chinese patients with cerebral ischemia.

#### METHODS AND MATERIALS

One hundred and ten patients who experienced ischemic events underwent 3T cardiovascular magnetic resonance vessel wall scanning for the evaluation of intracranial atherosclerotic disease. Each plaque was classified according to its likelihood of causing a stroke (as culprit, uncertain, or non-culprit). The outer wall area (OWA) and lumen area of the lesion and reference sites were measured, and the wall and plaque areas, remodeling ratio, and plaque burden (characterized by a normalized wall index) were further calculated. The composition (T1 hyperintensity, enhancement) and morphology (surface irregularity) of each plaque were analyzed. Sex differences in intracranial plaque characteristics were compared between male and female patient groups.

#### RESULTS

Overall, 311 plaques were detected in 110 patients with ischemic stroke (81 and 29 male and female patients, respectively). The OWA ( $P < 0.001$ ) and wall area ( $P < 0.001$ ) of intracranial arterial lesions were significantly larger in male patients. Regarding culprit plaques, the plaque burden in male patients was similar to that in female patients ( $P = 0.178$ , odds ratio [OR]: 0.168, 95% confidence interval [CI]: -0.020 to 0.107). However, the prevalence of plaque T1 hyperintensity was significantly higher than that in female patients ( $P = 0.005$ , OR: 15.362, 95% CI: 2.280 to 103.49). In the overall ischemic stroke sample, intracranial T1 hyperintensity was associated with male sex (OR: 13.480, 95% CI: 2.444-74.354,  $P = 0.003$ ), systolic blood pressure (OR: 1.019, 95% CI: 1.002-1.036,  $P = 0.031$ ), and current smoker (OR: 3.245, 95% CI: 1.097-9.598,  $P = 0.033$ ).

#### CONCLUSION

For patients with ischemic stroke, the intracranial plaque burden in male patients was similar to that in female patients; however, the plaque characteristics in male patients are associated with higher risk, especially in culprit plaques.

#### CLINICAL RELEVANCE/APPLICATION

Our findings highlight the sex-specific characteristics of intracranial atherosclerotic plaques. The results suggest that men with ischemic stroke, while having a similar intracranial plaque burden to women, have a higher plaque risk profile, especially for culprit plaques. multi-contrast CMR vessel wall imaging can help stroke patients of different sexes better understand their atherosclerosis risk and further optimize their clinical management.

Printed on: 02/07/23

## Abstract Archives of the RSNA, 2022

M5B-SPNR-15

### Assessing Management of Acute Ischemic Stroke Using DICOM-Timestamps

Monday, Nov. 28 12:45PM - 1:15PM Room: Learning Center - NR DPS

#### Participants

Alexander Rau, MD, Freiburg, Germany (*Presenter*) Nothing to Disclose

#### PURPOSE

Since the management of acute stroke is time crucial, time data are relevant for both research and quality management. In routine clinical practice, these time data are often not reliably captured and documented. We investigated the value of image-based time data as captured automatically in the DICOM format.

#### METHODS AND MATERIALS

We enrolled data from two independent stroke centres (n=3.151 and n=2.092). Data from the first centre was assessed whether cases with large-vessel-occlusion (LVO, n=1.095), small-vessel-occlusions (SVO, n=422) and no occlusion (n=1634) show different arrival times at the hospital. The DICOM-tag StudyTime was used to analyse the distribution of scan times throughout the day. A convolutional probabilistic model for the distribution was generated with the following assumptions: (A) probability of stroke is uniform throughout the day, (B) people go to sleep at 21:00+/-3h and wake up at 7:00+/-3h, (C) ambulance transport follows combined gaussian and exponential distribution (Fig. 1).

#### RESULTS

The temporal distribution at both centres was exceptionally consistent with a peak around 10:00 AM. No relevant difference was found between vascular occlusion groups (large, small, and no occlusions) regarding their arrival time at the hospital. The real-world data and the simulation using a probabilistic model showed very good agreement.

#### CONCLUSION

s DICOM-timestamps can be used to assess the time course of management of acute ischemic stroke. Using this data we observed a peak of scans at 10.00 AM which can be explained with a probabilistic model describing a patient waking up, realising new symptoms, calling an ambulance and being transported to hospital. Furthermore, patients with large vessel occlusion do not seem to wake up earlier due to their stroke.

#### CLINICAL RELEVANCE/APPLICATION

DICOM-timestamp analysis has the potential to serve as a tool for quality control, optimised resource management, and stroke research in general since they are always automatically captured by the imaging devices as opposed to manual data collection in routine clinical practice.

Printed on: 02/07/23

## Abstract Archives of the RSNA, 2022

M5B-SPNR-16

### Assessment of Intracranial Atherosclerotic Disease Using PETRA-MRA: Comparison of 3D-TOF and CTA with DSA

Monday, Nov. 28 12:45PM - 1:15PM Room: Learning Center - NR DPS

#### Participants

Junxia Niu, MD, (Presenter) Nothing to Disclose

#### PURPOSE

Noninvasive assessment of intracranial atherosclerotic disease is important to manage ischemic stroke patients. 3D pointwise encoding time reduction magnetic resonance angiography (PETRA-MRA) is a promising non-contrast magnetic resonance angiography (MRA) technique for intracranial stenosis assessment. However, few previous studies have compared the diagnostic performance of PETRA-MRA with digital subtraction angiography (DSA) for intracranial atherosclerotic assessment relative to 3D time-of-flight (TOF), magnetic resonance angiography (MRA) and computed tomography angiography (CTA). The study's aim was to evaluate the diagnostic performance of PETRA-MRA, TOF-MRA and CTA, using DSA as a reference standard in patients with intracranial arterial stenosis.

#### METHODS AND MATERIALS

Thirty-eight patients with 66 intracranial arterial plaques (age  $56 \pm 10$  years, 25males) underwent PETRA-MRA, TOF-MRA, CTA and DSA within 1 month. The image quality of MRAs and CTA were graded on a 1-4 scale (1= poor, 4 = excellent) independently by three radiologists. The degree of stenosis and lesion length were measured by two radiologists independently on all imaging modalities.

#### RESULTS

There was an excellent interreader agreement for the stenosis and lesion length assessment on PETRA-MRA, TOF-MRA, CTA and DSA (ICCs > 0.95). PETRA-MRA, TOF-MRA and CTA had excellent image quality ( $3.98 \pm 0.12$ ,  $3.95 \pm 0.21$ ,  $3.94 \pm 0.24$ ,  $P=0.249$ ). PETRA-MRA had better agreement with DSA for stenosis measurements comparing with TOF-MRA and CTA (ICC = 0.92 vs. 0.88, 0.81). PETRA-MRA had higher sensitivity and specificity for detecting stenosis >50% than TOF-MRA and CTA; TOF-MRA had higher sensitivity and specificity for detecting stenosis >75% than PETRA-MRA and CTA, using DSA as the standard. CTA overestimated the degree of stenosis compared to DSA ( $64.3 \pm 20.0$  vs.  $53.3 \pm 18.9\%$ ,  $p = 0.001$ ), while PETRA-MRA and TOF-MRA didn't ( $54.9 \pm 18.1$  vs.  $53.3 \pm 18.9\%$ ,  $p = 0.41$ ;  $55.9 \pm 17.7$  vs.  $53.3 \pm 18.9\%$ ,  $p = 0.68$ ). PETRA-MRA and TOF-MRA had better agreement with DSA for lesion length measurements compared with CTA (ICC = 0.98, 0.97 vs. 0.74).

#### CONCLUSION

s PETRA-MRA is accurate for quantifying intracranial arterial stenosis compared with DSA and performs better than TOF-MRA and CTA in stenosis >50%. TOF-MRA performs better than PETRA-MRA and CTA in stenosis >70%. CTA overestimated the degree of stenosis compared to DSA. In lesion length, all 3 images perform well with DSA.

#### CLINICAL RELEVANCE/APPLICATION

Comparing with TOF-MRA and CTA, PETRA-MRA is less sensitive to motion effects, can improve flow dephasing to better demonstrate the artery lumina and has the acoustic noise attenuation which is beneficial to the child, the pregnant and the manic patient vulnerable to the noise.

Printed on: 02/07/23

## Abstract Archives of the RSNA, 2022

M5B-SPNR-17

### Optimal Scan Number of Whole-brain CT Perfusion in Patients with Acute Ischemic Stroke

Monday, Nov. 28 12:45PM - 1:15PM Room: Learning Center - NR DPS

#### Participants

Sentaro Takada, MD, Kumamoto, Japan (*Presenter*) Nothing to Disclose

#### PURPOSE

Computed tomographic perfusion (CTP) imaging is useful for determining the treatment strategy of acute ischemic stroke. The optimal scanning protocol of CTP to obtain reliable lesion volumes with CTP has not been fully established. We aimed to investigate the optimal scanning protocol of CTP in patients with acute ischemic stroke.

#### METHODS AND MATERIALS

This study included 29 consecutive patients with acute ischemic stroke (13 men, 26 women; mean age 77.5 years) who underwent whole-brain CTP on a 320-slice multidetector CT scanner. The data acquisition parameters for dynamic volume scanning were 320 × 0.5-mm detector collimation, 1.0-s tube rotation time, 100-mA tube current, and 80-kVp tube voltage. Twenty-three sampling scans were performed at the following varied intervals: 2 passes every 3 seconds intended for the prearrival baseline, 16 passes every 1.5 seconds targeting the rise and fall of enhancement, and 5 passes at 5-second intervals to complete and extend the temporal sampling window for 70.5 seconds. The penumbra and core volumes obtained from full imaging data were compared to those obtained from 3/4 and 1/2 imaging data. RAPID was used for penumbra and core quantification; their thresholds were 6-second increase in T<sub>max</sub> compared to healthy side for penumbra and 30% reduction in cerebral blood flow compared to healthy side for core. Spearman correlation coefficient and Bland-Altman analysis were used for the statistical analysis.

#### RESULTS

The penumbra and core volumes obtained from the full, the 3/4, and 1/2 data were 103.9 ± 69.7 ml and 13.3 ± 24.0 ml, 102.2 ± 72.0 ml and 13.7 ± 24.2 ml, and 102.3 ± 69.9 ml and 13.3 ± 24.9 ml, respectively. There was no significant difference between the three groups in penumbra and core volume (penumbra, P = 0.99 and core, P = 0.097). Spearman correlation coefficient showed a good agreement between the penumbra and core volumes generated from full and 1/2 data (penumbra, R = 0.991 and core, R = 0.999). Bland-Altman analysis showed the mean difference (± 2SD) for 1/2 data of penumbra and ischemic core volume against full data was 1.6 ml (± 18.7) and 0.1 ml (± 2.6).

#### CONCLUSION

s In patients with acute ischemic stroke, whole-brain CTP images with half scan data may provide equivalent diagnostic value compared with full scan data.

#### CLINICAL RELEVANCE/APPLICATION

Whole-brain CTP can reduce scan data by half and may reduce radiation exposure.

Printed on: 02/07/23



## Abstract Archives of the RSNA, 2022

M5B-SPNR-18

### Anterior Ischemic Stroke: Analysis of the Multivariable CT-Based Models for Prediction of Clinical Outcome

Monday, Nov. 28 12:45PM - 1:15PM Room: Learning Center - NR DPS

#### Participants

Aleksandr Drozdov, MD, El Paso, TX (*Presenter*) Nothing to Disclose

#### PURPOSE

To determine the predictive value of multiple CT- based measurements, individually and collectively, including arterial collateral filling (AC), tissue perfusion parameters, as well as cortical (CV) and medullary venous (MV) outflow, in patients with acute ischemic stroke (AIS).

#### METHODS AND MATERIALS

We retrospectively reviewed a database of patients with AIS in the middle cerebral artery distribution, who were evaluated by multiphase CT-angiography and perfusion. AC pial filling was evaluated using a scoring system described by Menon et al. The CV system was scored by the adopted PRECISE system as described by Parthasarathy et al. The MV status was evaluated using a method described by Drozdov et al. The perfusion parameters were calculated using the FDA-approved automated software. A good clinical outcome was defined as a Modified Rankin Scale of 0-2 at 90 days.

#### RESULTS

A total of 64 patients were included. Each of the CT-based measurements were able to predict clinical outcome independently ( $P < 0.05$ ). AC pial filling model did slightly better compared to other measurement models (AUC = 0.659, OR 4.11 (1.35-12.54)) vs CV (AUC=0.644, OR 3.29 (1.16 - 9.3)) vs MV (AUC=0.609 OR 6.17 (1.76 - 21.64)). Among perfusion parameters, the best prediction model was core size  $< 30$  ml vs  $\geq 30$  ml (AUC=0.629 OR 4.64 (1.13 - 17.7)). In multivariable modeling with two variables, AC combined with MV had the highest predictive value (AUC=0.721) followed by MV and CV (AUC=0.711). For other combinations, the AUC ranged from 0.684 to 0.698. Multivariable modeling with all 4 variables resulted in the highest predictive value AUC=0.763.

#### CONCLUSION

A model using the combination of multiple CT- based measurements is highly predictive of clinical outcomes in acute ischemic stroke and does better compared to the individual measurements alone

#### CLINICAL RELEVANCE/APPLICATION

The combination of arterial collateral flow, tissue perfusion, and venous outflow provides a more accurate prediction of clinical outcomes in AIS and performs better than each variable on its own. This additive effect of these techniques suggests that the information collected by each of these methods is only partially overlapping.

Printed on: 02/07/23

## Abstract Archives of the RSNA, 2022

M5B-SPNR-19

### Recurrent IDH-wild-type Glioblastoma: Association of Baseline Restricted Diffusion Pattern and Tumor Enhancement Volume with Repeat Resection Free Survival

Monday, Nov. 28 12:45PM - 1:15PM Room: Learning Center - NR DPS

#### Participants

David Timaran Montenegro, MD, Houston, TX (*Presenter*) Nothing to Disclose

#### PURPOSE

Despite advances in therapeutical options for glioblastoma, the overall prognosis remains poor with only 5.1% of patients surviving 5 years. Standard regimens include surgery and chemoradiation therapy. Repeat resection is a potential treatment option for recurrence aimed to control neurological symptoms and extend overall survival (OS). Recent studies, however, have reported that repeat resection may increase complications and may not benefit OS. Therefore, we aim to evaluate if baseline MRI may predict repeat resection free survival among patients with recurrent IDH-wild-type glioblastoma

#### METHODS AND MATERIALS

A single center, retrospective study of a prospectively maintained database of 161 patients with glioblastomas was performed. Fifteen (9.3%) subjects with IDH mutant glioblastomas were excluded. Overall, 146 patients, 86 men (59%) and 60 women (41%), with a median age of 61 years (interquartile range [IQR], 52-68 years) treated with surgical resection were enrolled. Baseline brain MRIs were assessed using the VASARI criteria and semiautomated tumoral segmentation. Linear regression analysis was used to assess associations between tumor volumes and time to repeat resection. Kaplan Meir curve and Long Rank test were used for survival analysis

#### RESULTS

In total, 37 patients (25%) required repeat resection at a median time of 6.4 months (IQR,3.9-10.9 months) due to tumor recurrence. Out of the 25 VASARI criteria, only restricted diffusion was found to affect repeat resection free survival. At 3, 6, 12 and 24 months, overall repeat resection free survival for patients with restricted diffusion was 94%, 29%, 0% and 0% versus 86%, 42%,28% and 14% for patients with mixed restricted/facilitated diffusion and 92%, 77%, 38% and 7% in patients with facilitated diffusion, respectively (Log-rank/Mantel-Cox estimate, 9.09) ( $p=0.01$ ). In addition, regression analysis revealed that tumor enhancement volumes were associated with repeat resection free survival ( $p=0.04$ ). Patients with tumor enhancement volumes equal or greater than 32 ml had resection free survival rates of 100%, 75%, 50% and 37% at 3, 6, 12 and 24 months, respectively, versus patients with lower tumor enhancement volumes with survival rates of 93%, 44%, 10% and 0%

#### CONCLUSION

s Patients with IDH-wild-type glioblastomas that had intralesional restricted diffusion and lower enhancing volumes were associated with lower repeat resection rates at 3, 6, 12 and 24 months compared to patients with tumoral facilitated diffusion and larger tumor enhancement volumes

#### CLINICAL RELEVANCE/APPLICATION

Our results provide information that will help to determine prognosis of patients with wild type glioblastomas.

Printed on: 02/07/23

## Abstract Archives of the RSNA, 2022

M5B-SPNR-20

### The Statin Medication Efficacy on Intracranial Atherosclerotic Plaque and Its Influencing Factors: A Magnetic Resonance Vessel Wall Imaging Study

Monday, Nov. 28 12:45PM - 1:15PM Room: Learning Center - NR DPS

#### Participants

Cong Liu, (*Presenter*) Nothing to Disclose

#### PURPOSE

To investigate the value of magnetic resonance vessel wall imaging (VWI) in evaluating the efficacy of statins on intracranial atherosclerotic plaque, and analyze the clinical and plaque characteristics that may be related with the treatment efficacy.

#### METHODS AND MATERIALS

A total of 53 patients with intracranial atherosclerotic disease and treated with statins were enrolled in this study. All patients underwent VWI scans during the baseline and follow-up period. The plaque characteristics, including plaque length, plaque thickness, plaque burden, the degree of vascular stenosis, the degree of plaque enhancement, vascular remodeling and plaque location were measured. The patient's clinical information at baseline was also collected. The patients were divided into two groups according to the tri-sectional quantiles of rate change of every plaque characteristic (good responder and poor responder). The difference of patient's clinical and plaque characteristics at baseline between the two groups was analyzed with t test, rank sum test or Chi-square test, and the relationship between patient's clinical and plaque characteristics and medication efficacy was assessed with multiple linear regression.

#### RESULTS

Compared with the baseline, the plaque thickness (1.30[1.05-1.50]mm vs. 1.30[1.20-1.50]mm,  $p=0.016$ ), plaque burden (51.42[33.47-76.98]% vs. 61.39[38.81-83.74]%,  $p=0.001$ ), vessel stenosis (30.00[18.00-54.50]% vs. 39.39[21.00-63.04]%,  $p=0.001$ ) and plaque enhancement (122.3±49.7% vs. 148.8±43.1%,  $p<0.001$ ) were significantly reduced in patients after treated with statins, especially in patients treated with statins for more than 6 months. The history of hypertension ( $B=0.188$ ,  $SE=0.086$ ,  $P=0.034$ ) and baseline BMI ( $kg/m^2$ ,  $B=0.043$ ,  $SE=0.013$ ,  $P=0.002$ ) were negatively correlated with the reduction of plaque enhancement, while the medication period (month,  $B=-0.03$ ,  $SE=0.011$ ,  $P=0.008$ ) and baseline plaque enhancement ( $B=-0.215$ ,  $SE=0.103$ ,  $P=0.043$ ) were positively correlated with the reduction of plaque enhancement.

#### CONCLUSION

In this study, we confirmed with VWI that statins can stabilize intracranial atherosclerotic plaques, and the therapeutic effects of statins on intracranial atherosclerotic plaques may have relationship with some of the patient's clinical and plaque characteristics at baseline.

#### CLINICAL RELEVANCE/APPLICATION

Compared with conventional luminal imaging techniques, VWI can directly provide more detailed plaque morphological information and help assess the statin medication efficacy on intracranial atherosclerotic plaque.

Printed on: 02/07/23

## Abstract Archives of the RSNA, 2022

M5B-SPNR-4

### Comparison of High-Resolution Vessel Wall Magnetic Resonance Imaging with Time of Flight Angiography to Detect Luminal Stenosis in Ischemic Stroke

Monday, Nov. 28 12:45PM - 1:15PM Room: Learning Center - NR DPS

#### Participants

Joel Samuel, MBBS, MD, (*Presenter*) Nothing to Disclose

#### PURPOSE

Ischemic stroke inflicts a major disease burden worldwide. Assessment of the lumen of intracranial vasculature using magnetic resonance angiography or CT angiography is the conventional method for evaluating pathology in the culprit vessel. High-resolution vessel wall magnetic resonance imaging is an emerging method which allows direct visualization of the vessel wall pathology. In addition, vessel wall imaging sequences can also be used to detect the extent of luminal stenosis. We compare the diagnostic performance of time-of-flight magnetic resonance angiography against vessel wall imaging sequences for detecting luminal stenosis in patients presenting with ischemic stroke. Vessel wall imaging was taken as the reference test. We further determine the correlation between the degree of stenosis in time-of-flight MR angiography and vessel wall imaging sequences.

#### METHODS AND MATERIALS

A prospective observational study conducted from 2019 - 2020, with a sample size of 150. The study group was patients with a clinical diagnosis of stroke, without hemorrhage on computed tomography, within the age of 18 - 70. Time of flight magnetic resonance angiography and vessel wall images were obtained using a 1.5T MRI system. The images were analyzed by a single observer. The presence of stenosis in the vascular territory of the infarcted region was determined, and the most stenotic lesion was taken as the culprit plaque. The percentage of stenosis was calculated by WASID criteria.

#### RESULTS

Time of flight magnetic resonance angiography had acceptable performance (AUC 0.896, sensitivity 85.9% and specificity 93.3%) but poor negative predictive value (42.1%) for detection of stenosis with vessel wall imaging as the reference standard. Spearman rank order correlation between degree of stenosis on vessel wall imaging and time-of-flight angiography showed statistically significant but moderate correlation ( $r = 0.715$ ).

#### CONCLUSION

Vessel wall imaging has superior diagnostic power to detect and quantify luminal stenosis compared to time-of-flight magnetic resonance angiography. Vessel wall imaging has a unique ability to detect non stenotic vulnerable plaques.

#### CLINICAL RELEVANCE/APPLICATION

The conventional time-of-flight angiography sequence in MR stroke protocols can be replaced by a vessel wall imaging sequence, yielding greater diagnostic information without significant increase in acquisition times.

Printed on: 02/07/23

## Abstract Archives of the RSNA, 2022

M5B-SPNR-5

### The Clinical Significance of the Hyperintense Acute Reperfusion Marker Sign in Subacute Stroke

Monday, Nov. 28 12:45PM - 1:15PM Room: Learning Center - NR DPS

#### Participants

Ji Young Lee, MD, Seoul, Korea, Republic Of (*Presenter*) Nothing to Disclose

#### PURPOSE

The hyperintense acute reperfusion marker (HARM) is characterized by the delayed enhancement of the subarachnoid or subpial space observed on postcontrast fluid-attenuated inversion recovery (FLAIR) images, and is considered a cerebral reperfusion marker for various brain disorders, including infarction. In this study, we evaluated the cerebral distribution patterns of HARM for discriminating between an enhancing subacute infarction and an enhancing mass located in the cortex and subcortical white matter.

#### METHODS AND MATERIALS

We analyzed consecutive patients who experienced a subacute ischemic stroke, were hospitalized, and underwent conventional brain magnetic resonance imaging including postcontrast FLAIR within 14 days from symptom onset, as well as those who had lesions corresponding to a clinical sign detected by diffusion-weighted imaging and postcontrast T1-weighted imaging between May 2019 and May 2021. A total of 199 patients were included in the study. Of them, 94 were finally included in the subacute infarction group. During the same period, 76 enhancing masses located in the cortex or subcortical white matter, which were subcategorized as metastasis, malignant glioma, and lymphoma, were analyzed. We analyzed the overall incidence of HARM in subacute ischemic stroke cases, and compared the enhancement patterns between cortical infarctions and cortical masses.

#### RESULTS

Among 94 patients with subacute stroke, 78 patients (83%) presented HARM, and among 76 patients with subcortical masses, 48 patients (63%) presented peripheral rim enhancement. Of 170 subcortical enhancing lesions, 88 (51.8%) showed HARM, and 78 (88.6%) were determined to be subacute infarction. Among 94 patients with subacute stroke, 48 patients (51%) had diffusion restrictions, and HARM was found in 39 patients (81.2%). Of the 46 patients (49%) without diffusion restriction, 39 patients (84.8%) showed HARM.

#### CONCLUSION

The presence of HARM was significantly associated with subacute infarctions. For the masses, a peripheral rim enhancement pattern was observed around the mass rather than the cerebral sulci on postcontrast FLAIR.

#### CLINICAL RELEVANCE/APPLICATION

We found that HARM with enhancing subcortical nodules was highly suggestive of subacute infarctions, and recommended a postcontrast FLAIR sequence for differentiating the ischemic subcortical infarctions from malignant lesions such as small metastasis.

Printed on: 02/07/23

## Abstract Archives of the RSNA, 2022

M5B-SPNR-7

### **Towards Personalized Radiotherapy: Tumor Growth Modeling May Supplement Traditional Radiotherapy Planning in Glioblastoma**

Monday, Nov. 28 12:45PM - 1:15PM Room: Learning Center - NR DPS

#### **Participants**

Marie-Christin Metz, MD, (*Presenter*) Nothing to Disclose

#### **PURPOSE**

One of the main challenges in the treatment of glioblastoma is the prediction of their individual growth behavior to guide more accurate radiotherapy after resection. Here, we introduce a new, deep learning - based tumor growth model which partially exceeds standard radiotherapy plans in covering the recurrence area.

#### **METHODS AND MATERIALS**

Our recently developed tumor growth model is based on a novel deep learning solver of the inverse problem in a Fisher-Kolmogorov growth model. We applied it to 30 cases of our prospective glioma cohort by utilizing FLAIR-, T2-, T1-, and T1-CE-data and compared volume and recurrence coverage with standard radiotherapy plans that were registered to the recurrence image. Statistical analysis was performed by applying Wilcoxon Signed Rank Test.

#### **RESULTS**

Depending on the chosen cut-off value of the predicted tumor cell density we saw a comparable target volume ( $p = 0.769$ ) with slight improvement of the covered recurrence area (mean improvement was 0.8% for a cut-off value of 50% for predicted tumor cell density with no significant difference due to the small sample size,  $p = 0.797$ ). The growth maps especially performed better in tumors with a highly diffuse growth pattern which exceed the traditional radiotherapy margins but are well captured in the estimated tumor spread from the growth model.

#### **CONCLUSION**

Here, we showed that utilizing a novel, deep learning - based tumor growth model for glioblastoma performed at least equally well to traditional radiotherapy plans in terms of recurrence coverage in our cohort, showing promise to improve in particular the planning of radiotherapy for highly infiltrative tumors. In a next step, we aim to correlate the calculated values with biological markers of proliferation and infiltration and validate our assumptions on larger data sets.

#### **CLINICAL RELEVANCE/APPLICATION**

Deep learning- based tumor growth modeling in glioblastoma carries potential to inform more personalized radiotherapy plans by predicting individual tumor spread. This may improve patient outcome in the future.

Printed on: 02/07/23

## Abstract Archives of the RSNA, 2022

M5B-SPNR-9

### Evaluation of A Deep Learning Model For The Detection Of Ischemic Acute Stroke Lesions And Assessment Of ASPECTS On Non-contrast CT Scans: A Multicenter Study

Monday, Nov. 28 12:45PM - 1:15PM Room: Learning Center - NR DPS

#### Participants

Weidao Chen, Beijing, China (*Presenter*) Nothing to Disclose

#### PURPOSE

Early detection of ischemia and assessing Alberta Stroke Project Early CT Score (ASPECTS) on non-contrast computed tomography (NCCT) plays a crucial role in the treatment of acute ischemic stroke (AIS). We aim to develop a robust deep learning (DL) model for automated detection of AIS lesions and assessment of ASPECTS based on NCCT images

#### METHODS AND MATERIALS

From January 2013 to December 2017, NCCT images of 1391 AIS patients (<6h from symptom onset to CT) from 5 hospitals were retrospectively collected and divided into the training dataset (n=1179) and internal validation dataset (n=212). Another 85 AIS patients from other three stroke centers were used as external validation dataset. All patients underwent follow-up diffusion-weighted (DW) MRI (within 24h after AIS), and the infarction regions on NCCT were manually contoured on DW MRI scans. A DL model was proposed for assessing ASPECTS, and model performance was evaluated with receiver operating characteristic (ROC) curve. The diagnostic performance of DL model was also compared with that of four experienced radiologists in the external validation dataset

#### RESULTS

In total 4240 (212 patients × 20 regions) and 1700 (85 patients × 20 regions) ASPECT regions in the internal and external validation datasets were scored. The AUC of the DL model was 0.876 (95% CI, 0.846-0.907) in the internal validation dataset. The DL model exhibited good performance in the external dataset with AUC achieving 0.729 (95% CI, 0.679-0.779), and the performance was non-inferior to that of four experienced radiologists (all p values > 0.05). The diagnostic accuracy of four radiologists was improved after DL model assistance with average sensitivity and specificity increased from 25.4% and 89.6%, to 33.3% and 91.5%, while the average diagnostic time per-case was reduced from 219.0 sec to 175.7 sec (p < 0.01), respectively

#### CONCLUSION

The NCCT-based DL model shows favorable performance and good robustness in multi-center validation datasets and can assist radiologists to achieve better performance for the early diagnosis of AIS

#### CLINICAL RELEVANCE/APPLICATION

This multicenter study demonstrated the deep learning model for detection of infarction and assessment of ASPECTS score on non-contrast CT had good feasibility and reliability for AIS patients

Printed on: 02/07/23

## Abstract Archives of the RSNA, 2022

M5B-SPOB

### OB/Gynecology Monday Poster Discussions - B

Monday, Nov. 28 12:45PM - 1:15PM Room: Learning Center - OB DPS

#### Participants

Cinthia Cruz, MD, Newton, MA (*Moderator*) Nothing to Disclose

#### Sub-Events

### M5B-SPOB-1 Whole-Volume MRI Radiomic Tumor Profiles Predict Survival in Uterine Cervical Cancer

#### Participants

Kari Wagner-Larsen, Bergen, Norway (*Presenter*) Nothing to Disclose

#### PURPOSE

To investigate whether pretreatment MRI-based radiomic tumor features predict disease-specific survival (DSS) in uterine cervical cancer (CC).

#### METHODS AND MATERIALS

This retrospective study included 135 (training set: n=90; validation set: n=45) histologically confirmed CC patients diagnosed in 2009-2017 who had pretreatment pelvic MRI depicting visible CC tumor. MRI included axial (oblique) T2-weighted MRI (T2WI) and axial (oblique) diffusion-weighted imaging (DWI). The primary tumors were manually segmented on T2WI, and the tumor masks were used to extract radiomic features from T2WI, high b-value DWI, and apparent diffusion coefficient (ADC) maps. LASSO Cox analysis was used to select significant features from T2WI only and from both T2WI and DWI (with ADC) to construct prediction models for DSS. The radiomic signature from T2WI only (T2rad) included tumor volume, gray level size zone matrix (GLSZM) feature (n=1), and shape-based features (n=3). The radiomic signature from both T2WI and DWI (T2+DWIrad) included tumor volume, GLSZM (n=2)-, neighboring gray tone difference matrix (NGTDM) (n=1)-, and gray level co-occurrence matrix (GLCM) (n=1) features. Prognostic performance of the radiomic signatures and MRI-measured maximum tumor diameter (tumormax) was evaluated by area under time-dependent receiver operating characteristics (tdROC) curves (AUC) in the training- (AUCT) and validation (AUCV) set. Survival was analyzed using Kaplan-Meier with log-rank test and Cox proportional hazard model.

#### RESULTS

The tdROC curves for predicting DSS at 5 years yielded AUCT/AUCV for tumormax, T2rad, and T2+DWIrad of 0.69/0.66, 0.75/0.71, and 0.82/0.72, respectively. High radiomic score for T2rad and T2+DWIrad was associated with reduced DSS in the training- (P < 0.001 for both) and validation (P = 0.09 and P = 0.03, respectively) set. Both radiomic signatures significantly predicted DSS with hazard ratios (HR) of 1.8-2.0 in the validation set (P = 0.006). After adjusting for 2018 FIGO stage (I-II vs. III-IV), T2rad independently predicted DSS (HR 1.6, P = 0.03), whereas T2+DWIrad only tended to the same (HR 1.7, P = 0.06).

#### CONCLUSION

The MRI-based whole-volume radiomic signatures, T2rad and T2+DWIrad, both yield high AUCs for predicting DSS in CC in the training- and validation set. Both radiomic signatures yield higher AUCs than tumormax and independently predict DSS after adjusting for 2018 FIGO stage.

#### CLINICAL RELEVANCE/APPLICATION

Whole-volume MRI radiomic tumor profiles may aid in pretreatment prognostication in CC patients.

### M5B-SPOB-2 Deep Myometrial Invasion of Endometrial Cancer - Sensitivity and Specificity of Fused T2 - Diffusion Weighted, Dynamic Contrast-Enhanced and T2 Weighed Magnetic Resonance Imaging

#### Participants

Jaromir Kargol, MD, (*Presenter*) Nothing to Disclose

#### PURPOSE

To evaluate and compare the sensitivity and specificity of fused T2 weighted - diffusion weighted magnetic resonance images, dynamic contrast enhanced (DCE) images and standard T2 weighted (T2WI) images in the diagnosis of deep myometrial invasion in patients with endometrial cancer.

#### METHODS AND MATERIALS

This is a single-center prospective study in a group of 83 consecutive patients (aged 36-86, median age 65), diagnosed with primary endometrial cancer after dilatation and curettage procedure. All patients underwent preoperative staging using the 1.5T magnetic resonance system. The images were evaluated by experienced radiologists blinded to histopathological and clinical data, using T2WI images, fused T2WI-DWI images and DCE images, to detect the depth of myometrial invasion of more than 50%. The findings were compared with the data from the histopathological analysis of surgical specimens.

## **RESULTS**

Deep myometrial invasions were confirmed in 41 of the 83 (49.4%) cases. The fused T2WI-DWI images provided better sensitivity (85.4% vs. 73.2%) and specificity (88.1% vs. 85.7%) in the detection of deep myometrial invasion than morphological T2WI alone. Contrast administration provided better diagnostic performance compared to T2WI images (78.0% vs. 73.2% for sensitivity and 90.5% vs. 85.7% for specificity). Fused imaging had higher sensitivity than DCE imaging (85.4% vs. 78.0%), although it had lower specificity (88.1% vs. 90.5%).

## **CONCLUSION**

s Magnetic resonance imaging has a high diagnostic performance for preoperative staging of endometrial cancer. Both fused T2WI-DWI and DCE magnetic resonance images have better sensitivity and specificity in the diagnosis of deep myometrial invasion than T2WI images. Utilizing fused T2WI-DWI may be a way to avoid the need for use of contrast medium.

## **CLINICAL RELEVANCE/APPLICATION**

Adherence of fused T2WI-DWI images to the preoperative MRI protocol improves the percentage of correctly diagnosed deep myometrial invasion cases among patients with endometrial cancer.

Printed on: 02/07/23

## Abstract Archives of the RSNA, 2022

M5B-SPOB-1

### Whole-Volume MRI Radiomic Tumor Profiles Predict Survival in Uterine Cervical Cancer

Monday, Nov. 28 12:45PM - 1:15PM Room: Learning Center - OB DPS

#### Participants

Kari Wagner-Larsen, Bergen, Norway (*Presenter*) Nothing to Disclose

#### PURPOSE

To investigate whether pretreatment MRI-based radiomic tumor features predict disease-specific survival (DSS) in uterine cervical cancer (CC).

#### METHODS AND MATERIALS

This retrospective study included 135 (training set: n=90; validation set: n=45) histologically confirmed CC patients diagnosed in 2009-2017 who had pretreatment pelvic MRI depicting visible CC tumor. MRI included axial (oblique) T2-weighted MRI (T2WI) and axial (oblique) diffusion-weighted imaging (DWI). The primary tumors were manually segmented on T2WI, and the tumor masks were used to extract radiomic features from T2WI, high b-value DWI, and apparent diffusion coefficient (ADC) maps. LASSO Cox analysis was used to select significant features from T2WI only and from both T2WI and DWI (with ADC) to construct prediction models for DSS. The radiomic signature from T2WI only (T2rad) included tumor volume, gray level size zone matrix (GLSZM) feature (n=1), and shape-based features (n=3). The radiomic signature from both T2WI and DWI (T2+DWIrad) included tumor volume, GLSZM (n=2)-, neighboring gray tone difference matrix (NGTDM) (n=1)-, and gray level co-occurrence matrix (GLCM) (n=1) features. Prognostic performance of the radiomic signatures and MRI-measured maximum tumor diameter (tumormax) was evaluated by area under time-dependent receiver operating characteristics (tdROC) curves (AUC) in the training- (AUCT) and validation (AUCV) set. Survival was analyzed using Kaplan-Meier with log-rank test and Cox proportional hazard model.

#### RESULTS

The tdROC curves for predicting DSS at 5 years yielded AUCT/AUCV for tumormax, T2rad, and T2+DWIrad of 0.69/0.66, 0.75/0.71, and 0.82/0.72, respectively. High radiomic score for T2rad and T2+DWIrad was associated with reduced DSS in the training- (P < 0.001 for both) and validation (P = 0.09 and P = 0.03, respectively) set. Both radiomic signatures significantly predicted DSS with hazard ratios (HR) of 1.8-2.0 in the validation set (P = 0.006). After adjusting for 2018 FIGO stage (I-II vs. III-IV), T2rad independently predicted DSS (HR 1.6, P = 0.03), whereas T2+DWIrad only tended to the same (HR 1.7, P = 0.06).

#### CONCLUSION

The MRI-based whole-volume radiomic signatures, T2rad and T2+DWIrad, both yield high AUCs for predicting DSS in CC in the training- and validation set. Both radiomic signatures yield higher AUCs than tumormax and independently predict DSS after adjusting for 2018 FIGO stage.

#### CLINICAL RELEVANCE/APPLICATION

Whole-volume MRI radiomic tumor profiles may aid in pretreatment prognostication in CC patients.

Printed on: 02/07/23

## Abstract Archives of the RSNA, 2022

M5B-SPOB-2

### Deep Myometrial Invasion of Endometrial Cancer - Sensitivity and Specificity of Fused T2 - Diffusion Weighted, Dynamic Contrast-Enhanced and T2 Weighted Magnetic Resonance Imaging

Monday, Nov. 28 12:45PM - 1:15PM Room: Learning Center - OB DPS

#### Participants

Jaromir Kargol, MD, (*Presenter*) Nothing to Disclose

#### PURPOSE

To evaluate and compare the sensitivity and specificity of fused T2 weighted - diffusion weighted magnetic resonance images, dynamic contrast enhanced (DCE) images and standard T2 weighted (T2WI) images in the diagnosis of deep myometrial invasion in patients with endometrial cancer.

#### METHODS AND MATERIALS

This is a single-center prospective study in a group of 83 consecutive patients (aged 36-86, median age 65), diagnosed with primary endometrial cancer after dilatation and curettage procedure. All patients underwent preoperative staging using the 1.5T magnetic resonance system. The images were evaluated by experienced radiologists blinded to histopathological and clinical data, using T2WI images, fused T2WI-DWI images and DCE images, to detect the depth of myometrial invasion of more than 50%. The findings were compared with the data from the histopathological analysis of surgical specimens.

#### RESULTS

Deep myometrial invasions were confirmed in 41 of the 83 (49.4%) cases. The fused T2WI-DWI images provided better sensitivity (85.4% vs. 73.2%) and specificity (88.1% vs. 85.7%) in the detection of deep myometrial invasion than morphological T2WI alone. Contrast administration provided better diagnostic performance compared to T2WI images (78.0% vs. 73.2% for sensitivity and 90.5% vs. 85.7% for specificity). Fused imaging had higher sensitivity than DCE imaging (85.4% vs. 78.0%), although it had lower specificity (88.1% vs. 90.5%).

#### CONCLUSION

s Magnetic resonance imaging has a high diagnostic performance for preoperative staging of endometrial cancer. Both fused T2WI-DWI and DCE magnetic resonance images have better sensitivity and specificity in the diagnosis of deep myometrial invasion than T2WI images. Utilizing fused T2WI-DWI may be a way to avoid the need for use of contrast medium.

#### CLINICAL RELEVANCE/APPLICATION

Adherence of fused T2WI-DWI images to the preoperative MRI protocol improves the percentage of correctly diagnosed deep myometrial invasion cases among patients with endometrial cancer.

Printed on: 02/07/23



## Abstract Archives of the RSNA, 2022

M5B-SPPD

### **Pediatric Monday Poster Discussions - B**

Monday, Nov. 28 12:45PM - 1:15PM Room: Learning Center - PD DPS

#### **Participants**

Gary Schooler, MD, Dallas, TX (*Moderator*) Nothing to Disclose

Printed on: 02/07/23



## Abstract Archives of the RSNA, 2022

M5B-SPPH

### Physics Monday Poster Discussions - B

Monday, Nov. 28 12:45PM - 1:15PM Room: Learning Center - PH DPS

#### Participants

James M. Kofler JR, PhD, Jacksonville, FL (*Moderator*) Nothing to Disclose

#### Sub-Events

### **M5B-SPPH-1 Newly Developed Deep Learning Reconstruction (DLR) for Dynamic Contrast-Enhanced CT Angiography: Comparison of Capability for Image Quality Improvements and Abdominal Arteries Assessments among DLR, Hybrid-Type and Model-Based Iterative Reconstructions (IRs) in Patients with Hepatic and Pancreatic Malignant Tumors**

#### Participants

Yoshiharu Ohno, MD, PhD, Toyooka, Japan (*Presenter*) Research Grant, Canon Medical Systems Corporation; Research Grant, Daiichi Sankyo Co, Ltd; Research Grant, Ministry of Education, Culture, Sports, Science and Technology

#### PURPOSE

To determine the capability of newly developed deep learning reconstruction (nDLR) for dynamic contrast-enhanced CT angiography (CE-CTA) for image quality improvement and vascular assessment as compared with conventional deep learning reconstruction for abdomen (cDLR), hybrid-type and model-based iterative reconstruction (IRs).

#### METHODS AND MATERIALS

Forty patients suspected of hepatic and pancreatic malignant tumors underwent dynamic CE-CTA at 320-detector row CTs. To compare quantitative image quality improvement among all methods, region of interests (ROIs) were placed over liver, aorta, celiac artery, proper, right and left hepatic arteries, cystic artery, dorsal pancreatic artery and fat for determination of CT values, signal-to-noise ratios (SNRs) and contrast-to-noise ratios (CNRs) of on all CT data. To compare qualitative image quality among all methods, two board-certified abdominal radiologists assessed overall image quality and depiction of all above-mentioned arteries on each CT data by means of 5-point scale, and final value of each quantitative index were determined by consensus of two readers on each CT data set. For comparison of quantitative image quality, all indexes were compared among all methods by Tukey's HSD test. To evaluate inter-observer agreements of overall image quality and all above-mentioned arteries, kappa statistics with ?2 tests were performed. On comparison of qualitative indexes, each index was also compared among all methods by Wilcoxon signed-rank test.

#### RESULTS

On quantitative image quality comparisons, SNR and CNR of nDLR at all arteries except cystic artery were significantly higher than those of hybrid-type IR ( $p < 0.05$ ). In addition, SNRs and CNRs of nDLR at aorta and celiac artery were significantly higher than those of model-based IR ( $p < 0.05$ ) or cDLR ( $p < 0.05$ ). Inter-observer agreement of overall image quality and all arteries on all methods were determined as significantly substantial or almost perfect ( $0.73 \leq \kappa \leq 1.0$ ,  $p < 0.0001$ ). On qualitative image quality comparisons, overall image qualities of nDLR, cDLR and MBIR were significantly higher than that of hybrid-type IR ( $p < 0.05$ ). Depictions of bilateral hepatic arteries and cystic artery of nDLR, cDLR and MBIR were significantly higher than those of hybrid-type IR ( $p < 0.05$ ).

#### CONCLUSION

Newly developed DLR for dynamic CE-CTA has equal or superior capability to other methods, especially hybrid-type IR, for improving image quality and vasculature assessment in routine clinical practice.

#### CLINICAL RELEVANCE/APPLICATION

Newly developed DLR for dynamic CE-CTA has equal or superior capability to other methods, especially hybrid-type IR, for improving image quality and vasculature assessment in routine clinical practice.

### **M5B-SPPH-2 3D Context-Aware Deep Learning Network in Detection of Pulmonary Mass-Like Lesions: A Preliminary Study**

#### Participants

Yan Zhang, Beijing, China (*Presenter*) Nothing to Disclose

#### PURPOSE

To explore the feasibility and reliability of 3D context-aware deep learning method in detection of pulmonary mass-like lesions by comparisons with radiologists.

#### METHODS AND MATERIALS

We built Context-aware DL network for detection of slice-level mass-like lesion based on deep learning 2722 CT scanning dataset,

with 2601 slice-level annotations confirmed by experienced pathologists. For the modeling of 3D context, this network took three consecutive slices from axial view as input. For the modeling of 2D context, we implemented an Atrous Spatial Pyramid Pooling (ASPP) module. During inference, the detected slice-level 2D lesion region were aggregated to 3D detection results based on their spatial continuity. Then, all the chest CT examinations were analyzed by Context-aware automatic mass detection (CAMD) from January of 2018 to March of 2019 as group A, and the results were compared with two experienced radiologists (group B). Statistical analysis were made with  $P < 0.05$ .

## RESULTS

A total of 563 CT scans were tested, with 176 mass-like lesions detected in group A and 159 in group B. Compared with radiologists, CAMD demonstrates 19 missed lesions, with 12 of which located at lung hilum. Besides, 36 cases were misdiagnosed, including 18 cases of pulmonary patchy infiltrates and consolidations, 7 cases of atelectasis, 6 cases of encapsulated effusion, 5 cases of hilar lymph nodes or pulmonary arteries and/or veins. The detection rate of CAMD in mass-like lesions was 76.2%, with 20.5% false rate and 8.2% missed rate.

## CONCLUSION

s Compared with experienced radiologists, context-aware automatic mass detection (CAMD) demonstrates potential feasibility in detection of pulmonary mass-like lesions.

## CLINICAL RELEVANCE/APPLICATION

with the further development of artificial intelligence, CAMD will help radiologists quickly locate lesions for diagnosis and generate structured reports.

### **M5B-SPPH-4 Photon-Counting Computed Tomography: Influence of Focal Spot Size on High Spatial Resolution Imaging**

Participants

Trevor Vent, (*Presenter*) Nothing to Disclose

## PURPOSE

Photon-Counting Computed Tomography (PCCT) has potential to provide significant benefits in diagnostic imaging, including high spatial resolution imaging. A limited x-ray flux at small focal spot sizes imposes limitations on attainable spatial resolution. This study examines the effects of the focal spot size of the x-ray tube on high spatial resolution imaging of a first-generation clinical dual source PCCT.

## METHODS AND MATERIALS

To evaluate the spatial resolution of a clinical PCCT scanner (Naeotom Alpha, Siemens Healthineers), a high-contrast lead foil Siemens Star (Type 9/10/360-003, Supertech) was placed with a 3D-printed adapter into a technical CT phantom (Multi-Energy CT Phantom, Sun Nuclear) to simulate realistic patient sizes. The phantom was scanned with a high-resolution protocol at two radiation dose levels (10, 16 mGy) that corresponded to two focal spot sizes (small:  $0.4 \times 0.4 \text{ mm}^2$ , large:  $0.6 \times 0.7 \text{ mm}^2$ ). Scans were repeated three times, and slices were reconstructed with 0.2 mm slice thickness, 0.1 mm slice spacing, and three different reconstruction kernels (Hr72, Hr84, Hr98). Images were evaluated using a contrast transfer function (CTF) analysis. Limiting spatial resolution (LSR) was measured at 50% and 10% modulation.

## RESULTS

LSR varied with focal spot size and reconstruction kernel. LSR increased with increasing reconstruction kernel for the small focal spot size: 25, 31.5, and 93 lp/cm (10% modulation), respectively. LSR was limited by the larger focal spot size at higher reconstruction kernels: 25, 30.5, and 30.5 lp/cm, respectively. There are no discernible differences between the Hr84 and Hr98 reconstruction kernels suggesting that the larger focal spot size was the limiting factor of resolution.

## CONCLUSION

s In this study, the resolution capabilities of a clinical PCCT system were evaluated based on reconstruction mode and focal spot size. The X-ray tube flux constraints must be overcome to fully unfold the high-resolution capabilities to all anatomical regions and patient sizes. In all modes, the PCCT system outperforms existing conventional CT technology in terms of spatial resolution achievable.

## CLINICAL RELEVANCE/APPLICATION

In clinical practice, high-resolution PCCT has the potential to aid in the diagnosis of diseases by providing visualization of small structures that may be difficult to identify on conventional CT.

### **M5B-SPPH-5 Differences in Noise Reduction Performance Between Two Deep-Learning CT Image Reconstruction Techniques: A Novel Textured Phantom Approach**

Participants

Hiroki Kawashima, PhD, RT, Kanazawa, Japan (*Presenter*) Nothing to Disclose

## PURPOSE

To characterize the noise reduction performance between two deep-learning image reconstruction (DLIR) techniques, using a phantom containing a simple uniform region and a complex non-uniform region.

## METHODS AND MATERIALS

A water-bath phantom with a diameter of 300 mm was used as a base phantom. A textured phantom with a diameter of 128 mm, which was made of two materials, one equivalent to water and the other being 12 mg/mL diluted iodine, irregularly mixed to create a complex texture (non-uniform region), was placed in the base phantom. Thirty repeated phantom scans were performed using two CT scanners (GE, Revolution CT with Apex Edition; Canon, Aquilion One PRISM Edition) at two dose levels (CTDI: 5 and 15 mGy). Images were reconstructed with each CT system's filtered back projection (FBP) and DLIR [GE, TrueFidelity (TF); Canon, Advanced intelligent Clear-IQ Engine Body Sharp (AC)] for three process strengths. For basic characteristics of noise, the standard deviation (SD) and noise power spectrum (NPS) were measured for the uniform (water) region. A noise magnitude map was generated by

calculating the inter-image SD at each pixel position across the 30 images. Then, a noise reduction map (NRM), which visualizes the relative differences in noise magnitude between FBP and DLIR, was calculated. The NRM values ranged from 0.0 to 1.0. A low NRM value represents a less aggressive noise reduction. The histograms of the NRM value were analyzed for the uniform and non-uniform regions.

## RESULTS

The reduction in noise magnitude compared with FBP tended to be greater with AC (45%-85%) than with TF (32%-65%). The average NPS frequencies of TF and AC were almost comparable to those of FBP, except for the low-dose condition and the high noise reduction strength for AC. The NRM values of TF and AC were higher in the uniform region than in the non-uniform region. In the non-uniform region, TF's average NRM values (0.21-0.48) tended to be lower than AC's (0.39-0.78). The histograms for TF showed a small overlap between the uniform and the non-uniform regions; in contrast, those for AC showed a greater overlap. This difference seems to indicate that TF processes the uniform and non-uniform regions more differently than AC does.

## CONCLUSION

This study has revealed a distinct difference in characteristics between the two DLIR techniques: TF tends to offer less aggressive noise reduction in non-uniform regions and preserve the original signals, whereas AC tends to prioritize noise filtering over edge-preservation, especially at the low-dose condition and with the high noise reduction strength.

## CLINICAL RELEVANCE/APPLICATION

An appropriate combination of strength and dose level should be selected for clinical use of each DLIR technique.

### **M5B-SPPH-6 Discriminability of Frequency-Dependent Non-Gaussian Noise Properties in CT and the Limitation of the Noise Power Spectrum to Describe Noise Texture with Non-Linear Reconstruction Algorithms.**

#### Participants

Daniel Shin, MS, Los Angeles, CA (*Presenter*) Employee, Canon Medical Systems Corporation

#### PURPOSE

To demonstrate the impact of frequency-dependent higher order, non-Gaussian noise properties on perceived noise texture via a human observer study using abdominal CT reconstruction algorithms as a use case.

#### METHODS AND MATERIALS

A 32 cm water phantom was scanned at two tube current levels on an Aquilion ONE Genesis CT system (Canon Medical Systems, Otawara, Japan). The raw data was reconstructed with three abdominal reconstruction algorithms: a model-based iterative reconstruction (MBIR) algorithm (FIRST), a deep-learning reconstruction (DLR) algorithm (AiCE), and, for one tube current, filtered backprojection (FBP) as a control. First, quantitative analysis of the noise in the resulting reconstructions was performed by extracting regions of interest (ROIs) (100x100 pixels) from the image data and assessing the 4th order statistics of each ROI via a global and frequency-binned excess kurtosis measurement. To evaluate the detectability of the non-Gaussian characteristics of these noise images, pure Gaussian noise counterpart image datasets with the same mean, standard deviation (SD), and Noise Power Spectrum (NPS) as each acquired data condition were also generated by convolving random white noise with the root-NPS of the acquired data. Then, using a two-alternative forced choice experiment, nine naïve observers were tasked with distinguishing the acquired noise image from its pure Gaussian counterpart.

## RESULTS

Excess kurtosis in the image ROIs was 0.01 for FBP, 0.74-0.85 for FIRST, and -0.13-0.21 for AiCE. Excess kurtosis trends differ with frequency band. From the observer study, it was found that FBP images appear indistinguishable from their pure Gaussian counterparts (AUC=.54), while MBIR images were readily distinguishable from Gaussian ones (AUC=.98-1). DLR images are more difficult to distinguish from their pure Gaussian counterparts (AUC 0.56-.85), which indicates that perceived noise texture is more similar to Gaussian noise.

## CONCLUSION

This work demonstrates that the appearance of CT noise texture may be dependent on frequency-dependent higher-order statistics not captured by the NPS. In some cases, noise textures with identical NPS and SD can be distinguished based on non-Gaussian properties. Deep-learning reconstruction has lower levels of excess kurtosis and is less readily discriminable from Gaussian noise, despite having a similar NPS to MBIR.

## CLINICAL RELEVANCE/APPLICATION

Noise texture can influence the acceptability of a reconstruction algorithm to the radiologist and thus full characterization of the noise is key to understanding and describing reconstruction algorithm performance.

### **M5B-SPPH-7A Multi Decade Study of CT Protocol Optimization underneath the Influence of Physicists, Radiologists and Improving Scanner Technologies**

#### Participants

Joseph Meier, PhD, Madison, WI (*Presenter*) Nothing to Disclose

#### PURPOSE

Adjusting CT protocols for optimization of image quality across a large site requires a multidisciplinary effort. Optimizing the performance of Automatic Tube Current Control (AEC) avoids acquiring images with high amounts of noise or with too low noise when the tube current (mA) is maxing or minning out respectively. This study investigates the longitudinal impact that protocol optimization by a team of medical physicists and radiologists and improvements in scanner technology have on the performance of the site's AEC.

#### METHODS AND MATERIALS

We analyzed 536 exams from either routine chest or routine abdomen from early protocol optimization (2007-2008) and 739 from current protocol optimization (2021-2022). Proper AEC function was measured for each examination by calculating the percentage of images at the maximum mA (%imgmax\_mA) and minimum (%imgmin\_mA). Examinations were classified as suboptimal if the

%imgmax\_mA or %imgmin\_mA was greater than 20%.

## RESULTS

For the chest exams, the mean %imgmax\_mA decreased from  $31.9 \pm 32.6\%$  to  $10.3 \pm 8.5\%$  ( $p < 0.001$ ) from the early to current protocol periods. Similarly, for the abdominal exams the mean %imgmax\_mA decreased from  $35.4 \pm 35.5\%$  to  $14.3 \pm 16.6\%$  ( $p < 0.001$ ). For the chest exams, the mean %imgmin\_mA decreased from  $19.0 \pm 32.1\%$  to  $3.6 \pm 4.2\%$  ( $p < 0.001$ ). Similarly, for the abdominal exams, the mean %imgmin\_mA decreased from  $21.8 \pm 35.1\%$  to  $3.6 \pm 13.4\%$  ( $p < 0.001$ ). The percent of suboptimal chest exams for %imgmax\_mA(%imgmin\_mA) decreased from 46.4(21.6)% to 8.2(1.1)%. Similarly, the percent of suboptimal abdominal exams for %imgmax\_mA(%imgmin\_mA), decreased from 44.3(27.4)% to 12.0(3.0)%.

## CONCLUSION

s This work shows that the incidence of suboptimal routine chest and abdominal examinations as measured by the percentage of images at the maximum or minimum mA, was greatly reduced through protocol optimization by medical physicists and radiologists as well as emerging scanner technology.

## CLINICAL RELEVANCE/APPLICATION

A multidecade analysis of CT tube current modulation data shows that the efforts of medical physicists and radiologists combined with evolving scanner technology has greatly reduced the number of suboptimal CT exams.

## M5B-SPPH-8 Clinical Thorax CT Image Quality Assessment Using Spectral and Spatial Features

Participants

Zahra Passand, MSc, (*Presenter*) Nothing to Disclose

## PURPOSE

The quality of computed tomography (CT) images is affected by different parameters such as patient motion and anatomy, detector design, scatter, the reconstruction algorithm and others. Patient CT images are not automatically analyzed by the scanner software during clinical routine. Introducing continuous monitoring of CT image quality would be beneficial for diagnostic purposes. As a consequence of such a broader analysis, the applied dose could be reduced while maintaining sufficient image quality level. Since most of the existing image quality analysis approaches are based on dedicated phantoms, we propose a method which combines the modulation transfer function (MTF), the frequency spectrum and the noise power spectrum (NPS) in a predefined regions of interest (ROI) to compute various image quality features. A classifier was trained using these features to distinguish different level of image quality.

## METHODS AND MATERIALS

The thorax CT images which were acquired from 30 patients were annotated by different radiologists. In this initial study, two quality levels (either "low" or "high") were used. For each CT image, an ROI containing the major fissure of the left lung was manually selected and was used to estimate the image quality. The outer edges of the major fissure were automatically detected using an active contour algorithm. The MTF was computed using the edge and line scan functions of the major fissure within the selected ROI. In addition to the MTF, the frequency power spectrum was estimated in the same ROI. The NPS was estimated from a homogenous area close to the ROI of the major fissure. Based on the parameters, several other frequency domain features were derived to determine the image quality. A classifier was trained using these features.

## RESULTS

Using the estimated features, a classification accuracy of 89% was achieved using the validation data set.

## CONCLUSION

s Using the image quality features which were defined for this work, CT images were classified in one of the two image quality categories. The classification results were in high agreement with the manual annotation performed by radiologists. Future work will include additional features and CT images to further improve and validate this approach.

## CLINICAL RELEVANCE/APPLICATION

The developed method has the potential to be used during clinical routine for image quality analysis and documentation. Long term studies would be required to analyze the quality over a larger population to investigate potential dose reduction strategies.

## M5B-SPPH-9 Deep Scatter Estimation (DSE) for High Scatter Frequencies caused by Coarse Anti Scatter Grids in Clinical CT

Participants

Julien Erath, Forchheim, Germany (*Presenter*) Employee, Siemens AG

## PURPOSE

To estimate and correct for high frequencies in scatter signals transmitted through coarse anti scatter grids (ASGs) as used in photon counting CT.

## METHODS AND MATERIALS

CT detectors with very small pixels, such as in photon-counting CT, may have anti scatter grids with a grid spacing being an integer multiple of the detector pixel size. For example, an ASG field may comprise a 2x3 matrix of detector pixels. The shading of the scattered radiation caused by the grid affects each of the six pixels within a grid field differently. Although scatter is a low frequency effect, this pixel-dependent shading results in high frequencies in the scatter signal transmitted through the ASG. These may cause moiré artifacts in the reconstructed images. We trained a deep learning-based scatter estimation (DSE) network to estimate that scatter signal, which can then be used to correct the measured data (e.g. by subtraction). To train DSE, scatter signals were obtained by Monte Carlo simulation of patient CT data. The geometry of the CT and of the coarse ASG matches the one of a clinical photon-counting CT (Naeotom Alpha, Siemens Healthineers). To adapt the network architecture to the coarse ASG, the network receives the six different pixel locations as separate input channels and is trained to predict six different output channels of the pixel locations, which can then be merged to obtain the scatter estimation for the whole detector. The DSE-corrected data are then reconstructed and evaluated in image domain.

## **RESULTS**

With the proposed neural network, the high frequency components of the scatter signal can be estimated and corrected very efficiently. DSE reduces scatter artifacts across all patients from a mean absolute error of about 10 HU to below 1 HU. DSE reduces scatter artifacts across all patients from a mean absolute error of about 10 HU to below 1 HU. The amplitude of the moiré artifacts can be reduced from about 15 HU to below 2 HU. With the proposed algorithm the moiré artifacts can be significantly reduced and the diagnostic image quality improved.

## **CONCLUSION**

s DSE can estimate ASG-modulated scatter frequencies in CT data and correct both for the scatter artifacts and for the moiré artifacts caused by the coarse ASG.

## **CLINICAL RELEVANCE/APPLICATION**

DSE leads to an accurate scatter correction of the moiré artifacts and can be crucial for accurate diagnostic CT image quality.

Printed on: 02/07/23

## Abstract Archives of the RSNA, 2022

M5B-SPPH-1

### **Newly Developed Deep Learning Reconstruction (DLR) for Dynamic Contrast-Enhanced CT Angiography: Comparison of Capability for Image Quality Improvements and Abdominal Arteries Assessments among DLR, Hybrid-Type and Model-Based Iterative Reconstructions (IRs) in Patients with Hepatic and Pancreatic Malignant Tumors**

Monday, Nov. 28 12:45PM - 1:15PM Room: Learning Center - PH DPS

#### **Participants**

Yoshiharu Ohno, MD, PhD, Toyoake, Japan (*Presenter*) Research Grant, Canon Medical Systems Corporation; Research Grant, Daiichi Sankyo Co, Ltd; Research Grant, Ministry of Education, Culture, Sports, Science and Technology

#### **PURPOSE**

To determine the capability of newly developed deep learning reconstruction (nDLR) for dynamic contrast-enhanced CT angiography (CE-CTA) for image quality improvement and vascular assessment as compared with conventional deep learning reconstruction for abdomen (cDLR), hybrid-type and model-based iterative reconstruction (IRs).

#### **METHODS AND MATERIALS**

Forty patients suspected of hepatic and pancreatic malignant tumors underwent dynamic CE-CTA at 320-detector row CTs. To compare quantitative image quality improvement among all methods, region of interests (ROIs) were placed over liver, aorta, celiac artery, proper, right and left hepatic arteries, cystic artery, dorsal pancreatic artery and fat for determination of CT values, signal-to-noise ratios (SNRs) and contrast-to-noise ratios (CNRs) of on all CT data. To compare qualitative image quality among all methods, two board-certified abdominal radiologists assessed overall image quality and depiction of all above-mentioned arteries on each CT data by means of 5-point scale, and final value of each quantitative index were determined by consensus of two readers on each CT data set. For comparison of quantitative image quality, all indexes were compared among all methods by Tukey's HSD test. To evaluate inter-observer agreements of overall image quality and all above-mentioned arteries, kappa statistics with ?2 tests were performed. On comparison of qualitative indexes, each index was also compared among all methods by Wilcoxon signed-rank test.

#### **RESULTS**

On quantitative image quality comparisons, SNR and CNR of nDLR at all arteries except cystic artery were significantly higher than those of hybrid-type IR ( $p < 0.05$ ). In addition, SNRs and CNRs of nDLR at aorta and celiac artery were significantly higher than those of mode-based IR ( $p < 0.05$ ) or cDLR ( $p < 0.05$ ). Inter-observer agreement of overall image quality and all arteries on all methods were determined as significantly substantial or almost perfect ( $0.73 \leq \kappa \leq 1.0$ ,  $p < 0.0001$ ). On qualitative image quality comparisons, overall image qualities of nDLR, cDLR and MBIR were significantly higher than that of hybrid-type IR ( $p < 0.05$ ). Depictions of bilateral hepatic arteries and cystic artery of nDLR, cDLR and MBIR were significantly higher than those of hybrid-type IR ( $p < 0.05$ ).

#### **CONCLUSION**

s Newly developed DLR for dynamic CE-CTA has equal or superior capability to other methods, especially hybrid-type IR, for improving image quality and vasculature assessment in routine clinical practice.

#### **CLINICAL RELEVANCE/APPLICATION**

Newly developed DLR for dynamic CE-CTA has equal or superior capability to other methods, especially hybrid-type IR, for improving image quality and vasculature assessment in routine clinical practice.

Printed on: 02/07/23

## Abstract Archives of the RSNA, 2022

M5B-SPPH-2

### 3D Context-Aware Deep Learning Network in Detection of Pulmonary Mass-Like Lesions: A Preliminary Study

Monday, Nov. 28 12:45PM - 1:15PM Room: Learning Center - PH DPS

#### Participants

Yan Zhang, Beijing, China (*Presenter*) Nothing to Disclose

#### PURPOSE

To explore the feasibility and reliability of 3D context-aware deep learning method in detection of pulmonary mass-like lesions by comparisons with radiologists.

#### METHODS AND MATERIALS

We built Context-aware DL network for detection of slice-level mass-like lesion based on deep learning 2722 CT scanning dataset, with 2601 slice-level annotations confirmed by experienced pathologists. For the modeling of 3D context, this network took three consecutive slices from axial view as input. For the modeling of 2D context, we implemented an Atrous Spatial Pyramid Pooling (ASPP) module. During inference, the detected slice-level 2D lesion region were aggregated to 3D detection results based on their spatial continuity. Then, all the chest CT examinations were analyzed by Context-aware automatic mass detection (CAMD) from January of 2018 to March of 2019 as group A, and the results were compared with two experienced radiologists (group B). Statistical analysis were made with  $P < 0.05$ .

#### RESULTS

A total of 563 CT scans were tested, with 176 mass-like lesions detected in group A and 159 in group B. Compared with radiologists, CAMD demonstrates 19 missed lesions, with 12 of which located at lung hilum. Besides, 36 cases were misdiagnosed, including 18 cases of pulmonary patchy infiltrates and consolidations, 7 cases of atelectasis, 6 cases of encapsulated effusion, 5 cases of hilar lymph nodes or pulmonary arteries and/or veins. The detection rate of CAMD in mass-like lesions was 76.2%, with 20.5% false rate and 8.2% missed rate.

#### CONCLUSION

s Compared with experienced radiologists, context-aware automatic mass detection (CAMD) demonstrates potential feasibility in detection of pulmonary mass-like lesions.

#### CLINICAL RELEVANCE/APPLICATION

with the further development of artificial intelligence, CAMD will help radiologists quickly locate lesions for diagnosis and generate structured reports.

Printed on: 02/07/23



## Abstract Archives of the RSNA, 2022

M5B-SPPH-4

### Photon-Counting Computed Tomography: Influence of Focal Spot Size on High Spatial Resolution Imaging

Monday, Nov. 28 12:45PM - 1:15PM Room: Learning Center - PH DPS

#### Participants

Trevor Vent, (*Presenter*) Nothing to Disclose

#### PURPOSE

Photon-Counting Computed Tomography (PCCT) has potential to provide significant benefits in diagnostic imaging, including high spatial resolution imaging. A limited x-ray flux at small focal spot sizes imposes limitations on attainable spatial resolution. This study examines the effects of the focal spot size of the x-ray tube on high spatial resolution imaging of a first-generation clinical dual source PCCT.

#### METHODS AND MATERIALS

To evaluate the spatial resolution of a clinical PCCT scanner (Naeotom Alpha, Siemens Healthineers), a high-contrast lead foil Siemens Star (Type 9/10/360-003, Supertech) was placed with a 3D-printed adapter into a technical CT phantom (Multi-Energy CT Phantom, Sun Nuclear) to simulate realistic patient sizes. The phantom was scanned with a high-resolution protocol at two radiation dose levels (10, 16 mGy) that corresponded to two focal spot sizes (small: 0.4 x 0.4 mm<sup>2</sup>, large: 0.6 x 0.7 mm<sup>2</sup>). Scans were repeated three times, and slices were reconstructed with 0.2 mm slice thickness, 0.1 mm slice spacing, and three different reconstruction kernels (Hr72, Hr84, Hr98). Images were evaluated using a contrast transfer function (CTF) analysis. Limiting spatial resolution (LSR) was measured at 50% and 10% modulation.

#### RESULTS

LSR varied with focal spot size and reconstruction kernel. LSR increased with increasing reconstruction kernel for the small focal spot size: 25, 31.5, and 93 lp/cm (10% modulation), respectively. LSR was limited by the larger focal spot size at higher reconstruction kernels: 25, 30.5, and 30.5 lp/cm, respectively. There are no discernible differences between the Hr84 and Hr98 reconstruction kernels suggesting that the larger focal spot size was the limiting factor of resolution.

#### CONCLUSION

In this study, the resolution capabilities of a clinical PCCT system were evaluated based on reconstruction mode and focal spot size. The X-ray tube flux constraints must be overcome to fully unfold the high-resolution capabilities to all anatomical regions and patient sizes. In all modes, the PCCT system outperforms existing conventional CT technology in terms of spatial resolution achievable.

#### CLINICAL RELEVANCE/APPLICATION

In clinical practice, high-resolution PCCT has the potential to aid in the diagnosis of diseases by providing visualization of small structures that may be difficult to identify on conventional CT.

Printed on: 02/07/23

## Abstract Archives of the RSNA, 2022

M5B-SPPH-5

### Differences in Noise Reduction Performance Between Two Deep-Learning CT Image Reconstruction Techniques: A Novel Textured Phantom Approach

Monday, Nov. 28 12:45PM - 1:15PM Room: Learning Center - PH DPS

#### Participants

Hiroki Kawashima, PhD, RT, Kanazawa, Japan (*Presenter*) Nothing to Disclose

#### PURPOSE

To characterize the noise reduction performance between two deep-learning image reconstruction (DLIR) techniques, using a phantom containing a simple uniform region and a complex non-uniform region.

#### METHODS AND MATERIALS

A water-bath phantom with a diameter of 300 mm was used as a base phantom. A textured phantom with a diameter of 128 mm, which was made of two materials, one equivalent to water and the other being 12 mg/mL diluted iodine, irregularly mixed to create a complex texture (non-uniform region), was placed in the base phantom. Thirty repeated phantom scans were performed using two CT scanners (GE, Revolution CT with Apex Edition; Canon, Aquilion One PRISM Edition) at two dose levels (CTDI: 5 and 15 mGy). Images were reconstructed with each CT system's filtered back projection (FBP) and DLIR [GE, TrueFidelity (TF); Canon, Advanced intelligent Clear-IQ Engine Body Sharp (AC)] for three process strengths. For basic characteristics of noise, the standard deviation (SD) and noise power spectrum (NPS) were measured for the uniform (water) region. A noise magnitude map was generated by calculating the inter-image SD at each pixel position across the 30 images. Then, a noise reduction map (NRM), which visualizes the relative differences in noise magnitude between FBP and DLIR, was calculated. The NRM values ranged from 0.0 to 1.0. A low NRM value represents a less aggressive noise reduction. The histograms of the NRM value were analyzed for the uniform and non-uniform regions.

#### RESULTS

The reduction in noise magnitude compared with FBP tended to be greater with AC (45%-85%) than with TF (32%-65%). The average NPS frequencies of TF and AC were almost comparable to those of FBP, except for the low-dose condition and the high noise reduction strength for AC. The NRM values of TF and AC were higher in the uniform region than in the non-uniform region. In the non-uniform region, TF's average NRM values (0.21-0.48) tended to be lower than AC's (0.39-0.78). The histograms for TF showed a small overlap between the uniform and the non-uniform regions; in contrast, those for AC showed a greater overlap. This difference seems to indicate that TF processes the uniform and non-uniform regions more differently than AC does.

#### CONCLUSION

s This study has revealed a distinct difference in characteristics between the two DLIR techniques: TF tends to offer less aggressive noise reduction in non-uniform regions and preserve the original signals, whereas AC tends to prioritize noise filtering over edge-preservation, especially at the low-dose condition and with the high noise reduction strength.

#### CLINICAL RELEVANCE/APPLICATION

An appropriate combination of strength and dose level should be selected for clinical use of each DLIR technique.

Printed on: 02/07/23

## Abstract Archives of the RSNA, 2022

M5B-SPPH-6

### **Discriminability of Frequency-Dependent Non-Gaussian Noise Properties in CT and the Limitation of the Noise Power Spectrum to Describe Noise Texture with Non-Linear Reconstruction Algorithms.**

Monday, Nov. 28 12:45PM - 1:15PM Room: Learning Center - PH DPS

#### **Participants**

Daniel Shin, MS, Los Angeles, CA (*Presenter*) Employee, Canon Medical Systems Corporation

#### **PURPOSE**

To demonstrate the impact of frequency-dependent higher order, non-Gaussian noise properties on perceived noise texture via a human observer study using abdominal CT reconstruction algorithms as a use case.

#### **METHODS AND MATERIALS**

A 32 cm water phantom was scanned at two tube current levels on an Aquilion ONE Genesis CT system (Canon Medical Systems, Otawara, Japan). The raw data was reconstructed with three abdominal reconstruction algorithms: a model-based iterative reconstruction (MBIR) algorithm (FIRST), a deep-learning reconstruction (DLR) algorithm (AiCE), and, for one tube current, filtered backprojection (FBP) as a control. First, quantitative analysis of the noise in the resulting reconstructions was performed by extracting regions of interest (ROIs) (100x100 pixels) from the image data and assessing the 4th order statistics of each ROI via a global and frequency-binned excess kurtosis measurement. To evaluate the detectability of the non-Gaussian characteristics of these noise images, pure Gaussian noise counterpart image datasets with the same mean, standard deviation (SD), and Noise Power Spectrum (NPS) as each acquired data condition were also generated by convolving random white noise with the root-NPS of the acquired data. Then, using a two-alternative forced choice experiment, nine naïve observers were tasked with distinguishing the acquired noise image from its pure Gaussian counterpart.

#### **RESULTS**

Excess kurtosis in the image ROIs was 0.01 for FBP, 0.74-0.85 for FIRST, and -0.13-0.21 for AiCE. Excess kurtosis trends differ with frequency band. From the observer study, it was found that FBP images appear indistinguishable from their pure Gaussian counterparts (AUC=.54), while MBIR images were readily distinguishable from Gaussian ones (AUC=.98-1). DLR images are more difficult to distinguish from their pure Gaussian counterparts (AUC 0.56-.85), which indicates that perceived noise texture is more similar to Gaussian noise.

#### **CONCLUSION**

s This work demonstrates that the appearance of CT noise texture may be dependent on frequency-dependent higher-order statistics not captured by the NPS. In some cases, noise textures with identical NPS and SD can be distinguished based on non-Gaussian properties. Deep-learning reconstruction has lower levels of excess kurtosis and is less readily discriminable from Gaussian noise, despite having a similar NPS to MBIR.

#### **CLINICAL RELEVANCE/APPLICATION**

Noise texture can influence the acceptability of a reconstruction algorithm to the radiologist and thus full characterization of the noise is key to understanding and describing reconstruction algorithm performance.

Printed on: 02/07/23

## Abstract Archives of the RSNA, 2022

M5B-SPPH-7

### A Multi Decade Study of CT Protocol Optimization underneath the Influence of Physicists, Radiologists and Improving Scanner Technologies

Monday, Nov. 28 12:45PM - 1:15PM Room: Learning Center - PH DPS

#### Participants

Joseph Meier, PhD, Madison, WI (*Presenter*) Nothing to Disclose

#### PURPOSE

Adjusting CT protocols for optimization of image quality across a large site requires a multidisciplinary effort. Optimizing the performance of Automatic Tube Current Control (AEC) avoids acquiring images with high amounts of noise or with too low noise when the tube current (mA) is maxxing or minning out respectively. This study investigates the longitudinal impact that protocol optimization by a team of medical physicists and radiologists and improvements in scanner technology have on the performance of the site's AEC.

#### METHODS AND MATERIALS

We analyzed 536 exams from either routine chest or routine abdomen from early protocol optimization(2007-2008) and 739 from current protocol optimization(2021-2022). Proper AEC function was measured for each examination by calculating the percentage of images at the maximum mA (%imgmax\_mA)and minimum(%imgmin\_mA). Examinations were classified as suboptimal if the %imgmax\_mA or %imgmin\_mA was greater than 20%.

#### RESULTS

For the chest exams, the mean %imgmax\_mA decreased from  $31.9 \pm 32.6\%$  to  $10.3 \pm 8.5\%$ ( $p<0.001$ ) from the early to current protocol periods. Similarly, for the abdominal exams the mean %imgmax\_mA decreased from  $35.4 \pm 35.5\%$  to  $14.3 \pm 16.6\%$  ( $p<0.001$ ). For the chest exams, the mean %imgmin\_mA decreased from  $19.0 \pm 32.1\%$  to  $3.6 \pm 4.2\%$ ( $p<0.001$ ). Similarly, for the abdominal exams, the mean %imgmin\_mA decreased from  $21.8 \pm 35.1\%$  to  $3.6 \pm 13.4\%$ ( $p<0.001$ ). The percent of suboptimal chest exams for %imgmax\_mA(%imgmin\_mA) decreased from 46.4(21.6)% to 8.2(1.1)%. Similarly, the percent of suboptimal abdominal exams for %imgmax\_mA(%imgmin\_mA), decreased from 44.3(27.4)% to 12.0(3.0)%.

#### CONCLUSION

s This work shows that the incidence of suboptimal routine chest and abdominal examinations as measured by the percentage of images at the maximum or minimum mA, was greatly reduced through protocol optimization by medical physicists and radiologists as well as emerging scanner technology.

#### CLINICAL RELEVANCE/APPLICATION

A multidecade analysis of CT tube current modulation data shows that the efforts of medical physicists and radiologists combined with evolving scanner technology has greatly reduced the number of suboptimal CT exams.

Printed on: 02/07/23



## Abstract Archives of the RSNA, 2022

M5B-SPPH-8

### Clinical Thorax CT Image Quality Assessment Using Spectral and Spatial Features

Monday, Nov. 28 12:45PM - 1:15PM Room: Learning Center - PH DPS

#### Participants

Zahra Passand, MSc, (*Presenter*) Nothing to Disclose

#### PURPOSE

The quality of computed tomography (CT) images is affected by different parameters such as patient motion and anatomy, detector design, scatter, the reconstruction algorithm and others. Patient CT images are not automatically analyzed by the scanner software during clinical routine. Introducing continuous monitoring of CT image quality would be beneficial for diagnostic purposes. As a consequence of such a broader analysis, the applied dose could be reduced while maintaining sufficient image quality level. Since most of the existing image quality analysis approaches are based on dedicated phantoms, we propose a method which combines the modulation transfer function (MTF), the frequency spectrum and the noise power spectrum (NPS) in a predefined regions of interest (ROI) to compute various image quality features. A classifier was trained using these features to distinguish different level of image quality.

#### METHODS AND MATERIALS

The thorax CT images which were acquired from 30 patients were annotated by different radiologists. In this initial study, two quality levels (either "low" or "high") were used. For each CT image, an ROI containing the major fissure of the left lung was manually selected and was used to estimate the image quality. The outer edges of the major fissure were automatically detected using an active contour algorithm. The MTF was computed using the edge and line scan functions of the major fissure within the selected ROI. In addition to the MTF, the frequency power spectrum was estimated in the same ROI. The NPS was estimated from a homogenous area close to the ROI of the major fissure. Based on the parameters, several other frequency domain features were derived to determine the image quality. A classifier was trained using these features.

#### RESULTS

Using the estimated features, a classification accuracy of 89% was achieved using the validation data set.

#### CONCLUSION

Using the image quality features which were defined for this work, CT images were classified in one of the two image quality categories. The classification results were in high agreement with the manual annotation performed by radiologists. Future work will include additional features and CT images to further improve and validate this approach.

#### CLINICAL RELEVANCE/APPLICATION

The developed method has the potential to be used during clinical routine for image quality analysis and documentation. Long term studies would be required to analyze the quality over a larger population to investigate potential dose reduction strategies.

Printed on: 02/07/23

## Abstract Archives of the RSNA, 2022

M5B-SPPH-9

### Deep Scatter Estimation (DSE) for High Scatter Frequencies caused by Coarse Anti Scatter Grids in Clinical CT

Monday, Nov. 28 12:45PM - 1:15PM Room: Learning Center - PH DPS

#### Participants

Julien Erath, Forchheim, Germany (*Presenter*) Employee, Siemens AG

#### PURPOSE

To estimate and correct for high frequencies in scatter signals transmitted through coarse anti scatter grids (ASGs) as used in photon counting CT.

#### METHODS AND MATERIALS

CT detectors with very small pixels, such as in photon-counting CT, may have anti scatter grids with a grid spacing being an integer multiple of the detector pixel size. For example, an ASG field may comprise a 2x3 matrix of detector pixels. The shading of the scattered radiation caused by the grid affects each of the six pixels within a grid field differently. Although scatter is a low frequency effect, this pixel-dependent shading results in high frequencies in the scatter signal transmitted through the ASG. These may cause moiré artifacts in the reconstructed images. We trained a deep learning-based scatter estimation (DSE) network to estimate that scatter signal, which can then be used to correct the measured data (e.g. by subtraction). To train DSE, scatter signals were obtained by Monte Carlo simulation of patient CT data. The geometry of the CT and of the coarse ASG matches the one of a clinical photon-counting CT (Naeotom Alpha, Siemens Healthineers). To adapt the network architecture to the coarse ASG, the network receives the six different pixel locations as separate input channels and is trained to predict six different output channels of the pixel locations, which can then be merged to obtain the scatter estimation for the whole detector. The DSE-corrected data are then reconstructed and evaluated in image domain.

#### RESULTS

With the proposed neural network, the high frequency components of the scatter signal can be estimated and corrected very efficiently. DSE reduces scatter artifacts across all patients from a mean absolute error of about 10 HU to below 1 HU. DSE reduces scatter artifacts across all patients from a mean absolute error of about 10 HU to below 1 HU. The amplitude of the moiré artifacts can be reduced from about 15 HU to below 2 HU. With the proposed algorithm the moiré artifacts can be significantly reduced and the diagnostic image quality improved.

#### CONCLUSION

DSE can estimate ASG-modulated scatter frequencies in CT data and correct both for the scatter artifacts and for the moiré artifacts caused by the coarse ASG.

#### CLINICAL RELEVANCE/APPLICATION

DSE leads to an accurate scatter correction of the moiré artifacts and can be crucial for accurate diagnostic CT image quality.

Printed on: 02/07/23



## Abstract Archives of the RSNA, 2022

M5B-SPVA

### Vascular Monday Poster Discussions - B

Monday, Nov. 28 12:45PM - 1:15PM Room: Learning Center - VA DPS

#### Sub-Events

#### M5B-SPVA-1 Noise-Optimized Virtual Monoenergetic Reconstruction Improves Diagnostic Accuracy and Image Quality of Dual-Energy CT Angiography in Peripheral Arterial Occlusive Disease

##### Participants

Philipp Gruschwitz, Wuerzburg, Germany (*Presenter*) Nothing to Disclose

##### PURPOSE

The aim of this study was to evaluate the influence of a noise optimized virtual monoenergetic reconstruction algorithm (VMI+) on the image quality and diagnostic accuracy of dual-energy (DE) computed tomography angiography (CTA) of the lower extremity runoff.

##### METHODS AND MATERIALS

A total of 118 lower extremity runoff CTA performed on a 3rd generation DE-CT scanner in 109 patients (54 females;  $75.6 \pm 9.5$  years) were included in this IRB-approved, HIPAA-compliant retrospective study. Axial image stacks were reconstructed with standard 120 kV setting and VMI+ of different keV levels. Objective image quality criteria (contrast attenuation, signal-to-noise [SNR] and contrast-to-noise ratio [CNR]) were measured and subjective image quality was evaluated. Diagnostic accuracy for significant stenosis (>75%) and vessel occlusion was assessed for 120 kV and 50 keV VMI+ images. In all patients, a digital subtraction angiography (DSA) served as standard of reference.

##### RESULTS

Intraluminal attenuation was highest in 40/50 keV VMI+ while SNR were similar to 120 kV images. In subjective assessment, intraluminal contrast of 50 keV images was deemed superior compared to 120 kV despite higher image noise. Sensitivity, specificity and accuracy of the detection of a vessel occlusion were superior in 50 keV VMI+, especially for the lower leg runoff (70%/92%/84%; 70%/91%/83%;  $p < 0.001$ ). 13 of 118 (11%) lower leg runoffs were only assessable with 50 keV VMI+. Relevant stenosis (> 75%) was found with 100% accuracy on VMI+.

##### CONCLUSION

s VMI+ reconstructions improve objective and subjective image quality and diagnostic accuracy of DE-CTA, allowing also the evaluation of lower leg runoffs inassessable with standard images.

##### CLINICAL RELEVANCE/APPLICATION

We could show that virtual monoenergetic reconstructions facilitate superior diagnostic accuracy compared to conventional linear blended images for significant artery stenosis and also allows for correct assessment of lower leg runoffs with pronounced arteriosclerosis that are not assessable with standard reformatting, first with sufficient patient number (109) using digital subtraction angiography as reference standard. These results underline that 50 keV should be used for routine evaluation of DE-CTA.

Printed on: 02/07/23

## Abstract Archives of the RSNA, 2022

M5B-SPVA-1

### Noise-Optimized Virtual Monoenergetic Reconstruction Improves Diagnostic Accuracy and Image Quality of Dual-Energy CT Angiography in Peripheral Arterial Occlusive Disease

Monday, Nov. 28 12:45PM - 1:15PM Room: Learning Center - VA DPS

#### Participants

Philipp Gruschwitz, Wuerzburg, Germany (*Presenter*) Nothing to Disclose

#### PURPOSE

The aim of this study was to evaluate the influence of a noise optimized virtual monoenergetic reconstruction algorithm (VMI+) on the image quality and diagnostic accuracy of dual-energy (DE) computed tomography angiography (CTA) of the lower extremity runoff.

#### METHODS AND MATERIALS

A total of 118 lower extremity runoff CTA performed on a 3rd generation DE-CT scanner in 109 patients (54 females;  $75.6 \pm 9.5$  years) were included in this IRB-approved, HIPAA-compliant retrospective study. Axial image stacks were reconstructed with standard 120 kV setting and VMI+ of different keV levels. Objective image quality criteria (contrast attenuation, signal-to-noise [SNR] and contrast-to-noise ratio [CNR]) were measured and subjective image quality was evaluated. Diagnostic accuracy for significant stenosis (>75%) and vessel occlusion was assessed for 120 kV and 50 keV VMI+ images. In all patients, a digital subtraction angiography (DSA) served as standard of reference.

#### RESULTS

Intraluminal attenuation was highest in 40/50 keV VMI+ while SNR were similar to 120 kV images. In subjective assessment, intraluminal contrast of 50 keV images was deemed superior compared to 120 kV despite higher image noise. Sensitivity, specificity and accuracy of the detection of a vessel occlusion were superior in 50 keV VMI+, especially for the lower leg runoff (70%/92%/84%; 70%/91%/83%;  $p < 0.001$ ). 13 of 118 (11%) lower leg runoffs were only assessable with 50 keV VMI+. Relevant stenosis (> 75%) was found with 100% accuracy on VMI+.

#### CONCLUSION

s VMI+ reconstructions improve objective and subjective image quality and diagnostic accuracy of DE-CTA, allowing also the evaluation of lower leg runoffs inassessable with standard images.

#### CLINICAL RELEVANCE/APPLICATION

We could show that virtual monoenergetic reconstructions facilitate superior diagnostic accuracy compared to conventional linear blended images for significant artery stenosis and also allows for correct assessment of lower leg runoffs with pronounced arteriosclerosis that are not assessable with standard reformatting, first with sufficient patient number (109) using digital subtraction angiography as reference standard. These results underline that 50 keV should be used for routine evaluation of DE-CTA.

Printed on: 02/07/23

## Abstract Archives of the RSNA, 2022

R2-SPBR

### Breast Thursday Poster Discussions

Thursday, Dec. 1 9:00AM - 9:30AM Room: Learning Center - BR DPS

#### Participants

Phoebe Freer, MD, Park City, UT (*Moderator*) Nothing to Disclose

#### Sub-Events

#### **R2-SPBR-1 Assessing the necessity of implant included mammography in women with breast implants.**

#### Participants

Hee Jeong Kim, MD, Seoul, Korea, Republic Of (*Presenter*) Nothing to Disclose

#### PURPOSE

To investigate the necessity of implant full (IF) views in mammography for women with breast implants.

#### METHODS AND MATERIALS

Screening and diagnostic augmentation mammography performed in 748 women (mean age  $\pm$  standard deviation, 46.4  $\pm$  8.9 years) with no prior history of breast cancer from January 2009 to December 2019 were retrospectively identified. Routine mammography included four IF views and four implant displaced (ID) views. Breast cancer detection rate, sensitivity, mean glandular dose per breast, and implant rupture detection rate were evaluated and compared between routine eight views, four IF views and four ID views. Between-group differences were evaluated statistically using the t-test or paired t-test for continuous variables and the chi-square test for categorical variables. Cancer detection rate and sensitivity were compared using McNemar's test. A p-value less than 0.05 was considered statistically significant.

#### RESULTS

Incidence of breast cancer was 17.6% (132/748) and 15% (20/132) were mammographically occult. Breast cancer detection rate of routine eight views (15%; 95% CI: 12.6%, 17.7%) was higher than that of IF views (8.8%; 95% CI: 7.0%, 11.1%;  $p < 0.0001$ ), while not different from that of ID views (15%; 95% CI: 12.5%, 17.6%;  $p > 0.999$ ). The sensitivity of routine eight views (84.8%; 95% CI: 77.8%, 90.0%) was significantly higher than that of IF views (50%; 95% CI: 41.6%, 58.4%;  $p < 0.0001$ ), while not different from that of ID views (84.8%; 95% CI: 77.8%, 90.0%;  $p > 0.999$ ). Mean glandular dose was 1.05 mGy in routine eight views and 0.99 mGy in ID views ( $p < 0.0001$ ). Implant rupture was found in 2.1% (16/748). Implant rupture detection rate was 81.3% (13/16) in routine eight views and IF views and 12.5% (2/16) in ID views.

#### CONCLUSION

Routine eight-view mammography and four ID views showed similar performance for detecting breast cancer and the diagnostic gain of four IF views was low.

#### CLINICAL RELEVANCE/APPLICATION

Considering the low clinical impact and cumulative radiation, the necessity IF views in mammography need to be reconsidered in women with breast implants.

#### **R2-SPBR-2 Comparing the Performance of Full-Field Digital Mammography (FFDM) and Digital Breast Tomosynthesis (DBT) in the Post-Treatment Surveillance of Patients with a History of Breast Cancer: A Retrospective Study**

#### Participants

Emily Nia, MD, Houston, TX (*Presenter*) Nothing to Disclose

#### PURPOSE

Guidelines for imaging follow-up in patients with a history of breast cancer vary among different medical societies. However, all recommend annual screening mammography. The purpose of our study was to compare the performance of full-field digital mammography (FFDM) alone against FFDM plus digital breast tomosynthesis (DBT) in the post-treatment surveillance of asymptomatic patients with a history of breast cancer.

#### METHODS AND MATERIALS

In this institutional review board (IRB) approved retrospective review study, a comprehensive list of women with a history of breast cancer who underwent screening with either FFDM or FFDM plus DBT at our institution from 5/2017 to 5/2020 was retrieved. A total of 20,211 exams were identified and screening performance metrics were compared.

#### RESULTS

There was no significant difference in cancer detection rate (CDR) (9.4/1000 vs. 8.2/1000,  $P = 0.38$ ), recall rate (RR) (7.5% vs.

6.9%,  $P=0.087$ ), or positive predictive value (PPV) (12.5% vs. 11.9%,  $P=0.74$ ) between FFDM alone vs. FFDM plus DBT. Stratification by breast tissue identified no significant difference in CDR ( $P=0.581$  and  $P=0.428$ ), RR ( $P=0.230$  and  $P=0.205$ ), or PPV ( $P=0.908$  and  $P=0.721$ ) between fatty/scattered and heterogeneous/extremely dense breast tissue when comparing FFDM alone vs. FFDM plus DBT. Stratification by age did not identify a significant difference in RR or PPV between the two groups. However, CDR was significantly increased with FFDM alone vs. FFDM plus DBT in the 60-69 years group ( $P=0.021$ ). Stratification by race did not identify a significant difference in RR or PPV between the two groups. However, CDR was significantly increased with FFDM plus DBT vs. FFDM alone in white women ( $P=0.036$ ). Stratification by laterality (bilateral vs. unilateral exams post mastectomy) did not identify a significant difference in RR or PPV between the two groups. However, CDR was significantly increased in FFDM alone vs. FFDM plus DBT in unilateral exams ( $P=0.009$ ).

## CONCLUSION

In general, the addition of DBT to FFDM does not improve CDR, RR, or PPV for asymptomatic women with a history of breast cancer.

## CLINICAL RELEVANCE/APPLICATION

Supplemental screening modalities are needed beyond DBT for patients with a history of breast cancer.

### R2-SPBR-3 Mammographic compression and its association with lesion conspicuity for calcification-only lesions

Participants

Melissa L. Hill, PHD, (*Presenter*) Consultant, Volpara Health Technologies Limited

## PURPOSE

To investigate associations between modifiable mammographic image factors and conspicuity for lesions detectable by calcification only.

## METHODS AND MATERIALS

OPTIMAM database cases were selected among 2343 with raw images and lesion conspicuity scores. Expert readers at two sites where screening was originally performed retrospectively marked regions of interest (ROI) and classified conspicuity for biopsy-proven lesions. After exclusions (bilateral lesions, implants, missing data) and selection of cases with lesions whose only mammographic features were calcifications, 586 cases (37 benign, 547 malignant) were included with obvious (OC;  $n=349$ ), subtle (SC;  $n=201$ ), or very subtle (VSC;  $n=36$ ) conspicuity. Volumetric breast density (VBD), breast volume, compression pressure, contact area, and breast positioning measures were derived using Volpara Imaging Software (v3.4). Other factors were extracted from DICOM metadata (compression force, breast thickness, paddle type). VBD was computed as the mean from contralateral breast views, with all other image parameters from the affected breast MLO view only. Lesion ROI size, image-based lesion features, and histopathological characteristics were collected. Univariate analysis was performed to test non-modifiable parameters for associations with conspicuity. A multinomial logistic regression model was fit to predict lesion conspicuity for calcification-only lesions using Akaike Information Criterion for predictor selection among modifiable image factors and the parameters identified in univariate testing.

## RESULTS

After adjusting for confounders, the longest ROI side length, compression pressure and screening site were significantly associated with the risk of SC and VSC vs OC, with odds ratios (OR) and 95% confidence intervals (CI) of 0.96 (0.94-0.97), 0.85 (0.78-0.92) and 0.52 (0.36-0.77), respectively for SC vs OC, and 0.93 (0.90-0.97), 0.81 (0.67-0.97) and 0.21 (0.08-0.53), respectively for VSC vs OC. Compression force was significantly associated with only SC vs OC, with OR and 95% CI of 1.01 (1.00-1.02).

## CONCLUSION

Among modifiable mammographic image factors in the MLO view, multinomial modelling demonstrated compression pressure to be predictive of calcification-only lesion conspicuity, with greater pressure reducing the risk of lower conspicuity. These results suggest that pressure-based compression targets may be effective towards achieving good diagnostic performance.

## CLINICAL RELEVANCE/APPLICATION

The conspicuity of lesions visible on mammography by calcification only are associated with mammographic compression pressure. Screening program performance may benefit from ensuring adequate compression pressure.

### R2-SPBR-4 Artificial Intelligence (AI) Comparison of Synthetic Mammography (SM) and Full Field Digital Mammography (FFDM) in Malignancy Detection

Participants

Laura Heacock, MD, MS, New York, NY (*Presenter*) Nothing to Disclose

## PURPOSE

To evaluate the strengths and weaknesses of AI systems trained separately on synthetic mammography (SM) and full field digital mammography (FFDM).

## METHODS AND MATERIALS

This was a retrospective, IRB-approved study. We trained two identical AI systems separately on paired FFDM and SM images, respectively, on a dataset of 1,239,272 combination (FFDM + DBT) screening mammography exams consecutively acquired from patients between 2017-2020. These examinations were separated with a 60/10/30 training/validation/test set split. Ground truth was either pathology-proven diagnosis or stability on imaging over time. Additionally, the images were supplemented with radiologist-annotated segmentation labels and classification for these segmentations (malignant/benign, distortion/non-distortion). The model is trained to localize lesions by generating the location of suspicious areas in the exam with bounding boxes. These detections are then used to generate a final score of malignancy for each mammogram. Preset false-positive (FP) rates were chosen for analysis. Location of bounding boxes on false negatives (FN) and high-scoring (high discrepancy between SM and FFDM AI scores) FP exams were reviewed and compared for both SM and FFDM models. Area under the curve (AUC) and chi-squared tests were used for statistical analysis.

## RESULTS

The AI system achieved an AUC of 0.933 on SM and 0.909 on FFDM for identifying exams with malignant lesions. At a preset FP rate of 20%, there was a SM FN rate of 0.007% (9/121858) and a FFDM rate of 0.009% (12/121858). On review of bounding boxes, 58.3% (7/12) FN findings on FFDM were detected by the model but did not meet AI score criteria for malignancy. 66.7% (6/9) of SM findings were detected by the model but did not meet AI score criteria ( $p=0.34$ ). SM FN were more likely to be masses compared to FFDM FN (7/9 vs 0/12;  $p<0.001$ ); FFDM FN were more likely to be distortion (50%; 6/12) or calcifications (25%; 3/12). There was no significant correlation between FN in either modality and breast density, size, presence/absence of distortion, or presence/absence of calcifications. High-scoring FFDM FP were more likely to be asymmetries or circumscribed masses. High-scoring SM FP were more likely to be pseudo-distortion or pseudo-calcifications on review of corresponding DBT.

## CONCLUSION

s AI systems highlight different areas of concern on FFDM and SM images, but demonstrate better performance on SM images.

## CLINICAL RELEVANCE/APPLICATION

Most AI systems are trained on FFDM images. Radiologists using AI systems as a second reader should be aware that the strengths and weaknesses of these systems may vary when used on DBT-generated SM views.

### R2-SPBR-5 Evaluation of The Impact of Sociodemographic Status on Breast Screening Volumes During The COVID-19 Pandemic In a Provincial, Population-based Organized Breast Screening Program

Participants

Tracee Wee, MD, BSc, Vancouver, BC (*Presenter*) Nothing to Disclose

## PURPOSE

We sought to assess the impact of sociodemographic status on breast screening volumes (BSVs) during the COVID-19 pandemic in a large, population-based breast screening program which exclusively serves a provincial population of over 5 million.

## METHODS AND MATERIALS

The BC Cancer Breast Screening database, a population-based database, was the primary dataset accessed. All patients who completed breast screening between April 1st, 2017 and March 31st, 2021 were eligible to participate. An average of three annual periods between April 1st, 2017 and March 31st, 2020 was utilized as the pre-COVID period to limit the effect of annual variation while the period between April 1st, 2020 and March 31st, 2021 was utilized as the COVID-impacted period. Residential postal codes were utilized to impute sociodemographic variables. The Postal CodeOM Conversion File Plus was utilized to map residential postal codes to 2016 Census standard geographical areas, which provided information on community size, income quintile and dissemination areas. Dissemination areas were subsequently linked to the Canadian Index of Multiple Deprivation (CIMD), which assigns a level of deprivation for each dissemination area in four dimensions.

## RESULTS

Overall BSV was reduced by 23.0% during the COVID-impacted period as compared to the pre-COVID period. Percent reduction in BSV was greatest among younger patients 40 to 49 years of age (-31.3%) and patients residing in communities with a population of less than 10 000 (-27.0%). Percent reduction in BSV was greatest among patients in the lowest income quintile (-28.1%). Percent reduction in BSV was greatest for patients in the most deprived quintiles across all four dimensions of the CIMD: ethnocultural composition (-28.1%), situational vulnerability (-26.7%), economic dependency (-24.5%), and residential instability (-23.7%).

## CONCLUSION

s Disproportionate reductions in BSVs were observed among younger patients, patients residing in rural communities, patients in lower income quintiles, and patients in quintiles which were most deprived during the COVID-19 pandemic.

## CLINICAL RELEVANCE/APPLICATION

Identification of the exacerbation of underlying inequities in access to breast screening during the COVID-19 pandemic provides the opportunity to improve equitable access to breast screening for vulnerable populations.

### R2-SPBR-6 Racial Disparities in Proportion of Patients Returning for Annual Screening Mammograms

Participants

Mina Moussavi, BSc, PhD, (*Presenter*) Employee, RadNet, Inc

## PURPOSE

Screening guidelines are increasingly being scrutinized for appropriateness for all racial groups, as evidence suggests that cancer incidence and mortality may differ by race. Any such changes might need to consider adherence to current guidelines among these racial groups to more realistically address cancer disparities. We sought to compare the percentage of patients returning for recommended annual screening by race/ethnicity in a large and diverse population across the USA.

## METHODS AND MATERIALS

Screening mammography data was retrospectively collected from 186 clinical sites across the United States from 2017-2021. Screening exams from 1,391,248 patients above the age of 35 years (mean age 58.2+/- 11.0 years) were collected. We reviewed patients with an initial exam prior to June 2019 and a subsequent screening exam 9-30 months later. The interval between initial and subsequent screening mammograms was defined as annual if they were 9-18 months apart and biennial if they were 19-30 months apart. We then analyzed the proportion of returning patients who were screened at the recommended annual cadence broken down by self-reported race and ethnicity. Confidence intervals were calculated using the adjusted Wald method.

## RESULTS

White patients ( $n=396,372$ ) returned annually more often than Black ( $n=159,823$ ) and Asian ( $n=81,276$ ) patients at 75.8%, 71.4%, and 71.8%, respectively. The proportion of Hispanic/Latino ( $n=152,126$ ), Native Hawaiian/Pacific Islander ( $n=6,066$ ), and American Indian/Alaska Native patients ( $n=4,332$ ) returning annually was the lowest of all ethnic groups at 69.6%, 69.1%, and 68.3%, respectively.

## CONCLUSION

s Black, Asian, and women from other non-White populations return for screening at a meaningfully lower rate than White women. As revisions to guidelines are being considered, these data on real-world adherence to existing guidelines might better inform any changes.

## CLINICAL RELEVANCE/APPLICATION

Racial disparities in breast cancer screening adherence continue to persist and should be considered when updating mammography screening guidelines.

## R2-SPBR-7 Visibility Trends and Tumor Characteristics of Malignant Architectural Distortion on Synthesized 2D and Tomosynthesis Mammograms: Can We Move Away From Surgery For A Low Risk AD Subset?

Participants

Cedric Pluguez-Turull, MD, Miami, FL (*Presenter*) Consultant, INFOTECHSoft, Inc

## PURPOSE

Explore visibility trends of tomography-detected (TOMO) architectural distortion (AD) on synthesized 2D (s2D) mammography (MMG) and digital breast tomosynthesis (DBT) as well as other imaging and clinical parameters that predict pathology.

## METHODS AND MATERIALS

Clinical and imaging data was extracted from our EMR and PACS for 1.7 years of biopsied AD with both DBT and s2D at diagnosis yielding 297 cases. A retrospective review of clinical and imaging parameters on MMG, MRI and US was performed. Visibility analysis by consensus read was performed by three breast radiologists documenting AD on one view (CC or ML/MLO), two views or no views for s2D, and one view or two views on DBT. Other clinical and imaging parameters were also analyzed for statistical associations to pathologic outcomes. Tumor size, hormone receptor, Her2 and Ki67 for invasive breast cancer (IBC) were analyzed by consensus visibility.

## RESULTS

297 biopsied AD detected by s2d + TOMO, 99 were malignant (33%), 89 were high-risk (30%), and 109 were benign (37%). PPV3 for malignancy was 33%. The most common outcome by sub-group is: IDC (54%) for malignancy, radial scar (88%) for high-risk, and stromal fibrosis (52%) for benign. The presence of an US correlate increases the likelihood of malignancy by 2.4x (PLR) with PPV=88%. A positive MRI increases malignancy likelihood by 4.2x (PLR) with PPV= 83% and the absence decreases the likelihood by 0.04x (NLR) with NPV=96%. Interreader agreement is fair (k=0.4) for tomo AD and fair (k=0.35) for s2D AD. Visibility analysis demonstrates more s2D-occult AD correspond to benign and high-risk subsets compared to s2D visible AD. There is a linear trend (p=0.03) for benign AD manifesting as s2D-occult or one view finding on TOMO. A loose trend of increasing malignant AD findings as s2D+TOMO visibility increases was not significant (p=0.93). The 2D-occult iBC size (median, IQR: 12,15) is smaller compared to 2D-visible iBC (median, IQR: 20,25) (p=0.04). No differences were found for tumor markers and molecular subtype.

## CONCLUSION

s Interreader analysis shows there is poor agreement on AD detection for both s2D and TOMO AD. Negative MRI is suitable for downgrading AD to low suspicion for malignancy and perhaps defer biopsy. A higher proportion of benign and high-risk s2D-occult AD explains a decreased PPV for malignancy arising from AD in the DBT era. iBC arising from 2D-occult TOMO AD that were previously undetectable by 2D MMG are similar in tumor biology than their 2D-visible counterparts, but smaller in size.

## CLINICAL RELEVANCE/APPLICATION

DBT finds identical, yet smaller, iBC than s2D mammography. Pertinent clinical and imaging factors could sway the breast imager to consider short-term follow-up or pre-biopsy Breast MRI for a particular subset of low-risk AD and patients.

Printed on: 02/07/23

## Abstract Archives of the RSNA, 2022

R2-SPBR-1

### Assessing the necessity of implant included mammography in women with breast implants.

Thursday, Dec. 1 9:00AM - 9:30AM Room: Learning Center - BR DPS

#### Participants

Hee Jeong Kim, MD, Seoul, Korea, Republic Of (*Presenter*) Nothing to Disclose

#### PURPOSE

To investigate the necessity of implant full (IF) views in mammography for women with breast implants.

#### METHODS AND MATERIALS

Screening and diagnostic augmentation mammography performed in 748 women (mean age  $\pm$  standard deviation, 46.4  $\pm$  8.9 years) with no prior history of breast cancer from January 2009 to December 2019 were retrospectively identified. Routine mammography included four IF views and four implant displaced (ID) views. Breast cancer detection rate, sensitivity, mean glandular dose per breast, and implant rupture detection rate were evaluated and compared between routine eight views, four IF views and four ID views. Between-group differences were evaluated statistically using the t-test or paired t-test for continuous variables and the chi-square test for categorical variables. Cancer detection rate and sensitivity were compared using McNemar's test. A p-value less than 0.05 was considered statistically significant.

#### RESULTS

Incidence of breast cancer was 17.6% (132/748) and 15% (20/132) were mammographically occult. Breast cancer detection rate of routine eight views (15%; 95% CI: 12.6%, 17.7%) was higher than that of IF views (8.8%; 95% CI: 7.0%, 11.1%;  $p < 0.0001$ ), while not different from that of ID views (15%; 95% CI: 12.5%, 17.6%;  $p > 0.999$ ). The sensitivity of routine eight views (84.8%; 95% CI: 77.8%, 90.0%) was significantly higher than that of IF views (50%; 95% CI: 41.6%, 58.4%;  $p < 0.0001$ ), while not different from that of ID views (84.8%; 95% CI: 77.8%, 90.0%;  $p > 0.999$ ). Mean glandular dose was 1.05 mGy in routine eight views and 0.99 mGy in ID views ( $p < 0.0001$ ). Implant rupture was found in 2.1% (16/748). Implant rupture detection rate was 81.3% (13/16) in routine eight views and IF views and 12.5% (2/16) in ID views.

#### CONCLUSION

s Routine eight-view mammography and four ID views showed similar performance for detecting breast cancer and the diagnostic gain of four IF views was low.

#### CLINICAL RELEVANCE/APPLICATION

Considering the low clinical impact and cumulative radiation, the necessity IF views in mammography need to be reconsidered in women with breast implants.

Printed on: 02/07/23



## Abstract Archives of the RSNA, 2022

R2-SPBR-2

### Comparing the Performance of Full-Field Digital Mammography (FFDM) and Digital Breast Tomosynthesis (DBT) in the Post-Treatment Surveillance of Patients with a History of Breast Cancer: A Retrospective Study

Thursday, Dec. 1 9:00AM - 9:30AM Room: Learning Center - BR DPS

#### Participants

Emily Nia, MD, Houston, TX (*Presenter*) Nothing to Disclose

#### PURPOSE

Guidelines for imaging follow-up in patients with a history of breast cancer vary among different medical societies. However, all recommend annual screening mammography. The purpose of our study was to compare the performance of full-field digital mammography (FFDM) alone against FFDM plus digital breast tomosynthesis (DBT) in the post-treatment surveillance of asymptomatic patients with a history of breast cancer.

#### METHODS AND MATERIALS

In this institutional review board (IRB) approved retrospective review study, a comprehensive list of women with a history of breast cancer who underwent screening with either FFDM or FFDM plus DBT at our institution from 5/2017 to 5/2020 was retrieved. A total of 20,211 exams were identified and screening performance metrics were compared.

#### RESULTS

There was no significant difference in cancer detection rate (CDR) (9.4/1000 vs. 8.2/1000,  $P=0.38$ ), recall rate (RR) (7.5% vs. 6.9%,  $P=0.087$ ), or positive predictive value (PPV) (12.5% vs. 11.9%,  $P=0.74$ ) between FFDM alone vs. FFDM plus DBT. Stratification by breast tissue identified no significant difference in CDR ( $P=0.581$  and  $P=0.428$ ), RR ( $P=0.230$  and  $P=0.205$ ), or PPV ( $P=0.908$  and  $P=0.721$ ) between fatty/scattered and heterogeneous/extremely dense breast tissue when comparing FFDM alone vs. FFDM plus DBT. Stratification by age did not identify a significant difference in RR or PPV between the two groups. However, CDR was significantly increased with FFDM alone vs. FFDM plus DBT in the 60-69 years group ( $P=0.021$ ). Stratification by race did not identify a significant difference in RR or PPV between the two groups. However, CDR was significantly increased with FFDM plus DBT vs. FFDM alone in white women ( $P=0.036$ ). Stratification by laterality (bilateral vs. unilateral exams post mastectomy) did not identify a significant difference in RR or PPV between the two groups. However, CDR was significantly increased in FFDM alone vs. FFDM plus DBT in unilateral exams ( $P=0.009$ ).

#### CONCLUSION

s In general, the addition of DBT to FFDM does not improve CDR, RR, or PPV for asymptomatic women with a history of breast cancer.

#### CLINICAL RELEVANCE/APPLICATION

Supplemental screening modalities are needed beyond DBT for patients with a history of breast cancer.

Printed on: 02/07/23

## Abstract Archives of the RSNA, 2022

R2-SPBR-3

### Mammographic compression and its association with lesion conspicuity for calcification-only lesions

Thursday, Dec. 1 9:00AM - 9:30AM Room: Learning Center - BR DPS

#### Participants

Melissa L. Hill, PHD, (*Presenter*) Consultant, Volpara Health Technologies Limited

#### PURPOSE

To investigate associations between modifiable mammographic image factors and conspicuity for lesions detectable by calcification only.

#### METHODS AND MATERIALS

OPTIMAM database cases were selected among 2343 with raw images and lesion conspicuity scores. Expert readers at two sites where screening was originally performed retrospectively marked regions of interest (ROI) and classified conspicuity for biopsy-proven lesions. After exclusions (bilateral lesions, implants, missing data) and selection of cases with lesions whose only mammographic features were calcifications, 586 cases (37 benign, 547 malignant) were included with obvious (OC; n=349), subtle (SC; n=201), or very subtle (VSC; n=36) conspicuity. Volumetric breast density (VBD), breast volume, compression pressure, contact area, and breast positioning measures were derived using Volpara Imaging Software (v3.4). Other factors were extracted from DICOM metadata (compression force, breast thickness, paddle type). VBD was computed as the mean from contralateral breast views, with all other image parameters from the affected breast MLO view only. Lesion ROI size, image-based lesion features, and histopathological characteristics were collected. Univariate analysis was performed to test non-modifiable parameters for associations with conspicuity. A multinomial logistic regression model was fit to predict lesion conspicuity for calcification-only lesions using Akaike Information Criterion for predictor selection among modifiable image factors and the parameters identified in univariate testing.

#### RESULTS

After adjusting for confounders, the longest ROI side length, compression pressure and screening site were significantly associated with the risk of SC and VSC vs OC, with odds ratios (OR) and 95% confidence intervals (CI) of 0.96 (0.94-0.97), 0.85 (0.78-0.92) and 0.52 (0.36-0.77), respectively for SC vs OC, and 0.93 (0.90-0.97), 0.81 (0.67-0.97) and 0.21 (0.08-0.53), respectively for VSC vs OC. Compression force was significantly associated with only SC vs OC, with OR and 95% CI of 1.01 (1.00-1.02).

#### CONCLUSION

Among modifiable mammographic image factors in the MLO view, multinomial modelling demonstrated compression pressure to be predictive of calcification-only lesion conspicuity, with greater pressure reducing the risk of lower conspicuity. These results suggest that pressure-based compression targets may be effective towards achieving good diagnostic performance.

#### CLINICAL RELEVANCE/APPLICATION

The conspicuity of lesions visible on mammography by calcification only are associated with mammographic compression pressure. Screening program performance may benefit from ensuring adequate compression pressure.

Printed on: 02/07/23



## Abstract Archives of the RSNA, 2022

R2-SPBR-4

### Artificial Intelligence (AI) Comparison of Synthetic Mammography (SM) and Full Field Digital Mammography (FFDM) in Malignancy Detection

Thursday, Dec. 1 9:00AM - 9:30AM Room: Learning Center - BR DPS

#### Participants

Laura Heacock, MD, MS, New York, NY (*Presenter*) Nothing to Disclose

#### PURPOSE

To evaluate the strengths and weaknesses of AI systems trained separately on synthetic mammography (SM) and full field digital mammography (FFDM).

#### METHODS AND MATERIALS

This was a retrospective, IRB-approved study. We trained two identical AI systems separately on paired FFDM and SM images, respectively, on a dataset of 1,239,272 combination (FFDM + DBT) screening mammography exams consecutively acquired from patients between 2017-2020. These examinations were separated with a 60/10/30 training/validation/test set split. Ground truth was either pathology-proven diagnosis or stability on imaging over time. Additionally, the images were supplemented with radiologist-annotated segmentation labels and classification for these segmentations (malignant/benign, distortion/non-distortion). The model is trained to localize lesions by generating the location of suspicious areas in the exam with bounding boxes. These detections are then used to generate a final score of malignancy for each mammogram. Preset false-positive (FP) rates were chosen for analysis. Location of bounding boxes on false negatives (FN) and high-scoring (high discrepancy between SM and FFDM AI scores) FP exams were reviewed and compared for both SM and FFDM models. Area under the curve (AUC) and chi-squared tests were used for statistical analysis.

#### RESULTS

The AI system achieved an AUC of 0.933 on SM and 0.909 on FFDM for identifying exams with malignant lesions. At a preset FP rate of 20%, there was a SM FN rate of 0.007% (9/121858) and a FFDM rate of 0.009% (12/121858). On review of bounding boxes, 58.3% (7/12) FN findings on FFDM were detected by the model but did not meet AI score criteria for malignancy. 66.7% (6/9) of SM findings were detected by the model but did not meet AI score criteria ( $p=0.34$ ). SM FN were more likely to be masses compared to FFDM FN (7/9 vs 0/12;  $p<0.001$ ); FFDM FN were more likely to be distortion (50%; 6/12) or calcifications (25%; 3/12). There was no significant correlation between FN in either modality and breast density, size, presence/absence of distortion, or presence/absence of calcifications. High-scoring FFDM FP were more likely to be asymmetries or circumscribed masses. High-scoring SM FP were more likely to be pseudo-distortion or pseudo-calcifications on review of corresponding DBT.

#### CONCLUSION

s AI systems highlight different areas of concern on FFDM and SM images, but demonstrate better performance on SM images.

#### CLINICAL RELEVANCE/APPLICATION

Most AI systems are trained on FFDM images. Radiologists using AI systems as a second reader should be aware that the strengths and weaknesses of these systems may vary when used on DBT-generated SM views.

Printed on: 02/07/23



## Abstract Archives of the RSNA, 2022

R2-SPBR-5

### Evaluation of The Impact of Sociodemographic Status on Breast Screening Volumes During The COVID-19 Pandemic In a Provincial, Population-based Organized Breast Screening Program

Thursday, Dec. 1 9:00AM - 9:30AM Room: Learning Center - BR DPS

#### Participants

Tracee Wee, MD, BSc, Vancouver, BC (*Presenter*) Nothing to Disclose

#### PURPOSE

We sought to assess the impact of sociodemographic status on breast screening volumes (BSVs) during the COVID-19 pandemic in a large, population-based breast screening program which exclusively serves a provincial population of over 5 million.

#### METHODS AND MATERIALS

The BC Cancer Breast Screening database, a population-based database, was the primary dataset accessed. All patients who completed breast screening between April 1st, 2017 and March 31st, 2021 were eligible to participate. An average of three annual periods between April 1st, 2017 and March 31st, 2020 was utilized as the pre-COVID period to limit the effect of annual variation while the period between April 1st, 2020 and March 31st, 2021 was utilized as the COVID-impacted period. Residential postal codes were utilized to impute sociodemographic variables. The Postal CodeOM Conversion File Plus was utilized to map residential postal codes to 2016 Census standard geographical areas, which provided information on community size, income quintile and dissemination areas. Dissemination areas were subsequently linked to the Canadian Index of Multiple Deprivation (CIMD), which assigns a level of deprivation for each dissemination area in four dimensions.

#### RESULTS

Overall BSV was reduced by 23.0% during the COVID-impacted period as compared to the pre-COVID period. Percent reduction in BSV was greatest among younger patients 40 to 49 years of age (-31.3%) and patients residing in communities with a population of less than 10 000 (-27.0%). Percent reduction in BSV was greatest among patients in the lowest income quintile (-28.1%). Percent reduction in BSV was greatest for patients in the most deprived quintiles across all four dimensions of the CIMD: ethnocultural composition (-28.1%), situational vulnerability (-26.7%), economic dependency (-24.5%), and residential instability (-23.7%).

#### CONCLUSION

Disproportionate reductions in BSVs were observed among younger patients, patients residing in rural communities, patients in lower income quintiles, and patients in quintiles which were most deprived during the COVID-19 pandemic.

#### CLINICAL RELEVANCE/APPLICATION

Identification of the exacerbation of underlying inequities in access to breast screening during the COVID-19 pandemic provides the opportunity to improve equitable access to breast screening for vulnerable populations.

Printed on: 02/07/23



## Abstract Archives of the RSNA, 2022

R2-SPBR-6

### Racial Disparities in Proportion of Patients Returning for Annual Screening Mammograms

Thursday, Dec. 1 9:00AM - 9:30AM Room: Learning Center - BR DPS

#### Participants

Mina Moussavi, BSc, PhD, (*Presenter*) Employee, RadNet, Inc

#### PURPOSE

Screening guidelines are increasingly being scrutinized for appropriateness for all racial groups, as evidence suggests that cancer incidence and mortality may differ by race. Any such changes might need to consider adherence to current guidelines among these racial groups to more realistically address cancer disparities. We sought to compare the percentage of patients returning for recommended annual screening by race/ethnicity in a large and diverse population across the USA.

#### METHODS AND MATERIALS

Screening mammography data was retrospectively collected from 186 clinical sites across the United States from 2017-2021. Screening exams from 1,391,248 patients above the age of 35 years (mean age 58.2+/- 11.0 years) were collected. We reviewed patients with an initial exam prior to June 2019 and a subsequent screening exam 9-30 months later. The interval between initial and subsequent screening mammograms was defined as annual if they were 9-18 months apart and biennial if they were 19-30 months apart. We then analyzed the proportion of returning patients who were screened at the recommended annual cadence broken down by self-reported race and ethnicity. Confidence intervals were calculated using the adjusted Wald method.

#### RESULTS

White patients (n=396,372) returned annually more often than Black (n=159,823) and Asian (n=81,276) patients at 75.8%, 71.4%, and 71.8%, respectively. The proportion of Hispanic/Latino (n=152,126), Native Hawaiian/Pacific Islander (n=6,066), and American Indian/Alaska Native patients (n=4,332) returning annually was the lowest of all ethnic groups at 69.6%, 69.1%, and 68.3%, respectively.

#### CONCLUSION

Black, Asian, and women from other non-White populations return for screening at a meaningfully lower rate than White women. As revisions to guidelines are being considered, these data on real-world adherence to existing guidelines might better inform any changes.

#### CLINICAL RELEVANCE/APPLICATION

Racial disparities in breast cancer screening adherence continue to persist and should be considered when updating mammography screening guidelines.

Printed on: 02/07/23

## Abstract Archives of the RSNA, 2022

R2-SPBR-7

### Visibility Trends and Tumor Characteristics of Malignant Architectural Distortion on Synthesized 2D and Tomosynthesis Mammograms: Can We Move Away From Surgery For A Low Risk AD Subset?

Thursday, Dec. 1 9:00AM - 9:30AM Room: Learning Center - BR DPS

#### Participants

Cedric Pluguez-Turull, MD, Miami, FL (*Presenter*) Consultant, INFOTECHSoft, Inc

#### PURPOSE

Explore visibility trends of tomography-detected (TOMO) architectural distortion (AD) on synthesized 2D (s2D) mammography (MMG) and digital breast tomosynthesis (DBT) as well as other imaging and clinical parameters that predict pathology.

#### METHODS AND MATERIALS

Clinical and imaging data was extracted from our EMR and PACS for 1.7 years of biopsied AD with both DBT and s2D at diagnosis yielding 297 cases. A retrospective review of clinical and imaging parameters on MMG, MRI and US was performed. Visibility analysis by consensus read was performed by three breast radiologists documenting AD on one view (CC or ML/MLO), two views or no views for s2D, and one view or two views on DBT. Other clinical and imaging parameters were also analyzed for statistical associations to pathologic outcomes. Tumor size, hormone receptor, Her2 and Ki67 for invasive breast cancer (IBC) were analyzed by consensus visibility.

#### RESULTS

297 biopsied AD detected by s2d + TOMO, 99 were malignant (33%), 89 were high-risk (30%), and 109 were benign (37%). PPV3 for malignancy was 33%. The most common outcome by sub-group is: IDC (54%) for malignancy, radial scar (88%) for high-risk, and stromal fibrosis (52%) for benign. The presence of an US correlate increases the likelihood of malignancy by 2.4x (PLR) with PPV=88%. A positive MRI increases malignancy likelihood by 4.2x (PLR) with PPV= 83% and the absence decreases the likelihood by 0.04x (NLR) with NPV=96%. Interreader agreement is fair (k=0.4) for tomo AD and fair (k=0.35) for s2D AD. Visibility analysis demonstrates more s2D-occult AD correspond to benign and high-risk subsets compared to s2D visible AD. There is a linear trend (p=0.03) for benign AD manifesting as s2D-occult or one view finding on TOMO. A loose trend of increasing malignant AD findings as s2D+TOMO visibility increases was not significant (p=0.93). The 2D-occult iBC size (median, IQR: 12,15) is smaller compared to 2D-visible iBC (median, IQR: 20,25) (p=0.04). No differences were found for tumor markers and molecular subtype.

#### CONCLUSION

s Interreader analysis shows there is poor agreement on AD detection for both s2D and TOMO AD. Negative MRI is suitable for downgrading AD to low suspicion for malignancy and perhaps defer biopsy. A higher proportion of benign and high-risk s2D-occult AD explains a decreased PPV for malignancy arising from AD in the DBT era. iBC arising from 2D-occult TOMO AD that were previously undetectable by 2D MMG are similar in tumor biology than their 2D-visible counterparts, but smaller in size.

#### CLINICAL RELEVANCE/APPLICATION

DBT finds identical, yet smaller, iBC than s2D mammography. Pertinent clinical and imaging factors could sway the breast imager to consider short-term follow-up or pre-biopsy Breast MRI for a particular subset of low-risk AD and patients.

Printed on: 02/07/23

## Abstract Archives of the RSNA, 2022

R2-SPCA

### Cardiac Thursday Poster Discussions

Thursday, Dec. 1 9:00AM - 9:30AM Room: Learning Center - CA DPS

#### Sub-Events

#### R2-SPCA-1 Comparison Study of Myocardial Radiomics Feature Properties on Energy-Integrating and Photon-Counting Detector CT

##### Participants

Matthias Froelich, MD, Mannheim, Germany (*Presenter*) Consultant, Smart Reporting GmbH; Consultant, Guerbet SA

##### PURPOSE

The implementation of radiomics-based, quantitative imaging parameters is hampered by lack of stability and standardization. Photon-Counting computed tomography (PCCT), compared to Energy-Integrating computed tomography (EICT), does rely on an entirely novel detector technology and promises better spatial resolution, lower beam hardening artefacts and better contrast-to-noise ratio. However, its effect on radiomics feature properties is yet unknown. This work investigates this topic in myocardial imaging.

##### METHODS AND MATERIALS

In this retrospective, single-center IRB-approved study, the left ventricular myocardium was segmented on short axis reconstructions of CT and radiomics features were extracted using pyradiomics. To compare features between scanners, t-test for non-paired samples and F-test was performed with a threshold of 0.05 set as a benchmark for significance. Feature correlations were calculated by Pearson correlation coefficient. Visualization was performed with unclustered and clustered heatmaps.

##### RESULTS

A total of 50 patients (56 % male, 44 % female, mean age 56) were enrolled in this study with equal proportions on PCCT and EICT. First-order features were nearly totally comparable between both groups. However, higher-order features showed a partially significant difference between PCCT and EICT.

##### CONCLUSION

While first-order radiomics features of left ventricular myocardium show comparability between PCCT and EICT, detected differences of higher-order features may indicate a possible impact of improved spatial resolution, better detection of lower-energy photons, and better signal-to-noise ratio on texture analysis on PCCT.

##### CLINICAL RELEVANCE/APPLICATION

The implementation of photon-counting detector CT may novel cardiac CT imaging by lower beam-hardening artefacts, better spatial resolution and contrast-to-noise ratio and paves the way for radiomics analysis of left ventricular myocardium in CT imaging.

#### R2-SPCA-2 Multicenter Consistency Assessment of Rapid CMR Strain Quantification

##### Participants

Moritz Halfmann, MD, Mainz, Germany (*Presenter*) Nothing to Disclose

##### PURPOSE

Strain parameters have been under scrutiny for their reproducibility and generalizability, partly due to the black-box model used for the calculation. This multicenter study evaluated the interobserver agreement of a simplified rapid-strain algorithm depending solely on longitudinal ventricular shortening in a real-world setting.

##### METHODS AND MATERIALS

A total of 4 sites each retrospectively identified 20 patients with various cardiomyopathies and 20 healthy controls who had undergone cardiac MRI at their respective centers using locally available scanners from 2 manufacturers with both 1.5 and 3T field strengths and local imaging protocols. First, conventional and rapid longitudinal strains were evaluated at each site and then independently re-evaluated by a core lab. The core lab did not contribute data in order to reduce potential bias towards their own data. Intraclass correlation coefficients (ICC) and Bland-Altman plots were used to assess interobserver agreement. Pearson's correlation was used to evaluate agreement with conventional strain.

##### RESULTS

ICCs demonstrated excellent agreement between sites for left ventricular rapid strains (ICC =0.95 for all sites). Bland-Altman plots showed no significant bias between site and core lab readings and limits of agreement (LoA) were well within clinically acceptable margins (Mean difference: -0.06%, 95% CI: -3.8 to 3.7%). In addition, there was a strong-to-excellent correlation between conventional and rapid ventricular longitudinal strain measurements ( $r=0.89$ ). Regression analyses showed that neither field strengths nor scanner vendors were significant confounders for the simplified ventricular strain algorithm.

## CONCLUSION

s Independently of scanner manufacturers, field strengths, and local imaging protocols, the simplified rapid ventricular strain algorithm could reliably assess left ventricular strain longitudinal strain.

## CLINICAL RELEVANCE/APPLICATION

Advanced post-processing imaging biomarkers such as strain need careful reproducibility-assessment in real-world scenarios using different scanners, field strengths and local imaging protocols.

## R2-SPCA-3 Missed Patent Foramen Ovale Using Coronary CT Angiography in Patients with Cardiac Symptoms

Participants

Hui Zhou, MD, (*Presenter*) Nothing to Disclose

## PURPOSE

The purpose of this study was to determine the proportion of patent foramen ovale (PFO) in patients with cardiac symptoms who received coronary CT angiography (CCTA) imaging and to examine whether PFO were missed using CCTA.

## METHODS AND MATERIALS

This population-based retrospective cohort study assessed patients with cardiac symptoms who received CCTA imaging in a large-scale comprehensive university hospital, July 2018 to May 2020. CT findings of PFO were defined as follows: (a) distinct left atrial flap in expected location of septum primum, (b) channel-like appearance of the interatrial septum (IAS) and (c) a contrast agent jet from left atrium (LA) to right atrium (RA). The CCTA images and the initial radiology reports were retrospectively reinterpreted by two subspecialty cardiovascular radiologists with more than 5 years' experience. The morphological quantitative features and potential causes for missed diagnosis of PFO were recorded.

## RESULTS

Among 5715 qualifying patients, 455(8.0%)met all three CT criteria of PFO. None of the 455 patients were diagnosed with PFO in the initial CCTA report. In 288 patients who underwent both echocardiography and CCTA, only 11 (3.8%) cases were diagnosed with PFO by echocardiography. The lengths of channel-like appearance of IAS, distinct left atrial flap, and the contrast agent jet from LA to RA were  $8.54\pm 3.27$  mm,  $12.59\pm 3.80$  mm, and  $10.62\pm 4.00$  mm, respectively. The width of the LA opening, middle and RA openings of channel-like appearance of IAS were  $1.77\pm 0.65$  mm,  $1.98\pm 0.74$  mm,  $1.73\pm 0.63$  mm, respectively. Atrial septal aneurysm (ASA) accompanying PFO were present in 5 patients (1.1%). Neurological symptoms of migraine or syncope were observed in 16 (3.5%) patients, and cerebral infarction were detected by brain MRI in 7 (1.5%) patients.

## CONCLUSION

s There were a large number of missed PFO in CCTA which could be avoided. Increased recognition of the manifestations of PFO and concomitant ASA in CCTA are recommended to minimize missed diagnosis of PFO.

## CLINICAL RELEVANCE/APPLICATION

PFO diagnosed by CCTA are frequently missed, which appeared to be due to a lack of recognition of the CT criteria for the diagnosis of PFO. Increased education among radiologists and clinicians regarding these imaging pitfalls should be encouraged.

Printed on: 02/07/23

## Abstract Archives of the RSNA, 2022

R2-SPCA-1

### Comparison Study of Myocardial Radiomics Feature Properties on Energy-Integrating and Photon-Counting Detector CT

Thursday, Dec. 1 9:00AM - 9:30AM Room: Learning Center - CA DPS

#### Participants

Matthias Froelich, MD, Mannheim, Germany (*Presenter*) Consultant, Smart Reporting GmbH; Consultant, Guerbet SA

#### PURPOSE

The implementation of radiomics-based, quantitative imaging parameters is hampered by lack of stability and standardization. Photon-Counting computed tomography (PCCT), compared to Energy-Integrating computed tomography (EICT), does rely on an entirely novel detector technology and promises better spatial resolution, lower beam hardening artefacts and better contrast-to-noise ratio. However, its effect on radiomics feature properties is yet unknown. This work investigates this topic in myocardial imaging.

#### METHODS AND MATERIALS

In this retrospective, single-center IRB-approved study, the left ventricular myocardium was segmented on short axis reconstructions of CT and radiomics features were extracted using pyradiomics. To compare features between scanners, t-test for non-paired samples and F-test was performed with a threshold of 0.05 set as a benchmark for significance. Feature correlations were calculated by Pearson correlation coefficient. Visualization was performed with unclustered and clustered heatmaps.

#### RESULTS

A total of 50 patients (56 % male, 44 % female, mean age 56) were enrolled in this study with equal proportions on PCCT and EICT. First-order features were nearly totally comparable between both groups. However, higher-order features showed a partially significant difference between PCCT and EICT.

#### CONCLUSION

While first-order radiomics features of left ventricular myocardium show comparability between PCCT and EICT, detected differences of higher-order features may indicate a possible impact of improved spatial resolution, better detection of lower-energy photons, and better signal-to-noise ratio on texture analysis on PCCT.

#### CLINICAL RELEVANCE/APPLICATION

The implementation of photon-counting detector CT may novel cardiac CT imaging by lower beam-hardening artefacts, better spatial resolution and contrast-to-noise ratio and paves the way for radiomics analysis of left ventricular myocardium in CT imaging.

Printed on: 02/07/23



## Abstract Archives of the RSNA, 2022

R2-SPCA-2

### Multicenter Consistency Assessment of Rapid CMR Strain Quantification

Thursday, Dec. 1 9:00AM - 9:30AM Room: Learning Center - CA DPS

#### Participants

Moritz Halfmann, MD, Mainz, Germany (*Presenter*) Nothing to Disclose

#### PURPOSE

Strain parameters have been under scrutiny for their reproducibility and generalizability, partly due to the black-box model used for the calculation. This multicenter study evaluated the interobserver agreement of a simplified rapid-strain algorithm depending solely on longitudinal ventricular shortening in a real-world setting.

#### METHODS AND MATERIALS

A total of 4 sites each retrospectively identified 20 patients with various cardiomyopathies and 20 healthy controls who had undergone cardiac MRI at their respective centers using locally available scanners from 2 manufacturers with both 1.5 and 3T field strengths and local imaging protocols. First, conventional and rapid longitudinal strains were evaluated at each site and then independently re-evaluated by a core lab. The core lab did not contribute data in order to reduce potential bias towards their own data. Intraclass correlation coefficients (ICC) and Bland-Altman plots were used to assess interobserver agreement. Pearson's correlation was used to evaluate agreement with conventional strain.

#### RESULTS

ICCs demonstrated excellent agreement between sites for left ventricular rapid strains (ICC =0.95 for all sites). Bland-Altman plots showed no significant bias between site and core lab readings and limits of agreement (LoA) were well within clinically acceptable margins (Mean difference: -0.06%, 95% CI: -3.8 to 3.7%). In addition, there was a strong-to-excellent correlation between conventional and rapid ventricular longitudinal strain measurements ( $r= 0.89$ ). Regression analyses showed that neither field strengths nor scanner vendors were significant confounders for the simplified ventricular strain algorithm.

#### CONCLUSION

Independently of scanner manufacturers, field strengths, and local imaging protocols, the simplified rapid ventricular strain algorithm could reliably assess left ventricular strain longitudinal strain.

#### CLINICAL RELEVANCE/APPLICATION

Advanced post-processing imaging biomarkers such as strain need careful reproducibility-assessment in real-world scenarios using different scanners, field strengths and local imaging protocols.

Printed on: 02/07/23

## Abstract Archives of the RSNA, 2022

R2-SPCA-3

### Missed Patent Foramen Ovale Using Coronary CT Angiography in Patients with Cardiac Symptoms

Thursday, Dec. 1 9:00AM - 9:30AM Room: Learning Center - CA DPS

#### Participants

Hui Zhou, MD, (*Presenter*) Nothing to Disclose

#### PURPOSE

The purpose of this study was to determine the proportion of patent foramen ovale (PFO) in patients with cardiac symptoms who received coronary CT angiography (CCTA) imaging and to examine whether PFO were missed using CCTA.

#### METHODS AND MATERIALS

This population-based retrospective cohort study assessed patients with cardiac symptoms who received CCTA imaging in a large-scale comprehensive university hospital, July 2018 to May 2020. CT findings of PFO were defined as follows: (a) distinct left atrial flap in expected location of septum primum, (b) channel-like appearance of the interatrial septum (IAS) and (c) a contrast agent jet from left atrium (LA) to right atrium (RA). The CCTA images and the initial radiology reports were retrospectively reinterpreted by two subspecialty cardiovascular radiologists with more than 5 years' experience. The morphological quantitative features and potential causes for missed diagnosis of PFO were recorded.

#### RESULTS

Among 5715 qualifying patients, 455(8.0%) met all three CT criteria of PFO. None of the 455 patients were diagnosed with PFO in the initial CCTA report. In 288 patients who underwent both echocardiography and CCTA, only 11 (3.8%) cases were diagnosed with PFO by echocardiography. The lengths of channel-like appearance of IAS, distinct left atrial flap, and the contrast agent jet from LA to RA were  $8.54\pm 3.27$  mm,  $12.59\pm 3.80$  mm, and  $10.62\pm 4.00$  mm, respectively. The width of the LA opening, middle and RA openings of channel-like appearance of IAS were  $1.77\pm 0.65$  mm,  $1.98\pm 0.74$  mm,  $1.73\pm 0.63$  mm, respectively. Atrial septal aneurysm (ASA) accompanying PFO were present in 5 patients (1.1%). Neurological symptoms of migraine or syncope were observed in 16 (3.5%) patients, and cerebral infarction were detected by brain MRI in 7 (1.5%) patients.

#### CONCLUSION

s There were a large number of missed PFO in CCTA which could be avoided. Increased recognition of the manifestations of PFO and concomitant ASA in CCTA are recommended to minimize missed diagnosis of PFO.

#### CLINICAL RELEVANCE/APPLICATION

PFO diagnosed by CCTA are frequently missed, which appeared to be due to a lack of recognition of the CT criteria for the diagnosis of PFO. Increased education among radiologists and clinicians regarding these imaging pitfalls should be encouraged.

Printed on: 02/07/23

## Abstract Archives of the RSNA, 2022

R2-SPCH

### Chest Thursday Poster Discussions

Thursday, Dec. 1 9:00AM - 9:30AM Room: Learning Center - CH DPS

#### Participants

Matthew Cham, MD, Kenmore, WA (*Moderator*) Nothing to Disclose

#### Sub-Events

### R2-SPCH-1 Automatic Detection of Enlarged Chest Lymph Nodes in Contrast Non-Contrast Chest CT: An External Evaluation

#### Participants

Dazhou Guo, Columbia, SC (*Presenter*) Nothing to Disclose

#### PURPOSE

Accurate determination of lymph node (LN) status directly affects the treatment strategy and prognosis of patients with different diseases. We developed a deep learning system to detect enlarged chest LNs in CT. In this study, we evaluate its generalizability on external data of diverse sources.

#### METHODS AND MATERIALS

Our algorithm is a two-stage detector (Fig. a). We trained it on two private datasets and a public dataset with 262 patients and 4338 annotated LNs in total. Mediastinal, hilar, and supraclavicular LNs were annotated on contrast-enhanced (CE) CTs, and non-contrast (NC) training data are added by registering the NC CT to its CE counterpart. To improve robustness, we added intensive data augmentation in training. We selected test data from 4 external cohorts: 100 random in-house CTs without filtering patients' diseases, 40 esophageal cancer patients, 35 lung cancer patients from TCIA public data, and 12 COVID patients from TCIA. One radiologist (more than 10 years of experience in thoracic imaging) read the CT scans and verified the detection results with a short axial diameter of at least 5 mm. Detections are classified into LN requiring follow-up, LN not requiring follow-up (e.g. LNs with necrosis, calcification, and short diameter less than 1cm), and non-LN. LNs not detected were manually added.

#### RESULTS

A total of 1733 LNs were labeled on 187 images. At 2 FPs per patient, our algorithm achieves lesion-level detection sensitivity (Sens) of 93.1%, 82.7%, 82.9%, and 73.1% for the in-house, esophageal, lung, and COVID cohorts, respectively, (Fig. b). The accuracy is better in in-house but worse in COVID cohort, probably because fewer patients have severe diseases in the in-house cohort, while the COVID CTs have more pathological changes (e.g. mediastinitis) which interfered with the algorithm. The model performs similarly on CE vs. NC CT (Sens=84.7% vs. 87.5%@2FP, Fig. c), meanwhile more accurately in CTs with thick than with thin slices (Sens=96.4% vs. 87.2%@2FP, Fig. d). LNs annotated in thick-slice CTs are fewer and in average larger thus easier to detect, which partially explains its higher accuracy. Our algorithm works well at LNs in the aortic and subcarinal regions. Clusters of LNs can also be detected. FPs come from cervical/mediastinal vessels (39.3%), partial volume effects in mediastinum and bronchial wall at the bifurcation (16.3% and 16.0%), esophagus or esophageal tumors (11.2%), etc.

#### CONCLUSION

The algorithm shows good accuracy and generalizability. It has room to improve on images with severe pathological changes.

#### CLINICAL RELEVANCE/APPLICATION

Our algorithm can be widely applied in chest CT examination (e.g. tumor and COVID patients) to help radiologists with the challenging LN detection task, reducing their workload and missing rate.

### R2-SPCH-2 CT Features of Interstitial Lung Disease Associated with Systemic Lupus Erythematosus

#### Participants

Marie-Pierre Debray, MD, Paris, France (*Presenter*) Speaker, Boehringer Ingelheim GmbH

#### PURPOSE

To describe the initial and follow-up CT features of interstitial lung disease associated with systemic lupus erythematosus (SLE-ILD)

#### METHODS AND MATERIALS

Multicentric retrospective study of SLE-ILD extending from 2005 to 2021, including 67 patients (24 patients without and 43 patients with another connective tissue disease (CTD) associated with SLE, mainly Sjögren syndrome, n=25, and systemic sclerosis, n=12). The chest CT performed closest to the time of SLE-ILD diagnosis was analyzed by one thoracic radiologist specialized in ILD, for the pattern and extent of ILD. Evolution of CT signs of fibrosis (increase or decrease in extent, change in texture or lung volume) and overall disease extent was analyzed on the latest available chest CT in 45 patients (median follow-up 78 months, IQR [51; 130]).

#### RESULTS

Significant ground-glass opacities, reticulations, traction bronchiectasis, honeycombing and cysts were observed in 41/67 (61%), 54/67 (81%), 39/67 (58%), 28/67 (42%) and 28/67 (42%) patients, respectively. Lesions showed a basal and subpleural predominant distribution in 55/67 (82%) and 36/67 (54%) patients. Chest CT was most often classified as indeterminate, in 18/67 (27%), or evocative of non specific interstitial pneumonia, in 28/67 (42%) patients with organizing pneumonia features in 7 of the latter. The pattern was typical of usual interstitial pneumonia in 10/67 (15%) patients, among those 7 patients showed exuberant honeycombing. There was no significant difference in CT pattern distribution between patients without and patients with another associated CTD. The latest available chest CT showed an increase of CT signs of fibrosis, in 29/45 (64%) patients, whereas lesions appeared unchanged or decreased in 13/67 (19%) patients.

## CONCLUSION

s SLE-ILD most often shows an indeterminate or a non specific interstitial pneumonia pattern. After a median follow-up of 78 months, two thirds of patients have an increase of CT signs of fibrosis.

## CLINICAL RELEVANCE/APPLICATION

ILD is a rare manifestation of SLE, frequently showing progressive signs of fibrosis. In this series, no distinctive CT features were observed between isolated SLE and other CTD associated SLE.

## R2-SPCH-3 Application of CT Lymphangiography in Diagnosing Chest Complex Lymphatic Anomaly

### Participants

Yan Zhang, Beijing, China (*Presenter*) Nothing to Disclose

### PURPOSE

To explore the clinical value of CT lymphangiography (CTL) in diagnosing chest complex lymphatic anomaly.

### METHODS AND MATERIALS

59 patients diagnosed as chest complex lymphatic anomaly (CLA) clinically were analyzed retrospectively. All patients underwent CTL. All patients underwent CTL (Somatom Sensation Cardiac 16, Siemens Healthcare or Brilliance iCT, Philips Medical Healthcare, Best, the Netherlands). All CTL and chest CT images were double-blind reviewed by two radiologists with 15 years of experience. The contrast agent (lipiodol) reflux and abnormal deposition of lymphatic vessels in the chest were observed. After the contrast agent (lipiodol) has been injected into the superficial lymphatic vessels of the unilateral foot, the lipiodol follows the lymphatic fluid up the lumbar trunk and converges into the cisterna chyli, then into the thoracic duct, and finally into the blood at the angle of the left jugular vein. During this process, it is considered abnormal distribution if lipiodol deposits in any other part of the body, such as the diaphragm, peritracheal region, pericardium, pleura, and hilum. Such deposits represent the presence of dilated lymphatic vessels hyperplasia, reflux, or fistula.

### RESULTS

CTL showed contrast agent abnormally deposited in all 59 patients: the end of thoracic duct was seen in 42 cases (71.2%), the end of right lymphatic duct in 13 cases (22.0%), mediastinum in 34 cases (57.6%), hilar in 19 cases (32.2%), pleura in 18 cases (30.5%), lung in 10 cases (16.9%), above the diaphragm in 4 cases (6.8%). Abnormal CT changes including: the thickening of bronchovascular bundle in 21 cases (35.6%), the thickening of interlobular septum in 15 cases (25.4%), ground glass opacity in 30 cases (50.8%), atelectasis in 17 cases (28.8%), consolidation in 1 case (1.7%), the crazy-paving sign in 3 cases (5.1%), cystic low-density foci in mediastinum in 44 cases (74.6%), pleural effusion in 36 cases (61.0%), pericardial effusion in 14 cases (23.7%), above the diaphragm in 4 cases (6.8%).

## CONCLUSION

s CT L can show lymphatic abnormalities of chest CLA and other chest CT abnormalities. This method provides an important imaging basis for the diagnosis and differentiation of the disease.

## CLINICAL RELEVANCE/APPLICATION

CT L can show lymphatic abnormalities of chest CLA and other chest CT abnormalities. This method provides an important imaging basis for the diagnosis and differentiation of the disease.

## R2-SPCH-5 Topology-aware Aortic Lumen and Wall Segmentation on Computed Tomography Scans

### Participants

Prateek Prasanna, PhD, Stony Brook, NY (*Presenter*) Nothing to Disclose

### PURPOSE

Accurate assessment of the aorta via imaging is important for downstream morphological assessment tasks. The wall is often very thin in aneurysmal portions of the aorta and cannot be accurately segmented by current deep learning (DL) models. The simultaneous segmentation of the lumen and the wall is a multi-class semantic segmentation problem involving a topological constraint driven by organ anatomy, i.e., the wall completely separates the lumen from the background. DL methods have achieved impressive performances, but are limited in their ability to encode topological interactions/constraints among different classes; here the topological constraint is that the aortic lumen is always enclosed by the wall. To address this we propose a novel method to encode such interactions, w.r.t fine-scale aortic anatomy, into deep neural networks (DNNs). The efficacy of our method is validated on a proprietary aorta dataset.

### METHODS AND MATERIALS

28 CT scans were obtained from an institutional database of patients with thoracic and/or abdominal aortic aneurysm. Inclusion criteria for patients included known aneurysmal disease of the aorta and history of undergoing contrast-enhanced CT with arterial-phase contrast injection. Ground truth lumen and wall annotations were obtained by 4 expert readers working in consensus. We developed a novel method to learn the topological interactions for multi-class segmentation DNNs. Key observation is that lumen and background voxels can never be adjacent. Our method has two stages - a convolution-based method which generates a critical voxels map, followed by a custom loss function. Fig 1b gives an overview of the proposed DL framework.

## RESULTS

Our proposed method improves segmentation results both qualitatively (Fig 1a) and quantitatively (Fig 1c). It fixes the interaction errors by forcing the lumen to always be enclosed by the wall. We see in Fig 1a that we are able to reconstruct broken lumen and wall structures, and also improve quantitative measures for both. The measures used are Dice, Hausdorff distance (HD), Avg. Symmetric Surface Distance (ASSD) and a proposed metric called percentage-violations which is the number of voxels violating the constraint as a fraction of the total number of foreground voxels.

## CONCLUSION

s We propose a new method for multi-class segmentation that focuses on topological interactions. By incorporating our method into the training of DNNs, we enforce them to learn better feature representations, resulting in improved segmentation quality.

## CLINICAL RELEVANCE/APPLICATION

Accurate aorta segmentation is crucial to downstream analysis tasks such as measurement of diameter and tortuosity, and assessment of aneurysms. Our method can improve aorta segmentation quality in both 2D and 3D settings.

## R2-SPCH-6 Development and Validation of Deep Learning-based Computer-aided Detection System for Pulmonary Embolism on Chest Computed Tomography

Participants  
YeRa Choi, MD, Seoul, Korea, Republic Of (*Presenter*) Nothing to Disclose

## PURPOSE

To develop and validate a deep learning-based computer-aided detection system (DL-CAD) to detect pulmonary embolism (PE) on chest computed tomography (CT) images.

## METHODS AND MATERIALS

For the development of CAD, CT pulmonary angiographies (CTPAs) of patients with PE were retrospectively collected from two institutions. Two thoracic radiologists made voxel-wise annotations for areas of PE on each transverse CT image. The DL-CAD consisted of three elements based on convolutional neural networks (CNNs): 1) segmentation of pulmonary arteries for extraction of regions of interest, 2) detection of candidate lesions for PE, and 3) reduction of false-positive detections. For the evaluation of DL-CAD, a separate test dataset was built, comprising CT images from the same institutions without overlap in patients with the developmental dataset. The CT images for test dataset were conveniently collected to exhibit 1:1 ratio between 1) CTs with and without PE, 2) CTPAs and general contrast-enhanced chest CT (CECT)s, and 3) CT with thin-slice (<1.5 mm slice thickness) and thick-slice images. The performance of DL CAD was evaluated with examination-level sensitivity, specificity, PPV (positive predictive value), and NPV (negative predictive value) for discrimination of CTs with and without PE.

## RESULTS

A total of 370 CTPA examinations with PE were used for the development of DL-CAD. The test dataset included 320 CT examinations (160 with PE; 160 CTPAs and 160 general CECTs; 160 with thin-slice images). The DL-CAD exhibited sensitivity, specificity, PPV, and NPV of 88.8%, 85.0%, 85.5%, and 88.3%, respectively for identification of CT examinations with PE. The DL-CAD exhibited slightly higher sensitivity in CTPAs compared to general CECT (92.5% vs. 85.0%;  $P=.133$ ) at the same specificity (85.0%). Meanwhile, the DL-CAD exhibited significantly higher sensitivity in CTs with thin-slice images (97.5% vs. 80.0%;  $P<.001$ ) and lower specificity (77.5% vs. 92.5%;  $P=.008$ ) compared to CTs with thick-slice images.

## CONCLUSION

s The DL-CAD could successfully identify PE not only in CTPA images but also in general CECT images.

## CLINICAL RELEVANCE/APPLICATION

Automated detection of PE on chest CTs can improve the quality and efficiency of interpretation and help timely treatment for patients.

## R2-SPCH-7 Accuracy of Airway Thickness Measurements in Low-dose High-resolution photon-counting-detector CT

Participants  
Chelsea Dunning, DPHIL, Rochester, MN (*Presenter*) Nothing to Disclose

## PURPOSE

To evaluate the accuracy of bronchial airway thickness in low-dose chest CT using a clinical photon-counting-detector (PCD) CT compared to conventional energy-integrating-detector (EID) CT.

## METHODS AND MATERIALS

Twelve 3D-printed acrylic tubes of assorted wall thicknesses (0.33 - 1.6 mm) and inner diameters (0.42 - 3.4 mm) were placed throughout an anthropomorphic chest phantom (Lungman, Kyoto Kagaku). The phantom was scanned on a whole-body PCD-CT (NAEOTOM Alpha, Siemens) at 100 kV with an additional tin filter (Sn100) in single-source ultra-high-resolution mode (detector configuration: 120 x 0.2 mm) at three dose levels (volume CT dose index (CTDI<sub>vol</sub>): 0.2, 0.4, and 0.8 mGy). The phantom was also scanned on a conventional EID-CT scanner (SOMATOM Force, Siemens) using Sn100 kV in single-source mode (detector configuration: 96 x 0.6 mm). A reference high-dose scan was also acquired at 120 kV and 12 mGy for both scanners. All images were reconstructed with quantitative kernels and iterative reconstruction with a strength setting of 3; Qr54-3 for standard resolution (SR) EID-CT, Qr56-3 for SR PCD-CT, and Qr89-3 for ultra-high-resolution (UHR) PCD-CT. The image noise was measured as the standard deviation in a region of interest within the mediastinum. The wall thickness of each tube was measured by taking the radial profile in multiple slices and measuring the average full width at half maximum (FWHM). The airway thickness accuracy was expressed using linear regression ( $R^2$  and RMSE) between the measured wall thickness at each dose level.

## RESULTS

At matched spatial resolution (Qr54 for EID-CT and Qr56 for PCD-CT), PCD-CT reduced image noise by 53%, 57%, and 56% at 0.2 mGy, 0.4 mGy, and 0.8 mGy dose levels compared to EID-CT. At 0.2 mGy, 0.4 mGy, and 0.8 mGy, the wall thickness RMSE values

were 0.37, 0.36, and 0.57 mm for EID-CT ; 0.49, 0.46, and 0.47 mm for SR PCD-CT; and 0.18, 0.15, and 0.11 mm for UHR PCD-CT. The UHR PCD-CT had the closest  $R^2$  values to unity across all dose levels ( $R^2 > 0.963$ ), compared to EID-CT ( $R^2 > 0.816$ ) and SR PCD-CT ( $R^2 > 0.823$ ).

## CONCLUSION

More accurate airway wall thickness measurements can be achieved for UHR PCD-CT compared to EID-CT or SR PCD-CT at radiation dose levels at or lower than in lung cancer screening exams.

## CLINICAL RELEVANCE/APPLICATION

High accuracy measurements of bronchial airway wall thickness in high-resolution low-dose PCD-CT can enable reliable diagnosis of lung diseases such as COPD or cystic fibrosis.

## R2-SPCH-8 Value-added Opportunistic Screening: Prediction Model of Arterial Stiffness Based on Clinical and Thoracic Aorta Imaging Risk Factors

Participants

Jinrong Yang, (*Presenter*) Nothing to Disclose

## PURPOSE

This study is to establish and verify a nomogram model based on clinical and thoracic aorta imaging risk factors for predicting the risk of arterial stiffness (AS).

## METHODS AND MATERIALS

This is a cross-sectional study. A total of 815 patients were enrolled and the baseline clinical data, biochemical indicators, concomitant diseases and AI data (the diameter, area at 9 levels and volume, length at two adjacent levels of thoracic aorta recommended by AHA Guidelines (2010)) of them were collected. They were randomly divided into the training set of 570 cases (70%) and the validation set of 245 cases (30%). Based on the recommendations of the Committee on Physiological Diagnostic Criteria for Vascular Failure,  $8 \leq$  cardio-ankle vascular index (CAVI)  $< 9$  indicates pre-AS, CAVI  $\geq 9$  indicates AS. In the training set, variance, t-test (for normal distribution) /Mann-Whitney U-test (for non-normal distribution), least absolute shrinkage and selection operator (LASSO) were used for selecting thoracic aorta imaging risk factors to construct AI measurement score and multivariate logistic backward stepwise regression were used to analyze the influencing factors of hypertension. According to the clinical application for different data conditions, five nomogram prediction models were constructed, named AIMeasure model, BasicClinical model, TotalClinical model, AIBasicClinical model, AITotalClinical model. Moreover, receiver operating characteristic (ROC) curve, calibration curve and decision curve analyses (DCA) were used to test the distinction, accuracy and clinical applicability of the model both in training set and validation set.

## RESULTS

The results showed age, BMI, systolic blood pressure (SBP), smoking, serum sodium, serum magnesium and thoracic aortic dilatation were all related to the occurrence of AS. The area under the ROC curve of the above five models was 0.763, 0.826, 0.842, 0.831, 0.843 in the training set and was 0.794, 0.793, 0.803, 0.819, 0.827 in the verification set, respectively. Moreover, the calibration curves and DCAs performed well on accuracy and clinical practicality.

## CONCLUSION

The risk prediction nomogram models have good predictive ability and clinical value, which could be used as an effective tool for the risk prediction of arterial stiffness. Furthermore, they would facilitate earlier intervention to prevent the future development of arterial stiffness.

## CLINICAL RELEVANCE/APPLICATION

Based on clinical data and thoracic aorta data measured by AI on non-contrast enhanced chest CT, prediction models were constructed for different clinical scenarios, so as to carry out opportunistic screening of arterial stiffness.

Printed on: 02/07/23

## Abstract Archives of the RSNA, 2022

R2-SPCH-1

### Automatic Detection of Enlarged Chest Lymph Nodes in Contrast Non-Contrast Chest CT: An External Evaluation

Thursday, Dec. 1 9:00AM - 9:30AM Room: Learning Center - CH DPS

#### Participants

Dazhou Guo, Columbia, SC (*Presenter*) Nothing to Disclose

#### PURPOSE

Accurate determination of lymph node (LN) status directly affects the treatment strategy and prognosis of patients with different diseases. We developed a deep learning system to detect enlarged chest LNs in CT. In this study, we evaluate its generalizability on external data of diverse sources.

#### METHODS AND MATERIALS

Our algorithm is a two-stage detector (Fig. a). We trained it on two private datasets and a public dataset with 262 patients and 4338 annotated LNs in total. Mediastinal, hilar, and supraclavicular LNs were annotated on contrast-enhanced (CE) CTs, and non-contrast (NC) training data are added by registering the NC CT to its CE counterpart. To improve robustness, we added intensive data augmentation in training. We selected test data from 4 external cohorts: 100 random in-house CTs without filtering patients' diseases, 40 esophageal cancer patients, 35 lung cancer patients from TCIA public data, and 12 COVID patients from TCIA. One radiologist (more than 10 years of experience in thoracic imaging) read the CT scans and verified the detection results with a short axial diameter of at least 5 mm. Detections are classified into LN requiring follow-up, LN not requiring follow-up (e.g. LNs with necrosis, calcification, and short diameter less than 1cm), and non-LN. LNs not detected were manually added.

#### RESULTS

A total of 1733 LNs were labeled on 187 images. At 2 FPs per patient, our algorithm achieves lesion-level detection sensitivity (Sens) of 93.1%, 82.7%, 82.9%, and 73.1% for the in-house, esophageal, lung, and COVID cohorts, respectively, (Fig. b). The accuracy is better in in-house but worse in COVID cohort, probably because fewer patients have severe diseases in the in-house cohort, while the COVID CTs have more pathological changes (e.g. mediastinitis) which interfered with the algorithm. The model performs similarly on CE vs. NC CT (Sens=84.7% vs. 87.5%@2FP, Fig. c), meanwhile more accurately in CTs with thick than with thin slices (Sens=96.4% vs. 87.2%@2FP, Fig. d). LNs annotated in thick-slice CTs are fewer and in average larger thus easier to detect, which partially explains its higher accuracy. Our algorithm works well at LNs in the aortic and subcarinal regions. Clusters of LNs can also be detected. FPs come from cervical/mediastinal vessels (39.3%), partial volume effects in mediastinum and bronchial wall at the bifurcation (16.3% and 16.0%), esophagus or esophageal tumors (11.2%), etc.

#### CONCLUSION

The algorithm shows good accuracy and generalizability. It has room to improve on images with severe pathological changes.

#### CLINICAL RELEVANCE/APPLICATION

Our algorithm can be widely applied in chest CT examination (e.g. tumor and COVID patients) to help radiologists with the challenging LN detection task, reducing their workload and missing rate.

Printed on: 02/07/23

## Abstract Archives of the RSNA, 2022

R2-SPCH-2

### CT Features of Interstitial Lung Disease Associated with Systemic Lupus Erythematosus

Thursday, Dec. 1 9:00AM - 9:30AM Room: Learning Center - CH DPS

#### Participants

Marie-Pierre Debray, MD, Paris, France (*Presenter*) Speaker, Boehringer Ingelheim GmbH

#### PURPOSE

To describe the initial and follow-up CT features of interstitial lung disease associated with systemic lupus erythematosus (SLE-ILD)

#### METHODS AND MATERIALS

Multicentric retrospective study of SLE-ILD extending from 2005 to 2021, including 67 patients (24 patients without and 43 patients with another connective tissue disease (CTD) associated with SLE, mainly Sjögren syndrome, n=25, and systemic sclerosis, n=12). The chest CT performed closest to the time of SLE-ILD diagnosis was analyzed by one thoracic radiologist specialized in ILD, for the pattern and extent of ILD. Evolution of CT signs of fibrosis (increase or decrease in extent, change in texture or lung volume) and overall disease extent was analyzed on the latest available chest CT in 45 patients (median follow-up 78 months, IQR [51; 130]).

#### RESULTS

Significant ground-glass opacities, reticulations, traction bronchiectasis, honeycombing and cysts were observed in 41/67 (61%), 54/67 (81%), 39/67 (58%), 28/67 (42%) and 28/67 (42%) patients, respectively. Lesions showed a basal and subpleural predominant distribution in 55/67 (82%) and 36/67 (54%) patients. Chest CT was most often classified as indeterminate, in 18/67 (27%), or evocative of non specific interstitial pneumonia, in 28/67 (42%) patients with organizing pneumonia features in 7 of the latter. The pattern was typical of usual interstitial pneumonia in 10/67 (15%) patients, among those 7 patients showed exuberant honeycombing. There was no significant difference in CT pattern distribution between patients without and patients with another associated CTD. The latest available chest CT showed an increase of CT signs of fibrosis, in 29/45 (64%) patients, whereas lesions appeared unchanged or decreased in 13/67 (19%) patients.

#### CONCLUSION

s SLE-ILD most often shows an indeterminate or a non specific interstitial pneumonia pattern. After a median follow-up of 78 months, two thirds of patients have an increase of CT signs of fibrosis.

#### CLINICAL RELEVANCE/APPLICATION

ILD is a rare manifestation of SLE, frequently showing progressive signs of fibrosis. In this series, no distinctive CT features were observed between isolated SLE and other CTD associated SLE.

Printed on: 02/07/23

## Abstract Archives of the RSNA, 2022

R2-SPCH-3

### Application of CT Lymphangiography in Diagnosing Chest Complex Lymphatic Anomaly

Thursday, Dec. 1 9:00AM - 9:30AM Room: Learning Center - CH DPS

#### Participants

Yan Zhang, Beijing, China (*Presenter*) Nothing to Disclose

#### PURPOSE

To explore the clinical value of CT lymphangiography (CTL) in diagnosing chest complex lymphatic anomaly.

#### METHODS AND MATERIALS

59 patients diagnosed as chest complex lymphatic anomaly (CLA) clinically were analyzed retrospectively. All patients underwent CTL. All patients underwent CTL (Somatom Sensation Cardiac 16, Siemens Healthcare or Brilliance iCT, Philips Medical Healthcare, Best, the Netherlands). All CTL and chest CT images were double-blind reviewed by two radiologists with 15 years of experience. The contrast agent (lipiodol) reflux and abnormal deposition of lymphatic vessels in the chest were observed. After the contrast agent (lipiodol) has been injected into the superficial lymphatic vessels of the unilateral foot, the lipiodol follows the lymphatic fluid up the lumbar trunk and converges into the cisterna chyli, then into the thoracic duct, and finally into the blood at the angle of the left jugular vein. During this process, it is considered abnormal distribution if lipiodol deposits in any other part of the body, such as the diaphragm, peritracheal region, pericardium, pleura, and hilum. Such deposits represent the presence of dilated lymphatic vessels hyperplasia, reflux, or fistula.

#### RESULTS

CTL showed contrast agent abnormally deposited in all 59 patients: the end of thoracic duct was seen in 42 cases (71.2%), the end of right lymphatic duct in 13 cases (22.0%), mediastinum in 34 cases (57.6%), hilar in 19 cases (32.2%), pleura in 18 cases (30.5%), lung in 10 cases (16.9%), above the diaphragm in 4 cases (6.8%). Abnormal CT changes including: the thickening of bronchovascular bundle in 21 cases (35.6%), the thickening of interlobular septum in 15 cases (25.4%), ground glass opacity in 30 cases (50.8%), atelectasis in 17 cases (28.8%), consolidation in 1 case (1.7%), the crazy-paving sign in 3 cases (5.1%), cystic low-density foci in mediastinum in 44 cases (74.6%), pleural effusion in 36 cases (61.0%), pericardial effusion in 14 cases (23.7%), above the diaphragm in 4 cases (6.8%).

#### CONCLUSION

s CT L can show lymphatic abnormalities of chest CLA and other chest CT abnormalities. This method provides an important imaging basis for the diagnosis and differentiation of the disease.

#### CLINICAL RELEVANCE/APPLICATION

CT L can show lymphatic abnormalities of chest CLA and other chest CT abnormalities. This method provides an important imaging basis for the diagnosis and differentiation of the disease.

Printed on: 02/07/23



## Abstract Archives of the RSNA, 2022

R2-SPCH-5

### Topology-aware Aortic Lumen and Wall Segmentation on Computed Tomography Scans

Thursday, Dec. 1 9:00AM - 9:30AM Room: Learning Center - CH DPS

#### Participants

Prateek Prasanna, PhD, Stony Brook, NY (*Presenter*) Nothing to Disclose

#### PURPOSE

Accurate assessment of the aorta via imaging is important for downstream morphological assessment tasks. The wall is often very thin in aneurysmal portions of the aorta and cannot be accurately segmented by current deep learning (DL) models. The simultaneous segmentation of the lumen and the wall is a multi-class semantic segmentation problem involving a topological constraint driven by organ anatomy, i.e., the wall completely separates the lumen from the background. DL methods have achieved impressive performances, but are limited in their ability to encode topological interactions/constraints among different classes; here the topological constraint is that the aortic lumen is always enclosed by the wall. To address this we propose a novel method to encode such interactions, w.r.t fine-scale aortic anatomy, into deep neural networks (DNNs). The efficacy of our method is validated on a proprietary aorta dataset.

#### METHODS AND MATERIALS

28 CT scans were obtained from an institutional database of patients with thoracic and/or abdominal aortic aneurysm. Inclusion criteria for patients included known aneurysmal disease of the aorta and history of undergoing contrast-enhanced CT with arterial-phase contrast injection. Ground truth lumen and wall annotations were obtained by 4 expert readers working in consensus. We developed a novel method to learn the topological interactions for multi-class segmentation DNNs. Key observation is that lumen and background voxels can never be adjacent. Our method has two stages - a convolution-based method which generates a critical voxels map, followed by a custom loss function. Fig 1b gives an overview of the proposed DL framework.

#### RESULTS

Our proposed method improves segmentation results both qualitatively (Fig 1a) and quantitatively (Fig 1c). It fixes the interaction errors by forcing the lumen to always be enclosed by the wall. We see in Fig 1a that we are able to reconstruct broken lumen and wall structures, and also improve quantitative measures for both. The measures used are Dice, Hausdorff distance (HD), Avg. Symmetric Surface Distance (ASSD) and a proposed metric called percentage-violations which is the number of voxels violating the constraint as a fraction of the total number of foreground voxels.

#### CONCLUSION

s We propose a new method for multi-class segmentation that focuses on topological interactions. By incorporating our method into the training of DNNs, we enforce them to learn better feature representations, resulting in improved segmentation quality.

#### CLINICAL RELEVANCE/APPLICATION

Accurate aorta segmentation is crucial to downstream analysis tasks such as measurement of diameter and tortuosity, and assessment of aneurysms. Our method can improve aorta segmentation quality in both 2D and 3D settings.

Printed on: 02/07/23

## Abstract Archives of the RSNA, 2022

R2-SPCH-6

### Development and Validation of Deep Learning-based Computer-aided Detection System for Pulmonary Embolism on Chest Computed Tomography

Thursday, Dec. 1 9:00AM - 9:30AM Room: Learning Center - CH DPS

#### Participants

YeRa Choi, MD, Seoul, Korea, Republic Of (*Presenter*) Nothing to Disclose

#### PURPOSE

To develop and validate a deep learning-based computer-aided detection system (DL-CAD) to detect pulmonary embolism (PE) on chest computed tomography (CT) images.

#### METHODS AND MATERIALS

For the development of CAD, CT pulmonary angiographies (CTPAs) of patients with PE were retrospectively collected from two institutions. Two thoracic radiologists made voxel-wise annotations for areas of PE on each transverse CT image. The DL-CAD consisted of three elements based on convolutional neural networks (CNNs): 1) segmentation of pulmonary arteries for extraction of regions of interest, 2) detection of candidate lesions for PE, and 3) reduction of false-positive detections. For the evaluation of DL-CAD, a separate test dataset was built, comprising CT images from the same institutions without overlap in patients with the developmental dataset. The CT images for test dataset were conveniently collected to exhibit 1:1 ratio between 1) CTs with and without PE, 2) CTPAs and general contrast-enhanced chest CT (CECT)s, and 3) CT with thin-slice (<1.5 mm slice thickness) and thick-slice images. The performance of DL CAD was evaluated with examination-level sensitivity, specificity, PPV (positive predictive value), and NPV (negative predictive value) for discrimination of CTs with and without PE.

#### RESULTS

A total of 370 CTPA examinations with PE were used for the development of DL-CAD. The test dataset included 320 CT examinations (160 with PE; 160 CTPAs and 160 general CECTs; 160 with thin-slice images). The DL-CAD exhibited sensitivity, specificity, PPV, and NPV of 88.8%, 85.0%, 85.5%, and 88.3%, respectively for identification of CT examinations with PE. The DL-CAD exhibited slightly higher sensitivity in CTPAs compared to general CECT (92.5% vs. 85.0%;  $P=.133$ ) at the same specificity (85.0%). Meanwhile, the DL-CAD exhibited significantly higher sensitivity in CTs with thin-slice images (97.5% vs. 80.0%;  $P<.001$ ) and lower specificity (77.5% vs. 92.5%;  $P=.008$ ) compared to CTs with thick-slice images.

#### CONCLUSION

s The DL-CAD could successfully identify PE not only in CTPA images but also in general CECT images.

#### CLINICAL RELEVANCE/APPLICATION

Automated detection of PE on chest CTs can improve the quality and efficiency of interpretation and help timely treatment for patients.

Printed on: 02/07/23

## Abstract Archives of the RSNA, 2022

R2-SPCH-7

### Accuracy of Airway Thickness Measurements in Low-dose High-resolution photon-counting-detector CT

Thursday, Dec. 1 9:00AM - 9:30AM Room: Learning Center - CH DPS

#### Participants

Chelsea Dunning, DPHIL, Rochester, MN (*Presenter*) Nothing to Disclose

#### PURPOSE

To evaluate the accuracy of bronchial airway thickness in low-dose chest CT using a clinical photon-counting-detector (PCD) CT compared to conventional energy-integrating-detector (EID) CT.

#### METHODS AND MATERIALS

Twelve 3D-printed acrylic tubes of assorted wall thicknesses (0.33 - 1.6 mm) and inner diameters (0.42 - 3.4 mm) were placed throughout an anthropomorphic chest phantom (Lungman, Kyoto Kagaku). The phantom was scanned on a whole-body PCD-CT (NAEOTOM Alpha, Siemens) at 100 kV with an additional tin filter (Sn100) in single-source ultra-high-resolution mode (detector configuration: 120 x 0.2 mm) at three dose levels (volume CT dose index (CTDIvol): 0.2, 0.4, and 0.8 mGy). The phantom was also scanned on a conventional EID-CT scanner (SOMATOM Force, Siemens) using Sn100 kV in single-source mode (detector configuration: 96 x 0.6 mm). A reference high-dose scan was also acquired at 120 kV and 12 mGy for both scanners. All images were reconstructed with quantitative kernels and iterative reconstruction with a strength setting of 3; Qr54-3 for standard resolution (SR) EID-CT, Qr56-3 for SR PCD-CT, and Qr89-3 for ultra-high-resolution (UHR) PCD-CT. The image noise was measured as the standard deviation in a region of interest within the mediastinum. The wall thickness of each tube was measured by taking the radial profile in multiple slices and measuring the average full width at half maximum (FWHM). The airway thickness accuracy was expressed using linear regression ( $R^2$  and RMSE) between the measured wall thickness at each dose level.

#### RESULTS

At matched spatial resolution (Qr54 for EID-CT and Qr56 for PCD-CT), PCD-CT reduced image noise by 53%, 57%, and 56% at 0.2 mGy, 0.4 mGy, and 0.8 mGy dose levels compared to EID-CT. At 0.2 mGy, 0.4 mGy, and 0.8 mGy, the wall thickness RMSE values were 0.37, 0.36, and 0.57 mm for EID-CT; 0.49, 0.46, and 0.47 mm for SR PCD-CT; and 0.18, 0.15, and 0.11 mm for UHR PCD-CT. The UHR PCD-CT had the closest  $R^2$  values to unity across all dose levels ( $R^2 > 0.963$ ), compared to EID-CT ( $R^2 > 0.816$ ) and SR PCD-CT ( $R^2 > 0.823$ ).

#### CONCLUSION

More accurate airway wall thickness measurements can be achieved for UHR PCD-CT compared to EID-CT or SR PCD-CT at radiation dose levels at or lower than in lung cancer screening exams.

#### CLINICAL RELEVANCE/APPLICATION

High accuracy measurements of bronchial airway wall thickness in high-resolution low-dose PCD-CT can enable reliable diagnosis of lung diseases such as COPD or cystic fibrosis.

Printed on: 02/07/23

## Abstract Archives of the RSNA, 2022

R2-SPCH-8

### Value-added Opportunistic Screening: Prediction Model of Arterial Stiffness Based on Clinical and Thoracic Aorta Imaging Risk Factors

Thursday, Dec. 1 9:00AM - 9:30AM Room: Learning Center - CH DPS

#### Participants

Jinrong Yang, (*Presenter*) Nothing to Disclose

#### PURPOSE

This study is to establish and verify a nomogram model based on clinical and thoracic aorta imaging risk factors for predicting the risk of arterial stiffness (AS).

#### METHODS AND MATERIALS

This is a cross-sectional study. A total of 815 patients were enrolled and the baseline clinical data, biochemical indicators, concomitant diseases and AI data (the diameter, area at 9 levels and volume, length at two adjacent levels of thoracic aorta recommended by AHA Guidelines (2010)) of them were collected. They were randomly divided into the training set of 570 cases (70%) and the validation set of 245 cases (30%). Based on the recommendations of the Committee on Physiological Diagnostic Criteria for Vascular Failure, 8= cardio-ankle vascular index (CAVI) < 9 indicates pre-AS, CAVI=9 indicates AS. In the training set, variance, t-test (for normal distribution) /Mann-Whitney U-test (for non-normal distribution), least absolute shrinkage and selection operator (LASSO) were used for selecting thoracic aorta imaging risk factors to construct AI measurement score and multivariate logistic backward stepwise regression were used to analyze the influencing factors of hypertension. According to the clinical application for different data conditions, five nomogram prediction models were constructed, named AIMeasure model, BasicClinical model, TotalClinical model, AIBasicClinical model, AITotalClinical model. Moreover, receiver operating characteristic (ROC) curve, calibration curve and decision curve analyses (DCA) were used to test the distinction, accuracy and clinical applicability of the model both in training set and validation set.

#### RESULTS

The results showed age, BMI, systolic blood pressure (SBP), smoking, serum sodium, serum magnesium and thoracic aortic dilatation were all related to the occurrence of AS. The area under the ROC curve of the above five models was 0.763, 0.826, 0.842, 0.831, 0.843 in the training set and was 0.794, 0.793, 0.803, 0.819, 0.827 in the verification set, respectively. Moreover, the calibration curves and DCAs performed well on accuracy and clinical practicality.

#### CONCLUSION

The risk prediction nomogram models have good predictive ability and clinical value, which could be used as an effective tool for the risk prediction of arterial stiffness. Furthermore, they would facilitate earlier intervention to prevent the future development of arterial stiffness.

#### CLINICAL RELEVANCE/APPLICATION

Based on clinical data and thoracic aorta data measured by AI on non-contrast enhanced chest CT, prediction models were constructed for different clinical scenarios, so as to carry out opportunistic screening of arterial stiffness.

Printed on: 02/07/23



## Abstract Archives of the RSNA, 2022

R2-SPER

### Emergency Thursday Poster Discussions

Thursday, Dec. 1 9:00AM - 9:30AM Room: Learning Center - ER DPS

#### Participants

Scott Steenburg, MD, Indianapolis, IN (*Moderator*) Nothing to Disclose

#### Sub-Events

#### R2-SPER-1 Subcostal And Right Lateral Views Are Not Equivalent in Obtaining IVC Measurements Using Ultrasound in Healthy Adults

#### Participants

Fadi Haroun, BS, (*Presenter*) Nothing to Disclose

#### PURPOSE

The objective of this study is to assess concordance between the subcostal and right lateral view for ultrasonographic inferior vena cava (IVC) measurements including the end-inspiratory diameter, end-expiratory diameter, and respiratory variation represented by the caval index in spontaneously breathing healthy adults.

#### METHODS AND MATERIALS

We recruited a convenience sample of 33 healthy adults. A phased array ultrasound probe was used to obtain IVC measurements from a subcostal view in the sagittal plane and from a right lateral view in the coronal plane with B mode ultrasound. End-inspiratory diameter, end-expiratory diameter, and caval index were obtained for each view. A two-tailed t-test was performed to compare the caval indices obtained by the two views. Bland-Altman analysis was used to obtain the limits of agreement for the IVC diameter and caval index across the two views.

#### RESULTS

Subcostal and right lateral caval indices across all participants were significantly different according to a paired t-test ( $p < 0.0001$ ). The Bland-Altman analysis showed wide limits of agreement in end-inspiratory diameter (-0.97 and 0.50 cm) and in end-expiratory diameter (-0.94 and 0.90 cm). The right lateral view underestimated the IVC caval index relative to the subcostal view.

#### CONCLUSION

The subcostal and right lateral views are not equivalent in obtaining IVC measurements in spontaneously breathing healthy adults. Current cut off values for measurement-based applications of IVC ultrasound, including fluid responsiveness using caval indices, may not be accurate when values are obtained from the right lateral view in the coronal plane of the IVC in patients.

#### CLINICAL RELEVANCE/APPLICATION

Though previous studies have demonstrated the discordance between measurements of the IVC obtained from the subcostal and right lateral views, our study is the first study to demonstrate this in adult non-ICU populations. This expands to a new population the conclusion that cut-off values for measurement-based applications of IVC ultrasound should not be used interchangeably for these two views since most of these cut-offs were established using the subcostal view only.

Printed on: 02/07/23

## Abstract Archives of the RSNA, 2022

R2-SPER-1

### Subcostal And Right Lateral Views Are Not Equivalent in Obtaining IVC Measurements Using Ultrasound in Healthy Adults

Thursday, Dec. 1 9:00AM - 9:30AM Room: Learning Center - ER DPS

#### Participants

Fadi Haroun, BS, (*Presenter*) Nothing to Disclose

#### PURPOSE

The objective of this study is to assess concordance between the subcostal and right lateral view for ultrasonographic inferior vena cava (IVC) measurements including the end-inspiratory diameter, end-expiratory diameter, and respiratory variation represented by the caval index in spontaneously breathing healthy adults.

#### METHODS AND MATERIALS

We recruited a convenience sample of 33 healthy adults. A phased array ultrasound probe was used to obtain IVC measurements from a subcostal view in the sagittal plane and from a right lateral view in the coronal plane with B mode ultrasound. End-inspiratory diameter, end-expiratory diameter, and caval index were obtained for each view. A two-tailed t-test was performed to compare the caval indices obtained by the two views. Bland-Altman analysis was used to obtain the limits of agreement for the IVC diameter and caval index across the two views.

#### RESULTS

Subcostal and right lateral caval indices across all participants were significantly different according to a paired t-test ( $p < 0.0001$ ). The Bland-Altman analysis showed wide limits of agreement in end-inspiratory diameter (-0.97 and 0.50 cm) and in end-expiratory diameter (-0.94 and 0.90 cm). The right lateral view underestimated the IVC caval index relative to the subcostal view.

#### CONCLUSION

The subcostal and right lateral views are not equivalent in obtaining IVC measurements in spontaneously breathing healthy adults. Current cut off values for measurement-based applications of IVC ultrasound, including fluid responsiveness using caval indices, may not be accurate when values are obtained from the right lateral view in the coronal plane of the IVC in patients.

#### CLINICAL RELEVANCE/APPLICATION

Though previous studies have demonstrated the discordance between measurements of the IVC obtained from the subcostal and right lateral views, our study is the first study to demonstrate this in adult non-ICU populations. This expands to a new population the conclusion that cut-off values for measurement-based applications of IVC ultrasound should not be used interchangeably for these two views since most of these cut-offs were established using the subcostal view only.

Printed on: 02/07/23

## Abstract Archives of the RSNA, 2022

R2-SPGI

### Gastrointestinal Thursday Poster Discussions

Thursday, Dec. 1 9:00AM - 9:30AM Room: Learning Center - GI DPS

#### Participants

Senta Berggruen, MD, Shorewood, IL (*Moderator*) Nothing to Disclose

#### Sub-Events

#### **R2-SPGI-1 Pancreatic Ductal Adenocarcinoma (PDAC) Regional Nodal Disease: Is MRI Accurate for identifying node-positive patients?**

#### Participants

Sami Adham, MD, (*Presenter*) Nothing to Disclose

#### PURPOSE

Multiple studies have demonstrated that metastatic regional lymph nodes have prognostic value in patients with PDAC. The purpose of this study is to determine the diagnostic accuracy of MRI for evaluating the presence of regional nodal disease in patients with biopsy-confirmed PDAC.

#### METHODS AND MATERIALS

With IRB approval, all adult patients with pancreatic MRI performed from 2011 to 2021 within 3 months of a Whipple resection including regional nodal dissection at our institution were eligible for inclusion in this single-centre retrospective cohort study. Patients with an incomplete MRI or those who received neoadjuvant therapy were excluded. Each MRI was independently reviewed by two experienced fellowship-trained abdominal radiologists. The following characteristics were evaluated at the patient level: primary tumour size, largest regional lymph node short and long axes length, number of regional lymph nodes, and an apparent diffusion coefficient (ADC) node-to-spleen signal index was calculated and absolute ADC values were documented. Additionally, the presence of the following lymph node characteristics was evaluated: round shape, indistinct margin, peri-nodal fat-stranding, the presence of one or more regional lymph nodes with heterogeneous T2 signal, or restricted diffusion greater than the spleen, and Radiologists documented subjectively whether or not they believed a patient was node positive. Surgical pathology was the reference standard.

#### RESULTS

Of 75 included patients, 85% (64/75) were positive for regional nodal disease. None of the categorical variables evaluated on MRI were associated with pathologic regional nodes including the presence of one or more node with heterogeneous T2-weighted signal, a round shape, indistinct margin, peri-nodal fat stranding, restricted diffusion greater than the spleen, or subjective radiologist opinion ( $P > 0.05$  each). Median primary tumor maximum diameter was slightly larger for patients with pathologic regional lymph nodes compared to those without, 18 mm (10-42 mm) vs. 16 mm (9-22 mm),  $P = 0.027$ . None of the other continuous variables evaluated on MRI were associated with pathologic regional nodes.

#### CONCLUSION

Pre-operative MRI has low accuracy for evaluating regional nodal disease in patients with PDAC. A larger median primary tumour maximum diameter was the only feature that was associated with regional nodal disease.

#### CLINICAL RELEVANCE/APPLICATION

Multiple lymph node morphologic features routinely assessed on MRI for malignancies elsewhere in the body are likely not applicable when assessing for PDAC regional nodal disease.

#### **R2-SPGI-10 Inter-rater agreement of tumor measurements for assessment of neoadjuvant treatment response in pancreatic ductal adenocarcinoma**

#### Participants

Jon Heiselman, (*Presenter*) Nothing to Disclose

#### PURPOSE

To evaluate inter-rater variability of pancreatic ductal adenocarcinoma (PDAC) diameters and volumes on baseline and restaging CT after neoadjuvant therapy.

#### METHODS AND MATERIALS

Thirty patients with resectable PDAC enrolled in an IRB-approved Phase II clinical trial for neoadjuvant chemotherapy were retrospectively analyzed. For each patient, three raters independently segmented whole tumor and pancreas volumes of interest from contrast-enhanced CT images acquired pre- and post-neoadjuvant treatment. Each rater also measured axial plane lesion diameters in both images to evaluate treatment response (PR: partial response, SD: stable disease, PD: progressive disease) according to the response evaluation criteria in solid tumors guidelines (RECIST v1.1). Variability in spatial overlap was quantified

via generalized conformity index (GCI) and compared with Wilcoxon signed rank tests. Volume and diameter measurements were compared by intra-class correlation coefficient (ICC), and variations in RECIST groups assessed with Fleiss' Kappa (k).

## RESULTS

Inter-rater agreement of pancreas segmentations was moderate (pre-treatment GCI 0.60, ICC 0.52; post-treatment GCI 0.57, ICC 0.61), while tumor segmentations showed significantly lower spatial overlap ( $p < 0.005$ ) despite concordant gross volumes (pre-treatment GCI 0.46, ICC 0.63; post-treatment GCI 0.38, ICC 0.81). GCI of tumor segmentations were significantly lower in post-treatment pre-treatment imaging ( $p < 0.01$ ). When evaluating pre- to post-treatment differences in tumor volume identified by each rater, agreement was very poor (ICC 0.12). Similarly, the percent change in the sum of longest diameters measured by individual raters agreed poorly (ICC 0.25). RECIST category across each patient was found to depend on the reader, with only slight agreement observed ( $k = 0.18$ ). Complete agreement of RECIST group between all three raters occurred in only 60% of patients (18 of 30; 0 PR, 17 SD, 1 PD); raters disagreed between PR/SD in 8 of 12 remaining patients, between SD/PD in 3 of 12, and between PR/SD/PD in 1 patient.

## CONCLUSION

s Longitudinal changes in PDAC tumor size are associated with high measurement variability, which suggests more reliable methods for measuring treatment response are needed.

## CLINICAL RELEVANCE/APPLICATION

PDAC often presents with ill-defined radiographic borders, yet standard methods for assessing therapeutic response require dimensional measurement of tumor diameters or volumes throughout treatment. The high variability we observe suggests more precise quantitative measures of longitudinal treatment response should be pursued to better inform PDAC treatment course and improve outcome prediction.

## R2-SPGI-2 CT characteristics of recurrent acute pancreatitis at different onset times

Participants

Ju Zhang, MMed, Chengdu, Sichuan, China (*Presenter*) Nothing to Disclose

## PURPOSE

To investigate the CT characteristic of recurrent acute pancreatitis (RAP) at different onset times.

## METHODS AND MATERIALS

RAP data were obtained over the past 5 years. RAP patients were divided into five subgroups according to the time from RAP onset to performing CT examination: 1-3 days, 4-7 days, 8-14 days, 15-30 days, and after 30 days. RAP was categorized into the early phase (first week) and late phase (after the first week) based on the 2012 revised Atlanta classification (RAC). Evaluation and pairwise comparison of patients' demographic data, RAC, CT findings, CT severity index (CTSI) score, and extrapancreatic inflammation on CT (EPIC) score were conducted.

## RESULTS

In the 690 patients with RAP, hypertriglyceridemia was the most common cause. The proportion of mild RAP patients on both RAC and CTSI in the early stage of onset was higher than those in the late stage of onset (both  $P < .005$ ). The proportion of moderately severe RAP and NP patients on CT at 15-30 days of onset was higher than those in the early phase of onset (both  $P < .005$ ), and the percentage of severe RAP patients after 14 days of onset was higher than that in the early stage of onset.

## CONCLUSION

s In the 690 patients with RAP, hypertriglyceridemia was the most common cause. The proportion of mild RAP patients on both RAC and CTSI in the early stage of onset was higher than those in the late stage of onset (both  $P < .005$ ). The proportion of moderately severe RAP and NP patients on CT at 15-30 days of onset was higher than those in the early phase of onset (both  $P < .005$ ), and the percentage of severe RAP patients after 14 days of onset was higher than that in the early stage of onset.

## CLINICAL RELEVANCE/APPLICATION

Recognizing the characteristics of RAP at different onset times, and accurately grasping the changes in the condition of RAP patients can help clinicians to give reasonable treatment according to the changes of the disease, and then effectively prevent the onset of chronic pancreatitis.

## R2-SPGI-3 Diagnostic value of pancreatic ECV in patients with diabetes: a comparative study of HU value and iodine density method

Participants

Xiaoyi Cai, MBBS, (*Presenter*) Nothing to Disclose

## PURPOSE

To investigate the correlation between extracellular volume (ECV) fraction and HbA1c value in patients with diabetes mellitus, and compare absolute contrast enhancement (ECV-HU) method and dual-energy iodine density (ECV-ID) method.

## METHODS AND MATERIALS

In this study, 92 patients with suspected abdominal diseases were retrospectively enrolled, all of whom received abdominal CT precontrast scan (120kV) and dual-energy CT enhanced scan. Patients were divided into two groups according to HbA1c value: the diabetes group ( $HbA1c \geq 6.5\%$ , 39 patients) and the non-diabetes group ( $HbA1c < 6.5\%$ , 53 patients). ECV fraction of pancreas was calculated using two methods: ECV-HU method,  $ECV-HU = (HU_{pancreas-equilibrium\ phase} - HU_{pancreas} - precontrast) / (HU_{abdominal\ aorta} - equilibrium\ phase - HU_{abdominal\ aorta} - precontrast) \times (100 - Hct)$ ; ECV-ID method,  $ECV-ID = (ID_{pancreas} - equilibrium\ phase / ID_{abdominal\ aorta} - equilibrium\ phase) \times (100 - Hct)$ . Independent sample T-test was used to analyze the differences in ECV between two groups, and Spearman correlation analysis was performed to analyze the correlation between ECV and HbA1c value. The diagnostic performance of pancreatic ECV-HU and ECV-ID in differentiating diabetic mellitus was evaluated by receiver operating characteristic (ROC) curve analysis.

## RESULTS

HbA1c value was positively correlated with ECV-HU and ECV-ID in whole patients ( $r_s=0.571$ ,  $r_s=0.629$ , respectively; both  $P<0.001$ ). ECV-HU and ECV-ID in diabetes group were significantly higher than those in non-diabetes group ( $25.03\pm 2.13$  vs.  $22.33\pm 2.40$ ,  $34.58\pm 2.03$  vs.  $31.59\pm 2.23$ , respectively; both  $P<0.05$ ). For diabetes differentiation, the area under the curve (AUC) of ECV-ID was higher than that of ECV-HU ( $0.835$  vs.  $0.808$ ,  $P=0.418$ ). When the cut-off value was set at 32.70%, the sensitivity and specificity of ECV-ID were 87.2% and 66.0%, respectively.

## CONCLUSION

Both ECV-ID and ECV-HU of pancreas are potential indices to diagnose diabetes mellitus and can reflect the status of HbA1c value.

## CLINICAL RELEVANCE/APPLICATION

Pancreatic ECV obtained by CT is a reliable index which can not only monitor HbA1c for patients with diabetes, but also assist in diagnosis of diabetes mellitus.

## R2-SPGI-4 Texture analysis of IVIM-DWI in early postoperative MRI to predict post-pancreatectomy acute pancreatitis after pancreaticoduodenectomy.

Participants

Giulia A. Zamboni, MD, Verona, Italy (*Presenter*) Nothing to Disclose

## PURPOSE

Pancreaticoduodenectomy can be burdened by significant morbidity and mortality. Post-pancreatectomy acute pancreatitis (PPAP) is one of the most common complications and can lead to more severe complications such as postoperative fistula, with prolonged hospitalization and poor outcome. The purpose of this study is to assess if early postoperative MRI after pancreaticoduodenectomy can predict post-pancreatectomy acute pancreatitis (PPAP) by identifying early microstructural changes that lead to inflammation and microcirculation changes.

## METHODS AND MATERIALS

In this IRB-approved prospective study, 65 patients underwent MRI on a 1.5 T scanner (Philips Ingenia) on postoperative day 3 (POD3) after pancreaticoduodenectomy. The scan protocol included a combination of standard sequences, post-gadolinium acquisitions, and IVIM DWI. The IVIM DICOM images were analyzed with in-house software that produced F, D and  $D^*$  maps and allowed to calculate the texture parameters of the ROIs. One reader drew 3 ROIs on the pancreatic stump on each MRI: adjacent to the resection margin, on the tail further from the margin, and on the entire pancreatic remnant. The 2021 ISGPS definition of PPAP was used to dichotomize patients into a group with POH/PPAP and a group without that complication. Texture parameters and radiological findings were compared between the two groups.

## RESULTS

20 patients developed POH and 6 of these PPAP grade B or C. Significant differences in texture analysis results were identified between the POH/PPAP and the non-POH/PPAP group for mean ADC value ( $(1.33 \pm 0.22) \times 10^{-3}$  vs  $(1.56 \pm 0.28) \times 10^{-3}$  mm<sup>2</sup>/s;  $p=0.006$ ), mean D value ( $0.11 \pm 0.14$  vs  $0.22 \pm 0.15$ ;  $p=0.03$ ), F entropy ( $4.5$ , SE 0.10 vs  $4.1$ , SE 0.08;  $p=0.004$ ) and  $D^*$  ( $2.7$ , SE 0.73 vs  $1.3$ , SE 0.38;  $p=0.01$ ) entropy of ROIs including the pancreatic stump. Similar results were obtained for the ROIs of the tail and the entire pancreatic remnant. No imaging findings consistent with PPAP were identified at MRI in the POH/PPAP group.

## CONCLUSION

Texture analysis of IVIM-derived parameters on early postoperative MRI after pancreaticoduodenectomy can help identify patients who will develop PPAP.

## CLINICAL RELEVANCE/APPLICATION

Earlier identification of patients who will develop POH/PPAD can lead to a better treatment and patient outcome

## R2-SPGI-6 Role of preoperative regional lymph node metastasis detected on CT and/or FDG-PET scans in the prediction of early recurrence of pancreatic adenocarcinoma after curative resection

Participants

Ja Kyung Yoon, (*Presenter*) Nothing to Disclose

## PURPOSE

This study aimed to evaluate the role of regional lymph node (LN) metastasis detected on preoperative CT and/or 18F-fluoro-2-deoxyglucose-positron emission tomography (FDG-PET) scans in the prediction of early tumor recurrence after curative surgical resection of pancreatic ductal adenocarcinoma (PDAC).

## METHODS AND MATERIALS

This retrospective study included 137 patients who underwent upfront surgery with R0 resection of PDAC between 2013 and 2016. Regional LN metastasis was identified using two criteria: both preoperative CT and FDG-PET scans (LNAND) or preoperative CT or FDG-PET scans (LNOR). Cox proportional hazard regression analysis was used to determine the preoperative risk factors for early tumor recurrence. The significant risk factors for early tumor recurrence were used to create a predictive nomogram for early tumor recurrence.

## RESULTS

Fifty-five patients had early tumor recurrence within 12 months after curative resection. Regional LN metastasis (both LNOR and LNAND criteria), preoperative carbohydrate antigen 19-9 (CA19-9) levels, and preoperative locally advanced status were significant risk factors for early tumor recurrence. Compared with the LNAND criteria, the LNOR criteria provided higher sensitivity (22.4% vs. 15.5%,  $p = 0.046$ ) and a higher negative predictive value (61.9% vs. 59.8%,  $p = 0.046$ ). LNOR, preoperative CA19-9 level, and resectability were included in the predictive nomogram with an adjusted C-index of 0.589.

## CONCLUSION

s The preoperative LN metastasis on CT or FDG-PET scans, elevated serum CA19-9 levels, and locally advanced status were significant risk factors for early recurrence of PDAC after surgery. The predictive nomogram, including these factors, may help guide the first-line treatment of PDAC.

## CLINICAL RELEVANCE/APPLICATION

Preoperative LN metastasis identified on CT or FDG-PET scans may help predict early recurrence of pancreatic adenocarcinoma after curative resection.

## R2-SPGI-7 MRI vs. CT for pancreatic adenocarcinoma vascular invasion and resectability: Comparative diagnostic test accuracy systematic review and meta-analysis

### Participants

Ankush Jajodia, MD, MBBS, New Delhi, India (*Presenter*) Nothing to Disclose

### PURPOSE

To perform a systematic review evaluating the diagnostic test accuracy of MRI vs CT for assessing pancreatic ductal adenocarcinoma (PDAC) vascular invasion and resectability.

### METHODS AND MATERIALS

MEDLINE, EMBASE, Cochrane Central Register of Controlled Trials (CENTRAL) and Scopus were searched until December 2021 for all studies directly comparing the accuracy of MRI vs CT for vascular invasion and resectability of pathologically confirmed PDAC in the same patients. Findings on curative resection or exploratory laparotomy were the preferred reference standard. Data extraction, risk of bias and applicability assessment was performed by two authors using QUADAS-C, a tool for assessing risk of bias in comparative diagnostic accuracy studies. A bivariate random-effects model was used with meta-regression for test comparison and covariate analysis with 95% confidence intervals (95%CI). Hierarchical summary receiver operating characteristic (ROC) curves and coupled forest plots were generated.

### RESULTS

Five studies met inclusion criteria consisting of 215 patients, 635 vessels and 124 resectable tumors. There was no difference between MRI and CT for diagnosing PDAC vascular invasion: MRI sensitivity/specificity were 73% (95%CI: 50-88%)/97% (94-99%) and for CT, 75% (56-88%)/97% (94-98%). Similarly, no difference was seen between MRI and CT for resectability assessment: MRI sensitivity/specificity were 85% (77-90%)/67% (46-82%) and for CT, 84% (75-90%)/75% (60-86%). Sources of bias included selection bias from a subset of CT patients undergoing MRI, and verification bias for patients with unresectable disease not proceeding to surgical confirmation. Study risk of bias did not impact MRI or CT performance on meta-regression.

### CONCLUSION

s Limited data suggest there is no difference between MRI and CT for assessing PDAC vascular invasion or resectability; however, further research is needed to improve confidence in this finding.

## CLINICAL RELEVANCE/APPLICATION

MRI is more sensitive than CT for detecting PDAC liver metastases; if also more accurate at assessing vascular invasion and resectability, then it could be a "one-stop shop" for PDAC detection and staging.

## R2-SPGI-8 Development and validation of a radiomics model for predicting malignant IPMN compared with the revised Fukuoka guidelines

### Participants

Doo Young Lee, MD, MS, Seoul, Korea, Republic Of (*Presenter*) Nothing to Disclose

### PURPOSE

The revised international consensus Fukuoka guidelines (Fukuoka guidelines) are commonly used for evaluating pancreatic intraductal papillary mucinous neoplasms (IPMNs). However, assessment of radiomics model in comparison with Fukuoka guidelines by radiologists has been lacking. Thus, this study aimed to evaluate CT-based radiomics model for determining malignant IPMNs and compare its performance with Fukuoka guidelines.

### METHODS AND MATERIALS

This retrospective study included a total of 194 consecutive patients with surgically resected pancreatic IPMNs from January 2008 to December 2020. Surgical histopathologic analysis was the reference standard for malignancy. Radiomic features were extracted from preoperative contrast-enhanced CT, and radiomics model was built using the least absolute shrinkage and selection operator with fivefold cross-validation. CT and MR images were independently reviewed based on Fukuoka guidelines by two board-certified abdominal radiologists, who arrived at a consensus in cases of discrepancy. The performance of Fukuoka guidelines was compared with that of the radiomics model. Areas under the curve (AUCs) were compared by using the DeLong method.

### RESULTS

A total of 194 patients with pancreatic IPMNs (benign, 83 [43%], malignant, 111 [57%]) were included. The patients were chronologically divided into training set (n = 141; mean age 65 + SD 8.6; men 88) and temporal validation set (n = 53; mean age 66 + SD 9.7; men 31). The diagnostic performance of Fukuoka guidelines was not statistically different between CT and MRI (AUC 0.71 vs. 0.71, P = 0.93). Thus, CT was selected for further comparison between Fukuoka guidelines and radiomics model. The CT radiomics model showed higher diagnostic performance (AUC, 0.85 vs 0.71 [P = 0.038]), specificity (84.6% vs 61.5% [P = 0.041]), and positive predictive value (84.0% vs 66.7% [P = 0.044]) than Fukuoka guidelines in the validation set.

### CONCLUSION

s A CT radiomics model exhibited better diagnostic performance than the revised Fukuoka guidelines by experienced radiologists for classifying malignant IPMNs.

## CLINICAL RELEVANCE/APPLICATION

The CT radiomics model performed better than the revised Fukuoka guidelines in determining the malignancy of IPMN. Therefore, the radiomics model will facilitate proper treatment decision making.

## R2-SPGI-9 Vascular involvement and resectability of pancreatic ductal adenocarcinoma on contrast-enhanced MRI: comparison with pancreatic protocol CT

Participants

Yukako Iritani, MD, Gifu, Japan (*Presenter*) Nothing to Disclose

## PURPOSE

To compare the diagnostic performance for detecting vascular involvement and determining resectability differences regarding pancreatic ductal adenocarcinoma (PDAC) between contrast-enhanced CT and MRI.

## METHODS AND MATERIALS

This retrospective study evaluated 82 patients (73 years, 46 men) with PDAC who underwent both preoperative contrast-enhanced CT and MRI from January 2008 to March 2021. Two radiologists independently categorized vascular involvements for celiac, superior mesenteric, splenic, and common hepatic arteries, and portal, superior mesenteric, and splenic veins into no tumor contact, solid soft-tissue contact  $\leq 180^\circ$ , or solid soft-tissue contact  $>180^\circ$ . The radiologists also classified resectability into resectable, borderline resectable, or locally advanced. Receiver-operating-characteristic (ROC) analysis was conducted to evaluate the diagnostic performances for detecting vascular involvements which were confirmed by pathological or intraoperative findings. The proportion of resectability classifications was compared between CT and MRI by the Fisher's exact test.

## RESULTS

No statistical difference was found in the diagnostic performances for detecting vascular involvement in CT (area under the ROC curve [AUC], 0.50-0.89) and MRI (AUC, 0.51-0.75) ( $P = .06$ - $>.99$ ). Resectabilities on CT were 79% and 68%, 20% and 26%, and 1% and 6% for resectable, borderline resectable, and locally advanced tumors for reviewers 1 and 2; those on MRI were 87% and 81%, 12% and 13%, and 1% and 6%, respectively. The proportion of resectability was not different between CT and MRI ( $P = .48$  and  $= .15$  for reviewers 1 and 2, respectively).

## CONCLUSION

The diagnostic performance for detecting vascular involvement and determining resectability of PDAC on contrast-enhanced MRI were comparable with pancreatic protocol CT.

## CLINICAL RELEVANCE/APPLICATION

Diagnostic performance for detecting vascular involvement and determining resectability of pancreatic ductal adenocarcinoma on contrast-enhanced MRI were statistically comparable with pancreatic protocol CT.

Printed on: 02/07/23

## Abstract Archives of the RSNA, 2022

R2-SPGI-1

### **Pancreatic Ductal Adenocarcinoma (PDAC) Regional Nodal Disease: Is MRI Accurate for identifying node-positive patients?**

Thursday, Dec. 1 9:00AM - 9:30AM Room: Learning Center - GI DPS

#### **Participants**

Sami Adham, MD, (*Presenter*) Nothing to Disclose

#### **PURPOSE**

Multiple studies have demonstrated that metastatic regional lymph nodes have prognostic value in patients with PDAC. The purpose of this study is to determine the diagnostic accuracy of MRI for evaluating the presence of regional nodal disease in patients with biopsy-confirmed PDAC.

#### **METHODS AND MATERIALS**

With IRB approval, all adult patients with pancreatic MRI performed from 2011 to 2021 within 3 months of a Whipple resection including regional nodal dissection at our institution were eligible for inclusion in this single-centre retrospective cohort study. Patients with an incomplete MRI or those who received neoadjuvant therapy were excluded. Each MRI was independently reviewed by two experienced fellowship-trained abdominal radiologists. The following characteristics were evaluated at the patient level: primary tumour size, largest regional lymph node short and long axes length, number of regional lymph nodes, and an apparent diffusion coefficient (ADC) node-to-spleen signal index was calculated and absolute ADC values were documented. Additionally, the presence of the following lymph node characteristics was evaluated: round shape, indistinct margin, peri-nodal fat-stranding, the presence of one or more regional lymph nodes with heterogeneous T2 signal, or restricted diffusion greater than the spleen, and Radiologists documented subjectively whether or not they believed a patient was node positive. Surgical pathology was the reference standard.

#### **RESULTS**

Of 75 included patients, 85% (64/75) were positive for regional nodal disease. None of the categorical variables evaluated on MRI were associated with pathologic regional nodes including the presence of one or more node with heterogeneous T2-weighted signal, a round shape, indistinct margin, peri-nodal fat stranding, restricted diffusion greater than the spleen, or subjective radiologist opinion ( $P > 0.05$  each). Median primary tumor maximum diameter was slightly larger for patients with pathologic regional lymph nodes compared to those without, 18 mm (10-42 mm) vs. 16 mm (9-22 mm),  $P = 0.027$ . None of the other continuous variables evaluated on MRI were associated with pathologic regional nodes.

#### **CONCLUSION**

Pre-operative MRI has low accuracy for evaluating regional nodal disease in patients with PDAC. A larger median primary tumour maximum diameter was the only feature that was associated with regional nodal disease.

#### **CLINICAL RELEVANCE/APPLICATION**

Multiple lymph node morphologic features routinely assessed on MRI for malignancies elsewhere in the body are likely not applicable when assessing for PDAC regional nodal disease.

Printed on: 02/07/23

## Abstract Archives of the RSNA, 2022

R2-SPGI-10

### Inter-rater agreement of tumor measurements for assessment of neoadjuvant treatment response in pancreatic ductal adenocarcinoma

Thursday, Dec. 1 9:00AM - 9:30AM Room: Learning Center - GI DPS

#### Participants

Jon Heiselman, (*Presenter*) Nothing to Disclose

#### PURPOSE

To evaluate inter-rater variability of pancreatic ductal adenocarcinoma (PDAC) diameters and volumes on baseline and restaging CT after neoadjuvant therapy.

#### METHODS AND MATERIALS

Thirty patients with resectable PDAC enrolled in an IRB-approved Phase II clinical trial for neoadjuvant chemotherapy were retrospectively analyzed. For each patient, three raters independently segmented whole tumor and pancreas volumes of interest from contrast-enhanced CT images acquired pre- and post-neoadjuvant treatment. Each rater also measured axial plane lesion diameters in both images to evaluate treatment response (PR: partial response, SD: stable disease, PD: progressive disease) according to the response evaluation criteria in solid tumors guidelines (RECIST v1.1). Variability in spatial overlap was quantified via generalized conformity index (GCI) and compared with Wilcoxon signed rank tests. Volume and diameter measurements were compared by intra-class correlation coefficient (ICC), and variations in RECIST groups assessed with Fleiss' Kappa ( $k$ ).

#### RESULTS

Inter-rater agreement of pancreas segmentations was moderate (pre-treatment GCI 0.60, ICC 0.52; post-treatment GCI 0.57, ICC 0.61), while tumor segmentations showed significantly lower spatial overlap ( $p < 0.005$ ) despite concordant gross volumes (pre-treatment GCI 0.46, ICC 0.63; post-treatment GCI 0.38, ICC 0.81). GCI of tumor segmentations were significantly lower in post- than pre-treatment imaging ( $p < 0.01$ ). When evaluating pre- to post-treatment differences in tumor volume identified by each rater, agreement was very poor (ICC 0.12). Similarly, the percent change in the sum of longest diameters measured by individual raters agreed poorly (ICC 0.25). RECIST category across each patient was found to depend on the reader, with only slight agreement observed ( $k = 0.18$ ). Complete agreement of RECIST group between all three raters occurred in only 60% of patients (18 of 30; 0 PR, 17 SD, 1 PD); raters disagreed between PR/SD in 8 of 12 remaining patients, between SD/PD in 3 of 12, and between PR/SD/PD in 1 patient.

#### CONCLUSION

Longitudinal changes in PDAC tumor size are associated with high measurement variability, which suggests more reliable methods for measuring treatment response are needed.

#### CLINICAL RELEVANCE/APPLICATION

PDAC often presents with ill-defined radiographic borders, yet standard methods for assessing therapeutic response require dimensional measurement of tumor diameters or volumes throughout treatment. The high variability we observe suggests more precise quantitative measures of longitudinal treatment response should be pursued to better inform PDAC treatment course and improve outcome prediction.

Printed on: 02/07/23

## Abstract Archives of the RSNA, 2022

R2-SPGI-2

### CT characteristics of recurrent acute pancreatitis at different onset times

Thursday, Dec. 1 9:00AM - 9:30AM Room: Learning Center - GI DPS

#### Participants

Ju Zhang, MMed, Chengdu, Sichuan, China (*Presenter*) Nothing to Disclose

#### PURPOSE

To investigate the CT characteristic of recurrent acute pancreatitis (RAP) at different onset times.

#### METHODS AND MATERIALS

RAP data were obtained over the past 5 years. RAP patients were divided into five subgroups according to the time from RAP onset to performing CT examination: 1-3 days, 4-7 days, 8-14 days, 15-30 days, and after 30 days. RAP was categorized into the early phase (first week) and late phase (after the first week) based on the 2012 revised Atlanta classification (RAC). Evaluation and pairwise comparison of patients' demographic data, RAC, CT findings, CT severity index (CTSI) score, and extrapancreatic inflammation on CT (EPIC) score were conducted.

#### RESULTS

In the 690 patients with RAP, hypertriglyceridemia was the most common cause. The proportion of mild RAP patients on both RAC and CTSI in the early stage of onset was higher than those in the late stage of onset (both  $P < .005$ ). The proportion of moderately severe RAP and NP patients on CT at 15-30 days of onset was higher than those in the early phase of onset (both  $P < .005$ ), and the percentage of severe RAP patients after 14 days of onset was higher than that in the early stage of onset.

#### CONCLUSION

s In the 690 patients with RAP, hypertriglyceridemia was the most common cause. The proportion of mild RAP patients on both RAC and CTSI in the early stage of onset was higher than those in the late stage of onset (both  $P < .005$ ). The proportion of moderately severe RAP and NP patients on CT at 15-30 days of onset was higher than those in the early phase of onset (both  $P < .005$ ), and the percentage of severe RAP patients after 14 days of onset was higher than that in the early stage of onset.

#### CLINICAL RELEVANCE/APPLICATION

Recognizing the characteristics of RAP at different onset times, and accurately grasping the changes in the condition of RAP patients can help clinicians to give reasonable treatment according to the changes of the disease, and then effectively prevent the onset of chronic pancreatitis.

Printed on: 02/07/23

## Abstract Archives of the RSNA, 2022

R2-SPGI-3

### Diagnostic value of pancreatic ECV in patients with diabetes: a comparative study of HU value and iodine density method

Thursday, Dec. 1 9:00AM - 9:30AM Room: Learning Center - GI DPS

#### Participants

Xiaoyi Cai, MBBS, (*Presenter*) Nothing to Disclose

#### PURPOSE

To investigate the correlation between extracellular volume (ECV) fraction and HbA1c value in patients with diabetes mellitus, and compare absolute contrast enhancement (ECV-HU) method and dual-energy iodine density (ECV-ID) method.

#### METHODS AND MATERIALS

In this study, 92 patients with suspected abdominal diseases were retrospectively enrolled, all of whom received abdominal CT precontrast scan (120kV) and dual-energy CT enhanced scan. Patients were divided into two groups according to HbA1c value: the diabetes group (HbA1c=6.5%,39 patients) and the non-diabetes group (HbA1<6.5%,53 patients). ECV fraction of pancreas was calculated using two methods: ECV-HU method,  $ECV-HU = \frac{HU \text{ pancreas-equilibrium phase} - HU \text{ pancreas} - \text{precontrast}}{HU \text{ abdominal aorta} - \text{equilibrium phase} - HU \text{ abdominal aorta} - \text{precontrast}} \times (100 - Hct)$ ; ECV-ID method,  $ECV-ID = \frac{ID \text{ pancreas} - \text{equilibrium phase}}{ID \text{ abdominal aorta} - \text{equilibrium phase}} \times (100 - Hct)$ . Independent sample T-test was used to analyze the differences in ECV between two groups, and Spearman correlation analysis was performed to analyze the correlation between ECV and HbA1c value. The diagnostic performance of pancreatic ECV-HU and ECV-ID in differentiating diabetic mellitus was evaluated by receiver operating characteristic (ROC) curve analysis.

#### RESULTS

HbA1c value was positively correlated with ECV-HU and ECV-ID in whole patients ( $r_s=0.571$ ,  $r_s=0.629$ , respectively; both  $P<0.001$ ). ECV-HU and ECV-ID in diabetes group were significantly higher than those in non-diabetes group ( $25.03 \pm 2.13$  vs.  $22.33 \pm 2.40$ ,  $34.58 \pm 2.03$  vs.  $31.59 \pm 2.23$ , respectively; both  $P<0.05$ ). For diabetes differentiation, the area under the curve (AUC) of ECV-ID was higher than that of ECV-HU (0.835 vs. 0.808,  $P=0.418$ ). When the cut-off value was set at 32.70%, the sensitivity and specificity of ECV-ID were 87.2% and 66.0%, respectively.

#### CONCLUSION

s Both ECV-ID and ECV-HU of pancreas are potential indices to diagnose diabetes mellitus and can reflect the status of HbA1c value.

#### CLINICAL RELEVANCE/APPLICATION

Pancreatic ECV obtained by CT is a reliable index which can not only monitor HbA1c for patients with diabetes, but also assist in diagnosis of diabetes mellitus.

Printed on: 02/07/23

## Abstract Archives of the RSNA, 2022

R2-SPGI-4

### Texture analysis of IVIM-DWI in early postoperative MRI to predict post-pancreatectomy acute pancreatitis after pancreaticoduodenectomy.

Thursday, Dec. 1 9:00AM - 9:30AM Room: Learning Center - GI DPS

#### Participants

Giulia A. Zamboni, MD, Verona, Italy (*Presenter*) Nothing to Disclose

#### PURPOSE

Pancreaticoduodenectomy can be burdened by significant morbidity and mortality. Post-pancreatectomy acute pancreatitis (PPAP) is one of the most common complications and can lead to more severe complications such as postoperative fistula, with prolonged hospitalization and poor outcome. The purpose of this study is to assess if early postoperative MRI after pancreaticoduodenectomy can predict post-pancreatectomy acute pancreatitis (PPAP) by identifying early microstructural changes that lead to inflammation and microcirculation changes.

#### METHODS AND MATERIALS

In this IRB-approved prospective study, 65 patients underwent MRI on a 1.5 T scanner (Philips Ingenia) on postoperative day 3 (POD3) after pancreaticoduodenectomy. The scan protocol included a combination of standard sequences, post-gadolinium acquisitions, and IVIM DWI. The IVIM DICOM images were analyzed with in-house software that produced F, D and D\* maps and allowed to calculate the texture parameters of the ROIs. One reader drew 3 ROIs on the pancreatic stump on each MRI: adjacent to the resection margin, on the tail further from the margin, and on the entire pancreatic remnant. The 2021 ISGPS definition of PPAP was used to dichotomize patients into a group with POH/PPAP and a group without that complication. Texture parameters and radiological findings were compared between the two groups.

#### RESULTS

20 patients developed POH and 6 of these PPAP grade B or C. Significant differences in texture analysis results were identified between the POH/PPAP and the non-POH/PPAP group for mean ADC value ( $(1.33 \pm 0.22) \times 10^{-3}$  vs  $(1.56 \pm 0.28) \times 10^{-3}$  mm<sup>2</sup>/s; p=0.006), mean D value ( $0.11 \pm 0.14$  vs  $0.22 \pm 0.15$ ; p=0.03), F entropy (4.5, SE 0.10 vs 4.1, SE 0.08; p=0.004) and D\* (2.7, SE 0.73 vs 1.3, SE 0.38; p=0.01) entropy of ROIs including the pancreatic stump. Similar results were obtained for the ROIs of the tail and the entire pancreatic remnant. No imaging findings consistent with PPAP were identified at MRI in the POH/PPAP group.

#### CONCLUSION

s Texture analysis of IVIM-derived parameters on early postoperative MRI after pancreaticoduodenectomy can help identify patients who will develop PPAP.

#### CLINICAL RELEVANCE/APPLICATION

earlier identification of patients who will develop POH/PPAD can lead to a better treatment and patient outcome

Printed on: 02/07/23

## Abstract Archives of the RSNA, 2022

R2-SPGI-6

### Role of preoperative regional lymph node metastasis detected on CT and/or FDG-PET scans in the prediction of early recurrence of pancreatic adenocarcinoma after curative resection

Thursday, Dec. 1 9:00AM - 9:30AM Room: Learning Center - GI DPS

#### Participants

Ja Kyung Yoon, (*Presenter*) Nothing to Disclose

#### PURPOSE

This study aimed to evaluate the role of regional lymph node (LN) metastasis detected on preoperative CT and/or 18F-fluoro-2-deoxyglucose-positron emission tomography (FDG-PET) scans in the prediction of early tumor recurrence after curative surgical resection of pancreatic ductal adenocarcinoma (PDAC).

#### METHODS AND MATERIALS

This retrospective study included 137 patients who underwent upfront surgery with R0 resection of PDAC between 2013 and 2016. Regional LN metastasis was identified using two criteria: both preoperative CT and FDG-PET scans (LNAND) or preoperative CT or FDG-PET scans (LNOR). Cox proportional hazard regression analysis was used to determine the preoperative risk factors for early tumor recurrence. The significant risk factors for early tumor recurrence were used to create a predictive nomogram for early tumor recurrence.

#### RESULTS

Fifty-five patients had early tumor recurrence within 12 months after curative resection. Regional LN metastasis (both LNOR and LNAND criteria), preoperative carbohydrate antigen 19-9 (CA19-9) levels, and preoperative locally advanced status were significant risk factors for early tumor recurrence. Compared with the LNAND criteria, the LNOR criteria provided higher sensitivity (22.4% vs. 15.5%,  $p = 0.046$ ) and a higher negative predictive value (61.9% vs. 59.8%,  $p = 0.046$ ). LNOR, preoperative CA19-9 level, and resectability were included in the predictive nomogram with an adjusted C-index of 0.589.

#### CONCLUSION

The preoperative LN metastasis on CT or FDG-PET scans, elevated serum CA19-9 levels, and locally advanced status were significant risk factors for early recurrence of PDAC after surgery. The predictive nomogram, including these factors, may help guide the first-line treatment of PDAC.

#### CLINICAL RELEVANCE/APPLICATION

Preoperative LN metastasis identified on CT or FDG-PET scans may help predict early recurrence of pancreatic adenocarcinoma after curative resection.

Printed on: 02/07/23

## Abstract Archives of the RSNA, 2022

R2-SPGI-7

### **MRI vs. CT for pancreatic adenocarcinoma vascular invasion and resectability: Comparative diagnostic test accuracy systematic review and meta-analysis**

Thursday, Dec. 1 9:00AM - 9:30AM Room: Learning Center - GI DPS

#### **Participants**

Ankush Jajodia, MD, MBBS, New Delhi, India (*Presenter*) Nothing to Disclose

#### **PURPOSE**

To perform a systematic review evaluating the diagnostic test accuracy of MRI vs CT for assessing pancreatic ductal adenocarcinoma (PDAC) vascular invasion and resectability.

#### **METHODS AND MATERIALS**

MEDLINE, EMBASE, Cochrane Central Register of Controlled Trials (CENTRAL) and Scopus were searched until December 2021 for all studies directly comparing the accuracy of MRI vs CT for vascular invasion and resectability of pathologically confirmed PDAC in the same patients. Findings on curative resection or exploratory laparotomy were the preferred reference standard. Data extraction, risk of bias and applicability assessment was performed by two authors using QUADAS-C, a tool for assessing risk of bias in comparative diagnostic accuracy studies. A bivariate random-effects model was used with meta-regression for test comparison and covariate analysis with 95% confidence intervals (95%CI). Hierarchical summary receiver operating characteristic (ROC) curves and coupled forest plots were generated.

#### **RESULTS**

Five studies met inclusion criteria consisting of 215 patients, 635 vessels and 124 resectable tumors. There was no difference between MRI and CT for diagnosing PDAC vascular invasion: MRI sensitivity/specificity were 73% (95%CI: 50-88%)/97% (94-99%) and for CT, 75% (56-88%)/97% (94-98%). Similarly, no difference was seen between MRI and CT for resectability assessment: MRI sensitivity/specificity were 85% (77-90%)/67% (46-82%) and for CT, 84% (75-90%)/75% (60-86%). Sources of bias included selection bias from a subset of CT patients undergoing MRI, and verification bias for patients with unresectable disease not proceeding to surgical confirmation. Study risk of bias did not impact MRI or CT performance on meta-regression.

#### **CONCLUSION**

Limited data suggest there is no difference between MRI and CT for assessing PDAC vascular invasion or resectability; however, further research is needed to improve confidence in this finding.

#### **CLINICAL RELEVANCE/APPLICATION**

MRI is more sensitive than CT for detecting PDAC liver metastases; if also more accurate at assessing vascular invasion and resectability, then it could be a "one-stop shop" for PDAC detection and staging.

Printed on: 02/07/23

## Abstract Archives of the RSNA, 2022

R2-SPGI-8

### Development and validation of a radiomics model for predicting malignant IPMN compared with the revised Fukuoka guidelines

Thursday, Dec. 1 9:00AM - 9:30AM Room: Learning Center - GI DPS

#### Participants

Doo Young Lee, MD, MS, Seoul, Korea, Republic Of (*Presenter*) Nothing to Disclose

#### PURPOSE

The revised international consensus Fukuoka guidelines (Fukuoka guidelines) are commonly used for evaluating pancreatic intraductal papillary mucinous neoplasms (IPMNs). However, assessment of radiomics model in comparison with Fukuoka guidelines by radiologists has been lacking. Thus, this study aimed to evaluate CT-based radiomics model for determining malignant IPMNs and compare its performance with Fukuoka guidelines.

#### METHODS AND MATERIALS

This retrospective study included a total of 194 consecutive patients with surgically resected pancreatic IPMNs from January 2008 to December 2020. Surgical histopathologic analysis was the reference standard for malignancy. Radiomic features were extracted from preoperative contrast-enhanced CT, and radiomics model was built using the least absolute shrinkage and selection operator with fivefold cross-validation. CT and MR images were independently reviewed based on Fukuoka guidelines by two board-certified abdominal radiologists, who arrived at a consensus in cases of discrepancy. The performance of Fukuoka guidelines was compared with that of the radiomics model. Areas under the curve (AUCs) were compared by using the DeLong method.

#### RESULTS

A total of 194 patients with pancreatic IPMNs (benign, 83 [43%], malignant, 111 [57%]) were included. The patients were chronologically divided into training set (n = 141; mean age 65 + SD 8.6; men 88) and temporal validation set (n = 53; mean age 66 + SD 9.7; men 31). The diagnostic performance of Fukuoka guidelines was not statistically different between CT and MRI (AUC 0.71 vs. 0.71, P = 0.93). Thus, CT was selected for further comparison between Fukuoka guidelines and radiomics model. The CT radiomics model showed higher diagnostic performance (AUC, 0.85 vs 0.71 [P = 0.038]), specificity (84.6% vs 61.5% [P = 0.041]), and positive predictive value (84.0% vs 66.7% [P = 0.044]) than Fukuoka guidelines in the validation set.

#### CONCLUSION

A CT radiomics model exhibited better diagnostic performance than the revised Fukuoka guidelines by experienced radiologists for classifying malignant IPMNs.

#### CLINICAL RELEVANCE/APPLICATION

The CT radiomics model performed better than the revised Fukuoka guidelines in determining the malignancy of IPMN. Therefore, the radiomics model will facilitate proper treatment decision making.

Printed on: 02/07/23

## Abstract Archives of the RSNA, 2022

R2-SPGI-9

### **Vascular involvement and resectability of pancreatic ductal adenocarcinoma on contrast-enhanced MRI: comparison with pancreatic protocol CT**

Thursday, Dec. 1 9:00AM - 9:30AM Room: Learning Center - GI DPS

#### **Participants**

Yukako Iritani, MD, Gifu, Japan (*Presenter*) Nothing to Disclose

#### **PURPOSE**

To compare the diagnostic performance for detecting vascular involvement and determining resectability differences regarding pancreatic ductal adenocarcinoma (PDAC) between contrast-enhanced CT and MRI.

#### **METHODS AND MATERIALS**

This retrospective study evaluated 82 patients (73 years, 46 men) with PDAC who underwent both preoperative contrast-enhanced CT and MRI from January 2008 to March 2021. Two radiologists independently categorized vascular involvements for celiac, superior mesenteric, splenic, and common hepatic arteries, and portal, superior mesenteric, and splenic veins into no tumor contact, solid soft-tissue contact  $\leq 180^\circ$ , or solid soft-tissue contact  $>180^\circ$ . The radiologists also classified resectability into resectable, borderline resectable, or locally advanced. Receiver-operating-characteristic (ROC) analysis was conducted to evaluate the diagnostic performances for detecting vascular involvements which were confirmed by pathological or intraoperative findings. The proportion of resectability classifications was compared between CT and MRI by the Fisher's exact test.

#### **RESULTS**

No statistical difference was found in the diagnostic performances for detecting vascular involvement in CT (area under the ROC curve [AUC], 0.50-0.89) and MRI (AUC, 0.51-0.75) ( $P = .06$ - $>.99$ ). Resectabilities on CT were 79% and 68%, 20% and 26%, and 1% and 6% for resectable, borderline resectable, and locally advanced tumors for reviewers 1 and 2; those on MRI were 87% and 81%, 12% and 13%, and 1% and 6%, respectively. The proportion of resectability was not different between CT and MRI ( $P = .48$  and  $= .15$  for reviewers 1 and 2, respectively).

#### **CONCLUSION**

The diagnostic performance for detecting vascular involvement and determining resectability of PDAC on contrast-enhanced MRI were comparable with pancreatic protocol CT.

#### **CLINICAL RELEVANCE/APPLICATION**

Diagnostic performance for detecting vascular involvement and determining resectability of pancreatic ductal adenocarcinoma on contrast-enhanced MRI were statistically comparable with pancreatic protocol CT.

Printed on: 02/07/23

## Abstract Archives of the RSNA, 2022

R2-SPGU

### Genitourinary Thursday Poster Discussions

Thursday, Dec. 1 9:00AM - 9:30AM Room: Learning Center - GU DPS

#### Sub-Events

#### R2-SPGU-1 Preoperative prediction of pathological grade of bladder cancer with low VI-RADS score by decision tree model

Participants

Bohong Cao, Shanghai, China (*Presenter*) Nothing to Disclose

#### PURPOSE

To explore a new model to predict the pathological high-grade (HG) of low VI-RADS (=2) bladder cancer (BC). Meanwhile, the diagnostic efficiency of VI-RADS in predicting muscular-invasive BC (MIBC) will be prospectively validated.

#### METHODS AND MATERIALS

From March 2020 to February 2022, prospective, preoperative multiparametric MRI was performed on primary patients. VI-RADS scores were performed on the whole group. The pathological findings were considered to be the gold standard of diagnostic assessment. The low VI-RADS group was isolated from the entire cohort. The diagnostic efficiency of the whole group and the subgroup in predicting HGBC, and the whole group in predicting MIBC was assessed. In the subgroup, the correlation of the VI-RADS score main points, which also included other baseline clinical data and imaging characteristics, with the pathological grade of BC were analyzed. Univariate and multivariable logistic regression analysis was used to obtain independent significant factors. The decision tree algorithm was used to construct the prediction model and the ROC curve is used to analyze diagnostic efficiency for the subgroup.

#### RESULTS

A total of 89 patients were enrolled. The sensitivity, specificity, positive predictive value (PPV), and negative predictive value (NPV) for predicting HGBC in the whole group were 38.7%, 100.0%, 100.0% and 41.5%; the AUC was 0.697. For the subgroup, the sensitivity, specificity, PPV, and NPV were 79.0%, 22.2%, 58.8% and 42.9%; the AUC was 0.506. For predicting MIBC in the whole group, sensitivity, specificity, PPV, and NPV were 94.7%, 91.4%, 75.0%, and 98.5%; the AUC was 0.965. The four independent significant factors obtained by logistic regression analysis, gender, age, maximum tumor diameter and tumor contact length accounted for 0.138, 0.339, 0.298 and 0.224, respectively. The AUC of the decision tree model is 0.892

#### CONCLUSION

For primary patients, VI-RADS is worthy of promotion as a preoperative standard T-staging method. When VI-RADS = 3, it has excellent positive predictive efficiency for the diagnosis of HGBC. The decision tree model can potentially provide a good preoperative imaging grading method for low VI-RADS primary BC and should be investigated further.

#### CLINICAL RELEVANCE/APPLICATION

The majority of BC with VI-RADS =3 were high-grade. The decision tree model has good diagnostic efficacy for predicting high-grade BC with VI-RADS =2, and the treatment threshold can be moved forward.

#### R2-SPGU-2 Diagnosis of Lipid-poor Adrenal Adenomas: Performance Comparison between Non-contrast Spectral CT versus Chemical-Shift MRI

Participants

Yasunori Nagayama, MD, Kumamoto, Japan (*Presenter*) Nothing to Disclose

#### PURPOSE

To compare the diagnostic performance of noncontrast spectral CT and chemical-shift MRI for the discrimination of lipid-poor adrenal adenomas (>10 HU) from nonadenomas.

#### METHODS AND MATERIALS

This retrospective study included 96 patients with indeterminate adrenal lesions (67 patients with lipid-poor adenomas and 29 patients with nonadenomas [14 metastases, 9 pheochromocytomas (PHEOs), 2 hematomas, 1 adrenocortical carcinoma, 1 cyst, 1 schwannoma, and 1 medullary hyperplasia]) who underwent noncontrast abdominal CT on a dual-layer spectral-detector scanner and chemical-shift MRI on 3-T systems. For each lesion, noncontrast attenuation on conventional 120-kVp images (HUconv) and MonoE 40- and 140-keV images (HUMono40 and HUMono140, respectively) was quantified.  $\Delta$ HU index ( $= \{[HUMono140 - HUMono40]/HUconv\} \times 100$ ) were calculated as a possible parameter for the adenoma diagnoses (a high  $\Delta$ HU index indicated lipid-poor adenomas). For chemical-shift MRI, the signal intensity (SI) index was calculated as follows:  $([SI \text{ on in phase} - SI \text{ on opposed phase}]/SI \text{ on in phase}) \times 100$ . Each imaging parameter was compared between lipid-poor adenomas and nonadenomas using the Mann-Whitney U test. Receiver operating characteristic (ROC) analysis was performed to determine the area under the ROC curve (AUC) for the diagnosis of lipid-poor adenomas. The AUC of each parameter was compared using the DeLong method.

## RESULTS

HUconv was significantly lower in adenomas than in nonadenomas ( $23.7 \pm 7.9$  vs.  $33.5 \pm 8.4$  HU,  $P < 0.001$ ), whereas adenomas showed higher  $\rho$ HU index ( $135 \pm 105$  vs.  $12.4 \pm 21.5$ ) and SI index ( $41.4 \pm 20.2$  vs.  $7.0 \pm 7.9$ ) than nonadenomas (both  $P < 0.01$ ). The AUC of  $\rho$ HU index was significantly higher than that of HUconv (0.93 [95% confidence interval (CI), 0.86-0.97] vs. 0.80 [95% CI, 0.71-0.88],  $P < 0.01$ ) and almost equivalent to that of SI index (0.94 [95% CI, 0.87-0.98],  $P = 0.88$ ).

## CONCLUSION

s Noncontrast spectral CT allowed the discrimination of lipid-poor adenomas from nonadenomas with diagnostic performance almost equivalent to chemical-shift MRI.

## CLINICAL RELEVANCE/APPLICATION

The use of spectral CT technology can eliminate the need for chemical-shift MRI and adrenal washout CT for most lipid-poor adrenal lesions identified on noncontrast CT.

## R2-SPGU-3 Impact of dynamic contrast-enhanced MRI in 1.5T versus 3T MRI for clinically significant prostate cancer detection

### Participants

Lars Schimmoeller, MD, Dusseldorf, Germany (*Presenter*) Nothing to Disclose

## PURPOSE

This study analyzes the value of dynamic contrast-enhanced MRI (DCE) of the prostate on 1.5T and 3T examinations in patients within PI-RADS category 4.

## METHODS AND MATERIALS

In this retrospective, bi-centric, cohort study all consecutive patients classified as PI-RADS 4 in mpMRI with 100 verified prostate cancers (PCa) in subsequent MRI/US-guided fusion biopsy were included for 1.5T and 3T, each. PCa detection in peripheral zone (PZ) lesions upgraded to PI-RADS 4 based on positive DCE findings was compared between 1.5T and 3T. Secondary objectives are the comparison of false positive lesions and distribution of ISUP groups.

## RESULTS

In total, 293 patients within PI-RADS category 4, including 152 (mean  $66 \pm 8$ y; median PSA 6.4ng/ml) in the 1.5T group and 141 (mean  $65 \pm 8$ y; median PSA 7.2ng/ml) in the 3T group were included. Overall amount of PCa (66%vs.71%;  $p=0.346$ ) and portion of upgraded lesions (28%vs.21%;  $p=0.126$ ) did not differ significantly. At 1.5T PCa detection was higher in upgraded lesions compared to 3T (67%vs.48%) with fewer false positives (33%vs.52%). The amount of clinically significant (cs)PCa positive, upgraded lesions was significantly higher at 1.5T versus 3T (11%vs.2.8%;  $p=0.002$ ). 28% (12/43; 1.5T) and 34% (10/29; 3T) of the upgraded lesions were ISUP1 PCa.

## CONCLUSION

s DCE enabled the detection of a substantial amount of additional csPCA in prostate mpMRI at 1.5T. Although, DCE also allowed the detection of additional csPCA at 3T, the effect was smaller at the higher field strength and was accompanied by a higher risk of overdiagnosis due to detection of additional low-risk PCa.

## CLINICAL RELEVANCE/APPLICATION

At 1.5 T, DCE still has great impact in diagnosing prostate cancer, as especially csPCA often show increased perfusion. Whereas cancer was often already obvious after T2w- and DWI-imaging at 3T, DCE plays an important role for the detection when imaging is conducted at lower field strength.

Printed on: 02/07/23

## Abstract Archives of the RSNA, 2022

R2-SPGU-1

### Preoperative prediction of pathological grade of bladder cancer with low VI-RADS score by decision tree model

Thursday, Dec. 1 9:00AM - 9:30AM Room: Learning Center - GU DPS

#### Participants

Bohong Cao, Shanghai, China (*Presenter*) Nothing to Disclose

#### PURPOSE

To explore a new model to predict the pathological high-grade (HG) of low VI-RADS (=2) bladder cancer (BC). Meanwhile, the diagnostic efficiency of VI-RADS in predicting muscular-invasive BC (MIBC) will be prospectively validated.

#### METHODS AND MATERIALS

From March 2020 to February 2022, prospective, preoperative multiparametric MRI was performed on primary patients. VI-RADS scores were performed on the whole group. The pathological findings were considered to be the gold standard of diagnostic assessment. The low VI-RADS group was isolated from the entire cohort. The diagnostic efficiency of the whole group and the subgroup in predicting HGBC, and the whole group in predicting MIBC was assessed. In the subgroup, the correlation of the VI-RADS score main points, which also included other baseline clinical data and imaging characteristics, with the pathological grade of BC were analyzed. Univariate and multivariable logistic regression analysis was used to obtain independent significant factors. The decision tree algorithm was used to construct the prediction model and the ROC curve is used to analyze diagnostic efficiency for the subgroup.

#### RESULTS

A total of 89 patients were enrolled. The sensitivity, specificity, positive predictive value (PPV), and negative predictive value (NPV) for predicting HGBC in the whole group were 38.7%, 100.0%, 100.0% and 41.5%; the AUC was 0.697. For the subgroup, the sensitivity, specificity, PPV, and NPV were 79.0%, 22.2%, 58.8% and 42.9%; the AUC was 0.506. For predicting MIBC in the whole group, sensitivity, specificity, PPV, and NPV were 94.7%, 91.4%, 75.0%, and 98.5%; the AUC was 0.965. The four independent significant factors obtained by logistic regression analysis, gender, age, maximum tumor diameter and tumor contact length accounted for 0.138, 0.339, 0.298 and 0.224, respectively. The AUC of the decision tree model is 0.892

#### CONCLUSION

For primary patients, VI-RADS is worthy of promotion as a preoperative standard T-staging method. When VI-RADS = 3, it has excellent positive predictive efficiency for the diagnosis of HGBC. The decision tree model can potentially provide a good preoperative imaging grading method for low VI-RADS primary BC and should be investigated further.

#### CLINICAL RELEVANCE/APPLICATION

The majority of BC with VI-RADS =3 were high-grade. The decision tree model has good diagnostic efficacy for predicting high-grade BC with VI-RADS =2, and the treatment threshold can be moved forward.

Printed on: 02/07/23

## Abstract Archives of the RSNA, 2022

R2-SPGU-2

### Diagnosis of Lipid-poor Adrenal Adenomas: Performance Comparison between Non-contrast Spectral CT versus Chemical-Shift MRI

Thursday, Dec. 1 9:00AM - 9:30AM Room: Learning Center - GU DPS

#### Participants

Yasunori Nagayama, MD, Kumamoto, Japan (*Presenter*) Nothing to Disclose

#### PURPOSE

To compare the diagnostic performance of noncontrast spectral CT and chemical-shift MRI for the discrimination of lipid-poor adrenal adenomas (>10 HU) from nonadenomas.

#### METHODS AND MATERIALS

This retrospective study included 96 patients with indeterminate adrenal lesions (67 patients with lipid-poor adenomas and 29 patients with nonadenomas [14 metastases, 9 pheochromocytomas (PHEOs), 2 hematomas, 1 adrenocortical carcinoma, 1 cyst, 1 schwannoma, and 1 medullary hyperplasia]) who underwent noncontrast abdominal CT on a dual-layer spectral-detector scanner and chemical-shift MRI on 3-T systems. For each lesion, noncontrast attenuation on conventional 120-kVp images (HUconv) and MonoE 40- and 140-keV images (HUMono40 and HUMono140, respectively) was quantified. ?HU index (= {[HUMono140 - HUMono40]/HUconv} × 100) were calculated as a possible parameter for the adenoma diagnoses (a high ?HU index indicated lipid-poor adenomas). For chemical-shift MRI, the signal intensity (SI) index was calculated as follows: ([SI on in phase - SI on opposed phase]/SI on in phase) × 100. Each imaging parameter was compared between lipid-poor adenomas and nonadenomas using the Mann-Whitney U test. Receiver operating characteristic (ROC) analysis was performed to determine the area under the ROC curve (AUC) for the diagnosis of lipid-poor adenomas. The AUC of each parameter was compared using the DeLong method.

#### RESULTS

HUconv was significantly lower in adenomas than in nonadenomas ( $23.7 \pm 7.9$  vs.  $33.5 \pm 8.4$  HU,  $P < 0.001$ ), whereas adenomas showed higher ?HU index ( $135 \pm 105$  vs.  $12.4 \pm 21.5$ ) and SI index ( $41.4 \pm 20.2$  vs.  $7.0 \pm 7.9$ ) than nonadenomas (both  $P < 0.01$ ). The AUC of ?HU index was significantly higher than that of HUconv (0.93 [95% confidence interval (CI), 0.86-0.97] vs. 0.80 [95% CI, 0.71-0.88],  $P < 0.01$ ) and almost equivalent to that of SI index (0.94 [95% CI, 0.87-0.98],  $P = 0.88$ ).

#### CONCLUSION

Noncontrast spectral CT allowed the discrimination of lipid-poor adenomas from nonadenomas with diagnostic performance almost equivalent to chemical-shift MRI.

#### CLINICAL RELEVANCE/APPLICATION

The use of spectral CT technology can eliminate the need for chemical-shift MRI and adrenal washout CT for most lipid-poor adrenal lesions identified on noncontrast CT.

Printed on: 02/07/23

## Abstract Archives of the RSNA, 2022

R2-SPGU-3

### Impact of dynamic contrast-enhanced MRI in 1.5T versus 3T MRI for clinically significant prostate cancer detection

Thursday, Dec. 1 9:00AM - 9:30AM Room: Learning Center - GU DPS

#### Participants

Lars Schimmoeller, MD, Dusseldorf, Germany (*Presenter*) Nothing to Disclose

#### PURPOSE

This study analyzes the value of dynamic contrast-enhanced MRI (DCE) of the prostate on 1.5T and 3T examinations in patients within PI-RADS category 4.

#### METHODS AND MATERIALS

In this retrospective, bi-centric, cohort study all consecutive patients classified as PI-RADS 4 in mpMRI with 100 verified prostate cancers (PCa) in subsequent MRI/US-guided fusion biopsy were included for 1.5T and 3T, each. PCa detection in peripheral zone (PZ) lesions upgraded to PI-RADS 4 based on positive DCE findings was compared between 1.5T and 3T. Secondary objectives are the comparison of false positive lesions and distribution of ISUP groups.

#### RESULTS

In total, 293 patients within PI-RADS category 4, including 152 (mean 66±8y; median PSA 6.4ng/ml) in the 1.5T group and 141 (mean 65±8y; median PSA 7.2ng/ml) in the 3T group were included. Overall amount of PCa (66%vs.71%; p=0.346) and portion of upgraded lesions (28%vs.21%; p=0.126) did not differ significantly. At 1.5T PCa detection was higher in upgraded lesions compared to 3T (67%vs.48%) with fewer false positives (33%vs.52%). The amount of clinically significant (cs)PCa positive, upgraded lesions was significantly higher at 1.5T versus 3T (11%vs.2.8%; p=0.002). 28% (12/43; 1.5T) and 34% (10/29; 3T) of the upgraded lesions were ISUP1 PCa.

#### CONCLUSION

s DCE enabled the detection of a substantial amount of additional csPCA in prostate mpMRI at 1.5T. Although, DCE also allowed the detection of additional csPCA at 3T, the effect was smaller at the higher field strength and was accompanied by a higher risk of overdiagnosis due to detection of additional low-risk PCa.

#### CLINICAL RELEVANCE/APPLICATION

At 1.5 T, DCE still has great impact in diagnosing prostate cancer, as especially csPCA often show increased perfusion. Whereas cancer was often already obvious after T2w- and DWI-imaging at 3T, DCE plays an important role for the detection when imaging is conducted at lower field strength.

Printed on: 02/07/23

## Abstract Archives of the RSNA, 2022

R2-SPHN

### Head and Neck Thursday Poster Discussions

Thursday, Dec. 1 9:00AM - 9:30AM Room: Learning Center - HN DPS

#### Sub-Events

#### R2-SPHN-1 Development of A Machine Learning-based Fine-grained Risk Stratification System for Thyroid Nodules Using Predefined Clinicoradiological Features

Participants

Jayoung Moon, MD, Suwon, Korea, Republic Of (*Presenter*) Nothing to Disclose

#### PURPOSE

An explainable artificial intelligence-based fine-grained risk stratification is necessary to improve diagnostic specificity and personalized management of thyroid nodules. We constructed and validated a machine learning-based malignancy risk estimation model using ultrasonography, and evaluate its clinical utility for personalized management of thyroid nodules.

#### METHODS AND MATERIALS

In total, 5,708 biopsy-proven benign ( $n = 4,597$ ) and malignant ( $n = 1,111$ ) thyroid nodules were collected from 5,081 consecutive patients from 26 institutions. Seventeen experienced radiologists evaluated nodule composition, echogenicity, orientation, margin, and calcifications on ultrasonographic images. Eight predictive models were used to stratify thyroid nodules according to malignancy risk; model performance was assessed via nested 10-fold cross-validation. The best-performing algorithm was externally validated using 454 thyroid nodules from a tertiary hospital, then compared to the Thyroid Imaging Reporting and Data System (TIRADS)-based interpretations of experienced radiologists.

#### RESULTS

The area under the receiver operating characteristic (AUROC) curves of the new algorithms ranged from 0.773 to 0.862. The sensitivities, specificities, positive predictive values, and negative predictive values of the best-performing models were 73.6-75.9%, 81.5-83.8%, 49.8-52.4%, and 92.9-93.3%, respectively. For the external validation set, the ElasticNet values were 83.2%, 89.2%, 81.8%, and 90.1%, respectively. The corresponding TIRADS values (generated by radiologists) were 76.0-85.0%, 61.3-80.8%, 53.4-72.1%, and 81.5-90.3%, respectively. The new model exhibited a significantly higher AUROC and specificity than did the TIRADS risk stratification, although its sensitivity was similar. An interactive version of our algorithm can be found at <http://tirads.cdss.co.kr>.

#### CONCLUSION

We developed a reliable machine learning-based predictive model that demonstrated enhanced specificity when stratifying thyroid nodules according to malignancy risk. This system will contribute to improved personalized management of thyroid nodules.

#### CLINICAL RELEVANCE/APPLICATION

1. The AUROC, sensitivity, and specificity of our model were 0.914, 83.2%, and 89.2%, respectively (derived from the validation data set). 2. Compared to the TIRADS values, the AUROC and specificity are significantly higher, while the sensitivity is similar. 3. An interactive version of our AI algorithm is at <http://tirads.cdss.co.kr>. 4. On the basis of our findings, an explainable AI-based risk stratification system based on the predefined US features could enhance clinical applicability alongside the radiologists.

#### R2-SPHN-3 Can Ultrasonography Be Used to Differentiate Parathyroid Masses Abutting Thyroid Gland and Thyroid Masses Extending into Parathyroid Area?

Participants

Chae Woon Lee, MD, Seoul, Korea, Republic Of (*Presenter*) Nothing to Disclose

#### PURPOSE

To determine the ultrasonographic (US) features that could help to distinguish between parathyroid masses abutting thyroid gland and thyroid masses extending into parathyroid area.

#### METHODS AND MATERIALS

Two blinded readers retrospectively evaluated the US images of histopathologically confirmed 76 parathyroid masses abutting thyroid gland and 34 thyroid masses extending into parathyroid area. Maximal diameter, transverse diameter/anterior-posterior diameter (T/AP) ratio, longitudinal diameter/AP diameter (L/AP) ratio, margin, shape, echogenicity, echotexture, and echogenic interface were evaluated and compared between the two groups.

#### RESULTS

The echogenic interface ( $p < 0.0001$ ) and L/AP ratio ( $p < 0.0005$ ) were identified as statistically significant US features in the differentiation between parathyroid and thyroid masses. Other US features did not show any statistical significance in both groups.

Interobserver agreements were excellent for all US features. The sensitivity/specificity of the presence of echogenic interface and L/AP ratio > 2.0 were 85.5%/100% and 43.2%/82.4% in distinguishing parathyroid from thyroid masses, respectively.

#### **CONCLUSION**

s The presence of echogenic interface and L/AP ratio > 2.0 were useful US features of parathyroid masses abutting thyroid gland in differentiating from thyroid masses extending into parathyroid area.

#### **CLINICAL RELEVANCE/APPLICATION**

In US differentiation between parathyroid masses abutting thyroid gland and thyroid masses extending into parathyroid area, echogenic interface sign and L/AP ratio > 2.0 would be helpful.

Printed on: 02/07/23

## Abstract Archives of the RSNA, 2022

R2-SPHN-1

### Development of A Machine Learning-based Fine-grained Risk Stratification System for Thyroid Nodules Using Predefined Clinicoradiological Features

Thursday, Dec. 1 9:00AM - 9:30AM Room: Learning Center - HN DPS

#### Participants

Jayoung Moon, MD, Suwon, Korea, Republic Of (*Presenter*) Nothing to Disclose

#### PURPOSE

An explainable artificial intelligence-based fine-grained risk stratification is necessary to improve diagnostic specificity and personalized management of thyroid nodules. We constructed and validated a machine learning-based malignancy risk estimation model using ultrasonography, and evaluate its clinical utility for personalized management of thyroid nodules.

#### METHODS AND MATERIALS

In total, 5,708 biopsy-proven benign ( $n = 4,597$ ) and malignant ( $n = 1,111$ ) thyroid nodules were collected from 5,081 consecutive patients from 26 institutions. Seventeen experienced radiologists evaluated nodule composition, echogenicity, orientation, margin, and calcifications on ultrasonographic images. Eight predictive models were used to stratify thyroid nodules according to malignancy risk; model performance was assessed via nested 10-fold cross-validation. The best-performing algorithm was externally validated using 454 thyroid nodules from a tertiary hospital, then compared to the Thyroid Imaging Reporting and Data System (TIRADS)-based interpretations of experienced radiologists.

#### RESULTS

The area under the receiver operating characteristic (AUROC) curves of the new algorithms ranged from 0.773 to 0.862. The sensitivities, specificities, positive predictive values, and negative predictive values of the best-performing models were 73.6-75.9%, 81.5-83.8%, 49.8-52.4%, and 92.9-93.3%, respectively. For the external validation set, the ElasticNet values were 83.2%, 89.2%, 81.8%, and 90.1%, respectively. The corresponding TIRADS values (generated by radiologists) were 76.0-85.0%, 61.3-80.8%, 53.4-72.1%, and 81.5-90.3%, respectively. The new model exhibited a significantly higher AUROC and specificity than did the TIRADS risk stratification, although its sensitivity was similar. An interactive version of our algorithm can be found at <http://tirads.cdss.co.kr>.

#### CONCLUSION

s We developed a reliable machine learning-based predictive model that demonstrated enhanced specificity when stratifying thyroid nodules according to malignancy risk. This system will contribute to improved personalized management of thyroid nodules.

#### CLINICAL RELEVANCE/APPLICATION

1. The AUROC, sensitivity, and specificity of our model were 0.914, 83.2%, and 89.2%, respectively (derived from the validation data set). 2. Compared to the TIRADS values, the AUROC and specificity are significantly higher, while the sensitivity is similar. 3. An interactive version of our AI algorithm is at <http://tirads.cdss.co.kr>. 4. On the basis of our findings, an explainable AI-based risk stratification system based on the predefined US features could enhance clinical applicability alongside the radiologists.

Printed on: 02/07/23

## Abstract Archives of the RSNA, 2022

R2-SPHN-3

### Can Ultrasonography Be Used to Differentiate Parathyroid Masses Abutting Thyroid Gland and Thyroid Masses Extending into Parathyroid Area?

Thursday, Dec. 1 9:00AM - 9:30AM Room: Learning Center - HN DPS

#### Participants

Chae Woon Lee, MD, Seoul, Korea, Republic Of (*Presenter*) Nothing to Disclose

#### PURPOSE

To determine the ultrasonographic (US) features that could help to distinguish between parathyroid masses abutting thyroid gland and thyroid masses extending into parathyroid area.

#### METHODS AND MATERIALS

Two blinded readers retrospectively evaluated the US images of histopathologically confirmed 76 parathyroid masses abutting thyroid gland and 34 thyroid masses extending into parathyroid area. Maximal diameter, transverse diameter/anterior-posterior diameter (T/AP) ratio, longitudinal diameter/AP diameter (L/AP) ratio, margin, shape, echogenicity, echotexture, and echogenic interface were evaluated and compared between the two groups.

#### RESULTS

The echogenic interface ( $p < 0.0001$ ) and L/AP ratio ( $p < 0.0005$ ) were identified as statistically significant US features in the differentiation between parathyroid and thyroid masses. Other US features did not show any statistical significance in both groups. Interobserver agreements were excellent for all US features. The sensitivity/specificity of the presence of echogenic interface and L/AP ratio  $> 2.0$  were 85.5%/100% and 43.2%/82.4% in distinguishing parathyroid from thyroid masses, respectively.

#### CONCLUSION

s The presence of echogenic interface and L/AP ratio  $> 2.0$  were useful US features of parathyroid masses abutting thyroid gland in differentiating from thyroid masses extending into parathyroid area.

#### CLINICAL RELEVANCE/APPLICATION

In US differentiation between parathyroid masses abutting thyroid gland and thyroid masses extending into parathyroid area, echogenic interface sign and L/AP ratio  $> 2.0$  would be helpful.

Printed on: 02/07/23

## Abstract Archives of the RSNA, 2022

R2-SPIN

### Informatics Thursday Poster Discussions

Thursday, Dec. 1 9:00AM - 9:30AM Room: Learning Center - IN DPS

#### Sub-Events

#### R2-SPIN-1 Functional MRI Data Analysis by Large-scale Kernelized Granger Causality for Identification of Schizophrenia Patients

##### Participants

Ali Vosoughi, Rochester, NY (*Presenter*) Nothing to Disclose

##### PURPOSE

To develop and evaluate a novel machine learning method for identifying patients with schizophrenia using large-scale Kernelized Granger Causality (IsKGC) by capturing connectivity differences in resting-state functional MRI (rsfMRI).

##### METHODS AND MATERIALS

From the publicly available Centers of Biomedical Research Excellence (COBRE) fMRI data repository on 146 subjects (72 schizophrenia patients, 62 controls), we included the subsample of all 62 subjects under the age of 32 years (29 schizophrenia patients, 33 controls) using standard preprocessing by the Nilearn Python library and the NIAK resting-state pipeline, with functional parcellation into 122 brain regions [Bellec, NIAK, 2016]. For calculating directed functional connectivity between brain regions, we have recently developed the large-scale Kernelized Granger Causality (IsKGC) algorithm [Citation blinded for review] that combines nonlinear dimension reduction with multivariate predictive causal modeling in high-dimensional fMRI time series. A 100-iteration cross-validation approach with 80%/20% train/test ratio was applied, where feature selection was performed on each training set using Kendall's tau rank correlation, followed by support vector machine classification. To quantitatively evaluate diagnostic accuracy of IsKGC for correctly classifying schizophrenia patients and normal controls, we compare its performance with both a recent state-of-the-art causal discovery method (PCMCI, [Runge et al., Science, 2019]), and the current clinical fMRI analysis standard of cross-correlation (CC), reporting accuracy, area under ROC curve (AUC), and f1-score.

##### RESULTS

The IsKGC rsfMRI analysis method significantly outperformed both PCMCI and the clinical standard CC techniques at classifying schizophrenia patients from healthy subjects, with accuracy/AUC/f1 score of 100%/1.0/100% for IsKGC, 86.4%/0.81/78.4% for PCMCI, and 65.8%/0.62/60.4% for CC, respectively.

##### CONCLUSION

Our results suggest that IsKGC significantly improves the diagnostic accuracy of correctly identifying patients with schizophrenia from rsfMRI neuroimaging. We conclude that, when compared to both conventional CC analysis and state-of-the-art PCMCI, IsKGC is better suited to capture disease-related brain network connectivity changes in schizophrenia patients.

##### CLINICAL RELEVANCE/APPLICATION

The IsKGC method classifies schizophrenia subjects and controls by identifying relevant changes in fMRI connectivity, suggesting its potential use as a diagnostic imaging biomarker for neurologic disease.

#### R2-SPIN-2 A Machine Learning (ML) Model Based on Radiomic Feature From Pre-treatment CT to Predict Response to 1st-line single agent Immunotherapy in Advanced Non-Small Cell Lung Cancer (NSCLC) with High PDL1 Expression

##### Participants

Ian Janzen, BSc, Vancouver, BC (*Presenter*) Nothing to Disclose

##### PURPOSE

Lung cancer is the leading cancer-caused death globally, mainly due to most diagnoses being made at incurable advanced stages. More than 75% advanced stage patients have no driver mutation therefore cytotoxic chemotherapy is the primary treatment option. Recent trials have shown immunotherapy (IO) pembrolizumab (Pem) is superior to chemotherapy in the 1st-line setting. Identifying patients most likely respond to IO remains challenging as no convincing clinicopathological features or biomarkers are available; including PDL1, the most widely used biomarker. Patient pre-selection is more critical in the cohort of similar high PDL1 levels (gt;=50%), as half of this sub-cohort can benefit best from single agent Pem, but others may require combined Pem and chemotherapy. The objective of this study is to develop a ML model trained on radiomic features extracted from baseline CT to predict response to Pem in advanced NSCLC with PDL1gt;=50%.

##### METHODS AND MATERIALS

This study included 97 stage IIIB/IV NSCLC patients with PDL1=50%, no driver mutations, and received 1st-line Pem (56F:41M, 73±6 yo; 96% smoker; 40±26 py; ECOG range: 0-4). All had CT at baseline and the 1st FU occurred 9-12 weeks after starting treatment. Response was assessed using RECIST 1.1 standard definitions (n=60 "disease control, DC"; n=37 "progressive disease,

PD"). Radiologists quantified "disease burden" at baseline CT using the largest dimension of target lung tumor and the total number of organs with metastases. An in-house radiomic feature extraction pipeline calculated radiomic features from lung tumor lesions. 5-fold cross validated ML models (Linear Discriminant Analysis) were trained using clinical- and radiomic-based feature sets to predict response (i.e., DC vs. PD). Models were compared using ROC and the model with the highest AUC was used to classify patients into "high- vs. "low-probability responder" using the predicted response probability. Time-to-progression and time-to-death was compared between two groups using Kaplan-Meier plots.

## RESULTS

The ML model including both lung tumor radiomics and clinical factors demonstrates optimal performance in classifying treatment response (AUC: 0.94). The OS and PFS prediction is significantly different between the model's predicted "high- vs. low- probability responders" ( $p < 0.0001$ ).

## CONCLUSION

An LDA model trained on clinical features and radiomic features derived from lung tumors on the baseline CT images prior to treatment start can predict NSCLC treatment response to Pem.

## CLINICAL RELEVANCE/APPLICATION

A ML model can serve as a decision-making tool in choosing the optimal 1st- line treatment for advanced NSCLC with PDL1  $\geq 50\%$ , which is currently an unresolved clinical dilemma.

## R2-SPIN-3 Modeling Pulmonary Nodule Growth in CT over Time using Spatio-Temporal Neural Network

Participants

Prince Wang, BA, Berkeley, CA (*Presenter*) Nothing to Disclose

## PURPOSE

Deep learning-based lung nodule risk stratification is a well-established topic of study, but most existing convolutional neural network models are restricted to a single time point. Doubling time is an important predictor of malignancy risk of a nodule. This study aims to develop and validate a radiology-specific Spatio-Temporal Convolutional-Long Short Term Memory (ST-ConvLSTM) model that can analyze changes in 3D radiological images across two time points, specifically doubling time and steady growth, thus enabling improved risk stratification.

## METHODS AND MATERIALS

A synthetic 3D-transformed MNIST handwritten digit pairs dataset with doubling time labels and a real-world longitudinal nodule image pairs dataset with volumetric segmentations from the National Lung Cancer Screening (NLST) CT dataset were created using commercial software. The ST-ConvLSTM architecture was modified and optimized using the synthetic 3D-MNIST dataset, originally adapted from the convolutional LSTM architecture to allow for 3D image and temporal input. The model was trained for both regression and classification tasks of predicting doubling times and growth at a specific range of rates. Evaluation metrics on the holdout test set included Mean Squared Error (MSE) for regression and AUC-ROC for classification.

## RESULTS

The ST-ConvLSTM was trained and optimized on 10,000 3D-MNIST digit pairs with known doubling times. The optimal model was tested on 1,000 holdout digit pairs set, achieving a test-time averaged Mean Squared Error (MSE) of 43.2 (error range:  $\pm 6.57$  days). The model was then adapted to the NLST training data of 4,274 nodule image pairs. Doubling time of 60-1,000 days was labeled as 'steady growth' and others were considered 'not steady growth' to model typical malignant lung nodule behavior. The model achieved test-time accuracy of 95.27% for correctly predicting steady growth on the test sequence of 300 pairs. Our test-time result also achieved a ROC AUC of 0.986. All code is to be made available at presentation.

## CONCLUSION

We have developed and optimized an ST-ConvLSTM neural network model that can analyze visual and temporal trends in image pairs and then evaluated it on synthetic 3D digit pairs and NLST lung nodule pairs datasets.

## CLINICAL RELEVANCE/APPLICATION

We developed and validated a neural network model that can compare two CT images of pulmonary nodules to assess interval growth, allowing for more accurate risk stratification.

## R2-SPIN-4 Focal Loss Improves Clinical Deployability of Deep Learning Models

Participants

Syed Rakin Ahmed, (*Presenter*) Nothing to Disclose

## PURPOSE

Deep learning (DL) models for clinical diagnosis, prognosis and treatment need to be trustworthy and robust for clinical deployment, given that model predictions often directly inform a subsequent course of action, where individual patient lives are at stake. Central to model robustness is repeatability, or the ability of a model to generate near-identical predictions under identical conditions. The purpose of this study is to utilize focal loss, with and without the presence of Monte Carlo (MC) Dropout in order to improve model repeatability.

## METHODS AND MATERIALS

We conduct our experiments on two datasets: the publicly available longitudinal Multicenter Osteoarthritis Study (MOST) dataset for knee osteoarthritis grading, and the Digital Mammographic Imaging Screening Trial (DMIST) dataset, a multi-institutional screening dataset for breast density classification; both represent clinically important classification tasks. We begin with two baseline models optimized for classification performance in each dataset, utilizing cross-entropy loss for (A) MOST, and (B) DMIST, with or without MC dropout and all other parameters identical for each corresponding dataset. We subsequently train models with focal loss, using parameters  $\gamma=2$  and  $\alpha=0.25$  following hyperparameter tuning, with and without MC dropout. We compare each focal loss experimental result with the corresponding MC or non-MC versions of the baseline.

## RESULTS

We find that, in all instances, focal loss improves repeatability from the respective baseline, reflected in statistically significant decreases in the 95% limits of agreement (LoA) on the Bland-Altman plots, while not affecting classification performance, reflected in no statistically significant difference in the corresponding accuracy.

## CONCLUSION

Given that small changes in an image can produce significantly different DL model predictions, it is essential that models designed for clinical deployment be specifically optimized for improved repeatability. Our demonstration that focal loss improves model repeatability without harming classification performance is a critical result, facilitating reliability and trust on clinical DL models.

## CLINICAL RELEVANCE/APPLICATION

Improved repeatability utilizing focal loss leads to robust, reliable predictions from clinically deployed deep learning models, preventing incorrect courses of action that might jeopardize patients.

## R2-SPIN-5 Generative Adversarial Networks with Dual Discriminator in Image and Fourier Domains for Denoising of Low Dose CT

### Participants

Sunggu Kyung, MS, Seoul, Korea, Republic Of (*Presenter*) Nothing to Disclose

## PURPOSE

Reduced radiation dosage causes more noise and artifacts, which makes the CT scan more difficult to interpret. Deep learning-based denoising has recently emerged as a potential solution for low-dose CT (LDCT) denoising. However, there are still no satisfactory results due to the over-denoising and artifacts. In this study, we attempted to achieve high denoising metrics using a generative adversarial network (GAN) with dual discriminators in image and Fourier domains.

## METHODS AND MATERIALS

The head and neck CT scans for Low Dose training dataset were retrospectively obtained by Asan Medical Center. First, unlike other existing methods, we did not apply the windowing in data preprocessing but used windowing in the discriminator for the applications in the real world. Second, we used the generative adversarial network framework which consists of a generator and two discriminators. We constructed the generator with a Fourier transform convolution to perform more effective denoising and adopted the U-Net structure as a discriminator for concentrating on the image's contexts from global to local details. Third, we combined a discriminator in the Fourier domain to compensate for the information not recognized in the image domain.

## RESULTS

In the test set, the proposed model outperformed other models in all metrics, including peak signal-to-noise ratio (PSNR), structural similarity index measure (SSIM), and root mean square error (RMSE) of 33.327, 0.901, and 0.033, respectively. In visualized images, our proposed model showed domain unspecific and high-quality denoising image reconstruction for the brain CT scans. We can analyze that the outputs from low-dose images preserved clinically important signals like the sulcus and gyrus in the brain with high qualities.

## CONCLUSION

Introducing the Fourier domain to the existing GAN of the image domain improved denoising performances. In this study, the Fourier transform convolution in the generator and the discriminator in the Fourier domain were helpful for denoising GAN training. The evaluation results showed that our framework achieved state-of-the-art denoising results compared with existing methods.

## CLINICAL RELEVANCE/APPLICATION

Unlike existing methods, our model is robust to windowing preprocessing and achieve high performance in denoising task. Thus, our model can be applied to the real medical world and high PSNR low-dose images can be helpful for patients and radiologists.

Printed on: 02/07/23

## Abstract Archives of the RSNA, 2022

R2-SPIN-1

### Functional MRI Data Analysis by Large-scale Kernelized Granger Causality for Identification of Schizophrenia Patients

Thursday, Dec. 1 9:00AM - 9:30AM Room: Learning Center - IN DPS

#### Participants

Ali Vosoughi, Rochester, NY (*Presenter*) Nothing to Disclose

#### PURPOSE

To develop and evaluate a novel machine learning method for identifying patients with schizophrenia using large-scale Kernelized Granger Causality (IsKGC) by capturing connectivity differences in resting-state functional MRI (rsfMRI).

#### METHODS AND MATERIALS

From the publicly available Centers of Biomedical Research Excellence (COBRE) fMRI data repository on 146 subjects (72 schizophrenia patients, 62 controls), we included the subsample of all 62 subjects under the age of 32 years (29 schizophrenia patients, 33 controls) using standard preprocessing by the Nilearn Python library and the NIAK resting-state pipeline, with functional parcellation into 122 brain regions [Bellec, NIAK, 2016]. For calculating directed functional connectivity between brain regions, we have recently developed the large-scale Kernelized Granger Causality (IsKGC) algorithm [Citation blinded for review] that combines nonlinear dimension reduction with multivariate predictive causal modeling in high-dimensional fMRI time series. A 100-iteration cross-validation approach with 80%/20% train/test ratio was applied, where feature selection was performed on each training set using Kendall's tau rank correlation, followed by support vector machine classification. To quantitatively evaluate diagnostic accuracy of IsKGC for correctly classifying schizophrenia patients and normal controls, we compare its performance with both a recent state-of-the-art causal discovery method (PCMCI, [Runge et al., Science, 2019]), and the current clinical fMRI analysis standard of cross-correlation (CC), reporting accuracy, area under ROC curve (AUC), and f1-score.

#### RESULTS

The IsKGC rsfMRI analysis method significantly outperformed both PCMCI and the clinical standard CC techniques at classifying schizophrenia patients from healthy subjects, with accuracy/AUC/f1 score of 100%/1.0/100% for IsKGC, 86.4%/0.81/78.4% for PCMCI, and 65.8%/0.62/60.4% for CC, respectively.

#### CONCLUSION

Our results suggest that IsKGC significantly improves the diagnostic accuracy of correctly identifying patients with schizophrenia from rsfMRI neuroimaging. We conclude that, when compared to both conventional CC analysis and state-of-the-art PCMCI, IsKGC is better suited to capture disease-related brain network connectivity changes in schizophrenia patients.

#### CLINICAL RELEVANCE/APPLICATION

The IsKGC method classifies schizophrenia subjects and controls by identifying relevant changes in fMRI connectivity, suggesting its potential use as a diagnostic imaging biomarker for neurologic disease.

Printed on: 02/07/23

## Abstract Archives of the RSNA, 2022

R2-SPIN-2

### **A Machine Learning (ML) Model Based on Radiomic Feature From Pre-treatment CT to Predict Response to 1st-line single agent Immunotherapy in Advanced Non-Small Cell Lung Cancer (NSCLC) with High PDL1 Expression**

Thursday, Dec. 1 9:00AM - 9:30AM Room: Learning Center - IN DPS

#### **Participants**

Ian Janzen, BSc, Vancouver, BC (*Presenter*) Nothing to Disclose

#### **PURPOSE**

Lung cancer is the leading cancer-caused death globally, mainly due to most diagnoses being made at incurable advanced stages. More than 75% advanced stage patients have no driver mutation therefore cytotoxic chemotherapy is the primary treatment option. Recent trials have shown immunotherapy (IO) pembrolizumab (Pem) is superior to chemotherapy in the 1st-line setting. Identifying patients most likely respond to IO remains challenging as no convincing clinicopathological features or biomarkers are available; including PDL1, the most widely used biomarker. Patient pre-selection is more critical in the cohort of similar high PDL1 levels ( $gt;=50\%$ ), as half of this sub-cohort can benefit best from single agent Pem, but others may require combined Pem and chemotherapy. The objective of this study is to develop a ML model trained on radiomic features extracted from baseline CT to predict response to Pem in advanced NSCLC with PDL1 $gt;=50\%$ .

#### **METHODS AND MATERIALS**

This study included 97 stage IIIB/IV NSCLC patients with PDL1 $=50\%$ , no driver mutations, and received 1st-line Pem (56F:41M, 73 $\pm$ 6 yo; 96% smoker; 40 $\pm$ 26 py; ECOG range: 0-4). All had CT at baseline and the 1st FU occurred 9-12 weeks after starting treatment. Response was assessed using RECIST 1.1 standard definitions (n=60 "disease control, DC"; n=37 "progressive disease, PD"). Radiologists quantified "disease burden" at baseline CT using the largest dimension of target lung tumor and the total number organs with metastases. An in-house radiomic feature extraction pipeline calculated radiomic features from lung tumor lesions. 5-fold cross validated ML models (Linear Discriminant Analysis) were trained using clinical- and radiomic-based feature sets to predict response (i.e., DC vs. PD). Models were compared using ROC and the model with the highest AUC was used to classify patients into "high- vs. "low-probability responder" using the predicted response probability. Time-to-progression and time-to-death was compared between two groups using Kaplan-Meier plots.

#### **RESULTS**

The ML model including both lung tumor radiomics and clinical factors demonstrates optimal performance in classifying treatment response (AUC: 0.94). The OS and PFS prediction is significantly different between the model's predicted "high- vs. low- probability responders" ( $plt;0.0001$ ).

#### **CONCLUSION**

s An LDA model trained on clinical features and radiomic features derived from lung tumors on the baseline CT images prior to treatment start can predict NSCLC treatment response to Pem.

#### **CLINICAL RELEVANCE/APPLICATION**

A ML model can serve as a decision-making tool in choosing the optimal 1st- line treatment for advanced NSCLC with PDL1  $gt;=50\%$ , which is a currently an unresolved clinical dilemma.

Printed on: 02/07/23

## Abstract Archives of the RSNA, 2022

R2-SPIN-3

### Modeling Pulmonary Nodule Growth in CT over Time using Spatio-Temporal Neural Network

Thursday, Dec. 1 9:00AM - 9:30AM Room: Learning Center - IN DPS

#### Participants

Prince Wang, BA, Berkeley, CA (*Presenter*) Nothing to Disclose

#### PURPOSE

Deep learning-based lung nodule risk stratification is a well-established topic of study, but most existing convolutional neural network models are restricted to a single time point. Doubling time is an important predictor of malignancy risk of a nodule. This study aims to develop and validate a radiology-specific Spatio-Temporal Convolutional-Long Short Term Memory (ST-ConvLSTM) model that can analyze changes in 3D radiological images across two time points, specifically doubling time and steady growth, thus enabling improved risk stratification.

#### METHODS AND MATERIALS

A synthetic 3D-transformed MNIST handwritten digit pairs dataset with doubling time labels and a real-world longitudinal nodule image pairs dataset with volumetric segmentations from the National Lung Cancer Screening (NLST) CT dataset were created using commercial software. The ST-ConvLSTM architecture was modified and optimized using the synthetic 3D-MNIST dataset, originally adapted from the convolutional LSTM architecture to allow for 3D image and temporal input. The model was trained for both regression and classification tasks of predicting doubling times and growth at a specific range of rates. Evaluation metrics on the holdout test set included Mean Squared Error (MSE) for regression and AUC-ROC for classification.

#### RESULTS

The ST-ConvLSTM was trained and optimized on 10,000 3D-MNIST digit pairs with known doubling times. The optimal model was tested on 1,000 holdout digit pairs set, achieving a test-time averaged Mean Squared Error (MSE) of 43.2 (error range:  $\pm 6.57$  days). The model was then adapted to the NLST training data of 4,274 nodule image pairs. Doubling time of 60-1,000 days was labeled as 'steady growth' and others were considered 'not steady growth' to model typical malignant lung nodule behavior. The model achieved test-time accuracy of 95.27% for correctly predicting steady growth on the test sequence of 300 pairs. Our test-time result also achieved a ROC AUC of 0.986. All code is to be made available at presentation.

#### CONCLUSION

s We have developed and optimized an ST-ConvLSTM neural network model that can analyze visual and temporal trends in image pairs and then evaluated it on synthetic 3D digit pairs and NLST lung nodule pairs datasets.

#### CLINICAL RELEVANCE/APPLICATION

We developed and validated a neural network model that can compare two CT images of pulmonary nodules to assess interval growth, allowing for more accurate risk stratification.

Printed on: 02/07/23



## Abstract Archives of the RSNA, 2022

R2-SPIN-4

### Focal Loss Improves Clinical Deployability of Deep Learning Models

Thursday, Dec. 1 9:00AM - 9:30AM Room: Learning Center - IN DPS

#### Participants

Syed Rakin Ahmed, (*Presenter*) Nothing to Disclose

#### PURPOSE

Deep learning (DL) models for clinical diagnosis, prognosis and treatment need to be trustworthy and robust for clinical deployment, given that model predictions often directly inform a subsequent course of action, where individual patient lives are at stake. Central to model robustness is repeatability, or the ability of a model to generate near-identical predictions under identical conditions. The purpose of this study is to utilize focal loss, with and without the presence of Monte Carlo (MC) Dropout in order to improve model repeatability.

#### METHODS AND MATERIALS

We conduct our experiments on two datasets: the publicly available longitudinal Multicenter Osteoarthritis Study (MOST) dataset for knee osteoarthritis grading, and the Digital Mammographic Imaging Screening Trial (DMIST) dataset, a multi-institutional screening dataset for breast density classification; both represent clinically important classification tasks. We begin with two baseline models optimized for classification performance in each dataset, utilizing cross-entropy loss for (A) MOST, and (B) DMIST, with or without MC dropout and all other parameters identical for each corresponding dataset. We subsequently train models with focal loss, using parameters  $\gamma=2$  and  $\alpha=0.25$  following hyperparameter tuning, with and without MC dropout. We compare each focal loss experimental result with the corresponding MC or non-MC versions of the baseline.

#### RESULTS

We find that, in all instances, focal loss improves repeatability from the respective baseline, reflected in statistically significant decreases in the 95% limits of agreement (LoA) on the Bland-Altman plots, while not affecting classification performance, reflected in no statistically significant difference in the corresponding accuracy.

#### CONCLUSION

Given that small changes in an image can produce significantly different DL model predictions, it is essential that models designed for clinical deployment be specifically optimized for improved repeatability. Our demonstration that focal loss improves model repeatability without harming classification performance is a critical result, facilitating reliability and trust on clinical DL models.

#### CLINICAL RELEVANCE/APPLICATION

Improved repeatability utilizing focal loss leads to robust, reliable predictions from clinically deployed deep learning models, preventing incorrect courses of action that might jeopardize patients.

Printed on: 02/07/23

## Abstract Archives of the RSNA, 2022

R2-SPIN-5

### Generative Adversarial Networks with Dual Discriminator in Image and Fourier Domains for Denoising of Low Dose CT

Thursday, Dec. 1 9:00AM - 9:30AM Room: Learning Center - IN DPS

#### Participants

Sunggu Kyung, MS, Seoul, Korea, Republic Of (*Presenter*) Nothing to Disclose

#### PURPOSE

Reduced radiation dosage causes more noise and artifacts, which makes the CT scan more difficult to interpret. Deep learning-based denoising has recently emerged as a potential solution for low-dose CT (LDCT) denoising. However, there are still no satisfactory results due to the over-denoising and artifacts. In this study, we attempted to achieve high denoising metrics using a generative adversarial network (GAN) with dual discriminators in image and Fourier domains.

#### METHODS AND MATERIALS

The head and neck CT scans for Low Dose training dataset were retrospectively obtained by Asan Medical Center. First, unlike other existing methods, we did not apply the windowing in data preprocessing but used windowing in the discriminator for the applications in the real world. Second, we used the generative adversarial network framework which consists of a generator and two discriminators. We constructed the generator with a Fourier transform convolution to perform more effective denoising and adopted the U-Net structure as a discriminator for concentrating on the image's contexts from global to local details. Third, we combined a discriminator in the Fourier domain to compensate for the information not recognized in the image domain.

#### RESULTS

In the test set, the proposed model outperformed other models in all metrics, including peak signal-to-noise ratio (PSNR), structural similarity index measure (SSIM), and root mean square error (RMSE) of 33.327, 0.901, and 0.033, respectively. In visualized images, our proposed model showed domain unspecific and high-quality denoising image reconstruction for the brain CT scans. We can analyze that the outputs from low-dose images preserved clinically important signals like the sulcus and gyrus in the brain with high qualities.

#### CONCLUSION

Introducing the Fourier domain to the existing GAN of the image domain improved denoising performances. In this study, the Fourier transform convolution in the generator and the discriminator in the Fourier domain were helpful for denoising GAN training. The evaluation results showed that our framework achieved state-of-the-art denoising results compared with existing methods.

#### CLINICAL RELEVANCE/APPLICATION

Unlike existing methods, our model is robust to windowing preprocessing and achieve high performance in denoising task. Thus, our model can be applied to the real medical world and high PSNR low-dose images can be helpful for patients and radiologists.

Printed on: 02/07/23

## Abstract Archives of the RSNA, 2022

R2-SPIR

### Interventional Thursday Poster Discussions

Thursday, Dec. 1 9:00AM - 9:30AM Room: Learning Center - IR DPS

#### Sub-Events

#### **R2-SPIR-1 Efficacy of Selective Transarterial Chemoembolization with Radiotherapy Versus Y-90 Transarterial Radioembolization in Hepatocellular Carcinoma with Portal Vein Tumor Thrombus**

Participants

Yanisa Jarusyingdumrong, MD, (*Presenter*) Nothing to Disclose

#### **PURPOSE**

To compare the efficacy of selective transarterial chemoembolization (TACE) combined with radiotherapy (RT) and Y-90 transarterial radioembolization (TARE) in the treatment of hepatocellular carcinoma (HCC) with portal vein tumor thrombosis (PVTT).

#### **METHODS AND MATERIALS**

In retrospective cohort study, patients received treatment from January 2011 to October 2019 in a single center were recruited. The overall survival (OS) rate and median survival time were compared between the two groups. Survival curves were constructed using the Kaplan-Meier method and were compared using the log rank test. The confounding factors were adjusted using Laplace regression.

#### **RESULTS**

A total of 82 patients with HCC and PVTT received either selective TACE combined with radiotherapy (n = 48) or Y-90 TARE alone (n = 34). The OS rate was significantly lower (1-year HR 3.19; 95%CI 1.22, 8.31; p-value 0.012; 2-year HR 4.00; 95%CI 1.79, 8.94; p-value <0.001) and the median survival time was significantly shorter (4.5 vs 21.1 months, respectively; p-value 0.004) in combined selective TACE and RT group than in Y-90 TARE alone group.

#### **CONCLUSION**

s Group receiving selective TACE combined with RT has shorter survival time than group receiving Y-90 TARE alone in patients with HCC and PVTT.

#### **CLINICAL RELEVANCE/APPLICATION**

In many countries with limited resources, the systemic treatment recommended for treating advanced stage HCC may not be available. Therefore, a safe and effective alternative should be explored.

#### **R2-SPIR-2 Nanoscale CaO<sub>2</sub> Materials Provides a New Perspective for Trans-arterial Chemoembolization Therapy in VX2 Orthotopic Rabbit Liver Cancer Model**

Participants

Yingliang Wang, (*Presenter*) Nothing to Disclose

#### **PURPOSE**

Transcatheter arterial chemoembolization (TACE) is extensively used in the treatment of liver cancer. However, the efficacy of TACE is usually limited to secondary tumor hypoxia and other progressive exacerbation of the abnormal tumor microenvironment (TME). Herein, we synthesized CaO<sub>2</sub> nanoparticles (nano-CaO<sub>2</sub>) and applied them as a synergistic agent to improve the antitumor efficacy of TACE. Being injected into the tumor, nano-CaO<sub>2</sub> would react with water to generate abundant oxygen, hydroxyl ions (OH<sup>-</sup>), and calcium ions (Ca<sup>2+</sup>), enabling relieve tumor hypoxia, neutralization of acidic TME, and Ca<sup>2+</sup> overloading mediated antitumor, respectively. Moreover, the effect of chemotherapeutic drug within the TACE would be improved due to the improved TME.

#### **METHODS AND MATERIALS**

The nano-CaO<sub>2</sub> was fabricated by the CaCl<sub>2</sub>-H<sub>2</sub>O<sub>2</sub> reaction at alkaline pH and stabilized by polyvinyl pyrrolidone. The characteristics of the nanoparticle were evaluated by X-ray diffraction, X-ray photoelectron spectroscopy, Field Emission Transmission Electron Microscopy, and Dynamic light scattering. Measurement of dissolved O<sub>2</sub> concentration, pH value and GSH content in solution. In vitro test was used to evaluate the cytotoxicity, apoptosis, intracellular O<sub>2</sub>, GSH, HIF-1 $\alpha$  and VEGF level. In vivo test, twenty-five rabbits with VX2 liver tumor were randomly divided into five groups and injected different agents via hepatic artery (group A: normal saline; group B: lipiodol; group C: lipiodol + doxorubicin; group D: lipiodol + nano-CaO<sub>2</sub>; group E: lipiodol + nano-CaO<sub>2</sub> + doxorubicin). The tumor growth rate, necrosis rate, proliferation index and apoptosis index, histological markers associated with angiogenesis (HIF- $\alpha$ , VEGF, MVD) and immune response (CD8+ T cell) were assessed by imaging and histopathology. Biosafety was evaluated by testing the hepatic and renal function (AST, ALT, BUN, and Cr) and HE staining of main organs in each group.

#### **RESULTS**

In vitro, nano-CaO<sub>2</sub> could efficiently regulate the TME and improve the antitumor effect of doxorubicin under hypoxia condition. In vivo, compared to other groups, group E achieved lower tumor growth rate, higher tumor necrosis rate, lower expression of histological markers associated with hypoxia and angiogenesis, and higher CD8<sup>+</sup> T cell recruitment. All rabbits in group B-E undergo temporary liver injury and recovered later.

## CONCLUSION

s Nano-CaO<sub>2</sub> could significantly improve the efficacy of TACE in the treatment of rabbit VX2 liver tumors.

## CLINICAL RELEVANCE/APPLICATION

Nano-CaO<sub>2</sub> could significantly improve the efficacy of TACE in the treatment of rabbit VX2 liver tumors and could recruit CD8<sup>+</sup> T cell which may serve as a synergistic agent with immune checkpoint inhibitors. Thus, it has a broad clinical application prospect.

## R2-SPIR-3 Gene Expression and DNA Methylation Patterns Highlight Disparities in Ethno-racial Status and Treatment Response in Hepatocellular Carcinoma Patients

### Participants

Vishwaarth Vijayakumar, MD, Dunlap, IL (*Presenter*) Nothing to Disclose

## PURPOSE

Since 85% of hepatocellular carcinoma (HCC) patients are ineligible for surgical resection or liver transplantation, Interventional Radiology offers locoregional therapies (LRT) as an additional option. However, response rates are modest and the biological factors that underlie tumor response are unclear. HCC rates vary based on ethno-racial status with little information about how these differences may correspond to tumor biology. Therefore, this study performed HCC epigenetic profiling to investigate tumor biology associated with ethno-racial patient populations and LRT response.

## METHODS AND MATERIALS

DNA and RNA was extracted from formalin-fixed paraffin-embedded tumor samples representing 47 HCC patients (n=15 Black, n=22 White, n=10 Hispanic). Treatment response was determined using CT/MRI imaging 3 months post-treatment (n=24 complete response, n=15 retreatment candidates). RNA expression (RNA-seq) and DNA methylation (reduced representation bisulfite sequencing) levels were used to stratify patients based on ethno-racial status and treatment response using partial least-squares discriminant analysis (PLS-DA) with 300 runs of bootstrap subsampling. Results were validated using hierarchical clustering. Ingenuity pathway analysis was performed to identify upstream regulators and pathways enriched for identified genes.

## RESULTS

PLS-DA identified 100 genes and 12 methylated regions that successfully differentiated between Black and White/Hispanic patients. Hierarchical clustering based on either the top 16 genes identified in >80% of the models or the top 5 methylation regions identified in >60% of the models resulted in successful clustering of Black from White and Hispanic patients. These genes were associated with pathways and upstream regulators related to metabolic regulation and protein translation. PLS-DA identified 100 genes and 150 methylated regions that successfully differentiated between complete responders and retreatment candidates. Hierarchical clustering based on either the top 30 genes identified in >50% of the models or the top 13 methylation regions identified in >85% of the models resulted in successful clustering of patients based on response. These genes, relevant upstream activators, and pathways were related to p53 signaling, DNA repair, and metabolism.

## CONCLUSION

s Epigenetic profiles of HCC patients show that differences in metabolic regulation, protein translation, p53 signaling, and DNA repair may correspond to differences in ethno-racial status and treatment response.

## CLINICAL RELEVANCE/APPLICATION

This study identified epigenetic profiles, upstream regulators, and enriched pathways which could be useful for identification of precision therapeutic targets for HCC.

## R2-SPIR-4 Making a Mark: Follow-up of Outcomes for Combined Methylene Blue and Embolization Coil Marking for Lung Nodule Localization

### Participants

Joe Khoury, DO, MBA, Manhasset, NY (*Presenter*) Nothing to Disclose

## PURPOSE

To study the efficacy of lung nodule localization with a combined technique utilizing both methylene blue and embolization coils.

## METHODS AND MATERIALS

This study was a retrospective mono-centric review of 93 patients who underwent amalgam technique of utilizing methylene blue and embolization coils for lung nodule marking. Inclusion criteria was limited to any patient who underwent lung marking utilizing this technique from 2010 to 2020.

## RESULTS

Of the patients undergoing lung marking, 34% (32/93) were male and 66% (61/93) were female. The average age was 65 years, ranging from 3 to 88 years. One patient was excluded due to unavailability of operative documentation. One patient had two nodules that were marked. In these 92 patients, 100% (93/93) of the lung nodules were localized. Both methylene blue and the coil marker were identified in 88/92 (95.7%) patients. In the remaining 4 patients (4.3%), only methylene blue was noted in the pathology and operative reports. 93/93 (100%) of the marked nodules were successfully resected and confirmed by pathology. All of the nodules were successfully excised via VATS, with 0% (0/92) requiring conversion to open thoracotomy. Three patients had difficulties with coil deployment, which did not result in any patient morbidity. In one patient, the embolization coil was dislodged but methylene blue was administered and the nodule was resected. Two patients had coil migratory complications, which involved the coil extending proximally through the trocar tract. Eight patients developed pneumothoraces, with three requiring chest tubes.

## CONCLUSION

s This study further supports our hypothesis that lung nodule localization utilizing both methylene blue and embolization microcoils is safe and allows for successful identification and resection of nodules utilizing VATS technique.

## CLINICAL RELEVANCE/APPLICATION

Along with the advent of high resolution computed tomography, there has been increasing detection of small pulmonary nodules. These nodules are often not well visualized or palpable during minimally invasive wedge resection with Video Assisted Thoracic Surgery (VATS), which has historically led to an increased rate of conversion to open thoracotomy, as well as increased morbidity. The rate of conversion from VATS to open thoracotomy has been noted to be as high as 23% secondary to inability to properly locate these small nodules. The solution to this problem has been preoperative localization of these nodules with either hook wires, methylene blue, or embolization coils. This study aims to evaluate a combined technique of utilizing both methylene blue and embolization coils, with minimal additional technical effort, that may increase the detection of small pulmonary nodules and decrease perioperative morbidity.

## R2-SP1R-5 Experience of Two Referral Centers in The Embolization of The Parenchymal Tract After Percutaneous Portal Vein Catheterization: What's the Best?

Participants  
Francesco Carbone, MD, Bergamo, Italy (*Presenter*) Nothing to Disclose

## PURPOSE

The aim of this study is to compare the outcomes, in terms of safety and efficacy, of different embolization techniques of the parenchymal tract after percutaneous catheterization of the portal vein.

## METHODS AND MATERIALS

We retrospectively analyzed all the interventional procedures with percutaneous transhepatic or transplenic access to the portal vein from January 2010 to July 2021 in two tertiary hospitals; procedures of portal vein embolization were excluded. The following data were evaluated: access site, technique of embolization, technical success in terms of immediate thrombosis of the tract, safety and clinical efficacy in terms of hemorrhagic and thrombotic complications absence.

## RESULTS

A total of 161 patients (80 females; median age 35.7 years, IQR 40.7) underwent 220 (range 1-6 procedures per patient) percutaneous transhepatic or transplenic portal vein catheterization procedures. The main indications were pancreatic islet transplantation, portal anastomotic stenosis after liver transplantation, and portal vein thrombosis recanalization. As embolic materials gelfoam was used in 105 cases, metallic micro-coils in 54 cases, and cyanoacrylic glue plus lipiodol in 44 cases; in 17 cases the parenchymal tract was not embolized. Technical success was 97.5% (100% gelfoam; 98.1% coils; 97.8% glue; 94% without embolization;  $p = 0.45$ ). 18 abdominal post-procedural bleedings (8/105 gelfoam; 7/54 coils; 1/44 glue; 2/17 without embolization) occurred, but the difference among groups was not statistically significant ( $p = 0.25$ ). We detected 12 intrahepatic portal branch thromboses not strictly related to an embolization technique (1/105 gelfoam, 4/54 coils, 3/44 glue, 4/17 without embolization;  $p = 0.001$ ). Only 1 case of peripheral non-target embolization was documented with glue, without clinical consequences. Comparable technical success rates and clinical outcomes were observed among the transhepatic and the transplenic approaches.

## CONCLUSION

s Embolization of the parenchymal tract after percutaneous portal catheterization is technically safe and effective. The use of cyanoacrylic glue in higher caliber accesses allows a better control of periprocedural bleeding, without adding significant embolic complications.

## CLINICAL RELEVANCE/APPLICATION

Percutaneous access site hemostasis after percutaneous portal vein catheterization is a sensitive issue in IR suite, with several techniques described, but no global consensus on their effectiveness.

## R2-SP1R-6 Risk Factors for Failure of Endovascular Aneurysm Repair with Acute Conversion to Open Aortic Repair

Participants  
Waseem Wahood, MS, Burr Ridge, IL (*Presenter*) Nothing to Disclose

## PURPOSE

Patients with abdominal aortic aneurysms who undergo failure of endovascular aneurysm repair and acute conversion to open aortic repair (EVAR-c) have a higher 30-day mortality than those treated with open repair alone. The purpose of this study was to identify patients at risk for EVAR-c.

## METHODS AND MATERIALS

The National Surgical Quality Improvement Project Vascular-targeted database was queried from 2011 to 2019 for EVAR patients. Patient demographics were analyzed between EVAR and EVAR-c groups using chi-square and student t-tests. Multivariable logistic regression was conducted for risk factor assessment and 30-day reoperations.

## RESULTS

18,387 underwent EVAR and 146 underwent EVAR-c. There was no statistical difference in age ( $p=0.47$ ), gender ( $p=0.32$ ), race ( $p=0.75$ ) or BMI ( $p=0.61$ ). The average aneurysm diameter was 5.83 cm (SD=1.69) in the EVAR group, and 6.43 cm (SD=1.65) in the EVAR-c group ( $p<0.001$ ). Aneurysm diameter (OR: 1.07 per 1 cm increase; 95% CI: 1.01-1.14;  $p<0.001$ ), distal extension involving the common iliac (OR: 2.38, 95% CI: 1.43-3.98,  $p=0.001$ ), and distal extension inferior to the common iliac (OR: 2.40; 95% CI: 1.24-4.63;  $p=0.009$ ) were associated with higher odds of EVAR-c. EVAR-c was associated with similar odds of 30-day reoperations compared to EVAR (OR: 1.57; 95% CI: 0.61-4.05;  $p=0.35$ ).

## CONCLUSION

s This study suggests that aneurysm morphology plays a dominant and important role when predicting patients who are at risk for failure of endovascular therapy. These results may help guide patient selection for interventional radiologists.

#### **CLINICAL RELEVANCE/APPLICATION**

The lack of patient demographic association with EVAR-c in the current study may be secondary to a decrease in access-related issues in patients with complex anatomy, as well as technological advancement and improved operator skillset leading to more successful EVAR procedures in patients with increased comorbidities.

#### **R2-SPIR-7 Radiofrequency Ablation in Combination with Kyphoplasty for the Treatment of Painful Spine Metastases-Evaluation of VAS Pain Scale**

Participants  
Kenneth Richardson, Miami, FL (*Presenter*) Nothing to Disclose

#### **PURPOSE**

To determine the efficacy in pain improvement and safety of radiofrequency ablation (RF) in conjunction with kyphoplasty in treatment of patients with painful spinal metastases

#### **METHODS AND MATERIALS**

Between 3/2019 and 10/2021, a total of 51 painful spine tumors were treated among 43 patients and were reviewed retrospectively. The median age of the cohort was 64 years old (range, 33-79) with male-to-female ratio of 0.82. The primary neoplastic disease metastatic to spine were as follows: multiple myeloma (n=16, 31.4%), metastatic breast adenocarcinoma (n=13, 25.5%), metastatic prostate cancer (n=5, 9.8%), small cell lung cancer (n=4, 7.8%), colon adenocarcinoma, follicular lymphoma, pancreatic adenocarcinoma, squamous cell lung cancer (n=2, 3.9%), melanoma, renal cell carcinoma, metastatic thyroid cancer, urothelial cancer, and metastatic adenoid cystic tumor (n=1, 2%). Pain relief was evaluated by the visual analogue scale (VAS) score before and within 3-months after the procedure. The highest documented VAS pre- and post-procedure was recorded. A neurologic exam was also performed immediately before and immediately after the procedure. A two tailed P value <0.05 was considered statistically significant.

#### **RESULTS**

Technical success was achieved in all patients. Kyphoplasty and RF ablation was performed on thoracic vertebral bodies in 21 patients (41.2%), lumbar vertebral bodies in 25 patients (49%), and thoracolumbar vertebral bodies on 5 patients (9.8%). 32 patients (62.75%) had kyphoplasty at one vertebral level, 13 patients (25.49%) had two-level kyphoplasty, 5 patients (9.8%) had three-level kyphoplasty, and one patient (1.96%) had a four-level spinal kyphoplasty. The median VAS score decreased from 10 (IQR, 8-10) to 4 (IQR, 2-5) in 3 months after procedure (median change -6 (IQR, -7 to -4), P <0.001). The median VAS score change was -6 (IQR, -7 to -4) for single level procedures and -6 (IQR, -7 to -4.25) for multilevel procedures (P= 0.85). Median VAS score change was -6 (IQR, -7 to -5) for thoracic procedures, -5 (IQR, -7 to -4) for lumbar procedures, and -5.5 (IQR, -7.5 to -3.75) for thoracolumbar procedures (P= 0.85). During one kyphoplasty procedure, the anterior margin of the vertebral body was inadvertently breached, but the procedure was completed successfully with no long-term sequelae.

#### **CONCLUSION**

s RFA in conjunction with Kyphoplasty appears to be safe and provides meaningful clinical improvement in VAS pain scale scores in patients with pain due to metastatic disease to the spine, when measured at post procedure follow up within 3 months of the procedure.

#### **CLINICAL RELEVANCE/APPLICATION**

These results highlight the role of kyphoplasty with RFA in the management of patients with painful spinal metastases and functional decline.

#### **R2-SPIR-8 Safety and Efficacy of Provocative Visceral Angiography with tPA in Patient's With GI Bleed**

Participants  
Susan Win, MD, (*Presenter*) Nothing to Disclose

#### **PURPOSE**

To evaluate the efficacy and safety of provocative visceral angiography with catheter directed tPA in the diagnosis and management of patients presenting with occult GI bleed that could not be localized with routine diagnostic work-up.

#### **METHODS AND MATERIALS**

Radiology reports from a single institution were reviewed to identify patients who underwent provocative visceral angiography for GI bleed from 10/2015 to 7/2021. Clinical information was then collected regarding prior diagnostic studies, intra-procedural medications, immediate technical clinical outcomes, and long term outcomes.

#### **RESULTS**

A total of 44 provocative visceral angiograms were performed for both acute and chronic GI bleeds with an unidentified source despite traditional diagnostic work-up. Two cases were excluded as the patient did not receive catheter directed tPA during the procedure, for a total of 42 cases across 37 patients. Patients received up to 24 mg of catheter directed tPA and a combination of up to 5000u of IV heparin and/or 600 mcg Nitroglycerin. Bleeding was successfully induced in 36% (15/42) of patients who, on average, received 16.8 mg of tPA, 5000u of heparin, and 400 mcg Nitroglycerin. Of those, 87% (13/15) underwent intervention (12 IR embolization, 1 GI band ligation), with technical success achieved in all cases. Clinical success, as defined by no recurrent bleeding beyond the perioperative (30 day) period, was achieved in 85% (11/13) of cases. This includes 2 cases where the patient had a single remote episode of self-limited GI bleed following the initiation of systemic anticoagulation. Of the cases where embolization was not performed or was not clinically successful, all patients (4/4) required subsequent surgical intervention. The patients who underwent successful provocative angiography on average had 4 prior GI studies (endoscopy, colonoscopy, or capsule endoscopy). 8/15 had at least 1 prior CTA, 11/15 had a prior RBC scan, 3/15 underwent prior negative provocative angiograms, and 6/15 underwent prior negative non-provoked visceral angiograms. Importantly, no post-procedural complications were identified across all patients.

## **CONCLUSION**

s Provocative visceral angiography with tPA was capable of inducing GI bleed in approximately 1/3 of patients studied. In patients where a bleed was induced, intervention resulted in clinical success in 73% (11/15) of patients. No procedure related complications were identified in this study, suggesting that provocative visceral angiography is a safe and efficacious option for the management of GI bleeds.

## **CLINICAL RELEVANCE/APPLICATION**

This study adds to the limited body of evidence demonstrating that provocative visceral angiogram is a safe and efficacious tool for the management of occult GI bleeds.

Printed on: 02/07/23

## Abstract Archives of the RSNA, 2022

R2-SP1R-1

### **Efficacy of Selective Transarterial Chemoembolization with Radiotherapy Versus Y-90 Transarterial Radioembolization in Hepatocellular Carcinoma with Portal Vein Tumor Thrombus**

Thursday, Dec. 1 9:00AM - 9:30AM Room: Learning Center - IR DPS

#### **Participants**

Yanisa Jarusyingdumrong, MD, (*Presenter*) Nothing to Disclose

#### **PURPOSE**

To compare the efficacy of selective transarterial chemoembolization (TACE) combined with radiotherapy (RT) and Y-90 transarterial radioembolization (TARE) in the treatment of hepatocellular carcinoma (HCC) with portal vein tumor thrombosis (PVTT).

#### **METHODS AND MATERIALS**

In retrospective cohort study, patients received treatment from January 2011 to October 2019 in a single center were recruited. The overall survival (OS) rate and median survival time were compared between the two groups. Survival curves were constructed using the Kaplan-Meier method and were compared using the log rank test. The confounding factors were adjusted using Laplace regression.

#### **RESULTS**

A total of 82 patients with HCC and PVTT received either selective TACE combined with radiotherapy (n = 48) or Y-90 TARE alone (n = 34). The OS rate was significantly lower (1-year HR 3.19; 95%CI 1.22, 8.31; p-value 0.012; 2-year HR 4.00; 95%CI 1.79, 8.94; p-value <0.001) and the median survival time was significantly shorter (4.5 vs 21.1 months, respectively; p-value 0.004) in combined selective TACE and RT group than in Y-90 TARE alone group.

#### **CONCLUSION**

s Group receiving selective TACE combined with RT has shorter survival time than group receiving Y-90 TARE alone in patients with HCC and PVTT.

#### **CLINICAL RELEVANCE/APPLICATION**

In many countries with limited resources, the systemic treatment recommended for treating advanced stage HCC may not be available. Therefore, a safe and effective alternative should be explored.

Printed on: 02/07/23

## Abstract Archives of the RSNA, 2022

R2-SP1R-2

### Nanoscale CaO<sub>2</sub> Materials Provides a New Perspective for Trans-arterial Chemoembolization Therapy in VX2 Orthotopic Rabbit Liver Cancer Model

Thursday, Dec. 1 9:00AM - 9:30AM Room: Learning Center - IR DPS

#### Participants

Yingliang Wang, (*Presenter*) Nothing to Disclose

#### PURPOSE

Transcatheter arterial chemoembolization (TACE) is extensively used in the treatment of liver cancer. However, the efficacy of TACE is usually limited to secondary tumor hypoxia and other progressive exacerbation of the abnormal tumor microenvironment (TME). Herein, we synthesized CaO<sub>2</sub> nanoparticles (nano-CaO<sub>2</sub>) and applied them as a synergistic agent to improve the antitumor efficacy of TACE. Being injected into the tumor, nano-CaO<sub>2</sub> would react with water to generate abundant oxygen, hydroxyl ions (OH<sup>-</sup>), and calcium ions (Ca<sup>2+</sup>), enabling relieve tumor hypoxia, neutralization of acidic TME, and Ca<sup>2+</sup> overloading mediated antitumor, respectively. Moreover, the effect of chemotherapeutic drug within the TACE would be improved due to the improved TME.

#### METHODS AND MATERIALS

The nano-CaO<sub>2</sub> was fabricated by the CaCl<sub>2</sub>-H<sub>2</sub>O<sub>2</sub> reaction at alkaline pH and stabilized by polyvinyl pyrrolidone. The characteristics of the nanoparticle were evaluated by X-ray diffraction, X-ray photoelectron spectroscopy, Field Emission Transmission Electron Microscopy, and Dynamic light scattering. Measurement of dissolved O<sub>2</sub> concentration, pH value and GSH content in solution. In vitro test was used to evaluate the cytotoxicity, apoptosis, intracellular O<sub>2</sub>, GSH, HIF-1 $\alpha$  and VEGF level. In vivo test, twenty-five rabbits with VX2 liver tumor were randomly divided into five groups and injected different agents via hepatic artery (group A: normal saline; group B: lipiodol; group C: lipiodol + doxorubicin; group D: lipiodol + nano-CaO<sub>2</sub>; group E: lipiodol + nano-CaO<sub>2</sub> + doxorubicin). The tumor growth rate, necrosis rate, proliferation index and apoptosis index, histological markers associated with angiogenesis (HIF- $\alpha$ , VEGF, MVD) and immune response (CD8+ T cell) were assessed by imaging and histopathology. Biosafety was evaluated by testing the hepatic and renal function (AST, ALT, BUN, and Cr) and HE staining of main organs in each group.

#### RESULTS

In vitro, nano-CaO<sub>2</sub> could efficiently regulate the TME and improve the antitumor effect of doxorubicin under hypoxia condition. In vivo, compared to other groups, group E achieved lower tumor growth rate, higher tumor necrosis rate, lower expression of histological markers associated with hypoxia and angiogenesis, and higher CD8+ T cell recruitment. All rabbits in group B-E undergo temporary liver injury and recovered later.

#### CONCLUSION

s Nano-CaO<sub>2</sub> could significantly improve the efficacy of TACE in the treatment of rabbit VX2 liver tumors.

#### CLINICAL RELEVANCE/APPLICATION

Nano-CaO<sub>2</sub> could significantly improve the efficacy of TACE in the treatment of rabbit VX2 liver tumors and could recruit CD8+ T cell which may serve as a synergistic agent with immune checkpoint inhibitors. Thus, it has a broad clinical application prospect.

Printed on: 02/07/23

## Abstract Archives of the RSNA, 2022

R2-SPIR-3

### Gene Expression and DNA Methylation Patterns Highlight Disparities in Ethno-racial Status and Treatment Response in Hepatocellular Carcinoma Patients

Thursday, Dec. 1 9:00AM - 9:30AM Room: Learning Center - IR DPS

#### Participants

Vishwaarth Vijayakumar, MD, Dunlap, IL (*Presenter*) Nothing to Disclose

#### PURPOSE

Since 85% of hepatocellular carcinoma (HCC) patients are ineligible for surgical resection or liver transplantation, Interventional Radiology offers locoregional therapies (LRT) as an additional option. However, response rates are modest and the biological factors that underlie tumor response are unclear. HCC rates vary based on ethno-racial status with little information about how these differences may correspond to tumor biology. Therefore, this study performed HCC epigenetic profiling to investigate tumor biology associated with ethno-racial patient populations and LRT response.

#### METHODS AND MATERIALS

DNA and RNA was extracted from formalin-fixed paraffin-embedded tumor samples representing 47 HCC patients (n=15 Black, n=22 White, n=10 Hispanic). Treatment response was determined using CT/MRI imaging 3 months post-treatment (n=24 complete response, n=15 retreatment candidates). RNA expression (RNA-seq) and DNA methylation (reduced representation bisulfite sequencing) levels were used to stratify patients based on ethno-racial status and treatment response using partial least-squares discriminant analysis (PLS-DA) with 300 runs of bootstrap subsampling. Results were validated using hierarchical clustering. Ingenuity pathway analysis was performed to identify upstream regulators and pathways enriched for identified genes.

#### RESULTS

PLS-DA identified 100 genes and 12 methylated regions that successfully differentiated between Black and White/Hispanic patients. Hierarchical clustering based on either the top 16 genes identified in >80% of the models or the top 5 methylation regions identified in >60% of the models resulted in successful clustering of Black from White and Hispanic patients. These genes were associated with pathways and upstream regulators related to metabolic regulation and protein translation. PLS-DA identified 100 genes and 150 methylated regions that successfully differentiated between complete responders and retreatment candidates. Hierarchical clustering based on either the top 30 genes identified in >50% of the models or the top 13 methylation regions identified in >85% of the models resulted in successful clustering of patients based on response. These genes, relevant upstream activators, and pathways were related to p53 signaling, DNA repair, and metabolism.

#### CONCLUSION

Epigenetic profiles of HCC patients show that differences in metabolic regulation, protein translation, p53 signaling, and DNA repair may correspond to differences in ethno-racial status and treatment response.

#### CLINICAL RELEVANCE/APPLICATION

This study identified epigenetic profiles, upstream regulators, and enriched pathways which could be useful for identification of precision therapeutic targets for HCC.

Printed on: 02/07/23



## Abstract Archives of the RSNA, 2022

R2-SP1R-4

### **Making a Mark: Follow-up of Outcomes for Combined Methylene Blue and Embolization Coil Marking for Lung Nodule Localization**

Thursday, Dec. 1 9:00AM - 9:30AM Room: Learning Center - IR DPS

#### **Participants**

Joe Khoury, DO, MBA, Manhasset, NY (*Presenter*) Nothing to Disclose

#### **PURPOSE**

To study the efficacy of lung nodule localization with a combined technique utilizing both methylene blue and embolization coils.

#### **METHODS AND MATERIALS**

This study was a retrospective mono-centric review of 93 patients who underwent amalgam technique of utilizing methylene blue and embolization coils for lung nodule marking. Inclusion criteria was limited to any patient who underwent lung marking utilizing this technique from 2010 to 2020.

#### **RESULTS**

Of the patients undergoing lung marking, 34% (32/93) were male and 66% (61/93) were female. The average age was 65 years, ranging from 3 to 88 years. One patient was excluded due to unavailability of operative documentation. One patient had two nodules that were marked. In these 92 patients, 100% (93/93) of the lung nodules were localized. Both methylene blue and the coil marker were identified in 88/92 (95.7%) patients. In the remaining 4 patients (4.3%), only methylene blue was noted in the pathology and operative reports. 93/93 (100%) of the marked nodules were successfully resected and confirmed by pathology. All of the nodules were successfully excised via VATS, with 0% (0/92) requiring conversion to open thoracotomy. Three patients had difficulties with coil deployment, which did not result in any patient morbidity. In one patient, the embolization coil was dislodged but methylene blue was administered and the nodule was resected. Two patients had coil migratory complications, which involved the coil extending proximally through the trocar tract. Eight patients developed pneumothoraces, with three requiring chest tubes.

#### **CONCLUSION**

s This study further supports our hypothesis that lung nodule localization utilizing both methylene blue and embolization microcoils is safe and allows for successful identification and resection of nodules utilizing VATS technique.

#### **CLINICAL RELEVANCE/APPLICATION**

Along with the advent of high resolution computed tomography, there has been increasing detection of small pulmonary nodules. These nodules are often not well visualized or palpable during minimally invasive wedge resection with Video Assisted Thoracic Surgery (VATS), which has historically led to an increased rate of conversion to open thoracotomy, as well as increased morbidity. The rate of conversion from VATS to open thoracotomy has been noted to be as high as 23% secondary to inability to properly locate these small nodules. The solution to this problem has been preoperative localization of these nodules with either hook wires, methylene blue, or embolization coils. This study aims to evaluate a combined technique of utilizing both methylene blue and embolization coils, with minimal additional technical effort, that may increase the detection of small pulmonary nodules and decrease perioperative morbidity.

Printed on: 02/07/23

## Abstract Archives of the RSNA, 2022

R2-SPIR-5

### Experience of Two Referral Centers in The Embolization of The Parenchymal Tract After Percutaneous Portal Vein Catheterization: What's the Best?

Thursday, Dec. 1 9:00AM - 9:30AM Room: Learning Center - IR DPS

#### Participants

Francesco Carbone, MD, Bergamo, Italy (*Presenter*) Nothing to Disclose

#### PURPOSE

The aim of this study is to compare the outcomes, in terms of safety and efficacy, of different embolization techniques of the parenchymal tract after percutaneous catheterization of the portal vein.

#### METHODS AND MATERIALS

We retrospectively analyzed all the interventional procedures with percutaneous transhepatic or transsplenic access to the portal vein from January 2010 to July 2021 in two tertiary hospitals; procedures of portal vein embolization were excluded. The following data were evaluated: access site, technique of embolization, technical success in terms of immediate thrombosis of the tract, safety and clinical efficacy in terms of hemorrhagic and thrombotic complications absence.

#### RESULTS

A total of 161 patients (80 females; median age 35.7 years, IQR 40.7) underwent 220 (range 1-6 procedures per patient) percutaneous transhepatic or transsplenic portal vein catheterization procedures. The main indications were pancreatic islet transplantation, portal anastomotic stenosis after liver transplantation, and portal vein thrombosis recanalization. As embolic materials gelfoam was used in 105 cases, metallic micro-coils in 54 cases, and cyanoacrylic glue plus lipiodol in 44 cases; in 17 cases the parenchymal tract was not embolized. Technical success was 97.5% (100% gelfoam; 98.1% coils; 97.8% glue; 94% without embolization;  $p = 0.45$ ). 18 abdominal post-procedural bleedings (8/105 gelfoam; 7/54 coils; 1/44 glue; 2/17 without embolization) occurred, but the difference among groups was not statistically significant ( $p = 0.25$ ). We detected 12 intrahepatic portal branch thromboses not strictly related to an embolization technique (1/105 gelfoam, 4/54 coils, 3/44 glue, 4/17 without embolization;  $p = 0.001$ ). Only 1 case of peripheral non-target embolization was documented with glue, without clinical consequences. Comparable technical success rates and clinical outcomes were observed among the transhepatic and the transsplenic approaches.

#### CONCLUSION

s Embolization of the parenchymal tract after percutaneous portal catheterization is technically safe and effective. The use of cyanoacrylic glue in higher caliber accesses allows a better control of periprocedural bleeding, without adding significant embolic complications.

#### CLINICAL RELEVANCE/APPLICATION

Percutaneous access site hemostasis after percutaneous portal vein catheterization is a sensitive issue in IR suite, with several techniques described, but no global consensus on their effectiveness.

Printed on: 02/07/23

## Abstract Archives of the RSNA, 2022

R2-SPIR-6

### Risk Factors for Failure of Endovascular Aneurysm Repair with Acute Conversion to Open Aortic Repair

Thursday, Dec. 1 9:00AM - 9:30AM Room: Learning Center - IR DPS

#### Participants

Waseem Wahood, MS, Burr Ridge, IL (*Presenter*) Nothing to Disclose

#### PURPOSE

Patients with abdominal aortic aneurysms who undergo failure of endovascular aneurysm repair and acute conversion to open aortic repair (EVAR-c) have a higher 30-day mortality than those treated with open repair alone. The purpose of this study was to identify patients at risk for EVAR-c.

#### METHODS AND MATERIALS

The National Surgical Quality Improvement Project Vascular-targeted database was queried from 2011 to 2019 for EVAR patients. Patient demographics were analyzed between EVAR and EVAR-c groups using chi-square and student t-tests. Multivariable logistic regression was conducted for risk factor assessment and 30-day reoperations.

#### RESULTS

18,387 underwent EVAR and 146 underwent EVAR-c. There was no statistical difference in age ( $p=0.47$ ), gender ( $p=0.32$ ), race ( $p=0.75$ ) or BMI ( $p=0.61$ ). The average aneurysm diameter was 5.83 cm ( $SD=1.69$ ) in the EVAR group, and 6.43 cm ( $SD=1.65$ ) in the EVAR-c group ( $p<0.001$ ). Aneurysm diameter (OR: 1.07 per 1 cm increase; 95% CI: 1.01-1.14;  $p<0.001$ ), distal extension involving the common iliac (OR: 2.38, 95% CI: 1.43-3.98,  $p=0.001$ ), and distal extension inferior to the common iliac (OR: 2.40; 95% CI: 1.24-4.63;  $p=0.009$ ) were associated with higher odds of EVAR-c. EVAR-c was associated with similar odds of 30-day reoperations compared to EVAR (OR: 1.57; 95% CI: 0.61-4.05;  $p=0.35$ ).

#### CONCLUSION

s This study suggests that aneurysm morphology plays a dominant and important role when predicting patients who are at risk for failure of endovascular therapy. These results may help guide patient selection for interventional radiologists.

#### CLINICAL RELEVANCE/APPLICATION

The lack of patient demographic association with EVAR-c in the current study may be secondary to a decrease in access-related issues in patients with complex anatomy, as well as technological advancement and improved operator skillset leading to more successful EVAR procedures in patients with increased comorbidities.

Printed on: 02/07/23

## Abstract Archives of the RSNA, 2022

R2-SP1R-7

### Radiofrequency Ablation in Combination with Kyphoplasty for the Treatment of Painful Spine Metastases- Evaluation of VAS Pain Scale

Thursday, Dec. 1 9:00AM - 9:30AM Room: Learning Center - IR DPS

#### Participants

Kenneth Richardson, Miami, FL (*Presenter*) Nothing to Disclose

#### PURPOSE

To determine the efficacy in pain improvement and safety of radiofrequency ablation (RF) in conjunction with kyphoplasty in treatment of patients with painful spinal metastases

#### METHODS AND MATERIALS

Between 3/2019 and 10/2021, a total of 51 painful spine tumors were treated among 43 patients and were reviewed retrospectively. The median age of the cohort was 64 years old (range, 33-79) with male-to-female ratio of 0.82. The primary neoplastic disease metastatic to spine were as follows: multiple myeloma (n=16, 31.4%), metastatic breast adenocarcinoma (n=13, 25.5%), metastatic prostate cancer (n=5, 9.8%), small cell lung cancer (n=4, 7.8%), colon adenocarcinoma, follicular lymphoma, pancreatic adenocarcinoma, squamous cell lung cancer (n=2, 3.9%), melanoma, renal cell carcinoma, metastatic thyroid cancer, urothelial cancer, and metastatic adenoid cystic tumor (n=1, 2%). Pain relief was evaluated by the visual analogue scale (VAS) score before and within 3-months after the procedure. The highest documented VAS pre- and post-procedure was recorded. A neurologic exam was also performed immediately before and immediately after the procedure. A two tailed P value <0.05 was considered statistically significant.

#### RESULTS

Technical success was achieved in all patients. Kyphoplasty and RF ablation was performed on thoracic vertebral bodies in 21 patients (41.2%), lumbar vertebral bodies in 25 patients (49%), and thoracolumbar vertebral bodies on 5 patients (9.8%). 32 patients (62.75%) had kyphoplasty at one vertebral level, 13 patients (25.49%) had two-level kyphoplasty, 5 patients (9.8%) had three-level kyphoplasty, and one patient (1.96%) had a four-level spinal kyphoplasty. The median VAS score decreased from 10 (IQR, 8-10) to 4 (IQR, 2-5) in 3 months after procedure (median change -6 (IQR, -7 to -4), P <0.001). The median VAS score change was -6 (IQR, -7 to -4) for single level procedures and -6 (IQR, -7 to -4.25) for multilevel procedures (P= 0.85). Median VAS score change was -6 (IQR, -7 to -5) for thoracic procedures, -5 (IQR, -7 to -4) for lumbar procedures, and -5.5 (IQR, -7.5 to -3.75) for thoracolumbar procedures (P= 0.85). During one kyphoplasty procedure, the anterior margin of the vertebral body was inadvertently breached, but the procedure was completed successfully with no long-term sequelae.

#### CONCLUSION

s RFA in conjunction with Kyphoplasty appears to be safe and provides meaningful clinical improvement in VAS pain scale scores in patients with pain due to metastatic disease to the spine, when measured at post procedure follow up within 3 months of the procedure.

#### CLINICAL RELEVANCE/APPLICATION

These results highlight the role of kyphoplasty with RFA in the management of patients with painful spinal metastases and functional decline.

Printed on: 02/07/23

## Abstract Archives of the RSNA, 2022

R2-SP1R-8

### Safety and Efficacy of Provocative Visceral Angiography with tPA in Patient's With GI Bleed

Thursday, Dec. 1 9:00AM - 9:30AM Room: Learning Center - IR DPS

#### Participants

Susan Win, MD, (*Presenter*) Nothing to Disclose

#### PURPOSE

To evaluate the efficacy and safety of provocative visceral angiography with catheter directed tPA in the diagnosis and management of patients presenting with occult GI bleed that could not be localized with routine diagnostic work-up.

#### METHODS AND MATERIALS

Radiology reports from a single institution were reviewed to identify patients who underwent provocative visceral angiography for GI bleed from 10/2015 to 7/2021. Clinical information was then collected regarding prior diagnostic studies, intra-procedural medications, immediate technical clinical outcomes, and long term outcomes.

#### RESULTS

A total of 44 provocative visceral angiograms were performed for both acute and chronic GI bleeds with an unidentified source despite traditional diagnostic work-up. Two cases were excluded as the patient did not receive catheter directed tPA during the procedure, for a total of 42 cases across 37 patients. Patients received up to 24 mg of catheter directed tPA and a combination of up to 5000u of IV heparin and/or 600 mcg Nitroglycerin. Bleeding was successfully induced in 36% (15/42) of patients who, on average, received 16.8 mg of tPA, 5000u of heparin, and 400 mcg Nitroglycerin. Of those, 87% (13/15) underwent intervention (12 IR embolization, 1 GI band ligation), with technical success achieved in all cases. Clinical success, as defined by no recurrent bleeding beyond the perioperative (30 day) period, was achieved in 85% (11/13) of cases. This includes 2 cases where the patient had a single remote episode of self-limited GI bleed following the initiation of systemic anticoagulation. Of the cases where embolization was not performed or was not clinically successful, all patients (4/4) required subsequent surgical intervention. The patients who underwent successful provocative angiography on average had 4 prior GI studies (endoscopy, colonoscopy, or capsule endoscopy). 8/15 had at least 1 prior CTA, 11/15 had a prior RBC scan, 3/15 underwent prior negative provocative angiograms, and 6/15 underwent prior negative non-provoked visceral angiograms. Importantly, no post-procedural complications were identified across all patients.

#### CONCLUSION

s Provocative visceral angiography with tPA was capable of inducing GI bleed in approximately 1/3 of patients studied. In patients where a bleed was induced, intervention resulted in clinical success in 73% (11/15) of patients. No procedure related complications were identified in this study, suggesting that provocative visceral angiography is a safe and efficacious option for the management of GI bleeds.

#### CLINICAL RELEVANCE/APPLICATION

This study adds to the limited body of evidence demonstrating that provocative visceral angiogram is a safe and efficacious tool for the management of occult GI bleeds.

Printed on: 02/07/23

## Abstract Archives of the RSNA, 2022

R2-SPMK

### Musculoskeletal Thursday Poster Discussions

Thursday, Dec. 1 9:00AM - 9:30AM Room: Learning Center - MK DPS

#### Participants

Shivani Ahlawat, MD, Ellicott City, MD (*Moderator*) Nothing to Disclose

#### Sub-Events

#### R2-SPMK-1 Can Radiographic Changes of The Humerus Greater Tubercle Predict Superior Cuff Tear?

#### Participants

Hyemin Park, Seoul, Korea, Republic Of (*Presenter*) Nothing to Disclose

#### PURPOSE

The aim of this study was to assess the diagnostic value of radiographic findings at humerus greater tubercle (GT) to predict various degrees of superior cuff tear (SCT).

#### METHODS AND MATERIALS

From January to March of 2019, 255 consecutive patients with shoulder pain who underwent radiographic evaluation followed by ultrasound (US) or magnetic resonance imaging (MRI) were included. Radiographs were reviewed by two musculoskeletal radiologists who were blinded to the US or MRI results for the following findings: sclerosis, erosion, spur and femoralization of humerus GT. Consensus was made in discordant cases. The odds ratio of each radiographic finding to predict the presence of SCT, high grade or more severe tear, full thickness tear (FTT), and FTT over 1cm in anteroposterior (AP) dimension was calculated. Also, the value of using at least one radiographic finding, or two or more findings to predict SCT was assessed.

#### RESULTS

Sclerosis, erosion, spur and femoralization of GT were all predictive of the presence of superior cuff tear (odds ratio [OR] = 5.95, OR = 15.7948, OR = 6.0992, OR = 8.6035, respectively), high grade or more severe degree of tear (OR = 4.3636, OR = 13.9703, OR = 9.6416, OR = 18.482, respectively), FTT (OR = 3.6959, OR = 25.3881, OR = 25.3881, OR = 36.7284, respectively) and FTT over 1cm in AP dimension (OR = 4.2895, OR = 18.3045, OR = 28.875, OR = 47.4923, respectively). GT sclerosis showed the lowest diagnostic accuracy (69.41%), and GT erosion showed the highest diagnostic accuracy (80.00%) to predict the presence of SCT. Femoralization showed the highest diagnostic accuracy (87.45%) to predict the FTT over 1cm in AP dimension and showed 100% of specificity to diagnose any degree of SCT. When two or more imaging findings were found, there was more solid association between the radiographic findings and SCT regardless of degree (OR = 9.1829, OR = 7.0707, OR = 6.9726, respectively, all p = 0.0001).

#### CONCLUSION

s Radiographic findings at humerus GT can predict SCT on US or MR. GT erosion showed the highest diagnostic accuracy (80.00%) to predict the presence of SCT.

#### CLINICAL RELEVANCE/APPLICATION

Radiograph of the shoulder can be used for the screening of SCT and can help the physician to identify the candidates for further examination of the rotator cuff with US or MRI.

#### R2-SPMK-3 Inter-Rater Reliability and Correlation of L1 Hounsfield Unit Measurements with DXA Scores

#### Participants

Steven Rothenberg, MD, Birmingham, AL (*Presenter*) Founder, Empower Therapeutics Inc ;Member, Translation Holdings LLC;Consultant, Radiostics LLC

#### PURPOSE

The opportunistic use of computed tomography (CT) in screening for osteoporosis has been previously reported; however, its broad applicability has yet to be demonstrated. Hounsfield units (HUs) are known to correlate well with dual-energy X-ray absorptiometry (DXA) based bone assessments and offer a clinically applicable method of estimating bone quality. While prior studies have generally reported rigorous protocols using prespecified CT scanner settings for HU measurements, the present study sought to report on the correlation between DXA and HUs recorded using several CT scanners with varying sequences, simulating measurements performed in "real-world" hospital and Emergency Department (ED) settings.

#### METHODS AND MATERIALS

Forty consecutive patients who underwent DXA and two abdominal CT scans, each on a Phillips and General Electric (GE) scanner within six months between the years of 2017 and 2021 at a level 1 tertiary care academic medical center were included in this study. Six raters performed HU measurements of trabecular bone at the L1 vertebral body for each patient on the two separate scanners. Inter-rater reliability of the HU measurements and their correlations with recorded DXA-based bone assessments were

determined on each scanner brand. Correlation coefficients were calculated for the HU measurements between scanner brands as well as for the CT HUs with each DXA measurement (femoral neck, total femur, L1 vertebra and total spine). Results were reported using the intraclass coefficient (ICC) statistic for reliability and Pearson's R for correlations.

## RESULTS

The ICC for L1 HUs read on the Phillips and GE scanners were 0.85 and 0.82, respectively, indicating excellent agreement. The correlation coefficient for the mean HUs on the Phillips and GE scanners was 0.92, also indicating excellent correlation. For both scanner brands, the HU values most closely correlated with the total femur (Phillips:  $Rho = 0.52$ ,  $p < 0.001$ ; GE:  $Rho = 0.45$ ,  $p = 0.003$ ) and femoral neck (Phillips:  $Rho = 0.46$ ,  $p = 0.003$ ; GE:  $Rho = 0.38$ ,  $p = 0.02$ ) T-scores, respectively. L1 and total spine T-scores correlated less with L1 HU values.

## CONCLUSION

s HU values recorded on a Phillips and GE scanner both demonstrated excellent inter-rater reliability. Correlations were strongest between L1 HU values and total femur DXA T-scores.

## CLINICAL RELEVANCE/APPLICATION

Abdominal CT imaging across multiple hospital settings demonstrates reliable identification of patients with osteoporosis and represents an opportunity for minimizing radiation exposure and cost.

## R2-SPMK-4 Electron Density As A Quantitative CT Metric To Evaluate Lumbar Intervertebral Disc Degeneration

### Participants

Tsubasa Nakano, Kagoshima, Japan (*Presenter*) Nothing to Disclose

### PURPOSE

To preliminarily evaluate the usefulness of electron density (ED) as a quantitative CT metric to detect lumbar intervertebral disc degeneration.

### METHODS AND MATERIALS

This study included 338 discs in 100 patients who underwent CT examination and MRI within one month. CT was performed using a spectral detector CT scanner, and images of conventional poly-energetic CT value (CTconv) and ED were obtained. Severity of degeneration for each disc was determined using modified Pfirrmann grade (mPG) based on T2-weighted MRI. In each disc, three ROIs were drawn in the anterior and posterior annulus fibrosis (AAF and PAF) as well as in the nucleus pulposus (NP). Mean CTconv and ED for each ROI were correlated with mPG using Spearman's rank correlation coefficient. The CTconv and ED values in the 3 ROIs as well as their differences between AAF and NP (?AAF-NP) and between PAF and NP (?PAF-NP) were compared between normal (mPG1 and 2) and degenerated discs (mPG3-7) using the Mann-Whitney U test. ROC curve analysis was used to assess the diagnostic abilities of CTconv and ED values. The sensitivity, specificity, and accuracy for differentiating mPG3-7 from mPG1 and 2 were calculated using a threshold criterion determined by the largest Youden's index.

### RESULTS

The mean CTconv was significantly positively correlated with mPG in NP ( $r=0.239$ ,  $P<0.001$ ), while it was significantly negatively correlated with mPG in AAF and PAF ( $r=-0.332$ ,  $-0.287$ ,  $P<0.001$ ). The mean ED was more closely correlated with mPG than CTconv both in NP ( $r=0.446$ ,  $P<0.001$ ) and in AAF and PAF ( $r=-0.357$ ,  $-0.291$ ,  $P<0.001$  for each). The CTconv and ED of NP in degenerated discs were significantly higher than those of normal discs ( $P<0.001$ ). In addition, the CTconv and ED of AF as well as ?AAF-NP and ?PAF-NP were significantly lower than those of normal discs ( $P<0.001$  for each). The AUC values for CTconv and ED of AAF, PAF, and NP ranged from 0.617 to 0.758, those for ?AAF-NP and ?PAF-NP of CTconv and ED ranged from 0.765 to 0.915. The AUC value for ?AAF-NP of ED performed best (AUC = 0.915) among all indices.

### CONCLUSION

s ED may be a useful quantitative CT metric to evaluate lumbar intervertebral disc degeneration.

### CLINICAL RELEVANCE/APPLICATION

Our results demonstrated the potential of ED as a quantitative metric to evaluate lumbar intervertebral disc degeneration.

Printed on: 02/07/23

## Abstract Archives of the RSNA, 2022

R2-SPMK-1

### Can Radiographic Changes of The Humerus Greater Tubercle Predict Superior Cuff Tear?

Thursday, Dec. 1 9:00AM - 9:30AM Room: Learning Center - MK DPS

#### Participants

Hyemin Park, Seoul, Korea, Republic Of (*Presenter*) Nothing to Disclose

#### PURPOSE

The aim of this study was to assess the diagnostic value of radiographic findings at humerus greater tubercle (GT) to predict various degrees of superior cuff tear (SCT).

#### METHODS AND MATERIALS

From January to March of 2019, 255 consecutive patients with shoulder pain who underwent radiographic evaluation followed by ultrasound (US) or magnetic resonance imaging (MRI) were included. Radiographs were reviewed by two musculoskeletal radiologists who were blinded to the US or MRI results for the following findings: sclerosis, erosion, spur and femoralization of humerus GT. Consensus was made in discordant cases. The odds ratio of each radiographic finding to predict the presence of SCT, high grade or more severe tear, full thickness tear (FTT), and FTT over 1cm in anteroposterior (AP) dimension was calculated. Also, the value of using at least one radiographic finding, or two or more findings to predict SCT was assessed.

#### RESULTS

Sclerosis, erosion, spur and femoralization of GT were all predictive of the presence of superior cuff tear (odds ratio [OR] = 5.95, OR = 15.7948, OR = 6.0992, OR = 8.6035, respectively), high grade or more severe degree of tear (OR = 4.3636, OR = 13.9703, OR = 9.6416, OR = 18.482, respectively), FTT (OR = 3.6959, OR = 25.3881, OR = 25.3881, OR = 36.7284, respectively) and FTT over 1cm in AP dimension (OR = 4.2895, OR = 18.3045, OR = 28.875, OR = 47.4923, respectively). GT sclerosis showed the lowest diagnostic accuracy (69.41%), and GT erosion showed the highest diagnostic accuracy (80.00%) to predict the presence of SCT. Femoralization showed the highest diagnostic accuracy (87.45%) to predict the FTT over 1cm in AP dimension and showed 100% of specificity to diagnose any degree of SCT. When two or more imaging findings were found, there was more solid association between the radiographic findings and SCT regardless of degree (OR = 9.1829, OR = 7.0707, OR = 6.9726, respectively, all p = 0.0001).

#### CONCLUSION

s Radiographic findings at humerus GT can predict SCT on US or MR. GT erosion showed the highest diagnostic accuracy (80.00%) to predict the presence of SCT.

#### CLINICAL RELEVANCE/APPLICATION

Radiograph of the shoulder can be used for the screening of SCT and can help the physician to identify the candidates for further examination of the rotator cuff with US or MRI.

Printed on: 02/07/23



## Abstract Archives of the RSNA, 2022

R2-SPMK-3

### Inter-Rater Reliability and Correlation of L1 Hounsfield Unit Measurements with DXA Scores

Thursday, Dec. 1 9:00AM - 9:30AM Room: Learning Center - MK DPS

#### Participants

Steven Rothenberg, MD, Birmingham, AL (*Presenter*) Founder, Empower Therapeutics Inc ;Member, Translation Holdings LLC;Consultant, Radiostics LLC

#### PURPOSE

The opportunistic use of computed tomography (CT) in screening for osteoporosis has been previously reported; however, its broad applicability has yet to be demonstrated. Hounsfield units (HUs) are known to correlate well with dual-energy X-ray absorptiometry (DXA) based bone assessments and offer a clinically applicable method of estimating bone quality. While prior studies have generally reported rigorous protocols using prespecified CT scanner settings for HU measurements, the present study sought to report on the correlation between DXA and HUs recorded using several CT scanners with varying sequences, simulating measurements performed in "real-world" hospital and Emergency Department (ED) settings.

#### METHODS AND MATERIALS

Forty consecutive patients who underwent DXA and two abdominal CT scans, each on a Phillips and General Electric (GE) scanner within six months between the years of 2017 and 2021 at a level 1 tertiary care academic medical center were included in this study. Six raters performed HU measurements of trabecular bone at the L1 vertebral body for each patient on the two separate scanners. Inter-rater reliability of the HU measurements and their correlations with recorded DXA-based bone assessments were determined on each scanner brand. Correlation coefficients were calculated for the HU measurements between scanner brands as well as for the CT HUs with each DXA measurement (femoral neck, total femur, L1 vertebra and total spine). Results were reported using the intraclass coefficient (ICC) statistic for reliability and Pearson's R for correlations.

#### RESULTS

The ICC for L1 HUs read on the Phillips and GE scanners were 0.85 and 0.82, respectively, indicating excellent agreement. The correlation coefficient for the mean HUs on the Phillips and GE scanners was 0.92, also indicating excellent correlation. For both scanner brands, the HU values most closely correlated with the total femur (Phillips:  $Rho = 0.52$ ,  $p < 0.001$ ; GE:  $Rho = 0.45$ ,  $p = 0.003$ ) and femoral neck (Phillips:  $Rho = 0.46$ ,  $p = 0.003$ ; GE:  $Rho = 0.38$ ,  $p = 0.02$ ) T-scores, respectively. L1 and total spine T-scores correlated less with L1 HU values.

#### CONCLUSION

s HU values recorded on a Phillips and GE scanner both demonstrated excellent inter-rater reliability. Correlations were strongest between L1 HU values and total femur DXA T-scores.

#### CLINICAL RELEVANCE/APPLICATION

Abdominal CT imaging across multiple hospital settings demonstrates reliable identification of patients with osteoporosis and represents an opportunity for minimizing radiation exposure and cost.

Printed on: 02/07/23

## Abstract Archives of the RSNA, 2022

R2-SPMK-4

### Electron Density As A Quantitative CT Metric To Evaluate Lumbar Intervertebral Disc Degeneration

Thursday, Dec. 1 9:00AM - 9:30AM Room: Learning Center - MK DPS

#### Participants

Tsubasa Nakano, Kagoshima, Japan (*Presenter*) Nothing to Disclose

#### PURPOSE

To preliminarily evaluate the usefulness of electron density (ED) as a quantitative CT metric to detect lumbar intervertebral disc degeneration.

#### METHODS AND MATERIALS

This study included 338 discs in 100 patients who underwent CT examination and MRI within one month. CT was performed using a spectral detector CT scanner, and images of conventional poly-energetic CT value (CTconv) and ED were obtained. Severity of degeneration for each disc was determined using modified Pfirrmann grade (mPG) based on T2-weighted MRI. In each disc, three ROIs were drawn in the anterior and posterior annulus fibrosis (AAF and PAF) as well as in the nucleus pulposus (NP). Mean CTconv and ED for each ROI were correlated with mPG using Spearman's rank correlation coefficient. The CTconv and ED values in the 3 ROIs as well as their differences between AAF and NP (?AAF-NP) and between PAF and NP (?PAF-NP) were compared between normal (mPG1 and 2) and degenerated discs (mPG3-7) using the Mann-Whitney U test. ROC curve analysis was used to assess the diagnostic abilities of CTconv and ED values. The sensitivity, specificity, and accuracy for differentiating mPG3-7 from mPG1 and 2 were calculated using a threshold criterion determined by the largest Youden's index.

#### RESULTS

The mean CTconv was significantly positively correlated with mPG in NP (?=0.239,  $P<0.001$ ), while it was significantly negatively correlated with mPG in AAF and PAF (?=-0.332, -0.287,  $P<0.001$ ). The mean ED was more closely correlated with mPG than CTconv both in NP (?=0.446,  $P<0.001$ ) and in AAF and PAF (?=-0.357, -0.291,  $P<0.001$  for each). The CTconv and ED of NP in degenerated discs were significantly higher than those of normal discs ( $P<0.001$ ). In addition, the CTconv and ED of AF as well as ?AAF-NP and ?PAF-NP were significantly lower than those of normal discs ( $P<0.001$  for each). The AUC values for CTconv and ED of AAF, PAF, and NP ranged from 0.617 to 0.758, those for ?AAF-NP and ?PAF-NP of CTconv and ED ranged from 0.765 to 0.915. The AUC value for ?AAF-NP of ED performed best (AUC = 0.915) among all indices.

#### CONCLUSION

s ED may be a useful quantitative CT metric to evaluate lumbar intervertebral disc degeneration.

#### CLINICAL RELEVANCE/APPLICATION

Our results demonstrated the potential of ED as a quantitative metric to evaluate lumbar intervertebral disc degeneration.

Printed on: 02/07/23

## Abstract Archives of the RSNA, 2022

R2-SPMS

### Multisystem Thursday Poster Discussion

Thursday, Dec. 1 9:00AM - 9:30AM Room: Learning Center - MS DPS

#### Sub-Events

#### R2-SPMS-1 Sarcoidosis Like Reaction Mimics Progression in Patients Treated With Immune Checkpoint Inhibitors

##### Participants

Samy Ammari, MD, PhD, Villejuif, France (*Presenter*) Nothing to Disclose

##### PURPOSE

The use of immune checkpoint inhibitors (ICI), has revealed a new panel of unconventional immune-related phenomena in terms of tumor response or progression, and adverse events. Immune-related sarcoidosis-like reactions is frequently misdiagnosed as progressive or recurrent disease. This study aims to decipher the diagnosis hallmark of immune-related sarcoidosis-like reactions as well as its association with patients' outcome.

##### METHODS AND MATERIALS

we retrospectively included all patients with histologically proven immune-related sarcoidosis-like reaction from a single institution registry centralizing all immune-related adverse events in metastatic cancer patients treated with ICI in monotherapy or combination (anti-PD-1, anti-PD-L1, anti-PD-1 + anti-CTLA-4, anti-PD-L1 + anti-CTLA-4). Fifty-four variables were retrospectively recorded: clinical (n=17), biological (n=11) and radiological (CT and PET-CT scans) (n=26), as well as the percentage of objective response to treatment using the best overall response according to iRECIST.

##### RESULTS

Out of 3,200 patients treated with ICI, a total of 18 histologically proven sarcoidosis were diagnosed. In these 18 patients, the majority were female patients (n=11/18) treated for melanoma (n=14/18) or clear renal cell carcinoma (n=3/18). The median [range] time to diagnosis of a sarcoidosis-like reaction was 30 [5-126] weeks after ICI treatment initiation. On CT-scans, the most common radiological findings were: absence of radiographical progression of the primary tumor per RECIST1.1 (100%), bilateral symmetrical mediastinal lymphadenopathy (100%), symmetrical hilar lymphadenopathy (84%), and micronodules with lymphatic distribution (15%). On PET-CT, an extramediastinal and/or extrathoracic glucose uptake was observed in 65% of patients. The sites involved were pleural involvement, abdominal lymph nodes, liver, and spleen. Patients with immune-related sarcoidosis-like reactions were objective responders according to iRECIST in 84% (n=15/18) of patients, while only 15% had stable disease.

##### CONCLUSION

s In our series, immune-related sarcoidosis is characterized by the appearance of new mediastinal and/or pulmonary lesions, usually at 30 weeks after initiation of treatment, with stability of baseline target lesions. PET/CT demonstrated extramediastinal and/or extrathoracic uptake in 65% of patients. This should not be misinterpreted as disease progressive since 84% of patients will show an objective response to ICI.

##### CLINICAL RELEVANCE/APPLICATION

This study is a message for oncologists and radiologists who need to be aware of the different clinical and radiological aspects of sarcoidosis in order not to be misdiagnosed with tumor progression.

Printed on: 02/07/23

## Abstract Archives of the RSNA, 2022

R2-SPMS-1

### Sarcoidosis Like Reaction Mimics Progression in Patients Treated With Immune Checkpoint Inhibitors

Thursday, Dec. 1 9:00AM - 9:30AM Room: Learning Center - MS DPS

#### Participants

Samy Ammari, MD, PhD, Villejuif, France (*Presenter*) Nothing to Disclose

#### PURPOSE

The use of immune checkpoint inhibitors (ICI), has revealed a new panel of unconventional immune-related phenomena in terms of tumor response or progression, and adverse events. Immune-related sarcoidosis-like reactions is frequently misdiagnosed as progressive or recurrent disease. This study aims to decipher the diagnosis hallmark of immune-related sarcoidosis-like reactions as well as its association with patients' outcome.

#### METHODS AND MATERIALS

we retrospectively included all patients with histologically proven immune-related sarcoidosis-like reaction from a single institution registry centralizing all immune-related adverse events in metastatic cancer patients treated with ICI in monotherapy or combination (anti-PD-1, anti-PD-L1, anti-PD-1 + anti-CTLA-4, anti-PD-L1 + anti-CTLA-4). Fifty-four variables were retrospectively recorded: clinical (n=17), biological (n=11) and radiological (CT and PET-CT scans) (n=26), as well as the percentage of objective response to treatment using the best overall response according to iRECIST.

#### RESULTS

Out of 3,200 patients treated with ICI, a total of 18 histologically proven sarcoidosis were diagnosed. In these 18 patients, the majority were female patients (n=11/18) treated for melanoma (n=14/18) or clear renal cell carcinoma (n=3/18). The median [range] time to diagnosis of a sarcoidosis-like reaction was 30 [5-126] weeks after ICI treatment initiation. On CT-scans, the most common radiological findings were: absence of radiographical progression of the primary tumor per RECIST1.1 (100%), bilateral symmetrical mediastinal lymphadenopathy (100%), symmetrical hilar lymphadenopathy (84%), and micronodules with lymphatic distribution (15%). On PET-CT, an extramediastinal and/or extrathoracic glucose uptake was observed in 65% of patients. The sites involved were pleural involvement, abdominal lymph nodes, liver, and spleen. Patients with immune-related sarcoidosis-like reactions were objective responders according to iRECIST in 84% (n=15/18) of patients, while only 15% had stable disease.

#### CONCLUSION

s In our series, immune-related sarcoidosis is characterized by the appearance of new mediastinal and/or pulmonary lesions, usually at 30 weeks after initiation of treatment, with stability of baseline target lesions. PET/CT demonstrated extramediastinal and/or extrathoracic uptake in 65% of patients. This should not be misinterpreted as disease progressive since 84% of patients will show an objective response to ICI.

#### CLINICAL RELEVANCE/APPLICATION

This study is a message for oncologists and radiologists who need to be aware of the different clinical and radiological aspects of sarcoidosis in order not to be misdiagnosed with tumor progression.

Printed on: 02/07/23

## Abstract Archives of the RSNA, 2022

R2-SPNMMI

### Nuclear Medicine/Molecular Imaging Thursday Poster Discussion

Thursday, Dec. 1 9:00AM - 9:30AM Room: Learning Center - NMMI DPS

#### Participants

Ashwin Parihar, MBBS, MD, Saint Louis, MO (*Moderator*) Nothing to Disclose

#### Sub-Events

### R2-SPNMMI- Metabolic Tumor Volume and Sites of Organ Involvement Predict Outcome in NSCLC Patients Receiving Immune-Checkpoint Inhibitor Therapy-a Prospective - Single-Center Study<sup>1</sup>

#### Participants

Daria Kifjak, MD, Worcester, MA (*Presenter*) Nothing to Disclose

#### PURPOSE

To evaluate the ability of pre-treatment PET parameters and peripheral blood biomarkers for predicting progression free survival (PFS) and overall survival (OS) in NSCLC patients treated with immune-checkpoint inhibitor therapy (ICIT).

#### METHODS AND MATERIALS

This prospective, single-centre study included 87 patients who underwent a [18F]-FDG PET/CT before ICIT initiation. Organ specific and total metabolic tumor burden were measured using a semiautomatic software. The association between clinical, laboratory and imaging parameters with PFS and OS was assessed using the Log-rank test and cox-regression analysis.

#### RESULTS

Patients were followed-up for a median of 11 months (range 1-63 months). Metabolic tumor volume (MTV) increased with the sites of organ involvement (SOI) and was correlated with peripheral blood biomarkers including the neutrophil and lymphocyte cell count (Spearman's rho=.0272 or .32; p=.02 or .003; respectively). After adjusting for risk factors (e.g., PD-L1 expression and neutrophil cell count) the MTV and the SOI were independent risk factors for progression (per 100cm<sup>3</sup>; adjusted hazard ratio [aHR]: 1.13; 95% confidence interval [95%CI]: 1.0128; p=.04; single SOI vs. = 4 SOI: [aHR]: 2.26, [95%CI]: 1.0494; p=.04). MTV and the SOI were independent risk factors for OS (per 100cm<sup>3</sup> [aHR]: 1.11, [95%CI]: 1.0123; p=.03; single SOI vs. = 4 SOI: [aHR]: 4.54, [95%CI]: 1.64.58; p=.04). The combination of MTV and SOI improved the risk stratification for PFS and OS (lognk test p<.001).

#### CONCLUSION

Our study supports the prognostic value of [18F]FDG-PET/CT in NSCLC patients receiving ICIT. It further demonstrates the complementary value of MTV and metric of organ metastasis for risk assessment of disease progression and mortality.

#### CLINICAL RELEVANCE/APPLICATION

Incorporation of simple radiological parameters like MTV and SOI could greatly aid the risk assessment of NSCLC patients scheduled for ICIT treatment.

### R2-SPNMMI- 18F-FDG PET/CT Features of SMARCA4-deficient Non-small Cell Lung Cancer (SMARCA4-dNSCLC): Comparative Analysis of SMARCA4-dNSCLC and Non-SMARCA4-dNSCLC in Resection Specimens<sup>2</sup>

#### Participants

Zhao Long, MD, (*Presenter*) Nothing to Disclose

#### PURPOSE

The SMARCA4-deficient non-small cell lung cancer (SMARCA4-dNSCLCs) does not overlap with SMARCA4-thoracic sarcoma. There is limited knowledge on the Clinicopathological and 18F-FDG PET/CT features of these SMARCA4-dNSCLCs. This study aimed to retrospectively compare features of SMARCA4-dNSCLC and non-SMARCA4-dNSCLC.

#### METHODS AND MATERIALS

SMARCA4-dNSCLCs were retrospectively identified in 53 patients from June 2020 to January 2022. Additionally, as a comparative cohort, we consecutively enrolled patients who underwent surgical resection with newly diagnosed of non-SMARCA4-dNSCLC in July 2021. All diagnoses were histopathologic confirmed by surgical samples. The SUVmax of 18F-FDG uptake were calculated for the primary lesion.

#### RESULTS

A total of 53 SMARCA4-dNSCLC patients and 137 non-SMARCA4-dNSCLC patients were compared. The SMARCA4-dNSCLC occurred more frequently in males (92.5%, P < 0.001) and in smoker (86.8%, P < 0.001). The comparison of smoking history did not remain statistically significant by stratified analysis according to gender. Maximum diameter had no statistically significant difference among subgroups (P=0.910). The SMARCA4-dNSCLC was more frequently observed with higher SUVmax values (P = 0.001). For

predicting SMARCA4-dNSCLC, the receiver operating characteristic curve analysis showed that the area under the curve (AUC) values of the SUVmax and two factors (SUVmax and Male) was 0.663 (95%CI, 0.578-0.748; P = 0.001) and 0.727 (95%CI, 0.653-0.801; P < 0.001).

## CONCLUSION

s The SMARCA4-dNSCLC tumors tend to be higher 18F-FDG uptake compared with non-SMARCA4-dNSCLC tumors.

## CLINICAL RELEVANCE/APPLICATION

For the first time, we demonstrated that the metabolic characteristic was different between SMARCA4-dNSCLC and non-SMARCA4-dNSCLC. The implications for clinical practice and future research are valuable.

## R2-SPNMMI- Low-Power MRgFUS Tumor Ablation upon Controlled Accumulation of Magnetic Nanoparticles by Cascade-Activated DNA Cross Linkers

Participants

Yi Zhu, Shanghai, China (*Presenter*) Nothing to Disclose

## PURPOSE

Conventional MRgFUS requires high energy when used for tumor treatment and may cause damage to healthy tissue. We developed a new DNA strand surface-modified SPIO nanoparticle to act as a sensitizer to enhance MRgFUS ablation.

## METHODS AND MATERIALS

It has been reported that the magnetic Fe<sub>3</sub>O<sub>4</sub> nanoparticles can act as a dual-sensitizer to strengthen both MRI and ultrasound ablation. Herein, in order to reinforce such a dual-enhancing effect of Fe<sub>3</sub>O<sub>4</sub> nanoparticle, a surface modification strategy is developed to prolong its blood circulation and tumor-environment-triggered accumulation and retention at the tumor site. Especially, DNA was selected as the pH-responsive motif because of its superior biocompatibility as well as the fast and sensitive responsive capability.

## RESULTS

A DNA linker that can sensitively respond to the weak acidity of 6.5-6.8, corresponding to the extracellular pH of tumor tissues, is screened by DNA sequence optimization. Finally, the double-insured activation process significantly enhanced the delivery and retention amount of the magnetic nanoparticles at the tumor site; as a consequence, the MRI sensitivity was enhanced by 2.4 folds, and a comparable thermal ablation effect could be reached by lowering the ultrasound power by half.

## CONCLUSION

s In summary, a modified Fe<sub>3</sub>O<sub>4</sub> nanoparticle, FSIC5P, is designed and synthesized in order to reinforce the dual-enhancing effect of Fe<sub>3</sub>O<sub>4</sub> nanoparticles for MRgFUS treatment application. The dual modifications with the ROS-responsive TK-PEG and pH-responsive DNA cross-linker were demonstrated to lead the Fe<sub>3</sub>O<sub>4</sub> nanoparticles with improved MRI sensitivity by 1.7 folds and significantly enhanced the thermal ablation efficacy.

## CLINICAL RELEVANCE/APPLICATION

Overall, this investigation demonstrates a feasible resolution to promote the MRgFUS treatment by enhancing the therapeutic efficacy and reducing the side effects, which will be helpful to guide the clinical practice in the future.

Printed on: 02/07/23

## Abstract Archives of the RSNA, 2022

R2-SPNMMI-1

### Metabolic Tumor Volume and Sites of Organ Involvement Predict Outcome in NSCLC Patients Receiving Immune-Checkpoint Inhibitor Therapy-a Prospective - Single-Center Study

Thursday, Dec. 1 9:00AM - 9:30AM Room: Learning Center - NMMI DPS

#### Participants

Daria Kifjak, MD, Worcester, MA (*Presenter*) Nothing to Disclose

#### PURPOSE

To evaluate the ability of pre-treatment PET parameters and peripheral blood biomarkers for predicting progression free survival (PFS) and overall survival (OS) in NSCLC patients treated with immune-checkpoint inhibitor therapy (ICIT).

#### METHODS AND MATERIALS

This prospective, single-centre study included 87 patients who underwent a [18F]-FDG PET/CT before ICIT initiation. Organ specific and total metabolic tumor burden were measured using a semiautomatic software. The association between clinical, laboratory and imaging parameters with PFS and OS was assessed using the Log-rank test and cox-regression analysis.

#### RESULTS

Patients were followed-up for a median of 11 months (range 1-63 months). Metabolic tumor volume (MTV) increased with the sites of organ involvement (SOI) and was correlated with peripheral blood biomarkers including the neutrophil and lymphocyte cell count (Spearman's rho=.0272 or .32; p=.02 or .003; respectively). After adjusting for risk factors (e.g., PD-L1 expression and neutrophil cell count) the MTV and the SOI were independent risk factors for progression (per 100cm<sup>3</sup>; adjusted hazard ratio [aHR]: 1.13; 95% confidence interval [95%CI]: 1.0128; p=.04; single SOI vs. = 4 SOI: [aHR]: 2.26, [95%CI]: 1.0494; p=.04). MTV and the SOI were independent risk factors for OS (per 100cm<sup>3</sup> [aHR]: 1.11, [95%CI]: 1.0123; p=.03; single SOI vs. = 4 SOI: [aHR]: 4.54, [95%CI]: 1.64.58; p=.04). The combination of MTV and SOI improved the risk stratification for PFS and OS (lognk test p<.001).

#### CONCLUSION

s Our study supports the prognostic value of [18F]FDG-PET/CT in NSCLC patients receiving ICIT. It further demonstrates the complementary value of MTV and metric of organ metastasis for risk assessment of disease progression and mortality.

#### CLINICAL RELEVANCE/APPLICATION

Incorporation of simple radiological parameters like MTV and SOI could greatly aid the risk assessment of NSCLC patients scheduled for ICIT treatment.

Printed on: 02/07/23

## Abstract Archives of the RSNA, 2022

R2-SPNMMI-2

### **18F-FDG PET/CT Features of SMARCA4-deficient Non-small Cell Lung Cancer (SMARCA4-dNSCLC): Comparative Analysis of SMARCA4-dNSCLC and Non-SMARCA4-dNSCLC in Resection Specimens**

Thursday, Dec. 1 9:00AM - 9:30AM Room: Learning Center - NMMI DPS

#### **Participants**

Zhao Long, MD, (*Presenter*) Nothing to Disclose

#### **PURPOSE**

The SMARCA4-deficient non-small cell lung cancer (SMARCA4-dNSCLCs) does not overlap with SMARCA4-thoracic sarcoma. There is limited knowledge on the Clinicopathological and 18F-FDG PET/CT features of these SMARCA4-dNSCLCs. This study aimed to retrospectively compare features of SMARCA4-dNSCLC and non-SMARCA4-dNSCLC.

#### **METHODS AND MATERIALS**

SMARCA4-dNSCLCs were retrospectively identified in 53 patients from June 2020 to January 2022. Additionally, as a comparative cohort, we consecutively enrolled patients who underwent surgical resection with newly diagnosed of non-SMARCA4-dNSCLC in July 2021. All diagnoses were histopathologic confirmed by surgical samples. The SUVmax of 18F-FDG uptake were calculated for the primary lesion.

#### **RESULTS**

A total of 53 SMARCA4-dNSCLC patients and 137 non-SMARCA4-dNSCLC patients were compared. The SMARCA4-dNSCLC occurred more frequently in males (92.5%,  $P < 0.001$ ) and in smoker (86.8%,  $P < 0.001$ ). The comparison of smoking history did not remain statistically significant by stratified analysis according to gender. Maximum diameter had no statistically significant difference among subgroups ( $P=0.910$ ). The SMARCA4-dNSCLC was more frequently observed with higher SUVmax values ( $P = 0.001$ ). For predicting SMARCA4-dNSCLC, the receiver operating characteristic curve analysis showed that the area under the curve (AUC) values of the SUVmax and two factors (SUVmax and Male) was 0.663 (95%CI, 0.578-0.748;  $P = 0.001$ ) and 0.727 (95%CI, 0.653-0.801;  $P < 0.001$ ).

#### **CONCLUSION**

s The SMARCA4-dNSCLC tumors tend to be higher 18F-FDG uptake compared with non-SMARCA4-dNSCLC tumors.

#### **CLINICAL RELEVANCE/APPLICATION**

For the first time, we demonstrated that the metabolic characteristic was different between SMARCA4-dNSCLC and non-SMARCA4-dNSCLC. The implications for clinical practice and future research are valuable.

Printed on: 02/07/23



## Abstract Archives of the RSNA, 2022

R2-SPNMMI-3

### Low-Power MRgFUS Tumor Ablation upon Controlled Accumulation of Magnetic Nanoparticles by Cascade-Activated DNA Cross Linkers

Thursday, Dec. 1 9:00AM - 9:30AM Room: Learning Center - NMMI DPS

#### Participants

Yi Zhu, Shanghai, China (*Presenter*) Nothing to Disclose

#### PURPOSE

Conventional MRgFUS requires high energy when used for tumor treatment and may cause damage to healthy tissue. We developed a new DNA strand surface-modified SPIO nanoparticle to act as a sensitizer to enhance MRgFUS ablation.

#### METHODS AND MATERIALS

It has been reported that the magnetic Fe<sub>3</sub>O<sub>4</sub> nanoparticles can act as a dual-sensitizer to strengthen both MRI and ultrasound ablation. Herein, in order to reinforce such a dual-enhancing effect of Fe<sub>3</sub>O<sub>4</sub> nanoparticle, a surface modification strategy is developed to prolong its blood circulation and tumor-environment-triggered accumulation and retention at the tumor site. Especially, DNA was selected as the pH-responsive motif because of its superior biocompatibility as well as the fast and sensitive responsive capability.

#### RESULTS

A DNA linker that can sensitively respond to the weak acidity of 6.5-6.8, corresponding to the extracellular pH of tumor tissues, is screened by DNA sequence optimization. Finally, the double-insured activation process significantly enhanced the delivery and retention amount of the magnetic nanoparticles at the tumor site; as a consequence, the MRI sensitivity was enhanced by 2.4 folds, and a comparable thermal ablation effect could be reached by lowering the ultrasound power by half.

#### CONCLUSION

In summary, a modified Fe<sub>3</sub>O<sub>4</sub> nanoparticle, FSIC5P, is designed and synthesized in order to reinforce the dual-enhancing effect of Fe<sub>3</sub>O<sub>4</sub> nanoparticles for MRgFUS treatment application. The dual modifications with the ROS-responsive TK-PEG and pH-responsive DNA cross-linker were demonstrated to lead the Fe<sub>3</sub>O<sub>4</sub> nanoparticles with improved MRI sensitivity by 1.7 folds and significantly enhanced the thermal ablation efficacy.

#### CLINICAL RELEVANCE/APPLICATION

Overall, this investigation demonstrates a feasible resolution to promote the MRgFUS treatment by enhancing the therapeutic efficacy and reducing the side effects, which will be helpful to guide the clinical practice in the future.

Printed on: 02/07/23



## Abstract Archives of the RSNA, 2022

R2-SPNPM

### Noninterpretive Skills/Quality Improvement/Practice Management Thursday Poster Discussions

Thursday, Dec. 1 9:00AM - 9:30AM Room: Learning Center - NPM DPS

#### Sub-Events

#### R2-SPNPM-1A Critical Appraisal of The Quality of Vertigo Practice Guidelines Using the AGREE II Tool: A EuroAIM Initiative

##### Participants

Moreno Zanardo, PhD, San Donato Milanese, Italy (*Presenter*) Nothing to Disclose

##### PURPOSE

Among the diagnostic tests aimed at the deepening of vertigo, an important role is played by neuroimaging. The aim of this review is to assess the methodological quality of guidelines for the management of vertigo and dizziness and to compare their recommendations, with specific focus on neuroimaging.

##### METHODS AND MATERIALS

No ethics committee approval was required for this systematic review. In May 2021, a systematic search was performed to find practice guidelines of management of vertigo and dizziness. Databases Reviewed: MEDLINE, EMBASE, National Guideline Clearinghouse, and National Institute for Health and Clinical Excellence database. The evaluation of guidelines quality was performed independently by four authors using the AGREE II tool. We excluded from the results those guidelines that were not primarily focused on vertigo and dizziness, such as national/international guidelines in which vertigo and dizziness were only briefly mentioned.

##### RESULTS

Our strategy of literature search identified 161 studies, and 15 guidelines published between 2012 and 2020 were selected for the appraisal. Only four guidelines reached the acceptance level in the overall result (at least 60%), with two of them reaching the highest scores (at least 80%). The highest scores were found in Domain 6 "Editorial Independence" (median value=65%) and Domain 4 "Clarity of presentation" (median value=61%). The remaining domains showed a low level of quality: Domain 2 "Stakeholder Involvement", Domain 3 "Rigor of development" and Domain 5 "Applicability" had median values of 21%, 26% and 22% respectively. Eight works out of 15 (53%) had authors coming from different subspecialties that composing the multidisciplinary group, while the other half had authors from a single specialty. The overall assessment of the guidelines correlates both with the number of authors ( $P = 0.003$ , Spearman's rho) and with the number of subspecialties involved in the author's group ( $P = 0.03$ , Spearman's rho). The quality of these guidelines was very low, because of low involvement of multidisciplinary teams in writing guidelines recommendations.

##### CONCLUSION

From our analysis, the quality of the guidelines for the management of vertigo in clinical practice resulted low. This result is attributable to the partial adoption of high-quality standards as suggested by the international indications of AGREE-II for guideline drafting, the lack of randomized controlled trials on the topic of vertigo and dizziness management, and the characteristics of the panels defining guidelines, which were small and heterogeneous.

##### CLINICAL RELEVANCE/APPLICATION

Future guidelines might take this into account to improve clinical applicability.

#### R2-SPNPM-2 Frozen or Not? AI Algorithm for Identifying Motion Artifacts on Chest CT

##### Participants

Giridhar Dasegowda, MBBS, Boston, MA (*Presenter*) Nothing to Disclose

##### PURPOSE

Motion artifacts recognized at the time of reporting can result in suboptimal diagnostic interpretation (with missed or misclassified lesions) and patient recall. We developed and tested a deep learning (DL) model for identifying substantial motion artifacts on chest CT images that has a negative impact on diagnostic interpretation.

##### METHODS AND MATERIALS

With IRB approval and HIPAA compliance, we queried our multicenter radiology report database (mPower, Nuance) for chest CT reports between July 2015 - March 2022 for the following terms "motion artifacts," "respiratory motion," "technically inadequate," and "suboptimal" or "limited exam." All CT reports belonged to one of the quaternary (Site A, n= 335; B, n= 199) or community (C, n= 259) hospitals. A thoracic radiologist reviewed CT images of all positive hits for motion artifacts (present or absent) and their severity (no diagnostic effect or major diagnostic impairment). Coronal multiplanar images (2-2.5 mm) belonging to 793 chest CT exams were deidentified and exported offline into a DL model building prototype (Cognex Vision Pro, Cognex Inc.) to create (70% training dataset, n= 554) and test (30% test dataset, n= 239) a DL model to perform two-class classification ("motion" or "no

motion"). Separately, CT from two sites were used for training and testing and later validated on the images from the third hospital. A 5-fold repeated cross-validation was performed to evaluate the model performance with accuracy and receiver operating characteristics analysis (ROC).

## **RESULTS**

Among the chest CT images from 793 patients (mean age  $63 \pm 17$  years; 391 males, 402 females), 372 had no motion artifacts and 421 had substantial motion artifacts. The statistics for the average performance of the DL model after 5-fold repeated cross-validation for the two-class classification included 94% sensitivity, 91% specificity, 93% accuracy and 0.93 area under the ROC curve (AUC: 95% CI 0.89-0.97). Among the training datasets from sites A and B, the DL had 96% sensitivity, 91% specificity, 93% accuracy, 0.94 AUC (95% CI 0.88-0.99). On the external validation dataset from site C, DL had 85% sensitivity, 90% specificity, 87% accuracy with 0.88 AUC (95% CI 0.83-0.92).

## **CONCLUSION**

s Our DL model can successfully identify chest CT exams with diagnostic interpretation limiting motion artifacts in multicenter training and test datasets.

## **CLINICAL RELEVANCE/APPLICATION**

Our DL model deployed on the scanner graphic user interface (GUI) can help alert the technologists about substantial motion artifacts where a repeat image acquisition can help salvage diagnostic information.

Printed on: 02/07/23

## Abstract Archives of the RSNA, 2022

R2-SPNPM-1

### A Critical Appraisal of The Quality of Vertigo Practice Guidelines Using the AGREE II Tool: A EuroAIM Initiative

Thursday, Dec. 1 9:00AM - 9:30AM Room: Learning Center - NPM DPS

#### Participants

Moreno Zanardo, PhD, San Donato Milanese, Italy (*Presenter*) Nothing to Disclose

#### PURPOSE

Among the diagnostic tests aimed at the deepening of vertigo, an important role is played by neuroimaging. The aim of this review is to assess the methodological quality of guidelines for the management of vertigo and dizziness and to compare their recommendations, with specific focus on neuroimaging.

#### METHODS AND MATERIALS

No ethics committee approval was required for this systematic review. In May 2021, a systematic search was performed to find practice guidelines of management of vertigo and dizziness. Databases Reviewed: MEDLINE, EMBASE, National Guideline Clearinghouse, and National Institute for Health and Clinical Excellence database. The evaluation of guidelines quality was performed independently by four authors using the AGREE II tool. We excluded from the results those guidelines that were not primarily focused on vertigo and dizziness, such as national/international guidelines in which vertigo and dizziness were only briefly mentioned.

#### RESULTS

Our strategy of literature search identified 161 studies, and 15 guidelines published between 2012 and 2020 were selected for the appraisal. Only four guidelines reached the acceptance level in the overall result (at least 60%), with two of them reaching the highest scores (at least 80%). The highest scores were found in Domain 6 "Editorial Independence" (median value=65%) and Domain 4 "Clarity of presentation" (median value=61%). The remaining domains showed a low level of quality: Domain 2 "Stakeholder Involvement", Domain 3 "Rigor of development" and Domain 5 "Applicability" had median values of 21%, 26% and 22% respectively. Eight works out of 15 (53%) had authors coming from different subspecialties that composing the multidisciplinary group, while the other half had authors from a single specialty. The overall assessment of the guidelines correlates both with the number of authors ( $P = 0.003$ , Spearman's rho) and with the number of subspecialties involved in the author's group ( $P = 0.03$ , Spearman's rho). The quality of these guidelines was very low, because of low involvement of multidisciplinary teams in writing guidelines recommendations.

#### CONCLUSION

From our analysis, the quality of the guidelines for the management of vertigo in clinical practice resulted low. This result is attributable to the partial adoption of high-quality standards as suggested by the international indications of AGREE-II for guideline drafting, the lack of randomized controlled trials on the topic of vertigo and dizziness management, and the characteristics of the panels defining guidelines, which were small and heterogeneous.

#### CLINICAL RELEVANCE/APPLICATION

Future guidelines might take this into account to improve clinical applicability.

Printed on: 02/07/23

## Abstract Archives of the RSNA, 2022

R2-SPNPM-2

### Frozen or Not? AI Algorithm for Identifying Motion Artifacts on Chest CT

Thursday, Dec. 1 9:00AM - 9:30AM Room: Learning Center - NPM DPS

#### Participants

Giridhar Dasegowda, MBBS, Boston, MA (*Presenter*) Nothing to Disclose

#### PURPOSE

Motion artifacts recognized at the time of reporting can result in suboptimal diagnostic interpretation (with missed or miscalled lesions) and patient recall. We developed and tested a deep learning (DL) model for identifying substantial motion artifacts on chest CT images that has a negative impact on diagnostic interpretation.

#### METHODS AND MATERIALS

With IRB approval and HIPAA compliance, we queried our multicenter radiology report database (mPower, Nuance) for chest CT reports between July 2015 - March 2022 for the following terms "motion artifacts," "respiratory motion," "technically inadequate," and "suboptimal" or "limited exam." All CT reports belonged to one of the quaternary (Site A, n= 335; B, n= 199) or community (C, n= 259) hospitals. A thoracic radiologist reviewed CT images of all positive hits for motion artifacts (present or absent) and their severity (no diagnostic effect or major diagnostic impairment). Coronal multiplanar images (2-2.5 mm) belonging to 793 chest CT exams were deidentified and exported offline into a DL model building prototype (Cognex Vision Pro, Cognex Inc.) to create (70% training dataset, n= 554) and test (30% test dataset, n= 239) a DL model to perform two-class classification ("motion" or "no motion"). Separately, CT from two sites were used for training and testing and later validated on the images from the third hospital. A 5-fold repeated cross-validation was performed to evaluate the model performance with accuracy and receiver operating characteristics analysis (ROC).

#### RESULTS

Among the chest CT images from 793 patients (mean age  $63 \pm 17$  years; 391 males, 402 females), 372 had no motion artifacts and 421 had substantial motion artifacts. The statistics for the average performance of the DL model after 5-fold repeated cross-validation for the two-class classification included 94% sensitivity, 91% specificity, 93% accuracy and 0.93 area under the ROC curve (AUC: 95% CI 0.89-0.97). Among the training datasets from sites A and B, the DL had 96% sensitivity, 91% specificity, 93% accuracy, 0.94 AUC (95% CI 0.88-0.99). On the external validation dataset from site C, DL had 85% sensitivity, 90% specificity, 87% accuracy with 0.88 AUC (95% CI 0.83-0.92).

#### CONCLUSION

Our DL model can successfully identify chest CT exams with diagnostic interpretation limiting motion artifacts in multicenter training and test datasets.

#### CLINICAL RELEVANCE/APPLICATION

Our DL model deployed on the scanner graphic user interface (GUI) can help alert the technologists about substantial motion artifacts where a repeat image acquisition can help salvage diagnostic information.

Printed on: 02/07/23



## Abstract Archives of the RSNA, 2022

R2-SPNR

### Neuroradiology Thursday Poster Discussions

Thursday, Dec. 1 9:00AM - 9:30AM Room: Learning Center - NR DPS

#### Participants

Christine J. Kim, MD, Los Angeles, CA (*Moderator*) Consultant, Bayer AG

#### Sub-Events

### R2-SPNR-1 Imaging Findings That Cause False Positive Predictions of Intracranial Hemorrhage by Artificial Intelligence, a Pictorial Review

#### Participants

Cody Savage, BS, Tuscaloosa, AL (*Presenter*) Nothing to Disclose

#### PURPOSE

To identify which imaging findings most often lead to false-positive predictions of intracranial hemorrhage (ICH) by artificial intelligence (AI).

#### METHODS AND MATERIALS

False-positive cases were collected from a single-center, prospective comparative effectiveness study of ICH detection by the FDA approved AI algorithm Aidoc. By evaluating written reports by the neuroradiologists, the cases marked positive for ICH by AI but read negative for ICH by the neuroradiologists were selected. A second neuroradiologist then reviewed the selected cases to establish ground truth. The second neuroradiologist's diagnosis was used as the gold standard of diagnosis. The false-positive cases by AI were then reviewed to detect the pattern of misclassification. Also, examples of false-positive cases are presented by pictorial review.

#### RESULTS

False positives by AI occurred in 223 ( 2.2%) of the 9978 cases, equating to a specificity of 97.5%. The sensitivity and accuracy were 96.9% and 95.2%, respectively. The most common imaging finding that resulted in a false positive was beam hardening under the skull ( 36.7%). Other imaging findings that resulted in false positives include hyperdensity of brain parenchyma by calcium deposition or mass (16.1 %), post-surgical changes ( 9.4% ), hyperdense dura matter (9%), dense vessels (8%), motion artifact (5%), meningioma (3%), Laminar necrosis (3%), leptomeningeal thickening (carcinomatosis or meningitis) (2.6%), cavernoma ( 2.6%), contrast staining ( 1.7%), and choroid plexus calcification (0.4%).

#### CONCLUSION

The beam-hardening CT artifact, hyperdense parenchymal structures, dural hyperdensity, iatrogenic imaging findings, dense vessels, and motion artifact are the most common cause of false-positive ICH predictions by AI algorithm. While less common, meningioma, laminar necrosis, leptomeningeal infiltration, cavernoma, and contrast staining can also contribute to false-positive predictions.

#### CLINICAL RELEVANCE/APPLICATION

The radiologists who use AI to screen the ICH should be aware of false-positive calls. Despite the sophisticated developing process of medical AI platforms, it seems that AI models for ICH detection work mainly by detecting hyperdensities that can end in false-positive calls.

### R2-SPNR-11 Iterative Labeling and Review with Consensus and Conditional Probability Can Be Utilized to Decrease Variability for Artificial Intelligence Data Curation

#### Participants

Simas Glinskis, Ithaca, NY (*Presenter*) Employee, Covera Health, Inc

#### PURPOSE

Machine learning model performance depends on high quality and consistent data annotation, which can be difficult to obtain in the presence of inherent inter-reader labeling variability amongst radiologists. Guidelines can help reduce ambiguity when grading a pathology's severity; however, guidelines themselves may contain ambiguous definitions. We hypothesized a labeling and review process for guidelines would minimize the inter-reader variability through an iterative process and implemented a method to test this hypothesis on a real life dataset.

#### METHODS AND MATERIALS

Cervical spine MRI studies were annotated independently for severity of cord compression, central canal stenosis, disc herniation, and neural foraminal stenosis by three subspecialty trained board certified radiologists with the same version of guidelines in batches of 25-50-50 randomly sampled studies. After completion of each batch, statistical methods based on conditional probability were used to measure the inter-reader pathology severity variability and agreement as a group and for each pair of annotators.

Pathology severities with high inter-reader variability or low agreement were targeted for guideline revision that was used in the next batch of MRI studies. The "measure-revise" process was repeated.

## RESULTS

Inter-reader variability decreased from 23% to 3% for spinal cord compression when we revised the guidelines and added more granularity, splitting the not-compressed severity into normal, indentend, and flattened cord. Similarly, inter-reader agreement improved from 57% to 75% for severe central canal stenosis, from 74% to 84% for none or small disc herniation, and from 59% to 65% for large disc herniation when we iteratively redefined our guidelines for these pathology severities.

## CONCLUSION

s Label agreement amongst our radiologists increased and generated more consistent training data for our machine learning models using the iterative labeling and review process. This approach is pathology agnostic and can be applied whenever clear severity definitions are required.

## CLINICAL RELEVANCE/APPLICATION

Iterative labeling as performed with this methodology has the potential to reduce the variation for grading of pathologies in medical images and may improve the performance of AI models.

## R2-SPNR-12 Brain Image Auto-Segmentation using 3D Capsule Networks

Participants  
Arman Avesta, MD, New Haven, CT (*Presenter*) Stockholder, Hyperfine Research, Inc;

## PURPOSE

To develop and validate 3D capsule networks (CapsNets) to segment brain images with features not represented in the training data.

## METHODS AND MATERIALS

We used 3430 brain MRIs acquired in a multi-institutional study. We compared our CapsNets with U-Nets, the current standard, based on the accuracy in segmenting various brain structures and those with spatial features not represented in the training data. We also assessed performance when the models are trained using limited data, memory requirements, and computation times.

## RESULTS

3D CapsNets segmented the third ventricle, thalamus, and hippocampus with Dice scores of 94%, 94%, and 91%, respectively. 3D CapsNets outperformed 3D U-Nets in segmenting brain images with features that were not represented in the training data, with Dice scores more than 30% higher (P-values < 0.01). 3D CapsNets had 93% fewer trainable parameters than 3D U-Nets. The 3D CapsNets were 25% faster to train compared with U-Nets. The two models were equally fast during testing.

## CONCLUSION

s 3D CapsNets segment brain structures with high accuracy, outperform U-Nets in segmenting brain images with features that were not represented during training, and are more efficient compared with U-Nets, achieving similar results while their size is an order of magnitude smaller.

## CLINICAL RELEVANCE/APPLICATION

In patients undergoing radiotherapy or neurosurgery, neuroanatomical segmentation is a critical aid that improves outcomes. 3D CapsNets outperformed current auto-segmentation methods in generalizability to brain images with features not represented in the training data.

## R2-SPNR-13 Artificial Intelligence (AI) Model Based on Automated Morphometry and Planimetric Data Obtained in Brain MRI, a Proof of Concepts: Lights Towards the Future for Differentiating Progressive Supranuclear Palsy From Parkinson's Disease

Participants  
Francisco Mendoza, MD, (*Presenter*) Nothing to Disclose

## PURPOSE

To develop an AI model to differentiate Progressive Supranuclear Palsy (PSP) from Parkinson's disease (PD) and healthy subjects (HS) using automated volumetry and non-automated planimetric assessment data obtained in Magnetic Resonance Imaging (MRI).

## METHODS AND MATERIALS

We retrospectively assessed a total of 141 patients with a clinical diagnosis of Parkinsonism paired by age and sex and with a group of HS (PSP n = 47, PD n = 68, HS = 26) between January 2003 and April 2021 and analyzed their brain MRI. Patients without T1 high resolution sequences were excluded, leaving 83 patients (PSP n = 29, PD n = 54). We included different clinical subtypes of PSP: PSP-RS (n = 19), PSP-P (n = 5), PSP-PGF (n = 4), and PSP-F (n = 1). Using automatized SyngoviaBrainMorphometry software (Siemens), we obtained 109 VOIs for each subject, including absolute and normalized values. Two independent radiologists blind to diagnosis performed a planimetric assessment (Massey ratio, Oba ratio, MPRI 1.0, and MRP 2.0). We developed a machine-learning model based on multivariate feature selection and an extreme gradient boosting (XGB) vs. univariate feature selection and random forest (RF) using both automated volumetric data and planimetric assessment to predict PSP, PD, and HS. All subjects were randomly divided into training (85%) and validation (15%) data sets with the same proportions for each clinical group. We assessed the diagnostic accuracy of the model and the most relevant features were ordered by importance score (F-score; where 1.0 represents perfect precision and recall). Additionally, we assessed the diagnostic accuracy of each feature using ROC curves.

## RESULTS

The global diagnostic performance of the model to differentiate between the three groups was 82.3%. The diagnostic accuracy of the model to predict PSP from the other groups was 81.82 and for PD was 82.35. The most relevant features of the AI model were the mesencephalic area (0.22), mesencephalic width (0.13), left frontal gray matter normalized volume (0.088), and the left

thalamus absolute volume (0.059), and Oba Ratio (0.044). The AUC to differentiate PSP from PD and HS was for the mesencephalic area =0.94, for the mesencephalic width = 0.99, the left frontal gray matter normalized volume =0.50, and the left thalamus absolute volume = 0.69.

## CONCLUSION

The developed AI model using data obtained from brain MRI automated volumetry and non-automated planimetric assessment, showed high accurate discrimination between PSP, PD, and HS, especially for PSP in our study population.

## CLINICAL RELEVANCE/APPLICATION

AI model using morphometry and planimetric data can differentiate patients with parkinsonism. It would be necessary to validate this model for its clinical application.

## R2-SPNR-15 Neural Architecture Search Based MRI Sequence Design

Participants

Hongjun An, (*Presenter*) Nothing to Disclose

## PURPOSE

Designing an MR sequence is very challenging, resulting that currently available sequences are constrained by human intuition. We proposed a new sequence design method using neural architecture search (NAS).

## METHODS AND MATERIALS

Our method is designed to produce an optimal sequence for given and target objectives. Hence, these properties are inputted to the Bloch simulator to generate MR signals. Using the signals, a loss function defined by the objective is calculated for optimization. Then the sequence scheduler determines the sequence design using NAS (Fig. 1). NAS was utilized to optimize a series of operations (i.e., sequence) by replacing a neural architecture and its weight parameters with a sequence design and its scan parameters, respectively. To test, two experiments were performed repeatedly to design FLAIR-like sequences and spin-echo-like sequences.

## RESULTS

In Experiment 1 (Fig. 1c1), a FLAIR-like sequence and non-intuitive sequence showing 4 RF pulses in place of inversion were generated while CSF signal suppression and gray/white matter signal recovery. In Experiment 2 (Fig. 1c2), a conventional spin echo (CPMG), Hann-echo-like sequence, and a less intuitive sequence with three or four RF pulse ( $12^\circ$ - $89^\circ$ - $168^\circ$  and  $5^\circ$ - $16^\circ$ - $85^\circ$ - $162^\circ$ ). In in-vivo experiment, the new three-RF sequence produced identical contrasts and similar SNR with the spin-echo images (new sequence SNR:  $297.1 \pm 70.1$  vs. spin-echo SNR:  $295.8 \pm 78.2$ ). The new sequences had reduced RF energy (90% of the spin-echo), while taking a longer duration (18.6 ms vs. 12.4 ms).

## CONCLUSION

A novel automatic sequence design method requiring no prior knowledge or training data was proposed, which successfully reproduced the conventional sequence and invented less-intuitive sequences. This study suggests a potential for automated sequence design that may explore possibilities beyond human intuition.

## CLINICAL RELEVANCE/APPLICATION

Using our method, a new sequence can be automatically developed in the clinical considerations with non-intuitive behavior.

## R2-SPNR-16 Age-Adjusted Atlas of Diffusion Metrics in Normal Neonatal Brains

Participants

Pratheek Bobba, BS, New Haven, CT (*Presenter*) Nothing to Disclose

## PURPOSE

Diffusion weighted imaging (DWI) and diffusion tensor imaging (DTI) are increasingly used in the diagnosis and prognostication of neonatal brain injury. However, rapid changes of apparent diffusion coefficient (ADC) values from DWI and fractional anisotropy (FA) and mean diffusivity (MD) values from DTI complicate the interpretation of DWI and DTI scans in neonates. Thus, robust characterization of these metrics in neonatal brains is required.

## METHODS AND MATERIALS

The medical and imaging records of all neonates (0-3 months) born since 2013 at our institution were analyzed. Subjects with normal MRI scans on both clinical report and visual inspection were included. DWI (and associated ADC maps) and DTI scans (and associated FA/MD maps) were then coregistered to a pediatric standard brain space. Voxel-wise general linear models (GLM) were applied to analyze the age-related changes of ADC values throughout the brain. Tract-based spatial statistics of DTI metrics was also applied along white matter tracts in the brain. Linear regression models were used to calculate the rate of change in ADC, FA, and MD values across 5mm cubic voxels. Age adjusted normative atlases of these metrics were generated by calculating the mean and standard deviation in each voxel.

## RESULTS

565 neonates with DWI scans, of whom 162 also had DTI scans were included. The mean  $\pm$ SD gestational age (GA) at scan for the DWI cohort was  $39.67 \pm 2.79$  weeks and for the DTI cohort was  $38.53 \pm 1.94$  weeks. Increasing GA at scan was associated with significant reduction of ADC values throughout the brain and significant increase of FA and reduction of MD values throughout white matter tracts. The highest temporal rate of decline in ADC values was seen in the subcortical and cerebellar white matter and vermis. The highest temporal rate of increase in FA and rate of decrease in MD values was seen throughout the cortical white matter (Figure 1). After correcting for GA at scan, greater GA at birth was associated with significant reduction of ADC values in the corpus callosum and convexity cortex and significantly higher FA and lower MD values in the corpus callosum. Online interactive atlases displaying age-specific normative values of ADC (34.5-46.5 weeks), and DTI metrics (35-41 weeks) were developed.

## CONCLUSION

There is significant age-related reduction of ADC values throughout the neonatal brain with steepest decline in the

There is significant age-related reduction of ADC values throughout the neonatal brain, with steepest decline in the periventricular white matter. Similar trends in FA and MD values indicate that changes in ADC values are likely related to myelination of white matter in neonatal brains.

#### **CLINICAL RELEVANCE/APPLICATION**

Our age-adjusted normative atlases can aid neuroradiologists in identification and diagnosis of subtle developmental anomalies and ischemic brain injury in neonates.

#### **R2-SPNR-17 Clinical Feasibility of Reverse Encoding Distortion Correction for Brain DWI: Comparison With Conventional DWI**

Participants

Atsushi Nakamoto, MD, PhD, Suita, Japan (*Presenter*) Nothing to Disclose

#### **PURPOSE**

Single-shot echo-planar imaging is a widely used conventional diffusion-weighted imaging (C-DWI) technique, owing to its high speed, but is susceptible to magnetic field inhomogeneities which causes high image distortion. This study was conducted to evaluate whether reverse encoding distortion correction DWI (RDC-DWI), which acquires a pair of two opposite phase encoding polarities, can reduce image distortion for DWI of the brain.

#### **METHODS AND MATERIALS**

This study included 50 patients who underwent both RDC-DWI and C-DWI of the brain. Both DW images were obtained by two excitations with acquisition times of 121 and 107 seconds, respectively. Using a five-point scale, two neuroradiologists qualitatively evaluated the image distortion of the pons, cerebellum, temporal skull bases and frontal skull base, and the overall image quality. For quantitative analysis, distortion ratios (DR), the apparent diffusion coefficients (ADC) values, and signal-to-noise ratios (SNR) of the pons and frontal lobe were measured. For the pathologies, we qualitatively evaluated image distortion and measured the ADC values.

#### **RESULTS**

The scores for image distortions of all evaluated sites were significantly lower for RDC-DWI than for C-DWI ( $p < 0.01$ ), and those for overall image quality were significantly higher for RDC-DWI than for C-DWI ( $p < 0.01$ ). The DR of the pons and frontal lobe were significantly lower for RDC-DWI than for C-DWI ( $p < 0.01$ ). SNR of these sites were significantly higher for RDC-DWI than for C-DWI ( $p = 0.03$  and  $p = 0.01$ , respectively). Mean ADC values of these sites did not significantly differ between the two techniques ( $p = 0.62$  and  $p = 0.66$ , respectively). The scores for image distortions of intracranial lesions ( $n = 22$ ) did not differ significantly between the two techniques ( $p = 0.25$ ), whereas those of sinonasal lesions ( $n = 7$ ) was significantly lower for RDC-DWI than for C-DWI ( $p = 0.03$ ). Mean ADC values of both intracranial and sinonasal lesions did not differ between the two techniques ( $p = 0.16$  and  $p = 0.80$ , respectively).

#### **CONCLUSION**

RDC-DWI can significantly reduce image distortion and increase SNR with minimal additional acquisition time, compared with C-DWI.

#### **CLINICAL RELEVANCE/APPLICATION**

RDC-DWI can reduce image distortion in the tissue-air interface and improve delineation of sinonasal pathologies.

#### **R2-SPNR-18 Diffusion Weighted Imaging with and without Reverse Encoding Distortion Correction (RDC): Influence to Image Quality and ADC Evaluation in Patients with Skull-based Brain Tumors**

Participants

Kazuhiro Murayama, MD, Toyooka, Japan (*Presenter*) Research Grant, Canon Medical Systems Corporation

#### **PURPOSE**

To evaluate influences of newly developed reverse encoding distortion correction (RDC) method for reducing image distortion to image quality and ADC evaluation on diffusion-weighted imaging (DWI) in patients with skull-based brain tumors.

#### **METHODS AND MATERIALS**

26 patients with suspected skull-based various brain tumors underwent DWIs with and without RDC at 3T systems. To compare image distortion between DWIs with and without RDC, the deformation ratio (DR) of each tumor was calculated from each tumor area difference between DWI and T2-weighted images. To compare image quality and ADC values between DWIs with and without RDC, the signal to noise ratio (SNR) of normal appearance white matter (NAWM) and ADC values of tumor were determined by ROI measurements in each patient. Moreover, overall image quality, lesion distortion and lesion conspicuity of each tumor were assessed by 5-point visual scoring system by two board-certified radiologists. For quantitative and qualitative image quality comparisons, DR and SNR were compared between DWIs with and without RDC by paired t-test. Kappa statistics with  $\chi^2$  test was performed for each interobserver agreement evaluations. Then, each score was compared between DWIs with and without RDC by Wilcoxon's signed sum test. To determine the influence of RDC to ADC measurement, ADC value was correlated between DWIs with and without RDC by Spearman's correlation. Then, the limits of agreement of ADC between both DWIs were also determined.

#### **RESULTS**

DR of DWI with RDC technique was significantly smaller than that without RDC ( $p < 0.05$ ), although others had no significant differences between DWIs with and without RDC. Interobserver agreement for each image quality score was significantly substantial or excellent ( $0.70 \leq \kappa \leq 0.92$ ,  $p < 0.001$ ). Moreover, each image quality score of DWI with RDC was significantly higher than that without RDC ( $p < 0.05$ ). ADC had a significant and good correction between DWIs with and without RDC ( $r = 0.98$ ,  $p < 0.0001$ ). The limits of agreement between DWIs with and without RDC was  $0.00 \pm 0.13 \times 10^{-3} \text{ s/mm}^2$ .

#### **CONCLUSION**

Newly developed RDC method has no influence to ADC evaluation and makes it possible to improve image quality on DWI in patients with skull-based brain tumors.

## CLINICAL RELEVANCE/APPLICATION

Newly developed RDC method has no influence to ADC evaluation and makes it possible to improve image quality on DWI in patients with skull-based brain tumors.

## R2-SPNR-19 Histogram Analysis Based on Neurite Orientation Dispersion and Density Imaging for Differentiation Between Solitary Brain Metastasis and Glioblastoma Multiforme: A Comparison of Two Different ROI Placements

Participants

Jinbo Qi, MD, (*Presenter*) Nothing to Disclose

### PURPOSE

To explore the value of histogram analysis based on NODDI in differentiating between solitary brain metastasis (SBM) and glioblastoma multiforme (GBM), and to compare the diagnostic performance of two different region of interest (ROI) placements.

### METHODS AND MATERIALS

NODDI data were prospectively obtained from 109 patients with pathologically confirmed GBM (n = 57) and SBM (n = 52) were included. Two ROIs—the peritumoral edema area and whole-tumor area—were delineated across all slices. Eleven histogram parameters of intra-cellular volume fraction (ICVF), isotropic volume fraction (ISOVF) and orientation dispersion index (ODI) from both ROIs were extracted. The parameters of the histogram analysis were compared between SBM and GBM, using independent sample t-test or rank sum test, and then to make meaningful parameters based on logistic regression modeling. Receiver operating characteristic (ROC) analyses were conducted to evaluate the differential diagnosis performance and their performances were compared using DeLong's test.

### RESULTS

In peritumoral edema area, ICVF<sub>minimum</sub>, ICVF<sub>max</sub>, ICVF<sub>kurtosis</sub>, ISOVF<sub>skewness</sub>, ISOVF<sub>kurtosis</sub>, ODI<sub>10</sub>, ODI<sub>25</sub> and ODI<sub>minimum</sub> were significantly higher for GBM than for SBM. ISOVF<sub>10</sub>, ISOVF<sub>25</sub>, ISOVF<sub>50</sub>, ISOVF<sub>75</sub>, ISOVF<sub>mean</sub> and ISOVF<sub>skewness</sub> were significantly lower for GBM than for SBM. The sensitivity of the corresponding logistic regression differential diagnosis model was 80.7%, specificity was 80.7%, and area under the curve (AUC) was 0.851. In whole-tumor area, ICVF<sub>max</sub>, ICVF<sub>skewness</sub>, ICVF<sub>kurtosis</sub>, ISOVF<sub>skewness</sub>, ISOVF<sub>kurtosis</sub> and ODI<sub>kurtosis</sub> were significantly lower for GBM than for SBM. ISOVF<sub>10</sub>, ISOVF<sub>25</sub>, ISOVF<sub>50</sub>, ISOVF<sub>75</sub>, ISOVF<sub>minimum</sub>, ODI<sub>10</sub>, ODI<sub>25</sub>, ODI<sub>50</sub>, ODI<sub>75</sub>, ODI<sub>90</sub>, ODI<sub>mean</sub>, ODI<sub>variance</sub>, and ODI<sub>skewness</sub> were significantly lower for GBM than for SBM. The sensitivity of the corresponding logistic regression differential diagnosis model was 96.1%, specificity was 86%, and the area under curve (AUC) was 0.958. DeLong's test showed significant difference (P=0.014) in differential performance between two different ROI placements.

### CONCLUSION

s GBM and SBM can be differentiated using the NODDI-based histogram analysis and the ROI on whole-tumor area would exhibit better performance.

## CLINICAL RELEVANCE/APPLICATION

The NODDI compartment model theoretically distinguishes three types of water diffusion behavior (i.e., intracellular, extracellular, and CSF), it is more sensitive to microstructural changes, which might demonstrate the difference in water diffusion between tumor infiltration and vasogenic edema. Furthermore, NODDI techniques can identify more different tissue components within tumors than conventional imaging for differentiating the heterogeneity of GBM and SBM.

## R2-SPNR-2 Successful Implementation of a Comprehensive CT Brain Artificial Intelligence Assist Device Improves Radiologist Performance

Participants

Peter R. Brotchie, MBBS, PhD, Fitzroy, Australia (*Presenter*) Consultant, Annalise-AI Pty Ltd

### PURPOSE

To assess the effect on accuracy when radiologists are assisted by a comprehensive CT Brain (CTB) artificial intelligence device.

### METHODS AND MATERIALS

CTB are one of the most common CT investigations in clinical radiology. Despite the extensive training of radiologists, missed diagnosis remains a problem. To assist radiologists in reducing errors, many artificial intelligence devices have been developed. However, most of these tools are capable of only detecting a single finding. With the aim to improve a radiologist's performance across a full range of findings on CTB, a comprehensive AI assist device capable of detecting 144 findings was developed. The deep learning model was trained on 212,484 CTB images and tested on a dataset of 2,848 images. The test set was ground truthed by at least 3 radiologists and adjudicated by a neuroradiologist. The performance of 32 radiologists was measured when reviewing the test dataset with and without AI assistance across several metrics including area under the receiver operating characteristic curve (AUC).

### RESULTS

The radiologists AUC averaged 0.79 when assisted by the AI compared to 0.73 when unassisted. Significant improvement in AUC was observed across 91 findings. 17 findings showed decreases in AUC. Many of the largest gains in performance by the radiologists when using the AI, were for clinically critical findings, including findings signifying mass effect (basal cistern effacement, tonsillar and uncus herniation, midline shift, sulcal and ventricular effacement), intracranial haemorrhage (especially aneurysmal and convexity subarachnoid haemorrhage), trauma (intracranial haemorrhage and fractures), obstructive hydrocephalus, intra-axial lesions, aggressive extra-axial masses, orbital cellulitis and acute infarction.

### CONCLUSION

s The use of a comprehensive CTB assist device significantly improved radiologist performance across a majority of clinical findings on CTB, demonstrating the potential safety improvements of comprehensive AI.

## CLINICAL RELEVANCE/APPLICATION

The comprehensive AI device for CTB, after testing with a large selection of radiologists, showed improved performance by the assisted radiologist, and indicates a potential use case in a radiologists workflow.

## R2-SPNR-20 Reliability of Functional and Diffusion Magnetic Resonance Imaging Near Cerebral Cavernous Malformations

Participants  
Marco Colasurdo, MD, Pescara, Italy (*Presenter*) Nothing to Disclose

### PURPOSE

Surgical resection of cerebral cavernous malformations (CCMs) routinely employs fMRI and DTI for surgical planning to best preserve neurological function. However, hemosiderin-rich lesions such as CCMs may cause artefactual distortion of MRI signals in close proximity. This study investigates the reliability of fMRI and DTI near CCMs.

### METHODS AND MATERIALS

Consecutive patients with CCMs undergoing pre-surgical fMRI and DTI mapping were identified from June 2002 to June 2019 at an academic medical centre. Each CCM lesion was hand-contoured using T2 sequences, and two sequential 4-mm expansion shells (S1 and S2) were created, generating three ROIs; every ROI was then flipped to the contralateral hemisphere to obtain control ROIs. Fractional anisotropy (FA) and Regional Homogeneity (ReHo) measurements were then extracted from each ROI. FA and ReHo values were compared with contralateral controls to calculate percentage error. Reliability, accuracy, and precision within ROIs were compared using Welch's t-tests, F-tests and Wilcoxon matched-pairs signed rank tests; p-values were adjusted for multiple comparisons as appropriate.

### RESULTS

61 patients were identified and included. Overall, errors of FA were significantly lower than ReHo in S1 and S2 ( $p=0.0001$  for both), suggesting that FA is more reliable than ReHo near CCMs. Proximity to CCM lesions significantly worsened the reliability of ReHo (S1 vs. S2,  $p=0.0007$ ), but not FA ( $p=0.24$ ). Further investigations of sources of error revealed that while FA was not significantly biased in any ROI ( $p>0.05$  for all), ReHo was biased towards lower signals in CCMs, S1 and S2 ( $p<0.05$ ), an effect that was attenuated with distance from CCMs ( $p<0.05$ ). FA measurements were also more precise than ReHo in S1 and S2 ( $p<0.0001$  for both), though proximity to CCMs did not impact precision of either modality ( $p>0.05$  for both).

### CONCLUSION

Our findings suggest that DTI imaging is significantly more reliable than fMRI near CCMs. This difference appears largely driven by the negative bias of ReHo measurements near CCMs, a finding consistent with the hypothesis that hemosiderin-rich lesions may lead to artefactual depression of fMRI signals in a distance-dependent manner, phenomenon not seen with DTI in our study. Regardless of proximity to CCMs, DTI was also more precise than fMRI, a difference that may be intrinsic to the imaging modality itself and not due to CCM-related artifacts.

## CLINICAL RELEVANCE/APPLICATION

Pre-surgical advanced MRI mapping near vascular rich lesion such as CCMs should be interpreted with caution. Clinicians should be aware that based on our findings, fMRI may not be reliable up to an 8 mm distance from CCMs while DTI appears to be consistently reliable even in close proximity.

## R2-SPNR-3 Automated Detection of Cerebral Aneurysms on Time of Flight MR-Angiography using a Deep Learning Approach

Participants  
Daniel Paech, MD, PhD, Heidelberg, Germany (*Presenter*) Nothing to Disclose

### PURPOSE

To evaluate the diagnostic performance of an AI-based software solution designed to automatically detect intracranial aneurysms on time-of-flight MR angiography.

### METHODS AND MATERIALS

191 MRI data sets were analyzed using the AI software solution mbrain (Mediaire, Berlin, Germany) for the presence of intracranial aneurysms on 3D time-of-flight MR angiography obtained using two 3T MRI scanners or a 1.5T MRI scanner according to our clinical standard protocol. The results were compared to the expert reading of an experienced radiologist as a gold standard to measure sensitivity, specificity, positive and negative predictive values as well as the accuracy of the software solution. Additionally, detection rates depending on size, morphology and location of the aneurysms were evaluated.

### RESULTS

A total of 54 aneurysms were detected by the expert reader. The software's overall sensitivity for the detection of cerebral aneurysms was 72.6%, the specificity was 87.2%, the accuracy was 82.6%. The positive predictive value was 67.9%, the negative predictive value was 88.5%. We observed high detection rates of 100% for saccular aneurysms larger than 5 mm with no signs of thrombosis, and low detection rates for fusiform and/or partially thrombosed aneurysms of 33.3% and 16.7%, respectively. Out of eight aneurysms that were not included in the initial written reports but that were detected by the expert reader retrospectively, four were detected by the software solution.

### CONCLUSION

Our data suggest that the software can be of assistance to radiologists reporting on time-of-flight MR angiograms. We found the software to be highly reliable in the case of saccular aneurysms, while fusiform aneurysms or aneurysms with partial thrombosis cannot be ruled out by the software. Further studies are needed to investigate the software's impact on detection rates, interrater reliability and reading times.

## CLINICAL RELEVANCE/APPLICATION

The software solution we investigated is a CE-labelled product that has not yet been reported on in terms of diagnostic accuracy. Thus, our findings are of importance to radiologists using the software to understand its capabilities, but also its limitations.

## **R2-SPNR-4 ML-based Prediction of Tumor Etiology in Brain Metastases using Radiomic Features**

Participants

Christopher Atkins, MD, New Haven, CT (*Presenter*) Nothing to Disclose

### **PURPOSE**

Brain metastases (BM) are the most common adult brain malignancies. Upon diagnosis, the site of primary tumor is not known in up to 15% of patients. Knowing the likely primary however could alter patient management, and we proposed to create a machine learning-and radiomics-based approach to provide a non-invasive way to facilitate diagnosis.

### **METHODS AND MATERIALS**

Contrast-enhanced T1w MR and FLAIR imaging from 164 patients with a total number of 584 treatment-naive brain metastases were collected. Volumetric segmentations were generated semiautomatically and were reviewed by a board-certified neuroradiologist. Radiomic features were extracted with PyRadiomics. Filter-based feature selection and XGBoost classification were performed in a nested cross-validation (CV) scheme. Classification performance (CP) was evaluated with "One-vs-Rest"-AUC, comparing each class prediction against the sum of all others, and class-weighted macro-AUC.

### **RESULTS**

Most common primary cancers were non-small-cell-lung-cancer (NSCLC, n=88), melanoma (n=33), breast-cancer (n=13), gastrointestinal-cancers (n=13), small-cell-lung-cancer (both n=13), renal-cell-carcinoma (n=7), and others (n=10). XGBoost reached an AUC of 0.64 in internal 5-fold-CV and 0.46 in an external validation set (143 lesions in 42 patients). Best label-wise classification was achieved for NSCLC (One-vs-Rest-AUC=0.71). Integrating individual lesion predictions to predict patient-level outcomes via hard ensemble voting did not lead to improved CP. The clinical performance of the model was not significantly different for metastases with volumes larger versus smaller than a 10-mm-diameter sphere ( $P > 0.05$ ).

### **CONCLUSION**

s This study underlines the challenging nature of predicting the site of the primary tumor in brain metastases by using radiomic features alone. Diagnosis might require the addition of further functional image analysis and/or incorporation of clinical data.

### **CLINICAL RELEVANCE/APPLICATION**

The technology detailed here could one day be applied to brain metastasis of unknown primary in order to more quickly target treatment and improve patient outcomes or survival rates.

## **R2-SPNR-5 Deep Learning Applied to Cranial Ultrasound for Prediction of Neurodevelopmental Impairment in Preterm Babies: Lessons Learned**

Participants

Tahani Ahmad, MD, (*Presenter*) Nothing to Disclose

### **PURPOSE**

Cranial ultrasound (CUS) is widely used as a screening tool to assess brain injury in preterm infants. Severe abnormalities on CUS are known to be associated with Neurodevelopmental impairment (NDI) while, for less severe changes or apparently "normal" scans the prognostic outcome is variable. This study aims to train a deep learning prognostic model based on CUS to early assess NDI outcomes.

### **METHODS AND MATERIALS**

Each CUS image was anonymized, pixels intensities were normalized, and resized to a standard 224x224 resolution. Regions outside of the brain were masked and set to intensity zero. The NDI outcome (i.e. patient outcome) and CUS diagnostic outcome (i.e. timepoint outcome) were imported based on the clinical assessment. The dataset is split into stratified training/test sets (90:10 percent split) grouped by the patient. The total number of patients is 619 with 4180 images. We trained the model using different deep learning approaches: from simple classic CNN to more advanced strategies (e.g. multi-view CNNs, to multiple instance learning).

### **RESULTS**

We tested different CNN architectures and strategies. Preliminary results indicate an average of 0.722 AUC (0.664- 0.779 C.I.) using 10 bootstraps stratified sampling strategies using DenseNet169.

### **CONCLUSION**

s This is a preliminary work to provide a tool to assist clinicians during early NDI assessment. During the preparation of this study, many challenges came to our attention (e.g. images acquired from multiple manufacturers, high presence of clinical confounding variables, scanty literature in this field) and we deployed different strategies to address each of them learning valuable lessons. Finally, although prognostic modeling is difficult, we expect the model performance to improve by including the clinical variable in the next stage.

### **CLINICAL RELEVANCE/APPLICATION**

Prediction of NeuroDevelopmental Impairment (NDI) in preterm infants enables early identification and referral of high-risk infants to intervention programs that have the potential to improve mobility and cognitive development.

## **R2-SPNR-6 Cost-Effectiveness of AI-Based Opportunistic Screening for Osteoporotic Compression Fractures on Existing Radiographs**

Participants

Patti Curl, MD, (*Presenter*) Nothing to Disclose

## PURPOSE

Osteoporotic compression fractures (OCFs) are a highly prevalent source of morbidity and mortality, and preventative treatment has been demonstrated to be both effective and cost effective. Still, many patients with OCFs remain undiagnosed, and there is potential value in identifying undiagnosed fractures on radiographs obtained for other indications. Our study group is developing software to access existing radiographs for OCFs with high sensitivity and specificity using an established artificial intelligence deep learning algorithm. The purpose of this analysis is to assess the potential cost-effectiveness of implementing this software.

## METHODS AND MATERIALS

Analysis was performed using TreeAge Pro Healthcare software. A deterministic expected-value cost-utility model, combining tree model and Markov model, was used to compare the strategies of opportunistic screening for osteoporotic compression fractures against usual care. The tree model was used to determine the likelihood a patient would receive treatment, and the expected value of each path was calculated with a separate Markov model. Total costs and total quality adjusted life years (QALYS) were calculated for each strategy. The baseline analysis assumed a population of women age 75, and a lifetime time horizon was used. Screening and treatment costs were considered from a societal perspective, at 2022 prices.

## RESULTS

In the base case, assuming a cost of software implantation of 10 dollars per patient screened, the screening strategy dominated the non-screening strategy: it resulted in lower cost and increased QALYS. The lower cost was primarily due to the decreased costs associated with fracture treatment and decreased probability of requiring long-term care in patients who received preventative treatment. The screening strategy was dominant up to a cost of \$156 per patient screened. At \$157, screening was cost effective with an incremental cost effectiveness ratio of \$100/QALY (Screening \$5389/1.19 QALY No-screening \$5388/1.18 QALY).

## CONCLUSION

s Opportunistic screening for OCFs can be cost-effective from a societal perspective.

## CLINICAL RELEVANCE/APPLICATION

Given the substantial population of patients with OCFs not receiving treatment, opportunistic diagnosis provides an opportunity to add value while also decreasing costs for the health care system as a whole.

## R2-SPNR-7 Development and Validation of a Deep Learning-Based Automatic Classification Algorithm for the Medial Temporal Lobe Atrophy Scale Using a Multi-Modality Cascade Transformer

Participants

Dongsoo Lee, MPH, MPH, Seoul, Korea, Republic Of (*Presenter*) Nothing to Disclose

## PURPOSE

Although medial temporal lobe atrophy (MTA) has been incorporated into the diagnostic criteria for Alzheimer's disease (AD) and mild cognitive impairment (MCI) in the NIA-AA guidelines, there might be concerns regarding interobserver variability because the MTA scale is a visual semi-quantitative method that requires training of the readers for confident uses. We aimed to develop and validate a deep learning-based automatic classification algorithm for the MTA scale in patients with cognitive impairment.

## METHODS AND MATERIALS

We developed a multi-modality cascade transformer using Vision Transformer (ViT) and TabNet classifier that were used to handle tabular and image data simultaneously. This observational study included consecutive patients with cognitive impairment from a tertiary hospital. 793 patients for the training dataset and 150 patients for the test dataset in the first model were included from March 2017 to June 2018. To improve accuracy, we devised a second model by applying transfer learning with a large cohort to the first model. 1200 patients for the training dataset and 100 patients for the test dataset in the second model were included from June 2018 to June 2021. We clustered the MTA scales into 3 groups (0,1), (2), (3,4) by clinical significance. After analyzing both sides, the higher scale was determined. To compare the performance of the two models, the test dataset of each model and the ADNI dataset were applied and compared.

## RESULTS

In first training dataset, group 0, 1, and 2 were 261 (33%), 202 (26%), and 330 (42%) patients, respectively. In the first test dataset, groups 0, 1, and 2 were all 50 (33%) patients, respectively. In second training dataset, group 0, 1, and 2 were 216 (18%), 586 (49%) and 398 (33%) patients, respectively. In second test dataset, group 0, 1 and 2 were 28 (28%), 37 (37%), and 35 (35%) patients, respectively. We conducted an ablation study to compare with various baseline models, and our proposed model achieved the best performance (precision 0.801, recall 0.787, and AUC 0.923). In the first model, the accuracy using the test dataset was 0.787. The accuracy of the second model using the same test dataset applied to the first model was 0.833. In ADNI test dataset, group 0, 1, and 2 were 67 (17%), 198 (50%), and 135 (34%), respectively. The accuracies of both models were 0.613 and 0.642 (the first model and second model), respectively.

## CONCLUSION

s The deep learning-based automatic classification algorithm using a multi-modality cascade transformer may allow accurate classification of the MTA scale.

## CLINICAL RELEVANCE/APPLICATION

It may be possible to reduce the inter/intra-observer variation in measuring the MTA scale using the deep learning model that we proposed.

## R2-SPNR-8 Development and Validation of a Deep Learning-based Automatic Segmentation and Classification of Cerebral White Matter Hyperintensities

Participants

Wooseok Jung, MSc, Seoul, Korea, Republic Of (*Presenter*) Nothing to Disclose

## PURPOSE

White matter hyperintensities (WMH) commonly attribute to vascular dementia and represent neuroimaging markers of cerebral small vessel disease. Fazekas scale is used to quantify WMH severity in radiology research. An automatic quantification model covering both WMH segmentation and Fazekas scale classification has not yet been explored in depth. We aimed to develop and validate a deep learning-based automatic segmentation and classification of cerebral white matter hyperintensities in patients with cognitive impairment.

## **METHODS AND MATERIALS**

This observational study included consecutive patients with cognitive impairment from a tertiary hospital. A segmentation model using the 2D UNet for training and validation was performed on the dataset of 511 and 64, respectively. An input FLAIR and the corresponding output mask of the segmentation model are concatenated to generate 2-channel input of Fazekas classification model. Two separated classification models for each WMH subtypes using 3D EfficientNetv2 for training and validation were performed on the dataset of 1661 and 110, respectively. Test of segmentation model was performed on the 278 the ADNI dataset. Test of the Fazekas scale classification model was performed on 100 ADNI dataset and 178 dataset of the tertiary hospital included. For the evaluation of the Fazekas scale classification, the datasets used in the test model were evaluated by four experienced neuroradiologists. Classification according to the Fazekas scale was divided into three categories (normal/mild, moderate, and severe), and locations were separately reported as periventricular (PWMH) and deep white matter (DWMH).

## **RESULTS**

Dice score performance of the segmentation model on test dataset by target location subtype were  $0.744 \pm 0.108$ ,  $0.904 \pm 0.054$ ,  $0.851 \pm 0.068$  (PWMH and DWMH, PWMH only, DWMH only), respectively. Dice score only concerning PWMH on test dataset by the three categories were  $0.907 \pm 0.044$ ,  $0.948 \pm 0.011$ , and  $0.957 \pm 0.014$ , respectively. Dice score only concerning DWMH on the same test dataset by the three categories were  $0.844 \pm 0.057$ ,  $0.946 \pm 0.023$ , and  $0.954 \pm 0.015$ , respectively. The accuracy of performance of the Fazekas scale classification model by single rater were 0.86 and 0.87 at PWMH and DWMH, respectively. The accuracy evaluated against mean of multi-rater labels were 0.76 and 0.69 at PWMH and DWMH, respectively.

## **CONCLUSION**

s These results demonstrate the excellent segmentation and classification performance of our models and their potential for deployment as accurate diagnostic support tools for quantified evaluation of WMH.

## **CLINICAL RELEVANCE/APPLICATION**

It may be possible to segment and classify white matter hyperintensities using a deep learning model that we proposed.

Printed on: 02/07/23

## Abstract Archives of the RSNA, 2022

R2-SPNR-1

### Imaging Findings That Cause False Positive Predictions of Intracranial Hemorrhage by Artificial Intelligence, a Pictorial Review

Thursday, Dec. 1 9:00AM - 9:30AM Room: Learning Center - NR DPS

#### Participants

Cody Savage, BS, Tuscaloosa, AL (*Presenter*) Nothing to Disclose

#### PURPOSE

To identify which imaging findings most often lead to false-positive predictions of intracranial hemorrhage (ICH) by artificial intelligence (AI).

#### METHODS AND MATERIALS

False-positive cases were collected from a single-center, prospective comparative effectiveness study of ICH detection by the FDA approved AI algorithm Aidoc. By evaluating written reports by the neuroradiologists, the cases marked positive for ICH by AI but read negative for ICH by the neuroradiologists were selected. A second neuroradiologist then reviewed the selected cases to establish ground truth. The second neuroradiologist's diagnosis was used as the gold standard of diagnosis. The false-positive cases by AI were then reviewed to detect the pattern of misclassification. Also, examples of false-positive cases are presented by pictorial review.

#### RESULTS

False positives by AI occurred in 223 ( 2.2%) of the 9978 cases, equating to a specificity of 97.5%. The sensitivity and accuracy were 96.9% and 95.2%, respectively. The most common imaging finding that resulted in a false positive was beam hardening under the skull ( 36.7%). Other imaging findings that resulted in false positives include hyperdensity of brain parenchyma by calcium deposition or mass (16.1 %), post-surgical changes ( 9.4% ), hyperdense dura matter (9%), dense vessels (8%), motion artifact (5%), meningioma (3%), Laminar necrosis (3%), leptomeningeal thickening (carcinomatosis or meningitis) (2.6%), cavernoma ( 2.6%), contrast staining ( 1.7%), and choroid plexus calcification (0.4%).

#### CONCLUSION

s The beam-hardening CT artifact, hyperdense parenchymal structures, dural hyperdensity, iatrogenic imaging findings, dense vessels, and motion artifact are the most common cause of false-positive ICH predictions by AI algorithm. While less common, meningioma, laminar necrosis, leptomeningeal infiltration, cavernoma, and contrast staining can also contribute to false-positive predictions.

#### CLINICAL RELEVANCE/APPLICATION

The radiologists who use AI to screen the ICH should be aware of false-positive calls. Despite the sophisticated developing process of medical AI platforms, it seems that AI models for ICH detection work mainly by detecting hyperdensities that can end in false-positive calls.

Printed on: 02/07/23

## Abstract Archives of the RSNA, 2022

R2-SPNR-11

### **Iterative Labeling and Review with Consensus and Conditional Probability Can Be Utilized to Decrease Variability for Artificial Intelligence Data Curation**

Thursday, Dec. 1 9:00AM - 9:30AM Room: Learning Center - NR DPS

#### **Participants**

Simas Glinskis, Ithaca, NY (*Presenter*) Employee, Covera Health, Inc

#### **PURPOSE**

Machine learning model performance depends on high quality and consistent data annotation, which can be difficult to obtain in the presence of inherent inter-reader labeling variability amongst radiologists. Guidelines can help reduce ambiguity when grading a pathology's severity; however, guidelines themselves may contain ambiguous definitions. We hypothesized a labeling and review process for guidelines would minimize the inter-reader variability through an iterative process and implemented a method to test this hypothesis on a real life dataset.

#### **METHODS AND MATERIALS**

Cervical spine MRI studies were annotated independently for severity of cord compression, central canal stenosis, disc herniation, and neural foraminal stenosis by three subspecialty trained board certified radiologists with the same version of guidelines in batches of 25-50-50 randomly sampled studies. After completion of each batch, statistical methods based on conditional probability were used to measure the inter-reader pathology severity variability and agreement as a group and for each pair of annotators. Pathology severities with high inter-reader variability or low agreement were targeted for guideline revision that was used in the next batch of MRI studies. The "measure-revise" process was repeated.

#### **RESULTS**

Inter-reader variability decreased from 23% to 3% for spinal cord compression when we revised the guidelines and added more granularity, splitting the not-compressed severity into normal, indentend, and flattened cord. Similarly, inter-reader agreement improved from 57% to 75% for severe central canal stenosis, from 74% to 84% for none or small disc herniation, and from 59% to 65% for large disc herniation when we iteratively redefined our guidelines for these pathology severities.

#### **CONCLUSION**

s Label agreement amongst our radiologists increased and generated more consistent training data for our machine learning models using the iterative labeling and review process. This approach is pathology agnostic and can be applied whenever clear severity definitions are required.

#### **CLINICAL RELEVANCE/APPLICATION**

Iterative labeling as performed with this methodology has the potential to reduce the variation for grading of pathologies in medical images and may improve the performance of AI models.

Printed on: 02/07/23



## Abstract Archives of the RSNA, 2022

R2-SPNR-12

### Brain Image Auto-Segmentation using 3D Capsule Networks

Thursday, Dec. 1 9:00AM - 9:30AM Room: Learning Center - NR DPS

#### Participants

Arman Avesta, MD, New Haven, CT (*Presenter*) Stockholder, Hyperfine Research, Inc;

#### PURPOSE

To develop and validate 3D capsule networks (CapsNets) to segment brain images with features not represented in the training data.

#### METHODS AND MATERIALS

We used 3430 brain MRIs acquired in a multi-institutional study. We compared our CapsNets with U-Nets, the current standard, based on the accuracy in segmenting various brain structures and those with spatial features not represented in the training data. We also assessed performance when the models are trained using limited data, memory requirements, and computation times.

#### RESULTS

3D CapsNets segmented the third ventricle, thalamus, and hippocampus with Dice scores of 94%, 94%, and 91%, respectively. 3D CapsNets outperformed 3D U-Nets in segmenting brain images with features that were not represented in the training data, with Dice scores more than 30% higher ( $P$ -values  $< 0.01$ ). 3D CapsNets had 93% fewer trainable parameters than 3D U-Nets. The 3D CapsNets were 25% faster to train compared with U-Nets. The two models were equally fast during testing.

#### CONCLUSION

s 3D CapsNets segment brain structures with high accuracy, outperform U-Nets in segmenting brain images with features that were not represented during training, and are more efficient compared with U-Nets, achieving similar results while their size is an order of magnitude smaller.

#### CLINICAL RELEVANCE/APPLICATION

In patients undergoing radiotherapy or neurosurgery, neuroanatomical segmentation is a critical aid that improves outcomes. 3D CapsNets outperformed current auto-segmentation methods in generalizability to brain images with features not represented in the training data.

Printed on: 02/07/23

## Abstract Archives of the RSNA, 2022

R2-SPNR-13

### Artificial Intelligence (AI) Model Based on Automatized Morphometry and Planimetric Data Obtained in Brain MRI, a Proof of Concepts: Lights Towards the Future for Differentiating Progressive Supranuclear Palsy From Parkinson's Disease

Thursday, Dec. 1 9:00AM - 9:30AM Room: Learning Center - NR DPS

#### Participants

Francisco Mendoza, MD, (Presenter) Nothing to Disclose

#### PURPOSE

To develop an AI model to differentiate Progressive Supranuclear Palsy (PSP) from Parkinson's disease (PD) and healthy subjects (HS) using automated volumetry and non-automated planimetric assessment data obtained in Magnetic Resonance Imaging (MRI).

#### METHODS AND MATERIALS

We retrospectively assessed a total of 141 patients with a clinical diagnosis of Parkinsonism paired by age and sex and with a group of HS (PSP n = 47, PD n = 68, HS = 26) between January 2003 and April 2021 and analyzed their brain MRI. Patients without T1 high resolution sequences were excluded, leaving 83 patients (PSP n = 29, PD n = 54). We included different clinical subtypes of PSP: PSP-RS (n = 19), PSP-P (n = 5), PSP-PGF (n = 4), and PSP-F (n = 1). Using automatized SyngoviaBrainMorphometry software (Siemens), we obtained 109 VOIs for each subject, including absolute and normalized values. Two independent radiologists blind to diagnosis performed a planimetric assessment (Massey ratio, Oba ratio, MPRI 1.0, and MRP 2.0). We developed a machine-learning model based on multivariate feature selection and an extreme gradient boosting (XGB) vs. univariate feature selection and random forest (RF) using both automated volumetric data and planimetric assessment to predict PSP, PD, and HS. All subjects were randomly divided into training (85%) and validation (15%) data sets with the same proportions for each clinical group. We assessed the diagnostic accuracy of the model and the most relevant features were ordered by importance score (F-score; where 1.0 represents perfect precision and recall). Additionally, we assessed the diagnostic accuracy of each feature using ROC curves.

#### RESULTS

The global diagnostic performance of the model to differentiate between the three groups was 82.3%. The diagnostic accuracy of the model to predict PSP from the other groups was 81.82 and for PD was 82.35. The most relevant features of the AI model were the mesencephalic area (0.22), mesencephalic width (0.13), left frontal gray matter normalized volume (0.088), and the left thalamus absolute volume (0.059), and Oba Ratio (0.044). The AUC to differentiate PSP from PD and HS was for the mesencephalic area = 0.94, for the mesencephalic width = 0.99, the left frontal gray matter normalized volume = 0.50, and the left thalamus absolute volume = 0.69.

#### CONCLUSION

The developed AI model using data obtained from brain MRI automated volumetry and non-automated planimetric assessment, showed high accurate discrimination between PSP, PD, and HS, especially for PSP in our study population.

#### CLINICAL RELEVANCE/APPLICATION

AI model using morphometry and planimetric data can differentiate patients with parkinsonism. It would be necessary to validate this model for its clinical application.

Printed on: 02/07/23

## Abstract Archives of the RSNA, 2022

R2-SPNR-15

### Neural Architecture Search Based MRI Sequence Design

Thursday, Dec. 1 9:00AM - 9:30AM Room: Learning Center - NR DPS

#### Participants

Hongjun An, (*Presenter*) Nothing to Disclose

#### PURPOSE

Designing an MR sequence is very challenging, resulting that currently available sequences are constrained by human intuition. We proposed a new sequence design method using neural architecture search (NAS).

#### METHODS AND MATERIALS

Our method is designed to produce an optimal sequence for given and target objectives. Hence, these properties are inputted to the Bloch simulator to generate MR signals. Using the signals, a loss function defined by the objective is calculated for optimization. Then the sequence scheduler determines the sequence design using NAS (Fig. 1). NAS was utilized to optimize a series of operations (i.e., sequence) by replacing a neural architecture and its weight parameters with a sequence design and its scan parameters, respectively. To test, two experiments were performed repeatedly to design FLAIR-like sequences and spin-echo-like sequences.

#### RESULTS

In Experiment 1 (Fig. 1c1), a FLAIR-like sequence and non-intuitive sequence showing 4 RF pulses in place of inversion were generated while CSF signal suppression and gray/white matter signal recovery. In Experiment 2 (Fig. 1c2), a conventional spin echo (CPMG), Hann-echo-like sequence, and a less intuitive sequence with three or four RF pulses ( $12^\circ$ - $89^\circ$ - $168^\circ$  and  $5^\circ$ - $16^\circ$ - $85^\circ$ - $162^\circ$ ). In in-vivo experiment, the new three-RF sequence produced identical contrasts and similar SNR with the spin-echo images (new sequence SNR:  $297.1 \pm 70.1$  vs. spin-echo SNR:  $295.8 \pm 78.2$ ). The new sequences had reduced RF energy (90% of the spin-echo), while taking a longer duration (18.6 ms vs. 12.4 ms).

#### CONCLUSION

A novel automatic sequence design method requiring no prior knowledge or training data was proposed, which successfully reproduced the conventional sequence and invented less-intuitive sequences. This study suggests a potential for automated sequence design that may explore possibilities beyond human intuition.

#### CLINICAL RELEVANCE/APPLICATION

Using our method, a new sequence can be automatically developed in the clinical considerations with non-intuitive behavior.

Printed on: 02/07/23

## Abstract Archives of the RSNA, 2022

R2-SPNR-16

### Age-Adjusted Atlas of Diffusion Metrics in Normal Neonatal Brains

Thursday, Dec. 1 9:00AM - 9:30AM Room: Learning Center - NR DPS

#### Participants

Pratheek Bobba, BS, New Haven, CT (*Presenter*) Nothing to Disclose

#### PURPOSE

Diffusion weighted imaging (DWI) and diffusion tensor imaging (DTI) are increasingly used in the diagnosis and prognostication of neonatal brain injury. However, rapid changes of apparent diffusion coefficient (ADC) values from DWI and fractional anisotropy (FA) and mean diffusivity (MD) values from DTI complicate the interpretation of DWI and DTI scans in neonates. Thus, robust characterization of these metrics in neonatal brains is required.

#### METHODS AND MATERIALS

The medical and imaging records of all neonates (0-3 months) born since 2013 at our institution were analyzed. Subjects with normal MRI scans on both clinical report and visual inspection were included. DWI (and associated ADC maps) and DTI scans (and associated FA/MD maps) were then coregistered to a pediatric standard brain space. Voxel-wise general linear models (GLM) were applied to analyze the age-related changes of ADC values throughout the brain. Tract-based spatial statistics of DTI metrics was also applied along white matter tracts in the brain. Linear regression models were used to calculate the rate of change in ADC, FA, and MD values across 5mm cubic voxels. Age adjusted normative atlases of these metrics were generated by calculating the mean and standard deviation in each voxel.

#### RESULTS

565 neonates with DWI scans, of whom 162 also had DTI scans were included. The mean±SD gestational age (GA) at scan for the DWI cohort was 39.67±2.79 weeks and for the DTI cohort was 38.53±1.94 weeks. Increasing GA at scan was associated with significant reduction of ADC values throughout the brain and significant increase of FA and reduction of MD values throughout white matter tracts. The highest temporal rate of decline in ADC values was seen in the subcortical and cerebellar white matter and vermis. The highest temporal rate of increase in FA and rate of decrease in MD values was seen throughout the cortical white matter (Figure 1). After correcting for GA at scan, greater GA at birth was associated with significant reduction of ADC values in the corpus callosum and convexity cortex and significantly higher FA and lower MD values in the corpus callosum. Online interactive atlases displaying age-specific normative values of ADC (34.5-46.5 weeks), and DTI metrics (35-41 weeks) were developed.

#### CONCLUSION

There is significant age-related reduction of ADC values throughout the neonatal brain, with steepest decline in the periventricular white matter. Similar trends in FA and MD values indicate that changes in ADC values are likely related to myelination of white matter in neonatal brains.

#### CLINICAL RELEVANCE/APPLICATION

Our age adjusted normative atlases can aid neuroradiologists in identification and diagnosis of subtle developmental anomalies and ischemic brain injury in neonates.

Printed on: 02/07/23

## Abstract Archives of the RSNA, 2022

R2-SPNR-17

### Clinical Feasibility of Reverse Encoding Distortion Correction for Brain DWI: Comparison With Conventional DWI

Thursday, Dec. 1 9:00AM - 9:30AM Room: Learning Center - NR DPS

#### Participants

Atsushi Nakamoto, MD, PhD, Suita, Japan (*Presenter*) Nothing to Disclose

#### PURPOSE

Single-shot echo-planar imaging is a widely used conventional diffusion-weighted imaging (C-DWI) technique, owing to its high speed, but is susceptible to magnetic field inhomogeneities which causes high image distortion. This study was conducted to evaluate whether reverse encoding distortion correction DWI (RDC-DWI), which acquires a pair of two opposite phase encoding polarities, can reduce image distortion for DWI of the brain.

#### METHODS AND MATERIALS

This study included 50 patients who underwent both RDC-DWI and C-DWI of the brain. Both DW images were obtained by two excitations with acquisition times of 121 and 107 seconds, respectively. Using a five-point scale, two neuroradiologists qualitatively evaluated the image distortion of the pons, cerebellum, temporal skull bases and frontal skull base, and the overall image quality. For quantitative analysis, distortion ratios (DR), the apparent diffusion coefficients (ADC) values, and signal-to-noise ratios (SNR) of the pons and frontal lobe were measured. For the pathologies, we qualitatively evaluated image distortion and measured the ADC values.

#### RESULTS

The scores for image distortions of all evaluated sites were significantly lower for RDC-DWI than for C-DWI ( $p < 0.01$ ), and those for overall image quality were significantly higher for RDC-DWI than for C-DWI ( $p < 0.01$ ). The DR of the pons and frontal lobe were significantly lower for RDC-DWI than for C-DWI ( $p < 0.01$ ). SNR of these sites were significantly higher for RDC-DWI than for C-DWI ( $p = 0.03$  and  $p = 0.01$ , respectively). Mean ADC values of these sites did not significantly differ between the two techniques ( $p = 0.62$  and  $p = 0.66$ , respectively). The scores for image distortions of intracranial lesions ( $n = 22$ ) did not differ significantly between the two techniques ( $p = 0.25$ ), whereas those of sinonasal lesions ( $n = 7$ ) was significantly lower for RDC-DWI than for C-DWI ( $p = 0.03$ ). Mean ADC values of both intracranial and sinonasal lesions did not differ between the two techniques ( $p = 0.16$  and  $p = 0.80$ , respectively).

#### CONCLUSION

s RDC-DWI can significantly reduce image distortion and increase SNR with minimal additional acquisition time, compared with C-DWI.

#### CLINICAL RELEVANCE/APPLICATION

RDC-DWI can reduce image distortion in the tissue-air interface and improve delineation of sinonasal pathologies.

Printed on: 02/07/23

## Abstract Archives of the RSNA, 2022

R2-SPNR-18

### Diffusion Weighted Imaging with and without Reverse Encoding Distortion Correction (RDC): Influence to Image Quality and ADC Evaluation in Patients with Skull-based Brain Tumors

Thursday, Dec. 1 9:00AM - 9:30AM Room: Learning Center - NR DPS

#### Participants

Kazuhiro Murayama, MD, Toyoake, Japan (*Presenter*) Research Grant, Canon Medical Systems Corporation

#### PURPOSE

To evaluate influences of newly developed reverse encoding distortion correction (RDC) method for reducing image distortion to image quality and ADC evaluation on diffusion-weighted imaging (DWI) in patients with skull-based brain tumors.

#### METHODS AND MATERIALS

26 patients with suspected skull-based various brain tumors underwent DWIs with and without RDC at 3T systems. To compare image distortion between DWIs with and without RDC, the deformation ratio (DR) of each tumor was calculated from each tumor area difference between DWI and T2-weighted images. To compare image quality and ADC values between DWIs with and without RDC, the signal to noise ratio (SNR) of normal appearance white matter (NAWM) and ADC values of tumor were determined by ROI measurements in each patient. Moreover, overall image quality, lesion distortion and lesion conspicuity of each tumor were assessed by 5-point visual scoring system by two board-certified radiologists. For quantitative and qualitative image quality comparisons, DR and SNR were compared between DWIs with and without RDC by paired t-test. Kappa statistics with  $\chi^2$  test was performed for each interobserver agreement evaluations. Then, each score was compared between DWIs with and without RDC by Wilcoxon's signed sum test. To determine the influence of RDC to ADC measurement, ADC value was correlated between DWIs with and without RDC by Spearman's correlation. Then, the limits of agreement of ADC between both DWIs were also determined.

#### RESULTS

DR of DWI with RDC technique was significantly smaller than that without RDC ( $p < 0.05$ ), although others had no significant differences between DWIs with and without RDC. Interobserver agreement for each image quality score was significantly substantial or excellent ( $0.70 \leq \kappa \leq 0.92$ ,  $p < 0.001$ ). Moreover, each image quality score of DWI with RDC was significantly higher than that without RDC ( $p < 0.05$ ). ADC had a significant and good correction between DWIs with and without RDC ( $r = 0.98$ ,  $p < 0.0001$ ). The limits of agreement between DWIs with and without RDC was  $0.00 \pm 0.13 \times 10^{-3} \text{ s/mm}^2$ .

#### CONCLUSION

Newly developed RDC method has no influence to ADC evaluation and makes it possible to improve image quality on DWI in patients with skull-based brain tumors.

#### CLINICAL RELEVANCE/APPLICATION

Newly developed RDC method has no influence to ADC evaluation and makes it possible to improve image quality on DWI in patients with skull-based brain tumors.

Printed on: 02/07/23

## Abstract Archives of the RSNA, 2022

R2-SPNR-19

### **Histogram Analysis Based on Neurite Orientation Dispersion and Density Imaging for Differentiation Between Solitary Brain Metastasis and Glioblastoma Multiforme: A Comparison of Two Different ROI Placements**

Thursday, Dec. 1 9:00AM - 9:30AM Room: Learning Center - NR DPS

#### **Participants**

Jinbo Qi, MD, (*Presenter*) Nothing to Disclose

#### **PURPOSE**

To explore the value of histogram analysis based on NODDI in differentiating between solitary brain metastasis (SBM) and glioblastoma multiforme (GBM), and to compare the diagnostic performance of two different region of interest (ROI) placements.

#### **METHODS AND MATERIALS**

NODDI data were prospectively obtained from 109 patients with pathologically confirmed GBM (n = 57) and SBM (n = 52) were included. Two ROIs—the peritumoral edema area and whole-tumor area—were delineated across all slices. Eleven histogram parameters of intra-cellular volume fraction (ICVF), isotropic volume fraction (ISOVF) and orientation dispersion index (ODI) from both ROIs were extracted. The parameters of the histogram analysis were compared between SBM and GBM, using independent sample t-test or rank sum test, and then to make meaningful parameters based on logistic regression modeling. Receiver operating characteristic (ROC) analyses were conducted to evaluate the differential diagnosis performance and their performances were compared using DeLong's test.

#### **RESULTS**

In peritumoral edema area, ICVF<sub>minimum</sub>, ICVF<sub>max</sub>, ICVF<sub>kurtosis</sub>, ISOVF<sub>skewness</sub>, ISOVF<sub>kurtosis</sub>, ODI<sub>10</sub>, ODI<sub>25</sub> and ODI<sub>minimum</sub> were significantly higher for GBM than for SBM. ISOVF<sub>10</sub>, ISOVF<sub>25</sub>, ISOVF<sub>50</sub>, ISOVF<sub>75</sub>, ISOVF<sub>mean</sub> and ISOVF<sub>skewness</sub> were significantly lower for GBM than for SBM. The sensitivity of the corresponding logistic regression differential diagnosis model was 80.7%, specificity was 80.7%, and area under the curve (AUC) was 0.851. In whole-tumor area, ICVF<sub>max</sub>, ICVF<sub>skewness</sub>, ICVF<sub>kurtosis</sub>, ISOVF<sub>skewness</sub>, ISOVF<sub>kurtosis</sub> and ODI<sub>kurtosis</sub> were significantly lower for GBM than for SBM. ISOVF<sub>10</sub>, ISOVF<sub>25</sub>, ISOVF<sub>50</sub>, ISOVF<sub>75</sub>, ISOVF<sub>minimum</sub>, ODI<sub>10</sub>, ODI<sub>25</sub>, ODI<sub>50</sub>, ODI<sub>75</sub>, ODI<sub>90</sub>, ODI<sub>mean</sub>, ODI<sub>variance</sub>, and ODI<sub>skewness</sub> were significantly lower for GBM than for SBM. The sensitivity of the corresponding logistic regression differential diagnosis model was 96.1%, specificity was 86%, and the area under curve (AUC) was 0.958. DeLong's test showed significant difference (P=0.014) in differential performance between two different ROI placements.

#### **CONCLUSION**

s GBM and SBM can be differentiated using the NODDI-based histogram analysis and the ROI on whole-tumor area would exhibit better performance.

#### **CLINICAL RELEVANCE/APPLICATION**

The NODDI compartment model theoretically distinguishes three types of water diffusion behavior (i.e., intracellular, extracellular, and CSF), it is more sensitive to microstructural changes, which might demonstrate the difference in water diffusion between tumor infiltration and vasogenic edema. Furthermore, NODDI techniques can identify more different tissue components within tumors than conventional imaging for differentiating the heterogeneity of GBM and SBM.

Printed on: 02/07/23



## Abstract Archives of the RSNA, 2022

R2-SPNR-2

### Successful Implementation of a Comprehensive CT Brain Artificial Intelligence Assist Device Improves Radiologist Performance

Thursday, Dec. 1 9:00AM - 9:30AM Room: Learning Center - NR DPS

#### Participants

Peter R. Brotchie, MBBS, PhD, Fitzroy, Australia (*Presenter*) Consultant, Annalise-AI Pty Ltd

#### PURPOSE

To assess the effect on accuracy when radiologists are assisted by a comprehensive CT Brain (CTB) artificial intelligence device.

#### METHODS AND MATERIALS

CTB are one of the most common CT investigations in clinical radiology. Despite the extensive training of radiologists, missed diagnosis remains a problem. To assist radiologists in reducing errors, many artificial intelligence devices have been developed. However, most of these tools are capable of only detecting a single finding. With the aim to improve a radiologist's performance across a full range of findings on CTB, a comprehensive AI assist device capable of detecting 144 findings was developed. The deep learning model was trained on 212,484 CTB images and tested on a dataset of 2,848 images. The test set was ground truthed by at least 3 radiologists and adjudicated by a neuroradiologist. The performance of 32 radiologists was measured when reviewing the test dataset with and without AI assistance across several metrics including area under the receiver operating characteristic curve (AUC).

#### RESULTS

The radiologists AUC averaged 0.79 when assisted by the AI compared to 0.73 when unassisted. Significant improvement in AUC was observed across 91 findings. 17 findings showed decreases in AUC. Many of the largest gains in performance by the radiologists when using the AI, were for clinically critical findings, including findings signifying mass effect (basal cistern effacement, tonsillar and uncal herniation, midline shift, sulcal and ventricular effacement), intracranial haemorrhage (especially aneurysmal and convexity subarachnoid haemorrhage), trauma (intracranial haemorrhage and fractures), obstructive hydrocephalus, intra-axial lesions, aggressive extra-axial masses, orbital cellulitis and acute infarction.

#### CONCLUSION

The use of a comprehensive CTB assist device significantly improved radiologist performance across a majority of clinical findings on CTB, demonstrating the potential safety improvements of comprehensive AI.

#### CLINICAL RELEVANCE/APPLICATION

The comprehensive AI device for CTB, after testing with a large selection of radiologists, showed improved performance by the assisted radiologist, and indicates a potential use case in a radiologists workflow.

Printed on: 02/07/23

## Abstract Archives of the RSNA, 2022

R2-SPNR-20

### Reliability of Functional and Diffusion Magnetic Resonance Imaging Near Cerebral Cavernous Malformations

Thursday, Dec. 1 9:00AM - 9:30AM Room: Learning Center - NR DPS

#### Participants

Marco Colasurdo, MD, Pescara, Italy (*Presenter*) Nothing to Disclose

#### PURPOSE

Surgical resection of cerebral cavernous malformations (CCMs) routinely employs fMRI and DTI for surgical planning to best preserve neurological function. However, hemosiderin-rich lesions such as CCMs may cause artefactual distortion of MRI signals in close proximity. This study investigates the reliability of fMRI and DTI near CCMs.

#### METHODS AND MATERIALS

Consecutive patients with CCMs undergoing pre-surgical fMRI and DTI mapping were identified from June 2002 to June 2019 at an academic medical centre. Each CCM lesion was hand-contoured using T2 sequences, and two sequential 4-mm expansion shells (S1 and S2) were created, generating three ROIs; every ROI was then flipped to the contralateral hemisphere to obtain control ROIs. Fractional anisotropy (FA) and Regional Homogeneity (ReHo) measurements were then extracted from each ROI. FA and ReHo values were compared with contralateral controls to calculate percentage error. Reliability, accuracy, and precision within ROIs were compared using Welch's t-tests, F-tests and Wilcoxon matched-pairs signed rank tests; p-values were adjusted for multiple comparisons as appropriate.

#### RESULTS

61 patients were identified and included. Overall, errors of FA were significantly lower than ReHo in S1 and S2 ( $p=0.0001$  for both), suggesting that FA is more reliable than ReHo near CCMs. Proximity to CCM lesions significantly worsened the reliability of ReHo (S1 vs. S2,  $p=0.0007$ ), but not FA ( $p=0.24$ ). Further investigations of sources of error revealed that while FA was not significantly biased in any ROI ( $p>0.05$  for all), ReHo was biased towards lower signals in CCMs, S1 and S2 ( $p<0.05$ ), an effect that was attenuated with distance from CCMs ( $p<0.05$ ). FA measurements were also more precise than ReHo in S1 and S2 ( $p<0.0001$  for both), though proximity to CCMs did not impact precision of either modality ( $p>0.05$  for both).

#### CONCLUSION

Our findings suggest that DTI imaging is significantly more reliable than fMRI near CCMs. This difference appears largely driven by the negative bias of ReHo measurements near CCMs, a finding consistent with the hypothesis that hemosiderin-rich lesions may lead to artefactual depression of fMRI signals in a distance-dependent manner, phenomenon not seen with DTI in our study. Regardless of proximity to CCMs, DTI was also more precise than fMRI, a difference that may be intrinsic to the imaging modality itself and not due to CCM-related artifacts.

#### CLINICAL RELEVANCE/APPLICATION

Pre-surgical advanced MRI mapping near vascular rich lesion such as CCMs should be interpreted with caution. Clinicians should be aware that based on our findings, fMRI may not be reliable up to an 8 mm distance from CCMs while DTI appears to be consistently reliable even in close proximity.

Printed on: 02/07/23



## Abstract Archives of the RSNA, 2022

R2-SPNR-3

### Automated Detection of Cerebral Aneurysms on Time of Flight MR-Angiography using a Deep Learning Approach

Thursday, Dec. 1 9:00AM - 9:30AM Room: Learning Center - NR DPS

#### Participants

Daniel Paech, MD, PhD, Heidelberg, Germany (*Presenter*) Nothing to Disclose

#### PURPOSE

To evaluate the diagnostic performance of an AI-based software solution designed to automatically detect intracranial aneurysms on time-of-flight MR angiography.

#### METHODS AND MATERIALS

191 MRI data sets were analyzed using the AI software solution mbrain (Mediaire, Berlin, Germany) for the presence of intracranial aneurysms on 3D time-of-flight MR angiography obtained using two 3T MRI scanners or a 1.5T MRI scanner according to our clinical standard protocol. The results were compared to the expert reading of an experienced radiologist as a gold standard to measure sensitivity, specificity, positive and negative predictive values as well as the accuracy of the software solution. Additionally, detection rates depending on size, morphology and location of the aneurysms were evaluated.

#### RESULTS

A total of 54 aneurysms were detected by the expert reader. The software's overall sensitivity for the detection of cerebral aneurysms was 72.6%, the specificity was 87.2%, the accuracy was 82.6%. The positive predictive value was 67.9%, the negative predictive value was 88.5%. We observed high detection rates of 100% for saccular aneurysms larger than 5 mm with no signs of thrombosis, and low detection rates for fusiform and/or partially thrombosed aneurysms of 33.3% and 16.7%, respectively. Out of eight aneurysms that were not included in the initial written reports but that were detected by the expert reader retrospectively, four were detected by the software solution.

#### CONCLUSION

Our data suggest that the software can be of assistance to radiologists reporting on time-of-flight MR angiograms. We found the software to be highly reliable in the case of saccular aneurysms, while fusiform aneurysms or aneurysms with partial thrombosis cannot be ruled out by the software. Further studies are needed to investigate the software's impact on detection rates, interrater reliability and reading times.

#### CLINICAL RELEVANCE/APPLICATION

The software solution we investigated is a CE-labelled product that has not yet been reported on in terms of diagnostic accuracy. Thus, our findings are of importance to radiologists using the software to understand its capabilities, but also its limitations.

Printed on: 02/07/23

## Abstract Archives of the RSNA, 2022

R2-SPNR-4

### ML-based Prediction of Tumor Etiology in Brain Metastases using Radiomic Features

Thursday, Dec. 1 9:00AM - 9:30AM Room: Learning Center - NR DPS

#### Participants

Christopher Atkins, MD, New Haven, CT (*Presenter*) Nothing to Disclose

#### PURPOSE

Brain metastases (BM) are the most common adult brain malignancies. Upon diagnosis, the site of primary tumor is not known in up to 15% of patients. Knowing the likely primary however could alter patient management, and we proposed to create a machine learning- and radiomics-based approach to provide a non-invasive way to facilitate diagnosis.

#### METHODS AND MATERIALS

Contrast-enhanced T1w MR and FLAIR imaging from 164 patients with a total number of 584 treatment-naive brain metastases were collected. Volumetric segmentations were generated semiautomatically and were reviewed by a board-certified neuroradiologist. Radiomic features were extracted with PyRadiomics. Filter-based feature selection and XGBoost classification were performed in a nested cross-validation (CV) scheme. Classification performance (CP) was evaluated with "One-vs-Rest"-AUC, comparing each class prediction against the sum of all others, and class-weighted macro-AUC.

#### RESULTS

Most common primary cancers were non-small-cell-lung-cancer (NSCLC, n=88), melanoma (n=33), breast-cancer (n=13), gastrointestinal-cancers (n=13), small-cell-lung-cancer (both n=13), renal-cell-carcinoma (n=7), and others (n=10). XGBoost reached an AUC of 0.64 in internal 5-fold-CV and 0.46 in an external validation set (143 lesions in 42 patients). Best label-wise classification was achieved for NSCLC (One-vs-Rest-AUC=0.71). Integrating individual lesion predictions to predict patient-level outcomes via hard ensemble voting did not lead to improved CP. The clinical performance of the model was not significantly different for metastases with volumes larger versus smaller than a 10-mm-diameter sphere ( $P > 0.05$ ).

#### CONCLUSION

s This study underlines the challenging nature of predicting the site of the primary tumor in brain metastases by using radiomic features alone. Diagnosis might require the addition of further functional image analysis and/or incorporation of clinical data.

#### CLINICAL RELEVANCE/APPLICATION

The technology detailed here could one day be applied to brain metastasis of unknown primary in order to more quickly target treatment and improve patient outcomes or survival rates.

Printed on: 02/07/23



## Abstract Archives of the RSNA, 2022

R2-SPNR-5

### Deep Learning Applied to Cranial Ultrasound for Prediction of Neurodevelopmental Impairment in Preterm Babies: Lessons Learned

Thursday, Dec. 1 9:00AM - 9:30AM Room: Learning Center - NR DPS

#### Participants

Tahani Ahmad, MD, (*Presenter*) Nothing to Disclose

#### PURPOSE

Cranial ultrasound (CUS) is widely used as a screening tool to assess brain injury in preterm infants. Severe abnormalities on CUS are known to be associated with Neurodevelopmental impairment (NDI) while, for less severe changes or apparently "normal" scans the prognostic outcome is variable. This study aims to train a deep learning prognostic model based on CUS to early assess NDI outcomes.

#### METHODS AND MATERIALS

Each CUS image was anonymized, pixels intensities were normalized, and resized to a standard 224x224 resolution. Regions outside of the brain were masked and set to intensity zero. The NDI outcome (i.e. patient outcome) and CUS diagnostic outcome (i.e. timepoint outcome) were imported based on the clinical assessment. The dataset is split into stratified training/test sets (90:10 percent split) grouped by the patient. The total number of patients is 619 with 4180 images. We trained the model using different deep learning approaches: from simple classic CNN to more advanced strategies (e.g. multi-view CNNs, to multiple instance learning).

#### RESULTS

We tested different CNN architectures and strategies. Preliminary results indicate an average of 0.722 AUC (0.664- 0.779 C.I.) using 10 bootstraps stratified sampling strategies using DenseNet169.

#### CONCLUSION

s This is a preliminary work to provide a tool to assist clinicians during early NDI assessment. During the preparation of this study, many challenges came to our attention (e.g. images acquired from multiple manufacturers, high presence of clinical confounding variables, scanty literature in this field) and we deployed different strategies to address each of them learning valuable lessons. Finally, although prognostic modeling is difficult, we expect the model performance to improve by including the clinical variable in the next stage.

#### CLINICAL RELEVANCE/APPLICATION

Prediction of NeuroDevelopmental Impairment (NDI) in preterm infants enables early identification and referral of high-risk infants to intervention programs that have the potential to improve mobility and cognitive development.

Printed on: 02/07/23



## Abstract Archives of the RSNA, 2022

R2-SPNR-6

### Cost-Effectiveness of AI-Based Opportunistic Screening for Osteoporotic Compression Fractures on Existing Radiographs

Thursday, Dec. 1 9:00AM - 9:30AM Room: Learning Center - NR DPS

#### Participants

Patti Curl, MD, (*Presenter*) Nothing to Disclose

#### PURPOSE

Osteoporotic compression fractures (OCFs) are a highly prevalent source of morbidity and mortality, and preventative treatment has been demonstrated to be both effective and cost effective. Still, many patients with OCFs remain undiagnosed, and there is potential value in identifying undiagnosed fractures on radiographs obtained for other indications. Our study group is developing software to access existing radiographs for OCFs with high sensitivity and specificity using an established artificial intelligence deep learning algorithm. The purpose of this analysis is to assess the potential cost-effectiveness of implementing this software.

#### METHODS AND MATERIALS

Analysis was performed using TreeAge Pro Healthcare software. A deterministic expected-value cost-utility model, combining tree model and Markov model, was used to compare the strategies of opportunistic screening for osteoporotic compression fractures against usual care. The tree model was used to determine the likelihood a patient would receive treatment, and the expected value of each path was calculated with a separate Markov model. Total costs and total quality adjusted life years (QALYS) were calculated for each strategy. The baseline analysis assumed a population of women age 75, and a lifetime time horizon was used. Screening and treatment costs were considered from a societal perspective, at 2022 prices.

#### RESULTS

In the base case, assuming a cost of software implantation of 10 dollars per patient screened, the screening strategy dominated the non-screening strategy: it resulted in lower cost and increased QALYS. The lower cost was primarily due to the decreased costs associated with fracture treatment and decreased probability of requiring long-term care in patients who received preventative treatment. The screening strategy was dominant up to a cost of \$156 per patient screened. At \$157, screening was cost effective with an incremental cost effectiveness ratio of \$100/QALY (Screening \$5389/1.19 QALY No-screening \$5388/1.18 QALY).

#### CONCLUSION

s Opportunistic screening for OCFs can be cost-effective from a societal perspective.

#### CLINICAL RELEVANCE/APPLICATION

Given the substantial population of patients with OCFs not receiving treatment, opportunistic diagnosis provides an opportunity to add value while also decreasing costs for the health care system as a whole.

Printed on: 02/07/23

## Abstract Archives of the RSNA, 2022

R2-SPNR-7

### Development and Validation of a Deep Learning-Based Automatic Classification Algorithm for the Medial Temporal Lobe Atrophy Scale Using a Multi-Modality Cascade Transformer

Thursday, Dec. 1 9:00AM - 9:30AM Room: Learning Center - NR DPS

#### Participants

Dongsoo Lee, MPH, MPH, Seoul, Korea, Republic Of (*Presenter*) Nothing to Disclose

#### PURPOSE

Although medial temporal lobe atrophy (MTA) has been incorporated into the diagnostic criteria for Alzheimer's disease (AD) and mild cognitive impairment (MCI) in the NIA-AA guidelines, there might be concerns regarding interobserver variability because the MTA scale is a visual semi-quantitative method that requires training of the readers for confident uses. We aimed to develop and validate a deep learning-based automatic classification algorithm for the MTA scale in patients with cognitive impairment.

#### METHODS AND MATERIALS

We developed a multi-modality cascade transformer using Vision Transformer (ViT) and TabNet classifier that were used to handle tabular and image data simultaneously. This observational study included consecutive patients with cognitive impairment from a tertiary hospital. 793 patients for the training dataset and 150 patients for the test dataset in the first model were included from March 2017 to June 2018. To improve accuracy, we devised a second model by applying transfer learning with a large cohort to the first model. 1200 patients for the training dataset and 100 patients for the test dataset in the second model were included from June 2018 to June 2021. We clustered the MTA scales into 3 groups (0,1), (2), (3,4) by clinical significance. After analyzing both sides, the higher scale was determined. To compare the performance of the two models, the test dataset of each model and the ADNI dataset were applied and compared.

#### RESULTS

In first training dataset, group 0, 1, and 2 were 261 (33%), 202 (26%), and 330 (42%) patients, respectively. In the first test dataset, groups 0, 1, and 2 were all 50 (33%) patients, respectively. In second training dataset, group 0, 1, and 2 were 216 (18%), 586 (49%) and 398 (33%) patients, respectively. In second test dataset, group 0, 1 and 2 were 28 (28%), 37 (37%), and 35 (35%) patients, respectively. We conducted an ablation study to compare with various baseline models, and our proposed model achieved the best performance (precision 0.801, recall 0.787, and AUC 0.923). In the first model, the accuracy using the test dataset was 0.787. The accuracy of the second model using the same test dataset applied to the first model was 0.833. In ADNI test dataset, group 0, 1, and 2 were 67 (17%), 198 (50%), and 135 (34%), respectively. The accuracies of both models were 0.613 and 0.642 (the first model and second model), respectively.

#### CONCLUSION

The deep learning-based automatic classification algorithm using a multi-modality cascade transformer may allow accurate classification of the MTA scale.

#### CLINICAL RELEVANCE/APPLICATION

It may be possible to reduce the inter/intra-observer variation in measuring the MTA scale using the deep learning model that we proposed.

Printed on: 02/07/23

## Abstract Archives of the RSNA, 2022

R2-SPNR-8

### Development and Validation of a Deep Learning-based Automatic Segmentation and Classification of Cerebral White Matter Hyperintensities

Thursday, Dec. 1 9:00AM - 9:30AM Room: Learning Center - NR DPS

#### Participants

Wooseok Jung, MSc, Seoul, Korea, Republic Of (*Presenter*) Nothing to Disclose

#### PURPOSE

White matter hyperintensities (WMH) commonly attribute to vascular dementia and represent neuroimaging markers of cerebral small vessel disease. Fazekas scale is used to quantify WMH severity in radiology research. An automatic quantification model covering both WMH segmentation and Fazekas scale classification has not yet been explored in depth. We aimed to develop and validate a deep learning-based automatic segmentation and classification of cerebral white matter hyperintensities in patients with cognitive impairment.

#### METHODS AND MATERIALS

This observational study included consecutive patients with cognitive impairment from a tertiary hospital. A segmentation model using the 2D UNet for training and validation was performed on the dataset of 511 and 64, respectively. An input FLAIR and the corresponding output mask of the segmentation model are concatenated to generate 2-channel input of Fazekas classification model. Two separated classification models for each WMH subtypes using 3D EfficientNetv2 for training and validation were performed on the dataset of 1661 and 110, respectively. Test of segmentation model was performed on the 278 the ADNI dataset. Test of the Fazekas scale classification model was performed on 100 ADNI dataset and 178 dataset of the tertiary hospital included. For the evaluation of the Fazekas scale classification, the datasets used in the test model were evaluated by four experienced neuroradiologists. Classification according to the Fazekas scale was divided into three categories (normal/mild, moderate, and severe), and locations were separately reported as periventricular (PVMH) and deep white matter (DWMH).

#### RESULTS

Dice score performance of the segmentation model on test dataset by target location subtype were  $0.744 \pm 0.108$ ,  $0.904 \pm 0.054$ ,  $0.851 \pm 0.068$  (PVMH and DWMH, PVMH only, DWMH only), respectively. Dice score only concerning PVMH on test dataset by the three categories were  $0.907 \pm 0.044$ ,  $0.948 \pm 0.011$ , and  $0.957 \pm 0.014$ , respectively. Dice score only concerning DWMH on the same test dataset by the three categories were  $0.844 \pm 0.057$ ,  $0.946 \pm 0.023$ , and  $0.954 \pm 0.015$ , respectively. The accuracy of performance of the Fazekas scale classification model by single rater were 0.86 and 0.87 at PVMH and DWMH, respectively. The accuracy evaluated against mean of multi-rater labels were 0.76 and 0.69 at PVMH and DWMH, respectively.

#### CONCLUSION

s These results demonstrate the excellent segmentation and classification performance of our models and their potential for deployment as accurate diagnostic support tools for quantified evaluation of WMH.

#### CLINICAL RELEVANCE/APPLICATION

It may be possible to segment and classify white matter hyperintensities using a deep learning model that we proposed.

Printed on: 02/07/23

## Abstract Archives of the RSNA, 2022

R2-SPOB

### OB/Gynecology Thursday Poster Discussions

Thursday, Dec. 1 9:00AM - 9:30AM Room: Learning Center - OB DPS

#### Participants

Hanna M. Zafar, MD, Philadelphia, PA (*Moderator*) Nothing to Disclose

#### Sub-Events

### R2-SPOB-1 Comparison of Capability for Image Quality Improvements between Women's Pelvic Diffusion-Weighted Imaging with and without Reverse Encoding Distortion Correction at a 1.5 T MR System

#### Participants

Yoshiharu Ohno, MD, PhD, Toyoake, Japan (*Presenter*) Research Grant, Canon Medical Systems Corporation; Research Grant, Daiichi Sankyo Co, Ltd; Research Grant, Ministry of Education, Culture, Sports, Science and Technology

#### PURPOSE

To determine the capability for image quality improvements between women's pelvic diffusion weighted imaging (DWI) with and without reverse encoding distortion correction (RDC) at a 1.5 T MR system.

#### METHODS AND MATERIALS

Thirty-one consecutive female patients with various pelvic diseases underwent DWIs with and without RDC at a 1.5T MR system, and each ADC map was reconstructed. For quantitative image quality assessments, signal-to-noise ratio (SNR) on each DWI at b value as 1000mm<sup>2</sup>/s and ADC value of gluteal muscle were determined by ROI measurement. For qualitative image quality assessments, two board certified radiologists assessed overall image quality (OIQ), deformation severity (DS) and diagnostic confidence level (DCL) by 5-point scales, and each final score was determined as consensus of two readers. On quantitative image quality evaluations, SNR was compared between both DWIs by paired t-test. Correlation of ADC value between both DWIs were evaluated by Spearman's rank correlation coefficient. The limits of agreement of ADC between both DWIs were determined by Bland-Altman analysis. For qualitative image quality evaluations, inter-observer agreement on each DWI was assessed by ? statistics followed by ?2 test. Finally, both indexes were compared between two DWIs by Wilcoxon signed-rank test.

#### RESULTS

There was no significant difference of SNR between both DWIs ( $p>0.05$ ). There were significant correlations of ADC values between DWIs with and without RDC ( $r=0.92$ ,  $p<0.001$ ). There were no significant differences of ADC values between two methods ( $p>0.05$ ), the limits of agreement in the gluteal muscle were determined as  $0.009 \pm 0.017$ s/mm<sup>2</sup>. Inter-observer agreements for all qualitative indexes were determined as 'substantial' or 'excellent' ( $0.78 < r < 0.97$ ,  $p < 0.0001$ ). OIQ and DCL of DWI with RDC (OIQ: Median 5, IQR 4-5; DCL: Median 5, IQR 5-5) were significantly higher than those without RDC (OIQ: Median 4, IQR 3-5,  $p=0.0004$ ; DCL: Median 5, IQR 4-5,  $p=0.03$ ). DS of DWI with RDC (Median 1, IQR 1-2) was significantly lower than that without RDC (Median 2, IQR 1-3,  $p=0.0004$ ).

#### CONCLUSION

s RDC is able to improve image quality without any influence on ADC evaluation on women's pelvic DWI at 1.5 T system.

#### CLINICAL RELEVANCE/APPLICATION

RDC is useful for image quality improvement with reducing image deformation on women's pelvic DWI at 1.5 T system.

Printed on: 02/07/23

## Abstract Archives of the RSNA, 2022

R2-SPOB-1

### Comparison of Capability for Image Quality Improvements between Women's Pelvic Diffusion-Weighted Imaging with and without Reverse Encoding Distortion Correction at a 1.5 T MR System

Thursday, Dec. 1 9:00AM - 9:30AM Room: Learning Center - OB DPS

#### Participants

Yoshiharu Ohno, MD, PhD, Toyoake, Japan (*Presenter*) Research Grant, Canon Medical Systems Corporation; Research Grant, Daiichi Sankyo Co, Ltd; Research Grant, Ministry of Education, Culture, Sports, Science and Technology

#### PURPOSE

To determine the capability for image quality improvements between women's pelvic diffusion weighted imaging (DWI) with and without reverse encoding distortion correction (RDC) at a 1.5 T MR system.

#### METHODS AND MATERIALS

Thirty-one consecutive female patients with various pelvic diseases underwent DWIs with and without RDC at a 1.5T MR system, and each ADC map was reconstructed. For quantitative image quality assessments, signal-to-noise ratio (SNR) on each DWI at b value as 1000mm<sup>2</sup>/s and ADC value of gluteal muscle were determined by ROI measurement. For qualitative image quality assessments, two board certified radiologists assessed overall image quality (OIQ), deformation severity (DS) and diagnostic confidence level (DCL) by 5-point scales, and each final score was determined as consensus of two readers. On quantitative image quality evaluations, SNR was compared between both DWIs by paired t-test. Correlation of ADC value between both DWIs were evaluated by Spearman's rank correlation coefficient. The limits of agreement of ADC between both DWIs were determined by Bland-Altman analysis. For qualitative image quality evaluations, inter-observer agreement on each DWI was assessed by ? statistics followed by ?2 test. Finally, both indexes were compared between two DWIs by Wilcoxon signed-rank test.

#### RESULTS

There was no significant difference of SNR between both DWIs ( $p>0.05$ ). There were significant correlations of ADC values between DWIs with and without RDC ( $r=0.92$ ,  $p<0.001$ ). There were no significant differences of ADC values between two methods ( $p>0.05$ ), the limits of agreement in the gluteal muscle were determined as  $0.009 \pm 0.017$ s/mm<sup>2</sup>. Inter-observer agreements for all qualitative indexes were determined as 'substantial' or 'excellent' ( $0.78<r<0.97$ ,  $p<0.0001$ ). OIQ and DCL of DWI with RDC (OIQ: Median 5, IQR 4-5; DCL: Median 5, IQR 5-5) were significantly higher than those without RDC (OIQ: Median 4, IQR 3-5,  $p=0.0004$ ; DCL: Median 5, IQR 4-5,  $p=0.03$ ). DS of DWI with RDC (Median 1, IQR 1-2) was significantly lower than that without RDC (Median 2, IQR 1-3,  $p=0.0004$ ).

#### CONCLUSION

s RDC is able to improve image quality without any influence on ADC evaluation on women's pelvic DWI at 1.5 T system.

#### CLINICAL RELEVANCE/APPLICATION

RDC is useful for image quality improvement with reducing image deformation on women's pelvic DWI at 1.5 T system.

Printed on: 02/07/23

## Abstract Archives of the RSNA, 2022

R2-SPPD

### Pediatric Thursday Poster Discussions

Thursday, Dec. 1 9:00AM - 9:30AM Room: Learning Center - PD DPS

#### Participants

Jonathan D. Samet, MD, Chicago, IL (*Moderator*) Nothing to Disclose

#### Sub-Events

#### R2-SPPD-1 Neurological Consequences of COVID-19 in Children

#### Participants

Yunuen Rojas, CIUDAD NEZAHUALCOYOTL, Mexico (*Presenter*) Nothing to Disclose

#### PURPOSE

Long term neurological symptoms associated to COVID19 had been reported in adults ("Long Covid"). However, there is little information about possible neurological consequences in children. Speculations about the difficulties detecting neurological symptoms associated to COVID19 in this early stage of the neurological development had been made, pointing that these could be easily mislead towards other pathologies.

#### METHODS AND MATERIALS

We employed Resting State fMRI (rs-fMRI) to observe the underlying behavior of the brains of a cohort of 14 post-COVID19 patients, with no record of other illness prior to infection, the scans were acquired at least 3 months after hospital discharge. The results were compared to those of a control cohort of 31 healthy volunteers without record of COVID19 at scan acquirement. Scans were analyzed using CONN: functional connectivity toolbox (Version 20.b).

#### RESULTS

The acquired results showed that the children who survived COVID19 has a higher temporal correlation when compared to controls in regions Vermis 3 (Culmen) and Middle Temporal Gyrus, Temporo-occipital part (toMTG).

#### CONCLUSION

s Results suggests that post-COVID19 children could be demanding more resources while activating regions associated to visual processing mechanism. Empirical data about the asociated symptoms.

#### CLINICAL RELEVANCE/APPLICATION

Employing functional Magnetic Resonance Imaging (fMRI), an study in post-COVID19 children was driven seeking after functional differences in the basal behavior of their brains directly correlated to the virus.

Printed on: 02/07/23



## Abstract Archives of the RSNA, 2022

R2-SPPD-1

### Neurological Consequences of COVID-19 in Children

Thursday, Dec. 1 9:00AM - 9:30AM Room: Learning Center - PD DPS

#### Participants

Yunuen Rojas, CIUDAD NEZAHUALCOYOTL, Mexico (*Presenter*) Nothing to Disclose

#### PURPOSE

Long term neurological symptoms associated to COVID19 had been reported in adults ("Long Covid"). However, there is little information about possible neurological consequences in children. Speculations about the difficulties detecting neurological symptoms associated to COVID19 in this early stage of the neurological development had been made, pointing that these could be easily mislead towards other pathologies.

#### METHODS AND MATERIALS

We employed Resting State fMRI (rs-fMRI) to observe the underlying behavior of the brains of a cohort of 14 post-COVID19 patients, with no record of other illness prior to infection, the scans were acquired at least 3 months after hospital discharge. The results were compared to those of a control cohort of 31 healthy volunteers without record of COVID19 at scan acquirement. Scans were analyzed using CONN: functional connectivity toolbox (Version 20.b).

#### RESULTS

The acquired results showed that the children who survived COVID19 has a higher temporal correlation when compared to controls in regions Vermis 3 (Culmen) and Middle Temporal Gyrus, Temporo-occipital part (toMTG).

#### CONCLUSION

s Results suggests that post-COVID19 children could be demanding more resources while activating regions associated to visual processing mechanism. Empirical data about the asociated symptoms.

#### CLINICAL RELEVANCE/APPLICATION

Employing functional Magnetic Resonance Imaging (fMRI), an study in post-COVID19 children was driven seeking after functional differences in the basal behavior of their brains directly correlated to the virus.

Printed on: 02/07/23

## Abstract Archives of the RSNA, 2022

R2-SPPH

### Physics Thursday Poster Discussions

Thursday, Dec. 1 9:00AM - 9:30AM Room: Learning Center - PH DPS

#### Participants

Scott Hsieh, Rochester, MN (*Moderator*) Nothing to Disclose

#### Sub-Events

#### R2-SPPH-1 Local Diagnostic Reference Levels in North of Mexico

##### Participants

Maria del Carmen Franco, MS, Monterrey, Mexico (*Presenter*) Nothing to Disclose

#### PURPOSE

To establish local diagnostic reference levels (DRL) from adult patients in chest and abdominal CT.

#### METHODS AND MATERIALS

Observational, descriptive, and retrospective study, limited to the technical factors obtained in four different private and public hospitals in the north of Mexico. The data was obtained during a 9-month period using RIS/PACS system. Only examinations with complete patient information, older than 16 years old, and with normal CT abdominal or thorax protocol were included. Those with more than one body part scan and the ones with contrast materials were excluded. The size of the patient was determined by measuring thickness and anteroposterior diameters in the axial images. The water-equivalent diameter was used to determine the Size Specific Dose Estimate from volume CT dose index.

#### RESULTS

Local DRL for CT DIvol, SSDE and Dose-length product as the median value of each variable. For all CT scans, the DRL and SSDE were higher for patients of larger size than those of smaller size. The local DRLs were comparable to current published values in the United States.

#### CONCLUSION

We were able to establish local DRLs for the most frequent CT scans in our institutions. These are within US DRL, which suggests that patient doses with our current protocols (yielding acceptable image quality) are within a typical practice in that Country. To our knowledge, this represents the first time in our country that DRLs are used in patients using their size.

#### CLINICAL RELEVANCE/APPLICATION

This study shows that in our country, other hospitals can adopt DRLs to their practice, which benefits the patient and protects the ALARA concept.

#### R2-SPPH-2 Setting Local Dose Reference Levels in Pediatric CT With a Dose Management Software

##### Participants

Maria Perez Fernandez, MSc, (*Presenter*) Nothing to Disclose

#### PURPOSE

To compare the doses administered in pediatric CT examinations with published dose reference levels (DRLs) and to establish local dose reference levels for a public hospital that provides care to a population of 400,000 people.

#### METHODS AND MATERIALS

The CT DIvol and DLP of all examinations performed between 2016 and 2020 in three CT scanners were collected with a dose management software. The data corresponding to pediatric patients were divided by age ranges and types of CTs procedures including "Head" (854 patients), "Thorax" (91 patients), "Abdomen" (62 patients) and "Joints" (183 patients). Other types of examinations were discarded. The 50th and 75th percentiles of each group were obtained. The 50th percentiles were compared to RP185 EDRLs to verify if the clinical practice is adequate in terms of patient's radiological protection. The 75th percentiles obtained were set as local DRLs when their value were lower than the published DRL and the number of CT scans analyzed were more than 20.

#### RESULTS

The median CT DIvol and DLP obtained for each type of examination and age group are lower than the corresponding published DRL, with the exception of the head DLP of the older age group, which is slightly higher. This indicates the clinical practice is adequate. The following DRLs were set: HEAD Age group under 3 months: CT DIvol =12mGy, DLP=199mGy.cm; age group between 3 months and 1 year: CT DIvol =10mGy, DLP=159mGy.cm; age group between 1 and 6 years: CT DIvol=21mGy, DLP=345mGy.cm; age group over 6 years: CT DIvol=49mGy. THORAX Age group between 1 month and 4 years: CT DIvol=1,3mGy, DLP=31mGy; age group

between 4 and 10 years: CTDIvol=2,4mGy.ABDOMEN Age group between 14 and 18 years: CTDIvol=7mGy, DLP= 323mGy.JOINTS Age group between 4 and 10 years: CTDIvol=4,8mGy, DLP=82mGy.cm; age group between 10 and 14 years: CTDIvol=4,8mGy, DLP=90mGy.cm; age group between 14 and 18 years: CTDIvol=4,8mGy, DLP=97mGy.cm.

## CONCLUSION

s The scarce number of CT scans performed in children complicates setting reliable local DRLs. However, with a dose management software acceptable statistics can be obtained in a reasonable period of time.

## CLINICAL RELEVANCE/APPLICATION

In this work, reliable local DRLs have been obtained with updated data for pediatric most common CT examinations with acceptable statistics thanks to the dose management software.

### R2-SPPH-4 Multi-Parametric Diagnostic Reference Levels (DRL) For CT: Data From 4648 Patients From 12 Sites in Brazil

Participants

Shadi Ebrahimian, MD, Boston, MA (*Presenter*) Nothing to Disclose

## PURPOSE

Diagnostic reference levels (DRL) can help in radiation dose optimization and monitoring. We conducted a prospective study on establishing multi-parametric, multi-site national (Brazil) DRL for CT exams based on patient gender, size, body regions, and clinical indications.

## METHODS AND MATERIALS

With institutional review board approvals, we prospectively included 4648 adult patients (18-99 years; male: female 2674:1974) who underwent CT at 12 sites in Brazil between January and October 2021 including: head (n=1511 patients), chest (n=1227), and abdomen-pelvis [AP] (n=842). Following information was recorded: hospital name, patient age, gender, weight, height, body mass index [BMI], clinical indications, scanner information (vendor, scanner name, slice profile), scan parameters (number of scan phases, kV, mA, pitch) and dose indices (phase-specific CT dose index volume [CTDIvol] and phase-specific and total dose length products [DLP]). Patients were divided into under-, over-, normal- and obese-BMI groups per the WHO classification. Median and 75th percentile CTDIvol and DLP values were estimated and compared for different patient groups (gender and size), body region, clinical indications.

## RESULTS

The estimated 75th percentile CTDIvol and DLP were head (46mGy, 1016mGy.cm), paranasal sinus (19mGy, 362mGy.cm), cervical spine (26mGy, 679mGy.cm), chest (11mGy, 362mGy.cm), and AP (14mGy, 753mGy.cm). The highest DLP were recorded for carotid CTA (1450mGy.cm), pulmonary CTA (602mGy.cm), oncologic abdomen CT (4667mGy.cm) ( $p<0.001$ ). For identical body part, gender, BMI, and clinical indications, there were significant and several-fold differences in both CTDIvol and DLP values across the 12 Brazilian hospitals ( $p<0.001$ ).

## CONCLUSION

s In this study most Brazilian DRL (CTDIvol and DLP) were lower or similar to the US and European reported DRLs for corresponding CT exams and protocols with variations based on clinical indications and patient size.

## CLINICAL RELEVANCE/APPLICATION

Substantial inter-site variations in radiation doses for similar BMI, body-region and clinical indications suggest an urgent need for CT technology upgrade and protocol optimization.

### R2-SPPH-5 Skin Dosimetry Model for CT Acquisitions

Participants

Mahta Mazloumi, MA, (*Presenter*) Nothing to Disclose

## PURPOSE

Skin is the first organ that is exposed to X-ray during a CT scan and it can receive a relatively high radiation dose in CT procedures with repeated exposure to the same skin area such as interventional or perfusion CT. The aim of this study is to provide a skin dose model based on CT acquisition parameters to allow dose follow-up for this organ at risk.

## METHODS AND MATERIALS

A virtual cylindrical phantom was generated (32cm,L=20cm,pixel size=0.5mm<sup>2</sup>) in DICOM format. The phantom was used as a 3D geometrical model for Monte Carlo (MC) simulations with ImpactMC (Advanced Breast-CT). The impact of acquisition parameters including tube voltage (70,80,100,120, and 140kVp), bow-tie filter (medium filter, large filter), and position in the gantry (+14, +11, +7, +3, 0, -5, and -9cm along the y-axis) on skin dose were investigated with the MC simulations. The first layer at the surface of the phantom was considered as skin (thickness 0.5mm<sup>2</sup>). The dose values were normalized to CTDIvol (D\_CTDI). In addition, the model was validated with experimental TLD measurements and MC simulations on the humanoid Rando Alderson (RA) phantom for the large filter at 120kVp and 80-mm collimation.

## RESULTS

Results show increase in the skin dose for decreasing distance to the isocenter. For distances smaller than 120mm, four curves were fitted to the data based on high tube voltage (HV) at 100,120, and 140kVp, low tube voltage (LV) at 70 and 80kVp, medium filter (MF), and large (LF) with the equation  $D\_CTDI=A*x(mm)^2+B*x(mm)+C$ . The values of A, B, and C for the investigated tube voltages and filters are as follows; for HV-MF:  $A=4.71E-05$ ,  $B=92.95E-05$ ,  $C=2.09$ , for LV-MF:  $A=6.92E-05$ ,  $B=240E-05$ ,  $C=2.59$ , for HV-LF:  $A=3.96E-05$ ,  $B=62.58E-05$ ,  $C=1.80$  and for LV-LF:  $A=4.75E-05$ ,  $B=25.49E-05$ ,  $C=1.96$ . For distances larger than 120mm, the curves for the various kVp selections differ marginally, and one fitting formula is sufficient ( $A=3.74E-05$ ,  $B=-0.02$ ,  $C=2.79$ ) to estimate skin dose for all combinations with an average error of 4.3% between this estimation and estimations of the exact equations. Additionally, the skin dose values of RA phantom were in good agreement with our model at 120kVp and LF. The average deviation between the experimental TLD measurement on the RA phantom and the MC simulations of the phantom was 9%.

## CONCLUSION

s The developed skin dose model can estimate skin dose as a function of filter type, tube voltage, and skin-isocenter distance in CT imaging.

## CLINICAL RELEVANCE/APPLICATION

The developed skin dose model in this study has the potential to enable the implementation of a systematic skin dose assessment and registration in clinical CT imaging. Additionally, it can estimate skin dose prior to the CT scan based on the localizer scan in combination with selected acquisition parameters.

## R2-SPPH-6 Application of Deep Learning Image Reconstruction (DLIR) Algorithm to Improve Image Quality in CT Angiography of Children With Takayasu Arteritis

Participants

Ji Hang Sun, Beijing, China (*Presenter*) Nothing to Disclose

## PURPOSE

Objective: To evaluate the image quality improvement in CT angiography (CTA) of children with Takayasu arteritis (TAK) using a deep learning image reconstruction (DLIR) in comparison to other reconstruction algorithms.

## METHODS AND MATERIALS

32 patients (9.14±4.51 years old) with TAK underwent abdominal CTA with 100kVp were enrolled. Images were reconstructed at 0.625mm slice thickness using Filtered Back-Projection (FBP), 50% adaptive statistical iterative reconstruction-V (50%ASIR-V), 100%ASIR-V and DLIR with high setting (DLIR-H). The CT number and standard deviation (SD) of the descending aorta and back muscle were measured and contrast-to-noise ratio (CNR) for aorta was calculated. The vessel visualization, overall image noise and diagnostic confidence were evaluated using a 5-point scale (5, excellent; 3, acceptable) by 2 observers.

## RESULTS

There was no significant difference in CT number across all reconstructions. The image noise values (in HU) were 31.36±6.01, 24.96±4.69, 18.46±3.91 and 15.58±3.65, and CNR values for aorta were 11.93±2.12, 15.66±2.37, 22.54±3.34 and 24.02±4.55 with FBP, 50%ASIR-V, 100%ASIR-V and DLIR-H, respectively. The DLIR-H images had the lowest image noise and highest CNR among all reconstructions. The subjective evaluation suggested that all images were diagnostic for large arteries, but only 50%ASIR-V and DLIR-H met the diagnostic requirement for small arteries (3.03±0.18 and 3.53±0.51) with the combination of image noise and spatial resolution.

## CONCLUSION

s DLIR-H improves the CTA image quality and diagnostic confidence for TAK patients compared with 50%ASIR-V, and best balances image noise and spatial resolution compared with 100%ASIR-V.

## CLINICAL RELEVANCE/APPLICATION

DLIR-H can be used in CTA for patients with Takayasu's arteritis to improve overall image quality and the identification of small vessels.

## R2-SPPH-7 Model-Specific Benchmarks for Non-contrast Head and Brain CT Imaging

Participants

Jered Wells, PhD, Glenwood, IL (*Presenter*) Employee, LANDAUER, Inc;Consultant, Vaxa Medical Physics;Research Consultant, Agfa-Gevaert Group

## PURPOSE

Effective computed tomography (CT) protocol review includes comparison of average CTDIvol per protocol against available (national) benchmarks. While comparisons to benchmarks can be an effective gauge of individual system performance relative to the general practice of CT imaging, these benchmarks do not account for potential differences between CT scanner models and system implementation preferences. This work investigates the utility of model-specific CT benchmarks for non-contrast head and brain imaging and compares this against the variability in site-specific implementation.

## METHODS AND MATERIALS

Anonymized adult CT HEAD BRAIN WO IVCON exposure data from calendar year 2021 were collected using LANDAUER OPTIMIZE dose monitoring software. Thirteen CT scanner models (70 individual scanners installed at 50 imaging facilities) qualified for analysis based on 66,057 eligible non-contrast head exams. A CT scanner model qualified for analysis if at least four scanners from at least two imaging facilities had at least 50 eligible image series per scanner. A two-way ANOVA test with significance threshold  $\alpha = 0.05$  was performed to analyze the effects of CT scanner model and imaging facility (i.e. site-specific implementation) on CTDIvol.

## RESULTS

The overall median CTDIvol was 48.12 mGy (IQR = 43.92-52.79 mGy) which is comparable to established national benchmarks for CT HEAD BRAIN WO IVCON derived from Kanal, et. al. (2017) who report median CTDIvol (achievable dose) of 49 mGy and upper quartile (diagnostic reference level) of 56 mGy for this protocol. Two-way ANOVA analysis of CTDIvol showed that scanner model had a significant effect ( $p = 0.022$ ), and imaging facility had a highly significant effect ( $p << 0.001$ ). Interaction effects between CT scanner model and imaging facility were not statistically significant ( $p = 0.109$ ).

## CONCLUSION

s Scanner model is an important determinant of achievable CTDIvol for non-contrast head and brain CT imaging. Furthermore, site-specific scanner implementation was found to be an even greater source of CTDIvol variability than scanner model. This suggests that scanner options and institutional imaging protocol preferences have an outsized influence on CT dose over scanner base model. Even so, model-specific CT benchmarks are merited for better CT dose management in accordance with scanner model capabilities.

## CLINICAL RELEVANCE/APPLICATION

Comparison of CT DIvol to national benchmarks is the current gold standard for CT dose management, but variation between scanner models and implementation preferences make it difficult to determine when protocols are truly optimized.

## R2-SPPH-8 Potential CT Radiation Dose Reduction to the Female Breast by a Novel Risk-Minimizing Tube Current Modulation

Participants

Laura Klein, Heidelberg, Germany (*Presenter*) Nothing to Disclose

## PURPOSE

To compare riskTCM, a recently proposed tube current modulation technique intended to minimize the patient radiation risk, with a conventional mAs-minimizing TCM (mAsTCM) and an established organ-specific TCM (osTCM) with special focus on the female breast.

## METHODS AND MATERIALS

To reduce dose to the female breast in CT, different TCM methods are available. Typical methods used in clinical systems are the mAs-minimizing TCM (mAsTCM) as well as organ-specific TCMs (osTCM). Both methodologies do not account for the actual patient risk but minimize physical quantities. While mAsTCM minimizes the mAs-product at constant image quality, osTCM reduces the mAs for anterior views to spare the female breast. Herein, osTCM is implemented to be similar to the X-Care algorithm (Siemens Healthineers) which reduces the mAs for 120° in front of the patient compared to a reference value. We consider two cases: in the first case, the mAs in front of the patient is reduced to 25% (osTCM25%), in the other case it is reduced to 0% (osTCM0%) while keeping the total mAs-product constant. The actual patient risk is only considered in the riskTCM method. This is done by minimizing the effective dose to the patient. The prior knowledge required to do so can, e.g., be obtained by using a coarse reconstruction from topogram(s). The three TCM methods are retrospectively applied to thorax scans of seven patients using a tube voltage of 70 kV. The effective dose reduction for mAsTCM, osTCM0%, osTCM25%, and riskTCM are compared to a case with constant tube current (noTCM).

## RESULTS

On average, the reduction of total effective dose for the entire chest compared to the case of noTCM is 14% for mAsTCM, 18% for osTCM25%, 21% for osTCM0%, and 33% for riskTCM. The reduction of dose delivered to breast tissue compared to noTCM is about 7% for mAsTCM, 28% for osTCM25%, 36% for osTCM0%, and 55% for riskTCM.

## CONCLUSION

The proposed riskTCM method allows for the highest reduction of effective dose and, surprisingly, of dose to the breast amongst all investigated TCMs.

## CLINICAL RELEVANCE/APPLICATION

riskTCM can potentially further reduce the effective dose in CT examinations of the female breast compared to current clinically used algorithms.

Printed on: 02/07/23

## Abstract Archives of the RSNA, 2022

R2-SPPH-1

### Local Diagnostic Reference Levels in North of Mexico

Thursday, Dec. 1 9:00AM - 9:30AM Room: Learning Center - PH DPS

#### Participants

Maria del Carmen Franco, MS, Monterrey, Mexico (*Presenter*) Nothing to Disclose

#### PURPOSE

To establish local diagnostic reference levels (DRL) from adult patients in chest and abdominal CT.

#### METHODS AND MATERIALS

Observational, descriptive, and retrospective study, limited to the technical factors obtained in four different private and public hospitals in the north of Mexico. The data was obtained during a 9-month period using RIS/PACS system. Only examinations with complete patient information, older than 16 years old, and with normal CT abdominal or thorax protocol were included. Those with more than one body part scan and the ones with contrast materials were excluded. The size of the patient was determined by measuring thickness and anteroposterior diameters in the axial images. The water-equivalent diameter was used to determine the Size Specific Dose Estimate from volume CT dose index.

#### RESULTS

Local DRL for CT DIvol, SSDE and Dose-length product as the median value of each variable. For all CT scans, the DRL and SSDE were higher for patients of larger size than those of smaller size. The local DRLs were comparable to current published values in the United States.

#### CONCLUSION

s We were able to establish local DRLs for the most frequent CT scans in our institutions. These are within US DRL, which suggests that patient doses with our current protocols (yielding acceptable image quality) are within a typical practice in that Country. To our knowledge, this represents the first time in our country that DRLs are used in patients using their size.

#### CLINICAL RELEVANCE/APPLICATION

This study shows that in our country, other hospitals can adopt DRLs to their practice, which benefits the patient and protects the ALARA concept.

Printed on: 02/07/23

## Abstract Archives of the RSNA, 2022

R2-SPPH-2

### Setting Local Dose Reference Levels in Pediatric CT With a Dose Management Software

Thursday, Dec. 1 9:00AM - 9:30AM Room: Learning Center - PH DPS

#### Participants

Maria Perez Fernandez, MSc, (*Presenter*) Nothing to Disclose

#### PURPOSE

To compare the doses administered in pediatric CT examinations with published dose reference levels (DRLs) and to establish local dose reference levels for a public hospital that provides care to a population of 400,000 people.

#### METHODS AND MATERIALS

The CT DIvol and DLP of all examinations performed between 2016 and 2020 in three CT scanners were collected with a dose management software. The data corresponding to pediatric patients were divided by age ranges and types of CTs procedures including "Head" (854 patients), "Thorax" (91 patients), "Abdomen" (62 patients) and "Joints" (183 patients). Other types of examinations were discarded. The 50th and 75th percentiles of each group were obtained. The 50th percentiles were compared to RP185 EDRLs to verify if the clinical practice is adequate in terms of patient's radiological protection. The 75th percentiles obtained were set as local DRLs when their value were lower than the published DRL and the number of CT scans analyzed were more than 20.

#### RESULTS

The median CT DIvol and DLP obtained for each type of examination and age group are lower than the corresponding published DRL, with the exception of the head DLP of the older age group, which is slightly higher. This indicates the clinical practice is adequate. The following DRLs were set: HEAD Age group under 3 months: CT DIvol =12mGy, DLP=199mGy.cm; age group between 3 months and 1 year: CT DIvol =10mGy, DLP=159mGy.cm; age group between 1 and 6 years: CT DIvol=21mGy, DLP=345mGy.cm; age group over 6 years: CT DIvol=49mGy. THORAX Age group between 1 month and 4 years: CT DIvol=1,3mGy, DLP=31mGy; age group between 4 and 10 years: CT DIvol=2,4mGy. ABDOMEN Age group between 14 and 18 years: CT DIvol=7mGy, DLP= 323mGy. JOINTS Age group between 4 and 10 years: CT DIvol=4,8mGy, DLP=82mGy.cm; age group between 10 and 14 years: CT DIvol=4,8mGy, DLP=90mGy.cm; age group between 14 and 18 years: CT DIvol=4,8mGy, DLP=97mGy.cm.

#### CONCLUSION

s The scarce number of CT scans performed in children complicates setting reliable local DRLs. However, with a dose management software acceptable statistics can be obtained in a reasonable period of time.

#### CLINICAL RELEVANCE/APPLICATION

In this work, reliable local DRLs have been obtained with updated data for pediatric most common CT examinations with acceptable statistics thanks to the dose management software.

Printed on: 02/07/23

## Abstract Archives of the RSNA, 2022

R2-SPPH-4

### Multi-Parametric Diagnostic Reference Levels (DRL) For CT: Data From 4648 Patients From 12 Sites in Brazil

Thursday, Dec. 1 9:00AM - 9:30AM Room: Learning Center - PH DPS

#### Participants

Shadi Ebrahimi, MD, Boston, MA (*Presenter*) Nothing to Disclose

#### PURPOSE

Diagnostic reference levels (DRL) can help in radiation dose optimization and monitoring. We conducted a prospective study on establishing multi-parametric, multi-site national (Brazil) DRL for CT exams based on patient gender, size, body regions, and clinical indications.

#### METHODS AND MATERIALS

With institutional review board approvals, we prospectively included 4648 adult patients (18-99 years; male: female 2674:1974) who underwent CT at 12 sites in Brazil between January and October 2021 including: head (n=1511 patients), chest (n=1227), and abdomen-pelvis [AP] (n=842). Following information was recorded: hospital name, patient age, gender, weight, height, body mass index [BMI], clinical indications, scanner information (vendor, scanner name, slice profile), scan parameters (number of scan phases, kV, mA, pitch) and dose indices (phase-specific CT dose index volume [CTDIvol] and phase-specific and total dose length products [DLP]). Patients were divided into under-, over-, normal- and obese-BMI groups per the WHO classification. Median and 75th percentile CTDIvol and DLP values were estimated and compared for different patient groups (gender and size), body region, clinical indications.

#### RESULTS

The estimated 75th percentile CTDIvol and DLP were head (46mGy, 1016mGy.cm), paranasal sinus (19mGy, 362mGy.cm), cervical spine (26mGy, 679mGy.cm), chest (11mGy, 362mGy.cm), and AP (14mGy, 753mGy.cm). The highest DLP were recorded for carotid CTA (1450mGy.cm), pulmonary CTA (602mGy.cm), oncologic abdomen CT (4667mGy.cm) ( $p<0.001$ ). For identical body part, gender, BMI, and clinical indications, there were significant and several-fold differences in both CTDIvol and DLP values across the 12 Brazilian hospitals ( $p<0.001$ ).

#### CONCLUSION

In this study most Brazilian DRL (CTDIvol and DLP) were lower or similar to the US and European reported DRLs for corresponding CT exams and protocols with variations based on clinical indications and patient size.

#### CLINICAL RELEVANCE/APPLICATION

Substantial inter-site variations in radiation doses for similar BMI, body-region and clinical indications suggest an urgent need for CT technology upgrade and protocol optimization.

Printed on: 02/07/23

## Abstract Archives of the RSNA, 2022

R2-SPPH-5

### Skin Dosimetry Model for CT Acquisitions

Thursday, Dec. 1 9:00AM - 9:30AM Room: Learning Center - PH DPS

#### Participants

Mahta Mazloumi, MA, (*Presenter*) Nothing to Disclose

#### PURPOSE

Skin is the first organ that is exposed to X-ray during a CT scan and it can receive a relatively high radiation dose in CT procedures with repeated exposure to the same skin area such as interventional or perfusion CT. The aim of this study is to provide a skin dose model based on CT acquisition parameters to allow dose follow-up for this organ at risk.

#### METHODS AND MATERIALS

A virtual cylindrical phantom was generated (32cm,L=20cm, pixel size=0.5mm<sup>2</sup>) in DICOM format. The phantom was used as a 3D geometrical model for Monte Carlo (MC) simulations with ImpactMC (Advanced Breast-CT). The impact of acquisition parameters including tube voltage (70,80,100,120, and 140kVp), bow-tie filter (medium filter, large filter), and position in the gantry (+14, +11, +7, +3, 0, -5, and -9cm along the y-axis) on skin dose were investigated with the MC simulations. The first layer at the surface of the phantom was considered as skin (thickness 0.5mm<sup>2</sup>). The dose values were normalized to CTDIvol (D<sub>CTDI</sub>). In addition, the model was validated with experimental TLD measurements and MC simulations on the humanoid Rando Alderson (RA) phantom for the large filter at 120kVp and 80-mm collimation.

#### RESULTS

Results show increase in the skin dose for decreasing distance to the isocenter. For distances smaller than 120mm, four curves were fitted to the data based on high tube voltage (HV) at 100,120, and 140kVp, low tube voltage (LV) at 70 and 80kVp, medium filter (MF), and large (LF) with the equation  $D_{CTDI}=A*x(mm)^2+B*x(mm)+C$ . The values of A, B, and C for the investigated tube voltages and filters are as follows; for HV-MF: A=-4.71E-05, B=-92.95E-05, C=2.09, for LV-MF: A=6.92E-05, B=-240E-05, C=2.59, for HV-LF: A=-3.96E-05, B=62.58E-05, C=1.80 and for LV-LF: A=-4.75E-05, B=25.49E-05, C=1.96. For distances larger than 120mm, the curves for the various kVp selections differ marginally, and one fitting formula is sufficient (A=3.74E-05, B=-0.02, C=2.79) to estimate skin dose for all combinations with an average error of 4.3% between this estimation and estimations of the exact equations. Additionally, the skin dose values of RA phantom were in good agreement with our model at 120kVp and LF. The average deviation between the experimental TLD measurement on the RA phantom and the MC simulations of the phantom was 9%.

#### CONCLUSION

The developed skin dose model can estimate skin dose as a function of filter type, tube voltage, and skin-isocenter distance in CT imaging.

#### CLINICAL RELEVANCE/APPLICATION

The developed skin dose model in this study has the potential to enable the implementation of a systematic skin dose assessment and registration in clinical CT imaging. Additionally, it can estimate skin dose prior to the CT scan based on the localizer scan in combination with selected acquisition parameters.

Printed on: 02/07/23

## Abstract Archives of the RSNA, 2022

R2-SPPH-6

### Application of Deep Learning Image Reconstruction (DLIR) Algorithm to Improve Image Quality in CT Angiography of Children With Takayasu Arteritis

Thursday, Dec. 1 9:00AM - 9:30AM Room: Learning Center - PH DPS

#### Participants

Ji Hang Sun, Beijing, China (*Presenter*) Nothing to Disclose

#### PURPOSE

Objective: To evaluate the image quality improvement in CT angiography (CTA) of children with Takayasu arteritis (TAK) using a deep learning image reconstruction (DLIR) in comparison to other reconstruction algorithms.

#### METHODS AND MATERIALS

32 patients (9.14±4.51 years old) with TAK underwent abdominal CTA with 100kVp were enrolled. Images were reconstructed at 0.625mm slice thickness using Filtered Back-Projection (FBP), 50% adaptive statistical iterative reconstruction-V (50%ASIR-V), 100%ASIR-V and DLIR with high setting (DLIR-H). The CT number and standard deviation (SD) of the descending aorta and back muscle were measured and contrast-to-noise ratio (CNR) for aorta was calculated. The vessel visualization, overall image noise and diagnostic confidence were evaluated using a 5-point scale (5, excellent; 3, acceptable) by 2 observers.

#### RESULTS

There was no significant difference in CT number across all reconstructions. The image noise values (in HU) were 31.36±6.01, 24.96±4.69, 18.46±3.91 and 15.58±3.65, and CNR values for aorta were 11.93±2.12, 15.66±2.37, 22.54±3.34 and 24.02±4.55 with FBP, 50%ASIR-V, 100%ASIR-V and DLIR-H, respectively. The DLIR-H images had the lowest image noise and highest CNR among all reconstructions. The subjective evaluation suggested that all images were diagnostic for large arteries, but only 50%ASIR-V and DLIR-H met the diagnostic requirement for small arteries (3.03±0.18 and 3.53±0.51) with the combination of image noise and spatial resolution.

#### CONCLUSION

s DLIR-H improves the CTA image quality and diagnostic confidence for TAK patients compared with 50%ASIR-V, and best balances image noise and spatial resolution compared with 100%ASIR-V.

#### CLINICAL RELEVANCE/APPLICATION

DLIR-H can be used in CTA for patients with Takayasu's arteritis to improve overall image quality and the identification of small vessels.

Printed on: 02/07/23

## Abstract Archives of the RSNA, 2022

R2-SPPH-7

### Model-Specific Benchmarks for Non-contrast Head and Brain CT Imaging

Thursday, Dec. 1 9:00AM - 9:30AM Room: Learning Center - PH DPS

#### Participants

Jered Wells, PhD, Glenwood, IL (*Presenter*) Employee, LANDAUER, Inc; Consultant, Vaxa Medical Physics; Research Consultant, Agfa-Gevaert Group

#### PURPOSE

Effective computed tomography (CT) protocol review includes comparison of average CTDIvol per protocol against available (national) benchmarks. While comparisons to benchmarks can be an effective gauge of individual system performance relative to the general practice of CT imaging, these benchmarks do not account for potential differences between CT scanner models and system implementation preferences. This work investigates the utility of model-specific CT benchmarks for non-contrast head and brain imaging and compares this against the variability in site-specific implementation.

#### METHODS AND MATERIALS

Anonymized adult CT HEAD BRAIN WO IVCON exposure data from calendar year 2021 were collected using LANDAUER OPTIMIZE dose monitoring software. Thirteen CT scanner models (70 individual scanners installed at 50 imaging facilities) qualified for analysis based on 66,057 eligible non-contrast head exams. A CT scanner model qualified for analysis if at least four scanners from at least two imaging facilities had at least 50 eligible image series per scanner. A two-way ANOVA test with significance threshold  $\alpha = 0.05$  was performed to analyze the effects of CT scanner model and imaging facility (i.e. site-specific implementation) on CTDIvol.

#### RESULTS

The overall median CTDIvol was 48.12 mGy (IQR = 43.92-52.79 mGy) which is comparable to established national benchmarks for CT HEAD BRAIN WO IVCON derived from Kanal, et. al. (2017) who report median CTDIvol (achievable dose) of 49 mGy and upper quartile (diagnostic reference level) of 56 mGy for this protocol. Two-way ANOVA analysis of CTDIvol showed that scanner model had a significant effect ( $p = 0.022$ ), and imaging facility had a highly significant effect ( $p \ll 0.001$ ). Interaction effects between CT scanner model and imaging facility were not statistically significant ( $p = 0.109$ ).

#### CONCLUSION

Scanner model is an important determinant of achievable CTDIvol for non-contrast head and brain CT imaging. Furthermore, site-specific scanner implementation was found to be an even greater source of CTDIvol variability than scanner model. This suggests that scanner options and institutional imaging protocol preferences have an outsized influence on CT dose over scanner base model. Even so, model-specific CT benchmarks are merited for better CT dose management in accordance with scanner model capabilities.

#### CLINICAL RELEVANCE/APPLICATION

Comparison of CTDIvol to national benchmarks is the current gold standard for CT dose management, but variation between scanner models and implementation preferences make it difficult to determine when protocols are truly optimized.

Printed on: 02/07/23

## Abstract Archives of the RSNA, 2022

R2-SPPH-8

### Potential CT Radiation Dose Reduction to the Female Breast by a Novel Risk-Minimizing Tube Current Modulation

Thursday, Dec. 1 9:00AM - 9:30AM Room: Learning Center - PH DPS

#### Participants

Laura Klein, Heidelberg, Germany (*Presenter*) Nothing to Disclose

#### PURPOSE

To compare riskTCM, a recently proposed tube current modulation technique intended to minimize the patient radiation risk, with a conventional mAs-minimizing TCM (mAsTCM) and an established organ-specific TCM (osTCM) with special focus on the female breast.

#### METHODS AND MATERIALS

To reduce dose to the female breast in CT, different TCM methods are available. Typical methods used in clinical systems are the mAs-minimizing TCM (mAsTCM) as well as organ-specific TCMs (osTCM). Both methodologies do not account for the actual patient risk but minimize physical quantities. While mAsTCM minimizes the mAs-product at constant image quality, osTCM reduces the mAs for anterior views to spare the female breast. Herein, osTCM is implemented to be similar to the X-Care algorithm (Siemens Healthineers) which reduces the mAs for 120° in front of the patient compared to a reference value. We consider two cases: in the first case, the mAs in front of the patient is reduced to 25% (osTCM25%), in the other case it is reduced to 0% (osTCM0%) while keeping the total mAs-product constant. The actual patient risk is only considered in the riskTCM method. This is done by minimizing the effective dose to the patient. The prior knowledge required to do so can, e.g., be obtained by using a coarse reconstruction from topogram(s). The three TCM methods are retrospectively applied to thorax scans of seven patients using a tube voltage of 70 kV. The effective dose reduction for mAsTCM, osTCM0%, osTCM25%, and riskTCM are compared to a case with constant tube current (noTCM).

#### RESULTS

On average, the reduction of total effective dose for the entire chest compared to the case of noTCM is 14% for mAsTCM, 18% for osTCM25%, 21% for osTCM0%, and 33% for riskTCM. The reduction of dose delivered to breast tissue compared to noTCM is about 7% for mAsTCM, 28% for osTCM25%, 36% for osTCM0%, and 55% for riskTCM.

#### CONCLUSION

s The proposed riskTCM method allows for the highest reduction of effective dose and, surprisingly, of dose to the breast amongst all investigated TCMs.

#### CLINICAL RELEVANCE/APPLICATION

riskTCM can potentially further reduce the effective dose in CT examinations of the female breast compared to current clinically used algorithms.

Printed on: 02/07/23

## Abstract Archives of the RSNA, 2022

R2-SPRO

### Radiation Oncology Thursday Poster Discussions

Thursday, Dec. 1 9:00AM - 9:30AM Room: Learning Center - RO DPS

#### Participants

Tracy M. Sherertz, MD, Seattle, WA (*Moderator*) Nothing to Disclose

#### Sub-Events

#### R2-SPRO-1 Racial Disparities in Patients Referred to Radiation Oncology for Palliation of Acute Pain Symptom

#### Participants

Elana Benishay, BS, (*Presenter*) Nothing to Disclose

#### PURPOSE

Despite the breadth of options available to treat pain symptoms, cancer patients are often under-treated for their level of pain. Further, there are known racial disparities in pain management. Studies have shown that patients identifying as Black or African American are significantly less likely to be prescribed pain medication or adequate doses of pain medications. The aim of this study is to investigate potential racial disparities in patients referred to the Radiation Oncology department for acute pain management.

#### METHODS AND MATERIALS

This retrospective review analyzed patients seen in consultation in the Radiation Oncology department for acute pain management between July 23, 2020, and July 23, 2021. Clinical data including patient and treatment characteristics, cancer type, pain scores and medication lists were abstracted for all identified patients. Statistical analysis was performed using univariate and multivariate logistic regression models to assess patient characteristics associated with severe pain.

#### RESULTS

The mean overall pain score was 5.95 (SD 2.53). In African American patients, the mean pain score was 6.72 (SD 2.54), while Caucasian patients had a mean pain score of 5.55 (SD 2.45). African American patients (OR 3.35,  $p=0.008$ ) were more likely to present with severe pain compared to Caucasian patients. Amongst African American patients, 40% ( $n=10$ ) reported mild to moderate pain (pain score 1-6) and 60% ( $n=15$ ) reported severe pain (pain score 7-10). Comparatively, 69% ( $n=51$ ) of Caucasian patients had mild to moderate pain and 31% ( $n=23$ ) had severe pain.

#### CONCLUSION

Patients referred to Radiation Oncology for management of acute pain are often under treated for their pain. Patients identifying as African American present with higher rates of severe pain in comparison to Caucasian patients. The findings of this study should promote the continued exposure of unjust delivery of care. Standardized practice and implicit bias training can help eliminate these disparities.

#### CLINICAL RELEVANCE/APPLICATION

Inadequate treatment of pain may lead to racial disparities, poor quality of life, and higher healthcare costs.

Printed on: 02/07/23



## Abstract Archives of the RSNA, 2022

R2-SPRO-1

### Racial Disparities in Patients Referred to Radiation Oncology for Palliation of Acute Pain Symptom

Thursday, Dec. 1 9:00AM - 9:30AM Room: Learning Center - RO DPS

#### Participants

Elana Benishay, BS, (*Presenter*) Nothing to Disclose

#### PURPOSE

Despite the breadth of options available to treat pain symptoms, cancer patients are often under-treated for their level of pain. Further, there are known racial disparities in pain management. Studies have shown that patients identifying as Black or African American are significantly less likely to be prescribed pain medication or adequate doses of pain medications. The aim of this study is to investigate potential racial disparities in patients referred to the Radiation Oncology department for acute pain management.

#### METHODS AND MATERIALS

This retrospective review analyzed patients seen in consultation in the Radiation Oncology department for acute pain management between July 23, 2020, and July 23, 2021. Clinical data including patient and treatment characteristics, cancer type, pain scores and medication lists were abstracted for all identified patients. Statistical analysis was performed using univariate and multivariate logistic regression models to assess patient characteristics associated with severe pain.

#### RESULTS

The mean overall pain score was 5.95 (SD 2.53). In African American patients, the mean pain score was 6.72 (SD 2.54), while Caucasian patients had a mean pain score of 5.55 (SD 2.45). African American patients (OR 3.35,  $p=0.008$ ) were more likely to present with severe pain compared to Caucasian patients. Amongst African American patients, 40% ( $n=10$ ) reported mild to moderate pain (pain score 1-6) and 60% ( $n=15$ ) reported severe pain (pain score 7-10). Comparatively, 69% ( $n=51$ ) of Caucasian patients had mild to moderate pain and 31% ( $n=23$ ) had severe pain.

#### CONCLUSION

Patients referred to Radiation Oncology for management of acute pain are often under treated for their pain. Patients identifying as African American present with higher rates of severe pain in comparison to Caucasian patients. The findings of this study should promote the continued exposure of unjust delivery of care. Standardized practice and implicit bias training can help eliminate these disparities.

#### CLINICAL RELEVANCE/APPLICATION

Inadequate treatment of pain may lead to racial disparities, poor quality of life, and higher healthcare costs.

Printed on: 02/07/23

## Abstract Archives of the RSNA, 2022

R5A-SPBR

### Breast Thursday Poster Discussions - A

Thursday, Dec. 1 12:15PM - 12:45PM Room: Learning Center - BR DPS

#### Participants

Stamatia Destounis, MD, Rochester, NY (*Moderator*) Medical Advisory Board, iCad, Inc

#### Sub-Events

### R5A-SPBR-1 Benefits of Reading Artificial Intelligence-enhanced Synthetic Thick Slabs Instead of Standard Thin Slices in Digital Breast Tomosynthesis

#### Participants

Stephanie Sauer, Wuerzburg, 97080, Germany (*Presenter*) Nothing to Disclose

#### PURPOSE

Digital breast tomosynthesis provides additional value over standard mammography, albeit at the cost of longer reading time. The aim of this study was to investigate the impact of reading synthetic 6-mm slabs instead of conventional 1-mm slices on interpretation time, diagnostic confidence and accuracy.

#### METHODS AND MATERIALS

For this retrospective study, radiologists with 6 (R1), 4 (R2), and 2 (R3) years of breast imaging experience reviewed 111 digital breast tomosynthesis scans in either craniocaudal (21), mediolateral (12) or mediolateral oblique orientation (78). Two datasets were interpreted independently for each examination, with one set containing standard 1-mm slices, while the other set comprised artificial intelligence-enhanced synthetic 6-mm slabs with 3-mm overlap. Blinded to histologic results and follow-up imaging, readers noted the estimated BIRADS score, maximum lesion diameter, and diagnostic confidence, while reading time was recorded. Among 111 tomosynthesis examinations, 70 findings had histologic follow-up, including 56 malignancies (4 DCIS, 42 NST, 7 lobular, and 3 other carcinomas).

#### RESULTS

Diagnostic accuracy was comparable for 6-mm thick slab and 1-mm slice readings (R1: 87.0% vs. 87.0%; R2: 86.1% vs. 87.0%; R3: 80.0% vs. 84.4%;  $p=0.125$ ), with 1 of 3 radiologists reporting higher confidence when interpreting 1-mm slices (R1:  $p=0.033$ ). Correspondingly, a significant measurement discrepancy between slabs and slices was ascertained for 1 of 3 readers (R1: mean difference of 0.8 mm;  $p=0.010$ ). No difference was found between the BIRADS scores assigned with access to 1-mm and 6-mm datasets ( $p=0.317$ ), while interrater agreement was comparably high for slabs and slices (ICC 0.848 vs. 0.865). Reading time was substantially shorter when interpreting synthetic 6-mm slabs compared to 1-mm slices (R1: 33.5 vs. 46.2 sec; R2: 49.1 vs. 64.8 sec; R3: 39.5 vs. 67.2 sec; all  $p<0.001$ ).

#### CONCLUSION

Employing a reconstruction protocol with artificial intelligence-enhanced 6-mm slabs instead of 1-mm slices for digital breast tomosynthesis facilitates similar diagnostic performance with reduced interpretation time.

#### CLINICAL RELEVANCE/APPLICATION

Interpretation of synthetic thick slabs instead of standard thin slices allows for substantial time saving without decreasing the diagnostic accuracy of radiologists.

### R5A-SPBR-2 Distinction Between Benign and Malignant Breast Masses of Digital Breast Tomosynthesis Using Deep Learning Method with Mask-R Convolutional Neural Network

#### Participants

Huizhi Cao, PhD, (*Presenter*) Nothing to Disclose

#### PURPOSE

We aimed to use deep learning with Mask-R convolutional neural network (Mask-R-CNN) to discriminate between benign and malignant breast mass images from digital breast tomosynthesis.

#### METHODS AND MATERIALS

In total, 2000 patients (1196 benign masses and 804 malignant masses) were randomly divided into the training cohort (1600 patients) and the two validation cohorts (200 patients for each cohort). Deep learning model was constructed using Mask-R-CNN architecture in two views (craniocaudal, CC and mediolateral oblique, MLO). The performance of the trained neural network was tested with this one validation cohort. Four radiologists (2 senior and 2 junior) interpreted the test data set. In a second step, the neural network was re-trained with all cases and then was tested with another validation cohort. Sensitivity, specificity, accuracy, positive predictive value (PPV), negative predictive value (NPV) and area under the receiver operating characteristic curve (AUC) were compared between readers and the neural network.

## RESULTS

For initially constructed Mask-R-CNN model, the Sensitivity, specificity, accuracy, PPV, NPV and AUC in CC view and MLO view were 92.30% Vs. 96.20%, 85.40% Vs. 81.30%, 89% Vs. 89%, 85.70% Vs. 87.40%, 91.90% Vs. 95.10%, 0.845 Vs. 0.858, respectively. The proposed model achieved better classification performance than the junior radiologists and inferior to that of senior radiologists ( $P < 0.05$ ). With the re-trained Mask-R-CNN model, the Sensitivity, specificity, accuracy, PPV, NPV and AUC in CC view and MLO view were 96.10% Vs. 96.10%, 95.90% Vs. 91.80%, 96% Vs. 94%, 96.10% Vs. 92.50%, 95.90% Vs. 95.70%, 0.949 Vs. 0.908, respectively. There was no significant difference in classification performance between AI model and senior radiologists ( $P < 0.05$ ).

## CONCLUSION

The results obtained demonstrate that the proposed Mask-R convolutional neural network is performant and can indeed be used to predict if the mass lesions are benign or malignant.

## CLINICAL RELEVANCE/APPLICATION

The study demonstrates that deep learning with Mask-R-CNN have higher performance in classifying mass lesions of digital breast tomosynthesis.

## R5A-SPBR-3 Breast Cancer Screening in the Real-World: A Multi-Site Database of Women Screened for Breast Cancer

### Participants

Emily F. Conant, MD, Philadelphia, PA (*Presenter*) Research Grant, Hologic, Inc; Advisory Panel, Hologic, Inc; Research Grant, OM1, Inc; Research Grant, iCad, Inc; Advisory Panel, iCad, Inc; Speaker, WebMD LLC

### PURPOSE

Mammographic imaging is the standard for early detection of breast cancer (BC). Digital breast tomosynthesis (DBT) improves recall and cancer detection rates over digital mammography (DM). Yet few studies describe benefits and risks of these imaging modalities in a real-world setting, including in underrepresented patient subgroups. This study provides real-world evidence (RWE) for BC screening outcomes in a large population of women in the United States (US) receiving DBT or DM screenings.

### METHODS AND MATERIALS

This retrospective, observational study included women who received routine DM or DBT screenings between 2014 and 2020 at five large healthcare organizations. Integrated electronic medical record, radiology information system, and tumor registry data were used. Women 40-79 years old with  $>1$  screening and no history of BC were included. Outcomes of recall rate (RR), cancer detection rate (CDR), positive predictive value of recall (PPV1), and biopsy rate, and corresponding 95% confidence intervals (CI), were assessed overall and by screening modality. Logistic regression models adjusted for age, breast density, site, and exam year.

### RESULTS

The cohort included 1,100,447 women and 2,528,063 screenings (2,071,741 from women with  $>2$  observed screens). Women were on average 57.3 (standard deviation 10.3) years of age, primarily white (74.5%), and post-menopausal (66.8%) with a breast density of 'scattered fibroglandular densities' (47.5%). DBT screens led to significantly reduced RR (DBT 8.9%, DM 10.3%,  $p < 0.001$ ), and increased CDR (DBT 4.3/1000, DM 4.9/1000,  $p < 0.001$ ), PPV1 (DBT 5.5%, DM 4.2%,  $p < 0.001$ ), and biopsy rates (DBT 18.1/1000, DM 14.8/1000,  $p < 0.001$ ) (see Figure). These associations remained in adjusted analyses, and were consistent across patient subgroups defined by age, race, breast density, and risk status.

### CONCLUSION

This ongoing US study of over 2.5 million mammograms offers a rich platform to explore outstanding questions around the real-world benefits and risks of breast cancer screening, particularly in key patient subgroups. In this cohort, DBT screenings were associated with reduced RR and increased CDR, PPV1, and rate of biopsy.

### CLINICAL RELEVANCE/APPLICATION

Routine screening with DBT, compared to DM, may reduce recall and increase cancer detection, biopsy rates and positive predictive value of recall.

## R5A-SPBR-4 Improved Cancer Detection with Digital Breast Tomosynthesis compared to Digital Mammography using Deep Learning Model

### Participants

Ray Mayo III, MD, Houston, TX (*Presenter*) Nothing to Disclose

### PURPOSE

There is evidence of improved reader performance using digital breast tomosynthesis (DBT) compared to full field digital mammograms (FFDM). We compared the performance of an artificial intelligence-based computer aided detection (AI-CAD) software on a set of patients who had both DBT and FFDM exams.

### METHODS AND MATERIALS

We tested performance of an AI-CAD (cmAssist™, CureMetrix, Inc, La Jolla, CA). The test set is composed of 933 patients (age range: 30-88, average 56 years) who underwent both DBT and FFDM at their screening exams, obtained between 2012 and 2018 from 2 sites in Northeastern and Southeastern United States and using 2 equipment vendors. There were 508 patients with biopsy confirmed cancer and 425 normal patients who had at least one year of followup as confirmation of benignity. Of the cancer patients, 156 had calcification lesions and 352 had mass or architectural distortion lesions. Bootstrap analysis was used to generate area under the curve (AUC) of the receiver operating characteristic which was measured at 95% confidence interval (CI) for both FFDM and DBT exams.

### RESULTS

For FFDM, cmAssist has an AUC of 0.95 [CI: 0.93 - 0.96] for calcifications. For mass and architectural distortion lesions, the AUC is 0.75 [CI: 0.72 - 0.78]. For DBT, cmAssist has an AUC of 0.96 [CI: 0.95 - 0.97] for calcifications. For mass and architectural

distortions, the AUC is 0.89 [CI: 0.87 - 0.91].

## CONCLUSION

s There was improved performance of cmAssist AI-CAD using DBT compared to FFDM. The improvement was more robust for mass and architectural distortions as expected; many of the cancers were only visible on DBT in this cancer-enriched sample of patients who underwent both FFDM and DBT. For calcifications, this AI-CAD achieves similar high performance for DBT and FFDM.

## CLINICAL RELEVANCE/APPLICATION

AI-CAD (cmAssist) shows improved performance with digital breast tomosynthesis compared to full field digital mammography and appears to be a promising aid to the radiologist in enhancing cancer detection.

## R5A-SPBR-5 Analysis of False Negative Digital BreastTomosynthesisScreening Exams

Participants

Sydney Payne, MD, BS, Palo Alto, CA (*Presenter*) Nothing to Disclose

## PURPOSE

To determine reasons for false negative (FN) digital breast tomosynthesis (DBT) screening mammograms (MG).

## METHODS AND MATERIALS

2 MQSA-certified radiologists classified FN DBT screenings from 3/31/2014- 3/31/2022 as negative studies (NS) or detectable, listing factors contributing to non-detection. We queried the EMR for patient breast cancer risk factors and cancer presentation/characteristics.

## RESULTS

There were 69,594 screens with 416 screen-detected cancers (CDR 6/1000, 416/69,592) and 56 FN (0.8/1000, 56/69,594) studies. 7/56 FN were excluded for no DBT, leaving 49 women (age 28-82 years old, mean 60 yo) with 51 cancers comprising the study (11 DCIS, 11 IDC, 24 ILC, 1 IDC/ILC and 4 other cancers) found at an average 7.5 months (range 0.5-12 mo) post screening. Most women (61%,30/49) had risk factors and dense tissue (46.9%,23/49 heterogeneously dense; 26.6%,13/49 extremely dense). Detection was by screening MRI (24/51,47%), clinical findings (23/51,45%; 19 palpation, 2 pain, 2 palpation/pain), or imaging (1 screening MG,1 screening US, 1 PET-CT, 1 CT). 35/51(57%) cancers were NS, and 16/51 (31%) were non-detected masses (14/16,87.5%) or calcifications (2/16,12.5%). Screening MRI found DCIS more often (9/11,81.2%) than palpation and/or pain (2/11,18.2%). ILC was markedly represented in the pathology (24/51,47%) and was detected more often clinically (15/24,62.5%) than on screening MRI (8/24,33.3%) or US (1/24,0.4%). Factors contributing to non-detection were dense tissue (8/16,50%), one view findings (6/16,37.5%),developing asymmetries (4/16,25%), distracting findings (3/16,18.8%), post-surgical changes (2/16,12.5%), benign appearing mass (2/16,12.5%), at image edge (2/16,12.5%), positioning (1/16,0.1%),too few calcifications (1/16,0.1%) or poor image quality (1/16,0.1%).

## CONCLUSION

s Almost half of cancers not detected by DBT were found on screening breast MRI (47%) and were ILC pathology (47%). Dense tissue and one-view findings were the most common factors contributing to non-detection.

## CLINICAL RELEVANCE/APPLICATION

The most common reason for missed cancers on DBT is dense breast tissue or one-view findings, with a predominance of ILC. Screening breast MRI found almost half of the missed cancers.

## R5A-SPBR-6 Screening Tomosynthesis Detected Breast Cancer in Women with Dense Tissue

Participants

Stamatia Destounis, MD, Rochester, NY (*Presenter*) Medical Advisory Board, iCad, Inc

## PURPOSE

To report the cancer detection rate and tumor characteristics in women with dense breast tissue having screening Digital Breast Tomosynthesis (DBT).

## METHODS AND MATERIALS

This retrospective review identified patients with dense breast tissue who had a breast cancer diagnosis that was detected on a screening Digital Breast Tomosynthesis (DBT) examination between the years of 2016 and 2021. This resulted in an analysis of 194,340 exams in 60,884 patients. VolparaDensity was utilized in real time to assess breast density versions (v1.5.3 - v4.2.2). Lesion type, lymph node status, stage, and grade were collected.

## RESULTS

Overall, 1076 cancers were detected in 913 patients by screening DBT between the years of 2016 and 2021. Most of these cancers were masses (576/1076, 54%). Of the 1076 cancers 79% (n=855) were invasive cancers and 221 (21%) were ductal carcinoma in situ. DBT was able to detect nine lymph nodes that were pathologically proven to be metastatic. In the 913 patients that were diagnosed, the cancers were Grade 1 or Grade 2 (298 (33%) and 297 (32.5%), respectively), and a majority were of early stage (Stage 0, Stage 1) (855/1076, 79%). At surgery, 73% (n=665) patients had negative nodes.

## CONCLUSION

s This retrospective review demonstrated that DBT found lower grade and early-stage malignancies in women with dense breast tissue. DBT was also able to detect metastatic lymph nodes.

## CLINICAL RELEVANCE/APPLICATION

Some facilities are only offering DBT as a diagnostic tool. Utilizing DBT for screening can aid in the detection of breast cancer in patients with dense tissue as thus far it has been shown to detect lower grade, and early-stage cancers. Greater adoption will occur with proven utility of DBT in this population.

## **R5A-SPBR-7 Automated Breast Ultrasound vs Handheld Ultrasound in Moderate Risk Breast Cancer Women With Dense Breast**

### Participants

MARIA TERESA FERNANDEZ-TARANILLA, PhD, Madrid, Spain (*Presenter*) Nothing to Disclose

### **PURPOSE**

To determine if Automated Breast UltraSound (ABUS) is at least as effective as handheld ultrasound (HHUS) in detecting lesions in intermediate risk breast cancer patients with dense breast. To compare the degree of interobserver agreement between BI-RADS categorization with ABUS vs HHUS.

### **METHODS AND MATERIALS**

200 patients (350 breast) were evaluated the same day with ABUS and HHUS between June 2020 to July 2021 in a tertiary hospital. Women with dense breast C or D according to the American College Radiology and intermediate risk were included. Previous personal breast cancer (pBC), known family history of BC (fBC), prior lesion of uncertain malignant potential (B3 lesions) and certain syndromes and gene mutations were considered as intermediate risk subcategories. BI-RADS categorization was used to determine the agreement between both techniques with Kappa index.

### **RESULTS**

Mean age of women were 47 years old, 45% had type C and 55% type D breast densities. The most frequent group of patients were the pBC (67%) and mostly were BI-RADS 2. The mean time of ABUS lecture were 4 minutes. The Kappa index was almost perfect (0.84) in the radiologist interpretation with BI-RADS between ABUS vs HHUS ( $p < 0,001$ ). Moderate agreement (0.52) was observed on pBC ( $p < 0,005$ ) always referring to the remaining breast after radical surgery. Excellent agreement (0.89) was observed on patients with fBC ( $p < 0,001$ ) and on syndromes with intermediate risk ( $p < 0,005$ ). On B3 lesions the results were not significant ( $p < 0,07$ ).

### **CONCLUSION**

s ABUS could be a valuable and cost-effective screening tool for women with dense breast and moderate risk in combination with mammography.

### **CLINICAL RELEVANCE/APPLICATION**

The screening for breast cancer on patients with dense breast is still a challenge, even more if those patients had an increased risk of cancer (15-20%). Our proposal is to introduce a cost-effective tool like ABUS in the routine screening programs to increase sensibility and specificity on patients with dense breast and moderate risk cancer.

Printed on: 02/07/23

## Abstract Archives of the RSNA, 2022

R5A-SPBR-1

### Benefits of Reading Artificial Intelligence-enhanced Synthetic Thick Slabs Instead of Standard Thin Slices in Digital Breast Tomosynthesis

Thursday, Dec. 1 12:15PM - 12:45PM Room: Learning Center - BR DPS

#### Participants

Stephanie Sauer, Wuerzburg, 97080, Germany (*Presenter*) Nothing to Disclose

#### PURPOSE

Digital breast tomosynthesis provides additional value over standard mammography, albeit at the cost of longer reading time. The aim of this study was to investigate the impact of reading synthetic 6-mm slabs instead of conventional 1-mm slices on interpretation time, diagnostic confidence and accuracy.

#### METHODS AND MATERIALS

For this retrospective study, radiologists with 6 (R1), 4 (R2), and 2 (R3) years of breast imaging experience reviewed 111 digital breast tomosynthesis scans in either craniocaudal (21), mediolateral (12) or mediolateral oblique orientation (78). Two datasets were interpreted independently for each examination, with one set containing standard 1-mm slices, while the other set comprised artificial intelligence-enhanced synthetic 6-mm slabs with 3-mm overlap. Blinded to histologic results and follow-up imaging, readers noted the estimated BIRADS score, maximum lesion diameter, and diagnostic confidence, while reading time was recorded. Among 111 tomosynthesis examinations, 70 findings had histologic follow-up, including 56 malignancies (4 DCIS, 42 NST, 7 lobular, and 3 other carcinomas).

#### RESULTS

Diagnostic accuracy was comparable for 6-mm thick slab and 1-mm slice readings (R1: 87.0% vs. 87.0%; R2: 86.1% vs. 87.0%; R3: 80.0% vs. 84.4%;  $p=0.125$ ), with 1 of 3 radiologists reporting higher confidence when interpreting 1-mm slices (R1:  $p=0.033$ ). Correspondingly, a significant measurement discrepancy between slabs and slices was ascertained for 1 of 3 readers (R1: mean difference of 0.8 mm;  $p=0.010$ ). No difference was found between the BIRADS scores assigned with access to 1-mm and 6-mm datasets ( $p=0.317$ ), while interrater agreement was comparably high for slabs and slices (ICC 0.848 vs. 0.865). Reading time was substantially shorter when interpreting synthetic 6-mm slabs compared to 1-mm slices (R1: 33.5 vs. 46.2 sec; R2: 49.1 vs. 64.8 sec; R3: 39.5 vs. 67.2 sec; all  $p<0.001$ ).

#### CONCLUSION

Employing a reconstruction protocol with artificial intelligence-enhanced 6-mm slabs instead of 1-mm slices for digital breast tomosynthesis facilitates similar diagnostic performance with reduced interpretation time.

#### CLINICAL RELEVANCE/APPLICATION

Interpretation of synthetic thick slabs instead of standard thin slices allows for substantial time saving without decreasing the diagnostic accuracy of radiologists.

Printed on: 02/07/23



## Abstract Archives of the RSNA, 2022

R5A-SPBR-2

### Distinction Between Benign and Malignant Breast Masses of Digital Breast Tomosynthesis Using Deep Learning Method with Mask-R Convolutional Neural Network

Thursday, Dec. 1 12:15PM - 12:45PM Room: Learning Center - BR DPS

#### Participants

Huizhi Cao, PhD, (Presenter) Nothing to Disclose

#### PURPOSE

We aimed to use deep learning with Mask-R convolutional neural network (Mask-R-CNN) to discriminate between benign and malignant breast mass images from digital breast tomosynthesis.

#### METHODS AND MATERIALS

In total, 2000 patients (1196 benign masses and 804 malignant masses) were randomly divided into the training cohort (1600 patients) and the two validation cohorts (200 patients for each cohort). Deep learning model was constructed using Mask-R-CNN architecture in two views (craniocaudal, CC and mediolateral oblique, MLO). The performance of the trained neural network was tested with this one validation cohort. Four radiologists (2 senior and 2 junior) interpreted the test data set. In a second step, the neural network was re-trained with all cases and then was tested with another validation cohort. Sensitivity, specificity, accuracy, positive predictive value (PPV), negative predictive value (NPV) and area under the receiver operating characteristic curve (AUC) were compared between readers and the neural network.

#### RESULTS

For initially constructed Mask-R-CNN model, the Sensitivity, specificity, accuracy, PPV, NPV and AUC in CC view and MLO view were 92.30% Vs. 96.20%, 85.40% Vs. 81.30%, 89% Vs. 89%, 85.70% Vs. 87.40%, 91.90% Vs. 95.10%, 0.845 Vs. 0.858, respectively. The proposed model achieved better classification performance than the junior radiologists and inferior to that of senior radiologists ( $P < 0.05$ ). With the re-trained Mask-R-CNN model, the Sensitivity, specificity, accuracy, PPV, NPV and AUC in CC view and MLO view were 96.10% Vs. 96.10%, 95.90% Vs. 91.80%, 96% Vs. 94%, 96.10% Vs. 92.50%, 95.90% Vs. 95.70%, 0.949 Vs. 0.908, respectively. There was no significant difference in classification performance between AI model and senior radiologists ( $P < 0.05$ ).

#### CONCLUSION

The results obtained demonstrate that the proposed Mask-R convolutional neural network is performant and can indeed be used to predict if the mass lesions are benign or malignant.

#### CLINICAL RELEVANCE/APPLICATION

The study demonstrates that deep learning with Mask-R-CNN have higher performance in classifying mass lesions of digital breast tomosynthesis.

Printed on: 02/07/23



## Abstract Archives of the RSNA, 2022

R5A-SPBR-3

### Breast Cancer Screening in the Real-World: A Multi-Site Database of Women Screened for Breast Cancer

Thursday, Dec. 1 12:15PM - 12:45PM Room: Learning Center - BR DPS

#### Participants

Emily F. Conant, MD, Philadelphia, PA (*Presenter*) Research Grant, Hologic, Inc; Advisory Panel, Hologic, Inc; Research Grant, OM1, Inc; Research Grant, iCad, Inc; Advisory Panel, iCad, Inc; Speaker, WebMD LLC

#### PURPOSE

Mammographic imaging is the standard for early detection of breast cancer (BC). Digital breast tomosynthesis (DBT) improves recall and cancer detection rates over digital mammography (DM). Yet few studies describe benefits and risks of these imaging modalities in a real-world setting, including in underrepresented patient subgroups. This study provides real-world evidence (RWE) for BC screening outcomes in a large population of women in the United States (US) receiving DBT or DM screenings.

#### METHODS AND MATERIALS

This retrospective, observational study included women who received routine DM or DBT screenings between 2014 and 2020 at five large healthcare organizations. Integrated electronic medical record, radiology information system, and tumor registry data were used. Women 40-79 years old with >1 screening and no history of BC were included. Outcomes of recall rate (RR), cancer detection rate (CDR), positive predictive value of recall (PPV1), and biopsy rate, and corresponding 95% confidence intervals (CI), were assessed overall and by screening modality. Logistic regression models adjusted for age, breast density, site, and exam year.

#### RESULTS

The cohort included 1,100,447 women and 2,528,063 screenings (2,071,741 from women with >2 observed screens). Women were on average 57.3 (standard deviation 10.3) years of age, primarily white (74.5%), and post-menopausal (66.8%) with a breast density of 'scattered fibroglandular densities' (47.5%). DBT screens led to significantly reduced RR (DBT 8.9%, DM 10.3%,  $p < 0.001$ ), and increased CDR (DBT 4.3/1000, DM 4.9/1000,  $p < 0.001$ ), PPV1 (DBT 5.5%, DM 4.2%,  $p < 0.001$ ), and biopsy rates (DBT 18.1/1000, DM 14.8/1000,  $p < 0.001$ ) (see Figure). These associations remained in adjusted analyses, and were consistent across patient subgroups defined by age, race, breast density, and risk status.

#### CONCLUSION

This ongoing US study of over 2.5 million mammograms offers a rich platform to explore outstanding questions around the real-world benefits and risks of breast cancer screening, particularly in key patient subgroups. In this cohort, DBT screenings were associated with reduced RR and increased CDR, PPV1, and rate of biopsy.

#### CLINICAL RELEVANCE/APPLICATION

Routine screening with DBT, compared to DM, may reduce recall and increase cancer detection, biopsy rates and positive predictive value of recall.

Printed on: 02/07/23

## Abstract Archives of the RSNA, 2022

R5A-SPBR-4

### Improved Cancer Detection with Digital Breast Tomosynthesis compared to Digital Mammography using Deep Learning Model

Thursday, Dec. 1 12:15PM - 12:45PM Room: Learning Center - BR DPS

#### Participants

Ray Mayo III, MD, Houston, TX (*Presenter*) Nothing to Disclose

#### PURPOSE

There is evidence of improved reader performance using digital breast tomosynthesis (DBT) compared to full field digital mammograms (FFDM). We compared the performance of an artificial intelligence-based computer aided detection (AI-CAD) software on a set of patients who had both DBT and FFDM exams.

#### METHODS AND MATERIALS

We tested performance of an AI-CAD (cmAssist™, CureMetrix, Inc, La Jolla, CA). The test set is composed of 933 patients (age range: 30-88, average 56 years) who underwent both DBT and FFDM at their screening exams, obtained between 2012 and 2018 from 2 sites in Northeastern and Southeastern United States and using 2 equipment vendors. There were 508 patients with biopsy confirmed cancer and 425 normal patients who had at least one year of followup as confirmation of benignity. Of the cancer patients, 156 had calcification lesions and 352 had mass or architectural distortion lesions. Bootstrap analysis was used to generate area under the curve (AUC) of the receiver operating characteristic which was measured at 95% confidence interval (CI) for both FFDM and DBT exams.

#### RESULTS

For FFDM, cmAssist has an AUC of 0.95 [CI: 0.93 - 0.96] for calcifications. For mass and architectural distortion lesions, the AUC is 0.75 [CI: 0.72 - 0.78]. For DBT, cmAssist has an AUC of 0.96 [CI: 0.95 - 0.97] for calcifications. For mass and architectural distortions, the AUC is 0.89 [CI: 0.87 - 0.91].

#### CONCLUSION

There was improved performance of cmAssist AI-CAD using DBT compared to FFDM. The improvement was more robust for mass and architectural distortions as expected; many of the cancers were only visible on DBT in this cancer-enriched sample of patients who underwent both FFDM and DBT. For calcifications, this AI-CAD achieves similar high performance for DBT and FFDM.

#### CLINICAL RELEVANCE/APPLICATION

AI-CAD (cmAssist) shows improved performance with digital breast tomosynthesis compared to full field digital mammography and appears to be a promising aid to the radiologist in enhancing cancer detection.

Printed on: 02/07/23

## Abstract Archives of the RSNA, 2022

R5A-SPBR-5

### Analysis of False Negative Digital Breast Tomosynthesis Screening Exams

Thursday, Dec. 1 12:15PM - 12:45PM Room: Learning Center - BR DPS

#### Participants

Sydney Payne, MD, BS, Palo Alto, CA (*Presenter*) Nothing to Disclose

#### PURPOSE

To determine reasons for false negative (FN) digital breast tomosynthesis (DBT) screening mammograms (MG).

#### METHODS AND MATERIALS

2 MQSA-certified radiologists classified FN DBT screenings from 3/31/2014- 3/31/2022 as negative studies (NS) or detectable, listing factors contributing to non-detection. We queried the EMR for patient breast cancer risk factors and cancer presentation/characteristics.

#### RESULTS

There were 69,594 screens with 416 screen-detected cancers (CDR 6/1000, 416/69,592) and 56 FN (0.8/1000, 56/69,594) studies. 7/56 FN were excluded for no DBT, leaving 49 women (age 28-82 years old, mean 60 yo) with 51 cancers comprising the study (11 DCIS, 11 IDC, 24 ILC, 1 IDC/ILC and 4 other cancers) found at an average 7.5 months (range 0.5-12 mo) post screening. Most women (61%, 30/49) had risk factors and dense tissue (46.9%, 23/49 heterogeneously dense; 26.6%, 13/49 extremely dense). Detection was by screening MRI (24/51, 47%), clinical findings (23/51, 45%; 19 palpation, 2 pain, 2 palpation/pain), or imaging (1 screening MG, 1 screening US, 1 PET-CT, 1 CT). 35/51 (69%) cancers were NS, and 16/51 (31%) were non-detected masses (14/16, 87.5%) or calcifications (2/16, 12.5%). Screening MRI found DCIS more often (9/11, 81.2%) than palpation and/or pain (2/11, 18.2%). ILC was markedly represented in the pathology (24/51, 47%) and was detected more often clinically (15/24, 62.5%) than on screening MRI (8/24, 33.3%) or US (1/24, 0.4%). Factors contributing to non-detection were dense tissue (8/16, 50%), one view findings (6/16, 37.5%), developing asymmetries (4/16, 25%), distracting findings (3/16, 18.8%), post-surgical changes (2/16, 12.5%), benign appearing mass (2/16, 12.5%), at image edge (2/16, 12.5%), positioning (1/16, 0.1%), too few calcifications (1/16, 0.1%) or poor image quality (1/16, 0.1%).

#### CONCLUSION

Almost half of cancers not detected by DBT were found on screening breast MRI (47%) and were ILC pathology (47%). Dense tissue and one-view findings were the most common factors contributing to non-detection.

#### CLINICAL RELEVANCE/APPLICATION

The most common reason for missed cancers on DBT is dense breast tissue or one-view findings, with a predominance of ILC. Screening breast MRI found almost half of the missed cancers.

Printed on: 02/07/23



## Abstract Archives of the RSNA, 2022

R5A-SPBR-6

### Screening Tomosynthesis Detected Breast Cancer in Women with Dense Tissue

Thursday, Dec. 1 12:15PM - 12:45PM Room: Learning Center - BR DPS

#### Participants

Stamatia Destounis, MD, Rochester, NY (*Presenter*) Medical Advisory Board, iCad, Inc

#### PURPOSE

To report the cancer detection rate and tumor characteristics in women with dense breast tissue having screening Digital Breast Tomosynthesis (DBT).

#### METHODS AND MATERIALS

This retrospective review identified patients with dense breast tissue who had a breast cancer diagnosis that was detected on a screening Digital Breast Tomosynthesis (DBT) examination between the years of 2016 and 2021. This resulted in an analysis of 194,340 exams in 60,884 patients. VolparaDensity was utilized in real time to assess breast density versions (v1.5.3 - v4.2.2). Lesion type, lymph node status, stage, and grade were collected.

#### RESULTS

Overall, 1076 cancers were detected in 913 patients by screening DBT between the years of 2016 and 2021. Most of these cancers were masses (576/1076, 54%). Of the 1076 cancers 79% (n=855) were invasive cancers and 221 (21%) were ductal carcinoma in situ. DBT was able to detect nine lymph nodes that were pathologically proven to be metastatic. In the 913 patients that were diagnosed, the cancers were Grade 1 or Grade 2 (298 (33%) and 297 (32.5%), respectively), and a majority were of early stage (Stage 0, Stage 1) (855/1076, 79%). At surgery, 73% (n=665) patients had negative nodes.

#### CONCLUSION

s This retrospective review demonstrated that DBT found lower grade and early-stage malignancies in women with dense breast tissue. DBT was also able to detect metastatic lymph nodes.

#### CLINICAL RELEVANCE/APPLICATION

Some facilities are only offering DBT as a diagnostic tool. Utilizing DBT for screening can aid in the detection of breast cancer in patients with dense tissue as thus far it has been shown to detect lower grade, and early-stage cancers. Greater adoption will occur with proven utility of DBT in this population.

Printed on: 02/07/23

## Abstract Archives of the RSNA, 2022

R5A-SPBR-7

### Automated Breast Ultrasound vs Handheld Ultrasound in Moderate Risk Breast Cancer Women With Dense Breast

Thursday, Dec. 1 12:15PM - 12:45PM Room: Learning Center - BR DPS

#### Participants

MARIA TERESA FERNANDEZ-TARANILLA, PhD, Madrid, Spain (*Presenter*) Nothing to Disclose

#### PURPOSE

To determine if Automated Breast UltraSound (ABUS) is at least as effective as handheld ultrasound (HHUS) in detecting lesions in intermediate risk breast cancer patients with dense breast. To compare the degree of interobserver agreement between BI-RADS categorization with ABUS vs HHUS.

#### METHODS AND MATERIALS

200 patients (350 breast) were evaluated the same day with ABUS and HHUS between June 2020 to July 2021 in a tertiary hospital. Women with dense breast C or D according the American College Radiology and intermediate risk were included. Previous personal breast cancer (pBC), known family history of BC (fBC), prior lesion of uncertain malignant potential (B3 lesions) and certain syndromes and gene mutations were considered as intermediate risk subcategories. BI-RADS categorization was used to determine the agreement between both techniques with Kappa index.

#### RESULTS

Mean age of women were 47 years old, 45% had type C and 55% type D breast densities. The most frequent group of patients were the pBC (67%) and mostly were BI-RADS 2. The mean time of ABUS lecture were 4 minutes. The Kappa index was almost perfect (0.84) in the radiologist interpretation with BI-RADS between ABUS vs HHUS ( $p < 0,001$ ). Moderate agreement (0.52) was observed on pBC ( $p < 0,005$ ) always referring to the remaining breast after radical surgery. Excellent agreement (0.89) was observed on patients with fBC ( $p < 0,001$ ) and on syndromes with intermediate risk ( $p < 0,005$ ). On B3 lesions the results were not significant ( $p < 0,07$ ).

#### CONCLUSION

s ABUS could be a valuable and cost-effective screening tool for women with dense breast and moderate risk in combination with mammography.

#### CLINICAL RELEVANCE/APPLICATION

The screening for breast cancer on patients with dense breast is still a challenge, even more if those patients had an increased risk of cancer (15-20%). Our proposal is to introduce a cost-effective tool like ABUS in the routine screening programs to increase sensibility and specificity on patients with dense breast and moderate risk cancer.

Printed on: 02/07/23

## Abstract Archives of the RSNA, 2022

R5A-SPCA

### Cardiac Thursday Poster Discussions - A

Thursday, Dec. 1 12:15PM - 12:45PM Room: Learning Center - CA DPS

#### Sub-Events

#### R5A-SPCA-1 Cardiac Resonance Imaging Parameters Show Association Between Myocardial Abnormalities and Severity of Chronic Kidney Disease

##### Participants

Xi Jia, Wuhan, China (*Presenter*) Nothing to Disclose

##### PURPOSE

To investigate the relationship between myocardial abnormalities and the severity of chronic kidney disease (CKD), as well as the effects of hemodialysis, using cardiac magnetic resonance (CMR) imaging.

##### METHODS AND MATERIALS

We enrolled 84 patients with various stages of CKD (group I: CKD stages 1-3, n = 23; group II: CKD stages 4-5, n = 20; group III: hemodialysis patients, n = 41) and 32 healthy subjects. The demographics and biochemical parameters of the study subjects were evaluated. All subjects underwent non-contrast CMR scans. Myocardial strain, native T1, and T2 values were calculated from the scanning results. Analysis of covariance (ANCOVA) was used to compare the CMR imaging parameters between group I-III and the controls.

##### RESULTS

The left ventricular ejection fraction (LVEF), global radial strain (GRS) and global circumferential strain (GCS) values were significantly lower in group III patients compared with the controls (LVEF: 49% vs. 56%, p = 0.021; GRS: 29 vs. 37, p = 0.019; GCS: -17.4 vs. -20.6, p < 0.001). Furthermore, the global longitudinal strain (GLS) values were significantly lower in group II and III patients compared with the controls (-13.7 and -12.9 vs. -16.2, p < 0.05). Compared with the controls, the native T1 values were significantly higher in groups II and III patients (1041±7 and 1053±6 vs. 1009±6, p < 0.05), and T2 values were obviously higher in group I-III CKD patients (49.9±0.6 and 53.2±0.7 and 50.1±0.5 vs. 46.6±0.5, p < 0.001). The advanced CKD stages showed significant positive correlation with GLS (r = 0.436, p < 0.001), GCS (r = 0.386, p < 0.001), native T1 (r = 0.5, p < 0.001) and T2 (r = 0.467, p < 0.001) values. In comparison with the group II patients, hemodialysis patients showed significantly lower T2 values (53.2±0.7 vs. 50.1±0.5, p = 0.002), and higher T1 values (1041±7 vs. 1053±6) without significant difference.

##### CONCLUSION

Our study showed that myocardial strain, native T1, and T2 values were associated with the CKD stages. Furthermore, CMR image parameters demonstrated that hemodialysis improved myocardial edema but did not ameliorate myocardial fibrosis.

##### CLINICAL RELEVANCE/APPLICATION

Non-contrast CMR can be used to non-invasively estimate the cardiac pathologic changes in CKD patients and improve constant medical attention to prevent an early occurrence of CVD.

#### R5A-SPCA-3 Cardiac Magnetic Resonance for Diagnosing Heart Failure with Preserved Ejection Fraction

##### Participants

Ming-Yen Ng, MBBS, Hong Kong, Hong Kong (*Presenter*) Education Grant, General Electric Company; Education Grant, Bayer AG; Education Grant, Circle Cardiovascular Imaging Inc; Education Grant, TeraRecon, Inc; Education Grant, Arterys Inc; Speakers Bureau, Boehringer Ingelheim GmbH

##### PURPOSE

Cardiac magnetic resonance (CMR) feature tracking (CMR-FT), PC imaging, tagging extracellular volume (ECV) have long been suggested as having potential to diagnose heart failure with preserved ejection fraction (HFpEF) potentially complement echocardiography especially when echocardiography is indeterminate for HFpEF. However, data is limited or absent. We conducted a prospective case-control study assessing diagnostic accuracy of cardiac magnetic resonance (CMR) feature tracking (CMR-FT), phase contrast (PC) imaging, tagging ECV to diagnose HFpEF.

##### METHODS AND MATERIALS

121 suspected HFpEF patients, 26 angina patients and 26 normal volunteers were recruited into this study from four centres. Patients and volunteers underwent echocardiography, CMR and NT-proBNP measurements within 24 hours. After initial examinations with or without catheter pressure measurements or stress echocardiography to confirm HFpEF, there were 48 HFpEF, 23 angina, 17 normal volunteers, and 14 deconditioned patients. HFpEF patients were confirmed using the European Society of Cardiology 2019 expert recommendations. For patients suspected of having HFpEF but were indeterminate after echo and NT-proBNP, left ventricular pressure measurements or stress echocardiography was performed. As per guidelines, if pressure measurements or stress echocardiography confirmed diastolic dysfunction, HFpEF was confirmed otherwise patients were diagnosed as

deconditioned.

## **RESULTS**

CMR-FT radial early diastolic strain rate (SR), radial systolic SR circumferential strain showed the highest accuracy (Area under the curve (AUC) 0.734, 0.731, 0.731 respectively) to differentiate HFpEF and non-HFpEF patients indicating acceptable power of discrimination. PC had relatively poor to reasonable diagnostic power with E/A ratio (AUC 0.536), septal and lateral wall  $e'$  AUC 0.514, 0.601 respectively), E/ $e'$  ratio (AUC 0.597), S/D ratio (AUC 0.555). CMR tagging circumferential radial strain had reasonable power of discrimination (AUC values of 0.693 and 0.611 respectively). CMR left atrial volume indexed had the highest AUC 0.795. ECV had poor discrimination (AUC 0.534).

## **CONCLUSION**

s CMR-FT parameters radial early diastolic SR, radial systolic SR and circumferential strain show potential in being utilised for identifying HFpEF. PC imaging, tagging and ECV had low to reasonable diagnostic accuracy to diagnose HFpEF. CMR left atrial volume indexed had the highest AUC. CMR-FT holds promise in being able to help identify patients with HFpEF.

## **CLINICAL RELEVANCE/APPLICATION**

CMR-FT shows promise in diagnosing HFpEF. However, the best CMR parameter for HFpEF diagnosis was left atrial volume indexed. PC imaging tagging may not be as useful as initially thought at diagnosing HFpEF.

Printed on: 02/07/23

## Abstract Archives of the RSNA, 2022

R5A-SPCA-1

### Cardiac Resonance Imaging Parameters Show Association Between Myocardial Abnormalities and Severity of Chronic Kidney Disease

Thursday, Dec. 1 12:15PM - 12:45PM Room: Learning Center - CA DPS

#### Participants

Xi Jia, Wuhan, China (*Presenter*) Nothing to Disclose

#### PURPOSE

To investigate the relationship between myocardial abnormalities and the severity of chronic kidney disease (CKD), as well as the effects of hemodialysis, using cardiac magnetic resonance (CMR) imaging.

#### METHODS AND MATERIALS

We enrolled 84 patients with various stages of CKD (group I: CKD stages 1-3, n = 23; group II: CKD stages 4-5, n = 20; group III: hemodialysis patients, n = 41) and 32 healthy subjects. The demographics and biochemical parameters of the study subjects were evaluated. All subjects underwent non-contrast CMR scans. Myocardial strain, native T1, and T2 values were calculated from the scanning results. Analysis of covariance (ANCOVA) was used to compare the CMR imaging parameters between group I-III and the controls.

#### RESULTS

The left ventricular ejection fraction (LVEF), global radial strain (GRS) and global circumferential strain (GCS) values were significantly lower in group III patients compared with the controls (LVEF: 49% vs. 56%, p = 0.021; GRS: 29 vs. 37, p = 0.019; GCS: -17.4 vs. -20.6, p < 0.001). Furthermore, the global longitudinal strain (GLS) values were significantly lower in group II and III patients compared with the controls (-13.7 and -12.9 vs. -16.2, p < 0.05). Compared with the controls, the native T1 values were significantly higher in groups II and III patients (1041±7 and 1053±6 vs. 1009±6, p < 0.05), and T2 values were obviously higher in group I-III CKD patients (49.9±0.6 and 53.2±0.7 and 50.1±0.5 vs. 46.6±0.5, p < 0.001). The advanced CKD stages showed significant positive correlation with GLS (r = 0.436, p < 0.001), GCS (r = 0.386, p < 0.001), native T1 (r = 0.5, p < 0.001) and T2 (r = 0.467, p < 0.001) values. In comparison with the group II patients, hemodialysis patients showed significantly lower T2 values (53.2±0.7 vs. 50.1±0.5, p = 0.002), and higher T1 values (1041±7 vs. 1053±6) without significant difference.

#### CONCLUSION

Our study showed that myocardial strain, native T1, and T2 values were associated with the CKD stages. Furthermore, CMR image parameters demonstrated that hemodialysis improved myocardial edema but did not ameliorate myocardial fibrosis.

#### CLINICAL RELEVANCE/APPLICATION

Non-contrast CMR can be used to non-invasively estimate the cardiac pathologic changes in CKD patients and improve constant medical attention to prevent an early occurrence of CVD.

Printed on: 02/07/23

## Abstract Archives of the RSNA, 2022

R5A-SPCA-3

### Cardiac Magnetic Resonance for Diagnosing Heart Failure with Preserved Ejection Fraction

Thursday, Dec. 1 12:15PM - 12:45PM Room: Learning Center - CA DPS

#### Participants

Ming-Yen Ng, MBBS, Hong Kong, Hong Kong (*Presenter*) Education Grant, General Electric Company; Education Grant, Bayer AG; Education Grant, Circle Cardiovascular Imaging Inc; Education Grant, TeraRecon, Inc; Education Grant, Arterys Inc; Speakers Bureau, Boehringer Ingelheim GmbH

#### PURPOSE

Cardiac magnetic resonance (CMR) feature tracking (CMR-FT), PC imaging, tagging extracellular volume (ECV) have long been suggested as having potential to diagnose heart failure with preserved ejection fraction (HFpEF) potentially complement echocardiography especially when echocardiography is indeterminate for HFpEF. However, data is limited or absent. We conducted a prospective case-control study assessing diagnostic accuracy of cardiac magnetic resonance (CMR) feature tracking (CMR-FT), phase contrast (PC) imaging, tagging ECV to diagnose HFpEF.

#### METHODS AND MATERIALS

121 suspected HFpEF patients, 26 angina patients and 26 normal volunteers were recruited into this study from four centres. Patients and volunteers underwent echocardiography, CMR and NT-proBNP measurements within 24 hours. After initial examinations with or without catheter pressure measurements or stress echocardiography to confirm HFpEF, there were 48 HFpEF, 23 angina, 17 normal volunteers, and 14 deconditioned patients. HFpEF patients were confirmed using the European Society of Cardiology 2019 expert recommendations. For patients suspected of having HFpEF but were indeterminate after echo and NT-proBNP, left ventricular pressure measurements or stress echocardiography was performed. As per guidelines, if pressure measurements or stress echocardiography confirmed diastolic dysfunction, HFpEF was confirmed otherwise patients were diagnosed as deconditioned.

#### RESULTS

CMR-FT radial early diastolic strain rate (SR), radial systolic SR circumferential strain showed the highest accuracy (Area under the curve (AUC) 0.734, 0.731, 0.731 respectively) to differentiate HFpEF and non-HFpEF patients indicating acceptable power of discrimination. PC had relatively poor to reasonable diagnostic power with E/A ratio (AUC 0.536), septal and lateral wall  $e'$  AUC 0.514, 0.601 respectively),  $E/e'$  ratio (AUC 0.597), S/D ratio (AUC 0.555). CMR tagging circumferential radial strain had reasonable power of discrimination (AUC values of 0.693 and 0.611 respectively). CMR left atrial volume indexed had the highest AUC 0.795. ECV had poor discrimination (AUC 0.534).

#### CONCLUSION

s CMR-FT parameters radial early diastolic SR, radial systolic SR and circumferential strain show potential in being utilised for identifying HFpEF. PC imaging, tagging and ECV had low to reasonable diagnostic accuracy to diagnose HFpEF. CMR left atrial volume indexed had the highest AUC. CMR-FT holds promise in being able to help identify patients with HFpEF.

#### CLINICAL RELEVANCE/APPLICATION

CMR-FT shows promise in diagnosing HFpEF. However, the best CMR parameter for HFpEF diagnosis was left atrial volume indexed. PC imaging tagging may not be as useful as initially thought at diagnosing HFpEF.

Printed on: 02/07/23

## Abstract Archives of the RSNA, 2022

R5A-SPCH

### Chest Thursday Poster Discussions - A

Thursday, Dec. 1 12:15PM - 12:45PM Room: Learning Center - CH DPS

#### Participants

Ryan Short, MD, Saint Louis, MO (*Moderator*) Co-founder, Scanslated, Inc; Officer, Scanslated, Inc

#### Sub-Events

### R5A-SPCH-1 Non-ECG-gated Low-dose Chest CT-based DL Model for Coronary Calcification Scoring Predicts Subjective Radiologist Grading and Agatston Scores from ECG-gated Coronary Calcium Scoring CT

#### Participants

Lina Karout, MD, Boston, MA (*Presenter*) Nothing to Disclose

#### PURPOSE

Coronary arterial calcification (CAC) on low-dose chest CT (LDCT) is an important, reportable finding in lung cancer screening patients. We assessed if non-ECG-gated low-dose chest CT-based CAC scoring with a deep learning (DL) model with three HU thresholds (90, 110, 130 HU) can predict subjective radiologist CAC grading and Agatston scores from ECG-gated coronary calcium scoring CT (CCS-CT).

#### METHODS AND MATERIALS

With IRB approval, we processed thin-section LDCT chest images (<1.25mm) of 107 adults patients (age >55 years; male: female 66:38) with a DL model (Riverain Tech) to obtain separate CAC scores at 90, 110, and 130 HU thresholds since LDCTs are acquired at different KV (80-120) unlike CCS-CT (120 kV). Each patient also had a CCS-CT within one year of LDCT, from which we obtained Agatston scores. In addition, two thoracic radiologists graded CAC subjectively as none, mild (<1/3 of coronary length calcified), moderate (1/3-2/3 calcified), and heavy (>2/3 calcified) as per prior recommendation. Data were analyzed with Pearson correlation and area under precision-recall curve (AUPRC) analysis for asymmetric data distribution.

#### RESULTS

Each of the three HU thresholds could differentiate between the radiologists' CAC grading into mild (90HU: 282±1106; 110HU: 752 ±383, 130HU: 4762 ±3787), moderate (90HU: 242 ±965; 110HU: 653 ±330, 130HU: 4187 ±3356), and heavy (90HU: 203 ±821; 110HU: 560±278, 130HU: 3685±3000) categories ( $p<0.001$ ). There was a strong linear, direct correlation between DL-CAC from LDCT and Agatston score from CCS-CT ( $r=0.939$ ;  $p<0.001$ ). The AUPRC for DL-CAC in differentiating mild, moderate, and severe subjective CAC grading was 0.82 ( $p<0.001$ ).

#### CONCLUSION

s DL-CAC scoring can help automate subjective grading of CAC on non-ECG-gated, low-dose chest CT with high performance; it has an excellent linear correlation with Agatston score.

#### CLINICAL RELEVANCE/APPLICATION

Estimation of DL-CAC scores can replace subjective CAC grading and decrease the need for dedicated CCS-CT in patients who have undergone LDCT of the chest.

### R5A-SPCH-3 Diagnostic Evaluation of Pseudo-continuous ASL-MRI for The Detection of Pulmonary Embolism: A Prospective Single Center Trial

#### Participants

Ferdinand Seith, MD, BSc, Tübingen, Germany (*Presenter*) Nothing to Disclose

#### PURPOSE

To prospectively evaluate pseudo-continuous ASL-MRI (PCASL-MRI) for the detection of acute pulmonary embolism (PE).

#### METHODS AND MATERIALS

Within 12 months, 97 hemodynamically stable adult patients (48f, median age 61) with suspected PE, CT pulmonary angiography (CTPA) within the last 72h and without MRI-contraindications were prospectively included. PCASL-MRI was performed in three orthogonal planes under free breathing at 1.5T: labeling the pulmonary trunk during systole, post-labeling delay 1000ms, bSSFP image acquisition. Additionally, multi-slice coronal bSSFP imaging of the whole lungs was performed. Two radiologists performed a blinded assessment regarding overall image quality, artifacts and diagnostic confidence (5-point Likert-scale, 5=best). The readers categorized patients as positive or negative for PE and conducted a lobe-wise assessment (5 lobes per patient) of PCASL-MRI and CTPA. Sensitivity and specificity were calculated for MRI on patient-level with final clinical diagnosis serving as reference standard. Furthermore, interchangeability between MRI and CTPA was tested using the individual equivalence index and defined as discordant judgement of less than 5% in the lobe-wise analyses.

## RESULTS

PCASL-MRI was performed successfully in all included patients with excellent scores for image quality, artifact and diagnostic confidence (median scores=5; inter-rater agreement:  $k > 0.74$ ). 38/97 Patients were positive for PE. PCASL-MRI detected PE correctly in 35/38 patients and yielded 3 false positive and 3 false negative findings resulting in a sensitivity of 0.921 (95%-CI 0.808-0.980) and a specificity of 0.949 (95%-CI 0.873-0.978). A high degree of interchangeability between MRI and CTPA was detected with an individual equivalency index of 2.58% (95%-CI 1.20-3.82%).

## CONCLUSION

s PCASL-MRI can reliably detect deficits in lung perfusion caused by acute pulmonary embolism and should be considered as a radiation- and contrast-agent free alternative for individual patients.

## CLINICAL RELEVANCE/APPLICATION

PCASL-MRI could be a radiation- and contrast-agent free alternative to diagnose PE in individual patients.

## R5A-SPCH-4 The Evaluation of The Variation Pattern of The Pulmonary Vein: Preoperative Identification by Thin-section CT and 3D-CTPA

Participants  
Makiko Murota, MD, Kitagun, Japan (*Presenter*) Nothing to Disclose

## PURPOSE

Understanding pulmonary vein (PV) branches and their variations is a key to successful anatomical lung resection. The right top PV is defined as an anomalous branch of the right superior PV (SPV) draining into the left atrium (LA). There have been a few reports of the right top PV, but no detail reports of the left top PV. The aim of the present study was to evaluate the PV variations including right and left top PV using thin-section CT (TSCT) images and 3D-CTPA.

## METHODS AND MATERIALS

The study included 1437 patients in right side and 1454 patients in left side consecutive patients who were suspected with lung cancer and underwent CTPA. We assessed the presence of the PV variations including the right and left top PV on TSCT and 3D-CTPA images.

## RESULTS

The most common PV variation draining into the LA on the right side was the PV of the middle lobe draining into the right inferior PV (IPV) in 4.2% (61/1437), whereas the common trunk of the left PV in 14.4% (210/1454). The left IPV receiving venous branch from the lingula segment was found in 6.9% (100/1454). The right top PV was found in 9.1% (131/1437) ( $p = 0.88$ ), whereas the left top PV in 2.9% (42/1454) ( $p = 0.45$ ).

## CONCLUSION

s The variations of the PV branching pattern could be evaluated using TSCT and 3D-CTPA images. They provided precise preoperative information.

## CLINICAL RELEVANCE/APPLICATION

The most common variation of PV is the common trunk of the left PV. The right top PV is not so rare, and the left top PV should also be recognized.

## R5A-SPCH-5 Prognostic Value of Vascular Abnormalities in Dual Energy CT Compared with Visual CT Severity Score in Patients Suspected of COVID-19 and Acute Pulmonary Artery Embolism

Participants  
Abass Noor, MD, Philadelphia, PA (*Presenter*) Nothing to Disclose

## PURPOSE

High prevalence of pulmonary iodine distribution abnormalities on DECT has been reported as a feature of COVID19 pneumonia. The objective of this study was to evaluate the added benefit of using iodine maps from dual energy chest CT in patients suspected of COVID-19 and acute pulmonary artery embolism. The null hypothesis was that DECT iodine maps offered no additional clinical value in evaluating patients.

## METHODS AND MATERIALS

This IRB-approved retrospective study was developed as part of a quality improvement project evaluating the use of DECT in patients suspected of COVID-19 and pulmonary artery embolism. In a single hospital, 100 consecutive patients were examined with DECT using a protocol including iodine distribution maps between December 2020- March 2021. Two subspecialty trained thoracic radiologists examined iodine map abnormalities and pulmonary opacities. Visual lung damage CT score was calculated. Percent of lung involved by either increased or decreased pulmonary iodine density was visually estimated and categorized into quartiles. Statistical analysis included kappa statistics for inter-observer agreements and Cox proportional survival analysis.

## RESULTS

Patients with positive SARS-CoV-2 RT PCR were more likely to present with fever, myalgia, and fatigue ( $p < 0.05$ ). Pulmonary embolism was observed in 12 patients (12%), with no difference observed in prevalence of pulmonary embolism between patients with and without positive PCR result ( $p = 0.985$ ). Overall, 70 (70%) patients were admitted to the hospital, with 25 (25%) admitted to the Intensive Care Unit (ICU)—15 (15%) of whom demonstrated a positive SARS-CoV-2 RT PCR on the date of admission. Patients with positive SARS-CoV-2 RT PCR had longer hospital ( $p = 0.019$ ) and ICU stays ( $p = 0.047$ ). No significant difference was observed in occurrence of intubation ( $p = 0.866$ ) or mortality ( $p = 0.368$ ). There was moderate agreement for visual lung damage CT score ( $k: 0.695$ ; CI 95%: 0.611 to 0.780), and little agreement observed in evaluation of pulmonary iodine density ( $k: 0.056$ ; CI 95% -0.045 to 0.158). There was a significant decrease in overall survival with increased visual lung damage CT score for both raters ( $p = 0.002$  and  $p = 0.001$ ). Percent increased or decreased pulmonary iodine density was not related to overall survival.

## CONCLUSION

s Our study has redemonstrated correlation between survival and visual CT severity score but did not show correlation with pulmonary iodine density on DECT.

## CLINICAL RELEVANCE/APPLICATION

Vascular abnormalities on DECT in patients with COVID-19 is of uncertain clinical significance. This study has shown disagreement among interpreters regarding iodine distribution map findings and may not offer more clinical value than observing the severity of pneumonia.

## R5A-SPCH-6 Prospective Comparative Effectiveness Study of Radiologist Performance With and Without AI for Incidental PE Detection

### Participants

Steven Rothenberg, MD, Birmingham, AL (*Presenter*) Founder, Empower Therapeutics Inc ;Member, Translation Holdings LLC;Consultant, Radiostics LLC

### PURPOSE

To compare the effectiveness of radiologist performance at detecting incidental PE on CT images with and without AI triage (CADt).

### METHODS AND MATERIALS

For this IRB-approved prospective single center study, 4652 consecutive patients who underwent cross sectional imaging of the chest or abdomen were recruited in two phases. Patients who underwent CT angiography with a PE protocol were excluded. In phase 1, consecutive CTs (N=1467) were evaluated independently by a radiologist and by a FDA-cleared AI triage algorithm. This data was used to establish a baseline for unassisted radiologist and AI interpretations. Following this, all radiologists interpreting CT (N=??) were trained to review the results of the AI algorithm and triage system concurrently during image evaluation and reporting. In phase 2, consecutive CTs (N=3185) were evaluated by radiologists using AI assistance for all cases. Reports and addendums were manually reviewed for the presence or absence of PE. A chest radiologist determined the number of missed incidental PEs by reviewing the image data and reports of all potential misses. The miss rate of iPE was calculated along with the sensitivity, specificity, and accuracy of the AI algorithm.

### RESULTS

In phase 1 and 2, 1.4% (21/1467) and 1.8% (57/3185) of CTs were positive for PE, respectively ( $p=0.374$ ). In phase 1 and 2, 19.0% (4/21) and 1.8% (1/57) of incidental PEs were missed ( $p=0.006$ ). The percentage of missed iPEs per exam decreased from 0.27% to 0.03% ( $p=0.019$ ). The triage algorithm's accuracy, sensitivity, and specificity was 0.993, 0.628, and 0.999 respectively.

## CONCLUSION

s In a single-center prospective real-world study, the miss rate for detection of iPE on CT was statistically higher than the miss rate of radiologists assisted by an algorithm for detection and triage.

## CLINICAL RELEVANCE/APPLICATION

Incidental pulmonary emboli (iPE) are easily missed when the purpose of an examination is for an alternative indication, however, the presence of a PE is critical finding that often changes clinical management.

## R5A-SPCH-7 Added Value of An Artificial Intelligence Tool For Prioritization of Incidental Pulmonary Embolism on Chest CT

### Participants

Laurens Topff, MD, (*Presenter*) Nothing to Disclose

### PURPOSE

To evaluate the diagnostic efficacy of commercially available artificial intelligence (AI) software to detect incidental pulmonary embolism (IPE) on chest CT and shorten the time to diagnosis using worklist prioritization.

### METHODS AND MATERIALS

In this prospective study, AI software was deployed in a clinical environment to analyze routinely acquired chest CT scans of adult oncology patients. Three time periods of 15 weeks each were compared: routine workflow without AI, manual triage without AI, and worklist prioritization with AI. Diagnostic accuracy of the tool was evaluated on both prospectively and retrospectively collected data. Temporal endpoints including Detection and Notification Times (DNT) were assessed.

### RESULTS

A total of 11 736 CT scans were evaluated. Prevalence of IPE was 1.2% (n=143). The AI software detected 131 true positives, 12 false negatives, 31 false positives, and 11559 true negatives. Sensitivity was 91.6%, specificity 99.7%, NPV 99.9%, and PPV 80.9%. When applied retrospectively, the AI software found IPEs in 47 CTs (44.8%) that were missed in the radiology report. The median DNT for IPE positive examinations was 7714, 4973, 87 min for the respective time periods. The difference in DNT between positive and negative CTs was largest when using AI assistance and was significantly different from both workflows without AI. In contrast, no statistically significant difference was found between routine workflow and manual triage without AI.

## CONCLUSION

s A commercially available AI tool was found to have a high diagnostic efficacy in detecting IPE on CT of oncology patients. AI assisted worklist prioritization was shown to be effective in significantly reducing the time to diagnosis of IPE cases compared to the routine clinical workflow.

## CLINICAL RELEVANCE/APPLICATION

Incidental pulmonary embolism is a common comorbidity in oncology patients. Despite being clinically unsuspected, IPE can be an urgent and life-threatening event. AI based worklist prioritization can assist the radiologist to shorten the time to diagnosis of

critical imaging findings.

Printed on: 02/07/23

## Abstract Archives of the RSNA, 2022

R5A-SPCH-1

### Non-ECG-gated Low-dose Chest CT-based DL Model for Coronary Calcification Scoring Predicts Subjective Radiologist Grading and Agatston Scores from ECG-gated Coronary Calcium Scoring CT

Thursday, Dec. 1 12:15PM - 12:45PM Room: Learning Center - CH DPS

#### Participants

Lina Karout, MD, Boston, MA (*Presenter*) Nothing to Disclose

#### PURPOSE

Coronary arterial calcification (CAC) on low-dose chest CT (LDCT) is an important, reportable finding in lung cancer screening patients. We assessed if non-ECG-gated low-dose chest CT-based CAC scoring with a deep learning (DL) model with three HU thresholds (90, 110, 130 HU) can predict subjective radiologist CAC grading and Agatston scores from ECG-gated coronary calcium scoring CT (CCS-CT).

#### METHODS AND MATERIALS

With IRB approval, we processed thin-section LDCT chest images (<1.25mm) of 107 adults patients (age >55 years; male: female 66:38) with a DL model (Riverain Tech) to obtain separate CAC scores at 90, 110, and 130 HU thresholds since LDCTs are acquired at different KV (80-120) unlike CCS-CT (120 kV). Each patient also had a CCS-CT within one year of LDCT, from which we obtained Agatston scores. In addition, two thoracic radiologists graded CAC subjectively as none, mild (<1/3 of coronary length calcified), moderate (1/3-2/3 calcified), and heavy (>2/3 calcified) as per prior recommendation. Data were analyzed with Pearson correlation and area under precision-recall curve (AUPRC) analysis for asymmetric data distribution.

#### RESULTS

Each of the three HU thresholds could differentiate between the radiologists' CAC grading into mild (90HU: 282±1106; 110HU: 752 ±383, 130HU: 4762 ±3787), moderate (90HU: 242 ±965; 110HU: 653 ±330, 130HU: 4187 ±3356), and heavy (90HU: 203 ±821; 110HU: 560±278, 130HU: 3685±3000) categories ( $p<0.001$ ). There was a strong linear, direct correlation between DL-CAC from LDCT and Agatston score from CCS-CT ( $r=0.939$ ;  $p<0.001$ ). The AUPRC for DL-CAC in differentiating mild, moderate, and severe subjective CAC grading was 0.82 ( $p<0.001$ ).

#### CONCLUSION

s DL-CAC scoring can help automate subjective grading of CAC on non-ECG-gated, low-dose chest CT with high performance; it has an excellent linear correlation with Agatston score.

#### CLINICAL RELEVANCE/APPLICATION

Estimation of DL-CAC scores can replace subjective CAC grading and decrease the need for dedicated CCS-CT in patients who have undergone LDCT of the chest.

Printed on: 02/07/23

## Abstract Archives of the RSNA, 2022

R5A-SPCH-3

### Diagnostic Evaluation of Pseudo-continuous ASL-MRI for The Detection of Pulmonary Embolism: A Prospective Single Center Trial

Thursday, Dec. 1 12:15PM - 12:45PM Room: Learning Center - CH DPS

#### Participants

Ferdinand Seith, MD, BSc, Tübingen, Germany (*Presenter*) Nothing to Disclose

#### PURPOSE

To prospectively evaluate pseudo-continuous ASL-MRI (PCASL-MRI) for the detection of acute pulmonary embolism (PE).

#### METHODS AND MATERIALS

Within 12 months, 97 hemodynamically stable adult patients (48f, median age 61) with suspected PE, CT pulmonary angiography (CTPA) within the last 72h and without MRI-contraindications were prospectively included. PCASL-MRI was performed in three orthogonal planes under free breathing at 1.5T: labeling the pulmonary trunk during systole, post-labeling delay 1000ms, bSSFP image acquisition. Additionally, multi-slice coronal bSSFP imaging of the whole lungs was performed. Two radiologists performed a blinded assessment regarding overall image quality, artifacts and diagnostic confidence (5-point Likert-scale, 5=best). The readers categorized patients as positive or negative for PE and conducted a lobe-wise assessment (5 lobes per patient) of PCASL-MRI and CTPA. Sensitivity and specificity were calculated for MRI on patient-level with final clinical diagnosis serving as reference standard. Furthermore, interchangeability between MRI and CTPA was tested using the individual equivalence index and defined as discordant judgement of less than 5% in the lobe-wise analyses.

#### RESULTS

PCASL-MRI was performed successfully in all included patients with excellent scores for image quality, artifact and diagnostic confidence (median scores=5; inter-rater agreement:  $k > 0.74$ ). 38/97 Patients were positive for PE. PCASL-MRI detected PE correctly in 35/38 patients and yielded 3 false positive and 3 false negative findings resulting in a sensitivity of 0.921 (95%-CI 0.808-0.980) and a specificity of 0.949 (95%-CI 0.873-0.978). A high degree of interchangeability between MRI and CTPA was detected with an individual equivalency index of 2.58% (95%-CI 1.20-3.82%).

#### CONCLUSION

PCASL-MRI can reliably detect deficits in lung perfusion caused by acute pulmonary embolism and should be considered as a radiation- and contrast-agent free alternative for individual patients.

#### CLINICAL RELEVANCE/APPLICATION

PCASL-MRI could be a radiation- and contrast-agent free alternative to diagnose PE in individual patients.

Printed on: 02/07/23

## Abstract Archives of the RSNA, 2022

R5A-SPCH-4

### The Evaluation of The Variation Pattern of The Pulmonary Vein: Preoperative Identification by Thin-section CT and 3D-CTPA

Thursday, Dec. 1 12:15PM - 12:45PM Room: Learning Center - CH DPS

#### Participants

Makiko Murota, MD, Kitagun, Japan (*Presenter*) Nothing to Disclose

#### PURPOSE

Understanding pulmonary vein (PV) branches and their variations is a key to successful anatomical lung resection. The right top PV is defined as an anomalous branch of the right superior PV (SPV) draining into the left atrium (LA). There have been a few reports of the right top PV, but no detail reports of the left top PV. The aim of the present study was to evaluate the PV variations including right and left top PV using thin-section CT (TSCT) images and 3D-CTPA.

#### METHODS AND MATERIALS

The study included 1437 patients in right side and 1454 patients in left side consecutive patients who were suspected with lung cancer and underwent CTPA. We assessed the presence of the PV variations including the right and left top PV on TSCT and 3D-CTPA images.

#### RESULTS

The most common PV variation draining into the LA on the right side was the PV of the middle lobe draining into the right inferior PV (IPV) in 4.2% (61/1437), whereas the common trunk of the left PV in 14.4% (210/1454). The left IPV receiving venous branch from the lingula segment was found in 6.9% (100/1454). The right top PV was found in 9.1% (131/1437) ( $p=0.88$ ), whereas the left top PV in 2.9% (42/1454) ( $p=0.45$ ).

#### CONCLUSION

The variations of the PV branching pattern could be evaluated using TSCT and 3D-CTPA images. They provided precise preoperative information.

#### CLINICAL RELEVANCE/APPLICATION

The most common variation of PV is the common trunk of the left PV. The right top PV is not so rare, and the left top PV should also be recognized.

Printed on: 02/07/23

## Abstract Archives of the RSNA, 2022

R5A-SPCH-5

### Prognostic Value of Vascular Abnormalities in Dual Energy CT Compared with Visual CT Severity Score in Patients Suspected of COVID-19 and Acute Pulmonary Artery Embolism

Thursday, Dec. 1 12:15PM - 12:45PM Room: Learning Center - CH DPS

#### Participants

Abass Noor, MD, Philadelphia, PA (*Presenter*) Nothing to Disclose

#### PURPOSE

High prevalence of pulmonary iodine distribution abnormalities on DECT has been reported as a feature of COVID19 pneumonia. The objective of this study was to evaluate the added benefit of using iodine maps from dual energy chest CT in patients suspected of COVID-19 and acute pulmonary artery embolism. The null hypothesis was that DECT iodine maps offered no additional clinical value in evaluating patients.

#### METHODS AND MATERIALS

This IRB-approved retrospective study was developed as part of a quality improvement project evaluating the use of DECT in patients suspected of COVID-19 and pulmonary artery embolism. In a single hospital, 100 consecutive patients were examined with DECT using a protocol including iodine distribution maps between December 2020- March 2021. Two subspecialty trained thoracic radiologists examined iodine map abnormalities and pulmonary opacities. Visual lung damage CT score was calculated. Percent of lung involved by either increased or decreased pulmonary iodine density was visually estimated and categorized into quartiles. Statistical analysis included kappa statistics for inter-observer agreements and Cox proportional survival analysis.

#### RESULTS

Patients with positive SARS-CoV-2 RT PCR were more likely to present with fever, myalgia, and fatigue ( $p < 0.05$ ). Pulmonary embolism was observed in 12 patients (12%), with no difference observed in prevalence of pulmonary embolism between patients with and without positive PCR result ( $p = 0.985$ ). Overall, 70 (70%) patients were admitted to the hospital, with 25 (25%) admitted to the Intensive Care Unit (ICU)—15 (15%) of whom demonstrated a positive SARS-CoV-2 RT PCR on the date of admission. Patients with positive SARS-CoV-2 RT PCR had longer hospital ( $p = 0.019$ ) and ICU stays ( $p = 0.047$ ). No significant difference was observed in occurrence of intubation ( $p = 0.866$ ) or mortality ( $p = 0.368$ ). There was moderate agreement for visual lung damage CT score ( $k: 0.695$ ; CI 95%: 0.611 to 0.780), and little agreement observed in evaluation of pulmonary iodine density ( $k: 0.056$ ; CI 95% -0.045 to 0.158). There was a significant decrease in overall survival with increased visual lung damage CT score for both raters ( $p = 0.002$  and  $p = 0.001$ ). Percent increased or decreased pulmonary iodine density was not related to overall survival.

#### CONCLUSION

Our study has redemonstrated correlation between survival and visual CT severity score but did not show correlation with pulmonary iodine density on DECT.

#### CLINICAL RELEVANCE/APPLICATION

Vascular abnormalities on DECT in patients with COVID-19 is of uncertain clinical significance. This study has shown disagreement among interpreters regarding iodine distribution map findings and may not offer more clinical value than observing the severity of pneumonia.

Printed on: 02/07/23



## Abstract Archives of the RSNA, 2022

R5A-SPCH-6

### Prospective Comparative Effectiveness Study of Radiologist Performance With and Without AI for Incidental PE Detection

Thursday, Dec. 1 12:15PM - 12:45PM Room: Learning Center - CH DPS

#### Participants

Steven Rothenberg, MD, Birmingham, AL (*Presenter*) Founder, Empower Therapeutics Inc ;Member, Translation Holdings LLC;Consultant, Radiostics LLC

#### PURPOSE

To compare the effectiveness of radiologist performance at detecting incidental PE on CT images with and without AI triage (CADt).

#### METHODS AND MATERIALS

For this IRB-approved prospective single center study, 4652 consecutive patients who underwent cross sectional imaging of the chest or abdomen were recruited in two phases. Patients who underwent CT angiography with a PE protocol were excluded. In phase 1, consecutive CTs (N=1467) were evaluated independently by a radiologist and by a FDA-cleared AI triage algorithm. This data was used to establish a baseline for unassisted radiologist and AI interpretations. Following this, all radiologists interpreting CT (N=??) were trained to review the results of the AI algorithm and triage system concurrently during image evaluation and reporting. In phase 2, consecutive CTs (N=3185) were evaluated by radiologists using AI assistance for all cases. Reports and addendums were manually reviewed for the presence or absence of PE. A chest radiologist determined the number of missed incidental PEs by reviewing the image data and reports of all potential misses. The miss rate of iPE was calculated along with the sensitivity, specificity, and accuracy of the AI algorithm.

#### RESULTS

In phase 1 and 2, 1.4% (21/1467) and 1.8% (57/3185) of CTs were positive for PE, respectively ( $p=0.374$ ). In phase 1 and 2, 19.0% (4/21) and 1.8% (1/57) of incidental PEs were missed ( $p=0.006$ ). The percentage of missed iPEs per exam decreased from 0.27% to 0.03% ( $p=0.019$ ). The triage algorithm's accuracy, sensitivity, and specificity was 0.993, 0.628, and 0.999 respectively.

#### CONCLUSION

s In a single-center prospective real-world study, the miss rate for detection of iPE on CT was statistically higher than the miss rate of radiologists assisted by an algorithm for detection and triage.

#### CLINICAL RELEVANCE/APPLICATION

Incidental pulmonary emboli (iPE) are easily missed when the purpose of an examination is for an alternative indication, however, the presence of a PE is critical finding that often changes clinical management.

Printed on: 02/07/23

## Abstract Archives of the RSNA, 2022

R5A-SPCH-7

### Added Value of An Artificial Intelligence Tool For Prioritization of Incidental Pulmonary Embolism on Chest CT

Thursday, Dec. 1 12:15PM - 12:45PM Room: Learning Center - CH DPS

#### Participants

Laurens Topff, MD, (*Presenter*) Nothing to Disclose

#### PURPOSE

To evaluate the diagnostic efficacy of commercially available artificial intelligence (AI) software to detect incidental pulmonary embolism (IPE) on chest CT and shorten the time to diagnosis using worklist prioritization.

#### METHODS AND MATERIALS

In this prospective study, AI software was deployed in a clinical environment to analyze routinely acquired chest CT scans of adult oncology patients. Three time periods of 15 weeks each were compared: routine workflow without AI, manual triage without AI, and worklist prioritization with AI. Diagnostic accuracy of the tool was evaluated on both prospectively and retrospectively collected data. Temporal endpoints including Detection and Notification Times (DNT) were assessed.

#### RESULTS

A total of 11 736 CT scans were evaluated. Prevalence of IPE was 1.2% (n=143). The AI software detected 131 true positives, 12 false negatives, 31 false positives, and 11559 true negatives. Sensitivity was 91.6%, specificity 99.7%, NPV 99.9%, and PPV 80.9%. When applied retrospectively, the AI software found IPEs in 47 CTs (44.8%) that were missed in the radiology report. The median DNT for IPE positive examinations was 7714, 4973, 87 min for the respective time periods. The difference in DNT between positive and negative CTs was largest when using AI assistance and was significantly different from both workflows without AI. In contrast, no statistically significant difference was found between routine workflow and manual triage without AI.

#### CONCLUSION

A commercially available AI tool was found to have a high diagnostic efficacy in detecting IPE on CT of oncology patients. AI assisted worklist prioritization was shown to be effective in significantly reducing the time to diagnosis of IPE cases compared to the routine clinical workflow.

#### CLINICAL RELEVANCE/APPLICATION

Incidental pulmonary embolism is a common comorbidity in oncology patients. Despite being clinically unsuspected, IPE can be an urgent and life-threatening event. AI based worklist prioritization can assist the radiologist to shorten the time to diagnosis of critical imaging findings.

Printed on: 02/07/23

## Abstract Archives of the RSNA, 2022

R5A-SPER

### Emergency Thursday Poster Discussions - A

Thursday, Dec. 1 12:15PM - 12:45PM Room: Learning Center - ER DPS

#### Participants

Scott Steenburg, MD, Indianapolis, IN (*Moderator*) Nothing to Disclose

#### Sub-Events

### R5A-SPER-1 Investigating the Sonographic Murphy Sign and the Diagnosis of Acute Cholecystitis After Non-Opioid Analgesia Administration

#### Participants

Karina Marcelo, MD, Triper AMC, HI (*Presenter*) Nothing to Disclose

#### PURPOSE

There is no single clinical, laboratory, or radiology exam sufficient to diagnose acute cholecystitis (AC). This increases reliance on highly correlated findings such as maximum abdominal pain elicited by a probe during right upper quadrant ultrasound (RUQUS), also known as the sonographic Murphy sign (SMS). Controversy exists regarding the effect of premedication with opioid analgesia on the SMS. The purpose of this study was to examine the use of non-opioid analgesia (NOA), such as acetaminophen or non-steroidal anti-inflammatory drugs, prior to RUQUS and the effect on the SMS and the radiologic accuracy of diagnosing AC.

#### METHODS AND MATERIALS

The research subjects (n=682) consisted of adult emergency department patients at a tertiary hospital who underwent a RUQUS over a 21 month period. A retrospective cohort chart review analyzed the SMS in patients who received NOA prior to RUQUS versus patients who did not (control) and the effect on diagnosis of AC. Radiology results were compared to final pathology diagnosis as a gold standard.

#### RESULTS

The average age of patients at the time of their RUQUS was 38.5 years. Four hundred forty-nine patients (65.8%) were female and 233 (34.2%) were male. The racial/ethnic composition of the study participants were as follows: Caucasian 43.1%, African American/Black 13.5%, Asian/Pacific Islander 16.3%, Native American 0.4%, Other 19%, Unknown 7.6%. Patients receiving NOA prior to RUQUS (n=248), when compared to the control group (n=434), did not experience significantly different rates of positive (31 cases vs 54 cases, respectively), negative (174 cases vs 332 cases, respectively), or indeterminate (43 cases vs 48 cases, respectively) SMS (p=0.06). There was no significant difference between NOA vs control in SMS sensitivity (33.3% [17.3%-52.8%] vs. 46.2% [32.2%-60.5%], respectively), specificity (90.4% [85.6%-93.9%] vs 92.1% [89.0%-94.6%], respectively), positive predictive value (PPV; 32.2% [19.9%-47.7%] vs 44.4% [33.7%-55.7%], respectively), or negative predictive value (NPV; 90.7% [88.4%-92.7%] vs 92.6% [90.7%-94.2%], respectively) in diagnosing AC.

#### CONCLUSION

s NOA administration prior to RUQUS does not affect the rate of finding a positive, negative or indeterminate SMS. Additionally, NOA does not significantly change the sensitivity, specificity, PPV, or NPV of the SMS in diagnosing AC. Future investigative opportunities include evaluating the effects of NOA administration timing, route (oral vs intravenous), dosing, and type.

#### CLINICAL RELEVANCE/APPLICATION

Despite controversy surrounding opioid premedication on the SMS, these results suggest that NOA prior to RUQUS in patients under evaluation for AC is of little diagnostic consequence.

Printed on: 02/07/23



## Abstract Archives of the RSNA, 2022

R5A-SPER-1

### Investigating the Sonographic Murphy Sign and the Diagnosis of Acute Cholecystitis After Non-Opioid Analgesia Administration

Thursday, Dec. 1 12:15PM - 12:45PM Room: Learning Center - ER DPS

#### Participants

Karina Marcelo, MD, Triper AMC, HI (*Presenter*) Nothing to Disclose

#### PURPOSE

There is no single clinical, laboratory, or radiology exam sufficient to diagnose acute cholecystitis (AC). This increases reliance on highly correlated findings such as maximum abdominal pain elicited by a probe during right upper quadrant ultrasound (RUQUS), also known as the sonographic Murphy sign (SMS). Controversy exists regarding the effect of premedication with opioid analgesia on the SMS. The purpose of this study was to examine the use of non-opioid analgesia (NOA), such as acetaminophen or non-steroidal anti-inflammatory drugs, prior to RUQUS and the effect on the SMS and the radiologic accuracy of diagnosing AC.

#### METHODS AND MATERIALS

The research subjects (n=682) consisted of adult emergency department patients at a tertiary hospital who underwent a RUQUS over a 21 month period. A retrospective cohort chart review analyzed the SMS in patients who received NOA prior to RUQUS versus patients who did not (control) and the effect on diagnosis of AC. Radiology results were compared to final pathology diagnosis as a gold standard.

#### RESULTS

The average age of patients at the time of their RUQUS was 38.5 years. Four hundred forty-nine patients (65.8%) were female and 233 (34.2%) were male. The racial/ethnic composition of the study participants were as follows: Caucasian 43.1%, African American/Black 13.5%, Asian/Pacific Islander 16.3%, Native American 0.4%, Other 19%, Unknown 7.6%. Patients receiving NOA prior to RUQUS (n=248), when compared to the control group (n=434), did not experience significantly different rates of positive (31 cases vs 54 cases, respectively), negative (174 cases vs 332 cases, respectively), or indeterminate (43 cases vs 48 cases, respectively) SMS (p=0.06). There was no significant difference between NOA vs control in SMS sensitivity (33.3% [17.3%-52.8%] vs. 46.2% [32.2%-60.5%], respectively), specificity (90.4% [85.6%-93.9%] vs 92.1% [89.0%-94.6%], respectively), positive predictive value (PPV; 32.2% [19.9%-47.7%] vs 44.4% [33.7%-55.7%], respectively), or negative predictive value (NPV; 90.7% [88.4%-92.7%] vs 92.6% [90.7%-94.2%], respectively) in diagnosing AC.

#### CONCLUSION

s NOA administration prior to RUQUS does not affect the rate of finding a positive, negative or indeterminate SMS. Additionally, NOA does not significantly change the sensitivity, specificity, PPV, or NPV of the SMS in diagnosing AC. Future investigative opportunities include evaluating the effects of NOA administration timing, route (oral vs intravenous), dosing, and type.

#### CLINICAL RELEVANCE/APPLICATION

Despite controversy surrounding opioid premedication on the SMS, these results suggest that NOA prior to RUQUS in patients under evaluation for AC is of little diagnostic consequence.

Printed on: 02/07/23

## Abstract Archives of the RSNA, 2022

R5A-SPGI

### Gastrointestinal Thursday Poster Discussions - A

Thursday, Dec. 1 12:15PM - 12:45PM Room: Learning Center - GI DPS

#### Participants

Neeraj Lalwani, MD, Glen Allen, VA (*Moderator*) Educator, MRI Online, LLC; Speaker, MRI Online, LLC; Author, RELX

#### Sub-Events

### R5A-SPGI-1 Multiparametric MRI for prediction of tumor response to systemic chemotherapy in pancreatic ductal adenocarcinoma

#### Participants

Yoshihiko Fukukura, MD, PhD, Kagoshima, Japan (*Presenter*) Nothing to Disclose

#### PURPOSE

Despite recent advances in diagnostic techniques, >80% of patients with PDAC are diagnosed at an advanced surgically unresectable stage and systemic chemotherapy is the mainstay of life-prolonging treatment. In recent years, neoadjuvant chemotherapy has emerged as a new alternative approach for patients with resectable diseases. Therefore, systemic chemotherapy is considered an essential first-line treatment for all stages of PDAC, in both the neoadjuvant and palliative settings. However, patients with PDAC respond differently to chemotherapy. There is a critical need for reliable predictive biomarkers to predict the treatment response is required for selecting the optimal therapeutic option. Therefore, this study aimed to identify multiparametric MRI biomarkers to predict the tumor response to chemotherapy in PDAC.

#### METHODS AND MATERIALS

This retrospective study included 81 consecutive patients (50 men, 31 women; mean age, 68.5 years; range, 47-83) with histologically confirmed PDAC who underwent multiparametric MRI including T1, T2, T2\* mappings, diffusion-weighted imaging (DWI), and dynamic contrast-enhanced MRI (DCE-MRI) before gemcitabine-based first-line chemotherapy. T1, T2, and T2\* relaxation times, apparent diffusion coefficient (ADC) obtained with DWI, and pharmacokinetic parameters ( $k_{trans}$ ,  $kep$ ,  $ve$ , and  $iAUC$ ) calculated with DCE-MRI were measured using ROI measurements within PDAC. Clinical factors and multiparametric MRI parameters to predict the responders determined after the third cycle of gemcitabine-based chemotherapy and those to predict progression-free survival (PFS) and overall survival (OS) were evaluated using multivariable logistic regression and the Cox proportional hazard model.

#### RESULTS

Among the clinical factors and MRI parameters, tumor size and pharmacokinetic parameter ( $ve$ ) of DCE-MRI were independent predictors for tumor response. The area under the receiver operating characteristic curve of combined use of the tumor size and pharmacokinetic parameter ( $ve$ ) was 0.842 with a sensitivity of 78.8% and specificity of 79.2% (cut off, <26 mm for tumor size and <21% for  $ve$ ). The pharmacokinetic parameter ( $ve$ ) was also identified as one of the independent predictors for PFS and OS.

#### CONCLUSION

Tumor pharmacokinetic parameters calculated with DCE-MRI may be useful to predict tumor response and survival in patients with PDAC receiving chemotherapy.

#### CLINICAL RELEVANCE/APPLICATION

DCE-MRI allows for the prediction of favorable tumor response and patient survival after chemotherapy.

### R5A-SPGI-10 Characterization of Non-alcoholic Fatty Liver Disease using Ultrasound Texture Parameters with Various Beamforming Sound Speeds

#### Participants

Kibo Nam, PhD, Philadelphia, PA (*Presenter*) Equipment support, Canon Medical Systems Corporation; Equipment support, General Electric Company ; Support, Lantheus Medical Imaging; Research funded, Canon Medical Systems Corporation

#### PURPOSE

To investigate if ultrasound texture features extracted using various beamforming speed of sounds (SOSs) can improve the characterization of non-alcoholic fatty liver disease (NAFLD).

#### METHODS AND MATERIALS

Patients with suspected NAFLD undergoing liver biopsy or MRI-PDFF, have been prospectively enrolled. Subjects were imaged with a C1-6 probe on a Logiq E9 scanner (GE Healthcare). The radio-frequency data from subjects' right and left lobes were collected using 9 beamforming SOSs: 1300, 1350, 1400, 1450, 1500, 1540, 1600, 1650, and 1700 m/s and analyzed offline using Matlab (MathWorks). The texture parameters, i.e. contrast, correlation, energy, and homogeneity from gray-level co-occurrence matrix of normalized envelope were obtained from the liver parenchyma. The diagnostic accuracy of texture parameters from each

beamforming SOS was assessed independently and in combination (using a generalized linear regression) by ROC analyses.

## RESULTS

64 subjects were included in the analysis. 43 subjects were diagnosed of steatosis (27 by biopsy steatosis = 5% and 16 by MRI-PDFF = 6.5%) and 28 of them had fibrosis (grade 1-4). 21 subjects had no steatosis (7 by biopsy and 14 by MRI-PDFF) and 6 of them had fibrosis. In detecting steatosis, homogeneity showed the AUC of 0.73-0.82 and 0.58-0.81 for left and right lobes, respectively with varying beamforming SOSs. The combined homogeneity over 1300-1700 m/s from left and right lobes showed the AUC 0.92 and 0.84, respectively. Moreover, the combined homogeneity from left and right lobes over 1300-1700 m/s improved the AUC to 0.96. In detecting fibrosis, correlation showed the AUC of 0.52-0.60 and 0.50-0.70 for left and right lobes, respectively with varying beamforming SOSs. The combined correlation over 1300-1700 m/s from left and right lobes showed the AUC 0.77 and 0.80, respectively. Finally, the combination of correlation from left and right lobes over 1300-1700 m/s showed the AUC of 0.86. However, no independent or combined value differentiated all 4 groups, i.e., normal liver, steatosis only, fibrosis only, and steatosis with fibrosis.

## CONCLUSION

s The diagnostic reliability of ultrasound texture parameter in NAFLD patients was improved with various beamforming SOSs.

## CLINICAL RELEVANCE/APPLICATION

Ultrasound texture parameters extracted from the images acquired with various beamforming SOSs may improve the characterization of NAFLD.

## R5A-SPGI-2 Dual-energy CT with virtual monoenergetic images iodine maps improve tumor conspicuity in patients with pancreatic ductal adenocarcinoma

Participants

Yongmei Li, Chongqing, China (*Presenter*) Nothing to Disclose

## PURPOSE

To evaluate the value of monoenergetic images (MEI [+]) and iodine maps in dual-source dual-energy computed tomography (DECT) for assessing pancreatic ductal adenocarcinoma (PDAC), including the visually isoattenuating PDAC.

## METHODS AND MATERIALS

Seventy-five patients with PDAC underwent contrast-enhanced DECT were retrospectively included in this study. Conventional polyenergetic image (PEI) and 40-80 keV MEI (+) (10-keV increments) were reconstructed. The tumor contrast, contrast-to-noise ratio (CNR) of the tumor and peripancreatic vessels, the signal-to-noise ratio (SNR) of the pancreas and tumor, and the tumor diameters were quantified. On iodine maps, the normalized iodine concentration (NIC) in the tumor and parenchyma were quantified and compared. For subjective analysis, two radiologists independently evaluated images on a 5-point scale.

## RESULTS

All the quantitative parameters were maximized at 40-keV MEI (+) and decreased gradually with increasing energy. The tumor contrast, SNR of pancreas and CNRs in 40-60 keV MEI (+) were significantly higher than those in PEI ( $p < 0.05$ ). For visually isoattenuating PDAC, 40-50 keV MEI (+) provided significantly higher CNR of the tumor compared to PEI ( $p < 0.05$ ). The reproducibility in tumor measurements were highest in 40-keV MEI (+) between the two radiologists. The NIC value of tumor and parenchyma were  $1.28 \pm 0.65$  and  $3.38 \pm 0.72$  mg/mL, respectively ( $p < 0.001$ ). 40-50 keV MEI (+) provided the highest subjective scores for all criteria, compared to PEI ( $p < 0.001$ ).

## CONCLUSION

s Low-keV MEI (+) of DECT substantially improve the subjective and objective image quality and tumor conspicuity in patients with PDAC. Combining the low-keV MEI (+) and iodine maps may be allowed for earlier diagnosis of PDAC.

## CLINICAL RELEVANCE/APPLICATION

- Low-keV MEI (+) increases subjective and objective image quality compared with PEI in patients with PDAC.
- Tumor conspicuity and reproducibility in tumor sizes were maximized at 40-keV MEI (+) in patients with PDAC.
- Combining low-keV MEI (+) and iodine maps may achieve earlier diagnosis and thus improve PDAC prognosis.

## R5A-SPGI-3 How Often Is Pancreatic Cancer Missed on CT or MRI Imaging? A Novel Root Cause Analysis System To Establish the Most Plausible Explanation for Post Imaging Pancreatic Cancer.

Participants

Melisa Sia, FRCR, MBChB, (*Presenter*) Nothing to Disclose

## PURPOSE

Pancreatic cancer (PC) often has a short time window for curative surgery. Missing PC on cross-sectional imaging (post imaging pancreatic cancer or PIPC) may therefore result in worse clinical outcomes in a cancer with already poor outcomes. We have undertaken root cause analysis of potentially missed PIPC to establish the most plausible explanations if imaging signs of PC were missed.

## METHODS AND MATERIALS

Electronic records of adults diagnosed with PC between 2019-21 at two NHS providers were examined. PIPC was defined as a PC diagnosed 6 to 18 months after abdominal cross-sectional imaging (CT or MRI) that did not diagnose PC. The imaging that did not diagnose the PC and the later diagnostic imaging were reviewed by two radiologists independently. An algorithm was developed to categorise PIPC and identify the most plausible explanation.

## RESULTS

Of 600 PC studied, 47 (7.8%) were categorised as PIPC. 47% of PIPC were located in the pancreatic head, 23.4% in the body, 21.3% in the body and tail, 6.40% in the head and neck and 2% in the entire pancreas. 44 CT and four MRI scans in PIPC patients

performed within 6 to 18 months of PC diagnosis were reviewed. Of 44 CT scans reviewed, 15 were CT thorax abdomen and pelvis, 17 were CT abdomen and pelvis, 2 CT colons, 4 CT thorax, 2 CT Pancreas, 1 CT Urogram, 1 CT neck, thorax, abdomen and pelvis, 1 CT lumbar spine and 1 CT neck and thorax. 7 CT scans were without contrast. MRI scans were MRI liver, MRI renal, MRI abdomen and MRCP. PIPC were categorised as: Type 1 - missed PC lesion, imaging inadequate to exclude lesion (10.6%); Type 2 - missed PC lesion, adequate imaging and lesion visible on review - perceptual error (25.5%); Type 3 - PC associated abnormality detected (e.g. pancreatic or bile duct dilatation but no focal lesion) but inadequate follow up plan - management error (10.6%); Type 4 - PC associated abnormality detected, with adequate subsequent management, but still PIPC (12.8%); Type 5 - Genuine new PC lesion - no abnormality detected on initial imaging and imaging adequate to exclude lesion (40.4%). 36% of PIPC were considered potentially avoidable.

## CONCLUSION

This is the first study to undertake detailed root cause analysis of potentially missed PC on imaging. Missed opportunities to potentially avoid PIPC were identified in 36%.

## CLINICAL RELEVANCE/APPLICATION

This root cause analysis system can standardize future investigation of PIPC and guide quality improvement efforts to improve outcomes in PC.

## R5A-SPGI-5 Predictors for Proton Density Fat Fraction (PDFF) Reduction in Patients Undergoing Very Low Calorie Liquid Diet in a Weight Loss Study

### Participants

Patricia Burns, MD, San Diego, CA (*Presenter*) Nothing to Disclose

### PURPOSE

Nonalcoholic fatty liver disease (NAFLD) is the hepatic manifestation of metabolic syndrome. MRI-derived proton density fat fraction (PDFF) is a non-invasive quantitative imaging biomarker that depicts distribution of hepatic steatosis. It has been suggested that metabolic derangements are responsible for the rapid reduction of PDFF early in the intense caloric restriction and surgery treatment option. Previous studies have investigated the effect of intense caloric restriction on PDFF, however, predictors for the amount of PDFF reduction while undergoing intense caloric restriction are not known. Thus, the purpose of this study is to identify predictors for PDFF reduction during a low caloric liquid diet period in a Weight Loss Study population with obesity assigned to a caloric restriction model.

### METHODS AND MATERIALS

Twenty-nine adults with obesity (26 female, 3 male, mean age 48 yrs) scheduled for bariatric surgery were recruited prospectively to participate in an ongoing pilot research study which includes collection of age, sex, BMI, waist/hip ratio (a marker of abdominal adiposity), lipid panel, and HbA1C. MR exams were performed on a 3T scanner (GE Signa Premier, or GE Discovery MR750, GE Healthcare, Waukesha WI) at baseline (visit 1) and 2-3 days prior to surgery (visit 2). Mean hepatic PDFF was calculated by a 9-ROI approach as previously described. Rates of PDFF change were estimated for each subject between visits 1 and 2. Bayesian Information Criterion (BIC)-based stepwise linear regression was used to search for baseline predictors of change for each of these periods. Clinical, serological, and imaging predictors were considered.

### RESULTS

PDFF decreased (-2.849 PDFF%/month,  $p < 0.001$ ) from 9.64% to 6.66%. PDFF at baseline (regression coefficient = -0.56,  $p < 0.001$ ) and waist/hip ratio at baseline (regression coefficient = 16.40,  $p < 0.001$ ) were selected as best predictors of change during the diet period.

### CONCLUSION

PDFF decreased after a period of low caloric liquid diet. Prediction models support that baseline PDFF and waist/hip ratio are associated with rate of PDFF change. A higher baseline PDFF predicts a more rapid decline in PDFF, but a higher baseline waist/hip ratio predicts a slower decline of PDFF. This suggests that increased abdominal adiposity, as assessed by waist/hip ratio, may result in resistance to fat mobilization from the liver during intense caloric restriction. Further research is needed to validate our findings, ideally including populations with a more equal male:female distribution and less severe caloric restriction.

### CLINICAL RELEVANCE/APPLICATION

Abdominal adiposity may be a marker of resistance to fat mobilization from the liver during intense caloric restriction weight loss.

## R5A-SPGI-6 The value of constructing a nomogram model based on preoperative contrast-enhanced CT to predict R0 resection of pancreatic ductal adenocarcinoma

### Participants

Zhengxiao Li, (*Presenter*) Nothing to Disclose

### PURPOSE

To investigate the value of preoperative enhanced CT scan features combined with clinical features to construct a nomogram model to predict R0 resection of pancreatic ductal adenocarcinoma (PDAC).

### METHODS AND MATERIALS

The preoperative contrast-enhanced CT imaging data of 106 patients with PDAC who were confirmed by surgery and pathology and whose resection margin status was evaluated from January 2015 to November 2021 in our hospital were retrospectively analyzed. According to the resection margin status, they were divided into R0 resection group and R1 resection group. The preoperative CA199, CA125, CEA and other clinical data of the patients were analyzed; the tumor location, the transverse diameter of the tumor, and the maximum angle between the tumor and the surrounding blood vessels (T/arterial angle, T/portal vein angle, T/super mesenteric angle) were observed. Vein, peritumoral fat space, and lymph node metastasis. Then, univariate and multivariate Logistic regression was used to construct a nomogram model to predict the value of preoperative PDAC tumor R0 resection.

### RESULTS

There were significant differences between the R0 resection group and the R1 resection group in tumor transverse diameter, CA199, CA125, CEA, T/arterial angle, T/portal vein angle, T/superior mesenteric vein and lymph node metastasis ( $p < 0.05$ ). Univariate and multivariate logistic regression analysis of lymph node metastasis [OR: 0.205 (CI: 0.043-0.972),  $p < 0.05$ ], T/arterial angle [OR: 0.085 (CI: 0.017-0.434),  $p < 0.01$ ], T/Portal vein angle [OR: 0.155 (CI: 0.031-0.783),  $p < 0.05$ ], tumor diameter [OR: 1.073 (CI: 1.004-1.146),  $p < 0.05$ ], CA199 [OR: 1.003 (CI: 1.001) -1.005),  $p < 0.01$ ] was an independent risk factor for R0 resection. The model constructed by multivariate logistic regression can effectively predict the R0 resection of PDAC tumors. The calibration curve shows that the predicted probability of the nomogram model can better fit the actual probability, and the calibration degree is high.

## CONCLUSION

Preoperative lower level of CA199, shorter tumor transverse diameter, T/arterial angle and T/portal vein angle  $< 180^\circ$ , and non-lymph node metastasis status were independent predictors of R0 resection of PDAC tumors, and the nomogram model can effectively predict R0 resection status for PDAC tumors.

## CLINICAL RELEVANCE/APPLICATION

To investigate the value of preoperative enhanced CT scan features combined with clinical features to construct a nomogram model to predict R0 resection of pancreatic ductal adenocarcinoma (PDAC).

## R5A-SPGI-7 Pancreatic neuroendocrine tumors: Correlation between dynamic contrast enhanced ultrasound and pathological tumor grades

Participants  
Yi Dong, MD, PhD, Shanghai, China (*Presenter*) Nothing to Disclose

## PURPOSE

Tumor grade is one of the major prognostic factors for pancreatic neuroendocrine tumors' (pNETs). Pathologically, pNETs are classified into Grade 1 (G1), Grade 2 (G2), and Grade 3 (G3) tumors based on the Ki-67 proliferation index and the mitotic activity. Early differential diagnosis between G1 and G2/G3 is important on therapeutic strategy and survival duration. The aim of this study was to investigate whether the dynamic contrast enhanced ultrasound (D-CEUS) features with quantitative parameters could effectively predicting pNETs grades before operation according to WHO classification.

## METHODS AND MATERIALS

This prospective study was approved by the institutional review board of our institution. Informed consent was waived before CEUS examination. Patients suspected of pNETs underwent D-CEUS of pancreas within one week prior to the surgery. Time intensity curves (TICs) were created and quantitative indexes of D-CEUS were analyzed. Patient demographics, CEUS findings, and quantitative parameters were compared to histopathological features using the Mann-Whitney U test. Diagnostic accuracy was assessed by ROC-AUC analysis, sensitivity and specificity were assessed for each quantitative parameter.

## RESULTS

Finally, a total of 36 patients with histopathologically confirmed pNETs met the inclusion criteria, including 12 cases of G1, 16 cases of G2, and 8 cases of G3 patients. Compared with G1, G2/G3 pNETs showed ill-defined margin (62.5 %) and hypoenhancement during the late phase (41.6 %). Liver metastases were detected in 15 G2/G3 patients during the late phase scan of the whole liver. Among all CEUS quantitative indexes, area under curve (AUC) was significantly higher in G2/G3 pNETs with ROC-AUC 0.731, sensitivity 81.8 % (95 % CI: 62.2-91.3) and specificity 65.2 % (95 % CI: 43.7-80.1) ( $P < 0.05$ ).

## CONCLUSION

D-CEUS analysis might be helpful in preoperative predicting tumor grades and liver metastases of pNETs. AUC is the potential D-CEUS parameter for identification of G2/G3 from G1 pNETs.

## CLINICAL RELEVANCE/APPLICATION

Dynamic CEUS analysis and quantitative parameters could be used as non-invasive imaging method to predict tumor histological grades of pNETs.

## R5A-SPGI-8 Correlations between POPF and delayed imaging findings in Patients who underwent Distal Pancreatectomy

Participants  
Giulia A. Zamboni, MD, Verona, Italy (*Presenter*) Nothing to Disclose

## PURPOSE

To analyze correlations between the presence of delayed fluid collections (FC) and postoperative pancreatic fistula (POPF), as defined by the International Study Group of Pancreatic Fistula (ISGPF), in patients who underwent Distal Pancreatectomy (DP).

## METHODS AND MATERIALS

This is a IRB approved prospective study. Patients who underwent DP between 2018 and 2020 and had a contrast-enhanced postoperative MR 1 month after surgery were included. They were divided into 3 groups based on ISGPF grade: 0: no fistula; B: persistent drainage for more than 3 weeks, need for clinical management changes, percutaneous or endoscopic drainage, angiographic procedures for bleeding and development of signs of infection; C: reoperation, organ failure, death. Group 0 was further subdivided in patients without fistula and patients with biochemical leak (BL), who had drainage amylase  $> 3$  times the upper limit of normal serum amylase value. BL is not considered a fistula as no intervention is required to improve clinical outcome. Two readers in consensus analyzed the MRI scans and logged presence of: pancreatic enhancement inhomogeneity; main pancreatic duct (MPD) dilation; presence of fluid collections adjacent to pancreatic stump, their content and major dimensions.

## RESULTS

107 patients (51 males, 56 females; mean age 60 years) who underwent DP in our Institution from August 2018 to August 2020 were included. 91 patients (86%) were classified as grade 0 (30 patients -29% had BL), 14 patients (12%) as grade B and 2

patients (2%) as grade C. Group C was too small to be analyzed significantly. 4 patients (3.7%) presented with inhomogenous pancreatic stump enhancement and MPD dilation, without correlation to ISGPF grade. 87 Patients (83%) had a FC one month after DP. No statistically significant correlation between POPF and the presence of FCs, collection signal intensity, inhomogeneity in T1 and T2 weighted sequences and FC size was found.

## CONCLUSION

s Delayed FCs are a common finding after DPs. They do not correlate with the presence of POPF and their relevance is still unclear.

## CLINICAL RELEVANCE/APPLICATION

The aim of this preliminary study is to investigate the features of different) delayed findings after pancreatic resections and their clinical relevance in patients' management. FCs are common postoperative findings and may persist for more than one month, but their clinical significance is unclear. Excluding a correlation between POPF and delayed FCs formation may help clinicians in the patient follow-up. Further multidisciplinary studies are required to describe which clinical symptoms and biochemical alterations could lead to delayed FCs development and their clinical importance.

## R5A-SPGI-9 CT Texture-analysis of pancreatic adenocarcinoma after neo-adjuvant treatment: can we predict pathological response?

Participants

Giulia A. Zamboni, MD, Verona, Italy (*Presenter*) Nothing to Disclose

## PURPOSE

Standard imaging criteria for pancreatic adenocarcinoma (PDAC) have been demonstrated to perform poorly after neoadjuvant treatment in predicting resectability and response to treatment. Our purpose was to assess if texture analysis of CT images after neoadjuvant treatment can predict response at pathology.

## METHODS AND MATERIALS

Standard imaging criteria for pancreatic adenocarcinoma (PDAC) have been demonstrated to perform poorly after neoadjuvant treatment in predicting resectability and response to treatment. Our purpose was to assess if texture analysis of CT images after neoadjuvant treatment can predict response at pathology. MM This is a retrospective study on patients collected in our institutional registry; informed consent for the utilization of clinical and radiologic data had been provided by all patients (PAD-R registry, n1101CESC). We included resected patients with histologically confirmed PDAC for which we had contrast-enhanced CT before and after neoadjuvant treatment, and for which the tumor regression grade (TRG) had been calculated on the resected specimen using three scores (Evans, CAP, MD Anderson). Two radiologists in consensus reviewed the scans for tumor size, location, margins, indirect signs (MPD, CBD dilation), vascular infiltration, resectability according to NCCN criteria, and overall disease assessment at post-NAT CT (response, stable disease, progression). One radiologist performed CT-Texture analysis on all post-NAT scans using commercially available software (LifeX) and derived first and second-order parameters. Texture parameters were compared with TRG scores by using ANOVA.

## RESULTS

Qualitative imaging features and NCCN criteria were not correlated with TRG scores. TRG expressed by CAP was significantly correlated with asymmetry ( $p < 0.0001$ ), kurtosis ( $p < 0.0001$ ), and energy ( $p < 0.0430$ ). Energy was also significantly correlated with TRG according to the MD Anderson score ( $p < 0.0465$ ). Among the second-order features, only GLCM\_entropy\_log 10 was correlated with the CAP score ( $p < 0.0382$ ). No first or second-order parameter correlated with the Evans score.

## CONCLUSION

s CT-derived texture parameters may correlate with tumor regression grade at pathology and therefore provide a preoperative noninvasive prediction of tumor response and, ultimately patient prognosis.

## CLINICAL RELEVANCE/APPLICATION

a more accurate preoperative prediction of response to treatment could aid in better treatment selection, for example sparing from surgery patients who have not responded and whose prognosis would not be improved by resection

Printed on: 02/07/23

## Abstract Archives of the RSNA, 2022

R5A-SPGI-1

### Multiparametric MRI for prediction of tumor response to systemic chemotherapy in pancreatic ductal adenocarcinoma

Thursday, Dec. 1 12:15PM - 12:45PM Room: Learning Center - GI DPS

#### Participants

Yoshihiko Fukukura, MD, PhD, Kagoshima, Japan (*Presenter*) Nothing to Disclose

#### PURPOSE

Despite recent advances in diagnostic techniques, >80% of patients with PDAC are diagnosed at an advanced surgically unresectable stage and systemic chemotherapy is the mainstay of life-prolonging treatment. In recent years, neoadjuvant chemotherapy has emerged as a new alternative approach for patients with resectable diseases. Therefore, systemic chemotherapy is considered an essential first-line treatment for all stages of PDAC, in both the neoadjuvant and palliative settings. However, patients with PDAC respond differently to chemotherapy. There is a critical need for reliable predictive biomarkers to predict the treatment response is required for selecting the optimal therapeutic option. Therefore, this study aimed to identify multiparametric MRI biomarkers to predict the tumor response to chemotherapy in PDAC.

#### METHODS AND MATERIALS

This retrospective study included 81 consecutive patients (50 men, 31 women; mean age, 68.5 years; range, 47-83) with histologically confirmed PDAC who underwent multiparametric MRI including T1, T2, T2\* mappings, diffusion-weighted imaging (DWI), and dynamic contrast-enhanced MRI (DCE-MRI) before gemcitabine-based first-line chemotherapy. T1, T2, and T2\* relaxation times, apparent diffusion coefficient (ADC) obtained with DWI, and pharmacokinetic parameters (k<sub>trans</sub>, k<sub>ep</sub>, v<sub>e</sub>, and iAUC) calculated with DCE-MRI were measured using ROI measurements within PDAC. Clinical factors and multiparametric MRI parameters to predict the responders determined after the third cycle of gemcitabine-based chemotherapy and those to predict progression-free survival (PFS) and overall survival (OS) were evaluated using multivariable logistic regression and the Cox proportional hazard model.

#### RESULTS

Among the clinical factors and MRI parameters, tumor size and pharmacokinetic parameter (v<sub>e</sub>) of DCE-MRI were independent predictors for tumor response. The area under the receiver operating characteristic curve of combined use of the tumor size and pharmacokinetic parameter (v<sub>e</sub>) was 0.842 with a sensitivity of 78.8% and specificity of 79.2% (cut off, <26 mm for tumor size and <21% for v<sub>e</sub>). The pharmacokinetic parameter (v<sub>e</sub>) was also identified as one of the independent predictors for PFS and OS.

#### CONCLUSION

s Tumor pharmacokinetic parameters calculated with DCE-MRI may be useful to predict tumor response and survival in patients with PDAC receiving chemotherapy.

#### CLINICAL RELEVANCE/APPLICATION

DCE-MRI allows for the prediction of favorable tumor response and patient survival after chemotherapy.

Printed on: 02/07/23

## Abstract Archives of the RSNA, 2022

R5A-SPGI-10

### Characterization of Non-alcoholic Fatty Liver Disease using Ultrasound Texture Parameters with Various Beamforming Sound Speeds

Thursday, Dec. 1 12:15PM - 12:45PM Room: Learning Center - GI DPS

#### Participants

Kibo Nam, PhD, Philadelphia, PA (*Presenter*) Equipment support, Canon Medical Systems Corporation; Equipment support, General Electric Company ; Support, Lantheus Medical Imaging; Research funded, Canon Medical Systems Corporation

#### PURPOSE

To investigate if ultrasound texture features extracted using various beamforming speed of sounds (SOSs) can improve the characterization of non-alcoholic fatty liver disease (NAFLD).

#### METHODS AND MATERIALS

Patients with suspected NAFLD undergoing liver biopsy or MRI-PDFF, have been prospectively enrolled. Subjects were imaged with a C1-6 probe on a Logiq E9 scanner (GE Healthcare). The radio-frequency data from subjects' right and left lobes were collected using 9 beamforming SOSs: 1300, 1350, 1400, 1450, 1500, 1540, 1600, 1650, and 1700 m/s and analyzed offline using Matlab (MathWorks). The texture parameters, i.e. contrast, correlation, energy, and homogeneity from gray-level co-occurrence matrix of normalized envelope were obtained from the liver parenchyma. The diagnostic accuracy of texture parameters from each beamforming SOS was assessed independently and in combination (using a generalized linear regression) by ROC analyses.

#### RESULTS

64 subjects were included in the analysis. 43 subjects were diagnosed of steatosis (27 by biopsy steatosis = 5% and 16 by MRI-PDFF = 6.5%) and 28 of them had fibrosis (grade 1-4). 21 subjects had no steatosis (7 by biopsy and 14 by MRI-PDFF) and 6 of them had fibrosis. In detecting steatosis, homogeneity showed the AUC of 0.73-0.82 and 0.58-0.81 for left and right lobes, respectively with varying beamforming SOSs. The combined homogeneity over 1300-1700 m/s from left and right lobes showed the AUC 0.92 and 0.84, respectively. Moreover, the combined homogeneity from left and right lobes over 1300-1700 m/s improved the AUC to 0.96. In detecting fibrosis, correlation showed the AUC of 0.52-0.60 and 0.50-0.70 for left and right lobes, respectively with varying beamforming SOSs. The combined correlation over 1300-1700 m/s from left and right lobes showed the AUC 0.77 and 0.80, respectively. Finally, the combination of correlation from left and right lobes over 1300-1700 m/s showed the AUC of 0.86. However, no independent or combined value differentiated all 4 groups, i.e., normal liver, steatosis only, fibrosis only, and steatosis with fibrosis.

#### CONCLUSION

s The diagnostic reliability of ultrasound texture parameter in NAFLD patients was improved with various beamforming SOSs.

#### CLINICAL RELEVANCE/APPLICATION

Ultrasound texture parameters extracted from the images acquired with various beamforming SOSs may improve the characterization of NAFLD.

Printed on: 02/07/23

## Abstract Archives of the RSNA, 2022

R5A-SPGI-2

### Dual-energy CT with virtual monoenergetic images iodine maps improve tumor conspicuity in patients with pancreatic ductal adenocarcinoma

Thursday, Dec. 1 12:15PM - 12:45PM Room: Learning Center - GI DPS

#### Participants

Yongmei Li, Chongqing, China (*Presenter*) Nothing to Disclose

#### PURPOSE

To evaluate the value of monoenergetic images (MEI [+]) and iodine maps in dual-source dual-energy computed tomography (DECT) for assessing pancreatic ductal adenocarcinoma (PDAC), including the visually isoattenuating PDAC.

#### METHODS AND MATERIALS

Seventy-five patients with PDAC underwent contrast-enhanced DECT were retrospectively included in this study. Conventional polyenergetic image (PEI) and 40-80 keV MEI (+) (10-keV increments) were reconstructed. The tumor contrast, contrast-to-noise ratio (CNR) of the tumor and peripancreatic vessels, the signal-to-noise ratio (SNR) of the pancreas and tumor, and the tumor diameters were quantified. On iodine maps, the normalized iodine concentration (NIC) in the tumor and parenchyma were quantified and compared. For subjective analysis, two radiologists independently evaluated images on a 5-point scale.

#### RESULTS

All the quantitative parameters were maximized at 40-keV MEI (+) and decreased gradually with increasing energy. The tumor contrast, SNR of pancreas and CNRs in 40-60 keV MEI (+) were significantly higher than those in PEI ( $p<0.05$ ). For visually isoattenuating PDAC, 40-50 keV MEI (+) provided significantly higher CNR of the tumor compared to PEI ( $p<0.05$ ). The reproducibility in tumor measurements were highest in 40-keV MEI (+) between the two radiologists. The NIC value of tumor and parenchyma were  $1.28\pm 0.65$  and  $3.38\pm 0.72$  mg/mL, respectively ( $p<0.001$ ). 40-50 keV MEI (+) provided the highest subjective scores for all criteria, compared to PEI ( $p<0.001$ ).

#### CONCLUSION

Low-keV MEI (+) of DECT substantially improve the subjective and objective image quality and tumor conspicuity in patients with PDAC. Combining the low-keV MEI (+) and iodine maps may be allowed for earlier diagnosis of PDAC.

#### CLINICAL RELEVANCE/APPLICATION

- Low-keV MEI (+) increases subjective and objective image quality compared with PEI in patients with PDAC.
- Tumor conspicuity and reproducibility in tumor sizes were maximized at 40-keV MEI (+) in patients with PDAC.
- Combining low-keV MEI (+) and iodine maps may achieve earlier diagnosis and thus improve PDAC prognosis.

Printed on: 02/07/23

## Abstract Archives of the RSNA, 2022

R5A-SPGI-3

### How Often Is Pancreatic Cancer Missed on CT or MRI Imaging? A Novel Root Cause Analysis System To Establish the Most Plausible Explanation for Post Imaging Pancreatic Cancer.

Thursday, Dec. 1 12:15PM - 12:45PM Room: Learning Center - GI DPS

#### Participants

Melisa Sia, FRCR, MBChB, (Presenter) Nothing to Disclose

#### PURPOSE

Pancreatic cancer (PC) often has a short time window for curative surgery. Missing PC on cross-sectional imaging (post imaging pancreatic cancer or PIPC) may therefore result in worse clinical outcomes in a cancer with already poor outcomes. We have undertaken root cause analysis of potentially missed PIPC to establish the most plausible explanations if imaging signs of PC were missed.

#### METHODS AND MATERIALS

Electronic records of adults diagnosed with PC between 2019-21 at two NHS providers were examined. PIPC was defined as a PC diagnosed 6 to 18 months after abdominal cross-sectional imaging (CT or MRI) that did not diagnose PC. The imaging that did not diagnose the PC and the later diagnostic imaging were reviewed by two radiologists independently. An algorithm was developed to categorise PIPC and identify the most plausible explanation.

#### RESULTS

Of 600 PC studied, 47 (7.8%) were categorised as PIPC. 47% of PIPC were located in the pancreatic head, 23.4% in the body, 21.3% in the body and tail, 6.40% in the head and neck and 2% in the entire pancreas. 44 CT and four MRI scans in PIPC patients performed within 6 to 18 months of PC diagnosis were reviewed. Of 44 CT scans reviewed, 15 were CT thorax abdomen and pelvis, 17 were CT abdomen and pelvis, 2 CT colons, 4 CT thorax, 2 CT Pancreas, 1 CT Urogram, 1 CT neck, thorax, abdomen and pelvis, 1 CT lumbar spine and 1 CT neck and thorax. 7 CT scans were without contrast. MRI scans were MRI liver, MRI renal, MRI abdomen and MRCP. PIPC were categorised as: Type 1 - missed PC lesion, imaging inadequate to exclude lesion (10.6%); Type 2 - missed PC lesion, adequate imaging and lesion visible on review - perceptual error (25.5%); Type 3 - PC associated abnormality detected (e.g. pancreatic or bile duct dilatation but no focal lesion) but inadequate follow up plan - management error (10.6%); Type 4 - PC associated abnormality detected, with adequate subsequent management, but still PIPC (12.8%); Type 5 - Genuine new PC lesion - no abnormality detected on initial imaging and imaging adequate to exclude lesion (40.4%). 36% of PIPC were considered potentially avoidable.

#### CONCLUSION

This is the first study to undertake detailed root cause analysis of potentially missed PC on imaging. Missed opportunities to potentially avoid PIPC were identified in 36%.

#### CLINICAL RELEVANCE/APPLICATION

This root cause analysis system can standardize future investigation of PIPC and guide quality improvement efforts to improve outcomes in PC.

Printed on: 02/07/23

## Abstract Archives of the RSNA, 2022

R5A-SPGI-5

### **Predictors for Proton Density Fat Fraction (PDFF) Reduction in Patients Undergoing Very Low Calorie Liquid Diet in a Weight Loss Study**

Thursday, Dec. 1 12:15PM - 12:45PM Room: Learning Center - GI DPS

#### **Participants**

Patricia Burns, MD, San Diego, CA (*Presenter*) Nothing to Disclose

#### **PURPOSE**

Nonalcoholic fatty liver disease (NAFLD) is the hepatic manifestation of metabolic syndrome. MRI-derived proton density fat fraction (PDFF) is a non-invasive quantitative imaging biomarker that depicts distribution of hepatic steatosis. It has been suggested that metabolic derangements are responsible for the rapid reduction of PDFF early in the intense caloric restriction and surgery treatment option. Previous studies have investigated the effect of intense caloric restriction on PDFF, however, predictors for the amount of PDFF reduction while undergoing intense caloric restriction are not known. Thus, the purpose of this study is to identify predictors for PDFF reduction during a low caloric liquid diet period in a Weight Loss Study population with obesity assigned to a caloric restriction model.

#### **METHODS AND MATERIALS**

Twenty-nine adults with obesity (26 female, 3 male, mean age 48 yrs) scheduled for bariatric surgery were recruited prospectively to participate in an ongoing pilot research study which includes collection of age, sex, BMI, waist/hip ratio (a marker of abdominal adiposity), lipid panel, and HbA1C. MR exams were performed on a 3T scanner (GE Signa Premier, or GE Discovery MR750, GE Healthcare, Waukesha WI) at baseline (visit 1) and 2-3 days prior to surgery (visit 2). Mean hepatic PDFF was calculated by a 9-ROI approach as previously described. Rates of PDFF change were estimated for each subject between visits 1 and 2. Bayesian Information Criterion (BIC)-based stepwise linear regression was used to search for baseline predictors of change for each of these periods. Clinical, serological, and imaging predictors were considered.

#### **RESULTS**

PDFF decreased (-2.849 PDFF%/month,  $p < 0.001$ ) from 9.64% to 6.66%. PDFF at baseline (regression coefficient = -0.56,  $p < 0.001$ ) and waist/hip ratio at baseline (regression coefficient = 16.40,  $p < 0.001$ ) were selected as best predictors of change during the diet period.

#### **CONCLUSION**

s PDFF decreased after a period of low caloric liquid diet. Prediction models support that baseline PDFF and waist/hip ratio are associated with rate of PDFF change. A higher baseline PDFF predicts a more rapid decline in PDFF, but a higher baseline waist/hip ratio predicts a slower decline of PDFF. This suggests that increased abdominal adiposity, as assessed by waist/hip ratio, may result in resistance to fat mobilization from the liver during intense caloric restriction. Further research is needed to validate our findings, ideally including populations with a more equal male:female distribution and less severe caloric restriction.

#### **CLINICAL RELEVANCE/APPLICATION**

Abdominal adiposity may be a marker of resistance to fat mobilization from the liver during intense caloric restriction weight loss.

Printed on: 02/07/23

## Abstract Archives of the RSNA, 2022

R5A-SPGI-6

### The value of constructing a nomogram model based on preoperative contrast-enhanced CT to predict R0 resection of pancreatic ductal adenocarcinoma

Thursday, Dec. 1 12:15PM - 12:45PM Room: Learning Center - GI DPS

#### Participants

Zhengxiao Li, (*Presenter*) Nothing to Disclose

#### PURPOSE

To investigate the value of preoperative enhanced CT scan features combined with clinical features to construct a nomogram model to predict R0 resection of pancreatic ductal adenocarcinoma (PDAC).

#### METHODS AND MATERIALS

The preoperative contrast-enhanced CT imaging data of 106 patients with PDAC who were confirmed by surgery and pathology and whose resection margin status was evaluated from January 2015 to November 2021 in our hospital were retrospectively analyzed. According to the resection margin status, they were divided into R0 resection group and R1 resection group. . The preoperative CA199, CA125, CEA and other clinical data of the patients were analyzed; the tumor location, the transverse diameter of the tumor, and the maximum angle between the tumor and the surrounding blood vessels (T/arterial angle, T/portal vein angle, T/superior mesenteric angle) were observed. Vein), peritumoral fat space, and lymph node metastasis. Then, univariate and multivariate Logistic regression was used to construct a nomogram model to predict the value of preoperative PDAC tumor R0 resection.

#### RESULTS

There were significant differences between the R0 resection group and the R1 resection group in tumor transverse diameter, CA199, CA125, CEA, T/arterial angle, T/portal vein angle, T/superior mesenteric vein and lymph node metastasis ( $p < 0.05$ ). Univariate and multivariate logistic regression analysis of lymph node metastasis [OR: 0.205 (CI: 0.043-0.972),  $p < 0.05$ ], T/arterial angle [OR: 0.085 (CI: 0.017-0.434),  $p < 0.01$ ], T /Portal vein angle [OR: 0.155 (CI: 0.031-0.783),  $p < 0.05$ ], tumor diameter [OR: 1.073 (CI: 1.004-1.146),  $p < 0.05$ ], CA199 [OR: 1.003 (CI: 1.001] -1.005),  $p < 0.01$ ] was an independent risk factor for R0 resection. The model constructed by multivariate logistic regression can effectively predict the R0 resection of PDAC tumors. The calibration curve shows that the predicted probability of the nomogram model can better fit the actual probability, and the calibration degree is high.

#### CONCLUSION

s Preoperative lower level of CA199, shorter tumor transverse diameter, T/arterial angle and T/portal vein angle  $< 180^\circ$ , and non-lymph node metastasis status were independent predictors of R0 resection of PDAC tumors, and the nomogram model can effectively Prediction of preoperative R0 resection status for PDAC tumors.

#### CLINICAL RELEVANCE/APPLICATION

To investigate the value of preoperative enhanced CT scan features combined with clinical features to construct a nomogram model to predict R0 resection of pancreatic ductal adenocarcinoma (PDAC).

Printed on: 02/07/23

## Abstract Archives of the RSNA, 2022

R5A-SPGI-7

### **Pancreatic neuroendocrine tumors: Correlation between dynamic contrast enhanced ultrasound and pathological tumor grades**

Thursday, Dec. 1 12:15PM - 12:45PM Room: Learning Center - GI DPS

#### **Participants**

Yi Dong, MD, PhD, Shanghai, China (*Presenter*) Nothing to Disclose

#### **PURPOSE**

Tumor grade is one of the major prognostic factors for pancreatic neuroendocrine tumors' (pNETs). Pathologically, pNETs are classified into Grade 1 (G1), Grade 2 (G2), and Grade 3 (G3) tumors based on the Ki-67 proliferation index and the mitotic activity. Early differential diagnosis between G1 and G2/G3 is important on therapeutic strategy and survival duration. The aim of this study was to investigate whether the dynamic contrast enhanced ultrasound (D-CEUS) features with quantitative parameters could effectively predicting pNETs grades before operation according to WHO classification.

#### **METHODS AND MATERIALS**

This prospective study was approved by the institutional review board of our institution. Informed consent was waived before CEUS examination. Patients suspected of pNETs underwent D-CEUS of pancreas within one week prior to the surgery. Time intensity curves (TICs) were created and quantitative indexes of D-CEUS were analyzed. Patient demographics, CEUS findings, and quantitative parameters were compared to histopathological features using the Mann-Whitney U test. Diagnostic accuracy was assessed by ROC-AUC analysis, sensitivity and specificity were assessed for each quantitative parameter.

#### **RESULTS**

Finally, a total of 36 patients with histopathologically confirmed pNETs met the inclusion criteria, including 12 cases of G1, 16 cases of G2, and 8 cases of G3 patients. Compared with G1, G2/G3 pNETs showed ill-defined margin (62.5 %) and hypoenhancement during the late phase (41.6 %). Liver metastases were detected in 15 G2/G3 patients during the late phase scan of the whole liver. Among all CEUS quantitative indexes, area under curve (AUC) was significantly higher in G2/G3 pNETs with ROC-AUC 0.731, sensitivity 81.8 % (95 % CI: 62.2-91.3) and specificity 65.2 % (95 % CI: 43.7-80.1) ( $P < 0.05$ ).

#### **CONCLUSION**

s D-CEUS analysis might be helpful in preoperative predicting tumor grades and liver metastases of pNETs. AUC is the potential D-CEUS parameter for identification of G2/G3 from G1 pNETs.

#### **CLINICAL RELEVANCE/APPLICATION**

Dynamic CEUS analysis and quantitative parameters could be used as non-invasive imaging method to predict tumor histological grades of pNETs.

Printed on: 02/07/23

## Abstract Archives of the RSNA, 2022

R5A-SPGI-8

### Correlations between POPF and delayed imaging findings in Patients who underwent Distal Pancreatectomy

Thursday, Dec. 1 12:15PM - 12:45PM Room: Learning Center - GI DPS

#### Participants

Giulia A. Zamboni, MD, Verona, Italy (*Presenter*) Nothing to Disclose

#### PURPOSE

To analyze correlations between the presence of delayed fluid collections (FC) and postoperative pancreatic fistula (POPF), as defined by the International Study Group of Pancreatic Fistula (ISGPF), in patients who underwent Distal Pancreatectomy (DP).

#### METHODS AND MATERIALS

This is a IRB approved prospective study. Patients who underwent DP between 2018 and 2020 and had a contrast-enhanced postoperative MR 1 month after surgery were included. They were divided into 3 groups based on ISGPF grade: 0: no fistula; B: persistent drainage for more than 3 weeks, need for clinical management changes, percutaneous or endoscopic drainage, angiographic procedures for bleeding and development of signs of infection; C: reoperation, organ failure, death. Group 0 was further subdivided in patients without fistula and patients with biochemical leak (BL), who had drainage amylase >3 times the upper limit of normal serum amylase value. BL is not considered a fistula as no intervention is required to improve clinical outcome. Two readers in consensus analyzed the MRI scans and logged presence of: pancreatic enhancement inhomogeneity; main pancreatic duct (MPD) dilation; presence of fluid collections adjacent to pancreatic stump, their content and major dimensions.

#### RESULTS

107 patients (51 males, 56 females; mean age 60 years) who underwent DP in our Institution from August 2018 to August 2020 were included. 91 patients (86%) were classified as grade 0 (30 patients -29%- had BL), 14 patients (12%) as grade B and 2 patients (2%) as grade C. Group C was too small to be analyzed significantly. 4 patients (3.7%) presented with inhomogenous pancreatic stump enhancement and MPD dilation, without correlation to ISGPF grade. 87 Patients (83%) had a FC one month after DP. No statistically significant correlation between POPF and the presence of FCs, collection signal intensity, inhomogeneity in T1 and T2 weighted sequences and FC size was found.

#### CONCLUSION

s Delayed FCs are a common finding after DPs. They do not correlate with the presence of POPF and their relevance is still unclear.

#### CLINICAL RELEVANCE/APPLICATION

The aim of this preliminary study is to investigate the features of different) delayed findings after pancreatic resections and their clinical relevance in patients' management. FCs are common postoperative findings and may persist for more than one month, but their clinical significance is unclear. Excluding a correlation between POPF and delayed FCs formation may help clinicians in the patient follow-up. Further multidisciplinary studies are required to describe which clinical symptoms and biochemical alterations could lead to delayed FCs development and their clinical importance.

Printed on: 02/07/23

## Abstract Archives of the RSNA, 2022

R5A-SPGI-9

### CT Texture-analysis of pancreatic adenocarcinoma after neo-adjuvant treatment: can we predict pathological response?

Thursday, Dec. 1 12:15PM - 12:45PM Room: Learning Center - GI DPS

#### Participants

Giulia A. Zamboni, MD, Verona, Italy (*Presenter*) Nothing to Disclose

#### PURPOSE

Standard imaging criteria for pancreatic adenocarcinoma (PDAC) have been demonstrated to perform poorly after neoadjuvant treatment in predicting resectability and response to treatment. Our purpose was to assess if texture analysis of CT images after neoadjuvant treatment can predict response at pathology.

#### METHODS AND MATERIALS

Standard imaging criteria for pancreatic adenocarcinoma (PDAC) have been demonstrated to perform poorly after neoadjuvant treatment in predicting resectability and response to treatment. Our purpose was to assess if texture analysis of CT images after neoadjuvant treatment can predict response at pathology. MM This is a retrospective study on patients collected in our institutional registry; informed consent for the utilization of clinical and radiologic data had been provided by all patients (PAD-R registry, n1101CESC). We included resected patients with histologically confirmed PDAC for which we had contrast-enhanced CT before and after neoadjuvant treatment, and for which the tumor regression grade (TRG) had been calculated on the resected specimen using three scores (Evans, CAP, MD Anderson). Two radiologists in consensus reviewed the scans for tumor size, location, margins, indirect signs (MPD, CBD dilation), vascular infiltration, resectability according to NCCN criteria, and overall disease assessment at post-NAT CT (response, stable disease, progression). One radiologist performed CT-Texture analysis on all post-NAT scans using commercially available software (LifeX) and derived first and second-order parameters. Texture parameters were compared with TRG scores by using ANOVA.

#### RESULTS

Qualitative imaging features and NCCN criteria were not correlated with TRG scores. TRG expressed by CAP was significantly correlated with asymmetry ( $p < 0.0001$ ), kurtosis ( $p < 0.0001$ ), and energy ( $p < 0.0430$ ). Energy was also significantly correlated with TRG according to the MD Anderson score ( $p < 0.0465$ ). Among the second-order features, only GLCM\_entropy\_log 10 was correlated with the CAP score ( $p < 0.0382$ ). No first or second-order parameter correlated with the Evans score.

#### CONCLUSION

s CT-derived texture parameters may correlate with tumor regression grade at pathology and therefore provide a preoperative noninvasive prediction of tumor response and, ultimately patient prognosis.

#### CLINICAL RELEVANCE/APPLICATION

a more accurate preoperative prediction of response to treatment could aid in better treatment selection, for example sparing from surgery patients who have not responded and whose prognosis would not be improved by resection

Printed on: 02/07/23

## Abstract Archives of the RSNA, 2022

R5A-SPGU

### Genitourinary Thursday Poster Discussions - A

Thursday, Dec. 1 12:15PM - 12:45PM Room: Learning Center - GU DPS

#### Sub-Events

#### **R5A-SPGU-1 The learning curve in bladder MRI using VIRADS assessment score during an interactive dedicated training program.**

Participants

Emanuele Messina, MD, Roma, Italy (*Presenter*) Nothing to Disclose

#### **PURPOSE**

The purpose of the study was to evaluate the effect of an interactive training program on the learning curve of radiology residents for bladder MRI interpretation using the VI-RADS score.

#### **METHODS AND MATERIALS**

Three radiology residents with minimal experience in bladder MRI served as readers. They blindly evaluated 200 studies divided into 4 subsets of 50 cases over a 3-month period. After 2 months, the first subset was reassessed, resulting in a total of 250 evaluations. An interactive training program was provided and included educational lessons and case-based practice. The learning curve was constructed by plotting mean agreement as the ratio of correct evaluations per batch. Inter-reader agreement and diagnostic performance analysis were performed with kappa statistics and ROC analysis.

#### **RESULTS**

As for the VI-RADS scoring agreement, the kappa differences between pre-training and post-training evaluation of the same group of cases were 0.555 to 0.852 for reader 1, 0.522 to 0.695 for reader 2, and 0.481 to 0.794 for reader 3. Using VI-RADS = 3 as cut-off for muscle invasion, sensitivity ranged from 84 to 89% and specificity from 91 to 94%, while the AUCs from 0.89 (95% CI:0.84, 0.94) to 0.90 (95% CI:0.86, 0.95). Mean evaluation time decreased from 5.21 ± 1.12 to 3.52 ± 0.69 min in subsets 1 and 5. Mean grade of confidence improved from 3.31 ± 0.93 to 4.21 ± 0.69, in subsets 1 and 5.

#### **CONCLUSION**

An interactive dedicated education program on bladder MRI and the VI-RADS score led to a significant increase in readers' diagnostic performance over time, with a general improvement observed after 100-150 cases.

#### **CLINICAL RELEVANCE/APPLICATION**

These findings may represent a useful experience to improve and shape future fellowship programs and radiology curricula.

#### **R5A-SPGU-2 Yield of second-round targeted multi-parametric MRI (mpMRI) Ultrasound (US) guided fusion prostate biopsy after initial first-round biopsy: factors associated with second-round clinically significant prostate cancer diagnosis**

Participants

Yashmin Nisha, MD, (*Presenter*) Nothing to Disclose

#### **PURPOSE**

To determine the yield of second-round mpMRI-US fusion biopsy and factors which may predict eventual clinically significant (CS) PCa diagnosis

#### **METHODS AND MATERIALS**

The retrospective cross-sectional study identified 940 men with MRI before prostate biopsy at a single institution from Jan 1 2013 to Dec 30 2021. 106 patients with negative MRI were excluded. 85 men underwent second-round mpMRI-US fusion biopsy of 92 lesions (47.8% [44/92] peripheral zone and 52.2% [48/92] transition zone). Patient age, PSA, PSA density (PSAD), PI-RADS score, size and location of lesions were retrieved and compared to histopathological diagnosis (any PCa and CS-PCa=Gleason Score =7 on target or on template biopsy) using multi-variate logistic regression.

#### **RESULTS**

Mean patient age, PSA, PSAD were: 64±7 years, 8.5±7.0 ng/mL, 0.17±0.11. Clinical indications were: active surveillance 21.2% (18/85), previous negative biopsy 42.4% (36/85) and 36.5% (31/85) biopsy naïve. Results from first-round targeted biopsy were: 63.0% (58/92) negative and 37.0% (34/92) Gleason 6 PCa. The time interval between first-round and second-round biopsy was 42 ± 1428 days. Second-round targeted biopsy identified 25.0% (23/92) CS-PCa (Gleason score 3+4=7 N=19, Gleason score 4+3=7 N=4) and an additional eight Gleason 3+3=6 PCa on targeted biopsy. Multivariate logistic regression showed no difference in age (p=0.101), psa (p=0.381), psad (p=0.268), PI-RADS score (p=0.491), size (p=0.235) or location (p=0.293) of lesions by eventual CS-PCa diagnosis.

## CONCLUSION

s Repeat second-round targeted mpMRI-US fusion biopsy yielded clinically significant PCa diagnosis in the targeted biopsy specimen in approximately one-quarter of patients in our study. There was no variable which was significantly associated with second round CS-PCa diagnosis

## CLINICAL RELEVANCE/APPLICATION

Clinically significant PCa diagnosed in approximately one-quarter of patients on repeat second-round targeted mpMRI-US fusion biopsy suggest the need for repeat biopsy.

## R5A-SPGU-3 CT-based preoperative risk assessment of prolonged urine leak in patients undergoing partial nephrectomy for renal tumor

Participants

Hyojeong Lee, Seoul, Korea, Republic Of (*Presenter*) Nothing to Disclose

## PURPOSE

To evaluate risk factors of prolonged urine leak following partial nephrectomy, in order to identify objective imaging characteristics on preoperative CT.

## METHODS AND MATERIALS

865 patients who underwent partial nephrectomy for renal tumor were included. The RENAL nephrometry scoring system was used to characterize the CT features of renal tumor. Perioperative findings including ischemic time during the surgery and tumor pathology were compared between the groups with or without urine leak. As we intended to identify an imaging parameters other than tumor size and location, we set two fold tumor-size matched control group without urine leak, with all tumor located  $\geq 4$  mm to the collecting system. Four CT parameters that depicts the relationship of tumor and collecting system were analyzed; curvilinear border length, protruding distance, margin at the interface and pelvicalyceal contact. Multivariate logistic regression analyses were performed to identify significant predictors of urine leak. The sensitivity, specificity, and accuracy of significant variables were calculated.

## RESULTS

53 of 865 patients (6.1%) demonstrated urine leak. The urine leak group had significantly larger tumor size (4.75 vs. 2.88 cm) and were more likely to have close proximity to renal sinus. The curvilinear border length and protruding distance were significantly longer in urine leak group (28.32 vs. 16.82 and 12.48 vs. 6.27, respectively). The frequencies of urine leak were higher with the tumor has non-smooth contact interface (18.9%) and direct pelvicalyceal contact (71.7%). In the multivariate analysis pelvicalyceal contact was the significant predictor of urine leak (OR = 2.612). Ischemic time was longer in the urine leak group (1423.0 vs. 1105.0 sec). Ischemic time was positively correlated with curvilinear border length, protruding distance and tumor size. For diagnostic accuracy, combined the CT parameters obtained AUC of 0.70 with a sensitivity of 58.5% and a specificity of 79.2%.

## CONCLUSION

s The four preoperative CT features were significantly associated with increased risk of urine leak, and should be considered as predictor of urine leak before partial nephrectomy.

## CLINICAL RELEVANCE/APPLICATION

A comprehensive preoperative imaging evaluation of the relationship between the tumor and renal sinus may provide advantages to select the optimal surgical options and afford better patient counselling of complication risk.

Printed on: 02/07/23

## Abstract Archives of the RSNA, 2022

R5A-SPGU-1

### The learning curve in bladder MRI using VIRADS assessment score during an interactive dedicated training program.

Thursday, Dec. 1 12:15PM - 12:45PM Room: Learning Center - GU DPS

#### Participants

Emanuele Messina, MD, Roma, Italy (*Presenter*) Nothing to Disclose

#### PURPOSE

The purpose of the study was to evaluate the effect of an interactive training program on the learning curve of radiology residents for bladder MRI interpretation using the VI-RADS score.

#### METHODS AND MATERIALS

Three radiology residents with minimal experience in bladder MRI served as readers. They blindly evaluated 200 studies divided into 4 subsets of 50 cases over a 3-month period. After 2 months, the first subset was reassessed, resulting in a total of 250 evaluations. An interactive training program was provided and included educational lessons and case-based practice. The learning curve was constructed by plotting mean agreement as the ratio of correct evaluations per batch. Inter-reader agreement and diagnostic performance analysis were performed with kappa statistics and ROC analysis.

#### RESULTS

As for the VI-RADS scoring agreement, the kappa differences between pre-training and post-training evaluation of the same group of cases were 0.555 to 0.852 for reader 1, 0.522 to 0.695 for reader 2, and 0.481 to 0.794 for reader 3. Using VI-RADS = 3 as cut-off for muscle invasion, sensitivity ranged from 84 to 89% and specificity from 91 to 94%, while the AUCs from 0.89 (95% CI:0.84, 0.94) to 0.90 (95% CI:0.86, 0.95). Mean evaluation time decreased from  $5.21 \pm 1.12$  to  $3.52 \pm 0.69$  min in subsets 1 and 5. Mean grade of confidence improved from  $3.31 \pm 0.93$  to  $4.21 \pm 0.69$ , in subsets 1 and 5.

#### CONCLUSION

An interactive dedicated education program on bladder MRI and the VI-RADS score led to a significant increase in readers' diagnostic performance over time, with a general improvement observed after 100-150 cases.

#### CLINICAL RELEVANCE/APPLICATION

These findings may represent a useful experience to improve and shape future fellowship programs and radiology curricula.

Printed on: 02/07/23

## Abstract Archives of the RSNA, 2022

R5A-SPGU-2

### **Yield of second-round targeted multi-parametric MRI (mpMRI) Ultrasound (US) guided fusion prostate biopsy after initial first-round biopsy: factors associated with second-round clinically significant prostate cancer diagnosis**

Thursday, Dec. 1 12:15PM - 12:45PM Room: Learning Center - GU DPS

#### **Participants**

Yashmin Nisha, MD, (*Presenter*) Nothing to Disclose

#### **PURPOSE**

To determine the yield of second-round mpMRI-US fusion biopsy and factors which may predict eventual clinically significant (CS) PCa diagnosis

#### **METHODS AND MATERIALS**

The retrospective cross-sectional study identified 940 men with MRI before prostate biopsy at a single institution from Jan 1 2013 to Dec 30 2021. 106 patients with negative MRI were excluded. 85 men underwent second-round mpMRI-US fusion biopsy of 92 lesions (47.8% [44/92] peripheral zone and 52.2% [48/92] transition zone). Patient age, PSA, PSA density (PSAD), PI-RADS score, size and location of lesions were retrieved and compared to histopathological diagnosis (any PCa and CS-PCa=Gleason Score =7 on target or on template biopsy) using multi-variate logistic regression.

#### **RESULTS**

Mean patient age, PSA, PSAD were: 64±7 years, 8.5±7.0 ng/mL, 0.17±0.11. Clinical indications were: active surveillance 21.2% (18/85), previous negative biopsy 42.4% (36/85) and 36.5% (31/85) biopsy naïve. Results from first-round targeted biopsy were: 63.0% (58/92) negative and 37.0% (34/92) Gleason 6 PCa. The time interval between first-round and second-round biopsy was 42 ± 1428 days. Second-round targeted biopsy identified 25.0% (23/92) CS-PCa (Gleason score 3+4=7 N=19, Gleason score 4+3=7 N=4) and an additional eight Gleason 3+3=6 PCa on targeted biopsy. Multivariate logistic regression showed no difference in age (p=0.101), psa (p=0.381), psad (p=0.268), PI-RADS score (p=0.491), size (p=0.235) or location (p=0.293) of lesions by eventual CS-PCa diagnosis.

#### **CONCLUSION**

s Repeat second-round targeted mpMRI-US fusion biopsy yielded clinically significant PCa diagnosis in the targeted biopsy specimen in approximately one-quarter of patients in our study. There was no variable which was significantly associated with second round CS-PCa diagnosis

#### **CLINICAL RELEVANCE/APPLICATION**

Clinically significant PCa diagnosed in approximately one-quarter of patients on repeat second-round targeted mpMRI-US fusion biopsy suggest the need for repeat biopsy.

Printed on: 02/07/23

## Abstract Archives of the RSNA, 2022

R5A-SPGU-3

### CT-based preoperative risk assessment of prolonged urine leak in patients undergoing partial nephrectomy for renal tumor

Thursday, Dec. 1 12:15PM - 12:45PM Room: Learning Center - GU DPS

#### Participants

Hyojeong Lee, Seoul, Korea, Republic Of (*Presenter*) Nothing to Disclose

#### PURPOSE

To evaluate risk factors of prolonged urine leak following partial nephrectomy, in order to identify objective imaging characteristics on preoperative CT.

#### METHODS AND MATERIALS

865 patients who underwent partial nephrectomy for renal tumor were included. The RENAL nephrometry scoring system was used to characterize the CT features of renal tumor. Perioperative findings including ischemic time during the surgery and tumor pathology were compared between the groups with or without urine leak. As we intended to identify an imaging parameters other than tumor size and location, we set two fold tumor-size matched control group without urine leak, with all tumor located  $\leq 4$  mm to the collecting system. Four CT parameters that depicts the relationship of tumor and collecting system were analyzed; curvilinear border length, protruding distance, margin at the interface and pelvicalyceal contact. Multivariate logistic regression analyses were performed to identify significant predictors of urine leak. The sensitivity, specificity, and accuracy of significant variables were calculated.

#### RESULTS

53 of 865 patients (6.1%) demonstrated urine leak. The urine leak group had significantly larger tumor size (4.75 vs. 2.88 cm) and were more likely to have close proximity to renal sinus. The curvilinear border length and protruding distance were significantly longer in urine leak group (28.32 vs. 16.82 and 12.48 vs. 6.27, respectively). The frequencies of urine leak were higher with the tumor has non-smooth contact interface (18.9%) and direct pelvicalyceal contact (71.7%). In the multivariate analysis pelvicalyceal contact was the significant predictor of urine leak (OR = 2.612). Ischemic time was longer in the urine leak group (1423.0 vs. 1105.0 sec). Ischemic time was positively correlated with curvilinear border length, protruding distance and tumor size. For diagnostic accuracy, combined the CT parameters obtained AUC of 0.70 with a sensitivity of 58.5% and a specificity of 79.2%.

#### CONCLUSION

The four preoperative CT features were significantly associated with increased risk of urine leak, and should be considered as predictor of urine leak before partial nephrectomy.

#### CLINICAL RELEVANCE/APPLICATION

A comprehensive preoperative imaging evaluation of the relationship between the tumor and renal sinus may provide advantages to select the optimal surgical options and afford better patient counselling of complication risk.

Printed on: 02/07/23

## Abstract Archives of the RSNA, 2022

R5A-SPHN

### Head and Neck Thursday Poster Discussions - A

Thursday, Dec. 1 12:15PM - 12:45PM Room: Learning Center - HN DPS

#### Sub-Events

#### **R5A-SPHN-1 Ultra-sonographic Prediction of Tumor Invasiveness in Follicular Thyroid Carcinoma: Based on The WHO Classification and TERT Promoter Mutation**

Participants

Myoung Kyoung Kim, seoul, Korea, Republic Of (*Presenter*) Nothing to Disclose

#### **PURPOSE**

The purpose of this study was to assess the role of ultrasound (US) in predicting tumor invasiveness in follicular thyroid carcinoma (FTC) based on the World Health Organization (WHO) classification and telomerase reverse transcriptase (TERT) promoter mutation.

#### **METHODS AND MATERIALS**

This retrospective study included 54 surgically confirmed FTC patients who underwent preoperative US and TERT mutation analysis. The WHO classification consisted of minimally invasive (MI-FTC), encapsulated angioinvasive (EA-FTC), and widely invasive (WI-FTC) types. The alternative classification was composed as follows: Group 1 (MI-FTC; EA-FTC with wild type [WT]-TERT), Group 2 (WI-FTC with WT-TERT), and Group 3 (EA-FTC with mutant [M]-TERT; WI-FTC with M-TERT). Each nodule was categorized based on the US pattern according to the K-TIRADS and ACR-TIRADS. For statistical analysis, the Jonckheere-Terpstra and Cochran-Armitage tests were used.

#### **RESULTS**

Among the 54 FTCs, there were 29 (53.7%) MI-FTCs, 16 (29.6%) EA-FTCs, and 9 (16.6%) WI-FTCs. The alternative classification included 42 (77.8%) Group 1, 5 (9.3%) Group 2, and 7 (13.0%) Group 3. Neither benign nor low suspicion US category was assigned to WI-FTC and alternative groups 2 and 3. In both classification groups, lobulation, irregular margin, and final assessment category showed significant differences (all  $p < 0.04$ ) and incidences of lobulation, irregular margin, and high suspicion category had a trend to increase with the increasing tumor invasiveness (all  $p$  for trend  $< 0.006$ ). In the WHO groups, hypoechogenicity differed significantly among the groups ( $p = 0.0112$ ) and tended to increase in proportion as tumor invasiveness increased ( $p$  for trend = 0.0145). Meanwhile, in the alternative groups, so did punctate echogenic foci ( $p = 0.0256$ ,  $p$  for trend = 0.0245).

#### **CONCLUSION**

Increasing tumor invasiveness in FTC based on the WHO classification and TERT promoter mutation is significantly correlated with the probability of displaying malignant US features using both K-TIRADS and ACR-TIRADS.

#### **CLINICAL RELEVANCE/APPLICATION**

A recent study proposed molecular marker-based risk stratification of FTC using TERT promoter mutations and WHO classification to better predict clinical outcome. Our study suggests that US prediction of tumor invasiveness in FTC is highly correlated with the WHO morphological classification as well as newly proposed TERT promoter mutation-based risk stratification.

#### **R5A-SPHN-3 Risk Stratification of Thyroid Nodules Initially Diagnosed as Atypia/Follicular Lesion of Undetermined Significance Cytology with Thyroid Imaging Reporting and Data System, Cytology Subcategory, and Nodule Size**

Participants

Hye Shin Ahn, MD, (*Presenter*) Nothing to Disclose

#### **PURPOSE**

To stratify the malignancy risk of thyroid nodules initially diagnosed as atypia/follicular lesion of undetermined significance (AUS/FLUS) cytology with Thyroid Imaging Reporting and Data System (TIRADS), cytology subcategory, and nodule size.

#### **METHODS AND MATERIALS**

This study included 320 consecutive nodules with final diagnoses among 504 thyroid nodules (= 1 cm) initially diagnosed as AUS/FLUS from January 2010 to December 2014. The malignancy risk was assessed according to US patterns by TIRADS (ATA guideline, KSThR(KT) guideline, AACE/ACE/AME guideline, ETA guideline, and ACR guideline), cytology subtype (AUS or FLUS), and nodule size. We investigated if TIRADS guidelines could predict malignancy at each cytology subcategory of AUS/FLUS nodules.

#### **RESULTS**

The overall malignancy rate was 20.6% (AUS, 22.4% and FLUS, 14.7%,  $p = 0.145$ ). The large nodules (= 3 cm) showed a higher malignancy rate than small nodules ( $< 3$  cm) in overall and AUS/FLUS subcategory nodule ( $p = 0.057$ ). The malignancy rate of all nodules was significantly different in all of TIRADS guidelines ( $p = 0.004$ ) and there was a trend towards an increasing malignancy

rate as the score of each guideline increased ( $p = 0.003$ ). The malignancy rates of AUS nodules and FLUS nodules were significantly different according to the US pattern and there was a trend towards an increasing malignancy rate as the guideline score increased in both of AUS nodules and FLUS nodules except FLUS nodules in ETA and AACE guidelines. Malignancy was not found in KT3/FLUS, ATA3/FLUS, ETA3/FLUS, ACR3/FLUS nodules less than 3 cm, and the malignancy rate of large nodules ( $\geq 3$  cm) was at least 16.7% in these guidelines.

#### **CONCLUSION**

s Malignancy risk can be stratified by TIRADS guidelines in both AUS and FLUS subcategory nodules. Small nodules ( $< 3$  cm) diagnosed as FLUS on initial cytology with mild or low suspicious US feature could be managed conservatively with US follow-up.

#### **CLINICAL RELEVANCE/APPLICATION**

AUS/FLUS is represented by cytology that is not easily classified as benign, suspicious, or malignant. In a recent Bethesda system, the estimated malignancy risk of this category is 10% to 30% and repeat FNA, molecular test, or lobectomy was recommended for management, even though the nodule was benign. According to the result of this study, small FLUS nodules can be observed by follow-up US instead of further invasive diagnostic procedure.

Printed on: 02/07/23

## Abstract Archives of the RSNA, 2022

R5A-SPHN-1

### Ultra-sonographic Prediction of Tumor Invasiveness in Follicular Thyroid Carcinoma: Based on The WHO Classification and TERT Promoter Mutation

Thursday, Dec. 1 12:15PM - 12:45PM Room: Learning Center - HN DPS

#### Participants

Myoung Kyoung Kim, seoul, Korea, Republic Of (*Presenter*) Nothing to Disclose

#### PURPOSE

The purpose of this study was to assess the role of ultrasound (US) in predicting tumor invasiveness in follicular thyroid carcinoma (FTC) based on the World Health Organization (WHO) classification and telomerase reverse transcriptase (TERT) promoter mutation.

#### METHODS AND MATERIALS

This retrospective study included 54 surgically confirmed FTC patients who underwent preoperative US and TERT mutation analysis. The WHO classification consisted of minimally invasive (MI-FTC), encapsulated angioinvasive (EA-FTC), and widely invasive (WI-FTC) types. The alternative classification was composed as follows: Group 1 (MI-FTC; EA-FTC with wild type [WT]-TERT), Group 2 (WI-FTC with WT-TERT), and Group 3 (EA-FTC with mutant [M]-TERT; WI-FTC with M-TERT). Each nodule was categorized based on the US pattern according to the K-TIRADS and ACR-TIRADS. For statistical analysis, the Jonckheere-Terpstra and Cochran-Armitage tests were used.

#### RESULTS

Among the 54 FTCs, there were 29 (53.7%) MI-FTCs, 16 (29.6%) EA-FTCs, and 9 (16.6%) WI-FTCs. The alternative classification included 42 (77.8%) Group 1, 5 (9.3%) Group 2, and 7 (13.0%) Group 3. Neither benign nor low suspicion US category was assigned to WI-FTC and alternative groups 2 and 3. In both classification groups, lobulation, irregular margin, and final assessment category showed significant differences (all  $p < 0.04$ ) and incidences of lobulation, irregular margin, and high suspicion category had a trend to increase with the increasing tumor invasiveness (all  $p$ s for trend  $< 0.006$ ). In the WHO groups, hypoechogenicity differed significantly among the groups ( $p = 0.0112$ ) and tended to increase in proportion as tumor invasiveness increased ( $p$  for trend = 0.0145). Meanwhile, in the alternative groups, so did punctate echogenic foci ( $p = 0.0256$ ,  $p$  for trend = 0.0245).

#### CONCLUSION

Increasing tumor invasiveness in FTC based on the WHO classification and TERT promoter mutation is significantly correlated with the probability of displaying malignant US features using both K-TIRADS and ACR-TIRADS.

#### CLINICAL RELEVANCE/APPLICATION

A recent study proposed molecular marker-based risk stratification of FTC using TERT promoter mutations and WHO classification to better predict clinical outcome. Our study suggests that US prediction of tumor invasiveness in FTC is highly correlated with the WHO morphological classification as well as newly proposed TERT promoter mutation-based risk stratification.

Printed on: 02/07/23

## Abstract Archives of the RSNA, 2022

R5A-SPHN-3

### **Risk Stratification of Thyroid Nodules Initially Diagnosed as Atypia/Follicular Lesion of Undetermined Significance Cytology with Thyroid Imaging Reporting and Data System, Cytology Subcategory, and Nodule Size**

Thursday, Dec. 1 12:15PM - 12:45PM Room: Learning Center - HN DPS

#### **Participants**

Hye Shin Ahn, MD, (*Presenter*) Nothing to Disclose

#### **PURPOSE**

To stratify the malignancy risk of thyroid nodules initially diagnosed as atypia/follicular lesion of undetermined significance (AUS/FLUS) cytology with Thyroid Imaging Reporting and Data System (TIRADS), cytology subcategory, and nodule size.

#### **METHODS AND MATERIALS**

This study included 320 consecutive nodules with final diagnoses among 504 thyroid nodules (= 1 cm) initially diagnosed as AUS/FLUS from January 2010 to December 2014. The malignancy risk was assessed according to US patterns by TIRADS (ATA guideline, KSThR(KT) guideline, AACE/ACE/AME guideline, ETA guideline, and ACR guideline), cytology subtype (AUS or FLUS), and nodule size. We investigated if TIRADS guidelines could predict malignancy at each cytology subcategory of AUS/FLUS nodules.

#### **RESULTS**

The overall malignancy rate was 20.6% (AUS, 22.4% and FLUS, 14.7%,  $p = 0.145$ ). The large nodules (= 3 cm) showed a higher malignancy rate than small nodules (< 3 cm) in overall and AUS/FLUS subcategory nodule ( $p = 0.057$ ). The malignancy rate of all nodules was significantly different in all of TIRADS guidelines ( $p = 0.004$ ) and there was a trend towards an increasing malignancy rate as the score of each guideline increased ( $p = 0.003$ ). The malignancy rates of AUS nodules and FLUS nodules were significantly different according to the US pattern and there was a trend towards an increasing malignancy rate as the guideline score increased in both of AUS nodules and FLUS nodules except FLUS nodules in ETA and AACE guidelines. Malignancy was not found in KT3/FLUS, ATA3/FLUS, ETA3/FLUS, ACR3/FLUS nodules less than 3 cm, and the malignancy rate of large nodules (= 3 cm) was at least 16.7% in these guidelines.

#### **CONCLUSION**

s Malignancy risk can be stratified by TIRADS guidelines in both AUS and FLUS subcategory nodules. Small nodules (< 3 cm) diagnosed as FLUS on initial cytology with mild or low suspicious US feature could be managed conservatively with US follow-up.

#### **CLINICAL RELEVANCE/APPLICATION**

AUS/FLUS is represented by cytology that is not easily classified as benign, suspicious, or malignant. In a recent Bethesda system, the estimated malignancy risk of this category is 10% to 30% and repeat FNA, molecular test, or lobectomy was recommended for management, even though the nodule was benign. According to the result of this study, small FLUS nodules can be observed by follow-up US instead of further invasive diagnostic procedure.

Printed on: 02/07/23

## Abstract Archives of the RSNA, 2022

R5A-SPIN

### Informatics Thursday Poster Discussions - A

Thursday, Dec. 1 12:15PM - 12:45PM Room: Learning Center - IN DPS

#### Sub-Events

#### R5A-SPIN-1 Fully Automated Volumetry of Living Donor Liver Transplantations Incorporating the Central Hepatic Vein

##### Participants

Sven Koitka, Essen, Germany (*Presenter*) Nothing to Disclose

##### PURPOSE

For major liver resections and living donor liver transplantations, a pre-operative calculation of the liver volume is essential. The aim of this retrospective study was to develop a fully-automated, reproducible, and quantitative 3D volumetry of the right and left liver lobes from standard CT scans of the abdomen.

##### METHODS AND MATERIALS

In this work, a dataset consisting of 100 in-house contrast-enhanced venous phase CT scans for training, as well as 30 ex-house contrast-enhanced venous phase CT scans for testing, were collected. All CT images were resampled to a common slice thickness of 5mm and were annotated with background, right lobe, and left lobe labels. The training images were annotated only once, but the testing images were annotated by three experienced annotators and, additionally, a standard of reference (SoR) was derived for evaluation by employing a majority voting. Voxels with tie votes were marked with an ignore label and were not included in the metrics calculation. An ensemble of 3D Multi-resolution U-Nets was trained using 5-fold cross-validation.

##### RESULTS

When compared against the SoR annotations, the ensemble achieves a Sørensen-Dice coefficient of 0.9726 for the liver, 0.9639 for the right lobe, and 0.9223 for the left lobe on the ex-house test dataset. The mean volume differences are 32.12ml for the liver, 22.68ml for the right lobe, and 9.44ml for the left lobe.

##### CONCLUSION

The developed system implements a fully automated, reproducible, fast, and accurate volumetry of right and left liver lobes.

##### CLINICAL RELEVANCE/APPLICATION

The fully automated liver volumetry can reduce the workload for radiologist while increasing the standardization and reproducibility of the volumetry for liver transplantations.

#### R5A-SPIN-2 Data Augmentation Can Cause Class Bias in Medical Image Classification

##### Participants

Hansang Lee, Daejeon, Korea, Republic Of (*Presenter*) Nothing to Disclose

##### PURPOSE

Data augmentation (DA) plays an important role in preventing overfitting for classifier learning by diversifying the amount and the pattern of the training data. However, it has recently been reported that the effect of DA on the computer vision task is not only class-dependent but also shows the class bias that decreases the classifier performance for some classes. We aim to observe whether the DA exhibits the class bias characteristics in the medical image classification tasks.

##### METHODS AND MATERIALS

To validate whether DA causes class bias, we used a dataset of 1290 CT liver lesion images consisting of 681 training, 302 validation, and 307 test images of 3 disease classes. In DA, we applied scaling, rotation, or translation DA with various parameters. In network training, we trained ResNet-18 CNN. From these trained networks, we observed the change in test accuracy and class-wise AUCs according to the selection of DA parameter. In order to verify that our observation is not limited to a specific dataset, we also perform experiments on the public ISIC skin lesion classification dataset.

##### RESULTS

In experiments, we observed that the trend of the test accuracy and the trends of class-wise performances according to the DA parameter do not match. This means that the DA with the best test accuracy does not guarantee the best performances in every class. In the CT dataset, the hemangiomas show different AUC trends from those of cysts, metastases, and the test accuracy. Thus, at the "optimal" DA with the best test accuracy, the AUC of hemangiomas is degraded by 2.05% lower than the best AUC of hemangiomas. In the ISIC dataset, the melanomas and the vascular lesions show opposite class sensitivity trends according to the DA parameters and the class bias on the melanomas was also observed at the "optimal" DA settings.

## CONCLUSION

s We generally optimize the DA parameters by maximizing the accuracy of the entire validation data. This is based on the assumption that the effect of the DA will appear nearly uniformly for the entire data. However, we observed that the effect of DA improved the performance of only some class data or even reinforced the class bias by decreasing the performance of other classes. Our observation suggests two future directions. First, we need to optimize DA by considering the performance of each class as well as the accuracy of the entire data. Second, it can be helpful to design a novel DA technique that applies different levels of transformation for each class. (This work was supported by the National Research Foundation of Korea grant funded by the Korea government (MSIT) (No. 2020R1A2C1102140))

## CLINICAL RELEVANCE/APPLICATION

Our observation and discussions are expected to be valid for other medical image classification problems and other DA techniques.

## R5A-SPIN-3 Application Of Artificial Intelligence for Evaluation Of Neuroradiology Emergencies; Clinical Workflow

Participants

Delaram Shakoor, MD, (*Presenter*) Nothing to Disclose

## PURPOSE

The goal of this study was to assess the user-interface of radiologists with an artificial-intelligence (AI) algorithm to detect intracranial hematoma (ICH) and cervical spine fracture (CSFX).

## METHODS AND MATERIALS

Over 12 month period, positive consecutive head and cervical spine CTs performed at our institution were reviewed and user-interaction data with our AI algorithm (AiDOC) were obtained. These interaction variables were extracted (Figure 1): Notification Image Review (NIR), representing the number of scans in which the key image of a positive notification was reviewed on the desktop application, upon receiving the prioritization notification. Panel image review (PIR) was defined as the number of positive scans which was reviewed by a reader from the main panel. Positive dictated cases (PDC) represented the number of positive notifications which were received by the readers upon interpreting the positive study. Positive reviewed cases (PRC) were the number of positive studies which dictating reader reviewed the key image of a positive case from the notification. Usage variable was defined as division of PRC over the PDC to evaluate the usage of Aidoc key images by the reader. Wilcoxon-Mann-Whitney test was used to compare median and interquartile range (IQR) of interaction variables. Linear and binary logistic regressions were performed to assess for presence of factors associated with higher usage.

## RESULTS

Data from interactions of 86 residents, 19 neuroradiology fellows, 36 ED and 15 neuroradiology attendings were collected. All interactions except for usage (ICH: median: 28.8%, IQR:34.3%; CSFX: median:21.8%, IQR:62.5%, P-value=0.9) were significantly higher for head CT (Figure 2). Linear regression did not show any statistically significant association between usage and scan type (Coefficient: 2.18, 95% CI: -4.7, 9.1, P-value 0.6), trainees versus attendings (Coefficient: -1.8, 95%CI: -9.3, 5.6, P-value=0.6), ED versus neuroradiology (Coefficient: -5.8, 95% CI: -12.9, 1.3, P-value:0.1). Comparing the interactions of trainees versus attendings for head CTs, median of PDC was significantly higher for faculty (Trainee: median:16, IQR:31; Faculty: median:40, IQR:63, P-value:0.004) while the remaining interactions were not statistically significantly different. No significant difference was noted between ED and neuroradiology attendings.

## CONCLUSION

s The results of our preliminary study imply that approximately two third of our readers don't interact with Aidoc while interpreting head and cervical spine CTs.

## CLINICAL RELEVANCE/APPLICATION

Further studies with survey analysis are recommended to recognize the reasons for low interactions and means to increase radiologist interface with AI in a busy radiology practice.

## R5A-SPIN-4 Pretraining using Masked Image Reconstruction Improves Deep Learning Performance in Disease Classification and Segmentation

Participants

Joseph Bae, MS, BS, Chino Hills, CA (*Presenter*) Nothing to Disclose

## PURPOSE

Deep learning (DL) analysis in medical imaging suffers from the absence of large datasets for model pretraining analogous to those for natural images (eg: ImageNet). To improve computational modeling of small medical image datasets, self-supervised training can be utilized to improve feature learning. Here we analyze Masked Autoencoder (MAE) self-pretraining to improve medical segmentation and classification performance. Self-pretraining refers to the pretraining of a DL network on the same dataset studied in downstream classification/segmentation tasks. By self-pretraining a Vision Transformer (ViT) to reconstruct images after masking a subset of regions in the original image, we hypothesize that the model will learn to exploit the regional interdependencies inherent to anatomical structures and the physiological environments that they cohabitate.

## METHODS AND MATERIALS

We applied MAE self-pretraining to 3 common medical imaging tasks using public datasets. The ChestX-ray14 (CXr14) dataset was studied for thoracic disease classification, the Multi-Atlas Labeling Beyond the Cranial Vault (BTCV) was studied for organ segmentation, and the Brain Tumor Segmentation (BRATS) dataset was studied for tumor segmentation. CXr14 contains 112,120 frontal CXRs, BTCV contains 30 abdominal CT scans, and BRATS contains 484 multi-sequence brain MRIs. For MAE self-pretraining, CXRs were split into 16x16 pixel patches. CTs and MRIs were split into 16x16x16 voxel patches. For each dataset, a fraction of image patches were masked and input into a ViT. A decoder was trained to reconstruct whole images from ViT outputs. After the completion of self-pretraining, the ViT was used for dataset-specific downstream tasks in either classification (CXr14) or segmentation (BTCV, BRATS). Performance was compared with state of the art (SOTA) approaches. Classification and segmentation performance were assessed using AUC and dice score (DSC), respectively.

## RESULTS

A masked patch ratio of 12.5% was found to be optimal for the downstream tasks. CXR14 classification yielded an AUC of 81.5% (SOTA: 80.7%). BTCV abdominal organ segmentation resulted in a DSC of 83.5 (SOTA: 79.7). BRATS brain tumor segmentation resulted in a DSC of 78.9% (SOTA: 77.8).

## CONCLUSION

s MAE self-pretraining can improve image classification and segmentation tasks for a variety of imaging modalities and anatomical sites. MAE enforces the learning of spatial relationships between anatomical regions and can improve performance on datasets as small as N=30.

## CLINICAL RELEVANCE/APPLICATION

MAE self-pretraining can be leveraged for the analysis of pathologies and images that might be too rare or costly for large-scale data collection while also achieving clinically impactful performance.

## R5A-SPIN-5 MAGIC: Multitask Synthesis of Contrast-free CT Perfusion Maps via Generative Adversarial Network

Participants

Garrett Fullerton, BS, Gainesville, FL (*Presenter*) Nothing to Disclose

## PURPOSE

CTP is a popular imaging modality used to evaluate the micro circulatory structures of the brain and is commonly used in the detection of abnormalities in the brain parenchyma. Contrast imaging is generally safe, but it can present adverse side effects with increased procedure time and monetary cost. Here, we introduce a multi-task automated generation framework (MAGIC) model for contrast-free CTP brain imaging generation via physiology-inspired deep learning. By applying this framework, we predict contrast-free CTP maps with only non-contrast CT (NCCT) comparable to those generated by commercial software from contrast-enhanced images.

## METHODS AND MATERIALS

Neuroimaging data were retrospectively retrieved from 12,186 (7.76 TB) patients at UF Health between 2013 and 2020 with Institutional Review Board approval. The perfusion studies were conducted using iodinated contrast injection, and the collected data were analyzed using RAPID CT Perfusion analysis software (iSchemaView, Menlo Park, CA., USA), termed as "RAPID" below. Subjects with both NCCT imaging and RAPID-generated perfusion maps were included, resulting in 493 subjects. 431 subjects were selected for training and the remainder were reserved for testing. Model MAGIC was implemented using PyTorch v1.5.0 in Python v3.6.10 and NVIDIA CUDA v7.6.5. Model MAGIC was trained for 50 epochs on an NVIDIA TITAN X GPU.

## RESULTS

Three experienced radiologists evaluated MAGIC- and RAPID-generated CTP maps from 62 subjects in a double-blinded fashion via a 4-part questionnaire. Raters determined that there was no physiologically distinguishable difference between the synthetic and real CTP maps ( $p < 0.05$ ) and found 81% accuracy in diagnostic outcomes in the synthetic and real CTP maps. The further quantitative evaluation confirmed the high structural fidelity between the synthetic and real CTP maps. It was determined that the MAGIC-generated CTP maps were both physiologically and diagnostically acceptable and consistent.

## CONCLUSION

s The proposed framework MAGIC can generate contrast-free brain perfusion imaging from solely non-contrast, structural imaging that exhibits comparable analytical and diagnostic results to the ground-truth perfusion imaging, reducing the time, cost, and patient risk associated with CTP brain imaging.

## CLINICAL RELEVANCE/APPLICATION

The proposed artificial intelligence (AI) model enables the diagnostically competitive synthesis of CT perfusion (CTP) maps from non-contrast-enhanced imaging alone, reducing the cost, time, and radiation dose associated with perfusion imaging.

Printed on: 02/07/23

## Abstract Archives of the RSNA, 2022

R5A-SPIN-1

### Fully Automated Volumetry of Living Donor Liver Transplantations Incorporating the Central Hepatic Vein

Thursday, Dec. 1 12:15PM - 12:45PM Room: Learning Center - IN DPS

#### Participants

Sven Koitka, Essen, Germany (*Presenter*) Nothing to Disclose

#### PURPOSE

For major liver resections and living donor liver transplantations, a pre-operative calculation of the liver volume is essential. The aim of this retrospective study was to develop a fully-automated, reproducible, and quantitative 3D volumetry of the right and left liver lobes from standard CT scans of the abdomen.

#### METHODS AND MATERIALS

In this work, a dataset consisting of 100 in-house contrast-enhanced venous phase CT scans for training, as well as 30 ex-house contrast-enhanced venous phase CT scans for testing, were collected. All CT images were resampled to a common slice thickness of 5mm and were annotated with background, right lobe, and left lobe labels. The training images were annotated only once, but the testing images were annotated by three experienced annotators and, additionally, a standard of reference (SoR) was derived for evaluation by employing a majority voting. Voxels with tie votes were marked with an ignore label and were not included in the metrics calculation. An ensemble of 3D Multi-resolution U-Nets was trained using 5-fold cross-validation.

#### RESULTS

When compared against the SoR annotations, the ensemble achieves a Sørensen-Dice coefficient of 0.9726 for the liver, 0.9639 for the right lobe, and 0.9223 for the left lobe on the ex-house test dataset. The mean volume differences are 32.12ml for the liver, 22.68ml for the right lobe, and 9.44ml for the left lobe.

#### CONCLUSION

The developed system implements a fully automated, reproducible, fast, and accurate volumetry of right and left liver lobes.

#### CLINICAL RELEVANCE/APPLICATION

The fully automated liver volumetry can reduce the workload for radiologist while increasing the standardization and reproducibility of the volumetry for liver transplantations.

Printed on: 02/07/23



## Abstract Archives of the RSNA, 2022

R5A-SPIN-2

### Data Augmentation Can Cause Class Bias in Medical Image Classification

Thursday, Dec. 1 12:15PM - 12:45PM Room: Learning Center - IN DPS

#### Participants

Hansang Lee, Daejeon, Korea, Republic Of (*Presenter*) Nothing to Disclose

#### PURPOSE

Data augmentation (DA) plays an important role in preventing overfitting for classifier learning by diversifying the amount and the pattern of the training data. However, it has recently been reported that the effect of DA on the computer vision task is not only class-dependent but also shows the class bias that decreases the classifier performance for some classes. We aim to observe whether the DA exhibits the class bias characteristics in the medical image classification tasks.

#### METHODS AND MATERIALS

To validate whether DA causes class bias, we used a dataset of 1290 CT liver lesion images consisting of 681 training, 302 validation, and 307 test images of 3 disease classes. In DA, we applied scaling, rotation, or translation DA with various parameters. In network training, we trained ResNet-18 CNN. From these trained networks, we observed the change in test accuracy and class-wise AUCs according to the selection of DA parameter. In order to verify that our observation is not limited to a specific dataset, we also perform experiments on the public ISIC skin lesion classification dataset.

#### RESULTS

In experiments, we observed that the trend of the test accuracy and the trends of class-wise performances according to the DA parameter do not match. This means that the DA with the best test accuracy does not guarantee the best performances in every class. In the CT dataset, the hemangiomas show different AUC trends from those of cysts, metastases, and the test accuracy. Thus, at the "optimal" DA with the best test accuracy, the AUC of hemangiomas is degraded by 2.05% lower than the best AUC of hemangiomas. In the ISIC dataset, the melanomas and the vascular lesions show opposite class sensitivity trends according to the DA parameters and the class bias on the melanomas was also observed at the "optimal" DA settings.

#### CONCLUSION

s We generally optimize the DA parameters by maximizing the accuracy of the entire validation data. This is based on the assumption that the effect of the DA will appear nearly uniformly for the entire data. However, we observed that the effect of DA improved the performance of only some class data or even reinforced the class bias by decreasing the performance of other classes. Our observation suggests two future directions. First, we need to optimize DA by considering the performance of each class as well as the accuracy of the entire data. Second, it can be helpful to design a novel DA technique that applies different levels of transformation for each class. (This work was supported by the National Research Foundation of Korea grant funded by the Korea government (MSIT) (No. 2020R1A2C1102140))

#### CLINICAL RELEVANCE/APPLICATION

Our observation and discussions are expected to be valid for other medical image classification problems and other DA techniques.

Printed on: 02/07/23



## Abstract Archives of the RSNA, 2022

R5A-SPIN-3

### Application Of Artificial Intelligence for Evaluation Of Neuroradiology Emergencies; Clinical Workflow

Thursday, Dec. 1 12:15PM - 12:45PM Room: Learning Center - IN DPS

#### Participants

Delaram Shakoor, MD, (*Presenter*) Nothing to Disclose

#### PURPOSE

The goal of this study was to assess the user-interface of radiologists with an artificial-intelligence (AI) algorithm to detect intracranial hematoma (ICH) and cervical spine fracture (CSFX).

#### METHODS AND MATERIALS

Over 12 month period, positive consecutive head and cervical spine CTs performed at our institution were reviewed and user-interaction data with our AI algorithm (AiDOC) were obtained. These interaction variables were extracted (Figure 1): Notification Image Review (NIR), representing the number of scans in which the key image of a positive notification was reviewed on the desktop application, upon receiving the prioritization notification. Panel image review (PIR) was defined as the number of positive scans which was reviewed by a reader from the main panel. Positive dictated cases (PDC) represented the number of positive notifications which were received by the readers upon interpreting the positive study. Positive reviewed cases (PRC) were the number of positive studies which dictating reader reviewed the key image of a positive case from the notification. Usage variable was defined as division of PRC over the PDC to evaluate the usage of Aidoc key images by the reader. Wilcoxon-Mann-Whitney test was used to compare median and interquartile range (IQR) of interaction variables. Linear and binary logistic regressions were performed to assess for presence of factors associated with higher usage.

#### RESULTS

Data from interactions of 86 residents, 19 neuroradiology fellows, 36 ED and 15 neuroradiology attendings were collected. All interactions except for usage (ICH: median: 28.8%, IQR:34.3%; CSFX: median:21.8%, IQR:62.5%, P-value=0.9) were significantly higher for head CT (Figure 2). Linear regression did not show any statistically significant association between usage and scan type (Coefficient: 2.18, 95% CI: -4.7, 9.1, P-value 0.6), trainees versus attendings (Coefficient: -1.8, 95%CI: -9.3, 5.6, P-value=0.6), ED versus neuroradiology (Coefficient: -5.8, 95% CI: -12.9, 1.3, P-value:0.1). Comparing the interactions of trainees versus attendings for head CTs, median of PDC was significantly higher for faculty (Trainee: median:16, IQR:31; Faculty: median:40, IQR:63, P-value:0.004) while the remaining interactions were not statistically significantly different. No significant difference was noted between ED and neuroradiology attendings.

#### CONCLUSION

The results of our preliminary study imply that approximately two third of our readers don't interact with Aidoc while interpreting head and cervical spine CTs.

#### CLINICAL RELEVANCE/APPLICATION

Further studies with survey analysis are recommended to recognize the reasons for low interactions and means to increase radiologist interface with AI in a busy radiology practice.

Printed on: 02/07/23



## Abstract Archives of the RSNA, 2022

R5A-SPIN-4

### Pretraining using Masked Image Reconstruction Improves Deep Learning Performance in Disease Classification and Segmentation

Thursday, Dec. 1 12:15PM - 12:45PM Room: Learning Center - IN DPS

#### Participants

Joseph Bae, MS, BS, Chino Hills, CA (*Presenter*) Nothing to Disclose

#### PURPOSE

Deep learning (DL) analysis in medical imaging suffers from the absence of large datasets for model pretraining analogous to those for natural images (eg: ImageNet). To improve computational modeling of small medical image datasets, self-supervised training can be utilized to improve feature learning. Here we analyze Masked Autoencoder (MAE) self-pretraining to improve medical segmentation and classification performance. Self-pretraining refers to the pretraining of a DL network on the same dataset studied in downstream classification/segmentation tasks. By self-pretraining a Vision Transformer (ViT) to reconstruct images after masking a subset of regions in the original image, we hypothesize that the model will learn to exploit the regional interdependencies inherent to anatomical structures and the physiological environments that they cohabitate.

#### METHODS AND MATERIALS

We applied MAE self-pretraining to 3 common medical imaging tasks using public datasets. The ChestX-ray14 (CXR14) dataset was studied for thoracic disease classification, the Multi-Atlas Labeling Beyond the Cranial Vault (BTCV) was studied for organ segmentation, and the Brain Tumor Segmentation (BRATS) dataset was studied for tumor segmentation. CXR14 contains 112,120 frontal CXRs, BTCV contains 30 abdominal CT scans, and BRATS contains 484 multi-sequence brain MRIs. For MAE self-pretraining, CXRs were split into 16x16 pixel patches. CTs and MRIs were split into 16x16x16 voxel patches. For each dataset, a fraction of image patches were masked and input into a ViT. A decoder was trained to reconstruct whole images from ViT outputs. After the completion of self-pretraining, the ViT was used for dataset-specific downstream tasks in either classification (CXR14) or segmentation (BTCV, BRATS). Performance was compared with state of the art (SOTA) approaches. Classification and segmentation performance were assessed using AUC and dice score (DSC), respectively.

#### RESULTS

A masked patch ratio of 12.5% was found to be optimal for the downstream tasks. CXR14 classification yielded an AUC of 81.5% (SOTA: 80.7%). BTCV abdominal organ segmentation resulted in a DSC of 83.5 (SOTA: 79.7). BRATS brain tumor segmentation resulted in a DSC of 78.9% (SOTA: 77.8).

#### CONCLUSION

MAE self-pretraining can improve image classification and segmentation tasks for a variety of imaging modalities and anatomical sites. MAE enforces the learning of spatial relationships between anatomical regions and can improve performance on datasets as small as N=30.

#### CLINICAL RELEVANCE/APPLICATION

MAE self-pretraining can be leveraged for the analysis of pathologies and images that might be too rare or costly for large-scale data collection while also achieving clinically impactful performance.

Printed on: 02/07/23

## Abstract Archives of the RSNA, 2022

R5A-SPIN-5

### **MAGIC: Multitask Synthesis of Contrast-free CT Perfusion Maps via Generative Adversarial Network**

Thursday, Dec. 1 12:15PM - 12:45PM Room: Learning Center - IN DPS

#### **Participants**

Garrett Fullerton, BS, Gainesville, FL (*Presenter*) Nothing to Disclose

#### **PURPOSE**

CTP is a popular imaging modality used to evaluate the micro circulatory structures of the brain and is commonly used in the detection of abnormalities in the brain parenchyma. Contrast imaging is generally safe, but it can present adverse side effects with increased procedure time and monetary cost. Here, we introduce a multi-task automated generation framework (MAGIC) model for contrast-free CTP brain imaging generation via physiology-inspired deep learning. By applying this framework, we predict contrast-free CTP maps with only non-contrast CT (NCCT) comparable to those generated by commercial software from contrast-enhanced images.

#### **METHODS AND MATERIALS**

Neuroimaging data were retrospectively retrieved from 12,186 (7.76 TB) patients at UF Health between 2013 and 2020 with Institutional Review Board approval. The perfusion studies were conducted using iodinated contrast injection, and the collected data were analyzed using RAPID CT Perfusion analysis software (iSchemaView, Menlo Park, CA., USA), termed as "RAPID" below. Subjects with both NCCT imaging and RAPID-generated perfusion maps were included, resulting in 493 subjects. 431 subjects were selected for training and the remainder were reserved for testing. Model MAGIC was implemented using PyTorch v1.5.0 in Python v3.6.10 and NVIDIA CUDA v7.6.5. Model MAGIC was trained for 50 epochs on an NVIDIA TITAN X GPU.

#### **RESULTS**

Three experienced radiologists evaluated MAGIC- and RAPID-generated CTP maps from 62 subjects in a double-blinded fashion via a 4-part questionnaire. Raters determined that there was no physiologically distinguishable difference between the synthetic and real CTP maps ( $p < 0.05$ ) and found 81% accuracy in diagnostic outcomes in the synthetic and real CTP maps. The further quantitative evaluation confirmed the high structural fidelity between the synthetic and real CTP maps. It was determined that the MAGIC-generated CTP maps were both physiologically and diagnostically acceptable and consistent.

#### **CONCLUSION**

The proposed framework MAGIC can generate contrast-free brain perfusion imaging from solely non-contrast, structural imaging that exhibits comparable analytical and diagnostic results to the ground-truth perfusion imaging, reducing the time, cost, and patient risk associated with CTP brain imaging.

#### **CLINICAL RELEVANCE/APPLICATION**

The proposed artificial intelligence (AI) model enables the diagnostically competitive synthesis of CT perfusion (CTP) maps from non-contrast-enhanced imaging alone, reducing the cost, time, and radiation dose associated with perfusion imaging.

Printed on: 02/07/23

## Abstract Archives of the RSNA, 2022

R5A-SPIR

### Interventional Thursday Poster Discussions - A

Thursday, Dec. 1 12:15PM - 12:45PM Room: Learning Center - IR DPS

#### Sub-Events

#### R5A-SPIR-1 Imaging Implications of Extracellular Matrix Stiffness on Liver Cancer Vascular Phenotypes

Participants

Ryosuke Taiji, MD, Kashihara, Japan (*Presenter*) Nothing to Disclose

#### PURPOSE

Interplay between liver tumor stiffness and microvascular phenotypes has not been fully elucidated. The goal of this study is to characterize impact of matrix stiffness signatures on vascular histology and dynamic contrast-enhancement imaging in a rat HCC model.

#### METHODS AND MATERIALS

Buffalo-McA-RH7777 (n=12) and Sprague Dawley-N1S1 (n=8) tumor models were used to evaluate tumor stiffness by shear wave elastography (SWE), along with tumor perfusion by dynamic CEUS and CECT. Atomic force microscopy (AFM) was used to calculate tumor stiffness at a sub-micron scale. Computer-aided image analyses were performed using Aperio-microvessel and GENIE pattern-recognition algorithms. Arbitrary 2(au) and Hounsfield units (HU) were used for peak intensity or attenuation, respectively. Pearson product-moment correlation coefficient, linear mixed model, and Wilcoxon signed-rank were used to evaluate pairwise correlations and differences between models.

#### RESULTS

Results of linear mixed model showed distinct tissue signatures between models according to the distribution of the stiffness values ( $P < 0.05$ ). Higher stiffness values were attributed to SD-N1S1 tumors, with a positive coefficient for AFM ( $P = 0.048$ ) and marginally significant for SWE ( $P = 0.07$ ), using AFM as reference. The stiffer N1S1 model was associated with scant microvascular network and with mean % of CD34+microvessel coverage of  $2.9 \pm 1.2$  compared to  $8.7 \pm 1.6$  in McA-RH7777 ( $P = 0.001$ ). Moreover, a higher % of vessels were located on the tumor periphery compared to tumor center ( $P = 0.03$ ). Opposite results were observed in McA-RH7777 model, exhibiting richer tumor vasculature with predominantly central distribution ( $P = 0.02$ ). Consistently with these findings, tumor enhancement was significantly greater in McA-RH7777 tumors than N1S1 on both CEUS ( $P = 0.014$ ) and CECT (HU increase;  $P = 0.003$ , AUCarterial;  $P < 0.001$ ; AUCtotal au\*s;  $P = 0.02$  and HU\*s;  $P < 0.001$ ). Significant positive correlation between tumor perfusion and % microvessel coverage was observed (CEUS;  $P = 0.043$  and CECT;  $P = 0.006$ ). Enhancement features were closely correlated with between CEUS and CECT;  $P < 0.05$

#### CONCLUSION

s Stiffness signatures translated into different tumor vascular phenotypes. These differences displayed unique imaging perfusion parameters with significantly greater contrast enhancement observed in softer McA-RH7777 tumors

#### CLINICAL RELEVANCE/APPLICATION

Matrix stiffness represents a barrier to effective drug delivery and can negatively impact the outcome of local treatments. Elastography can provide helpful information about the tumor microenvironment, particularly the matrix and its modification by stromal cells

#### R5A-SPIR-2 Percutaneous Combined Chemical and Mechanical Necrosectomy for Walled-Off Pancreatic Necrosis: A Retrospective Analysis

Participants

Kamyar Ghabili, MD, New Haven, CT (*Presenter*) Nothing to Disclose

#### PURPOSE

The management of walled-off pancreatic necrosis (WOPN) as a complication of acute necrotic pancreatitis necessitates a multidisciplinary step-up approach. However, the current level of evidence for percutaneous necrosectomy by interventional radiology in treating WOPN is limited. We aimed to study the feasibility, safety, and efficacy of percutaneous combined chemical and mechanical necrosectomy using a Malecot anchor drain and Arrow-Trerotola Percutaneous Thrombolytic device in patients with WOPN by comparing the results with a historical control group.

#### METHODS AND MATERIALS

In a retrospective analysis, patients with pancreatitis complicated by WOPN not amenable to endoscopic-guided cystogastrostomy were studied in case and historical control groups. Patients in the case group underwent percutaneous combined chemical (using hydrogen peroxide) and mechanical necrosectomy using the Malecot anchor drain and/or Arrow-Trerotola percutaneous thrombolytic device from December 2020 through September 2021. The controls underwent mechanical necrosectomy alone without chemical necrosectomy. Clinical success was defined as complete resolution of the cavity on follow up sinogram or noncontract CT

scans with subsequent drain removal.

## RESULTS

Thirteen patients (median age, 40 years; 11 men) in the case group and 11 control patients (median age, 60 years; 10 men) underwent CT or US guided percutaneous drain placement followed by percutaneous combined chemical and mechanical necrosectomy (case group) or mechanical necrosectomy only (control group) for WOPN. Drain placement and necrosectomy were technically successful in all studied patients. One case patient developed bleeding from a small branch of the jejunal artery on post-necrosectomy day 9, which was successfully embolized by interventional radiology. No pancreaticocutaneous fistula was reported on 3-month follow-up of our patients. The clinical success rate in the case and control groups was 100% and 38.4%, respectively ( $p=0.002$ ).

## CONCLUSION

s Percutaneous combined chemical and mechanical necrosectomy performed by interventional radiology is a feasible, safe, and effective treatment approach of WOPN.

## CLINICAL RELEVANCE/APPLICATION

Percutaneous chemical plus mechanical necrosectomy using Malecot catheter and Arrow-Trerotola thrombolytic device is a feasible, safe and effective treatment of walled-off pancreatic necrosis.

## R5A-SPIR-3 The Bariatric Embolization of Arteries with Imaging Visible Embolics (BEATLES) Trial: Pilot Phase

Participants

Adham Khalil, MD, Baltimore, MD (*Presenter*) Research Grant, Siemens AG

## PURPOSE

To evaluate the feasibility, safety and efficacy of bariatric artery embolization (BAE) in patients with obesity using customized tightly calibrated 100-200 $\mu$ m radiopaque embolic microspheres, "BTG-001933" (Biocompatibles UK Ltd).

## METHODS AND MATERIALS

BEATLES is an IRB and FDA-approved physician-initiated investigational device exemption prospective clinical trial. The pilot phase of this study started in October 2020, with 10 participants currently enrolled. Key inclusion criteria include: age 21-70 years, BMI  $\geq 35$  kg/m<sup>2</sup> and weight  $\geq 400$  lb. Absolute exclusion criteria include: taking hypoglycemic agents (except metformin), inability to undergo MRI, allergy to iodinated contrast and renal insufficiency. After initial screening, participants have a six-week "run-in" to complete pre-BAE screening for psychiatric disorders and dietary coaching. Eligible participants undergo a rapid whole-body MRI for volumetric measurement of body adiposity, and an upper endoscopy with gastric mucosal biopsy to rule out pathologies such as peptic ulcer disease or gastritis, which may exclude them from the study. Seven participants (6 women and 1 man; mean age  $39.7 \pm 10.5$  years) with obesity who underwent BAE were included in the preliminary analysis. Participants were followed up for 12 months after embolization. Changes in body weight and BMI at 1, 3, 6, and 12-months follow-up as well as the 30-day adverse events (AEs) were recorded. Feasibility was assessed based on ability to visualize the microspheres under fluoroscopy and extent of embolic fundal coverage on post-procedural MDCT.

## RESULTS

In seven participants, the LGA ( $n=7$ ), with or without the gastroepiploic artery (GEA;  $n=4$ ), was embolized, with a 100% technical success rate. There were no major AEs. One minor AE (mucosal ulcer) was observed and healed at 5-month endoscopy. All participants were admitted for routine supportive care for  $<48$  hours post-BAE. Pre-procedural mean weight was  $124.6 \pm 21.2$  kg and mean BMI  $42.7 \pm 4.5$  kg/m<sup>2</sup>. Table 1 shows the changes in body weight and BMI at different follow-ups.

## CONCLUSION

s BAE using customized tightly calibrated radiopaque 100-200 $\mu$ m microspheres "BTG-001933" is feasible and appears to be well tolerated by participants with severe obesity. Preliminary analysis of weight loss outcomes demonstrates promising efficacy.

## CLINICAL RELEVANCE/APPLICATION

BEATLES is the first clinical study to evaluate using "BTG-001933", a novel customized tightly calibrated radiopaque microspheres of the 100-200 $\mu$ m size, for bariatric artery embolization.

## R5A-SPIR-4 Ethanol Embolization Combined or Not with Surgery and Close Clinical Follow-up Can Effectively Control Extracranial Arterio-venous Malformations (AVMS)

Participants

Ke Chen, MD, (*Presenter*) Nothing to Disclose

## PURPOSE

Arteriovenous malformations (AVM) are congenital high flow lesions that have a wide range of clinical manifestations, varying from asymptomatic to high-output heart failure. We looked at the long-term outcome of patients with extra-cranial AVMs following different types of treatment.

## METHODS AND MATERIALS

A retrospective study was performed, collecting data on all cases of proven extracranial AVMs at two university hospitals from 1985 to 2021. We documented whether the patient received conservative, endovascular, surgical, or combined treatments. The clinical response of treatments was assessed using the Schobinger's classification. Our primary endpoint was to evaluate evolution of Schobinger class in patients of our cohort.

## RESULTS

A total of 190 proven cases of extracranial AVMs were included in the study. Mean follow up time was 7.0 years [0.0-28.0 years]. The mean Schobinger stage was 2.11 at baseline and 1.32 at final follow-up ( $p<0.001$ ). For the cohort, 52 patients were treated conservatively, 104 patients received endovascular treatment alone, 3 patients received surgical treatment alone, and 31 patients

received combined therapy. Overall, 71 patients (37%) achieved complete remission of the disease, 34 patients (18%) achieved improvement of symptoms, 81 patients (42%) remained stable, and 4 patients (2%) worsened. No clinical worsening was observed in the 52 patients (Schobinger stage 1-2) that did not receive any endovascular or surgical treatment.

## CONCLUSION

s Ethanol embolization with or without surgery is efficient for long term control of extracranial AVMs. We observed that not all patients evolve from Schobinger stage 1-2 to a further stage, and clinical observation without treatment can be suitable and appropriate for asymptomatic patients.

## CLINICAL RELEVANCE/APPLICATION

Since extracranial AVMs are rare, there is a lack of empirical evidence in the literature to assess if ethanol embolization with or without surgery can successfully and safely achieve lifelong control of extracranial AVMs. It was also thought that all these lesions inevitably progress with time. Our study demonstrates the effectiveness and safety of ethanol embolization to treat extracranial AVMs. We also show that not all patients with AVMs evolve to a further stage.

## R5A-SPIR-6 The Reproducibility of Interventional Radiology Randomized Controlled Trials

Participants

Assala Aslan, MD, Shreveport, LA (*Presenter*) Nothing to Disclose

## PURPOSE

Numerous randomized controlled trials (RCTs) relevant to the Interventional Radiology field have been performed within the last decade. The fragility index was recently developed to complement the P value and measure the robustness and reproducibility of clinical findings of RCTs. Low fragility index indicates that the study hinges on only a few events for statistical significance. In this study we evaluate the fragility index for key Interventional Radiology RCTs.

## METHODS AND MATERIALS

Interventional Radiology RCTs published between 2000 and 2021 were reviewed. Six key areas were specifically targeted in relation to transjugular intrahepatic portosystemic shunt, trans-arterial chemoembolization, preoperative embolization, needle biopsy, gastrostomy tube insertion, and nephrostomy tube insertion. RCTs related to cardiovascular or neurosurgical intervention were not included as they were reported in prior studies.

## RESULTS

A total of 84 RCTs that reported significant differences between both study groups in terms of the primary outcome were included. The median fragility index of those studies was 4. Studies related to trans-arterial chemoembolization were associated with a higher fragility index compared to other fields.

## CONCLUSION

s The median fragility index related to Intervention Radiology is low compared to other surgical fields. Therefore, one should exercise caution with interpreting the results of those RCTs, especially when the sample size and events numbers are small and there is a high number of patients who were lost to follow up.

## CLINICAL RELEVANCE/APPLICATION

Fragility index is a reflex of the robustness and reproducibility of clinical trials. A fragility index of 1 means that if only 1 patient did not reach the primary outcome in the study group the results will not be statistically significant. Trials with low fragility index are less reproducible and, thus, should not be included in clinical guidelines.

## R5A-SPIR-7 Short and Mid Term Follow-up of Sympathetic Chain Block with Botox in PAOD and CRPS Patients

Participants

Benjamin Reichardt, Hattingen, Germany (*Presenter*) Nothing to Disclose

## PURPOSE

To analyze the duration of therapeutic success in PAOD and CRPS patients in lumbar sympathetic chain block using botulinum toxin as an alternative to definitive sympathectomy.

## METHODS AND MATERIALS

We analyzed 126 Patients 66 with CRPS of the foot and 60 pat. with PAOD grade 3 4 from 2015 - 2022. 49 patients were treated bilaterally in the case of PAOD. Initial pain scale was between 7 and 10. PAOD patients with 67% had small dermal ulcerations. CRPS patients 40% with CRPS type 1; 60% type 2. PAOD patients were treated with medication, interventional or vascular surgery. Sympathectomy was indicated to improve micro-vascular perfusion. CRPS patients suffered on average for more than 3 mo. from chronically maintained pain that could not be assigned to a nerve supply area. CT-guided lumbar sympathetic blocks. The target region was the ventrolateral ganglion at the level of the upper edge of the 4th lumbar vertebral body of the affected side. Temperature probes were applied to feet soles before intervention. The injection is performed placing a 22G myelography needle into the target region with 100 mouse units botulinum toxin in 1ml NaCl. 1h, 24h, 1 week, 4 weeks, 3, 6 and 12 months the patients were evaluated by questionnaire about their symptoms, pain and walking distance.

## RESULTS

CRPS patients showed a rapid increase in temperature and a significant reduction in pain. The improvement of symptoms in CRPS patients lasted up to 12 months and after follow up. PAOD patients showed a slight increase in temperature and delayed improvement in micro-vascular perfusion within the first hour after intervention. Pain improved from 7-10 to 1-4 in the first 24 h. Dermal ulcerations healed within the first week. The longer observation period between 6 and 12 months showed worsening of walking distance and pain as well as microvascularization. The median pain value: 7.

## CONCLUSION

s Botox is a potent agent for lumbar sympathetic blocks. The results for the treatment of CRPS are promising and showed no risks.

There was no worsening of symptoms during the observation period. In contrast, botox showed only a medium-term improvement in microvascularization and pain reduction in PAOD. Symptom worsening was accompanied by physiological degradation of the product. Nevertheless, no clear distinction could be made whether there was worsening of the underlying PAOD, therapy changes etc..

#### **CLINICAL RELEVANCE/APPLICATION**

Botox can be used as a potent therapeutics in CRPS in sympathetic chain blocks. In PAOD it is a usefull and in a Dosis of 100MU a harmless therapeutic with effective improvement of mikrovasculature and pain reduction between 6 and 12 Months. It might also be used as bridging therapy for support of dermal ulcer healing or before definitive intervention or bypass surgery.

#### **R5A-SP1R-8 Trends in Inferior Vena Cava Filter Placement, Repositioning, and Retrieval Rates in the Medicare Population**

Participants  
Nidhi Ramesh, (*Presenter*) Nothing to Disclose

#### **PURPOSE**

To analyze trends in the procedural volume of inferior vena cava (IVC) filter placements, retrievals, and repositionings in the Medicare beneficiary population between the years 2015 and 2019.

#### **METHODS AND MATERIALS**

The nationwide Medicare Physician/Supplier Procedure Summary Master Files were used to determine the volume of IVC filter placements, repositionings, and retrievals, which correspond to Current Procedural Terminology (CPT) codes 37191, 37192, and 37193, respectively. A regression analysis of each of these trends was additionally performed.

#### **RESULTS**

The total volume of Medicare IVC filter placement decreased from 44,378 in 2015 to 25,557 in 2019. The total volume of Medicare IVC filter repositionings in 2015 was 38 and increased to 46 in 2017, and then decreased to 35 in 2019. The total retrieval of IVC filters increased from 6,166 removals in 2015 to 7,490 in 2019. Placement rate per 100,000 Medicare beneficiaries decreased from 81.73 in 2015 to 42.42 in 2019. Retrieval rate per 100,000 Medicare beneficiaries increased from 11.36 in 2015 to 12.43 in 2019.

#### **CONCLUSION**

s In the Medicare population between 2015 and 2019, the number of IVC filter placements per 100,000 enrollees decreased by 48% while the number of IVC filter retrievals per 100,00 enrollees increased by 9.3%. The number of IVC repositionings remained relatively constant throughout this period. These data support the FDA's 2014 recommendation to remove retrievable IVC filters once a patient's risk for acute pulmonary embolism has passed, given that these types of filters are not always removed expeditiously.

#### **CLINICAL RELEVANCE/APPLICATION**

In analyzing IVC filter trends in the Medicare population, we are able to gain valuable insight into physician preferences for utilizing IVC filters as well as the success of efforts to improve filter retrievals.

#### **R5A-SP1R-9 Emergency Trans-jugular Intrahepatic Portosystemic Shunt Creation (TIPS): Hybrid Intervention (tri-modal) and Image Fusion**

Participants  
Jonathan Nadjiri, MD, (*Presenter*) Nothing to Disclose

#### **PURPOSE**

Emergency transjugular intrahepatic portosystemic shunt (TIPS) creation is associated with high peri-interventional mortality. It remains the only treatment in patients with portal hypertension and oesophageal bleedings and unsuccessful endoscopic treatment. The reasons for the high mortality are often post-interventional liver bleedings because of incorrect puncture. In the last years hybrid intervention suites are emerging. They combine CT-imaging with conventional angiography allowing to project 3D information into the conventional 2D imaging and further CT-fluoroscopic puncture of the portal vein. The purpose of this prospective study was to assess survival rate in emergency TIPS patients treated with a hybrid intervention using image fusion in comparison to outcome of TIPS using standard intervention.

#### **METHODS AND MATERIALS**

All emergency TIPS patients from 2021 and 2022 were included (n=11). Six patients were treated with the standard technique and 5 patients in the hybrid angiography suite. Jugular access was done with sonography guidance for both groups. For the hybrid intervention a contrast enhanced CT was performed on the angiography table. The 3D information was registered to the patient. Portal vein access point and preferred liver vein were marked. The lower liver capsule was marked. From the CT a 3D volume was created using virtual rendering technique (VRT). The VRT as well as the above-mentioned markings were blended into the conventional angiography image and used as guidance for the TIPS-needle.

#### **RESULTS**

Hybrid TIPS did lead to a significantly shorter fluoroscopy time ( $p = 0.038$ ). Mean radiation exposure was significantly reduced by the factor 6 ( $p = 0.014$ ). Furthermore, the mortality rate was lower in patients who underwent the hybrid intervention (0% vs 33%).

#### **CONCLUSION**

s Emergency TIPS using hybrid intervention technique improves survival for this high-risk procedure. Further, this technique the procedure is quicker and reduces radiation exposure for the patient and the interventionalist.

#### **CLINICAL RELEVANCE/APPLICATION**

In daily clinical practice hybrid TIPS creation using image fusion should be preferred over a conventional approach when ever possible.



## Abstract Archives of the RSNA, 2022

R5A-SP1R-1

### Imaging Implications of Extracellular Matrix Stiffness on Liver Cancer Vascular Phenotypes

Thursday, Dec. 1 12:15PM - 12:45PM Room: Learning Center - IR DPS

#### Participants

Ryosuke Taiji, MD, Kashihara, Japan (*Presenter*) Nothing to Disclose

#### PURPOSE

Interplay between liver tumor stiffness and microvascular phenotypes has not been fully elucidated. The goal of this study is to characterize impact of matrix stiffness signatures on vascular histology and dynamic contrast-enhancement imaging in a rat HCC model.

#### METHODS AND MATERIALS

Buffalo-McA-RH7777 (n=12) and Sprague Dawley-N1S1 (n=8) tumor models were used to evaluate tumor stiffness by shear wave elastography (SWE), along with tumor perfusion by dynamic CEUS and CECT. Atomic force microscopy (AFM) was used to calculate tumor stiffness at a sub-micron scale. Computer-aided image analyses were performed using Aperio-microvessel and GENIE pattern-recognition algorithms. Arbitrary 2(au) and Hounsfield units (HU) were used for peak intensity or attenuation, respectively. Pearson product-moment correlation coefficient, linear mixed model, and Wilcoxon signed-rank were used to evaluate pairwise correlations and differences between models.

#### RESULTS

Results of linear mixed model showed distinct tissue signatures between models according to the distribution of the stiffness values ( $P < 0.05$ ). Higher stiffness values were attributed to SD-N1S1 tumors, with a positive coefficient for AFM ( $P = 0.048$ ) and marginally significant for SWE ( $P = 0.07$ ), using AFM as reference. The stiffer N1S1 model was associated with scant microvascular network and with mean % of CD34+microvessel coverage of  $2.9 \pm 1.2$  compared to  $8.7 \pm 1.6$  in McA-RH7777 ( $P = 0.001$ ). Moreover, a higher % of vessels were located on the tumor periphery compared to tumor center ( $P = 0.03$ ). Opposite results were observed in McA-RH7777 model, exhibiting richer tumor vasculature with predominantly central distribution ( $P = 0.02$ ). Consistently with these findings, tumor enhancement was significantly greater in McA-RH7777 tumors than N1S1 on both CEUS ( $P = 0.014$ ) and CECT (HU increase;  $P = 0.003$ , AUCarterial;  $P < 0.001$ ; AUCtotal au\*s;  $P = 0.02$  and HU\*s;  $P < 0.001$ ). Significant positive correlation between tumor perfusion and % microvessel coverage was observed (CEUS;  $P = 0.043$  and CECT;  $P = 0.006$ ). Enhancement features were closely correlated with between CEUS and CECT;  $P < 0.05$

#### CONCLUSION

s Stiffness signatures translated into different tumor vascular phenotypes. These differences displayed unique imaging perfusion parameters with significantly greater contrast enhancement observed in softer McA-RH7777 tumors

#### CLINICAL RELEVANCE/APPLICATION

Matrix stiffness represents a barrier to effective drug delivery and can negatively impact the outcome of local treatments. Elastography can provide helpful information about the tumor microenvironment, particularly the matrix and its modification by stromal cells

Printed on: 02/07/23

## Abstract Archives of the RSNA, 2022

R5A-SPIR-2

### **Percutaneous Combined Chemical and Mechanical Necrosectomy for Walled-Off Pancreatic Necrosis: A Retrospective Analysis**

Thursday, Dec. 1 12:15PM - 12:45PM Room: Learning Center - IR DPS

#### **Participants**

Kamyar Ghabili, MD, New Haven, CT (*Presenter*) Nothing to Disclose

#### **PURPOSE**

The management of walled-off pancreatic necrosis (WOPN) as a complication of acute necrotic pancreatitis necessitates a multidisciplinary step-up approach. However, the current level of evidence for percutaneous necrosectomy by interventional radiology in treating WOPN is limited. We aimed to study the feasibility, safety, and efficacy of percutaneous combined chemical and mechanical necrosectomy using a Malecot anchor drain and Arrow-Trerotola Percutaneous Thrombolytic device in patients with WOPN by comparing the results with a historical control group.

#### **METHODS AND MATERIALS**

In a retrospective analysis, patients with pancreatitis complicated by WOPN not amenable to endoscopic-guided cystogastrostomy were studied in case and historical control groups. Patients in the case group underwent percutaneous combined chemical (using hydrogen peroxide) and mechanical necrosectomy using the Malecot anchor drain and/or Arrow-Trerotola percutaneous thrombolytic device from December 2020 through September 2021. The controls underwent mechanical necrosectomy alone without chemical necrosectomy. Clinical success was defined as complete resolution of the cavity on follow up sinogram or noncontract CT scans with subsequent drain removal.

#### **RESULTS**

Thirteen patients (median age, 40 years; 11 men) in the case group and 11 control patients (median age, 60 years; 10 men) underwent CT or US guided percutaneous drain placement followed by percutaneous combined chemical and mechanical necrosectomy (case group) or mechanical necrosectomy only (control group) for WOPN. Drain placement and necrosectomy were technically successful in all studied patients. One case patient developed bleeding from a small branch of the jejunal artery on post-necrosectomy day 9, which was successfully embolized by interventional radiology. No pancreaticocutaneous fistula was reported on 3-month follow-up of our patients. The clinical success rate in the case and control groups was 100% and 38.4%, respectively ( $p=0.002$ ).

#### **CONCLUSION**

Percutaneous combined chemical and mechanical necrosectomy performed by interventional radiology is a feasible, safe, and effective treatment approach of WOPN.

#### **CLINICAL RELEVANCE/APPLICATION**

Percutaneous chemical plus mechanical necrosectomy using Malecot catheter and Arrow-Trerotola thrombolytic device is a feasible, safe and effective treatment of walled-off pancreatic necrosis.

Printed on: 02/07/23

## Abstract Archives of the RSNA, 2022

R5A-SP1R-3

### The Bariatric Embolization of Arteries with Imaging Visible Embolics (BEATLES) Trial: Pilot Phase

Thursday, Dec. 1 12:15PM - 12:45PM Room: Learning Center - IR DPS

#### Participants

Adham Khalil, MD, Baltimore, MD (*Presenter*) Research Grant, Siemens AG

#### PURPOSE

To evaluate the feasibility, safety and efficacy of bariatric artery embolization (BAE) in patients with obesity using customized tightly calibrated 100-200 $\mu$ m radiopaque embolic microspheres, "BTG-001933" (Biocompatibles UK Ltd).

#### METHODS AND MATERIALS

BEATLES is an IRB and FDA-approved physician-initiated investigational device exemption prospective clinical trial. The pilot phase of this study started in October 2020, with 10 participants currently enrolled. Key inclusion criteria include: age 21-70 years, BMI  $\geq$ 35 kg/m<sup>2</sup> and weight  $\geq$ 400 lb. Absolute exclusion criteria include: taking hypoglycemic agents (except metformin), inability to undergo MRI, allergy to iodinated contrast and renal insufficiency. After initial screening, participants have a six-week "run-in" to complete pre-BAE screening for psychiatric disorders and dietary coaching. Eligible participants undergo a rapid whole-body MRI for volumetric measurement of body adiposity, and an upper endoscopy with gastric mucosal biopsy to rule out pathologies such as peptic ulcer disease or gastritis, which may exclude them from the study. Seven participants (6 women and 1 man; mean age 39.7 $\pm$ 10.5 years) with obesity who underwent BAE were included in the preliminary analysis. Participants were followed up for 12 months after embolization. Changes in body weight and BMI at 1, 3, 6, and 12-months follow-up as well as the 30-day adverse events (AEs) were recorded. Feasibility was assessed based on ability to visualize the microspheres under fluoroscopy and extent of embolic fundal coverage on post-procedural MDCT.

#### RESULTS

In seven participants, the LGA (n=7), with or without the gastroepiploic artery (GEA; n=4), was embolized, with a 100% technical success rate. There were no major AEs. One minor AE (mucosal ulcer) was observed and healed at 5-month endoscopy. All participants were admitted for routine supportive care for <48 hours post-BAE. Pre-procedural mean weight was 124.6 $\pm$ 21.2 kg and mean BMI 42.7 $\pm$ 4.5 kg/m<sup>2</sup>. Table 1 shows the changes in body weight and BMI at different follow-ups.

#### CONCLUSION

s BAE using customized tightly calibrated radiopaque 100-200 $\mu$ m microspheres "BTG-001933" is feasible and appears to be well tolerated by participants with severe obesity. Preliminary analysis of weight loss outcomes demonstrates promising efficacy.

#### CLINICAL RELEVANCE/APPLICATION

BEATLES is the first clinical study to evaluate using "BTG-001933", a novel customized tightly calibrated radiopaque microspheres of the 100-200 $\mu$ m size, for bariatric artery embolization.

Printed on: 02/07/23

## Abstract Archives of the RSNA, 2022

R5A-SPIR-4

### **Ethanol Embolization Combined or Not with Surgery and Close Clinical Follow-up Can Effectively Control Extracranial Arterio-venous Malformations (AVMS)**

Thursday, Dec. 1 12:15PM - 12:45PM Room: Learning Center - IR DPS

#### **Participants**

Ke Chen, MD, (*Presenter*) Nothing to Disclose

#### **PURPOSE**

Arteriovenous malformations (AVM) are congenital high flow lesions that have a wide range of clinical manifestations, varying from asymptomatic to high-output heart failure. We looked at the long-term outcome of patients with extra-cranial AVMS following different types of treatment.

#### **METHODS AND MATERIALS**

A retrospective study was performed, collecting data on all cases of proven extracranial AVMS at two university hospitals from 1985 to 2021. We documented whether the patient received conservative, endovascular, surgical, or combined treatments. The clinical response of treatments was assessed using the Schobinger's classification. Our primary endpoint was to evaluate evolution of Schobinger class in patients of our cohort.

#### **RESULTS**

A total of 190 proven cases of extracranial AVMS were included in the study. Mean follow up time was 7.0 years [0.0-28.0 years]. The mean Schobinger stage was 2.11 at baseline and 1.32 at final follow-up ( $p < 0.001$ ). For the cohort, 52 patients were treated conservatively, 104 patients received endovascular treatment alone, 3 patients received surgical treatment alone, and 31 patients received combined therapy. Overall, 71 patients (37%) achieved complete remission of the disease, 34 patients (18%) achieved improvement of symptoms, 81 patients (42%) remained stable, and 4 patients (2%) worsened. No clinical worsening was observed in the 52 patients (Schobinger stage 1-2) that did not receive any endovascular or surgical treatment.

#### **CONCLUSION**

s Ethanol embolization with or without surgery is efficient for long term control of extracranial AVMS. We observed that not all patients evolve from Schobinger stage 1-2 to a further stage, and clinical observation without treatment can be suitable and appropriate for asymptomatic patients.

#### **CLINICAL RELEVANCE/APPLICATION**

Since extracranial AVMS are rare, there is a lack of empirical evidence in the literature to assess if ethanol embolization with or without surgery can successfully and safely achieve lifelong control of extracranial AVMS. It was also thought that all these lesions inevitably progress with time. Our study demonstrates the effectiveness and safety of ethanol embolization to treat extracranial AVMS. We also show that not all patients with AVMS evolve to a further stage.

Printed on: 02/07/23



## Abstract Archives of the RSNA, 2022

R5A-SPIR-6

### The Reproducibility of Interventional Radiology Randomized Controlled Trials

Thursday, Dec. 1 12:15PM - 12:45PM Room: Learning Center - IR DPS

#### Participants

Assala Aslan, MD, Shreveport, LA (*Presenter*) Nothing to Disclose

#### PURPOSE

Numerous randomized controlled trials (RCTs) relevant to the Interventional Radiology field have been performed within the last decade. The fragility index was recently developed to complement the P value and measure the robustness and reproducibility of clinical findings of RCTs. Low fragility index indicates that the study hinges on only a few events for statistical significance. In this study we evaluate the fragility index for key Interventional Radiology RCTs.

#### METHODS AND MATERIALS

Interventional Radiology RCTs published between 2000 and 2021 were reviewed. Six key areas were specifically targeted in relation to transjugular intrahepatic portosystemic shunt, trans-arterial chemoembolization, preoperative embolization, needle biopsy, gastrostomy tube insertion, and nephrostomy tube insertion. RCTs related to cardiovascular or neurosurgical intervention were not included as they were reported in prior studies.

#### RESULTS

A total of 84 RCTs that reported significant differences between both study groups in terms of the primary outcome were included. The median fragility index of those studies was 4. Studies related to trans-arterial chemoembolization were associated with a higher fragility index compared to other fields.

#### CONCLUSION

The median fragility index related to Intervention Radiology is low compared to other surgical fields. Therefore, one should exercise caution with interpreting the results of those RCTs, especially when the sample size and events numbers are small and there is a high number of patients who were lost to follow up.

#### CLINICAL RELEVANCE/APPLICATION

Fragility index is a reflex of the robustness and reproducibility of clinical trials. A fragility index of 1 means that if only 1 patient did not reach the primary outcome in the study group the results will not be statistically significant. Trials with low fragility index are less reproducible and, thus, should not be included in clinical guidelines.

Printed on: 02/07/23

## Abstract Archives of the RSNA, 2022

R5A-SPIR-7

### Short and Mid Term Follow-up of Sympathetic Chain Block with Botox in PAOD and CRPS Patients

Thursday, Dec. 1 12:15PM - 12:45PM Room: Learning Center - IR DPS

#### Participants

Benjamin Reichardt, Hattingen, Germany (*Presenter*) Nothing to Disclose

#### PURPOSE

To analyze the duration of therapeutic success in PAOD and CRPS patients in lumbar sympathetic chain block using botulinum toxin as an alternative to definitive sympathiccolysis.

#### METHODS AND MATERIALS

We analyzed 126 Patients 66 with CRPS of the foot and 60 pat. with PAOD grade 3 4 from 2015 - 2022. 49 patients were treated bilaterally in the case of PAOD. Initial pain scale was between 7 and 10. PAOD patients with 67% had small dermal ulcerations. CRPS patients 40% with CRPS type 1; 60% type 2. PAOD patients were treated with medication, interventional or vascular surgery. Sympathiccolysis was indicated to improve micro-vascular perfusion. CRPS patients suffered on average for more than 3 mo. from chronically maintained pain that could not be assigned to a nerve supply area. CT-guided lumbar sympathetic blocks. The target region was the ventrolateral ganglion at the level of the upper edge of the 4th lumbar vertebral body of the affected side. Temperature probes were applied to feootsoles before intervention . The injection is performed placing a 22G myelography needle into the target region with 100 mouse units botulinum toxin in 1ml NaCl. 1h, 24h, 1 week, 4 weeks, 3, 6 and 12 months the patients were evaluated by questionnaire about their symptoms, pain and walking distance.

#### RESULTS

CRPS patients showed a rapid increase in temperature and a significant reduction in pain. The improvement of symptoms in CRPS patients lasted up to 12 months and after follow up. PAOD patients showed a slight increase in temperature and delayed improvement in micro-vascular perfusion within the first hour after intervention. Pain improved from 7-10 to 1-4 in the first 24 h. Dermal ulcerations healed within the first week. The longer observation period between 6 and 12 months showed worsening of walking distance and pain as well as microvascularization. The median pain value: 7.

#### CONCLUSION

s Botox is a potent agent for lumbar sympathetic blocks. The results for the treatment of CRPS are promising and showed no risks. There was no worsening of symptoms during the observation period. In contrast, botox showed only a medium-term improvement in microvascularization and pain reduction in PAOD. Symptom worsening was accompanied by physiological degradation of the product. Nevertheless, no clear distinction could be made whether there was worsening of the underlying PAOD, therapy changes etc..

#### CLINICAL RELEVANCE/APPLICATION

Botox can be used as a potent therapeutics in CRPS in sympathetic chain blocks. In PAOD it is a usefull and in a Dosis of 100MU a harmless therapeutic with effective improvement of mikrovasculature and pain reduction between 6 and 12 Months. It might also be used as bridging therapy for support of dermal ulcer healing or before definitive intervention or bypass surgery.

Printed on: 02/07/23



## Abstract Archives of the RSNA, 2022

R5A-SPIR-8

### Trends in Inferior Vena Cava Filter Placement, Repositioning, and Retrieval Rates in the Medicare Population

Thursday, Dec. 1 12:15PM - 12:45PM Room: Learning Center - IR DPS

#### Participants

Nidhi Ramesh, (*Presenter*) Nothing to Disclose

#### PURPOSE

To analyze trends in the procedural volume of inferior vena cava (IVC) filter placements, retrievals, and repositionings in the Medicare beneficiary population between the years 2015 and 2019.

#### METHODS AND MATERIALS

The nationwide Medicare Physician/Supplier Procedure Summary Master Files were used to determine the volume of IVC filter placements, repositionings, and retrievals, which correspond to Current Procedural Terminology (CPT) codes 37191, 37192, and 37193, respectively. A regression analysis of each of these trends was additionally performed.

#### RESULTS

The total volume of Medicare IVC filter placement decreased from 44,378 in 2015 to 25,557 in 2019. The total volume of Medicare IVC filter repositionings in 2015 was 38 and increased to 46 in 2017, and then decreased to 35 in 2019. The total retrieval of IVC filters increased from 6,166 removals in 2015 to 7,490 in 2019. Placement rate per 100,000 Medicare beneficiaries decreased from 81.73 in 2015 to 42.42 in 2019. Retrieval rate per 100,000 Medicare beneficiaries increased from 11.36 in 2015 to 12.43 in 2019.

#### CONCLUSION

In the Medicare population between 2015 and 2019, the number of IVC filter placements per 100,000 enrollees decreased by 48% while the number of IVC filter retrievals per 100,00 enrollees increased by 9.3%. The number of IVC repositionings remained relatively constant throughout this period. These data support the FDA's 2014 recommendation to remove retrievable IVC filters once a patient's risk for acute pulmonary embolism has passed, given that these types of filters are not always removed expeditiously.

#### CLINICAL RELEVANCE/APPLICATION

In analyzing IVC filter trends in the Medicare population, we are able to gain valuable insight into physician preferences for utilizing IVC filters as well as the success of efforts to improve filter retrievals.

Printed on: 02/07/23

## Abstract Archives of the RSNA, 2022

R5A-SPIR-9

### Emergency Trans-jugular Intrahepatic Portosystemic Shunt Creation (TIPS): Hybrid Intervention (tri-modal) and Image Fusion

Thursday, Dec. 1 12:15PM - 12:45PM Room: Learning Center - IR DPS

#### Participants

Jonathan Nadjiri, MD, (*Presenter*) Nothing to Disclose

#### PURPOSE

Emergency transjugular intrahepatic portosystemic shunt (TIPS) creation is associated with high peri-interventional mortality. It remains the only treatment in patients with portal hypertension and oesophageal bleedings and unsuccessful endoscopic treatment. The reasons for the high mortality are often post-interventional liver bleedings because of incorrect puncture. In the last years hybrid intervention suites are emerging. They combine CT-imaging with conventional angiography allowing to project 3D information into the conventional 2D imaging and further CT-fluoroscopic puncture of the portal vein. The purpose of this prospective study was to assess survival rate in emergency TIPS patients treated with a hybrid intervention using image fusion in comparison to outcome of TIPS using standard intervention.

#### METHODS AND MATERIALS

All emergency TIPS patients from 2021 and 2022 were included (n=11). Six patients were treated with the standard technique and 5 patients in the hybrid angiography suite. Jugular access was done with sonography guidance for both groups. For the hybrid intervention a contrast enhanced CT was performed on the angiography table. The 3D information was registered to the patient. Portal vein access point and preferred liver vein were marked. The lower liver capsule was marked. From the CT a 3D volume was created using virtual rendering technique (VRT). The VRT as well as the above-mentioned markings were blended into the conventional angiography image and used as guidance for the TIPS-needle.

#### RESULTS

Hybrid TIPS did lead to a significantly shorter fluoroscopy time ( $p = 0.038$ ). Mean radiation exposure was significantly reduced by the factor 6 ( $p = 0.014$ ). Furthermore, the mortality rate was lower in patients who underwent the hybrid intervention (0% vs 33%).

#### CONCLUSION

Emergency TIPS using hybrid intervention technique improves survival for this high-risk procedure. Further, this technique the procedure is quicker and reduces radiation exposure for the patient and the interventionalist.

#### CLINICAL RELEVANCE/APPLICATION

In daily clinical practice hybrid TIPS creation using image fusion should be preferred over a conventional approach when ever possible.

Printed on: 02/07/23

## Abstract Archives of the RSNA, 2022

R5A-SPMK

### Musculoskeletal Thursday Poster Discussions - A

Thursday, Dec. 1 12:15PM - 12:45PM Room: Learning Center - MK DPS

#### Participants

Jacob Mandell, MD, Waltham, MA (*Moderator*) Author with royalties, Cambridge University Press

#### Sub-Events

### R5A-SPMK-1 Radiomic Nomogram for Predicting High-Risk Cytogenetic Status in Multiple Myeloma Based on Fat-Suppressed T2-Weighted Magnetic Resonance Imaging

#### Participants

Suwei Liu, (*Presenter*) Nothing to Disclose

#### PURPOSE

To establish and validate clinical fat-suppressed T2-weighted magnetic resonance imaging (FS-T2WI) radiomic nomograms of MM HRC status for pre-treatment decision making and prognostic assessment.

#### METHODS AND MATERIALS

A cohort of 159 patients with MM (71 HRC, 88 non-HRC), The region of interest of the largest tumor lesions on FS-T2WI images was manually outlined, and 1688 features were obtained. Fourteen radiomic features were selected by 10-fold cross-validation using feature selection variance thresholds, Student's t test, redundancy analysis, and least absolute shrinkage and selection operator methods. Logistic regression was used to establish a clinical prediction model (model 1), a FS-T2WI radiomic prediction model (model 2), and a clinical-radiomic prediction model (model 3). Receiver operating characteristic (ROC) curves were used to evaluate and compare their diagnostic performance. Kaplan-Meier survival analysis and logrank tests were used to assess the prognostic value of the radiomic nomograms.

#### RESULTS

Models 2 and 3 showed significantly higher diagnostic efficacy than model 1 (both  $p < 0.05$ ). The area under the ROC curve of models 1, 2, and 3 was (training set: 0.65, 0.83, and 0.85; validation set: 0.70, 0.73, and 0.76, respectively). Kaplan-Meier survival analysis showed similar prognostic values for the radiomic nomogram and MM cytogenetic status (logrank test, both  $p < 0.05$ ; C-index, 0.651 and 0.659, respectively; z-score test,  $p = 0.153$ ).

#### CONCLUSION

s Radiomic nomograms can predict the HRC status of MM, potentially contributing to pre-treatment clinical decision making and prognostic assessment.

#### CLINICAL RELEVANCE/APPLICATION

Radiomics has shown promise for predicting the cytogenetic status of multiple myeloma (MM). However, few studies have investigated the role of single sequence radiomic nomograms in predicting the high-risk cytogenetic (HRC) status of MM.

### R5A-SPMK-2 Deep Learning-based Automated Compression Fracture Analysis Algorithm On Spine Radiography for Onsite Application

#### Participants

Hongjun Yoon, Seoul, Korea, Republic Of (*Presenter*) Nothing to Disclose

#### PURPOSE

To develop a deep-learning-based algorithm that conducts reliable measuring of compression ratio (CR) for compression fracture (CF) diagnosis in lateral X-rays.

#### METHODS AND MATERIALS

We, retrospectively, collected 7,650 spine X-ray images which has been sent to the government agency under ministry of health and welfare responsible for claims review and quality assessment of the Health Insurance. We used four classification models, view, body part, posture, and assistant device, to classify whether the input radiography is a subject for CF analysis. With U-Net model, trained with 1,040 lateral TL-spine X-rays and annotations, we segment vertebra body (VB) to calculate the compression ratio by each subject's front height over average of the two adjacent ones. We calculated CR by the subject VB's front height over average of the two adjacent VB's front heights.

#### RESULTS

For evaluating performance of our algorithm, we used 250 spine X-ray images, included 145 TL-Spine X-ray images suitable for CR measurement ( $44.18\% \pm 13.04\%$ , min: 20%, max: 74.72%). The sequential CF subject classification model show an accuracy of

94.8% (95% CI: 0.912–0.972). Mean Absolute Error (MAE) between ground truth and the predicted CR was 6.04% with standard deviation of 8.86%. By evaluating the above performance by ground truth's severity, the mild, moderate, and, severe fracture performances were 6.54%±7.64%, 4%±3.78% and 7.2%±10.74% respectively.

## CONCLUSION

In practice, it is essential to check whether the input image is suitable for specific analysis algorithms. Unsuitable input could give false result, potentially misguide medical practitioner, and even slow down the process, which is the opposite of the purpose of automated system. Result of this study shows that our automatic algorithm could not only provide an efficient change in process of measuring CR with high performance, but also be an objective solution by selecting subject analysis images.

## CLINICAL RELEVANCE/APPLICATION

To apply deep learning based automated analysis algorithm into actual practice, we propose a sequential classification model to select the subject image for analysis of CF, which is required to be plain lateral TL-spine x-ray image.

### R5A-SPMK-3 A Study for Measuring Vertebral Bone Structure by Generated Micro-CT-like Images: An Approach Based on FUNIT Conditional Generative Adversarial Network Mapping

#### Participants

Dan Jin, Beijing, China (*Presenter*) Nothing to Disclose

#### PURPOSE

To investigate the quality of micro-CT-like images generated by FUNIT models based on conditional generative adversarial networks (CGAN) and their value in vertebral bone structure measurements.

#### METHODS AND MATERIALS

The same anatomical areas of 25 human lumbar spine specimens were scanned using MDCT and micro-CT for normalization, resulting in 6,250 MDCT images (slice thickness 0.6 mm, slice spacing 0.1 mm) and 12,500 micro-CT images (slice thickness 0.052 mm, slice spacing 0.052 mm). 80% of the MDCT and micro-CT images are randomly selected as the training set, and 20% image in the previous section are used as the test set in this part. Image mapping is performed by three unsupervised methods, where FUNIT is the experimental model and StarGAN and CycleGAN control models. Image quality evaluation of vertebral images was performed using Friedman test to compare the differences in SSIM and FID values between the original MDCT and three groups of unsupervised model-generated micro-CT-like images. The paired t-test and linear regression were used to compare the differences and correlations of bone structural indices (BV/TV, Tb.Th and Tb.Sp) between FUNIT-like micro-CT and micro-CT. ICCs were used to analyze the consistency between bone structure indexes between FUNIT micro-CT-like and micro-CT image.

#### RESULTS

The image quality scores (SSIM/FID) of original MDCT and micro-CT-like images generated by FUNIT, starGAN and cycleGAN models were 0.519±0.030/ 201.737±15.031, 0.437±0.025/ 289.503±18.037, 0.377±0.035/ 347.311±25.051, and 0.238±0.031/ 453.425±39.081 respectively. The bone structure measurements measured by FUNIT micro-CT-like and micro-CT were images as follows, BV/TV (%) 0.143±0.018 and 0.180±0.016, Tb.Th (mm) 0.158±0.021 and 0.218±0.015, Tb.Sp (mm) 1.144±0.166 and 0.934±0.126, respectively. The BV/TV and Tb.Th measured by FUNIT micro-CT-like images were smaller than that of micro-CT ( $P < 0.05$ ), while Tb.Sp was larger than that of micro-CT ( $P < 0.05$ ). The correlations of bone structure indexes between FUNIT micro-CT-like and micro-CT were BV/TV ( $R^2=0.667$ ), Tb.Th ( $R^2=0.613$ ) and Tb.Sp ( $R^2=0.603$ ), respectively ( $P < 0.001$ ). The ICC of bone structure measurements between FUNIT micro-CT-like and the micro-CT images were BV/TV (0.809), Tb.Th (0.753) and Tb.Sp (0.753), respectively ( $P < 0.001$ ).

## CONCLUSION

The CGAN-based unsupervised FUNIT-micro-CT-like images were highly similar to micro-CT, and the bone structure indexes measured by FUNIT-micro-CT-like images this image are highly correlated with those of micro-CT.

## CLINICAL RELEVANCE/APPLICATION

The CGAN-based unsupervised FUNIT-micro-CT-like image may provides an in-vivo and non-invasive solution for bone structure measurement.

### R5A-SPMK-4 A Deep Learning Model for Classification of Chondroid Tumors on CT-Images

#### Participants

Felix Gassert, MD, MBA, Munich, Germany (*Presenter*) Consultant, SmartReporting GmbH

#### PURPOSE

Differentiation between enchondromas, atypical cartilaginous tumors (ACT) and high-grade chondrosarcomas is crucial for adequate patient management. Although, several imaging features have been identified, differentiating enchondromas from ACTs radiologically remains challenging. Therefore, the goal of this study was to develop a deep learning model (DLM) for the classification of chondroid tumors based on CT images.

#### METHODS AND MATERIALS

Patients from two independent cohorts ( $n=344$ ; age= $50.3 \pm 14.3$  years; 175 women) who were diagnosed with either an enchondroma ( $n=124$ ), an ACT ( $n=92$ ) or a high-grade chondrosarcoma ( $n=128$ ) and had undergone CT imaging as well as clinical and histological assessment of the tumor, were included in this study. The final diagnosis was based on the consensus of an interdisciplinary tumor board. The tumors were segmented on the CT images. The major cohort was split into training and validation sets ( $n=168/76$ ), and the smaller cohort was used for external testing ( $n=100$ ). A 2D convolutional neural network (CNN) was trained for classification. The mean squared error loss was used for optimization. For comparison, blinded readings were performed on the external test-set by three radiologists (3, 4, 10 years of experience).

#### RESULTS

The DL model achieved an area under the curve (AUC) of 0.87 for the differentiation between benign, intermediate and malignant cartilaginous tumors on CT images. The AUC of the readers was at 0.77/0.81/0.83. For the differentiation between enchondromas

and ACTs performed by the DLM, the AUC was at 0.80, whereas the readings of the residents resulted in an AUC of 0.72 and 0.76 and the readings of the musculoskeletal fellowship-trained radiologist in an AUC of 0.79 for this analysis. The ROC of the DLM was significantly better than the ROC of resident 1 for the differentiation between benign and malignant lesions ( $P=0.012$ ). Sensitivity, specificity and accuracy are displayed in the figure.

#### **CONCLUSION**

s Compared to resident radiologists, the DLM showed better results for the differentiation of benign, intermediate and malignant chondroid bone tumors, whereas there was no significant difference found compared to the musculoskeletal fellowship-trained radiologist. A DLM may therefore improve and standardize diagnosis of chondroid tumors especially for the differentiation between enchondromas and ACTs.

#### **CLINICAL RELEVANCE/APPLICATION**

Classification of chondroid tumors - especially the differentiation between enchondromas and ACTs is challenging on CT images and is crucial for proper patient management. A DLM assessing CT images of the tumor may therefore support the decision making of the radiologists and improve patient outcome.

Printed on: 02/07/23

## Abstract Archives of the RSNA, 2022

R5A-SPMK-1

### **Radiomic Nomogram for Predicting High-Risk Cytogenetic Status in Multiple Myeloma Based on Fat-Suppressed T2-Weighted Magnetic Resonance Imaging**

Thursday, Dec. 1 12:15PM - 12:45PM Room: Learning Center - MK DPS

#### **Participants**

Suwei Liu, (*Presenter*) Nothing to Disclose

#### **PURPOSE**

To establish and validate clinical fat-suppressed T2-weighted magnetic resonance imaging (FS-T2WI) radiomic nomograms of MM HRC status for pre-treatment decision making and prognostic assessment.

#### **METHODS AND MATERIALS**

A cohort of 159 patients with MM (71 HRC, 88 non-HRC), The region of interest of the largest tumor lesions on FS-T2WI images was manually outlined, and 1688 features were obtained. Fourteen radiomic features were selected by 10-fold cross-validation using feature selection variance thresholds, Student's t test, redundancy analysis, and least absolute shrinkage and selection operator methods. Logistic regression was used to establish a clinical prediction model (model 1), a FS-T2WI radiomic prediction model (model 2), and a clinical-radiomic prediction model (model 3). Receiver operating characteristic (ROC) curves were used to evaluate and compare their diagnostic performance. Kaplan-Meier survival analysis and logrank tests were used to assess the prognostic value of the radiomic nomograms.

#### **RESULTS**

Models 2 and 3 showed significantly higher diagnostic efficacy than model 1 (both  $p < 0.05$ ). The area under the ROC curve of models 1, 2, and 3 was (training set: 0.65, 0.83, and 0.85; validation set: 0.70, 0.73, and 0.76, respectively). Kaplan-Meier survival analysis showed similar prognostic values for the radiomic nomogram and MM cytogenetic status (logrank test, both  $p < 0.05$ ; C-index, 0.651 and 0.659, respectively; z-score test,  $p = 0.153$ ).

#### **CONCLUSION**

s Radiomic nomograms can predict the HRC status of MM, potentially contributing to pre-treatment clinical decision making and prognostic assessment.

#### **CLINICAL RELEVANCE/APPLICATION**

Radiomics has shown promise for predicting the cytogenetic status of multiple myeloma (MM). However, few studies have investigated the role of single sequence radiomic nomograms in predicting the high-risk cytogenetic (HRC) status of MM.

Printed on: 02/07/23

## Abstract Archives of the RSNA, 2022

R5A-SPMK-2

### Deep Learning-based Automated Compression Fracture Analysis Algorithm On Spine Radiography for Onsite Application

Thursday, Dec. 1 12:15PM - 12:45PM Room: Learning Center - MK DPS

#### Participants

Hongjun Yoon, Seoul, Korea, Republic Of (*Presenter*) Nothing to Disclose

#### PURPOSE

To develop a deep-learning-based algorithm that conducts reliable measuring of compression ratio (CR) for compression fracture (CF) diagnosis in lateral X-rays.

#### METHODS AND MATERIALS

We, retrospectively, collected 7,650 spine X-ray images which has been sent to the government agency under ministry of health and welfare responsible for claims review and quality assessment of the Health Insurance. We used four classification models, view, body part, posture, and assistant device, to classify whether the input radiography is a subject for CF analysis. With U-Net model, trained with 1,040 lateral TL-spine X-rays and annotations, we segment vertebra body (VB) to calculate the compression ratio by each subject's front height over average of the two adjacent ones. We calculated CR by the subject VB's front height over average of the two adjacent VB's front heights.

#### RESULTS

For evaluating performance of our algorithm, we used 250 spine X-ray images, included 145 TL-Spine X-ray images suitable for CR measurement ( $44.18\% \pm 13.04\%$ , min: 20%, max: 74.72%). The sequential CF subject classification model show an accuracy of 94.8% (95% CI: 0.912= $p=0.972$ ). Mean Absolute Error (MAE) between ground truth and the predicted CR was 6.04% with standard deviation of 8.86%. By evaluating the above performance by ground truth's severity, the mild, moderate, and, severe fracture performances were  $6.54\% \pm 7.64\%$ ,  $4\% \pm 3.78\%$  and  $7.2\% \pm 10.74\%$  respectively.

#### CONCLUSION

s In practice, it is essential to check whether the input image is suitable for specific analysis algorithms. Unsuitable input could give false result, potentially misguide medical practitioner, and even slow down the process, which is the opposite of the purpose of automated system. Result of this study shows that our automatic algorithm could not only provide an efficient change in process of measuring CR with high performance, but also be an objective solution by selecting subject analysis images.

#### CLINICAL RELEVANCE/APPLICATION

To apply deep learning based automated analysis algorithm into actual practice, we propose a sequential classification model to select the subject image for analysis of CF, which is required to be plain lateral TL-spine x-ray image.

Printed on: 02/07/23

## Abstract Archives of the RSNA, 2022

R5A-SPMK-3

### A Study for Measuring Vertebral Bone Structure by Generated Micro-CT-like Images: An Approach Based on FUNIT Conditional Generative Adversarial Network Mapping

Thursday, Dec. 1 12:15PM - 12:45PM Room: Learning Center - MK DPS

#### Participants

Dan Jin, Beijing, China (*Presenter*) Nothing to Disclose

#### PURPOSE

To investigate the quality of micro-CT-like images generated by FUNIT models based on conditional generative adversarial networks (CGAN) and their value in vertebral bone structure measurements.

#### METHODS AND MATERIALS

The same anatomical areas of 25 human lumbar spine specimens were scanned using MDCT and micro-CT for normalization, resulting in 6,250 MDCT images (slice thickness 0.6 mm, slice spacing 0.1 mm) and 12,500 micro-CT images (slice thickness 0.052 mm, slice spacing 0.052 mm). 80% of the MDCT and micro-CT images are randomly selected as the training set, and 20% image in the previous section are used as the test set in this part. Image mapping is performed by three unsupervised methods, where FUNIT is the experimental model and StarGAN and CycleGAN control models. Image quality evaluation of vertebral images was performed using Friedman test to compare the differences in SSIM and FID values between the original MDCT and three groups of unsupervised model-generated micro-CT-like images. The paired t-test and linear regression were used to compare the differences and correlations of bone structural indices (BV/TV, Tb.Th and Tb.Sp) between FUNIT-like micro-CT and micro-CT. ICCs were used to analyze the consistency between bone structure indexes between FUNIT micro-CT-like and micro-CT image.

#### RESULTS

The image quality scores (SSIM/FID) of original MDCT and micro-CT-like images generated by FUNIT, starGAN and cycleGAN models were  $0.519 \pm 0.030 / 201.737 \pm 15.031$ ,  $0.437 \pm 0.025 / 289.503 \pm 18.037$ ,  $0.377 \pm 0.035 / 347.311 \pm 25.051$ , and  $0.238 \pm 0.031 / 453.425 \pm 39.081$  respectively. The bone structure measurements measured by FUNIT micro-CT-like and micro-CT were images as follows, BV/TV (%)  $0.143 \pm 0.018$  and  $0.180 \pm 0.016$ , Tb.Th (mm)  $0.158 \pm 0.021$  and  $0.218 \pm 0.015$ , Tb.Sp (mm)  $1.144 \pm 0.166$  and  $0.934 \pm 0.126$ , respectively. The BV/TV and Tb.Th measured by FUNIT micro-CT-like images were smaller than that of micro-CT ( $P < 0.05$ ), while Tb.Sp was larger than that of micro-CT ( $P < 0.05$ ). The correlations of bone structure indexes between FUNIT micro-CT-like and micro-CT were BV/TV ( $R^2=0.667$ ), Tb.Th ( $R^2=0.613$ ) and Tb.Sp ( $R^2=0.603$ ), respectively ( $P < 0.001$ ). The ICC of bone structure measurements between FUNIT micro-CT-like and the micro-CT images were BV/TV (0.809), Tb.Th (0.753) and Tb.Sp (0.753), respectively ( $P < 0.001$ ).

#### CONCLUSION

The CGAN-based unsupervised FUNIT-micro-CT-like images were highly similar to micro-CT, and the bone structure indexes measured by FUNIT-micro-CT-like images this image are highly correlated with those of micro-CT.

#### CLINICAL RELEVANCE/APPLICATION

The CGAN-based unsupervised FUNIT-micro-CT-like image may provides an in-vivo and non-invasive solution for bone structure measurement.

Printed on: 02/07/23

## Abstract Archives of the RSNA, 2022

R5A-SPMK-4

### A Deep Learning Model for Classification of Chondroid Tumors on CT-Images

Thursday, Dec. 1 12:15PM - 12:45PM Room: Learning Center - MK DPS

#### Participants

Felix Gassert, MD, MBA, Munich, Germany (*Presenter*) Consultant, SmartReporting GmbH

#### PURPOSE

Differentiation between enchondromas, atypical cartilaginous tumors (ACT) and high-grade chondrosarcomas is crucial for adequate patient management. Although, several imaging features have been identified, differentiating enchondromas from ACTs radiologically remains challenging. Therefore, the goal of this study was to develop a deep learning model (DLM) for the classification of chondroid tumors based on CT images.

#### METHODS AND MATERIALS

Patients from two independent cohorts (n=344; age=50.3±14.3 years; 175 women) who were diagnosed with either an enchondroma (n=124), an ACT (n=92) or a high-grade chondrosarcoma (n=128) and had undergone CT imaging as well as clinical and histological assessment of the tumor, were included in this study. The final diagnosis was based on the consensus of an interdisciplinary tumor board. The tumors were segmented on the CT images. The major cohort was split into training and validation sets (n=168/76), and the smaller cohort was used for external testing (n=100). A 2D convolutional neural network (CNN) was trained for classification. The mean squared error loss was used for optimization. For comparison, blinded readings were performed on the external test-set by three radiologists (3, 4, 10 years of experience).

#### RESULTS

The DL model achieved an area under the curve (AUC) of 0.87 for the differentiation between benign, intermediate and malignant cartilaginous tumors on CT images. The AUC of the readers was at 0.77/0.81/0.83. For the differentiation between enchondromas and ACTs performed by the DLM, the AUC was at 0.80, whereas the readings of the residents resulted in an AUC of 0.72 and 0.76 and the readings of the musculoskeletal fellowship-trained radiologist in an AUC of 0.79 for this analysis. The ROC of the DLM was significantly better than the ROC of resident 1 for the differentiation between benign and malignant lesions (P=0.012). Sensitivity, specificity and accuracy are displayed in the figure.

#### CONCLUSION

Compared to resident radiologists, the DLM showed better results for the differentiation of benign, intermediate and malignant chondroid bone tumors, whereas there was no significant difference found compared to the musculoskeletal fellowship-trained radiologist. A DLM may therefore improve and standardize diagnosis of chondroid tumors especially for the differentiation between enchondromas and ACTs.

#### CLINICAL RELEVANCE/APPLICATION

Classification of chondroid tumors - especially the differentiation between enchondromas and ACTs is challenging on CT images and is crucial for proper patient management. A DLM assessing CT images of the tumor may therefore support the decision making of the radiologists and improve patient outcome.

Printed on: 02/07/23



## Abstract Archives of the RSNA, 2022

R5A-SPMS

### Multisystem Thursday Poster Discussion - A

Thursday, Dec. 1 12:15PM - 12:45PM Room: Learning Center - MS DPS

#### Sub-Events

#### R5A-SPMS-1 Inter-reader Reliability of Immune-specific Response Criteria (irRECIST iRECIST)

##### Participants

Kathleen Ruchalski, MD, Santa Monica, CA (*Presenter*) Nothing to Disclose

##### PURPOSE

RECIST 1.1 can underestimate treatment benefits of immunotherapy, with irRECIST and iRECIST accounting for atypical responses. Inter-reader discordances are known to occur in a dual reader paradigm. Our objective is to compare inter-reader reliability between RECIST 1.1, irRECIST, and iRECIST.

##### METHODS AND MATERIALS

This is a retrospective analysis of advanced Non-small cell lung cancer (NSCLC) patients treated with pembrolizumab at our institution as part of the KEYNOTE-001 study. All trial imaging was interpreted by two radiologists. RECIST 1.1, irRECIST, and iRECIST categorical responses and agreement for progressive disease (PD) was compared by kappa statistic. Time to progression (TTP) or time to censor was compared between readers by paired t test. Relationship to disease progression and overall survival (OS) was assessed by log rank.

##### RESULTS

Of 98 patients, 77 had baseline and subsequent imaging available for 5.8 mean timepoints with 42.9 weeks of follow up. From this group, 44 patients had imaging beyond iUPD (unconfirmed-PD) for confirmation and were analyzed. PD occurred by reader 1, reader 2 in 34, 33 patients by RECIST 1.1 ( $k = 0.562$ ,  $CI = 0.275-0.850$ ), 31, 29 patients by irRECIST ( $k = 0.477$ ,  $CI = 0.201-0.754$ ), and 27, 22 patients by iRECIST iCPD (confirmed-PD) ( $k = 0.682$ ,  $CI = 0.471-0.892$ ). There was no significant difference in reader agreement of time to PD by RECIST 1.1, irRECIST, iRECIST ( $p = 0.38, 0.60, 0.26$ ). There was a significant difference in time to progression between RECIST 1.1, irRECIST and iRECIST, with median PFS 3.4 months (2.6-4.6), 4.7 (3.5-6.8) and 8.7 (6.9-14.5) ( $p < 0.0001$ ). PD by any criteria was not significantly correlated with OS.

##### CONCLUSION

s PD confirmation by iRECIST resulted in substantial reader agreement compared to moderate reader agreement by RECIST 1.1 and irRECIST. There were significant differences in TTP between the criteria, with iRECIST having the longest TTP. PD by each criteria did not correlate with a significant difference in OS.

##### CLINICAL RELEVANCE/APPLICATION

While iRECIST provides improved reader agreement compared to irRECIST and RECIST 1.1, there were no significant differences in reader agreement of TTP for each criteria.

Printed on: 02/07/23

## Abstract Archives of the RSNA, 2022

R5A-SPMS-1

### Inter-reader Reliability of Immune-specific Response Criteria (irRECIST iRECIST)

Thursday, Dec. 1 12:15PM - 12:45PM Room: Learning Center - MS DPS

#### Participants

Kathleen Ruchalski, MD, Santa Monica, CA (*Presenter*) Nothing to Disclose

#### PURPOSE

RECIST 1.1 can underestimate treatment benefits of immunotherapy, with irRECIST and iRECIST accounting for atypical responses. Inter-reader discordances are known to occur in a dual reader paradigm. Our objective is to compare inter-reader reliability between RECIST 1.1, irRECIST, and iRECIST.

#### METHODS AND MATERIALS

This is a retrospective analysis of advanced Non-small cell lung cancer (NSCLC) patients treated with pembrolizumab at our institution as part of the KEYNOTE-001 study. All trial imaging was interpreted by two radiologists. RECIST 1.1, irRECIST, and iRECIST categorical responses and agreement for progressive disease (PD) was compared by kappa statistic. Time to progression (TTP) or time to censor was compared between readers by paired t test. Relationship to disease progression and overall survival (OS) was assessed by log rank.

#### RESULTS

Of 98 patients, 77 had baseline and subsequent imaging available for 5.8 mean timepoints with 42.9 weeks of follow up. From this group, 44 patients had imaging beyond iUPD (unconfirmed-PD) for confirmation and were analyzed. PD occurred by reader 1, reader 2 in 34, 33 patients by RECIST 1.1 ( $k = 0.562$ ,  $CI = 0.275-0.850$ ), 31, 29 patients by irRECIST ( $k = 0.477$ ,  $CI = 0.201-0.754$ ), and 27, 22 patients by iRECIST iCPD (confirmed-PD) ( $k = 0.682$ ,  $CI = 0.471-0.892$ ). There was no significant difference in reader agreement of time to PD by RECIST 1.1, irRECIST, iRECIST ( $p = 0.38, 0.60, 0.26$ ). There was a significant difference in time to progression between RECIST 1.1, irRECIST and iRECIST, with median PFS 3.4 months (2.6-4.6), 4.7 (3.5-6.8) and 8.7 (6.9-14.5) ( $p < 0.0001$ ). PD by any criteria was not significantly correlated with OS.

#### CONCLUSION

s PD confirmation by iRECIST resulted in substantial reader agreement compared to moderate reader agreement by RECIST 1.1 and irRECIST. There were significant differences in TTP between the criteria, with iRECIST having the longest TTP. PD by each criteria did not correlate with a significant difference in OS.

#### CLINICAL RELEVANCE/APPLICATION

While iRECIST provides improved reader agreement compared to irRECIST and RECIST 1.1, there were no significant differences in reader agreement of TTP for each criteria.

Printed on: 02/07/23

## Abstract Archives of the RSNA, 2022

R5A-SPNMMI

### Nuclear Medicine/Molecular Imaging Thursday Poster Discussion - A

Thursday, Dec. 1 12:15PM - 12:45PM Room: Learning Center - NMMI DPS

#### Participants

Ashwin Parihar, MBBS, MD, Saint Louis, MO (*Moderator*) Nothing to Disclose

#### Sub-Events

#### R5A-SPNMMI-1 Assessment of Bone Metastases Response to Lu177-PSMA in mCRPC Patients

Participants

Sarah Boughdad, (*Presenter*) Nothing to Disclose

#### PURPOSE

Prostate cancer (PC) is the most frequent cancer in males and progressive metastatic castrate-resistance PC (mCRPC) is defined as an incurable disease. Recently, Lu-177-PSMA has been validated as a valid therapeutic option by the Vision trial (Sartor et al. 2021). Most patients have a predominant bone disease, but to our knowledge there is no consensus for bone radiological response assessment. Thus, we investigated bone metastasis response using 68Ga-PSMA PET/CT, taking as a reference PSA changes.

#### METHODS AND MATERIALS

In our retrospective and single-center study, we included mCRPC patients eligible for Lu-177-PSMA after screening for 68Ga-PSMA PET/CT positivity and who received at least 4 Lu-177-PSMA cycles. Responders (PSA-R)/non-responders (PSA-NR) were defined as  $>50\%/=50\%$  decrease in PSA levels between baseline and at the 4th cycle. For each patient, 3 bone target lesions were assessed with SUVmax/SUVmean/Tumor lesion activity (TLA)/Metabolic tumor volume (MTV) evaluated by PET and the lesion biggest diameter and density (HU) by CT. Percent changes were compared between PSA-R and PSA-NR in a per-lesion analysis using Mann-Whitney test. We assessed the association between PET and CT response parameters using Spearman correlation. We also compared PSA changes as a function of the presence of visceral disease.

#### RESULTS

We included 18 mCRPC patients with a total of 55 bone lesions. Thirteen patients (72%) were classified as PSA-R. There was significantly drop in PSA-R in SUVmax ( $-64\pm 45\%$  vs.  $-42\pm 24\%$ ;  $p=0.001$ ), SUVmean ( $-64\pm 45\%$  vs.  $-43\pm 25\%$ ;  $p<0.001$ ) and TLA ( $-24\pm 141\%$  vs.  $96\pm 281\%$ ;  $p=0.002$ ). By contrast, changes in MTV, CT-size or -density were not significant ( $p=0.1$ ,  $p=0.37$  and  $p=0.19$ , respectively). There was no significant correlation between PET and CT response parameters. We found a trend for a negative correlation between SUVmax and CT density changes ( $p=0.095$ ). There was a significant association between CT-size and -density variations ( $\rho=0.29$ ;  $p=0.03$ ) and no difference in PSA variation as a function of the presence of visceral disease.

#### CONCLUSION

In a small but homogenous population of mCRPC pts treated with Lu-177-PSMA, PSA response was associated with Ga-68-PSMA PET metabolic changes whereas changes in lesion size or density were not significant. Those findings suggest that metabolic changes better reflect tumor response in mCRPC patients and could help for the follow-up in this population. Indeed, mCRPC patients presenting with PSA increase after Lu-177-PSMA might benefit from additional cycles of Lu-177-PSMA in case of Ga-68-PSMA PET positive metastases.

#### CLINICAL RELEVANCE/APPLICATION

Most patients have a predominantly bone metastatic disease but to our knowledge there is few data on assessment of bone response.

#### R5A-SPNMMI-2 Validation of SSTR-RADS 1.0 for SSTR-PET/CT in the Diagnosis and Treatment Planning of NET Patients

Participants

Johannes Ruebenthaler, MD, Munich, Germany (*Presenter*) Nothing to Disclose

#### PURPOSE

The recently proposed standardized reporting and data system for somatostatin receptor (SSTR)-targeted PET/CT SSTR-RADS 1.0 showed promising first results in the assessment of diagnosis and treatment planning with peptide receptor radionuclide therapy (PRRT) in patients with neuroendocrine tumors (NET). This study aims to determine the intra- and interobserver agreement of SSTR-RADS 1.0 in the interpretation of SSTR-PET/CTs in NET patients.

#### METHODS AND MATERIALS

SSTR-PET/CT scans of 100 patients were independently evaluated by an experienced (E1, E2) and inexperienced (I1, I2) nuclear medicine physician and radiologist, respectively, according to SSTR-RADS 1.0 criteria at two time points with 6 weeks in between. For each scan, a maximum of five target lesions were freely chosen by the readers (not more than three lesions per organ) and

assigned to the SSTR-RADS 1.0 criteria. Moreover, an overall scan score and binary decision on PRRT was assessed. Intra- and interobserver agreement was assessed using the intraclass correlation coefficient (ICC).

## **RESULTS**

The interobserver agreement using SSTR-RADS 1.0 for identical target lesions (ICC = 0.89) and for the overall scan score was excellent (ICC = 0.91). The decision to use PRRT also demonstrated excellent agreement (ICC = 0.80). No significant differences between E1/E2 and I1/I2 for overall scan impression were achieved ( $p = 0.11$ ). All four readers showed excellent intraobserver agreement even among different experience levels (ICC 0.836 - 0.986) when comparing target lesion-based scores and decision for PRRT.

## **CONCLUSION**

s SSTR-RADS 1.0 represents a highly reproducible and accurate system for stratifying SSTR-targeted PET imaging scans with high intra- and interobserver agreement. The system is a promising approach to standardize the diagnosis and treatment planning in NET patients.

## **CLINICAL RELEVANCE/APPLICATION**

The reporting and data system SSTR-RADS 1.0 is a promising approach to standardize diagnosis and treatment planning of NET patients using hybrid imaging and can be a useful tool for simplifying and improving the management of NET patients in clinical practice.

Printed on: 02/07/23

## Abstract Archives of the RSNA, 2022

R5A-SPNMMI-1

### Assessment of Bone Metastases Response to Lu177-PSMA in mCRPC Patients

Thursday, Dec. 1 12:15PM - 12:45PM Room: Learning Center - NMMI DPS

#### Participants

Sarah Boughdad, (*Presenter*) Nothing to Disclose

#### PURPOSE

Prostate cancer (PC) is the most frequent cancer in males and progressive metastatic castrate-resistance PC (mCRPC) is defined as an incurable disease. Recently, Lu-177-PSMA has been validated as a valid therapeutic option by the Vision trial (Sartor et al. 2021). Most patients have a predominant bone disease, but to our knowledge there is no consensus for bone radiological response assessment. Thus, we investigated bone metastasis response using 68Ga-PSMA PET/CT, taking as a reference PSA changes.

#### METHODS AND MATERIALS

In our retrospective and single-center study, we included mCRPC patients eligible for Lu-177-PSMA after screening for 68Ga-PSMA PET/CT positivity and who received at least 4 Lu-177-PSMA cycles. Responders (PSA-R)/non-responders (PSA-NR) were defined as >50%/=50% decrease in PSA levels between baseline and at the 4th cycle. For each patient, 3 bone target lesions were assessed with SUV<sub>max</sub>/SUV<sub>mean</sub>/Tumor lesion activity (TLA)/Metabolic tumor volume (MTV) evaluated by PET and the lesion biggest diameter and density (HU) by CT. Percent changes were compared between PSA-R and PSA-NR in a per-lesion analysis using Mann-Whitney test. We assessed the association between PET and CT response parameters using Spearman correlation. We also compared PSA changes as a function of the presence of visceral disease.

#### RESULTS

We included 18 mCRPC patients with a total of 55 bone lesions. Thirteen patients (72%) were classified as PSA-R. There was significantly drop in PSA-R in SUV<sub>max</sub> (-64±45% vs. -42±24%; p=0.001), SUV<sub>mean</sub> (-64±45% vs. -43±25%; p<0.001) and TLA (-24±141% vs. 96%±281%; p=0.002). By contrast, changes in MTV, CT-size or -density were not significant (p=0.1, p=0.37 and p=0.19, respectively). There was no significant correlation between PET and CT response parameters. We found a trend for a negative correlation between SUV<sub>max</sub> and CT density changes (p=0.095). There was a significant association between CT-size and -density variations (rho=0.29; p=0.03) and no difference in PSA variation as a function of the presence of visceral disease.

#### CONCLUSION

In a small but homogenous population of mCRPC pts treated with Lu-177-PSMA, PSA response was associated with Ga-68-PSMA PET metabolic changes whereas changes in lesion size or density were not significant. Those findings suggest that metabolic changes better reflect tumor response in mCRPC patients and could help for the follow-up in this population. Indeed, mCRPC patients presenting with PSA increase after Lu-177-PSMA might benefit from additional cycles of Lu-177-PSMA in case of Ga-68-PSMA PET positive metastases.

#### CLINICAL RELEVANCE/APPLICATION

Most patients have a predominantly bone metastatic disease but to our knowledge there is few data on assessment of bone response.

Printed on: 02/07/23

## Abstract Archives of the RSNA, 2022

R5A-SPNMMI-2

### Validation of SSTR-RADS 1.0 for SSTR-PET/CT in the Diagnosis and Treatment Planning of NET Patients

Thursday, Dec. 1 12:15PM - 12:45PM Room: Learning Center - NMMI DPS

#### Participants

Johannes Ruebenthaler, MD, Munich, Germany (*Presenter*) Nothing to Disclose

#### PURPOSE

The recently proposed standardized reporting and data system for somatostatin receptor (SSTR)-targeted PET/CT SSTR-RADS 1.0 showed promising first results in the assessment of diagnosis and treatment planning with peptide receptor radionuclide therapy (PRRT) in patients with neuroendocrine tumors (NET). This study aims to determine the intra- and interobserver agreement of SSTR-RADS 1.0 in the interpretation of SSTR-PET/CTs in NET patients.

#### METHODS AND MATERIALS

SSTR-PET/CT scans of 100 patients were independently evaluated by an experienced (E1, E2) and inexperienced (I1, I2) nuclear medicine physician and radiologist, respectively, according to SSTR-RADS 1.0 criteria at two time points with 6 weeks in between. For each scan, a maximum of five target lesions were freely chosen by the readers (not more than three lesions per organ) and assigned to the SSTR-RADS 1.0 criteria. Moreover, an overall scan score and binary decision on PRRT was assessed. Intra- and interobserver agreement was assessed using the intraclass correlation coefficient (ICC).

#### RESULTS

The interobserver agreement using SSTR-RADS 1.0 for identical target lesions (ICC = 0.89) and for the overall scan score was excellent (ICC = 0.91). The decision to use PRRT also demonstrated excellent agreement (ICC = 0.80). No significant differences between E1/E2 and I1/I2 for overall scan impression were achieved ( $p = 0.11$ ). All four readers showed excellent intraobserver agreement even among different experience levels (ICC 0.836 - 0.986) when comparing target lesion-based scores and decision for PRRT.

#### CONCLUSION

SSTR-RADS 1.0 represents a highly reproducible and accurate system for stratifying SSTR-targeted PET imaging scans with high intra- and interobserver agreement. The system is a promising approach to standardize the diagnosis and treatment planning in NET patients.

#### CLINICAL RELEVANCE/APPLICATION

The reporting and data system SSTR-RADS 1.0 is a promising approach to standardize diagnosis and treatment planning of NET patients using hybrid imaging and can be a useful tool for simplifying and improving the management of NET patients in clinical practice.

Printed on: 02/07/23



## Abstract Archives of the RSNA, 2022

R5A-SPNPM

### Noninterpretive Skills/Quality Improvement/Practice Management Thursday Poster Discussions - A

Thursday, Dec. 1 12:15PM - 12:45PM Room: Learning Center - NPM DPS

#### Participants

Cynthia S. Santillan, MD, San Diego, CA (*Moderator*) Consultant, Alimientiv Health Trust

#### Sub-Events

#### R5A-SPNPM-Focused Assessment with Sonography for Trauma: Bridging the Resource Gap

1

Participants

Scott Rohren, Houston, TX (*Presenter*) Nothing to Disclose

#### PURPOSE

In resource-constrained regions, ultrasound serves as a portable and available diagnostic modality. Particularly in emergent cases such as trauma, ultrasound is often the only imaging available. There is limited evidence on the impact and cost benefits of ultrasound in resource-constrained settings. The purpose of this study is to identify the utility and applicability of ultrasound in trauma settings within low-and-middle-income countries (LMICs).

#### METHODS AND MATERIALS

Electronic databases were queried from 2012 to 2022, to identify stakeholders and trends in ultrasound use. Two categories were created, one for reported applications of ultrasound use in LMICs and another for novel ultrasound studies. Articles were characterized by (1) the geographic and specialty-specific use of ultrasound in LMICs, (2) the innovative applications and the accompanying research findings, and (3) the development of associated educational and training programs. Trend analysis was conducted based on grouping, noting temporal changes, similar uses in varying regions, and differential outcomes.

#### RESULTS

A total of 6,276 articles were identified with 287 studies describing original applications of ultrasound for trauma uses in LMICs. 72% of studies involved ultrasound usage originating from Southeast Asia and sub-Saharan Africa, the latter being the region with the highest number of innovative ultrasound use. Research about ultrasound use has increased by 70% and geographically expanded by 32% in the past decade. Overwhelmingly, ultrasounds have improved outcomes for trauma patients, with a 28% decrease in mortality. Additionally, there has been an 80% increase in sonographer training programs. The use of ultrasounds in sub-Saharan Africa has significantly increased at a rate faster than other LMICs.

#### CONCLUSION

Ultrasound has growing utilization for its use as low-cost portable imaging technology. The increased interest in training and prehospital utilization has led to improved health outcomes in many resource-limited regions. Point-of-care ultrasound has particularly been useful for assessing patients in areas that would have otherwise lacked imaging capabilities. There is a growing use of ultrasound for diagnosing life-threatening conditions in trauma such as pneumothorax, vascular status, musculoskeletal injuries, and testicular injuries. While training programs have increased, there is still a deficit in formal education amongst sonographers in LMICs.

#### CLINICAL RELEVANCE/APPLICATION

The use of ultrasound in trauma settings within LMICs has not previously been quantified for overall usage or trends. This study provides new insights on how and where ultrasounds are being used while highlighting key areas for improvement.

#### R5A-SPNPM-Risk Factors for Acute Adverse Reactions to Gadolinium-Based Contrast Agents

2

Participants

Yasuhiro Fukushima, RT, PhD, (*Presenter*) Endowed Chair, Siemens AG

#### PURPOSE

Multiple gadolinium-based contrast agents (GBCAs) are classified according to the chelate structure (macrocyclic or linear, and ionic or nonionic). Macrocyclic GBCAs are recommended as possible for the prevention of nephrogenic systemic fibrosis (NSF), but it is also clinically important to consider acute adverse effects (AARs). The purpose of this study was to compare the incidence of AARs among the widely used five types of GBCAs and identify both the GBCA-related and patient-related risk factors.

#### METHODS AND MATERIALS

All intravenous GBCA injections in MRI studies (n=61 147) at a single institution between January 2008 and September 2019 were retrospectively evaluated. All AARs for the five types of GBCAs (gadoteridol, gadoterate meglumine, gadopentetate dimeglumine, gadobutrol, and gadoxetate disodium [hepatocyte specific GBCA]) were classified into allergic-like or physiologic reactions, and their severity was classified into mild, moderate and severe. GBCA-related and patient-related risk factors were evaluated by logistic regression models using generalized estimating equations.

## RESULTS

AARs occurred in 238 GBCA injections (0.39%), with an incidence of 0.22% for allergic-like and 0.20% for physiologic reactions. The highest OR for allergic-like reactions with the reference of gadoterate meglumine was 4.5 for gadoteridol (95% confidence interval [CI]: 3.5, 8.1;  $p < .001$ ), followed by 3.6 for gadobutrol (1.3, 10;  $p = .015$ ) and 2.6 for gadopentetate dimeglumine (1.4, 4.8;  $p = .003$ ). The OR for physiologic with the reference of gadoterate meglumine was 3.5 for gadoteridol (1.8, 6.9;  $p < .001$ ). For allergic-like reactions, younger age (21-40 years) was the risk factor, and for physiologic reactions, men, inpatient, younger age (21-40 years), face/neck and breast MRI examinations were the risk factors.

## CONCLUSION

s There was a significant difference in the AAR incidence between five types of GBCAs, particularly in the allergic-like reaction, and the incidence was also related to age. The incidence of physiologic reaction was related to age, gender, in/outpatient, and examination type.

## CLINICAL RELEVANCE/APPLICATION

Not only the risk of NSF, but also the risk of AARs should be considered in selecting GBCA.

## R5A-SPNPM-Reduced Body Gd Exposure Over 5 Months After a Single Human Equivalent Dose of Gadopicolenol as Compared to Gadobutrol in Healthy Rats

Participants  
Philippe Robert, Roissy CDG CEDEX, France (*Presenter*) Employee, Guerbet SA

## PURPOSE

Gadopicolenol is a high relaxivity macrocyclic Gadolinium-Based Contrast Agent (GBCA) under review by health authorities. The phase 3 clinical trials demonstrated that gadopicolenol at 0.05 mmol/kg results in the same diagnostic performance as gadobutrol at 0.1 mmol/kg in CNS and body MRI. In this context, the aim of this study was to evaluate the body gadolinium (Gd) exposure over a period of 5 months in healthy rats after a single injection of gadopicolenol or gadobutrol both administered at the Human Equivalent Dose (HED).

## METHODS AND MATERIALS

Healthy female rats ( $n=60$ ) received a single injection at the HED of gadobutrol (0.6 mmol/kg) or gadopicolenol (0.3 mmol/kg), and were euthanized after 1, 4 or 20 weeks (W1, W4, W20) ( $n=10$ /group). Cerebellum, subcortical brain, liver, kidney medulla, kidney cortex and femur diaphysis were sampled at the time of sacrifice. In group W1, blood was sampled each day. Skin biopsies were performed at 1, 3 and 7 days and at 1, 2, 3, 4 and 5 months. Gd dosing was performed by Inductively Coupled Plasma-Mass Spectrometry (ICP-MS) and compared with a Mann-Whitney non-parametric t-test. Total Gd exposition in all organs between the first sampling point to the sacrifice was estimated by integrating the Area Under the concentration Curve (AUC) based on a mono-exponential fitting of the time-dependent Gd concentrations.

## RESULTS

In all tissues except bone, Gd concentrations after gadopicolenol are lower than after gadobutrol administration during the first month after injection (see Figure, log scale). The higher Gd concentration is observed in the kidney cortex for both contrast agents with 1.5 to 1.8-fold lower levels for gadopicolenol (at 1 week,  $194 \pm 65$  nmol/g vs  $109 \pm 32$  nmol/g for gadobutrol and gadopicolenol respectively). A strong washout for both contrast agents is observed in all tissues during the period of follow-up. In femur, residual gadolinium concentration is higher or equal after gadopicolenol as compared to gadobutrol, and no washout is observed for both GBCAs, making mono-exponential fitting not possible. The global Gd exposition (AUC) over 5 months is 1.2 to 2.6-times lower after gadopicolenol as compared to gadobutrol.

## CONCLUSION

s For the same diagnostic efficacy (demonstrated by phase 3 clinical trials), the exposition of Gd after gadopicolenol is lower than that of gadobutrol, thanks to the half dose injected.

## CLINICAL RELEVANCE/APPLICATION

Gadopicolenol, a high relaxivity GBCA (2 to 2.5-fold higher than gadobutrol), allows to reduce the Gd exposure by injecting half dose.

Printed on: 02/07/23



## Abstract Archives of the RSNA, 2022

R5A-SPNPM-1

### Focused Assessment with Sonography for Trauma: Bridging the Resource Gap

Thursday, Dec. 1 12:15PM - 12:45PM Room: Learning Center - NPM DPS

#### Participants

Scott Rohren, Houston, TX (*Presenter*) Nothing to Disclose

#### PURPOSE

In resource-constrained regions, ultrasound serves as a portable and available diagnostic modality. Particularly in emergent cases such as trauma, ultrasound is often the only imaging available. There is limited evidence on the impact and cost benefits of ultrasound in resource-constrained settings. The purpose of this study is to identify the utility and applicability of ultrasound in trauma settings within low-and-middle-income countries (LMICs).

#### METHODS AND MATERIALS

Electronic databases were queried from 2012 to 2022, to identify stakeholders and trends in ultrasound use. Two categories were created, one for reported applications of ultrasound use in LMICs and another for novel ultrasound studies. Articles were characterized by (1) the geographic and specialty-specific use of ultrasound in LMICs, (2) the innovative applications and the accompanying research findings, and (3) the development of associated educational and training programs. Trend analysis was conducted based on grouping, noting temporal changes, similar uses in varying regions, and differential outcomes.

#### RESULTS

A total of 6,276 articles were identified with 287 studies describing original applications of ultrasound for trauma uses in LMICs. 72% of studies involved ultrasound usage originating from Southeast Asia and sub-Saharan Africa, the latter being the region with the highest number of innovative ultrasound use. Research about ultrasound use has increased by 70% and geographically expanded by 32% in the past decade. Overwhelmingly, ultrasounds have improved outcomes for trauma patients, with a 28% decrease in mortality. Additionally, there has been an 80% increase in sonographer training programs. The use of ultrasounds in sub-Saharan Africa has significantly increased at a rate faster than other LMICs.

#### CONCLUSION

Ultrasound has growing utilization for its use as low-cost portable imaging technology. The increased interest in training and prehospital utilization has led to improved health outcomes in many resource-limited regions. Point-of-care ultrasound has particularly been useful for assessing patients in areas that would have otherwise lacked imaging capabilities. There is a growing use of ultrasound for diagnosing life-threatening conditions in trauma such as pneumothorax, vascular status, musculoskeletal injuries, and testicular injuries. While training programs have increased, there is still a deficit in formal education amongst sonographers in LMICs.

#### CLINICAL RELEVANCE/APPLICATION

The use of ultrasound in trauma settings within LMICs has not previously been quantified for overall usage or trends. This study provides new insights on how and where ultrasounds are being used while highlighting key areas for improvement.

Printed on: 02/07/23

## Abstract Archives of the RSNA, 2022

R5A-SPNPM-2

### Risk Factors for Acute Adverse Reactions to Gadolinium-Based Contrast Agents

Thursday, Dec. 1 12:15PM - 12:45PM Room: Learning Center - NPM DPS

#### Participants

Yasuhiro Fukushima, RT, PhD, (*Presenter*) Endowed Chair, Siemens AG

#### PURPOSE

Multiple gadolinium-based contrast agents (GBCAs) are classified according to the chelate structure (macrocyclic or linear, and ionic or nonionic). Macrocyclic GBCAs are recommended as possible for the prevention of nephrogenic systemic fibrosis (NSF), but it is also clinically important to consider acute adverse effects (AARs). The purpose of this study was to compare the incidence of AARs among the widely used five types of GBCAs and identify both the GBCA-related and patient-related risk factors.

#### METHODS AND MATERIALS

All intravenous GBCA injections in MRI studies (n=61 147) at a single institution between January 2008 and September 2019 were retrospectively evaluated. All AARs for the five types of GBCAs (gadoteridol, gadoterate meglumine, gadopentetate dimeglumine, gadobutrol, and gadoxetate disodium [hepatocyte specific GBCA]) were classified into allergic-like or physiologic reactions, and their severity was classified into mild, moderate and severe. GBCA-related and patient-related risk factors were evaluated by logistic regression models using generalized estimating equations.

#### RESULTS

AARs occurred in 238 GBCA injections (0.39%), with an incidence of 0.22% for allergic-like and 0.20% for physiologic reactions. The highest OR for allergic-like reactions with the reference of gadoterate meglumine was 4.5 for gadoteridol (95% confidence interval [CI]: 3.5, 8.1;  $p < .001$ ), followed by 3.6 for gadobutrol (1.3, 10;  $p = .015$ ) and 2.6 for gadopentetate dimeglumine (1.4, 4.8;  $p = .003$ ). The OR for physiologic with the reference of gadoterate meglumine was 3.5 for gadoteridol (1.8, 6.9;  $p < .001$ ). For allergic-like reactions, younger age (21-40 years) was the risk factor, and for physiologic reactions, men, inpatient, younger age (21-40 years), face/neck and breast MRI examinations were the risk factors.

#### CONCLUSION

s There was a significant difference in the AAR incidence between five types of GBCAs, particularly in the allergic-like reaction, and the incidence was also related to age. The incidence of physiologic reaction was related to age, gender, in/outpatient, and examination type.

#### CLINICAL RELEVANCE/APPLICATION

Not only the risk of NSF, but also the risk of AARs should be considered in selecting GBCA.

Printed on: 02/07/23

## Abstract Archives of the RSNA, 2022

R5A-SPNPM-3

### Reduced Body Gd Exposure Over 5 Months After a Single Human Equivalent Dose of Gadopicolenol as Compared to Gadobutrol in Healthy Rats

Thursday, Dec. 1 12:15PM - 12:45PM Room: Learning Center - NPM DPS

#### Participants

Philippe Robert, Roissy CDG CEDEX, France (*Presenter*) Employee, Guerbet SA

#### PURPOSE

Gadopicolenol is a high relaxivity macrocyclic Gadolinium-Based Contrast Agent (GBCA) under review by health authorities. The phase 3 clinical trials demonstrated that gadopicolenol at 0.05 mmol/kg results in the same diagnostic performance as gadobutrol at 0.1 mmol/kg in CNS and body MRI. In this context, the aim of this study was to evaluate the body gadolinium (Gd) exposure over a period of 5 months in healthy rats after a single injection of gadopicolenol or gadobutrol both administered at the Human Equivalent Dose (HED).

#### METHODS AND MATERIALS

Healthy female rats (n=60) received a single injection at the HED of gadobutrol (0.6 mmol/kg) or gadopicolenol (0.3 mmol/kg), and were euthanized after 1, 4 or 20 weeks (W1, W4, W20) (n=10/group). Cerebellum, subcortical brain, liver, kidney medulla, kidney cortex and femur diaphysis were sampled at the time of sacrifice. In group W1, blood was sampled each day. Skin biopsies were performed at 1, 3 and 7 days and at 1, 2, 3, 4 and 5 months. Gd dosing was performed by Inductively Coupled Plasma-Mass Spectrometry (ICP-MS) and compared with a Mann-Whitney non-parametric t-test. Total Gd exposition in all organs between the first sampling point to the sacrifice was estimated by integrating the Area Under the concentration Curve (AUC) based on a mono-exponential fitting of the time-dependent Gd concentrations.

#### RESULTS

In all tissues except bone, Gd concentrations after gadopicolenol are lower than after gadobutrol administration during the first month after injection (see Figure, log scale). The higher Gd concentration is observed in the kidney cortex for both contrast agents with 1.5 to 1.8-fold lower levels for gadopicolenol (at 1 week,  $194 \pm 65$  nmol/g vs  $109 \pm 32$  nmol/g for gadobutrol and gadopicolenol respectively). A strong washout for both contrast agents is observed in all tissues during the period of follow-up. In femur, residual gadolinium concentration is higher or equal after gadopicolenol as compared to gadobutrol, and no washout is observed for both GBCAs, making mono-exponential fitting not possible. The global Gd exposition (AUC) over 5 months is 1.2 to 2.6-times lower after gadopicolenol as compared to gadobutrol.

#### CONCLUSION

For the same diagnostic efficacy (demonstrated by phase 3 clinical trials), the exposition of Gd after gadopicolenol is lower than that of gadobutrol, thanks to the half dose injected.

#### CLINICAL RELEVANCE/APPLICATION

Gadopicolenol, a high relaxivity GBCA (2 to 2.5-fold higher than gadobutrol), allows to reduce the Gd exposure by injecting half dose.

Printed on: 02/07/23



## Abstract Archives of the RSNA, 2022

R5A-SPNR

### Neuroradiology Thursday Poster Discussions - A

Thursday, Dec. 1 12:15PM - 12:45PM Room: Learning Center - NR DPS

#### Participants

Sam Payabvash, MD, NEW HAVEN, CT (*Moderator*) Nothing to Disclose

#### Sub-Events

### R5A-SPNR-1 A Fully Automated and Quantifiable Visual Grading System for WMH Utilizing a Rule-Based Algorithm: The Modified Fazekas Scale Using T2-Fluid Attenuated Inversion Recovery Magnetic Resonance Imaging

#### Participants

ZunHyan Rieu, BS, Seoul, Korea, Republic Of (*Presenter*) Employee, NEUROPHET, Inc

#### PURPOSE

White matter hyperintensities (WMH) have become the primary biomarker for small-vessel cerebrovascular diseases and brain atrophy. The Fazekas and Scheltens scales are the most conventional visual grading system for WMH and have been practiced by radiologists worldwide. However, in clinical practice, it is still challenged by the labor-intensive process and non-standardized criteria for measuring the irregular shapes of WMHs, which tend to be evaluated with one's subjective opinion. Therefore, we aim to fully automate the visual grading system for WMH with only the numerically quantifiable measurement using the modified Fazekas scale, Clinical Research Center for Dementia of South Korea (CREDOS) criteria, which suggests the visual grading system for WMH with the combination of diameter measurements between deep white matter hyperintensity (DWMH) and periventricular hyperintensity (PVMH).

#### METHODS AND MATERIALS

Our approach involves four stages, including brain tissue and WMH segmentation using the deep learning algorithm, WMH separation into periventricular hyperintensity and deep white matter hyperintensity using a rule-based algorithm, diameter measurement of WMH, and Fazekas scale prediction. For validation, we compared the performances of our proposed method and that of the CREDOS criteria-based visual grading system for WMH done by three certified radiologists using a total of 404 subjects with T2-fluid attenuated inversion recovery magnetic resonance imaging (T2-FLAIR) utilized from a clinical site in Korea.

#### RESULTS

The inter-rater agreements using Krippendorff's alpha were comparable between the radiologists (R) and all methods (A), including our approach. The agreements were substantial (R, 0.732 vs. A, 0.694), substantial (R, 0.671 vs. A, 0.658), and moderate (R, 0.586 vs. A, 0.579) for the modified Fazekas scale, the DWMH scale, and the PVMH scale, respectively. In addition, the total mean of areas under the receiver operating characteristic curve between radiologists (G) and radiologists against our approach (P) showed comparable performance (G,  $0.80 \pm 0.09$  vs. P,  $0.80 \pm 0.03$ ).

#### CONCLUSION

Our approach, a fully automated and quantifiable visual grading system for WMH, demonstrated comparable results against the radiologists.

#### CLINICAL RELEVANCE/APPLICATION

We believe our approach has a great potential to assist the radiologist in clinical findings.

### R5A-SPNR-10 Optimization of 3D Head SNAP Angiography Based on Compression Sensing Technology

#### Participants

Yukun Zhang, Dalian, China (*Presenter*) Nothing to Disclose

#### PURPOSE

To optimize simultaneous non-contrast angiography and intraplaque hemorrhage (SNAP), we combined SNAP and compressed sensing (CS SNAP) and identified the optimal acceleration factors (AFs) for clinical use to obtain high-quality MRA and vascular wall images capable of whole brain coverage in a short time.

#### METHODS AND MATERIALS

30 healthy volunteers (13 males, 17 females, mean age  $43.33 \pm 18.76$  years) were prospectively recruited in this study. Among them, 10 volunteers performed the pre-scan for selecting a precise head 3D SNAP parameters (Table.1) at 3.0 Tesla (Philips Ingenia CX 3.0T MRI); The remaining 20 volunteers scanned with different CS AFs of 2,2.5,3,4,5 on the basis of the optimized pre-scan sequence (Table.2). Two radiologists delineated the region of interest (ROI) on all of the original images, measured the signal intensity (SI) and standard deviation (SD) for the vascular lumen, vascular wall and white matter (Fig.1). Signal to noise ratio (SNR) and contrast to noise ratio (CNR) of vascular lumen, contrast-to-tissue ratio (CTR) and CTR efficiency (CTR<sub>eff</sub>) of the

vascular wall were further calculated; at the same time, The image quality of each dataset was scored subjectively by two radiologists (Table.3). The consistency of measurements and subjective scores of the two observers was analyzed using Kappa and intraclass correlation coefficient (ICC) test. Compare and analyze the differences in measurement parameters and subjective scores between different AFs.

## RESULTS

The measured data and subjective scores of the two observers were in good agreement (Kappa: 0.568-0.884, ICC: 0.602-0.968). when CS AF=4, the SNR and CNR of vascular lumen, and subjective score were significantly different from SNAP without CS ( $p<0.05$ ). When CS AF =2.5, 3, 4, 5, the CT<sub>Reff</sub> of vascular wall were significantly different compared with SNAP without CS ( $p<0.05$ ) (Table.4, Fig.2).

## CONCLUSION

s 3D CS SNAP can obtain whole cerebrovascular MRA and vascular wall images in a relatively short period of time, and AF of 3 is recommended as its optimized sequence (Fig.5).

## CLINICAL RELEVANCE/APPLICATION

3D CS SNAP technology has the potential to apply to multi-contrast blood imaging protocols, allowing for the acquisition of whole cerebral angiography and vascular wall images in relatively short periods of time.

## R5A-SPNR-11 Pharmacokinetics, Safety and Tolerability of the Novel Tetrameric, High Relaxivity, Macrocyclic Gadolinium-based Contrast Agent Gadoquatrane for CE-MRI

Participants

Birte Hofmann, DVM, PhD, Berlin, Germany (*Presenter*) Employee, Bayer AG

## PURPOSE

Gadoquatrane (BAY 1747846) is a novel tetrameric, macrocyclic gadolinium (Gd)-based contrast agent (GBCA) featuring a unique tetrameric structure and high relaxivity. The present study investigated its pharmacokinetics (PK) including excretion pathways, safety and tolerability in healthy volunteers.

## METHODS AND MATERIALS

This first-in-human study was conducted as a randomized, single-blind, placebo-controlled, single dose study with 6 consecutive dose cohorts consisting of 8 to 9 healthy young women and men (N=49 total). Gadoquatrane or matching placebo (NaCl 0.9%) were intravenously administered by either infusion (doses of 0.025, 0.05, or 0.1 mmol Gd/kg bw) or bolus injection (doses of 0.03, 0.1 or 0.2 mmol Gd/kg bw). Safety and tolerability were assessed over 7 days post injection (p.i.) including adverse events, cardiac and respiratory function and safety laboratory analyses. Plasma PK and excretion in urine and feces were investigated over 72 h p.i. by ICP-MS as well as HPLC-ICP-MS.

## RESULTS

Demographics were well balanced, with no notable differences between cohorts (24 ?, 25 ?; mean age ( $\pm$ SD) of 34.6 $\pm$ 6.3 years; mean BMI ( $\pm$ SD) of 23.4 $\pm$ 2.57 kg/m<sup>2</sup>). Plasma concentrations declined rapidly due to fast extracellular distribution and elimination, with no relevant gender differences. AUC and C<sub>max</sub> increased dose proportionally, volume of distribution (0.21-0.24 L/kg) and plasma clearance (0.09-0.1 L/h/kg) remained constant. Excretion via the kidneys was essentially complete (80-100%) within 12 h p.i.. No metabolites were detected in plasma or urine. Incidence and severity of treatment emergent adverse events (TEAEs) were similar in all dose groups incl. placebo. Intensity of most study drug related TEAE was mild, few were of moderate intensity, and none severe; all were recovered or recovering at 7 days p.i..

## CONCLUSION

s The novel high relaxivity, tetrameric, macrocyclic GBCA gadoquatrane was very well tolerated at all doses. The PK profile is essentially the same as for other extracellular macrocyclic GBCAs (like gadobutrol or gadoterate meglumine). Gadoquatrane has the potential to be used at substantially lower Gd doses in clinical routine compared to currently marketed extracellular GBCAs.

## CLINICAL RELEVANCE/APPLICATION

The novel, tetrameric gadoquatrane is a promising GBCA in development for MRI and its profile incl PK, safety, high relaxivity and stability meets the clinical demand to reduce the gadolinium dose.

## R5A-SPNR-13 Investigation of Image Quality of Different Monochromatic Energy Images in Spectral CT Scan: A Phantom Study

Participants

Yaoming Ma, (*Presenter*) Nothing to Disclose

## PURPOSE

Objective to explore the influence of different monochromatic energy images on the quality of energy spectrum images.

## METHODS AND MATERIALS

A polypropylene cylindrical phantom (QSP Phantom dimension) with five tubes containing different concentrations of iodine (0, 2.5, 5, 10, 20 mg/ml) was scanned using a spectral CT (Revolution CT, GE Healthcare) in gemstone spectral imaging (GSI) mode using fast kV switch (80/140 kV), the tube current was 485mA, the layer thickness was 1.25mm, the collimation width was 80mm, noise index (NI) 9, pitch 0.992:1. The CT and SD values were measured at 11 different central planes., the region of interest (ROI) of the phantom tube with iodine concentration of 20% was delineated, The area of ROI was 1 / 2-1 / 3 of the cross-sectional area of the phantom tube. The CT values and noise of 40 keV, 70 keV, 100 keV and 130 keV groups were measured and recorded by GSI viewer. One way ANOVA was used to compare the CT value and noise of iodine 20 phantom tube under different keV. LSD-t test was used to compare the two groups.

## RESULTS

With the increase of monochromatic energy level the CT value and noise of the images gradually decreased. The CT value of 40

with the increase of monochromatic energy level, the CT value and noise of the images gradually decreased. The CT value of 40 keV, 70 keV, 100 keV and 130 keV groups were  $1546.34 \pm 3.13\text{HU}$ ,  $490.13 \pm 1.60\text{HU}$ ,  $215.71 \pm 1.28\text{HU}$ ,  $121.52 \pm 18\text{HU}$ , the difference was statistically significant ( $P < 0.05$ ); The noise of 40 keV, 70 keV, 100 keV and 130 keV groups was  $25.46 \pm 2.89\text{HU}$ ,  $11.44 \pm 1.3\text{HU}$ ,  $7.83 \pm 0.92\text{HU}$ ,  $6.62 \pm 0.75\text{HU}$ , the difference was statistically significant ( $P < 0.05$ ).

## CONCLUSION

s With the increase of monochromatic energy level, the CT value and noise of the images gradually decrease, and monochromatic energy images in spectral CT scan can optimize the image quality.

## CLINICAL RELEVANCE/APPLICATION

Through the basic research of phantom, compared with conventional kVp scanning, energy spectrum CT scanning can provide the same image quality scanning radiation dose. At the same time, compared with conventional kVp scanning, energy spectrum CT scanning can provide different levels (40-140keV) of single energy and effective atomic coefficient, and more energy spectrum information of base material. This study has guiding significance for the application of energy spectrum scanning in different clinical scenes.

## R5A-SPNR-15 Study on the Image Quality of Head and Neck CTA With Energy Spectrum Combined With Iterative Reconstruction Method

Participants

Deng Jie, (*Presenter*) Nothing to Disclose

## PURPOSE

To investigate the influence and application value of spectral CT single-energy imaging combined with adaptive iterative reconstruction (ASIR) technology on head and neck CT angiography (CTA).

## METHODS AND MATERIALS

88 patients undergoing head and neck CTA examination were compared using energy spectrum combined with adaptive iterative 40% ASIR scanning, and reconstructed single-energy 40keV, 60 keV, 80 keV, and performed vascular surface reconstruction (CPR) and maximum density projection on the three groups of images. Processing (MIP). The effects of different reconstruction methods on the image quality of head and neck CTA were evaluated from the two aspects of objective measurement and subjective score.

## RESULTS

Objective evaluation: The CT values, SD values, SNR values, and CNR values of the aortic arch, common carotid artery, middle cerebral artery, vertebral artery, and basilar artery measured under the three reconstruction methods were all statistically different ( $P < 0.05$ ). Subjective evaluation: The Kappa value of the subjective evaluation of the image reconstruction quality by the physicians of the two diagnosis groups in each group was 0.75, showing strong consistency. There was no statistical difference in the scores of MIP reconstruction images among the groups ( $P = 0.467$ ). There was a statistically significant difference in the scores of CPR reconstruction images among the groups ( $P < 0.05$ ).

## CONCLUSION

s In the image quality of head and neck CTA examination, the single energy spectrum of 60keV combined with adaptive iterative 40% ASIR scanning can reduce image noise and improve the image signal-to-noise ratio. be applied.

## CLINICAL RELEVANCE/APPLICATION

When applied to head and neck CTA, the single energy spectrum of 60keV combined with adaptive iterative 40% ASIR scan has the best image quality, which can be used in clinical practice.

## R5A-SPNR-16 Predicting Early Glioma Recurrence With Peritumoral Radiomic Features From Amide Proton Transfer Weighted MR Images

Participants

Shanshan Jiang, MD, PhD, Baltimore, MD (*Presenter*) Nothing to Disclose

## PURPOSE

Because of the basement membrane barrier effect, diffuse infiltration of tumor cells into surrounding brain tissue has been proved a significant factor for migration/invasion of malignant gliomas. However, the peritumoral areas have been rarely studied for post-surgery/chemoradiation malignant gliomas. Amide proton transfer-weighted (APT<sub>w</sub>) MRI, a method generating the MRI contrast dominated by endogenous cellular proteins, has showed an encouraging diagnostic performance for gliomas. The goal was to evaluate the power of APT<sub>w</sub>-based peritumoral radiomics for classification of treatment effects and tumor recurrence.

## METHODS AND MATERIALS

A total of 90 patients with post-treatment malignant gliomas were retrospectively re-assessed. Diagnosis of tumor recurrence vs. treatment effects was based on the integrated clinical pathologic results or the updated RANO criteria. The sequences included T1w, T2w, FLAIR, APT<sub>w</sub>, and gadolinium contrast-enhanced T1w (T1w-Gd). After imaging preprocessing, radiomic features were extracted from the peritumoral regions, which were segmented manually covering abnormal FLAIR/T2w signal intensities outside the gadolinium-enhancing tumor core. A current reality tree (CRT) model was constructed to identify the most critical features when differentiating tumor recurrence from treatment effects. The alpha level of all tests was set at  $P < 0.05$ .

## RESULTS

29 vs. 61 patients were confirmed, respectively, as treatment effect or tumor recurrence. The CRT model achieved accuracies of 83.3% with radiomic features extracted from FLAIR, 90.0% with those from APT<sub>w</sub>, and 91.1% with those from both FLAIR and APT<sub>w</sub>. The 90 percentile APT<sub>w</sub> value was listed as the most important feature to distinguish these two entities in both decision trees based on APT<sub>w</sub> and FLAIRAPT<sub>w</sub> MRI models.

## CONCLUSION

s APT<sub>w</sub>-derived radiomic features are capable of capturing the progressive pattern in peritumoral areas, aiding in the accurate

treatment response assessment in post-treatment malignant gliomas by increasing detection specificity.

#### CLINICAL RELEVANCE/APPLICATION

Our results suggest that the use of APTw MR images radiomic features from peritumoral area can add important value to structural MRI to assess the early treatment response.

#### R5A-SPNR-18 **Newly Developed Iterative Motion Correction (IMC) for Brain MRI: Utility for Reducing Motion Artifacts and Improving Image Quality without Any Affection to Examination Time in Uncooperative Patients**

Participants

Kazuhiro Murayama, MD, Toyoake, Japan (*Presenter*) Research Grant, Canon Medical Systems Corporation

#### PURPOSE

To determine the utility of newly developed iterative motion correction (IMC) method for reducing motion artifact and improve image quality without any affection to examination time in uncooperative patients.

#### METHODS AND MATERIALS

65 patients suspected of cerebrovascular disease obtained fluid attenuated inversion recovery (FLAIR) images with and without IMC at 3T systems. Based on FLAIR image without IMC results, all patients were divided into cooperative (n=19) and uncooperative (n=46) patient groups. To compare examination and reconstruction time differences, these times were recorded in all patients. To assess the capability for image quality improvement between FLAIR images with and without IMC, SNR of normal appearance white matter (NAWM), CNR between gray matter and NAWM, and CNR between NAWM and deep and subcortical white matter hyper intensity (DSWMH) abnormalities were determined by ROI measurements on each FLAIR. Moreover, overall image quality, artifact and lesion conspicuity in each group were assessed by 5-point scales by two board-certified radiologists. To compare examination and reconstruction time between two methods, Wilcoxon signed-rank test was performed. For image quality comparisons, SNR and CNRs were compared between FLAIRs with and without IMC in cooperative and uncooperative groups by Student's t-test. To determine interobserver agreements for all indexes, kappa statistics with  $\chi^2$  test were performed. Then, each qualitative score was also compared between FLAIRs with and without IMC by Wilcoxon's signed sum test.

#### RESULTS

Mean examination and reconstruction times of FLAIR with IMC ( $256.3 \pm 2.7$  sec) were significantly longer than those of FLAIR without IMC ( $217.0 \pm 0.59$  sec,  $p < 0.0001$ ). SNR and CNRs of FLAIRs with IMC was significantly higher than that without IMC in uncooperative group ( $p < 0.05$ ). Interobserver agreements for each qualitative image quality score were assessed as substantial or excellent in each group ( $0.74 \leq \kappa \leq 0.91$ ,  $p < 0.001$ ). Each qualitative image quality score of FLAIR with IMC was significantly higher than that without IMC in uncooperative group ( $p < 0.05$ ).

#### CONCLUSION

The IMC technique has a potential for reducing motion artifacts and improving image quality on brain MRI with less than 1 minute prolongation of examination and reconstruction times in uncooperative patients.

#### CLINICAL RELEVANCE/APPLICATION

The IMC technique has a potential for reducing motion artifacts and improving image quality on brain MRI in uncooperative patients.

#### R5A-SPNR-19 **Natural Language Processing for Extraction of Glioblastoma and Patient Characteristics from Radiology Reports**

Participants

Ahmad Amer, BS, North Chicago, IL (*Presenter*) Nothing to Disclose

#### PURPOSE

Glioblastoma (GBM) is an aggressive primary brain tumor with a median survival of 15 months. To assist with data extraction and evaluation of potential prognostic factors, natural language processing (NLP) was applied to automate extraction of patient and tumor data from one of the largest GBM patient populations at MD Anderson Cancer Center (MDACC).

#### METHODS AND MATERIALS

The radiology information system (RIS) was used to identify 4511 patients with a pathology-confirmed GBM diagnosis presenting to MDACC from 2006-2021. 50,202 corresponding radiology reports were identified, and Python was used for report processing. Identification of specific strings and aggregation by MRN allowed for determination of tumor multicentricity, extent of resection, and patient handedness. A similar approach was applied to extract tumor location, with separate strings used for lobe and laterality. Primary and secondary lobe were determined based on occurrence frequency of lobe-specific strings. Patient survival was estimated by determining the time difference between patients' first report mentioning GBM and last report. Extraction of pre-op tumor volume first required isolation of pre-op reports. A subset of such reports were extracted by selecting reports with pre-op-specific phrases in the examination section. Next, reports nearest to and within a week prior to intra-op dates were extracted. Intra-op dates were determined by searching reports' examination sections for intra-op-specific strings and extracting surgery dates with Regex. Reports occurring prior to suspicion or diagnosis of GBM were excluded. The syntax of remaining reports were then analyzed using a pre-trained SciSpacy model, and sentences without tumor-related strings were excluded. Tumor dimensions were extracted using Regex and used to calculate tumor volume. Manual validation was performed for OS, volume, and location.

#### RESULTS

NLP characterized patients as long-term survivors with 94.7% sensitivity, 97.6% specificity, and an ROC-AUC of .953. Quantitative analysis yielded a mean absolute error of 19.40%. Lobe and laterality were 98% and 90% accurate respectively. Successful extraction of all tumor dimensions for volume calculation was achieved in 72.5% of cases.

#### CONCLUSION

Automated extraction of tumor lobe, laterality, multicentricity, extent of resection, volume, and OS and handedness was

accomplished. OS and location data were highly accurate.

#### **CLINICAL RELEVANCE/APPLICATION**

NLP was successfully applied to extract data for the investigation of prognostic factors of GBM, which could lead to improvements in patient management and inform expectations of care.

#### **R5A-SPNR-2 A Novel Connectomic Analysis Framework for Personalised Presurgical Planning using Multimodal Neuroimaging**

Participants

Ruchi Sharma, MS,BS, Bhopal, madhya Pradesh, India (*Presenter*) Nothing to Disclose

#### **PURPOSE**

The traditional method of surgical selection and planning in brain tumours was based mostly on the topography of the tumour. With recent advances, connectomics promises to provide comprehensive information by integrating the inferences from network mapping, tractography, and tumour segmentation. This information helps neurosurgeons develop new insights and an optimal strategy for tumour resection. We present a novel, automated connectomic analysis framework that integrates rs-fMRI, DWI and sMRI (T1w, FLAIR, and T1CE) modalities to determine the effect of a tumor on the individual's structural and functional connectivity, assisting in presurgical planning.

#### **METHODS AND MATERIALS**

A study was conducted on 15 tumor subjects who underwent the above mentioned MR modalities prior to surgery. Three groups of five subjects underwent tb-fMRI for Motor, Visual, and Language tasks. For each subject, our framework analysed the multiple modalities using the following techniques - multivariate statistical analysis on rs-fMR images to generate major functional networks, deep learning-based segmentation strategy on sMR images for tumour demarcation, and whole-brain probabilistic tractography on DWI for generation of major fibre tracts. Additionally, the framework reports the tumor's proximity to the generated functional network and white matter tracts using a heuristic algorithm.

#### **RESULTS**

Connectomic profiles were generated for all the subjects. For the five subjects that underwent tb-fMRI, all the network maps produced by rs-fMRI and tb-fMRI yielded similar activations in the corresponding network regions. The heuristic algorithm used to report the distance between the tumours, network maps, and tracts were highly useful in deciding the trajectory of operation.

#### **CONCLUSION**

s The connectomic profile for the clinical cases using network maps, fibre tracts, and tumor demarcation proved to be highly beneficial in the personalised presurgical planning. The validation of rs-fMRI against tb-fMRI also helped to mindfully perform the surgery to avoid functional loss of major networks.

#### **CLINICAL RELEVANCE/APPLICATION**

This study proposes a multimodal connectomic analysis method to produce personalised presurgical insights for tumor patients which helps in taking critical decisions for operating the tumor with a better understanding of the anatomical, functional and surgical complexities which is highly beneficial.

#### **R5A-SPNR-20 Perfusion-Based Radiomics Enable to Predict Thrombolysis/Thrombectomy Related Hemorrhagic Transformation in Patients With Acute Stroke: Development and Validation**

Participants

Yunhwa Roh, (*Presenter*) Nothing to Disclose

#### **PURPOSE**

Prompt diagnosis and early detection of hemorrhagic transformation (HT) may prevent dismal prognosis in acute stroke patients. We aimed to develop and validate a radiomics-based model for predicting thrombolysis/thrombectomy-related HT in patients with acute ischemic stroke using multiparametric MRI of conventional, diffusion-, and perfusion-weighted imaging.

#### **METHODS AND MATERIALS**

In this retrospective study, a radiomics model was developed in a consecutive 462 patients diagnosed with acute ischemic stroke and who underwent multiparametric MRI between 2017 to 2018 and tested in an independent validation set of 276 patients between 2019 to 2021. For each patient, 140 radiomics features were extracted from FLAIR and GRE image, DWI, and perfusion-weighted imaging including CBF, CBV, K2, MTT, Tmax, and TTP maps. HT was classified as either presence of HT (HT) or the presence of parenchymal hemorrhage (PH). Radiomics features for predicting outcomes were selected using random forest, and the model was developed by using logistic regression classifier. The diagnostic performance was calculated and compared among imaging sequences in the independent validation set using the area under the curve (AUC) from a receiver operating characteristic curve analysis, sensitivity, specificity, and accuracy.

#### **RESULTS**

For predicting HT, 8 out of 10 top features were from perfusion-weighted imaging using variable importance including TTP, CBF, and Tmax. For predicting PH, 8 out of 10 top features were from perfusion-weighted imaging including CBV, CBF, MTT, and K2. Volume and compactness of DWI and FLAIR also become significant predictors. In the test cohort, the perfusion-based radiomics model significantly improved performance (AUC 0.725) compared with DWI or FLAIR alone (AUC 0.665 and 0.679, respectively) for predicting HT. For predicting PH, the perfusion-based radiomics model also significantly improved performance (AUC 0.732) compared with DWI or FLAIR alone (AUC, 0.693 and 0.702, respectively).

#### **CONCLUSION**

s Utilizing perfusion-weighted imaging for the radiomics model significantly improved the prediction of hemorrhagic transformation as well as parenchymal hemorrhage in patients with acute stroke.

#### **CLINICAL RELEVANCE/APPLICATION**

HT following cerebral ischemia has been postulated to result in a negative impact on the clinical course. A radiomics model that utilized perfusion-weighted imaging showed improved diagnostic performance for predicting hemorrhagic transformation than conventional imaging or diffusion-weighted imaging alone. These findings support the role of perfusion MRI in identifying patients who are at increased risk for secondary HT following acute ischemic stroke and may assist patient management for clinicians.

### **R5A-SPNR-3 Disorganized Subcortical Functional Gradients in Schizophrenia and the Treatment Effects After Administration of Antipsychotics**

Participants

Chengmin Yang, (*Presenter*) Nothing to Disclose

#### **PURPOSE**

Growing evidence indicates that subcortex is pivotal in the pathophysiology of schizophrenia, and changes in subcortical regions were also sensitive indicators of pharmacological treatments. However, how the subcortex embeds within the macroscale cortical system, and the structural constraints and functional emergences of spatial arrangements, remain unclear. The new concept of gradients focused on spatial relationships, which revealed that macroscale gradients integrated systematic information into more abstract representations. Exploring the subcortex in the broader cortical landscape as well as investigating its feature as treatment target in schizophrenia is promising for its extensive connections with the entire cerebral cortex.

#### **METHODS AND MATERIALS**

Leveraging connectome gradients, we systematically scrutinized abnormalities of functional connectome gradient in antipsychotic-naïve first-episode schizophrenia patients (FES0W, n = 57) at baseline, comparing to healthy controls (HCs, n = 64), as well as longitudinal comparisons of baseline with 6-week (FES6W, n = 19) and 12-month (FES12M, n = 57) follow-up, respectively. And further examined the reproducibility in an independent validation sample (vFES0W, n = 22; HCs, n = 25), and the patients with 6-week (vFES6W, n = 22) follow-up. Correlational analyses were conducted between the longitudinal functional gradient alterations and the psychopathological ratings, including Positive and Negative Syndrome Scale (PANSS) and Global Assessment of Functioning (GAF) scores.

#### **RESULTS**

In both primary and validation datasets, patients at baseline showed the higher gradients mainly in limbic system and lower gradients in thalamus and caudate, and the longitudinal functional gradients alterations showed the improved trend over time (all  $p < 0.001$ , Bonferroni corrected, Figure 1 and 2). Namely, in the period of antipsychotic treatment, the increased gradients were positively while the decreased gradients were negatively correlated with symptom improvement.

#### **CONCLUSION**

Our findings provided a novel insight into the functional system hierarchy alterations of subcortical organization, which were sensitive to illness and treatment effects. This might extend our understanding of the functional connectome organization of subcortex in schizophrenia, and this measure makes a promising indicator of treatment response.

#### **CLINICAL RELEVANCE/APPLICATION**

This study provided the new perspective on the abnormal subcortical hierarchy organization in schizophrenia and its longitudinal gradient changes could be sensitive to reflect the antipsychotic treatment effect.

### **R5A-SPNR-5 Use of Real Life Safety Data From International Pharmacovigilance Databases to Assess the Importance of Symptoms Associated With Gadolinium Exposure**

Participants

Imran Shahid, (*Presenter*) Nothing to Disclose

#### **PURPOSE**

Recent scientific publications have reported cases of patients who complained from a variety of symptoms after they received a gadolinium-based contrast agent (GBCA). The aim of this study was to appreciate the importance of these clinical manifestations in the overall population by assessing the weight of "symptoms associated with gadolinium exposure" (SAGE) among the bulk of safety experiences reported to major health authorities.

#### **METHODS AND MATERIALS**

SAGE symptoms were identified from a review of the scientific literature, and the corresponding preferred terms (PTs) were searched in each system organ class (SOC) category recorded in the European and North American pharmacovigilance databases, EudraVigilance (EV) and FDA Adverse Event Reporting System (FAERS), respectively. The numbers of SAGE symptoms per PT, and cumulatively per SOC, were recorded and their weights in the overall spectrum of AEs was determined for each GBCA.

#### **RESULTS**

The literature search led to identify 11 articles from which the most prevalent SAGE symptoms were selected. The extraction and analysis of such AEs in EV and FAERS revealed a significantly higher SAGE weight for gadobenate dimeglumine (EV: 25.83%, FAERS: 32.24%) than for gadoteridol (EV: 15.51%; FAERS: 21.13%), and significantly lower SAGE weights for gadobutrol (EV: 7.75%; FAERS: 13.31%) and gadoterate meglumine (EV: 8.66%; FAERS: 12.99%). The SOCs "skin and subcutaneous tissue disorders", "musculoskeletal and connective tissue disorders", "general disorders and administration site conditions" and "psychiatric disorders" were consistent with this ranking, with gadoteridol showing alternately a SAGE profile aligned on the linear GBCA or on the other macrocyclic GBCAs.

#### **CONCLUSION**

This study showed that SAGE symptoms represent a significant percentage of the bulk of adverse events reported to the health authorities for each GBCA. It provided real-life arguments suggesting that SAGE symptoms may be more prevalent with linear than macrocyclic GBCAs, and that gadoteridol may present a higher SAGE risk than the other macrocyclic contrast agents.

#### **CLINICAL RELEVANCE/APPLICATION**

This study investigates, in EMA and FDA pharmacovigilance databases, the proclivity of symptoms associated with gadolinium

This study investigated, in a multi-center, retrospective analysis, the presence of symptoms associated with gadolinium exposure (SAGE) in patients exposed to gadolinium-based MRI contrast agents.

### **R5A-SPNR-6 Variation in Prices for Outpatient Brain MRI in the US**

Participants

Kinpritma Sangha, PhD, MPH, (*Presenter*) Employee, Siemens AG

#### **PURPOSE**

The 2021 Hospital Price Transparency Rule was implemented to require hospitals to publish payer-specific negotiated commercial prices for medical services. Payer-negotiated prices vary across the country and are based on hospital and state characteristics, with the greatest markup from mean negotiated prices compared with Medicare reimbursement to be for magnetic resonance imaging (MRI). The objective of this study was to analyze the variation in MRI brain exam prices and to estimate the association between state characteristics and the median MRI brain exam price in the US.

#### **METHODS AND MATERIALS**

This cross-sectional study examined MRI brain exam prices in the hospitals across US using payer-negotiated prices from the Turquoise Health dataset. MRI brain exam, as a billable service, was identified using the Current Procedural Terminology (CPT) code of 70551. Price variance analysis was performed for all states and characteristics including Herfindahl-Hirschman Index (HHI) and certificate of need (CON) program in the state. Multivariable regression analyses were conducted to determine factors that impact brain MRI exam price among the states.

#### **RESULTS**

A total of 2504 hospitals disclosed the payer-negotiated prices in 2021 Turquoise Health dataset for brain MRI exams. The greatest price variation in brain MRI exams was for commercial payers with median price of \$1531, ranging from \$3230 to \$611.57. Alaska, with the least number of hospitals, has the highest median price of \$3230, while New York, with 84 hospitals has the lowest median price of \$611.57. States with the CON program had a higher median price (by \$164) than states without the CON program and states with a high HHI index (HHI>6000), indicating a less competitive market, have a higher median price (by \$412) than states with a more competitive market. Both the number of health systems in the state ( $p=0.001$ ) and having commercial payers ( $p=0.000$ ) were found to be statistically significant in affecting impact the median MRI brain exam prices.

#### **CONCLUSION**

While MRI brain exam prices vary throughout the US, more health systems and commercial payers in the state drive the prices higher.

#### **CLINICAL RELEVANCE/APPLICATION**

This study helps to understand the factors affecting price variation in brain MRIs in the US.

### **R5A-SPNR-7 Clinical Evaluation of Scout Accelerated Motion Estimation and Reduction (SAMER) For Brain MRI in an Emergency and Inpatient Setting**

Participants

Azadeh Tabari, MD, Boston, MA (*Presenter*) Nothing to Disclose

#### **PURPOSE**

A navigation-free retrospective motion-correction method (SAMER) has been developed to achieve rapid motion estimation and correction. In this work, we performed an initial evaluation of SAMER in a clinical setting

#### **METHODS AND MATERIALS**

In this prospective IRB approved and HIPAA compliant study, 97 patients from emergency and inpatient care settings were scanned on a 3T system (MAGNETOM Skyra, Siemens) using a 20-channel head-neck coil, between August 2021 and January 2022. The imaging protocol included a 4-fold accelerated T1-weighted MPRAGE sequence, which was acquired using a custom linear+checkered sequence reordering. This sequence was incorporated into routine brain MRI to assess the performance of motion correction on non-contrast and contrast-enhanced exams. Retrospective reconstructions of the MPRAGE data were performed with and without SAMER motion correction. All 97 cases were reviewed by two neuroradiologists in a blinded manner to rate the impact of motion artifacts on diagnostic image quality using a previously published 5-tier scale (None, minimal, mild, moderate, severe). Discrepancies in the two neuroradiologists' scores were adjudicated by a third neuroradiologist

#### **RESULTS**

There was no significant difference in the performance of motion correction between the contrast-enhanced ( $n=58$ ) and non-contrast ( $n=42$ ) exams ( $p>0.05$ ). Six (6.1%) of cases showed no motion, 46 (47.4%) showed minimal motion, 30 (31%) showed mild motion, 8 (8.2%) showed moderate motion, and 10 (10.3%) showed severe motion. The prevalence of repeat sequences was 3% of total MRI examinations. Following motion correction with SAMER, there was a significant improvement in motion score ( $P<0.005$  for both raters). The motion score improvement was defined as the pre-correction motion score minus the post-correction score. For cases with motion scores of "none" or "minimal", SAMER had negligible impact on the motion score. For cases with "mild", "moderate", and "severe" motion, SAMER improved the motion score by an average score of 0.36, 1.1, and 1.2 points, respectively

#### **CONCLUSION**

SAMER improves diagnostic image quality of clinical brain MR exams in the presence of motion, and the improvement is most pronounced when motion is moderate or severe

#### **CLINICAL RELEVANCE/APPLICATION**

Motion artifacts are common in emergency and inpatient brain MRI exams. SAMER demonstrates utility in a clinical setting to reduce motion artifacts in these studies, which may facilitate timely diagnosis and require fewer repeat sequences and callbacks for critically ill patients

### **R5A-SPNR-8 Preoperative Visualization of the Transverse and Sigmoid Sinuses Using Non-contrast Virtual**

## Monochromatic CT Images for the Lateral Suboccipital Retrosigmoid Approach

Participants

Tomomi Omura, Akita, Japan (*Presenter*) Nothing to Disclose

### PURPOSE

In the surgical planning of suboccipital retrosigmoid craniotomy, it is important for neurosurgeons to recognize tortuosity of the transverse and sigmoid sinuses and their relationship to superficial landmarks including asterion. This study aimed to improve the depiction of those venous sinuses in preoperative non-contrast (NC) virtual monochromatic images (VMIs).

### METHODS AND MATERIALS

Thirty-one patients (24 women and 7 men; mean age, 63 ± 19 years) who underwent NCCT retrosigmoid craniotomy were included. The NCCT was scanned using dual-source CT (SOMATOM Drive, Siemens Healthineers, Forchheim, Germany). The NC-DECT images were acquired at a kV-pair of 80 kV and 140 kV with tin-filtration at about 70 mGy using automatic exposure control. Mixed-120 kV images were synthesized by compositing both kV images. The native VMIs were generated at 40, 70, 100, 130, 160, and 190 keV using a CT vendor's workstation. In the reconstructed sagittal section of each image, a circular region of interest (ROI) was set in the transverse sinus and cerebral cortex as a reference. Standard deviation (SD) and attenuation value (HU) were measured in each ROI to obtain the difference in HU values between the transverse sinus and cerebral cortex ( $\Delta$ HU) and contrast-to-noise ratio (CNR).

### RESULTS

The median  $\Delta$ HU for each VMI was increased with higher keV, and each  $\Delta$ HU for 100, 130, 160, and 190 keV was significantly higher than that for Mixed-120 kV (9.6, 10.3, 10.5, and 11.0 HU for 100, 130, 160, and 190 keV respectively, and 8.8 HU for Mixed-120 kV,  $P < 0.001$  for each). The median CNR for each VMI was also increased with higher keV, and each CNR for 100, 130, 160, and 190 keV was significantly higher than that for Mixed-120 kV (6.8, 6.8, 6.7, and 7.3 for 100, 130, 160, and 190 keV respectively, and 3.2 for Mixed-120 kV,  $P < 0.001$  for each).

### CONCLUSION

Both  $\Delta$ HU and CNR of transverse sinuses were improved at VMIs above 100 keV. The results suggest that high keV VMIs improve visualization of the transverse sinus and are useful in surgical planning for suboccipital retrosigmoid craniotomy.

### CLINICAL RELEVANCE/APPLICATION

High keV VMI is less susceptible to beam hardening, so structures and findings adjacent to bone are clearly delineated.

## R5A-SPNR-9 Blood-Brain Barrier Dysfunction in Patients with Heart Failure

Participants

Kamlesh Jobanputra, MD, Birmingham, AL (*Presenter*) Nothing to Disclose

### PURPOSE

Heart failure (HF) patients show brain tissue injury in sites that mediate autonomic, cognitive, and mood functions, which are deficient in HF and are linked with increased morbidity and mortality and poor quality of life in the condition. However, the pathological mechanisms that may contribute to brain tissue injury in HF are unclear, but blood brain barrier (BBB) disruption might be one of the processes that contribute to brain injury. Our aim was to examine BBB function, based on diffusion-weighted pseudo-continuous arterial spin labeling (DW-pCASL) procedures, in HF and healthy control subjects.

### METHODS AND MATERIALS

We performed DW-pCASL imaging in 25 HF [age, 55.4±7.4 years; body-mass-index (BMI), 27.2±4.3 kg/m<sup>2</sup>; 18 male; NYHA functional class II/III, LVEF <40%] and 56 healthy controls (age, 51.7±9.0 years; BMI, 26.8±3.7 kg/m<sup>2</sup>; 31 male) using a 3.0-Tesla MRI scanner (Siemens, Magnetom, Prisma Fit). Using DW-pCASL data, arterial transit time (ATT, an index of large artery integrity) and water exchange rate across the BBB (K<sub>w</sub>, BBB function) were quantified and whole-brain ATT and K<sub>w</sub> maps were generated. Whole-brain ATT and K<sub>w</sub> maps were normalized to Montreal neurological institute space, smoothed, and compared voxel-by-voxel between HF and control groups using analysis of covariance (ANCOVA; covariates: age, sex; SPM12, uncorrected  $p < 0.005$ ). Brain clusters with significant differences between groups were overlaid onto background images for structural identification.

### RESULTS

No significant differences in age ( $p = 0.08$ ), sex ( $p = 0.16$ ), or BMI ( $p = 0.65$ ) appeared between groups. Multiple brain areas, which are involved in cognitive, mood, autonomic functions, showed altered K<sub>w</sub> and ATT values in HF over health controls. Increased K<sub>w</sub> values were observed in the insular cortices, hippocampus, thalamus, occipital cortices, cerebellar vermis, and other cortices and white matters regions. ATT values were decreased in the prefrontal, temporal, and occipital cortices, and mid brain, and increased in few areas, including the insular cortices and cerebellum in HF patients.

### CONCLUSION

HF patients show compromised BBB function and altered large artery integrity. BBB alterations may introduce neural damage in autonomic, mood, and cognitive regulatory areas, contributing to abnormal functions in HF. The findings suggest a need to repair BBB function in HF with strategies commonly used in other acute and chronic conditions.

### CLINICAL RELEVANCE/APPLICATION

Management of neurologic symptoms in patients with heart failure is complex. Translational research focused on need for blood brain barrier repairing strategies in HF patients with brain injury may open new avenues of disease prevention and limiting progression.

Printed on: 02/07/23



## Abstract Archives of the RSNA, 2022

R5A-SPNR-1

### A Fully Automated and Quantifiable Visual Grading System for WMH Utilizing a Rule-Based Algorithm: The Modified Fazekas Scale Using T2-Fluid Attenuated Inversion Recovery Magnetic Resonance Imaging

Thursday, Dec. 1 12:15PM - 12:45PM Room: Learning Center - NR DPS

#### Participants

ZunHyan Rieu, BS, Seoul, Korea, Republic Of (*Presenter*) Employee, NEUROPHET, Inc

#### PURPOSE

White matter hyperintensities (WMH) have become the primary biomarker for small-vessel cerebrovascular diseases and brain atrophy. The Fazekas and Scheltens scales are the most conventional visual grading system for WMH and have been practiced by radiologists worldwide. However, in clinical practice, it is still challenged by the labor-intensive process and non-standardized criteria for measuring the irregular shapes of WMHs, which tend to be evaluated with one's subjective opinion. Therefore, we aim to fully automate the visual grading system for WMH with only the numerically quantifiable measurement using the modified Fazekas scale, Clinical Research Center for Dementia of South Korea (CREDOS) criteria, which suggests the visual grading system for WMH with the combination of diameter measurements between deep white matter hyperintensity (DWMH) and periventricular hyperintensity (PVMH).

#### METHODS AND MATERIALS

Our approach involves four stages, including brain tissue and WMH segmentation using the deep learning algorithm, WMH separation into periventricular hyperintensity and deep white matter hyperintensity using a rule-based algorithm, diameter measurement of WMH, and Fazekas scale prediction. For validation, we compared the performances of our proposed method and that of the CREDOS criteria-based visual grading system for WMH done by three certified radiologists using a total of 404 subjects with T2-fluid attenuated inversion recovery magnetic resonance imaging (T2-FLAIR) utilized from a clinical site in Korea.

#### RESULTS

The inter-rater agreements using Krippendorff's alpha were comparable between the radiologists (R) and all methods (A), including our approach. The agreements were substantial (R, 0.732 vs. A, 0.694), substantial (R, 0.671 vs. A, 0.658), and moderate (R, 0.586 vs. A, 0.579) for the modified Fazekas scale, the DWMH scale, and the PVMH scale, respectively. In addition, the total mean of areas under the receiver operating characteristic curve between radiologists (G) and radiologists against our approach (P) showed comparable performance (G,  $0.80 \pm 0.09$  vs. P,  $0.80 \pm 0.03$ ).

#### CONCLUSION

Our approach, a fully automated and quantifiable visual grading system for WMH, demonstrated comparable results against the radiologists.

#### CLINICAL RELEVANCE/APPLICATION

We believe our approach has a great potential to assist the radiologist in clinical findings.

Printed on: 02/07/23

## Abstract Archives of the RSNA, 2022

R5A-SPNR-10

### Optimization of 3D Head SNAP Angiography Based on Compression Sensing Technology

Thursday, Dec. 1 12:15PM - 12:45PM Room: Learning Center - NR DPS

#### Participants

Yukun Zhang, Dalian, China (*Presenter*) Nothing to Disclose

#### PURPOSE

To optimize simultaneous non-contrast angiography and intraplaque hemorrhage (SNAP), we combined SNAP and compressed sensing (CS SNAP) and identified the optimal acceleration factors (AFs) for clinical use to obtain high-quality MRA and vascular wall images capable of whole brain coverage in a short time.

#### METHODS AND MATERIALS

30 healthy volunteers (13 males, 17 females, mean age 43.33 ±18.76 years) were prospectively recruited in this study. Among them, 10 volunteers performed the pre-scan for selecting a precise head 3D SNAP parameters (Table.1) at 3.0 Tesla (Philips Ingenia CX 3.0T MRI); The remaining 20 volunteers scanned with different CS AFs of 2,2.5,3,4,5 on the basis of the optimized pre-scan sequence (Table.2). Two radiologists delineated the region of interest (ROI) on all of the original images, measured the signal intensity (SI) and standard deviation (SD) for the vascular lumen, vascular wall and white matter (Fig.1). Signal to noise ratio (SNR) and contrast to noise ratio (CNR) of vascular lumen, contrast-to-tissue ratio (CTR) and CTR efficiency (CTReff) of the vascular wall were further calculated; at the same time, The image quality of each dataset was scored subjectively by two radiologists (Table.3). The consistency of measurements and subjective scores of the two observers was analyzed using Kappa and intraclass correlation coefficient (ICC) test. Compare and analyze the differences in measurement parameters and subjective scores between different AFs.

#### RESULTS

The measured data and subjective scores of the two observers were in good agreement (Kappa: 0.568-0.884, ICC: 0.602-0.968). when CS AF=4, the SNR and CNR of vascular lumen, and subjective score were significantly different from SNAP without CS ( $p<0.05$ ). When CS AF =2.5, 3, 4, 5, the CTReff of vascular wall were significantly different compared with SNAP without CS ( $p<0.05$ ) (Table.4, Fig.2).

#### CONCLUSION

s 3D CS SNAP can obtain whole cerebrovascular MRA and vascular wall images in a relatively short period of time, and AF of 3 is recommended as its optimized sequence (Fig.5).

#### CLINICAL RELEVANCE/APPLICATION

3D CS SNAP technology has the potential to apply to multi-contrast blood imaging protocols, allowing for the acquisition of whole cerebral angiography and vascular wall images in relatively short periods of time.

Printed on: 02/07/23

## Abstract Archives of the RSNA, 2022

R5A-SPNR-11

### Pharmacokinetics, Safety and Tolerability of the Novel Tetrameric, High Relaxivity, Macrocyclic Gadolinium-based Contrast Agent Gadoquatrane for CE-MRI

Thursday, Dec. 1 12:15PM - 12:45PM Room: Learning Center - NR DPS

#### Participants

Birte Hofmann, DVM, PhD, Berlin, Germany (*Presenter*) Employee, Bayer AG

#### PURPOSE

Gadoquatrane (BAY 1747846) is a novel tetrameric, macrocyclic gadolinium (Gd)-based contrast agent (GBCA) featuring a unique tetrameric structure and high relaxivity. The present study investigated its pharmacokinetics (PK) including excretion pathways, safety and tolerability in healthy volunteers.

#### METHODS AND MATERIALS

This first-in-human study was conducted as a randomized, single-blind, placebo-controlled, single dose study with 6 consecutive dose cohorts consisting of 8 to 9 healthy young women and men (N=49 total). Gadoquatrane or matching placebo (NaCl 0.9%) were intravenously administered by either infusion (doses of 0.025, 0.05, or 0.1 mmol Gd/kg bw) or bolus injection (doses of 0.03, 0.1 or 0.2 mmol Gd/kg bw). Safety and tolerability were assessed over 7 days post injection (p.i.) including adverse events, cardiac and respiratory function and safety laboratory analyses. Plasma PK and excretion in urine and feces were investigated over 72 h p.i. by ICP-MS as well as HPLC-ICP-MS.

#### RESULTS

Demographics were well balanced, with no notable differences between cohorts (24 ♀, 25 ♂; mean age ( $\pm$ SD) of 34.6 $\pm$ 6.3 years; mean BMI ( $\pm$ SD) of 23.4 $\pm$ 2.57 kg/m<sup>2</sup>). Plasma concentrations declined rapidly due to fast extracellular distribution and elimination, with no relevant gender differences. AUC and C<sub>max</sub> increased dose proportionally, volume of distribution (0.21-0.24 L/kg) and plasma clearance (0.09-0.1 L/h/kg) remained constant. Excretion via the kidneys was essentially complete (80-100%) within 12 h p.i.. No metabolites were detected in plasma or urine. Incidence and severity of treatment emergent adverse events (TEAEs) were similar in all dose groups incl. placebo. Intensity of most study drug related TEAE was mild, few were of moderate intensity, and none severe; all were recovered or recovering at 7 days p.i..

#### CONCLUSION

The novel high relaxivity, tetrameric, macrocyclic GBCA gadoquatrane was very well tolerated at all doses. The PK profile is essentially the same as for other extracellular macrocyclic GBCAs (like gadobutrol or gadoterate meglumine). Gadoquatrane has the potential to be used at substantially lower Gd doses in clinical routine compared to currently marketed extracellular GBCAs.

#### CLINICAL RELEVANCE/APPLICATION

The novel, tetrameric gadoquatrane is a promising GBCA in development for MRI and its profile incl PK, safety, high relaxivity and stability meets the clinical demand to reduce the gadolinium dose.

Printed on: 02/07/23

## Abstract Archives of the RSNA, 2022

R5A-SPNR-13

### Investigation of Image Quality of Different Monochromatic Energy Images in Spectral CT Scan: A Phantom Study

Thursday, Dec. 1 12:15PM - 12:45PM Room: Learning Center - NR DPS

#### Participants

Yaoping Ma, (*Presenter*) Nothing to Disclose

#### PURPOSE

Objective to explore the influence of different monochromatic energy images on the quality of energy spectrum images.

#### METHODS AND MATERIALS

A polypropylene cylindrical phantom (QSP Phantom dimension) with five tubes containing different concentrations of iodine (0, 2.5, 5, 10, 20 mg/ml) was scanned using a spectral CT (Revolution CT, GE Healthcare) in gemstone spectral imaging (GSI) mode using fast kV switch (80/140 kV), the tube current was 485mA, the layer thickness was 1.25mm, the collimation width was 80mm, noise index (NI) 9, pitch 0.992:1. The CT and SD values were measured at 11 different central planes, the region of interest (ROI) of the phantom tube with iodine concentration of 20% was delineated, The area of ROI was 1 / 2-1 / 3 of the cross-sectional area of the phantom tube. The CT values and noise of 40 keV, 70 keV, 100 keV and 130 keV groups were measured and recorded by GSI viewer. One way ANOVA was used to compare the CT value and noise of iodine 20 phantom tube under different keV. LSD-t test was used to compare the two groups.

#### RESULTS

With the increase of monochromatic energy level, the CT value and noise of the images gradually decreased. The CT value of 40 keV, 70 keV, 100 keV and 130 keV groups were 1546.34±3.13HU, 490.13±1.60HU, 215.71±1.28HU, 121.52±18HU, the difference was statistically significant ( $P < 0.05$ ); The noise of 40 keV, 70 keV, 100 keV and 130 keV groups was 25.46±2.89HU, 11.44±1.3HU, 7.83±0.92HU, 6.62±0.75HU, the difference was statistically significant ( $P < 0.05$ ).

#### CONCLUSION

s With the increase of monochromatic energy level, the CT value and noise of the images gradually decrease, and monochromatic energy images in spectral CT scan can optimize the image quality.

#### CLINICAL RELEVANCE/APPLICATION

Through the basic research of phantom, compared with conventional kVp scanning, energy spectrum CT scanning can provide the same image quality scanning radiation dose. At the same time, compared with conventional kVp scanning, energy spectrum CT scanning can provide different levels (40-140keV) of single energy and effective atomic coefficient, and more energy spectrum information of base material. This study has guiding significance for the application of energy spectrum scanning in different clinical scenes.

Printed on: 02/07/23

## Abstract Archives of the RSNA, 2022

R5A-SPNR-15

### Study on the Image Quality of Head and Neck CTA With Energy Spectrum Combined With Iterative Reconstruction Method

Thursday, Dec. 1 12:15PM - 12:45PM Room: Learning Center - NR DPS

#### Participants

Deng Jie, (*Presenter*) Nothing to Disclose

#### PURPOSE

To investigate the influence and application value of spectral CT single-energy imaging combined with adaptive iterative reconstruction (ASIR) technology on head and neck CT angiography (CTA).

#### METHODS AND MATERIALS

88 patients undergoing head and neck CTA examination were compared using energy spectrum combined with adaptive iterative 40% ASIR scanning, and reconstructed single-energy 40keV, 60 keV, 80 keV, and performed vascular surface reconstruction (CPR) and maximum density projection on the three groups of images. Processing (MIP). The effects of different reconstruction methods on the image quality of head and neck CTA were evaluated from the two aspects of objective measurement and subjective score.

#### RESULTS

Objective evaluation: The CT values, SD values, SNR values, and CNR values of the aortic arch, common carotid artery, middle cerebral artery, vertebral artery, and basilar artery measured under the three reconstruction methods were all statistically different ( $P<0.05$ ). Subjective evaluation: The Kappa value of the subjective evaluation of the image reconstruction quality by the physicians of the two diagnosis groups in each group was 0.75, showing strong consistency. There was no statistical difference in the scores of MIP reconstruction images among the groups ( $P=0.467$ ). There was a statistically significant difference in the scores of CPR reconstruction images among the groups ( $P<0.05$ ).

#### CONCLUSION

s In the image quality of head and neck CTA examination, the single energy spectrum of 60keV combined with adaptive iterative 40% ASIR scanning can reduce image noise and improve the image signal-to-noise ratio. be applied.

#### CLINICAL RELEVANCE/APPLICATION

When applied to head and neck CTA, the single energy spectrum of 60keV combined with adaptive iterative 40% ASIR scan has the best image quality, which can be used in clinical practice.

Printed on: 02/07/23

## Abstract Archives of the RSNA, 2022

R5A-SPNR-16

### Predicting Early Glioma Recurrence With Peritumoral Radiomic Features From Amide Proton Transfer Weighted MR Images

Thursday, Dec. 1 12:15PM - 12:45PM Room: Learning Center - NR DPS

#### Participants

Shanshan Jiang, MD, PhD, Baltimore, MD (*Presenter*) Nothing to Disclose

#### PURPOSE

Because of the basement membrane barrier effect, diffuse infiltration of tumor cells into surrounding brain tissue has been proved a significant factor for migration/invasion of malignant gliomas. However, the peritumoral areas have been rarely studied for post-surgery/chemoradiation malignant gliomas. Amide proton transfer-weighted (APT<sub>w</sub>) MRI, a method generating the MRI contrast dominated by endogenous cellular proteins, has showed an encouraging diagnostic performance for gliomas. The goal was to evaluate the power of APT<sub>w</sub>-based peritumoral radiomics for classification of treatment effects and tumor recurrence.

#### METHODS AND MATERIALS

A total of 90 patients with post-treatment malignant gliomas were retrospectively re-assessed. Diagnosis of tumor recurrence vs. treatment effects was based on the integrated clinical pathologic results or the updated RANO criteria. The sequences included T1<sub>w</sub>, T2<sub>w</sub>, FLAIR, APT<sub>w</sub>, and gadolinium contrast-enhanced T1<sub>w</sub> (T1<sub>w</sub>-Gd). After imaging preprocessing, radiomic features were extracted from the peritumoral regions, which were segmented manually covering abnormal FLAIR/T2<sub>w</sub> signal intensities outside the gadolinium-enhancing tumor core. A current reality tree (CRT) model was constructed to identify the most critical features when differentiating tumor recurrence from treatment effects. The alpha level of all tests was set at  $P < 0.05$ .

#### RESULTS

29 vs. 61 patients were confirmed, respectively, as treatment effect or tumor recurrence. The CRT model achieved accuracies of 83.3% with radiomic features extracted from FLAIR, 90.0% with those from APT<sub>w</sub>, and 91.1% with those from both FLAIR and APT<sub>w</sub>. The 90 percentile APT<sub>w</sub> value was listed as the most important feature to distinguish these two entities in both decision trees based on APT<sub>w</sub> and FLAIRAPT<sub>w</sub> MRI models.

#### CONCLUSION

s APT<sub>w</sub>-derived radiomic features are capable of capturing the progressive pattern in peritumoral areas, aiding in the accurate treatment response assessment in post-treatment malignant gliomas by increasing detection specificity.

#### CLINICAL RELEVANCE/APPLICATION

Our results suggest that the use of APT<sub>w</sub> MR images radiomic features from peritumoral area can add important value to structural MRI to assess the early treatment response.

Printed on: 02/07/23

## Abstract Archives of the RSNA, 2022

R5A-SPNR-18

### Newly Developed Iterative Motion Correction (IMC) for Brain MRI: Utility for Reducing Motion Artifacts and Improving Image Quality without Any Affection to Examination Time in Uncooperative Patients

Thursday, Dec. 1 12:15PM - 12:45PM Room: Learning Center - NR DPS

#### Participants

Kazuhiro Murayama, MD, Toyoake, Japan (*Presenter*) Research Grant, Canon Medical Systems Corporation

#### PURPOSE

To determine the utility of newly developed iterative motion correction (IMC) method for reducing motion artifact and improve image quality without any affection to examination time in uncooperative patients.

#### METHODS AND MATERIALS

65 patients suspected of cerebrovascular disease obtained fluid attenuated inversion recovery (FLAIR) images with and without IMC at 3T systems. Based on FLAIR image without IMC results, all patients were divided into cooperative (n=19) and uncooperative (n=46) patient groups. To compare examination and reconstruction time differences, these times were recorded in all patients. To assess the capability for image quality improvement between FLAIR images with and without IMC, SNR of normal appearance white matter (NAWM), CNR between gray matter and NAWM, and CNR between NAWM and deep and subcortical white matter hyper intensity (DSWMH) abnormalities were determined by ROI measurements on each FLAIR. Moreover, overall image quality, artifact and lesion conspicuity in each group were assessed by 5-point scales by two board-certified radiologists. To compare examination and reconstruction time between two methods, Wilcoxon signed-rank test was performed. For image quality comparisons, SNR and CNRs were compared between FLAIRs with and without IMC in cooperative and uncooperative groups by Student's t-test. To determine interobserver agreements for all indexes, kappa statistics with ?2 test were performed. Then, each qualitative score was also compared between FLAIRs with and without IMC by Wilcoxon's signed sum test.

#### RESULTS

Mean examination and reconstruction times of FLAIR with IMC ( $256.3 \pm 2.7$  sec) were significantly longer than those of FLAIR without IMC ( $217.0 \pm 0.59$  sec,  $p < 0.0001$ ). SNR and CNRs of FLAIRs with IMC was significantly higher than that without IMC in uncooperative group ( $p < 0.05$ ). Interobserver agreements for each qualitative image quality score were assessed as substantial or excellent in each group ( $0.74 \leq \kappa \leq 0.91$ ,  $p < 0.001$ ). Each qualitative image quality score of FLAIR with IMC was significantly higher than that without IMC in uncooperative group ( $p < 0.05$ ).

#### CONCLUSION

The IMC technique has a potential for reducing motion artifacts and improving image quality on brain MRI with less than 1 minute prolongation of examination and reconstruction times in uncooperative patients.

#### CLINICAL RELEVANCE/APPLICATION

The IMC technique has a potential for reducing motion artifacts and improving image quality on brain MRI in uncooperative patients.

Printed on: 02/07/23



## Abstract Archives of the RSNA, 2022

R5A-SPNR-19

### Natural Language Processing for Extraction of Glioblastoma and Patient Characteristics from Radiology Reports

Thursday, Dec. 1 12:15PM - 12:45PM Room: Learning Center - NR DPS

#### Participants

Ahmad Amer, BS, North Chicago, IL (*Presenter*) Nothing to Disclose

#### PURPOSE

Glioblastoma (GBM) is an aggressive primary brain tumor with a median survival of 15 months. To assist with data extraction and evaluation of potential prognostic factors, natural language processing (NLP) was applied to automate extraction of patient and tumor data from one of the largest GBM patient populations at MD Anderson Cancer Center (MDACC).

#### METHODS AND MATERIALS

The radiology information system (RIS) was used to identify 4511 patients with a pathology-confirmed GBM diagnosis presenting to MDACC from 2006-2021. 50,202 corresponding radiology reports were identified, and Python was used for report processing. Identification of specific strings and aggregation by MRN allowed for determination of tumor multicentricity, extent of resection, and patient handedness. A similar approach was applied to extract tumor location, with separate strings used for lobe and laterality. Primary and secondary lobe were determined based on occurrence frequency of lobe-specific strings. Patient survival was estimated by determining the time difference between patients' first report mentioning GBM and last report. Extraction of pre-op tumor volume first required isolation of pre-op reports. A subset of such reports were extracted by selecting reports with pre-op-specific phrases in the examination section. Next, reports nearest to and within a week prior to intra-op dates were extracted. Intra-op dates were determined by searching reports' examination sections for intra-op-specific strings and extracting surgery dates with Regex. Reports occurring prior to suspicion or diagnosis of GBM were excluded. The syntax of remaining reports were then analyzed using a pre-trained SciSpacy model, and sentences without tumor-related strings were excluded. Tumor dimensions were extracted using Regex and used to calculate tumor volume. Manual validation was performed for OS, volume, and location.

#### RESULTS

NLP characterized patients as long-term survivors with 94.7% sensitivity, 97.6% specificity, and an ROC-AUC of .953. Quantitative analysis yielded a mean absolute error of 19.40%. Lobe and laterality were 98% and 90% accurate respectively. Successful extraction of all tumor dimensions for volume calculation was achieved in 72.5% of cases.

#### CONCLUSION

s Automated extraction of tumor lobe, laterality, multicentricity, extent of resection, volume, and OS and handedness was accomplished. OS and location data were highly accurate.

#### CLINICAL RELEVANCE/APPLICATION

NLP was successfully applied to extract data for the investigation of prognostic factors of GBM, which could lead to improvements in patient management and inform expectations of care.

Printed on: 02/07/23

## Abstract Archives of the RSNA, 2022

R5A-SPNR-2

### A Novel Connectomic Analysis Framework for Personalised Presurgical Planning using Multimodal Neuroimaging

Thursday, Dec. 1 12:15PM - 12:45PM Room: Learning Center - NR DPS

#### Participants

Ruchi Sharma, MS,BS, Bhopal, madhya Pradesh, India (*Presenter*) Nothing to Disclose

#### PURPOSE

The traditional method of surgical selection and planning in brain tumours was based mostly on the topography of the tumour. With recent advances, connectomics promises to provide comprehensive information by integrating the inferences from network mapping, tractography, and tumour segmentation. This information helps neurosurgeons develop new insights and an optimal strategy for tumour resection. We present a novel, automated connectomic analysis framework that integrates rs-fMRI, DWI and sMRI (T1w, FLAIR, and T1CE) modalities to determine the effect of a tumor on the individual's structural and functional connectivity, assisting in presurgical planning.

#### METHODS AND MATERIALS

A study was conducted on 15 tumor subjects who underwent the above mentioned MR modalities prior to surgery. Three groups of five subjects underwent tb-fMRI for Motor, Visual, and Language tasks. For each subject, our framework analysed the multiple modalities using the following techniques - multivariate statistical analysis on rs-fMR images to generate major functional networks, deep learning-based segmentation strategy on sMR images for tumour demarcation, and whole-brain probabilistic tractography on DWI for generation of major fibre tracts. Additionally, the framework reports the tumor's proximity to the generated functional network and white matter tracts using a heuristic algorithm.

#### RESULTS

Connectomic profiles were generated for all the subjects. For the five subjects that underwent tb-fMRI, all the network maps produced by rs-fMRI and tb-fMRI yielded similar activations in the corresponding network regions. The heuristic algorithm used to report the distance between the tumours, network maps, and tracts were highly useful in deciding the trajectory of operation.

#### CONCLUSION

s The connectomic profile for the clinical cases using network maps, fibre tracts, and tumor demarcation proved to be highly beneficial in the personalised presurgical planning. The validation of rs-fMRI against tb-fMRI also helped to mindfully perform the surgery to avoid functional loss of major networks.

#### CLINICAL RELEVANCE/APPLICATION

This study proposes a multimodal connectomic analysis method to produce personalised presurgical insights for tumor patients which helps in taking critical decisions for operating the tumor with a better understanding of the anatomical, functional and surgical complexities which is highly beneficial.

Printed on: 02/07/23

## Abstract Archives of the RSNA, 2022

R5A-SPNR-20

### Perfusion-Based Radiomics Enable to Predict Thrombolysis/Thrombectomy Related Hemorrhagic Transformation in Patients With Acute Stroke: Development and Validation

Thursday, Dec. 1 12:15PM - 12:45PM Room: Learning Center - NR DPS

#### Participants

Yunhwa Roh, (*Presenter*) Nothing to Disclose

#### PURPOSE

Prompt diagnosis and early detection of hemorrhagic transformation (HT) may prevent dismal prognosis in acute stroke patients. We aimed to develop and validate a radiomics-based model for predicting thrombolysis/thrombectomy-related HT in patients with acute ischemic stroke using multiparametric MRI of conventional, diffusion-, and perfusion-weighted imaging.

#### METHODS AND MATERIALS

In this retrospective study, a radiomics model was developed in a consecutive 462 patients diagnosed with acute ischemic stroke and who underwent multiparametric MRI between 2017 to 2018 and tested in an independent validation set of 276 patients between 2019 to 2021. For each patient, 140 radiomics features were extracted from FLAIR and GRE image, DWI, and perfusion-weighted imaging including CBF, CBV, K2, MTT, Tmax, and TTP maps. HT was classified as either presence of HT (HT) or the presence of parenchymal hemorrhage (PH). Radiomics features for predicting outcomes were selected using random forest, and the model was developed by using logistic regression classifier. The diagnostic performance was calculated and compared among imaging sequences in the independent validation set using the area under the curve (AUC) from a receiver operating characteristic curve analysis, sensitivity, specificity, and accuracy.

#### RESULTS

For predicting HT, 8 out of 10 top features were from perfusion-weighted imaging using variable importance including TTP, CBF, and Tmax. For predicting PH, 8 out of 10 top features were from perfusion-weighted imaging including CBV, CBF, MTT, and K2. Volume and compactness of DWI and FLAIR also become significant predictors. In the test cohort, the perfusion-based radiomics model significantly improved performance (AUC 0.725) compared with DWI or FLAIR alone (AUC 0.665 and 0.679, respectively) for predicting HT. For predicting PH, the perfusion-based radiomics model also significantly improved performance (AUC 0.732) compared with DWI or FLAIR alone (AUC, 0.693 and 0.702, respectively).

#### CONCLUSION

s Utilizing perfusion-weighted imaging for the radiomics model significantly improved the prediction of hemorrhagic transformation as well as parenchymal hemorrhage in patients with acute stroke.

#### CLINICAL RELEVANCE/APPLICATION

HT following cerebral ischemia has been postulated to result in a negative impact on the clinical course. A radiomics model that utilized perfusion-weighted imaging showed improved diagnostic performance for predicting hemorrhagic transformation than conventional imaging or diffusion-weighted imaging alone. These findings support the role of perfusion MRI in identifying patients who are at increased risk for secondary HT following acute ischemic stroke and may assist patient management for clinicians.

Printed on: 02/07/23

## Abstract Archives of the RSNA, 2022

R5A-SPNR-3

### Disorganized Subcortical Functional Gradients in Schizophrenia and the Treatment Effects After Administration of Antipsychotics

Thursday, Dec. 1 12:15PM - 12:45PM Room: Learning Center - NR DPS

#### Participants

Chengmin Yang, (*Presenter*) Nothing to Disclose

#### PURPOSE

Growing evidence indicates that subcortex is pivotal in the pathophysiology of schizophrenia, and changes in subcortical regions were also sensitive indicators of pharmacological treatments. However, how the subcortex embeds within the macroscale cortical system, and the structural constraints and functional emergences of spatial arrangements, remain unclear. The new concept of gradients focused on spatial relationships, which revealed that macroscale gradients integrated systematic information into more abstract representations. Exploring the subcortex in the broader cortical landscape as well as investigating its feature as treatment target in schizophrenia is promising for its extensive connections with the entire cerebral cortex.

#### METHODS AND MATERIALS

Leveraging connectome gradients, we systematically scrutinized abnormalities of functional connectome gradient in antipsychotic-naïve first-episode schizophrenia patients (FES0W, n = 57) at baseline, comparing to healthy controls (HCs, n = 64), as well as longitudinal comparisons of baseline with 6-week (FES6W, n = 19) and 12-month (FES12M, n = 57) follow-up, respectively. And further examined the reproducibility in an independent validation sample (vFES0W, n = 22; HCs, n = 25), and the patients with 6-week (vFES6W, n = 22) follow-up. Correlational analyses were conducted between the longitudinal functional gradient alterations and the psychopathological ratings, including Positive and Negative Syndrome Scale (PANSS) and Global Assessment of Functioning (GAF) scores.

#### RESULTS

In both primary and validation datasets, patients at baseline showed the higher gradients mainly in limbic system and lower gradients in thalamus and caudate, and the longitudinal functional gradients alterations showed the improved trend over time (all  $p < 0.001$ , Bonferroni corrected, Figure 1 and 2). Namely, in the period of antipsychotic treatment, the increased gradients were positively while the decreased gradients were negatively correlated with symptom improvement.

#### CONCLUSION

Our findings provided a novel insight into the functional system hierarchy alterations of subcortical organization, which were sensitive to illness and treatment effects. This might extend our understanding of the functional connectome organization of subcortex in schizophrenia, and this measure makes a promising indicator of treatment response.

#### CLINICAL RELEVANCE/APPLICATION

This study provided the new perspective on the abnormal subcortical hierarchy organization in schizophrenia and its longitudinal gradient changes could be sensitive to reflect the antipsychotic treatment effect.

Printed on: 02/07/23

## Abstract Archives of the RSNA, 2022

R5A-SPNR-5

### Use of Real Life Safety Data From International Pharmacovigilance Databases to Assess the Importance of Symptoms Associated With Gadolinium Exposure

Thursday, Dec. 1 12:15PM - 12:45PM Room: Learning Center - NR DPS

#### Participants

Imran Shahid, (*Presenter*) Nothing to Disclose

#### PURPOSE

Recent scientific publications have reported cases of patients who complained from a variety of symptoms after they received a gadolinium-based contrast agent (GBCA). The aim of this study was to appreciate the importance of these clinical manifestations in the overall population by assessing the weight of "symptoms associated with gadolinium exposure" (SAGE) among the bulk of safety experiences reported to major health authorities.

#### METHODS AND MATERIALS

SAGE symptoms were identified from a review of the scientific literature, and the corresponding preferred terms (PTs) were searched in each system organ class (SOC) category recorded in the European and North American pharmacovigilance databases, EudraVigilance (EV) and FDA Adverse Event Reporting System (FAERS), respectively. The numbers of SAGE symptoms per PT, and cumulatively per SOC, were recorded and their weights in the overall spectrum of AEs was determined for each GBCA.

#### RESULTS

The literature search led to identify 11 articles from which the most prevalent SAGE symptoms were selected. The extraction and analysis of such AEs in EV and FAERS revealed a significantly higher SAGE weight for gadobenate dimeglumine (EV: 25.83%, FAERS: 32.24%) than for gadoteridol (EV: 15.51%; FAERS: 21.13%), and significantly lower SAGE weights for gadobutrol (EV: 7.75%; FAERS: 13.31%) and gadoterate meglumine (EV: 8.66%; FAERS: 12.99%). The SOCs "skin and subcutaneous tissue disorders", "musculoskeletal and connective tissue disorders", "general disorders and administration site conditions" and "psychiatric disorders" were consistent with this ranking, with gadoteridol showing alternately a SAGE profile aligned on the linear GBCA or on the other macrocyclic GBCAs.

#### CONCLUSION

This study showed that SAGE symptoms represent a significant percentage of the bulk of adverse events reported to the health authorities for each GBCA. It provided real-life arguments suggesting that SAGE symptoms may be more prevalent with linear than macrocyclic GBCAs, and that gadoteridol may present a higher SAGE risk than the other macrocyclic contrast agents.

#### CLINICAL RELEVANCE/APPLICATION

This study investigates, in EMA and FDA pharmacovigilance databases, the proclivity of symptoms associated with gadolinium exposure (SAGE) in patients exposed to gadolinium-based MRI contrast agents.

Printed on: 02/07/23



## Abstract Archives of the RSNA, 2022

R5A-SPNR-6

### Variation in Prices for Outpatient Brain MRI in the US

Thursday, Dec. 1 12:15PM - 12:45PM Room: Learning Center - NR DPS

#### Participants

Kinpritma Sangha, PhD, MPH, (*Presenter*) Employee, Siemens AG

#### PURPOSE

The 2021 Hospital Price Transparency Rule was implemented to require hospitals to publish payer-specific negotiated commercial prices for medical services. Payer-negotiated prices vary across the country and are based on hospital and state characteristics, with the greatest markup from mean negotiated prices compared with Medicare reimbursement to be for magnetic resonance imaging (MRI). The objective of this study was to analyze the variation in MRI brain exam prices and to estimate the association between state characteristics and the median MRI brain exam price in the US.

#### METHODS AND MATERIALS

This cross-sectional study examined MRI brain exam prices in the hospitals across US using payer-negotiated prices from the Turquoise Health dataset. MRI brain exam, as a billable service, was identified using the Current Procedural Terminology (CPT) code of 70551. Price variance analysis was performed for all states and characteristics including Herfindahl-Hirschman Index (HHI) and certificate of need (CON) program in the state. Multivariable regression analyses were conducted to determine factors that impact brain MRI exam price among the states.

#### RESULTS

A total of 2504 hospitals disclosed the payer-negotiated prices in 2021 Turquoise Health dataset for brain MRI exams. The greatest price variation in brain MRI exams was for commercial payers with median price of \$1531, ranging from \$3230 to \$611.57. Alaska, with the least number of hospitals, has the highest median price of \$3230, while New York, with 84 hospitals has the lowest median price of \$611.57. States with the CON program had a higher median price (by \$164) than states without the CON program and states with a high HHI index ( $HHI > 6000$ ), indicating a less competitive market, have a higher median price (by \$412) than states with a more competitive market. Both the number of health systems in the state ( $p=0.001$ ) and having commercial payers ( $p=0.000$ ) were found to be statistically significant in affecting impact the median MRI brain exam prices.

#### CONCLUSION

While MRI brain exam prices vary throughout the US, more health systems and commercial payers in the state drive the prices higher.

#### CLINICAL RELEVANCE/APPLICATION

This study helps to understand the factors affecting price variation in brain MRIs in the US.

Printed on: 02/07/23

## Abstract Archives of the RSNA, 2022

R5A-SPNR-7

### Clinical Evaluation of Scout Accelerated Motion Estimation and Reduction (SAMER) For Brain MRI in an Emergency and Inpatient Setting

Thursday, Dec. 1 12:15PM - 12:45PM Room: Learning Center - NR DPS

#### Participants

Azadeh Tabari, MD, Boston, MA (*Presenter*) Nothing to Disclose

#### PURPOSE

A navigation-free retrospective motion-correction method (SAMER) has been developed to achieve rapid motion estimation and correction. In this work, we performed an initial evaluation of SAMER in a clinical setting

#### METHODS AND MATERIALS

In this prospective IRB approved and HIPAA compliant study, 97 patients from emergency and inpatient care settings were scanned on a 3T system (MAGNETOM Skyra, Siemens) using a 20-channel head-neck coil, between August 2021 and January 2022. The imaging protocol included a 4-fold accelerated T1-weighted MPRAGE sequence, which was acquired using a custom linear+checkered sequence reordering. This sequence was incorporated into routine brain MRI to assess the performance of motion correction on non-contrast and contrast-enhanced exams. Retrospective reconstructions of the MPRAGE data were performed with and without SAMER motion correction. All 97 cases were reviewed by two neuroradiologists in a blinded manner to rate the impact of motion artifacts on diagnostic image quality using a previously published 5-tier scale (None, minimal, mild, moderate, severe). Discrepancies in the two neuroradiologists' scores were adjudicated by a third neuroradiologist

#### RESULTS

There was no significant difference in the performance of motion correction between the contrast-enhanced (n=58) and non-contrast (n=42) exams ( $p>0.05$ ). Six (6.1%) of cases showed no motion, 46 (47.4%) showed minimal motion, 30 (31%) showed mild motion, 8 (8.2%) showed moderate motion, and 10 (10.3%) showed severe motion. The prevalence of repeat sequences was 3% of total MRI examinations. Following motion correction with SAMER, there was a significant improvement in motion score ( $P<0.005$  for both raters). The motion score improvement was defined as the pre-correction motion score minus the post-correction score. For cases with motion scores of "none" or "minimal", SAMER had negligible impact on the motion score. For cases with "mild", "moderate", and "severe" motion, SAMER improved the motion score by an average score of 0.36, 1.1, and 1.2 points, respectively

#### CONCLUSION

s SAMER improves diagnostic image quality of clinical brain MR exams in the presence of motion, and the improvement is most pronounced when motion is moderate or severe

#### CLINICAL RELEVANCE/APPLICATION

Motion artifacts are common in emergency and inpatient brain MRI exams. SAMER demonstrates utility in a clinical setting to reduce motion artifacts in these studies, which may facilitate timely diagnosis and require fewer repeat sequences and callbacks for critically ill patients

Printed on: 02/07/23

## Abstract Archives of the RSNA, 2022

R5A-SPNR-8

### Preoperative Visualization of the Transverse and Sigmoid Sinuses Using Non-contrast Virtual Monochromatic CT Images for the Lateral Suboccipital Retrosigmoid Approach

Thursday, Dec. 1 12:15PM - 12:45PM Room: Learning Center - NR DPS

#### Participants

Tomomi Omura, Akita, Japan (*Presenter*) Nothing to Disclose

#### PURPOSE

In the surgical planning of suboccipital retrosigmoid craniotomy, it is important for neurosurgeons to recognize tortuosity of the transverse and sigmoid sinuses and their relationship to superficial landmarks including asterion. This study aimed to improve the depiction of those venous sinuses in preoperative non-contrast (NC) virtual monochromatic images (VMIs).

#### METHODS AND MATERIALS

Thirty-one patients (24 women and 7 men; mean age,  $63 \pm 19$  years) who underwent NCCT retrosigmoid craniotomy were included. The NCCT was scanned using dual-source CT (SOMATOM Drive, Siemens Healthineers, Forchheim, Germany). The NC-DECT images were acquired at a kV-pair of 80 kV and 140 kV with tin-filtration at about 70 mGy using automatic exposure control. Mixed-120 kV images were synthesized by compositing both kV images. The native VMIs were generated at 40, 70, 100, 130, 160, and 190 keV using a CT vendor's workstation. In the reconstructed sagittal section of each image, a circular region of interest (ROI) was set in the transverse sinus and cerebral cortex as a reference. Standard deviation (SD) and attenuation value (HU) were measured in each ROI to obtain the difference in HU values between the transverse sinus and cerebral cortex ( $\Delta$ HU) and contrast-to-noise ratio (CNR).

#### RESULTS

The median  $\Delta$ HU for each VMI was increased with higher keV, and each  $\Delta$ HU for 100, 130, 160, and 190 keV was significantly higher than that for Mixed-120 kV (9.6, 10.3, 10.5, and 11.0 HU for 100, 130, 160, and 190 keV respectively, and 8.8 HU for Mixed-120 kV,  $P < 0.001$  for each). The median CNR for each VMI was also increased with higher keV, and each CNR for 100, 130, 160, and 190 keV was significantly higher than that for Mixed-120 kV (6.8, 6.8, 6.7, and 7.3 for 100, 130, 160, and 190 keV respectively, and 3.2 for Mixed-120 kV,  $P < 0.001$  for each).

#### CONCLUSION

s Both  $\Delta$ HU and CNR of transverse sinuses were improved at VMIs above 100 keV. The results suggest that high keV VMIs improve visualization of the transverse sinus and are useful in surgical planning for suboccipital retrosigmoid craniotomy.

#### CLINICAL RELEVANCE/APPLICATION

High keV VMI is less susceptible to beam hardening, so structures and findings adjacent to bone are clearly delineated.

Printed on: 02/07/23

## Abstract Archives of the RSNA, 2022

R5A-SPNR-9

### Blood-Brain Barrier Dysfunction in Patients with Heart Failure

Thursday, Dec. 1 12:15PM - 12:45PM Room: Learning Center - NR DPS

#### Participants

Kamlesh Jobanputra, MD, Birmingham, AL (*Presenter*) Nothing to Disclose

#### PURPOSE

Heart failure (HF) patients show brain tissue injury in sites that mediate autonomic, cognitive, and mood functions, which are deficient in HF and are linked with increased morbidity and mortality and poor quality of life in the condition. However, the pathological mechanisms that may contribute to brain tissue injury in HF are unclear, but blood brain barrier (BBB) disruption might be one of the processes that contribute to brain injury. Our aim was to examine BBB function, based on diffusion-weighted pseudo-continuous arterial spin labeling (DW-pCASL) procedures, in HF and healthy control subjects.

#### METHODS AND MATERIALS

We performed DW-pCASL imaging in 25 HF [age, 55.4±7.4 years; body-mass-index (BMI), 27.2±4.3 kg/m<sup>2</sup>; 18 male; NYHA functional class II/III, LVEF <40%] and 56 healthy controls (age, 51.7±9.0 years; BMI, 26.8±3.7 kg/m<sup>2</sup>; 31 male) using a 3.0-Tesla MRI scanner (Siemens, Magnetom, Prisma Fit). Using DW-pCASL data, arterial transit time (ATT, an index of large artery integrity) and water exchange rate across the BBB (K<sub>w</sub>, BBB function) were quantified and whole-brain ATT and K<sub>w</sub> maps were generated. Whole-brain ATT and K<sub>w</sub> maps were normalized to Montreal neurological institute space, smoothed, and compared voxel-by-voxel between HF and control groups using analysis of covariance (ANCOVA; covariates: age, sex; SPM12, uncorrected p<0.005). Brain clusters with significant differences between groups were overlaid onto background images for structural identification.

#### RESULTS

No significant differences in age (p=0.08), sex (p=0.16), or BMI (p=0.65) appeared between groups. Multiple brain areas, which are involved in cognitive, mood, autonomic functions, showed altered K<sub>w</sub> and ATT values in HF over health controls. Increased K<sub>w</sub> values were observed in the insular cortices, hippocampus, thalamus, occipital cortices, cerebellar vermis, and other cortices and white matters regions. ATT values were decreased in the prefrontal, temporal, and occipital cortices, and mid brain, and increased in few areas, including the insular cortices and cerebellum in HF patients.

#### CONCLUSION

HF patients show compromised BBB function and altered large artery integrity. BBB alterations may introduce neural damage in autonomic, mood, and cognitive regulatory areas, contributing to abnormal functions in HF. The findings suggest a need to repair BBB function in HF with strategies commonly used in other acute and chronic conditions.

#### CLINICAL RELEVANCE/APPLICATION

Management of neurologic symptoms in patients with heart failure is complex. Translational research focused on need for blood brain barrier repairing strategies in HF patients with brain injury may open new avenues of disease prevention and limiting progression.

Printed on: 02/07/23

## Abstract Archives of the RSNA, 2022

R5A-SPOB

### OB/Gynecology Thursday Poster Discussions - A

Thursday, Dec. 1 12:15PM - 12:45PM Room: Learning Center - OB DPS

#### Participants

Nancy Kim, MD, Washington, DC (*Moderator*) Nothing to Disclose

#### Sub-Events

### R5A-SPOB-1 Deep Learning Image Reconstruction Algorithm for Submillisievert Female Pelvic Computed Tomography: Impact on Image Quality and Lesion Detection

#### Awards

##### Trainee Research Prize - Medical Student

#### Participants

Jing Ren, MD, Beijing, China (*Presenter*) Nothing to Disclose

#### PURPOSE

To assess the impact of a new deep learning reconstruction (DLR) algorithm on image quality and lesion detection in submillisievert female pelvic CT, with standard dose (SD) hybrid-iterative reconstruction (IR) images as the reference.

#### METHODS AND MATERIALS

Fifty consecutive female patients who underwent contrast-enhanced abdominal pelvic CT for indications were enrolled. SD and subsequent low-dose (LD) portal venous phase scans were obtained 60 s after contrast agent injection. A noise index of 15 was set for LD scans to acquire submillisievert pelvic images reconstructed with DLR (body and body sharp kernels), hybrid-IR, and model-based IR (MBIR). SD scans with a noise index of 7.5 were reconstructed using hybrid-IR. Radiation dose, quantitative image quality (noise value, signal-to-noise ratio [SNR], and contrast-to-noise ratio [CNR]), and qualitative image quality (overall image quality and image appearance) using a 5-point Likert scale with 5 being the best were evaluated and compared. Clinically significant pelvic lesions were detected and evaluated by two board-certified radiologists.

#### RESULTS

The CT dose index volume in submillisievert pelvic CT was reduced by 54.2-70.6% compared to SD scans. Among LD images, DLR (body sharp) provided the best quantitative image quality, followed by DLR (body), MBIR, and hybrid-IR. LD DLR (both body and body sharp kernel) images showed lower noise, and higher SNR and CNR than SD images. Compared to SD hybrid-IR, LD DLR (body kernel) and LD hybrid-IR were considered to have natural appearance ( $p=0.209$  and  $0.070$ ). Only LD DLR (body kernel) was rated comparable scores with SD hybrid-IR on overall image quality ( $p=0.084$ ). In total, 40 pelvic lesions were detected in both SD and LD images. LD DLR (body) and LD DLR (body sharp) exhibited equivalent enhancement characteristic ratings ( $p=0.655$  and  $0.372$ ) and diagnostic confidence ( $p=0.317$  and  $0.096$ ) with SD hybrid-IR.

#### CONCLUSION

A DLR algorithm providing comparable image quality and detectability is considered feasible in submillisievert female pelvic CT. DLR (body kernel) with favorable image appearance and overall image quality is more recommended for clinical settings.

#### CLINICAL RELEVANCE/APPLICATION

Submillisievert female pelvic CT with deep learning reconstruction exhibited non-inferior image quality and detectability, so it can reduce the radiation burden for patients requiring multiple screenings and long-term follow-up.

### R5A-SPOB-2 Differential Diagnosis Value of Contrast-Enhanced Ultrasound in the Diagnosis of Pediatric Ovarian Torsion

#### Participants

Zehang Hu, Shenzhen, China (*Presenter*) Nothing to Disclose

#### PURPOSE

Ovarian torsion is a common concern in girls presenting to emergency care with pelvic or abdominal pain, threatening their future fertility. Conventional ultrasound (US) is the imaging modality of choice. We sought to describe contrast enhanced ultrasound (CEUS) characteristics of ovarian torsion in girls, and to assess the potential diagnostic advantages and limitations of method.

#### METHODS AND MATERIALS

We retrospectively analyzed all cases with clinically suspected ovarian torsion and underwent explorative surgery in Shenzhen children's hospital between 2019 and 2022, all of them were previously evaluated by US and CEUS. Those CEUS ovarian images were retrospectively analyzed with the software SonoLiver®, and the time-intensity curve (TIC) was generated to compare the bilateral ovarian time to peak (TTP) and maximum intensity (IMAX).

## **RESULTS**

Our study included 13 cases with age range 4 months~13 years old (median age 10 years), We identified 3/13 torsion-confirmed cases and 10/13 torsion-absent cases by surgical confirmation. Of those torsion-absent cases, 6/13 cases with ovarian tumors ,3/13 cases with hemorrhagic corpus luteum, and 1/13 case with normal ovaries. US identified 4/13 cases with torsion (2 torsion-confirmed cases; 2 torsion-absent cases); 9/13 cases without torsion (8 torsion-absent cases, 1 torsion-confirmed case). In this study, the sensitivity, specificity and overall accuracy of US in the diagnosis of ovarian torsion were 66.7%, 81.4% and 76.9% respectively. US combined with CEUS identified 4/13 cases with torsion (3 torsion-confirmed cases, all torsion ovaries appeared hypo-enhancing or non-enhancing compared with healthy ovaries, and showed prolonged TTP and lower IMAX; 1 case proven without torsion); CEUS identified 9/13 cases without torsion (9 torsion-absent cases). In this study, the sensitivity, specificity and overall accuracy of CEUS in the detection of ovarian torsion were 100%, 90% and 92.3% respectively.

## **CONCLUSION**

s US combined with CEUS has a higher sensitivity, specificity and overall accuracy than US in the detection of ovarian torsion.

## **CLINICAL RELEVANCE/APPLICATION**

CEUS may be used as a supplementary means of US to increase the diagnostic accuracy of ovarian torsion.

Printed on: 02/07/23

## Abstract Archives of the RSNA, 2022

R5A-SPOB-1

### Deep Learning Image Reconstruction Algorithm for Submillisievert Female Pelvic Computed Tomography: Impact on Image Quality and Lesion Detection

Thursday, Dec. 1 12:15PM - 12:45PM Room: Learning Center - OB DPS

#### Awards

Trainee Research Prize - Medical Student

#### Participants

Jing Ren, MD, Beijing, China (*Presenter*) Nothing to Disclose

#### PURPOSE

To assess the impact of a new deep learning reconstruction (DLR) algorithm on image quality and lesion detection in submillisievert female pelvic CT, with standard dose (SD) hybrid-iterative reconstruction (IR) images as the reference.

#### METHODS AND MATERIALS

Fifty consecutive female patients who underwent contrast-enhanced abdominal pelvic CT for indications were enrolled. SD and subsequent low-dose (LD) portal venous phase scans were obtained 60 s after contrast agent injection. A noise index of 15 was set for LD scans to acquire submillisievert pelvic images reconstructed with DLR (body and body sharp kernels), hybrid-IR, and model-based IR (MBIR). SD scans with a noise index of 7.5 were reconstructed using hybrid-IR. Radiation dose, quantitative image quality (noise value, signal-to-noise ratio [SNR], and contrast-to-noise ratio [CNR]), and qualitative image quality (overall image quality and image appearance) using a 5-point Likert scale with 5 being the best were evaluated and compared. Clinically significant pelvic lesions were detected and evaluated by two board-certified radiologists.

#### RESULTS

The CT dose index volume in submillisievert pelvic CT was reduced by 54.2-70.6% compared to SD scans. Among LD images, DLR (body sharp) provided the best quantitative image quality, followed by DLR (body), MBIR, and hybrid-IR. LD DLR (both body and body sharp kernel) images showed lower noise, and higher SNR and CNR than SD images. Compared to SD hybrid-IR, LD DLR (body kernel) and LD hybrid-IR were considered to have natural appearance ( $p=0.209$  and  $0.070$ ). Only LD DLR (body kernel) was rated comparable scores with SD hybrid-IR on overall image quality ( $p=0.084$ ). In total, 40 pelvic lesions were detected in both SD and LD images. LD DLR (body) and LD DLR (body sharp) exhibited equivalent enhancement characteristic ratings ( $p=0.655$  and  $0.372$ ) and diagnostic confidence ( $p=0.317$  and  $0.096$ ) with SD hybrid-IR.

#### CONCLUSION

A DLR algorithm providing comparable image quality and detectability is considered feasible in submillisievert female pelvic CT. DLR (body kernel) with favorable image appearance and overall image quality is more recommended for clinical settings.

#### CLINICAL RELEVANCE/APPLICATION

Submillisievert female pelvic CT with deep learning reconstruction exhibited non-inferior image quality and detectability, so it can reduce the radiation burden for patients requiring multiple screenings and long-term follow-up.

Printed on: 02/07/23

## Abstract Archives of the RSNA, 2022

R5A-SPOB-2

### Differential Diagnosis Value of Contrast-Enhanced Ultrasound in the Diagnosis of Pediatric Ovarian Torsion

Thursday, Dec. 1 12:15PM - 12:45PM Room: Learning Center - OB DPS

#### Participants

Zehang Hu, Shenzhen, China (*Presenter*) Nothing to Disclose

#### PURPOSE

Ovarian torsion is a common concern in girls presenting to emergency care with pelvic or abdominal pain, threatening their future fertility. Conventional ultrasound (US) is the imaging modality of choice. We sought to describe contrast enhanced ultrasound (CEUS) characteristics of ovarian torsion in girls, and to assess the potential diagnostic advantages and limitations of method.

#### METHODS AND MATERIALS

We retrospectively analyzed all cases with clinically suspected ovarian torsion and underwent explorative surgery in Shenzhen children's hospital between 2019 and 2022, all of them were previously evaluated by US and CEUS. Those CEUS ovarian images were retrospectively analyzed with the software SonoLiver®, and the time-intensity curve (TIC) was generated to compare the bilateral ovarian time to peak (TTP) and maximum intensity (IMAX).

#### RESULTS

Our study included 13 cases with age range 4 months~13 years old (median age 10 years), We identified 3/13 torsion-confirmed cases and 10/13 torsion-absent cases by surgical confirmation. Of those torsion-absent cases, 6/13 cases with ovarian tumors, 3/13 cases with hemorrhagic corpus luteum, and 1/13 case with normal ovaries. US identified 4/13 cases with torsion (2 torsion-confirmed cases; 2 torsion-absent cases); 9/13 cases without torsion (8 torsion-absent cases, 1 torsion-confirmed case). In this study, the sensitivity, specificity and overall accuracy of US in the diagnosis of ovarian torsion were 66.7%, 81.4% and 76.9% respectively. US combined with CEUS identified 4/13 cases with torsion (3 torsion-confirmed cases, all torsion ovaries appeared hypo-enhancing or non-enhancing compared with healthy ovaries, and showed prolonged TTP and lower IMAX; 1 case proven without torsion); CEUS identified 9/13 cases without torsion (9 torsion-absent cases). In this study, the sensitivity, specificity and overall accuracy of CEUS in the detection of ovarian torsion were 100%, 90% and 92.3% respectively.

#### CONCLUSION

US combined with CEUS has a higher sensitivity, specificity and overall accuracy than US in the detection of ovarian torsion.

#### CLINICAL RELEVANCE/APPLICATION

CEUS may be used as a supplementary means of US to increase the diagnostic accuracy of ovarian torsion.

Printed on: 02/07/23

## Abstract Archives of the RSNA, 2022

R5A-SPPD

### Pediatric Thursday Poster Discussions - A

Thursday, Dec. 1 12:15PM - 12:45PM Room: Learning Center - PD DPS

#### Participants

Cara Morin, PhD, Memphis, TN (*Moderator*) Nothing to Disclose

#### Sub-Events

### R5A-SPPD-1 Application of Deep Learning Reconstruction in Low-Dose Brain CT of Children With Cerebral Trauma for Image Quality Improvement

#### Participants

Wei Weian, (*Presenter*) Nothing to Disclose

#### PURPOSE

To explore the application value of deep learning reconstruction (DLR) in low-dose brain CT imaging for children with acute cerebral trauma by comparing with ASIR-V.

#### METHODS AND MATERIALS

51 children with cerebral trauma complicated with intracerebral hemorrhage who experienced low dose brain CT were retrospectively collected. Scanning parameters: axial scan, rotation speed: 0.5s/rotation, 100 kVp and 250 mAs for children younger than 1.5 years old (y), 120 kVp and 250 mAs for children of 1.5 to 7y, 120 kVp and 300 mAs for those older than 7y. All images were reconstructed at 1.25 mm and 5 mm slice thickness utilizing two reconstruction algorithms with different strengths and divided into six subgroups: ASIR-V0%, ASIR-V50%, ASIR-V100%, DLR-L, DLR-M and DLR-H. The CT attenuation, SNR and CNR of dorsal thalamus, white matter of frontal lobe and hemorrhage lesion, as well as skull base artifact noise, background noise, and overall subjective image quality score of DLR and ASIR-V images were compared by one-way ANOVA and Kruskal-Wallis H test. Two-sample t and Mann Whitney U were used for comparison between two groups.

#### RESULTS

The average CTDIvol and DLP of head CT were  $16.79 \pm 0.55$  mGy and  $240.79 \pm 11.49$  mGy\*cm. At the same thickness, the subjective scores of DLR images were better than those of ASIR-V ( $p < 0.05$ ), and a higher reconstruction grade of ASIR-V and DLR led to higher SNR and CNR values of each structure as well as lower SD value ( $p < 0.05$ ). Among them, the SD artifact and SD background of DLR-H images ( $3.55 \pm 0.83$  HU and  $2.87 \pm 0.59$  HU for 5mm;  $5.21 \pm 1.24$  HU and  $4.63 \pm 1.20$  HU for 1.25 mm) and ASIR-V100% ( $3.32 \pm 0.74$  HU and  $2.74 \pm 0.55$  HU for 5mm;  $5.22 \pm 1.16$  HU and  $4.78 \pm 1.09$  HU for 1.25 mm) were the lowest and similar ( $p > 0.05$ ), but at 1.25mm thickness, CNR value for gray and white matter of DLR-H images was higher than that of ASIR-V100% ( $1.95 \pm 0.69$  vs.  $1.63 \pm 0.60$ ,  $p < 0.05$ ). With the decrease of slice thickness, the image quality was decreased, but the average subjective scores of 1.25mm DLR images were still more than 3 points, while those of ASIR-V images were less than 3 points and could not fully meet the needs of diagnosis. In addition, the scoring of 1.25mm DLR-H was similar with that of 5mm ASIR-V50% ( $3.93 \pm 0.22$  vs.  $3.17 \pm 0.39$ ,  $p > 0.05$ ), but the DLR group improved the spatial resolution and the detection capability of micro-hemorrhagic foci.

#### CONCLUSION

In children's low-dose cerebral CT, DLR shows powerful ability to reduce noise and artifacts, also improve the display of general structure and microhemorrhagic foci, therein DLR-H has the best performance.

#### CLINICAL RELEVANCE/APPLICATION

In head CT for children, DLR holds great potential in decline of radiation dose and improvement of image quality, valuable for the diagnosis of brain disease especially for microhemorrhagic foci.

Printed on: 02/07/23

## Abstract Archives of the RSNA, 2022

R5A-SPPD-1

### Application of Deep Learning Reconstruction in Low-Dose Brain CT of Children With Cerebral Trauma for Image Quality Improvement

Thursday, Dec. 1 12:15PM - 12:45PM Room: Learning Center - PD DPS

#### Participants

Wei Weian, (*Presenter*) Nothing to Disclose

#### PURPOSE

To explore the application value of deep learning reconstruction (DLR) in low-dose brain CT imaging for children with acute cerebral trauma by comparing with ASIR-V.

#### METHODS AND MATERIALS

51 children with cerebral trauma complicated with intracerebral hemorrhage who experienced low dose brain CT were retrospectively collected. Scanning parameters: axial scan, rotation speed: 0.5s/rotation, 100 kVp and 250 mAs for children younger than 1.5 years old (y), 120 kVp and 250 mAs for children of 1.5 to 7y, 120 kVp and 300 mAs for those older than 7y. All images were reconstructed at 1.25 mm and 5 mm slice thickness utilizing two reconstruction algorithms with different strengths and divided into six subgroups: ASIR-V0%, ASIR-V50%, ASIR-V100%, DLR-L, DLR-M and DLR-H. The CT attenuation, SNR and CNR of dorsal thalamus, white matter of frontal lobe and hemorrhage lesion, as well as skull base artifact noise, background noise, and overall subjective image quality score of DLR and ASIR-V images were compared by one-way ANOVA and Kruskal-Wallis H test. Two-sample t and Mann Whitney U were used for comparison between two groups.

#### RESULTS

The average CTDI<sub>vol</sub> and DLP of head CT were  $16.79 \pm 0.55$  mGy and  $240.79 \pm 11.49$  mGy\*cm. At the same thickness, the subjective scores of DLR images were better than those of ASIR-V ( $p < 0.05$ ), and a higher reconstruction grade of ASIR-V and DLR led to higher SNR and CNR values of each structure as well as lower SD value ( $p < 0.05$ ). Among them, the SD<sub>artifact</sub> and SD<sub>background</sub> of DLR-H images ( $3.55 \pm 0.83$  HU and  $2.87 \pm 0.59$  HU for 5mm;  $5.21 \pm 1.24$  HU and  $4.63 \pm 1.20$  HU for 1.25 mm) and ASIR-V100% ( $3.32 \pm 0.74$  HU and  $2.74 \pm 0.55$  HU for 5mm;  $5.22 \pm 1.16$  HU and  $4.78 \pm 1.09$  HU for 1.25 mm) were the lowest and similar ( $p > 0.05$ ), but at 1.25mm thickness, CNR value for gray and white matter of DLR-H images was higher than that of ASIR-V100% ( $1.95 \pm 0.69$  vs.  $1.63 \pm 0.60$ ,  $p < 0.05$ ). With the decrease of slice thickness, the image quality was decreased, but the average subjective scores of 1.25mm DLR images were still more than 3 points, while those of ASIR-V images were less than 3 points and could not fully meet the needs of diagnosis. In addition, the scoring of 1.25mm DLR-H was similar with that of 5mm ASIR-V50% ( $3.93 \pm 0.22$  vs.  $3.17 \pm 0.39$ ,  $p > 0.05$ ), but the DLR group improved the spatial resolution and the detection capability of micro-hemorrhagic foci.

#### CONCLUSION

In children's low-dose cerebral CT, DLR shows powerful ability to reduce noise and artifacts, also improve the display of general structure and microhemorrhagic foci, therein DLR-H has the best performance.

#### CLINICAL RELEVANCE/APPLICATION

In head CT for children, DLR holds great potential in decline of radiation dose and improvement of image quality, valuable for the diagnosis of brain disease especially for microhemorrhagic foci.

Printed on: 02/07/23

## Abstract Archives of the RSNA, 2022

R5A-SPPH

### Physics Thursday Poster Discussions - A

Thursday, Dec. 1 12:15PM - 12:45PM Room: Learning Center - PH DPS

#### Participants

Liqiang Ren, PhD, Rochester, MN (*Moderator*) Nothing to Disclose

#### Sub-Events

### R5A-SPPH-1 Comparison of Computed Tomographic Dose Data of Tin Filter With Conventional Scanning Protocols Using Thermoluminescence Dosimeter Measurements

#### Participants

Simone Schuele, (*Presenter*) Nothing to Disclose

#### PURPOSE

We aim to investigate whether there are differences in the applied dose (TLD measurements (thermoluminescence dosimeter)) between different scanning protocols in computed tomography for the same CTDIvol (Computed Tomography Dose Index). Special focus is on the tin filter technique (Sn).

#### METHODS AND MATERIALS

Sixteen TLD measurements (3 measurement repetitions each) were performed in a water phantom (diameter 32 cm) using five different scan protocols (Sn 150 kV, 150 kV, 120 kV, 100 kV, Sn 100 kV) at three (CTDIvol: 29 mGy, 8.5 mGy, and 2.8 mGy) dose settings on a 3-generation dual source CT scanner. With the Sn 100 kV protocol, limited by the scanner, irradiations were only possible up to 6.4 mGy (CTDIvol). The TLDs were positioned centrally in the water phantom. TLD measurement results and the slope of the linear regression of the different protocols were compared. ANOVA or Kruskal-Wallis-test was used for statistical testing, where applicable.

#### RESULTS

Compared to the 100 kV, 120 kV, and 150 kV protocols, the tin filter protocols (Sn 150 kV, Sn 100 kV) applied higher doses (average dose difference: 16% +/- 4%) at all dose settings studied ( $p < 0.01$ ) except for the comparison between the Sn 150 kV and 150 kV protocols at a CTDIvol of 29 mGy ( $p = 0.072$ ). The Sn 150 kV protocol showed a steeper slope of the linear regression than the 100 kV and 120 kV protocols ( $p < 0.05$ ).

#### CONCLUSION

s The CTDIvol information from the scanner underestimates the dose of the Sn 150 kV and Sn 100 kV protocols compared to protocols without tin filtration.

#### CLINICAL RELEVANCE/APPLICATION

Tin filter protocols expose patients to higher radiation doses than standard protocols at the same CTDIvol. This must be taken into account when using the tin filter technique in computed tomography for radiation protection reasons.

### R5A-SPPH-2 Multicenter, International Study of CT Practices and Radiation Doses from 5 African Countries: An International Atomic Energy Agency (IAEA) Baseline Study

#### Participants

Giridhar Dasegowda, MBBS, Boston, MA (*Presenter*) Nothing to Disclose

#### PURPOSE

There are few studies on CT practices from Africa to inform about the implementation of justification and optimization principles for radiation protection of patients. Therefore, under the framework of the IAEA Technical Cooperation Regional Project RAF9/064 entitled "a comprehensive baseline study was conducted to under to assess CT practices and radiation doses from multiple hospitals across several African countries and better determine the needs for improved radiation protection of patients.

#### METHODS AND MATERIALS

Six hospitals from Mauritius, Tunisia, Kenya, Sudan, Burkina Faso contributed information on 20-30 consecutive patients who underwent head, chest, and/or abdomen-pelvis CT examinations. Prior to the data recording step, all sites had a mandatory one-hour training on best practices in recording the relevant data elements without any personal health identifiers. The recorded data elements included patient age, gender, weight, height, CT protocol name, scanner information, scan factors (tube current, automatic exposure control, tube potential, number and names of scan phases), and radiation dose metrics including series-specific CT dose index volume (CTDIvol in mGy) and dose length product (DLP in mGy.cm). Information was recorded by either on-site CT technologists or medical physicists and radiologists between January-April 2022. For statistical analysis, we estimated median and interquartile range of body-region specific CTDIvol and DLP and compared data with Kruskal Wallis H test.

## RESULTS

There were substantial variations in radiation doses between the different hospitals with minimum and maximum CT DIvol and DLP of 33-81mGy and 638-1891mGy.cm for head CT, 6-25mGy and 192-974mGy.cm for chest CT, and 6-15mGy and 303-1375mGy.cm for abdomen-pelvis CT ( $p < 0.01$ ). There was no significant difference between body mass index (BMI) or age across the different sites. Most sites used multiphase CT protocols for chest-abdomen-pelvis (6/6 sites) and chest CT (3/6 sites), regardless of clinical indications. Total DLP values for head, chest, abdomen, and chest-abdomen-pelvis CT at 3/6, 4/6, 4/6, and 5/6 sites were above the American College of Radiology and European reference dose levels.

## CONCLUSION

There are concerning variations in CT practices and protocols across several hospitals in Africa emphasizing need for protocol optimization to improve radiation protection of patients.

## CLINICAL RELEVANCE/APPLICATION

Use of higher than recommended CT radiation doses in several African sites underscore critical need for optimization and oversight of CT practices.

## R5A-SPPH-3 Effect of Hormone Therapy on Target Volume in Radio-therapy of Localized Prostate Cancer

Participants

Ayşe Daglı, Istanbul, Turkey (*Presenter*) Nothing to Disclose

## PURPOSE

To determine the extent of tumor volume reduction and normal organ doses in prostate cancer (PCa) patients, with large prostate volumes that are geometrically unsuitable, treated with radiotherapy (RT) and combined androgen deprivation therapy (ADT).

## METHODS AND MATERIALS

Ten patients with localized PCa included into the study. Median patient age was 71.6. (60-76). Patients underwent neoadjuvant ADT at least three months (3-36 months). Simulation CT images were obtained before the initiation of ADT (Plan 1) and 2 months after ADT (Plan 2). All patients were simulated in supine position with full bladder and empty rectum. RT treatment plans were done on each image set. All plans were done with VMAT using two full arcs. Prescribed dose was 76 Gy with 2 Gy/day in 38 fractions. Tumor volume and normal organ doses were dosimetrically compared. Maximum target doses (D<sub>max</sub>), homogeneity index (HI) and conformity index (CI), bladder, rectum and penile bulb doses were compared between two plans. Statistical analysis was done using paired t test.  $P < 0.05$  was accepted as statistically significant.

## RESULTS

The median prostate volume was 77 cc (range: 51-113 cc) in Plan 1 images and the median prostate volume was 56 cc (range: 35-90 cc) in the Plan 2 images. Median prostate volume reduction with ADT was 17 cc, representing a 23% reduction in the target volume ( $p < 0.001$ ). The D<sub>max</sub> ( $p = 0.77$ ), HI ( $p = 0.16$ ) and CI ( $p = 0.66$ ) was not statistically different in two plans. Bladder ( $p = 0.48$ ) and rectum ( $p = 0.07$ ) volumes were not significantly different between two plans. Bladder volumes receiving 30 Gy (V<sub>30</sub>), 40 Gy (V<sub>40</sub>), 50 Gy (V<sub>50</sub>), 56 Gy (V<sub>56</sub>), 65 Gy (V<sub>65</sub>), 75 Gy (V<sub>75</sub>) decreased 14%, 8%, 7%, 4%, 4%, 1%, respectively combined ADT. Bladder D<sub>max</sub> was decreased 7% but D<sub>mean</sub> did not change. Rectum volumes receiving 30 Gy (V<sub>30</sub>), 40 Gy (V<sub>40</sub>), 50 Gy (V<sub>50</sub>), 56 Gy (V<sub>56</sub>), 60 Gy (V<sub>60</sub>), 70 Gy (V<sub>70</sub>), 75 Gy (V<sub>75</sub>) decreased 21% 26%, 34%, 35%, 34%, 33%, 35%, respectively combined ADT. Rectum D<sub>mean</sub> was decreased 19% but D<sub>max</sub> did not change. Doses to 90 ml (D<sub>90</sub>) penile bulb was decreased 8%; mean and maximum penile bulb doses were decreased 9% and 2%, respectively.

## CONCLUSION

Prostate shrinkage after combined ADT provides significant reduction in normal organ doses in PCa RT. This benefit may result in fewer acute and late radiotherapy complications. Clinical studies are needed to supported this data.

## CLINICAL RELEVANCE/APPLICATION

It may be necessary to revise target volume in treatment planning, as it provides significant reduction in prostate volume after combined ADT.

## R5A-SPPH-4 Cumulative Radiation Exposure in Covid-19 Patients Admitted to the Intensive Care Unit

Participants

Lama HADID, (*Presenter*) Nothing to Disclose

## PURPOSE

Medical imaging plays a major role in coronavirus disease-2019 (COVID-19) patient diagnosis and management. However, the radiation dose received from medical procedures by these patients has been poorly investigated. We aimed to estimate the cumulative effective dose (CED) related to medical exposure in COVID-19 patients admitted to the intensive care unit (ICU) in comparison to the usual critically ill patients.

## METHODS AND MATERIALS

We designed a descriptive cohort study including 90 successive ICU COVID-19 patients admitted between March and May 2020 and 90 successive non-COVID 19 patients admitted between March and May 2019. In this study, the CED resulting from all radiological examinations was calculated and clinical characteristics predictive of higher exposure risk identified.

## RESULTS

The number of radiological examinations was 12.0 (5.0-26.0) [median (interquartile range) in COVID-19 vs. 4.0 (2.0-8.0) in non-COVID-19 patient ( $P < 0.001$ )]. The CED during a fourmonth period was 4.2 mSv (1.9-11.2) in the COVID-19 vs. 1.2 mSv (0.13-6.19) in the non-COVID-19 patients ( $P < 0.001$ ). In the survivors, the CED in COVID-19 vs. non-COVID-19 patients was =100 mSv in 3% vs. 0%, 10-100 mSv in 23% vs. 15%, 1-10 mSv in 56% vs. 30% and ,1 mSv in 18% vs. 55%. The CED ( $P < 0.001$ ) and CED per ICU hospitalization day ( $P = 0.004$ ) were significantly higher in COVID-19 than non-COVID-19 patients. The CED correlated significantly with the hospitalization duration ( $r = 0.45$ ,  $P < 0.001$ ) and the number of conventional radiological examinations ( $r =$

0.8,  $P < 0.001$ ).

## CONCLUSION

To conclude, more radiological examinations were performed in critically ill COVID-19 patients than non-COVID-19 patients resulting in higher CED. In COVID-19 patients, contribution of strategies to limit CED should be investigated in the future.

## CLINICAL RELEVANCE/APPLICATION

This study is relevant for Covid-19 patients cared for in radiology departments and intensive care units.

## R5A-SPPH-5 Patient-Specific Analysis of Dose Metrics and Organ Doses Based on Monte Carlo Simulation in Multiphase Abdominal CT Examinations

Participants

Keisuke Fujii, PhD, Nagoya, Japan (*Presenter*) Nothing to Disclose

## PURPOSE

The aims of this study are to determine organ doses based on Monte Carlo (MC) simulations for individual patients in multiphase abdominal CT examinations and to evaluate the correlations between the organ doses and dose metrics.

## METHODS AND MATERIALS

The voxelized models of 30 adults (15 normal weight patients with body mass index (BMI) of 18.5-25.0 and 15 overweight patients with BMI more than 25.0) undergoing four phase abdominal CT examinations with Aquilion ONE VISION (n=10) and Aquilion Precision (n=20) (Canon Medical Systems) were created by inputting the CT images into MC simulation software ImpactMC (Advanced Breast CT, GmbH). MC simulations for each voxelized phantom were performed by inputting the detailed descriptions of the CT scanners and scanning parameters into ImpactMC. The scan range for pre-contrast, arterial phase, and delayed phase and for portal phase was set to upper abdomen and chest-abdomen-pelvis, respectively. Next, region of interests (ROIs) of seven radiosensitive organs (thyroid, lung, esophagus, breast, liver, stomach, and bladder) were created by delineating each organ on the CT images. Each ROI was set on the dose distribution images obtained as the simulation results and organ doses for each organ were evaluated as average doses within each organ ROI. For dose metrics, volume CT dose index (CTDIvol) and size-specific dose estimates (SSDE) were collected, and organ-specific SSDE were calculated using the average CTDIvol and water equivalent diameter over each organ position.

## RESULTS

Organ doses for liver and stomach within scan range at all phase in abdominal CT examinations were approximately 17-48 mGy at each phase and 70-190 mGy in total. The doses had strong linear relationships with organ-specific SSDE, and the doses for overweight patients in the CT examinations with one of the CT scanners were approximately 60-70% higher than those for normal weight patients. Organ doses in lung and esophagus partially included in scan range at the pre-contrast, arterial and delayed phase were approximately 6-32 mGy at each phase, and the doses accounted for approximately 50-70% of 30-140 mGy in total at the four phases.

## CONCLUSION

Organ doses for organs within or partially included in scan range in multiphase abdominal CT examinations will widely vary depending on the types of CT scanners and patient size. Organ-specific SSDE can be useful for total organ dose estimations for organs within scan range in the CT examinations.

## CLINICAL RELEVANCE/APPLICATION

The reduction of organ doses for individual patients in multiphase abdominal CT examinations will require the optimization of scanning parameters including tube current modulation for each CT scanner.

## R5A-SPPH-6 Patient-Specific Organ Dose and Cancer Risk Estimation in Adult Computed Tomography: Impact of a 7 Years Dose Optimization Process

Participants

Benoit Dufour, Sion, Switzerland (*Presenter*) Nothing to Disclose

## PURPOSE

To estimate the impact of dose optimization on cancer risks from adult computed tomography (CT).

## METHODS AND MATERIALS

From 2016 to 2022, after a phase (P0) of protocol harmonization according to clinical indication, three successive phases of dose optimization were implemented at our institution (9 centers). P1 (first dose optimization round); P2 (second dose optimization round with the introduction of new generation CT scanners); P3 (third dose optimization round with the introduction of deep learning reconstruction). To estimate cancer risk for each patient and phase, patient-specific organ doses, age at exposure and sex were needed. Patient-specific organ doses were computed using the organ dosimetry module of a dose monitoring system (DoseWatch, GE Healthcare). Finally, lifetime risk and organ-specific risk of developing cancer were estimated using RadRAT (version 4.2.1). Results from each phase were compared by using the mean risk (Kruskal-Wallis test, significance  $p < 0.05$ ). Data were also stratified per anatomical region and clinical indication (chest (emphysema, pulmonary embolism and pneumonia) and abdomen (appendicitis, diverticulitis, kidney stones, liver, pancreas tumor, renal tumor and infection)).

## RESULTS

Preliminary results on comparing P3 (4698 examinations) and P1 (678 examinations) showed an overall reduction of 49.5% lifetime risk of developing cancer. Stratifying per anatomical region, the reduction was 53.7%/27.6% for abdomen/thorax respectively. The highest excessive risk reduction was observed for the pancreas tumor (66.7%), diverticulitis (62.7%), and kidney stone (50.4%) protocols. The lowest impact was on the pneumonia and renal infection protocols, with 11.4% and 23.6% respectively. Statistical analyses for P0 and P4 and stratification per organ are ongoing.

## CONCLUSION

s Patient-specific lifetime risk of developing cancer from CT imaging have been estimated for adult patients. The continuous process of CT protocol optimization allowed for a significant reduction of cancer risk associated with ionizing radiation.

#### **CLINICAL RELEVANCE/APPLICATION**

Excess of radiation-induced cancer cases can be reduced by fostering continuous dose optimization and avoiding scanner obsolescence.

#### **R5A-SPPH-7 Establishment of CT Local Diagnostic Reference Levels at King Faisal Specialist Hospital and Research Centre**

Participants

Omar Mohamed Noor, MSc, (*Presenter*) Nothing to Disclose

#### **PURPOSE**

To establish local diagnostic reference levels at KFSHRC for computed tomography examinations of adults and identify the need for optimization.

#### **METHODS AND MATERIALS**

Data for over 4500 patients who have undergone CT scans in 2021 were analyzed. Four anatomical regions were considered for this study, namely head, head neck, chest, and abdomen-pelvis. In total, there are six CT scanners with multislice capability at KFSHRC. Sectra Dose Track management system was used to extract patient dose information. CT-dose index (CTDIvol, mGy) and dose length product (DLP, mGy.cm) were the selected dose matrices for the study. The 25th, 50th and 75th percentiles of these two quantities were calculated for each scanner. The local DRL values were then determined by calculating the 75th percentile of the distribution of median values. The results were compared with national and international DRL values.

#### **RESULTS**

The determined CTDIvol/DLP for the head, head neck, chest, and abdomen-pelvis protocols were 51.93/1054, 17/564, 7/244 and 13/891, respectively.

#### **CONCLUSION**

s The established local DRL values have shown appreciable improvement compared to prior estimated values in 2018, up to 30% improvement for some protocols. Also, the established values are relatively lower than the national DRL values by an average of 12% and are comparable to international values.

#### **CLINICAL RELEVANCE/APPLICATION**

Diagnostic reference levels are a great quality control tool to ensure optimal diagnostic imaging radiation doses and adherence to international best practices.

#### **R5A-SPPH-8 Fluoroscopic X-Ray Beam Optimization for Improved Radiation Safety in Neurosurgery Imaging**

Participants

Xinhua Li, PhD, Boston, MA (*Presenter*) Employee, MorphoSys AG ;Employee, Elevation Oncology

#### **PURPOSE**

Fluoroscopic-guided neurosurgery may be associated with prolonged procedure time, intensive use of radiation, and notable adverse radiation effects. This study examines x-ray spectral optimization to achieve dose reduction and improved safety for patients and operators.

#### **METHODS AND MATERIALS**

Through this retrospective cohort study, radiation exposure to consecutive patients who underwent neurosurgery in two biplane procedure rooms, each with Artis zee replaced by Artis icono (Siemens Healthineers), was analyzed. Tests with anthropomorphic phantom (ATOM 701-B, CIRS Inc., VA; Weight 73 kg, height 173 cm) on Artis icono were conducted and effective x-ray beam filtration was characterized with x-ray spectral modeling.

#### **RESULTS**

No. of procedures was 716 (median age at procedure, 58; range 7-95) on Artis zee (Jan-Nov,2021) and 415 (59; 7-95) on Artis icono (Oct,2021-Apr,2022),with insignificant difference in age ( $p=0.098$ , two-tailed t test) between them. Dosage was 881.4 (838.5-924.3) mGy [mean (95% CI)] for air kerma at the reference point, 110.9 (105.1-116.7) Gy·cm<sup>2</sup> for air kerma-area product, and 26.0 (24.4-27.5) minutes for fluoroscopic time on Artis zee and it was 402.3 (361.2-443.4) mGy, 54.8 (49.7-59.9) Gy·cm<sup>2</sup>, and 25.0 (22.9-27.2) minutes on Artis icono. In phantom tests [FL Neuro Sharp, mag1 (40 cm), 7.5 P/S], AP plane used 66-67 kV, Cu filters of 0.9, 0.6 and 0.3 mm and LAT plane used 64-68 kV, Cu filters of 0.6, 0.6 and 0.3 mm for low, normal, and high dose modes. Half value layer (HVL) was 7.19, 6.42 and 5.25 mmAl (effective energy 51,48,43 keV; FWHM 19.5, 22, 24.5 keV) (AP) and 5.86, 6.27, and 5.08 mmAl (effective energy 46,47,42 keV; FWHM 21.5, 23.2, 25.2 keV) (LAT).

#### **CONCLUSION**

s Substantial (=50.6%) dose reduction is achieved in neurosurgery imaging by optimizing x-ray beam spectrum.

#### **CLINICAL RELEVANCE/APPLICATION**

Optimization of x-ray beam filtration and spectrum can facilitate radiation dose reduction in neurosurgery imaging for improved radiation safety for patients and the staff.

#### **R5A-SPPH-9 Usefulness of Generative Adversarial Network-Based Low-Dose Digital Breast Tomosynthesis for Image Quality Improvement**

Participants

Tsutomu Gomi, PhD, (*Presenter*) Nothing to Disclose

## PURPOSE

To evaluate the image quality improvement in digital breast tomosynthesis under low-radiation-dose conditions of prereconstruction processing using conditional generative adversarial networks (cGAN [pix2pix]).

## METHODS AND MATERIALS

The pix2pix prereconstruction processing (p2p) with filtered back projection (FBP) and simultaneous algebraic reconstruction technique total variation first-iterative shrinkage-thresholding algorithm (SART-TV-FISTA) was compared with and without multiscale bilateral filtering. Noise reduction and preserve contrast rates were compared using full width at half-maximum (FWHM), contrast-to-noise ratio, peak signal-to-noise ratio (PSNR), and structural similarity (SSIM) in the in-focus plane using a BR3D phantom at various radiation doses (reference-dose [automatic exposure control reference dose: AECrd]; average glandular dose [AGD] 1.36 mGy, 50% [AGD; 0.66 mGy] and 75% [AGD; 0.31 mGy] reduced AECrd).

## RESULTS

The overall performance of p2p-FBP in FWHM, PSNR, and SSIM was effective for both with and without MSBF prereconstruction processing with FBP and SART-TV-FISTA. At ~75% radiation-dose reduction, p2p-FBP in FWHM yielded good results independent of microcalcification (MC) sizes equivalent to that of the reference images, but without significant difference in statistical results (FBP p2p of 0.196 mm [ $p = 0.98$ ], 0.23 mm [ $p = 0.72$ ], and 0.29 mm [ $p = 0.60$ ]; FBP with MSBF of 0.196 mm [ $p = 0.11$ ], 0.23 mm [ $p < 0.05$ ], and 0.29 mm [ $p < 0.05$ ]; FBP without MSBF of 0.196 mm [ $p = 0.74$ ], 0.23 mm [ $p = 1.00$ ], and 0.29 mm [ $p = 0.99$ ]; SART-TV-FISTA p2p of 0.196 mm [ $p = 1.00$ ], 0.23 mm [ $p = 0.80$ ], and 0.29 mm [ $p = 0.55$ ]; SART-TV-FISTA with MSBF of 0.196 mm [ $p = 0.91$ ], 0.23 mm [ $p < 0.05$ ], and 0.29 mm [ $p < 0.05$ ]; SART-TV-FISTA without MSBF of 0.196 mm [ $p = 0.82$ ], 0.23 mm, [ $p = 0.91$ ], and 0.29 mm, [ $p = 0.96$ ]) in preserving the MC structure and mass contrast. PSNR results showed that p2p-FBP demonstrated the minimum error with reference images at a ~75% reduction in radiation dose. SSIM analysis indicated that p2p-FBP yielded superior similarity at ~75% radiation-dose reduction, with features most similar to the reference images.

## CONCLUSION

s This phantom study revealed that a ~75% reduction in radiation dose is feasible using our proposed p2p-FBP.

## CLINICAL RELEVANCE/APPLICATION

The p2p-FBP can significantly reduce noise with preserved contrast and radiation-dose reduction in clinical practice.

Printed on: 02/07/23

## Abstract Archives of the RSNA, 2022

R5A-SPPH-1

### Comparison of Computed Tomographic Dose Data of Tin Filter With Conventional Scanning Protocols Using Thermoluminescence Dosimeter Measurements

Thursday, Dec. 1 12:15PM - 12:45PM Room: Learning Center - PH DPS

#### Participants

Simone Schuele, (*Presenter*) Nothing to Disclose

#### PURPOSE

We aim to investigate whether there are differences in the applied dose (TLD measurements (thermoluminescence dosimeter)) between different scanning protocols in computed tomography for the same CTDIvol (Computed Tomography Dose Index). Special focus is on the tin filter technique (Sn).

#### METHODS AND MATERIALS

Sixteen TLD measurements (3 measurement repetitions each) were performed in a water phantom (diameter 32 cm) using five different scan protocols (Sn 150 kV, 150 kV, 120 kV, 100 kV, Sn 100 kV) at three (CTDIvol: 29 mGy, 8.5 mGy, and 2.8 mGy) dose settings on a 3-generation dual source CT scanner. With the Sn 100 kV protocol, limited by the scanner, irradiations were only possible up to 6.4 mGy (CTDIvol). The TLDs were positioned centrally in the water phantom. TLD measurement results and the slope of the linear regression of the different protocols were compared. ANOVA or Kruskal-Wallis-test was used for statistical testing, where applicable.

#### RESULTS

Compared to the 100 kV, 120 kV, and 150 kV protocols, the tin filter protocols (Sn 150 kV, Sn 100 kV) applied higher doses (average dose difference: 16% +/- 4%) at all dose settings studied ( $p < 0.01$ ) except for the comparison between the Sn 150 kV and 150 kV protocols at a CTDIvol of 29 mGy ( $p = 0.072$ ). The Sn 150 kV protocol showed a steeper slope of the linear regression than the 100 kV and 120 kV protocols ( $p < 0.05$ ).

#### CONCLUSION

s The CTDIvol information from the scanner underestimates the dose of the Sn 150 kV and Sn 100 kV protocols compared to protocols without tin filtration.

#### CLINICAL RELEVANCE/APPLICATION

Tin filter protocols expose patients to higher radiation doses than standard protocols at the same CTDIvol. This must be taken into account when using the tin filter technique in computed tomography for radiation protection reasons.

Printed on: 02/07/23

## Abstract Archives of the RSNA, 2022

R5A-SPPH-2

### Multicenter, International Study of CT Practices and Radiation Doses from 5 African Countries: An International Atomic Energy Agency (IAEA) Baseline Study

Thursday, Dec. 1 12:15PM - 12:45PM Room: Learning Center - PH DPS

#### Participants

Giridhar Dasegowda, MBBS, Boston, MA (*Presenter*) Nothing to Disclose

#### PURPOSE

There are few studies on CT practices from Africa to inform about the implementation of justification and optimization principles for radiation protection of patients. Therefore, under the framework of the IAEA Technical Cooperation Regional Project RAF9/064 entitled "a comprehensive baseline study was conducted to under to assess CT practices and radiation doses from multiple hospitals across several African countries and better determine the needs for improved radiation protection of patients.

#### METHODS AND MATERIALS

Six hospitals from Mauritius, Tunisia, Kenya, Sudan, Burkina Faso contributed information on 20-30 consecutive patients who underwent head, chest, and/or abdomen-pelvis CT examinations. Prior to the data recording step, all sites had a mandatory one-hour training on best practices in recording the relevant data elements without any personal health identifiers. The recorded data elements included patient age, gender, weight, height, CT protocol name, scanner information, scan factors (tube current, automatic exposure control, tube potential, number and names of scan phases), and radiation dose metrics including series-specific CT dose index volume (CTDIvol in mGy) and dose length product (DLP in mGy.cm). Information was recorded by either on-site CT technologists or medical physicists and radiologists between January-April 2022. For statistical analysis, we estimated median and interquartile range of body-region specific CTDIvol and DLP and compared data with Kruskal Wallis H test.

#### RESULTS

There were substantial variations in radiation doses between the different hospitals with minimum and maximum CTDIvol and DLP of 33-81mGy and 638-1891mGy.cm for head CT, 6-25mGy and 192-974mGy.cm for chest CT, and 6-15mGy and 303-1375mGy.cm for abdomen-pelvis CT ( $p < 0.01$ ). There was no significant difference between body mass index (BMI) or age across the different sites. Most sites used multiphase CT protocols for chest-abdomen-pelvis (6/6 sites) and chest CT (3/6 sites), regardless of clinical indications. Total DLP values for head, chest, abdomen, and chest-abdomen-pelvis CT at 3/6, 4/6, 4/6, and 5/6 sites were above the American College of Radiology and European reference dose levels.

#### CONCLUSION

There are concerning variations in CT practices and protocols across several hospitals in Africa emphasizing need for protocol optimization to improve radiation protection of patients.

#### CLINICAL RELEVANCE/APPLICATION

Use of higher than recommended CT radiation doses in several African sites underscore critical need for optimization and oversight of CT practices.

Printed on: 02/07/23

## Abstract Archives of the RSNA, 2022

R5A-SPPH-3

### Effect of Hormone Therapy on Target Volume in Radio-therapy of Localized Prostate Cancer

Thursday, Dec. 1 12:15PM - 12:45PM Room: Learning Center - PH DPS

#### Participants

Ayşe Dagi, Istanbul, Turkey (*Presenter*) Nothing to Disclose

#### PURPOSE

To determine the extent of tumor volume reduction and normal organ doses in prostate cancer (PCa) patients, with large prostate volumes that are geometrically unsuitable, treated with radiotherapy (RT) and combined androgen deprivation therapy (ADT).

#### METHODS AND MATERIALS

Ten patients with localized PCa included into the study. Median patient age was 71.6. (60-76). Patients underwent neoadjuvant ADT at least three months (3-36 months). Simulation CT images were obtained before the initiation of ADT (Plan 1) and 2 months after ADT (Plan 2). All patients were simulated in supine position with full bladder and empty rectum. RT treatment plans were done on each image set. All plans were done with VMAT using two full arcs. Prescribed dose was 76 Gy with 2 Gy/day in 38 fractions. Tumor volume and normal organ doses were dosimetrically compared. Maximum target doses (Dmax), homogeneity index (HI) and conformity index (CI), bladder, rectum and penile bulb doses were compared between two plans. Statistical analysis was done using paired t test. P<0.05 was accepted as statistically significant.

#### RESULTS

The median prostate volume was 77 cc (range: 51-113 cc) in Plan 1 images and the median prostate volume was 56 cc (range: 35-90 cc) in the Plan 2 images. Median prostate volume reduction with ADT was 17 cc, representing a 23% reduction in the target volume (p<0.001). The Dmax (p=0.77), HI (p=0.16) and CI (p=0.66) was not statistically different in two plans. Bladder (p=0.48) and rectum (p=0.07) volumes were not significantly different between two plans. Bladder volumes receiving 30 Gy (V30), 40 Gy (V40), 50 Gy (V50), 56 Gy (V56), 65 Gy (V65), 75 Gy (V75) decreased 14%, 8%, 7%, 4%, 4%, 1%, respectively combined ADT. Bladder Dmax was decreased 7% but Dmean did not change. Rectum volumes receiving 30 Gy (V30), 40 Gy (V40), 50 Gy (V50), 56 Gy (V56), 60 Gy (V60), 70 Gy (V70), 75 Gy (V75) decreased 21%, 26%, 34%, 35%, 34%, 33%, 35%, respectively combined ADT. Rectum Dmean was decreased 19% but Dmax did not change. Doses to 90 ml (D90) penile bulb was decreased 8%; mean and maximum penile bulb doses were decreased 9% and 2%, respectively.

#### CONCLUSION

Prostate shrinkage after combined ADT provides significant reduction in normal organ doses in PCa RT. This benefit may result in fewer acute and late radiotherapy complications. Clinical studies are needed to support this data.

#### CLINICAL RELEVANCE/APPLICATION

It may be necessary to revise target volume in treatment planning, as it provides significant reduction in prostate volume after combined ADT.

Printed on: 02/07/23

## Abstract Archives of the RSNA, 2022

R5A-SPPH-4

### Cumulative Radiation Exposure in Covid-19 Patients Admitted to the Intensive Care Unit

Thursday, Dec. 1 12:15PM - 12:45PM Room: Learning Center - PH DPS

#### Participants

Lama HADID, (*Presenter*) Nothing to Disclose

#### PURPOSE

Medical imaging plays a major role in coronavirus disease-2019 (COVID-19) patient diagnosis and management. However, the radiation dose received from medical procedures by these patients has been poorly investigated. We aimed to estimate the cumulative effective dose (CED) related to medical exposure in COVID-19 patients admitted to the intensive care unit (ICU) in comparison to the usual critically ill patients.

#### METHODS AND MATERIALS

We designed a descriptive cohort study including 90 successive ICU COVID-19 patients admitted between March and May 2020 and 90 successive non-COVID-19 patients admitted between March and May 2019. In this study, the CED resulting from all radiological examinations was calculated and clinical characteristics predictive of higher exposure risk identified.

#### RESULTS

The number of radiological examinations was 12.0 (5.0-26.0) [median (interquartile range) in COVID-19 vs. 4.0 (2.0-8.0) in non-COVID-19 patient ( $P < 0.001$ )]. The CED during a fourmonth period was 4.2 mSv (1.9-11.2) in the COVID-19 vs. 1.2 mSv (0.13-6.19) in the non-COVID-19 patients ( $P < 0.001$ ). In the survivors, the CED in COVID-19 vs. non-COVID-19 patients was  $\geq 100$  mSv in 3% vs. 0%, 10-100 mSv in 23% vs. 15%, 1-10 mSv in 56% vs. 30% and  $\leq 1$  mSv in 18% vs. 55%. The CED ( $P < 0.001$ ) and CED per ICU hospitalization day ( $P = 0.004$ ) were significantly higher in COVID-19 than non-COVID-19 patients. The CED correlated significantly with the hospitalization duration ( $r = 0.45$ ,  $P < 0.001$ ) and the number of conventional radiological examinations ( $r = 0.8$ ,  $P < 0.001$ ).

#### CONCLUSION

To conclude, more radiological examinations were performed in critically ill COVID-19 patients than non-COVID-19 patients resulting in higher CED. In COVID-19 patients, contribution of strategies to limit CED should be investigated in the future.

#### CLINICAL RELEVANCE/APPLICATION

This study is relevant for Covid-19 patients cared for in radiology departments and intensive care units.

Printed on: 02/07/23

## Abstract Archives of the RSNA, 2022

R5A-SPPH-5

### Patient-Specific Analysis of Dose Metrics and Organ Doses Based on Monte Carlo Simulation in Multiphase Abdominal CT Examinations

Thursday, Dec. 1 12:15PM - 12:45PM Room: Learning Center - PH DPS

#### Participants

Keisuke Fujii, PhD, Nagoya, Japan (*Presenter*) Nothing to Disclose

#### PURPOSE

The aims of this study are to determine organ doses based on Monte Carlo (MC) simulations for individual patients in multiphase abdominal CT examinations and to evaluate the correlations between the organ doses and dose metrics.

#### METHODS AND MATERIALS

The voxelized models of 30 adults (15 normal weight patients with body mass index (BMI) of 18.5-25.0 and 15 overweight patients with BMI more than 25.0) undergoing four phase abdominal CT examinations with Aquilion ONE VISION (n=10) and Aquilion Precision (n=20) (Canon Medical Systems) were created by inputting the CT images into MC simulation software ImpactMC (Advanced Breast CT, GmbH). MC simulations for each voxelized phantom were performed by inputting the detailed descriptions of the CT scanners and scanning parameters into ImpactMC. The scan range for pre-contrast, arterial phase, and delayed phase and for portal phase was set to upper abdomen and chest-abdomen-pelvis, respectively. Next, region of interests (ROIs) of seven radiosensitive organs (thyroid, lung, esophagus, breast, liver, stomach, and bladder) were created by delineating each organ on the CT images. Each ROI was set on the dose distribution images obtained as the simulation results and organ doses for each organ were evaluated as average doses within each organ ROI. For dose metrics, volume CT dose index (CTDIvol) and size-specific dose estimates (SSDE) were collected, and organ-specific SSDE were calculated using the average CTDIvol and water equivalent diameter over each organ position.

#### RESULTS

Organ doses for liver and stomach within scan range at all phase in abdominal CT examinations were approximately 17-48 mGy at each phase and 70-190 mGy in total. The doses had strong linear relationships with organ-specific SSDE, and the doses for overweight patients in the CT examinations with one of the CT scanners were approximately 60-70% higher than those for normal weight patients. Organ doses in lung and esophagus partially included in scan range at the pre-contrast, arterial and delayed phase were approximately 6-32 mGy at each phase, and the doses accounted for approximately 50-70% of 30-140 mGy in total at the four phases.

#### CONCLUSION

Organ doses for organs within or partially included in scan range in multiphase abdominal CT examinations will widely vary depending on the types of CT scanners and patient size. Organ-specific SSDE can be useful for total organ dose estimations for organs within scan range in the CT examinations.

#### CLINICAL RELEVANCE/APPLICATION

The reduction of organ doses for individual patients in multiphase abdominal CT examinations will require the optimization of scanning parameters including tube current modulation for each CT scanner.

Printed on: 02/07/23

## Abstract Archives of the RSNA, 2022

R5A-SPPH-6

### Patient-Specific Organ Dose and Cancer Risk Estimation in Adult Computed Tomography: Impact of a 7 Years Dose Optimization Process

Thursday, Dec. 1 12:15PM - 12:45PM Room: Learning Center - PH DPS

#### Participants

Benoit Dufour, Sion, Switzerland (*Presenter*) Nothing to Disclose

#### PURPOSE

To estimate the impact of dose optimization on cancer risks from adult computed tomography (CT).

#### METHODS AND MATERIALS

From 2016 to 2022, after a phase (P0) of protocol harmonization according to clinical indication, three successive phases of dose optimization were implemented at our institution (9 centers). P1 (first dose optimization round); P2 (second dose optimization round with the introduction of new generation CT scanners); P3 (third dose optimization round with the introduction of deep learning reconstruction). To estimate cancer risk for each patient and phase, patient-specific organ doses, age at exposure and sex were needed. Patient-specific organ doses were computed using the organ dosimetry module of a dose monitoring system (DoseWatch, GE Healthcare). Finally, lifetime risk and organ-specific risk of developing cancer were estimated using RadRAT (version 4.2.1). Results from each phase were compared by using the mean risk (Kruskal-Wallis test, significance  $p < 0.05$ ). Data were also stratified per anatomical region and clinical indication (chest (emphysema, pulmonary embolism and pneumonia) and abdomen (appendicitis, diverticulitis, kidney stones, liver, pancreas tumor, renal tumor and infection)).

#### RESULTS

Preliminary results on comparing P3 (4698 examinations) and P1 (678 examinations) showed an overall reduction of 49.5% lifetime risk of developing cancer. Stratifying per anatomical region, the reduction was 53.7%/27.6% for abdomen/thorax respectively. The highest excessive risk reduction was observed for the pancreas tumor (66.7%), diverticulitis (62.7%), and kidney stone (50.4%) protocols. The lowest impact was on the pneumonia and renal infection protocols, with 11.4% and 23.6% respectively. Statistical analyses for P0 and P4 and stratification per organ are ongoing.

#### CONCLUSION

s Patient-specific lifetime risk of developing cancer from CT imaging have been estimated for adult patients. The continuous process of CT protocol optimization allowed for a significant reduction of cancer risk associated with ionizing radiation.

#### CLINICAL RELEVANCE/APPLICATION

Excess of radiation-induced cancer cases can be reduced by fostering continuous dose optimization and avoiding scanner obsolescence.

Printed on: 02/07/23



## Abstract Archives of the RSNA, 2022

R5A-SPPH-7

### Establishment of CT Local Diagnostic Reference Levels at King Faisal Specialist Hospital and Research Centre

Thursday, Dec. 1 12:15PM - 12:45PM Room: Learning Center - PH DPS

#### Participants

Omar Mohamed Noor, MSc, (*Presenter*) Nothing to Disclose

#### PURPOSE

To establish local diagnostic reference levels at KFSHRC for computed tomography examinations of adults and identify the need for optimization.

#### METHODS AND MATERIALS

Data for over 4500 patients who have undergone CT scans in 2021 were analyzed. Four anatomical regions were considered for this study, namely head, head neck, chest, and abdomen-pelvis. In total, there are six CT scanners with multislice capability at KFSHRC. Sectra Dose Track management system was used to extract patient dose information. CT-dose index (CTDIvol, mGy) and dose length product (DLP, mGy.cm) were the selected dose matrices for the study. The 25th, 50th and 75th percentiles of these two quantities were calculated for each scanner. The local DRL values were then determined by calculating the 75th percentile of the distribution of median values. The results were compared with national and international DRL values.

#### RESULTS

The determined CTDIvol/DLP for the head, head neck, chest, and abdomen-pelvis protocols were 51.93/1054, 17/564, 7/244 and 13/891, respectively.

#### CONCLUSION

s The established local DRL values have shown appreciable improvement compared to prior estimated values in 2018, up to 30% improvement for some protocols. Also, the established values are relatively lower than the national DRL values by an average of 12% and are comparable to international values.

#### CLINICAL RELEVANCE/APPLICATION

Diagnostic reference levels are a great quality control tool to ensure optimal diagnostic imaging radiation doses and adherence to international best practices.

Printed on: 02/07/23

## Abstract Archives of the RSNA, 2022

R5A-SPPH-8

### Fluoroscopic X-Ray Beam Optimization for Improved Radiation Safety in Neurosurgery Imaging

Thursday, Dec. 1 12:15PM - 12:45PM Room: Learning Center - PH DPS

#### Participants

Xinhua Li, PhD, Boston, MA (*Presenter*) Employee, MorphoSys AG ;Employee, Elevation Oncology

#### PURPOSE

Fluoroscopic-guided neurosurgery may be associated with prolonged procedure time, intensive use of radiation, and notable adverse radiation effects. This study examines x-ray spectral optimization to achieve dose reduction and improved safety for patients and operators.

#### METHODS AND MATERIALS

Through this retrospective cohort study, radiation exposure to consecutive patients who underwent neurosurgery in two biplane procedure rooms, each with Artis zee replaced by Artis icono (Siemens Healthineers), was analyzed. Tests with anthropomorphic phantom (ATOM 701-B, CIRS Inc., VA; Weight 73 kg, height 173 cm) on Artis icono were conducted and effective x-ray beam filtration was characterized with x-ray spectral modeling.

#### RESULTS

No. of procedures was 716 (median age at procedure, 58; range 7-95) on Artis zee (Jan-Nov,2021) and 415 (59; 7-95) on Artis icono (Oct,2021-Apr,2022),with insignificant difference in age ( $p=0.098$ , two-tailed t test) between them. Dosage was 881.4 (838.5-924.3) mGy [mean (95% CI)] for air kerma at the reference point, 110.9 (105.1-116.7) Gy·cm<sup>2</sup> for air kerma-area product, and 26.0 (24.4-27.5) minutes for fluoroscopic time on Artis zee and it was 402.3 (361.2-443.4) mGy, 54.8 (49.7-59.9) Gy·cm<sup>2</sup>, and 25.0 (22.9-27.2) minutes on Artis icono. In phantom tests [FL Neuro Sharp, mag1 (40 cm), 7.5 P/S], AP plane used 66-67 kV, Cu filters of 0.9, 0.6 and 0.3 mm and LAT plane used 64-68 kV, Cu filters of 0.6, 0.6 and 0.3 mm for low, normal, and high dose modes. Half value layer (HVL) was 7.19, 6.42 and 5.25 mmAl (effective energy 51,48,43 keV; FWHM 19.5, 22, 24.5 keV) (AP) and 5.86, 6.27, and 5.08 mmAl (effective energy 46,47,42 keV; FWHM 21.5, 23.2, 25.2 keV) (LAT).

#### CONCLUSION

s Substantial (=50.6%) dose reduction is achieved in neurosurgery imaging by optimizing x-ray beam spectrum.

#### CLINICAL RELEVANCE/APPLICATION

Optimization of x-ray beam filtration and spectrum can facilitate radiation dose reduction in neurosurgery imaging for improved radiation safety for patients and the staff.

Printed on: 02/07/23

## Abstract Archives of the RSNA, 2022

R5A-SPPH-9

### Usefulness of Generative Adversarial Network-Based Low-Dose Digital Breast Tomosynthesis for Image Quality Improvement

Thursday, Dec. 1 12:15PM - 12:45PM Room: Learning Center - PH DPS

#### Participants

Tsutomu Gomi, PhD, (*Presenter*) Nothing to Disclose

#### PURPOSE

To evaluate the image quality improvement in digital breast tomosynthesis under low-radiation-dose conditions of prereconstruction processing using conditional generative adversarial networks (cGAN [pix2pix]).

#### METHODS AND MATERIALS

The pix2pix prereconstruction processing (p2p) with filtered back projection (FBP) and simultaneous algebraic reconstruction technique total variation first-iterative shrinkage-thresholding algorithm (SART-TV-FISTA) was compared with and without multiscale bilateral filtering. Noise reduction and preserve contrast rates were compared using full width at half-maximum (FWHM), contrast-to-noise ratio, peak signal-to-noise ratio (PSNR), and structural similarity (SSIM) in the in-focus plane using a BR3D phantom at various radiation doses (reference-dose [automatic exposure control reference dose: AECrd]; average glandular dose [AGD] 1.36 mGy, 50% [AGD; 0.66 mGy] and 75% [AGD; 0.31 mGy] reduced AECrd).

#### RESULTS

The overall performance of p2p-FBP in FWHM, PSNR, and SSIM was effective for both with and without MSBF prereconstruction processing with FBP and SART-TV-FISTA. At ~75% radiation-dose reduction, p2p-FBP in FWHM yielded good results independent of microcalcification (MC) sizes equivalent to that of the reference images, but without significant difference in statistical results (FBP p2p of 0.196 mm [ $p = 0.98$ ], 0.23 mm [ $p = 0.72$ ], and 0.29 mm [ $p = 0.60$ ]; FBP with MSBF of 0.196 mm [ $p = 0.11$ ], 0.23 mm [ $p < 0.05$ ], and 0.29 mm [ $p < 0.05$ ]; FBP without MSBF of 0.196 mm [ $p = 0.74$ ], 0.23 mm [ $p = 1.00$ ], and 0.29 mm [ $p = 0.99$ ]; SART-TV-FISTA p2p of 0.196 mm [ $p = 1.00$ ], 0.23 mm [ $p = 0.80$ ], and 0.29 mm [ $p = 0.55$ ]; SART-TV-FISTA with MSBF of 0.196 mm [ $p = 0.91$ ], 0.23 mm [ $p < 0.05$ ], and 0.29 mm [ $p < 0.05$ ]; SART-TV-FISTA without MSBF of 0.196 mm [ $p = 0.82$ ], 0.23 mm, [ $p = 0.91$ ], and 0.29 mm, [ $p = 0.96$ ]) in preserving the MC structure and mass contrast. PSNR results showed that p2p-FBP demonstrated the minimum error with reference images at a ~75% reduction in radiation dose. SSIM analysis indicated that p2p-FBP yielded superior similarity at ~75% radiation-dose reduction, with features most similar to the reference images.

#### CONCLUSION

s This phantom study revealed that a ~75% reduction in radiation dose is feasible using our proposed p2p-FBP.

#### CLINICAL RELEVANCE/APPLICATION

The p2p-FBP can significantly reduce noise with preserved contrast and radiation-dose reduction in clinical practice.

Printed on: 02/07/23



## Abstract Archives of the RSNA, 2022

R5A-SPVA

### Vascular Thursday Poster Discussions - A

Thursday, Dec. 1 12:15PM - 12:45PM Room: Learning Center - VA DPS

#### Sub-Events

#### R5A-SPVA-1 Investigation of Metal Artifact Reduction Applications: Comparing Four Different Angiographic Systems

##### Participants

Mitsuharu Osawa, RT, MA, (*Presenter*) Nothing to Disclose

##### PURPOSE

Cone-beam CT as an indispensable tool for endovascular treatment has a big pitfall, the degradation of image quality due to the metal artifacts with coils and other highly absorptive materials. The applications for metal artifact reduction (MAR) have been usually installed in any angiography machines. We studied the usefulness of this tools based on the comparison between the angiography systems of four makers about the effect and difference of artifact reduction (reduction effect).

##### METHODS AND MATERIALS

Angiography systems used for this study are follows: Artis Q (Siemens, Germany), Azurion7 (Philips, Netherlands), Alphenix (Canon, Japan), and Innova IGS 630 (GE, the United States America). A cylindrical water phantom was used to evaluate artifacts with six patterns of various CT values of iodine contrast agents for CT (2300, 3300, 4500, 5000, 6000, and 8300) and a metal clip as high absorbing artifact sources. The CBCT protocol for the head was used for imaging of each device. The acquired images were subjected to MAR processing, and the artifacts were compared quantitatively and isotropically between the images with and without MAR by extreme value statistical analysis using the Gumbel evaluation method (Imai's index).

##### RESULTS

Azurion7 showed a reduction effect in the image with a CT value of more than 3300, while the other three showed it from the value of more than 6000. Although the threshold in recognizing metals was clear in MARs of Alphenix and Artis Q, Azurion7 had lower threshold than those of the others. Innova IGS 630 has a special function, automatic detection and MAR process for coils and clips using AI technology. It enabled to recognize clips regardless of the size of the CT value and to realize the useful reduction processing.

##### CONCLUSION

s We found that the difference of MAR reduction effect between angiographic systems of 4 makers depending on the CT value including clips. It is necessary to understand the difference of the effect of MAR by each machine on the evaluation of images of embolized patients, particularly the ones undergoing the embolization with medium density materials of approximately 3000 to 5000, such as NBCA and Onyx. Also we must know that some machines have less effects of MAR around the clips.

##### CLINICAL RELEVANCE/APPLICATION

Metal artifact reduction system for highly absorbent materials with high density, such as coils is applied in any angiographic systems. However, some machines have weak points to realize the effect of MAR, so the adequate machines should be used to get the higher quality image by each case with embolization.

Printed on: 02/07/23

## Abstract Archives of the RSNA, 2022

R5A-SPVA-1

### Investigation of Metal Artifact Reduction Applications: Comparing Four Different Angiographic Systems

Thursday, Dec. 1 12:15PM - 12:45PM Room: Learning Center - VA DPS

#### Participants

Mitsuharu Osawa, RT, MA, (*Presenter*) Nothing to Disclose

#### PURPOSE

Cone-beam CT as an indispensable tool for endovascular treatment has a big pitfall, the degradation of image quality due to the metal artifacts with coils and other highly absorptive materials. The applications for metal artifact reduction (MAR) have been usually installed in any angiography machines. We studied the usefulness of this tools based on the comparison between the angiography systems of four makers about the effect and difference of artifact reduction (reduction effect).

#### METHODS AND MATERIALS

Angiography systems used for this study are follows: Artis Q (Siemens, Germany), Azurion7 (Philips, Netherlands), Alphenix (Canon, Japan), and Innova IGS 630 (GE, the United States America). A cylindrical water phantom was used to evaluate artifacts with six patterns of various CT values of iodine contrast agents for CT (2300, 3300, 4500, 5000, 6000, and 8300) and a metal clip as high absorbing artifact sources. The CBCT protocol for the head was used for imaging of each device. The acquired images were subjected to MAR processing, and the artifacts were compared quantitatively and isotropically between the images with and without MAR by extreme value statistical analysis using the Gumbel evaluation method (Imai's index).

#### RESULTS

Azurion7 showed a reduction effect in the image with a CT value of more than 3300, while the other three showed it from the value of more than 6000. Although the threshold in recognizing metals was clear in MARs of Alphenix and Artis Q, Azurion7 had lower threshold than those of the others. Innova IGS 630 has a special function, automatic detection and MAR process for coils and clips using AI technology. It enabled to recognize clips regardless of the size of the CT value and to realize the useful reduction processing.

#### CONCLUSION

s We found that the difference of MAR reduction effect between angiographic systems of 4 makers depending on the CT value including clips. It is necessary to understand the difference of the effect of MAR by each machine on the evaluation of images of embolized patients, particularly the ones undergoing the embolization with medium density materials of approximately 3000 to 5000, such as NBCA and Onyx. Also we must know that some machines have less effects of MAR around the clips.

#### CLINICAL RELEVANCE/APPLICATION

Metal artifact reduction system for highly absorbent materials with high density, such as coils is applied in any angiographic systems. However, some machines have weak points to realize the effect of MAR, so the adequate machines should be used to get the higher quality image by each case with embolization.

Printed on: 02/07/23

## Abstract Archives of the RSNA, 2022

R5B-SPBR

### Breast Thursday Poster Discussions - B

Thursday, Dec. 1 12:45PM - 1:15PM Room: Learning Center - BR DPS

#### Participants

Paola Clauser, MD, Vienna, (*Moderator*) Speaker, Siemens AG

#### Sub-Events

### R5B-SPBR-2 Improved Breast 2D-SWE Algorithm to Eliminate False Negative Cases

#### Participants

Richard G. Barr, MD, PhD, Canfield, OH (*Presenter*) Consultant, Siemens AG; Speakers Bureau, Siemens AG; Research Grant, Siemens AG; Consultant, Koninklijke Philips NV; Speakers Bureau, Koninklijke Philips NV; Consultant, Canon Medical Systems Corporation; Advisor, Hologic, Inc; Research Grant, Hologic, Inc

#### PURPOSE

To evaluate a new breast 2D-SWE algorithm and compare to the existing algorithm.

#### METHODS AND MATERIALS

This prospective, single-center study was approved by our local IRB and HIPAA compliant. From 4/25/19 to 1/18/22 raw shear wave data was saved to a hard drive on patients having an examination on a research Siemens Sequoia ultrasound unit. After removing benign lesions <2-year follow-up (80), cysts (44), scars (10), not breast lesion (16), and artifacts (9), there were 210 patients with 268 lesions for analysis with biopsy proven pathology or >2-year follow-up. Raw data from these lesions were processed using the standard algorithm (SA) and a new algorithm (NA). 3mm ROIs were placed in the highest stiffness in the lesion or adjacent 3mm on the SA. Stiffness values (SWS, Max) in this location from both algorithms were recorded. The 3mm ROI was then placed in the highest SWS area on the NA. Statistics were calculated for each ROI location.

#### RESULTS

The mean patient age was 55.8±9.9 years (range 20-91). The mean lesion size was 12.6±12.0mm (range 4-43mm). There were 129 benign (>2-year follow-up) and 139 biopsied lesions (38 benign; 101 malignant). Max stiffness for benign lesions were (2.07±1.20, 3.07±1.74, 3.03±1.86) m/s and for malignant lesions (4.74±1.79, 8.10±1.65, 8.35±1.38) m/s for the SA, NA with the SA ROI, and NA respectively. The AUROC was 0.90 SA and 0.97 NA (both ROI placements). Using a cut-off value of 4.5m/s the sensitivity increased from 0.54 to 1.0 and the specificity changed from 0.95 to 0.82. For the NA the PPV was 0.77 and the NPV was 1.0 and a NLR or 0.00. Using the SA in cancers there were 30 (30.4%) color filled, 36 (35.3%) with high SWV ring, and 35 (34.3%) with no elevated SWS. With the NA there were 95 (93.1%) color filled, 7 (6.9%) with high SWV ring and 0% with no SWS elevation.

#### CONCLUSION

Using a new breast SWE algorithm significantly improve the sensitivity of the technique with a small decrease in specificity, virtually eliminating the "soft" cancer issue.

#### CLINICAL RELEVANCE/APPLICATION

Breast SWE has been limited due to artifactual false negative cases; a new algorithm significantly decreases these false negative cases increasing sensitivity to 99%.

### R5B-SPBR-3 Positive Predictive Value of Axillary Lymph Node Cortical Thickness and Nodal, Clinical and Tumor Characteristics in Newly Diagnosed Breast Cancer Patients

#### Participants

Anne-Sophie Loonis, MD, MSc, Boston, MA (*Presenter*) Nothing to Disclose

#### PURPOSE

To determine the positive predictive value (PPV) of cortical thickness of abnormal axillary lymph nodes (LNs) in newly diagnosed breast cancer patients and identify nodal, clinical and tumor characteristics associated with likelihood of axillary metastasis.

#### METHODS AND MATERIALS

IRB-approved, retrospective review of all axillary LN fine needle aspirations (FNAs) performed 1/1/2018-12/31/2019 was completed. Patients with contralateral breast cancer, no subsequent axillary surgery, male sex, or lymphoma were excluded. There were 135 ipsilateral axillary FNAs in 134 patients with newly diagnosed breast cancer. Patient demographics, clinical characteristics, histopathology results, and imaging features were obtained from medical records. Hypothesis testing was performed using independent samples t-tests and multivariable binary logistic regression to identify statistically significant predictors of axillary LN metastasis.

#### RESULTS

Of 135 axillary LN FNAs, cytology was positive in 72 (53.3%), negative in 61 (45.2%), and nondiagnostic in 2 (1.5%). At axillary surgery, histopathology was positive in 84 (62.2%) and negative in 51 (37.8%). Lymph node cortices were thicker in metastatic compared to negative nodes ( $p < 0.0001$ ). PPV of axillary LNs with cortical thickness greater than 3mm, 3.5 mm, 4 mm and 4.25 mm was 0.62 (95% CI 0.53, 0.70), 0.63 (0.54, 0.72), 0.67 (0.57, 0.76) and 0.74 (0.64, 0.83), respectively. At multivariable analysis, abnormal hilum was statistically significantly associated with nodal metastasis (OR=3.44,  $p=0.016$ ) while focal/eccentric cortical thickening was inversely associated with metastasis (OR=0.35,  $p=0.038$ ). Other nodal, clinical, and tumor characteristics were not associated with increased likelihood of axillary LN metastasis.

## CONCLUSION

Increasing axillary LN cortical thickness is associated with likelihood of nodal metastasis in newly diagnosed cancer patients. PPV of axillary LN cortical thickness  $>3$  mm and  $>3.5$  mm is similar, but PPV is statistically significantly higher for cortical thickness  $>4$  mm and  $>4.25$  mm. Higher likelihood of metastasis is associated with axillary LNs with abnormal fatty hilum and diffuse cortical thickening.

## CLINICAL RELEVANCE/APPLICATION

FNA of axillary LNs with cortical thickness  $>4$  mm should be performed. FNA of axillary lymph nodes with cortical thickness  $<4$  mm may be unnecessary for some patients undergoing sentinel LN biopsy.

## R5B-SPBR-4 Comparison of Digital Breast Tomosynthesis-Guided Biopsy versus Ultrasound-Guided Biopsy of Non-Calcified Breast Lesions

Participants

Masoud Baikpour, MD, (Presenter) Nothing to Disclose

## PURPOSE

Historically, mammographic-guided core needle biopsy is performed almost exclusively for calcifications. Increasingly centers are shifting to mammographic-guided biopsy for non-calcified breast lesions given improved efficiency and comfort with new approaches of digital breast tomosynthesis-guided biopsy (DBT-bx). This study aims to compare the characteristics and cancer rates of non-calcified breast lesions that underwent DBT-bx vs. ultrasound-guided biopsy (US-bx).

## METHODS AND MATERIALS

This retrospective study included consecutive patients who underwent DBT-bx and US-bx of non-calcified breast lesions between 4/1/2016 and 3/31/2018. Lesions without mammographic findings were excluded. Medical records were reviewed for patient demographics, mammographic breast density, imaging findings, and final pathology results. Mann-Whitney U test and Pearson's Chi-squared test were used to compare the DBT-bx and US-bx groups.

## RESULTS

The study cohort consisted of 1211 patients with 1279 biopsies (226 DBT-bx in 217 patients [58.6 $\pm$ 12.2 years, range 23-88] and 1053 US-bx in 994 patients [56.7 $\pm$ 14.6 years, range 25-96]). DBT-bx was performed in more women with non-dense breasts (65%) compared to US-bx (48%,  $p < .001$ ). Distributions of non-calcified mammographic findings sampled in the DBT-bx and US-bx groups differed significantly ( $p < .001$ ), with DBT-bx more commonly performed for asymmetry (44.7% vs. 30.8%) and architectural distortion (33.2% vs. 1.3%) compared to US-bx. The positive predictive value (PPV3) of DBT-bx (32.7%, 74/226) was lower than that of US-bx (44.7%, 471/1053,  $p = .001$ ). Specifically, PPV3 was significantly lower for asymmetry (26.7% vs. 50.9%;  $p < .001$ ) and architectural distortion (30.7% vs. 71.4%;  $p = .004$ ) in the DBT-bx group vs. the US-bx group. Among malignant outcomes, DBT-bx yielded higher proportions of invasive lobular carcinoma (24.3% vs. 14.2%,  $p = .026$ ) and ductal carcinoma in situ (17.6% vs. 4.1%,  $p < .001$ ) than US-bx.

## CONCLUSION

While the malignancy rates of asymmetry and distortion sampled via DBT-bx were significantly lower than those sampled under US, the PPVs remain high and warrant biopsy.

## CLINICAL RELEVANCE/APPLICATION

Ultrasound (US) evaluation and biopsy of breast asymmetry and architectural distortion remain vital even with improved mammographic-guided biopsy, which should be performed for suspicious non-calcified lesions without definitive US correlates.

## R5B-SPBR-5 AI-Radiologist Disagreement on Ultrasound Examinations: Predictors of Malignancy

Participants

Sarah Ricklan, MD, (Presenter) Nothing to Disclose

## PURPOSE

To examine an artificial intelligence system's (AIS) ability to diagnose breast cancer on ultrasound (US) in a dataset of discordant predictions between the AIS and radiologists. Our AIS shows high accuracy in diagnosing breast cancer on US. We evaluated exams in which the AIS and an expert radiologist consensus disagreed on the probability of malignancy (POM).

## METHODS AND MATERIALS

This is an IRB approved retrospective study of an AIS using 288,767 US exams (AUC 0.976). We selected reader cases in which a consensus of ten board-certified radiologists and the AIS provided contradictory POM predictions. The full reader set was 663 exams (644 patients, 1,048 areas of interest (cases)). Of these, 10.8% (113/1048) (109 exams, 108 patients, 113 cases, mean age 54.1  $\pm$  14.1 yrs) had discordant benign-malignant determinations between the AIS and the radiologists; AIS was correct in 47.8% (54/113) of cases. 4.4% (5/113) of cases had a biopsy-determined malignancy. We compared demographic and US features including age, mean POM, mammographic breast density, and mass features between AI correct and AI incorrect discordant cases using t-, Mann-Whitney, and chi-square tests. Ground truth was tissue diagnosis or imaging stability.

## RESULTS

The AIS correctly designated 54/113 (47.8%) discordant cases as benign or malignant. 94.5% (52/55) of cases called by the AIS

as benign but the radiologist as malignant were true negatives; 5.5% (3/55) of AI-benign cases were false negatives. Of 113 cases, 78.8% (89/113) had lesions described as masses; 21.2% (24/113) had no or non-mass lesions (e.g. cysts, scars). The AIS was correct in 49/89 (55.1%) of masses. The AIS was more likely to be correct than the radiologist in cases with dense breasts ( $p=0.001$ ) and irregular ( $p<0.001$ ) and non-circumscribed ( $p<0.0001$ ) masses. Age, orientation, and posterior features were non-significant.

## CONCLUSION

s Compared to breast radiologists, the AIS may be more accurate in dense breasts. The AIS is more likely to correctly identify masses with concerning features (non-circumscribed margins) as benign or malignant. Further research should incorporate these strengths and weaknesses into a hybrid AI/radiologist workflow.

## CLINICAL RELEVANCE/APPLICATION

Hybrid AI-radiologist US systems may be more accurate in identifying findings in dense breasts and in downgrading benign lesions that radiologists initially find concerning.

## R5B-SPBR-7 Diagnostic Performance of Supplemental Breast US Screening to Digital Breast Tomosynthesis and to Digital Mammography in Women with Dense Breasts: A Matched Cohort Study

### Participants

Jung Min Chang, MD, Seoul, (*Presenter*) Research Consultant, Genoray Co, Ltd

## PURPOSE

Comparative screening performance of supplemental breast US after digital breast tomosynthesis (DBT) versus digital mammography (DM) in women with dense breasts is not well-known. This study was to evaluate and compare the performance of supplemental US screening following DBT and DM in women with dense breasts.

## METHODS AND MATERIALS

A retrospective database search identified consecutive asymptomatic women with dense breasts who underwent breast cancer screening with DBT or DM and whole-breast US simultaneously between June 2016 and July 2019. Combined DBT with US (DBT+US) and DM with US (DM+US) were matched 1:2 according to mammographic density, age, menopausal status, hormone replacement therapy, and family history of breast cancer. Cancer detection rate (CDR) per 1000 screening examination, sensitivity, specificity, and abnormal interpretation rate were compared.

## RESULTS

A total of 863 women in DBT+US group were matched with 1726 women in DM+US group (mean age 53 years). 26 breast cancers (DBT+US group, 4 ductal carcinoma in situ [DCIS] and 5 invasive ductal carcinoma [IDC]; DM+US group, 7 DCIS and 10 IDC) were identified. The CDRs were not significantly different in DBT+US and DM+US groups (10.4 vs. 9.8;  $P = .89$  [overall], 4.0 vs. 3.3 per 1000 examinations;  $P = .80$  [negative DBT or DM]), with higher abnormal interpretation in DBT+US than DM+US group (32% vs. 22%;  $P < .001$  [overall], 24% vs. 16%;  $P < .001$  [negative DBT or DM]). Sensitivities in both DBT+US and DM+US groups were 100% without interval cancers. Supplemental US contributed more cancer detection after negative DBT (1 DCIS and 2 IDC) or DM (1 DCIS and 4 IDC), especially invasive cancers, however, there was no statistical significant difference in terms of pathological results between both DBT+US and DM+US groups.

## CONCLUSION

s Supplemental US examination after negative DBT or DM yielded additional cancer detection in asymptomatic women with dense breasts, however, no significant improvement in diagnostic performances was noted in DBT+US than DM+US screening.

## CLINICAL RELEVANCE/APPLICATION

In asymptomatic women with dense breasts planned to be screened with the whole-breast US, baseline screening with DBT has no benefit over DM in regard to diagnostic performance.

Printed on: 02/07/23



## Abstract Archives of the RSNA, 2022

R5B-SPBR-2

### Improved Breast 2D-SWE Algorithm to Eliminate False Negative Cases

Thursday, Dec. 1 12:45PM - 1:15PM Room: Learning Center - BR DPS

#### Participants

Richard G. Barr, MD, PhD, Canfield, OH (*Presenter*) Consultant, Siemens AG;Speakers Bureau, Siemens AG;Research Grant, Siemens AG;Consultant, Koninklijke Philips NV;Speakers Bureau, Koninklijke Philips NV;Consultant, Canon Medical Systems Corporation;Advisor, Hologic, Inc;Research Grant, Hologic, Inc

#### PURPOSE

To evaluate a new breast 2D-SWE algorithm and compare to the existing algorithm.

#### METHODS AND MATERIALS

This prospective, single-center study was approved by our local IRB and HIPAA compliant. From 4/25/19 to 1/18/22 raw shear wave data was saved to a hard drive on patients having an examination on a research Siemens Sequoia ultrasound unit. After removing benign lesions <2-year follow-up (80), cysts (44), scars (10), not breast lesion (16), and artifacts (9), there were 210 patients with 268 lesions for analysis with biopsy proven pathology or >2-year follow-up. Raw data from these lesions were proceeded using the standard algorithm (SA) and a new algorithm (NA). 3mm ROIs were placed in the highest stiffness in the lesion or adjacent 3mm on the SA. Stiffness values (SWS, Max) in this location from both algorithms were recorded. The 3mm ROI was then placed in the highest SWS area on the NA. Statistics were calculated for each ROI location.

#### RESULTS

The mean patient age was 55.8±9.9 years (range 20-91). The mean lesion size was 12.6±12.0mm (range 4-43mm). There were 129 benign (>2-year follow-up) and 139 biopsied lesions (38 benign; 101 malignant). Max stiffness for benign lesions were (2.07±1.20, 3.07±1.74, 3.03±1.86) m/s and for malignant lesions (4.74±1.79, 8.10±1.65, 8.35±1.38) m/s for the SA, NA with the SA ROI, and NA respectively. The AUROC was 0.90 SA and 0.97 NA (both ROI placements). Using a cut-off value of 4.5m/s the sensitivity increased from 0.54 to 1.0 and the specificity changed from 0.95 to 0.82. For the NA the PPV was 0.77 and the NPV was 1.0 and a NLR or 0.00. Using the SA in cancers there were 30 (30.4%) color filled, 36 (35.3%) with high SWV ring, and 35 (34.3%) with no elevated SWS. With the NA there were 95 (93.1%) color filled, 7 (6.9%) with high SWV ring and 0% with no SWS elevation.

#### CONCLUSION

s Using a new breast SWE algorithm significantly improve the sensitivity of the technique with a small decrease in specificity, virtually eliminating the "soft" cancer issue.

#### CLINICAL RELEVANCE/APPLICATION

Breast SWE has been limited due to artifactual false negative cases; a new algorithm significantly decreases these false negative cases increasing sensitivity to 99%.

Printed on: 02/07/23

## Abstract Archives of the RSNA, 2022

R5B-SPBR-3

### Positive Predictive Value of Axillary Lymph Node Cortical Thickness and Nodal, Clinical and Tumor Characteristics in Newly Diagnosed Breast Cancer Patients

Thursday, Dec. 1 12:45PM - 1:15PM Room: Learning Center - BR DPS

#### Participants

Anne-Sophie Loonis, MD, MSc, Boston, MA (*Presenter*) Nothing to Disclose

#### PURPOSE

To determine the positive predictive value (PPV) of cortical thickness of abnormal axillary lymph nodes (LNs) in newly diagnosed breast cancer patients and identify nodal, clinical and tumor characteristics associated with likelihood of axillary metastasis.

#### METHODS AND MATERIALS

IRB-approved, retrospective review of all axillary LN fine needle aspirations (FNAs) performed 1/1/2018-12/31/2019 was completed. Patients with contralateral breast cancer, no subsequent axillary surgery, male sex, or lymphoma were excluded. There were 135 ipsilateral axillary FNAs in 134 patients with newly diagnosed breast cancer. Patient demographics, clinical characteristics, histopathology results, and imaging features were obtained from medical records. Hypothesis testing was performed using independent samples t-tests and multivariable binary logistic regression to identify statistically significant predictors of axillary LN metastasis.

#### RESULTS

Of 135 axillary LN FNAs, cytology was positive in 72 (53.3%), negative in 61 (45.2%), and nondiagnostic in 2 (1.5%). At axillary surgery, histopathology was positive in 84 (62.2%) and negative in 51 (37.8%). Lymph node cortices were thicker in metastatic compared to negative nodes ( $p < 0.0001$ ). PPV of axillary LNs with cortical thickness greater than 3mm, 3.5 mm, 4 mm and 4.25 mm was 0.62 (95% CI 0.53, 0.70), 0.63 (0.54, 0.72), 0.67 (0.57, 0.76) and 0.74 (0.64, 0.83), respectively. At multivariable analysis, abnormal hilum was statistically significantly associated with nodal metastasis (OR=3.44,  $p=0.016$ ) while focal/eccentric cortical thickening was inversely associated with metastasis (OR=0.35,  $p=0.038$ ). Other nodal, clinical, and tumor characteristics were not associated with increased likelihood of axillary LN metastasis.

#### CONCLUSION

Increasing axillary LN cortical thickness is associated with likelihood of nodal metastasis in newly diagnosed cancer patients. PPV of axillary LN cortical thickness  $>3$  mm and  $>3.5$  mm is similar, but PPV is statistically significantly higher for cortical thickness  $>4$  mm and  $>4.25$  mm. Higher likelihood of metastasis is associated with axillary LNs with abnormal fatty hilum and diffuse cortical thickening.

#### CLINICAL RELEVANCE/APPLICATION

FNA of axillary LNs with cortical thickness  $>4$  mm should be performed. FNA of axillary lymph nodes with cortical thickness  $<4$  mm may be unnecessary for some patients undergoing sentinel LN biopsy.

Printed on: 02/07/23

## Abstract Archives of the RSNA, 2022

R5B-SPBR-4

### Comparison of Digital Breast Tomosynthesis-Guided Biopsy versus Ultrasound-Guided Biopsy of Non-Calcified Breast Lesions

Thursday, Dec. 1 12:45PM - 1:15PM Room: Learning Center - BR DPS

#### Participants

Masoud Baikpour, MD, (*Presenter*) Nothing to Disclose

#### PURPOSE

Historically, mammographic-guided core needle biopsy is performed almost exclusively for calcifications. Increasingly centers are shifting to mammographic-guided biopsy for non-calcified breast lesions given improved efficiency and comfort with new approaches of digital breast tomosynthesis-guided biopsy (DBT-bx). This study aims to compare the characteristics and cancer rates of non-calcified breast lesions that underwent DBT-bx vs. ultrasound-guided biopsy (US-bx).

#### METHODS AND MATERIALS

This retrospective study included consecutive patients who underwent DBT-bx and US-bx of non-calcified breast lesions between 4/1/2016 and 3/31/2018. Lesions without mammographic findings were excluded. Medical records were reviewed for patient demographics, mammographic breast density, imaging findings, and final pathology results. Mann-Whitney U test and Pearson's Chi-squared test were used to compare the DBT-bx and US-bx groups.

#### RESULTS

The study cohort consisted of 1211 patients with 1279 biopsies (226 DBT-bx in 217 patients [58.6±12.2 years, range 23-88] and 1053 US-bx in 994 patients [56.7±14.6 years, range 25-96]). DBT-bx was performed in more women with non-dense breasts (65%) compared to US-bx (48%,  $p<.001$ ). Distributions of non-calcified mammographic findings sampled in the DBT-bx and US-bx groups differed significantly ( $p<.001$ ), with DBT-bx more commonly performed for asymmetry (44.7% vs. 30.8%) and architectural distortion (33.2% vs. 1.3%) compared to US-bx. The positive predictive value (PPV3) of DBT-bx (32.7%, 74/226) was lower than that of US-bx (44.7%, 471/1053,  $p=.001$ ). Specifically, PPV3 was significantly lower for asymmetry (26.7% vs. 50.9%;  $p<.001$ ) and architectural distortion (30.7% vs. 71.4%;  $p=.004$ ) in the DBT-bx group vs. the US-bx group. Among malignant outcomes, DBT-bx yielded higher proportions of invasive lobular carcinoma (24.3% vs. 14.2%,  $p=.026$ ) and ductal carcinoma in situ (17.6% vs. 4.1%,  $p<.001$ ) than US-bx.

#### CONCLUSION

While the malignancy rates of asymmetry and distortion sampled via DBT-bx were significantly lower than those sampled under US, the PPVs remain high and warrant biopsy.

#### CLINICAL RELEVANCE/APPLICATION

Ultrasound (US) evaluation and biopsy of breast asymmetry and architectural distortion remain vital even with improved mammographic-guided biopsy, which should be performed for suspicious non-calcified lesions without definitive US correlates.

Printed on: 02/07/23



## Abstract Archives of the RSNA, 2022

R5B-SPBR-5

### AI-Radiologist Disagreement on Ultrasound Examinations: Predictors of Malignancy

Thursday, Dec. 1 12:45PM - 1:15PM Room: Learning Center - BR DPS

#### Participants

Sarah Ricklan, MD, (Presenter) Nothing to Disclose

#### PURPOSE

To examine an artificial intelligence system's (AIS) ability to diagnose breast cancer on ultrasound (US) in a dataset of discordant predictions between the AIS and radiologists. Our AIS shows high accuracy in diagnosing breast cancer on US. We evaluated exams in which the AIS and an expert radiologist consensus disagreed on the probability of malignancy (POM).

#### METHODS AND MATERIALS

This is an IRB approved retrospective study of an AIS using 288,767 US exams (AUC 0.976). We selected reader cases in which a consensus of ten board-certified radiologists and the AIS provided contradictory POM predictions. The full reader set was 663 exams (644 patients, 1,048 areas of interest (cases)). Of these, 10.8% (113/1048) (109 exams, 108 patients, 113 cases, mean age  $54.1 \pm 14.1$  yrs) had discordant benign-malignant determinations between the AIS and the radiologists; AIS was correct in 47.8% (54/113) of cases. 4.4% (5/113) of cases had a biopsy-determined malignancy. We compared demographic and US features including age, mean POM, mammographic breast density, and mass features between AI correct and AI incorrect discordant cases using t-, Mann-Whitney, and chi-square tests. Ground truth was tissue diagnosis or imaging stability.

#### RESULTS

The AIS correctly designated 54/113 (47.8%) discordant cases as benign or malignant. 94.5% (52/55) of cases called by the AIS as benign but the radiologist as malignant were true negatives; 5.5% (3/55) of AI-benign cases were false negatives. Of 113 cases, 78.8% (89/113) had lesions described as masses; 21.2% (24/113) had no or non-mass lesions (e.g. cysts, scars). The AIS was correct in 49/89 (55.1%) of masses. The AIS was more likely to be correct than the radiologist in cases with dense breasts ( $p=0.001$ ) and irregular ( $p<0.001$ ) and non-circumscribed ( $p<0.0001$ ) masses. Age, orientation, and posterior features were non-significant.

#### CONCLUSION

Compared to breast radiologists, the AIS may be more accurate in dense breasts. The AIS is more likely to correctly identify masses with concerning features (non-circumscribed margins) as benign or malignant. Further research should incorporate these strengths and weaknesses into a hybrid AI/radiologist workflow.

#### CLINICAL RELEVANCE/APPLICATION

Hybrid AI-radiologist US systems may be more accurate in identifying findings in dense breasts and in downgrading benign lesions that radiologists initially find concerning.

Printed on: 02/07/23

## Abstract Archives of the RSNA, 2022

R5B-SPBR-7

### Diagnostic Performance of Supplemental Breast US Screening to Digital Breast Tomosynthesis and to Digital Mammography in Women with Dense Breasts: A Matched Cohort Study

Thursday, Dec. 1 12:45PM - 1:15PM Room: Learning Center - BR DPS

#### Participants

Jung Min Chang, MD, Seoul, (*Presenter*) Research Consultant, Genoray Co, Ltd

#### PURPOSE

Comparative screening performance of supplemental breast US after digital breast tomosynthesis (DBT) versus digital mammography (DM) in women with dense breasts is not well-known. This study was to evaluate and compare the performance of supplemental US screening following DBT and DM in women with dense breasts.

#### METHODS AND MATERIALS

A retrospective database search identified consecutive asymptomatic women with dense breasts who underwent breast cancer screening with DBT or DM and whole-breast US simultaneously between June 2016 and July 2019. Combined DBT with US (DBT+US) and DM with US (DM+US) were matched 1:2 according to mammographic density, age, menopausal status, hormone replacement therapy, and family history of breast cancer. Cancer detection rate (CDR) per 1000 screening examination, sensitivity, specificity, and abnormal interpretation rate were compared.

#### RESULTS

A total of 863 women in DBT+US group were matched with 1726 women in DM+US group (mean age 53 years). 26 breast cancers (DBT+US group, 4 ductal carcinoma in situ [DCIS] and 5 invasive ductal carcinoma [IDC]; DM+US group, 7 DCIS and 10 IDC) were identified. The CDRs were not significantly different in DBT+US and DM+US groups (10.4 vs. 9.8;  $P = .89$  [overall], 4.0 vs. 3.3 per 1000 examinations;  $P = .80$  [negative DBT or DM]), with higher abnormal interpretation in DBT+US than DM+US group (32% vs. 22%;  $P < .001$  [overall], 24% vs. 16%;  $P < .001$  [negative DBT or DM]). Sensitivities in both DBT+US and DM+US groups were 100% without interval cancers. Supplemental US contributed more cancer detection after negative DBT (1 DCIS and 2 IDC) or DM (1 DCIS and 4 IDC), especially invasive cancers, however, there was no statistical significant difference in terms of pathological results between both DBT+US and DM+US groups.

#### CONCLUSION

Supplemental US examination after negative DBT or DM yielded additional cancer detection in asymptomatic women with dense breasts, however, no significant improvement in diagnostic performances was noted in DBT+US than DM+US screening.

#### CLINICAL RELEVANCE/APPLICATION

In asymptomatic women with dense breasts planned to be screened with the whole-breast US, baseline screening with DBT has no benefit over DM in regard to diagnostic performance.

Printed on: 02/07/23

## Abstract Archives of the RSNA, 2022

R5B-SPCA

### Cardiac Thursday Poster Discussions - B

Thursday, Dec. 1 12:45PM - 1:15PM Room: Learning Center - CA DPS

#### Sub-Events

#### R5B-SPCA-1 Hemodynamic Signatures of Aortic Root and Ascending Aorta Aneurysm by 4D Flow MRI

##### Participants

Joe Juffermans, MSc, Leiden, Netherlands (*Presenter*) Nothing to Disclose

##### PURPOSE

Thoracic aortic aneurysms (TAA) are found in the aortic root and ascending aorta in patients with tricuspid aortic valves (TAV). Since aorta hemodynamic changes have been associated with aneurysm formation, the aim of this study was to determine hemodynamic signatures of aortic root and ascending aorta aneurysms in TAV patients.

##### METHODS AND MATERIALS

Eighty TAV patients underwent aortic 4D flow MRI. Left ventricular stroke volume, normalized flow displacement, flow jet angle, wall shear stress (WSS) magnitude, axial WSS, circumferential WSS, WSS angle, vorticity magnitude, absolute helicity and aortic diameter were assessed at peak systole in the aortic root and ascending aorta. Root and ascending z-scores were calculated and used to categorize the aneurysm type according to the Della Corte's classification (i.e., root, ascending or no aneurysm). To assess hemodynamic differences between the aneurysm cohorts, Kruskal-Wallis test was performed with subsequent Mann-Whitney U-tests for post-hoc analysis. Hemodynamics signatures were illustrated by radial plots.

##### RESULTS

After classification, three aneurysm cohorts were identified: aortic root aneurysm (n=40), ascending aorta aneurysm (n=19), and no aorta aneurysm (n=21) (48±11years, 54±11years, and 49±10years, respectively; p=0.25). Root aneurysm patients presented a significantly higher stroke volume compared to patients with ascending or no aneurysm (both p<0.05). Ascending aneurysm patients presented a significantly higher normalized flow displacement, flow jet angle and WSS angle together with lower WSS magnitude and axial WSS compared to patients with root or no aneurysms (all p<0.01; see Figure 1). Patients with no aneurysm demonstrated a significantly higher vorticity magnitude and absolute helicity at the ascending aorta compared to patients with root or ascending aneurysm (all p=0.01).

##### CONCLUSION

Patients with root or ascending aneurysm demonstrated two distinct hemodynamic signatures, as compared to patients without an aneurysm. Root aneurysm patients have a significantly higher left ventricular stroke volume and ascending aneurysm patients have a significantly higher normalized flow displacement, flow jet angle and WSS angle.

##### CLINICAL RELEVANCE/APPLICATION

Aortic 4D flow MRI revealed two distinct hemodynamic signatures in patients with aortic root or ascending aorta aneurysm, as compared to patients without aneurysm.

#### R5B-SPCA-2 Impact on Clinical Outcome of High-pitch non-ECG-gated CT Angiography for Transcatheter Aortic Valve Implantation Planning as Compared to An ECG-gated CTA Protocol

##### Participants

Martin Sinn, Hamburg, Germany (*Presenter*) Nothing to Disclose

##### PURPOSE

The question of whether to use ECG-guided or non-ECG-guided high-pitch CT angiography (CTA) in planning transcatheter aortic valve implantation (TAVI) has been controversial, with ECG-guided CTA currently recommended. However, the impact on clinical outcome, including post-interventional paravalvular leakage (PVL), remains unclear. Therefore, the aim of this study was to compare a retrospective ECG-guided CTA protocol with a non-ECG-guided high-pitch CTA protocol for TAVI planning and the associated impact on clinical outcome.

##### METHODS AND MATERIALS

This retrospective, institutional review board-approved study included 231 subjects (age 80±7 years) who underwent implantation of an Evolut R (Medtronic, Minneapolis, USA) self-expandable transcatheter heart valve. Thereof, 48 subjects received retrospective ECG-guided CTA (group A) prior intervention, and 183 subjects received non-ECG-guided high-pitch CTA (group B). The amount of aortic valve calcification (Agatston score), aortic annulus diameter, and circumferential area were measured using commercially available software tools. Visual motion scoring of the aortic root and valve was performed by two radiologists. For each patient, the cover index was calculated  $100 \times \left( \frac{\text{prosthesis diameter} - \text{annulus diameter}}{\text{prosthesis diameter}} \right)$ . Clinical outcome parameters were assessed 30 days after TAVI following the Valve Academic Research Consortium-3 consensus document. Paired and unpaired two-sided t-test and Chi-squared test were utilized to compare continuous and categorical

variables, respectively.

## RESULTS

There were no significant differences in motion artefacts of the aortic root or aortic valve calcification between both groups ( $p > .05$ ). A significant difference in cover index was observed, with a higher cover index for group A (group A:  $6.6 \pm 8.6$  vs. group B:  $-1.3 \pm 10.4$ ;  $p = .001$ ). However, this difference did not lead to significantly different rates of PVL post TAVI ( $p = .399$ ). Further, there were no significant differences in major adverse cardiac events (MACE) between both groups ( $p = .49$ ).

## CONCLUSION

Although the cover index for TAVR planning of a high-pitch non-ECG-gated CTA was lower compared to an ECG-gated CTA protocol, rates of PVL and MACE were comparable between groups.

## CLINICAL RELEVANCE/APPLICATION

A high-pitch non-ECG-gated CTA protocol may be suitable for TAVI planning.

## R5B-SPCA-3 Ex-vivo Swine Model Reveals Characteristic Aortic Flow Alterations After Different Aortic Valve Replacement Strategies

Participants

Maren Balks, (*Presenter*) Nothing to Disclose

## PURPOSE

Aortic hemodynamics can be altered by aortic valve replacement (AVR) with studies suggesting differences in flow alterations after different types of replacement. Ozaki aortic valve neocuspidization is a new, promising procedure for reconstructing the aortic valve using the patient's own pericardium. In order to perform any open AVR, an incision in the ascending aorta (aortotomy) is obligatory to gain access to the valve. Little is known about impact of the surgical incision itself on aortic flow. The purpose of this work was to establish a biological model to comprehensively evaluate the impact of the surgical pathway alone and in combination with different valve replacement strategies on aortic hemodynamics.

## METHODS AND MATERIALS

Six fresh swine aortas were anastomosed to an in-house developed piston pump pumping blood-mimicking fluid at 3l/min and 60bpm. 4D Flow MRI was acquired at 3Tesla (Achieva, Philips, The Netherlands). Each aorta was imaged with the native valve, after aortotomy, and after valve replacement with either a mechanical valve (MecValve,  $n=2$ ; Standard Masters, St. Jude Medical, USA), a biological valve (BioValve  $n=2$ ; Perimount Magna Ease, Edwards Lifesciences, USA) or Ozaki procedure (Ozaki,  $n=2$ ). Peak velocity was quantified using GTFLOW (GyroTools, Switzerland). Secondary flow patterns such as vortices and helices were visualized. They were graded according to their diameter relative to the vessel diameter as small, medium, or large.

## RESULTS

Physiological flow without secondary flow patterns was detected in all native aortas. After aortotomy one secondary flow pattern developed in the ascending aorta in every specimen. AVR induced more pronounced changes in aortic hemodynamics: The mechanical valve induced the least secondary flow patterns ( $n=1$ ) followed by the Ozaki procedure ( $n=2$ ). Biological valve replacement induced the most secondary flow patterns ( $n=3$ ) and an increase in peak velocity.

## CONCLUSION

The surgical pathway alone alters aortic hemodynamics. The new Ozaki procedure induced more secondary flow patterns than mechanical valves but fewer than biological valves. This makes it a promising alternative to biological valves that profoundly alter aortic hemodynamics.

## CLINICAL RELEVANCE/APPLICATION

Flow changes after various aortic valve replacement procedures should be monitored in patients because altered hemodynamics may affect valve function and aortic wall integrity.

Printed on: 02/07/23

## Abstract Archives of the RSNA, 2022

R5B-SPCA-1

### Hemodynamic Signatures of Aortic Root and Ascending Aorta Aneurysm by 4D Flow MRI

Thursday, Dec. 1 12:45PM - 1:15PM Room: Learning Center - CA DPS

#### Participants

Joe Juffermans, MSc, Leiden, Netherlands (*Presenter*) Nothing to Disclose

#### PURPOSE

Thoracic aortic aneurysms (TAA) are found in the aortic root and ascending aorta in patients with tricuspid aortic valves (TAV). Since aorta hemodynamic changes have been associated with aneurysm formation, the aim of this study was to determine hemodynamic signatures of aortic root and ascending aorta aneurysms in TAV patients.

#### METHODS AND MATERIALS

Eighty TAV patients underwent aortic 4D flow MRI. Left ventricular stroke volume, normalized flow displacement, flow jet angle, wall shear stress (WSS) magnitude, axial WSS, circumferential WSS, WSS angle, vorticity magnitude, absolute helicity and aortic diameter were assessed at peak systole in the aortic root and ascending aorta. Root and ascending z-scores were calculated and used to categorize the aneurysm type according to the Della Corte's classification (i.e., root, ascending or no aneurysm). To assess hemodynamic differences between the aneurysm cohorts, Kruskal-Wallis test was performed with subsequent Mann-Whitney U-tests for post-hoc analysis. Hemodynamics signatures were illustrated by radial plots.

#### RESULTS

After classification, three aneurysm cohorts were identified: aortic root aneurysm (n=40), ascending aorta aneurysm (n=19), and no aorta aneurysm (n=21) (48±11years, 54±11years, and 49±10years, respectively; p=0.25). Root aneurysm patients presented a significantly higher stroke volume compared to patients with ascending or no aneurysm (both p<0.05). Ascending aneurysm patients presented a significantly higher normalized flow displacement, flow jet angle and WSS angle together with lower WSS magnitude and axial WSS compared to patients with root or no aneurysms (all p<0.01; see Figure 1). Patients with no aneurysm demonstrated a significantly higher vorticity magnitude and absolute helicity at the ascending aorta compared to patients with root or ascending aneurysm (all p=0.01).

#### CONCLUSION

Patients with root or ascending aneurysm demonstrated two distinct hemodynamic signatures, as compared to patients without an aneurysm. Root aneurysm patients have a significantly higher left ventricular stroke volume and ascending aneurysm patients have a significantly higher normalized flow displacement, flow jet angle and WSS angle.

#### CLINICAL RELEVANCE/APPLICATION

Aortic 4D flow MRI revealed two distinct hemodynamic signatures in patients with aortic root or ascending aorta aneurysm, as compared to patients without aneurysm.

Printed on: 02/07/23

## Abstract Archives of the RSNA, 2022

R5B-SPCA-2

### Impact on Clinical Outcome of High-pitch non-ECG-gated CT Angiography for Transcatheter Aortic Valve Implantation Planning as Compared to An ECG-gated CTA Protocol

Thursday, Dec. 1 12:45PM - 1:15PM Room: Learning Center - CA DPS

#### Participants

Martin Sinn, Hamburg, Germany (*Presenter*) Nothing to Disclose

#### PURPOSE

The question of whether to use ECG-guided or non-ECG-guided high-grid CT angiography (CTA) in planning transcatheter aortic valve implantation (TAVI) has been controversial, with ECG-guided CTA currently recommended. However, the impact on clinical outcome, including post-interventional paravalvular leakage (PVL), remains unclear. Therefore, the aim of this study was to compare a retrospective ECG-guided CTA protocol with a non-ECG-guided high-pitch CTA protocol for TAVI planning and the associated impact on clinical outcome.

#### METHODS AND MATERIALS

This retrospective, institutional review board-approved study included 231 subjects (age  $80 \pm 7$  years) who underwent implantation of an Evolut R (Medtronic, Minneapolis, USA) self-expandable transcatheter heart valve. Thereof, 48 subjects received retrospective ECG-guided CTA (group A) prior intervention, and 183 subjects received non-ECG-guided high-pitch CTA (group B). The amount of aortic valve calcification (Agatston score), aortic annulus diameter, and circumferential area were measured using commercially available software tools. Visual motion scoring of the aortic root and valve was performed by two radiologists. For each patient, the cover index was calculated  $100 \times ([\text{prosthesis diameter} - \text{annulus diameter}] / \text{prosthesis diameter})$ . Clinical outcome parameters were assessed 30 days after TAVI following the Valve Academic Research Consortium-3 consensus document. Paired and unpaired two-sided t-test and Chi-squared test were utilized to compare continuous and categorical variables, respectively.

#### RESULTS

There were no significant differences in motion artefacts of the aortic root or aortic valve calcification between both groups ( $p > .05$ ). A significant difference in cover index was observed, with a higher cover index for group A (group A:  $6.6 \pm 8.6$  vs. group B:  $-1.3 \pm 10.4$ ;  $p = .001$ ). However, this difference did not lead to significantly different rates of PVL post TAVI ( $p = .399$ ). Further, there were no significant differences in major adverse cardiac events (MACE) between both groups ( $p = .49$ ).

#### CONCLUSION

Although the cover index for TAVR planning of a high-pitch non-ECG-gated CTA was lower compared to an ECG-gated CTA protocol, rates of PVL and MACE were comparable between groups.

#### CLINICAL RELEVANCE/APPLICATION

A high-pitch non-ECG-gated CTA protocol may be suitable for TAVI planning.

Printed on: 02/07/23

## Abstract Archives of the RSNA, 2022

R5B-SPCA-3

### Ex-vivo Swine Model Reveals Characteristic Aortic Flow Alterations After Different Aortic Valve Replacement Strategies

Thursday, Dec. 1 12:45PM - 1:15PM Room: Learning Center - CA DPS

#### Participants

Maren Balks, (*Presenter*) Nothing to Disclose

#### PURPOSE

Aortic hemodynamics can be altered by aortic valve replacement (AVR) with studies suggesting differences in flow alterations after different types of replacement. Ozaki aortic valve neocuspidization is a new, promising procedure for reconstructing the aortic valve using the patient's own pericardium. In order to perform any open AVR, an incision in the ascending aorta (aortotomy) is obligatory to gain access to the valve. Little is known about impact of the surgical incision itself on aortic flow. The purpose of this work was to establish a biological model to comprehensively evaluate the impact of the surgical pathway alone and in combination with different valve replacement strategies on aortic hemodynamics.

#### METHODS AND MATERIALS

Six fresh swine aortas were anastomosed to an in-house developed piston pump pumping blood-mimicking fluid at 3l/min and 60bpm. 4D Flow MRI was acquired at 3Tesla (Achieva, Philips, The Netherlands). Each aorta was imaged with the native valve, after aortotomy, and after valve replacement with either a mechanical valve (MecValve, n=2; Standard Masters, St. Jude Medical, USA), a biological valve (BioValve n=2; Perimount Magna Ease, Edwards Lifesciences, USA) or Ozaki procedure (Ozaki, n=2). Peak velocity was quantified using GTFlow (GyroTools, Switzerland). Secondary flow patterns such as vortices and helices were visualized. They were graded according to their diameter relative to the vessel diameter as small, medium, or large.

#### RESULTS

Physiological flow without secondary flow patterns was detected in all native aortas. After aortotomy one secondary flow pattern developed in the ascending aorta in every specimen. AVR induced more pronounced changes in aortic hemodynamics: The mechanical valve induced the least secondary flow patterns (n=1) followed by the Ozaki procedure (n=2). Biological valve replacement induced the most secondary flow patterns (n=3) and an increase in peak velocity.

#### CONCLUSION

The surgical pathway alone alters aortic hemodynamics. The new Ozaki procedure induced more secondary flow patterns than mechanical valves but fewer than biological valves. This makes it a promising alternative to biological valves that profoundly alter aortic hemodynamics.

#### CLINICAL RELEVANCE/APPLICATION

Flow changes after various aortic valve replacement procedures should be monitored in patients because altered hemodynamics may affect valve function and aortic wall integrity.

Printed on: 02/07/23



## Abstract Archives of the RSNA, 2022

R5B-SPCH

### Chest Thursday Poster Discussions - B

Thursday, Dec. 1 12:45PM - 1:15PM Room: Learning Center - CH DPS

#### Participants

Ryan Short, MD, Saint Louis, MO (*Moderator*) Co-founder, Scanslated, Inc; Officer, Scanslated, Inc

#### Sub-Events

### R5B-SPCH-1 Clinical Outcome of Incidental Pulmonary Embolism Detected by Artificial Intelligence Software: A Retrospective Analysis

#### Participants

Nahyun Jo, MD, Galveston, TX (*Presenter*) Nothing to Disclose

#### PURPOSE

The purpose of this study is to evaluate the clinical outcomes in retrospectively screened patients for incidental pulmonary embolism (iPE) by Artificial Intelligence (AI) algorithm on standard contrast-enhanced Chest Computed Tomography (Chest CT).

#### METHODS AND MATERIALS

The iPE algorithm was applied to 2793 consecutive patients undergoing Chest CT between 05/2020 to 01/2021 and AI results were compared to the original radiology report. Concordant cases between the original report and AI were considered ground truth. Discordant cases deemed positive by AI and negative by the report were reassessed by an experienced Chest Radiologist to establish the true diagnosis. Clinical outcomes were determined by a retrospective review of the medical record, including readmission, outpatient encounters, follow-up imaging, or death.

#### RESULTS

The prevalence of iPE was 2.3% (65/2792). 45 cases were found to be positive by both AI and radiologist report. AI detected 23 additional discordant positive cases. Of these, 87% (20/23) were considered true positive on the Chest Radiologist's secondary review. The AI-enhanced detection rate was 44.4% (20/45). 10% (2/20) were chronic PE, while 90% (18/20) were acute/subacute PE. 70% (14/20) were subsegmental PE. No follow-up imaging was found in 60% (12/20). 40% (8/20) had follow-up imaging: 5% (1/20) was a patient with known PE under treatment in whom resolution was noted on follow-up CT. In 50% (4/8), iPE spontaneously resolved. In 38% (3/8), iPE was noticed on follow-up and reported. In all 3, anticoagulation therapy was initiated. The average treatment delay in these patients was 132 days. As for the discrepant cases, in 35% (3/20) anticoagulation was given for other reasons. In the remaining 65% (13/20), iPE was unnoticed by radiologists or clinicians and the patient did not receive any treatment. No clear direct negative outcome from iPE was found in these patients. 25% (5/20) of patients died of unrelated causes.

#### CONCLUSION

A substantial number of patients with retrospectively confirmed iPE by AI appeared to have had limited clinical implications. However, the improved detection rate of iPE by AI may bring significant benefits for prompt management in selected individuals, especially the ones at risk for recurrent thromboembolic events.

#### CLINICAL RELEVANCE/APPLICATION

The advantages of AI for PE detection had been demonstrated when actively searching for thromboembolic disease. We retrospectively explored the potential added benefit of scrutinizing CT contrast studies, other than Pulmonary CT Angiograms, for iPE diagnosis, management, and outcome implications. Future prospective studies utilizing AI in daily practice would provide additional information, particularly in the assessment of high-risk populations.

### R5B-SPCH-2 Prospective Real-world Comparison of Standard of Care vs AI Assistance for Detection and Triage of Acute Pulmonary Emboli on CTPA

#### Participants

Steven Rothenberg, MD, Birmingham, AL (*Presenter*) Founder, Empower Therapeutics Inc ;Member, Translation Holdings LLC; Consultant, Radiostics LLC

#### PURPOSE

To compare the accuracy and efficiency of radiologists at detection and triage of PE on CTPA using standard of care vs. AI detection and triage.

#### METHODS AND MATERIALS

For this IRB-approved prospective single center study, 1529 consecutive adult patients with suspected PE who underwent a CTPA were included. The study was conducted in two phases in a real-world clinical practice setting. In phase 1, consecutive CTPAs (N=503) were evaluated independently by radiologists and by an FDA-cleared AI detection and triage system (CADt), with the CADt

results blocked from interacting with the interpreting radiologists. In phase 2, consecutive CTPAs (N=1026) were evaluated by radiologists interpreting the exams while using CADt. Five radiologists independently re-reviewed all positive, discrepant, and 20% of negative CTPA exams. All exams with discrepancies between the primary radiologist report, AI algorithm, and secondary radiologist interpretation were adjudicated by a committee of chest radiologists to determine ground truth.

## RESULTS

In phase 1 and 2, 14.3% (72/503) and 15.6% (160/1026) CTPA exams were positive for any PE ( $p=0.512$ ), and 10.3% (52/503) and 9.5% (97/1026) were positive for clinically-significant PE ( $p=0.622$ ). The radiologist miss rate for any PE was 11.1% in phase 1 and 5.00% in phase 2 ( $p=0.089$ ). The radiologist miss rate for clinically-significant PE was 3.9% in phase 1 and 1.0% in phase 2 ( $p=0.244$ ). The accuracy, sensitivity, specificity, PPV, and NPV of the radiologist for any PE was 97.8%, 88.9%, 99.3%, 95.5%, and 98.2% in phase 1 and 98.8%, 95.0%, 99.5%, 97.4%, and 99.1% in phase 2. Mean exam TAT (turnaround time; from exam order to final report) was 210.7 min in phase 1 and 212.1 min in phase 2 ( $p=0.523$ ). Mean interpretation TAT (from resident/radiologist opening imaging exam to final report) was 34.0 min in phase 1 and 30.0 min in phase 2 ( $p=0.2824$ ). Mean interpretation TAT for positive cases was 34.9 min in phase 1 and 33.0 min in phase 2 ( $p=0.267$ ).

## CONCLUSION

In a single-center prospective real-world study, the miss rate and accuracy of radiologists for detection of PE on CTPA and exam and report TATs did not significantly change when radiologists used AI detection and triage.

## CLINICAL RELEVANCE/APPLICATION

The accurate and efficient detection and triage of an acute pulmonary embolus (PE) on a CT pulmonary angiogram (CTPA) has the potential to be augmented using an AI algorithm and triage system.

### R5B-SPCH-3 Feasibility of Pulmonary Artery Pulse Wave Velocity Measurements Using Phase-resolved Functional Lung (PREFUL) Magnetic Resonance Imaging in Chronic Obstructive Disease

Participants

Gesa Helen Pohler, Hannover, Germany (*Presenter*) Nothing to Disclose

## PURPOSE

To measure pulmonary arterial pulse wave velocity using phase-resolved functional lung (PREFUL) MRI, its repeatability and compare with main pulmonary artery distensibility.

## METHODS AND MATERIALS

Twenty-three COPD patients underwent MRI of three coronal slices with 2D PREFUL technique (Spoiled gradient echo sequence, 128 x128 matrix, 15 mm) at baseline and after 14 days. After flexible registration, cardiac cycle with 15 phases was reconstructed. Based on this, a pulmonary pulse transit time map (ms) was calculated as the time the pulse wave travels from main pulmonary artery to the microvasculature. Then, the distance in m between two regions of interest (ROI) of the main pulmonary artery and a distal in-plane located pulmonary arterial segment was calculated. Mean pulse wave velocity in m/s of each patient was defined as the distance difference (distanceROI) divided by difference of the two above defined pulsetransit time ROI's. Relative cross-sectional area change (%) of the main pulmonary artery was computed with magnitude-images of phase contrast cine MRI. Each parameter's median (25-75% quartile) of scan 1 and 2 were assessed by Wilcoxon sign rank test, Bland-Altman analysis, coefficient of variation, Spearman r.

## RESULTS

There were no bias and no significant differences between both MRI's for all parameters (all  $p>0.2$ ). Pulse wave velocity of scan 1 was 3.1 (2-8) m/s, distanceROI was 2.8 (2.4-3.6) cm, proximal and distal pulmonary arterial pulse transit times were 8.4 (-3-26) ms and 21 (2-35) ms, pulmonary pulse transit times' difference was 11 (7-17) ms. Pulse wave velocities coefficient of variation was 9.3 (3.6-12.7) %. Relative cross-sectional area change was 40.7 (32.8-65.5) %. Pulse wave velocity of scan 1 and 2 correlated inversely to relative area change ( $r:-0.64, -0.67$ ;  $p=0.0009, p=0.0004$ ).

## CONCLUSION

PREFUL MRI pulse wave velocity was good repeatable over two scans and increases with main pulmonary artery stiffness in COPD patients.

## CLINICAL RELEVANCE/APPLICATION

PREFUL MRI pulse wave velocity offers a contrast agent-free tool for monitoring pulmonary arterial distensibility in chronic lung disease, which may be relevant for clinical decision-making in the future.

### R5B-SPCH-4 Myocardial Extracellular Volume Assessment at Computed Tomography Novel Coronavirus Disease (COVID-19) Patients with Regards to Pulmonary Embolism

Participants

Caterina Monti, MD, PhD, Milan, Italy (*Presenter*) Travel support, Bracco Group

## PURPOSE

to assess myocardial extracellular volume (ECV) in patients with novel coronavirus disease (COVID-19) with regards to the presence of pulmonary embolism (PE).

## METHODS AND MATERIALS

We retrospectively reviewed consecutive patients who underwent contrast-enhanced computed tomography (CT) for the assessment of PE, and whose CT scans included at least one unenhanced and one venous phase acquisition performed at 1 minute after contrast administration for evaluating the mediastinum. Included patients were also to have hematocrit values obtained at most one day from the CT scan. Regions of interest were placed in the myocardium and ventricular blood pool of both the unenhanced and venous phase scan, and ECV was subsequently calculated.

## RESULTS

our final population counted 94 patients, 63 (67%) of whom males, with a median age of 70 years (interquartile range, IQR, 56-76 years), 28 of whom with PE visible at CT. Median hematocrit was 39% (IQR 35-43%). Median overall ECV was 31% (IQR 26-35%), whereas median ECV in patients with PE was 34% (IQR 29-38%), significantly higher than in those without PE (30%, IQR 25-34%,  $P=0.010$ ).

#### **CONCLUSION**

s myocardial ECV is high in COVID-19 patients, possibly indicating a likelihood of underlying myocardial damage. The higher ECV in patients with PE may relate to the ventricular overload rising from subsequent pulmonary hypertension.

#### **CLINICAL RELEVANCE/APPLICATION**

CT-derived myocardial ECV could be used as a biomarker of cardiovascular involvement in COVID-19 patients, obtaining further data from an investigation that is already part of clinical workflows.

Printed on: 02/07/23

## Abstract Archives of the RSNA, 2022

R5B-SPCH-1

### Clinical Outcome of Incidental Pulmonary Embolism Detected by Artificial Intelligence Software: A Retrospective Analysis

Thursday, Dec. 1 12:45PM - 1:15PM Room: Learning Center - CH DPS

#### Participants

Nahyun Jo, MD, Galveston, TX (*Presenter*) Nothing to Disclose

#### PURPOSE

The purpose of this study is to evaluate the clinical outcomes in retrospectively screened patients for incidental pulmonary embolism (iPE) by Artificial Intelligence (AI) algorithm on standard contrast-enhanced Chest Computed Tomography (Chest CT).

#### METHODS AND MATERIALS

The iPE algorithm was applied to 2793 consecutive patients undergoing Chest CT between 05/2020 to 01/2021 and AI results were compared to the original radiology report. Concordant cases between the original report and AI were considered ground truth. Discordant cases deemed positive by AI and negative by the report were reassessed by an experienced Chest Radiologist to establish the true diagnosis. Clinical outcomes were determined by a retrospective review of the medical record, including readmission, outpatient encounters, follow-up imaging, or death.

#### RESULTS

The prevalence of iPE was 2.3% (65/2792). 45 cases were found to be positive by both AI and radiologist report. AI detected 23 additional discordant positive cases. Of these, 87% (20/23) were considered true positive on the Chest Radiologist's secondary review. The AI-enhanced detection rate was 44.4% (20/45). 10% (2/20) were chronic PE, while 90% (18/20) were acute/subacute PE. 70% (14/20) were subsegmental PE. No follow-up imaging was found in 60% (12/20). 40% (8/20) had follow-up imaging: 5% (1/20) was a patient with known PE under treatment in whom resolution was noted on follow-up CT. In 50% (4/8), iPE spontaneously resolved. In 38% (3/8), iPE was noticed on follow-up and reported. In all 3, anticoagulation therapy was initiated. The average treatment delay in these patients was 132 days. As for the discrepant cases, in 35% (3/20) anticoagulation was given for other reasons. In the remaining 65% (13/20), iPE was unnoticed by radiologists or clinicians and the patient did not receive any treatment. No clear direct negative outcome from iPE was found in these patients. 25% (5/20) of patients died of unrelated causes.

#### CONCLUSION

A substantial number of patients with retrospectively confirmed iPE by AI appeared to have had limited clinical implications. However, the improved detection rate of iPE by AI may bring significant benefits for prompt management in selected individuals, especially the ones at risk for recurrent thromboembolic events.

#### CLINICAL RELEVANCE/APPLICATION

The advantages of AI for PE detection had been demonstrated when actively searching for thromboembolic disease. We retrospectively explored the potential added benefit of scrutinizing CT contrast studies, other than Pulmonary CT Angiograms, for iPE diagnosis, management, and outcome implications. Future prospective studies utilizing AI in daily practice would provide additional information, particularly in the assessment of high-risk populations.

Printed on: 02/07/23

## Abstract Archives of the RSNA, 2022

R5B-SPCH-2

### Prospective Real-world Comparison of Standard of Care vs AI Assistance for Detection and Triage of Acute Pulmonary Emboli on CTPA

Thursday, Dec. 1 12:45PM - 1:15PM Room: Learning Center - CH DPS

#### Participants

Steven Rothenberg, MD, Birmingham, AL (*Presenter*) Founder, Empower Therapeutics Inc ;Member, Translation Holdings LLC;Consultant, Radiostics LLC

#### PURPOSE

To compare the accuracy and efficiency of radiologists at detection and triage of PE on CTPA using standard of care vs. AI detection and triage.

#### METHODS AND MATERIALS

For this IRB-approved prospective single center study, 1529 consecutive adult patients with suspected PE who underwent a CTPA were included. The study was conducted in two phases in a real-world clinical practice setting. In phase 1, consecutive CTPAs (N=503) were evaluated independently by radiologists and by an FDA-cleared AI detection and triage system (CADt), with the CADt results blocked from interacting with the interpreting radiologists. In phase 2, consecutive CTPAs (N=1026) were evaluated by radiologists interpreting the exams while using CADt. Five radiologists independently re-reviewed all positive, discrepant, and 20% of negative CTPA exams. All exams with discrepancies between the primary radiologist report, AI algorithm, and secondary radiologist interpretation were adjudicated by a committee of chest radiologists to determine ground truth.

#### RESULTS

In phase 1 and 2, 14.3% (72/503) and 15.6% (160/1026) CTPA exams were positive for any PE ( $p=0.512$ ), and 10.3% (52/503) and 9.5% (97/1026) were positive for clinically-significant PE ( $p=0.622$ ). The radiologist miss rate for any PE was 11.1% in phase 1 and 5.00% in phase 2 ( $p=0.089$ ). The radiologist miss rate for clinically-significant PE was 3.9% in phase 1 and 1.0% in phase 2 ( $p=0.244$ ). The accuracy, sensitivity, specificity, PPV, and NPV of the radiologist for any PE was 97.8%, 88.9%, 99.3%, 95.5%, and 98.2% in phase 1 and 98.8%, 95.0%, 99.5%, 97.4%, and 99.1% in phase 2. Mean exam TAT (turnaround time; from exam order to final report) was 210.7 min in phase 1 and 212.1 min in phase 2 ( $p=0.523$ ). Mean interpretation TAT (from resident/radiologist opening imaging exam to final report) was 34.0 min in phase 1 and 30.0 min in phase 2 ( $p=0.2824$ ). Mean interpretation TAT for positive cases was 34.9 min in phase 1 and 33.0 min in phase 2 ( $p=0.267$ ).

#### CONCLUSION

In a single-center prospective real-world study, the miss rate and accuracy of radiologists for detection of PE on CTPA and exam and report TATs did not significantly change when radiologists used AI detection and triage.

#### CLINICAL RELEVANCE/APPLICATION

The accurate and efficient detection and triage of an acute pulmonary embolus (PE) on a CT pulmonary angiogram (CTPA) has the potential to be augmented using an AI algorithm and triage system.

Printed on: 02/07/23

## Abstract Archives of the RSNA, 2022

R5B-SPCH-3

### Feasibility of Pulmonary Artery Pulse Wave Velocity Measurements Using Phase-resolved Functional Lung (PREFUL) Magnetic Resonance Imaging in Chronic Obstructive Disease

Thursday, Dec. 1 12:45PM - 1:15PM Room: Learning Center - CH DPS

#### Participants

Gesa Helen Pohler, Hannover, Germany (*Presenter*) Nothing to Disclose

#### PURPOSE

To measure pulmonary arterial pulse wave velocity using phase-resolved functional lung (PREFUL) MRI, its repeatability and compare with main pulmonary artery distensibility.

#### METHODS AND MATERIALS

Twenty-three COPD patients underwent MRI of three coronal slices with 2D PREFUL technique (Spoiled gradient echo sequence, 128 x128 matrix, 15 mm) at baseline and after 14 days. After flexible registration, cardiac cycle with 15 phases was reconstructed. Based on this, a pulmonary pulse transit time map (ms) was calculated as the time the pulse wave travels from main pulmonary artery to the microvasculature. Then, the distance in m between two regions of interest (ROI) of the main pulmonary artery and a distal in-plane located pulmonary arterial segment was calculated. Mean pulse wave velocity in m/s of each patient was defined as the distance difference (distanceROI) divided by difference of the two above defined pulsetransit time ROI's. Relative cross-sectional area change (%) of the main pulmonary artery was computed with magnitude-images of phase contrast cine MRI. Each parameter's median (25-75% quartile) of scan 1 and 2 were assessed by Wilcoxon sign rank test, Bland-Altman analysis, coefficient of variation, Spearman r.

#### RESULTS

There were no bias and no significant differences between both MRI's for all parameters (all  $p > 0.2$ ). Pulse wave velocity of scan 1 was 3.1 (2-8) m/s, distanceROI was 2.8 (2.4-3.6) cm, proximal and distal pulmonary arterial pulse transit times were 8.4 (-3-26) ms and 21 (2-35) ms, pulmonary pulse transit times' difference was 11 (7-17) ms. Pulse wave velocities coefficient of variation was 9.3 (3.6-12.7) %. Relative cross-sectional area change was 40.7 (32.8-65.5) %. Pulse wave velocity of scan 1 and 2 correlated inversely to relative area change ( $r: -0.64, -0.67; p=0.0009, p=0.0004$ ).

#### CONCLUSION

s PREFUL MRI pulse wave velocity was good repeatable over two scans and increases with main pulmonary artery stiffness in COPD patients.

#### CLINICAL RELEVANCE/APPLICATION

PREFUL MRI pulse wave velocity offers a contrast agent-free tool for monitoring pulmonary arterial distensibility in chronic lung disease, which may be relevant for clinical decision-making in the future.

Printed on: 02/07/23

## Abstract Archives of the RSNA, 2022

R5B-SPCH-4

### **Myocardial Extracellular Volume Assessment at Computed Tomography Novel Coronavirus Disease (COVID-19) Patients with Regards to Pulmonary Embolism**

Thursday, Dec. 1 12:45PM - 1:15PM Room: Learning Center - CH DPS

#### **Participants**

Caterina Monti, MD, PhD, Milan, Italy (*Presenter*) Travel support, Bracco Group

#### **PURPOSE**

to assess myocardial extracellular volume (ECV) in patients with novel coronavirus disease (COVID-19) with regards to the presence of pulmonary embolism (PE).

#### **METHODS AND MATERIALS**

we retrospectively reviewed consecutive patients who underwent contrast-enhanced computed tomography (CT) for the assessment of PE, and whose CT scans included at least one unenhanced and one venous phase acquisition performed at 1 minute after contrast administration for evaluating the mediastinum. Included patients were also to have hematocrit values obtained at most one day from the CT scan. Regions of interest were placed in the myocardium and ventricular blood pool of both the unenhanced and venous phase scan, and ECV was subsequently calculated.

#### **RESULTS**

our final population counted 94 patients, 63 (67%) of whom males, with a median age of 70 years (interquartile range, IQR, 56-76 years), 28 of whom with PE visible at CT. Median hematocrit was 39% (IQR 35-43%). Median overall ECV was 31% (IQR 26-35%), whereas median ECV in patients with PE was 34% (IQR 29-38%), significantly higher than in those without PE (30%, IQR 25-34%,  $P=0.010$ ).

#### **CONCLUSION**

s myocardial ECV is high in COVID-19 patients, possibly indicating a likelihood of underlying myocardial damage. The higher ECV in patients with PE may relate to the ventricular overload rising from subsequent pulmonary hypertension.

#### **CLINICAL RELEVANCE/APPLICATION**

CT-derived myocardial ECV could be used as a biomarker of cardiovascular involvement in COVID-19 patients, obtaining further data from an investigation that is already part of clinical workflows.

Printed on: 02/07/23

## Abstract Archives of the RSNA, 2022

R5B-SPGI

### Gastrointestinal Thursday Poster Discussions - B

Thursday, Dec. 1 12:45PM - 1:15PM Room: Learning Center - GI DPS

#### Participants

Sonia Lee, MD, Irvine, CA (*Moderator*) Nothing to Disclose

#### Sub-Events

### R5B-SPGI-1 Hepatic and Pancreatic Extracellular Volume Fraction Using Contrast-Enhanced CT in Patients with Impaired Glucose Tolerance

#### Participants

Takashi Ota, MD, PhD, Suita, Japan (*Presenter*) Nothing to Disclose

#### PURPOSE

Liver fibrosis and pancreatic fibrosis are each associated with impaired glucose tolerance (IGT). Furthermore, liver fibrosis can be associated with pancreatic fibrosis. The purpose of the present study was to investigate the relationship between hepatic and pancreatic extracellular volume fraction (fECV) that correlates with tissue fibrosis and their relationships with IGT.

#### METHODS AND MATERIALS

The study included 100 consecutive patients with known or suspected liver and/or pancreatic diseases who underwent contrast-enhanced CT, including the precontrast and the equilibrium phase (62 males and 38 females; median age, 62 years; range, 28-93 years). Patients were classified into three groups based on the American Diabetes Association criteria: non-diabetes subjects, HbA1c < 5.7% or fasting plasma glucose (FPG) < 100 mg/dL; pre-diabetes, 5.7% ≤ HbA1c < 6.5% or 100 ≤ FPG < 125 mg/dL; and type 2 diabetes mellitus (T2DM), HbA1c ≥ 6.5% or FPG ≥ 125 mg/dL. Subtraction images between unenhanced and equilibrium phase images were prepared using a new subtraction algorithm. The liver and the pancreas were automatically extracted excluding focal lesions, major vascular branches and ducts using a high-speed 3D image analysis system and mean CT values for them were calculated, respectively. The enhancement degree of the aorta (Aorta) was also measured. fECV was calculated using the following equation:  $fECV = (100 - \text{hematocrit}) \times \frac{\text{Pancreas}}{\text{Aorta}}$ . We investigated the differences in hepatic fECV and pancreatic fECV among the three patient groups using Kruskal-Wallis and Dwass-Steel-Crichlow-Fligner multiple comparisons statistical test and the correlation between the each two in hepatic fECV, pancreatic fECV and HbA1c using Spearman's rho coefficient.

#### RESULTS

Pancreatic fECV positively correlated with hepatic fECV and HbA1c ( $r = 0.51$ ,  $P < 0.001$  and  $r = 0.51$ ,  $P < 0.001$ , respectively). Pancreatic fECV differed significantly among the three groups ( $P < 0.001$ ). Pancreatic fECV was significantly greater in T2DM compared with pre-diabetes or no-diabetes subjects and in pre-diabetes compared with no-diabetes subjects ( $P < 0.001$ ). Hepatic fECV was significantly greater in T2DM compared with non-diabetes subjects ( $P < 0.05$ ).

#### CONCLUSION

There is a close relationship between hepatic fECV, pancreatic fECV and IGT.

#### CLINICAL RELEVANCE/APPLICATION

Hepatic fECV is associated with pancreatic fECV and diabetes mellitus. Hepatic fECV may be possible to use for the assessment of IGT in conjunction with pancreatic fECV.

### R5B-SPGI-3 3-Dimensional Dual-Frequency Magnetic Resonance Elastography Derived Viscosity as a Surrogate of Hepatic Inflammation, Independent of Simultaneously Measured Stiffness

#### Participants

Jenna Feeley, BS, (*Presenter*) Nothing to Disclose

#### PURPOSE

The traditional Magnetic Resonance Elastography (MRE) method that is used to detect liver inflammation utilizes the damping ratio (DR) which factors stiffness (Gd) into the calculation. Hence, the purpose of this study is to identify a surrogate of liver inflammation, independent of stiffness, using 3-Dimensional (3D) dual-frequency (2F-MRE).

#### METHODS AND MATERIALS

45 patients with chronic liver disease (Hepatitis C or Steatohepatitis) were included in this prospective study. 3D 2F-MRE was performed at 56 and 28 Hz on a 3T scanner. Liver viscosity (Gl) and stiffness (Gd) were measured at both frequencies. The difference in tissue viscosity and stiffness derived from the two frequencies was calculated ( $\Delta Gl$ ,  $\Delta Gd$ ). All patients had liver biopsies for ISHAK scoring (inflammation range 0-18, fibrosis range 0-6). Statistical analysis was used to evaluate the degree of correlation between inflammation and fibrosis scores obtained from biopsy versus Gl and Gd, respectively (28 Hz and 56 Hz separately), and  $\Delta Gl$  and  $\Delta Gd$  obtained from 3D 2F-MRE. Lastly, diagnostic performance was evaluated by Receiver Operating Characteristic (ROC)

curves.

## RESULTS

The average patient age and BMI were  $56.16 \pm 9.26$  years and  $27.82 \pm 3.98$  kg/m<sup>2</sup>, respectively, and 11 were women. Of the three viscosity parameters measured (GI<sub>28</sub>, GI<sub>56</sub>, and ?GI), ?GI showed the most significant correlation with ISHAK inflammation scores ( $P=0.0041$ ). Stepwise multilinear regression analysis revealed that ?GI was the only significant surrogate of hepatic inflammation ( $R^2 = 0.1975$ ,  $P = 0.0025$ ) and excluded all GI and Gd values (from both frequencies) from the model. ?GI also showed a strong diagnostic performance for detecting moderate/severe hepatic inflammation (ISHAK > 8: AUC = 0.8, Sensitivity 80%, Specificity 73.5%,  $P = 0.0001$ ). All Gd values correlated similarly with fibrosis and no difference in diagnostic performance was found.

## CONCLUSION

These results indicate that the difference in liver viscosity, ?GI, obtained by 3D 2F-MRE is a significant and independent surrogate of liver inflammation and has a robust diagnostic performance for detecting moderate/severe liver inflammation. Unlike other MRE methods, ?GI derived from 3D 2F-MRE is an independent measurement that does not rely on the DR which factors in liver stiffness.

## CLINICAL RELEVANCE/APPLICATION

3D 2F-MRE-derived ?GI is an independent surrogate marker of liver inflammation. This non-invasive measure provides early detection of liver inflammation and, with monitored treatment, may help mitigate the progression to fibrosis.

## R5B-SPGI-4 Ultrasound shear wave elastography and shear wave dispersion imaging for diagnosis and staging of hepatic fibrosis

### Participants

Kibo Nam, PhD, Philadelphia, PA (*Presenter*) Equipment support, Canon Medical Systems Corporation; Equipment support, General Electric Company ; Support, Lantheus Medical Imaging; Research funded, Canon Medical Systems Corporation

### PURPOSE

To compare ultrasound shear wave elastography (SWE) and shear wave dispersion slope (SWDS) values to the fibrosis diagnosis and staging by a liver biopsy or MRE in non-alcoholic fatty liver disease (NAFLD) suspected patients.

### METHODS AND MATERIALS

Subjects underwent a liver biopsy or MRE for suspected NAFLD and were scanned with an i8C1 probe on the Aplio i800 scanner (Canon Medical Systems). Five SWE (in kPa) and five SWDS (in m/s/KHz) values were obtained from the right liver lobe of each patient using built-in software. A circular region of interest (ROI) with a 1 cm diameter was placed =1 cm below the liver capsule manually in the liver parenchyma, referring to the shear wave propagation map. The obtained values met the criteria of IQR/median = 0.30 for SWE and =0.15 for SWDS. The mean SWE and SWDS values were compared with the reference results using a t-test and Pearson's correlation coefficient ( $r$ ).

### RESULTS

Among 54 patients, 30 underwent liver biopsy and 24 had MRE. Fibrosis was diagnosed in 27 patients (18 by biopsy and 9 by MRE; 10 stage 1, 6 stage 1 to 2, 1 stage 2, 5 stage 2 to 3, 1 stage 3, and 4 stage 4), while 27 patients showed stage 0 (12 by biopsy and 15 by MRE). The SWE and SWDS values were significantly higher in fibrotic livers compared to normal livers ( $7.1 \pm 1.7$  vs.  $5.5 \pm 1.2$  kPa;  $p < 0.0001$  and  $12.1 \pm 2.8$  vs.  $10.5 \pm 2.3$  m/s/kHz;  $p = 0.012$ , respectively). There was a fair correlation between fibrosis stage and mean SWE and SWDS values among all patients regardless of the reported clinical reference standard ( $r = 0.69$  and  $r = 0.52$ , respectively). Liver biopsy fibrosis staging was moderately correlated with SWE and SWDS ( $r = 0.70$  and  $r = 0.60$ , respectively). The correlation between MRE stiffness values (in kPa) with SWE and SWDS was weaker ( $r = 0.63$  and  $r = 0.34$ , respectively).

### CONCLUSION

Ultrasound SWE showed a higher correlation with the diagnosis and staging of liver fibrosis by biopsy and/or MRE compared to SWDS.

### CLINICAL RELEVANCE/APPLICATION

Ultrasound SWE has more potential for diagnosis and staging of liver fibrosis in NAFLD compared to SWDS values.

## R5B-SPGI-5 Preoperative ultrasound radiomics for predicting clinically relevant postoperative pancreatic fistula after pancreatectomy

### Participants

Yi Dong, MD, PhD, Shanghai, China (*Presenter*) Nothing to Disclose

### PURPOSE

To evaluate the efficacy of the radiomics model based on preoperative grayscale ultrasound and shear wave elastography (SWE) in predicting the occurrence of clinically relevant postoperative pancreatic fistula (CR-POPF) after pancreatectomy.

### METHODS AND MATERIALS

This prospective study was conducted from Jan 2020 to Nov 2021. Patients who scheduled to undergo pancreatectomy were initially enrolled and received ultrasound assessment within one week before surgery. The risk factors of POPF (grades B and C) were analyzed. Preoperative grayscale ultrasound images, ultrasound SWE values of pancreatic lesions and their surrounding parenchyma were used to build preoperative prediction radiomics model. Radiomic signatures were extracted and constructed using a minimal Redundancy Maximal Relevance (mRMR) algorithm and a L1 penalized logistic regression. Combined model was built using multivariate regression which incorporating radiomics signatures and clinical variables.

### RESULTS

Finally, 147 patients (median age 62.0 y) were prospectively enrolled. Among which, 85 patients underwent distal pancreatectomy, and 62 patients underwent pancreaticoduodenectomy. During the three-weeks follow-up after pancreatectomy, the incidence rates

of grade B/C POPF were 28.6% (42/147 patients). Radiomic signatures constructed from grayscale ultrasound images of pancreas parenchymal regions (panRS) achieved an AUC of 0.75, accuracy of 68.7%, sensitivity of 85.7 % and specificity of 61.9 % in preoperative noninvasive prediction of CR-POPF. AUC of radiomics model increased to 0.81 when panRS was used for the prediction of CR-POPF after pancreaticoduodenectomy.

## CONCLUSION

s Radiomics model based on ultrasound images was potentially useful for preoperative noninvasively predicting of CR-POPF.

## CLINICAL RELEVANCE/APPLICATION

Patients with high-risk factors of CR-POPF could be closely monitored during the postoperative period.

## R5B-SPGI-6 Longitudinal Changes in Liver Imaging Biomarkers Following Low Calorie Liquid Diet

Participants

Jake Weeks, La Jolla, CA (*Presenter*) Nothing to Disclose

## PURPOSE

Low calorie liquid diet (LCLD) prior to bariatric surgery has been shown to reduce liver volume by ~20% on average, resulting in improved outcomes by reducing the technical difficulty of the operation. The effect of LCLD on liver volume has been well-documented, but relationships between liver shrinkage and other liver biomarkers are poorly understood. Changes to liver stiffness could also explain improved outcomes in bariatric surgery, but the effects of preparatory diet on liver stiffness have not been reported. This study describes changes in automated MR-based liver volume, steatosis, and stiffness after LCLD to elucidate the mechanisms of improved bariatric surgery outcomes.

## METHODS AND MATERIALS

Forty-five adults with obesity scheduled for bariatric surgery were prospectively recruited to participate in an ongoing research study which includes two non-contrast MR imaging exams at 3.0T (GE Signa Premier, or GE Discovery MR750, GE Healthcare, Waukesha WI) at baseline and 2-3 days prior to surgery. LCLD was prescribed for 14-21 days during this interval. Imaging biomarkers included MRI-PDFF (IDEAL-IQ), liver volume based on MR imaging (3D convolutional neural network developed at our institution), and 2D SE-EPI MR Elastography. Mean PDFF was quantified by a 9-segment ROI analysis. Elastography was analyzed manually using the MRE Quant™ software (Resoundant, Inc., Minnesota, USA). BMI was examined for correlation with these parameters.

## RESULTS

Following LCLD, mean liver volume decreased 414.36 cm<sup>3</sup> (2098.32 cm<sup>3</sup> to 1683.96 cm<sup>3</sup>). Mean liver PDFF decreased 3.45% (8.51% to 5.06%). Mean liver stiffness decreased by 0.09 kPa (2.07 kPa to 1.98 kPa). Mean BMI decreased by 2.13kg/m<sup>2</sup> (46.15 kg/m<sup>2</sup> to 44.02 kg/m<sup>2</sup>). Rate of change of volume demonstrated moderate, statistically significant correlations with the rates of change for MRE ( $r = 0.43$ ,  $p = 0.004$ ), PDFF ( $r = 0.38$ ,  $p = 0.013$ ), and BMI ( $r = 0.32$ ,  $p = 0.040$ ).

## CONCLUSION

s The results of this study agree with previous data showing reductions in liver volume and steatosis following LCLD. We also found that liver stiffness is reduced during the dieting phase. MRE-derived liver stiffness change is correlated with liver volume change following LCLD. Reduced liver stiffness may affect outcomes in bariatric surgery, but the sample size was small and requires additional investigation. Further research within larger cohorts is needed to validate these findings.

## CLINICAL RELEVANCE/APPLICATION

Longitudinal changes in MRI biomarkers following preparatory diet in bariatric surgery patients may help explain mechanisms underlying improved surgical outcomes.

## R5B-SPGI-7 Splenic Volume is Associated with Survival in Patients Receiving Immunotherapy for Advanced Hepatocellular Carcinoma

Participants

Bang Bin Chen, MD, (*Presenter*) Nothing to Disclose

## PURPOSE

To investigate the association of splenic volume and its changes with survival outcomes among patients who underwent immunotherapy for advanced hepatocellular carcinoma (HCC).

## METHODS AND MATERIALS

In this retrospective analysis, patients who initiated immunotherapy for advanced HCC were included. The baseline splenic volume and its relative changes after 1~3 months (median 55 days) on CT or MRI were measured by volumetric segmentation using 3D slicer software. The association between splenic volume at baseline and its relative change [(posttherapy - baseline)/baseline] and progression-free survival (PFS) or overall survival (OS) were evaluated using univariate and multivariate Cox analyses.

## RESULTS

A total of 134 patients were included (men/women = 118/16; mean age, 59.5 ± 11.5 years (standard deviation)). The median follow-up duration was 30.5 months (95% confidence interval (CI) = 20.7-40.3). The overall response rate was 30.6%, and the disease control rate was 68.7%. The median PFS was 4 months (95% CI = 2.9-5.1), and the median OS was 17.2 months (95% CI = 10.9-23.5). After treatment, splenic volume was increased in 95 (70.9%) patients, and decreased in 39 (29.1%) patients. At baseline, patients with splenomegaly exhibited significantly shorter PFS (median, 4.0 vs. 5.4 months,  $P = 0.019$ ) and OS (median, 11.2 vs. 19.3 months,  $P < 0.001$ ) than patients without splenomegaly. After treatment, patients with increased splenic volume exhibited significantly better PFS (median, 2.6 vs. 6.7 months,  $P = 0.003$ ) and OS (median, 12.0 vs. 23.1 months,  $P = 0.001$ ) than patients with decreased splenic volume. In multivariate analysis adjusting for patient demographics, tumor extent, immunotherapy line, and liver function reserve, splenic volume change remained an independent predictor of PFS (hazard ratio (HR) 0.59; 95% CI: 0.37-0.94,  $P = 0.025$ ) and OS (HR 0.46; 95% CI: 0.28-0.75,  $P = 0.002$ ).

## CONCLUSION

s Splenic volume may be used as a prognostic marker in patients who received immunotherapy for advanced HCC.

## CLINICAL RELEVANCE/APPLICATION

Follow-up splenic volume after 1~3 months post-therapy may help clinicians predict clinical outcomes in HCC patients receiving immunotherapy.

## R5B-SPGI-8 Synergistic Anticancer Effect of Pulsed Focused Ultrasound with Ultrasound-Sensitive Nanoparticle IMP301 on Pancreas Cancer Xenograft Model.

Participants

Soojin Kim, MD, (*Presenter*) Nothing to Disclose

## PURPOSE

Focused ultrasound (FUS) has been widely investigated for use in drug delivery system as a noninvasive synergistic modality. The purpose of this study was to investigate synergistic anticancer effect of FUS with a novel ultrasound-sensitive nanoparticle IMP 301 (doxorubicin-loaded) on pancreas cancer xenograft model.

## METHODS AND MATERIALS

Nude mice were subcutaneously inoculated with human pancreatic cancer cell PANC-1 and randomly divided into six different groups (n=5 per group) for study 1 and 2 respectively. Ectopic pancreatic tumors were conditionally exposed to pHIFU with pre-studied parameters (acoustic power = 72 Watt, gap = 2mm x 2mm, total time = 20 second/spot, duty cycle = 2%, pulse repetition frequency = 250Hz). In Study 1, mice were assigned to 1) control, 2) gemcitabine only (200mg intraperitoneal), 3) doxil (4mg/kg) with FUS, and 4-6) three groups treated with different doses of IMP301 (2,4,6mg/kg) with FUS. In Study 2, mice were assigned to 1) control, 2) FUS only, 3) gemcitabine only, 4) doxil (4mg/kg) with FUS, and 5-6) two groups treated with IMP 301 (4mg/kg) with or without FUS. The presence of synergistic effect of IMP 301 when combined with FUS was evaluated by comparison with other groups in terms of tumor growth suppression.

## RESULTS

In Study 1, IMP301 with FUS group showed significantly lower tumor volume ( $121 \text{ mm}^3 \pm 28 \text{ mm}^3$ ) and growth rate ( $12.1 \text{ mm}^3/\text{week} \pm 5.2 \text{ mm}^3/\text{week}$ ) when dose exceeded 4mg/kg, compared to gemcitabine only ( $244.7 \text{ mm}^3 \pm 47.6 \text{ mm}^3$ ,  $30.5 \text{ mm}^3/\text{week} \pm 11.7 \text{ mm}^3/\text{week}$ ) and doxil with FUS group ( $208 \text{ mm}^3 \pm 25 \text{ mm}^3$ ,  $25.6 \text{ mm}^3/\text{week} \pm 7.7 \text{ mm}^3/\text{week}$ ) [ $p < 0.05$ ]. In Study 2, IMP301 with FUS group showed significantly lower tumor volume ( $98 \text{ mm}^3 \pm 42 \text{ mm}^3$ ) and growth rate ( $9.2 \text{ mm}^3/\text{week} \pm 6.5 \text{ mm}^3/\text{week}$ ;  $p < 0.05$ ) than gemcitabine only ( $323 \text{ mm}^3 \pm 158 \text{ mm}^3$ ,  $46.7 \text{ mm}^3/\text{week} \pm 29.1 \text{ mm}^3/\text{week}$ ) and doxil with FUS group ( $236 \text{ mm}^3 \pm 60 \text{ mm}^3$ ,  $32.2 \text{ mm}^3/\text{week} \pm 11.9 \text{ mm}^3/\text{week}$ ) [ $p < 0.05$ ]. However, IMP301 without FUS group ( $256 \text{ mm}^3 \pm 107 \text{ mm}^3$ ,  $35.6 \text{ mm}^3/\text{week} \pm 18.8 \text{ mm}^3/\text{week}$ ) showed no significant difference with gemcitabine only and doxil with FUS group.

## CONCLUSION

s In conclusion, IMP301 combined with short duty cycle FUS exhibited significantly higher and persistent tumor suppression effect, compared to the single use of conventional drug or IMP 301 or the combined use of conventional drug and FUS, showing the potential of IMP 301 with FUS for the treatment of pancreatic cancer.

## CLINICAL RELEVANCE/APPLICATION

Ultrasound-sensitive drug release by FUS can be applied in treatment for nonoperative pancreatic cancer patients as a highly effective noninvasive localized therapeutic modality.

## R5B-SPGI-9 An Attention-Based Convolutional Neural Network for Differentiating Benign from Malignant Focal Liver Lesions in Wash-In and Wash-Out Contrast-Enhanced Ultrasonography

Participants

Thodsawit Tiyarattanachai, (*Presenter*) Nothing to Disclose

## PURPOSE

Contrast-enhanced ultrasound (CEUS) is increasingly used to characterize focal liver lesions (FLLs). We have previously developed deep learning models to support interpretation of wash-in CEUS data in FLL characterization. In this work, we investigated whether including wash-out data into our models can improve differentiation of benign from malignant FLLs.

## METHODS AND MATERIALS

This study used CEUS data from an ongoing multi-institutional IRB-approved study and informed consent was obtained from all patients. A wash-in cine was used as input into a "wash-in subnetwork" based on a three-dimensional (3D) convolutional neural network (CNN). Variable instances of wash-out images were used as inputs into six "wash-out subnetworks" based on two-dimensional (2D) CNNs. Since wash-out data are usually acquired as an ambiguous number of images and not cines, an attention module was built on top of the wash-in and wash-out subnetworks to deal with such variable instances of wash-out images. To evaluate the add-on utility of the attention module, the following three models were compared: 1) a simple 3D CNN, which was inspired by previously published works, receiving as input a wash-in cine (Model A); 2) a simple 3D CNN receiving as input a wash-in cine temporally appended with wash-out images (Model B); and 3) the model with attention module built on top of wash-in and wash-out subnetworks (Model C). 5-fold cross validation was performed. Mean SD of performance results across all folds were reported. Area under receiver operating characteristic curve (AUROC), sensitivity and specificity were used as evaluation metrics.

## RESULTS

A total of 158 FLLs from 130 patients were included. Of these, 31 (19.6%) FLLs were benign, and 127 (80.4%) FLLs were malignant based on a composite reference standard of pathology, CT and MRI. Model A achieved AUROC of  $0.75 \pm 0.10$ , sensitivity of  $76.9\% \pm 14.5\%$  and specificity of  $78.6\% \pm 24.2\%$ . Model B achieved AUROC of  $0.76 \pm 0.10$ , sensitivity of  $74.9\% \pm 9.7\%$  and specificity of  $84.3\% \pm 15.6\%$ . With incorporation of the attention module, Model C achieved the highest AUROC of  $0.86 \pm 0.08$ , sensitivity of  $84.2\% \pm 8.1\%$  and specificity of  $87.1\% \pm 7.3\%$ .

## CONCLUSION

s The attention module improved performance of CNN in differentiating benign from malignant FLLs on wash-in and wash-out CEUS.

#### **CLINICAL RELEVANCE/APPLICATION**

The Attention-based CNN can be used to characterize FLLs on CEUS acquired in clinical practice, where the number of recorded wash-out instances is variable.

Printed on: 02/07/23

## Abstract Archives of the RSNA, 2022

R5B-SPGI-1

### Hepatic and Pancreatic Extracellular Volume Fraction Using Contrast-Enhanced CT in Patients with Impaired Glucose Tolerance

Thursday, Dec. 1 12:45PM - 1:15PM Room: Learning Center - GI DPS

#### Participants

Takashi Ota, MD, PhD, Suita, Japan (*Presenter*) Nothing to Disclose

#### PURPOSE

Liver fibrosis and pancreatic fibrosis are each associated with impaired glucose tolerance (IGT). Furthermore, liver fibrosis can be associated with pancreatic fibrosis. The purpose of the present study was to investigate the relationship between hepatic and pancreatic extracellular volume fraction (fECV) that correlates with tissue fibrosis and their relationships with IGT.

#### METHODS AND MATERIALS

The study included 100 consecutive patients with known or suspected liver and/or pancreatic diseases who underwent contrast-enhanced CT, including the precontrast and the equilibrium phase (62 males and 38 females; median age, 62 years; range, 28-93 years). Patients were classified into three groups based on the American Diabetes Association criteria: non-diabetes subjects, HbA1c < 5.7% or fasting plasma glucose (FPG) < 100 mg/dL; pre-diabetes, 5.7% ≤ HbA1c < 6.5% or 100 ≤ FPG < 125 mg/dL; and type 2 diabetes mellitus (T2DM), HbA1c ≥ 6.5% or FPG ≥ 125 mg/dL. Subtraction images between unenhanced and equilibrium phase images were prepared using a new subtraction algorithm. The liver and the pancreas were automatically extracted excluding focal lesions, major vascular branches and ducts using a high-speed 3D image analysis system and mean CT values for them were calculated, respectively. The enhancement degree of the aorta (Aorta) was also measured. fECV was calculated using the following equation:  $fECV = (100 - \text{hematocrit}) \times \frac{\text{Pancreas} - \text{Aorta}}{\text{Aorta}}$ . We investigated the differences in hepatic fECV and pancreatic fECV among the three patient groups using Kruskal-Wallis and Dwass-Steel-Crichlow-Fligner multiple comparisons statistical test and the correlation between the each two in hepatic fECV, pancreatic fECV and HbA1c using Spearman's rho coefficient.

#### RESULTS

Pancreatic fECV positively correlated with hepatic fECV and HbA1c ( $r = 0.51$ ,  $P < 0.001$  and  $r = 0.51$ ,  $P < 0.001$ , respectively). Pancreatic fECV differed significantly among the three groups ( $P < 0.001$ ). Pancreatic fECV was significantly greater in T2DM compared with pre-diabetes or no-diabetes subjects and in pre-diabetes compared with no-diabetes subjects ( $P < 0.001$ ). Hepatic fECV was significantly greater in T2DM compared with non-diabetes subjects ( $P < 0.05$ ).

#### CONCLUSION

There is a close relationship between hepatic fECV, pancreatic fECV and IGT.

#### CLINICAL RELEVANCE/APPLICATION

Hepatic fECV is associated with pancreatic fECV and diabetes mellitus. Hepatic fECV may be possible to use for the assessment of IGT in conjunction with pancreatic fECV.

Printed on: 02/07/23

## Abstract Archives of the RSNA, 2022

R5B-SPGI-3

### 3-Dimensional Dual-Frequency Magnetic Resonance Elastography Derived Viscosity as a Surrogate of Hepatic Inflammation, Independent of Simultaneously Measured Stiffness

Thursday, Dec. 1 12:45PM - 1:15PM Room: Learning Center - GI DPS

#### Participants

Jenna Feeley, BS, (*Presenter*) Nothing to Disclose

#### PURPOSE

The traditional Magnetic Resonance Elastography (MRE) method that is used to detect liver inflammation utilizes the damping ratio (DR) which factors stiffness (Gd) into the calculation. Hence, the purpose of this study is to identify a surrogate of liver inflammation, independent of stiffness, using 3-Dimensional (3D) dual-frequency (2F-MRE).

#### METHODS AND MATERIALS

45 patients with chronic liver disease (Hepatitis C or Steatohepatitis) were included in this prospective study. 3D 2F-MRE was performed at 56 and 28 Hz on a 3T scanner. Liver viscosity (GI) and stiffness (Gd) were measured at both frequencies. The difference in tissue viscosity and stiffness derived from the two frequencies was calculated ( $\Delta$ GI,  $\Delta$ Gd). All patients had liver biopsies for ISHAK scoring (inflammation range 0-18, fibrosis range 0-6). Statistical analysis was used to evaluate the degree of correlation between inflammation and fibrosis scores obtained from biopsy versus GI and Gd, respectively (28 Hz and 56 Hz separately), and  $\Delta$ GI and  $\Delta$ Gd obtained from 3D 2F-MRE. Lastly, diagnostic performance was evaluated by Receiver Operating Characteristic (ROC) curves.

#### RESULTS

The average patient age and BMI were  $56.16 \pm 9.26$  years and  $27.82 \pm 3.98$  kg/m<sup>2</sup>, respectively, and 11 were women. Of the three viscosity parameters measured (GI<sub>28</sub>, GI<sub>56</sub>, and  $\Delta$ GI),  $\Delta$ GI showed the most significant correlation with ISHAK inflammation scores ( $P=0.0041$ ). Stepwise multilinear regression analysis revealed that  $\Delta$ GI was the only significant surrogate of hepatic inflammation ( $R^2 = 0.1975$ ,  $P = 0.0025$ ) and excluded all GI and Gd values (from both frequencies) from the model.  $\Delta$ GI also showed a strong diagnostic performance for detecting moderate/severe hepatic inflammation (ISHAK > 8: AUC = 0.8, Sensitivity 80%, Specificity 73.5%,  $P = 0.0001$ ). All Gd values correlated similarly with fibrosis and no difference in diagnostic performance was found.

#### CONCLUSION

These results indicate that the difference in liver viscosity,  $\Delta$ GI, obtained by 3D 2F-MRE is a significant and independent surrogate of liver inflammation and has a robust diagnostic performance for detecting moderate/severe liver inflammation. Unlike other MRE methods,  $\Delta$ GI derived from 3D 2F-MRE is an independent measurement that does not rely on the DR which factors in liver stiffness.

#### CLINICAL RELEVANCE/APPLICATION

3D 2F-MRE-derived  $\Delta$ GI is an independent surrogate marker of liver inflammation. This non-invasive measure provides early detection of liver inflammation and, with monitored treatment, may help mitigate the progression to fibrosis.

Printed on: 02/07/23

## Abstract Archives of the RSNA, 2022

R5B-SPGI-4

### Ultrasound shear wave elastography and shear wave dispersion imaging for diagnosis and staging of hepatic fibrosis

Thursday, Dec. 1 12:45PM - 1:15PM Room: Learning Center - GI DPS

#### Participants

Kibo Nam, PhD, Philadelphia, PA (*Presenter*) Equipment support, Canon Medical Systems Corporation; Equipment support, General Electric Company ; Support, Lantheus Medical Imaging; Research funded, Canon Medical Systems Corporation

#### PURPOSE

To compare ultrasound shear wave elastography (SWE) and shear wave dispersion slope (SWDS) values to the fibrosis diagnosis and staging by a liver biopsy or MRE in non-alcoholic fatty liver disease (NAFLD) suspected patients.

#### METHODS AND MATERIALS

Subjects underwent a liver biopsy or MRE for suspected NAFLD and were scanned with an i8C1 probe on the Aplio i800 scanner (Canon Medical Systems). Five SWE (in kPa) and five SWDS (in m/s/KHz) values were obtained from the right liver lobe of each patient using built-in software. A circular region of interest (ROI) with a 1 cm diameter was placed =1 cm below the liver capsule manually in the liver parenchyma, referring to the shear wave propagation map. The obtained values met the criteria of IQR/median= 0.30 for SWE and =0.15 for SWDS. The mean SWE and SWDS values were compared with the reference results using a t-test and Pearson's correlation coefficient (r).

#### RESULTS

Among 54 patients, 30 underwent liver biopsy and 24 had MRE. Fibrosis was diagnosed in 27 patients (18 by biopsy and 9 by MRE; 10 stage 1, 6 stage 1 to 2, 1 stage 2, 5 stage 2 to 3, 1 stage 3, and 4 stage 4), while 27 patients showed stage 0 (12 by biopsy and 15 by MRE). The SWE and SWDS values were significantly higher in fibrotic livers compared to normal livers (7.1±1.7 vs. 5.5±1.2 kPa;  $p<0.0001$  and 12.1±2.8 vs. 10.5±2.3 m/s/kHz;  $p=0.012$ , respectively). There was a fair correlation between fibrosis stage and mean SWE and SWDS values among all patients regardless of the reported clinical reference standard ( $r=0.69$  and  $r=0.52$ , respectively). Liver biopsy fibrosis staging was moderately correlated with SWE and SWDS ( $r=0.70$  and  $r=0.60$ , respectively). The correlation between MRE stiffness values (in kPa) with SWE and SWDS was weaker ( $r=0.63$  and  $r=0.34$ , respectively).

#### CONCLUSION

s Ultrasound SWE showed a higher correlation with the diagnosis and staging of liver fibrosis by biopsy and/or MRE compared to SWDS.

#### CLINICAL RELEVANCE/APPLICATION

Ultrasound SWE has more potential for diagnosis and staging of liver fibrosis in NAFLD compared to SWDS values.

Printed on: 02/07/23

## Abstract Archives of the RSNA, 2022

R5B-SPGI-5

### Preoperative ultrasound radiomics for predicting clinically relevant postoperative pancreatic fistula after pancreatectomy

Thursday, Dec. 1 12:45PM - 1:15PM Room: Learning Center - GI DPS

#### Participants

Yi Dong, MD, PhD, Shanghai, China (*Presenter*) Nothing to Disclose

#### PURPOSE

To evaluate the efficacy of the radiomics model based on preoperative grayscale ultrasound and shear wave elastography (SWE) in predicting the occurrence of clinically relevant postoperative pancreatic fistula (CR-POPF) after pancreatectomy.

#### METHODS AND MATERIALS

This prospective study was conducted from Jan 2020 to Nov 2021. Patients who scheduled to undergo pancreatectomy were initially enrolled and received ultrasound assessment within one week before surgery. The risk factors of POPF (grades B and C) were analyzed. Preoperative grayscale ultrasound images, ultrasound SWE values of pancreatic lesions and their surrounding parenchyma were used to build preoperative prediction radiomics model. Radiomic signatures were extracted and constructed using a minimal Redundancy Maximal Relevance (mRMR) algorithm and a L1 penalized logistic regression. Combined model was built using multivariate regression which incorporating radiomics signatures and clinical variables.

#### RESULTS

Finally, 147 patients (median age 62.0 y) were prospectively enrolled. Among which, 85 patients underwent distal pancreatectomy, and 62 patients underwent pancreaticoduodenectomy. During the three-weeks follow-up after pancreatectomy, the incidence rates of grade B/C POPF were 28.6% (42/147 patients). Radiomic signatures constructed from grayscale ultrasound images of pancreas parenchymal regions (panRS) achieved an AUC of 0.75, accuracy of 68.7%, sensitivity of 85.7 % and specificity of 61.9 % in preoperative noninvasive prediction of CR-POPF. AUC of radiomics model increased to 0.81 when panRS was used for the prediction of CR-POPF after pancreaticoduodenectomy.

#### CONCLUSION

s Radiomics model based on ultrasound images was potentially useful for preoperative noninvasively predicting of CR-POPF.

#### CLINICAL RELEVANCE/APPLICATION

Patients with high-risk factors of CR-POPF could be closely monitored during the postoperative period.

Printed on: 02/07/23

## Abstract Archives of the RSNA, 2022

R5B-SPGI-6

### Longitudinal Changes in Liver Imaging Biomarkers Following Low Calorie Liquid Diet

Thursday, Dec. 1 12:45PM - 1:15PM Room: Learning Center - GI DPS

#### Participants

Jake Weeks, La Jolla, CA (*Presenter*) Nothing to Disclose

#### PURPOSE

Low calorie liquid diet (LCLD) prior to bariatric surgery has been shown to reduce liver volume by ~20% on average, resulting in improved outcomes by reducing the technical difficulty of the operation. The effect of LCLD on liver volume has been well-documented, but relationships between liver shrinkage and other liver biomarkers are poorly understood. Changes to liver stiffness could also explain improved outcomes in bariatric surgery, but the effects of preparatory diet on liver stiffness have not been reported. This study describes changes in automated MR-based liver volume, steatosis, and stiffness after LCLD to elucidate the mechanisms of improved bariatric surgery outcomes.

#### METHODS AND MATERIALS

Forty-five adults with obesity scheduled for bariatric surgery were prospectively recruited to participate in an ongoing research study which includes two non-contrast MR imaging exams at 3.0T (GE Signa Premier, or GE Discovery MR750, GE Healthcare, Waukesha WI) at baseline and 2-3 days prior to surgery. LCLD was prescribed for 14-21 days during this interval. Imaging biomarkers included MRI-PDFF (IDEAL-IQ), liver volume based on MR imaging (3D convolutional neural network developed at our institution), and 2D SE-EPI MR Elastography. Mean PDFF was quantified by a 9-segment ROI analysis. Elastography was analyzed manually using the MRE Quant™ software (Resoundant, Inc., Minnesota, USA). BMI was examined for correlation with these parameters.

#### RESULTS

Following LCLD, mean liver volume decreased 414.36 cm<sup>3</sup> (2098.32 cm<sup>3</sup> to 1683.96 cm<sup>3</sup>). Mean liver PDFF decreased 3.45% (8.51% to 5.06%). Mean liver stiffness decreased by 0.09 kPa (2.07 kPa to 1.98 kPa). Mean BMI decreased by 2.13kg/m<sup>2</sup> (46.15 kg/m<sup>2</sup> to 44.02 kg/m<sup>2</sup>). Rate of change of volume demonstrated moderate, statistically significant correlations with the rates of change for MRE ( $r = 0.43$ ,  $p = 0.004$ ), PDFF ( $r = 0.38$ ,  $p = 0.013$ ), and BMI ( $r = 0.32$ ,  $p = 0.040$ ).

#### CONCLUSION

The results of this study agree with previous data showing reductions in liver volume and steatosis following LCLD. We also found that liver stiffness is reduced during the dieting phase. MRE-derived liver stiffness change is correlated with liver volume change following LCLD. Reduced liver stiffness may affect outcomes in bariatric surgery, but the sample size was small and requires additional investigation. Further research within larger cohorts is needed to validate these findings.

#### CLINICAL RELEVANCE/APPLICATION

Longitudinal changes in MRI biomarkers following preparatory diet in bariatric surgery patients may help explain mechanisms underlying improved surgical outcomes.

Printed on: 02/07/23

## Abstract Archives of the RSNA, 2022

R5B-SPGI-7

### Splenic Volume is Associated with Survival in Patients Receiving Immunotherapy for Advanced Hepatocellular Carcinoma

Thursday, Dec. 1 12:45PM - 1:15PM Room: Learning Center - GI DPS

#### Participants

Bang Bin Chen, MD, (*Presenter*) Nothing to Disclose

#### PURPOSE

To investigate the association of splenic volume and its changes with survival outcomes among patients who underwent immunotherapy for advanced hepatocellular carcinoma (HCC).

#### METHODS AND MATERIALS

In this retrospective analysis, patients who initiated immunotherapy for advanced HCC were included. The baseline splenic volume and its relative changes after 1~3 months (median 55 days) on CT or MRI were measured by volumetric segmentation using 3D slicer software. The association between splenic volume at baseline and its relative change  $[(\text{posttherapy} - \text{baseline})/\text{baseline}]$  and progression-free survival (PFS) or overall survival (OS) were evaluated using univariate and multivariate Cox analyses.

#### RESULTS

A total of 134 patients were included (men/women = 118/16; mean age,  $59.5 \pm 11.5$  years (standard deviation)). The median follow-up duration was 30.5 months (95% confidence interval (CI) = 20.7-40.3). The overall response rate was 30.6%, and the disease control rate was 68.7%. The median PFS was 4 months (95% CI = 2.9-5.1), and the median OS was 17.2 months (95% CI = 10.9-23.5). After treatment, splenic volume was increased in 95 (70.9%) patients, and decreased in 39 (29.1%) patients. At baseline, patients with splenomegaly exhibited significantly shorter PFS (median, 4.0 vs. 5.4 months,  $P = 0.019$ ) and OS (median, 11.2 vs. 19.3 months,  $P < 0.001$ ) than patients without splenomegaly. After treatment, patients with increased splenic volume exhibited significantly better PFS (median, 2.6 vs. 6.7 months,  $P = 0.003$ ) and OS (median, 12.0 vs. 23.1 months,  $P = 0.001$ ) than patients with decreased splenic volume. In multivariate analysis adjusting for patient demographics, tumor extent, immunotherapy line, and liver function reserve, splenic volume change remained an independent predictor of PFS (hazard ratio (HR) 0.59; 95% CI: 0.37-0.94,  $P = 0.025$ ) and OS (HR 0.46; 95% CI: 0.28-0.75,  $P = 0.002$ ).

#### CONCLUSION

Splenic volume may be used as a prognostic marker in patients who received immunotherapy for advanced HCC.

#### CLINICAL RELEVANCE/APPLICATION

Follow-up splenic volume after 1~3 months post-therapy may help clinicians predict clinical outcomes in HCC patients receiving immunotherapy.

Printed on: 02/07/23

## Abstract Archives of the RSNA, 2022

R5B-SPGI-8

### **Synergistic Anticancer Effect of Pulsed Focused Ultrasound with Ultrasound-Sensitive Nanoparticle IMP301 on Pancreas Cancer Xenograft Model.**

Thursday, Dec. 1 12:45PM - 1:15PM Room: Learning Center - GI DPS

#### **Participants**

Soojin Kim, MD, (*Presenter*) Nothing to Disclose

#### **PURPOSE**

Focused ultrasound (FUS) has been widely investigated for use in drug delivery system as a noninvasive synergistic modality. The purpose of this study was to investigate synergistic anticancer effect of FUS with a novel ultrasound-sensitive nanoparticle IMP 301 (doxorubicin-loaded) on pancreas cancer xenograft model.

#### **METHODS AND MATERIALS**

Nude mice were subcutaneously inoculated with human pancreatic cancer cell PANC-1 and randomly divided into six different groups (n=5 per group) for study 1 and 2 respectively. Ectopic pancreatic tumors were conditionally exposed to pHIFU with pre-studied parameters (acoustic power = 72 Watt, gap = 2mm x 2mm, total time = 20 second/spot, duty cycle = 2%, pulse repetition frequency = 250Hz). In Study 1, mice were assigned to 1) control, 2) gemcitabine only (200mg intraperitoneal), 3) doxil (4mg/kg) with FUS, and 4-6) three groups treated with different doses of IMP301 (2,4,6mg/kg) with FUS. In Study 2, mice were assigned to 1) control, 2) FUS only, 3) gemcitabine only, 4) doxil (4mg/kg) with FUS, and 5-6) two groups treated with IMP 301 (4mg/kg) with or without FUS. The presence of synergistic effect of IMP 301 when combined with FUS was evaluated by comparison with other groups in terms of tumor growth suppression.

#### **RESULTS**

In Study 1, IMP301 with FUS group showed significantly lower tumor volume ( $121 \text{ mm}^3 \pm 28 \text{ mm}^3$ ) and growth rate ( $12.1 \text{ mm}^3/\text{week} \pm 5.2 \text{ mm}^3/\text{week}$ ) when dose exceeded 4mg/kg, compared to gemcitabine only ( $244.7 \text{ mm}^3 \pm 47.6 \text{ mm}^3$ ,  $30.5 \text{ mm}^3/\text{week} \pm 11.7 \text{ mm}^3/\text{week}$ ) and doxil with FUS group ( $208 \text{ mm}^3 \pm 25 \text{ mm}^3$ ,  $25.6 \text{ mm}^3/\text{week} \pm 7.7 \text{ mm}^3/\text{week}$ ) [ $p < 0.05$ ]. In Study 2, IMP301 with FUS group showed significantly lower tumor volume ( $98 \text{ mm}^3 \pm 42 \text{ mm}^3$ ) and growth rate ( $9.2 \text{ mm}^3/\text{week} \pm 6.5 \text{ mm}^3/\text{week}$ ;  $p < 0.05$ ) than gemcitabine only ( $323 \text{ mm}^3 \pm 158 \text{ mm}^3$ ,  $46.7 \text{ mm}^3/\text{week} \pm 29.1 \text{ mm}^3/\text{week}$ ) and doxil with FUS group ( $236 \text{ mm}^3 \pm 60 \text{ mm}^3$ ,  $32.2 \text{ mm}^3/\text{week} \pm 11.9 \text{ mm}^3/\text{week}$ ) [ $p < 0.05$ ]. However, IMP301 without FUS group ( $256 \text{ mm}^3 \pm 107 \text{ mm}^3$ ,  $35.6 \text{ mm}^3/\text{week} \pm 18.8 \text{ mm}^3/\text{week}$ ) showed no significant difference with gemcitabine only and doxil with FUS group.

#### **CONCLUSION**

In conclusion, IMP301 combined with short duty cycle FUS exhibited significantly higher and persistent tumor suppression effect, compared to the single use of conventional drug or IMP 301 or the combined use of conventional drug and FUS, showing the potential of IMP 301 with FUS for the treatment of pancreatic cancer.

#### **CLINICAL RELEVANCE/APPLICATION**

Ultrasound-sensitive drug release by FUS can be applied in treatment for nonoperative pancreatic cancer patients as a highly effective noninvasive localized therapeutic modality.

Printed on: 02/07/23

## Abstract Archives of the RSNA, 2022

R5B-SPGI-9

### An Attention-Based Convolutional Neural Network for Differentiating Benign from Malignant Focal Liver Lesions in Wash-In and Wash-Out Contrast-Enhanced Ultrasonography

Thursday, Dec. 1 12:45PM - 1:15PM Room: Learning Center - GI DPS

#### Participants

Thodsawit Tiyarattanachai, (*Presenter*) Nothing to Disclose

#### PURPOSE

Contrast-enhanced ultrasound (CEUS) is increasingly used to characterize focal liver lesions (FLLs). We have previously developed deep learning models to support interpretation of wash-in CEUS data in FLL characterization. In this work, we investigated whether including wash-out data into our models can improve differentiation of benign from malignant FLLs.

#### METHODS AND MATERIALS

This study used CEUS data from an ongoing multi-institutional IRB-approved study and informed consent was obtained from all patients. A wash-in cine was used as input into a "wash-in subnetwork" based on a three-dimensional (3D) convolutional neural network (CNN). Variable instances of wash-out images were used as inputs into six "wash-out subnetworks" based on two-dimensional (2D) CNNs. Since wash-out data are usually acquired as an ambiguous number of images and not cines, an attention module was built on top of the wash-in and wash-out subnetworks to deal with such variable instances of wash-out images. To evaluate the add-on utility of the attention module, the following three models were compared: 1) a simple 3D CNN, which was inspired by previously published works, receiving as input a wash-in cine (Model A); 2) a simple 3D CNN receiving as input a wash-in cine temporally appended with wash-out images (Model B); and 3) the model with attention module built on top of wash-in and wash-out subnetworks (Model C). 5-fold cross validation was performed. Mean SD of performance results across all folds were reported. Area under receiver operating characteristic curve (AUROC), sensitivity and specificity were used as evaluation metrics.

#### RESULTS

A total of 158 FLLs from 130 patients were included. Of these, 31 (19.6%) FLLs were benign, and 127 (80.4%) FLLs were malignant based on a composite reference standard of pathology, CT and MRI. Model A achieved AUROC of 0.75±0.10, sensitivity of 76.9%±14.5% and specificity of 78.6%±24.2%. Model B achieved AUROC of 0.76±0.10, sensitivity of 74.9%±9.7% and specificity of 84.3%±15.6%. With incorporation of the attention module, Model C achieved the highest AUROC of 0.86±0.08, sensitivity of 84.2%±8.1% and specificity of 87.1%±7.3%.

#### CONCLUSION

The attention module improved performance of CNN in differentiating benign from malignant FLLs on wash-in and wash-out CEUS.

#### CLINICAL RELEVANCE/APPLICATION

The Attention-based CNN can be used to characterize FLLs on CEUS acquired in clinical practice, where the number of recorded wash-out instances is variable.

Printed on: 02/07/23

## Abstract Archives of the RSNA, 2022

R5B-SPGU

### Genitourinary Thursday Poster Discussions - B

Thursday, Dec. 1 12:45PM - 1:15PM Room: Learning Center - GU DPS

#### Sub-Events

#### **R5B-SPGU-1 Proportion of malignancy in Bosniak Classification of Cystic Renal Masses version 2019 (v2019) Classes: Systematic Review and Meta-Analysis**

Participants

Nicola Schieda, MD, Ottawa, ON (*Presenter*) Nothing to Disclose

#### PURPOSE

To determine the proportion of malignancy within Bosniak v2019 Classes.

#### METHODS AND MATERIALS

MEDLINE and EMBASE were searched. Eligible studies contained patients with cystic renal masses undergoing CT or MRI renal protocol examinations with pathology confirmation, applying Bosniak v2019. Proportion of malignancy was estimated within Bosniak v2019 Class. Risk of bias was assessed using QUADAS-2.

#### RESULTS

We included 471 patients with 480 cystic renal masses. No Class I malignant masses were observed. Pooled proportion of malignancy were: Class II, 12% (6/51, 95%CI 5-24%), Class IIF, 46% (37/85, 95%CI 28-66%), Class III, 79% (138/173, 95%CI 68-88%), Class IV, 84% (114/135, 95%CI 77-90%). Proportion of malignancy differed between Bosniak v2019 II-IV classes ( $p=0.004$ ). Four studies reported the proportion of malignancy by wall/septa feature. The pooled proportion of malignancy with 95%CI were: Class III thick smooth wall/septa, 77% (41/56, 95%CI 53-91%), Class III obtuse protrusion  $\geq 3$  mm (irregularity), 83% (97/117, 95%CI 75-89%), Class IV nodule with acute angulation, 86% (50/58, 95%CI 75-93%) or obtuse angulation  $\geq 4$  mm, 83%, (64/77, 95%CI 73-90%). Subgroup analysis by wall/septa feature was limited by small sample size; however, no differences were found comparing Class III masses with irregularity to Class IV masses ( $p=0.74$ ) or between Class IV masses by acute versus obtuse angles ( $p=0.62$ ).

#### CONCLUSION

Preliminary data suggest Bosniak v2019 Class IIF masses have higher proportion of malignancy compared to the original Classification and there are no differences in proportion of malignancy comparing Class III masses with irregularities to Class IV masses with acute or obtuse nodules.

#### CLINICAL RELEVANCE/APPLICATION

Our results suggest a potential opportunity for simplification of the Bosniak v2019 Classification, where cystic masses that show any wall or septa protrusion could be considered as Class IV and those with smooth wall or septa thickness considered as Class III.

#### **R5B-SPGU-2 Assessment of muscle invasion in bladder urothelial carcinoma with variant histology using the Vesical Imaging-Reporting and Data System: a multi-institutional multi-reader pair-matched cohort study**

#### Awards

**Trainee Research Prize - Fellow**

Participants

Yuki Arita, MD, (*Presenter*) Nothing to Disclose

#### PURPOSE

Recent studies demonstrated high accuracy of the Vesicle Imaging-Reporting and Data System (VI-RADS) for diagnosing muscle-invasive bladder cancer (MIBC), especially for the pure urothelial carcinoma (PUC) patients. However, the diagnostic performance of VI-RADS for variant histology urothelial carcinoma (VUC) remains unknown. This study aimed to investigate the utility of the VI-RADS for muscle-invasion assessment in VUC by comparing its diagnostic performance with that of PUC.

#### METHODS AND MATERIALS

This multi-institutional study included consecutive treatment-naïve patients with pathologically proven PUC or VUC who underwent bladder multiparametric magnetic resonance imaging (mpMRI) before transurethral bladder tumor resection between 2011 and 2019. Four board-certified radiologists (two fellowship-trained and two fellowship-training), blinded to the clinical information including histopathological findings, independently reviewed the mpMRI data according to the VI-RADS criteria. Histopathological results were used as reference standard. Receiver operating characteristic curve analysis, Z-test, and Wald test were used to evaluate the diagnostic performance.

## RESULTS

Of the 122 pair-matched patients (PUC cohort: 61, VUC cohort: 61), 34 (55.7%) and 33 (54.1%) had pathologically confirmed MIBC, while 27 (44.3%) and 28 (45.9%) had non-MIBC (NMIBC), respectively. The areas under the curves (AUCs) of the VI-RADS overall scores for MIBC diagnosis in PUC/VUC were 0.94/0.89-0.92. There were no significant differences between the PUC and VUC cohorts in the AUC, sensitivity, and specificity for muscle invasion of the VI-RADS overall scores for all readers ( $p>0.05$  for all). In the evaluation by fellowship-training radiologists using diffusion-weighted imaging (DWI) scores alone with a cutoff score of 4, the sensitivity, but not specificity, was significantly lower for VUC than for PUC (54.5/89.3-92.9% vs. 82.4/92.6%,  $p=0.01/0.67-0.97$ ). However, the sensitivity and specificity did not significantly differ between the two cohorts using the VI-RADS overall scores with a cutoff score of 4 (85.3/92.6% vs. 75.8-78.8/85.7-89.3%,  $p=0.32-0.49/0.41-0.67$ ).

## CONCLUSION

s VI-RADS overall scores have comparably high diagnostic performance for muscle invasion detection in PUC and VUC regardless of the readers' experience. However, when DWI scores alone are used, there may be a risk of less experienced radiologists underestimating muscle invasion in VUC.

## CLINICAL RELEVANCE/APPLICATION

VI-RADS is useful for muscle-invasion assessment both in VUC and PUC. Less experienced radiologists can better assess muscle invasion in VUC using the VI-RADS overall classification algorithm owing to the effect of dynamic contrast-enhanced MRI scores.

Printed on: 02/07/23

## Abstract Archives of the RSNA, 2022

R5B-SPGU-1

### Proportion of malignancy in Bosniak Classification of Cystic Renal Masses version 2019 (v2019) Classes: Systematic Review and Meta-Analysis

Thursday, Dec. 1 12:45PM - 1:15PM Room: Learning Center - GU DPS

#### Participants

Nicola Schieda, MD, Ottawa, ON (*Presenter*) Nothing to Disclose

#### PURPOSE

To determine the proportion of malignancy within Bosniak v2019 Classes.

#### METHODS AND MATERIALS

MEDLINE and EMBASE were searched. Eligible studies contained patients with cystic renal masses undergoing CT or MRI renal protocol examinations with pathology confirmation, applying Bosniak v2019. Proportion of malignancy was estimated within Bosniak v2019 Class. Risk of bias was assessed using QUADAS-2.

#### RESULTS

We included 471 patients with 480 cystic renal masses. No Class I malignant masses were observed. Pooled proportion of malignancy were: Class II, 12% (6/51, 95%CI 5-24%), Class IIF, 46% (37/85, 95%CI 28-66%), Class III, 79% (138/173, 95%CI 68-88%), Class IV, 84% (114/135, 95%CI 77-90%). Proportion of malignancy differed between Bosniak v2019 II-IV classes ( $p=0.004$ ). Four studies reported the proportion of malignancy by wall/septa feature. The pooled proportion of malignancy with 95%CI were: Class III thick smooth wall/septa, 77% (41/56, 95%CI 53-91%), Class III obtuse protrusion =3 mm (irregularity), 83% (97/117, 95%CI 75-89%), Class IV nodule with acute angulation, 86% (50/58, 95%CI 75-93%) or obtuse angulation =4 mm, 83%, (64/77, 95%CI 73-90%). Subgroup analysis by wall/septa feature was limited by small sample size; however, no differences were found comparing Class III masses with irregularity to Class IV masses ( $p=0.74$ ) or between Class IV masses by acute versus obtuse angles ( $p=0.62$ ).

#### CONCLUSION

s Preliminary data suggest Bosniak v2019 Class IIF masses have higher proportion of malignancy compared to the original Classification and there are no differences in proportion of malignancy comparing Class III masses with irregularities to Class IV masses with acute or obtuse nodules.

#### CLINICAL RELEVANCE/APPLICATION

Our results suggest a potential opportunity for simplification of the Bosniak v2019 Classification, where cystic masses that show any wall or septa protrusion could be considered as Class IV and those with smooth wall or septa thickness considered as Class III.

Printed on: 02/07/23

## Abstract Archives of the RSNA, 2022

R5B-SPGU-2

### Assessment of muscle invasion in bladder urothelial carcinoma with variant histology using the Vesical Imaging-Reporting and Data System: a multi-institutional multi-reader pair-matched cohort study

Thursday, Dec. 1 12:45PM - 1:15PM Room: Learning Center - GU DPS

#### Awards

Trainee Research Prize - Fellow

#### Participants

Yuki Arita, MD, (*Presenter*) Nothing to Disclose

#### PURPOSE

Recent studies demonstrated high accuracy of the Vesicle Imaging-Reporting and Data System (VI-RADS) for diagnosing muscle-invasive bladder cancer (MIBC), especially for the pure urothelial carcinoma (PUC) patients. However, the diagnostic performance of VI-RADS for variant histology urothelial carcinoma (VUC) remains unknown. This study aimed to investigate the utility of the VI-RADS for muscle-invasion assessment in VUC by comparing its diagnostic performance with that of PUC.

#### METHODS AND MATERIALS

This multi-institutional study included consecutive treatment-naïve patients with pathologically proven PUC or VUC who underwent bladder multiparametric magnetic resonance imaging (mpMRI) before transurethral bladder tumor resection between 2011 and 2019. Four board-certified radiologists (two fellowship-trained and two fellowship-training), blinded to the clinical information including histopathological findings, independently reviewed the mpMRI data according to the VI-RADS criteria. Histopathological results were used as reference standard. Receiver operating characteristic curve analysis, Z-test, and Wald test were used to evaluate the diagnostic performance.

#### RESULTS

Of the 122 pair-matched patients (PUC cohort: 61, VUC cohort: 61), 34 (55.7%) and 33 (54.1%) had pathologically confirmed MIBC, while 27 (44.3%) and 28 (45.9%) had non-MIBC (NMIBC), respectively. The areas under the curves (AUCs) of the VI-RADS overall scores for MIBC diagnosis in PUC/VUC were 0.94/0.89-0.92. There were no significant differences between the PUC and VUC cohorts in the AUC, sensitivity, and specificity for muscle invasion of the VI-RADS overall scores for all readers ( $p > 0.05$  for all). In the evaluation by fellowship-training radiologists using diffusion-weighted imaging (DWI) scores alone with a cutoff score of 4, the sensitivity, but not specificity, was significantly lower for VUC than for PUC (54.5/89.3-92.9% vs. 82.4/92.6%,  $p = 0.01/0.67-0.97$ ). However, the sensitivity and specificity did not significantly differ between the two cohorts using the VI-RADS overall scores with a cutoff score of 4 (85.3/92.6% vs. 75.8-78.8/85.7-89.3%,  $p = 0.32-0.49/0.41-0.67$ ).

#### CONCLUSION

s VI-RADS overall scores have comparably high diagnostic performance for muscle invasion detection in PUC and VUC regardless of the readers' experience. However, when DWI scores alone are used, there may be a risk of less experienced radiologists underestimating muscle invasion in VUC.

#### CLINICAL RELEVANCE/APPLICATION

VI-RADS is useful for muscle-invasion assessment both in VUC and PUC. Less experienced radiologists can better assess muscle invasion in VUC using the VI-RADS overall classification algorithm owing to the effect of dynamic contrast-enhanced MRI scores.

Printed on: 02/07/23



## Abstract Archives of the RSNA, 2022

R5B-SPHN

### Head and Neck Thursday Poster Discussions - B

Thursday, Dec. 1 12:45PM - 1:15PM Room: Learning Center - HN DPS

#### Sub-Events

#### R5B-SPHN-2 TI-RADS: Improving Patient Care or Just Pain in The Neck: A Retrospective Review

##### Participants

Tyler Rogers, BA, MMedSc, CHAPEL HILL, NC (*Presenter*) Nothing to Disclose

##### PURPOSE

The purpose of this study was to evaluate the American College of Radiology Thyroid Imaging Reporting and Data Systems (TI-RADS) by correlating TI-RADS score with biopsy results to validate or reaffirm the recommendation of fine needle aspiration (FNA) in the higher scoring nodules. Other covariables investigated included patient age, gender, FDG avidity on Positron Emission Tomography (PET), and echogenic foci as possible independent predictors of malignancy.

##### METHODS AND MATERIALS

This was a retrospective study performed at a large academic institution. 624 nodules underwent ultrasound (US) examination and US-guided FNA over a three-year period. Chart review included: age, gender, TI-RADS score, presence of echogenic foci, nodule size, pathology from FNA, and method of detection. Both TI-RADS scoring and FNA of nodules were performed by abdominal fellowship trained radiologists. Results were categorized as benign, indeterminate, or malignant based on the Bethesda System for Reporting Thyroid Cytopathology or non-diagnostic. The study implemented a multinomial logistic regression model where the TI-RADS category was the main independent variable, with the following control variables: gender, age, echogenic foci, and PET detection. Additionally, the study evaluated all possible 2-way interactions of control variables using a backwards elimination strategy to remove interactions with  $p < 0.05$ . An ordinal logistic regression was used to determine if higher TI-RADS scores were associated with higher probability of malignancy.

##### RESULTS

The percentage of malignant nodules in each TI-RADS (TR) category were as follows: TR 2- 0%, TR 3-4.9%, TR 4-3.6%, TR 5-16.3%. The odds ratio for a 1-unit increase in TIRADS was 3.16 [95% CI: 1.25, 7.98,  $p=0.015$ ] for malignant pathology, consistent with increasing malignant risk with increasing TI-RADS score. No control variables or 2-way interactions were significant.

##### CONCLUSION

The study supports the use of the TI-RADS model at our institution. The higher TI-RADS scores were significantly associated with malignant pathology on FNA. This validates the recommendation of FNA in nodules with higher TI-RADS scores.

##### CLINICAL RELEVANCE/APPLICATION

The higher TIRADS scores were associated with higher probability of malignant pathology at FNA. The decision to biopsy thyroid nodules should continue to be based on TIRADS score.

Printed on: 02/07/23

## Abstract Archives of the RSNA, 2022

R5B-SPHN-2

### TI-RADS: Improving Patient Care or Just Pain in The Neck: A Retrospective Review

Thursday, Dec. 1 12:45PM - 1:15PM Room: Learning Center - HN DPS

#### Participants

Tyler Rogers, BA, MMedSc, CHAPEL HILL, NC (*Presenter*) Nothing to Disclose

#### PURPOSE

The purpose of this study was to evaluate the American College of Radiology Thyroid Imaging Reporting and Data Systems (TI-RADS) by correlating TI-RADS score with biopsy results to validate or reaffirm the recommendation of fine needle aspiration (FNA) in the higher scoring nodules. Other covariables investigated included patient age, gender, FDG avidity on Positron Emission Tomography (PET), and echogenic foci as possible independent predictors of malignancy.

#### METHODS AND MATERIALS

This was a retrospective study performed at a large academic institution. 624 nodules underwent ultrasound (US) examination and US-guided FNA over a three-year period. Chart review included: age, gender, TI-RADS score, presence of echogenic foci, nodule size, pathology from FNA, and method of detection. Both TI-RADS scoring and FNA of nodules were performed by abdominal fellowship trained radiologists. Results were categorized as benign, indeterminate, or malignant based on the Bethesda System for Reporting Thyroid Cytopathology or non-diagnostic. The study implemented a multinomial logistic regression model where the TI-RADS category was the main independent variable, with the following control variables: gender, age, echogenic foci, and PET detection. Additionally, the study evaluated all possible 2-way interactions of control variables using a backwards elimination strategy to remove interactions with  $p < 0.05$ . An ordinal logistic regression was used to determine if higher TI-RADS scores were associated with higher probability of malignancy.

#### RESULTS

The percentage of malignant nodules in each TI-RADS (TR) category were as follows: TR 2- 0%, TR 3-4.9%, TR 4-3.6%, TR 5-16.3%. The odds ratio for a 1-unit increase in TIRADS was 3.16 [95% CI: 1.25, 7.98,  $p=0.015$ ] for malignant pathology, consistent with increasing malignant risk with increasing TI-RADS score. No control variables or 2-way interactions were significant.

#### CONCLUSION

The study supports the use of the TI-RADS model at our institution. The higher TI-RADS scores were significantly associated with malignant pathology on FNA. This validates the recommendation of FNA in nodules with higher TI-RADS scores.

#### CLINICAL RELEVANCE/APPLICATION

The higher TIRADS scores were associated with higher probability of malignant pathology at FNA. The decision to biopsy thyroid nodules should continue to be based on TIRADS score.

Printed on: 02/07/23

## Abstract Archives of the RSNA, 2022

R5B-SPIN

### Informatics Thursday Poster Discussions - B

Thursday, Dec. 1 12:45PM - 1:15PM Room: Learning Center - IN DPS

#### Sub-Events

#### R5B-SPIN-1 A Robustly Optimized Natural Language Processing Model for Label Extraction in Mammography Report

Participants

Yuxing Tang, Bethesda, MD (*Presenter*) Nothing to Disclose

#### PURPOSE

To explore RoBERTa (robustly retrained BERT model, namely the Bidirectional Encoder Representations from Transformers) in classifying mammography diagnostic text reports to facilitate large-scale weakly-supervised learning for image-based mammography diagnosis systems.

#### METHODS AND MATERIALS

Weakly-supervised learning from mammogram images requires binary labels for each view to indicate the presence of a lesion type. Previously these labels were either manually labeled by experienced radiologists, or obtained from the diagnostic reports by applying text processing rules or relatively simple natural language processing (NLP) models. We formulate this task as a text classification problem and propose Mammo-RoBERTa by fine-tuning the pre-trained RoBERTa on our large-scale mammogram report data with whole word masking. Mammo-RoBERTa treats each text report as a sample and takes both the description and impression parts of a report as the input. It consists of 12 encoding layers with 768 hidden units and 12 attention heads. We use the final hidden vector corresponding to the first input token as the aggregate representation of the input sequence. A linear classification layer and a softmax function are applied to predict the probability that a lesion type is present in a mammogram. A large-scale dataset containing 33,630 mammogram studies with diagnostic reports from 30,495 patients was collected, among which 3,753 studies were manually labeled by radiologists.

#### RESULTS

We perform three-fold cross-validation on 3,753 mammography studies. Mammo-RoBERTa achieves very high accuracy ( $98.72\% \pm 0.24\%$  and  $98.19\% \pm 0.27\%$  for left and right breasts, respectively) in predicting the presence of a specified lesion type in the mammogram images from the corresponding text reports, far exceeding the previous rule-based text processing approaches ( $p < 0.05$ ). The F1 scores (left:  $0.973 \pm 0.005$ , right:  $0.958 \pm 0.006$ ) and weighted F1 scores (left  $0.987 \pm 0.005$ , right:  $0.982 \pm 0.005$ ) also show that the performance of our Mammo-RoBERTa is very robust in general.

#### CONCLUSION

We proposed Mammo-RoBERTa, a RoBERTa model fine-tuned on mammogram report data, which can be used to predict the presence of specific lesion types (e.g., mass) in mammograms with very high accuracy, with input from the text report.

#### CLINICAL RELEVANCE/APPLICATION

The advanced NLP models, such as RoBERTa, can be fine-tuned on clinical text report data to substantially improve the system performance in automatically understanding the content of pervasive clinical diagnostic reports.

#### R5B-SPIN-2 Machine Learning Methods Based on Injection Pressure to Detect the Contrast Material Extravasation During CT

Participants

Takeshi Nakaura, MD, Kumamoto, Japan (*Presenter*) Nothing to Disclose

#### PURPOSE

To evaluate the performance of a machine learning (ML) method to detect the contrast material extravasation based on injection pressure during computed tomography (CT).

#### METHODS AND MATERIALS

We enrolled 46,666 patients who underwent contrast enhanced CT examination in one hospital. We chose an 8:2 training-to-validation ratio and developed ML software to predict the risk of contrast material extravasation based on injection pressure of first 6 seconds with 0.25 second interval and injection rate settings. This ML software contains ML classifiers for time series data (kNN, ROCKET, TSF, RISE) and the stacking ensemble ML (LightGBM) using the outputs of other ML classifiers as input data. We trained and evaluated ML classifiers using 5-fold cross-validation using the training data ( $n = 37,336$ ), and we evaluated the performance of best model in the test data ( $n = 9,330$ ) using areas under the receiver operating characteristic curves (AUCs).

#### RESULTS

The contrast material extravasation occurred in 0.20% (94/46,666) of the patients. The stacking ensemble ML gave the highest

THE CONTRAST MATERIAL EXTRAVASATION OCCURRED IN 0.2076 (24/10,000) OF THE PATIENTS. THE STACKING ENSEMBLE ML GAVE THE HIGHEST PERFORMANCE (AUC = 0.748), FOLLOWED BY THE KNN (AUC = 0.728), ROCKET (AUC = 0.71), TSF (AUC = 0.648), AND RISE (AUC = 0.654). THE PERFORMANCE OF STACKING ENSEMBLE ML DID NOT DECREASE IN THE TEST GROUP (AUC = 0.761).

## CONCLUSION

s The stacking ensemble ML offered high performance to detect the contrast material extravasation based on injection pressure during CT as compared with ML methods for time series data.

## CLINICAL RELEVANCE/APPLICATION

The stacking ensemble ML based on injection pressure might be the useful tool for the early detection of the contrast material extravasation during CT.

## R5B-SPIN-3 F-18 FDG Uptake in Axillary Lymph Nodes after Vaccination Against COVID-19

Participants

Kaoru Maruyama, Osaka, Japan (*Presenter*) Nothing to Disclose

## PURPOSE

Little is known about the frequency and duration of increased F-18 fluorodeoxyglucose (FDG) uptake in lymph nodes after vaccination. Increased FDG uptake may be mistaken for a sign of malignancy. We assessed the frequency of increased FDG uptake in axillary lymph nodes after vaccination against the coronavirus disease 2019 (COVID-19).

## METHODS AND MATERIALS

We collected vaccination data for all individuals at the time FDG positron emission tomography/computed tomography (PET/CT) imaging. Unilateral FDG uptake in axillary lymph node on side (arm) of last vaccination (or, if individual was not sure about side, higher uptake on either side) was examined.

## RESULTS

We used data from 181 vaccinated individuals (including 51 healthy individuals and 130 patients) who received one or two dose of the two type of mRNA Covid-19 vaccines (either Pfizer or Moderna). The frequency of increased FDG uptake was 22% (39/181 individuals), occurred within 1 day, and lasted 122 days after vaccination. No uptake in axillary lymph node was detected from 3 days after the first dose, and from 4 days after the second dose. The median onset of local reactions was 17 days after first dose and 18 days after the second dose. Axillary lymph node FDG positive rate was: 63% (12 of 19) of individuals at 3-96 days of vaccination after the first dose; 14% (20 of 147) of individuals at 2-135 days after the second dose; and 47% (7 of 15) of individuals at 1-63 days in the unknown (first or second) dose.

## CONCLUSION

s Results are consistent with as many as 22% of individuals and long-lasting of increased FDG uptake in lymph node of COVID-19 vaccination, but waning with time. This potential pitfalls in PET/CT should be borne in mind during current COVID-19 vaccination programs.

## CLINICAL RELEVANCE/APPLICATION

As COVID-19 vaccination programs expand worldwide, it will be important for oncologists and radiologists to include history of vaccination in interpreting the results of PET imaging studies.

## R5B-SPIN-4 Effect of inter-slice resolution improvement for orbital bone segmentation of facial 3D CT images with different slice thicknesses

Participants

Jinseo An, BS, Seoul, Korea, Republic Of (*Presenter*) Nothing to Disclose

## PURPOSE

To make a customized bone template for reconstruction of fractured orbital bone in cranio-maxillofacial surgery, it is necessary to accurately segment and model the orbital bone on facial CT images. However, it is limited by the aliasing effect due to the thick slice thickness and the partial volume effects in the thin bone area. The purpose of this study is to improve the z-axis resolution of the CT images to 1mm and to validate the effect of improved inter-slice resolution on segmentation of orbital bone with thin bone structures.

## METHODS AND MATERIALS

To improve the inter-slice resolution downsampled to 2~3mm, a 2D CNN-based network that considers intensity, gradient, and perceptual differences in the sagittal and axial planes is applied. To accurately segment the orbital bone with thin bone structures, 3D U-Net-based segmentation and post-processing are performed according to the characteristics of the bone by dividing it into cortical and thin bones with different intensity ranges. In the experiment, 355 facial CT images with a resolution of 512 x 512, pixel spacing of 0.4~0.619mm, slice thickness of 1mm were randomly divided into 228 training, 56 validation, and 71 test sets, and evaluation ROIs were defined globally and regionally, including whole orbital bone, medial wall, and floor area. Bilinear and bicubic interpolation were used as comparative methods, and the segmentation results were evaluated using the original images with a slice thickness of 1mm and inter-slice resolution improved images from a slice thickness of 2~3mm.

## RESULTS

In the interpolation-based methods, the orbital bone region tends to be under-segmented because it is generated by considering only the intensity values without information on the bone shape. On the other hand, the proposed CNN-based method shows improved segmentation performance because it generates a CT image similar to the original image while maintaining shape information. Especially, the jagged-shaped aliasing effect remains in the generated image of the interpolation-based method at the orbital floor with a horizontally gentle slope and shows the results of segmentation of the broken structure, while the proposed CNN-based method produces a reconstruction image similar to that of the original images.

## CONCLUSION

s Our method improved the z-axis resolution of CT images with slice thicknesses greater than 1mm and showed similar segmentation performance to the original CT images, which helped to reduce the aliasing effect of the 3D reconstructed orbital bone. (Project Number: 9991007552, K MDF\_PR\_20200901\_0270)

#### **CLINICAL RELEVANCE/APPLICATION**

Our method can be used to provide a customized bone template like a slice thickness of 1 mm, even on facial 3D CT images with a thick slice thickness of 2~3mm.

Printed on: 02/07/23

## Abstract Archives of the RSNA, 2022

R5B-SPIN-1

### A Robustly Optimized Natural Language Processing Model for Label Extraction in Mammography Report

Thursday, Dec. 1 12:45PM - 1:15PM Room: Learning Center - IN DPS

#### Participants

Yuxing Tang, Bethesda, MD (*Presenter*) Nothing to Disclose

#### PURPOSE

To explore RoBERTa (robustly retrained BERT model, namely the Bidirectional Encoder Representations from Transformers) in classifying mammography diagnostic text reports to facilitate large-scale weakly-supervised learning for image-based mammography diagnosis systems.

#### METHODS AND MATERIALS

Weakly-supervised learning from mammogram images requires binary labels for each view to indicate the presence of a lesion type. Previously these labels were either manually labeled by experienced radiologists, or obtained from the diagnostic reports by applying text processing rules or relatively simple natural language processing (NLP) models. We formulate this task as a text classification problem and propose Mammo-RoBERTa by fine-tuning the pre-trained RoBERTa on our large-scale mammogram report data with whole word masking. Mammo-RoBERTa treats each text report as a sample and takes both the description and impression parts of a report as the input. It consists of 12 encoding layers with 768 hidden units and 12 attention heads. We use the final hidden vector corresponding to the first input token as the aggregate representation of the input sequence. A linear classification layer and a softmax function are applied to predict the probability that a lesion type is present in a mammogram. A large-scale dataset containing 33,630 mammogram studies with diagnostic reports from 30,495 patients was collected, among which 3,753 studies were manually labeled by radiologists.

#### RESULTS

We perform three-fold cross-validation on 3,753 mammography studies. Mammo-RoBERTa achieves very high accuracy ( $98.72\% \pm 0.24\%$  and  $98.19\% \pm 0.27\%$  for left and right breasts, respectively) in predicting the presence of a specified lesion type in the mammogram images from the corresponding text reports, far exceeding the previous rule-based text processing approaches ( $p < 0.05$ ). The F1 scores (left:  $0.973 \pm 0.005$ , right:  $0.958 \pm 0.006$ ) and weighted F1 scores (left  $0.987 \pm 0.005$ , right:  $0.982 \pm 0.005$ ) also show that the performance of our Mammo-RoBERTa is very robust in general.

#### CONCLUSION

s We proposed Mammo-RoBERTa, a RoBERTa model fine-tuned on mammogram report data, which can be used to predict the presence of specific lesion types (e.g., mass) in mammograms with very high accuracy, with input from the text report.

#### CLINICAL RELEVANCE/APPLICATION

The advanced NLP models, such as RoBERTa, can be fine-tuned on clinical text report data to substantially improve the system performance in automatically understanding the content of pervasive clinical diagnostic reports.

Printed on: 02/07/23

## Abstract Archives of the RSNA, 2022

R5B-SPIN-2

### Machine Learning Methods Based on Injection Pressure to Detect the Contrast Material Extravasation During CT

Thursday, Dec. 1 12:45PM - 1:15PM Room: Learning Center - IN DPS

#### Participants

Takeshi Nakaura, MD, Kumamoto, Japan (*Presenter*) Nothing to Disclose

#### PURPOSE

To evaluate the performance of a machine learning (ML) method to detect the contrast material extravasation based on injection pressure during computed tomography (CT).

#### METHODS AND MATERIALS

We enrolled 46,666 patients who underwent contrast enhanced CT examination in one hospital. We chose an 8:2 training-to-validation ratio and developed ML software to predict the risk of contrast material extravasation based on injection pressure of first 6 seconds with 0.25 second interval and injection rate settings. This ML software contains ML classifiers for time series data (kNN, ROCKET, TSF, RISE) and the stacking ensemble ML (LightGBM) using the outputs of other ML classifiers as input data. We trained and evaluated ML classifiers using 5-fold cross-validation using the training data (n = 37,336), and we evaluated the performance of best model in the test data (n = 9,330) using areas under the receiver operating characteristic curves (AUCs).

#### RESULTS

The contrast material extravasation occurred in 0.20% (94/46,666) of the patients. The stacking ensemble ML gave the highest performance (AUC = 0.748), followed by the kNN (AUC = 0.728), ROCKET (AUC = 0.71), TSF (AUC = 0.648), and RISE (AUC = 0.654). The performance of stacking ensemble ML did not decrease in the test group (AUC = 0.761).

#### CONCLUSION

The stacking ensemble ML offered high performance to detect the contrast material extravasation based on injection pressure during CT as compared with ML methods for time series data.

#### CLINICAL RELEVANCE/APPLICATION

The stacking ensemble ML based on injection pressure might be the useful tool for the early detection of the contrast material extravasation during CT.

Printed on: 02/07/23

## Abstract Archives of the RSNA, 2022

R5B-SPIN-3

### F-18 FDG Uptake in Axillary Lymph Nodes after Vaccination Against COVID-19

Thursday, Dec. 1 12:45PM - 1:15PM Room: Learning Center - IN DPS

#### Participants

Kaoru Maruyama, Osaka, Japan (*Presenter*) Nothing to Disclose

#### PURPOSE

Little is known about the frequency and duration of increased F-18 fluorodeoxyglucose (FDG) uptake in lymph nodes after vaccination. Increased FDG uptake may be mistaken for a sign of malignancy. We assessed the frequency of increased FDG uptake in axillary lymph nodes after vaccination against the coronavirus disease 2019 (COVID-19).

#### METHODS AND MATERIALS

We collected vaccination data for all individuals at the time FDG positron emission tomography/computed tomography (PET/CT) imaging. Unilateral FDG uptake in axillary lymph node on side (arm) of last vaccination (or, if individual was not sure about side, higher uptake on either side) was examined.

#### RESULTS

We used data from 181 vaccinated individuals (including 51 healthy individuals and 130 patients) who received one or two dose of the two type of mRNA Covid-19 vaccines (either Pfizer or Moderna). The frequency of increased FDG uptake was 22% (39/181 individuals), occurred within 1 day, and lasted 122 days after vaccination. No uptake in axillary lymph node was detected from 3 days after the first dose, and from 4 days after the second dose. The median onset of local reactions was 17 days after first dose and 18 days after the second dose. Axillary lymph node FDG positive rate was: 63% (12 of 19) of individuals at 3-96 days of vaccination after the first dose; 14% (20 of 147) of individuals at 2-135 days after the second dose; and 47% (7 of 15) of individuals at 1-63 days in the unknown (first or second) dose.

#### CONCLUSION

Results are consistent with as many as 22% of individuals and long-lasting of increased FDG uptake in lymph node of COVID-19 vaccination, but waning with time. This potential pitfall in PET/CT should be borne in mind during current COVID-19 vaccination programs.

#### CLINICAL RELEVANCE/APPLICATION

As COVID-19 vaccination programs expand worldwide, it will be important for oncologists and radiologists to include history of vaccination in interpreting the results of PET imaging studies.

Printed on: 02/07/23

## Abstract Archives of the RSNA, 2022

R5B-SPIN-4

### Effect of inter-slice resolution improvement for orbital bone segmentation of facial 3D CT images with different slice thicknesses

Thursday, Dec. 1 12:45PM - 1:15PM Room: Learning Center - IN DPS

#### Participants

Jinseo An, BS, Seoul, Korea, Republic Of (*Presenter*) Nothing to Disclose

#### PURPOSE

To make a customized bone template for reconstruction of fractured orbital bone in cranio-maxillofacial surgery, it is necessary to accurately segment and model the orbital bone on facial CT images. However, it is limited by the aliasing effect due to the thick slice thickness and the partial volume effects in the thin bone area. The purpose of this study is to improve the z-axis resolution of the CT images to 1mm and to validate the effect of improved inter-slice resolution on segmentation of orbital bone with thin bone structures.

#### METHODS AND MATERIALS

To improve the inter-slice resolution downsampled to 2~3mm, a 2D CNN-based network that considers intensity, gradient, and perceptual differences in the sagittal and axial planes is applied. To accurately segment the orbital bone with thin bone structures, 3D U-Net-based segmentation and post-processing are performed according to the characteristics of the bone by dividing it into cortical and thin bones with different intensity ranges. In the experiment, 355 facial CT images with a resolution of 512 x 512, pixel spacing of 0.4~0.619mm, slice thickness of 1mm were randomly divided into 228 training, 56 validation, and 71 test sets, and evaluation ROIs were defined globally and regionally, including whole orbital bone, medial wall, and floor area. Bilinear and bicubic interpolation were used as comparative methods, and the segmentation results were evaluated using the original images with a slice thickness of 1mm and inter-slice resolution improved images from a slice thickness of 2~3mm.

#### RESULTS

In the interpolation-based methods, the orbital bone region tends to be under-segmented because it is generated by considering only the intensity values without information on the bone shape. On the other hand, the proposed CNN-based method shows improved segmentation performance because it generates a CT image similar to the original image while maintaining shape information. Especially, the jagged-shaped aliasing effect remains in the generated image of the interpolation-based method at the orbital floor with a horizontally gentle slope and shows the results of segmentation of the broken structure, while the proposed CNN-based method produces a reconstruction image similar to that of the original images.

#### CONCLUSION

Our method improved the z-axis resolution of CT images with slice thicknesses greater than 1mm and showed similar segmentation performance to the original CT images, which helped to reduce the aliasing effect of the 3D reconstructed orbital bone. (Project Number: 9991007552, KMDF\_PR\_20200901\_0270)

#### CLINICAL RELEVANCE/APPLICATION

Our method can be used to provide a customized bone template like a slice thickness of 1 mm, even on facial 3D CT images with a thick slice thickness of 2~3mm.

Printed on: 02/07/23

## Abstract Archives of the RSNA, 2022

R5B-SPIR

### Interventional Thursday Poster Discussions - B

Thursday, Dec. 1 12:45PM - 1:15PM Room: Learning Center - IR DPS

#### Sub-Events

#### R5B-SPIR-1 The Interim Report of B-RTO Using Candis System

##### Participants

Masakatsu Tsurusaki, MD, PhD, (*Presenter*) Nothing to Disclose

##### PURPOSE

Balloon-occluded retrograde transvenous obliteration (B-RTO) has become widely accepted in Japan as a minimally invasive, highly effective treatment for gastric varices (GV). However, in some cases that involve complex types of afferent or draining veins, the use of standard B-RTO for the treatment of GV is associated with difficulties that can lead to unfavorable results. In such cases, additional techniques are required for successful treatment. A new coaxial balloon catheter system (CANDIS system) developed in Japan by Tanoue et al. (CVIR 2016) that is characterized by a 5 Fr catheter has a high flexibility and can be coaxially inserted into the guiding catheter in advance. The purpose of this study is to evaluate the midterm results of B-RTO for gastric varices using the CANDIS system.

##### METHODS AND MATERIALS

Between 2012 and 2018, 24 cases (male 8 cases, average age 70 years) were treated by B-RTO with CANDIS system for GV. The procedures, including technical success rate (maneuverability of the catheter and successfully injected sclerosing agent), fluoroscopy time, clinical success rate (disappearance of gastric varices after 6 months), complications, and Child-Pugh score were evaluated retrospectively. We compared to 23 cases treated with a single balloon system in the past.

##### RESULTS

The etiology was HBV 4, HCV 8, NBNC 13 (alcohol 4, NASH 2, PBC 2, IPNB 1, Blue liver syndrome 1, polycystic liver 1, unknown 2) cases. Four cases to improve shunt encephalopathy. Three cases had been treated with a single balloon system in the past. The average fluoroscopy time was 30.7 minutes (v.s. 39.2 minutes in a single balloon system) and the average amount of EOI used was 15.7 mL (v.s. 15.2mL). Pre B-RTO Hirota grade 1/2/3/4/5 was 3/6/7/8/0 cases, and post B-RTO Hirota grade 1/2/3/4/5 was 15/9/0/0/0 cases. The technical success rate was 100% (24/24 cases), the cases which the CANDIS system was effective was 81.8% (18/22), the clinical success rate was 92% (22/24). Minor vascular injuries occurred at 17% (4/24). Development of esophageal varices were seen at 29% (7/24). Child-Pugh score improved at 33% (8/24).

##### CONCLUSION

s CANDIS system was useful for single balloon B-RTO failure cases. B-RTO could not only reduce GV but also improve liver function for some cases.

##### CLINICAL RELEVANCE/APPLICATION

There are still insufficient reports that B-RTO with double interruption system leads to the improvement of mid-term and long-term hepatic functional reserve compared with the conventional methods. In the present study, we retrospectively compared and evaluated the outcomes and the long-term effects on liver functional reserve in patients treated with B-RTO for GVs using conventional and double interruption system.

#### R5B-SPIR-2 Clinical Outcomes of Prophylactic Perioperative IVC Filter Utility in Patients Undergoing Oncological Surgery

##### Participants

Mensur Koso, BS, (*Presenter*) Nothing to Disclose

##### PURPOSE

This study evaluated the clinical outcomes of inferior vena cava (IVC) filter use for pulmonary embolism (PE) prophylaxis in patients undergoing cancer-related surgery.

##### METHODS AND MATERIALS

This single-center retrospective study analyzed characteristics and outcomes of oncological surgery patients from January 2007 to December 2021 who received perioperative prophylactic IVC filters at a large academic medical center. Inclusion criteria included patients with an active malignancy who were undergoing surgery to either cure or palliate cancer. Dual clinical outcomes were assessed, relating to both venous thromboembolism (VTE) occurrence as well as filter retrieval complications. Any definitive VTE events were evaluated from time of placement until at least 3 months post-surgery, to the time of filter retrieval, or until the most current date of available information if no retrieval occurred. Complications were classified according to the Society of Interventional Radiology (SIR) classification system as major or minor. Clinical outcomes were aggregated using mean and value counts as well as relative frequencies (%) for categorical data.

## RESULTS

A total of 252 consecutive oncological surgery patients (female 51%/male 49%; median age, 59) received IVC filters for the perioperative prevention of PE. Average filter dwell time for removed filters was 7.5 months (range, 1-39 mo). 36% of IVC filters were ultimately retrieved. Complications involved 1% (two total) of retrievals and were all classified as minor. 15% of patients experienced DVTs and other extremity VTE events in the post-placement pre-retrieval period, while 2% (n=6) experienced definitive PEs. There were 21 noted incidences of thrombi entrapped within or close to the IVC filters (8%). Primary surgical sites included spine (n=91, 36%), orthopedic extremity/joint (n=49, 19%), genitourinary (n=47, 19%), brain/cranial (n=40, 16%), abdominal (n=18, 7%), mixed locations (n=4, 2%), and chest (n=3, 1%).

## CONCLUSION

s IVC filters in an oncological surgery cohort resulted in a low complication rate, demonstrated capture of PE-potential thrombi, and ultimately accomplished a low incidence of PE as well as DVT relative to values reported in the literature.

## CLINICAL RELEVANCE/APPLICATION

Cancer patients undergoing surgery represent an at-risk population for VTE, although the role of IVC filter prophylaxis has been underexplored and no filter guidelines exist for this population.

## R5B-SPiR-3 Proximal Splenic Artery Embolization in Grade IV or V Splenic Trauma - A Single Centre 11-Year Experience

Participants

Kevin Eng, MD, (*Presenter*) Nothing to Disclose

## PURPOSE

1. Assess the effectiveness of proximal splenic artery embolization (SAE) with a vascular plug at stopping bleeding and achieving splenic salvage in patients with American Association for the Surgery of Trauma (AAST) grade IV or V splenic injuries. 2. Compare complication and mortality rates between patients receiving single embolization (vascular plug alone) versus combined embolization (vascular plug and coils).

## METHODS AND MATERIALS

A retrospective review was performed. Adult trauma patients with AAST grade IV or V splenic injury who underwent proximal SAE with a vascular plug at our level 1 trauma center between November 2010 and January 2021 were included. Data extracted included: splenic injury grade, presence/size of splenic artery pseudoaneurysms, and type and diameter of the plug and coils (if used). Technical success was defined as successful proximal occlusion of the splenic artery, and clinical success was defined as cessation of bleeding or resolution of pseudoaneurysm within 30 days of embolization. Follow-up imaging and clinical notes were reviewed to determine the rate of moderate to severe adverse events (as defined by the Society of Interventional Radiology Adverse Event Classification), new left pleural effusion, and death. The Chi-square test and T-test were used for hypothesis testing, and a p value of <0.05 was considered statistically significant.

## RESULTS

76 patients were included. The rates of technical success, clinical success, and splenic salvage were 100% (76/76), 95% (72/26), and 96% (73/76) respectively. The complication rate was 10% (6/58) in the single embolization group and 33% (6/18) in the combined embolization group; the difference was statistically significant (p=0.03). Complications included: splenic infarction, persistent bleeding/pseudoaneurysm necessitating splenectomy, splenic hematoma, and puncture site pseudoaneurysm. The mortality rate was 2% (1/58) in the single embolization group and 6% (1/18) in the combined embolization group (p >0.05). The rate of new left pleural effusions was comparable between the two groups.

## CONCLUSION

s Technical success was achieved in all patients with grade IV or V splenic trauma. Clinical success rate and splenic preservation rate was high and comparable to results from literature. Combined embolization has a higher complication rate than single embolization; mortality rates were not significantly different.

## CLINICAL RELEVANCE/APPLICATION

In patients with high grade splenic injury, proximal SAE with a vascular plug is highly effective. Additional coils are often deployed if there is inadequate coverage of the dorsal pancreatic artery origin, however higher complication rates with combined embolization support the use of a vascular plug alone when possible.

## R5B-SPiR-4 Contrast Medium Free Selective Adrenal Vein Sampling in The Management of Primary Aldosteronism

Participants

Lars Schimmoeller, MD, Dusseldorf, Germany (*Presenter*) Nothing to Disclose

## PURPOSE

To analyse contrast free adrenal vein sampling (AVS) for differentiating unilateral from bilateral disease in patients diagnosed with hypertension due to primary aldosteronism (PA).

## METHODS AND MATERIALS

Consecutive patients diagnosed with PA and subsequent contrast medium free AVS between 04/2015 and 12/2020 were retrospectively included in this study. Cross-sectional imaging (CSI), AVS data, and clinical data were analysed regarding diagnostic performance of CSI and AVS. In addition, in subgroup analysis patients with lateralisation receiving adrenalectomy were compared to a control group treated with mineralocorticoid antagonists regarding clinical outcome parameters.

## RESULTS

In total 193 patients with contrast medium free AVS were included. A success rate of 88% for bilateral catheterization with a median effective dose of 2.9 mSv was observed. CSI had an accuracy of 60% (95%-CI: 0.52-0.67) in the detection of lateralization when compared with AVS as the reference standard. Patients diagnosed with bilateral adrenal hyperplasia and those

with aldosterone-producing adenoma did not differ in clinical data as systolic blood pressure (sBP) ( $p=0.63$ ) or number of antihypertensive drugs (NAD) ( $p=0.11$ ) at baseline examination. In the adrenalectomy group, 28 patients were cured (51%; sBP =130mmHg, no antihypertensive drugs), 18 were improved (33%; decrease of sBP =20mmHg and decreased NAD), and 16 were unchanged (16%; unchanged sBP or decrease <20mmHg with increased NAD or increased sBP <20mmHg and decreased NAD). Both groups differed significantly at follow up examination in sBP (median sBP 130mmHg vs. 140mmHg), NAD (median NAD 0 vs. 2), serum potassium (mean 4.3mmol/l vs. 4.1mmol/l), and serum aldosterone (mean 101pg/ml vs. 349pg/ml) ( $p<0.05$ ).

## CONCLUSION

s Contrast medium free AVS is a reliable procedure in the diagnostic management of patients with PA with high technical success rate. The accordance between CSI and results from AVS was only moderate indicating the central role of AVS in the diagnostic work-up of patients with PA. Patients with predominant disease diagnosed with AVS had a high cure rate and/or significant improvement after adrenalectomy.

## CLINICAL RELEVANCE/APPLICATION

Contrast medium is not needed at all for adrenal vein sampling in patients with primary hyperaldosteronism. AVS still has an important role in the diagnostic pathway as the accordance with CT scans for detecting unilateral disease was only moderate.

## R5B-SPiR-5 Retrospective Review of Optimal Catheter to Vein Size Ratio of Peripherally Inserted Central Catheters (PICC) Line Procedures to Prevent the Symptomatic Deep Venous Thrombosis (DVT) in Pediatric Oncology Patients

Participants

Parth Patel, Germantown, TN (*Presenter*) Nothing to Disclose

## PURPOSE

To investigate the effects of catheter to vein size (CV) ratio (ratio comparing the diameter of catheter inserted to the vein diameter at the needle puncture site) on incidences of symptomatic DVT corresponding to PICC line insertion in pediatric oncology patients and to identify the optimal CV size ratio as a threshold ratio to prevent PICC related DVT.

## METHODS AND MATERIALS

This retrospective, observational cohort study reviewed pediatric oncology patients at our hospital between January 2019 to December 2021 who had a PICC line placed. Vein diameter was measured at the site of needle access at the time of PICC line placement. A tourniquet was placed around the arm just below the shoulder before PICC placement in each patient. Patient demographics and medical history was collected from the Electronic Medical Record System (EMR). PICC line procedure and technique specific data (Date of procedure, arm placement, PICC lumens, Size of PICC line, Size of Catheter, Vein accessed) were also collected.

## RESULTS

Data from 207 pediatric oncology patients (18% Leukemia, 20% Lymphoma, 62% Other) who had PICC line placed was reviewed. Median age was 11 years with 61% males. Study had 14 cases symptomatic DVT related to PICC placement. Receiver Operator Characteristic Curve and Regression Model (ROC) identified that a 49% CV ratio made for an optimal threshold point to maximize sensitivity and specificity (AUC=0.8031, 95% CI-0.7189-0.8873). It was found that the patients with a CV ratio of >49% were 20 times more likely to suffer DVT ( $p=0.001$ ). On univariate analyses, age, sex, race, catheter size, number of lumens, site of vein or arm for PICC line placement did not reveal any significance.

## CONCLUSION

s The study found that a CV ratio of 49% in PICC line procedure was the optimal threshold point with high sensitivity and specificity to reduce risk of PICC related DVT in pediatric oncology patients.

## CLINICAL RELEVANCE/APPLICATION

Application of the optimal CV ratio during PICC line insertion procedures could significantly decrease the incidences of PICC line related symptomatic DVTs in pediatric oncology patients.

## R5B-SPiR-8 Transjugular Intrahepatic Portosystemic Shunts: A Retrospective Comparative Study of Primary Outcomes Between 6mm, 8mm, 10mm and 12mm Diameter Stents

Participants

Howard Dabbous, MD, Atlanta, GA (*Presenter*) Nothing to Disclose

## PURPOSE

To compare differences in primary and clinical outcomes between the different stent diameter sizes utilized in Transjugular intrahepatic portosystemic shunts (TIPS).

## METHODS AND MATERIALS

We conducted a retrospective analysis of patients who underwent TIPS placement of sizes 6mm, 8mm, 10mm, and 12mm between 2004 and 2022. Data was collected on baseline characteristics (age, gender, race, MELD-score, Child Pugh score, comorbidities predisposing to thrombosis, liver disease etiology, and indication for TIPS) and on peri- and post-procedural variables (stent size, angioplasty balloon size, adjunct procedures, e.g., embolization, paracentesis and thoracentesis). Measured outcomes consisted of technical success, pre- and post- TIPS portosystemic gradient (PSG), clinical resolution of the indication, hepatic encephalopathy (HE) symptoms. Primary outcomes were patency, liver transplant (LT), death, TIPS revision, and TIPS occlusion and analyzed at 1 year.

## RESULTS

A total of 331 patients were evaluated with 30, 111, 118, and 72 patients for sizes 6mm, 8mm, 10mm, and 12mm respectively. TIPS creation was technically successful in all 331 patients (100%). The average percent reduction in PSG for the 4 different stent sizes were -40.5%, -54.8%, -63%, and -71.5% respectively. Resolution of variceal hemorrhage was achieved in 6/9 (67%), 39/45 (87%),

36/38 (95%), and 31/32 (97%) patients who received size 6mm, 8mm, 10mm, and 12mm, respectively. Between the above stent sizes, respectively, decreased ascites/hydrothorax was observed in 8/14 (57%), 32/37 (86%), 31/42 (74%), and 22/25 (88%) patients, and new or worsening HE was seen in 10/21 (48%), 23/73 (32%), 23/87 (26%), and 27/55 (49%) patients. At 1-year, patency was 1/6, 26/30, 46/52, and 47/47 of remaining patients. By 1 year, 4/30, 6/111, 7/118, and 3/72 patients underwent LT and 5/30 (17%), 21/111 (19%), 21/118 (18%), and 4/72 (6%) patients were deceased. Additionally, 12/30, 12/111, 18/118, and 10/72 patients received a TIPS revision and a further 5/30, 4/111, 6/118, and 0/72 found to have TIPS occlusion.

#### **CONCLUSION**

s The various stent sizes overall had similar clinical resolution rates. 1-year mortality rates were similar but lowest for the 12mm size.

#### **CLINICAL RELEVANCE/APPLICATION**

For patients receiving TIPS, the varying sizes offer similar resolution of symptoms and 1-year mortality rates.

Printed on: 02/07/23



## Abstract Archives of the RSNA, 2022

R5B-SP1R-1

### The Interim Report of B-RTO Using Candis System

Thursday, Dec. 1 12:45PM - 1:15PM Room: Learning Center - IR DPS

#### Participants

Masakatsu Tsurusaki, MD, PhD, (*Presenter*) Nothing to Disclose

#### PURPOSE

Balloon-occluded retrograde transvenous obliteration (B-RTO) has become widely accepted in Japan as a minimally invasive, highly effective treatment for gastric varices (GV). However, in some cases that involve complex types of afferent or draining veins, the use of standard B-RTO for the treatment of GV is associated with difficulties that can lead to unfavorable results. In such cases, additional techniques are required for successful treatment. A new coaxial balloon catheter system (CANDIS system) developed in Japan by Tanoue et al. (CVIR 2016) that is characterized by a 5 Fr catheter has a high flexibility and can be coaxially inserted into the guiding catheter in advance. The purpose of this study is to evaluate the midterm results of B-RTO for gastric varices using the CANDIS system.

#### METHODS AND MATERIALS

Between 2012 and 2018, 24 cases (male 8 cases, average age 70 years) were treated by B-RTO with CANDIS system for GV. The procedures, including technical success rate (maneuverability of the catheter and successfully injected sclerosing agent), fluoroscopy time, clinical success rate (disappearance of gastric varices after 6 months), complications, and Child-Pugh score were evaluated retrospectively. We compared to 23 cases treated with a single balloon system in the past.

#### RESULTS

The etiology was HBV 4, HCV 8, NBNC 13 (alcohol 4, NASH 2, PBC 2, IPNB 1, Blue liver syndrome 1, polycystic liver 1, unknown 2) cases. Four cases to improve shunt encephalopathy. Three cases had been treated with a single balloon system in the past. The average fluoroscopy time was 30.7 minutes (v.s. 39.2 minutes in a single balloon system) and the average amount of EOI used was 15.7 mL (v.s. 15.2mL). Pre B-RTO Hirota grade 1/2/3/4/5 was 3/6/7/8/0 cases, and post B-RTO Hirota grade 1/2/3/4/5 was 15/9/0/0/0 cases. The technical success rate was 100% (24/24 cases), the cases which the CANDIS system was effective was 81.8% (18/22), the clinical success rate was 92% (22/24). Minor vascular injuries occurred at 17% (4/24). Development of esophageal varices were seen at 29% (7/24). Child-Pugh score improved at 33% (8/24).

#### CONCLUSION

s CANDIS system was useful for single balloon B-RTO failure cases. B-RTO could not only reduce GV but also improve liver function for some cases.

#### CLINICAL RELEVANCE/APPLICATION

There are still insufficient reports that B-RTO with double interruption system leads to the improvement of mid-term and long-term hepatic functional reserve compared with the conventional methods. In the present study, we retrospectively compared and evaluated the outcomes and the long-term effects on liver functional reserve in patients treated with B-RTO for GVs using conventional and double interruption system.

Printed on: 02/07/23

## Abstract Archives of the RSNA, 2022

R5B-SPIR-2

### Clinical Outcomes of Prophylactic Perioperative IVC Filter Utility in Patients Undergoing Oncological Surgery

Thursday, Dec. 1 12:45PM - 1:15PM Room: Learning Center - IR DPS

#### Participants

Mensur Koso, BS, (*Presenter*) Nothing to Disclose

#### PURPOSE

This study evaluated the clinical outcomes of inferior vena cava (IVC) filter use for pulmonary embolism (PE) prophylaxis in patients undergoing cancer-related surgery.

#### METHODS AND MATERIALS

This single-center retrospective study analyzed characteristics and outcomes of oncological surgery patients from January 2007 to December 2021 who received perioperative prophylactic IVC filters at a large academic medical center. Inclusion criteria included patients with an active malignancy who were undergoing surgery to either cure or palliate cancer. Dual clinical outcomes were assessed, relating to both venous thromboembolism (VTE) occurrence as well as filter retrieval complications. Any definitive VTE events were evaluated from time of placement until at least 3 months post-surgery, to the time of filter retrieval, or until the most current date of available information if no retrieval occurred. Complications were classified according to the Society of Interventional Radiology (SIR) classification system as major or minor. Clinical outcomes were aggregated using mean and value counts as well as relative frequencies (%) for categorical data.

#### RESULTS

A total of 252 consecutive oncological surgery patients (female 51%/male 49%; median age, 59) received IVC filters for the perioperative prevention of PE. Average filter dwell time for removed filters was 7.5 months (range, 1-39 mo). 36% of IVC filters were ultimately retrieved. Complications involved 1% (two total) of retrievals and were all classified as minor. 15% of patients experienced DVTs and other extremity VTE events in the post-placement pre-retrieval period, while 2% (n=6) experienced definitive PEs. There were 21 noted incidences of thrombi entrapped within or close to the IVC filters (8%). Primary surgical sites included spine (n=91, 36%), orthopedic extremity/joint (n=49, 19%), genitourinary (n=47, 19%), brain/cranial (n=40, 16%), abdominal (n=18, 7%), mixed locations (n=4, 2%), and chest (n=3, 1%).

#### CONCLUSION

s IVC filters in an oncological surgery cohort resulted in a low complication rate, demonstrated capture of PE-potential thrombi, and ultimately accomplished a low incidence of PE as well as DVT relative to values reported in the literature.

#### CLINICAL RELEVANCE/APPLICATION

Cancer patients undergoing surgery represent an at-risk population for VTE, although the role of IVC filter prophylaxis has been underexplored and no filter guidelines exist for this population.

Printed on: 02/07/23

## Abstract Archives of the RSNA, 2022

R5B-SP1R-3

### Proximal Splenic Artery Embolization in Grade IV or V Splenic Trauma - A Single Centre 11-Year Experience

Thursday, Dec. 1 12:45PM - 1:15PM Room: Learning Center - IR DPS

#### Participants

Kevin Eng, MD, (*Presenter*) Nothing to Disclose

#### PURPOSE

1. Assess the effectiveness of proximal splenic artery embolization (SAE) with a vascular plug at stopping bleeding and achieving splenic salvage in patients with American Association for the Surgery of Trauma (AAST) grade IV or V splenic injuries. 2. Compare complication and mortality rates between patients receiving single embolization (vascular plug alone) versus combined embolization (vascular plug and coils).

#### METHODS AND MATERIALS

A retrospective review was performed. Adult trauma patients with AAST grade IV or V splenic injury who underwent proximal SAE with a vascular plug at our level 1 trauma center between November 2010 and January 2021 were included. Data extracted included: splenic injury grade, presence/size of splenic artery pseudoaneurysms, and type and diameter of the plug and coils (if used). Technical success was defined as successful proximal occlusion of the splenic artery, and clinical success was defined as cessation of bleeding or resolution of pseudoaneurysm within 30 days of embolization. Follow-up imaging and clinical notes were reviewed to determine the rate of moderate to severe adverse events (as defined by the Society of Interventional Radiology Adverse Event Classification), new left pleural effusion, and death. The Chi-square test and T-test were used for hypothesis testing, and a p value of <0.05 was considered statistically significant.

#### RESULTS

76 patients were included. The rates of technical success, clinical success, and splenic salvage were 100% (76/76), 95% (72/26), and 96% (73/76) respectively. The complication rate was 10% (6/58) in the single embolization group and 33% (6/18) in the combined embolization group; the difference was statistically significant (p=0.03). Complications included: splenic infarction, persistent bleeding/pseudoaneurysm necessitating splenectomy, splenic hematoma, and puncture site pseudoaneurysm. The mortality rate was 2% (1/58) in the single embolization group and 6% (1/18) in the combined embolization group (p >0.05). The rate of new left pleural effusions was comparable between the two groups.

#### CONCLUSION

s Technical success was achieved in all patients with grade IV or V splenic trauma. Clinical success rate and splenic preservation rate was high and comparable to results from literature. Combined embolization has a higher complication rate than single embolization; mortality rates were not significantly different.

#### CLINICAL RELEVANCE/APPLICATION

In patients with high grade splenic injury, proximal SAE with a vascular plug is highly effective. Additional coils are often deployed if there is inadequate coverage of the dorsal pancreatic artery origin, however higher complication rates with combined embolization support the use of a vascular plug alone when possible.

Printed on: 02/07/23

## Abstract Archives of the RSNA, 2022

R5B-SP1R-4

### Contrast Medium Free Selective Adrenal Vein Sampling in The Management of Primary Aldosteronism

Thursday, Dec. 1 12:45PM - 1:15PM Room: Learning Center - IR DPS

#### Participants

Lars Schimmoeller, MD, Dusseldorf, Germany (*Presenter*) Nothing to Disclose

#### PURPOSE

To analyse contrast free adrenal vein sampling (AVS) for differentiating unilateral from bilateral disease in patients diagnosed with hypertension due to primary aldosteronism (PA).

#### METHODS AND MATERIALS

Consecutive patients diagnosed with PA and subsequent contrast medium free AVS between 04/2015 and 12/2020 were retrospectively included in this study. Cross-sectional imaging (CSI), AVS data, and clinical data were analysed regarding diagnostic performance of CSI and AVS. In addition, in subgroup analysis patients with lateralisation receiving adrenalectomy were compared to a control group treated with mineralocorticoid antagonists regarding clinical outcome parameters.

#### RESULTS

In total 193 patients with contrast medium free AVS were included. A success rate of 88% for bilateral catheterization with a median effective dose of 2.9 mSv was observed. CSI had an accuracy of 60% (95%-CI: 0.52-0.67) in the detection of lateralization when compared with AVS as the reference standard. Patients diagnosed with bilateral adrenal hyperplasia and those with aldosterone-producing adenoma did not differ in clinical data as systolic blood pressure (sBP) ( $p=0.63$ ) or number of antihypertensive drugs (NAD) ( $p=0.11$ ) at baseline examination. In the adrenalectomy group, 28 patients were cured (51%; sBP =130mmHg, no antihypertensive drugs), 18 were improved (33%; decrease of sBP =20mmHg and decreased NAD), and 16 were unchanged (16%; unchanged sBP or decrease <20mmHg with increased NAD or increased sBP <20mmHg and decreased NAD). Both groups differed significantly at follow up examination in sBP (median sBP 130mmHg vs. 140mmHg), NAD (median NAD 0 vs. 2), serum potassium (mean 4.3mmol/l vs. 4.1mmol/l), and serum aldosterone (mean 101pg/ml vs. 349pg/ml) ( $p<0.05$ ).

#### CONCLUSION

s Contrast medium free AVS is a reliable procedure in the diagnostic management of patients with PA with high technical success rate. The accordance between CSI and results from AVS was only moderate indicating the central role of AVS in the diagnostic work-up of patients with PA. Patients with predominant disease diagnosed with AVS had a high cure rate and/or significant improvement after adrenalectomy.

#### CLINICAL RELEVANCE/APPLICATION

Contrast medium is not needed at all for adrenal vein sampling in patients with primary hyperaldosteronism. AVS still has an important role in the diagnostic pathway as the accordance with CT scans for detecting unilateral disease was only moderate.

Printed on: 02/07/23



## Abstract Archives of the RSNA, 2022

R5B-SP1R-5

### Retrospective Review of Optimal Catheter to Vein Size Ratio of Peripherally Inserted Central Catheters (PICC) Line Procedures to Prevent the Symptomatic Deep Venous Thrombosis (DVT) in Pediatric Oncology Patients

Thursday, Dec. 1 12:45PM - 1:15PM Room: Learning Center - IR DPS

#### Participants

Parth Patel, Germantown, TN (*Presenter*) Nothing to Disclose

#### PURPOSE

To investigate the effects of catheter to vein size (CV) ratio (ratio comparing the diameter of catheter inserted to the vein diameter at the needle puncture site) on incidences of symptomatic DVT corresponding to PICC line insertion in pediatric oncology patients and to identify the optimal CV size ratio as a threshold ratio to prevent PICC related DVT.

#### METHODS AND MATERIALS

This retrospective, observational cohort study reviewed pediatric oncology patients at our hospital between January 2019 to December 2021 who had a PICC line placed. Vein diameter was measured at the site of needle access at the time of PICC line placement. A tourniquet was placed around the arm just below the shoulder before PICC placement in each patient. Patient demographics and medical history was collected from the Electronic Medical Record System (EMR). PICC line procedure and technique specific data (Date of procedure, arm placement, PICC lumens, Size of PICC line, Size of Catheter, Vein accessed) were also collected.

#### RESULTS

Data from 207 pediatric oncology patients (18% Leukemia, 20% Lymphoma, 62% Other) who had PICC line placed was reviewed. Median age was 11 years with 61% males. Study had 14 cases symptomatic DVT related to PICC placement. Receiver Operator Characteristic Curve and Regression Model (ROC) identified that a 49% CV ratio made for an optimal threshold point to maximize sensitivity and specificity (AUC=0.8031, 95% CI-0.7189-0.8873). It was found that the patients with a CV ratio of >49% were 20 times more likely to suffer DVT (p=0.001). On univariate analyses, age, sex, race, catheter size, number of lumens, site of vein or arm for PICC line placement did not reveal any significance.

#### CONCLUSION

The study found that a CV ratio of 49% in PICC line procedure was the optimal threshold point with high sensitivity and specificity to reduce risk of PICC related DVT in pediatric oncology patients.

#### CLINICAL RELEVANCE/APPLICATION

Application of the optimal CV ratio during PICC line insertion procedures could significantly decrease the incidences of PICC line related symptomatic DVTs in pediatric oncology patients.

Printed on: 02/07/23

## Abstract Archives of the RSNA, 2022

R5B-SPIR-8

### Transjugular Intrahepatic Portosystemic Shunts: A Retrospective Comparative Study of Primary Outcomes Between 6mm, 8mm, 10mm and 12mm Diameter Stents

Thursday, Dec. 1 12:45PM - 1:15PM Room: Learning Center - IR DPS

#### Participants

Howard Dabbous, MD, Atlanta, GA (*Presenter*) Nothing to Disclose

#### PURPOSE

To compare differences in primary and clinical outcomes between the different stent diameter sizes utilized in Transjugular intrahepatic portosystemic shunts (TIPS).

#### METHODS AND MATERIALS

We conducted a retrospective analysis of patients who underwent TIPS placement of sizes 6mm, 8mm, 10mm, and 12mm between 2004 and 2022. Data was collected on baseline characteristics (age, gender, race, MELD-score, Child Pugh score, comorbidities predisposing to thrombosis, liver disease etiology, and indication for TIPS) and on peri- and post-procedural variables (stent size, angioplasty balloon size, adjunct procedures, e.g., embolization, paracentesis and thoracentesis). Measured outcomes consisted of technical success, pre- and post- TIPS portosystemic gradient (PSG), clinical resolution of the indication, hepatic encephalopathy (HE) symptoms. Primary outcomes were patency, liver transplant (LT), death, TIPS revision, and TIPS occlusion and analyzed at 1 year.

#### RESULTS

A total of 331 patients were evaluated with 30, 111, 118, and 72 patients for sizes 6mm, 8mm, 10mm, and 12mm respectively. TIPS creation was technically successful in all 331 patients (100%). The average percent reduction in PSG for the 4 different stent sizes were -40.5%, -54.8%, -63%, and -71.5% respectively. Resolution of variceal hemorrhage was achieved in 6/9 (67%), 39/45 (87%), 36/38 (95%), and 31/32 (97%) patients who received size 6mm, 8mm, 10mm, and 12mm, respectively. Between the above stent sizes, respectively, decreased ascites/hydrothorax was observed in 8/14(57%), 32/37 (86%), 31/42 (74%), and 22/25 (88%) patients, and new or worsening HE was seen in 10/21 (48%), 23/73 (32%), 23/87 (26%), and 27/55 (49%) patients. At 1-year, patency was 1/6, 26/30, 46/52, and 47/47 of remaining patients. By 1 year, 4/30, 6/111, 7/118, and 3/72 patients underwent LT and 5/30 (17%), 21/111(19%), 21/118 (18%), and 4/72 (6%) patients were deceased. Additionally, 12/30, 12/111, 18/118, and 10/72 patients received a TIPS revision and a further 5/30, 4/111, 6/118, and 0/72 found to have TIPS occlusion.

#### CONCLUSION

The various stent sizes overall had similar clinical resolution rates. 1-year mortality rates were similar but lowest for the 12mm size.

#### CLINICAL RELEVANCE/APPLICATION

For patients receiving TIPS, the varying sizes offer similar resolution of symptoms and 1-year mortality rates.

Printed on: 02/07/23

## Abstract Archives of the RSNA, 2022

R5B-SPMK

### Musculoskeletal Thursday Poster Discussions - B

Thursday, Dec. 1 12:45PM - 1:15PM Room: Learning Center - MK DPS

#### Participants

Lawrence Lo, MD, Baltimore, MD (*Moderator*) Nothing to Disclose

#### Sub-Events

### R5B-SPMK-1 Fast kVp-Switching Dual-energy Computed Tomography Water-hydroxyapatite Decomposition Technique for Detection of Vertebral Compression Fractures Related Bone Marrow Edema in Comparison with Magnetic Resonance Imaging

#### Participants

Xuee Zhu, MD, (*Presenter*) Nothing to Disclose

#### PURPOSE

To assess the fast kVp - switching dual-energy computed tomography (DECT) water-hydroxyapatite (HAP) decomposition technique for detection of traumatic bone marrow edema (BME) in patients with vertebral compression fractures (VCFs) compared with that on magnetic resonance imaging (MRI).

#### METHODS AND MATERIALS

A total of 53 consecutive patients with 338 vertebrae who underwent both DECT and MRI of the spine within 3 days after trauma were retrospectively enrolled. All vertebral bodies were blindly evaluated for the presence of BME on sagittal water-(HAP) images by using color-coded maps. Water concentration and maximum area of BME were measured in those edematous vertebral bodies. Water concentration was also assessed in either chronic VCFs or normal vertebrae. An experienced radiologist blindly evaluated the presence of BME on MR images( reference standard) and calculated the maximum area of it. One-way ANOVA was used to compare water concentration among different groups. The receiver operating characteristic (ROC) curve analysis was conducted and the threshold of water concentration was calculated. Bland Altman analysis was performed to evaluate the consistency of the maximum area of BME measured on CT and MRI.

#### RESULTS

MRI depicted 53 acute VCFs, 37 chronic VCFs and 248 normal vertebrae. In the visual analysis of VCFs, DECT had an overall sensitivity of 98.1%, specificity of 99.6%, accuracy of 99.4%, positive predictive value of 98.1%, and negative predictive value of 99.6%, respectively. The water concentration had a significant difference between acute and chronic VCFs ( $P<0.01$ ) and between acute VCFs and normal vertebrae ( $P<0.01$ ), but had no significant difference between chronic VCFs and normal vertebrae bodies ( $P=0.86$ ). The ROC analysis of water concentration achieved an AUC of 0.994, and the optimal threshold of 992.5mg/cm<sup>3</sup> provided a sensitivity of 96.2% and specificity of 93.0%. Bland-Altman plots indicated that the maximum area of BME measured on CT and MRI was highly consistent.

#### CONCLUSION

s Fast kVp-switching DECT water-(HAP) decomposition technique had an excellent diagnostic performance for distinguishing acute VCFs from chronic ones both in visual and quantitative analyses. The depicted areas of BME on DECT and MR were almost the same.

#### CLINICAL RELEVANCE/APPLICATION

Single-energy CT of the spine is the standard examination for fast exclusion or closer assessment of vertebral compression fractures (VCFs). However, it is sometimes difficult to distinguish between acute and chronic VCFs. Although MRI is the reference standard to distinguish acute and old VCFs, it is contraindicated in many patients. DECT can quickly depict the areas of bone marrow edema to identify acute VCFs from chronic ones with a high sensitivity and specificity.

Printed on: 02/07/23

## Abstract Archives of the RSNA, 2022

R5B-SPMK-1

### Fast kVp-Switching Dual-energy Computed Tomography Water-hydroxyapatite Decomposition Technique for Detection of Vertebral Compression Fractures Related Bone Marrow Edema in Comparison with Magnetic Resonance Imaging

Thursday, Dec. 1 12:45PM - 1:15PM Room: Learning Center - MK DPS

#### Participants

Xuee Zhu, MD, (*Presenter*) Nothing to Disclose

#### PURPOSE

To assess the fast kVp - switching dual-energy computed tomography (DECT) water-hydroxyapatite (HAP) decomposition technique for detection of traumatic bone marrow edema (BME) in patients with vertebral compression fractures (VCFs) compared with that on magnetic resonance imaging (MRI).

#### METHODS AND MATERIALS

A total of 53 consecutive patients with 338 vertebrae who underwent both DECT and MRI of the spine within 3 days after trauma were retrospectively enrolled. All vertebral bodies were blindly evaluated for the presence of BME on sagittal water-(HAP) images by using color-coded maps. Water concentration and maximum area of BME were measured in those edematous vertebral bodies. Water concentration was also assessed in either chronic VCFs or normal vertebrae. An experienced radiologist blindly evaluated the presence of BME on MR images( reference standard) and calculated the maximum area of it. One-way ANOVA was used to compare water concentration among different groups. The receiver operating characteristic (ROC) curve analysis was conducted and the threshold of water concentration was calculated. Bland Altman analysis was performed to evaluate the consistency of the maximum area of BME measured on CT and MRI.

#### RESULTS

MRI depicted 53 acute VCFs, 37 chronic VCFs and 248 normal vertebrae. In the visual analysis of VCFs, DECT had an overall sensitivity of 98.1%, specificity of 99.6%, accuracy of 99.4%, positive predictive value of 98.1%, and negative predictive value of 99.6%, respectively. The water concentration had a significant difference between acute and chronic VCFs ( $P<0.01$ ) and between acute VCFs and normal vertebrae ( $P<0.01$ ), but had no significant difference between chronic VCFs and normal vertebrae bodies ( $P=0.86$ ). The ROC analysis of water concentration achieved an AUC of 0.994, and the optimal threshold of 992.5mg/cm<sup>3</sup> provided a sensitivity of 96.2% and specificity of 93.0%. Bland-Altman plots indicated that the maximum area of BME measured on CT and MRI was highly consistent.

#### CONCLUSION

s Fast kVp-switching DECT water-(HAP) decomposition technique had an excellent diagnostic performance for distinguishing acute VCFs from chronic ones both in visual and quantitative analyses. The depicted areas of BME on DECT and MR were almost the same.

#### CLINICAL RELEVANCE/APPLICATION

Single-energy CT of the spine is the standard examination for fast exclusion or closer assessment of vertebral compression fractures (VCFs). However, it is sometimes difficult to distinguish between acute and chronic VCFs. Although MRI is the reference standard to distinguish acute and old VCFs, it is contraindicated in many patients. DECT can quickly depict the areas of bone marrow edema to identify acute VCFs from chronic ones with a high sensitivity and specificity.

Printed on: 02/07/23

## Abstract Archives of the RSNA, 2022

R5B-SPNMMI

### Nuclear Medicine/Molecular Imaging Thursday Poster Discussion - B

Thursday, Dec. 1 12:45PM - 1:15PM Room: Learning Center - NMMI DPS

#### Participants

Ashwin Parihar, MBBS, MD, Saint Louis, MO (*Moderator*) Nothing to Disclose

#### Sub-Events

#### **R5B-SPNMMI-1** Incidental Detection of Focal FDG Uptake in Major Organs of Oncologic Patients on the FDG PET/CT

#### Participants

Kyung Hoon Hwang, MD, PhD, Incheon, Korea, Republic Of (*Presenter*) Nothing to Disclose

#### PURPOSE

In this study, we presented our experiences on incidental focal colorectal, thyroid and prostate hypermetabolism to justify the application of F-18 FDG PET/CT imaging to the oncologic patients and the subjects at high risk of developing cancer.

#### METHODS AND MATERIALS

The final reports of a total of 16,010 F-18 FDG PET/CT scans performed at our hospital between January 2016 and January 2022 were retrospectively reviewed to identify unexpectedly observed focal colorectal or thyroid or prostate FDG uptake. They are classified as malignant, premalignant (for colon/rectum), and benign according to their histopathological reports. The effective dose from FDG PET/CT was estimated and the hypermetabolic uptake was measured and compared amongst the groups to confirm whether the PET parameters were useful in distinguishing malignant from benign lesions and to identify cut-offs.

#### RESULTS

The estimated average effective dose from a F-18 FDG PET/CT scan was  $7.3 \pm 0.8\text{mSv}$ , which was comparable to that of pre- and post-contrast chest or abdominal pelvic CT. Overall, 61.6% of the focal colorectal uptake were malignant/premalignant lesions and 59.6% of the focal thyroid uptake were malignant lesions. 56.4% of the focal prostate uptake were malignant lesions. Maximum SUV was an independent diagnostic parameter to differentiate malignant (and premalignant) from benign lesions in both incidental focal colorectal and thyroid FDG uptake.

#### CONCLUSION

With advances in hardware and software technology related to PET/CT equipment, radiation exposure during a F-18 FDG PET/CT scan is gradually decreasing. Incidentally observed focal hypermetabolic colon/rectum or thyroid uptake showed a high rate (approximately 60%) of malignant (or premalignant for colon/rectum) lesions. Hence, these findings justify the encouraged application of PET imaging to the oncologic patients and the subjects at high risk of developing cancer.

#### CLINICAL RELEVANCE/APPLICATION

Unexpected incidental focal F-18 FDG activity is not an uncommon finding in the clinical PET studies. Due to high malignancy/premalignancy rate in the colorectal or thyroid lesions with incidental focal uptake, authors recommend further active assessment.

#### **R5B-SPNMMI-2** Pre- to Post-Treatment Evolution of PET-CT Parameters in CAR-T Cell Treatment of Lymphoma

#### Participants

Michael Winkelmann, MD, Munich, Germany (*Presenter*) Nothing to Disclose

#### PURPOSE

Chimeric antigen receptor (CAR) T-cell therapy with patient-derived T cells against tumor cells are approved for relapsed or refractory (r/r) diffuse large B-cell lymphoma (DLBCL). Anti-tumor activity differs from conventional treatment strategies with so far undefined response criteria. We evaluated changes in morphologic and metabolic parameters from baseline to 3 months and their prognostic value for overall survival (OS).

#### METHODS AND MATERIALS

Consecutive r/r DLBCL patients with PET-CT imaging at baseline and at 3 months after CAR T-cell transfusion were selected. Overall response was determined based on Lugano criteria with up to 6 target lesions. The sum of the product of diameters (SPD) was used to represent tumor burden and its percent reduction over time (depth of response, DoR). Maximum standard uptake value percent reduction between baseline and 3 months (?SUV) was applied as metabolic response parameter.

#### RESULTS

22 patients were included (median age: 67 years, 64% male) with median baseline SPD of 6088 mm<sup>2</sup> and SUV<sub>max</sub> of 25.8. According to Lugano criteria, 12 patients (55%) were in complete metabolic remission at 3 months. A color-coded waterfall plot

shows DoR together with the Lugano response category (Figure 1). The median tumor burden and metabolism were reduced in DoR by 81.5% and in  $\Delta$ SUV by 62.1%. Among patients with reduction in tumor burden and metabolism, DoR and  $\Delta$ SUV showed good correlation ( $r=0.71$ ,  $p<0.001$ , Figure 2A). DoR=50%,  $\Delta$ SUV=40% and complete metabolic response per Lugano showed significant stratification of OS (each with  $p=0.05$ ; Figure 2B-D).

#### **CONCLUSION**

s For r/r DLBCL patients undergoing CAR T-cell therapy, morphologic and metabolic parameters represent different properties. Our preliminary data indicate that both DoR and  $\Delta$ SUV at 3 months may have prognostic information. Further studies should determine which individual parameter or combination is most suitable for survival prognostication after CAR T-cell therapy.

#### **CLINICAL RELEVANCE/APPLICATION**

CAR T-cell therapy has emerged as a new effective antigen-driven cell-based immunotherapy to treat patients with r/r DLBCL. Identifying early prognostic parameters is crucial to guide patient care.

Printed on: 02/07/23



## Abstract Archives of the RSNA, 2022

R5B-SPNMMI-1

### Incidental Detection of Focal FDG Uptake in Major Organs of Oncologic Patients on the FDG PET/CT

Thursday, Dec. 1 12:45PM - 1:15PM Room: Learning Center - NMMI DPS

#### Participants

Kyung Hoon Hwang, MD, PhD, Incheon, Korea, Republic Of (*Presenter*) Nothing to Disclose

#### PURPOSE

In this study, we presented our experiences on incidental focal colorectal, thyroid and prostate hypermetabolism to justify the application of F-18 FDG PET/CT imaging to the oncologic patients and the subjects at high risk of developing cancer.

#### METHODS AND MATERIALS

The final reports of a total of 16,010 F-18 FDG PET/CT scans performed at our hospital between January 2016 and January 2022 were retrospectively reviewed to identify unexpectedly observed focal colorectal or thyroid or prostate FDG uptake. They are classified as malignant, premalignant (for colon/rectum), and benign according to their histopathological reports. The effective dose from FDG PET/CT was estimated and the hypermetabolic uptake was measured and compared amongst the groups to confirm whether the PET parameters were useful in distinguishing malignant from benign lesions and to identify cut-offs.

#### RESULTS

The estimated average effective dose from a F-18 FDG PET/CT scan was  $7.3 \pm 0.8\text{mSv}$ , which was comparable to that of pre- and post-contrast chest or abdominal pelvic CT. Overall, 61.6% of the focal colorectal uptake were malignant/premalignant lesions and 59.6% of the focal thyroid uptake were malignant lesions. 56.4% of the focal prostate uptake were malignant lesions. Maximum SUV was an independent diagnostic parameter to differentiate malignant (and premalignant) from benign lesions in both incidental focal colorectal and thyroid FDG uptake.

#### CONCLUSION

With advances in hardware and software technology related to PET/CT equipment, radiation exposure during a F-18 FDG PET/CT scan is gradually decreasing. Incidentally observed focal hypermetabolic colon/rectum or thyroid uptake showed a high rate (approximately 60%) of malignant (or premalignant for colon/rectum) lesions. Hence, these findings justify the encouraged application of PET imaging to the oncologic patients and the subjects at high risk of developing cancer.

#### CLINICAL RELEVANCE/APPLICATION

Unexpected incidental focal F-18 FDG activity is not an uncommon finding in the clinical PET studies. Due to high malignancy/premalignancy rate in the colorectal or thyroid lesions with incidental focal uptake, authors recommend further active assessment.

Printed on: 02/07/23

## Abstract Archives of the RSNA, 2022

R5B-SPNMMI-2

### Pre- to Post-Treatment Evolution of PET-CT Parameters in CAR-T Cell Treatment of Lymphoma

Thursday, Dec. 1 12:45PM - 1:15PM Room: Learning Center - NMMI DPS

#### Participants

Michael Winkelmann, MD, Munich, Germany (*Presenter*) Nothing to Disclose

#### PURPOSE

Chimeric antigen receptor (CAR) T-cell therapy with patient-derived T cells against tumor cells are approved for relapsed or refractory (r/r) diffuse large B-cell lymphoma (DLBCL). Anti-tumor activity differs from conventional treatment strategies with so far undefined response criteria. We evaluated changes in morphologic and metabolic parameters from baseline to 3 months and their prognostic value for overall survival (OS).

#### METHODS AND MATERIALS

Consecutive r/r DLBCL patients with PET-CT imaging at baseline and at 3 months after CAR T-cell transfusion were selected. Overall response was determined based on Lugano criteria with up to 6 target lesions. The sum of the product of diameters (SPD) was used to represent tumor burden and its percent reduction over time (depth of response, DoR). Maximum standard uptake value percent reduction between baseline and 3 months (?SUV) was applied as metabolic response parameter.

#### RESULTS

22 patients were included (median age: 67 years, 64% male) with median baseline SPD of 6088 mm<sup>2</sup> and SUV<sub>max</sub> of 25.8. According to Lugano criteria, 12 patients (55%) were in complete metabolic remission at 3 months. A color-coded waterfall plot shows DoR together with the Lugano response category (Figure 1). The median tumor burden and metabolism were reduced in DoR by 81.5% and in ?SUV by 62.1%. Among patients with reduction in tumor burden and metabolism, DoR and ?SUV showed good correlation ( $r=0.71$ ,  $p<0.001$ , Figure 2A). DoR=50%, ?SUV=40% and complete metabolic response per Lugano showed significant stratification of OS (each with  $p=0.05$ ; Figure 2B-D).

#### CONCLUSION

s For r/r DLBCL patients undergoing CAR T-cell therapy, morphologic and metabolic parameters represent different properties. Our preliminary data indicate that both DoR and ?SUV at 3 months may have prognostic information. Further studies should determine which individual parameter or combination is most suitable for survival prognostication after CAR T-cell therapy.

#### CLINICAL RELEVANCE/APPLICATION

CAR T-cell therapy has emerged as a new effective antigen-driven cell-based immunotherapy to treat patients with r/r DLBCL. Identifying early prognostic parameters is crucial to guide patient care.

Printed on: 02/07/23



## Abstract Archives of the RSNA, 2022

R5B-SPNPM

### Noninterpretive Skills/Quality Improvement/Practice Management Thursday Poster Discussions - B

Thursday, Dec. 1 12:45PM - 1:15PM Room: Learning Center - NPM DPS

#### Participants

Cynthia S. Santillan, MD, San Diego, CA (*Moderator*) Consultant, Alimientiv Health Trust

#### Sub-Events

#### **R5B-SPNPM- Gadolinium-Based Contrast Agent Guideline Considering Serum Bilirubin Level in Patients With Impaired Renal Function for Rapid Elimination and Minimal Retention of Gadolinium**<sup>1</sup>

#### Participants

Jeong Woo Kim, MD, PhD, Seoul, Korea, Republic Of (*Presenter*) Nothing to Disclose

#### PURPOSE

In our institution, a gadolinium-based contrast agent (GBCA) guideline for patients with impaired renal function was devised by the consensus of radiologists and nephrologists. This study aimed to evaluate clinical outcomes after following the guideline for seven years in a tertiary hospital.

#### METHODS AND MATERIALS

This retrospective study identified all patients who were referred to the radiology department due to elevated serum creatinine level among patients scheduled for GBCA-enhanced MRI between January 2012 and December 2018. GBCAs have different concentrations of gadolinium [0.25 M for gadoteric acid (GA); 0.5 M for gadoterate meglumine (GM); 1.0 M for gadobutrol (GB)] and excretion pathways [dual pathways (50% renal and 50% biliary excretion) for GA; 100% renal excretion for GM and GB]. Considering these characteristics of GBCAs, hemodialysis, estimated glomerular filtration rate (eGFR), serum bilirubin level, and previous GBCA-enhanced MRI examination, patients underwent MRI with the contrast medium and dose recommended in the guideline. GA was recommended for patients with normal serum bilirubin level, and GM or GB was recommended for patients with elevated serum bilirubin level at an adjusted dose. A search of electronic medical records was performed to assess NSF occurrence. In patients who underwent brain MRI during the follow-up period, gadolinium depositions (high signal intensity within dentate nucleus and globus pallidus on precontrast T1-weighted image) were evaluated.

#### RESULTS

Of the 313 referred patients, a total of 298 patients underwent GBCA-enhanced MRI according to the guideline. These included 76 patients with eGFR of 15-29 mL/min/1.73 m<sup>2</sup> (CKD stage 4) and 126 patients with eGFR <15 mL/min/1.73 m<sup>2</sup> (CKD stage 5). There were 106 patients on hemodialysis and 178 patients underwent two or more GBCA-enhanced MRI examinations. Ninety-seven patients with eGFR less than 30 mL/min/1.73m<sup>2</sup> or undergoing hemodialysis underwent MRI using GA. During the follow-up period, there was no reported NSF case. In addition, there was no evidence of gadolinium deposition in brain tissues (in 12 patients with CKD stage 5 and 3 patients with CKD stage 4).

#### CONCLUSION

The GBCA guideline for the use of different GBCAs at an adjusted dose according to serum bilirubin level may be safe with respect to NSF and gadolinium deposition in brain tissues, although further studies are needed to confirm this.

#### CLINICAL RELEVANCE/APPLICATION

In consideration of the gadolinium concentration and excretion pathway of GBCAs, the GBCA guideline which recommended different GBCAs at an adjusted dose according to serum bilirubin level, can be safely used for patients with impaired renal function by enabling rapid elimination and minimal retention of gadolinium.

#### **R5B-SPNPM- Automatic Diagnosis Extraction Using NLP to Monitor the Impact of Clinical Decision Support on CT for Diagnosis of Pulmonary Embolism**<sup>2</sup>

#### Participants

Abdullah Khan, MD, Sacramento, CA (*Presenter*) Nothing to Disclose

#### PURPOSE

CMS recently mandated that ordering clinicians consult Clinical Decision Support (CDS) when ordering certain high value imaging tests, including CT Pulmonary Angiography (CTPA) for suspected acute pulmonary embolism (PE). The assumption is that CTPA is overutilized and has a low diagnostic yield, and that CDS will decrease utilization and increase the percentage of CTPA exams that are positive for PE. We developed and validated an NLP-based pipeline to identify whether CTPA reports confirmed the presence of PE, and applied it to a corpus of 6953 reports obtained before and after implementing CDS in December 2019.

#### METHODS AND MATERIALS

Final radiology report impressions for all CTPA exams ordered from the Emergency Department of our quaternary care hospital

between July 2016 and April 2022 were obtained and manually classified as either confirming the presence of PE or not. The report impressions were also processed through a custom NLP pipeline based on the Clinical Text and Knowledge Extraction System (CTAKES), an open-source biomedical NLP toolset. We applied the CTAKES NegexAnnotator to identify negation status, identified a set of UMLS Concept Unique Identifiers (CUIs) that covered the variety of phrases commonly understood to indicate the presence of pulmonary thromboemboli, and applied a custom heuristic to handle lexical complexities common in radiology reports. We compared the accuracy of the NLP pipeline to the manual annotations using a 2x2 contingency table to measure sensitivity, specificity, and F1 score.

## **RESULTS**

The CTAKES-based NLP pipeline correctly classified 888 exams as true positive, 5909 exams as true negatives, and incorrectly predicted 68 false positives and 88 false negatives, yielding sensitivity=0.91, specificity=0.99, accuracy 0.98, and F1-score 0.92. Monthly aggregate exam positivity is very similar between the manual and NLP-derived classification.

## **CONCLUSION**

s An NLP pipeline based on the open-source CTAKES system is accurate in classifying CTPA reports as positive or negative for PE. Such an automated classification system is useful in monitoring the effectiveness of CDS and other quality-improvement initiatives that purport to improve utilization.

## **CLINICAL RELEVANCE/APPLICATION**

Automatic diagnostic accuracy classification is useful in monitoring the impact of CDS and other efforts that purport to improve healthcare utilization.

Printed on: 02/07/23

## Abstract Archives of the RSNA, 2022

R5B-SPNPM-1

### Gadolinium-Based Contrast Agent Guideline Considering Serum Bilirubin Level in Patients With Impaired Renal Function for Rapid Elimination and Minimal Retention of Gadolinium

Thursday, Dec. 1 12:45PM - 1:15PM Room: Learning Center - NPM DPS

#### Participants

Jeong Woo Kim, MD, PhD, Seoul, Korea, Republic Of (*Presenter*) Nothing to Disclose

#### PURPOSE

In our institution, a gadolinium-based contrast agent (GBCA) guideline for patients with impaired renal function was devised by the consensus of radiologists and nephrologists. This study aimed to evaluate clinical outcomes after following the guideline for seven years in a tertiary hospital.

#### METHODS AND MATERIALS

This retrospective study identified all patients who were referred to the radiology department due to elevated serum creatinine level among patients scheduled for GBCA-enhanced MRI between January 2012 and December 2018. GBCAs have different concentrations of gadolinium [0.25 M for gadoxetic acid (GA); 0.5 M for gadoterate meglumine (GM); 1.0 M for gadobutrol (GB)] and excretion pathways [dual pathways (50% renal and 50% biliary excretion) for GA; 100% renal excretion for GM and GB]. Considering these characteristics of GBCAs, hemodialysis, estimated glomerular filtration rate (eGFR), serum bilirubin level, and previous GBCA-enhanced MRI examination, patients underwent MRI with the contrast medium and dose recommended in the guideline. GA was recommended for patients with normal serum bilirubin level, and GM or GB was recommended for patients with elevated serum bilirubin level at an adjusted dose. A search of electronic medical records was performed to assess NSF occurrence. In patients who underwent brain MRI during the follow-up period, gadolinium depositions (high signal intensity within dentate nucleus and globus pallidus on precontrast T1-weighted image) were evaluated.

#### RESULTS

Of the 313 referred patients, a total of 298 patients underwent GBCA-enhanced MRI according to the guideline. These included 76 patients with eGFR of 15-29 mL/min/1.73 m<sup>2</sup> (CKD stage 4) and 126 patients with eGFR <15 mL/min/1.73 m<sup>2</sup> (CKD stage 5). There were 106 patients on hemodialysis and 178 patients underwent two or more GBCA-enhanced MRI examinations. Ninety-seven patients with eGFR less than 30 mL/min/1.73m<sup>2</sup> or undergoing hemodialysis underwent MRI using GA. During the follow-up period, there was no reported NSF case. In addition, there was no evidence of gadolinium deposition in brain tissues (in 12 patients with CKD stage 5 and 3 patients with CKD stage 4).

#### CONCLUSION

s The GBCA guideline for the use of different GBCAs at an adjusted dose according to serum bilirubin level may be safe with respect to NSF and gadolinium deposition in brain tissues, although further studies are needed to confirm this.

#### CLINICAL RELEVANCE/APPLICATION

In consideration of the gadolinium concentration and excretion pathway of GBCAs, the GBCA guideline which recommended different GBCAs at an adjusted dose according to serum bilirubin level, can be safely used for patients with impaired renal function by enabling rapid elimination and minimal retention of gadolinium.

Printed on: 02/07/23



## Abstract Archives of the RSNA, 2022

R5B-SPNPM-2

### Automatic Diagnosis Extraction Using NLP to Monitor the Impact of Clinical Decision Support on CT for Diagnosis of Pulmonary Embolism

Thursday, Dec. 1 12:45PM - 1:15PM Room: Learning Center - NPM DPS

#### Participants

Abdullah Khan, MD, Sacramento, CA (*Presenter*) Nothing to Disclose

#### PURPOSE

CMS recently mandated that ordering clinicians consult Clinical Decision Support (CDS) when ordering certain high value imaging tests, including CT Pulmonary Angiography (CTPA) for suspected acute pulmonary embolism (PE). The assumption is that CTPA is overutilized and has a low diagnostic yield, and that CDS will decrease utilization and increase the percentage of CTPA exams that are positive for PE. We developed and validated an NLP-based pipeline to identify whether CTPA reports confirmed the presence of PE, and applied it to a corpus of 6953 reports obtained before and after implementing CDS in December 2019.

#### METHODS AND MATERIALS

Final radiology report impressions for all CTPA exams ordered from the Emergency Department of our quaternary care hospital between July 2016 and April 2022 were obtained and manually classified as either confirming the presence of PE or not. The report impressions were also processed through a custom NLP pipeline based on the Clinical Text and Knowledge Extraction System (CTAKES), an open-source biomedical NLP toolset. We applied the CTAKES NegexAnnotator to identify negation status, identified a set of UMLS Concept Unique Identifiers (CUIs) that covered the variety of phrases commonly understood to indicate the presence of pulmonary thromboemboli, and applied a custom heuristic to handle lexical complexities common in radiology reports. We compared the accuracy of the NLP pipeline to the manual annotations using a 2x2 contingency table to measure sensitivity, specificity, and F1 score.

#### RESULTS

The CTAKES-based NLP pipeline correctly classified 888 exams as true positive, 5909 exams as true negatives, and incorrectly predicted 68 false positives and 88 false negatives, yielding sensitivity=0.91, specificity=0.99, accuracy 0.98, and F1-score 0.92. Monthly aggregate exam positivity is very similar between the manual and NLP-derived classification.

#### CONCLUSION

An NLP pipeline based on the open-source CTAKES system is accurate in classifying CTPA reports as positive or negative for PE. Such an automated classification system is useful in monitoring the effectiveness of CDS and other quality-improvement initiatives that purport to improve utilization.

#### CLINICAL RELEVANCE/APPLICATION

Automatic diagnostic accuracy classification is useful in monitoring the impact of CDS and other efforts that purport to improve healthcare utilization.

Printed on: 02/07/23

## Abstract Archives of the RSNA, 2022

R5B-SPNR

### Neuroradiology Thursday Poster Discussions - B

Thursday, Dec. 1 12:45PM - 1:15PM Room: Learning Center - NR DPS

#### Participants

Ryan Peterson, MD, Atlanta, GA (*Moderator*) Nothing to Disclose

Ryan Peterson, MD, Atlanta, GA (*Moderator*) Nothing to Disclose

Jennifer Soun, MD, Irvine, CA (*Moderator*) Research Grant, Canon Medical Systems Corporation

Jennifer Soun, MD, Irvine, CA (*Moderator*) Research Grant, Canon Medical Systems Corporation

#### Sub-Events

### R5B-SPNR-1 Effective Atomic Number as a Quantitative CT Marker for Myelin Content: A Validation Study Using Synthetic MRI

#### Participants

Tomohito Hasegawa, Kagoshima, Japan (*Presenter*) Nothing to Disclose

#### PURPOSE

The effective atomic number (Zeff) reflects the elemental composition in biological tissues. Our purpose was to validate Zeff as a quantitative CT marker for myelin content in vivo.

#### METHODS AND MATERIALS

Fifteen patients (5 males and 10 females, age range from 35 to 84 years) with apparently normal cerebral parenchyma who underwent MRI scan and spectral detector CT scan within 1 month were included in this retrospective study. Images of myelin volume fraction (Vmy) were generated from synthetic MRI data using the multiparametric model based on the longitudinal and transverse relaxation rates and proton density. Whole brain spectral detector CT scans were performed using a dual-layer CT system, and images of the conventional CT value (CTconv), electron density (ED), and Zeff were obtained. The CT images were coregistered to the corresponding MR images using SPM12. Two independent observers placed elliptical ROIs in 12 gray matter (GM) and 12 white matter (WM) regions in each brain. Correlations between Vmy and CT parameters were evaluated using the Spearman's rank correlation coefficient for GM, WM, and altogether (GM+WM). The interobserver agreement was evaluated using the intraclass correlation coefficient (ICC).

#### RESULTS

The Vmy ranged from 0.881% to 32.06% in GM and from 25.34% to 48.32% in WM. CTconv, Zeff, and ED were significantly negatively correlated with Vmy for GM+WM. Zeff showed a strong negative correlation with Vmy ( $r=-0.783$ ,  $P<0.001$ ), which was stronger than CTconv ( $r=-0.715$ ,  $P<0.001$ ). ED showed only a moderate negative correlation with Vmy ( $r=-0.448$ ,  $P<0.001$ ). Only Zeff showed significant correlation with Vmy both in GM ( $r=-0.407$ ,  $P<0.001$ ) and WM ( $r=-0.215$ ,  $P=0.004$ ). The interobserver agreement was excellent for all measurement (ICC ranged from 0.897 to 0.984).

#### CONCLUSION

s Myelin content was more strongly reflected in Zeff than ED and CTconv. The negative correlation between Zeff and Vmy may be related to elemental composition of WM which is characterized by higher carbon and lower oxygen mass fractions than GM. The Zeff may serve as a quantitative CT marker for myelin content.

#### CLINICAL RELEVANCE/APPLICATION

The effective atomic number may serve as a quantitative CT marker for myelin content.

### R5B-SPNR-10 Investigation on Pre ASiR-v on Image Quality and Radiation Dose of Non Spectral Scanning: A Phantom Study

#### Participants

Yaoping Ma, (*Presenter*) Nothing to Disclose

#### PURPOSE

To investigate the influence of different pre adaptive statistical iterative reconstruction - Veo (ASiR-V) level on the image quality and radiation dose of non spectral scanning.

#### METHODS AND MATERIALS

A polypropylene cylindrical phantom (QSP Phantom) with nine tubes containing different concentrations of iodine (0, 2.5, 5, 10, 20 mgI/ml) was scanned in using spectral CT (Revolution, GE Healthcare) gemstone spectral imaging (GSI) mode using fast kV switch (80/140 kV), the tube current was 485mA, the layer thickness was 1.25mm, the collimation width was 80mm, noise index (NI) 5HU, pitch 0.992:1. Three groups of pre-ASiR-V level (30%, 40%, 50%) was used for spectral CT scanning. Eleven groups of images were selected from the scan center and five layers above and below. CT value and the area of ROI were measured. The CT dose

index (CTDI) of different pre ASiR-V level scans was recorded. The dose length product (DLP), CT value and noise (SD) of the tube were recorded. Signal noise ratio (SNR) and contrast to noise ratio (CNR) of tubes was calculated. The DLP across three groups were analyzed by simple linear regression analysis. SD, SNR and CNR across three groups were analyzed by one-way ANOVA.

## RESULTS

With the increase of pre-selected ASiR-V level, DLP showed decreasing trend. There was significant difference in DLP among groups (9.24mSv, 7.55mSv, 6.00mSv for 30%, 40%, 50% pre-ASiR-V, respectively.  $P < 0.05$ ). There were no significant differences in SD among groups ( $10.85 \pm 0.80$  (I20),  $8.38 \pm 0.29$  (I10),  $8.10 \pm 0.41$  (H2O), for 30% pre-ASiR-V,  $10.86 \pm 0.74$  (I20),  $8.42 \pm 0.29$  (I10),  $8.05 \pm 0.46$  (H2O) 40% pre-ASiR-V,  $11.36 \pm 0.76$  (I20),  $7.97 \pm 0.29$  (I10),  $7.76 \pm 0.34$  (H2O), 50% pre-ASiR-V,  $F = 2.130$ ,  $p > 0.05$ ).

## CONCLUSION

With the increase of pre-ASiR-V from 30%, 40%, 50%, radiation dose was reduced effectively, while the image quality was not changed significantly.

## CLINICAL RELEVANCE/APPLICATION

Radiation dose is reduced with the increase of pre-ASiR-V and image quality keeps no change. Correlation of clinical application: through the basic research of phantom, compared with conventional kVp scanning, energy spectrum CT scanning can provide the same image quality scanning radiation dose, at the same time, energy spectrum CT scanning can provide different levels (40-140keV) of single energy and effective atomic number, and more energy spectrum information of base material than conventional kVp scanning. This study has guiding significance for the application of energy spectrum scanning in different clinical scenarios.

## R5B-SPNR- Effects of Different Weighted Iterative Reconstruction on the Image Quality of Head and Neck CTA

13

Participants

Deng Jie, (Presenter) Nothing to Disclose

## PURPOSE

To investigate the effect of adaptive statistical iterative reconstruction (ASIR-V) algorithm on image quality and application value of head and neck CTA scanning.

## METHODS AND MATERIALS

A total of 88 patients underwent head and neck CTA. Image reconstruction was performed using Filtered Back Projection (FBP), 20% ASIR-V algorithm, 40% ASIR-V algorithm, 60% ASIR-V algorithm and 80% ASIR-V algorithm, and perform volume projection and maximum density projection processing on the five groups of images. The effects of different reconstruction methods on the image quality of head and neck CTA were evaluated from the two aspects of objective measurement and subjective score.

## RESULTS

Comparison of five groups of different reconstruction methods (filtered back projection method) FBP, 20% ASIR, 40% ASIR, 60% ASIR and 80% ASIR in the blood vessels of the head and neck (aortic arch, left common carotid artery, right common carotid artery) Artery, left middle cerebral artery, right middle cerebral artery, left vertebral artery, right vertebral artery, basilar artery) image quality parameter comparison, there is no statistical difference in CT value and SD value among the five groups of images among each blood vessel ( $P > 0.05$ ); when comparing SNR and CNR, the blood vessels in the eight groups were  $80\% \text{ASIR} > 60\% \text{ASIR} > 40\% \text{ASIR} > 20\% \text{ASIR} > \text{FBP}$  ( $P < 0.05$ ). The Kappa value of the subjective rating of quality is 0.75, with strong consistency. The subjective scores were ( $4.13 \pm 1.669$ ), ( $4.30 \pm 2.607$ ), and ( $4.93 \pm 2.640$ ), respectively, and there was no significant difference in the subjective scores among the three groups ( $F = 0.876$ ,  $P > 0.05$ ).

## CONCLUSION

With the gradual increase of the pre-ASIR-V weight, the CT value did not change significantly, and the image noise gradually increased. At the pre-ASIR-V level of 0~40%, the subjective image score was basically stable, and there was no significant difference in image quality. 60%~80% of the pre-ASIR-V level, the subjective scores in each group showed a gradually decreasing trend, and the image quality decreased obviously and gradually.

## CLINICAL RELEVANCE/APPLICATION

When the ASIR value of different weights applied to head and neck CTA scans is 40%, the image quality is the best, which can be used in clinical practice.

## R5B-SPNR- Description of Magnetic Resonance Fingerprinting in Patients with Amyotrophic Lateral Sclerosis

14

Participants

Philipp Moser, MD, PhD, (Presenter) Nothing to Disclose

## PURPOSE

Applicability of 3T Magnetic Resonance Fingerprinting (MRF) T1 and T2 mapping for quantitative analysis of the capsula interna in patients with amyotrophic lateral sclerosis (ALS)

## METHODS AND MATERIALS

3T single-step MRF T1 and MRF T2 map data acquisition in addition to conventional multi-step MRI image acquisition was performed in patients diagnosed with ALS. In addition, DTI (b-values 0-2500) was analyzed in seven patients. A ROI-based analysis of relaxation times of the left and right capsula interna was performed. Interclass correlation (ICC, 3 repeats) and Pearson correlation coefficient were done for statistical analysis. Data presented as mean  $\pm$  SD.

## RESULTS

Eighteen patients (mean age 63.7  $\pm$  12.7 years, male 61%) were included. We found excellent intra-observer ICC values for MRF T1R 0.985 (0.98-0.99, CI 95%) and MRF T2R 0.998 (0.99-1.0, CI 95%). The mean relaxation time of MRF T1R was 103634.1 ms and of MRF T2R was 2742308 ms. We observed a correlation between the MRF T1R values of the left and right capsula interna ( $R = 0.65$ ,

p=0.003) and the MRF T2R values of the left and right capsula interna (R=0.96, p<0.0001). In addition, we found a correlation between MRF T1R and DTI values (R= -0.54, p=0.044) but no correlation between MRF T1R and ADC nor between MRF T2R and ADC or DTI.

## CONCLUSION

s MRF T1 and T2 mapping of the capsula interna was successfully performed in patients with ALS and quantitative assessment may provide additional support in the diagnosis of upper motoneuron involvement.

## CLINICAL RELEVANCE/APPLICATION

MRF may assist in the assessment of upper motoneuron involvement and disease progression in patients with ALS.

## R5B-SPNR- 15 **A Clinical Application of 3D High-Resolution Contrast Enhanced MR Neurography With Precise Fat Suppression in Lumbosacral Plexus**

Participants  
Xiangchuang Kong, Wuhan, China (*Presenter*) Nothing to Disclose

## PURPOSE

The purpose of this study was to investigate the clinical application of precise fat suppression for 3D high-resolution contrast-enhanced MR neurography of lumbosacral plexus.

## METHODS AND MATERIALS

32 patients were prospectively selected: 14 patients (group A) with preset TI, and 22 patients (group B) with accurately calculated TI values. All patients were scanned using a 3.0 T MR scanner (Ingenia CX, Philips Healthcare, the Netherlands) with a 32-element phased-array coil. After intravenous injection of Gd-DTPA (0.15mmol/kg), patients were scanned using the 3D NerveView sequence: TI=220ms in group A and calculated TI in group B by a low resolution and fast 3D NerveView scanning with different TI values (TI=180 200 220 230 250 260 270 280 300 320 ms, TR=2200ms). Images were reconstructed on the scanner by the vendor-supplied software package (Compressed SENSE, Philips Healthcare). The signal intensity of fat, and nerve was measured on the original graph and the MIP graph respectively and the signal intensity ratio of nerve to fat was calculated for evaluation of fat suppression. Then the nerve/fat signal ratio (NFR) was calculated. The IBM SPSS22.0 software was used for statistical analysis, and NFR between the two groups was compared by unpaired sample t-test. P<0.05 indicated a statistically significant difference.

## RESULTS

1. The proposed TI scout method could improve fat suppression in MRN dramatically. The calculated NFR (precise fat suppression) (13.26±5.47) was about 425.4% higher than that in the preset TI situation (220ms) (2.39±0.55). The difference between the two groups was statistically significant (t=26.495, P<0.05). 2. The detection rates of nerve roots and trunks by the two methods were 100% (18/18,14/14); The detection rates of the nerve tracts and branches in precise fat-suppression sequence were 94.4% (17/18) and 83.3% (15/18), respectively. The detection rates of nerve tracts and branches in the preset method were 92.9% (13/14) and 71.4% (10/14), respectively. There was no statistically significant difference between the two methods in the detection rate of nerve tracts and branches (P=1.00, 0.67).

## CONCLUSION

s A fast and easy TI scout-based strategy was proposed to improve the fat suppression in 3D MRN of the lumbosacral plexus, which enhanced the image quality significantly. The NFR was increased by about 425.4% more than that in the vendor-provided preset TI scheme.

## CLINICAL RELEVANCE/APPLICATION

A fast and easy TI scout-based strategy was proposed to improve the fat suppression in 3D MR neurography of lumbosacral plexus, which enhanced the image quality significantly. The nerve fat signal intensity ratio was increased by about 425.4% than that in vendor-provided preset TI scheme.

## R5B-SPNR- 16 **Rapid Susceptibility-Weighted Imaging using Wave CAIPI for Differentiation of Diamagnetic and Paramagnetic Signal**

Participants  
Parker Lawson, MD, (*Presenter*) Nothing to Disclose

## PURPOSE

Susceptibility-weighted imaging (SWI) is primarily used for the detection of paramagnetic and diamagnetic substances, typically hemorrhage and calcifications respectively. Differentiation between the two can be difficult on post-processed SWI images as both create a similar magnitude of susceptibility and appearance; however, SWI phase imaging can often distinguish the two as their phase shifts and resultant signals are opposite of each other. Unfortunately, differentiation is not always achievable for larger lesions. Wave CAIPI SWI has been recently developed as an alternative to conventional SWI with reduced scan times. Prior to this investigation, Wave CAIPI SWI phase had not been evaluated for its ability to differentiate between paramagnetic and diamagnetic susceptibility.

## METHODS AND MATERIALS

126 Brain MRI studies were prospectively selected with the inclusion of a Wave CAIPI SWI sequence at 1.5T and 3T MR units. The images were evaluated by two radiologists for presence and characterization of susceptibility on both conventional SWI (scan time: 4.8 minutes) and Wave CAIPI (scan time: 1.14 minutes) phase and confirmed with head CTs.

## RESULTS

Of the 126 studies, 64 demonstrated a focus of susceptibility on conventional SWI and Wave CAIPI SWI. All 64 were identifiable as diamagnetic or paramagnetic on Wave CAIPI phase with homogeneous black or white signal. There were a total of 31 cases in which larger lesions demonstrated heterogeneous or dipole signal on conventional SWI phase, making interpretation difficult; however, Wave CAIPI SWI phase demonstrated homogenous signal facilitating interpretation that was confirmed by CT.

## CONCLUSION

s Wave CAIPI SWI phase is a non-inferior alternative to conventional SWI phase in differentiating between paramagnetic and diamagnetic signal and aids interpretation of larger lesions. The findings of this study, coupled with reduced scan times, support the inclusion of Wave CAIPI SWI sequences into routine brain imaging.

## CLINICAL RELEVANCE/APPLICATION

Wave CAIPI SWI phase images offer a non-inferior alternative to conventional SWI for differentiating between intracranial hemorrhage and calcification that can be acquired within less than 1/4th of the scan time.

## R5B-SPNR-17 **Aberrant Spontaneous Brain Activity in Patients with Dyshyroid Optic Neuropathy: A Resting-State Functional MRI Study**

Participants

Ping Liu, MS, (*Presenter*) Nothing to Disclose

## PURPOSE

Increasing evidence indicated that DON is not only a disease limited to the visual system, it is an eye-brain disease involves multiple brain regions. The purpose of the study was to investigate the brain functional alteration in patients with DON by evaluating the spontaneous neural activity changes using resting-state functional magnetic resonance imaging (rs-fMRI) with the regional homogeneity (ReHo).

## METHODS AND MATERIALS

Forty-seven TAO patients, including 20 with neuropathy (DON) and 27 without neuropathy, and 28 healthy controls (HCs) were recruited, matched for weight, height, age, sex, and educational level. All participants underwent resting-state functional nuclear resonance imaging, and the characteristics of spontaneous brain activity were evaluated employing the regional homogeneity (ReHo) method. Each patient with dyshyroid optic neuropathy also completed the ophthalmopathy examination. The ReHo values were compared among groups. Correlations between ReHo values and clinical metrics were assessed.

## RESULTS

Compared with TAOs, DON showed significantly decreased ReHo values in the left insula and right superior temporal gyrus, and increased ReHo values in left posterior cingulum and left precentral cuneus. Compared with HCs, TAOs also showed significantly decreased ReHo values in the left posterior cingulum. Additionally, the changed ReHo values were correlated visual acuity, mean deviation (MD) and pattern standard deviation (PSD) of visual field, and the amplitude and absolute latency of P100 of the visual-evoked potentials (VEPs).

## CONCLUSION

s DON patients had altered spontaneous brain activities in the left insula, right superior temporal gyrus, left posterior cingulum and left precentral cuneus. And these brain functional abnormalities associated with the visual function.

## CLINICAL RELEVANCE/APPLICATION

The abnormal spontaneous brain activities may be related to the pathological mechanism of DON, which may provide a valuable basis for further research on the clinical management of DON. Moreover, regional homogeneity has the potential for early diagnosis and prevent DON.

## R5B-SPNR-18 **Identification of Autism Spectrum Disorder (ASD) Patients Using Functional MRI - Nonlinear, Directed, Multivariate Brain Connectivity Analysis by Non-Linear Large-scale Granger Causality (IsNGC)**

Participants

Ali Vosoughi, Rochester, NY (*Presenter*) Nothing to Disclose

## PURPOSE

To develop and evaluate a novel machine learning method for identifying patients with Autism Spectrum Disorder (ASD) using large-scale Nonlinear Granger Causality (IsNGC) by capturing connectivity differences in resting-state functional MRI (rsfMRI).

## METHODS AND MATERIALS

We included the subset of all 93 rsfMRI data sets acquired from ASD patients and healthy controls from two institutions (36 from Olin, Institute of Living at Hartford Hospital, and 57 from University of Pittsburgh School of Medicine: Longitudinal Sample) represented in the publicly available preprocessed Autism Brain Imaging Data Exchange I (ABIDE I) data repository. For calculating directed functional connectivity between brain regions, we have recently developed the large-scale Nonlinear Granger Causality (IsNGC) algorithm [Citation blinded for review] that leverages radial basis function kernel transformation for causal modeling in high-dimensional fMRI time series. A 100-iteration cross-validation approach with 80%/20% train/test ratio was applied, where feature selection was performed on each training set using Kendall's tau rank correlation, followed by support vector machine classification. To quantitatively evaluate diagnostic accuracy of IsNGC for correctly classifying ASD patients and normal controls, we compare its performance with both a recent state-of-the-art causal discovery method (PCMCI, [Runge et al., Science, 2019]), and the current clinical fMRI analysis standard of cross-correlation (CC), reporting accuracy, area under ROC curve (AUC), and f1-score.

## RESULTS

The IsNGC rsfMRI analysis method significantly outperformed both PCMCI and the clinical standard CC techniques at classifying ASD patients from healthy subjects, with accuracy/AUC/f1 score of 100%/1.0/100% for IsNGC, 75.4%/0.69/70.0% for PCMCI, and 65.8%/0.61/62.4% for CC, respectively.

## CONCLUSION

s Our results suggest that IsNGC significantly improves the diagnostic accuracy of correctly identifying patients with ASD from rsfMRI neuroimaging. We conclude that, when compared to both conventional CC analysis and state-of-the-art PCMCI, IsNGC is better suited to capture disease-related brain network connectivity changes in ASD patients.

## CLINICAL RELEVANCE/APPLICATION

The IsNGC method classifies Autism Spectrum Disorder (ASD) patients and controls by identifying relevant changes in fMRI connectivity, suggesting its potential usefulness as a novel diagnostic imaging biomarker for neurologic disease.

## R5B-SPNR-19 Three-vessel Selective Pseudo-continuous Arterial Spin Labeling Using Designed Metal Artifacts: A Feasibility Study

Participants  
Keizo Tanitame, MD, Hiroshima, Japan (*Presenter*) Nothing to Disclose

### PURPOSE

Arterial spin labeling (ASL) of magnetic resonance (MR) imaging is a noninvasive evaluation method for assessing cerebral perfusion, and delineation of individual perfusion territories of cerebral arteries can help in the evaluation of the collateral pathway development in cerebrovascular disease patients. We evaluated the feasibility of three-vessel selective pseudo-continuous ASL (pCASL) using designed metal artifacts.

### METHODS AND MATERIALS

We recruited fifteen healthy volunteers, and firstly obtained MR angiography of the brain and whole brain perfusion maps of all the cerebral arteries using three-dimensional pCASL. Then while confirming the anatomical location of common carotid arteries (CCAs), we placed one or two small insulated metals on the skin surface near the right, left or bilateral CCAs at the labeling plane, and performed vessel-selective pCASL using three different kinds of local labeling suppression. From analysis of the perfusion maps of all the cerebral arteries, the right CCA and vertebrobasilar artery (VBA), the left CCA and VBA, and only the VBA, two independent observers inferred and drew the cerebral arterial atlases, and another assessed the coincidence of the schematic atlas and MRA image in each subject.

### RESULTS

Three-vessel selective pCASL imaging could be performed in all subjects, and no subjects complained of local heat sensation related to the insulated metals. The coincidence rate of inferred cerebral arterial atlases and MRA images was 86.7% in each observer. In five subjects with incomplete circle of Willis, contralateral routes from well-developed communicating arteries could be inferred from the vessel-selective pCASL images. In a subject with an aberrant branch of the left posterior artery, the perfusion territory of the branch was shown in the vessel-selective pCASL images. Interobserver agreement was 100%. In two subjects, two observers independently suspected anterior to posterior circulation through well-developed bilateral posterior communicating arteries from the vessel-selective pCASL images, but MRA showed that the arteries were absent. These misunderstandings were thought to be due to unexpected suppression effect of the metals on VBA labeling.

### CONCLUSION

s We presented a three-vessel selective pCASL using designed metal artifacts. The perfusion territories of individual cerebral arteries could be delineated differently, but attention is needed for the depth of the vertebral arteries.

## CLINICAL RELEVANCE/APPLICATION

Three-vessel selective pseudo-continuous arterial spin labeling using designed metal artifacts can be used to obtain individual perfusion maps of bilateral carotid and vertebrobasilar arteries.

## R5B-SPNR-2 Feasibility of Ultrashort Echo Time Quantitative Susceptibility Mapping (UTE-QSM) With a 3D Cones Trajectory in the Human Brain

Participants  
Sam Sedaghat, MD, La Jolla, CA (*Presenter*) Nothing to Disclose

### PURPOSE

Over the past decade, quantitative susceptibility mapping (QSM) has emerged as a promising quantitative MR imaging technique to assess the microenvironment in the brain. In literatures, many new QSM techniques have been proposed, but non-Cartesian ultrashort echo time (UTE) sequences have not been explored. In this study, the feasibility of UTE-QSM based on a 3D spiral cones trajectory is demonstrated in the brain.

### METHODS AND MATERIALS

The UTE-QSM sequence based on a 3D cones trajectory was implemented on a 3T clinical MRI scanner (MR 750, GE Healthcare). To show the feasibility, an ex vivo experiment was performed on 3 fresh human brain samples using an 8-ch head coil with the following imaging parameters: TR = 50 ms, TE = 0.032, 4.4, 8.8, 13.2, 17.6, and 22 ms, FA = 20°, FOV = 220x220x80 mm<sup>3</sup>, matrix = 256x256x80, and readout bandwidth = 166.6 kHz. The scan was repeated with 8 different stretching factors (SFs) of the 3D cones spiral arms: 1.0, 1.1, 1.2, 1.3, 1.4, 1.5, 1.6, and 1.7 with the corresponding scan times of 1383, 1229, 1099, 1005, 920, 857, 794, and 745 sec (acceleration factors (AFs) of 1.00, 1.13, 1.26, 1.38, 1.50, 1.62, 1.74, and 1.86), respectively. An in vivo UTE-QSM was performed on five healthy volunteers (37.6 ± 6.7 years old) using the same imaging protocol except for: matrix = 220x220x80, FOV = 220x220x160 mm<sup>3</sup>, SF = 1.7 (AF = 1.86), and scan time = 645 sec. The reconstructed complex MR images were processed with a UTE-QSM pipeline established based on a MEDI toolbox.

### RESULTS

In the ex vivo experiment, a very high correlation in pixelwise QSM values (i.e., susceptibility) was found between SF of 1.0 and SFs from 1.1 to 1.7: Pearson's correlation 0.987, 0.981, 0.976, 0.972, 0.970, 0.962, and 0.953, respectively with all p-values < 0.05. In the in vivo experiment, the measured QSM values in cortical gray matter, juxtacortical white matter, corpus callosum, caudate, and putamen were 25.4 ± 4.0, -21.8 ± 3.2, -22.6 ± 10.0, 77.5 ± 18.8, and 53.8 ± 7.1 ppb in five volunteers, which correspond well with the values reported in literatures.

### CONCLUSION

s In this study, we demonstrated the clinical feasibility of 3D UTE-QSM in the brain for the first time. UTE-QSM with a stretched cones trajectory (i.e., acceleration up to 1.86x) showed reliable estimation of susceptibility in the brain.

## CLINICAL RELEVANCE/APPLICATION

The proposed UTE-QSM technique based on an efficient cones trajectory allows whole brain susceptibility mapping in a clinically feasible scan time of ~11 min. UTE-QSM is likely to provide more accurate assessment of calcification, hemorrhage, iron overload, and tumor vascularization as UTE acquisition allows direct imaging of short T2 tissues and robust mapping of their susceptibilities. Moreover, the non-Cartesian UTE-QSM is likely to be more robust to patient motion.

## R5B-SPNR- The Value of Deep Learning Reconstruction Algorithm in CT Whole Brain Perfusion in Patients with Ischemic Stroke

Participants

Limin Lei, Zhengzhou, China (*Presenter*) Nothing to Disclose

### PURPOSE

To compare deep learning-based image reconstruction (DLIR) algorithm and adaptive statistical iterative reconstruction-Veo (ASIR-V) algorithm on the image quality and brain perfusion parameters of whole brain CT perfusion scanning in patients with ischemic stroke due to large vessel occlusion.

### METHODS AND MATERIALS

A total of 27 patients with ischemic stroke due to large vessel occlusion were collected prospectively in this study, including 15 cases of acute and 12 cases of chronic, consisted of 22 males and 5 females with a median age of 54(range 30-79 years). All patients underwent whole brain perfusion imaging using latest-generation 16 cm detector coverage CT scanner (APEX CT, GE Healthcare). CT datasets were reconstructed using ASIR-V at a level of 80% (80%ASIR-V) and DLIR with high reconstruction strength level (DLIR-H) with 1.25-mm slice thickness. The volumetric CT dose index (CTDIvol) and dose length product (DLP) for each patient scan were recorded. Objective parameters including CT values and standard deviation (SD) in frontotemporal lobe, gray matter nucleus (caudate lobe, lenticular, thalamus) and posterior limb of internal capsule on the contralateral side, as well as the signal-to-noise ratio (SNR) and contrast-to-noise ratio (CNR) of gray matter nucleus were compared. We performed brain perfusion analysis based on CT Perfusion 4D package and calculated the perfusion parameters such as CBF, CBV, MTT and TTP at the same site as the CT values were measured. Moreover, the functional analysis of ipsilateral cerebral infarction including the brain tissue volume, Tmax average value, CBV average value were conducted with the threshold as CBV beyond 1ml/100g while Tmax within 6 seconds. Differences between continuous data were tested using paired t test or Wilcoxon rank test.

### RESULTS

DLIR-H had a lower image noise in frontotemporal lobe, gray matter nucleus and posterior limb of internal capsule than 80% ASIR-V (all  $P < 0.001$ ), while higher SNR and CNR of gray matter nucleus(all  $P < 0.001$ ) without changing the CT values. Moreover, there was no significant difference between DLIR-H and 80% ASIR-V in the perfusion parameters including CBF, CBV, MTT and TTP of gray matter and white matter as well as the Tmax average value, CBV average value with the threshold as CBV beyond 1ml/100g while Tmax within 6 seconds.

### CONCLUSION

In cerebral perfusion scan of patients with ischemic stroke, DLIR-H reconstruction algorithm can effectively improve image quality without changing perfusion parameters and functional parameters.

## CLINICAL RELEVANCE/APPLICATION

Deep learning reconstruction algorithm can reduce image noise without changing the vital diagnostic parameters, which throws light on low-dose CT acquisition protocol of clinical cerebral perfusion scans.

## R5B-SPNR-3 Label-Free Spectral X-Ray Method for Non-invasively Quantifying Amyloid Burden in the Human Brain

Participants

Eshan Dahal, (*Presenter*) Nothing to Disclose

### PURPOSE

To describe a spectral x-ray method based on the small-angle elastic scattering of photons for measuring amyloid burden in the human brain.

### METHODS AND MATERIALS

We built a prototype system capable of probing an intact human head using a polychromatic x-ray source with tungsten anode in the diagnostic x-ray energy range and a 2D spectroscopic photon-counting detector (80 x 80, 250-micron pixels) with a 1-mm cadmium telluride (HEXITEC) to record energy (in 1-keV bins) and location of each scattered photons. An energy-dependent transmission correction factor was calculated using spectroscopic measurements of the primary beam. The x-ray beam was pinhole collimated to create a 2-mm pencil beam to irradiate the human head phantom with and without embedded targets. We used a commercially available tissue-mimicking (brain and skull) phantom with slabs and an anthropomorphic human head phantom to assess the recovery of the scattering signature for targets with varying concentrations. By comparing the scattering profiles for areas with and without targets, we report amyloid burden as the area-under-the-peak for the characteristic target peaks which correlates with the mass fraction of amyloid plaques.

### RESULTS

Measurements of the head phantom with embedded caffeine targets show well-defined characteristic Bragg peaks at momentum transfer of 8.4 and 18.7 nm<sup>-1</sup>. We recovered the characteristic peaks with exposure times as low as 60 s. Measurements investigating the effect of sample thickness up to 16 cm and spectral x-ray energies from 30 to 120 keV was evaluated to maximize the scattering signal from the targets.

### CONCLUSION

The findings of the study suggest that the spectral x-ray-based method for non-invasively detecting and quantifying amyloid-like targets embedded within a human head has promise.

## CLINICAL RELEVANCE/APPLICATION

Amyloid burden can be used to monitor onset and progression of Alzheimer's disease. The spectral small-angle method described in this study has potential to facilitate more efficient therapeutic clinical trials by providing a fast and label-free amyloid plaque quantification tool as an alternative to amyloid-specific positron emission tomography.

#### **R5B-SPNR-4 How Confident Are You - Contrast-Enhanced T1-weighted SPACE Versus 3D FLASH Sequences for the Detection of Brain Metastases**

Participants

Maria Gule-Monroe, MD, Houston, TX (*Presenter*) Nothing to Disclose

##### **PURPOSE**

This study aimed to evaluate the utility of contrast-enhanced (CE) T1-weighted 3D fast spin-echo-based SPACE sequence, by comparing to the gradient-echo-based 3D-FLASH sequence (without inversion recovery, IR) for the detection of brain metastases at 3T.

##### **METHODS AND MATERIALS**

220 patients at a single institution who were scheduled for brain MRI underwent optimized CE T1-weighted SPACE and 3D-FLASH sequences at 3T as part of a practice quality improvement project. Each scan took approximately 4 minutes, and the order of the two sequences was balanced among the patients. The medical records were retrospectively reviewed, and 79 patients found to have brain metastases at the time of imaging were included. Images were evaluated by 5 CAQ certified neuroradiologists, with at least 2-week separation between scoring sequences for the same patient and 20 patients scored by 2 radiologists. Parameters evaluated included number of metastatic lesions, number of indeterminate lesions, visual assessment of lesion margin, visual assessment of contrast to noise ratio (CNR), presence of image artifact, and overall image quality. In addition, CNR was quantified for solidly enhancing lesions greater than 1 cm.

##### **RESULTS**

SPACE detected more lesions than 3D-FLASH in 35 patients, while 3D-FLASH detected more lesions in 10 patients. A greater number of indeterminate lesions were seen on 3D-FLASH (27 patients) vs SPACE (9 patients), mostly related to presence of vascular enhancement seen in 3D-FLASH images. When rating overall image quality, lesion margin and CNR on a Likert scale, SPACE performed better than 3D-FLASH with more image artifact seen on 3D-FLASH. Higher quantitative CNR was found in SPACE than 3D-FLASH images (mean=26.9 vs. 19.8, respectively, n=16, p=0.054).

##### **CONCLUSION**

This is the first study to date comparing the performance of CE T1-weighted SPACE to non-IR 3D-FLASH sequence for the detection of brain metastases. The SPACE sequence detects a greater number of metastatic lesions and is rated higher for image quality, lesion margin and CNR with less artifact. Gradient Echo are the most commonly used sequences for detection and radiation treatment planning of brain metastases. Superiority of SPACE for lesion detection and confidence has implications across the diagnostic and therapeutic imaging journey.

##### **CLINICAL RELEVANCE/APPLICATION**

This is the first study to date evaluating the performance of CE T1-weighted SPACE to non-IR 3D-FLASH for the detection of brain metastases. Superiority of SPACE for lesion detection and confidence has implications across the diagnostic and therapeutic imaging journey.

#### **R5B-SPNR-5 Characterization of Lenticulostriate Arteries by Combining High Resolution Black-blood T1-weighted with Variable Flip Angles Compressed Sensitivity Encoding at 3.0 Tesla**

Participants

Yukun Zhang, Dalian, China (*Presenter*) Nothing to Disclose

##### **PURPOSE**

To visualize and characterize lenticulostriate arteries (LSAs) in a short period time on a 3.0T MR scanner, we investigated the feasibility of high resolution black-blood T1-weighted with variable flip angles (T1w TSE-VFA) accelerated by compressed sensitivity encoding (CS-T1w TSE-VFA) and further identify the optimal acceleration factors (AFs) for clinical use.

##### **METHODS AND MATERIALS**

14 healthy volunteers (6 males, mean age 29.57±6.17 years) and 7 patients with cerebral infarction (4 males, mean age 50.06±20.13 years) were prospectively included and divided into the volunteer group and patient group. T1w TSE-VFA images with different AFs (Parallel imaging (PI) AF=3, CS AF=3,4,5,6) (Table 1) were acquired on a 3.0T scanner (uMR Omega, Imaging Healthcare, Shanghai, China). For objective evaluation, the regions of interest (ROIs) of the middle cerebral artery (MCA), the longest LSA, and corresponding white matter on the original or reformatted images were delineated (Fig.1 a-b). Then the signal intensity (SI) and standard deviation (SD) were measured and contrast-to-noise ratio (CNR): (SILSA/MCA-SIWM)/SDWM was further calculated. For subjective evaluation, the the number and length of LSAs of T1w (Fig.1 c) and subjective scoring (Fig.1 d-f) of T1w TSE-VFA with different AFs were measured. Paired t-test were used to compare CNR of MCA and LSA, number and length of LSAs, and image quality between T1w TSE-VFA with PI AF=3 and with CS AF=3 to 6.

##### **RESULTS**

For the volunteer group, when CS AF=6, the number of LSAs were significantly different from that of PI-T1w TSE-VFA (p<0.05); when CS AF=5, the length of LSAs and subjective scoring were significantly different from PI-T1w TSE-VFA (p<0.05)(Table.3 , Figs.2 and 4). For the patient group, when CS AF=6, the CNR of LSA and subjective scoring were significantly different from PI-T1w TSE-VFA (p<0.05); when CS AF=5, length and number of LSAs were significantly different from PI-T1w TSE-VFA (p<0.05)(Table 2, Figs. 3 and 4).

##### **CONCLUSION**

CS-T1w TSE-VFA with AF of 3 can provide a better LSA display but time longer; with AF of 4 can balance visualization of LSAs and acquisition time. These sequences had the potential to be used in clinical to provide diagnostic information for preventive medicine at 3 Tesla.

## CLINICAL RELEVANCE/APPLICATION

CS-T1w TSE-VFA can be used as a non-invasive head microvasculature examination in asymptomatic subjects and patients with cerebrovascular disease, which will be an important asset in preventive medicine.

## R5B-SPNR-6 Reproducible Brain MRI Radiomics Features Achieving Test-Retest, Multi-Scanner, and Computational Reproducibility: A Phantom Study

Participants

Yunhwa Roh, (*Presenter*) Nothing to Disclose

### PURPOSE

The image biomarker standardization initiative helped improving computational reproducibility of radiomics features on CT. Nonetheless, reproducible multiparametric MRI sequences across multi-scanner and different algorithms are yet to be standardized. We aimed to determine reproducible radiomic features in multiparametric sequences with multi-scanner and computational methods setting.

### METHODS AND MATERIALS

A phantom was scanned twice on a clinical 3 T system (Philips, Siemens, and GE) with T1-weighted (T1w), T2-weighted (T2w), and diffusion-weighted imaging (DWI) sequences. Radiomic features were extracted using pyradiomics (110 features) and MITK (the Medical Imaging Interaction Toolkit) (364 features) from each test-retest and multi-scanner setting. Stable radiomics features were calculated when maintaining 5% cut-off of averaging features among different imaging methods (test-retest and multi-scanner) and computational methods. The stable features were calculated concordance- and intraclass correlation coefficients (CCC and ICC) and compared among sequences.

### RESULTS

The number of robust features (CCC = 0.90) was higher for features calculated from DWI than from T1w and T2w images in test-retest analysis. From imaging reproducibility, a total of 79 (23.9%) of 330 features from pyradiomics and 473 (43.3%) of 1092 MITK features showed excellent robustness (ICC = 0.90). Applying both imaging and computational reproducibility cut-off, total 58 (17.5% from pyradiomics and 5.3% from MITK) features showed robustness across test-retest, multi-scanner, and computational methods. DWI images provided the highest percentage of robust features (23 out of 58, 39.6%), followed by T2w (19 out of 58, 32.7%) and T1w (16 out of 58, 27.6%).

### CONCLUSION

s Only between 5.3% and 17.5% radiomics features from multiparametric MRI showed excellent robustness from both imaging with computational reproducibility. Diffusion-weighted imaging showed best robustness, and care must be taken in the interpretation of clinical studies using non-robust features.

## CLINICAL RELEVANCE/APPLICATION

A recent multi-center study from the image biomarker standardization initiative (IBSI) helped improving computational reproducibility of radiomics features on CT. Nonetheless, reproducible multiparametric MRI sequences across multi-scanner and different algorithms are yet to be standardized. In this study, we found only between 5.3% and 17.5% radiomics features from multiparametric MRI showed excellent robustness from both imaging with computational reproducibility. Diffusion-weighted imaging showed best robustness, and care must be taken in the interpretation of clinical studies using non-robust features.

## R5B-SPNR-7 Novel Technique of Simultaneous Non-contrast MR Angiography and Multi-contrast Vessel Wall Imaging (Simul-MRA+VWI) Using Multi-Shot Gradient-echo EPI (MSG-EPI) for Carotid Artery Evaluation

Participants

Yasuhiro Nagai, RT, Osaka, Japan (*Presenter*) Nothing to Disclose

### PURPOSE

MRI for carotid artery has been widely used to assess the luminal stenosis and plaque characterization. However, separate acquisition of MR Angiography (MRA) and vessel wall imaging (VWI) require the long scan time and cause the misregistration. The hybrid of multi-shot gradient-echo EPI with modification of Look-Locker method enable to obtain the Simultaneous MRA and VWI (Simul-MRA+VWI) in a single scan. This study aims to compare the qualitative and quantitative image analysis for carotid artery between Simul-MRA+VWI and conventional scans.

### METHODS AND MATERIALS

We obtained the carotid artery MRI with Simul-MRA+VWI and conventional sequences (TOF and IR-GRE) in 10 healthy volunteers using 3T-MRI. The phantom of simulated plaque (blueberry jam:T1=300msec) was scanned together with volunteers. Simul-MRA-VWI provide multi-contrast images with different inversion time (TI) after IR pulse. Images with short TI yield MRA as bright blood imaging and images with null TI of blood yield VWI as dark blood T1 weighted images. The image quality of MRA and VWI were evaluated using the 4-point scale. In MRA, SNR of blood and contrast ratio (CR) between blood and muscle were measured. In VWI, CR between blood and muscle and CR between plaque and muscle were measured. Then, we compared these parameters between Simul-MRA-VWI and conventional sequences.

### RESULTS

The mean acquisition time of Simul-MRA-VWI sequence was 213sec, which was 60.7% shorter than the conventional two scans. There were no significant differences in image quality of MRA and VWI between Simul-MRA-VWI and conventional scans. In MRA, Simul-MRA-VWI had slightly higher SNR of blood and significantly higher CR between blood and muscle compared with TOF. In VWI, CR between blood and muscle (as black blood effect) tended to be higher in Simul-MRA-VWI than in IR-GRE but showed the no significant difference. CR between plaque and muscle (T1 contrast) was significantly higher in Simul-MRA-VWI than in IR-GRE with moderate correlation between two methods ( $r=0.78$ )

### CONCLUSION

s Simul-MRA-VWI is a promising technique for shortening scan time with equivalent image quality to conventional sequences and

Similar that VWI is a promising technique for shortening scan time with equivalent image quality to conventional sequences and yielding higher contrast MRA and VWI of carotid artery.

#### **CLINICAL RELEVANCE/APPLICATION**

Simul-MRA-VWI enable the simultaneous imaging of both carotid artery lumen and vessel wall with equivalent image quality to conventional methods. Our proposed method is practical approach for the reduction of scan time and the integrated assessment of both MRA and VWI without misregistration due to separate acquisition. Further, MRA and VWI obtained by this method can provide the higher contrast and permit the optimal contrast by determination from multiple TI images.

#### **R5B-SPNR-8 Real Time Augmented Reality (AR) Navigation Technology From Medical Images: Toward Medical Metaverse Era**

Participants

Yun-Sik Dho, Cheonju, Korea, Republic Of (*Presenter*) Stock options, Medical IP Co, Ltd

#### **PURPOSE**

Augmented reality is the essential underlying technology for metaverse implementation. Concomitant with the significant advances in computing technology, the novel concept of augmented reality (AR) registration and tracking have become possible. We introduce our newly developed real-time inside-out (RTIO) tracking AR navigation system.

#### **METHODS AND MATERIALS**

We developed RTIO tracking based on visual inertial odometry and a visual inertial simultaneous localization and mapping algorithm. The cube quick response (QR) marker and depth data obtained from light detection and ranging (LiDAR) sensors are used for continuous tracking. The registration accuracy was validated by both the intuitive method through visualization by the virtual 3-dimensional (3D) patient model for AR and the life-size 3D-printed patient model, and the quantitative method of identifying coordinates by matching errors. For depth realization, order-independent transparency (OIT), clipping, and annotation and measurement functions were developed. To validate depth realization technology, the AR model of a brain tumor patient was applied to its life-size 3D printed model.

#### **RESULTS**

By using RTIO tracking, we confirmed that the AR model remained consistent with the 3D-printed patient model without flutter, regardless of the movement of the visualization device. The red fiducial markers of the AR and the blue fiducial markers of the 3D-printed model were superimposed precisely at all locations. The registration accuracy was quantified using coordinates, and the average moving errors of the X-axis and Y-axis before and after the movement of visualization device were  $0.34 \pm 0.21$  and  $0.04 \pm 0.08$  mm (before) and  $0.39 \pm 0.22$  and  $0.05 \pm 0.09$  mm (after), respectively. Further, the application of OIT with multi-layer alpha blending (MLAB) and filtered alpha composites (FAC) improved the perception of overlapping internal brain structures. Clipping and annotation and measurement functions were also developed to aid depth perception, and worked perfectly during real-time coordination. We named this system METAMEDIP navigation.

#### **CONCLUSION**

s With these novel technologies developed for continuous tracking and depth perception in AR environments, we are able to overcome the critical obstacles in the development of clinically applicable AR neuronavigation in the metaverse era.

#### **CLINICAL RELEVANCE/APPLICATION**

It is verified augmented reality navigation can be used for brain tumor surgery planning and surgery and can be performed while checking anatomical structures intuitively compare to MRI-based neuro-navigation.

#### **R5B-SPNR-9 Association of Brain Viscoelastic Properties With Age and Glymphatic Function in Neurologically Normal Subjects: An Exploratory Study of MR Elastography Using a Novel Transducer**

Participants

Bio Joo, MD, Seoul, Korea, Republic Of (*Presenter*) Nothing to Disclose

#### **PURPOSE**

Magnetic resonance elastography (MRE) can image viscoelastic properties of tissues by measuring propagation of mechanical waves generated by a MRE transducer. The purpose of this study was to investigate the relationship between viscoelastic properties of the brain measured by MRE with a novel MRE transducer and normal aging and glymphatic function in neurologically normal subjects.

#### **METHODS AND MATERIALS**

A total of 52 neurologically normal subjects (mean age:  $48.1 \pm 15.5$  years, age range: 23 - 74, male:female = 23:29) were enrolled in this prospective study. MRE was conducted by using a transducer based on a rotational eccentric mass. Viscoelastic parameters, including storage modulus  $G'$ , loss modulus  $G''$ , magnitude of the complex shear modulus  $|G^*|$ , and phase angle  $\phi$ , were assessed in the centrum semiovale region. Glymphatic function was assessed using Diffusion Tensor Image Analysis Along the Perivascular Space index (ALPS-index). The viscoelastic parameters were compared with age and ALPS-index by Pearson correlation coefficient ( $r$ ).

#### **RESULTS**

All the viscoelastic parameters showed significantly negative correlations with age ( $G'$ :  $r = -0.44$ ,  $P < 0.01$ ;  $G''$ :  $r = -0.44$ ,  $P < 0.01$ ;  $|G^*|$ :  $r = -0.33$ ,  $P = 0.02$ ;  $\phi$ :  $r = -0.29$ ,  $P = 0.04$ ). ALPS-index showed significantly positive correlations with  $G'$  ( $r = 0.35$ ,  $P = 0.02$ ),  $G''$  ( $r = 0.37$ ,  $P = 0.02$ ), and  $|G^*|$  ( $r = 0.37$ ,  $P = 0.01$ ), but not with  $\phi$  ( $r = 0.25$ ,  $P = 0.11$ ).

#### **CONCLUSION**

s This study demonstrated the applicability of the brain MRE using a novel transducer and the relationship between brain viscoelastic properties and glymphatic function in healthy subjects over a wide range of age. The brain MRE with the gravitational transducer can potentially play a role in various neurological conditions by providing additional information of the brain.

#### **CLINICAL RELEVANCE/APPLICATION**

MRE using a gravitational transducer can assess brain viscoelastic properties, which may be associated with normal aging as well as glymphatic function.

Printed on: 02/07/23

## Abstract Archives of the RSNA, 2022

R5B-SPNR-1

### Effective Atomic Number as a Quantitative CT Marker for Myelin Content: A Validation Study Using Synthetic MRI

Thursday, Dec. 1 12:45PM - 1:15PM Room: Learning Center - NR DPS

#### Participants

Tomohito Hasegawa, Kagoshima, Japan (*Presenter*) Nothing to Disclose

#### PURPOSE

The effective atomic number (Zeff) reflects the elemental composition in biological tissues. Our purpose was to validate Zeff as a quantitative CT marker for myelin content in vivo.

#### METHODS AND MATERIALS

Fifteen patients (5 males and 10 females, age range from 35 to 84 years) with apparently normal cerebral parenchyma who underwent MRI scan and spectral detector CT scan within 1 month were included in this retrospective study. Images of myelin volume fraction (Vmy) were generated from synthetic MRI data using the multiparametric model based on the longitudinal and transverse relaxation rates and proton density. Whole brain spectral detector CT scans were performed using a dual-layer CT system, and images of the conventional CT value (CTconv), electron density (ED), and Zeff were obtained. The CT images were coregistered to the corresponding MR images using SPM12. Two independent observers placed elliptical ROIs in 12 gray matter (GM) and 12 white matter (WM) regions in each brain. Correlations between Vmy and CT parameters were evaluated using the Spearman's rank correlation coefficient for GM, WM, and altogether (GM+WM). The interobserver agreement was evaluated using the intraclass correlation coefficient (ICC).

#### RESULTS

The Vmy ranged from 0.881% to 32.06% in GM and from 25.34% to 48.32% in WM. CTconv, Zeff, and ED were significantly negatively correlated with Vmy for GM+WM. Zeff showed a strong negative correlation with Vmy ( $r=-0.783$ ,  $P<0.001$ ), which was stronger than CTconv ( $r=-0.715$ ,  $P<0.001$ ). ED showed only a moderate negative correlation with Vmy ( $r=-0.448$ ,  $P<0.001$ ). Only Zeff showed significant correlation with Vmy both in GM ( $r=-0.407$ ,  $P<0.001$ ) and WM ( $r=-0.215$ ,  $P=0.004$ ). The interobserver agreement was excellent for all measurement (ICC ranged from 0.897 to 0.984).

#### CONCLUSION

s Myelin content was more strongly reflected in Zeff than ED and CTconv. The negative correlation between Zeff and Vmy may be related to elemental composition of WM which is characterized by higher carbon and lower oxygen mass fractions than GM. The Zeff may serve as a quantitative CT marker for myelin content.

#### CLINICAL RELEVANCE/APPLICATION

The effective atomic number may serve as a quantitative CT marker for myelin content.

Printed on: 02/07/23

## Abstract Archives of the RSNA, 2022

R5B-SPNR-10

### Investigation on Pre ASiR-v on Image Quality and Radiation Dose of Non Spectral Scanning: A Phantom Study

Thursday, Dec. 1 12:45PM - 1:15PM Room: Learning Center - NR DPS

#### Participants

Yaoming Ma, (Presenter) Nothing to Disclose

#### PURPOSE

To investigate the influence of different pre adaptive statistical iterative reconstruction - Veo (ASiR-V) level on the image quality and radiation dose of non spectral scanning.

#### METHODS AND MATERIALS

A polypropylene cylindrical phantom (QSP Phantom) with nine tubes containing different concentrations of iodine (0, 2.5, 5, 10, 20 mgI/ml) was scanned in using spectral CT (Revolution, GE Healthcare) gemstone spectral imaging (GSI) mode using fast kV switch (80/140 kV), the tube current was 485mA, the layer thickness was 1.25mm, the collimation width was 80mm, noise index (NI) 5HU, pitch 0.992:1. Three groups of pre-ASiR-V level (30%, 40%, 50%) was used for spectral CT scanning. Eleven groups of images were selected from the scan center and five layers above and below. CT value and the area of ROI were measured. The CT dose index (CTDI) of different pre ASiR-V level scans was recorded. The dose length product (DLP), CT value and noise (SD) of the tube were recorded. Signal noise ratio (SNR) and contrast to noise ratio (CNR) of tubes was calculated. The DLP across three groups were analyzed by simple linear regression analysis. SD, SNR and CNR across three groups were analyzed by one-way ANOVA.

#### RESULTS

With the increase of pre-selected ASiR-V level, DLP showed decreasing trend. There was significant difference in DLP among groups (9.24mSv, 7.55mSv, 6.00mSv for 30%, 40%, 50% pre-ASiR-V, respectively.  $P < 0.05$ ). There were no significant differences in SD among groups (10.85±0.80(I20), 8.38±0.29(I10), 8.10±0.41(H2O), for 30% pre-ASiR-V, 10.86±0.74(I20), 8.42±0.29(I10), 8.05±0.46(H2O) 40% pre-ASiR-V, 11.36±0.76(I20), 7.97±0.29(I10), 7.76±0.34(H2O), 50% pre-ASiR-V,  $F = 2.130$ ,  $p > 0.05$ ).

#### CONCLUSION

s With the increase of pre-ASiR-V from 30%, 40%, 50%, radiation dose was reduced effectively, while the image quality was not changed significantly.

#### CLINICAL RELEVANCE/APPLICATION

Radiation dose is reduced with the increase of pre-ASiR-V and image quality keeps no change. Correlation of clinical application: through the basic research of phantom, compared with conventional kVp scanning, energy spectrum CT scanning can provide the same image quality scanning radiation dose, at the same time, energy spectrum CT scanning can provide different levels (40-140keV) of single energy and effective atomic number, and more energy spectrum information of base material than conventional kVp scanning, This study has guiding significance for the application of energy spectrum scanning in different clinical scenarios.

Printed on: 02/07/23

## Abstract Archives of the RSNA, 2022

R5B-SPNR-13

### Effects of Different Weighted Iterative Reconstruction on the Image Quality of Head and Neck CTA

Thursday, Dec. 1 12:45PM - 1:15PM Room: Learning Center - NR DPS

#### Participants

Deng Jie, (*Presenter*) Nothing to Disclose

#### PURPOSE

To investigate the effect of adaptive statistical iterative reconstruction (ASIR-V) algorithm on image quality and application value of head and neck CTA scanning.

#### METHODS AND MATERIALS

A total of 88 patients underwent head and neck CTA. Image reconstruction was performed using Filtered Back Projection (FBP), 20% ASIR-V algorithm, 40% ASIR-V algorithm, 60% ASIR-V algorithm and 80% ASIR-V algorithm, and perform volume projection and maximum density projection processing on the five groups of images. The effects of different reconstruction methods on the image quality of head and neck CTA were evaluated from the two aspects of objective measurement and subjective score.

#### RESULTS

Comparison of five groups of different reconstruction methods (filtered back projection method) FBP, 20% ASIR, 40% ASIR, 60% ASIR and 80% ASIR in the blood vessels of the head and neck (aortic arch, left common carotid artery, right common carotid artery) Artery, left middle cerebral artery, right middle cerebral artery, left vertebral artery, right vertebral artery, basilar artery) image quality parameter comparison, there is no statistical difference in CT value and SD value among the five groups of images among each blood vessel ( $P>0.05$ ); when comparing SNR and CNR, the blood vessels in the eight groups were  $80\%ASIR>60\%ASIR>40\%ASIR>20\%ASIR>FBP$  ( $P<0.05$ ). The Kappa value of the subjective rating of quality is 0.75, with strong consistency. The subjective scores were  $(4.13\pm 1.669)$ ,  $(4.30\pm 2.607)$ , and  $(4.93\pm 2.640)$ , respectively, and there was no significant difference in the subjective scores among the three groups ( $F=0.876$ ,  $P>0.05$ ).

#### CONCLUSION

With the gradual increase of the pre-ASIR-V weight, the CT value did not change significantly, and the image noise gradually increased. At the pre-ASIR-V level of 0~40%, the subjective image score was basically stable, and there was no significant difference in image quality. 60%~80% of the pre-ASIR-V level, the subjective scores in each group showed a gradually decreasing trend, and the image quality decreased obviously and gradually.

#### CLINICAL RELEVANCE/APPLICATION

When the ASIR value of different weights applied to head and neck CTA scans is 40%, the image quality is the best, which can be used in clinical practice.

Printed on: 02/07/23



## Abstract Archives of the RSNA, 2022

R5B-SPNR-14

### Description of Magnetic Resonance Fingerprinting in Patients with Amyotrophic Lateral Sclerosis

Thursday, Dec. 1 12:45PM - 1:15PM Room: Learning Center - NR DPS

#### Participants

Philipp Moser, MD, PhD, (*Presenter*) Nothing to Disclose

#### PURPOSE

Applicability of 3T Magnetic Resonance Fingerprinting (MRF) T1 and T2 mapping for quantitative analysis of the capsula interna in patients with amyotrophic lateral sclerosis (ALS)

#### METHODS AND MATERIALS

3T single-step MRF T1 and MRF T2 map data acquisition in addition to conventional multi-step MRI image acquisition was performed in patients diagnosed with ALS. In addition, DTI (b-values 0-2500) was analyzed in seven patients. A ROI-based analysis of relaxation times of the left and right capsula interna was performed. Interclass correlation (ICC, 3 repeats) and Pearson correlation coefficient were done for statistical analysis. Data presented as mean +/- SD.

#### RESULTS

Eighteen patients (mean age 63.712.7 years, male 61%) were included. We found excellent intra-observer ICC values for MRF T1R 0.985 (0.98-0.99, CI 95%) and MRF T2R 0.998 (0.99-1.0, CI 95%). The mean relaxation time of MRF T1R was 103634.1 ms and of MRF T2R was 2742308 ms. We observed a correlation between the MRF T1R values of the left and right capsula interna ( $R=0.65$ ,  $p=0.003$ ) and the MRF T2R values of the left and right capsula interna ( $R=0.96$ ,  $p<0.0001$ ). In addition, we found a correlation between MRF T1R and DTI values ( $R= -0.54$ ,  $p=0.044$ ) but no correlation between MRF T1R and ADC nor between MRF T2R and ADC or DTI.

#### CONCLUSION

s MRF T1 and T2 mapping of the capsula interna was successfully performed in patients with ALS and quantitative assessment may provide additional support in the diagnosis of upper motoneuron involvement.

#### CLINICAL RELEVANCE/APPLICATION

MRF may assist in the assessment of upper motoneuron involvement and disease progression in patients with ALS.

Printed on: 02/07/23

## Abstract Archives of the RSNA, 2022

R5B-SPNR-15

### A Clinical Application of 3D High-Resolution Contrast Enhanced MR Neurography With Precise Fat Suppression in Lumbosacral Plexus

Thursday, Dec. 1 12:45PM - 1:15PM Room: Learning Center - NR DPS

#### Participants

Xiangchuang Kong, Wuhan, China (*Presenter*) Nothing to Disclose

#### PURPOSE

The purpose of this study was to investigate the clinical application of precise fat suppression for 3D high-resolution contrast-enhanced MR neurography of lumbosacral plexus.

#### METHODS AND MATERIALS

32 patients were prospectively selected: 14 patients (group A) with preset TI, and 22 patients (group B) with accurately calculated TI values. All patients were scanned using a 3.0 T MR scanner (Ingenia CX, Philips Healthcare, the Netherlands) with a 32-element phased-array coil. After intravenous injection of Gd-DTPA (0.15mmol/kg), patients were scanned using the 3D NerveView sequence: TI=220ms in group A and calculated TI in group B by a low resolution and fast 3D NerveView scanning with different TI values (TI=180 200 220 230 250 260 270 280 300 320 ms, TR=2200ms). Images were reconstructed on the scanner by the vendor-supplied software package (Compressed SENSE, Philips Healthcare). The signal intensity of fat, and nerve was measured on the original graph and the MIP graph respectively and the signal intensity ratio of nerve to fat was calculated for evaluation of fat suppression. Then the nerve/fat signal ratio (NFR) was calculated. The IBM SPSS22.0 software was used for statistical analysis, and NFR between the two groups was compared by unpaired sample t-test. P<0.05 indicated a statistically significant difference.

#### RESULTS

1. The proposed TI scout method could improve fat suppression in MRN dramatically. The calculated NFR (precise fat suppression) ( $13.26\pm 5.47$ ) was about 425.4% higher than that in the preset TI situation (220ms) ( $2.39\pm 0.55$ ). The difference between the two groups was statistically significant ( $t=26.495$ ,  $P<0.05$ ). 2. The detection rates of nerve roots and trunks by the two methods were 100% (18/18, 14/14); The detection rates of the nerve tracts and branches in precise fat-suppression sequence were 94.4% (17/18) and 83.3% (15/18), respectively. The detection rates of nerve tracts and branches in the preset method were 92.9% (13/14) and 71.4% (10/14), respectively. There was no statistically significant difference between the two methods in the detection rate of nerve tracts and branches ( $P=1.00$ , 0.67).

#### CONCLUSION

A fast and easy TI scout-based strategy was proposed to improve the fat suppression in 3D MRN of the lumbosacral plexus, which enhanced the image quality significantly. The NFR was increased by about 425.4% more than that in the vendor-provided preset TI scheme.

#### CLINICAL RELEVANCE/APPLICATION

A fast and easy TI scout-based strategy was proposed to improve the fat suppression in 3D MR neurography of lumbosacral plexus, which enhanced the image quality significantly. The nerve fat signal intensity ratio was increased by about 425.4% than that in vendor-provided preset TI scheme.

Printed on: 02/07/23



## Abstract Archives of the RSNA, 2022

R5B-SPNR-16

### Rapid Susceptibility-Weighted Imaging using Wave CAIPI for Differentiation of Diamagnetic and Paramagnetic Signal

Thursday, Dec. 1 12:45PM - 1:15PM Room: Learning Center - NR DPS

#### Participants

Parker Lawson, MD, (*Presenter*) Nothing to Disclose

#### PURPOSE

Susceptibility-weighted imaging (SWI) is primarily used for the detection of paramagnetic and diamagnetic substances, typically hemorrhage and calcifications respectively. Differentiation between the two can be difficult on post-processed SWI images as both create a similar magnitude of susceptibility and appearance; however, SWI phase imaging can often distinguish the two as their phase shifts and resultant signals are opposite of each other. Unfortunately, differentiation is not always achievable for larger lesions. Wave CAIPI SWI has been recently developed as an alternative to conventional SWI with reduced scan times. Prior to this investigation, Wave CAIPI SWI phase had not been evaluated for its ability to differentiate between paramagnetic and diamagnetic susceptibility.

#### METHODS AND MATERIALS

126 Brain MRI studies were prospectively selected with the inclusion of a Wave CAIPI SWI sequence at 1.5T and 3T MR units. The images were evaluated by two radiologists for presence and characterization of susceptibility on both conventional SWI (scan time: 4.8 minutes) and Wave CAIPI (scan time: 1.14 minutes) phase and confirmed with head CTs.

#### RESULTS

Of the 126 studies, 64 demonstrated a focus of susceptibility on conventional SWI and Wave CAIPI SWI. All 64 were identifiable as diamagnetic or paramagnetic on Wave CAIPI phase with homogeneous black or white signal. There were a total of 31 cases in which larger lesions demonstrated heterogeneous or dipole signal on conventional SWI phase, making interpretation difficult; however, Wave CAIPI SWI phase demonstrated homogenous signal facilitating interpretation that was confirmed by CT.

#### CONCLUSION

s Wave CAIPI SWI phase is a non-inferior alternative to conventional SWI phase in differentiating between paramagnetic and diamagnetic signal and aids interpretation of larger lesions. The findings of this study, coupled with reduced scan times, support the inclusion of Wave CAIPI SWI sequences into routine brain imaging.

#### CLINICAL RELEVANCE/APPLICATION

Wave CAIPI SWI phase images offer a non-inferior alternative to conventional SWI for differentiating between intracranial hemorrhage and calcification that can be acquired within less than 1/4th of the scan time.

Printed on: 02/07/23

## Abstract Archives of the RSNA, 2022

R5B-SPNR-17

### Aberrant Spontaneous Brain Activity in Patients with Dysthyroid Optic Neuropathy: A Resting-State Functional MRI Study

Thursday, Dec. 1 12:45PM - 1:15PM Room: Learning Center - NR DPS

#### Participants

Ping Liu, MS, (*Presenter*) Nothing to Disclose

#### PURPOSE

Increasing evidence indicated that DON is not only a disease limited to the visual system, it is an eye-brain disease involves multiple brain regions. The purpose of the study was to investigate the brain functional alteration in patients with DON by evaluating the spontaneous neural activity changes using resting-state functional magnetic resonance imaging (rs-fMRI) with the regional homogeneity (ReHo).

#### METHODS AND MATERIALS

Forty-seven TAO patients, including 20 with neuropathy (DON) and 27 without neuropathy, and 28 healthy controls (HCs) were recruited, matched for weight, height, age, sex, and educational level. All participants underwent resting-state functional nuclear resonance imaging, and the characteristics of spontaneous brain activity were evaluated employing the regional homogeneity (ReHo) method. Each patient with dysthyroid optic neuropathy also completed the ophthalmopathy examination. The ReHo values were compared among groups. Correlations between ReHo values and clinical metrics were assessed.

#### RESULTS

Compared with TAOs, DON showed significantly decreased ReHo values in the left insula and right superior temporal gyrus, and increased ReHo values in left posterior cingulum and left precentral cuneus. Compared with HCs, TAOs also showed significantly decreased ReHo values in the left posterior cingulum. Additionally, the changed ReHo values were correlated visual acuity, mean deviation (MD) and pattern standard deviation (PSD) of visual field, and the amplitude and absolute latency of P100 of the visual-evoked potentials (VEPs).

#### CONCLUSION

DON patients had altered spontaneous brain activities in the left insula, right superior temporal gyrus, left posterior cingulum and left precentral cuneus. And these brain functional abnormalities associated with the visual function.

#### CLINICAL RELEVANCE/APPLICATION

The abnormal spontaneous brain activities may be related to the pathological mechanism of DON, which may provide a valuable basis for further research on the clinical management of DON. Moreover, regional homogeneity has the potential for early diagnosis and prevent DON.

Printed on: 02/07/23



## Abstract Archives of the RSNA, 2022

R5B-SPNR-18

### Identification of Autism Spectrum Disorder (ASD) Patients Using Functional MRI - Nonlinear, Directed, Multivariate Brain Connectivity Analysis by Non-Linear Large-scale Granger Causality (IsNGC)

Thursday, Dec. 1 12:45PM - 1:15PM Room: Learning Center - NR DPS

#### Participants

Ali Vosoughi, Rochester, NY (*Presenter*) Nothing to Disclose

#### PURPOSE

To develop and evaluate a novel machine learning method for identifying patients with Autism Spectrum Disorder (ASD) using large-scale Nonlinear Granger Causality (IsNGC) by capturing connectivity differences in resting-state functional MRI (rsfMRI).

#### METHODS AND MATERIALS

We included the subset of all 93 rsfMRI data sets acquired from ASD patients and healthy controls from two institutions (36 from Olin, Institute of Living at Hartford Hospital, and 57 from University of Pittsburgh School of Medicine: Longitudinal Sample) represented in the publicly available preprocessed Autism Brain Imaging Data Exchange I (ABIDE I) data repository. For calculating directed functional connectivity between brain regions, we have recently developed the large-scale Nonlinear Granger Causality (IsNGC) algorithm [Citation blinded for review] that leverages radial basis function kernel transformation for causal modeling in high-dimensional fMRI time series. A 100-iteration cross-validation approach with 80%/20% train/test ratio was applied, where feature selection was performed on each training set using Kendall's tau rank correlation, followed by support vector machine classification. To quantitatively evaluate diagnostic accuracy of IsNGC for correctly classifying ASD patients and normal controls, we compare its performance with both a recent state-of-the-art causal discovery method (PCMCI, [Runge et al., Science, 2019]), and the current clinical fMRI analysis standard of cross-correlation (CC), reporting accuracy, area under ROC curve (AUC), and f1-score.

#### RESULTS

The IsNGC rsfMRI analysis method significantly outperformed both PCMCI and the clinical standard CC techniques at classifying ASD patients from healthy subjects, with accuracy/AUC/f1 score of 100%/1.0/100% for IsNGC, 75.4%/0.69/70.0% for PCMCI, and 65.8%/0.61/62.4% for CC, respectively.

#### CONCLUSION

Our results suggest that IsNGC significantly improves the diagnostic accuracy of correctly identifying patients with ASD from rsfMRI neuroimaging. We conclude that, when compared to both conventional CC analysis and state-of-the-art PCMCI, IsNGC is better suited to capture disease-related brain network connectivity changes in ASD patients.

#### CLINICAL RELEVANCE/APPLICATION

The IsNGC method classifies Autism Spectrum Disorder (ASD) patients and controls by identifying relevant changes in fMRI connectivity, suggesting its potential usefulness as a novel diagnostic imaging biomarker for neurologic disease.

Printed on: 02/07/23

## Abstract Archives of the RSNA, 2022

R5B-SPNR-19

### Three-vessel Selective Pseudo-continuous Arterial Spin Labeling Using Designed Metal Artifacts: A Feasibility Study

Thursday, Dec. 1 12:45PM - 1:15PM Room: Learning Center - NR DPS

#### Participants

Keizo Tanitame, MD, Hiroshima, Japan (*Presenter*) Nothing to Disclose

#### PURPOSE

Arterial spin labeling (ASL) of magnetic resonance (MR) imaging is a noninvasive evaluation method for assessing cerebral perfusion, and delineation of individual perfusion territories of cerebral arteries can help in the evaluation of the collateral pathway development in cerebrovascular disease patients. We evaluated the feasibility of three-vessel selective pseudo-continuous ASL (pCASL) using designed metal artifacts.

#### METHODS AND MATERIALS

We recruited fifteen healthy volunteers, and firstly obtained MR angiography of the brain and whole brain perfusion maps of all the cerebral arteries using three-dimensional pCASL. Then while confirming the anatomical location of common carotid arteries (CCAs), we placed one or two small insulated metals on the skin surface near the right, left or bilateral CCAs at the labeling plane, and performed vessel-selective pCASL using three different kinds of local labeling suppression. From analysis of the perfusion maps of all the cerebral arteries, the right CCA and vertebrobasilar artery (VBA), the left CCA and VBA, and only the VBA, two independent observers inferred and drew the cerebral arterial atlases, and another assessed the coincidence of the schematic atlas and MRA image in each subject.

#### RESULTS

Three-vessel selective pCASL imaging could be performed in all subjects, and no subjects complained of local heat sensation related to the insulated metals. The coincidence rate of inferred cerebral arterial atlases and MRA images was 86.7% in each observer. In five subjects with incomplete circle of Willis, contralateral routes from well-developed communicating arteries could be inferred from the vessel-selective pCASL images. In a subject with an aberrant branch of the left posterior artery, the perfusion territory of the branch was shown in the vessel-selective pCASL images. Interobserver agreement was 100%. In two subjects, two observers independently suspected anterior to posterior circulation through well-developed bilateral posterior communicating arteries from the vessel-selective pCASL images, but MRA showed that the arteries were absent. These misunderstandings were thought to be due to unexpected suppression effect of the metals on VBA labeling.

#### CONCLUSION

s We presented a three-vessel selective pCASL using designed metal artifacts. The perfusion territories of individual cerebral arteries could be delineated differently, but attention is needed for the depth of the vertebral arteries.

#### CLINICAL RELEVANCE/APPLICATION

Three-vessel selective pseudo-continuous arterial spin labeling using designed metal artifacts can be used to obtain individual perfusion maps of bilateral carotid and vertebrobasilar arteries.

Printed on: 02/07/23

## Abstract Archives of the RSNA, 2022

R5B-SPNR-2

### Feasibility of Ultrashort Echo Time Quantitative Susceptibility Mapping (UTE-QSM) With a 3D Cones Trajectory in the Human Brain

Thursday, Dec. 1 12:45PM - 1:15PM Room: Learning Center - NR DPS

#### Participants

Sam Sedaghat, MD, La Jolla, CA (*Presenter*) Nothing to Disclose

#### PURPOSE

Over the past decade, quantitative susceptibility mapping (QSM) has emerged as a promising quantitative MR imaging technique to assess the microenvironment in the brain. In literatures, many new QSM techniques have been proposed, but non-Cartesian ultrashort echo time (UTE) sequences have not been explored. In this study, the feasibility of UTE-QSM based on a 3D spiral cones trajectory is demonstrated in the brain.

#### METHODS AND MATERIALS

The UTE-QSM sequence based on a 3D cones trajectory was implemented on a 3T clinical MRI scanner (MR 750, GE Healthcare). To show the feasibility, an ex vivo experiment was performed on 3 fresh human brain samples using an 8-ch head coil with the following imaging parameters: TR = 50 ms, TE = 0.032, 4.4, 8.8, 13.2, 17.6, and 22 ms, FA = 20°, FOV = 220x220x80 mm<sup>3</sup>, matrix = 256x256x80, and readout bandwidth = 166.6 kHz. The scan was repeated with 8 different stretching factors (SFs) of the 3D cones spiral arms: 1.0, 1.1, 1.2, 1.3, 1.4, 1.5, 1.6, and 1.7 with the corresponding scan times of 1383, 1229, 1099, 1005, 920, 857, 794, and 745 sec (acceleration factors (AFs) of 1.00, 1.13, 1.26, 1.38, 1.50, 1.62, 1.74, and 1.86), respectively. An in vivo UTE-QSM was performed on five healthy volunteers (37.6 ± 6.7 years old) using the same imaging protocol except for: matrix = 220x220x80, FOV = 220x220x160 mm<sup>3</sup>, SF = 1.7 (AF = 1.86), and scan time = 645 sec. The reconstructed complex MR images were processed with a UTE-QSM pipeline established based on a MEDI toolbox.

#### RESULTS

In the ex vivo experiment, a very high correlation in pixelwise QSM values (i.e., susceptibility) was found between SF of 1.0 and SFs from 1.1 to 1.7: Pearson's correlation 0.987, 0.981, 0.976, 0.972, 0.970, 0.962, and 0.953, respectively with all p-values < 0.05. In the in vivo experiment, the measured QSM values in cortical gray matter, juxtacortical white matter, corpus callosum, caudate, and putamen were 25.4 ± 4.0, -21.8 ± 3.2, -22.6 ± 10.0, 77.5 ± 18.8, and 53.8 ± 7.1 ppb in five volunteers, which correspond well with the values reported in literatures.

#### CONCLUSION

In this study, we demonstrated the clinical feasibility of 3D UTE-QSM in the brain for the first time. UTE-QSM with a stretched cones trajectory (i.e., acceleration up to 1.86x) showed reliable estimation of susceptibility in the brain.

#### CLINICAL RELEVANCE/APPLICATION

The proposed UTE-QSM technique based on an efficient cones trajectory allows whole brain susceptibility mapping in a clinically feasible scan time of ~11 min. UTE-QSM is likely to provide more accurate assessment of calcification, hemorrhage, iron overload, and tumor vascularization as UTE acquisition allows direct imaging of short T2 tissues and robust mapping of their susceptibilities. Moreover, the non-Cartesian UTE-QSM is likely to be more robust to patient motion.

Printed on: 02/07/23

## Abstract Archives of the RSNA, 2022

R5B-SPNR-20

### The Value of Deep Learning Reconstruction Algorithm in CT Whole Brain Perfusion in Patients with Ischemic Stroke

Thursday, Dec. 1 12:45PM - 1:15PM Room: Learning Center - NR DPS

#### Participants

Limin Lei, Zhengzhou, China (*Presenter*) Nothing to Disclose

#### PURPOSE

To compare deep learning-based image reconstruction (DLIR) algorithm and adaptive statistical iterative reconstruction-Veo (ASIR-V) algorithm on the image quality and brain perfusion parameters of whole brain CT perfusion scanning in patients with ischemic stroke due to large vessel occlusion.

#### METHODS AND MATERIALS

A total of 27 patients with ischemic stroke due to large vessel occlusion were collected prospectively in this study, including 15 cases of acute and 12 cases of chronic, consisted of 22 males and 5 females with a median age of 54(range 30-79 years). All patients underwent whole brain perfusion imaging using latest-generation 16 cm detector coverage CT scanner (APEX CT, GE Healthcare). CT datasets were reconstructed using ASIR-V at a level of 80% (80%ASIR-V) and DLIR with high reconstruction strength level (DLIR-H) with 1.25-mm slice thickness. The volumetric CT dose index (CTDIvol) and dose length product (DLP) for each patient scan were recorded. Objective parameters including CT values and standard deviation (SD) in frontotemporal lobe, gray matter nucleus (caudate lobe, lenticular, thalamus) and posterior limb of internal capsule on the contralateral side, as well as the signal-to-noise ratio (SNR) and contrast-to-noise ratio (CNR) of gray matter nucleus were compared. We performed brain perfusion analysis based on CT Perfusion 4D package and calculated the perfusion parameters such as CBF, CBV, MTT and TTP at the same site as the CT values were measured. Moreover, the functional analysis of ipsilateral cerebral infarction including the brain tissue volume, Tmax average value, CBV average value were conducted with the threshold as CBV beyond 1ml/100g while Tmax within 6 seconds. Differences between continuous data were tested using paired t test or Wilcoxon rank test.

#### RESULTS

DLIR-H had a lower image noise in frontotemporal lobe, gray matter nucleus and posterior limb of internal capsule than 80% ASIR-V (all  $P < 0.001$ ), while higher SNR and CNR of gray matter nucleus(all  $P < 0.001$ ) without changing the CT values. Moreover, there was no significant difference between DLIR-H and 80% ASIR-V in the perfusion parameters including CBF, CBV, MTT and TTP of gray matter and white matter as well as the Tmax average value, CBV average value with the threshold as CBV beyond 1ml/100g while Tmax within 6 seconds.

#### CONCLUSION

In cerebral perfusion scan of patients with ischemic stroke, DLIR-H reconstruction algorithm can effectively improve image quality without changing perfusion parameters and functional parameters.

#### CLINICAL RELEVANCE/APPLICATION

Deep learning reconstruction algorithm can reduce image noise without changing the vital diagnostic parameters, which throws light on low-dose CT acquisition protocol of clinical cerebral perfusion scans.

Printed on: 02/07/23

## Abstract Archives of the RSNA, 2022

R5B-SPNR-3

### Label-Free Spectral X-Ray Method for Non-invasively Quantifying Amyloid Burden in the Human Brain

Thursday, Dec. 1 12:45PM - 1:15PM Room: Learning Center - NR DPS

#### Participants

Eshan Dahal, (*Presenter*) Nothing to Disclose

#### PURPOSE

To describe a spectral x-ray method based on the small-angle elastic scattering of photons for measuring amyloid burden in the human brain.

#### METHODS AND MATERIALS

We built a prototype system capable of probing an intact human head using a polychromatic x-ray source with tungsten anode in the diagnostic x-ray energy range and a 2D spectroscopic photon-counting detector (80 x 80, 250-micron pixels) with a 1-mm cadmium telluride (HEXITEC) to record energy (in 1-keV bins) and location of each scattered photons. An energy-dependent transmission correction factor was calculated using spectroscopic measurements of the primary beam. The x-ray beam was pinhole collimated to create a 2-mm pencil beam to irradiate the human head phantom with and without embedded targets. We used a commercially available tissue-mimicking (brain and skull) phantom with slabs and an anthropomorphic human head phantom to assess the recovery of the scattering signature for targets with varying concentrations. By comparing the scattering profiles for areas with and without targets, we report amyloid burden as the area-under-the-peak for the characteristic target peaks which correlates with the mass fraction of amyloid plaques.

#### RESULTS

Measurements of the head phantom with embedded caffeine targets show well-defined characteristic Bragg peaks at momentum transfer of 8.4 and 18.7 nm<sup>-1</sup>. We recovered the characteristic peaks with exposure times as low as 60 s. Measurements investigating the effect of sample thickness up to 16 cm and spectral x-ray energies from 30 to 120 keV was evaluated to maximize the scattering signal from the targets.

#### CONCLUSION

s The findings of the study suggest that the spectral x-ray-based method for non-invasively detecting and quantifying amyloid-like targets embedded within a human head has promise.

#### CLINICAL RELEVANCE/APPLICATION

Amyloid burden can be used to monitor onset and progression of Alzheimer's disease. The spectral small-angle method described in this study has potential to facilitate more efficient therapeutic clinical trials by providing a fast and label-free amyloid plaque quantification tool as an alternative to amyloid-specific positron emission tomography.

Printed on: 02/07/23

## Abstract Archives of the RSNA, 2022

R5B-SPNR-4

### How Confident Are You - Contrast-Enhanced T1-weighted SPACE Versus 3D FLASH Sequences for the Detection of Brain Metastases

Thursday, Dec. 1 12:45PM - 1:15PM Room: Learning Center - NR DPS

#### Participants

Maria Gule-Monroe, MD, Houston, TX (*Presenter*) Nothing to Disclose

#### PURPOSE

This study aimed to evaluate the utility of contrast-enhanced (CE) T1-weighted 3D fast spin-echo-based SPACE sequence, by comparing to the gradient-echo-based 3D-FLASH sequence (without inversion recovery, IR) for the detection of brain metastases at 3T.

#### METHODS AND MATERIALS

220 patients at a single institution who were scheduled for brain MRI underwent optimized CE T1-weighted SPACE and 3D-FLASH sequences at 3T as part of a practice quality improvement project. Each scan took approximately 4 minutes, and the order of the two sequences was balanced among the patients. The medical records were retrospectively reviewed, and 79 patients found to have brain metastases at the time of imaging were included. Images were evaluated by 5 CAQ certified neuroradiologists, with at least 2-week separation between scoring sequences for the same patient and 20 patients scored by 2 radiologists. Parameters evaluated included number of metastatic lesions, number of indeterminate lesions, visual assessment of lesion margin, visual assessment of contrast to noise ratio (CNR), presence of image artifact, and overall image quality. In addition, CNR was quantified for solidly enhancing lesions greater than 1 cm.

#### RESULTS

SPACE detected more lesions than 3D-FLASH in 35 patients, while 3D-FLASH detected more lesions in 10 patients. A greater number of indeterminate lesions were seen on 3D-FLASH (27 patients) vs SPACE (9 patients), mostly related to presence of vascular enhancement seen in 3D-FLASH images. When rating overall image quality, lesion margin and CNR on a Likert scale, SPACE performed better than 3D-FLASH with more image artifact seen on 3D-FLASH. Higher quantitative CNR was found in SPACE than 3D FLASH images (mean=26.9 vs. 19.8, respectively, n=16, p=0.054).

#### CONCLUSION

s This is the first study to date comparing the performance of CE T1-weighted SPACE to non-IR 3D-FLASH sequence for the detection of brain metastases. The SPACE sequence detects a greater number of metastatic lesions and is rated higher for image quality, lesion margin and CNR with less artifact. Gradient Echo are the most commonly used sequences for detection and radiation treatment planning of brain metastases. Superiority of SPACE for lesion detection and confidence has implications across the diagnostic and therapeutic imaging journey.

#### CLINICAL RELEVANCE/APPLICATION

This is the first study to date evaluating the performance of CE T1-weighted SPACE to non-IR 3D-FLASH for the detection of brain metastases. Superiority of SPACE for lesion detection and confidence has implications across the diagnostic and therapeutic imaging journey.

Printed on: 02/07/23

## Abstract Archives of the RSNA, 2022

R5B-SPNR-5

### Characterization of Lenticulostriate Arteries by Combining High Resolution Black-blood T1-weighted with Variable Flip Angles Compressed Sensitivity Encoding at 3.0 Tesla

Thursday, Dec. 1 12:45PM - 1:15PM Room: Learning Center - NR DPS

#### Participants

Yukun Zhang, Dalian, China (*Presenter*) Nothing to Disclose

#### PURPOSE

To visualize and characterize lenticulostriate arteries (LSAs) in a short period time on a 3.0T MR scanner, we investigated the feasibility of high resolution black-blood T1-weighted with variable flip angles (T1w TSE-VFA) accelerated by compressed sensitivity encoding (CS-T1w TSE-VFA) and further identify the optimal acceleration factors (AFs) for clinical use.

#### METHODS AND MATERIALS

14 healthy volunteers (6 males, mean age 29.57±6.17 years) and 7 patients with cerebral infarction (4 males, mean age 50.06±20.13 years) were prospectively included and divided into the volunteer group and patient group. T1w TSE-VFA images with different AFs (Parallel imaging (PI) AF=3, CS AF=3,4,5,6) (Table 1) were acquired on a 3.0T scanner (uMR Omega, Imaging Healthcare, Shanghai, China). For objective evaluation, the regions of interest (ROIs) of the middle cerebral artery (MCA), the longest LSA, and corresponding white matter on the original or reformatted images were delineated (Fig.1 a-b). Then the signal intensity (SI) and standard deviation (SD) were measured and contrast-to-noise ratio (CNR): (SILSA/MCA-SIWM)/SDWM was further calculated. For subjective evaluation, the the number and length of LSAs of T1w (Fig.1 c) and subjective scoring (Fig.1 d-f) of T1w TSE-VFA with different AFs were measured. Paired t-test were used to compare CNR of MCA and LSA, number and length of LSAs, and image quality between T1w TSE-VFA with PI AF=3 and with CS AF=3 to 6.

#### RESULTS

For the volunteer group, when CS AF=6, the number of LSAs were significantly different from that of PI-T1w TSE-VFA ( $p<0.05$ ); when CS AF=5, the length of LSAs and subjective scoring were significantly different from PI-T1w TSE-VFA ( $p<0.05$ ) (Table.3 , Figs.2 and 4). For the patient group, when CS AF=6, the CNR of LSA and subjective scoring were significantly different from PI-T1w TSE-VFA ( $p<0.05$ ); when CS AF=5, length and number of LSAs were significantly different from PI-T1w TSE-VFA ( $p<0.05$ ) (Table 2, Figs. 3 and 4).

#### CONCLUSION

s CS-T1w TSE-VFA with AF of 3 can provide a better LSA display but time longer; with AF of 4 can balance visualization of LSAs and acquisition time. These sequences had the potential to be used in clinical to provide diagnostic information for preventive medicine at 3 Tesla.

#### CLINICAL RELEVANCE/APPLICATION

CS-T1w TSE-VFA can be used as a non-invasive head microvasculature examination in asymptomatic subjects and patients with cerebrovascular disease, which will be an important asset in preventive medicine.

Printed on: 02/07/23



## Abstract Archives of the RSNA, 2022

R5B-SPNR-6

### Reproducible Brain MRI Radiomics Features Achieving Test-Retest, Multi-Scanner, and Computational Reproducibility: A Phantom Study

Thursday, Dec. 1 12:45PM - 1:15PM Room: Learning Center - NR DPS

#### Participants

Yunhwa Roh, (*Presenter*) Nothing to Disclose

#### PURPOSE

The image biomarker standardization initiative helped improving computational reproducibility of radiomics features on CT. Nonetheless, reproducible multiparametric MRI sequences across multi-scanner and different algorithms are yet to be standardized. We aimed to determine reproducible radiomic features in multiparametric sequences with multi-scanner and computational methods setting.

#### METHODS AND MATERIALS

A phantom was scanned twice on a clinical 3 T system (Philips, Siemens, and GE) with T1-weighted (T1w), T2-weighted (T2w), and diffusion-weighted imaging (DWI) sequences. Radiomic features were extracted using pyradiomics (110 features) and MITK (the Medical Imaging Interaction Toolkit) (364 features) from each test-retest and multi-scanner setting. Stable radiomics features were calculated when maintaining 5% cut-off of averaging features among different imaging methods (test-retest and multi-scanner) and computational methods. The stable features were calculated concordance- and intraclass correlation coefficients (CCC and ICC) and compared among sequences.

#### RESULTS

The number of robust features (CCC = 0.90) was higher for features calculated from DWI than from T1w and T2w images in test-retest analysis. From imaging reproducibility, a total of 79 (23.9%) of 330 features from pyradiomics and 473 (43.3%) of 1092 MITK features showed excellent robustness (ICC = 0.90). Applying both imaging and computational reproducibility cut-off, total 58 (17.5% from pyradiomics and 5.3% from MITK) features showed robustness across test-retest, multi-scanner, and computational methods. DWI images provided the highest percentage of robust features (23 out of 58, 39.6%), followed by T2w (19 out of 58, 32.7%) and T1w (16 out of 58, 27.6%).

#### CONCLUSION

Only between 5.3% and 17.5% radiomics features from multiparametric MRI showed excellent robustness from both imaging with computational reproducibility. Diffusion-weighted imaging showed best robustness, and care must be taken in the interpretation of clinical studies using non-robust features.

#### CLINICAL RELEVANCE/APPLICATION

A recent multi-center study from the image biomarker standardization initiative (IBSI) helped improving computational reproducibility of radiomics features on CT. Nonetheless, reproducible multiparametric MRI sequences across multi-scanner and different algorithms are yet to be standardized. In this study, we found only between 5.3% and 17.5% radiomics features from multiparametric MRI showed excellent robustness from both imaging with computational reproducibility. Diffusion-weighted imaging showed best robustness, and care must be taken in the interpretation of clinical studies using non-robust features.

Printed on: 02/07/23

## Abstract Archives of the RSNA, 2022

R5B-SPNR-7

### Novel Technique of Simultaneous Non-contrast MR Angiography and Multi-contrast Vessel Wall Imaging (Simul-MRA+VWI) Using Multi-Shot Gradient-echo EPI (MSG-EPI) for Carotid Artery Evaluation

Thursday, Dec. 1 12:45PM - 1:15PM Room: Learning Center - NR DPS

#### Participants

Yasuhiro Nagai, RT, Osaka, Japan (*Presenter*) Nothing to Disclose

#### PURPOSE

MRI for carotid artery has been widely used to assess the luminal stenosis and plaque characterization. However, separate acquisition of MR Angiography (MRA) and vessel wall imaging (VWI) require the long scan time and cause the misregistration. The hybrid of multi-shot gradient-echo EPI with modification of Look-Locker method enable to obtain the Simultaneous MRA and VWI (Simul-MRA+VWI) in a single scan. This study aims to compare the qualitative and quantitative image analysis for carotid artery between Simul-MRA+VWI and conventional scans.

#### METHODS AND MATERIALS

We obtained the carotid artery MRI with Simul-MRA+VWI and conventional sequences (TOF and IR-GRE) in 10 healthy volunteers using 3T-MRI. The phantom of simulated plaque (blueberry jam: T1=300msec) was scanned together with volunteers. Simul-MRA+VWI provide multi-contrast images with different inversion time (TI) after IR pulse. Images with short TI yield MRA as bright blood imaging and images with null TI of blood yield VWI as dark blood T1 weighted images. The image quality of MRA and VWI were evaluated using the 4-point scale. In MRA, SNR of blood and contrast ratio (CR) between blood and muscle were measured. In VWI, CR between blood and muscle and CR between plaque and muscle were measured. Then, we compared these parameters between Simul-MRA+VWI and conventional sequences.

#### RESULTS

The mean acquisition time of Simul-MRA+VWI sequence was 213sec, which was 60.7% shorter than the conventional two scans. There were no significant differences in image quality of MRA and VWI between Simul-MRA+VWI and conventional scans. In MRA, Simul-MRA+VWI had slightly higher SNR of blood and significantly higher CR between blood and muscle compared with TOF. In VWI, CR between blood and muscle (as black blood effect) tended to be higher in Simul-MRA+VWI than in IR-GRE but showed the no significant difference. CR between plaque and muscle (T1 contrast) was significantly higher in Simul-MRA+VWI than in IR-GRE with moderate correlation between two methods ( $r=0.78$ )

#### CONCLUSION

Simul-MRA+VWI is a promising technique for shortening scan time with equivalent image quality to conventional sequences and yielding higher contrast MRA and VWI of carotid artery.

#### CLINICAL RELEVANCE/APPLICATION

Simul-MRA+VWI enable the simultaneous imaging of both carotid artery lumen and vessel wall with equivalent image quality to conventional methods. Our proposed method is practical approach for the reduction of scan time and the integrated assessment of both MRA and VWI without misregistration due to separate acquisition. Further, MRA and VWI obtained by this method can provide the higher contrast and permit the optimal contrast by determination from multiple TI images.

Printed on: 02/07/23



## Abstract Archives of the RSNA, 2022

R5B-SPNR-8

### Real Time Augmented Reality (AR) Navigation Technology From Medical Images: Toward Medical Metaverse Era

Thursday, Dec. 1 12:45PM - 1:15PM Room: Learning Center - NR DPS

#### Participants

Yun-Sik Dho, Cheonju, Korea, Republic Of (*Presenter*) Stock options, Medical IP Co, Ltd

#### PURPOSE

Augmented reality is the essential underlying technology for metaverse implementation. Concomitant with the significant advances in computing technology, the novel concept of augmented reality (AR) registration and tracking have become possible. We introduce our newly developed real-time inside-out (RTIO) tracking AR navigation system.

#### METHODS AND MATERIALS

We developed RTIO tracking based on visual inertial odometry and a visual inertial simultaneous localization and mapping algorithm. The cube quick response (QR) marker and depth data obtained from light detection and ranging (LiDAR) sensors are used for continuous tracking. The registration accuracy was validated by both the intuitive method through visualization by the virtual 3-dimensional (3D) patient model for AR and the life-size 3D-printed patient model, and the quantitative method of identifying coordinates by matching errors. For depth realization, order-independent transparency (OIT), clipping, and annotation and measurement functions were developed. To validate depth realization technology, the AR model of a brain tumor patient was applied to its life-size 3D printed model.

#### RESULTS

By using RTIO tracking, we confirmed that the AR model remained consistent with the 3D-printed patient model without flutter, regardless of the movement of the visualization device. The red fiducial markers of the AR and the blue fiducial markers of the 3D-printed model were superimposed precisely at all locations. The registration accuracy was quantified using coordinates, and the average moving errors of the X-axis and Y-axis before and after the movement of visualization device were  $0.34 \pm 0.21$  and  $0.04 \pm 0.08$  mm (before) and  $0.39 \pm 0.22$  and  $0.05 \pm 0.09$  mm (after), respectively. Further, the application of OIT with multi-layer alpha blending (MLAB) and filtered alpha composites (FAC) improved the perception of overlapping internal brain structures. Clipping and annotation and measurement functions were also developed to aid depth perception, and worked perfectly during real-time coordination. We named this system METAMEDIP navigation.

#### CONCLUSION

s With these novel technologies developed for continuous tracking and depth perception in AR environments, we are able to overcome the critical obstacles in the development of clinically applicable AR neuronavigation in the metaverse era.

#### CLINICAL RELEVANCE/APPLICATION

It is verified augmented reality navigation can be used for brain tumor surgery planning and surgery and can be performed while checking anatomical structures intuitively compare to MRI-based neuro-navigation.

Printed on: 02/07/23

## Abstract Archives of the RSNA, 2022

R5B-SPNR-9

### Association of Brain Viscoelastic Properties With Age and Glymphatic Function in Neurologically Normal Subjects: An Exploratory Study of MR Elastography Using a Novel Transducer

Thursday, Dec. 1 12:45PM - 1:15PM Room: Learning Center - NR DPS

#### Participants

Bio Joo, MD, Seoul, Korea, Republic Of (*Presenter*) Nothing to Disclose

#### PURPOSE

Magnetic resonance elastography (MRE) can image viscoelastic properties of tissues by measuring propagation of mechanical waves generated by a MRE transducer. The purpose of this study was to investigate the relationship between viscoelastic properties of the brain measured by MRE with a novel MRE transducer and normal aging and glymphatic function in neurologically normal subjects.

#### METHODS AND MATERIALS

A total of 52 neurologically normal subjects (mean age:  $48.1 \pm 15.5$  years, age range: 23 - 74, male:female = 23:29) were enrolled in this prospective study. MRE was conducted by using a transducer based on a rotational eccentric mass. Viscoelastic parameters, including storage modulus  $G'$ , loss modulus  $G''$ , magnitude of the complex shear modulus  $|G^*|$ , and phase angle  $\delta$ , were assessed in the centrum semiovale region. Glymphatic function was assessed using Diffusion Tensor Image Analysis Along the Perivascular Space index (ALPS-index). The viscoelastic parameters were compared with age and ALPS-index by Pearson correlation coefficient ( $r$ ).

#### RESULTS

All the viscoelastic parameters showed significantly negative correlations with age ( $G'$ :  $r=-0.44$ ,  $P<0.01$ ;  $G''$ :  $r=-0.44$ ,  $P<0.01$ ;  $|G^*|$ :  $r=-0.33$ ,  $P=0.02$ ;  $\delta$ :  $r=-0.29$ ,  $P=0.04$ ). ALPS-index showed significantly positive correlations with  $G'$  ( $r=0.35$ ,  $P=0.02$ ),  $G''$  ( $r=0.37$ ,  $P=0.02$ ), and  $|G^*|$  ( $r=0.37$ ,  $P=0.01$ ), but not with  $\delta$  ( $r=0.25$ ,  $P=0.11$ ).

#### CONCLUSION

s This study demonstrated the applicability of the brain MRE using a novel transducer and the relationship between brain viscoelastic properties and glymphatic function in healthy subjects over a wide range of age. The brain MRE with the gravitational transducer can potentially play a role in various neurological conditions by providing additional information of the brain.

#### CLINICAL RELEVANCE/APPLICATION

MRE using a gravitational transducer can assess brain viscoelastic properties, which may be associated with normal aging as well as glymphatic function.

Printed on: 02/07/23

## Abstract Archives of the RSNA, 2022

R5B-SPOB

### OB/Gynecology Thursday Poster Discussions - B

Thursday, Dec. 1 12:45PM - 1:15PM Room: Learning Center - OB DPS

#### Participants

Nancy Kim, MD, Washington, DC (*Moderator*) Nothing to Disclose

#### Sub-Events

### R5B-SPOB-1 Re-envisioning Pelvic Organ Prolapse (POP): Comparing Clinical and Imaging Assessments of Pelvic Organ Prolapse

#### Participants

Daniel Heller, BA, Lincolnwood, IL (*Presenter*) Nothing to Disclose

#### PURPOSE

To correlate Pelvic Organ Prolapse Quantification (POP-Q) clinical staging with MR defecography (MRD) assessment using correlative anatomical points, and compare staging using different reference line methods.

#### METHODS AND MATERIALS

IRB-approved, retrospective single-institution study of patients that underwent MRD and POP-Q staging by gynecologists from 2016 to 2022. Exclusion criteria: patients without POP-Q score, incomplete or poor quality MRD. POP-Q scores and clinical presenting complaints were documented. One fellowship-trained radiologist reviewed MRD and documented the following: H-line, and M-line at rest, and evacuation phase; different compartment POP grades based on pubococcygeal line (PCL) and mid pubic line (MPL), and POP-Q variables replicated on MRD. Statistical analysis was performed using weighted kappa tests.

#### RESULTS

A total of 116 patients with POP underwent MRD from 1/2016 to 4/2022, of which 24 met our inclusion criteria. Levator plate angle (LPA) was abnormal in 23/24 patients, and abnormal urethrovesical angle (UVA) in 19/24. Although PCL is more comparable to clinical staging of POP, both MPL and PCL were not comparable to clinical staging using weighted kappa analysis. MPL consistently overstaged POP, similar to literature. POP-Q variables replicated on MRD: better correlation with points D (16/20), Gh (14/19) and PB (13/20) with an allowed 2-3 cm difference between clinical and MR techniques. POP-Q clinical staging: stage 0 (1/24), stage 1 (8/24), stage 2 (13/24), stage 3 (2/24), stage 4 (0/24). POP staging by MRD was stage 0 (19/24); stage 1 (5/24). Although there is a better correlation of individual points, the overall score is underestimated by MRD. Limitations of the study include small sample size and a single radiologist review. The study can be improved with a multicenter trial, a prolonged study period, and additional radiologists reviewing the images with interreader agreement calculation in the future.

#### CONCLUSION

Abnormal LPA and UVA measurements can serve as complementary tools to assess pelvic floor dysfunction. PCL had higher agreement than MPL with POP-Q clinic staging. We recommend a reassessment of the MPL staging criteria to avoid overstaging of POP and to better reflect clinical staging. Although overall POP-Q staging replication on MRD is not representative, individual measurement points can be replicated with confidence and help guide POP management.

#### CLINICAL RELEVANCE/APPLICATION

Diagnosis and management of pelvic organ prolapse (POP) requires a multidisciplinary approach with radiologists involvement. To date, there is limited radiographic and clinical concordance in POP staging.

Printed on: 02/07/23

## Abstract Archives of the RSNA, 2022

R5B-SPOB-1

### Re-envisioning Pelvic Organ Prolapse (POP): Comparing Clinical and Imaging Assessments of Pelvic Organ Prolapse

Thursday, Dec. 1 12:45PM - 1:15PM Room: Learning Center - OB DPS

#### Participants

Daniel Heller, BA, Lincolnwood, IL (*Presenter*) Nothing to Disclose

#### PURPOSE

To correlate Pelvic Organ Prolapse Quantification (POP-Q) clinical staging with MR defecography (MRD) assessment using correlative anatomical points, and compare staging using different reference line methods.

#### METHODS AND MATERIALS

IRB-approved, retrospective single-institution study of patients that underwent MRD and POP-Q staging by gynecologists from 2016 to 2022. Exclusion criteria: patients without POP-Q score, incomplete or poor quality MRD. POP-Q scores and clinical presenting complaints were documented. One fellowship-trained radiologist reviewed MRD and documented the following: H-line, and M-line at rest, and evacuation phase; different compartment POP grades based on pubococcygeal line (PCL) and mid pubic line (MPL), and POP-Q variables replicated on MRD. Statistical analysis was performed using weighted kappa tests.

#### RESULTS

A total of 116 patients with POP underwent MRD from 1/2016 to 4/2022, of which 24 met our inclusion criteria. Levator plate angle (LPA) was abnormal in 23/24 patients, and abnormal urethrovesical angle (UVA) in 19/24. Although PCL is more comparable to clinical staging of POP, both MPL and PCL were not comparable to clinical staging using weighted kappa analysis. MPL consistently overstaged POP, similar to literature. POP-Q variables replicated on MRD: better correlation with points D (16/20), Gh (14/19) and PB (13/20) with an allowed 2-3 cm difference between clinical and MR techniques. POP-Q clinical staging: stage 0 (1/24), stage 1 (8/24), stage 2 (13/24), stage 3 (2/24), stage 4 (0/24). POP staging by MRD was stage 0 (19/24); stage 1 (5/24). Although there is a better correlation of individual points, the overall score is underestimated by MRD. Limitations of the study include small sample size and a single radiologist review. The study can be improved with a multicenter trial, a prolonged study period, and additional radiologists reviewing the images with interreader agreement calculation in the future.

#### CONCLUSION

Abnormal LPA and UVA measurements can serve as complementary tools to assess pelvic floor dysfunction. PCL had higher agreement than MPL with POP-Q clinic staging. We recommend a reassessment of the MPL staging criteria to avoid overstaging of POP and to better reflect clinical staging. Although overall POP-Q staging replication on MRD is not representative, individual measurement points can be replicated with confidence and help guide POP management.

#### CLINICAL RELEVANCE/APPLICATION

Diagnosis and management of pelvic organ prolapse (POP) requires a multidisciplinary approach with radiologists involvement. To date, there is limited radiographic and clinical concordance in POP staging.

Printed on: 02/07/23



## Abstract Archives of the RSNA, 2022

R5B-SPPD

### Pediatric Thursday Poster Discussions - B

Thursday, Dec. 1 12:45PM - 1:15PM Room: Learning Center - PD DPS

#### Participants

Patricia Acharya, MD, Monrovia, CA (*Moderator*) Nothing to Disclose

#### Sub-Events

### R5B-SPPD-1 Comparison of Image Quality, Contrast Administration, and Radiation Dose of Pediatric Abdominal Dual-Energy CT in Actual Usage

#### Participants

Yeseul Kang, MD, Gyeonggi-do, Korea, Republic Of (*Presenter*) Nothing to Disclose

#### PURPOSE

To compare the image quality, injected amount of iodine contrast and radiation dose of single-energy CT (SECT) and dual-energy CT (DECT) for pediatric abdominal CT.

#### METHODS AND MATERIALS

From April to December 2021, pediatric patients ( $\geq 18$  years old) who underwent abdominal SECT or DECT were retrospectively included in this study. Patients were classified into the SECT or DECT group after propensity-score matching. For the DECT group, the amount of iodine contrast was reduced to 10-30% of the routine dose. CT images were obtained at the hepatic venous phase with a routine reconstruction method (iDose4) and DECT was additionally reconstructed with a virtual monochromatic image (VMI) at 40 keV. To compare image quality quantitatively, the contrast-to-noise ratio (CNR) and signal-to-noise ratio (SNR) of the liver, pancreas, and portal vein were compared. The total amount of injected iodine contrast and radiation dose were compared using the Mann-Whitney U test.

#### RESULTS

Among 318 patients, 116 patients were included after propensity-score matching (median 16 years old, range 9-18 years, 58 patients in each group). Compared with the SECT group, CNR and SNR were significantly lower in the DECT group using the routine reconstruction method, but no significant differences were observed using VMI at 40 keV. The total amount of injected contrast was significantly lower in the DECT group (median 90 cc vs. 76 cc,  $p=0.007$ ), with a 15.6% reduction from the routine dose. The CT dose index volume did not differ between the two groups (median 2.9 mGy vs. 2.8 mGy,  $p=0.714$ ).

#### CONCLUSION

Pediatric abdominal DECT can reduce the amount of iodine contrast, without significant difference in image quality and radiation dose compared to SECT in our study population of 9-18 years old.

#### CLINICAL RELEVANCE/APPLICATION

This study demonstrated actual clinical impact of DECT on pediatric abdominal CT and approved that DECT could be used for pediatric patients without degradation of image quality or increasing radiation dose, even with lower iodine contrast amount.

Printed on: 02/07/23

## Abstract Archives of the RSNA, 2022

R5B-SPPD-1

### Comparison of Image Quality, Contrast Administration, and Radiation Dose of Pediatric Abdominal Dual-Energy CT in Actual Usage

Thursday, Dec. 1 12:45PM - 1:15PM Room: Learning Center - PD DPS

#### Participants

Yeseul Kang, MD, Gyeonggi-do, Korea, Republic Of (*Presenter*) Nothing to Disclose

#### PURPOSE

To compare the image quality, injected amount of iodine contrast and radiation dose of single-energy CT (SECT) and dual-energy CT (DECT) for pediatric abdominal CT.

#### METHODS AND MATERIALS

From April to December 2021, pediatric patients ( $\leq 18$  years old) who underwent abdominal SECT or DECT were retrospectively included in this study. Patients were classified into the SECT or DECT group after propensity-score matching. For the DECT group, the amount of iodine contrast was reduced to 10-30% of the routine dose. CT images were obtained at the hepatic venous phase with a routine reconstruction method (iDose4) and DECT was additionally reconstructed with a virtual monochromatic image (VMI) at 40 keV. To compare image quality quantitatively, the contrast-to-noise ratio (CNR) and signal-to-noise ratio (SNR) of the liver, pancreas, and portal vein were compared. The total amount of injected iodine contrast and radiation dose were compared using the Mann-Whitney U test.

#### RESULTS

Among 318 patients, 116 patients were included after propensity-score matching (median 16 years old, range 9-18 years, 58 patients in each group). Compared with the SECT group, CNR and SNR were significantly lower in the DECT group using the routine reconstruction method, but no significant differences were observed using VMI at 40 keV. The total amount of injected contrast was significantly lower in the DECT group (median 90 cc vs. 76 cc,  $p=0.007$ ), with a 15.6% reduction from the routine dose. The CT dose index volume did not differ between the two groups (median 2.9 mGy vs. 2.8 mGy,  $p=0.714$ ).

#### CONCLUSION

Pediatric abdominal DECT can reduce the amount of iodine contrast, without significant difference in image quality and radiation dose compared to SECT in our study population of 9-18 years old.

#### CLINICAL RELEVANCE/APPLICATION

This study demonstrated actual clinical impact of DECT on pediatric abdominal CT and approved that DECT could be used for pediatric patients without degradation of image quality or increasing radiation dose, even with lower iodine contrast amount.

Printed on: 02/07/23

## Abstract Archives of the RSNA, 2022

R5B-SPPH

### Physics Thursday Poster Discussions - B

Thursday, Dec. 1 12:45PM - 1:15PM Room: Learning Center - PH DPS

#### Participants

Ran Zhang, PhD, Madison, WI (*Moderator*) Nothing to Disclose

#### Sub-Events

### R5B-SPPH-1 Task-Based Image Quality Assessments of Super-Resolution Deep-Learning Reconstruction for Coronary CT Angiography

#### Participants

Yasunori Nagayama, MD, Kumamoto, Japan (*Presenter*) Nothing to Disclose

#### PURPOSE

To evaluate the task-based image quality of novel super-resolution deep-learning reconstruction (SR-DLR) designed for coronary CT angiography and compare it with those of hybrid iterative reconstruction (HIR), model-based iterative reconstruction (MBIR), and normal-resolution DLR (NR-DLR) algorithms.

#### METHODS AND MATERIALS

A cylindrical physical evaluation phantom (Catphan 700) was scanned on a 320-row scanner at seven tube currents (100-700 mA; CTDIvol, 1.9-10.2 mGy) with a tube voltage of 120 kVp and rotation time of 0.275 s. Raw data were reconstructed with HIR (AIDR 3D), MBIR (FIRST), NR-DLR (AiCE), and SR-DLR (PIQE) at 0.5-mm section thickness using dedicated cardiac parameters. Noise power spectrum (NPS) was evaluated on CTP712 homogeneous module; the noise magnitude and average NPS frequencies were quantified. The spatial resolution at given dose and contrast levels were evaluated with task-based transfer function (TTF) on CTP682 sensitometry module. The values of TTF at 50% (TTF50%) for Delrin (approximately 340 HU), polyethylene (approximately 30 HU), and Bone-50% (approximately 630 HU) inserts were quantified. The detectability index for the simulated coronary lumen (300 HU with a 2-mm diameter), soft plaque (40 HU with a 1-mm diameter), and calcified plaque (500 HU with a 1-mm diameter) were calculated by synthesizing the NPS and TTF outcomes. Five readers subjectively ranked the algorithms in terms of the visibility of fine high-contrast objects, delineation of small low-contrast objects, blooming artifact, noise magnitude, and noise texture on a 4-point scale.

#### RESULTS

Throughout the entire dose levels, SR-DLR yielded the lowest noise magnitude, highest average NPS frequency, and highest TTF50% for all inserts. The detectability index for all task objects were higher in SR-DLR than in HIR, MBIR, and NR-DLR. At each dose setting, the best subjective scores for all evaluation criteria were attained with SR-DLR.

#### CONCLUSION

Compared with HIR, MBIR, and NR-DLR algorithms, newly introduced SR-DLR improved the task-based image quality and detectability for low- and high-contrast objects relevant to coronary CT angiography.

#### CLINICAL RELEVANCE/APPLICATION

SR-DLR provides CT images with excellent spatial resolution, preferable noise texture, and object detectability, potentially facilitating the interpretation of coronary artery diseases.

### R5B-SPPH-3 Physical Properties of a New Deep Learning Reconstruction in Ultra-High-Resolution Images: Comparison with Model-Based Iterative Reconstruction

#### Participants

Shun Muramatsu, RT, Fukushima, Japan (*Presenter*) Nothing to Disclose

#### PURPOSE

In this study, we physically evaluated ultra-high resolution (U-HR) images reconstructed with model-based iterative reconstruction (MBIR) and deep learning reconstruction (DLR), and demonstrated the usefulness of U-HR images with DLR.

#### METHODS AND MATERIALS

The U-HRCT system used in this study was Aquilion Precision (Canon Medical Systems, Otawara, Tochigi, Japan). This scanner is characterized by 0.25 mm collimation (160 detector rows) in the z axis, and 1792 channels (0.25 mm detectors in the x-y plane). The phantom was 180 mm in diameter and 250 mm in height and consisted of a water-only part and a part in which fiber rods (Wilmington, DE, USA) with different CT numbers were inserted into the water. The data acquired were reconstructed with forward-projected MBIR solution (FIRST), which was MBIR, and Advanced Intelligent Clear-IQ Engine (AiCE), which was DLR. Both images were reconstructed with a slice thickness of 0.25 mm and an image matrix size of 1024 × 1024 pixels. For physical evaluation, the modulation transfer function (MTF) and noise power spectrum (NPS) of MBIR and DLR were compared.

## RESULTS

The MTFs of MBIR and DLR were comparable. The NPS of DLR was lower than that of MBIR. The NPS had less noise in DLR than MBIR in all frequency ranges. Therefore, DLR would be more useful than MBIR in terms of physical performance.

## CONCLUSION

There was no difference in the resolution characteristics of MBIR and DLR. DLR had better noise characteristics than MBIR. DLR is more useful than MBIR for with U-HR images.

## CLINICAL RELEVANCE/APPLICATION

DLR would be more useful than MBIR for obtaining U-HR images. In contrast to a normal CT images (matrix size:  $512 \times 512$ , slice thickness: 0.5 mm), a high-resolution images (matrix size:  $1024 \times 1024$ , slice thickness: 0.25 mm) has a smaller voxel size. Therefore, if we consider only the statistics of photon detection, the noise in the image is about four times larger. In other words, in order to achieve a noise level equivalent to that of a conventional image, the dose needs to be increased by a factor of 16. Fine sampling requires a combined image noise suppression technique, and, as mentioned above, DLR may be effective in reducing image noise. To achieve higher spatial resolution and less image noise, DLR would be more useful than MBIR.

## R5B-SPPH-4 Combined digital twin and deep learning approach to scatter correction in head cone-beam CT: Use of MC-GPU and patient-derived head voxel phantom

Participants

AHYEONG LEE, BEng, (*Presenter*) Nothing to Disclose

## PURPOSE

A digital twin refers to a digital replica of the physician system that could predict how the system will perform by making simulations. This study explores the potential of combined digital twin and deep learning approach in performance improvement of Cone-beam CT (CBCT).

## METHODS AND MATERIALS

A digital twin CBCT platform was constructed by using a Monte Carlo-based CBCT simulator and patient-derived 3D voxel phantoms. From the publicly available CQ500 dataset of head scans, 20 sets of patient-derived 3D head voxel phantoms were generated that mimicked the patient's anatomy and material property of human tissues. MC-GPU was used for accurate simulation of CBCT imaging for the patient-derived voxel phantoms with an accelerated graphics processing unit (GPU) based computing speed including generation of synthetic radiographic images and reconstruction of CT scans reflecting the real-world hardware component and geometry of CBCT systems. Pairs of scattered and corresponding non-scattered images were generated by calculating the interaction of photon transport in voxel phantom through MC-GPU that reflected the real CBCT geometry. The projection images were reconstructed and then, a CNN-based deep learning model was trained to predict the non-scattered CT image from the input scattered CT image. The 20 simulated CT cases were divided into 15 training and 5 test set. The quality improvement with deep learning-based scatter correction was evaluated with cupping artifact index (CAI) and CT number uniformity index (CUI). CAI was defined as the difference between the average HU values in the peripheral area and middle area, while CUI was defined as the difference between maximum and minimum HU values on the homogeneous brain parenchyma.

## RESULTS

CAI was 39.59 in the scattered image, 5.03 in non-scattered image, and 8.15 in scatter-corrected image, respectively, showing about 90% reduction of cupping artifacts in the scatter-corrected image. CUI was 14.76 in scattered image, 6.26 in scatter-corrected image showing about 42% improved of CT number uniformity in the scatter-corrected image.

## CONCLUSION

Our combined digital twin with a deep learning model could reduce scatter artifacts and has a potential to improve the imaging performance of CBCT.

## CLINICAL RELEVANCE/APPLICATION

Reconstructed images using digital twin phantom and MC-GPU are feasible with deep convolutional neural network for CBCT scatter correction, potentially applicable to real CBCT images.

## R5B-SPPH-5 Evaluation of Zero TE Imaging for MR-only Catheter Detection in Interstitial Gynecologic HDR Brachytherapy

Participants

Habib Al Saleh, PhD, (*Presenter*) Nothing to Disclose

## PURPOSE

One of the main challenges for MR-only interstitial brachytherapy treatment planning is that the implanted plastic needles cannot be detected with acceptable accuracy using conventional MR T1 and T2 weighted images. While it might not also be clearly visible in CT images, our current workflow requires acquisition of CT images with marker-filled catheters for registration with MR images and needle reconstruction. Eventual changes between MR and CT scans could lead to registration errors and affect the calculated dose. In this work, the feasibility of using ZTE images for detection and reconstruction of interstitial needles as an alternative to CT approach was evaluated.

## METHODS AND MATERIALS

Two ProGuide (Elekta Brachytherapy, Stockholm, Sweden) 6Fx294mm interstitial plastic needles (one rounded and one sharp) were inserted into a melon and scanned with and without CT marker in a 3.0T GE Signa Premier MRI system (GE Healthcare, Milwaukee, WI) and a Philips Brilliance Big Bore CT (Philips, Netherland). The rounded needle was slightly moved out of its first insertion to demonstrate the ability of detecting needle tip from scanned images. The phantom was CT scanned and subsequently coronal 3D MR images were acquired with MPRAGE T1W (TR/TE 2308/4 ms, FOV 200, matrix 288), CUBE T2W (TR/TE 3000/108 ms, FOV 200, matrix 288) and ZTE (TR/TE 647/0.016, FOV 200, matrix 288). Scan time was approximately identical for all MR sequences. MR images were registered to CT images for comparison.

## RESULTS

T1w and T2w images demonstrate susceptibility-induced distortions around the empty needles, and the distortion increased in the presence of the CT-marker. ZTE image of empty needles showed clear depiction of the catheters with no artifacts. With CT marker, ZTE image present less artifact and a uniform distortion around the top part of the marker. ZTE-CT fusion showed very good positional agreement between top bright part of the marker in CT image with the metal-induced susceptibility artifact in the ZTE image.

## CONCLUSION

In this work we showed that ZTE sequence with near zero echo time has the potential to localize empty needles more accurately than T1 and T2 weighted images and can be used with CT-marker for catheter reconstruction in MR-only brachytherapy workflow. Future clinical investigation is required to confirm these initial results for clinical workflow.

## CLINICAL RELEVANCE/APPLICATION

Magnetic Resonance Zero Echo Time (ZTE) imaging has the potential to improve interstitial gynecologic HDR brachytherapy dose estimation and MR-guided treatment planning workflow.

## R5B-SPPH-6 Evaluation of Multi-Criteria Optimization for Improving RapidPlan Model Based Treatment Planning for Prostate Cancer

Participants

Vishruta Dumane, PhD, (*Presenter*) Nothing to Disclose

## PURPOSE

To investigate the ability of multicriteria optimization (MCO) to improve the dosimetric sparing of the rectum and bladder in RapidPlan based plans for prostate cancer and to compare the results with clinical plans.

## METHODS AND MATERIALS

A total of 93 patient plans treated at our institution with radiation using volumetric modulated arc therapy with 2-3 coplanar arcs and 6 MV photons were used to build a dose volume histogram (DVH) estimation model for organs at risk (OARs, essentially the bladder, bladder wall, rectum, rectal wall, bowel and femoral heads). Prescription dose to the PTV was 45 Gy. Dose constraints for the rectal wall and the bladder wall were  $V40Gy \leq 30\%$ ,  $V30Gy \leq 50\%$ , bowel maximum  $\leq 50Gy$ , femoral head maximum  $\leq 45Gy$  and  $V30Gy \leq 50\%$ . Dose heterogeneity to the PTV was expected to be within 110% and the PTV D95 at least 98%. The model generated was tested on 10 patient cases that were not originally used in training or testing. After application of the RapidPlan model, MCO was utilized to explore tradeoffs to see if the organ at risk (OAR) sparing could be improved without compromising on the coverage or other OAR doses. Dosimetric parameters between the MCO + Rapidplan were compared to both the RapidPlan alone and the clinical plan. Parameters were compared using the Wilcoxon sign-rank test for statistical significance.

## RESULTS

Compared to the clinical plan, combination of MCO and RapidPlan helped reduce the rectum  $V30Gy$ ,  $V25Gy$ ,  $V20Gy$ ,  $V15Gy$  and  $V10Gy$  by 6.2%, 10.5%, 18.3%, 26.6% and 10.2% ( $p \leq 0.01$ ) respectively without a significant change in PTV D95 and V95 or the rectal wall maximum dose. The improvement in sparing of the rectum with MCO over RapidPlan alone for these dosimetric parameters was as much as 16.8% ( $p \leq 0.01$ ). Compared to the clinical plan, combination of MCO and RapidPlan was also reduced the bladder  $V30Gy$ ,  $V25Gy$ ,  $V20Gy$ ,  $V15Gy$  and  $V10Gy$  by as much as 8.5%. MCO+RapidPlan did not significantly improve bladder sparing compared to RapidPlan alone. The change in the maximum dose to the bladder wall was insignificant as a result of using MCO+RapidPlan

## CONCLUSION

Although both the clinical and the RapidPlan based plans can meet dose constraints, MCO can potentially significantly improve the sparing of OARs and has the potential to improve our RapidPlan model for intact prostate.

## CLINICAL RELEVANCE/APPLICATION

Development of optimal treatment plans for patient specific anatomy requires a significant intervention from the treatment planner. This work shows not only the potential of MCO + RapidPlan to meet constraints but also significantly improve OAR sparing that could be clinically impactful.

## R5B-SPPH-7 Carbon Nanotube-Based Wide-Slot Long-Length Tomosynthesis for Whole Body Skeletal Imaging

Participants

Diwash Thapa, BS, Wake Forest, NC (*Presenter*) Nothing to Disclose

## PURPOSE

The purpose of this work is to demonstrate the feasibility of cone beam geometry-based reconstruction for long length tomosynthesis in a system comprising carbon nanotube (CNT) x-ray sources and to characterize the scatter and radiation associated with the system.

## METHODS AND MATERIALS

CNT-based long length tomosynthesis or orthogonal tomosynthesis (OT) consists of a linear x-ray tube positioned orthogonally to a small field-of-view (FOV) area detector. Sources are collimated to a  $5 \times 30 \text{ cm}^2$  rectangular strip on the detector and projections are acquired in a step-and-shoot scheme (figure 1 a). In preprocessing, all projections from a given source were stitched using weighted addition. Reconstructions were performed with two algorithms: simultaneous iterative reconstruction technique (SIRT) and simultaneous algebraic reconstruction technique (SART). Entrance dose at 100 cm source to detector distance was measured using the RaySafe X2 R/F sensor (figure 1 b) and the dose area product (DAP) within the FOV was calculated. Projection space scatter to primary ratio (S/P) and scatter degradation factor (SDF) was calculated.

## RESULTS

Reconstruction images using SIRT and SART are displayed in figure 1 c, d. The compiled SIRT algorithm took 3.44 s while SART took

21.6 s for completion. Both reconstructions were found to be anatomically correct and provided good resolution of all osseous structures. With collimation, DAP was calculated to be 170.0 mGy whereas without collimation DAP was 207.1 mGy to image the 540 cm<sup>2</sup> FOV of the chest phantom reconstructions. The average S/P and SDF with collimation across sources was 0.31 and 0.77 while the same was 0.69 and 0.59 respectively without collimation.

## CONCLUSION

This work demonstrates the feasibility of cone beam geometry based algebraic reconstruction for OT. Due to collimation, this system has significantly reduced scatter (> 50% decrease in S/P) and radiation (18% decrease in DAP) burden compared to conventional tomosynthesis.

## CLINICAL RELEVANCE/APPLICATION

Conventional tomosynthesis is performed with specific anatomy within a limited FOV. Extended FOV tomosynthesis is beneficial for whole-body skeletal imaging in austere environments due to tomosynthesis' increased fracture detection sensitivity. Current research and commercial long-length tomosynthesis systems are built on large gantries making them unsuitable for mobile applications. The OT system presented here can be mounted on a single small unit and fits on the back of an ambulance or a helicopter. Patients could be scanned as they are loaded into the transport vehicle without the tube/detector ever moving. The reduced scatter and radiation hazard also makes OT suitable for repetitive use such as scoliosis imaging.

## R5B-SPPH-8 Deep learning denoising and assessment of detectability of microcalcifications in digital breast tomosynthesis: A task-based image evaluation approach using CNN

Participants

Mingjie Gao, (*Presenter*) Nothing to Disclose

## PURPOSE

Deep learning (DL) denoising for digital breast tomosynthesis (DBT) has the potential to reduce dose and improve microcalcification (MC) detection. This study proposed two convolutional neural network (CNN) models to assess image noise (CNN-ns) and MC detectability (CNN-mc) and guide the development of denoising techniques.

## METHODS AND MATERIALS

For the CNN-ns for noise estimation, we extracted 52,526 128×128×3-pixel patches from virtual DBTs of a wide range of noise levels simulated by the VICTRE software as training set and calculated the root-mean-square variations of pixel values as training labels to fine-tune the ImageNet pre-trained ConvNeXt-T. For the CNN-mc for MC vs background classification, we collected with IRB approval 231 views of DBTs from 116 human subjects who had biopsy proven MCs and split the set by case into 127 views for training/validation and 104 views for testing. We reconstructed the DBTs with (1) simultaneous algebraic reconstruction technique (SART), (2) SART with DL-denoised projections, and (3) DL-denoiser regularized plug-and-play reconstruction. For each condition, we extracted 751 128×128×3-pixel MC patches (6,008 after flipping and rotation augmentation) and 6,305 MC-free patches as training/validation set, and 709 MC and 777 MC-free patches as test set. Maximum intensity projection of the 3 slices was applied to all patches to emphasize the MCs. We adopted a multi-stage transfer learning strategy of first fine-tuning the ConvNeXt-T to CNN-ns, which was then further fine-tuned to CNN-mc. We used the area under ROC curve (AUC) of the CNN-mc as an MC detectability measure.

## RESULTS

Our DL denoising methods reduced image noise and improved AUC. The AUC increased with MC signal strengths when the CNN-ns estimated noise was comparable. DL-denoiser regularized reconstruction with additional post-reconstruction denoising resulted in the lowest CNN-ns estimated noise and highest AUC. The AUC and noise rankings matched our visual judgement on the images.

## CONCLUSION

The CNN-mc and CNN-ns provided task-based measures for image assessment, which may be useful for comparison of the detectability of clustered MCs in DBTs obtained with different denoising or reconstruction techniques.

## CLINICAL RELEVANCE/APPLICATION

The CNN image assessment tools can help develop better DBT denoising or reconstruction methods, which may lead to lower dose and higher sensitivity and specificity for MC detection in screening.

Printed on: 02/07/23

## Abstract Archives of the RSNA, 2022

R5B-SPPH-1

### Task-Based Image Quality Assessments of Super-Resolution Deep-Learning Reconstruction for Coronary CT Angiography

Thursday, Dec. 1 12:45PM - 1:15PM Room: Learning Center - PH DPS

#### Participants

Yasunori Nagayama, MD, Kumamoto, Japan (*Presenter*) Nothing to Disclose

#### PURPOSE

To evaluate the task-based image quality of novel super-resolution deep-learning reconstruction (SR-DLR) designed for coronary CT angiography and compare it with those of hybrid iterative reconstruction (HIR), model-based iterative reconstruction (MBIR), and normal-resolution DLR (NR-DLR) algorithms.

#### METHODS AND MATERIALS

A cylindrical physical evaluation phantom (Catphan 700) was scanned on a 320-row scanner at seven tube currents (100-700 mA; CTDIvol, 1.9-10.2 mGy) with a tube voltage of 120 kVp and rotation time of 0.275 s. Raw data were reconstructed with HIR (AIDR 3D), MBIR (FIRST), NR-DLR (AiCE), and SR-DLR (PIQE) at 0.5-mm section thickness using dedicated cardiac parameters. Noise power spectrum (NPS) was evaluated on CTP712 homogeneous module; the noise magnitude and average NPS frequencies were quantified. The spatial resolution at given dose and contrast levels were evaluated with task-based transfer function (TTF) on CTP682 sensitometry module. The values of TTF at 50% (TTF50%) for Delrin (approximately 340 HU), polyethylene (approximately 30 HU), and Bone-50% (approximately 630 HU) inserts were quantified. The detectability index for the simulated coronary lumen (300 HU with a 2-mm diameter), soft plaque (40 HU with a 1-mm diameter), and calcified plaque (500 HU with a 1-mm diameter) were calculated by synthesizing the NPS and TTF outcomes. Five readers subjectively ranked the algorithms in terms of the visibility of fine high-contrast objects, delineation of small low-contrast objects, blooming artifact, noise magnitude, and noise texture on a 4-point scale.

#### RESULTS

Throughout the entire dose levels, SR-DLR yielded the lowest noise magnitude, highest average NPS frequency, and highest TTF50% for all inserts. The detectability index for all task objects were higher in SR-DLR than in HIR, MBIR, and NR-DLR. At each dose setting, the best subjective scores for all evaluation criteria were attained with SR-DLR.

#### CONCLUSION

Compared with HIR, MBIR, and NR-DLR algorithms, newly introduced SR-DLR improved the task-based image quality and detectability for low- and high-contrast objects relevant to coronary CT angiography.

#### CLINICAL RELEVANCE/APPLICATION

SR-DLR provides CT images with excellent spatial resolution, preferable noise texture, and object detectability, potentially facilitating the interpretation of coronary artery diseases.

Printed on: 02/07/23

## Abstract Archives of the RSNA, 2022

R5B-SPPH-3

### Physical Properties of a New Deep Learning Reconstruction in Ultra-High-Resolution Images: Comparison with Model-Based Iterative Reconstruction

Thursday, Dec. 1 12:45PM - 1:15PM Room: Learning Center - PH DPS

#### Participants

Shun Muramatsu, RT, Fukushima, Japan (*Presenter*) Nothing to Disclose

#### PURPOSE

In this study, we physically evaluated ultra-high resolution (U-HR) images reconstructed with model-based iterative reconstruction (MBIR) and deep learning reconstruction (DLR), and demonstrated the usefulness of U-HR images with DLR.

#### METHODS AND MATERIALS

The U-HRCT system used in this study was Aquilion Precision (Canon Medical Systems, Otawara, Tochigi, Japan). This scanner is characterized by 0.25 mm collimation (160 detector rows) in the z axis, and 1792 channels (0.25 mm detectors in the x-y plane). The phantom was 180 mm in diameter and 250 mm in height and consisted of a water-only part and a part in which five rods (Wilmington, DE, USA) with different CT numbers were inserted into the water. The data acquired were reconstructed with forward-projected MBIR solution (FIRST), which was MBIR, and Advanced Intelligent Clear-IQ Engine (AiCE), which was DLR. Both images were reconstructed with a slice thickness of 0.25 mm and an image matrix size of 1024 × 1024 pixels. For physical evaluation, the modulation transfer function (MTF) and noise power spectrum (NPS) of MBIR and DLR were compared.

#### RESULTS

The MTFs of MBIR and DLR were comparable. The NPS of DLR was lower than that of MBIR. The NPS had less noise in DLR than MBIR in all frequency ranges. Therefore, DLR would be more useful than MBIR in terms of physical performance.

#### CONCLUSION

There was no difference in the resolution characteristics of MBIR and DLR. DLR had better noise characteristics than MBIR. DLR is more useful than MBIR for with U-HR images.

#### CLINICAL RELEVANCE/APPLICATION

DLR would be more useful than MBIR for obtaining U-HR images. In contrast to a normal CT images (matrix size: 512 × 512, slice thickness: 0.5 mm), a high-resolution images (matrix size: 1024 × 1024, slice thickness: 0.25 mm) has a smaller voxel size. Therefore, if we consider only the statistics of photon detection, the noise in the image is about four times larger. In other words, in order to achieve a noise level equivalent to that of a conventional image, the dose needs to be increased by a factor of 16. Fine sampling requires a combined image noise suppression technique, and, as mentioned above, DLR may be effective in reducing image noise. To achieve higher spatial resolution and less image noise, DLR would be more useful than MBIR.

Printed on: 02/07/23

## Abstract Archives of the RSNA, 2022

R5B-SPPH-4

### Combined digital twin and deep learning approach to scatter correction in head cone-beam CT: Use of MC-GPU and patient-derived head voxel phantom

Thursday, Dec. 1 12:45PM - 1:15PM Room: Learning Center - PH DPS

#### Participants

AHYEONG LEE, BEng, (Presenter) Nothing to Disclose

#### PURPOSE

A digital twin refers to a digital replica of the physician system that could predict how the system will perform by making simulations. This study explores the potential of combined digital twin and deep learning approach in performance improvement of Cone-beam CT (CBCT).

#### METHODS AND MATERIALS

A digital twin CBCT platform was constructed by using a Monte Carlo-based CBCT simulator and patient-derived 3D voxel phantoms. From the publicly available CQ500 dataset of head scans, 20 sets of patient-derived 3D head voxel phantoms were generated that mimicked the patient's anatomy and material property of human tissues. MC-GPU was used for accurate simulation of CBCT imaging for the patient-derived voxel phantoms with an accelerated graphics processing unit (GPU) based computing speed including generation of synthetic radiographic images and reconstruction of CT scans reflecting the real-world hardware component and geometry of CBCT systems. Pairs of scattered and corresponding non-scattered images were generated by calculating the interaction of photon transport in voxel phantom through MC-GPU that reflected the real CBCT geometry. The projection images were reconstructed and then, a CNN-based deep learning model was trained to predict the non-scattered CT image from the input scattered CT image. The 20 simulated CT cases were divided into 15 training and 5 test set. The quality improvement with deep learning-based scatter correction was evaluated with cupping artifact index (CAI) and CT number uniformity index (CUI). CAI was defined as the difference between the average HU values in the peripheral area and middle area, while CUI was defined as the difference between maximum and minimum HU values on the homogeneous brain parenchyma.

#### RESULTS

CAI was 39.59 in the scattered image, 5.03 in non-scattered image, and 8.15 in scatter-corrected image, respectively, showing about 90% reduction of cupping artifacts in the scatter-corrected image. CUI was 14.76 in scattered image, 6.26 in scatter-corrected image showing about 42% improved of CT number uniformity in the scatter-corrected image.

#### CONCLUSION

Our combined digital twin with a deep learning model could reduce scatter artifacts and has a potential to improve the imaging performance of CBCT.

#### CLINICAL RELEVANCE/APPLICATION

Reconstructed images using digital twin phantom and MC-GPU are feasible with deep convolutional neural network for CBCT scatter correction, potentially applicable to real CBCT images.

Printed on: 02/07/23

## Abstract Archives of the RSNA, 2022

R5B-SPPH-5

### Evaluation of Zero TE Imaging for MR-only Catheter Detection in Interstitial Gynecologic HDR Brachytherapy

Thursday, Dec. 1 12:45PM - 1:15PM Room: Learning Center - PH DPS

#### Participants

Habib Al Saleh, PhD, (*Presenter*) Nothing to Disclose

#### PURPOSE

One of the main challenges for MR-only interstitial brachytherapy treatment planning is that the implanted plastic needles cannot be detected with acceptable accuracy using conventional MR T1 and T2 weighted images. While it might not also be clearly visible in CT images, our current workflow requires acquisition of CT images with marker-filled catheters for registration with MR images and needle reconstruction. Eventual changes between MR and CT scans could lead to registration errors and affect the calculated dose. In this work, the feasibility of using ZTE images for detection and reconstruction of interstitial needles as an alternative to CT approach was evaluated.

#### METHODS AND MATERIALS

Two ProGuide (Elekta Brachytherapy, Stockholm, Sweden) 6Fx294mm interstitial plastic needles (one rounded and one sharp) were inserted into a melon and scanned with and without CT marker in a 3.0T GE Signa Premier MRI system (GE Healthcare, Milwaukee, WI) and a Philips Brilliance Big Bore CT (Philips, Netherland). The rounded needle was slightly moved out of its first insertion to demonstrate the ability of detecting needle tip from scanned images. The phantom was CT scanned and subsequently coronal 3D MR images were acquired with MPRAGE T1W (TR/TE 2308/4 ms, FOV 200, matrix 288), CUBE T2W (TR/TE 3000/108 ms, FOV 200, matrix 288) and ZTE (TR/TE 647/0.016, FOV 200, matrix 288). Scan time was approximately identical for all MR sequences. MR images were registered to CT images for comparison.

#### RESULTS

T1w and T2w images demonstrate susceptibility-induced distortions around the empty needles, and the distortion increased in the presence of the CT-marker. ZTE image of empty needles showed clear depiction of the catheters with no artifacts. With CT marker, ZTE image present less artifact and a uniform distortion around the top part of the marker. ZTE-CT fusion showed very good positional agreement between top bright part of the marker in CT image with the metal-induced susceptibility artifact in the ZTE image.

#### CONCLUSION

s In this work we showed that ZTE sequence with near zero echo time has the potential to localize empty needles more accurately than T1 and T2 weighted images and can be used with CT-marker for catheter reconstruction in MR-only brachytherapy workflow. Future clinical investigation is required to confirm these initial results for clinical workflow.

#### CLINICAL RELEVANCE/APPLICATION

Magnetic Resonance Zero Echo Time (ZTE) imaging has the potential to improves interstitial gynecologic HDR brachytherapy dose estimation and MR-guided treatment planning workflow.

Printed on: 02/07/23

## Abstract Archives of the RSNA, 2022

R5B-SPPH-6

### Evaluation of Multi-Criteria Optimization for Improving RapidPlan Model Based Treatment Planning for Prostate Cancer

Thursday, Dec. 1 12:45PM - 1:15PM Room: Learning Center - PH DPS

#### Participants

Vishruta Dumane, PhD, (*Presenter*) Nothing to Disclose

#### PURPOSE

To investigate the ability of multicriteria optimization (MCO) to improve the dosimetric sparing of the rectum and bladder in RapidPlan based plans for prostate cancer and to compare the results with clinical plans.

#### METHODS AND MATERIALS

A total of 93 patient plans treated at our institution with radiation using volumetric modulated arc therapy with 2-3coplanar arcs and 6 MV photons were used to build a dose volume histogram (DVH) estimation model for organs at risk (OARs, essentially the bladder, bladder wall, rectum, rectal wall, bowel and femoral heads). Prescription dose to the PTV was 45 Gy. Dose constraints for the rectal wall and the bladder wall were  $V40Gy \leq 30\%$ ,  $V30Gy \leq 50\%$ , bowel maximum  $\leq 50Gy$ , femoral head maximum  $\leq 45Gy$  and  $V30Gy \leq 50\%$ . Dose heterogeneity to the PTV was expected to be within 110% and the PTV D95 at least 98%. The model generated was tested on 10 patient cases that were not originally used in training or testing. After application of the RapidPlan model, MCO was utilized to explore tradeoffs to see if the organ at risk (OAR) sparing could be improved without compromising on the coverage or other OAR doses. Dosimetric parameters between the MCO + Rapidplan were compared to both the RapidPlan alone and the clinical plan. Parameters were compared using the Wilcoxon sign-rank test for statistical significance.

#### RESULTS

Compared to the clinical plan, combination of MCO and RapidPlan helped reduce the rectum  $V30Gy$ ,  $V25Gy$ ,  $V20Gy$ ,  $V15Gy$  and  $V10Gy$  by 6.2%, 10.5%, 18.3%, 26.6% and 10.2% ( $p \leq 0.01$ ) respectively without a significant change in PTV D95 and V95 or the rectal wall maximum dose. The improvement in sparing of the rectum with MCO over RapidPlan alone for these dosimetric parameters was as much as 16.8% ( $p \leq 0.01$ ). Compared to the clinical plan, combination of MCO and RapidPlan was also reduced the bladder  $V30Gy$ ,  $V25Gy$ ,  $V20Gy$ ,  $V15Gy$  and  $V10Gy$  by as much as 8.5%. MCO+RapidPlan did not significantly improve bladder sparing compared to RapidPlan alone. The change in the maximum dose to the bladder wall was insignificant as a result of using MCO+RapidPlan

#### CONCLUSION

Although both the clinical and the RapidPlan based plans can meet dose constraints, MCO can potentially significantly improve the sparing of OARs and has the potential to improve our RapidPlan model for intact prostate.

#### CLINICAL RELEVANCE/APPLICATION

Development of optimal treatment plans for patient specific anatomy requires a significant intervention from the treatment planner. This work shows not only the potential of MCO + RapidPlan to meet constraints but also significantly improve OAR sparing that could be clinically impactful.

Printed on: 02/07/23

## Abstract Archives of the RSNA, 2022

R5B-SPPH-7

### Carbon Nanotube-Based Wide-Slot Long-Length Tomosynthesis for Whole Body Skeletal Imaging

Thursday, Dec. 1 12:45PM - 1:15PM Room: Learning Center - PH DPS

#### Participants

Diwash Thapa, BS, Wake Forest, NC (*Presenter*) Nothing to Disclose

#### PURPOSE

The purpose of this work is to demonstrate the feasibility of cone beam geometry-based reconstruction for long length tomosynthesis in a system comprising carbon nanotube (CNT) x-ray sources and to characterize the scatter and radiation associated with the system.

#### METHODS AND MATERIALS

CNT-based long length tomosynthesis or orthogonal tomosynthesis (OT) consists of a linear x-ray tube positioned orthogonally to a small field-of-view (FOV) area detector. Sources are collimated to a 5 X 30 cm<sup>2</sup> rectangular strip on the detector and projections are acquired in a step-and-shoot scheme (figure 1 a). In preprocessing, all projections from a given source were stitched using weighted addition. Reconstructions were performed with two algorithms: simultaneous iterative reconstruction technique (SIRT) and simultaneous algebraic reconstruction technique (SART). Entrance dose at 100 cm source to detector distance was measured using the RaySafe X2 R/F sensor (figure 1 b) and the dose area product (DAP) within the FOV was calculated. Projection space scatter to primary ratio (S/P) and scatter degradation factor (SDF) was calculated.

#### RESULTS

Reconstruction images using SIRT and SART are displayed in figure 1 c, d. The compiled SIRT algorithm took 3.44 s while SART took 21.6 s for completion. Both reconstructions were found to be anatomically correct and provided good resolution of all osseous structures. With collimation, DAP was calculated to be 170.0 mGy whereas without collimation DAP was 207.1 mGy to image the 540 cm<sup>2</sup> FOV of the chest phantom reconstructions. The average S/P and SDF with collimation across sources was 0.31 and 0.77 while the same was 0.69 and 0.59 respectively without collimation.

#### CONCLUSION

s This work demonstrates the feasibility of cone beam geometry based algebraic reconstruction for OT. Due to collimation, this system has significantly reduced scatter (> 50% decrease in S/P) and radiation (18% decrease in DAP) burden compared to conventional tomosynthesis.

#### CLINICAL RELEVANCE/APPLICATION

Conventional tomosynthesis is performed with specific anatomy within a limited FOV. Extended FOV tomosynthesis is beneficial for whole-body skeletal imaging in austere environments due to tomosynthesis' increased fracture detection sensitivity. Current research and commercial long-length tomosynthesis systems are built on large gantries making them unsuitable for mobile applications. The OT system presented here can be mounted on a single small unit and fits on the back of an ambulance or a helicopter. Patients could be scanned as they are loaded into the transport vehicle without the tube/detector ever moving. The reduced scatter and radiation hazard also makes OT suitable for repetitive use such as scoliosis imaging.

Printed on: 02/07/23

## Abstract Archives of the RSNA, 2022

R5B-SPPH-8

### Deep learning denoising and assessment of detectability of microcalcifications in digital breast tomosynthesis: A task-based image evaluation approach using CNN

Thursday, Dec. 1 12:45PM - 1:15PM Room: Learning Center - PH DPS

#### Participants

Mingjie Gao, (*Presenter*) Nothing to Disclose

#### PURPOSE

Deep learning (DL) denoising for digital breast tomosynthesis (DBT) has the potential to reduce dose and improve microcalcification (MC) detection. This study proposed two convolutional neural network (CNN) models to assess image noise (CNN-ns) and MC detectability (CNN-mc) and guide the development of denoising techniques.

#### METHODS AND MATERIALS

For the CNN-ns for noise estimation, we extracted 52,526  $128 \times 128 \times 3$ -pixel patches from virtual DBTs of a wide range of noise levels simulated by the VICTRE software as training set and calculated the root-mean-square variations of pixel values as training labels to fine-tune the ImageNet pre-trained ConvNeXt-T. For the CNN-mc for MC vs background classification, we collected with IRB approval 231 views of DBTs from 116 human subjects who had biopsy proven MCs and split the set by case into 127 views for training/validation and 104 views for testing. We reconstructed the DBTs with (1) simultaneous algebraic reconstruction technique (SART), (2) SART with DL-denoised projections, and (3) DL-denoiser regularized plug-and-play reconstruction. For each condition, we extracted 751  $128 \times 128 \times 3$ -pixel MC patches (6,008 after flipping and rotation augmentation) and 6,305 MC-free patches as training/validation set, and 709 MC and 777 MC-free patches as test set. Maximum intensity projection of the 3 slices was applied to all patches to emphasize the MCs. We adopted a multi-stage transfer learning strategy of first fine-tuning the ConvNeXt-T to CNN-ns, which was then further fine-tuned to CNN-mc. We used the area under ROC curve (AUC) of the CNN-mc as an MC detectability measure.

#### RESULTS

Our DL denoising methods reduced image noise and improved AUC. The AUC increased with MC signal strengths when the CNN-ns estimated noise was comparable. DL-denoiser regularized reconstruction with additional post-reconstruction denoising resulted in the lowest CNN-ns estimated noise and highest AUC. The AUC and noise rankings matched our visual judgement on the images.

#### CONCLUSION

The CNN-mc and CNN-ns provided task-based measures for image assessment, which may be useful for comparison of the detectability of clustered MCs in DBTs obtained with different denoising or reconstruction techniques.

#### CLINICAL RELEVANCE/APPLICATION

The CNN image assessment tools can help develop better DBT denoising or reconstruction methods, which may lead to lower dose and higher sensitivity and specificity for MC detection in screening.

Printed on: 02/07/23

## Abstract Archives of the RSNA, 2022

S3A-SPBR

### Breast Sunday Poster Discussions - A

Sunday, Nov. 27 11:45AM - 12:15PM Room: Learning Center - BR DPS

#### Participants

Beatriz Adrada, MD, Houston, TX (*Moderator*) Nothing to Disclose

#### Sub-Events

### S3A-SPBR-1 Use of Artificial Intelligence in Women with Mammographic Abnormality Reduces Screening Recalls

#### Participants

Jung Min Chang, MD, Seoul, (*Presenter*) Research Consultant, Genoray Co, Ltd

#### PURPOSE

Potential benefit of using artificial intelligence (AI) in reducing screening mammography recalls has not been well investigated in the past. This study was to evaluate whether artificial intelligence (AI)-aided reviews of mammographic findings can reduce unnecessary recall while maintaining cancer detection ability in mammography screening.

#### METHODS AND MATERIALS

A retrospective reader study was performed with screening mammography from women who were recalled for mammography-detected abnormalities between January 2016 and December 2019 at two screening centers. Exams were sequentially interpreted in two sessions, with and without AI aid, by three radiologists providing their decision on whether it should be recalled. The area under the receiver operating characteristic curve (AUC), sensitivity, specificity, and recall rates were compared.

#### RESULTS

A total of 793 women (mean age  $\pm$  standard deviation, 49.8 years  $\pm$  8.9), 54 cancer and 739 benign cases, were included. The AI standalone per-examination AUC was significantly higher than that of all three radiologists (0.94 [95% CI, 0.92-0.97] vs. 0.76 [95% CI, 0.69-0.83]; 0.80 [95% CI, 0.74-0.86]; 0.86 [95% CI, 0.82-0.91];  $P < .001$ , respectively). The per-examination and per-lesion reader-averaged AUC improved after AI aid (0.80 [95% CI, 0.71-0.90] vs. 0.91 [95% CI, 0.83-0.99];  $P = .02$ ; 0.79 [95% CI, 0.70-0.89] vs. 0.89 [95% CI, 0.83-0.96];  $P = .03$ ). In both the per-examination and per-lesion analyses, average specificities of all radiologists improved after AI aid (41.9% [95% CI, 4.3%-79.5%] vs. 53.9% [95% CI, 27.1%-80.7%];  $P = .04$ ), whereas the sensitivities only improved for the least experienced radiologist with AI aid (79.6%, 43 of 54 [95% CI, 66.5%-89.4%] vs. 90.7%, 49 of 54 [95% CI, 79.7%-96.9%];  $P = .03$ ). With AI aid, the average recall rate decreased from 60.4% (95% CI, 23.9%-96.8%) to 49.5% (95% CI, 23.9%-75.0%) with marginal significance ( $P = .05$ ).

#### CONCLUSION

The use of an AI system in women with screening recalls reduces the need for supplemental mammographic views and improves the overall diagnostic performance.

#### CLINICAL RELEVANCE/APPLICATION

In women recalled for mammographic abnormalities, the use of an AI system could improve the diagnostic performance of screening mammography, and provide an efficient way of diagnosing negative cases, which ultimately leads to a reduction of unnecessary recall and the workload.

### S3A-SPBR-2 Deep Learning-enabled Fully Automated Pipeline for Segmentation and Classification of Breast Lesions using Contrast Enhanced Mammography

#### Participants

Ning Mao, Yantai, China (*Presenter*) Nothing to Disclose

#### PURPOSE

We aimed to develop a deep learning - enabled fully automated pipeline for segmentation and classification of breast lesions using contrast enhanced mammography (CEM).

#### METHODS AND MATERIALS

In this study, we retrospectively collected 1710 preoperative CEM images of breast lesions from a hospital for the fully automated pipeline development and test. We adopted RefineNet and Xception as sub-networks of the pipeline system to perform segmentation and classification tasks, respectively. The segmentation performance was assessed using dice similarity coefficient (DSC) in test set. For classification task, we compared our system with the classification performance of four radiologists using the area under the receiver operating characteristic curve (AUROC). Finally, we also explored the performance of radiologists assisted by artificial intelligence (AI) and the changes in the amount of fine needle aspiration biopsy under the AI-assisted Breast Imaging Reporting and Data System (BI-RADS) category in view of clinical application.

## RESULTS

The automated pipeline for tumor segmentation achieved a DSC 0.888 in test cohort, the classification task performed by the Xception yielded an AUC of 0.906 (95%CI=0.857-0.955) in the CC+MLO view on test set, which is higher than CC view (0.876, 95%CI=0.819-0.933) and MLO view (0.850, 95%CI=0.784-0.916). And it also was significantly higher than those of radiologists (0.846, 95%CI=0.784-0.916). Furthermore, AI-assisted strategy improved the pooled AUC of the radiologists from 0.741 (95%CI=0.657-0.855) when diagnosing without AI to 0.874 (95%CI=0.757-0.921) with AI for the performance of classification in test set. The number of fine needle aspiration biopsies also reduced from 162 to 120 in the case of AI assisting BI-RADS category in test set.

## CONCLUSION

Our fully automated pipeline system based on CEM demonstrated the potential for segmentation and classification of breast lesions, and also had good clinical applicability.

## CLINICAL RELEVANCE/APPLICATION

The fully automated pipeline system that we developed can be well applied to the segmentation and classification of breast lesions as a non-invasive method. In addition, it also contributes greatly in assisting radiologists in making BI-RADS classification and reduces unnecessary biopsies, which could alleviate patient healthcare burden and promote the reallocation of healthcare resources.

### S3A-SPBR-3 Artificial Intelligence (AI) for Ultrasound (US) MicroFlow Imaging (MFI) in Breast Cancer Diagnosis

#### Participants

Ji Hyun Youk, MD, Seoul, Korea, Republic Of (*Presenter*) Nothing to Disclose

#### PURPOSE

To develop and evaluate AI algorithms for US MFI in breast cancer diagnosis

#### METHODS AND MATERIALS

We retrospectively collected a dataset consisting of 516 breast lesions (364 benign, 152 malignant) in 471 women who underwent B-mode US and MFI. BI-RADS category assigned by board-certified breast radiologists on B-mode US were noted. Pathology or at least 2-year follow up was used as the reference standard. To develop AI algorithms based on deep CNNs for MFI, the internal dataset was split into training (n=410, 79%) and test dataset (n=106, 21%). AI algorithms were trained to provide malignancy risk (0-100%). The developed AI algorithms were further validated with an independent external dataset consisting of 238 breast lesions (208 benign, 27 malignant). To evaluate and compare the diagnostic performance of B-mode US, AI algorithms, or their combination, the area under the receiver operating characteristic curve (AUROC) was calculated. Logistic regression analysis was used to calculate the malignancy risk of lesions in combined B-mode US and AI algorithms.

## RESULTS

The AUROC of developed three AI algorithms were 0.966, 0.964, and 0.955, respectively, and higher than that of B-mode US (0.842,  $P < .0001$ ). AI algorithms had higher specificity (93-95% vs. 72%) and accuracy (93% vs. 79%) than B-mode US ( $P < .003$ ). No significant difference was found in sensitivity between AI algorithms (88-91%) and B-mode US (97%). The performance metrics of the AI algorithms on the external validation dataset were similar to those of the test dataset (AUROC of 0.892-0.920, sensitivity of 82-89%, specificity of 92-98%, and accuracy of 91-96%). Among AI algorithms, no significant difference was found in all performance metrics with or without combination of B-mode US. Combined B-mode US and AI algorithms had higher performance than B-mode US (AUROC of 0.963-0.972, specificity of 96%, and accuracy of 94%,  $P = .0001$ ) except sensitivity (91%). By combining B-mode US and AI algorithms, false-positive rate of BI-RADS category 4A lesions significantly decreased from 87% to 13% ( $P < .0001$ ).

## CONCLUSION

AI-based MFI diagnosed breast cancers with better performance than B-mode US. Combined B-mode US and AI algorithm could eliminate 74% of false-positive diagnosis in BI-RADS category 4A lesions.

## CLINICAL RELEVANCE/APPLICATION

AI-based MFI can improve diagnostic accuracy of breast US by decreasing false positives diagnosis, and thus reducing unnecessary biopsies of benign lesions.

### S3A-SPBR-4 Detailed External Validation of A Commercial AI Algorithm for Breast Cancer Detection in The Setting of An Organized Population-based Breast Screening

#### Participants

Janette Sam, RT, Vancouver, BC (*Presenter*) Nothing to Disclose

#### PURPOSE

Evaluate the performance of a commercial Artificial Intelligence (AI) system for breast cancer detection using the digital mammograms from the BC Cancer Breast Screening Program

#### METHODS AND MATERIALS

Digital screening mammograms and associated outcomes, including mammographic findings (features), demographics, and risk factors were extracted for 136,700 women who underwent breast screening in British Columbia, Canada during the period February 1, 2019 - January 31, 2020. The outcome data were extracted on March 18, 2022. The images were de-identified and fed to the Lunit MMG AI algorithm version 1.1.2.0 running on a GeForce RTX 2080 GPU with 11 GB VRAM. The AI model performance was evaluated using Area Under the Curve (AUC) of Receiver Operating Characteristic (ROC) methodology.

## RESULTS

The overall performance of the AI algorithm measured with AUC was 0.938 (CI: 0.927-0.949). However, once binary classification is performed using the 10% cut-off value used by the algorithm, the AUC dropped to 0.846 (0.836-0.856) compared to the

radiologists performance at 0.937 (0.929-0.944). The AI AUC for BIRAD breast density categories assigned by the radiologists were: A: 0.964 (0.934-0.993); B: 0.946 (0.932-0.961); C: 0.934 (0.916-0.952) and D: 0.831 (0.752-0.911). For women with family history of breast cancer, the AI AUC was 0.919 (0.895-0.943) whereas for women with no family history, 0.945 (0.933-0.957). The algorithm performance for cancers with any architectural distortion was 0.961 (0.944-0.978) whereas for cancers with any calcifications was 0.878 (0.855-0.900).

## CONCLUSION

The tested commercial AI algorithm is generalizable for a large external cohort from Canada. However, the performance of the AI algorithm fell short of that of the well-qualified screening program radiologists. Performance of the algorithm for women with family history of breast cancer and for cancers manifesting as calcifications was found to be weaker.

## CLINICAL RELEVANCE/APPLICATION

Commercial AI algorithms well trained with datasets from multiple countries for breast cancer detection can be generalizable to cohorts in other countries. However, further improvements may be needed to match the performance of radiologists from well-organized population based breast screening programs.

## S3A-SPBR-6 Investigating a Stand-alone AI System Prompt Accuracy for Interval Cancer Detection in Screening Mammography

### Awards

**Trainee Research Prize - Fellow**

### Participants

Sarah Hickman, MBBS, Cambridge, United Kingdom (*Presenter*) Research collaboration, Vara; Research collaboration, ScreenPoint Medical BV; Research collaboration, Lunit Inc; Research collaboration, Kheiron Medical Technologies Ltd; Research collaboration, Alphabet Inc; Research collaboration, Volpara Health Technologies Limited

## PURPOSE

To evaluate the accuracy of prompts from a commercial artificial intelligence (AI) system in interval cancer detection.

## METHODS AND MATERIALS

An enriched dataset of screening mammograms of 1548 normals and 514 interval cancers diagnosed between 2011 and 2018 was analyzed with a commercial AI algorithm. This provided a continuous per-lesion, per-image, per-breast and per-case score (0-10), and prompts for suspicious lesion location. A pre-defined threshold specificity of 96%, (prompt score 6.8) was used. Each case is assigned an overall risk score representing the highest per-lesion score. Interval cancers were classified as either true negatives, minimal signs, or false negatives by a consensus panel. The cancer cases were reviewed (radiologist, 7 years' experience) to determine the accuracy of prompt location (prompt within boundary of cancer) with consensus (two breast radiologists) for indeterminate cases. The ground truth was histopathology for cancers and a three yearly normal screen for normals.

## RESULTS

The algorithm prompted 122/514 cancer cases, with an average prompt score of 8.5 (6.8-9.9) and correct localisation in 93/122 cases (76.2%). The highest prompt score was given for the cancer in 91/93 (97.8%) of the correctly localised cases. Overall interval cancer detection rate was 93/514 (18%). AI detected 12.6% of true negatives, 46% with minimal signs and 50% false negatives ( $p < 0.01$ ). There were 49 false positive prompts (0.09 per cancer case). For normal cases, the AI algorithm provided 61 false-positive recalls (3.9%) with an average prompt score of 8.1 (6.8-9.9). The overall sensitivity, specificity, and accuracy was 18%, 96%, and 76.6%, respectively. At alternative thresholds of 30% sensitivity and 90% specificity, the correct cancer localisation detection rate increased to 21.9%, and 25.4%, respectively. This corresponded to 7.5% and 9.6% false-positive recalls.

## CONCLUSION

Standalone AI set at the 96% specificity threshold can identify 23.7% of interval cancers with accurate localisation in three-quarters of cases.

## CLINICAL RELEVANCE/APPLICATION

High accuracy of AI localisation prompts provides a layer of explainability, providing required information for cases not detected by human readers to target supplemental imaging or clinic assessment biopsy.

## S3A-SPBR-7 AI-based Computer Assisted Diagnosis/Detection Systems Can Be Used for Upgrade Prediction of DCIS Diagnosed with Percutaneous Biopsy

### Participants

Jung Hyun Yoon, MD, PhD, Seoul, Korea, Republic Of (*Presenter*) Nothing to Disclose

## PURPOSE

To evaluate whether mammographic features and the abnormality scores provided by artificial intelligence (AI)-based computer assisted detection/diagnosis (AI-CAD) system can be used in predicting upgrade in ductal carcinoma in situ (DCIS).

## METHODS AND MATERIALS

This retrospective study had approval from our institutional review board (IRB). From Jan. 2015 to Dec. 2019, 440 DCIS diagnosed via percutaneous biopsy in 420 women (mean age, 52.8±10.6 years, range: 28-85) were included. Prebiopsy routine 4-view digital mammograms were analyzed using a commercially-available AI-CAD to obtain an abnormality score (range, 0-100%). Radiologic features were assessed according to mammographic features of the proven DCIS (negative, soft tissue lesions, calcifications with/without soft tissue lesions) and BI-RADS final assessment. Optimal cutoff for AI-CAD score was calculated using Youden J index. Uni-/multivariable regression analysis was used to calculate the association between clinical, radiologic, and pathologic factors to DCIS upgrade after surgery.

## RESULTS

Of the 440 DCIS, 117 (26.6%) were upgraded to invasive cancers. Mean AI-CAD score was significantly higher in those with upgrade (96.6% vs. 58.6%,  $P=0.0006$ ). Optimal cutoff of AI-CAD score for DCIS upgrade was calculated as 82.87%. Among radiologic features, BI-RADS assessment, presence of calcifications, and AI-CAD score showed significance on univariable analysis (all  $P<0.05$ ). BI-RADS 4c (OR: 2.509 (95% CI: 1.154-5.455),  $P=0.020$ ) and 5 (OR: 5.266 (95% CI: 2.215-12.519),  $P=0.0002$ ), presence of calcifications (OR: 2.198 (95% CI: 1.075-4.485),  $P=0.031$ ), AI-CAD score (at cutoff of 82.87%) (OR: 2.272 (95% CI: 1.340-3.853),  $P=0.002$ ), and vacuum-assisted biopsy for diagnosis (0.465 (95% CI: 0.248-0.871),  $P=0.016$ ) were factors showing significance in multivariable analysis.

#### **CONCLUSION**

s Mammographic features assessed by radiologists and AI-CAD can be used as significant predictors of DCIS upgrade.

#### **CLINICAL RELEVANCE/APPLICATION**

Noninvasive imaging features including results from AI-based cancer detection and diagnosis system have the potential in predicting DCIS upgrade that may be beneficial in patient management including surgical extent.

Printed on: 02/07/23

## Abstract Archives of the RSNA, 2022

S3A-SPBR-1

### Use of Artificial Intelligence in Women with Mammographic Abnormality Reduces Screening Recalls

Sunday, Nov. 27 11:45AM - 12:15PM Room: Learning Center - BR DPS

#### Participants

Jung Min Chang, MD, Seoul, (*Presenter*) Research Consultant, Genoray Co, Ltd

#### PURPOSE

Potential benefit of using artificial intelligence (AI) in reducing screening mammography recalls has not been well investigated in the past. This study was to evaluate whether artificial intelligence (AI)-aided reviews of mammographic findings can reduce unnecessary recall while maintaining cancer detection ability in mammography screening.

#### METHODS AND MATERIALS

A retrospective reader study was performed with screening mammography from women who were recalled for mammography-detected abnormalities between January 2016 and December 2019 at two screening centers. Exams were sequentially interpreted in two sessions, with and without AI aid, by three radiologists providing their decision on whether it should be recalled. The area under the receiver operating characteristic curve (AUC), sensitivity, specificity, and recall rates were compared.

#### RESULTS

A total of 793 women (mean age  $\pm$  standard deviation, 49.8 years  $\pm$  8.9), 54 cancer and 739 benign cases, were included. The AI standalone per-examination AUC was significantly higher than that of all three radiologists (0.94 [95% CI, 0.92-0.97] vs. 0.76 [95% CI, 0.69-0.83]; 0.80 [95% CI, 0.74-0.86]; 0.86 [95% CI, 0.82-0.91];  $P < .001$ , respectively). The per-examination and per-lesion reader-averaged AUC improved after AI aid (0.80 [95% CI, 0.71-0.90] vs. 0.91 [95% CI, 0.83-0.99];  $P = .02$ ; 0.79 [95% CI, 0.70-0.89] vs. 0.89 [95% CI, 0.83-0.96];  $P = .03$ ). In both the per-examination and per-lesion analyses, average specificities of all radiologists improved after AI aid (41.9% [95% CI, 4.3%-79.5%] vs. 53.9% [95% CI, 27.1%-80.7%];  $P = .04$ ), whereas the sensitivities only improved for the least experienced radiologist with AI aid (79.6%, 43 of 54 [95% CI, 66.5%-89.4%] vs. 90.7%, 49 of 54 [95% CI, 79.7%-96.9%];  $P = .03$ ). With AI aid, the average recall rate decreased from 60.4% (95% CI, 23.9%-96.8%) to 49.5% (95% CI, 23.9%-75.0%) with marginal significance ( $P = .05$ ).

#### CONCLUSION

The use of an AI system in women with screening recalls reduces the need for supplemental mammographic views and improves the overall diagnostic performance.

#### CLINICAL RELEVANCE/APPLICATION

In women recalled for mammographic abnormalities, the use of an AI system could improve the diagnostic performance of screening mammography, and provide an efficient way of diagnosing negative cases, which ultimately leads to a reduction of unnecessary recall and the workload.

Printed on: 02/07/23

## Abstract Archives of the RSNA, 2022

S3A-SPBR-2

### Deep Learning-enabled Fully Automated Pipeline for Segmentation and Classification of Breast Lesions using Contrast Enhanced Mammography

Sunday, Nov. 27 11:45AM - 12:15PM Room: Learning Center - BR DPS

#### Participants

Ning Mao, Yantai, China (*Presenter*) Nothing to Disclose

#### PURPOSE

We aimed to develop a deep learning - enabled fully automated pipeline for segmentation and classification of breast lesions using contrast enhanced mammography (CEM).

#### METHODS AND MATERIALS

In this study, we retrospectively collected 1710 preoperative CEM images of breast lesions from a hospital for the fully automated pipeline development and test. We adopted RefineNet and Xception as sub-networks of the pipeline system to perform segmentation and classification tasks, respectively. The segmentation performance was assessed using dice similarity coefficient (DSC) in test set. For classification task, we compared our system with the classification performance of four radiologists using the area under the receiver operating characteristic curve (AUROC). Finally, we also explored the performance of radiologists assisted by artificial intelligence (AI) and the changes in the amount of fine needle aspiration biopsy under the AI-assisted Breast Imaging Reporting and Data System (BI-RADS) category in view of clinical application.

#### RESULTS

The automated pipeline for tumor segmentation achieved a DSC 0.888 in test cohort, the classification task performed by the Xception yielded an AUC of 0.906 (95%CI=0.857-0.955) in the CC+MLO view on test set, which is higher than CC view (0.876, 95%CI=0.819-0.933) and MLO view (0.850, 95%CI=0.784-0.916). And it also was significantly higher than those of radiologists (0.846, 95%CI=0.784-0.916). Furthermore, AI-assisted strategy improved the pooled AUC of the radiologists from 0.741(95%CI=0.657-0.855) when diagnosing without AI to 0.874 (95%CI=0.757-0.921) with AI for the performance of classification in test set. The number of fine needle aspiration biopsies also reduced from 162 to 120 in the case of AI assisting BI-RADS category in test set.

#### CONCLUSION

Our fully automated pipeline system based on CEM demonstrated the potential for segmentation and classification of breast lesions, and also had good clinical applicability.

#### CLINICAL RELEVANCE/APPLICATION

The fully automated pipeline system that we developed can be well applied to the segmentation and classification of breast lesions as a non-invasive method, In addition, it also contributes greatly in assisting radiologists in making BI-RADS classification and reduces unnecessary biopsies, which could alleviate patient healthcare burden and promote the reallocation of healthcare resources.

Printed on: 02/07/23

## Abstract Archives of the RSNA, 2022

S3A-SPBR-3

### Artificial Intelligence (AI) for Ultrasound (US) MicroFlow Imaging (MFI) in Breast Cancer Diagnosis

Sunday, Nov. 27 11:45AM - 12:15PM Room: Learning Center - BR DPS

#### Participants

Ji Hyun Youk, MD, Seoul, Korea, Republic Of (*Presenter*) Nothing to Disclose

#### PURPOSE

To develop and evaluate AI algorithms for US MFI in breast cancer diagnosis

#### METHODS AND MATERIALS

We retrospectively collected a dataset consisting of 516 breast lesions (364 benign, 152 malignant) in 471 women who underwent B-mode US and MFI. BI-RADS category assigned by board-certified breast radiologists on B-mode US were noted. Pathology or at least 2-year follow up was used as the reference standard. To develop AI algorithms based on deep CNNs for MFI, the internal dataset was split on into training (n=410, 79%) and test dataset (n=106, 21%). AI algorithms were trained to provide malignancy risk (0-100%). The developed AI algorithms were further validated with an independent external dataset consisting of 238 breast lesions (208 benign, 27 malignant). To evaluate and compare the diagnostic performance of B-mode US, AI algorithms, or their combination, the area under the receiver operating characteristic curve (AUROC) was calculated. Logistic regression analysis was used to calculate the malignancy risk of lesions in combined B-mode US and AI algorithms.

#### RESULTS

The AUROC of developed three AI algorithms were 0.966, 0.964, and 0.955, respectively, and higher than that of B-mode US (0.842,  $P < .0001$ ). AI algorithms had higher specificity (93-95% vs. 72%) and accuracy (93% vs. 79%) than B-mode US ( $P < .003$ ). No significant difference was found in sensitivity between AI algorithms (88-91%) and B-mode US (97%). The performance metrics of the AI algorithms on the external validation dataset were similar to those of the test dataset (AUROC of 0.892-0.920, sensitivity of 82-89%, specificity of 92-98%, and accuracy of 91-96%). Among AI algorithms, no significant difference was found in all performance metrics with or without combination of B-mode US. Combined B-mode US and AI algorithms had higher performance than B-mode US (AUROC of 0.963-0.972, specificity of 96%, and accuracy of 94%,  $P = .0001$ ) except sensitivity (91%). By combining B-mode US and AI algorithms, false-positive rate of BI-RADS category 4A lesions significantly decreased from 87% to 13% ( $P < .0001$ ).

#### CONCLUSION

s AI-based MFI diagnosed breast cancers with better performance than B-mode US. Combined B-mode US and AI algorithm could eliminate 74% of false-positive diagnosis in BI-RADS category 4A lesions.

#### CLINICAL RELEVANCE/APPLICATION

AI-based MFI can improve diagnostic accuracy of breast US by decreasing false positives diagnosis, and thus reducing unnecessary biopsies of benign lesions.

Printed on: 02/07/23

## Abstract Archives of the RSNA, 2022

S3A-SPBR-4

### Detailed External Validation of A Commercial AI Algorithm for Breast Cancer Detection in The Setting of An Organized Population-based Breast Screening

Sunday, Nov. 27 11:45AM - 12:15PM Room: Learning Center - BR DPS

#### Participants

Janette Sam, RT, Vancouver, BC (*Presenter*) Nothing to Disclose

#### PURPOSE

Evaluate the performance of a commercial Artificial Intelligence (AI) system for breast cancer detection using the digital mammograms from the BC Cancer Breast Screening Program

#### METHODS AND MATERIALS

Digital screening mammograms and associated outcomes, including mammographic findings (features), demographics, and risk factors were extracted for 136,700 women who underwent breast screening in British Columbia, Canada during the period February 1, 2019 - January 31, 2020. The outcome data were extracted on March 18, 2022. The images were de-identified and fed to the Lunit MMG AI algorithm version 1.1.2.0 running on a GeForce RTX 2080 GPU with 11 GB VRAM. The AI model performance was evaluated using Area Under the Curve (AUC) of Receiver Operating Characteristic (ROC) methodology.

#### RESULTS

The overall performance of the AI algorithm measured with AUC was 0.938 (CI: 0.927-0.949). However, once binary classification is performed using the 10% cut-off value used by the algorithm, the AUC dropped to 0.846 (0.836-0.856) compared to the radiologists performance at 0.937 (0.929-0.944). The AI AUC for BIRAD breast density categories assigned by the radiologists were: A: 0.964 (0.934-0.993); B: 0.946 (0.932-0.961); C: 0.934 (0.916-0.952) and D: 0.831 (0.752-0.911). For women with family history of breast cancer, the AI AUC was 0.919 (0.895-0.943) whereas for women with no family history, 0.945 (0.933-0.957). The algorithm performance for cancers with any architectural distortion was 0.961 (0.944-0.978) whereas for cancers with any calcifications was 0.878 (0.855-0.900).

#### CONCLUSION

The tested commercial AI algorithm is generalizable for a large external cohort from Canada. However, the performance of the AI algorithm fell short of that of the well-qualified screening program radiologists. Performance of the algorithm for women with family history of breast cancer and for cancers manifesting as calcifications was found to be weaker.

#### CLINICAL RELEVANCE/APPLICATION

Commercial AI algorithms well trained with datasets from multiple countries for breast cancer detection can be generalizable to cohorts in other countries. However, further improvements may be needed to match the performance of radiologists from well-organized population based breast screening programs.

Printed on: 02/07/23

## Abstract Archives of the RSNA, 2022

S3A-SPBR-6

### Investigating a Stand-alone AI System Prompt Accuracy for Interval Cancer Detection in Screening Mammography

Sunday, Nov. 27 11:45AM - 12:15PM Room: Learning Center - BR DPS

#### Awards

**Trainee Research Prize - Fellow**

#### Participants

Sarah Hickman, MBBS, Cambridge, United Kingdom (*Presenter*) Research collaboration, Vara; Research collaboration, ScreenPoint Medical BV; Research collaboration, Lunit Inc; Research collaboration, Kheiron Medical Technologies Ltd; Research collaboration, Alphabet Inc; Research collaboration, Volpara Health Technologies Limited

#### PURPOSE

To evaluate the accuracy of prompts from a commercial artificial intelligence (AI) system in interval cancer detection.

#### METHODS AND MATERIALS

An enriched dataset of screening mammograms of 1548 normals and 514 interval cancers diagnosed between 2011 and 2018 was analyzed with a commercial AI algorithm. This provided a continuous per-lesion, per-image, per-breast and per-case score (0-10), and prompts for suspicious lesion location. A pre-defined threshold specificity of 96%, (prompt score 6.8) was used. Each case is assigned an overall risk score representing the highest per-lesion score. Interval cancers were classified as either true negatives, minimal signs, or false negatives by a consensus panel. The cancer cases were reviewed (radiologist, 7 years' experience) to determine the accuracy of prompt location (prompt within boundary of cancer) with consensus (two breast radiologists) for indeterminate cases. The ground truth was histopathology for cancers and a three yearly normal screen for normals.

#### RESULTS

The algorithm prompted 122/514 cancer cases, with an average prompt score of 8.5 (6.8-9.9) and correct localisation in 93/122 cases (76.2%). The highest prompt score was given for the cancer in 91/93 (97.8%) of the correctly localised cases. Overall interval cancer detection rate was 93/514 (18%). AI detected 12.6% of true negatives, 46% with minimal signs and 50% false negatives ( $p < 0.01$ ). There were 49 false positive prompts (0.09 per cancer case). For normal cases, the AI algorithm provided 61 false-positive recalls (3.9%) with an average prompt score of 8.1 (6.8-9.9). The overall sensitivity, specificity, and accuracy was 18%, 96%, and 76.6%, respectively. At alternative thresholds of 30% sensitivity and 90% specificity, the correct cancer localisation detection rate increased to 21.9%, and 25.4%, respectively. This corresponded to 7.5% and 9.6% false-positive recalls.

#### CONCLUSION

Standalone AI set at the 96% specificity threshold can identify 23.7% of interval cancers with accurate localisation in three-quarters of cases.

#### CLINICAL RELEVANCE/APPLICATION

High accuracy of AI localisation prompts provides a layer of explainability, providing required information for cases not detected by human readers to target supplemental imaging or clinic assessment biopsy.

Printed on: 02/07/23

## Abstract Archives of the RSNA, 2022

S3A-SPBR-7

### AI-based Computer Assisted Diagnosis/Detection Systems Can Be Used for Upgrade Prediction of DCIS Diagnosed with Percutaneous Biopsy

Sunday, Nov. 27 11:45AM - 12:15PM Room: Learning Center - BR DPS

#### Participants

Jung Hyun Yoon, MD, PhD, Seoul, Korea, Republic Of (*Presenter*) Nothing to Disclose

#### PURPOSE

To evaluate whether mammographic features and the abnormality scores provided by artificial intelligence (AI)-based computer assisted detection/diagnosis (AI-CAD) system can be used in predicting upgrade in ductal carcinoma in situ (DCIS).

#### METHODS AND MATERIALS

This retrospective study had approval from our institutional review board (IRB). From Jan. 2015 to Dec. 2019, 440 DCIS diagnosed via percutaneous biopsy in 420 women (mean age, 52.8±10.6 years, range: 28-85) were included. Prebiopsy routine 4-view digital mammograms were analyzed using a commercially-available AI-CAD to obtain an abnormality score (range, 0-100%). Radiologic features were assessed according to mammographic features of the proven DCIS (negative, soft tissue lesions, calcifications with/without soft tissue lesions) and BI-RADS final assessment. Optimal cutoff for AI-CAD score was calculated using Youden J index. Uni-/multivariable regression analysis was used to calculate the association between clinical, radiologic, and pathologic factors to DCIS upgrade after surgery.

#### RESULTS

Of the 440 DCIS, 117 (26.6%) were upgraded to invasive cancers. Mean AI-CAD score was significantly higher in those with upgrade (96.6% vs. 58.6%,  $P=0.0006$ ). Optimal cutoff of AI-CAD score for DCIS upgrade was calculated as 82.87%. Among radiologic features, BI-RADS assessment, presence of calcifications, and AI-CAD score showed significance on univariable analysis (all  $P<0.05$ ). BI-RADS 4c (OR: 2.509 (95% CI: 1.154-5.455),  $P=0.020$ ) and 5 (OR: 5.266 (95% CI: 2.215-12.519),  $P=0.0002$ ), presence of calcifications (OR: 2.198 (95% CI: 1.075-4.485),  $P=0.031$ ), AI-CAD score (at cutoff of 82.87%) (OR: 2.272 (95% CI: 1.340-3.853),  $P=0.002$ ), and vacuum-assisted biopsy for diagnosis (0.465 (95% CI: 0.248-0.871),  $P=0.016$ ) were factors showing significance in multivariable analysis.

#### CONCLUSION

s Mammographic features assessed by radiologists and AI-CAD can be used as significant predictors of DCIS upgrade.

#### CLINICAL RELEVANCE/APPLICATION

Noninvasive imaging features including results from AI-based cancer detection and diagnosis system have the potential in predicting DCIS upgrade that may be beneficial in patient management including surgical extent.

Printed on: 02/07/23

## Abstract Archives of the RSNA, 2022

S3A-SPCA

### Cardiac Sunday Poster Discussions - A

Sunday, Nov. 27 11:45AM - 12:15PM Room: Learning Center - CA DPS

#### Sub-Events

#### **S3A-SPCA-1 Improvement of Coronary Stent CT Imaging with Super-Resolution Deep-Learning Reconstruction: An Initial In Vivo Experience**

##### Participants

Yasunori Nagayama, MD, Kumamoto, Japan (*Presenter*) Nothing to Disclose

##### PURPOSE

To evaluate the subjective and objective image qualities of novel super-resolution deep-learning reconstruction (SR-DLR) algorithm for in vivo coronary stents and compare them with those of iterative reconstruction (IR) and normal-resolution DLR (NR-DLR) algorithms.

##### METHODS AND MATERIALS

This retrospective study included 17 patients with 24 coronary stents who underwent ECG-gated coronary CT angiography on a 320-row scanner. Raw data were reconstructed with hybrid IR (HIR, AIDR 3D), model-based IR (MBIR, FIRST), NR-DLR (AiCE), and SR-DLR (PIQE) using dedicated cardiac parameters at a slice thickness of 0.5 mm. The external and internal diameters of the stents were measured to quantify the degree of blooming artifacts (defined as [measured external stent diameter - measured internal stent diameter]/measured external stent diameter). CT attenuation in the lumen of the stent (HUstent) and that of upstream coronary artery (HUcoronary) was measured. The stent-induced beam hardening artifacts were quantified as HUstent-HUcoronary. The image noise and contrast-to-noise ratio (CNR) of the coronary arteries were quantified. The delineation of the coronary wall before the stent, stent lumen, stent strut, calcifications surrounding the stent, beam-hardening artifacts, image noise, and overall quality were subjectively scored on a 5-point scale (1, inadequate; 5, excellent).

##### RESULTS

Among all reconstructions, SR-DLR images showed the largest internal diameters of the stents, for which blooming artifact was considerably reduced relative to HIR, MBIR, and NR-DLR images (all  $p < 0.05$ ). SR-DLR also provided lower stent-induced beam hardening artifacts, lower image noise, and higher CNR than HIR, MBIR, and NR-DLR (all  $p < 0.05$ ). In the subjective assessments, SR-DLR images received the best scores for all evaluation criteria (all  $p < 0.05$ ).

##### CONCLUSION

SR-DLR improves the objective and subjective qualities of coronary stent imaging compared with HIR, MBIR, and NR-DLR algorithms.

##### CLINICAL RELEVANCE/APPLICATION

Novel SR-DLR algorithm allows improvement of coronary stent evaluation because of excellent spatial resolution, lower blooming artifact, and stent-induced beam-hardening artifacts.

#### **S3A-SPCA-2 High Fidelity Coronary CT Angiography Generated by Deep Learning Based Post Hoc Denoising Method Improved the Diagnostic Performance of the Coronary Perivascular Fat Attenuation Index**

##### Participants

Tatsuya Nishii, MD, PhD, Suita, Japan (*Presenter*) Speakers Bureau, Guerbet SA; Speakers Bureau, General Electric Company; Speakers Bureau, Siemens AG; Research Grant, Canon Medical Systems Corporation

##### PURPOSE

Coronary inflammation related to vulnerable hemorrhagic plaques can be captured by the perivascular fat attenuation index (FAI) using coronary CT angiography (CCTA). Since FAI is susceptible to image noise, we believed that deep learning (DL) based post hoc noise reduction could improve diagnostic capability. We aimed to assess the diagnosis performance of FAI in DL-based denoised high fidelity CCTA images using coronary plaque MR imaging as a reference.

##### METHODS AND MATERIALS

We retrospectively reviewed 64 patients who examined standard CCTA and coronary plaque MR imaging (MPRAGE) within 2-month intervals from April 2017 to June 2019. Those examined with non-3T MRIs and those with stents or obstructions at proximal right coronary artery (RCA) were excluded. We generated the high fidelity CCTA images by denoising the standard CCTA images using a residual dense network supervised the denoising task by averaging CCTA images. In the original and denoised CCTA, we measured the FAIs as the mean CT value of all voxels (range of -190 to -30 HU) located within a radial distance from the outer proximal RCA wall using dedicated software. The diagnostic reference was defined using MRI with the consensus reading of 2 board-certified radiologists. We specified high-intensity plaques (HIP; vulnerable hemorrhagic plaque) as those with a plaque-to-myocardium signal ratio  $\geq 1.4$ . The diagnostic performance of FAI in the original and denoised image was assessed using ROC analysis with regarded

presence of HIPs.

## RESULTS

Of 45 cases (37 males, median 65 years), 12 cases had HIPs. The FAIs in the denoised CCTA image were correlated ( $r=0.97$ ,  $P<.001$ ) but were higher than those of the original (mean difference, 4.3 [95%CI 0.64-0.92],  $P<.001$ ). FAI in the denoised CCTA improved the area under the ROC curve (0.87 [95%CI 0.77-0.98]) compared with FAI in the original image (0.78 [95%CI 0.64-0.92],  $P=.013$ ). The optimal cutoff value for predicting HIPs in denoised CCTA was -69HU with 0.83 sensitivity, 0.79 specificities, and 0.80 accuracies.

## CONCLUSION

s DL-based denoised high fidelity CCTA improved the diagnosis performance of FAI for predicting vulnerable hemorrhagic plaques.

## CLINICAL RELEVANCE/APPLICATION

The DL-based post hoc denoising method, which does not require CT projection data nor additional radiation exposure, can improve the diagnostic performance of FAI for vulnerable hemorrhagic plaques in CCTA.

## S3A-SPCA-3 Photon Counting Detector-CT Angiography of The Coronary Arteries: Intra-individual Comparison of Image Quality to Conventional Energy-integrating Detector-CT Angiography

Participants

Joseph Griffith III, Charleston, SC (*Presenter*) Nothing to Disclose

## PURPOSE

The aim of this study was the intra-individual evaluation of objective image quality for CT angiography of the coronary arteries on a photon counting detector CT (PCD-CCTA) in comparison to a conventional energy-integrating detector CT (EID-CCTA).

## METHODS AND MATERIALS

Twenty prospectively included patients ( $59.2\pm 13.2$  years, 65% male) with PCD- and EID-CCTA were examined at an interval of  $9 \pm 4$  days. Contrast agent protocol and radiation dose were matched between PCD and EID CCTA. Polychromatic images were reconstructed for both EID and PCD CCTA (T3D). In addition, virtual monoenergetic images at 40, 50, 60, and 70 keV were reconstructed on the PCD-CT. Signal, contrast and noise were measured in the aorta, coronary arteries, and myocardium, and the contrast-to-noise ratio (CNR) was calculated for each anatomical structure. Differences were compared using a paired t-test and a Bonferroni-corrected p-value of 0.008 was considered significant.

## RESULTS

The mean CNR of the left coronary artery was  $13.3\pm 5.4$  for the EID-CCTA and  $31.8\pm 12.1$ ,  $28.4\pm 9.7$ ,  $23.5\pm 7.1$ ,  $21.2\pm 6.7$  and  $21.9\pm 6.7$  for the PCD-CCTA at 40, 50, 60, 70 keV and T3D, respectively. CNR was significantly higher in all virtual monoenergetic reconstructions of PCD-CT than EID-CT (all  $P<0.008$ ).

## CONCLUSION

s PCD-CCTA with monoenergetic reconstructions leads to a significantly increased CNR compared to EID-CCTA.

## CLINICAL RELEVANCE/APPLICATION

The improved image quality of PCD-CCTA may be translated into clinical advantages including low-dose scanning or improved detection of coronary artery disease.

## S3A-SPCA-4 Super-Resolution Deep Learning Reconstruction for Cardiac CT: Comparison of Stenosis Evaluation Accuracy, Image Quality, Stenosis Confidence Level at Coronary Arteries and CAD-RADS Classification with Hybrid-Type and Model-Based Iterative Reconstructions and Deep Learning Reconstruction at In Vivo and In Vitro Studies

Participants

Yoshiharu Ohno, MD, PhD, Toyooka, Japan (*Presenter*) Research Grant, Canon Medical Systems Corporation; Research Grant, Daiichi Sankyo Co, Ltd; Research Grant, Ministry of Education, Culture, Sports, Science and Technology

## PURPOSE

Super-resolution deep learning reconstruction (SR-DLR) for cardiac CT scans is recently set in routine clinical practice, which can maximize spatial resolution of area-detector CT (ADCT) ( $0.5\text{mm}\times 320$  rows/896 channels) as super-high-resolution CT ( $0.25\text{mm}\times 160$  rows/1792 channels) without reducing low-contrast detectability or increasing dose. The purpose of this study was to compare stenosis evaluation accuracy, image quality, stenosis confidence level and CAD-RADS classification on cardiac ADCT among hybrid-type and model-based iterative reconstructions (i.e. hybrid-type IR and MBIR), deep learning reconstruction (DLR) and SR-DLR at in vivo and in vitro studies.

## METHODS AND MATERIALS

On in vitro study, a commercially available pulsating cardiac phantom with 3mm and 4 mm coronary artery phantoms, which had simulated 0, 25, 50 and 75% stenoses, were firstly scanned with standard protocol on a ADCT at five times and reconstructed with each method. Then, inner diameter of each coronary artery phantom was automatically measured. On in vivo study, 31 patients who suspected ischemic heart disease and underwent cardiac ADCT with standard protocol and coronary arteriography (CAG) were selected, and each cardiac ADCT data was also reconstructed with all methods. To compare stenosis evaluation accuracy among all methods, Spearman's correlations and Bland-Altman analyses were performed. To compare overall image quality, stenosis confidence level and CAD-RADS evaluations at all coronary arteries, each index was assessed by 5-points scoring systems and CAD-RADS classification and compared among all methods by Wilcoxon's signed rank test. Moreover, accuracy of CAD-RADS classification with standard reference generated from CAG by cardiologists were compared among all methods by McNemar's test.

## RESULTS

On in vitro study, each methods showed excellent correlation (hybrid-type IR:  $\rho=0.93$ ,  $p<0.0001$ ; others:  $\rho=0.94$ ,  $p<0.0001$ ). The

limits of agreements for SR-DLR ( $0.7\pm 0.4\text{mm}$ ) and DLR ( $0.7\pm 0.4\text{mm}$ ) were smaller than those for hybrid-type IR ( $0.8\pm 0.5\text{mm}$ ) and MBIR ( $0.8\pm 0.4\text{mm}$ ). On in vivo study, overall image quality and stenosis confidence level of SR-DLR were significantly higher than those of others ( $p<0.05$ ). Moreover, both indexes of DLR were significantly higher than those of hybrid-type IR ( $p<0.05$ ). On the other hand, CAD-RADS classification accuracy had no significant difference among all methods ( $p>0.05$ ).

#### **CONCLUSION**

s SR-DLR has a potential to improve stenosis evaluation accuracy, image quality and stenosis confidence level on cardiac CT than others at in vivo and in vitro studies.

#### **CLINICAL RELEVANCE/APPLICATION**

SR-DLR has a potential to improve stenosis evaluation accuracy, image quality and stenosis confidence level than others on cardiac ADCT.

Printed on: 02/07/23

## Abstract Archives of the RSNA, 2022

S3A-SPCA-1

### Improvement of Coronary Stent CT Imaging with Super-Resolution Deep-Learning Reconstruction: An Initial In Vivo Experience

Sunday, Nov. 27 11:45AM - 12:15PM Room: Learning Center - CA DPS

#### Participants

Yasunori Nagayama, MD, Kumamoto, Japan (*Presenter*) Nothing to Disclose

#### PURPOSE

To evaluate the subjective and objective image qualities of novel super-resolution deep-learning reconstruction (SR-DLR) algorithm for in vivo coronary stents and compare them with those of iterative reconstruction (IR) and normal-resolution DLR (NR-DLR) algorithms.

#### METHODS AND MATERIALS

This retrospective study included 17 patients with 24 coronary stents who underwent ECG-gated coronary CT angiography on a 320-row scanner. Raw data were reconstructed with hybrid IR (HIR, AIDR 3D), model-based IR (MBIR, FIRST), NR-DLR (AiCE), and SR-DLR (PIQE) using dedicated cardiac parameters at a slice thickness of 0.5 mm. The external and internal diameters of the stents were measured to quantify the degree of blooming artifacts (defined as [measured external stent diameter - measured internal stent diameter]/measured external stent diameter). CT attenuation in the lumen of the stent (HUstent) and that of upstream coronary artery (HUcoronary) was measured. The stent-induced beam hardening artifacts were quantified as HUstent-HUcoronary. The image noise and contrast-to-noise ratio (CNR) of the coronary arteries were quantified. The delineation of the coronary wall before the stent, stent lumen, stent strut, calcifications surrounding the stent, beam-hardening artifacts, image noise, and overall quality were subjectively scored on a 5-point scale (1, inadequate; 5, excellent).

#### RESULTS

Among all reconstructions, SR-DLR images showed the largest internal diameters of the stents, for which blooming artifact was considerably reduced relative to HIR, MBIR, and NR-DLR images (all  $p < 0.05$ ). SR-DLR also provided lower stent-induced beam hardening artifacts, lower image noise, and higher CNR than HIR, MBIR, and NR-DLR (all  $p < 0.05$ ). In the subjective assessments, SR-DLR images received the best scores for all evaluation criteria (all  $p < 0.05$ ).

#### CONCLUSION

SR-DLR improves the objective and subjective qualities of coronary stent imaging compared with HIR, MBIR, and NR-DLR algorithms.

#### CLINICAL RELEVANCE/APPLICATION

Novel SR-DLR algorithm allows improvement of coronary stent evaluation because of excellent spatial resolution, lower blooming artifact, and stent-induced beam-hardening artifacts.

Printed on: 02/07/23

## Abstract Archives of the RSNA, 2022

S3A-SPCA-2

### High Fidelity Coronary CT Angiography Generated by Deep Learning Based Post Hoc Denoising Method Improved the Diagnostic Performance of the Coronary Perivascular Fat Attenuation Index

Sunday, Nov. 27 11:45AM - 12:15PM Room: Learning Center - CA DPS

#### Participants

Tatsuya Nishii, MD, PhD, Suita, Japan (*Presenter*) Speakers Bureau, Guerbet SA; Speakers Bureau, General Electric Company; Speakers Bureau, Siemens AG; Research Grant, Canon Medical Systems Corporation

#### PURPOSE

Coronary inflammation related to vulnerable hemorrhagic plaques can be captured by the perivascular fat attenuation index (FAI) using coronary CT angiography (CCTA). Since FAI is susceptible to image noise, we believed that deep learning (DL) based post hoc noise reduction could improve diagnostic capability. We aimed to assess the diagnosis performance of FAI in DL-based denoised high fidelity CCTA images using coronary plaque MR imaging as a reference.

#### METHODS AND MATERIALS

We retrospectively reviewed 64 patients who examined standard CCTA and coronary plaque MR imaging (MPRAGE) within 2-month intervals from April 2017 to June 2019. Those examined with non-3T MRIs and those with stents or obstructions at proximal right coronary artery (RCA) were excluded. We generated the high fidelity CCTA images by denoising the standard CCTA images using a residual dense network supervised the denoising task by averaging CCTA images. In the original and denoised CCTA, we measured the FAIs as the mean CT value of all voxels (range of -190 to -30 HU) located within a radial distance from the outer proximal RCA wall using dedicated software. The diagnostic reference was defined using MRI with the consensus reading of 2 board-certified radiologists. We specified high-intensity plaques (HIP; vulnerable hemorrhagic plaque) as those with a plaque-to-myocardium signal ratio  $\geq 1.4$ . The diagnostic performance of FAI in the original and denoised image was assessed using ROC analysis with regarded presence of HIPs.

#### RESULTS

Of 45 cases (37 males, median 65 years), 12 cases had HIPs. The FAIs in the denoised CCTA image were correlated ( $r=0.97$ ,  $P<.001$ ) but were higher than those of the original (mean difference, 4.3 [95%CI 0.64-0.92],  $P<.001$ ). FAI in the denoised CCTA improved the area under the ROC curve (0.87 [95%CI 0.77-0.98]) compared with FAI in the original image (0.78 [95%CI 0.64-0.92],  $P=.013$ ). The optimal cutoff value for predicting HIPs in denoised CCTA was -69HU with 0.83 sensitivity, 0.79 specificities, and 0.80 accuracies.

#### CONCLUSION

s DL-based denoised high fidelity CCTA improved the diagnosis performance of FAI for predicting vulnerable hemorrhagic plaques.

#### CLINICAL RELEVANCE/APPLICATION

The DL-based post hoc denoising method, which does not require CT projection data nor additional radiation exposure, can improve the diagnostic performance of FAI for vulnerable hemorrhagic plaques in CCTA.

Printed on: 02/07/23

## Abstract Archives of the RSNA, 2022

S3A-SPCA-3

### Photon Counting Detector-CT Angiography of The Coronary Arteries: Intra-individual Comparison of Image Quality to Conventional Energy-integrating Detector-CT Angiography

Sunday, Nov. 27 11:45AM - 12:15PM Room: Learning Center - CA DPS

#### Participants

Joseph Griffith III, Charleston, SC (*Presenter*) Nothing to Disclose

#### PURPOSE

The aim of this study was the intra-individual evaluation of objective image quality for CT angiography of the coronary arteries on a photon counting detector CT (PCD-CCTA) in comparison to a conventional energy-integrating detector CT (EID-CCTA).

#### METHODS AND MATERIALS

Twenty prospectively included patients ( $59.2 \pm 13.2$  years, 65% male) with PCD- and EID-CCTA were examined at an interval of  $9 \pm 4$  days. Contrast agent protocol and radiation dose were matched between PCD and EID CCTA. Polychromatic images were reconstructed for both EID and PCD CCTA (T3D). In addition, virtual monoenergetic images at 40, 50, 60, and 70 keV were reconstructed on the PCD-CT. Signal, contrast and noise were measured in the aorta, coronary arteries, and myocardium, and the contrast-to-noise ratio (CNR) was calculated for each anatomical structure. Differences were compared using a paired t-test and a Bonferroni-corrected p-value of 0.008 was considered significant.

#### RESULTS

The mean CNR of the left coronary artery was  $13.3 \pm 5.4$  for the EID-CCTA and  $31.8 \pm 12.1$ ,  $28.4 \pm 9.7$ ,  $23.5 \pm 7.1$ ,  $21.2 \pm 6.7$  and  $21.9 \pm 6.7$  for the PCD-CCTA at 40, 50, 60, 70 keV and T3D, respectively. CNR was significantly higher in all virtual monoenergetic reconstructions of PCD-CT than EID-CT (all  $P < 0.008$ ).

#### CONCLUSION

s PCD-CCTA with monoenergetic reconstructions leads to a significantly increased CNR compared to EID-CCTA.

#### CLINICAL RELEVANCE/APPLICATION

The improved image quality of PCD-CCTA may be translated into clinical advantages including low-dose scanning or improved detection of coronary artery disease.

Printed on: 02/07/23

## Abstract Archives of the RSNA, 2022

S3A-SPCA-4

### Super-Resolution Deep Learning Reconstruction for Cardiac CT: Comparison of Stenosis Evaluation Accuracy, Image Quality, Stenosis Confidence Level at Coronary Arteries and CAD-RADS Classification with Hybrid-Type and Model-Based Iterative Reconstructions and Deep Learning Reconstruction at In Vivo and In Vitro Studies

Sunday, Nov. 27 11:45AM - 12:15PM Room: Learning Center - CA DPS

#### Participants

Yoshiharu Ohno, MD, PhD, Toyoake, Japan (*Presenter*) Research Grant, Canon Medical Systems Corporation; Research Grant, Daiichi Sankyo Co, Ltd; Research Grant, Ministry of Education, Culture, Sports, Science and Technology

#### PURPOSE

Super-resolution deep learning reconstruction (SR-DLR) for cardiac CT scans is recently set in routine clinical practice, which can maximize spatial resolution of area-detector CT (ADCT) (0.5mm×320 rows/896 channels) as super-high-resolution CT (0.25mm×160 rows/1792 channels) without reducing low-contrast detectability or increasing dose. The purpose of this study was to compare stenosis evaluation accuracy, image quality, stenosis confidence level and CAD-RADS classification on cardiac ADCT among hybrid-type and model-based iterative reconstructions (i.e. hybrid-type IR and MBIR), deep learning reconstruction (DLR) and SR-DLR at in vivo and in vitro studies.

#### METHODS AND MATERIALS

On in vitro study, a commercially available pulsating cardiac phantom with 3mm and 4 mm coronary artery phantoms, which had simulated 0, 25, 50 and 75% stenoses, were firstly scanned with standard protocol on a ADCT at five times and reconstructed with each method. Then, inner diameter of each coronary artery phantom was automatically measured. On in vivo study, 31 patients who suspected ischemic heart disease and underwent cardiac ADCT with standard protocol and coronary arteriography (CAG) were selected, and each cardiac ADCT data was also reconstructed with all methods. To compare stenosis evaluation accuracy among all methods, Spearman's correlations and Bland-Altman analyses were performed. To compare overall image quality, stenosis confidence level and CAD-RADS evaluations at all coronary arteries, each index was assessed by 5-points scoring systems and CAD-RADS classification and compared among all methods by Wilcoxon's signed rank test. Moreover, accuracy of CAD-RADS classification with standard reference generated from CAG by cardiologists were compared among all methods by McNemar's test.

#### RESULTS

On in vitro study, each methods showed excellent correlation (hybrid-type IR:  $r=0.93$ ,  $p<0.0001$ ; others:  $r=0.94$ ,  $p<0.0001$ ). The limits of agreements for SR-DLR ( $0.7\pm0.4$ mm) and DLR ( $0.7\pm0.4$ mm) were smaller than those for hybrid-type IR ( $0.8\pm0.5$ mm) and MBIR ( $0.8\pm0.4$ mm). On in vivo study, overall image quality and stenosis confidence level of SR-DLR were significantly higher than those of others ( $p<0.05$ ). Moreover, both indexes of DLR were significantly higher than those of hybrid-type IR ( $p<0.05$ ). On the other hand, CAD-RADS classification accuracy had no significant difference among all methods ( $p>0.05$ ).

#### CONCLUSION

SR-DLR has a potential to improve stenosis evaluation accuracy, image quality and stenosis confidence level on cardiac CT than others at in vivo and in vitro studies.

#### CLINICAL RELEVANCE/APPLICATION

SR-DLR has a potential to improve stenosis evaluation accuracy, image quality and stenosis confidence level than others on cardiac ADCT.

Printed on: 02/07/23

## Abstract Archives of the RSNA, 2022

S3A-SPCH

### Chest Sunday Poster Discussions - A

Sunday, Nov. 27 11:45AM - 12:15PM Room: Learning Center - CH DPS

#### Participants

Ryoko Egashira, MD, PhD, Saga, (*Moderator*) Speakers Bureau, Boehringer Ingelheim GmbH; Speakers Bureau, AstraZeneca PLC; Speakers Bureau, Shionogi & Co, Ltd; Speakers Bureau, KYORIN Holdings, Inc; Speakers Bureau, DAIICHI SANKYO Group; Speakers Bureau, Bayer AG; Speakers Bureau, Otsuka Holdings Co, Ltd;

#### Sub-Events

### S3A-SPCH-2 Clinical Value of Dual Layer Spectral Detector CT in Differential Diagnosis of Primary Malignant Chronic Lung Inflammation and Pulmonary Tuberculosis

#### Participants

Xiaoxia Zheng, MD, (*Presenter*) Nothing to Disclose

#### PURPOSE

To explore the clinical value of dual-layer detector spectral CT (DLCT) in differential diagnosis of lung primary malignant tumor, chronic inflammation and pulmonary tuberculosis using conventional CT signs and spectral multi-parameters.

#### METHODS AND MATERIALS

From August 2020 to June 2021, 345 patients with pathologically confirmed of pulmonary diseases who underwent DLCT chest enhanced scan in our hospital were retrospective enrolled for this study. The patients were divided into three groups: primary lung malignant tumor group (n = 187, 88 adenocarcinoma, 51 squamous cell carcinoma and 34 small cell lung cancer and 14 other malignant tumors), chronic inflammation group (n = 101) and tuberculosis group (n = 57). The conventional CT signs and spectral CT parameters of the three groups were analyzed. Logistic regression analysis was performed for parameters with statistically significant differences, and conventional CT diagnostic model, spectral CT parameter diagnostic model and combined diagnostic model were established. The diagnostic efficiency of each model was compared with the Area under the Receiver Operating characteristic (AUC).

#### RESULTS

In the three groups, the distance from pleura (P=0.009), morphology (P<0.001), density (P=0.001), separation from lung tissue (P=0.001), lobulation (P<0.001), liquefaction necrosis (P=0.003), vascular cluster sign (P<0.001), halo sign (P=0.003), satellite focus (P=0.045), pleural effusion (P=0.002), Mediastinal lymph node enlargement (P<0.001), effective atomic number, iodine density, normalization iodine density, energy spectrum curve slope both in the arterial and venous phase, arterial enhancement fraction (P<0.001). The areas under ROC curve for the diagnosis of primary lung malignant tumor, chronic inflammation and pulmonary tuberculosis by conventional CT diagnostic model were 0.827, 0.753 and 0.770. The areas under ROC curve by spectral CT parameters were 0.905, 0.824 and 0.909. The areas under ROC curve by combining conventional CT signs and spectral CT parameters were 0.929, 0.889 and 0.942.

#### CONCLUSION

Spectral CT parameters combined with conventional CT signs can improve the differential diagnosis efficiency of pulmonary malignant tumor, chronic inflammation and pulmonary tuberculosis.

#### CLINICAL RELEVANCE/APPLICATION

Spectral CT parameters combined with conventional CT diagnosis can significantly improve the differential diagnosis efficiency of pulmonary primary malignant tumor, chronic inflammation and tuberculosis, which has high clinical application value. Reduce the probability of unnecessary surgery and biopsy for benign lesions due to difficulties in preoperative diagnosis.

### S3A-SPCH-3 Dual-Source vs. Twin-Beam CT in Dual-Energy Lung Perfusion Assessment for Emphysema Patients

#### Participants

Quirin Strotzer, MD, Regensburg, Germany (*Presenter*) Nothing to Disclose

#### PURPOSE

This study is the first to compare dual-source dual-energy chest computed tomography (DECT) vs. twin-beam DECT to assess lung perfusion in emphysema patients with planned lung volume reduction therapy. Single-photon emission computed tomography (SPECT) was used as the gold standard.

#### METHODS AND MATERIALS

Sixty-two lung emphysema patients assessed for lung volume reduction therapy were included. All patients received a SPECT scan. Additionally, dual-source (two X-ray source/detector systems) DECT (thirty-two patients) or twin-beam (X-ray beam from a single source split with two filters into high and low energy spectra) DECT (thirty patients) was acquired. SPECT acquisitions were semi-

manually segmented, and the relative lung perfusion was calculated on a lobar level. On the DECTs, the lung lobes were automatically segmented using a U-Net, and segmentations were manually verified. The relative lung perfusion of each lobe was derived from iodine maps computed from the dual-energy data using a three-material decomposition algorithm.

## RESULTS

Statistical analysis included the Pearson correlation coefficient to test the correlation between DECT and SPECT assessed lobar relative lung perfusion. While both methods showed a significant correlation with the SPECT acquisitions ( $p < .001$ ), the correlation was higher for dual-source DECT ( $r = .861$ ) than for twin-beam DECT ( $r = .766$ ). Bland-Altman analysis showed a slightly better agreement for the dual-source data. No bias was observed.

## CONCLUSION

We conclude that both dual-source and twin-beam DECT are capable of assessing lung perfusion on a lobar level compared to SPECT. However, correlation and agreement are higher for dual-source DECT.

## CLINICAL RELEVANCE/APPLICATION

Currently, patients undergoing assessment for lung volume reduction therapy require both structural computed tomography and evaluation of lung perfusion by single-photon emission computed tomography. With lung perfusion computed from dual-energy computed tomography data more readily available, the necessary information could be obtained from a single examination, saving time and money, and reducing the patients' radiation dose.

### S3A-SPCH-4 Chest CT Angiography in Daily Practice With a Photon Counting CT Equipment: Comparison of Image Quality with Dual-source CT in 142 Patients

#### Participants

Martine J. Remy-Jardin, MD, PhD, Lille, France (*Presenter*) Research Grant, Siemens AG; Speaker, Siemens AG

#### PURPOSE

To compare the image quality of chest CT angiographic (CTA) examinations between photon-counting CT (PCCT) and dual-source CT (DSCT) in paired populations.

#### METHODS AND MATERIALS

The study population included 71 consecutive patients scanned with PCCT (Naeotom Alpha; Siemens Healthineers; Germany), compared to a paired population of 71 patients scanned with a 3rd-generation DSCT scanner (Somatom Force; Siemens Healthineers; Germany) selected on the basis of similar (a) injection protocols (80 mL of a 40% contrast agent; 4 mL/s); (b) age ( $\pm 5$  years) and weight ( $\pm 5$  kg). The scanning parameters included (a) for DSCT (Group 1): collimation of 64x0.6x2 mm; pitch of 0.55; reconstruction of averaged images from both tubes; kernel: Br36; level of iterative reconstruction: ADMIRE 3; (b) for PCCT (Group 2): collimation of 144 x 0.4mm; pitch of 1.5; single-source acquisition; reconstruction of images at 70 keV; kernel: Br 36; level of iterative reconstruction: QIR 3. Comparative analysis of image quality of morphologic and perfusion images was undertaken.

## RESULTS

Compared to Group 1: (a) the mean DLP of Group 2 acquisitions was significantly lower ( $172.6 \pm 55.14$  vs  $339.4 \pm 75.64$  mGy.cm;  $p < 0.0001$ ) (52% dose reduction); (b) the duration of data acquisition in Group 2 was significantly shorter ( $0.93 \pm 0.1s$  vs  $3.98 \pm 0.35s$ ;  $p < 0.0001$ ). On mediastinal images, there was (a) no significant difference in the mean ( $\pm$ SD) attenuation value within central pulmonary arteries (Group 1:  $420.0 \pm 131.3$  HU; Group 2:  $398.0 \pm 144.4$  HU;  $p = 0.32$ ) nor at the level of the aorta (Group 1:  $394.7 \pm 92.34$  HU; Group 2:  $375.2 \pm 90.34$  HU;  $p = 0.15$ ); (b) a higher level of background noise, measured in the air around the patient (Group 2:  $9.55 \pm 1.86$  HU; Group 1:  $6.88 \pm 1.56$  HU;  $p < 0.0001$ ). On perfusion images (a) the mean level of attenuation did not differ between the two groups (Group 1:  $89.99 \pm 28.86$  HU; Group 2:  $80.37 \pm 30.07$  HU;  $p = 0.05$ ) nor did the rating of subjective image noise (Group 1: mild:  $n = 69$ ; 97.2%, moderate:  $n = 2$ ; 2.8%; Group 2: mild:  $n = 64$ ; 90.1%, moderate:  $n = 7$ ; 9.9%;  $p = 0.16$ ); (b) the distribution of scores of fissure visualization significantly differed between the 2 groups ( $p < 0.0001$ ) with a higher proportion of fissures sharply delineated in Group 2 ( $n = 60$ ; 84.5%) than in Group 1 ( $n = 26$ ; 26.6%); (c) the rating of motion artifacts in the vicinity of the left ventricle differed between the 2 groups ( $p < 0.0001$ ) with a higher percentage of mild artifacts in Group 2 ( $n = 69$ ; 97.2%) than in Group 1 ( $n = 19$ ; 26.8%).

## CONCLUSION

PCCT acquisitions provided similar morphologic image quality and superior perfusion imaging at lower radiation dose.

## CLINICAL RELEVANCE/APPLICATION

Photon-counting CT has the potential to improve perfusion imaging while maintaining morphologic image quality with a radiation dose reduced by 50%.

### S3A-SPCH-6 Strain Analysis in Patients with Obstructive Ventilation Dysfunction Using Four It Dimensional Dynamic > Ventilation CT

#### Participants

Yanyan Xu, MD, Beijing, China (*Presenter*) Nothing to Disclose

#### PURPOSE

To quantitatively identify abnormal lung motion in COPD using strain analysis, and further clarify the potential differences of deformation in COPD with different severity of airflow limitation.

#### METHODS AND MATERIALS

A total of 53 patients with suspected COPD were enrolled in this study. All CT examinations were performed on a 320 It row MDCT scanner, and dynamic It ventilation CT data was continuously reconstructed every 0.2 seconds (total 41 frames per patient). Strain measurement was performed using dynamic It ventilation CT data with a computational fluid dynamics analysis software (Micro Vec V3.6.2). The strain parameters derived from the whole expiration phase, the first 2s of expiration phase were divided respectively by the changes in lung volume to adjust for the degree of expiration. Spearman rank correlation analysis was used to evaluate associations between the adjusted strain parameters and various spirometric parameters. Comparisons of the strain

parameters between COPD and non It COPD patients, between GOLD I and GOLD II-IV were made using the Mann It Whitney U test. Then, receiver-operating characteristic (ROC) analysis was performed to evaluate the diagnostic performance of the adjusted strain parameters for COPD.  $P < 0.05$  was considered statistically significant.

## RESULTS

Strain-related parameters were significantly correlated with forced expiratory volume in one second/forced vital capacity ( $r = 0.450 \sim 0.687$ ,  $P < 0.001$ ), maximum mid-expiratory flow rate ( $r = 0.364 \sim 0.643$ ,  $P < 0.05$ ), and peak expiratory flow ( $r = 0.275 \sim 0.456$ ,  $P < 0.05$ ), suggesting that heterogeneity in lung motion are related to abnormal spirometric results, and patients with obstructive ventilation dysfunction demonstrated lower strain values ( $P < 0.001$ ). According to the ROC curve, the strain-related parameters showed moderate diagnostic significance with the AUC values range from 0.821 to 0.894. The strain parameters derived from the whole expiration phase (PSmax-all, Speedmax-all) showed statistical differences between GOLD I and GOLD II-IV patients ( $z = -2.782$ ,  $P = 0.005$ ;  $z = -2.053$ ,  $P = 0.04$ ).

## CONCLUSION

s Strain parameters basing on dynamic It ventilation CT data associated with lung function impairment in COPD, reflecting the severity of airflow limitation in some degree, even though its utility in severe COPD patients remains to be investigated.

## CLINICAL RELEVANCE/APPLICATION

Strain measurements provides a promisingly quantitative method for monitoring disease progression in COPD.

### **S3A-SPCH-7 Dynamic Contrast-Enhanced Whole-Lung Perfusion Area-Detector CT: Capability for Lung Structure Change and Pulmonary Functional Loss Evaluations in Operated Stage I Lung Cancer Patients**

#### Participants

Yoshiharu Ohno, MD, PhD, Toyoake, Japan (*Presenter*) Research Grant, Canon Medical Systems Corporation; Research Grant, Daiichi Sankyo Co, Ltd; Research Grant, Ministry of Education, Culture, Sports, Science and Technology

#### PURPOSE

To determine the capability of dynamic contrast-enhanced (CE-) whole-lung perfusion area-detector CT (ADCT) for pathological change and pulmonary functional loss evaluations in operated Stage I lung cancer patients.

#### METHODS AND MATERIALS

Sixty-three consecutive stage I lung cancer patients underwent dynamic CE-perfusion ADCT performed at two or three different positions as single examination, pulmonary function test, surgical treatment, and pathological examination. From perfusion ADCT data in each patient, whole lung total perfusion (TP), pulmonary arterial perfusion (PAP) and systemic arterial perfusion (SAP) maps were computationally generated based on dual-input maximum slope method by pixel-by-pixel analyses with commercially available software. Then, ROIs were placed within operated lung based on pathological examination results. In this study, all ROIs within operated lung were divided into following four structure groups: normal lung, emphysema, fibrotic changes without honeycombing (non-honeycombing), and honeycombing. To determine the capability of each perfusion parameter for pulmonary functional loss, Pearson's correlation was performed. To compare each perfusion parameter among all structure groups, Tukey's HSD test was performed. Finally, discrimination accuracy for structure change evaluation was compared among all perfusion parameters by McNemar's test.

#### RESULTS

%FEV1, %VC and %DLCO/VA had significant correlations with TP ( $0.47 < r < 0.60$ ,  $p < 0.0001$ ) and PAP ( $0.43 < r < 0.58$ ,  $p < 0.0001$ ). All perfusion parameters had significant differences between normal lung and other groups ( $p < 0.05$ ), between emphysema and non-honeycombing groups ( $p < 0.0001$ ) and between emphysema and honeycombing groups ( $p < 0.0001$ ). Moreover, SAP had significant difference between non-honeycombing and honeycombing groups ( $p < 0.0001$ ). Finally, discrimination accuracy of TP (71.0%) was significantly higher than that of others (PAP: 45.8%,  $p < 0.0001$ , SAP: 52.4%,  $p < 0.0001$ ).

#### CONCLUSION

s Whole-lung dynamic first-pass CE-perfusion ADCT is useful for pathological change and pulmonary functional loss evaluations in operated stage I lung cancer patients.

#### CLINICAL RELEVANCE/APPLICATION

Whole-lung dynamic first-pass CE-perfusion ADCT is useful for pathological change and pulmonary functional loss evaluations in operated stage I lung cancer patients.

### **S3A-SPCH-8 Diagnostic Performance of Extracellular Volume Fraction (ECV) Measured by Dual-Energy CT: Prediction for Programmed Death-ligand 1 (PD-L1) Expression in Invasive Pulmonary Adenocarcinoma**

#### Participants

Masahiro Yanagawa, MD, PhD, Suita, Japan (*Presenter*) Nothing to Disclose

#### PURPOSE

To examine the association between quantitative data measured by dual-energy CT and expression of programmed death-ligand 1 (PD-L1) using immunostaining methods.

#### METHODS AND MATERIALS

37 patients with invasive pulmonary adenocarcinoma were scanned by dual-energy CT (Revolution CT; GE) with fast kV (80- and 140-kVp) switching mode for examining solitary pulmonary nodules. Enhanced dual-energy CT images in the 180s late phase were obtained with 1.25 mm thickness, 20 cm field of view and 512×512 matrix using a standard kernel and 30% adaptive statistical iterative reconstruction. The dose of contrast material (IOHEXOL300mgI) per patient was decided on the basis of 2 ml per weight. Volume of interest on three dimensional (3D) iodine density mapping was set in each nodule and aorta as large as possible. Extracellular volume fraction (ECV) was calculated using the following formula:  $ECV = (1 - \text{hematocrit}) \times (\text{iodine density in each}$

odule / iodine density in each aorta). 3D iodine density histogram texture analysis was performed for each nodule: 7 texture features (max, min, median, average, standard deviation, skewness, and kurtosis) were also obtained. A pathologist evaluated a tumor proportion score (TPS, %) using PD-L1 immunostaining: PD-L1 strong positive (TPS =50 %) (first line criteria for immune checkpoint inhibitors). Associations between expression of PD-L1(TPS =50%) and 8 parameters were evaluated using univariate and multivariate logistic regression analyses. Diagnostic performance was evaluated by sensitivity, specificity, and an area under the receiver operator characteristic curve (AUC). P values < 0.05 were considered significant.

## **RESULTS**

Volume of 37 nodules (15 part-solid and 22 solid) showed 5.46 cc  $\pm$ 16.33 (mean  $\pm$  SD). The number of PD-L1(TPS =50 %) was 11. Univariate logistic regression analysis revealed that the average >1.39 mg/cc, skewness =-2.28, kurtosis >6.17, and ECV >21.23 % were significant indicators ( $p < 0.032$ ). Multivariate logistic regression analysis revealed that skewness =-2.28 and ECV >21.23% were independent indicators associated with PD-L1(TPS =50 %) (odds ratio, 7.11 and 6.57; 95% confidence interval, 1.11-45.6 and 1.12-38.4;  $p = 0.039$  and  $0.037$ , respectively). The diagnostic performance of these two findings combined were as follows: sensitivity of 64 % (7/11) specificity of 86 % (25/26) and AUC of 0.83.

## **CONCLUSION**

s Skewness and ECV from dual-energy CT in the 180s late phase may predict high expression of PD-L1 in invasive pulmonary adenocarcinoma.

## **CLINICAL RELEVANCE/APPLICATION**

Dual-energy CT may be a noninvasive method for chemotherapy strategy such as immune checkpoint inhibitors in invasive adenocarcinoma.

Printed on: 02/07/23

## Abstract Archives of the RSNA, 2022

S3A-SPCH-2

### Clinical Value of Dual Layer Spectral Detector CT in Differential Diagnosis of Primary Malignant Chronic Lung Inflammation and Pulmonary Tuberculosis

Sunday, Nov. 27 11:45AM - 12:15PM Room: Learning Center - CH DPS

#### Participants

Xiaoxia Zheng, MD, (*Presenter*) Nothing to Disclose

#### PURPOSE

To explore the clinical value of dual-layer detector spectral CT (DLCT) in differential diagnosis of lung primary malignant tumor, chronic inflammation and pulmonary tuberculosis using conventional CT signs and spectral multi-parameters.

#### METHODS AND MATERIALS

From August 2020 to June 2021, 345 patients with pathologically confirmed of pulmonary diseases who underwent DLCT chest enhanced scan in our hospital were retrospective enrolled for this study. The patients were divided into three groups: primary lung malignant tumor group (n = 187, 88 adenocarcinoma, 51squamous cell carcinoma and 34 small cell lung cancer and 14 other malignant tumors), chronic inflammation group (n = 101) and tuberculosis group (n = 57) . The conventional CT signs and spectral CT parameters of the three groups were analyzed. Logistic regression analysis was performed for parameters with statistically significant differences, and conventional CT diagnostic model, spectral CT parameter diagnostic model and combined diagnostic model were established The diagnostic efficiency of each model was compared with the Area under the Receiver Operating characteristic (AUC).

#### RESULTS

In the three groups, the distance from pleura (P=0.009), morphology (P<0.001), density (P=0.001), separation from lung tissue (P=0.001), lobulation (P<0.001), liquefaction necrosis (P=0.003), vascular cluster sign (P<0.001), halo sign (P=0.003), satellite focus (P=0.045), pleural effusion (P=0.002), Mediastinal lymph node enlargement(P<0.001),effective atomic number, iodine density, normalization iodine density, energy spectrum curve slope both in the arterial and venous phase,arterial enhancement fraction (P<0.001). The areas under ROC curve for the diagnosis of primary lung malignant tumor, chronic inflammation and pulmonary tuberculosis by conventional CT diagnostic model were 0.827, 0.753 and 0.770. The areas under ROC curve by spectral CT parameters were 0.905 0.824 and 0.909. The areas under ROC curve by combining conventional CT signs and spectral CT parameters were 0.929, 0.889 and 0.942.

#### CONCLUSION

Spectral CT parameters combined with conventional CT signs can improve the differential diagnosis efficiency of pulmonary malignant tumor, chronic inflammation and pulmonary tuberculosis.

#### CLINICAL RELEVANCE/APPLICATION

Spectral CT parameters combined with conventional CT diagnosis can significantly improve the differential diagnosis efficiency of pulmonary primary malignant tumor, chronic inflammation and tuberculosis, which has high clinical application value. Reduce the probability of unnecessary surgery and biopsy for benign lesions due to difficulties in preoperative diagnosis.

Printed on: 02/07/23

## Abstract Archives of the RSNA, 2022

S3A-SPCH-3

### Dual-Source vs. Twin-Beam CT in Dual-Energy Lung Perfusion Assessment for Emphysema Patients

Sunday, Nov. 27 11:45AM - 12:15PM Room: Learning Center - CH DPS

#### Participants

Quirin Strotzer, MD, Regensburg, Germany (*Presenter*) Nothing to Disclose

#### PURPOSE

This study is the first to compare dual-source dual-energy chest computed tomography (DECT) vs. twin-beam DECT to assess lung perfusion in emphysema patients with planned lung volume reduction therapy. Single-photon emission computed tomography (SPECT) was used as the gold standard.

#### METHODS AND MATERIALS

Sixty-two lung emphysema patients assessed for lung volume reduction therapy were included. All patients received a SPECT scan. Additionally, dual-source (two X-ray source/detector systems) DECT (thirty-two patients) or twin-beam (X-ray beam from a single source split with two filters into high and low energy spectra) DECT (thirty patients) was acquired. SPECT acquisitions were semi-manually segmented, and the relative lung perfusion was calculated on a lobar level. On the DECTs, the lung lobes were automatically segmented using a U-Net, and segmentations were manually verified. The relative lung perfusion of each lobe was derived from iodine maps computed from the dual-energy data using a three-material decomposition algorithm.

#### RESULTS

Statistical analysis included the Pearson correlation coefficient to test the correlation between DECT and SPECT assessed lobar relative lung perfusion. While both methods showed a significant correlation with the SPECT acquisitions ( $p < .001$ ), the correlation was higher for dual-source DECT ( $r = .861$ ) than for twin-beam DECT ( $r = .766$ ). Bland-Altman analysis showed a slightly better agreement for the dual-source data. No bias was observed.

#### CONCLUSION

s We conclude that both dual-source and twin-beam DECT are capable of assessing lung perfusion on a lobar level compared to SPECT. However, correlation and agreement are higher for dual-source DECT.

#### CLINICAL RELEVANCE/APPLICATION

Currently, patients undergoing assessment for lung volume reduction therapy require both structural computed tomography and evaluation of lung perfusion by single-photon emission computed tomography. With lung perfusion computed from dual-energy computed tomography data more readily available, the necessary information could be obtained from a single examination, saving time and money, and reducing the patients' radiation dose.

Printed on: 02/07/23

## Abstract Archives of the RSNA, 2022

S3A-SPCH-4

### Chest CT Angiography in Daily Practice With a Photon Counting CT Equipment: Comparison of Image Quality with Dual-source CT in 142 Patients

Sunday, Nov. 27 11:45AM - 12:15PM Room: Learning Center - CH DPS

#### Participants

Martine J. Remy-Jardin, MD, PhD, Lille, France (*Presenter*) Research Grant, Siemens AG; *Speaker*, Siemens AG

#### PURPOSE

To compare the image quality of chest CT angiographic (CTA) examinations between photon-counting CT (PCCT) and dual-source CT (DSCT) in paired populations.

#### METHODS AND MATERIALS

The study population included 71 consecutive patients scanned with PCCT (Naeotom Alpha; Siemens Healthineers; Germany), compared to a paired population of 71 patients scanned with a 3rd-generation DSCT scanner (Somatom Force; Siemens Healthineers; Germany) selected on the basis of similar (a) injection protocols (80 mL of a 40% contrast agent; 4 mL/s); (b) age ( $\pm 5$  years) and weight ( $\pm 5$  kg). The scanning parameters included (a) for DSCT (Group 1): collimation of 64x0.6x2 mm; pitch of 0.55; reconstruction of averaged images from both tubes; kernel: Br36; level of iterative reconstruction: ADMIRE 3; (b) for PCCT (Group 2): collimation of 144 x 0.4mm; pitch of 1.5; single-source acquisition; reconstruction of images at 70 keV; kernel: Br 36; level of iterative reconstruction: QIR 3. Comparative analysis of image quality of morphologic and perfusion images was undertaken.

#### RESULTS

Compared to Group 1: (a) the mean DLP of Group 2 acquisitions was significantly lower ( $172.6 \pm 55.14$  vs  $339.4 \pm 75.64$  mGy.cm;  $p < 0.0001$ ) (52% dose reduction); (b) the duration of data acquisition in Group 2 was significantly shorter ( $0.93 \pm 0.1$ s vs  $3.98 \pm 0.35$ s;  $p < 0.0001$ ). On mediastinal images, there was (a) no significant difference in the mean ( $\pm$ SD) attenuation value within central pulmonary arteries (Group 1:  $420.0 \pm 131.3$  HU; Group 2:  $398.0 \pm 144.4$  HU;  $p = 0.32$ ) nor at the level of the aorta (Group 1:  $394.7 \pm 92.34$  HU; Group 2:  $375.2 \pm 90.34$  HU;  $p = 0.15$ ); (b) a higher level of background noise, measured in the air around the patient (Group 2:  $9.55 \pm 1.86$  HU; Group 1:  $6.88 \pm 1.56$  HU;  $p < 0.0001$ ). On perfusion images (a) the mean level of attenuation did not differ between the two groups (Group 1:  $89.99 \pm 28.86$  HU; Group 2:  $80.37 \pm 30.07$  HU;  $p = 0.05$ ) nor did the rating of subjective image noise (Group 1: mild:  $n = 69$ ; 97.2%, moderate:  $n = 2$ ; 2.8%; Group 2: mild:  $n = 64$ ; 90.1%, moderate:  $n = 7$ ; 9.9%;  $p = 0.16$ ); (b) the distribution of scores of fissure visualization significantly differed between the 2 groups ( $p < 0.0001$ ) with a higher proportion of fissures sharply delineated in Group 2 ( $n = 60$ ; 84.5%) than in Group 1 ( $n = 26$ ; 26.6%); (c) the rating of motion artifacts in the vicinity of the left ventricle differed between the 2 groups ( $p < 0.0001$ ) with a higher percentage of mild artifacts in Group 2 ( $n = 69$ ; 97.2%) than in Group 1 ( $n = 19$ ; 26.8%).

#### CONCLUSION

s PCCT acquisitions provided similar morphologic image quality and superior perfusion imaging at lower radiation dose.

#### CLINICAL RELEVANCE/APPLICATION

Photon-counting CT has the potential to improve perfusion imaging while maintaining morphologic image quality with a radiation dose reduced by 50%.

Printed on: 02/07/23

## Abstract Archives of the RSNA, 2022

S3A-SPCH-6

### Strain Analysis in Patients with Obstructive Ventilation Dysfunction Using Four Dimensional Dynamic Ventilation CT >

Sunday, Nov. 27 11:45AM - 12:15PM Room: Learning Center - CH DPS

#### Participants

Yanyan Xu, MD, Beijing, China (*Presenter*) Nothing to Disclose

#### PURPOSE

To quantitatively identify abnormal lung motion in COPD using strain analysis, and further clarify the potential differences of deformation in COPD with different severity of airflow limitation.

#### METHODS AND MATERIALS

A total of 53 patients with suspected COPD were enrolled in this study. All CT examinations were performed on a 320 It row MDCT scanner, and dynamic It ventilation CT data was continuously reconstructed every 0.2 seconds (total 41 frames per patient). Strain measurement was performed using dynamic It ventilation CT data with a computational fluid dynamics analysis software (Micro Vec V3.6.2). The strain parameters derived from the whole expiration phase, the first 2s of expiration phase were divided respectively by the changes in lung volume to adjust for the degree of expiration. Spearman rank correlation analysis was used to evaluate associations between the adjusted strain parameters and various spirometric parameters. Comparisons of the strain parameters between COPD and non It COPD patients, between GOLD I and GOLD II-IV were made using the Mann It Whitney U test. Then, receiver-operating characteristic (ROC) analysis was performed to evaluate the diagnostic performance of the adjusted strain parameters for COPD.  $P < 0.05$  was considered statistically significant.

#### RESULTS

Strain-related parameters were significantly correlated with forced expiratory volume in one second/forced vital capacity ( $r = 0.450 \sim 0.687$ ,  $P < 0.001$ ), maximum mid-expiratory flow rate ( $r = 0.364 \sim 0.643$ ,  $P < 0.05$ ), and peak expiratory flow ( $r = 0.275 \sim 0.456$ ,  $P < 0.05$ ), suggesting that heterogeneity in lung motion are related to abnormal spirometric results, and patients with obstructive ventilation dysfunction demonstrated lower strain values ( $P < 0.001$ ). According to the ROC curve, the strain-related parameters showed moderate diagnostic significance with the AUC values range from 0.821 to 0.894. The strain parameters derived from the whole expiration phase (PSmax-all, Speedmax-all) showed statistical differences between GOLD I and GOLD II-IV patients ( $z = -2.782$ ,  $P = 0.005$ ;  $z = -2.053$ ,  $P = 0.04$ ).

#### CONCLUSION

Strain parameters basing on dynamic It ventilation CT data associated with lung function impairment in COPD, reflecting the severity of airflow limitation in some degree, even though its utility in severe COPD patients remains to be investigated.

#### CLINICAL RELEVANCE/APPLICATION

Strain measurements provides a promisingly quantitative method for monitoring disease progression in COPD.

Printed on: 02/07/23

## Abstract Archives of the RSNA, 2022

S3A-SPCH-7

### Dynamic Contrast-Enhanced Whole-Lung Perfusion Area-Detector CT: Capability for Lung Structure Change and Pulmonary Functional Loss Evaluations in Operated Stage I Lung Cancer Patients

Sunday, Nov. 27 11:45AM - 12:15PM Room: Learning Center - CH DPS

#### Participants

Yoshiharu Ohno, MD, PhD, Toyoake, Japan (*Presenter*) Research Grant, Canon Medical Systems Corporation; Research Grant, Daiichi Sankyo Co, Ltd; Research Grant, Ministry of Education, Culture, Sports, Science and Technology

#### PURPOSE

To determine the capability of dynamic contrast-enhanced (CE-) whole-lung perfusion area-detector CT (ADCT) for pathological change and pulmonary functional loss evaluations in operated Stage I lung cancer patients.

#### METHODS AND MATERIALS

Sixty-three consecutive stage I lung cancer patients underwent dynamic CE-perfusion ADCT performed at two or three different positions as single examination, pulmonary function test, surgical treatment, and pathological examination. From perfusion ADCT data in each patient, whole lung total perfusion (TP), pulmonary arterial perfusion (PAP) and systemic arterial perfusion (SAP) maps were computationally generated based on dual-input maximum slope method by pixel-by-pixel analyses with commercially available software. Then, ROIs were placed within operated lung based on pathological examination results. In this study, all ROIs within operated lung were divided into following four structure groups: normal lung, emphysema, fibrotic changes without honeycombing (non-honeycombing), and honeycombing. To determine the capability of each perfusion parameter for pulmonary functional loss, Pearson's correlation was performed. To compare each perfusion parameter among all structure groups, Tukey's HSD test was performed. Finally, discrimination accuracy for structure change evaluation was compared among all perfusion parameters by McNemar's test.

#### RESULTS

%FEV1, %VC and %DLCO/VA had significant correlations with TP ( $0.47 < r < 0.60$ ,  $p < 0.0001$ ) and PAP ( $0.43 < r < 0.58$ ,  $p < 0.0001$ ). All perfusion parameters had significant differences between normal lung and other groups ( $p < 0.05$ ), between emphysema and non-honeycombing groups ( $p < 0.0001$ ) and between emphysema and honeycombing groups ( $p < 0.0001$ ). Moreover, SAP had significant difference between non-honeycombing and honeycombing groups ( $p < 0.0001$ ). Finally, discrimination accuracy of TP (71.0%) was significantly higher than that of others (PAP: 45.8%,  $p < 0.0001$ , SAP: 52.4%,  $p < 0.0001$ ).

#### CONCLUSION

s Whole-lung dynamic first-pass CE-perfusion ADCT is useful for pathological change and pulmonary functional loss evaluations in operated stage I lung cancer patients.

#### CLINICAL RELEVANCE/APPLICATION

Whole-lung dynamic first-pass CE-perfusion ADCT is useful for pathological change and pulmonary functional loss evaluations in operated stage I lung cancer patients.

Printed on: 02/07/23

## Abstract Archives of the RSNA, 2022

S3A-SPCH-8

### Diagnostic Performance of Extracellular Volume Fraction (ECV) Measured by Dual-Energy CT: Prediction for Programmed Death-ligand 1 (PD-L1) Expression in Invasive Pulmonary Adenocarcinoma

Sunday, Nov. 27 11:45AM - 12:15PM Room: Learning Center - CH DPS

#### Participants

Masahiro Yanagawa, MD, PhD, Suita, Japan (*Presenter*) Nothing to Disclose

#### PURPOSE

To examine the association between quantitative data measured by dual-energy CT and expression of programmed death-ligand 1 (PD-L1) using immunostaining methods.

#### METHODS AND MATERIALS

37 patients with invasive pulmonary adenocarcinoma were scanned by dual-energy CT (Revolution CT; GE) with fast kV (80- and 140-kVp) switching mode for examining solitary pulmonary nodules. Enhanced dual-energy CT images in the 180s late phase were obtained with 1.25 mm thickness, 20 cm field of view and 512×512 matrix using a standard kernel and 30% adaptive statistical iterative reconstruction. The dose of contrast material (IOHEXOL300mgI) per patient was decided on the basis of 2 ml per weight. Volume of interest on three dimensional (3D) iodine density mapping was set in each nodule and aorta as large as possible. Extracellular volume fraction (ECV) was calculated using the following formula:  $ECV = (1 - \text{hematocrit}) \times (\text{iodine density in each nodule} / \text{iodine density in each aorta})$ . 3D iodine density histogram texture analysis was performed for each nodule: 7 texture features (max, min, median, average, standard deviation, skewness, and kurtosis) were also obtained. A pathologist evaluated a tumor proportion score (TPS, %) using PD-L1 immunostaining: PD-L1 strong positive (TPS =50 %) (first line criteria for immune checkpoint inhibitors). Associations between expression of PD-L1(TPS =50%) and 8 parameters were evaluated using univariate and multivariate logistic regression analyses. Diagnostic performance was evaluated by sensitivity, specificity, and an area under the receiver operator characteristic curve (AUC). P values < 0.05 were considered significant.

#### RESULTS

Volume of 37 nodules (15 part-solid and 22 solid) showed 5.46 cc ±16.33 (mean ± SD). The number of PD-L1(TPS =50 %) was 11. Univariate logistic regression analysis revealed that the average >1.39 mg/cc, skewness =-2.28, kurtosis >6.17, and ECV >21.23 % were significant indicators (p < 0.032). Multivariate logistic regression analysis revealed that skewness =-2.28 and ECV >21.23% were independent indicators associated with PD-L1(TPS =50 %) (odds ratio, 7.11 and 6.57; 95% confidence interval, 1.11-45.6 and 1.12-38.4; p = 0.039 and 0.037, respectively). The diagnostic performance of these two findings combined were as follows: sensitivity of 64 % (7/11) specificity of 86 % (25/26) and AUC of 0.83.

#### CONCLUSION

Skewness and ECV from dual-energy CT in the 180s late phase may predict high expression of PD-L1 in invasive pulmonary adenocarcinoma.

#### CLINICAL RELEVANCE/APPLICATION

Dual-energy CT may be a noninvasive method for chemotherapy strategy such as immune checkpoint inhibitors in invasive adenocarcinoma.

Printed on: 02/07/23



## Abstract Archives of the RSNA, 2022

S3A-SPER

### Emergency Sunday Poster Discussions - A

Sunday, Nov. 27 11:45AM - 12:15PM Room: Learning Center - ER DPS

#### Participants

Vanessa M. Zayas-Colon, MD, Webster, NY (*Moderator*) Nothing to Disclose

#### Sub-Events

### S3A-SPER-1 Jointly Optimized Deep Neural Networks to Synthesize Monoenergetic Images from CT Angiography for Improving Classification of Pulmonary Embolism

#### Participants

Matthias Fink, MD, BSc, Heidelberg, Germany (*Presenter*) Nothing to Disclose

#### PURPOSE

To develop a jointly optimized deep learning framework based on dual-energy CT pulmonary angiography (DE-CTPA) data to generate synthetic monoenergetic images (SMI) for improving automatic pulmonary embolism (PE) detection in single-energy CTPA scans.

#### METHODS AND MATERIALS

We used two data sets: our institutional DE-CTPA data set D1 comprising polyenergetic arterial series and the corresponding VMI at low-energy levels (40 keV) with 7,892 image pairs, and a 10% subset of the 2020 RSNA Pulmonary Embolism Detection Challenge data set D2, which consisted of 161,253 polyenergetic images with binary slice-wise annotations (PE/no PE). We trained a fully convolutional encoder-decoder on D1 to generate SMI from single-energy CTPA scans of D2, which were then fed into a ResNet50 network for training of the downstream PE classification task. We evaluated our VMI reconstruction results in terms of Peak-Signal-to-Noise-Ratio (PSNR) and Structural Similarity Index Measure (SSIM). For PE identification, we performed a binary classification on slice level and report the area under the curve (AUC).

#### RESULTS

The quantitative results on the reconstruction ability of our framework revealed high-quality visual SMI predictions with reconstruction results of  $0.984 \pm 0.002$  (structural similarity) and  $41.706 \pm 0.547$  dB (peak-signal-to-noise ratio). PE classification resulted in an AUC of 0.84 for our model, which achieved improved performance compared to other naïve approaches with AUCs up to 0.81.

#### CONCLUSION

Using joint optimization strategies for deep learning algorithms allows training of translating polyenergetic into monoenergetic images without losing features necessary for automatic PE classification. Our model hereby improves noticeably over straight forward classification while outperforming existing methods.

#### CLINICAL RELEVANCE/APPLICATION

The proposed pipeline may prove to be beneficial for computer-aided detection systems and could help rescue CTPA studies with suboptimal contrast attenuation of the pulmonary arteries from single-energy CT scanners.

Printed on: 02/07/23



## Abstract Archives of the RSNA, 2022

S3A-SPER-1

### Jointly Optimized Deep Neural Networks to Synthesize Monoenergetic Images from CT Angiography for Improving Classification of Pulmonary Embolism

Sunday, Nov. 27 11:45AM - 12:15PM Room: Learning Center - ER DPS

#### Participants

Matthias Fink, MD, BSc, Heidelberg, Germany (*Presenter*) Nothing to Disclose

#### PURPOSE

To develop a jointly optimized deep learning framework based on dual-energy CT pulmonary angiography (DE-CTPA) data to generate synthetic monoenergetic images (SMI) for improving automatic pulmonary embolism (PE) detection in single-energy CTPA scans.

#### METHODS AND MATERIALS

We used two data sets: our institutional DE-CTPA data set D1 comprising polyenergetic arterial series and the corresponding VMI at low-energy levels (40 keV) with 7,892 image pairs, and a 10% subset of the 2020 RSNA Pulmonary Embolism Detection Challenge data set D2, which consisted of 161,253 polyenergetic images with binary slice-wise annotations (PE/no PE). We trained a fully convolutional encoder-decoder on D1 to generate SMI from single-energy CTPA scans of D2, which were then fed into a ResNet50 network for training of the downstream PE classification task. We evaluated our VMI reconstruction results in terms of Peak-Signal-to-Noise-Ratio (PSNR) and Structural Similarity Index Measure (SSIM). For PE identification, we performed a binary classification on slice level and report the area under the curve (AUC).

#### RESULTS

The quantitative results on the reconstruction ability of our framework revealed high-quality visual SMI predictions with reconstruction results of  $0.984 \pm 0.002$  (structural similarity) and  $41.706 \pm 0.547$  dB (peak-signal-to-noise ratio). PE classification resulted in an AUC of 0.84 for our model, which achieved improved performance compared to other naive approaches with AUCs up to 0.81.

#### CONCLUSION

Using joint optimization strategies for deep learning algorithms allows training of translating polyenergetic into monoenergetic images without losing features necessary for automatic PE classification. Our model hereby improves noticeably over straight forward classification while outperforming existing methods.

#### CLINICAL RELEVANCE/APPLICATION

The proposed pipeline may prove to be beneficial for computer-aided detection systems and could help rescue CTPA studies with suboptimal contrast attenuation of the pulmonary arteries from single-energy CT scanners.

Printed on: 02/07/23

## Abstract Archives of the RSNA, 2022

S3A-SPGI

### Gastrointestinal Sunday Poster Discussions - A

Sunday, Nov. 27 11:45AM - 12:15PM Room: Learning Center - GI DPS

#### Participants

Ott Le, MD, Sugar Land, TX (*Moderator*) Nothing to Disclose

#### Sub-Events

### S3A-SPGI-1 PACS-integrated Artificial Intelligence-based Analysis of Body Composition in Exocrine Pancreatic Cancer: Skeletal Muscle Index and Sarcopenia Predict Survival

#### Participants

Nick Beetz, MD, Berlin, Germany (*Presenter*) Nothing to Disclose

#### PURPOSE

Worldwide, pancreatic cancer is the seventh leading cause of cancer death in both sexes. Because of its poor prognosis, pancreatic cancer accounts for almost as many deaths as cases even if curative intended surgery is performed. The aim of this study is to analyze baseline CT body composition using artificial intelligence (AI)-based tissue segmentation to identify possible imaging predictors of survival.

#### METHODS AND MATERIALS

We retrospectively included 103 patients with exocrine pancreatic cancer for whom baseline CT imaging datasets were available. Body composition at the third lumbar vertebra level was analyzed using an AI-based software tool. Patient and survival data were obtained from medical records. Forty-six patients underwent surgery. First, presence of surgical treatment and cut-off values for sarcopenia and obesity served as independent variates. Second, presence of surgery, skeletal muscle index (SMI), visceral adipose tissue (VAT), and subcutaneous adipose tissue (SAT) served as independent variates. Cox regression analysis was performed for 1-year, 2-year, and 3-year survival after baseline CT. Additionally, possible differences between patients undergoing surgical versus nonsurgical treatment were analyzed.

#### RESULTS

Presence of surgery significantly predicted 1-year, 2-year, and 3-year survival ( $p=0.01$ ,  $<0.001$ , and  $<0.001$ , respectively). Across the follow-up periods of 1-year, 2-year, and 3-year survival, the presence of sarcopenia became an equally important predictor of survival ( $p=0.2$ , 1.66, and  $<0.001$ , respectively). Additionally, increased VAT predicted 2-year and 3-year survival ( $p=0.02$  and 0.04, respectively). The impact of sarcopenia on 3-year survival was higher in the surgical treatment group ( $p=0.02$  and  $OR=2.61$ ) compared to the nonsurgical treatment group ( $p=0.05$  and  $OR=1.85$ ). Fittingly, a lower SMI significantly affected 3-year survival only in patients who underwent surgery ( $p=0.02$ ).

#### CONCLUSION

This study for the first time uses a PACS-integrated AI-based body composition analysis tool to predict survival in patients with pancreatic cancer. Besides the already known influence of sarcopenia on survival, our results provide evidence that increased visceral fat is a negative predictor of survival. Moreover, we show that sarcopenia has a greater impact in patients who undergo surgery compared to patients undergoing nonsurgical treatment only.

#### CLINICAL RELEVANCE/APPLICATION

AI-based body composition analysis in pancreatic cancer provides important metabolic information for predicting patient survival. Especially if surgery is performed, sarcopenia and reduced muscle mass are unfavorable imaging predictors and should warrant additional special care to improve survival.

### S3A-SPGI-2 Development and Validation of Deep Learning-based Automatic Detection and Grading of Motion-related Artifacts on Gadoteric Acid-enhanced Liver MRI

#### Participants

Dong Wook Kim, MD, PhD, Seoul, Korea, Republic Of (*Presenter*) Nothing to Disclose

#### PURPOSE

To develop and validate deep learning algorithm (DLA) for automatic detection and grading of motion-related artifact on arterial phase of gadoteric acid-enhanced liver MRI

#### METHODS AND MATERIALS

Multi-step DLA for detection and grading of motion-related artifact, based on modified ResNet-101 and U-net, were trained using 336 arterial-phase images of gadoteric acid-enhanced liver MRI obtained in 2017 (development dataset; 68.6-years [range, 18-95]; 254 men). Motion-related artifact was evaluated in 4 different MRI slices using 3-tier grading systems. In the validation datasets, 313 from the same institution obtained in 2018 (internal validation dataset; 67.2-years [range, 21-87], 228 men) and 329 from

three different institutions (external validation dataset; 64.0-years [range, 23-90], 214 men), per-slice and per-exam diagnostic performances for detection of motion-related artifact were evaluated.

## RESULTS

Per-slice sensitivity and specificity for detecting grade 3 motion-related artifact were 91.5% (97/106) and 96.8% (1134/1172) in the internal validation dataset, and were 93.3% (265/284) and 91.6% (948/1035) in the external validation dataset. Per-exam sensitivity and specificity were 92.0% (23/25) and 99.7% (287/288) in the internal validation dataset, and were 90.0% (72/80) and 96.0% (239/249) in the external validation dataset. The average processing time of DLA for automatic grading of motion-related artifact was 4.15 seconds per MRI examination.

## CONCLUSION

s DLA enables automatic and instant detection and grading of the motion-related artifact on arterial-phase gadoteric acid-enhanced liver MRI.

## CLINICAL RELEVANCE/APPLICATION

Implementation of DLA in liver MRI examination would potentially reduce repeat examination and additional cost caused by nondiagnostic image from motion-related artifact.

### S3A-SPGI-3 Predicting tumor deposits in rectal cancer: A combined deep learning model using T2WI-MR imaging< and gtclinical features

Participants

Jin Yumei, (*Presenter*) Nothing to Disclose

## PURPOSE

To develop and validate a deep learning (DL)based combined model incorporating T2-MR image and clinical factors for preoperatively predicting tumor deposits (TDs) in rectal cancer (RC) patients.

## METHODS AND MATERIALS

A total of 327 RC patients from December 2017 to July 2021 was retrospectively collected and the TDs status was pathologically confirmed. Both tumoral and peritumoral regions were labeled on the preoperative T2-MR images. Patients were randomly divided into a development dataset (143 non-TDs and 103 TDs) and an independent testing set (47 non-TDs and 34 TDs). Three DL models were proposed: a single-channel deep learning (single-DL) model using only the tumoral regions as input, a multi-channel deep learning (multi-DL) model using both the tumoral and peri-tumoral regions as input, and a hybrid deep learning (hybrid-DL) model that incorporating both tumoral and peri-tumoral regions as well as the selected clinical variables. A clinical model was also constructed via multivariate logistic regression analysis. The performance of these predictive models was evaluated with respect to discrimination, calibration and clinical usefulness.

## RESULTS

The AUCs of the clinical, single-DL, multi-DL and hybrid-DL models were 0.734 (95% CI, 0.674-0.788), 0.710 (95% CI, 0.649-0.766), 0.767 (95% CI, 0.710-0.819) and 0.857 (95% CI, 0.807-0.898) in the development dataset, respectively. Similar performance of these models was observed in the testing dataset with AUCs achieving 0.726 (95% CI, 0.615-0.819), 0.676 (95% CI, 0.563-0.776), 0.738 (95% CI, 0.628-0.829) and 0.839 (95% CI, 0.741-0.911), respectively. DeLong's test indicated the hybrid-DL model showed improved performance than the clinical model ( $p = 0.134$ ), single-DL model ( $p=0.028$ ) and multi-DL model ( $p = 0.066$ ) in the testing dataset. All models showed good calibration, and decision curve analysis confirmed net benefit of the hybrid-DL model was higher than other models across majority range of threshold probabilities

## CONCLUSION

s The proposed hybrid-DL model incorporating T2-MR images and clinical risk factors achieved good predictive efficacy and could be used to predict tumor deposits in rectal cancer.

## CLINICAL RELEVANCE/APPLICATION

We developed a deep learning model based on both T2-MR images and clinical risk factors with favorable performance, which could be used for preoperative prediction of tumor deposits in rectal cancer.

### S3A-SPGI-4 Prognostic value of preoperative CT-based radiomics in grade 1-2 pancreatic neuroendocrine tumors: a multi-institutional study

Participants

Subin Heo, MD, Suwon, Korea, Republic Of (*Presenter*) Nothing to Disclose

## PURPOSE

To develop and validate a radiomics-based model for predicting postsurgical outcomes using preoperative CT in patients with grade 1-2 pancreatic neuroendocrine tumors (PNETs), and to evaluate the incremental prognostic value of radiomics analysis to the current staging system.

## METHODS AND MATERIALS

This multicenter retrospective study included patients who underwent dynamic CT and subsequent curative resection for grade 1-2 PNETs. In the training cohort (441 patients from one institution), radiomics features were extracted from the segmented tumor of the arterial and portal-venous phase images. A radiomics score (R-score) for predicting recurrence-free survival (RFS) was built using the least absolute shrinkage and selection operator-Cox regression analysis. A model consisting of age and the 8th American Joint Committee on Cancer staging system (AJCC)-based tumor stage, and another model combining the R-score, age and AJCC stage were built to predict RFS and overall survival (OS) using the multivariable Cox regression analysis. Models were tested in an external cohort (159 patients from another institution) using Harrell's C-index. The incremental difference of the models was evaluated using the net reclassification improvement (NRI) and integrated discrimination improvement (IDI).

## RESULTS

In the training cohort, 63 patients (14.3 %) experienced recurrence, and 35 (7.9 %) died. In the test cohort, recurrence occurred in 19 (11.9 %) and 12 (7.5 %) died. The median follow-up was 68.3 and 59.7 months in training and test cohort, respectively. In the test cohort, R-score had C-index of 0.716 for RFS and 0.674 for OS. The combined model outperformed the model without R-score in predicting outcomes in the test cohort (for RFS, C-index, 0.73 vs 0.66,  $p = 0.01$ ; for OS, 0.78 vs 0.68,  $p = 0.04$ ). By integrating the R-score, the combined model achieved improvement in classification and discrimination in predicting RFS at 3 years (NRI, 0.33; IDI, 0.07 [ $p < 0.001$  for both]).

## CONCLUSION

s Radiomics analysis adds incremental value beyond current tumor staging system in predicting RFS and OS in resected grade 1-2 PNETs.

## CLINICAL RELEVANCE/APPLICATION

CT radiomics analysis improves prognostic performance when added to the current staging system in grade 1-2 PNETs, thus enables better patient assessment and individualized treatment decision-making.

## S3A-SPGI-5 Multi-scale sampling method adapted for the detection of small hepatic lesions on gadoxetic acid-enhanced hepatobiliary phase MR images

Participants

Tatsuya Yamaguchi, Kawasaki-Shi, Japan (*Presenter*) Nothing to Disclose

## PURPOSE

Gadoxetic acid-enhanced hepatobiliary phase (HBP) magnetic resonance (MR) images are highly sensitive for the detection of liver lesions. However, small lesions, especially those near hepatic vessels, may be missed because they and the vessels are low signal intense on HBP images. Our new multi-scale sampling method is adapted for their detection. We investigated the feasibility of our method for the detection of small liver lesions on HBP images.

## METHODS AND MATERIALS

We propose a new method based on multi-scale (6-, 12-, and 24 mm) sampling patch images. The patch images were converted from 3D- to 2D images via the minimum intensity projection of 3 orthogonal planes (axial, coronal, and sagittal). Areas harboring malignant hepatic tumors, hemangiomas, or cysts were sampled from the HBP images of 17 patients. A board-certified radiologist annotated 460 lesions. The VGG-16 convolutional neural network was used for their binary classification (hepatic lesion yes/no). Of the 460 lesions, 32 (7%) were used for evaluation and the other 328 for learning. True positive was recorded when the particle obtained by integrating the detection results acquired at each scale even partially overlapped the lesion. False positive was recorded when the particle showed no overlap. Free-response receiver operating characteristic (FROC) analysis was used to evaluate the performance of our method.

## RESULTS

From FROC evaluation, the sensitivity of our method was 78% (25/32 lesions) at 9 false positives per volume (FP/vol); it was 80% (8/10 lesions) when limited to lesions less than 10 mm. Our method was more sensitive than single-scale methods used in related studies.

## CONCLUSION

s Regardless of the target size, our multi-scale sampling method is highly sensitive for liver lesions on HBP images.

## CLINICAL RELEVANCE/APPLICATION

Our multi-scale sampling method can detect small liver lesions with high sensitivity on HBP images regardless of the target size. Our method may be useful in patients with small, possibly metastatic hepatic lesions.

## S3A-SPGI-6 Image Quality Improvement of Liver Ultrasound Using Unsupervised Deep Learning

Participants

Jaeyoung Huh, MS, Daejeon, Korea, Republic Of (*Presenter*) Nothing to Disclose

## PURPOSE

To evaluate image quality improvement of liver ultrasound (US) obtained by an old equipment through a deep learning approach.

## METHODS AND MATERIALS

The neural network was trained using low-quality images as inputs and high-quality images as targets. Since there is no matched low-high quality paired dataset, unsupervised learning using cyclic consistency and adaptive instance normalization (AdaIN) was utilized. We consecutively enrolled and randomly selected liver US to prepared two categories of datasets for training our deep learning-based algorithm, i.e., 1) liver US obtained by an aged US machine more than 10 years served as inputs or students (All 500sets, training sets: test sets = 400:100); 2) liver us obtained by a high-end US machine manufactured within 5 years, served as targets or teacher (400 sets, all training sets). The image quality was evaluated by 5 categories by two reviewers, i.e., brightness, contrast, resolution, reverberation artifact and overall quality, using 5-scored system. Additionally, the reviewers assessed the presence of liver cirrhosis (LC), fatty liver, solid hepatic focal lesion detection, gallbladder polyp and gallstones in each US set. We use paired simple t test to assess five categories of image quality improvement and weighted kappa analysis for inter-reader agreement. To compare diagnostic performance, the Fisher exact test was used and inter-reader diagnostic difference was evaluated by McNemar test.

## RESULTS

Liver US reconstructed by the proposed algorithm showed a significantly higher value in most categories such as brightness, contrast and overall quality ( $p < 0.0001$ ) by both reviewers. On the other hand, there was a slight increase in resolution and reverberation categories, but with no significant difference. The weighted kappa values of the image quality and diagnostic performance categories were calculated as 0.225 to 0.838, showing fair to almost perfect inter reader agreement. All reviewers called significantly more LC at post-processed sets and the diagnostic performance of LC increased at post-processed sets in both

reviewers ( $p < 0.05$ ), based on clinical diagnosis made by physicians with other imaging and laboratory studies.

## CONCLUSION

The proposed algorithm enhances the low-quality liver US images to high-quality, thereby helping early diagnosis and intervention for liver cirrhosis.

## CLINICAL RELEVANCE/APPLICATION

The proposed algorithm enhances the low-quality liver US images to high-quality, thereby helping early diagnosis and intervention for liver cirrhosis.

### **33A-SPGI-7 Concordance between fully automated Computed Tomography-based and bioimpedance-based analysis of body composition in a prospective study**

#### Participants

Uli Fehrenbach, MD, Berlin, Germany (*Presenter*) Grant, Siemens AG; Grant, Bayer AG; Grant, Ipsen SA; Grant, Asahi Intecc Co, Ltd; Grant, ESGAR; Grant, General Electric Company

#### PURPOSE

Body composition is increasingly recognized as an important indicator of patient frailty. Apart from the established bioimpedance analysis (BIA), computed tomography (CT)-based body composition assessment is increasingly used to identify patients at risk. The aim of this prospective study was to compare body composition parameters obtained from BIA and CT using a fully automated artificial intelligence (AI)-based segmentation method.

#### METHODS AND MATERIALS

We prospectively included 210 randomly selected patients who underwent contrast-enhanced CT imaging of the abdomen at our institution. Immediately prior the CT scan, all patients underwent BIA (InBody 770, InBody Europe B.V.). CT body composition was assessed with an AI-based single-slice segmentation tool (Visage Imaging) at the level of the third lumbar vertebra with automated detection and segmentation. BIA-derived parameters, body fat mass (BFM) and skeletal muscle mass (SMM), as well as the CT parameters subcutaneous and visceral adipose tissue area (SATA and VATA) and skeletal muscle area (SMA) were obtained. Body Fat Percentage (BFP) and Skeletal Muscle Index (SMI) were calculated by normalizing the BIA and CT parameters to patient's weight (BFP) or height (SMI). Pearson correlation coefficient was used to compare muscle and fat tissue parameters by sex. Linear regression models were used to analyse indices.

#### RESULTS

Fat and muscle tissue parameters, BIA-based BFM and CT-based SATA+VATA, as well as BIA-based SMM and CT-based SMA, showed strong correlations in female (fat:  $r=0.95$ ; muscle:  $r=0.72$ ; both  $p < 0.001$ ) and male (fat:  $r=0.91$ ; muscle:  $r=0.71$ ; both  $p < 0.001$ ) patients. Linear regression analysis was statistically significant and showed that BFPCT and LSMICT could predict BFPBIA and SMIBIA for female (BFP:  $b_1=5.29$ ; CI95 [4.62-5.95]; SMI:  $b_1=0.11$ ; CI95 [0.09-0.13]; both  $p < 0.001$ ) and male (BFP:  $b_1=4.47$ ; CI95 [3.97-4.97]; SMI:  $b_1=0.09$ ; CI95 [0.08-0.11]; both  $p < 0.001$ ) patients.

## CONCLUSION

Fully automated, AI-based CT body composition parameters strongly correlate with BIA measurements and allow quantification of body fat percentage and skeletal muscle index comparable to the measurements gleaned from the existing gold standard. Thus, an additional BIA appears unnecessary in patients who have received an abdominal CT scan as part of their clinical workup.

## CLINICAL RELEVANCE/APPLICATION

The data obtained from CT-body composition analysis allows for assessment of patient frailty (e.g., sarcopenia). Our study shows that CT body composition is comparable to BIA and so it seems feasible that CT body composition assessment could replace BIA as the new standard in clinical practice.

### **33A-SPGI-8 Can Deep Learning Reconstruction Effectively Reduce The Number Of Excitations In Fast Spin-Echo T2-Weighted MRI Of The Liver?**

#### Participants

Takashi Ota, MD, PhD, Suita, Japan (*Presenter*) Nothing to Disclose

#### PURPOSE

Deep learning reconstruction (DLR) can reduce noise and allow number of excitations (NEX) to be reduced in MRI. However, it remains unknown if DLR can effectively reduce NEX in fast spin-echo T2-weighted imaging (FSE-T2WI) of the liver because reducing NEX might exacerbate motion artifacts. The purpose of this study was to intra-individually compare the image quality of liver FSE-T2WI obtained with NEX 1 along with DLR (NEX1-DLR) versus that with NEX 2 along with conventional reconstruction (NEX2-CR).

#### METHODS AND MATERIALS

Forty-seven patients were included in this study who were followed-up in our hospital and underwent liver MRI examinations before and after an introduction of DLR into our 3T-MR system. Respiratory-triggered FSE-T2WI was obtained with NEX2-CR and NEX1-DLR before and after the introduction of DLR, respectively. One radiologist measured the signal-to-noise-ratio (SNR) and the relative contrast. Two radiologists assessed the two sets of T2WI in a random order regarding noise, ghost artifacts, homogeneity, sharpness, liver conspicuity, lesion conspicuity, and overall image quality. After reviewing each image separately, they compared the two series side-to-side and selected better series considering the total visual quality. The results were compared using the paired t-test or Wilcoxon signed-rank test.

#### RESULTS

The mean acquisition time was 136 and 197 sec with NEX1-DLR and NEX2-CR, respectively. NEX1-DLR provided significantly higher SNR of the liver than NEX2-CR (mean, 10.13 and 8.60, respectively,  $p < .001$ ). There was no significant difference in liver-to-focal liver lesion contrast between them. Qualitative analyses showed that the score of noise was significantly better with NEX1-DLR than with NEX2-CR in both reviewers ( $p < .001$ ). There were no significant differences in the other evaluations except that one

reviewer rated significantly better scores for NEX2-CR than for NEX1-DLR regarding homogeneity. In the side-to-side comparisons, NEX1-DLR was preferred in 21 and 20 patients while NEX2-CR was preferred in 20 and 18 patients by the two reviewers.

## **CONCLUSION**

s Liver FSE-T2WI with NEX1-DLR and NEX2-CR showed almost the same image quality.

## **CLINICAL RELEVANCE/APPLICATION**

DLR can effectively reduce the scan time of liver FSE-T2WI by reducing NEX without diminishing the image quality.

## **S3A-SPGI-9 The Automatic diagnosis model for acute appendicitis in CT images based on deep learning**

Participants

Kexin Wang, (*Presenter*) Nothing to Disclose

## **PURPOSE**

To train a model based on 3D Residual Network for the triage of acute appendicitis with emergency CT images.

## **METHODS AND MATERIALS**

991 sets of emergency plain CT scans from July 1st, 2019 to December 31st, 2020 were used. The clinical diagnosis was archived from the electronic medical recording system. 492 patients were diagnosed with acute appendicitis, and the other 499 patients were diagnosed without acute appendicitis. The images were allocated into three datasets. There was no overlap among the three datasets. In dataset 1, 100 of the images were annotated in the appendix area. A 3D UNet model (model 1) was trained to segment the area of the appendix. In dataset 2, 800 of the images were used to train a 3D ResNet (model 2) to classify acute appendicitis, within the predicted area of model 1. In dataset 3, 91 of the images were used to test the detection rate of acute appendicitis, sequentially by model 1 and model 2.

## **RESULTS**

For model 1, the average Dice coefficient of the predicted appendix area was 0.87. For model 2, the accuracy, sensitivity, specificity, and F1-score of the classification of acute appendicitis were 0.82, 0.86, 0.88, and 0.81, respectively. In dataset 3, all the appendix areas were predicted by model 1 and the classification accuracy was 0.79 by model 2.

## **CONCLUSION**

s It is possible to use deep learning models to establish a triage system for acute appendicitis in emergency radiology department.

## **CLINICAL RELEVANCE/APPLICATION**

Automatic and rapid detection of patients with acute appendicitis after CT examinations in ER, facilitating patient management and improving safety.

Printed on: 02/07/23

## Abstract Archives of the RSNA, 2022

S3A-SPGI-1

### **PACS-integrated Artificial Intelligence-based Analysis of Body Composition in Exocrine Pancreatic Cancer: Skeletal Muscle Index and Sarcopenia Predict Survival**

Sunday, Nov. 27 11:45AM - 12:15PM Room: Learning Center - GI DPS

#### **Participants**

Nick Beetz, MD, Berlin, Germany (*Presenter*) Nothing to Disclose

#### **PURPOSE**

Worldwide, pancreatic cancer is the seventh leading cause of cancer death in both sexes. Because of its poor prognosis, pancreatic cancer accounts for almost as many deaths as cases even if curative intended surgery is performed. The aim of this study is to analyze baseline CT body composition using artificial intelligence (AI)-based tissue segmentation to identify possible imaging predictors of survival.

#### **METHODS AND MATERIALS**

We retrospectively included 103 patients with exocrine pancreatic cancer for whom baseline CT imaging datasets were available. Body composition at the third lumbar vertebra level was analyzed using an AI-based software tool. Patient and survival data were obtained from medical records. Forty-six patients underwent surgery. First, presence of surgical treatment and cut-off values for sarcopenia and obesity served as independent variates. Second, presence of surgery, skeletal muscle index (SMI), visceral adipose tissue (VAT), and subcutaneous adipose tissue (SAT) served as independent variates. Cox regression analysis was performed for 1-year, 2-year, and 3-year survival after baseline CT. Additionally, possible differences between patients undergoing surgical versus nonsurgical treatment were analyzed.

#### **RESULTS**

Presence of surgery significantly predicted 1-year, 2-year, and 3-year survival ( $p=0.01$ ,  $<0.001$ , and  $<0.001$ , respectively). Across the follow-up periods of 1-year, 2-year, and 3-year survival, the presence of sarcopenia became an equally important predictor of survival ( $p=0.2$ ,  $1.66$ , and  $<0.001$ , respectively). Additionally, increased VAT predicted 2-year and 3-year survival ( $p=0.02$  and  $0.04$ , respectively). The impact of sarcopenia on 3-year survival was higher in the surgical treatment group ( $p=0.02$  and  $OR=2.61$ ) compared to the nonsurgical treatment group ( $p=0.05$  and  $OR=1.85$ ). Fittingly, a lower SMI significantly affected 3-year survival only in patients who underwent surgery ( $p=0.02$ ).

#### **CONCLUSION**

This study for the first time uses a PACS-integrated AI-based body composition analysis tool to predict survival in patients with pancreatic cancer. Besides the already known influence of sarcopenia on survival, our results provide evidence that increased visceral fat is a negative predictor of survival. Moreover, we show that sarcopenia has a greater impact in patients who undergo surgery compared to patients undergoing nonsurgical treatment only.

#### **CLINICAL RELEVANCE/APPLICATION**

AI-based body composition analysis in pancreatic cancer provides important metabolic information for predicting patient survival. Especially if surgery is performed, sarcopenia and reduced muscle mass are unfavorable imaging predictors and should warrant additional special care to improve survival.

Printed on: 02/07/23

## Abstract Archives of the RSNA, 2022

S3A-SPGI-2

### Development and Validation of Deep Learning-based Automatic Detection and Grading of Motion-related Artifacts on Gadoteric Acid-enhanced Liver MRI

Sunday, Nov. 27 11:45AM - 12:15PM Room: Learning Center - GI DPS

#### Participants

Dong Wook Kim, MD, PhD, Seoul, Korea, Republic Of (*Presenter*) Nothing to Disclose

#### PURPOSE

To develop and validate deep learning algorithm (DLA) for automatic detection and grading of motion-related artifact on arterial phase of gadoteric acid-enhanced liver MRI

#### METHODS AND MATERIALS

Multi-step DLA for detection and grading of motion-related artifact, based on modified ResNet-101 and U-net, were trained using 336 arterial-phase images of gadoteric acid-enhanced liver MRI obtained in 2017 (development dataset; 68.6-years [range, 18-95]; 254 men). Motion-related artifact was evaluated in 4 different MRI slices using 3-tier grading systems. In the validation datasets, 313 from the same institution obtained in 2018 (internal validation dataset; 67.2-years [range, 21-87], 228 men) and 329 from three different institutions (external validation dataset; 64.0-years [range, 23-90], 214 men), per-slice and per-exam diagnostic performances for detection of motion-related artifact were evaluated.

#### RESULTS

Per-slice sensitivity and specificity for detecting grade 3 motion-related artifact were 91.5% (97/106) and 96.8% (1134/1172) in the internal validation dataset, and were 93.3% (265/284) and 91.6% (948/1035) in the external validation dataset. Per-exam sensitivity and specificity were 92.0% (23/25) and 99.7% (287/288) in the internal validation dataset, and were 90.0% (72/80) and 96.0% (239/249) in the external validation dataset. The average processing time of DLA for automatic grading of motion-related artifact was 4.15 seconds per MRI examination.

#### CONCLUSION

s DLA enables automatic and instant detection and grading of the motion-related artifact on arterial-phase gadoteric acid-enhanced liver MRI.

#### CLINICAL RELEVANCE/APPLICATION

Implementation of DLA in liver MRI examination would potentially reduce repeat examination and additional cost caused by nondiagnostic image from motion-related artifact.

Printed on: 02/07/23

## Abstract Archives of the RSNA, 2022

S3A-SPGI-3

### Predicting tumor deposits in rectal cancer: A combined deep learning model using T2WI-MR imaging and clinical features

Sunday, Nov. 27 11:45AM - 12:15PM Room: Learning Center - GI DPS

#### Participants

Jin Yumei, (*Presenter*) Nothing to Disclose

#### PURPOSE

To develop and validate a deep learning (DL) based combined model incorporating T2-MR image and clinical factors for preoperatively predicting tumor deposits (TDs) in rectal cancer (RC) patients.

#### METHODS AND MATERIALS

A total of 327 RC patients from December 2017 to July 2021 was retrospectively collected and the TDs status was pathologically confirmed. Both tumoral and peritumoral regions were labeled on the preoperative T2-MR images. Patients were randomly divided into a development dataset (143 non-TDs and 103 TDs) and an independent testing set (47 non-TDs and 34 TDs). Three DL models were proposed: a single-channel deep learning (single-DL) model using only the tumoral regions as input, a multi-channel deep learning (multi-DL) model using both the tumoral and peri-tumoral regions as input, and a hybrid deep learning (hybrid-DL) model that incorporating both tumoral and peri-tumoral regions as well as the selected clinical variables. A clinical model was also constructed via multivariate logistic regression analysis. The performance of these predictive models was evaluated with respect to discrimination, calibration and clinical usefulness.

#### RESULTS

The AUCs of the clinical, single-DL, multi-DL and hybrid-DL models were 0.734 (95% CI, 0.674-0.788), 0.710 (95% CI, 0.649-0.766), 0.767 (95% CI, 0.710-0.819) and 0.857 (95% CI, 0.807-0.898) in the development dataset, respectively. Similar performance of these models was observed in the testing dataset with AUCs achieving 0.726 (95% CI, 0.615-0.819), 0.676 (95% CI, 0.563-0.776), 0.738 (95% CI, 0.628-0.829) and 0.839 (95% CI, 0.741-0.911), respectively. Delong's test indicated the hybrid-DL model showed improved performance than the clinical model ( $p = 0.134$ ), single-DL model ( $p = 0.028$ ) and multi-DL model ( $p = 0.066$ ) in the testing dataset. All models showed good calibration, and decision curve analysis confirmed net benefit of the hybrid-DL model was higher than other models across majority range of threshold probabilities

#### CONCLUSION

The proposed hybrid-DL model incorporating T2-MR images and clinical risk factors achieved good predictive efficacy and could be used to predict tumor deposits in rectal cancer.

#### CLINICAL RELEVANCE/APPLICATION

We developed a deep learning model based on both T2-MR images and clinical risk factors with favorable performance, which could be used for preoperative prediction of tumor deposits in rectal cancer.

Printed on: 02/07/23

## Abstract Archives of the RSNA, 2022

S3A-SPGI-4

### Prognostic value of preoperative CT-based radiomics in grade 1-2 pancreatic neuroendocrine tumors: a multi-institutional study

Sunday, Nov. 27 11:45AM - 12:15PM Room: Learning Center - GI DPS

#### Participants

Subin Heo, MD, Suwon, Korea, Republic Of (*Presenter*) Nothing to Disclose

#### PURPOSE

To develop and validate a radiomics-based model for predicting postsurgical outcomes using preoperative CT in patients with grade 1-2 pancreatic neuroendocrine tumors (PNETs), and to evaluate the incremental prognostic value of radiomics analysis to the current staging system.

#### METHODS AND MATERIALS

This multicenter retrospective study included patients who underwent dynamic CT and subsequent curative resection for grade 1-2 PNETs. In the training cohort (441 patients from one institution), radiomics features were extracted from the segmented tumor of the arterial and portal-venous phase images. A radiomics score (R-score) for predicting recurrence-free survival (RFS) was built using the least absolute shrinkage and selection operator-Cox regression analysis. A model consisting of age and the 8th American Joint Committee on Cancer staging system (AJCC)-based tumor stage, and another model combining the R-score, age and AJCC stage were built to predict RFS and overall survival (OS) using the multivariable Cox regression analysis. Models were tested in an external cohort (159 patients from another institution) using Harrell's C-index. The incremental difference of the models was evaluated using the net reclassification improvement (NRI) and integrated discrimination improvement (IDI).

#### RESULTS

In the training cohort, 63 patients (14.3 %) experienced recurrence, and 35 (7.9 %) died. In the test cohort, recurrence occurred in 19 (11.9 %) and 12 (7.5 %) died. The median follow-up was 68.3 and 59.7 months in training and test cohort, respectively. In the test cohort, R-score had C-index of 0.716 for RFS and 0.674 for OS. The combined model outperformed the model without R-score in predicting outcomes in the test cohort (for RFS, C-index, 0.73 vs 0.66,  $p = 0.01$ ; for OS, 0.78 vs 0.68,  $p = 0.04$ ). By integrating the R-score, the combined model achieved improvement in classification and discrimination in predicting RFS at 3 years (NRI, 0.33; IDI, 0.07 [ $p < 0.001$  for both]).

#### CONCLUSION

s Radiomics analysis adds incremental value beyond current tumor staging system in predicting RFS and OS in resected grade 1-2 PNETs.

#### CLINICAL RELEVANCE/APPLICATION

CT radiomics analysis improves prognostic performance when added to the current staging system in grade 1-2 PNETs, thus enables better patient assessment and individualized treatment decision-making.

Printed on: 02/07/23

## Abstract Archives of the RSNA, 2022

S3A-SPGI-5

### Multi-scale sampling method adapted for the detection of small hepatic lesions on gadoxetic acid-enhanced hepatobiliary phase MR images

Sunday, Nov. 27 11:45AM - 12:15PM Room: Learning Center - GI DPS

#### Participants

Tatsuya Yamaguchi, Kawasaki-Shi, Japan (*Presenter*) Nothing to Disclose

#### PURPOSE

Gadoxetic acid-enhanced hepatobiliary phase (HBP) magnetic resonance (MR) images are highly sensitive for the detection of liver lesions. However, small lesions, especially those near hepatic vessels, may be missed because they and the vessels are low signal intense on HBP images. Our new multi-scale sampling method is adapted for their detection. We investigated the feasibility of our method for the detection of small liver lesions on HBP images.

#### METHODS AND MATERIALS

We propose a new method based on multi-scale (6-, 12-, and 24 mm) sampling patch images. The patch images were converted from 3D- to 2D images via the minimum intensity projection of 3 orthogonal planes (axial, coronal, and sagittal). Areas harboring malignant hepatic tumors, hemangiomas, or cysts were sampled from the HBP images of 17 patients. A board-certified radiologist annotated 460 lesions. The VGG-16 convolutional neural network was used for their binary classification (hepatic lesion yes/no). Of the 460 lesions, 32 (7%) were used for evaluation and the other 328 for learning. True positive was recorded when the particle obtained by integrating the detection results acquired at each scale even partially overlapped the lesion. False positive was recorded when the particle showed no overlap. Free-response receiver operating characteristic (FROC) analysis was used to evaluate the performance of our method.

#### RESULTS

From FROC evaluation, the sensitivity of our method was 78% (25/32 lesions) at 9 false positives per volume (FP/vol); it was 80% (8/10 lesions) when limited to lesions less than 10 mm. Our method was more sensitive than single-scale methods used in related studies.

#### CONCLUSION

Regardless of the target size, our multi-scale sampling method is highly sensitive for liver lesions on HBP images.

#### CLINICAL RELEVANCE/APPLICATION

Our multi-scale sampling method can detect small liver lesions with high sensitivity on HBP images regardless of the target size. Our method may be useful in patients with small, possibly metastatic hepatic lesions.

Printed on: 02/07/23

## Abstract Archives of the RSNA, 2022

S3A-SPGI-6

### Image Quality Improvement of Liver Ultrasound Using Unsupervised Deep Learning

Sunday, Nov. 27 11:45AM - 12:15PM Room: Learning Center - GI DPS

#### Participants

Jaeyoung Huh, MS, Daejeon, Korea, Republic Of (*Presenter*) Nothing to Disclose

#### PURPOSE

To evaluate image quality improvement of liver ultrasound (US) obtained by an old equipment through a deep learning approach.

#### METHODS AND MATERIALS

The neural network was trained using low-quality images as inputs and high-quality images as targets. Since there is no matched low-high quality paired dataset, unsupervised learning using cyclic consistency and adaptive instance normalization (AdaIN) was utilized. We consecutively enrolled and randomly selected liver US to prepared two categories of datasets for training our deep learning-based algorithm, i.e., 1) liver US obtained by an aged US machine more than 10 years served as inputs or students (All 500sets, training sets: test sets = 400:100); 2) liver us obtained by a high-end US machine manufactured within 5 years, served as targets or teacher (400 sets, all training sets). The image quality was evaluated by 5 categories by two reviewers, i.e., brightness, contrast, resolution, reverberation artifact and overall quality, using 5-scored system. Additionally, the reviewers assessed the presence of liver cirrhosis (LC), fatty liver, solid hepatic focal lesion detection, gallbladder polyp and gallstones in each US set. We use paired simple t test to assess five categories of image quality improvement and weighted kappa analysis for inter-reader agreement. To compare diagnostic performance, the Fisher exact test was used and inter-reader diagnostic difference was evaluated by McNemar test.

#### RESULTS

Liver US reconstructed by the proposed algorithm showed a significantly higher value in most categories such as brightness, contrast and overall quality ( $p < 0.0001$ ) by both reviewers. On the other hand, there was a slight increase in resolution and reverberation categories, but with no significant difference. The weighted kappa values of the image quality and diagnostic performance categories were calculated as 0.225 to 0.838, showing fair to almost perfect inter reader agreement. All reviewers called significantly more LC at post-processed sets and the diagnostic performance of LC increased at post-processed sets in both reviewers ( $p < 0.05$ ), based on clinical diagnosis made by physicians with other imaging and laboratory studies.

#### CONCLUSION

s The proposed algorithm enhances the low-quality liver US images to high-quality, thereby helping early diagnosis and intervention for liver cirrhosis.

#### CLINICAL RELEVANCE/APPLICATION

The proposed algorithm enhances the low-quality liver US images to high-quality, thereby helping early diagnosis and intervention for liver cirrhosis.

Printed on: 02/07/23

## Abstract Archives of the RSNA, 2022

S3A-SPGI-7

### Concordance between fully automated Computed Tomography-based and bioimpedance-based analysis of body composition in a prospective study

Sunday, Nov. 27 11:45AM - 12:15PM Room: Learning Center - GI DPS

#### Participants

Uli Fehrenbach, MD, Berlin, Germany (*Presenter*) Grant, Siemens AG; Grant, Bayer AG; Grant, Ipsen SA; Grant, Asahi Intecc Co, Ltd; Grant, ESGAR; Grant, General Electric Company

#### PURPOSE

Body composition is increasingly recognized as an important indicator of patient frailty. Apart from the established bioimpedance analysis (BIA), computed tomography (CT)-based body composition assessment is increasingly used to identify patients at risk. The aim of this prospective study was to compare body composition parameters obtained from BIA and CT using a fully automated artificial intelligence (AI)-based segmentation method.

#### METHODS AND MATERIALS

We prospectively included 210 randomly selected patients who underwent contrast-enhanced CT imaging of the abdomen at our institution. Immediately prior the CT scan, all patients underwent BIA (InBody 770, InBody Europe B.V.). CT body composition was assessed with an AI-based single-slice segmentation tool (Visage Imaging) at the level of the third lumbar vertebra with automated detection and segmentation. BIA-derived parameters, body fat mass (BFM) and skeletal muscle mass (SMM), as well as the CT parameters subcutaneous and visceral adipose tissue area (SATA and VATA) and skeletal muscle area (SMA) were obtained. Body Fat Percentage (BFP) and Skeletal Muscle Index (SMI) were calculated by normalizing the BIA and CT parameters to patient's weight (BFP) or height (SMI). Pearson correlation coefficient was used to compare muscle and fat tissue parameters by sex. Linear regression models were used to analyse indices.

#### RESULTS

Fat and muscle tissue parameters, BIA-based BFM and CT-based SATA+VATA, as well as BIA-based SMM and CT-based SMA, showed strong correlations in female (fat:  $r=0.95$ ; muscle:  $r=0.72$ ; both  $p<0.001$ ) and male (fat:  $r=0.91$ ; muscle:  $r=0.71$ ; both  $p<0.001$ ) patients. Linear regression analysis was statistically significant and showed that BFPCT and LSMICT could predict BFPBIA and SMIBIA for female (BFP:  $b1=5.29$ ; CI95 [4.62-5.95]; SMI:  $b1=0.11$ ; CI95 [0.09-0.13]; both  $p<0.001$ ) and male (BFP:  $b1=4.47$ ; CI95 [3.97-4.97]; SMI:  $b1=0.09$ ; CI95 [0.08-0.11]; both  $p<0.001$ ) patients.

#### CONCLUSION

Fully automated, AI-based CT body composition parameters strongly correlate with BIA measurements and allow quantification of body fat percentage and skeletal muscle index comparable to the measurements gleaned from the existing gold standard. Thus, an additional BIA appears unnecessary in patients who have received an abdominal CT scan as part of their clinical workup.

#### CLINICAL RELEVANCE/APPLICATION

The data obtained from CT-body composition analysis allows for assessment of patient frailty (e.g., sarcopenia). Our study shows that CT body composition is comparable to BIA and so it seems feasible that CT body composition assessment could replace BIA as the new standard in clinical practice.

Printed on: 02/07/23

## Abstract Archives of the RSNA, 2022

S3A-SPGI-8

### Can Deep Learning Reconstruction Effectively Reduce The Number Of Excitations In Fast Spin-Echo T2-Weighted MRI Of The Liver?

Sunday, Nov. 27 11:45AM - 12:15PM Room: Learning Center - GI DPS

#### Participants

Takashi Ota, MD, PhD, Suita, Japan (*Presenter*) Nothing to Disclose

#### PURPOSE

Deep learning reconstruction (DLR) can reduce noise and allow number of excitations (NEX) to be reduced in MRI. However, it remains unknown if DLR can effectively reduce NEX in fast spin-echo T2-weighted imaging (FSE-T2WI) of the liver because reducing NEX might exacerbate motion artifacts. The purpose of this study was to intra-individually compare the image quality of liver FSE-T2WI obtained with NEX 1 along with DLR (NEX1-DLR) versus that with NEX 2 along with conventional reconstruction (NEX2-CR).

#### METHODS AND MATERIALS

Forty-seven patients were included in this study who were followed-up in our hospital and underwent liver MRI examinations before and after an introduction of DLR into our 3T-MR system. Respiratory-triggered FSE-T2WI was obtained with NEX2-CR and NEX1-DLR before and after the introduction of DLR, respectively. One radiologist measured the signal-to-noise-ratio (SNR) and the relative contrast. Two radiologists assessed the two sets of T2WI in a random order regarding noise, ghost artifacts, homogeneity, sharpness, liver conspicuity, lesion conspicuity, and overall image quality. After reviewing each image separately, they compared the two series side-to-side and selected better series considering the total visual quality. The results were compared using the paired t-test or Wilcoxon signed-rank test.

#### RESULTS

The mean acquisition time was 136 and 197 sec with NEX1-DLR and NEX2-CR, respectively. NEX1-DLR provided significantly higher SNR of the liver than NEX2-CR (mean, 10.13 and 8.60, respectively,  $p < .001$ ). There was no significant difference in liver-to-focal liver lesion contrast between them. Qualitative analyses showed that the score of noise was significantly better with NEX1-DLR than with NEX2-CR in both reviewers ( $p < .001$ ). There were no significant differences in the other evaluations except that one reviewer rated significantly better scores for NEX2-CR than for NEX1-DLR regarding homogeneity. In the side-to-side comparisons, NEX1-DLR was preferred in 21 and 20 patients while NEX2-CR was preferred in 20 and 18 patients by the two reviewers.

#### CONCLUSION

Liver FSE-T2WI with NEX1-DLR and NEX2-CR showed almost the same image quality.

#### CLINICAL RELEVANCE/APPLICATION

DLR can effectively reduce the scan time of liver FSE-T2WI by reducing NEX without diminishing the image quality.

Printed on: 02/07/23



## Abstract Archives of the RSNA, 2022

S3A-SPGI-9

### The Automatic diagnosis model for acute appendicitis in CT images based on deep learning

Sunday, Nov. 27 11:45AM - 12:15PM Room: Learning Center - GI DPS

#### Participants

Kexin Wang, (*Presenter*) Nothing to Disclose

#### PURPOSE

To train a model based on 3D Residual Network for the triage of acute appendicitis with emergency CT images.

#### METHODS AND MATERIALS

991 sets of emergency plain CT scans from July 1st, 2019 to December 31st, 2020 were used. The clinical diagnosis was archived from the electronic medical recording system. 492 patients were diagnosed with acute appendicitis, and the other 499 patients were diagnosed without acute appendicitis. The images were allocated into three datasets. There was no overlap among the three datasets. In dataset 1, 100 of the images were annotated in the appendix area. A 3D UNet model (model 1) was trained to segment the area of the appendix. In dataset 2, 800 of the images were used to train a 3D ResNet (model 2) to classify acute appendicitis, within the predicted area of model 1. In dataset 3, 91 of the images were used to test the detection rate of acute appendicitis, sequentially by model 1 and model 2.

#### RESULTS

For model 1, the average Dice coefficient of the predicted appendix area was 0.87. For model 2, the accuracy, sensitivity, specificity, and F1-score of the classification of acute appendicitis were 0.82, 0.86, 0.88, and 0.81, respectively. In dataset 3, all the appendix areas were predicted by model 1 and the classification accuracy was 0.79 by model 2.

#### CONCLUSION

It is possible to use deep learning models to establish a triage system for acute appendicitis in emergency radiology department.

#### CLINICAL RELEVANCE/APPLICATION

Automatic and rapid detection of patients with acute appendicitis after CT examinations in ER, facilitating patient management and improving safety.

Printed on: 02/07/23

## Abstract Archives of the RSNA, 2022

S3A-SPGU

### Genitourinary Sunday Poster Discussions - A

Sunday, Nov. 27 11:45AM - 12:15PM Room: Learning Center - GU DPS

#### Sub-Events

#### **S3A-SPGU-1 Thin-slice T2-weighted TSE prostate MRI including deep learning image reconstruction: improvement of image quality without increase of acquisition time**

##### Participants

Sebastian Gassenmaier, MD, Tuebingen, Germany (*Presenter*) Nothing to Disclose

##### PURPOSE

To investigate the impact of a thin-slice deep learning reconstructed T2-weighted (w) TSE imaging sequence (T2DL) of the prostate without increase of acquisition time as compared to conventional T2w TSE imaging (T2S).

##### METHODS AND MATERIALS

Thirty patients were included in this prospective study at one university center after obtaining written informed consent. T2S (3 mm slice thickness) was acquired first in three orthogonal planes. Afterwards, the thin-slice T2DL consisting of a 2 mm slice thickness was acquired in axial plane. Regular acquisition time of T2S was 4:12 min compared to 4:11 min of T2DL due to reduction of signal averages in T2DL. Afterwards, the remaining sequences (DWI, T1, DCE) of the multiparametric imaging protocol were obtained in standard manner. Imaging datasets were evaluated by two radiologists independently consisting of axial T2w TSE imaging (T2S and T2DL), DWI, and DCE imaging in a blinded random order reading. T2w TSE imaging was evaluated using a Likert-scale ranging from 1 - 4 with 4 being the best regarding the following parameters: noise, sharpness, lesion detectability, artifacts, overall image quality, and diagnostic confidence. Furthermore, T2 as well as PI-RADS scoring was obtained.

##### RESULTS

Mean patient age was  $68 \pm 8$  years (range, 49-85 years). Noise levels were evaluated to be significantly improved in T2DL versus T2S by both readers with a median of 4 versus a median of 3.5 ( $p < 0.001$  for both readers). The extent of artifacts was also assessed to be superior in T2DL with a median 4 in comparison to a median of 3 in T2S ( $p < 0.001$  for both readers). Sharpness of images and lesion detectability were rated better in T2DL with a median of 4 versus a median of 3 in T2S ( $p < 0.001$  for both readers). Consequently, overall image quality was also evaluated to be superior in T2DL versus T2S with a median of 4 versus 3 ( $p < 0.001$  for both readers). Diagnostic confidence was significantly higher in T2DL as compared to T2S for reader 1 with a median of 4 versus 3 as well as for reader 2 with a median of 4 for both ( $p < 0.001$  and  $p = 0.004$ , respectively).

##### CONCLUSION

s Thin-slice T2DL of the prostate provides a significant improvement of image quality without prolongation of acquisition time.

##### CLINICAL RELEVANCE/APPLICATION

Apart from acquisition time reduction, deep learning image reconstruction can be applied successfully for improvement of diagnostic image quality without extension of examination times. Application of these techniques might lead to higher diagnostic accuracy in prostate MRI.

#### **S3A-SPGU-3 Fully Automated Longitudinal Assessment of Volumetric Renal Stone Burden on Computed Tomography Using Deep Learning**

##### Participants

Pritam Mukherjee, PhD, Bethesda, MD (*Presenter*) Nothing to Disclose

##### PURPOSE

To develop and evaluate a fully automated deep learning based pipeline for assessing and tracking total renal stone burden in serial computed tomography (CT) scans.

##### METHODS AND MATERIALS

This retrospective study included 177 subjects (median age 56; male 66%) who underwent CT colonography between 2004 and 2016, had an initial noncontrast scan with slice thickness less than 2 mm, at least one follow-up, and were confirmed to have at least one renal calculus in the initial scan by a board-certified radiologist. A deep learning model was used to detect and segment stones, and measure their volumes on the initial and follow-up scans. The true (predicted) volumetric total stone burden (SB) was the sum of the volumes of all true (predicted) stones on a scan. The segmentation performance of the deep learning algorithm was evaluated using the Dice similarity coefficient (DSC). Given the initial and first follow-up (FU1) scans of the same patient, we computed the difference  $SBC = SBFU1 - SB_{initial}$ , and the relative change  $SBR = SBC/SB_{initial}$  for the true and the predicted stones. We evaluated the agreement between the ground truth and predictions for SB, SBC, and SBR using the Lin's concordance correlation coefficient (CCC).

## RESULTS

The sensitivity for our deep learning model was 100%, the mean number of false positives (FPs) per scan was 0.3 (max: 8, IQR: [0,0]), and the median DSC for a random sample of 30 true stones was 100% (100% in 29 stones and 94% on 1 stone). The median number of true stones per scan was 1 (max: 12, IQR: [1,2]). In total, 272 true stones and 40 FPs were present in the initial scans, and 265 true stones and 53 FPs were found in the follow-up scan. The mean SB increased from 57.3 mm<sup>3</sup> in the initial scan to 69.7 mm<sup>3</sup> in the follow-up scan. The CCC for SB, SBC and SBR were 77% (73% - 80%), 66% (59% - 72%) and 87% (83% - 90%), respectively. On removing 8 outliers which lie beyond the 1st and 99th percentile, the CCC improves to 96% (95% - 97%), 95% (94% - 97%) and 98% (98% - 99%) for SB, SBC, and SBR, respectively.

## CONCLUSION

The predictions of the deep learning based pipeline shows strong agreement with the ground truth when assessing the volumetric total stone burden on a scan and tracking its change on longitudinal CT scans.

## CLINICAL RELEVANCE/APPLICATION

Automating the longitudinal assessment of renal stone burden on CTs can facilitate the opportunistic screening and follow-up of renal stones, reduce physician burden, and help improve patient care.

### **S3A-SPGU-4 High diagnostic accuracy of Transperineal Multiparametric Magnetic Resonance Imaging-Ultrasound Fusion Targeted Prostate Biopsy**

Participants

Ryan Ward, MD, (*Presenter*) Nothing to Disclose

## PURPOSE

Although transrectal (TR) prostate biopsy remains the gold standard, there is growing interest in the use of transperineal (TP) biopsy. The main aim of this study was to assess the performance of MRI in distinguishing patients with and without cancer, among those who received transperineal (TP) biopsy.

## METHODS AND MATERIALS

Using an IRB-approved, HIPPA compliant prostate MRI registry, we identified all men who underwent transperineal biopsy from February 2019 to March 2021. Patients were excluded who had no MRI recorded prior to biopsy or the MRI was obtained more than 6 months prior to the biopsy. Patients with prior treatment were also excluded. We extracted the relevant clinical data and Prostate Imaging Reporting Data System (PI-RADS) scores from the associated prostate MRI reports.

## RESULTS

The initial sample consisted of 296 TP biopsies. A total of 194 TP biopsies (from 192 patients) were included in the final sample. A summary of the MRI and TP biopsy results is provided in Table 1. Estimates of intrinsic accuracy and predictive values when MRI results are used to distinguish cases that are positive and negative at TP biopsy are provided in table 2. A positive MRI (PI-RADS $\geq$ 3) combined with TP biopsy rendered positive predictive values of 89-97%, increasing with higher PI-RADS scores.

## CONCLUSION

In patients with positive MRI, TP MRI-US fusion guided biopsy has high diagnostic performance in the diagnosis of prostate cancer.

## CLINICAL RELEVANCE/APPLICATION

TP biopsy offers advantages over conventional TR biopsy. Our data supports the growing evidence that TP biopsy is at least as good as TR biopsy and may have advantages in certain patient populations.

Printed on: 02/07/23

## Abstract Archives of the RSNA, 2022

S3A-SPGU-1

### Thin-slice T2-weighted TSE prostate MRI including deep learning image reconstruction: improvement of image quality without increase of acquisition time

Sunday, Nov. 27 11:45AM - 12:15PM Room: Learning Center - GU DPS

#### Participants

Sebastian Gassenmaier, MD, Tuebingen, Germany (*Presenter*) Nothing to Disclose

#### PURPOSE

To investigate the impact of a thin-slice deep learning reconstructed T2-weighted (w) TSE imaging sequence (T2DL) of the prostate without increase of acquisition time as compared to conventional T2w TSE imaging (T2S).

#### METHODS AND MATERIALS

Thirty patients were included in this prospective study at one university center after obtaining written informed consent. T2S (3 mm slice thickness) was acquired first in three orthogonal planes. Afterwards, the thin-slice T2DL consisting of a 2 mm slice thickness was acquired in axial plane. Regular acquisition time of T2S was 4:12 min compared to 4:11 min of T2DL due to reduction of signal averages in T2DL. Afterwards, the remaining sequences (DWI, T1, DCE) of the multiparametric imaging protocol were obtained in standard manner. Imaging datasets were evaluated by two radiologists independently consisting of axial T2w TSE imaging (T2S and T2DL), DWI, and DCE imaging in a blinded random order reading. T2w TSE imaging was evaluated using a Likert-scale ranging from 1 - 4 with 4 being the best regarding the following parameters: noise, sharpness, lesion detectability, artifacts, overall image quality, and diagnostic confidence. Furthermore, T2 as well as PI-RADS scoring was obtained.

#### RESULTS

Mean patient age was  $68 \pm 8$  years (range, 49-85 years). Noise levels were evaluated to be significantly improved in T2DL versus T2S by both readers with a median of 4 versus a median of 3.5 ( $p < 0.001$  for both readers). The extent of artifacts was also assessed to be superior in T2DL with a median 4 in comparison to a median of 3 in T2S ( $p < 0.001$  for both readers). Sharpness of images and lesion detectability were rated better in T2DL with a median of 4 versus a median of 3 in T2S ( $p < 0.001$  for both readers). Consequently, overall image quality was also evaluated to be superior in T2DL versus T2S with a median of 4 versus 3 ( $p < 0.001$  for both readers). Diagnostic confidence was significantly higher in T2DL as compared to T2S for reader 1 with a median of 4 versus 3 as well as for reader 2 with a median of 4 for both ( $p < 0.001$  and  $p = 0.004$ , respectively).

#### CONCLUSION

s Thin-slice T2DL of the prostate provides a significant improvement of image quality without prolongation of acquisition time.

#### CLINICAL RELEVANCE/APPLICATION

Apart from acquisition time reduction, deep learning image reconstruction can be applied successfully for improvement of diagnostic image quality without extension of examination times. Application of these techniques might lead to higher diagnostic accuracy in prostate MRI.

Printed on: 02/07/23

## Abstract Archives of the RSNA, 2022

S3A-SPGU-3

### Fully Automated Longitudinal Assessment of Volumetric Renal Stone Burden on Computed Tomography Using Deep Learning

Sunday, Nov. 27 11:45AM - 12:15PM Room: Learning Center - GU DPS

#### Participants

Pritam Mukherjee, PhD, Bethesda, MD (*Presenter*) Nothing to Disclose

#### PURPOSE

To develop and evaluate a fully automated deep learning based pipeline for assessing and tracking total renal stone burden in serial computed tomography (CT) scans.

#### METHODS AND MATERIALS

This retrospective study included 177 subjects (median age 56; male 66%) who underwent CT colonography between 2004 and 2016, had an initial noncontrast scan with slice thickness less than 2 mm, at least one follow-up, and were confirmed to have at least one renal calculus in the initial scan by a board-certified radiologist. A deep learning model was used to detect and segment stones, and measure their volumes on the initial and follow-up scans. The true (predicted) volumetric total stone burden (SB) was the sum of the volumes of all true (predicted) stones on a scan. The segmentation performance of the deep learning algorithm was evaluated using the Dice similarity coefficient (DSC). Given the initial and first follow-up (FU1) scans of the same patient, we computed the difference  $SBC = SBFU1 - SB_{initial}$ , and the relative change  $SBR = SBC/SB_{initial}$  for the true and the predicted stones. We evaluated the agreement between the ground truth and predictions for SB, SBC, and SBR using the Lin's concordance correlation coefficient (CCC).

#### RESULTS

The sensitivity for our deep learning model was 100%, the mean number of false positives (FPs) per scan was 0.3 (max: 8, IQR: [0,0]), and the median DSC for a random sample of 30 true stones was 100% (100% in 29 stones and 94% on 1 stone). The median number of true stones per scan was 1 (max: 12, IQR: [1,2]). In total, 272 true stones and 40 FPs were present in the initial scans, and 265 true stones and 53 FPs were found in the follow-up scan. The mean SB increased from 57.3 mm<sup>3</sup> in the initial scan to 69.7 mm<sup>3</sup> in the follow-up scan. The CCC for SB, SBC and SBR were 77% (73% - 80%), 66% (59% - 72%) and 87% (83% - 90%), respectively. On removing 8 outliers which lie beyond the 1st and 99th percentile, the CCC improves to 96% (95% - 97%), 95% (94% - 97%) and 98% (98% - 99%) for SB, SBC, and SBR, respectively.

#### CONCLUSION

The predictions of the deep learning based pipeline shows strong agreement with the ground truth when assessing the volumetric total stone burden on a scan and tracking its change on longitudinal CT scans.

#### CLINICAL RELEVANCE/APPLICATION

Automating the longitudinal assessment of renal stone burden on CTs can facilitate the opportunistic screening and follow-up of renal stones, reduce physician burden, and help improve patient care.

Printed on: 02/07/23



## Abstract Archives of the RSNA, 2022

S3A-SPGU-4

### High diagnostic accuracy of Transperineal Multiparametric Magnetic Resonance Imaging-Ultrasound Fusion Targeted Prostate Biopsy

Sunday, Nov. 27 11:45AM - 12:15PM Room: Learning Center - GU DPS

#### Participants

Ryan Ward, MD, (*Presenter*) Nothing to Disclose

#### PURPOSE

Although transrectal (TR) prostate biopsy remains the gold standard, there is growing interest in the use of transperineal (TP) biopsy. The main aim of this study was to assess the performance of MRI in distinguishing patients with and without cancer, among those who received transperineal (TP) biopsy.

#### METHODS AND MATERIALS

Using an IRB-approved, HIPPA compliant prostate MRI registry, we identified all men who underwent transperineal biopsy from February 2019 to March 2021. Patients were excluded who had no MRI recorded prior to biopsy or the MRI was obtained more than 6 months prior to the biopsy. Patients with prior treatment were also excluded. We extracted the relevant clinical data and Prostate Imaging Reporting Data System (PI-RADS) scores from the associated prostate MRI reports.

#### RESULTS

The initial sample consisted of 296 TP biopsies. A total of 194 TP biopsies (from 192 patients) were included in the final sample. A summary of the MRI and TP biopsy results is provided in Table 1. Estimates of intrinsic accuracy and predictive values when MRI results are used to distinguish cases that are positive and negative at TP biopsy are provided in table 2. A positive MRI (PI-RADS $\geq$ 3) combined with TP biopsy rendered positive predictive values of 89-97%, increasing with higher PI-RADS scores.

#### CONCLUSION

In patients with positive MRI, TP MRI-US fusion guided biopsy has high diagnostic performance in the diagnosis of prostate cancer.

#### CLINICAL RELEVANCE/APPLICATION

TP biopsy offers advantages over conventional TR biopsy. Our data supports the growing evidence that TP biopsy is at least as good as TR biopsy and may have advantages in certain patient populations.

Printed on: 02/07/23

## Abstract Archives of the RSNA, 2022

S3A-SPHN

### Head and Neck Sunday Poster Discussions - A

Sunday, Nov. 27 11:45AM - 12:15PM Room: Learning Center - HN DPS

#### Sub-Events

#### S3A-SPHN-1 Utility of the Echo Planar Imaging with Compressed SENSE (EPICS) for the Evaluation in Head and Neck

Participants

Yuya Hirano, Sapporo, Japan (*Presenter*) Nothing to Disclose

#### PURPOSE

To compare the image quality between echo-planar imaging (EPI) with compressed SENSE (EPICS)-based diffusion weighted imaging (DWI) and conventional parallel imaging (PI)-based DWI of the head and neck.

#### METHODS AND MATERIALS

This prospective study was approved by our institutional review board, and written informed consent was obtained from all participants. Ten healthy volunteers (10 men,  $30.5 \pm 2.9$  years) participated in this study. EPICS-DWI was acquired based on the axial spin-echo EPI sequence with the EPICS acceleration factor of 2, 3, and 4 respectively, with two b-values of 0 and 1000 sec/mm<sup>2</sup>. Conventional PI-DWI was also acquired using the same acceleration factors (2, 3, and 4) and b-values (0 and 1000 sec/mm<sup>2</sup>) as the EPICS-DWI. The quantitative assessments were performed by measuring the value of SNR and apparent diffusion coefficient (ADC) by placing the circular region of interest (ROI) on the parotid gland tissue. For qualitative evaluation, three-point grading system was used for the visual assessment in 1) the overall image quality (1; poor, 2; moderate, 3; good) and 2) degree of the image distortion (1; moderate-severe distortion, 2; slight distortion, 3 almost no distortion); these qualitative assessments were performed by board-certified neuroradiologist.

#### RESULTS

In quantitative assessment, the value of SNR in EPICS-DWI was significantly higher than that in PI-DWI for acceleration factors of 3 and 4 ( $p < 0.05$ , respectively). The value of ADC was revealed slightly lower in EPICS-DWI compared to PI-DWI. In qualitative assessment, overall image quality in EPICS-DWI was significantly higher than PI-DWI for acceleration factor of 3 ( $p < 0.01$ ). The degree of image distortion was significantly larger in EPICS-DWI with acceleration factor of 2 than that of 3 and 4 ( $p < 0.01$ , respectively).

#### CONCLUSION

With the appropriate setting of the acceleration factor, EPICS-DWI demonstrated the higher quantitative SNR and better qualitative overall image quality than PI-DWI without the increase of image distortion in acquiring the head and neck DWI.

#### CLINICAL RELEVANCE/APPLICATION

EPICS can provide improved image quality with high SNR even in DWI of the head and neck, where poor image quality due to the magnetic field inhomogeneity is frequently problematic.

#### S3A-SPHN-2 The Value of Dual-Energy CT in the Diagnosis and Localization of Middle Ear and External Acoustic Meatus Cholesteatoma.

Participants

MINGYUE HUO, (*Presenter*) Nothing to Disclose

#### PURPOSE

To evaluate the diagnostic accuracy of the dual-energy CT (DECT) for cholesteatoma qualitatively and quantitatively, and assess the accuracy of DECT for cholesteatoma tissues localization.

#### METHODS AND MATERIALS

This prospective study included 40 consecutive patients (44 ears) who received preoperative DECT and surgery with a clinical suspicion of cholesteatoma from July 2021 to January 2022. Two radiologists (both with more than 5 years of experience) evaluated the presence or absence of cholesteatoma randomly and independently on DECT then measured four parameters including CT value, Water [hydroxyapatite (Hap)] concentration, Hap (Water) concentration, and the effective Z (Eff-Z) value for statistical analysis. The receiver operating characteristic curves (ROCs) were used for finding out the parameter with the best diagnostic performance for cholesteatoma. The localization accuracy of DECT for cholesteatoma was evaluated ultimately by dividing the external acoustic meatus and middle ear into 7 anatomic sites (external acoustic meatus, tympanic antrum, mastoid cavity, epitympanum, mesotympanum, hypotympanum, posterior tympanum).

#### RESULTS

Taking the surgical results as the reference standard, the sensitivity, specificity, PPV, and NPV of visual evaluation on DECT for

Taking the surgical results as the reference standard, the sensitivity, specificity, PPV, and NPV of visual evaluation on DECT for cholesteatoma were 95.8%, 80.0%, 85.2%, and 94.1% respectively, and the Kappa value was 0.764. Water (Hap) concentration was the best parameter for diagnosis of cholesteatoma with the area under the curve (AUC) of 0.898, the corresponding sensitivity, specificity, PPV and NPV were 91.67%, 80%, 84.6%, and 88.9% respectively when the Water (Hap) concentration was more than 1040.82 mg/cm<sup>3</sup>. The overall accuracy of DECT in evaluating cholesteatoma localization was 91.7%.

## CONCLUSION

s DECT can be capable of diagnosing cholesteatoma qualitatively and quantitatively, and evaluating the localization accurately, to help clinicians to choose a reasonable surgical plan.

## CLINICAL RELEVANCE/APPLICATION

We hypothesized that the difference in histological composition between cholesteatoma and non-cholesteatoma would lead to characteristics of the DECT that can be visualized and quantified. The present study confirmed that DECT technique can be used to identify cholesteatoma qualitatively and quantitatively, and assess the localization of cholesteatoma precisely.

## S3A-SPHN-3 Application of Multi-Shot Echo Planar Imaging Diffusion Weighted Imaging of the Skull Base

Participants

HEDAN LUO, DALIAN, China (*Presenter*) Nothing to Disclose

## PURPOSE

Exploring the performance of Image Reconstruction Using Image-space Sampling (IRIS)-based multi-shot echo planar imaging diffusion weighted imaging (MS-EPI DWI) for the skull base region.

## METHODS AND MATERIALS

31 healthy volunteers were recruited, with an average age of 38.23±18.99 years old. All patients were scanned using a 3.0 T MR scanner (Ingenia CX, Philips Healthcare, the Netherlands) with a thirty-two-channel bilateral phase-array brain coil. All subjects underwent conventional single-shot Echo Planar Imaging Diffusion Weighted Imaging (SS-EPI DWI) and IRIS-based multiple-shot diffusion-weighted imaging (8, 6, 4, and 2 shots, respectively), scan parameters were shown in Table 1. The ADC values, Signal to Noise Ratio (SNR) and Contrast to Noise Ratio (CNR) of bilateral cerebellum, brainstem and pons were measured or calculated. A five-point scoring method was used by two observers to subjectively evaluate the image quality (Table 2). The Kappa test was adopted to evaluate the consistency of the scores by the two observers. The differences of ADC, SNR, CNR and subjective scores among MS-EPI DWI with different number of shots and SS-EPI DWI were analyzed using Friedman test. If the differences were statistically significant, perform multiple comparisons.

## RESULTS

The scores by the two observers were in good agreement ( $\kappa=0.806, 0.874, 0.843, 0.805, 0.850$ ). Comparing MS-EPI DWI with different the number of shots, there was no significant difference in ADC of bilateral cerebellum and CNR of right brainstem and pons. Pairwise comparison of the Bonferroni test results showed that when the number of shots was 4, the ADC difference of the right brainstem and pons was statistically significant compared with SS-EPI DWI. When the number of shots was 2, the left brainstem and pons ADC difference was statistically significant compared with SS-EPI DWI ( $p<0.05$ ). The SNR and CNR of both sides of the cerebellum, brainstem and pons on MS-EPI DWI were greater than those on SS-EPI DWI. When the number of shots was 6, the left cerebellum, brainstem and pons SNR, CNR, right cerebellum SNR, CNR, right brainstem and pons SNR and subjective scores were significantly different than SS-EPI DWI ( $p<0.05$ ). (Table 3, 4)

## CONCLUSION

s Compared with SS-EPI DWI, MS-EPI DWI based on IRIS that showed higher SNR and lower geometric distortion compared with SS-EPI DWI. MS-EPI DWI shots 6 is recommended for clinical skull base between imaging time and image quality.

## CLINICAL RELEVANCE/APPLICATION

IRIS-based MS-EPI DWI technology can significantly reduce the geometric distortion of the skull base and high signal artifacts, it can be applied to MS-EPI DWI when the skull base needs to be observed or suspected of lesions, and has broad clinical application prospects.

Printed on: 02/07/23

## Abstract Archives of the RSNA, 2022

S3A-SPHN-1

### Utility of the Echo Planar Imaging with Compressed SENSE (EPICS) for the Evaluation in Head and Neck

Sunday, Nov. 27 11:45AM - 12:15PM Room: Learning Center - HN DPS

#### Participants

Yuya Hirano, Sapporo, Japan (*Presenter*) Nothing to Disclose

#### PURPOSE

To compare the image quality between echo-planar imaging (EPI) with compressed SENSE (EPICS)-based diffusion weighted imaging (DWI) and conventional parallel imaging (PI)-based DWI of the head and neck.

#### METHODS AND MATERIALS

This prospective study was approved by our institutional review board, and written informed consent was obtained from all participants. Ten healthy volunteers (10 men,  $30.5 \pm 2.9$  years) participated in this study. EPICS-DWI was acquired based on the axial spin-echo EPI sequence with the EPICS acceleration factor of 2, 3, and 4 respectively, with two b-values of 0 and 1000 sec/mm<sup>2</sup>. Conventional PI-DWI was also acquired using the same acceleration factors (2, 3, and 4) and b-values (0 and 1000 sec/mm<sup>2</sup>) as the EPICS-DWI. The quantitative assessments were performed by measuring the value of SNR and apparent diffusion coefficient (ADC) by placing the circular region of interest (ROI) on the parotid gland tissue. For qualitative evaluation, three-point grading system was used for the visual assessment in 1) the overall image quality (1; poor, 2; moderate, 3; good) and 2) degree of the image distortion (1; moderate-severe distortion, 2; slight distortion, 3 almost no distortion); these qualitative assessments were performed by board-certified neuroradiologist.

#### RESULTS

In quantitative assessment, the value of SNR in EPICS-DWI was significantly higher than that in PI-DWI for acceleration factors of 3 and 4 ( $p < 0.05$ , respectively). The value of ADC was revealed slightly lower in EPICS-DWI compared to PI-DWI. In qualitative assessment, overall image quality in EPICS-DWI was significantly higher than PI-DWI for acceleration factor of 3 ( $p < 0.01$ ). The degree of image distortion was significantly larger in EPICS-DWI with acceleration factor of 2 than that of 3 and 4 ( $p < 0.01$ , respectively).

#### CONCLUSION

s With the appropriate setting of the acceleration factor, EPICS-DWI demonstrated the higher quantitative SNR and better qualitative overall image quality than PI-DWI without the increase of image distortion in acquiring the head and neck DWI.

#### CLINICAL RELEVANCE/APPLICATION

EPICS can provide improved image quality with high SNR even in DWI of the head and neck, where poor image quality due to the magnetic field inhomogeneity is frequently problematic.

Printed on: 02/07/23

## Abstract Archives of the RSNA, 2022

S3A-SPHN-2

### The Value of Dual-Energy CT in the Diagnosis and Localization of Middle Ear and External Acoustic Meatus Cholesteatoma.

Sunday, Nov. 27 11:45AM - 12:15PM Room: Learning Center - HN DPS

#### Participants

MINGYUE HUO, (*Presenter*) Nothing to Disclose

#### PURPOSE

To evaluate the diagnostic accuracy of the dual-energy CT(DECT) for cholesteatoma qualitatively and quantitatively, and assess the accuracy of DECT for cholesteatoma tissues localization.

#### METHODS AND MATERIALS

This prospective study included 40 consecutive patients (44 ears) who received preoperative DECT and surgery with a clinical suspicion of cholesteatoma from July 2021 to January 2022. Two radiologists (both with more than 5 years of experience) evaluated the presence or absence of cholesteatoma randomly and independently on DECT then measured four parameters including CT value, Water [hydroxyapatite (Hap)] concentration, Hap (Water) concentration, and the effective Z (Eff-Z) value for statistical analysis. The receiver operating characteristic curves (ROCs) were used for finding out the parameter with the best diagnostic performance for cholesteatoma. The localization accuracy of DECT for cholesteatoma was evaluated ulteriorly by dividing the external acoustic meatus and middle ear into 7 anatomic sites (external acoustic meatus, tympanic antrum, mastoid cavity, epitympanum, mesotympanum, hypotympanum, posterior tympanum).

#### RESULTS

Taking the surgical results as the reference standard, the sensitivity, specificity, PPV, and NPV of visual evaluation on DECT for cholesteatoma were 95.8%, 80.0%, 85.2%, and 94.1% respectively, and the Kappa value was 0.764. Water (Hap) concentration was the best parameter for diagnosis of cholesteatoma with the area under the curve (AUC) of 0.898, the corresponding sensitivity, specificity, PPV and NPV were 91.67%, 80%, 84.6%, and 88.9% respectively when the Water (Hap) concentration was more than 1040.82 mg/cm<sup>3</sup>. The overall accuracy of DECT in evaluating cholesteatoma localization was 91.7%.

#### CONCLUSION

s DECT can be capable of diagnosing cholesteatoma qualitatively and quantitatively, and evaluating the localization accurately, to help clinicians to choose a reasonable surgical plan.

#### CLINICAL RELEVANCE/APPLICATION

We hypothesized that the difference in histological composition between cholesteatoma and non-cholesteatoma would lead to characteristics of the DECT that can be visualized and quantified. The present study confirmed that DECT technique can be used to identify cholesteatoma qualitatively and quantitatively, and assess the localization of cholesteatoma precisely.

Printed on: 02/07/23

## Abstract Archives of the RSNA, 2022

S3A-SPHN-3

### Application of Multi-Shot Echo Planar Imaging Diffusion Weighted Imaging of the Skull Base

Sunday, Nov. 27 11:45AM - 12:15PM Room: Learning Center - HN DPS

#### Participants

HEDAN LUO, DALIAN, China (*Presenter*) Nothing to Disclose

#### PURPOSE

Exploring the performance of Image Reconstruction Using Image-space Sampling (IRIS)-based multi-shot echo planar imaging diffusion weighted imaging (MS-EPI DWI) for the skull base region.

#### METHODS AND MATERIALS

31 healthy volunteers were recruited, with an average age of  $38.23 \pm 18.99$  years old. All patients were scanned using a 3.0 T MR scanner (Ingenia CX, Philips Healthcare, the Netherlands) with a thirty-two-channel bilateral phase-array brain coil. All subjects underwent conventional single-shot Echo Planar Imaging Diffusion Weighted Imaging (SS-EPI DWI) and IRIS-based multiple-shot diffusion-weighted imaging (8, 6, 4, and 2 shots, respectively), scan parameters were shown in Table 1. The ADC values, Signal to Noise Ratio (SNR) and Contrast to Noise Ratio (CNR) of bilateral cerebellum, brainstem and pons were measured or calculated. A five-point scoring method was used by two observers to subjectively evaluate the image quality (Table 2). The Kappa test was adopted to evaluate the consistency of the scores by the two observers. The differences of ADC, SNR, CNR and subjective scores among MS-EPI DWI with different number of shots and SS-EPI DWI were analyzed using Friedman test. If the differences were statistically significant, perform multiple comparisons.

#### RESULTS

The scores by the two observers were in good agreement ( $\kappa = 0.806, 0.874, 0.843, 0.805, 0.850$ ). Comparing MS-EPI DWI with different the number of shots, there was no significant difference in ADC of bilateral cerebellum and CNR of right brainstem and pons. Pairwise comparison of the Bonferroni test results showed that when the number of shots was 4, the ADC difference of the right brainstem and pons was statistically significant compared with SS-EPI DWI. When the number of shots was 2, the left brainstem and pons ADC difference was statistically significant compared with SS-EPI DWI ( $p < 0.05$ ). The SNR and CNR of both sides of the cerebellum, brainstem and pons on MS-EPI DWI were greater than those on SS-EPI DWI. When the number of shots was 6, the left cerebellum, brainstem and pons SNR, CNR, right cerebellum SNR, CNR, right brainstem and pons SNR and subjective scores were significantly different than SS-EPI DWI ( $p < 0.05$ ). (Table 3, 4)

#### CONCLUSION

Compared with SS-EPI DWI, MS-EPI DWI based on IRIS that showed higher SNR and lower geometric distortion compared with SS-EPI DWI. MS-EPI DWI shots 6 is recommended for clinical skull base between imaging time and image quality.

#### CLINICAL RELEVANCE/APPLICATION

IRIS-based MS-EPI DWI technology can significantly reduce the geometric distortion of the skull base and high signal artifacts, it can be applied to MS-EPI DWI when the skull base needs to be observed or suspected of lesions, and has broad clinical application prospects.

Printed on: 02/07/23

## Abstract Archives of the RSNA, 2022

S3A-SPIN

### Informatics Sunday Poster Discussions - A

Sunday, Nov. 27 11:45AM - 12:15PM Room: Learning Center - IN DPS

#### Sub-Events

#### **S3A-SPIN-1 Significantly Accelerated Longitudinal Assessment of Imaging Findings on CT and MRI with Deep Learning Identification of Relevant Prior Exams and Finding Locations**

##### Participants

Thomas Weikert, MD, (*Presenter*) Nothing to Disclose

##### PURPOSE

Comparison to relevant prior studies is a requisite component in the assessment of radiology imaging findings. It is the aim of this study to evaluate the impact of a deep learning tool identifying relevant prior images, time lens (TL), on the longitudinal assessment of lesions on CT and MRI.

##### METHODS AND MATERIALS

The algorithm pipeline used in this retrospective study is based on natural language processing (NLP) and a descriptor-based image matching algorithm. The dataset used for testing comprised 3872 series of 246 radiology examinations from 75 patients (189 CTs, 95 MRIs, time period: 06/2010-06/2021). Five finding types were included: Aortic Aneurysm, Intracranial Aneurysm, Kidney Lesion, Meningioma, Pulmonary Nodule. After a standardized training session, nine radiologists from three university hospitals (2x U.S.A, 1x Switzerland) performed two reading sessions in which the finding of interest was measured on two or more exams: first without use of the tool, and a second session at a 21-day interval with the use of the tool. All user actions were logged for each round, including time needed to measure the finding at all timepoints, number of mouse clicks, and mouse distance travelled. Mouse movement patterns were analyzed with heatmaps. To assess the effect of habituation to the cases, a third round of readings was performed without the tool. A standardized 5-item questionnaire was used to assess user experience.

##### RESULTS

Across scenarios, time needed to assess a finding at all time-points was reduced by 39.0 % (107 vs. 65 seconds;  $p < 0.001$ ). Largest accelerations were demonstrated for assessment of pulmonary nodules (47.0%;  $p < 0.001$ ), and for less experienced readers (44.3%;  $p = 0.02$ ). Less mouse-clicks (-39.0%,  $p < 0.001$ ) and mouse-meters (-25.8%,  $p < 0.001$ ) were needed for finding evaluation with TL. The heatmaps showed consistently simplified mouse-movement-patterns with TL. The habituation effect was not decisive. Overall, user satisfaction was high (4.2/5).

##### CONCLUSION

s TL significantly reduces time needed to assess findings of interest on cross-sectional imaging at multiple timepoints.

##### CLINICAL RELEVANCE/APPLICATION

Because comparison to relevant prior studies is routinely performed in radiology departments, the time-saving potential by computer assistance is tremendous, and more so for cross-sectional imaging.

#### **S3A-SPIN-2 Effect of Deep Learning Image Reconstruction Algorithm on Image Quality and Detectability of Hypovascular Hepatic Metastases at Different Radiation Dose Levels**

##### Participants

Nana Liu, Zhengzhou, China (*Presenter*) Nothing to Disclose

##### PURPOSE

To investigate the effects of deep learning image reconstruction algorithm by comparing with adaptive statistical iterative construction-V on detecting and diagnosis of hypovascular hepatic metastases and image quality under different radiation doses.

##### METHODS AND MATERIALS

Fifty-six patients with suspected liver disease who underwent abdominal enhanced CT scans were collected prospectively. According to the second venous phase currents, the selected patients were randomly assigned into three groups A, B and C. Patients in each group received conventional radiation dose with tube current-time products of 400mAs CT scans in the first vein phase, low-dose CT scans in the second vein phase, which were set as tube current-time products of were 280mAs for group A, 200mAs for group B and 120mAs for group C. The images of first vein phase and second vein phase were reconstructed with ASIR-V60% and DLIR-H. Quantitative parameters [image noise, contrast to noise ratio (CNR), liver and portal vein signal to noise ratio (SNR)] and qualitative parameters [overall image quality, lesion conspicuity, diagnostic confidence] of ASIR-V60% and DLIR-H images were compared, and the effective radiation dose of each group was recorded. Quantitative parameters and effective radiation doses were compared by paired t test, and qualitative parameters were compared by Wilcoxon test.

##### RESULTS

The radiation dose of each group decreased with the decreasing of tube current, the effective radiation doses (ED) were significantly different between the first vein phase and the second vein phase ( $P < 0.001$ ). Compared with the conventional dose first vein phase, the effective radiation dose of group A, B and C decreased by about 30%, 50% and 70%, respectively. The quantitative and qualitative scores of the conventional dose first vein phase were the best. Moreover, with the decrease of radiation dose, the noise gradually increased, and the CNR<sub>lesions</sub>, SNR<sub>liver</sub> and SNR<sub>portal vein</sub> gradually decreased. Notably, under the same radiation dose condition, the quantitative scores of DLIR-H images were statistically better than those of ASiR-V60% (all  $P < 0.001$ ). Furthermore, the qualitative parameters of each group decreased with the decrease of radiation dose. Under the same radiation dose, the overall image quality, lesion conspicuity and diagnostic confidence of DLIR-H were higher than those of ASiR-V60% (all  $P < 0.001$ ).

## CONCLUSION

Compared with ASiR-V60%, DLIR-H could reduce image noise, improve overall image quality and lesion conspicuity of liver metastasis, as well as increase diagnostic confidence under different radiation doses.

## CLINICAL RELEVANCE/APPLICATION

Compared with ASiR-V60%, DLIR can reduce image noise, improve image quality and lesion conspicuity of liver metastasis.

## S3A-SPIN-3 Can We Combine the Best of Two Worlds? Artifact Reduction from Dental Implants in Photon-Counting Detector CT Datasets Based on high-keV Monoenergetic Reconstructions and Iterative Metal Artifact Reduction (iMAR) Reconstructions

Participants

Franka Risch, MSc, Augsburg, Germany (*Presenter*) Nothing to Disclose

## PURPOSE

This study assessed the effect of virtual monoenergetic imaging (VMI) settings, the use of iterative metal artifact reduction (iMAR), and kernel choice on metal artifacts caused by dental fillings/ implants on photon-counting detector CT (PCD-CT) datasets.

## METHODS AND MATERIALS

Patients with dental fillings or implants undergoing staging CT including the neck region on a PCD-CT were screened for study inclusion. A standard and sharp quantitative kernel were reconstructed with and without iterative metal artifact reduction (Qr40, Qr40 iMAR, Qr60, Qr60 iMAR) in nine different virtual monoenergetic keV-levels (range: 40-190 keV). On four selected slices, two with and two without metal artifacts caused by dental fillings/implants, six regions of interest (ROIs) were positioned in air and various defined soft tissues. For each ROI, the mean and standard deviation of CT values were recorded in all series at identical positions. The mean absolute error of CT values and an artifact index were calculated. Statistical analyses focused on differences in artifact index between VMI levels (low vs. high keV), between kernels (standard vs. sharp) and between reconstructions with vs. without iMAR.

## RESULTS

Fifty consecutive patients (age  $71.7 \pm 10.8$  years; 15 female) were included. For each patient, 4 image series for 9 different VMIs were reconstructed, resulting in 36 series per patient. The artifact index severely increased for lower VMI levels ( $< 50$  keV) but did not exhibit significant changes in the 60 - 190 keV range. Overall, the effect of keV settings on noise parameters was relatively small. Sharp kernels increased artifact index moderately ( $\sim 35\%$ ). By using iMAR, the most pronounced reduction of both calculated indices was observed for the standard and sharp kernel as well as in all measured regions of interest (Qr40/Qr60 vs. Qr40 iMAR/Qr60 iMAR, reduction in ?HU: 57 % - 79 %, reduction in AI: 55 % - 88 %).

## CONCLUSION

Metal artifacts caused by dental fillings/ implants are profoundly reduced using iMAR for standard and sharp kernels. Unlike reported for artifacts around orthopedic surgical material, VMI levels had very little effect on artifacts by dental implants.

## CLINICAL RELEVANCE/APPLICATION

Metal artifacts can significantly affect image quality and reduce diagnostic value. iMAR offers effective and reliable reduction of metal artifacts from dental implants.

## S3A-SPIN-4 AI Enabled Automatic CNR Measurement: Development and Evaluation using Multi-energy Images in Abdomen Dual-Energy Contrast-Enhanced CT

Participants

Sihwan Kim, BS, Seoul, Korea, Republic Of (*Presenter*) Nothing to Disclose

## PURPOSE

To develop a system automatically measuring contrast-to-noise ratio (CNR) for evaluating image quality of different dual-energy CT (DECT) scan protocols.

## METHODS AND MATERIALS

The system consists of three stages - deep learning (DL) based liver segmentation, extraction of homogenous ROIs and structure ROIs, and calculation of CNR. For the DL-based segmentation model, U-net architecture with multi-planar reconstruction (MPR) approach was used. The model was trained with contrast and non-contrast CT images of three-hundred patients. For the evaluation of the segmentation model, 131 contrast-enhanced CT (CECT) from Decathlon open-challenge dataset was used. The performance of liver segmentation model was evaluated with dice-coefficient. To extract homogeneous and structure edge regions on CT images, structure coherence map was analyzed using gradient and hessian images. For the evaluation of system performance, twenty-four abdominal DECT scans were retrospectively investigated. The evaluation was performed on four different reconstructed image types; 40-keV VMI image (40-keV VMI), 50-keV VMI image (50-keV VMI), 80-kVp image and linearly blended images simulating 100-kVp image (100-kVp). All the reconstructed images were automatically evaluated with three evaluation metrics; noise, signal-to-noise (SNR) and contrast-to-noise ratio (CNR). In addition, one radiologist visually assessed the successive of CNR measurement with five-point scale.

## RESULTS

The dice value of liver segmentation model was  $0.090 \pm 0.08$  (Mean $\pm$ S.D.) in open challenge dataset. The system presented SNR values as  $8.73 \pm 2.12$  in 40-keV VMI,  $9.08 \pm 2.05$  in 50-keV VMI,  $9.29 \pm 1.67$  in 80-kVp, and  $10.79 \pm 2.04$  in linearly blended 100-kVp. CNR values were  $3.98 \pm 1.53$  in 40-keV VMI,  $3.32 \pm 1.16$  in 50-keV VMI,  $2.80 \pm 1.15$  in 80-kVp, and  $2.15 \pm 1.00$  in linearly blended 100-kVp. Measured noises of each energy-level images had  $20.09 \pm 2.83$  HU,  $14.50 \pm 1.81$  HU,  $11.92 \pm 1.32$  HU, and  $8.51 \pm 0.72$  HU in 40-keV VMI, 50-keV VMI, 80-kVp, and linearly blended 100-kVp, respectively. The five-scale visual assessment result by the radiologist was  $4.08 \pm 0.72$  in 40-keV VMI,  $4.00 \pm 0.72$  in 50-keV VMI,  $4.13 \pm 0.74$  in 80-kVp, and  $3.96 \pm 0.62$  in linearly blended 100-kVp.

## CONCLUSION

We developed a deep learning-assisted CNR measurement system to evaluate the image quality of different DECT scan protocols. We believe that developed system can contribute to the monitoring of CT machine maintenance and optimization of CT scan protocols in clinical practice.

## CLINICAL RELEVANCE/APPLICATION

Image Quality Assessment in Dual-energy CT

### **S3A-SPIN-6 A Unified Framework for Accurate and Robust Lesion RECIST Diameter Prediction and Segmentation with Transformers**

Participants

Youbao Tang, PhD, Bethesda, MD (*Presenter*) Nothing to Disclose

## PURPOSE

Accurately measuring lesion/tumor size with RECIST (Response Evaluation Criteria In Solid Tumors) diameters and segmentation is important for assessing the lesion growth rates and making therapeutic plan. Manually annotating them is tedious, time-consuming, and prone to observer-inconsistency. To overcome these issues, we propose a transformer-based unified framework (MeaFormer) for lesion RECIST diameter prediction and segmentation on CT scans automatically and accurately.

## METHODS AND MATERIALS

MeaFormer formulates LRDPs as three correlative and complementary sub-tasks: lesion segmentation, heatmap prediction, and keypoint regression. It employs transformers to model the long-range dependencies of the high-resolution deep features extracted by a small convolutional neural network. Two consistency losses are introduced to explicitly build relationships among these sub-tasks for multi-task learning and joint optimization. Only requiring a single click operation within the lesion region from clinicians, MeaFormer can output accurate RECIST diameter predictions and 2D mask of the lesion on the key slice where the lesion has the largest spatial extent. Besides, a 3D mask can be obtained by segmenting the lesion slice-by-slice where the center point of the segmented mask on the previous slice is considered as the click point on the current slice. It was evaluated on the DeepLesion dataset containing 32,735 lesions from 10,594 studies of 4,427 patients. 200/1,000 lesion images from 500 patients are manually segmented with 3D/2D masks for testing. The rest patient data are used for training (80%) and validation (20%). Also, 480 lesion pairs from the test set are used for a downstream task evaluation (i.e., longitudinal RECIST assessment based on the predicted diameters).

## RESULTS

Compared to the best previous work on each sub-task, MeaFormer achieved the best performance. For RECIST diameter prediction, the long/short diameter error between the automatic results and manual reference standard is  $1.6 \pm 1.3$  mm/ $1.4 \pm 1.5$  mm. For lesion segmentation, a 2D/3D Dice score of  $0.927 \pm 0.043$ / $0.856 \pm 0.065$  is obtained. On the 480 test lesion pairs, it achieved an accuracy of 91.7% for the tumor response classification (4 classes based on RECIST version 1.1).

## CONCLUSION

We proposed a transformer-based deep learning framework to annotate tumor sizes automatically and accurately with RECIST diameters and segmentations via a simple click operation. It achieved comparable accuracies to manual annotations, but improved efficiency with greatly reduced time and effort.

## CLINICAL RELEVANCE/APPLICATION

It can serve as a useful tool for clinicians to accurately measure tumor sizes with minimal effort and may provide high positive values on clinical workflows.

Printed on: 02/07/23

## Abstract Archives of the RSNA, 2022

S3A-SPIN-1

### Significantly Accelerated Longitudinal Assessment of Imaging Findings on CT and MRI with Deep Learning Identification of Relevant Prior Exams and Finding Locations

Sunday, Nov. 27 11:45AM - 12:15PM Room: Learning Center - IN DPS

#### Participants

Thomas Weikert, MD, (*Presenter*) Nothing to Disclose

#### PURPOSE

Comparison to relevant prior studies is a requisite component in the assessment of radiology imaging findings. It is the aim of this study to evaluate the impact of a deep learning tool identifying relevant prior images, time lens (TL), on the longitudinal assessment of lesions on CT and MRI.

#### METHODS AND MATERIALS

The algorithm pipeline used in this retrospective study is based on natural language processing (NLP) and a descriptor-based image matching algorithm. The dataset used for testing comprised 3872 series of 246 radiology examinations from 75 patients (189 CTs, 95 MRIs, time period: 06/2010-06/2021). Five finding types were included: Aortic Aneurysm, Intracranial Aneurysm, Kidney Lesion, Meningioma, Pulmonary Nodule. After a standardized training session, nine radiologists from three university hospitals (2x U.S.A, 1x Switzerland) performed two reading sessions in which the finding of interest was measured on two or more exams: first without use of the tool, and a second session at a 21-day interval with the use of the tool. All user actions were logged for each round, including time needed to measure the finding at all timepoints, number of mouse clicks, and mouse distance travelled. Mouse movement patterns were analyzed with heatmaps. To assess the effect of habituation to the cases, a third round of readings was performed without the tool. A standardized 5-item questionnaire was used to assess user experience.

#### RESULTS

Across scenarios, time needed to assess a finding at all time-points was reduced by 39.0 % (107 vs. 65 seconds;  $p < 0.001$ ). Largest accelerations were demonstrated for assessment of pulmonary nodules (47.0%;  $p < 0.001$ ), and for less experienced readers (44.3%;  $p = 0.02$ ). Less mouse-clicks (-39.0%,  $p < 0.001$ ) and mouse-meters (-25.8%,  $p < 0.001$ ) were needed for finding evaluation with TL. The heatmaps showed consistently simplified mouse-movement-patterns with TL. The habituation effect was not decisive. Overall, user satisfaction was high (4.2/5).

#### CONCLUSION

s TL significantly reduces time needed to assess findings of interest on cross-sectional imaging at multiple timepoints.

#### CLINICAL RELEVANCE/APPLICATION

Because comparison to relevant prior studies is routinely performed in radiology departments, the time-saving potential by computer assistance is tremendous, and more so for cross-sectional imaging.

Printed on: 02/07/23

## Abstract Archives of the RSNA, 2022

S3A-SPIN-2

### Effect of Deep Learning Image Reconstruction Algorithm on Image Quality and Detectability of Hypovascular Hepatic Metastases at Different Radiation Dose Levels

Sunday, Nov. 27 11:45AM - 12:15PM Room: Learning Center - IN DPS

#### Participants

Nana Liu, Zhengzhou, China (*Presenter*) Nothing to Disclose

#### PURPOSE

To investigate the effects of deep learning image reconstruction algorithm by comparing with adaptive statistical iterative construction-V on detecting and diagnosis of hypovascular hepatic metastases and image quality under different radiation doses.

#### METHODS AND MATERIALS

Fifty-six patients with suspected liver disease who underwent abdominal enhanced CT scans were collected prospectively. According to the second venous phase currents, the selected patients were randomly assigned into three groups A, B and C. Patients in each group received conventional radiation dose with tube current-time products of 400mAs CT scans in the first vein phase, low-dose CT scans in the second vein phase, which were set as tube current-time products of 280mAs for group A, 200mAs for group B and 120mAs for group C. The images of first vein phase and second vein phase were reconstructed with ASiR-V60% and DLIR-H. Quantitative parameters [image noise, contrast to noise ratio (CNR), liver and portal vein signal to noise ratio (SNR)] and qualitative parameters [overall image quality, lesion conspicuity, diagnostic confidence] of ASiR-V60% and DLIR-H images were compared, and the effective radiation dose of each group was recorded. Quantitative parameters and effective radiation doses were compared by paired t test, and qualitative parameters were compared by Wilcoxon test.

#### RESULTS

The radiation dose of each group decreased with the decreasing of tube current, the effective radiation doses (ED) were significantly different between the first vein phase and the second vein phase ( $P < 0.001$ ). Compared with the conventional dose first vein phase, the effective radiation dose of group A, B and C decreased by about 30%, 50% and 70%, respectively. The quantitative and qualitative scores of the conventional dose first vein phase were the best. Moreover, with the decrease of radiation dose, the noise gradually increased, and the CNR<sub>lesions</sub>, SNR<sub>liver</sub> and SNR<sub>portal vein</sub> gradually decreased. Notably, under the same radiation dose condition, the quantitative scores of DLIR-H images were statistically better than those of ASiR-V60% (all  $P < 0.001$ ). Furthermore, the qualitative parameters of each group decreased with the decrease of radiation dose. Under the same radiation dose, the overall image quality, lesion conspicuity and diagnostic confidence of DLIR-H were higher than those of ASiR-V60% (all  $P < 0.001$ ).

#### CONCLUSION

Compared with ASiR-V60%, DLIR-H could reduce image noise, improve overall image quality and lesion conspicuity of liver metastasis, as well as increase diagnostic confidence under different radiation doses.

#### CLINICAL RELEVANCE/APPLICATION

Compared with ASiR-V60%, DLIR can reduce image noise, improve image quality and lesion conspicuity of liver metastasis.

Printed on: 02/07/23

## Abstract Archives of the RSNA, 2022

S3A-SPIN-3

### Can We Combine the Best of Two Worlds? Artifact Reduction from Dental Implants in Photon-Counting Detector CT Datasets Based on high-keV Monoenergetic Reconstructions and Iterative Metal Artifact Reduction (iMAR) Reconstructions

Sunday, Nov. 27 11:45AM - 12:15PM Room: Learning Center - IN DPS

#### Participants

Franka Risch, MSc, Augsburg, Germany (*Presenter*) Nothing to Disclose

#### PURPOSE

This study assessed the effect of virtual monoenergetic imaging (VMI) settings, the use of iterative metal artifact reduction (iMAR), and kernel choice on metal artifacts caused by dental fillings/ implants on photon-counting detector CT (PCD-CT) datasets.

#### METHODS AND MATERIALS

Patients with dental fillings or implants undergoing staging CT including the neck region on a PCD-CT were screened for study inclusion. A standard and sharp quantitative kernel were reconstructed with and without iterative metal artifact reduction (Qr40, Qr40 iMAR, Qr60, Qr60 iMAR) in nine different virtual monoenergetic keV-levels (range: 40-190 keV). On four selected slices, two with and two without metal artifacts caused by dental fillings/implants, six regions of interest (ROIs) were positioned in air and various defined soft tissues. For each ROI, the mean and standard deviation of CT values were recorded in all series at identical positions. The mean absolute error of CT values and an artifact index were calculated. Statistical analyses focused on differences in artifact index between VMI levels (low vs. high keV), between kernels (standard vs. sharp) and between reconstructions with vs. without iMAR.

#### RESULTS

Fifty consecutive patients (age  $71.7 \pm 10.8$  years; 15 female) were included. For each patient, 4 image series for 9 different VMIs were reconstructed, resulting in 36 series per patient. The artifact index severely increased for lower VMI levels ( $< 50$  keV) but did not exhibit significant changes in the 60 - 190 keV range. Overall, the effect of keV settings on noise parameters was relatively small. Sharp Kernels increased artifact index moderately ( $\sim 35\%$ ). By using iMAR, the most pronounced reduction of both calculated indices was observed for the standard and sharp kernel as well as in all measured regions of interest (Qr40/Qr60 vs. Qr40 iMAR/ Qr60 iMAR, reduction in  $\rho$ HU: 57 % - 79 %, reduction in AI: 55 % - 88 %).

#### CONCLUSION

s Metal artifacts caused by dental fillings/ implants are profoundly reduced using iMAR for standard and sharp kernels. Unlike reported for artifacts around orthopedic surgical material, VMI levels had very little effect on artifacts by dental implants.

#### CLINICAL RELEVANCE/APPLICATION

Metal artifacts can significantly affect image quality and reduce diagnostic value. iMAR offers effective and reliable reduction of metal artifacts from dental implants.

Printed on: 02/07/23

## Abstract Archives of the RSNA, 2022

S3A-SPIN-4

### AI Enabled Automatic CNR Measurement: Development and Evaluation using Multi-energy Images in Abdomen Dual-Energy Contrast-Enhanced CT

Sunday, Nov. 27 11:45AM - 12:15PM Room: Learning Center - IN DPS

#### Participants

Sihwan Kim, BS, Seoul, Korea, Republic Of (*Presenter*) Nothing to Disclose

#### PURPOSE

To develop a system automatically measuring contrast-to-noise ratio (CNR) for evaluating image quality of different dual-energy CT (DECT) scan protocols.

#### METHODS AND MATERIALS

The system consists of three stages - deep learning (DL) based liver segmentation, extraction of homogenous ROIs and structure ROIs, and calculation of CNR. For the DL-based segmentation model, U-net architecture with multi-planar reconstruction (MPR) approach was used. The model was trained with contrast and non-contrast CT images of three-hundred patients. For the evaluation of the segmentation model, 131 contrast-enhanced CT (CECT) from Decathlon open-challenge dataset was used. The performance of liver segmentation model was evaluated with dice-coefficient. To extract homogeneous and structure edge regions on CT images, structure coherence map was analyzed using gradient and hessian images. For the evaluation of system performance, twenty-four abdominal DECT scans were retrospectively investigated. The evaluation was performed on four different reconstructed image types; 40-keV VMI image (40-keV VMI), 50-keV VMI image (50-keV VMI), 80-kVp image and linearly blended images simulating 100-kVp image (100-kVp). All the reconstructed images were automatically evaluated with three evaluation metrics; noise, signal-to-noise (SNR) and contrast-to-noise ratio (CNR). In addition, one radiologist visually assessed the successive of CNR measurement with five-point scale.

#### RESULTS

The dice value of liver segmentation model was  $0.90 \pm 0.08$  (Mean $\pm$ S.D.) in open challenge dataset. The system presented SNR values as  $8.73 \pm 2.12$  in 40-keV VMI,  $9.08 \pm 2.05$  in 50-keV VMI,  $9.29 \pm 1.67$  in 80-kVp, and  $10.79 \pm 2.04$  in linearly blended 100-kVp. CNR values were  $3.98 \pm 1.53$  in 40-keV VMI,  $3.32 \pm 1.16$  in 50-keV VMI,  $2.80 \pm 1.15$  in 80-kVp, and  $2.15 \pm 1.00$  in linearly blended 100-kVp. Measured noises of each energy-level images had  $20.09 \pm 2.83$  HU,  $14.50 \pm 1.81$  HU,  $11.92 \pm 1.32$  HU, and  $8.51 \pm 0.72$  HU in 40-keV VMI, 50-keV VMI, 80-kVp, and linearly blended 100-kVp, respectively. The five-scale visual assessment result by the radiologist was  $4.08 \pm 0.72$  in 40-keV VMI,  $4.00 \pm 0.72$  in 50-keV VMI,  $4.13 \pm 0.74$  in 80-kVp, and  $3.96 \pm 0.62$  in linearly blended 100-kVp.

#### CONCLUSION

s We developed a deep learning-assisted CNR measurement system to evaluate the image quality of different DECT scan protocols. We believe that developed system can contribute to the monitoring of CT machine maintenance and optimization of CT scan protocols in clinical practice.

#### CLINICAL RELEVANCE/APPLICATION

Image Quality Assessment in Dual-energy CT

Printed on: 02/07/23

## Abstract Archives of the RSNA, 2022

S3A-SPIN-6

### A Unified Framework for Accurate and Robust Lesion RECIST Diameter Prediction and Segmentation with Transformers

Sunday, Nov. 27 11:45AM - 12:15PM Room: Learning Center - IN DPS

#### Participants

Youbao Tang, PhD, Bethesda, MD (*Presenter*) Nothing to Disclose

#### PURPOSE

Accurately measuring lesion/tumor size with RECIST (Response Evaluation Criteria In Solid Tumors) diameters and segmentation is important for assessing the lesion growth rates and making therapeutic plan. Manually annotating them is tedious, time-consuming, and prone to observer-inconsistency. To overcome these issues, we propose a transformer-based unified framework (MeaFormer) for lesion RECIST diameter prediction and segmentation on CT scans automatically and accurately.

#### METHODS AND MATERIALS

MeaFormer formulates LRDPs as three correlative and complementary sub-tasks: lesion segmentation, heatmap prediction, and keypoint regression. It employs transformers to model the long-range dependencies of the high-resolution deep features extracted by a small convolutional neural network. Two consistency losses are introduced to explicitly build relationships among these sub-tasks for multi-task learning and joint optimization. Only requiring a single click operation within the lesion region from clinicians, MeaFormer can output accurate RECIST diameter predictions and 2D mask of the lesion on the key slice where the lesion has the largest spatial extent. Besides, a 3D mask can be obtained by segmenting the lesion slice-by-slice where the center point of the segmented mask on the previous slice is considered as the click point on the current slice. It was evaluated on the DeepLesion dataset containing 32,735 lesions from 10,594 studies of 4,427 patients. 200/1,000 lesion images from 500 patients are manually segmented with 3D/2D masks for testing. The rest patient data are used for training (80%) and validation (20%). Also, 480 lesion pairs from the test set are used for a downstream task evaluation (i.e., longitudinal RECIST assessment based on the predicted diameters).

#### RESULTS

Compared to the best previous work on each sub-task, MeaFormer achieved the best performance. For RECIST diameter prediction, the long/short diameter error between the automatic results and manual reference standard is  $1.6\pm 1.3$  mm/ $1.4\pm 1.5$  mm. For lesion segmentation, a 2D/3D Dice score of  $0.927\pm 0.043$ / $0.856\pm 0.065$  is obtained. On the 480 test lesion pairs, it achieved an accuracy of 91.7% for the tumor response classification (4 classes based on RECIST version 1.1).

#### CONCLUSION

s We proposed a transformer-based deep learning framework to annotate tumor sizes automatically and accurately with RECIST diameters and segmentations via a simple click operation. It achieved comparable accuracies to manual annotations, but improved efficiency with greatly reduced time and effort.

#### CLINICAL RELEVANCE/APPLICATION

It can serve as a useful tool for clinicians to accurately measure tumor sizes with minimal effort and may provide high positive values on clinical workflows.

Printed on: 02/07/23



## Abstract Archives of the RSNA, 2022

S3A-SPIR

### Interventional Sunday Poster Discussions - A

Sunday, Nov. 27 11:45AM - 12:15PM Room: Learning Center - IR DPS

#### Sub-Events

#### S3A-SPIR-1 Systematic Assessment of Formulation Parameters Affecting Stability of Sclerosing Foams: Implications for Image Guided Sclerotherapy

Participants

Felipe Berg, (*Presenter*) Nothing to Disclose

#### PURPOSE

Sodium tetradecyl sulfate (STS) is a commonly utilized sclerosant used to treat various pathologies including vascular malformations and venous disease. It is often utilized as a foam, created by mixing STS with air and various contrast agents using the Tessari Method. Reported ratios of STS, contrast and air used to create sclerosing foam vary widely, and the impact of various ratios on foam stability are not well described. The purpose of this study is to evaluate the effect of various STS, air to Lipiodol® volume ratios on sclerosing foam stability.

#### METHODS AND MATERIALS

Different sclerosing foam combinations were generated with different ratios of Sodium tetradecyl sulfate, air and contrast. STS 30 mg/mL was used as a surfactant; and foam was created using various air:STS:Lipiodol ratios including 1:1.5:0; 1:2:0; 1:3:0; 1:4:0, 1:1.5:1, 1:2:1, 1:3:1, and 1:4:1. Each mixture was agitated 30 times at room temperature using Tessari Method for each trial by the same researcher. Foam decay rates were recorded with a camera system for 45min or until all the foam had returned to its liquid phase. For trials with a contrast agent, 1 mL of Lipiodol® ethiodized oil (Guerbet LLC®) was added to the mixture. The drainage time and drainage rate were recorded for each trial.

#### RESULTS

In the trials with only STS, smaller air:STS with an average foam half-life of 1.8 min for the 4:1 ratio and 3.2 min for the 1.5 ratios, the foam has drained completely in 5 min for all trials. By adding Lipiodol to the mixture the foam stability increased significantly with an average foam half-life of 7.5 min and foam was present for more than 45min. No difference was observed within trials with Lipiodol related to the varying of the air:STS ratio.

#### CONCLUSION

Increasing the air-to-liquid ratio reduces foam stability. Addition of Lipiodol significantly increases the foam stability. The air-to-liquid ratio could be used as a simple, and reproducible strategy to produce foams with stability suitable to the clinical scenario. Furthermore, the use of oil-based contrast agents (e.g. Lipiodol) can be used to produce foams with extended stability and radio-opacity, which may be appropriate for specific clinical indications.

#### CLINICAL RELEVANCE/APPLICATION

Sclerotherapy plays an important role in management of various pathologic processes including vascular malformation, venous insufficiency, and variceal gastrointestinal bleeding. A stable foam may increase efficacy due to a longer duration of contact with the targeted structure, and yet it may also act as a more effective and therefore dangerous vascular embolic in the setting of non-target embolization. Characterization of basic foam properties, including stability, created during a procedure is key for an effective and safe procedure.

#### S3A-SPIR-2 Differences in Outcomes Between Patients with Lower Gastrointestinal Bleeding Undergoing Primary Endovascular vs Primary Endoscopic Interventions

Participants

Alexander Villalobos, MD, (*Presenter*) Nothing to Disclose

#### PURPOSE

To compare outcomes in patients with lower gastrointestinal bleeding (LGIB) treated with primary endovascular vs endoscopic interventions.

#### METHODS AND MATERIALS

All LGIB encounters and associated procedures in the 2005-2015 National Inpatient Sample databases were identified using ICD-9 codes. Encounters initially treated with surgery or conservative management were excluded. Those initially treated with angiography and/or embolization (IR-PEI) vs diagnostic and/or therapeutic endoscopy (GI-PEI) were evaluated. Afterwards, encounters initially treated with only diagnostic angiography and/or endoscopy were excluded and those initially treated with transarterial embolization (IR-ITE) vs therapeutic endoscopy (GI-ITE) evaluated. Odds ratios (OR) for mortality and prolonged (>7 days) length of stay (LOS) were evaluated using multivariate logistic regression after propensity score matching of clinically relevant baseline covariates.

## RESULTS

Of 617,735 LGIB encounters, 8,514 underwent an IR intervention, 5,987 IR-PEI, 2,172 IR-ITE, 193,476 GI-PEI, and 58,957 GI-ITE. Overall mean age, gender, and race/ethnicity was 69 years, 54% female, and 73% Caucasian. Any IR intervention usage was associated with increased risk of mortality (OR=1.4 [95%CI 1.3-1.5],  $p<0.001$ ) and prolonged LOS (OR=2.5 [95%CI 2.4-2.6],  $p<0.001$ ). With GI-PEI as reference, IR-PEI was associated with increased mortality (OR=3.2 [95%CI 2.9-3.4],  $p<0.001$ ) and prolonged LOS (OR=3.6 [95%CI 3.1-4.2],  $p<0.001$ ). With GI-ITE as reference, IR-ITE was associated with increased mortality (OR=8.5 [95%CI 6.4-11.2],  $p<0.001$ ) and prolonged LOS (OR=3.57 [95%CI 3.05-4.18],  $p<0.001$ ).

## CONCLUSION

s Compared to endoscopic interventions, endovascular interventions for LGIB were associated with an increased mortality and prolonged LOS.

## CLINICAL RELEVANCE/APPLICATION

Primary endovascular interventions for the management of lower gastrointestinal bleeding are associated with an increased risk of mortality and prolonged hospital length of stay as compared to standard-of-care primary endoscopic interventions.

### S3A-SPIR-3 Prediction of Oncologic Outcomes Following CT-guided Thermal Ablation of Colorectal Liver Metastasis

#### Participants

Iwan Paolucci, PhD, (*Presenter*) Stockholder, Intuitive Surgical, Inc ;Stockholder, SOPHiA GENETICS

#### PURPOSE

To build and evaluate predictive models for local tumor progression (LTP) and intrahepatic progression outside the ablation zone (IHP) following CT-guided thermal (TA) ablation of colorectal liver metastasis (CLM).

#### METHODS AND MATERIALS

A single-center retrospective evaluation of a liver ablation registry was surveyed to identify patients with CLM submitted to CT-guided TA between 10/2015 to 03/2020. Patients with  $\leq$ 1-year imaging follow-up, combined treatment with other local therapies, insufficient image quality for tumor depiction, and repeat ablations (IHP model only) were excluded. Oncologic outcomes (LTP/IHP) were determined prior to prediction model development by two radiologists. Definition for the Assessment of Time-to-Event End Points in Cancer Trials was applied for LTP- and IHP-free survival (LTPFS/IHPFS) assessment. The data was split into a training and test set (80%/20% split) on a patient level and ensuring similar LTPFS and IHPFS. LTPFS and IHPFS were truncated at 36 and 18 months respectively. A Bayesian parametric Weibull survival model was used with the following prognosticators: CLM diameter, nr of ablated CLM, TP53 mutation, CEA, NLR, extrahepatic metastasis, hepatic steatosis (only for IHP), RAS mutation (only for LTP), and software-based minimum ablation margin (only for LTP). Tumors/patients were stratified into High and Low risk of progression using the median predicted survival on the training set. Model performance was reported with positive predictive value (PPV), negative predictive value (NPV), and Kaplan-Meier curves of LTPFS and IHPFS of High and Low risk groups.

## RESULTS

For the LTP model, training/testing comprised of 217/54 CLM, respectively. In testing, 9 CLM (16.6%) had LTP within 3 years and all of them were classified as High risk. The LTP model had a PPV 31% and an NPV of 100%. The risk of LTP within 36 months was 34.2% (CI95% = [11.8, 50.8]) vs. 0% in the High vs. Low risk group respectively ( $p=0.003$ ). For the IHP model, training/testing comprised of 101/25 ablation naïve patients, respectively. In testing, 16/25 (64%) of patients had IHP within 18 months and 15 of those were classified as High risk. The IHP model had a PPV of 83.3% and an NPV of 85.7%. The risk of IHP within 18 months was 14.3% (CI95% = [0, 36.7]) vs. 83.3% (CI95% = [53.2, 94.1]) in the High vs. Low risk group respectively ( $p=0.007$ ).

## CONCLUSION

s Both models showed good performance in identifying patients and CLM that are unlikely to progress following TA. However, the LTP model shows a low PPV suggesting that there are more patient-/ablation-related factors that protect from LTP.

## CLINICAL RELEVANCE/APPLICATION

Prediction models could be used to tailor treatment strategies for patients with CLM based on a per-tumor and -patient's prognosis.

### S3A-SPIR-5 Influence of Pelvic Magnetic Resonance Angiography for Prostatic Artery Embolization Planning and Technical Success

#### Participants

Matthias Boschheidgen, Dusseldorf, Germany (*Presenter*) Nothing to Disclose

#### PURPOSE

Knowledge about anatomical details seems to facilitate the procedure of prostatic artery embolization (PAE) in patients with benign prostatic hyperplasia (BPH). We analysed pre-interventional MR angiography (MRA) of prostatic vessels to identify anatomical parameters which may influence procedural factors and technical success.

#### METHODS AND MATERIALS

MRA and digital subtraction angiography (DSA) of patients with PAE between 04/2018 and 03/2021 were analysed retrospectively regarding prostatic artery (PA) visibility, PA type, vessel elongation, and defined angles. These parameters were correlated with the DSA (intervention time, fluoroscopy time, dose area product (DAP), cumulative air kerma (CAK), contrast media (CM) dose) and technical success of embolization. T-test, ANOVA, Pearson correlation, and Kruskal-Wallis test were applied to check for statistical significance.

## RESULTS

Seventy-eight patients (mean age 71 years) were included. MRA identified PA in 126 of 147 cases (accuracy 86%). PA had similar origin on both sides only in 57% of the patients. PA type showed no significant effect on DSA parameters. Contrarily, vessel elongation affected time for catheterization of right PA ( $p=0.02$ ), fluoroscopy time ( $p=0.05$ ), and CM dose ( $p=0.02$ ) significantly.

Moderate correlation was observed for iliac bifurcation angles with DAP ( $r=0.30$  left;  $r=0.34$  right;  $p=0.01$ ) and CAK ( $r=0.32$  left;  $r=0.36$  right;  $p=0.01$ ) on both sides.

## CONCLUSION

s Pre-interventional MRA could reliably identify PA origin, offering a good anatomic orientation before performing PAE. PA type did not have an influence on procedural complexity of PAE and technical success while vessel elongation prolonged the intervention preceding to longer intervention times and higher doses of contrast media. MRA could not predict technical success for selective PA catheterization.

## CLINICAL RELEVANCE/APPLICATION

Pre-interventional MRA can provide useful information on anatomic details of patients undergoing PAE. This can facilitate the intervention and has the potential to save time and resources as well as radiation dose.

### S3A-SPIR-6 Clinical and Imaging Outcomes of Percutaneous Sclerotherapy for the Management of Lymphatic Malformations

#### Participants

Tushar Garg, MD, Baltimore, MD (*Presenter*) Conference Travel, Siemens Healthineers

#### PURPOSE

To evaluate the safety and outcomes of percutaneous sclerotherapy (PS) for lymphatic malformations (LMs) involving any part of the body.

#### METHODS AND MATERIALS

We reviewed all patients who underwent PS for the management of LMs between 4/2003 to 3/2022. Clinical and imaging findings were assessed to evaluate clinical response, lesion size changes, and complication rates. Fisher's Exact Tests were used for statistical analysis. Clinical symptoms response was classified as resolved, improved and stable and/or worsened. The LM size change was assessed by calculating the difference between pre- and post-procedure MRI of the largest lesion diameter in one plane, comparable to the response evaluation criteria in solid tumors (RECIST): complete response (CR, 100% reduction), partial response (PR, 30% reduction), stable disease (SD,  $\leq 30\%$  reduction or  $\leq 20\%$  enlargement), and progressive disease (PD,  $\geq 20\%$  VM size increase). Adverse events were classified by SIR classification criteria.

#### RESULTS

158 patients (49.4% F,  $14.9 \pm 18.4$  years) underwent 241 PS (average  $1.7 \pm 1.1$ ) sessions with a technical success rate of 97.1% (234/241). Most of the LMs presented after birth (43.7%; 69/158) with swelling (55%; 87/158) and pain (21.5%; 34/158) being the most common symptoms. 53.8% (85/158) of the LMs were in the head and neck and rest were almost equally distributed throughout the body. 38.6% (61/158) of the patients received previous outside PS, surgery or medical management. Doxycycline (80.5%; 191/241) was the most common sclerosant used, followed by bleomycin foam and liquid (12%; 29/241), ethanol (10.7%; 26/241), sotradecol foam (1.7%; 4/241) and n-BCA (0.4%; 4/241). A cosmetic deformity was seen in 77.2% (122/158) and functional deficit was seen in 24.8% (45/158) of the patients. For these patients with adequate follow-up, PS significantly improved cosmetic symptoms with 12.9% (13/101) resolved, 70.3% (71/101) improved, and 16.8% (17/101) stable or worsened ( $p < 0.0001$ ) and functional deficits with 20.7% (6/29) resolved, 69% (20/29) improved, and 10.3% (3/29) stable or worsened ( $p < 0.0001$ ). PS also significantly decreased LM size on imaging ( $p = 0.0001$ ). Of the 140 (58.5%) procedures with both pre- and post-MRI imaging, 2 patients saw CR (1.4%), 51 patients (36.2%) experienced PR, 67 patients (47.5%) experienced SD and 19 patients (13.5%) saw PD. Early (30-day) post-procedural complications occurred after 30 of 241 procedures (12.4%), the majority of which were hyperpigmentation (23.3%; 7/30) and mild in severity (56.7%; 17/30).

#### CONCLUSION

s PS significantly decreases lesion size and improves clinical symptoms in LMs.

## CLINICAL RELEVANCE/APPLICATION

PS is a safe and effective treatment option for the management of patients with LMs.

### S3A-SPIR-7 Prospective Study of Different Embolic Agents for Pulmonary Arteriovenous Malformation (PAVM) Embolization: Technical Results, Time Saved, and Financial Costs

#### Participants

Anna Gong, Baltimore, MD (*Presenter*) Nothing to Disclose

#### PURPOSE

While embolization of PAVMs with Micro Vascular Plug Systems (MVP™ systems) has been shown to have a 0-2% PAVM persistence rate, few attempts have been made to understand the technical features, time and costs of embolization with MVP™ systems versus other embolics.

#### METHODS AND MATERIALS

We evaluated 34 patients with PAVMs who underwent embolization with at least one MVP™ systems, Amplatzer vascular plug (AVP) or coil between 4/2019 and 2/2022. All data was collected in real time by dedicated scribes. Technical success, occlusion time, room-time, and costs were analyzed. Occlusion time was evaluated immediately after device deployment and in two-minute intervals until occlusion occurred or until another embolic was delivered. We extracted cost information from the electronic medical record. Mann-Whitney U tests (Bonferroni correction factor: adjusted significance value  $p < 0.01667$ ) were used for statistical analyses.

#### RESULTS

In 34 patients, 64 PAVMs and 81 feeding arteries were treated: 58 with at least one MVP™ systems, 20 with coils alone, and 3 with AVP. The per-feeding artery technical success rates were 100% for all cases. Median occlusion time was 1.0 min (Range  $<1$  to 30 min) for feeding arteries treated with at least one MVP™ systems, 9.0 min (Range 3.0 to 25.0 min) for coils, and 5.0 min (Range 4.0 to 6.0 min) for AVP). Embolization with MVP™ systems achieves a significantly shorter occlusion time than embolization with coils

(median 8.0 min saved per feeding artery) ( $P < 0.0001$ ). When compared to embolization with coils, embolization with MVP™ systems reduce room costs by a median of \$429.77 per feeding artery ( $p < 0.0001$ ). Device costs for embolization with MVP™ systems versus coils were not significantly different per feeding artery (MVP™ systems: \$2790.45; Coils: \$3531: Median difference \$740.55) ( $p = 0.1718$ ).

## CONCLUSION

When compared to coils, MVP™ systems have an equivalently high technical success rate and significant time and cost savings in addition to a known 0-2% PAVM persistence rate.

## CLINICAL RELEVANCE/APPLICATION

MVP™ systems should be considered as a first-line agent for embolization of PAVMs for eligible patients.

### **S3A-SPIR-8 Application and Potential Benefits of Color-coded Digital Variance Angiography in Prostatic Artery Embolization**

Participants

Leona Alizadeh, MD, Frankfurt, Germany (*Presenter*) Nothing to Disclose

## PURPOSE

Color-coded digital variance angiography (ccDVA) is a recently developed image processing technology capable of visualization of hemodynamic conditions in 2D X-ray angiography setting. Our aim was to explore the potential advantages of ccDVA in prostatic artery embolization (PAE).

## METHODS AND MATERIALS

This retrospective study evaluated 108 angiographic acquisitions from 30 patients (mean  $\pm$  SD age  $68.0 \pm 8.9$ , range 41-87) undergoing PAE between May and October 2020. DSA and ccDVA images were generated from the same unsubtracted acquisition. Visual evaluation of ccDVA and DSA images was performed by four experienced interventional. The diagnostic value of DSA and ccDVA images was evaluated using clinically relevant criteria (visibility of small [ $< 2.5$  mm] and large arteries [ $> 2.5$  mm], feeding arteries and tissue blush) in a paired comparison. Data were analysed by the binomial test, the interrater agreement was determined by the Fleiss Kappa analysis.

## RESULTS

The preference of ccDVA images was significantly higher in all criteria. The preference of ccDVA images was the highest in the tissue blush category (quality agreement [QA] 89%, interrater agreement [IR] 79%, followed by the small arteries (QA: 79%, IR: 70%), feeding arteries (QA: 79%, IR: 65%) and large arteries (QA: 63%, IR: 58%). The Fleiss Kappa range was 0.02-0.18, significant in all criteria except large vessels.

## CONCLUSION

Our data show that ccDVA significantly improves the diagnostic evaluation of tissue blush, small arteries and feeding arteries in PAE. As these structures are critically important in the procedure, the ccDVA technology might help the decision-making process in PAE interventions, although these benefits have to be validated in further prospective clinical studies.

## CLINICAL RELEVANCE/APPLICATION

Color-coded DVA (ccDVA) significantly improves the visualization of small arteries, feeding arteries and tissue blush, thereby provides more information for PAE procedures than DSA in 79-89 % of comparisons.

### **S3A-SPIR-9 The Role of Machine Learning Algorithms in Predicting the Treatment Outcome of High-Intensity Focused Ultrasound Ablation of Uterine Fibroids with an Immediate Nonperfused Volume Ratio of at least 90%**

Participants

Bilgin Keserci, PhD, (*Presenter*) Nothing to Disclose

## PURPOSE

To investigate the role of machine learning (ML) classifiers to find the most informative multiparametric (mp) magnetic resonance imaging (MRI) features in predicting the treatment outcome of high intensity focused ultrasound (HIFU) ablation with an immediate nonperfused volume (NPV) ratio of at least 90%.

## METHODS AND MATERIALS

This retrospective study was approved by the institutional review board, and informed consent was obtained in all participants. Seventy-three women who underwent HIFU treatment were divided into groups A ( $n=47$ ), and B ( $n=26$ ), comprising patients with an NPV ratio of at least 90% and less than 90%, respectively. An ensemble feature ranking model was introduced based on the score values assigned to the 37 features by five different ML classifiers including Logistic Regression (LR), Support Vector Classifier (SVC), Random Forest (RF), Adaptive Boosting (Adaboost), Gradient Boosting (GBM), to find the most informative mpMRI features. The relationship between the mpMRI features and the immediate NPV ratio of 90% was evaluated using Pearson's correlation coefficients. The diagnostic ability of ML classifiers was performed by means of standard performance metrics, including the area under the receiver operating characteristic curve (AUROC), accuracy, sensitivity, and specificity in eight folds cross-validation.

## RESULTS

For all the 12 most informative features, the AUROC ranged from 0.5 to 0.97, accuracy ranged from 0.34 to 0.97, specificity ranged from 0.56 to 1.0, and sensitivity ranged from 0.87 to 1.0. The GBM classifier showed the best predictive performance with an AUROC of 0.95 and accuracy of 0.92, followed by the RF, Adaboost, LR, and SVC classifiers, which yielded an AUROC of 0.92, 0.92, 0.83 and 0.78, and accuracy of 0.96, 0.88, 0.84 and 0.84, respectively. The best classifier performance with the best-performing features from each mpMRI group, Ktrans ratio of the fibroid to the myometrium, the ratio of AUC of the fibroid to the myometrium, subcutaneous fat thickness, the ratio of ADC value of fibroid to the myometrium, and T2-signal intensity (SI) of fibroid, was

achieved using GBM.

#### **CONCLUSION**

s The preliminary findings in this study suggest that the most informative 12 and best performing features from each mpMRI group should be considered in predicting the treatment outcome of HIFU ablation to achieve an immediate NPV ratio of 90%.

#### **CLINICAL RELEVANCE/APPLICATION**

The best classifier performance with the best-performing features from each mpMRI group should be considered by the treating physician in the screening phase to predict the treatment outcome of HIFU ablation to achieve an immediate NPV ratio of 90%.

Printed on: 02/07/23

## Abstract Archives of the RSNA, 2022

S3A-SPIR-1

### Systematic Assessment of Formulation Parameters Affecting Stability of Sclerosing Foams: Implications for Image Guided Sclerotherapy

Sunday, Nov. 27 11:45AM - 12:15PM Room: Learning Center - IR DPS

#### Participants

Felipe Berg, (*Presenter*) Nothing to Disclose

#### PURPOSE

Sodium tetradecyl sulfate (STS) is a commonly utilized sclerosant used to treat various pathologies including vascular malformations and venous disease. It is often utilized as a foam, created by mixing STS with air and various contrast agents using the Tessari Method. Reported ratios of STS, contrast and air used to create sclerosing foam vary widely, and the impact of various ratios on foam stability are not well described. The purpose of this study is to evaluate the effect of various STS, air to Lipiodol® volume ratios on sclerosing foam stability.

#### METHODS AND MATERIALS

Different sclerosing foam combinations were generated with different ratios of Sodium tetradecyl sulfate, air and contrast. STS 30 mg/mL was used as a surfactant; and foam was created using various air:STS:Lipiodol ratios including 1:1.5:0; 1:2:0; 1:3:0; 1:4:0, 1:1.5:1, 1:2:1, 1:3:1, and 1:4:1. Each mixture was agitated 30 times at room temperature using Tessari Method for each trial by the same researcher. Foam decay rates were recorded with a camera system for 45min or until all the foam had returned to its liquid phase. For trials with a contrast agent, 1 mL of Lipiodol® ethiodized oil (Guerbet LLC®) was added to the mixture. The drainage time and drainage rate were recorded for each trial.

#### RESULTS

In the trials with only STS, smaller air:STS with an average foam half-life of 1.8 min for the 4:1 ratio and 3.2 min for the 1.5 ratios, the foam has drained completely in 5 min for all trials. By adding Lipiodol to the mixture the foam stability increased significantly with an average foam half-life of 7.5 min and foam was present for more than 45min. No difference was observed within trials with Lipiodol related to the varying of the air:STS ratio.

#### CONCLUSION

Increasing the air-to-liquid ratio reduces foam stability. Addition of Lipiodol significantly increases the foam stability. The air-to-liquid ratio could be used as a simple, and reproducible strategy to produce foams with stability suitable to the clinical scenario. Furthermore, the use of oil-based contrast agents (e.g. Lipiodol) can be used to produce foams with extended stability and radio-opacity, which may be appropriate for specific clinical indications.

#### CLINICAL RELEVANCE/APPLICATION

Sclerotherapy plays an important role in management of various pathologic processes including vascular malformation, venous insufficiency, and variceal gastrointestinal bleeding. A stable foam may increase efficacy due to a longer duration of contact with the targeted structure, and yet it may also act as a more effective and therefore dangerous vascular embolic in the setting of non-target embolization. Characterization of basic foam properties, including stability, created during a procedure is key for an effective and safe procedure.

Printed on: 02/07/23

## Abstract Archives of the RSNA, 2022

S3A-SPIR-2

### Differences in Outcomes Between Patients with Lower Gastrointestinal Bleeding Undergoing Primary Endovascular vs Primary Endoscopic Interventions

Sunday, Nov. 27 11:45AM - 12:15PM Room: Learning Center - IR DPS

#### Participants

Alexander Villalobos, MD, (*Presenter*) Nothing to Disclose

#### PURPOSE

To compare outcomes in patients with lower gastrointestinal bleeding (LGIB) treated with primary endovascular vs endoscopic interventions.

#### METHODS AND MATERIALS

All LGIB encounters and associated procedures in the 2005-2015 National Inpatient Sample databases were identified using ICD-9 codes. Encounters initially treated with surgery or conservative management were excluded. Those initially treated with angiography and/or embolization (IR-PEI) vs diagnostic and/or therapeutic endoscopy (GI-PEI) were evaluated. Afterwards, encounters initially treated with only diagnostic angiography and/or endoscopy were excluded and those initially treated with transarterial embolization (IR-ITE) vs therapeutic endoscopy (GI-ITE) evaluated. Odds ratios (OR) for mortality and prolonged (>7 days) length of stay (LOS) were evaluated using multivariate logistic regression after propensity score matching of clinically relevant baseline covariates.

#### RESULTS

Of 617,735 LGIB encounters, 8,514 underwent an IR intervention, 5,987 IR-PEI, 2,172 IR-ITE, 193,476 GI-PEI, and 58,957 GI-ITE. Overall mean age, gender, and race/ethnicity was 69 years, 54% female, and 73% Caucasian. Any IR intervention usage was associated with increased risk of mortality (OR=1.4 [95%CI 1.3-1.5],  $p<0.001$ ) and prolonged LOS (OR=2.5 [95%CI 2.4-2.6],  $p<0.001$ ). With GI-PEI as reference, IR-PEI was associated with increased mortality (OR=3.2 [95%CI 2.9-3.4],  $p<0.001$ ) and prolonged LOS (OR=3.6 [95%CI 3.1-4.2],  $p<0.001$ ). With GI-ITE as reference, IR-ITE was associated with increased mortality (OR=8.5 [95%CI 6.4-11.2],  $p<0.001$ ) and prolonged LOS (OR=3.57 [95%CI 3.05-4.18],  $p<0.001$ ).

#### CONCLUSION

Compared to endoscopic interventions, endovascular interventions for LGIB were associated with an increased mortality and prolonged LOS.

#### CLINICAL RELEVANCE/APPLICATION

Primary endovascular interventions for the management of lower gastrointestinal bleeding are associated with an increased risk of mortality and prolonged hospital length of stay as compared to standard-of-care primary endoscopic interventions.

Printed on: 02/07/23

## Abstract Archives of the RSNA, 2022

S3A-SP1R-3

### Prediction of Oncologic Outcomes Following CT-guided Thermal Ablation of Colorectal Liver Metastasis

Sunday, Nov. 27 11:45AM - 12:15PM Room: Learning Center - IR DPS

#### Participants

Iwan Paolucci, PhD, (Presenter) Stockholder, Intuitive Surgical, Inc ;Stockholder, SOPHiA GENETICS

#### PURPOSE

To build and evaluate predictive models for local tumor progression (LTP) and intrahepatic progression outside the ablation zone (IHP) following CT-guided thermal (TA) ablation of colorectal liver metastasis (CLM).

#### METHODS AND MATERIALS

A single-center retrospective evaluation of a liver ablation registry was surveyed to identify patients with CLM submitted to CT-guided TA between 10/2015 to 03/2020. Patients with  $\leq$ 1-year imaging follow-up, combined treatment with other local therapies, insufficient image quality for tumor depiction, and repeat ablations (IHP model only) were excluded. Oncologic outcomes (LTP/IHP) were determined prior to prediction model development by two radiologists. Definition for the Assessment of Time-to-Event End Points in Cancer Trials was applied for LTP- and IHP-free survival (LTPFS/IHPFS) assessment. The data was split into a training and test set (80%/20% split) on a patient level and ensuring similar LTPFS and IHPFS. LTPFS and IHPFS were truncated at 36 and 18 months respectively. A Bayesian parametric Weibull survival model was used with the following prognosticators: CLM diameter, nr of ablated CLM, TP53 mutation, CEA, NLR, extrahepatic metastasis, hepatic steatosis (only for IHP), RAS mutation (only for LTP), and software-based minimum ablation margin (only for LTP). Tumors/patients were stratified into High and Low risk of progression using the median predicted survival on the training set. Model performance was reported with positive predictive value (PPV), negative predictive value (NPV), and Kaplan-Meier curves of LTPFS and IHPFS of High and Low risk groups.

#### RESULTS

For the LTP model, training/testing comprised of 217/54 CLM, respectively. In testing, 9 CLM (16.6%) had LTP within 3 years and all of them were classified as High risk. The LTP model had a PPV 31% and an NPV of 100%. The risk of LTP within 36 months was 34.2% (CI95% = [11.8, 50.8]) vs. 0% in the High vs. Low risk group respectively (p=0.003). For the IHP model, training/testing comprised of 101/25 ablation naïve patients, respectively. In testing, 16/25 (64%) of patients had IHP within 18 months and 15 of those were classified as High risk. The IHP model had a PPV of 83.3% and an NPV of 85.7%. The risk of IHP within 18 months was 14.3% (CI95% = [0, 36.7]) vs. 83.3% (CI95% = [53.2, 94.1]) in the High vs. Low risk group respectively (p=0.007).

#### CONCLUSION

Both models showed good performance in identifying patients and CLM that are unlikely to progress following TA. However, the LTP model shows a low PPV suggesting that there are more patient-/ablation-related factors that protect from LTP.

#### CLINICAL RELEVANCE/APPLICATION

Prediction models could be used to tailor treatment strategies for patients with CLM based on a per-tumor and -patient's prognosis.

Printed on: 02/07/23

## Abstract Archives of the RSNA, 2022

S3A-SP1R-5

### **Influence of Pelvic Magnetic Resonance Angiography for Prostatic Artery Embolization Planning and Technical Success**

Sunday, Nov. 27 11:45AM - 12:15PM Room: Learning Center - IR DPS

#### **Participants**

Matthias Boschheidgen, Dusseldorf, Germany (*Presenter*) Nothing to Disclose

#### **PURPOSE**

Knowledge about anatomical details seems to facilitate the procedure of prostatic artery embolization (PAE) in patients with benign prostatic hyperplasia (BPH). We analysed pre-interventional MR angiography (MRA) of prostatic vessels to identify anatomical parameters which may influence procedural factors and technical success.

#### **METHODS AND MATERIALS**

MRA and digital subtraction angiography (DSA) of patients with PAE between 04/2018 and 03/2021 were analysed retrospectively regarding prostatic artery (PA) visibility, PA type, vessel elongation, and defined angles. These parameters were correlated with the DSA (intervention time, fluoroscopy time, dose area product (DAP), cumulative air kerma (CAK), contrast media (CM) dose) and technical success of embolization. T-test, ANOVA, Pearson correlation, and Kruskal-Wallis test were applied to check for statistical significance.

#### **RESULTS**

Seventy-eight patients (mean age 71 years) were included. MRA identified PA in 126 of 147 cases (accuracy 86%). PA had similar origin on both sides only in 57% of the patients. PA type showed no significant effect on DSA parameters. Contrarily, vessel elongation affected time for catheterization of right PA ( $p=0.02$ ), fluoroscopy time ( $p=0.05$ ), and CM dose ( $p=0.02$ ) significantly. Moderate correlation was observed for iliac bifurcation angles with DAP ( $r=0.30$  left;  $r=0.34$  right;  $p=0.01$ ) and CAK ( $r=0.32$  left;  $r=0.36$  right;  $p=0.01$ ) on both sides.

#### **CONCLUSION**

s Pre-interventional MRA could reliably identify PA origin, offering a good anatomic orientation before performing PAE. PA type did not have an influence on procedural complexity of PAE and technical success while vessel elongation prolonged the intervention preceding to longer intervention times and higher doses of contrast media. MRA could not predict technical success for selective PA catheterization.

#### **CLINICAL RELEVANCE/APPLICATION**

Pre-interventional MRA can provide useful information on anatomic details of patients undergoing PAE. This can facilitate the intervention and has the potential to save time and resources as well as radiation dose.

Printed on: 02/07/23

## Abstract Archives of the RSNA, 2022

S3A-SPIR-6

### Clinical and Imaging Outcomes of Percutaneous Sclerotherapy for the Management of Lymphatic Malformations

Sunday, Nov. 27 11:45AM - 12:15PM Room: Learning Center - IR DPS

#### Participants

Tushar Garg, MD, Baltimore, MD (*Presenter*) Conference Travel, Siemens Healthineers

#### PURPOSE

To evaluate the safety and outcomes of percutaneous sclerotherapy (PS) for lymphatic malformations (LMs) involving any part of the body.

#### METHODS AND MATERIALS

We reviewed all patients who underwent PS for the management of LMs between 4/2003 to 3/2022. Clinical and imaging findings were assessed to evaluate clinical response, lesion size changes, and complication rates. Fisher's Exact Tests were used for statistical analysis. Clinical symptoms response was classified as resolved, improved and stable and/or worsened. The LM size change was assessed by calculating the difference between pre-and post-procedure MRI of the largest lesion diameter in one plane, comparable to the response evaluation criteria in solid tumors (RECIST): complete response (CR, 100% reduction), partial response (PR, 30% reduction), stable disease (SD, =30% reduction or =20% enlargement), and progressive disease (PD, =20% VM size increase). Adverse events were classified by SIR classification criteria.

#### RESULTS

158 patients (49.4% F, 14.9 ± 18.4 years) underwent 241 PS (average 1.7 ± 1.1) sessions with a technical success rate of 97.1% (234/241). Most of the LMs presented after birth (43.7%; 69/158) with swelling (55%; 87/158) and pain (21.5%; 34/158) being the most common symptoms. 53.8% (85/158) of the LMs were in the head and neck and rest were almost equally distributed throughout the body. 38.6% (61/158) of the patients received previous outside PS, surgery or medical management. Doxycycline (80.5%; 191/241) was the most common sclerosant used, followed by bleomycin foam and liquid (12%; 29/241), ethanol (10.7%; 26/241), sotradecol foam (1.7%; 4/241) and n-BCA (0.4%; 4/241). A cosmetic deformity was seen in 77.2% (122/158) and functional deficit was seen in 24.8% (45/158) of the patients. For these patients with adequate follow-up, PS significantly improved cosmetic symptoms with 12.9% (13/101) resolved, 70.3% (71/101) improved, and 16.8% (17/101) stable or worsened ( $p < 0.0001$ ) and functional deficits with 20.7% (6/29) resolved, 69% (20/29) improved, and 10.3% (3/29) stable or worsened ( $p < 0.0001$ ). PS also significantly decreased LM size on imaging ( $p = 0.0001$ ). Of the 140 (58.5%) procedures with both pre-and post-MRI imaging, 2 patients saw CR (1.4%), 51 patients (36.2%) experienced PR, 67 patients (47.5%) experienced SD and 19 patients (13.5%) saw PD. Early (30-day) post-procedural complications occurred after 30 of 241 procedures (12.4%), the majority of which were hyperpigmentation (23.3%; 7/30) and mild in severity (56.7%; 17/30).

#### CONCLUSION

PS significantly decreases lesion size and improves clinical symptoms in LMs.

#### CLINICAL RELEVANCE/APPLICATION

PS is a safe and effective treatment option for the management of patients with LMs.

Printed on: 02/07/23

## Abstract Archives of the RSNA, 2022

S3A-SP1R-7

### **Prospective Study of Different Embolic Agents for Pulmonary Arteriovenous Malformation (PAVM) Embolization: Technical Results, Time Saved, and Financial Costs**

Sunday, Nov. 27 11:45AM - 12:15PM Room: Learning Center - IR DPS

#### **Participants**

Anna Gong, Baltimore, MD (*Presenter*) Nothing to Disclose

#### **PURPOSE**

While embolization of PAVMs with Micro Vascular Plug Systems (MVP™ systems) has been shown to have a 0-2% PAVM persistence rate, few attempts have been made to understand the technical features, time and costs of embolization with MVP™ systems versus other embolics.

#### **METHODS AND MATERIALS**

We evaluated 34 patients with PAVMs who underwent embolization with at least one MVP™ systems, Amplatzer vascular plug (AVP) or coil between 4/2019 and 2/2022. All data was collected in real time by dedicated scribes. Technical success, occlusion time, room-time, and costs were analyzed. Occlusion time was evaluated immediately after device deployment and in two-minute intervals until occlusion occurred or until another embolic was delivered. We extracted cost information from the electronic medical record. Mann-Whitney U tests (Bonferroni correction factor: adjusted significance value  $p < 0.01667$ ) were used for statistical analyses.

#### **RESULTS**

In 34 patients, 64 PAVMs and 81 feeding arteries were treated: 58 with at least one MVP™ systems, 20 with coils alone, and 3 with AVP. The per-feeding artery technical success rates were 100% for all cases. Median occlusion time was 1.0 min (Range <1 to 30 min) for feeding arteries treated with at least one MVP™ systems, 9.0 min (Range 3.0 to 25.0 min) for coils, and 5.0 min (Range 4.0 to 6.0 min) for AVP). Embolization with MVP™ systems achieves a significantly shorter occlusion time than embolization with coils (median 8.0 min saved per feeding artery) ( $P < 0.0001$ ). When compared to embolization with coils, embolization with MVP™ systems reduce room costs by a median of \$429.77 per feeding artery ( $p < 0.0001$ ). Device costs for embolization with MVP™ systems versus coils were not significantly different per feeding artery (MVP™ systems: \$2790.45; Coils: \$3531; Median difference \$740.55) ( $p = 0.1718$ ).

#### **CONCLUSION**

s When compared to coils, MVP™ systems have an equivalently high technical success rate and significant time and cost savings in addition to a known 0-2% PAVM persistence rate.

#### **CLINICAL RELEVANCE/APPLICATION**

MVP™ systems should be considered as a first-line agent for embolization of PAVMs for eligible patients.

Printed on: 02/07/23

## Abstract Archives of the RSNA, 2022

S3A-SP1R-8

### Application and Potential Benefits of Color-coded Digital Variance Angiography in Prostatic Artery Embolization

Sunday, Nov. 27 11:45AM - 12:15PM Room: Learning Center - IR DPS

#### Participants

Leona Alizadeh, MD, Frankfurt, Germany (*Presenter*) Nothing to Disclose

#### PURPOSE

Color-coded digital variance angiography (ccDVA) is a recently developed image processing technology capable of visualization of hemodynamic conditions in 2D X-ray angiography setting. Our aim was to explore the potential advantages of ccDVA in prostatic artery embolization (PAE).

#### METHODS AND MATERIALS

This retrospective study evaluated 108 angiographic acquisitions from 30 patients (mean  $\pm$  SD age 68.0  $\pm$  8.9, range 41-87) undergoing PAE between May and October 2020. DSA and ccDVA images were generated from the same unsubtracted acquisition. Visual evaluation of ccDVA and DSA images was performed by four experienced interventional. The diagnostic value of DSA and ccDVA images was evaluated using clinically relevant criteria (visibility of small [ $<$  2.5 mm] and large arteries [ $>$  2.5 mm], feeding arteries and tissue blush) in a paired comparison. Data were analysed by the binomial test, the interrater agreement was determined by the Fleiss Kappa analysis.

#### RESULTS

The preference of ccDVA images was significantly higher in all criteria. The preference of ccDVA images was the highest in the tissue blush category (quality agreement [QA] 89%, interrater agreement [IR] 79%, followed by the small arteries (QA: 79%, IR: 70%), feeding arteries (QA: 79%, IR: 65%) and large arteries (QA: 63%, IR: 58%). The Fleiss Kappa range was 0.02-0.18, significant in all criteria except large vessels.

#### CONCLUSION

Our data show that ccDVA significantly improves the diagnostic evaluation of tissue blush, small arteries and feeding arteries in PAE. As these structures are critically important in the procedure, the ccDVA technology might help the decision-making process in PAE interventions, although these benefits have to be validated in further prospective clinical studies.

#### CLINICAL RELEVANCE/APPLICATION

Color-coded DVA (ccDVA) significantly improves the visualization of small arteries, feeding arteries and tissue blush, thereby provides more information for PAE procedures than DSA in 79-89 % of comparisons.

Printed on: 02/07/23

## Abstract Archives of the RSNA, 2022

S3A-SP1R-9

### The Role of Machine Learning Algorithms in Predicting the Treatment Outcome of High-Intensity Focused Ultrasound Ablation of Uterine Fibroids with an Immediate Nonperfused Volume Ratio of at least 90%

Sunday, Nov. 27 11:45AM - 12:15PM Room: Learning Center - IR DPS

#### Participants

Bilgin Keserci, PhD, (*Presenter*) Nothing to Disclose

#### PURPOSE

To investigate the role of machine learning (ML) classifiers to find the most informative multiparametric (mp) magnetic resonance imaging (MRI) features in predicting the treatment outcome of high intensity focused ultrasound (HIFU) ablation with an immediate nonperfused volume (NPV) ratio of at least 90%.

#### METHODS AND MATERIALS

This retrospective study was approved by the institutional review board, and informed consent was obtained in all participants. Seventy-three women who underwent HIFU treatment were divided into groups A (n=47), and B (n=26), comprising patients with an NPV ratio of at least 90% and less than 90%, respectively. An ensemble feature ranking model was introduced based on the score values assigned to the 37 features by five different ML classifiers including Logistic Regression (LR), Support Vector Classifier (SVC), Random Forest (RF), Adaptive Boosting (Adaboost), Gradient Boosting (GBM), to find the most informative mpMRI features. The relationship between the mpMRI features and the immediate NPV ratio of 90% was evaluated using Pearson's correlation coefficients. The diagnostic ability of ML classifiers was performed by means of standard performance metrics, including the area under the receiver operating characteristic curve (AUROC), accuracy, sensitivity, and specificity in eight folds cross-validation.

#### RESULTS

For all the 12 most informative features, the AUROC ranged from 0.5 to 0.97, accuracy ranged from 0.34 to 0.97, specificity ranged from 0.56 to 1.0, and sensitivity ranged from 0.87 to 1.0. The GBM classifier showed the best predictive performance with an AUROC of 0.95 and accuracy of 0.92, followed by the RF, Adaboost, LR, and SVC classifiers, which yielded an AUROC of 0.92, 0.92, 0.83 and 0.78, and accuracy of 0.96, 0.88, 0.84 and 0.84, respectively. The best classifier performance with the best-performing features from each mpMRI group, Ktrans ratio of the fibroid to the myometrium, the ratio of AUC of the fibroid to the myometrium, subcutaneous fat thickness, the ratio of ADC value of fibroid to the myometrium, and T2-signal intensity (SI) of fibroid, was achieved using GBM.

#### CONCLUSION

The preliminary findings in this study suggest that the most informative 12 and best performing features from each mpMRI group should be considered in predicting the treatment outcome of HIFU ablation to achieve an immediate NPV ratio of 90%.

#### CLINICAL RELEVANCE/APPLICATION

The best classifier performance with the best-performing features from each mpMRI group should be considered by the treating physician in the screening phase to predict the treatment outcome of HIFU ablation to achieve an immediate NPV ratio of 90%.

Printed on: 02/07/23

## Abstract Archives of the RSNA, 2022

S3A-SPMK

### Musculoskeletal Sunday Poster Discussions - A

Sunday, Nov. 27 11:45AM - 12:15PM Room: Learning Center - MK DPS

#### Sub-Events

#### S3A-SPMK-1 Does the dGEMRIC Index Recover 3 Years After Fai Surgery Following an Initial Decrease at 1 Year Follow-up? A Controlled Prospective Study

##### Participants

Florian Schmaranzer, MD, Bern, Switzerland (*Presenter*) Nothing to Disclose

##### PURPOSE

Delayed gadolinium-enhanced MRI of cartilage (dGEMRIC) allows objective and noninvasive assessment of cartilage quality. An interim analysis 1 year after correction of femoroacetabular impingement previously showed that the dGEMRIC index decreased despite good clinical outcome. Our aim was to evaluate dGEMRIC indices longitudinally in patients with FAI correction and in a control group undergoing non-operative therapy for FAI.

##### METHODS AND MATERIALS

Prospective, comparative longitudinal study. 39 patients (40 hips) who received either surgical FAI correction (n=20) or non-operative therapy (n=20) were included. Baseline demographics and presence of osseous deformities did not differ between groups. All patients received indirect MR arthrography at all three time points (baseline, 1 and 3 year follow-up [FU]). The 3D cartilage models were created using a custom-developed deep learning-based software and were manually corrected if necessary. The dGEMRIC indices were determined separately for acetabular and femoral cartilage. A mixed-effects model was used for statistical analysis in repeated measures.

##### RESULTS

The surgical group showed an initial (preoperative to 1-year FU) decrease of dGEMRIC indices: acetabular cartilage 512±174 ms to 392±123 ms; femoral cartilage 530±173 ms to 411±117 ms (both  $p < 0.001$ ). From 1-year to 3-year FU, dGEMRIC indices increased: acetabular cartilage 392±123 ms to 456±163 ms; femoral cartilage 411±117 ms to 477±169 ms (both  $p < 0.001$ ). The nonoperative group showed no significant changes in dGEMRIC indices of acetabular and femoral cartilage between the 3 timepoints (all  $p > 0.6$ ).

##### CONCLUSION

Three years after FAI correction, an improvement in dGEMRIC indices was found compared to short-term 1-year FU. This may be due to normalized joint biomechanics or regressive postoperative activation of the inflammatory cascade at mid-term following intra-articular surgery.

##### CLINICAL RELEVANCE/APPLICATION

This study shows the potential of deep learning based analysis of quantitative cartilage mapping techniques to detect adaptive changes in cartilage composition following therapeutic interventions.

#### S3A-SPMK-3 Enthesis Assessment Using Ultrashort Echo Time Magnetic Resonance Imaging (UTE-MRI) T1 And Magnetization Transfer (MT) Modeling in Psoriatic Arthritis

##### Participants

Dina Moazamian, San Diego, CA (*Presenter*) Nothing to Disclose

##### PURPOSE

This study uses ultrashort echo time (UTE) magnetic resonance imaging (MRI) techniques to quantify the collagen proton content and T1 values of Achilles tendon entheses, and evaluates differences between patients with psoriatic arthritis disease (PSA) and healthy controls.

##### METHODS AND MATERIALS

Seventeen PSA patients (59±15 years old, 41% female) and twenty-one healthy control participants (33 ±11 years old, 47% female) were scanned with newly developed 3D UTE Cones sequences, including T1 and MT modeling on a 3T clinical scanner (MR750, GE) employing a 3-inch surface coil. The entheses region between the Achilles tendon and the calcaneus bone was imaged in the sagittal plane. To conduct UTE-MT modeling, T1 was measured with an actual variable flip angle (AFI-VFA) sequence (AFI: TE=0.032ms, TRs=20,100ms, FA=45°; VFA: TE=0.032ms, TR=18ms, FAs=5, 12, and 24°). A 3D-UTE-Cones-MT sequence (pulse power=350°, 750°; frequency offset=2, 5, 10, 20, and 50kHz; FA=7°; 11 spokes per MT preparation) was performed for the two-pool MT modeling. MT modeling estimates collagen proton content (i.e., macromolecular proton fraction, MMF). The total scan time was 25 mins. Two different regions of interest (ROIs) for each participant were drawn, one on the entheses (close to the calcaneus bone) and the other one on the tensile Achilles tendon (Fig.1A). UTE-MRI markers were calculated for the two groups and were compared using the Mann-Whitney-U test. P values <0.05 were considered significant.

## RESULTS

T1 and MMF pixel maps of a representative patient and a healthy control are presented in Fig.1 B-C and Fig.1 D-E, respectively. Average and standard deviation of T1 and MMF and their statistical significance are presented in Fig.1F. Significant differences in T1 and MMF values between entheses and tendon regions were found between the PSA and control groups. MMF difference between the control and PSA groups (23.8%) was higher than the T1 difference (12.1%).

## CONCLUSION

s UTE-T1 and MMF from UTE-MT modeling can be used as quantitative methods for assessing entheses. As MMF values were significantly lower and T1 levels significantly higher in the entheses of PSA patients, this suggests a lower macromolecular content (collagen and proteoglycan) in the entheses of PSA patients compared with the control group.

## CLINICAL RELEVANCE/APPLICATION

UTE-MT and T1 sequences are capable of evaluating entheses and tendons and may be able to detect abnormalities in PSA patients in order to improve the diagnosis and monitoring of PSA patients.

## S3A-SPMK-4 The Abnormal Calcified Layer of Articular Cartilage of Knee (CLC) In 3D Ultrashort Echo Time MRI Correlating With Cartilage Degeneration in Proton Density Spin-Echo Sequence With Fat Suppression (PDFS)

Participants

Sunmin Lee, MD, (*Presenter*) Nothing to Disclose

## PURPOSE

To evaluate the association between the abnormal calcified layer of articular cartilage of the knee (CLC) in 3D ultrashort echo time MRI (UTE) and cartilage degeneration in proton density spin-echo sequence with fat suppression (PDFS).

## METHODS AND MATERIALS

96 knees were performed sagittal 3D UTE (TR = 16.1ms TE = 0.028ms and 6.6ms) and sagittal proton density spin-echo sequence with fat suppression (PDFS). Two musculoskeletal radiologists evaluated cartilage using Modified Noyer's chondromalacia grading system and subchondral bone change (SBC) in seven zones of the knee (mid, and posterior portion of the medial femoral condyle, medial tibial plateau, anterior, mid, and posterior portion of the lateral femoral condyle, lateral tibial plateau). CLC was analyzed in the same zone and divided into normal and abnormal (irregularity, thickening, thinning, and defect). The grade of chondromalacia and the presence of SBC were compared with the morphology of CLC using Kendall's tau b correlation and linear by linear correlation.

## RESULTS

The zones of abnormal CLC were found 3 of 526 grade 0 (7%), 16 of 44 grade 1 (36%), 8 of 37 grade 2a (22%), 13 of 22 grade 2b (59%) and 33 of 41 grade 3 (80%) and 2 of 2 osteochondral defect (100%). The higher grade of chondromalacia, the higher frequency of abnormal CLC with statistical significance ( $P < 0.001$ ). In the same grade, the area with SBC was more frequently accompanied by abnormal CLC than the area without SBC ( $P < 0.05$ ).

## CONCLUSION

s The CLC abnormality can be successfully visualized in 3D UTE and may be associated with cartilage degeneration.

## CLINICAL RELEVANCE/APPLICATION

The calcified layer of cartilage has been expected to play an important role in cartilage damage. However, the Conventional PDFS could not see the calcified cartilage layer. Our study proves that 3D UTE can visualize abnormalities in the calcified cartilage layer and correlates with the degree of Noyer's chondromalacia in PDFS, which is expected to help understand the pathophysiology and early detection of cartilage damage and may affect treatment and cartilage surgery in the future.

Printed on: 02/07/23

## Abstract Archives of the RSNA, 2022

S3A-SPMK-1

### Does the dGEMRIC Index Recover 3 Years After Fai Surgery Following an Initial Decrease at 1 Year Follow-up? A Controlled Prospective Study

Sunday, Nov. 27 11:45AM - 12:15PM Room: Learning Center - MK DPS

#### Participants

Florian Schmaranzer, MD, Bern, Switzerland (*Presenter*) Nothing to Disclose

#### PURPOSE

Delayed gadolinium-enhanced MRI of cartilage (dGEMRIC) allows objective and noninvasive assessment of cartilage quality. An interim analysis 1 year after correction of femoroacetabular impingement previously showed that the dGEMRIC index decreased despite good clinical outcome. Our aim was to evaluate dGEMRIC indices longitudinally in patients with FAI correction and in a control group undergoing non-operative therapy for FAI.

#### METHODS AND MATERIALS

Prospective, comparative longitudinal study. 39 patients (40 hips) who received either surgical FAI correction (n=20) or non-operative therapy (n=20) were included. Baseline demographics and presence of osseous deformities did not differ between groups. All patients received indirect MR arthrography at all three time points (baseline, 1 and 3 year follow-up [FU]). The 3D cartilage models were created using a custom-developed deep learning-based software and were manually corrected if necessary. The dGEMRIC indices were determined separately for acetabular and femoral cartilage. A mixed-effects model was used for statistical analysis in repeated measures.

#### RESULTS

The surgical group showed an initial (preoperative to 1-year FU) decrease of dGEMRIC indices: acetabular cartilage 512±174 ms to 392±123 ms; femoral cartilage 530±173 ms to 411±117 ms (both  $p < 0.001$ ). From 1-year to 3-year FU, dGEMRIC indices increased: acetabular cartilage 392±123 ms to 456±163 ms; femoral cartilage 411±117 ms to 477±169 ms (both  $p < 0.001$ ). The nonoperative group showed no significant changes in dGEMRIC indices of acetabular and femoral cartilage between the 3 timepoints (all  $p > 0.6$ ).

#### CONCLUSION

s Three years after FAI correction, an improvement in dGEMRIC indices was found compared to short-term 1-year FU. This may be due to normalized joint biomechanics or regressive postoperative activation of the inflammatory cascade at mid-term following intra-articular surgery.

#### CLINICAL RELEVANCE/APPLICATION

This study shows the potential of deep learning based analysis of quantitative cartilage mapping techniques to detect adaptive changes in cartilage composition following therapeutic interventions.

Printed on: 02/07/23

## Abstract Archives of the RSNA, 2022

S3A-SPMK-3

### Enthesis Assessment Using Ultrashort Echo Time Magnetic Resonance Imaging (UTE-MRI) T1 And Magnetization Transfer (MT) Modeling in Psoriatic Arthritis

Sunday, Nov. 27 11:45AM - 12:15PM Room: Learning Center - MK DPS

#### Participants

Dina Moazamian, San Diego, CA (Presenter) Nothing to Disclose

#### PURPOSE

This study uses ultrashort echo time (UTE) magnetic resonance imaging (MRI) techniques to quantify the collagen proton content and T1 values of Achilles tendon entheses, and evaluates differences between patients with psoriatic arthritis disease (PSA) and healthy controls.

#### METHODS AND MATERIALS

Seventeen PSA patients (59±15 years old, 41% female) and twenty-one healthy control participants (33 ±11 years old, 47% female) were scanned with newly developed 3D UTE Cones sequences, including T1 and MT modeling on a 3T clinical scanner (MR750, GE) employing a 3-inch surface coil. The entheses region between the Achilles tendon and the calcaneus bone was imaged in the sagittal plane. To conduct UTE-MT modeling, T1 was measured with an actual variable flip angle (AFI-VFA) sequence (AFI: TE=0.032ms, TRs=20,100ms, FA=45°; VFA: TE=0.032ms, TR=18ms, FAs=5, 12, and 24°). A 3D-UTE-Cones-MT sequence (pulse power=350°, 750°; frequency offset=2, 5, 10, 20, and 50kHz; FA=7°; 11 spokes per MT preparation) was performed for the two-pool MT modeling. MT modeling estimates collagen proton content (i.e., macromolecular proton fraction, MMF). The total scan time was 25 mins. Two different regions of interest (ROIs) for each participant were drawn, one on the entheses (close to the calcaneus bone) and the other one on the tensile Achilles tendon (Fig.1A). UTE-MRI markers were calculated for the two groups and were compared using the Mann-Whitney-U test. P values <0.05 were considered significant.

#### RESULTS

T1 and MMF pixel maps of a representative patient and a healthy control are presented in Fig.1 B-C and Fig.1 D-E, respectively. Average and standard deviation of T1 and MMF and their statistical significance are presented in Fig.1F. Significant differences in T1 and MMF values between entheses and tendon regions were found between the PSA and control groups. MMF difference between the control and PSA groups (23.8%) was higher than the T1 difference (12.1%).

#### CONCLUSION

s UTE-T1 and MMF from UTE-MT modeling can be used as quantitative methods for assessing entheses. As MMF values were significantly lower and T1 levels significantly higher in the entheses of PSA patients, this suggests a lower macromolecular content (collagen and proteoglycan) in the entheses of PSA patients compared with the control group.

#### CLINICAL RELEVANCE/APPLICATION

UTE-MT and T1 sequences are capable of evaluating entheses and tendons and may be able to detect abnormalities in PSA patients in order to improve the diagnosis and monitoring of PSA patients.

Printed on: 02/07/23

## Abstract Archives of the RSNA, 2022

S3A-SPMK-4

### **The Abnormal Calcified Layer of Articular Cartilage of Knee (CLC) In 3D Ultrashort Echo Time MRI Correlating With Cartilage Degeneration in Proton Density Spin-Echo Sequence With Fat Suppression (PDFS)**

Sunday, Nov. 27 11:45AM - 12:15PM Room: Learning Center - MK DPS

#### **Participants**

Sunmin Lee, MD, (*Presenter*) Nothing to Disclose

#### **PURPOSE**

To evaluate the association between the abnormal calcified layer of articular cartilage of the knee (CLC) in 3D ultrashort echo time MRI (UTE) and cartilage degeneration in proton density spin-echo sequence with fat suppression (PDFS).

#### **METHODS AND MATERIALS**

96 knees were performed sagittal 3D UTE (TR = 16.1ms TE = 0.028ms and 6.6ms) and sagittal proton density spin-echo sequence with fat suppression (PDFS). Two musculoskeletal radiologists evaluated cartilage using Modified Noyer's chondromalacia grading system and subchondral bone change (SBC) in seven zones of the knee (mid, and posterior portion of the medial femoral condyle, medial tibial plateau, anterior, mid, and posterior portion of the lateral femoral condyle, lateral tibial plateau). CLC was analyzed in the same zone and divided into normal and abnormal (irregularity, thickening, thinning, and defect). The grade of chondromalacia and the presence of SBC were compared with the morphology of CLC using Kendall's tau b correlation and linear by linear correlation.

#### **RESULTS**

The zones of abnormal CLC were found 3 of 526 grade 0 (7%), 16 of 44 grade 1 (36%), 8 of 37 grade 2a (22%), 13 of 22 grade 2b (59%) and 33 of 41 grade 3 (80%) and 2 of 2 osteochondral defect (100%). The higher grade of chondromalacia, the higher frequency of abnormal CLC with statistical significance ( $P < 0.001$ ). In the same grade, the area with SBC was more frequently accompanied by abnormal CLC than the area without SBC ( $P < 0.05$ ).

#### **CONCLUSION**

s The CLC abnormality can be successfully visualized in 3D UTE and may be associated with cartilage degeneration.

#### **CLINICAL RELEVANCE/APPLICATION**

The calcified layer of cartilage has been expected to play an important role in cartilage damage. However, the Conventional PDFS could not see the calcified cartilage layer. Our study proves that 3D UTE can visualize abnormalities in the calcified cartilage layer and correlates with the degree of Noyer's chondromalacia in PDFS, which is expected to help understand the pathophysiology and early detection of cartilage damage and may affect treatment and cartilage surgery in the future.

Printed on: 02/07/23

## Abstract Archives of the RSNA, 2022

S3A-SPMS

### Multisystem Sunday Poster Discussions - A

Sunday, Nov. 27 11:45AM - 12:15PM Room: Learning Center - MS DPS

#### Sub-Events

#### S3A-SPMS-1 Thickening of The Parotid Facial Process As a Sign of Hypertrophy and/or Inflammation in Patients with Sjogren's or Sicca syndrome

##### Participants

Andrea Portella Alegre, MD, Barcelona, Spain (*Presenter*) Nothing to Disclose

##### PURPOSE

Primary Sjögren's syndrome (pSS) is an autoimmune exocrinopathy which often manifests with asthenia, musculoskeletal and sicca syndrome (xerostomia and xerophthalmia). The salivary gland ultrasound (SGUS) is a simple and non-invasive procedure that is readily available and supplies important information on the major salivary glands. The score that assesses the heterogeneity of the glandular parenchyma has shown similar weight compared to minor items of the last set of criteria (2016 ACR/EULAR criteria) established to classify pSS patients. Our objective is to define new sonographic (US) features that can be included in a sonographic scoring system for the diagnosis of pSS.

##### METHODS AND MATERIALS

SGUS were conducted on 53 pSS and 26 sicca patients and 15 healthy controls (HC). The criteria for pSS was based on the 2016 ACR-EULAR classification, and the non-Sjögren's sicca patients presented symptoms but the score was less than 4. The US features that were examined were the maximum thickness of the facial process of the PG (FPPG) and Stensen's duct (SD) width. The analysis of continuous variables was made with Student's test and receiver operating characteristic (ROC) curve was employed to evaluate the performance of the width of the FPPG and the best cut-off value was determined.

##### RESULTS

There were no statistically significant differences between the thickness of the FPPG between pSS and sicca patients, although were significantly higher compared with the control group of both pSS and sicca patients independently. Consequently, the pSS and sicca patients were clustered into a single group and compared with HC, obtaining statistically significant differences with a mean value of  $4.49 \pm 1.61$  mm for pSS+sicca and  $2.93 \pm 0.84$  mm HC,  $p < 0.001$ . ROC curves was performed to obtain a cut-off point between pSS+sicca patients and HC that would allow discriminating which thickness can be considered pathological, obtaining an AUC value of 0.8/0.037 and confidence interval (CI) of (0.73-0.87) with sensitivity of 0.67 (67%) CI (0.59-0.75) and specificity of 0.79 (79%) CI (0.60-0.92). The cut-off width of FPPG was 4mm. SD thickness was also significantly higher in the group of pSS+sicca patients versus HC with a value of  $1.05 \pm 0.52$ mm and  $0.72 \pm 0.22$  mm, respectively.

##### CONCLUSION

s The width of FPPG may be an US feature to take into account to assess hypertrophies or signs of inflammation in patients with pSS or sicca versus HC, with a pathological cut-off point of =4mm, as well as the assessment of the thickness of SD.

##### CLINICAL RELEVANCE/APPLICATION

SGUS may be a candidate diagnostic test to be included in the ACR/EULAR criteria for the diagnosis of pSS. These new ultrasound features can help to make a score that can be incorporated as an item within the diagnostic criteria.

Printed on: 02/07/23

## Abstract Archives of the RSNA, 2022

S3A-SPMS-1

### Thickening of The Parotid Facial Process As a Sign of Hypertrophy and/or Inflammation in Patients with Sjogren's or Sicca syndrome

Sunday, Nov. 27 11:45AM - 12:15PM Room: Learning Center - MS DPS

#### Participants

Andrea Portella Alegre, MD, Barcelona, Spain (*Presenter*) Nothing to Disclose

#### PURPOSE

Primary Sjögren's syndrome (pSS) is an autoimmune exocrinopathy which often manifests with asthenia, musculoskeletal and sicca syndrome (xerostomia and xerophthalmia). The salivary gland ultrasound (SGUS) is a simple and non-invasive procedure that is readily available and supplies important information on the major salivary glands. The score that assesses the heterogeneity of the glandular parenchyma has shown similar weight compared to minor items of the last set of criteria (2016 ACR/EULAR criteria) established to classify pSS patients. Our objective is to define new sonographic (US) features that can be included in a sonographic scoring system for the diagnosis of pSS.

#### METHODS AND MATERIALS

SGUS were conducted on 53 pSS and 26 sicca patients and 15 healthy controls (HC). The criteria for pSS was based on the 2016 ACR-EULAR classification, and the non-Sjögren's sicca patients presented symptoms but the score was less than 4. The US features that were examined were the maximum thickness of the facial process of the PG (FPPG) and Stensen's duct (SD) width. The analysis of continuous variables was made with Student's test and receiver operating characteristic (ROC) curve was employed to evaluate the performance of the width of the FPPG and the best cut-off value was determined.

#### RESULTS

There were no statistically significant differences between the thickness of the FPPG between pSS and sicca patients, although were significantly higher compared with the control group of both pSS and sicca patients independently. Consequently, the pSS and sicca patients were clustered into a single group and compared with HC, obtaining statistically significant differences with a mean value of  $4.49 \pm 1.61$  mm for pSS+sicca and  $2.93 \pm 0.84$  mm HC,  $p < 0.001$ . ROC curves was performed to obtain a cut-off point between pSS+sicca patients and HC that would allow discriminating which thickness can be considered pathological, obtaining an AUC value of 0.8/0.037 and confidence interval (CI) of (0.73-0.87) with sensitivity of 0.67 (67%) CI (0.59-0.75) and specificity of 0.79 (79%) CI (0.60-0.92). The cut-off width of FPPG was 4mm. SD thickness was also significantly higher in the group of pSS+sicca patients versus HC with a value of  $1.05 \pm 0.52$ mm and  $0.72 \pm 0.22$  mm, respectively.

#### CONCLUSION

s The width of FPPG may be an US feature to take into account to assess hypertrophies or signs of inflammation in patients with pSS or sicca versus HC, with a pathological cut-off point of  $\geq 4$ mm, as well as the assessment of the thickness of SD.

#### CLINICAL RELEVANCE/APPLICATION

SGUS may be a candidate diagnostic test to be included in the ACR/EULAR criteria for the diagnosis of pSS. These new ultrasound features can help to make a score that can be incorporated as an item within the diagnostic criteria.

Printed on: 02/07/23

## Abstract Archives of the RSNA, 2022

S3A-SPNMMI

### Nuclear Medicine/Molecular Imaging Sunday Poster Discussion - A

Sunday, Nov. 27 11:45AM - 12:15PM Room: Learning Center - NMMI DPS

#### Participants

Nadine Mallak, MD, Portland, OR (*Moderator*) Nothing to Disclose  
Nadine Mallak, MD, Portland, OR (*Moderator*) Nothing to Disclose  
Ashwin Parihar, MBBS, MD, Saint Louis, MO (*Moderator*) Nothing to Disclose  
Ashwin Parihar, MBBS, MD, Saint Louis, MO (*Moderator*) Nothing to Disclose

#### Sub-Events

#### S3A-SPNMMI-1 Screening of Optimal Concentration of Magnetic Labeled Placental Mesenchymal Stem Cells

##### Participants

Hua He, MMedSc, MMedSc, Yinchuan, China (*Presenter*) Nothing to Disclose

#### PURPOSE

To determine the optimal magnetic labeling concentration range of human placental mesenchymal stem cells (hPMSCs) labeled with Ultrasmall Superparamagnetic Iron Oxides (USPIO), is critical to the realization of the external dynamic imaging and clinical application of the MR in vivo.

#### METHODS AND MATERIALS

hPMSCs were isolated and cultured, Polylysine(PLL) were transfected into USPIO to form PLL-USPIO complex, then label hPMSCs and investigate the labeling efficiency. Detect biological characteristics of labeled hPMSCs: cell survival rate calculated by trypan blue exclusion test, cell proliferation detected by Cell count (CCK-8) kit, and flow cytometry was used to judge the apoptosis of the cells. the difference of cell proliferation ability was analyzed by one way ANOVA or Kruskal Wallis testing, and the cell survival rate and apoptosis rate were compared by chi-square test.

#### RESULTS

Prussian blue staining in the experimental group showed that a large number of iron particles existed in the cytoplasm, and no iron particles stained blue were found in or outside the cells of the experimental group, the labeling rate was more than 95%, When the concentration of magnetic labeling was 15, 20 and 25  $\mu\text{g}\cdot\text{mL}^{-1}$ , the survival rate of hPMSCs was  $87.06\pm 2.11$ ,  $87.06\pm 2.11$ ,  $80.95\pm 0.28$ , which were all lower than those of the control group ( $P < 0.05$ ). on the 7th day of culture, the OD value of the labeling concentration of 25  $\mu\text{g}\cdot\text{mL}^{-1}$  group was  $1.068\pm 0.134$ , which was lower than that of the control group ( $P=0.047$ ); There was no significant difference in late apoptosis rate between labeled cells and unlabeled cells (all  $P>0.05$ , the early apoptosis rate increased with the increase of marker concentration, the early apoptosis rate was higher than that of the control group when the concentration of labeling was  $\approx 15 \mu\text{g}\cdot\text{mL}^{-1}$

#### CONCLUSION

When the concentration range of PLL-USPIO is 5 $\mu\text{g}/\text{ml}$ -15 $\mu\text{g}/\text{ml}$ , hPMSCs can be effectively labeled and has no significant effect on its activity, proliferation and apoptosis rate.

#### CLINICAL RELEVANCE/APPLICATION

This study provides basic research data for the realization of hPMSCs in vivo MRI dynamic imaging and clinical application.

#### S3A-SPNMMI-2 Simultaneous 18F-FDG PET/MRI for the Prediction of Early Response to Neoadjuvant Chemotherapy in Breast Cancer

##### Participants

Valeria Romeo, MD, PhD, Naples, Italy (*Presenter*) Nothing to Disclose

#### PURPOSE

To assess whether pre- and intra-treatment simultaneous 18F-FDG PET/MRI could be useful in the prediction of the response to neoadjuvant chemotherapy (NAC) in breast cancer (BC) patients.

#### METHODS AND MATERIALS

Between January 2017 and January 2020, 37 consecutive patients (mean age  $45 \pm 15$  yrs) with 41 histologically proven BC lesions, candidate to anthracycline- and taxane-based NAC were prospectively enrolled. Simultaneous breast 18F-FDG PET/MRI examination was performed twice in each patient, one week before NAC and after the second anthracycline administration. PET/MRI images were analyzed to extract quantitative diffusion ( $\text{ADC}_{\text{min}}$ ,  $\text{ADC}_{\text{mean}}$ ), perfusion ( $K_{\text{trans}}$ ,  $K_{\text{ep}}$ ,  $V_e$ ,  $\text{IAUC}$ ) and metabolic ( $\text{SUV}_{2\text{D}}$ ,  $\text{SUV}_{3\text{D}}$ ,  $\text{MTV}$ ) parameters. The variation of each parameter ( $\Delta$ , %) after the second anthracycline cycle was then calculated. Univariate analysis through Mann-Whitney U test was performed to assess differences in terms of pre-treatment and  $\Delta$  parameters between patients who showed complete and partial response (CR, PR) at histological examination after NAC. Multivariate logistic

regression analysis was then used to identify imaging parameters predictive of CR.

## **RESULTS**

At Mann Mann-Whitney U test, significant differences were found between patients with PR and CR after NAC in terms of  $\beta$ -Ve ( $p=0.016$ ), SUV3D ( $p=0.022$ ) and SUV2D ( $p=0.043$ ). In detail, the early post-treatment variation of Ve was significantly higher in patients who showed CR after NAC. Furthermore, patients with CR showed higher pre-treatment SUV3D and SUV2D compared to patient with PR after NAC. At multivariate logistic regression, both  $\beta$ -Ve and SUV3D resulted independent predictors of complete response to NAC, with p values of 0.013 and 0.021, respectively.

## **CONCLUSION**

s Simultaneous breast PET/MRI could be useful to early predict the response to NAC in patients with BC. Our preliminary observations show that functional parameters (i.e. perfusion and metabolic) may identify patients who will respond completely, particularly using both pre-treatment and the variation of quantitative parameters early after the second cycle of NAC.

## **CLINICAL RELEVANCE/APPLICATION**

Simultaneous breast PET/MRI may be useful for early identification of BC patients who would benefit from continuing NAC or for whom surgical excision could be optionally considered.

Printed on: 02/07/23

## Abstract Archives of the RSNA, 2022

S3A-SPNMMI-1

### Screening of Optimal Concentration of Magnetic Labeled Placental Mesenchymal Stem Cells

Sunday, Nov. 27 11:45AM - 12:15PM Room: Learning Center - NMMI DPS

#### Participants

Hua He, MMedSc, MMedSc, Yinchuan, China (*Presenter*) Nothing to Disclose

#### PURPOSE

To determine the optimal magnetic labeling concentration range of human placental mesenchymal stem cells (hPMSCs) labeled with Ultrasmall Superparamagnetic Iron Oxides (USPIO), is critical to the realization of the external dynamic imaging and clinical application of the MR in vivo.

#### METHODS AND MATERIALS

hPMSCs were isolated and cultured , Polylysine(PLL) were transfected into USPIO to form PLL-USPIO complex, then label hPMSCs and investigate the labeling efficiency . Detect biological characteristics of labeled hPMSCs: cell survival rate calculated by trypan blue exclusion test, cell proliferation detected by Cell count (CCK-8) kit, and flow cytometry was used to judge the apoptosis of the cells. the difference of cell proliferation ability was analyzed by one way ANOVA or Kruskal Wallis testing, and the cell survival rate and apoptosis rate were compared by chi-square test.

#### RESULTS

Prussian blue staining in the experimental group showed that a large number of iron particles existed in the cytoplasm, and no iron particles stained blue were found in or outside the cells of the experimental group,the labeling rate was more than 95% , When the concentration of magnetic labeling was 15, 20 and 25  $\mu\text{g}\cdot\text{mL}^{-1}$ , the survival rate of hPMSCs was  $87.06\pm 2.11$ ,  $87.06\pm 2.11$ ,  $80.95\pm 0.28$ , which were all lower than those of the control group ( $P < 0.05$ ). on the 7th day of culture, the OD value of the labeling concentration of 25  $\mu\text{g}\cdot\text{mL}^{-1}$  group was  $1.068\pm 0.134$ , which was lower than that of the control group ( $P=0.047$ ); There was no significant difference in late apoptosis rate between labeled cells and unlabeled cells (all  $P>0.05$ , the early apoptosis rate increased with the increase of marker concentration, the early apoptosis rate was higher than that of the control group when the concentration of labeling was  $\approx 15 \mu\text{g}\cdot\text{mL}^{-1}$

#### CONCLUSION

s When the concentration range of PLL-USPIO is 5ug/ml-15ug/ml-1, hPMSCs can be effectively labeled and has no significant effect on its activity, proliferation and apoptosis rate.

#### CLINICAL RELEVANCE/APPLICATION

This study provides basic research data for the realization of hPMSCs in vivo MRI dynamic imaging and clinical application.

Printed on: 02/07/23

## Abstract Archives of the RSNA, 2022

S3A-SPNMMI-2

### Simultaneous 18F-FDG PET/MRI for the Prediction of Early Response to Neoadjuvant Chemotherapy in Breast Cancer

Sunday, Nov. 27 11:45AM - 12:15PM Room: Learning Center - NMMI DPS

#### Participants

Valeria Romeo, MD, PhD, Naples, Italy (*Presenter*) Nothing to Disclose

#### PURPOSE

To assess whether pre- and intra-treatment simultaneous 18F-FDG PET/MRI could be useful in the prediction of the response to neoadjuvant chemotherapy (NAC) in breast cancer (BC) patients.

#### METHODS AND MATERIALS

Between January 2017 and January 2020, 37 consecutive patients (mean age  $45 \pm 15$  yrs) with 41 histologically proven BC lesions, candidate to anthracycline- and taxane-based NAC were prospectively enrolled. Simultaneous breast 18F-FDG PET/MRI examination was performed twice in each patient, one week before NAC and after the second anthracycline administration. PET/MRI images were analyzed to extract quantitative diffusion (ADC<sub>min</sub>, ADC<sub>mean</sub>), perfusion (K<sub>trans</sub>, K<sub>ep</sub>, V<sub>e</sub>, IAUC) and metabolic (SUV<sub>2D</sub>, SUV<sub>3D</sub>, MTV) parameters. The variation of each parameter (delta,  $\Delta$ ) after the second anthracycline cycle was then calculated. Univariate analysis through Mann-Whitney U test was performed to assess differences in terms of pre-treatment and  $\Delta$  parameters between patients who showed complete and partial response (CR, PR) at histological examination after NAC. Multivariate logistic regression analysis was then used to identify imaging parameters predictive of CR.

#### RESULTS

At Mann Mann-Whitney U test, significant differences were found between patients with PR and CR after NAC in terms of  $\Delta$ -V<sub>e</sub> (p=0.016), SUV<sub>3D</sub> (p=0.022) and SUV<sub>2D</sub> (p=0.043). In detail, the early post-treatment variation of V<sub>e</sub> was significantly higher in patients who showed CR after NAC. Furthermore, patients with CR showed higher pre-treatment SUV<sub>3D</sub> and SUV<sub>2D</sub> compared to patient with PR after NAC. At multivariate logistic regression, both  $\Delta$ -V<sub>e</sub> and SUV<sub>3D</sub> resulted independent predictors of complete response to NAC, with p values of 0.013 and 0.021, respectively.

#### CONCLUSION

Simultaneous breast PET/MRI could be useful to early predict the response to NAC in patients with BC. Our preliminary observations show that functional parameters (i.e. perfusion and metabolic) may identify patients who will respond completely, particularly using both pre-treatment and the variation of quantitative parameters early after the second cycle of NAC.

#### CLINICAL RELEVANCE/APPLICATION

Simultaneous breast PET/MRI may be useful for early identification of BC patients who would benefit from continuing NAC or for whom surgical excision could be optionally considered.

Printed on: 02/07/23



## Abstract Archives of the RSNA, 2022

S3A-SPNPM

### Noninterpretive Skills/Quality Improvement/Practice Management Sunday Poster Discussions - A

Sunday, Nov. 27 11:45AM - 12:15PM Room: Learning Center - NPM DPS

#### Participants

Stefanie Woodard, DO, Birmingham, AL (*Moderator*) Investigator, Bracco Group Institutional research support, Bracco Group

#### Sub-Events

#### S3A-SPNPM-Financial Toxicity Analysis of Virtual Versus In-Person Radiation Oncology Residency Interviews<sup>1</sup>

##### Participants

Yorlery Vicioso Mora, MD, PhD, (*Presenter*) Nothing to Disclose

#### PURPOSE

Recent work has indicated that medical students may take loans of up to \$7,000 to offset costs related to the residency match interview process. Because of the COVID-19 pandemic, US residency programs starting with the 2021 match cycle have adopted virtual interviews as replacements for in-person interviews. The financial toxicity of virtual versus in-person interviews for Radiation Oncology is addressed in the following cost analysis.

#### METHODS AND MATERIALS

Previous literature (including national 2019-2022 Radiation Oncology residency match statistics) was assessed to identify the average number of interviews per applicant ( $n = 14$ ). Using these data, the cost of Electronic Residency Application Services (ERAS) applications, transportation (flight costs, Uber rides), and hotel stay was analyzed to estimate the total cost of in-person or virtual interviews. The cost of interviewing at 14 programs and at 20 programs (maximum rank list size without increased ERAS financial toxicity) was calculated regionally and broadly throughout the US.

#### RESULTS

The estimated total cost of interviewing at 14 programs in-person is \$8,151 compared to \$944 virtually, yielding a per-interview cost of \$582.21 in-person versus \$67.43 virtually. For applicants desiring to interview at 20 programs, the cost of in-person interviews increases to \$10,986 while remaining at \$944 virtually. This translates to a per-interview cost of \$549.30 in-person versus \$47.20 virtually to maximize rank list size.

#### CONCLUSION

The financial toxicity for applicants applying to the average number of radiation oncology interviews is nearly 9 times more for in-person versus virtual interviews; this increases to nearly 12 times more toxicity for applicants interviewing at 20 programs.

#### CLINICAL RELEVANCE/APPLICATION

The virtual interview process substantially decreases financial toxicity, allowing applicants to interview at approximately 10 programs virtually per one program in-person. This sizeable increase in opportunity has the potential to increase the diversity, equity, and inclusion of medicine by decreasing the longstanding financial limitations facing residency applicants of lower socioeconomic status.

#### S3A-SPNPM-Predictors of Workforce Paid Time-off and Productivity Lost After COVID MRNA Vaccination Within a Department of Radiology at a Large Academic Hospital<sup>2</sup>

##### Participants

Moses Flash, Boston, MA (*Presenter*) Nothing to Disclose

#### PURPOSE

Hospitals have implemented COVID vaccination requirements for employees. The BNT162b2 (Pfizer) and mRNA-1273 (Moderna) mRNA vaccines have demonstrated high effectiveness but cause transient reactogenicity that can require time off work to recover. We aimed to identify predictors of requiring post-vaccination sick leave and to determine the cost of productivity loss with mandatory vaccination of hospital employees.

#### METHODS AND MATERIALS

An IRB-approved, HIPAA-compliant survey was sent to all 2,655 employees of the radiology department of a large academic hospital to assess vaccine side effects and whether sick leave was required. Logistic regression identified factors associated with requiring sick leave. A budget impact analysis compared productivity loss with mandatory vs non-mandatory vaccination over the course of one year. Sick leave duration, vaccine efficacy, and vaccine uptake were varied in a sensitivity analysis.

#### RESULTS

Among the 477 (18%) employees who completed surveys, the majority experienced symptoms after each dose (dose 1, 81.3%;

dose 2, 89.5%). 188 (39.4%) employees required a total of 339.5 days of sick leave (0.74 days/employee among all respondents; Table 1). On multivariate logistic regression, factors associated with taking sick leave were receiving the Moderna vaccine (odds ratio [OR], 1.89; P=.01), the number of symptoms after dose 1 (1-2: OR, 2.57; P=.006; 5+: 2.46, P=.05) and dose 2 (3-4: OR, 7.99; P=.001; 5+: OR, 23.34; P<.001), underreporting symptoms to the employer (OR, 0.10; P<.001) and injection site symptoms after dose 1 (OR, 0.50; P=.01). At the base rates of vaccine-related sick leave, vaccine uptake, and vaccine efficacy, annual productivity losses were \$115,647 with mandatory vaccination and \$128,594 without mandatory vaccination, yielding a cost benefit of \$12,947 with mandatory vaccination among the 352 employees with available salary data. Sensitivity analyses demonstrated a cost benefit with mandatory vaccination across a wide range of vaccine efficacies, uptakes, and sick-leave durations.

## **CONCLUSION**

s Despite the high rate of reactogenicity after vaccination requiring 339.5 days of sick leave, mandatory vaccination of healthcare employees was associated with an annual cost benefit across a wide range of sick leave durations, vaccine efficacies, and uptakes.

## **CLINICAL RELEVANCE/APPLICATION**

With COVID now endemic, seasonal vaccination may be necessary for hospital workers. However, vaccine reactogenicity places strain on staffing productivity, affecting patient care. We evaluated productivity loss with mandatory vs non-mandatory vaccination for hospital workers.

Printed on: 02/07/23



## Abstract Archives of the RSNA, 2022

S3A-SPNPM-1

### Financial Toxicity Analysis of Virtual Versus In-Person Radiation Oncology Residency Interviews

Sunday, Nov. 27 11:45AM - 12:15PM Room: Learning Center - NPM DPS

#### Participants

Yorleny Vicioso Mora, MD, PhD, (*Presenter*) Nothing to Disclose

#### PURPOSE

Recent work has indicated that medical students may take loans of up to \$7,000 to offset costs related to the residency match interview process. Because of the COVID-19 pandemic, US residency programs starting with the 2021 match cycle have adopted virtual interviews as replacements for in-person interviews. The financial toxicity of virtual versus in-person interviews for Radiation Oncology is addressed in the following cost analysis.

#### METHODS AND MATERIALS

Previous literature (including national 2019-2022 Radiation Oncology residency match statistics) was assessed to identify the average number of interviews per applicant ( $n = 14$ ). Using these data, the cost of Electronic Residency Application Services (ERAS) applications, transportation (flight costs, Uber rides), and hotel stay was analyzed to estimate the total cost of in-person or virtual interviews. The cost of interviewing at 14 programs and at 20 programs (maximum rank list size without increased ERAS financial toxicity) was calculated regionally and broadly throughout the US.

#### RESULTS

The estimated total cost of interviewing at 14 programs in-person is \$8,151 compared to \$944 virtually, yielding a per-interview cost of \$582.21 in-person versus \$67.43 virtually. For applicants desiring to interview at 20 programs, the cost of in-person interviews increases to \$10,986 while remaining at \$944 virtually. This translates to a per-interview cost of \$549.30 in-person versus \$47.20 virtually to maximize rank list size.

#### CONCLUSION

The financial toxicity for applicants applying to the average number of radiation oncology interviews is nearly 9 times more for in-person versus virtual interviews; this increases to nearly 12 times more toxicity for applicants interviewing at 20 programs.

#### CLINICAL RELEVANCE/APPLICATION

The virtual interview process substantially decreases financial toxicity, allowing applicants to interview at approximately 10 programs virtually per one program in-person. This sizeable increase in opportunity has the potential to increase the diversity, equity, and inclusion of medicine by decreasing the longstanding financial limitations facing residency applicants of lower socioeconomic status.

Printed on: 02/07/23



## Abstract Archives of the RSNA, 2022

S3A-SPNPM-2

### Predictors of Workforce Paid Time-off and Productivity Lost After COVID mRNA Vaccination Within a Department of Radiology at a Large Academic Hospital

Sunday, Nov. 27 11:45AM - 12:15PM Room: Learning Center - NPM DPS

#### Participants

Moses Flash, Boston, MA (*Presenter*) Nothing to Disclose

#### PURPOSE

Hospitals have implemented COVID vaccination requirements for employees. The BNT162b2 (Pfizer) and mRNA-1273 (Moderna) mRNA vaccines have demonstrated high effectiveness but cause transient reactogenicity that can require time off work to recover. We aimed to identify predictors of requiring post-vaccination sick leave and to determine the cost of productivity loss with mandatory vaccination of hospital employees.

#### METHODS AND MATERIALS

An IRB-approved, HIPAA-compliant survey was sent to all 2,655 employees of the radiology department of a large academic hospital to assess vaccine side effects and whether sick leave was required. Logistic regression identified factors associated with requiring sick leave. A budget impact analysis compared productivity loss with mandatory vs non-mandatory vaccination over the course of one year. Sick leave duration, vaccine efficacy, and vaccine uptake were varied in a sensitivity analysis.

#### RESULTS

Among the 477 (18%) employees who completed surveys, the majority experienced symptoms after each dose (dose 1, 81.3%; dose 2, 89.5%). 188 (39.4%) employees required a total of 339.5 days of sick leave (0.74 days/employee among all respondents; Table 1). On multivariate logistic regression, factors associated with taking sick leave were receiving the Moderna vaccine (odds ratio [OR], 1.89;  $P=.01$ ), the number of symptoms after dose 1 (1-2: OR, 2.57;  $P=.006$ ; 5+: 2.46,  $P=.05$ ) and dose 2 (3-4: OR, 7.99;  $P=.001$ ; 5+: OR, 23.34;  $P<.001$ ), underreporting symptoms to the employer (OR, 0.10;  $P<.001$ ) and injection site symptoms after dose 1 (OR, 0.50;  $P=.01$ ). At the base rates of vaccine-related sick leave, vaccine uptake, and vaccine efficacy, annual productivity losses were \$115,647 with mandatory vaccination and \$128,594 without mandatory vaccination, yielding a cost benefit of \$12,947 with mandatory vaccination among the 352 employees with available salary data. Sensitivity analyses demonstrated a cost benefit with mandatory vaccination across a wide range of vaccine efficacies, uptakes, and sick-leave durations.

#### CONCLUSION

Despite the high rate of reactogenicity after vaccination requiring 339.5 days of sick leave, mandatory vaccination of healthcare employees was associated with an annual cost benefit across a wide range of sick leave durations, vaccine efficacies, and uptakes.

#### CLINICAL RELEVANCE/APPLICATION

With COVID now endemic, seasonal vaccination may be necessary for hospital workers. However, vaccine reactogenicity places strain on staffing productivity, affecting patient care. We evaluated productivity loss with mandatory vs non-mandatory vaccination for hospital workers.

Printed on: 02/07/23

## Abstract Archives of the RSNA, 2022

S3A-SPNR

### Neuroradiology Sunday Poster Discussions - A

Sunday, Nov. 27 11:45AM - 12:15PM Room: Learning Center - NR DPS

#### Sub-Events

#### S3A-SPNR-1 Morphologic, Microstructural, and Connectomic Correlates of Attention-Deficit/Hyperactivity Disorder in Adolescents

Participants

Huang Lin, New Haven, CT (*Presenter*) Nothing to Disclose

#### PURPOSE

To investigate microstructural, morphological, and functional connectivity correlates of ADHD on brain MRI of adolescents.

#### METHODS AND MATERIALS

We retrieved the imaging and clinical information of 1,830 subjects with ADHD and 6,067 without ADHD from the ABCD (<https://abcdstudy.org/>) database of 11,876 adolescents - participants' average (SD) age was 118.94 (7.46) months. We excluded those with incomplete clinical information, history of traumatic brain injury, and failure to pass image quality control. In multivariate logistic regression adjusted for age and sex, we examined the association of ADHD with different neuroimaging metrics. The neuroimaging metrics included fractional anisotropy (FA), neurite density (ND), mean-(MD), radial-(RD) and axial diffusivity (AD) of white matter (WM) tracts, cortical region thickness and surface areas from T1-MPRAGE series, and functional network connectivity correlations from resting-state fMRI. We applied False Discovery Rate (FDR) to correct for multiple comparisons. We also optimized, trained, tested, and validated different combinations of machine learning classifiers and feature selection algorithms for prediction of ADHD.

#### RESULTS

Individuals with ADHD had a significantly (adjusted  $p < 0.05$ ) lower FA and ND but higher MD and RD -predominantly in left hemispheric WM tracts compared to those without ADHD. Presence of ADHD was associated with reduced cortical regions, especially in the right middle temporal gyrus (adjusted  $p < 0.001$ ). The auditory-, cingulo-parietal, ventral-/dorsal-attention and default-network differed between those with and without ADHD. In repeated 10-fold cross-validation, a combination of elastic net logistic regression with hierarchical clustering feature selection yielded the highest and most stable performance, attaining an AUC of 0.6085, 95% CI [0,5757, 0,6414], in predicting ADHD in an independent validation set.

#### CONCLUSION

Abnormal functional connectivity, involving networks related to memory processing, tonic alertness, and the auditory process, thinning of brain cortex, and WM tract neural fiber loss and microarchitectural disintegrality are markers of adolescents' ADHD. Multi-modal neuroimaging metrics can be used as input for machine learning models to support identification of at-risk children.

#### CLINICAL RELEVANCE/APPLICATION

Using a large population cohort, we elucidated the underlying neurobiology of adolescents' ADHD and suggest a possible role for neuroimage-based machine-learning models to assist with diagnosis.

#### S3A-SPNR-10 The Influence of Alcohol On In Utero Brain Development: A Structural Fetal MRI Study

Participants

Patric Kienast, Wien, Austria (*Presenter*) Nothing to Disclose

#### PURPOSE

Alcohol consumption during pregnancy affects brain development leading to a variety of behavioral and cognitive disorders. However, early structural alterations of fetal brain development have not yet been systematically studied. This prospective single center fetal MRI study aims to assess the effects of alcohol exposure on brain development.

#### METHODS AND MATERIALS

After inclusion of 20 fetal MRI studies of fetuses with prenatal alcohol exposure (PAE, 22+1 - 36+4 weeks of gestation (GW)) due to the standardized systematic questionnaires (TACE and PRAMS). These cases were 1:1 age-matched to a healthy control case. Brain maturation was assessed by using the fetal total maturation score (fTMS) (Vossough et al. 2013) based on superresolution-postprocessed T2-weighted/SSFP sequences in 3 planes (1.5T). In addition, the depth of temporal and occipital sulci and the expression of fetal brain asymmetry in the temporal lobe were quantified.

#### RESULTS

In PAE fetuses, the fTMS score was significantly lower ( $p = 0.007$ ) and the right superior temporal sulcus (STS) was shallower ( $p < 0.001$ ). Delayed fetal brain development could be specifically related to an age inappropriate/delayed stage of myelination and

less distinct gyrfication in the frontal and occipital lobes ( $p=0.04$ ).

## CONCLUSION

This fetal MRI study revealed an early impact of PAE on structural fetal brain maturation and development. In addition to alterations of the periventricular zone and the corpus callosum detectable by atlas based analysis (Stuempflen et al. RSNA 2021), this study emphasizes early and diffuse alterations to fetal structural brain development and delayed brain maturation in fetuses affected by maternal alcohol consumption.

## CLINICAL RELEVANCE/APPLICATION

Identification of the teratologic toxic effects on human brain development opens new diagnostic opportunities for fetal neuroradiology, allowing early postnatal support programs in these cases and stimulating the discussion of alcohol prevention during pregnancy to promote public health.

### S3A-SPNR-12 Evaluation of Glymphatic System Activity Using Diffusion Tensor Image Analysis Along the Perivascular Space (DTI-ALPS) in Cognitively Normal Older Adults: Correlation with Amyloid PET

Participants

Chae Jung Park, MD, (Presenter) Nothing to Disclose

## PURPOSE

Diffusion Tensor Image-Analysis aLong the Perivascular Space (DTI-ALPS) is a recently introduced method for the assessment of glymphatic system without need for contrast injection. In this study, we aimed to evaluate the glymphatic system in cognitively normal elderly adults using DTI-ALPS, by correlating it with amyloid PET.

## METHODS AND MATERIALS

In this prospective study, total 123 cognitively normal elderly adults with or without subjective cognitive decline (SCD) were recruited through advertisement in communities. They performed baseline cognitive test, MRI and PET. On DTI-MRI, the diffusivities along x-, y-, and z-axes were measured, and the ALPS-index was calculated. To measure the amyloid deposition from PET, standardized uptake value ratios (SUVR) were calculated from variable cortical regions. The differences in the ALPS-index between normal and SCD group were compared using the Mann-Whitney test. Pearson's correlation was used to analyze the correlation between ALPS-index and SUVRs. Multiple linear regression was performed to assess the association between ALPS-index and other relevant variables - age, duration of education, Mini-Mental State Examination score, presence of Apolipoprotein e4 allele and SUVRs.

## RESULTS

Among total 123 subjects, 63 were asymptomatic (mean age, 73.0 years  $\pm$  4.2 [standard deviation], 43 men) and 60 had SCD (mean age, 73.7 years  $\pm$  3.5, 41 men). The ALPS-index was not significantly different between the normal and SCD group ( $1.34 \pm 0.13$  vs.  $1.34 \pm 0.12$ ,  $P = 0.897$ ). Among SUVRs from variable cortices, SUVR from paracentral cortex was the only variable which was negatively correlated with ALPS-index ( $r = -0.218$ ,  $P = 0.016$ , figure). Multiple linear regression revealed that older age (coefficient,  $-0.007$ ) and increased SUVR from paracentral cortex (coefficient,  $-0.101$ ) were the two independent variables which had significant association with lower ALPS-index ( $P = 0.015$  and  $0.049$ , respectively).

## CONCLUSION

The ALPS-index was not significantly different between the normal and SCD group. Correlating DTI-ALPS with amyloid PET revealed that increased amyloid deposition in the paracentral cortex was significantly associated with lower ALPS-index, which gives the notion that the clearance in paracentral cortex might play an important role in the glymphatic system.

## CLINICAL RELEVANCE/APPLICATION

In this study, we correlated DTI-ALPS with amyloid PET in cognitively normal elderly adults for better understanding of glymphatic system. We found that older age and increased amyloid deposition in the paracentral cortex identified from PET were significantly associated with lower ALPS-index. It implies that the clearance in paracentral cortex might have a significant impact on glymphatic system.

### S3A-SPNR-13 Analysis of Neurite Orientation Dispersion and Density Imaging (NODDI) Parameters for Assessing the Hippocampal Neurodegenerative Progression in Early Alzheimer's Disease, Compared to Cerebrospinal Fluid (CSF) Level of Phosphorylated tau (P-tau)

Participants

Hiroto Takahashi, MD, Suita, Japan (Presenter) Nothing to Disclose

## PURPOSE

Cerebrospinal fluid (CSF) phosphorylated tau (p-tau) is sensitive to neurodegeneration in Alzheimer's disease (AD), but its measurement is invasive. Neurite orientation dispersion and density imaging (NODDI) is a diffusion magnetic resonance imaging (MRI) technique which assumes a three-compartment (intracellular, extracellular, and CSF) biophysical tissue model for each voxel, and can provide specific data on neuronal changes. We aimed to explore the imaging biomarker that supports the CSF biomarker for evaluating disease progression in early AD.

## METHODS AND MATERIALS

Sixty-nine patients with mild cognitive impairment underwent both CSF measurement of A $\beta$ 42 and p-tau and multi-shell diffusion MRI at 3T. Based on the CSF A $\beta$ 42 and p-tau values, 35 patients with AD pathology (group AD) were discriminated from 34 patients with non-AD pathology (group non-AD). The NODDI and diffusion tensor imaging (DTI) parametric maps were generated from the obtained diffusion MRI data. Two neuroradiologists created the region of interest (ROI) of each side of hippocampus, separately. The hippocampal values were calculated using the ROIs. Inter-ROI value correlations between two neuroradiologists were calculated for the intraclass correlation coefficients (ICCs). Correlations between each hippocampal value and the CSF p-tau value were assessed using Pearson's correlation analysis.

## RESULTS

Almost all the ICCs were substantial or almost perfect, besides the ICCs of the NODDI-derived isotropic volume fraction, throughout the group. There were significant correlations between the NODDI-derived orientation dispersion index (ODI) of the right hippocampal ROIs and the CSF p-tau value in the group AD ( $P < 0.05$ ), whereas no significant correlation was shown in any other hippocampal value. The NODDI-derived intracellular volume fraction, the DTI-derived fractional anisotropy and axial diffusivity correlated weakly with the CSF p-tau value in the group AD.

## CONCLUSION

s Present hippocampal ROI analysis indicated that diffusion MRI parameters, especially the right hippocampal ODI, might support the CSF p-tau measurement and be useful biomarker for evaluating disease progression in early AD.

## CLINICAL RELEVANCE/APPLICATION

The hippocampal NODDI parameter might be a useful imaging biomarker for assessing neurodegenerative progression with the CSF p-tau elevation in early AD.

## S3A-SPNR- Cognitive Impairment and Amygdala Sub-regions Atrophy in Patients with End-stage Renal Disease 14

Participants

Yuan Li, Dalian, China (*Presenter*) Nothing to Disclose

## PURPOSE

Cognitive dysfunction is prevalent in end-stage renal disease (ESRD) patients, and the amygdala plays an important role in cognition. This study aimed to compare the volume of the amygdala subregions between ESRD patients and healthy controls (HCs), and to analyze the correlations of subregion volumes with cognitive function.

## METHODS AND MATERIALS

Forty-nine ESRD patients and 41 age, gender, education matched HCs were recruited. All subjects were scanned using a 3T MRI to acquire 3D T1 anatomical images. Automatic volumetric measurement of the amygdala subregions was done using FreeSurfer 7.0. The amygdala was segmented, bilaterally, into the lateral nucleus, basal nucleus, accessory basal nucleus, anterior amygdaloid area, central nucleus, medial nucleus, cortical nucleus, corticoamygdaloid transition area, and paralamina nucleus (Figure 1). Thirty-four ESRD patients and 16 HCs underwent neuropsychological examinations. The amygdala subregion volumes and cognitive test results were compared between the two groups using an independent sample t-test. Partial correlation analysis was used to assess correlations between the amygdala subregion volumes and cognitive test scores in the ESRD group, with sex, age and education level as covariates.

## RESULTS

The volumes of the amygdala subregions were decreased in the ESRD group (Figure 2-3), especially the bilateral accessory basal nucleus (left:  $P=0.028$ , right:  $P=0.019$ ) and bilateral corticoamygdaloid transition area (left:  $P=0.033$ , right:  $P=0.009$ ) (Table 1). Compared with HCs, ESRD patients had lower MoCA ( $P<0.001$ ) and DSST ( $P=0.030$ ) scores but higher TMT-B ( $P=0.017$ ), HAMA ( $P=0.030$ ) and HAMD ( $P=0.001$ ) scores (Table 2). The partial correlation analysis showed that the volume of the right lateral nucleus was negatively correlated with TMT-A scores ( $P=0.010$ ,  $r=-0.390$ ), as well as those of the left paralamina nucleus, the right basal nucleus and the right paralamina nucleus were positively correlated with immediately recall scores ( $P=0.047$ ,  $r=0.305$ ;  $P=0.046$ ,  $r=0.306$ ;  $P=0.036$ ,  $r=0.321$ ).

## CONCLUSION

s ESRD patients are accompanied by cognitive impairment, anxiety and depression. Patients with ESRD develop atrophy of the amygdala subregions, which is related to impaired visuospatial function and short-term memory performance.

## CLINICAL RELEVANCE/APPLICATION

Previous studies were based on the overall amygdala structure, but since the amygdala consists of several subregions, it cannot accurately reflect the subtle changes by measuring the whole volume of the amygdala. Therefore, it is essential to further explore the effects of specific substructures by automatic volumetric segmentation of the amygdala subregions, which is a stable and reproducible quantitative measurement.

## S3A-SPNR- Correlation Hippocampal Subfields Alterations and Metabolic-neurologic Changes in Patients with Type 2 Diabetes Mellitus 15

Participants

Jiajun Cao, (*Presenter*) Nothing to Disclose

## PURPOSE

To explore the changes of the volume and asymmetry of hippocampal subfields in patients with type 2 diabetes mellitus and the correlation between the significantly atrophied regions of the hippocampal subfields and clinical data, laboratory indicators, cerebral small vessel diseases scores and cognitive scores was analyzed.

## METHODS AND MATERIALS

Thirty-one patients with T2DM and 24 volunteers as the control group were prospectively recruited into this present study. T1WI, T2WI, T2Flair and 3DT1WI sequences were performed using Philips Ingenia CX3.0T MRI scanner. The clinical data and laboratory indicators of all subjects were recorded, including gender, age, height, weight, waist circumference, hip circumference, systolic blood pressure, diastolic blood pressure, education level, insulin, fasting glucose, glycated hemoglobin, total cholesterol, triglyceride, low density lipoprotein, high density lipoprotein, homocysteine acid. Meanwhile, body mass index and waist hip ratio were calculated. CSVD MRI features of all subjects were scored quantitatively including: periventricular hyperintense and deep white matter hyperintense grades, basal ganglia enlarged perivascular space and centrum-semiovale enlarged perivascular space grades, the grade of lacune and the grade of cerebral microbleed, and the CSVD total burden scores were calculated. Detailed neuropsychological scale assessment was performed on all subjects, including the mini-mental state examination, Montreal cognitive assessment, California verbal learning test, symbol digit modalities test. FreeSurfer (version 6.0.0, <http://surfer.nmr.mgh.harvard.edu/>) software was used for imaging post-processing. The volume of all

subjects' hippocampal subfields and hippocampal asymmetry index were calculated.

## RESULTS

Compared with the control group, the volumes of left presubiculum, left fimbria and left hippocampal amygdala transition area were significantly decreased in the T2DM group ( $p=0.041, p=0.048, p=0.030$ ), HAI decreased in cornu ammonis 1, but increased in HATA area ( $p=0.029, p=0.023$ ). Partial correlation analysis was carried out between the volume of left presubiculum, left fimbria, left HATA volume and clinical data, laboratory indicators, cognitive score and CSVD quantitative score, age, gender and years of education were taken as covariates.

## CONCLUSION

The atrophy of hippocampal subfields is asymmetric, and the volume of hippocampal subfields is closely related to metabolic syndrome, increased burden of CSVD and decline of cognitive function.

## CLINICAL RELEVANCE/APPLICATION

The atrophy of hippocampal subfields is asymmetric, and the volume is closely related to metabolic syndrome, increased burden of CSVD and decline of cognitive function.

## S3A-SPNR- Connectome-based Models Predict Cognitive Functions in Systemic Lupus Erythematosus 17

Participants

Jiaying Mo, (*Presenter*) Nothing to Disclose

## PURPOSE

Systemic lupus erythematosus (SLE) is a mainly female inflammatory autoimmune disorder that can affect the central nervous system and cognitive functions in up to 80% of patients. This study aims to investigate whether the topological network of functional connectivity can predict the performance of neuropsychological tests in different domains, using connectome-based predictive modeling (CPM).

## METHODS AND MATERIALS

We evaluated 61 SLE patients who underwent a resting-state functional MRI scanning in a Philips Achieva 3T MRI system and a comprehensive neuropsychological assessment for the four cognitive domains of verbal, visuospatial, visual memory, and attention. According to the Brainnetome atlas, ROI-based functional connectivity analysis was employed to extract the whole-brain functional networks. CPM with leave-one-out cross-validation was conducted to identify different networks that predicted the performance of neuropsychological tests. The predictive ability of identified networks would be tested in an independent sample of patients who were scanned in a different 3T MRI system (uMR 780, United Imaging Healthcare, Shanghai, China).

## RESULTS

Four CPM models enabled prediction of neuropsychological scores for unseen subjects in cross-validation, with Pearson's correlation coefficients  $r$  of 0.40-0.48 (all  $p$  values  $< 0.001$ ). In these four cognitive function predictions, brain connectivities that show top contributing power commonly concentrated on the hippocampus, parahippocampal gyrus, superior frontal gyrus, medial frontal gyrus, inferior parietal lobule, and insula, which were the key nodes of the default-mode network and salience network. Moreover, the CPM models based on these important brain regions could predict overall cognitive ability (MoCA score;  $r = 0.45, p < 0.001$ ).

## CONCLUSION

Our results provide preliminary evidence that different functional networks with overlapping of important brain regions including frontal lobe, parietal lobe, insular lobe and several subcortical regions may contribute to cognitive ability of various domains and allow to predict the corresponding cognitive functions in SLE.

## CLINICAL RELEVANCE/APPLICATION

CPM identified brain networks that underlie different cognitive functions in individuals and these "neural fingerprints" could potentially assist the diagnosis of cognitive dysfunction in SLE.

## S3A-SPNR- Associations of Cortical Iron Accumulation with Cognition and Cerebral Atrophy in Alzheimer's 18 Disease

Participants

Aocai Yang, Beijing, China (*Presenter*) Nothing to Disclose

## PURPOSE

Cerebral iron accumulation is consistently observed in Alzheimer's disease and co-localizes with the pathological proteins—amyloid- $\beta$  and tau. We aimed to investigate the whole-brain distributional pattern of cortical iron deposition and its relationships with cognition and cortical thickness in Alzheimer's disease via Quantitative Susceptibility Mapping (QSM).

## METHODS AND MATERIALS

We prospectively recruited 30 participants with Alzheimer's disease (AD) and 26 age- and sex-matched healthy controls (HC) in this cross-sectional study. All the participants underwent QSM and structural T1 examinations on 3.0T MRI scanner. Mini-Mental State Examination (MMSE) and Montreal Cognitive Assessment (MoCA) were used to assess the global cognitive level. The whole-brain cross-sectional QSM analysis and the whole-brain QSM regression analyses against MMSE and MoCA scores were performed. Additionally, we conducted a surface-based morphometry analysis. Subsequently, in the significant atrophy regions, we compared the magnetic susceptibility between two groups and assessed the association of magnetic susceptibility with cortical thickness.

## RESULTS

The whole-brain QSM cross-sectional analysis demonstrated that widespread susceptibility increased in AD across the cortical ribbon, asymmetrically covering left hemisphere cerebral cortex, caudate nucleus, putamen and partial cerebellar cortex. The whole-brain QSM regression analyses showed increased susceptibility that covaried with lower MMSE and MoCA scores in AD, and was predominantly located in the right parietal cortex and lateral occipital cortex. The reduced cortical thickness was located in the

left superior temporal, right frontal pole, fusiform and pars opercularis in AD and the corresponding susceptibility increased in right frontal pole (AD:0.034±0.007ppm, HC:0.030±0.005ppm; P=0.016) and pars opercularis (AD:0.020±0.003ppm, HC:0.017±0.002ppm; P=0.002). Susceptibility was negatively correlated with cortical thickness in right pars opercularis in both entire cohort (r=-0.521, P<0.001) and AD (r=-0.510, P=0.005).

## CONCLUSION

Widespread cortical iron, measured by QSM, accumulated in Alzheimer's disease and was associated with poor cognitive performance. Increased iron content was associated with brain atrophy in AD. QSM may be a useful imaging biomarker to monitor the neurodegenerative progression of AD.

## CLINICAL RELEVANCE/APPLICATION

Increased iron content was associated with cortical atrophy and cognitive level in Alzheimer's disease. These may be useful to monitor the disease progression and cognitive severity of Alzheimer's disease at the whole brain level in vivo, and provide new insights into the application of QSM as a disease biomarker.

## S3A-SPNR-19 Classification of Major Depression Disorder Based on Integrated Temporal and Spatial Variability Features of Dynamic Brain Networks

Participants  
Qun Gai, (Presenter) Nothing to Disclose

## PURPOSE

The dynamics of brain networks has been a focus in the study of depression in recent years. However, most previous studies focused on single temporal dimension only, ignoring spatial dimension information. The present study aimed to integrate temporal and spatial variability features of dynamic brain networks to distinguish patients with major depressive disorder (MDD) from healthy controls (HC).

## METHODS AND MATERIALS

245 MDD subjects and 230 well-matched HC were recruited in this study (the discovery cohort: 119 MDD and 106 HC, the validation cohort: 126 MDD and 124 HC). Temporal and spatial variability features were extracted from dynamic brain networks as features. A two-level feature selection strategy and random forest (RF) were employed for classification. Two other classifiers were also applied to validate our model. Furthermore, a linear regression model for assessing MDD symptom severity was established based on above selected temporal and spatial features.

## RESULTS

Our model based on the integration of temporal and spatial variability features achieved the best performance with an accuracy of 93.33% (an accuracy of 83.40% for an independent sample). Moreover, features with high discriminative power to distinguish MDD from HC showed strong association with the visual network (VIS) and cognitive control network (CCN). Importantly, altered temporal and spatial variability could predict depression and anxiety severity of MDD.

## CONCLUSION

Our results demonstrate that integrating temporal and spatial variability features can discriminate MDD from HC with a high classification performance and suggest that spatiotemporal dynamics may explain underlying neurobiological mechanism of MDD symptoms.

## CLINICAL RELEVANCE/APPLICATION

Our findings provide direct evidence that spatiotemporal dynamics could be used as effective biomarkers for clinical diagnosis of MDD and may play an important role in detecting depression and anxiety symptom severity of MDD.

## S3A-SPNR-2 Evaluation and Clinical Validation of a Deep Learning Algorithm for Predicting Delayed Myelination in Infant Brains from MRI

Participants  
Gunvant Chaudhari, BS, San Francisco, CA (Presenter) Nothing to Disclose

## PURPOSE

Assisting diagnosis of infant delayed myelination by creating a convolutional neural network (CNN) capable of predicting delayed myelination based on routine clinical T1T2-weighted brain MRIs.

## METHODS AND MATERIALS

MRIs were obtained from our institutional clinical database. Patients aged 0-25 months with reportedly normal myelination from 1995-2019 (n=5028) and delayed myelination from 1995-2021 (n=426) were included. For normal myelination MRIs, exclusion criteria included uneven age distribution (N=2659), myelination at the lower limits of normal (N=46), missing gestationally corrected age (GCA, N=1352), poor automated skullstripping or registration (N=103), and lack of T1 or T2 imaging (N=252). For delayed myelination MRIs, MRIs missing GCA (N=162), with poor automated skullstripping or registration (N=19), and without T1 or T2 imaging (N=121) were excluded. The CNN had input of paired, registered T1 T2 MRIs and GCA and was trained to predict delayed myelination status. Results from 10-fold cross-validation are reported. For a clinical benchmark, 3 neuroradiologists with 3-24 years of experience in pediatric neuroradiology blindly interpreted 30 randomly sampled MRIs, 15 normal and 15 delayed myelination, and assigned numerical values corresponding to confidence of delayed myelination (Figure 1). Ground-truth myelination status was defined as the average of 3 radiologists' and report label values.

## RESULTS

The dataset consisted of 616 infant brain MRIs with normal myelination and 124 with delayed myelination. The CNN had an area under the receiver operator characteristic curve (AUC) of 0.77 (95% CI: 0.70-0.84) in cross-validation. In the subset of cases selected for the ready study, the CNN had an AUC of 0.83 (95% CI: 0.66-0.96) compared to 3 neuroradiologists with AUCs of 0.65 (0.45-0.84, p=0.19), 0.66 (0.46-0.85, p=0.19), and 0.78 (0.65-0.90, p=0.60), respectively.

## CONCLUSION

s A CNN can recognize infant delayed myelination using T1- and T2-weighted brain MRI and GCAs, with performance similar to clinical neuroradiologists.

## CLINICAL RELEVANCE/APPLICATION

Determining delayed myelination on infant brain MRI is subjective, especially for radiologists without high volume practice in pediatric neuroradiology. An AI system can aid radiologists in this task.

### S3A-SPNR- Hippocampal Atrophy in Neurofunctional Subfields in Chronic Insomnia 20

Participants

Yang Yang, (*Presenter*) Nothing to Disclose

## PURPOSE

To investigate the pattern of volume changes in neurofunctional hippocampal subfields in patients with chronic insomnia (PIs).

## METHODS AND MATERIALS

A total of 120 PIs (78 females, 42 males; mean age $\pm$  std, 43.74  $\pm$  13.02 years) and 120 good sleepers (60 females, 60 males; mean age, 42.69  $\pm$  12.24 years) were recruited. The left hippocampus was segmented into anterior (L1), middle (L2), and posterior (L3) subregions. The right hippocampus was segmented into top anterior (R1), second top anterior (R2), middle (R3), posterior (R4), and last posterior (R5) subregions. Multivariate Logistic regression was used to evaluate hippocampal subfields and the associations with the risk of chronic insomnia. Mediation analyses evaluated mediated associations with post-insomnia negative emotion, insomnia severity, and hippocampal atrophy. A visual easy-to-deploy risk nomogram was used for individual prediction of insomnia risk. All statistical analyses were performed using Matlab; P <0.05 was considered a statistically significant difference.

## RESULTS

Hippocampal atrophy was identified in the L1, R1, and R2. L1 and R2 atrophy each predisposed to an approximate 3-fold higher risk of chronic insomnia (L1, OR: 2.90, 95% CI: [1.24, 6.76], P= 0.014; R2, 2.72 [1.19, 6.20], P= 0.018). Anxiety fully mediates the causal insomnia path, leading to R1 volume atrophy on positive affect. We developed a practical and visual competing risk-nomogram tool for individual prediction of insomnia risk, which stratifies individuals into different levels of insomnia risk with the highest prediction accuracy of 97.4% and an average C-statistic of 0.83.

## CONCLUSION

s Chronic insomnia is associated with hippocampal atrophy in specific neurofunctional subfields that are risk factors for chronic insomnia.

## CLINICAL RELEVANCE/APPLICATION

These findings could broaden our understanding of the etiology of insomnia, help individuals identify their potential risk profile, and guide individuals to take precise actions promptly to prevent the future incidence of insomnia.

### S3A-SPNR-3 Synthetic MRI-based Fast Gray Matter Acquisition T1 Inversion Recovery (FGATIR) Contrasts Identify Neonatal Brainstem Pathways

Participants

Victor Schmidbauer, MD, Vienna, Austria (*Presenter*) Nothing to Disclose

## PURPOSE

Synthetic imaging allows to retrospectively reconstruct different MR contrasts using a single acquisition of a multi-dynamic multi-echo (MDME) sequence. This study aimed to investigate the feasibility of synthetic MRI-based fast gray matter acquisition T1 inversion recovery (FGATIR) contrasts for the qualitative identification of early myelinating neonatal brainstem pathways in vivo.

## METHODS AND MATERIALS

Thirty-one cases of neonatal MRI (median gestational age at birth: 27+0; range, 23+4-41+6) were collected, which included MDME sequences and conventional T1-weighted/T2-weighted sequence acquisitions as a standard-of-reference. MDME-based FGATIR contrasts (TR/TE/TI: 3000/5/410 ms) were generated using the MR data post-processing software SyMRI®. The identification of seven brainstem pathways/regions of interest was assessed on synthetic FGATIR contrasts and conventionally acquired T1-weighted/T2-weighted imaging data: decussation of superior cerebellar peduncle (DSCP); left/right medial lemniscus (ML); left/right central tegmental tract (CTT); and left/right longitudinal medial fascicle (LMF).

## RESULTS

SyMRI® provided FGATIR contrasts of diagnostic quality in 31/31 cases (100%). Based on MDME-based FGATIR contrasts, the DSCP [31/31 (100%)]; left/right ML [31/31 (100%)]; left/right CTT [20/31 (65%)]; and left/right LMF [31/31 (100%)] were reliably identified. Based on conventional T1-weighted contrasts, the DSCP [14/31 (45%)]; left/right ML [25/31 (81%)/23/31 (74%)]; left/right CTT [3/31 (10%)/7/31 (23%)]; and left/right LMF [15/31 (48%)] were reliably identified. Based on conventional T2-weighted contrasts, the DSCP [30/31 (97%)]; left/right ML [30/31 (97%)/29/31 (94%)]; left/right CTT [26/31 (84%)/25/31 (81%)]; and left/right LMF [30/31 (97%)] were reliably identified.

## CONCLUSION

s Synthetic generation of FGATIR contrasts enables reliable radiological identification of neonatal brainstem pathway anatomy in vivo. The investigated MR approach depicts early myelinating tracts more reliable than standard-of-reference contrasts.

## CLINICAL RELEVANCE/APPLICATION

Conventional, T1- and T2-weighted-based MRI currently lacks sensitivity for the reliable assessment of delayed brain myelination in former preterm neonates - therefore, MR approaches that utilize white matter signal suppression contribute to a more sensitive evaluation of myelination patterns at early stages of cerebral development.

### **S3A-SPNR-4 Development of The Orbitofrontal Cortex Through Childhood and Adolescence**

Participants

Zhe Guan, (*Presenter*) Nothing to Disclose

#### **PURPOSE**

The orbitofrontal cortex is an incompletely understood part of the prefrontal cortex linked to adaptive learning and executive processes and known to be key towards successful maturation through adolescence to adulthood. The purpose of this study is to evaluate age-dependence of orbitofrontal cortical volume in a large cohort of young, healthy individuals.

#### **METHODS AND MATERIALS**

High-resolution, structural T1-weighted imaging from 655 healthy individuals (8 to 21 years old) from the Human Connectome Project Development (HCP-D) Study were used. FreeSurfer v6.0.0 measures of orbitofrontal cortical volume provided as part of the HCP dataset were used as well as an investigational deep learning-based, automated segmentation tool, DenseUnet-based Automatic Rapid Tool (DARTS). Pearson correlation coefficients were calculated. Subset analysis of male and female cohorts was performed and size asymmetry was assessed using Student's t test.

#### **RESULTS**

Segmentation data are available from HCP (FreeSurfer) for 415 of the 655 subjects of this cohort. DARTS segmentation was performed in all subjects. 323 subjects (49.3%) were male. We found a significant negative correlation between total orbitofrontal volume and age ( $r = -0.360$ ,  $p < 0.00001$ ;  $r = -0.314$ ,  $p < 0.00001$  using FreeSurfer and DARTS, respectively). For subsegments of the orbitofrontal cortex, the correlations under FreeSurfer and DARTS respectively were  $r = -0.364$ ,  $p < 0.00001$ ;  $r = -0.407$ ,  $p < 0.00001$  (left lateral orbitofrontal),  $r = -0.200$ ,  $p < 0.00001$ ;  $r = -0.033$ ,  $p = 0.396$  (left medial orbitofrontal),  $r = -0.335$ ,  $p < 0.00001$ ;  $r = -0.283$ ,  $p < 0.00001$  (right lateral orbitofrontal), and  $r = -0.329$ ,  $p < 0.00001$ ;  $r = -0.099$ ,  $p = 0.011$  (right medial orbitofrontal). The standard deviation of the total orbitofrontal volumes was lower using DARTS (2.40 mL) compared with FreeSurfer (3.73 mL). Similar trends were observed across males and females. Size asymmetry was noted with the left lateral and medial orbitofrontal cortical volumes being larger than the right ( $p < 0.0001$  using FreeSurfer and DARTS).

#### **CONCLUSION**

s Orbitofrontal cortical volume as measured on MRI decreases with age during childhood and adolescence, suggesting that development of this area is complex and may involve cortical pruning or other anatomic refinement on the way to maturation.

#### **CLINICAL RELEVANCE/APPLICATION**

The orbitofrontal cortex is implicated in the development of adaptive learning and executive responses including stimulus-reinforcer associations. These functions undergo maturation and refinement during childhood and adolescence and unveiling anatomic changes to this area contribute to our understanding of how this process unfolds, potentially aiding identification of developmental aberrations.

### **S3A-SPNR-5 Development of Fetal Ventricular Volume Reference Norms Using nnUNet**

Participants

Minerva Zhou, MD, (*Presenter*) Nothing to Disclose

#### **PURPOSE**

To use deep learning methods to segment and measure ventricular volume of fetal brain MRIs across a wide range of gestational ages.

#### **METHODS AND MATERIALS**

We applied nnU-Net to segment the ventricular system of 91 nonpathologic and 9 pathologic fetal brain MRIs across a variety of gestational ages (19-36 weeks). Twenty fetal brain MRIs from our institution were reconstructed to a high-resolution 3D volume using slice-to-volume reconstruction and then manually segmented and combined with the MICCAI Fetal Tissue Annotation Challenge data to generate a dataset of 100 fetal brain MRI volumes, which were randomly split into 80 training studies and 20 test studies in a 5-fold cross-validation. Performance was assessed using Dice coefficients and volume comparison to manual reference segmentation. A normative reference of ventricular volume across gestational ages was generated using the 91 nonpathologic training studies.

#### **RESULTS**

The nnU-Net predicted segmentation of fetal ventricles across gestational ages with median Dice score of 0.90 (IQR 0.88-0.93; Fig 1A). The automatically computed ventricular volume measurements were highly correlated with manual measurements (Pearson's  $r=0.99$ ,  $P<0.001$ , Fig 1B). A normative range of ventricular volumes across gestational ages was developed using the automated segmentation volumes. All 9 patients with hydrocephalus were predicted to be greater than two standard deviations higher than the age-specific reference mean (Fig 1C).

#### **CONCLUSION**

s Deep learning techniques can be used to provide an objective measure of ventricular volume on fetal brain MRI and identify hydrocephalus based on a normative reference standard.

#### **CLINICAL RELEVANCE/APPLICATION**

This study explores using deep learning techniques to quickly and accurately quantify ventricular volume on fetal brain MRI and subsequently identify pathological volumes.

### **S3A-SPNR-6 Brain Gray Matter Connectome Disorganization in Social Anxiety Disorder**

Participants

Xun Zhang, (*Presenter*) Nothing to Disclose

#### **PURPOSE**

Phenotyping approaches grounded in structural network science can offer advanced insights into neurobiological substrates of psychosis, but this remains to be clarified at the individual level in social anxiety disorder (SAD). Herein, we aimed to investigate the topological organizations of individual structural covariance networks using a novel approach in a homogenous sample of SAD patients, and assess their potential clinical relationship and diagnostic value.

## **METHODS AND MATERIALS**

Forty-nine non-comorbid adult patients with SAD and fifty-three demographically-matched healthy controls (HC) were recruited to obtain clinical evaluation and 3.0-Tesla high-resolution T1-weighted images. We constructed single-subject structural covariance networks based on multivariate morphometry (i.e., cortical thickness, surface area, curvature, and gray matter volume) using a recent novel approach combining probability density estimation and Kullback-Leibler divergence, and estimated their global and nodal network properties via graph theory analysis. Network metrics were compared between SAD and HC groups, and the relationship to clinical characteristics was analyzed. Furthermore, exploratory support vector machine analyses were conducted to discriminate SAD from HC.

## **RESULTS**

Globally, SAD patients showed significantly altered topological characteristics, including higher global efficiency, shorter characteristic path length, and stronger small-worldness. Locally, SAD patients exhibited abnormal nodal degree and efficiency mainly involving left superior frontal gyrus, right superior parietal lobe, right paracentral gyrus, right lingual, right pericalcarine cortex, and left amygdala. Furthermore, altered global and nodal topological metrics were associated with the symptom severity and disease duration in SAD cohort, suggesting a pathophysiological relevance. Graph-based metrics allowed single-subject classification of SAD versus HC with significant accuracy, indicating potential diagnostic efficacy.

## **CONCLUSION**

The topological organization of structural covariance networks was disrupted in SAD in a way that suggests compensatory greater integration of information processing with a more randomly organized brain network, which may extend neurobiological understandings of a system-level brain maturational disruption in SAD.

## **CLINICAL RELEVANCE/APPLICATION**

These results provide structural network insights into the neurobiology of SAD, and may navigate the development of reliable and objective neuroanatomical biomarkers for clinical diagnosis, targeted intervention, and therapeutic efficacy evaluation in SAD.

## **S3A-SPNR-7 Pediatric Low-Grade Glioma Molecular Subtype Identification Based on 3D Probability Distributions of Tumor Location in MRI**

Participants

Farzad Khalvati, PhD, MSc, Toronto, ON (*Presenter*) Board of Directors, MESH Scheduling Inc

## **PURPOSE**

Genetic marker identification of pediatric Low-Grade Glioma (pLGG) is crucial for early prognostication and individualized treatment planning. We propose a method to exploit tumor location in MRI data to identify the most common pLGG subtypes (BRAF V600E mutation vs. BRAF fusion) without using any other information.

## **METHODS AND MATERIALS**

In this REB-approved retrospective study, Fluid-Attenuated Inversion Recovery (FLAIR) sequences of the baseline MRI from 200 patients with pLGG acquired between Jan. 2000 and Dec. 2018 were included. Tumor segmentations were provided by a pediatric neuroradiology fellow and verified by a senior pediatric neuroradiologist. The ground truth molecular subtype labels (BRAF V600E mutation and BRAF fusion) were obtained through biopsy. To build the probability density functions (PDF) of BRAF V600E mutation and BRAF fusion, the 3D binary masks of segmentation in FLAIR images for each class in the training dataset were added together and then normalized. In the test cohort, the probabilities of belonging to each class were calculated by a voxel-wise multiplication of the binary segmentation mask of the test case and the 3D PDF of the corresponding class in the training dataset. We repeated the data split (80/20 for training and test) 100 times and calculated the Area Under ROC Curve (AUROC).

## **RESULTS**

Using only location of the tumor in the FLAIR images, we achieved a mean AUROC of 0.783 with a 95% Confidence Interval (CI) of (0.769, 0.798) over 100 experiments for the classification of BRAF V600E mutation vs. BRAF fusion in pLGG.

## **CONCLUSION**

3D PDFs of tumor subtypes can help create a location-based pipeline for molecular subtype identification of pLGG. While location is ignored in the majority of radiomics and neural-network-based classification models, our results show BRAF V600E mutation and BRAF fusion in pLGG tumors follow different location distributions, which can be utilized for subtype identification.

## **CLINICAL RELEVANCE/APPLICATION**

The location-based subtype identification of pLGG can be used as a stand-alone classifier or as an adjunct to Artificial Intelligence based classification models to allow imaging-based molecular characterization.

## **S3A-SPNR-8 MRI Alterations in Patients with Psychogenic Non-epileptic Seizures: Prevalence, Distribution and Classification of The Findings**

Participants

Alex Jareno Badenas, MD, Sant Vicenc de Castellet, Spain (*Presenter*) Nothing to Disclose

## **PURPOSE**

Psychogenic non-epileptic seizures (PNES) are paroxysmic episodes that mimic epileptic seizures without electroencephalographic representation. Conversive psychiatric origin is attributed to this kind of episode. However, beyond this psychiatric perspective, the possible neurobiological basis of PNES has not received much attention. Some studies have documented structural and functional alterations in these patients, but without consistent results to support a causative hypothesis. The objectives of this study are:-

To evaluate the MRI findings in patients with PNES- To classify the results- To evaluate a possible structural basis of these episodes

## **METHODS AND MATERIALS**

We performed a retrospective analysis of the MRI studies conducted on patients of our epilepsy unit with a confirmed diagnosis of only PNES or PNES and epilepsy (PNES+epilepsy). A descriptive study of the findings in both groups was performed and compared with the incidental findings in the general population obtained from the literature. The radiologic findings were classified into: vascular, tumoral, posttraumatic/gliotic, small vessel, cortical, hippocampal sclerosis, unspecific or normal studies, as well as into epileptogenic and non-epileptogenic.

## **RESULTS**

Our study population was formed of 60 patients with a confirmed diagnosis of PNES and 16 patients with PNES+epilepsy (75% women, 25% men, mean age at diagnostic of 41 years). 55% of patients with PNES and 81% with PNES+epilepsy had a pathological finding. These findings were considered epileptogenic in 13% of the PNES group and in 31% of the PNES+epilepsy group. The most frequent findings in patients with were unspecific, vascular and hippocampal sclerosis, whilst in the PNES+epilepsy group were unspecific, hippocampal sclerosis and small vessel.

## **CONCLUSION**

s Patients with PNES have a higher prevalence of abnormalities in MRI than the general population (around 18% according to existing literature) and this prevalence is even higher when PNES are associated with epilepsy. There is a higher prevalence of PNES among women.

## **CLINICAL RELEVANCE/APPLICATION**

Our study shows higher prevalence of MRI structural findings in patients with PNES than in the general population, suggesting a neurobiological/structural basis in a pathology considered psychiatric.

## **S3A-SPNR-9 The Individual Association Between Functional and Morphological Asymmetry During Fetal Brain Development observed in In-utero MRI**

Participants

Georg Langs, Vienna, Austria (*Presenter*) Co-founder, contextflow GmbH Shareholder, contextflow GmbH

## **PURPOSE**

While function is shaped and constrained by brain structure, there is also possible impacts of functional activity on morphology. At the early stages of life, this relationship is particularly dynamic due to maturational processes and rapid conformational changes of the fetal brain. Cross-sectional studies in the early infancy and newborns suggest that the impaired development of cerebral morphology may promote the recruitment of alternative axonal pathways to sustain function, affecting the integration and specification of functional circuits at both cortical and sub-cortical levels. However, little is known about their complex interplay at the developmentally critical period in utero. Here, we assess the individual association of structural and functional brain development in the fetus.

## **METHODS AND MATERIALS**

Resting-state fMRI and consecutive T2-weighted scans were acquired for 72 singleton fetuses between 19 and 39 weeks of gestation. Data were processed by customized functional- and anatomical image processing pipelines including irregular fetal movement correction, age-specific segmentation, and atlas registration. Individualized functional connectivity (FC) matrices were obtained by correlating regional brain activity over time and individualized local surface folding was quantified by measuring gyrification index (GI). We calculated the morphological and functional laterality indices for each individual subject as the normalized difference of GI and of FC degree between the hemispheres, respectively. The P-values for all evaluations were corrected for multiple comparisons using Benjamini-Yekutieli procedure.

## **RESULTS**

After computational quality benchmarking, 24 cases were excluded and the final study cohort consisted of 48 fetuses that had no confirmed brain abnormalities (mean gestational age  $\pm$ SD: 28.97 $\pm$ 4.84 weeks). We found significant leftward laterality in Temporal-Superior ( $p=0.043$ ), Temporal-Medial ( $p=0.047$ ), and Temporal-Inferior ( $p=0.048$ ) regions after correcting for multiple comparisons. Statistical tests of the functional asymmetry did not reach statistical significance for the rest of cortical regions. Significant morphological asymmetry was found in medial wall ( $p=0.0089$ ) and mesial frontal region ( $p=0.003$ ). We observed significant individual association between functional- and morphological asymmetry in the limbic area ( $p<0.001$  corrected)

## **CONCLUSION**

s Our results support the hypothesis that a significant relationship between brain structure and function is present during prenatal brain development.

## **CLINICAL RELEVANCE/APPLICATION**

It may lead to a better understanding of the neural mechanisms involved in adverse outcomes.

Printed on: 02/07/23

## Abstract Archives of the RSNA, 2022

S3A-SPNR-1

### **Morphologic, Microstructural, and Connectomic Correlates of Attention-Deficit/Hyperactivity Disorder in Adolescents**

Sunday, Nov. 27 11:45AM - 12:15PM Room: Learning Center - NR DPS

#### **Participants**

Huang Lin, New Haven, CT (*Presenter*) Nothing to Disclose

#### **PURPOSE**

To investigate microstructural, morphological, and functional connectivity correlates of ADHD on brain MRI of adolescents.

#### **METHODS AND MATERIALS**

We retrieved the imaging and clinical information of 1,830 subjects with ADHD and 6,067 without ADHD from the ABCD (<https://abcdstudy.org/>) database of 11,876 adolescents - participants' average (SD) age was 118.94 (7.46) months. We excluded those with incomplete clinical information, history of traumatic brain injury, and failure to pass image quality control. In multivariate logistic regression adjusted for age and sex, we examined the association of ADHD with different neuroimaging metrics. The neuroimaging metrics included fractional anisotropy (FA), neurite density (ND), mean-(MD), radial-(RD) and axial diffusivity (AD) of white matter (WM) tracts, cortical region thickness and surface areas from T1-MPRAGE series, and functional network connectivity correlations from resting-state fMRI. We applied False Discovery Rate (FDR) to correct for multiple comparisons. We also optimized, trained, tested, and validated different combinations of machine learning classifiers and feature selection algorithms for prediction of ADHD.

#### **RESULTS**

Individuals with ADHD had a significantly (adjusted  $p < 0.05$ ) lower FA and ND but higher MD and RD -predominantly in left hemispheric WM tracts compared to those without ADHD. Presence of ADHD was associated with reduced cortical regions, especially in the right middle temporal gyrus (adjusted  $p < 0.001$ ). The auditory-, cingulo-parietal, ventral-/dorsal-attention and default-network differed between those with and without ADHD. In repeated 10-fold cross-validation, a combination of elastic net logistic regression with hierarchical clustering feature selection yielded the highest and most stable performance, attaining an AUC of 0.6085, 95% CI [0,5757, 0,6414], in predicting ADHD in an independent validation set.

#### **CONCLUSION**

Abnormal functional connectivity, involving networks related to memory processing, tonic alertness, and the auditory process, thinning of brain cortex, and WM tract neural fiber loss and microarchitectural disintegrity are markers of adolescents' ADHD. Multi-modal neuroimaging metrics can be used as input for machine learning models to support identification of at-risk children.

#### **CLINICAL RELEVANCE/APPLICATION**

Using a large population cohort, we elucidated the underlying neurobiology of adolescents' ADHD and suggest a possible role for neuroimage-based machine-learning models to assist with diagnosis.

Printed on: 02/07/23

## Abstract Archives of the RSNA, 2022

S3A-SPNR-10

### The Influence of Alcohol On In Utero Brain Development: A Structural Fetal MRI Study

Sunday, Nov. 27 11:45AM - 12:15PM Room: Learning Center - NR DPS

#### Participants

Patric Kienast, Wien, Austria (*Presenter*) Nothing to Disclose

#### PURPOSE

Alcohol consumption during pregnancy affects brain development leading to a variety of behavioral and cognitive disorders. However, early structural alterations of fetal brain development have not yet been systematically studied. This prospective single center fetal MRI study aims to assess the effects of alcohol exposure on brain development.

#### METHODS AND MATERIALS

After inclusion of 20 fetal MRI studies of fetuses with prenatal alcohol exposure (PAE, 22+1 - 36+4 weeks of gestation (GW)) due to the standardized systematic questionnaires (TACE and PRAMS). These cases were 1:1 age-matched to a healthy control case. Brain maturation was assessed by using the fetal total maturation score (fTMS) (Vossough et al. 2013) based on superresolution-postprocessed T2-weighted/SSFP sequences in 3 planes (1.5T). In addition, the depth of temporal and occipital sulci and the expression of fetal brain asymmetry in the temporal lobe were quantified.

#### RESULTS

In PAE fetuses, the fTMS score was significantly lower ( $p=0.007$ ) and the right superior temporal sulcus (STS) was shallower ( $p<0.001$ ). Delayed fetal brain development could be specifically related to an age inappropriate/delayed stage of myelination and less distinct gyrification in the frontal and occipital lobes ( $p=0.04$ ).

#### CONCLUSION

s This fetal MRI study revealed an early impact of PAE on structural fetal brain maturation and development. In addition to alterations of the periventricular zone and the corpus callosum detectable by atlas based analysis (Stuempflen et al. RSNA 2021), this study emphasizes early and diffuse alterations to fetal structural brain development and delayed brain maturation in fetuses affected by maternal alcohol consumption.

#### CLINICAL RELEVANCE/APPLICATION

Identification of the teratologic toxic effects on human brain development opens new diagnostic opportunities for fetal neuroradiology, allowing early postnatal support programs in these cases and stimulating the discussion of alcohol prevention during pregnancy to promote public health.

Printed on: 02/07/23

## Abstract Archives of the RSNA, 2022

S3A-SPNR-12

### Evaluation of Glymphatic System Activity Using Diffusion Tensor Image Analysis Along the Perivascular Space (DTI-ALPS) in Cognitively Normal Older Adults: Correlation with Amyloid PET

Sunday, Nov. 27 11:45AM - 12:15PM Room: Learning Center - NR DPS

#### Participants

Chae Jung Park, MD, (*Presenter*) Nothing to Disclose

#### PURPOSE

Diffusion Tensor Image-Analysis along the Perivascular Space (DTI-ALPS) is a recently introduced method for the assessment of glymphatic system without need for contrast injection. In this study, we aimed to evaluate the glymphatic system in cognitively normal elderly adults using DTI-ALPS, by correlating it with amyloid PET.

#### METHODS AND MATERIALS

In this prospective study, total 123 cognitively normal elderly adults with or without subjective cognitive decline (SCD) were recruited through advertisement in communities. They performed baseline cognitive test, MRI and PET. On DTI-MRI, the diffusivities along x-, y-, and z-axes were measured, and the ALPS-index was calculated. To measure the amyloid deposition from PET, standardized uptake value ratios (SUVR) were calculated from variable cortical regions. The differences in the ALPS-index between normal and SCD group were compared using the Mann-Whitney test. Pearson's correlation was used to analyze the correlation between ALPS-index and SUVRs. Multiple linear regression was performed to assess the association between ALPS-index and other relevant variables - age, duration of education, Mini-Mental State Examination score, presence of Apolipoprotein e4 allele and SUVRs.

#### RESULTS

Among total 123 subjects, 63 were asymptomatic (mean age, 73.0 years  $\pm$  4.2 [standard deviation], 43 men) and 60 had SCD (mean age, 73.7 years  $\pm$  3.5, 41 men). The ALPS-index was not significantly different between the normal and SCD group ( $1.34 \pm 0.13$  vs.  $1.34 \pm 0.12$ ,  $P = 0.897$ ). Among SUVRs from variable cortices, SUVR from paracentral cortex was the only variable which was negatively correlated with ALPS-index ( $r = -0.218$ ,  $P = 0.016$ , figure). Multiple linear regression revealed that older age (coefficient,  $-0.007$ ) and increased SUVR from paracentral cortex (coefficient,  $-0.101$ ) were the two independent variables which had significant association with lower ALPS-index ( $P = 0.015$  and  $0.049$ , respectively).

#### CONCLUSION

The ALPS-index was not significantly different between the normal and SCD group. Correlating DTI-ALPS with amyloid PET revealed that increased amyloid deposition in the paracentral cortex was significantly associated with lower ALPS-index, which gives the notion that the clearance in paracentral cortex might play an important role in the glymphatic system.

#### CLINICAL RELEVANCE/APPLICATION

In this study, we correlated DTI-ALPS with amyloid PET in cognitively normal elderly adults for better understanding of glymphatic system. We found that older age and increased amyloid deposition in the paracentral cortex identified from PET were significantly associated with lower ALPS-index. It implies that the clearance in paracentral cortex might have a significant impact on glymphatic system.

Printed on: 02/07/23

## Abstract Archives of the RSNA, 2022

S3A-SPNR-13

### **Analysis of Neurite Orientation Dispersion and Density Imaging (NODDI) Parameters for Assessing the Hippocampal Neurodegenerative Progression in Early Alzheimer's Disease, Compared to Cerebrospinal Fluid (CSF) Level of Phosphorylated tau (P-tau)**

Sunday, Nov. 27 11:45AM - 12:15PM Room: Learning Center - NR DPS

#### **Participants**

Hiroto Takahashi, MD, Suita, Japan (*Presenter*) Nothing to Disclose

#### **PURPOSE**

Cerebrospinal fluid (CSF) phosphorylated tau (p-tau) is sensitive to neurodegeneration in Alzheimer's disease (AD), but its measurement is invasive. Neurite orientation dispersion and density imaging (NODDI) is a diffusion magnetic resonance imaging (MRI) technique which assumes a three-compartment (intracellular, extracellular, and CSF) biophysical tissue model for each voxel, and can provide specific data on neuronal changes. We aimed to explore the imaging biomarker that supports the CSF biomarker for evaluating disease progression in early AD.

#### **METHODS AND MATERIALS**

Sixty-nine patients with mild cognitive impairment underwent both CSF measurement of A $\beta$ 42 and p-tau and multi-shell diffusion MRI at 3T. Based on the CSF A $\beta$ 42 and p-tau values, 35 patients with AD pathology (group AD) were discriminated from 34 patients with non-AD pathology (group non-AD). The NODDI and diffusion tensor imaging (DTI) parametric maps were generated from the obtained diffusion MRI data. Two neuroradiologists created the region of interest (ROI) of each side of hippocampus, separately. The hippocampal values were calculated using the ROIs. Inter-ROI value correlations between two neuroradiologists were calculated for the intraclass correlation coefficients (ICCs). Correlations between each hippocampal value and the CSF p-tau value were assessed using Pearson's correlation analysis.

#### **RESULTS**

Almost all the ICCs were substantial or almost perfect, besides the ICCs of the NODDI-derived isotropic volume fraction, throughout the group. There were significant correlations between the NODDI-derived orientation dispersion index (ODI) of the right hippocampal ROIs and the CSF p-tau value in the group AD ( $P < 0.05$ ), whereas no significant correlation was shown in any other hippocampal value. The NODDI-derived intracellular volume fraction, the DTI-derived fractional anisotropy and axial diffusivity correlated weakly with the CSF p-tau value in the group AD.

#### **CONCLUSION**

Present hippocampal ROI analysis indicated that diffusion MRI parameters, especially the right hippocampal ODI, might support the CSF p-tau measurement and be useful biomarker for evaluating disease progression in early AD.

#### **CLINICAL RELEVANCE/APPLICATION**

The hippocampal NODDI parameter might be a useful imaging biomarker for assessing neurodegenerative progression with the CSF p-tau elevation in early AD.

Printed on: 02/07/23

## Abstract Archives of the RSNA, 2022

S3A-SPNR-14

### Cognitive Impairment and Amygdala Sub-regions Atrophy in Patients with End-stage Renal Disease

Sunday, Nov. 27 11:45AM - 12:15PM Room: Learning Center - NR DPS

#### Participants

Yuan Li, Dalian, China (*Presenter*) Nothing to Disclose

#### PURPOSE

Cognitive dysfunction is prevalent in end-stage renal disease (ESRD) patients, and the amygdala plays an important role in cognition. This study aimed to compare the volume of the amygdala subregions between ESRD patients and healthy controls (HCs), and to analyze the correlations of subregion volumes with cognitive function.

#### METHODS AND MATERIALS

Forty-nine ESRD patients and 41 age, gender, education matched HCs were recruited. All subjects were scanned using a 3T MRI to acquire 3D T1 anatomical images. Automatic volumetric measurement of the amygdala subregions was done using FreeSurfer 7.0. The amygdala was segmented, bilaterally, into the lateral nucleus, basal nucleus, accessory basal nucleus, anterior amygdaloid area, central nucleus, medial nucleus, cortical nucleus, corticoamygdaloid transition area, and paralaminar nucleus (Figure 1). Thirty-four ESRD patients and 16 HCs underwent neuropsychological examinations. The amygdala subregion volumes and cognitive test results were compared between the two groups using an independent sample t-test. Partial correlation analysis was used to assess correlations between the amygdala subregion volumes and cognitive test scores in the ESRD group, with sex, age and education level as covariates.

#### RESULTS

The volumes of the amygdala subregions were decreased in the ESRD group (Figure 2-3), especially the bilateral accessory basal nucleus (left:  $P=0.028$ , right:  $P=0.019$ ) and bilateral corticoamygdaloid transition area (left:  $P=0.033$ , right:  $P=0.009$ ) (Table 1). Compared with HCs, ESRD patients had lower MoCA ( $P<0.001$ ) and DSST ( $P=0.030$ ) scores but higher TMT-B ( $P=0.017$ ), HAMA ( $P=0.030$ ) and HAMD ( $P=0.001$ ) scores (Table 2). The partial correlation analysis showed that the volume of the right lateral nucleus was negatively correlated with TMT-A scores ( $P=0.010$ ,  $r=-0.390$ ), as well as those of the left paralaminar nucleus, the right basal nucleus and the right paralaminar nucleus were positively correlated with immediately recall scores ( $P=0.047$ ,  $r=0.305$ ;  $P=0.046$ ,  $r=0.306$ ;  $P=0.036$ ,  $r=0.321$ ).

#### CONCLUSION

ESRD patients are accompanied by cognitive impairment, anxiety and depression. Patients with ESRD develop atrophy of the amygdala subregions, which is related to impaired visuospatial function and short-term memory performance.

#### CLINICAL RELEVANCE/APPLICATION

Previous studies were based on the overall amygdala structure, but since the amygdala consists of several subregions, it cannot accurately reflect the subtle changes by measuring the whole volume of the amygdala. Therefore, it is essential to further explore the effects of specific substructures by automatic volumetric segmentation of the amygdala subregions, which is a stable and reproducible quantitative measurement.

Printed on: 02/07/23

## Abstract Archives of the RSNA, 2022

S3A-SPNR-15

### Correlation Hippocampal Subfields Alterations and Metabolic-neurologic Changes in Patients with Type 2 Diabetes Mellitus

Sunday, Nov. 27 11:45AM - 12:15PM Room: Learning Center - NR DPS

#### Participants

Jiajun Cao, (Presenter) Nothing to Disclose

#### PURPOSE

To explore the changes of the volume and asymmetry of hippocampal subfields in patients with type 2 diabetes mellitus and the correlation between the significantly atrophied regions of the hippocampal subfields and clinical data, laboratory indicators, cerebral small vessel diseases scores and cognitive scores was analyzed.

#### METHODS AND MATERIALS

Thirty-one patients with T2DM and 24 volunteers as the control group were prospectively recruited into this present study. T1WI, T2WI, T2Flair and 3DT1WI sequences were performed using Philips Ingenia CX3.0T MRI scanner. The clinical data and laboratory indicators of all subjects were recorded, including gender, age, height, weight, waist circumference, hip circumference, systolic blood pressure, diastolic blood pressure, education level, insulin, fasting glucose, glycated hemoglobin, total cholesterol, triglyceride, low density lipoprotein, high density lipoprotein, homocysteic acid. Meanwhile, body mass index and waist hip ratio were calculated. CSVD MRI features of all subjects were scored quantitatively including: periventricular hyperintense and deep white matter hyperintense grades, basal ganglia enlarged perivascular space and centrum-semiovale enlarged perivascular space grades, the grade of lacune and the grade of cerebral microbleed, and the CSVD total burden scores were calculated. Detailed neuropsychological scale assessment was performed on all subjects, including the mini-mental state examination, Montreal cognitive assessment, California verbal learning test, symbol digit modalities test. FreeSurfer (version 6.0.0, <http://surfer.nmr.mgh.harvard.edu/>) software was used for imaging post-processing. The volume of all subjects' hippocampal subfields and hippocampal asymmetry index were calculated.

#### RESULTS

Compared with the control group, the volumes of left presubiculum, left fimbria and left hippocampal amygdala transition area were significantly decreased in the T2DM group ( $p=0.041$ ,  $p=0.048$ ,  $p=0.030$ ), HAI decreased in cornu ammonis 1, but increased in HATA area ( $p=0.029$ ,  $p=0.023$ ). Partial correlation analysis was carried out between the volume of left presubiculum, left fimbria, left HATA volume and clinical data, laboratory indicators, cognitive score and CSVD quantitative score, age, gender and years of education were taken as covariates.

#### CONCLUSION

The atrophy of hippocampal subfields is asymmetric, and the volume of hippocampal subfields is closely related to metabolic syndrome, increased burden of CSVD and decline of cognitive function.

#### CLINICAL RELEVANCE/APPLICATION

The atrophy of hippocampal subfields is asymmetric, and the volume is closely related to metabolic syndrome, increased burden of CSVD and decline of cognitive function.

Printed on: 02/07/23

## Abstract Archives of the RSNA, 2022

S3A-SPNR-17

### Connectome-based Models Predict Cognitive Functions in Systemic Lupus Erythematosus

Sunday, Nov. 27 11:45AM - 12:15PM Room: Learning Center - NR DPS

#### Participants

Jiaying Mo, (*Presenter*) Nothing to Disclose

#### PURPOSE

Systemic lupus erythematosus (SLE) is a mainly female inflammatory autoimmune disorder that can affect the central nervous system and cognitive functions in up to 80% of patients. This study aims to investigate whether the topological network of functional connectivity can predict the performance of neuropsychological tests in different domains, using connectome-based predictive modeling (CPM).

#### METHODS AND MATERIALS

We evaluated 61 SLE patients who underwent a resting-state functional MRI scanning in a Philips Achieva 3T MRI system and a comprehensive neuropsychological assessment for the four cognitive domains of verbal, visuospatial, visual memory, and attention. According to the Brainnetome atlas, ROI-based functional connectivity analysis was employed to extract the whole-brain functional networks. CPM with leave-one-out cross-validation was conducted to identify different networks that predicted the performance of neuropsychological tests. The predictive ability of identified networks would be tested in an independent sample of patients who were scanned in a different 3T MRI system (uMR 780, United Imaging Healthcare, Shanghai, China).

#### RESULTS

Four CPM models enabled prediction of neuropsychological scores for unseen subjects in cross-validation, with Pearson's correlation coefficients  $r$  of 0.40-0.48 (all  $p$  values  $< 0.001$ ). In these four cognitive function predictions, brain connectivities that show top contributing power commonly concentrated on the hippocampus, parahippocampal gyrus, superior frontal gyrus, medial frontal gyrus, inferior parietal lobule, and insula, which were the key nodes of the default-mode network and salience network. Moreover, the CPM models based on these important brain regions could predict overall cognitive ability (MoCA score;  $r = 0.45$ ,  $p < 0.001$ ).

#### CONCLUSION

Our results provide preliminary evidence that different functional networks with overlapping of important brain regions including frontal lobe, parietal lobe, insular lobe and several subcortical regions may contribute to cognitive ability of various domains and allow to predict the corresponding cognitive functions in SLE.

#### CLINICAL RELEVANCE/APPLICATION

CPM identified brain networks that underlie different cognitive functions in individuals and these "neural fingerprints" could potentially assist the diagnosis of cognitive dysfunction in SLE.

Printed on: 02/07/23

## Abstract Archives of the RSNA, 2022

S3A-SPNR-18

### Associations of Cortical Iron Accumulation with Cognition and Cerebral Atrophy in Alzheimer's Disease

Sunday, Nov. 27 11:45AM - 12:15PM Room: Learning Center - NR DPS

#### Participants

Aocai Yang, Beijing, China (*Presenter*) Nothing to Disclose

#### PURPOSE

Cerebral iron accumulation is consistently observed in Alzheimer's disease and co-localizes with the pathological proteins—amyloid- $\beta$  and tau. We aimed to investigate the whole-brain distributional pattern of cortical iron deposition and its relationships with cognition and cortical thickness in Alzheimer's disease via Quantitative Susceptibility Mapping (QSM).

#### METHODS AND MATERIALS

We prospectively recruited 30 participants with Alzheimer's disease (AD) and 26 age- and sex-matched healthy controls (HC) in this cross-sectional study. All the participants underwent QSM and structural T1 examinations on 3.0T MRI scanner. Mini-Mental State Examination (MMSE) and Montreal Cognitive Assessment (MoCA) were used to assess the global cognitive level. The whole-brain cross-sectional QSM analysis and the whole-brain QSM regression analyses against MMSE and MoCA scores were performed. Additionally, we conducted a surface-based morphometry analysis. Subsequently, in the significant atrophy regions, we compared the magnetic susceptibility between two groups and assessed the association of magnetic susceptibility with cortical thickness.

#### RESULTS

The whole-brain QSM cross-sectional analysis demonstrated that widespread susceptibility increased in AD across the cortical ribbon, asymmetrically covering left hemisphere cerebral cortex, caudate nucleus, putamen and partial cerebellar cortex. The whole-brain QSM regression analyses showed increased susceptibility that covaried with lower MMSE and MoCA scores in AD, and was predominantly located in the right parietal cortex and lateral occipital cortex. The reduced cortical thickness was located in the left superior temporal, right frontal pole, fusiform and pars opercularis in AD and the corresponding susceptibility increased in right frontal pole (AD:0.034 $\pm$ 0.007ppm, HC:0.030 $\pm$ 0.005ppm; P=0.016) and pars opercularis (AD:0.020 $\pm$ 0.003ppm, HC:0.017 $\pm$ 0.002ppm; P=0.002). Susceptibility was negatively correlated with cortical thickness in right pars opercularis in both entire cohort ( $r$ =-0.521, P<0.001) and AD ( $r$ =-0.510, P=0.005).

#### CONCLUSION

Widespread cortical iron, measured by QSM, accumulated in Alzheimer's disease and was associated with poor cognitive performance. Increased iron content was associated with brain atrophy in AD. QSM may be a useful imaging biomarker to monitor the neurodegenerative progression of AD.

#### CLINICAL RELEVANCE/APPLICATION

Increased iron content was associated with cortical atrophy and cognitive level in Alzheimer's disease. These may be useful to monitor the disease progression and cognitive severity of Alzheimer's disease at the whole brain level in vivo, and provide new insights into the application of QSM as a disease biomarker.

Printed on: 02/07/23

## Abstract Archives of the RSNA, 2022

S3A-SPNR-19

### Classification of Major Depression Disorder Based on Integrated Temporal and Spatial Variability Features of Dynamic Brain Networks

Sunday, Nov. 27 11:45AM - 12:15PM Room: Learning Center - NR DPS

#### Participants

Qun Gai, (*Presenter*) Nothing to Disclose

#### PURPOSE

The dynamics of brain networks has been a focus in the study of depression in recent years. However, most previous studies focused on single temporal dimension only, ignoring spatial dimension information. The present study aimed to integrate temporal and spatial variability features of dynamic brain networks to distinguish patients with major depressive disorder (MDD) from healthy controls (HC).

#### METHODS AND MATERIALS

245 MDD subjects and 230 well-matched HC were recruited in this study (the discovery cohort: 119 MDD and 106 HC, the validation cohort: 126 MDD and 124 HC). Temporal and spatial variability features were extracted from dynamic brain networks as features. A two-level feature selection strategy and random forest (RF) were employed for classification. Two other classifiers were also applied to validate our model. Furthermore, a linear regression model for assessing MDD symptom severity was established based on above selected temporal and spatial features.

#### RESULTS

Our model based on the integration of temporal and spatial variability features achieved the best performance with an accuracy of 93.33% (an accuracy of 83.40% for an independent sample). Moreover, features with high discriminative power to distinguish MDD from HC showed strong association with the visual network (VIS) and cognitive control network (CCN). Importantly, altered temporal and spatial variability could predict depression and anxiety severity of MDD.

#### CONCLUSION

Our results demonstrate that integrating temporal and spatial variability features can discriminate MDD from HC with a high classification performance and suggest that spatiotemporal dynamics may explain underlying neurobiological mechanism of MDD symptoms.

#### CLINICAL RELEVANCE/APPLICATION

Our findings provide direct evidence that spatiotemporal dynamics could be used as effective biomarkers for clinical diagnosis of MDD and may play an important role in detecting depression and anxiety symptom severity of MDD.

Printed on: 02/07/23

## Abstract Archives of the RSNA, 2022

S3A-SPNR-2

### Evaluation and Clinical Validation of a Deep Learning Algorithm for Predicting Delayed Myelination in Infant Brains from MRI

Sunday, Nov. 27 11:45AM - 12:15PM Room: Learning Center - NR DPS

#### Participants

Gunvant Chaudhari, BS, San Francisco, CA (*Presenter*) Nothing to Disclose

#### PURPOSE

Assisting diagnosis of infant delayed myelination by creating a convolutional neural network (CNN) capable of predicting delayed myelination based on routine clinical T1T2-weighted brain MRIs.

#### METHODS AND MATERIALS

MRIs were obtained from our institutional clinical database. Patients aged 0-25 months with reportedly normal myelination from 1995-2019 (n=5028) and delayed myelination from 1995-2021 (n=426) were included. For normal myelination MRIs, exclusion criteria included uneven age distribution (N=2659), myelination at the lower limits of normal (N=46), missing gestationally corrected age (GCA, N=1352), poor automated skullstripping or registration (N=103), and lack of T1 or T2 imaging (N=252). For delayed myelination MRIs, MRIs missing GCA (N=162), with poor automated skullstripping or registration (N=19), and without T1 or T2 imaging (N=121) were excluded. The CNN had input of paired, registered T1 T2 MRIs and GCA and was trained to predict delayed myelination status. Results from 10-fold cross-validation are reported. For a clinical benchmark, 3 neuroradiologists with 3-24 years of experience in pediatric neuroradiology blindly interpreted 30 randomly sampled MRIs, 15 normal and 15 delayed myelination, and assigned numerical values corresponding to confidence of delayed myelination (Figure 1). Ground-truth myelination status was defined as the average of 3 radiologists' and report label values.

#### RESULTS

The dataset consisted of 616 infant brain MRIs with normal myelination and 124 with delayed myelination. The CNN had an area under the receiver operator characteristic curve (AUC) of 0.77 (95% CI: 0.70-0.84) in cross-validation. In the subset of cases selected for the ready study, the CNN had an AUC of 0.83 (95% CI: 0.66-0.96) compared to 3 neuroradiologists with AUCs of 0.65 (0.45-0.84, p=0.19), 0.66 (0.46-0.85, p=0.19), and 0.78 (0.65-0.90, p=0.60), respectively.

#### CONCLUSION

s A CNN can recognize infant delayed myelination using T1- and T2-weighted brain MRI and GCAs, with performance similar to clinical neuroradiologists.

#### CLINICAL RELEVANCE/APPLICATION

Determining delayed myelination on infant brain MRI is subjective, especially for radiologists without high volume practice in pediatric neuroradiology. An AI system can aid radiologists in this task.

Printed on: 02/07/23

## Abstract Archives of the RSNA, 2022

S3A-SPNR-20

### Hippocampal Atrophy in Neurofunctional Subfields in Chronic Insomnia

Sunday, Nov. 27 11:45AM - 12:15PM Room: Learning Center - NR DPS

#### Participants

Yang Yang, (*Presenter*) Nothing to Disclose

#### PURPOSE

To investigate the pattern of volume changes in neurofunctional hippocampal subfields in patients with chronic insomnia (PIs).

#### METHODS AND MATERIALS

A total of 120 PIs (78 females, 42 males; mean age $\pm$  std, 43.74  $\pm$  13.02 years) and 120 good sleepers (60 females, 60 males; mean age, 42.69  $\pm$  12.24 years) were recruited. The left hippocampus was segmented into anterior (L1), middle (L2), and posterior (L3) subregions. The right hippocampus was segmented into top anterior (R1), second top anterior (R2), middle (R3), posterior (R4), and last posterior (R5) subregions. Multivariate Logistic regression was used to evaluate hippocampal subfields and the associations with the risk of chronic insomnia. Mediation analyses evaluated mediated associations with post-insomnia negative emotion, insomnia severity, and hippocampal atrophy. A visual easy-to-deploy risk nomogram was used for individual prediction of insomnia risk. All statistical analyses were performed using Matlab; P <0.05 was considered a statistically significant difference.

#### RESULTS

Hippocampal atrophy was identified in the L1, R1, and R2. L1 and R2 atrophy each predisposed to an approximate 3-fold higher risk of chronic insomnia (L1, OR: 2.90, 95% CI: [1.24, 6.76], P= 0.014; R2, 2.72 [1.19, 6.20], P= 0.018). Anxiety fully mediates the causal insomnia path, leading to R1 volume atrophy on positive affect. We developed a practical and visual competing risk-nomogram tool for individual prediction of insomnia risk, which stratifies individuals into different levels of insomnia risk with the highest prediction accuracy of 97.4% and an average C-statistic of 0.83.

#### CONCLUSION

s Chronic insomnia is associated with hippocampal atrophy in specific neurofunctional subfields that are risk factors for chronic insomnia.

#### CLINICAL RELEVANCE/APPLICATION

These findings could broaden our understanding of the etiology of insomnia, help individuals identify their potential risk profile, and guide individuals to take precise actions promptly to prevent the future incidence of insomnia.

Printed on: 02/07/23

## Abstract Archives of the RSNA, 2022

S3A-SPNR-3

### Synthetic MRI-based Fast Gray Matter Acquisition T1 Inversion Recovery (FGATIR) Contrasts identify Neonatal Brainstem Pathways

Sunday, Nov. 27 11:45AM - 12:15PM Room: Learning Center - NR DPS

#### Participants

Victor Schmidbauer, MD, Vienna, Austria (*Presenter*) Nothing to Disclose

#### PURPOSE

Synthetic imaging allows to retrospectively reconstruct different MR contrasts using a single acquisition of a multi-dynamic multi-echo (MDME) sequence. This study aimed to investigate the feasibility of synthetic MRI-based fast gray matter acquisition T1 inversion recovery (FGATIR) contrasts for the qualitative identification of early myelinating neonatal brainstem pathways in vivo.

#### METHODS AND MATERIALS

Thirty-one cases of neonatal MRI (median gestational age at birth: 27+0; range, 23+4-41+6) were collected, which included MDME sequences and conventional T1-weighted/T2-weighted sequence acquisitions as a standard-of-reference. MDME-based FGATIR contrasts (TR/TE/TI: 3000/5/410 ms) were generated using the MR data post-processing software SyMRI®. The identification of seven brainstem pathways/regions of interest was assessed on synthetic FGATIR contrasts and conventionally acquired T1-weighted/T2-weighted imaging data: decussation of superior cerebellar peduncle (DSCP); left/right medial lemniscus (ML); left/right central tegmental tract (CTT); and left/right longitudinal medial fascicle (LMF).

#### RESULTS

SyMRI® provided FGATIR contrasts of diagnostic quality in 31/31 cases (100%). Based on MDME-based FGATIR contrasts, the DSCP [31/31 (100%)]; left/right ML [31/31 (100%)]; left/right CTT [20/31 (65%)]; and left/right LMF [31/31 (100%)] were reliably identified. Based on conventional T1-weighted contrasts, the DSCP [14/31 (45%)]; left/right ML [25/31 (81%)/23/31 (74%)]; left/right CTT [3/31 (10%)/7/31 (23%)]; and left/right LMF [15/31 (48%)] were reliably identified. Based on conventional T2-weighted contrasts, the DSCP [30/31 (97%)]; left/right ML [30/31 (97%)/29/31 (94%)]; left/right CTT [26/31 (84%)/25/31 (81%)]; and left/right LMF [30/31 (97%)] were reliably identified.

#### CONCLUSION

Synthetic generation of FGATIR contrasts enables reliable radiological identification of neonatal brainstem pathway anatomy in vivo. The investigated MR approach depicts early myelinating tracts more reliable than standard-of-reference contrasts.

#### CLINICAL RELEVANCE/APPLICATION

Conventional, T1- and T2-weighted-based MRI currently lacks sensitivity for the reliable assessment of delayed brain myelination in former preterm neonates - therefore, MR approaches that utilize white matter signal suppression contribute to a more sensitive evaluation of myelination patterns at early stages of cerebral development.

Printed on: 02/07/23

## Abstract Archives of the RSNA, 2022

S3A-SPNR-4

### Development of The Orbitofrontal Cortex Through Childhood and Adolescence

Sunday, Nov. 27 11:45AM - 12:15PM Room: Learning Center - NR DPS

#### Participants

Zhe Guan, (*Presenter*) Nothing to Disclose

#### PURPOSE

The orbitofrontal cortex is an incompletely understood part of the prefrontal cortex linked to adaptive learning and executive processes and known to be key towards successful maturation through adolescence to adulthood. The purpose of this study is to evaluate age-dependence of orbitofrontal cortical volume in a large cohort of young, healthy individuals.

#### METHODS AND MATERIALS

High-resolution, structural T1-weighted imaging from 655 healthy individuals (8 to 21 years old) from the Human Connectome Project Development (HCP-D) Study were used. FreeSurfer v6.0.0 measures of orbitofrontal cortical volume provided as part of the HCP dataset were used as well as an investigational deep learning-based, automated segmentation tool, DenseUnet-based Automatic Rapid Tool (DARTS). Pearson correlation coefficients were calculated. Subset analysis of male and female cohorts was performed and size asymmetry was assessed using Student's t test.

#### RESULTS

Segmentation data are available from HCP (FreeSurfer) for 415 of the 655 subjects of this cohort. DARTS segmentation was performed in all subjects. 323 subjects (49.3%) were male. We found a significant negative correlation between total orbitofrontal volume and age ( $r = -0.360$ ,  $p < 0.00001$ ;  $r = -0.314$ ,  $p < 0.00001$  using FreeSurfer and DARTS, respectively). For subsegments of the orbitofrontal cortex, the correlations under FreeSurfer and DARTS respectively were  $r = -0.364$ ,  $p < 0.00001$ ;  $r = -0.407$ ,  $p < 0.00001$  (left lateral orbitofrontal),  $r = -0.200$ ,  $p < 0.00001$ ;  $r = -0.033$ ,  $p = 0.396$  (left medial orbitofrontal),  $r = -0.335$ ,  $p < 0.00001$ ;  $r = -0.283$ ,  $p < 0.00001$  (right lateral orbitofrontal), and  $r = -0.329$ ,  $p < 0.00001$ ;  $r = -0.099$ ,  $p = 0.011$  (right medial orbitofrontal). The standard deviation of the total orbitofrontal volumes was lower using DARTS (2.40 mL) compared with FreeSurfer (3.73 mL). Similar trends were observed across males and females. Size asymmetry was noted with the left lateral and medial orbitofrontal cortical volumes being larger than the right ( $p < 0.0001$  using FreeSurfer and DARTS).

#### CONCLUSION

s Orbitofrontal cortical volume as measured on MRI decreases with age during childhood and adolescence, suggesting that development of this area is complex and may involve cortical pruning or other anatomic refinement on the way to maturation.

#### CLINICAL RELEVANCE/APPLICATION

The orbitofrontal cortex is implicated in the development of adaptive learning and executive responses including stimulus-reinforcer associations. These functions undergo maturation and refinement during childhood and adolescence and unveiling anatomic changes to this area contribute to our understanding of how this process unfolds, potentially aiding identification of developmental aberrations.

Printed on: 02/07/23

## Abstract Archives of the RSNA, 2022

S3A-SPNR-5

### Development of Fetal Ventricular Volume Reference Norms Using nnUNet

Sunday, Nov. 27 11:45AM - 12:15PM Room: Learning Center - NR DPS

#### Participants

Minerva Zhou, MD, (*Presenter*) Nothing to Disclose

#### PURPOSE

To use deep learning methods to segment and measure ventricular volume of fetal brain MRIs across a wide range of gestational ages.

#### METHODS AND MATERIALS

We applied nnU-Net to segment the ventricular system of 91 nonpathologic and 9 pathologic fetal brain MRIs across a variety of gestational ages (19-36 weeks). Twenty fetal brain MRIs from our institution were reconstructed to a high-resolution 3D volume using slice-to-volume reconstruction and then manually segmented and combined with the MICCAI Fetal Tissue Annotation Challenge data to generate a dataset of 100 fetal brain MRI volumes, which were randomly split into 80 training studies and 20 test studies in a 5-fold cross-validation. Performance was assessed using Dice coefficients and volume comparison to manual reference segmentation. A normative reference of ventricular volume across gestational ages was generated using the 91 nonpathologic training studies.

#### RESULTS

The nnU-Net predicted segmentation of fetal ventricles across gestational ages with median Dice score of 0.90 (IQR 0.88-0.93; Fig 1A). The automatically computed ventricular volume measurements were highly correlated with manual measurements (Pearson's  $r=0.99$ ,  $P<0.001$ , Fig 1B). A normative range of ventricular volumes across gestational ages was developed using the automated segmentation volumes. All 9 patients with hydrocephalus were predicted to be greater than two standard deviations higher than the age-specific reference mean (Fig 1C).

#### CONCLUSION

Deep learning techniques can be used to provide an objective measure of ventricular volume on fetal brain MRI and identify hydrocephalus based on a normative reference standard.

#### CLINICAL RELEVANCE/APPLICATION

This study explores using deep learning techniques to quickly and accurately quantify ventricular volume on fetal brain MRI and subsequently identify pathological volumes.

Printed on: 02/07/23

## Abstract Archives of the RSNA, 2022

S3A-SPNR-6

### Brain Gray Matter Connectome Disorganization in Social Anxiety Disorder

Sunday, Nov. 27 11:45AM - 12:15PM Room: Learning Center - NR DPS

#### Participants

Xun Zhang, (*Presenter*) Nothing to Disclose

#### PURPOSE

Phenotyping approaches grounded in structural network science can offer advanced insights into neurobiological substrates of psychosis, but this remains to be clarified at the individual level in social anxiety disorder (SAD). Herein, we aimed to investigate the topological organizations of individual structural covariance networks using a novel approach in a homogenous sample of SAD patients, and assess their potential clinical relationship and diagnostic value.

#### METHODS AND MATERIALS

Forty-nine non-comorbid adult patients with SAD and fifty-three demographically-matched healthy controls (HC) were recruited to obtain clinical evaluation and 3.0-Tesla high-resolution T1-weighted images. We constructed single-subject structural covariance networks based on multivariate morphometry (i.e., cortical thickness, surface area, curvature, and gray matter volume) using a recent novel approach combining probability density estimation and Kullback-Leibler divergence, and estimated their global and nodal network properties via graph theory analysis. Network metrics were compared between SAD and HC groups, and the relationship to clinical characteristics was analyzed. Furthermore, exploratory support vector machine analyses were conducted to discriminate SAD from HC.

#### RESULTS

Globally, SAD patients showed significantly altered topological characteristics, including higher global efficiency, shorter characteristic path length, and stronger small-worldness. Locally, SAD patients exhibited abnormal nodal degree and efficiency mainly involving left superior frontal gyrus, right superior parietal lobe, right paracentral gyrus, right lingual, right pericalcarine cortex, and left amygdala. Furthermore, altered global and nodal topological metrics were associated with the symptom severity and disease duration in SAD cohort, suggesting a pathophysiological relevance. Graph-based metrics allowed single-subject classification of SAD versus HC with significant accuracy, indicating potential diagnostic efficacy.

#### CONCLUSION

s The topological organization of structural covariance networks was disrupted in SAD in a way that suggests compensatory greater integration of information processing with a more randomly organized brain network, which may extend neurobiological understandings of a system-level brain maturational disruption in SAD.

#### CLINICAL RELEVANCE/APPLICATION

These results provide structural network insights into the neurobiology of SAD, and may navigate the development of reliable and objective neuroanatomical biomarkers for clinical diagnosis, targeted intervention, and therapeutic efficacy evaluation in SAD.

Printed on: 02/07/23

## Abstract Archives of the RSNA, 2022

S3A-SPNR-7

### **Pediatric Low-Grade Glioma Molecular Subtype Identification Based on 3D Probability Distributions of Tumor Location in MRI**

Sunday, Nov. 27 11:45AM - 12:15PM Room: Learning Center - NR DPS

#### **Participants**

Farzad Khalvati, PhD, MSc, Toronto, ON (*Presenter*) Board of Directors, MESH Scheduling Inc

#### **PURPOSE**

Genetic marker identification of pediatric Low-Grade Glioma (pLGG) is crucial for early prognostication and individualized treatment planning. We propose a method to exploit tumor location in MRI data to identify the most common pLGG subtypes (BRAF V600E mutation vs. BRAF fusion) without using any other information.

#### **METHODS AND MATERIALS**

In this REB-approved retrospective study, Fluid-Attenuated Inversion Recovery (FLAIR) sequences of the baseline MRI from 200 patients with pLGG acquired between Jan. 2000 and Dec. 2018 were included. Tumor segmentations were provided by a pediatric neuroradiology fellow and verified by a senior pediatric neuroradiologist. The ground truth molecular subtype labels (BRAF V600E mutation and BRAF fusion) were obtained through biopsy. To build the probability density functions (PDF) of BRAF V600E mutation and BRAF fusion, the 3D binary masks of segmentation in FLAIR images for each class in the training dataset were added together and then normalized. In the test cohort, the probabilities of belonging to each class were calculated by a voxel-wise multiplication of the binary segmentation mask of the test case and the 3D PDF of the corresponding class in the training dataset. We repeated the data split (80/20 for training and test) 100 times and calculated the Area Under ROC Curve (AUROC).

#### **RESULTS**

Using only location of the tumor in the FLAIR images, we achieved a mean AUROC of 0.783 with a 95% Confidence Interval (CI) of (0.769, 0.798) over 100 experiments for the classification of BRAF V600E mutation vs. BRAF fusion in pLGG.

#### **CONCLUSION**

3D PDFs of tumor subtypes can help create a location-based pipeline for molecular subtype identification of pLGG. While location is ignored in the majority of radiomics and neural-network-based classification models, our results show BRAF V600E mutation and BRAF fusion in pLGG tumors follow different location distributions, which can be utilized for subtype identification.

#### **CLINICAL RELEVANCE/APPLICATION**

The location-based subtype identification of pLGG can be used as a stand-alone classifier or as an adjunct to Artificial Intelligence based classification models to allow imaging-based molecular characterization.

Printed on: 02/07/23

## Abstract Archives of the RSNA, 2022

S3A-SPNR-8

### MRI Alterations in Patients with Psychogenic Non-epileptic Seizures: Prevalence, Distribution and Classification of The Findings

Sunday, Nov. 27 11:45AM - 12:15PM Room: Learning Center - NR DPS

#### Participants

Aleix Jareno Badenas, MD, Sant Vicenc de Castellet, Spain (*Presenter*) Nothing to Disclose

#### PURPOSE

Psychogenic non-epileptic seizures (PNES) are paroxysmic episodes that mimic epileptic seizures without electroencephalographic representation. Conversive psychiatric origin is attributed to this kind of episode. However, beyond this psychiatric perspective, the possible neurobiological basis of PNES has not received much attention. Some studies have documented structural and functional alterations in these patients, but without consistent results to support a causative hypothesis. The objectives of this study are:- To evaluate the MRI findings in patients with PNES- To classify the results- To evaluate a possible structural basis of these episodes

#### METHODS AND MATERIALS

We performed a retrospective analysis of the MRI studies conducted on patients of our epilepsy unit with a confirmed diagnosis of only PNES or PNES and epilepsy (PNES+epilepsy). A descriptive study of the findings in both groups was performed and compared with the incidental findings in the general population obtained from the literature. The radiologic findings were classified into: vascular, tumoral, posttraumatic/gliotic, small vessel, cortical, hippocampal sclerosis, unspecific or normal studies, as well as into epileptogenic and non-epileptogenic.

#### RESULTS

Our study population was formed of 60 patients with a confirmed diagnosis of PNES and 16 patients with PNES+epilepsy (75% women, 25% men, mean age at diagnostic of 41 years). 55% of patients with PNES and 81% with PNES+epilepsy had a pathological finding. These findings were considered epileptogenic in 13% of the PNES group and in 31% of the PNES+epilepsy group. The most frequent findings in patients with were unspecific, vascular and hippocampal sclerosis, whilst in the PNES+epilepsy group were unspecific, hippocampal sclerosis and small vessel.

#### CONCLUSION

s Patients with PNES have a higher prevalence of abnormalities in MRI than the general population (around 18% according to existing literature) and this prevalence is even higher when PNES are associated with epilepsy. There is a higher prevalence of PNES among women.

#### CLINICAL RELEVANCE/APPLICATION

Our study shows higher prevalence of MRI structural findings in patients with PNES than in the general population, suggesting a neurobiological/structural basis in a pathology considered psychiatric.

Printed on: 02/07/23



## Abstract Archives of the RSNA, 2022

S3A-SPNR-9

### The Individual Association Between Functional and Morphological Asymmetry During Fetal Brain Development observed in In-utero MRI

Sunday, Nov. 27 11:45AM - 12:15PM Room: Learning Center - NR DPS

#### Participants

Georg Langs, Vienna, Austria (*Presenter*) Co-founder, contextflow GmbH Shareholder, contextflow GmbH

#### PURPOSE

While function is shaped and constrained by brain structure, there is also possible impacts of functional activity on morphology. At the early stages of life, this relationship is particularly dynamic due to maturational processes and rapid conformational changes of the fetal brain. Cross-sectional studies in the early infancy and newborns suggest that the impaired development of cerebral morphology may promote the recruitment of alternative axonal pathways to sustain function, affecting the integration and specification of functional circuits at both cortical and sub-cortical levels. However, little is known about their complex interplay at the developmentally critical period in utero. Here, we assess the individual association of structural and functional brain development in the fetus.

#### METHODS AND MATERIALS

Resting-state fMRI and consecutive T2-weighted scans were acquired for 72 singleton fetuses between 19 and 39 weeks of gestation. Data were processed by customized functional- and anatomical image processing pipelines including irregular fetal movement correction, age-specific segmentation, and atlas registration. Individualized functional connectivity (FC) matrices were obtained by correlating regional brain activity over time and individualized local surface folding was quantified by measuring gyrification index (GI). We calculated the morphological and functional laterality indices for each individual subject as the normalized difference of GI and of FC degree between the hemispheres, respectively. The P-values for all evaluations were corrected for multiple comparisons using Benjamini-Yekutieli procedure.

#### RESULTS

After computational quality benchmarking, 24 cases were excluded and the final study cohort consisted of 48 fetuses that had no confirmed brain abnormalities (mean gestational age  $\pm$ SD: 28.97 $\pm$ 4.84 weeks). We found significant leftward laterality in Temporal-Superior ( $p=0.043$ ), Temporal-Medial ( $p=0.047$ ), and Temporal-Inferior ( $p=0.048$ ) regions after correcting for multiple comparisons. Statistical tests of the functional asymmetry did not reach statistical significance for the rest of cortical regions. Significant morphological asymmetry was found in medial wall ( $p=0.0089$ ) and mesial frontal region ( $p=0.003$ ). We observed significant individual association between functional- and morphological asymmetry in the limbic area ( $p<0.001$  corrected)

#### CONCLUSION

Our results support the hypothesis that a significant relationship between brain structure and function is present during prenatal brain development.

#### CLINICAL RELEVANCE/APPLICATION

It may lead to a better understanding of the neural mechanisms involved in adverse outcomes.

Printed on: 02/07/23



## Abstract Archives of the RSNA, 2022

S3A-SPOB

### OB/Gynecology Sunday Poster Discussions - A

Sunday, Nov. 27 11:45AM - 12:15PM Room: Learning Center - OB DPS

#### Participants

Angela Tong, MD, New York, NY (*Moderator*) Equipment support, Siemens AG

Printed on: 02/07/23



## Abstract Archives of the RSNA, 2022

S3A-SPPD

### Pediatric Sunday Poster Discussions - A

Sunday, Nov. 27 11:45AM - 12:15PM Room: Learning Center - PD DPS

#### Participants

Judy Squires, MD, Pittsburgh, PA (*Moderator*) Nothing to Disclose

#### Sub-Events

### S3A-SPPD-1 Development and Validation of a Nomogram to Predict Intracranial Hemorrhage in Neonates

#### Participants

Siqi Zhang, Shanxi Children's Hospital, Taiyuan, China (*Presenter*) Nothing to Disclose

#### PURPOSE

The aim of this study was to evaluate the prevalence of neonatal intracranial hemorrhage (ICH) using susceptibility-weighted imaging (SWI) and to develop and externally validate a nomogram for predicting the probability of ICH in neonates.

#### METHODS AND MATERIALS

Retrospectively collect clinical data of 1018 neonates clinically suspected craniocerebral injury, including prenatal, intrapartum and postnatal risk factors of ICH. All neonates underwent SWI to determine if there is ICH. The nomogram was developed based on the variables identified by the univariate and multivariate logistic regression analyses. Then the nomogram was validated in another independent cohort of 106 neonates. The performance of the nomogram was evaluated in terms of discrimination by the area under the receiver-operating characteristic curve (AUC), calibration by the calibration curve and clinical net benefit by the decision curve analysis (DCA).

#### RESULTS

267(26.2%) neonates with ICH were detected by SWI in the primary cohort, and 31(29.3%) in the validation cohort. The nomogram comprised six variables: 1 minute Apgar score, heart rate, platelet, delivery method, jaundice, and mothers with/without gestational diabetes. The AUC of the nomogram in the primary and validation cohort were 0.734 and 0.743, respectively. The calibration curve showed a good correlation between the nomogram prediction and actual observation for ICH. DCA showed the nomogram was clinically useful.

#### CONCLUSION

We developed and validated an easy-to-use nomogram to predict ICH for neonates. This model could support individualized risk assessment and healthcare.

#### CLINICAL RELEVANCE/APPLICATION

We developed and validated a nomogram to predict the probability of neonatal ICH and confirmed its good performance. We believe that the application of the proposed model would enable clinicians to accurately assess the probability of neonatal ICH and make appropriate individualized risk assessment and healthcare.

Printed on: 02/07/23



## Abstract Archives of the RSNA, 2022

S3A-SPPD-1

### Development and Validation of a Nomogram to Predict Intracranial Hemorrhage in Neonates

Sunday, Nov. 27 11:45AM - 12:15PM Room: Learning Center - PD DPS

#### Participants

Siqi Zhang, Shanxi Children's Hospital, Taiyuan, China (*Presenter*) Nothing to Disclose

#### PURPOSE

The aim of this study was to evaluate the prevalence of neonatal intracranial hemorrhage (ICH) using susceptibility-weighted imaging (SWI) and to develop and externally validate a nomogram for predicting the probability of ICH in neonates.

#### METHODS AND MATERIALS

Retrospectively collect clinical data of 1018 neonates clinically suspected craniocerebral injury, including prenatal, intrapartum and postnatal risk factors of ICH. All neonates underwent SWI to determine if there is ICH. The nomogram was developed based on the variables identified by the univariate and multivariate logistic regression analyses. Then the nomogram was validated in another independent cohort of 106 neonates. The performance of the nomogram was evaluated in terms of discrimination by the area under the receiver-operating characteristic curve (AUC), calibration by the calibration curve and clinical net benefit by the decision curve analysis (DCA).

#### RESULTS

267(26.2%) neonates with ICH were detected by SWI in the primary cohort, and 31(29.3%) in the validation cohort. The nomogram comprised six variables: 1 minute Apgar score, heart rate, platelet, delivery method, jaundice, and mothers with/without gestational diabetes. The AUC of the nomogram in the primary and validation cohort were 0.734 and 0.743, respectively. The calibration curve showed a good correlation between the nomogram prediction and actual observation for ICH. DCA showed the nomogram was clinically useful.

#### CONCLUSION

s We developed and validated an easy-to-use nomogram to predict ICH for neonates. This model could support individualized risk assessment and healthcare.

#### CLINICAL RELEVANCE/APPLICATION

We developed and validated a nomogram to predict the probability of neonatal ICH and confirmed it's good performance. We believe that the application of the proposed model would enable clinicians to accurately assess the probability of neonatal ICH and make appropriate individualized risk assessment and healthcare.

Printed on: 02/07/23

## Abstract Archives of the RSNA, 2022

S3A-SPPH

### Physics Sunday Poster Discussions - A

Sunday, Nov. 27 11:45AM - 12:15PM Room: Learning Center - PH DPS

#### Participants

Emily Marshall, PhD, Chicago, IL (*Moderator*) Scientific Advisory Board, Bayer AG; Consultant, Bayer AG; Scientific Advisory Board, Radimetrics Dosimetry Services; Consultant, Radimetrics Dosimetry Services

#### Sub-Events

### S3A-SPPH-1 Development of a Deep Learning Method for Age Estimation of Cadavers Using Postmortem Vertebral CT Images

#### Participants

Ikuo Kawashita, PhD, Hiroshima, Japan (*Presenter*) Nothing to Disclose

#### PURPOSE

We developed an age estimation method for unidentified cadavers. It applies deep learning to postmortem computed tomography (PMCT) images of the vertebral bones. The purpose of this study was to determine the optimal image processing method and deep-learning model for age estimation.

#### METHODS AND MATERIALS

Our image database consisted of CT images of 1,120 cases (140 cases for each of 8 decades of age from the 20s to the 90s. The training set included 70 males and 70 females per decade. The evaluation set included 187 cases (112 males, 75 females; average age 64.4 years; 56 damaged, 131 undamaged). The training images were whole-body CT images obtained from positron emission tomography-CT scans; the test images were PMCT images. In preliminary experiments using 200 training images, CT-scanograms, curved planar reformation (CPR)-, maximum intensity projection (MIP)-, and curved MIP images were compared to identify suitable image processing methods for accurate age estimation. We selected the optimal models (GoogLeNet, VGG16, ResNet, DenseNet) as network structures for deep learning (Figure 1).

#### RESULTS

MIP was the optimal image processing method for age estimation (Figure 2). The others made little learning progress and all output the same age, only VGG16 was able to estimate the age. With combined MIP and VGG16, the intraclass correlation coefficient between the actual and estimated age of the 187 evaluation cadavers was 0.96 (95% CI: 0.95 - 0.97,  $p < 0.001$ ), reliability was excellent. The mean absolute error (MAE) and the standard error of the estimate (SEE) between the actual and estimated age was 4.27 and 5.39 years, respectively. Shapley additive explanations visualization (SHAP) suggested that with MIP age-related changes around the thoracolumbar spine, e.g. osteophytes, intervertebral spacing, bone density, and aortic calcification, were assessed correctly (Figure 3).

#### CONCLUSION

For age estimation using whole vertebral bone PMCT images, MIP yielded the best source image as the effects of gases due to decomposition were suppressed. VGG16 was the optimal network structure. The MAE was 4.27 years (margin of error +/- 10 years, 95% probability) and reliability was excellent.

#### CLINICAL RELEVANCE/APPLICATION

Our age estimation method using MIP images and VGG16 estimated the age of cadavers accurately. It may help to identify unknown cadavers.

### S3A-SPPH-2 A Fairtale of a Fair Comparison in Deep Learning MRI Reconstruction

#### Participants

Chungseok Oh, (*Presenter*) Nothing to Disclose

#### PURPOSE

Despite the recent success in medical imaging, deep learning suffers from a generalization issue: network performance degrades when the test data have different image characteristics (e.g. resolution, SNR, etc.) from training data. This issue suggests that diversity in dataset plays a critical role in the network performance. In medical imaging, however, many of the studies still utilize a "private" dataset because no "public" dataset is available. In this study, we demonstrated that the use of a private dataset can lead to an unfair comparison between networks.

#### METHODS AND MATERIALS

When comparing your network with a published network, there are two options: comparing with a pre-trained network or comparing with a re-trained network. When comparing with a pre-trained network, which was trained by a different private dataset from yours, the performance comparison may not be fair. To demonstrate it, two networks, designed to perform quantitative

susceptibility mapping (QSM), were trained by datasets with different image characteristics, either resolution or preprocessing method, and their performances were compared. When comparing with a re-trained network, the re-trained network may underperform because of inadequate hyperparameter set or random seeds. For this case, we re-trained a published network (i.e. QSMnet) with a new dataset and demonstrated that the re-trained network may require hyperparameter tuning or multiple seeds.

## RESULTS

[Comparison with pre-trained network] When comparing two networks trained by different datasets, each network outperformed when the training dataset has the same image characteristics as the test dataset. Therefore, the performance comparison result can easily be reversed by the image characteristics of the test dataset.[Comparison with re-trained network] When the re-trained network was hyperparameter-tuned, the performance was improved. Also, the network performances were different depending on the seed values. These results imply that the re-trained network may no longer retain its original network performance.

## CONCLUSION

s We demonstrated that the use of a private dataset can lead to an unfair comparison between networks. For a fair comparison, a common test dataset and a trained network with information for reproducibility are necessary. This conclusion may also be applicable to other medical image processing tasks using private datasets.

## CLINICAL RELEVANCE/APPLICATION

Performance comparison between networks is essential in academic research. This work suggests a lesson about the unfairness of comparison results which may be easily experienced in medical imaging.

### S3A-SPPH-3 Temporal Deep Learning for Adhesion Detection on Cine-MRI

Participants

Bram de Wilde, MSc, (*Presenter*) Nothing to Disclose

#### PURPOSE

To explore the benefit of deep learning video architectures for the challenging novel task of adhesion detection in the abdomen on cine-MRI.

#### METHODS AND MATERIALS

Adhesions are a common cause of chronic abdominal pain, with a prevalence of up to 20% after surgery. Adhesion diagnosis is a novel application of cine-MRI, where patients induce motion in the abdomen through the Valsalva maneuver. Adhesions connect bowel loops to the anterior abdominal wall, abdominal organs, or to other bowel loops. The radiologist must analyze the movement of organs through time, to determine adhesion presence. This is challenging and requires expertise, so AI assistance could help introduce this technique in more clinics worldwide. In this study, we aim to find out if deep neural network architectures developed for video data (2D+T) are able to extract temporal information essential to detect adhesions. Adhesions were annotated with bounding boxes on 196 2D+T cine-MRI series of 85 patients. A 2D ResNet-18 was trained using only the first frame of each series (image). A 2D+T ResNet-18 was trained using the full temporal information of each series (video). Both networks analyze 49x49 pixel patches, with a third dimension of 30 time frames for the 2D+T network. The training label for each patch is positive (1) if the center pixel is inside an annotated bounding box, otherwise negative (0). Diagnostic performance for each architecture is characterized by the area under the receiver operating characteristic curve (AUC). A permutation test compared the performances using 25 individually trained models for each architecture, in a nested 5-fold cross validation scheme.

#### RESULTS

The 2D+T ResNet-18 architecture (mean AUC 0.70 [0.55-0.84]), was significantly better ( $p=0.0011$ ) than the 2D ResNet-18 architecture (mean AUC 0.64 [0.52-0.77]).

#### CONCLUSION

s Adhesion detection is an exciting new problem for AI in medical imaging, because of the complex movement patterns that are featured in abdominal cine-MRI. This study provides evidence that deep learning video architectures can learn temporal patterns essential to analyze adhesions.

#### CLINICAL RELEVANCE/APPLICATION

Cine-MRI is a novel and uncommon modality for adhesion detection. This study paves the way for assisted diagnosis of adhesions, potentially lowering the barrier for wider adoption.

### S3A-SPPH-4 UK Biobank Application of Susceptibility Source Separation (Chi-Separation) Using Deep Neural Network

Participants

Hwihun Jeong, MD, Seoul, Korea, Republic Of (*Presenter*) Nothing to Disclose

#### PURPOSE

?-separation has been proposed for illustrating the distribution of iron and myelin in the brain. The requirement for an R2 map hampers a wide application of ?-separation. We propose a pipeline that allows us to apply ?-separation to UK Biobank (UKB) data using R2 maps from deep neural networks.

#### METHODS AND MATERIALS

We scanned 20 subjects (train/validation/test: 10/1/9) using the same sequences as the UKB protocol and additional sequences for the reference R2 and R2\* maps. The R2\* map of the UKB protocol datasets suffered from noise and artifacts, so we developed an additional network (R2\* denoising network) that infers reference R2\* values from UKB GRE data. A local field map is generated using the same protocol as the UKB QSM protocol. For R2 mapping, the neural network was trained using the input of MPRAGE and T2-FLAIR to generate an R2 map. Using local field and R2' maps, iLSQR-style ?-separation was conducted to reconstruct positive and negative susceptibility, and the result was compared to the reference. Deep neural networks share the same structure as Unet with fully connected layers on the backend. The training was conducted with an L1 loss between output and reference.

## RESULTS

The  $\gamma$ -separation maps of the proposed method demonstrate a good match to those of reference. (NRMSE =  $54.4 \pm 4.7$ , PSNR =  $21.9 \pm 0.8$ , and SSIM =  $0.989 \pm 0.008$ ). The zoomed-in  $\gamma_{pos}$  and  $\gamma_{neg}$  maps confirm that the results of the proposed method show similar structures to those of the references, revealing details of iron and myelin distribution in the brain. Particularly in the thalamus, which contains both iron and myelin, the results demonstrate details of subthalamic nuclei, agreeing with the reference.

## CONCLUSION

In this study, we developed a pipeline for reconstructing  $\gamma$ -separation maps from the UK Biobank protocol dataset by leveraging a deep neural network. Our results suggest that  $\gamma$ -separation can be applied to existing large-scale data including the UK Biobank dataset. Using this method, we will explore full UKB data, potentially benefiting from the large population dataset.

## CLINICAL RELEVANCE/APPLICATION

$\gamma$ -separation, which is a useful methodology for estimating the distribution of iron and myelin in the brain, can be applied to a large-scale dataset.

### S3A-SPPH-6 Test-Time Mix-up Augmentation for Uncertainty Estimation and Expert Assistance in Medical Image Classification

Participants

Helen Hong, PhD, Seoul, Korea, Republic Of (*Presenter*) Nothing to Disclose

## PURPOSE

Experts are often hesitant to fully trust the prediction results of deep neural networks on disease diagnosis which consists of only labels and probability values. Uncertainty estimation is a method to quantify the confidence of the network in the disease prediction. We propose a method of estimating more reliable uncertainty measure through test-time mixup augmentation.

## METHODS AND MATERIALS

We used an IDRid dataset consisting of 413 training and 103 validation color fundus images of 5 diabetic retinopathy (DR) disease grades. We first train a VGG-19 on the mixup-augmented training data. In test-time, a set of mixup test data is generated by applying mixup for each test data with the randomly sampled training data. The trained CNN is then applied to the mixup test data to obtain the mixup test labels. In lesion classification, the label of each test data is determined by majority voting on the mixup test labels. In uncertainty estimation, the uncertainty of each test data is computed by the entropy of the distribution of mixup test labels.

## RESULTS

In experiments, we compared the proposed TTMA method with the existing test-time affine-based augmentation (TTA) and the Monte-Carlo drop-out (MCDO) methods. The data uncertainty can be evaluated by two criteria. First, the rejection-accuracy curves can evaluate the reliability of the uncertainty by observing whether the accuracy is increasing as the uncertainty decreases. In DR grading, the proposed TTMA achieved 100% accuracy at a 95% rejection rate, meaning that the 5% of the test results with the lowest TTMA uncertainty are 100% accurate. In contrast, the TTA and MCDO achieved 68.0% and 71.6% accuracy even at a 95% rejection rate, respectively. Second, the histogram of uncertainty of correct and incorrect predictions can evaluate the uncertainty by observing whether the uncertainty distributions of two predictions are separable. In TTA and MCDO, both distributions are heavily overlapped around the zero uncertainty. However, in the proposed TTMA, the distributions are not only shifted to the higher uncertainty values thanks to the mixup perturbation, but also in relatively separable form.

## CONCLUSION

The proposed TTMA provides more reliable uncertainty measure than the existing TTA or MCDO methods thanks to the mixup perturbation. The proposed TTMA uncertainty can assist the experts to select the data requires additional review among the CNN prediction results. (This work was supported by the Korea Medical Device Development Fund grant funded by the Korea government (Project Number: 9991007550, KMDF\_PR\_20200901\_0269))

## CLINICAL RELEVANCE/APPLICATION

The proposed uncertainty measure can assist experts to decide whether to accept or revision the CNN prediction results.

### S3A-SPPH-8 Automatic Tracking of Prostate Fiducials in X-Ray Images With Deep-Learning Model During Radiation Treatment

Participants

Shuang Zhou, MS, Saint Louis, MO (*Presenter*) Nothing to Disclose

## PURPOSE

Automatic tracking of fiducials is needed in image-guided radiation treatments. We developed a deep-learning based fiducial detection method can automatically detect and track fiducials in x-ray images during radiation treatments.

## METHODS AND MATERIALS

Total of 1870 orthogonal x-ray images acquired from 63 patients during radiation treatments were used for training (90%) and validation (10%). Additional images from 12 additional patients were used for testing. The fiducials in the x-ray images were manually labeled with a rectangle bounding-box in Microsoft COCO format. Improved YOLOX deep-learning network developed for the object detection was trained with the manually labeled x-ray images. Mean average precision (mAP) was used as the evaluation metric.

## RESULTS

The YOLOX deep-learning network was able to detect fiducials in the prostate with reasonable accuracy. The average precision (AP) scores derived from the precision-recall curve range are 0.44 and 0.16 for anteroposterior and lateral x-ray, respectively. The discrepancy was due to the poor visibility of fiducials in lateral x-rays.

## CONCLUSION

s The YOLOX deep-learning network can detect most prostate fiducials in x-ray images with reasonable visibility and potentially can be used for automatic tracking of the target during radiation treatment delivery.

## CLINICAL RELEVANCE/APPLICATION

Automatic detection and tracking of fiducials in the treatment target can facilitate precise radiation treatment delivery.

## S3A-SPPH-9 Deep Learning Identification of Severe COVID Infection in Chest Radiographs Using Multi-Institutional Data

Participants

Andre Sobiecki, PhD, MSc, (*Presenter*) Nothing to Disclose

## PURPOSE

To develop a deep learning model for identifying severe COVID cases on chest radiographs (CXRs).

## METHODS AND MATERIALS

We are developing a deep-learning-based approach for identifying severe COVID infection on CXRs. Our processing pipeline mainly included two convolutional neural networks: a lung segmentation model (LS) followed by a severity assessment model (LD) that classified the COVID as severe or not severe. Two datasets were used in this study: M1 - from the RICORD set in the Medical Imaging Data Resource Center (MIDRC) and M2 - collected with IRB approval from our institution. The training and validation sets for both LS and LD were from M1. The training set included 425 cases, 582 images and 30 images with manual outlines of the lungs. The validation set included 50 cases, 68 images and 7 images with manual outlines. Two test sets were used: one from M1 with 26 cases, 173 images and 39 images with manual outlines, and the other from M2 with 235 cases and 250 images. The CXRs from M1 were rated by 3 radiologists as negative, mild, moderate or severe and those from M2 were rated by one radiologist. For the LS model, we used an ImageNet pre-trained U-Net. We manually outlined the lungs in a subset of the NIH ChestX-ray database and a subset from M1 for two-stage fine-tuning of the U-Net, and for validation and testing. The trained LS model was deployed to all images in M1 and M2. Jaccard Index (JI), Dice Coefficient (Dice), Hausdorff distance (HD) and average distance (AD) were used to evaluate the segmentation quality. For the severity assessment LD model, we used the InceptionV1 model. The segmented lung images pre-processed with mean shift and scaled by the standard deviation of the gray levels were used as input to LD model.

## RESULTS

For the LS model on the M1 test set , we achieved mean JI of 0.87, mean Dice of 0.93, mean HD of 28.2 mm and mean AD of 3.8 mm. For the LD model, we achieved an AUC of 0.86 on the M1 test set and 0.81 on the M2 test set.

## CONCLUSION

s Our approach shows promise in identifying lungs with severe COVID infection. The current model was limited by the small training sets with severity ratings. Further improvement is expected when larger training set becomes available.

## CLINICAL RELEVANCE/APPLICATION

Our deep learning approach demonstrated the potential for accurate assessment of severe COVID infection in chest x-rays, which may be useful for treatment decision support.

Printed on: 02/07/23

## Abstract Archives of the RSNA, 2022

S3A-SPPH-1

### Development of a Deep Learning Method for Age Estimation of Cadavers Using Postmortem Vertebral CT Images

Sunday, Nov. 27 11:45AM - 12:15PM Room: Learning Center - PH DPS

#### Participants

Ikuo Kawashita, PhD, Hiroshima, Japan (*Presenter*) Nothing to Disclose

#### PURPOSE

We developed an age estimation method for unidentified cadavers. It applies deep learning to postmortem computed tomography (PMCT) images of the vertebral bones. The purpose of this study was to determine the optimal image processing method and deep-learning model for age estimation.

#### METHODS AND MATERIALS

Our image database consisted of CT images of 1,120 cases (140 cases for each of 8 decades of age from the 20s to the 90s. The training set included 70 males and 70 females per decade. The evaluation set included 187 cases (112 males, 75 females; average age 64.4 years; 56 damaged, 131 undamaged). The training images were whole-body CT images obtained from positron emission tomography-CT scans; the test images were PMCT images. In preliminary experiments using 200 training images, CT-scanograms, curved planar reformation (CPR)-, maximum intensity projection (MIP)-, and curved MIP images were compared to identify suitable image processing methods for accurate age estimation. We selected the optimal models (GoogLeNet, VGG16, ResNet, DenseNet) as network structures for deep learning (Figure 1).

#### RESULTS

MIP was the optimal image processing method for age estimation (Figure 2). The others made little learning progress and all output the same age, only VGG16 was able to estimate the age. With combined MIP and VGG16, the intraclass correlation coefficient between the actual and estimated age of the 187 evaluation cadavers was 0.96 (95% CI: 0.95 - 0.97,  $p < 0.001$ ), reliability was excellent. The mean absolute error (MAE) and the standard error of the estimate (SEE) between the actual and estimated age was 4.27 and 5.39 years, respectively. Shapley additive explanations visualization (SHAP) suggested that with MIP age-related changes around the thoracolumbar spine, e.g. osteophytes, intervertebral spacing, bone density, and aortic calcification, were assessed correctly (Figure 3).

#### CONCLUSION

s For age estimation using whole vertebral bone PMCT images, MIP yielded the best source image as the effects of gases due to decomposition were suppressed. VGG16 was the optimal network structure. The MAE was 4.27 years (margin of error +/- 10 years, 95% probability) and reliability was excellent.

#### CLINICAL RELEVANCE/APPLICATION

Our age estimation method using MIP images and VGG16 estimated the age of cadavers accurately. It may help to identify unknown cadavers.

Printed on: 02/07/23



## Abstract Archives of the RSNA, 2022

S3A-SPPH-2

### A Fairytale of a Fair Comparison in Deep Learning MRI Reconstruction

Sunday, Nov. 27 11:45AM - 12:15PM Room: Learning Center - PH DPS

#### Participants

Chungseok Oh, (*Presenter*) Nothing to Disclose

#### PURPOSE

Despite the recent success in medical imaging, deep learning suffers from a generalization issue: network performance degrades when the test data have different image characteristics (e.g. resolution, SNR, etc.) from training data. This issue suggests that diversity in dataset plays a critical role in the network performance. In medical imaging, however, many of the studies still utilize a "private" dataset because no "public" dataset is available. In this study, we demonstrated that the use of a private dataset can lead to an unfair comparison between networks.

#### METHODS AND MATERIALS

When comparing your network with a published network, there are two options: comparing with a pre-trained network or comparing with a re-trained network. When comparing with a pre-trained network, which was trained by a different private dataset from yours, the performance comparison may not be fair. To demonstrate it, two networks, designed to perform quantitative susceptibility mapping (QSM), were trained by datasets with different image characteristics, either resolution or preprocessing method, and their performances were compared. When comparing with a re-trained network, the re-trained network may underperform because of inadequate hyperparameter set or random seeds. For this case, we re-trained a published network (i.e. QSMnet) with a new dataset and demonstrated that the re-trained network may require hyperparameter tuning or multiple seeds.

#### RESULTS

[Comparison with pre-trained network] When comparing two networks trained by different datasets, each network outperformed when the training dataset has the same image characteristics as the test dataset. Therefore, the performance comparison result can easily be reversed by the image characteristics of the test dataset.[Comparison with re-trained network] When the re-trained network was hyperparameter-tuned, the performance was improved. Also, the network performances were different depending on the seed values. These results imply that the re-trained network may no longer retain its original network performance.

#### CONCLUSION

s We demonstrated that the use of a private dataset can lead to an unfair comparison between networks. For a fair comparison, a common test dataset and a trained network with information for reproducibility are necessary. This conclusion may also be applicable to other medical image processing tasks using private datasets.

#### CLINICAL RELEVANCE/APPLICATION

Performance comparison between networks is essential in academic research. This work suggests a lesson about the unfairness of comparison results which may be easily experienced in medical imaging.

Printed on: 02/07/23

## Abstract Archives of the RSNA, 2022

S3A-SPPH-3

### Temporal Deep Learning for Adhesion Detection on Cine-MRI

Sunday, Nov. 27 11:45AM - 12:15PM Room: Learning Center - PH DPS

#### Participants

Bram de Wilde, MSc, (*Presenter*) Nothing to Disclose

#### PURPOSE

To explore the benefit of deep learning video architectures for the challenging novel task of adhesion detection in the abdomen on cine-MRI.

#### METHODS AND MATERIALS

Adhesions are a common cause of chronic abdominal pain, with a prevalence of up to 20% after surgery. Adhesion diagnosis is a novel application of cine-MRI, where patients induce motion in the abdomen through the Valsalva maneuver. Adhesions connect bowel loops to the anterior abdominal wall, abdominal organs, or to other bowel loops. The radiologist must analyze the movement of organs through time, to determine adhesion presence. This is challenging and requires expertise, so AI assistance could help introduce this technique in more clinics worldwide. In this study, we aim to find out if deep neural network architectures developed for video data (2D+T) are able to extract temporal information essential to detect adhesions. Adhesions were annotated with bounding boxes on 196 2D+T cine-MRI series of 85 patients. A 2D ResNet-18 was trained using only the first frame of each series (image). A 2D+T ResNet-18 was trained using the full temporal information of each series (video). Both networks analyze 49x49 pixel patches, with a third dimension of 30 time frames for the 2D+T network. The training label for each patch is positive (1) if the center pixel is inside an annotated bounding box, otherwise negative (0). Diagnostic performance for each architecture is characterized by the area under the receiver operating characteristic curve (AUC). A permutation test compared the performances using 25 individually trained models for each architecture, in a nested 5-fold cross validation scheme.

#### RESULTS

The 2D+T ResNet-18 architecture (mean AUC 0.70 [0.55-0.84]), was significantly better ( $p=0.0011$ ) than the 2D ResNet-18 architecture (mean AUC 0.64 [0.52-0.77]).

#### CONCLUSION

Adhesion detection is an exciting new problem for AI in medical imaging, because of the complex movement patterns that are featured in abdominal cine-MRI. This study provides evidence that deep learning video architectures can learn temporal patterns essential to analyze adhesions.

#### CLINICAL RELEVANCE/APPLICATION

Cine-MRI is a novel and uncommon modality for adhesion detection. This study paves the way for assisted diagnosis of adhesions, potentially lowering the barrier for wider adoption.

Printed on: 02/07/23

## Abstract Archives of the RSNA, 2022

S3A-SPPH-4

### UK Biobank Application of Susceptibility Source Separation (Chi-Separation) Using Deep Neural Network

Sunday, Nov. 27 11:45AM - 12:15PM Room: Learning Center - PH DPS

#### Participants

Hwihun Jeong, MD, Seoul, Korea, Republic Of (*Presenter*) Nothing to Disclose

#### PURPOSE

$\chi$ -separation has been proposed for illustrating the distribution of iron and myelin in the brain. The requirement for an R2 map hampers a wide application of  $\chi$ -separation. We propose a pipeline that allows us to apply  $\chi$ -separation to UK Biobank (UKB) data using R2 maps from deep neural networks.

#### METHODS AND MATERIALS

We scanned 20 subjects (train/validation/test: 10/1/9) using the same sequences as the UKB protocol and additional sequences for the reference R2 and R2\* maps. The R2\* map of the UKB protocol datasets suffered from noise and artifacts, so we developed an additional network (R2\* denoising network) that infers reference R2\* values from UKB GRE data. A local field map is generated using the same protocol as the UKB QSM protocol. For R2 mapping, the neural network was trained using the input of MPRAGE and T2-FLAIR to generate an R2 map. Using local field and R2' maps, iLSQR-style  $\chi$ -separation was conducted to reconstruct positive and negative susceptibility, and the result was compared to the reference. Deep neural networks share the same structure as Unet with fully connected layers on the backend. The training was conducted with an L1 loss between output and reference.

#### RESULTS

The  $\chi$ -separation maps of the proposed method demonstrate a good match to those of reference. (NRMSE =  $54.4 \pm 4.7$ , PSNR =  $21.9 \pm 0.8$ , and SSIM =  $0.989 \pm 0.008$ ). The zoomed-in  $\chi_{pos}$  and  $\chi_{neg}$  maps confirm that the results of the proposed method show similar structures to those of the references, revealing details of iron and myelin distribution in the brain. Particularly in the thalamus, which contains both iron and myelin, the results demonstrate details of subthalamic nuclei, agreeing with the reference.

#### CONCLUSION

In this study, we developed a pipeline for reconstructing  $\chi$ -separation maps from the UK Biobank protocol dataset by leveraging a deep neural network. Our results suggest that  $\chi$ -separation can be applied to existing large-scale data including the UK Biobank dataset. Using this method, we will explore full UKB data, potentially benefiting from the large population dataset.

#### CLINICAL RELEVANCE/APPLICATION

$\chi$ -separation, which is a useful methodology for estimating the distribution of iron and myelin in the brain, can be applied to a large-scale dataset.

Printed on: 02/07/23

## Abstract Archives of the RSNA, 2022

S3A-SPPH-6

### Test-Time Mix-up Augmentation for Uncertainty Estimation and Expert Assistance in Medical Image Classification

Sunday, Nov. 27 11:45AM - 12:15PM Room: Learning Center - PH DPS

#### Participants

Helen Hong, PhD, PhD, Seoul, Korea, Republic Of (*Presenter*) Nothing to Disclose

#### PURPOSE

Experts are often hesitant to fully trust the prediction results of deep neural networks on disease diagnosis which consists of only labels and probability values. Uncertainty estimation is a method to quantify the confidence of the network in the disease prediction. We propose a method of estimating more reliable uncertainty measure through test-time mixup augmentation.

#### METHODS AND MATERIALS

We used an IDRid dataset consisting of 413 training and 103 validation color fundus images of 5 diabetic retinopathy (DR) disease grades. We first train a VGG-19 on the mixup-augmented training data. In test-time, a set of mixup test data is generated by applying mixup for each test data with the randomly sampled training data. The trained CNN is then applied to the mixup test data to obtain the mixup test labels. In lesion classification, the label of each test data is determined by majority voting on the mixup test labels. In uncertainty estimation, the uncertainty of each test data is computed by the entropy of the distribution of mixup test labels.

#### RESULTS

In experiments, we compared the proposed TTMA method with the existing test-time affine-based augmentation (TTA) and the Monte-Carlo drop-out (MCDO) methods. The data uncertainty can be evaluated by two criteria. First, the rejection-accuracy curves can evaluate the reliability of the uncertainty by observing whether the accuracy is increasing as the uncertainty decreases. In DR grading, the proposed TTMA achieved 100% accuracy at a 95% rejection rate, meaning that the 5% of the test results with the lowest TTMA uncertainty are 100% accurate. In contrast, the TTA and MCDO achieved 68.0% and 71.6% accuracy even at a 95% rejection rate, respectively. Second, the histogram of uncertainty of correct and incorrect predictions can evaluate the uncertainty by observing whether the uncertainty distributions of two predictions are separable. In TTA and MCDO, both distributions are heavily overlapped around the zero uncertainty. However, in the proposed TTMA, the distributions are not only shifted to the higher uncertainty values thanks to the mixup perturbation, but also in relatively separable form.

#### CONCLUSION

The proposed TTMA provides more reliable uncertainty measure than the existing TTA or MCDO methods thanks to the mixup perturbation. The proposed TTMA uncertainty can assist the experts to select the data requires additional review among the CNN prediction results. (This work was supported by the Korea Medical Device Development Fund grant funded by the Korea government (Project Number: 9991007550, KMDF\_PR\_20200901\_0269))

#### CLINICAL RELEVANCE/APPLICATION

The proposed uncertainty measure can assist experts to decide whether to accept or revision the CNN prediction results.

Printed on: 02/07/23



## Abstract Archives of the RSNA, 2022

S3A-SPPH-8

### Automatic Tracking of Prostate Fiducials in X-Ray Images With Deep-Learning Model During Radiation Treatment

Sunday, Nov. 27 11:45AM - 12:15PM Room: Learning Center - PH DPS

#### Participants

Shuang Zhou, MS, Saint Louis, MO (*Presenter*) Nothing to Disclose

#### PURPOSE

Automatic tracking of fiducials is needed in image-guided radiation treatments. We developed a deep-learning based fiducial detection method can automatically detect and track fiducials in x-ray images during radiation treatments.

#### METHODS AND MATERIALS

Total of 1870 orthogonal x-ray images acquired from 63 patients during radiation treatments were used for training (90%) and validation (10%). Additional images from 12 additional patients were used for testing. The fiducials in the x-ray images were manually labeled with a rectangle bounding-box in Microsoft COCO format. Improved YOLOX deep-learning network developed for the object detection was trained with the manually labeled x-ray images. Mean average precision (mAP) was used as the evaluation metric.

#### RESULTS

The YOLOX deep-learning network was able to detect fiducials in the prostate with reasonable accuracy. The average precision (AP) scores derived from the precision-recall curve range are 0.44 and 0.16 for anteroposterior and lateral x-ray, respectively. The discrepancy was due to the poor visibility of fiducials in lateral x-rays.

#### CONCLUSION

s The YOLOX deep-learning network can detect most prostate fiducials in x-ray images with reasonable visibility and potentially can be used for automatic tracking of the target during radiation treatment delivery.

#### CLINICAL RELEVANCE/APPLICATION

Automatic detection and tracking of fiducials in the treatment target can facilitate precise radiation treatment delivery.

Printed on: 02/07/23



## Abstract Archives of the RSNA, 2022

S3A-SPPH-9

### Deep Learning Identification of Severe COVID Infection in Chest Radiographs Using Multi-Institutional Data

Sunday, Nov. 27 11:45AM - 12:15PM Room: Learning Center - PH DPS

#### Participants

Andre Sobiecki, PhD, MSc, (*Presenter*) Nothing to Disclose

#### PURPOSE

To develop a deep learning model for identifying severe COVID cases on chest radiographs (CXRs).

#### METHODS AND MATERIALS

We are developing a deep-learning-based approach for identifying severe COVID infection on CXRs. Our processing pipeline mainly included two convolutional neural networks: a lung segmentation model (LS) followed by a severity assessment model (LD) that classified the COVID as severe or not severe. Two datasets were used in this study: M1 - from the RICORD set in the Medical Imaging Data Resource Center (MIDRC) and M2 - collected with IRB approval from our institution. The training and validation sets for both LS and LD were from M1. The training set included 425 cases, 582 images and 30 images with manual outlines of the lungs. The validation set included 50 cases, 68 images and 7 images with manual outlines. Two test sets were used: one from M1 with 26 cases, 173 images and 39 images with manual outlines, and the other from M2 with 235 cases and 250 images. The CXRs from M1 were rated by 3 radiologists as negative, mild, moderate or severe and those from M2 were rated by one radiologist. For the LS model, we used an ImageNet pre-trained U-Net. We manually outlined the lungs in a subset of the NIH ChestX-ray database and a subset from M1 for two-stage fine-tuning of the U-Net, and for validation and testing. The trained LS model was deployed to all images in M1 and M2. Jaccard Index (JI), Dice Coefficient (Dice), Hausdorff distance (HD) and average distance (AD) were used to evaluate the segmentation quality. For the severity assessment LD model, we used the InceptionV1 model. The segmented lung images pre-processed with mean shift and scaled by the standard deviation of the gray levels were used as input to LD model.

#### RESULTS

For the LS model on the M1 test set, we achieved mean JI of 0.87, mean Dice of 0.93, mean HD of 28.2 mm and mean AD of 3.8 mm. For the LD model, we achieved an AUC of 0.86 on the M1 test set and 0.81 on the M2 test set.

#### CONCLUSION

Our approach shows promise in identifying lungs with severe COVID infection. The current model was limited by the small training sets with severity ratings. Further improvement is expected when larger training set becomes available.

#### CLINICAL RELEVANCE/APPLICATION

Our deep learning approach demonstrated the potential for accurate assessment of severe COVID infection in chest x-rays, which may be useful for treatment decision support.

Printed on: 02/07/23

## Abstract Archives of the RSNA, 2022

S3A-SPVA

### Vascular Sunday Poster Discussions - A

Sunday, Nov. 27 11:45AM - 12:15PM Room: Learning Center - VA DPS

#### Sub-Events

#### S3A-SPVA-1 Acceleration Motion Compensation Diffusion-weighted Imaging For Aortitis: Phantom and Clinical Studies

##### Participants

Tomoko Hyodo, MD, Osaka-sayama, Japan (*Presenter*) Nothing to Disclose

##### PURPOSE

To investigate the utility of acceleration motion compensation diffusion-weighted imaging (aMC-DWI) in assessing ascending aortitis.

##### METHODS AND MATERIALS

A phantom experiment and a clinical study were conducted on a 1.5 T MRI scanner. Qualitative comparisons were made between the aMC-DWI and conventional DWI (cDWI) (b factor=800 s/mm<sup>2</sup> for both) since the apparent diffusion coefficient value of aMC-DWI could not be compared in principle. In the phantom study, two experimenters independently manipulated the balloon to move the syringe filled with agar up and down in the 5mm range at 60 times per minute. The phantom images obtained using each DWI technique were graded on a 5-point scale (1=poor to 5=as good as a static image using cDWI). Mann-Whitney U tests with Bonferroni correction were used to assess differences among the sessions. The prospective clinical study was performed on patients with suspected aortitis undergoing FDG-PET/CT and whole-body diffusion-weighted MRI. Both DWI techniques were performed for the thorax in each patient. cDWI and aMC-DWI were visually scored for active inflammation of the ascending aorta (0=negative or 1=positive). Statistical analyses included calculation of diagnostic accuracy with FDG-PET/CT as the reference standard and a two-sided one-sample t-test (assuming mean difference score [aMC-DWI - cDWI]= 0).

##### RESULTS

In the phantom experiment, aMC-DWI showed a significantly higher median score than cDWI in both experimenters 1 (4 vs 3; P =.048) and 2 (3 vs 1; P =.048). In the clinical study, 21 patients (median age, 69 years [range, 19-84 years]; 15 women) were assessed. Eight patients were diagnosed with active arteritis (five with Takayasu's arteritis and the other with giant cell arteritis). Seven patients were found to have active ascending aortitis in FDG-PET/CT (with a median and range of maximum standardized uptake value, 3.5[2.2-4.4]). The sensitivity, specificity, and positive and negative predictive value, respectively, for detecting active inflammation in the ascending aorta were 1/7 (14 %), 13/14 (93 %), 1/2 (50 %), and 13/19(68 %) for cDWI; and 6/7 (86 %), 9/14 (64 %), 6/11 (55 %) and 9/10 (90 %) for aMC-DWI. Mean difference between two DWI techniques was significant in seven PET-positive cases (t = 3.873; P = .008; 95% CI = 0.26-1).

##### CONCLUSION

s The aMC technique promises to increase the utility of DWI in the assessment of ascending aortitis.

##### CLINICAL RELEVANCE/APPLICATION

The activity of thoracic aortitis is usually assessed by a segmental approach (the ascending, arch, and descending). With aMC-DWI, MRI may become an alternative to FDG-PET/CT.

Printed on: 02/07/23

## Abstract Archives of the RSNA, 2022

S3A-SPVA-1

### Acceleration Motion Compensation Diffusion-weighted Imaging For Aortitis: Phantom and Clinical Studies

Sunday, Nov. 27 11:45AM - 12:15PM Room: Learning Center - VA DPS

#### Participants

Tomoko Hyodo, MD, Osaka-sayama, Japan (*Presenter*) Nothing to Disclose

#### PURPOSE

To investigate the utility of acceleration motion compensation diffusion-weighted imaging (aMC-DWI) in assessing ascending aortitis.

#### METHODS AND MATERIALS

A phantom experiment and a clinical study were conducted on a 1.5 T MRI scanner. Qualitative comparisons were made between the aMC-DWI and conventional DWI (cDWI) (b factor=800 s/mm<sup>2</sup> for both) since the apparent diffusion coefficient value of aMC-DWI could not be compared in principle. In the phantom study, two experimenters independently manipulated the balloon to move the syringe filled with agar up and down in the 5mm range at 60 times per minute. The phantom images obtained using each DWI technique were graded on a 5-point scale (1=poor to 5=as good as a static image using cDWI). Mann-Whitney U tests with Bonferroni correction were used to assess differences among the sessions. The prospective clinical study was performed on patients with suspected aortitis undergoing FDG-PET/CT and whole-body diffusion-weighted MRI. Both DWI techniques were performed for the thorax in each patient. cDWI and aMC-DWI were visually scored for active inflammation of the ascending aorta (0=negative or 1=positive). Statistical analyses included calculation of diagnostic accuracy with FDG-PET/CT as the reference standard and a two-sided one-sample t-test (assuming mean difference score [aMC-DWI - cDWI]= 0).

#### RESULTS

In the phantom experiment, aMC-DWI showed a significantly higher median score than cDWI in both experimenters 1 (4 vs 3; P =.048) and 2 (3 vs 1; P =.048). In the clinical study, 21 patients (median age, 69 years [range, 19-84 years]; 15 women) were assessed. Eight patients were diagnosed with active arteritis (five with Takayasu's arteritis and the other with giant cell arteritis). Seven patients were found to have active ascending aortitis in FDG-PET/CT (with a median and range of maximum standardized uptake value, 3.5[2.2-4.4]). The sensitivity, specificity, and positive and negative predictive value, respectively, for detecting active inflammation in the ascending aorta were 1/7 (14 %), 13/14 (93 %), 1/2 (50 %), and 13/19(68 %) for cDWI; and 6/7 (86 %), 9/14 (64 %), 6/11 (55 %) and 9/10 (90 %) for aMC-DWI. Mean difference between two DWI techniques was significant in seven PET-positive cases (t = 3.873; P = .008; 95% CI = 0.26-1).

#### CONCLUSION

s The aMC technique promises to increase the utility of DWI in the assessment of ascending aortitis.

#### CLINICAL RELEVANCE/APPLICATION

The activity of thoracic aortitis is usually assessed by a segmental approach (the ascending, arch, and descending). With aMC-DWI, MRI may become an alternative to FDG-PET/CT.

Printed on: 02/07/23



## Abstract Archives of the RSNA, 2022

S3B-SPBR

### Breast Sunday Poster Discussions - B

Sunday, Nov. 27 12:15PM - 12:45PM Room: Learning Center - BR DPS

#### Participants

Katja Pinker-Domenig, MD, PhD, New York, NY (*Moderator*) Speakers Bureau, European Society of Breast Imaging; Speakers Bureau, Siemens AG; Speakers Bureau, IDKD; Speakers Bureau, Canon Medical Systems Corporation; Consultant, F. Hoffmann-La Roche Ltd; Consultant, Merantix Healthcare; Consultant, AURA Health

#### Sub-Events

### S3B-SPBR-1 Deep Learning with 3D Convolutional Neural Networks For Prediction of BRCA Gene Mutation in High-Risk Breast Cancer Patients

#### Participants

Sung Eun Song, MD, (*Presenter*) Nothing to Disclose

#### PURPOSE

Patients who carry a mutation in germline BRCA1/2 (gBRCA) genes might benefit from targeted therapy but genetic testing is costly. The purpose of this study was to determine the feasibility of using a deep learning (DL) approach for predicting the gBRCA mutation by using the three-dimensional (3D) MR images of breast cancer and clinical data in high-risk cancer patients.

#### METHODS AND MATERIALS

A total of 312 breast cancer patients who had high-risk factors and underwent gBRCA tests were retrospectively collected. A data set of 3D MR images of breast cancer from 312 subjects were manually segmented on contrast-enhanced T1-weighted subtraction images by an experienced breast radiologist. A 3D convolutional neural networks (CNNs)-based transformer architectures were trained on 80% of the data set and tested on the remaining 20%. Clinical data obtaining from biopsy were also used. The models' performances with or without clinical data were analyzed in terms of sensitivity, specificity, and areas under the receiver operating characteristic curve (AUCs) and compared by DeLong's test.

#### RESULTS

Among 312 patients, 112 (35.9%) had gBRCA 1/2 pathogenic mutation. For prediction of gBRCA mutation, a 3D CNNs-based transformer architectures achieved an AUC of 0.82 (95% confidence interval [CI]: 0.69, 0.96) in the train set and that of 0.81 (95%CI:0.69, 0.95) in the test set, respectively. Adding the clinical data did not improve an AUC of DL model (AUCs: 0.83 and 0.81 in both of train and test sets;  $P = .14$  and  $.15$ , respectively). The DL model achieved 72% sensitivity and 80% specificity in the train set and 74% sensitivity and 86% specificity in the test set.

#### CONCLUSION

Using 3D MR images, DL models can effectively predict the gBRCA mutation without clinical data.

#### CLINICAL RELEVANCE/APPLICATION

Artificial intelligence may provide an early detection of gBRCA mutation for breast cancer patients who had high-risk factors.

### S3B-SPBR-2 Automatic Assessment of The Quality of Breast Positioning in Mammography Using Deep Learning-based Methods

#### Participants

Huei-yi Tsai, MD, MS, (*Presenter*) Nothing to Disclose

#### PURPOSE

Breast positioning assessment is an important component of mammographic quality control. The aim of this study is to develop deep learning-based automated analytic tools to assess breast positioning, focusing on the completeness of breast tissue in the images.

#### METHODS AND MATERIALS

Assessing metrics: 1. Completeness of breast tissue, classifying into three degrees (inadequate, acceptable, and perfect); 2. Measuring the length of the posterior nipple line (PNL) on the CC view and MLO view; 3. Length of pectoral muscle to PNL. Datasets: Screening mammography were retrospectively enrolled. The images showing breast implant or breast distortion due to tumor or previous operation were excluded. A total of 479 mammography with 1,916 images (958 CC view and 958 MLO view) were labeled by two radiologists for the completeness of breast tissue after a consensus meeting. Manual annotation of nipple and pectoral muscle was also performed. The data was then randomly subdivided into training, validation, and test datasets. Model training and metrics computation: For classification of the completeness of breast tissue in the image, a ConvMixer model was used for patch embedding and feature extraction, followed by Random Forest classification. For MLO view, before ConvMixer model, the pectoral muscle was first localized by using You Only Look Once (YOLO)-v5 model and removed from the diagonal line of the bounding box. YOLO-v5 was trained to detect the nipple and pectoral muscle in mammograms. The length of PNL and the length

from the inferior extent of pectoral muscle to PNL were then calculated by automatic drawing a vertical line from nipple to the posterior image border/pectoral muscle. Intraclass correlation coefficient (ICC) was used to investigate the correlation between model and manual measurements.

## RESULTS

For classification of the completeness of breast tissue, the AUCs of the three degrees (inadequate, acceptable, and perfect) were 0.97 (95%CI: 0.96-0.98), 0.79 (95%CI: 0.77-0.81), and 0.92 (95%CI: 0.91-0.93). The mean average precisions of YOLO-v5 model for nipple and pectoral muscle detection were 0.995 and 0.863, respectively. The ICC for the length of PNL between model and manual measurements was 0.997 for CC view and 0.984 for MLO view. The ICC for the length of pectoral muscle to PNL between model and manual measurements was 0.981.

## CONCLUSION

The proposed deep learning-based methods allowed for automatic and accurate assessment of the quality of breast positioning in mammography.

## CLINICAL RELEVANCE/APPLICATION

The deep learning-based methods have the potential to be part of an automated image quality assessment system.

### S3B-SPBR-3 Attention-Based Deep Learning for Breast Lesions Classification on Contrast Enhanced Spectral Mammography: A Multicenter Study

Participants

Ning Mao, Yantai, China (*Presenter*) Nothing to Disclose

## PURPOSE

This study aims to develop an attention-based deep learning model for distinguishing benign from malignant breast lesions on Contrast Enhanced Spectral Mammography (CESM).

## METHODS AND MATERIALS

Preoperative CESM images of 1239 patients, which were definitely diagnosed on pathology in a multicenter cohort, were divided into training and validation sets, internal and external test sets. The regions of interest of the breast lesions were outlined manually by a senior radiologist. We adopted three conventional convolutional neural networks (CNNs), namely, DenseNet 121, Xception, and ResNet 50, as the backbone architectures and incorporated the convolutional block attention module (CBAM) into them for classification. The performance of the models was analyzed in terms of the receiver operating characteristic (ROC) curve, accuracy, the positive predictive value (PPV), the negative predictive value (NPV), the F1 score, the precision recall curve (PRC), and heat maps. The final models were compared with the diagnostic performance of conventional CNNs, radiomics models, and radiologists with specialized breast imaging experience.

## RESULTS

The best-performing deep learning model, that is, the CBAM-based Xception, achieved an area under the ROC curve (AUC) of 0.970, a sensitivity of 0.848, a specificity of 1.000, and an accuracy of 0.891 on the external test set, which was higher than those of other CNNs, radiomics models, and radiologists. The PRC and the heat maps also indicated the favorable predictive performance of the attention-based CNN model. The diagnostic performance of radiologists improved with deep learning assistance.

## CONCLUSION

Using an attention-based deep learning model based on CESM images can help to distinguish benign from malignant breast lesions, and the diagnostic performance of radiologists improved with deep learning assistance.

## CLINICAL RELEVANCE/APPLICATION

We developed an attention-based deep learning model using CESM to noninvasively distinguish between benign and malignant breast lesions. In addition, the diagnostic performance of radiologists improved with deep learning assistance. Therefore, it has high clinical applicability and promotion value.

### S3B-SPBR-4 A Regional Interpretation of Mammography Phantom Object by Evaluating ACR Phantom Images using a Deep Learning Model

Participants

Kyung Mi Lee, MD, PhD, Seoul, Korea, Republic Of (*Presenter*) Nothing to Disclose

## PURPOSE

Mammography is the initial examination to detect breast cancer symptoms, and quality control of mammography devices is crucial to maintain accurate diagnosis and to safeguard against degradation of performance. The objective of this study was to assist radiologists in mammography phantom image evaluation by developing and validating an interpretable deep learning model capable of objectively evaluating the quality of standard phantom images for mammography.

## METHODS AND MATERIALS

A total of 2,208 mammography phantom images were collected for periodic accreditation of the scanner from 1,755 institutions. The dataset was randomly split into training (1,808 images) and testing (400 images) datasets. To develop an interpretable model that contains two deep learning networks in series, five processing steps were performed: mammography phantom detection, phantom object detection, post-processing, score evaluation, and a report with a comment.

## RESULTS

For phantom detection, the accuracy and mean intersection over union (mIOU) were 1.00 and 0.938 in the test dataset, respectively. During phantom object detection, a total of 6,369 out of 6,400 objects were detected as the correct object class, and the accuracy and mIOU were 0.995 and 0.813, respectively. The predicted score for each object showed a consensus of 97.40% excluding fifth object in the fiber group, fourth object in the specks and mass groups. A score difference of 240 objects

was evaluated for the fiber group, 171 for the specks group, and 207 for the mass group. The highest difference in scores for the 0.5 point difference was found to be 145 objects at the fifth object in the fiber group (36.80% in itself), 149 objects at the fourth object of the specks (38.21%), and 163 objects in the fourth mass group (41.06%).

## CONCLUSION

The interpretable deep learning model using large-scale data from multiple centers shows high performance and reasonable object scoring, successfully validating the reliability and feasibility of mammography phantom image quality management.

## CLINICAL RELEVANCE/APPLICATION

Deep learning algorithm with phantom image evaluator can demonstrate to be used to assess quality control for mammography, CT and MRI as a practical method for early and precision diagnosis.

### **S3B-SPBR-5 Real-time Decision Support by Light-weighted AI Model Trained with Large-scale Data for Breast Cancer Diagnosis Using Ultrasound**

Participants

Jaehil Kim, PhD, Daegu, Korea, Republic Of (*Presenter*) Stockholder, BeamWorks, Inc.

## PURPOSE

Although many of artificial intelligence (AI) models for ultrasound (US) diagnosis have been introduced, real-time decision support by AI is still challenging, due to its high computation cost. We aimed to evaluate the technical feasibility of real-time decision support by light-weighted AI model trained with large-scale data for breast cancer diagnosis using US.

## METHODS AND MATERIALS

Using a large-scale data over 400,000 breast US images, we developed an AI decision support model based on weakly-supervised learning. In order to achieve the real-time processing of the developed AI model, we implemented a quantization method which can reduce inference time and memory usage while maintaining diagnostic accuracy. For the evaluation of the real-time decision support, US examinations were prospectively recorded from May 2021 in biopsy-proven breast cancer patients. A total of 8 video clips were simulated and tested with our light-weighted AI model. Diagnostic performance and inference time to return AI diagnosis were measured according to two hardware configurations (1: Intel Core i7 2.90 GHz with a GPU and 2: Intel Core i9 2.30Hz without GPU). Frame-wise ground truth labeling for malignancy/non-malignancy was performed by an experienced radiologist with reference to pathologic and radiologic reports.

## RESULTS

Our light-weighted AI model diagnosed breast US images in the video clips in real-time and simultaneously produced score for cancer with cancer-relevant maps. Of the 8 examinations with breast cancer patients, our maps correctly highlighted the cancer in all examinations. For a total of 19,231 images with 4,525 malignant images and 14,706 non-malignant images, extracted from the video clips, the diagnostic performance was 0.93 of AUC and sensitivity/specificity was 85.4%/85.2%, respectively. Mean time to return AI diagnosis for each image was 0.03 seconds in hardware configuration 1 with GPU and 0.06 seconds in configuration 2 without GPU.

## CONCLUSION

With our development of light-weighted AI model trained with a large-scale data, real-time decision support is feasible to diagnose breast cancer using US with high detection and diagnostic performances.

## CLINICAL RELEVANCE/APPLICATION

Real-time decision support for breast US diagnosis can help sonographers/radiologists to detect and differentiate the breast lesions among high volume of time-series images.

### **S3B-SPBR-6 Real-World Retrospective Cohort Studies of Artificial Intelligence (AI) Readers in Population Breast Cancer Screening**

Participants

Helen Frazer, FRANZCR, Fitzroy, Australia (*Presenter*) Nothing to Disclose

## PURPOSE

To assess an AI reader in various breast cancer screening operating modes in real-world retrospective cohort studies.

## METHODS AND MATERIALS

We curated two datasets from a population breast cancer screening program. First, we established a cancer-rich dataset comprising 10,917 cancer images from 4,680 screening episodes (4,647 clients) and 69,775 non-cancer images from 40,364 screening episodes (39,704 clients), which we used for AI model training and testing. Second, we compiled an independent two-year sequential population cohort of women screened in 2016-2017 comprising 497,288 screening episodes (494,246 clients) and 2,094,424 images. This second dataset was used for the retrospective cohort studies. Five candidate CNN models (ECAResNet269d, ResNet152d, ResNet200d, ResNet101d, Xception41) were trained and tested on the cancer-rich set. The ensemble of the five CNN models achieved an AUROC of 0.877 (95% CI 0.873, 0.881) on the 2016-2017 population dataset and was used for the retrospective cohort simulation study. The study assessed application of the AI model in three operating modes: i) first pass read to remove easy normal mammograms; ii) second reader replacement with comparable/better accuracy; iii) final pass read to detect missed cancers. The simulation included all 497,288 screening episodes of the 2016-2017 retrospective cohort, real-world reader and screening outcomes for comparison, and real-world unit costs. The simulation model produced key classification outcomes (TP, FP, TN, FN) for each retrospective AI operating mode with a range of thresholds, as well as cost implications.

## RESULTS

The best result was the operating mode of second reader replacement. It demonstrated superior performance to current screening outcomes with 396,173 fewer human reads, 3,103 fewer unnecessary recalls, 51 fewer missed cancers and a 16.9% reduction in reading and assessment costs (threshold set at 0.1).

## CONCLUSION

s Our retrospective cohort studies using the simulation model demonstrated that the use of an AI model for second reader replacement can achieve better screening outcomes, with fewer false negatives and fewer false positives at lower cost, than the current screening process.

## CLINICAL RELEVANCE/APPLICATION

Retrospective and prospective cohort studies with real-world clinical data and consideration of operating modes are necessary to evaluate AI readers in population breast cancer screening programs.

## S3B-SPBR-7 Comparison of Mammography Artificial Intelligence Algorithms for 5-year Breast Cancer Risk Prediction

Participants

Vignesh Arasu, MD, Vallejo, CA (*Presenter*) Nothing to Disclose

## PURPOSE

We examined the ability of mammography artificial intelligence (AI) algorithms, most trained for computer-aided detection (CAD) of visible breast cancer on mammograms, to predict 5-year future risk. We compared 5 AI algorithms -- 3 commercial CAD algorithms (representing 1/3 of the FDA/CE cleared devices) and 2 well known open source algorithms -- relative to the Breast Cancer Surveillance Consortium clinical risk model (BCSC v2)

## METHODS AND MATERIALS

In this case-cohort study, women with a screening mammogram in 2016 at a large managed care organization with no evidence of cancer on final imaging assessment were followed through September 2021. Women were excluded with a prior history of breast cancer or highly penetrant gene mutation. From the 324,009 eligible women, a random subcohort of 13,628 (4.2%) were selected; 193 had incident cancer. All 4,391 additional incident cancers were also included. AI scores were generated from the index 2016 mammogram. Discrimination was assessed with time-varying area under the curve [AUC(t)].

## RESULTS

For incident cancers at 0 to 1 year (interval cancer risk), the AUC(t) for BCSC was 0.62 (95% CI 0.59, 0.66), and AI algorithms all had significantly higher AUC(t)s, ranging from 0.67-0.71 ( $P < .05$ ). For incident cancers at >1 to 5 years (5-year future cancer risk), the BCSC AUC(t) was 0.61 (95% CI 0.60, 0.62), and the AI algorithms AUC(t)s ranged from 0.63 to 0.67, all significantly higher than BCSC. Combined BCSC and AI models demonstrated AUC(t)s for interval cancer risk of 0.67-0.73 and for 5-year future cancer risk of 0.66-0.68.

## CONCLUSION

s The evaluated AI mammography algorithms had significantly higher discrimination than the BCSC clinical risk model for interval and 5-year future cancer risk. Combined AI and BCSC models had slightly higher discrimination than AI alone.

## CLINICAL RELEVANCE/APPLICATION

Mammography AI algorithms provide a new approach for improving breast cancer risk prediction beyond clinical variables such as age, family history, or the traditional imaging risk biomarker of breast density. Most CAD algorithms, trained for detection at shorter time horizons can also predict longer-term risk. Breast imaging practices may incorporate CAD AI for both diagnostic assistance and future risk stratification.

Printed on: 02/07/23

## Abstract Archives of the RSNA, 2022

S3B-SPBR-1

### Deep Learning with 3D Convolutional Neural Networks For Prediction of BRCA Gene Mutation in High-Risk Breast Cancer Patients

Sunday, Nov. 27 12:15PM - 12:45PM Room: Learning Center - BR DPS

#### Participants

Sung Eun Song, MD, (*Presenter*) Nothing to Disclose

#### PURPOSE

Patients who carry a mutation in germline BRCA1/2 (gBRCA) genes might benefit from targeted therapy but genetic testing is costly. The purpose of this study was to determine the feasibility of using a deep learning (DL) approach for predicting the gBRCA mutation by using the three-dimensional (3D) MR images of breast cancer and clinical data in high-risk cancer patients.

#### METHODS AND MATERIALS

A total of 312 breast cancer patients who had high-risk factors and underwent gBRCA tests were retrospectively collected. A data set of 3D MR images of breast cancer from 312 subjects were manually segmented on contrast-enhanced T1-weighted subtraction images by an experienced breast radiologist. A 3D convolutional neural networks (CNNs)-based transformer architectures were trained on 80% of the data set and tested on the remaining 20%. Clinical data obtaining from biopsy were also used. The models' performances with or without clinical data were analyzed in terms of sensitivity, specificity, and areas under the receiver operating characteristic curve (AUCs) and compared by DeLong's test.

#### RESULTS

Among 312 patients, 112 (35.9%) had gBRCA 1/2 pathogenic mutation. For prediction of gBRCA mutation, a 3D CNNs-based transformer architectures achieved an AUC of 0.82 (95% confidence interval [CI]: 0.69, 0.96) in the train set and that of 0.81 (95%CI:0.69, 0.95) in the test set, respectively. Adding the clinical data did not improve an AUC of DL model (AUCs: 0.83 and 0.81 in both of train and test sets; P= .14 and .15, respectively). The DL model achieved 72% sensitivity and 80% specificity in the train set and 74% sensitivity and 86% specificity in the test set.

#### CONCLUSION

Using 3D MR images, DL models can effectively predict the gBRCA mutation without clinical data.

#### CLINICAL RELEVANCE/APPLICATION

Artificial intelligence may provide an early detection of gBRCA mutation for breast cancer patients who had high-risk factors.

Printed on: 02/07/23

## Abstract Archives of the RSNA, 2022

S3B-SPBR-2

### Automatic Assessment of The Quality of Breast Positioning in Mammography Using Deep Learning-based Methods

Sunday, Nov. 27 12:15PM - 12:45PM Room: Learning Center - BR DPS

#### Participants

Huei-yi Tsai, MD, MS, (*Presenter*) Nothing to Disclose

#### PURPOSE

Breast positioning assessment is an important component of mammographic quality control. The aim of this study is to develop deep learning-based automated analytic tools to assess breast positioning, focusing on the completeness of breast tissue in the images.

#### METHODS AND MATERIALS

Assessing metrics: 1. Completeness of breast tissue, classifying into three degrees (inadequate, acceptable, and perfect); 2. Measuring the length of the posterior nipple line (PNL) on the CC view and MLO view; 3. Length of pectoral muscle to PNL. Datasets: Screening mammography were retrospectively enrolled. The images showing breast implant or breast distortion due to tumor or previous operation were excluded. A total of 479 mammography with 1,916 images (958 CC view and 958 MLO view) were labeled by two radiologists for the completeness of breast tissue after a consensus meeting. Manual annotation of nipple and pectoral muscle was also performed. The data was then randomly subdivided into training, validation, and test datasets. Model training and metrics computation: For classification of the completeness of breast tissue in the image, a ConvMixer model was used for patch embedding and feature extraction, followed by Random Forest classification. For MLO view, before ConvMixer model, the pectoral muscle was first localized by using You Only Look Once (YOLO)-v5 model and removed from the diagonal line of the bounding box. YOLO-v5 was trained to detect the nipple and pectoral muscle in mammograms. The length of PNL and the length from the inferior extent of pectoral muscle to PNL were then calculated by automatic drawing a vertical line from nipple to the posterior image border/pectoral muscle. Intraclass correlation coefficient (ICC) was used to investigate the correlation between model and manual measurements.

#### RESULTS

For classification of the completeness of breast tissue, the AUCs of the three degrees (inadequate, acceptable, and perfect) were 0.97 (95%CI: 0.96-0.98), 0.79 (95%CI: 0.77-0.81), and 0.92 (95%CI: 0.91-0.93). The mean average precisions of YOLO-v5 model for nipple and pectoral muscle detection were 0.995 and 0.863, respectively. The ICC for the length of PNL between model and manual measurements was 0.997 for CC view and 0.984 for MLO view. The ICC for the length of pectoral muscle to PNL between model and manual measurements was 0.981.

#### CONCLUSION

The proposed deep learning-based methods allowed for automatic and accurate assessment of the quality of breast positioning in mammography.

#### CLINICAL RELEVANCE/APPLICATION

The deep learning-based methods have the potential to be part of an automated image quality assessment system.

Printed on: 02/07/23



## Abstract Archives of the RSNA, 2022

S3B-SPBR-3

### Attention-Based Deep Learning for Breast Lesions Classification on Contrast Enhanced Spectral Mammography: A Multicenter Study

Sunday, Nov. 27 12:15PM - 12:45PM Room: Learning Center - BR DPS

#### Participants

Ning Mao, Yantai, China (*Presenter*) Nothing to Disclose

#### PURPOSE

This study aims to develop an attention-based deep learning model for distinguishing benign from malignant breast lesions on Contrast Enhanced Spectral Mammography (CESM).

#### METHODS AND MATERIALS

Preoperative CESM images of 1239 patients, which were definitely diagnosed on pathology in a multicenter cohort, were divided into training and validation sets, internal and external test sets. The regions of interest of the breast lesions were outlined manually by a senior radiologist. We adopted three conventional convolutional neural networks (CNNs), namely, DenseNet 121, Xception, and ResNet 50, as the backbone architectures and incorporated the convolutional block attention module (CBAM) into them for classification. The performance of the models was analyzed in terms of the receiver operating characteristic (ROC) curve, accuracy, the positive predictive value (PPV), the negative predictive value (NPV), the F1 score, the precision recall curve (PRC), and heat maps. The final models were compared with the diagnostic performance of conventional CNNs, radiomics models, and radiologists with specialized breast imaging experience.

#### RESULTS

The best-performing deep learning model, that is, the CBAM-based Xception, achieved an area under the ROC curve (AUC) of 0.970, a sensitivity of 0.848, a specificity of 1.000, and an accuracy of 0.891 on the external test set, which was higher than those of other CNNs, radiomics models, and radiologists. The PRC and the heat maps also indicated the favorable predictive performance of the attention-based CNN model. The diagnostic performance of radiologists improved with deep learning assistance.

#### CONCLUSION

Using an attention-based deep learning model based on CESM images can help to distinguish benign from malignant breast lesions, and the diagnostic performance of radiologists improved with deep learning assistance.

#### CLINICAL RELEVANCE/APPLICATION

We developed an attention-based deep learning model using CESM to noninvasively distinguish between benign and malignant breast lesions. In addition, the diagnostic performance of radiologists improved with deep learning assistance. Therefore, it has high clinical applicability and promotion value.

Printed on: 02/07/23



## Abstract Archives of the RSNA, 2022

S3B-SPBR-4

### A Regional Interpretation of Mammography Phantom Object by Evaluating ACR Phantom Images using a Deep Learning Model

Sunday, Nov. 27 12:15PM - 12:45PM Room: Learning Center - BR DPS

#### Participants

Kyung Mi Lee, MD, PhD, Seoul, Korea, Republic Of (*Presenter*) Nothing to Disclose

#### PURPOSE

Mammography is the initial examination to detect breast cancer symptoms, and quality control of mammography devices is crucial to maintain accurate diagnosis and to safeguard against degradation of performance. The objective of this study was to assist radiologists in mammography phantom image evaluation by developing and validating an interpretable deep learning model capable of objectively evaluating the quality of standard phantom images for mammography.

#### METHODS AND MATERIALS

A total of 2,208 mammography phantom images were collected for periodic accreditation of the scanner from 1,755 institutions. The dataset was randomly split into training (1,808 images) and testing (400 images) datasets. To develop an interpretable model that contains two deep learning networks in series, five processing steps were performed: mammography phantom detection, phantom object detection, post-processing, score evaluation, and a report with a comment.

#### RESULTS

For phantom detection, the accuracy and mean intersection over union (mIOU) were 1.00 and 0.938 in the test dataset, respectively. During phantom object detection, a total of 6,369 out of 6,400 objects were detected as the correct object class, and the accuracy and mIOU were 0.995 and 0.813, respectively. The predicted score for each object showed a consensus of 97.40% excluding fifth object in the fiber group, fourth object in the specks and mass groups. A score difference of 240 objects was evaluated for the fiber group, 171 for the specks group, and 207 for the mass group. The highest difference in scores for the 0.5 point difference was found to be 145 objects at the fifth object in the fiber group (36.80% in itself), 149 objects at the fourth object of the specks (38.21%), and 163 objects in the fourth mass group (41.06%).

#### CONCLUSION

The interpretable deep learning model using large-scale data from multiple centers shows high performance and reasonable object scoring, successfully validating the reliability and feasibility of mammography phantom image quality management.

#### CLINICAL RELEVANCE/APPLICATION

Deep learning algorithm with phantom image evaluator can demonstrate to be used to assess quality control for mammography, CT and MRI as a practical method for early and precision diagnosis.

Printed on: 02/07/23

## Abstract Archives of the RSNA, 2022

S3B-SPBR-5

### Real-time Decision Support by Light-weighted AI Model Trained with Large-scale Data for Breast Cancer Diagnosis Using Ultrasound

Sunday, Nov. 27 12:15PM - 12:45PM Room: Learning Center - BR DPS

#### Participants

Jaeil Kim, PhD, Daegu, Korea, Republic Of (*Presenter*) Stockholder, BeamWorks, Inc.

#### PURPOSE

Although many of artificial intelligence (AI) models for ultrasound (US) diagnosis have been introduced, real-time decision support by AI is still challenging, due to its high computation cost. We aimed to evaluate the technical feasibility of real-time decision support by light-weighted AI model trained with large-scale data for breast cancer diagnosis using US.

#### METHODS AND MATERIALS

Using a large-scale data over 400,000 breast US images, we developed an AI decision support model based on weakly-supervised learning. In order to achieve the real-time processing of the developed AI model, we implemented a quantization method which can reduce inference time and memory usage while maintaining diagnostic accuracy. For the evaluation of the real-time decision support, US examinations were prospectively recorded from May 2021 in biopsy-proven breast cancer patients. A total of 8 video clips were simulated and tested with our light-weighted AI model. Diagnostic performance and inference time to return AI diagnosis were measured according to two hardware configurations (1: Intel Core i7 2.90 GHz with a GPU and 2: Intel Core i9 2.30Hz without GPU). Frame-wise ground truth labeling for malignancy/non-malignancy was performed by an experienced radiologist with reference to pathologic and radiologic reports.

#### RESULTS

Our light-weighted AI model diagnosed breast US images in the video clips in real-time and simultaneously produced score for cancer with cancer-relevant maps. Of the 8 examinations with breast cancer patients, our maps correctly highlighted the cancer in all examinations. For a total of 19,231 images with 4,525 malignant images and 14,706 non-malignant images, extracted from the video clips, the diagnostic performance was 0.93 of AUC and sensitivity/specificity was 85.4%/85.2%, respectively. Mean time to return AI diagnosis for each image was 0.03 seconds in hardware configuration 1 with GPU and 0.06 seconds in configuration 2 without GPU.

#### CONCLUSION

s With our development of light-weighted AI model trained with a large-scale data, real-time decision support is feasible to diagnose breast cancer using US with high detection and diagnostic performances.

#### CLINICAL RELEVANCE/APPLICATION

Real-time decision support for breast US diagnosis can help sonographers/radiologists to detect and differentiate the breast lesions among high volume of time-series images.

Printed on: 02/07/23



## Abstract Archives of the RSNA, 2022

S3B-SPBR-6

### Real-World Retrospective Cohort Studies of Artificial Intelligence (AI) Readers in Population Breast Cancer Screening

Sunday, Nov. 27 12:15PM - 12:45PM Room: Learning Center - BR DPS

#### Participants

Helen Frazer, FRANZCR, Fitzroy, Australia (*Presenter*) Nothing to Disclose

#### PURPOSE

To assess an AI reader in various breast cancer screening operating modes in real-world retrospective cohort studies.

#### METHODS AND MATERIALS

We curated two datasets from a population breast cancer screening program. First, we established a cancer-rich dataset comprising 10,917 cancer images from 4,680 screening episodes (4,647 clients) and 69,775 non-cancer images from 40,364 screening episodes (39,704 clients), which we used for AI model training and testing. Second, we compiled an independent two-year sequential population cohort of women screened in 2016-2017 comprising 497,288 screening episodes (494,246 clients) and 2,094,424 images. This second dataset was used for the retrospective cohort studies. Five candidate CNN models (ECAResNet269d, ResNet152d, ResNet200d, ResNet101d, Xception41) were trained and tested on the cancer-rich set. The ensemble of the five CNN models achieved an AUROC of 0.877 (95% CI 0.873, 0.881) on the 2016-2017 population dataset and was used for the retrospective cohort simulation study. The study assessed application of the AI model in three operating modes: i) first pass read to remove easy normal mammograms; ii) second reader replacement with comparable/better accuracy; iii) final pass read to detect missed cancers. The simulation included all 497,288 screening episodes of the 2016-2017 retrospective cohort, real-world reader and screening outcomes for comparison, and real-world unit costs. The simulation model produced key classification outcomes (TP, FP, TN, FN) for each retrospective AI operating mode with a range of thresholds, as well as cost implications.

#### RESULTS

The best result was the operating mode of second reader replacement. It demonstrated superior performance to current screening outcomes with 396,173 fewer human reads, 3,103 fewer unnecessary recalls, 51 fewer missed cancers and a 16.9% reduction in reading and assessment costs (threshold set at 0.1).

#### CONCLUSION

Our retrospective cohort studies using the simulation model demonstrated that the use of an AI model for second reader replacement can achieve better screening outcomes, with fewer false negatives and fewer false positives at lower cost, than the current screening process.

#### CLINICAL RELEVANCE/APPLICATION

Retrospective and prospective cohort studies with real-world clinical data and consideration of operating modes are necessary to evaluate AI readers in population breast cancer screening programs.

Printed on: 02/07/23

## Abstract Archives of the RSNA, 2022

S3B-SPBR-7

### Comparison of Mammography Artificial Intelligence Algorithms for 5-year Breast Cancer Risk Prediction

Sunday, Nov. 27 12:15PM - 12:45PM Room: Learning Center - BR DPS

#### Participants

Vignesh Arasu, MD, Vallejo, CA (*Presenter*) Nothing to Disclose

#### PURPOSE

We examined the ability of mammography artificial intelligence (AI) algorithms, most trained for computer-aided detection (CAD) of visible breast cancer on mammograms, to predict 5-year future risk. We compared 5 AI algorithms -- 3 commercial CAD algorithms (representing 1/3 of the FDA/CE cleared devices) and 2 well known open source algorithms -- relative to the Breast Cancer Surveillance Consortium clinical risk model (BCSC v2)

#### METHODS AND MATERIALS

In this case-cohort study, women with a screening mammogram in 2016 at a large managed care organization with no evidence of cancer on final imaging assessment were followed through September 2021. Women were excluded with a prior history of breast cancer or highly penetrant gene mutation. From the 324,009 eligible women, a random subcohort of 13,628 (4.2%) were selected; 193 had incident cancer. All 4,391 additional incident cancers were also included. AI scores were generated from the index 2016 mammogram. Discrimination was assessed with time-varying area under the curve [AUC(t)].

#### RESULTS

For incident cancers at 0 to 1 year (interval cancer risk), the AUC(t) for BCSC was 0.62 (95% CI 0.59, 0.66), and AI algorithms all had significantly higher AUC(t)s, ranging from 0.67-0.71 ( $P < .05$ ). For incident cancers at >1 to 5 years (5-year future cancer risk), the BCSC AUC(t) was 0.61 (95% CI 0.60, 0.62), and the AI algorithms AUC(t)s ranged from 0.63 to 0.67, all significantly higher than BCSC. Combined BCSC and AI models demonstrated AUC(t)s for interval cancer risk of 0.67-0.73 and for 5-year future cancer risk of 0.66-0.68.

#### CONCLUSION

The evaluated AI mammography algorithms had significantly higher discrimination than the BCSC clinical risk model for interval and 5-year future cancer risk. Combined AI and BCSC models had slightly higher discrimination than AI alone.

#### CLINICAL RELEVANCE/APPLICATION

Mammography AI algorithms provide a new approach for improving breast cancer risk prediction beyond clinical variables such as age, family history, or the traditional imaging risk biomarker of breast density. Most CAD algorithms, trained for detection at shorter time horizons can also predict longer-term risk. Breast imaging practices may incorporate CAD AI for both diagnostic assistance and future risk stratification.

Printed on: 02/07/23

## Abstract Archives of the RSNA, 2022

S3B-SPCA

### Cardiac Sunday Poster Discussions - B

Sunday, Nov. 27 12:15PM - 12:45PM Room: Learning Center - CA DPS

#### Sub-Events

#### S3B-SPCA-1 Diagnostic Performance of Myocardial Native T1 and T2 Mapping in Differentiating Between Acute Myocarditis, Acute Myocardial Infarction and Takotsubo

Participants

Giulia Cundari, MD, Rome, Italy (*Presenter*) Nothing to Disclose

#### PURPOSE

To evaluate the diagnostic performance of myocardial native T1 (nT1) and T2 mapping in the differentiation between three acute cardiac conditions causing acute chest pain (ACP): acute myocardial infarction (MI), acute myocarditis (AM) and Takotsubo syndrome (TTS) by using cardiac magnetic resonance (CMR).

#### METHODS AND MATERIALS

166 patients with ACP and troponin increase who underwent CMR within 30 days from the onset of symptoms were retrospectively enrolled: 76/166 (45.8%) AM, 29/166 (17.5%) early-MI (onset-to-CMR= 10 days), 37/166 (22.3%) late-MI (onset-to-CMR: 11-30 days) and 24/166 (14.5%) TTS. Thirty healthy controls were also included in the analysis. CMR protocol included MOLLI and T2-3pt-GRE for the evaluation of nT1 and T2 mapping respectively. For each patient, the maximum segmental value (Max-), the average value among all the segments with increased mapping values (Ave-) and the global value for all the segments (Glo-) were calculated both in nT1 and for T2 maps. nT1 and T2 thresholds were calculated as > 95th percentile of controls values. Statistical analysis was performed using SPSS and included ANOVA, Kruskal-Wallis, and ROC curve analysis. Parameters were considered statistically significant when <0.05.

#### RESULTS

Using ANOVA, the comparisons between the groups with each mapping parameter (Ave-,Max- and Glo-T1 and T2) were statistically significant ( $p<.001$ ). Significant differences have been found in the paired comparison between AM vs. controls and AM vs. e-MI/l-MI/TTS ( $p<.001$  for all). No significant difference was found in the paired comparison between e-MI, l-MI, and TTS ( $p>.05$ ). ROC curve analysis showed excellent performance in discriminating between ACP patients vs. controls for all the parameters ( $p<.001$  for all); fair in differentiating between AM vs e-MI/l-MI/TTS using glo-T1, Ave-T1, Ave-T2 and Max-T2, good for Max-T1 and poor for Glo-T2. Diagnostic performance was very good in distinguishing controls vs. AM for glo-T1, Ave-T1, Max-T1, Ave-T2 and Max-T2 and good for Glo-T2.

#### CONCLUSION

s nT1 and T2 mapping play a role in the detection of acute cardiac conditions, and differentiation between AM versus myocardial infarction or TTS. Max- and Ave-T1 and T2 showed a greater diagnostic performance as compared to Glo-T1 and T2.

#### CLINICAL RELEVANCE/APPLICATION

The use of mapping sequences can help in the diagnosis of MI, AM and TTS in the acute setting, even without the use of contrast agent.

#### S3B-SPCA-2 Efficacy of Super-Resolution Deep-Learning Reconstruction for the Assessments of Obstructive Coronary Artery Disease on Cardiac CT

Participants

Yasunori Nagayama, MD, Kumamoto, Japan (*Presenter*) Nothing to Disclose

#### PURPOSE

To evaluate the image quality of super-resolution deep-learning reconstruction (SR-DLR) for coronary CT angiography (CCTA) in patients with coronary artery disease (CAD).

#### METHODS AND MATERIALS

This retrospective study included 48 patients with obstructive CAD (=50% stenosis in at least one coronary vessel) who underwent CCTA on a 320-row scanner. The images were reconstructed with hybrid iterative reconstruction (HIR, AIDR 3D), model-based iterative reconstruction (MBIR, FIRST), normal-resolution DLR (NR-DLR, AiCE), and SR-DLR (PIQE) using dedicated cardiac parameters. For each image series, CT attenuation at the left main artery, proximal and distal segments of the right coronary artery, left anterior descending artery (LAD), and left circumflex artery was quantified. Image noise was quantified as the standard deviation of CT attenuation in the subcutaneous fat at the level of the proximal and distal coronary arteries. The contrast-to-noise ratio (CNR) was calculated as the ratio of the attenuation differences between the coronary lumen and adjacent pericoronary fat and image noise. At the coronary segments with calcified plaques, blooming artifact was quantified using following formula: [(measured external coronary section diameter with calcified plaque - measured lumen diameter)/measured external coronary

section diameter with calcified plaque]  $\times 100$ . The image sharpness, image noise, delineation of coronary lumens, calcified and noncalcified plaques, cardiac muscle, valves, and diagnostic confidence were subjectively scored on a 5-point scale (1, insufficient; 5, excellent). The quantitative parameters and qualitative scores were compared among the four reconstruction algorithms using the Kruskal-Wallis and Steel-Dwass tests.

## RESULTS

SR-DLR yielded significantly lower quantitative image noise and blooming artifact with higher CNR at all coronary segments relative to HIR, MBIR, and NR-DLR images (all  $P < 0.05$ ). The best subjective scores for all evaluation criteria were attained at SR-DLR images, with significant differences from all other reconstruction algorithms ( $P < 0.05$ ).

## CONCLUSION

s SR-DLR considerably improves the subjective and objective image qualities and diagnostic confidence of CCTA in patients with obstructive CAD.

## CLINICAL RELEVANCE/APPLICATION

SR-DLR improves the spatial resolution while reducing noise and blooming, thereby allowing the accurate interpretation of CCTA performed in patients with obstructive CAD.

## S3B-SPCA-3 A Pilot Study of combining 2nd Order Flow Compensated Diffusion and Computed DWI to Detect the Myocardial Infarction without Exogenous Contrast Agents

Participants

Rui Chen, Guangzhou, China (*Presenter*) Nothing to Disclose

## PURPOSE

Cardiac diffusion weighted imaging (DWI) could provide essential information for diagnosis and clinical decision in patients with myocardial infarction without exogenous contrast agents. Higher b-value DWI could improve the detection rate of myocardial infarction, but it is challenging for image acquisition in cardiac DWI because of the low signal-to-noise ratio. The present study aimed to combine the 2nd order motion compensated diffusion with computed DWI to overcome these challenges.

## METHODS AND MATERIALS

The graphical abstract (A) showed the proposed solution in the present study. To decrease the motion impact on cardiac DWI images, the 2nd order flow compensated diffusion (mcDWI) was used for image acquisition. Computed diffusion (cDWI) was implemented to generate higher b-value DWI images. To our knowledge, no published studies have combined mcDWI and cDWI in cardiac imaging. We called the combination of these two techniques as m2cDWI, and obtained the high b-value cardiac DWI images for the first time. To evaluate the feasibility of m2cDWI, we compared the m2cDWI images and origin DWI images with late gadolinium enhancement (LGE) imaging.

## RESULTS

In the graphical abstract (B), the subendocardial enhancement seen in LGE might be more clearly shown in the m2cDWI images ( $b = 800$ ,  $b=1200$ ,  $b = 1600$ ) than the origin DWI images ( $b = 400$ ). It showed that the m2cDWI images seemed to be more sensitive to myocardial infarction.

## CONCLUSION

s The m2cDWI could obtain higher b-value cardiac DWI images and improve the detection rate of myocardial infarction without exogenous contrast agents.

## CLINICAL RELEVANCE/APPLICATION

In the present study, a novel scheme m2cDWI was proposed to obtain higher b value cardiac diffusion by combining mcDWI and cDWI, which was more sensitive to myocardial infarction. It could also have the potential improve the detection rate of of other microscopic structural remodeling without exogenous contrast agents.

Printed on: 02/07/23

## Abstract Archives of the RSNA, 2022

S3B-SPCA-1

### Diagnostic Performance of Myocardial Native T1 and T2 Mapping in Differentiating Between Acute Myocarditis, Acute Myocardial Infarction and Takotsubo

Sunday, Nov. 27 12:15PM - 12:45PM Room: Learning Center - CA DPS

#### Participants

Giulia Cundari, MD, Rome, Italy (*Presenter*) Nothing to Disclose

#### PURPOSE

To evaluate the diagnostic performance of myocardial native T1 (nT1) and T2 mapping in the differentiation between three acute cardiac conditions causing acute chest pain (ACP): acute myocardial infarction (MI), acute myocarditis (AM) and Takotsubo syndrome (TTS) by using cardiac magnetic resonance (CMR).

#### METHODS AND MATERIALS

166 patients with ACP and troponin increase who underwent CMR within 30 days from the onset of symptoms were retrospectively enrolled: 76/166 (45.8%) AM, 29/166 (17.5%) early-MI (onset-to-CMR= 10 days), 37/166 (22.3%) late-MI (onset-to-CMR: 11-30 days) and 24/166 (14.5%) TTS. Thirty healthy controls were also included in the analysis. CMR protocol included MOLLI and T2-3pt-GRE for the evaluation of nT1 and T2 mapping respectively. For each patient, the maximum segmental value (Max-), the average value among all the segments with increased mapping values (Ave-) and the global value for all the segments (Glo-) were calculated both in nT1 and for T2 maps. nT1 and T2 thresholds were calculated as > 95th percentile of controls values. Statistical analysis was performed using SPSS and included ANOVA, Kruskal-Wallis, and ROC curve analysis. Parameters were considered statistically significant when <0.05.

#### RESULTS

Using ANOVA, the comparisons between the groups with each mapping parameter (Ave-,Max- and Glo-T1 and T2) were statistically significant ( $p<.001$ ). Significant differences have been found in the paired comparison between AM vs. controls and AM vs. e-MI/l-MI/TTS ( $p<.001$  for all). No significant difference was found in the paired comparison between e-MI, l-MI, and TTS ( $p>.05$ ). ROC curve analysis showed excellent performance in discriminating between ACP patients vs. controls for all the parameters ( $p<.001$  for all); fair in differentiating between AM vs e-MI/l-MI/TTS using glo-T1, Ave-T1, Ave-T2 and Max-T2, good for Max-T1 and poor for Glo-T2. Diagnostic performance was very good in distinguishing controls vs. AM for glo-T1, Ave-T1, Max-T1, Ave-T2 and Max-T2 and good for Glo-T2.

#### CONCLUSION

s nT1 and T2 mapping play a role in the detection of acute cardiac conditions, and differentiation between AM versus myocardial infarction or TTS. Max- and Ave-T1 and T2 showed a greater diagnostic performance as compared to Glo-T1 and T2.

#### CLINICAL RELEVANCE/APPLICATION

The use of mapping sequences can help in the diagnosis of MI, AM and TTS in the acute setting, even without the use of contrast agent.

Printed on: 02/07/23

## Abstract Archives of the RSNA, 2022

S3B-SPCA-2

### Efficacy of Super-Resolution Deep-Learning Reconstruction for the Assessments of Obstructive Coronary Artery Disease on Cardiac CT

Sunday, Nov. 27 12:15PM - 12:45PM Room: Learning Center - CA DPS

#### Participants

Yasunori Nagayama, MD, Kumamoto, Japan (*Presenter*) Nothing to Disclose

#### PURPOSE

To evaluate the image quality of super-resolution deep-learning reconstruction (SR-DLR) for coronary CT angiography (CCTA) in patients with coronary artery disease (CAD).

#### METHODS AND MATERIALS

This retrospective study included 48 patients with obstructive CAD ( $\geq 50\%$  stenosis in at least one coronary vessel) who underwent CCTA on a 320-row scanner. The images were reconstructed with hybrid iterative reconstruction (HIR, AIDR 3D), model-based iterative reconstruction (MBIR, FIRST), normal-resolution DLR (NR-DLR, AiCE), and SR-DLR (PIQE) using dedicated cardiac parameters. For each image series, CT attenuation at the left main artery, proximal and distal segments of the right coronary artery, left anterior descending artery (LAD), and left circumflex artery was quantified. Image noise was quantified as the standard deviation of CT attenuation in the subcutaneous fat at the level of the proximal and distal coronary arteries. The contrast-to-noise ratio (CNR) was calculated as the ratio of the attenuation differences between the coronary lumen and adjacent pericoronary fat and image noise. At the coronary segments with calcified plaques, blooming artifact was quantified using following formula:  $[(\text{measured external coronary section diameter with calcified plaque} - \text{measured lumen diameter}) / \text{measured external coronary section diameter with calcified plaque}] \times 100$ . The image sharpness, image noise, delineation of coronary lumens, calcified and noncalcified plaques, cardiac muscle, valves, and diagnostic confidence were subjectively scored on a 5-point scale (1, insufficient; 5, excellent). The quantitative parameters and qualitative scores were compared among the four reconstruction algorithms using the Kruskal-Wallis and Steel-Dwass tests.

#### RESULTS

SR-DLR yielded significantly lower quantitative image noise and blooming artifact with higher CNR at all coronary segments relative to HIR, MBIR, and NR-DLR images (all  $P < 0.05$ ). The best subjective scores for all evaluation criteria were attained at SR-DLR images, with significant differences from all other reconstruction algorithms ( $P < 0.05$ ).

#### CONCLUSION

SR-DLR considerably improves the subjective and objective image qualities and diagnostic confidence of CCTA in patients with obstructive CAD.

#### CLINICAL RELEVANCE/APPLICATION

SR-DLR improves the spatial resolution while reducing noise and blooming, thereby allowing the accurate interpretation of CCTA performed in patients with obstructive CAD.

Printed on: 02/07/23

## Abstract Archives of the RSNA, 2022

S3B-SPCA-3

### A Pilot Study of combining 2nd Order Flow Compensated Diffusion and Computed DWI to Detect the Myocardial Infarction without Exogenous Contrast Agents

Sunday, Nov. 27 12:15PM - 12:45PM Room: Learning Center - CA DPS

#### Participants

Rui Chen, Guangzhou, China (*Presenter*) Nothing to Disclose

#### PURPOSE

Cardiac diffusion weighted imaging (DWI) could provide essential information for diagnosis and clinical decision in patients with myocardial infarction without exogenous contrast agents. Higher b-value DWI could improve the detection rate of myocardial infarction, but it is challenging for image acquisition in cardiac DWI because of the low signal-to-noise ratio. The present study aimed to combine the 2nd order motion compensated diffusion with computed DWI to overcome these challenges.

#### METHODS AND MATERIALS

The graphical abstract (A) showed the proposed solution in the present study. To decrease the motion impact on cardiac DWI images, the 2nd order flow compensated diffusion (mCDWI) was used for image acquisition. Computed diffusion (cDWI) was implemented to generate higher b-value DWI images. To our knowledge, no published studies have combined mCDWI and cDWI in cardiac imaging. We called the combination of these two techniques as m2cDWI, and obtained the high b-value cardiac DWI images for the first time. To evaluate the feasibility of m2cDWI, we compared the m2cDWI images and origin DWI images with late gadolinium enhancement (LGE) imaging.

#### RESULTS

In the graphical abstract (B), the subendocardial enhancement seen in LGE might be more clearly shown in the m2cDWI images ( $b = 800$ ,  $b = 1200$ ,  $b = 1600$ ) than the origin DWI images ( $b = 400$ ). It showed that the m2cDWI images seemed to be more sensitive to myocardial infarction.

#### CONCLUSION

The m2cDWI could obtain higher b-value cardiac DWI images and improve the detection rate of myocardial infarction without exogenous contrast agents.

#### CLINICAL RELEVANCE/APPLICATION

In the present study, a novel scheme m2cDWI was proposed to obtain higher b value cardiac diffusion by combining mCDWI and cDWI, which was more sensitive to myocardial infarction. It could also have the potential improve the detection rate of other microscopic structural remodeling without exogenous contrast agents.

Printed on: 02/07/23

## Abstract Archives of the RSNA, 2022

S3B-SPCH

### Chest Sunday Poster Discussions - B

Sunday, Nov. 27 12:15PM - 12:45PM Room: Learning Center - CH DPS

#### Participants

Ryoko Egashira, MD, PhD, Saga, (*Moderator*) Speakers Bureau, Boehringer Ingelheim GmbH; Speakers Bureau, AstraZeneca PLC; Speakers Bureau, Shionogi & Co, Ltd; Speakers Bureau, KYORIN Holdings, Inc; Speakers Bureau, DAIICHI SANKYO Group; Speakers Bureau, Bayer AG; Speakers Bureau, Otsuka Holdings Co, Ltd;

#### Sub-Events

### S3B-SPCH-2 Quantitative Evaluation of Airway Disease in Rheumatoid Arthritis Using Ultra-high-resolution CT

#### Participants

Tae Iwasawa, MD, PhD, Yokohama, Japan (*Presenter*) Support, Canon Medical Systems Corporation; Support, Ziosoft Inc; Speaker, FUJIFILM Holdings Corporation; Speaker, Boehringer Ingelheim GmbH

#### PURPOSE

Airway disease is an important feature of rheumatoid arthritis (RA). In this study, we quantitatively evaluated bronchial dilatation in patients with RA using ultra-high-resolution CT (U-HRCT).

#### METHODS AND MATERIALS

This multicenter study was approved by the institutional review board, and the requirement for informed consent was waived. We collected clinical data, pulmonary function test results, and U-HRCT images of patients diagnosed with RA. All CT scans were performed using a 160-row U-HRCT scanner (Aquilion Precision, Canon Medical Systems, Otawara, Tochigi, Japan). CT scans were performed at 120 kVp, 0.25 × 160 collimation, using automatic exposure control. Two kinds of images were reconstructed: (1) U-HRCT mode (1024 × 1024 matrix size, 0.25-mm slice thickness, and deep learning reconstruction algorithm for the lung, Fig.1a) and (2) normal-resolution image (512 × 512 matrix size, 0.5-mm slice thickness, and iterative reconstruction method). We produced bronchial 3-dimensional images of U-HRCT using a workstation (Ziostation 2) (Fig.1.b), measured the airway volume in the right lower lobe (AWV<sub>rl</sub>), and calculated the ratio to the right lower lobe volume (AWV<sub>rl</sub>% = AWV<sub>rl</sub>/ volume of the right lower lobe × 100). We further measured the extension of interstitial lung diseases (ILD) in normal resolution images using a software (QZIP-ILD, Ziosoft, Inc, Tokyo, Japan) (Fig.1c). We compared AWV<sub>rl</sub>% with extension ILD, pulmonary function test results, and Krebs von den Lungen-6 (KL-6) using Spearman's rank correlation.

#### RESULTS

Overall, 151 patients (106 female) were enrolled, with a median age of 77. Fifty-one patients had a history of smoking and 119 had received with disease-modifying antirheumatic drugs and steroids at CT examinations. AWV<sub>rl</sub>% showed a significant negative correlation with forced vital capacity (%pred) ( $r = -0.383$ ), diffusing capacity of the lung for carbon monoxide (DLCO %pred) ( $r = 0.412$ ) (Fig.1d), and significant positive correlation with the extent of fibrotic lesion (%) ( $r = 0.742$ ), and KL-6 ( $r = 0.697$ ) (Fig.1e) ( $p < 0.001$ , respectively).

#### CONCLUSION

s AWV<sub>rl</sub>% is a useful parameter to evaluate airway disease in RA.

#### CLINICAL RELEVANCE/APPLICATION

Bronchiolitis and bronchiectasis are significant features of the RA lung. U-HRCT enables clinicians to extract peripheral bronchi and measure AWV<sub>rl</sub>%, which is easier than measuring intra-bronchial area and wall-thickness.

### S3B-SPCH-3 Limiting CT-based Severity Staging of COPD to a Single Inspiratory Acquisition Using Convolutional Neural Networks

#### Participants

Amanda Lee, (*Presenter*) Nothing to Disclose

#### PURPOSE

Several methods for computed tomography (CT)-based severity staging of chronic obstructive pulmonary disease (COPD) utilize both inspiratory and expiratory acquisitions, which are not the clinical standard and increase patients' exposure to ionizing radiation. We assess the feasibility of using a convolutional neural network (CNN) to stage COPD using only inspiratory images.

#### METHODS AND MATERIALS

This retrospective study is HIPAA-compliant and IRB-approved with waived requirement for written informed consent. We sampled 7,822 inspiratory lung CT series and spirometry measurements (forced expiratory volume in one second [FEV<sub>1</sub>], FEV<sub>1</sub> to forced vital capacity ratio [FEV<sub>1</sub>/FVC], percent predicted FEV<sub>1</sub> [FEV<sub>1</sub>pp]) from the COPD Gene Phase I cohort. Severity stages were determined according to the Global Initiative for Obstructive Lung Disease (GOLD) stages. A 3D residual attention network was trained to

predict spirometry measurements using inspiratory images as input. CNN-predicted spirometry measurements were then used to estimate GOLD stage. Agreement between CNN-predicted and true spirometry measurements was assessed using intraclass correlation (ICC) and Bland Altman analysis. Accuracy for predicting GOLD stage, within one GOLD stage, and GOLD 0 vs. 1-4 was calculated.

## RESULTS

FEV1, FEV1/FVC, and FEV1pp ICCs were 0.84, 0.85, and 0.79 and Bland Altman bias and limits of agreement were 0.01 [-0.97, 0.98]; gt; -0.01 [-0.17, 0.17]; and -1.03 [-32.21, 30.16], respectively. Accuracies were 0.63, 0.90, and 0.84 for GOLD stage, within one GOLD stage, and GOLD 0 vs. 1-4. Our model improves upon existing inspiratory models with accuracies of 0.51, 0.75, and 0.77, respectively, and achieves comparable accuracy to an existing inspiratory-expiratory model with GOLD 0 vs. 1-4 accuracy of 0.89.

## CONCLUSION

s Inspiratory images can be used to accurately stage COPD severity within one stage. Accuracies are comparable to those achieved by competing methods, which use both inspiratory and expiratory series, suggesting inspiratory series contain the majority of information needed for imaging-based staging.

## CLINICAL RELEVANCE/APPLICATION

The proposed model can be used to lower patients' CT radiation exposure, improve accessibility to CT-based staging, and align current methods to the clinical standard.

### S3B-SPCH-4 Narrowing the Differential Diagnosis of Cystic Lesions in Smoking Related Lung Diseases with Expiratory CT Acquisition

Participants

Matheus Zanon, MD, MSc, Porto Alegre, Brazil (*Presenter*) Nothing to Disclose

## PURPOSE

to assess the respiratory changes in the size of pulmonary cysts in paired inspiratory and expiratory CT scans from patients with cysts from honeycombing fibrosis, pulmonary Langerhans cell histiocytosis (PLCH), and paraseptal emphysema.

## METHODS AND MATERIALS

smokers with cystic we retrospectively reviewed inspiratory and expiratory CT scans from lesions from paraseptal emphysema, honeycombing, and PLCH. Diagnosis should have been confirmed by histopathology. Blinded to the final diagnosis, two senior thoracic radiologists measured the diameters of the three largest cysts on paired inspiratory and expiratory CT scans.

## RESULTS

A total of 72 patients and 216 lesions were included. The intraclass correlation coefficients demonstrated excellent reliability (ICC= 0.91). PLCH and honeycombing presented a decrease in the mean diameter of the cystic lesions (PLCH, d = 60.9%; p = 0.001; honeycombing, d = 47.5%; p = 0.014). Conversely, paraseptal emphysema did not show any changes (d = 5.2%; p = 0.34).

## CONCLUSION

s our results demonstrate that cysts in smokers with PLCH and honeycombing fibrosis get smaller during expiratory CT scans, whereas the size of cystic-like lesions due to paraseptal emphysema and bullae tend to remain constant during respiratory cycles.

## CLINICAL RELEVANCE/APPLICATION

presence of cyst-airway communication could narrow the differential diagnosis of cysts in smoking-related lung diseases, avoiding misinterpretation of honeycombing as paraseptal emphysema, and vice-versa.

### S3B-SPCH-6 HRCT and Post-lymphangiographic CT (PLCT) In Lymphangiomyomatosis: A Retrospective Study

Participants

Xingpeng Li, Beijing, China (*Presenter*) Nothing to Disclose

## PURPOSE

To investigate the imaging features and clinical value of chest high-resolution CT (HRCT) and post lymphangiographic CT (PLCT) in lymphangiomyomatosis.

## METHODS AND MATERIALS

Fifty-six patients diagnosed as lymphangiomyomatosis were recruited in this retrospective study from December of 2008 to April of 2019. All patients underwent HRCT, and 45 underwent PLCT. All the imaging data were blinded reviewed by two radiologists respectively, with the imaging features of abnormal thoracic, abdominal and pelvic manifestations, abnormal distribution of contrast agents throughout the whole body. Statistical analyses were performed with the constituent ratio in the classified variable data.

## RESULTS

HRCT findings of 56 patients showed diffuse thin-walled air cysts of different sizes in both lungs, the lung ground glass density 16 cases, 8 cases within the lung nodules, atelectasis 32 cases, bronchus enlargement of blood vessel bundle 12 cases, interlobular septal thickening 25 cases, mediastinal fat increased density 30 cases, pericardial effusion 6 cases, mediastinal lymph node enlargement 9 cases, pleural effusion 45 cases, pneumothorax 12 cases. PLCT findings of 45 patients showed abnormal iodine oil from different parts of the deposit: 24 cases of the end of thoracic duct, 7 cases with right lymphatic catheter, 7 cases were intrapulmonary and 7 cases were hilum, mediastinum 20 cases, pericardium 1 case, pleural cavity 7 cases, Intercostal 17 cases, axillary 6 cases, diaphragmatic around 32 cases, 27 cases of spinal column, abdominal pelvic 45 cases, double iliac 41 cases, bilateral inguinal 36 cases, perineum 3 cases. In addition, 3 patients had hepatic angiomyolipoma, 8 patients had renal angiomyolipoma, 4 patients had diffuse intestinal wall thickening, and 31 patients had abdominal and pelvic effusion.

## CONCLUSION

s HRCT and PLCT demonstrates capability in abnormalities of the thoracic, abdominal and pelvic and detection of location, distribution and range of abnormal lymphatics, which is useful for diagnosis and therapeutic adoptions for lymphangiomyomatosis.

#### **CLINICAL RELEVANCE/APPLICATION**

Lymphangiomyomatosis is an autoimmune disease involving multiple organs and systems. It is necessary to evaluate the systematic lymphatic circulation abnormality for with HRCT and PLCT in patients with SLE, which is very important for therapeutic options.

### **S3B-SPCH-7 Dark-Field Chest Radiography Outperforms Conventional Radiography for the Diagnosis and Staging of Pulmonary Emphysema**

#### **Awards**

**Trainee Research Prize - Resident**

Participants

Theresa Urban, MSc, Garching, Germany (*Presenter*) Nothing to Disclose

#### **PURPOSE**

Dark-field chest radiography visualizes the condition of the lungs' alveolar structure by measuring the coherent ultra-small-angle scattering of X-rays. Here, we compare dark-field chest radiography with conventional radiography for the diagnosis and staging of pulmonary emphysema.

#### **METHODS AND MATERIALS**

Subjects were included after a medically indicated CT scan of the thorax, showing either no lung impairments or different stages of emphysema. To establish a ground truth, all CTs were assessed separately by three radiologists assigning visual scores based on the Fleischner society classification scheme for emphysema severity (absent, trace, mild, moderate, confluent, advanced destructive). Participants were imaged at a commercial chest radiography device, yielding a conventional attenuation image, and at a clinical prototype for dark-field chest radiography, yielding both an attenuation and a dark-field image. Three independent blinded readers assessed the conventional attenuation image and both attenuation and dark-field image from the prototype for presence and severity of emphysema (no emphysema, mild emphysema, moderate emphysema, severe emphysema). Statistical analysis included evaluation of receiver-operator-characteristics and pair-wise comparison of adjacent Fleischner groups using an AUC-based z-test with a significance level of 0.05.

#### **RESULTS**

A total of 90 patients (56 males) were included, with a mean age of  $65 \pm 12$  years. The dark-field images show a distinct decrease of signal strength with emphysema severity. Compared to conventional images (AUC = 0.74), readers were significantly better able to identify emphysema with images from the dark-field prototype (AUC = 0.85,  $p < 0.05$ ). While ratings of adjacent emphysema severity groups with conventional radiographs were only different for trace and mild emphysema, ratings based on images from the dark-field prototype were different for trace and mild, mild and moderate, and moderate and confluent emphysema.

#### **CONCLUSION**

s Compared to conventional chest radiography, dark-field chest radiography provides improved capability for identification and staging of emphysema.

#### **CLINICAL RELEVANCE/APPLICATION**

Dark-field chest radiography improves the detection of emphysematous changes in the lung, demonstrating its high diagnostic value for lung assessment.

### **S3B-SPCH-8 Lung Imaging at 0.55T MRI for Interstitial Lung Disease Assessment in Patients with Pulmonary Sarcoidosis**

Participants

Hanns-Christian Breit, MD, Basel, Switzerland (*Presenter*) Nothing to Disclose

#### **PURPOSE**

To evaluate the potential of lung MR imaging at 0.55T in patients with pulmonary sarcoidosis.

#### **METHODS AND MATERIALS**

We performed a prospective study with 7 patients (4 male, 3 female,  $42 \pm 9$  years). All patients underwent a routine chest CT (SOMATOM Definition Edge, Siemens Healthineers, arms overhead position) followed by MRI on a 0.55T whole-body scanner (MAGNETOM Free.Max, Siemens Healthineers, gradient amplitude 26 mT/m, gradient slew rate 45 T/m/s) using a 6-channel chest array coil and a 6-channel spine coil. All patients had sarcoidosis with proven pulmonary involvement. Morphological lung imaging was performed by using a free-breathing 3D half-radial dual-echo sequence termed bSTAR (TA = 5:30 min, TE1/TE2/TR = 0.08/2.1/2.2 ms, field-of-view =  $34 \times 34 \times 34$  cm<sup>3</sup>, flip angle = 25°, bandwidth = 1002 Hz/pixel) with a 1.3 mm isotropic resolution, a commercial axial breath-hold balanced steady state free precession (bSSFP) (TA = 0:48 min, TE/TR = 2.3/4.6 ms, field-of-view = 380 x 304 mm, 6 mm slice thickness, flip angle = 90°). Furthermore, functional lung MRI using matrix pencil (MP) method for the evaluation of the fractional ventilation and pulmonary perfusion was performed using bSSFP (TA = 1:06 min, TE/TR = 1.20/2.66 ms, field-of-view =  $450 \times 450$  mm<sup>2</sup>, 12-mm slice thickness, flip angle = 80°).

#### **RESULTS**

In 4 patients, hilar and mediastinal lymphadenopathy was seen on both CT and MRI. All 7 patients showed CT findings compatible with pulmonary sarcoidosis (perilymphatic nodules with associated partially thickened interlobular septa, airspace opacities, signs of pulmonary fibrosis). All findings were delineable in the morphologic MRI sequences, although the resolution of the perilymphatic micronodules was inferior. In line with these findings, functional MRI images showed a reduced perfusion and ventilation in the affected areas.

#### **CONCLUSION**

s Lung imaging at 0.55T MRI is a promising tool for visualizing morphologic changes in patients with sarcoidosis. Additional

s Lung imaging at 0.55T MRI is a promising tool for visualizing morphologic changes in patients with sarcoidosis. Additional information on perfusion and ventilation can be obtained using functional imaging. Further quantitative analyzes might be performed in the further to assess the full potential of this new method.

#### **CLINICAL RELEVANCE/APPLICATION**

Pulmonary MRI may be an attractive alternative to CT for diagnosis and follow-up of pulmonary sarcoidosis. Unlike CT, pulmonary MRI can provide additional functional information on pulmonary perfusion and ventilation

Printed on: 02/07/23

## Abstract Archives of the RSNA, 2022

S3B-SPCH-2

### Quantitative Evaluation of Airway Disease in Rheumatoid Arthritis Using Ultra-high-resolution CT

Sunday, Nov. 27 12:15PM - 12:45PM Room: Learning Center - CH DPS

#### Participants

Tae Iwasawa, MD, PhD, Yokohama, Japan (*Presenter*) Support, Canon Medical Systems Corporation; Support, Ziosoft Inc; Speaker, FUJIFILM Holdings Corporation; Speaker, Boehringer Ingelheim GmbH

#### PURPOSE

Airway disease is an important feature of rheumatoid arthritis (RA). In this study, we quantitatively evaluated bronchial dilatation in patients with RA using ultra-high-resolution CT (U-HRCT).

#### METHODS AND MATERIALS

This multicenter study was approved by the institutional review board, and the requirement for informed consent was waived. We collected clinical data, pulmonary function test results, and U-HRCT images of patients diagnosed with RA. All CT scans were performed using a 160-row U-HRCT scanner (Aquilion Precision, Canon Medical Systems, Otawara, Tochigi, Japan). CT scans were performed at 120 kVp, 0.25 × 160 collimation, using automatic exposure control. Two kinds of images were reconstructed: (1) U-HRCT mode (1024 × 1024 matrix size, 0.25-mm slice thickness, and deep learning reconstruction algorithm for the lung, Fig.1a) and (2) normal-resolution image (512 × 512 matrix size, 0.5-mm slice thickness, and iterative reconstruction method). We produced bronchial 3-dimensional images of U-HRCT using a workstation (Ziostation 2) (Fig.1.b), measured the airway volume in the right lower lobe (AWV<sub>rl</sub>), and calculated the ratio to the right lower lobe volume (AWV<sub>rl</sub>% = AWV<sub>rl</sub>/ volume of the right lower lobe × 100). We further measured the extension of interstitial lung diseases (ILD) in normal resolution images using a software (QZIP-ILD, Ziosoft, Inc, Tokyo, Japan) (Fig.1c). We compared AWV<sub>rl</sub> with extension ILD, pulmonary function test results, and Krebs von den Lungen-6 (KL-6) using Spearman's rank correlation.

#### RESULTS

Overall, 151 patients (106 female) were enrolled, with a median age of 77. Fifty-one patients had a history of smoking and 119 had received with disease-modifying antirheumatic drugs and steroids at CT examinations. AWV<sub>rl</sub>% showed a significant negative correlation with forced vital capacity (%pred) ( $r=-0.383$ ), diffusing capacity of the lung for carbon monoxide (DLCO %pred) ( $r=-0.412$ ) (Fig.1d), and significant positive correlation with the extent of fibrotic lesion (%) ( $r=0.742$ ), and KL-6 ( $r=0.697$ ) (Fig.1e) ( $p<0.001$ , respectively).

#### CONCLUSION

s AWV<sub>rl</sub> is a useful parameter to evaluate airway disease in RA.

#### CLINICAL RELEVANCE/APPLICATION

Bronchiolitis and bronchiectasis are significant features of the RA lung. U-HRCT enables clinicians to extract peripheral bronchi and measure AWV<sub>rl</sub>%, which is easier than measuring intra-bronchial area and wall-thickness.

Printed on: 02/07/23

## Abstract Archives of the RSNA, 2022

S3B-SPCH-3

### Limiting CT-based Severity Staging of COPD to a Single Inspiratory Acquisition Using Convolutional Neural Networks

Sunday, Nov. 27 12:15PM - 12:45PM Room: Learning Center - CH DPS

#### Participants

Amanda Lee, (*Presenter*) Nothing to Disclose

#### PURPOSE

Several methods for computed tomography (CT)-based severity staging of chronic obstructive pulmonary disease (COPD) utilize both inspiratory and expiratory acquisitions, which are not the clinical standard and increase patients' exposure to ionizing radiation. We assess the feasibility of using a convolutional neural network (CNN) to stage COPD using only inspiratory images.

#### METHODS AND MATERIALS

This retrospective study is HIPAA-compliant and IRB-approved with waived requirement for written informed consent. We sampled 7,822 inspiratory lung CT series and spirometry measurements (forced expiratory volume in one second [FEV1], FEV1 to forced vital capacity ratio [FEV1/FVC], percent predicted FEV1 [FEV1pp]) from the COPDGen Phase I cohort. Severity stages were determined according to the Global Initiative for Obstructive Lung Disease (GOLD) stages. A 3D residual attention network was trained to predict spirometry measurements using inspiratory images as input. CNN-predicted spirometry measurements were then used to estimate GOLD stage. Agreement between CNN-predicted and true spirometry measurements was assessed using intraclass correlation (ICC) and Bland Altman analysis. Accuracy for predicting GOLD stage, within one GOLD stage, and GOLD 0 vs. 1-4 was calculated.

#### RESULTS

FEV1, FEV1/FVC, and FEV1pp ICCs were 0.84, 0.85, and 0.79 and Bland Altman bias and limits of agreement were 0.01 [-0.97, 0.98]; gt; -0.01 [-0.17, 0.17]; and -1.03 [-32.21, 30.16], respectively. Accuracies were 0.63, 0.90, and 0.84 for GOLD stage, within one GOLD stage, and GOLD 0 vs. 1-4. Our model improves upon existing inspiratory models with accuracies of 0.51, 0.75, and 0.77, respectively, and achieves comparable accuracy to an existing inspiratory-expiratory model with GOLD 0 vs. 1-4 accuracy of 0.89.

#### CONCLUSION

s Inspiratory images can be used to accurately stage COPD severity within one stage. Accuracies are comparable to those achieved by competing methods, which use both inspiratory and expiratory series, suggesting inspiratory series contain the majority of information needed for imaging-based staging.

#### CLINICAL RELEVANCE/APPLICATION

The proposed model can be used to lower patients' CT radiation exposure, improve accessibility to CT-based staging, and align current methods to the clinical standard.

Printed on: 02/07/23

## Abstract Archives of the RSNA, 2022

S3B-SPCH-4

### Narrowing the Differential Diagnosis of Cystic Lesions in Smoking Related Lung Diseases with Expiratory CT Acquisition

Sunday, Nov. 27 12:15PM - 12:45PM Room: Learning Center - CH DPS

#### Participants

Matheus Zanon, MD, MSc, Porto Alegre, Brazil (*Presenter*) Nothing to Disclose

#### PURPOSE

to assess the respiratory changes in the size of pulmonary cysts in paired inspiratory and expiratory CT scans from patients with cysts from honeycombing fibrosis, pulmonary Langerhans cell histiocytosis (PLCH), and paraseptal emphysema.

#### METHODS AND MATERIALS

smokers with cystic we retrospectively reviewed inspiratory and expiratory CT scans from lesions from paraseptal emphysema, honeycombing, and PLCH. Diagnosis should have been confirmed by histopathology. Blinded to the final diagnosis, two senior thoracic radiologists measured the diameters of the three largest cysts on paired inspiratory and expiratory CT scans.

#### RESULTS

A total of 72 patients and 216 lesions were included. The intraclass correlation coefficients demonstrated excellent reliability (ICC= 0.91). PLCH and honeycombing presented a decrease in the mean diameter of the cystic lesions (PLCH,  $d = 60.9\%$ ;  $p = 0.001$ ; honeycombing,  $d = 47.5\%$ ;  $p = 0.014$ ). Conversely, paraseptal emphysema did not show any changes ( $d = 5.2\%$ ;  $p = 0.34$ ).

#### CONCLUSION

s our results demonstrate that cysts in smokers with PLCH and honeycombing fibrosis get smaller during expiratory CT scans, whereas the size of cystic-like lesions due to paraseptal emphysema and bullae tend to remain constant during respiratory cycles.

#### CLINICAL RELEVANCE/APPLICATION

presence of cyst-airway communication could narrow the differential diagnosis of cysts in smoking-related lung diseases, avoiding misinterpretation of honeycombing as paraseptal emphysema, and vice-versa.

Printed on: 02/07/23

## Abstract Archives of the RSNA, 2022

S3B-SPCH-6

### HRCT and Post-lymphangiographic CT (PLCT) In Lymphangiomyomatosis: A Retrospective Study

Sunday, Nov. 27 12:15PM - 12:45PM Room: Learning Center - CH DPS

#### Participants

Xingpeng Li, Beijing, China (*Presenter*) Nothing to Disclose

#### PURPOSE

To investigate the imaging features and clinical value of chest high-resolution CT (HRCT) and post lymphangiographic CT (PLCT) in lymphangiomyomatosis.

#### METHODS AND MATERIALS

Fifty-six patients diagnosed as lymphangiomyomatosis were recruited in this retrospective study from December of 2008 to April of 2019. All patients underwent HRCT, and 45 underwent PLCT. All the imaging data were blinded reviewed by two radiologists respectively, with the imaging features of abnormal thoracic, abdominal and pelvic manifestations, abnormal distribution of contrast agents throughout the whole body. Statistical analyses were performed with the constituent ratio in the classified variable data.

#### RESULTS

HRCT findings of 56 patients showed diffuse thin-walled air cysts of different sizes in both lungs, the lung ground glass density 16 cases, 8 cases within the lung nodules, atelectasis 32 cases, bronchus enlargement of blood vessel bundle 12 cases, interlobular septal thickening 25 cases, mediastinal fat increased density 30 cases, pericardial effusion 6 cases, mediastinal lymph node enlargement 9 cases, pleural effusion 45 cases, pneumothorax 12 cases. PLCT findings of 45 patients showed abnormal iodine oil from different parts of the deposit: 24 cases of the end of thoracic duct, 7 cases with right lymphatic catheter, 7 cases were intrapulmonary and 7 cases were hilum, mediastinum 20 cases, pericardium 1 case, pleural cavity 7 cases, Intercostal 17 cases, axillary 6 cases, diaphragmatic around 32 cases, 27 cases of spinal column, abdominal pelvic 45 cases, double iliac 41 cases, bilateral inguinal 36 cases, perineum 3 cases. In addition, 3 patients had hepatic angiomyolipoma, 8 patients had renal angiomyolipoma, 4 patients had diffuse intestinal wall thickening, and 31 patients had abdominal and pelvic effusion.

#### CONCLUSION

s HRCT and PLCT demonstrates capability in abnormalities of the thoracic, abdominal and pelvic and detection of location, distribution and range of abnormal lymphatics, which is useful for diagnosis and therapeutic adoptions for lymphangiomyomatosis.

#### CLINICAL RELEVANCE/APPLICATION

Lymphangiomyomatosis is an autoimmune disease involving multiple organs and systems. It is necessary to evaluate the systematic lymphatic circulation abnormality for with HRCT and PLCT in patients with SLE, which is very important for therapeutic options.

Printed on: 02/07/23

## Abstract Archives of the RSNA, 2022

S3B-SPCH-7

### Dark-Field Chest Radiography Outperforms Conventional Radiography for the Diagnosis and Staging of Pulmonary Emphysema

Sunday, Nov. 27 12:15PM - 12:45PM Room: Learning Center - CH DPS

#### Awards

**Trainee Research Prize - Resident**

#### Participants

Theresa Urban, MSc, Garching, Germany (*Presenter*) Nothing to Disclose

#### PURPOSE

Dark-field chest radiography visualizes the condition of the lungs' alveolar structure by measuring the coherent ultra-small-angle scattering of X-rays. Here, we compare dark-field chest radiography with conventional radiography for the diagnosis and staging of pulmonary emphysema.

#### METHODS AND MATERIALS

Subjects were included after a medically indicated CT scan of the thorax, showing either no lung impairments or different stages of emphysema. To establish a ground truth, all CTs were assessed separately by three radiologists assigning visual scores based on the Fleischner society classification scheme for emphysema severity (absent, trace, mild, moderate, confluent, advanced destructive). Participants were imaged at a commercial chest radiography device, yielding a conventional attenuation image, and at a clinical prototype for dark-field chest radiography, yielding both an attenuation and a dark-field image. Three independent blinded readers assessed the conventional attenuation image and both attenuation and dark-field image from the prototype for presence and severity of emphysema (no emphysema, mild emphysema, moderate emphysema, severe emphysema). Statistical analysis included evaluation of receiver-operator-characteristics and pair-wise comparison of adjacent Fleischner groups using an AUC-based z-test with a significance level of 0.05.

#### RESULTS

A total of 90 patients (56 males) were included, with a mean age of  $65 \pm 12$  years. The dark-field images show a distinct decrease of signal strength with emphysema severity. Compared to conventional images (AUC = 0.74), readers were significantly better able to identify emphysema with images from the dark-field prototype (AUC = 0.85,  $p < 0.05$ ). While ratings of adjacent emphysema severity groups with conventional radiographs were only different for trace and mild emphysema, ratings based on images from the dark-field prototype were different for trace and mild, mild and moderate, and moderate and confluent emphysema.

#### CONCLUSION

Compared to conventional chest radiography, dark-field chest radiography provides improved capability for identification and staging of emphysema.

#### CLINICAL RELEVANCE/APPLICATION

Dark-field chest radiography improves the detection of emphysematous changes in the lung, demonstrating its high diagnostic value for lung assessment.

Printed on: 02/07/23

## Abstract Archives of the RSNA, 2022

S3B-SPCH-8

### Lung Imaging at 0.55T MRI for Interstitial Lung Disease Assessment in Patients with Pulmonary Sarcoidosis

Sunday, Nov. 27 12:15PM - 12:45PM Room: Learning Center - CH DPS

#### Participants

Hanns-Christian Breit, MD, Basel, Switzerland (*Presenter*) Nothing to Disclose

#### PURPOSE

To evaluate the potential of lung MR imaging at 0.55T in patients with pulmonary sarcoidosis.

#### METHODS AND MATERIALS

We performed a prospective study with 7 patients (4 male, 3 female, 42±9 years) . All patients underwent a routine chest CT (SOMATOM Definition Edge, Siemens Healthineers, arms overhead position) followed by MRI on a 0.55T whole-body scanner (MAGNETOM Free.Max, Siemens Healthineers, gradient amplitude 26 mT/m, gradient slew rate 45 T/m/s) using a 6-channel chest array coil and a 6-channel spine coil. All patients had sarcoidosis with proven pulmonary involvement. Morphological lung imaging was performed by using a free-breathing 3D half-radial dual-echo sequence termed bSTAR (TA = 5:30 min, TE1/TE2/TR = 0.08/2.1/2.2 ms, field-of-view = 34×34×34cm<sup>3</sup>, flip angle = 25°, bandwidth = 1002 Hz/pixel) with a 1.3 mm isotropic resolution, a commercial axial breath-hold balanced steady state free precession (bSSFP) (TA = 0:48min, TE/TR = 2.3/4.6 ms, field-of-view = 380 x 304 mm, 6 mm slice thickness, flip angle = 90°). Furthermore, functional lung MRI using matrix pencil (MP) method for the evaluation of the fractional ventilation and pulmonary perfusion was performed using bSSFP (TA = 1:06 min, TE/TR = 1.20/2.66ms, field-of-view=? 450×450?mm<sup>2</sup>, 12-mm slice thickness, flip angle = 80°).

#### RESULTS

In 4 patients, hilar and mediastinal lymphadenopathy was seen on both CT and MRI. All 7 patients showed CT findings compatible with pulmonary sarcoidosis (perilymphatic nodules with associated partially thickened interlobular septa, airspace opacities, signs of pulmonary fibrosis). All findings were delineable in the morphologic MRI sequences, although the resolution of the perilymphatic micronodules was inferior. In line with these findings, functional MRI images showed a reduced perfusion and ventilation in the affected areas.

#### CONCLUSION

Lung imaging at 0.55T MRI is a promising tool for visualizing morphologic changes in patients with sarcoidosis. Additional information on perfusion and ventilation can be obtained using functional imaging. Further quantitative analyzes might be performed in the future to assess the full potential of this new method.

#### CLINICAL RELEVANCE/APPLICATION

Pulmonary MRI may be an attractive alternative to CT for diagnosis and follow-up of pulmonary sarcoidosis. Unlike CT, pulmonary MRI can provide additional functional information on pulmonary perfusion and ventilation

Printed on: 02/07/23

## Abstract Archives of the RSNA, 2022

S3B-SPGI

### Gastrointestinal Sunday Poster Discussions - B

Sunday, Nov. 27 12:15PM - 12:45PM Room: Learning Center - GI DPS

#### Participants

Kevin Chang, MD, Sharon, MA (*Moderator*) Speaker, Anderson Publishing, Ltd; Speaker, Koninklijke Philips NV

#### Sub-Events

### S3B-SPGI-1 Fully automated 3D organ segmentation in assessing hepatic steatosis on pre-contrast and post-contrast abdominal CT: diagnostic performances of various CT attenuation-based parameters

#### Participants

Jeongin Yoo, Seoul, Korea, Republic Of (*Presenter*) Nothing to Disclose

#### PURPOSE

To investigate the clinical utility of fully automated 3D organ segmentation in assessing hepatic steatosis on pre-contrast and post-contrast CT images, using MR spectroscopy (MRS)-derived proton density fat fraction (PDFF) as the reference standard.

#### METHODS AND MATERIALS

This retrospective study included 489 potential living liver donors (291 men; mean age: 37.1 years) with abdominal CT scans and MRS-PDFF. Using a deep learning-based fully automated 3D organ segmentation algorithm, mean volumetric CT attenuation of the liver and spleen were measured on pre-contrast (liver(L)\_pre and spleen(S)\_pre) and post-contrast (portal venous phase) images (L\_post and S\_post), respectively. Mean attenuation of the liver and spleen were also quantified using a conventional method, 2D manually-defined circular region-of-interest (ROI)-based measurement, and their agreements with volumetric measurements were assessed using the Bland-Altman analysis and intraclass correlation coefficient (ICC). Diagnostic performances for detecting MRS-PDFF  $\geq 5\%$  or  $\geq 10\%$  of CT attenuation-based parameters (L\_pre, liver-minus-spleen(L-S)\_pre, L\_post, and L-S\_post) were evaluated using receiver operating characteristic (ROC) curve analysis, and compared between volumetric and manual measurements using z-statistics.

#### RESULTS

According to MRS-PDFF, 143 (29.2%) and 51 (10.4%) subjects had  $\geq 5\%$  and  $\geq 10\%$  hepatic steatosis, respectively. Volumetric and ROI-based attenuation measurements showed good agreements both for liver and spleen, with mean differences of -4.1 HU (ICC=0.980) and -3.4 HU (ICC=0.915) on pre-contrast CT; and -1.4 HU (ICC=0.992) and -7.7 HU (ICC=0.968) on post-contrast CT, respectively. L\_pre, L-S\_pre, L\_post, and L-S\_post of volumetric measurements showed areas under the ROC curve (AUCs) of 0.786, 0.827, 0.748, and 0.807 for  $\geq 5\%$  steatosis; and 0.893, 0.921, 0.842, and 0.883 for  $\geq 10\%$  steatosis, respectively, which were comparable to those of ROI-based measurements (AUCs: 0.748-0.828; and 0.837-0.908, all  $P_s > 0.05$ ).

#### CONCLUSION

Fully automated 3D segmentation analysis of the liver and spleen provides quantitative CT attenuation-based parameters that work well for assessing hepatic steatosis both on pre-contrast and post-contrast CT.

#### CLINICAL RELEVANCE/APPLICATION

Using the fully automated organ segmentation tool, CT volumetric attenuation data of liver and spleen can be obtained which can detect and grade hepatic steatosis. By allowing large population data collection on hepatic steatosis, it may be used for screening risk groups for metabolic disease and predicting the prognosis of various diseases.

### S3B-SPGI-10 The establishment of a classification model for the acute ileus and perforation on abdominal radiographic image based on deep learning

#### Participants

Kexin Wang, (*Presenter*) Nothing to Disclose

#### PURPOSE

Establish an automatic triage system to classify whether typical imaging features of ileus or perforation exists on an abdominal radiography based on deep learning neural network.

#### METHODS AND MATERIALS

In the study for establishment of classification model aimed to diagnose ileus in X-ray plain image, we included 1697 consecutive patients (median age, 55 years; men, 1154) from January 1st 2018 to August 30th 2020 in our PACS/RIS database, who were divided into training dataset (n=1355), validation dataset (n=169) and testing dataset (n=173). As the model for classify image about whether perforation is existed, 271 patients were included, separated into training dataset (n=214), validation dataset (n=30) and testing dataset (n=27) randomly. The above-mentioned data were used to train classification models based on MedicalNet. Accuracy, misclassification, recall, specificity, precision, and F1-score were calculated and used to evaluate the

performance of models.

## RESULTS

In the testing dataset of ileus model, 75 cases were classified as positive, while 98 cases were negative. The accuracy, misclassification, recall, specificity, precision, and F1-score were 94.8%, 4.3%, 0.949, 0.933, and 0.957, respectively. In the testing dataset of perforation diagnostic model, 11 cases were classified as positive, while 16 cases were negative. The accuracy, misclassification, recall, specificity, precision, and F1-score were 96.3%, 3.7%, 0.917, 1, 1, and 0.957, respectively.

## CONCLUSION

s For the abdomen radiographs of patients with acute abdomen, the AI algorithm can be used in triage of the patients suspected of ileus and perforation.

## CLINICAL RELEVANCE/APPLICATION

Automatic and rapid detection of patients with the acute abdomen on abdominal radiography in the ER, facilitating patient management and improving safety.

### S3B-SPGI-2 Prediction Histological Grades and Ki-67 Expression of Hepatocellular Carcinoma Based on Sonazoid Contrast Enhanced Ultrasound Radiomics Signatures

Participants

Yi Dong, MD, PhD, Shanghai, China (*Presenter*) Nothing to Disclose

## PURPOSE

Tumor histopathological grades and Ki-67 expression are key aspects concerning to prognosis of patients with hepatocellular carcinoma (HCC) lesions. The aim of this study is to investigate whether radiomics model derived from Sonazoid contrast enhanced (S-CEUS) images could predict histological grades and Ki-67 expression in HCC lesions.

## METHODS AND MATERIALS

This prospective study included 101 (training cohort: n = 71; validation cohort: n = 30) patients with surgical resection and histopathological confirmed HCC lesions. Radiomics features were extracted from B mode and Kupffer phase of S-CEUS images. Maximum relevance minimum redundancy (MRMR) and Least Absolute Shrinkage and Selection Operator (LASSO) were used for feature selection and stepwise multivariate logit regression model was trained for prediction. Model accuracy, sensitivity and specificity in both training and testing datasets were used to evaluate performance.

## RESULTS

Prediction model derived from Kupffer phase images (CE-model) displayed a significantly better performance for the prediction of stage III HCC patients, with an area under the receiver operating characteristic curve (AUROC) of 0.869 in the training dataset, and 0.865 in testing set. CE-model demonstrated well generalizability in identifying HCC patients with elevated Ki-67 expression (> 10 %) with a training AUROC of 0.873 and testing AUROC of 0.768, with noticeably higher specificity of 93.3% and 80.0% in training and testing datasets.

## CONCLUSION

s Radiomic model constructed from Kupffer phase of S-CEUS images have potential for predicting Ki-67 expression and histological stages in patients with HCC.

## CLINICAL RELEVANCE/APPLICATION

Radiomic model constructed from Kupffer phase of S-CEUS images could be used to provide valuable information for predicting histopathologic stages and Ki-67 expression in patients with HCC.

### S3B-SPGI-3 Detection of Colon Cancer on CT using Machine Learning

Participants

Robert Harris, PhD, (*Presenter*) Scientist, Virtual Radiologic Corporation

## PURPOSE

Colorectal cancer is among the most common cancers diagnosed in the U.S. The survival rate is greatly influenced by how early the disease is caught, with a 5-year survival rate of 91% in patients with localized cancer. However, less than half of patients are diagnosed at this early stage. Our teleradiology institution processes approximately 3 million CT studies each year, during which a small number of masses suspicious for colon cancer are missed on the initial CT read and discovered during quality assurance (QA) review. We hypothesized that we could train a machine learning algorithm to identify masses suspicious for colon cancer on CT images and use this model as part of a QA process to notify radiologists if a suspicious mass has been potentially missed.

## METHODS AND MATERIALS

Natural language processing (NLP) of radiology CT reports was used retrospectively to identify 99 studies containing colorectal masses suspicious for cancer. An axial image series from each of these studies was annotated by a Board Certified radiologist by segmenting masses suspicious for cancer. These segmentations were converted into bounding boxes, with 1,085 annotated images used as positives and 2,170 axial CT images with no colon masses used as negatives in the training dataset. A yolo-v3 bounding box model was used for training. A test dataset was created using 16 CT studies containing a suspicious colorectal mass that had been missed on the initial read and later found by QA, along with 16 CT studies with no suspicious pathology. The trained model was run on this test dataset. The model was also integrated with our teleradiology practice workflow to classify prospective studies during a four-week period.

## RESULTS

The model achieved an AUC of 0.930 on the test dataset, with a sensitivity of 50% and specificity of 100%. For prospective data, 17,451 abdominal CT studies were inferenced, of which 40 were NLP-positive for suspicion of colorectal cancer. The model correctly identified 22 of these for a sensitivity of 55.0% and specificity of 92.3%.

## CONCLUSION

s An artificial intelligence model was trained to identify masses suspicious for colorectal cancer on CT imaging. This model was able to identify half of our practice's previously missed suspicious colon masses and performs equally well on prospective data. This model is currently undergoing iterative retraining and will be used to screen CT data for missed findings.

## CLINICAL RELEVANCE/APPLICATION

At least 20 colorectal masses suspicious for cancer are missed on CT imaging each year at our practice due to our high volume of CT imaging. A machine learning model capable of identifying these missed findings shortly after image interpretation can be used to correct missed diagnoses and improve patient care.

### S3B-SPGI-5 Prior-judgement-based 2D Deep Transfer Learning Improves MRI Prediction of Preoperative T-staging in Rectal Cancer

Participants

Min Hou, (*Presenter*) Nothing to Disclose

## PURPOSE

To investigate whether the addition of expert radiologists' prior selection of imaging slice in 2D deep transfer learning model could achieve better predictive performance than the 2D model without prior information and subjective assessment of expert radiologists.

## METHODS AND MATERIALS

A total of 788 consecutive RC patients with pathologically proven T-staging results in our institution were retrospectively enrolled in this study. All patients were randomly divided into the training cohort (n = 670) and the testing cohort (n = 118). We established an ImageNet pre-trained ResNet18 model for the pretreatment prediction on tumor T-staging. Then two tumor-derived deep learning (DL) diagnostic models were developed: Model1 based on the slice selected by radiologists which they reckon to compromise the deepest invasion depth of the tumor, and Model2 based on the slice of maximum tumor cross-section. The diagnostic performance of the DL models were compared to each other and to the subjective assessment of expert radiologists by receiver operating characteristic (ROC). The sensitivity, specificity, and accuracy were calculated.

## RESULTS

The diagnostic performance of Model1 [the area under the curve (AUC) 91.7%, sensitivity 0.907, specificity 0.761, and accuracy 0.855] was significantly higher than that of Model2 (AUC 80.0%, sensitivity 0.815, specificity 0.693, and accuracy 0.772) for predicting RC T-staging (P<0.05). Both the DL models achieved superior predictive performance than the expert radiologists (P<0.05).

## CONCLUSION

s We introduced a novel 2D deep transfer learning model for preoperative assessing the T-staging category of rectal cancer, and found that the performance of the DL model was significantly improved based on expert radiologists' prior selected slice of the deepest invasion depth of tumor.

## CLINICAL RELEVANCE/APPLICATION

The accuracy of T-staging prediction among RC patients has been a prime concern in tailoring preoperative treatment strategy. We firstly established a 2D deep transfer learning model with satisfying predictive performance, and found that the performance could be significantly improved by using radiologists' prior judgment.

### S3B-SPGI-6 A Novel Multimodal Deep Learning Model for Preoperative Prediction of Microvascular Invasion and Outcome in Hepatocellular Carcinoma

Participants

Fang Wang, Hangzhou, China (*Presenter*) Nothing to Disclose

## PURPOSE

Accurate preoperative identification of the positive propensity of microvascular invasion (MVI) can relieve the pressure from personalized treatment adaptation and improve the poor prognosis for hepatocellular carcinoma (HCC). This study aimed to develop and validate a novel multimodal deep learning (DL) model for MVI status prediction based on contrast-enhanced computed tomography (CT) and multi-parameter magnetic resonance imaging (MRI).

## METHODS AND MATERIALS

This retrospective study enrolled 397 patients from two institutions with pathologically-confirmed HCC. All patients underwent both CT and MRI examinations preoperative. Patients from institution I (n = 297) were included as training cohort and patients from institution II (n = 100) served as an independent validation set. To predict the presence of MVI, the clinical model (C) and the CT/MRI radiological models (RCT, RMRI) were established by support vector machine (SVM), and DL models (DLCT\_ALL, DLMRI\_ALL, DLCT+MRI) based on single or multi-modality medical images were developed by convolutional neural network (CNN) ResNet18, and the comprehensive model (CALL) involving multi-modality DL features and clinical and radiological features was constructed using SVM algorithm. In addition, the prognostic value of the DL models for recurrence-free survival (RFS) was further explored.

## RESULTS

The DLCT+MRI model exhibited superior predicted efficiency over single-modality models, especially over the DLCT\_ALL model (area under receiver operating characteristics curve [AUC]: 0.819 vs. 0.742, net reclassification index [NRI] > 0, integrated discrimination improvement [IDI] > 0). Besides, the DLMRI\_ALL model improved the performance over the RMRI model (AUC: 0.794 vs. 0.766, NRI > 0, IDI < 0), but no such difference was found between the DLCT\_ALL model and the RCT model (AUC: 0.742 vs. 0.710, NRI < 0, IDI < 0). And the diagnostic performance of the C model was worse than any other models. Furthermore, both DLCT+MRI and CALL models revealed the prognostic power in the stratification of RFS (P<0.001).

## CONCLUSION

s The proposed DLCT+MRI model showed robust capability in predicting the risk of MVI occurrence and outcomes for HCC patients, which might help surgeons decide the extent of operation in precise medicine. Besides, the performance of multi-modality DL model was better than any single modality, especially for CT.

#### **CLINICAL RELEVANCE/APPLICATION**

MVI plays a crucial role in the personalized treatment strategy of HCC, yet a high level of diagnostic expertise tends to be localized in minority reference centers. One promising solution is the adoption of the deep learning model based on multi-modality medical images to improve the accuracy of preoperative prediction of MVI.

#### **S3B-SPGI-7 Prediction of Microvascular Invasion in Hepatocellular Carcinoma Using Artificial Intelligence: A systematic review and meta-analysis of 12,216 patients**

Participants

Pedram Keshavarz, MD, Los Angeles, CA (*Presenter*) Nothing to Disclose

#### **PURPOSE**

To review the developed microvascular invasion (MVI) predictive models using radiomics, non-radiomics, and Convolutional Neural Network (CNN) in patients with hepatocellular carcinoma (HCC).

#### **METHODS AND MATERIALS**

A systematic search of PubMed, Scopus, Embase, Web of Science, and Google Scholar was performed. The random-effect models were utilized to calculate pool sensitivity, specificity, predictive values, summary ROC curves, and AUC based on the "Standards for Reporting Diagnostic accuracy studies" (STARD) guidelines. The heterogeneity between studies was examined using Cochrane's Q and I<sup>2</sup> tests.

#### **RESULTS**

The meta-analysis study cohort included 47 studies comprising 12,216 cases including 15, 26 and 10 studies in the radiomics, non-radiomics, and CNN subcohorts respectively. Four studies reported two models. The pooled specificity, sensitivity, and AUC of the radiomics, non-radiomics and CNN subcohorts were 0.76 (95% CI: 0.69-0.82, I<sup>2</sup> = 87%), 0.79 (95% CI: 0.73-0.85, I<sup>2</sup> = 84%), 0.85 and 0.81 (95% CI: 0.76-0.85, I<sup>2</sup> = 79%), 0.73 (95% CI: 0.65-0.79, I<sup>2</sup> = 82%), 0.84 and 0.81 (95% CI: 0.76-0.85, I<sup>2</sup> = 49%, and 0.83 (95% CI: 0.78-0.88, I<sup>2</sup> = 60%), and AUC of 0.89, respectively. Meta-regression and sub-group analysis showed significant differences in performance of CNN models in patients with multiple vs single HCC tumors (specificity 0.78, 95% CI: 0.72-0.83, I<sup>2</sup> = 37%, sensitivity 0.82, 95% CI: 0.74-0.88, I<sup>2</sup> = 46%, AUC: 0.85) without significant differences between studies using different imaging modalities (MRI vs. CT).

#### **CONCLUSION**

s Based on the meta-analysis, the CNN subcohort had the best pooled prediction of MVI, compared to radiomics and non-radiomics sub-cohorts, especially in patients with multiple HCC lesions.

#### **CLINICAL RELEVANCE/APPLICATION**

CNN-based deep learning models have high performance for the prediction of MVI in HCC patients, although the long-term outcomes and multicenter validation are required to provide a reliable and robust prediction tool that translates into clinical utilization.

#### **S3B-SPGI-9 DeePSC - Automated decision support for the diagnosis of primary sclerosing cholangitis**

##### **Awards**

**Trainee Research Prize - Resident**

Participants

Haissam Ragab, MD, (*Presenter*) Nothing to Disclose

#### **PURPOSE**

To develop a deep learning-based clinical decision support system for the automated diagnosis of primary sclerosing cholangitis (PSC) on 2D-MRCP images that surpasses the predictive performance of the average radiologist.

#### **METHODS AND MATERIALS**

In this retrospective study, 2D-MRCP datasets of 342 patients with confirmed diagnosis of PSC and another 264 control subjects without any history of chronic liver disease obtained at 1.5 and 3 T were included. For external validation, another 37 MRCP datasets (20 PSC/17 non-PSC) from a different scanner and manufacturer (3 T, Siemens) were included. The binary classification task was performed with a multi-view deep convolutional neural network (CNN) specialized on simultaneously processing seven 2D-MRCP images taken from different rotational angles from the same patient. The diagnostic performance of our model was eventually compared to that of four board-certified radiologists at different levels of training and with varying experience in reading MRCP.

#### **RESULTS**

The model showed high performance with an accuracy, sensitivity, and specificity of 82 %, 81 %, and 83 % on the unseen 3 T test dataset, and 82 %, 82 %, and 82 % on the unseen 1.5 T test dataset, respectively. For comparison, the average diagnostic performance of the four radiologists was 75 %, 77 %, and 72 % for accuracy, sensitivity, and specificity, respectively, on the 3 T images as well as 72 %, 73 %, and 70 % on the 1.5 T images. When comparing individually, the model achieved similar values to the best radiologist in all metrics on the 1.5 T data as well as in 3 T sensitivity, and scored second best in 3 T accuracy and specificity. On the external dataset, the model achieved near perfect values for accuracy (94 %), sensitivity (100 %) and specificity (88 %).

#### **CONCLUSION**

s The proposed multi-view CNN outperformed the average predictions provided by four radiologists on all metrics and datasets and even performed on par with the best radiologist on the 1.5 T dataset. The high performance on the external dataset suggests generalizability of the developed algorithm. Our results show that automated classification of PSC-compatible findings based on 2D-MRCP is achievable with high accuracy for both 1.5 and 3 T.

#### **CLINICAL RELEVANCE/APPLICATION**

The proposed algorithm might serve as a clinical decision support system to improve the expert diagnosis of PSC-compatible features on 2D-MRCP image data.

Printed on: 02/07/23

## Abstract Archives of the RSNA, 2022

S3B-SPGI-1

### Fully automated 3D organ segmentation in assessing hepatic steatosis on pre-contrast and post-contrast abdominal CT: diagnostic performances of various CT attenuation-based parameters

Sunday, Nov. 27 12:15PM - 12:45PM Room: Learning Center - GI DPS

#### Participants

Jeongin Yoo, Seoul, Korea, Republic Of (*Presenter*) Nothing to Disclose

#### PURPOSE

To investigate the clinical utility of fully automated 3D organ segmentation in assessing hepatic steatosis on pre-contrast and post-contrast CT images, using MR spectroscopy (MRS)-derived proton density fat fraction (PDFF) as the reference standard.

#### METHODS AND MATERIALS

This retrospective study included 489 potential living liver donors (291 men; mean age: 37.1 years) with abdominal CT scans and MRS-PDFF. Using a deep learning-based fully automated 3D organ segmentation algorithm, mean volumetric CT attenuation of the liver and spleen were measured on pre-contrast (liver(L)\_pre and spleen(S)\_pre) and post-contrast (portal venous phase) images (L\_post and S\_post), respectively. Mean attenuation of the liver and spleen were also quantified using a conventional method, 2D manually-defined circular region-of-interest (ROI)-based measurement, and their agreements with volumetric measurements were assessed using the Bland-Altman analysis and intraclass correlation coefficient (ICC). Diagnostic performances for detecting MRS-PDFF  $\geq 5\%$  or  $\geq 10\%$  of CT attenuation-based parameters (L\_pre, liver-minus-spleen(L-S)\_pre, L\_post, and L-S\_post) were evaluated using receiver operating characteristic (ROC) curve analysis, and compared between volumetric and manual measurements using z-statistics.

#### RESULTS

According to MRS-PDFF, 143 (29.2%) and 51 (10.4%) subjects had  $\geq 5\%$  and  $\geq 10\%$  hepatic steatosis, respectively. Volumetric and ROI-based attenuation measurements showed good agreements both for liver and spleen, with mean differences of -4.1 HU (ICC=0.980) and -3.4 HU (ICC=0.915) on pre-contrast CT; and -1.4 HU (ICC=0.992) and -7.7 HU (ICC=0.968) on post-contrast CT, respectively. L\_pre, L-S\_pre, L\_post, and L-S\_post of volumetric measurements showed areas under the ROC curve (AUCs) of 0.786, 0.827, 0.748, and 0.807 for  $\geq 5\%$  steatosis; and 0.893, 0.921, 0.842, and 0.883 for  $\geq 10\%$  steatosis, respectively, which were comparable to those of ROI-based measurements (AUCs: 0.748-0.828; and 0.837-0.908, all  $P_s > 0.05$ ).

#### CONCLUSION

s Fully automated 3D segmentation analysis of the liver and spleen provides quantitative CT attenuation-based parameters that work well for assessing hepatic steatosis both on pre-contrast and post-contrast CT.

#### CLINICAL RELEVANCE/APPLICATION

Using the fully automated organ segmentation tool, CT volumetric attenuation data of liver and spleen can be obtained which can detect and grade hepatic steatosis. By allowing large population data collection on hepatic steatosis, it may be used for screening risk groups for metabolic disease and predicting the prognosis of various diseases.

Printed on: 02/07/23

## Abstract Archives of the RSNA, 2022

S3B-SPGI-10

### The establishment of a classification model for the acute ileus and perforation on abdominal radiographic image based on deep learning

Sunday, Nov. 27 12:15PM - 12:45PM Room: Learning Center - GI DPS

#### Participants

Kexin Wang, (*Presenter*) Nothing to Disclose

#### PURPOSE

Establish an automatic triage system to classify whether typical imaging features of ileus or perforation exists on an abdominal radiography based on deep learning neural network.

#### METHODS AND MATERIALS

In the study for establishment of classification model aimed to diagnose ileus in X-ray plain image, we included 1697 consecutive patients (median age, 55 years; men, 1154) from January 1st 2018 to August 30th 2020 in our PACS/RIS database, who were divided into training dataset (n=1355), validation dataset (n=169) and testing dataset (n=173). As the model for classify image about whether perforation is existed, 271 patients were included, separated into training dataset (n=214), validation dataset (n=30) and testing dataset (n=27) randomly. The above-mentioned data were used to train classification models based on MedicalNet. Accuracy, misclassification, recall, specificity, precision, and F1-score were calculated and used to evaluate the performance of models.

#### RESULTS

In the testing dataset of ileus model, 75 cases were classified as positive, while 98 cases were negative. The accuracy, misclassification, recall, specificity, precision, and F1-score were 94.8%, 4.3%, 0.949, 0.933, and 0.957, respectively. In the testing dataset of perforation diagnostic model, 11 cases were classified as positive, while 16 cases were negative. The accuracy, misclassification, recall, specificity, precision, and F1-score were 96.3%, 3.7%, 0.917, 1, 1, and 0.957, respectively.

#### CONCLUSION

s For the abdomen radiographs of patients with acute abdomen, the AI algorithm can be used in triage of the patients suspected of ileus and perforation.

#### CLINICAL RELEVANCE/APPLICATION

Automatic and rapid detection of patients with the acute abdomen on abdominal radiography in the ER, facilitating patient management and improving safety.

Printed on: 02/07/23

## Abstract Archives of the RSNA, 2022

S3B-SPGI-2

### **Prediction Histological Grades and Ki-67 Expression of Hepatocellular Carcinoma Based on Sonazoid Contrast Enhanced Ultrasound Radiomics Signatures**

Sunday, Nov. 27 12:15PM - 12:45PM Room: Learning Center - GI DPS

#### **Participants**

Yi Dong, MD, PhD, Shanghai, China (*Presenter*) Nothing to Disclose

#### **PURPOSE**

Tumor histopathological grades and Ki-67 expression are key aspects concerning to prognosis of patients with hepatocellular carcinoma (HCC) lesions. The aim of this study is to investigate whether radiomics model derived from Sonazoid contrast enhanced (S-CEUS) images could predict histological grades and Ki-67 expression in HCC lesions.

#### **METHODS AND MATERIALS**

This prospective study included 101 (training cohort: n = 71; validation cohort: n = 30) patients with surgical resection and histopathological confirmed HCC lesions. Radiomics features were extracted from B mode and Kupffer phase of S-CEUS images. Maximum relevance minimum redundancy (MRMR) and Least Absolute Shrinkage and Selection Operator (LASSO) were used for feature selection and stepwise multivariate logit regression model was trained for prediction. Model accuracy, sensitivity and specificity in both training and testing datasets were used to evaluate performance.

#### **RESULTS**

Prediction model derived from Kupffer phase images (CE-model) displayed a significantly better performance for the prediction of stage III HCC patients, with an area under the receiver operating characteristic curve (AUROC) of 0.869 in the training dataset, and 0.865 in testing set. CE-model demonstrated well generalizability in identifying HCC patients with elevated Ki-67 expression (> 10 %) with a training AUROC of 0.873 and testing AUROC of 0.768, with noticeably higher specificity of 93.3% and 80.0% in training and testing datasets.

#### **CONCLUSION**

s Radiomic model constructed from Kupffer phase of S-CEUS images have potential for predicting Ki-67 expression and histological stages in patients with HCC.

#### **CLINICAL RELEVANCE/APPLICATION**

Radiomic model constructed from Kupffer phase of S-CEUS images could be used to provide valuable information for predicting histopathologic stages and Ki-67 expression in patients with HCC.

Printed on: 02/07/23



## Abstract Archives of the RSNA, 2022

S3B-SPGI-3

### Detection of Colon Cancer on CT using Machine Learning

Sunday, Nov. 27 12:15PM - 12:45PM Room: Learning Center - GI DPS

#### Participants

Robert Harris, PhD, (*Presenter*) Scientist, Virtual Radiologic Corporation

#### PURPOSE

Colorectal cancer is among the most common cancers diagnosed in the U.S. The survival rate is greatly influenced by how early the disease is caught, with a 5-year survival rate of 91% in patients with localized cancer. However, less than half of patients are diagnosed at this early stage. Our teleradiology institution processes approximately 3 million CT studies each year, during which a small number of masses suspicious for colon cancer are missed on the initial CT read and discovered during quality assurance (QA) review. We hypothesized that we could train a machine learning algorithm to identify masses suspicious for colon cancer on CT images and use this model as part of a QA process to notify radiologists if a suspicious mass has been potentially missed.

#### METHODS AND MATERIALS

Natural language processing (NLP) of radiology CT reports was used retrospectively to identify 99 studies containing colorectal masses suspicious for cancer. An axial image series from each of these studies was annotated by a Board Certified radiologist by segmenting masses suspicious for cancer. These segmentations were converted into bounding boxes, with 1,085 annotated images used as positives and 2,170 axial CT images with no colon masses used as negatives in the training dataset. A yolo-v3 bounding box model was used for training. A test dataset was created using 16 CT studies containing a suspicious colorectal mass that had been missed on the initial read and later found by QA, along with 16 CT studies with no suspicious pathology. The trained model was run on this test dataset. The model was also integrated with our teleradiology practice workflow to classify prospective studies during a four-week period.

#### RESULTS

The model achieved an AUC of 0.930 on the test dataset, with a sensitivity of 50% and specificity of 100%. For prospective data, 17,451 abdominal CT studies were inferenced, of which 40 were NLP-positive for suspicion of colorectal cancer. The model correctly identified 22 of these for a sensitivity of 55.0% and specificity of 92.3%.

#### CONCLUSION

s An artificial intelligence model was trained to identify masses suspicious for colorectal cancer on CT imaging. This model was able to identify half of our practice's previously missed suspicious colon masses and performs equally well on prospective data. This model is currently undergoing iterative retraining and will be used to screen CT data for missed findings.

#### CLINICAL RELEVANCE/APPLICATION

At least 20 colorectal masses suspicious for cancer are missed on CT imaging each year at our practice due to our high volume of CT imaging. A machine learning model capable of identifying these missed findings shortly after image interpretation can be used to correct missed diagnoses and improve patient care.

Printed on: 02/07/23

## Abstract Archives of the RSNA, 2022

S3B-SPGI-5

### Prior-judgement-based 2D Deep Transfer Learning Improves MRI Prediction of Preoperative T-staging in Rectal Cancer

Sunday, Nov. 27 12:15PM - 12:45PM Room: Learning Center - GI DPS

#### Participants

Min Hou, (*Presenter*) Nothing to Disclose

#### PURPOSE

To investigate whether the addition of expert radiologists' prior selection of imaging slice in 2D deep transfer learning model could achieve better predictive performance than the 2D model without prior information and subjective assessment of expert radiologists.

#### METHODS AND MATERIALS

A total of 788 consecutive RC patients with pathologically proven T-staging results in our institution were retrospectively enrolled in this study. All patients were randomly divided into the training cohort (n = 670) and the testing cohort (n = 118). We established an ImageNet pre-trained ResNet18 model for the pretreatment prediction on tumor T-staging. Then two tumor-derived deep learning (DL) diagnostic models were developed: Model1 based on the slice selected by radiologists which they reckon to compromise the deepest invasion depth of the tumor, and Model2 based on the slice of maximum tumor cross-section. The diagnostic performance of the DL models were compared to each other and to the subjective assessment of expert radiologists by receiver operating characteristic (ROC). The sensitivity, specificity, and accuracy were calculated.

#### RESULTS

The diagnostic performance of Model1 [the area under the curve (AUC) 91.7%, sensitivity 0.907, specificity 0.761, and accuracy 0.855] was significantly higher than that of Model2 (AUC 80.0%, sensitivity 0.815, specificity 0.693, and accuracy 0.772) for predicting RC T-staging (P<0.05). Both the DL models achieved superior predictive performance than the expert radiologists (P<0.05).

#### CONCLUSION

s We introduced a novel 2D deep transfer learning model for preoperative assessing the T-staging category of rectal cancer, and found that the performance of the DL model was significantly improved based on expert radiologists' prior selected slice of the deepest invasion depth of tumor.

#### CLINICAL RELEVANCE/APPLICATION

The accuracy of T-staging prediction among RC patients has been a prime concern in tailoring preoperative treatment strategy. We firstly established a 2D deep transfer learning model with satisfying predictive performance, and found that the performance could be significantly improved by using radiologists' prior judgment.

Printed on: 02/07/23

## Abstract Archives of the RSNA, 2022

S3B-SPGI-6

### A Novel Multimodal Deep Learning Model for Preoperative Prediction of Microvascular Invasion and Outcome in Hepatocellular Carcinoma

Sunday, Nov. 27 12:15PM - 12:45PM Room: Learning Center - GI DPS

#### Participants

Fang Wang, Hangzhou, China (*Presenter*) Nothing to Disclose

#### PURPOSE

Accurate preoperative identification of the positive propensity of microvascular invasion (MVI) can relieve the pressure from personalized treatment adaptation and improve the poor prognosis for hepatocellular carcinoma (HCC). This study aimed to develop and validate a novel multimodal deep learning (DL) model for MVI status prediction based on contrast-enhanced computed tomography (CT) and multi-parameter magnetic resonance imaging (MRI).

#### METHODS AND MATERIALS

This retrospective study enrolled 397 patients from two institutions with pathologically-confirmed HCC. All patients underwent both CT and MRI examinations preoperative. Patients from institution I (n = 297) were included as training cohort and patients from institution II (n = 100) served as an independent validation set. To predict the presence of MVI, the clinical model (C) and the CT/MRI radiological models (RCT, RMRI) were established by support vector machine (SVM), and DL models (DLCT\_ALL, DLMRI\_ALL, DLCT+MRI) based on single or multi-modality medical images were developed by convolutional neural network (CNN) ResNet18, and the comprehensive model (CALL) involving multi-modality DL features and clinical and radiological features was constructed using SVM algorithm. In addition, the prognostic value of the DL models for recurrence-free survival (RFS) was further explored.

#### RESULTS

The DLCT+MRI model exhibited superior predicted efficiency over single-modality models, especially over the DLCT\_ALL model (area under receiver operating characteristics curve [AUC]: 0.819 vs. 0.742, net reclassification index [NRI] > 0, integrated discrimination improvement [IDI] > 0). Besides, the DLMRI\_ALL model improved the performance over the RMRI model (AUC: 0.794 vs. 0.766, NRI > 0, IDI < 0), but no such difference was found between the DLCT\_ALL model and the RCT model (AUC: 0.742 vs. 0.710, NRI < 0, IDI < 0). And the diagnostic performance of the C model was worse than any other models. Furthermore, both DLCT+MRI and CALL models revealed the prognostic power in the stratification of RFS (P < 0.001).

#### CONCLUSION

The proposed DLCT+MRI model showed robust capability in predicting the risk of MVI occurrence and outcomes for HCC patients, which might help surgeons decide the extent of operation in precise medicine. Besides, the performance of multi-modality DL model was better than any single modality, especially for CT.

#### CLINICAL RELEVANCE/APPLICATION

MVI plays a crucial role in the personalized treatment strategy of HCC, yet a high level of diagnostic expertise tends to be localized in minority reference centers. One promising solution is the adoption of the deep learning model based on multi-modality medical images to improve the accuracy of preoperative prediction of MVI.

Printed on: 02/07/23

## Abstract Archives of the RSNA, 2022

S3B-SPGI-7

### **Prediction of Microvascular Invasion in Hepatocellular Carcinoma Using Artificial Intelligence: A systematic review and meta-analysis of 12,216 patients**

Sunday, Nov. 27 12:15PM - 12:45PM Room: Learning Center - GI DPS

#### **Participants**

Pedram Keshavarz, MD, Los Angeles, CA (*Presenter*) Nothing to Disclose

#### **PURPOSE**

To review the developed microvascular invasion (MVI) predictive models using radiomics, non-radiomics, and Convolutional Neural Network (CNN) in patients with hepatocellular carcinoma (HCC).

#### **METHODS AND MATERIALS**

A systematic search of PubMed, Scopus, Embase, Web of Science, and Google Scholar was performed. The random-effect models were utilized to calculate pool sensitivity, specificity, predictive values, summary ROC curves, and AUC based on the "Standards for Reporting Diagnostic accuracy studies" (STARD) guidelines. The heterogeneity between studies was examined using Cochrane's Q and I2 tests.

#### **RESULTS**

The meta-analysis study cohort included 47 studies comprising 12,216 cases including 15, 26 and 10 studies in the radiomics, non-radiomics, and CNN subcohorts respectively. Four studies reported two models. The pooled specificity, sensitivity, and AUC of the radiomics, non-radiomics and CNN subcohorts were 0.76 (95% CI: 0.69-0.82, I2 = 87%), 0.79 (95% CI: 0.73-0.85, I2 = 84%), 0.85 and 0.81 (95% CI: 0.76-0.85, I2 = 79%), 0.73 (95% CI: 0.65-0.79, I2 = 82%), 0.84 and 0.81 (95% CI: 0.76-0.85, I2 = 49%, and 0.83 (95% CI: 0.78-0.88, I2 = 60%), and AUC of 0.89, respectively. Meta-regression and sub-group analysis showed significant differences in performance of CNN models in patients with multiple vs single HCC tumors (specificity 0.78, 95% CI: 0.72-0.83, I2 = 37%, sensitivity 0.82, 95% CI: 0.74-0.88, I2 = 46%, AUC: 0.85) without significant differences between studies using different imaging modalities (MRI vs. CT).

#### **CONCLUSION**

s Based on the meta-analysis, the CNN subcohort had the best pooled prediction of MVI, compared to radiomics and non-radiomics sub-cohorts, especially in patients with multiple HCC lesions.

#### **CLINICAL RELEVANCE/APPLICATION**

CNN-based deep learning models have high performance for the prediction of MVI in HCC patients, although the long-term outcomes and multicentral validation are required to provide a reliable and robust prediction tool that translates into clinical utilization.

Printed on: 02/07/23



## Abstract Archives of the RSNA, 2022

S3B-SPGI-9

### DeePSC - Automated decision support for the diagnosis of primary sclerosing cholangitis

Sunday, Nov. 27 12:15PM - 12:45PM Room: Learning Center - GI DPS

#### Awards

Trainee Research Prize - Resident

#### Participants

Haissam Ragab, MD, (*Presenter*) Nothing to Disclose

#### PURPOSE

To develop a deep learning-based clinical decision support system for the automated diagnosis of primary sclerosing cholangitis (PSC) on 2D-MRCP images that surpasses the predictive performance of the average radiologist.

#### METHODS AND MATERIALS

In this retrospective study, 2D-MRCP datasets of 342 patients with confirmed diagnosis of PSC and another 264 control subjects without any history of chronic liver disease obtained at 1.5 and 3 T were included. For external validation, another 37 MRCP datasets (20 PSC/17 non-PSC) from a different scanner and manufacturer (3 T, Siemens) were included. The binary classification task was performed with a multi-view deep convolutional neural network (CNN) specialized on simultaneously processing seven 2D-MRCP images taken from different rotational angles from the same patient. The diagnostic performance of our model was eventually compared to that of four board-certified radiologists at different levels of training and with varying experience in reading MRCP.

#### RESULTS

The model showed high performance with an accuracy, sensitivity, and specificity of 82 %, 81 %, and 83 % on the unseen 3 T test dataset, and 82 %, 82 %, and 82 % on the unseen 1.5 T test dataset, respectively. For comparison, the average diagnostic performance of the four radiologists was 75 %, 77 %, and 72 % for accuracy, sensitivity, and specificity, respectively, on the 3 T images as well as 72 %, 73 %, and 70 % on the 1.5 T images. When comparing individually, the model achieved similar values to the best radiologist in all metrics on the 1.5 T data as well as in 3 T sensitivity, and scored second best in 3 T accuracy and specificity. On the external dataset, the model achieved near perfect values for accuracy (94 %), sensitivity (100 %) and specificity (88 %).

#### CONCLUSION

The proposed multi-view CNN outperformed the average predictions provided by four radiologists on all metrics and datasets and even performed on par with the best radiologist on the 1.5 T dataset. The high performance on the external dataset suggests generalizability of the developed algorithm. Our results show that automated classification of PSC-compatible findings based on 2D-MRCP is achievable with high accuracy for both 1.5 and 3 T.

#### CLINICAL RELEVANCE/APPLICATION

The proposed algorithm might serve as a clinical decision support system to improve the expert diagnosis of PSC-compatible features on 2D-MRCP image data.

Printed on: 02/07/23

## Abstract Archives of the RSNA, 2022

S3B-SPGU

### Genitourinary Sunday Poster Discussions - B

Sunday, Nov. 27 12:15PM - 12:45PM Room: Learning Center - GU DPS

#### Sub-Events

#### S3B-SPGU-2 Improved Detection of Renal Stones using Photon Counting Detector (PCD) CT

Participants

Andrea Esquivel Mora, MD, San Jose, Costa Rica (*Presenter*) Nothing to Disclose

#### PURPOSE

To compare photon-counting detector (PCD) CT to dual-energy CT (DECT) with conventional energy-integrating detectors (EIDs) for renal stone detection.

#### METHODS AND MATERIALS

After IRB approval and informed written consent, patients with renal stones detected using DECT underwent a research PCD-CT exam using similar acquisition settings. Inclusion criteria: (1) archived DECT projection data, (2) no more than 10 renal stones, and (3) at least one stone with a maximum dimension of 3 mm or smaller. For each patient, two DECT mixed images were reconstructed via filtered backprojection (FBP) with (1) a 512 matrix, Qr40 kernel, slice thickness of 1 mm and (2), a 512 matrix, Br40 kernel, and slice thickness of 2 mm. Likewise, for each patient, two PCD-CT virtual monoenergetic images (VMIs) at 70 keV were reconstructed with (1) a 1024 matrix, Qr68 kernel with IR strength 3, and slice thickness of 2 mm and (2), a 1024 matrix, Br68 kernel with IR strength 4, and slice thickness of 0.4 mm. Two radiologists blinded to CT system, slice thickness, and kernel independently compared the de-identified, randomized images in a side-by-side manner to evaluate the visibility of each renal stone using a 4-point Likert score (1=Definitely present, 2=Probably present, 3=Questionably present, 4=Not seen), with disagreements resolved by a genitourinary radiologist. To generate a reference standard for stone presence, a stone was considered definitely present if a consensus score of 1 was assigned for at least one of the four reconstructions, and not present otherwise.

#### RESULTS

Twenty-one patients underwent a DECT exam with EID followed by a PCD CT (mean age 66 years [range, 48-74]; CTDIvol of PCD [15.65 ± 14.17 mGy], CTDIvol of DECT [15.93 ± 14.17 mGy]). 121 renal stones were characterized as definitely present (mean maximum dimension 2.84 ± 2.61 mm, interquartile range: [1.1 mm, 2.7 mm]); 86 of these stones were 3 mm or less. The sensitivity of conventional DECT was 61.2% (74/121; 95% CI: 51.9-69.9) at 2 mm and 65.3% (79/121; 95% CI: 56.1-73.7) at 1 mm. Sensitivity of PCD CT was 73.6% (89/121; 95% CI: 64.8-81.2) at 2 mm and 95.9% (116/121; 95% CI: 90.6-98.6) at 0.4 mm. For stones 3 mm or smaller, PCD at 0.4 mm slice thickness (sensitivity 94.2% [81/86]) was significantly more sensitive than DECT at either slice thickness (at 2 mm: 47.7% [41/86], P=.005; at 1 mm: 53.5% [46/86], P=.01) or PCD at 2 mm (62.8% [54/86], P <.001).

#### CONCLUSION

s PCD CT with high resolution reconstruction enabled detection of renal stones 3 mm and smaller that were not seen or characterized by DECT with conventional EIDs.

#### CLINICAL RELEVANCE/APPLICATION

PCD CT facilitates more accurate detection of small renal stones, which has implications for patient counseling and triage.

#### S3B-SPGU-3 Prostate Imaging-Reporting and Data System Version 2 Release Has Improved Biopsy Accuracy Regarding Tumor Grade: An Experience of Single, Tertiary Institution

Participants

Sung Yoon Park, (*Presenter*) Nothing to Disclose

#### PURPOSE

Before Prostate Imaging-Reporting and Data System Version 2 (PI-RADSv2) release, there was a significant discrepancy in tumor grade between prostate biopsy and surgery. We investigated changes of prostate biopsy accuracy regarding tumor grade before and after PI-RADSv2 release in single, tertiary institution.

#### METHODS AND MATERIALS

We retrospectively evaluated 1191 patients before (2013 cohort, n=394) and 5 years after PI-RADSv2 release (2020 cohort, n=797) who had biopsy-proven prostate cancer (PCa), magnetic resonance imaging (MRI), and surgery. The highest tumor grade of each biopsy and surgical specimens was recorded, respectively. We compared the concordant, underestimated, and overestimated biopsy rates regarding tumor grade compared to surgery between two cohorts, respectively. For patients who underwent both prostate MRI and biopsy at our institution, we investigated the proportion of prebiopsy MRI, age, and prostate-specific antigen of patients, and performed logistic regression for analyzing which parameters are associated with concordant biopsy.

## **RESULTS**

Concordant and underestimated biopsy rates were significantly different between two cohorts: concordance rates were 47.2% in 2013 and 54.5% in 2020 ( $p=.019$ ); underestimated rates were 46.3% in 2013 and 36.4% in 2020 ( $p=.003$ ). However, overestimated biopsy rates between two cohorts were similar ( $p=.993$ ). The proportion of prebiopsy MRI was significantly higher in 2020 than 2013 (80.9% versus 4.9%;  $p<.001$ ), and it was independently associated with concordant biopsy result in multivariate analysis (odds ratio=1.486; 95% confidence interval, 1.057-2.089;  $p=.022$ ).

## **CONCLUSION**

s There was a significant change in the proportion of prebiopsy MRI before and after PI-RADSv2 release in patients who underwent surgery for PCa. This change appears to improve biopsy accuracy regarding tumor grade by reducing underestimation.

## **CLINICAL RELEVANCE/APPLICATION**

We demonstrated the change in clinical pathway and improvement of biopsy accuracy before and after PI-RADSv2 release. Current data will serve as evidence for supporting MRI-directed biopsy pathway.

Printed on: 02/07/23

## Abstract Archives of the RSNA, 2022

S3B-SPGU-2

### Improved Detection of Renal Stones using Photon Counting Detector (PCD) CT

Sunday, Nov. 27 12:15PM - 12:45PM Room: Learning Center - GU DPS

#### Participants

Andrea Esquivel Mora, MD, San Jose, Costa Rica (*Presenter*) Nothing to Disclose

#### PURPOSE

To compare photon-counting detector (PCD) CT to dual-energy CT (DECT) with conventional energy-integrating detectors (EIDs) for renal stone detection.

#### METHODS AND MATERIALS

After IRB approval and informed written consent, patients with renal stones detected using DECT underwent a research PCD-CT exam using similar acquisition settings. Inclusion criteria: (1) archived DECT projection data, (2) no more than 10 renal stones, and (3) at least one stone with a maximum dimension of 3 mm or smaller. For each patient, two DECT mixed images were reconstructed via filtered backprojection (FBP) with (1) a 512 matrix, Qr40 kernel, slice thickness of 1 mm and (2), a 512 matrix, Br40 kernel, and slice thickness of 2 mm. Likewise, for each patient, two PCD-CT virtual monoenergetic images (VMIs) at 70 keV were reconstructed with (1) a 1024 matrix, Qr68 kernel with IR strength 3, and slice thickness of 2 mm and (2), a 1024 matrix, Br68 kernel with IR strength 4, and slice thickness of 0.4 mm. Two radiologists blinded to CT system, slice thickness, and kernel independently compared the de-identified, randomized images in a side-by-side manner to evaluate the visibility of each renal stone using a 4-point Likert score (1=Definitely present, 2=Probably present, 3=Questionably present, 4=Not seen), with disagreements resolved by a genitourinary radiologist. To generate a reference standard for stone presence, a stone was considered definitely present if a consensus score of 1 was assigned for at least one of the four reconstructions, and not present otherwise.

#### RESULTS

Twenty-one patients underwent a DECT exam with EID followed by a PCD CT (mean age 66 years [range, 48-74]; CTDIvol of PCD [15.65 ± 14.17 mGy], CTDIvol of DECT [15.93 ± 14.17 mGy]). 121 renal stones were characterized as definitely present (mean maximum dimension 2.84 ± 2.61 mm, interquartile range: [1.1 mm, 2.7 mm]); 86 of these stones were 3 mm or less. The sensitivity of conventional DECT was 61.2% (74/121; 95% CI: 51.9-69.9) at 2 mm and 65.3% (79/121; 95% CI: 56.1-73.7) at 1 mm. Sensitivity of PCD CT was 73.6% (89/121; 95% CI: 64.8-81.2) at 2 mm and 95.9% (116/121; 95% CI: 90.6-98.6) at 0.4 mm. For stones 3 mm or smaller, PCD at 0.4 mm slice thickness (sensitivity 94.2% [81/86]) was significantly more sensitive than DECT at either slice thickness (at 2 mm: 47.7% [41/86], P=.005; at 1 mm: 53.5% [46/86], P=.01) or PCD at 2 mm (62.8% [54/86], P <.001).

#### CONCLUSION

s PCD CT with high resolution reconstruction enabled detection of renal stones 3 mm and smaller that were not seen or characterized by DECT with conventional EIDs.

#### CLINICAL RELEVANCE/APPLICATION

PCD CT facilitates more accurate detection of small renal stones, which has implications for patient counseling and triage.

Printed on: 02/07/23



## Abstract Archives of the RSNA, 2022

S3B-SPGU-3

### Prostate Imaging-Reporting and Data System Version 2 Release Has Improved Biopsy Accuracy Regarding Tumor Grade: An Experience of Single, Tertiary Institution

Sunday, Nov. 27 12:15PM - 12:45PM Room: Learning Center - GU DPS

#### Participants

Sung Yoon Park, (*Presenter*) Nothing to Disclose

#### PURPOSE

Before Prostate Imaging-Reporting and Data System Version 2 (PI-RADSv2) release, there was a significant discrepancy in tumor grade between prostate biopsy and surgery. We investigated changes of prostate biopsy accuracy regarding tumor grade before and after PI-RADSv2 release in single, tertiary institution.

#### METHODS AND MATERIALS

We retrospectively evaluated 1191 patients before (2013 cohort, n=394) and 5 years after PI-RADSv2 release (2020 cohort, n=797) who had biopsy-proven prostate cancer (PCa), magnetic resonance imaging (MRI), and surgery. The highest tumor grade of each biopsy and surgical specimens was recorded, respectively. We compared the concordant, underestimated, and overestimated biopsy rates regarding tumor grade compared to surgery between two cohorts, respectively. For patients who underwent both prostate MRI and biopsy at our institution, we investigated the proportion of prebiopsy MRI, age, and prostate-specific antigen of patients, and performed logistic regression for analyzing which parameters are associated with concordant biopsy.

#### RESULTS

Concordant and underestimated biopsy rates were significantly different between two cohorts: concordance rates were 47.2% in 2013 and 54.5% in 2020 ( $p=.019$ ); underestimated rates were 46.3% in 2013 and 36.4% in 2020 ( $p=.003$ ). However, overestimated biopsy rates between two cohorts were similar ( $p=.993$ ). The proportion of prebiopsy MRI was significantly higher in 2020 than 2013 (80.9% versus 4.9%;  $p<.001$ ), and it was independently associated with concordant biopsy result in multivariate analysis (odds ratio=1.486; 95% confidence interval, 1.057-2.089;  $p=.022$ ).

#### CONCLUSION

s There was a significant change in the proportion of prebiopsy MRI before and after PI-RADSv2 release in patients who underwent surgery for PCa. This change appears to improve biopsy accuracy regarding tumor grade by reducing underestimation.

#### CLINICAL RELEVANCE/APPLICATION

We demonstrated the change in clinical pathway and improvement of biopsy accuracy before and after PI-RADSv2 release. Current data will serve as evidence for supporting MRI-directed biopsy pathway.

Printed on: 02/07/23

## Abstract Archives of the RSNA, 2022

S3B-SPHN

### Head and Neck Sunday Poster Discussions - B

Sunday, Nov. 27 12:15PM - 12:45PM Room: Learning Center - HN DPS

#### Sub-Events

#### S3B-SPHN-1 Spectral Shaping in Ultra-High-Resolution Photon-Counting and Energy-Integrating Detector CT of the Temporal Bone by Means of Tin Prefiltration

##### Participants

Henner Huflage, MD, Wuerzburg, Germany (*Presenter*) Nothing to Disclose

##### PURPOSE

To investigate the dose saving potential of spectral shaping via tin prefiltration in photon-counting detector CT (PCD-CT) of the temporal bone.

##### METHODS AND MATERIALS

Deploying dose-matched scan protocols with and without tin prefiltration on a PCD-CT and EID-CT system (low-/intermediate-/full-dose: 4.8/7.6-7.7/27.0-27.1 mGy), twelve ultra-high-resolution examinations were performed on each of five cadaveric heads. While 120 kVp were applied for standard imaging, the protocols with spectral shaping used the highest potential available with tin prefiltration (EID-CT: Sn 150 kVp, PCD-CT: Sn 140 kVp). Contrast-to-noise ratios and dose saving potential by spectral shaping were computed for each scanner. Three radiologists independently assessed the image quality of each examination.

##### RESULTS

Regardless of tin prefiltration, PCD-CT with low (171.2±10.3 HU) and intermediate dose (134.7±4.5 HU) produced less image noise than full-dose EID-CT (177.0±14.2 HU;  $p < 0.001$ ). Targeting matched image noise to 120 kVp EID-CT, mean dose reduction of 79.3±3.9% could be realized in 120 kVp PCD-CT. Subjective image quality of PCD-CT was better than EID-CT on each dose level ( $p < 0.050$ ). While no distinction was found between dose-matched PCD-CT with and without tin prefiltration ( $p = 0.928$ ), Sn 150 kVp EID-CT provided better image quality than 120 kVp EID-CT at high and intermediate dose levels ( $p > 0.050$ ). The majority of low-dose EID-CT examinations was considered not diagnostic, whereas PCD-CT scans of the same dose level received satisfactory or better ratings. Interrater reliability was excellent (ICC: 0.903).

##### CONCLUSION

s PCD-CT provides superior image quality and significant dose savings compared to EID-CT for ultra-high-resolution examinations of the temporal bone. Aiming for matched image noise, high-voltage scan protocols with tin prefiltration facilitate additional dose saving in EID-CT, whereas superior inherent denoising decreases the dose reduction potential of spectral shaping in PCD-CT.

##### CLINICAL RELEVANCE/APPLICATION

In ultra-high-resolution photon-counting detector CT of the temporal bone, the denoising effect of spectral shaping through tin prefiltration is less pronounced than in energy-integrating detector CT.

#### S3B-SPHN-2 Improved Cochlear Implant Electrode Localization Using Co-registration of Pre- and Post-Operative CT

##### Participants

Paul Farnsworth, DO, Saint Cloud, FL (*Presenter*) Nothing to Disclose

##### PURPOSE

A primary objective of cochlear implant surgery is an atraumatic electrode array insertion, preventing the implant from violating the basilar membrane and osseous spiral lamina with transscalar migration of the array from the scala tympani into the scala vestibuli, disrupting the cochlear duct. Accurate localization of electrode and can be difficult on post-operative imaging secondary to artifact. Here, we describe the use of co-registered pre- and post-operative multi-detector CT images to determine scalar location of the cochlear implant and determine depth of electrode insertion.

##### METHODS AND MATERIALS

Pre- and post-operative temporal bone CT examinations were retrospectively reviewed after co-registration and overlay of both exams. Images were evaluated by 2 neuroradiologists for scalar location of electrodes tip (+/- scalar translocation), tip fold over, and depth of insertion. Any disagreements between reviewers were resolved via consensus. Depth of insertion was expressed in radial degrees beyond the round window. For purposes of statistical analysis, depth of insertion was considered to represent agreement if the discrepancy was <90 degrees difference between reviewers. Electronic medical records of patients were searched for intra-operative and post-operative complications.

##### RESULTS

Thirty-four patients were included in the final cohort: Thirteen (38.2%) females and 21 (61.8%) males. Fourteen (41.2%) had right

thirty-four patients were included in the final cohort. Thirteen (38.2%) females and 21 (61.8%) males. Fourteen (41.2%) had right sided cochlear implants and 20 (58.8%) had left. Transscalar migration was present in 3 (8.8%) cases (one case demonstrated tip fold over), with initial disagreement between reviewers regarding transscalar migration in 1/34 patients (2.9%). Agreement regarding depth of insertion between the two reviewers was present in 31 (91.1%) cases. The average depth of insertion was 495° (range = 285-720).

## CONCLUSION

s Co-registration of pre- and post-operative CT examinations provides a useful technique for accurate localization of cochlear implant electrode arrays.

## CLINICAL RELEVANCE/APPLICATION

Fused co-registration of pre-operative and post-operative temporal bone CT images can reduce artifact and permit a more accurate localization of the electrode array with implications for improvement in surgical technique and electrode array design.

## S3B-SPHN-3 Comparison of 3D Virtual Surgical Planning and Conventional Methods for Mandibular and Maxillary Free Flap Reconstruction

Participants

Mohammad Khalil, MD, (Presenter) Nothing to Disclose

## PURPOSE

This study aims to compare the rate of bony union in 3D virtual surgical planning (VSP) and conventional methods (CM) for reconstruction.

## METHODS AND MATERIALS

The postoperative CT of patients who underwent mandibular or maxillary reconstruction with fibular or scapular free flap from 2014 to 2021 were retrospectively reviewed. The reconstruction was performed using either 3D VSP with 3D printed models and cutting guides derived from the preoperative CT or CM. A neuroradiologist and a neuroradiology fellow, blinded to the type of surgical planning and clinical outcomes, classified the radiographic union as complete, partial or non-union. Statistical significance was determined using chi-square test.

## RESULTS

124 patients were included with 55 patients in the VSP group and 69 patients in the CM group for a total of 325 appositions. When assessing appositions individually, complete and partial bony union was higher in the VSP group (74.8%; 17.9%, respectively) than in the CM group (64.9%; 16.1%, respectively) and non-union was higher in the CM group (33%) than in the VSP group (7.3%) ( $p < 0.01$ ). Patients in the VSP group had a higher rate of complete or partial union across all their appositions (85.5%) than in the CM group (69.6%) and non-union across all appositions was higher in patients in the CM group (30.4%) than in the VSP group (14.5%) ( $p = 0.04$ ).

## CONCLUSION

s 3D VSP is associated with better bony union rates. Thus, it has the potential to improve clinical outcomes and could be considered as part of the routine preoperative surgical planning.

## CLINICAL RELEVANCE/APPLICATION

The improvement of preoperative surgical planning techniques in mandibular and maxillary free flap reconstruction contributes to favorable functional and cosmetic outcomes. Virtual surgical planning and 3D printing of models and cutting guides allows for precise reconstruction to achieve adequate bony alignment and higher rate of union in comparison to conventional methods.

Printed on: 02/07/23

## Abstract Archives of the RSNA, 2022

S3B-SPHN-1

### Spectral Shaping in Ultra-High-Resolution Photon-Counting and Energy-Integrating Detector CT of the Temporal Bone by Means of Tin Prefiltration

Sunday, Nov. 27 12:15PM - 12:45PM Room: Learning Center - HN DPS

#### Participants

Henner Huflage, MD, Wuerzburg, Germany (*Presenter*) Nothing to Disclose

#### PURPOSE

To investigate the dose saving potential of spectral shaping via tin prefiltration in photon-counting detector CT (PCD-CT) of the temporal bone.

#### METHODS AND MATERIALS

Deploying dose-matched scan protocols with and without tin prefiltration on a PCD-CT and EID-CT system (low-/intermediate-/full-dose: 4.8/7.6-7.7/27.0-27.1 mGy), twelve ultra-high-resolution examinations were performed on each of five cadaveric heads. While 120 kVp were applied for standard imaging, the protocols with spectral shaping used the highest potential available with tin prefiltration (EID-CT: Sn 150 kVp, PCD-CT: Sn 140 kVp). Contrast-to-noise ratios and dose saving potential by spectral shaping were computed for each scanner. Three radiologists independently assessed the image quality of each examination.

#### RESULTS

Regardless of tin prefiltration, PCD-CT with low ( $171.2 \pm 10.3$  HU) and intermediate dose ( $134.7 \pm 4.5$  HU) produced less image noise than full-dose EID-CT ( $177.0 \pm 14.2$  HU;  $p < 0.001$ ). Targeting matched image noise to 120 kVp EID-CT, mean dose reduction of  $79.3 \pm 3.9\%$  could be realized in 120 kVp PCD-CT. Subjective image quality of PCD-CT was better than EID-CT on each dose level ( $p < 0.050$ ). While no distinction was found between dose-matched PCD-CT with and without tin prefiltration ( $p = 0.928$ ), Sn 150 kVp EID-CT provided better image quality than 120 kVp EID-CT at high and intermediate dose levels ( $p > 0.050$ ). The majority of low-dose EID-CT examinations was considered not diagnostic, whereas PCD-CT scans of the same dose level received satisfactory or better ratings. Interrater reliability was excellent (ICC: 0.903).

#### CONCLUSION

s PCD-CT provides superior image quality and significant dose savings compared to EID-CT for ultra-high-resolution examinations of the temporal bone. Aiming for matched image noise, high-voltage scan protocols with tin prefiltration facilitate additional dose saving in EID-CT, whereas superior inherent denoising decreases the dose reduction potential of spectral shaping in PCD-CT.

#### CLINICAL RELEVANCE/APPLICATION

In ultra-high-resolution photon-counting detector CT of the temporal bone, the denoising effect of spectral shaping through tin prefiltration is less pronounced than in energy-integrating detector CT.

Printed on: 02/07/23

## Abstract Archives of the RSNA, 2022

S3B-SPHN-2

### Improved Cochlear Implant Electrode Localization Using Co-registration of Pre- and Post-Operative CT

Sunday, Nov. 27 12:15PM - 12:45PM Room: Learning Center - HN DPS

#### Participants

Paul Farnsworth, DO, Saint Cloud, FL (*Presenter*) Nothing to Disclose

#### PURPOSE

A primary objective of cochlear implant surgery is an atraumatic electrode array insertion, preventing the implant from violating the basilar membrane and osseous spiral lamina with transscalar migration of the array from the scala tympani into the scala vestibuli, disrupting the cochlear duct. Accurate localization of electrode and can be difficult on post-operative imaging secondary to artifact. Here, we describe the use of co-registered pre- and post-operative multi-detector CT images to determine scalar location of the cochlear implant and determine depth of electrode insertion.

#### METHODS AND MATERIALS

Pre- and post-operative temporal bone CT examinations were retrospectively reviewed after co-registration and overlay of both exams. Images were evaluated by 2 neuroradiologists for scalar location of electrodes tip (+/- scalar translocation), tip fold over, and depth of insertion. Any disagreements between reviewers were resolved via consensus. Depth of insertion was expressed in radial degrees beyond the round window. For purposes of statistical analysis, depth of insertion was considered to represent agreement if the discrepancy was <90 degrees difference between reviewers. Electronic medical records of patients were searched for intra-operative and post-operative complications.

#### RESULTS

Thirty-four patients were included in the final cohort: Thirteen (38.2%) females and 21 (61.8%) males. Fourteen (41.2%) had right sided cochlear implants and 20 (58.8%) had left. Transscalar migration was present in 3 (8.8%) cases (one case demonstrated tip fold over), with initial disagreement between reviewers regarding transscalar migration in 1/34 patients (2.9%). Agreement regarding depth of insertion between the two reviewers was present in 31 (91.1%) cases. The average depth of insertion was 495° (range = 285-720).

#### CONCLUSION

s Co-registration of pre- and post-operative CT examinations provides a useful technique for accurate localization of cochlear implant electrode arrays.

#### CLINICAL RELEVANCE/APPLICATION

Fused co-registration of pre-operative and post-operative temporal bone CT images can reduce artifact and permit a more accurate localization of the electrode array with implications for improvement in surgical technique and electrode array design.

Printed on: 02/07/23

## Abstract Archives of the RSNA, 2022

S3B-SPHN-3

### Comparison of 3D Virtual Surgical Planning and Conventional Methods for Mandibular and Maxillary Free Flap Reconstruction

Sunday, Nov. 27 12:15PM - 12:45PM Room: Learning Center - HN DPS

#### Participants

Mohammad Khalil, MD, (*Presenter*) Nothing to Disclose

#### PURPOSE

This study aims to compare the rate of bony union in 3D virtual surgical planning (VSP) and conventional methods (CM) for reconstruction.

#### METHODS AND MATERIALS

The postoperative CT of patients who underwent mandibular or maxillary reconstruction with fibular or scapular free flap from 2014 to 2021 were retrospectively reviewed. The reconstruction was performed using either 3D VSP with 3D printed models and cutting guides derived from the preoperative CT or CM. A neuroradiologist and a neuroradiology fellow, blinded to the type of surgical planning and clinical outcomes, classified the radiographic union as complete, partial or non-union. Statistical significance was determined using chi-square test.

#### RESULTS

124 patients were included with 55 patients in the VSP group and 69 patients in the CM group for a total of 325 appositions. When assessing appositions individually, complete and partial bony union was higher in the VSP group (74.8%; 17.9%, respectively) than in the CM group (64.9%; 16.1%, respectively) and non-union was higher in the CM group (33%) than in the VSP group (7.3%) ( $p < 0.01$ ). Patients in the VSP group had a higher rate of complete or partial union across all their appositions (85.5%) than in the CM group (69.6%) and non-union across all appositions was higher in patients in the CM group (30.4%) than in the VSP group (14.5%) ( $p = 0.04$ ).

#### CONCLUSION

s 3D VSP is associated with better bony union rates. Thus, it has the potential to improve clinical outcomes and could be considered as part of the routine preoperative surgical planning.

#### CLINICAL RELEVANCE/APPLICATION

The improvement of preoperative surgical planning techniques in mandibular and maxillary free flap reconstruction contributes to favorable functional and cosmetic outcomes. Virtual surgical planning and 3D printing of models and cutting guides allows for precise reconstruction to achieve adequate bony alignment and higher rate of union in comparison to conventional methods.

Printed on: 02/07/23

## Abstract Archives of the RSNA, 2022

S3B-SPIN

### Informatics Sunday Poster Discussions - B

Sunday, Nov. 27 12:15PM - 12:45PM Room: Learning Center - IN DPS

#### Sub-Events

#### S3B-SPIN-1 Improvement of Radiomics Reproducibility using Deep Learning-based Image Conversion between CT Reconstruction Algorithms

##### Participants

Heejin Lee, BEng, Seongnam-Si, Korea, Republic Of (*Presenter*) Student, Seoul National University

##### PURPOSE

To evaluate the effect of deep learning-based image conversion between CT reconstruction algorithms, in improving radiomics reproducibility in hepatocellular carcinomas (HCC).

##### METHODS AND MATERIALS

This retrospective study included 78 patients who underwent four-phase liver CTs consisting of non-contrast, late arterial (LAP), portal venous (PVP), and delayed phase (DP) images, reconstructed using both filtered back projection (FBP) and advanced modeled iterative reconstruction (ADMIRE). PVP images of the first 34 consecutive patients were used in training the convolutional neural network (CNN) model to convert images from FBP to ADMIRE and vice versa. All LAP, PVP, and DP images of the following 14 and 30 consecutive patients with HCCs were used for validation and testing, respectively. The radiomic features were extracted from the largest HCC in each patient using a semi-automatic segmentation tool on original and converted images. We used concordance correlation coefficients (CCCs) to evaluate the radiomics reproducibility for original FBP (oFBP) vs. original ADMIRE (oADMIRE), oFBP vs. converted FBP (cFBP), and oADMIRE vs. converted ADMIRE (cADMIRE).

##### RESULTS

In the test group, the CCC and the proportion of reproducible features (CCC = 0.85) for oFBP vs. oADMIRE were 0.65 and 32.9% (524/1595) at LAP, 0.65 and 35.9% (573/1595) at PVP, and 0.69 and 43.8% (699/1595) at DP. For oFBP vs. cFBP, the values increased to 0.92 and 83.9% (1339/1595) at LAP, 0.89 and 71.0% (1133/1595) at PVP, and 0.90 and 79.7% (1271/1595) at DP. Likewise, for oADMIRE vs. cADMIRE, the values increased to 0.87 and 68.1% (1086/1595) at LAP, 0.91 and 82.1% (1309/1595) at PVP, and 0.89 and 76.2% (1216/1595) at DP.

##### CONCLUSION

The CNN-based image conversion between two different CT reconstruction algorithms improved the radiomics reproducibility for HCCs.

##### CLINICAL RELEVANCE/APPLICATION

This study promoted the reproducibility and generalizability of different CT reconstruction algorithms in radiomics research for clinical diagnosis and prediction of prognosis.

#### S3B-SPIN-2 Understanding the Role of Imaging Factors in The Variability of CT-based Texture Analysis (CTTA) Metrics

##### Participants

Bino A. Varghese, PhD, Los Angeles, CA (*Presenter*) Nothing to Disclose

##### PURPOSE

To assess the reproducibility of radiomic features derived from computed tomography (CT) images by varying dose, reconstruction algorithms and slice thickness using scans of a uniform water phantom, anthropomorphic liver phantom, and a human liver in vivo.

##### METHODS AND MATERIALS

Scans were acquired on a 16 cm detector GE Revolution CT scanner with variations across three different slice thicknesses: 0.625mm, 1.25mm and 2.5mm, three different dose levels: CTDIvol of 13,86 mGy for the standard dose, 40 % reduced dose and 60 % reduction and two different reconstruction algorithms: a deep learning image reconstruction (DLIR-high) algorithm and a hybrid iterative reconstruction (IR) algorithm ASiR-V50% (AV50) were explored, varying one at a time. To assess the effect of non-linear modifications of image by AV50 and DLIR-high, images of the water phantom were also reconstructed using filtered back projection. The texture panel comprised of 70 features belonging to first-order CT texture analysis (CTTA) metrics. Beta coefficients of each of the radiomic metrics were extracted from the images of all the ROIs across all scans.

##### RESULTS

Across all scans, imaging and reconstruction settings, CTTA metrics including but not limited to coefficient of variation (CV), inter-quartile range (IQR) and standard deviation (SD) showed statistically significant linear trend with reduction in dose and slice

thickness. For example, when the standard dose was reduced by 60% the IQR increased from 14.98±4.58 to 20.1±6.72 ( $p<0.01$ ). However, this trend was not reported in all features when using filtered back projection reconstruction. Lower values of CV, IQR and SD were observed in DLIR-high reconstructions compared to AV50 and FBP. The Poisson statistics were more stringently followed in FBP than DLIR-H and AV50.

## CONCLUSION

s Variation in image noise due to dose reduction algorithms, tube current, and slice thickness show a consistent trend across phantom and patient scans. Prospective evaluation across multiple centers, preferably with human subjects, is needed for establishing quality assurance and control required for the clinical translation of radiomics.

## CLINICAL RELEVANCE/APPLICATION

Understanding the relationships between radiomic metrics and imaging variables may help improving imaging quality by compensating one variable for another for e.g., increasing dose for reducing slice thickness etc.

### S3B-SPIN-3 Accurately Segment Rectal Tumor From Multi-parametric Magnetic Imaging: A Deep Learning Based Method

Participants

Meng Dou, Chengdu, China (*Presenter*) Nothing to Disclose

## PURPOSE

Accurate segmentation of rectal tumor from multi-parametric Magnetic Resonance Imaging (MRI) images is the basis of rectal cancer diagnosis. Multiparametric MRI images can also provide detailed information of the physical characteristics of rectum tumors. However, manual delineation of rectal tumors is a time-consuming procedure, as it requires a high level of expertise. In this study, we propose and evaluate a deep learning-based method for automatic segmentation of rectal cancers on multi-parametric MRI images.

## METHODS AND MATERIALS

In this retrospective study, 156 patients with locally advanced rectal cancer were collected and divided into a training cohort (100), a validation cohort (30), and a test cohort (26). For each patient, three types of MRIs including T2-weighted imaging, apparent diffusion coefficient-weighted (ADC), and diffusion-weighted MRI (DWI) were exported from the PACS system. All manual segmentations were performed by two radiologists with 10 years experience of diagnosis of rectal cancer using ITK-SNAP software. In addition, the DWI and ADC images were registered to T2 images using a rigid transformation. We explore three pretrained Convnext-tiny models as the backbone to extract different levels of semantic features for each type of MRI image. Then, an attention-based fusion module was proposed to fuse the semantic information from the different backbones. After that, this fusion feature was concatenated with the context feature, generated by fusing different levels of semantic feature, and was input into a self-attention module and generate the final probability map.

## RESULTS

As shown in Tab 1, compared with other methods, our method attains a performance of 0.845 in terms of dice value on the test set, which outperforms the Attention-UNet by 1.35%. The qualitative results of our method show that our method can produce accurate segmentation results with fewer mis-segmentation pixels.

## CONCLUSION

s In this study, we develop a deep learning-based model to accurately segment the primary tumor area from multi-parametric MRI images and evaluate its' performance with other advanced segmentation methods. The results proved that our method can produce accurate segmentation results, especially at the tumor margins.

## CLINICAL RELEVANCE/APPLICATION

Accurate segmentation of rectal tumor from multi-parametric MRI images is the basis of rectal cancer diagnosis. However, manual delineation of rectal tumors is a time-consuming and subjective procedure. Thus, there is a high demand for accurate and reliable automatic segmentation methods.

### S3B-SPIN-4 Multi-planar Deep Learning Pelvic MRI Segmentation using Geometric Conditional Loss Functions

Participants

Melina Hosseiny, MD, Los Angeles, CA (*Presenter*) Nothing to Disclose

## PURPOSE

Deep learning is a powerful tool for segmentation of anatomic structures in medical images, but typically requires substantial training data that can be time-consuming to obtain. For enhanced prostate MRI, we sought to develop a single algorithm accomplishing two tasks: 1) provide spatial orientation for oblique plane prescription, handled in sagittal sections, and 2) divide the prostate into central and peripheral zones, handled in axial sections. To that end, two datasets were aggregated by 3D image re-slicing to be used for training based on conditional loss functions to address missing labels and encode geometric relationships.

## METHODS AND MATERIALS

We retrospectively collected pelvic MRI from 656 patients. The urinary bladder, prostate, and point locations of the prostate's apex and base were annotated on T2 sagittal images in 391 patients. The prostate gland and its peripheral zone were segmented on T2 axial images in 265 patients. Datasets were then divided by patient, into train (80%), validation (10%) and test (10%) cohorts. Three modified U-Nets were trained: CNN1 using sagittal annotations, CNN2 using axial annotations, and the proposed CNN using both, while incorporating custom conditional loss functions. Model performance for segmentation and localization were assessed by Dice score and L2 distance error respectively.

## RESULTS

Median Dice for prostate segmentation improved from 80.3 (IQR 76.0-81.8) by CNN1 to 88.2 (IQR, 84.2-89.0) by the proposed CNN ( $p$ -value $<0.05$ , Wilcoxon test). Median L2 errors decreased from 5.7 (IQR 4.5-6.9) mm and 6.5 (IQR 5.6-7.7) mm by CNN1 to 3.6 (IQR 2.6-4.7) mm and 3.5 (IQR 2.4-4.5) mm by the proposed CNN. Results of central and peripheral zone segmentation on axial

sections did not significantly change between CNN2 and the proposed CNN.

## CONCLUSION

s Aggregating training data developed for multiple tasks in multiple imaging planes is possible by the use of 3D image re-slicing and conditional loss functions to handle missing labels and encode geometric relationships. These can be used to train a multi-task deep learning algorithm which surpasses the performance of CNNs trained only on data for individual tasks.

## CLINICAL RELEVANCE/APPLICATION

Deep learning algorithms can be trained with small, partially-annotated datasets for segmentation tasks in multiple planes, to potentially automate image analysis tasks.

### S3B-SPIN-5 Multi-site Brain MRI Analysis using Deep Learning-Harmonization Protocols

Participants

Zhifan Jiang, PhD, Washington, DC (*Presenter*) Nothing to Disclose

## PURPOSE

Insufficient training data can compromise the robustness of deep learning models trained on medical images. Rare pediatric diseases, such as optic pathway gliomas secondary to neurofibromatosis type 1 (NF1-OPGs), often have this challenge. Therefore, multiple sites must collaborate when acquiring imaging data like magnetic resonance imaging (MRI), even though they use different device manufacturers and protocols. We designed a deep learning framework to simultaneously address the challenges of MRI data harmonization and analysis, specially targeting segmentation of optic nerves, chiasm and optic tract, referred to as the anterior visual pathway (AVP), for children with NF1-OPG.

## METHODS AND MATERIALS

The proposed method builds a semi-supervised model based on multiple generative adversarial networks to: (i) harmonize images from multiple sources sharing latent spaces, (ii) generate a latent protocol, and (iii) segment anatomical structures, i.e., the AVP in this application. T1-weighted MRI data were collected from three institutions and acquired with different imaging protocols and scanners: Site A (General Electric), Site B (Siemens) and Site C (Philips). The average voxel size across sites was A (0.43×0.59×0.43 mm), B (0.91×0.83×0.83 mm) and C (0.63×0.96×0.62 mm). The framework was evaluated on MRIs from 180 subjects with NF1-OPG using manual segmentations as ground truth.

## RESULTS

The proposed framework demonstrated a strong performance in the AVP segmentation task. Results showed that the average Dice volume overlap was 80.63±6.17%. In comparison, the inter-observer variability for manual segmentations was 75.00±6.00%. The average normalized surface distance between our method and ground truth was 0.28±0.20 mm. The AVP volume was similar between the automatic segmentation and ground truth (p-value=0.14). Although this method was focused on the segmentation of AVP, however, the method can be applied to other quantitative imaging tasks with data resources from multiple sites.

## CONCLUSION

s We present a framework for harmonization of MRI acquired with different scanners and protocols, which demonstrated high quality segmentation of AVP. Deep learning models can help provide reliable data analysis on small and diverse imaging datasets by utilizing image harmonization.

## CLINICAL RELEVANCE/APPLICATION

Deep neural network-optimized protocols harmonize the presentation and analysis of multi-site MRI data, which may assist clinical trials and routine care with consistent data for their examination.

### S3B-SPIN-6 Contrast Media Dynamics Determine CT Radiomics Profiles and Machine-learning-based Tumor Identification in Oncologic Imaging

Participants

Martin Watzkenboeck, MD, Vienna, Austria (*Presenter*) Nothing to Disclose

## PURPOSE

The reproducibility of radiomics features extracted from CT examinations depends on several physiological and technical factors including inspiration depth, examination protocol, slice thickness and the reconstruction kernel. Particularly in oncologic imaging, the use of contrast-agent dynamics might affect the stability of radiomics features. Our aim was to evaluate the impact of contrast-agent timing on radiomics feature profiles using CT perfusion of prostate and lung cancers.

## METHODS AND MATERIALS

We extracted 1204 radiomics features from healthy prostate parenchyma and tumors in seven patients with biopsy-proven peripheral prostate cancer, and from tumors in seven patients with biopsy-proven NSCLC, who received dynamic contrast-enhanced perfusion CT with high temporal resolution. Features showing significant differences between contrast phases were identified using linear mixed models. We used a L2-penalized logistic regression classifier to predict class labels for tumor and healthy segments for patients with prostate cancer.

## RESULTS

The timing of the contrast enhancement peak in the reference vessel and tumor varied between patients. After normalizing for individual enhancement patterns by defining seven individual phases based on the reference vessel, 19, 467 and 128 features (1204 total features) showed significant temporal dynamics in healthy prostate parenchyma, prostate tumors and lung tumors, respectively. While machine learning classifiers could not differentiate well between healthy and tumor segments early after contrast-agent application (AUC 0.63, 95% CI 0.31-0.95), a high predictive accuracy was achieved during the arterial phase (AUC 0.92, 95% CI 0.76-1).

## CONCLUSION

s Radiomic profiles of tumor segments in prostate CT are highly dependent on contrast perfusion timing. Accordingly, machine

s radiomic profiles of tumor segments in prostate CT are highly dependent on contrast perfusion timing. Accordingly, machine learning based classification accuracy highly depends on contrast-agent phase.

#### **CLINICAL RELEVANCE/APPLICATION**

Our data highlights the need for careful design of radiomic studies when contrast media are involved, as a substantial number of radiomics features is contrast perfusion dependent and prone to bias. When using contrast enhanced scans for radiomics studies care should be taken to ensure a standardized perfusion timing for radiomics analysis, which is tumor specific.

Printed on: 02/07/23

## Abstract Archives of the RSNA, 2022

S3B-SPIN-1

### Improvement of Radiomics Reproducibility using Deep Learning-based Image Conversion between CT Reconstruction Algorithms

Sunday, Nov. 27 12:15PM - 12:45PM Room: Learning Center - IN DPS

#### Participants

Heejin Lee, BEng, Seongnam-Si, Korea, Republic Of (*Presenter*) Student, Seoul National University

#### PURPOSE

To evaluate the effect of deep learning-based image conversion between CT reconstruction algorithms, in improving radiomics reproducibility in hepatocellular carcinomas (HCC).

#### METHODS AND MATERIALS

This retrospective study included 78 patients who underwent four-phase liver CTs consisting of non-contrast, late arterial (LAP), portal venous (PVP), and delayed phase (DP) images, reconstructed using both filtered back projection (FBP) and advanced modeled iterative reconstruction (ADMIRE). PVP images of the first 34 consecutive patients were used in training the convolutional neural network (CNN) model to convert images from FBP to ADMIRE and vice versa. All LAP, PVP, and DP images of the following 14 and 30 consecutive patients with HCCs were used for validation and testing, respectively. The radiomic features were extracted from the largest HCC in each patient using a semi-automatic segmentation tool on original and converted images. We used concordance correlation coefficients (CCCs) to evaluate the radiomics reproducibility for original FBP (oFBP) vs. original ADMIRE (oADMIRE), oFBP vs. converted FBP (cFBP), and oADMIRE vs. converted ADMIRE (cADMIRE).

#### RESULTS

In the test group, the CCC and the proportion of reproducible features (CCC = 0.85) for oFBP vs. oADMIRE were 0.65 and 32.9% (524/1595) at LAP, 0.65 and 35.9% (573/1595) at PVP, and 0.69 and 43.8% (699/1595) at DP. For oFBP vs. cFBP, the values increased to 0.92 and 83.9% (1339/1595) at LAP, 0.89 and 71.0% (1133/1595) at PVP, and 0.90 and 79.7% (1271/1595) at DP. Likewise, for oADMIRE vs. cADMIRE, the values increased to 0.87 and 68.1% (1086/1595) at LAP, 0.91 and 82.1% (1309/1595) at PVP, and 0.89 and 76.2% (1216/1595) at DP.

#### CONCLUSION

The CNN-based image conversion between two different CT reconstruction algorithms improved the radiomics reproducibility for HCCs.

#### CLINICAL RELEVANCE/APPLICATION

This study promoted the reproducibility and generalizability of different CT reconstruction algorithms in radiomics research for clinical diagnosis and prediction of prognosis.

Printed on: 02/07/23

## Abstract Archives of the RSNA, 2022

S3B-SPIN-2

### Understanding the Role of Imaging Factors in The Variability of CT-based Texture Analysis (CTTA) Metrics

Sunday, Nov. 27 12:15PM - 12:45PM Room: Learning Center - IN DPS

#### Participants

Bino A. Varghese, PhD, Los Angeles, CA (*Presenter*) Nothing to Disclose

#### PURPOSE

To assess the reproducibility of radiomic features derived from computed tomography (CT) images by varying dose, reconstruction algorithms and slice thickness using scans of a uniform water phantom, anthropomorphic liver phantom, and a human liver in vivo.

#### METHODS AND MATERIALS

Scans were acquired on a 16 cm detector GE Revolution CT scanner with variations across three different slice thicknesses: 0.625mm, 1.25mm and 2.5mm, three different dose levels: CTDIvol of 13,86 mGy for the standard dose, 40 % reduced dose and 60 % reduction and two different reconstruction algorithms: a deep learning image reconstruction (DLIR-high) algorithm and a hybrid iterative reconstruction (IR) algorithm ASiR-V50% (AV50) were explored, varying one at a time. To assess the effect of non-linear modifications of image by AV50 and DLIR-high, images of the water phantom were also reconstructed using filtered back projection. The texture panel comprised of 70 features belonging to first-order CT texture analysis (CTTA) metrics. Beta coefficients of each of the radiomic metrics were extracted from the images of all the ROIs across all scans.

#### RESULTS

Across all scans, imaging and reconstruction settings, CTTA metrics including but not limited to coefficient of variation (CV), inter-quartile range (IQR) and standard deviation (SD) showed statistically significant linear trend with reduction in dose and slice thickness. For example, when the standard dose was reduced by 60% the IQR increased from  $14.98 \pm 4.58$  to  $20.1 \pm 6.72$  ( $p < 0.01$ ). However, this trend was not reported in all features when using filtered back projection reconstruction. Lower values of CV, IQR and SD were observed in DLIR-high reconstructions compared to AV50 and FBP. The Poisson statistics were more stringently followed in FBP than DLIR-H and AV50.

#### CONCLUSION

s Variation in image noise due to dose reduction algorithms, tube current, and slice thickness show a consistent trend across phantom and patient scans. Prospective evaluation across multiple centers, preferably with human subjects, is needed for establishing quality assurance and control required for the clinical translation of radiomics.

#### CLINICAL RELEVANCE/APPLICATION

Understanding the relationships between radiomic metrics and imaging variables may help improving imaging quality by compensating one variable for another for e.g., increasing dose for reducing slice thickness etc.

Printed on: 02/07/23

## Abstract Archives of the RSNA, 2022

S3B-SPIN-3

### Accurately Segment Rectal Tumor From Multi-parametric Magnetic Imaging: A Deep Learning Based Method

Sunday, Nov. 27 12:15PM - 12:45PM Room: Learning Center - IN DPS

#### Participants

Meng Dou, Chengdu, China (*Presenter*) Nothing to Disclose

#### PURPOSE

Accurate segmentation of rectal tumor from multi-parametric Magnetic Resonance Imaging (MRI) images is the basis of rectal cancer diagnosis. Multiparametric MRI images can also provide detailed information of the physical characteristics of rectum tumors. However, manual delineation of rectal tumors is a time-consuming procedure, as it requires a high level of expertise. In this study, we propose and evaluate a deep learning-based method for automatic segmentation of rectal cancers on multi-parametric MRI images.

#### METHODS AND MATERIALS

In this retrospective study, 156 patients with locally advanced rectal cancer were collected and divided into a training cohort (100), a validation cohort (30), and a test cohort (26). For each patient, three types of MRIs including T2-weighted imaging, apparent diffusion coefficient-weighted (ADC), and diffusion-weighted MRI (DWI) were exported from the PACS system. All manual segmentations were performed by two radiologists with 10 years experience of diagnosis of rectal cancer using ITK-SNAP software. In addition, the DWI and ADC images were registered to T2 images using a rigid transformation. We explore three pretrained Convnext-tiny models as the backbone to extract different levels of semantic features for each type of MRI image. Then, an attention-based fusion module was proposed to fuse the semantic information from the different backbones. After that, this fusion feature was concatenated with the context feature, generated by fusing different levels of semantic feature, and was input into a self-attention module and generate the final probability map.

#### RESULTS

As shown in Tab 1, compared with other methods, our method attains a performance of 0.845 in terms of dice value on the test set, which outperforms the Attention-UNet by 1.35%. The qualitative results of our method show that our method can produce accurate segmentation results with fewer mis-segmentation pixels.

#### CONCLUSION

In this study, we develop a deep learning-based model to accurately segment the primary tumor area from multi-parametric MRI images and evaluate its' performance with other advanced segmentation methods. The results proved that our method can produce accurate segmentation results, especially at the tumor margins.

#### CLINICAL RELEVANCE/APPLICATION

Accurate segmentation of rectal tumor from multi-parametric MRI images is the basis of rectal cancer diagnosis. However, manual delineation of rectal tumors is a time-consuming and subjective procedure. Thus, there is a high demand for accurate and reliable automatic segmentation methods.

Printed on: 02/07/23

## Abstract Archives of the RSNA, 2022

S3B-SPIN-4

### Multi-planar Deep Learning Pelvic MRI Segmentation using Geometric Conditional Loss Functions

Sunday, Nov. 27 12:15PM - 12:45PM Room: Learning Center - IN DPS

#### Participants

Melina Hosseiny, MD, Los Angeles, CA (*Presenter*) Nothing to Disclose

#### PURPOSE

Deep learning is a powerful tool for segmentation of anatomic structures in medical images, but typically requires substantial training data that can be time-consuming to obtain. For enhanced prostate MRI, we sought to develop a single algorithm accomplishing two tasks: 1) provide spatial orientation for oblique plane prescription, handled in sagittal sections, and 2) divide the prostate into central and peripheral zones, handled in axial sections. To that end, two datasets were aggregated by 3D image re-slicing to be used for training based on conditional loss functions to address missing labels and encode geometric relationships.

#### METHODS AND MATERIALS

We retrospectively collected pelvic MRI from 656 patients. The urinary bladder, prostate, and point locations of the prostate's apex and base were annotated on T2 sagittal images in 391 patients. The prostate gland and its peripheral zone were segmented on T2 axial images in 265 patients. Datasets were then divided by patient, into train (80%), validation (10%) and test (10%) cohorts. Three modified U-Nets were trained: CNN1 using sagittal annotations, CNN2 using axial annotations, and the proposed CNN using both, while incorporating custom conditional loss functions. Model performance for segmentation and localization were assessed by Dice score and L2 distance error respectively.

#### RESULTS

Median Dice for prostate segmentation improved from 80.3 (IQR 76.0-81.8) by CNN1 to 88.2 (IQR, 84.2-89.0) by the proposed CNN (p-value<0.05, Wilcoxon test). Median L2 errors decreased from 5.7 (IQR 4.5-6.9) mm and 6.5 (IQR 5.6-7.7) mm by CNN1 to 3.6 (IQR 2.6-4.7) mm and 3.5 (IQR 2.4-4.5) mm by the proposed CNN. Results of central and peripheral zone segmentation on axial sections did not significantly change between CNN2 and the proposed CNN.

#### CONCLUSION

s Aggregating training data developed for multiple tasks in multiple imaging planes is possible by the use of 3D image re-slicing and conditional loss functions to handle missing labels and encode geometric relationships. These can be used to train a multi-task deep learning algorithm which surpasses the performance of CNNs trained only on data for individual tasks.

#### CLINICAL RELEVANCE/APPLICATION

Deep learning algorithms can be trained with small, partially-annotated datasets for segmentation tasks in multiple planes, to potentially automate image analysis tasks.

Printed on: 02/07/23

## Abstract Archives of the RSNA, 2022

S3B-SPIN-5

### Multi-site Brain MRI Analysis using Deep Learning-Harmonization Protocols

Sunday, Nov. 27 12:15PM - 12:45PM Room: Learning Center - IN DPS

#### Participants

Zhifan Jiang, PhD, Washington, DC (*Presenter*) Nothing to Disclose

#### PURPOSE

Insufficient training data can compromise the robustness of deep learning models trained on medical images. Rare pediatric diseases, such as optic pathway gliomas secondary to neurofibromatosis type 1 (NF1-OPGs), often have this challenge. Therefore, multiple sites must collaborate when acquiring imaging data like magnetic resonance imaging (MRI), even though they use different device manufacturers and protocols. We designed a deep learning framework to simultaneously address the challenges of MRI data harmonization and analysis, specially targeting segmentation of optic nerves, chiasm and optic tract, referred to as the anterior visual pathway (AVP), for children with NF1-OPG.

#### METHODS AND MATERIALS

The proposed method builds a semi-supervised model based on multiple generative adversarial networks to: (i) harmonize images from multiple sources sharing latent spaces, (ii) generate a latent protocol, and (iii) segment anatomical structures, i.e., the AVP in this application. T1-weighted MRI data were collected from three institutions and acquired with different imaging protocols and scanners: Site A (General Electric), Site B (Siemens) and Site C (Philips). The average voxel size across sites was A (0.43×0.59×0.43 mm), B (0.91×0.83×0.83 mm) and C (0.63×0.96×0.62 mm). The framework was evaluated on MRIs from 180 subjects with NF1-OPG using manual segmentations as ground truth.

#### RESULTS

The proposed framework demonstrated a strong performance in the AVP segmentation task. Results showed that the average Dice volume overlap was 80.63±6.17%. In comparison, the inter-observer variability for manual segmentations was 75.00±6.00%. The average normalized surface distance between our method and ground truth was 0.28±0.20 mm. The AVP volume was similar between the automatic segmentation and ground truth (p-value=0.14). Although this method was focused on the segmentation of AVP, however, the method can be applied to other quantitative imaging tasks with data resources from multiple sites.

#### CONCLUSION

s We present a framework for harmonization of MRI acquired with different scanners and protocols, which demonstrated high quality segmentation of AVP. Deep learning models can help provide reliable data analysis on small and diverse imaging datasets by utilizing image harmonization.

#### CLINICAL RELEVANCE/APPLICATION

Deep neural network-optimized protocols harmonize the presentation and analysis of multi-site MRI data, which may assist clinical trials and routine care with consistent data for their examination.

Printed on: 02/07/23

## Abstract Archives of the RSNA, 2022

S3B-SPIN-6

### Contrast Media Dynamics Determine CT Radiomics Profiles and Machine-learning-based Tumor Identification in Oncologic Imaging

Sunday, Nov. 27 12:15PM - 12:45PM Room: Learning Center - IN DPS

#### Participants

Martin Watzenboeck, MD, Vienna, Austria (*Presenter*) Nothing to Disclose

#### PURPOSE

The reproducibility of radiomics features extracted from CT examinations depends on several physiological and technical factors including inspiration depth, examination protocol, slice thickness and the reconstruction kernel. Particularly in oncologic imaging, the use of contrast-agent dynamics might affect the stability of radiomics features. Our aim was to evaluate the impact of contrast-agent timing on radiomics feature profiles using CT perfusion of prostate and lung cancers.

#### METHODS AND MATERIALS

We extracted 1204 radiomics features from healthy prostate parenchyma and tumors in seven patients with biopsy-proven peripheral prostate cancer, and from tumors in seven patients with biopsy-proven NSCLC, who received dynamic contrast-enhanced perfusion CT with high temporal resolution. Features showing significant differences between contrast phases were identified using linear mixed models. We used a L2-penalized logistic regression classifier to predict class labels for tumor and healthy segments for patients with prostate cancer.

#### RESULTS

The timing of the contrast enhancement peak in the reference vessel and tumor varied between patients. After normalizing for individual enhancement patterns by defining seven individual phases based on the reference vessel, 19, 467 and 128 features (1204 total features) showed significant temporal dynamics in healthy prostate parenchyma, prostate tumors and lung tumors, respectively. While machine learning classifiers could not differentiate well between healthy and tumor segments early after contrast-agent application (AUC 0.63, 95% CI 0.31-0.95), a high predictive accuracy was achieved during the arterial phase (AUC 0.92, 95% CI 0.76-1).

#### CONCLUSION

s Radiomic profiles of tumor segments in prostate CT are highly dependent on contrast perfusion timing. Accordingly, machine learning based classification accuracy highly depends on contrast-agent phase.

#### CLINICAL RELEVANCE/APPLICATION

Our data highlights the need for careful design of radiomic studies when contrast media are involved, as a substantial number of radiomics features is contrast perfusion dependent and prone to bias. When using contrast enhanced scans for radiomics studies care should be taken to ensure a standardized perfusion timing for radiomics analysis, which is tumor specific.

Printed on: 02/07/23

## Abstract Archives of the RSNA, 2022

S3B-SPIR

### Interventional Sunday Poster Discussions - B

Sunday, Nov. 27 12:15PM - 12:45PM Room: Learning Center - IR DPS

#### Sub-Events

#### S3B-SPIR-1 Evaluation of The Prediction for The Change of Future Liver Volume after Portal Vein Embolization (PVE) using 2D Perfusion Angiography (2D-PA)

Participants

Hiroki Yano, MD, (*Presenter*) Nothing to Disclose

#### PURPOSE

2D-PA application equipped with the angiography unit can visualize the chronological flow of contrast through vessels as a color coded image and enables visible and quantitative blood flow evaluation. Among the several parameters of the 2D-PA, area under the curve (AUC) is considered as the total blood volume in the measured liver parenchyma. The purpose of this study is to investigate the relationship between the change of liver volume and the parameter of 2D-PA during pre and post PVE.

#### METHODS AND MATERIALS

Thirty six patients who underwent PVE between 2006 and 2022 were included in this retrospective case-control study. Percutaneous transhepatic portography was performed pre and post embolization with the same volume and rate of contrast injection as 2D-PA mode. Regions of interest (ROI) are placed in each lobes of the liver, and AUC (AUC-left ; remnant liver, -right ; embolized liver) are measured pre- and post-PVE, respectively. AUC ratio (AUCR =AUC pre-left/right) was calculated. In order to reflect each lobes blood flow in the liver parenchyma as purely as possible in 2D-PA, ROI were set on the right side outside the diaphragm and the left side outside the umbilical point. Enhanced CT examinations were performed before and 3 weeks after PVE for volumetry of liver parenchyma. Future remnant liver volume (FRLV), embolized liver volume (ELV), and total liver volume (TLV) were measured, and ELVR (=ELV/TLV), FRLVR (=FRLV/TLV), degree of hypertrophy (DH=FRLVR post/pre), degree of reduction (DR=1-ELVR post/pre) were calculated respectively. The relationships between the change of AUC and FRLR each live volume were also evaluated by Pearson's correlation coefficient (R, P<0.05).

#### RESULTS

Post AUC-left was significantly increased compared to pre AUC-left. No significant correlation was found between DH and AUCR. A positive correlation was found between DR and AUCR (R=0.418, p=0.0111), FRLVR post and AUCR (R=0.616, p=0.0000632). Furthermore, ROC analysis between AUCR and FRLVR post exceeds 40% or not, the area under the curve was 0.885 (sensitivity 78.8%, specificity 85.2%), when cutoff value of AUCR was 0.455.)

#### CONCLUSION

The AUC ratio of both liver lobes in 2D-PA before PVE correlates with the embolized liver volume rate and future remnant liver volume rate of 3 weeks after PVE.

#### CLINICAL RELEVANCE/APPLICATION

PVE is sometimes performed for hypertrophy before hepatectomy to avoid postoperative acute liver failure, but the precise prediction for the degree of hypertrophy of liver parenchyma is unclear. The AUC ratio of pre 2D-PA may help predicting the degree of future remnant liver volume.

#### S3B-SPIR-2 Genicular Artery Embolization as a Treatment for Symptomatic Knee Osteoarthritis: A Systematic Review and Meta-analysis

Participants

Yan Epelboym, MPH, (*Presenter*) Nothing to Disclose

#### PURPOSE

Genicular artery embolization (GAE) is a minimally invasive therapy for symptomatic osteoarthritis (OA) in patients with knee pain refractory to conservative management. The purpose of this study was to evaluate current evidence on the effectiveness of GAE for OA related knee pain.

#### METHODS AND MATERIALS

Using three databases (Embase, PubMed, and Web of Science), we performed a systematic review to identify studies evaluating treatment of knee OA with GAE. Studies were screened by 2 of the investigators independently, first by study title, and from those the abstracts were reviewed, followed by a full-text review to select the final cohort. Exclusion criteria included studies of hemarthrosis, review articles, or republished data in the case of already-included patients. The primary outcome measure was change in pain scale score at 6 months; changes at 1, 3, and 12 months were secondary outcomes. We computed Hedge's g as a measure of effect size, a version of standardized mean difference (change per standard deviation) that includes a correction for small samples, selecting Visual Analog Scale (VAS) first if available and Knee Injury and Osteoarthritis Outcome Score (KOOS) and

Western Ontario and McMaster Universities Osteoarthritis Index (WOMAC) if VAS was not available. To estimate pooled change in pain a meta-analysis was performed using a random effects model with restricted maximum likelihood.

## RESULTS

The initial search yielded 581 studies. After screening titles, abstracts, and the full text, 8 studies met the inclusion and exclusion criteria for this study. The inter-reader agreement at the title review stage was  $k = 0.681$  (substantial), abstract stage was  $k = 0.655$  (substantial), and full-text review stage was  $k = 0.94$  (almost perfect). Eight studies with 276 treated knees were included. Seven studies were cohort studies without control groups, categorized as level II evidence. One randomized controlled trial with a sham intervention group was categorized as level I evidence. Of the 276 treated knees, 241 (87%) demonstrated Kellgren Lawrence grade I-III OA. The estimated standardized mean change (Hedges'  $g$ ) from baseline to six months, was  $-1.4$  (95% CI:  $(-2.1, -0.8)$ ). The estimated standardized mean change in pain scores for secondary outcomes was  $-1.3$  (95% CI:  $(-1.6, -0.97)$ ) at one month,  $-1.2$  (95% CI:  $(-1.54, -0.84)$ ) at three months and  $-1.25$  (95% CI:  $(-2.0, -0.6)$ ) at twelve months.

## CONCLUSION

s GAE provides durable reductions in pain scores for patients with symptomatic knee OA. The effect size of GAE on pain appears to be greater than published effects for oral non-steroidal anti-inflammatories and intra-articular corticosteroid injections.

## CLINICAL RELEVANCE/APPLICATION

GAE is a promising treatment for OA related knee pain.

### S3B-SP1R-3 Impact of Computed Tomography Angiography on Lower Gastrointestinal Bleeding Primary Endovascular Intervention Outcomes

Participants

Olivia Little, BS, Savannah, GA (*Presenter*) Nothing to Disclose

## PURPOSE

To evaluate the impact of pre-procedural computed tomography angiography (CTA) on treatment success, hospitalization length of stay (LOS), and mortality of patients undergoing primary endovascular intervention (PEI) for lower gastrointestinal bleeding (LGIB).

## METHODS AND MATERIALS

Using ICD-9 codes, all LGIB encounters and associated procedures in the 2005-2015 National Inpatient Sample databases were identified. Patients treated with conservative management or those who received nuclear scintigraphy were excluded. LGIB encounters initially treated with either angiography and/or embolization (PEI) and were not re-treated with PEI or another intervention were classified as successfully treated. In patients that underwent pre-procedural CTA versus those who did not, differences in mortality, mean LOS, and successful LGIB treatment were assessed with chi-square test, ANOVA, and student's t-test.

## RESULTS

Of 224,640 LGIB encounters captured, 5,983 LGIB encounters treated with PEI met our inclusion/exclusion criteria. Overall mean age, gender, race/ethnicity was 69 years, 53% female, and 73% Caucasian. PEI definitively treated LGIB in 61.6% of LGIB encounters. Compared to patients who did not undergo CTA prior to PEI, pre-intervention CTA was associated with a greater incidence of definitive treatment success after PEI (70.8% vs 29.2%; Odds-Ratio (OR)=1.5 [95%CI 1.1-2.2],  $p < 0.02$ ). There was no significant difference in LOS ( $8.3 \pm 9.6$  vs  $7.7 \pm 8.8$  days;  $p = 0.5$ ) or mortality (6.9% vs 8.1%;  $p = 0.7$ ) between encounters involving vs. not involving CTA prior to PEI.

## CONCLUSION

s CTA utilization prior to LGIB PEI is associated with a higher incidence of successful treatment but does not impact LOS nor incidence of mortality.

## CLINICAL RELEVANCE/APPLICATION

When utilized for the management of lower gastrointestinal bleeding, pre-intervention CTA is associated with a higher incidence of definitive treatment success after primary endovascular intervention but does impact the length of hospital stay nor incidence of mortality.

### S3B-SP1R-4 Treatment Patterns in Chronic Venous Disease: Endovenous vs. Open Vein Stripping: Where Are We Today?

Participants

Brian D'Amore, BS, (*Presenter*) Nothing to Disclose

## PURPOSE

Chronic venous disease (CVD) affects over 30 million patients in the United States with an annual incidence of 1.9% in males and 2-6% in females. Advances in minimally-invasive treatments allow faster recovery times and lower complications with endovenous treatment options when compared to traditional vein stripping. Yet, surgical interventions persist both as primary and salvage CVD therapy. The purpose of this study was to compare the relative utilization of vein stripping and endovenous treatments, including thermal and laser ablation.

## METHODS AND MATERIALS

Endovenous treatment (including thermal and laser ablation) and vein stripping data was obtained from the American College of Surgeons - National Surgical Quality Improvement Program (NSQIP) based on CPT codes (36475-9, 37700, 37718, 37722, and 37735) between 2011-2017. Demographics were extracted for each patient, including race, gender and age. Utilization trends were computed, and percent change was calculated for each procedure.

## RESULTS

We identified 22,114 patients who underwent treatment for chronic superficial venous insufficiency between 2011-2017. Thermal

ablation was the most frequently performed procedure with 49.5% (n=10,941) patients receiving this treatment, followed by vein stripping at 35.0% (n=7744) and laser ablation at 15.5% (n=3429). Volume increased by 6.3% for thermal ablation and 1.1% for vein stripping, while it decreased by 18.5% for laser ablation. Lastly, thermal ablation increased in males by 24.6% and decreased in females by 1.3%. It also increased in patients aged 65 and older by 24.6% and decreased in patients less than 65 by 3.03%.

## CONCLUSION

Although thermal ablation was the most performed procedure for superficial CVD between 2011-2017, vein stripping volume was still greater than expected. Trends in thermal ablation increased significantly for males when compared to females and for patients aged 65 and older when compared to patients less than 65.

## CLINICAL RELEVANCE/APPLICATION

The transition from vein stripping to endovenous procedures may be slower than originally presumed and total volume of procedures is lower than expected based on disease prevalence.

### S3B-SP1R-5 The Role of Boosting Algorithms in Machine Learning in Predicting the Treatment Outcome of High-Intensity Focused Ultrasound Ablation of Uterine Fibroids: Most Informative Perfusion MRI Features

Participants

Bilgin Keserci, PhD, (*Presenter*) Nothing to Disclose

## PURPOSE

To comparatively evaluate the role of boosting algorithms in machine learning to find the most informative perfusion MRI features in predicting the treatment outcome of High-Intensity Focused Ultrasound (HIFU) ablation with an immediate nonperfused volume (NPV) ratio of at least 90%.

## METHODS AND MATERIALS

A total of 73 women with symptomatic uterine fibroids who underwent HIFU treatment were classified according to T1 perfusion-based classification as group A (n = 47, if the time-SI curve of lesion was lower than that of myometrium) and group B (n = 26, if the time-SI curve of lesion was equal to or higher than that of myometrium). In this study, myometrium was chosen as an internal reference. An ensemble feature ranking model was introduced based on the score values assigned to the 21 perfusion MRI features by three different boosting algorithms including Adaptive boosting (Adaboost), Category boosting (Catboost) and Gradient boosting (GBM), to find the most informative perfusion MRI features. The relationship between perfusion MRI features and the immediate NPV ratio of 90% was evaluated using Pearson's correlation coefficients. The diagnostic ability of Boosting algorithms was performed by means of standard performance metrics, including the area under the receiver operating characteristic curve (AUROC), accuracy, sensitivity, and specificity in eight folds cross-validation.

## RESULTS

For the most informative perfusion MRI features, the AUROC ranged from 0.838 to 0.916, accuracy ranged from 0.84 to 0.96, specificity of 0.833, and sensitivity ranged from 0.842 to 1.0. The GBM algorithm showed the best predictive performance with an AUROC of 0.95 and accuracy of 0.92, followed by the Catboost and Adaboost algorithms, which yielded an AUROC of 0.864 and 0.838, and accuracy of 0.88 and 0.84, respectively. The best classifier performance with the best-performing features from each perfusion MRI group, Ktrans ratio of fibroid to myometrium, The ratio of area under the curve of fibroid to myometrium, the ratio of maximum relative enhancement of fibroid to myometrium, the ratio of relative enhancement of fibroid to myometrium and the ratio of maximum enhancement of fibroid to myometrium, was achieved using GBM.

## CONCLUSION

The preliminary findings in this study suggest that the most informative perfusion MRI features should be considered in predicting the treatment outcome of HIFU ablation to achieve an immediate NPV ratio of 90%.

## CLINICAL RELEVANCE/APPLICATION

The best boosting algorithm performance with the best-performing perfusion MRI features should be considered by the treating physician in the screening phase to predict the treatment outcome of HIFU ablation to achieve an immediate NPV ratio of 90%.

### S3B-SP1R-6 Sustained Clinical Improvement After Prostate Artery Embolization (PAE) for Symptomatic Benign Prostate Hyperplasia (BPH): Results from a Single Center, Retrospective Analysis

Participants

Vijay Chockalingam, BS, (*Presenter*) Nothing to Disclose

## PURPOSE

To validate if short term clinical results of Prostate Artery Embolization (PAE) in Benign Prostate Hyperplasia (BPH) are sustained over time.

## METHODS AND MATERIALS

In an IRB approved, single center, retrospective study, 120 patients (Mean age 70.6 years  $\pm$ 9.7 years) who underwent PAE were identified. Technical success was defined as successful embolization on at least one side. Baseline IPSS (International Prostate Symptom Score) was obtained for each patient. Clinical success was evaluated as change in IPSS in short-term (< 1 year), medium-term (1-2 years) and long-term (3 or more years) follow-up. To determine change in IPSS between pre-PAE procedure and follow-up post-PAE procedure, IPSS was analyzed through a multilevel model using time as a fixed effect and patient ID as a random effect to account for within-patient correlations. Prostate shrinkage was also evaluated and changes in prostate size between baseline and post-PAE procedure were analyzed.

## RESULTS

Between February 2014 and May 2021, 56 patients were accounted for in the pre-procedure baseline measurement, which showed an average IPSS of 22.1 (95% CI 20.4-23.9). Technical success was seen in 90.1% of patients in the study. Short-term (n=21), mid-term (n=24), and long-term (n=11) follow-up of these patients showed average IPSS scores of 10.2 (95% CI 7.3-13.1), 9.7 (95% CI 6.7-12.7), and 6.1 (95% CI 4.2-8.0). The results show a statistically significant (p = 0.000) and dramatic drop in IPSS of

13.5 points in the short term. The trend post-embolization, although not statistically significant ( $p = 0.321$ ) shows that IPSS scores remain decreased over-time. Prostate size decreased from pre-PAE procedure ( $n=35$ ) to post-PAE procedure follow up ( $n=27$ ) from an average of 138.7 cc to 89.9 cc ( $p = 0.000$ ).

## CONCLUSION

The short term, statistically significant drop in IPSS after PAE appears to be sustained in the medium and long term study period in our study, with all available data. Although these results suggest a sustained long term clinical success of the procedure, large multi-center studies are needed.

## CLINICAL RELEVANCE/APPLICATION

PAE has emerged as a minimally invasive technique to treat BPH that involves a reduced hospital stay and less adverse effects compared to current gold standard approaches, all while maintaining significant symptom reduction over long term follow-up.

### S3B-SP1R-7 In-vitro Characterization of Drug Eluting Superabsorbent Polymer Microspheres: Absorption and Eluting Capacity of Contrast Material, Antibiotics and/or Analgesics

Participants

Akiko Narita, MD, PhD, Nagakute, Japan (*Presenter*) Nothing to Disclose

## PURPOSE

Superabsorbent polymer microspheres (SAP-MS) have a property of absorbing fluids to swell. Therefore, drug-loaded SAP-MS will become visible, antibacterial and/or analgesic. The purpose of this study was to examine the characteristics of drug-loaded SAP-MS.

## METHODS AND MATERIALS

SAP-MS were suspended in the drug solution (a) antibiotics (Cefazolin) (b) analgesics (Lidocaine) (c) contrast material (Iopamidol) and Cefazolin (d) Iopamidol and Lidocaine (e) Iopamidol, Cefazolin and Lidocaine. 1) Change of the diameter of each drug-loaded SAP-MS was observed by a stereomicroscope for three hours. 2) Absorption capacity of each drug-loaded SAP-MS were assessed by measuring the concentration of drug solution using high performance liquid chromatography (HPLC) sequentially. 3) Filtered each drug-loaded SAP-MS were mixed with 100ml of saline and drug eluting capacity of each drug-loaded SAP-MS were evaluated using HPLC over time.

## RESULTS

1) Diameter of drug-loaded SAP-MS increased for about 15 minutes and came to an equilibrium. Finally, the diameter was (a) 3.9 times (b) 5.0 times (c) 2.2 times (d) 5.5 times (e) 3.6 times larger than its original size. 2) The concentration of drug solution did not change and the amount of drug solution decreased. 3) Each drug was released into 10 minutes and came to an equilibrium. The concentration of each drug in the mixture was increased by (a) Cefazolin: 1.82 mg/ml (b) Lidocaine: 0.06 mg/ml (c) Iopamidol: 1.34 mg/ml, Cefazolin: 0.17 mg/ml (d) Iopamidol: 4.51 mg/ml, Lidocaine: 0.11 mg/ml (e) Iopamidol: 2.70 mg/ml, Cefazolin: 1.10 mg/ml, Lidocaine: 0.03 mg/ml.

## CONCLUSION

SAP-MS can absorb each drug as much as it swells. And drug-loaded SAP-MS release contrast material, antibiotics and analgesics.

## CLINICAL RELEVANCE/APPLICATION

Visible, antibiotic and/or analgesic microspheres will contribute to safe and useful embolization, in addition, relief of pain and prevention infection like abscess.

### S3B-SP1R-8 Bariatric Arterial Embolization with Radiopaque Hydrogel Microspheres Suppresses Weight Gain and Fundal Ghrelin Levels in Swine

Participants

Yingli Fu, Baltimore, MD (*Presenter*) Nothing to Disclose

## PURPOSE

Octreotide is a somatostatin analogue with beneficial effect on ghrelin suppression and weight loss. The purpose of this study is to evaluate the effect of octreotide-eluting, lipiodol-impregnated, alginate microspheres (OLMs) on the safety and efficacy of bariatric arterial embolization (BAE) in swine.

## METHODS AND MATERIALS

X-ray-visible OLMs were produced from lipiodol-impregnated alginate (2% w/v) solution containing 10 mg/ml octreotide using an electrostatic droplet generator. BAE was performed in 6 healthy, growing swine (mean weight: 22.2 kg) by selective infusion of X-ray-visible OLMs ( $n = 3$ ) or saline ( $n = 3$ ) into the right gastric artery (RGA) and the left gastroepiploic artery (LGEA) under X-ray guidance. Weight was obtained in all animals at baseline and weekly up to 8 weeks post embolization. Cone-beam CT (CBCT) images of the stomachs were acquired immediately after embolization and at 8 weeks prior to sacrifice to assess the embolization coverage of the fundus, and the visibility and distribution of OLMs. All animals were euthanized for gross and histological examination of stomach mucosal integrity at 8 weeks. Ghrelin-expressing cells (GECs) in the stomach were assessed immunohistochemically and analyzed using the Mann-Whitney U test.

## RESULTS

OLMs were monodispersed with diameter of  $185 \pm 6 \mu\text{m}$ . BAE with OLMs was successfully performed in all animals. The OLMs can be visualized both on fluoroscopy and CBCT images during the embolization procedure. The post-procedural percentage of weight gain was lower in BAE-treated animals as compared to controls (BAE vs. control:  $39.4\% \pm 12.9$  vs.  $61.0\% \pm 3.2$  at 8 weeks). The GECs were significantly decreased in the gastric fundus of OLM-embolized animals compared to control animals (BAE vs. control:  $14.9 \pm 3.6$  vs.  $24.3 \pm 5.4$ ,  $p < 0.0001$ ). Superficial healed mucosal ulcers were observed in one OLM-embolized animal along the stomach fundus and body.

## CONCLUSION

s BAE with octreotide-eluting, lipiodol/alginate microspheres can be safely performed in all animals and significantly suppress the percentage of weight gain and fundal ghrelin levels.

## CLINICAL RELEVANCE/APPLICATION

BAE with octreotide-eluting, lipiodol/alginate microspheres may be useful for treating obesity.

## S3B-SP1R-9 New TRUS Techniques and Imaging Features of PI-RADS 4 or 5: Influence on Tumor Targeting

Participants

Byung Kwan Park, MD, PhD, (*Presenter*) Nothing to Disclose

## PURPOSE

To determine if the new transrectal ultrasound (TRUS) techniques and imaging features contribute to targeting Prostate Imaging and Reporting and Data System (PI-RADS) 4 or 5.

## METHODS AND MATERIALS

Between December 2018 and February 2020, 115 men underwent cognitive biopsy by radiologist A, who was familiar with the new TRUS findings and biopsy techniques. During the same period, 179 men underwent magnetic resonance imaging-TRUS image fusion or cognitive biopsy by radiologist B, who was unfamiliar with the new biopsy techniques. Prior to biopsy, both radiologists knew MRI findings such as the location, size, and shape of PI-RADS 4 or 5. We recorded how many target biopsies were performed without systematic biopsy and how many of these detected higher Gleason score (GS) than those detected by systematic biopsy. The numbers of biopsy cores were also obtained. Fisher Exact or Mann-Whitney test was used for statistical analysis.

## RESULTS

For PI-RADS 4, target biopsy alone was performed in 0% (0/84) by radiologist A and 0.8% (1/127) by radiologist B ( $p > 0.9999$ ). Target biopsy yielded higher GSs in 57.7% (30/52) by radiologist A and 29.5% (23/78) by radiologist B ( $p = 0.0019$ ). For PI-RADS 5, target biopsy alone was performed in 29.0% (9/31) by radiologist A and 1.9% (1/52) by radiologist B ( $p = 0.0004$ ). Target biopsy yielded higher GSs in 50.0% (14/28) by radiologist A and 18.2% (8/44) by radiologist B ( $p = 0.0079$ ). Radiologist A sampled fewer biopsy cores than radiologist B ( $p = 0.0008$  and  $0.0023$  for PI-RADS 4 and 5), respectively.

## CONCLUSION

s PI-RADS 4 or 5 can be more precisely targeted if the new TRUS biopsy techniques are applied.

## CLINICAL RELEVANCE/APPLICATION

The new TRUS biopsy techniques help to not only target PI-RADS 4 or 5 lesions more precisely but also to reduce the number of biopsy cores needed. Moreover, systematic biopsy can be omitted in PI-RADS 5 patients who do not stop taking aspirin because of cardiovascular disease.

Printed on: 02/07/23

## Abstract Archives of the RSNA, 2022

S3B-SP1R-1

### Evaluation of The Prediction for The Change of Future Liver Volume after Portal Vein Embolization (PVE) using 2D Perfusion Angiography (2D-PA)

Sunday, Nov. 27 12:15PM - 12:45PM Room: Learning Center - IR DPS

#### Participants

Hiroki Yano, MD, (*Presenter*) Nothing to Disclose

#### PURPOSE

2D-PA application equipped with the angiography unit can visualize the chronological flow of contrast through vessels as a color coded image and enables visible and quantitative blood flow evaluation. Among the several parameters of the 2D-PA, area under the curve (AUC) is considered as the total blood volume in the measured liver parenchyma. The purpose of this study is to investigate the relationship between the change of liver volume and the parameter of 2D-PA during pre and post PVE.

#### METHODS AND MATERIALS

Thirty six patients who underwent PVE between 2006 and 2022 were included in this retrospective case-control study. Percutaneous transhepatic portography was performed pre and post embolization with the same volume and rate of contrast injection as 2D-PA mode. Regions of interest (ROI) are placed in each lobes of the liver, and AUC (AUC-left ; remnant liver, -right ; embolized liver) are measured pre- and post-PVE, respectively. AUC ratio (AUCR =AUC pre-left/right) was calculated. In order to reflect each lobes blood flow in the liver parenchyma as purely as possible in 2D-PA, ROI were set on the right side outside the diaphragm and the left side outside the umbilical point. Enhanced CT examinations were performed before and 3 weeks after PVE for volumetry of liver parenchyma. Future remnant liver volume (FRLV), embolized liver volume (ELV), and total liver volume (TLV) were measured, and ELVR (=ELV/TLV), FRLVR (=FRLV/TLV), degree of hypertrophy (DH=FRLVR post/pre), degree of reduction (DR=1-ELVR post/pre) were calculated respectively. The relationships between the change of AUC and FRLR each live volume were also evaluated by Pearson's correlation coefficient (R, P<0.05).

#### RESULTS

Post AUC-left was significantly increased compared to pre AUC-left. No significant correlation was found between DH and AUCR. A positive correlation was found between DR and AUCR (R=0.418, p=0.0111), FRLVR post and AUCR (R=0.616, p=0.0000632). Furthermore, ROC analysis between AUCR and FRLVR post exceeds 40% or not, the area under the curve was 0.885 (sensitivity 78.8%, specificity 85.2%), when cutoff value of AUCR was 0.455.)

#### CONCLUSION

The AUC ratio of both liver lobes in 2D-PA before PVE correlates with the embolized liver volume rate and future remnant liver volume rate of 3 weeks after PVE.

#### CLINICAL RELEVANCE/APPLICATION

PVE is sometimes performed for hypertrophy before hepatectomy to avoid postoperative acute liver failure, but the precise prediction for the degree of hypertrophy of liver parenchyma is unclear. The AUC ratio of pre 2D-PA may help predicting the degree of future remnant liver volume.

Printed on: 02/07/23

## Abstract Archives of the RSNA, 2022

S3B-SPIR-2

### Genicular Artery Embolization as a Treatment for Symptomatic Knee Osteoarthritis: A Systematic Review and Meta-analysis

Sunday, Nov. 27 12:15PM - 12:45PM Room: Learning Center - IR DPS

#### Participants

Yan Epelboym, MPH, (*Presenter*) Nothing to Disclose

#### PURPOSE

Genicular artery embolization (GAE) is a minimally invasive therapy for symptomatic osteoarthritis (OA) in patients with knee pain refractory to conservative management. The purpose of this study was to evaluate current evidence on the effectiveness of GAE for OA related knee pain.

#### METHODS AND MATERIALS

Using three databases (Embase, PubMed, and Web of Science), we performed a systematic review to identify studies evaluating treatment of knee OA with GAE. Studies were screened by 2 of the investigators independently, first by study title, and from those the abstracts were reviewed, followed by a full-text review to select the final cohort. Exclusion criteria included studies of hemarthrosis, review articles, or republished data in the case of already-included patients. The primary outcome measure was change in pain scale score at 6 months; changes at 1, 3, and 12 months were secondary outcomes. We computed Hedge's g as a measure of effect size, a version of standardized mean difference (change per standard deviation) that includes a correction for small samples, selecting Visual Analog Scale (VAS) first if available and Knee Injury and Osteoarthritis Outcome Score (KOOS) and Western Ontario and McMaster Universities Osteoarthritis Index (WOMAC) if VAS was not available. To estimate pooled change in pain a meta-analysis was performed using a random effects model with restricted maximum likelihood.

#### RESULTS

The initial search yielded 581 studies. After screening titles, abstracts, and the full text, 8 studies met the inclusion and exclusion criteria for this study. The inter-reader agreement at the title review stage was  $k = 0.681$  (substantial), abstract stage was  $k = 0.655$  (substantial), and full-text review stage was  $k = 0.94$  (almost perfect). Eight studies with 276 treated knees were included. Seven studies were cohort studies without control groups, categorized as level II evidence. One randomized controlled trial with a sham intervention group was categorized as level I evidence. Of the 276 treated knees, 241 (87%) demonstrated Kellgren Lawrence grade I-III OA. The estimated standardized mean change (Hedges' g) from baseline to six months, was -1.4 (95% CI: (-2.1, -0.8)). The estimated standardized mean change in pain scores for secondary outcomes was -1.3 (95% CI: (-1.6, -0.97)) at one month, -1.2 (95% CI: (-1.54, -0.84)) at three months and -1.25 (95% CI: (-2.0, -0.6)) at twelve months.

#### CONCLUSION

GAE provides durable reductions in pain scores for patients with symptomatic knee OA. The effect size of GAE on pain appears to be greater than published effects for oral non-steroidal anti-inflammatories and intra-articular corticosteroid injections.

#### CLINICAL RELEVANCE/APPLICATION

GAE is a promising treatment for OA related knee pain.

Printed on: 02/07/23

## Abstract Archives of the RSNA, 2022

S3B-SPIR-3

### Impact of Computed Tomography Angiography on Lower Gastrointestinal Bleeding Primary Endovascular Intervention Outcomes

Sunday, Nov. 27 12:15PM - 12:45PM Room: Learning Center - IR DPS

#### Participants

Olivia Little, BS, Savannah, GA (*Presenter*) Nothing to Disclose

#### PURPOSE

To evaluate the impact of pre-procedural computed tomography angiography (CTA) on treatment success, hospitalization length of stay (LOS), and mortality of patients undergoing primary endovascular intervention (PEI) for lower gastrointestinal bleeding (LGIB).

#### METHODS AND MATERIALS

Using ICD-9 codes, all LGIB encounters and associated procedures in the 2005-2015 National Inpatient Sample databases were identified. Patients treated with conservative management or those who received nuclear scintigraphy were excluded. LGIB encounters initially treated with either angiography and/or embolization (PEI) and were not re-treated with PEI or another intervention were classified as successfully treated. In patients that underwent pre-procedural CTA versus those who did not, differences in mortality, mean LOS, and successful LGIB treatment were assessed with chi-square test, ANOVA, and student's t-test.

#### RESULTS

Of 224,640 LGIB encounters captured, 5,983 LGIB encounters treated with PEI met our inclusion/exclusion criteria. Overall mean age, gender, race/ethnicity was 69 years, 53% female, and 73% Caucasian. PEI definitively treated LGIB in 61.6% of LGIB encounters. Compared to patients who did not undergo CTA prior to PEI, pre-intervention CTA was associated with a greater incidence of definitive treatment success after PEI (70.8% vs 29.2%; Odds-Ratio (OR)=1.5 [95%CI 1.1-2.2],  $p<0.02$ ). There was no significant difference in LOS ( $8.3\pm 9.6$  vs  $7.7\pm 8.8$  days;  $p=0.5$ ) or mortality (6.9% vs 8.1%;  $p=0.7$ ) between encounters involving vs. not involving CTA prior to PEI.

#### CONCLUSION

s CTA utilization prior to LGIB PEI is associated with a higher incidence of successful treatment but does not impact LOS nor incidence of mortality.

#### CLINICAL RELEVANCE/APPLICATION

When utilized for the management of lower gastrointestinal bleeding, pre-intervention CTA is associated with a higher incidence of definitive treatment success after primary endovascular intervention but does impact the length of hospital stay nor incidence of mortality.

Printed on: 02/07/23



## Abstract Archives of the RSNA, 2022

S3B-SPIR-4

### Treatment Patterns in Chronic Venous Disease: Endovenous vs. Open Vein Stripping: Where Are We Today?

Sunday, Nov. 27 12:15PM - 12:45PM Room: Learning Center - IR DPS

#### Participants

Brian D'Amore, BS, (*Presenter*) Nothing to Disclose

#### PURPOSE

Chronic venous disease (CVD) affects over 30 million patients in the United States with an annual incidence of 1.9% in males and 2-6% in females. Advances in minimally-invasive treatments allow faster recovery times and lower complications with endovenous treatment options when compared to traditional vein stripping. Yet, surgical interventions persist both as primary and salvage CVD therapy. The purpose of this study was to compare the relative utilization of vein stripping and endovenous treatments, including thermal and laser ablation.

#### METHODS AND MATERIALS

Endovenous treatment (including thermal and laser ablation) and vein stripping data was obtained from the American College of Surgeons - National Surgical Quality Improvement Program (NSQIP) based on CPT codes (36475-9, 37700, 37718, 37722, and 37735) between 2011-2017. Demographics were extracted for each patient, including race, gender and age. Utilization trends were computed, and percent change was calculated for each procedure.

#### RESULTS

We identified 22,114 patients who underwent treatment for chronic superficial venous insufficiency between 2011-2017. Thermal ablation was the most frequently performed procedure with 49.5% (n=10,941) patients receiving this treatment, followed by vein stripping at 35.0% (n=7744) and laser ablation at 15.5% (n=3429). Volume increased by 6.3% for thermal ablation and 1.1% for vein stripping, while it decreased by 18.5% for laser ablation. Lastly, thermal ablation increased in males by 24.6% and decreased in females by 1.3%. It also increased in patients aged 65 and older by 24.6% and decreased in patients less than 65 by 3.03%.

#### CONCLUSION

Although thermal ablation was the most performed procedure for superficial CVD between 2011-2017, vein stripping volume was still greater than expected. Trends in thermal ablation increased significantly for males when compared to females and for patients aged 65 and older when compared to patients less than 65.

#### CLINICAL RELEVANCE/APPLICATION

The transition from vein stripping to endovenous procedures may be slower than originally presumed and total volume of procedures is lower than expected based on disease prevalence.

Printed on: 02/07/23

## Abstract Archives of the RSNA, 2022

S3B-SP1R-5

### The Role of Boosting Algorithms in Machine Learning in Predicting the Treatment Outcome of High-Intensity Focused Ultrasound Ablation of Uterine Fibroids: Most Informative Perfusion MRI Features

Sunday, Nov. 27 12:15PM - 12:45PM Room: Learning Center - IR DPS

#### Participants

Bilgin Keserci, PhD, (*Presenter*) Nothing to Disclose

#### PURPOSE

To comparatively evaluate the role of boosting algorithms in machine learning to find the most informative perfusion MRI features in predicting the treatment outcome of High-Intensity Focused Ultrasound (HIFU) ablation with an immediate nonperfused volume (NPV) ratio of at least 90%.

#### METHODS AND MATERIALS

A total of 73 women with symptomatic uterine fibroids who underwent HIFU treatment were classified according to T1 perfusion-based classification as group A (n = 47, if the time-SI curve of lesion was lower than that of myometrium) and group B (n = 26, if the time-SI curve of lesion was equal to or higher than that of myometrium). In this study, myometrium was chosen as an internal reference. An ensemble feature ranking model was introduced based on the score values assigned to the 21 perfusion MRI features by three different boosting algorithms including Adaptive boosting (Adaboost), Category boosting (Catboost) and Gradient boosting (GBM), to find the most informative perfusion MRI features. The relationship between perfusion MRI features and the immediate NPV ratio of 90% was evaluated using Pearson's correlation coefficients. The diagnostic ability of Boosting algorithms was performed by means of standard performance metrics, including the area under the receiver operating characteristic curve (AUROC), accuracy, sensitivity, and specificity in eight folds cross-validation.

#### RESULTS

For the most informative perfusion MRI features, the AUROC ranged from 0.838 to 0.916, accuracy ranged from 0.84 to 0.96, specificity of 0.833, and sensitivity ranged from 0.842 to 1.0. The GBM algorithm showed the best predictive performance with an AUROC of 0.95 and accuracy of 0.92, followed by the Catboost and Adaboost algorithms, which yielded an AUROC of 0.864 and 0.838, and accuracy of 0.88 and 0.84, respectively. The best classifier performance with the best-performing features from each perfusion MRI group, Ktrans ratio of fibroid to myometrium, The ratio of area under the curve of fibroid to myometrium, the ratio of maximum relative enhancement of fibroid to myometrium, the ratio of relative enhancement of fibroid to myometrium and the ratio of maximum enhancement of fibroid to myometrium, was achieved using GBM.

#### CONCLUSION

The preliminary findings in this study suggest that the most informative perfusion MRI features should be considered in predicting the treatment outcome of HIFU ablation to achieve an immediate NPV ratio of 90%.

#### CLINICAL RELEVANCE/APPLICATION

The best boosting algorithm performance with the best-performing perfusion MRI features should be considered by the treating physician in the screening phase to predict the treatment outcome of HIFU ablation to achieve an immediate NPV ratio of 90%.

Printed on: 02/07/23

## Abstract Archives of the RSNA, 2022

S3B-SPIR-6

### **Sustained Clinical Improvement After Prostate Artery Embolization (PAE) for Symptomatic Benign Prostate Hyperplasia (BPH): Results from a Single Center, Retrospective Analysis**

Sunday, Nov. 27 12:15PM - 12:45PM Room: Learning Center - IR DPS

#### **Participants**

Vijay Chockalingam, BS, (*Presenter*) Nothing to Disclose

#### **PURPOSE**

To validate if short term clinical results of Prostate Artery Embolization (PAE) in Benign Prostate Hyperplasia (BPH) are sustained over time.

#### **METHODS AND MATERIALS**

In an IRB approved, single center, retrospective study, 120 patients (Mean age 70.6 years  $\pm$ 9.7 years) who underwent PAE were identified. Technical success was defined as successful embolization on at least one side. Baseline IPSS (International Prostate Symptom Score) was obtained for each patient. Clinical success was evaluated as change in IPSS in short-term (< 1 year), medium-term (1-2 years) and long-term (3 or more years) follow-up. To determine change in IPSS between pre-PAE procedure and follow-up post-PAE procedure, IPSS was analyzed through a multilevel model using time as a fixed effect and patient ID as a random effect to account for within-patient correlations. Prostate shrinkage was also evaluated and changes in prostate size between baseline and post-PAE procedure were analyzed.

#### **RESULTS**

Between February 2014 and May 2021, 56 patients were accounted for in the pre-procedure baseline measurement, which showed an average IPSS of 22.1 (95% CI 20.4-23.9). Technical success was seen in 90.1% of patients in the study. Short-term (n=21), mid-term (n=24), and long-term (n=11) follow-up of these patients showed average IPSS scores of 10.2 (95% CI 7.3-13.1), 9.7 (95% CI 6.7-12.7), and 6.1 (95% CI 4.2-8.0). The results show a statistically significant ( $p = 0.000$ ) and dramatic drop in IPSS of 13.5 points in the short term. The trend post-embolization, although not statistically significant ( $p = 0.321$ ) shows that IPSS scores remain decreased over-time. Prostate size decreased from pre-PAE procedure (n=35) to post-PAE procedure follow up (n=27) from an average of 138.7 cc to 89.9 cc ( $p = 0.000$ ).

#### **CONCLUSION**

The short term, statistically significant drop in IPSS after PAE appears to be sustained in the medium and long term study period in our study, with all available data. Although these results suggest a sustained long term clinical success of the procedure, large multi-center studies are needed.

#### **CLINICAL RELEVANCE/APPLICATION**

PAE has emerged as a minimally invasive technique to treat BPH that involves a reduced hospital stay and less adverse effects compared to current gold standard approaches, all while maintaining significant symptom reduction over long term follow-up.

Printed on: 02/07/23

## Abstract Archives of the RSNA, 2022

S3B-SP1R-7

### **In-vitro Characterization of Drug Eluting Superabsorbent Polymer Microspheres: Absorption and Eluting Capacity of Contrast Material, Antibiotics and/or Analgesics**

Sunday, Nov. 27 12:15PM - 12:45PM Room: Learning Center - IR DPS

#### **Participants**

Akiko Narita, MD, PhD, Nagakute, Japan (*Presenter*) Nothing to Disclose

#### **PURPOSE**

Superabsorbent polymer microspheres (SAP-MS) have a property of absorbing fluids to swell. Therefore, drug-loaded SAP-MS will become visible, antibacterial and/or analgesic. The purpose of this study was to examine the characteristics of drug-loaded SAP-MS.

#### **METHODS AND MATERIALS**

SAP-MS were suspended in the drug solution (a) antibiotics (Cefazolin) (b) analgesics (Lidocaine) (c) contrast material (Iopamidol) and Cefazolin (d) Iopamidol and Lidocaine (e) Iopamidol, Cefazolin and Lidocaine. 1) Change of the diameter of each drug-loaded SAP-MS was observed by a stereomicroscope for three hours. 2) Absorption capacity of each drug-loaded SAP-MS were assessed by measuring the concentration of drug solution using high performance liquid chromatography (HPLC) sequentially. 3) Filtered each drug-loaded SAP-MS were mixed with 100ml of saline and drug eluting capacity of each drug-loaded SAP-MS were evaluated using HPLC over time.

#### **RESULTS**

1) Diameter of drug-loaded SAP-MS increased for about 15 minutes and came to an equilibrium. Finally, the diameter was (a) 3.9 times (b) 5.0 times (c) 2.2 times (d) 5.5 times (e) 3.6 times larger than its original size. 2) The concentration of drug solution did not change and the amount of drug solution decreased. 3) Each drug was released into 10 minutes and came to an equilibrium. The concentration of each drug in the mixture was increased by (a) Cefazolin: 1.82 mg/ml (b) Lidocaine: 0.06 mg/ml (c) Iopamidol: 1.34 mg/ml, Cefazolin: 0.17 mg/ml (d) Iopamidol: 4.51 mg/ml, Lidocaine: 0.11 mg/ml (e) Iopamidol: 2.70 mg/ml, Cefazolin: 1.10 mg/ml, Lidocaine: 0.03 mg/ml.

#### **CONCLUSION**

s SAP-MS can absorb each drug as much as it swells. And drug-loaded SAP-MS release contrast material, antibiotics and analgesics.

#### **CLINICAL RELEVANCE/APPLICATION**

Visible, antibiotic and/or analgesic microspheres will contribute to safe and useful embolization, in addition, relief of pain and prevention infection like abscess.

Printed on: 02/07/23

## Abstract Archives of the RSNA, 2022

S3B-SPIR-8

### **Bariatric Arterial Embolization with Radiopaque Hydrogel Microspheres Suppresses Weight Gain and Fundal Ghrelin Levels in Swine**

Sunday, Nov. 27 12:15PM - 12:45PM Room: Learning Center - IR DPS

#### **Participants**

Yingli Fu, Baltimore, MD (*Presenter*) Nothing to Disclose

#### **PURPOSE**

Octreotide is a somatostatin analogue with beneficial effect on ghrelin suppression and weight loss. The purpose of this study is to evaluate the effect of octreotide-eluting, lipiodol-impregnated, alginate microspheres (OLMs) on the safety and efficacy of bariatric arterial embolization (BAE) in swine.

#### **METHODS AND MATERIALS**

X-ray-visible OLMs were produced from lipiodol-impregnated alginate (2% w/v) solution containing 10 mg/ml octreotide using an electrostatic droplet generator. BAE was performed in 6 healthy, growing swine (mean weight: 22.2 kg) by selective infusion of X-ray-visible OLMs (n = 3) or saline (n = 3) into the right gastric artery (RGA) and the left gastroepiploic artery (LGEA) under X-ray guidance. Weight was obtained in all animals at baseline and weekly up to 8 weeks post embolization. Cone-beam CT (CBCT) images of the stomachs were acquired immediately after embolization and at 8 weeks prior to sacrifice to assess the embolization coverage of the fundus, and the visibility and distribution of OLMs. All animals were euthanized for gross and histological examination of stomach mucosal integrity at 8 weeks. Ghrelin-expressing cells (GECs) in the stomach were assessed immunohistochemically and analyzed using the Mann-Whitney U test.

#### **RESULTS**

OLMs were monodispersed with diameter of  $185 \pm 6 \mu\text{m}$ . BAE with OLMs was successfully performed in all animals. The OLMs can be visualized both on fluoroscopy and CBCT images during the embolization procedure. The post-procedural percentage of weight gain was lower in BAE-treated animals as compared to controls (BAE vs. control:  $39.4\% \pm 12.9$  vs.  $61.0\% \pm 3.2$  at 8 weeks). The GECs were significantly decreased in the gastric fundus of OLM-embolized animals compared to control animals (BAE vs. control:  $14.9 \pm 3.6$  vs.  $24.3 \pm 5.4$ ,  $p < 0.0001$ ). Superficial healed mucosal ulcers were observed in one OLM-embolized animal along the stomach fundus and body.

#### **CONCLUSION**

s BAE with octreotide-eluting, lipiodol/alginate microspheres can be safely performed in all animals and significantly suppress the percentage of weight gain and fundal ghrelin levels.

#### **CLINICAL RELEVANCE/APPLICATION**

BAE with octreotide-eluting, lipiodol/alginate microspheres may be useful for treating obesity.

Printed on: 02/07/23

## Abstract Archives of the RSNA, 2022

S3B-SPIR-9

### New TRUS Techniques and Imaging Features of PI-RADS 4 or 5: Influence on Tumor Targeting

Sunday, Nov. 27 12:15PM - 12:45PM Room: Learning Center - IR DPS

#### Participants

Byung Kwan Park, MD, PhD, (*Presenter*) Nothing to Disclose

#### PURPOSE

To determine if the new transrectal ultrasound (TRUS) techniques and imaging features contribute to targeting Prostate Imaging and Reporting and Data System (PI-RADS) 4 or 5.

#### METHODS AND MATERIALS

Between December 2018 and February 2020, 115 men underwent cognitive biopsy by radiologist A, who was familiar with the new TRUS findings and biopsy techniques. During the same period, 179 men underwent magnetic resonance imaging-TRUS image fusion or cognitive biopsy by radiologist B, who was unfamiliar with the new biopsy techniques. Prior to biopsy, both radiologists knew MRI findings such as the location, size, and shape of PI-RADS 4 or 5. We recorded how many target biopsies were performed without systematic biopsy and how many of these detected higher Gleason score (GS) than those detected by systematic biopsy. The numbers of biopsy cores were also obtained. Fisher Exact or Mann-Whitney test was used for statistical analysis.

#### RESULTS

For PI-RADS 4, target biopsy alone was performed in 0% (0/84) by radiologist A and 0.8% (1/127) by radiologist B ( $p > 0.9999$ ). Target biopsy yielded higher GSs in 57.7% (30/52) by radiologist A and 29.5% (23/78) by radiologist B ( $p = 0.0019$ ). For PI-RADS 5, target biopsy alone was performed in 29.0% (9/31) by radiologist A and 1.9% (1/52) by radiologist B ( $p = 0.0004$ ). Target biopsy yielded higher GSs in 50.0% (14/28) by radiologist A and 18.2% (8/44) by radiologist B ( $p = 0.0079$ ). Radiologist A sampled fewer biopsy cores than radiologist B ( $p = 0.0008$  and  $0.0023$  for PI-RADS 4 and 5), respectively.

#### CONCLUSION

s PI-RADS 4 or 5 can be more precisely targeted if the new TRUS biopsy techniques are applied.

#### CLINICAL RELEVANCE/APPLICATION

The new TRUS biopsy techniques help to not only target PI-RADS 4 or 5 lesions more precisely but also to reduce the number of biopsy cores needed. Moreover, systematic biopsy can be omitted in PI-RADS 5 patients who do not stop taking aspirin because of cardiovascular disease.

Printed on: 02/07/23

## Abstract Archives of the RSNA, 2022

S3B-SPMK

### Musculoskeletal Sunday Poster Discussions - B

Sunday, Nov. 27 12:15PM - 12:45PM Room: Learning Center - MK DPS

#### Sub-Events

#### **S3B-SPMK-1 Impact of Non-steroidal Anti-inflammatory Drugs (NSAIDs) on Synovitis and The Progression of Osteoarthritis: Data From The Osteoarthritis Initiative (OAI)**

##### Participants

Johanna Luitjens, MD, San Francisco, CA (*Presenter*) Consultant, Smart Reporting

##### PURPOSE

Synovitis and associated inflammation have been shown to play a major role in promoting progression of osteoarthritis (OA). Non-steroidal anti-inflammatory drugs (NSAIDs) are commonly used to treat pain in OA patients and could also influence the progression of the disease through their anti-inflammatory effect. To investigate these mechanisms, the goals of this study were (1) to analyze the association between the use of NSAIDs and synovitis and (2) to assess how treatment with NSAIDs impacts structural outcomes over four years.

##### METHODS AND MATERIALS

Participants from the Osteoarthritis Initiative (OAI) cohort with moderate to severe OA (Kellgren-Lawrence (K/L) grades 2-4) and sustained NSAID treatment for =1 year between baseline and 4-year follow-up were included and compared with non-NSAID treated participants (controls). All participants underwent a 3T MRI of the knee at baseline and after 4 years. Images were semi-quantitatively scored for MR biomarkers of synovial inflammation (effusion-synovitis, size and signal intensity of infrapatellar fat pad (IFP), synovial proliferation score (SPS)). Cartilage thickness and T2-relaxation time measurements served as non-invasive biomarkers for evaluating OA progression. The associations between baseline and findings after 4 years were investigated with linear regression models (including adjustment for sex, BMI, age, pain, K/L grade).

##### RESULTS

A total of 721 participants matched the inclusion criteria (129 with and 592 participants without regular usage of NSAID). At baseline, significantly higher signal intensity in the IFP was observed in NSAID users as compared to controls (adjusted difference in score, 95% CI, p) (0.26; [-0.5, -0.129], 0.039). Additionally in the longitudinal analysis, there was a significantly higher increase in signal intensity of IFP (0.46; [0.2, 0.72], < 0.001) and higher increase in effusion-synovitis (0.27, [0.06, 0.47], 0.01) in NSAIDs users compared to controls. The size of IFP and SPS did not show a significant difference between groups at baseline and no significant change over time. NSAID users showed more degenerative changes regarding T2-relaxation time and cartilage thickness over time, but this did not reach statistical significance.

##### CONCLUSION

s NSAID users demonstrated higher signal intensity in IFP and more effusion/ synovitis than controls, suggesting that longtime NSAID usage is associated with more synovitis.

##### CLINICAL RELEVANCE/APPLICATION

In this study, no structural long-term benefit of NSAID use in patients with OA could be found. Furthermore, users showed more synovitis at baseline and change over 4 years, which may lead to an increase in pain and a decrease in joint function.

#### **S3B-SPMK-2 Contrast-enhanced 3D UTE MRI to Assess Active Inflammation of Sacroiliitis in Spondyloarthropathy: The Diagnostic Performance Compared with Contrast-enhanced fat-suppressed T1 Weighted Spin Echo Sequence**

##### Participants

Yeo Ju Kim, MD, Seoul, Korea, Republic Of (*Presenter*) Nothing to Disclose

##### PURPOSE

To evaluate the diagnostic performance of contrast-enhanced 3D ultrashort echo time MRI (CE-3DUTE) for active inflammation of sacroiliitis in spondyloarthropathy compared with contrast-enhanced T1 weighted spin-echo sequence with fat suppression (CE-T1).

##### METHODS AND MATERIALS

A total of 50 patients (mean age: 40.6 years old, age range: 20-79, 30 men, 20 women), composed of 30 patients with axial spondyloarthropathy (ASPA group), 7 patients with inflammatory back pain, and 13 patients with mechanical back pain were enrolled in this retrospective study. All patients performed oblique coronal CE-3DUTE and CE-T1 for sacroiliac joint, respectively. Active inflammation of the sacroiliac joint in MRI such as osteitis, synovitis, capsulitis, and enthesitis was semi-quantitatively scored by two musculoskeletal radiologists independently and compared between CE-3DUTE and CE-T1 using a one-way ANOVA test. Clinical inflammation activity such as the Bath Ankylosing Spondylitis Disease Activity Index (BASDAI), AS Disease Activity

Score (ASDAS), erythrocyte sedimentation rate (ESR), C-reactive protein (CRP) level were also documented and correlated with imaging inflammatory scores using bivariate correlation analysis.

## RESULTS

ASPA group showed higher scores of osteitis, synovitis, and enthesitis in both CE-3DUTE and CE-T1 than other groups ( $P < 0.05$ ). Among clinical inflammatory activity index, ESR was correlated with osteitis, synovitis, enthesitis in both CE-3DUTE and CE-T1, and with capsulitis in CE-3DUTE with statistical significance ( $P < 0.05$ ). CRP was correlated with osteitis in CE-3DUTE and CE-T1, synovitis in CE-3DUTE, and enthesitis in CE-T1 ( $P < 0.05$ ).

## CONCLUSION

s CE-3DUTE might differentiate ASPA from other non-specific inflammatory back pain and mechanical back pain and may reflect inflammatory activity as a complement to CE-T1.

## CLINICAL RELEVANCE/APPLICATION

UTE has been expected to better reflect the degree of inflammation in tissues with the majority of short T2 components such as ligaments and tendons, which show no signal in conventional MRI, but there have been few clinical studies in the meantime. Our study suggests that UTE may be useful in the diagnosis of spondyloarthropathy as well as many inflammatory diseases involving tissue with the majority of short T2 components and reflect the inflammatory activity.

## S3B-SPMK-3 Radiographic OA Progression Following Meniscus Surgery

Participants

Azad Darbandi, BS, MS, Chicago, IL (*Presenter*) Nothing to Disclose

## PURPOSE

Osteoarthritis (OA) is one of the most common joint disorders affecting over fifty-eight million individuals in the United States with an estimated annual cost of \$185 billion. Known risk factors include obesity, joint trauma, and overuse. Radiographic scoring and analysis are utilized to assess the progression on OA in patients and help assist with clinical management. To date, the effects of meniscus surgery on osteoarthritis have not been well studied. To help define the risk of meniscus surgery on osteoarthritis progression, we conducted a case-control study comparing radiographic markers of OA progression in patients with and without meniscus surgery by utilizing data from the Osteoarthritis Initiative.

## METHODS AND MATERIALS

Patients were identified based on the presence of imaging data and outcomes at baseline and at a 48-month period. Following exclusion criteria, 83 patients with meniscus surgery were matched against 83 controls. Patients were matched based on various confounding factors including age, sex, BMI, comorbidities, intraarticular injections, and semi-quantitative imaging outcomes at baseline. ANCOVA testing was done using imaging outcomes as dependent variables and confounding factors as covariates. Imaging outcomes included joint space narrowing, Kellgren Lawrence (KL) grade, osteophyte formation in tibia/femur medial/lateral compartment, and sclerosis in tibia/femur medial/lateral compartment.

## RESULTS

At 48M, a significant difference was found in medial compartment joint space narrowing ( $p < .001$ ) and osteophyte presentation in the femur medial compartment ( $p = .005$ ) between patients who received meniscus surgery and patients who did not. Sclerosis of the femur medial compartment ( $p = .02$ ) and sclerosis of the tibia lateral compartment ( $p = .02$ ) was found significant as well. KL Grade was  $2.04 \pm 1.08$  in patients who received meniscal surgery and  $1.22 \pm .96$  in control patients, with a significant difference between the two groups ( $p < .001$ ). Patients who had meniscus surgery scored higher in each significant radiological marker.

## CONCLUSION

s A significant increase in radiographic osteoarthritis progression was seen in patients receiving meniscus surgery compared to control patients. Patients with meniscus surgery had an increase in various radiographic markers including sclerosis, formation of osteophytes, and joint space narrowing. The risks of osteoarthritis following meniscus surgery should be discussed with patients and accounted for throughout clinical management.

## CLINICAL RELEVANCE/APPLICATION

Given the increased radiographic progression of osteoarthritis following meniscus surgery, providers should weigh the advantages and disadvantages of the intervention with their patients.

Printed on: 02/07/23

## Abstract Archives of the RSNA, 2022

S3B-SPMK-1

### Impact of Non-steroidal Anti-inflammatory Drugs (NSAIDs) on Synovitis and The Progression of Osteoarthritis: Data From The Osteoarthritis Initiative (OAI)

Sunday, Nov. 27 12:15PM - 12:45PM Room: Learning Center - MK DPS

#### Participants

Johanna Luitjens, MD, San Fransisco, CA (*Presenter*) Consultant, Smart Reporting

#### PURPOSE

Synovitis and associated inflammation have been shown to play a major role in promoting progression of osteoarthritis (OA). Non-steroidal anti-inflammatory drugs (NSAIDs) are commonly used to treat pain in OA patients and could also influence the progression of the disease through their anti-inflammatory effect. To investigate these mechanisms, the goals of this study were (1) to analyze the association between the use of NSAIDs and synovitis and (2) to assess how treatment with NSAIDs impacts structural outcomes over four years.

#### METHODS AND MATERIALS

Participants from the Osteoarthritis Initiative (OAI) cohort with moderate to severe OA (Kellgren-Lawrence (K/L) grades 2-4) and sustained NSAID treatment for  $\geq 1$  year between baseline and 4-year follow-up were included and compared with non-NSAID treated participants (controls). All participants underwent a 3T MRI of the knee at baseline and after 4 years. Images were semi-quantitatively scored for MR biomarkers of synovial inflammation (effusion-synovitis, size and signal intensity of infrapatellar fat pad (IFP), synovial proliferation score (SPS)). Cartilage thickness and T2-relaxation time measurements served as non-invasive biomarkers for evaluating OA progression. The associations between baseline and findings after 4 years were investigated with linear regression models (including adjustment for sex, BMI, age, pain, K/L grade).

#### RESULTS

A total of 721 participants matched the inclusion criteria (129 with and 592 participants without regular usage of NSAID). At baseline, significantly higher signal intensity in the IFP was observed in NSAID users as compared to controls (adjusted difference in score, 95% CI, p) (0.26; [-0.5, -0.129], 0.039). Additionally in the longitudinal analysis, there was a significantly higher increase in signal intensity of IFP (0.46; [0.2, 0.72],  $< 0.001$ ) and higher increase in effusion-synovitis (0.27, [0.06, 0.47], 0.01) in NSAIDs users compared to controls. The size of IFP and SPS did not show a significant difference between groups at baseline and no significant change over time. NSAID users showed more degenerative changes regarding T2-relaxation time and cartilage thickness over time, but this did not reach statistical significance.

#### CONCLUSION

s NSAID users demonstrated higher signal intensity in IFP and more effusion/ synovitis than controls, suggesting that longtime NSAID usage is associated with more synovitis.

#### CLINICAL RELEVANCE/APPLICATION

In this study, no structural long-term benefit of NSAID use in patients with OA could be found. Furthermore, users showed more synovitis at baseline and change over 4 years, which may lead to an increase in pain and a decrease in joint function.

Printed on: 02/07/23

## Abstract Archives of the RSNA, 2022

S3B-SPMK-2

### Contrast-enhanced 3D UTE MRI to Assess Active Inflammation of Sacroiliitis in Spondyloarthritis: The Diagnostic Performance Compared with Contrast-enhanced fat-suppressed T1 Weighted Spin Echo Sequence

Sunday, Nov. 27 12:15PM - 12:45PM Room: Learning Center - MK DPS

#### Participants

Yeo Ju Kim, MD, Seoul, Korea, Republic Of (*Presenter*) Nothing to Disclose

#### PURPOSE

To evaluate the diagnostic performance of contrast-enhanced 3D ultrashort echo time MRI (CE-3DUTE) for active inflammation of sacroiliitis in spondyloarthritis compared with contrast-enhanced T1 weighted spin-echo sequence with fat suppression (CE-T1).

#### METHODS AND MATERIALS

A total of 50 patients (mean age: 40.6 years old, age range: 20-79, 30 men, 20 women), composed of 30 patients with axial spondyloarthritis (ASPA group), 7 patients with inflammatory back pain, and 13 patients with mechanical back pain were enrolled in this retrospective study. All patients performed oblique coronal CE-3DUTE and CE-T1 for sacroiliac joint, respectively. Active inflammation of the sacroiliac joint in MRI such as osteitis, synovitis, capsulitis, and enthesitis was semi-quantitatively scored by two musculoskeletal radiologists independently and compared between CE-3DUTE and CE-T1 using a one-way ANOVA test. Clinical inflammation activity such as the Bath Ankylosing Spondylitis Disease Activity Index (BASDAI), AS Disease Activity Score (ASDAS), erythrocyte sedimentation rate (ESR), C-reactive protein (CRP) level were also documented and correlated with imaging inflammatory scores using bivariate correlation analysis.

#### RESULTS

ASPA group showed higher scores of osteitis, synovitis, and enthesitis in both CE-3DUTE and CE-T1 than other groups ( $P < 0.05$ ). Among clinical inflammatory activity index, ESR was correlated with osteitis, synovitis, enthesitis in both CE-3DUTE and CE-T1, and with capsulitis in CE-3DUTE with statistical significance ( $P < 0.05$ ). CRP was correlated with osteitis in CE-3DUTE and CE-T1, synovitis in CE-3DUTE, and enthesitis in CE-T1 ( $P < 0.05$ ).

#### CONCLUSION

CE-3DUTE might differentiate ASPA from other non-specific inflammatory back pain and mechanical back pain and may reflect inflammatory activity as a complement to CE-T1.

#### CLINICAL RELEVANCE/APPLICATION

UTE has been expected to better reflect the degree of inflammation in tissues with the majority of short T2 components such as ligaments and tendons, which show no signal in conventional MRI, but there have been few clinical studies in the meantime. Our study suggests that UTE may be useful in the diagnosis of spondyloarthritis as well as many inflammatory diseases involving tissue with the majority of short T2 components and reflect the inflammatory activity.

Printed on: 02/07/23

## Abstract Archives of the RSNA, 2022

S3B-SPMK-3

### Radiographic OA Progression Following Meniscus Surgery

Sunday, Nov. 27 12:15PM - 12:45PM Room: Learning Center - MK DPS

#### Participants

Azad Darbandi, BS, MS, Chicago, IL (*Presenter*) Nothing to Disclose

#### PURPOSE

Osteoarthritis (OA) is one of the most common joint disorders affecting over fifty-eight million individuals in the United States with an estimated annual cost of \$185 billion. Known risk factors include obesity, joint trauma, and overuse. Radiographic scoring and analysis are utilized to assess the progression on OA in patients and help assist with clinical management. To date, the effects of meniscus surgery on osteoarthritis have not been well studied. To help define the risk of meniscus surgery on osteoarthritis progression, we conducted a case-control study comparing radiographic markers of OA progression in patients with and without meniscus surgery by utilizing data from the Osteoarthritis Initiative.

#### METHODS AND MATERIALS

Patients were identified based on the presence of imaging data and outcomes at baseline and at a 48-month period. Following exclusion criteria, 83 patients with meniscus surgery were matched against 83 controls. Patients were matched based on various confounding factors including age, sex, BMI, comorbidities, intraarticular injections, and semi-quantitative imaging outcomes at baseline. ANCOVA testing was done using imaging outcomes as dependent variables and confounding factors as covariates. Imaging outcomes included joint space narrowing, Kellgren Lawrence (KL) grade, osteophyte formation in tibia/femur medial/lateral compartment, and sclerosis in tibia/femur medial/lateral compartment.

#### RESULTS

At 48M, a significant difference was found in medial compartment joint space narrowing ( $p < .001$ ) and osteophyte presentation in the femur medial compartment ( $p = .005$ ) between patients who received meniscus surgery and patients who did not. Sclerosis of the femur medial compartment ( $p = .02$ ) and sclerosis of the tibia lateral compartment ( $p = .02$ ) was found significant as well. KL Grade was  $2.04 \pm 1.08$  in patients who received meniscal surgery and  $1.22 \pm .96$  in control patients, with a significant difference between the two groups ( $p < .001$ ). Patients who had meniscus surgery scored higher in each significant radiological marker.

#### CONCLUSION

A significant increase in radiographic osteoarthritis progression was seen in patients receiving meniscus surgery compared to control patients. Patients with meniscus surgery had an increase in various radiographic markers including sclerosis, formation of osteophytes, and joint space narrowing. The risks of osteoarthritis following meniscus surgery should be discussed with patients and accounted for throughout clinical management.

#### CLINICAL RELEVANCE/APPLICATION

Given the increased radiographic progression of osteoarthritis following meniscus surgery, providers should weigh the advantages and disadvantages of the intervention with their patients.

Printed on: 02/07/23

## Abstract Archives of the RSNA, 2022

S3B-SPNMMI

### Nuclear Medicine/Molecular Imaging Sunday Poster Discussion - B

Sunday, Nov. 27 12:15PM - 12:45PM Room: Learning Center - NMMI DPS

#### Participants

Nadine Mallak, MD, Portland, OR (*Moderator*) Nothing to Disclose  
Nadine Mallak, MD, Portland, OR (*Moderator*) Nothing to Disclose  
Ashwin Parihar, MBBS, MD, Saint Louis, MO (*Moderator*) Nothing to Disclose  
Ashwin Parihar, MBBS, MD, Saint Louis, MO (*Moderator*) Nothing to Disclose

#### Sub-Events

#### S3B-SPNMMI-1 99mTc-pyrophosphate Scintigraphy and Clinical Findings Related to Early-Onset Patients With Wild-Type Transthyretin Cardiomyopathy

#### Participants

Kouji Ogasawara, Kumamoto, Japan (*Presenter*) Nothing to Disclose

#### PURPOSE

Wild-type transthyretin cardiomyopathy (ATTRwt-CM) is an increasingly recognized cause of heart failure especially in elderly patients, but there are a small number of early-onset ATTRwt-CM patients. We aimed to evaluate the status of amyloid deposition and clinical risk factors related to the early-onset ATTRwt-CM patients using 99mTc-pyrophosphate (PYP) scintigraphy with SPECT/CT examination.

#### METHODS AND MATERIALS

Our study included 111 patients who were clinically diagnosed with ATTRwt-CM and underwent PYP scintigraphy including SPECT/CT. Of all patients, 36 cases under 75 years were classified as early-onset group (Group 1), and 75 cases over 75 years were designated as late-onset group (Group 2). Heart-to-contralateral ratio (H/CL) was calculated from a planar image, and the uptake ratio of PYP in the septum (Se), posterior (Po), anterior (An), lateral (La), and apex (Ap) walls to the cavity pool (C) on SPECT/CT was calculated as Se/C, Po/C, An/C, La/C, and Ap/C, respectively. Clinical risk factors for heart disease included hypertension (HT), dyslipidemia (DL), diabetes mellitus (DM), chronic kidney disease (CKD), and smoking history. Univariate analysis and multiple logistic regression analysis were performed to evaluate the relationship between the scintigraphy and clinical findings and the patient's onset.

#### RESULTS

All indices of PYP scintigraphy were significantly higher for Group 1 than Group 2 ( $p < 0.01$ ). The proportion of male gender was significantly higher for Group 1 (94%) than Group 2 (79%) ( $p = 0.01$ ). Compared to Group 2, Group 1 had significantly higher DM prevalence (53% Group 1 vs 24% Group 2;  $p = 0.04$ ) and smoking history (73% Group 1 vs 44% Group 2;  $p < 0.01$ ). Multiple logistic regression analysis showed that independent, significant factors were An/C ( $p < 0.01$ ), DM ( $p < 0.01$ ), and smoking history ( $p = 0.05$ ).

#### CONCLUSION

s Myocardial accumulation of PYP was significantly higher in the early-onset patients with ATTRwt-CM than in the late-onset, suggesting that the rate of amyloid deposition may affect the age of onset. Also, the early-onset patients had a higher proportion of DM prevalence and smoking history, which may be factors accelerating amyloid deposition.

#### CLINICAL RELEVANCE/APPLICATION

Early-onset ATTRwt-CM patients have different scintigraphy and clinical findings compared to late-onset patients. Further investigation is needed as to whether treatment strategies should be considered according to the patient's onset.

#### S3B-SPNMMI-2 Multi-pool Model-based CEST Imaging Compared to IVIM and 11C-MET Uptake on PET/CT in Patients with Gliomas

#### Participants

Yasukage Takami, Mikicho, Japan (*Presenter*) Nothing to Disclose

#### PURPOSE

Although magnetization transfer ratio asymmetry (MTRAsym) analysis is often used as a chemical exchange saturation transfer (CEST), it is semiquantitative and entails some pitfalls. Recently, we developed the new parameters on CEST imaging by the multi-pool model (MPM). The MPM analysis can produce quantitative results and it may allow for a more detailed assessment of the tumors. The purpose of this study was to evaluate the clinical significance of the new parameters on CEST imaging by assessing the correlation among parameters on CEST imaging by MPM, intravoxel incoherent motion (IVIM) and 11C-methionine (MET) uptake on PET/CT in gliomas.

## METHODS AND MATERIALS

The preoperative MRI and 11C-MET PET/CT examinations of a total of 30 lesions from 17 patients with gliomas were examined. The magnetization transfer ratio asymmetry (MTR<sub>asym</sub>) value at 3.5 ppm downfield from the water signal was obtained by calculating the difference in signal intensity (SI) at  $\pm 3.5$  ppm on both sides of the water center frequency in the Z-spectrum. MPM assumes the magnetization transfer (MT) between free water pool, APT pool and binding water MT pool. "APT density" x "APT transfer rate" x ("Free water T1" or "T2") was visualized as APT\_T1 or APT\_T2, respectively. The MT image is obtained via MPM fitting. Firstly, the maximum values of the parameters (MTR<sub>asym</sub>, APT\_T1, APT\_T2, T2/T1 ratio, and MT) on CEST imaging were measured respectively by regions of interest (ROI) analysis. Secondly, ROIs of IVIM and 11C-MET PET/CT were placed in similar anatomical locations by visual assessment. ROIs were carefully placed in the solid component of a tumor and the best effort was given to avoid cystic components of the tumor. 11C-MET uptake was semiquantitatively assessed using tumor-to-contralateral normal brain tissue (T/N) ratio.

## RESULTS

There were significant positive correlations between APT\_T1 and MET T/N ratio ( $r = 0.86$ ,  $p < 0.01$ ), APT\_T2 and MET T/N ratio ( $r = 0.42$ ,  $p < 0.05$ ), T2/T1 and ADC ( $r = 0.36$ ,  $p = 0.05$ ), T2/T1 and D ( $r = 0.41$ ,  $p < 0.05$ ), and MTR<sub>asym</sub> and MET T/N ratio ( $r = 0.51$ ,  $p < 0.01$ ). There existed significant negative correlations between APT\_T1 and ADC ( $r = -0.64$ ,  $p < 0.01$ ), APT\_T1 and D ( $r = -0.67$ ,  $p < 0.01$ ), APT\_T2 and D\* ( $r = -0.46$ ,  $p = 0.01$ ), and T2/T1 and MET T/N ratio ( $r = -0.37$ ,  $p < 0.05$ ).

## CONCLUSION

These preliminary results suggest that parameters on CEST imaging by multi pool model seems to correlate with IVIM and 11C-MET uptake on PET/CT in patients with gliomas. Combining Multi-pool model-based CEST imaging, IVIM and 11C-MET PET/CT may improve the diagnostic ability of gliomas.

## CLINICAL RELEVANCE/APPLICATION

Combining Multi-pool model-based CEST imaging, IVIM and 11C-MET PET/CT may improve the diagnostic ability of gliomas.

## S3B-SPNMMI-3 Low-dose EDB Fibronectin Gd-DOTA Specific Probe for Pancreatic Cancer Targeting Magnetic-optical Dual-modality Imaging

Participants  
Wenjia Zhang, Beijing, China (*Presenter*) Nothing to Disclose

## PURPOSE

Pancreatic ductal adenocarcinoma (PDAC) is a lethal malignancy worldwide. PDAC is a hypovascular tumor surrounded by dense stroma, which is recognized as a vital factor of tumor progression. Multimodal molecular imaging of onco-proteins is a promising method for accurate, early detection of the disease. Extradomain-B fibronectin (EDB-FN), a high-expression onco-protein in the tumor extracellular matrix, can realize targeted and effective molecular imaging. Here, we prepared a novel Gd-based contrast agent of EDB-Cy7 to perform fluorescence molecular imaging (FMI) and molecular MRI, in order to realize accurate, early and safe detection of PDAC.

## METHODS AND MATERIALS

The EDB-FN targeting peptide and near infrared dye Cy7 were conjugated to the Gd-DOTA (EDB-Gd-Cy7) for the PDAC-targeting multimodality imaging. Five-week-old BALB/c nude mice were implanted with human pancreatic stellate cells (PSC) and human PDAC cell lines (Bxpc-3) to establish the subcutaneous and orthotopic PDAC models. Mice were intravenously injected with EDB-Gd-Cy7 or Gd-DOTA at the Gd concentration of 0.05 mmol/kg, which is merely a half of clinical dose. T1 mapping MRI and FMI were performed. The TBR (Tumor background ratio) of fluorescence intensity and the ratio of T1 value reduction (T1d%) were compared quantitatively. Histological and immunofluorescence analyses were used as references for ex vivo validation.

## RESULTS

The concentration of EDB-Gd-Cy7 showed a correlation with fluorescence intensity and T1 relaxation time in vitro. For in vivo MRI, the T1d% showed the most significant difference at 30 minutes post-injection in subcutaneous and orthotopic PDAC xenograft models. For in vivo FMI, at 30 minutes post-injection, the TBR of fluorescence intensity showed the most significant difference in subcutaneous models, while the TBR of fluorescence intensity showed no significant differences between two groups in orthotopic models. Immunofluorescence confirmed the targeting of EDB-Gd-Cy7 to EDB-FN in both PDAC models.

## CONCLUSION

Our dual-modal imaging findings indicate that FMI and molecular MRI could complement its advantages and translation of oncoprotein targeted dual-modal imaging with low-dose EDB-Gd-Cy7 to humans, which might provide a promising imaging technique to detect PDAC precisely. Moreover, these findings suggest that EDB-FN targeting MRI might have clinical application to evaluate the tumor extracellular matrix and chemo-therapy efficacy in the future.

## CLINICAL RELEVANCE/APPLICATION

Molecular MRI with the EDB-targeted probe provided robust detection of PDAC in two animal models and may enable non-invasive detection, precise staging and monitoring post-treatment fibrotic changes of PDAC compared to standard Gd-DOTA contrast agents.

Printed on: 02/07/23

## Abstract Archives of the RSNA, 2022

S3B-SPNMMI-1

### **99mTc-pyrophosphate Scintigraphy and Clinical Findings Related to Early-Onset Patients With Wild-Type Transthyretin Cardiomyopathy**

Sunday, Nov. 27 12:15PM - 12:45PM Room: Learning Center - NMMI DPS

#### **Participants**

Kouji Ogasawara, Kumamoto, Japan (*Presenter*) Nothing to Disclose

#### **PURPOSE**

Wild-type transthyretin cardiomyopathy (ATTRwt-CM) is an increasingly recognized cause of heart failure especially in elderly patients, but there are a small number of early-onset ATTRwt-CM patients. We aimed to evaluate the status of amyloid deposition and clinical risk factors related to the early-onset ATTRwt-CM patients using 99mTc-pyrophosphate (PYP) scintigraphy with SPECT/CT examination.

#### **METHODS AND MATERIALS**

Our study included 111 patients who were clinically diagnosed with ATTRwt-CM and underwent PYP scintigraphy including SPECT/CT. Of all patients, 36 cases under 75 years were classified as early-onset group (Group 1), and 75 cases over 75 years were designated as late-onset group (Group 2). Heart-to-contralateral ratio (H/CL) was calculated from a planar image, and the uptake ratio of PYP in the septum (Se), posterior (Po), anterior (An), lateral (La), and apex (Ap) walls to the cavity pool (C) on SPECT/CT was calculated as Se/C, Po/C, An/C, La/C, and Ap/C, respectively. Clinical risk factors for heart disease included hypertension (HT), dyslipidemia (DL), diabetes mellitus (DM), chronic kidney disease (CKD), and smoking history. Univariate analysis and multiple logistic regression analysis were performed to evaluate the relationship between the scintigraphy and clinical findings and the patient's onset.

#### **RESULTS**

All indices of PYP scintigraphy were significantly higher for Group 1 than Group 2 ( $p < 0.01$ ). The proportion of male gender was significantly higher for Group 1 (94%) than Group 2 (79%) ( $p = 0.01$ ). Compared to Group 2, Group 1 had significantly higher DM prevalence (53% Group 1 vs 24% Group 2;  $p = 0.04$ ) and smoking history (73% Group 1 vs 44% Group 2;  $p < 0.01$ ). Multiple logistic regression analysis showed that independent, significant factors were An/C ( $p < 0.01$ ), DM ( $p < 0.01$ ), and smoking history ( $p = 0.05$ ).

#### **CONCLUSION**

Myocardial accumulation of PYP was significantly higher in the early-onset patients with ATTRwt-CM than in the late-onset, suggesting that the rate of amyloid deposition may affect the age of onset. Also, the early-onset patients had a higher proportion of DM prevalence and smoking history, which may be factors accelerating amyloid deposition.

#### **CLINICAL RELEVANCE/APPLICATION**

Early-onset ATTRwt-CM patients have different scintigraphy and clinical findings compared to late-onset patients. Further investigation is needed as to whether treatment strategies should be considered according to the patient's onset.

Printed on: 02/07/23

## Abstract Archives of the RSNA, 2022

S3B-SPNMMI-2

### Multi-pool Model-based CEST Imaging Compared to IVIM and 11C-MET Uptake on PET/CT in Patients with Gliomas

Sunday, Nov. 27 12:15PM - 12:45PM Room: Learning Center - NMMI DPS

#### Participants

Yasukage Takami, Mikicho, Japan (*Presenter*) Nothing to Disclose

#### PURPOSE

Although magnetization transfer ratio asymmetry (MTR<sub>asym</sub>) analysis is often used as a chemical exchange saturation transfer (CEST), it is semiquantitative and entails some pitfalls. Recently, we developed the new parameters on CEST imaging by the multi-pool model (MPM). The MPM analysis can produce quantitative results and it may allow for a more detailed assessment of the tumors. The purpose of this study was to evaluate the clinical significance of the new parameters on CEST imaging by assessing the correlation among parameters on CEST imaging by MPM, intravoxel incoherent motion (IVIM) and 11C-methionine (MET) uptake on PET/CT in gliomas.

#### METHODS AND MATERIALS

The preoperative MRI and 11C-MET PET/CT examinations of a total of 30 lesions from 17 patients with gliomas were examined. The magnetization transfer ratio asymmetry (MTR<sub>asym</sub>) value at 3.5 ppm downfield from the water signal was obtained by calculating the difference in signal intensity (SI) at  $\pm 3.5$  ppm on both sides of the water center frequency in the Z-spectrum. MPM assumes the magnetization transfer (MT) between free water pool, APT pool and binding water MT pool. "APT density" x "APT transfer rate" x ("Free water T1" or "T2") was visualized as APT\_T1 or APT\_T2, respectively. The MT image is obtained via MPM fitting. Firstly, the maximum values of the parameters (MTR<sub>asym</sub>, APT\_T1, APT\_T2, T2/T1 ratio, and MT) on CEST imaging were measured respectively by regions of interest (ROI) analysis. Secondly, ROIs of IVIM and 11C-MET PET/CT were placed in similar anatomical locations by visual assessment. ROIs were carefully placed in the solid component of a tumor and the best effort was given to avoid cystic components of the tumor. 11C-MET uptake was semiquantitatively assessed using tumor-to-contralateral normal brain tissue (T/N) ratio.

#### RESULTS

There were significant positive correlations between APT\_T1 and MET T/N ratio ( $r = 0.86$ ,  $p < 0.01$ ), APT\_T2 and MET T/N ratio ( $r = 0.42$ ,  $p < 0.05$ ), T2/T1 and ADC ( $r = 0.36$ ,  $p = 0.05$ ), T2/T1 and D ( $r = 0.41$ ,  $p < 0.05$ ), and MTR<sub>asym</sub> and MET T/N ratio ( $r = 0.51$ ,  $p < 0.01$ ). There existed significant negative correlations between APT\_T1 and ADC ( $r = -0.64$ ,  $p < 0.01$ ), APT\_T1 and D ( $r = -0.67$ ,  $p < 0.01$ ), APT\_T2 and D\* ( $r = -0.46$ ,  $p = 0.01$ ), and T2/T1 and MET T/N ratio ( $r = -0.37$ ,  $p < 0.05$ ).

#### CONCLUSION

These preliminary results suggest that parameters on CEST imaging by multi pool model seems to correlate with IVIM and 11C-MET uptake on PET/CT in patients with gliomas. Combining Multi-pool model-based CEST imaging, IVIM and 11C-MET PET/CT may improve the diagnostic ability of gliomas.

#### CLINICAL RELEVANCE/APPLICATION

Combining Multi-pool model-based CEST imaging, IVIM and 11C-MET PET/CT may improve the diagnostic ability of gliomas.

Printed on: 02/07/23

## Abstract Archives of the RSNA, 2022

S3B-SPNMMI-3

### Low-dose EDB Fibronectin Gd-DOTA Specific Probe for Pancreatic Cancer Targeting Magnetic-optical Dual-modality Imaging

Sunday, Nov. 27 12:15PM - 12:45PM Room: Learning Center - NMMI DPS

#### Participants

Wenjia Zhang, Beijing, China (*Presenter*) Nothing to Disclose

#### PURPOSE

Pancreatic ductal adenocarcinoma (PDAC) is a lethal malignancy worldwide. PDAC is a hypovascular tumor surrounded by dense stroma, which is recognized as a vital factor of tumor progression. Multimodal molecular imaging of onco-proteins is a promising method for accurate, early detection of the disease. Extradomain-B fibronectin (EDB-FN), a high-expression onco-protein in the tumor extracellular matrix, can realize targeted and effective molecular imaging. Here, we prepared a novel Gd-based contrast agent of EDB-Cy7 to perform fluorescence molecular imaging (FMI) and molecular MRI, in order to realize accurate, early and safe detection of PDAC.

#### METHODS AND MATERIALS

The EDB-FN targeting peptide and near infrared dye Cy7 were conjugated to the Gd-DOTA (EDB-Gd-Cy7) for the PDAC-targeting multimodality imaging. Five-week-old BALB/c nude mice were implanted with human pancreatic stellate cells (PSC) and human PDAC cell lines (Bxpc-3) to establish the subcutaneous and orthotopic PDAC models. Mice were intravenously injected with EDB-Gd-Cy7 or Gd-DOTA at the Gd concentration of 0.05 mmol/kg, which is merely a half of clinical dose. T1 mapping MRI and FMI were performed. The TBR (Tumor background ratio) of fluorescence intensity and the ratio of T1 value reduction (T1d%) were compared quantitatively. Histological and immunofluorescence analyses were used as references for ex vivo validation.

#### RESULTS

The concentration of EDB-Gd-Cy7 showed a correlation with fluorescence intensity and T1 relaxation time in vitro. For in vivo MRI, the T1d% showed the most significant difference at 30 minutes post-injection in subcutaneous and orthotopic PDAC xenograft models. For in vivo FMI, at 30 minutes post-injection, the TBR of fluorescence intensity showed the most significant difference in subcutaneous models, while the TBR of fluorescence intensity showed no significant differences between two groups in orthotopic models. Immunofluorescence confirmed the targeting of EDB-Gd-Cy7 to EDB-FN in both PDAC models.

#### CONCLUSION

Our dual-modal imaging findings indicate that FMI and molecular MRI could complement its advantages and translation of oncoprotein targeted dual-modal imaging with low-dose EDB-Gd-Cy7 to humans, which might provide a promising imaging technique to detect PDAC precisely. Moreover, these findings suggest that EDB-FN targeting MRI might have clinical application to evaluate the tumor extracellular matrix and chemo-therapy efficacy in the future.

#### CLINICAL RELEVANCE/APPLICATION

Molecular MRI with the EDB-targeted probe provided robust detection of PDAC in two animal models and may enable non-invasive detection, precise staging and monitoring post-treatment fibrotic changes of PDAC compared to standard Gd-DOTA contrast agents.

Printed on: 02/07/23



## Abstract Archives of the RSNA, 2022

S3B-SPNPM

### Noninterpretive Skills/Quality Improvement/Practice Management Sunday Poster Discussions - B

Sunday, Nov. 27 12:15PM - 12:45PM Room: Learning Center - NPM DPS

#### Participants

Stefanie Woodard, DO, Birmingham, AL (*Moderator*) Investigator, Bracco Group Institutional research support, Bracco Group

#### Sub-Events

#### S3B-SPNPM-Artificial Intelligence Support in MR-Imaging of Renal Masses: A Primary Economic Evaluation<sup>1</sup>

##### Participants

Felix Gassert, MD, MBA, Munich, Germany (*Presenter*) Consultant, SmartReporting GmbH

#### PURPOSE

Unclear renal lesions often appear as incidental findings during various imaging procedures as they are common, especially in people over the age of 50. Correct differentiation between malignant and benign incidentally found renal lesions has critical implications for patient management. As shown in previous studies, modern artificial intelligence-based algorithms are on-par with or even exceed radiologists' performance in the differentiation of those lesions. Therefore, the aim of this study was to evaluate the cost-effectiveness of an AI-based system in the context of the evaluation of incidental renal masses based on MR images and define maximal possible costs for AI.

#### METHODS AND MATERIALS

For estimation of quality-adjusted life years (QALYs) and lifetime costs, a decision model was created, including the options MRI with and without applying an AI algorithm. For obtaining model input parameters, review of recent literature was performed. Willingness to pay (WTP) was set to \$100,000/QALY. Costs of \$0 were assumed in the base-case scenario and adapted accordingly in the sensitivity analysis. Model uncertainty and possible costs of the AI system were assessed using deterministic sensitivity analysis of diagnostic parameters and costs. Probabilistic sensitivity was determined using Monte Carlo modeling.

#### RESULTS

In the base-case scenario, total costs were at \$8054 for MRI and at \$7939 for the additional use of an AI-based algorithm, whereas the model yielded a cumulative effectiveness of 8.77 QALYs for both the use of MRI with and without the algorithm. Therefore, the incremental cost-effectiveness ratio was negative, and the use of AI was the dominant strategy from a cost-effectiveness point of view. Deterministic and probabilistic sensitivity analysis showed high robustness of the model with the incremental cost-effectiveness ratio remaining below the WTP for a wide range of variability of the input parameters. If increasing costs for the algorithm, the threshold of \$0 / QALY was exceeded at \$115, and the defined WTP was exceeded at \$667.

#### CONCLUSION

The use of AI-supported evaluation is feasible in classifying unclear renal masses using MRI from a cost-effectiveness point of view. Costs as high as \$667 for the algorithm can be accepted with high robustness of the model.

#### CLINICAL RELEVANCE/APPLICATION

The presented results have medical and economic impact on diagnostic workup of incidental renal masses and could help improve patient care by accelerating the translation of AI into clinical routine by proofing its cost-effectiveness.

#### S3B-SPNPM-To Explore the Effect of 70KVp Tube Voltage Coronary CTA Combined With Different Image Reconstruction Algorithms on the Image Quality of Overweight Patients<sup>2</sup>

##### Participants

Lijuan Zhu, (*Presenter*) Nothing to Disclose

#### PURPOSE

The purpose of this study was to investigate the effect of 70KV combined with DLIR and ASiR-V on the quality of CCTA images in overweight patients.

#### METHODS AND MATERIALS

A total of 48 overweight patients (24 kg/m<sup>2</sup> < BMI < 28.5 kg/m<sup>2</sup>) who underwent low-voltage CCTA with Revolution Apex CT in our hospital from September 2021 to January 2022 were selected, reconstructed with FBP, 40% weight, 80% weight ASiR-V and low-level (DLIR-L), medium-level (DLIR-M) and high-level respectively (DLIR-H) DLIR. The image noise of the aortic root and proximal main coronary artery of each group of images was recorded, and the SNR and CNR were calculated for subjective and objective images. Quality Evaluation. Subjective image quality was rated on a 5-point scale by two diagnostic radiologists with more than 5 years of experience.

#### RESULTS

1) The noise of FBP, ASiR-40%, ASiR-80%, DLIR-L, DLIR-M and DLIR-H decreased with the increase of reconstruction level (all  $P < 0.05$ ), and SNR and CNR gradually increased. For DLIR-H, it had an average increase of 13.81% and 79.23% compared with ASiR-80%. 2) For DLIR group, the scores of two observers, physician A and physician B, showed that the reconstruction weight increased with the increase of the reconstruction weight. Both observers believed that the best diagnostic effect was DLIR-H, which was better than DLIR-L increased by 20.32%, and the consistent Kappa value between the two observers was 0.857; for the ASiR-V, the two observers' scoring results showed that with the increase of the reconstruction weight, ASiR-80% On the contrary, the subjective image quality of ASiR-40% decreased by 4.47%, but the subjective image scores of both were higher than that of FBP, ASiR-40% increased by 43.28%, and ASiR-80% increased by 38.81% ( $P < 0.05$ ), and the consistent Kappa values between the two observers were greater than 0.8.

## **CONCLUSION**

As the weight of the ASiR-V reconstruction algorithm increases, the objective image evaluation improves. However, the excessive weight (ASiR-80%) changes the noise texture of the image, resulting in a decrease in the subjective score and affecting the diagnosis of the disease. Compared with the ASiR-V reconstruction algorithm, the DLIR algorithm can significantly reduce the noise of the CCTA image, improve the SNR and CNR of the image, and improve the subjective and objective image quality, without affecting the diagnosis of the disease. Overall, the DLIR algorithm has a high clinical application value.

## **CLINICAL RELEVANCE/APPLICATION**

By comparing the effects of ASiR-V and DLIR on conventional CCTA scan images of overweight patients under the condition of low tube voltage. The choice of reconstruction algorithms for patient CCTA scans offers more possibilities.

Printed on: 02/07/23

## Abstract Archives of the RSNA, 2022

S3B-SPNPM-1

### Artificial Intelligence Support in MR-Imaging of Renal Masses: A Primary Economic Evaluation

Sunday, Nov. 27 12:15PM - 12:45PM Room: Learning Center - NPM DPS

#### Participants

Felix Gassert, MD, MBA, Munich, Germany (*Presenter*) Consultant, SmartReporting GmbH

#### PURPOSE

Unclear renal lesions often appear as incidental findings during various imaging procedures as they are common, especially in people over the age of 50. Correct differentiation between malignant and benign incidentally found renal lesions has critical implications for patient management. As shown in previous studies, modern artificial intelligence-based algorithms are on-par with or even exceed radiologists' performance in the differentiation of those lesions. Therefore, the aim of this study was to evaluate the cost-effectiveness of an AI-based system in the context of the evaluation of incidental renal masses based on MR images and define maximal possible costs for AI.

#### METHODS AND MATERIALS

For estimation of quality-adjusted life years (QALYs) and lifetime costs, a decision model was created, including the options MRI with and without applying an AI algorithm. For obtaining model input parameters, review of recent literature was performed. Willingness to pay (WTP) was set to \$100,000/QALY. Costs of \$0 were assumed in the base-case scenario and adapted accordingly in the sensitivity analysis. Model uncertainty and possible costs of the AI system were assessed using deterministic sensitivity analysis of diagnostic parameters and costs. Probabilistic sensitivity was determined using Monte Carlo modeling.

#### RESULTS

In the base-case scenario, total costs were at \$8054 for MRI and at \$7939 for the additional use of an AI-based algorithm, whereas the model yielded a cumulative effectiveness of 8.77 QALYs for both the use of MRI with and without the algorithm. Therefore, the incremental cost-effectiveness ratio was negative, and the use of AI was the dominant strategy from a cost-effectiveness point of view. Deterministic and probabilistic sensitivity analysis showed high robustness of the model with the incremental cost-effectiveness ratio remaining below the WTP for a wide range of variability of the input parameters. If increasing costs for the algorithm, the threshold of \$0 / QALY was exceeded at \$115, and the defined WTP was exceeded at \$667.

#### CONCLUSION

The use of AI-supported evaluation is feasible in classifying unclear renal masses using MRI from a cost-effectiveness point of view. Costs as high as \$667 for the algorithm can be accepted with high robustness of the model.

#### CLINICAL RELEVANCE/APPLICATION

The presented results have medical and economic impact on diagnostic workup of incidental renal masses and could help improve patient care by accelerating the translation of AI into clinical routine by proofing its cost-effectiveness.

Printed on: 02/07/23

## Abstract Archives of the RSNA, 2022

S3B-SPNPM-2

### To Explore the Effect of 70KVp Tube Voltage Coronary CTA Combined With Different Image Reconstruction Algorithms on the Image Quality of Overweight Patients

Sunday, Nov. 27 12:15PM - 12:45PM Room: Learning Center - NPM DPS

#### Participants

Lijuan Zhu, (*Presenter*) Nothing to Disclose

#### PURPOSE

The purpose of this study was to investigate the effect of 70KV combined with DLIR and ASiR-V on the quality of CCTA images in overweight patients.

#### METHODS AND MATERIALS

A total of 48 overweight patients ( $24 \text{ kg/m}^2 < \text{BMI} < 28.5 \text{ kg/m}^2$ ) who underwent low-voltage CCTA with Revolution Apex CT in our hospital from September 2021 to January 2022 were selected, reconstructed with FBP, 40% weight, 80% weight ASiR-V and low-level (DLIR-L), medium-level (DLIR-M) and high-level respectively (DLIR-H) DLIR. The image noise of the aortic root and proximal main coronary artery of each group of images was recorded, and the SNR and CNR were calculated for subjective and objective images. Quality Evaluation. Subjective image quality was rated on a 5-point scale by two diagnostic radiologists with more than 5 years of experience.

#### RESULTS

1) The noise of FBP, ASiR-40%, ASiR-80%, DLIR-L, DLIR-M and DLIR-H decreased with the increase of reconstruction level (all  $P < 0.05$ ), and SNR and CNR gradually increased. For DLIR-H, it had an average increase of 13.81% and 79.23% compared with ASiR-80%. 2) For DLIR group, the scores of two observers, physician A and physician B, showed that the reconstruction weight increased with the increase of the reconstruction weight. Both observers believed that the best diagnostic effect was DLIR-H, which was better than DLIR-L increased by 20.32%, and the consistent Kappa value between the two observers was 0.857; for the ASiR-V, the two observers' scoring results showed that with the increase of the reconstruction weight, ASiR-80% On the contrary, the subjective image quality of ASiR-40% decreased by 4.47%, but the subjective image scores of both were higher than that of FBP, ASiR-40% increased by 43.28%, and ASiR-80% increased by 38.81% ( $P < 0.05$ ), and the consistent Kappa values between the two observers were greater than 0.8.

#### CONCLUSION

As the weight of the ASiR-V reconstruction algorithm increases, the objective image evaluation improves. However, the excessive weight (ASiR-80%) changes the noise texture of the image, resulting in a decrease in the subjective score and affecting the diagnosis of the disease. Compared with the ASiR-V reconstruction algorithm, the DLIR algorithm can significantly reduce the noise of the CCTA image, improve the SNR and CNR of the image, and improve the subjective and objective image quality, without affecting the diagnosis of the disease. Overall, the DLIR algorithm has a high clinical application value.

#### CLINICAL RELEVANCE/APPLICATION

By comparing the effects of ASiR-V and DLIR on conventional CCTA scan images of overweight patients under the condition of low tube voltage. The choice of reconstruction algorithms for patient CCTA scans offers more possibilities.

Printed on: 02/07/23

## Abstract Archives of the RSNA, 2022

S3B-SPNR

### Neuroradiology Sunday Poster Discussions - B

Sunday, Nov. 27 12:15PM - 12:45PM Room: Learning Center - NR DPS

#### Participants

Tanvir Rizvi, MD, MBBS, Charlottesville, VA (*Moderator*) Nothing to Disclose

#### Sub-Events

### S3B-SPNR-1 Volume and Permeability of White Matter Hyperintensity on Cognition: A DCE Imaging study in A Prospective Elderly Cohort

#### Participants

Hyeongwoo Kim, MD, Seoul, Korea, Republic Of (*Presenter*) Nothing to Disclose

#### PURPOSE

We aimed to evaluate the relationship between volume, permeability, and the effect of white matter pathology on cognition in elderly patients with mild to moderate WMH from a prospective elderly cohort.

#### METHODS AND MATERIALS

In this IRB-approved retrospective analysis of the prospective study, written informed consent was obtained from all participants. We selected 193 elderly participants of the age range (55-80 years) with minimal-to-moderate WMH from a prospective DCE MRI cohort (n=259) with normal and impaired cognition between August 2017 and June 2021. Periventricular WMH (PWMH), deep WMH (DWMH), and normal-appearing white matter (NAWM) were automatically segmented using a 3D T1-weighted sequence. Volume transfer constant [Ktrans] as BBB permeability was determined using DCE MRI. The effects of Ktrans of WMH and NAWM were evaluated using multivariable linear regression adjusted for demographic and volume measures.

#### RESULTS

and volume measures. 193 participants (age, 70.1±6.8 years; 128 women) include 44 with CDR=0, 119 with CDR=0.5, and 30 with CDR=1.0. The degree of WMH was minimal (n=87) and moderate (n=106). Higher Ktrans was observed in PWMH ( $0.598 \pm 0.509 \times 10^{-3} \text{ min}^{-1}$ ) compared to DWMH ( $0.496 \pm 0.478 \times 10^{-3} \text{ min}^{-1}$ ) and NAWM ( $0.476 \pm 0.398 \times 10^{-3} \text{ min}^{-1}$ ) ( $p < 0.001$ ). The strong negative correlation between Ktrans and the volume was noted in PWMH ( $\rho = -0.357$ ,  $p < 0.001$ ) and DWMH ( $\rho = -0.200$ ,  $p = 0.005$ ), but not in NAWM ( $\rho = 0.053$ ,  $p = 0.460$ ). After adjusting for age, sex, APOE4, education, cortex volume, PWMH volume (B = -0.0008, SE = 0.0002, beta = -0.363,  $p < 0.001$ ) and history of cardiovascular disease (B = 0.0066, SE = 0.0028, beta = 0.229,  $p < 0.021$ ) were predictive factors for Ktrans of PWMH ( $R^2 = 0.191$ ,  $F(2, 86) = 10.153$ ,  $p < 0.001$ ). After adjusting for covariates, only history of cardiovascular disease was the predictor for Ktrans of NAWM ( $R^2 = 0.036$ ,  $F(1, 153) = 5.740$ ,  $p < 0.018$ ). After adjusting covariates (age, sex, and APOE4 status), hippocampal volume ( $p < 0.001$ ), and PWMH volume (along with education level were independent predictors of worse cognition (CDR-SB = 3), whereas cortex volume and Ktrans of PWMH were not.

#### CONCLUSION

We found higher permeability of PWMH compared to DWMH and NAWM and a negative relationship between its permeability and volume. The volume of PWMH is the predictor of worse cognition in elderly individuals. Further, our finding suggests that WMH permeability and WMH volume change may be independent events.

#### CLINICAL RELEVANCE/APPLICATION

Our findings suggest the different underlying pathophysiology of PWMH and DWMH. In addition, the volume of PWMH predicts worse cognition in elderly individuals.

### S3B-SPNR-10 Assessment of White Matter Lesion Volume and Disability in Neuromyelitis Optica Spectrum Disorder

#### Participants

Jitlada Kusol, MD, Bangkok Noi, Thailand (*Presenter*) Nothing to Disclose

#### PURPOSE

Neuromyelitis optica spectrum disorder (NMOSD) is an aquaporin-4 (AQP4) antibody-mediated disease, affecting the white matter (WM). However, how burden of WM correlates to outcome is yet to be studied. The purposes of this study were to measure white matter lesion volume (WMLV) at locations with high AQP4 expression and to study its association to disability and disease progression.

#### METHODS AND MATERIALS

Retrospective review of 32 NMOSD patients who underwent two consecutive brain MRI scans with = 1-year interval were performed. Patients were categorized into low EDSS group (EDSS=3, n=15) and high EDSS group (EDSS=3.5, n=17). Disease progression (sustained increase in EDSS) was also significant parameter. WMLV were measured and categorized into five locations (diencephalic, dorsal brainstem, callosal/periventricular, hemispheric WM and corticospinal tract). Changes in WMLV in

mentioned locations were also defined.

## RESULTS

WMLV was significantly larger in the high EDSS group at the callosal/periventricular, hemispheric WM and corticospinal tract ( $p < 0.001$ ,  $0.041$  and  $0.025$ , respectively). In addition, the high EDSS group showed the lower change in the WMLV at hemispheric WM over the follow-up period ( $p = 0.044$ ). Patients with disease progression (6.3%) had higher WMLV at callosal/periventricular area than those without progression ( $p = 0.024$ ).

## CONCLUSION

Greater WMLV at callosal/periventricular, hemispheric WM and corticospinal tract related to the higher disability in NMOSD patients. In addition, higher WMLV at callosal/periventricular region may predict the development of disease progression. Our findings reflect that higher WMLV may correlate to worse clinical outcome.

## CLINICAL RELEVANCE/APPLICATION

Higher WMLV in NMOSD patients may correlate to worse clinical outcome, especially at callosal/periventricular, hemispheric WM and corticospinal tract.

## S3B-SPNR-11 Altered Vascular Permeability in Autoimmune Encephalitis: Region-based Evaluation with Dynamic Contrast-enhanced MRI and Automatic Whole Brain Segmentation

Participants  
Sohyun Ji, MD, MD, (Presenter) Nothing to Disclose

## PURPOSE

To evaluate the change in permeability of brain-blood barrier (BBB) in patients with autoimmune encephalitis, as compared with the healthy control group, by using dynamic contrast enhanced MRI (DCE-MRI) and to explore its predictive value for the treatment response in the patients.

## METHODS AND MATERIALS

In this retrospective study, a total of 38 patients with probable or possible autoimmune encephalitis and 15 healthy controls underwent DCE-MRI between April 2020 and May 2021. Automatic volumetric segmentation was performed on pre-/postcontrast T1-weighted images by using FreeSurfer, and encephalitis-associated brain region masks were extracted by using the software NordicICE. Ktrans maps, derived from DCE-MRI using Patlak model, were coregistered with the region-of-interest masks to calculate their mean values at the total volume of interest. The Wilcoxon rank sum test and Friedman test were used to compare Ktrans. Receiver operating characteristic curve analysis was used to assess the diagnostic performance.

## RESULTS

All brain regions showed significantly increased Ktrans in the patients, as compared with the controls ( $P < .05$ ). The right cerebral cortex ( $1.232$  vs.  $0.0003$   $\text{min}^{-1}$ ) and right nucleus accumbens ( $0.371$  vs.  $0.0002$   $\text{min}^{-1}$ ) had the largest mean difference of Ktrans between the patients and controls, followed by the right parahippocampus and right occipital lobe. The same trends were observed in each autoimmune encephalitis subtype (anti-LGI1, anti-NMDAR, and antibody-negative). No significant differences in Ktrans were found between the baseline and follow-up. Poor treatment response group had significantly higher baseline Ktrans in all brain regions ( $P < .05$ ), as compared with good treatment response group, except for the right nucleus accumbens ( $P = 0.33$ ) and right cerebral cortex ( $P = 0.08$ ). At the cutoff value of  $0.002$   $\text{min}^{-1}$ , sensitivity and specificity for the prediction of treatment response were 86% and 100%, respectively for the left cerebellar cortex.

## CONCLUSION

The BBB permeability was persistently increased in all brain regions in autoimmune encephalitis patients, as compared with controls, and baseline Ktrans were higher in patients with poor treatment outcome.

## CLINICAL RELEVANCE/APPLICATION

Autoimmune encephalitis patients showed increased BBB permeability in all brain regions, and the increased permeability of BBB was associated with treatment response.

## S3B-SPNR-13 A Review of The Appropriateness of Magnetic Resonance Imaging for Optic Neuritis in A Tertiary Referral Center in The West of Ireland

Participants  
Richard Faran, MBCh, BSc, (Presenter) Nothing to Disclose

## PURPOSE

Optic neuritis is a clinical condition which involves inflammation of the optic nerves. It is often seen concurrently with central nervous system (CNS) demyelination and there is well known link with multiple sclerosis. <sup>1</sup> The purpose of this study was to evaluate the appropriateness of magnetic resonance imaging of the CNS in patients with confirmed optic neuritis.

## METHODS AND MATERIALS

The study retrospectively reviewed MRI requests for patients with optic neuritis over a five-year period at University Hospital, Galway. Our institution is a tertiary referral center with neurology expertise in the west of Ireland. The study established which CNS imaging was requested by neurologists. Additionally, the final radiology reports were reviewed to establish if the imaging technique diagnosed any relevant positive findings.

## RESULTS

MRI brain and Orbits was the most commonly ordered investigation with neurologists requesting this study in 89 patients. Of these, 40 patients (44.9%) showed patterns consistent with optic neuritis. MRI orbits (alone) was the second most commonly requested imaging. 45 MRI patients underwent MRI orbits with relevant changes reported in 16 (35.6%) patients. MRI C-spine was performed on 47 patients with 12 (25.5%) showing significant changes. MRI T-spine was the least common investigation ordered with 10

patients undergoing such. From these, only 1 patient (10%) showed significant change on imaging.

## CONCLUSION

The purpose of this study was to establish how much imaging of the CNS is justified in patients with optic neuritis. MRI brain and orbits were the most prevalent imaging ordered. Their role in investigating patients with optic neuritis is largely justified with changes such as plaque accumulation and demyelination patterns noted in a significant portion of patients. Of note, only 10% of patients with optic neuritis had positive findings on MRI T-spine. This raises the question of whether MRI T-spine should be included in imaging work up for optic neuritis. Strengths of this study include relatively large sample size (n= 191), 5 year timeframe and significance of the hospital site as a tertiary referral center in the west of Ireland.

## CLINICAL RELEVANCE/APPLICATION

In conclusion, our study shows that MR imaging of brain and Orbits is justified when investigating patients with optic neuritis. Imaging the C-spine is justified in some circumstances. Our study shows that due to the low yield, MRI Thoracic spine is not justified in most cases. Requesting MRI T-Spine in most cases leads to unnecessary investigation and associated delay in patient flow and associated costs. We recommend that protocols should be in place to ensure MRI T-spine is only requested in very specific cases, upon discussion with senior neurologists.

## S3B-SPNR- Enlarged Choroid Plexus Related with Whole Brain Atrophy in Multiple Sclerosis 14

Participants  
Xiao Chen, MS,MS, Chongqing, China (*Presenter*) Nothing to Disclose

## PURPOSE

This study aims to investigate the alteration of choroid plexus volume and whole brain morphology in patients with MS and neuromyelitis optica spectrum diseases (NMOSD).

## METHODS AND MATERIALS

Fifty-one patients with MS, 42 patients with NMOSD and 56 healthy controls (HC) were recruited, of which 25 patients with MS and 20 patients with NMOSD were followed up. T2 FLAIR, 3DT1 image data and related clinical data were collected. The morphological changes of choroid plexus and whole brain tissue (ventricular system volume, sulcus cortex thickness, gyrus cortex thickness and deep gray matter volume) were compared between three groups and the correlation between choroid plexus volume and brain atrophy were further investigated.

## RESULTS

Compared with the HC group, the volume of choroid plexus was increased in the MS group ( $P<0.001$ ), but not in the NMOSD group. The MS group showed the whole-brain atrophy (increased ventricle system volume, reduced cortex thickness and deep gray matter volume) and the distribution of cortical atrophy in the sulcus area (61%, 41/67) was greater than that in the gyrus area (43%, 29/67). The NMOSD group showed mild brain atrophy related with increased third ventricle volume and decreased deep gray matter volume. In MS group ( $P<0.05$ ,  $r=-0.292\sim-0.538$ ) and NMOSD group ( $P<0.05$ ,  $r=-0.325\sim-0.572$ ), there were widespread correlations between choroid plexus volume and cerebral cortex thickness. In MS, compared with the baseline, the right nucleus accumbens and total deep gray matter brain volume were decreased ( $P<0.001$ ), and bilateral lateral ventricle volume were increased ( $P<0.001$ ) in follow-up. There was no significant alteration between baseline and follow-up in the NMOSD group.

## CONCLUSION

MS patients show enlarged choroid plexus related with whole brain atrophy, while the NMOSD patients show local brain atrophy. In the short-term follow-up, the brain atrophy in MS patients was gradually aggravated, and there was no obvious alteration in NMOSD patients.

## CLINICAL RELEVANCE/APPLICATION

A combined MRI and PET study showed that the increased choroid plexus tissue was significantly positively correlated with the expression of inflammatory factors, indicating that the mechanism based on the choroid plexus blood-cerebrospinal fluid barrier may play an important role in MS. The choroid plexus blood-cerebrospinal fluid barrier comprises a single layer of choroid plexus epithelial cells, which separates blood-borne substances from cerebrospinal fluid. Therefore, the choroid plexus blood-cerebrospinal fluid barrier may also play an important role in maintaining the stability of the brain environment.

## S3B-SPNR- Safety and Effectiveness of First-line Endovascular Management of Low-Grade Brain Arteriovenous Malformations: A Single Center Experience in 145 Patients 15

Participants  
Maichael MEKHAIL, (*Presenter*) Nothing to Disclose

## PURPOSE

Spetzler-Martin grade (SMG) I-II (low-grade) brain arteriovenous malformations (BAVMs) are often considered safe for microsurgical resection. However, the role of endovascular treatment (EVT) remains to be clarified in this indication, especially for unruptured BAVMs. The purpose of our study was to assess the safety and effectiveness of endovascular treatment as the first-line therapy for low-grade BAVMs.

## METHODS AND MATERIALS

From our local database, we retrospectively retrieved patients with low-grade BAVMs, either ruptured or unruptured, treated by embolization as first-line therapy in our department between January 2005 and January 2020. The primary endpoint was the total obliteration rate of BAVMs, and secondary endpoints were hemorrhagic complications, final clinical outcome, assessed through shift of the modified Rankin Scale, and mortality rate secondary to BAVM embolization.

## RESULTS

One hundred-forty-five patients meeting inclusion criteria and treated by EVT as first-line therapy were included in the study (82 ruptured and 63 unruptured BAVMs). Overall, complete exclusion of BAVMs was achieved in 110 patients (75.9%); 58 patients (70.7%) among ruptured BAVMs and 52 (82.5%) among unruptured ones, including 37.9% BAVMs excluded by EVT alone (35.5%

among ruptured BAVMs and 44.4% among unruptured ones) and 38% by combined treatment (EVT and surgery or EVT and SRS). There was no BAVM volume cut-off predictive for total obliteration by embolization alone. Early minor hemorrhagic complications were reported in 14 patients (9.6%) and early major hemorrhagic complications were reported in 5 patients (3.4%). No late hemorrhagic complications (0%) occurred; mortality rate was 0.7% (1/145 patients). Improved /unchanged mRS was reported in 137 patients (94.5%).

## CONCLUSION

s Endovascular treatment, alone or associated with others exclusion techniques, might be safe and effective for complete exclusion of low-grade brain arteriovenous malformations regardless of their volumes.

## CLINICAL RELEVANCE/APPLICATION

KEY WORDS Brain arteriovenous malformations, Endovascular treatment, Surgery, Pressure cooker technique.

## S3B-SPNR- Variations in Temperature Changes with SAR, B1+rms and Pulse Sequence: A Need for Caution? 16

Participants

David Gultekin, PhD, (*Presenter*) Nothing to Disclose

## PURPOSE

The applications of high field magnetic resonance imaging (MRI) are limited partly by considerations of radiofrequency (RF) safety and the design of RF systems. A current dilemma in moderate to high field MRI (3T to 9.4T) is how to optimize image quality and productivity while maintaining safety. Often one may be improved at the expense of other factors. There is growing interest in assessing the utility of temperature (T) and time (t) diagrams (T-t), specific absorption rate (SAR) and RF field (B1+rms) to monitor RF absorption and thermal hazards in tissues especially in the presence of conductive implants.

## METHODS AND MATERIALS

A phantom consisting of a conductive metallic wire in a tissue equivalent gel is used in this study. Any conductive wire such as a lead used for deep brain stimulation (DBS) with four electrodes or a half wavelength ( $l/2$ ) copper (Cu) or titanium (Ti) wires can be used as probes for monitoring the effects of RF using fiber optic temperature probes. Standard imaging sequences (functional, morphological, diffusion and perfusion) were implemented on a 3T Siemens Prisma MRI with a TEM RF transmit body coil interfaced with a 43.2 kW peak power transmitter amplifier and a 64-channel head and neck coil (64-H/N) for receiving the RF signals.

## RESULTS

The T-t diagrams can be used to assess different protocols for the scenario of slow imaging, allowing for cooling time between sequences, and of fast imaging, without allowing for cooling times. T-t diagrams were acquired for pairs of sequences with the same SAR and B1+rms but different RF exposure times (NA), different SAR, B1+rms and exposure time, and different SAR, B1+rms but the same exposure time. The functional, morphological, diffusion and perfusion MRI sequences show the utility of the each of T-t diagrams, B1+rms and SAR. The integration of T-t diagrams for the slow and fast imaging segments of the same fMRI series shows the conservation of thermal dose in two scenarios.

## CONCLUSION

s We show that T-t diagrams provide additional important information about thermal effects of RF heating that SAR and B1+rms alone cannot provide. By keeping SAR and B1+rms the same but increasing NA increases exposure time resulting in a substantially higher temperature rise with time. A practical method involving temperature and time diagrams can be used to evaluate, compare and optimize various imaging protocols to ensure patient safety.

## CLINICAL RELEVANCE/APPLICATION

This method can further be developed to scan patients with implants safely.

## S3B-SPNR- Dual-layer Detector Cone-beam CT Angiography Improves Intracranial Vessel Conspicuity and Reduces Artifacts 17

Participants

Fredrik Stahl, MD, (*Presenter*) Fredrik Ståhl has received reimbursements for conference travel expenses from Philips in 2022

## PURPOSE

To evaluate whether a dual-layer detector cone-beam CT prototype improves image quality in stroke patients, compared to reference standard single layer detector cone-beam CT angiography.

## METHODS AND MATERIALS

A prospective single center clinical trial (NCT04571099) enrolled consecutive patients, 50 years or older with ischemic or hemorrhagic stroke. Patients were subsequently imaged with the prototype system following an intravenous contrast media injection. Single layer (Front layer, FL) and 70 keV virtual monoenergetic images (VMI) derived from both detector layers were reconstructed and evaluated in a single-sequence two-period crossover design by two blinded neuroradiologists. Sixteen intracranial arterial segments were evaluated for vessel conspicuity and artifact presence on 5-point Likert scales (5: highest vessel conspicuity or fewest artifacts). The Wilcoxon matched-pairs signed-rank test was performed to determine significance ( $p < 0.05$ ), with Bonferroni correction for multiple tests.

## RESULTS

28 patients were enrolled. The median conspicuity of the sixteen FL and VMI arterial vessel segments for each patient was 3.5 (IQR 2-4) and 4 (IQR 3-5),  $p < 0.001$ . The median artifact ratings for FL and VMI were 3 (IQR 2-4) and 4 (IQR 3-5),  $p < 0.001$ . For individual segments the VMI showed superior conspicuity for the Basilar, SCA, M4- and P1- segment ( $p < 0.001$ ), as well as the P2- and M3- segment ( $p < 0.01$ ). The P1-segment ( $p < 0.001$ ) and Basilar, SCA, M1-, M3-, M4-, P2-, A1- and A2-segment ( $p < 0.01$ ) had a significantly lower degree of artifacts in VMI compared to FL.

## CONCLUSION

s Dual-layer detector cone-beam CT virtual monoenergetic images improves intracranial vessel conspicuity and reduces artifacts

s Dual-layer detector cone-beam CT virtual monoenergetic images improves intracranial vessel conspicuity and reduces artifacts compared to reference standard single layer detector cone-beam CT angiography.

#### **CLINICAL RELEVANCE/APPLICATION**

Cone-beam CT angiography is increasingly used in the primary diagnostic work-up of suspected ischemic stroke, and could be an alternative to CT angiography to shorten door to thrombectomy time. Our findings indicate that dual-layer detector cone-beam CT angiography improves intracranial image quality over standard single-layer cone-beam CT angiography.

#### **S3B-SPNR-18 Efficacy and Safety of Endovascular Trans-venous Embolization of Cerebrospinal Fluid-venous Fistulas Associated with Spontaneous Intracranial Hypotension**

Participants

Donna Parizadeh, MD, (*Presenter*) Nothing to Disclose

#### **PURPOSE**

To independently evaluate the efficacy and safety of endovascular transvenous embolization for treatment of patients with spontaneous intracranial hypotension (SIH) secondary to CSF-venous fistulas (CVF).

#### **METHODS AND MATERIALS**

We performed a retrospective review of a prospectively maintained database of patients with 1) clinical diagnosis of SIH and 2) definitive diagnosis of CVF on either lateral decubitus digital subtraction myelogram or CT myelogram who underwent 3) transvenous embolization for treatment of CVF at our institute between Dec. 2020 to Apr. 2022. To evaluate efficacy of the procedure, we assessed pre- and 3-month post-embolization clinical and imaging outcomes including Headache Impact Test (HIT-6) and Patient Global Impression of Change (PGIC) scores, and the Bern SIH score on brain MRI. Procedural and post-procedural complications were recorded. Post-embolization change in measures was assessed with Wilcoxon Signed rank test.

#### **RESULTS**

A total of 19 patients, median (IQR) age 60 (49-65) years, 74% female, underwent transvenous embolization. At 3-month follow-up, 18/19 (95%) of patients reported having either much or very much improved symptoms on PGIC. Follow-up HIT-6 and imaging were available for 18 and 15 patients, respectively. Among these patients, headache improved significantly from a median (IQR) HIT-6 score of 68 (58-72) pre-embolization to 36 (36-38) post-embolization ( $p = 0.001$ ). Bern SIH score improved significantly from median (IQR) of 8 (6-8) pre-embolization to 2 (1-3) post-embolization ( $p = 0.001$ ). One (5%) patient did not have improvement of clinical or imaging findings consistent with a treatment failure. There were no neurovascular complications. Side effects were localized back pain (84%) and rebound headache (74%) which resolved within one month with medical treatment in all cases.

#### **CONCLUSION**

s Transvenous embolization is a highly efficacious and safe treatment for CVF in SIH patients.

#### **CLINICAL RELEVANCE/APPLICATION**

Transvenous embolization is emerging as a novel highly efficacious, safe, and minimally invasive treatment for patients with spontaneous intracranial hypotension secondary to CSF-venous fistula.

#### **S3B-SPNR-19 Clinical and Imaging Outcomes of Percutaneous Sclerotherapy for Venous Malformations Affecting the Eye and Orbit**

Participants

Tushar Garg, MD, Baltimore, MD (*Presenter*) Conference Travel, Siemens Healthineers

#### **PURPOSE**

Sclerotherapy treatment can be used for patients with venous malformations (VMs) affecting the eye and orbit region. This study evaluates the safety and outcomes of these interventions.

#### **METHODS AND MATERIALS**

All patients who received sclerotherapy for VMs involving the eye and orbit between 12/2005 to 6/2021 were reviewed. The clinical and imaging findings of these patients were assessed. Clinical symptoms response was classified as resolved, improved and stable, or worsened. Differences between pre-and post-procedure MRI of the largest lesion diameter in one plane were used to calculate changes in VM size, similar to the response evaluation criteria in solid tumors: complete response (100% reduction), partial response (30% reduction), stable disease ( $=30\%$  reduction or  $=20\%$  enlargement), progressive disease ( $=20\%$  VM size increase) worse. SIR classification criteria were used to classify adverse events. Clinical response, lesion size changes, and complication rates were evaluated. Fisher's Exact Test- was used for statistical analysis.

#### **RESULTS**

13 patients (53.8% F) underwent a total of 32 embolization procedures with an average follow up period of 1344.5 days. The most common presenting symptoms were enlargement (6,46.2%) and functional deficit (6, 46.2%). Other common complications included pain (5; 38.5%), mass (4; 30.8%), cosmetic deformity (3; 23.1%), discoloration (3; 23.1%), bleeding/ discharge (1; 7.7%) or other (1, 7.7%). Patients had an average of 2.46 (med: 2) procedures with a technical success rate of 100% (32/32). Embolization did not significantly decrease VM size on imaging ( $p=0.4762$ ). 11 patients (11/13; 84.6%) had both pre- and post- MRI imaging measurements. Of these, zero patients saw complete response, 2 patients (18.2%) experienced partial response, 6 patients (54.5%) experienced no change in VM size, and 3 patients (27.3%) saw increased VM size. There was only one (3.1%) incident of early (30 days) post-procedural complications (delayed extubation) among a total of 32 procedures. The most common sclerosants used were bleomycin foam (8, 25.0%) and sotradecol (8, 25%). This was followed by ethanol (4, 12.5%), n-BCA (4, 12.5%), onyx (2, 6.3%) and coils (1, 3.1%). Some procedures used more than one agent. Sclerotherapy significantly improved clinical symptoms with 7.7% (1/13) resolved, 30.8% (4/13) improved, and 61.5% (8/13) stable or worsened ( $p = 0.0391$ ).

#### **CONCLUSION**

s This study shows that sclerotherapy of venous malformations within the eye and orbit is a safe and effective treatment.

## CLINICAL RELEVANCE/APPLICATION

The results of this study showed that sclerotherapy can be used for the management of VMs involving the eye and orbit without the need for more invasive surgical management.

### S3B-SPNR-20 Percutaneous Sclerotherapy for Superficial Venous Malformations Involving the Tongue: Clinical and Imaging Outcomes

Participants

Anna Gong, Baltimore, MD (*Presenter*) Nothing to Disclose

## PURPOSE

To assess the safety and effectiveness of percutaneous sclerotherapy (PS) of venous malformations (VMs) involving the tongue.

## METHODS AND MATERIALS

Between 7/2004 and 8/2021, we reviewed all patients who received PS for VMs of the tongue. Clinical response, lesion size changes, and complication rates were evaluated using clinical and imaging results. The type of sclerosant was used to sub-stratify analysis. For statistical analysis, Fisher's Exact Tests were applied. The severity of clinical symptoms was graded as resolved, improved, and stable/worsened. The difference between pre and post procedure MRI of the largest lesion diameter in one plane was used to calculate VM size change, similar to the response evaluation criteria in solid tumors: complete response (CR, 100% reduction), partial response (PR, 30% reduction), stable disease (SD, =30% reduction or =20% enlargement), progressive disease (PD, =20% VM enlargement) worse. Adverse events were scored using SIR classification criteria.

## RESULTS

A total of 58 embolization procedures were performed in 26 patients (80.8% F), with a mean follow-up duration of 975 days. Pain (14, 24.1%), enlargement (12, 20.7%), difficulty with mastication (7, 12.1%), difficulty with speaking (7, 12.1%), and difficulty swallowing (7, 12.1%) were the most prevalent presenting complaints. Patients underwent a median of 3 procedures (range:1-6) with a 100% technical success rate. Bleomycin foam (51, 64.5%) was the most commonly deployed sclerosant, followed by ethanol (26, 32.9%), and sotradecol foam (14, 17.7%), with some procedures using multiple agents. Sclerotherapy significantly improved clinical symptoms with 15.4% resolved (4, 15.4%), 53.8% improved (14, 53.8%), and (8,30.8%) stable or worsened ( $p < 0.0001$ ). On imaging, embolization demonstrated significant reduction in lesion size ( $p=0.0184$ ). Of the 17 (65.4%) patients who had both pre and post MR measurements, 0 patients had a complete response, 6 patients (35.3%) showed a PR, 11 patients (64.7%) showed no change in VM size, and 0 patients showed increased VM size. Early (30 day) post-procedural complications occurred after 3 of 58 procedures (5.2%), the majority of which were skin burns.

## CONCLUSION

s Percutaneous sclerotherapy significantly decreases lesion size and improves clinical symptoms of VMs involving the tongue.

## CLINICAL RELEVANCE/APPLICATION

Percutaneous, image-guide sclerotherapy is a safe and effective treatment for low-flow, venous malformations involving tongue.

### S3B-SPNR-3 Alterations of Cerebral Perfusion and Functional Connectivity in Children with Idiopathic Generalized Epilepsy

Participants

Guiqin Chen, (*Presenter*) Nothing to Disclose

## PURPOSE

Previous studies have demonstrated that adults with idiopathic generalized epilepsy (IGE) have functional abnormalities, however, the neuropathological pathogenesis differs between adults and children. This study aimed to explore the alterations of cerebral blood flow (CBF) and functional connectivity (FC) simultaneously to comprehensively understand the neuropathological mechanisms of IGE in children.

## METHODS AND MATERIALS

Arterial spin labeling (ASL) and blood oxygenation level-dependent magnetic resonance imaging data were acquired for 28 patients with IGE and 35 matched healthy controls (Table 1). Using ASL perfusion, we identified several regions of altered CBF in patients with IGE. Seed-based whole-brain FC analysis was then performed on regions with significant CBF changes. Multiple comparisons were corrected using a voxel-wise Gaussian random field method ( $P < 0.05$ , two tailed). The mean CBF and FC of each cluster with significant group differences were extracted and correlated with the clinical variables in the IGE group using Pearson's correlation analysis.

## RESULTS

Compared to controls, patients with IGE showed abnormalities in CBF, mainly located in the right middle temporal gyrus, right middle occipital gyrus (MOG), right superior frontal gyrus (SFG), and left inferior frontal gyrus, triangular part (IFGtriang) (Table 2, Figure 1). Based on these four regions, we constituted the whole-brain FC and observed that the FC between the left IFGtriang and calcarine fissure (CAL) was decreased, (Figure 2A) and the FC between the right MOG and bilateral CAL was decreased (Figure 2B). Correlation analyses indicated that hyperperfusion in the right SFG was correlated with IGE age of onset ( $r= -3.81$ ,  $P=0.045$ ) (Figure 3A), and decreased connectivity in the left CAL was correlated with the IGE patient's duration ( $r=-4.20$ ,  $P=0.026$ ) (Figure 3B).

## CONCLUSION

s The study findings suggest simultaneous alterations in both CBF and FC in the left IFGtriang and right MOG in children with IGE by combining ASL and rs-fMRI, and the abnormal brain area is associated with duration.

## CLINICAL RELEVANCE/APPLICATION

The combination of CBF and FC not only describe and track the progress of the disease, provide imaging basis for early diagnosis of IGE, but also can provide complementary information and comprehensive insights into the pathophysiology of IGE from the perspective of neuronal and vascular integration.

### **S3B-SPNR-4 Bitmap 3D Printing of Multimodal Imaging for Epilepsy Surgery**

Participants

Nicholas Jacobson, (*Presenter*) Nothing to Disclose

#### **PURPOSE**

Surgical Planning for epilepsy requires the sequential review of multiple volumetric and vector-based datasets. This data is viewed sequentially on a 2D screen, requiring significant visuospatial memory to composite and spatially reconstruct. The presurgical data review process has thus become increasingly inefficient and does not provide a holistic visualization of the data. This worrisome trajectory ignores the biggest promise of the information revolution: increased communication, connectivity, and interoperability. This cognitive load can be reduced by combining multimodal volumetric images with a 3D printed model. We present a method for creating a presurgical planning model that combines T1 MRI, CT SEEG data, tractography, and fMRI from pediatric epilepsy patients. The purpose is to reduce the cognitive load on surgeons and facilitate focused communication between the entire epilepsy team.

#### **METHODS AND MATERIALS**

16 bit image data, CT/MRI/fMRI, is mapped to color and opacity material mixing ratios corresponding to DICOM intensity values. 256 bit vector field data, Tractography/SEEG activation, is composited onto the image data in 3D voxel space. The composited multimodal 3D model is sliced for 3D printing in a voxel-based modeling program. The bitmap slices are printed at the spatial resolution of the images in a multi-material polyjet 3D printer. The model is reviewed during surgical conferences and used during a procedure in a clinical study (n=15).

#### **RESULTS**

Our method embeds vector-based features, representing dynamic physiology, within image-based models that represent gradients in biological tissue. The results leverage color-encoded data, displaying composited MRI, CT SEEG probes and activation, DWI tractography, and fMRI information. The models were used in discussion during case conferences and surgery. Preliminary survey results indicate increased spatial understanding and confidence in the surgical approach.

#### **CONCLUSION**

s We show that a variety of computationally derived physiologic datasets found in medical imaging can be directly 3D printed for neurosurgical epilepsy interventions. The relationships between data visualization, computer science, digital fabrication, and medicine are fostering an information revolution with the potential for increased communication, connectivity, and interoperability of data, bringing form and function together to improve health.

#### **CLINICAL RELEVANCE/APPLICATION**

The multimodal models unify and express more of the ever-increasing amount of data in surgical planning. The models are developing a platform that can be extended to study disease states that require information from multiple modalities of images.

### **S3B-SPNR-5 Clinical Significance of Hippocampal Asymmetry as a Sole Imaging Finding in Patients with Seizure**

Participants

Hasan Azeem Khan, MD, Galveston, WV (*Presenter*) Nothing to Disclose

#### **PURPOSE**

Hippocampal volume loss on MRI (Magnetic Resonance Imaging) is described as potential source or sequelae of seizure. Since the introduction of post processing automated volumetric techniques, there has been a reliable and objective method to assess hippocampus volume. Hippocampal asymmetry in the context of normal volume of individual hippocampi is an uncommon finding observed on volumetric studies of brain MRI performed for evaluation of seizure. The clinical significance and correlation of hippocampal asymmetry with seizures and EEG findings are lacking. We set out to create a study that evaluates the relationship between asymmetric otherwise normal hippocampi and seizures.

#### **METHODS AND MATERIALS**

We gathered data on 49 patients from 1257 brain MRIs performed for evaluation of seizure over the past 3 years. The total 49 patients are divided into two groups. A group of 25 patients with hippocampal asymmetry diagnosed on MRI using the Neuroquant protocol and a comparison group of 24 patients with symmetrical hippocampi. This included data of left/right hippocampal volume, asymmetry index reviewed and evaluated by a fellowship-trained neuroradiologist. EEG, clinical presentation and demographic characteristics were collected from the electronic medical record.

#### **RESULTS**

A total of 49 patients who presented with seizures were included in the study. All patients had normal hippocampal volumes on NeuroQuant volumetric analysis. 10 patients had epileptiform EEG findings and 39 patients had no epileptiform changes on EEG. 25 patients (51%) had hippocampal asymmetry, considered positive for volumetric analysis, while 24 (49%) were symmetric. Of the 25 patients with asymmetry, 6 patients (12%) had epileptiform findings on EEG, considered positive for EEG changes. Of the 24 patients with symmetric hippocampal volumes, 4 (8%) had positive EEG. Overall, in this population the likelihood of hippocampal asymmetry was 51% and the likelihood of epileptiform EEG findings was 20%. A McNemar's test for correlated proportions yielded a p-value of 0.003.

#### **CONCLUSION**

s Our study suggests that there may be an association between hippocampal asymmetry and EEG changes in the setting of otherwise normal-appearing hippocampi of normal volume. This could be considered an additional parameter in the assessment of patients with seizures.

#### **CLINICAL RELEVANCE/APPLICATION**

This finding should prompt follow-up imaging to assess the trajectory of the volume loss, which might have implications on patients' management and prognosis.

### **S3B-SPNR-6 Seed-to-Voxel Analysis of Resting-State fMRI Can Detect Functional Alterations in Seizure Onset and Spread Regions in Patients with Non-Lesional Temporal Lobe Epilepsy**

Participants  
India Shelley, BA, Philadelphia, PA (*Presenter*) Nothing to Disclose

#### **PURPOSE**

Temporal lobe epilepsy (TLE) can have severe clinical signs and symptoms. Abnormal neural seizure networks from underlying pathology may facilitate seizure spread and be involved in the manifestation of symptoms in TLE. Currently, stereotactic electroencephalography (sEEG) can detect correlations between zones of seizure onset (OZ) and early (ESZ) and late (LSZ) spread. We examined whether patient resting-state fMRI (rsfMRI) scans can detect similar correlations between the OZ, ESZ, and LSZ. We aimed to see whether noninvasive imaging techniques can uncover patterns of seizure spread to potentially demarcate areas for intervention.

#### **METHODS AND MATERIALS**

This is a retrospective study of 8 patients with refractory, non-lesional TLE (ages 25-53) and 10 controls (ages 22-35). The TLE patients were MRI- on routine diagnostics and subsequently received sEEG. The OZ, ESZ, and LSZ were calculated by generating regions around sEEG contacts that recorded seizure activity. The LSZ was only available for 3 patients. These regions and functional images were registered to MNI space using MIRTk. For each subject, we used dual regression to detect amplitude synchronization of the OZ with the rest of the brain and calculated the ratio of correlated voxels to the spread zone. The same process was done using the OZ, ESZ, and LSZ of each TLE patient for each control. TLE patients were compared to controls individually using a Wilcoxon test and as a group using a Student's t-test,  $\alpha = 0.05$ . The average BOLD signal over the time series was calculated in the onset and spread regions and compared using z-score analysis and a Student's t-test,  $\alpha = 0.05$ .

#### **RESULTS**

5/8 TLE patients showed decreased correlations from the OZ to the ESZ compared to controls. Only 1 TLE patient showed an increased correlation. 2/3 TLE patients showed decreased correlations between the OZ and LSZ. Group analysis showed TLE patients had lower overall connectivity with the ESZ compared to controls. TLE patients had higher average BOLD signal in the OZ and ESZ but not LSZ.

#### **CONCLUSION**

s TLE patients show decreased functional connectivity from the OZ to both ESZ and LSZ. TLE patients showed higher neuronal activity in the OZ and ESZ. These results indicate TLE patients show high levels of pathologic seizure activity but dysfunctional connections in seizure-related areas. Seed-to-voxel analysis of rsfMRI can detect functional network disruption that may expose pathophysiology underlying seizure propagation.

#### **CLINICAL RELEVANCE/APPLICATION**

fMRI analysis is a promising noninvasive method to detect correlated brain regions that may be involved in seizure propagation. It can explore underlying pathology and understanding of the disease.

### **S3B-SPNR-7 Automated Subfield Volumetric Analysis of Amygdala, Hippocampus, and Thalamic Nuclei in Mesial Temporal Lobe Epilepsy**

Participants  
India Shelley, BA, Philadelphia, PA (*Presenter*) Nothing to Disclose

#### **PURPOSE**

Identifying relationships between clinical features and quantitative characteristics of the amygdala-hippocampal and thalamic subregions in mesial temporal lobe epilepsy (mTLE) may offer insights into pathophysiology and the basis for imaging prognostic markers of treatment outcome.

#### **METHODS AND MATERIALS**

27 mTLE subjects with mesial temporal sclerosis (MTS) were scanned for conventional 3D T1w MPRAGE image and T2w scans. With respect to 12 months post-surgical seizure outcomes, 15 subjects reported seizure free and 12 had seizures. We performed quantitative automated segmentation and cortical parcellation using Freesurfer. Automatic labeling and volume estimation of hippocampal subfields, amygdala, and thalamic subnuclei were performed. Volume ratio (VR) for each label was computed and compared using linear regression analysis with significant FDR corrected p-value of  $<0.05$ . Additionally, we used age, sex, existence of tonic-clonic, age of seizure onset, and seizure class as confounding variables.

#### **RESULTS**

Amygdala: In the amygdala, the medial nucleus was the most significantly reduced in patients who were not seizure free when compared to patients who remained seizure free. Hippocampus: Comparison of volumes ipsilateral and contralateral with seizure outcomes showed volume loss was most noted in mesial hippocampal regions such as CA4 and hippocampal fissure. Volume loss was also most reduced in the presubiculum body in patients who were not seizure free at follow-up. Thalamus: VPL and PuL were the most significantly reduced thalamic nuclei in non-seizure free patients. In all statistically significant areas, volume reduction has been observed in the non-seizure free group.

#### **CONCLUSION**

s We demonstrated varying degrees of volume loss in the hippocampus, thalamus, and amygdala subregions of MTS, especially between patients who remained seizure-free and those who did not. These results can be used to further understand mTLE pathophysiology.

#### **CLINICAL RELEVANCE/APPLICATION**

In the future, we hope these results can be used to deepen the understanding of mTLE pathophysiology, leading to improved patient outcomes and treatments.

### **S3B-SPNR-8 Comparison of Functionally Versus Structurally-defined Nodes for Evaluation of DTI Connectome Edge Density (ED) in Infants with Autism Spectrum Disorder (ASD)**

Participants  
Clara Weber, New Haven, CT (*Presenter*) Nothing to Disclose

## **PURPOSE**

In our previous study, conventional DTI metrics and connectome ED based on structurally-defined nodes found significant ASD-related changes among adolescents and adults, but not pediatric cohorts. Here, we analyzed infants at risk of ASD and adults, to evaluate connectome ED based on tractography between functionally defined nodes that showed correlation with from ASD severity in a separate cohort.

## **METHODS AND MATERIALS**

We retrieved DTI from n=155 infants (Longitudinal MRI study of infants at Risk for Autism; median age at scan 7 months, ASD assessment at 24m) and n = 96 adults (Atypical Late Neurodevelopment in Autism, median age 230m) from the National Database of Autism Research. Lake et al. (Biol Psychiatry 2019;86(4):315-26) have previously identified cerebral regions (nodes) that showed significant positive, and respectively negative, functional correlation with symptom severity as measured by ADOS (Autism Diagnostic Observation Schedule) scores based on rs-fMRI from n=260 children. We subset these regions in two sensitivity levels and subsequently specified them as seed points in probabilistic tractography to generate ED maps. For statistical analysis, mean ED values within the JHU White Matter (WM) Labels atlas tracts were extracted.

## **RESULTS**

ED within major WM tracts shows pervasive correlation with ASD diagnosis (Figure 1) in both infants and adults. While present both for ED generated based on positively and negatively correlated cortical regions, positively correlated regions showed more widespread ASD-related changes. Comparing correlation coefficients between different sensitivity levels revealed that ED based on more sensitive nodes shows stronger correlation to ASD diagnosis than ED constructed from less sensitive nodes.

## **CONCLUSION**

s While tractography ED based on structural nodes could only find ASD-related differences in adults' cohort (but not infants), we showed that constructing ED based on functionally defined nodes could identify ASD-related changes in both infants' and adults' cohorts.

## **CLINICAL RELEVANCE/APPLICATION**

As alterations could only be detected in adolescent and adult cohorts in anatomy-based ED, our results imply benefits of combining functional and diffusion-weighted imaging for construction of connectome ED, especially in pediatric populations.

## **S3B-SPNR-9 Temporal Encephaloceles and Drug Resistant Epilepsy: Is There Radiological Correlation with The Epileptogenic Focus?**

Participants  
Aleix Jareno Badenas, MD, Sant Vicenc de Castellet, Spain (*Presenter*) Nothing to Disclose

## **PURPOSE**

Encephaloceles are protrusions of cerebral tissue through a skull defect. They are a possible cause of epilepsy, although their actual epileptogenic potential has not been assessed yet. Lately, with the improvement of MRI imaging, the identification of encephaloceles in patients with drug resistant epilepsy (DRE) has increased. The purposes of this study are: To correlate the location of encephaloceles with the epileptogenic focus in patients with DRE. To evaluate their characteristics and to correlate them with their epileptogenicity.

## **METHODS AND MATERIALS**

We performed a retrospective analysis of the MRI and neurofunctional studies of patients of our epilepsy unit with DRE and an MRI diagnosis of encephalocele. We evaluated the correlation between the encephalocele's location and the epileptogenic focus, as well as their characteristics (number, location, size and presence of gliosis). The location and characteristics of the encephaloceles were evaluated in the 3T MRI studies with a specific epilepsy protocol. The epileptogenic focus was evaluated in our epilepsy unit after the evaluation of different neurofunctional techniques (video-EEG, PET/SPECT and SEEG).

## **RESULTS**

We had a study population of 11 patients (7 women and 4 men) with a mean age of 24.6 years. Six (55%) patients had correlation between the epileptogenic focus and the location of the encephalocele, whilst in the other 5 (45%) they were not matching. 67% of the patients with correlation showed gliosis and a mean encephalocoeles volume of 0.25cc, while 40% of patients without correlation presented gliosis and a mean volume of 0.33cc.

## **CONCLUSION**

s Our results show that encephaloceles have to be considered as potentially epileptogenic lesions in patients with DRE. Gliosis may be an indicator of higher epileptogenicity. In our group of patients, the smaller encephaloceles were more epileptogenic, which is inconsistent with previous literature.

## **CLINICAL RELEVANCE/APPLICATION**

Our study shows that encephaloceles have epileptogenic potential and that some characteristics, such as the gliosis, may help to assess their epileptogenic potential.

Printed on: 02/07/23

## Abstract Archives of the RSNA, 2022

S3B-SPNR-1

### Volume and Permeability of White Matter Hyperintensity on Cognition: A DCE Imaging study in A Prospective Elderly Cohort

Sunday, Nov. 27 12:15PM - 12:45PM Room: Learning Center - NR DPS

#### Participants

Hyeonwoo Kim, MD, Seoul, Korea, Republic Of (*Presenter*) Nothing to Disclose

#### PURPOSE

We aimed to evaluate the relationship between volume, permeability, and the effect of white matter pathology on cognition in elderly patients with mild to moderate WMH from a prospective elderly cohort.

#### METHODS AND MATERIALS

In this IRB-approved retrospective analysis of the prospective study, written informed consent was obtained from all participants. We selected 193 elderly participants of the age range (55-80 years) with minimal-to-moderate WMH from a prospective DCE MRI cohort (n=259) with normal and impaired cognition between August 2017 and June 2021. Periventricular WMH (PWMH), deep WMH (DWMH), and normal-appearing white matter (NAWM) were automatically segmented using a 3D T1-weighted sequence. Volume transfer constant [K<sub>trans</sub>] as BBB permeability was determined using DCE MRI. The effects of K<sub>trans</sub> of WMH and NAWM were evaluated using multivariable linear regression adjusted for demographic and volume measures.

#### RESULTS

and volume measures. 193 participants (age, 70.1±6.8 years; 128 women) include 44 with CDR=0, 119 with CDR=0.5, and 30 with CDR=1.0. The degree of WMH was minimal (n=87) and moderate (n=106). Higher K<sub>trans</sub> was observed in PWMH (0.598 ± 0.509 x10<sup>-3</sup> min<sup>-1</sup>) compared to DWMH (0.496 ± 0.478 x10<sup>-3</sup> min<sup>-1</sup>) and NAWM (0.476 ± 0.398 x10<sup>-3</sup> min<sup>-1</sup>) (p<0.001). The strong negative correlation between K<sub>trans</sub> and the volume was noted in PWMH (rho=-0.357, p<0.001) and DWMH (rho = -0.200, p=0.005), but not in NAWM (rho = 0.053, p=0.460). After adjusting for age, sex, APOE4, education, cortex volume, PWMH volume (B = -0.0008, SE = 0.0002, beta = -0.363, p <0.001) and history of cardiovascular disease (B = 0.0066, SE = 0.0028, beta = 0.229, p <0.021) were predictive factors for K<sub>trans</sub> of PWMH (R<sup>2</sup>=0.191, F(2, 86) = 10.153, p<0.001). After adjusting for covariates, only history of cardiovascular disease was the predictor for K<sub>trans</sub> of NAWM (R<sup>2</sup>=0.036, F(1,153) =5.740, p<0.018). After adjusting covariates (age, sex, and APOE4 status), hippocampal volume (p<0.001), and PWMH volume (along with education level were independent predictors of worse cognition (CDR-SB = 3), whereas cortex volume and K<sub>trans</sub> of PWMH were not.

#### CONCLUSION

We found higher permeability of PWMH compared to DWMH and NAWM and a negative relationship between its permeability and volume. The volume of PWMH is the predictor of worse cognition in elderly individuals. Further, our finding suggests that WMH permeability and WMH volume change may be independent events.

#### CLINICAL RELEVANCE/APPLICATION

Our findings suggest the different underlying pathophysiology of PWMH and DWMH. In addition, the volume of PWMH predicts worse cognition in elderly individuals.

Printed on: 02/07/23

## Abstract Archives of the RSNA, 2022

S3B-SPNR-10

### Assessment of White Matter Lesion Volume and Disability in Neuromyelitis Optica Spectrum Disorder

Sunday, Nov. 27 12:15PM - 12:45PM Room: Learning Center - NR DPS

#### Participants

Jitlada Kusol, MD, Bangkok Noi, Thailand (*Presenter*) Nothing to Disclose

#### PURPOSE

Neuromyelitis optica spectrum disorder (NMOSD) is an aquaporin-4 (AQP4) antibody-mediated disease, affecting the white matter (WM). However, how burden of WM correlates to outcome is yet to be studied. The purposes of this study were to measure white matter lesion volume (WMLV) at locations with high AQP4 expression and to study its association to disability and disease progression.

#### METHODS AND MATERIALS

Retrospective review of 32 NMOSD patients who underwent two consecutive brain MRI scans with = 1-year interval were performed. Patients were categorized into low EDSS group (EDSS=3, n =15) and high EDSS group (EDSS=3.5, n=17). Disease progression (sustained increase in EDSS) was also significant parameter. WMLV were measured and categorized into five locations (diencephalic, dorsal brainstem, callosal/periventricular, hemispheric WM and corticospinal tract). Changes in WMLV in aforementioned locations were also defined.

#### RESULTS

WMLV was significantly larger in the high EDSS group at the callosal/periventricular, hemispheric WM and corticospinal tract ( $p < 0.001$ , 0.041 and 0.025, respectively). In addition, the high EDSS group showed the lower change in the WMLV at hemispheric WM over the follow-up period ( $p = 0.044$ ). Patients with disease progression (6.3%) had higher WMLV at callosal/periventricular area than those without progression ( $p = 0.024$ ).

#### CONCLUSION

Greater WMLV at callosal/periventricular, hemispheric WM and corticospinal tract related to the higher disability in NMOSD patients. In addition, higher WMLV at callosal/periventricular region may predict the development of disease progression. Our findings reflect that higher WMLV may correlate to worse clinical outcome.

#### CLINICAL RELEVANCE/APPLICATION

Higher WMLV in NMOSD patients may correlate to worse clinical outcome, especially at callosal/periventricular, hemispheric WM and corticospinal tract.

Printed on: 02/07/23

## Abstract Archives of the RSNA, 2022

S3B-SPNR-11

### Altered Vascular Permeability in Autoimmune Encephalitis: Region-based Evaluation with Dynamic Contrast-enhanced MRI and Automatic Whole Brain Segmentation

Sunday, Nov. 27 12:15PM - 12:45PM Room: Learning Center - NR DPS

#### Participants

Sohyun Ji, MD, MD, (Presenter) Nothing to Disclose

#### PURPOSE

To evaluate the change in permeability of brain-blood barrier (BBB) in patients with autoimmune encephalitis, as compared with the healthy control group, by using dynamic contrast enhanced MRI (DCE-MRI) and to explore its predictive value for the treatment response in the patients.

#### METHODS AND MATERIALS

In this retrospective study, a total of 38 patients with probable or possible autoimmune encephalitis and 15 healthy controls underwent DCE-MRI between April 2020 and May 2021. Automatic volumetric segmentation was performed on pre-/postcontrast T1-weighted images by using FreeSurfer, and encephalitis-associated brain region masks were extracted by using the software NordicICE. Ktrans maps, derived from DCE-MRI using Patlak model, were coregistered with the region-of-interest masks to calculate their mean values at the total volume of interest. The Wilcoxon rank sum test and Friedman test were used to compare Ktrans. Receiver operating characteristic curve analysis was used to assess the diagnostic performance.

#### RESULTS

All brain regions showed significantly increased Ktrans in the patients, as compared with the controls ( $P < .05$ ). The right cerebral cortex (1.232 vs. 0.0003 min<sup>-1</sup>) and right nucleus accumbens (0.371 vs. 0.0002 min<sup>-1</sup>) had the largest mean difference of Ktrans between the patients and controls, followed by the right parahippocampus and right occipital lobe. The same trends were observed in each autoimmune encephalitis subtype (anti-LGI1, anti-NMDAR, and antibody-negative). No significant differences in Ktrans were found between the baseline and follow-up. Poor treatment response group had significantly higher baseline Ktrans in all brain regions ( $P < .05$ ), as compared with good treatment response group, except for the right nucleus accumbens ( $P = 0.33$ ) and right cerebral cortex ( $P = 0.08$ ). At the cutoff value of 0.002 min<sup>-1</sup>, sensitivity and specificity for the prediction of treatment response were 86% and 100%, respectively for the left cerebellar cortex.

#### CONCLUSION

s The BBB permeability was persistently increased in all brain regions in autoimmune encephalitis patients, as compared with controls, and baseline Ktrans were higher in patients with poor treatment outcome.

#### CLINICAL RELEVANCE/APPLICATION

Autoimmune encephalitis patients showed increased BBB permeability in all brain regions, and the increased permeability of BBB was associated with treatment response.

Printed on: 02/07/23

## Abstract Archives of the RSNA, 2022

S3B-SPNR-13

### A Review of The Appropriateness of Magnetic Resonance Imaging for Optic Neuritis in A Tertiary Referral Center in The West of Ireland

Sunday, Nov. 27 12:15PM - 12:45PM Room: Learning Center - NR DPS

#### Participants

Richard Faman, BMBCh, BSc, (*Presenter*) Nothing to Disclose

#### PURPOSE

Optic neuritis is a clinical condition which involves inflammation of the optic nerves. It is often seen concurrently with central nervous system (CNS) demyelination and there is well known link with multiple sclerosis. <sup>1</sup> The purpose of this study was to evaluate the appropriateness of magnetic resonance imaging of the CNS in patients with confirmed optic neuritis.

#### METHODS AND MATERIALS

The study retrospectively reviewed MRI requests for patients with optic neuritis over a five-year period at University Hospital, Galway. Our institution is a tertiary referral center with neurology expertise in the west of Ireland. The study established which CNS imaging was requested by neurologists. Additionally, the final radiology reports were reviewed to establish if the imaging technique diagnosed any relevant positive findings.

#### RESULTS

MRI brain and Orbits was the most commonly ordered investigation with neurologists requesting this study in 89 patients. Of these, 40 patients (44.9%) showed patterns consistent with optic neuritis. MRI orbits (alone) was the second most commonly requested imaging. 45 MRI patients underwent MRI orbits with relevant changes reported in 16 (35.6%) patients. MRI C-spine was performed on 47 patients with 12 (25.5%) showing significant changes. MRI T-spine was the least common investigation ordered with 10 patients undergoing such. From these, only 1 patient (10%) showed significant change on imaging.

#### CONCLUSION

s The purpose of this study was to establish how much imaging of the CNS is justified in patients with optic neuritis. MRI brain and orbits were the most prevalent imaging ordered. Their role in investigating patients with optic neuritis is largely justified with changes such as plaque accumulation and demyelination patterns noted in a significant portion of patients. Of note, only 10% of patients with optic neuritis had positive findings on MRI T-spine. This raises the question of whether MRI T-spine should be included in imaging work up for optic neuritis. Strengths of this study include relatively large sample size (n= 191), 5 year timeframe and significance of the hospital site as a tertiary referral center in the west of Ireland.

#### CLINICAL RELEVANCE/APPLICATION

In conclusion, our study shows that MR imaging of brain and Orbits is justified when investigating patients with optic neuritis. Imaging the C-spine is justified in some circumstances. Our study shows that due to the low yield, MRI Thoracic spine is not justified in most cases. Requesting MRI T-Spine in most cases leads to unnecessary investigation and associated delay in patient flow and associated costs. We recommend that protocols should be in place to ensure MRI T-spine is only requested in very specific cases, upon discussion with senior neurologists.

Printed on: 02/07/23

## Abstract Archives of the RSNA, 2022

S3B-SPNR-14

### Enlarged Choroid Plexus Related with Whole Brain Atrophy in Multiple Sclerosis

Sunday, Nov. 27 12:15PM - 12:45PM Room: Learning Center - NR DPS

#### Participants

Xiao Chen, MS,MS, Chongqing, China (*Presenter*) Nothing to Disclose

#### PURPOSE

This study aims to investigate the alteration of choroid plexus volume and whole brain morphology in patients with MS and neuromyelitis optica spectrum diseases (NMOSD).

#### METHODS AND MATERIALS

Fifty-one patients with MS, 42 patients with NMOSD and 56 healthy controls (HC) were recruited, of which 25 patients with MS and 20 patients with NMOSD were followed up. T2 FLAIR, 3DT1 image data and related clinical data were collected. The morphological changes of choroid plexus and whole brain tissue (ventricular system volume, sulcus cortex thickness, gyrus cortex thickness and deep gray matter volume) were compared between three groups and the correlation between choroid plexus volume and brain atrophy were further investigated.

#### RESULTS

Compared with the HC group, the volume of choroid plexus was increased in the MS group ( $P < 0.001$ ), but not in the NMOSD group. The MS group showed the whole-brain atrophy (increased ventricle system volume, reduced cortex thickness and deep gray matter volume) and the distribution of cortical atrophy in the sulcus area (61%, 41/67) was greater than that in the gyrus area (43%, 29/67). The NMOSD group showed mild brain atrophy related with increased third ventricle volume and decreased deep gray matter volume. In MS group ( $P < 0.05$ ,  $r = -0.292 \sim -0.538$ ) and NMOSD group ( $P < 0.05$ ,  $r = -0.325 \sim -0.572$ ), there were widespread correlations between choroid plexus volume and cerebral cortex thickness. In MS, compared with the baseline, the right nucleus accumbens and total deep gray matter brain volume were decreased ( $P < 0.001$ ), and bilateral lateral ventricle volume were increased ( $P < 0.001$ ) in follow-up. There was no significant alteration between baseline and follow-up in the NMOSD group.

#### CONCLUSION

s MS patients show enlarged choroid plexus related with whole brain atrophy, while the NMOSD patients show local brain atrophy. In the short-term follow-up, the brain atrophy in MS patients was gradually aggravated, and there was no obvious alteration in NMOSD patients.

#### CLINICAL RELEVANCE/APPLICATION

A combined MRI and PET study showed that the increased choroid plexus tissue was significantly positively correlated with the expression of inflammatory factors, indicating that the mechanism based on the choroid plexus blood-cerebrospinal fluid barrier may play an important role in MS. The choroid plexus blood-cerebrospinal fluid barrier comprises a single layer of choroid plexus epithelial cells, which separates blood-borne substances from cerebrospinal fluid. Therefore, the choroid plexus blood-cerebrospinal fluid barrier may also play an important role in maintaining the stability of the brain environment.

Printed on: 02/07/23

## Abstract Archives of the RSNA, 2022

S3B-SPNR-15

### **Safety and Effectiveness of First-line Endovascular Management of Low-Grade Brain Arteriovenous Malformations: A Single Center Experience in 145 Patients**

Sunday, Nov. 27 12:15PM - 12:45PM Room: Learning Center - NR DPS

#### **Participants**

Maichael MEKHAIL, (*Presenter*) Nothing to Disclose

#### **PURPOSE**

Spetzler-Martin grade (SMG) I-II (low-grade) brain arteriovenous malformations (BAVMs) are often considered safe for microsurgical resection. However, the role of endovascular treatment (EVT) remains to be clarified in this indication, especially for unruptured BAVMs. The purpose of our study was to assess the safety and effectiveness of endovascular treatment as the first-line therapy for low-grade BAVMs.

#### **METHODS AND MATERIALS**

From our local database, we retrospectively retrieved patients with low-grade BAVMs, either ruptured or unruptured, treated by embolization as first-line therapy in our department between January 2005 and January 2020. The primary endpoint was the total obliteration rate of BAVMs, and secondary endpoints were hemorrhagic complications, final clinical outcome, assessed through shift of the modified Rankin Scale, and mortality rate secondary to BAVM embolization.

#### **RESULTS**

One hundred-forty-five patients meeting inclusion criteria and treated by EVT as first-line therapy were included in the study (82 ruptured and 63 unruptured BAVMs). Overall, complete exclusion of BAVMs was achieved in 110 patients (75.9%); 58 patients (70.7%) among ruptured BAVMs and 52 (82.5%) among unruptured ones, including 37.9% BAVMs excluded by EVT alone (35.5% among ruptured BAVMs and 44.4% among unruptured ones) and 38% by combined treatment (EVT and surgery or EVT and SRS). There was no BAVM volume cut-off predictive for total obliteration by embolization alone. Early minor hemorrhagic complications were reported in 14 patients (9.6%) and early major hemorrhagic complications were reported in 5 patients (3.4%). No late hemorrhagic complications (0%) occurred; mortality rate was 0.7% (1/145 patients). Improved /unchanged mRS was reported in 137 patients (94.5%).

#### **CONCLUSION**

s Endovascular treatment, alone or associated with others exclusion techniques, might be safe and effective for complete exclusion of low-grade brain arteriovenous malformations regardless of their volumes.

#### **CLINICAL RELEVANCE/APPLICATION**

KEY WORDS Brain arteriovenous malformations, Endovascular treatment, Surgery, Pressure cooker technique.

Printed on: 02/07/23

## Abstract Archives of the RSNA, 2022

S3B-SPNR-16

### Variations in Temperature Changes with SAR, B1+rms and Pulse Sequence: A Need for Caution?

Sunday, Nov. 27 12:15PM - 12:45PM Room: Learning Center - NR DPS

#### Participants

David Gultekin, PhD, (*Presenter*) Nothing to Disclose

#### PURPOSE

The applications of high field magnetic resonance imaging (MRI) are limited partly by considerations of radiofrequency (RF) safety and the design of RF systems. A current dilemma in moderate to high field MRI (3T to 9.4T) is how to optimize image quality and productivity while maintaining safety. Often one may be improved at the expense of other factors. There is growing interest in assessing the utility of temperature (T) and time (t) diagrams (T-t), specific absorption rate (SAR) and RF field (B1+rms) to monitor RF absorption and thermal hazards in tissues especially in the presence of conductive implants.

#### METHODS AND MATERIALS

A phantom consisting of a conductive metallic wire in a tissue equivalent gel is used in this study. Any conductive wire such as a lead used for deep brain stimulation (DBS) with four electrodes or a half wavelength ( $l/2$ ) copper (Cu) or titanium (Ti) wires can be used as probes for monitoring the effects of RF using fiber optic temperature probes. Standard imaging sequences (functional, morphological, diffusion and perfusion) were implemented on a 3T Siemens Prisma MRI with a TEM RF transmit body coil interfaced with a 43.2 kW peak power transmitter amplifier and a 64-channel head and neck coil (64-H/N) for receiving the RF signals.

#### RESULTS

The T-t diagrams can be used to assess different protocols for the scenario of slow imaging, allowing for cooling time between sequences, and of fast imaging, without allowing for cooling times. T-t diagrams were acquired for pairs of sequences with the same SAR and B1+rms but different RF exposure times (NA), different SAR, B1+rms and exposure time, and different SAR, B1+rms but the same exposure time. The functional, morphological, diffusion and perfusion MRI sequences show the utility of the each of T-t diagrams, B1+rms and SAR. The integration of T-t diagrams for the slow and fast imaging segments of the same fMRI series shows the conservation of thermal dose in two scenarios.

#### CONCLUSION

We show that T-t diagrams provide additional important information about thermal effects of RF heating that SAR and B1+rms alone cannot provide. By keeping SAR and B1+rms the same but increasing NA increases exposure time resulting in a substantially higher temperature rise with time. A practical method involving temperature and time diagrams can be used to evaluate, compare and optimize various imaging protocols to ensure patient safety.

#### CLINICAL RELEVANCE/APPLICATION

This method can further be developed to scan patients with implants safely.

Printed on: 02/07/23

## Abstract Archives of the RSNA, 2022

S3B-SPNR-17

### Dual-layer Detector Cone-beam CT Angiography Improves Intracranial Vessel Conspicuity and Reduces Artifacts

Sunday, Nov. 27 12:15PM - 12:45PM Room: Learning Center - NR DPS

#### Participants

Fredrik Stahl, MD, (*Presenter*) Fredrik Ståhl has received reimbursements for conference travel expenses from Philips in 2022

#### PURPOSE

To evaluate whether a dual-layer detector cone-beam CT prototype improves image quality in stroke patients, compared to reference standard single layer detector cone-beam CT angiography.

#### METHODS AND MATERIALS

A prospective single center clinical trial (NCT04571099) enrolled consecutive patients, 50 years or older with ischemic or hemorrhagic stroke. Patients were subsequently imaged with the prototype system following an intravenous contrast media injection. Single layer (Front layer, FL) and 70 keV virtual monoenergetic images (VMI) derived from both detector layers were reconstructed and evaluated in a single-sequence two-period crossover design by two blinded neuroradiologists. Sixteen intracranial arterial segments were evaluated for vessel conspicuity and artifact presence on 5-point Likert scales (5: highest vessel conspicuity or fewest artifacts). The Wilcoxon matched-pairs signed-rank test was performed to determine significance ( $p < 0.05$ ), with Bonferroni correction for multiple tests.

#### RESULTS

28 patients were enrolled. The median conspicuity of the sixteen FL and VMI arterial vessel segments for each patient was 3.5 (IQR 2-4) and 4 (IQR 3-5),  $p < 0.001$ . The median artifact ratings for FL and VMI were 3 (IQR 2-4) and 4 (IQR 3-5),  $p < 0.001$ . For individual segments the VMI showed superior conspicuity for the Basilar, SCA, M4- and P1- segment ( $p < 0.001$ ), as well as the P2- and M3- segment ( $p < 0.01$ ). The P1-segment ( $p < 0.001$ ) and Basilar, SCA, M1-, M3-, M4-, P2-, A1- and A2-segment ( $p < 0.01$ ) had a significantly lower degree of artifacts in VMI compared to FL.

#### CONCLUSION

Dual-layer detector cone-beam CT virtual monoenergetic images improves intracranial vessel conspicuity and reduces artifacts compared to reference standard single layer detector cone-beam CT angiography.

#### CLINICAL RELEVANCE/APPLICATION

Cone-beam CT angiography is increasingly used in the primary diagnostic work-up of suspected ischemic stroke, and could be an alternative to CT angiography to shorten door to thrombectomy time. Our findings indicate that dual-layer detector cone-beam CT angiography improves intracranial image quality over standard single-layer cone-beam CT angiography.

Printed on: 02/07/23

## Abstract Archives of the RSNA, 2022

S3B-SPNR-18

### **Efficacy and Safety of Endovascular Trans-venous Embolization of Cerebrospinal Fluid-venous Fistulas Associated with Spontaneous Intracranial Hypotension**

Sunday, Nov. 27 12:15PM - 12:45PM Room: Learning Center - NR DPS

#### **Participants**

Donna Parizadeh, MD, (*Presenter*) Nothing to Disclose

#### **PURPOSE**

To independently evaluate the efficacy and safety of endovascular transvenous embolization for treatment of patients with spontaneous intracranial hypotension (SIH) secondary to CSF-venous fistulas (CVF).

#### **METHODS AND MATERIALS**

We performed a retrospective review of a prospectively maintained database of patients with 1) clinical diagnosis of SIH and 2) definitive diagnosis of CVF on either lateral decubitus digital subtraction myelogram or CT myelogram who underwent 3) transvenous embolization for treatment of CVF at our institute between Dec. 2020 to Apr. 2022. To evaluate efficacy of the procedure, we assessed pre- and 3-month post-embolization clinical and imaging outcomes including Headache Impact Test (HIT-6) and Patient Global Impression of Change (PGIC) scores, and the Bern SIH score on brain MRI. Procedural and post-procedural complications were recorded. Post-embolization change in measures was assessed with Wilcoxon Signed rank test.

#### **RESULTS**

A total of 19 patients, median (IQR) age 60 (49-65) years, 74% female, underwent transvenous embolization. At 3-month follow-up, 18/19 (95%) of patients reported having either much or very much improved symptoms on PGIC. Follow-up HIT-6 and imaging were available for 18 and 15 patients, respectively. Among these patients, headache improved significantly from a median (IQR) HIT-6 score of 68 (58-72) pre-embolization to 36 (36-38) post-embolization ( $p = 0.001$ ). Bern SIH score improved significantly from median (IQR) of 8 (6-8) pre-embolization to 2 (1-3) post-embolization ( $p = 0.001$ ). One (5%) patient did not have improvement of clinical or imaging findings consistent with a treatment failure. There were no neurovascular complications. Side effects were localized back pain (84%) and rebound headache (74%) which resolved within one month with medical treatment in all cases.

#### **CONCLUSION**

s Transvenous embolization is a highly efficacious and safe treatment for CVF in SIH patients.

#### **CLINICAL RELEVANCE/APPLICATION**

Transvenous embolization is emerging as a novel highly efficacious, safe, and minimally invasive treatment for patients with spontaneous intracranial hypotension secondary to CSF-venous fistula.

Printed on: 02/07/23

## Abstract Archives of the RSNA, 2022

S3B-SPNR-19

### Clinical and Imaging Outcomes of Percutaneous Sclerotherapy for Venous Malformations Affecting the Eye and Orbit

Sunday, Nov. 27 12:15PM - 12:45PM Room: Learning Center - NR DPS

#### Participants

Tushar Garg, MD, Baltimore, MD (*Presenter*) Conference Travel, Siemens Healthineers

#### PURPOSE

Sclerotherapy treatment can be used for patients with venous malformations (VMs) affecting the eye and orbit region. This study evaluates the safety and outcomes of these interventions.

#### METHODS AND MATERIALS

All patients who received sclerotherapy for VMs involving the eye and orbit between 12/2005 to 6/2021 were reviewed. The clinical and imaging findings of these patients were assessed. Clinical symptoms response was classified as resolved, improved and stable, or worsened. Differences between pre-and post-procedure MRI of the largest lesion diameter in one plane were used to calculate changes in VM size, similar to the response evaluation criteria in solid tumors: complete response (100% reduction), partial response (30% reduction), stable disease ( $\leq 30\%$  reduction or  $\leq 20\%$  enlargement), progressive disease ( $\geq 20\%$  VM size increase) worse. SIR classification criteria were used to classify adverse events. Clinical response, lesion size changes, and complication rates were evaluated. Fisher's Exact Test- was used for statistical analysis.

#### RESULTS

13 patients (53.8% F) underwent a total of 32 embolization procedures with an average follow up period of 1344.5 days. The most common presenting symptoms were enlargement (6, 46.2%) and functional deficit (6, 46.2%). Other common complications included pain (5; 38.5%), mass (4; 30.8%), cosmetic deformity (3; 23.1%), discoloration (3; 23.1%), bleeding/ discharge (1; 7.7%) or other (1, 7.7%). Patients had an average of 2.46 (med: 2) procedures with a technical success rate of 100% (32/32). Embolization did not significantly decrease VM size on imaging ( $p=0.4762$ ). 11 patients (11/13; 84.6%) had both pre- and post- MRI imaging measurements. Of these, zero patients saw complete response, 2 patients (18.2%) experienced partial response, 6 patients (54.5%) experienced no change in VM size, and 3 patients (27.3%) saw increased VM size. There was only one (3.1%) incident of early (30 days) post-procedural complications (delayed extubation) among a total of 32 procedures. The most common sclerosants used were bleomycin foam (8, 25.0%) and sotradecol (8, 25%). This was followed by ethanol (4, 12.5%), n-BCA (4, 12.5%), onyx (2, 6.3%) and coils (1, 3.1%). Some procedures used more than one agent. Sclerotherapy significantly improved clinical symptoms with 7.7% (1/13) resolved, 30.8% (4/13) improved, and 61.5% (8/13) stable or worsened ( $p = 0.0391$ ).

#### CONCLUSION

This study shows that sclerotherapy of venous malformations within the eye and orbit is a safe and effective treatment.

#### CLINICAL RELEVANCE/APPLICATION

The results of this study showed that sclerotherapy can be used for the management of VMs involving the eye and orbit without the need for more invasive surgical management.

Printed on: 02/07/23

## Abstract Archives of the RSNA, 2022

S3B-SPNR-20

### **Percutaneous Sclerotherapy for Superficial Venous Malformations Involving the Tongue: Clinical and Imaging Outcomes**

Sunday, Nov. 27 12:15PM - 12:45PM Room: Learning Center - NR DPS

#### **Participants**

Anna Gong, Baltimore, MD (*Presenter*) Nothing to Disclose

#### **PURPOSE**

To assess the safety and effectiveness of percutaneous sclerotherapy (PS) of venous malformations (VMs) involving the tongue.

#### **METHODS AND MATERIALS**

Between 7/2004 and 8/2021, we reviewed all patients who received PS for VMs of the tongue. Clinical response, lesion size changes, and complication rates were evaluated using clinical and imaging results. The type of sclerosant was used to sub-stratify analysis. For statistical analysis, Fisher's Exact Tests were applied. The severity of clinical symptoms was graded as resolved, improved, and stable/worsened. The difference between pre and post procedure MRI of the largest lesion diameter in one plane was used to calculate VM size change, similar to the response evaluation criteria in solid tumors: complete response (CR, 100% reduction), partial response (PR, 30% reduction), stable disease (SD, =30% reduction or =20% enlargement), progressive disease (PD, =20% VM enlargement) worse. Adverse events were scored using SIR classification criteria.

#### **RESULTS**

A total of 58 embolization procedures were performed in 26 patients (80.8% F), with a mean follow-up duration of 975 days. Pain (14, 24.1%), enlargement (12, 20.7%), difficulty with mastication (7, 12.1%), difficulty with speaking (7, 12.1%), and difficulty swallowing (7, 12.1%) were the most prevalent presenting complaints. Patients underwent a median of 3 procedures (range:1-6) with a 100% technical success rate. Bleomycin foam (51, 64.5%) was the most commonly deployed sclerosant, followed by ethanol (26, 32.9%), and sotradecol foam (14, 17.7%), with some procedures using multiple agents. Sclerotherapy significantly improved clinical symptoms with 15.4% resolved (4, 15.4%), 53.8% improved (14, 53.8), and (8,30.8%) stable or worsened ( $p < 0.0001$ ). On imaging, embolization demonstrated significant reduction in lesion size ( $p=0.0184$ ). Of the 17 (65.4%) patients who had both pre and post MR measurements, 0 patients had a complete response, 6 patients (35.3%) showed a PR, 11 patients (64.7%) showed no change in VM size, and 0 patients showed increased VM size. Early (30 day) post-procedural complications occurred after 3 of 58 procedures (5.2%), the majority of which were skin burns.

#### **CONCLUSION**

s Percutaneous sclerotherapy significantly decreases lesion size and improves clinical symptoms of VMs involving the tongue.

#### **CLINICAL RELEVANCE/APPLICATION**

Percutaneous, image-guide sclerotherapy is a safe and effective treatment for low-flow, venous malformations involving tongue.

Printed on: 02/07/23

## Abstract Archives of the RSNA, 2022

S3B-SPNR-3

### Alterations of Cerebral Perfusion and Functional Connectivity in Children with Idiopathic Generalized Epilepsy

Sunday, Nov. 27 12:15PM - 12:45PM Room: Learning Center - NR DPS

#### Participants

Guiqin Chen, (*Presenter*) Nothing to Disclose

#### PURPOSE

Previous studies have demonstrated that adults with idiopathic generalized epilepsy (IGE) have functional abnormalities, however, the neuropathological pathogenesis differs between adults and children. This study aimed to explore the alterations of cerebral blood flow (CBF) and functional connectivity (FC) simultaneously to comprehensively understand the neuropathological mechanisms of IGE in children.

#### METHODS AND MATERIALS

Arterial spin labeling (ASL) and blood oxygenation level-dependent magnetic resonance imaging data were acquired for 28 patients with IGE and 35 matched healthy controls (Table 1). Using ASL perfusion, we identified several regions of altered CBF in patients with IGE. Seed-based whole-brain FC analysis was then performed on regions with significant CBF changes. Multiple comparisons were corrected using a voxel-wise Gaussian random field method ( $P < 0.05$ , two tailed). The mean CBF and FC of each cluster with significant group differences were extracted and correlated with the clinical variables in the IGE group using Pearson's correlation analysis.

#### RESULTS

Compared to controls, patients with IGE showed abnormalities in CBF, mainly located in the right middle temporal gyrus, right middle occipital gyrus (MOG), right superior frontal gyrus (SFG), and left inferior frontal gyrus, triangular part (IFGtriang) (Table 2, Figure 1). Based on these four regions, we constituted the whole-brain FC and observed that the FC between the left IFGtriang and calcarine fissure (CAL) was decreased, (Figure 2A) and the FC between the right MOG and bilateral CAL was decreased (Figure 2B). Correlation analyses indicated that hyperperfusion in the right SFG was correlated with IGE age of onset ( $r = -3.81$ ,  $P = 0.045$ ) (Figure 3A), and decreased connectivity in the left CAL was correlated with the IGE patient's duration ( $r = -4.20$ ,  $P = 0.026$ ) (Figure 3B).

#### CONCLUSION

The study findings suggest simultaneous alterations in both CBF and FC in the left IFGtriang and right MOG in children with IGE by combining ASL and rs-fMRI, and the abnormal brain area is associated with duration.

#### CLINICAL RELEVANCE/APPLICATION

The combination of CBF and FC not only describe and track the progress of the disease, provide imaging basis for early diagnosis of IGE, but also can provide complementary information and comprehensive insights into the pathophysiology of IGE from the perspective of neuronal and vascular integration.

Printed on: 02/07/23



## Abstract Archives of the RSNA, 2022

S3B-SPNR-4

### Bitmap 3D Printing of Multimodal Imaging for Epilepsy Surgery

Sunday, Nov. 27 12:15PM - 12:45PM Room: Learning Center - NR DPS

#### Participants

Nicholas Jacobson, (*Presenter*) Nothing to Disclose

#### PURPOSE

Surgical Planning for epilepsy requires the sequential review of multiple volumetric and vector-based datasets. This data is viewed sequentially on a 2D screen, requiring significant visuospatial memory to composite and spatially reconstruct. The presurgical data review process has thus become increasingly inefficient and does not provide a holistic visualization of the data. This worrisome trajectory ignores the biggest promise of the information revolution: increased communication, connectivity, and interoperability. This cognitive load can be reduced by combining multimodal volumetric images with a 3D printed model. We present a method for creating a presurgical planning model that combines T1 MRI, CT SEEG data, tractography, and fMRI from pediatric epilepsy patients. The purpose is to reduce the cognitive load on surgeons and facilitate focused communication between the entire epilepsy team.

#### METHODS AND MATERIALS

16 bit image data, CT/MRI/fMRI, is mapped to color and opacity material mixing ratios corresponding to DICOM intensity values. 256 bit vector field data, Tractography/SEEG activation, is composited onto the image data in 3D voxel space. The composited multimodal 3D model is sliced for 3D printing in a voxel-based modeling program. The bitmap slices are printed at the spatial resolution of the images in a multi-material polyjet 3D printer. The model is reviewed during surgical conferences and used during a procedure in a clinical study (n=15).

#### RESULTS

Our method embeds vector-based features, representing dynamic physiology, within image-based models that represent gradients in biological tissue. The results leverage color-encoded data, displaying composited MRI, CT SEEG probes and activation, DWI tractography, and fMRI information. The models were used in discussion during case conferences and surgery. Preliminary survey results indicate increased spatial understanding and confidence in the surgical approach.

#### CONCLUSION

We show that a variety of computationally derived physiologic datasets found in medical imaging can be directly 3D printed for neurosurgical epilepsy interventions. The relationships between data visualization, computer science, digital fabrication, and medicine are fostering an information revolution with the potential for increased communication, connectivity, and interoperability of data, bringing form and function together to improve health.

#### CLINICAL RELEVANCE/APPLICATION

The multimodal models unify and express more of the ever-increasing amount of data in surgical planning. The models are developing a platform that can be extended to study disease states that require information from multiple modalities of images.

Printed on: 02/07/23

## Abstract Archives of the RSNA, 2022

S3B-SPNR-5

### Clinical Significance of Hippocampal Asymmetry as a Sole Imaging Finding in Patients with Seizure

Sunday, Nov. 27 12:15PM - 12:45PM Room: Learning Center - NR DPS

#### Participants

Hasan Azeem Khan, MD, Galveston, WV (*Presenter*) Nothing to Disclose

#### PURPOSE

Hippocampal volume loss on MRI (Magnetic Resonance Imaging) is described as potential source or sequelae of seizure. Since the introduction of post processing automated volumetric techniques, there has been a reliable and objective method to assess hippocampus volume. Hippocampal asymmetry in the context of normal volume of individual hippocampi is an uncommon finding observed on volumetric studies of brain MRI performed for evaluation of seizure. The clinical significance and correlation of hippocampal asymmetry with seizures and EEG findings are lacking. We set out to create a study that evaluates the relationship between asymmetric otherwise normal hippocampi and seizures.

#### METHODS AND MATERIALS

We gathered data on 49 patients from 1257 brain MRIs performed for evaluation of seizure over the past 3 years. The total 49 patients are divided into two groups. A group of 25 patients with hippocampal asymmetry diagnosed on MRI using the Neuroquant protocol and a comparison group of 24 patients with symmetrical hippocampi. This included data of left/right hippocampal volume, asymmetry index reviewed and evaluated by a fellowship-trained neuroradiologist. EEG, clinical presentation and demographic characteristics were collected from the electronic medical record.

#### RESULTS

A total of 49 patients who presented with seizures were included in the study. All patients had normal hippocampal volumes on NeuroQuant volumetric analysis. 10 patients had epileptiform EEG findings and 39 patients had no epileptiform changes on EEG. 25 patients (51%) had hippocampal asymmetry, considered positive for volumetric analysis, while 24 (49%) were symmetric. Of the 25 patients with asymmetry, 6 patients (12%) had epileptiform findings on EEG, considered positive for EEG changes. Of the 24 patients with symmetric hippocampal volumes, 4 (8%) had positive EEG. Overall, in this population the likelihood of hippocampal asymmetry was 51% and the likelihood of epileptiform EEG findings was 20%. A McNemar's test for correlated proportions yielded a p-value of 0.003.

#### CONCLUSION

Our study suggests that there may be an association between hippocampal asymmetry and EEG changes in the setting of otherwise normal-appearing hippocampi of normal volume. This could be considered an additional parameter in the assessment of patients with seizures.

#### CLINICAL RELEVANCE/APPLICATION

This finding should prompt follow-up imaging to assess the trajectory of the volume loss, which might have implications on patients' management and prognosis.

Printed on: 02/07/23

## Abstract Archives of the RSNA, 2022

S3B-SPNR-6

### Seed-to-Voxel Analysis of Resting-State fMRI Can Detect Functional Alterations in Seizure Onset and Spread Regions in Patients with Non-Lesional Temporal Lobe Epilepsy

Sunday, Nov. 27 12:15PM - 12:45PM Room: Learning Center - NR DPS

#### Participants

India Shelley, BA, Philadelphia, PA (*Presenter*) Nothing to Disclose

#### PURPOSE

Temporal lobe epilepsy (TLE) can have severe clinical signs and symptoms. Abnormal neural seizure networks from underlying pathology may facilitate seizure spread and be involved in the manifestation of symptoms in TLE. Currently, stereotactic electroencephalography (sEEG) can detect correlations between zones of seizure onset (OZ) and early (ESZ) and late (LSZ) spread. We examined whether patient resting-state fMRI (rsfMRI) scans can detect similar correlations between the OZ, ESZ, and LSZ. We aimed to see whether noninvasive imaging techniques can uncover patterns of seizure spread to potentially demarcate areas for intervention.

#### METHODS AND MATERIALS

This is a retrospective study of 8 patients with refractory, non-lesional TLE (ages 25-53) and 10 controls (ages 22-35). The TLE patients were MRI- on routine diagnostics and subsequently received sEEG. The OZ, ESZ, and LSZ were calculated by generating regions around sEEG contacts that recorded seizure activity. The LSZ was only available for 3 patients. These regions and functional images were registered to MNI space using MIRTk. For each subject, we used dual regression to detect amplitude synchronization of the OZ with the rest of the brain and calculated the ratio of correlated voxels to the spread zone. The same process was done using the OZ, ESZ, and LSZ of each TLE patient for each control. TLE patients were compared to controls individually using a Wilcoxon test and as a group using a Student's t-test,  $\alpha = 0.05$ . The average BOLD signal over the time series was calculated in the onset and spread regions and compared using z-score analysis and a Student's t-test,  $\alpha = 0.05$ .

#### RESULTS

5/8 TLE patients showed decreased correlations from the OZ to the ESZ compared to controls. Only 1 TLE patient showed an increased correlation. 2/3 TLE patients showed decreased correlations between the OZ and LSZ. Group analysis showed TLE patients had lower overall connectivity with the ESZ compared to controls. TLE patients had higher average BOLD signal in the OZ and ESZ but not LSZ.

#### CONCLUSION

s TLE patients show decreased functional connectivity from the OZ to both ESZ and LSZ. TLE patients showed higher neuronal activity in the OZ and ESZ. These results indicate TLE patients show high levels of pathologic seizure activity but dysfunctional connections in seizure-related areas. Seed-to-voxel analysis of rsfMRI can detect functional network disruption that may expose pathophysiology underlying seizure propagation.

#### CLINICAL RELEVANCE/APPLICATION

fMRI analysis is a promising noninvasive method to detect correlated brain regions that may be involved in seizure propagation. It can explore underlying pathology and understanding of the disease.

Printed on: 02/07/23

## Abstract Archives of the RSNA, 2022

S3B-SPNR-7

### Automated Subfield Volumetric Analysis of Amygdala, Hippocampus, and Thalamic Nuclei in Mesial Temporal Lobe Epilepsy

Sunday, Nov. 27 12:15PM - 12:45PM Room: Learning Center - NR DPS

#### Participants

India Shelley, BA, Philadelphia, PA (*Presenter*) Nothing to Disclose

#### PURPOSE

Identifying relationships between clinical features and quantitative characteristics of the amygdala-hippocampal and thalamic subregions in mesial temporal lobe epilepsy (mTLE) may offer insights into pathophysiology and the basis for imaging prognostic markers of treatment outcome.

#### METHODS AND MATERIALS

27 mTLE subjects with mesial temporal sclerosis (MTS) were scanned for conventional 3D T1w MPRAGE image and T2w scans. With respect to 12 months post-surgical seizure outcomes, 15 subjects reported seizure free and 12 had seizures. We performed quantitative automated segmentation and cortical parcellation using Freesurfer. Automatic labeling and volume estimation of hippocampal subfields, amygdala, and thalamic subnuclei were performed. Volume ratio (VR) for each label was computed and compared using linear regression analysis with significant FDR corrected p-value of <0.05. Additionally, we used age, sex, existence of tonic-clonic, age of seizure onset, and seizure class as confounding variables.

#### RESULTS

Amygdala: In the amygdala, the medial nucleus was the most significantly reduced in patients who were not seizure free when compared to patients who remained seizure free. Hippocampus: Comparison of volumes ipsilateral and contralateral with seizure outcomes showed volume loss was most noted in mesial hippocampal regions such as CA4 and hippocampal fissure. Volume loss was also most reduced in the presubiculum body in patients who were not seizure free at follow-up. Thalamus: VPL and PuL were the most significantly reduced thalamic nuclei in non-seizure free patients. In all statistically significant areas, volume reduction has been observed in the non-seizure free group.

#### CONCLUSION

We demonstrated varying degrees of volume loss in the hippocampus, thalamus, and amygdala subregions of MTS, especially between patients who remained seizure-free and those who did not. These results can be used to further understand mTLE pathophysiology.

#### CLINICAL RELEVANCE/APPLICATION

In the future, we hope these results can be used to deepen the understanding of mTLE pathophysiology, leading to improved patient outcomes and treatments.

Printed on: 02/07/23

## Abstract Archives of the RSNA, 2022

S3B-SPNR-8

### Comparison of Functionally Versus Structurally-defined Nodes for Evaluation of DTI Connectome Edge Density (ED) in Infants with Autism Spectrum Disorder (ASD)

Sunday, Nov. 27 12:15PM - 12:45PM Room: Learning Center - NR DPS

#### Participants

Clara Weber, New Haven, CT (*Presenter*) Nothing to Disclose

#### PURPOSE

In our previous study, conventional DTI metrics and connectome ED based on structurally-defined nodes found significant ASD-related changes among adolescents and adults, but not pediatric cohorts. Here, we analyzed infants at risk of ASD and adults, to evaluate connectome ED based on tractography between functionally defined nodes that showed correlation with from ASD severity in a separate cohort.

#### METHODS AND MATERIALS

We retrieved DTI from n=155 infants (Longitudinal MRI study of infants at Risk for Autism; median age at scan 7 months, ASD assessment at 24m) and n = 96 adults (Atypical Late Neurodevelopment in Autism, median age 230m) from the National Database of Autism Research. Lake et al. (Biol Psychiatry 2019;86(4):315-26) have previously identified cerebral regions (nodes) that showed significant positive, and respectively negative, functional correlation with symptom severity as measured by ADOS (Autism Diagnostic Observation Schedule) scores based on rs-fMRI from n=260 children. We subset these regions in two sensitivity levels and subsequently specified them as seed points in probabilistic tractography to generate ED maps. For statistical analysis, mean ED values within the JHU White Matter (WM) Labels atlas tracts were extracted.

#### RESULTS

ED within major WM tracts shows pervasive correlation with ASD diagnosis (Figure 1) in both infants and adults. While present both for ED generated based on positively and negatively correlated cortical regions, positively correlated regions showed more widespread ASD-related changes. Comparing correlation coefficients between different sensitivity levels revealed that ED based on more sensitive nodes shows stronger correlation to ASD diagnosis than ED constructed from less sensitive nodes.

#### CONCLUSION

While tractography ED based on structural nodes could only find ASD-related differences in adults' cohort (but not infants), we showed that constructing ED based on functionally defined nodes could identify ASD-related changes in both infants' and adults' cohorts.

#### CLINICAL RELEVANCE/APPLICATION

As alterations could only be detected in adolescent and adult cohorts in anatomy-based ED, our results imply benefits of combining functional and diffusion-weighted imaging for construction of connectome ED, especially in pediatric populations.

Printed on: 02/07/23

## Abstract Archives of the RSNA, 2022

S3B-SPNR-9

### Temporal Encephaloceles and Drug Resistant Epilepsy: Is There Radiological Correlation with The Epileptogenic Focus?

Sunday, Nov. 27 12:15PM - 12:45PM Room: Learning Center - NR DPS

#### Participants

Aleix Jareno Badenas, MD, Sant Vicenc de Castellet, Spain (*Presenter*) Nothing to Disclose

#### PURPOSE

Encephaloceles are protrusions of cerebral tissue through a skull defect. They are a possible cause of epilepsy, although their actual epileptogenic potential has not been assessed yet. Lately, with the improvement of MRI imaging, the identification of encephaloceles in patients with drug resistant epilepsy (DRE) has increased. The purposes of this study are: To correlate the location of encephaloceles with the epileptogenic focus in patients with DRE. To evaluate their characteristics and to correlate them with their epileptogenicity.

#### METHODS AND MATERIALS

We performed a retrospective analysis of the MRI and neurofunctional studies of patients of our epilepsy unit with DRE and an MRI diagnosis of encephalocele. We evaluated the correlation between the encephalocele's location and the epileptogenic focus, as well as their characteristics (number, location, size and presence of gliosis). The location and characteristics of the encephaloceles were evaluated in the 3T MRI studies with a specific epilepsy protocol. The epileptogenic focus was evaluated in our epilepsy unit after the evaluation of different neurofunctional techniques (video-EEG, PET/SPECT and SEEG).

#### RESULTS

We had a study population of 11 patients (7 women and 4 men) with a mean age of 24.6 years. Six (55%) patients had correlation between the epileptogenic focus and the location of the encephalocele, whilst in the other 5 (45%) they were not matching. 67% of the patients with correlation showed gliosis and a mean encephaloceles volume of 0.25cc, while 40% of patients without correlation presented gliosis and a mean volume of 0.33cc.

#### CONCLUSION

Our results show that encephaloceles have to be considered as potentially epileptogenic lesions in patients with DRE. Gliosis may be an indicator of higher epileptogenicity. In our group of patients, the smaller encephaloceles were more epileptogenic, which is inconsistent with previous literature.

#### CLINICAL RELEVANCE/APPLICATION

Our study shows that encephaloceles have epileptogenic potential and that some characteristics, such as the gliosis, may help to assess their epileptogenic potential.

Printed on: 02/07/23

## Abstract Archives of the RSNA, 2022

S3B-SPOB

### OB/Gynecology Sunday Poster Discussions - B

Sunday, Nov. 27 12:15PM - 12:45PM Room: Learning Center - OB DPS

#### Participants

Angela Tong, MD, New York, NY (*Moderator*) Equipment support, Siemens AG

#### Sub-Events

### S3B-SPOB-1 A Multi-Parametric Quantitative Assessment of Fetuses With Growth Restriction Using Advanced MRI Methods

#### Participants

Dafna Ben Bashat, PhD, (*Presenter*) Nothing to Disclose

#### PURPOSE

To assess fetal - placental structural and functional parameters using multi-parametric MRI methods and their association with gestational age (GA) and with fetal growth restriction (FGR) caused by placental insufficiency.

#### METHODS AND MATERIALS

Subjects 76 fetuses (31-38 weeks); 60 appropriate for gestational age (AGA), and 16 FGR caused by placental insufficiency. MRI data: acquired on 3T MRI systems (Siemens, Prisma/Skyra), including high-resolution fetal brain and body T2-weighted MRI for structural assessment of the fetus and placenta; and Pseudo continuous arterial spin labeling (pCASL) and intra-voxel incoherent motion (IVIM) for placental perfusion assessment. Image analysis: Total fetal body, brain and placenta volumes were extracted using deep learning segmentation methods. The distance of the umbilical cord insertion from the center (CI) was quantified manually. Placental perfusion parameters were calculated from pCASL and IVIM. Radiomics analysis was performed on all structural and functional parameters. Statistical analysis: Correlations with gestational age (GA) were measured in the AGA group, and differences between AGA and FGR were assessed using ANCOVA controlling for GA. Statistical significance was set to  $p < 0.05$ .

#### RESULTS

Significant correlations with GA were detected within the AGA group for total body volume; brain volume; and placental flow (f) extracted from IVIM. FGR fetuses had smaller total body and brain volumes compared to AGA, as well as larger CI, i.e, more marginal cord insertion. No significant differences between groups were detected for mean values of placental perfusion parameters, however, few radiomics features relating to shape and heterogeneity differentiated between groups.

#### CONCLUSION

This study provides MRI quantitative structural and perfusion assessment of 3rd trimester fetuses and demonstrates differences between AGA and FGR fetuses.

#### CLINICAL RELEVANCE/APPLICATION

This study demonstrated an MRI multi-parametric approach, providing reference values for several structural and functional parameters at late GA, and may be used to improve differentiation between AGA and FGR fetuses.

### S3B-SPOB-2 Rhombencephalosynapsis: A Underdiagnosed Condition Behind Severe Ventriculomegaly

#### Awards

Trainee Research Prize - Fellow

#### Participants

Isabella Bertuol Kinoshita, MD, Sao Paulo, Brazil (*Presenter*) Nothing to Disclose

#### PURPOSE

To evaluate and emphasize the association of rhombencephalosynapsis and severe ventriculomegaly in fetal magnetic resonance imaging (MRI).

#### METHODS AND MATERIALS

Fetal MR examinations performed due to ventriculomegaly in a single academic hospital were retrospectively reviewed. Fetuses with severe hydrocephalus in sonographic evaluation (ventricular atrium size of at least 15,1 mm plus brain parenchymal thinning) were included. Neural tube defects and unilateral or non-obstructive ventriculomegaly were exclusion criteria. MRI was performed after 24 week's gestational age, when the vermis and cerebellar folia are clearly visible. Four millimeter sections (without intervals) MR images were obtained with a field-of-view (FOV) of 30 or less. A Skyra 3T or Espree 1.5T unit (Siemens Healthineers, Erlangen, Germany) with 8 channel body array coils was employed. MR pulse sequences included: HASTE (TR 1000; TE 117), TrueFISP (TR 4,3; TE 2,15) and T1-W Gradient Echo (TR 136; TE 4). A detailed evaluation of the cerebellum and posterior fossa was conducted. The findings were described by two experienced pediatric neuroradiologists using pre-established rhombencephalosynapsis grading

criteria.

## **RESULTS**

Of 201 fetuses referred to MR due to severe ventriculomegaly, 111 were included. In 24,3% of the cases, an association of aqueductal stenosis and rhombencephalosynapsis was seen. Aqueductal stenosis alone was identified in 27,9%. Other associated conditions were: posterior fossa anomalies (17,1%); holoprosencephaly (18,8%) and diencephalic-mesencephalic junction anomalies (2,7%). Extrinsic aqueductal obstruction was seen in 5 cases, due to interhemispheric cyst (2,7%) and diencephalic-mesencephalic tumors (1,8%). In all fetuses, the following were also depicted: transverse cerebellar diameter inferior to the 3rd percentile for the gestational age; fusion of the dentate nucleus and continuous cerebellar folia in at least one axial and one coronal slice.

## **CONCLUSION**

s Rhombencephalosynapsis is found in a high percentage of fetuses with aqueductal stenosis and hydrocephalus.

## **CLINICAL RELEVANCE/APPLICATION**

Few reports describe the diagnosis of rhombencephalosynapsis associated with aqueductal stenosis in fetal MRI. The study shed light on the imaging findings and provided tools for accurate diagnosis.

Printed on: 02/07/23

## Abstract Archives of the RSNA, 2022

S3B-SPOB-1

### A Multi-Parametric Quantitative Assessment of Fetuses With Growth Restriction Using Advanced MRI Methods

Sunday, Nov. 27 12:15PM - 12:45PM Room: Learning Center - OB DPS

#### Participants

Dafna Ben Bashat, PhD, (*Presenter*) Nothing to Disclose

#### PURPOSE

To assess fetal - placental structural and functional parameters using multi-parametric MRI methods and their association with gestational age (GA) and with fetal growth restriction (FGR) caused by placental insufficiency.

#### METHODS AND MATERIALS

Subjects 76 fetuses (31-38 weeks); 60 appropriate for gestational age (AGA), and 16 FGR caused by placental insufficiency. MRI data: acquired on 3T MRI systems (Siemens, Prisma/Skyra), including high-resolution fetal brain and body T2-weighted MRI for structural assessment of the fetus and placenta; and Pseudo continuous arterial spin labeling (pCASL) and intra-voxel incoherent motion (IVIM) for placental perfusion assessment. Image analysis: Total fetal body, brain and placenta volumes were extracted using deep learning segmentation methods. The distance of the umbilical cord insertion from the center (CI) was quantified manually. Placental perfusion parameters were calculated from pCASL and IVIM. Radiomics analysis was performed on all structural and functional parameters. Statistical analysis: Correlations with gestational age (GA) were measured in the AGA group, and differences between AGA and FGR were assessed using ANCOVA controlling for GA. Statistical significance was set to  $p < 0.05$ .

#### RESULTS

Significant correlations with GA were detected within the AGA group for total body volume; brain volume; and placental flow (f) extracted from IVIM. FGR fetuses had smaller total body and brain volumes compared to AGA, as well as larger CI, i.e, more marginal cord insertion. No significant differences between groups were detected for mean values of placental perfusion parameters, however, few radiomics features relating to shape and heterogeneity differentiated between groups.

#### CONCLUSION

s This study provides MRI quantitative structural and perfusion assessment of 3rd trimester fetuses and demonstrates differences between AGA and FGR fetuses.

#### CLINICAL RELEVANCE/APPLICATION

This study demonstrated an MRI multi-parametric approach, providing reference values for several structural and functional parameters at late GA, and may be used to improve differentiation between AGA and FGR fetuses.

Printed on: 02/07/23

## Abstract Archives of the RSNA, 2022

S3B-SPOB-2

### Rhombencephalosynapsis: A Underdiagnosed Condition Behind Severe Ventriculomegaly

Sunday, Nov. 27 12:15PM - 12:45PM Room: Learning Center - OB DPS

#### Awards

Trainee Research Prize - Fellow

#### Participants

Isabella Bertuol Kinoshita, MD, Sao Paulo, Brazil (*Presenter*) Nothing to Disclose

#### PURPOSE

To evaluate and emphasize the association of rhombencephalosynapsis and severe ventriculomegaly in fetal magnetic resonance imaging (MRI).

#### METHODS AND MATERIALS

Fetal MR examinations performed due to ventriculomegaly in a single academic hospital were retrospectively reviewed. Fetuses with severe hydrocephalus in sonographic evaluation (ventricular atrium size of at least 15,1 mm plus brain parenchymal thinning) were included. Neural tube defects and unilateral or non-obstructive ventriculomegaly were exclusion criteria. MRI was performed after 24 week's gestational age, when the vermis and cerebellar folia are clearly visible. Four millimeters sections (without intervals) MR images were obtained with a field-of-view (FOV) of 30 or less. A Skyra 3T or Espree 1.5T unit (Siemens Healthineers, Erlangen, Germany) with 8 channel body array coils was employed. MR pulse sequences included: HASTE (TR 1000; TE 117), TrueFISP (TR 4,3; TE 2,15) and T1-W Gradient Echo (TR 136; TE 4). A detailed evaluation of the cerebellum and posterior fossa was conducted. The findings were described by two experienced pediatric neuroradiologists using pre-established rhombencephalosynapsis grading criteria.

#### RESULTS

Of 201 fetuses referred to MR due to severe ventriculomegaly, 111 were included. In 24,3% of the cases, an association of aqueductal stenosis and rhombencephalosynapsis was seen. Aqueductal stenosis alone was identified in 27,9%. Other associated conditions were: posterior fossa anomalies (17,1%); holoprosencephaly (18,8%) and diencephalic-mesencephalic junction anomalies (2,7%). Extrinsic aqueductal obstruction was seen in 5 cases, due to interhemispheric cyst (2,7%) and diencephalic-mesencephalic tumors (1,8%). In all fetuses, the following were also depicted: transverse cerebellar diameter inferior to the 3rd percentile for the gestational age; fusion of the dentate nucleus and continuous cerebellar folia in at least one axial and one coronal slice.

#### CONCLUSION

s Rhombencephalosynapsis is found in a high percentage of fetuses with aqueductal stenosis and hydrocephalus.

#### CLINICAL RELEVANCE/APPLICATION

Few reports describe the diagnosis of rhombencephalosynapsis associated with aqueductal stenosis in fetal MRI. The study shed light on the imaging findings and provided tools for accurate diagnosis.

Printed on: 02/07/23

## Abstract Archives of the RSNA, 2022

S3B-SPPD

### Pediatric Sunday Poster Discussions - B

Sunday, Nov. 27 12:15PM - 12:45PM Room: Learning Center - PD DPS

#### Participants

David M. Mirsky, MD, Aurora, CO (*Moderator*) Nothing to Disclose  
David M. Mirsky, MD, Aurora, CO (*Moderator*) Nothing to Disclose  
Eva Rubio, MD, Washington, DC (*Moderator*) Nothing to Disclose  
Eva Rubio, MD, Washington, DC (*Moderator*) Nothing to Disclose

#### Sub-Events

### S3B-SPPD-1 Quantification of Liver Fat Using Ultrasound-Guided Attenuation Parameter for Assessment of Steatosis with Reference to MRI-PDFF in Pediatric Non-Alcoholic Fatty Liver Disease

#### Participants

Jake Weeks, La Jolla, CA (*Presenter*) Nothing to Disclose

#### PURPOSE

The rising incidence of NAFLD demands the development of widely available, non-invasive screening techniques for evaluating liver steatosis. Prior studies have shown that the attenuation coefficient, as measured by Ultrasound-Guided Attenuation Parameter (UGAP), demonstrates a strong correlation with MRI-PDFF in adults. However, no study has evaluated its correlation with MRI-PDFF in children, and its performance in this group remains a gap in knowledge. This prospective pilot study examines the correlation of UGAP to MRI-PDFF in children with known or suspected NAFLD.

#### METHODS AND MATERIALS

Eighteen children with biopsy-proven NAFLD or suspected NAFLD, ages 10-16, were prospectively enrolled in an ongoing pilot research study to investigate quantitative ultrasound (US) and MRI biomarkers of liver disease. Each research visit included two ultrasound exams using a GE LOGIQ E10 system (GE Healthcare, Waukesha WI) and, on the same day, two MR exams on a GE Discovery MR750 3.0T scanner. In each ultrasound exam, least 6 valid UGAP values were acquired in a homogeneous area of liver parenchyma in the right lobe; the median and interquartile range (IQR) values were recorded. If the IQR/median < 0.30, the exam was considered reliable. MRI-PDFF was measured in the liver using IDEAL-IQ. Median UGAP values were correlated to PDFF values, using all available data. The confidence interval and significance of the correlation coefficient were computed using initial and repeat exams by a non-parametric bootstrap with per-patient resampling to adjust for within-patient dependence.

#### RESULTS

All UGAP exams met reliability criteria. 3 children could not tolerate MRI. The median of the 6 UGAP measurements and mean PDFF for 25 pairs of US and MRI exams were tested for correlation. Median per-child UGAP values ranged from 0.49 to 0.88 dB/cm/MHz (mean, 0.72). Mean per-child PDFF values ranged from 1.4% to 34.2% (mean, 17.6%). Median UGAP values and mean PDFF values were correlated for all 25 pairs of available data: the Pearson correlation coefficient was  $r = 0.72$  ( $p < 0.001$ ; 95% CI: 0.34, 0.88).

#### CONCLUSION

s UGAP and MRI-PDFF are significantly correlated in this preliminary pilot study in children with known or suspected NAFLD. This correlation is of similar strength to that found in prior studies in adults, but the sample size is small and the confidence interval is wide. Future studies with larger cohorts will be necessary to validate these findings.

#### CLINICAL RELEVANCE/APPLICATION

In this pilot study, UGAP showed promising correlation with MRI-PDFF in evaluating hepatic steatosis in children.

Printed on: 02/07/23

## Abstract Archives of the RSNA, 2022

S3B-SPPD-1

### Quantification of Liver Fat Using Ultrasound-Guided Attenuation Parameter for Assessment of Steatosis with Reference to MRI-PDFF in Pediatric Non-Alcoholic Fatty Liver Disease

Sunday, Nov. 27 12:15PM - 12:45PM Room: Learning Center - PD DPS

#### Participants

Jake Weeks, La Jolla, CA (*Presenter*) Nothing to Disclose

#### PURPOSE

The rising incidence of NAFLD demands the development of widely available, non-invasive screening techniques for evaluating liver steatosis. Prior studies have shown that the attenuation coefficient, as measured by Ultrasound-Guided Attenuation Parameter (UGAP), demonstrates a strong correlation with MRI-PDFF in adults. However, no study has evaluated its correlation with MRI-PDFF in children, and its performance in this group remains a gap in knowledge. This prospective pilot study examines the correlation of UGAP to MRI-PDFF in children with known or suspected NAFLD.

#### METHODS AND MATERIALS

Eighteen children with biopsy-proven NAFLD or suspected NAFLD, ages 10-16, were prospectively enrolled in an ongoing pilot research study to investigate quantitative ultrasound (US) and MRI biomarkers of liver disease. Each research visit included two ultrasound exams using a GE LOGIQ E10 system (GE Healthcare, Waukesha WI) and, on the same day, two MR exams on a GE Discovery MR750 3.0T scanner. In each ultrasound exam, least 6 valid UGAP values were acquired in a homogeneous area of liver parenchyma in the right lobe; the median and interquartile range (IQR) values were recorded. If the IQR/median < 0.30, the exam was considered reliable. MRI-PDFF was measured in the liver using IDEAL-IQ. Median UGAP values were correlated to PDFF values, using all available data. The confidence interval and significance of the correlation coefficient were computed using initial and repeat exams by a non-parametric bootstrap with per-patient resampling to adjust for within-patient dependence.

#### RESULTS

All UGAP exams met reliability criteria. 3 children could not tolerate MRI. The median of the 6 UGAP measurements and mean PDFF for 25 pairs of US and MRI exams were tested for correlation. Median per-child UGAP values ranged from 0.49 to 0.88 dB/cm/MHz (mean, 0.72). Mean per-child PDFF values ranged from 1.4% to 34.2% (mean, 17.6%). Median UGAP values and mean PDFF values were correlated for all 25 pairs of available data: the Pearson correlation coefficient was  $r = 0.72$  ( $p < 0.001$ ; 95% CI: 0.34, 0.88).

#### CONCLUSION

s UGAP and MRI-PDFF are significantly correlated in this preliminary pilot study in children with known or suspected NAFLD. This correlation is of similar strength to that found in prior studies in adults, but the sample size is small and the confidence interval is wide. Future studies with larger cohorts will be necessary to validate these findings.

#### CLINICAL RELEVANCE/APPLICATION

In this pilot study, UGAP showed promising correlation with MRI-PDFF in evaluating hepatic steatosis in children.

Printed on: 02/07/23

## Abstract Archives of the RSNA, 2022

S3B-SPPH

### Physics Sunday Poster Discussions - B

Sunday, Nov. 27 12:15PM - 12:45PM Room: Learning Center - PH DPS

#### Participants

Jia Wang, PhD, Stanford, CA (*Moderator*) Nothing to Disclose

#### Sub-Events

### S3B-SPPH-1 Diagnostic Accuracy of Artificial Intelligence for Pediatric Pulmonary Nodule Detection in Computed Tomography of the Chest: Comparison at Standard and Simulated Lower Radiation Doses

#### Participants

Rida Salman, MD, Houston, TX (*Presenter*) Nothing to Disclose

#### PURPOSE

To determine the diagnostic accuracy of an adult pulmonary nodule detection AI algorithm in pediatric patients imaged with CT chest, at standard and simulated lower radiation doses.

#### METHODS AND MATERIALS

We performed a retrospective chart review of all patients between 12-18 years-old who underwent a chest CT with or without contrast, on the Siemens SOMATOM Force from 12/20/2021 to 4/12/2022. Simulated lower doses at 75%, 50% and 25% were reconstructed at 3 mm slice thickness and with lung kernel Bl64d using ReconCT (Siemens Healthineers, Forchheim, Germany) and imported to an existing AI software, Syngo CT Lung Computer Aided Design (CAD) (Siemens Healthineers, Forchheim, Germany). Two Board certified radiologists reviewed the CTs and their consensus read was considered the gold standard. A pediatric radiology fellow compared the Lung CAD results at each dose level to the gold standard on a nodule by nodule basis. Data analysis was done using descriptive statistics; the sensitivity (Sn), specificity (Sp), positive predictive value (PPV), and false positive rate (FPR) of lung nodule detection at different doses was reported.

#### RESULTS

30 patients were included. 164 nodules were identified by the two radiologists. At 100%, 75%, 50%, 25%, Lung CAD detected 60,62,58,62 nodules; 28,28,29,26 were true positive (Sn=17%,17%,18%,16%), 30,32,27,34 were false positive (PPV=52%,53%,48%,57%) and 2 were missed by radiologists in 2 patients (2/30, 7%), respectively. Lung CAD and radiologists agreed on 4,5,5,3 patients who did not have any nodule (true negative), respectively. The 30,32,27,34 false nodules were identified by Lung CAD in 15,14,13,16 patients; 4,3,3,5 of whom did not have any nodule by gold standard read (Sp=4/19=21%,26%,28%,16% and FPR=15/19=79%,74%,72%,84%), respectively.

#### CONCLUSION

The adult Lung CAD shows low sensitivity and specificity with high false positive rate at all simulated lower doses. However, the dose may be reduced by 50% without further compromise to the Lung CAD performance. Slice thickness of the reconstructed volumes could be a likely cause for the less than optimal performance and further evaluation with thinner slices and other kernels is planned as a future study.

#### CLINICAL RELEVANCE/APPLICATION

Evaluation of adult Lung CAD performance for pulmonary nodules detection in children at lower simulated doses might guide ongoing research focusing on algorithm improvements in children.

### S3B-SPPH-2 Accurate Liver Tumor Detection on Noncontrast CT Scans via Annotation-Efficient Semi-Supervised Learning

#### Participants

Jack Wang, (*Presenter*) Nothing to Disclose

#### PURPOSE

Noncontrast CT routinely performed for different clinical indications is good for opportunistic screening of liver cancer at no additional cost or radiation exposure. We aim to develop a deep learning tool to assist radiologists in detecting hepatocellular carcinoma (HCC) and other liver tumors.

#### METHODS AND MATERIALS

We collected multiphase liver CT images from 909 patients with HCC, 307 patients with nonHCC (cholangiocarcinoma, metastasis, hemangioma), and 280 patients with normal liver. All HCC and nonHCC were confirmed by pathology. To obtain mask-level annotations, we applied nnUNet and semi-supervised learning on five public abdomen CT datasets (BTCV and four MSD sub-datasets) to train an initial multi-class (liver, liver tumor, hepatic vessels, gallbladder, stomach, spleen) semantic segmentation model on venous phase CT images. It was then applied to the venous phase of our data to generate initial multi-class masks. The HCC masks

were reviewed and corrected by an experienced liver imaging specialist using a customized multiphase CT labeling tool with referring to medical reports. The masks were then registered to the noncontrast phase CT by DEEDS, to obtain annotations. We randomly split our data into training, validation, and testing sets according to a ratio of 64%, 16%, and 20%. A nnUNet was trained to segment the HCC, nonHCC, and other classes. A patient was classified as HCC, nonHCC, or normal based on these segmented tumor volumes, with the optimal cutoff determined on the validation set.

## RESULTS

The testing set included 190 HCCs, 62 nonHCCs, and 51 normals. Our model achieved an AUC = 0.977. With the optimal cutoff volume (HCC+nonHCC) of 1.5 cm<sup>3</sup>, the patient-level sensitivity is 94.5%, and specificity is 98.5%. Defining successful tumor detection as the overlapping between auto-segmentation and ground-truth > 0 voxels, the sensitivity is 91.2%. When considering the segmented tumor type with a larger volume as the patient-level tumor type, the classification accuracy of HCC vs. nonHCC is 85.3% vs. 46.8%.

## CONCLUSION

The annotation-efficient semi-supervised learning method enabled automated liver tumor detection from noncontrast CT scans with high sensitivity and specificity.

## CLINICAL RELEVANCE/APPLICATION

The developed model can help reduce missing rate with low false-positive rate in noncontrast CT scans. It can also be used as an opportunistic screening tool for liver cancer.

### S3B-SPPH-3 Development of a Moiré Free Two Dimensional Anti-scatter to Improve Image Quality in Cone-Beam Computed Tomography System

Participants

Jongkuk Kim, (*Presenter*) Nothing to Disclose

## PURPOSE

Conventional anti-scatter grid (ASG) has been rarely used in a cone-beam computed tomography (CBCT) system because it does not provide a sufficient effect on the scatter reduction and also can cause Moiré artifact. We have developed a two-dimensional anti-scatter grid (2D ASG) designed with Moiré free as a scatter reduction solution in CBCT system. We show how the 2D ASG is fabricated using sawing process method and demonstrate Moiré free image and the improvement of image quality compared with conventional ASGs.

## METHODS AND MATERIALS

In order to fabricate a Moiré free 2D ASG, a graphite plate was used as an interspace body and it was sawed by a diamond-coated blade to make septa focused on x-ray source. Line density of the 2D ASG was designed to match with a pixel pitch of a VIVIX-D 1212G flat panel detector (FPD) in our CBCT testbed. Projection images were acquired at 100 kV of tube voltage and 4 mA for Catphan700 phantom to analyze Moiré image qualitatively and they were reconstructed using Feldkamp-Davis-Kress (FDK) algorithm to evaluate the effect of 2D ASG compared to a conventional ASG. Quantitative analysis for ASGs was performed using uniformity index to measure cupping effect and contrast noise ratio (CNR) with respect to No-ASG.

## RESULTS

No Moiré artifact was shown in the projection image of the 2D ASG compared with an image of a conventional ASG, and the spatial frequency domain image also shows there are no frequency peaks that indicate Moiré artifact. The cupping artifact was reduced by about 42 % for the 2D ASG and about 28 % for the conventional ASG. CNR values for the two types of ASG were increased by 40% and 25 % respectively.

## CONCLUSION

The improvement of image quality for the 2D ASG was demonstrated by both measurement results of cupping and CNR compared to the conventional ASG. Also, the 2D ASG does not have to take a further step to remove Moiré artifact. Thus, the Moiré free 2D ASG can be a solution for scatter rejection in CBCT.

## CLINICAL RELEVANCE/APPLICATION

The Moiré free 2D ASG can be easily applied to improve image quality by reducing scatter radiation in clinical CBCT systems, such as image-guided radiation therapy.

### S3B-SPPH-4 Effective Doses Associated With Weight-Bearing Imaging of the Hip and Extremities on a New Dedicated Cone-Beam CT Scanner

Participants

Jaydev K. Dave, PhD, Philadelphia, PA (*Presenter*) Research Grant, Koninklijke Philips NV; Equipment support, Lantheus Medical Imaging; Equipment support, General Electric Company; Research Consultant, Curvebeam LLC; Consultant, Rayscan, Inc.

## PURPOSE

The purpose of this project was two-fold; first, to measure organ and effective doses associated with weight-bearing CT imaging of the hip with a new dedicated cone-beam CT (CBCT) scanner (HiRise, CurveBeam) and compare with hip imaging performed on a conventional multidetector CT (MDCT; iCT 256, Philips Healthcare) and second, to compare effective doses associated with hand/wrist imaging and weight-bearing imaging of knees and foot/ankle between HiRise CBCT and other CBCT scanner (LineUp, Curvebeam) designed for extremity imaging.

## METHODS AND MATERIALS

Sectional and customized anthropomorphic phantoms of the adult hip (ATOM 701-G, CIRS), and hand/wrist (Model-XA231P), knee (Model-XA245L), and foot/ankle (Model-XA241R; The Phantom Laboratory) were used. Organ dose measurements were performed with OSL dosimeters (screened nanoDots, Landauer) readout by a calibrated microStar reader (Landauer). Adult hip phantom was scanned on the HiRise and iCT scanners, and other phantoms were scanned on the HiRise and LineUp scanners for dose comparisons using routine and manufacturer-recommended protocols. CBCT scans were repeated to assess reproducibility and

rotational variability.

## RESULTS

For hip imaging, average tissue-absorbed doses were significantly higher with MDCT ( $11.7 \pm 5.1$  mGy) relative to CBCT ( $3.6 \pm 2.1$  mGy;  $p < 0.001$ ), yielding effective dose values of 3.5 mSv and 0.9 mSv, respectively. No differences were noted in dose measurements while assessing reproducibility ( $p = 0.89$ ) and rotational dependency ( $p = 0.26$ ). The effective doses for imaging of the hand/wrist, knees and foot/ankle were significantly higher ( $p = 0.001$ ) for the HiRise system ( $1.6$ - $6.8$   $\mu$ Sv) relative to the LineUp system ( $0.3$ - $3.2$   $\mu$ Sv).

## CONCLUSION

Effective doses for hip imaging with CBCT could be substantially lower than with MDCT. The reported effective dose values for weight-bearing imaging of the hip (0.9 mSv) and extremities (max 6.8  $\mu$ Sv) are low. Therefore, clinical appropriateness/applicability should be considered for imaging using dedicated CBCT scanners.

## CLINICAL RELEVANCE/APPLICATION

Weight-bearing imaging of the hip and extremities permits diagnosis and surgical management by assessing misalignment and concomitant deformities.

### S3B-SPPH-5 Photon Counting Detector: The First Human Images

Participants

Ibrahim Bechwati, Danvers, MA (*Presenter*) Employee, Samsung Electronics Co, Ltd

## PURPOSE

The main purpose is to demonstrate the clinical imaging capabilities of the new Photon Counting Detector (PCD) fitted on the OmniTom scanner built by Neurologica Corporation.

## METHODS AND MATERIALS

The OmniTom scanner fitted with PCD array becomes the second scanner to get FDA 510K approval. The scanner gets approved for full diagnostic imaging. The OmniTom is a battery operated 16 slice head mobile scanner. It supports axial and helical scanning modes. The PCD array is made of individual cells of  $0.19 \times 0.23$  mm<sup>2</sup>. The Cadmium Telluride (CdTe) cells are binned to match the EID scanner detector size. The array provides three overlapping energy bands generating three images. A full spectrum image, a medium energy image and a high energy image. The first PCD image generated by the full spectrum is equivalent to the current CT images of the EID array. Two OmniTom scanners equipped with a PCD and an EID detector array were used to compare the image quality. Three different volunteers were scanned using a low dose scan of 40 mGy. Two volunteers were scanned on both scanners. Images from three 10mm sections were compared. The scanned sections are taken at the sinus level, the orbital region, and the top of the skull. The third volunteer underwent a complete head scan using only the OmniTom PCD. The scan covers the entire brain starting from above the upper jaw.

## RESULTS

The scans clearly show that PCD detectors can generate diagnostically acceptable images. The images were reviewed by two independent radiologists who both agreed that the images from the PCD OmniTom are diagnostically equivalent to the EID scanner.

## CONCLUSION

The comparative studies show the similarity between the PCD and the EID detectors. The full head scan demonstrates the ability of the PCD in doing complete clinical scan as needed.

## CLINICAL RELEVANCE/APPLICATION

Although this study is focused on demonstrating equivalent image quality to the conventional CT, the PCD scanner shows better low contrast distinction between the white and grey matter in the brain images. The PCD images also show less beam hardening artifact as seen in the nasal and orbital images.

### S3B-SPPH-6 Spectral Physical Density Quantifications for Non-invasive, Real-Time Spectral CT Thermometry

Participants

Leening Liu, Philadelphia, PA (*Presenter*) Nothing to Disclose

## PURPOSE

Hepatocellular carcinoma (HCC) is typically treated with thermal ablation under the guidance of computed tomography (CT). Though it is the best performing procedure, the rate of local recurrence is high. Real-time temperature feedback may provide the means to ensure complete ablation while preventing damage to surrounding healthy tissue and critical structures. We assess the feasibility of non-invasive spectral CT thermometry by the principle of thermal volumetric expansion that relates temperature and physical density.

## METHODS AND MATERIALS

To evaluate the relationship between physical density and temperature, a fiber optic temperature sensor was placed within a specifically designed tissue mimicking phantom that emulates the attenuation and thermal properties of liver. The phantom was subjected to a range of temperatures through heating and cooling while simultaneously being scanned with a dual-layer spectral CT at varying radiation doses (5 - 56.8 mGy). Clinically available spectral results were then utilized to generate physical density maps. Physical density was measured in regions of interest corresponding to the temperature sensor every 5 °C for each dose. A linear fit based on thermal volumetric expansion was applied to assess the relationship, and temperature sensitivity was calculated for different reconstruction parameters to inform future protocol optimization.

## RESULTS

Physical density reflected thermal volumetric expansion with a slope of  $0.000491$  mL/g/°C and a R value of 0.9942, demonstrating a strong positively correlated relationship. Temperature sensitivity improved with larger slice thickness, a smooth iterative

reconstruction kernel, and higher iterative reconstruction level. With radiation dose, it varied from 6.0 to 1.6 °C/g/mL between 5 and 56.8 mGy.

## CONCLUSION

s Spectral physical density quantifications of the tissue mimicking phantom affirmed a strong relationship with temperature that corresponded to thermal volumetric expansion. With this relationship, changes in physical density can be utilized to determine changes in temperature to provide non-invasive, real-time thermometry in thermal ablation with a temperature sensitivity of 1.6 °C/g/mL.

## CLINICAL RELEVANCE/APPLICATION

Thermal ablation procedures, using spectral CT thermometry with physical density measurements, may be effectively carried out for reducing local tumor recurrences by providing non-invasive, real-time feedback.

### S3B-SPPH-7 The Performance of Using CT Value Distribution in Dual-Energy Spectral CT Images to Predict Osteoporosis

Participants  
Tongtong DU, Xian, China (*Presenter*) Nothing to Disclose

## PURPOSE

To investigate the performance of using CT value distribution in dual-energy spectral CT (DEsCT) images to predict osteoporosis.

## METHODS AND MATERIALS

This study was IRB approved and consented by patients. A total of 156 consecutive patients (81 females and 80 males; mean age: 57.43±5.95 years, range 50-83 years) for chest CT screening were prospectively enrolled. All patients underwent chest DEsCT and Dual energy X-ray absorptiometry (DXA). Patients were divided into 2 groups using the T-score for the 1st lumbar vertebra on DXA: non-osteoporosis with T>-2.5 (n=101) and Osteoporosis with T=-2.5 (n=55). The chest DEsCT was performed on a 256-row Revolution CT (GE Healthcare) using 80-140kVp switching, 200mA and 0.5s/r. All images were reconstructed with 1.25mm thickness and analyzed using the GSI Viewer software on an AW4.7 workstation. CT values of the 1st lumbar vertebra were measured on the 120kVp-like images. According to CT histogram, the CT values were divided into 4 levels: A, <100HU; B, 100-199HU; C, 200-299 HU; D, ≥300HU. The distribution percentage in each level was compared between osteoporosis and non-osteoporosis groups. The cutoff of CT value distribution percentage for differentiating osteoporosis from non-osteoporosis was obtained by drawing a receiver operating characteristic (ROC) curve. The sensitivity, specificity, positive predictive value (PPV), and negative predictive value (NPV) were calculated. All statistical analyses were performed using the IBM SPSS statistical software (version 22.0), and two-tailed p<0.05 was considered statistically significant.

## RESULTS

The CT value distribution percentages in all four levels in osteoporosis group were significant different from those in non-osteoporosis group (all p<0.05). Specifically, the percentage in level A showed the best diagnostic performance for osteoporosis, and provided the area-under-the-curve (AUC), sensitivity, specificity, PPV and NPV of 0.805, 0.818, 0.745, 0.654 and 0.748, respectively with a cutoff of 18.74%.

## CONCLUSION

s The distribution percentage of CT value based on spectral histogram could predict osteoporosis and have a good diagnostic performance.

## CLINICAL RELEVANCE/APPLICATION

CT value distribution percentage based on DEsCT could provide more information about osteoporosis.

### S3B-SPPH-9 Technical Performance Study of the First Mobile Photon-Counting Detector CT

Participants  
Junyoung Park, Suwon-Si, Korea, Republic Of (*Presenter*) Employee, Samsung Electronics Co, Ltd

## PURPOSE

The purpose of this study is to evaluate the unique applications of photon-counting detectors (PCD) CT. The first is ability to "on demand" changes the scanner spatial resolution. The second is the ability to do "simultaneous" multi-energy scanning for material decomposition.

## METHODS AND MATERIALS

In this study, the FDA 510(k) cleared mobile PCD-CT (OmniTom Elite) was used. The diagnostic performance of the scanner was proven using three clinical scans. The spatial resolution of the PCD-CT scanner was tested using the high contrast module of ACR accreditation phantom. The spatial resolutions of a large detector pitch of 0.71-mm (14 lp/cm) and a smaller pitch of 0.35-mm (28 lp/cm) for PCD-CT were tested. For multi-energy CT feasibility, Gammex phantom containing solid iodine and calcium inserts was scanned with three energy thresholds using PCD-CT. For material decomposition capability of PCD-CT, the iodine, calcium, and water maps were generated. Virtual mono-energetic images (VMI) from 40 keV to 120 keV were synthesized and the linear attenuation coefficients (LAC) of all the inserts of Gammex phantom were compared against manufacturer reference values.

## RESULTS

The small pitch acquisition mode shows the highest resolution pattern of 11 lp/cm while only the resolution pattern of 7 lp/cm is seen when the same kernel (Posterior Fossa-kernel) is used in large pitch acquisition mode. For the quantitative multi-energy CT performance, the measured LAC in VMI of inserts of Gammex phantom matched the manufacturer reference values with mean percent error of 0.986%. In addition, the decomposition results with PCD-CT show that the iodine, calcium, and water can be well separated and quantified.

## CONCLUSION

s We have shown that the PCD detector CT can accommodate a multiple resolution acquisition mode without physically changing

As we have shown that the PCD detector CT can accommodate a multiple resolution acquisition mode without physically changing the detector CT. The first clinical mobile PCD-CT can provide superior spatial resolution than large pitch acquisition mode which is equivalent with conventional mobile CT. Additionally, the results from quantitative multi-energy CT performance demonstrated that the PCD-CT was able to provide reliable simultaneous multi-energy images for material decomposition with single exposure.

#### **CLINICAL RELEVANCE/APPLICATION**

The validated unique characteristics of PCD-CT are highly desirable in clinical scanning. The ability to switch between different acquisition modes expands the clinical use of the scanner, e.g., high resolution temporal bone scans and lower resolution abdominal imaging. The capability of simultaneous multi-energy imaging leads to a precise registration that is needed to ensure the success of various multi-energy applications, including generation of material decomposition maps, VMI and virtual non-contrast images.

Printed on: 02/07/23



## Abstract Archives of the RSNA, 2022

S3B-SPPH-1

### Diagnostic Accuracy of Artificial Intelligence for Pediatric Pulmonary Nodule Detection in Computed Tomography of the Chest: Comparison at Standard and Simulated Lower Radiation Doses

Sunday, Nov. 27 12:15PM - 12:45PM Room: Learning Center - PH DPS

#### Participants

Rida Salman, MD, Houston, TX (*Presenter*) Nothing to Disclose

#### PURPOSE

To determine the diagnostic accuracy of an adult pulmonary nodule detection AI algorithm in pediatric patients imaged with CT chest, at standard and simulated lower radiation doses.

#### METHODS AND MATERIALS

We performed a retrospective chart review of all patients between 12-18 years-old who underwent a chest CT with or without contrast, on the Siemens SOMATOM Force from 12/20/2021 to 4/12/2022. Simulated lower doses at 75%, 50% and 25% were reconstructed at 3 mm slice thickness and with lung kernel Bl64d using ReconCT (Siemens Healthineers, Forchheim, Germany) and imported to an existing AI software, Syngo CT Lung Computer Aided Design (CAD) (Siemens Healthineers, Forchheim, Germany). Two Board certified radiologists reviewed the CTs and their consensus read was considered the gold standard. A pediatric radiology fellow compared the Lung CAD results at each dose level to the gold standard on a nodule by nodule basis. Data analysis was done using descriptive statistics; the sensitivity (Sn), specificity (Sp), positive predictive value (PPV), and false positive rate (FPR) of lung nodule detection at different doses was reported.

#### RESULTS

30 patients were included. 164 nodules were identified by the two radiologists. At 100%, 75%, 50%, 25%, Lung CAD detected 60,62,58,62 nodules; 28,28,29,26 were true positive (Sn=17%,17%,18%,16%), 30,32,27,34 were false positive (PPV=52%,53%,48%,57%) and 2 were missed by radiologists in 2 patients (2/30, 7%), respectively. Lung CAD and radiologists agreed on 4,5,5,3 patients who did not have any nodule (true negative), respectively. The 30,32,27,34 false nodules were identified by Lung CAD in 15,14,13,16 patients; 4,3,3,5 of whom did not have any nodule by gold standard read (Sp=4/19=21%,26%,28%,16% and FPR=15/19=79%,74%,72%,84%), respectively.

#### CONCLUSION

The adult Lung CAD shows low sensitivity and specificity with high false positive rate at all simulated lower doses. However, the dose may be reduced by 50% without further compromise to the Lung CAD performance. Slice thickness of the reconstructed volumes could be a likely cause for the less than optimal performance and further evaluation with thinner slices and other kernels is planned as a future study.

#### CLINICAL RELEVANCE/APPLICATION

Evaluation of adult Lung CAD performance for pulmonary nodules detection in children at lower simulated doses might guide ongoing research focusing on algorithm improvements in children.

Printed on: 02/07/23

## Abstract Archives of the RSNA, 2022

S3B-SPPH-2

### Accurate Liver Tumor Detection on Noncontrast CT Scans via Annotation-Efficient Semi-Supervised Learning

Sunday, Nov. 27 12:15PM - 12:45PM Room: Learning Center - PH DPS

#### Participants

Jack Wang, (*Presenter*) Nothing to Disclose

#### PURPOSE

Noncontrast CT routinely performed for different clinical indications is good for opportunistic screening of liver cancer at no additional cost or radiation exposure. We aim to develop a deep learning tool to assist radiologists in detecting hepatocellular carcinoma (HCC) and other liver tumors.

#### METHODS AND MATERIALS

We collected multiphase liver CT images from 909 patients with HCC, 307 patients with nonHCC (cholangiocarcinoma, metastasis, hemangioma), and 280 patients with normal liver. All HCC and nonHCC were confirmed by pathology. To obtain mask-level annotations, we applied nnUNet and semi-supervised learning on five public abdomen CT datasets (BTCV and four MSD sub-datasets) to train an initial multi-class (liver, liver tumor, hepatic vessels, gallbladder, stomach, spleen) semantic segmentation model on venous phase CT images. It was then applied to the venous phase of our data to generate initial multi-class masks. The HCC masks were reviewed and corrected by an experienced liver imaging specialist using a customized multiphase CT labeling tool with referring to medical reports. The masks were then registered to the noncontrast phase CT by DEEDS, to obtain annotations. We randomly split our data into training, validation, and testing sets according to a ratio of 64%, 16%, and 20%. A nnUNet was trained to segment the HCC, nonHCC, and other classes. A patient was classified as HCC, nonHCC, or normal based on these segmented tumor volumes, with the optimal cutoff determined on the validation set.

#### RESULTS

The testing set included 190 HCCs, 62 nonHCCs, and 51 normals. Our model achieved an AUC = 0.977. With the optimal cutoff volume (HCC+nonHCC) of 1.5 cm<sup>3</sup>, the patient-level sensitivity is 94.5%, and specificity is 98.5%. Defining successful tumor detection as the overlapping between auto-segmentation and ground-truth > 0 voxels, the sensitivity is 91.2%. When considering the segmented tumor type with a larger volume as the patient-level tumor type, the classification accuracy of HCC vs. nonHCC is 85.3% vs. 46.8%.

#### CONCLUSION

The annotation-efficient semi-supervised learning method enabled automated liver tumor detection from noncontrast CT scans with high sensitivity and specificity.

#### CLINICAL RELEVANCE/APPLICATION

The developed model can help reduce missing rate with low false-positive rate in noncontrast CT scans. It can also be used as an opportunistic screening tool for liver cancer.

Printed on: 02/07/23

## Abstract Archives of the RSNA, 2022

S3B-SPPH-3

### Development of a Moiré Free Two Dimensional Anti-scatter to Improve Image Quality in Cone-Beam Computed Tomography System

Sunday, Nov. 27 12:15PM - 12:45PM Room: Learning Center - PH DPS

#### Participants

Jongkuk Kim, (*Presenter*) Nothing to Disclose

#### PURPOSE

Conventional anti-scatter grid (ASG) has been rarely used in a cone-beam computed tomography (CBCT) system because it does not provide a sufficient effect on the scatter reduction and also can cause Moiré artifact. We have developed a two-dimensional anti-scatter grid (2D ASG) designed with Moiré free as a scatter reduction solution in CBCT system. We show how the 2D ASG is fabricated using sawing process method and demonstrate Moiré free image and the improvement of image quality compared with conventional ASGs.

#### METHODS AND MATERIALS

In order to fabricate a Moiré free 2D ASG, a graphite plate was used as an interspace body and it was sawed by a diamond-coated blade to make septa focused on x-ray source. Line density of the 2D ASG was designed to match with a pixel pitch of a VIVIX-D 1212G flat panel detector (FPD) in our CBCT testbed. Projection images were acquired at 100 kV of tube voltage and 4 mA for Catphan700 phantom to analyze Moiré image qualitatively and they were reconstructed using Feldkamp-Davis-Kress (FDK) algorithm to evaluate the effect of 2D ASG compared to a conventional ASG. Quantitative analysis for ASGs was performed using uniformity index to measure cupping effect and contrast noise ratio (CNR) with respect to No-ASG.

#### RESULTS

No Moiré artifact was shown in the projection image of the 2D ASG compared with an image of a conventional ASG, and the spatial frequency domain image also shows there are no frequency peaks that indicate Moiré artifact. The cupping artifact was reduced by about 42 % for the 2D ASG and about 28 % for the conventional ASG. CNR values for the two types of ASG were increased by 40% and 25 % respectively.

#### CONCLUSION

The improvement of image quality for the 2D ASG was demonstrated by both measurement results of cupping and CNR compared to the conventional ASG. Also, the 2D ASG does not have to take a further step to remove Moiré artifact. Thus, the Moiré free 2D ASG can be a solution for scatter rejection in CBCT.

#### CLINICAL RELEVANCE/APPLICATION

The Moiré free 2D ASG can be easily applied to improve image quality by reducing scatter radiation in clinical CBCT systems, such as image-guided radiation therapy.

Printed on: 02/07/23

## Abstract Archives of the RSNA, 2022

S3B-SPPH-4

### Effective Doses Associated With Weight-Bearing Imaging of the Hip and Extremities on a New Dedicated Cone-Beam CT Scanner

Sunday, Nov. 27 12:15PM - 12:45PM Room: Learning Center - PH DPS

#### Participants

Jaydev K. Dave, PhD, Philadelphia, PA (*Presenter*) Research Grant, Koninklijke Philips NV; Equipment support, Lantheus Medical Imaging; Equipment support, General Electric Company; Research Consultant, Curvebeam LLC; Consultant, Rayscan, Inc.

#### PURPOSE

The purpose of this project was two-fold; first, to measure organ and effective doses associated with weight-bearing CT imaging of the hip with a new dedicated cone-beam CT (CBCT) scanner (HiRise, CurveBeam) and compare with hip imaging performed on a conventional multidetector CT (MDCT; iCT 256, Philips Healthcare) and second, to compare effective doses associated with hand/wrist imaging and weight-bearing imaging of knees and foot/ankle between HiRise CBCT and other CBCT scanner (LineUp, Curvebeam) designed for extremity imaging.

#### METHODS AND MATERIALS

Sectional and customized anthropomorphic phantoms of the adult hip (ATOM 701-G, CIRS), and hand/wrist (Model-XA231P), knee (Model-XA245L), and foot/ankle (Model-XA241R; The Phantom Laboratory) were used. Organ dose measurements were performed with OSL dosimeters (screened nanoDots, Landauer) readout by a calibrated microStar reader (Landauer). Adult hip phantom was scanned on the HiRise and iCT scanners, and other phantoms were scanned on the HiRise and LineUp scanners for dose comparisons using routine and manufacturer-recommended protocols. CBCT scans were repeated to assess reproducibility and rotational variability.

#### RESULTS

For hip imaging, average tissue-absorbed doses were significantly higher with MDCT ( $11.7 \pm 5.1$  mGy) relative to CBCT ( $3.6 \pm 2.1$  mGy;  $p < 0.001$ ), yielding effective dose values of 3.5 mSv and 0.9 mSv, respectively. No differences were noted in dose measurements while assessing reproducibility ( $p = 0.89$ ) and rotational dependency ( $p = 0.26$ ). The effective doses for imaging of the hand/wrist, knees and foot/ankle were significantly higher ( $p = 0.001$ ) for the HiRise system ( $1.6$ - $6.8$   $\mu$ Sv) relative to the LineUp system ( $0.3$ - $3.2$   $\mu$ Sv).

#### CONCLUSION

Effective doses for hip imaging with CBCT could be substantially lower than with MDCT. The reported effective dose values for weight-bearing imaging of the hip (0.9 mSv) and extremities (max 6.8  $\mu$ Sv) are low. Therefore, clinical appropriateness/applicability should be considered for imaging using dedicated CBCT scanners.

#### CLINICAL RELEVANCE/APPLICATION

Weight-bearing imaging of the hip and extremities permits diagnosis and surgical management by assessing misalignment and concomitant deformities.

Printed on: 02/07/23

## Abstract Archives of the RSNA, 2022

S3B-SPPH-5

### Photon Counting Detector: The First Human Images

Sunday, Nov. 27 12:15PM - 12:45PM Room: Learning Center - PH DPS

#### Participants

Ibrahim Bechwati, Danvers, MA (*Presenter*) Employee, Samsung Electronics Co, Ltd

#### PURPOSE

The main purpose is to demonstrate the clinical imaging capabilities of the new Photon Counting Detector (PCD) fitted on the OmniTom scanner built by Neurologica Corporation.

#### METHODS AND MATERIALS

The OmniTom scanner fitted with PCD array becomes the second scanner to get FDA 510K approval. The scanner gets approved for full diagnostic imaging. The OmniTom is a battery operated 16 slice head mobile scanner. It supports axial and helical scanning modes. The PCD array is made of individual cells of 0.19x0.23 mm<sup>2</sup>. The Cadmium Telluride (CdTe) cells are binned to match the EID scanner detector size. The array provides three overlapping energy bands generating three images. A full spectrum image, a medium energy image and a high energy image. The first PCD image generated by the full spectrum is equivalent to the current CT images of the EID array. Two OmniTom scanners equipped with a PCD and an EID detector array were used to compare the image quality. Three different volunteers were scanned using a low dose scan of 40 mGy. Two volunteers were scanned on both scanners. Images from three 10mm sections were compared. The scanned sections are taken at the sinus level, the orbital region, and the top of the skull. The third volunteer underwent a complete head scan using only the OmniTom PCD. The scan covers the entire brain starting from above the upper jaw.

#### RESULTS

The scans clearly show that PCD detectors can generate diagnostically acceptable images. The images were reviewed by two independent radiologists who both agreed that the images from the PCD OmniTom are diagnostically equivalent to the EID scanner.

#### CONCLUSION

The comparative studies show the similarity between the PCD and the EID detectors. The full head scan demonstrates the ability of the PCD in doing complete clinical scan as needed.

#### CLINICAL RELEVANCE/APPLICATION

Although this study is focused on demonstrating equivalent image quality to the conventional CT, the PCD scanner shows better low contrast distinction between the white and grey matter in the brain images. The PCD images also show less beam hardening artifact as seen in the nasal and orbital images.

Printed on: 02/07/23

## Abstract Archives of the RSNA, 2022

S3B-SPPH-6

### Spectral Physical Density Quantifications for Non-invasive, Real-Time Spectral CT Thermometry

Sunday, Nov. 27 12:15PM - 12:45PM Room: Learning Center - PH DPS

#### Participants

Leening Liu, Philadelphia, PA (*Presenter*) Nothing to Disclose

#### PURPOSE

Hepatocellular carcinoma (HCC) is typically treated with thermal ablation under the guidance of computed tomography (CT). Though it is the best performing procedure, the rate of local recurrence is high. Real-time temperature feedback may provide the means to ensure complete ablation while preventing damage to surrounding healthy tissue and critical structures. We assess the feasibility of non-invasive spectral CT thermometry by the principle of thermal volumetric expansion that relates temperature and physical density.

#### METHODS AND MATERIALS

To evaluate the relationship between physical density and temperature, a fiber optic temperature sensor was placed within a specifically designed tissue mimicking phantom that emulates the attenuation and thermal properties of liver. The phantom was subjected to a range of temperatures through heating and cooling while simultaneously being scanned with a dual-layer spectral CT at varying radiation doses (5 - 56.8 mGy). Clinically available spectral results were then utilized to generate physical density maps. Physical density was measured in regions of interest corresponding to the temperature sensor every 5 °C for each dose. A linear fit based on thermal volumetric expansion was applied to assess the relationship, and temperature sensitivity was calculated for different reconstruction parameters to inform future protocol optimization.

#### RESULTS

Physical density reflected thermal volumetric expansion with a slope of 0.000491 mL/g/°C and a R value of 0.9942, demonstrating a strong positively correlated relationship. Temperature sensitivity improved with larger slice thickness, a smooth iterative reconstruction kernel, and higher iterative reconstruction level. With radiation dose, it varied from 6.0 to 1.6 °C/g/mL between 5 and 56.8 mGy.

#### CONCLUSION

Spectral physical density quantifications of the tissue mimicking phantom affirmed a strong relationship with temperature that corresponded to thermal volumetric expansion. With this relationship, changes in physical density can be utilized to determine changes in temperature to provide non-invasive, real-time thermometry in thermal ablation with a temperature sensitivity of 1.6 °C/g/mL.

#### CLINICAL RELEVANCE/APPLICATION

Thermal ablation procedures, using spectral CT thermometry with physical density measurements, may be effectively carried out for reducing local tumor recurrences by providing non-invasive, real-time feedback.

Printed on: 02/07/23

## Abstract Archives of the RSNA, 2022

S3B-SPPH-7

### The Performance of Using CT Value Distribution in Dual-Energy Spectral CT Images to Predict Osteoporosis

Sunday, Nov. 27 12:15PM - 12:45PM Room: Learning Center - PH DPS

#### Participants

Tongtong DU, Xian, China (*Presenter*) Nothing to Disclose

#### PURPOSE

To investigate the performance of using CT value distribution in dual-energy spectral CT (DEsCT) images to predict osteoporosis.

#### METHODS AND MATERIALS

This study was IRB approved and consented by patients. A total of 156 consecutive patients (81 females and 80 males; mean age: 57.43±5.95 years, range 50-83 years) for chest CT screening were prospectively enrolled. All patients underwent chest DEsCT and Dual energy X-ray absorptiometry (DXA). Patients were divided into 2 groups using the T-score for the 1st lumbar vertebra on DXA: non-osteoporosis with  $T > -2.5$  (n=101) and Osteoporosis with  $T \leq -2.5$  (n=55). The chest DEsCT was performed on a 256-row Revolution CT (GE Healthcare) using 80-140kVp switching, 200mA and 0.5s/r. All images were reconstructed with 1.25mm thickness and analyzed using the GSI Viewer software on an AW4.7 workstation. CT values of the 1st lumbar vertebra were measured on the 120kVp-like images. According to CT histogram, the CT values were divided into 4 levels: A, <100HU; B, 100-199HU; C, 200-299 HU; D, ≥300HU. The distribution percentage in each level was compared between osteoporosis and non-osteoporosis groups. The cutoff of CT value distribution percentage for differentiating osteoporosis from non-osteoporosis was obtained by drawing a receiver operating characteristic (ROC) curve. The sensitivity, specificity, positive predictive value (PPV), and negative predictive value (NPV) were calculated. All statistical analyses were performed using the IBM SPSS statistical software (version 22.0), and two-tailed  $p < 0.05$  was considered statistically significant.

#### RESULTS

The CT value distribution percentages in all four levels in osteoporosis group were significant different from those in non-osteoporosis group (all  $p < 0.05$ ). Specifically, the percentage in level A showed the best diagnostic performance for osteoporosis, and provided the area-under-the-curve (AUC), sensitivity, specificity, PPV and NPV of 0.805, 0.818, 0.745, 0.654 and 0.748, respectively with a cutoff of 18.74%.

#### CONCLUSION

The distribution percentage of CT value based on spectral histogram could predict osteoporosis and have a good diagnostic performance.

#### CLINICAL RELEVANCE/APPLICATION

CT value distribution percentage based on DEsCT could provide more information about osteoporosis.

Printed on: 02/07/23

## Abstract Archives of the RSNA, 2022

S3B-SPPH-9

### Technical Performance Study of the First Mobile Photon-Counting Detector CT

Sunday, Nov. 27 12:15PM - 12:45PM Room: Learning Center - PH DPS

#### Participants

Junyoung Park, Suwon-Si, Korea, Republic Of (*Presenter*) Employee, Samsung Electronics Co, Ltd

#### PURPOSE

The purpose of this study is to evaluate the unique applications of photon-counting detectors (PCD) CT. The first is ability to "on demand" changes the scanner spatial resolution. The second is the ability to do "simultaneous" multi-energy scanning for material decomposition.

#### METHODS AND MATERIALS

In this study, the FDA 510(k) cleared mobile PCD-CT (OmniTom Elite) was used. The diagnostic performance of the scanner was proven using three clinical scans. The spatial resolution of the PCD-CT scanner was tested using the high contrast module of ACR accreditation phantom. The spatial resolutions of a large detector pitch of 0.71-mm (14 lp/cm) and a smaller pitch of 0.35-mm (28 lp/cm) for PCD-CT were tested. For multi-energy CT feasibility, Gammex phantom containing solid iodine and calcium inserts was scanned with three energy thresholds using PCD-CT. For material decomposition capability of PCD-CT, the iodine, calcium, and water maps were generated. Virtual mono-energetic images (VMI) from 40 keV to 120 keV were synthesized and the linear attenuation coefficients (LAC) of all the inserts of Gammex phantom were compared against manufacturer reference values.

#### RESULTS

The small pitch acquisition mode shows the highest resolution pattern of 11 lp/cm while only the resolution pattern of 7 lp/cm is seen when the same kernel (Posterior Fossa-kernel) is used in large pitch acquisition mode. For the quantitative multi-energy CT performance, the measured LAC in VMI of inserts of Gammex phantom matched the manufacturer reference values with mean percent error of 0.986%. In addition, the decomposition results with PCD-CT show that the iodine, calcium, and water can be well separated and quantified.

#### CONCLUSION

s We have shown that the PCD detector CT can accommodate a multiple resolution acquisition mode without physically changing the detector CT. The first clinical mobile PCD-CT can provide superior spatial resolution than large pitch acquisition mode which is equivalent with conventional mobile CT. Additionally, the results from quantitative multi-energy CT performance demonstrated that the PCD-CT was able to provide reliable simultaneous multi-energy images for material decomposition with single exposure.

#### CLINICAL RELEVANCE/APPLICATION

The validated unique characteristics of PCD-CT are highly desirable in clinical scanning. The ability to switch between different acquisition modes expands the clinical use of the scanner, e.g., high resolution temporal bone scans and lower resolution abdominal imaging. The capability of simultaneous multi-energy imaging leads to a precise registration that is needed to ensure the success of various multi-energy applications, including generation of material decomposition maps, VMI and virtual non-contrast images.

Printed on: 02/07/23

## Abstract Archives of the RSNA, 2022

S3B-SPRO

### Radiation Oncology Sunday Poster Discussions - B

Sunday, Nov. 27 12:15PM - 12:45PM Room: Learning Center - RO DPS

#### Participants

Anna Shapiro, MD, Syracuse, NY (*Moderator*) Nothing to Disclose

#### Sub-Events

### S3B-SPRO-1 The Effects of Human Placental Mesenchymal Stem Cells Labelled With Ultra Small Superparamagnetic Iron Oxides on the Growth of Colorectal Cancer (CRC) Cells

#### Participants

Hua He, MMedSc, MMedSc, Yinchuan, China (*Presenter*) Nothing to Disclose

#### PURPOSE

To investigate the effects of human placental mesenchymal stem cells (PMSCs) labelled with ultrasmall superparamagnetic iron oxides (USPIO) on the growth of colorectal cancer (CRC) cells.

#### METHODS AND MATERIALS

PMSCs were labeled with USPIOs, and their biological characteristics were identified. A subcutaneous CRC HT-29 xenograft model in immunodeficient mice was established, and we attempted to consider the labeled cells as experimental group and the unlabeled cells as control group. USPIOs and poly-L-lysine (PLL) were mixed at a ratio of 1:0.03, placed in a vortex mixer at 2200 r/min, and shaken for 30 min to form PLL-USPIO complex. The number of Prussian blue-stained and unstained cells were counted using hemocytometer ( $\times 100$ ) under an inverted microscope and labeling efficiency is determined by percentage of Prussian blue-stained positive cells over total cells. The growth of xenograft tumors of nude mice was assessed, then, diameter of each transplanted tumor was measured every 3-4 days, and the growth curve was plotted to calculate the volume of tumor.

#### RESULTS

? USPIO labelled PMSCs had no significant influence on biological characteristics, such as cell viability, proliferation ability, and apoptosis rate ( $P > 0.05$ ). ?The low signal area can be seen in the experimental group on the first day, on the 7th day, the regions with low signal intensity were narrowed, and these regions in the tumor partly showed poor clarity, whereas the signal intensities did not significantly change. On the 14th day, the tumor volume was 420mm<sup>3</sup>, CD31 and CD34 is (65±15.7), (58±14.5), and the positive expression rate of Ki67 >50%. ?The T2\* mapping has the best tracking ability for USPIO-labeled cells.

#### CONCLUSION

s USPIO labeled PMSCs had high labeling efficiency, while cell viability, proliferation ability, and apoptotic rate were not markedly influenced. It has a certain inhibitory effect on the growth of the transplanted tumor volume, but has no obvious effect on the proliferation and angiogenesis of the tumor.

#### CLINICAL RELEVANCE/APPLICATION

Provide basic research data for the targeted therapy of placental mesenchymal stem cells in colorectal cancer.

Printed on: 02/07/23

## Abstract Archives of the RSNA, 2022

S3B-SPRO-1

### The Effects of Human Placental Mesenchymal Stem Cells Labelled With Ultra Small Superparamagnetic Iron Oxides on the Growth of Colorectal Cancer (CRC) Cells

Sunday, Nov. 27 12:15PM - 12:45PM Room: Learning Center - RO DPS

#### Participants

Hua He, MMedSc, MMedSc, Yinchuan, China (*Presenter*) Nothing to Disclose

#### PURPOSE

To investigate the effects of human placental mesenchymal stem cells (PMSCs) labelled with ultrasmall superparamagnetic iron oxides (USPIO) on the growth of colorectal cancer (CRC) cells.

#### METHODS AND MATERIALS

PMSCs were labeled with USPIOs, and their biological characteristics were identified. A subcutaneous CRC HT-29 xenograft model in immunodeficient mice was established, and we attempted to consider the labeled cells as experimental group and the unlabeled cells as control group. USPIOs and poly-L-lysine (PLL) were mixed at a ratio of 1:0.03, placed in a vortex mixer at 2200 r/min, and shaken for 30 min to form PLL-USPIO complex. The number of Prussian blue-stained and unstained cells were counted using hemocytometer ( $\times 100$ ) under an inverted microscope and labeling efficiency is determined by percentage of Prussian blue-stained positive cells over total cells. The growth of xenograft tumors of nude mice was assessed, then, diameter of each transplanted tumor was measured every 3-4 days, and the growth curve was plotted to calculate the volume of tumor.

#### RESULTS

? USPIO labelled PMSCs had no significant influence on biological characteristics, such as cell viability, proliferation ability, and apoptosis rate ( $P > 0.05$ ). ?The low signal area can be seen in the experimental group on the first day, on the 7th day, the regions with low signal intensity were narrowed, and these regions in the tumor partly showed poor clarity, whereas the signal intensities did not significantly change. On the 14th day, the tumor volume was  $420\text{mm}^3$ , CD31 and CD34 is  $(65 \pm 15.7)$ ,  $(58 \pm 14.5)$ , and the positive expression rate of Ki67  $> 50\%$ . ?The T2\* mapping has the best tracking ability for USPIO-labeled cells.

#### CONCLUSION

s USPIO labeled PMSCs had high labeling efficiency, while cell viability, proliferation ability, and apoptotic rate were not markedly influenced. It has a certain inhibitory effect on the growth of the transplanted tumor volume, but has no obvious effect on the proliferation and angiogenesis of the tumor.

#### CLINICAL RELEVANCE/APPLICATION

Provide basic research data for the targeted therapy of placental mesenchymal stem cells in colorectal cancer.

Printed on: 02/07/23

## Abstract Archives of the RSNA, 2022

T2-SPBR

### Breast Tuesday Poster Discussions

Tuesday, Nov. 29 9:00AM - 9:30AM Room: Learning Center - BR DPS

#### Participants

Valeria Romeo, MD, PhD, Naples, Italy (*Moderator*) Nothing to Disclose

#### Sub-Events

### T2-SPBR-1 Different Imaging Modalities for The Diagnosis of Axillary Lymph Node Metastases in Breast Cancer: A Systematic Review and Network Meta-analysis

#### Participants

Zhifan Li, (*Presenter*) Nothing to Disclose

#### PURPOSE

We conducted this network meta-analysis (NMA) to evaluate the diagnostic performance of different imaging modalities for the detection of axillary lymph node metastasis (ALNM) in patients with breast cancer.

#### METHODS AND MATERIALS

PubMed, EMBASE, Cochrane Library, and Web of Science were searched from inception to November 2021 to identify relevant studies. The Quality Assessment of Diagnostic Accuracy Studies-2 (QUADAS-2) tool was used to assess the methodological quality of the included studies. Meta-analyses of individual imaging modalities, pairwise meta-analyses and Bayesian network meta-analyses were applied for data analysis. Sensitivity and specificity, relative sensitivity and specificity, diagnostic odds ratio (DOR), and superiority index, and their associated 95% confidence intervals (CI) were used to assess the diagnostic value of different imaging modalities.

#### RESULTS

A total of 61 studies were identified, including 8011 participants across 9 imaging modalities. The 9 imaging modalities included US, MRI, MMG, PET/CT, UE, CT, PET, SMM, and PET/MRI. On patient-based level, network meta-analysis showed that UE had the highest superiority index (5.95) with the highest sensitivity of 0.75 (95%CI: 0.62-0.85) and moderate specificity of 0.85 (95%CI: 0.76-0.92). At the lymph node level, network meta-analysis revealed that MRI had the highest superiority index (6.91) with the highest sensitivity of 0.91 (95%CI: 0.82-0.97) and the highest specificity of 0.87 (95%CI: 0.75-0.95).

#### CONCLUSION

s UE and MRI were recommended for the diagnosis of ALNM in breast cancer patients at the patient level and at the lymph node level, respectively. Given the low quality of some diagnostic accuracy studies and the imbalance in the number of studies among different imaging methods, further studies are needed to provide strong evidence to validate the conclusions.

#### CLINICAL RELEVANCE/APPLICATION

Axillary lymph node metastasis (ALNM) is considered to be a significant prognostic indicator in breast cancer. Accurate diagnosis of axillary lymph node (ALN) status of breast cancer patients is critical to guide local and systemic treatment. In addition to US, imaging modalities such as MMG, MRI, PET, CT, PET/CT are also increasingly used to assess LN status in breast cancer patients. However, the jury is still out on which imaging method has the best diagnostic performance. Therefore, we conducted this network meta-analysis to evaluate the diagnostic performance of different imaging modalities for the ALNM in patients with breast cancer. Our results provide a comprehensive overview of the existing evidence on the imaging diagnosis of ALNM in breast cancer patients and have implications for clinicians, researchers, radiologists, and guideline committees.

### T2-SPBR-2 Prediction of Primary Tumour and Axillary Lymph Node Response to Neoadjuvant Systemic Therapy with Dedicated Breast [18F]FDG PET/MRI in Breast Cancer

#### Participants

Thiemo Van Nijnatten, Maastricht, Netherlands (*Presenter*) Nothing to Disclose

#### PURPOSE

To investigate whether sequential dedicated breast hybrid [18F]FDG PET/MRI can be used to predict pathologic response to neoadjuvant systemic therapy (NST) in breast cancer.

#### METHODS AND MATERIALS

Between February 2015 and July 2017, patients were planned for [18F]FDG PET/MRI before, halfway and following completion NST followed by surgery. Qualitative response evaluation following NST was based on [18F]FDG-activity on PET and residual enhancement on MRI. Quantitatively, maximum standardized uptake value (SUVmax) on PET and signal enhancement ratio (SER) on dynamic contrast enhanced (DCE)-MRI were determined on the primary tumour. For response of axillary lymph node metastases (ALNMs), SUVmax was determined on the most FDG-avid ALN. Receiver operating characteristic (ROC) curves were generated to

determine optimal cut-off values for absolute and percentage change in quantitative variables in predicting response. Diagnostic performance in predicting primary tumour response was assessed with the area under the ROC curve (AUC). Similar analyses were performed in clinically node-positive (cN+) patients for ALNM response.

## RESULTS

Forty-one breast cancer patients with 42 primary tumours and 26 pathologically proven cN+ axillae were prospectively included. Pathological complete response (pCR) of the primary tumour occurred in 16 of all patients and pCR of the ALNMs in 14 of cN+ patients. The AUC of the qualitative evaluation was 0.71 (95% CI 0.53 - 0.89) for primary tumour and 0.54 (95% CI 0.27 - 0.80) for ALNM response. For primary tumour response, combining the percentage decrease in SUVmax and SER halfway NST achieved an AUC of 0.78 (0.63 - 0.93). Additionally, combining the absolute as well as the percentage decrease in SUVmax halfway NST improved AUC for ALNM response prediction to 0.92 (0.79 - 1.00).

## CONCLUSION

s Qualitative PET/MRI following NST can predict final pathologic primary tumour but not ALNM response.

## CLINICAL RELEVANCE/APPLICATION

Combining quantitative variables from sequential imaging halfway NST can improve the diagnostic accuracy for final pathologic ALNM response prediction.

## T2-SPBR-3 Predicting Recurrence Risk of Breast Cancer with Machine Learning in Patients Receiving Adjuvant Tamoxifen/Aromatase Inhibitors

Participants

Saba Dadsetan, BSc, PhD, Pittsburgh, PA (*Presenter*) Nothing to Disclose

## PURPOSE

Clinical factors, radiomics, and deep learning (DL) were used to assess recurrence risk in women undergoing tamoxifen/aromatase inhibitor (AI) therapy in a retrospective cohort.

## METHODS AND MATERIALS

Baseline (before tamoxifen/AI) and follow-up (after tamoxifen/AI) processed digital mammograms for 679 women (aged 28-93) with unilateral breast cancer were reviewed under an IRB-approved protocol, including: 58 recurrences (16 in breast, 42 distant), 121 new primary cancers, and 500 "control" cases without recurrence and at least 5-year follow-up. Using radiomics extracted from dense/whole breast tissue (unaffected breast) and DL, we classified two binary tasks: Task 1) controls (500 cases) vs. new primary (121 cases), and Task 2) controls vs. any recurrence (179 cases). CC- and MLO-views were incorporated separately and together at baseline and follow-up. We evaluated 15 adding clinical variables (e.g., initial tumor T, N stage, receptors, etc.). We used logistic regression and LASSO to model radiomics. DL used InceptionResnetV2 as its backbone. Breast dense area was segmented using LIBRA and breast density was quantified. For each task, patients were randomly divided 70-15-15% for training, validation, and testing. We used area under the ROC curve (AUC) as evaluation metric.

## RESULTS

Clinical factors alone yielded AUCs of 0.68 (Task 1) and 0.69 (Task 2). By using both baseline and follow-up mammograms, MLO-view whole-breast radiomics produced AUCs of 0.75 (Task 1) and 0.63 (Task 2), while radiomics of the dense area revealed AUCs of 0.73 (Task 1) and 0.62 (Task 2). Combining radiomics and clinical factors increased AUC for Task 1 and Task 2 for the whole breast to 0.80 ( $p=0.03$ ) and 0.80 ( $p=0.001$ ), respectively, and for the dense area, AUCs rose to 0.79 ( $p=0.04$ ) and 0.75 ( $p=0.001$ ), respectively. With DL on whole-breast, Tasks 1 and 2 had AUCs of 0.86 and 0.74, respectively, when using baseline MLO-view only, and 0.77 and 0.79 when using both MLO- and CC-views at baseline and follow-up. DL outperformed (all  $p<0.03$ ) radiomics when compared at the same settings. Adding clinical factors did not improve DL results ( $p>0.05$ ). Quantitative change in breast density between baseline and follow-up was not predictive of recurrence risk (AUC=0.50 Task 1 and 0.52 Task 2).

## CONCLUSION

s In patients with tamoxifen/AI treatment, radiomics and DL of contralateral cancer-unaffected mammograms and clinical factors predicted risk of recurrence. DL outperformed radiomics. The baseline mammograms show the highest AUC with DL for predicting new primary cancers.

## CLINICAL RELEVANCE/APPLICATION

In patients undergoing tamoxifen/AI treatment, machine learning may enhance prediction of risk of recurrent breast cancer and provide model-based biomarkers of treatment responsiveness.

## T2-SPBR-4 Head-to Head Comparison of 18F-FDG and 18F-FEC PET/MRI in Breast Cancer Patients: What Is the Difference?

Participants

Nina Poetsch, MD, Wien, Austria (*Presenter*) Nothing to Disclose

## PURPOSE

18F-Fluoroethylcholine (18F-FEC) is a PET tracer able to evaluate choline metabolism. Its usefulness for breast cancer is underinvestigated, and no studies compared the performance with the current standard (18F-Fluorodesoxyglucose, 18F-FDG). We compared 18F-FDG to 18F-FEC in a matched PET/MRI cohort.

## METHODS AND MATERIALS

Local staging PET/MRI scans of patients > 18 years with histologically verified breast cancer were retrospectively analyzed. Patients were matched based on age, tumor size, nodal status, histologic- and molecular subtype. SUVmax and parenchyma uptake were measured by a nuclear medicine physician, tumor to background (T/B) was calculated. Tumor visibility was rated on a 5-point Likert scale (1-no tumor detectable; 5-excellent tumor visualization) by a breast radiology fellow. Mann-Whitney-U test was used to compare SUV and T/B with tumor characteristics.

## RESULTS

We investigated 104 patients with 106 malignant breast lesions matched in 52 pairs. On a 5-point Likert scale lesion visibility was rated equal in 18F-FEC and 18F-FDG studies (mean 4.6 and 4.4). SUVmax values were higher for 18F-FDG compared to 18F-FEC (4.6 vs. 3.7,  $p=0.037$ ). The T/B ratio was higher in 18F-FEC (6.2 vs. 13.3,  $p<0.001$ ). Both tracers showed higher SUVmax ( $p<0.001$ ) in tumors with a higher proliferation index (MIB  $>20\%$ ). 18F-FDG showed higher SUVmax in ER negative tumors ( $p=0.032$ ). No difference was observed in SUVmax for 18F-FDG and 18F-FEC regarding Her2 status and for 18F-FEC regarding ER status.

## CONCLUSION

s Tumor visibility and metabolic activity were equal between 18F-FDG and 18F-FEC. Both were higher in tumors with higher proliferation index. 18F-FDG showed higher metabolic activity in ER negative tumors while 18F-FEC performs diagnostically independent from receptor status.

## CLINICAL RELEVANCE/APPLICATION

These results confirm the in vivo equality of 18F-FEC to 18F-FDG as a potential alternative tracer for PET/MRI imaging in breast cancer patients. While 18F-FDG may indicate hormonal receptor status, 18F-FEC is applicable independent of receptor status.

## T2-SPBR-5 High-resolution Diffusion-weighted Breast MRI: Improved Lesion Visibility and Image Quality with Water-excitation and Inversion-Recovery Fat Suppression

Participants

Stephanie Sauer, Wuerzburg, 97080, Germany (*Presenter*) Nothing to Disclose

## PURPOSE

To investigate subjective and semiquantitative criteria of image quality in high-resolution breast MRI with different fat suppression techniques for diffusion-weighted imaging (DWI).

## METHODS AND MATERIALS

Three 5-minute echo-planar DWI sequences with different fat suppression techniques were acquired on a 3-Tesla MRI scanner in 83 patients (age  $50.1 \pm 12.6$  years). DWI methods included fat suppression with non-product optimized water-excitation with spectral fat saturation (WE), spectral attenuated inversion recovery (SPAIR), and standard spectral fat saturation (FS). Three radiologists assessed overall image quality and lesion visibility (28 malignant, 60 benign) on images with b value of 800 s/mm<sup>2</sup> and apparent diffusion coefficient (ADC) maps. For all fat suppression methods, the longest diameter, mean signal intensity in DWI, and average ADC value of each lesion were measured.

## RESULTS

Image quality and lesion visibility in WE and SPAIR DWI was considered better than in standard FS DWI ( $p<0.001$ ). Correspondingly, mean signal-intensity ratios of WE ( $3.0 \pm 2.2$ ) and SPAIR sequences ( $3.3 \pm 2.8$ ) were superior to DWI with spectral fat saturation ( $2.0 \pm 1.1$ ;  $p<0.001$ ). Estimated lesion size difference between DWI and contrast-enhanced subtraction T1 images was smaller in WE ( $0.5 \pm 2.6$  mm) and SPAIR DWI ( $0.4 \pm 2.5$  mm) compared to FS DWI ( $2.0 \pm 3.5$  mm; all  $p<0.001$ ). Differences in mean ADC values between malignant and benign lesions were comparable between all three DWI methods (WE  $0.524 \times 10^{-3}$ ; SPAIR  $0.509 \times 10^{-3}$ ; FS  $0.509 \times 10^{-3}$  mm<sup>2</sup>/s).

## CONCLUSION

s Both WE and SPAIR DWI provide better image quality, subjective lesion visibility, and signal-intensity ratios than DWI with standard spectral fat saturation, resulting in a more accurate estimation of lesion size.

## CLINICAL RELEVANCE/APPLICATION

The choice of fat suppression method may influence diagnostic assessment in diffusion-weighted breast MRI. Both water excitation and inversion recovery techniques allow for excellent depiction of benign and malignant lesions at 3 Tesla.

## T2-SPBR-6 Utility of Kaiser Score for Focal Incidental Breast Uptake In a Diagnosed Malignant Population Undergoing 18 FDG PET-CT

Participants

Ankush Jajodia, MD, MBBS, New Delhi, India (*Presenter*) Nothing to Disclose

## PURPOSE

We compared the diagnostic accuracies of ACR BIRADS, Kaiser score, and SUVmax in focal incidental breast uptake (FIBU) on 18FDG PET-CT in a diagnosed population with primary cancers excluding breast.

## METHODS AND MATERIALS

A retrospective analysis in 21,657 female subjects with "FIBU" on 18 FDG PET-CT imaging in two hundred six subjects, between January 2010 and January 2020, including mass and non-mass enhancement (NME). ACR-BI-RADS category, Kaiser score, and SUVmax was derived for each lesion. Upgrade or downgrade was tabulated in an excel sheet. Independent samples t-test, diagnostic test calculator, and MedCalc 12.2.1 were used for statistical analysis.

## RESULTS

According to the ACR lexicon, eighty lesions with eighteen BI-RADS 3 lesions, forty-seven BI-RADS 4, and fifteen BI-RADS 5 lesions with benign histology in 13% (10/80) and malignant in 87% (70/80). For benign lesions, SUV max range was 1.6-29.3, while for malignant lesions, it was 2.1-22.7 ( $p=0.257$ ). Kaiser score ( $p=0.002$ ) assignment was statistically significant between the two groups. Kaiser score AUC (0.878; 95% CI: 0.786-0.94) was significantly high than ACR BIRADS (0.610; 95% CI :0.494-0.717) and SUVmax (0.566; 95% CI:0.451-0.677). Ninety-four percent (48/51) of upgraded lesions were found to be malignant; benign histology was found in the remaining 5.9% percent (3/51). All (100%) of lesions (4/4) were correctly downgraded. All (100%) lesions (18/18) which were incorrectly classified as ACR BIRADS 3 were correctly classified now as suspicious 4/5 category. When we used a Kaiser score of  $>4$  as a cut-off for malignancy, we got 100% sensitivity. Using six as a cut-off score, sensitivity dropped to 85.7%, but specificity went up to 60% from 40%, with a positive likelihood ratio of 2.14. (vs. 1.67 with a cut-off score of 4).

When we used a high cut-off value  $>8$  to rule-in malignancy, we were correct in 96.4% of the cases (54/56), with a specificity of 80% and a positive likelihood ratio of 3.71. We were able to identify all four lesions that had been downgraded from suspicious (BIRADS 4/5 category) to benign (BIRADS 5) when we set a cut-off Kaiser score of 5, thus potentially avoiding biopsies 100% of the time.

## CONCLUSION

s Kaiser score has meaningfully better diagnostic accuracy than ACR BIRADS and SUVmax for focal incidentally breast uptake.

## CLINICAL RELEVANCE/APPLICATION

Kaiser score has highest diagnostic accuracy than ACR BIRADS and SUVmax for focal incidentally breast uptake. Our study validates the clinical benefit of Kaiser score in correctly assigning suspicious 4/5 category to lesions falsely classified as ACR BIRADS 3.

## T2-SPBR-7 Quantitative Analysis of Enhancement Characteristics of Contrast-enhanced Spectral Mammography in Differentiating Malignant from Benign Breast Lesions

Participants

Huizhi Cao, PhD, (*Presenter*) Nothing to Disclose

## PURPOSE

To quantitatively analyze the enhancement Characteristics of breast lesions on contrast-enhanced spectral mammography (CESM) to improve the diagnostic efficiency.

## METHODS AND MATERIALS

A total of 283 patients with breast lesions admitted from August 2021 to Feb 2022 were retrospectively analyzed. Quantitative analysis of all enhancing lesions was performed to measure the enhancement values of the lesion area of interest (ROI), tissue surrounding the lesion (ROI1), tissue away from the lesion and close to the chest (ROI2), and the tissue at the level of the maximum diameter of the normal pectoralis major muscle on the ipsilateral side of the lesion (ROI3). rROI1, rROI2 and rROI3 were relative enhancement value between (ROI1,ROI2 and ROI3) and ROI. Differences in enhancement values between different ROIs of benign and malignant lesions were compared. Taking the pathological results as the gold standard, we used the receiver operating characteristic (ROC) curve to evaluate the diagnostic efficacy of the ROI enhancement value and rROI for the lesions.

## RESULTS

A total of 299 lesions were found in 283 patients, including 101 benign lesions and 198 malignant lesions. The ROI enhancement value, rROI1, rROI2, and rROI3 of malignant lesions were all significantly greater than those of benign lesions. For enhancement values of benign and malignant lesions of ROI, rROI1, rROI2 and rROI3, AUC was 0.795, 0.833, 0.812 and 0.741, respectively. The statistically significant difference in the AUC was only found between rROI1 and ROI enhancement value, and rROI1 had the greatest diagnostic value.

## CONCLUSION

s The enhancement value of malignant breast lesions was higher than that of benign lesions. The quantitative analysis of the enhancement value was of great value in the differential diagnosis of benign and malignant breast lesions.

## CLINICAL RELEVANCE/APPLICATION

Quantitative analysis in Contrast-enhanced spectral mammography has the potential value in the differential diagnosis of benign and malignant breast lesions.

Printed on: 02/07/23

## Abstract Archives of the RSNA, 2022

T2-SPBR-1

### Different Imaging Modalities for The Diagnosis of Axillary Lymph Node Metastases in Breast Cancer: A Systematic Review and Network Meta-analysis

Tuesday, Nov. 29 9:00AM - 9:30AM Room: Learning Center - BR DPS

#### Participants

Zhifan Li, (*Presenter*) Nothing to Disclose

#### PURPOSE

We conducted this network meta-analysis (NMA) to evaluate the diagnostic performance of different imaging modalities for the detection of axillary lymph node metastasis (ALNM) in patients with breast cancer.

#### METHODS AND MATERIALS

PubMed, EMBASE, Cochrane Library, and Web of Science were searched from inception to November 2021 to identify relevant studies. The Quality Assessment of Diagnostic Accuracy Studies-2 (QUADAS-2) tool was used to assess the methodological quality of the included studies. Meta-analyses of individual imaging modalities, pairwise meta-analyses and Bayesian network meta-analyses were applied for data analysis. Sensitivity and specificity, relative sensitivity and specificity, diagnostic odds ratio (DOR), and superiority index, and their associated 95% confidence intervals (CI) were used to assess the diagnostic value of different imaging modalities.

#### RESULTS

A total of 61 studies were identified, including 8011 participants across 9 imaging modalities. The 9 imaging modalities included US, MRI, MMG, PET/CT, UE, CT, PET, SMM, and PET/MRI. On patient-based level, network meta-analysis showed that UE had the highest superiority index (5.95) with the highest sensitivity of 0.75 (95%CI: 0.62-0.85) and moderate specificity of 0.85 (95%CI: 0.76-0.92). At the lymph node level, network meta-analysis revealed that MRI had the highest superiority index (6.91) with the highest sensitivity of 0.91 (95%CI: 0.82-0.97) and the highest specificity of 0.87 (95%CI: 0.75-0.95).

#### CONCLUSION

s UE and MRI were recommended for the diagnosis of ALNM in breast cancer patients at the patient level and at the lymph node level, respectively. Given the low quality of some diagnostic accuracy studies and the imbalance in the number of studies among different imaging methods, further studies are needed to provide strong evidence to validate the conclusions.

#### CLINICAL RELEVANCE/APPLICATION

Axillary lymph node metastasis (ALNM) is considered to be a significant prognostic indicator in breast cancer. Accurate diagnosis of axillary lymph node (ALN) status of breast cancer patients is critical to guide local and systemic treatment. In addition to US, imaging modalities such as MMG, MRI, PET, CT, PET/CT are also increasingly used to assess LN status in breast cancer patients. However, the jury is still out on which imaging method has the best diagnostic performance. Therefore, we conducted this network meta-analysis to evaluate the diagnostic performance of different imaging modalities for the ALNM in patients with breast cancer. Our results provide a comprehensive overview of the existing evidence on the imaging diagnosis of ALNM in breast cancer patients and have implications for clinicians, researchers, radiologists, and guideline committees.

Printed on: 02/07/23

## Abstract Archives of the RSNA, 2022

T2-SPBR-2

### Prediction of Primary Tumour and Axillary Lymph Node Response to Neoadjuvant Systemic Therapy with Dedicated Breast [18F]FDG PET/MRI in Breast Cancer

Tuesday, Nov. 29 9:00AM - 9:30AM Room: Learning Center - BR DPS

#### Participants

Thiemo Van Nijnatten, Maastricht, Netherlands (*Presenter*) Nothing to Disclose

#### PURPOSE

To investigate whether sequential dedicated breast hybrid [18F]FDG PET/MRI can be used to predict pathologic response to neoadjuvant systemic therapy (NST) in breast cancer.

#### METHODS AND MATERIALS

Between February 2015 and July 2017, patients were planned for [18F]FDG PET/MRI before, halfway and following completion NST followed by surgery. Qualitative response evaluation following NST was based on [18F]FDG-activity on PET and residual enhancement on MRI. Quantitatively, maximum standardized uptake value (SUV<sub>max</sub>) on PET and signal enhancement ratio (SER) on dynamic contrast enhanced (DCE)-MRI were determined on the primary tumour. For response of axillary lymph node metastases (ALNMs), SUV<sub>max</sub> was determined on the most FDG-avid ALN. Receiver operating characteristic (ROC) curves were generated to determine optimal cut-off values for absolute and percentage change in quantitative variables in predicting response. Diagnostic performance in predicting primary tumour response was assessed with the area under the ROC curve (AUC). Similar analyses were performed in clinically node-positive (cN+) patients for ALNM response.

#### RESULTS

Forty-one breast cancer patients with 42 primary tumours and 26 pathologically proven cN+ axillae were prospectively included. Pathological complete response (pCR) of the primary tumour occurred in 16 of all patients and pCR of the ALNMs in 14 of cN+ patients. The AUC of the qualitative evaluation was 0.71 (95% CI 0.53 - 0.89) for primary tumour and 0.54 (95% CI 0.27 - 0.80) for ALNM response. For primary tumour response, combining the percentage decrease in SUV<sub>max</sub> and SER halfway NST achieved an AUC of 0.78 (0.63 - 0.93). Additionally, combining the absolute as well as the percentage decrease in SUV<sub>max</sub> halfway NST improved AUC for ALNM response prediction to 0.92 (0.79 - 1.00).

#### CONCLUSION

s Qualitative PET/MRI following NST can predict final pathologic primary tumour but not ALNM response.

#### CLINICAL RELEVANCE/APPLICATION

Combining quantitative variables from sequential imaging halfway NST can improve the diagnostic accuracy for final pathologic ALNM response prediction.

Printed on: 02/07/23

## Abstract Archives of the RSNA, 2022

T2-SPBR-3

### Predicting Recurrence Risk of Breast Cancer with Machine Learning in Patients Receiving Adjuvant Tamoxifen/Aromatase Inhibitors

Tuesday, Nov. 29 9:00AM - 9:30AM Room: Learning Center - BR DPS

#### Participants

Saba Dadsetan, BSc, PhD, Pittsburgh, PA (*Presenter*) Nothing to Disclose

#### PURPOSE

Clinical factors, radiomics, and deep learning (DL) were used to assess recurrence risk in women undergoing tamoxifen/aromatase inhibitor (AI) therapy in a retrospective cohort.

#### METHODS AND MATERIALS

Baseline (before tamoxifen/AI) and follow-up (after tamoxifen/AI) processed digital mammograms for 679 women (aged 28-93) with unilateral breast cancer were reviewed under an IRB-approved protocol, including: 58 recurrences (16 in breast, 42 distant), 121 new primary cancers, and 500 "control" cases without recurrence and at least 5-year follow-up. Using radiomics extracted from dense/whole breast tissue (unaffected breast) and DL, we classified two binary tasks: Task 1) controls (500 cases) vs. new primary (121 cases), and Task 2) controls vs. any recurrence (179 cases). CC- and MLO-views were incorporated separately and together at baseline and follow-up. We evaluated 15 adding clinical variables (e.g., initial tumor T, N stage, receptors, etc.). We used logistic regression and LASSO to model radiomics. DL used InceptionResnetV2 as its backbone. Breast dense area was segmented using LIBRA and breast density was quantified. For each task, patients were randomly divided 70-15-15% for training, validation, and testing. We used area under the ROC curve (AUC) as evaluation metric.

#### RESULTS

Clinical factors alone yielded AUCs of 0.68 (Task 1) and 0.69 (Task 2). By using both baseline and follow-up mammograms, MLO-view whole-breast radiomics produced AUCs of 0.75 (Task 1) and 0.63 (Task 2), while radiomics of the dense area revealed AUCs of 0.73 (Task 1) and 0.62 (Task 2). Combining radiomics and clinical factors increased AUC for Task 1 and Task 2 for the whole breast to 0.80 ( $p=0.03$ ) and 0.80 ( $p=0.001$ ), respectively, and for the dense area, AUCs rose to 0.79 ( $p=0.04$ ) and 0.75 ( $p=0.001$ ), respectively. With DL on whole-breast, Tasks 1 and 2 had AUCs of 0.86 and 0.74, respectively, when using baseline MLO-view only, and 0.77 and 0.79 when using both MLO- and CC-views at baseline and follow-up. DL outperformed (all  $p<0.03$ ) radiomics when compared at the same settings. Adding clinical factors did not improve DL results ( $p>0.05$ ). Quantitative change in breast density between baseline and follow-up was not predictive of recurrence risk (AUC=0.50 Task 1 and 0.52 Task 2).

#### CONCLUSION

s In patients with tamoxifen/AI treatment, radiomics and DL of contralateral cancer-unaffected mammograms and clinical factors predicted risk of recurrence. DL outperformed radiomics. The baseline mammograms show the highest AUC with DL for predicting new primary cancers.

#### CLINICAL RELEVANCE/APPLICATION

In patients undergoing tamoxifen/AI treatment, machine learning may enhance prediction of risk of recurrent breast cancer and provide model-based biomarkers of treatment responsiveness.

Printed on: 02/07/23



## Abstract Archives of the RSNA, 2022

T2-SPBR-4

### Head-to Head Comparison of 18F-FDG and 18F-FEC PET/MRI in Breast Cancer Patients: What Is the Difference?

Tuesday, Nov. 29 9:00AM - 9:30AM Room: Learning Center - BR DPS

#### Participants

Nina Poetsch, MD, Wien, Austria (*Presenter*) Nothing to Disclose

#### PURPOSE

18F-Fluoroethylcholine (18F-FEC) is a PET tracer able to evaluate choline metabolism. Its usefulness for breast cancer is underinvestigated, and no studies compared the performance with the current standard (18F-Fluorodesoxyglucose, 18F-FDG). We compared 18F-FDG to 18F-FEC in a matched PET/MRI cohort.

#### METHODS AND MATERIALS

Local staging PET/MRI scans of patients > 18 years with histologically verified breast cancer were retrospectively analyzed. Patients were matched based on age, tumor size, nodal status, histologic- and molecular subtype. SUVmax and parenchyma uptake were measured by a nuclear medicine physician, tumor to background (T/B) was calculated. Tumor visibility was rated on a 5-point Likert scale (1-no tumor detectable; 5-excellent tumor visualization) by a breast radiology fellow. Mann-Whitney-U test was used to compare SUV and T/B with tumor characteristics.

#### RESULTS

We investigated 104 patients with 106 malignant breast lesions matched in 52 pairs. On a 5-point Likert scale lesion visibility was rated equal in 18F-FEC and 18F-FDG studies (mean 4.6 and 4.4). SUVmax values were higher for 18F-FDG compared to 18F-FEC (4.6 vs. 3.7,  $p=0.037$ ). The T/B ratio was higher in 18F-FEC (6.2 vs. 13.3,  $p<0.001$ ). Both tracers showed higher SUVmax ( $p<0.001$ ) in tumors with a higher proliferation index (MIB >20%). 18F-FDG showed higher SUVmax in ER negative tumors ( $p=0.032$ ). No difference was observed in SUVmax for 18F-FDG and 18F-FEC regarding Her2 status and for 18F-FEC regarding ER status.

#### CONCLUSION

Tumor visibility and metabolic activity were equal between 18F-FDG and 18F-FEC. Both were higher in tumors with higher proliferation index. 18F-FDG showed higher metabolic activity in ER negative tumors while 18F-FEC performs diagnostically independent from receptor status.

#### CLINICAL RELEVANCE/APPLICATION

These results confirm the in vivo equality of 18F-FEC to 18F-FDG as a potential alternative tracer for PET/MRI imaging in breast cancer patients. While 18F-FDG may indicate hormonal receptor status, 18F-FEC is applicable independent of receptor status.

Printed on: 02/07/23

## Abstract Archives of the RSNA, 2022

T2-SPBR-5

### High-resolution Diffusion-weighted Breast MRI: Improved Lesion Visibility and Image Quality with Water-excitation and Inversion-Recovery Fat Suppression

Tuesday, Nov. 29 9:00AM - 9:30AM Room: Learning Center - BR DPS

#### Participants

Stephanie Sauer, Wuerzburg, 97080, Germany (*Presenter*) Nothing to Disclose

#### PURPOSE

To investigate subjective and semiquantitative criteria of image quality in high-resolution breast MRI with different fat suppression techniques for diffusion-weighted imaging (DWI).

#### METHODS AND MATERIALS

Three 5-minute echo-planar DWI sequences with different fat suppression techniques were acquired on a 3-Tesla MRI scanner in 83 patients (age  $50.1 \pm 12.6$  years). DWI methods included fat suppression with non-product optimized water-excitation with spectral fat saturation (WE), spectral attenuated inversion recovery (SPAIR), and standard spectral fat saturation (FS). Three radiologists assessed overall image quality and lesion visibility (28 malignant, 60 benign) on images with b value of 800 s/mm<sup>2</sup> and apparent diffusion coefficient (ADC) maps. For all fat suppression methods, the longest diameter, mean signal intensity in DWI, and average ADC value of each lesion were measured.

#### RESULTS

Image quality and lesion visibility in WE and SPAIR DWI was considered better than in standard FS DWI ( $p < .001$ ). Correspondingly, mean signal-intensity ratios of WE ( $3.0 \pm 2.2$ ) and SPAIR sequences ( $3.3 \pm 2.8$ ) were superior to DWI with spectral fat saturation ( $2.0 \pm 1.1$ ;  $p < .001$ ). Estimated lesion size difference between DWI and contrast-enhanced subtraction T1 images was smaller in WE ( $0.5 \pm 2.6$  mm) and SPAIR DWI ( $0.4 \pm 2.5$  mm) compared to FS DWI ( $2.0 \pm 3.5$  mm; all  $p < .001$ ). Differences in mean ADC values between malignant and benign lesions were comparable between all three DWI methods (WE  $0.524 \times 10^{-3}$ ; SPAIR  $0.509 \times 10^{-3}$ ; FS  $0.509 \times 10^{-3}$  mm<sup>2</sup>/s).

#### CONCLUSION

Both WE and SPAIR DWI provide better image quality, subjective lesion visibility, and signal-intensity ratios than DWI with standard spectral fat saturation, resulting in a more accurate estimation of lesion size.

#### CLINICAL RELEVANCE/APPLICATION

The choice of fat suppression method may influence diagnostic assessment in diffusion-weighted breast MRI. Both water excitation and inversion recovery techniques allow for excellent depiction of benign and malignant lesions at 3 Tesla.

Printed on: 02/07/23

## Abstract Archives of the RSNA, 2022

T2-SPBR-6

### Utility of Kaiser Score for Focal Incidental Breast Uptake In a Diagnosed Malignant Population Undergoing 18 FDG PET-CT

Tuesday, Nov. 29 9:00AM - 9:30AM Room: Learning Center - BR DPS

#### Participants

Ankush Jajodia, MD, MBBS, New Delhi, India (*Presenter*) Nothing to Disclose

#### PURPOSE

We compared the diagnostic accuracies of ACR BIRADS, Kaiser score, and SUVmax in focal incidental breast uptake (FIBU) on 18FDG PET-CT in a diagnosed population with primary cancers excluding breast.

#### METHODS AND MATERIALS

A retrospective analysis in 21,657 female subjects with "FIBU" on 18 FDG PET-CT imaging in two hundred six subjects, between January 2010 and January 2020, including mass and non-mass enhancement (NME). ACR-BI-RADS category, Kaiser score, and SUVmax was derived for each lesion. Upgrade or downgrade was tabulated in an excel sheet. Independent samples t-test, diagnostic test calculator, and MedCalc 12.2.1 were used for statistical analysis.

#### RESULTS

According to the ACR lexicon, eighty lesions with eighteen BI-RADS 3 lesions, forty-seven BI-RADS 4, and fifteen BI-RADS 5 lesions with benign histology in 13% (10/80) and malignant in 87% (70/80). For benign lesions, SUV max range was 1.6-29.3, while for malignant lesions, it was 2.1-22.7(p=0.257). Kaiser score (p=0.002) assignment was statistically significant between the two groups. Kaiser score AUC (0.878; 95% CI: 0.786-0.94) was significantly high than ACR BIRADS (0.610; 95% CI :0.494-0.717) and SUVmax (0.566;95% CI:0.451-0.677). Ninety-four percent (48/51) of upgraded lesions were found to be malignant; benign histology was found in the remaining 5.9% percent (3/51). All (100%) of lesions (4/4) were correctly downgraded. All (100 %) lesions (18/18) which were incorrectly classified as ACR BIRADS 3 were correctly classified now as suspicious 4/5 category. When we used a Kaiser score of >4 as a cut-off for malignancy, we got 100% sensitivity. Using six as a cut-off score, sensitivity dropped to 85.7%, but specificity went up to 60% from 40%, with a positive likelihood ratio of 2.14. (vs. 1.67 with a cut-off score of 4). When we used a high cut-off value >8 to rule-in malignancy, we were correct in 96.4% of the cases (54/56), with a specificity of 80% and a positive likelihood ratio of 3.71. We were able to identify all four lesions that had been downgraded from suspicious (BIRADS 4/5 category) to benign (BIRADS 5) when we set a cut-off Kaiser score of 5, thus potentially avoiding biopsies 100% of the time.

#### CONCLUSION

s Kaiser score has meaningfully better diagnostic accuracy than ACR BIRADS and SUVmax for focal incidentally breast uptake.

#### CLINICAL RELEVANCE/APPLICATION

Kaiser score has highest diagnostic accuracy than ACR BIRADS and SUVmax for focal incidentally breast uptake. Our study validates the clinical benefit of Kaiser score in correctly assigning suspicious 4/5 category to lesions falsely classified as ACR BIRADS 3.

Printed on: 02/07/23

## Abstract Archives of the RSNA, 2022

T2-SPBR-7

### Quantitative Analysis of Enhancement Characteristics of Contrast-enhanced Spectral Mammography in Differentiating Malignant from Benign Breast Lesions

Tuesday, Nov. 29 9:00AM - 9:30AM Room: Learning Center - BR DPS

#### Participants

Huizhi Cao, PhD, (Presenter) Nothing to Disclose

#### PURPOSE

To quantitatively analyze the enhancement Characteristics of breast lesions on contrast-enhanced spectral mammography (CESM) to improve the diagnostic efficiency.

#### METHODS AND MATERIALS

A total of 283 patients with breast lesions admitted from August 2021 to Feb 2022 were retrospectively analyzed. Quantitative analysis of all enhancing lesions was performed to measure the enhancement values of the lesion area of interest (ROI), tissue surrounding the lesion (ROI1), tissue away from the lesion and close to the chest (ROI2), and the tissue at the level of the maximum diameter of the normal pectoralis major muscle on the ipsilateral side of the lesion (ROI3). rROI1, rROI2 and rROI3 were relative enhancement value between (ROI1,ROI2 and ROI3) and ROI. Differences in enhancement values between different ROIs of benign and malignant lesions were compared. Taking the pathological results as the gold standard, we used the receiver operating characteristic (ROC) curve to evaluate the diagnostic efficacy of the ROI enhancement value and rROI for the lesions.

#### RESULTS

A total of 299 lesions were found in 283 patients, including 101 benign lesions and 198 malignant lesions. The ROI enhancement value, rROI1, rROI2, and rROI3 of malignant lesions were all significantly greater than those of benign lesions. For enhancement values of benign and malignant lesions of ROI, rROI1, rROI2 and rROI3, AUC was 0.795, 0.833, 0.812 and 0.741, respectively. The statistically significant difference in the AUC was only found between rROI1 and ROI enhancement value, and rROI1 had the greatest diagnostic value.

#### CONCLUSION

The enhancement value of malignant breast lesions was higher than that of benign lesions. The quantitative analysis of the enhancement value was of great value in the differential diagnosis of benign and malignant breast lesions.

#### CLINICAL RELEVANCE/APPLICATION

Quantitative analysis in Contrast-enhanced spectral mammography has the potential value in the differential diagnosis of benign and malignant breast lesions.

Printed on: 02/07/23



## Abstract Archives of the RSNA, 2022

T2-SPCA

### Cardiac Tuesday Poster Discussions

Tuesday, Nov. 29 9:00AM - 9:30AM Room: Learning Center - CA DPS

#### Sub-Events

#### T2-SPCA-1 Epicardial Adipose Tissue Radiomics Features May Help Predict the Presence of Coronary Artery Disease on Unenhanced Computed Tomography Scans

##### Participants

Francesco Secchi, MD, PhD, (*Presenter*) Nothing to Disclose

##### PURPOSE

our aim was to assess the potential of radiomics features of epicardial adipose tissue (EAT) quantified on unenhanced computed tomography (CT) scans for predicting the presence of coronary artery disease (CAD).

##### METHODS AND MATERIALS

Consecutive patients undergoing contrast enhanced cardiac CT were retrospectively included in this study. The pericardium was manually segmented on the most representative slice for EAT on unenhanced scans, and subsequently thresholded for the Hounsfield Units (HU) of adipose tissue to obtain a mask for EAT. The presence of CAD defined as at least one moderate or two mild stenoses in the coronary tree was assessed on contrast-enhanced, gated scans. Radiomics features were then extracted from the EAT mask, and utilized to construct a machine learning model to predict the presence of CAD at contrast-enhanced, cardiac CT.

##### RESULTS

our final study population was composed by 480 patients, 294 (61%) of whom males, with a median age of 66 years (interquartile range 56-73 years), 164 (34%) of whom presenting with CAD. Using a support vector machine-based model, trained on a 80:20 split with 10-fold cross validation, the area under the curve for predicting the presence of CAD on the testing was 77%.

##### CONCLUSION

s radiomics features of EAT may help predict the presence of CAD through the assessment of unenhanced CT scans for calcium scoring.

##### CLINICAL RELEVANCE/APPLICATION

the risk of CAD may also be predicted in patients undergoing unenhanced CT scans from the analysis of EAT features.

Printed on: 02/07/23



## Abstract Archives of the RSNA, 2022

T2-SPCA-1

### Epicardial Adipose Tissue Radiomics Features May Help Predict the Presence of Coronary Artery Disease on Unenhanced Computed Tomography Scans

Tuesday, Nov. 29 9:00AM - 9:30AM Room: Learning Center - CA DPS

#### Participants

Francesco Secchi, MD, PhD, (*Presenter*) Nothing to Disclose

#### PURPOSE

our aim was to assess the potential of radiomics features of epicardial adipose tissue (EAT) quantified on unenhanced computed tomography (CT) scans for predicting the presence of coronary artery disease (CAD).

#### METHODS AND MATERIALS

Consecutive patients undergoing contrast enhanced cardiac CT were retrospectively included in this study. The pericardium was manually segmented on the most representative slice for EAT on unenhanced scans, and subsequently thresholded for the Hounsfield Units (HU) of adipose tissue to obtain a mask for EAT. The presence of CAD defined as at least one moderate or two mild stenoses in the coronary tree was assessed on contrast-enhanced, gated scans. Radiomics features were then extracted from the EAT mask, and utilized to construct a machine learning model to predict the presence of CAD at contrast-enhanced, cardiac CT.

#### RESULTS

our final study population was composed by 480 patients, 294 (61%) of whom males, with a median age of 66 years (interquartile range 56-73 years), 164 (34%) of whom presenting with CAD. Using a support vector machine-based model, trained on a 80:20 split with 10-fold cross validation, the area under the curve for predicting the presence of CAD on the testing was 77%.

#### CONCLUSION

s radiomics features of EAT may help predict the presence of CAD through the assessment of unenhanced CT scans for calcium scoring.

#### CLINICAL RELEVANCE/APPLICATION

the risk of CAD may also be predicted in patients undergoing unenhanced CT scans from the analysis of EAT features.

Printed on: 02/07/23

## Abstract Archives of the RSNA, 2022

T2-SPCH

### Chest Tuesday Poster Discussions

Tuesday, Nov. 29 9:00AM - 9:30AM Room: Learning Center - CH DPS

#### Participants

Axel Wismueller, MD, PhD, Pittsford, NY (*Moderator*) Nothing to Disclose

#### Sub-Events

### T2-SPCH-1 Comparison of CT Findings of Coronavirus Disease 2019 (COVID-19) Pneumonia Caused by Different Major Variants

#### Participants

Shohei Inui, MD, (*Presenter*) Nothing to Disclose

#### PURPOSE

To explore the CT findings and progression pattern of the Alpha and Delta variants of COVID-19 by comparing them with the pre-existing wild type.

#### METHODS AND MATERIALS

In this retrospective comparative study, a total of 392 patients with COVID-19 were included: 118 patients with wild type (70 men,  $56.8 \pm 20.7$  years), 137 with Alpha variant (93 men,  $49.4 \pm 17$  years), and 137 with Delta variant (94 men,  $45.4 \pm 12.4$ ). Chest CT evaluation included opacities and repairing changes as well as lesion distribution and laterality. Chest CT severity score was also calculated. These parameters were statistically compared across the variants.

#### RESULTS

Ground glass opacity (GGO) with consolidation and repairing changes were more frequent in the order of Delta variant, Alpha variant, and wild type throughout the disease course. Delta variant showed GGO with consolidation more conspicuously than did the other two on days 1 to 4 (vs. wild type, Bonferroni corrected- $p=0.01$ ; vs. Alpha variant, Bonferroni corrected- $p=0.003$ ) and days 5 to 8 (vs. wild type, Bonferroni corrected- $p<0.001$ ; vs. Alpha variant, Bonferroni corrected- $p=0.003$ ). Total lung CT severity scores of Delta variant were higher than those of wild type on days 1 to 4 and 5 to 8 (Bonferroni corrected- $p=0.01$  and Bonferroni corrected- $p=0.005$ , respectively) and that of Alpha variant on days 1 to 4 (Bonferroni corrected- $p=0.002$ ). There were no differences in the CT findings between wild type and Alpha variant.

#### CONCLUSION

Delta variant of COVID-19 showed GGO with reticulation or consolidation and repairing changes more conspicuously than did wild type and Alpha variant in the early phase. Chest CT scores of Delta variant were also higher than those of wild type during day 1 to 8 and Alpha variant during day 1 to 4.

#### CLINICAL RELEVANCE/APPLICATION

Pneumonia progression of Delta variant may be more rapid and severe in the early stage than in the other two. In contrast, there was no evidence of any difference in the CT findings between wild type and Alpha variant. The results of this study may be valuable for the ongoing and future battle with COVID-19 variants, reminding that different CT patterns may predispose different subtype infection and different clinical course.

### T2-SPCH-2 Uncertainty Quantification in COVID-19 Detection Using Evidential Deep Learning

#### Participants

Shahriar Faghani, MD, BSc, Rochester, MN (*Presenter*) Nothing to Disclose

#### PURPOSE

One of the factors that hinders the adoption of deep learning (DL) in clinical settings is the presence of performance errors. Most studies in recent years have been focused on developing novel approaches to improve models' accuracy. However, current models lack the implicit ability to say "I don't know" when provided input data that is out-of-distribution for the training data; compared to radiologists who tend to be careful when unsure about the diagnosis. Therefore, measuring and reporting the uncertainty level of DL models can be an important factor in their application in medicine.

#### METHODS AND MATERIALS

We used evidential deep learning (EDL) to quantify the uncertainty of a DL model. In this approach, by replacing the softmax function with the parameters of a Dirichlet density distribution, the model learns to recognize data instances that contribute efficiently to the performance during training, while providing an uncertainty estimate. This model has a specific loss function that can be optimized through backpropagation. We first trained the model on anteroposterior (AP) pneumonia negative and typical COVID-19 pneumonia chest x-rays (CXRs) of the SIIM-FISABIO-RSNA dataset ( $n=4,531$ ; 90% train set, 10% test set) to detect typical COVID-19 CXRs. We used images of atypical ( $n=474$ ) and indeterminate ( $n=1049$ ) COVID-19 CXRs from the same dataset to

measure models' uncertainty on unseen data. We also trained another DL model with cross-entropy loss for performance comparison. All the evaluation metrics are reported based on model performance on the holdout test set.

## RESULTS

The EDL model reached a final accuracy of 88.77%, though training the same model with the cross-entropy loss yielded an accuracy of 87.22% over the test set. On the test set, the EDL model provided a median uncertainty score of 0.25 and 0.07 for normal and typical COVID-19 CXRs, respectively. The misclassified samples had higher uncertainty levels compared to the correctly classified ones. The EDL model was able to provide a wide range of uncertainty scores for CXRs with typical COVID-19 infection. Moreover, we tested our model on the indeterminate and atypical subsets and the median uncertainty scores were 0.32 and 0.35, respectively.

## CONCLUSION

Overall, this study demonstrates applicability of EDL in disease detection that could facilitate the use of DL in practice by providing uncertainty scores.

## CLINICAL RELEVANCE/APPLICATION

When a deep learning model is going to be used in clinical practice, it should convey how uncertain it is when making a prediction, especially in out-of-distribution samples. This study shows a proof of concept of EDL technique in quantifying the level of uncertainty in a classification task, which can help guide the physicians on when a model cannot be trusted.

### T2-SPCH-3 Results of Post-PCNB (Percutaneous Core Needle Biopsy) Sputum Cytology: Diagnostic Yield and Factors for Positive Prediction

Participants

Heejeong Yu, MD, Busan, Korea, Republic Of (*Presenter*) Nothing to Disclose

## PURPOSE

We evaluated the results of the post-PCNB sputum cytology for diagnosing malignancy.

## METHODS AND MATERIALS

This retrospective study included the 987 patients who underwent percutaneous CT or fluoroscopy guided PCNB from January 2014 to March 2022. Patients' demographics, lung lesions' characteristics including solid, subsolid, open-bronchus, necrosis, location, underlying pulmonary disease including COPD or fibrosis, histopathologic results of the biopsy specimens of PCNB, post-PCNB sputum and final diagnosis were reviewed.

## RESULTS

Total 182 consecutive patients whose sputum specimens were obtained after PCNB for the intrapulmonary lesions were enrolled. Mean time between the day of PCNB and the day sputum specimens were obtained was 2 days (range 0-13). Final diagnoses of the patients were primary or metastatic lung cancer (n=157), benign pulmonary tumor (n=2), infection including bacteria, mycobacterium, fungus or parasite (n=22), and pneumoconiosis (n=1). Sufficient sputum specimens were obtained in 88 patients. The sufficient sputum was defined as containing  $\geq 10$  leukocytes and  $< 25$  squamous epithelial cells per low-power field. The diagnostic sputum specimens with atypical or malignant cells were obtained in 12 patients. The mean size of the lesion was 57.1 mm (range 15-100) and the mean distance of the lesion from the pleura was 6.3 mm (range 0-38) in the diagnostic sputum specimens. The sensitivity, specificity, accuracy, PPV and NPV of post-PCNB sputum cytology were 7.64%, 100%, 20.33%, 100% and 14.71% respectively. There were no significant differences in the location, solidity, multiplicity, presence of mediastinal lymph node, necrosis and underlying pulmonary disease between the diagnostic and non-diagnostic sputum specimens. The lesion size ( $p=0.009$ ,  $OR=1.037$ ), open-bronchus ( $p=0.006$ ,  $OR=23.232$ ) and subtype of squamous cell ( $p=0.007$ ,  $OR=7.108$ ) were significantly related to diagnostic sputum results.

## CONCLUSION

Post-PCNB sputum cytology could be diagnostic in some peripheral lung cancer patients who have cell types of squamous cell, relatively large tumors and open-bronchi to the lesions.

## CLINICAL RELEVANCE/APPLICATION

In some cases of peripheral lung cancer, malignant or atypical cells in the sputum cytology after PCNB can appear. It could be affected by the tumor size, presence of the open-bronchus to the tumor and subtype of squamous cell.

### T2-SPCH-4 Worldwide Performance of Lung-RADS in Lung Cancer Screening: A Systematic Review and Meta-Analysis

Participants

Yifei Mao, (*Presenter*) Nothing to Disclose

## PURPOSE

After the publication of Lung CT Screening Reporting and Data System (Lung-RADS), several lung cancer screenings have reported its performance, but it hasn't been validated systematically. In addition, compared to the initial version 1.0, there are multiple changes in updated version 1.1. Our aim of this meta-analysis is to evaluate and compare the diagnostic performance of Lung-RADS protocols version 1.0 and 1.1, and thereby explore whether Lung-RADS could be applicable for lung cancer screening worldwide.

## METHODS AND MATERIALS

Literature search for original diagnostic studies of Lung-RADS in LDCT lung cancer screening was conducted in PubMed, Web of Science, Cochrane Library, and Embase databases up to June 1, 2021. Pooled sensitivity and specificity were calculated using a bivariate random-effects model. The potential cause of heterogeneity between studies was explored using stratified analysis and meta-regression analysis. The following covariates were evaluated: population type (high-risk population, or general population), geographic area (Asia, or Non-Asia), study design (retrospective or prospective), reference standard (pathology alone, or pathology and other methods), and lung cancer prevalence ( $>1.8\%$ , or  $\leq 1.8\%$ ).

## RESULTS

Twenty-seven studies with 90,635 participants were included. Pooled sensitivity and specificity of Lung-RADS version 1.0 (24 studies) were 0.81 (95% confidence interval [CI]: 0.74-0.88) and 0.91 (95%CI: 0.89-0.93), respectively. Pooled sensitivity and specificity of Lung-RADS version 1.1 (three studies) were 0.91(95%CI: 0.83-0.99) and 0.66 (95%CI: 0.46-0.86), respectively. Population type (high-risk Vs. general population,  $p = 0.02$ ), geographic area (Asia Vs. Non-Asia,  $p = 0.04$ ), and prevalence of lung cancer ( $>1.8\%$  Vs.  $=1.8\%$ ,  $p = 0.04$ ) were significant factors for substantial heterogeneity among studies using Lung-RADS version 1.0.

## CONCLUSION

s Substantial higher sensitivity and relatively smaller decrease in specificity of Lung-RADS version 1.0 were noted especially for studies with a high-risk population in Non-Asia areas. Lung-RADS version 1.1 might have higher sensitivity, but lower specificity than version 1.0 in LDCT lung cancer screening; however, there were only three studies using version 1.1. More evidence in Asia is still required to determine the worldwide applicability of Lung-RADS 1.1 protocol.

## CLINICAL RELEVANCE/APPLICATION

1. This meta-analysis provides a sight to the applicability of Lung-RADS protocol in lung cancer screening worldwide. 2. Lung-RADS version 1.0 might be more applicable for the high-risk population in Non-Asia areas. Specifically tailored algorithm for Lung-RADS protocol might be needed for general population in Asia.

## T2-SPCH-5 The Image Classification of Abnormal Lipiodol Distribution in Thoracic Lymphatic Reflux on MDCT Lymphangiography

Participants

Qi Hao, Beijing, China (*Presenter*) Nothing to Disclose

## PURPOSE

The aim of this study was to analyze the different types of lipiodol distribution and characteristic findings on MDCT lymphangiography in patients with thoracic lymphatic reflux.

## METHODS AND MATERIALS

151 patients (84 males and 67 females) with thoracic lymphatic reflux underwent MDCT lymphangiography and abnormal lipiodol distributions in chest were retrospectively reviewed. The diseases spectrum included chylothorax ( $n=58$ ) single or multiple lymphangiomas ( $n=46$ ), diffuse pulmonary lymphangiomatosis ( $n=16$ ), pulmonary lymphangoectasis ( $n=10$ ), pulmonary lymphedema ( $n=12$ ), pulmonary lymphangiomyomatosis ( $n=9$ ) and chyloplmonary disease ( $n=6$ ). There were 61 males and 90 females aged from 5.5 to 78 years (median age 35.8).

## RESULTS

These patients were classified into 4 types according to lipiodol abnormal distribution on MDCTL: (1) type A is central type in 16 cases, lipiodol spotted distribution along peribronchovascular interstitium; (2) type B is superficial type in 91 cases: lipiodol diffused in peripheral lung tissue and visceral pleura; (3) type C is Intercostal type in 15 cases, lipiodol spotted distribution in parietal pleura and thoracic wall; (4) type D is mixed type in 29 cases, two or more types were exhibited at the same time. MDCTL findings including thoracic duct abnormalities in 147 patients with thoracic duct outlet stenosis in 108. Thoracic duct partially visible in group C were higher than that in the other 3 groups, with an incidence of 60.0%. Other image findings: type A was found with the highest incidence of peribronchovascular interstitium thickening(93.8%) and hydropericardium(81.3%), but the lowest incidence of atelectasis(62.5%), parietal pleura thickening(0) and ascites(0). Type B showed the highest incidence of atelectasis(97.8%) and ascites(69.2%), but the lowest incidence of peribronchovascular interstitium thickening(26.4%). In type C, the highest incidence of parietal pleura thickening(66.7%) was found. However, there was no characteristic performance in group D.

## CONCLUSION

s This study summarized a classification of four different types according to the lipiodol deposition in patients with thoracic lymphatic reflux, which provide more information for clinical diagnosis.

## CLINICAL RELEVANCE/APPLICATION

The four types of lipiodol abnormal distribution on MDCT lymphangiography provide more information for clinical diagnosis Thoracic lymphatic reflux .

## T2-SPCH-6 Safe Zone to Avoid Pneumothorax in a CT-guided Lung Biopsy

Participants

Nour Maalouf, MD, (*Presenter*) Nothing to Disclose

## PURPOSE

Pneumothorax is one of the most frequent complications of a CT-guided lung biopsy. This study aims to define the safe window of the biopsy needle's angle to the pleura during a CT-guided lung biopsy to diminish the risk of Pneumothorax.

## METHODS AND MATERIALS

Forty-three patients underwent CT-guided lung biopsies between January 2020 and January 2022 (24 m, 19 f, median age 70 years). All the interventions were carried out with a semi-automatic 18G needle and a 17G trocar in a prone or supine position. Right and left angles were measured and correlated to the presence of pneumothorax as an intraprocedural or early postprocedural complication. The minimum delta was calculated as the absolute value of the difference between a 90-degree angle (perpendicular to the chest wall) and the right and left angles. T-test p-value for the minimum delta was calculated.

## RESULTS

Out of the 43 patients, 28 experienced pneumothorax; intraprocedural and transient, postprocedural with minimal symptoms, or postprocedural with pronounced symptoms and requiring a chest tube insertion. 27 of the 43 patients had a minimum delta = 10, while 17 of them had a minimum delta < 10 degrees. 35% of the patients with a minimum delta < 10 degrees had pneumothorax,

while 81% of the patients with a minimum delta = 10 degrees had a pneumothorax (two-sided t-test p-value = 0.0017). A needle angle deviating from the perpendicular by more than 10 degrees correlated with a higher risk of pneumothorax development.

## CONCLUSION

s The study results show that as the needle's angle deviates from the perpendicular with an absolute value of more than 10 degrees, the pleural surface area experiencing trauma increases, and the likelihood of pneumothorax occurrence increases significantly.

## CLINICAL RELEVANCE/APPLICATION

CT-guided lung biopsy is widely used to gather valuable diagnostic information. On the downside, it still puts the patient at risk of developing pneumothorax. The present study provides quantitative data proving that adjusting the angle between the needle and the pleura can diminish the pneumothorax risk associated with a CT-guided lung biopsy. Opting for an angle close to 90 degrees between the needle and the pleura has been shown to reduce the risk of developing pneumothorax.

## T2-SPCH-7 Four Efficacy Types of Chest CT Imaging Manifestations of Lung Metastasis of Digestive System Tumors after CART Treatment

### Participants

Yiting Liu, Beijing, China (*Presenter*) Nothing to Disclose

## PURPOSE

Chimeric antigen receptor T cells (CART) are more lethal and specific than other immunotherapies. However, the immune response of lung metastases has not been investigated. Here, we evaluated the efficacy of CART on the pulmonary CT immune response.

## METHODS AND MATERIALS

Fifteen patients were enrolled from clinical trial NCT03874897. Patients had digestive system cancer with lung metastases and received CART therapy together with complete plain chest CT before and after treatment. Tumor responses were assessed according to RECIST 1.1.

## RESULTS

Four response types to CART therapy were observed, ranked from best to worst: ? Immuno-enrichment of metastasis nodule (IE-MN) Three patients showed expanded metastasis foci 2-4 days after treatment suggestive of progressive disease. However, the foci shrank within 4-23 days, indicative of pseudoprogression. Halo signs (ground glass density shadows) and/or thickening of interlobular septa were observed around the nodules, forming a "paving stone" sign. These reactions were synchronous with pseudoprogression of the metastatic nodules. ? Immuno-enrichment of normal lung (IE-NL) This was seen in six patients, appeared similar to type 1, and was characterized by: diffuse ground glass shadow (6/6); interstitial thickening, with significant axial interstitial thickening (4/6); paving stone signs (3/6); consolidation (4/6). As with type 1, the timelines were synchronized with pseudoprogression. The OS was 149-546 days. ? No immuno-enrichment of normal lung (nIE-NL) None of the five patients showed signs of immune hyperplasia or immune pneumonia. Metastatic nodules progressed in two patients and remained stable in three patients. Survival was poorer than in 1 and 2. ? Immuno-enrichment of lymphangitic carcinomatosis (IE-LC) The two patients showed obvious axial interstitial thickening. Peri-lymphatic nodules were diffused along the broncho-vascular bundle, subpleural, and interlobular septa. Patchy ground-glass shadow signs caused by exudative changes were rare.

## CONCLUSION

s The first two types are indicative of treatment effectiveness. The response was better (60% vs 12.6%) and faster (median 13 d vs 84 d) compared with ICIs. Lymphangitic spread of carcinoma is often a sign of poor prognosis.

## CLINICAL RELEVANCE/APPLICATION

Imaging of the chest response after CART therapy for solid tumors was classified to elucidate the biological mechanism and judge the overall response according to different chest responses.

Printed on: 02/07/23

## Abstract Archives of the RSNA, 2022

T2-SPCH-1

### Comparison of CT Findings of Coronavirus Disease 2019 (COVID-19) Pneumonia Caused by Different Major Variants

Tuesday, Nov. 29 9:00AM - 9:30AM Room: Learning Center - CH DPS

#### Participants

Shohei Inui, MD, (*Presenter*) Nothing to Disclose

#### PURPOSE

To explore the CT findings and progression pattern of the Alpha and Delta variants of COVID-19 by comparing them with the pre-existing wild type.

#### METHODS AND MATERIALS

In this retrospective comparative study, a total of 392 patients with COVID-19 were included: 118 patients with wild type (70 men,  $56.8 \pm 20.7$  years), 137 with Alpha variant (93 men,  $49.4 \pm 17$  years), and 137 with Delta variant (94 men,  $45.4 \pm 12.4$ ). Chest CT evaluation included opacities and repairing changes as well as lesion distribution and laterality. Chest CT severity score was also calculated. These parameters were statistically compared across the variants.

#### RESULTS

Ground glass opacity (GGO) with consolidation and repairing changes were more frequent in the order of Delta variant, Alpha variant, and wild type throughout the disease course. Delta variant showed GGO with consolidation more conspicuously than did the other two on days 1 to 4 (vs. wild type, Bonferroni corrected- $p=0.01$ ; vs. Alpha variant, Bonferroni corrected- $p=0.003$ ) and days 5 to 8 (vs. wild type, Bonferroni corrected- $p<0.001$ ; vs. Alpha variant, Bonferroni corrected- $p=0.003$ ). Total lung CT severity scores of Delta variant were higher than those of wild type on days 1 to 4 and 5 to 8 (Bonferroni corrected- $p=0.01$  and Bonferroni corrected- $p=0.005$ , respectively) and that of Alpha variant on days 1 to 4 (Bonferroni corrected- $p=0.002$ ). There were no differences in the CT findings between wild type and Alpha variant.

#### CONCLUSION

s Delta variant of COVID-19 showed GGO with reticulation or consolidation and repairing changes more conspicuously than did wild type and Alpha variant in the early phase. Chest CT scores of Delta variant were also higher than those of wild type during day 1 to 8 and Alpha variant during day 1 to 4.

#### CLINICAL RELEVANCE/APPLICATION

Pneumonia progression of Delta variant may be more rapid and severe in the early stage than in the other two. In contrast, there was no evidence of any difference in the CT findings between wild type and Alpha variant. The results of this study may be valuable for the ongoing and future battle with COVID-19 variants, reminding that different CT patterns may predispose different subtype infection and different clinical course.

Printed on: 02/07/23

## Abstract Archives of the RSNA, 2022

T2-SPCH-2

### Uncertainty Quantification in COVID-19 Detection Using Evidential Deep Learning

Tuesday, Nov. 29 9:00AM - 9:30AM Room: Learning Center - CH DPS

#### Participants

Shahriar Faghani, MD, BSc, Rochester, MN (*Presenter*) Nothing to Disclose

#### PURPOSE

One of the factors that hinders the adoption of deep learning (DL) in clinical settings is the presence of performance errors. Most studies in recent years have been focused on developing novel approaches to improve models' accuracy. However, current models lack the implicit ability to say "I don't know" when provided input data that is out-of-distribution for the training data; compared to radiologists who tend to be careful when unsure about the diagnosis. Therefore, measuring and reporting the uncertainty level of DL models can be an important factor in their application in medicine.

#### METHODS AND MATERIALS

We used evidential deep learning (EDL) to quantify the uncertainty of a DL model. In this approach, by replacing the softmax function with the parameters of a Dirichlet density distribution, the model learns to recognize data instances that contribute efficiently to the performance during training, while providing an uncertainty estimate. This model has a specific loss function that can be optimized through backpropagation. We first trained the model on anteroposterior (AP) pneumonia negative and typical COVID-19 pneumonia chest x-rays (CXRs) of the SIIM-FISABIO-RSNA dataset (n=4,531; 90% train set, 10% test set) to detect typical COVID-19 CXRs. We used images of atypical (n=474) and indeterminate (n=1049) COVID-19 CXRs from the same dataset to measure models' uncertainty on unseen data. We also trained another DL model with cross-entropy loss for performance comparison. All the evaluation metrics are reported based on model performance on the holdout test set.

#### RESULTS

The EDL model reached a final accuracy of 88.77%, though training the same model with the cross-entropy loss yielded an accuracy of 87.22% over the test set. On the test set, the EDL model provided a median uncertainty score of 0.25 and 0.07 for normal and typical COVID-19 CXRs, respectively. The misclassified samples had higher uncertainty levels compared to the correctly classified ones. The EDL model was able to provide a wide range of uncertainty scores for CXRs with typical COVID-19 infection. Moreover, we tested our model on the indeterminate and atypical subsets and the median uncertainty scores were 0.32 and 0.35, respectively.

#### CONCLUSION

Overall, this study demonstrates applicability of EDL in disease detection that could facilitate the use of DL in practice by providing uncertainty scores.

#### CLINICAL RELEVANCE/APPLICATION

When a deep learning model is going to be used in clinical practice, it should convey how uncertain it is when making a prediction, especially in out-of-distribution samples. This study shows a proof of concept of EDL technique in quantifying the level of uncertainty in a classification task, which can help guide the physicians on when a model cannot be trusted.

Printed on: 02/07/23

## Abstract Archives of the RSNA, 2022

T2-SPCH-3

### Results of Post-PCNB (Percutaneous Core Needle Biopsy) Sputum Cytology: Diagnostic Yield and Factors for Positive Prediction

Tuesday, Nov. 29 9:00AM - 9:30AM Room: Learning Center - CH DPS

#### Participants

Heejeong Yu, MD, Busan, Korea, Republic Of (*Presenter*) Nothing to Disclose

#### PURPOSE

We evaluated the results of the post-PCNB sputum cytology for diagnosing malignancy.

#### METHODS AND MATERIALS

This retrospective study included the 987 patients who underwent percutaneous CT or fluoroscopy guided PCNB from January 2014 to March 2022. Patients' demographics, lung lesions' characteristics including solid, subsolid, open-bronchus, necrosis, location, underlying pulmonary disease including COPD or fibrosis, histopathologic results of the biopsy specimens of PCNB, post-PCNB sputum and final diagnosis were reviewed.

#### RESULTS

Total 182 consecutive patients whose sputum specimens were obtained after PCNB for the intrapulmonary lesions were enrolled. Mean time between the day of PCNB and the day sputum specimens were obtained was 2 days (range 0-13). Final diagnoses of the patients were primary or metastatic lung cancer (n=157), benign pulmonary tumor (n=2), infection including bacteria, mycobacterium, fungus or parasite (n=22), and pneumoconiosis (n=1). Sufficient sputum specimens were obtained in 88 patients. The sufficient sputum was defined as containing  $\geq 10$  leukocytes and  $< 25$  squamous epithelial cells per low-power field. The diagnostic sputum specimens with atypical or malignant cells were obtained in 12 patients. The mean size of the lesion was 57.1 mm (range 15-100) and the mean distance of the lesion from the pleura was 6.3 mm (range 0-38) in the diagnostic sputum specimens. The sensitivity, specificity, accuracy, PPV and NPV of post-PCNB sputum cytology were 7.64%, 100%, 20.33%, 100% and 14.71% respectively. There were no significant differences in the location, solidity, multiplicity, presence of mediastinal lymph node, necrosis and underlying pulmonary disease between the diagnostic and non-diagnostic sputum specimens. The lesion size ( $p=0.009$ , OR=1.037), open-bronchus ( $p=0.006$ , OR=23.232) and subtype of squamous cell ( $p=0.007$ , OR=7.108) were significantly related to diagnostic sputum results.

#### CONCLUSION

Post-PCNB sputum cytology could be diagnostic in some peripheral lung cancer patients who have cell types of squamous cell, relatively large tumors and open-bronchi to the lesions.

#### CLINICAL RELEVANCE/APPLICATION

In some cases of peripheral lung cancer, malignant or atypical cells in the sputum cytology after PCNB can appear. It could be affected by the tumor size, presence of the open-bronchus to the tumor and subtype of squamous cell.

Printed on: 02/07/23

## Abstract Archives of the RSNA, 2022

T2-SPCH-4

### Worldwide Performance of Lung-RADS in Lung Cancer Screening: A Systematic Review and Meta-Analysis

Tuesday, Nov. 29 9:00AM - 9:30AM Room: Learning Center - CH DPS

#### Participants

Yifei Mao, (*Presenter*) Nothing to Disclose

#### PURPOSE

After the publication of Lung CT Screening Reporting and Data System (Lung-RADS), several lung cancer screenings have reported its performance, but it hasn't been validated systematically. In addition, compared to the initial version 1.0, there are multiple changes in updated version 1.1. Our aim of this meta-analysis is to evaluate and compare the diagnostic performance of Lung-RADS protocols version 1.0 and 1.1, and thereby explore whether Lung-RADS could be applicable for lung cancer screening worldwide.

#### METHODS AND MATERIALS

Literature search for original diagnostic studies of Lung-RADS in LDCT lung cancer screening was conducted in PubMed, Web of Science, Cochrane Library, and Embase databases up to June 1, 2021. Pooled sensitivity and specificity were calculated using a bivariate random-effects model. The potential cause of heterogeneity between studies was explored using stratified analysis and meta-regression analysis. The following covariates were evaluated: population type (high-risk population, or general population), geographic area (Asia, or Non-Asia), study design (retrospective or prospective), reference standard (pathology alone, or pathology and other methods), and lung cancer prevalence ( $>1.8\%$ , or  $=1.8\%$ ).

#### RESULTS

Twenty-seven studies with 90,635 participants were included. Pooled sensitivity and specificity of Lung-RADS version 1.0 (24 studies) were 0.81 (95% confidence interval [CI]: 0.74-0.88) and 0.91 (95%CI: 0.89-0.93), respectively. Pooled sensitivity and specificity of Lung-RADS version 1.1 (three studies) were 0.91(95%CI: 0.83-0.99) and 0.66 (95%CI: 0.46-0.86), respectively. Population type (high-risk Vs. general population,  $p = 0.02$ ), geographic area (Asia Vs. Non-Asia,  $p = 0.04$ ), and prevalence of lung cancer ( $>1.8\%$  Vs.  $=1.8\%$ ,  $p = 0.04$ ) were significant factors for substantial heterogeneity among studies using Lung-RADS version 1.0.

#### CONCLUSION

Substantial higher sensitivity and relatively smaller decrease in specificity of Lung-RADS version 1.0 were noted especially for studies with a high-risk population in Non-Asia areas. Lung-RADS version 1.1 might have higher sensitivity, but lower specificity than version 1.0 in LDCT lung cancer screening; however, there were only three studies using version 1.1. More evidence in Asia is still required to determine the worldwide applicability of Lung-RADS 1.1 protocol.

#### CLINICAL RELEVANCE/APPLICATION

1. This meta-analysis provides a sight to the applicability of Lung-RADS protocol in lung cancer screening worldwide. 2. Lung-RADS version 1.0 might be more applicable for the high-risk population in Non-Asia areas. Specifically tailored algorithm for Lung-RADS protocol might be needed for general population in Asia.

Printed on: 02/07/23

## Abstract Archives of the RSNA, 2022

T2-SPCH-5

### The Image Classification of Abnormal Lipiodol Distribution in Thoracic Lymphatic Reflux on MDCT Lymphangiography

Tuesday, Nov. 29 9:00AM - 9:30AM Room: Learning Center - CH DPS

#### Participants

Qi Hao, Beijing, China (*Presenter*) Nothing to Disclose

#### PURPOSE

The aim of this study was to analyze the different types of lipiodol distribution and characteristic findings on MDCT lymphangiography in patients with thoracic lymphatic reflux.

#### METHODS AND MATERIALS

151 patients (84 males and 67 females) with thoracic lymphatic reflux underwent MDCT lymphangiography and abnormal lipiodol distributions in chest were retrospectively reviewed. The diseases spectrum included chylothorax (n=58) single or multiple lymphangiomas (n=46), diffuse pulmonary lymphangiomatosis (n=16), pulmonary lymphangioectasis (n=10), pulmonary lymphedema (n=12), pulmonary lymphangiomyomatosis (n=9) and chylopulmonary disease (n=6). There were 61 males and 90 females aged from 5.5 to 78 years (median age 35.8).

#### RESULTS

These patients were classified into 4 types according to lipiodol abnormal distribution on MDCTL: (1) type A is central type in 16 cases, lipiodol spotted distribution along peribronchovascular interstitium; (2) type B is superficial type in 91 cases: lipiodol diffused in peripheral lung tissue and visceral pleura; (3) type C is Intercostal type in 15 cases, lipiodol spotted distribution in parietal pleura and thoracic wall; (4) type D is mixed type in 29 cases, two or more types were exhibited at the same time. MDCTL findings including thoracic duct abnormalities in 147 patients with thoracic duct outlet stenosis in 108. Thoracic duct partially visible in group C were higher than that in the other 3 groups, with an incidence of 60.0%. Other image findings: type A was found with the highest incidence of peribronchovascular interstitium thickening(93.8%) and hydropericardium(81.3%), but the lowest incidence of atelectasis(62.5%), parietal pleura thickening(0) and ascites(0). Type B showed the highest incidence of atelectasis(97.8%) and ascites(69.2%), but the lowest incidence of peribronchovascular interstitium thickening(26.4%). In type C, the highest incidence of parietal pleura thickening(66.7%) was found. However, there was no characteristic performance in group D.

#### CONCLUSION

s This study summarized a classification of four different types according to the lipiodol deposition in patients with thoracic lymphatic reflux, which provide more information for clinical diagnosis.

#### CLINICAL RELEVANCE/APPLICATION

The four types of lipiodol abnormal distribution on MDCT lymphangiography provide more information for clinical diagnosis Thoracic lymphatic reflux .

Printed on: 02/07/23

## Abstract Archives of the RSNA, 2022

T2-SPCH-6

### Safe Zone to Avoid Pneumothorax in a CT-guided Lung Biopsy

Tuesday, Nov. 29 9:00AM - 9:30AM Room: Learning Center - CH DPS

#### Participants

Nour Maalouf, MD, (*Presenter*) Nothing to Disclose

#### PURPOSE

Pneumothorax is one of the most frequent complications of a CT-guided lung biopsy. This study aims to define the safe window of the biopsy needle's angle to the pleura during a CT-guided lung biopsy to diminish the risk of Pneumothorax.

#### METHODS AND MATERIALS

Forty-three patients underwent CT-guided lung biopsies between January 2020 and January 2022 (24 m, 19 f, median age 70 years). All the interventions were carried out with a semi-automatic 18G needle and a 17G trocar in a prone or supine position. Right and left angles were measured and correlated to the presence of pneumothorax as an intraprocedural or early postprocedural complication. The minimum delta was calculated as the absolute value of the difference between a 90-degree angle (perpendicular to the chest wall) and the right and left angles. T-test p-value for the minimum delta was calculated.

#### RESULTS

Out of the 43 patients, 28 experienced pneumothorax; intraprocedural and transient, postprocedural with minimal symptoms, or postprocedural with pronounced symptoms and requiring a chest tube insertion. 27 of the 43 patients had a minimum delta = 10, while 17 of them had a minimum delta < 10 degrees. 35% of the patients with a minimum delta < 10 degrees had pneumothorax, while 81% of the patients with a minimum delta = 10 degrees had a pneumothorax (two-sided t-test p-value = 0.0017). A needle angle deviating from the perpendicular by more than 10 degrees correlated with a higher risk of pneumothorax development.

#### CONCLUSION

s The study results show that as the needle's angle deviates from the perpendicular with an absolute value of more than 10 degrees, the pleural surface area experiencing trauma increases, and the likelihood of pneumothorax occurrence increases significantly.

#### CLINICAL RELEVANCE/APPLICATION

CT-guided lung biopsy is widely used to gather valuable diagnostic information. On the downside, it still puts the patient at risk of developing pneumothorax. The present study provides quantitative data proving that adjusting the angle between the needle and the pleura can diminish the pneumothorax risk associated with a CT-guided lung biopsy. Opting for an angle close to 90 degrees between the needle and the pleura has been shown to reduce the risk of developing pneumothorax.

Printed on: 02/07/23

## Abstract Archives of the RSNA, 2022

T2-SPCH-7

### Four Efficacy Types of Chest CT Imaging Manifestations of Lung Metastasis of Digestive System Tumors after CART Treatment

Tuesday, Nov. 29 9:00AM - 9:30AM Room: Learning Center - CH DPS

#### Participants

Yiting Liu, Beijing, China (*Presenter*) Nothing to Disclose

#### PURPOSE

Chimeric antigen receptor T cells (CART) are more lethal and specific than other immunotherapies. However, the immune response of lung metastases has not been investigated. Here, we evaluated the efficacy of CART on the pulmonary CT immune response.

#### METHODS AND MATERIALS

Fifteen patients were enrolled from clinical trial NCT03874897. Patients had digestive system cancer with lung metastases and received CART therapy together with complete plain chest CT before and after treatment. Tumor responses were assessed according to RECIST 1.1.

#### RESULTS

Four response types to CART therapy were observed, ranked from best to worst: ? Immuno-enrichment of metastasis nodule (IE-MN) Three patients showed expanded metastasis foci 2-4 days after treatment suggestive of progressive disease. However, the foci shrank within 4-23 days, indicative of pseudoprogression. Halo signs (ground glass density shadows) and/or thickening of interlobular septa were observed around the nodules, forming a "paving stone" sign. These reactions were synchronous with pseudoprogression of the metastatic nodules. ? Immuno-enrichment of normal lung (IE-NL) This was seen in six patients, appeared similar to type 1, and was characterized by: diffuse ground glass shadow (6/6); interstitial thickening, with significant axial interstitial thickening (4/6); paving stone signs (3/6); consolidation (4/6). As with type 1, the timelines were synchronized with pseudoprogression. The OS was 149-546 days. ? No immuno-enrichment of normal lung (nIE-NL) None of the five patients showed signs of immune hyperplasia or immune pneumonia. Metastatic nodules progressed in two patients and remained stable in three patients. Survival was poorer than in 1 and 2. ? Immuno-enrichment of lymphangitic carcinomatosis (IE-LC) The two patients showed obvious axial interstitial thickening. Peri-lymphatic nodules were diffused along the broncho-vascular bundle, subpleural, and interlobular septa. Patchy ground-glass shadow signs caused by exudative changes were rare.

#### CONCLUSION

s The first two types are indicative of treatment effectiveness. The response was better (60% vs 12.6%) and faster (median 13 d vs 84 d) compared with ICIs. Lymphangitic spread of carcinoma is often a sign of poor prognosis.

#### CLINICAL RELEVANCE/APPLICATION

Imaging of the chest response after CART therapy for solid tumors was classified to elucidate the biological mechanism and judge the overall response according to different chest responses.

Printed on: 02/07/23

## Abstract Archives of the RSNA, 2022

T2-SPER

### Emergency Tuesday Poster Discussions

Tuesday, Nov. 29 9:00AM - 9:30AM Room: Learning Center - ER DPS

#### Participants

Claire Sandstrom, MD, Seattle, WA (*Moderator*) Nothing to Disclose

#### Sub-Events

#### **T2-SPER-1 CT features provide additional predictive value to clinical factors in predicting outcomes for patients with spontaneous rectus sheath hematoma**

#### Participants

Hadiseh Kavandi, MD, Boston, MA (*Presenter*) Nothing to Disclose

#### PURPOSE

To identify clinical and radiological features that predict outcomes of patients with spontaneous rectus sheath hematoma (RSH).

#### METHODS AND MATERIALS

In this retrospective IRB-approved, HIPAA-compliant study, consecutive patients with the diagnosis of RSH on CT scan between 1/1/2000 and 8/30/2021 in a tertiary care hospital were included. Patients with recent trauma or abdominal laparotomy were excluded. Clinical information and radiological features (size of hematoma and presence of active extravasation) were collected. Outcomes assessed included endovascular embolization, hospital stay greater than 5 days, RBC transfusion, the incidence of adverse events (surgery, readmission, and death), and the incidence of acute kidney injury (AKI).

#### RESULTS

261 patients (age 69±14 years, 154/261 (59%) females) were included. 157/261 (59%) patients underwent contrast-enhanced CT. Active extravasation was detected in 60/157 (38%) patients. Epigastric artery embolization was performed for 35/261 (13%) patients. Adverse events occurred in 18/261 (7%): 6/261 (2%) undergoing surgery, 7/261 (3%) being readmitted, and 5/261 (2%) with rectus sheath hematoma related deaths. Female sex, number of comorbidities, and anticoagulation medications were associated with longer hospital stay and need for transfusion ( $p<0.05$ ). Lower diastolic pressure and lower hematocrit at presentation were associated with adverse events, transfusions, and longer hospital stay ( $p<0.002$  for all). Active extravasation on CT was associated with adverse events, embolization, and transfusion ( $p<0.003$  for all). Larger hematomas were associated with a longer hospital stay, embolization, and transfusions ( $p<0.02$  for all). Radiological features of bleeding provided added predictive value to clinical predictors for RBC transfusion ( $p=0.005$ , AUC=0.88 vs. 0.78) and adverse events ( $p=0.003$ , AUC=0.99 vs. 0.80). 40/261 (15%) patients developed AKI; however, it did not correlate with contrast administration,  $p=0.4$ .

#### CONCLUSION

Rectus sheath hematoma size and active extravasation on CT are associated with worse outcomes. Radiological features provided added predictive value to clinical predictors for future RBC transfusion and adverse events.

#### CLINICAL RELEVANCE/APPLICATION

In patients with spontaneous rectus sheath hematoma, CT features (size of hematoma and dimensions) provide additional predictive value to clinical predictors for adverse events and RBC transfusions.

Printed on: 02/07/23

## Abstract Archives of the RSNA, 2022

T2-SPER-1

### CT features provide additional predictive value to clinical factors in predicting outcomes for patients with spontaneous rectus sheath hematoma

Tuesday, Nov. 29 9:00AM - 9:30AM Room: Learning Center - ER DPS

#### Participants

Hadiseh Kavandi, MD, Boston, MA (*Presenter*) Nothing to Disclose

#### PURPOSE

To identify clinical and radiological features that predict outcomes of patients with spontaneous rectus sheath hematoma (RSH).

#### METHODS AND MATERIALS

In this retrospective IRB-approved, HIPAA-compliant study, consecutive patients with the diagnosis of RSH on CT scan between 1/1/2000 and 8/30/2021 in a tertiary care hospital were included. Patients with recent trauma or abdominal laparotomy were excluded. Clinical information and radiological features (size of hematoma and presence of active extravasation) were collected. Outcomes assessed included endovascular embolization, hospital stay greater than 5 days, RBC transfusion, the incidence of adverse events (surgery, readmission, and death), and the incidence of acute kidney injury (AKI).

#### RESULTS

261 patients (age  $69 \pm 14$  years, 154/261 (59%) females) were included. 157/261 (59%) patients underwent contrast-enhanced CT. Active extravasation was detected in 60/157 (38%) patients. Epigastric artery embolization was performed for 35/261 (13%) patients. Adverse events occurred in 18/261 (7%): 6/261 (2%) undergoing surgery, 7/261 (3%) being readmitted, and 5/261 (2%) with rectus sheath hematoma related deaths. Female sex, number of comorbidities, and anticoagulation medications were associated with longer hospital stay and need for transfusion ( $p < 0.05$ ). Lower diastolic pressure and lower hematocrit at presentation were associated with adverse events, transfusions, and longer hospital stay ( $p < 0.002$  for all). Active extravasation on CT was associated with adverse events, embolization, and transfusion ( $p < 0.003$  for all). Larger hematomas were associated with a longer hospital stay, embolization, and transfusions ( $p < 0.02$  for all). Radiological features of bleeding provided added predictive value to clinical predictors for RBC transfusion ( $p = 0.005$ , AUC=0.88 vs. 0.78) and adverse events ( $p = 0.003$ , AUC=0.99 vs. 0.80). 40/261 (15%) patients developed AKI; however, it did not correlate with contrast administration,  $p = 0.4$ .

#### CONCLUSION

Rectus sheath hematoma size and active extravasation on CT are associated with worse outcomes. Radiological features provided added predictive value to clinical predictors for future RBC transfusion and adverse events.

#### CLINICAL RELEVANCE/APPLICATION

In patients with spontaneous rectus sheath hematoma, CT features (size of hematoma and dimensions) provide additional predictive value to clinical predictors for adverse events and RBC transfusions.

Printed on: 02/07/23

## Abstract Archives of the RSNA, 2022

T2-SPGI

### Gastrointestinal Tuesday Poster Discussions

Tuesday, Nov. 29 9:00AM - 9:30AM Room: Learning Center - GI DPS

#### Participants

Jena Depetris, MD, LOS ANGELES, CA (*Moderator*) Nothing to Disclose

#### Sub-Events

#### T2-SPGI-1 Photon-counting CT vs conventional CT - Evaluation of incidental lesions in the liver and kidney.

#### Participants

Leonid Roshkovan, MD, Philadelphia, PA (*Presenter*) Nothing to Disclose

#### PURPOSE

Incidental liver and renal lesions are extremely common in clinical practice and are often difficult to fully characterize on a single-phase CT examination. We hypothesized that photon-counting CT (PCCT) would be able to characterize incidental hypoattenuating lesions more accurately in the liver and kidneys compared to conventional single-phase CT.

#### METHODS AND MATERIALS

Patients who had undergone a clinical CT scan of the abdomen and pelvis on a clinical PCCT scanner (Naeotom Alpha, Siemens Healthineers) and a conventional CT scan (Definition Edge, Definition AS+, Somatom Force, Siemens Healthineers) within six months were identified. Incidental hypoattenuating lesions that were visible on both scans were included, but lesions less than five pixels in size were excluded since their density could not be accurately determined. Mean Hounsfield units (HU) and standard deviation (SD) were recorded, and signal to noise ratio (SNR) was calculated. To characterize the spectral signature of the individual lesions, iodine density maps and virtual monoenergetic images (VMI, at 40, 70, 100, and 190 keV) were used to cluster low density lesions into subgroups using K-means clustering. Clinical and scan variables including patient BMI, radiation dose and contrast volume were also recorded.

#### RESULTS

30 patients with a total of 61 lesions (16 and 45 lesions from unenhanced and enhanced CT scans, respectively) were included in the analysis, with lesions averaging a diameter of  $3 \pm 2.1$  mm. Mean HU values and SD as well as SNR were similar between both groups when values were obtained from VMI 70 keV ( $19.0 \pm 17.5$  HU, SNR 1.5) compared to conventional CT ( $21.1 \pm 13.7$  HU, SNR 1.5). With the spectral information from PCCT, hypoattenuating lesions in the liver and kidneys were automatically separated into three groups that corresponded to 10 fat-containing, 46 water-containing, and 5 iodine-containing lesions.

#### CONCLUSION

No significant difference in SNR and mean HU was identified between conventional CT and VMI 70 keV images on PCCT. Based on the spectral data from PCCT, it was possible to separate lesions into subgroups. Our ongoing work will focus on expanding our cohort size, comparing PCCT lesion characterization to other spectral scanners, and potentially utilizing spectral data for developing automatic lesion characterization.

#### CLINICAL RELEVANCE/APPLICATION

PCCT can more accurately characterize incidental hypoattenuating lesions compared to conventional CT regardless of the presence of contrast, thus increasing confidence in interpretation.

#### T2-SPGI-10 Potential Predictors of Long-term Outcomes of the LI-RADS Equivocal Category after Locoregional Therapy of Hepatocellular Carcinoma

#### Participants

Mohamed Tantawi, MBBCh, (*Presenter*) Nothing to Disclose

#### PURPOSE

The Liver Imaging and Reporting Data System (LI-RADS) has introduced a treatment response algorithm to assess the viability of hepatocellular carcinoma (HCC) tumors after locoregional therapy (LRT). Treated tumors can be classified as viable, nonviable, equivocal, or non-evaluable. Equivocal viability is defined as enhancement atypical for treatment-specific expected enhancement pattern and not meeting the criteria for probably or definitely viable. This study aimed to identify the potential predictors of long-term viability outcome of lesions classified as equivocal following LRT.

#### METHODS AND MATERIALS

The study included 136 HCC lesions in 115 patients classified as equivocal at least once following LRT. Then, we excluded patients who were retreated, died, or were lost to follow-up before a viable/nonviable outcome. Clinical characteristics and imaging features were compared between tumors with later viable vs. nonviable outcomes. Viability outcomes were defined by the subsequent viable/nonviable evaluation on cross-sectional imaging or pathologic findings on explant. T-tests and chi-square tests were used to

compare the variables between the two outcome groups.

## RESULTS

Across all treatment types, 74 lesions (72.6%) were nonviable on later assessments, while 28 (27.4%) were viable. A shorter time between treatment and LI-RADS equivocal read was significantly associated with a longer-term nonviable outcome ( $p=0.004$ ). Recurrent tumors after previous LRT were significantly more likely to have a viable outcome than those treated for the first time ( $p<0.001$ ). No single imaging feature or treatment type was associated with a longer-term definite viability outcome.

## CONCLUSION

s History of recurrence after LRT and time between treatment and equivocal read can be indicators of long-term viability outcome of HCC after LRTs.

## CLINICAL RELEVANCE/APPLICATION

In recently treated patients, equivocal findings on LI-RADS tend to represent evolving posttreatment changes and eventually become nonviable. Alternatively, equivocal findings in patients with a prior history of recurrence trend towards longer term viability.

### T2-SPGI-2 Application of selective photon shield on image quality and radiation dose of dual energy CT-Enterography

Participants

Zengmiao Xu, Xian, China (*Presenter*) Nothing to Disclose

## PURPOSE

To investigate the influence of selective photon shield on image quality and radiation dose of dual-energy CT enterography (CTE).

## METHODS AND MATERIALS

A total of 70 patients, 37 females and 33 males, aged (mean  $48.19\pm 15.53$  years, range 15~81 years) between January 2019 and April 2022 were retrospectively and consecutively enrolled. Exclusion criteria: 1) small bowel preparation failure; 2) Poor image quality or scanning failure; 3) Contrast agent allergy. All patients were divided into control group (SP group) of 36 patients (19 females, 17 males, mean age  $46.75\pm 14.69$  years) and experimental group (TF group) of 34 patients, (18 females, 16 males, mean age  $49.62\pm 16.88$  years), CTE were performed with SOMATOM Force 256 CT (SOMATOM). SP group used standard CTE scheme with 100kV, CARE Dose 4D, a pitch of 0.6. TF group used ultra-low-dose CTE scheme with 100/Sn150kV, CARE Dose 4D, a pitch of 0.6. The CT dose index (CTDI) and dose-length product (DLP) of the two groups were compared, and the signal-to-noise ratio (SNR) and contrast-to-noise ratio (CNR) of the two groups were calculated, respectively. All images were evaluated independently by two radiologists, who were blinded by clinical diagnosis. Any disagreements were resolved by consensus.

## RESULTS

1)The DLP, CTDI and ED of TF group were  $236.75\pm 11.90\text{mGy}\cdot\text{cm}$ ,  $6.02\pm 0.25\text{mGy}$ ,  $3.55\pm 0.19\text{mSv}$ , respectively, which were significantly lower than those of SP group ( $1540.58\pm 66.58\text{mGy}\cdot\text{cm}$ ,  $40.48\pm 1.26\text{mGy}$ ,  $23.11\pm 0.99\text{mSv}$ , all  $p<0.001$ ). (Table 2)  
2)There was no significant difference in the SNR and CNR of the abdominal aorta, superior mesenteric artery and superior mesenteric vein between TF group and SP group. ( $p>0.01$ )  
3)There was no significant difference in the subjective scores of image quality between the TF group and SP group.

## CONCLUSION

s Compared with standard CTE, selective photon shield of dual-energy CTE could significantly reduce radiation dose and obtain similar imaging quality. Clinical application: Selective photon shield of dual-energy CTE could be widely used in clinic instead of standard CTE.

## CLINICAL RELEVANCE/APPLICATION

### T2-SPGI-3 An evaluation of photon counting computed tomography of the abdomen and pelvis compared to dual energy CT in clinical routine

Participants

Manoj Mathew, MD, Philadelphia, PA (*Presenter*) Nothing to Disclose

## PURPOSE

This work presents a direct comparison of the image quality, contrast attenuation, and radiation dose of photon-counting computed tomography (PCCT) and dual-energy computed tomography (DECT) on contrast-enhanced abdomen and pelvic scans obtained in routine clinical practice.

## METHODS AND MATERIALS

In this institutional review board-approved retrospective study, we identified patients ( $n = 30$ ) who had undergone a routine contrast enhanced CT of the abdomen and pelvis on a clinical PCCT scanner (Naeotom Alpha, Siemens Healthineers) and who had also undergone a DECT (Somatom Force, Siemens Healthineers) within twelve months. The following patient and scan characteristics were recorded: the patient's weight, radiation dose (CTDIvol), and contrast volume. For quantitative comparison, we calculated contrast to noise ratio (CNR), signal to noise ratio (SNR), and image noise for organ parenchyma as well as the great vessels for both PCCT and DECT exams.

## RESULTS

Average BMI of patients undergoing contrast enhanced PCCT was 25.9 (range: 14.1 to 41.8). Average BMI change between contrast enhanced PCCT and DECT was 1.7 (range: 0 to 5.8). Average time between contrast enhanced PCCT and DECT was 50 days (range: 1 to 355 days). There was a statistically significant decrease in CTDIvol in PCCT compared to DECT of 11.1 versus 13.9, respectively ( $p=0.01$ ). There was no significant difference in CNR or SNR for organ parenchyma or vessels on contrast enhanced PCCT compared to DECT.

## CONCLUSION

Our early, real-world, comparison of routine contrast enhanced abdomen and pelvis studies on PCCT and DECT indicates decreased radiation exposure (CTDIvol) can be achieved on clinical PCCT with comparable image quality (CNR and SNR). Future planned analysis will focus on rigorous comparison of qualitative and quantitative metrics of image quality utilizing direct comparison of spectral data from both PCCT and DECT.

## CLINICAL RELEVANCE/APPLICATION

The introduction of PCCT has opened the opportunity of providing diagnostic image quality for contrast enhanced scans that are as good or better than conventional DECT at a reduced radiation dose.

### T2-SPGI-4 Quantitative Multi-Parameters Derived From Contrast-Enhanced Dual Layer Spectral CT on Predicting the Aggressiveness in Single Hepatocellular Carcinoma

Participants

Anqi Li, Guangzhou, China (*Presenter*) Nothing to Disclose

#### PURPOSE

Microvascular invasion (MVI) and vessels encapsulating tumor clusters (VETC) pattern of HCC are associated with aggressive biological behavior and early recurrent after liver surgery. We aim to evaluate the potential diagnostic performance of quantitative multi-parameters obtained from contrast-enhanced Dual Layer Spectral CT (DLSCT) to non-invasively predict MVI and VETC in single HCC.

#### METHODS AND MATERIALS

Fifty-seven histopathology-proven HCC patients with preoperative DLSCT examinations (+/-MVI, n = 17/40; +/-VETC, n=14/43) before liver resection were enrolled retrospectively from 06/2020 to 07/2021. The CT attenuation values on virtual monoenergetic images (VMIs) at 40keV, 70keV and 120keV, effective atomic number (Zeff), iodine density (ID) and the normalized iodine density (NID) values of tumor areas (without hemorrhage or necrosis regions) in both arterial phase (AP) and portal venous phase (PVP) were measured. NID was calculated by taking the ratio of iodine density between the tumor and the aorta of the same scan slice. Differences and ratios of CT attenuation values at different VMIs, Zeff, ID and NID values between AP and PVP were also calculated. The area under the receiver operating characteristic curve (AUC) was used to assess the diagnostic performance of quantitative multi-parameters for predicting MVI and VETC.

#### RESULTS

Among the twenty-four quantitative parameters, CT attenuation values at 40keV (AUC:0.73) and 70keV (AUC:0.71), Zeff (AUC:0.77) and ID (AUC: 0.76) in PVP showed good performances in identifying positive-MVI (all p<0.05), but without significantly different AUCs. Only Zeff (AUC:0.71) and ID (AUC: 0.69) values in PVP were found that could identify positive-VETC (all p<0.05).

## CONCLUSION

Zeff and ID values in PVP derived from DLSCT were promising biomarkers for identifying the status of MVI and VETC in single HCC, and CT attenuation values at 40keV and 70keV in PVP could predict positive MVI.

## CLINICAL RELEVANCE/APPLICATION

Zeff and ID values in PVP may be more suitable to be recommended as the effective quantitative parameters for predicting the aggressiveness in patients with HCC.

### T2-SPGI-5 Application value of enhanced CT based Radiomics in prognosis assessment of patients with gastric neuroendocrine neoplasm

Participants

Yi Jing Han, (*Presenter*) Nothing to Disclose

#### PURPOSE

The present study aimed to investigate the clinical prognostic significance of radiomics signature (R-signature) in patients with gastric neuroendocrine neoplasm(GNEN).

#### METHODS AND MATERIALS

A retrospective study of 182 patients with GNEN who underwent dual-phase enhanced scanning at two tertiary health-care institutions was conducted. LASSO-Cox regression analysis was used to screen the features and establish the arterial, venous and the arteriovenous phase combined radiomics model respectively. The radiomics model with the best prognostic performance was selected for subsequent analysis by calculating Harrell's concordance index (C-index). The association between the optimal R-signature and overall survival (OS) was assessed in the training group and verified in the validation group. Furthermore, the performance of a nomogram integrating the R-signature and significant clinicopathological risk factors was evaluated.

#### RESULTS

The arteriovenous phase combined radiomics model had the best performance in predicting OS, and its C-index values was better than the independent arterial and venous phase radiomics model (0.803 vs 0.784 and 0.803 vs 0.756, P<0.001, respectively). The combined radiomics model of the arteriovenous phase included 14 radiomics features, and the corresponding R-signature was significantly associated with OS in the training group and validation group. GNEN patients could be successfully divided into high and low prognostic risk groups with radiomics score median. The combined radiomics-clinical model combining this R-signature and independent clinicopathological risk factors (sex, age, treatment methods, T stage, N stage, M stage, tumor boundary, Ki67, CD56) exhibited significant prognostic superiority over clinical model, R-signature alone, and traditional TNM staging system (C-index, 0.882 vs 0.861, 882 vs 0.803, and 0.882 vs 0.870 respectively, P<0.001). All calibration curves showed remarkable consistency between predicted and actual survival, and decision curve analysis verified the usefulness of the combined radiomics-clinical nomogram for clinical practice.

## CONCLUSION

s The R-signature could be used to stratify patients with GNEB into high and low risk groups. Furthermore, the combined radiomics-clinical nomogram provided better predictive accuracy than other predictive models and might aid clinicians with therapeutic decision-making and patient counseling.

#### **CLINICAL RELEVANCE/APPLICATION**

The newly developed combined radiomics-clinical nomogram is a powerful predictor of OS for GNEB patients, which demonstrated incremental value of the R-signature to the traditional staging system for individualized survival estimation.

#### **T2-SPGI-6 Combination of clinical and spectral-CT parameters in evaluating the lymphovascular and perineural invasion of gastric cancer**

Participants

Tiezhu Ren, (*Presenter*) Nothing to Disclose

#### **PURPOSE**

The purpose of this study was to investigate the utility of combining clinical and spectral computed tomography (CT) parameters in the preoperative evaluation of lymphovascular invasion (LVI) and perineural invasion (PNI) in gastric cancer (GC).

#### **METHODS AND MATERIALS**

We retrospectively analysed 121 patients with GC. All cases were confirmed by pathology, underwent spectral-CT examination, and were divided into positive group (n=87) and negative group (n=34) depending on LVI/PNI occurrence. Clinical characteristics, including demographic information, serum tumour markers, and gastroscopic pathological information, were collected. The effective atomic number (Zeff), iodine concentration (IC), and water concentration were measured in the arterial (AP) and venous (VP) phases. Parameter differences between the two groups were compared, and diagnostic performance was evaluated.

#### **RESULTS**

The LVI/PNI-positive group's serum tumour marker CA125, histological grade, Borrmann type, Zeff, and IC were substantially greater than those of the negative group (CA125, 16.29±14.95 vs 8.45±2.53; AP-Zeff, 8.73±0.41 vs 8.40±0.24; VP-Zeff, 8.78±0.26 vs 8.54±0.20; AP-IC, 19.77±8.17 vs 13.43±4.31; VP-IC, 20.53±5.34 vs 15.88±3.66, all p<0.05). Predictive efficacy analysis demonstrated that CA125 exhibited a favourable performance (AUC=0.714), and the VP parameters' diagnostic efficacy was superior to that of the AP parameters (all AUC>0.75). The evaluated efficiency of the combination of clinical and spectral-CT parameters was superior to that of individual parameters (all AUC>0.85). The clinical parameters combined with Zeff and IC in AP and VP exhibited good evaluation efficacy (AUC=0.890, F1 score=0.888, accuracy=0.843, sensitivity=86.2%, specificity=79.4%, +RL=10.71, and -RL=0.44).

#### **CONCLUSION**

s Clinical and energy spectral-CT parameters exhibited considerable value in the preoperative evaluation of LVI and PNI in GC. The combination of clinical and spectral-CT parameters exhibited a favourable performance in predicting LVI and PNI in GC.

#### **CLINICAL RELEVANCE/APPLICATION**

The combination of clinical parameters and spectral-CT is a valuable approach to predicting LVI and PNI in GC.

#### **T2-SPGI-7 Dual source CT-based dual energy radiomics model in diagnosis of enlarged benign and malignant lymph nodes for gastric adenocarcinoma**

Participants

Yan Wang, Shijiazhuang, Hebei Province, China (*Presenter*) Nothing to Disclose

#### **PURPOSE**

To evaluate the efficacy of a radiomics model derived from dual energy image for discriminating benign and malignant enlarged lymph nodes (LNs) in gastric adenocarcinoma.

#### **METHODS AND MATERIALS**

This study retrospectively collected 62 gastric adenocarcinoma patients including 37 patients with postoperative pathological findings of pN3(Pathological N3 stage)and 25 pN0 patients. LNs with a short-axis diameter (SAD)=6 mm were divided into a metastasis group and a non-metastasis group according to pathological result. The LNs were randomly allocated into the training (n = 126) and test (n = 54) cohort. The region of interest (ROI) segmentation and radiomic feature extraction were performed on the slice of LNs with maximum diameter in 120kv-equivalent mixed image and automatically synchronized with iodine image in a dedicated radiomic software. Intraclass correlation coefficient (ICC) and Boruta were used for feature dimension reduction for the Random Forest radiomics model construction. Traditional features including clinical, CT features of primary lesion and LNs, and quantitative features were collected by two physicians. The clinical and combined model integrating the radiomic and traditional features were developed by univariate and multivariate analysis using Generalized Estimating Equations (GEE). The diagnostic performance of models was evaluated by receiver operating characteristic (ROC) and decision curve analysis (DCA) curve.

#### **RESULTS**

A total of 115 and 65 LNs were included in the metastatic group and the non-metastatic group.188 features with ICC>0.75 and the 8 radiomic features with highest importance selected by Boruta were utilized for radiomics model construction. The radiomics model yields an AUC 0.96(95% confidence interval [CI]:0.93, 0.99) and 0.95(95% CI: 0.89, 1) in training and test cohort, it showed significant improved discrimination efficacy compared to the clinical model in training (AUC, 0.88 [95% CI: 0.81, 0.94]; P = 0.02) and test (AUC, 0.76 [95% CI: 0.63, 0.89]; P=0.01). The combined model integrating the radiomic features and traditional (primary lesion axial maximum diameter and LNs fat fraction) performed well in training (AUC ,0.965[95% CI:0.939-0.991]), test (AUC , 0.929[95% CI:0.862-0.997]).

#### **CONCLUSION**

s Dual energy radiomics model showed higher diagnostic efficacy of benign and malignant enlarged LNs in gastric adenocarcinoma compared to the clinical model.

## CLINICAL RELEVANCE/APPLICATION

Accurate preoperative identification of metastatic LNs is important for the scope of surgery in patients with gastric adenocarcinoma. The combination of dual energy and radiomics has shown high diagnostic value for quantitative assessment and prediction of benign and malignant enlarged LNs.

### T2-SPGI-8 Predictive value of iodine mixed map of dual-source dual-energy enhanced CT in esophagogastric variceal bleeding in liver cirrhosis

Participants

Jiang Changqin, (Presenter) Nothing to Disclose

#### PURPOSE

To investigate the clinical value of iodine mixed map of dual-source dual-energy CT in diagnosing EV(esophagogastric varices) and predicting EVB (esophagogastric variceal bleeding) in patients with liver cirrhosis.

#### METHODS AND MATERIALS

Patients with liver cirrhosis were included and divided into significant EV group and non-significant EV group according to the gastroscopy, they were also divided into EVB group and non-EVB group. All patients underwent enhanced CT examination of the upper abdomen. Dual-energy post-processing software "syngo. Via" was used to obtain the iodine mixed map. Two doctors evaluated the EV and draw ROIs from the mixed map by a blind way. The IC (iodine concentration), iodine overlay value, relative IC and relative overlay value at the lower end plane of esophagus were measured. Kappa test was used to evaluate the consistency of two doctors' evaluation of EV. Spearman test was used to detect the consistency of iodine map and gastroscopy for EV. Pearson correlation test was used to evaluate the correlation between relative IC and relative overlay value. ROC was drawn to evaluate the diagnosis power of iodine parameters.

#### RESULTS

Eighty-eight patients with liver cirrhosis were finally enrolled, including 50 males and 38 females, aged 38 ~ 67 years. Forty one cases in significant EV group and 47 cases in non-significant EV group, 36 cases with EVB and 52 cases without EVB. Comparison of iodine parameters between non-significant EV group and significant group were IC ( $1.44 \pm 0.31\text{mg/ml}$ ,  $1.76 \pm 0.32\text{mg/ml}$ ,  $P < 0.05$ ), iodine overlay value ( $26.7 \pm 5.1$ ,  $31.9 \pm 7.3$ ,  $P < 0.001$ ), relative IC ( $0.76 \pm 0.20$ ,  $1.09 \pm 0.25$ ,  $P < 0.001$ ), relative iodine overlay value ( $0.84 \pm 0.22$ ,  $1.0 \pm 0.29$ ,  $P < 0.001$ ). Comparison of iodine parameters between non-EVB and EVB groups were IC ( $1.44 \pm 0.31\text{mg/ml}$ ,  $1.80 \pm 0.30\text{mg/ml}$ ,  $P < 0.001$ ), iodine overlay value ( $25.7 \pm 4.1$ ,  $34.1 \pm 6.7$ ,  $P < 0.001$ ), relative IC ( $0.75 \pm 0.21$ ,  $1.20 \pm 0.23$ ,  $P < 0.001$ ), relative overlay value ( $0.80 \pm 0.16$ ,  $1.18 \pm 0.27$ ,  $P < 0.001$ ). The Kappa value of the consistency of two observers in evaluating EV was 0.84. The consistency between iodine map and gastroscopy in the evaluation of EV was 0.728. The AUC of ROC curve for the diagnosis of significant EV was 0.844, with sensitivity of 78.0% and specificity of 80.9%. The AUC of relative IC in predicting EVB was 0.940, with sensitivity of 91.7% and specificity of 84.6%.

#### CONCLUSION

s The iodine mixed map of dual-source dual-energy CT can be used to diagnose EV and be a predicted method for EVB in patients with liver cirrhosis.

## CLINICAL RELEVANCE/APPLICATION

Iodine mixed map shows preferable clinical value in diagnosing EV and predicting EVB in liver cirrhosis patients.

### T2-SPGI-9 NEW INSIGHTS INTO THE RELATIONSHIP BETWEEN GASTRIC EMPTYING CUT-OFF, ETIOLOGY OF GASTROPARESIS AND THE CORRELATION WITH CLINICAL SYMPTOMS

Participants

Jesus R. Diaz, MD, (Presenter) Nothing to Disclose

#### PURPOSE

Gastric emptying scintigraphy (GES) is the gold standard for the diagnosis of gastric motility disorders such as gastroparesis (GP). However, current literature suggests that GES results and symptom scores do not correlate. This may warrant a further investigation into reassessing cut-off values.

#### METHODS AND MATERIALS

Different isotope retention values at 4 hours were assessed in an effort to explain the difficulty in correlating the reliability of GES with symptom scores. Additionally, diabetic and idiopathic patients were separated in order to assess differences between symptom scores and GES values. Data was collected via a retrospective review of 386 GES conducted at our institution between 2013 and 2021. Patients with rapid GES or those with insufficient data were excluded. A total of 89 patients were evaluated by separating them into groups based on their GES results ( $>25\%$  or  $<10\%$  retention) and their symptoms (nausea/vomiting, post-prandial fullness/early satiety, and bloating), were graded based on the gastroparesis cardinal symptom index (GCSI) scale in addition to retching, loss of appetite and belly enlargement. The mean of the symptoms between the groups was compared and a p-value of  $<0.05$  was considered statistically significant.

#### RESULTS

Patients with diabetic GP with retention  $\geq 25\%$  had significantly higher overall mean scores compared to idiopathic GP patients with  $\geq 25\%$  retention at 4 hours ( $p < 0.05$ ). Of note, diabetic patients with normal GES had a higher symptom score compared to non-diabetics with normal GES. However, patients with idiopathic GP ( $>10\%$  at 4hrs) had higher symptom scores than non-diabetics with normal GES. Data shows that diabetic GP patients with  $\geq 25\%$  retention on GES at 4 hours had a higher overall mean symptom score than patients with idiopathic GP when the cut-off point of  $\geq 25\%$  retention on GES at 4 hours was utilized. Additionally, in diabetic patients, GES results, whether normal or delayed, do not correlate with their symptoms in contrast to the idiopathic patients whose symptoms worsened with worsening GES.

#### CONCLUSION

s These results demonstrate the need to separate the diabetic and idiopathic GP etiologies in order to correct discrepancies found

when utilizing GES to grade symptoms.

**CLINICAL RELEVANCE/APPLICATION**

When analyzing GES data, the interpreting physician should consider the etiology of GP for the explanation of symptoms.

Printed on: 02/07/23

## Abstract Archives of the RSNA, 2022

T2-SPGI-1

### Photon-counting CT vs conventional CT - Evaluation of incidental lesions in the liver and kidney.

Tuesday, Nov. 29 9:00AM - 9:30AM Room: Learning Center - GI DPS

#### Participants

Leonid Roshkovan, MD, Philadelphia, PA (*Presenter*) Nothing to Disclose

#### PURPOSE

Incidental liver and renal lesions are extremely common in clinical practice and are often difficult to fully characterize on a single-phase CT examination. We hypothesized that photon-counting CT (PCCT) would be able to characterize incidental hypoattenuating lesions more accurately in the liver and kidneys compared to conventional single-phase CT.

#### METHODS AND MATERIALS

Patients who had undergone a clinical CT scan of the abdomen and pelvis on a clinical PCCT scanner (Naeotom Alpha, Siemens Healthineers) and a conventional CT scan (Definition Edge, Definition AS+, Somatom Force, Siemens Healthineers) within six months were identified. Incidental hypoattenuating lesions that were visible on both scans were included, but lesions less than five pixels in size were excluded since their density could not be accurately determined. Mean Hounsfield units (HU) and standard deviation (SD) were recorded, and signal to noise ratio (SNR) was calculated. To characterize the spectral signature of the individual lesions, iodine density maps and virtual monoenergetic images (VMI, at 40, 70, 100, and 190 keV) were used to cluster low density lesions into subgroups using K-means clustering. Clinical and scan variables including patient BMI, radiation dose and contrast volume were also recorded.

#### RESULTS

30 patients with a total of 61 lesions (16 and 45 lesions from unenhanced and enhanced CT scans, respectively) were included in the analysis, with lesions averaging a diameter of  $3 \pm 2.1$  mm. Mean HU values and SD as well as SNR were similar between both groups when values were obtained from VMI 70 keV ( $19.0 \pm 17.5$  HU, SNR 1.5) compared to conventional CT ( $21.1 \pm 13.7$  HU, SNR 1.5). With the spectral information from PCCT, hypoattenuating lesions in the liver and kidneys were automatically separated into three groups that corresponded to 10 fat-containing, 46 water-containing, and 5 iodine-containing lesions.

#### CONCLUSION

No significant difference in SNR and mean HU was identified between conventional CT and VMI 70 keV images on PCCT. Based on the spectral data from PCCT, it was possible to separate lesions into subgroups. Our ongoing work will focus on expanding our cohort size, comparing PCCT lesion characterization to other spectral scanners, and potentially utilizing spectral data for developing automatic lesion characterization.

#### CLINICAL RELEVANCE/APPLICATION

PCCT can more accurately characterize incidental hypoattenuating lesions compared to conventional CT regardless of the presence of contrast, thus increasing confidence in interpretation.

Printed on: 02/07/23



## Abstract Archives of the RSNA, 2022

T2-SPGI-10

### Potential Predictors of Long-term Outcomes of the LI-RADS Equivocal Category after Locoregional Therapy of Hepatocellular Carcinoma

Tuesday, Nov. 29 9:00AM - 9:30AM Room: Learning Center - GI DPS

#### Participants

Mohamed Tantawi, MBBCh, (*Presenter*) Nothing to Disclose

#### PURPOSE

The Liver Imaging and Reporting Data System (LI-RADS) has introduced a treatment response algorithm to assess the viability of hepatocellular carcinoma (HCC) tumors after locoregional therapy (LRT). Treated tumors can be classified as viable, nonviable, equivocal, or non-evaluable. Equivocal viability is defined as enhancement atypical for treatment-specific expected enhancement pattern and not meeting the criteria for probably or definitely viable. This study aimed to identify the potential predictors of long-term viability outcome of lesions classified as equivocal following LRT.

#### METHODS AND MATERIALS

The study included 136 HCC lesions in 115 patients classified as equivocal at least once following LRT. Then, we excluded patients who were retreated, died, or were lost to follow-up before a viable/nonviable outcome. Clinical characteristics and imaging features were compared between tumors with later viable vs. nonviable outcomes. Viability outcomes were defined by the subsequent viable/nonviable evaluation on cross-sectional imaging or pathologic findings on explant. T-tests and chi-square tests were used to compare the variables between the two outcome groups.

#### RESULTS

Across all treatment types, 74 lesions (72.6%) were nonviable on later assessments, while 28 (27.4%) were viable. A shorter time between treatment and LI-RADS equivocal read was significantly associated with a longer-term nonviable outcome ( $p=0.004$ ). Recurrent tumors after previous LRT were significantly more likely to have a viable outcome than those treated for the first time ( $p<0.001$ ). No single imaging feature or treatment type was associated with a longer-term definite viability outcome.

#### CONCLUSION

s History of recurrence after LRT and time between treatment and equivocal read can be indicators of long-term viability outcome of HCC after LRTs.

#### CLINICAL RELEVANCE/APPLICATION

In recently treated patients, equivocal findings on LI-RADS tend to represent evolving posttreatment changes and eventually become nonviable. Alternatively, equivocal findings in patients with a prior history of recurrence trend towards longer term viability.

Printed on: 02/07/23

## Abstract Archives of the RSNA, 2022

T2-SPGI-2

### Application of selective photon shield on image quality and radiation dose of dual energy CT-Enterography

Tuesday, Nov. 29 9:00AM - 9:30AM Room: Learning Center - GI DPS

#### Participants

Zengmiao Xu, Xian, China (*Presenter*) Nothing to Disclose

#### PURPOSE

To investigate the influence of selective photon shield on image quality and radiation dose of dual-energy CT enterography (CTE).

#### METHODS AND MATERIALS

A total of 70 patients, 37 females and 33 males, aged (mean  $48.19 \pm 15.53$  years, range 15~81 years) between January 2019 and April 2022 were retrospectively and consecutively enrolled. Exclusion criteria: 1) small bowel preparation failure; 2) Poor image quality or scanning failure; 3) Contrast agent allergy. All patients were divided into control group (SP group) of 36 patients (19 females, 17 males, mean age  $46.75 \pm 14.69$  years) and experimental group (TF group) of 34 patients, (18 females, 16 males, mean aged  $49.62 \pm 16.88$  years), CTE were performed with SOMATOM Force 256 CT (SOMATOM). SP group used standard CTE scheme with 100kV, CARE Dose 4D, a pitch of 0.6. TF group used ultra-low-dose CTE scheme with 100/Sn150kV, CARE Dose 4D, a pitch of 0.6. The CT dose index (CTDI) and dose-length product (DLP) of the two groups were compared, and the signal-to-noise ratio (SNR) and contrast-to-noise ratio (CNR) of the two groups were calculated, respectively. All images were evaluated independently by two radiologists, who were blinded by clinical diagnosis. Any disagreements were resolved by consensus.

#### RESULTS

1)The DLP, CTDI and ED of TF group were  $236.75 \pm 11.90 \text{mGy}\cdot\text{cm}$ ,  $6.02 \pm 0.25 \text{mGy}$ ,  $3.55 \pm 0.19 \text{mSv}$ , respectively, which were significantly lower than those of SP group ( $1540.58 \pm 66.58 \text{mGy}\cdot\text{cm}$ ,  $40.48 \pm 1.26 \text{mGy}$ ,  $23.11 \pm 0.99 \text{mSv}$ , all  $p < 0.001$ ). (Table 2)  
2)There was no significant difference in the SNR and CNR of the abdominal aorta, superior mesenteric artery and superior mesenteric vein between TF group and SP group. ( $p > 0.01$ )  
3)There was no significant difference in the subjective scores of image quality between the TF group and SP group.

#### CONCLUSION

Compared with standard CTE, selective photon shield of dual-energy CTE could significantly reduce radiation dose and obtain similar imaging quality. Clinical application: Selective photon shield of dual-energy CTE could be widely used in clinic instead of standard CTE.

#### CLINICAL RELEVANCE/APPLICATION

Printed on: 02/07/23

## Abstract Archives of the RSNA, 2022

T2-SPGI-3

### An evaluation of photon counting computed tomography of the abdomen and pelvis compared to dual energy CT in clinical routine

Tuesday, Nov. 29 9:00AM - 9:30AM Room: Learning Center - GI DPS

#### Participants

Manoj Mathew, MD, Philadelphia, PA (*Presenter*) Nothing to Disclose

#### PURPOSE

This work presents a direct comparison of the image quality, contrast attenuation, and radiation dose of photon-counting computed tomography (PCCT) and dual-energy computed tomography (DECT) on contrast-enhanced abdomen and pelvic scans obtained in routine clinical practice.

#### METHODS AND MATERIALS

In this institutional review board-approved retrospective study, we identified patients (n = 30) who had undergone a routine contrast enhanced CT of the abdomen and pelvis on a clinical PCCT scanner (Naeotom Alpha, Siemens Healthineers) and who had also undergone a DECT (Somatom Force, Siemens Healthineers) within twelve months. The following patient and scan characteristics were recorded: the patient's weight, radiation dose (CTDIvol), and contrast volume. For quantitative comparison, we calculated contrast to noise ratio (CNR), signal to noise ratio (SNR), and image noise for organ parenchyma as well as the great vessels for both PCCT and DECT exams.

#### RESULTS

Average BMI of patients undergoing contrast enhanced PCCT was 25.9 (range: 14.1 to 41.8). Average BMI change between contrast enhanced PCCT and DECT was 1.7 (range: 0 to 5.8). Average time between contrast enhanced PCCT and DECT was 50 days (range: 1 to 355 days). There was a statistically significant decrease in CTDIvol in PCCT compared to DECT of 11.1 versus 13.9, respectively (p=0.01). There was no significant difference in CNR or SNR for organ parenchyma or vessels on contrast enhanced PCCT compared to DECT.

#### CONCLUSION

Our early, real-world, comparison of routine contrast enhanced abdomen and pelvis studies on PCCT and DECT indicates decreased radiation exposure (CTDIvol) can be achieved on clinical PCCT with comparable image quality (CNR and SNR). Future planned analysis will focus on rigorous comparison of qualitative and quantitative metrics of image quality utilizing direct comparison of spectral data from both PCCT and DECT.

#### CLINICAL RELEVANCE/APPLICATION

The introduction of PCCT has opened the opportunity of providing diagnostic image quality for contrast enhanced scans that are as good or better than conventional DECT at a reduced radiation dose.

Printed on: 02/07/23

## Abstract Archives of the RSNA, 2022

T2-SPGI-4

### Quantitative Multi-Parameters Derived From Contrast-Enhanced Dual Layer Spectral CT on Predicting the Aggressiveness in Single Hepatocellular Carcinoma

Tuesday, Nov. 29 9:00AM - 9:30AM Room: Learning Center - GI DPS

#### Participants

Anqi Li, Guangzhou, China (*Presenter*) Nothing to Disclose

#### PURPOSE

Microvascular invasion (MVI) and vessels encapsulating tumor clusters (VETC) pattern of HCC are associated with aggressive biological behavior and early recurrent after liver surgery. We aim to evaluate the potential diagnostic performance of quantitative multi-parameters obtained from contrast-enhanced Dual Layer Spectral CT (DLST) to non-invasively predict MVI and VETC in single HCC.

#### METHODS AND MATERIALS

Fifty-seven histopathology-proven HCC patients with preoperative DLST examinations (+/-MVI, n = 17/40; +/-VETC, n=14/43) before liver resection were enrolled retrospectively from 06/2020 to 07/2021. The CT attenuation values on virtual monoenergetic images (VMIs) at 40keV, 70keV and 120keV, effective atomic number (Zeff), iodine density (ID) and the normalized iodine density (NID) values of tumor areas (without hemorrhage or necrosis regions) in both arterial phase (AP) and portal venous phase (PVP) were measured. NID was calculated by taking the ratio of iodine density between the tumor and the aorta of the same scan slice. Differences and ratios of CT attenuation values at different VMIs, Zeff, ID and NID values between AP and PVP were also calculated. The area under the receiver operating characteristic curve (AUC) was used to assess the diagnostic performance of quantitative multi-parameters for predicting MVI and VETC.

#### RESULTS

Among the twenty-four quantitative parameters, CT attenuation values at 40keV (AUC:0.73) and 70keV (AUC:0.71), Zeff (AUC:0.77) and ID (AUC: 0.76) in PVP showed good performances in identifying positive-MVI (all p<0.05), but without significantly different AUCs. Only Zeff (AUC:0.71) and ID (AUC: 0.69) values in PVP were found that could identify positive-VETC (all p<0.05).

#### CONCLUSION

s Zeff and ID values in PVP derived from DLST were promising biomarkers for identifying the status of MVI and VETC in single HCC, and CT attenuation values at 40keV and 70keV in PVP could predict positive MVI.

#### CLINICAL RELEVANCE/APPLICATION

Zeff and ID values in PVP may be more suitable to be recommended as the effective quantitative parameters for predicting the aggressiveness in patients with HCC.

Printed on: 02/07/23

## Abstract Archives of the RSNA, 2022

T2-SPGI-5

### Application value of enhanced CT based Radiomics in prognosis assessment of patients with gastric neuroendocrine neoplasm

Tuesday, Nov. 29 9:00AM - 9:30AM Room: Learning Center - GI DPS

#### Participants

Yi Jing Han, (*Presenter*) Nothing to Disclose

#### PURPOSE

The present study aimed to investigate the clinical prognostic significance of radiomics signature (R-signature) in patients with gastric neuroendocrine neoplasm (GNEN).

#### METHODS AND MATERIALS

A retrospective study of 182 patients with GNEN who underwent dual-phase enhanced scanning at two tertiary health-care institutions was conducted. LASSO-Cox regression analysis was used to screen the features and establish the arterial, venous and the arteriovenous phase combined radiomics model respectively. The radiomics model with the best prognostic performance was selected for subsequent analysis by calculating Harrell's concordance index (C-index). The association between the optimal R-signature and overall survival (OS) was assessed in the training group and verified in the validation group. Furthermore, the performance of a nomogram integrating the R-signature and significant clinicopathological risk factors was evaluated.

#### RESULTS

The arteriovenous phase combined radiomics model had the best performance in predicting OS, and its C-index values was better than the independent arterial and venous phase radiomics model (0.803 vs 0.784 and 0.803 vs 0.756,  $P < 0.001$ , respectively). The combined radiomics model of the arteriovenous phase included 14 radiomics features, and the corresponding R-signature was significantly associated with OS in the training group and validation group. GNEN patients could be successfully divided into high and low prognostic risk groups with radiomics score median. The combined radiomics-clinical model combining this R-signature and independent clinicopathological risk factors (sex, age, treatment methods, T stage, N stage, M stage, tumor boundary, Ki67, CD56) exhibited significant prognostic superiority over clinical model, R-signature alone, and traditional TNM staging system (C-index, 0.882 vs 0.861, 882 vs 0.803, and 0.882 vs 0.870 respectively,  $P < 0.001$ ). All calibration curves showed remarkable consistency between predicted and actual survival, and decision curve analysis verified the usefulness of the combined radiomics-clinical nomogram for clinical practice.

#### CONCLUSION

The R-signature could be used to stratify patients with GNEN into high and low risk groups. Furthermore, the combined radiomics-clinical nomogram provided better predictive accuracy than other predictive models and might aid clinicians with therapeutic decision-making and patient counseling.

#### CLINICAL RELEVANCE/APPLICATION

The newly developed combined radiomics-clinical nomogram is a powerful predictor of OS for GNEN patients, which demonstrated incremental value of the R-signature to the traditional staging system for individualized survival estimation.

Printed on: 02/07/23

## Abstract Archives of the RSNA, 2022

T2-SPGI-6

### Combination of clinical and spectral-CT parameters in evaluating the lymphovascular and perineural invasion of gastric cancer

Tuesday, Nov. 29 9:00AM - 9:30AM Room: Learning Center - GI DPS

#### Participants

Tiezhu Ren, (*Presenter*) Nothing to Disclose

#### PURPOSE

The purpose of this study was to investigate the utility of combining clinical and spectral computed tomography (CT) parameters in the preoperative evaluation of lymphovascular invasion (LVI) and perineural invasion (PNI) in gastric cancer (GC).

#### METHODS AND MATERIALS

We retrospectively analysed 121 patients with GC. All cases were confirmed by pathology, underwent spectral-CT examination, and were divided into positive group (n=87) and negative group (n=34) depending on LVI/PNI occurrence. Clinical characteristics, including demographic information, serum tumour markers, and gastroscopic pathological information, were collected. The effective atomic number (Zeff), iodine concentration (IC), and water concentration were measured in the arterial (AP) and venous (VP) phases. Parameter differences between the two groups were compared, and diagnostic performance was evaluated.

#### RESULTS

The LVI/PNI-positive group's serum tumour marker CA125, histological grade, Borrmann type, Zeff, and IC were substantially greater than those of the negative group (CA125, 16.29±14.95 vs 8.45±2.53; AP-Zeff, 8.73±0.41 vs 8.40±0.24; VP-Zeff, 8.78±0.26 vs 8.54±0.20; AP-IC, 19.77±8.17 vs 13.43±4.31; VP-IC, 20.53±5.34 vs 15.88±3.66, all p<0.05). Predictive efficacy analysis demonstrated that CA125 exhibited a favourable performance (AUC=0.714), and the VP parameters' diagnostic efficacy was superior to that of the AP parameters (all AUC>0.75). The evaluated efficiency of the combination of clinical and spectral-CT parameters was superior to that of individual parameters (all AUC>0.85). The clinical parameters combined with Zeff and IC in AP and VP exhibited good evaluation efficacy (AUC=0.890, F1 score=0.888, accuracy=0.843, sensitivity=86.2%, specificity=79.4%, +RL=10.71, and -RL=0.44).

#### CONCLUSION

Clinical and energy spectral-CT parameters exhibited considerable value in the preoperative evaluation of LVI and PNI in GC. The combination of clinical and spectral-CT parameters exhibited a favourable performance in predicting LVI and PNI in GC.

#### CLINICAL RELEVANCE/APPLICATION

The combination of clinical parameters and spectral-CT is a valuable approach to predicting LVI and PNI in GC.

Printed on: 02/07/23

## Abstract Archives of the RSNA, 2022

T2-SPGI-7

### Dual source CT-based dual energy radiomics model in diagnosis of enlarged benign and malignant lymph nodes for gastric adenocarcinoma

Tuesday, Nov. 29 9:00AM - 9:30AM Room: Learning Center - GI DPS

#### Participants

Yan Wang, Shijiazhuang, Hebei Province, China (*Presenter*) Nothing to Disclose

#### PURPOSE

To evaluate the efficacy of a radiomics model derived from dual energy image for discriminating benign and malignant enlarged lymph nodes (LNs) in gastric adenocarcinoma.

#### METHODS AND MATERIALS

This study retrospectively collected 62 gastric adenocarcinoma patients including 37 patients with postoperative pathological findings of pN3(Pathological N3 stage)and 25 pN0 patients. LNs with a short-axis diameter (SAD)=6 mm were divided into a metastasis group and a non-metastasis group according to pathological result. The LNs were randomly allocated into the training (n = 126) and test (n = 54) cohort. The region of interest (ROI) segmentation and radiomic feature extraction were performed on the slice of LNs with maximum diameter in 120kv-equivalent mixed image and automatically synchronized with iodine image in a dedicated radiomic software. Intraclass correlation coefficient (ICC) and Boruta were used for feature dimension reduction for the Random Forest radiomics model construction. Traditional features including clinical, CT features of primary lesion and LNs, and quantitative features were collected by two physicians. The clinical and combined model integrating the radiomic and traditional features were developed by univariate and multivariate analysis using Generalized Estimating Equations (GEE). The diagnostic performance of models was evaluated by receiver operating characteristic (ROC) and decision curve analysis (DCA) curve.

#### RESULTS

A total of 115 and 65 LNs were included in the metastatic group and the non-metastatic group.188 features with ICC>0.75 and the 8 radiomic features with highest importance selected by Boruta were utilized for radiomics model construction. The radiomics model yields an AUC 0.96(95% confidence interval [CI]:0.93, 0.99) and 0.95(95% CI: 0.89, 1) in training and test cohort, it showed significant improved discrimination efficacy compared to the clinical model in training (AUC, 0.88 [95% CI: 0.81, 0.94]; P = 0.02) and test (AUC, 0.76 [95% CI: 0.63, 0.89]; P=0.01). The combined model integrating the radiomic features and traditional (primary lesion axial maximum diameter and LNs fat fraction) performed well in training (AUC ,0.965[95% CI:0.939-0.991]), test (AUC , 0.929[95% CI:0.862-0.997]).

#### CONCLUSION

s Dual energy radiomics model showed higher diagnostic efficacy of benign and malignant enlarged LNs in gastric adenocarcinoma compared to the clinical model.

#### CLINICAL RELEVANCE/APPLICATION

Accurate preoperative identification of metastatic LNs is important for the scope of surgery in patients with gastric adenocarcinoma. The combination of dual energy and radiomics has shown high diagnostic value for quantitative assessment and prediction of benign and malignant enlarged LNs.

Printed on: 02/07/23

## Abstract Archives of the RSNA, 2022

T2-SPGI-8

### Predictive value of iodine mixed map of dual-source dual-energy enhanced CT in esophagogastric variceal bleeding in liver cirrhosis

Tuesday, Nov. 29 9:00AM - 9:30AM Room: Learning Center - GI DPS

#### Participants

Jiang Changqin, (*Presenter*) Nothing to Disclose

#### PURPOSE

To investigate the clinical value of iodine mixed map of dual-source dual-energy CT in diagnosing EV(esophagogastric varices) and predicting EVB (esophagogastric variceal bleeding) in patients with liver cirrhosis.

#### METHODS AND MATERIALS

Patients with liver cirrhosis were included and divided into significant EV group and non-significant EV group according to the gastroscopy, they were also divided into EVB group and non-EVB group. All patients underwent enhanced CT examination of the upper abdomen. Dual-energy post-processing software "syngo. Via" was used to obtain the iodine mixed map. Two doctors evaluated the EV and draw ROIs from the mixed map by a blind way. The IC (iodine concentration), iodine overlay value, relative IC and relative overlay value at the lower end plane of esophagus were measured. Kappa test was used to evaluate the consistency of two doctors' evaluation of EV. Spearman test was used to detect the consistency of iodine map and gastroscopy for EV. Pearson correlation test was used to evaluate the correlation between relative IC and relative overlay value. ROC was drawn to evaluate the diagnosis power of iodine parameters.

#### RESULTS

Eighty-eight patients with liver cirrhosis were finally enrolled, including 50 males and 38 females, aged 38 ~ 67 years. Forty one cases in significant EV group and 47 cases in non-significant EV group, 36 cases with EVB and 52 cases without EVB. Comparison of iodine parameters between non-significant EV group and significant group were IC ( $1.44 \pm 0.31\text{mg/ml}$ ,  $1.76 \pm 0.32\text{mg/ml}$ ,  $P < 0.05$ ), iodine overlay value ( $26.7 \pm 5.1$ ,  $31.9 \pm 7.3$ ,  $P < 0.001$ ), relative IC( $0.76 \pm 0.20$ ,  $1.09 \pm 0.25$ ,  $P < 0.001$ ), relative iodine overlay value ( $0.84 \pm 0.22$ ,  $1.0 \pm 0.29$ ,  $P < 0.001$ ). Comparison of iodine parameters between non EVB and EVB groups were IC ( $1.44 \pm 0.31\text{mg/ml}$ ,  $1.80 \pm 0.30\text{mg/ml}$ ,  $P < 0.001$ ), iodine overlay value ( $25.7 \pm 4.1$ ,  $34.1 \pm 6.7$ ,  $P < 0.001$ ), relative IC ( $0.75 \pm 0.21$ ,  $1.20 \pm 0.23$ ,  $P < 0.001$ ), relative overlay value ( $0.80 \pm 0.16$ ,  $1.18 \pm 0.27$ ,  $P < 0.001$ ). The Kappa value of the consistency of two observers in evaluating EV was 0.84. The consistency between iodine map and gastroscopy in the evaluation of EV was 0.728. The AUC of ROC curve for the diagnosis of significant EV was 0.844, with sensitivity of 78.0% and specificity of 80.9%. The AUC of relative IC in predicting EVB was 0.940, with sensitivity of 91.7% and specificity of 84.6%.

#### CONCLUSION

The iodine mixed map of dual-source dual-energy CT can be used to diagnose EV and be a predicted method for EVB in patients with liver cirrhosis.

#### CLINICAL RELEVANCE/APPLICATION

Iodine mixed map shows preferable clinical value in diagnosing EV and predicting EVB in liver cirrhosis patients.

Printed on: 02/07/23

## Abstract Archives of the RSNA, 2022

T2-SPGI-9

### NEW INSIGHTS INTO THE RELATIONSHIP BETWEEN GASTRIC EMPTYING CUT-OFF, ETIOLOGY OF GASTROPARESIS AND THE CORRELATION WITH CLINICAL SYMPTOMS

Tuesday, Nov. 29 9:00AM - 9:30AM Room: Learning Center - GI DPS

#### Participants

Jesus R. Diaz, MD, (*Presenter*) Nothing to Disclose

#### PURPOSE

Gastric emptying scintigraphy (GES) is the gold standard for the diagnosis of gastric motility disorders such as gastroparesis (GP). However, current literature suggests that GES results and symptom scores do not correlate. This may warrant a further investigation into reassessing cut-off values.

#### METHODS AND MATERIALS

Different isotope retention values at 4 hours were assessed in an effort to explain the difficulty in correlating the reliability of GES with symptom scores. Additionally, diabetic and idiopathic patients were separated in order to assess differences between symptom scores and GES values. Data was collected via a retrospective review of 386 GES conducted at our institution between 2013 and 2021. Patients with rapid GES or those with insufficient data were excluded. A total of 89 patients were evaluated by separating them into groups based on their GES results (>25% or <10% retention) and their symptoms (nausea/vomiting, post-prandial fullness/early satiety, and bloating), were graded based on the gastroparesis cardinal symptom index (GCSI) scale in addition to retching, loss of appetite and belly enlargement. The mean of the symptoms between the groups was compared and a p-value of <0.05 was considered statistically significant.

#### RESULTS

Patients with diabetic GP with retention =25% had significantly higher overall mean scores compared to idiopathic GP patients with =25% retention at 4 hours ( $p < 0.05$ ). Of note, diabetic patients with normal GES had a higher symptom score compared to non-diabetics with normal GES. However, patients with idiopathic GP (>10% at 4hrs) had higher symptom scores than non-diabetics with normal GES. Data shows that diabetic GP patients with =25% retention on GES at 4 hours had a higher overall mean symptom score than patients with idiopathic GP when the cut-off point of =25% retention on GES at 4 hours was utilized. Additionally, in diabetic patients, GES results, whether normal or delayed, do not correlate with their symptoms in contrast to the idiopathic patients whose symptoms worsened with worsening GES.

#### CONCLUSION

These results demonstrate the need to separate the diabetic and idiopathic GP etiologies in order to correct discrepancies found when utilizing GES to grade symptoms.

#### CLINICAL RELEVANCE/APPLICATION

When analyzing GES data, the interpreting physician should consider the etiology of GP for the explanation of symptoms.

Printed on: 02/07/23

## Abstract Archives of the RSNA, 2022

T2-SPGU

### Genitourinary Tuesday Poster Discussions

Tuesday, Nov. 29 9:00AM - 9:30AM Room: Learning Center - GU DPS

#### Sub-Events

#### **T2-SPGU-1 Comparison between Conventional Cystourethrography and MRI with Voiding MR-cystourethrography in the Evaluation of Male Urethral Strictures**

Participants

Marco Di Girolamo, MD, (*Presenter*) Nothing to Disclose

#### **PURPOSE**

To evaluate the accuracy of conventional retrograde and voiding cystourethrography and MRI together with voiding MR-cystourethrography in the evaluation of male urethral strictures.

#### **METHODS AND MATERIALS**

We evaluated 39 male patients with urethral strictures diagnosed with urine flow velocity recording and conventional retrograde and voiding cystourethrography. All these patients underwent MRI and voiding MR-cystourethrography using a 1.5T superconductive magnet. The patients had urine-filled bladders and high-resolution sagittal TSE T2-weighted scans were performed (TR:6250ms; TE:90ms;sl.thick.:3mm; acq.time:3'38"). Voiding MR-cystourethrography was performed with T1-weighted spoiled 3D gradient-echo acquisitions on sagittal plane (TR:12ms; TE:2,7ms; flip-angle:40°; sl.thickness: 2mm; acq.time:12s) after the filling of bladder lumen with contrast-material-enhanced urine obtained by the i.v administration 20 mg of furosemide followed by ¾ of the normal dose of a paramagnetic contrast agent (Magnevist, Bayer Pharma, Germany). After micturition high-resolution coronal TSE T2-weighted scans were performed at the level of the stenosis. Two radiologists in consensus evaluated the morphology and length of the urethral stenosis with the two modalities and with MRI the entity and the site of spongio-fibrosis was assessed.

#### **RESULTS**

6 patients were not able to perform voiding MR-cystourethrography. In 33 patients evaluated with two imaging modalities 42 urethral strictures were detected. The measurement of the stenosis length was equal or superior with voiding MR cystourethrography and the analysis of 3D sagittal scans allowed a better evaluation of the morphology of the urethral strictures in comparison with conventional cystourethrography. 32 strictures with Spongio-fibrosis were found (76%). The site of spongio-fibrosis was always assessed with MRI (dorsal, ventral, dorsal and ventral and circular fibrosis).

#### **CONCLUSION**

s MRI with voiding MR-cystourethrography shows the morphology and the length of the urethral strictures better than conventional cystourethrography and allows the detection and site of spongio-fibrosis, avoiding radiation exposure to the gonads and urinary catheterization.

#### **CLINICAL RELEVANCE/APPLICATION**

MRI could be proposed as all-in-one technique for the evaluation of urethral stenosis, allowing their detection and length assessment and determining the presence and site of spongiofibrosis.

#### **T2-SPGU-2 MR defecography revisited. Pelvic floor measurements with and without rectal gel. Is there a difference.**

Participants

Charles Myers, DO, Lexington, KY (*Presenter*) Nothing to Disclose

#### **PURPOSE**

To test if there is a difference in pelvic floor measurements (H-line, M-line and anorectal angle) before and after rectal gel administration during MR defecography and if this difference can affect the degree of pelvic floor grading.

#### **METHODS AND MATERIALS**

After IRB approval was obtained, we conducted a retrospective review of patients who had MR defecography at our institution from January 2018 to June 2021. An abdominal fellow, trained in the interpretation of MRI defecography, reviewed all studies and performed measurements of the M-line, H-line and anorectal angle for each patient, on sagittal midline T2-weighted sequences, before and after the instillation of rectal gel. Statistical analysis was conducted using two-tailed t-tests to determine the significance of the observed differences.

#### **RESULTS**

A total of 111 scans were reviewed. All patients were female. 64% (71) of the patients had at least mild pelvic floor widening (defined as an H-line of greater than 5 cm) without rectal gel. This increased to 67.6% (75) after rectal gel administration. 14.4 %

(16) had at least mild pelvic floor descent (defined as an M-line of greater than 2 cm) before rectal gel which increased to 38.7% (43) after the administration of gel. The anorectal angle was noted to be on average wider by 3.2 degrees after the administration of rectal gel. Also, 67.6% (75) of patients were found to have an anorectal angle outside the normal range (108-127 degrees) before gel versus 58.6% (65) after gel. P-values for the before and after effect of rectal gel on the H-line, M-line and anorectal angle measurements were 0.08, 0.0000085 and 0.07 respectively.

## **CONCLUSION**

The filling of the rectum with gel during MR defecography increases the H-line, M-line and anorectal angle measurements and influences pelvic floor grading. A standardized manner of obtaining these measurements should be implemented to allow better reproducibility and by extension, patient management.

## **CLINICAL RELEVANCE/APPLICATION**

The administration of rectal gel may alter the obtained measurements during dynamic pelvic floor imaging.

## **T2-SPGU-3 Comparison of three methods for lesion detection and classification on biparametric prostate MRI**

### **Participants**

Maria Sainz de Cea, PhD, Cambridge, MA (*Presenter*) Nothing to Disclose

### **PURPOSE**

Detection of lesions in bi-parametric MRI (bp-MRI) and their classification according to PIRADS guidelines is part of the clinical workflow for patients identified to be at risk of prostate cancer. We propose a method for segmentation and classification of prostate lesions in bp-MRI based on semantic segmentation of lesions and compare it with two state-of-the-art methods based on RetinaNet object detection and Panoptic Segmentation.

### **METHODS AND MATERIALS**

We propose the first multi-task deep convolutional model that performs lesion segmentation and classification. To improve the performance, we leverage information from prostate and zone by training the model to also predict their segmentation masks. Additionally, we include convolutional LSTM blocks to model the relationship between consecutive slices. The network training (on a large dataset) includes pre-processing and data augmentation. Performance was evaluated with five-fold cross validation and on a held-out test set. We report sensitivity, specificity, and accuracy for lesion classification for two classes: PIRADS 3 and PIRADS 4-5. Separately, we evaluate the lesion detection performance for both classes for our proposed network and the other two state-of-the-art methods.

### **RESULTS**

Our model was trained on 2940 studies from 9 different providers across Europe, United States, South America, and Asia. The studies were acquired with different protocols and manufacturers and contain bi-parametric MRI. The algorithm was trained using T2-w series, high b-value DWI and ADC maps. When we fix the number of FPs in the FROC curve the sensitivity of our proposed multi-task network is 91%, higher than other methods (74% for RetinaNet and 89.3% for Panoptic Segmentation). The classification accuracy for the validation set is 76% and 73% for PIRADS 3 and PIRADS 4-5 lesions respectively (74% and 68% for RetinaNet). For PIRADS 4-5 lesions, we obtain a sensitivity of 76% and a specificity of 61% (66% and 76% for RetinaNet).

## **CONCLUSION**

We present a deep learning system for automated lesion segmentation and classification that also performs gland and prostate segmentation. The incorporation of multi-task learning has been shown to boost the performance of lesion detection achieving a high classification accuracy on a large multi-center dataset.

## **CLINICAL RELEVANCE/APPLICATION**

Automated lesion segmentation and classification is clinically relevant and can be used for prostate cancer identification, biopsy, and treatment guidance.

Printed on: 02/07/23

## Abstract Archives of the RSNA, 2022

T2-SPGU-1

### Comparison between Conventional Cystourethrography and MRI with Voiding MR-cystourethrography in the Evaluation of Male Urethral Strictures

Tuesday, Nov. 29 9:00AM - 9:30AM Room: Learning Center - GU DPS

#### Participants

Marco Di Girolamo, MD, (*Presenter*) Nothing to Disclose

#### PURPOSE

To evaluate the accuracy of conventional retrograde and voiding cystourethrography and MRI together with voiding MR-cystourethrography in the evaluation of male urethral strictures.

#### METHODS AND MATERIALS

We evaluated 39 male patients with urethral strictures diagnosed with urine flow velocity recording and conventional retrograde and voiding cystourethrography. All these patients underwent MRI and voiding MR-cystourethrography using a 1.5T superconductive magnet. The patients had urine-filled bladders and high-resolution sagittal TSE T2-weighted scans were performed (TR:6250ms; TE:90ms;sl.thick.:3mm; acq.time:3'38"). Voiding MR-cystourethrography was performed with T1-weighted spoiled 3D gradient-echo acquisitions on sagittal plane (TR:12ms; TE:2,7ms; flip-angle:40°; sl.thickness: 2mm; acq.time:12s) after the filling of bladder lumen with contrast-material-enhanced urine obtained by the i.v administration 20 mg of furosemide followed by  $\frac{3}{4}$  of the normal dose of a paramagnetic contrast agent (Magnevist, Bayer Pharma, Germany). After micturition high-resolution coronal TSE T2-weighted scans were performed at the level of the stenosis. Two radiologists in consensus evaluated the morphology and length of the urethral stenosis with the two modalities and with MRI the entity and the site of spongio-fibrosis was assessed.

#### RESULTS

6 patients were not able to perform voiding MR-cystourethrography. In 33 patients evaluated with two imaging modalities 42 urethral strictures were detected. The measurement of the stenosis length was equal or superior with voiding MR cystourethrography and the analysis of 3D sagittal scans allowed a better evaluation of the morphology of the urethral strictures in comparison with conventional cystourethrography. 32 strictures with Spongio-fibrosis were found (76%). The site of spongio-fibrosis was always assessed with MRI (dorsal, ventral, dorsal and ventral and circular fibrosis).

#### CONCLUSION

s MRI with voiding MR-cystourethrography shows the morphology and the length of the urethral strictures better than conventional cystourethrography and allows the detection and site of spongio-fibrosis, avoiding radiation exposure to the gonads and urinary catheterization.

#### CLINICAL RELEVANCE/APPLICATION

MRI could be proposed as all-in-one technique for the evaluation of urethral stenosis, allowing their detection and length assessment and determining the presence and site of spongiofibrosis.

Printed on: 02/07/23



## Abstract Archives of the RSNA, 2022

T2-SPGU-2

**MR defecography revisited. Pelvic floor measurements with and without rectal gel. Is there a difference.**

Tuesday, Nov. 29 9:00AM - 9:30AM Room: Learning Center - GU DPS

### Participants

Charles Myers, DO, Lexington, KY (*Presenter*) Nothing to Disclose

### PURPOSE

To test if there is a difference in pelvic floor measurements (H-line, M-line and anorectal angle) before and after rectal gel administration during MR defecography and if this difference can affect the degree of pelvic floor grading.

### METHODS AND MATERIALS

After IRB approval was obtained, we conducted a retrospective review of patients who had MR defecography at our institution from January 2018 to June 2021. An abdominal fellow, trained in the interpretation of MRI defecography, reviewed all studies and performed measurements of the M-line, H-line and anorectal angle for each patient, on sagittal midline T2-weighted sequences, before and after the instillation of rectal gel. Statistical analysis was conducted using two-tailed t-tests to determine the significance of the observed differences.

### RESULTS

A total of 111 scans were reviewed. All patients were female. 64% (71) of the patients had at least mild pelvic floor widening (defined as an H-line of greater than 5 cm) without rectal gel. This increased to 67.6% (75) after rectal gel administration. 14.4 % (16) had at least mild pelvic floor descent (defined as an M-line of greater than 2 cm) before rectal gel which increased to 38.7% (43) after the administration of gel. The anorectal angle was noted to be on average wider by 3.2 degrees after the administration of rectal gel. Also, 67.6% (75) of patients were found to have an anorectal angle outside the normal range (108-127 degrees) before gel versus 58.6% (65) after gel. P-values for the before and after effect of rectal gel on the H-line, M-line and anorectal angle measurements were 0.08, 0.000085 and 0.07 respectively.

### CONCLUSION

The filling of the rectum with gel during MR defecography increases the H-line, M-line and anorectal angle measurements and influences pelvic floor grading. A standardized manner of obtaining these measurements should be implemented to allow better reproducibility and by extension, patient management.

### CLINICAL RELEVANCE/APPLICATION

The administration of rectal gel may alter the obtained measurements during dynamic pelvic floor imaging.

Printed on: 02/07/23



## Abstract Archives of the RSNA, 2022

T2-SPGU-3

### Comparison of three methods for lesion detection and classification on biparametric prostate MRI

Tuesday, Nov. 29 9:00AM - 9:30AM Room: Learning Center - GU DPS

#### Participants

Maria Sainz de Cea, PhD, Cambridge, MA (*Presenter*) Nothing to Disclose

#### PURPOSE

Detection of lesions in bi-parametric MRI (bp-MRI) and their classification according to PIRADS guidelines is part of the clinical workflow for patients identified to be at risk of prostate cancer. We propose a method for segmentation and classification of prostate lesions in bp-MRI based on semantic segmentation of lesions and compare it with two state-of-the-art methods based on RetinaNet object detection and Panoptic Segmentation.

#### METHODS AND MATERIALS

We propose the first multi-task deep convolutional model that performs lesion segmentation and classification. To improve the performance, we leverage information from prostate and zone by training the model to also predict their segmentation masks. Additionally, we include convolutional LSTM blocks to model the relationship between consecutive slices. The network training (on a large dataset) includes pre-processing and data augmentation. Performance was evaluated with five-fold cross validation and on a held-out test set. We report sensitivity, specificity, and accuracy for lesion classification for two classes: PIRADS 3 and PIRADS 4-5. Separately, we evaluate the lesion detection performance for both classes for our proposed network and the other two state-of-the-art methods.

#### RESULTS

Our model was trained on 2940 studies from 9 different providers across Europe, United States, South America, and Asia. The studies were acquired with different protocols and manufacturers and contain bi-parametric MRI. The algorithm was trained using T2-w series, high b-value DWI and ADC maps. When we fix the number of FPs in the FROC curve the sensitivity of our proposed multi-task network is 91%, higher than other methods (74% for RetinaNet and 89.3% for Panoptic Segmentation). The classification accuracy for the validation set is 76% and 73% for PIRADS 3 and PIRADS 4-5 lesions respectively (74% and 68% for RetinaNet). For PIRADS 4-5 lesions, we obtain a sensitivity of 76% and a specificity of 61% (66% and 76% for RetinaNet).

#### CONCLUSION

s We present a deep learning system for automated lesion segmentation and classification that also performs gland and prostate segmentation. The incorporation of multi-task learning has been shown to boost the performance of lesion detection achieving a high classification accuracy on a large multi-center dataset.

#### CLINICAL RELEVANCE/APPLICATION

Automated lesion segmentation and classification is clinically relevant and can be used for prostate cancer identification, biopsy, and treatment guidance.

Printed on: 02/07/23

## Abstract Archives of the RSNA, 2022

T2-SPHN

### Head and Neck Tuesday Poster Discussions

Tuesday, Nov. 29 9:00AM - 9:30AM Room: Learning Center - HN DPS

#### Sub-Events

#### T2-SPHN-1 Preliminary Evidence for Trans-synaptic Axonal Degeneration in Dysthyroid ) Optic Neuropathy Due to Thyroid-associated Ophthalmopathy

##### Participants

Ping Liu, MS, (*Presenter*) Nothing to Disclose

##### PURPOSE

Diffusion tensor imaging (DTI) provides a noninvasive tool to detect the microstructure of the entire visual pathway. To assess the microstructural changes of the whole visual pathway associated with DON and to investigate the potential mechanism of trans-synaptic degeneration pathogenesis in DON by DTI.

##### METHODS AND MATERIALS

A total of 64 bilateral thyroid-associated ophthalmopathy (TAO) patients with and without DON, and 30 healthy controls were included. All of the subjects underwent DTI examination, DTI parameters of each segment of the whole visual pathway (optic nerve, optic tract, optic radiation, including fractional anisotropy) (FA), mean diffusivity (MD), axial diffusivity (AD) and radial diffusivity (RD), were calculated and compared among the three groups using one-way analysis of variance (ANOVA) with post-hoc testing. Optical coherence tomography were finished to measure the mean retinal nerve fiber layer(mRNFL). The associations between the ophthalmological measures and DTI metrics were analyzed using correlation analysis.

##### RESULTS

DON patients showed significantly reduced mRNFL thickness ( $P = 0.008$ ) and abnormal visual evoked potential (VEP, delayed P100 latent time and/or reduced P100 amplitude,  $P = 0.001$  and  $0.064$ , respectively). There was a tendency for gradually reduced fractional anisotropy and increased diffusion in each segment of the whole visual pathway from overt DON and non-DON to HCs. For DON, the FA and MD of almost all segments of the visual pathway showed correlations with abnormal VEP.

##### CONCLUSION

s DTI is a useful tool for detecting microstructural changes in the entire visual pathway of DON due to TAO. Trans-synaptic degeneration may be a potential pathogenic mechanism of DON.

##### CLINICAL RELEVANCE/APPLICATION

Bidirectional trans-synaptic degeneration can be as a potential target for the neuroprotective treatment to DON. Additionally, DON is also an eye-brain neuropathy that is not confined to the eye but involves the entire visual pathway, providing evidence for a better understanding of the neuropathy mechanism of DON and the development of novel therapeutic regimens to slow or prevent the progression of neuropathy.

#### T2-SPHN-3 Clinical Value of 3D CT in Diagnosis of Unilateral Cricoarytenoid Joint Dislocation

##### Participants

Xueming Zeng, Nanjing City, China (*Presenter*) Nothing to Disclose

##### PURPOSE

To investigate the value of 3D CT in diagnosis of unilateral cricoarytenoid joint dislocation, and evaluate the different types of cricoarytenoid joint dislocation, in order to improve the understanding of this disease.

##### METHODS AND MATERIALS

31 patients who had been diagnosed with unilateral cricoarytenoid joint dislocation retrospectively reviewed, all patients were treated by reduction forceps, the voice returned to normal or significantly improved in all patients. CT scans were made during rest(respiratory phase) and phonation(phonation phase).In phonation phase, each patient was asked to sustain the vowel /e/. Thin-layer CT images were reconstructed as volume imaging (3d VR). Two radiologists analysed all the CT images independently and subjectively. If there was any disagreement, the third senior radiologist made the final judgment.On 3D VR images, the arytenoid articular surface of cricoid cartilage exposed completely means total dislocation,exposed partially means subluxation; The posterior part of the arytenoid articular surface of cricoid cartilage exposed means anterior dislocation, the anterior part exposed means posterior dislocation; In phonation phase, the lateral part of the arytenoid articular surface of cricoid cartilage exposed means external dislocation, the medial part exposed means medial dislocation.

##### RESULTS

There were 28 cases of cricoarytenoid subluxation (90.3%, 28 / 31) and 3 cases of complete dislocation (9.7%, 3 / 31); 26 cases

(83.9%, 26 / 31) of left cricoarytenoid dislocation and 5 cases (16.1%, 5 / 31) of right dislocation; Posterior dislocation in 28 cases (90.3%, 28 / 31), anterior dislocation in 3 cases (9.7%, 3 / 31); There were 23 cases of medial dislocation (74.2%, 23 / 31), 2 cases of external dislocation (6.4%, 2 / 31), and 6 cases without obvious internal and external dislocation (19.4%, 6 / 31). Three cases of complete dislocation were left posterior internal dislocation; Among the 28 cases of subluxation, there were 24 cases of left posterior dislocation (77.4%, 24 / 31), 4 cases of right posterior dislocation (12.9%, 4 / 31), 2 cases of left anterior dislocation (6.4%, 2 / 31) and 1 case of right anterior dislocation (3.2%, 1 / 31).

#### **CONCLUSION**

s 3D CT is a reliable method for the diagnosis of cricoarytenoid dislocation.

#### **CLINICAL RELEVANCE/APPLICATION**

3D CT is a reliable method for the diagnosis of cricoarytenoid dislocation, it tell the accurate dislocation orientation reliably, and may have a guidance effect in reduction forceps.

Printed on: 02/07/23

## Abstract Archives of the RSNA, 2022

T2-SPHN-1

### **Preliminary Evidence for Trans-synaptic Axonal Degeneration in Dysthyroid ) Optic Neuropathy Due to Thyroid-associated Ophthalmopathy**

Tuesday, Nov. 29 9:00AM - 9:30AM Room: Learning Center - HN DPS

#### **Participants**

Ping Liu, MS, (*Presenter*) Nothing to Disclose

#### **PURPOSE**

Diffusion tensor imaging (DTI) provides a noninvasive tool to detect the microstructure of the entire visual pathway. To assess the microstructural changes of the whole visual pathway associated with DON and to investigate the potential mechanism of trans-synaptic degeneration pathogenesis in DON by DTI.

#### **METHODS AND MATERIALS**

A total of 64 bilateral thyroid-associated ophthalmopathy (TAO) patients with and without DON, and 30 healthy controls were included. All of the subjects underwent DTI examination, DTI parameters of each segment of the whole visual pathway (optic nerve, optic tract, optic radiation, including fractional anisotropy) (FA), mean diffusivity (MD), axial diffusivity (AD) and radial diffusivity (RD), were calculated and compared among the three groups using one-way analysis of variance (ANOVA) with post-hoc testing. Optical coherence tomography were finished to measure the mean retinal nerve fiber layer(mRNFL). The associations between the ophthalmological measures and DTI metrics were analyzed using correlation analysis.

#### **RESULTS**

DON patients showed significantly reduced mRNFL thickness ( $P = 0.008$ ) and abnormal visual evoked potential (VEP, delayed P100 latent time and/or reduced P100 amplitude,  $P = 0.001$  and  $0.064$ , respectively). There was a tendency for gradually reduced fractional anisotropy and increased diffusion in each segment of the whole visual pathway from overt DON and non-DON to HCs. For DON, the FA and MD of almost all segments of the visual pathway showed correlations with abnormal VEP.

#### **CONCLUSION**

s DTI is a useful tool for detecting microstructural changes in the entire visual pathway of DON due to TAO. Trans-synaptic degeneration may be a potential pathogenic mechanism of DON.

#### **CLINICAL RELEVANCE/APPLICATION**

Bidirectional trans-synaptic degeneration can be as a potential target for the neuroprotective treatment to DON. Additionally, DON is also an eye-brain neuropathy that is not confined to the eye but involves the entire visual pathway, providing evidence for a better understanding of the neuropathy mechanism of DON and the development of novel therapeutic regimens to slow or prevent the progression of neuropathy.

Printed on: 02/07/23

## Abstract Archives of the RSNA, 2022

T2-SPHN-3

### Clinical Value of 3D CT in Diagnosis of Unilateral Cricoarytenoid Joint Dislocation

Tuesday, Nov. 29 9:00AM - 9:30AM Room: Learning Center - HN DPS

#### Participants

Xueming Zeng, Nanjing City, China (*Presenter*) Nothing to Disclose

#### PURPOSE

To investigate the value of 3D CT in diagnosis of unilateral cricoarytenoid joint dislocation, and evaluate the different types of cricoarytenoid joint dislocation, in order to improve the understanding of this disease.

#### METHODS AND MATERIALS

31 patients who had been diagnosed with unilateral cricoarytenoid joint dislocation retrospectively reviewed, all patients were treated by reduction forceps, the voice returned to normal or significantly improved in all patients. CT scans were made during rest (respiratory phase) and phonation (phonation phase). In phonation phase, each patient was asked to sustain the vowel /e/. Thin-layer CT images were reconstructed as volume imaging (3D VR). Two radiologists analysed all the CT images independently and subjectively. If there was any disagreement, the third senior radiologist made the final judgment. On 3D VR images, the arytenoid articular surface of cricoid cartilage exposed completely means total dislocation, exposed partially means subluxation; The posterior part of the arytenoid articular surface of cricoid cartilage exposed means anterior dislocation, the anterior part exposed means posterior dislocation; In phonation phase, the lateral part of the arytenoid articular surface of cricoid cartilage exposed means external dislocation, the medial part exposed means medial dislocation.

#### RESULTS

There were 28 cases of cricoarytenoid subluxation (90.3%, 28 / 31) and 3 cases of complete dislocation (9.7%, 3 / 31); 26 cases (83.9%, 26 / 31) of left cricoarytenoid dislocation and 5 cases (16.1%, 5 / 31) of right dislocation; Posterior dislocation in 28 cases (90.3%, 28 / 31), anterior dislocation in 3 cases (9.7%, 3 / 31); There were 23 cases of medial dislocation (74.2%, 23 / 31), 2 cases of external dislocation (6.4%, 2 / 31), and 6 cases without obvious internal and external dislocation (19.4%, 6 / 31). Three cases of complete dislocation were left posterior internal dislocation; Among the 28 cases of subluxation, there were 24 cases of left posterior dislocation (77.4%, 24 / 31), 4 cases of right posterior dislocation (12.9%, 4 / 31), 2 cases of left anterior dislocation (6.4%, 2 / 31) and 1 case of right anterior dislocation (3.2%, 1 / 31).

#### CONCLUSION

3D CT is a reliable method for the diagnosis of cricoarytenoid dislocation.

#### CLINICAL RELEVANCE/APPLICATION

3D CT is a reliable method for the diagnosis of cricoarytenoid dislocation, it tells the accurate dislocation orientation reliably, and may have a guidance effect in reduction forceps.

Printed on: 02/07/23



## Abstract Archives of the RSNA, 2022

T2-SPIN

### Informatics Tuesday Poster Discussions

Tuesday, Nov. 29 9:00AM - 9:30AM Room: Learning Center - IN DPS

#### Sub-Events

#### T2-SPIN-1 Curation of the CANDID-II Dataset for Deep Learning Algorithm Development on Adult Chest Radiographs

Participants

Sijing Feng, MBChB, BMedSc, Mosgiel, New Zealand (*Presenter*) Nothing to Disclose

#### PURPOSE

One of the main barriers to artificial intelligence (AI) development in clinical radiology is the lack of high quality publicly available datasets, often due to significant time and labor costs. MIMIC-CXR, NIH-CXR, and CheXpert datasets are examples of large public chest radiograph datasets that have significantly advanced chest radiograph AI development. However, the number of radiological findings identified in these datasets are limited. The CANDID-II (Chest x-ray Anonymized Dataset In [location]) dataset aims to build on this by presenting a more comprehensively manually labeled multi-classification dataset. This dataset can be used for training and testing of a wide range of deep learning algorithms.

#### METHODS AND MATERIALS

295,613 chest radiographs were exported in DICOM format from the [location] Hospital PACS with their corresponding free text reports between January 2010 and April 2020. This was followed by algorithmic anonymization. Inclusion criteria included images of both frontal and lateral orientations, of patients aged at least 16 years old, images that were free of pre-annotations, and that had complete field coverage of both lungs. Preservation of temporal relationships between studies and anonymized patient grouping of studies were performed. Reports of included images were randomized and sampled with equal weighting across 11 years. Selected reports were then manually labeled for 45 radiographic findings in seven categories over six months and then were double read to ensure accuracy and quality of labels. All 45 labels were mapped to Unified Medical System Language (UMLS) and RadLex ontologies for consistency and standardization of their definitions.

#### RESULTS

53,235 adult frontal (67%) and lateral (33%) anonymized chest radiographs are included in the final CANDID-II dataset with 35,200 corresponding anonymized free-text reports. These images derive from 23,706 unique patients, with a gender proportion of 1.1:1.0 (M: F). The mean age of patients in the CANDID-II dataset is 64 years with a standard deviation of 19 years.

#### CONCLUSION

The current project presents the curation of a large, publicly available anonymized comprehensively labeled chest radiograph dataset with corresponding free-text reports. After completion of ethics documentations, this dataset can be accessed at DOI: 10.17608/k6.auckland.19606921.

#### CLINICAL RELEVANCE/APPLICATION

The CANDID-II dataset can be used to train, test, and validate deep learning algorithms designed for a variety of clinical radiology applications including chest radiograph triaging, lung cancer screening, automated longitudinal follow up of abnormalities on chest radiographs as well as automated preliminary report generation.

#### T2-SPIN-2 Deep Learning for Pulmonary Embolism Response: A Validation of Artificial Intelligence-Guided RV/LV Analysis in Detecting and Predicting Outcomes

Participants

Anna Hu, BS, (*Presenter*) Nothing to Disclose

#### PURPOSE

Maximum right ventricle/left ventricle (RV/LV) ratio measurements from chest CT pulmonary angiograms (CTPA) and pulmonary embolism severity index (PESI) scoring are key risk indicators for life-threatening venous thromboembolic events (VTE), such as pulmonary embolism (PE). In practice, however, these indicators alone have limited prognostic value. This retrospective study was conducted using Imbio's artificial intelligence (AI)-guided RV/LV analysis software to assess its ability to evaluate success of Endovascular Thrombectomy (ET) and to predict the need for extracorporeal membrane oxygenation (ECMO) for treating PE.

#### METHODS AND MATERIALS

We retrospectively reviewed moderate to severe PE cases that were treated with Inari FlowTrieve ET at our institution between December 2018 and March 2022. Out of 73 total cases, those that had both pre- and post-procedural CTPA were included (31 total cases, 12 patients who were placed on ECMO and 19 who were not). Selected patients were evaluated using PESI scoring and Imbio's RV/LV software was utilized to measure ventricular dilation. Clinical success was defined as an improvement of RV/LV ratio and no VTE or ET related complications.

## RESULTS

Among the 31 patients included, the average PESI score was higher in patients who were placed on ECMO ( $130.2 \pm 40.8$  (ECMO) vs  $100.9 \pm 15.5$  (non-ECMO),  $P < 0.05$ ). Similarly, the average change in pre- vs post-procedural RV/LV ratios was higher in patients who were placed on ECMO ( $0.936 \pm 0.420$  (ECMO) vs  $0.430 \pm 0.273$  (non-ECMO),  $P < 0.005$ ). While the average post-procedural RV/LV ratios were not significantly different ( $P = 0.484$ ), average pre-procedural RV/LV ratios were significantly higher in patients who were placed on ECMO ( $1.977 \pm 0.370$  (ECMO) vs  $1.480 \pm 0.312$  (non-ECMO),  $P < 0.0005$ ). There was no significant difference in peak troponin levels prior to ET between the two groups ( $P = 0.186$ ). No complications were reported for any patients in both groups within 90 days post-operatively.

## CONCLUSION

Results from this study suggest that Inari FlowTrier ET is an effective therapy for patients with moderate to severe PE. Furthermore, AI-guided RV/LV analysis paired with PESI scoring can more reliably assess the need for ECMO therapy following ET than evaluating peak troponin values or radiologist-guided CTPA interpretations.

## CLINICAL RELEVANCE/APPLICATION

PE are among the most fatal cardiovascular diseases, where acute and rapid diagnosis is essential to improve prognosis. AI-guided RV/LV analysis software can improve risk stratification and shorten treatment initiation time for patients with moderate to severe PE.

## T2-SPIN-3 On-Demand Realistic Creation of Synthetic Chest Radiographs

Participants

Nicholas Primiano, MD, Buffalo, NY (*Presenter*) Nothing to Disclose

## PURPOSE

Deep convolutional neural networks (dCNNs) have recently shown accuracy in identifying and quantifying disease on chest radiographs. Unfortunately, dCNNs require large amounts of labeled training data to yield desirable results. Labeling by expert radiologists is a costly and time-intensive process. Furthermore, there are a limited number of high quality public datasets and many of these datasets do not contain a variety of diseases. For example, only 2.4% of the CheXpert dataset and 1.2% of the NIH CXR-14 dataset is labeled "Pneumonia". A generative adversarial network (GAN) can be used to create synthetic images that address these issues.

## METHODS AND MATERIALS

A class conditional implementation of StyleGan3 was trained on a subset of the CheXpert dataset consisting of 191,027 frontal chest radiographs. It was trained on an Nvidia RTX 3090 GPU. Similarity metrics, Fréchet inception distance and kernel inception distance, were calculated with StyleGan3's built-in metric generation tool. To determine if augmenting the dataset with synthetic images could improve the performance of a classification model, a DenseNet201 dCNN was trained on CheXpert as well as CheXpert augmented with 2,000 synthetic images per class label.

## RESULTS

Synthetic chest radiographs with the following characteristics were generated: Atelectasis, Cardiomegaly, Consolidation, Edema, Enlarged Cardiomediastinum, Fracture, Lung Lesion, Lung Opacity, No Finding, Pleural Effusion, Pleural Other, Pneumonia, and Pneumothorax. The network performed well, yielding a Fréchet inception distance of 11.92 and a kernel inception distance of 0.0089. The DenseNet201 model, trained on the CheXpert dataset alone achieved an AUC of 0.80 on a multi-label classification task of the CheXpert validation dataset. Another DenseNet201 model was trained on the CheXpert dataset augmented with synthetic images and achieved an AUC of 0.87 on the same classification task.

## CONCLUSION

After training the network, high quality images of a particular disease state or radiographic finding can be produced on-demand. These images can augment existing datasets, resulting in improved classification of disease on chest radiographs.

## CLINICAL RELEVANCE/APPLICATION

A large number of diverse synthetic chest radiographs can be created with a GAN. In contrast to real radiographs, GAN-generated radiographs do not require labeling or de-identification, making them ideal for deep learning research. In addition, they can be used to augment existing datasets to improve classification models that automatically classify disease. Finally, these techniques may be valuable educational tools, as they can be used to create on-demand realistic examples of rare pathologies with fine control over disease severity.

## T2-SPIN-4 Not So Black and White: Convolutional Neural Networks and Vision Transformers Demonstrate Sex and Race-Based Bias For Chest Radiograph Diagnosis In Inconsistent Ways

Participants

Paul Yi, MD, Baltimore, MD (*Presenter*) Consultant, FH Orthopedics SAS; Consultant, BunkerHill Health

## PURPOSE

Although convolutional neural networks (CNN) for thoracic disease diagnosis on chest radiographs (CXR) have demonstrated underperformance bias against underrepresented sex and racial groups, it is unclear if this is the case for vision transformers (VT), an emerging type of deep learning (DL) architecture with a fundamentally different mechanism of computer vision. We compared the presence and direction of bias based on sex and race in VT and CNN models trained to diagnose thoracic disease on CXR.

## METHODS AND MATERIALS

We compared DenseNet 121 CNN and Data-efficient Image Transformer (DeiT) VT architectures, which have demonstrated state-of-the-art results in radiology and general computer vision tasks, respectively. We fine-tuned these models on the NIH CXR14 dataset of 112,120 CXRs annotated for 14 disease labels. There were more males than females (56% male); race was not reported. Data were randomly split into 70/10/20% train/validation/test splits with maintained sex/disease distributions. Hyperparameter optimization was performed via grid search. Test performance was assessed on the internal test set and external dataset of 25,000

images from Stanford's CheXpert dataset (56% male; 67% white). For each test set, we calculated AUROCs for each disease label, which were compared between demographic groups based on sex (both datasets) and race (CheXpert only).

## RESULTS

AUROCs were significantly different between males and females for all disease labels in both test sets, as well as between white and non-white patients for all disease labels in CheXpert. However, the 'direction' of bias (group with worse diagnosis) was inconsistent between disease labels, datasets, and DL model type. For sex-based biases, in the NIH test set, the VT and CNN models had biases favoring males (higher AUROC) in 8/14 and 5/14 disease labels, respectively; in the CheXpert test set, they had biases favoring males in 1/7 and 3/7 disease labels, respectively (note CheXpert shares only 7 disease labels with the NIH dataset). For race-based biases, the VT and CNN models both had biases favoring white over non-white patients in 2/7 disease labels.

## CONCLUSION

s Although CNN and VT models demonstrated biases based on sex and race, these biases were inconsistent between disease labels, testing datasets, and DL model architectures. Surprisingly, biases did not consistently disadvantage underrepresented groups, suggesting that bias in DL models stems from multiple and interacting factors that require further analysis and characterization.

## CLINICAL RELEVANCE/APPLICATION

The widespread use of deep learning (DL) models for CXR diagnosis demands careful validation that controls for bias in under-represented groups, and these biases do not translate among different DL architectures.

## T2-SPIN-5 Deep Learning Classification Model Can Predict Upgrade of DCIS Lesions To Invasive Breast Cancer

Participants

John Mayfield, MD, MS, Lithia, FL (*Presenter*) Nothing to Disclose

## PURPOSE

A subset of ductal carcinoma in-situ (DCIS) lesions diagnosed on core biopsy will be upgraded to invasive breast cancer on surgical excision. Pre-operative identification of these lesions would inform clinical and surgical management of patients. The goal of our study was to train a Deep Convolutional Neural Network (DCNN) to classify DCIS lesions as non-upgraded or upgraded to invasive malignancy utilizing dynamic contrast-enhanced (DCE) breast MRI images, without the use of lesion segmentation.

## METHODS AND MATERIALS

113 DCIS lesions (95 non-upgraded and 18 upgraded post-excision) were evaluated on pre-operative DCE-MRI. A board-certified breast radiologist identified each DCIS lesion. Subsequently, a single image of each lesion from the most delayed contrast-enhanced T1-weighted sequence was cropped to exclude the mediastinum and contralateral breast. To handle the class imbalance, a Deep Convolutional Generative Adversarial Network (DCGAN) created an additional 77 upgraded images (Fig. 1a). Images were randomly split 20 times into training, validation, and testing with a 60:20:20 ratio (Fig. 1b). Binary classification accuracy was separately reported with model loss. Bootstrap resampling was used to estimate the model confidence intervals.

## RESULTS

The DCNN model was trained on 504,211,841 parameters with a dropout rate of 0.5 to reduce overfitting. Training and validation converged in 20 epochs with final reported validation accuracy of 78.2% (95% CI: 76.3 - 80.0). Testing on heldout DCIS images produced an 80.0% accuracy.

## CONCLUSION

s Nonsegmented DCIS lesions can be classified into non-upgraded or upgraded predictive categorization prior to surgery using a DCNN. Given the class imbalance, next steps will include testing on a larger and independent dataset.

## CLINICAL RELEVANCE/APPLICATION

Deep learning can assist in classifying DCIS lesions on DCE-MRI, impacting clinical and surgical management of patients. Application of the DCNN can be performed without the use of lesion segmentation, eliminating the interobserver variability encountered with manual or semi-automated segmentation methods.

## T2-SPIN-6 Generalization of AI Analysis for Prostate Cancer Diagnostic Imaging to Multiple Centres and Scanners

Participants

Antony Rix, MEng, PhD, Cambridge, United Kingdom (*Presenter*) Stockholder, Lucida Medical Ltd; Director, Lucida Medical Ltd

## PURPOSE

There has been little validation of AI to detect clinically significant prostate cancer (csPCa) beyond single site, mainly 3T, datasets, limiting translation to clinical practice. We evaluate how an AI system can generalise to real-world data from multiple sites, scanners, protocols, and field strengths, to provide stronger evidence to support clinical use.

## METHODS AND MATERIALS

AI-based software (Lucida Medical, PI v2) was developed using PROSTATEx and retrospective data from three UK NHS sites (PAIR-1 study), 458 patients total, to assess generality of the AI. Data included 5 scanner models, 1.5T/3.0T field strengths, and different acquisition protocols. Data was split, balanced per site, 274 patients for training, 91 patients for development-validation, 94 patients for held-out-test. The software automatically outputs scores and ROIs intended to identify GS=3+4 csPCa per-patient, for biopsy selection, and per-lesion, for biopsy targeting. csPCa was confirmed by biopsy, with PI-RADS1/2 patients/lesions that did not receive a biopsy assumed negative.

## RESULTS

For selecting patients for biopsy, the AI identified patients with csPCa with sensitivity 93% (95% CI 83-100%), specificity 41% (28-54%), NPV 92% (81-100%), and AUC 0.86 (0.76-0.93) using multiparametric MRI (mpMRI) data from the PROSTATEx/PAIR-1 held-out-test set (94 patients, 35% csPCa). On the whole PAIR-1 set (255 patients, PI-RADS=3), the reporting radiologists had

per-patient sensitivity 100% (95% CI 100-100%) due to the assumed ground truth, specificity 52% (44-60%), NPV 100% (100-100%), and AUC 0.93 (0.90-0.96). In meta-analysis of 12 major studies (37% csPCa), radiologists identified patients with GS=3+4 csPCa with sensitivity 86% and specificity 42%. For biopsy targeting (per-lesion), the AI identified csPCa lesions in the held-out-test set (140 lesions, 42% csPCa) with sensitivity 91% (82-98%), specificity 55% (45-65%), NPV 92% (85-98%), and AUC 0.82 (0.74-0.90) using mpMRI data. On the whole PAIR-1 set (344 lesions, PI-RADS=3), the reporting radiologists had per-lesion sensitivity 98% (95% CI 95-100%), specificity 49% (42-57%), NPV 98% (95-100%), and AUC 0.91 (0.88-0.94). The AI system has comparable sensitivity and specificity to radiologists in the PAIR-1 study, major radiology studies and AI literature, over this varied dataset.

#### **CONCLUSION**

s The proposed AI model shows promising results with both open and real-world multi-centre retrospective data with different field strengths and imaging.

#### **CLINICAL RELEVANCE/APPLICATION**

AI could support prostate cancer detection in diverse imaging settings including both 1.5T and 3T scanners, with sensitivity and specificity comparable to major radiology studies.

Printed on: 02/07/23



## Abstract Archives of the RSNA, 2022

T2-SPIN-1

### Curation of the CANDID-II Dataset for Deep Learning Algorithm Development on Adult Chest Radiographs

Tuesday, Nov. 29 9:00AM - 9:30AM Room: Learning Center - IN DPS

#### Participants

Sijing Feng, MBChB, BMedSc, Mosgiel, New Zealand (*Presenter*) Nothing to Disclose

#### PURPOSE

One of the main barriers to artificial intelligence (AI) development in clinical radiology is the lack of high quality publicly available datasets, often due to significant time and labor costs. MIMIC-CXR, NIH-CXR, and CheXpert datasets are examples of large public chest radiograph datasets that have significantly advanced chest radiograph AI development. However, the number of radiological findings identified in these datasets are limited. The CANDID-II (Chest x-ray Anonymized Dataset In [location]) dataset aims to build on this by presenting a more comprehensively manually labeled multi-classification dataset. This dataset can be used for training and testing of a wide range of deep learning algorithms.

#### METHODS AND MATERIALS

295,613 chest radiographs were exported in DICOM format from the [location] Hospital PACS with their corresponding free text reports between January 2010 and April 2020. This was followed by algorithmic anonymization. Inclusion criteria included images of both frontal and lateral orientations, of patients aged at least 16 years old, images that were free of pre-annotations, and that had complete field coverage of both lungs. Preservation of temporal relationships between studies and anonymized patient grouping of studies were performed. Reports of included images were randomized and sampled with equal weighting across 11 years. Selected reports were then manually labeled for 45 radiographic findings in seven categories over six months and then were double read to ensure accuracy and quality of labels. All 45 labels were mapped to Unified Medical System Language (UMLS) and RadLex ontologies for consistency and standardization of their definitions.

#### RESULTS

53,235 adult frontal (67%) and lateral (33%) anonymized chest radiographs are included in the final CANDID-II dataset with 35,200 corresponding anonymized free-text reports. These images derive from 23,706 unique patients, with a gender proportion of 1.1:1.0 (M: F). The mean age of patients in the CANDID-II dataset is 64 years with a standard deviation of 19 years.

#### CONCLUSION

The current project presents the curation of a large, publicly available anonymized comprehensively labeled chest radiograph dataset with corresponding free-text reports. After completion of ethics documentations, this dataset can be accessed at DOI: 10.17608/k6.auckland.19606921.

#### CLINICAL RELEVANCE/APPLICATION

The CANDID-II dataset can be used to train, test, and validate deep learning algorithms designed for a variety of clinical radiology applications including chest radiograph triaging, lung cancer screening, automated longitudinal follow up of abnormalities on chest radiographs as well as automated preliminary report generation.

Printed on: 02/07/23

## Abstract Archives of the RSNA, 2022

T2-SPIN-2

### Deep Learning for Pulmonary Embolism Response: A Validation of Artificial Intelligence-Guided RV/LV Analysis in Detecting and Predicting Outcomes

Tuesday, Nov. 29 9:00AM - 9:30AM Room: Learning Center - IN DPS

#### Participants

Anna Hu, BS, (*Presenter*) Nothing to Disclose

#### PURPOSE

Maximum right ventricle/left ventricle (RV/LV) ratio measurements from chest CT pulmonary angiograms (CTPA) and pulmonary embolism severity index (PESI) scoring are key risk indicators for life-threatening venous thromboembolic events (VTE), such as pulmonary embolism (PE). In practice, however, these indicators alone have limited prognostic value. This retrospective study was conducted using Imbio's artificial intelligence (AI)-guided RV/LV analysis software to assess its ability to evaluate success of Endovascular Thrombectomy (ET) and to predict the need for extracorporeal membrane oxygenation (ECMO) for treating PE.

#### METHODS AND MATERIALS

We retrospectively reviewed moderate to severe PE cases that were treated with Inari FlowTrierer ET at our institution between December 2018 and March 2022. Out of 73 total cases, those that had both pre- and post-procedural CTPA were included (31 total cases, 12 patients who were placed on ECMO and 19 who were not). Selected patients were evaluated using PESI scoring and Imbio's RV/LV software was utilized to measure ventricular dilation. Clinical success was defined as an improvement of RV/LV ratio and no VTE or ET related complications.

#### RESULTS

Among the 31 patients included, the average PESI score was higher in patients who were placed on ECMO ( $130.2 \pm 40.8$  (ECMO) vs  $100.9 \pm 15.5$  (non-ECMO),  $P < 0.05$ ). Similarly, the average change in pre- vs post-procedural RV/LV ratios was higher in patients who were placed on ECMO ( $0.936 \pm 0.420$  (ECMO) vs  $0.430 \pm 0.273$  (non-ECMO),  $P < 0.005$ ). While the average post-procedural RV/LV ratios were not significantly different ( $P = 0.484$ ), average pre-procedural RV/LV ratios were significantly higher in patients who were placed on ECMO ( $1.977 \pm 0.370$  (ECMO) vs  $1.480 \pm 0.312$  (non-ECMO),  $P < 0.0005$ ). There was no significant difference in peak troponin levels prior to ET between the two groups ( $P = 0.186$ ). No complications were reported for any patients in both groups within 90 days post-operatively.

#### CONCLUSION

Results from this study suggest that Inari FlowTrierer ET is an effective therapy for patients with moderate to severe PE. Furthermore, AI-guided RV/LV analysis paired with PESI scoring can more reliably assess the need for ECMO therapy following ET than evaluating peak troponin values or radiologist-guided CTPA interpretations.

#### CLINICAL RELEVANCE/APPLICATION

PE are among the most fatal cardiovascular diseases, where acute and rapid diagnosis is essential to improve prognosis. AI-guided RV/LV analysis software can improve risk stratification and shorten treatment initiation time for patients with moderate to severe PE.

Printed on: 02/07/23

## Abstract Archives of the RSNA, 2022

T2-SPIN-3

### On-Demand Realistic Creation of Synthetic Chest Radiographs

Tuesday, Nov. 29 9:00AM - 9:30AM Room: Learning Center - IN DPS

#### Participants

Nicholas Primiano, MD, Buffalo, NY (*Presenter*) Nothing to Disclose

#### PURPOSE

Deep convolutional neural networks (dCNNs) have recently shown accuracy in identifying and quantifying disease on chest radiographs. Unfortunately, dCNNs require large amounts of labeled training data to yield desirable results. Labeling by expert radiologists is a costly and time-intensive process. Furthermore, there are a limited number of high quality public datasets and many of these datasets do not contain a variety of diseases. For example, only 2.4% of the CheXpert dataset and 1.2% of the NIH CXR-14 dataset is labeled "Pneumonia". A generative adversarial network (GAN) can be used to create synthetic images that address these issues.

#### METHODS AND MATERIALS

A class conditional implementation of StyleGan3 was trained on a subset of the CheXpert dataset consisting of 191,027 frontal chest radiographs. It was trained on an Nvidia RTX 3090 GPU. Similarity metrics, Fréchet inception distance and kernel inception distance, were calculated with StyleGan3's built-in metric generation tool. To determine if augmenting the dataset with synthetic images could improve the performance of a classification model, a DenseNet201 dCNN was trained on CheXpert as well as CheXpert augmented with 2,000 synthetic images per class label.

#### RESULTS

Synthetic chest radiographs with the following characteristics were generated: Atelectasis, Cardiomegaly, Consolidation, Edema, Enlarged Cardiomeastinum, Fracture, Lung Lesion, Lung Opacity, No Finding, Pleural Effusion, Pleural Other, Pneumonia, and Pneumothorax. The network performed well, yielding a Fréchet inception distance of 11.92 and a kernel inception distance of 0.0089. The DenseNet201 model, trained on the CheXpert dataset alone achieved an AUC of 0.80 on a multi-label classification task of the CheXpert validation dataset. Another DenseNet201 model was trained on the CheXpert dataset augmented with synthetic images and achieved an AUC of 0.87 on the same classification task.

#### CONCLUSION

s After training the network, high quality images of a particular disease state or radiographic finding can be produced on-demand. These images can augment existing datasets, resulting in improved classification of disease on chest radiographs.

#### CLINICAL RELEVANCE/APPLICATION

A large number of diverse synthetic chest radiographs can be created with a GAN. In contrast to real radiographs, GAN-generated radiographs do not require labeling or de-identification, making them ideal for deep learning research. In addition, they can be used to augment existing datasets to improve classification models that automatically classify disease. Finally, these techniques may be valuable educational tools, as they can be used to create on-demand realistic examples of rare pathologies with fine control over disease severity.

Printed on: 02/07/23



## Abstract Archives of the RSNA, 2022

T2-SPIN-4

### Not So Black and White: Convolutional Neural Networks and Vision Transformers Demonstrate Sex and Race-Based Bias For Chest Radiograph Diagnosis In Inconsistent Ways

Tuesday, Nov. 29 9:00AM - 9:30AM Room: Learning Center - IN DPS

#### Participants

Paul Yi, MD, Baltimore, MD (*Presenter*) Consultant, FH Orthopedics SAS; Consultant, BunkerHill Health

#### PURPOSE

Although convolutional neural networks (CNN) for thoracic disease diagnosis on chest radiographs (CXR) have demonstrated underperformance bias against underrepresented sex and racial groups, it is unclear if this is the case for vision transformers (VT), an emerging type of deep learning (DL) architecture with a fundamentally different mechanism of computer vision. We compared the presence and direction of bias based on sex and race in VT and CNN models trained to diagnose thoracic disease on CXR.

#### METHODS AND MATERIALS

We compared DenseNet 121 CNN and Data-efficient Image Transformer (DeiT) VT architectures, which have demonstrated state-of-the-art results in radiology and general computer vision tasks, respectively. We fine-tuned these models on the NIH CXR14 dataset of 112,120 CXRs annotated for 14 disease labels. There were more males than females (56% male); race was not reported. Data were randomly split into 70/10/20% train/validation/test splits with maintained sex/disease distributions. Hyperparameter optimization was performed via grid search. Test performance was assessed on the internal test set and external dataset of 25,000 images from Stanford's CheXpert dataset (56% male; 67% white). For each test set, we calculated AUROCs for each disease label, which were compared between demographic groups based on sex (both datasets) and race (CheXpert only).

#### RESULTS

AUROCs were significantly different between males and females for all disease labels in both test sets, as well as between white and non-white patients for all disease labels in CheXpert. However, the 'direction' of bias (group with worse diagnosis) was inconsistent between disease labels, datasets, and DL model type. For sex-based biases, in the NIH test set, the VT and CNN models had biases favoring males (higher AUROC) in 8/14 and 5/14 disease labels, respectively; in the CheXpert test set, they had biases favoring males in 1/7 and 3/7 disease labels, respectively (note CheXpert shares only 7 disease labels with the NIH dataset). For race-based biases, the VT and CNN models both had biases favoring white over non-white patients in 2/7 disease labels.

#### CONCLUSION

s Although CNN and VT models demonstrated biases based on sex and race, these biases were inconsistent between disease labels, testing datasets, and DL model architectures. Surprisingly, biases did not consistently disadvantage underrepresented groups, suggesting that bias in DL models stems from multiple and interacting factors that require further analysis and characterization.

#### CLINICAL RELEVANCE/APPLICATION

The widespread use of deep learning (DL) models for CXR diagnosis demands careful validation that controls for bias in underrepresented groups, and these biases do not translate among different DL architectures.

Printed on: 02/07/23

## Abstract Archives of the RSNA, 2022

T2-SPIN-5

### Deep Learning Classification Model Can Predict Upgrade of DCIS Lesions To Invasive Breast Cancer

Tuesday, Nov. 29 9:00AM - 9:30AM Room: Learning Center - IN DPS

#### Participants

John Mayfield, MD, MS, Lithia, FL (*Presenter*) Nothing to Disclose

#### PURPOSE

A subset of ductal carcinoma in-situ (DCIS) lesions diagnosed on core biopsy will be upgraded to invasive breast cancer on surgical excision. Pre-operative identification of these lesions would inform clinical and surgical management of patients. The goal of our study was to train a Deep Convolutional Neural Network (DCNN) to classify DCIS lesions as non-upgraded or upgraded to invasive malignancy utilizing dynamic contrast-enhanced (DCE) breast MRI images, without the use of lesion segmentation.

#### METHODS AND MATERIALS

113 DCIS lesions (95 non-upgraded and 18 upgraded post-excision) were evaluated on pre-operative DCE-MRI. A board-certified breast radiologist identified each DCIS lesion. Subsequently, a single image of each lesion from the most delayed contrast-enhanced T1-weighted sequence was cropped to exclude the mediastinum and contralateral breast. To handle the class imbalance, a Deep Convolutional Generative Adversarial Network (DCGAN) created an additional 77 upgraded images (Fig. 1a). Images were randomly split 20 times into training, validation, and testing with a 60:20:20 ratio (Fig. 1b). Binary classification accuracy was separately reported with model loss. Bootstrap resampling was used to estimate the model confidence intervals.

#### RESULTS

The DCNN model was trained on 504,211,841 parameters with a dropout rate of 0.5 to reduce overfitting. Training and validation converged in 20 epochs with final reported validation accuracy of 78.2% (95% CI: 76.3 - 80.0). Testing on heldout DCIS images produced an 80.0% accuracy.

#### CONCLUSION

Nonsegmented DCIS lesions can be classified into non-upgraded or upgraded predictive categorization prior to surgery using a DCNN. Given the class imbalance, next steps will include testing on a larger and independent dataset.

#### CLINICAL RELEVANCE/APPLICATION

Deep learning can assist in classifying DCIS lesions on DCE-MRI, impacting clinical and surgical management of patients. Application of the DCNN can be performed without the use of lesion segmentation, eliminating the interobserver variability encountered with manual or semi-automated segmentation methods.

Printed on: 02/07/23

## Abstract Archives of the RSNA, 2022

T2-SPIN-6

### Generalization of AI Analysis for Prostate Cancer Diagnostic Imaging to Multiple Centres and Scanners

Tuesday, Nov. 29 9:00AM - 9:30AM Room: Learning Center - IN DPS

#### Participants

Antony Rix, MEng, PhD, Cambridge, United Kingdom (*Presenter*) Stockholder, Lucida Medical Ltd; Director, Lucida Medical Ltd

#### PURPOSE

There has been little validation of AI to detect clinically significant prostate cancer (csPCa) beyond single site, mainly 3T, datasets, limiting translation to clinical practice. We evaluate how an AI system can generalise to real-world data from multiple sites, scanners, protocols, and field strengths, to provide stronger evidence to support clinical use.

#### METHODS AND MATERIALS

AI-based software (Lucida Medical, PI v2) was developed using PROSTATEx and retrospective data from three UK NHS sites (PAIR-1 study), 458 patients total, to assess generality of the AI. Data included 5 scanner models, 1.5T/3.0T field strengths, and different acquisition protocols. Data was split, balanced per site, 274 patients for training, 91 patients for development-validation, 94 patients for held-out-test. The software automatically outputs scores and ROIs intended to identify GS=3+4 csPCa per-patient, for biopsy selection, and per-lesion, for biopsy targeting. csPCa was confirmed by biopsy, with PI-RADS1/2 patients/lesions that did not receive a biopsy assumed negative.

#### RESULTS

For selecting patients for biopsy, the AI identified patients with csPCa with sensitivity 93% (95% CI 83-100%), specificity 41% (28-54%), NPV 92% (81-100%), and AUC 0.86 (0.76-0.93) using multiparametric MRI (mpMRI) data from the PROSTATEx/PAIR-1 held-out-test set (94 patients, 35% csPCa). On the whole PAIR-1 set (255 patients, PI-RADS=3), the reporting radiologists had per-patient sensitivity 100% (95% CI 100-100%) due to the assumed ground truth, specificity 52% (44-60%), NPV 100% (100-100%), and AUC 0.93 (0.90-0.96). In meta-analysis of 12 major studies (37% csPCa), radiologists identified patients with GS=3+4 csPCa with sensitivity 86% and specificity 42%. For biopsy targeting (per-lesion), the AI identified csPCa lesions in the held-out-test set (140 lesions, 42% csPCa) with sensitivity 91% (82-98%), specificity 55% (45-65%), NPV 92% (85-98%), and AUC 0.82 (0.74-0.90) using mpMRI data. On the whole PAIR-1 set (344 lesions, PI-RADS=3), the reporting radiologists had per-lesion sensitivity 98% (95% CI 95-100%), specificity 49% (42-57%), NPV 98% (95-100%), and AUC 0.91 (0.88-0.94). The AI system has comparable sensitivity and specificity to radiologists in the PAIR-1 study, major radiology studies and AI literature, over this varied dataset.

#### CONCLUSION

s The proposed AI model shows promising results with both open and real-world multi-centre retrospective data with different field strengths and imaging.

#### CLINICAL RELEVANCE/APPLICATION

AI could support prostate cancer detection in diverse imaging settings including both 1.5T and 3T scanners, with sensitivity and specificity comparable to major radiology studies.

Printed on: 02/07/23

## Abstract Archives of the RSNA, 2022

T2-SPIR

### Interventional Tuesday Poster Discussions

Tuesday, Nov. 29 9:00AM - 9:30AM Room: Learning Center - IR DPS

#### Sub-Events

#### T2-SPIR-1 Safety and Effectiveness of Uterine Fibroid Embolization in Patients with Scarred Uterus

Participants

Saeblyol Ma, MD, (*Presenter*) Nothing to Disclose

#### PURPOSE

To evaluate the safety and effectiveness of uterine fibroid embolization (UFE) in patients with a scarred uterus caused by a previous myomectomy or cesarean section

#### METHODS AND MATERIALS

A total of 140 patients who underwent embolization for symptomatic fibroids were included in this retrospective study. The patients were divided into two groups, those with a history of myomectomy and/or cesarean section (scarred uterus group, n = 56), and those without surgical history involving the uterus (no-scar group, n = 84). Demographics, embolization details, outcomes, and complications were analyzed and compared between the two groups.

#### RESULTS

The overall clinical success rate was 89.28% in the scarred uterus group and 95.24% in the no-scar group. There was no statistical difference in infarction rate or change in fibroid volume in follow-up magnetic resonance imaging (MRI) between the groups. There was one major complication in the no-scar group, but there was no statistical difference in minor and major complications between the groups. The mean follow-up period was 25.9 months. The mean symptom-free time was 27.2 months in the scarred uterus group and 21.9 months in the no-scar group without a significant difference. There were no statistically significant differences in symptom changes, recurrence, and complication rates between the groups. Recurrence seen on imaging or regrowth was more common in the group with myomectomy history (36.8% vs. 15.9%, P = 0.052). However, there was no significant difference in symptom recurrence rates (15.8% vs. 12.5%, P = 0.713).

#### CONCLUSION

No statistically significant difference in technical and clinical outcomes was observed between the two groups. There was no significant increase in UFE complication rates in patients with a scarred uterus.

#### CLINICAL RELEVANCE/APPLICATION

UFE did not increase the risk of complications after myomectomy or cesarean section. Patients with a scarred uterus showed similar technical and clinical outcomes compared to the no-scar group in this study. Although caution should be taken, UFE can be a good option for symptomatic fibroid treatment in patients with a scarred uterus.

#### T2-SPIR-2 Cost Comparison of Prostatic Artery Embolization Between In-Hospital and Outpatient Lab Settings

Participants

Lucas Cusumano, MD, MPH, (*Presenter*) Nothing to Disclose

#### PURPOSE

To determine the costs associated with prostatic artery embolization (PAE) performed for treatment of benign prostatic hyperplasia (BPH) in hospital and outpatient-based lab (OBL) settings.

#### METHODS AND MATERIALS

Patients evaluated underwent outpatient PAE between January 2021 and December 2021, utilizing right common femoral artery access. Procedures were performed in similarly-equipped procedure suites located within a tertiary hospital or OBL. Costs were determined utilizing time-driven activity-based costing (TDABC), a micro-costing methodology for calculating procedural costs incurred by the institution. Process maps were created describing personnel, space, equipment, and materials. Time duration of each procedural step was recorded independently by a nurse caring for the patient at the time of the procedure and mean values were included in our model. Costs and capacity cost rates were determined using institutional and publicly available financial data.

#### RESULTS

37 PAE procedures met inclusion criteria with a mean patient age of 70.4 (+/- 6.7) years and mean prostate gland size of 129.7 (+/- 56.4) cc. 26 procedures were performed within the hospital setting and 11 procedures were performed within the OBL. Reduction in International Prostate Symptom Score (IPSS) was not significantly different following hospital and OBL procedures (57.2% vs. 81.8%, P=0.1850). Mean procedural time was not significantly different between the hospital and OBL settings (132.0 vs. 147.4 minutes, P=0.1574). However, duration between admission to discharge was significantly longer for procedures performed

in a hospital setting (468.8 vs. 325.4 minutes,  $P < 0.0001$ ). Total costs for hospital-based procedures were marginally higher (\$3,858.28 vs. \$3,642.67). Personnel and material costs constitute the largest proportion costs of 54.7% and 41.6%, respectively.

## CONCLUSION

s Total PAE cost was similar between the hospital and OBL settings. However, longer periprocedural times for hospital-based procedures and differences in reimbursement may favor performance of PAE in an OBL setting.

## CLINICAL RELEVANCE/APPLICATION

PAE is a safe and effective treatment for BPH. However, there is a paucity of data regarding costs, especially comparing hospital and OBL settings. The ongoing shift towards value-based incentive models requires accurate assessment of cost drivers and cost inefficiencies.

## T2-SPIR-3 SpaceOAR Hydrogel Distribution and Early Complications in Patients Undergoing Radiation Therapy for Prostate Cancer

Participants

Andrew Yates, MBBCh, BSc, Dublin 7, Ireland (*Presenter*) Nothing to Disclose

## PURPOSE

Hydrogel spacers aim to separate the rectum from the prostate before radiation therapy for patients with prostate cancer to decrease the radiation dose to the rectum. The aim of this study was to evaluate the distribution of the hydrogel spacer between the rectum and the prostate, to assess for hydrogel rectal wall infiltration and to assess for immediate complications

## METHODS AND MATERIALS

Retrospective study of 161 patients that underwent hydrogel spacer injection was performed. Symmetry and distribution of the hydrogel were assessed on planning MRI, as was the separation of the rectum and prostate. The MRI was reviewed for rectal wall injection or other malplacement of gel. Immediate post-procedure complications were recorded.

## RESULTS

117 (72.7%) patients had a symmetrical distribution of the hydrogel spacer with 44 (27.3%) patients having some asymmetry of the spacer. The mean anteroposterior rectoprostatic separation was  $10.2 \pm 3.7$  mm with a range of 0 - 27 mm. Eight (5.0%) patients had some rectal wall infiltration on the MRI; 7 (4.3%) patients had minimal infiltration and one (0.6%) patient had moderate infiltration. One (0.6%) patient had intraprostatic injection of gel. Two (1.2%) patients required treatment in the emergency department after the procedure; one for urinary retention and one for pain.

## CONCLUSION

s Hydrogel injection effectively separates the prostate from the rectum with a symmetrical distribution in the majority of cases prior to radiation therapy with a low rate of rectal wall injection and immediate complications.

## CLINICAL RELEVANCE/APPLICATION

This study informs clinicians regarding the technique, outcomes and complications related to hydrogel spacer injection prior to radiation therapy.

## T2-SPIR-5 Embolization Treatment of Primary Chylous Reflux Disease of Genitalia (PCRG)

Participants

Hee Eun Moon, MD, (*Presenter*) Nothing to Disclose

## PURPOSE

Primary chylous reflux disease of genitalia (PCRG) is a rare but devastating clinical condition manifested as genital chylolymphorrhea caused by the gravity-dependent reflux of abdominal chylous lymphatic fluid and consequent lymphatic dermal/mucosal backflow through megalymphatic vessels with incompetent valve. The purpose of this study is to evaluate the clinical efficacy and safety of lymphatic embolization as treatment of PCRG.

## METHODS AND MATERIALS

This is a retrospective study conducted from May 2016 to January 2022 at two advanced lymphatic centers (Seoul National University Hospital, Hospital of the University of Pennsylvania). Lymphoscintigraphy, dynamic contrast MR lymphangiography (DCMRL) and lipiodol lymphangiography were used to confirm the lymphatic backflow to inguinal, genital and medial thigh area. Diseased lymphatic vessels were selectively embolized using N-butyl cyanoacrylate (NBCA) glue to stop the lymphatic reflux.

## RESULTS

In total, 13 embolization procedures were performed. Three patients underwent additional treatments, two for residual symptoms and one for recurrent symptoms. The technical and clinical success rate were 100% (13/13) and 90% (9/10), respectively. Major complication occurred in one patient (1/10), in whom leg lymphedema worsened without improvement of genital lymphorrhea. 9 patients (out of 10) experienced immediate symptom improvement after initial embolization. 3 patients underwent additional embolization, 2 for residual and 1 for recurrent symptoms.

## CONCLUSION

s Overall, lymphatic embolization provided high clinical success rate with relatively low complication rate. We propose lymphatic embolization as a treatment option for PCRG that can significantly improve quality of life when performed with appropriate techniques in selected patients.

## CLINICAL RELEVANCE/APPLICATION

Same as conclusions.

## T2-SPIR-8 Simultaneous Portal Vein Embolization and Percutaneous Transhepatic Biliary Drainage Prior to Major

## Hepatectomy Is Feasible and Safe

Participants

Mohamed Soliman, MD, (*Presenter*) Nothing to Disclose

### PURPOSE

Demonstrate the feasibility and safety of simultaneous Percutaneous Transhepatic Biliary Drainage (PTBD) and Portal Vein Embolization (PVE) for pre-operative optimization prior to major hepatectomy for an obstructive hilar malignancy.

### METHODS AND MATERIALS

Following IRB approval, all patients with a resectable obstructive hilar malignancy who underwent both PVE and biliary drainage for pre-operative optimization were retrospectively identified. Type of initial drainage attempt (Endoscopic vs. PTBD), type, indication and number of subsequent drainage procedures, PVE-to-biliary drainage (BD) time interval, and drainage complications were recorded. Number of PVE procedures, embolic agent, degree of future liver remnant (FLR) hypertrophy, PVE-to-resection interval, and complications were recorded. Three groups were devised based on the PVE-BD interval in days (Group 1:  $t=0$ ,  $n=5$ ; Group 2:  $t=7$  to  $t=30$ ,  $n=12$ ; Group 3:  $t>30$ ,  $n=18$ ). All patients in group 1 underwent PTBD. Primary endpoint was the rate of Grade B/C Post-Hepatectomy Liver Failure (PHLF). Secondary outcomes included assessment of rates of surgical resection, complications, and comparison of initial biliary drainage techniques.

### RESULTS

A total of 35 patients (males  $n=25$ , females  $n=10$ , average age=64 years old) underwent both BD and PVE prior to major hepatectomy for either hilar cholangiocarcinoma ( $n=31$ ) or gallbladder carcinoma ( $n=4$ ). Rates of surgical resection were comparable among the three groups: Group 1: 4/5 [80%], Group 2: 6/12 [50%], Group 3: 8/18 [44%],  $p=0.87$ ). There was no statistical difference between the groups in incidence of grade B/C PHLF ( $p=0.56$ ). Initial biliary decompression was more commonly performed with an endoscopic stent (20/35, 57%) or PTBD 12/35, 34%). The former was associated with higher rates of post-procedural complications (11/20 [55%] vs. 4/12 [33%],  $p=0.03$ ). In addition, 13/20 (65%) patients who underwent initial endoscopic drainage required subsequent PTBD due to inadequate drainage of the FLR.

### CONCLUSION

Simultaneous BD and PVE for pre-operative optimization is safe and feasible. PTBD may be the optimal initial biliary drainage strategy.

### CLINICAL RELEVANCE/APPLICATION

Patients with a hilar mass suspicious for malignancy often undergo initial endoscopic biopsy with plastic stent placement for obstructive jaundice relief. Plastic stents often result in inadequate drainage of the FLR requiring subsequent endoscopic and percutaneous procedures to achieve optimal drainage. Additionally, patients who are surgical candidates require a major hepatectomy necessitating pre-surgical optimization with PVE to reduce the risk of PHLF. This paper examines the feasibility and safety of simultaneous PVE and PTBD on postoperative outcomes.

## T2-SPiR-9 Quantitative Evaluation and Spatial-visual Imaging of Liver Tissue Shrinkage Ex Vivo by Thermal Microwave Ablation Using Dynamic CT

Participants

Stefan Niehues, MD, Berlin, Germany (*Presenter*) Speaker, Bracco Group; Speaker, Guerbet SA; Speaker, Canon Medical Systems Corporation; Speaker, Teleflex Incorporated

### PURPOSE

Microwave ablation of liver tissue has gained importance in recent years. However, ablations may show tissue shrinkage immediately after ablation, which complicates the evaluation of ablation and can lead to an incorrect assessment of ablation success. Knowing about the typical shrinkage progression could allow for better assessment of ablation zone, but has not been systematically described yet. This study aimed to experimentally characterize and visualize the spatial distribution of liver tissue shrinkage during microwave ablation using computed tomography (CT) with 2D and 3D post-processing.

### METHODS AND MATERIALS

Eight injections of CT contrast agent were positioned in each of the six ex vivo bovine liver samples to form a three-dimensional reference grid around a microwave ablation antenna. Ablation was performed for 5 min at 100 W. CT scans of the liver sample were acquired every 30s during ablation and every 60s during subsequent cooling for an additional 10 min. 2D and 3D motion of the reference grid was tracked and used to calculate measures and spatial dimensions of enclosed tissue.

### RESULTS

Spatial distortion of the reference-grid indicated volume change of liver tissue resulting in a total volume reduction of 8.0% ( $p<0.001$ ) with a maximum extent located centrally. 6.6% of volume reduction appears during ablation ( $p<0.001$ ) with an additional 1.4% during the cooling phase. After 5 min no further tissue change could be measured. Two-dimensional radius reduction ranged from -18% to -2% with random distribution.

### CONCLUSION

In microwave ablation significant tissue shrinking of up to -8% can occur. Shrinkage predominantly occurs during the ablation phase but also shows a random distribution making it challenging to predict.

### CLINICAL RELEVANCE/APPLICATION

This study provides a better understanding of shrinkage after liver ablation, which is important for planning or evaluation. Because of its randomness, shrinkage cannot be systematically accounted for in post-ablation evaluation.

Printed on: 02/07/23

## Abstract Archives of the RSNA, 2022

T2-SPIR-1

### Safety and Effectiveness of Uterine Fibroid Embolization in Patients with Scarred Uterus

Tuesday, Nov. 29 9:00AM - 9:30AM Room: Learning Center - IR DPS

#### Participants

Saebiyol Ma, MD, (Presenter) Nothing to Disclose

#### PURPOSE

To evaluate the safety and effectiveness of uterine fibroid embolization (UFE) in patients with a scarred uterus caused by a previous myomectomy or cesarean section

#### METHODS AND MATERIALS

A total of 140 patients who underwent embolization for symptomatic fibroids were included in this retrospective study. The patients were divided into two groups, those with a history of myomectomy and/or cesarean section (scarred uterus group, n = 56), and those without surgical history involving the uterus (no-scar group, n = 84). Demographics, embolization details, outcomes, and complications were analyzed and compared between the two groups.

#### RESULTS

The overall clinical success rate was 89.28% in the scarred uterus group and 95.24% in the no-scar group. There was no statistical difference in infarction rate or change in fibroid volume in follow-up magnetic resonance imaging (MRI) between the groups. There was one major complication in the no-scar group, but there was no statistical difference in minor and major complications between the groups. The mean follow-up period was 25.9 months. The mean symptom-free time was 27.2 months in the scarred uterus group and 21.9 months in the no-scar group without a significant difference. There were no statistically significant differences in symptom changes, recurrence, and complication rates between the groups. Recurrence seen on imaging or regrowth was more common in the group with myomectomy history (36.8% vs. 15.9%, P = 0.052). However, there was no significant difference in symptom recurrence rates (15.8% vs. 12.5%, P = 0.713).

#### CONCLUSION

No statistically significant difference in technical and clinical outcomes was observed between the two groups. There was no significant increase in UFE complication rates in patients with a scarred uterus.

#### CLINICAL RELEVANCE/APPLICATION

UFE did not increase the risk of complications after myomectomy or cesarean section. Patients with a scarred uterus showed similar technical and clinical outcomes compared to the no-scar group in this study. Although caution should be taken, UFE can be a good option for symptomatic fibroid treatment in patients with a scarred uterus.

Printed on: 02/07/23



## Abstract Archives of the RSNA, 2022

T2-SPIR-2

### Cost Comparison of Prostatic Artery Embolization Between In-Hospital and Outpatient Lab Settings

Tuesday, Nov. 29 9:00AM - 9:30AM Room: Learning Center - IR DPS

#### Participants

Lucas Cusumano, MD, MPH, (*Presenter*) Nothing to Disclose

#### PURPOSE

To determine the costs associated with prostatic artery embolization (PAE) performed for treatment of benign prostatic hyperplasia (BPH) in hospital and outpatient-based lab (OBL) settings.

#### METHODS AND MATERIALS

Patients evaluated underwent outpatient PAE between January 2021 and December 2021, utilizing right common femoral artery access. Procedures were performed in similarly-equipped procedure suites located within a tertiary hospital or OBL. Costs were determined utilizing time-driven activity-based costing (TDABC), a micro-costing methodology for calculating procedural costs incurred by the institution. Process maps were created describing personnel, space, equipment, and materials. Time duration of each procedural step was recorded independently by a nurse caring for the patient at the time of the procedure and mean values were included in our model. Costs and capacity cost rates were determined using institutional and publicly available financial data.

#### RESULTS

37 PAE procedures met inclusion criteria with a mean patient age of 70.4 (+/- 6.7) years and mean prostate gland size of 129.7 (+/- 56.4) cc. 26 procedures were performed within the hospital setting and 11 procedures were performed within the OBL. Reduction in International Prostate Symptom Score (IPSS) was not significantly different following hospital and OBL procedures (57.2% vs. 81.8%, P=0.1850). Mean procedural time was not significantly different between the hospital and OBL settings (132.0 vs. 147.4 minutes, P=0.1574). However, duration between admission to discharge was significantly longer for procedures performed in a hospital setting (468.8 vs. 325.4 minutes, P<0.0001). Total costs for hospital-based procedures were marginally higher (\$3,858.28 vs. \$3,642.67). Personnel and material costs constitute the largest proportion costs of 54.7% and 41.6%, respectively.

#### CONCLUSION

s Total PAE cost was similar between the hospital and OBL settings. However, longer periprocedural times for hospital-based procedures and differences in reimbursement may favor performance of PAE in an OBL setting.

#### CLINICAL RELEVANCE/APPLICATION

PAE is a safe and effective treatment for BPH. However, there is a paucity of data regarding costs, especially comparing hospital and OBL settings. The ongoing shift towards value-based incentive models requires accurate assessment of cost drivers and cost inefficiencies.

Printed on: 02/07/23

## Abstract Archives of the RSNA, 2022

T2-SPIR-3

### SpaceOAR Hydrogel Distribution and Early Complications in Patients Undergoing Radiation Therapy for Prostate Cancer

Tuesday, Nov. 29 9:00AM - 9:30AM Room: Learning Center - IR DPS

#### Participants

Andrew Yates, MBBCh, BSc, Dublin 7, Ireland (*Presenter*) Nothing to Disclose

#### PURPOSE

Hydrogel spacers aim to separate the rectum from the prostate before radiation therapy for patients with prostate cancer to decrease the radiation dose to the rectum. The aim of this study was to evaluate the distribution of the hydrogel spacer between the rectum and the prostate, to assess for hydrogel rectal wall infiltration and to assess for immediate complications

#### METHODS AND MATERIALS

Retrospective study of 161 patients that underwent hydrogel spacer injection was performed. Symmetry and distribution of the hydrogel were assessed on planning MRI, as was the separation of the rectum and prostate. The MRI was reviewed for rectal wall injection or other malplacement of gel. Immediate post-procedure complications were recorded.

#### RESULTS

117 (72.7%) patients had a symmetrical distribution of the hydrogel spacer with 44 (27.3%) patients having some asymmetry of the spacer. The mean anteroposterior rectoprostatic separation was  $10.2 \pm 3.7$  mm with a range of 0 - 27 mm. Eight (5.0%) patients had some rectal wall infiltration on the MRI; 7 (4.3%) patients had minimal infiltration and one (0.6%) patient had moderate infiltration. One (0.6%) patient had intraprostatic injection of gel. Two (1.2%) patients required treatment in the emergency department after the procedure; one for urinary retention and one for pain.

#### CONCLUSION

Hydrogel injection effectively separates the prostate from the rectum with a symmetrical distribution in the majority of cases prior to radiation therapy with a low rate of rectal wall injection and immediate complications.

#### CLINICAL RELEVANCE/APPLICATION

This study informs clinicians regarding the technique, outcomes and complications related to hydrogel spacer injection prior to radiation therapy.

Printed on: 02/07/23

## Abstract Archives of the RSNA, 2022

T2-SPIR-5

### Embolization Treatment of Primary Chylous Reflux Disease of Genitalia (PCRG)

Tuesday, Nov. 29 9:00AM - 9:30AM Room: Learning Center - IR DPS

#### Participants

Hee Eun Moon, MD, (*Presenter*) Nothing to Disclose

#### PURPOSE

Primary chylous reflux disease of genitalia (PCRG) is a rare but devastating clinical condition manifested as genital chylolymphorrhea caused by the gravity-dependent reflux of abdominal chylous lymphatic fluid and consequent lymphatic dermal/mucosal backflow through megalymphatic vessels with incompetent valve. The purpose of this study is to evaluate the clinical efficacy and safety of lymphatic embolization as treatment of PCRG.

#### METHODS AND MATERIALS

This is a retrospective study conducted from May 2016 to January 2022 at two advanced lymphatic centers (Seoul National University Hospital, Hospital of the University of Pennsylvania). Lymphoscintigraphy, dynamic contrast MR lymphangiography (DCMRL) and lipiodol lymphangiography were used to confirm the lymphatic backflow to inguinal, genital and medial thigh area. Diseased lymphatic vessels were selectively embolized using N-butyl cyanoacrylate (NBCA) glue to stop the lymphatic reflux.

#### RESULTS

In total, 13 embolization procedures were performed. Three patients underwent additional treatments, two for residual symptoms and one for recurred symptoms. The technical and clinical success rate were 100% (13/13) and 90% (9/10), respectively. Major complication occurred in one patient (1/10), in whom leg lymphedema worsened without improvement of genital lymphorrhea. 9 patients (out of 10) experienced immediate symptom improvement after initial embolization. 3 patients underwent additional embolization, 2 for residual and 1 for recurred symptoms.

#### CONCLUSION

Overall, lymphatic embolization provided high clinical success rate with relatively low complication rate. We propose lymphatic embolization as a treatment option for PCRG that can significantly improve quality of life when performed with appropriate techniques in selected patients.

#### CLINICAL RELEVANCE/APPLICATION

Same as conclusions.

Printed on: 02/07/23

## Abstract Archives of the RSNA, 2022

T2-SPIR-8

### Simultaneous Portal Vein Embolization and Percutaneous Transhepatic Biliary Drainage Prior to Major Hepatectomy Is Feasible and Safe

Tuesday, Nov. 29 9:00AM - 9:30AM Room: Learning Center - IR DPS

#### Participants

Mohamed Soliman, MD, (Presenter) Nothing to Disclose

#### PURPOSE

Demonstrate the feasibility and safety of simultaneous Percutaneous Transhepatic Biliary Drainage (PTBD) and Portal Vein Embolization (PVE) for pre-operative optimization prior to major hepatectomy for an obstructive hilar malignancy.

#### METHODS AND MATERIALS

Following IRB approval, all patients with a resectable obstructive hilar malignancy who underwent both PVE and biliary drainage for pre-operative optimization were retrospectively identified. Type of initial drainage attempt (Endoscopic vs. PTBD), type, indication and number of subsequent drainage procedures, PVE-to-biliary drainage (BD) time interval, and drainage complications were recorded. Number of PVE procedures, embolic agent, degree of future liver remnant (FLR) hypertrophy, PVE-to-resection interval, and complications were recorded. Three groups were devised based on the PVE-BD interval in days (Group 1:  $t=0$ ,  $n=5$ ; Group 2:  $t=7$  to  $t=30$ ,  $n=12$ ; Group 3:  $t>30$ ,  $n=18$ ). All patients in group 1 underwent PTBD. Primary endpoint was the rate of Grade B/C Post-Hepatectomy Liver Failure (PHLF). Secondary outcomes included assessment of rates of surgical resection, complications, and comparison of initial biliary drainage techniques.

#### RESULTS

A total of 35 patients (males  $n=25$ , females  $n=10$ , average age=64 years old) underwent both BD and PVE prior to major hepatectomy for either hilar cholangiocarcinoma ( $n=31$ ) or gallbladder carcinoma ( $n=4$ ). Rates of surgical resection were comparable among the three groups: Group 1: 4/5 [80%], Group 2: 6/12 [50%], Group 3: 8/18 [44%],  $p=0.87$ ). There was no statistical difference between the groups in incidence of grade B/C PHLF ( $p=0.56$ ). Initial biliary decompression was more commonly performed with an endoscopic stent (20/35, 57%) or PTBD 12/35, 34%). The former was associated with higher rates of post-procedural complications (11/20 [55%] vs. 4/12 [33%],  $p=0.03$ ). In addition, 13/20 (65%) patients who underwent initial endoscopic drainage required subsequent PTBD due to inadequate drainage of the FLR.

#### CONCLUSION

Simultaneous BD and PVE for pre-operative optimization is safe and feasible. PTBD may be the optimal initial biliary drainage strategy.

#### CLINICAL RELEVANCE/APPLICATION

Patients with a hilar mass suspicious for malignancy often undergo initial endoscopic biopsy with plastic stent placement for obstructive jaundice relief. Plastic stents often result in inadequate drainage of the FLR requiring subsequent endoscopic and percutaneous procedures to achieve optimal drainage. Additionally, patients who are surgical candidates require a major hepatectomy necessitating pre-surgical optimization with PVE to reduce the risk of PHLF. This paper examines the feasibility and safety of simultaneous PVE and PTBD on postoperative outcomes.

Printed on: 02/07/23

## Abstract Archives of the RSNA, 2022

T2-SPIR-9

### Quantitative Evaluation and Spatial-visual Imaging of Liver Tissue Shrinkage Ex Vivo by Thermal Microwave Ablation Using Dynamic CT

Tuesday, Nov. 29 9:00AM - 9:30AM Room: Learning Center - IR DPS

#### Participants

Stefan Niehues, MD, Berlin, Germany (*Presenter*) Speaker, Bracco Group; Speaker, Guerbet SA; Speaker, Canon Medical Systems Corporation; Speaker, Teleflex Incorporated

#### PURPOSE

Microwave ablation of liver tissue has gained importance in recent years. However, ablations may show tissue shrinkage immediately after ablation, which complicates the evaluation of ablation and can lead to an incorrect assessment of ablation success. Knowing about the typical shrinkage progression could allow for better assessment of ablation zone, but has not been systematically described yet. This study aimed to experimentally characterize and visualize the spatial distribution of liver tissue shrinkage during microwave ablation using computed tomography (CT) with 2D and 3D post-processing.

#### METHODS AND MATERIALS

Eight injections of CT contrast agent were positioned in each of the six ex vivo bovine liver samples to form a three-dimensional reference grid around a microwave ablation antenna. Ablation was performed for 5 min at 100 W. CT scans of the liver sample were acquired every 30s during ablation and every 60s during subsequent cooling for an additional 10 min. 2D and 3D motion of the reference grid was tracked and used to calculate measures and spatial dimensions of enclosed tissue.

#### RESULTS

Spatial distortion of the reference-grid indicated volume change of liver tissue resulting in a total volume reduction of 8.0% ( $p < 0.001$ ) with a maximum extent located centrally. 6.6% of volume reduction appears during ablation ( $p < 0.001$ ) with an additional 1.4% during the cooling phase. After 5 min no further tissue change could be measured. Two-dimensional radius reduction ranged from -18% to -2% with random distribution.

#### CONCLUSION

In microwave ablation significant tissue shrinking of up to -8% can occur. Shrinkage predominantly occurs during the ablation phase but also shows a random distribution making it challenging to predict.

#### CLINICAL RELEVANCE/APPLICATION

This study provides a better understanding of shrinkage after liver ablation, which is important for planning or evaluation. Because of its randomness, shrinkage cannot be systematically accounted for in post-ablation evaluation.

Printed on: 02/07/23

## Abstract Archives of the RSNA, 2022

T2-SPMK

### Musculoskeletal Tuesday Poster Discussions

Tuesday, Nov. 29 9:00AM - 9:30AM Room: Learning Center - MK DPS

#### Participants

Derik L. Davis, MD, Baltimore, MD (*Moderator*) Nothing to Disclose  
Derik L. Davis, MD, Baltimore, MD (*Moderator*) Nothing to Disclose  
Mohamed Jarraya, MD, Boston, MA (*Moderator*) Nothing to Disclose  
Mohamed Jarraya, MD, Boston, MA (*Moderator*) Nothing to Disclose

#### Sub-Events

### T2-SPMK-1 Clinical Evaluation of 3D Elbow Joint MRI with Deep Learning-based Reconstruction: Diagnostic Performance of Tendon and Ligament Injury

#### Participants

Young Hwa Suh, MD, Busan, Korea, Republic Of (*Presenter*) Nothing to Disclose

#### PURPOSE

To assess the diagnostic performance of 3D elbow joint MRI with deep learning-based reconstruction (DLR) compared with 2D 1mm slice thickness MRI (1mm MRI) and 3D MRI with conventional reconstruction (CR) to evaluate tendon and ligament injury of elbow joint.

#### METHODS AND MATERIALS

This retrospective study included 22 patients with 23 elbows (12 men, 8 women; mean age,  $53.6 \pm 8.9$  [SD] years) between October 2021 and February 2022. They underwent 3T elbow MRI with the protocol including T2-weighted fat saturated (T2FS) coronal 1mm MRI with DLR, and 3D proton-density weighted fat saturated (PDFS) coronal MRI with CR and DLR. One musculoskeletal radiologist with 9-year experience assessed three sequences for subjective image quality and artifacts and identified pathologies of the proximal common extensor tendon (CET) and common flexor tendon (CFT), radial collateral ligament (RCL), lateral ulnar collateral ligament (LUCL), and ulnar collateral ligament (UCL). In 10 patients who underwent operation, diagnostic performance was calculated using surgical records as a reference standard.

#### RESULTS

Mean subjective image quality scores of 2D T2FS 1mm MRI, 3D PDFS MRI with CR and DLR were  $2.9 \pm 0.4$ ,  $2.1 \pm 0.6$ , and  $2.9 \pm 0.3$ , respectively. There were significant differences between 2D T2FS 1mm MRI and 3D PDFS MRI with CR, between 3D PDFS MRI with CR and DLR. Mean artifact scores were  $3.3 \pm 0.6$ ,  $3.9 \pm 0.3$ , and  $3.9 \pm 0.3$ , respectively. There were significant differences between 2D T2FS 1mm MRI and 3D PDFS MRI with CR, between 2D T2FS 1mm MRI with 3D PDFS MRI with DLR. For three sequences, the diagnostic performance using area under the receiver operating characteristic curve of 2D T2FS 1mm MRI, 3D PDFS MRI with CR and DLR were 0.841, 0.773, and 0.818, respectively. The diagnostic performance of 3D PDFS coronal MRI with adding axial reformation, 3D PDFS coronal MRI with adding axial and sagittal reformation were both 0.886.

#### CONCLUSION

By multiplanar reformation, 3D elbow joint MRI with deep learning-based reconstruction showed comparable diagnostic performance than 2D 1mm MRI for the evaluation of tendon and ligament injuries of elbow joint with similar subjective image qualities and artifacts.

#### CLINICAL RELEVANCE/APPLICATION

3D elbow joint MRI with deep learning-based reconstruction can help detect tendon and ligament pathologies of small joints by multiplanar reformation.

### T2-SPMK-2 Operative Management of Advanced Wrist Arthritis: The Current Role of Preoperative Imaging and Intraoperative Inspection

#### Participants

Shelby Payne, MD, Stanford, CA (*Presenter*) Nothing to Disclose

#### PURPOSE

Our objectives are to (1) analyze the influence of preoperative imaging (radiography, CT, MRI) on surgical decision-making for wrist arthrodesis and carpectomy procedures, (2) assess the frequency of intraoperative inspection to determine arthritis distribution, and (3) determine the most common surgical procedures for end-stage wrist arthritis.

#### METHODS AND MATERIALS

A systematic search of peer-reviewed literature on the role of preoperative imaging and intraoperative inspection in the selection of carpal bone fusion and carpectomy procedures was performed in three databases (Pubmed, Embase, Scopus) using established

criteria (PRISMA Extension for Scoping Reviews). Included studies reported at least 3 adult patients with advanced wrist arthritis and were published within the past 11 years (1/1/2011-4/6/2022). Procedures at the trapezometacarpal and distal radioulnar joints were excluded.

## RESULTS

From a total of 307 publications, eligibility criteria were satisfied by 48 articles. A total of 1,823 patients (1,886 wrists) received surgical intervention (age mean 51 [SD 10] yrs; 63% men, 37% women). Of 13 different arthrodesis and carpectomy procedures reported, the four most common were: four-corner fusion with scaphoid excision (845/1886, 45%), total wrist arthrodesis (457/1886, 24%), proximal row carpectomy (256/1886, 14%), and scaphocapitate fusion (79/1886, 4%). All articles reported preoperative radiography, but only a small number of articles reported preoperative CT (3/48, 6%) or MRI (2/48, 4%). Only 16 articles (33%) reported intraoperative inspection of the cartilage.

## CONCLUSION

All articles reported that the selection of a surgical procedure was influenced by the radiographic distribution of advanced arthritis in the carpus. Preoperative advanced imaging and intraoperative evaluation was not commonly performed, despite the current widespread availability of CT/MRI and wrist arthroscopy. Of 13 different surgical procedures, the most commonly reported was a 4-corner fusion with scaphoidectomy. Future research should address the unresolved controversy regarding any added value of CT, MRI, and diagnostic arthroscopy for optimizing surgical decision making.

## CLINICAL RELEVANCE/APPLICATION

Despite the widespread use of CT, MRI, and diagnostic arthroscopy, radiography is generally the only technique used to assess the distribution of advanced arthritis prior to wrist surgery.

### T2-SPMK-3 Chronic Pain After Arthroplasty: Major Contributions of Magnetic Resonance Imaging with Metal Artifact Reduction Sequences.

Participants

Ronald M. Trindade, MD, (*Presenter*) Nothing to Disclose

## PURPOSE

To determine the association between resorption at interfaces, using MAVRIC-SL (multiacquisition with variable resonance image combination-selective) sequences in Magnetic Resonance (MR), and the clinical severity of patients undergoing Total Knee Arthroplasties (TKA) and Total Hip Arthroplasties (THA); to describe areas affected by bone resorption in each component of the prostheses; to determine intra and interobserver agreement in the diagnosis of partial loosening of the prosthetic components and to compare fibrous membrane and osteolysis in this context.

## METHODS AND MATERIALS

A cross-sectional study was carried out between March 2019 and August 2020, with 47 patients (49 arthroplasties). Postoperative follow-up of knee or hip arthroplasties, with chronic pain 03 months after surgery, who answered the WOMAC questionnaire. The interfaces of the components of arthroplasties were defined as: osseointegration, partial loosening (fibrous membrane-type reabsorption or osteolysis) or non-diagnostic.

## RESULTS

When the loosening criterion is based only on the presence of osteolysis, there is a significant difference in the WOMAC means ( $p=0.010$ ). When the loosening criteria include osteolysis and fibrous membrane, there are no differences between groups, except in the stiffness subdomain ( $p=0,026$ ). The images obtained by MAVRIC-SL showed slight correlation between the number of osteolytic zones and clinical severity in most analysis. In the hip, there was a predominance of resorption (osteolysis) in the proximal femoral region (Gruen zones 1, 7, 8, 13 and 14), corresponding to 53.2% of the total. In the knee, the zones most affected by resorption (fibrous membrane) were those related to the tibial plateaus and its stem (zones 1, 2, 3, 4 e 5), corresponding to 64.3% of the total. There was substantial inter-reader reliability for most components (THA: acetabulum with  $k=0.72$  and femur with  $k=0,77$ ; TKA: tibia with  $k=0,72$ ). The intraobserver analysis showed moderate and substantial agreement for most components (THA: acetabulum with  $k=0.57$  and femur with  $k=0,64$ ; TKA: femur with  $k=0,76$  and tibia with  $k=0.62$ ).

## CONCLUSION

MR with MAVRIC-SL sequences demonstrated that in this sample, consisting of metal-on-metal type prosthesis, the characterization of periprosthetic osteolysis, may play an important role in clinical complaints and loss of joint function, with substantial interobserver and inter-rater reliability. In THA, partial loosening occurs mainly in the proximal part of the femoral component, while in TKA it occurs mainly in the plateau and stem region of the tibial component.

## CLINICAL RELEVANCE/APPLICATION

MRI with metal artifact reduction sequences as an additional tool for chronic pain evaluation in patients after arthroplasties.

### T2-SPMK-4 Identification of Bone Marrow Edema in Spondylodiscitis of The Dorso-lumbar Spine: Diagnostic Accuracy of Dual-energy CT Versus MRI

Participants

Giovanni Foti, MD, Negrar, Italy (*Presenter*) Nothing to Disclose

## PURPOSE

To evaluate the diagnostic accuracy values of dual-energy Computed Tomography (DECT) in identifying bone marrow edema (BME) in spondylodiscitis of the dorso-lumbar spine.

## METHODS AND MATERIALS

This prospective institutional review board-approved study included 40 consecutive patients (24 males and 16 females; mean age of 66.4, range 22-79 years) studied between January 2020 and January 2022. All patients underwent DECT (80 kV and tin filter 150 kV) and MRI within 7 days. DECT data were post-processed on a dedicated offline workstation (SyngoVia® VB20) by using a three-material decomposition algorithm for generating non-calcium images. Two radiologists (16 and 8 years of experience, respectively),

blinded to clinical data, evaluated the presence of BME on dedicated color-coded maps, endplate erosions and peri-vertebral inflammation. Diagnostic accuracy values of DECT were calculated by using MRI images as standard of reference. DECT numbers were assessed by using a region of interest (quantitative assessment). Receiver operator curves (ROC) and relative area under the curve (AUC) were calculated. Inter-observer and intra-observer agreement were calculated with k-statistics. Continuous and categorical variables were evaluated by using t test and  $\chi^2$  or Fisher exact test, as appropriate. A value of  $p < 0.05$  was considered statistically significant.

## **RESULTS**

MRI revealed the presence of spondylodiscitis in 32/40 patients (80.0%), located at the level of dorsal (n=15) and lumbar spine (n=25), respectively. The sensitivity, specificity, and AUC of DECT were 87.5% (28/32), 75.0% (6/8) with an AUC of 0.886 (95% CI: 0.771-0.915) for R1, and 75% (24/32) and 100% (8/8) with an AUC of 0.862 (95% CI: 0.748-0.909) for R2. DECT numbers were significantly different between positive (mean  $-11.4 \pm 22.5$  HU) and negative cases (mean  $-77.3 \pm 32.3$  HU) with a p value  $< 0.001$ . The interobserver and intraobserver agreements were near perfect ( $k=0.87$  and  $k=0.89$ , respectively).

## **CONCLUSION**

s DECT is an accurate imaging tool for the diagnosis of spondylodiscitis.

## **CLINICAL RELEVANCE/APPLICATION**

DECT represents a fast and accurate imaging tool for demonstration of BME, erosions and peri-vertebral inflammation in dorso-lumbar spondylodiscitis, virtually free from motion artifacts and with the additional advantage to yield high resolution bone window images.

Printed on: 02/07/23

## Abstract Archives of the RSNA, 2022

T2-SPMK-1

### Clinical Evaluation of 3D Elbow Joint MRI with Deep Learning-based Reconstruction: Diagnostic Performance of Tendon and Ligament Injury

Tuesday, Nov. 29 9:00AM - 9:30AM Room: Learning Center - MK DPS

#### Participants

Young Hwa Suh, MD, Busan, Korea, Republic Of (*Presenter*) Nothing to Disclose

#### PURPOSE

To assess the diagnostic performance of 3D elbow joint MRI with deep learning-based reconstruction (DLR) compared with 2D 1mm slice thickness MRI (1mm MRI) and 3D MRI with conventional reconstruction (CR) to evaluate tendon and ligament injury of elbow joint.

#### METHODS AND MATERIALS

This retrospective study included 22 patients with 23 elbows (12 men, 8 women; mean age,  $53.6 \pm 8.9$  [SD] years) between October 2021 and February 2022. They underwent 3T elbow MRI with the protocol including T2-weighted fat saturated (T2FS) coronal 1mm MRI with DLR, and 3D proton-density weighted fat saturated (PDFS) coronal MRI with CR and DLR. One musculoskeletal radiologist with 9-year experience assessed three sequences for subjective image quality and artifacts and identified pathologies of the proximal common extensor tendon (CET) and common flexor tendon (CFT), radial collateral ligament (RCL), lateral ulnar collateral ligament (LUCL), and ulnar collateral ligament (UCL). In 10 patients who underwent operation, diagnostic performance was calculated using surgical records as a reference standard.

#### RESULTS

Mean subjective image quality scores of 2D T2FS 1mm MRI, 3D PDFS MRI with CR and DLR were  $2.9 \pm 0.4$ ,  $2.1 \pm 0.6$ , and  $2.9 \pm 0.3$ , respectively. There were significant differences between 2D T2FS 1mm MRI and 3D PDFS MRI with CR, between 3D PDFS MRI with CR and DLR. Mean artifact scores were  $3.3 \pm 0.6$ ,  $3.9 \pm 0.3$ , and  $3.9 \pm 0.3$ , respectively. There were significant differences between 2D T2FS 1mm MRI and 3D PDFS MRI with CR, between 2D T2FS 1mm MRI with 3D PDFS MRI with DLR. For three sequences, the diagnostic performance using area under the receiver operating characteristic curve of 2D T2FS 1mm MRI, 3D PDFS MRI with CR and DLR were 0.841, 0.773, and 0.818, respectively. The diagnostic performance of 3D PDFS coronal MRI with adding axial reformation, 3D PDFS coronal MRI with adding axial and sagittal reformation were both 0.886.

#### CONCLUSION

By multiplanar reformation, 3D elbow joint MRI with deep learning-based reconstruction showed comparable diagnostic performance than 2D 1mm MRI for the evaluation of tendon and ligament injuries of elbow joint with similar subjective image qualities and artifacts.

#### CLINICAL RELEVANCE/APPLICATION

3D elbow joint MRI with deep learning-based reconstruction can help detect tendon and ligament pathologies of small joints by multiplanar reformation.

Printed on: 02/07/23



## Abstract Archives of the RSNA, 2022

T2-SPMK-2

### Operative Management of Advanced Wrist Arthritis: The Current Role of Preoperative Imaging and Intraoperative Inspection

Tuesday, Nov. 29 9:00AM - 9:30AM Room: Learning Center - MK DPS

#### Participants

Shelby Payne, MD, Stanford, CA (*Presenter*) Nothing to Disclose

#### PURPOSE

Our objectives are to (1) analyze the influence of preoperative imaging (radiography, CT, MRI) on surgical decision-making for wrist arthrodesis and carpectomy procedures, (2) assess the frequency of intraoperative inspection to determine arthritis distribution, and (3) determine the most common surgical procedures for end-stage wrist arthritis.

#### METHODS AND MATERIALS

A systematic search of peer-reviewed literature on the role of preoperative imaging and intraoperative inspection in the selection of carpal bone fusion and carpectomy procedures was performed in three databases (Pubmed, Embase, Scopus) using established criteria (PRISMA Extension for Scoping Reviews). Included studies reported at least 3 adult patients with advanced wrist arthritis and were published within the past 11 years (1/1/2011-4/6/2022). Procedures at the trapeziometacarpal and distal radioulnar joints were excluded.

#### RESULTS

From a total of 307 publications, eligibility criteria were satisfied by 48 articles. A total of 1,823 patients (1,886 wrists) received surgical intervention (age mean 51 [SD 10] yrs; 63% men, 37% women). Of 13 different arthrodesis and carpectomy procedures reported, the four most common were: four-corner fusion with scaphoid excision (845/1886, 45%), total wrist arthrodesis (457/1886, 24%), proximal row carpectomy (256/1886, 14%), and scaphocapitate fusion (79/1886, 4%). All articles reported preoperative radiography, but only a small number of articles reported preoperative CT (3/48, 6%) or MRI (2/48, 4%). Only 16 articles (33%) reported intraoperative inspection of the cartilage.

#### CONCLUSION

s All articles reported that the selection of a surgical procedure was influenced by the radiographic distribution of advanced arthritis in the carpus. Preoperative advanced imaging and intraoperative evaluation was not commonly performed, despite the current widespread availability of CT/MRI and wrist arthroscopy. Of 13 different surgical procedures, the most commonly reported was a 4-corner fusion with scaphoidectomy. Future research should address the unresolved controversy regarding any added value of CT, MRI, and diagnostic arthroscopy for optimizing surgical decision making.

#### CLINICAL RELEVANCE/APPLICATION

Despite the widespread use of CT, MRI, and diagnostic arthroscopy, radiography is generally the only technique used to assess the distribution of advanced arthritis prior to wrist surgery.

Printed on: 02/07/23

## Abstract Archives of the RSNA, 2022

T2-SPMK-3

### Chronic Pain After Arthroplasty: Major Contributions of Magnetic Resonance Imaging with Metal Artifact Reduction Sequences.

Tuesday, Nov. 29 9:00AM - 9:30AM Room: Learning Center - MK DPS

#### Participants

Ronald M. Trindade, MD, (*Presenter*) Nothing to Disclose

#### PURPOSE

To determine the association between resorption at interfaces, using MAVRIC-SL (multiacquisition with variable resonance image combination-selective) sequences in Magnetic Resonance (MR), and the clinical severity of patients undergoing Total Knee Arthroplasties (TKA) and Total Hip Arthroplasties (THA); to describe areas affected by bone resorption in each component of the prostheses; to determine intra and interobserver agreement in the diagnosis of partial loosening of the prosthetic components and to compare fibrous membrane and osteolysis in this context.

#### METHODS AND MATERIALS

A cross-sectional study was carried out between March 2019 and August 2020, with 47 patients (49 arthroplasties). Postoperative follow-up of knee or hip arthroplasties, with chronic pain 03 months after surgery, who answered the WOMAC questionnaire. The interfaces of the components of arthroplasties were defined as: osseointegration, partial loosening (fibrous membrane-type reabsorption or osteolysis) or non-diagnostic.

#### RESULTS

When the loosening criterion is based only on the presence of osteolysis, there is a significant difference in the WOMAC means ( $p=0.010$ ). When the loosening criteria include osteolysis and fibrous membrane, there are no differences between groups, except in the stiffness subdomain ( $p=0,026$ ). The images obtained by MAVRIC-SL showed slight correlation between the number of osteolytic zones and clinical severity in most analysis. In the hip, there was a predominance of resorption (osteolysis) in the proximal femoral region (Gruen zones 1, 7, 8, 13 and 14), corresponding to 53.2% of the total. In the knee, the zones most affected by resorption (fibrous membrane) were those related to the tibial plateaus and its stem (zones 1, 2, 3, 4 e 5), corresponding to 64.3% of the total. There was substantial inter-reader reliability for most components (THA: acetabulum with  $k=0.72$  and femur with  $k=0,77$ ; TKA: tibia with  $k=0,72$ ). The intraobserver analysis showed moderate and substantial agreement for most components (THA: acetabulum with  $k=0.57$  and femur with  $k=0,64$ ; TKA: femur with  $k=0,76$  and tibia with  $k=0.62$ ).

#### CONCLUSION

s MR with MAVRIC-SL sequences demonstrated that in this sample, consisting of metal-on-metal type prosthesis, the characterization of periprosthetic osteolysis, may play an important role in clinical complaints and loss of joint function, with substantial interobserver and inter-rater reliability. In THA, partial loosening occurs mainly in the proximal part of the femoral component, while in TKA it occurs mainly in the plateau and stem region of the tibial component.

#### CLINICAL RELEVANCE/APPLICATION

MRI with metal artifact reduction sequences as an additional tool for chronic pain evaluation in patients after arthroplasties.

Printed on: 02/07/23

## Abstract Archives of the RSNA, 2022

T2-SPMK-4

### Identification of Bone Marrow Edema in Spondylodiscitis of The Dorso-lumbar Spine: Diagnostic Accuracy of Dual-energy CT Versus MRI

Tuesday, Nov. 29 9:00AM - 9:30AM Room: Learning Center - MK DPS

#### Participants

Giovanni Foti, MD, Negrar, Italy (*Presenter*) Nothing to Disclose

#### PURPOSE

To evaluate the diagnostic accuracy values of dual-energy Computed Tomography (DECT) in identifying bone marrow edema (BME) in spondylodiscitis of the dorso-lumbar spine.

#### METHODS AND MATERIALS

This prospective institutional review board-approved study included 40 consecutive patients (24 males and 16 females; mean age of 66.4, range 22-79 years) studied between January 2020 and January 2022. All patients underwent DECT (80 kV and tin filter 150 kV) and MRI within 7 days. DECT data were post-processed on a dedicated offline workstation (SyngoVia® VB20) by using a three-material decomposition algorithm for generating non-calcium images. Two radiologists (16 and 8 years of experience, respectively), blinded to clinical data, evaluated the presence of BME on dedicated color-coded maps, endplate erosions and peri-vertebral inflammation. Diagnostic accuracy values of DECT were calculated by using MRI images as standard of reference. DECT numbers were assessed by using a region of interest (quantitative assessment). Receiver operator curves (ROC) and relative area under the curve (AUC) were calculated. Inter-observer and intra-observer agreement were calculated with k-statistics. Continuous and categorical variables were evaluated by using t test and  $\chi^2$  or Fisher exact test, as appropriate. A value of  $p < 0.05$  was considered statistically significant.

#### RESULTS

MRI revealed the presence of spondylodiscitis in 32/40 patients (80.0%), located at the level of dorsal (n=15) and lumbar spine (n=25), respectively. The sensitivity, specificity, and AUC of DECT were 87.5% (28/32), 75.0 % (6/8) with an AUC of 0.886 (95% CI: 0.771-0.915) for R1, and 75% (24/32) and 100% (8/8) with an AUC of 0.862 (95% CI: 0.748-0.909) for R2. DECT numbers were significantly different between positive (mean  $-11.4 \pm 22.5$  HU) and negative cases (mean  $-77.3 \pm 32.3$  HU) with a p value  $< 0.001$ . The interobserver and intraobserver agreements were near perfect ( $k=0.87$  and  $k=0.89$ , respectively).

#### CONCLUSION

s DECT is an accurate imaging tool for the diagnosis of spondylodiscitis.

#### CLINICAL RELEVANCE/APPLICATION

DECT represents a fast and accurate imaging tool for demonstration of BME, erosions and peri-vertebral inflammation in dorso-lumbar spondylodiscitis, virtually free from motion artifacts and with the additional advantage to yield high resolution bone window images.

Printed on: 02/07/23

## Abstract Archives of the RSNA, 2022

T2-SPNMMI

### Nuclear Medicine/Molecular Imaging Tuesday Poster Discussion

Tuesday, Nov. 29 9:00AM - 9:30AM Room: Learning Center - NMMI DPS

#### Participants

Georges El Fakhri, PhD, Boston, MA (*Moderator*) Nothing to Disclose

#### Sub-Events

### T2-SPNMMI- Bone Scan versus F-18 Fluciclovine PET/CT at Different PSA Levels: A Single-center Comparison 1 Study

#### Participants

Hatice Savas, MD, Chicago, IL (*Presenter*) Nothing to Disclose

#### PURPOSE

To compare the diagnostic performance of bone scintigraphy (BS) and F-18 Fluciclovine PET/CT in detecting bone metastasis in prostate cancer patients at different PSA levels.

#### METHODS AND MATERIALS

This IRB-approved retrospective study included 267 prostate cancer subjects. We evaluated the detection of bone metastasis using both F-18 Fluciclovine PET/CT and BS. Each scan was performed within less than a three-month period. Subjects with other known malignancies were excluded from this study. Concordance among imaging modalities detecting bone metastasis was assessed at five PSA levels: = 0.5, 0.5-2, 2-5, 5-10, and >10. In addition, positive cases were confirmed with six months follow-up assessments or bone biopsies.

#### RESULTS

Concordance between both scans was observed in 70% of all cases (203/267). 164 from 203 patients had both scans negative, whereas the remaining 39 from 203 patients had both scans positive. Within the discordant group, 26 of 64 patients were positive on F-18 Fluciclovine PET/CT and negative on BS. On the contrary, 38 from 64 scans were positive on BS and negative on F-18 Fluciclovine. The BS had an overall sensitivity of 66.1%, specificity of 81.7%, PPV of 50.6%, and NPV of 89.4%. F-18 Fluciclovine PET/CT had a sensitivity of 93.2%, specificity of 95.1%, PPV of 84.6%, and NPV of 98%.

#### CONCLUSION

Our data shows that F-18 Fluciclovine is diagnostically superior to BS in detecting bone metastasis. We found a higher concordance rate between both imaging modalities at lower PSA values.

#### CLINICAL RELEVANCE/APPLICATION

The literature is scarce when it comes to studies comparing the diagnostic performance of Fluciclovine PET/CT and bone scan evaluating metastatic prostate cancer. The largest available study only assessed 106 patients. They did not report the concordance between scans at various PSA levels or even the correlation with other sites of recurrence.

### T2-SPNMMI- The Impact of PSMA PET on the Treatment and Outcomes of Men with Biochemical Recurrence of 2 Prostate Cancer: a Systematic Review and Meta-Analysis

#### Participants

Alex Pozdnyakov, MD, Hamilton, ON (*Presenter*) Nothing to Disclose

#### PURPOSE

Prostate-specific membrane antigen (PSMA) PET is highly sensitive in identifying disease recurrence in men with biochemical recurrence of prostate cancer (BCR) after primary therapy and is rapidly being adopted in clinical practice. The purpose of this systematic review and meta-analysis was to assess the documented impact of PSMA-PET on patient management and outcomes, including prostate-specific antigen (PSA) response, and intermediate and long-term outcome measures.

#### METHODS AND MATERIALS

MBASE, PubMed, Web of Science, Cochrane and OVID databases were searched for studies reporting on the impact of PSMA-PET on the management and outcomes of patients with BCR after definitive primary therapy. Outcome measures assessed included biochemical response to therapy after PET and BCR-free survival (BRFS). The proportions of patients in whom management changed, and the proportion of patients in whom each outcome measure was obtained were tabulated and pooled into meta-analysis using DerSimonian-Laird method.

#### RESULTS

A total of 34 studies with 3680 men reported change in management after PSMA-PET and 27 studies with 2639 men reported on at

least one outcome measure and had follow-up data. PSMA-PET was positive in 2508/3680 (68.2%). The pooled proportion of change in management after PSMA-PET was 56.4% (95% CI, 48.0-63.9%). A decrease in serum PSA was documented in 72.4% of men (95% CI, 63.4-81.5%), and complete biochemical response in 23.3% (95% CI, 14.6-32.0%) at a median follow-up of 8.1 and 11 months, respectively. The pooled BRFS rate was 60.2% (95% CI, 49.1-71.4%) at a median follow-up of 20 months.

## CONCLUSION

In conclusion, PSMA PET is positive in more than 2/3 of men with BCR and impacts patient management in more than half of the men. BRFS after PET-directed management is 60% at a median of 20 months after salvage therapy, and complete biochemical response may be achieved in up to a quarter of men.

## CLINICAL RELEVANCE/APPLICATION

The findings of this meta-analysis further confirm the crucial role of PSMA PET in biochemical recurrence of prostate cancer and highlight the clinical implications of this molecular imaging technique.

## T2-SPNMMI- A Pilot Study of 68Ga-PSMA11 and 68Ga-RM2 PET/MRI for Biopsy Guidance in Patients with Suspected Prostate Cancer

Participants

Heying Duan, MD, (Presenter) Nothing to Disclose

## PURPOSE

Targeting of lesions seen on multiparametric MRI (mpMRI) improves prostate cancer (PC) detection at biopsy. However, 20-65% of highly suspicious lesions on mpMRI (PI-RADS 4 or 5) are false positives (FP), while 5-10% of clinically significant PC (csPC) are missed. Prostate specific membrane antigen (PSMA) and gastrin-releasing peptide receptors (GRPR) are both overexpressed in PC. We therefore aimed to evaluate the potential utility of 68Ga-PSMA11 and 68Ga-RM2 PET/MRI for biopsy guidance in patients with suspected PC.

## METHODS AND MATERIALS

Thirteen men, aged 58.00±7.13 years, with suspected PC were prospectively enrolled to undergo 68Ga-PSMA11 and 68Ga-RM2 PET/MRI. PET/MRI included whole-body and dedicated delayed pelvic imaging. All patients had standard 12-core biopsy, and additional targeted biopsy of any lesions seen on PET. Maximum and peak standardized uptake values (SUV<sub>max</sub> and SUV<sub>peak</sub>) of suspected PC lesions were collected and compared to gold standard biopsy.

## RESULTS

PSA and PSA density at enrollment were 9.80±5.97 (range 1.50-25.46) ng/mL and 0.20±0.18 (range 0.06-0.68) ng/mL<sup>2</sup>, respectively. Biopsy revealed a total of 14 PC in 8 participants: 6 were csPC and 8 were non-clinically significant PC (ncsPC). 68Ga-PSMA11 identified 25 lesions, of which 11 (44%) were true positive (TP) (5 csPC). 68Ga-RM2 showed 27 lesions, of which 14 (52%) were TP, identifying all 6 csPC and 8 ncsPC. There were 17 concordant lesions in 11 patients vs. 14 discordant lesions in 7 patients between PSMA and RM2. Incongruent lesions had the highest rate of FP (12 FP vs. 2 TP). PET/MRI guided biopsy led to the additional finding of 8 cancers of which 5 were csPC. Median SUV<sub>max</sub> was significantly higher for TP than FP lesions in delayed pelvic imaging for 68Ga-PSMA11 (6.49±4.14 vs. 4.05±1.55, P=0.023) but not for whole body images, nor for 68Ga-RM2. Sensitivity and specificity were 83% and 67% for 68Ga-RM2 63% and 86% for 68Ga-PSMA11, and 30% and 95% for mpMRI, respectively.

## CONCLUSION

Our results show that both 68Ga-PSMA11 and 68Ga-RM2 PET/MRI are feasible for biopsy guidance in suspected PC. Both radiopharmaceuticals detected additional clinically significant cancers not seen on mpMRI, 68Ga-RM2 PET/MRI identified all csPC confirmed at biopsy.

## CLINICAL RELEVANCE/APPLICATION

68Ga-PSMA11 and 68Ga-RM2 guided prostate biopsy help detecting csPC and might therefore avoid unnecessary biopsies and associated risks.

Printed on: 02/07/23

## Abstract Archives of the RSNA, 2022

T2-SPNMMI-1

### Bone Scan versus F-18 Fluciclovine PET/CT at Different PSA Levels: A Single-center Comparison Study

Tuesday, Nov. 29 9:00AM - 9:30AM Room: Learning Center - NMMI DPS

#### Participants

Hatice Savas, MD, Chicago, IL (*Presenter*) Nothing to Disclose

#### PURPOSE

To compare the diagnostic performance of bone scintigraphy (BS) and F-18 Fluciclovine PET/CT in detecting bone metastasis in prostate cancer patients at different PSA levels.

#### METHODS AND MATERIALS

This IRB-approved retrospective study included 267 prostate cancer subjects. We evaluated the detection of bone metastasis using both F-18 Fluciclovine PET/CT and BS. Each scan was performed within less than a three-month period. Subjects with other known malignancies were excluded from this study. Concordance among imaging modalities detecting bone metastasis was assessed at five PSA levels: = 0.5, 0.5-2, 2-5, 5-10, and >10. In addition, positive cases were confirmed with six months follow-up assessments or bone biopsies.

#### RESULTS

Concordance between both scans was observed in 70% of all cases (203/267). 164 from 203 patients had both scans negative, whereas the remaining 39 from 203 patients had both scans positive. Within the discordant group, 26 of 64 patients were positive on F-18 Fluciclovine PET/CT and negative on BS. On the contrary, 38 from 64 scans were positive on BS and negative on F-18 Fluciclovine. The BS had an overall sensitivity of 66.1%, specificity of 81.7%, PPV of 50.6%, and NPV of 89.4%. F-18 Fluciclovine PET/CT had a sensitivity of 93.2%, specificity of 95.1%, PPV of 84.6%, and NPV of 98%.

#### CONCLUSION

Our data shows that F-18 Fluciclovine is diagnostically superior to BS in detecting bone metastasis. We found a higher concordance rate between both imaging modalities at lower PSA values.

#### CLINICAL RELEVANCE/APPLICATION

The literature is scarce when it comes to studies comparing the diagnostic performance of Fluciclovine PET/CT and bone scan evaluating metastatic prostate cancer. The largest available study only assessed 106 patients. They did not report the concordance between scans at various PSA levels or even the correlation with other sites of recurrence.

Printed on: 02/07/23



## Abstract Archives of the RSNA, 2022

T2-SPNMMI-2

### The Impact of PSMA PET on the Treatment and Outcomes of Men with Biochemical Recurrence of Prostate Cancer: a Systematic Review and Meta-Analysis

Tuesday, Nov. 29 9:00AM - 9:30AM Room: Learning Center - NMMI DPS

#### Participants

Alex Pozdnyakov, MD, Hamilton, ON (*Presenter*) Nothing to Disclose

#### PURPOSE

Prostate-specific membrane antigen (PSMA) PET is highly sensitive in identifying disease recurrence in men with biochemical recurrence of prostate cancer (BCR) after primary therapy and is rapidly being adopted in clinical practice. The purpose of this systematic review and meta-analysis was to assess the documented impact of PSMA-PET on patient management and outcomes, including prostate-specific antigen (PSA) response, and intermediate and long-term outcome measures.

#### METHODS AND MATERIALS

MBASE, PubMed, Web of Science, Cochrane and OVID databases were searched for studies reporting on the impact of PSMA-PET on the management and outcomes of patients with BCR after definitive primary therapy. Outcome measures assessed included biochemical response to therapy after PET and BCR-free survival (BRFS). The proportions of patients in whom management changed, and the proportion of patients in whom each outcome measure was obtained were tabulated and pooled into meta-analysis using DerSimonian-Laird method.

#### RESULTS

A total of 34 studies with 3680 men reported change in management after PSMA-PET and 27 studies with 2639 men reported on at least one outcome measure and had follow-up data. PSMA-PET was positive in 2508/3680 (68.2%). The pooled proportion of change in management after PSMA-PET was 56.4% (95% CI, 48.0-63.9%). A decrease in serum PSA was documented in 72.4% of men (95% CI, 63.4-81.5%), and complete biochemical response in 23.3% (95% CI, 14.6-32.0%) at a median follow-up of 8.1 and 11 months, respectively. The pooled BRFS rate was 60.2% (95% CI, 49.1-71.4%) at a median follow-up of 20 months.

#### CONCLUSION

In conclusion, PSMA PET is positive in more than 2/3 of men with BCR and impacts patient management in more than half of the men. BRFS after PET-directed management is 60% at a median of 20 months after salvage therapy, and complete biochemical response may be achieved in up to a quarter of men.

#### CLINICAL RELEVANCE/APPLICATION

The findings of this meta-analysis further confirm the crucial role of PSMA PET in biochemical recurrence of prostate cancer and highlight the clinical implications of this molecular imaging technique.

Printed on: 02/07/23

## Abstract Archives of the RSNA, 2022

T2-SPNMMI-3

### A Pilot Study of 68Ga-PSMA11 and 68Ga-RM2 PET/MRI for Biopsy Guidance in Patients with Suspected Prostate Cancer

Tuesday, Nov. 29 9:00AM - 9:30AM Room: Learning Center - NMMI DPS

#### Participants

Heying Duan, MD, (Presenter) Nothing to Disclose

#### PURPOSE

Targeting of lesions seen on multiparametric MRI (mpMRI) improves prostate cancer (PC) detection at biopsy. However, 20-65% of highly suspicious lesions on mpMRI (PI-RADS 4 or 5) are false positives (FP), while 5-10% of clinically significant PC (csPC) are missed. Prostate specific membrane antigen (PSMA) and gastrin-releasing peptide receptors (GRPR) are both overexpressed in PC. We therefore aimed to evaluate the potential utility of 68Ga-PSMA11 and 68Ga-RM2 PET/MRI for biopsy guidance in patients with suspected PC.

#### METHODS AND MATERIALS

Thirteen men, aged 58.00±7.13 years, with suspected PC were prospectively enrolled to undergo 68Ga-PSMA11 and 68Ga-RM2 PET/MRI. PET/MRI included whole-body and dedicated delayed pelvic imaging. All patients had standard 12-core biopsy, and additional targeted biopsy of any lesions seen on PET. Maximum and peak standardized uptake values (SUV<sub>max</sub> and SUV<sub>peak</sub>) of suspected PC lesions were collected and compared to gold standard biopsy.

#### RESULTS

PSA and PSA density at enrollment were 9.80±5.97 (range 1.50-25.46) ng/mL and 0.20±0.18 (range 0.06-0.68) ng/mL<sup>2</sup>, respectively. Biopsy revealed a total of 14 PC in 8 participants: 6 were csPC and 8 were non-clinically significant PC (ncsPC). 68Ga-PSMA11 identified 25 lesions, of which 11 (44%) were true positive (TP) (5 csPC). 68Ga-RM2 showed 27 lesions, of which 14 (52%) were TP, identifying all 6 csPC and 8 ncsPC. There were 17 concordant lesions in 11 patients vs. 14 discordant lesions in 7 patients between PSMA and RM2. Incongruent lesions had the highest rate of FP (12 FP vs. 2 TP). PET/MRI guided biopsy led to the additional finding of 8 cancers of which 5 were csPC. Median SUV<sub>max</sub> was significantly higher for TP than FP lesions in delayed pelvic imaging for 68Ga-PSMA11 (6.49±4.14 vs. 4.05±1.55, P=0.023) but not for whole body images, nor for 68Ga-RM2. Sensitivity and specificity were 83% and 67% for 68Ga-RM2 63% and 86% for 68Ga-PSMA11, and 30% and 95% for mpMRI, respectively.

#### CONCLUSION

Our results show that both 68Ga-PSMA11 and 68Ga-RM2 PET/MRI are feasible for biopsy guidance in suspected PC. Both radiopharmaceuticals detected additional clinically significant cancers not seen on mpMRI, 68Ga-RM2 PET/MRI identified all csPC confirmed at biopsy.

#### CLINICAL RELEVANCE/APPLICATION

68Ga-PSMA11 and 68Ga-RM2 guided prostate biopsy help detecting csPC and might therefore avoid unnecessary biopsies and associated risks.

Printed on: 02/07/23



## Abstract Archives of the RSNA, 2022

T2-SPNPM

### Noninterpretive Skills/Quality Improvement/Practice Management Tuesday Poster Discussions

Tuesday, Nov. 29 9:00AM - 9:30AM Room: Learning Center - NPM DPS

#### Participants

Melissa Davis, MD, MBA, Atlanta, GA (*Moderator*) Nothing to Disclose

#### Sub-Events

#### T2-SPNPM-1 Recent Cuts in Reimbursement by Medicare for Interventional Radiology Procedures

#### Participants

Kenneth Huynh, BS, Orange, CA (*Presenter*) Nothing to Disclose

#### PURPOSE

To study recent trends in total charges of 20 common interventional radiology procedures by Medicare from 2012 to 2020.

#### METHODS AND MATERIALS

A list of common interventional radiology procedures was elicited from the Society for Interventional Radiology, similar to the methodology in Schwartz and Young 2021. The Medicare Part B Physician/Supplier Procedure Summary (PSPS) Master Files from 2012 through 2020 were used to extract reimbursement data. Compound annual growth rates (CAGRs) for three segments were compared: 2012-2016, 2016-2019, 2019-2020. The overall time interval was divided into segments based on significant events that would affect physician practice patterns, such as the MACRA act of 2015 and the COVID-19 pandemic beginning in 2020.

#### RESULTS

The average CAGR of total charges from 2012-2016 was 11.4% [-8.9% to 31.7%], from 2016-2019 was -3.2% [-8.2% to 1.8%], and from 2019-2020 was -13.2% [-20.4% to -6.0%]. The top three individual procedure CAGRs in 2012-2016 were for percutaneous catheter placement, visceral (194.3%), retrieval of IVC filter (36.3%), and radiofrequency ablation of hepatic tumor (22.4%). The three lowest individual procedure CAGRs for 2012-2016 were vascular embolization, tumors or ischemia (-18.5%), carotid artery stent placement (-16.3%), and external biliary drain placement (-15.2%). The top three individual procedure CAGRs in 2016-2019 were for carotid artery stent placement (30.1%), radiofrequency ablation renal tumor (11.0%), and radiofrequency ablation of hepatic tumor (5.7%). The three lowest individual procedure CAGRs for 2016-2019 were venous mechanical thrombectomy (-21.9%), insertion of IVC filter (-16.7%), and non-tunneled central venous line (-16.3%). The COVID-19 pandemic significantly decreased the total charges for IR procedures performed, as all procedures analyzed in this study exhibited significant decreases except for vascular embolization, tumors or ischemia (+29.9%) and venous mechanical thrombectomy (+19.0%).

#### CONCLUSION

Since 2016, the total charges for IR procedures have been cut by Medicare considerably. There continues to be steady decline in total charges for the most IR procedures, including those with relatively high complication rates, rate of revision, and prolonged operative time. The COVID-19 pandemic has negatively impacted reimbursement for IR procedures.

#### CLINICAL RELEVANCE/APPLICATION

Knowledge of these trends in total charges for interventional radiology procedures are important when formulating future reimbursement plans to facilitate and sustain the growth of interventional radiology.

#### T2-SPNPM-2 Inaugural Pan-Canadian RADGames: Results from a Successful Approach to Radiology Education for Medical Students

#### Participants

Aidan Canil, Kingston, ON (*Presenter*) Nothing to Disclose

#### PURPOSE

A goal in radiology recruitment is to improve medical student exposure to the field through activities such as networking and medical education events. Numerous studies have looked at gamification and game-based approaches to increase attendance at such events. In 2022, the Canadian Association of Radiologists' Medical Student Network hosted for the first time "RADGames", an interactive image interpretation contest for medical students across Canada. This program was aimed to spark medical student interest in radiology and improve their image interpretation skills with expert guidance. An evaluation from participants is presented.

#### METHODS AND MATERIALS

Volunteers from radiology interest groups in Canadian medical schools worked in team to set up a virtual session using breakout rooms and an interactive quiz platform for the competition. Recruitment was through social media and advertisement by medical student associations. Participants were surveyed anonymously for feedback following the event. Data about previous exposure to and knowledge of radiology and an evaluation of the event including self-perceived impact on participants' understanding of the field were collected.

## **RESULTS**

87 medical students from 15 of Canada's 17 medical schools competed against one another virtually. 47 (54%) responded to the post-event evaluation survey. All respondents responded favourably about the event itself. Respondents overwhelmingly indicated that the RADGames event increased their interest in radiology (38, 81%) and their understanding of the work of a radiologist (31, 66%), increased their knowledge about imaging principles (46, 98%), and improved their confidence in basic imaging interpretation (36, 77%).

## **CONCLUSION**

s The Canadian Association of Radiologists' Medical Student Network hosted Canada's first national image interpretation competition for medical students, RADGames. Feedback was overwhelmingly positive, with perceived benefits to participants on their understanding of and interest in radiology.

## **CLINICAL RELEVANCE/APPLICATION**

While medical students are underexposed to radiology, we present a new initiative using gamification and a game-based approach to promote radiology for medical students on a pan-Canadian scale.

Printed on: 02/07/23



## Abstract Archives of the RSNA, 2022

T2-SPNPM-1

### Recent Cuts in Reimbursement by Medicare for Interventional Radiology Procedures

Tuesday, Nov. 29 9:00AM - 9:30AM Room: Learning Center - NPM DPS

#### Participants

Kenneth Huynh, BS, Orange, CA (*Presenter*) Nothing to Disclose

#### PURPOSE

To study recent trends in total charges of 20 common interventional radiology procedures by Medicare from 2012 to 2020.

#### METHODS AND MATERIALS

A list of common interventional radiology procedures was elicited from the Society for Interventional Radiology, similar to the methodology in Schwartz and Young 2021. The Medicare Part B Physician/Supplier Procedure Summary (PSPS) Master Files from 2012 through 2020 were used to extract reimbursement data. Compound annual growth rates (CAGRs) for three segments were compared: 2012-2016, 2016-2019, 2019-2020. The overall time interval was divided into segments based on significant events that would affect physician practice patterns, such as the MACRA act of 2015 and the COVID-19 pandemic beginning in 2020.

#### RESULTS

The average CAGR of total charges from 2012-2016 was 11.4% [-8.9% to 31.7%], from 2016-2019 was -3.2% [-8.2% to 1.8%], and from 2019-2020 was -13.2% [-20.4% to -6.0%]. The top three individual procedure CAGRs in 2012-2016 were for percutaneous catheter placement, visceral (194.3%), retrieval of IVC filter (36.3%), and radiofrequency ablation of hepatic tumor (22.4%). The three lowest individual procedure CAGRs for 2012-2016 were vascular embolization, tumors or ischemia (-18.5%), carotid artery stent placement (-16.3%), and external biliary drain placement (-15.2%). The top three individual procedure CAGRs in 2016-2019 were for carotid artery stent placement (30.1%), radiofrequency ablation renal tumor (11.0%), and radiofrequency ablation of hepatic tumor (5.7%). The three lowest individual procedure CAGRs for 2016-2019 were venous mechanical thrombectomy (-21.9%), insertion of IVC filter (-16.7%), and non-tunneled central venous line (-16.3%). The COVID-19 pandemic significantly decreased the total charges for IR procedures performed, as all procedures analyzed in this study exhibited significant decreases except for vascular embolization, tumors or ischemia (+29.9%) and venous mechanical thrombectomy (+19.0%).

#### CONCLUSION

Since 2016, the total charges for IR procedures have been cut by Medicare considerably. There continues to be steady decline in total charges for the most IR procedures, including those with relatively high complication rates, rate of revision, and prolonged operative time. The COVID-19 pandemic has negatively impacted reimbursement for IR procedures.

#### CLINICAL RELEVANCE/APPLICATION

Knowledge of these trends in total charges for interventional radiology procedures are important when formulating future reimbursement plans to facilitate and sustain the growth of interventional radiology.

Printed on: 02/07/23



## Abstract Archives of the RSNA, 2022

T2-SPNPM-2

### Inaugural Pan-Canadian RADGames: Results from a Successful Approach to Radiology Education for Medical Students

Tuesday, Nov. 29 9:00AM - 9:30AM Room: Learning Center - NPM DPS

#### Participants

Aidan Canil, Kingston, ON (*Presenter*) Nothing to Disclose

#### PURPOSE

A goal in radiology recruitment is to improve medical student exposure to the field through activities such as networking and medical education events. Numerous studies have looked at gamification and game-based approaches to increase attendance at such events. In 2022, the Canadian Association of Radiologists' Medical Student Network hosted for the first time "RADGames", an interactive image interpretation contest for medical students across Canada. This program was aimed to spark medical student interest in radiology and improve their image interpretation skills with expert guidance. An evaluation from participants is presented.

#### METHODS AND MATERIALS

Volunteers from radiology interest groups in Canadian medical schools worked in team to set up a virtual session using breakout rooms and an interactive quiz platform for the competition. Recruitment was through social media and advertisement by medical student associations. Participants were surveyed anonymously for feedback following the event. Data about previous exposure to and knowledge of radiology and an evaluation of the event including self-perceived impact on participants' understanding of the field were collected.

#### RESULTS

87 medical students from 15 of Canada's 17 medical schools competed against one another virtually. 47 (54%) responded to the post-event evaluation survey. All respondents responded favourably about the event itself. Respondents overwhelmingly indicated that the RADGames event increased their interest in radiology (38, 81%) and their understanding of the work of a radiologist (31, 66%), increased their knowledge about imaging principles (46, 98%), and improved their confidence in basic imaging interpretation (36, 77%).

#### CONCLUSION

The Canadian Association of Radiologists' Medical Student Network hosted Canada's first national image interpretation competition for medical students, RADGames. Feedback was overwhelmingly positive, with perceived benefits to participants on their understanding of and interest in radiology.

#### CLINICAL RELEVANCE/APPLICATION

While medical students are underexposed to radiology, we present a new initiative using gamification and a game-based approach to promote radiology for medical students on a pan-Canadian scale.

Printed on: 02/07/23



## Abstract Archives of the RSNA, 2022

T2-SPNR

### Neuroradiology Tuesday Poster Discussions

Tuesday, Nov. 29 9:00AM - 9:30AM Room: Learning Center - NR DPS

#### Sub-Events

#### T2-SPNR-1 Deep Learning-based Infarct Core And Penumbra Quantification In Perfusion CT Data: Comparison with DWI Final Infarct Volume and RAPID

##### Participants

Peter Chang, MD, Irvine, CA (*Presenter*) Co-founder, Avicenna.ai; Stockholder, Avicenna.ai; Research Grant, Canon Medical Systems Corporation; Speakers Bureau, Canon Medical Systems Corporation; Research Grant, General Electric Company

##### PURPOSE

The primary objective of this study was to evaluate the accuracy of deep learning-based CT perfusion (CTP) core volume estimation when compared with diffusion-weighted imaging (DWI). The secondary objective of this study was to evaluate deep learning-based (DL) core and penumbra volume values with those obtained with a commercially-available threshold-based CTP analysis.

##### METHODS AND MATERIALS

A total of 38 consecutive adult patients for suspected acute ischemic stroke were retrospectively identified between 12/2020 - 06/2021 for whom CTP and 24-48 hour follow-up DWI MRI were obtained as part of the clinical workflow. Images of non-diagnostic quality or with missing data required for the DL analysis were excluded. The core volume was manually segmented on DWI images by a neuroradiologist with 5 years of experience. CTP images were analyzed for core and penumbra volumes with: (1) standard RAPID processing; (2) a DL-based method as part of Arterys Neuro AI (Arterys Inc.). Data normality distribution was checked using the Shapiro-Wilk test. Descriptive statistics were reported as median and interquartile range (IQR) values. Spearman correlation coefficients were used to compare core volumes. Two-sided Wilcoxon tests were used to compare automatically derived core and penumbra volumes. A P-value of 0.05 was deemed as statistically significant.

##### RESULTS

A total of 33 patients met all inclusion criteria for final analysis. Median (IQR) core volume from DWI images was 3.1 (0.1 - 15.2) ml. Median (IQR) difference between DWI and CTP core volumes was 3.0 (0.08 - 7.1) and 0.64 (0 - 6.5) ml for RAPID and Arterys software, respectively. Spearman correlation with DWI core volumes were 0.51 ( $p < 0.05$ ) and 0.61 ( $p < 0.001$ ) for RAPID and Arterys, respectively. A statistically significant difference was found between automatically derived core volumes ( $p = 0.023$ ) but not for penumbra.

##### CONCLUSION

Deep learning-based CTP analysis showed higher correlation with DWI-defined core values than traditional threshold-based CTP analysis. The presence of patients with embolic infarcts, which are too small to cause perfusion changes, might have contributed to the discrepancies between software packages. Further studies on a larger and heterogeneous patient cohort are needed to confirm these preliminary findings.

##### CLINICAL RELEVANCE/APPLICATION

Deep learning CTP may provide a more accurate estimate of DWI-defined core infarct volume than traditional threshold-based CTP analysis.

#### T2-SPNR-11 COVID-19 Effect on Mortality of Patients with Pulmonary Embolism

##### Participants

Miranda Rougelot, BS, (*Presenter*) Nothing to Disclose

##### PURPOSE

The purpose of this research was to determine if COVID-19 diagnosis within the past ninety days increased severity of PE. COVID diagnosis does not take into consideration specific strain.

##### METHODS AND MATERIALS

In this retrospective study 903 patients with pulmonary embolism and had tested positive for COVID in the last ninety days were observed. Risk was analyzed and patients were given PESI scores. PESI scores are a point system based on risk factors such as age, gender, medical history, symptoms, etc. Points categorize into Classes I-V with Class V being the highest risk. Class IV and V PESI scores were eligible for thrombectomy.

##### RESULTS

PE patient PESI scores increased by one class with COVID-19 diagnoses. Of the 903 patients, 1.9% had a standard PESI of Class I

while PESI + COVID was 1.4%. Class II jumped from a standard score of 4.9% to 10.9% with the inclusion of COVID diagnoses. Class III had 8.0% standard and 14.2% with COVID. Class IV had 14.2% standard and 22.4% with COVID. Finally class V had 23.6% standard and 27.2% with COVID diagnoses. These results are a significant difference from standard risk stratification ( $p=0.03$ ).

## CONCLUSION

s COVID-19 diagnosis significantly increases mortality in patients with Pulmonary Embolism in regards to PESI Score.

## CLINICAL RELEVANCE/APPLICATION

COVID-19 exposure increases thirty day mortality in patients with pulmonary embolism (PE). A Pulmonary Embolism Severity Index (PESI) score is given to patients based on age and predictors present. A patient's PESI score increases in class with the diagnosis of COVID-19 within 90 days of admission.

## T2-SPNR-12 Association of White Matter Hyperintensity Burden and Ischemic Core Growth in Large-Vessel Occlusion Stroke

Participants

Jia-Ying Zhou, (*Presenter*) Nothing to Disclose

## PURPOSE

To assess whether heavier white matter hyperintensity (WMH) burden is associated with faster ischemic core growth in acute stroke patients with large vessel occlusion.

## METHODS AND MATERIALS

In this retrospective study, we reviewed anterior circulation large-vessel-involved acute stroke patients who had baseline CT perfusion within 24 hours after symptom onset and had an MRI scan five days after admission from October 1, 2018, to October 31, 2021 at two stroke center. Core growth rate was calculated by the following equation: The core growth rate = Acute core volume on CT perfusion / Time from stroke onset to CT perfusion. The WMH volumes were assessed with semiautomated volumetric analysis at fluid-attenuated inversion recovery MRI by readers who were blinded to clinical data. The WMH index was calculated by the ratio of WMH volume within whole brain tissue volume and then categorized into tertiles: for each tertile, the core growth rate was summarized as median and inter-quartile range. Simple linear regressions were then performed to measure the predictive power of WMH volume and WMH index in core growth rate.

## RESULTS

A total of 154 patients in center 1 and 46 patients in center 2 were included (mean age, 69 years  $\pm$  19 [standard deviation]; 121 women [57.6%]). For patients allocated to slight WMH burden (tertile 1 of WMH index), moderate WMH burden (tertile 2), and heavy WMH burden (tertile 3), the median core growth rate was 3.15 ml/hour (1.05-6.24), 8.21 ml/hour (5.33-16.27), and 22.67 ml/hour (10.82-39.89) respectively. Increments in the WMH index by 1% resulted in an increase of core growth by 0.49 ml/hour (coefficient=0.49, 95% confidence interval=[0.41, 0.57],  $p<0.001$ ). The relationship of core growth and WMH index was validated in center 2. An increment in WMH index by 1% resulted in an increase of core growth by 0.54 ml/hour (coefficient=0.54 [0.42, 0.67],  $p<0.001$ ) in center 2.

## CONCLUSION

s WMH burden was associated with ischemic core growth for large-vessel occlusion stroke. Acute ischemic stroke patients with heavier white matter hyperintensity burden have faster ischemic core growth.

## CLINICAL RELEVANCE/APPLICATION

Acute ischemic stroke patients with heavier white matter hyperintensity burden have faster ischemic core growth. This study recommends considering WMH burden when making treatment decisions for acute ischemic stroke patients on the tissue-based level.

## T2-SPNR-13 Development of a Nomogram Based on DWI and Clinical Information to Predict DEACMP

Participants

Wenxuan Han, XI'AN, China (*Presenter*) Nothing to Disclose

## PURPOSE

Prevention of delayed encephalopathy after carbon monoxide poisoning (DEACMP), one of the most serious complications of acute carbon monoxide poisoning (ACOP), remains challenging. Hence, the purpose of this study was to identify the independent risk factors for DEACMP and to establish a nomogram to predict the probability of DEACMP.

## METHODS AND MATERIALS

Data of patients diagnosed with ACOP between September 2015 and June 2021 were retrospectively analyzed. According to the prognosis results, they were divided into the DEACMP group and the non-DEACMP group. Univariate analysis and multivariate logistic regression analysis were used to assess the risk factors of DEACMP, and a nomogram was constructed to predict the risk of DEACMP. The receiver operating characteristic curve (ROC) and calibration curves were used to evaluate the performance of this model.

## RESULTS

A total of 122 patients were enrolled in this study, of whom 30(24.6%) developed DEACMP. Multivariate logistic regression analysis showed that acute high-signal lesions on DWI, CO exposure time, and GCS score were independent risk factors for DEACMP (Odds Ratio=6.230, 1.323, 0.714,  $P<0.05$ ). The predictive nomogram was established according to the above indicators. The model reached an area under the curve (AUC) of the according receiver operating characteristic (ROC) curve of 0.959. The calibration curve of a nomogram showed a satisfactory consistency between prediction and observation.

## CONCLUSION

s In this study, a nomogram to predict DEACMP based on high-signal lesions on DWI and clinical indicators was constructed, which

may be a reliable tool to distinguish high-risk patients and then provide them with personalized treatment to reduce the incidence of DEACMP.

#### **CLINICAL RELEVANCE/APPLICATION**

We believe the nomogram may be a potential tool for identifying high-risk patients of DEACMP.

### **T2-SPNR-14 3D Chemical Exchange Saturation Transfer (CEST) Imaging: Differentiating Capability of Malignant from Benign Intracranial Meningiomas**

Participants

Kazuhiro Murayama, MD, Toyoake, Japan (*Presenter*) Research Grant, Canon Medical Systems Corporation

#### **PURPOSE**

To determine the capability of 3D chemical exchange saturation transfer (CEST) imaging at 3.5 ppm, which provides amide proton transfer (APT) weighted information in the entire brain, for differentiating malignant from benign intracranial meningiomas.

#### **METHODS AND MATERIALS**

36 patients with pathologically diagnosed intracranial meningiomas (mean age, 61.1 years) underwent CEST imaging using 3D gradient-echo based sequences at a 3T MR system. According to pathological and follow-up examination results, all tumors were divided into benign (grade 1, n = 24) and malignant (grade 2 or 3, n = 12) meningioma groups. In each lesion, magnetization transfer ratio asymmetry (MTRasym) at 3.5 ppm was computationally calculated from z spectra from each CEST data, and the MTRasym map was generated by pixel-by-pixel analysis. Then, MTRasym in the solid component of a tumor was determined by ROI measurements. To evaluate cell proliferation in each meningioma, MIB-1 index was also pathologically evaluated. To compare MTRasym between malignant and benign meningiomas, Student's t-test was performed. To evaluate the relationship between amide proton transfer and cell proliferation within each tumor, Spearman's correlations was performed between MTRasym and MIB-1 index. To assess the capability of MTRasym for distinguishing malignant from benign meningiomas, a ROC-based positive test was performed for determine the feasible threshold value. Finally, sensitivity, specificity and accuracy were assessed.

#### **RESULTS**

MTRasym of malignant meningiomas was significantly higher than that of benign meningiomas (malignant:  $2.61 \pm 0.79\%$ , benign:  $1.19 \pm 0.58$ ,  $p < 0.0001$ ). MTRasym was significantly and positively correlated with MIB-1 index ( $r = 0.51$ ,  $p < 0.05$ ). When applied feasible threshold value of MTRasym in this setting, sensitivity (SE), specificity (SP) and accuracy (AC) were determined as follows: SE, 91.7 (11/12) %; SP, 95.8 (23/24) %; AC, 94.4 (34/36) %, respectively.

#### **CONCLUSION**

s 3D CEST imaging has a good potential for differentiating malignant from benign meningiomas. APT-weighted imaging may provide regional cell proliferation difference within meningioma in routine clinical practice.

#### **CLINICAL RELEVANCE/APPLICATION**

3D CEST imaging has a good potential for differentiating malignant from benign meningiomas. APT-weighted imaging may provide regional cell proliferation difference within meningioma in routine clinical practice.

### **T2-SPNR-15 Association Between Auditory fMRI And Clinical Outcomes in Mild Traumatic Brain Injury**

Participants

Priya Santhanam, PhD, (*Presenter*) Nothing to Disclose

#### **PURPOSE**

This study assesses the relationship between auditory functional magnetic resonance imaging (fMRI) findings and clinical outcomes of patients diagnosed with mild traumatic brain injury (mTBI).

#### **METHODS AND MATERIALS**

Civilian patients (n=221) diagnosed with mTBI underwent auditory fMRI with separate auditory tasks performed on the right ear, the left ear, and bilaterally. Quantification of blood-oxygen-level dependent (BOLD) signal activation was performed, and a laterality index was calculated for each series. Clinical data relating to presentation and resolution of post-concussive symptoms were obtained via retrospective chart review. To account for inherent variability and uncertainty in symptom onset and resolution, data were right-censored and interval-censored. Clinical data were compared to the fMRI laterality index, overall asymmetry, and total activation.

#### **RESULTS**

Intensity and laterality of auditory fMRI activation were not significantly associated ( $p > 0.05$ ) with incidence of any surveyed post-concussive symptoms. Post-concussive headaches persisted significantly ( $p = 0.038$ ) longer in patients with a right-biased laterality during bilateral auditory stimulation. For left-sided auditory stimulation, longevity of post-concussive anxiety ( $p = 0.043$ ) and depression ( $p < 0.001$ ) were found to associate with activation signal intensity for subjects in the bottom 10th percentile of overall activation. For the right-sided auditory stimulation, longevity of post-concussive anxiety ( $p < 0.001$ ) and depression ( $p < 0.001$ ) were found to associate with activation signal intensity for subjects in bottom and top 10th percentiles of overall activation as well as asymmetry for those subjects in the top 10th percentile of activation asymmetry.

#### **CONCLUSION**

s Our results suggest that auditory fMRI may be a viable quantitative predictor of mTBI symptom persistence for the clinical assessment and management of mTBI. Further studies more explicitly assessing the relationship between fMRI activation and post-concussive headache, anxiety, and depression are warranted.

#### **CLINICAL RELEVANCE/APPLICATION**

Auditory functional magnetic resonance imaging could serve as a predictor of symptom persistence and recovery in patients with mild traumatic brain injury.

## **T2-SPNR-16 Follow-up Imaging of Clipped Intracranial Aneurysms With 3-T MRI: Comparison Between 3D Time-Of-Flight Mrangiography and Pointwise Encoding Time Reduction Withradial Acquisition Subtraction-Based MR Angiography**

Participants

Inyoung Kim, MD, (*Presenter*) Nothing to Disclose

### **PURPOSE**

Metallic susceptibility artifact due to implanted clips is a major limitation of using 3D time-of-flight magnetic resonance angiography (TOF-MRA) for follow-up imaging of clipped aneurysms (CAs). The purpose of this study was to compare pointwise encoding time reduction with radial acquisition (PETRA) subtraction-based MRA with TOF-MRA in terms of imaging quality and visibility of clip-adjacent arteries for use in follow-up imaging of CAs.

### **METHODS AND MATERIALS**

Sixty-two patients with 73 CAs were included retrospectively in this comparative study. All patients underwent PETRA-MRA after TOF-MRA performed simultaneously with 3-T MRI between September 2019 and March 2020. Two neuroradiologists independently compared images obtained with both MRA modalities to evaluate overall image quality using a 4-point scale and visibility of the parent artery and branching vessels near the clips using a 3-point scale. Subgroup analysis was performed according to the number of clips (less-clipped [1-2 clips] vs more-clipped [= 3 clips] aneurysms). The ability to detect aneurysm recurrence was also assessed.

### **RESULTS**

Compared with TOF-MRA, PETRA-MRA showed acceptable image quality (score of  $3.97 \pm 0.18$  for TOFMRA vs  $3.73 \pm 0.53$  for PETRA-MRA) and had greater visibility of the adjacent vessels near the CAs (score of  $1.25 \pm 0.59$  for TOF-MRA vs  $2.27 \pm 0.75$  for PETRA-MRA,  $p < 0.0001$ ). PETRA-MRA had greater visibility of vessels adjacent to less-clipped aneurysms (score of  $2.39 \pm 0.75$  for less-clipped aneurysms vs  $2.09 \pm 0.72$  for more-clipped aneurysms,  $p = 0.014$ ). Of 73 CAs, aneurysm recurrence in 4 cases was detected using PETRA-MRA.

### **CONCLUSION**

This study demonstrated that PETRA-MRA is superior to TOF-MRA for visualizing adjacent vessels near clips and can be an advantageous alternative to TOF-MRA for follow-up imaging of CAs.

### **CLINICAL RELEVANCE/APPLICATION**

PETRA-MRA may be an effective alternative for follow-up imaging of CAs.

## **T2-SPNR-18 Characterization of Thalamic Subregions Over 1-2 Years in Small Vessel Disease Using MR-Based Quantitative Susceptibility Mapping and Free-Water Mapping**

Participants

Yawen Sun, Shanghai, China (*Presenter*) Nothing to Disclose

### **PURPOSE**

The aim of this study was to evaluate the characteristics of the thalamic subregions using quantitative susceptibility mapping and free-water (FW) mapping in small vessel disease (SVD) over 1-2 years.

### **METHODS AND MATERIALS**

Fifty-one SVD patients underwent brain MRI scans and neuropsychological evaluations both at baseline and at follow-up, composed of 28 SVD patients with mild cognitive impairment (VaMCI) and 23 with no cognitive impairment (NCI). Quantitative susceptibility (QS) values, FW values, and volumes within thalamic subregions, i.e., the anterior nuclei, the median nuclei, the lateral nuclei (TL-LT), the pulvinar (TL-PLV) and the internal medullary lamina (TL-IML), were calculated for each individual. Temporal (baseline vs. follow-up) and cross-sectional (VaMCI vs. NCI) differences were studied using mixed factorial ANOVA analysis and appropriate t-tests. Partial correlations were used to assess the relationship between the MRI indices changes (i.e.,  $\Delta$ FW<sub>followup-baseline</sub>/FW<sub>baseline</sub>) and cognitive function changes (i.e.,  $\Delta$ MoCA<sub>followup-baseline</sub>/MoCA<sub>baseline</sub>).

### **RESULTS**

The Group effect resulted in greater mean FW values (index of neuroinflammation) in the left TL-PLV, bilateral TL-LT, and bilateral TL-IML for VaMCI compared with NCI, as well as resulted in higher mean QS values (index of iron deposition) in the left TL-PL and lower volumes in the left TL-IML ( $p < 0.05$ ). The Group $\times$ Time interaction identified increased mean QS values in the left TL-PLV for VaMCI over time. In addition, there were no significant effects for the FW values across Time. Furthermore, we observed significant negative associations between the FW values changes in the left TL-PLV and the right TL-LT and MoCA scores changes in VaMCI group over 1-2 years.

### **CONCLUSION**

Our results demonstrate that elevated FW and QS values in the thalamic subregions have the potential to be used as an indicator in the progression of SVD. The FW values changes in the TL-PLV and the TL-LT might be the biomarkers for the mechanism of cognitive decline in the evolution of SVD.

### **CLINICAL RELEVANCE/APPLICATION**

QSM and FW mapping when combined, can be considered as a specific and sensitive tool for the monitoring of the complex pathologies such as neuroinflammation and iron deposition in SVD. Our results might contribute to understanding the pathogenesis and progression of SVD.

## **T2-SPNR-19 Multiparametric Quantitative Evaluation Using Synthetic MRI in Normal-Appearing Brain Parenchyma in Adult Moyamoya Disease**

Participants

Kazufumi Kikuchi, MD, PhD, (*Presenter*) Nothing to Disclose

## PURPOSE

Moyamoya disease (MMD) is a progressive, steno-occlusive cerebrovascular disease affecting the arteries of the circle of the Willis. Few studies have examined the correlation between brain volume and function in patients with MMD. The purpose of this study was to investigate whether multiparametric brain volumes measured by synthetic MRI (SyMRI) correlate with cerebral blood flow (CBF) and brain function (BF) in MMD.

## METHODS AND MATERIALS

This retrospective study was approved by our institutional review boards and conducted on 18 MMD patients (3 men, 15 women; median age, 43 years; range, 20-72 years). SyMRI was performed using the 3D-QALAS sequence by a 3T scanner. Quantification map acquisition and raw data processing were performed with SyMRI software (Version 21.4; SyMRI, Linköping, Sweden). CBF was measured using 123I-IMP SPECT, including the acetazolamide challenge. BFs were measured using WAIS-III/IV and WMS-R tests. Quantitative evaluations, including grey matter (GM), white matter (WM), and myelin correlated volume (MyC), were measured and corrected with total brain volume in normal-appearing brain parenchyma in six areas (bilateral anterior, middle, posterior cerebral arterial [ACA/MCA/PCA] territories). These three parameters and their correlations with corrected CBF and BF were evaluated by Spearman's rank-order correlation test.

## RESULTS

Resting CBFs were correlated with GM fractions in the right ACA/MCA territories ( $r=0.524, 0.632; P=0.039, 0.018$ , respectively). Cerebrovascular reactivity to an acetazolamide challenge was correlated with GM fraction in the left PCA territory ( $r=0.574, P=0.018$ ). FSIQ/VCI derived from WAIS were correlated with GM fraction in the left PCA territory ( $r=0.625, 0.615; P=0.009, 0.001$ , respectively). PSI derived from WAIS was correlated with GM fraction in the right MCA territory ( $r=0.665, P=0.011$ ). There was no correlation between brain volume fractions and WMS-R indices.

## CONCLUSION

S Synthetic MRI could noninvasively evaluate multiparametric brain volumes that correlate with CBF and BF in MMD.

## CLINICAL RELEVANCE/APPLICATION

Synthetic MRI can quantitatively assess brain volume loss in patients with Moyamoya disease, which correlates with cerebral blood flow and brain function, and may help determine the disease severity.

## T2-SPNR-2 NCCT Image-based Automated Intracranial Hemorrhage Classification Using A Deep Learning Model: Is the Intracranial Hemorrhage Classification of Very Small Volume Hematoma Cases Reliable?

Participants

Myeong Jin Kim, MD, PhD, (*Presenter*) Nothing to Disclose

## PURPOSE

Intracranial hemorrhage (ICH) is a fatal disease that significantly affects the patient's life and prognosis over time. Patients with small-volume ICH (SICH) with small hematoma are more likely to have a benign clinical course and tend to experience hematoma expansion and have worse outcomes. In this study, we evaluate the classification performance for SICH cases using AI software (cHS-Heuron) for ICH diagnosis.

## METHODS AND MATERIALS

We evaluated the SICH classification performance by testing the target group SICH data and the control group non-small volume ICH (Non-SICH) data using cHS-Heuron. As the evaluation data, RSNA ICH Challenge 2019 test dataset and clinical data from single institute were used. The number of data was 397 patients in ICH (250 SICH, 147 non-SICH) and 130 patients in the control group (Non-ICH). The gold standard was generated by a stroke expert by evaluating the hematoma volume of each slice. SICH data were defined as hematoma volume less than 0.65ml and diameter of 2mm or more and 5mm or less. The classifying performance was evaluated through the sensitivity and specificity compared to gold standard.

## RESULTS

As the classifying performance of ICH patients, the sensitivity and specificity were 0.9748 and 0.9692, respectively. Among ICH patients, the true positive rate of SICH was 0.9600 in patient-wise classification. However, in slice-wise classification, the sensitivity and specificity were 0.8801 and 0.9890 for SICH group, and, in Non-SICH group, it was 0.9600 and 0.9867, respectively.

## CONCLUSION

As a result of the ICH classification study using cHS-Heuron, the SICH group showed slightly lower sensitivity than the Non-SICH group, but in the patient-wise and slice-wise tests, the SICH group, the Non-SICH group all showed very high ICH classification performance.

## CLINICAL RELEVANCE/APPLICATION

In the diagnosis of patients with ICH containing a very small volume hematoma area of less than 5 mm in diameter on NCCT images, cHS-Heuron can be utilized as a reliable pre-diagnosis tool for clinicians to quickly and accurately diagnose and make treatment decisions.

## T2-SPNR-3 Diagnostic Yield of CTA Head After Stroke Protocol Standardization: A Retrospective Study

Participants

Dane Weinert, MD, (*Presenter*) Nothing to Disclose

## PURPOSE

CT Angiography (CTA) of the head and neck is useful in the imaging of suspected stroke for identifying patients eligible for endovascular therapies. Acute stroke protocols may vary by when CTA is performed in the imaging algorithm. At our institution, a protocol was implemented which standardized CTA imaging to be obtained only as indicated after an initial non-contrast CT (NCCT)

head per American Heart Association stroke guidelines. The objective of our study is to investigate how often relevant diagnostic findings were found in CTA imaging as part of the acute stroke protocol when obtained only after NCCT head imaging and an appropriate neurological exam raised high clinical suspicion for acute ischemia, compared to when CTA head was obtained along with NCCT head imaging immediately upon activation of the stroke protocol and without a neurological exam.

## **METHODS AND MATERIALS**

CTA head reports were reviewed from April 2021 to Jan 2022. Patients with stroke-related indications in the image-requisition were included. A study was classified as "positive" if a large vessel occlusion was identified on imaging. Studies were then divided into "pre-intervention" (April through Aug 2021) and "post-intervention" (Sept 2021 through Jan 2022) groups to demarcate before and after the acute stroke protocol standardization to obtain CTA imaging after NCCT head imaging and an appropriate neurological exam raised high clinical suspicion for acute ischemia.

## **RESULTS**

Results identified 428 studies in the pre-intervention group and 280 in the post-intervention group. There were 21 positive CTA exams in the pre-intervention group (4.9%) and 23 positive exams in the post-intervention group (8.2%) ( $p < 0.05$ ). Additionally, the number of studies ordered for stroke-related reasons decreased by 34.6% compared to the pre-intervention period.

## **CONCLUSION**

The diagnostic yield of CTA was significantly improved after standardizing the acute stroke protocol to obtain CTA only after ischemic stroke was confirmed on NCCT. Adherence to standard practice guidelines in conjunction with judicious decision making when ordering imaging for stroke diagnosis is critical for limiting unnecessary radiation exposure and efficacious CT utilization.

## **CLINICAL RELEVANCE/APPLICATION**

This study supports guideline-directed imaging protocol for stroke diagnosis vis a vis higher diagnostic yield, limiting unnecessary radiation exposure, and efficient resource utilization.

## **T2-SPNR-4 The Application of Proton Exchange rate (kex) MRI in Ischemic Stroke Patients**

Participants

Yiran Zhou, (*Presenter*) Nothing to Disclose

## **PURPOSE**

Proton exchange rate (kex) MRI has recently been developed and preliminarily shown its potential value for evaluating reactive oxygen species of tissues in vivo. This study aimed to investigate the change of kex in different stroke stages and its correlation with stroke severity and prognosis.

## **METHODS AND MATERIALS**

96 ischemic stroke patients were divided into 3 groups (acute, subacute and chronic) based on the stroke phases. A spin-echo echo-planar imaging sequence with pre-saturation chemical exchange saturation power of 1.5, 2.5, and 3.5  $\mu\text{T}$  was implemented to obtain Z-spectra which were fitted to remove the water direct saturation (DS) effect. kex maps were constructed from DS-removed omega plots. Relative kex (rkex) and relative apparent diffusion coefficient (rADC) were calculated by taking the ratio of kex or ADC in the infarcts over that of the mirrored contralateral tissue, respectively. Pearson's correlation analysis was implemented to evaluate the correlations between kex rkex and the National Institute of Health Stroke Scale (NIHSS). The predictive performance of kex, rkex, rADC, and lesion volume for acute stroke outcome was evaluated through receiver operating characteristic curve.

## **RESULTS**

The kex of ischemic lesions was significantly higher compared to the mirrored contralateral tissue at the three stages (acute: ischemic lesion 935.08  $s^{-1}$  vs contralateral tissue 777.26  $s^{-1}$ ,  $P < 0.001$ ; subacute: ischemic lesion 881.42  $s^{-1}$  vs contralateral tissue 762.17  $s^{-1}$ ,  $P < 0.001$ ; chronic: ischemic lesion 866.93  $s^{-1}$  vs contralateral tissue 756.34  $s^{-1}$ ,  $P < 0.001$ ). Besides, the kex of acute lesions was significantly higher than subacute and chronic lesions ( $P < 0.05$ ,  $P < 0.01$ , respectively). However, the difference between the subacute and chronic lesions was not significant. Lesion's kex and rkex significantly correlated with the NIHSS score only for the acute cases ( $r = 0.406$ ,  $P = 0.016$ ;  $r = 0.531$ ,  $P = 0.001$ ). Acute patients with poor prognosis had significantly higher kex rkex of lesion compared to patients with good prognosis (991.08 vs. 893.08  $s^{-1}$ ,  $P < 0.001$ ; 1.28 vs. 1.15,  $P < 0.001$ ). These measures showed favorable predictive performance for acute stroke outcome with area under the curve (AUC) of 0.837 and 0.880, slightly while not significantly higher than lesion volume (AUC: 0.730) and rADC (AUC: 0.673).

## **CONCLUSION**

kex-MRI could identify ischemic lesions at different stages with markedly elevated intensity on the kex maps. It showed potential capability to reflect the stroke severity and predict the prognosis for acute stroke patients.

## **CLINICAL RELEVANCE/APPLICATION**

kex-MRI is promising for ischemic stroke diagnosis and management as it may reflect oxidative stress of stroke lesions at different stages and predict the acute stroke outcome.

## **T2-SPNR-5 Clinical, Imaging Correlates and Prognostic Implications of Asymmetric Perivascular Spaces in Acute Ischemic Stroke**

Participants

Jinhao Lyu, Beijing, China (*Presenter*) Nothing to Disclose

## **PURPOSE**

Perivascular spaces (PVSs) have been considered a key element of the glymphatic system of the central nervous system and played a role in the mechanism of small vessel disease. Asymmetric PVSs is reported to be correlated with post-stroke depression and seizure. The incidence, mechanism, and prognostic implication of asymmetric PVSs have yet to be determined. We aimed to determine the associations of asymmetric PVSs with stroke presentations, cerebral hemodynamics and functional independence in acute ischemic stroke (AIS).

## **METHODS AND MATERIALS**

We included 26 AIS patients with unilateral internal carotid artery and middle cerebral artery occlusion, who had undergone baseline routine head MRI and dynamic susceptibility contrast (DSC). Collateral circulation was graded 0-3 based on DSC source imaging (a higher value indicated better collaterals). The burden of PVSs was assessed by using a semi-quantitative scale. The scale selected 3 representative locations (midbrain [MB], basal ganglia [BG], and centrum semiovale [CS]) based on axial T2-weighted imaging slices and scored based on the number of PVSs (details please see Fig 1). The total score of PVSs in each hemisphere was calculated as: Stotal = SBG+ SCS+ SMB. Lesion side dominant asymmetry PVSs were defined as: Stotal of the infarct hemisphere - Stotal of the contralateral hemisphere > 0. The full baseline clinical and imaging features were listed in Table 1 in Fig 1. Binary logistic regression was used to identify predictors of lesion side dominant asymmetry PVSs and poor outcome defined as 3-month modified Rankin Scale > 2.

## **RESULTS**

In them, 17/26 presented lesion side dominant asymmetry PVSs, 9/26 presented symmetry distribution of PVSs, and 0/26 presented contralateral side dominant asymmetry PVSs. Collateral circulation grade was significantly associated with the presence of lesion side dominant asymmetry PVSs (unadjusted odds ratio [OR], 0.07; 95% confidence interval [CI], 0.01-0.53; P=0.01). In binary logistic regression, lesion side dominant asymmetry PVSs (OR, 12.06; 95% CI, 1.16-125.91; P=0.038) was independent predictors of stroke outcomes after adjusted for age. The total burden of PVSs showed no significant association with stroke outcomes.

## **CONCLUSION**

s In acute large vessel occlusion stroke, lesion side dominant asymmetry PVSs suggest the rapid impairments of the glymphatic system after ischemia, and hypoperfusion due to collateral circulation insufficiency may be one critical mechanism in the process.

## **CLINICAL RELEVANCE/APPLICATION**

Lesion side dominant asymmetry PVSs negatively associated with stroke outcomes in acute ischemic stroke. Global estimation of PVSs is feasible and the asymmetry appearance may provide helpful and insightful information.

Printed on: 02/07/23



## Abstract Archives of the RSNA, 2022

T2-SPNR-1

### Deep Learning-based Infarct Core And Penumbra Quantification In Perfusion CT Data: Comparison with DWI Final Infarct Volume and RAPID

Tuesday, Nov. 29 9:00AM - 9:30AM Room: Learning Center - NR DPS

#### Participants

Peter Chang, MD, Irvine, CA (*Presenter*) Co-founder, Avicenna.ai; Stockholder, Avicenna.ai; Research Grant, Canon Medical Systems Corporation; Speakers Bureau, Canon Medical Systems Corporation; Research Grant, General Electric Company

#### PURPOSE

The primary objective of this study was to evaluate the accuracy of deep learning-based CT perfusion (CTP) core volume estimation when compared with diffusion-weighted imaging (DWI). The secondary objective of this study was to evaluate deep learning-based (DL) core and penumbra volume values with those obtained with a commercially-available threshold-based CTP analysis.

#### METHODS AND MATERIALS

A total of 38 consecutive adult patients for suspected acute ischemic stroke were retrospectively identified between 12/2020 - 06/2021 for whom CTP and 24-48 hour follow-up DWI MRI were obtained as part of the clinical workflow. Images of non-diagnostic quality or with missing data required for the DL analysis were excluded. The core volume was manually segmented on DWI images by a neuroradiologist with 5 years of experience. CTP images were analyzed for core and penumbra volumes with: (1) standard RAPID processing; (2) a DL-based method as part of Arterys Neuro AI (Arterys Inc.). Data normality distribution was checked using the Shapiro-Wilk test. Descriptive statistics were reported as median and interquartile range (IQR) values. Spearman correlation coefficients were used to compare core volumes. Two-sided Wilcoxon tests were used to compare automatically derived core and penumbra volumes. A P-value of 0.05 was deemed as statistically significant.

#### RESULTS

A total of 33 patients met all inclusion criteria for final analysis. Median (IQR) core volume from DWI images was 3.1 (0.1 - 15.2) ml. Median (IQR) difference between DWI and CTP core volumes was 3.0 (0.08 - 7.1) and 0.64 (0 - 6.5) ml for RAPID and Arterys software, respectively. Spearman correlation with DWI core volumes were 0.51 ( $p < 0.05$ ) and 0.61 ( $p < 0.001$ ) for RAPID and Arterys, respectively. A statistically significant difference was found between automatically derived core volumes ( $p = 0.023$ ) but not for penumbra.

#### CONCLUSION

Deep learning-based CTP analysis showed higher correlation with DWI-defined core values than traditional threshold-based CTP analysis. The presence of patients with embolic infarcts, which are too small to cause perfusion changes, might have contributed to the discrepancies between software packages. Further studies on a larger and heterogeneous patient cohort are needed to confirm these preliminary findings.

#### CLINICAL RELEVANCE/APPLICATION

Deep learning CTP may provide a more accurate estimate of DWI-defined core infarct volume than traditional threshold-based CTP analysis.

Printed on: 02/07/23



## Abstract Archives of the RSNA, 2022

T2-SPNR-11

### COVID-19 Effect on Mortality of Patients with Pulmonary Embolism

Tuesday, Nov. 29 9:00AM - 9:30AM Room: Learning Center - NR DPS

#### Participants

Miranda Rougelot, BS, (*Presenter*) Nothing to Disclose

#### PURPOSE

The purpose of this research was to determine if COVID-19 diagnosis within the past ninety days increased severity of PE. COVID diagnosis does not take into consideration specific strain.

#### METHODS AND MATERIALS

In this retrospective study 903 patients with pulmonary embolism and had tested positive for COVID in the last ninety days were observed. Risk was analyzed and patients were given PESI scores. PESI scores are a point system based on risk factors such as age, gender, medical history, symptoms, etc. Points categorize into Classes I-V with Class V being the highest risk. Class IV and V PESI scores were eligible for thrombectomy.

#### RESULTS

PE patient PESI scores increased by one class with COVID-19 diagnoses. Of the 903 patients, 1.9% had a standard PESI of Class I while PESI + COVID was 1.4%. Class II jumped from a standard score of 4.9% to 10.9% with the inclusion of COVID diagnoses. Class III had 8.0% standard and 14.2% with COVID. Class IV had 14.2% standard and 22.4% with COVID. Finally class V had 23.6% standard and 27.2% with COVID diagnoses. These results are a significant difference from standard risk stratification ( $p=0.03$ ).

#### CONCLUSION

s COVID-19 diagnosis significantly increases mortality in patients with Pulmonary Embolism in regards to PESI Score.

#### CLINICAL RELEVANCE/APPLICATION

COVID- 19 exposure increases thirty day mortality in patients with pulmonary embolism (PE). A Pulmonary Embolism Severity Index (PESI) score is given to patients based on age and predictors present. A patient's PESI score increases in class with the diagnosis of COVID-19 within 90 days of admission.

Printed on: 02/07/23

## Abstract Archives of the RSNA, 2022

T2-SPNR-12

### Association of White Matter Hyperintensity Burden and Ischemic Core Growth in Large-Vessel Occlusion Stroke

Tuesday, Nov. 29 9:00AM - 9:30AM Room: Learning Center - NR DPS

#### Participants

Jia-Ying Zhou, (*Presenter*) Nothing to Disclose

#### PURPOSE

To assess whether heavier white matter hyperintensity (WMH) burden is associated with faster ischemic core growth in acute stroke patients with large vessel occlusion.

#### METHODS AND MATERIALS

In this retrospective study, we reviewed anterior circulation large-vessel-involved acute stroke patients who had baseline CT perfusion within 24 hours after symptom onset and had an MRI scan five days after admission from October 1, 2018, to October 31, 2021 at two stroke center. Core growth rate was calculated by the following equation: The core growth rate = Acute core volume on CT perfusion / Time from stroke onset to CT perfusion. The WMH volumes were assessed with semiautomated volumetric analysis at fluid-attenuated inversion recovery MRI by readers who were blinded to clinical data. The WMH index was calculated by the ratio of WMH volume within whole brain tissue volume and then categorized into tertiles: for each tertile, the core growth rate was summarized as median and inter-quartile range. Simple linear regressions were then performed to measure the predictive power of WMH volume and WMH index in core growth rate.

#### RESULTS

A total of 154 patients in center 1 and 46 patients in center 2 were included (mean age, 69 years  $\pm$  19 [standard deviation]; 121 women [57.6%]). For patients allocated to slight WMH burden (tertile 1 of WMH index), moderate WMH burden (tertile 2), and heavy WMH burden (tertile 3), the median core growth rate was 3.15 ml/hour (1.05-6.24), 8.21 ml/hour (5.33-16.27), and 22.67 ml/hour (10.82-39.89) respectively. Increments in the WMH index by 1% resulted in an increase of core growth by 0.49 ml/hour (coefficient=0.49, 95% confidence interval=[0.41, 0.57],  $p<0.001$ ). The relationship of core growth and WMH index was validated in center 2. An increment in WMH index by 1% resulted in an increase of core growth by 0.54 ml/hour (coefficient=0.54 [0.42, 0.67],  $p<0.001$ ) in center 2.

#### CONCLUSION

s WMH burden was associated with ischemic core growth for large-vessel occlusion stroke. Acute ischemic stroke patients with heavier white matter hyperintensity burden have faster ischemic core growth.

#### CLINICAL RELEVANCE/APPLICATION

Acute ischemic stroke patients with heavier white matter hyperintensity burden have faster ischemic core growth. This study recommends considering WMH burden when making treatment decisions for acute ischemic stroke patients on the tissue-based level.

Printed on: 02/07/23



## Abstract Archives of the RSNA, 2022

T2-SPNR-13

### Development of a Nomogram Based on DWI and Clinical Information to Predict DEACMP

Tuesday, Nov. 29 9:00AM - 9:30AM Room: Learning Center - NR DPS

#### Participants

Wenxuan Han, XI'AN, China (*Presenter*) Nothing to Disclose

#### PURPOSE

Prevention of delayed encephalopathy after carbon monoxide poisoning (DEACMP), one of the most serious complications of acute carbon monoxide poisoning (ACOP), remains challenging. Hence, the purpose of this study was to identify the independent risk factors for DEACMP and to establish a nomogram to predict the probability of DEACMP.

#### METHODS AND MATERIALS

Data of patients diagnosed with ACOP between September 2015 and June 2021 were retrospectively analyzed. According to the prognosis results, they were divided into the DEACMP group and the non-DEACMP group. Univariate analysis and multivariate logistic regression analysis were used to assess the risk factors of DEACMP, and a nomogram was constructed to predict the risk of DEACMP. The receiver operating characteristic curve (ROC) and calibration curves were used to evaluate the performance of this model.

#### RESULTS

A total of 122 patients were enrolled in this study, of whom 30(24.6%) developed DEACMP. Multivariate logistic regression analysis showed that acute high-signal lesions on DWI, CO exposure time, and GCS score were independent risk factors for DEACMP (Odds Ratio=6.230,1.323,0.714,  $P<0.05$ ). The predictive nomogram was established according to the above indicators. The model reached an area under the curve (AUC) of the according receiver operating characteristic (ROC) curve of 0.959. The calibration curve of a nomogram showed a satisfactory consistency between prediction and observation.

#### CONCLUSION

s In this study, a nomogram to predict DEACMP based on high-signal lesions on DWI and clinical indicators was constructed, which may be a reliable tool to distinguish high-risk patients and then provide them with personalized treatment to reduce the incidence of DEACMP.

#### CLINICAL RELEVANCE/APPLICATION

We believe the nomogram may be a potential tool for identifying high-risk patients of DEACMP.

Printed on: 02/07/23

## Abstract Archives of the RSNA, 2022

T2-SPNR-14

### 3D Chemical Exchange Saturation Transfer (CEST) Imaging: Differentiating Capability of Malignant from Benign Intracranial Meningiomas

Tuesday, Nov. 29 9:00AM - 9:30AM Room: Learning Center - NR DPS

#### Participants

Kazuhiro Murayama, MD, Toyoake, Japan (*Presenter*) Research Grant, Canon Medical Systems Corporation

#### PURPOSE

To determine the capability of 3D chemical exchange saturation transfer (CEST) imaging at 3.5 ppm, which provides amide proton transfer (APT) weighted information in the entire brain, for differentiating malignant from benign intracranial meningiomas.

#### METHODS AND MATERIALS

36 patients with pathologically diagnosed intracranial meningiomas (mean age, 61.1 years) underwent CEST imaging using 3D gradient-echo based sequences at a 3T MR system. According to pathological and follow-up examination results, all tumors were divided into benign (grade 1, n = 24) and malignant (grade 2 or 3, n = 12) meningioma groups. In each lesion, magnetization transfer ratio asymmetry (MTRasym) at 3.5 ppm was computationally calculated from z spectra from each CEST data, and the MTRasym map was generated by pixel-by-pixel analysis. Then, MTRasym in the solid component of a tumor was determined by ROI measurements. To evaluate cell proliferation in each meningioma, MIB-1 index was also pathologically evaluated. To compare MTRasym between malignant and benign meningiomas, Student's t-test was performed. To evaluate the relationship between amide proton transfer and cell proliferation within each tumor, Spearman's correlations was performed between MTRasym and MIB-1 index. To assess the capability of MTRasym for distinguishing malignant from benign meningiomas, a ROC-based positive test was performed for determine the feasible threshold value. Finally, sensitivity, specificity and accuracy were assessed.

#### RESULTS

MTRasym of malignant meningiomas was significantly higher than that of benign meningiomas (malignant:  $2.61 \pm 0.79\%$ , benign:  $1.19 \pm 0.58$ ,  $p < 0.0001$ ). MTRasym was significantly and positively correlated with MIB-1 index ( $r = 0.51$ ,  $p < 0.05$ ). When applied feasible threshold value of MTRasym in this setting, sensitivity (SE), specificity (SP) and accuracy (AC) were determined as follows: SE, 91.7 (11/12) %; SP, 95.8 (23/24) %; AC, 94.4 (34/36) %, respectively.

#### CONCLUSION

3D CEST imaging has a good potential for differentiating malignant from benign meningiomas. APT-weighted imaging may provide regional cell proliferation difference within meningioma in routine clinical practice.

#### CLINICAL RELEVANCE/APPLICATION

3D CEST imaging has a good potential for differentiating malignant from benign meningiomas. APT-weighted imaging may provide regional cell proliferation difference within meningioma in routine clinical practice.

Printed on: 02/07/23

## Abstract Archives of the RSNA, 2022

T2-SPNR-15

### Association Between Auditory fMRI And Clinical Outcomes in Mild Traumatic Brain Injury

Tuesday, Nov. 29 9:00AM - 9:30AM Room: Learning Center - NR DPS

#### Participants

Priya Santhanam, PhD, (*Presenter*) Nothing to Disclose

#### PURPOSE

This study assesses the relationship between auditory functional magnetic resonance imaging (fMRI) findings and clinical outcomes of patients diagnosed with mild traumatic brain injury (mTBI).

#### METHODS AND MATERIALS

Civilian patients (n=221) diagnosed with mTBI underwent auditory fMRI with separate auditory tasks performed on the right ear, the left ear, and bilaterally. Quantification of blood-oxygen-level dependent (BOLD) signal activation was performed, and a laterality index was calculated for each series. Clinical data relating to presentation and resolution of post-concussive symptoms were obtained via retrospective chart review. To account for inherent variability and uncertainty in symptom onset and resolution, data were right-censored and interval-censored. Clinical data were compared to the fMRI laterality index, overall asymmetry, and total activation.

#### RESULTS

Intensity and laterality of auditory fMRI activation were not significantly associated ( $p>0.05$ ) with incidence of any surveyed post-concussive symptoms. Post-concussive headaches persisted significantly ( $p=0.038$ ) longer in patients with a right-biased laterality during bilateral auditory stimulation. For left-sided auditory stimulation, longevity of post-concussive anxiety ( $p=0.043$ ) and depression ( $p<0.001$ ) were found to associate with activation signal intensity for subjects in the bottom 10th percentile of overall activation. For the right-sided auditory stimulation, longevity of post-concussive anxiety ( $p<0.001$ ) and depression ( $p<0.001$ ) were found to associate with activation signal intensity for subjects in bottom and top 10th percentiles of overall activation as well as asymmetry for those subjects in the top 10th percentile of activation asymmetry.

#### CONCLUSION

Our results suggest that auditory fMRI may be a viable quantitative predictor of mTBI symptom persistence for the clinical assessment and management of mTBI. Further studies more explicitly assessing the relationship between fMRI activation and post-concussive headache, anxiety, and depression are warranted.

#### CLINICAL RELEVANCE/APPLICATION

Auditory functional magnetic resonance imaging could serve as a predictor of symptom persistence and recovery in patients with mild traumatic brain injury.

Printed on: 02/07/23

## Abstract Archives of the RSNA, 2022

T2-SPNR-16

### Follow-up Imaging of Clipped Intracranial Aneurysms With 3-T MRI: Comparison Between 3D Time-Of-Flight Mrangiography and Pointwise Encoding Time Reduction Withradial Acquisition Subtraction-Based MR Angiography

Tuesday, Nov. 29 9:00AM - 9:30AM Room: Learning Center - NR DPS

#### Participants

Inyoung Kim, MD, (*Presenter*) Nothing to Disclose

#### PURPOSE

Metallic susceptibility artifact due to implanted clips is a major limitation of using 3D time-of-flight magnetic resonance angiography (TOF-MRA) for follow-up imaging of clipped aneurysms (CAs). The purpose of this study was to compare pointwise encoding time reduction with radial acquisition (PETRA) subtraction-based MRA with TOF-MRA in terms of imaging quality and visibility of clip-adjacent arteries for use in follow-up imaging of CAs.

#### METHODS AND MATERIALS

Sixty-two patients with 73 CAs were included retrospectively in this comparative study. All patients underwent PETRA-MRA after TOF-MRA performed simultaneously with 3-T MRI between September 2019 and March 2020. Two neuroradiologists independently compared images obtained with both MRA modalities to evaluate overall image quality using a 4-point scale and visibility of the parent artery and branching vessels near the clips using a 3-point scale. Subgroup analysis was performed according to the number of clips (less-clipped [1-2 clips] vs more-clipped [= 3 clips] aneurysms). The ability to detect aneurysm recurrence was also assessed.

#### RESULTS

Compared with TOF-MRA, PETRA-MRA showed acceptable image quality (score of  $3.97 \pm 0.18$  for TOFMRA vs  $3.73 \pm 0.53$  for PETRA-MRA) and had greater visibility of the adjacent vessels near the CAs (score of  $1.25 \pm 0.59$  for TOF-MRA vs  $2.27 \pm 0.75$  for PETRA-MRA,  $p < 0.0001$ ). PETRA-MRA had greater visibility of vessels adjacent to less-clipped aneurysms (score of  $2.39 \pm 0.75$  for less-clipped aneurysms vs  $2.09 \pm 0.72$  for more-clipped aneurysms,  $p = 0.014$ ). Of 73 CAs, aneurysm recurrence in 4 cases was detected using PETRA-MRA.

#### CONCLUSION

This study demonstrated that PETRA-MRA is superior to TOF-MRA for visualizing adjacent vessels near clips and can be an advantageous alternative to TOF-MRA for follow-up imaging of CAs.

#### CLINICAL RELEVANCE/APPLICATION

PETRA-MRA may be an effective alternative for follow-up imaging of CAs.

Printed on: 02/07/23

## Abstract Archives of the RSNA, 2022

T2-SPNR-18

### Characterization of Thalamic Subregions Over 1-2 Years in Small Vessel Disease Using MR-Based Quantitative Susceptibility Mapping and Free-Water Mapping

Tuesday, Nov. 29 9:00AM - 9:30AM Room: Learning Center - NR DPS

#### Participants

Yawen Sun, Shanghai, China (*Presenter*) Nothing to Disclose

#### PURPOSE

The aim of this study was to evaluate the characteristics of the thalamic subregions using quantitative susceptibility mapping and free-water (FW) mapping in small vessel disease (SVD) over 1-2 years.

#### METHODS AND MATERIALS

Fifty-one SVD patients underwent brain MRI scans and neuropsychological evaluations both at baseline and at follow-up, composed of 28 SVD patients with mild cognitive impairment (VaMCI) and 23 with no cognitive impairment (NCI). Quantitative susceptibility (QS) values, FW values, and volumes within thalamic subregions, i.e., the anterior nuclei, the median nuclei, the lateral nuclei (TL-LT), the pulvinar (TL-PLV) and the internal medullary lamina (TL-IML), were calculated for each individual. Temporal (baseline vs. follow-up) and cross-sectional (VaMCI vs. NCI) differences were studied using mixed factorial ANOVA analysis and appropriate t-tests. Partial correlations were used to assess the relationship between the MRI indices changes (i.e.,  $\Delta$ FW<sub>followup-baseline</sub>/FW<sub>baseline</sub>) and cognitive function changes (i.e.,  $\Delta$ MoCA<sub>followup-baseline</sub>/MoCA<sub>baseline</sub>).

#### RESULTS

The Group effect resulted in greater mean FW values (index of neuroinflammation) in the left TL-PLV, bilateral TL-LT, and bilateral TL-IML for VaMCI compared with NCI, as well as resulted in higher mean QS values (index of iron deposition) in the left TL-PL and lower volumes in the left TL-IML ( $p < 0.05$ ). The Group $\times$ Time interaction identified increased mean QS values in the left TL-PLV for VaMCI over time. In addition, there were no significant effects for the FW values across Time. Furthermore, we observed significant negative associations between the FW values changes in the left TL-PLV and the right TL-LT and MoCA scores changes in VaMCI group over 1-2 years.

#### CONCLUSION

Our results demonstrate that elevated FW and QS values in the thalamic subregions have the potential to be used as an indicator in the progression of SVD. The FW values changes in the TL-PLV and the TL-LT might be the biomarkers for the mechanism of cognitive decline in the evolution of SVD.

#### CLINICAL RELEVANCE/APPLICATION

QSM and FW mapping when combined, can be considered as a specific and sensitive tool for the monitoring of the complex pathologies such as neuroinflammation and iron deposition in SVD. Our results might contribute to understanding the pathogenesis and progression of SVD.

Printed on: 02/07/23

## Abstract Archives of the RSNA, 2022

T2-SPNR-19

### Multiparametric Quantitative Evaluation Using Synthetic MRI in Normal-Appearing Brain Parenchyma in Adult Moyamoya Disease

Tuesday, Nov. 29 9:00AM - 9:30AM Room: Learning Center - NR DPS

#### Participants

Kazufumi Kikuchi, MD, PhD, (*Presenter*) Nothing to Disclose

#### PURPOSE

Moyamoya disease (MMD) is a progressive, steno-occlusive cerebrovascular disease affecting the arteries of the circle of the Willis. Few studies have examined the correlation between brain volume and function in patients with MMD. The purpose of this study was to investigate whether multiparametric brain volumes measured by synthetic MRI (SyMRI) correlate with cerebral blood flow (CBF) and brain function (BF) in MMD.

#### METHODS AND MATERIALS

This retrospective study was approved by our institutional review boards and conducted on 18 MMD patients (3 men, 15 women; median age, 43 years; range, 20-72 years). SyMRI was performed using the 3D-QALAS sequence by a 3T scanner. Quantification map acquisition and raw data processing were performed with SyMRI software (Version 21.4; SyMRI, Linköping, Sweden). CBF was measured using 123I-IMP SPECT, including the acetazolamide challenge. BFs were measured using WAIS-III/IV and WMS-R tests. Quantitative evaluations, including grey matter (GM), white matter (WM), and myelin correlated volume (MyC), were measured and corrected with total brain volume in normal-appearing brain parenchyma in six areas (bilateral anterior, middle, posterior cerebral arterial [ACA/MCA/PCA] territories). These three parameters and their correlations with corrected CBF and BF were evaluated by Spearman's rank-order correlation test.

#### RESULTS

Resting CBFs were correlated with GM fractions in the right ACA/MCA territories ( $r=0.524$ ,  $0.632$ ;  $P=0.039$ ,  $0.018$ , respectively). Cerebrovascular reactivity to an acetazolamide challenge was correlated with GM fraction in the left PCA territory ( $r=0.574$ ,  $P=0.018$ ). FSIQ/VCI derived from WAIS were correlated with GM fraction in the left PCA territory ( $r=0.625$ ,  $0.615$ ;  $P=0.009$ ,  $0.001$ , respectively). PSI derived from WAIS was correlated with GM fraction in the right MCA territory ( $r=0.665$ ,  $P=0.011$ ). There was no correlation between brain volume fractions and WMS-R indices.

#### CONCLUSION

S Synthetic MRI could noninvasively evaluate multiparametric brain volumes that correlate with CBF and BF in MMD.

#### CLINICAL RELEVANCE/APPLICATION

Synthetic MRI can quantitatively assess brain volume loss in patients with Moyamoya disease, which correlates with cerebral blood flow and brain function, and may help determine the disease severity.

Printed on: 02/07/23

## Abstract Archives of the RSNA, 2022

T2-SPNR-2

### **NCCT Image-based Automated Intracranial Hemorrhage Classification Using A Deep Learning Model: Is the Intracranial Hemorrhage Classification of Very Small Volume Hematoma Cases Reliable?**

Tuesday, Nov. 29 9:00AM - 9:30AM Room: Learning Center - NR DPS

#### **Participants**

Myeong Jin Kim, MD, PhD, (*Presenter*) Nothing to Disclose

#### **PURPOSE**

Intracranial hemorrhage (ICH) is a fatal disease that significantly affects the patient's life and prognosis over time. Patients with small-volume ICH (SICH) with small hematoma are more likely to have a benign clinical course and tend to experience hematoma expansion and have worse outcomes. In this study, we evaluate the classification performance for SICH cases using AI software (cHS-Heuron) for ICH diagnosis.

#### **METHODS AND MATERIALS**

We evaluated the SICH classification performance by testing the target group SICH data and the control group non-small volume ICH (Non-SICH) data using cHS-Heuron. As the evaluation data, RSNA ICH Challenge 2019 test dataset and clinical data from single institute were used. The number of data was 397 patients in ICH (250 SICH, 147 non-SICH) and 130 patients in the control group (Non-ICH). The gold standard was generated by a stroke expert by evaluating the hematoma volume of each slice. SICH data were defined as hematoma volume less than 0.65ml and diameter of 2mm or more and 5mm or less. The classifying performance was evaluated through the sensitivity and specificity compared to gold standard.

#### **RESULTS**

As the classifying performance of ICH patients, the sensitivity and specificity were 0.9748 and 0.9692, respectively. Among ICH patients, the true positive rate of SICH was 0.9600 in patient-wise classification. However, in slice-wise classification, the sensitivity and specificity were 0.8801 and 0.9890 for SICH group, and, in Non-SICH group, it was 0.9600 and 0.9867, respectively.

#### **CONCLUSION**

As a result of the ICH classification study using cHS-Heuron, the SICH group showed slightly lower sensitivity than the Non-SICH group, but in the patient-wise and slice-wise tests, the SICH group, the Non-SICH group all showed very high ICH classification performance.

#### **CLINICAL RELEVANCE/APPLICATION**

In the diagnosis of patients with ICH containing a very small volume hematoma area of less than 5 mm in diameter on NCCT images, cHS-Heuron can be utilized as a reliable pre-diagnosis tool for clinicians to quickly and accurately diagnose and make treatment decisions.

Printed on: 02/07/23

## Abstract Archives of the RSNA, 2022

T2-SPNR-3

### Diagnostic Yield of CTA Head After Stroke Protocol Standardization: A Retrospective Study

Tuesday, Nov. 29 9:00AM - 9:30AM Room: Learning Center - NR DPS

#### Participants

Dane Weinert, MD, (*Presenter*) Nothing to Disclose

#### PURPOSE

CT Angiography (CTA) of the head and neck is useful in the imaging of suspected stroke for identifying patients eligible for endovascular therapies. Acute stroke protocols may vary by when CTA is performed in the imaging algorithm. At our institution, a protocol was implemented which standardized CTA imaging to be obtained only as indicated after an initial non-contrast CT (NCCT) head per American Heart Association stroke guidelines. The objective of our study is to investigate how often relevant diagnostic findings were found in CTA imaging as part of the acute stroke protocol when obtained only after NCCT head imaging and an appropriate neurological exam raised high clinical suspicion for acute ischemia, compared to when CTA head was obtained along with NCCT head imaging immediately upon activation of the stroke protocol and without a neurological exam.

#### METHODS AND MATERIALS

CTA head reports were reviewed from April 2021 to Jan 2022. Patients with stroke-related indications in the image-requisition were included. A study was classified as "positive" if a large vessel occlusion was identified on imaging. Studies were then divided into "pre-intervention" (April through Aug 2021) and "post-intervention" (Sept 2021 through Jan 2022) groups to demarcate before and after the acute stroke protocol standardization to obtain CTA imaging after NCCT head imaging and an appropriate neurological exam raised high clinical suspicion for acute ischemia.

#### RESULTS

Results identified 428 studies in the pre-intervention group and 280 in the post-intervention group. There were 21 positive CTA exams in the pre-intervention group (4.9%) and 23 positive exams in the post-intervention group (8.2%) ( $p < 0.05$ ). Additionally, the number of studies ordered for stroke-related reasons decreased by 34.6% compared to the pre-intervention period.

#### CONCLUSION

The diagnostic yield of CTA was significantly improved after standardizing the acute stroke protocol to obtain CTA only after ischemic stroke was confirmed on NCCT. Adherence to standard practice guidelines in conjunction with judicious decision making when ordering imaging for stroke diagnosis is critical for limiting unnecessary radiation exposure and efficacious CT utilization.

#### CLINICAL RELEVANCE/APPLICATION

This study supports guideline-directed imaging protocol for stroke diagnosis via a higher diagnostic yield, limiting unnecessary radiation exposure, and efficient resource utilization.

Printed on: 02/07/23

## Abstract Archives of the RSNA, 2022

T2-SPNR-4

### The Application of Proton Exchange rate (kex) MRI in Ischemic Stroke Patients

Tuesday, Nov. 29 9:00AM - 9:30AM Room: Learning Center - NR DPS

#### Participants

Yiran Zhou, (*Presenter*) Nothing to Disclose

#### PURPOSE

Proton exchange rate (kex) MRI has recently been developed and preliminarily shown its potential value for evaluating reactive oxygen species of tissues in vivo. This study aimed to investigate the change of kex in different stroke stages and its correlation with stroke severity and prognosis.

#### METHODS AND MATERIALS

96 ischemic stroke patients were divided into 3 groups (acute, subacute and chronic) based on the stroke phases. A spin-echo echo-planar imaging sequence with pre-saturation chemical exchange saturation power of 1.5, 2.5, and 3.5  $\mu\text{T}$  was implemented to obtain Z-spectra which were fitted to remove the water direct saturation (DS) effect. kex maps were constructed from DS-removed omega plots. Relative kex (rkex) and relative apparent diffusion coefficient (rADC) were calculated by taking the ratio of kex or ADC in the infarcts over that of the mirrored contralateral tissue, respectively. Pearson's correlation analysis was implemented to evaluate the correlations between kex rkex and the National Institute of Health Stroke Scale (NIHSS). The predictive performance of kex, rkex, rADC, and lesion volume for acute stroke outcome was evaluated through receiver operating characteristic curve.

#### RESULTS

The kex of ischemic lesions was significantly higher compared to the mirrored contralateral tissue at the three stages (acute: ischemic lesion 935.08 s<sup>-1</sup> vs contralateral tissue 777.26 s<sup>-1</sup>,  $P < 0.001$ ; subacute: ischemic lesion 881.42 s<sup>-1</sup> vs contralateral tissue 762.17 s<sup>-1</sup>,  $P < 0.001$ ; chronic: ischemic lesion 866.93 s<sup>-1</sup> vs contralateral tissue 756.34 s<sup>-1</sup>,  $P < 0.001$ ). Besides, the kex of acute lesions was significantly higher than subacute and chronic lesions ( $P < 0.05$ ,  $P < 0.01$ , respectively). However, the difference between the subacute and chronic lesions was not significant. Lesion's kex and rkex significantly correlated with the NIHSS score only for the acute cases ( $r = 0.406$ ,  $P = 0.016$ ;  $r = 0.531$ ,  $P = 0.001$ ). Acute patients with poor prognosis had significantly higher kex rkex of lesion compared to patients with good prognosis (991.08 vs. 893.08 s<sup>-1</sup>,  $P < 0.001$ ; 1.28 vs. 1.15,  $P < 0.001$ ). These measures showed favorable predictive performance for acute stroke outcome with area under the curve (AUC) of 0.837 and 0.880, slightly while not significantly higher than lesion volume (AUC: 0.730) and rADC (AUC: 0.673).

#### CONCLUSION

s kex-MRI could identify ischemic lesions at different stages with markedly elevated intensity on the kex maps. It showed potential capability to reflect the stroke severity and predict the prognosis for acute stroke patients.

#### CLINICAL RELEVANCE/APPLICATION

kex-MRI is promising for ischemic stroke diagnosis and management as it may reflect oxidative stress of stroke lesions at different stages and predict the acute stroke outcome.

Printed on: 02/07/23

## Abstract Archives of the RSNA, 2022

T2-SPNR-5

### Clinical, Imaging Correlates and Prognostic Implications of Asymmetric Perivascular Spaces in Acute Ischemic Stroke

Tuesday, Nov. 29 9:00AM - 9:30AM Room: Learning Center - NR DPS

#### Participants

Jinhao Lyu, Beijing, China (*Presenter*) Nothing to Disclose

#### PURPOSE

Perivascular spaces (PVSs) have been considered a key element of the glymphatic system of the central nervous system and played a role in the mechanism of small vessel disease. Asymmetric PVSs is reported to be correlated with post-stroke depression and seizure. The incidence, mechanism, and prognostic implication of asymmetric PVSs have yet to be determined. We aimed to determine the associations of asymmetric PVSs with stroke presentations, cerebral hemodynamics and functional independence in acute ischemic stroke (AIS).

#### METHODS AND MATERIALS

We included 26 AIS patients with unilateral internal carotid artery and middle cerebral artery occlusion, who had undergone baseline routine head MRI and dynamic susceptibility contrast (DSC). Collateral circulation was graded 0-3 based on DSC source imaging (a higher value indicated better collaterals). The burden of PVSs was assessed by using a semi-quantitative scale. The scale selected 3 representative locations (midbrain [MB], basal ganglia [BG], and centrum semiovale [CS]) based on axial T2-weighted imaging slices and scored based on the number of PVSs (details please see Fig 1). The total score of PVSs in each hemisphere was calculated as: Stotal = SBG+ SCS+ SMB. Lesion side dominant asymmetry PVSs were defined as: Stotal of the infarct hemisphere - Stotal of the contralateral hemisphere > 0. The full baseline clinical and imaging features were listed in Table 1 in Fig 1. Binary logistic regression was used to identify predictors of lesion side dominant asymmetry PVSs and poor outcome defined as 3-month modified Rankin Scale > 2.

#### RESULTS

In them, 17/26 presented lesion side dominant asymmetry PVSs, 9/26 presented symmetry distribution of PVSs, and 0/26 presented contralateral side dominant asymmetry PVSs. Collateral circulation grade was significantly associated with the presence of lesion side dominant asymmetry PVSs (unadjusted odds ratio [OR], 0.07; 95% confidence interval [CI], 0.01-0.53; P=0.01). In binary logistic regression, lesion side dominant asymmetry PVSs (OR, 12.06; 95% CI, 1.16-125.91; P=0.038) was independent predictors of stroke outcomes after adjusted for age. The total burden of PVSs showed no significant association with stroke outcomes.

#### CONCLUSION

s In acute large vessel occlusion stroke, lesion side dominant asymmetry PVSs suggest the rapid impairments of the glymphatic system after ischemia, and hypoperfusion due to collateral circulation insufficiency may be one critical mechanism in the process.

#### CLINICAL RELEVANCE/APPLICATION

Lesion side dominant asymmetry PVSs negatively associated with stroke outcomes in acute ischemic stroke. Global estimation of PVSs is feasible and the asymmetry appearance may provide helpful and insightful information.

Printed on: 02/07/23

## Abstract Archives of the RSNA, 2022

T2-SPOB

### OB/Gynecology Tuesday Poster Discussions

Tuesday, Nov. 29 9:00AM - 9:30AM Room: Learning Center - OB DPS

#### Participants

Krupa Patel-Lippmann, MD, Nashville, TN (*Moderator*) Nothing to Disclose

#### Sub-Events

#### T2-SPOB-1 Pregnancy Following Hysterosalpingography: From Research to Reality

#### Participants

Anne P. Hemingway, MBBS, (*Presenter*) Consultant, Guerbet SA

#### PURPOSE

An RCT published in the NEJM in 2017 concluded that women under the age of 39 with unexplained subfertility had an improved spontaneous conception and live birth rate following hysterosalpingography (HSG) and that this benefit was greater when the HSG was undertaken with Oil-soluble contrast media (OSCM) compared to Water soluble contrast media (WSCM). Studies have shown that patients who participate in RCTs, whether in the intervention or control group, have a better outcome than those who do not. We wished to determine if the conception rates following HSG with either WSCM or OSCM in routine clinical practice mirrored those reported in the published RCT.

#### METHODS AND MATERIALS

The imaging and medical records relating to 667 consecutive HSGs undertaken between January 2020 and December 2021 were retrospectively reviewed. Research Ethics committee approval was granted for this study. Demographic, medical, imaging and reproductive data was collected. Pregnancy outcomes, mode of conception (spontaneous or assisted reproductive therapy (ART)), time to conception from HSG and type of contrast used was recorded.

#### RESULTS

667 consecutive hysterosalpingograms (HSG) in women aged between 19 and 51 years, mean 35.5 years were reviewed. 133 (23.6%) conceptions occurred following HSG with WSCM, 92 (69%) spontaneous, 36 (27%) following ART. 13 of the spontaneous pregnancies and 8 of the ART pregnancies occurred in women aged 39 or over. 77 of the pregnancies (57 spontaneous and 18 ART, 2 unspecified) occurred in HSGs reported as normal, 56 (35 spontaneous, 18 ART, 3 unspecified) in HSGs reported as abnormal. 31 (30%) conceptions followed an HSG with OSCM, 25 (81%) spontaneous, 6 (19%) following ART. 24 pregnancies followed an HSG reported as normal, 6 in HSGs reported as abnormal. 4 spontaneous pregnancies occurred in women aged 39 years or over.

#### CONCLUSION

The study remains ongoing, women continue to be followed up. Preliminary data however fully supports the hypothesis that in everyday routine HSG practice the procedure is associated with an enhanced conception rate and that OSCM is superior to WSCM in this respect. Research does indeed translate to reality.

#### CLINICAL RELEVANCE/APPLICATION

The management of subfertility is complex. Detailed investigation to determine cause is critical to appropriate management. Assisted reproductive therapies (ART) are demanding of the patients involved physically, emotionally and often financially. Any safe intervention that improves the chances of successful spontaneous conception is desirable. From both published RCTs, meta-analyses and observational studies such as this, it is clear that an HSG with either WSCM or OSCM is advantageous in this respect and that OSCM has a significant advantage over WSCM.

Printed on: 02/07/23



## Abstract Archives of the RSNA, 2022

T2-SPOB-1

### Pregnancy Following Hysterosalpingography: From Research to Reality

Tuesday, Nov. 29 9:00AM - 9:30AM Room: Learning Center - OB DPS

#### Participants

Anne P. Hemingway, MBBS, (*Presenter*) Consultant, Guerbet SA

#### PURPOSE

An RCT published in the NEJM in 2017 concluded that women under the age of 39 with unexplained subfertility had an improved spontaneous conception and live birth rate following hysterosalpingography (HSG) and that this benefit was greater when the HSG was undertaken with Oil-soluble contrast media (OSCM) compared to Water soluble contrast media (WSCM). Studies have shown that patients who participate in RCTs, whether in the intervention or control group, have a better outcome than those who do not. We wished to determine if the conception rates following HSG with either WSCM or OSCM in routine clinical practice mirrored those reported in the published RCT.

#### METHODS AND MATERIALS

The imaging and medical records relating to 667 consecutive HSGs undertaken between January 2020 and December 2021 were retrospectively reviewed. Research Ethics committee approval was granted for this study. Demographic, medical, imaging and reproductive data was collected. Pregnancy outcomes, mode of conception (spontaneous or assisted reproductive therapy (ART)), time to conception from HSG and type of contrast used was recorded.

#### RESULTS

667 consecutive hysterosalpingograms (HSG) in women aged between 19 and 51 years, mean 35.5 years were reviewed. 133 (23.6%) conceptions occurred following HSG with WSCM, 92 (69%) spontaneous, 36 (27%) following ART. 13 of the spontaneous pregnancies and 8 of the ART pregnancies occurred in women aged 39 or over. 77 of the pregnancies (57 spontaneous and 18 ART, 2 unspecified) occurred in HSGs reported as normal, 56 (35 spontaneous, 18 ART, 3 unspecified) in HSGs reported as abnormal. 31 (30%) conceptions followed an HSG with OSCM, 25 (81%) spontaneous, 6 (19%) following ART. 24 pregnancies followed an HSG reported as normal, 6 in HSGs reported as abnormal. 4 spontaneous pregnancies occurred in women aged 39 years or over.

#### CONCLUSION

The study remains ongoing, women continue to be followed up. Preliminary data however fully supports the hypothesis that in everyday routine HSG practice the procedure is associated with an enhanced conception rate and that OSCM is superior to WSCM in this respect. Research does indeed translate to reality.

#### CLINICAL RELEVANCE/APPLICATION

The management of subfertility is complex. Detailed investigation to determine cause is critical to appropriate management. Assisted reproductive therapies (ART) are demanding of the patients involved physically, emotionally and often financially. Any safe intervention that improves the chances of successful spontaneous conception is desirable. From both published RCTs, meta-analyses and observational studies such as this, it is clear that an HSG with either WSCM or OSCM is advantageous in this respect and that OSCM has a significant advantage over WSCM.

Printed on: 02/07/23

## Abstract Archives of the RSNA, 2022

T2-SPPD

### Pediatric Tuesday Poster Discussions

Tuesday, Nov. 29 9:00AM - 9:30AM Room: Learning Center - PD DPS

#### Participants

Rama Ayyala, MD, Cincinnati, OH (*Moderator*) Nothing to Disclose

#### Sub-Events

#### **T2-SPPD-1 Neuroradiological Imaging in Newborns: A Standardized Brain MRI Protocol With Non-invasive Sedation Using a Melatonin-Based Solution**

#### Participants

Simone Marziali, MD, Rome, Italy (*Presenter*) Nothing to Disclose

#### PURPOSE

MRI is the best technique to investigate newborn neurological pathologies, particularly affecting preterm infants, in both acute setting and follow-up of late sequelae. Given the increasing use of neonatal brain MRI, great interest is developing in obtaining diagnostic images without profound sedation, which requires logistic accommodations and trained personnel in neonatal anesthesia, often difficult to achieve. Melatonin is known as a sleep inducer in children and used in neurophysiological and neuroimaging procedures. Our aim was to assess the efficacy of a melatonin-based solution for non-invasive sedation in a standardized neonatal brain MRI protocol.

#### METHODS AND MATERIALS

110 newborns (37 term and 73 preterm) which underwent brain MRI between 2017 and 2019 were enrolled in this study. Sedation was induced with one, two or three administrations of an oral solution of melatonin, tryptophan, and vitamin B6 (Melamil Tripto®). 30 minutes before the exam, 2 mg of melatonin was administered. If the neonate was still awake after 20 minutes, and additional 1 mg was administered. Additional 1 mg was administered if the baby was not sleeping after further 15 minutes. A neonatologist was present at each examination and both heart rate and oxygen saturation were monitored. We used a vacuum mattress to contain the little patients and mini muffs to reduce the noise. MRI was performed on a 1.5T scanner and basic protocol included multi-planar spin-echo (SE) T1-weighted, turbo-spin-echo (TSE) T2-weighted sequences, T2\* gradient echo sequences (GRE), diffusion weighted imaging (DWI) and susceptibility weighted imaging (SWI). Evaluation was performed by two different neuroradiologists experienced in neonatal neuroimaging.

#### RESULTS

In 106 patients we obtained sufficient sedation to perform an adequate quality MRI, with a median time of 25min to reach sleeping. In 3 patients MRI could not be performed due to complete wakefulness. One patient was excluded for consent withdrawn. Higher melatonin dose was necessary in patients with higher weight and in all the patients who took 3 shots of the solution, difficulty in performing the MRI was reported. However, this did not significantly affect the total length of the acquisition and no side effects have been reported up to 4 mg.

#### CONCLUSION

In patients with higher tendency to wakefulness, the acquisition of high resolution sequences was not possible due to longer acquisition time leading to increasing motion artifacts. However, in most cases our method was able to achieve sufficient sedation to perform MRI, avoiding the use of anesthetics and obtaining good quality images.

#### CLINICAL RELEVANCE/APPLICATION

These initial results may be helpful for future development of non-invasive neuroimaging protocols in neonates.

Printed on: 02/07/23

## Abstract Archives of the RSNA, 2022

T2-SPPD-1

### Neuroradiological Imaging in Newborns: A Standardized Brain MRI Protocol With Non-invasive Sedation Using a Melatonin-Based Solution

Tuesday, Nov. 29 9:00AM - 9:30AM Room: Learning Center - PD DPS

#### Participants

Simone Marziali, MD, Rome, Italy (*Presenter*) Nothing to Disclose

#### PURPOSE

MRI is the best technique to investigate newborn neurological pathologies, particularly affecting preterm infants, in both acute setting and follow-up of late sequelae. Given the increasing use of neonatal brain MRI, great interest is developing in obtaining diagnostic images without profound sedation, which requires logistic accommodations and trained personnel in neonatal anesthesia, often difficult to achieve. Melatonin is known as a sleep inducer in children and used in neurophysiological and neuroimaging procedures. Our aim was to assess the efficacy of a melatonin-based solution for non-invasive sedation in a standardized neonatal brain MRI protocol.

#### METHODS AND MATERIALS

110 newborns (37 term and 73 preterm) which underwent brain MRI between 2017 and 2019 were enrolled in this study. Sedation was induced with one, two or three administrations of an oral solution of melatonin, tryptophan, and vitamin B6 (Melamil Tripto®). 30 minutes before the exam, 2 mg of melatonin was administered. If the neonate was still awake after 20 minutes, and additional 1 mg was administered. Additional 1 mg was administered if the baby was not sleeping after further 15 minutes. A neonatologist was present at each examination and both heart rate and oxygen saturation were monitored. We used a vacuum mattress to contain the little patients and mini muffs to reduce the noise. MRI was performed on a 1.5T scanner and basic protocol included multi-planar spin-echo (SE) T1-weighted, turbo-spin-echo (TSE) T2-weighted sequences, T2\* gradient echo sequences (GRE), diffusion weighted imaging (DWI) and susceptibility weighted imaging (SWI). Evaluation was performed by two different neuroradiologists experienced in neonatal neuroimaging.

#### RESULTS

In 106 patients we obtained sufficient sedation to perform an adequate quality MRI, with a median time of 25min to reach sleeping. In 3 patients MRI could not be performed due to complete wakefulness. One patient was excluded for consent withdrawn. Higher melatonin dose was necessary in patients with higher weight and in all the patients who took 3 shots of the solution, difficulty in performing the MRI was reported. However, this did not significantly affect the total length of the acquisition and no side effects have been reported up to 4 mg.

#### CONCLUSION

In patients with higher tendency to wakefulness, the acquisition of high resolution sequences was not possible due to longer acquisition time leading to increasing motion artifacts. However, in most cases our method was able to achieve sufficient sedation to perform MRI, avoiding the use of anesthetics and obtaining good quality images.

#### CLINICAL RELEVANCE/APPLICATION

These initial results may be helpful for future development of non-invasive neuroimaging protocols in neonates.

Printed on: 02/07/23

## Abstract Archives of the RSNA, 2022

T2-SPPH

### Physics Tuesday Poster Discussions

Tuesday, Nov. 29 9:00AM - 9:30AM Room: Learning Center - PH DPS

#### Participants

Sarah McKenney, PhD, Stanford, CA (*Moderator*) Nothing to Disclose

#### Sub-Events

### T2-SPPH-1 **Soft Tissue Image Quality in Computed Tomography Using an Anthropomorphic Phantom: Model Observer Comparison Between Dual-Energy and Photon-Counting Scanners**

#### Participants

Dimitar Petrov, Leuven, Belgium (*Presenter*) Nothing to Disclose

#### PURPOSE

Study the soft tissue image quality (IQ) using an anthropomorphic phantom on a dual-energy CT scanner (DE-CT) and a newly installed photon-counting CT scanner (PC-CT). Investigate the differences in monoenergetic reconstructions and compare the performance between the two scanners.

#### METHODS AND MATERIALS

An anthropomorphic abdomen phantom producing clinically relevant soft tissue Hounsfield units (HU) was scanned 12 times on both a Siemens DE-CT and PC-CT scanners with  $CTDI_{vol}=8mGy$ . A custom insert containing 45 low-contrast (-20HU) spheres grouped into 3 sizes of 4, 6, and 8mm diameter was placed in the phantom for task-based IQ estimation. The acquisitions were reconstructed for 7 ascending monoenergetic X-ray spectra ranging between 60keV and 85keV, each of them reconstructed with iterative (IR) and filtered-back projection (FBP) reconstruction algorithms. The conventional polychromatic reconstructions were also added to the comparison. For each condition, 30 signal present and 90 signal absent regions of interest (ROI) were extracted from the phantom images. The image quality analysis was performed using a two-layer channelized Hotelling observer (CHO) performing a four-alternative forced-choice (4AFC) reading. The percentage correct (PC) values for each sphere size and condition were fitted with a psychometric fit and the sphere threshold detectability diameter ( $D_{tr}$ ) at 62.5 PC was used as a final IQ figure of merit.

#### RESULTS

The  $D_{tr}$  for each system was compared against the corresponding scanner type and reconstruction algorithm type (figure). The analysis showed that there is no significant difference between FBP and IR ( $p>0.11$ ). The performance of the DE-CT compared to the PC-CT for the polychromatic settings was, for both reconstruction algorithms, not significantly different ( $p=0.44$ ). For the two scanners, optimal low-contrast detectability occurred at different keV settings, for the PC-CT, at 67keV, and for DE-CT at 80keV. The PC-CT reached a monoenergetic threshold detectability diameter of  $5.3\pm 0.12$  mm, and the DE-CT a significantly higher value of  $5.5\pm 0.10$  mm ( $p=0.57$ ). Both scanners reach similar monoenergetic performance at 74keV ( $p>0.32$ ).

#### CONCLUSION

The CHO results show that the two scanners perform similarly for the standard polychromatic settings. The PC-CT outperforms the DE-CT for the lower monoenergetic reconstructions.

#### CLINICAL RELEVANCE/APPLICATION

The soft tissue image quality of PC-CT was optimal at 67keV. As most abdominal CT exams use contrast agents that also benefit from low keV values, the PC-CT may clinically outperform conventional DE-CTs.

### T2-SPPH-2 **Human Observer Detection of Liver Metastases in Patients vs. Model Observer Detection (D') In a Liver Phantom**

#### Participants

Emma Thingstad, MSc, Oslo, Norway (*Presenter*) Research collaboration, The Phantom Laboratory

#### PURPOSE

Detection and characterization of liver lesions is essential in oncological imaging, with decisive implication on patient care. Quantitative methods to evaluate diagnostic performance are aspired in clinical practice to tailor protocols. This study compares the detectability of liver metastasis by radiologists in a clinical setting (human observer) to performance of a tailored software applied to CT images of a liver phantom containing lesions (model observer).

#### METHODS AND MATERIALS

20 patients were scanned with standard abdominal CT protocol for detection of liver metastases (median  $CTDI_{vol} = 12.2$  mGy). 11 of these were additionally scanned with 60% and 40% dose and 9 were scanned with 50% and 30% dose. Images were reconstructed with ASiR-V (AV) 50% and True-Fidelity - high (TF). Detectability of liver metastases was assessed by two

radiologists and compared to a gold standard (evaluation using high dose and clinical information of the patient). CT scans of a liver phantom (The Phantom Laboratory) containing inserts with various iodine concentrations and diameters at corresponding conditions were analyzed using the ImQuest software (Duke University), and a detectability index ( $d'$ ) was calculated for each configuration. Results from the human observer method were compared to those of the model observer method.

## RESULTS

The model observer  $d'$  followed the same trend as lesions detected by human observers in patient images when changing dose level. When changing reconstruction algorithm TF improved  $d'$  compared to AV. In the patient group with 30/50% dose, results show that AV may be beneficial compared to TF, while in the patient group with 40/60% dose, this trend is not as clear. This may be because of different lesion sizes in the two groups. Dependence of lesion size and contrast is work in progress.

## CONCLUSION

The behavior of the detectability in patient vs.  $d'$  in the phantom coincides at different dose levels. However, when changing reconstruction algorithm the tests do not correlate to the same degree. Dependence on lesion size and contrast may be the reason for this.

## CLINICAL RELEVANCE/APPLICATION

Quality assessment of CT protocols is time consuming. Model observers in imaging phantoms could save radiologists both time and cost. But does the model observer correlate well with lesion detection?

### T2-SPPH-3 Comparison of Low-Contrast Object Detectability in Deep Learning and Conventional Reconstructions: AAPM TG-233 Phantom Evaluation

Participants

Chang Yong Heo, BS, Seoul, Korea, Republic Of (*Presenter*) Nothing to Disclose

## PURPOSE

To measure the detectability of low-contrast objects on CT according to AAPM TG-233 report and examine if deep learning-based technique could improve the detectability of low-contrast objects over conventional reconstructions in low-dose CT imaging.

## METHODS AND MATERIALS

ACR phantom was scanned at 120kV with SD (100mAs) and LD (25mAs) settings and reconstructed with two different scanners (GE: Discovery 750 HD, FBP and ASiR-V 30%; Siemens: Somatom Force, FBP and ADMIRE 2). A deep learning-based CT denoising model (DLM; ClariCT.AI™, ClariPi) was applied to all FBP images. Low-contrast detectability was measured according to AAPM TG-233 report using imQuest soft (Duke University) and compared for the different scan and reconstruction settings. Noise power spectrum (NPS) was measured on uniform section of module 3, and task-based transfer function (TTF) was analyzed on acrylic disk of module 1. Detectability index ( $d'$ ) was computed for a 5 mm low contrast disk object with 7 HU.

## RESULTS

Detectability index ( $d'$ ) improved markedly with DLM (GE, 1.90; Siemens, 2.17) from that of FBP (GE, 0.99; Siemens, 1.11), and was comparable with IR (GE, 1.03; Siemens, 1.22) in LD scans of both scanners. The detectability indices with DLM in LD scans were superior to those with FBP in HD scans (GE, 1.77; Siemens, 2.08) which translated to the dose reduction potential more than 75%.

## CONCLUSION

Measurement of low-contrast detectability on ACR phantom provided an objective comparison of image quality in conventional and DL reconstructions. Deep learning-based denoising model was shown to improve detectability of low-contrast objects while conventional IR was not.

## CLINICAL RELEVANCE/APPLICATION

Detectability measurement according to AAPM TG-233 report can be an objective way of examining image quality with newly developed reconstruction techniques in comparison with conventional reconstructions.

### T2-SPPH-4 Impact of an Artificial Intelligence Deep-Learning Reconstruction Algorithm for CT on Image Quality and Potential Dose Reduction: A Phantom Study

Participants

Joel Greffier, PhD, Nimes, France (*Presenter*) Nothing to Disclose

## PURPOSE

To assess the impact of a artificial intelligence deep-learning reconstruction (AI-DLR) algorithm on image quality and dose reduction compared with a hybrid IR algorithm in chest CT for different clinical indications.

## METHODS AND MATERIALS

Acquisitions on the CT ACR 464 and CT Torso CTU-41 phantoms were performed at five dose levels (CTDIvol: 9.5/7.5/6/2.5/0.4mGy) used for chest CT conditions. Raw data were reconstructed using filtered back projection (FBP), two levels of IR (iDose4 levels 4 (i4) and 7 (i7)), and five levels of AI-DLR (Precise Image; Smoother, Smooth, Standard, Sharp, Sharper). Noise power spectrum (NPS), task-based transfer function (TTF) and detectability index ( $d'$ ) were computed:  $d'$  modelled detection of a soft tissue mediastinal nodule, ground-glass opacity, or high-contrast pulmonary lesion. Subjective image quality of chest anthropomorphic phantom images was independently evaluated by two radiologists. They have assessed image noise, image smoothing, contrast between the vessels and fat in the mediastinum for mediastinal images, visual border detection between bronchus and lung parenchyma for parenchymal images and overall image quality using a commonly-used four or five-point scale.

## RESULTS

From Standard to Smoother levels, the noise magnitude decreased, the average NPS spatial frequency decreased and the detectability ( $d'$ ) of the three lesions increased. The opposite pattern was found from Standard to Sharper levels. From Smoother to Sharper levels, the spatial resolution increased for the low contrast polyethylene insert and the opposite for the high contrast air

insert. Compared to the i4 used in clinical practice,  $d'$  values were higher using Smoother, Smooth and Standard levels for mediastinal images and Smoother and Smooth levels for parenchymal images. Radiologists considered the images satisfactory for clinical use at these levels, but adaptation to the dose level of the protocol is required.

## CONCLUSION

s With AI-DLR, the smoothest levels reduced the noise and improved the detectability of chest lesions but increased the image smoothing. The opposite was found with the sharpest levels. The choice of level depends on the dose level and type of image: mediastinal or parenchymal.

## CLINICAL RELEVANCE/APPLICATION

For the first time, we assessed the impact of the new artificial intelligence deep-learning reconstruction algorithm developed by Philips Healthcare and called Precise Image, compared to a standard clinical protocol using either FBP or IR reconstruction algorithms.

## T2-SPPH-5 A Novel Detector Geometry for Third Generation CT

Participants

Jiang Hsieh, PhD, (*Presenter*) Former Employee, General Electric Company

## PURPOSE

State-of-the-art CT scanners employ conventional detector geometry that forms an arc concentric to the x-ray source. The collected projection samples form an equiangular dataset, but their distance to the isocenter is nonuniformly spaced. When CT scanners employ steps to convert cone-beam datasets to parallel-beam datasets prior to the reconstruction, both channel- and view-wise rebinning are required. Such approach potentially leads to a degraded spatial resolution and an increased aliasing artifact.

## METHODS AND MATERIALS

We propose a novel detector geometry that acquires projection samples with an evenly spaced distance to the isocenter. To ensure that the detector cell size is independent of the cell position, the source-to-detector distance varies as a function of the detector fan-angle. To guarantee detector surface being normal to the x-ray beam, each detector module (16 channels) is tilted relative to each other. This design requires only view-rebinning to form a parallel dataset. In addition, the detector surface area (arc-length) is reduced compared to the conventional design and a smaller cell size can be employed.

## RESULTS

Extensive computer simulations were used to demonstrate the efficacy of our design, utilizing a wire phantom, water phantom, Shepp-Logan head phantom, and a specially designed aliasing phantom. Spatial resolution was measured with modulation transfer function (MTF) and the proposed design offers 12.6% increase compared to the conventional design, resulting from the smaller detector cell and removal of the channel-wise interpolation. In addition, aliasing artifact is significantly improved at locations away from the isocenter. At matched spatial resolution (by modifying the reconstruction kernel for the conventional design), image noise for the proposed system is 8.8% lower.

## CONCLUSION

s Compared to the conventional geometry, the proposed detector geometry offers improved performance in spatial resolution and artifact reduction, and exhibits better noise performance at a matching resolution. Further research on this design is warranted to fully explore other systems parameters such as the compactness of the gantry design.

## CLINICAL RELEVANCE/APPLICATION

This research is relevant to improve the clinical performance of a CT system.

## T2-SPPH-6 Robust High Precision Nonlinear CT Reconstruction Two Orders of Magnitude Faster than Competing Iterative Reconstruction

Participants

Wolfram Jarisch, PhD, (*Presenter*) Nothing to Disclose

## PURPOSE

A new method for Tomographic reconstructions potentially makes highest quality diagnostic CT imaging available to all patients. The new method continues to evolve in competition to existing nonlinear iterative and deep learning methods that are overly sensitive to small data changes (Vegard Antuna, et al., 2020). Here we focus on a new iterative approach combining filtered backprojection (FBP), logarithmic and exponential transformations (LET), matching linearizations, and voxel state expansion. The nonlinear iterative approach provides high stability, accuracy, and computational speed. The method surpasses performance of other methods in terms of accuracy with two orders of magnitude higher speed.

## METHODS AND MATERIALS

The method was first implemented in a high level program language at an NIH laboratory using publicly available program components for projection and backprojection. Accuracy and speed exceeded results over a state-of-the-art OS-SART implementation (Ander Biguri, 2017, GitHub).

## RESULTS

On a 3D skull model, development of new Python code, showed half the residual-sum-of-squares on central slices and between 80 and 150 fold higher speed than OS-SART (Figure). Both algorithms used the same array processor.

## CONCLUSION

s The high imaging quality and speed of the new algorithm allows to compute 3D angiographic images from a sequence of 6 moving projections. Similarly, movie-like 3D tomograms may be estimated motion parameters during the reconstruction process (Levenber-Marquardt; 1944, 1963; not shown). The high imaging quality of the new algorithm follows from its relation to minimum variance

estimation and structural similarity to Maximum Entropy estimation.

#### **CLINICAL RELEVANCE/APPLICATION**

The combined noise resilience, high imaging quality, modeling of movement, and speed, can reduce several barriers to the effective use of CT: cost per procedures, radiation, procedure time, and movement of patients.

#### **T2-SPPH-7 CT Number Stability in Clinical Photon-Counting Virtual Monoenergetic Imaging**

Participants

Jessica Flores, MS, (*Presenter*) Nothing to Disclose

#### **PURPOSE**

In the quantitative assessment of pathology in sequential and inter-patient studies, robust attenuation estimation of materials is essential for clinical applications of computed tomography (CT). Current standards in CT technology rely on energy-integrating detectors in single-energy CT (SECT) and dual-energy CT (DECT). With the introduction of photon-counting CT (PCCT) into clinical practice, there is the potential to improve HU stability. Therefore, this work aimed to study CT number stability to elucidate differences in CT systems and to highlight the strengths of clinical PCCT.

#### **METHODS AND MATERIALS**

Data was acquired on a clinical PCCT scanner, Siemens NAEOTOM Alpha, and a SECT/DECT scanner, Siemens SOMATOM Drive. HU variation was investigated in the CIRS 662 phantom with material-equivalent inserts, like iodine in water (15.0 mg/mL), adipose, bone (200 mg/mL) and muscle. Two factory protocols and phantom size configurations were used to demonstrate stability across CTDIvol and size. Protocols were adjusted to sweep across kVp and define a constant CTDIvol. Standard IR strengths and a single reconstruction kernel were used to create volume images. Virtual monoenergetic images in the PCCT scanner were produced at 70 keV, corresponding closest to the mean energy of a 120 kVp spectrum. Circular ROI masks were applied over regions containing inserts in volume images and used to determine mean HU per material. Percent relative standard deviation is reported as a metric to quantify HU variation in each material.

#### **RESULTS**

Preliminary studies show that the clinical PCCT scanner produces more consistent measurements than the SECT/DECT scanner in SECT mode for the same material across phantom size, CTDIvol and kVp. For all material inserts, percent relative standard deviation varied between 4.6% and 26.2% in the SECT scanner and between 0.7% and 2.6% in the PCCT scanner. Differences in performance between scanners are particularly apparent in higher HU materials such as bone and iodine inserts, where measurements from the PCCT scanner show less variation. For 15.0 mg/mL iodine in water, HU estimations showed 26.2% and 0.7% relative standard deviation in the SECT and PCCT scanners, respectively.

#### **CONCLUSION**

s Compared to SECT, clinical PCCT produces more stable and consistent CT number measurements.

#### **CLINICAL RELEVANCE/APPLICATION**

Comparing a new clinical PCCT scanner to other scanners that are already familiar, this work highlights the strength of PCCT in the clinic to facilitate the quantitative assessment of pathology.

#### **T2-SPPH-8 Quality Comparison of Single-Energy CT at Low Tube Voltages and Virtual Monochromatic Imaging at Low Energies by Dual-Energy CT With Deep Learning Reconstruction**

Participants

Shingo Harashima, Tokyo, Japan (*Presenter*) Nothing to Disclose

#### **PURPOSE**

To compare quality of single-energy CT (SECT) at low tube voltages and virtual monochromatic imaging (VMI) at low energies by dual-energy CT (DECT) with deep learning reconstruction (DLR) in phantom experiments to simulate routine abdominal contrast-enhanced CT (CECT).

#### **METHODS AND MATERIALS**

We performed SECT and DECT scanning of a water phantom (GE), a phantom to assess beam-hardening artifact (BHA) (QSP-1 phantom; FUYO, Tokyo), and our original phantom to measure task-based modulation transfer function (TTF) using a state-of-the-art 256-gemstone-detector CT scanner (Revolution Apex, GE) at the similar volume CT dose index of approximately 10 mGy. For SECT scanning, tube voltage/current was 70 kVp/750 mA and 80 kVp/470 mA. For DECT scanning, tube voltage was rapidly switched from 80 to 140 kVp and tube current was 200 mA. SECT at 70 and 80 kVp and VMI at 40 and 50 keV were reconstructed using thickness of 1.25 mm and DLR (TrueFidelity, GE). We measured standard deviation of CT value as image noise and noise power spectrum (NPS) using the water phantom; CT value using the QSP-1 phantom with and without surrounding 350-mg iodine contrast media (CM), iohexol (Omnipaque 350, GE), at dilution factor of 10 for simulating bone attenuation to calculate its absolute difference as an index of BHA; contrast-noise ratio (CNR) and TTF using the TTF phantom with the CM at dilution factors of 30 and 60 for simulating arterial and hepatic attenuations, respectively; and thus compared these results among SECT at 70 and 80 kVp and VMI at 40 and 50 keV using one-way ANOVA and Tukey tests.

#### **RESULTS**

Whereas image noise significantly decreased from 40 keV to 50 keV to SECT ( $P < 0.05$ ), CNR significantly increased from SECT to 50 keV to 40 keV ( $P < 0.05$ ). NPS peaked at lower frequency by DECT than by SECT. BHA was significantly less by DECT than by SECT ( $P < 0.05$ ). TTF was lower by DECT than by SECT by approximately 12%.

#### **CONCLUSION**

s Using DLR at the similar radiation dose, VMI at the low energies degrade noise characteristics and decrease spatial resolution by approximately 12% but increase CNR and reduce BHA compared with SECT at the low tube voltages in routine abdominal CECT.

#### **CLINICAL RELEVANCE/APPLICATION**

When decreased spatial resolution by approximately 12% is acceptable, combined with DLR, VMI at 40-50 keV by DECT are clinically more beneficial than SECT at 70-80 kVp in routine abdominal CECT.

## **T2-SPPH-9 Evaluation of Pulse Pileup on a Clinical Photon-Counting CT Scanner**

Participants

Mridul Bhattarai, MS, BS, Durham, NC (*Presenter*) Nothing to Disclose

### **PURPOSE**

To evaluate the significance of pulse pileup on clinical photon-counting CT (PCCT) in terms of task-generic image quality metrics.

### **METHODS AND MATERIALS**

An ACR phantom was scanned on a commercial PCCT (NAEOTOM Alpha, Siemens). Tube current was varied from 240 - 980 mA to study the effects of the flux to the detector on pulse pileup. Helical scans were done at 120 kV without tube current modulation (TCM) under eleven tube currents (240 - 980 mA), rotation time of 0.5 s, and pitch of 1. The dose levels corresponded to CTDIvol (32 cm phantom) of 9.5 - 38.7 mGy. Images were reconstructed using QIR-off mode (FBP) with Br44 kernel and voxel size of  $0.4102 \times 0.4102 \times 3$  mm<sup>3</sup>. imQuest, an open-source MATLAB-based software package, was used to calculate noise power spectrum (NPS), modulation transfer function (MTF), contrast-to-noise ratio (CNR), and CT number according to AAPM task group 233.

### **RESULTS**

The shape of MTF did not change with mA. The relationship between noise magnitude and mA, noise proportional to  $\text{mA}^{-1/2}$ , deviated up to 24.5% at the higher dose levels. The average frequency of NPS decreased from 0.31 (at 240 mA) to 0.27 mm<sup>-1</sup> (at 980 mA), insignificant compared to the increase in dose. CNR increased monotonically up to 880 mA, then it decreased to 980 mA, demonstrating detector saturation due to high flux. CT numbers were consistent across all tube currents with ranges of  $\pm 0.8$ ,  $\pm 1.1$ ,  $\pm 3.4$ ,  $\pm 4.6$ ,  $\pm 1.0$  HU for water, polyethylene, bone, air, and acrylic inserts, respectively.

### **CONCLUSION**

Results demonstrate that the pulse pileup does not affect the spatial resolution, noise texture, and CT number accuracy, but has a modest influence on the noise magnitude and CNR. The significant effects were seen for only extremely high tube currents ( $> 880$  mA = CTDIvol of 34.7 mGy) when used to scan a 20-cm ACR phantom, which is not clinically applicable. In addition, generally, in clinical practices, TCM is used to control the exposure level decreasing the variation of flux on the detector and alleviating the chance of detector saturation due to high count rates. Thus, pulse pileup does not affect the image quality of commercial PCCT when clinically relevant tube currents are used.

### **CLINICAL RELEVANCE/APPLICATION**

High tube current causes high flux to the photon-counting detectors resulting in piling up of pulses formed by concurrent photons. Theoretically, pulse pileup causes count loss and energy resolution degradation, affecting image quality and HU number accuracy in PCCT. Several studies have been done previously to study the effects of pulse pileup through simulations or use of non-clinical detectors. In the tests performed, pulse pileup proved to be inconsequential in clinical PCCT as implemented.

Printed on: 02/07/23

## Abstract Archives of the RSNA, 2022

T2-SPPH-1

### Soft Tissue Image Quality in Computed Tomography Using an Anthropomorphic Phantom: Model Observer Comparison Between Dual-Energy and Photon-Counting Scanners

Tuesday, Nov. 29 9:00AM - 9:30AM Room: Learning Center - PH DPS

#### Participants

Dimitar Petrov, Leuven, Belgium (*Presenter*) Nothing to Disclose

#### PURPOSE

Study the soft tissue image quality (IQ) using an anthropomorphic phantom on a dual-energy CT scanner (DE-CT) and a newly installed photon-counting CT scanner (PC-CT). Investigate the differences in monoenergetic reconstructions and compare the performance between the two scanners.

#### METHODS AND MATERIALS

An anthropomorphic abdomen phantom producing clinically relevant soft tissue Hounsfield units (HU) was scanned 12 times on both a Siemens DE-CT and PC-CT scanners with  $CTDI_{vol}=8mGy$ . A custom insert containing 45 low-contrast (-20HU) spheres grouped into 3 sizes of 4, 6, and 8mm diameter was placed in the phantom for task-based IQ estimation. The acquisitions were reconstructed for 7 ascending monoenergetic X-ray spectra ranging between 60keV and 85keV, each of them reconstructed with iterative (IR) and filtered-back projection (FBP) reconstruction algorithms. The conventional polychromatic reconstructions were also added to the comparison. For each condition, 30 signal present and 90 signal absent regions of interest (ROI) were extracted from the phantom images. The image quality analysis was performed using a two-layer channelized Hotelling observer (CHO) performing a four-alternative forced-choice (4AFC) reading. The percentage correct (PC) values for each sphere size and condition were fitted with a psychometric fit and the sphere threshold detectability diameter (Dtr) at 62.5 PC was used as a final IQ figure of merit.

#### RESULTS

The Dtr for each system was compared against the corresponding scanner type and reconstruction algorithm type (figure). The analysis showed that there is no significant difference between FBP and IR ( $p>0.11$ ). The performance of the DE-CT compared to the PC-CT for the polychromatic settings was, for both reconstruction algorithms, not significantly different ( $p=0.44$ ). For the two scanners, optimal low-contrast detectability occurred at different keV settings, for the PC-CT, at 67keV, and for DE-CT at 80keV. The PC-CT reached a monoenergetic threshold detectability diameter of  $5.3\pm 0.12$  mm, and the DE-CT a significantly higher value of  $5.5\pm 0.10$  mm ( $p=0.57$ ). Both scanners reach similar monoenergetic performance at 74keV ( $p>0.32$ ).

#### CONCLUSION

The CHO results show that the two scanners perform similarly for the standard polychromatic settings. The PC-CT outperforms the DE-CT for the lower monoenergetic reconstructions.

#### CLINICAL RELEVANCE/APPLICATION

The soft tissue image quality of PC-CT was optimal at 67keV. As most abdominal CT exams use contrast agents that also benefit from low keV values, the PC-CT may clinically outperform conventional DE-CTs.

Printed on: 02/07/23

## Abstract Archives of the RSNA, 2022

T2-SPPH-2

### Human Observer Detection of Liver Metastases in Patients vs. Model Observer Detection ( $d'$ ) In a Liver Phantom

Tuesday, Nov. 29 9:00AM - 9:30AM Room: Learning Center - PH DPS

#### Participants

Emma Thingstad, MSc, Oslo, Norway (*Presenter*) Research collaboration, The Phantom Laboratory

#### PURPOSE

Detection and characterization of liver lesions is essential in oncological imaging, with decisive implication on patient care. Quantitative methods to evaluate diagnostic performance are aspired in clinical practice to tailor protocols. This study compares the detectability of liver metastasis by radiologists in a clinical setting (human observer) to performance of a tailored software applied to CT images of a liver phantom containing lesions (model observer).

#### METHODS AND MATERIALS

20 patients were scanned with standard abdominal CT protocol for detection of liver metastases (median CTDIvol = 12.2 mGy). 11 of these were additionally scanned with 60% and 40% dose and 9 were scanned with 50% and 30% dose. Images were reconstructed with ASiR-V (AV) 50% and True-Fidelity - high (TF). Detectability of liver metastases was assessed by two radiologists and compared to a gold standard (evaluation using high dose and clinical information of the patient). CT scans of a liver phantom (The Phantom Laboratory) containing inserts with various iodine concentrations and diameters at corresponding conditions were analyzed using the ImQuest software (Duke University), and a detectability index ( $d'$ ) was calculated for each configuration. Results from the human observer method were compared to those of the model observer method.

#### RESULTS

The model observer  $d'$  followed the same trend as lesions detected by human observers in patient images when changing dose level. When changing reconstruction algorithm TF improved  $d'$  compared to AV. In the patient group with 30/50% dose, results show that AV may be beneficial compared to TF, while in the patient group with 40/60% dose, this trend is not as clear. This may be because of different lesion sizes in the two groups. Dependence of lesion size and contrast is work in progress.

#### CONCLUSION

The behavior of the detectability in patient vs.  $d'$  in the phantom coincides at different dose levels. However, when changing reconstruction algorithm the tests do not correlate to the same degree. Dependence on lesion size and contrast may be the reason for this.

#### CLINICAL RELEVANCE/APPLICATION

Quality assessment of CT protocols is time consuming. Model observers in imaging phantoms could save radiologists both time and cost. But does the model observer correlate well with lesion detection?

Printed on: 02/07/23



## Abstract Archives of the RSNA, 2022

T2-SPPH-3

### Comparison of Low-Contrast Object Detectability in Deep Learning and Conventional Reconstructions: AAPM TG-233 Phantom Evaluation

Tuesday, Nov. 29 9:00AM - 9:30AM Room: Learning Center - PH DPS

#### Participants

Chang Yong Heo, BS, Seoul, Korea, Republic Of (*Presenter*) Nothing to Disclose

#### PURPOSE

To measure the detectability of low-contrast objects on CT according to AAPM TG-233 report and examine if deep learning-based technique could improve the detectability of low-contrast objects over conventional reconstructions in low-dose CT imaging.

#### METHODS AND MATERIALS

ACR phantom was scanned at 120kV with SD (100mAs) and LD (25mAs) settings and reconstructed with two different scanners (GE: Discovery 750 HD, FBP and ASiR-V 30%; Siemens: Somatom Force, FBP and ADMIRE 2). A deep learning-based CT denoising model (DLM; ClariCT.AI™, ClariPi) was applied to all FBP images. Low-contrast detectability was measured according to AAPM TG-233 report using imQuest soft (Duke University) and compared for the different scan and reconstruction settings. Noise power spectrum (NPS) was measured on uniform section of module 3, and task-based transfer function (TTF) was analyzed on acrylic disk of module 1. Detectability index ( $d'$ ) was computed for a 5 mm low contrast disk object with 7 HU.

#### RESULTS

Detectability index ( $d'$ ) improved markedly with DLM (GE, 1.90; Siemens, 2.17) from that of FBP (GE, 0.99; Siemens, 1.11), and was comparable with IR (GE, 1.03; Siemens, 1.22) in LD scans of both scanners. The detectability indices with DLM in LD scans were superior to those with FBP in HD scans (GE, 1.77; Siemens, 2.08) which translated to the dose reduction potential more than 75%.

#### CONCLUSION

s Measurement of low-contrast detectability on ACR phantom provided an objective comparison of image quality in conventional and DL reconstructions. Deep learning-based denoising model was shown to improve detectability of low-contrast objects while conventional IR was not.

#### CLINICAL RELEVANCE/APPLICATION

Detectability measurement according to AAPM TG-233 report can be an objective way of examining image quality with newly developed reconstruction techniques in comparison with conventional reconstructions.

Printed on: 02/07/23

## Abstract Archives of the RSNA, 2022

T2-SPPH-4

### Impact of an Artificial Intelligence Deep-Learning Reconstruction Algorithm for CT on Image Quality and Potential Dose Reduction: A Phantom Study

Tuesday, Nov. 29 9:00AM - 9:30AM Room: Learning Center - PH DPS

#### Participants

Joel Greffier, PhD, Nimes, France (*Presenter*) Nothing to Disclose

#### PURPOSE

To assess the impact of a artificial intelligence deep-learning reconstruction (AI-DLR) algorithm on image quality and dose reduction compared with a hybrid IR algorithm in chest CT for different clinical indications.

#### METHODS AND MATERIALS

Acquisitions on the CT ACR 464 and CT Torso CTU-41 phantoms were performed at five dose levels (CTDIvol: 9.5/7.5/6/2.5/0.4mGy) used for chest CT conditions. Raw data were reconstructed using filtered back projection (FBP), two levels of IR (iDose4 levels 4 (i4) and 7 (i7)), and five levels of AI-DLR (Precise Image; Smoother, Smooth, Standard, Sharp, Sharper). Noise power spectrum (NPS), task-based transfer function (TTF) and detectability index ( $d'$ ) were computed:  $d'$  modelled detection of a soft tissue mediastinal nodule, ground-glass opacity, or high-contrast pulmonary lesion. Subjective image quality of chest anthropomorphic phantom images was independently evaluated by two radiologists. They have assessed image noise, image smoothing, contrast between the vessels and fat in the mediastinum for mediastinal images, visual border detection between bronchus and lung parenchyma for parenchymal images and overall image quality using a commonly-used four or five-point scale.

#### RESULTS

From Standard to Smoother levels, the noise magnitude decreased, the average NPS spatial frequency decreased and the detectability ( $d'$ ) of the three lesions increased. The opposite pattern was found from Standard to Sharper levels. From Smoother to Sharper levels, the spatial resolution increased for the low contrast polyethylene insert and the opposite for the high contrast air insert. Compared to the i4 used in clinical practice,  $d'$  values were higher using Smoother, Smooth and Standard levels for mediastinal images and Smoother and Smooth levels for parenchymal images. Radiologists considered the images satisfactory for clinical use at these levels, but adaptation to the dose level of the protocol is required.

#### CONCLUSION

s With AI-DLR, the smoothest levels reduced the noise and improved the detectability of chest lesions but increased the image smoothing. The opposite was found with the sharpest levels. The choice of level depends on the dose level and type of image: mediastinal or parenchymal.

#### CLINICAL RELEVANCE/APPLICATION

For the first time, we assessed the impact of the new artificial intelligence deep-learning reconstruction algorithm developed by Philips Healthcare and called Precise Image, compared to a standard clinical protocol using either FBP or IR reconstruction algorithms.

Printed on: 02/07/23



## Abstract Archives of the RSNA, 2022

T2-SPPH-5

### A Novel Detector Geometry for Third Generation CT

Tuesday, Nov. 29 9:00AM - 9:30AM Room: Learning Center - PH DPS

#### Participants

Jiang Hsieh, PhD, (*Presenter*) Former Employee, General Electric Company

#### PURPOSE

State-of-the-art CT scanners employ conventional detector geometry that forms an arc concentric to the x-ray source. The collected projection samples form an equiangular dataset, but their distance to the isocenter is nonuniformly spaced. When CT scanners employ steps to convert cone-beam datasets to parallel-beam datasets prior to the reconstruction, both channel- and view-wise rebinning are required. Such approach potentially leads to a degraded spatial resolution and an increased aliasing artifact.

#### METHODS AND MATERIALS

We propose a novel detector geometry that acquires projection samples with an evenly spaced distance to the isocenter. To ensure that the detector cell size is independent of the cell position, the source-to-detector distance varies as a function of the detector fan-angle. To guarantee detector surface being normal to the x-ray beam, each detector module (16 channels) is tilted relative to each other. This design requires only view-rebinning to form a parallel dataset. In addition, the detector surface area (arc-length) is reduced compared to the conventional design and a smaller cell size can be employed.

#### RESULTS

Extensive computer simulations were used to demonstrate the efficacy of our design, utilizing a wire phantom, water phantom, Shepp-Logan head phantom, and a specially designed aliasing phantom. Spatial resolution was measured with modulation transfer function (MTF) and the proposed design offers 12.6% increase compared to the conventional design, resulting from the smaller detector cell and removal of the channel-wise interpolation. In addition, aliasing artifact is significantly improved at locations away from the isocenter. At matched spatial resolution (by modifying the reconstruction kernel for the conventional design), image noise for the proposed system is 8.8% lower.

#### CONCLUSION

Compared to the conventional geometry, the proposed detector geometry offers improved performance in spatial resolution and artifact reduction, and exhibits better noise performance at a matching resolution. Further research on this design is warranted to fully explore other systems parameters such as the compactness of the gantry design.

#### CLINICAL RELEVANCE/APPLICATION

This research is relevant to improve the clinical performance of a CT system.

Printed on: 02/07/23



## Abstract Archives of the RSNA, 2022

T2-SPPH-6

### Robust High Precision Nonlinear CT Reconstruction Two Orders of Magnitude Faster than Competing Iterative Reconstruction

Tuesday, Nov. 29 9:00AM - 9:30AM Room: Learning Center - PH DPS

#### Participants

Wolfram Jarisch, PhD, (*Presenter*) Nothing to Disclose

#### PURPOSE

A new method for Tomographic reconstructions potentially makes highest quality diagnostic CT imaging available to all patients. The new method continues to evolve in competition to existing nonlinear iterative and deep learning methods that are overly sensitive to small data changes (Vegard Antuna, et al., 2020). Here we focus on a new iterative approach combining filtered backprojection (FBP), logarithmic and exponential transformations (LET), matching linearizations, and voxel state expansion. The nonlinear iterative approach provides high stability, accuracy, and computational speed. The method surpasses performance of other methods in terms of accuracy with two orders of magnitude higher speed.

#### METHODS AND MATERIALS

The method was first implemented in a high level program language at an NIH laboratory using publicly available program components for projection and backprojection. Accuracy and speed exceeded results over a state-of-the-art OS-SART implementation (Ander Biguri, 2017, GitHub).

#### RESULTS

On a 3D skull model, development of new Python code, showed half the residual-sum-of squares on central slices and between 80 and 150 fold higher speed than OS-SART (Figure). Both algorithms used the same array processor.

#### CONCLUSION

The high imaging quality and speed of the new algorithm allows to compute 3D angiographic images from a sequence of 6 moving projections. Similarly, movie-like 3D tomograms may be estimated motion parameters during the reconstruction process (Levenberg-Marquardt; 1944, 1963; not shown). The high imaging quality of the new algorithm follows from its relation to minimum variance estimation and structural similarity to Maximum Entropy estimation.

#### CLINICAL RELEVANCE/APPLICATION

The combined noise resilience, high imaging quality, modeling of movement, and speed, can reduce several barriers to the effective use of CT: cost per procedure, radiation, procedure time, and movement of patients.

Printed on: 02/07/23

## Abstract Archives of the RSNA, 2022

T2-SPPH-7

### CT Number Stability in Clinical Photon-Counting Virtual Monoenergetic Imaging

Tuesday, Nov. 29 9:00AM - 9:30AM Room: Learning Center - PH DPS

#### Participants

Jessica Flores, MS, (*Presenter*) Nothing to Disclose

#### PURPOSE

In the quantitative assessment of pathology in sequential and inter-patient studies, robust attenuation estimation of materials is essential for clinical applications of computed tomography (CT). Current standards in CT technology rely on energy-integrating detectors in single-energy CT (SECT) and dual-energy CT (DECT). With the introduction of photon-counting CT (PCCT) into clinical practice, there is the potential to improve HU stability. Therefore, this work aimed to study CT number stability to elucidate differences in CT systems and to highlight the strengths of clinical PCCT.

#### METHODS AND MATERIALS

Data was acquired on a clinical PCCT scanner, Siemens NAEOTOM Alpha, and a SECT/DECT scanner, Siemens SOMATOM Drive. HU variation was investigated in the CIRS 662 phantom with material-equivalent inserts, like iodine in water (15.0 mg/mL), adipose, bone (200 mg/mL) and muscle. Two factory protocols and phantom size configurations were used to demonstrate stability across CT DIvol and size. Protocols were adjusted to sweep across kVp and define a constant CT DIvol. Standard IR strengths and a single reconstruction kernel were used to create volume images. Virtual monoenergetic images in the PCCT scanner were produced at 70 keV, corresponding closest to the mean energy of a 120 kVp spectrum. Circular ROI masks were applied over regions containing inserts in volume images and used to determine mean HU per material. Percent relative standard deviation is reported as a metric to quantify HU variation in each material.

#### RESULTS

Preliminary studies show that the clinical PCCT scanner produces more consistent measurements than the SECT/DECT scanner in SECT mode for the same material across phantom size, CT DIvol and kVp. For all material inserts, percent relative standard deviation varied between 4.6% and 26.2% in the SECT scanner and between 0.7% and 2.6% in the PCCT scanner. Differences in performance between scanners are particularly apparent in higher HU materials such as bone and iodine inserts, where measurements from the PCCT scanner show less variation. For 15.0 mg/mL iodine in water, HU estimations showed 26.2% and 0.7% relative standard deviation in the SECT and PCCT scanners, respectively.

#### CONCLUSION

Compared to SECT, clinical PCCT produces more stable and consistent CT number measurements.

#### CLINICAL RELEVANCE/APPLICATION

Comparing a new clinical PCCT scanner to other scanners that are already familiar, this work highlights the strength of PCCT in the clinic to facilitate the quantitative assessment of pathology.

Printed on: 02/07/23

## Abstract Archives of the RSNA, 2022

T2-SPPH-8

### Quality Comparison of Single-Energy CT at Low Tube Voltages and Virtual Monochromatic Imaging at Low Energies by Dual-Energy CT With Deep Learning Reconstruction

Tuesday, Nov. 29 9:00AM - 9:30AM Room: Learning Center - PH DPS

#### Participants

Shingo Harashima, Tokyo, Japan (*Presenter*) Nothing to Disclose

#### PURPOSE

To compare quality of single-energy CT (SECT) at low tube voltages and virtual monochromatic imaging (VMI) at low energies by dual-energy CT (DECT) with deep learning reconstruction (DLR) in phantom experiments to simulate routine abdominal contrast-enhanced CT (CECT).

#### METHODS AND MATERIALS

We performed SECT and DECT scanning of a water phantom (GE), a phantom to assess beam-hardening artifact (BHA) (QSP-1 phantom; FUYO, Tokyo), and our original phantom to measure task-based modulation transfer function (TTF) using a state-of-the-art 256-gemstone-detector CT scanner (Revolution Apex, GE) at the similar volume CT dose index of approximately 10 mGy. For SECT scanning, tube voltage/current was 70 kVp/750 mA and 80 kVp/470 mA. For DECT scanning, tube voltage was rapidly switched from 80 to 140 kVp and tube current was 200 mA. SECT at 70 and 80 kVp and VMI at 40 and 50 keV were reconstructed using thickness of 1.25 mm and DLR (TrueFidelity, GE). We measured standard deviation of CT value as image noise and noise power spectrum (NPS) using the water phantom; CT value using the QSP-1 phantom with and without surrounding 350-mg iodine contrast media (CM), iohexol (Omnipaque 350, GE), at dilution factor of 10 for simulating bone attenuation to calculate its absolute difference as an index of BHA; contrast-noise ratio (CNR) and TTF using the TTF phantom with the CM at dilution factors of 30 and 60 for simulating arterial and hepatic attenuations, respectively; and thus compared these results among SECT at 70 and 80 kVp and VMI at 40 and 50 keV using one-way ANOVA and Tukey tests.

#### RESULTS

Whereas image noise significantly decreased from 40 keV to 50 keV to SECT ( $P < 0.05$ ), CNR significantly increased from SECT to 50 keV to 40 keV ( $P < 0.05$ ). NPS peaked at lower frequency by DECT than by SECT. BHA was significantly less by DECT than by SECT ( $P < 0.05$ ). TTF was lower by DECT than by SECT by approximately 12%.

#### CONCLUSION

s Using DLR at the similar radiation dose, VMI at the low energies degrade noise characteristics and decrease spatial resolution by approximately 12% but increase CNR and reduce BHA compared with SECT at the low tube voltages in routine abdominal CECT.

#### CLINICAL RELEVANCE/APPLICATION

When decreased spatial resolution by approximately 12% is acceptable, combined with DLR, VMI at 40-50 keV by DECT are clinically more beneficial than SECT at 70-80 kVp in routine abdominal CECT.

Printed on: 02/07/23

## Abstract Archives of the RSNA, 2022

T2-SPPH-9

### Evaluation of Pulse Pileup on a Clinical Photon-Counting CT Scanner

Tuesday, Nov. 29 9:00AM - 9:30AM Room: Learning Center - PH DPS

#### Participants

Mridul Bhattarai, MS, BS, Durham, NC (*Presenter*) Nothing to Disclose

#### PURPOSE

To evaluate the significance of pulse pileup on clinical photon-counting CT (PCCT) in terms of task-generic image quality metrics.

#### METHODS AND MATERIALS

An ACR phantom was scanned on a commercial PCCT (NAEOTOM Alpha, Siemens). Tube current was varied from 240 - 980 mA to study the effects of the flux to the detector on pulse pileup. Helical scans were done at 120 kV without tube current modulation (TCM) under eleven tube currents (240 - 980 mA), rotation time of 0.5 s, and pitch of 1. The dose levels corresponded to CTDIvol (32 cm phantom) of 9.5 - 38.7 mGy. Images were reconstructed using QIR-off mode (FBP) with Br44 kernel and voxel size of 0.4102 x 0.4102 x 3 mm<sup>3</sup>. imQuest, an open-source MATLAB-based software package, was used to calculate noise power spectrum (NPS), modulation transfer function (MTF), contrast-to-noise ratio (CNR), and CT number according to AAPM task group 233.

#### RESULTS

The shape of MTF did not change with mA. The relationship between noise magnitude and mA, noise proportional to mA<sup>-1/2</sup>, deviated up to 24.5% at the higher dose levels. The average frequency of NPS decreased from 0.31 (at 240 mA) to 0.27 mm<sup>-1</sup> (at 980 mA), insignificant compared to the increase in dose. CNR increased monotonically up to 880 mA, then it decreased to 980 mA, demonstrating detector saturation due to high flux. CT numbers were consistent across all tube currents with ranges of  $\pm 0.8$ ,  $\pm 1.1$ ,  $\pm 3.4$ ,  $\pm 4.6$ ,  $\pm 1.0$  HU for water, polyethylene, bone, air, and acrylic inserts, respectively.

#### CONCLUSION

Results demonstrate that the pulse pileup does not affect the spatial resolution, noise texture, and CT number accuracy, but has a modest influence on the noise magnitude and CNR. The significant effects were seen for only extremely high tube currents (> 880 mA = CTDIvol of 34.7 mGy) when used to scan a 20-cm ACR phantom, which is not clinically applicable. In addition, generally, in clinical practices, TCM is used to control the exposure level decreasing the variation of flux on the detector and alleviating the chance of detector saturation due to high count rates. Thus, pulse pileup does not affect the image quality of commercial PCCT when clinically relevant tube currents are used.

#### CLINICAL RELEVANCE/APPLICATION

High tube current causes high flux to the photon-counting detectors resulting in piling up of pulses formed by concurrent photons. Theoretically, pulse pileup causes count loss and energy resolution degradation, affecting image quality and HU number accuracy in PCCT. Several studies have been done previously to study the effects of pulse pileup through simulations or use of non-clinical detectors. In the tests performed, pulse pileup proved to be inconsequential in clinical PCCT as implemented.

Printed on: 02/07/23



## Abstract Archives of the RSNA, 2022

T2-SPRO

### Radiation Oncology Tuesday Poster Discussions

Tuesday, Nov. 29 9:00AM - 9:30AM Room: Learning Center - RO DPS

#### Participants

Anna Shapiro, MD, Syracuse, NY (*Moderator*) Nothing to Disclose

Printed on: 02/07/23

## Abstract Archives of the RSNA, 2022

T5A-SPBR

### Breast Tuesday Poster Discussions - A

Tuesday, Nov. 29 12:15PM - 12:45PM Room: Learning Center - BR DPS

#### Participants

Michael Linver, MD, Alexandria, VA (*Moderator*) Medical Advisory Board, Three Palm Software LLC;Scientific Advisory Board, Seno Medical Instruments, Inc

Michael Linver, MD, Alexandria, VA (*Moderator*) Medical Advisory Board, Three Palm Software LLC;Scientific Advisory Board, Seno Medical Instruments, Inc

Eric L. Rosen, MD, Seattle, WA (*Moderator*) Nothing to Disclose

Eric L. Rosen, MD, Seattle, WA (*Moderator*) Nothing to Disclose

#### Sub-Events

### T5A-SPBR-1 Racial Disparities Associated with Suboptimal Preoperative Breast MRI Use in Recently Diagnosed Breast Cancer Patients

#### Participants

Sarah Eskreis-Winkler, MD, New York, NY (*Presenter*) Nothing to Disclose

#### PURPOSE

To evaluate racial disparities in preoperative breast MRI utilization among recently diagnosed breast cancer patients.

#### METHODS AND MATERIALS

Breast cancer patients presenting to our institution between 2008 and 2020, and who underwent breast surgery (either total or partial mastectomy) as part of their cancer treatment and self-identified as either non-Hispanic white or non-Hispanic Black, were included in this IRB approved, HIPAA-compliant retrospective study. Patients were divided into two cohorts: those who received an MRI before surgery (MRI cohort), and those who did not (No MRI cohort). Rates of MRI use were calculated for all patients, as well as for white and black racial subgroups, which were compared using a Chi-square test. For patients who underwent partial mastectomy, the rate of positive surgical margins (ink on tumor) was calculated for all patients, for those in the MRI cohort, for those in the No MRI cohort, as well as for white and black racial subgroups in the MRI and No MRI cohorts.

#### RESULTS

Of 28,384 eligible breast cancer patients (90% white, 10% Black), 9,305 (33%) received an MRI and 19,079 (67%) did not. White patients had a higher MRI use rate than Black patients (33% v. 30%,  $p < 0.001$ ). Patients in the MRI cohort had lower rates of positive surgical margins than those in the No MRI cohort (2.9% v. 4.8%,  $p = .029$ ). Black patients in the No MRI cohort had a higher positive margin rate compared to white patients in the No MRI cohort (6.2% v. 4.6%,  $p = .028$ ), however, this difference was not observed within the MRI cohort, with Black patients having a similar positive margin rate to white patients (3.2% v. 2.9%,  $p = 0.9$ ).

#### CONCLUSION

Compared to white patients, Black breast cancer patients were less likely to receive a breast MRI prior to breast surgery. Black patients who received a breast MRI had similar rates of positive surgical margins compared to white patients, while Black patients who did not receive an MRI had higher rates of positive surgical margins. This suggests that racial disparities exist in the utilization of preoperative breast MRI, which warrants further investigation to improve surgical outcomes for Black patients.

#### CLINICAL RELEVANCE/APPLICATION

Racial disparities exist in preoperative breast MRI use, which may be caused by a variety of factors, potentially leading to poor surgical outcomes for minority patients, representing an urgent need for unbiased data-driven triaging of MRI prior to breast surgery.

### T5A-SPBR-2 A Study on The Utility of Minimum ADC in Decreasing Unnecessary Biopsy Rate of Suspected Breast MRI Lesions

#### Participants

Fang Wu, MMedSc, (*Presenter*) Nothing to Disclose

#### PURPOSE

This study aimed to evaluate the ability of minimum apparent diffusion coefficient (ADC<sub>min</sub>) in decreasing the unnecessary biopsy rate of breast suspected lesions, to determine the ADC<sub>min</sub> threshold to facilitate clinical implementation, and to compare the results with the utility of mean ADC (ADC<sub>mean</sub>).

#### METHODS AND MATERIALS

Totally, 523 female patients with 548 MRI-detected BI-RADS 3, 4, or 5 lesions confirmed by surgical pathology were recruited in

this retrospective study. A training set (344 lesions) and a validation set (204 lesions) were determined according to the time sequence of collection. Variations including lesion size, morphology (mass, non-mass), minimum ADC (ADC<sub>min</sub>) and mean ADC (ADC<sub>mean</sub>) of each lesion were collected for analysis. The diagnostic performance indices were calculated by Receiver Operating Characteristics (ROC) analysis, and the Hanley and McNeil test was used for further performance comparison. Under the negative likelihood ratio (-LR) of 0.1, the ADC threshold with the highest specificity was selected as the clinical ADC threshold (ADC<sub>cl</sub>). The ability to decrease the biopsy rate of suspected lesions were compared by contingency table analysis.

## RESULTS

ADC<sub>min</sub> and ADC<sub>mean</sub> of malignant lesions were significantly lower than that of benign ones. ADC<sub>min</sub> showed comparable performance with ADC<sub>mean</sub> in the diagnosis of benign and malignant breast lesions ( $P > 0.05$  for all comparisons). According to the results of training set, the value of  $1.39 \times 10^{-3} \text{ mm}^2/\text{s}$  and the value of  $1.52 \times 10^{-3} \text{ mm}^2/\text{s}$  were determined as the cut-off for ADC<sub>min</sub> (ADC<sub>cl-min</sub>) and ADC<sub>mean</sub> (ADC<sub>cl-mean</sub>) in the diagnosis of benign and malignant breast lesions. Application of ADC<sub>cl</sub> to the validation set, -LR < 0.1, resulted in 26.2% (95%CL: 20.2~33.9%) and 26.7% (95%CL: 19.7~35.1%) reduction of the biopsy rate to BI-RADS 4 and 5 lesions. Compared with ADC<sub>cl-min</sub> and ADC<sub>cl-mean</sub>, there was no significant difference among all subsets in reduction of the biopsy rate of BI-RADS 4 and 5 lesions ( $P > 0.05$  for all comparisons).

## CONCLUSION

Almost 1/4 unnecessary biopsies classified as BI-RADS 4 and BI-RADS 5 could be avoided by using an ADC<sub>cl-min</sub> of  $1.39 \times 10^{-3} \text{ mm}^2/\text{s}$  or an ADC<sub>cl-mean</sub> of  $1.52 \times 10^{-3} \text{ mm}^2/\text{s}$ .

## CLINICAL RELEVANCE/APPLICATION

Using the ADC<sub>min</sub> of  $1.39 \times 10^{-3} \text{ mm}^2/\text{s}$  can avoid 1/4 unnecessary biopsies, the result was favorably compared with ADC<sub>mean</sub> by using a threshold of  $1.52 \times 10^{-3} \text{ mm}^2/\text{s}$ , and obtained a high sensitivity, so as to improve the overall accuracy of breast MRI.

## T5A-SPBR-4 Image Quality and Diagnostic Performance of A Next-generation Low-field MRI Scanner in The Clinical Setting: First Experience in Breast Imaging at 0.55T

Participants

Sabine Ohlmeyer, PhD, MD, Erlangen, Germany (*Presenter*) Nothing to Disclose

## PURPOSE

Breast-MRI is essential for state-of-the-art breast imaging. However, broader clinical use is limited due to high procedural costs, technical complexity, limited availability and substantial requirements on local-infrastructure. Low-field breast-MRI may compensate for some of these disadvantages. We optimized sequence parameters for a dedicated breast imaging protocol on a next-generation 0.55T scanner and report on our first ten patients in clinical routine examination settings.

## METHODS AND MATERIALS

We examined 5 healthy woman and 10 patients with indication for breast MRI (5 with breast Cup size A/B, 5 with Cup size = C) on a low-field MRI unit (MAGNETOM Free.Max, Siemens Healthcare, Erlangen/Germany; multichannel breast-coil, Noras, Höchberg/Germany). An adapted protocol including the following standard sequences was used: diffusion weighted imaging (DWI), T2w TSE, T2w Dixon and T1w VIBE with dynamic contrast enhancement (CE). Three independent MRI experts rated all sequences for signal-to-noise (SNR), contrast, resolution and overall diagnostic impression using a 5-point Likert scale (1 = very good to 5 = very bad). One expert in breast imaging blinded to further patients' history and MRI indication categorized a BI-RADS score to each breast.

## RESULTS

Diagnostic image quality, SNR, contrast and resolution were rated as very good to moderate (Likert score 1-3) by the 3 readers for almost all individual sequences. Only in one woman, DWI was rated to be poor (Likert Score 4) by one reader. The mean Likert scores were as follows: DWI 1.92, T2w TSE 1.67, T2w TSE Dixon 1.77, T1w VIBE 1.82. The study doctor (not blinded to patients' history) was able to reproduce all findings in the low-field MRI known from conventional breast diagnostics (mammography and ultrasound) and evaluated all datasets with a mean Likert Score of 1.23, regardless of breast size. Patient reports were as follows: 8 × BI-RADS 1, 6 × BI-RADS 2 (fibroadenomas, cystic lesions, intramammary lymph node), 6 × BI-RADS 6 (breast cancer under NAC). The blinded breast expert correctly categorized all benign reports. Three breast cancers were reported correctly, one as BI-RADS 4, two were missed and categorized as benign because of only residual DWI signal alterations and completely regressive CE of the breast cancer under NAC.

## CONCLUSION

The image quality with a next-generation low-field breast-MRI system with tailored sequences was diagnostic in the clinical setting in our first patients.

## CLINICAL RELEVANCE/APPLICATION

Breast imaging with a 0.55T MRI is possible. Our datasets showed diagnostic image quality that resulted in high sensitivity in our study group. This, together with the easier availability of a low-field scanner, could be an interesting aspect for MRI-based breast screening.

## T5A-SPBR-5 The Association Between the Ultrafast and Conventional Dynamic Contrast-enhanced MRI Parameters of Breast Cancer and the Histologic Prognostic Markers

Participants

Seong Gwang Kim, MD, Seongnam, Korea, Republic Of (*Presenter*) Nothing to Disclose

## PURPOSE

To compare the ultrafast and conventional dynamic contrast-enhanced MRI (DCE-MRI) parameters of breast cancer with their histologic characteristics.

## METHODS AND MATERIALS

This retrospective study included 102 patients who were diagnosed with breast cancer between Mar 2021 and Mar 2022 (98

patients with unilateral cancer and 4 patients with bilateral cancer, a total of 106 cancer lesions). The kinetic and morphologic features on ultrafast and conventional DCE-MRI were compared with histologic prognostic markers.

## RESULTS

Ninety-seven tumors were invasive cancer and 9 tumors were in situ cancers. 80 tumors were luminal cancer, 9 were HER2-enriched, and 11 were triple-negative. ER positivity was associated with a lower percentage of delayed washout ( $p=0.022$ ), smaller tumor size ( $p=0.043$ ), multiplicity ( $p=0.039$ ), and negative lymph node metastasis ( $p=0.007$ ). HER2 positivity and high histologic grade were associated with lymph node metastasis ( $p=0.018$  and  $p=0.002$ ). Ki-67 positivity ( $>14\%$ ) was associated with higher maximum enhancement (ME) on ultrafast imaging. Non-luminal cancers showed a higher percentage of delayed washout ( $p=0.047$ ), lymph node metastasis ( $p=0.04$ ), and single lesion ( $p=0.024$ ). Ultrafast imaging kinetic parameters were not significantly different according to molecular subtype of breast cancer. Invasive breast cancer showed higher ME ( $p<0.001$ ), slope ( $p=0.007$ ), maximum slope ( $p=0.013$ ), and area under the kinetic curve ( $p=0.014$ ) on ultrafast imaging, and delayed washout kinetics ( $p=0.01$ ) on conventional kinetic curve, and lesion type-mass ( $p=0.035$ ). In regression analysis using lesion type, delayed kinetics, and slope on ultrafast kinetics, delayed washout kinetics and slope higher than  $4.5\%/s$  were independent predictors of invasive breast cancer.

## CONCLUSION

s Ki-67 positivity was associated with a higher ME on ultrafast imaging, but there was no significant difference on ultrafast imaging parameters according to other histologic markers and molecular subtype. Histologic invasiveness of breast cancer was associated with a higher and faster enhancement on ultrafast imaging, delayed washout kinetics on conventional dynamic imaging, and lesion type-mass.

## CLINICAL RELEVANCE/APPLICATION

A higher and faster enhancement of breast cancer on ultrafast MR imaging can predict Ki-67 positivity and histologic invasiveness.

### T5A-SPBR-6 Not Detected Breast Malignancy in Dynamic Contrast-enhanced MRI: Frequency and Causes

Participants

Dong-Hun Song, MD, Seoul, Korea, Republic Of (*Presenter*) Nothing to Disclose

## PURPOSE

To investigate the frequency and main causes of malignant lesions not-detected in dynamic contrast-enhanced (DCE) breast MRI

## METHODS AND MATERIALS

A total 1707 cases of preoperative breast MR performed between 2020 and 2021 were included in this study. Of these 1707 cases, the final 13 malignancy cases not-detected in DCE MR were selected, based on the consensus between three radiologists. They also reviewed the final pathology reports to estimate the frequency, and evaluated the imaging findings including DCE MR with diffusion weighted image (DWI), ultrasound, mammography, and if available contrast enhanced chest CT. Then, each cases were classified into three main causes; rare but known non-enhancing pathological feature ( $n = 7$ ), peripherally located tumor ( $n = 3$ ), and underlying background parenchymal enhancement (BPE) ( $n = 3$ ).

## RESULTS

The final pathology and frequency of 13 cases were as follows; invasive ductal carcinoma (IDC) (4/1253, 0.3%), invasive lobular carcinoma (ILC) (3/58, 5.2%), mucinous carcinoma (3/50, 6%), ductal carcinoma in situ (DCIS) (1/233, 0.4%), metaplastic carcinoma (1/10, 10%), and primary breast lymphoma (1/2, 50%). Seven cases were not-detected due to non-enhancing pathological feature; mucinous carcinoma ( $n = 3$ ), ILC ( $n = 2$ ), metaplastic carcinoma ( $n = 1$ ) and lymphoma ( $n = 1$ ). In three cases, tumors were located in the breast periphery. They showed non-enhancement in MR due to compression, but showed homogeneous enhancement at corresponding lesion in chest CT. In the remaining three cases, malignant lesions were not identified due to underlying marked level of BPE. Although these cases were not-detected in DCE-MR, 7 cases were visible in mammography, 10 cases in DWI, 12 cases in ultrasound, and all 13 cases in ultrasound and DWI combination.

## CONCLUSION

s The frequency of not-detected malignancy in DCE-MR is very rare (13/1707, 0.76%). Knowing the causes of each case and correlating it with other imaging modalities could be helpful in diagnosis of breast malignancy.

## CLINICAL RELEVANCE/APPLICATION

MR is known to have the highest sensitivity in diagnosing breast malignancy among various imaging modalities, but some lesions are not-detected in DCE-MR. In this retrospective study, we evaluated the frequency and causes of these cases.

### T5A-SPBR-7 Impact of Pre-operative Breast MRI in Patient with N2 or N3 Stage Breast Cancer Using Propensity Score Matching

Participants

Minah Lee, MD, Seoul, Korea, Republic Of (*Presenter*) Nothing to Disclose

## PURPOSE

To investigate the association between preoperative breast magnetic resonance (MR) imaging and surgical nodal outcomes in patients with invasive breast carcinoma by using propensity score matching to decide whether MR examination is beneficial in avoiding unexpected N2 or N3 stage and the number of axillary lymph node dissection.

## METHODS AND MATERIALS

Patients diagnosed with invasive breast cancer and clinically N0 stage between 2006 and 2011 who had or had not undergone preoperative MRI and sentinel lymph node biopsy during breast surgery were retrospectively identified. We used propensity score matching using 17 variables and created matched groups with MRI and without MRI. Surgical outcomes of axillary nodes were compared by using chi-square and McNemar's test.

## RESULTS

Among 2054 Patients (mean age  $\pm$  standard deviation, 50 years $\pm$ 10), 1402 had undergone preoperative MRI (mean age, 49 $\pm$ 10) and

Among 2034 patients (mean age  $\pm$  standard deviation, 50 years $\pm$ 10), 1402 had undergone preoperative MRI (mean age, 47 $\pm$ 10) and 652 (mean age, 52 years  $\pm$ 11) had not. Any stage N positive disease was found in 303 in the MRI group, and 204 of the 652 patients in the non-MRI group (21.6% vs 31.3%,  $P < 0.001$ ). Stage N2 or N3 disease was found in 52 patients in the MRI group, and 45 patients in the non-MRI group (3.7% vs 6.9% in any N stage,  $P = 0.002$ ). The rate of axillary lymph node dissection was higher in non-MRI group ( $n=391$ ) than MRI group ( $n=402$ ; 60.4% vs 28.7%,  $P < 0.001$ ). After PS matching, Stage N2 or N3 disease was found in 14 of 363 patients in the MRI group, and 26 of 363 patients in the non-MRI group (3.9% vs 7.2% in any N stage,  $P = 0.072$ ). The axillary dissection rate was 104 patients in the MRI group and 217 patients in the non-MRI group (28.7% vs. 59.8%,  $P < 0.001$ ).

#### **CONCLUSION**

Preoperative MRI in patients with breast cancer is a useful method to predict the high tumor burden of axillary lymph nodes prior to sentinel biopsy and to decrease the axillary lymph node dissection surgery due to unexpected lymph node metastasis.

#### **CLINICAL RELEVANCE/APPLICATION**

Preoperative MRI is a useful method for avoiding the axillary lymph node dissection surgery due to unexpected lymph node metastasis.

Printed on: 02/07/23

## Abstract Archives of the RSNA, 2022

T5A-SPBR-1

### Racial Disparities Associated with Suboptimal Preoperative Breast MRI Use in Recently Diagnosed Breast Cancer Patients

Tuesday, Nov. 29 12:15PM - 12:45PM Room: Learning Center - BR DPS

#### Participants

Sarah Eskreis-Winkler, MD, New York, NY (*Presenter*) Nothing to Disclose

#### PURPOSE

To evaluate racial disparities in preoperative breast MRI utilization among recently diagnosed breast cancer patients.

#### METHODS AND MATERIALS

Breast cancer patients presenting to our institution between 2008 and 2020, and who underwent breast surgery (either total or partial mastectomy) as part of their cancer treatment and self-identified as either non-Hispanic white or non-Hispanic Black, were included in this IRB approved, HIPAA-compliant retrospective study. Patients were divided into two cohorts: those who received an MRI before surgery (MRI cohort), and those who did not (No MRI cohort). Rates of MRI use were calculated for all patients, as well as for white and black racial subgroups, which were compared using a Chi-square test. For patients who underwent partial mastectomy, the rate of positive surgical margins (ink on tumor) was calculated for all patients, for those in the MRI cohort, for those in the No MRI cohort, as well as for white and black racial subgroups in the MRI and No MRI cohorts.

#### RESULTS

Of 28,384 eligible breast cancer patients (90% white, 10% Black), 9,305 (33%) received an MRI and 19,079 (67%) did not. White patients had a higher MRI use rate than Black patients (33% v. 30%,  $p < 0.001$ ). Patients in the MRI cohort had lower rates of positive surgical margins than those in the No MRI cohort (2.9% v. 4.8%,  $p = .029$ ). Black patients in the No MRI cohort had a higher positive margin rate compared to white patients in the No MRI cohort (6.2% v. 4.6%,  $p = .028$ ), however, this difference was not observed within the MRI cohort, with Black patients having a similar positive margin rate to white patients (3.2% v. 2.9%,  $p = 0.9$ ).

#### CONCLUSION

Compared to white patients, Black breast cancer patients were less likely to receive a breast MRI prior to breast surgery. Black patients who received a breast MRI had similar rates of positive surgical margins compared to white patients, while Black patients who did not receive an MRI had higher rates of positive surgical margins. This suggests that racial disparities exist in the utilization of preoperative breast MRI, which warrants further investigation to improve surgical outcomes for Black patients.

#### CLINICAL RELEVANCE/APPLICATION

Racial disparities exist in preoperative breast MRI use, which may be caused by a variety of factors, potentially leading to poor surgical outcomes for minority patients, representing an urgent need for unbiased data-driven triaging of MRI prior to breast surgery.

Printed on: 02/07/23

## Abstract Archives of the RSNA, 2022

T5A-SPBR-2

### A Study on The Utility of Minimum ADC in Decreasing Unnecessary Biopsy Rate of Suspected Breast MRI Lesions

Tuesday, Nov. 29 12:15PM - 12:45PM Room: Learning Center - BR DPS

#### Participants

Fang Wu, MMedSc, (Presenter) Nothing to Disclose

#### PURPOSE

This study aimed to evaluate the ability of minimum apparent diffusion coefficient (ADC<sub>min</sub>) in decreasing the unnecessary biopsy rate of breast suspected lesions, to determine the ADC<sub>min</sub> threshold to facilitate clinical implementation, and to compare the results with the utility of mean ADC (ADC<sub>mean</sub>).

#### METHODS AND MATERIALS

Totally, 523 female patients with 548 MRI-detected BI-RADS 3, 4, or 5 lesions confirmed by surgical pathology were recruited in this retrospective study. A training set (344 lesions) and a validation set (204 lesions) were determined according to the time sequence of collection. Variations including lesion size, morphology (mass, non-mass), minimum ADC (ADC<sub>min</sub>) and mean ADC (ADC<sub>mean</sub>) of each lesion were collected for analysis. The diagnostic performance indices were calculated by Receiver Operating Characteristics (ROC) analysis, and the Hanley and McNeil test was used for further performance comparison. Under the negative likelihood ratio (-LR) of 0.1, the ADC threshold with the highest specificity was selected as the clinical ADC threshold (ADC<sub>cl</sub>). The ability to decrease the biopsy rate of suspected lesions were compared by contingency table analysis.

#### RESULTS

ADC<sub>min</sub> and ADC<sub>mean</sub> of malignant lesions were significantly lower than that of benign ones. ADC<sub>min</sub> showed comparable performance with ADC<sub>mean</sub> in the diagnosis of benign and malignant breast lesions ( $P > 0.05$  for all comparisons). According to the results of training set, the value of  $1.39 \times 10^{-3} \text{ mm}^2/\text{s}$  and the value of  $1.52 \times 10^{-3} \text{ mm}^2/\text{s}$  were determined as the cut-off for ADC<sub>min</sub> (ADC<sub>cl</sub>-min) and ADC<sub>mean</sub> (ADC<sub>cl</sub>-mean) in the diagnosis of benign and malignant breast lesions. Application of ADC<sub>cl</sub> to the validation set, -LR < 0.1, resulted in 26.2% (95%CL: 20.2~33.9%) and 26.7% (95%CL: 19.7~35.1%) reduction of the biopsy rate to BI-RADS 4 and 5 lesions. Compared with ADC<sub>cl</sub>-min and ADC<sub>cl</sub>-mean, there was no significant difference among all subsets in reduction of the biopsy rate of BI-RADS 4 and 5 lesions ( $P > 0.05$  for all comparisons).

#### CONCLUSION

Almost 1/4 unnecessary biopsies classified as BI-RADS 4 and BI-RADS 5 could be avoided by using an ADC<sub>cl</sub>-min of  $1.39 \times 10^{-3} \text{ mm}^2/\text{s}$  or an ADC<sub>cl</sub>-mean of  $1.52 \times 10^{-3} \text{ mm}^2/\text{s}$ .

#### CLINICAL RELEVANCE/APPLICATION

Using the ADC<sub>min</sub> of  $1.39 \times 10^{-3} \text{ mm}^2/\text{s}$  can avoid 1/4 unnecessary biopsies, the result was favorably compared with ADC<sub>mean</sub> by using a threshold of  $1.52 \times 10^{-3} \text{ mm}^2/\text{s}$ , and obtained a high sensitivity, so as to improve the overall accuracy of breast MRI.

Printed on: 02/07/23

## Abstract Archives of the RSNA, 2022

T5A-SPBR-4

### Image Quality and Diagnostic Performance of A Next-generation Low-field MRI Scanner in The Clinical Setting: First Experience in Breast Imaging at 0.55T

Tuesday, Nov. 29 12:15PM - 12:45PM Room: Learning Center - BR DPS

#### Participants

Sabine Ohlmeyer, PhD, MD, Erlangen, Germany (*Presenter*) Nothing to Disclose

#### PURPOSE

Breast-MRI is essential for state-of-the-art breast imaging. However, broader clinical use is limited due to high procedural costs, technical complexity, limited availability and substantial requirements on local-infrastructure. Low-field breast-MRI may compensate for some of these disadvantages. We optimized sequence parameters for a dedicated breast imaging protocol on a next-generation 0.55T scanner and report on our first ten patients in clinical routine examination settings.

#### METHODS AND MATERIALS

We examined 5 healthy woman and 10 patients with indication for breast MRI (5 with breast Cup size A/B, 5 with Cup size = C) on a low-field MRI unit (MAGNETOM Free.Max, Siemens Healthcare, Erlangen/Germany; multichannel breast-coil, Noras, Höchberg/Germany). An adapted protocol including the following standard sequences was used: diffusion weighted imaging (DWI), T2w TSE, T2w Dixon and T1w VIBE with dynamic contrast enhancement (CE). Three independent MRI experts rated all sequences for signal-to-noise (SNR), contrast, resolution and overall diagnostic impression using a 5-point Likert scale (1 = very good to 5 = very bad). One expert in breast imaging blinded to further patients' history and MRI indication categorized a BI-RADS score to each breast.

#### RESULTS

Diagnostic image quality, SNR, contrast and resolution were rated as very good to moderate (Likert score 1-3) by the 3 readers for almost all individual sequences. Only in one woman, DWI was rated to be poor (Likert Score 4) by one reader. The mean Likert scores were as follows: DWI 1.92, T2w TSE 1.67, T2w TSE Dixon 1.77, T1w VIBE 1.82. The study doctor (not blinded to patients' history) was able to reproduce all findings in the low-field MRI known from conventional breast diagnostics (mammography and ultrasound) and evaluated all datasets with a mean Likert Score of 1.23, regardless of breast size. Patient reports were as follows: 8 × BI-RADS 1, 6 × BI-RADS 2 (fibroadenomas, cystic lesions, intramammary lymph node), 6 × BI-RADS 6 (breast cancer under NAC). The blinded breast expert correctly categorized all benign reports. Three breast cancers were reported correctly, one as BI-RADS 4, two were missed and categorized as benign because of only residual DWI signal alterations and completely regressive CE of the breast cancer under NAC.

#### CONCLUSION

s The image quality with a next-generation low-field breast-MRI system with tailored sequences was diagnostic in the clinical setting in our first patients.

#### CLINICAL RELEVANCE/APPLICATION

Breast imaging with a 0.55T MRI is possible. Our datasets showed diagnostic image quality that resulted in high sensitivity in our study group. This, together with the easier availability of a low-field scanner, could be an interesting aspect for MRI-based breast screening.

Printed on: 02/07/23

## Abstract Archives of the RSNA, 2022

T5A-SPBR-5

### The Association Between the Ultrafast and Conventional Dynamic Contrast-enhanced MRI Parameters of Breast Cancer and the Histologic Prognostic Markers

Tuesday, Nov. 29 12:15PM - 12:45PM Room: Learning Center - BR DPS

#### Participants

Seong Gwang Kim, MD, Seongnam, Korea, Republic Of (*Presenter*) Nothing to Disclose

#### PURPOSE

To compare the ultrafast and conventional dynamic contrast-enhanced MRI (DCE-MRI) parameters of breast cancer with their histologic characteristics.

#### METHODS AND MATERIALS

This retrospective study included 102 patients who were diagnosed with breast cancer between Mar 2021 and Mar 2022 (98 patients with unilateral cancer and 4 patients with bilateral cancer, a total of 106 cancer lesions). The kinetic and morphologic features on ultrafast and conventional DCE-MRI were compared with histologic prognostic markers.

#### RESULTS

Ninety-seven tumors were invasive cancer and 9 tumors were in situ cancers. 80 tumors were luminal cancer, 9 were HER2-enriched, and 11 were triple-negative. ER positivity was associated with a lower percentage of delayed washout ( $p=0.022$ ), smaller tumor size ( $p=0.043$ ), multiplicity ( $p=0.039$ ), and negative lymph node metastasis ( $p=0.007$ ). HER2 positivity and high histologic grade were associated with lymph node metastasis ( $p=0.018$  and  $p=0.002$ ). Ki-67 positivity ( $>14\%$ ) was associated with higher maximum enhancement (ME) on ultrafast imaging. Non-luminal cancers showed a higher percentage of delayed washout ( $p=0.047$ ), lymph node metastasis ( $p=0.04$ ), and single lesion ( $p=0.024$ ). Ultrafast imaging kinetic parameters were not significantly different according to molecular subtype of breast cancer. Invasive breast cancer showed higher ME ( $p<0.001$ ), slope ( $p=0.007$ ), maximum slope ( $p=0.013$ ), and area under the kinetic curve ( $p=0.014$ ) on ultrafast imaging, and delayed washout kinetics ( $p=0.01$ ) on conventional kinetic curve, and lesion type-mass ( $p=0.035$ ). In regression analysis using lesion type, delayed kinetics, and slope on ultrafast kinetics, delayed washout kinetics and slope higher than 4.5%/s were independent predictors of invasive breast cancer.

#### CONCLUSION

s Ki-67 positivity was associated with a higher ME on ultrafast imaging, but there was no significant difference on ultrafast imaging parameters according to other histologic markers and molecular subtype. Histologic invasiveness of breast cancer was associated with a higher and faster enhancement on ultrafast imaging, delayed washout kinetics on conventional dynamic imaging, and lesion type-mass.

#### CLINICAL RELEVANCE/APPLICATION

A higher and faster enhancement of breast cancer on ultrafast MR imaging can predict Ki-67 positivity and histologic invasiveness.

Printed on: 02/07/23

## Abstract Archives of the RSNA, 2022

T5A-SPBR-6

### Not Detected Breast Malignancy in Dynamic Contrast-enhanced MRI: Frequency and Causes

Tuesday, Nov. 29 12:15PM - 12:45PM Room: Learning Center - BR DPS

#### Participants

Dong-Hun Song, MD, Seoul, Korea, Republic Of (*Presenter*) Nothing to Disclose

#### PURPOSE

To investigate the frequency and main causes of malignant lesions not-detected in dynamic contrast-enhanced (DCE) breast MRI

#### METHODS AND MATERIALS

A total 1707 cases of preoperative breast MR performed between 2020 and 2021 were included in this study. Of these 1707 cases, the final 13 malignancy cases not-detected in DCE MR were selected, based on the consensus between three radiologists. They also reviewed the final pathology reports to estimate the frequency, and evaluated the imaging findings including DCE MR with diffusion weighted image (DWI), ultrasound, mammography, and if available contrast enhanced chest CT. Then, each cases were classified into three main causes; rare but known non-enhancing pathological feature (n = 7), peripherally located tumor (n = 3), and underlying background parenchymal enhancement (BPE) (n = 3).

#### RESULTS

The final pathology and frequency of 13 cases were as follows; invasive ductal carcinoma (IDC) (4/1253, 0.3%), invasive lobular carcinoma (ILC) (3/58, 5.2%), mucinous carcinoma (3/50, 6%), ductal carcinoma in situ (DCIS) (1/233, 0.4%), metaplastic carcinoma (1/10, 10%), and primary breast lymphoma (1/2, 50%). Seven cases were not-detected due to non-enhancing pathological feature; mucinous carcinoma (n = 3), ILC (n = 2), metaplastic carcinoma (n = 1) and lymphoma (n = 1). In three cases, tumors were located in the breast periphery. They showed non-enhancement in MR due to compression, but showed homogeneous enhancement at corresponding lesion in chest CT. In the remaining three cases, malignant lesions were not identified due to underlying marked level of BPE. Although these cases were not-detected in DCE-MR, 7 cases were visible in mammography, 10 cases in DWI, 12 cases in ultrasound, and all 13 cases in ultrasound and DWI combination.

#### CONCLUSION

s The frequency of not-detected malignancy in DCE-MR is very rare (13/1707, 0.76%). Knowing the causes of each case and correlating it with other imaging modalities could be helpful in diagnosis of breast malignancy.

#### CLINICAL RELEVANCE/APPLICATION

MR is known to have the highest sensitivity in diagnosing breast malignancy among various imaging modalities, but some lesions are not-detected in DCE-MR. In this retrospective study, we evaluated the frequency and causes of these cases.

Printed on: 02/07/23

## Abstract Archives of the RSNA, 2022

T5A-SPBR-7

### Impact of Pre-operative Breast MRI in Patient with N2 or N3 Stage Breast Cancer Using Propensity Score Matching

Tuesday, Nov. 29 12:15PM - 12:45PM Room: Learning Center - BR DPS

#### Participants

Minah Lee, MD, Seoul, Korea, Republic Of (*Presenter*) Nothing to Disclose

#### PURPOSE

To investigate the association between preoperative breast magnetic resonance (MR) imaging and surgical nodal outcomes in patients with invasive breast carcinoma by using propensity score matching to decide whether MR examination is beneficial in avoiding unexpected N2 or N3 stage and the number of axillary lymph node dissection.

#### METHODS AND MATERIALS

Patients diagnosed with invasive breast cancer and clinically N0 stage between 2006 and 2011 who had or had not undergone preoperative MRI and sentinel lymph node biopsy during breast surgery were retrospectively identified. We used propensity score matching using 17 variables and created matched groups with MRI and without MRI. Surgical outcomes of axillary nodes were compared by using chi-square and McNemar's test.

#### RESULTS

Among 2054 Patients (mean age  $\pm$  standard deviation, 50 years $\pm$ 10), 1402 had undergone preoperative MRI (mean age, 49 $\pm$ 10) and 652 (mean age, 52 years  $\pm$ 11) had not. Any stage N positive disease was found in 303 in the MRI group, and 204 of the 652 patients in the non-MRI group (21.6% vs 31.3%,  $P < 0.001$ ). Stage N2 or N3 disease was found in 52 patients in the MRI group, and 45 patients in the non-MRI group (3.7% vs 6.9% in any N stage,  $P = 0.002$ ). The rate of axillary lymph node dissection was higher in non-MRI group ( $n=391$ ) than MRI group ( $n=402$ ; 60.4% vs 28.7%,  $P < 0.001$ ). After PS matching, Stage N2 or N3 disease was found in 14 of 363 patients in the MRI group, and 26 of 363 patients in the non-MRI group (3.9% vs 7.2% in any N stage,  $P = 0.072$ ). The axillary dissection rate was 104 patients in the MRI group and 217 patient in the non-MRI group (28.7% vs. 59.8 %,  $P < 0.001$ ).

#### CONCLUSION

s Preoperative MRI in patients with breast cancer is a useful method to predict the high tumor burden of axillary lymph nodes prior to sentinel biopsy and to decrease the axillary lymph node dissection surgery due to unexpected lymph node metastasis.

#### CLINICAL RELEVANCE/APPLICATION

Preoperative MRI is useful method for avoiding the axillary lymph node dissection surgery due to unexpected lymph node metastasis.

Printed on: 02/07/23

## Abstract Archives of the RSNA, 2022

T5A-SPCA

### Cardiac Tuesday Poster Discussions - A

Tuesday, Nov. 29 12:15PM - 12:45PM Room: Learning Center - CA DPS

#### Sub-Events

#### **T5A-SPCA-1 Non-contrast-enhanced High-resolution REACT MR Angiography of The Great Vessels in Young Children with Complex Congenital Heart Disease**

##### Participants

Alexander Isaak, MD, Bonn, Germany (*Presenter*) Nothing to Disclose

##### PURPOSE

High-resolution MR angiography (MRA) in small children with congenital heart disease (CHD) is challenging and generally requires contrast agent administration. This study aimed to evaluate the great vessels in young children with complex CHD using native 3D Relaxation-Enhanced Angiography without Contrast (REACT) in comparison to high-resolution contrast-enhanced MRA.

##### METHODS AND MATERIALS

In this retrospective study from April to July 2021, respiratory- and electrocardiogram-gated REACT MRA was compared to contrast-enhanced single-phase MRA in young children with CHD (<10 years) that underwent cardiac MRI at 3T for pre- or postsurgical follow-up. Vascular assessment at predefined landmarks of the great vessels and proximal coronary arteries included (i) image quality (1=non-diagnostic, 5=excellent), (ii) vessel size, (iii) artifact burden, and (iv) diagnostic findings. For statistical analysis, paired t-test, Pearson correlation, Bland-Altman analysis, Wilcoxon test, and intraclass correlation coefficients (ICC) were applied.

##### RESULTS

36 children with complex CHD (median age, 4 years, interquartile range, 2-5; 20 males) who had undergone cardiac MRI under deep sedation were included. Native REACT MRA (mean scan time: 4:22±1:44min) demonstrated comparable overall image quality to contrast-enhanced MRA (3.9±1.0 vs 3.8±0.9, P=0.018). REACT MRA achieved better image quality at the ascending aorta (4.8±0.5 vs 4.3±0.8, P<0.001), proximal coronary arteries (e.g., left: 4.1±1.0 vs 3.3±1.1, P=0.001), and inferior vena cava (4.6±0.5 vs 3.2±0.8, P<0.001). Overall vessel diameters correlated strongly between both MRA methods (Pearson r=0.99; bias=0.04±0.61mm) with high interobserver reproducibility (ICCs: 0.99). Six new vascular findings were detected equally with native REACT MRA and the contrast-enhanced reference standard.

##### CONCLUSION

In young children with complex CHD undergoing preoperative or postoperative follow-up, non-contrast enhanced REACT MRA provides high image quality, accurate vascular measurements, and equivalent diagnostic quality of the great vessels and proximal coronary arteries compared to standard contrast-enhanced MRA.

##### CLINICAL RELEVANCE/APPLICATION

The use of REACT MRA can provide gadolinium-free vascular assessment in young children with CHD, eliminating potential risks of contrast-associated complications, reducing examination costs, and expediting clinical workflow.

#### **T5A-SPCA-2 Doppler Ultrasound-gated Fetal Cardiac MRI in Complex Congenital Heart Disease: Clinical Feasibility and Comparison to Echocardiography**

##### Participants

Thomas Vollbrecht, Bonn, Germany (*Presenter*) Nothing to Disclose

##### PURPOSE

To evaluate the feasibility of fetal cardiac MRI using recently introduced Doppler ultrasound (DUS)-based direct gating in clinical routine and to investigate its diagnostic performance in complex congenital heart disease (CHD) compared to fetal echocardiography.

##### METHODS AND MATERIALS

In this prospective study (ClinicalTrials.gov identifier: NCT05066399) from May 2021 to March 2022, female participants with CHD of the fetus underwent fetal echocardiography and DUS-gated fetal cardiac MRI on the same day. For fetal cardiac MRI, balanced steady-state free precession cine images were acquired in continuous axial and optional sagittal and/or coronal orientation (slice thickness: 4 mm). Overall image quality and cardiovascular structure delineability for cine MRI were assessed (4-point Likert scale; 1=non-diagnostic image quality - 4=good image quality). Abnormalities of 20 fetal cardiovascular features previously defined in a study evaluation form were independently assessed for both modalities (abnormality present: yes or no). The reference standard was the result of postnatal examinations. Differences in sensitivities and specificities were calculated with McNemar's test.

##### RESULTS

23 participants (mean gestational age, 36 weeks  $\pm$  1) were included. Fetal cardiac MRI could be completed in all participants. Median overall image quality of DUS-gated cine images was 3 (interquartile range, 2.5-4). In 21 of 23 participants (91%) the underlying CHD was correctly assumed by fetal cardiac MRI. One case with situs inversus but levocardia and congenitally corrected transposition of the great arteries was correctly diagnosed only with MRI. No differences were found regarding sensitivities (88.2%, 95% confidence interval [CI]: 81.4%-92.7% vs. 90.6%, 95% CI: 84.2%-94.5%;  $P=0.581$ ) and specificities (99.1%, 95% CI: 97.4%-99.7% vs. 99.4%, 95% CI: 97.8%-99.8%;  $P=0.999$ ) for the detection of abnormal fetal cardiovascular features between echocardiography and MRI.

## CONCLUSION

s DUS-gated fetal cine cardiac MRI can reliably diagnose even complex forms of CHD and might be implemented as an adjunct diagnostic tool for prenatal assessment of congenital heart disease.

## CLINICAL RELEVANCE/APPLICATION

As echocardiography may be limited especially in late gestation, DUS-gated fetal cardiac MRI could become a diagnostic tool for CHD assessment and further expand the applications of cardiac MRI.

## T5A-SPCA-3 Microvascular Dysfunction Predicts Outcomes in Hypertrophic Cardiomyopathy: Insights from the Intravoxel Incoherent Motion MRI

Participants

Xiaorui Xiang, MD, Beijing, China (*Presenter*) Nothing to Disclose

## PURPOSE

Although intravoxel incoherent motion (IVIM) magnetic resonance imaging (MRI) has emerged as an in vivo marker of microvascular dysfunction, its role in predicting outcomes of patients with hypertrophic cardiomyopathy (HCM) remains unclear. This study aimed to investigate the prognostic value of IVIM-MRI in patients with HCM.

## METHODS AND MATERIALS

A total of 112 consecutive patients with HCM underwent cardiac MRI were enrolled in this study. The imaging protocol consisted of cine, IVIM, and late gadolinium enhancement (LGE). IVIM derived parameters (D, D\* and f) were quantitatively analyzed to assess microvascular dysfunction, and the relationship of IVIM derived parameters and LGE extent were analyzed based on 16 American Heart Association segments. All patients were followed up prospectively, the endpoint was set as major adverse cardiac events (MACEs) including cardiac death, aborted sudden death, heart transplantation, and unplanned rehospitalization for heart failure. The MACEs were examined with univariable and multivariable Cox proportional hazards models. Log-rank test and Kaplan-Meier survival analysis were performed to identify the association between variables and outcomes.

## RESULTS

During an average follow-up of 40.84 $\pm$ 10.47 months, 19 patients (16.9%) reached endpoints. Patients with MACEs showed a trend towards impaired D\* value (43.02  $\pm$  14.24 $\mu$ m<sup>2</sup>/ms,  $p = 0.01$ ), lower f value (10.57  $\pm$  1.72%,  $p=0.02$ ), and more extensive LGE (19.95  $\pm$  8.99%,  $p < 0.001$ ) than those without events, while D value (4.75  $\pm$  1.63 $\mu$ m<sup>2</sup>/ms,  $p = 0.285$ ) was preserved. Significant correlations were demonstrated between D\* value, f value and LGE extent. In the stepwise multivariate Cox regression analysis, D\* value (HR 0.93, 95% CI 0.88-0.98,  $p = 0.001$ ) and f value (HR 0.65, 95% CI 0.45-0.92,  $p = 0.002$ ) emerged as independent predictors of MACEs, even after adjustment for other relevant disease variables. In the Kaplan-Meier survival analysis, the incidence of MACEs was significantly higher in patients with decreased D\* value and f value (all,  $p < 0.001$ ).

## CONCLUSION

s Microvascular dysfunction assessed by IVIM is associated with adverse clinical outcomes in patients with HCM, D\* value and f value are independent predictors in addition to LGE.

## CLINICAL RELEVANCE/APPLICATION

This is the first study to apply IVIM-MRI to predict clinical outcomes in HCM patients, providing real world evidence for the use of non-contrast IVIM-MRI to aid in assessing microvascular dysfunction in routine practice.

## T5A-SPCA-4 Cardiac Magnetic Resonance Native T1 mapping for Risk Stratification in Pulmonary Arterial Hypertension

Participants

Yue Wang, MD, (*Presenter*) Nothing to Disclose

## PURPOSE

To investigate the value of cardiac magnetic resonance (CMR) native T1 mapping for risk stratification in patients with pulmonary arterial hypertension (PAH)

## METHODS AND MATERIALS

A total of 59 patients with diagnosed PAH who received CMR examination at our institution was retrospectively included. Patients were subdivided into two groups based on the clinically-assessed risk status: low-risk group and intermediate- or high-risk group. Thirty healthy individuals were included as normal controls. Anterior right ventricular insertion point (ARVIP), interventricular septum (IVS) and inferior right ventricular insertion point (IRVIP) native T1 times were evaluated manually. CMR-based cardiac functional parameters such as ejection fraction (EF), end diastolic ventricular volume index (EDV-index) and end systolic ventricular volume index (ESV index) of left ventricular (LV) and right ventricular (RV) were also measured and recorded. Native T1 times at ARVIP, IVS and IRVIP as well as CMR-based functional parameters were compared between groups. Receiver operating characteristics (ROC) curves and area under the curves (AUC) were calculated.

## RESULTS

ARVIP, IVS and IRVIP native T1 times were significantly higher in PAH patients as compared with normal controls. Patients in intermediate- or high-risk status showed higher native T1 times in ARVIP and IRVIP. The AUC for ARVIP and IRVIP native T1 times

for discriminating patients with different risk status were 0.741 and 0.702, respectively. LV EDV index, LV ESV index, RVEF, RV EDV index, RV ESV index were also obviously differed between patients with different risk status, with AUC ranged between 0.701 to 0.801. The combining model which integrated ARVIP and IRVIP native T1 times as well as CMR-based cardiac functional parameters showed an AUC of 0.846 for discriminating patients with intermediate- or high-risk status.

#### **CONCLUSION**

s ARVIP, and IRVIP native T1 times hold promise for discriminating PAH patients with different risk status.

#### **CLINICAL RELEVANCE/APPLICATION**

The combining model integrating native T1 times and CMR-based cardiac functional parameters may supplement the evaluation of the risk status in PAH patients.

Printed on: 02/07/23

## Abstract Archives of the RSNA, 2022

T5A-SPCA-1

### Non-contrast-enhanced High-resolution REACT MR Angiography of The Great Vessels in Young Children with Complex Congenital Heart Disease

Tuesday, Nov. 29 12:15PM - 12:45PM Room: Learning Center - CA DPS

#### Participants

Alexander Isaak, MD, Bonn, Germany (*Presenter*) Nothing to Disclose

#### PURPOSE

High-resolution MR angiography (MRA) in small children with congenital heart disease (CHD) is challenging and generally requires contrast agent administration. This study aimed to evaluate the great vessels in young children with complex CHD using native 3D Relaxation-Enhanced Angiography without Contrast (REACT) in comparison to high-resolution contrast-enhanced MRA.

#### METHODS AND MATERIALS

In this retrospective study from April to July 2021, respiratory- and electrocardiogram-gated REACT MRA was compared to contrast-enhanced single-phase MRA in young children with CHD (<10 years) that underwent cardiac MRI at 3T for pre- or postsurgical follow-up. Vascular assessment at predefined landmarks of the great vessels and proximal coronary arteries included (i) image quality (1=non-diagnostic, 5=excellent), (ii) vessel size, (iii) artifact burden, and (iv) diagnostic findings. For statistical analysis, paired t-test, Pearson correlation, Bland-Altman analysis, Wilcoxon test, and intraclass correlation coefficients (ICC) were applied.

#### RESULTS

36 children with complex CHD (median age, 4 years, interquartile range, 2-5; 20 males) who had undergone cardiac MRI under deep sedation were included. Native REACT MRA (mean scan time: 4:22±1:44min) demonstrated comparable overall image quality to contrast-enhanced MRA (3.9±1.0 vs 3.8±0.9, P=0.018). REACT MRA achieved better image quality at the ascending aorta (4.8±0.5 vs 4.3±0.8, P<0.001), proximal coronary arteries (e.g., left: 4.1±1.0 vs 3.3±1.1, P=0.001), and inferior vena cava (4.6±0.5 vs 3.2±0.8, P<0.001). Overall vessel diameters correlated strongly between both MRA methods (Pearson r=0.99; bias=0.04±0.61mm) with high interobserver reproducibility (ICCs: 0.99). Six new vascular findings were detected equally with native REACT MRA and the contrast-enhanced reference standard.

#### CONCLUSION

In young children with complex CHD undergoing preoperative or postoperative follow-up, non-contrast enhanced REACT MRA provides high image quality, accurate vascular measurements, and equivalent diagnostic quality of the great vessels and proximal coronary arteries compared to standard contrast-enhanced MRA.

#### CLINICAL RELEVANCE/APPLICATION

The use of REACT MRA can provide gadolinium-free vascular assessment in young children with CHD, eliminating potential risks of contrast-associated complications, reducing examination costs, and expediting clinical workflow.

Printed on: 02/07/23

## Abstract Archives of the RSNA, 2022

T5A-SPCA-2

### Doppler Ultrasound-gated Fetal Cardiac MRI in Complex Congenital Heart Disease: Clinical Feasibility and Comparison to Echocardiography

Tuesday, Nov. 29 12:15PM - 12:45PM Room: Learning Center - CA DPS

#### Participants

Thomas Vollbrecht, Bonn, Germany (*Presenter*) Nothing to Disclose

#### PURPOSE

To evaluate the feasibility of fetal cardiac MRI using recently introduced Doppler ultrasound (DUS)-based direct gating in clinical routine and to investigate its diagnostic performance in complex congenital heart disease (CHD) compared to fetal echocardiography.

#### METHODS AND MATERIALS

In this prospective study (ClinicalTrials.gov identifier: NCT05066399) from May 2021 to March 2022, female participants with CHD of the fetus underwent fetal echocardiography and DUS-gated fetal cardiac MRI on the same day. For fetal cardiac MRI, balanced steady-state free precession cine images were acquired in continuous axial and optional sagittal and/or coronal orientation (slice thickness: 4 mm). Overall image quality and cardiovascular structure delineability for cine MRI were assessed (4-point Likert scale; 1=non-diagnostic image quality - 4=good image quality). Abnormalities of 20 fetal cardiovascular features previously defined in a study evaluation form were independently assessed for both modalities (abnormality present: yes or no). The reference standard was the result of postnatal examinations. Differences in sensitivities and specificities were calculated with McNemar's test.

#### RESULTS

23 participants (mean gestational age, 36 weeks  $\pm$  1) were included. Fetal cardiac MRI could be completed in all participants. Median overall image quality of DUS-gated cine images was 3 (interquartile range, 2.5-4). In 21 of 23 participants (91%) the underlying CHD was correctly assumed by fetal cardiac MRI. One case with situs inversus but levocardia and congenitally corrected transposition of the great arteries was correctly diagnosed only with MRI. No differences were found regarding sensitivities (88.2%, 95% confidence interval [CI]: 81.4%-92.7% vs. 90.6%, 95% CI: 84.2%-94.5%;  $P=0.581$ ) and specificities (99.1%, 95% CI: 97.4%-99.7% vs. 99.4%, 95% CI: 97.8%-99.8%;  $P=0.999$ ) for the detection of abnormal fetal cardiovascular features between echocardiography and MRI.

#### CONCLUSION

s DUS-gated fetal cine cardiac MRI can reliably diagnose even complex forms of CHD and might be implemented as an adjunct diagnostic tool for prenatal assessment of congenital heart disease.

#### CLINICAL RELEVANCE/APPLICATION

As echocardiography may be limited especially in late gestation, DUS-gated fetal cardiac MRI could become a diagnostic tool for CHD assessment and further expand the applications of cardiac MRI.

Printed on: 02/07/23

## Abstract Archives of the RSNA, 2022

T5A-SPCA-3

### Microvascular Dysfunction Predicts Outcomes in Hypertrophic Cardiomyopathy: Insights from the Intravoxel Incoherent Motion MRI

Tuesday, Nov. 29 12:15PM - 12:45PM Room: Learning Center - CA DPS

#### Participants

Xiaorui Xiang, MD, Beijing, China (*Presenter*) Nothing to Disclose

#### PURPOSE

Although intravoxel incoherent motion (IVIM) magnetic resonance imaging (MRI) has emerged as an in vivo marker of microvascular dysfunction, its role in predicting outcomes of patients with hypertrophic cardiomyopathy (HCM) remains unclear. This study aimed to investigate the prognostic value of IVIM-MRI in patients with HCM.

#### METHODS AND MATERIALS

A total of 112 consecutive patients with HCM underwent cardiac MRI were enrolled in this study. The imaging protocol consisted of cine, IVIM, and late gadolinium enhancement (LGE). IVIM derived parameters (D, D\* and f) were quantitatively analyzed to assess microvascular dysfunction, and the relationship of IVIM derived parameters and LGE extent were analyzed based on 16 American Heart Association segments. All patients were followed up prospectively, the endpoint was set as major adverse cardiac events (MACEs) including cardiac death, aborted sudden death, heart transplantation, and unplanned rehospitalization for heart failure. The MACEs were examined with univariable and multivariable Cox proportional hazards models. Log-rank test and Kaplan-Meier survival analysis were performed to identify the association between variables and outcomes.

#### RESULTS

During an average follow-up of 40.84±10.47 months, 19 patients (16.9%) reached endpoints. Patients with MACEs showed a trend towards impaired D\* value ( $43.02 \pm 14.24 \mu\text{m}^2/\text{ms}$ ,  $p = 0.01$ ), lower f value ( $10.57 \pm 1.72\%$ ,  $p=0.02$ ), and more extensive LGE ( $19.95 \pm 8.99\%$ ,  $p < 0.001$ ) than those without events, while D value ( $4.75 \pm 1.63 \mu\text{m}^2/\text{ms}$ ,  $p = 0.285$ ) was preserved. Significant correlations were demonstrated between D\* value, f value and LGE extent. In the stepwise multivariate Cox regression analysis, D\* value (HR 0.93, 95% CI 0.88-0.98,  $p = 0.001$ ) and f value (HR 0.65, 95% CI 0.45-0.92,  $p = 0.002$ ) emerged as independent predictors of MACEs, even after adjustment for other relevant disease variables. In the Kaplan-Meier survival analysis, the incidence of MACEs was significantly higher in patients with decreased D\* value and f value (all,  $p < 0.001$ ).

#### CONCLUSION

s Microvascular dysfunction assessed by IVIM is associated with adverse clinical outcomes in patients with HCM, D\* value and f value are independent predictors in addition to LGE.

#### CLINICAL RELEVANCE/APPLICATION

This is the first study to apply IVIM-MRI to predict clinical outcomes in HCM patients, providing real world evidence for the use of non-contrast IVIM-MRI to aid in assessing microvascular dysfunction in routine practice.

Printed on: 02/07/23

## Abstract Archives of the RSNA, 2022

T5A-SPCA-4

### Cardiac Magnetic Resonance Native T1 mapping for Risk Stratification in Pulmonary Arterial Hypertension

Tuesday, Nov. 29 12:15PM - 12:45PM Room: Learning Center - CA DPS

#### Participants

Yue Wang, MD, (*Presenter*) Nothing to Disclose

#### PURPOSE

To investigate the value of cardiac magnetic resonance (CMR) native T1 mapping for risk stratification in patients with pulmonary arterial hypertension (PAH)

#### METHODS AND MATERIALS

A total of 59 patients with diagnosed PAH who received CMR examination at our institution was retrospectively included. Patients were subdivided into two groups based on the clinically-assessed risk status: low-risk group and intermediate- or high-risk group. Thirty healthy individuals were included as normal controls. Anterior right ventricular insertion point (ARVIP), interventricular septum (IVS) and inferior right ventricular insertion point (IRVIP) native T1 times were evaluated manually. CMR-based cardiac functional parameters such as ejection fraction (EF), end diastolic ventricular volume index (EDV-index) and end systolic ventricular volume index (ESV index) of left ventricular (LV) and right ventricular (RV) were also measured and recorded. Native T1 times at ARVIP, IVS and IRVIP as well as CMR-based functional parameters were compared between groups. Receiver operating characteristics (ROC) curves and area under the curves (AUC) were calculated.

#### RESULTS

ARVIP, IVS and IRVIP native T1 times were significantly higher in PAH patients as compared with normal controls. Patients in intermediate- or high-risk status showed higher native T1 times in ARVIP and IRVIP. The AUC for ARVIP and IRVIP native T1 times for discriminating patients with different risk status were 0.741 and 0.702, respectively. LV EDV index, LV ESV index, RVEF, RV EDV index, RV ESV index were also obviously differed between patients with different risk status, with AUC ranged between 0.701 to 0.801. The combining model which integrated ARVIP and IRVIP native T1 times as well as CMR-based cardiac functional parameters showed an AUC of 0.846 for discriminating patients with intermediate- or high-risk status.

#### CONCLUSION

s ARVIP, and IRVIP native T1 times hold promise for discriminating PAH patients with different risk status.

#### CLINICAL RELEVANCE/APPLICATION

The combining model integrating native T1 times and CMR-based cardiac functional parameters may supplement the evaluation of the risk status in PAH patients.

Printed on: 02/07/23

## Abstract Archives of the RSNA, 2022

T5A-SPCH

### Chest Tuesday Poster Discussions - A

Tuesday, Nov. 29 12:15PM - 12:45PM Room: Learning Center - CH DPS

#### Participants

Joon Beom Seo, MD, PhD, Seoul, (*Moderator*) Stockholder, Promedius Inc; Stockholder, Coreline Soft, Co Ltd; Stockholder, Anymedi Inc

#### Sub-Events

### T5A-SPCH-1 Magnitude and Characteristics of Missed Lung Nodules during COVID-19 Pandemic

#### Participants

Arpit Kothari, Indore, India (*Presenter*) Research Consultant, Qure.ai; Research Consultant, Subtle Medical, Inc; Research Consultant, Lunit Inc; Research Consultant, FUJIFILM Holdings Corporation; Research Consultant, Level42AI; Director, Kothari Diagnostics Pvt Ltd; CEO, Kothari Diagnostics Pvt Ltd

#### PURPOSE

Lung cancer is the leading cause of cancer deaths. CT scans can identify cancer in early stages. During Coronavirus Pandemic, lot of CT scans were taken. It is possible that the already strained radiologists were only looking to either confirm or rule out COVID and missed nodules. The purpose of this study is to estimate the magnitude of such misses and assess the role of a Deep Learning (DL) software in aiding the detection of nodules.

#### METHODS AND MATERIALS

2432 CT scans taken during the second and third wave of COVID from two radiology diagnosis chains were processed by qCT Lung-a DL software for nodules. The radiologist report of the scan which the DL flagged were reviewed for nodules. Cases for which nodules not mentioned were re-read by an independent radiologist with qCT assistance. This radiologist was asked to either confirm or refute the flagged abnormality as nodule. If a nodule is confirmed, the radiologist rated its malignancy potential in a 5-point positive directed Likert scale. The radiologist gave an alternative finding for false flag.

#### RESULTS

The DL system flagged 653 scans as having nodules. Of this 80 were identified in radiologist report. The remaining 573 scans were re-read, 111 (19.4%) were confirmed as having nodules. 44 of these scans had more than one nodule flagged. The median of the longest diameter was 14 mm (range: 6 to 48 mm) and 62.8% of them were solid nodules. The distribution of localization of the nodule was similar between upper and lower lobes. Common cause of false flags was ground-glass opacity with consolidation (94.8%) followed peripheral vessel (1.9%). 92 of the 111 scans were given a malignancy rating of 1 or 2 (non-malignant or probably non-malignant). 17 were given a rating of 3 (could be malignant or non-malignant) and 2 were rated as probably malignant. Spiculation was more likely in DLs output for those with higher rating..

#### CONCLUSION

111 scans with nodules were not reported. Looking at the independent radiologist malignancy rating, it is possible for some cases the initial radiologist did not report it due perceived risk. 19 of these cases would have been eligible for follow-up investigations. The presence of ground-glass opacity in COVID can explain some of the errors of this DL.

#### CLINICAL RELEVANCE/APPLICATION

Radiologist report only the findings which are relevant to the radiology request form and their perceived risk of incidental findings. A conservative approach would be to report all findings irrespective of the perceived risk so that the treating physician can take appropriate action.

### T5A-SPCH-10 Acceptability of NLST Image Data for Modern Quantitative Algorithm Development

#### Participants

Artit Jirapatnakul, PhD, New York, NY (*Presenter*) Nothing to Disclose

#### PURPOSE

To assess the applicability of CT images from the National Lung Screening Trial (NLST) to current lung cancer screening recommendations

#### METHODS AND MATERIALS

The NLST provides a public database of all CT images performed during the trial. With 73,118 studies and 203,099 image series, this is the largest publicly available database of chest CT images and is being used for the development and testing of quantitative algorithms, such as lung nodule measurement, detection, and diagnosis. However, the NLST screened participants between 2002 and 2006; these CT scans are now 15-20 years old. Minimum quality guidelines for scan acquisition and reconstruction have been developed by the Quantitative Imaging Biomarker Alliance (QIBA) of the Radiological Society of North America for tasks related to

quantitative measurements in the context of LDCT. We downloaded all available NLST images from the Cancer Imaging Archive, excluding localizer or topogram images, or incomplete series. We analyzed DICOM header information of the remaining series to extract the scanner and protocol information. As a measure of modern quantitative image standards, we determined the proportion of scans meeting protocol recommendations of QIBA Small Nodule Committee.

## RESULTS

70486 CT image series containing <20 images were excluded. Of the remaining 132613 CT series, 10321 (7.8%) were acquired with a slice thickness (ST)  $\leq 1.25$  mm, the current QIBA Small Lung Nodule recommendation. Of this group, the 10 most frequent combinations account for 97.8% (10098/10321) of the CT series. After eliminating scans with edge-enhancing kernels (4185) and from scanners in which spatial warping has been identified (4649), only 1487 meet QIBA eligibility criteria. There were 4447 CT images series for NLST participants with lung cancer, of which only 399 CT image series in 139 participants were acquired with a slice thickness  $\leq 1.25$  mm.

## CONCLUSION

s With advances in image processing, quantitation, and artificial intelligence, there is a need for high quality image databases for software development for automation and standardization of screening CT image analysis. The NLST CT images have been made openly available for this purpose, but over 95% of the images do not meet the image acquisition and reconstruction quality standards required for optimizing algorithm performance. New databases and distribution approaches are necessary for progression of software development; various organizations are now in the process of developing newer databases that will be made available.

## CLINICAL RELEVANCE/APPLICATION

Databases of modern, clinically relevant images are critical for continued development of AI algorithms; care must be taken in the interpretation of results of studies using outdated CT scans.

### **T5A-SPCH-2 Transfer-learning deep radiomics and binary dilation for predicting PET-positive thoracic lymph nodes from contrast enhanced computed tomography in lung cancer.**

Participants

Fabian Laqua, (*Presenter*) Research Grant, Koninklijke Philips NV

## PURPOSE

Positron emission tomography (PET) is currently the non-invasive reference standard for staging of lymph nodes in lung cancer. However, due to high costs, limited availability, and additional radiation exposure, not all patients can undergo this diagnostic procedure. Purpose of this study was to build a classification model, that predicts the PET result from traditional contrast-enhanced computed tomography (CT) and to test different feature extraction strategies.

## METHODS AND MATERIALS

All thoracic lymph nodes of consecutive lung cancer patients in a single center, that underwent routine contrast-enhanced thoracic CT and subsequent PET for staging between 2014 and 2019, were segmented. Penalized ('elastic') logistic regression models were trained to predict whether a lymph node shows 18-fluorodeoxyglucose uptake in the subsequent PET-scan. Radiomics features were extracted i) as traditional hand-crafted radiomics features from the segmented lymph nodes, ii) from segmentations dilated by varying radiuses around the original segmentation, iii) by applying the first k layers of a EfficientNet-CNN pretrained on ImageNet database on the segmented lymph nodes and iv) a hybrid approach that combines the features of iii) with traditional shape and first-order features.

## RESULTS

In total, 2734 lymph nodes [555 (20.3 %) PET-positive] from 100 patients [49% female, median age 67 (IQR: 60-71)] with lung cancer (60% adeno carcinoma, 21% plate epithelial carcinoma, 8% small cell lung cancer) were included in this study. The Area-under-the-receiver-operating-characteristics (AUC) was slightly but significantly [ $z=4.2$ ,  $p<0.001$ ; 0.881 (95% CI 0.873-0.889) vs. 0.873 (0.865-0.882)] netter for the features extracted from segmentations dilated by 1 pixel compared to the original segmentation. The combination of the features of iii) and shape and first-order features yielded best results [AUC 0.890 (0.881 - 0.902)], that were significantly better than i) traditional ( $z=3.8$ ,  $p=0.02$ ) and iii) transfer-learning CNN features ( $z=10.4$ ,  $p<0.001$ ).

## CONCLUSION

s Minor binary dilatation of lymph node segmentation improves machine learning classification of lymph nodes. Both, traditional radiomics features and transfer-learning deep radiomics features provide relevant and complimentary information for classification of lymph nodes in lung cancer staging.

## CLINICAL RELEVANCE/APPLICATION

Prediction of thoracic nodal status using radiomics and machine learning techniques on standard contrast-enhanced CT provides very good classification performance compared to PET. Even in absence of available PET, exploitation of the available information by the approach presented in this study may be a good alternative for non-invasive nodal staging in lung cancer.

### **T5A-SPCH-3 Clinicopathological and CT Features of Tumor Spread Through Air Space in Invasive Lung Adenocarcinoma**

Participants

Lili Qin, (*Presenter*) Nothing to Disclose

## PURPOSE

Tumor spread through air spaces (STAS) has recently been reported as a novel invasive pattern in lung adenocarcinoma, the aim of this study was to investigate the clinical/pathological and radiological features in invasive lung adenocarcinoma with tumor spread through air space(STAS).

## METHODS AND MATERIALS

Data of 503 invasive lung adenocarcinoma who underwent operation between January1,2015 and December 31,2021 were collected. The correlations of STAS presence and clinicopathological and radiological characteristics were analyzed. Statistical

analysis was performed using SPSS 22.0.

## RESULTS

Among the 503 patients with invasive adenocarcinoma, 247(47.9%) were positive for STAS and 262(52.1%) were negative for STAS. STAS were more common in papillary, micropapillary and solid tumors ( $P < 0.01$ ). STAS was associated with advanced pN ( $P < 0.001$ ) and pTNM ( $P < 0.001$ ) stage, more lymph node metastases ( $P < 0.01$ ), more pleural invasion ( $P < 0.01$ ), more neurovascular invasion ( $P = 0.025$ ). The maximum diameter ( $P < 0.01$ ), the maximum diameters of the solid component ( $P < 0.01$ ), the consolidation/tumor ratio (CTR,  $P < 0.01$ ) was significantly larger in STAS-positive than in STAS-negative adenocarcinoma. Other common CT features of adenocarcinomas, ie, lobulation ( $P < 0.01$ ), spiculation ( $P < 0.01$ ), vacuole ( $P < 0.01$ ), air bronchogram ( $P = 0.020$ ), vascular convergence ( $P < 0.01$ ), pleural indentation ( $P < 0.01$ ) were shown to be significantly associated with STAS. In a multivariable analysis, maximum diameter of solid component was an independent predictor of STAS (odds ratio, 2.505; 95% confidence interval: 1.886, 3.329) and a cut-off value of 1.18cm showed a discriminatory power with a sensitivity of 73.9% and a specificity of 69.1%.

## CONCLUSION

s STAS was significantly correlated with several invasive clinicopathological and radiological characteristics, the maximum diameter was an independent predictor of STAS. These results will prove helpful in identifying STAS-positive adenocarcinoma by CT before surgical resection.

## CLINICAL RELEVANCE/APPLICATION

As a newly named and pathologically diagnosed tumour invasion pattern in lung adenocarcinoma, STAS not only has an impact on the determination of the degree of invasion on its pathological tissues, but also has a significant impact on the selection and assessment of surgical treatment modalities for lung adenocarcinoma patients and the intervention of patient prognosis. The results of this study show that the largest diameter of solid component in lung adenocarcinoma lesions on CT and CRT are important signs for predicting STAS, and other common signs of malignancies also have some predictive value.

## T5A-SPCH-4 Progression of Bronchiectasis during Five or More years Follow-up in Low-Dose CT Screening for Lung Cancer

Participants

Qiang Cai, PhD, MD, New York, NY (*Presenter*) Nothing to Disclose

## PURPOSE

To assess the frequency of development of bronchiectasis among participants without previous bronchiectasis as well as the progression of bronchiectasis in participants with bronchiectasis on the baseline LDCT for five or more years after enrollment in a screening program.

## METHODS AND MATERIALS

Changes in the ELCAP Bronchiectasis Score between baseline and the last LDCT were reviewed for smokers aged 40-90 years who had five or more years of follow-up screening after the baseline LDCT in the Mount Sinai ELCAP screening study between 2010 and 2019. MANOVA was used to assess the change in the four ELCAP Bronchiectasis component scores (severity and extent of bronchial dilatation, bronchial wall thickening (BWT), and mucoid impaction (MI)) as well as the total score.

## RESULTS

Of the 2191 participants at baseline, 534 participants had five or more years of follow-up LDCTs. Among the 534 participants, baseline LDCT showed 408 (76.4%) without bronchiectasis while it was present in 126 (23.6%). Development of bronchiectasis was found in 9 (2.2%) of the 408 participants without bronchiectasis on baseline LDCT, with subsequent ELCAP Bronchiectasis Scores ranging from 2 to 20. Progression was present in 25 (19.8%) of the 126 with bronchiectasis on baseline LDCT and the increase in the ELCAP Bronchiectasis Scores ranged from 1 to 8. Progression of severity in bronchial dilatation was associated with increasing age ( $p = 0.006$ ) and self-reported stroke ( $p = 0.01$ ) at baseline enrollment, as well as progression in the extent of bronchial dilatation ( $p = 0.01$ ), BWT ( $p = 0.04$ ) and MI ( $p < 0.0001$ ). Progression of extent was associated with increasing age ( $p = 0.03$ ) and higher MI score ( $p = 0.0001$ ) on baseline CT. Progression of BWT was associated with increasing pack-years of smoking ( $p = 0.0007$ ), self-reported COPD ( $p = 0.047$ ), and lower BWT ( $p = 0.03$ ) on baseline LDCT. An increase in MI was a significant predictor of increasing age, increase in severity and extent of bronchial dilatation ( $p = 0.001$ ).

## CONCLUSION

s Awareness of bronchiectasis in LDCT screening for lung cancer is necessary as one-fifth of participants during long-term follow-up had progression compared to those without bronchiectasis on initial LDCT screening.

## CLINICAL RELEVANCE/APPLICATION

The ELCAP Bronchiectasis Score provides a useful assessment of the progression of bronchiectasis. Reporting of bronchiectasis findings and continued assessment over the period of participation in the LDCT screening allows for documentation of change for future assessment of the benefit of early treatment.

## T5A-SPCH-5 CT on Lung Cancer Screening is Useful for Adjuvant Comorbidity Diagnosis in Developing Countries

Participants

Bruno Hochegger, PhD, Gainesville, FL (*Presenter*) Nothing to Disclose

## PURPOSE

To analyze and quantify the prevalence of comorbidities derived from chest computed tomography (CT) of patients undergoing lung cancer screening in a developing country.

## METHODS AND MATERIALS

For this retrospective study, low-dose CT scans ( $n = 775$ ) from patients undergoing LCS in a tertiary hospital between 2016 and 2020 were examined. A group of controls with similar age and gender but undergoing chest CT for other indications was also used for comparison ( $n = 370$ ). CT images were evaluated by experienced radiologists regarding coronary artery calcium (CAC) score, skeletal muscle area (SMA), interstitial lung abnormalities (ILA), presence of emphysema, osteoporosis, and hepatic steatosis using

a dedicated software. Prevalence of abnormalities and clinical characteristics of the groups were compared using t-test and chi-squared tests. Interclass correlation coefficient (ICCs) and kappa coefficients for interobserver agreement were also calculated. The level of significance was set at 0.05.

## RESULTS

One or more comorbidities were identified on imaging in 86.6% of patients undergoing LCS and in 40% of the controls. The most prevalent comorbidity was osteoporosis, present in 44.2% of patients and 24.8% of controls. CAC was identified in 41.9% of cases (vs. 23.7% of controls), emphysema in 66.3% (vs. 8.9% of controls), and osteoporosis in 44.2% (vs. 24.8% of controls). Compared to information retrieved from the medical records, CAC, emphysema, and osteoporosis were newly diagnosed in 25%, 7%, and 46% of the LCS patients, respectively. Sarcopenia was identified on 9.9% of LCS patients (vs. 3.5% controls) and hepatic steatosis in 40.7% (vs. 15.9% of controls). The kappa coefficient for CAC was 0.906, while ICC for measurements in the liver, spleen, and bone density were 0.88, 0.93, and 0.96, respectively.

## CONCLUSION

s Data derived from the CT of patients undergoing LCS may lead to the identification of potentially undiagnosed comorbidities in more than 80% of patients.

## CLINICAL RELEVANCE/APPLICATION

Smoking-related comorbidities (CAC, emphysema, ILA, sarcopenia, osteoporosis, and hepatic steatosis) are highly prevalent in patients undergoing low-dose CT for LCS. Integrated assessment of the CT in LCS for features other than nodule screening may lead to the identification of these comorbidities early and increase the chances of a favorable outcome for patients.

## T5A-SPCH-6 Is It Time to Replace Low-dose CT with Ultra-low-dose CT in Lung Cancer Screening?

Participants

Matheus Zanon, MD, MSc, Porto Alegre, Brazil (*Presenter*) Nothing to Disclose

## PURPOSE

To assess the agreement between ultra-low-dose CT (ULDCT) and low-dose CT (LDCT) in the evaluation of pulmonary findings in smokers undergoing lung cancer screening (LCS).

## METHODS AND MATERIALS

For one month, we prospectively included eligible patients for LCS that underwent both chest ULDCT and LDCT for one month. Eligibility for LCS followed the 2021 guidelines by the United States Preventive Services Task Force. Patients should be adults, aged 50 to 80 years, with a 20 pack-year smoking history, currently smoking or former smokers that had quit within the past 15 years. Images were acquired in a 64-detector CT scanner as follows: LDCT: 100kVp/25mAs; ULDCT: 80kVp/15mAs. Two independent senior radiologists evaluated the presence of consolidation, ground-glass opacification (GGO), septal thickening, pulmonary nodule, bronchial wall thickening (BWT), pleural effusion, emphysema, bronchiectasis, and atelectasis.

## RESULTS

From the 265 patients enrolled, 58 (21.9%) had abnormal CT scans. Mean effective radiation doses (ERD) for LDCT and ULDCT were  $1.21 \pm 0.34$  mSv and  $0.39 \pm 0.15$  mSv, respectively, representing a reduction in the mean ERD of 67.8%. Agreement was almost perfect for emphysema ( $\kappa=0.92$ ) and nodules ( $\kappa=0.91$ ). BWT, bronchiectasis, and atelectasis presented a strong agreement ( $\kappa, 0.80-0.90$ ), and consolidation, septal thickening, and pleural effusion presented substantial agreement ( $\kappa, 0.60-0.80$ ). Conversely, GGO presented a poor agreement ( $\kappa=0.37$ ).

## CONCLUSION

s Although the mean ERD reduced dropped to almost a third from LDCT to ULDCT, inter-reader agreement was poor for significant findings, such as consolidation and GGO, that may represent other types of lung cancer (e.g., lepidic adenocarcinoma).

## CLINICAL RELEVANCE/APPLICATION

Despite the exciting agreement for some pulmonary findings, these results question whether using an ULDCT protocol for LCS would be adequate, as many subsolid or GGO lesions could be missed. Also, despite the significant reduction in the RED, it is questionable whether there is a patient benefit from going to 1.2 to 0.39 mSv.

## T5A-SPCH-7 Screening for the Screeners: Our Institutional Experience with Double Reading of CT Lung Cancer Screening

Participants

Padma Manapragada, MD, MBBS, Birmingham, AL (*Presenter*) Nothing to Disclose

## PURPOSE

Our institution participated in the NLST and continued to offer screening. Post approval by the USPSTF and the CMS, patient volume and the number of readers increased. With faculty turnover, the participating readers also kept changing. This study evaluates if double reading would increase adherence to screening requirements, consistent Lung RADS interpretation and unify follow up recommendations.

## METHODS AND MATERIALS

The local IRB approved this retrospective study and written informed consent was waived. All lung cancer screening [LCS] cases from 2015 to through 2021 [2347 cases] were evaluated. Patients met the 2015 CMS criteria for inclusion: age 55-77, 30 pack years, current smoker or less than 15 years since quitting. A separate LCS PACS reading list was established. In rotation two radiologists were assigned to read the list each day. The first reader dictated the templated report and placed it in draft status. The second reader reviewed the study and the draft report, made any changes needed, signed the report, recorded if there was a discrepancy and, if present, the type of discrepancy. An Excel sheet recorded patient screened, Lung-RADS score, yes/no discrepancy, and category of discrepancy. Retrospectively the discrepancies were graded as: Significant-1: Changed L-RADS status or coronary artery calcification [CAC] score, other cancers, or major vascular aneurysm. Equivocal-2: Additional nodules but no L-RADS score change, other lung disease. Incidental-3: Non-cancer potentially significant findings (cirrhosis, renal stones,

Pulmonary Artery HTN, AVM).

## RESULTS

The majority of the 190 discrepancies were significant-109/190. Equivocal cases were 48/109 and incidental cases were 28/109. 5 cases were classified in more than one category. In eight cases the LR category changed from negative [1, 2] to positive [3,4]. The percentage of discrepancies initially increased as the number of cases increased, a new reader was added or new L-RADS introduced then decreased.

## CONCLUSION

Double reading improved consistency in evaluation of LCS CTs and the application of LungRADS. This provides more uniform patient care over time and when patient care is escalated to biopsy or treatment.

## CLINICAL RELEVANCE/APPLICATION

Double reading in evaluation of LCS CTs provides consistent high quality reports and consistent application of LungRADS. This provides uniform high quality patient care over time and when patient care is escalated to biopsy or treatment.

## T5A-SPCH-8 Risk of Exacerbations in Participants with Bronchiectasis in a Program of Low-dose CT Screening

Participants

Natthaya Triphuridet, MD, PhD, New York, NY (*Presenter*) Nothing to Disclose

## PURPOSE

To predict future exacerbations during the two years following the initial LDCT in screening participants with bronchiectasis based on the LDCT findings including emphysema, and self-reported co-morbidities.

## METHODS AND MATERIALS

Electronic medical record (EMR) review of prospectively enrolled participants who smoked in Early Lung and Cardiac Action Program, a LDCT screening program from 2010 to 2019. EMR were reviewed to identify participants with respiratory symptoms and exacerbations during two years before and two years after initial LDCT screening. Uni- and multivariable regression analysis were performed to identify predictors of future exacerbations using LDCT findings and self-reported co-morbidities at the time of screening.

## RESULTS

Of 2191 participants, 504(23%) had bronchiectasis and EMR had available records on 300 (median age,69 years;154(51%) women). Emphysema was identified on LDCT in 152(51%). Exacerbations were identified during two years after LDCT screening in 84(28%) participants. Participants with emphysema, compared to those without emphysema, had significantly higher median ELCAP Bronchiectasis Score (13.0 vs. 11.5,  $p=.02$ ), higher frequency of respiratory symptoms [97(64%) vs. 75(51%),  $p=.02$ ] and exacerbations [49(32%) vs. 35(24%),  $p=.10$ ]. Multivariable analyses showed that the ELCAP Bronchiectasis Score (OR=1.12, $p<.001$ ), self-reported COPD (OR=2.69, $p<.001$ ) and asthma (OR=2.47, $p=.006$ ) were independent predictors of exacerbations, but not emphysema. Considering ELCAP Bronchiectasis component scales instead of the total score, severity of bronchial dilatation (OR=1.30, $p=.001$ ) and bronchial wall thickening (OR=1.29, $p=.004$ ) were significant predictors. When including prior respiratory symptoms and exacerbations during two years prior to screening as predictors, ELCAP Bronchiectasis Score remained as an independent predictor of future exacerbations.

## CONCLUSION

High ELCAP Bronchiectasis Score, self-reported COPD and asthma are independent predictors of exacerbations. This type of information is needed to develop preventive management protocols.

## CLINICAL RELEVANCE/APPLICATION

Among 300 participants with bronchiectasis and available electronic medical records, 84(28.0%) had exacerbations during two years following initial LDCT screening. Significant predictors of future exacerbations were: ELCAP Bronchiectasis Score [OR=1.12,  $p<.001$ ], self-reported COPD [OR=2.69,  $p<.001$ ] and asthma [OR=2.47,  $p=0.006$ ].

## T5A-SPCH-9 Computational Risk Stratification: A Deep Learning Approach to Predicting a Major Lung Biopsy Complication

Participants

Alexander Lindqwister, BS,MS, Lebanon, NH (*Presenter*) Nothing to Disclose

## PURPOSE

CT-guided core needle biopsies (CT-CNB) are a major component of the diagnostic work-up of lung lesions. The most common associated risk is iatrogenic pneumothorax (PTX) which may require tube thoracostomy and subsequent hospitalization. The ability to predict PTX requiring tube thoracostomy in the pre-procedural setting would allow radiologists to make more individualized recommendations in patient management, improve the informed consent process, and augment care delivery through risk stratification.

## METHODS AND MATERIALS

A retrospective study of 502 patients who underwent CT-CNB of the lung was performed. Procedural, patient demographic, and outcomes data were collected and descriptive statistics were performed to determine significant distinguishing features between patients who required chest tubes and those who did not. Six parameters (age, sex, emphysema, projected length of needle path, greatest dimension of lung lesion, lung lobe) encoded through 12 features were utilized by a deep neural network to create a predictive model. Exhaustive 5-fold cross validation in addition to an external dataset consisting of 449 patients was used to validate the model.

## RESULTS

Deep learning models were highly successful in predicting PTX requiring tube thoracostomy, with a receiver operating characteristic

area under the curve (ROC-AUC) of 0.961 [± 0.033] averaged across 2,000 simulations. The model had consistent performance with the external dataset, achieving an ROC-AUC of 0.886 [± 0.059]. Testing metrics revealed a sensitivity of 0.879, specificity of 0.924, and a negative predictive value of 0.986 after adjusting for incidence of chest tube placement.

#### **CONCLUSION**

The strong performance of deep learning models to predict chest tube placement demonstrates the possible clinical utility of machine learning in predicting post-procedural complications in this setting. The model performed well on data collected from two different patient cohorts, which suggests generalizability and the potential for broad application.

#### **CLINICAL RELEVANCE/APPLICATION**

Neural networks and other data-driven approaches may be useful in predicting adverse post-procedural complications in the setting of lung CT-CNB.

Printed on: 02/07/23

## Abstract Archives of the RSNA, 2022

T5A-SPCH-1

### Magnitude and Characteristics of Missed Lung Nodules during COVID-19 Pandemic

Tuesday, Nov. 29 12:15PM - 12:45PM Room: Learning Center - CH DPS

#### Participants

Arpit Kothari, Indore, India (*Presenter*) Research Consultant, Qure.ai; Research Consultant, Subtle Medical, Inc; Research Consultant, Lunit Inc; Research Consultant, FUJIFILM Holdings Corporation; Research Consultant, Level42AI; Director, Kothari Diagnostics Pvt Ltd; CEO, Kothari Diagnostics Pvt Ltd

#### PURPOSE

Lung cancer is the leading cause of cancer deaths. CT scans can identify cancer in early stages. During Coronavirus Pandemic, lot of CT scans were taken. It is possible that the already strained radiologists were only looking to either confirm or rule out COVID and missed nodules. The purpose of this study is to estimate the magnitude of such misses and assess the role of a Deep Learning (DL) software in aiding the detection of nodules.

#### METHODS AND MATERIALS

2432 CT scans taken during the second and third wave of COVID from two radiology diagnosis chains were processed by qCT Lung-a DL software for nodules. The radiologist report of the scan which the DL flagged were reviewed for nodules. Cases for which nodules not mentioned were re-read by an independent radiologist with qCT assistance. This radiologist was asked to either confirm or refute the flagged abnormality as nodule. If a nodule is confirmed, the radiologist rated its malignancy potential in a 5-point positive directed Likert scale. The radiologist gave an alternative finding for false flag.

#### RESULTS

The DL system flagged 653 scans as having nodules. Of this 80 were identified in radiologist report. The remaining 573 scans were re-read, 111 (19.4%) were confirmed as having nodules. 44 of these scans had more than one nodule flagged. The median of the longest diameter was 14 mm (range: 6 to 48 mm) and 62.8% of them were solid nodules. The distribution of localization of the nodule was similar between upper and lower lobes. Common cause of false flags was ground-glass opacity with consolidation (94.8%) followed peripheral vessel (1.9%). 92 of the 111 scans were given a malignancy rating of 1 or 2 (non-malignant or probably non-malignant). 17 were given a rating of 3 (could be malignant or non-malignant) and 2 were rated as probably malignant. Spiculation was more likely in DLs output for those with higher rating..

#### CONCLUSION

s 111 scans with nodules were not reported. Looking at the independent radiologist malignancy rating, it is possible for some cases the initial radiologist did not report it due perceived risk. 19 of these cases would have been eligible for follow-up investigations. The presence of ground-glass opacity in COVID can explain some of the errors of this DL.

#### CLINICAL RELEVANCE/APPLICATION

Radiologist report only the findings which are relevant to the radiology request form and their perceived risk of incidental findings. A conservative approach would be to report all findings irrespective of the perceived risk so that the treating physician can take appropriate action.

Printed on: 02/07/23



## Abstract Archives of the RSNA, 2022

T5A-SPCH-10

### Acceptability of NLST Image Data for Modern Quantitative Algorithm Development

Tuesday, Nov. 29 12:15PM - 12:45PM Room: Learning Center - CH DPS

#### Participants

Artit Jirapatnakul, PhD, New York, NY (*Presenter*) Nothing to Disclose

#### PURPOSE

To assess the applicability of CT images from the National Lung Screening Trial (NLST) to current lung cancer screening recommendations

#### METHODS AND MATERIALS

The NLST provides a public database of all CT images performed during the trial. With 73,118 studies and 203,099 image series, this is the largest publicly available database of chest CT images and is being used for the development and testing of quantitative algorithms, such as lung nodule measurement, detection, and diagnosis. However, the NLST screened participants between 2002 and 2006; these CT scans are now 15-20 years old. Minimum quality guidelines for scan acquisition and reconstruction have been developed by the Quantitative Imaging Biomarker Alliance (QIBA) of the Radiological Society of North America for tasks related to quantitative measurements in the context of LDCT. We downloaded all available NLST images from the Cancer Imaging Archive, excluding localizer or topogram images, or incomplete series. We analyzed DICOM header information of the remaining series to extract the scanner and protocol information. As a measure of modern quantitative image standards, we determined the proportion of scans meeting protocol recommendations of QIBA Small Nodule Committee.

#### RESULTS

70486 CT image series containing <20 images were excluded. Of the remaining 132613 CT series, 10321 (7.8%) were acquired with a slice thickness (ST)  $\leq 1.25$  mm, the current QIBA Small Lung Nodule recommendation. Of this group, the 10 most frequent combinations account for 97.8% (10098/10321) of the CT series. After eliminating scans with edge-enhancing kernels (4185) and from scanners in which spatial warping has been identified (4649), only 1487 meet QIBA eligibility criteria. There were 4447 CT images series for NLST participants with lung cancer, of which only 399 CT image series in 139 participants were acquired with a slice thickness  $\leq 1.25$  mm.

#### CONCLUSION

s With advances in image processing, quantitation, and artificial intelligence, there is a need for high quality image databases for software development for automation and standardization of screening CT image analysis. The NLST CT images have been made openly available for this purpose, but over 95% of the images do not meet the image acquisition and reconstruction quality standards required for optimizing algorithm performance. New databases and distribution approaches are necessary for progression of software development; various organizations are now in the process of developing newer databases that will be made available.

#### CLINICAL RELEVANCE/APPLICATION

Databases of modern, clinically relevant images are critical for continued development of AI algorithms; care must be taken in the interpretation of results of studies using outdated CT scans.

Printed on: 02/07/23

## Abstract Archives of the RSNA, 2022

T5A-SPCH-2

### Transfer-learning deep radiomics and binary dilation for predicting PET-positive thoracic lymph nodes from contrast enhanced computed tomography in lung cancer.

Tuesday, Nov. 29 12:15PM - 12:45PM Room: Learning Center - CH DPS

#### Participants

Fabian Laqua, (*Presenter*) Research Grant, Koninklijke Philips NV

#### PURPOSE

Positron emission tomography (PET) is currently the non-invasive reference standard for staging of lymph nodes in lung cancer. However, due to high costs, limited availability, and additional radiation exposure, not all patients can undergo this diagnostic procedure. Purpose of this study was to build a classification model, that predicts the PET result from traditional contrast-enhanced computed tomography (CT) and to test different feature extraction strategies.

#### METHODS AND MATERIALS

All thoracic lymph nodes of consecutive lung cancer patients in a single center, that underwent routine contrast-enhanced thoracic CT and subsequent PET for staging between 2014 and 2019, were segmented. Penalized ('elastic') logistic regression models were trained to predict whether a lymph node shows 18-fluorodeoxyglucose uptake in the subsequent PET-scan. Radiomics features were extracted i) as traditional hand-crafted radiomics features from the segmented lymph nodes, ii) from segmentations dilated by varying radiuses around the original segmentation, iii) by applying the first k layers of a EfficientNet-CNN pretrained on ImageNet database on the segmented lymph nodes and iv) a hybrid approach that combines the features of iii) with traditional shape and first-order features.

#### RESULTS

In total, 2734 lymph nodes [555 (20.3 %) PET-positive] from 100 patients [49% female, median age 67 (IQR: 60-71)] with lung cancer (60% adeno carcinoma, 21% plate epithelial carcinoma, 8% small cell lung cancer) were included in this study. The Area-under-the-receiver-operating-characteristics (AUC) was slightly but significantly [ $z=4.2$ ,  $p<0.001$ ; 0.881 (95% CI 0.873-0.889) vs. 0.873 (0.865-0.882)] netter for the features extracted from segmentations dilated by 1 pixel compared to the original segmentation. The combination of the features of iii) and shape and first-order features yielded best results [AUC 0.890 (0.881 - 0.902)], that were significantly better than i) traditional ( $z=3.8$ ,  $p=0.02$ ) and iii) transfer-learning CNN features ( $z=10.4$ ,  $p<0.001$ ).

#### CONCLUSION

s Minor binary dilatation of lymph node segmentation improves machine learning classification of lymph nodes. Both, traditional radiomics features and transfer-learning deep radiomics features provide relevant and complimentary information for classification of lymph nodes in lung cancer staging.

#### CLINICAL RELEVANCE/APPLICATION

Prediction of thoracic nodal status using radiomics and machine learning techniques on standard contrast-enhanced CT provides very good classification performance compared to PET. Even in absence of available PET, exploitation of the available information by the approach presented in this study may be a good alternative for non-invasive nodal staging in lung cancer.

Printed on: 02/07/23

## Abstract Archives of the RSNA, 2022

T5A-SPCH-3

### Clinicopathological and CT Features of Tumor Spread Through Air Space in Invasive Lung Adenocarcinoma

Tuesday, Nov. 29 12:15PM - 12:45PM Room: Learning Center - CH DPS

#### Participants

Lili Qin, (*Presenter*) Nothing to Disclose

#### PURPOSE

Tumor spread through air spaces (STAS) has recently been reported as a novel invasive pattern in lung adenocarcinoma, the aim of this study was to investigate the clinicopathological and radiological features in invasive lung adenocarcinoma with tumor spread through air space (STAS).

#### METHODS AND MATERIALS

Data of 503 invasive lung adenocarcinoma who underwent operation between January 1, 2015 and December 31, 2021 were collected. The correlations of STAS presence and clinicopathological and radiological characteristics were analyzed. Statistical analysis was performed using SPSS 22.0.

#### RESULTS

Among the 503 patients with invasive adenocarcinoma, 247 (47.9%) were positive for STAS and 262 (52.1%) were negative for STAS. STAS were more common in papillary, micropapillary and solid tumors ( $P < 0.01$ ). STAS was associated with advanced pN ( $P < 0.001$ ) and pTNM ( $P < 0.001$ ) stage, more lymph node metastases ( $P < 0.01$ ), more pleural invasion ( $P < 0.01$ ), more neurovascular invasion ( $P = 0.025$ ). The maximum diameter ( $P < 0.01$ ), the maximum diameters of the solid component ( $P < 0.01$ ), the consolidation/tumor ratio (CTR,  $P < 0.01$ ) was significantly larger in STAS-positive than in STAS-negative adenocarcinoma. Other common CT features of adenocarcinomas, ie, lobulation ( $P < 0.01$ ), spiculation ( $P < 0.01$ ), vacuole ( $P < 0.01$ ), air bronchogram ( $P = 0.020$ ), vascular convergence ( $P < 0.01$ ), pleural indentation ( $P < 0.01$ ) were shown to be significantly associated with STAS. In a multivariable analysis, maximum diameter of solid component was an independent predictor of STAS (odds ratio, 2.505; 95% confidence interval: 1.886, 3.329) and a cut-off value of 1.18cm showed a discriminatory power with a sensitivity of 73.9% and a specificity of 69.1%.

#### CONCLUSION

STAS was significantly correlated with several invasive clinicopathological and radiological characteristics, the maximum diameter was an independent predictor of STAS. These results will prove helpful in identifying STAS-positive adenocarcinoma by CT before surgical resection.

#### CLINICAL RELEVANCE/APPLICATION

As a newly named and pathologically diagnosed tumour invasion pattern in lung adenocarcinoma, STAS not only has an impact on the determination of the degree of invasion on its pathological tissues, but also has a significant impact on the selection and assessment of surgical treatment modalities for lung adenocarcinoma patients and the intervention of patient prognosis. The results of this study show that the largest diameter of solid component in lung adenocarcinoma lesions on CT and CRT are important signs for predicting STAS, and other common signs of malignancies also have some predictive value.

Printed on: 02/07/23

## Abstract Archives of the RSNA, 2022

T5A-SPCH-4

### Progression of Bronchiectasis during Five or More years Follow-up in Low-Dose CT Screening for Lung Cancer

Tuesday, Nov. 29 12:15PM - 12:45PM Room: Learning Center - CH DPS

#### Participants

Qiang Cai, PhD, MD, New York, NY (*Presenter*) Nothing to Disclose

#### PURPOSE

To assess the frequency of development of bronchiectasis among participants without previous bronchiectasis as well as the progression of bronchiectasis in participants with bronchiectasis on the baseline LDCT for five or more years after enrollment in a screening program.

#### METHODS AND MATERIALS

Changes in the ELCAP Bronchiectasis Score between baseline and the last LDCT were reviewed for smokers aged 40-90 years who had five or more years of follow-up screening after the baseline LDCT in the Mount Sinai ELCAP screening study between 2010 and 2019. MANOVA was used to assess the change in the four ELCAP Bronchiectasis component scores (severity and extent of bronchial dilatation, bronchial wall thickening (BWT), and mucoid impaction (MI)) as well as the total score.

#### RESULTS

Of the 2191 participants at baseline, 534 participants had five or more years of follow-up LDCTs. Among the 534 participants, baseline LDCT showed 408 (76.4%) without bronchiectasis while it was present in 126 (23.6%). Development of bronchiectasis was found in 9 (2.2%) of the 408 participants without bronchiectasis on baseline LDCT, with subsequent ELCAP Bronchiectasis Scores ranging from 2 to 20. Progression was present in 25 (19.8%) of the 126 with bronchiectasis on baseline LDCT and the increase in the ELCAP Bronchiectasis Scores ranged from 1 to 8. Progression of severity in bronchial dilatation was associated with increasing age ( $p=0.006$ ) and self-reported stroke ( $p=0.01$ ) at baseline enrollment, as well as progression in the extent of bronchial dilatation ( $p=0.01$ ), BWT ( $p=0.04$ ) and MI ( $p<.0001$ ). Progression of extent was associated with increasing age ( $p=0.03$ ) and higher MI score ( $p=.0001$ ) on baseline CT. Progression of BWT was associated with increasing pack-years of smoking ( $p=0.0007$ ), self-reported COPD ( $p=0.047$ ), and lower BWT ( $p=0.03$ ) on baseline LDCT. An increase in MI was a significant predictor of increasing age, increase in severity and extent of bronchial dilatation ( $p=.001$ ).

#### CONCLUSION

Awareness of bronchiectasis in LDCT screening for lung cancer is necessary as one-fifth of participants during long-term follow-up had progression compared to those without bronchiectasis on initial LDCT screening.

#### CLINICAL RELEVANCE/APPLICATION

The ELCAP Bronchiectasis Score provides a useful assessment of the progression of bronchiectasis. Reporting of bronchiectasis findings and continued assessment over the period of participation in the LDCT screening allows for documentation of change for future assessment of the benefit of early treatment.

Printed on: 02/07/23

## Abstract Archives of the RSNA, 2022

T5A-SPCH-5

### CT on Lung Cancer Screening is Useful for Adjuvant Comorbidity Diagnosis in Developing Countries

Tuesday, Nov. 29 12:15PM - 12:45PM Room: Learning Center - CH DPS

#### Participants

Bruno Hochhegger, PhD, Gainesville, FL (*Presenter*) Nothing to Disclose

#### PURPOSE

To analyze and quantify the prevalence of comorbidities derived from chest computed tomography (CT) of patients undergoing lung cancer screening in a developing country.

#### METHODS AND MATERIALS

For this retrospective study, low-dose CT scans (n=775) from patients undergoing LCS in a tertiary hospital between 2016 and 2020 were examined. A group of controls with similar age and gender but undergoing chest CT for other indications was also used for comparison (n=370). CT images were evaluated by experienced radiologists regarding coronary artery calcium (CAC) score, skeletal muscle area (SMA), interstitial lung abnormalities (ILA), presence of emphysema, osteoporosis, and hepatic steatosis using a dedicated software. Prevalence of abnormalities and clinical characteristics of the groups were compared using t-test and chi-squared tests. Interclass correlation coefficient (ICCs) and kappa coefficients for interobserver agreement were also calculated. The level of significance was set at 0.05.

#### RESULTS

One or more comorbidities were identified on imaging in 86.6% of patients undergoing LCS and in 40% of the controls. The most prevalent comorbidity was osteoporosis, present in 44.2% of patients and 24.8% of controls. CAC was identified in 41.9% of cases (vs. 23.7% of controls), emphysema in 66.3% (vs. 8.9% of controls), and osteoporosis in 44.2% (vs. 24.8% of controls). Compared to information retrieved from the medical records, CAC, emphysema, and osteoporosis were newly diagnosed in 25%, 7%, and 46% of the LCS patients, respectively. Sarcopenia was identified on 9.9% of LCS patients (vs. 3.5% controls) and hepatic steatosis in 40.7% (vs. 15.9% of controls). The kappa coefficient for CAC was 0.906, while ICC for measurements in the liver, spleen, and bone density were 0.88, 0.93, and 0.96, respectively.

#### CONCLUSION

s Data derived from the CT of patients undergoing LCS may lead to the identification of potentially undiagnosed comorbidities in more than 80% of patients.

#### CLINICAL RELEVANCE/APPLICATION

Smoking-related comorbidities (CAC, emphysema, ILA, sarcopenia, osteoporosis, and hepatic steatosis) are highly prevalent in patients undergoing low-dose CT for LCS. Integrated assessment of the CT in LCS for features other than nodule screening may lead to the identification of these comorbidities early and increase the chances of a favorable outcome for patients.

Printed on: 02/07/23

## Abstract Archives of the RSNA, 2022

T5A-SPCH-6

### Is It Time to Replace Low-dose CT with Ultra-low-dose CT in Lung Cancer Screening?

Tuesday, Nov. 29 12:15PM - 12:45PM Room: Learning Center - CH DPS

#### Participants

Matheus Zanon, MD, MSc, Porto Alegre, Brazil (*Presenter*) Nothing to Disclose

#### PURPOSE

To assess the agreement between ultra-low-dose CT (ULDCT) and low-dose CT (LDCT) in the evaluation of pulmonary findings in smokers undergoing lung cancer screening (LCS).

#### METHODS AND MATERIALS

For one month, we prospectively included eligible patients for LCS that underwent both chest ULDCT and LDCT for one month. Eligibility for LCS followed the 2021 guidelines by the United States Preventive Services Task Force. Patients should be adults, aged 50 to 80 years, with a 20 pack-year smoking history, currently smoking or former smokers that had quit within the past 15 years. Images were acquired in a 64-detector CT scanner as follows: LDCT: 100kVp/25mAs; ULDCT: 80kVp/15mAs. Two independent senior radiologists evaluated the presence of consolidation, ground-glass opacification (GGO), septal thickening, pulmonary nodule, bronchial wall thickening (BWT), pleural effusion, emphysema, bronchiectasis, and atelectasis.

#### RESULTS

From the 265 patients enrolled, 58 (21.9%) had abnormal CT scans. Mean effective radiation doses (ERD) for LDCT and ULDCT were  $1.21 \pm 0.34$  mSv and  $0.39 \pm 0.15$  mSv, respectively, representing a reduction in the mean ERD of 67.8%. Agreement was almost perfect for emphysema ( $\kappa=0.92$ ) and nodules ( $\kappa=0.91$ ). BWT, bronchiectasis, and atelectasis presented a strong agreement ( $\kappa, 0.80-0.90$ ), and consolidation, septal thickening, and pleural effusion presented substantial agreement ( $\kappa, 0.60-0.80$ ). Conversely, GGO presented a poor agreement ( $\kappa=0.37$ ).

#### CONCLUSION

Although the mean ERD reduced dropped to almost a third from LDCT to ULDCT, inter-reader agreement was poor for significant findings, such as consolidation and GGO, that may represent other types of lung cancer (e.g., lepidic adenocarcinoma).

#### CLINICAL RELEVANCE/APPLICATION

Despite the exciting agreement for some pulmonary findings, these results question whether using an ULDCT protocol for LCS would be adequate, as many subsolid or GGO lesions could be missed. Also, despite the significant reduction in the RED, it is questionable whether there is a patient benefit from going to 1.2 to 0.39 mSv.

Printed on: 02/07/23



## Abstract Archives of the RSNA, 2022

T5A-SPCH-7

### Screening for the Screeners: Our Institutional Experience with Double Reading of CT Lung Cancer Screening

Tuesday, Nov. 29 12:15PM - 12:45PM Room: Learning Center - CH DPS

#### Participants

Padma Manapragada, MD, MBBS, Birmingham, AL (*Presenter*) Nothing to Disclose

#### PURPOSE

Our institution participated in the NLST and continued to offer screening. Post approval by the USPSTF and the CMS, patient volume and the number of readers increased. With faculty turnover, the participating readers also kept changing. This study evaluates if double reading would increase adherence to screening requirements, consistent Lung RADS interpretation and unify follow up recommendations.

#### METHODS AND MATERIALS

The local IRB approved this retrospective study and written informed consent was waived. All lung cancer screening [LCS] cases from 2015 to through 2021 [2347 cases] were evaluated. Patients met the 2015 CMS criteria for inclusion: age 55-77, 30 pack years, current smoker or less than 15 years since quitting. A separate LCS PACS reading list was established. In rotation two radiologists were assigned to read the list each day. The first reader dictated the templated report and placed it in draft status. The second reader reviewed the study and the draft report, made any changes needed, signed the report, recorded if there was a discrepancy and, if present, the type of discrepancy. An Excel sheet recorded patient screened, Lung-RADS score, yes/no discrepancy, and category of discrepancy. Retrospectively the discrepancies were graded as: Significant-1: Changed L-RADS status or coronary artery calcification [CAC] score, other cancers, or major vascular aneurysm. Equivocal-2: Additional nodules but no L-RADS score change, other lung disease. Incidental-3: Non-cancer potentially significant findings (cirrhosis, renal stones, Pulmonary Artery HTN, AVM).

#### RESULTS

The majority of the 190 discrepancies were significant-109/190. Equivocal cases were 48/190 and incidental cases were 28/190. 5 cases were classified in more than one category. In eight cases the LR category changed from negative [1, 2] to positive [3,4]. The percentage of discrepancies initially increased as the number of cases increased, a new reader was added or new L-RADS introduced then decreased.

#### CONCLUSION

Double reading improved consistency in evaluation of LCS CTs and the application of LungRADS. This provides more uniform patient care over time and when patient care is escalated to biopsy or treatment.

#### CLINICAL RELEVANCE/APPLICATION

Double reading in evaluation of LCS CTs provides consistent high quality reports and consistent application of LungRADS. This provides uniform high quality patient care over time and when patient care is escalated to biopsy or treatment.

Printed on: 02/07/23

## Abstract Archives of the RSNA, 2022

T5A-SPCH-8

### Risk of Exacerbations in Participants with Bronchiectasis in a Program of Low-dose CT Screening

Tuesday, Nov. 29 12:15PM - 12:45PM Room: Learning Center - CH DPS

#### Participants

Natthaya Triphuridet, MD, PhD, New York, NY (*Presenter*) Nothing to Disclose

#### PURPOSE

To predict future exacerbations during the two years following the initial LDCT in screening participants with bronchiectasis based on the LDCT findings including emphysema, and self-reported co-morbidities.

#### METHODS AND MATERIALS

Electronic medical record (EMR) review of prospectively enrolled participants who smoked in Early Lung and Cardiac Action Program, a LDCT screening program from 2010 to 2019. EMR were reviewed to identify participants with respiratory symptoms and exacerbations during two years before and two years after initial LDCT screening. Uni- and multivariable regression analysis were performed to identify predictors of future exacerbations using LDCT findings and self-reported co-morbidities at the time of screening.

#### RESULTS

Of 2191 participants, 504(23%) had bronchiectasis and EMR had available records on 300 (median age,69 years;154(51%) women). Emphysema was identified on LDCT in 152(51%). Exacerbations were identified during two years after LDCT screening in 84(28%) participants. Participants with emphysema, compared to those without emphysema, had significantly higher median ELCAP Bronchiectasis Score (13.0 vs. 11.5,  $p=.02$ ), higher frequency of respiratory symptoms [97(64%) vs. 75(51%),  $p=.02$ ] and exacerbations [49(32%) vs. 35(24%),  $p=.10$ ]. Multivariable analyses showed that the ELCAP Bronchiectasis Score ( $OR=1.12, p<.001$ ), self-reported COPD ( $OR=2.69, p<.001$ ) and asthma ( $OR=2.47, p=.006$ ) were independent predictors of exacerbations, but not emphysema. Considering ELCAP Bronchiectasis component scales instead of the total score, severity of bronchial dilatation ( $OR=1.30, p=.001$ ) and bronchial wall thickening ( $OR=1.29, p=.004$ ) were significant predictors. When including prior respiratory symptoms and exacerbations during two years prior to screening as predictors, ELCAP Bronchiectasis Score remained as an independent predictor of future exacerbations.

#### CONCLUSION

High ELCAP Bronchiectasis Score, self-reported COPD and asthma are independent predictors of exacerbations. This type of information is needed to develop preventive management protocols.

#### CLINICAL RELEVANCE/APPLICATION

Among 300 participants with bronchiectasis and available electronic medical records, 84(28.0%) had exacerbations during two years following initial LDCT screening. Significant predictors of future exacerbations were: ELCAP Bronchiectasis Score [ $OR=1.12, p<.001$ ], self-reported COPD [ $OR=2.69, p<.001$ ] and asthma [ $OR=2.47, p=0.006$ ].

Printed on: 02/07/23

## Abstract Archives of the RSNA, 2022

T5A-SPCH-9

### Computational Risk Stratification: A Deep Learning Approach to Predicting a Major Lung Biopsy Complication

Tuesday, Nov. 29 12:15PM - 12:45PM Room: Learning Center - CH DPS

#### Participants

Alexander Lindqwister, BS,MS, Lebanon, NH (*Presenter*) Nothing to Disclose

#### PURPOSE

CT-guided core needle biopsies (CT-CNB) are a major component of the diagnostic work-up of lung lesions. The most common associated risk is iatrogenic pneumothorax (PTX) which may require tube thoracostomy and subsequent hospitalization. The ability to predict PTX requiring tube thoracostomy in the pre-procedural setting would allow radiologists to make more individualized recommendations in patient management, improve the informed consent process, and augment care delivery through risk stratification.

#### METHODS AND MATERIALS

A retrospective study of 502 patients who underwent CT-CNB of the lung was performed. Procedural, patient demographic, and outcomes data were collected and descriptive statistics were performed to determine significant distinguishing features between patients who required chest tubes and those who did not. Six parameters (age, sex, emphysema, projected length of needle path, greatest dimension of lung lesion, lung lobe) encoded through 12 features were utilized by a deep neural network to create a predictive model. Exhaustive 5-fold cross validation in addition to an external dataset consisting of 449 patients was used to validate the model.

#### RESULTS

Deep learning models were highly successful in predicting PTX requiring tube thoracostomy, with a receiver operating characteristic area under the curve (ROC-AUC) of 0.961 [ $\pm$  0.033] averaged across 2,000 simulations. The model had consistent performance with the external dataset, achieving an ROC-AUC of 0.886 [ $\pm$  0.059]. Testing metrics revealed a sensitivity of 0.879, specificity of 0.924, and a negative predictive value of 0.986 after adjusting for incidence of chest tube placement.

#### CONCLUSION

The strong performance of deep learning models to predict chest tube placement demonstrates the possible clinical utility of machine learning in predicting post procedural complications in this setting. The model performed well on data collected from two different patient cohorts, which suggests generalizability and the potential for broad application.

#### CLINICAL RELEVANCE/APPLICATION

Neural networks and other data-driven approaches may be useful in predicting adverse post-procedural complications in the setting of lung CT-CNB.

Printed on: 02/07/23

## Abstract Archives of the RSNA, 2022

T5A-SPER

### Emergency Tuesday Poster Discussions - A

Tuesday, Nov. 29 12:15PM - 12:45PM Room: Learning Center - ER DPS

#### Participants

Waleed Abdellatif, MD, MSc, Richardson, TX (*Moderator*) Nothing to Disclose

#### Sub-Events

### T5A-SPER-1 Spot and Leakage Signs: Predicting Intracerebral Hemorrhage Expansion

#### Participants

Maria del Carmen Gonzalez Dominguez, MD, (*Presenter*) Nothing to Disclose

#### PURPOSE

To describe the acquisition protocol, the diagnostic criteria, and the utility of "spot sign" and "leakage sign" as predicting factors for intracerebral hemorrhage expansion. To assess the consequences and the impact on clinical factors such as neurologic impairment and in-hospital mortality.

#### METHODS AND MATERIALS

A prospective study was performed on 117 patients with spontaneous intracerebral hemorrhagic (ICH) stroke. These patients underwent non-enhanced computed tomography (NECT) and computed tomography angiogram (CTA), which were acquired in both arterial (35 seconds) and delayed (300 seconds) phases. The initial study obtained the hematoma volume, location (lobar or in basal ganglia), and attenuation values. We consider active bleeding the presence of a "spot sign" and/or "leakage sign". Spot sign was defined as a focal accumulation of contrast within the hematoma in the arterial phase). Leakage sign was established as increased contrast extravasation from the early phase or its onset in the delayed phase. Later, hematoma volume was recalculated in follow-up NECT. We defined hematoma expansion as a >15% increase in hematoma size. Other variables were also evaluated, particularly neurological deterioration (increase in National Institute of Health (NIH) stroke score) and in-hospital mortality.

#### RESULTS

Spot sign [OR: 4,27 (1,55-11,75)] and Leakage sign [OR: 4,80 (1,82-12,68)] were independently associated with hematoma volume expansion. In the neurologic impairment course group, a positive spot sign was present in 68,75 % of patients, and a positive leakage sign was present in 75% of patients with a independently statistically significant association [OR: 2,95 (1,28-6,77)] and [OR: 3,26 (1,42-7,51)], respectively. The presentation of active bleeding signs was also independently associated with a significant increase in-hospital deaths, for Leakage sign [OR: 6,86 (2,73-17,25)] and Spot sign [OR: 9,31 (3,50-24,80)].

#### CONCLUSION

s Determining active bleeding signs in two phases improves the prediction of intraparenchymal hematoma volume expansion, neurologic impairment, and hospital deaths.

#### CLINICAL RELEVANCE/APPLICATION

Patients with positive leakage signs were associated with worse clinical prognoses and increased probability of in-hospital mortality. The possibility of surgical evacuation or strict control of blood pressure of intraparenchymal hematomas with positive leakage signs was proposed in our hospital, and they are currently being carried out in selected patients. So, in our study, imaging tools play a key role in the diagnosis and prognosis of ICH stroke patients and provide therapeutic decision support.

Printed on: 02/07/23

## Abstract Archives of the RSNA, 2022

T5A-SPER-1

### Spot and Leakage Signs: Predicting Intracerebral Hemorrhage Expansion

Tuesday, Nov. 29 12:15PM - 12:45PM Room: Learning Center - ER DPS

#### Participants

Maria del Carmen Gonzalez Dominguez, MD, (*Presenter*) Nothing to Disclose

#### PURPOSE

To describe the acquisition protocol, the diagnostic criteria, and the utility of "spot sign" and "leakage sign" as predicting factors for intracerebral hemorrhage expansion. To assess the consequences and the impact on clinical factors such as neurologic impairment and in-hospital mortality.

#### METHODS AND MATERIALS

A prospective study was performed on 117 patients with spontaneous intracerebral hemorrhagic (ICH) stroke. These patients underwent non-enhanced computed tomography (NECT) and computed tomography angiogram (CTA), which were acquired in both arterial (35 seconds) and delayed (300 seconds) phases. The initial study obtained the hematoma volume, location (lobar or in basal ganglia), and attenuation values. We consider active bleeding the presence of a "spot sign" and/or "leakage sign". Spot sign was defined as a focal accumulation of contrast within the hematoma in the arterial phase). Leakage sign was established as increased contrast extravasation from the early phase or its onset in the delayed phase. Later, hematoma volume was recalculated in follow-up NECT. We defined hematoma expansion as a >15% increase in hematoma size. Other variables were also evaluated, particularly neurological deterioration (increase in National Institute of Health (NIH) stroke score) and in-hospital mortality.

#### RESULTS

Spot sign [OR: 4,27 (1,55-11,75)] and Leakage sign [OR: 4,80 (1,82-12,68)] were independently associated with hematoma volume expansion. In the neurologic impairment course group, a positive spot sign was present in 68,75 % of patients, and a positive leakage sign was present in 75% of patients with a independently statistically significant association [OR: 2,95 (1,28-6,77)] and [OR: 3,26 (1,42-7,51)], respectively. The presentation of active bleeding signs was also independently associated with a significant increase in-hospital deaths, for Leakage sign [OR: 6,86 (2,73-17,25)] and Spot sign [OR: 9,31 (3,50-24,80)].

#### CONCLUSION

s Determining active bleeding signs in two phases improves the prediction of intraparenchymal hematoma volume expansion, neurologic impairment, and hospital deaths.

#### CLINICAL RELEVANCE/APPLICATION

Patients with positive leakage signs were associated with worse clinical prognoses and increased probability of in-hospital mortality. The possibility of surgical evacuation or strict control of blood pressure of intraparenchymal hematomas with positive leakage signs was proposed in our hospital, and they are currently being carried out in selected patients. So, in our study, imaging tools play a key role in the diagnosis and prognosis of ICH stroke patients and provide therapeutic decision support.

Printed on: 02/07/23

## Abstract Archives of the RSNA, 2022

T5A-SPGI

### Gastrointestinal Tuesday Poster Discussions - A

Tuesday, Nov. 29 12:15PM - 12:45PM Room: Learning Center - GI DPS

#### Participants

Amita Kamath, MD, MPH, Short Hills, NY (*Moderator*) Nothing to Disclose

#### Sub-Events

### T5A-SPGI-1 Laparoscopic Cholecystectomy and Percutaneous Cholecystostomy: An Analysis of Trends in Procedure Volume Among Medicare Patients from 2010-2018.

#### Participants

Abdullah Khan, MD, Sacramento, CA (*Presenter*) Nothing to Disclose

#### PURPOSE

Cholecystectomies represent the most common procedure performed by general surgeons, with hundreds of thousands being performed annually. Percutaneous image-guided cholecystostomy is an alternative option for acute cholecystitis, particularly in patients that are high risk surgical candidates. Currently, minimal data exists on national trends in the utilization of these techniques including procedure volume, inpatient status, and procedural costs.

#### METHODS AND MATERIALS

This study utilized data derived from publicly available databases provided by the Center for Medicare and Medicaid Services (CMS). Billing data from the CMS Physicians/Supplier Procedure Summary (PSPS) Master Files from 2010 to 2018 were obtained. Billing codes 47562, 47563, 47564 were combined to designate laparoscopic cholecystectomy. Code 47490 was used to capture data for percutaneous cholecystostomy tube placement. The Mann-Kendall test was used to analyze for statistically significant trends in procedure volume and cost.

#### RESULTS

The volume of annual laparoscopic cholecystectomy surgeries decreased significantly over the study period, from 218637 performed in 2010 to 173845 performed in 2018 (-20.0%,  $p < 0.001$ ). Conversely, the volume of annual percutaneous cholecystostomy tube placements increased significantly, rising from 7225 in 2010 to 12135 in 2018 (+68.0%,  $p < 0.001$ ). Mean submitted charge increased from 2240 to 2620 for cholecystectomy (17%,  $p < 0.001$ ) and from 1490 to 1560 for cholecystostomy (4.7%,  $p = 0.11$ ). 91.5% of cholecystostomy tube placements and 41.3% of cholecystectomies were completed in an inpatient setting, which remained stable over the study period.

#### CONCLUSION

s Medicare data demonstrates an increasing trend in percutaneous cholecystostomy tube placement between 2010 and 2018, and a decreasing trend in the number of charges for laparoscopic cholecystectomy. Increasing cholecystostomy procedures may reflect trends in the aging patient population as well as increased provider familiarity with the procedure. Concurrently, the decreasing numbers of laparoscopic cholecystectomy performed may represent increasingly cautious surgical risk stratification and associated changes in the treatment algorithms for acute cholecystitis.

#### CLINICAL RELEVANCE/APPLICATION

Data from Medicare demonstrates an increasing number of percutaneous cholecystostomy tube placements with a concurrent decrease in laparoscopic cholecystectomies, which may reflect trends associated with an aging patient population and changing treatment algorithms.

### T5A-SPGI-10 Radiomic Features of Hepatocellular Carcinoma at Ultra-High-Resolution CT with a 1024 Matrix: Dependencies on Matrix Size and Reconstruction Algorithm

#### Participants

Masatoshi Hori, MD, Kobe, Japan (*Presenter*) Research Grant, Canon Medical Systems Corporation

#### PURPOSE

Ultra-high-resolution (UHR) CT yields 1024-matrix CT images of higher spatial resolution compared to conventional 512-matrix images. However, the role of UHR CT in radiomics is not well understood. Thus, the aim was to determine the effects of CT matrix size and reconstruction algorithm on the quantification of UHR CT radiomic features to characterize hepatocellular carcinoma.

#### METHODS AND MATERIALS

This retrospective study included 27 patients (14 men and 13 women; median age, 71 years) with hepatocellular carcinoma who underwent contrast-enhanced multi-phasic CT during the late arterial and the portal venous phase (LAP and PVP) in super-high-resolution mode using a UHR CT scanner (Aquilion Precision; Canon). The mean size of lesions was  $48.3 \pm 37.0$  mm (range, 11-129 mm). UHR CT images with a 1024- and 512-matrix were reconstructed using filtered back projection (FBP) and hybrid iterative

reconstruction (hybrid IR). The slice thickness was 1 mm. A representative tumor was three-dimensionally segmented in each patient. Then, 120 radiomic features were calculated for each image set. Features were categorized as first order (n=19), shape (26), and texture features (75). A linear mixed-effects model was used to assess the effect of matrix size and reconstruction algorithm on features. A P value less than 0.05 divided by 120 was considered significant (approximately 0.00041; Bonferroni correction for the 120 responses).

## RESULTS

The matrix size had a significant effect on 94 features (78.3 %) in LAP and 90 features (75.0 %) in PVP out of 120 features ( $P < 0.00041$  for all). It showed significant effects on 17 first-order features (89.5 %) for LAP and 17 features (89.5 %) for PVP, 12 shape features (46.2 %) for LAP and 10 features (38.5 %) for PVP, and 65 texture features (86.7 %) for LAP and 63 features (84.0 %) for PVP ( $P < 0.00041$  for all). Reconstruction algorithm had a significant effect on 44 (36.7 %) in LAP and 43 (35.8 %) in PVP out of 120 features ( $P < 0.00041$  for all). No significant effect of the reconstruction algorithm was observed for 26 shape features and 5 neighboring gray-tone difference matrix (NGTDM) texture features for both LAP and PVP.

## CONCLUSION

Both matrix size and reconstruction algorithm affect the radiomic features in hepatocellular carcinoma at UHR CT. Above all, 1024-matrix size had a significant effect on approximately 90 % of the first-order features and texture features.

## CLINICAL RELEVANCE/APPLICATION

It should be noted that radiomics from UHR CT with a 1024 matrix have different properties than those from conventional CT with a 512 matrix.

### **T5A-SPGI-2 MR Guided Liver Biopsies - Depiction Of The Biopsy Site On Immediate Postinterventional Contrast Enhanced MRI**

#### Participants

Guenther K. Schneider, MD, PhD, Homburg, Germany (*Presenter*) Research Grant, Siemens AG; Speakers Bureau, Siemens AG; Speakers Bureau, Bracco Group; Research Grant, Bracco Group

#### PURPOSE

Sampling errors in image guided biopsies of primary, hypervascular focal liver lesions are a common problem in clinical routine, resulting in unnecessary delay or even inadequate treatment of patients. The purpose of our study was to evaluate as if immediate post biopsy MRI may detect the exact location where a liver biopsy was taken and confirm or exclude sampling of representative tissue.

#### METHODS AND MATERIALS

MRI guided liver biopsy was performed in 68 patients with primary liver tumors (HCC, FNH, Adenoma, NRH) using a 18G core biopsy device. Lesion size ranged from 7 mm to 2.7 cm. Following tissue sampling the biopsy tract was closed with gelatin foam pledgets. Immediately post biopsy a diagnostic MRI was performed in order to detect possible complications and to depict the exact area, where the biopsy was sampled. Imaging included T1-/T2-weighted unenhanced sequences (T2 TSE, HASTE, T1w flash 2D and 3D VIBE-DIXON Sequences) as well as dynamic 3D VIBE-DIXON imaging post bolus CM injection (0.05 mmol/kg MultiHance) in the arterial and portalvenous phase. Furthermore T1w images with and without fat suppression in the equilibrium and hepatobiliary phase (hb-phase) were acquired.

## RESULTS

In all patients the biopsy tract could be depicted at least in one sequence. On unenhanced images the biopsy tract was best detected on T1w flash-2D sequences (57/68) followed by the 3D VIBE-DIXON sequence (51/68). T2w (12/68) and HASTE images (28/68) could not delineate the biopsy tract sufficiently. On CE images the biopsy tract together with the lesion was depicted best in the arterial phase both on the T1w flash 2D and 3D VIBE DIXON sequence (61/68). In the biliary phase depiction of the sampling area together with the lesion was possible in 59 of 61 patients. In 63 of 68 patients MRI confirmed that tissue was taken from the lesions and facilitated histologic diagnosis. In 5 cases lesions were missed, both based on findings in MRI and histology and biopsy was repeated.

## CONCLUSION

Immediate post liver biopsy MRI allows for depiction of the biopsy tract both on unenhanced and CE MRI with advantages seen for CE images. T2w imaging did not reliably depict the biopsy tract. By identifying the biopsy area, sampling errors can be detected post biopsy what is of special importance in small lesions, lesions which are similar to normal liver tissue on histology like FNH or regenerative nodules and in lesions in a cirrhotic liver, where findings of regenerating tissue might imply correct tissue sampling in cases in which an HCC was missed.

## CLINICAL RELEVANCE/APPLICATION

MRI immediately post liver biopsy reliably depicts biopsy tracts and thus can confirm or exclude sampling of representative tissue and avoid unnecessary delay in diagnosis.

### **T5A-SPGI-3 Automated AI-Based Splenic Segmentation for Predicting Survival and Estimating the Risk of Hepatic Decompensation in TACE Patients With HCC**

#### Participants

Lukas Mueller, MD, Mainz, Germany (*Presenter*) Nothing to Disclose

#### PURPOSE

Splenic volume was proposed as a relevant prognostic factor for patients with hepatocellular carcinoma (HCC). We trained a deep-learning algorithm to fully-automatically assess splenic volume based on computed tomography (CT) scans. Then, we investigated splenic volume as a prognostic factor for patients with HCC undergoing transarterial chemoembolization (TACE).

#### METHODS AND MATERIALS

This retrospective study included 327 treatment-naïve patients with HCC undergoing initial TACE at our tertiary care center

between 2010 and 2020. A convolutional neural network was trained and validated on the first 100 consecutive cases for spleen segmentation. Then, we used the algorithm to evaluate splenic volume in all 327 patients. Subsequently, we evaluated correlations between splenic volume and survival as well as the risk of hepatic decompensation during TACE.

## RESULTS

The algorithm showed Sørensen Dice Scores of 0.96 during both training and validation. In the remaining 227 patients assessed with the algorithm, spleen segmentation was visually approved in 223 patients (98.2%) and failed in four patients (1.8%), which required manual re-assessments. Mean splenic volume was 551ml. Median survival was significantly lower in patients with high splenic volume (10.9 months), compared to low splenic volume (22.0 months,  $p=0.001$ ). In contrast, overall survival was not significantly predicted by axial and craniocaudal spleen diameter. Furthermore, patients with a hepatic decompensation after TACE had significantly higher splenic volumes ( $p<0.001$ ).

## CONCLUSION

s Automated splenic volume assessments showed superior survival predictions in patients with HCC undergoing TACE compared to two-dimensional spleen size estimates and identified patients at risk of hepatic decompensation.

## CLINICAL RELEVANCE/APPLICATION

Thus, splenic volume could serve as an automatically available, currently underappreciated imaging biomarker.

### **T5A-SPGI-4 Performance of LI-RADS Major Feature Combinations within the CT/MRI Diagnostic Algorithm: Individual Patient Data Meta-analysis**

Participants

Jean-Paul Salameh, MSc, (*Presenter*) Nothing to Disclose

## PURPOSE

The Liver Imaging Reporting and Data System (LI-RADS) assigns a risk for hepatocellular carcinoma (HCC) to imaging observations. The purpose of this study is to perform an individual-patient data (IPD) meta-analysis to establish the percentage of HCC for combinations of LI-RADS major features using the CT/MRI LI-RADS diagnostic algorithm in high-risk patients

## METHODS AND MATERIALS

Multiple databases (MEDLINE, Embase, Cochrane Central Register of Controlled Trials, and Scopus) were searched for studies from January 2014 to September 2019 that evaluated the accuracy of CT/MRI using LI-RADS (v2014/17/18). IPD were pooled to compute the percentage of HCC for each major feature combination using a random-effects model. Percentage of HCC with 95% confidence intervals (95%CI) are presented. Heterogeneity was quantified using the I-squared statistic. Risk of bias was assessed using Quality Assessment of Diagnostic Accuracy Studies 2

## RESULTS

Thirty-one studies (2602 patients; 3350 observations) were included. Pooled percentage of HCC for combinations of LI-RADS major features ranged between 15.5% (95%CI 6.0%-34.5%) and 50.7% (95%CI 27.5%-73.6%) for LR3 combinations, 56.7% (95%CI 34.2%-76.8%) and 100% (95%CI 20.3%-100%) for LR4 combinations, and 81.8% (95%CI 61.7%-92.6%) and 96.1% (95%CI 83.4%-99.2%) for LR5 combinations (Figure 1). Twenty-five studies (78%) had high risk of bias due to reporting ambiguity or study design flaws

## CONCLUSION

s Our findings document increasing percentage of HCC with each LI-RADS category; however, substantial variability exists within each category depending on feature combination. This data will inform updates of the LI-RADS diagnostic algorithms to better align feature combinations with intended percentage of HCC in each LI-RADS category

## CLINICAL RELEVANCE/APPLICATION

Our findings will help determine which observations are definite HCC based on feature combinations. This will impact patient care by providing timely access to treatment and avoiding unnecessary biopsy

### **T5A-SPGI-5 Extracellular Volume Fraction Using Contrast Enhanced CT Is Useful In Differentiating Intrahepatic Cholangiocellular Carcinoma From Hepatocellular Carcinoma**

Participants

Takashi Ota, MD, PhD, Suita, Japan (*Presenter*) Nothing to Disclose

## PURPOSE

To evaluate whether extracellular volume fraction (fECV) of the tumors using contrast-enhanced computed tomography (CT) aids in the differentiation of hepatocellular carcinoma (HCC) and intrahepatic cholangiocellular carcinoma (ICC).

## METHODS AND MATERIALS

In this retrospective study, 113 patients with pathologically confirmed HCC ( $n = 74$ ) or ICC ( $n = 39$ ) who had undergone preoperative contrast-enhanced CT examinations were enrolled. Enhancement values of the tumor (Etumor) and aorta (Eaorta) were obtained based on the precontrast and equilibrium phase CT images. The fECV was calculated using the following equation:  $fECV [\%] = Etumor/Eaorta \times (100 - Hematocrit [\%])$ . The fECVs were compared between HCC and ICC groups using Welch's t-test. The diagnostic performance of fECV in the differentiation of HCC and ICC was assessed using receiver operating characteristic (ROC) analysis. The imaging features including tumor demarcation, shape, arterial enhancement pattern, washout pattern, bile duct dilatation, and tortuous tumoral vessels were evaluated by two radiologists and were examined by the  $\chi^2$  test or Fisher's exact test (when  $n<5$ ). A multivariate logistic regression analysis was also performed to identify factors predicting a diagnosis of ICC; variables with a P-value of  $<0.1$  were entered into the final model.

## RESULTS

The mean fECV of ICCs ( $43.8\pm 13.2\%$ ) was significantly higher than that of HCCs ( $31.6\pm 9.0\%$ ,  $P < .001$ ). The area under the curve

was 0.763. Lobulated and irregular shape, indistinct margin, peripheral rim enhancement in the arterial phase, and the presence of bile duct dilatation were CT features favoring ICC, whereas a round shape, distinct margin, non-rim enhancement in the arterial phase, and washout pattern were CT features favoring HCC in the univariate analysis ( $P < .001$ ). In the multivariate analysis, fECV and a washout pattern were independent CT features for distinguishing between the two types. ( $P = 0.03$ ,  $P < .001$ , respectively).

## CONCLUSION

s A higher value of fECV and a washout pattern were respectively independent factors of multivariate analysis in distinguishing between ICC and HCC and more indicative of ICC than HCC on contrast-enhanced CT.

## CLINICAL RELEVANCE/APPLICATION

The addition of extracellular volume fraction analysis to the imaging features evaluation on contrast-enhanced CT may allow more accurately differentiating ICC from HCC.

## T5A-SPGI-7 Tomoelastography-based Viscoelastic Signatures for Prediction of Proliferative Phenotype in Hepatocellular Carcinoma

Participants

Gui Liu, (*Presenter*) Nothing to Disclose

## PURPOSE

To investigate the biomechanical signatures of proliferative hepatocellular carcinoma (HCC) and the value of tomoelastography in characterizing the proliferative HCC phenotype.

## METHODS AND MATERIALS

A total of 121 patients with 124 pathologically confirmed HCC lesions (63 proliferative and 61 non-proliferative HCC) were included in this prospective study. All participants underwent preoperative MRI and tomoelastography. Rim arterial phase hyperenhancement [APHE], nonperipheral washout, enhancing capsule and LI-RADS categorization were evaluated. Tumor and liver viscoelasticity were quantified as shear wave speed ( $c$ , m/s), representing tissue stiffness, and loss angle ( $f$ , rad), indicating fluidity. Univariate and multivariate logistic regression analyses were used to determine predictors of proliferative HCC. A prediction nomogram of proliferative HCC was constructed.

## RESULTS

Multivariate logistic regression analysis results showed that tumor  $c$  (OR: 0.24, 95%CI: 0.089-0.63;  $P = 0.0037$ ), tumor  $f$  (OR: 39.12, 95%CI: 2.72-561.94;  $P=0.007$ ), liver  $c$  (OR: 0.12, 95%CI: 0.027- 0.54;  $P = 0.0056$ ), liver  $f$  (OR: 540.64, 95%CI:6.72 - 43521.86;  $P = 0.0049$ ) and rim APHE (OR: 15.32, 95%CI: 2.87- 81.87;  $P=0.0014$ ) were independent predictors of proliferative HCC. Combining these variables yielded an AUC of 0.77 (95%CI: 0.69-0.84), sensitivity of 73.02% (95%CI: 0.64-0.86), specificity of 68.85% (95%CI: 0.54-0.79), and accuracy of 70.97% (95%CI: 0.62-0.79), respectively, for predicting proliferative HCC. The C-index of the corresponding nomogram was 0.77 (95%CI: 0.69-0.84).

## CONCLUSION

s Proliferative HCC reveals decreased stiffness and increased fluidity for both tumor and liver. Combining biomechanical signature and viscoelasticity could predicate proliferative HCC.

## CLINICAL RELEVANCE/APPLICATION

The proliferation class accounts for about 50% of HCCs, which has strong invasiveness and poor prognosis. Therefore, predicting proliferative HCC was urgent and important to characterize morpho-molecular subtypes for the prediction of prognosis and therapeutic response in clinical practice. We investigated the diagnostic ability of the biomechanical parameters quantified by in vivo tomoelastography for predicting proliferative HCC subtypes. To our knowledge, this is the first study to connect biomechanical properties with the proliferative nature of HCCs. Based on our data, Proliferative HCC may be softer, more liquid like and more bioinvasive than non-proliferative HCC. Additionally, proliferative HCC could be predicted with good accuracy by combining stiffness and fluidity of both the tumor and the liver.

## T5A-SPGI-9 Preliminary Radiogenomic Study of Hepatitis B-related Hepatocellular Carcinoma: Associations between MR Features and Mutations

Participants

Ruofan Sheng, MD, Shanghai, China (*Presenter*) Nothing to Disclose

## PURPOSE

Hepatocellular carcinoma (HCC) is the most common primary liver cancer, and radiogenomics plays an important role in providing accurate imaging substitutes which are associated with genetic expression. This study aimed to investigate associations between MR features and the high-frequency mutations of hepatitis B virus (HBV) related hepatocellular carcinoma (HCC).

## METHODS AND MATERIALS

This retrospective study included 58 HCC patients who underwent abdominal contrast-enhanced MRI prior to surgical resection and genome sequencing. MR imaging features and mutation information were evaluated. Associations between MR features and the high-frequency mutations as well as tumor mutation burden (TMB) level were tested by using Pearson's chi-squared test or Fisher exact test.

## RESULTS

The top 5 most frequently mutated genes of HCC were TP53 (53.45%), TAF1(24.14%), PDE4DIP (22.41%), ABCA13 (18.97%), LRP1B (17.24%). Mutations of TP53 were associated with the presence of tumor necrosis ( $P=0.035$ ). Mutations of ABCA13 were associated with the presence of mosaic architecture ( $P=0.025$ ) and necrosis ( $P=0.010$ ). Mutations of LRP1B were associated with the presence of mosaic architecture ( $P=0.015$ ). MR features were not correlated to the TMB level ( $P=0.945$  to  $P>0.99$ ).

## CONCLUSION

s This preliminary radiogenomic analysis revealed associations between MR features and the high frequency mutations in HBV

5 This preliminary radiogenomic analysis revealed associations between MR features and the high-frequency mutations in HBV-related HCC.

#### **CLINICAL RELEVANCE/APPLICATION**

This preliminary radiogenomics analysis showed associations between MR features and the high-frequency mutations in HBV-related HCCs, which demonstrated potential clinical value of imaging traits as surrogate markers of molecular portraits in HCC.

Printed on: 02/07/23



## Abstract Archives of the RSNA, 2022

T5A-SPGI-1

### Laparoscopic Cholecystectomy and Percutaneous Cholecystostomy: An Analysis of Trends in Procedure Volume Among Medicare Patients from 2010-2018.

Tuesday, Nov. 29 12:15PM - 12:45PM Room: Learning Center - GI DPS

#### Participants

Abdullah Khan, MD, Sacramento, CA (*Presenter*) Nothing to Disclose

#### PURPOSE

Cholecystectomies represent the most common procedure performed by general surgeons, with hundreds of thousands being performed annually. Percutaneous image-guided cholecystostomy is an alternative option for acute cholecystitis, particularly in patients that are high risk surgical candidates. Currently, minimal data exists on national trends in the utilization of these techniques including procedure volume, inpatient status, and procedural costs.

#### METHODS AND MATERIALS

This study utilized data derived from publicly available databases provided by the Center for Medicare and Medicaid Services (CMS). Billing data from the CMS Physicians/Supplier Procedure Summary (PSPS) Master Files from 2010 to 2018 were obtained. Billing codes 47562, 47563, 47564 were combined to designate laparoscopic cholecystectomy. Code 47490 was used to capture data for percutaneous cholecystostomy tube placement. The Mann-Kendall test was used to analyze for statistically significant trends in procedure volume and cost.

#### RESULTS

The volume of annual laparoscopic cholecystectomy surgeries decreased significantly over the study period, from 218637 performed in 2010 to 173845 performed in 2018 (-20.0%,  $p < 0.001$ ). Conversely, the volume of annual percutaneous cholecystostomy tube placements increased significantly, rising from 7225 in 2010 to 12135 in 2018 (+68.0%,  $p < 0.001$ ). Mean submitted charge increased from 2240 to 2620 for cholecystectomy (17%,  $p < 0.001$ ) and from 1490 to 1560 for cholecystostomy (4.7%,  $p = 0.11$ ). 91.5% of cholecystostomy tube placements and 41.3% of cholecystectomies were completed in an inpatient setting, which remained stable over the study period.

#### CONCLUSION

s Medicare data demonstrates an increasing trend in percutaneous cholecystostomy tube placement between 2010 and 2018, and a decreasing trend in the number of charges for laparoscopic cholecystectomy. Increasing cholecystostomy procedures may reflect trends in the aging patient population as well as increased provider familiarity with the procedure. Concurrently, the decreasing numbers of laparoscopic cholecystectomy performed may represent increasingly cautious surgical risk stratification and associated changes in the treatment algorithms for acute cholecystitis.

#### CLINICAL RELEVANCE/APPLICATION

Data from Medicare demonstrates an increasing number of percutaneous cholecystostomy tube placements with a concurrent decrease in laparoscopic cholecystectomies, which may reflect trends associated with an aging patient population and changing treatment algorithms.

Printed on: 02/07/23

## Abstract Archives of the RSNA, 2022

T5A-SPGI-10

### Radiomic Features of Hepatocellular Carcinoma at Ultra-High-Resolution CT with a 1024 Matrix: Dependencies on Matrix Size and Reconstruction Algorithm

Tuesday, Nov. 29 12:15PM - 12:45PM Room: Learning Center - GI DPS

#### Participants

Masatoshi Hori, MD, Kobe, Japan (*Presenter*) Research Grant, Canon Medical Systems Corporation

#### PURPOSE

Ultra-high-resolution (UHR) CT yields 1024-matrix CT images of higher spatial resolution compared to conventional 512-matrix images. However, the role of UHR CT in radiomics is not well understood. Thus, the aim was to determine the effects of CT matrix size and reconstruction algorithm on the quantification of UHR CT radiomic features to characterize hepatocellular carcinoma.

#### METHODS AND MATERIALS

This retrospective study included 27 patients (14 men and 13 women; median age, 71 years) with hepatocellular carcinoma who underwent contrast-enhanced multi-phasic CT during the late arterial and the portal venous phase (LAP and PVP) in super-high-resolution mode using a UHR CT scanner (Aquilion Precision; Canon). The mean size of lesions was  $48.3 \pm 37.0$  mm (range, 11?129 mm). UHR CT images with a 1024- and 512-matrix were reconstructed using filtered back projection (FBP) and hybrid iterative reconstruction (hybrid IR). The slice thickness was 1 mm. A representative tumor was three-dimensionally segmented in each patient. Then, 120 radiomic features were calculated for each image set. Features were categorized as first order (n=19), shape (26), and texture features (75). A linear mixed-effects model was used to assess the effect of matrix size and reconstruction algorithm on features. A P value less than 0.05 divided by 120 was considered significant (approximately 0.00041; Bonferroni correction for the 120 responses).

#### RESULTS

The matrix size had a significant effect on 94 features (78.3 %) in LAP and 90 features (75.0 %) in PVP out of 120 features ( $P < 0.00041$  for all). It showed significant effects on 17 first-order features (89.5 %) for LAP and 17 features (89.5 %) for PVP, 12 shape features (46.2 %) for LAP and 10 features (38.5 %) for PVP, and 65 texture features (86.7 %) for LAP and 63 features (84.0 %) for PVP ( $P < 0.00041$  for all). Reconstruction algorithm had a significant effect on 44 (36.7 %) in LAP and 43 (35.8 %) in PVP out of 120 features ( $P < 0.00041$  for all). No significant effect of the reconstruction algorithm was observed for 26 shape features and 5 neighboring gray-tone difference matrix (NGTDM) texture features for both LAP and PVP.

#### CONCLUSION

s Both matrix size and reconstruction algorithm affect the radiomic features in hepatocellular carcinoma at UHR CT. Above all, 1024-matrix size had a significant effect on approximately 90 % of the first-order features and texture features.

#### CLINICAL RELEVANCE/APPLICATION

It should be noted that radiomics from UHR CT with a 1024 matrix have different properties than those from conventional CT with a 512 matrix.

Printed on: 02/07/23

## Abstract Archives of the RSNA, 2022

T5A-SPGI-2

### MR Guided Liver Biopsies - Depiction Of The Biopsy Site On Immediate Postinterventional Contrast Enhanced MRI

Tuesday, Nov. 29 12:15PM - 12:45PM Room: Learning Center - GI DPS

#### Participants

Guenther K. Schneider, MD, PhD, Homburg, Germany (*Presenter*) Research Grant, Siemens AG; Speakers Bureau, Siemens AG; Speakers Bureau, Bracco Group; Research Grant, Bracco Group

#### PURPOSE

Sampling errors in image guided biopsies of primary, hypervascular focal liver lesions are a common problem in clinical routine, resulting in unnecessary delay or even inadequate treatment of patients. The purpose of our study was to evaluate as if immediate post biopsy MRI may detect the exact location where a liver biopsy was taken and confirm or exclude sampling of representative tissue.

#### METHODS AND MATERIALS

MRI guided liver biopsy was performed in 68 patients with primary liver tumors (HCC, FNH, Adenoma, NRH) using a 18G core biopsy device. Lesion size ranged from 7 mm to 2.7 cm. Following tissue sampling the biopsy tract was closed with gelatin foam pledgets. Immediately post biopsy a diagnostic MRI was performed in order to detect possible complications and to depict the exact area, where the biopsy was sampled. Imaging included T1-/T2-weighted unenhanced sequences (T2 TSE, HASTE, T1w flash 2D and 3D VIBE-DIXON Sequences) as well as dynamic 3D VIBE-DIXON imaging post bolus CM injection (0.05 mmol/kg MultiHance) in the arterial and portalvenous phase. Furthermore T1w images with and without fat suppression in the equilibrium and hepatobiliary phase (hb-phase) were acquired.

#### RESULTS

In all patients the biopsy tract could be depicted at least in one sequence. On unenhanced images the biopsy tract was best detected on T1w flash-2D sequences (57/68) followed by the 3D VIBE-DIXON sequence (51/68). T2w (12/68) and HASTE images (28/68) could not delineate the biopsy tract sufficiently. On CE images the biopsy tract together with the lesion was depicted best in the arterial phase both on the T1w flash 2D and 3D VIBE DIXON sequence (61/68). In the biliary phase depiction of the sampling area together with the lesion was possible in 59 of 41 patients. In 63 of 68 patients MRI confirmed that tissue was taken from the lesions and facilitated histologic diagnosis. In 5 cases lesions were missed, both based on findings in MRI and histology and biopsy was repeated.

#### CONCLUSION

s Immediate post liver biopsy MRI allows for depiction of the biopsy tract both on unenhanced and CE MRI with advantages seen for CE images. T2w imaging did not reliably depict the biopsy tract. By identifying the biopsy area, sampling errors can be detected post biopsy what is of special importance in small lesions, lesions which are similar to normal liver tissue on histology like FNH or regenerative nodules and in lesions in a cirrhotic liver, where findings of regenerating tissue might imply correct tissue sampling in cases in which an HCC was missed.

#### CLINICAL RELEVANCE/APPLICATION

MRI immediately post liver biopsy reliably depicts biopsy tracts and thus can confirm or exclude sampling of representative tissue and avoid unnecessary delay in diagnosis.

Printed on: 02/07/23

## Abstract Archives of the RSNA, 2022

T5A-SPGI-3

### Automated AI-Based Splenic Segmentation for Predicting Survival and Estimating the Risk of Hepatic Decompensation in TACE Patients With HCC

Tuesday, Nov. 29 12:15PM - 12:45PM Room: Learning Center - GI DPS

#### Participants

Lukas Mueller, MD, Mainz, Germany (*Presenter*) Nothing to Disclose

#### PURPOSE

Splenic volume was proposed as a relevant prognostic factor for patients with hepatocellular carcinoma (HCC). We trained a deep-learning algorithm to fully-automatically assess splenic volume based on computed tomography (CT) scans. Then, we investigated splenic volume as a prognostic factor for patients with HCC undergoing transarterial chemoembolization (TACE).

#### METHODS AND MATERIALS

This retrospective study included 327 treatment-naïve patients with HCC undergoing initial TACE at our tertiary care center between 2010 and 2020. A convolutional neural network was trained and validated on the first 100 consecutive cases for spleen segmentation. Then, we used the algorithm to evaluate splenic volume in all 327 patients. Subsequently, we evaluated correlations between splenic volume and survival as well as the risk of hepatic decompensation during TACE.

#### RESULTS

The algorithm showed Sørensen Dice Scores of 0.96 during both training and validation. In the remaining 227 patients assessed with the algorithm, spleen segmentation was visually approved in 223 patients (98.2%) and failed in four patients (1.8%), which required manual re-assessments. Mean splenic volume was 551ml. Median survival was significantly lower in patients with high splenic volume (10.9 months), compared to low splenic volume (22.0 months,  $p=0.001$ ). In contrast, overall survival was not significantly predicted by axial and craniocaudal spleen diameter. Furthermore, patients with a hepatic decompensation after TACE had significantly higher splenic volumes ( $p<0.001$ ).

#### CONCLUSION

s Automated splenic volume assessments showed superior survival predictions in patients with HCC undergoing TACE compared to two-dimensional spleen size estimates and identified patients at risk of hepatic decompensation.

#### CLINICAL RELEVANCE/APPLICATION

Thus, splenic volume could serve as an automatically available, currently underappreciated imaging biomarker.

Printed on: 02/07/23

## Abstract Archives of the RSNA, 2022

T5A-SPGI-4

### Performance of LI-RADS Major Feature Combinations within the CT/MRI Diagnostic Algorithm: Individual Patient Data Meta-analysis

Tuesday, Nov. 29 12:15PM - 12:45PM Room: Learning Center - GI DPS

#### Participants

Jean-Paul Salameh, MSc, (*Presenter*) Nothing to Disclose

#### PURPOSE

The Liver Imaging Reporting and Data System (LI-RADS) assigns a risk for hepatocellular carcinoma (HCC) to imaging observations. The purpose of this study is to perform an individual-patient data (IPD) meta-analysis to establish the percentage of HCC for combinations of LI-RADS major features using the CT/MRI LI-RADS diagnostic algorithm in high-risk patients

#### METHODS AND MATERIALS

Multiple databases (MEDLINE, Embase, Cochrane Central Register of Controlled Trials, and Scopus) were searched for studies from January 2014 to September 2019 that evaluated the accuracy of CT/MRI using LI-RADS (v2014/17/18). IPD were pooled to compute the percentage of HCC for each major feature combination using a random-effects model. Percentage of HCC with 95% confidence intervals (95%CI) are presented. Heterogeneity was quantified using the I-squared statistic. Risk of bias was assessed using Quality Assessment of Diagnostic Accuracy Studies 2

#### RESULTS

Thirty-one studies (2602 patients; 3350 observations) were included. Pooled percentage of HCC for combinations of LI-RADS major features ranged between 15.5% (95%CI 6.0%-34.5%) and 50.7% (95%CI 27.5%-73.6%) for LR3 combinations, 56.7% (95%CI 34.2%-76.8%) and 100% (95%CI 20.3%-100%) for LR4 combinations, and 81.8% (95%CI 61.7%-92.6%) and 96.1% (95%CI 83.4%-99.2%) for LR5 combinations (Figure 1). Twenty-five studies (78%) had high risk of bias due to reporting ambiguity or study design flaws

#### CONCLUSION

Our findings document increasing percentage of HCC with each LI-RADS category; however, substantial variability exists within each category depending on feature combination. This data will inform updates of the LI-RADS diagnostic algorithms to better align feature combinations with intended percentage of HCC in each LI-RADS category

#### CLINICAL RELEVANCE/APPLICATION

Our findings will help determine which observations are definite HCC based on feature combinations. This will impact patient care by providing timely access to treatment and avoiding unnecessary biopsy

Printed on: 02/07/23

## Abstract Archives of the RSNA, 2022

T5A-SPGI-5

### Extracellular Volume Fraction Using Contrast Enhanced CT Is Useful In Differentiating Intrahepatic Cholangiocellular Carcinoma From Hepatocellular Carcinoma

Tuesday, Nov. 29 12:15PM - 12:45PM Room: Learning Center - GI DPS

#### Participants

Takashi Ota, MD, PhD, Suita, Japan (*Presenter*) Nothing to Disclose

#### PURPOSE

To evaluate whether extracellular volume fraction (fECV) of the tumors using contrast-enhanced computed tomography (CT) aids in the differentiation of hepatocellular carcinoma (HCC) and intrahepatic cholangiocellular carcinoma (ICC).

#### METHODS AND MATERIALS

In this retrospective study, 113 patients with pathologically confirmed HCC (n = 74) or ICC (n = 39) who had undergone preoperative contrast-enhanced CT examinations were enrolled. Enhancement values of the tumor (E<sub>tumor</sub>) and aorta (E<sub>aorta</sub>) were obtained based on the precontrast and equilibrium phase CT images. The fECV was calculated using the following equation: fECV [%] = E<sub>tumor</sub>/E<sub>aorta</sub> × (100 - Hematocrit [%]). The fECVs were compared between HCC and ICC groups using Welch's t-test. The diagnostic performance of fECV in the differentiation of HCC and ICC was assessed using receiver operating characteristic (ROC) analysis. The imaging features including tumor demarcation, shape, arterial enhancement pattern, washout pattern, bile duct dilatation, and tortuous tumoral vessels were evaluated by two radiologists and were examined by the  $\chi^2$  test or Fisher's exact test (when n < 5). A multivariate logistic regression analysis was also performed to identify factors predicting a diagnosis of ICC; variables with a P-value of < 0.1 were entered into the final model.

#### RESULTS

The mean fECV of ICCs (43.8 ± 13.2%) was significantly higher than that of HCCs (31.6 ± 9.0%, P < .001). The area under the curve was 0.763. Lobulated and irregular shape, indistinct margin, peripheral rim enhancement in the arterial phase, and the presence of bile duct dilatation were CT features favoring ICC, whereas a round shape, distinct margin, non-rim enhancement in the arterial phase, and washout pattern were CT features favoring HCC in the univariate analysis (P < .001). In the multivariate analysis, fECV and a washout pattern were independent CT features for distinguishing between the two types. (P = 0.03, P < .001, respectively).

#### CONCLUSION

A higher value of fECV and a washout pattern were respectively independent factors of multivariate analysis in distinguishing between ICC and HCC and more indicative of ICC than HCC on contrast-enhanced CT.

#### CLINICAL RELEVANCE/APPLICATION

The addition of extracellular volume fraction analysis to the imaging features evaluation on contrast-enhanced CT may allow more accurately differentiating ICC from HCC.

Printed on: 02/07/23

## Abstract Archives of the RSNA, 2022

T5A-SPGI-7

### **Tomoelastography-based Viscoelastic Signatures for Prediction of Proliferative Phenotype in Hepatocellular Carcinoma**

Tuesday, Nov. 29 12:15PM - 12:45PM Room: Learning Center - GI DPS

#### **Participants**

Gui Liu, (*Presenter*) Nothing to Disclose

#### **PURPOSE**

To investigate the biomechanical signatures of proliferative hepatocellular carcinoma (HCC) and the value of tomoelastography in characterizing the proliferative HCC phenotype.

#### **METHODS AND MATERIALS**

A total of 121 patients with 124 pathologically confirmed HCC lesions (63 proliferative and 61 non-proliferative HCC) were included in this prospective study. All participants underwent preoperative MRI and tomoelastography. Rim arterial phase hyperenhancement [APHE], nonperipheral washout, enhancing capsule and LI-RADS categorization were evaluated. Tumor and liver viscoelasticity were quantified as shear wave speed ( $c$ , m/s), representing tissue stiffness, and loss angle ( $f$ , rad), indicating fluidity. Univariate and multivariate logistic regression analyses were used to determine predictors of proliferative HCC. A prediction nomogram of proliferative HCC was constructed.

#### **RESULTS**

Multivariate logistic regression analysis results showed that tumor  $c$  (OR: 0.24, 95%CI: 0.089-0.63;  $P = 0.0037$ ), tumor  $f$  (OR: 39.12, 95%CI: 2.72-561.94;  $P=0.007$ ), liver  $c$  (OR: 0.12, 95%CI: 0.027- 0.54;  $P = 0.0056$ ), liver  $f$  (OR: 540.64, 95%CI: 6.72 - 43521.86;  $P = 0.0049$ ) and rim APHE (OR: 15.32, 95%CI: 2.87- 81.87;  $P=0.0014$ ) were independent predictors of proliferative HCC. Combining these variables yielded an AUC of 0.77 (95%CI: 0.69-0.84), sensitivity of 73.02% (95%CI: 0.64-0.86), specificity of 68.85% (95%CI: 0.54-0.79), and accuracy of 70.97% (95%CI: 0.62-0.79), respectively, for predicting proliferative HCC. The C-index of the corresponding nomogram was 0.77 (95%CI: 0.69-0.84).

#### **CONCLUSION**

s Proliferative HCC reveals decreased stiffness and increased fluidity for both tumor and liver. Combining biomechanical signature and viscoelasticity could predicate proliferative HCC.

#### **CLINICAL RELEVANCE/APPLICATION**

The proliferation class accounts for about 50% of HCCs, which has strong invasiveness and poor prognosis. Therefore, predicting proliferative HCC was urgent and important to characterize morpho-molecular subtypes for the prediction of prognosis and therapeutic response in clinical practice. We investigated the diagnostic ability of the biomechanical parameters quantified by in vivo tomoelastography for predicting proliferative HCC subtypes. To our knowledge, this is the first study to connect biomechanical properties with the proliferative nature of HCCs. Based on our data, Proliferative HCC may be softer, more liquid like and more bioinvasive than non-proliferative HCC. Additionally, proliferative HCC could be predicted with good accuracy by combining stiffness and fluidity of both the tumor and the liver.

Printed on: 02/07/23

## Abstract Archives of the RSNA, 2022

T5A-SPGI-9

### **Preliminary Radiogenomic Study of Hepatitis B-related Hepatocellular Carcinoma: Associations between MR Features and Mutations**

Tuesday, Nov. 29 12:15PM - 12:45PM Room: Learning Center - GI DPS

#### **Participants**

Ruofan Sheng, MD, Shanghai, China (*Presenter*) Nothing to Disclose

#### **PURPOSE**

Hepatocellular carcinoma (HCC) is the most common primary liver cancer, and radiogenomics plays an important role in providing accurate imaging substitutes which are associated with genetic expression. This study aimed to investigate associations between MR features and the high-frequency mutations of hepatitis B virus (HBV) related hepatocellular carcinoma (HCC).

#### **METHODS AND MATERIALS**

This retrospective study included 58 HCC patients who underwent abdominal contrast-enhanced MRI prior to surgical resection and genome sequencing. MR imaging features and mutation information were evaluated. Associations between MR features and the high-frequency mutations as well as tumor mutation burden (TMB) level were tested by using Pearson's chi-squared test or Fisher exact test.

#### **RESULTS**

The top 5 most frequently mutated genes of HCC were TP53 (53.45%), TAF1(24.14%), PDE4DIP (22.41%), ABCA13 (18.97%), LRP1B (17.24%). Mutations of TP53 were associated with the presence of tumor necrosis ( $P=0.035$ ). Mutations of ABCA13 were associated with the presence of mosaic architecture ( $P=0.025$ ) and necrosis ( $P=0.010$ ). Mutations of LRP1B were associated with the presence of mosaic architecture ( $P=0.015$ ). MR features were not correlated to the TMB level ( $P=0.945$  to  $P>0.99$ ).

#### **CONCLUSION**

s This preliminary radiogenomic analysis revealed associations between MR features and the high-frequency mutations in HBV-related HCC.

#### **CLINICAL RELEVANCE/APPLICATION**

This preliminary radiogenomics analysis showed associations between MR features and the high-frequency mutations in HBV-related HCCs, which demonstrated potential clinical value of imaging traits as surrogate markers of molecular portraits in HCC.

Printed on: 02/07/23

## Abstract Archives of the RSNA, 2022

T5A-SPGU

### Genitourinary Tuesday Poster Discussions - A

Tuesday, Nov. 29 12:15PM - 12:45PM Room: Learning Center - GU DPS

#### Sub-Events

#### **T5A-SPGU-1 MRI guided focused ultrasound ablation (MRgFUS) for localized intermediate-risk prostate cancer - results of a phase II trial**

##### Participants

Sangeet Ghai, MD, Toronto, ON (*Presenter*) Research Grant, INSIGHTEC Ltd

##### PURPOSE

To explore oncologic and functional outcomes at 2 years following targeted focal therapy performed under MRI guided focused ultrasound (MRgFUS) for intermediate-risk csPCa

##### METHODS AND MATERIALS

In this prospective phase II trial, between February 2016 and July 2019, men with MRI visible unifocal csPCa were treated by transrectal MRgFUS. Real time ablation monitoring was performed by MR thermography. Non-perfused volume was measured at treatment completion. Peri-procedural complications were recorded. Follow-up included International Prostate Symptom Score (IPSS) and International Index of Erectile Function (IIEF-15) at 24 months, and mpMRI and biopsy at 6 and 24 months. LQMM models were used to model median change from baseline.

##### RESULTS

Treatment was successfully completed in all 44 men, 36 with Grade Group (GG) 2 and 8 with GG3 disease (median age [IQR]: 67 years [62-70]). Median (IQR) prostate volume and tumor length 40cc (31.5-50.8) and 9mm (7-12.5) respectively. 17 PCa sites were in peripheral zone and 6 in transition zone. Median (IQR) non perfused volumes were 6.1cc (3.5-8.0). No major treatment-related adverse events occurred. 40 of 44 (91%) sites of PCa (=6mm GG1 disease or any volume =GG2 disease) were free of disease at treatment site at study conclusion (24 months). Additional 3 of 44 participants (7%) had out of field new site of csPCa at 2 years. 37 men (84%) remained free of disease (=6mm GG1 or any volume GG2) at 2 years. Median (IQR) IPSS and IIEF-15 were similar at baseline and 24 months (3.5 [IQR: 2.0-7.0] vs. 4.5 [IQR: 1.0-8.0],  $p=0.84$ ; 59.5 [25.2-65.0] vs. 31.5 [IQR: 16.2-61.0],  $p=0.34$ , respectively). 3 of 7 men with recurrent disease underwent salvage treatment (2 underwent salvage focal treatment by MRI laser therapy and 1 participant underwent radical prostatectomy with negative margins). The remaining 41 of 44 (93%) men including 4 with small volume MR invisible csPCa remain on active surveillance.

##### CONCLUSION

Targeted focal therapy of intermediate-risk prostate cancer performed under MRgFUS is safe with very encouraging 2 year oncological and functional outcomes.

##### CLINICAL RELEVANCE/APPLICATION

MRI guided targeted focal therapy by MRgFUS is a feasible treatment option in men with localized clinically significant prostate cancer (csPCa).

#### **T5A-SPGU-2 Fat-containing adnexal masses on MRI: solid tissue volume and fat distribution as a guide for O-RADS Score assignment**

##### Participants

Monica Cheng, MD, (*Presenter*) Nothing to Disclose

##### PURPOSE

To evaluate the O-RADS MRI scoring system for fat-containing adnexal masses, by investigating the optimal method for quantifying volume of solid tissue and the associations between fat distribution and malignant histology.

##### METHODS AND MATERIALS

This retrospective single-center study included consecutive patients with fat-containing ovarian masses on MRI during 2008-2021. Two radiologists (R1, R2) independently reviewed MRI for overall size, size of any solid tissue, size of solid tissue that was not a Rokitansky nodule (RN), and distribution of fat (fat only, fat-fluid level, fat balls, focal, scattered). Reference standard was pathology or follow-up >6 months. Wilcoxon rank sum test, Fisher exact test, and ROC curve tests were used for statistical analysis. Data are presented as median (interquartile ranges).

##### RESULTS

205 women (age 35years; range 25-46) with 180 benign lesions (including 172 mature teratomas) and 25 malignant lesions (10 immature teratomas, 5 teratomas with malignant transformation, 6 mixed germ cell tumors, and 4 others) were included. Overall size

(9.9 cm [8.4-14.8] vs 5.6 cm [3.7-8.1] for R1; 12.4 cm [8.5-15.2] vs 5.7 cm [3.8-8.1] for R2), size of any solid tissue (5.1 cm [2-10] vs 1.2 cm [0-2.1] for R1; 3.2 cm [1.5-6.7] vs 0 cm [0-1.5] for R2), size of non-RN solid tissue (5.1 cm [0-10] vs 0 cm [0-0] for R1; 3.1 cm [1.0-6.7] vs 0 cm [0-0] for R2), and distribution of fat were all significantly different between malignant and benign lesions ( $p < 0.01$ ). The area under the ROC was greatest for size of non-RN solid tissue (0.84 [95%CI 0.74-0.93] for R1; 0.86 [95%CI 0.77-0.95] for R2) compared to overall size of mass (0.80 [95%CI 0.69-0.91] for R1; 0.83 [95%CI 0.73-0.92] for R2) and size of any solid tissue (0.80 [0.69-0.91] for R1; 0.81 [95% CI, 0.71-0.92] for R2). Optimal cutoffs using non-RN solid tissue were  $\geq 1.2$  cm (R1) and  $\geq 1.0$  cm (R2), yielding sensitivities and specificities of 0.72 (95%CI 0.51-0.88) and 0.93 (95%CI 0.89-0.97) for R1 and 0.76 (95%CI 0.55-0.91) and 0.95 (95%CI 0.91-0.98) for R2. Scattered fat was present in most (9/10) immature teratomas and mixed germ cell tumors for both R1 and R2.

## CONCLUSION

In patients with fat-containing ovarian masses, size of overall mass, size of solid tissue, and distribution of fat were significantly different between benign and malignant lesions.

## CLINICAL RELEVANCE/APPLICATION

To refine O-RADS, a simple approach assessing size of solid tissue that is not a Rokitansky nodule and scattered fat may be useful for determining ovarian malignancy.

## T5A-SPGU-3 Investigation of multiparametric magnetic resonance imaging applied in evaluating bladder cancer pathological response after neoadjuvant immunotherapy.

### Participants

Lingmin Kong, Guangdong, China (*Presenter*) Nothing to Disclose

## PURPOSE

To investigate the diagnostic performance of T2WI, dynamic contrast-enhanced (DCE) and diffusion-weighted (DW) MRI in discriminating bladder cancer (BCa) pathological changes after neoadjuvant chemotherapy (NAC) plus immunotherapy.

## METHODS AND MATERIALS

This prospective study included 13 patients with pathologically confirmed BCa, who underwent both pre- and post treatment (at least two cycles of NAC plus immunotherapy that is Cisplatin-based NAC in combination with immunotherapy, including Tislelizumab, Toripalimab or Sintilimab Injection) MR imaging and subsequent cystectomy or transurethral resection. MRI examinations included conventional MRI sequences (T1 weighted, T2 weighted imaging) and functional MRI sequences (DCE, DW imaging) on a 3.0T scanner (Signa Pioneer, GE, Milwaukee, WI, USA). The tumor response was assessed by two senior radiologists through three steps (figure 1). The results (table 1) were compared with the findings at histopathology specimens obtained after NAC.

## RESULTS

On post neoadjuvant immunotherapy cystectomy or transurethral resection specimens, pathological complete response (pCR) was confirmed in 7 patients (53.8%, 7/13). The diagnostic accuracy of multiparametric magnetic resonance imaging (mp MRI) in distinguishing complete response (CR) from non-CR was 100%.

## CONCLUSION

mp MRI can be a potential noninvasive technique for evaluating BCa pathological response after NAC plus immunotherapy.

## CLINICAL RELEVANCE/APPLICATION

Immune checkpoint inhibitors (ICIs), especially PD-1/PD-L1 inhibitors, emerged as an important treatment strategy in muscle invasive bladder cancer and cisplatin-based NAC plus immunotherapy becomes research focus recently. This study first investigate the diagnostic potential of multiparametric magnetic resonance imaging (mp MRI) in evaluating BCa pathological response after NAC plus immunotherapy and showed that the combination of T2WI, dynamic contrast-enhanced MR (DCE-MR) and diffusion-weighted MR (DW-MR) had significant advantages in discriminating pathological changes. The results indicated that mp MRI may be a useful non-invasive imaging biomarker that can not only evaluate pathological response but also select BCa patients who are suitable for conservative therapy, to further salvage unnecessary operation and improve patients' life quality.

Printed on: 02/07/23

## Abstract Archives of the RSNA, 2022

T5A-SPGU-1

### **MRI guided focused ultrasound ablation (MRgFUS) for localized intermediate-risk prostate cancer -results of a phase II trial**

Tuesday, Nov. 29 12:15PM - 12:45PM Room: Learning Center - GU DPS

#### **Participants**

Sangeet Ghai, MD, Toronto, ON (*Presenter*) Research Grant, INSIGHTEC Ltd

#### **PURPOSE**

To explore oncologic and functional outcomes at 2 years following targeted focal therapy performed under MRI guided focused ultrasound (MRgFUS) for intermediate-risk csPCa

#### **METHODS AND MATERIALS**

In this prospective phase II trial, between February 2016 and July 2019, men with MRI visible unifocal csPCa were treated by transrectal MRgFUS. Real time ablation monitoring was performed by MR thermography. Non-perfused volume was measured at treatment completion. Peri-procedural complications were recorded. Follow-up included International Prostate Symptom Score (IPSS) and International Index of Erectile Function (IIEF-15) at 24 months, and mpMRI and biopsy at 6 and 24 months. LQMM models were used to model median change from baseline.

#### **RESULTS**

Treatment was successfully completed in all 44 men, 36 with Grade Group (GG) 2 and 8 with GG3 disease (median age [IQR]: 67 years [62-70]). Median (IQR) prostate volume and tumor length 40cc (31.5-50.8) and 9mm (7-12.5) respectively. 17 PCa sites were in peripheral zone and 6 in transition zone. Median (IQR) non perfused volumes were 6.1cc (3.5-8.0). No major treatment-related adverse events occurred. 40 of 44 (91%) sites of PCa (=6mm GG1 disease or any volume =GG2 disease) were free of disease at treatment site at study conclusion (24 months). Additional 3 of 44 participants (7%) had out of field new site of csPCa at 2 years. 37 men (84%) remained free of disease (=6mm GG1 or any volume GG2) at 2 years. Median (IQR) IPSS and IIEF-15 were similar at baseline and 24 months (3.5 [IQR: 2.0-7.0] vs. 4.5 [IQR: 1.0-8.0],  $p=0.84$ ; 59.5 [25.2-65.0] vs. 31.5 [IQR: 16.2-61.0],  $p=0.34$ , respectively). 3 of 7 men with recurrent disease underwent salvage treatment (2 underwent salvage focal treatment by MRI laser therapy and 1 participant underwent radical prostatectomy with negative margins). The remaining 41 of 44 (93%) men including 4 with small volume MR invisible csPCa remain on active surveillance.

#### **CONCLUSION**

s Targeted focal therapy of intermediate-risk prostate cancer performed under MRgFUS is safe with very encouraging 2 year oncological and functional outcomes.

#### **CLINICAL RELEVANCE/APPLICATION**

MRI guided targeted focal therapy by MRgFUS is a feasible treatment option in men with localized clinically significant prostate cancer (csPCa).

Printed on: 02/07/23

## Abstract Archives of the RSNA, 2022

T5A-SPGU-2

### Fat-containing adnexal masses on MRI: solid tissue volume and fat distribution as a guide for O-RADS Score assignment

Tuesday, Nov. 29 12:15PM - 12:45PM Room: Learning Center - GU DPS

#### Participants

Monica Cheng, MD, (*Presenter*) Nothing to Disclose

#### PURPOSE

To evaluate the O-RADS MRI scoring system for fat-containing adnexal masses, by investigating the optimal method for quantifying volume of solid tissue and the associations between fat distribution and malignant histology.

#### METHODS AND MATERIALS

This retrospective single-center study included consecutive patients with fat-containing ovarian masses on MRI during 2008-2021. Two radiologists (R1, R2) independently reviewed MRI for overall size, size of any solid tissue, size of solid tissue that was not a Rokitansky nodule (RN), and distribution of fat (fat only, fat-fluid level, fat balls, focal, scattered). Reference standard was pathology or follow-up >6 months. Wilcoxon rank sum test, Fisher exact test, and ROC curve tests were used for statistical analysis. Data are presented as median (interquartile ranges).

#### RESULTS

205 women (age 35years; range 25-46) with 180 benign lesions (including 172 mature teratomas) and 25 malignant lesions (10 immature teratomas, 5 teratomas with malignant transformation, 6 mixed germ cell tumors, and 4 others) were included. Overall size (9.9 cm [8.4-14.8] vs 5.6 cm [3.7-8.1] for R1; 12.4 cm [8.5-15.2] vs 5.7 cm [3.8-8.1] for R2), size of any solid tissue (5.1 cm [2-10] vs 1.2 cm [0-2.1] for R1; 3.2 cm [1.5-6.7] vs 0 cm [0-1.5] for R2), size of non-RN solid tissue (5.1 cm [0-10] vs 0 cm [0-0] for R1; 3.1 cm [1.0-6.7] vs 0 cm [0-0] for R2), and distribution of fat were all significantly different between malignant and benign lesions ( $p < 0.01$ ). The area under the ROC was greatest for size of non-RN solid tissue (0.84 [95%CI 0.74-0.93] for R1; 0.86 [95%CI 0.77-0.95] for R2) compared to overall size of mass (0.80 [95%CI 0.69-0.91] for R1; 0.83 [95%CI 0.73-0.92] for R2) and size of any solid tissue (0.80 [0.69-0.91] for R1; 0.81 [95% CI, 0.71-0.92] for R2). Optimal cutoffs using non-RN solid tissue were =1.2 cm (R1) and =1.0 cm (R2), yielding sensitivities and specificities of 0.72 (95%CI 0.51-0.88) and 0.93 (95%CI 0.89-0.97) for R1 and 0.76 (95%CI 0.55-0.91) and 0.95 (95%CI 0.91-0.98) for R2. Scattered fat was present in most (9/10) immature teratomas and mixed germ cell tumors for both R1 and R2.

#### CONCLUSION

In patients with fat-containing ovarian masses, size of overall mass, size of solid tissue, and distribution of fat were significantly different between benign and malignant lesions.

#### CLINICAL RELEVANCE/APPLICATION

To refine O-RADS, a simple approach assessing size of solid tissue that is not a Rokitansky nodule and scattered fat may be useful for determining ovarian malignancy.

Printed on: 02/07/23

## Abstract Archives of the RSNA, 2022

T5A-SPGU-3

### Investigation of multiparametric magnetic resonance imaging applied in evaluating bladder cancer pathological response after neoadjuvant immunotherapy.

Tuesday, Nov. 29 12:15PM - 12:45PM Room: Learning Center - GU DPS

#### Participants

Lingmin Kong, Guangdong, China (*Presenter*) Nothing to Disclose

#### PURPOSE

To investigate the diagnostic performance of T2WI, dynamic contrast-enhanced (DCE) and diffusion-weighted (DW) MRI in discriminating bladder cancer (BCa) pathological changes after neoadjuvant chemotherapy (NAC) plus immunotherapy.

#### METHODS AND MATERIALS

This prospective study included 13 patients with pathologically confirmed BCa, who underwent both pre- and post treatment (at least two cycles of NAC plus immunotherapy that is Cisplatin-based NAC in combination with immunotherapy, including Tislelizumab, Toripalimab or Sintilimab Injection) MR imaging and subsequent cystectomy or transurethral resection. MRI examinations included conventional MRI sequences (T1 weighted, T2 weighted imaging) and functional MRI sequences (DCE, DW imaging) on a 3.0T scanner (Signa Pioneer, GE, Milwaukee, WI, USA). The tumor response was assessed by two senior radiologists through three steps (figure 1). The results (table 1) were compared with the findings at histopathology specimens obtained after NAC.

#### RESULTS

On post neoadjuvant immunotherapy cystectomy or transurethral resection specimens, pathological complete response (pCR) was confirmed in 7 patients (53.8%, 7/13). The diagnostic accuracy of multiparametric magnetic resonance imaging (mp MRI) in distinguishing complete response (CR) from non-CR was 100%.

#### CONCLUSION

mp MRI can be a potential noninvasive technique for evaluating BCa pathological response after NAC plus immunotherapy.

#### CLINICAL RELEVANCE/APPLICATION

Immune checkpoint inhibitors (ICIs), especially PD-1/PD-L1 inhibitors, emerged as an important treatment strategy in muscle invasive bladder cancer and cisplatin-based NAC plus immunotherapy becomes research focus recently. This study first investigate the diagnostic potential of multiparametric magnetic resonance imaging (mp MRI) in evaluating BCa pathological response after NAC plus immunotherapy and showed that the combination of T2WI, dynamic contrast-enhanced MR (DCE-MR) and diffusion-weighted MR (DW-MR) had significant advantages in discriminating pathological changes. The results indicated that mp MRI may be a useful non-invasive imaging biomarker that can not only evaluate pathological response but also select BCa patients who are suitable for conservative therapy, to further salvage unnecessary operation and improve patients' life quality.

Printed on: 02/07/23

## Abstract Archives of the RSNA, 2022

T5A-SPHN

### Head and Neck Tuesday Poster Discussions - A

Tuesday, Nov. 29 12:15PM - 12:45PM Room: Learning Center - HN DPS

#### Sub-Events

#### **T5A-SPHN-1 Application Value of Radiomic Nomogram Based on Preoperative HRCT in Predicting Fallopian Canal Involvement in Cholesteatoma**

Participants

Xiaoxue Fan, PhD, (*Presenter*) Nothing to Disclose

#### **PURPOSE**

Cholesteatoma growth pattern predicts frequent involvement of the tympanic segment of the fallopian canal, and fallopian canal dehiscence is a major risk factor for facial nerve injury during middle ear mastoid surgery. The purpose of this study was to establish and validate a non-contrast HRCT based radiomic nomogram for predicting fallopian canal involvement in patients with cholesteatoma.

#### **METHODS AND MATERIALS**

214 consecutive patients (157 in the training set and 57 in the test set) who underwent surgery and had pathologically confirmed cholesteatoma were retrospectively included. Open-source radiomics software was used to select and extract features on the HRCT. A radiomics signature model was constructed to fallopian canal involvement using the least absolute shrinkage and selection operator (LASSO). Radiomic features, clinically independent risk factors were incorporated into multivariate logistic regression analysis and presented in the formation of a nomogram for predicting fallopian canal involvement in both the training and test sets, which were evaluated by its discrimination, calibration, and clinical usefulness.

#### **RESULTS**

A radiomics model consisting of seven radiomic features with a good prognostic ability in the training set with the area under the curve (AUC) of 0.85 (95%CI, 0.78-0.90), which was also confirmed in the test set with an AUC of 0.81 (95%CI, 0.68-0.90). Multivariate logistic regression identifies cerebral plate hypoplasia and stapes destruction as independent risk factors for fallopian canal involvement in cholesteatoma. The nomogram consisting of the radiomics scores and cerebral plate hypoplasia and stapes destruction showed good discrimination ability in the training and test sets with an AUC of 0.91 (95%CI, 0.85-0.95) and an AUC of 0.83 (95%CI, 0.71-0.92), respectively. Decision curve analysis showed that the radiomic nomogram was clinically useful.

#### **CONCLUSION**

s Radiomic nomogram based on the non-contrast HRCT is a useful tool for the prediction of fallopian canal involvement in patients with cholesteatoma, which can assist clinicians for optimized risk stratification of patients preoperatively and take effective measures to prevent intraoperative facial nerve injury.

#### **CLINICAL RELEVANCE/APPLICATION**

This study developed and validated the efficacy of preoperative individualized prediction of fallopian canal involvement in patients with cholesteatoma based on radiomics nomogram of HRCT scans. The radiomics nomogram drawings include the radiomic model, stapes involvement, and low cerebral plate. The easy-to-use radiomics nomogram showed good discrimination in both the training set (AUC, 0.910) and the test set (AUC, 0.828), outperforming traditional clinical factors.

#### **T5A-SPHN-3 Otomastoiditis: A Potentially Overused and Unnecessarily Alarmist Term in the Reporting of Non-contrast Head CT**

Participants

Jimmy Swanson, MD, Winston Salem, NC (*Presenter*) Nothing to Disclose

#### **PURPOSE**

Otomastoiditis is a rare, clinically diagnosed infection with potential for life-threatening intracranial complications. Middle ear and mastoid opacification are common, nonspecific imaging findings. Some radiologists attribute middle ear and mastoid opacification to otomastoiditis, even in the absence of supportive clinical features. This approach is potentially problematic and may result in unnecessary antibiotic use and otolaryngology consults. Among inpatients and emergency department (ED) patients undergoing noncontrast head CT for reasons unrelated to suspected temporal bone pathology whose radiology report includes the term "otomastoiditis," we hypothesize a low prevalence of true, clinically diagnosed otomastoiditis. Our purpose is to determine the true otomastoiditis prevalence in this population and to characterize downstream effects of radiologist "otomastoiditis" usage.

#### **METHODS AND MATERIALS**

Inpatients and ED patients undergoing noncontrast head CT between February 2018 and August 2021 were retrospectively reviewed. The following inclusion criteria were applied: 1) age 18+ years, 2) indication unrelated to temporal bone pathology, 3) no known temporal bone pathology or prior surgery, 4) "otomastoiditis" used in the radiology report. Patient demographics and relevant

clinical information were collected from the electronic health record. Among patients with clinically diagnosed otomastoiditis, CT imaging was reviewed to assess for imaging features specific for otomastoiditis (e.g., coalescence, epidural abscess).

## **RESULTS**

A total of 92 patients (54 male, 38 female, mean age 63 years) formed the study cohort. Otolaryngology was consulted to evaluate possible otomastoiditis in 7 (8%), antibiotics were initiated prior to consultation in 3 (3%), and a clinical diagnosis of otomastoiditis was established in 1 (1%) patient whose head CT demonstrated mastoid erosion, pneumocephalus, and temporal lobe edema.

## **CONCLUSION**

s Although the term "otomastoiditis" was used in 100% of our cohort's radiology reports, the true prevalence was only 1%. Importantly, no patients with sole imaging findings of middle ear and mastoid opacification received a clinical diagnosis of otomastoiditis. Absent clinical suspicion for infection or imaging evidence of an infectious complication, we recommend the descriptive term "opacification" over "otomastoiditis" to minimize the risk of unwarranted otolaryngology consults and unnecessary antibiotic usage.

## **CLINICAL RELEVANCE/APPLICATION**

The clinical relevance of this study is that the data provide justification for using the term "opacification" over "otomastoiditis" in the absence of clinical suspicion for infection or imaging evidence of an infectious complication.

Printed on: 02/07/23

## Abstract Archives of the RSNA, 2022

T5A-SPHN-1

### Application Value of Radiomic Nomogram Based on Preoperative HRCT in Predicting Fallopian Canal Involvement in Cholesteatoma

Tuesday, Nov. 29 12:15PM - 12:45PM Room: Learning Center - HN DPS

#### Participants

Xiaoxue Fan, PhD, (*Presenter*) Nothing to Disclose

#### PURPOSE

Cholesteatoma growth pattern predicts frequent involvement of the tympanic segment of the fallopian canal, and fallopian canal dehiscence is a major risk factor for facial nerve injury during middle ear mastoid surgery. The purpose of this study was to establish and validate a non-contrast HRCT based radiomic nomogram for predicting fallopian canal involvement in patients with cholesteatoma.

#### METHODS AND MATERIALS

214 consecutive patients (157 in the training set and 57 in the test set) who underwent surgery and had pathologically confirmed cholesteatoma were retrospectively included. Open-source radiomics software was used to select and extract features on the HRCT. A radiomics signature model was constructed to fallopian canal involvement using the least absolute shrinkage and selection operator (LASSO). Radiomic features, clinically independent risk factors were incorporated into multivariate logistic regression analysis and presented in the formation of a nomogram for predicting fallopian canal involvement in both the training and test sets, which were evaluated by its discrimination, calibration, and clinical usefulness.

#### RESULTS

A radiomics model consisting of seven radiomic features with a good prognostic ability in the training set with the area under the curve (AUC) of 0.85 (95%CI, 0.78-0.90), which was also confirmed in the test set with an AUC of 0.81 (95%CI, 0.68-0.90). Multivariate logistic regression identifies cerebral plate hypoplasia and stapes destruction as independent risk factors for fallopian canal involvement in cholesteatoma. The nomogram consisting of the radiomics scores and cerebral plate hypoplasia and stapes destruction showed good discrimination ability in the training and test sets with an AUC of 0.91 (95%CI, 0.85-0.95) and an AUC of 0.83 (95%CI, 0.71-0.92), respectively. Decision curve analysis showed that the radiomic nomogram was clinically useful.

#### CONCLUSION

s Radiomic nomogram based on the non-contrast HRCT is a useful tool for the prediction of fallopian canal involvement in patients with cholesteatoma, which can assist clinicians for optimized risk stratification of patients preoperatively and take effective measures to prevent intraoperative facial nerve injury.

#### CLINICAL RELEVANCE/APPLICATION

This study developed and validated the efficacy of preoperative individualized prediction of fallopian canal involvement in patients with cholesteatoma based on radiomics nomogram of HRCT scans. The radiomics nomogram drawings include the radiomic model, stapes involvement, and low cerebral plate. The easy-to-use radiomics nomogram showed good discrimination in both the training set (AUC, 0.910) and the test set (AUC, 0.828), outperforming traditional clinical factors.

Printed on: 02/07/23

## Abstract Archives of the RSNA, 2022

T5A-SPHN-3

### Otomastoiditis: A Potentially Overused and Unnecessarily Alarmist Term in the Reporting of Non-contrast Head CT

Tuesday, Nov. 29 12:15PM - 12:45PM Room: Learning Center - HN DPS

#### Participants

Jimmy Swanson, MD, Winston Salem, NC (*Presenter*) Nothing to Disclose

#### PURPOSE

Otomastoiditis is a rare, clinically diagnosed infection with potential for life-threatening intracranial complications. Middle ear and mastoid opacification are common, nonspecific imaging findings. Some radiologists attribute middle ear and mastoid opacification to otomastoiditis, even in the absence of supportive clinical features. This approach is potentially problematic and may result in unnecessary antibiotic use and otolaryngology consults. Among inpatients and emergency department (ED) patients undergoing noncontrast head CT for reasons unrelated to suspected temporal bone pathology whose radiology report includes the term "otomastoiditis," we hypothesize a low prevalence of true, clinically diagnosed otomastoiditis. Our purpose is to determine the true otomastoiditis prevalence in this population and to characterize downstream effects of radiologist "otomastoiditis" usage.

#### METHODS AND MATERIALS

Inpatients and ED patients undergoing noncontrast head CT between February 2018 and August 2021 were retrospectively reviewed. The following inclusion criteria were applied: 1) age 18+ years, 2) indication unrelated to temporal bone pathology, 3) no known temporal bone pathology or prior surgery, 4) "otomastoiditis" used in the radiology report. Patient demographics and relevant clinical information were collected from the electronic health record. Among patients with clinically diagnosed otomastoiditis, CT imaging was reviewed to assess for imaging features specific for otomastoiditis (e.g., coalescence, epidural abscess).

#### RESULTS

A total of 92 patients (54 male, 38 female, mean age 63 years) formed the study cohort. Otolaryngology was consulted to evaluate possible otomastoiditis in 7 (8%), antibiotics were initiated prior to consultation in 3 (3%), and a clinical diagnosis of otomastoiditis was established in 1 (1%) patient whose head CT demonstrated mastoid erosion, pneumocephalus, and temporal lobe edema.

#### CONCLUSION

Although the term "otomastoiditis" was used in 100% of our cohort's radiology reports, the true prevalence was only 1%. Importantly, no patients with sole imaging findings of middle ear and mastoid opacification received a clinical diagnosis of otomastoiditis. Absent clinical suspicion for infection or imaging evidence of an infectious complication, we recommend the descriptive term "opacification" over "otomastoiditis" to minimize the risk of unwarranted otolaryngology consults and unnecessary antibiotic usage.

#### CLINICAL RELEVANCE/APPLICATION

The clinical relevance of this study is that the data provide justification for using the term "opacification" over "otomastoiditis" in the absence of clinical suspicion for infection or imaging evidence of an infectious complication.

Printed on: 02/07/23



## Abstract Archives of the RSNA, 2022

T5A-SPIN

### Informatics Tuesday Poster Discussions - A

Tuesday, Nov. 29 12:15PM - 12:45PM Room: Learning Center - IN DPS

#### Sub-Events

#### T5A-SPIN-1 Intelligent Denoising

##### Participants

Marina Manso Jimeno, New York, NY (*Presenter*) Nothing to Disclose

##### PURPOSE

To accelerate the Alzheimer's disease (AD) screening MRI protocol employed at our institution by trading off signal-to-noise ratio (SNR) for faster acquisition time. SNR is recovered post-acquisition via image denoising using deep learning (DL). We aim to (i) improve imaging throughput; (ii) guarantee image quality using DL denoising, measured by peak SNR (PSNR, dB) and structural similarity index (SSIM) compared to the unaccelerated acquisitions.

##### METHODS AND MATERIALS

Intelligent protocolling The routine protocol (gold standard, GS) consisted of two T1 sagittal sequences and five axial sequences: T2, DWI, T2 FLAIR, T2\*, and T1, totaling 19:47 (minutes: seconds). The accelerated protocol (Fastest) was constructed by consulting sequence-specific Look Up Tables similarly to Ravi et al., MRI, 2020, to obtain acquisition parameters yielding the shortest acquisition times and highest relative SNRs. Two experiments were performed to investigate: (1) improvement in throughput (measured by table time; 1 volunteer); (2) repeatability across 5 sessions (5 volunteers). All healthy volunteers were imaged on a GE 3T Premier scanner, and 26 datasets were acquired in total. Image denoising using deep learning Contrast-specific baseline deep learning (DL) models and subject-specific DL (DL-SS) models were trained on publicly available datasets for image denoising. The noise was forward simulated similarly to Geethanath et al., ISMRM, 2021. All models utilized a common network architecture and were trained for 75 epochs. DL-SS were obtained by fine-tuning the DL models on the worst SNR data acquired across all repeats from experiment #2. Additionally, DL-based unsharp masking was performed. The four methods (GS, Fastest, DL, DL-SS) were evaluated on PSNR, SSIM over 5 contrasts, and volumetry values for 99 regions obtained from T1 data using the tool described in Thomas et al., IEEE BIBE, 2020.

##### RESULTS

The table times measured from experiment 1 were 19:12 and 9:52 for the GS and Fastest protocols, respectively. This was a 1.94x gain in imaging throughput. The mean improvement in PSNR/SSIM across contrasts were 3.943/0.083 (DL) and 5.570/0.100 (DL-SS). The mean RMSE of 12 T1 volumetry measures from GS data were 12.335 (Fastest), 6.607 (DL), and 4.293 (DL-SS), respectively. On-going work involves evaluating these methods on clinically relevant metrics for the remaining contrasts.

##### CONCLUSION

The Fastest protocol resulted in a 1.94x gain in imaging throughput. The DL-SS models outperformed the baseline DL models, yielding a mean improvement of 7.1813 dB/0.1256 (PSNR/SSIM).

##### CLINICAL RELEVANCE/APPLICATION

Intelligent protocolling can improve AD screening throughput and DL-based image denoising can guarantee image quality.

#### T5A-SPIN-3 Automated AI Pipeline for Brain Lesion Classification using Dual-Energy Computed Tomography

##### Participants

Colin Schaeffer, MS, (*Presenter*) Nothing to Disclose

##### PURPOSE

The current protocol for patients presenting with stroke-like symptoms is a CT scan with iodinated contrast. If it is then determined that the patient is having an ischemic stroke, the patient is treated with blood thinners; however, blood thinners put the patient at further risk of hemorrhagic transformation. Therefore, it is hospital protocol to rescan the patient using dual-energy CT (DECT) within 24 hours to monitor for bleeds. The problem with rescanning in such a short period of time is that it is possible for residual iodine contrast to still be present in the brain. Discriminating between hemorrhages and residual contrast is a difficult task for radiologists. What we propose in this study is a form of computer aided diagnosis system that uses a three step A.I. pipeline to identify images with lesions, segment the lesion, and then classify it as either residual contrast or an intracranial hemorrhage. This project presents the first two steps in the pipeline: 1) Lesion identification and 2) Lesion segmentation.

##### METHODS AND MATERIALS

For our identification model, with IRB approval, we obtained 11,547 head CT scans (10,000 without lesions and 1,547 with lesions). This dataset was filtered and stratified into a training set of 7,490 images and a test set of 1,873 images. We then used a five-fold cross validation method on the training set for hyperparameter tuning and model selection. For our segmentation algorithm, the image volumes were co-registered and skull stripped before training both an unsupervised anomaly detection algorithm and a

supervised U-net architecture for segmentation. These models were tested and compared on a set of manually segmented images.

## RESULTS

Our model to identify brain volumes containing lesions obtained an average area under the curve (AUC) of 0.942 when evaluated using a five-fold cross validation method.

## CONCLUSION

s We have developed an automated A.I. pipeline that can be used to identify and segment brain lesions in follow-up stroke DECT imaging. This pipeline can be used to extract quantitative information about the lesions from DECT data which can then be used to classify the lesion.

## CLINICAL RELEVANCE/APPLICATION

An A.I. pipeline such as the one proposed in this study addresses the clinical problem of residual contrast in follow-up stroke imaging. Residual iodine contrast can hinder diagnosis. While reader studies using DECT iodine maps have been published addressing this problem, no quantitative model to differentiate blood from iodine has been published.

### **T5A-SPIN-4 Gender Disparity in Developing a Convolutional Neural Network Specific for The Identification of Infrarenal Abdominal Aortic Aneurysms**

Participants

Justin Camara, MD, Loma Linda, CA (*Presenter*) Nothing to Disclose

## PURPOSE

To determine if gender training and testing factors affect the accuracy of a convolutional neural network (CNN) for infrarenal abdominal aortic aneurysms (AAA) identification on computed tomography angiogram (CTA) scans.

## METHODS AND MATERIALS

From 2015 to 2020, a HIPAA-compliant, IRB-approved, retrospective study analyzed 400 abdominopelvic CTA scans. Utilizing a previously reported methodology to develop a foundational AAA-specific trained CNN, 6 new CNN models were created under varying gender training and testing conditions to assess overall accuracy: male-only training/male-only testing, female-only training/female-only testing, male-only training/all testing, female-only training/all testing, all training/male-only testing, all training/female-only testing. Model accuracy and AUC were analyzed and reported. Misjudgments were analyzed by review of heatmaps, via gradient weighted class activation, overlaid on CTA images.

## RESULTS

Similar to our previously reported custom CNN model for AAA on CTA images, five of six of the new gender-restricted training/testing CNN models also demonstrated high levels of sensitivities (96.6% - 99.1%), specificities (98.4% - 99.6%), and overall accuracies (98.0% - 99.1%). However, the gender model that was trained with female-only cases and tested on both male and female cases demonstrated a significantly reduced level of specificity (87.7%) and reduced overall accuracy (93.0%). Interestingly, the companion gender model (male-only cases and tested on both male and female cases) maintained a high level of specificity (99.5%) and overall accuracy (98.0%). A preliminary subanalysis of misjudgements in the female-only trained model demonstrates aneurysm size and mural thrombus to be predominant factors in false negative misjudgment cases and errors in segmentation to be the predominant factor in false positive misjudgements.

## CONCLUSION

s Preliminary analysis determined that female-only gender training has a reduced accuracy in the development of CNN for AAA identification on CT angiograms. Further investigation is needed to elucidate the reason for the gender disparity to rectify any future AI AAA modeling for real-world application and deployment.

## CLINICAL RELEVANCE/APPLICATION

Gender disparity in medicine and radiology needs further investigation. Although not deeply studied in machine learning, such studies are important to reduce any gender bias/disparity in any future AI modeling for real-world application and deployment.

### **T5A-SPIN-5 Deep Transfer Learning Strategy For Whole-body Aorta Segmentation Using CT Angiography Image of Two Acquisition Protocols**

Participants

Seung-Won Yang, MS, (*Presenter*) Nothing to Disclose

## PURPOSE

To develop a deep learning algorithm for whole-body aorta segmentation on CT angiography (CTA) images in normal population, utilizing transfer learning strategy across two CT acquisition protocols of coronary and whole-body aorta.

## METHODS AND MATERIALS

In order for the whole-body aorta segmentation task to leverage the benefit of coronary CTA (CCTA) with high-resolution features by dedicated acquisition protocol and its relatively lower labeling cost, we enrolled two kinds of CTA scans separately: CT scans of 368 patients who underwent ECG-gated CCTA were included for the pre-training of aortic root and ascending aorta segmentation, and CT scans of 100 patients who underwent ECG-gated aorta CTA using high-pitch helical mode were used for the whole-body aorta segmentation. Non-experts labeled aorta by using a manual toolkit, and an expert radiologist examined its validity before the data were enrolled. The labeled dataset was finally refined by applying preprocessing algorithms of equalization, denoising, interpolation, and normalization (and divided into train and test sets with a ratio of 9:1). The pre-training model adopted U-shape architecture as a backbone network, and is fed with augmented data under the RandAugment strategy of an automated augmentation method. In the whole-body segmentation, we built a Swin-Transformer based encoder-decoder network of which backbone layers are initialized by the pre-trained weights. As for loss function, we used a combo loss that is weighted summation of distribution-based and overlap-based losses.

## RESULTS

To assess model performance, we introduced the dice score coefficient (DSC) and the averaged Hausdorff distance (AHD) in mm. The pre-trained model achieved high performance with DSC of  $0.969\pm 0.0223$  and AHD of  $1.80\pm 1.06$  for aortic root and ascending aorta segmentation. The proposed model for the whole-body aorta segmentation also showed improvement compared to a non-transferred model, so that the metrics were improved from  $0.929\pm 0.0231$  and  $7.53\pm 4.76$  to  $0.935\pm 0.0125$  and  $5.71\pm 2.35$ . Particularly, we witnessed the knowledge transfer makes the aortic root segmentation in whole-body CTA more accurate, yielding better DSC and AHD from  $0.896\pm 0.102$  and  $13.1\pm 8.82$  to  $0.921\pm 0.0712$  and  $11.2\pm 9.15$ .

## CONCLUSION

Our approach is able to improve performance of the whole-body aorta segmentation model to be comparable to radiologists, utilizing the CCTA that has detail anatomic information and lower labeling cost.

## CLINICAL RELEVANCE/APPLICATION

The proposed model can be built with less effort in data collection, and is practical enough to provide geometric parameters of the whole-body aorta that can be used for further medical applications, such as follow-up of aortic aneurysm or planning for catheter treatment.

## T5A-SPIN-6 A Deep-learning Method for Intracranial Aneurysm Detection on Computed Tomographic Angiography Images

### PURPOSE

Computed tomographic angiography (CTA) is preferred for intracranial aneurysms (IAs) screening. Recently, deep learning-based algorithms show the potential to detect IAs in CTA. However, low diagnostic accuracy and high false-positive results were found in these models. The aim of this study is to develop a deep learning model with improved diagnostic accuracy and validated in real-world data.

### METHODS AND MATERIALS

The model consisted of a U-Net based segmentation network and a refine network. It differentiated voxels being potential IAs on 3D patches of CTA images. Only the patches that contained positive voxels were proceeded by the refine network, and the possibilities of these patches having IAs were computed. By focusing on the positive patches from the segmentation results, the refine network screened discriminative features and reduced false-positive results. The model was trained and validated using a public dataset with 1338 CTA scans. Then, the model was tested in a dataset of 38 patients with IAs who have both CTA and DSA results. Finally, two radiologists with more than 10 years' experience reviewed the dataset with and without the assistance of AI.

### RESULTS

For the public dataset, after applying the refine network, the precision on lesion level surged from 45.5% to 69.4% without sacrificing the diagnostic sensitivity (96% vs. 95.2%) (Figure 1-A). On the patient level, the precision increased from 89.5% to 94.8% with a similar diagnostic sensitivity of (97.3% versus 96.7%). For the real-world dataset, with the assistance of AI, radiologists obtained higher diagnostic accuracy compared to without AI (Figure 1-B). In detail, diagnostic sensitivity increased from 64.9% to 91% and precision increased from 83.8% to 97.3%.

## CONCLUSION

The refine network improved the diagnostic precision for CTA detection of IAs. With the assistance of this model, radiologists improved diagnostic accuracy for IAs.

## CLINICAL RELEVANCE/APPLICATION

The proposed deep learning method may help make clinical diagnoses of IAs. It may improve the diagnostic accuracy for IAs screening in CTA.

Printed on: 02/07/23

## Abstract Archives of the RSNA, 2022

T5A-SPIN-1

### Intelligent Denoising

Tuesday, Nov. 29 12:15PM - 12:45PM Room: Learning Center - IN DPS

#### Participants

Marina Manso Jimeno, New York, NY (*Presenter*) Nothing to Disclose

#### PURPOSE

To accelerate the Alzheimer's disease (AD) screening MRI protocol employed at our institution by trading off signal-to-noise ratio (SNR) for faster acquisition time. SNR is recovered post-acquisition via image denoising using deep learning (DL). We aim to (i) improve imaging throughput; (ii) guarantee image quality using DL denoising, measured by peak SNR (PSNR, dB) and structural similarity index (SSIM) compared to the unaccelerated acquisitions.

#### METHODS AND MATERIALS

Intelligent protocolling The routine protocol (gold standard, GS) consisted of two T1 sagittal sequences and five axial sequences: T2, DWI, T2 FLAIR, T2\*, and T1, totaling 19:47 (minutes: seconds). The accelerated protocol (Fastest) was constructed by consulting sequence-specific Look Up Tables similarly to Ravi et al., MRI, 2020, to obtain acquisition parameters yielding the shortest acquisition times and highest relative SNRs. Two experiments were performed to investigate: (1) improvement in throughput (measured by table time; 1 volunteer); (2) repeatability across 5 sessions (5 volunteers). All healthy volunteers were imaged on a GE 3T Premier scanner, and 26 datasets were acquired in total. Image denoising using deep learning Contrast-specific baseline deep learning (DL) models and subject-specific DL (DL-SS) models were trained on publicly available datasets for image denoising. The noise was forward simulated similarly to Geethanath et al., ISMRM, 2021. All models utilized a common network architecture and were trained for 75 epochs. DL-SS were obtained by fine-tuning the DL models on the worst SNR data acquired across all repeats from experiment #2. Additionally, DL-based unsharp masking was performed. The four methods (GS, Fastest, DL, DL-SS) were evaluated on PSNR, SSIM over 5 contrasts, and volumetry values for 99 regions obtained from T1 data using the tool described in Thomas et al., IEEE BIBE, 2020.

#### RESULTS

The table times measured from experiment 1 were 19:12 and 9:52 for the GS and Fastest protocols, respectively. This was a 1.94x gain in imaging throughput. The mean improvement in PSNR/SSIM across contrasts were 3.943/0.083 (DL) and 5.570/0.100 (DL-SS). The mean RMSE of 12 T1 volumetry measures from GS data were 12.335 (Fastest), 6.607 (DL), and 4.293 (DL-SS), respectively. On-going work involves evaluating these methods on clinically relevant metrics for the remaining contrasts.

#### CONCLUSION

s The Fastest protocol resulted in a 1.94x gain in imaging throughput. The DL-SS models outperformed the baseline DL models, yielding a mean improvement of 7.1813 dB/0.1256 (PSNR/SSIM).

#### CLINICAL RELEVANCE/APPLICATION

Intelligent protocolling can improve AD screening throughput and DL-based image denoising can guarantee image quality.

Printed on: 02/07/23

## Abstract Archives of the RSNA, 2022

T5A-SPIN-3

### Automated AI Pipeline for Brain Lesion Classification using Dual-Energy Computed Tomography

Tuesday, Nov. 29 12:15PM - 12:45PM Room: Learning Center - IN DPS

#### Participants

Colin Schaeffer, MS, (*Presenter*) Nothing to Disclose

#### PURPOSE

The current protocol for patients presenting with stroke-like symptoms is a CT scan with iodinated contrast. If it is then determined that the patient is having an ischemic stroke, the patient is treated with blood thinners; however, blood thinners put the patient at further risk of hemorrhagic transformation. Therefore, it is hospital protocol to rescan the patient using dual-energy CT (DECT) within 24 hours to monitor for bleeds. The problem with rescanning in such a short period of time is that it is possible for residual iodine contrast to still be present in the brain. Discriminating between hemorrhages and residual contrast is a difficult task for radiologists. What we propose in this study is a form of computer aided diagnosis system that uses a three step A.I. pipeline to identify images with lesions, segment the lesion, and then classify it as either residual contrast or an intracranial hemorrhage. This project presents the first two steps in the pipeline: 1) Lesion identification and 2) Lesion segmentation.

#### METHODS AND MATERIALS

For our identification model, with IRB approval, we obtained 11,547 head CT scans (10,000 without lesions and 1,547 with lesions). This dataset was filtered and stratified into a training set of 7,490 images and a test set of 1,873 images. We then used a five-fold cross validation method on the training set for hyperparameter tuning and model selection. For our segmentation algorithm, the image volumes were co-registered and skull stripped before training both an unsupervised anomaly detection algorithm and a supervised U-net architecture for segmentation. These models were tested and compared on a set of manually segmented images.

#### RESULTS

Our model to identify brain volumes containing lesions obtained an average area under the curve (AUC) of 0.942 when evaluated using a five-fold cross validation method.

#### CONCLUSION

s We have developed an automated A.I. pipeline that can be used to identify and segment brain lesions in follow-up stroke DECT imaging. This pipeline can be used to extract quantitative information about the lesions from DECT data which can then be used to classify the lesion.

#### CLINICAL RELEVANCE/APPLICATION

An A.I. pipeline such as the one proposed in this study addresses the clinical problem of residual contrast in follow-up stroke imaging. Residual iodine contrast can hinder diagnosis. While reader studies using DECT iodine maps have been published addressing this problem, no quantitative model to differentiate blood from iodine has been published.

Printed on: 02/07/23

## Abstract Archives of the RSNA, 2022

T5A-SPIN-4

### Gender Disparity in Developing a Convolutional Neural Network Specific for The Identification of Infrarenal Abdominal Aortic Aneurysms

Tuesday, Nov. 29 12:15PM - 12:45PM Room: Learning Center - IN DPS

#### Participants

Justin Camara, MD, Loma Linda, CA (*Presenter*) Nothing to Disclose

#### PURPOSE

To determine if gender training and testing factors affect the accuracy of a convolutional neural network (CNN) for infrarenal abdominal aortic aneurysms (AAA) identification on computed tomography angiogram (CTA) scans.

#### METHODS AND MATERIALS

From 2015 to 2020, a HIPAA-compliant, IRB-approved, retrospective study analyzed 400 abdominopelvic CTA scans. Utilizing a previously reported methodology to develop a foundational AAA-specific trained CNN, 6 new CNN models were created under varying gender training and testing conditions to assess overall accuracy: male-only training/male-only testing, female-only training/female-only testing, male-only training/all testing, female-only training/all testing, all training/male-only testing, all training/female-only testing. Model accuracy and AUC were analyzed and reported. Misjudgments were analyzed by review of heatmaps, via gradient weighted class activation, overlaid on CTA images.

#### RESULTS

Similar to our previously reported custom CNN model for AAA on CTA images, five of six of the new gender-restricted training/testing CNN models also demonstrated high levels of sensitivities (96.6% - 99.1%), specificities (98.4% - 99.6%), and overall accuracies (98.0% - 99.1%). However, the gender model that was trained with female-only cases and tested on both male and female cases demonstrated a significantly reduced level of specificity (87.7%) and reduced overall accuracy (93.0%). Interestingly, the companion gender model (male-only cases and tested on both male and female cases) maintained a high level of specificity (99.5%) and overall accuracy (98.0%). A preliminary subanalysis of misjudgements in the female-only trained model demonstrates aneurysm size and mural thrombus to be predominant factors in false negative misjudgment cases and errors in segmentation to be the predominant factor in false positive misjudgements.

#### CONCLUSION

s Preliminary analysis determined that female-only gender training has a reduced accuracy in the development of CNN for AAA identification on CT angiograms. Further investigation is needed to elucidate the reason for the gender disparity to rectify any future AI AAA modeling for real-world application and deployment.

#### CLINICAL RELEVANCE/APPLICATION

Gender disparity in medicine and radiology needs further investigation. Although not deeply studied in machine learning, such studies are important to reduce any gender bias/disparity in any future AI modeling for real-world application and deployment.

Printed on: 02/07/23

## Abstract Archives of the RSNA, 2022

T5A-SPIN-5

### Deep Transfer Learning Strategy For Whole-body Aorta Segmentation Using CT Angiography Image of Two Acquisition Protocols

Tuesday, Nov. 29 12:15PM - 12:45PM Room: Learning Center - IN DPS

#### Participants

Seung-Won Yang, MS, (*Presenter*) Nothing to Disclose

#### PURPOSE

To develop a deep learning algorithm for whole-body aorta segmentation on CT angiography (CTA) images in normal population, utilizing transfer learning strategy across two CT acquisition protocols of coronary and whole-body aorta.

#### METHODS AND MATERIALS

In order for the whole-body aorta segmentation task to leverage the benefit of coronary CTA (CCTA) with high-resolution features by dedicated acquisition protocol and its relatively lower labeling cost, we enrolled two kinds of CTA scans separately: CT scans of 368 patients who underwent ECG-gated CCTA were included for the pre-training of aortic root and ascending aorta segmentation, and CT scans of 100 patients who underwent ECG-gated aorta CTA using high-pitch helical mode were used for the whole-body aorta segmentation. Non-experts labeled aorta by using a manual toolkit, and an expert radiologist examined its validity before the data were enrolled. The labeled dataset was finally refined by applying preprocessing algorithms of equalization, denoising, interpolation, and normalization (and divided into train and test sets with a ratio of 9:1). The pre-training model adopted U-shape architecture as a backbone network, and is fed with augmented data under the RandAugment strategy of an automated augmentation method. In the whole-body segmentation, we built a Swin-Transformer based encoder-decoder network of which backbone layers are initialized by the pre-trained weights. As for loss function, we used a combo loss that is weighted summation of distribution-based and overlap-based losses.

#### RESULTS

To assess model performance, we introduced the dice score coefficient (DSC) and the averaged Hausdorff distance (AHD) in mm. The pre-trained model achieved high performance with DSC of  $0.969 \pm 0.0223$  and AHD of  $1.80 \pm 1.06$  for aortic root and ascending aorta segmentation. The proposed model for the whole-body aorta segmentation also showed improvement compared to a non-transferred model, so that the metrics were improved from  $0.929 \pm 0.0231$  and  $7.53 \pm 4.76$  to  $0.935 \pm 0.0125$  and  $5.71 \pm 2.35$ . Particularly, we witnessed the knowledge transfer makes the aortic root segmentation in whole-body CTA more accurate, yielding better DSC and AHD from  $0.896 \pm 0.102$  and  $13.1 \pm 8.82$  to  $0.921 \pm 0.0712$  and  $11.2 \pm 9.15$ .

#### CONCLUSION

Our approach is able to improve performance of the whole-body aorta segmentation model to be comparable to radiologists, utilizing the CCTA that has detail anatomic information and lower labeling cost.

#### CLINICAL RELEVANCE/APPLICATION

The proposed model can be built with less effort in data collection, and is practical enough to provide geometric parameters of the whole-body aorta that can be used for further medical applications, such as follow-up of aortic aneurysm or planning for catheter treatment.

Printed on: 02/07/23

## Abstract Archives of the RSNA, 2022

T5A-SPIN-6

### A Deep-learning Method for Intracranial Aneurysm Detection on Computed Tomographic Angiography Images

Tuesday, Nov. 29 12:15PM - 12:45PM Room: Learning Center - IN DPS

#### PURPOSE

Computed tomographic angiography (CTA) is preferred for intracranial aneurysms (IAs) screening. Recently, deep learning-based algorithms show the potential to detect IAs in CTA. However, low diagnostic accuracy and high false-positive results were found in these models. The aim of this study is to develop a deep learning model with improved diagnostic accuracy and validated in real-world data.

#### METHODS AND MATERIALS

The model consisted of a U-Net based segmentation network and a refine network. It differentiated voxels being potential IAs on 3D patches of CTA images. Only the patches that contained positive voxels were proceeded by the refine network, and the possibilities of these patches having IAs were computed. By focusing on the positive patches from the segmentation results, the refine network screened discriminative features and reduced false-positive results. The model was trained and validated using a public dataset with 1338 CTA scans. Then, the model was tested in a dataset of 38 patients with IAs who have both CTA and DSA results. Finally, two radiologists with more than 10 years' experience reviewed the dataset with and without the assistance of AI.

#### RESULTS

For the public dataset, after applying the refine network, the precision on lesion level surged from 45.5% to 69.4% without sacrificing the diagnostic sensitivity (96% vs. 95.2%) (Figure 1-A). On the patient level, the precision increased from 89.5% to 94.8% with a similar diagnostic sensitivity of (97.3% versus 96.7%). For the real-world dataset, with the assistance of AI, radiologists obtained higher diagnostic accuracy compared to without AI (Figure 1-B). In detail, diagnostic sensitivity increased from 64.9% to 91% and precision increased from 83.8% to 97.3%.

#### CONCLUSION

The refine network improved the diagnostic precision for CTA detection of IAs. With the assistance of this model, radiologists improved diagnostic accuracy for IAs.

#### CLINICAL RELEVANCE/APPLICATION

The proposed deep learning method may help make clinical diagnoses of IAs. It may improve the diagnostic accuracy for IAs screening in CTA.

Printed on: 02/07/23

## Abstract Archives of the RSNA, 2022

T5A-SPIR

### Interventional Tuesday Poster Discussions - A

Tuesday, Nov. 29 12:15PM - 12:45PM Room: Learning Center - IR DPS

#### Sub-Events

#### T5A-SPIR-1 Cryoablation of Breast Cancer in Metastatic Patients. A Single Institutional Experience

Participants

Claudio Pusceddu, MD, (*Presenter*) Nothing to Disclose

#### PURPOSE

to evaluate the safety and efficacy of breast cryoablation (CRA) as local therapy for patient with metastatic breast cancer.

#### METHODS AND MATERIALS

thirty-nine breast lesions, mean size 2,1 (range 1 - 6,7 cm) in twenty-nine consecutive patients, mean age 51 (36-81) with core-needle biopsy-proven breast carcinoma and metastases were included in this study. Twenty-three patients had one lesion, 4 patients two lesions, 1 patient three lesions and 1 patient five lesions. Under local anaesthesia and mild conscious sedation, the tumour and surrounding breast tissue were ablated with percutaneous CT-guided CRA. Cryoablation consisted of 2 cycles each of 10 minutes of freezing followed by a 4-min active and 4-min passive thawing phase for each one. Twenty-four patients underwent one CRA session, four patients 2 CRA sessions and one patient underwent 3 CRA sessions.

#### RESULTS

all CRA sessions were successfully completed and all breast tumours were ablated. Morbidity consisted in transient and mild ecchymotic changes and post-procedural oedema seen in ten cases. The therapeutic outcomes were evaluated by contrast-enhanced TC or MRI at 2-, 6-, 12-, and 18-month intervals. The absence of tumour enhancement TC or MR image was considered as indicating complete tumour necrosis. During the mean follow-up of 15 months (6- 28 months) 26 patients had shown complete response to the treatment. Only 3 patients out 29 (10%) showed relapse close to the treated lesion.

#### CONCLUSION

s CRA of metastatic breast cancer is a safe and effective method which allows local control of the disease.

#### CLINICAL RELEVANCE/APPLICATION

This method can effectively be used with good local control of the disease in patients who present with metastases at the beginning of the illness.

#### T5A-SPIR-2 Outcomes of Percutaneous Cholangioscopy Directed Biopsies for Suspicious Biliary Lesions

Participants

Tushar Garg, MD, Baltimore, MD (*Presenter*) Conference Travel, Siemens Healthineers

#### PURPOSE

To evaluate the safety and effectiveness of percutaneous cholangioscopy (PC)-directed biopsies for the evaluation of biliary pathology.

#### METHODS AND MATERIALS

This was an IRB-approved, retrospective study evaluating patients who underwent PC-directed biopsy for biliary pathology from July 2013 and January 2022. Fifteen patients (10 male; mean age 61 [range 48-84] years) underwent 15 PC-directed biopsies for various indications. The technical success was defined as successful access with endoscope and visualization of the biliary system, while procedural success was defined as successful biopsy of the lesion if present.

#### RESULTS

Out of the 15 PC-directed biopsies, 8 (53.3%) were performed to rule out recurrence of malignancy, 3 (20%) to evaluate a mass lesion, 2 (13.3%) to evaluate a filling defect, and 1(6.6%) to evaluate the extent of malignancy. The technical and procedural success rate for the procedure was 100% (15/15), however, there was failure to obtain a clamshell biopsy in one procedure for which successful brush biopsy was performed. Clamshell biopsy (1.6 mm forceps) was done in 86.6% (13/15) of procedures with a median of 3 samples per procedure and brush biopsy (1.72 mm or 3 mm cytology brush) was taken in 6 (40%) procedures with a median of 2.5 samples per procedure. All samples obtained were adequate to make a pathological diagnosis and led to change in patient management. No complications were seen during the procedure and up to 30-days post-procedure.

#### CONCLUSION

s This study supports the safety and effectiveness of PC-directed biopsies in patients with suspicious biliary pathologies.

## CLINICAL RELEVANCE/APPLICATION

PC-directed biopsies can be used for the diagnostic evaluation of patients with biliary lesions which otherwise cannot be evaluated with the help of non-invasive imaging techniques or laboratory evaluation.

### **T5A-SPIR-3 Biodegradable Stents in The Management of Biliary Strictures After Pediatric Split Liver Transplantation**

Participants  
Paolo Marra, Bergamo, Italy (*Presenter*) Nothing to Disclose

#### **PURPOSE**

To present the preliminary experience with biodegradable biliary stents as adjuvant treatment to percutaneous transhepatic cholangiography (PTC), bilioplasty and internal-external biliary drainage (IEBD), in the management of biliary strictures after split liver transplantation (SLT).

#### **METHODS AND MATERIALS**

In addition to the standard treatment, 10 pediatric patients (6 males; median age 8 years) with SLT underwent percutaneous transhepatic implantation of an innovative 10F helical-shaped biodegradable biliary stent, featuring a slow degradation profile of 11 weeks. To our knowledge the device is unique and the first to be CE-marked for the use in this indication. Feasibility of percutaneous implantation and short-term clinical outcomes were assessed.

#### **RESULTS**

Percutaneous stent implantation was technically successful in all 10 patients. In 6 patients a single stent was placed across the anastomotic stricture; in 3 patients two stents were used in parallel to achieve larger sizes. In the first performed case early stent dislodgement and migration in the bowel was demonstrated with X-rays after 72 hours, without sequelae. In the other cases correct stent position and progressive degradation was confirmed by serial X-rays. No complications occurred during a median follow up of 6 months. Two patients presented stricture relapse 8 months after treatment.

#### **CONCLUSION**

Preliminary data suggest that implantation of biodegradable biliary stents is feasible and safe, to be considered in the management of post SLT cholestasis in pediatric patients. This device may prolong biliary drainage and may relieve discomfort of long-term IEBD.

## CLINICAL RELEVANCE/APPLICATION

Pediatric split liver transplantation is burdened by a relatively high rate of biliary complications and biodegradable biliary stents may improve the interventional radiological management.

### **T5A-SPIR-4 Effect of Transarterial Chemoembolization Selectivity Treatment Modality in Hepatocellular Carcinoma Patients over 12 Months Follow Up**

Participants  
Shin Yin Ooi, MBBS, MRCS, (*Presenter*) Nothing to Disclose

#### **PURPOSE**

Transarterial chemoembolization (TACE) is a widely used palliative treatment for liver cancer worldwide. However, it is commonly associated with post embolization syndrome which causes fever, nausea, lethargy and pain. The purpose of this study is to assess the effect of TACE selectivity treatment modality on quality of life in palliative hepatocellular carcinoma patients.

#### **METHODS AND MATERIALS**

This is a prospective study carried out in Vascular and Interventional Radiology Department of Singapore General Hospital from September 2018 till February 2019. Patients who were diagnosed with hepatocellular carcinoma based on American Association for the Study of Liver Diseases (AASLD) imaging criteria or histology were included. The patients' quality of life (QOL) were assessed at pre-treatment, 2 weeks, 4 weeks, 3 months, 6 months and 12 months post-treatment using Functional Assessment of Cancer Therapy-Hepatobiliary (FACT-Hep) questionnaire.

#### **RESULTS**

Twenty-six patients (male:20, female: 6) with primary hepatocellular carcinoma, good ECOG performance status (ECOG 0 or 1) and preserved liver function (84.6% Child A, 15.4% Child B) were enrolled in the study. Majority of the study population has multiple liver tumours (57.7%) compared to single large liver tumour (42.3%). The FACT-G scores were different in selectivity treatment modality group at 6 months (p-value: 0.040) and 12 months (p-value: 0.038). Patients who underwent superselective and ultrasensitive TACE were reported to have better QOL compared to the selective group.

#### **CONCLUSION**

In this prospective study, patients who received superselective and ultrasensitive TACE treatment were reported having statistically significant improvement in QOL composite scores at 6 months and 12 months. Patients without hepatitis have better liver function and QOL scores compared to Hepatitis C patients. The limitation of this study is the small sample size, but the strength is it reflects the actual clinical practice in local population.

## CLINICAL RELEVANCE/APPLICATION

Increase use of superselectivity and ultrasensitivity treatment modality in TACE can improve the quality of life in palliative hepatocellular cancer patients.

### **T5A-SPIR-5 Prediction of Future Remnant Liver Hypertrophy After Portal Vein Embolization**

Participants  
Max Masthoff, MD, Muenster, Germany (*Presenter*) Nothing to Disclose

## PURPOSE

To evaluate the predictive value of baseline computed-tomography (CT) data for future remnant liver (FRL) hypertrophy after portal vein embolization (PVE) prior to major hepatectomy.

## METHODS AND MATERIALS

In this retrospective study all consecutive patients undergoing right-sided PVE with or without liver vein embolization (LVE) between 2018 and 2021 were included. CT-volumetry was performed before and 2-5 weeks after PVE to assess standardized FRL volume (sFRLV). Radiomic features (RF) were extracted from baseline CT after segmenting liver and spleen volume and a standardized region of interest (ROI) from the L1 vertebra, representing bone marrow. For selecting features that allow classification of response (hypertrophy=1.33), a stepwise dimension reduction was performed. Logistic regression models were fitted and selected features were tested for their predictive value.

## RESULTS

A total of n=53 patients (f= 21, m=32; mean age 64±10.5y (range 22-82y)) with primary or secondary liver cancer were included in this study. sFRLV increased significantly from 20.8±7.7% to 30.4±8.7% after PVE (p<0.001), resulting in a mean hypertrophy of FRL by 1.5 ± 0.3 fold. There was no significant difference in hypertrophy after PVE with or without LVE. sFRLV hypertrophy =1.33 was reached in n=35 (66%) patients. Three independent radiomic features, one each liver-, spleen- and bone-associated, differentiated well between responders and non-responders. A logistic regression model including the features MaximumProbability\_liver, Skewness\_spleen and TotalEnergy\_bone revealed highest accuracy (AUC=0.875) for the prediction of response.

## CONCLUSION

s This proof-of-concept study provides first evidence on a potential predictive value of baseline CT imaging data for FRL hypertrophy after portal vein embolization.

## CLINICAL RELEVANCE/APPLICATION

Baseline imaging data may allow for early prediction of future remnant liver hypertrophy after portal vein embolization and may thus enable individualized patient selection and avoidance of ineffective interventions to optimize treatment strategies in liver cancer.

## T5A-SPiR-6 Reduction in 30 Day Readmissions by Initial Insertion of Larger Bore Biliary Drainage Catheters

Participants

Muhammad Malik, MD, Boston, MA (*Presenter*) Nothing to Disclose

## PURPOSE

Prior data has shown that 30-day readmissions after biliary drainage (PTBD) is common (46%) when initial drainage is performed with 8 Fr drains. The current study evaluated for differences in readmissions when initial drainage was performed with a larger bore drainage catheter.

## METHODS AND MATERIALS

In an IRB approved, retrospective, single center study all PTBD procedures between 01-2014 to 11-2021 (n=3015) were analyzed. Procedures through pre-existing access (n=2430), multiple initial access biliary procedures (n=211), and patients dying during the index admission (n=44) were excluded. For each patient, the first 30-day readmission was used to determine cause of readmission. Readmissions were categorized as planned or unplanned, and unplanned causes as related to or unrelated to interventional radiology.

## RESULTS

Patients (n=330, age: 66 (IQR: 26-98) years; 52% men) fit criteria and underwent 330 PTBD. PTBD was performed for malignant obstruction in 161/330 (48%), benign obstruction in 136/330 (41%), and biliary leakage in 33/330 (10%). Catheters were placed in the right duct (170/330 [52%]), in the left duct (79/330 [24%]), bilaterally (65/330 [20%]), trilaterally (13/330 [4%]) and via trans-cholecystic approach (3/330 [1%]). Mean length of index hospitalization was 14±15 days (1-115). After discharge, 30-day readmission was 118/330 (36%) and 30-day death was 29/330 (9%). Of all readmissions, 25/118 (21%) were planned and 93/118 (79%) were unplanned. A majority of unplanned readmissions (65/93; 70%) were related to interventional radiology. Overall, initial access used 8 Fr catheters in 79/330 (24%) and gt;8 Fr catheters in 251/330 (76%) procedures. In years when 8 Fr catheters were more commonly used (25/38; 66% vs 13/38; 34% for gt;8 Fr) the readmission rate was 20/38 (53%). In years when gt;8 Fr were used more commonly (223/292; 76% vs 54/292; 18% for 8 Fr) the readmission rates was 98/292 (33%). 30-day readmission was more common in 8 Fr years compared to gt;8 Fr years (53% vs. 33%, p=0.02).

## CONCLUSION

s Increased usage of gt;8 Fr initial PTBD catheters for initial access was associated with lower 30-day readmission rates compared to 8 Fr initial PTBD catheters.

## CLINICAL RELEVANCE/APPLICATION

Thirty day readmissions after percutaneous biliary drainage procedures can be reduced by using larger bore (gt;8 Fr) catheters during initial access.

## T5A-SPiR-7 Complications in 2290 Percutaneous Biliary Procedures: Single Institution Experience

Participants

Ahsun Riaz, MD, Chicago, IL (*Presenter*) Consultant, Boston Scientific Corporation

## PURPOSE

Examine complication rates of percutaneous biliary interventions performed by Interventional Radiology (IR) in 452 patients.

## METHODS AND MATERIALS

We analysed retrospective data from 452 consecutive patients that underwent 2290 percutaneous biliary procedures at our center

from January 2010 to April 2020. The procedures included drain placement/exchange, cholangioplasty, and stent placement. Data regarding peri-catheter leak, catheter malposition, catheter occlusion, bleeding, perforation, sepsis requiring intensive care treatment (ICU), sepsis not requiring ICU treatment and death were collected.

## RESULTS

Complications were observed in 707 procedures (31%), of which 75% were minor complications; peri-catheter leak (47%), catheter occlusion (15%) and drain malposition (13%). The mean duration of drain was 79 days (range:1-2404 days). The mean number of exchanges per drain was 3.9 (range: 1-32). On sub-stratification analysis, complications occurred more frequently in cases with malignant indications; 22% vs 9.7% ( $p<.00001$ ). Intraprocedural bleeding was observed in 7 cases and post-procedural bleeding secondary to pseudoaneurysm formation in 30; 1% and 4.2% of all complications, respectively. 63% of all bleeds were managed by embolization. Sepsis occurred in 5.4% of cases, of which 1.1% required ICU treatment. Two percent of patients undergoing biliary drainage for a malignant indication developed sepsis compared to one in benign. Bowel perforation was a rare observation noted in only 2 cases. Death within 30 days occurred in 4 patients; three of these patients had a malignant etiology.

## CONCLUSION

Over 10 years, an overall complication rate of 31% was observed in 2290 consecutive biliary procedures. Most were minor with peri-catheter leak, drain malposition, and catheter occlusion accounting for 47%, 13% and 15% of complications, respectively. Sepsis was the most frequent major complication occurring in 5.4% of cases, followed by bleeding in 5.2%. IR should make efforts to internalize drains as soon as clinically possible to minimize minor complications.

## CLINICAL RELEVANCE/APPLICATION

Percutaneous management of biliary pathologies is routinely performed by Interventional Radiology. The majority of post-procedural complications are minor which can be decreased by an effort to internalize biliary drains as soon as clinically possible.

## T5A-SPIR-9 Development of A Three-Dimensional Multi-Modal Perfusion-Thermal Electrode System for Complete Tumor Eradication

Participants

Hui Zheng, MD, (*Presenter*) Nothing to Disclose

## PURPOSE

To develop a novel three-dimensional (3D) multi-modal perfusion-thermal electrode system for complete eradication of medium-to-large malignancies.

## METHODS AND MATERIALS

This study included five steps: (i) design of the new system; (ii) production of the new system; (iii) ex-vivo evaluation of the perfusion-thermal functions; (iv) mathematic simulation to confirm its accurate temperature profiles; and (iv) in-vivo technical validation using living animal models with orthotopic liver tumors.

## RESULTS

In ex-vivo experiments, gross pathology and optical imaging demonstrated the successful distribution/deposition of the motexafin gadolinium (MGd) at a sphere shape through the new electrode, with a temperature gradient from the electrode core at 80° to its periphery at 42°. An excellent consistence of temperature profiles at varying spots, from center to periphery of the liver tumor, was found between the mathematic simulation and actual animal tumor models (Pearson coefficient=0.977). For in-vivo technical validation, indocyanine green (ICG) was directly delivered into the peritumoral zones while simultaneous generation of central tumoral lethal radiofrequency (RF) heat (> 60°) with peritumoral sublethal RF hyperthermia (< 60°). Both optical imaging and fluorescent microscopy confirmed successful peritumoral ICG distribution/deposition with increased heat shock protein 70 expression.

## CONCLUSION

This new 3D perfusion-thermal electrode system enabled simultaneously delivery of agents and RF hyperthermia into the difficult-to-treat peritumoral zones, which may open the new avenues to solve the critical clinical problems, the incomplete eradication of medium-to-larger tumors with current image-guided percutaneous thermal ablation techniques.

## CLINICAL RELEVANCE/APPLICATION

This study has established ground works for developing a new 3D perfusion-thermal electrode system, to solve the clinical problem on incomplete eradication of medium-to-larger tumors with current thermal ablations.

Printed on: 02/07/23

## Abstract Archives of the RSNA, 2022

T5A-SPIR-1

### Cryoablation of Breast Cancer in Metastatic Patients. A Single Institutional Experience

Tuesday, Nov. 29 12:15PM - 12:45PM Room: Learning Center - IR DPS

#### Participants

Claudio Pusceddu, MD, (*Presenter*) Nothing to Disclose

#### PURPOSE

to evaluate the safety and efficacy of breast cryoablation (CRA) as local therapy for patient with metastatic breast cancer.

#### METHODS AND MATERIALS

thirty-nine breast lesions, mean size 2,1 (range 1 - 6,7 cm) in twenty-nine consecutive patients, mean age 51 (36-81) with core-needle biopsy-proven breast carcinoma and metastases were included in this study. Twenty-three patients had one lesion, 4 patients two lesions, 1 patient three lesions and 1 patient five lesions. Under local anaesthesia and mild conscious sedation, the tumour and surrounding breast tissue were ablated with percutaneous CT-guided CRA. Cryoablation consisted of 2 cycles each of 10 minutes of freezing followed by a 4-min active and 4-min passive thawing phase for each one. Twenty-four patients underwent one CRA session, four patients 2 CRA sessions and one patient underwent 3 CRA sessions.

#### RESULTS

all CRA sessions were successfully completed and all breast tumours were ablated. Morbidity consisted in transient and mild ecchymotic changes and post-procedural oedema seen in ten cases. The therapeutic outcomes were evaluated by contrast-enhanced TC or MRI at 2-, 6-, 12-, and 18-month intervals. The absence of tumour enhancement TC or MR image was considered as indicating complete tumour necrosis. During the mean follow-up of 15 months (6- 28 months) 26 patients had shown complete response to the treatment. Only 3 patients out 29 (10%) showed relapse close to the treated lesion.

#### CONCLUSION

s CRA of metastatic breast cancer is a safe and effective method which allows local control of the disease.

#### CLINICAL RELEVANCE/APPLICATION

This method can effectively be used with good local control of the disease in patients who present with metastases at the beginning of the illness.

Printed on: 02/07/23

## Abstract Archives of the RSNA, 2022

T5A-SPIR-2

### Outcomes of Percutaneous Cholangioscopy Directed Biopsies for Suspicious Biliary Lesions

Tuesday, Nov. 29 12:15PM - 12:45PM Room: Learning Center - IR DPS

#### Participants

Tushar Garg, MD, Baltimore, MD (*Presenter*) Conference Travel, Siemens Healthineers

#### PURPOSE

To evaluate the safety and effectiveness of percutaneous cholangioscopy (PC)-directed biopsies for the evaluation of biliary pathology.

#### METHODS AND MATERIALS

This was an IRB-approved, retrospective study evaluating patients who underwent PC-directed biopsy for biliary pathology from July 2013 and January 2022. Fifteen patients (10 male; mean age 61 [range 48-84] years) underwent 15 PC-directed biopsies for various indications. The technical success was defined as successful access with endoscope and visualization of the biliary system, while procedural success was defined as successful biopsy of the lesion if present.

#### RESULTS

Out of the 15 PC-directed biopsies, 8 (53.3%) were performed to rule out recurrence of malignancy, 3 (20%) to evaluate a mass lesion, 2 (13.3%) to evaluate a filling defect, and 1(6.6%) to evaluate the extent of malignancy. The technical and procedural success rate for the procedure was 100% (15/15), however, there was failure to obtain a clamshell biopsy in one procedure for which successful brush biopsy was performed. Clamshell biopsy (1.6 mm forceps) was done in 86.6% (13/15) of procedures with a median of 3 samples per procedure and brush biopsy (1.72 mm or 3 mm cytology brush) was taken in 6 (40%) procedures with a median of 2.5 samples per procedure. All samples obtained were adequate to make a pathological diagnosis and led to change in patient management. No complications were seen during the procedure and up to 30-days post-procedure.

#### CONCLUSION

s This study supports the safety and effectiveness of PC-directed biopsies in patients with suspicious biliary pathologies.

#### CLINICAL RELEVANCE/APPLICATION

PC-directed biopsies can be used for the diagnostic evaluation of patients with biliary lesions which otherwise cannot be evaluated with the help of non-invasive imaging techniques or laboratory evaluation.

Printed on: 02/07/23

## Abstract Archives of the RSNA, 2022

T5A-SPIR-3

### Biodegradable Stents in The Management of Biliary Strictures After Pediatric Split Liver Transplantation

Tuesday, Nov. 29 12:15PM - 12:45PM Room: Learning Center - IR DPS

#### Participants

Paolo Marra, Bergamo, Italy (*Presenter*) Nothing to Disclose

#### PURPOSE

To present the preliminary experience with biodegradable biliary stents as adjuvant treatment to percutaneous transhepatic cholangiography (PTC), bilioplasty and internal-external biliary drainage (IEBD), in the management of biliary strictures after split liver transplantation (SLT).

#### METHODS AND MATERIALS

In addition to the standard treatment, 10 pediatric patients (6 males; median age 8 years) with SLT underwent percutaneous transhepatic implantation of an innovative 10F helical-shaped biodegradable biliary stent, featuring a slow degradation profile of 11 weeks. To our knowledge the device is unique and the first to be CE-marked for the use in this indication. Feasibility of percutaneous implantation and short-term clinical outcomes were assessed.

#### RESULTS

Percutaneous stent implantation was technically successful in all 10 patients. In 6 patients a single stent was placed across the anastomotic stricture; in 3 patients two stents were used in parallel to achieve larger sizes. In the first performed case early stent dislodgement and migration in the bowel was demonstrated with X-rays after 72 hours, without sequelae. In the other cases correct stent position and progressive degradation was confirmed by serial X-rays. No complications occurred during a median follow up of 6 months. Two patients presented stricture relapse 8 months after treatment.

#### CONCLUSION

s Preliminary data suggest that implantation of biodegradable biliary stents is feasible and safe, to be considered in the management of post SLT cholestasis in pediatric patients. This device may prolong biliary drainage and may relieve discomfort of long-term IEBD.

#### CLINICAL RELEVANCE/APPLICATION

Pediatric split liver transplantation is burdened by a relatively high rate of biliary complications and biodegradable biliary stents may improve the interventional radiological management.

Printed on: 02/07/23

## Abstract Archives of the RSNA, 2022

T5A-SPIR-4

### Effect of Transarterial Chemoembolization Selectivity Treatment Modality in Hepatocellular Carcinoma Patients over 12 Months Follow Up

Tuesday, Nov. 29 12:15PM - 12:45PM Room: Learning Center - IR DPS

#### Participants

Shin Yin Ooi, MBBS, MRCS, (*Presenter*) Nothing to Disclose

#### PURPOSE

Transarterial chemoembolization (TACE) is a widely used palliative treatment for liver cancer worldwide. However, it is commonly associated with post embolization syndrome which causes fever, nausea, lethargy and pain. The purpose of this study is to assess the effect of TACE selectivity treatment modality on quality of life in palliative hepatocellular carcinoma patients.

#### METHODS AND MATERIALS

This is a prospective study carried out in Vascular and Interventional Radiology Department of Singapore General Hospital from September 2018 till February 2019. Patients who were diagnosed with hepatocellular carcinoma based on American Association for the Study of Liver Diseases (AASLD) imaging criteria or histology were included. The patients' quality of life (QOL) were assessed at pre-treatment, 2 weeks, 4 weeks, 3 months, 6 months and 12 months post-treatment using Functional Assessment of Cancer Therapy-Hepatobiliary (FACT-Hep) questionnaire.

#### RESULTS

Twenty-six patients (male:20, female: 6) with primary hepatocellular carcinoma, good ECOG performance status (ECOG 0 or 1) and preserved liver function (84.6% Child A, 15.4% Child B) were enrolled in the study. Majority of the study population has multiple liver tumours (57.7%) compared to single large liver tumour (42.3%). The FACT-G scores were different in selectivity treatment modality group at 6 months (p-value: 0.040) and 12 months (p-value: 0.038). Patients who underwent superselective and ultrasensitive TACE were reported to have better QOL compared to the selective group.

#### CONCLUSION

In this prospective study, patients who received superselective and ultrasensitive TACE treatment were reported having statistically significant improvement in QOL composite scores at 6 months and 12 months. Patients without hepatitis have better liver function and QOL scores compared to Hepatitis C patients. The limitation of this study is the small sample size, but the strength is it reflects the actual clinical practice in local population.

#### CLINICAL RELEVANCE/APPLICATION

Increase use of superselectivity and ultrasensitivity treatment modality in TACE can improve the quality of life in palliative hepatocellular cancer patients.

Printed on: 02/07/23

## Abstract Archives of the RSNA, 2022

T5A-SPIR-5

### Prediction of Future Remnant Liver Hypertrophy After Portal Vein Embolization

Tuesday, Nov. 29 12:15PM - 12:45PM Room: Learning Center - IR DPS

#### Participants

Max Masthoff, MD, Muenster, Germany (*Presenter*) Nothing to Disclose

#### PURPOSE

To evaluate the predictive value of baseline computed-tomography (CT) data for future remnant liver (FRL) hypertrophy after portal vein embolization (PVE) prior to major hepatectomy.

#### METHODS AND MATERIALS

In this retrospective study all consecutive patients undergoing right-sided PVE with or without liver vein embolization (LVE) between 2018 and 2021 were included. CT-volumetry was performed before and 2-5 weeks after PVE to assess standardized FRL volume (sFRLV). Radiomic features (RF) were extracted from baseline CT after segmenting liver and spleen volume and a standardized region of interest (ROI) from the L1 vertebra, representing bone marrow. For selecting features that allow classification of response (hypertrophy=1.33), a stepwise dimension reduction was performed. Logistic regression models were fitted and selected features were tested for their predictive value.

#### RESULTS

A total of n=53 patients (f= 21, m=32; mean age 64±10.5y (range 22-82y)) with primary or secondary liver cancer were included in this study. sFRLV increased significantly from 20.8±7.7% to 30.4±8.7% after PVE (p<0.001), resulting in a mean hypertrophy of FRL by 1.5 ± 0.3 fold. There was no significant difference in hypertrophy after PVE with or without LVE. sFRLV hypertrophy =1.33 was reached in n=35 (66%) patients. Three independent radiomic features, one each liver-, spleen- and bone-associated, differentiated well between responders and non-responders. A logistic regression model including the features MaximumProbability\_liver, Skewness\_spleen and TotalEnergy\_bone revealed highest accuracy (AUC=0.875) for the prediction of response.

#### CONCLUSION

This proof-of-concept study provides first evidence on a potential predictive value of baseline CT imaging data for FRL hypertrophy after portal vein embolization.

#### CLINICAL RELEVANCE/APPLICATION

Baseline imaging data may allow for early prediction of future remnant liver hypertrophy after portal vein embolization and may thus enable individualized patient selection and avoidance of ineffective interventions to optimize treatment strategies in liver cancer.

Printed on: 02/07/23

## Abstract Archives of the RSNA, 2022

T5A-SPIR-6

### Reduction in 30 Day Readmissions by Initial Insertion of Larger Bore Biliary Drainage Catheters

Tuesday, Nov. 29 12:15PM - 12:45PM Room: Learning Center - IR DPS

#### Participants

Muhammad Malik, MD, Boston, MA (*Presenter*) Nothing to Disclose

#### PURPOSE

Prior data has shown that 30-day readmissions after biliary drainage (PTBD) is common (46%) when initial drainage is performed with 8 Fr drains. The current study evaluated for differences in readmissions when initial drainage was performed with a larger bore drainage catheter.

#### METHODS AND MATERIALS

In an IRB approved, retrospective, single center study all PTBD procedures between 01-2014 to 11-2021 (n=3015) were analyzed. Procedures through pre-existing access (n=2430), multiple initial access biliary procedures (n=211), and patients dying during the index admission (n=44) were excluded. For each patient, the first 30-day readmission was used to determine cause of readmission. Readmissions were categorized as planned or unplanned, and unplanned causes as related to or unrelated to interventional radiology.

#### RESULTS

Patients (n=330, age: 66 (IQR: 26-98) years; 52% men) fit criteria and underwent 330 PTBD. PTBD was performed for malignant obstruction in 161/330 (48%), benign obstruction in 136/330 (41%), and biliary leakage in 33/330 (10%). Catheters were placed in the right duct (170/330 [52%]), in the left duct (79/330 [24%]), bilaterally (65/330 [20%]), trilaterally (13/330 [4%]) and via trans-cholecystic approach (3/330 [1%]). Mean length of index hospitalization was 14±15 days (1-115). After discharge, 30-day readmission was 118/330 (36%) and 30-day death was 29/330 (9%). Of all readmissions, 25/118 (21%) were planned and 93/118 (79%) were unplanned. A majority of unplanned readmissions (65/93; 70%) were related to interventional radiology. Overall, initial access used 8 Fr catheters in 79/330 (24%) and gt;8 Fr catheters in 251/330 (76%) procedures. In years when 8 Fr catheters were more commonly used (25/38; 66% vs 13/38; 34% for gt;8 Fr) the readmission rate was 20/38 (53%). In years when gt;8 Fr were used more commonly (223/292; 76% vs 54/292; 18% for 8 Fr) the readmission rates was 98/292 (33%). 30-day readmission was more common in 8 Fr years compared to gt;8 Fr years (53% vs. 33%, p=0.02).

#### CONCLUSION

Increased usage of gt;8 Fr initial PTBD catheters for initial access was associated with lower 30-day readmission rates compared to 8 Fr initial PTBD catheters.

#### CLINICAL RELEVANCE/APPLICATION

Thirty day readmissions after percutaneous biliary drainage procedures can be reduced by using larger bore (gt;8 Fr) catheters during initial access.

Printed on: 02/07/23



## Abstract Archives of the RSNA, 2022

T5A-SPIR-7

### Complications in 2290 Percutaneous Biliary Procedures: Single Institution Experience

Tuesday, Nov. 29 12:15PM - 12:45PM Room: Learning Center - IR DPS

#### Participants

Ahsun Riaz, MD, Chicago, IL (*Presenter*) Consultant, Boston Scientific Corporation

#### PURPOSE

Examine complication rates of percutaneous biliary interventions performed by Interventional Radiology (IR) in 452 patients.

#### METHODS AND MATERIALS

We analysed retrospective data from 452 consecutive patients that underwent 2290 percutaneous biliary procedures at our center from January 2010 to April 2020. The procedures included drain placement/exchange, cholangioplasty, and stent placement. Data regarding peri-catheter leak, catheter malposition, catheter occlusion, bleeding, perforation, sepsis requiring intensive care treatment (ICU), sepsis not requiring ICU treatment and death were collected.

#### RESULTS

Complications were observed in 707 procedures (31%), of which 75% were minor complications; peri-catheter leak (47%), catheter occlusion (15%) and drain malposition (13%). The mean duration of drain was 79 days (range:1-2404 days). The mean number of exchanges per drain was 3.9 (range: 1-32). On sub-stratification analysis, complications occurred more frequently in cases with malignant indications; 22% vs 9.7% ( $p<.00001$ ). Intraprocedural bleeding was observed in 7 cases and post-procedural bleeding secondary to pseudoaneurysm formation in 30; 1% and 4.2% of all complications, respectively. 63% of all bleeds were managed by embolization. Sepsis occurred in 5.4% of cases, of which 1.1% required ICU treatment. Two percent of patients undergoing biliary drainage for a malignant indication developed sepsis compared to one in benign. Bowel perforation was a rare observation noted in only 2 cases. Death within 30 days occurred in 4 patients; three of these patients had a malignant etiology.

#### CONCLUSION

Over 10 years, an overall complication rate of 31% was observed in 2290 consecutive biliary procedures. Most were minor with peri-catheter leak, drain malposition, and catheter occlusion accounting for 47%, 13% and 15% of complications, respectively. Sepsis was the most frequent major complication occurring in 5.4% of cases, followed by bleeding in 5.2%. IR should make efforts to internalize drains as soon as clinically possible to minimize minor complications.

#### CLINICAL RELEVANCE/APPLICATION

Percutaneous management of biliary pathologies is routinely performed by Interventional Radiology. The majority of post-procedural complications are minor which can be decreased by an effort to internalize biliary drains as soon as clinically possible.

Printed on: 02/07/23

## Abstract Archives of the RSNA, 2022

T5A-SPIR-9

### Development of A Three-Dimensional Multi-Modal Perfusion-Thermal Electrode System for Complete Tumor Eradication

Tuesday, Nov. 29 12:15PM - 12:45PM Room: Learning Center - IR DPS

#### Participants

Hui Zheng, MD, (*Presenter*) Nothing to Disclose

#### PURPOSE

To develop a novel three-dimensional (3D) multi-modal perfusion-thermal electrode system for complete eradication of medium-to-large malignancies.

#### METHODS AND MATERIALS

This study included five steps: (i) design of the new system; (ii) production of the new system; (iii) ex-vivo evaluation of the perfusion-thermal functions; (iv) mathematic simulation to confirm its accurate temperature profiles; and (iv) in-vivo technical validation using living animal models with orthotopic liver tumors.

#### RESULTS

In ex-vivo experiments, gross pathology and optical imaging demonstrated the successful distribution/deposition of the motexafin gadolinium (MGd) at a sphere shape through the new electrode, with a temperature gradient from the electrode core at 80° to its periphery at 42°. An excellent consistence of temperature profiles at varying spots, from center to periphery of the liver tumor, was found between the mathematic simulation and actual animal tumor models (Pearson coefficient=0.977). For in-vivo technical validation, indocyanine green (ICG) was directly delivered into the peritumoral zones while simultaneous generation of central tumoral lethal radiofrequency (RF) heat (> 60°) with peritumoral sublethal RF hyperthermia (< 60°). Both optical imaging and fluorescent microscopy confirmed successful peritumoral ICG distribution/deposition with increased heat shock protein 70 expression.

#### CONCLUSION

s This new 3D perfusion-thermal electrode system enabled simultaneously delivery of agents and RF hyperthermia into the difficult-to-treat peritumoral zones, which may open the new avenues to solve the critical clinical problems, the incomplete eradication of medium-to-larger tumors with current image-guided percutaneous thermal ablation techniques.

#### CLINICAL RELEVANCE/APPLICATION

This study has established ground works for developing a new 3D perfusion-thermal electrode system, to solve the clinical problem on incomplete eradication of medium-to-larger tumors with current thermal ablations.

Printed on: 02/07/23

## Abstract Archives of the RSNA, 2022

T5A-SPMK

### Musculoskeletal Tuesday Poster Discussions - A

Tuesday, Nov. 29 12:15PM - 12:45PM Room: Learning Center - MK DPS

#### Sub-Events

#### **T5A-SPMK-1 Comparison of Isotropic MAVRIC-SL and Conventional MAVRIC-SL in the Evaluation of Symptomatic Hip Arthroplasties at 3T**

Participants

Kathryn Stevens, MBBS, FRCR, Stanford, CA (*Presenter*) Nothing to Disclose

#### **PURPOSE**

To compare isotropic MAVRIC-SL with conventional MAVRIC-SL in patients with symptomatic hip implants at 3T.

#### **METHODS AND MATERIALS**

39 symptomatic patients with 59 total hip implants were imaged on a 3T MRI scanner including conventional proton density-weighted coronal MAVRIC-SL (6m58s scan time, 1.25x1.6x4mm resolution) and isotropic coronal MAVRIC-SL (4m10s scan time, 1.6x1.6x1.6mm resolution) employing robust principal component analysis for accelerated scanning. Two MSK radiologists graded overall image quality on acquired coronal images, as well as reformatted axial and sagittal images, overall metal artifact, and visualization around the femoral and acetabular components using a 3-point scale (3: diagnostic, 2: moderately diagnostic, 1: non-diagnostic). Images were examined for different pathologies, including effusion, synovitis, osteolysis, loosening, pseudotumor, fracture, gluteal tendon abnormalities, with degree of confidence. Reformatted images were evaluated to see if they lead to a change in diagnostic confidence or diagnosis of new pathology that could potentially contribute to hip pain.

#### **RESULTS**

No significant difference was demonstrated between coronal MAVRIC-SL and isotropic MAVRIC-SL for overall image quality, metal artifact suppression, or visualization around the acetabular or femoral components, but image quality on axial and sagittal reformats was significantly higher with the isotropic sequence ( $p < 0.01$ ). Interobserver agreement for was substantial ( $k = 0.798$ ). Isotropic MAVRIC-SL achieved a comparable degree of diagnostic confidence for most types of pathology ( $p < 0.05$ ). Inclusion of axial and sagittal reformats changed the diagnosis or increased diagnostic confidence in 7.6% cases on conventional imaging, compared to 42.4% on isotropic imaging ( $p < 0.01$ ). A new diagnosis based on reformatted images that may contribute to hip symptoms was made in 22.9% cases on conventional imaging, compared to 50.8% on isotropic imaging ( $p < 0.01$ ).

#### **CONCLUSION**

s Coronal isotropic and conventional MAVRIC-SL images were comparable, with similar degrees of diagnostic confidence for most types of pathology. However, image quality of isotropic reformatted images was significantly better and revealed abnormalities that were either obscured or not as well seen in the coronal acquisition plane, as well as other findings that could contribute to hip pain.

#### **CLINICAL RELEVANCE/APPLICATION**

This fast RPCA MAVRIC-SL isotropic acquisition shows promise for improved visualization of hardware complications with diagnostically acceptable image quality and has the potential to significantly decrease overall clinical scan time, both by eliminating the need to scan in multiple planes and through use of accelerated scanning.

#### **T5A-SPMK-2 Hip Impingement in Flexion Did Not Involve Cam-deformity and Is Located on Anterior-inferior Proximal Femur in Cam and Pincer FAI Patients with Decreased Femoral Version**

Participants

Till Lerch, MD, PhD, Bern, Switzerland (*Presenter*) Nothing to Disclose

#### **PURPOSE**

Symptomatic FAI patients have limitations in daily activities and sports and report exacerbation of hip pain in deep flexion or while sitting. But exact impingement location in deep flexion is unknown. Hypothesis/Purpose We aimed to investigate impingement-free maximal flexion, location of hip impingement and if cam-deformity causes impingement in flexion in symptomatic cam and pincer FAI patients with decreased femoral version(FV).

#### **METHODS AND MATERIALS**

An IRB-approved retrospective study involving 24 patients (37 hips) with decreased femoral version( $FV < 5^\circ$ ) was performed. All FAI patients were symptomatic(mean age  $33 \pm 10$  years) and had anterior hip/groin pain and a positive anterior-impingement-test. Subgroups of patients with cam-type deformity(16 hips), patients with pincer-type deformity(7 hips) and patients with mixed-type FAI(6 hips) were compared. All patients underwent pelvic CT scans and were evaluated with individual CT-based 3D-models and validated software for patient-specific impingement-simulation using equidistant-method.

#### **RESULTS**

(1) Mean impingement-free flexion of patients with pincer-type FAI ( $113 \pm 10^\circ$ ) and patients with mixed-type FAI ( $114 \pm 11^\circ$ ) was significantly ( $p < 0.001$ ) lower compared to patients with cam-type FAI ( $122 \pm 13^\circ$ ). (2) Patients with mixed-type FAI (67%) and patients with pincer-type FAI (57%) had significantly ( $p < 0.001$ ) increased prevalence of intraarticular impingement compared to cam-type FAI (33%) in  $115^\circ$  of flexion. Patients with pincer-type FAI (57%) had significantly ( $p < 0.001$ ) higher prevalence of extraarticular subspine hip impingement compared to cam-type FAI (22%) in  $125^\circ$  of flexion. (3) Femoral impingement in maximal flexion was located anterior-inferior at 4 o'clock (71% of pincer-type FAI, 50% of mixed-type FAI) and 5 o'clock (61% of cam-type FAI). Cam-deformity was not involved in maximal flexion (0% 1-3 o'clock). Acetabular impingement in maximal flexion was located anterior-superior (2 o'clock) of all patients.

## CONCLUSION

Femoral impingement conflict in flexion was located anterior-inferior and did not involve the cam-deformity. This is different compared to previous studies that reported anterior-superior femoral impingement location during the anterior-impingement-test.

## CLINICAL RELEVANCE/APPLICATION

This could be important for FAI patients to avoid exacerbation of hip pain in deep flexion. This could be important for radiologists to better understand FAI and the cam-deformity.

## T5A-SPMK-3 3D Printed Model and Guide for Decompression and Stem-Cell Treatment of Avascular Necrosis of the Femoral Head

Participants

Alborz Feizi, New Haven, CT (*Presenter*) Nothing to Disclose

## PURPOSE

Avascular necrosis (AVN) is a condition characterized by bone tissue necrosis as a result of poor blood supply. The disease progresses in stages, and the treatment depends on the stage and location of AVN. One of the most common locations of AVN is at the femoral head. During the early stages of the disease, treatment options such as core decompression and cellular therapies can diminish further necrosis and avoid hip collapse. However, current treatment protocols lack the means to accurately guide a therapeutic device to the precise location of necrotic tissue. Furthermore, existing modes of treatment delivery can be complicated by postoperative infection and fracture. Here, we present a technique and device that has the potential to improve therapy outcomes by precisely targeting lesions, and placing stem cells in the optimal environment to induce revascularization.

## METHODS AND MATERIALS

A foam cortical shell femur was scanned using computed tomography (CT) and segmented in Synopsys Simpleware ScanIP software to create a 3D femur model. From the model, a femur-specific drill-guide was designed based on a preoperatively planned ideal drill trajectory for the placement of the decompression device and for the delivery of stem-cells to the core of the necrotic region. A delivery cannula and a needle were drilled into the foam cortical shell femur using the 3D-printed drill-guide. After placement of the delivery cannula and needle using the custom guide, a second CT scan was performed to evaluate the accuracy and precision of the 3D-printed guide in delivering treatment to the ideal drill tip location.

## RESULTS

In our model, the post-drilling 3D reconstruction showed a maximum of 2-degree deviation from the theoretical model. The needle tip was also between 0.257 and 2.149 mm away from the theoretical needle tip.

## CONCLUSION

3D printed devices have the potential to improve positioning of treatment instruments. Consequently, this technique can allow for more precise localized decompression and stem-cell treatment of necrotic tissue.

## CLINICAL RELEVANCE/APPLICATION

Approximately 50% percent of patients with femoral AVN experience hip collapse. This procedure has the potential to improve outcomes of decompression and stem-cell treatment and reduce the need for hip replacement surgery.

Printed on: 02/07/23

## Abstract Archives of the RSNA, 2022

T5A-SPMK-1

### Comparison of Isotropic MAVRIC-SL and Conventional MAVRIC-SL in the Evaluation of Symptomatic Hip Arthroplasties at 3T

Tuesday, Nov. 29 12:15PM - 12:45PM Room: Learning Center - MK DPS

#### Participants

Kathryn Stevens, MBBS, FRCR, Stanford, CA (*Presenter*) Nothing to Disclose

#### PURPOSE

To compare isotropic MAVRIC-SL with conventional MAVRIC-SL in patients with symptomatic hip implants at 3T.

#### METHODS AND MATERIALS

39 symptomatic patients with 59 total hip implants were imaged on a 3T MRI scanner including conventional proton density-weighted coronal MAVRIC-SL (6m58s scan time, 1.25x1.6x4mm resolution) and isotropic coronal MAVRIC-SL (4m10s scan time, 1.6x1.6x1.6mm resolution) employing robust principal component analysis for accelerated scanning. Two MSK radiologists graded overall image quality on acquired coronal images, as well as reformatted axial and sagittal images, overall metal artifact, and visualization around the femoral and acetabular components using a 3-point scale (3: diagnostic, 2: moderately diagnostic, 1: non-diagnostic). Images were examined for different pathologies, including effusion, synovitis, osteolysis, loosening, pseudotumor, fracture, gluteal tendon abnormalities, with degree of confidence. Reformatted images were evaluated to see if they lead to a change in diagnostic confidence or diagnosis of new pathology that could potentially contribute to hip pain.

#### RESULTS

No significant difference was demonstrated between coronal MAVRIC-SL and isotropic MAVRIC-SL for overall image quality, metal artifact suppression, or visualization around the acetabular or femoral components, but image quality on axial and sagittal reformats was significantly higher with the isotropic sequence ( $p < 0.01$ ). Interobserver agreement for was substantial ( $k = 0.798$ ). Isotropic MAVRIC-SL achieved a comparable degree of diagnostic confidence for most types of pathology ( $p < 0.05$ ). Inclusion of axial and sagittal reformats changed the diagnosis or increased diagnostic confidence in 7.6% cases on conventional imaging, compared to 42.4% on isotropic imaging ( $p < 0.01$ ). A new diagnosis based on reformatted images that may contribute to hip symptoms was made in 22.9% cases on conventional imaging, compared to 50.8% on isotropic imaging ( $p < 0.01$ ).

#### CONCLUSION

s Coronal isotropic and conventional MAVRIC-SL images were comparable, with similar degrees of diagnostic confidence for most types of pathology. However, image quality of isotropic reformatted images was significantly better and revealed abnormalities that were either obscured or not as well seen in the coronal acquisition plane, as well as other findings that could contribute to hip pain.

#### CLINICAL RELEVANCE/APPLICATION

This fast RPCA MAVRIC-SL isotropic acquisition shows promise for improved visualization of hardware complications with diagnostically acceptable image quality and has the potential to significantly decrease overall clinical scan time, both by eliminating the need to scan in multiple planes and through use of accelerated scanning.

Printed on: 02/07/23

## Abstract Archives of the RSNA, 2022

T5A-SPMK-2

### **Hip Impingement in Flexion Did Not Involve Cam-deformity and Is Located on Anterior-inferior Proximal Femur in Cam and Pincer FAI Patients with Decreased Femoral Version**

Tuesday, Nov. 29 12:15PM - 12:45PM Room: Learning Center - MK DPS

#### **Participants**

Till Lerch, MD, PhD, Bern, Switzerland (*Presenter*) Nothing to Disclose

#### **PURPOSE**

Symptomatic FAI patients have limitations in daily activities and sports and report exacerbation of hip pain in deep flexion or while sitting. But exact impingement location in deep flexion is unknown. Hypothesis/Purpose We aimed to investigate impingement-free maximal flexion, location of hip impingement and if cam-deformity causes impingement in flexion in symptomatic cam and pincer FAI patients with decreased femoral version(FV).

#### **METHODS AND MATERIALS**

An IRB-approved retrospective study involving 24 patients (37 hips) with decreased femoral version(FV<5°) was performed. All FAI patients were symptomatic(mean age 33±10 years) and had anterior hip/groin pain and a positive anterior-impingement-test. Subgroups of patients with cam-type deformity(16 hips), patients with pincer-type deformity(7 hips) and patients with mixed-type FAI(6 hips) were compared. All patients underwent pelvic CT scans and were evaluated with individual CT-based 3D-models and validated software for patient-specific impingement-simulation using equidistant-method.

#### **RESULTS**

(1)Mean impingement-free flexion of patients with pincer-type FAI(113±10°) and patients with mixed-type FAI(114±11°) was significantly(p<0.001) lower compared to patients with cam-type FAI(122±13°). (2)Patients with mixed-type FAI(67%) and patients with pincer-type FAI(57%) had significantly(p<0.001) increased prevalence of intraarticular impingement compared to cam-type FAI(33%) in 115° of flexion. Patients with pincer-type FAI (57%) had significantly(p<0.001) higher prevalence of extraarticular subspine hip impingement compared to cam-type FAI(22%)in 125° of flexion. (3)Femoral impingement in maximal flexion was located anterior-inferior at 4 o'clock(71% of pincer-type FAI, 50% of mixed-type FAI) and 5 o'clock (61% of cam-type FAI). Cam-deformity was not involved in maximal flexion (0% 1-3 o'clock). Acetabular impingement in maximal flexion was located anterior-superior(2 o'clock) of all patients.

#### **CONCLUSION**

s Femoral impingement conflict in flexion was located anterior-inferior and did not involve the cam-deformity. This is different compared to previous studies that reported anterior-superior femoral impingement location during the anterior-impingement-test.

#### **CLINICAL RELEVANCE/APPLICATION**

This could be important for FAI patients to avoid exacerbation of hip pain in deep flexion. This could be important for radiologists to better understand FAI and the cam-deformity.

Printed on: 02/07/23

## Abstract Archives of the RSNA, 2022

T5A-SPMK-3

### 3D Printed Model and Guide for Decompression and Stem-Cell Treatment of Avascular Necrosis of the Femoral Head

Tuesday, Nov. 29 12:15PM - 12:45PM Room: Learning Center - MK DPS

#### Participants

Alborz Feizi, New Haven, CT (*Presenter*) Nothing to Disclose

#### PURPOSE

Avascular necrosis (AVN) is a condition characterized by bone tissue necrosis as a result of poor blood supply. The disease progresses in stages, and the treatment depends on the stage and location of AVN. One of the most common locations of AVN is at the femoral head. During the early stages of the disease, treatment options such as core decompression and cellular therapies can diminish further necrosis and avoid hip collapse. However, current treatment protocols lack the means to accurately guide a therapeutic device to the precise location of necrotic tissue. Furthermore, existing modes of treatment delivery can be complicated by postoperative infection and fracture. Here, we present a technique and device that has the potential to improve therapy outcomes by precisely targeting lesions, and placing stem cells in the optimal environment to induce revascularization.

#### METHODS AND MATERIALS

A foam cortical shell femur was scanned using computed tomography (CT) and segmented in Synopsys Simpleware ScanIP software to create a 3D femur model. From the model, a femur-specific drill-guide was designed based on a preoperatively planned ideal drill trajectory for the placement of the decompression device and for the delivery of stem-cells to the core of the necrotic region. A delivery cannula and a needle were drilled into the foam cortical shell femur using the 3D-printed drill-guide. After placement of the delivery cannula and needle using the custom guide, a second CT scan was performed to evaluate the accuracy and precision of the 3D-printed guide in delivering treatment to the ideal drill tip location.

#### RESULTS

In our model, the post-drilling 3D reconstruction showed a maximum of 2-degree deviation from the theoretical model. The needle tip was also between 0.257 and 2.149 mm away from the theoretical needle tip.

#### CONCLUSION

3D printed devices have the potential to improve positioning of treatment instruments. Consequently, this technique can allow for more precise localized decompression and stem-cell treatment of necrotic tissue.

#### CLINICAL RELEVANCE/APPLICATION

Approximately 50% percent of patients with femoral AVN experience hip collapse. This procedure has the potential to improve outcomes of decompression and stem-cell treatment and reduce the need for hip replacement surgery.

Printed on: 02/07/23

## Abstract Archives of the RSNA, 2022

T5A-SPMS

### Multisystem Tuesday Poster Discussion - A

Tuesday, Nov. 29 12:15PM - 12:45PM Room: Learning Center - MS DPS

#### Sub-Events

#### **T5A-SPMS-1 The Changes of Brain Function and Psychological Activity in Patients with Crohn's Disease: A Prospective Case-control Study**

Participants

Ruonan Zhang, Guangzhou, China (*Presenter*) Nothing to Disclose

#### **PURPOSE**

Recent studies point to the brain-gut axis dysfunction as a key player in the occurrence and development of Crohn's disease (CD). Disclosing neuropsychological characteristics of CD patients may help shed light on its pathogenesis and provide potential therapeutic target. However, little is known about neuropsychological changes in CD patients. The aim of this study is to investigate the alterations in brain function in CD patients and to explore the relationship between psychological changes and CD activity.

#### **METHODS AND MATERIALS**

43 CD patients who underwent brain functional MRI-bold (fMRI-bold) , Diffusion Tensor Imaging (DTI) , 3D T1 MPRAG and intestinal MRI and 22 matched healthy controls (HCs) who only received brain fMRI and 3D T1 MPRAG were prospectively recruited. Psychological activities (depression, anxiety, stress) and CD bowel activity (simplified Magnetic Resonance Index of Activity (MaRIAs) and Crohn's Disease Activity Index (CDAI)) were evaluated. Differences in brain function and psychological activity between CD patients and HCs were analyzed. The correlation between psychological activities and both CDAI and MaRIAs were investigated.

#### **RESULTS**

CD patients had significantly higher amplitude of low frequency fluctuations in thalamus, higher regional homogeneity in cerebellar, higher fractional anisotropy in seven fiber bundles (eg, body of corpus callosum, and inferior fronto-occipital fasciculus, etc), but lower gray matter signal in right orbitofrontal cortex than those of HCs (all  $P < 0.05$ ). Moreover, there were significant differences in psychological activities between HCs and CD patients ( $P < 0.05$ ). We found a positive and statistically significant correlation between MaRIAs and CDAI in CD patients ( $n = 43$ ,  $r = 0.397$ ,  $p < 0.05$ ). However, no significant association was found between bowel activity (MaRIAs and CDAI) and psychological activities (all  $P > 0.05$ ).

#### **CONCLUSION**

s CD patients demonstrated abnormal neural activity that associated with emotional, pain and cognitive-related functions, which may relate to their poor psychological activities.

#### **CLINICAL RELEVANCE/APPLICATION**

Although our preliminary results are not yet sufficient to support a close relationship between psychological status and bowel activity, clinicians still should pay more attention to these neuropsychological changes of CD patients as they might be potential therapeutic targets.

Printed on: 02/07/23

## Abstract Archives of the RSNA, 2022

T5A-SPMS-1

### The Changes of Brain Function and Psychological Activity in Patients with Crohn's Disease: A Prospective Case-control Study

Tuesday, Nov. 29 12:15PM - 12:45PM Room: Learning Center - MS DPS

#### Participants

Ruonan Zhang, Guangzhou, China (*Presenter*) Nothing to Disclose

#### PURPOSE

Recent studies point to the brain-gut axis dysfunction as a key player in the occurrence and development of Crohn's disease (CD). Disclosing neuropsychological characteristics of CD patients may help shed light on its pathogenesis and provide potential therapeutic target. However, little is known about neuropsychological changes in CD patients. The aim of this study is to investigate the alterations in brain function in CD patients and to explore the relationship between psychological changes and CD activity.

#### METHODS AND MATERIALS

43 CD patients who underwent brain functional MRI-bold (fMRI-bold) , Diffusion Tensor Imaging (DTI) , 3D T1 MPRAG and intestinal MRI and 22 matched healthy controls (HCs) who only received brain fMRI and 3D T1 MPRAG were prospectively recruited. Psychological activities (depression, anxiety, stress) and CD bowel activity (simplified Magnetic Resonance Index of Activity (MaRIAs) and Crohn's Disease Activity Index (CDAI)) were evaluated. Differences in brain function and psychological activity between CD patients and HCs were analyzed. The correlation between psychological activities and both CDAI and MaRIAs were investigated.

#### RESULTS

CD patients had significantly higher amplitude of low frequency fluctuations in thalamus, higher regional homogeneity in cerebellar, higher fractional anisotropy in seven fiber bundles (eg, body of corpus callosum, and inferior fronto-occipital fasciculus, etc), but lower gray matter signal in right orbitofrontal cortex than those of HCs (all  $P < 0.05$ ). Moreover, there were significant differences in psychological activities between HCs and CD patients ( $P < 0.05$ ). We found a positive and statistically significant correlation between MaRIAs and CDAI in CD patients ( $n = 43$ ,  $r = 0.397$ ,  $p < 0.05$ ). However, no significant association was found between bowel activity (MaRIAs and CDAI) and psychological activities (all  $P > 0.05$ ).

#### CONCLUSION

s CD patients demonstrated abnormal neural activity that associated with emotional, pain and cognitive-related functions, which may relate to their poor psychological activities.

#### CLINICAL RELEVANCE/APPLICATION

Although our preliminary results are not yet sufficient to support a close relationship between psychological status and bowel activity, clinicians still should pay more attention to these neuropsychological changes of CD patients as they might be potential therapeutic targets.

Printed on: 02/07/23

## Abstract Archives of the RSNA, 2022

T5A-SPNMMI

### Nuclear Medicine/Molecular Imaging Tuesday Poster Discussion - A

Tuesday, Nov. 29 12:15PM - 12:45PM Room: Learning Center - NMMI DPS

#### Participants

Georges El Fakhri, PhD, Boston, MA (*Moderator*) Nothing to Disclose

#### Sub-Events

#### **T5A-SPNMMI-1 A Pilot Study of 68Ga-PSMA11 and 68Ga-RM2 PET/MRI for Evaluation of Prostate Cancer Response to High Intensity Focused Ultrasound (HIFU) Therapy**

#### Participants

Heying Duan, MD, (*Presenter*) Nothing to Disclose

#### PURPOSE

Focal therapy for localized prostate cancer (PC) using high intensity focused ultrasound (HIFU) is gaining in popularity as it is non-invasive and associated with fewer side effects than standard whole-gland treatments. However, better methods to evaluate response to HIFU are an unmet need. Prostate specific membrane antigen (PSMA) and gastrin-releasing peptide receptors (GRPR) are both overexpressed in PC. In this study, we evaluated a novel approach of using both 68Ga-RM2 and 68Ga-PSMA11 PET/MRI in each patient before and after HIFU treatment to assess accuracy of target tumor localization and response to treatment.

#### METHODS AND MATERIALS

Fourteen men, 64.5±8.0 (range 48 - 78) years-old, with newly diagnosed PC were prospectively enrolled. Pre-HIFU, patients underwent prostate biopsy, multiparametric MRI (mpMRI), 68Ga-PSMA11 and 68Ga-RM2 PET/MRI. Response to treatment was assessed at a minimum of 6 months after HIFU with prostate biopsy (n=9), as well as 68Ga-PSMA11 and 68Ga-RM2 PET/MRI (n=14). Maximum and peak standardized uptake values (SUV<sub>max</sub> and SUV<sub>peak</sub>) of known or suspected PC lesions were collected.

#### RESULTS

Pre-HIFU biopsy revealed 17 cancers of which 14 were clinically significant (Gleason score =3+4). mpMRI identified 18 lesions, 14 of them =PI-RADS 4. 68Ga-PSMA11 and 68Ga-RM2 PET/MRI each showed 23 positive intraprostatic lesions, of which 21 were congruent in 13 patients and 5 were incongruent in 5 patients. In the pre-HIFU workup, 68Ga-PSMA11 identified all target tumors while 68Ga-RM2 PET/MRI missed 2 tumors. Post-HIFU, 68Ga-RM2 PET/MRI was negative in the treatment zones, whereas 68Ga-PSMA11 showed persistent uptake in one lesion which proved to be non-clinically significant cancer on biopsy. Three new ipsilateral lesions were seen with both radiopharmaceuticals, which were verified by prostate biopsy and patients were subsequently treated with a repeat HIFU. Pre-treatment prostate specific antigen (PSA) decreased significantly after HIFU by 66%. Concordantly, SUV<sub>max</sub> decreased significantly after HIFU for 68Ga-PSMA11 (P=0.003) and 68Ga-RM2 (P=0.000).

#### CONCLUSION

Our results show that 68Ga-PSMA11 and 68Ga-RM2 PET/MRI identified the target tumor for HIFU in 100% and 86%, respectively, and accurately verified response to treatment. This suggests that PET might be a useful tool in the guidance and monitoring of treatment success in patients receiving focal therapy for PC.

#### CLINICAL RELEVANCE/APPLICATION

68Ga-PSMA11 and 68Ga-RM2 PET/MRI were feasible for monitoring HIFU treatment success and might avoid re-biopsies for treatment verification with its associated risks.

#### **T5A-SPNMMI-2 Impact of 18F-fluciclovine PET/CT on Failure-free Survival in Biochemical Recurrence of Prostate Cancer Following Salvage Radiation Therapy**

#### Participants

Charles Marcus, MD, Atlanta, GA (*Presenter*) Nothing to Disclose

#### PURPOSE

To evaluate the correlation between 18F-fluciclovine PET/CT findings and failure-free survival (FFS) in patients with biochemical recurrence of prostate cancer, status post radical prostatectomy who underwent salvage radiation therapy (RT)

#### METHODS AND MATERIALS

79 prostate cancer patients enrolled in the study arm of a single center, randomized controlled trial (NCT01666808) in which salvage RT guided by fluciclovine PET/CT findings (including radiotherapy target volume design) were included. 4 patients with extrapelvic disease (M1) were excluded. Treatment failure was defined as a serum prostate specific antigen (PSA) level of =0.2ng/mL above the nadir after salvage RT, confirmed with an additional measurement, requiring systemic treatment or clinical progression. All patients were followed at regular intervals up to 48 months. Kaplan-Meier plot was generated and FFS were compared between patients with no uptake, prostate bed only and/or pelvic nodal uptake using the Z test at 3 years and 4

## **RESULTS**

80% (60/75) of patients had a positive M0 fluciclovine PET/CT, of which 57% (34/60) of the patients had prostate bed only uptake, while 43% (26/60) had pelvic nodal  $\pm$  bed uptake. RT planning decision was changed in 32% of patients. Following RT, disease failure was detected in 36% (27/75) patients. There was a significant difference in FFS between patients who had a positive vs negative scan (62% vs 93%;  $p<0.001$ ) at 36 months and (59% vs 93%;  $p<0.001$ ) at 48 months. Similarly, there was a significant difference in FFS between patients with uptake in pelvic nodes  $\pm$  bed vs prostate bed only at 36 months (50% vs 71%;  $p=0.003$ ) and at 48 months (50% vs 66%;  $p=0.040$ ) (Figures 1-3),

## **CONCLUSION**

s 18F-fluciclovine PET/CT findings are predictive of failure-free survival in post-prostatectomy patients with biochemical recurrence status post salvage radiation therapy. Difference in failure-free survival despite targeted salvage radiotherapy based on the PET/CT findings may indicate the complex biology of these tumors and its relationship to metabolic tumor burden.

## **CLINICAL RELEVANCE/APPLICATION**

18F-fluciclovine PET/CT findings can predict failure-free survival outcomes in patients with biochemical recurrence of prostate cancer.

Printed on: 02/07/23

## Abstract Archives of the RSNA, 2022

T5A-SPNMMI-1

### A Pilot Study of 68Ga-PSMA11 and 68Ga-RM2 PET/MRI for Evaluation of Prostate Cancer Response to High Intensity Focused Ultrasound (HIFU) Therapy

Tuesday, Nov. 29 12:15PM - 12:45PM Room: Learning Center - NMMI DPS

#### Participants

Heying Duan, MD, (Presenter) Nothing to Disclose

#### PURPOSE

Focal therapy for localized prostate cancer (PC) using high intensity focused ultrasound (HIFU) is gaining in popularity as it is non-invasive and associated with fewer side effects than standard whole-gland treatments. However, better methods to evaluate response to HIFU are an unmet need. Prostate specific membrane antigen (PSMA) and gastrin-releasing peptide receptors (GRPR) are both overexpressed in PC. In this study, we evaluated a novel approach of using both 68Ga-RM2 and 68Ga-PSMA11 PET/MRI in each patient before and after HIFU treatment to assess accuracy of target tumor localization and response to treatment.

#### METHODS AND MATERIALS

Fourteen men, 64.5±8.0 (range 48 - 78) years-old, with newly diagnosed PC were prospectively enrolled. Pre-HIFU, patients underwent prostate biopsy, multiparametric MRI (mpMRI), 68Ga-PSMA11 and 68Ga-RM2 PET/MRI. Response to treatment was assessed at a minimum of 6 months after HIFU with prostate biopsy (n=9), as well as 68Ga-PSMA11 and 68Ga-RM2 PET/MRI (n=14). Maximum and peak standardized uptake values (SUVmax and SUVpeak) of known or suspected PC lesions were collected.

#### RESULTS

Pre-HIFU biopsy revealed 17 cancers of which 14 were clinically significant (Gleason score =3+4). mpMRI identified 18 lesions, 14 of them =PI-RADS 4. 68Ga-PSMA11 and 68Ga-RM2 PET/MRI each showed 23 positive intraprostatic lesions, of which 21 were congruent in 13 patients and 5 were incongruent in 5 patients. In the pre-HIFU workup, 68Ga-PSMA11 identified all target tumors while 68Ga-RM2 PET/MRI missed 2 tumors. Post-HIFU, 68Ga-RM2 PET/MRI was negative in the treatment zones, whereas 68Ga-PSMA11 showed persistent uptake in one lesion which proved to be non-clinically significant cancer on biopsy. Three new ipsilateral lesions were seen with both radiopharmaceuticals, which were verified by prostate biopsy and patients were subsequently treated with a repeat HIFU. Pre-treatment prostate specific antigen (PSA) decreased significantly after HIFU by 66%. Concordantly, SUVmax decreased significantly after HIFU for 68Ga-PSMA11 (P=0.003) and 68Ga-RM2 (P=0.000).

#### CONCLUSION

Our results show that 68Ga-PSMA11 and 68Ga-RM2 PET/MRI identified the target tumor for HIFU in 100% and 86%, respectively, and accurately verified response to treatment. This suggests that PET might be a useful tool in the guidance and monitoring of treatment success in patients receiving focal therapy for PC.

#### CLINICAL RELEVANCE/APPLICATION

68Ga-PSMA11 and 68Ga-RM2 PET/MRI were feasible for monitoring HIFU treatment success and might avoid re-biopsies for treatment verification with its associated risks.

Printed on: 02/07/23

## Abstract Archives of the RSNA, 2022

T5A-SPNMMI-2

### Impact of 18F-fluciclovine PET/CT on Failure-free Survival in Biochemical Recurrence of Prostate Cancer Following Salvage Radiation Therapy

Tuesday, Nov. 29 12:15PM - 12:45PM Room: Learning Center - NMMI DPS

#### Participants

Charles Marcus, MD, Atlanta, GA (*Presenter*) Nothing to Disclose

#### PURPOSE

To evaluate the correlation between 18F-fluciclovine PET/CT findings and failure-free survival (FFS) in patients with biochemical recurrence of prostate cancer, status post radical prostatectomy who underwent salvage radiation therapy (RT)

#### METHODS AND MATERIALS

79 prostate cancer patients enrolled in the study arm of a single center, randomized controlled trial (NCT01666808) in which salvage RT guided by fluciclovine PET/CT findings (including radiotherapy target volume design) were included. 4 patients with extrapelvic disease (M1) were excluded. Treatment failure was defined as a serum prostate specific antigen (PSA) level of  $\geq 0.2$  ng/mL above the nadir after salvage RT, confirmed with an additional measurement, requiring systemic treatment or clinical progression. All patients were followed at regular intervals up to 48 months. Kaplan-Meier plot was generated and FFS were compared between patients with no uptake, prostate bed only and/or pelvic nodal uptake using the Z test at 3 years and 4 years. Funding Information: National Institutes of Health/National Cancer Institute, Blue Earth Diagnostics

#### RESULTS

80% (60/75) of patients had a positive M0 fluciclovine PET/CT, of which 57% (34/60) of the patients had prostate bed only uptake, while 43% (26/60) had pelvic nodal  $\pm$  bed uptake. RT planning decision was changed in 32% of patients. Following RT, disease failure was detected in 36% (27/75) patients. There was a significant difference in FFS between patients who had a positive vs negative scan (62% vs 93%;  $p < 0.001$ ) at 36 months and (59% vs 93%;  $p < 0.001$ ) at 48 months. Similarly, there was a significant difference in FFS between patients with uptake in pelvic nodes  $\pm$  bed vs prostate bed only at 36 months (50% vs 71%;  $p = 0.003$ ) and at 48 months (50% vs 66%;  $p = 0.040$ ) (Figures 1-3),

#### CONCLUSION

s 18F-fluciclovine PET/CT findings are predictive of failure-free survival in post-prostatectomy patients with biochemical recurrence status post salvage radiation therapy. Difference in failure-free survival despite targeted salvage radiotherapy based on the PET/CT findings may indicate the complex biology of these tumors and its relationship to metabolic tumor burden.

#### CLINICAL RELEVANCE/APPLICATION

18F-fluciclovine PET/CT findings can predict failure-free survival outcomes in patients with biochemical recurrence of prostate cancer.

Printed on: 02/07/23

## Abstract Archives of the RSNA, 2022

T5A-SPNPM

### Noninterpretive Skills/Quality Improvement/Practice Management Tuesday Poster Discussions - A

Tuesday, Nov. 29 12:15PM - 12:45PM Room: Learning Center - NPM DPS

#### Participants

Shaun A. Wahab, MD, Mason, OH (*Moderator*) Consultant, GlaxoSmithKline plc; Consultant, BioClinica, Inc; Consultant, Mersana Therapeutics, Inc

#### Sub-Events

#### T5A-SPNPM- Efficacy of Low-Cost Gelatin Models to Teach Vascular Anatomy and Intravascular Access Techniques 1

##### Participants

Kenneth Richardson, Miami, FL (*Presenter*) Nothing to Disclose

#### PURPOSE

Ultrasound (US) guided vascular access has become increasingly popular due to its reduced complications and higher success rates. Commercial training phantoms have grown in popularity due to their advantage in allowing providers to develop tactile skills in a low risk setting. However, such models are expensive and thus poorly accessible. This study analyzes the efficacy of homemade, low-cost reusable gelatin-based central line vascular models to teach vascular anatomy and intravascular access techniques in training physicians.

#### METHODS AND MATERIALS

Medical students from all years were recruited from the University of Miami to participate in a 90-minute simulation workshop led by Interventional Radiology residents. Participants completed pre- and post-surveys that assessed knowledge acquisition and subjective confidence levels related to the procedure. After a brief orientation, participants practiced US guided central line access using two different homemade gelatin models that simulated the anatomical positioning of the internal jugular (IJ) and femoral veins. The sternocleidomastoid muscle and femoral nerve were simulated using tofu and a cord of hotdog, respectively. Balloons and latex tubing injected with red food coloring simulated veins and arteries, respectively. The mold was created using a mixture of 90 mg gelatin, 500 mL water, 2 tbsp Metamucil, 30 mL rubbing alcohol, and food coloring. Statistical analysis was performed using IBM SPSS statistics.

#### RESULTS

A total of 20 medical students were recruited, with a 100% response rate in both the pre- and post-surveys. There was a statistically significant increase in self-reported confidence in basic US use (adjusting gain, depth, probe manipulation), localizing major anatomical structures, using ultrasound for vessel access ( $p=0.013$ ,  $p<0.001$ ,  $p<0.001$ ), and reported ease in identifying muscle, nerves, and major blood vessels under US ( $p<0.001$ ,  $p<0.001$ ,  $p<0.001$ ). There was also a significant increase in correctly identified anatomical landmarks following the workshop, including the sternocleidomastoid muscle, IJ, carotid artery, femoral nerve, femoral artery, and femoral vein ( $p<0.001$ ,  $p=0.008$ ,  $p=0.004$ ,  $p<0.001$ ,  $p<0.001$ ,  $p<0.001$ ).

#### CONCLUSION

Our findings suggest our homemade low-cost reusable gelatin-based models were effective in teaching vascular anatomy and US guided vascular access techniques to training physicians. Limitations include a small sample size from a single institution, and quantitative survey research design.

#### CLINICAL RELEVANCE/APPLICATION

Low-cost gelatin models represent an alternative to expensive commercial US phantoms to teach vascular anatomy and access techniques. These models have the potential to be adapted to many US guided procedures.

#### T5A-SPNPM- Motivations of Canadian Medical Students, Resident Physicians, and Fellows to Participate in a National Radiology Mentorship Program: Potential for Mutual Benefit? 2

##### Participants

Mohamed Abu-Nada, (*Presenter*) Nothing to Disclose

#### PURPOSE

To determine the reasons why mentees (medical students) and mentors (radiology residents and fellows) believe participating in a radiology mentorship program will be beneficial.

#### METHODS AND MATERIALS

A pan-Canadian survey was distributed to Canadian medical students and radiology trainees as a needs assessment to launch a longitudinal radiology mentorship program. The survey was shared through the Canadian Association of Radiologists and radiology residency programs. Medical students were categorized as mentees and trainees as mentors.

## RESULTS

161 participants (67 mentors and 94 mentees) responded from Canadian medical schools. Despite being underrepresented in radiology, most mentors were women (55%). Women also represented 47% of mentees. Additionally, 26% of mentors and 37% of mentees identified as visible minorities. Mentors' top reasons for participating in mentorship were to aid in the development of future radiologists (85%) and to enhance their own mentoring/teaching skills (84%). Additionally, 42% of mentors who previously had a mentor themselves believed it positively influenced their radiology application and 95% believed mentoring was beneficial to trainees. Mentees' top reasons for participating were to learn more about radiology (82%), they were considering applying to radiology (82%), or were looking to get involved in radiology research projects (79%).

## CONCLUSION

This data can be used to inform the creation of a targeted radiology mentorship program since mentors and mentees have either benefitted or believe they can benefit from such a program. This data also shows the motivation of radiology trainees to improve their mentoring skills, which could also be acquired by creating intentional mentoring training.

## CLINICAL RELEVANCE/APPLICATION

Due to the lack of exposure to radiology in the medical teaching curricula, radiology is often poorly understood by medical students. Currently, no Canadian radiology-specific mentorship program exists for medical students. Literature suggests that students with mentors have an increased sense of personal accomplishment, feel more confident in their careers, and have reduced burnout rates. Mentors benefit from mentorship programs with internal gratification, personal enrichment, and job satisfaction. Also, being a mentor provides the opportunity to develop leadership, communication, and collaboration skills. Additionally, in Canada, there exists a gender gap in radiology where women are under-represented and visible minorities also seem less represented. Studies have also shown that females and minorities are less likely to have mentors in radiology. Hence, a Canadian radiology mentorship program offered to all medical students could help increase diversity in radiology.

## T5A-SPNPM- Formal Wellness Training of Academic Radiology Leaders Raises Awareness and Improved Teamwork Scores of Their Faculty

Participants  
Jay R. Parikh, MD, West University Place, TX (*Presenter*) Nothing to Disclose

## PURPOSE

To investigate the effect of formal leadership training of academic radiology leaders within an academic center on their faculty burnout and professional fulfillment.

## METHODS AND MATERIALS

The study cohort were academic radiologists within one of the largest academic organizations of academic radiologists within the United States. All academic radiologists within the organization were electronically mailed a weblink to a confidential IRB-approved survey in April 2021. The survey included validated questions from the Stanford Professional Fulfillment Index (PFI), values alignment, teamwork, overload, and work family conflict. Academic leaders were invited in May 2021 to participate in instructor-led formal training on leading wellness focusing on 5 core leadership skills - emotional intelligence, self-care, resilience support, demonstrating care, and managing burnout. An identical follow-up survey was electronically mailed to their faculty 6 months after initial training in November 2021.

## RESULTS

The overall response rate of academic radiologists was 13 % (24/178). There was high internal consistency (Cronbach's  $\alpha = 0.88$  for work exhaustion and  $\alpha = 0.93$  for fulfillment). The inverse association between professional fulfillment and work exhaustion was significant ( $r = -0.83$ ,  $p < 0.01$ ). There was statistically significant improvement in one aspect of teamwork scores; assuming positive intent (5.36 vs 4.64;  $p = 0.03$ ). No statistically significant differences were identified for fulfillment, work exhaustion, alignment, work overload and work family conflict scores after training.

## CONCLUSION

Formal instruction of academic radiology leaders in leading wellness improved teamwork scores in their academic faculty. There was no significant change in work exhaustion, fulfillment nor organizational alignment of the faculty.

## CLINICAL RELEVANCE/APPLICATION

Formal instruction of academic radiology leaders in leading wellness raised awareness and improved teamwork scores of their faculty.

Printed on: 02/07/23



## Abstract Archives of the RSNA, 2022

T5A-SPNPM-1

### Efficacy of Low-Cost Gelatin Models to Teach Vascular Anatomy and Intravascular Access Techniques

Tuesday, Nov. 29 12:15PM - 12:45PM Room: Learning Center - NPM DPS

#### Participants

Kenneth Richardson, Miami, FL (*Presenter*) Nothing to Disclose

#### PURPOSE

Ultrasound (US) guided vascular access has become increasingly popular due to its reduced complications and higher success rates. Commercial training phantoms have grown in popularity due to their advantage in allowing providers to develop tactile skills in a low risk setting. However, such models are expensive and thus poorly accessible. This study analyzes the efficacy of homemade, low-cost reusable gelatin-based central line vascular models to teach vascular anatomy and intravascular access techniques in training physicians.

#### METHODS AND MATERIALS

Medical students from all years were recruited from the University of Miami to participate in a 90-minute simulation workshop led by Interventional Radiology residents. Participants completed pre- and post-surveys that assessed knowledge acquisition and subjective confidence levels related to the procedure. After a brief orientation, participants practiced US guided central line access using two different homemade gelatin models that simulated the anatomical positioning of the internal jugular (IJ) and femoral veins. The sternocleidomastoid muscle and femoral nerve were simulated using tofu and a cord of hotdog, respectively. Balloons and latex tubing injected with red food coloring simulated veins and arteries, respectively. The mold was created using a mixture of 90 mg gelatin, 500 mL water, 2 tbsp Metamucil, 30 mL rubbing alcohol, and food coloring. Statistical analysis was performed using IBM SPSS statistics.

#### RESULTS

A total of 20 medical students were recruited, with a 100% response rate in both the pre- and post-surveys. There was a statistically significant increase in self-reported confidence in basic US use (adjusting gain, depth, probe manipulation), localizing major anatomical structures, using ultrasound for vessel access ( $p=0.013$ ,  $p<0.001$ ,  $p<0.001$ ), and reported ease in identifying muscle, nerves, and major blood vessels under US ( $p<0.001$ ,  $p<0.001$ ,  $p<0.001$ ). There was also a significant increase in correctly identified anatomical landmarks following the workshop, including the sternocleidomastoid muscle, IJ, carotid artery, femoral nerve, femoral artery, and femoral vein ( $p<0.001$ ,  $p=0.008$ ,  $p=0.004$ ,  $p<0.001$ ,  $p<0.001$ ,  $p<0.001$ ).

#### CONCLUSION

Our findings suggest our homemade low-cost reusable gelatin-based models were effective in teaching vascular anatomy and US guided vascular access techniques to training physicians. Limitations include a small sample size from a single institution, and quantitative survey research design.

#### CLINICAL RELEVANCE/APPLICATION

Low-cost gelatin models represent an alternative to expensive commercial US phantoms to teach vascular anatomy and access techniques. These models have the potential to be adapted to many US guided procedures.

Printed on: 02/07/23



## Abstract Archives of the RSNA, 2022

T5A-SPNPM-2

### Motivations of Canadian Medical Students, Resident Physicians, and Fellows to Participate in a National Radiology Mentorship Program: Potential for Mutual Benefit?

Tuesday, Nov. 29 12:15PM - 12:45PM Room: Learning Center - NPM DPS

#### Participants

Mohamed Abu-Nada, (*Presenter*) Nothing to Disclose

#### PURPOSE

To determine the reasons why mentees (medical students) and mentors (radiology residents and fellows) believe participating in a radiology mentorship program will be beneficial.

#### METHODS AND MATERIALS

A pan-Canadian survey was distributed to Canadian medical students and radiology trainees as a needs assessment to launch a longitudinal radiology mentorship program. The survey was shared through the Canadian Association of Radiologists and radiology residency programs. Medical students were categorized as mentees and trainees as mentors.

#### RESULTS

161 participants (67 mentors and 94 mentees) responded from Canadian medical schools. Despite being underrepresented in radiology, most mentors were women (55%). Women also represented 47% of mentees. Additionally, 26% of mentors and 37% of mentees identified as visible minorities. Mentors' top reasons for participating in mentorship were to aid in the development of future radiologists (85%) and to enhance their own mentoring/teaching skills (84%). Additionally, 42% of mentors who previously had a mentor themselves believed it positively influenced their radiology application and 95% believed mentoring was beneficial to trainees. Mentees' top reasons for participating were to learn more about radiology (82%), they were considering applying to radiology (82%), or were looking to get involved in radiology research projects (79%).

#### CONCLUSION

s This data can be used to inform the creation of a targeted radiology mentorship program since mentors and mentees have either benefitted or believe they can benefit from such a program. This data also shows the motivation of radiology trainees to improve their mentoring skills, which could also be acquired by creating intentional mentoring training.

#### CLINICAL RELEVANCE/APPLICATION

Due to the lack of exposure to radiology in the medical teaching curricula, radiology is often poorly understood by medical students. Currently, no Canadian radiology-specific mentorship program exists for medical students. Literature suggests that students with mentors have an increased sense of personal accomplishment, feel more confident in their careers, and have reduced burnout rates. Mentors benefit from mentorship programs with internal gratification, personal enrichment, and job satisfaction. Also, being a mentor provides the opportunity to develop leadership, communication, and collaboration skills. Additionally, in Canada, there exists a gender gap in radiology where women are under-represented and visible minorities also seem less represented. Studies have also shown that females and minorities are less likely to have mentors in radiology. Hence, a Canadian radiology mentorship program offered to all medical students could help increase diversity in radiology.

Printed on: 02/07/23



## Abstract Archives of the RSNA, 2022

T5A-SPNPM-3

### Formal Wellness Training of Academic Radiology Leaders Raises Awareness and Improved Teamwork Scores of Their Faculty

Tuesday, Nov. 29 12:15PM - 12:45PM Room: Learning Center - NPM DPS

#### Participants

Jay R. Parikh, MD, West University Place, TX (*Presenter*) Nothing to Disclose

#### PURPOSE

To investigate the effect of formal leadership training of academic radiology leaders within an academic center on their faculty burnout and professional fulfillment.

#### METHODS AND MATERIALS

The study cohort were academic radiologists within one of the largest academic organizations of academic radiologists within the United States. All academic radiologists within the organization were electronically mailed a weblink to a confidential IRB-approved survey in April 2021. The survey included validated questions from the Stanford Professional Fulfillment Index (PFI), values alignment, teamwork, overload, and work family conflict. Academic leaders were invited in May 2021 to participate in instructor-led formal training on leading wellness focusing on 5 core leadership skills - emotional intelligence, self-care, resilience support, demonstrating care, and managing burnout. An identical follow-up survey was electronically mailed to their faculty 6 months after initial training in November 2021.

#### RESULTS

The overall response rate of academic radiologists was 13 % (24/178). There was high internal consistency (Cronbach's  $\alpha = 0.88$  for work exhaustion and  $\alpha = 0.93$  for fulfillment). The inverse association between professional fulfillment and work exhaustion was significant ( $r = -0.83$ ,  $p < 0.01$ ). There was statistically significant improvement in one aspect of teamwork scores; assuming positive intent (5.36 vs 4.64;  $p = 0.03$ ). No statistically significant differences were identified for fulfillment, work exhaustion, alignment, work overload and work family conflict scores after training.

#### CONCLUSION

Formal instruction of academic radiology leaders in leading wellness improved teamwork scores in their academic faculty. There was no significant change in work exhaustion, fulfillment nor organizational alignment of the faculty.

#### CLINICAL RELEVANCE/APPLICATION

Formal instruction of academic radiology leaders in leading wellness raised awareness and improved teamwork scores of their faculty.

Printed on: 02/07/23

## Abstract Archives of the RSNA, 2022

T5A-SPNR

### Neuroradiology Tuesday Poster Discussions - A

Tuesday, Nov. 29 12:15PM - 12:45PM Room: Learning Center - NR DPS

#### Participants

Birgit Ertl-Wagner, MD, Toronto, ON (*Moderator*) Spouse, Employee, Siemens AG

#### Sub-Events

### T5A-SPNR-1 MRI Radiogenomics Analysis Predicts KRAS, EGFR and MET Mutational Status in Non-Small Cell Lung Carcinoma Brain Metastasis

#### Participants

Murat AK, MD, Pittsburgh, PA (*Presenter*) Nothing to Disclose

#### PURPOSE

Non-small cell lung cancer (NSCLC) has the highest incidence of metastases to the brain. Targetable alterations are often present in brain metastasis (BM) not found in the primary tumor. A non-invasive strategy is needed to detect brain-specific alterations. This study was conducted to assess the potential of radiogenomics to predict KRAS, EGFR and MET mutation status in BM from NSCLC patients.

#### METHODS AND MATERIALS

We retrospectively identified 159 NSCLC with BM both imaging and genomic annotation available. For each lesion, we segmented edema, contrast enhancement, and necrosis volume of interest (VOI) on both T2 FLAIR and T1 post-contrast sequences. Additionally, contralateral white matter (cWM) was also segmented for feature normalization. 10 histogram based first-order features and 195 second-order gray level co-occurrence matrix features were extracted from each VOI. After normalization, we divided the 195 second order features by the volumes of each VOI to produce another 195 volume-independent features per VOI for a total of 2,400 extracted features per lesions. We performed feature selection with Least Absolute Shrinkage and Selection Operator (LASSO). We split the cohort into 70% training and 30% testing sets for KRAS and EGFR and 80% training and 20% testing sets for MET models. We report the area under the curve (AUC) for classifying mutation status of each lesion and XGBoost was used to generate radiomics model.

#### RESULTS

Out of the 2,400 total features, LASSO identified 32 features for the EGFR mutant (mt) prediction model; of which the 20 most relevant were used for model building. The model achieved 78% accuracy, 77% sensitivity and 100% specificity. For the KRAS mt prediction model, LASSO defined 91 features and the model was generated with the top 30 features attaining 71% accuracy, 82% sensitivity and 60% specificity. Similarly, LASSO determined 90 features for MET mt prediction model, of which the top 15 features were used for the model demonstrating 77% accuracy, 76% sensitivity and 83% specificity.

#### CONCLUSION

This study demonstrates that radiomics-based signatures can predict brain-specific molecular alterations including KRAS, EGFR and MET mutations.

#### CLINICAL RELEVANCE/APPLICATION

While further validation is warranted in a larger cohort, the proposed predictive radiomics-based approach is cost-effective, non-invasive and will help identify NSCLC patients with BM that are likely to respond to targeted treatments.

### T5A-SPNR-10 The Role of Susceptibility-Weighted Imaging as an Accessory Diagnostic Tool of Global Cerebral Anoxia in the Post Cardiac Arrest Setting

#### Participants

Alyssa Ionno, Syracuse, NY (*Presenter*) Nothing to Disclose

#### PURPOSE

To examine the utility of Susceptibility-Weighted Imaging (SWI) in patients with concern for acute hypoxic-ischemic injury (HII) to the brain in the post cardiac arrest setting. It is well known that Diffusion-Weighted Imaging is our most sensitive MR sequence to detect a hypoxic-ischemic event, however it is our goal to demonstrate SWI as an effective accessory tool that should be utilized to assist in qualifying the degree of ischemic injury.

#### METHODS AND MATERIALS

Retrospective chart review was conducted in our tertiary care center. A total of 50 adult patients were selected at random with a history of acute cardiac arrest and MRI evaluation with concern for anoxic brain injury. With an independent review from a board-certified Neuroradiologist, SWI sequences were evaluated with an emphasis on the appearance of the superficial cortical veins. The great cerebral vein along with visualized arterial vasculature was also evaluated. The appearance of these vessels was quantified

using a scale of 0 - 3, 0 for absent or not seen, 1 for diminished appearance, 2 for present and normal, 3 for dilated. These findings were correlated with DWI results.

## RESULTS

Of the 50 patients initially chart reviewed 37 demonstrated MR findings consistent with anoxic brain injury on either T2-weighted or DWI imaging. Within those 37 cases 26 had DWI findings consistent with acute anoxic brain injury (70%). SWI was unavailable or suboptimal in 6 cases leaving a total of 44 cases for complete analysis. Within the SWI subset, 34 of the 44 available cases demonstrated absent (0) or diminished (1) superficial cortical veins (77%). Importantly, only 5 of the 37 patients (14%) with any MRI findings characteristic of anoxic brain injury did not show any form of diminished superficial venous vasculature on SWI. Additionally, the great cerebral vein was absent or diminished in 30 of the 44 available cases (68%). In comparison to DWI, only 5 of the 26 (19%) cases with DWI findings consistent with HII did not show any form of diminished superficial or great venous vasculature on SWI. Interestingly, of the 13 available cases with no additional MR findings to suggest anoxic brain injury 4 demonstrated diminished or absent superficial cortical veins.

## CONCLUSION

s In SWI, the amount of deoxy-hemoglobin content within the cortical veins directly correlates with their prominence. This can therefore be applied to episodes HII, which is secondary to a decrease in overall cerebral oxygen metabolism. Our data demonstrates a significant correlation with decreased vascular prominence on SWI in this setting.

## CLINICAL RELEVANCE/APPLICATION

To further reinforce the use and addition of susceptibility weighted imaging in protocols for acute anoxic brain injury.

### **T5A-SPNR- Predictors of Intracranial Aneurysm Wall Enhancement on High Resolution MR Vessel Wall Imaging** 11

Participants

Abhinav Patel, MBBS, Chicago, IL (*Presenter*) Nothing to Disclose

## PURPOSE

MR Vessel Wall Imaging (VWI) is an increasingly utilized modality for evaluation of neurovascular pathologies like Intracranial aneurysms (IAs) and atherosclerotic plaques. Multiple studies have evaluated the associations between intracranial aneurysm wall enhancement (AWE), risk of rupture, and aneurysm growth on follow-up. In our study, we aim to identify predictors for AWE.

## METHODS AND MATERIALS

IRB approval was obtained for a retrospective study. Patients with IAs greater or equal to 2mm and VWI imaging were included. AWE was evaluated qualitatively, and a quantitative assessment of the percentage increase in signal intensity (SI) was also performed using means of three point ROIs placed on aneurysm wall on pre and post-contrast axial T1-SPACE sequences. The increase in SI was normalized to white matter SI on pre and post-contrast images. Patient demographics, risk factors and IA size and morphology were recorded. IAs were grouped into small (<3.9mm), medium (4-7mm), and large (>7.1mm) sizes. Spearman rank test, linear regression, and one way ANOVA were used to assess statistical associations between an increase in signal intensity, size, and other variables using SPSS v28.

## RESULTS

A total of 174 patients (Mean age = 62.5 (24-87), 74% females) with 214 IAs (Mean size = 5.149 mm (2-30 mm) were assessed. 18/174 (10.34%) patients presented with subarachnoid hemorrhage. On qualitative evaluation, AWE was observed in 112/214 ICAs (52.3%). IA size demonstrated a moderate correlation ( $r = 0.5$ ,  $p < 0.001$ , 95% CI, 0.372-0.609) to percentage increase in SI. There was a statistically significant ( $p < 0.001$ ) increase in percentage SI, 24.75%, 46.35%, and 79.69%, in small ( $n = 78$ ), medium ( $n = 96$ ), and large ( $n = 40$ ) aneurysm groups. Thrombosis of the aneurysm sac ( $r = 0.238$ ,  $p = 0.002$ , 95% CI, 0.085-0.381) and SAH demonstrated a statistically significant albeit weak correlation ( $r = 0.188$ ,  $p = 0.015$ , 95% CI, 0.032-0.0335) with AWE. There was no correlation between demographics, risk factors (HTN, HLD, family history, smoking) and AWE.

## CONCLUSION

s Destabilizing IA factors that may increase permeability appear to be associated with AWE or uptake, including large size, mural thrombus, and rupture.

## CLINICAL RELEVANCE/APPLICATION

VWI holds an advantage over traditional vascular imaging techniques that are restricted to visualizing the vessel lumen. This study supports the hypothesis that AWE on MR VWI could be an indicator of aneurysm wall instability while lack of enhancement could correlate to wall stability.

### **T5A-SPNR- Characterization of Normal-Appearing White Matter Over 1-2 Years in Small Vessel Disease Using** 12 **Quantitative Susceptibility Mapping and Free-Water Mapping**

Participants

Yawen Sun, Shanghai, China (*Presenter*) Nothing to Disclose

## PURPOSE

The aim of this study was to investigate alterations in the normal-appearing white matter (NAWM) with small vessel disease (SVD) over 1-2 years using quantitative susceptibility mapping and free-water (FW) mapping.

## METHODS AND MATERIALS

Fifty-one SVD patients were included in this prospective study. Clinical testing and brain MRI scans were performed both at baseline and follow-up. Quantitative susceptibility (QS), fractional anisotropy (FA), mean diffusivity (MD), FW, FW-corrected FA (FAT), and FW-corrected MD (MDT) maps within white matter lesions (WMLs) and NAWM were generated for comparison. We also used the Johns Hopkins University Inventory of Cognitive Bias in Medicine (ICBM)-DTI-81 white matter (WM) label atlas as an anatomic guide and calculated the NAWM part in each of the WM tracts. The average regional values were extracted and paired t-test was used to analyze the longitudinal change. Partial correlations were used to assess the relationship between the MRI indices changes (e.g. ?QSfollowup-baseline/QSbaseline) and Montreal Cognitive Assessment (MoCA) scores changes (?MoCAfollowup-

baseline/MoCABaseline) which represent the cognitive function.

## RESULTS

Over 1-2 years, no significant difference was found in these MRI indices between baseline and follow-up in the WMLs region. In contrast, the QS values (index of demyelination) increased significantly in the NAWM at follow-up. Among WM tracts, we found the QS values in the NAWM part of the left superior frontal blade (SF), left occipital blade, right uncinate fasciculus, and right corticospinal tract (CST) were higher at follow-up than those at baseline. Results of FW (index of neuroinflammation/edema) analysis revealed that SVD patients at follow-up had increased FW in the NAWM part of the right CST and decreased FW in the NAWM part of the right inferior frontal blade (IF). The right SF and the right IF demonstrated significantly decreased FAT (indices of axonal loss) at follow-up compared to baseline. The degree of FAT changes in the NAWM part of the right IF were positively correlated with MoCA scores changes.

## CONCLUSION

Our study revealed how WMLs and NAWM may change over the years. The results supported that SVD is a dynamic chronic disease and the NAWM in SVD is still in the progressive injury process. Distinguishing among demyelination, neuronal degeneration, and neuroinflammation in the NAWM in vivo may provide a better understanding of the progression of SVD.

## CLINICAL RELEVANCE/APPLICATION

QSM and FW mapping can provide complementary information in the NAWM of SVD patients.

### T5A-SPNR-13 **Structural Disconnection Is Associated With Disease Severity in Neuromyelitis Optica Spectrum Disorder**

Participants

Ji Young Woo, Seoul, Korea, Republic Of (*Presenter*) Nothing to Disclose

## PURPOSE

Neuromyelitis optica spectrum disorder (NMOSD) is an autoimmune inflammatory and demyelinating disorder of the central nervous system (CNS). Accumulating evidence suggest that distinct pattern of MRI lesions characteristic of NMOSD exists and the brain MRI have potential prognostic implications. However, we do not fully understand how this brain lesions in NMOSD is associated to its rather severe and distinct clinical course. Here, we tried to investigate the association via brain structural disconnection.

## METHODS AND MATERIALS

20 patients diagnosed with NMOSD with AQP4-IgG according to the 2015 International Panel for NMO Diagnosis (IPND) criteria. The white matter lesion ROIs were manually drawn section by section on the 3D FLAIR sequence. Structural disconnection was estimated using the Lesion Quantification Toolkit. Connectome-based predictive modeling (CPM) was used to predict patient's EDSS (Expanded Disability Status Scale) from their disconnection severity matrix. In addition, correlational tractography using 32 direction diffusion weighted image was conducted to reveal local connection associated with disease severity.

## RESULTS

CPM successfully predicted the EDSS using the disconnection severity matrix ( $r = 0.506$ ,  $p = 0.028$ ;  $q2 = 0.274$ ). Among important edges in the prediction process, 19 edges were connecting the Motor - frontoparietal network, followed by 16 edges connecting the nodes within motor network and 15 edges connecting within frontoparietal network. Correlational tractography revealed local connectome in the periependymal area is associated with EDSS score.

## CONCLUSION

The structural disconnection within and between the motor and frontoparietal networks emerged as being most informative in predictions. In other words, the more severe disconnections involving these networks is predictive of severe EDSS score. Also, local disconnectome in the periependymal region is associated with EDSS score

## CLINICAL RELEVANCE/APPLICATION

Using state-of the art imaging techniques and multivariate machine learning approach, we show that structural disconnection due to brain lesions, especially motor and fronto-parietal network, is predictive of disease severity in NMOSD.

### T5A-SPNR-14 **Spatial Similarity of MRI-Visible Perivascular Spaces in Healthy Young Adult Twins**

Participants

Boeun Lee, (*Presenter*) Nothing to Disclose

## PURPOSE

This study aims to determine whether genetic factors affect the location of dilated perivascular spaces (dPVS) by comparing healthy young twins and non-twin (NT) siblings.

## METHODS AND MATERIALS

A total of 700 healthy young adult twins and NT siblings (138 monozygotic (MZ) twin pairs, 79 dizygotic (DZ) twin pairs, and 133 NT sibling pairs) were collected from the Human Connectome Project dataset. dPVS was automatically segmented and normalized to standard space. Then, spatial similarity indices (mean squared error [MSE], structural similarity [SSIM], and dice similarity [DS]) were calculated for dPVS in the basal ganglia (BGdPVS) and white matter (WMdPVS) between paired subjects before and after propensity score matching of dPVS volumes between groups. Within-pair correlations for the regional volumes of dPVS were also assessed using the intraclass correlation coefficient (ICC).

## RESULTS

The spatial similarity of dPVS was significantly higher in MZ twins (higher DS [median, 0.382 and 0.310] and SSIM [0.963 and 0.887] and lower MSE [0.005 and 0.005] for BGdPVS and WMdPVS, respectively) than DZ twins (DS [0.121 and 0.119], SSIM [0.941 and 0.868], and MSE [0.010 and 0.011]) and NT siblings (DS [0.106 and 0.097], SSIM [0.924 and 0.848], and MSE [0.016 and 0.017]). No significant difference was found between DZ twins and NT siblings. Similar results were found even after subjects were matched

according to dPVS volume. Regional dPVS volumes were also more correlated within pairs in MZ twins than DZ twins and NT siblings.

## CONCLUSION

s Our results suggest that genetic factors affect the location of dPVS.

## CLINICAL RELEVANCE/APPLICATION

We demonstrated that location of dPVS as well as its overall burden might be genetically determined to some extent using high quality images of healthy young twins and NT siblings from a large dataset.

### **T5A-SPNR-15 Characterization of White Matter Microstructural Abnormalities Associated With Cognitive Dysfunction in Cerebral Small Vessel Disease With Cerebral Microbleeds**

Participants

Haotian Xin, Jinan, China (*Presenter*) Nothing to Disclose

## PURPOSE

To characterize white matter (WM) microstructural abnormalities with diffusion tensor imaging (DTI) and their relationship with cognitive dysfunction in cerebral small vessel disease (CSVD) patients with cerebral microbleeds (CMBs) at the group and individual levels.

## METHODS AND MATERIALS

Fractional anisotropy (FA), mean diffusivity (MD), axial diffusivity (AD) and radial diffusivity (RD) images from 49 CSVD patients with CMBs (CSVD-c), 114 CSVD patients without CMBs (CSVD-n), and 83 controls were analyzed using DTI-derived tract-based spatial statistics (TBSS) to detect WM diffusion changes among groups. Pearson's correlations between regional diffusion changes and cognitive performance were investigated for all groups. Furthermore, machine learning and multivariate pattern analysis (MVPA) were applied for group classification and identifying the discriminative WM diffusion features for predicting CSVD patients with CMBs.

## RESULTS

The CSVD-c group showed significant FA decrease, AD, RD and MD increases mainly in the bilateral superior longitudinal fasciculus (SLF), inferior fronto-occipital fasciculus (IFOF), anterior thalamic radiation (ATR), inferior longitudinal fasciculus (ILF), corticospinal tract (CST), corpus callosum, external capsule and right anterior limb of internal capsule (ALIC) compared with the CSVD-n and control groups. There was no significant difference in any diffusion metric between the CSVD-n and control groups. In addition, the widespread regional diffusion alterations among groups were significantly correlated with cognitive parameters in both the CSVD-c and CSVD-n groups. Notably, we applied the multiple kernel learning (MKL) technique in MVPA to combine regional diffusion features, yielding an average of >77% accuracy for three binary classifications, which shows a considerable improvement over the individual modality approach.

## CONCLUSION

s Our findings revealed that CSVD patients with CMBs have extensive WM microstructural deterioration and suggested a key role of CMBs in causing vascular cognitive impairment involved in auditory verbal, symbol digit and executive control. Combining DTI-derived diffusivity and anisotropy metrics can provide complementary information for assessing WM alterations associated with cognitive dysfunction and serve as a potential discriminative pattern to detect CSVD at the individual level.

## CLINICAL RELEVANCE/APPLICATION

Our study may help to understand the pathology of CSVD and develop new objective neuroimaging biomarkers for diagnosis, monitoring the progression of disease or evaluating treatment efficacy.

### **T5A-SPNR-16 Quantitative Evaluation of White Matter Injury after Acute Carbon Monoxide Poisoning by Diffusion Tensor Imaging**

Participants

Wenxuan Han, XI'AN, China (*Presenter*) Nothing to Disclose

## PURPOSE

Carbon monoxide (CO) poisoning is one of the leading causes of poisoning death worldwide. At present, the brain injury mechanism of CO poisoning is still unclear, which may be related to ischemic brain tissue injury and white matter (WM) demyelination. Still, there is no consistent conclusion in existing studies. Therefore, DTI was used in this study to evaluate the microstructural integrity of white matter in patients with acute CO poisoning, and to provide evidence for the characteristics of early DTI in patients with acute CO poisoning.

## METHODS AND MATERIALS

Twenty-four patients with acute CO poisoning were received MRI within 7 days after CO poisoning. Meanwhile, 25 age- and sex-matched healthy subjects were enrolled as controls for the study. MRI was performed using a 3.0-T scanner with a 24 channels head coil. MRI sequences included T1-weighted image (T1WI), T2WI and DTI were acquired. DTI data were processed using the FMRI Software Library (FSL) Diffusion Toolkit. Tract-Based Spatial Statistics (TBSS) was used to perform voxel-wise analysis. The differences between the two groups of demographic data were analyzed. Statistical analysis of DTI data was implemented using the permutation-based (non-parametric) randomize tool within FSL. A restrictive statistical threshold was used (Threshold-Free Cluster Enhancement threshold,  $p < 0.05$ , corrected for multiple comparisons).

## RESULTS

Of the 24 analyzed patients, the median age was  $53.4 \pm 16.2$  years, and there were 5 male patients (20.8%). The median age of healthy controls was  $53.4 \pm 14.2$  years and there were 9 males (36.0%). There were no significant differences in sex or age between patients and controls ( $p = 0.24$ ,  $p = 0.99$ ). Fractional anisotropy (FA) value of genu, body and splenium of corpus callosum, bilateral frontal corona radiata and bilateral posterior WM in acute CO poisoning patients was significantly lower than that in the control group, while mean diffusivity (MD), axial diffusivity (AD), radial diffusivity (RD) was significantly higher than that in the control group. The spatial extents were relatively similar in all 4 DTI statistical maps.

## CONCLUSION

s This study suggests that DTI can provide a basis for quantitative assessment of brain injury after acute CO poisoning.

## CLINICAL RELEVANCE/APPLICATION

DTI may be a biomarker for varying injury severity in acute CO poisoning.

## **T5A-SPNR-17 Interaction Effect Between White Matter Hyperintensity Burden and Cognitive Status on the Grey Matter Volume: A Large Scale Cross-Sectional T1 and T2 Multi-Modal Study Using Automated Segmentation Tool**

Participants  
Regina Ey Kim, (*Presenter*) Researcher, NEUROPHET, Inc

## PURPOSE

The correlation between the white matter hyperintensity (WMH) and brain atrophy has been increasingly recognized as the biomarker of conversion from mild cognitive impairment (MCI) to Alzheimer's disease (AD). However, due to the studies with limited subject ( $n < 100$ ), the related findings are debatable. In addition, the detailed WMH analysis, such as periventricular hyperintensity (PWMH) and deep white matter hyperintensity (DWMH), has not been investigated previously. To better understand the association between WM burden and grey matter (GM) atrophy, the interaction effect between WMH burden (both PWMH and DWMH) and cognitive status on the GM volume was investigated.

## METHODS AND MATERIALS

A total of 3060 paired images of T1-weighted (T1w) MRI and T2- Fluid Attenuated Inversion Recovery (T2-FLAIR) MRI were utilized from seven research or clinical sites in Korea. Participants were categorized into cognitively normal ( $N=1540$ ), mild cognitive impairment (MCI,  $N=1099$ ), and dementia ( $N=421$ ) group based on their clinical assessments. T1w and T2-FLAIR images were processed and extracted their outcomes (seven GM volumes and three WMH ratio to WM) using previously developed tools. Multivariate linear regression analysis was then performed to identify interaction effect between WMH ratio to WM and cognitive status after adjusting for corresponding WMH ratio, GM volume, age, and sex.

## RESULTS

Our results indicated the higher WMH burden was associated with the lower cingulate volume in MCI ( $-9.5\text{mL}$ ,  $p=0.022$ ) when compared to the control groups. This interaction effect was mainly driven by the PWMH ( $-9.6\text{mL}$ ,  $p=0.039$ ) rather than the DWMH ( $-0.1\text{mL}$ ,  $p=0.248$ ). For the dementia group, the larger GMV with increased WMH was observed for frontal ( $+69.9\text{mL}$ ,  $p=0.022$ ) and parietal GM ( $+55.7\text{mL}$ ,  $p=0.018$ ). The parietal result was mostly driven by the PWMH ( $80.2\text{mL}$ ,  $p=0.018$ ) too.

## CONCLUSION

s Our research demonstrated the significant interaction effect between the WMH burden and the cognitive type, highlighting the importance of observing WMH burden in details (e.g., PWMH vs. DWMH) for cognitive decline status.

## CLINICAL RELEVANCE/APPLICATION

The WMH burden in association with cognitive decline, including MCI and dementia, should be closely monitored for their effect on brain atrophy.

## **T5A-SPNR-18 What Causes Us to Fail and What Happens Afterwards? A Retrospective Analysis of Failed Fluoroscopic Guided Lumbar Punctures at a Large Tertiary Medical Center**

Participants  
Myroslav Gerasymchuk, MD, (*Presenter*) Nothing to Disclose

## PURPOSE

Fluoroscopic guided lumbar punctures (FGLP) is an image guided procedure performed to obtain cerebrospinal fluid (CSF). Rarely, FGLPs can be unsuccessful for variety of reasons including inability to enter the spinal canal or inability to collect CSF, even though the needle tip is seen in the spinal canal on fluoroscopy. To our knowledge, no published data on FGLP failure rates, causes of failures, and immediate outcomes of patients with failed FGLPs exists. We hypothesize that FGLPs have a high success rate, majority of failed FGLPs are due to inadequate egress of CSF through the needle, and majority of patients with failed FGLPs return and undergo a successful FGLP.

## METHODS AND MATERIALS

We retrospectively reviewed charts of patients with failed FGLPs from 6/1/2018-3/31/2022 to collect demographic data and determine cause of FGLP failure (inability to collect CSF), if patient had a successful repeat FGLP, and if no further FGLP attempt was made, if the patient was successfully discharged.

## RESULTS

From 6/1/2018-3/31/2022,  $n=922$  FGLPs were performed on inpatient/ER patients. 46/922 (5.0%) of patients had failed initial attempts by 30 trainees at obtaining CSF. 23/46 (50%) of failures were due to lack of egress of CSF through the LP needle, though the needle tip was within the spinal canal. 10/23 patients (43%) returned to undergo FGLP on another date (mean 6.3 days (range 1-28 days) after 1st attempt) of which 70% underwent documented IV hydration prior to the FGLP and 90% were successful. 14/46 (30%) of failures were due to inability to access the spinal canal either due to degenerative changes ( $n=10$ ), high BMI ( $>35$ ) ( $n=3$ ), or postsurgical scarring ( $n=1$ ). 3/14 of patients returned to undergo another FGLP of which 2 were successful and 1 failed again. 17/46 (35%) of patients did not undergo further FGLP attempt as they improved clinically or other reasons for symptomatology were revealed and 100% of these patients were successfully discharged.

## CONCLUSION

s In our large sample, FGLPs had a success rate of 95%. Majority of the FGLPs failures were due to inability to collect CSF presumably due to low CSF pressure. Majority of these patients subsequently underwent a successful FGLP after hydration. Of patients who returned for a repeat FGLP after an initial FGLP failure due to degenerative bony changes or high BMI, 66% were

successful. Few patients did not return for a repeat FGLP and were successfully discharged.

#### CLINICAL RELEVANCE/APPLICATION

FGLPs have a high success rate in obtaining CSF and majority of the FGLP failures are due to presumed low CSF pressure. Assurance of proper hydration may obviate a need for repeat FGLP. Physicians should also be aware that FGLPs can still fail and some patients will eventually be discharged without requiring CSF sampling.

#### T5A-SPNR- In Vitro and In Vivo Evaluation of US-Triggered Release from Novel Spinal Device 19

Participants

Flemming Forsberg, PhD, Philadelphia, PA (*Presenter*) Research Grant, Canon Medical Systems Corporation; Research support, Canon Medical Systems Corporation; Research support, General Electric Company; Speaker, General Electric Company; Research support, Siemens AG; Research Grant, Butterfly Network, Inc; Research support, Lantheus Medical Imaging, Inc; Research support, Bracco Group

#### PURPOSE

Bacterial infection following spinal fusion is a major clinical concern, with up to 15% incidence, despite aggressive peri-operative antibiotic treatments. To serve this need, we have designed and evaluated an US-activated bulk release system to combat post-surgical bacterial survival.

#### METHODS AND MATERIALS

Poly(lactic acid) (PLA) clips with a 0.79 cm<sup>3</sup> drug-loading reservoir were 3D printed, loaded with the appropriate payload, and sealed with a PLA film (0.05 ± 0.01 mm thick). Clips evaluated in vitro were loaded with 150 µL vancomycin (VAN, 400 mg/mL, Athenex) and 50 µL Sonazoid (GE Healthcare), and those tested in vivo with 150 µL methylene blue (MeB) solution and 50 µL Sonazoid. Long-term stability of Sonazoid in distilled water and VAN was determined over a 14-day incubation at 4°C. Microbubble counts were obtained via flow cytometry. Contrast enhancement was visualized with a Logiq E10 scanner (GE). VAN-loaded clips were submerged in 37°C water and insonated for 10 minutes using a curvilinear C6 probe. Power Doppler imaging (1.8 MHz, 6.5 kHz PRF, ISPTA 146.2 ± 1.4 mW/cm<sup>2</sup>) induced VAN release, quantified using spectrophotometry. MeB-loaded clips were implanted into a rabbit along the spinal midline at L2 and L5, as well as a pig at L1 and L3, then insonated in Doppler mode at 1.7 MHz for 20 minutes using the C6 probe (5.4 kHz PRF, ISPTA < 146 mW/cm<sup>2</sup>). Animals were sacrificed 2 hours post-insonation for evaluation.

#### RESULTS

VAN had a conservatory effect on Sonazoid ( $p = 0.007$ ) over the 14 days, since the number of Sonazoid microbubbles in distilled water had reduced by ~90% (from  $7.3 \pm 1.4 \times 10^7$ /mL to  $7.3 \pm 1.6 \times 10^6$ /mL), while those incubated in the VAN solution reduced by ~60% (from  $8.9 \pm 6.7 \times 10^6$ /mL to  $3.3 \pm 9.3 \times 10^6$ /mL). Contrast enhancement was observed from both solutions at 14 days, indicating retained cavitation ability. Insonated clips had an average cumulative VAN release of  $81.4 \pm 2.8$  mg at 72 hours. Uninsonated clips had only  $0.3 \pm 0.1$  mg average cumulative VAN release ( $p < 0.0001$ ). Clips retrieved from the rabbit showed no signs of PLA film rupture nor MeB staining on surrounding tissues. Following physical puncture of the PLA film, release of MeB solution was visible. The pig clip PLA film was visibly ruptured, and demonstrated some MeB staining of the overlying tissues.

#### CONCLUSION

s These results demonstrate the ability to produce US-triggered release of an encapsulated prophylactic solution, and an important proof of concept for continuing large animal model in vivo evaluations.

#### CLINICAL RELEVANCE/APPLICATION

Existing methods are only partially successful in preventing infection after spinal fusion surgery. We designed an US-activated system for release of prophylactics to combat post-surgical infection.

#### T5A-SPNR-2 Intraorbital Findings in Giant Cell Arteritis on Black Blood MRI

Participants

Konstanze Guggenberger, MD, Wuerzburg, Germany (*Presenter*) Nothing to Disclose

#### PURPOSE

An expedient and accurate diagnosis of giant cell arteritis (GCA) is critical as blindness is an irreversible complication. Little is known about the spectrum of orbital imaging findings in GCA. We determined the prevalence of inflammatory changes of the intraorbital structures using high-resolution black blood MRI (BB-MRI) in patients with GCA compared to age-matched controls.

#### METHODS AND MATERIALS

A retrospective multicenter case-control study was performed screening for patients who underwent a BB-MRI on a 3 Tesla MR scanner, a clinical or histologic diagnosis of GCA, as well as age-matched controls. The BB-MRI pulse sequence was a post-contrast compressed-sensing (CS) T1-weighted sampling perfection with application-optimized contrasts using different flip angle evolution sequence. Two radiologists, blinded to clinical history, independently assessed for enhancement of the optic nerve, optic nerve sheath, ophthalmic artery vessel wall, optic chiasm, intraconal fat and extraocular muscle. Descriptive statistics were used to report percentages. Association of intraorbital BB-MRI findings with orbital symptoms was tested by Chi-Square analysis

#### RESULTS

56 patients (N=41 females; mean age 74 years) with GCA and 50 age-matched controls (17 female; mean age 70) met inclusion criteria. At the time of BB-MRI, 20 patients were steroid-naïve and 36 patients received a mean of 70 days (SD 133 days) of steroids. 32% of GCA patients showed inflammatory changes of at least one intraorbital structure. In GCA patients, optic nerve sheath enhancement (23%) was the most common BB-MRI finding, followed by ophthalmic artery vessel wall enhancement (OA-VWE) (14%). OA-VWE was unilateral in 9% and bilateral in 5%. Optic nerve enhancement was observed in one GCA patient. There was no significant correlation between patient reported orbital symptoms and pathologic enhancement of an intraorbital structure ( $p=0.10$ ). None of the age-matched control patients showed any inflammatory changes of intraorbital structures.

#### CONCLUSION

s BB-MRI revealed inflammatory findings in the orbits in up to 32% of patients with GCA independent of patient reported orbital

symptoms. Optic nerve sheath enhancement was the most common intraorbital inflammatory change.

#### CLINICAL RELEVANCE/APPLICATION

BB-MRI is a promising imaging technique to assess early inflammatory orbital changes in patients with GCA and may have a diagnostic and prognostic role for ophthalmologic complications.

#### T5A-SPNR-3 Multimodal Imaging of Lateral Branch Circulation and Cerebral Hemodynamic Correlation in Moyamoya Disease

Participants

Yao Lu, Beijing, China (*Presenter*) Nothing to Disclose

#### PURPOSE

To investigate the relationship between collateral circulation and cerebral hemodynamics in patients with moyamoya disease and moyamoya syndrome using 4D CTA-CTP imaging.

#### METHODS AND MATERIALS

The clinical and imaging data of 32 patients with moyamoya disease and moyamoya syndrome in Beijing Hospital from January 2017 to January 2022 were retrospectively analyzed. 4D-CTA images were scored by ASPECTS multi-phases scoring system, and DSA images were scored by ASITN/SIR score. The patients were divided into good collateral circulation group, medium collateral circulation group and poor collateral circulation group based on collateral circulation score. The consistency and correlation of the two collateral scores were compared. The perfusion parameters including cerebral blood volume (CBV), cerebral blood flow (CBF), mean transit time (MTT), mean transit time (TTP) and delay time (DLY) were obtained at basal ganglia level. The regions of interest (ROI) were plotted in the frontal, temporal and occipital lobes of both hemispheres respectively. Total of 192 measurements were obtained for each perfusion parameter. The differences of perfusion parameters among the three groups were compared.

#### RESULTS

1. The consistency of the two collateral circulation scores was moderate ( $Kappa=0.693$ ,  $P<0.001$ ). Spearman correlation analysis showed the correlation was good ( $r=0.805$ ,  $P<0.001$ ). 2. There were statistically significant differences in CBF, MTT and TTP among the three groups [CBF (38.2 ml /100g/min vs 40.6 ml /100g/min vs 42.1 ml /100g/min,  $P=0.019$ ), MTT (4.9s vs 4.9s vs 4.5s), TTP (20.0s vs 18.3s vs 16.4s,  $P=0.012$ ). The CBF value of the poor collateral circulation group was lower than that of the good collateral circulation group ( $P=0.015$  after Bonferroni correction). The MTT value of the moderate collateral circulation group was higher than that of the good collateral circulation group ( $P=0.005$  after Bonferroni correction). The TTP value of the poor collateral circulation group was higher than that of the good collateral circulation group ( $P=0.015$  after Bonferroni correction).

#### CONCLUSION

s 4D CTA-CTP is equivalent to DSA in evaluating collateral circulation in patients with moyamoya disease and moyamoya syndrome, and the cerebral hemodynamics can be assessed simultaneously, which has high clinical significance for disease monitoring.

#### CLINICAL RELEVANCE/APPLICATION

Multi-modal imaging can be used to monitor the cerebral hemodynamics of patients with moyamoya disease in a non-invasive manner, provide effective guidance for treatment, and observe the disease progression in real time.

#### T5A-SPNR-5 To Achieve Dramatic Radiation Dose and Contrast Dose Reduction with 70kVp Tube Voltage and Iterative Reconstruction for Head and Neck CT Angiography on Wide-detector CT: Comparison with Conventional CT Using 120kVp

Participants

Yanan Zhu, Ankang, China (*Presenter*) Nothing to Disclose

#### PURPOSE

To evaluate the clinical value of using 70kVp and new generation adaptive statistical iterative reconstruction (ASIR-V) for reducing radiation dose and contrast dose in head and neck computed tomographic angiography (CTA) on a 16cm wide-detector CT.

#### METHODS AND MATERIALS

Sixteen patients (Group A) were prospectively enrolled to undergo low radiation and contrast dose head and neck CTA using 70 kVp tube voltage and 25 mL contrast medium (CM) on a 16cm wide-detector CT system. Images were reconstructed using ASIR-V at 80% level. These images were compared with the historic data of 16 consecutive patients (Group B) who were scanned on a 64 slices CT scanner using conventional doses with 120 kVp and 50 mL CM. CT values and noise of the internal carotid artery (ICA), basilar artery (BA), middle cerebral artery (MCA), left thalamus, left centrum ovale and left cerebellar hemisphere were measured. The signal-to-noise ratio (SNR) and the contrast-to-noise ratio (CNR) for targeted arteries and brain parenchyma were calculated. Subjective image quality in terms of bone-brain interface, beam hardening artifact and gray matter and white matter contrast was evaluated. The volumetric CT dose index (CTDIvol) was recorded. Measurements from the two groups were statistically compared.

#### RESULTS

Group A reduced radiation dose by 94% ( $1.94\pm 0.0mGy$  vs.  $33.16\pm 4.92mGy$ ,  $p<0.001$ ) and used half the contrast medium dose (25mL vs. 50mL) compared with Group B. There was no difference in the mean CT values of ICA, BA and MCA between Group A ( $507.95\pm 171.06HU$ ,  $430.43\pm 169.20HU$ ,  $431.06\pm 152.85HU$ , respectively) and Group B ( $427.09\pm 97.01HU$ ,  $341.88\pm 79.17HU$ ,  $328.40\pm 84.74HU$ , respectively) There were no differences in SNR and the CNR for the targeted arteries and brain parenchyma and no difference in subjective image quality between the two groups (all  $P > 0.05$ ).

#### CONCLUSION

s The use of 70kVp and ASIR-V in head and neck CTA on a wide-detector CT system significantly reduces both radiation dose and contrast dose while providing excellent image quality, compared to the use of conventional protocols .

#### CLINICAL RELEVANCE/APPLICATION

Image quality of the head and neck CTA were not impaired at the low dose of 70kVp and 25mL indicated contrast agent on wide

image quality of the head and neck CTA were not impaired at the low dose of 70kVp and 25ml iodinated contrast agent on wide-detector CT, allowing for radiation and contrast medium reduction.

## **T5A-SPNR-6 Positive Correlation Between Cerebral Amyloid Angiopathy (CAA) And Transverse Relaxation Rate (R2): An Analysis of Ex-vivo MRI and Neuropathology**

Participants

Md Tahmid Yasar, (*Presenter*) Nothing to Disclose

### **PURPOSE**

Cerebral amyloid angiopathy (CAA) is identified by deposition of amyloid in the cortical and meningeal vessel walls. In this work, the association of CAA with the transverse relaxation rate R2 values in a large community-based cohort of older adults was investigated.

### **METHODS AND MATERIALS**

Cerebral hemispheres from 797 older adult participants of three cohort studies, the Rush Memory and Aging Project, the Minority Aging Research Study, and the Religious Orders Study were utilized in this work. All hemispheres were imaged ex-vivo at approximately 30 days postmortem using 3T clinical MRI scanners. Each scan included a multi-echo spin-echo sequence. The signals from different echoes were used to fit a mono-exponential T2 decay function (R2 is the reciprocal of T2) in each voxel. The obtained R2 maps were registered to an ex-vivo hemisphere template using ANTS. Following the MRI scan, each hemisphere underwent thorough neuropathologic evaluation. The assessed pathologies were: CAA, Alzheimer's pathology, LATE-NC, hippocampal sclerosis, Lewy bodies, arteriolosclerosis, atherosclerosis, gross and microscopic infarcts. Voxel-wise linear regression was carried out to determine the association of CAA with R2, controlling for all other pathologies listed above, demographics (age at death, sex, education), postmortem interval to fixation and imaging and scanner covariates. Statistical analysis was done using PALM with tail-accelerated 1000 permutations, threshold-free cluster enhancement, and family-wise error rate correction. Statistical significance was set at  $p < 0.05$ .

### **RESULTS**

The analysis showed a spatial pattern of higher R2 values for elevated CAA scores. The pattern comprised of structures such as the caudate, putamen, nucleus accumbens, hippocampus, insula, anterior cingulate cortex, orbitofrontal cortex, and superior frontal cortex. Negative association between R2 values and CAA scores were not found.

### **CONCLUSION**

Our work showed that CAA is associated with higher R2 among older adults, independent of demographic covariates and other neuropathologies. The spatial pattern included basal ganglia and frontal lobe structures.

### **CLINICAL RELEVANCE/APPLICATION**

Our work demonstrates the association of CAA with relaxation rate R2 in older adults. The findings can be used to generate features for MRI-based classifier that can detect the CAA pathology.

## **T5A-SPNR-7 Migraine-Associated Vascular Changes on Structural 7T-MRI**

**Awards**

**Trainee Research Prize - Medical Student**

Participants

Wilson Xu, Los Angeles, CA (*Presenter*) Nothing to Disclose

### **PURPOSE**

Migraine is a complex medical disorder which might be associated with vascular-related changes in the brain, such as white matter hyperintensities (WMH), and in some cases cerebral microbleeds (CMB). The association between migraine and enlarged perivascular spaces (EPVS) has not been thoroughly investigated. Our study utilizes ultra-high field 7T MRI to compare structural microvascular changes in different types of migraine, comparing them for the first time to headache-free healthy controls (HC).

### **METHODS AND MATERIALS**

Participants included 10 chronic migraine (CM), 10 episodic migraine without aura (EMWoA), and 5 age-matched HC. Inclusion criteria were ages 25-60 years and ongoing CM/EMWoA. Exclusion criteria were overt cognitive impairment, brain tumor, prior intracranial surgery, contraindications to MRI, and claustrophobia. Neuroimaging data were collected using 7T MRI scans utilizing T1, T2, FLAIR, and SWI/QSM sequences. We calculated EPVS in centrum semiovale (CSO) and basal ganglia (BG), WMH using the Fazekas scale, and CMB using the microbleed anatomical rating scale. We also collected clinical data such as disease duration and severity, symptoms at time of scan, presence of aura, and side of headache. Regression analysis compared neuroimaging data among CM, EMWoA, and HC.

### **RESULTS**

Preliminary statistical analysis reveals that the number of EPVS in the CSO, but not in the BG, was significantly higher with migraine compared to HC ( $p=0.04$ ). Frequency of WMH and CMB in migraine did not differ significantly from that of HC. However, migraine patients showed a significant correlation between EPVS quantity in CSO and deep WMH severity ( $p=0.04$ ).

### **CONCLUSION**

Significant differences in the EPVS in migraine compared to HC might be suggestive of glymphatic disruption within the brain, but whether such changes affect migraine development or result from migraine is unknown. EPVS may influence other vascular-related changes in migraine, suggesting a pathophysiological mechanism or possible use as an early imaging biomarker. Continued study with larger case populations and longitudinal follow-up will better establish the relationship between structural changes and migraine development and type.

### **CLINICAL RELEVANCE/APPLICATION**

7T MRI allows us to measure EPVS in migraine more accurately, advancing our knowledge on the effect of vascular/glymphatic

changes on various types of migraine for future disease-specific therapy.

## **T5A-SPNR-8 Migraine-Associated Perfusion Changes on 7T MRI**

Participants

Brendon Chou, Arcadia, CA (*Presenter*) Nothing to Disclose

### **PURPOSE**

Perfusion studies using Arterial Spin Labeling (ASL) in migraines have had conflicting results. However, these studies were limited by image resolution of 1.5 and 3T MRI scanners. Our study utilizes ultra-high field 7T MRI to investigate perfusion changes in different types of migraine with comparison to healthy controls (HC) for the first time to improve our understanding of migraine pathophysiology and guide diagnosis and treatment.

### **METHODS AND MATERIALS**

Participants were recruited as 10 chronic migraine (CM), 10 episodic migraine without aura (EMWoA), and 5 age-matched HC. Inclusion criteria were ages 25-60 years and ongoing CM/EMWoA. Exclusion criteria were overt cognitive impairment, brain tumor, prior intracranial surgery, contraindications to MRI, and claustrophobia. Neuroimaging data were acquired using the Human Connectome Project protocol implemented on a 7T MRI scanner. For the quantification of cerebral blood flow, we adopted a 3D gradient and spin-echo (GRASE) pseudo-continuous ASL (pCASL) sequence with background suppression. We also collected clinical data such as disease duration and severity, symptoms at time of scan, presence of aura, and side of headache. Cerebral blood flow (CBF) maps were generated by performing pairwise subtraction of motion-corrected label and control images from pCASL data, which were subsequently averaged across the time series.

### **RESULTS**

We observed a trend for higher cerebral blood flow (CBF) in the cortex and white matter of CM patients compared with HC or EMWoA patients ( $p=0.07$ ).

### **CONCLUSION**

s This study is novel in its usage of 7T MRI pCASL to assess perfusion changes in migraine patients. CBF increase within the cortex and white matter may reflect the lasting effects of cerebral hyperperfusion in chronic migraine or can be secondary to repetitive and frequent cortical hyperactivity. In order to understand the underlying mechanism of these changes, further studies are required to investigate the relationship between CBF and functional connectivity changes in different migraine types and phases.

### **CLINICAL RELEVANCE/APPLICATION**

Increase in CBF in CM migraine compared to EMWoA or HC can be suggestive of more extensive vascular dysregulation in this group, which may help us understand the underlying mechanism, differentiate specific types of migraine and guide further treatment.

Printed on: 02/07/23



## Abstract Archives of the RSNA, 2022

T5A-SPNR-1

### MRI Radiogenomics Analysis Predicts KRAS, EGFR and MET Mutational Status in Non-Small Cell Lung Carcinoma Brain Metastasis

Tuesday, Nov. 29 12:15PM - 12:45PM Room: Learning Center - NR DPS

#### Participants

Murat AK, MD, Pittsburgh, PA (*Presenter*) Nothing to Disclose

#### PURPOSE

Non-small cell lung cancer (NSCLC) has the highest incidence of metastases to the brain. Targetable alterations are often present in brain metastasis (BM) not found in the primary tumor. A non-invasive strategy is needed to detect brain-specific alterations. This study was conducted to assess the potential of radiogenomics to predict KRAS, EGFR and MET mutation status in BM from NSCLC patients.

#### METHODS AND MATERIALS

We retrospectively identified 159 NSCLC with BM both imaging and genomic annotation available. For each lesion, we segmented edema, contrast enhancement, and necrosis volume of interest (VOI) on both T2 FLAIR and T1 post-contrast sequences. Additionally, contralateral white matter (cWM) was also segmented for feature normalization. 10 histogram based first-order features and 195 second-order gray level co-occurrence matrix features were extracted from each VOI. After normalization, we divided the 195 second order features by the volumes of each VOI to produce another 195 volume-independent features per VOI for a total of 2,400 extracted features per lesions. We performed feature selection with Least Absolute Shrinkage and Selection Operator (LASSO). We split the cohort into 70% training and 30% testing sets for KRAS and EGFR and 80% training and 20% testing sets for MET models. We report the area under the curve (AUC) for classifying mutation status of each lesion and XGBoost was used to generate radiomics model.

#### RESULTS

Out of the 2,400 total features, LASSO identified 32 features for the EGFR mutant (mt) prediction model; of which the 20 most relevant were used for model building. The model achieved 78% accuracy, 77% sensitivity and 100% specificity. For the KRAS mt prediction model, LASSO defined 91 features and the model was generated with the top 30 features attaining 71% accuracy, 82% sensitivity and 60% specificity. Similarly, LASSO determined 90 features for MET mt prediction model, of which the top 15 features were used for the model demonstrating 77% accuracy, 76% sensitivity and 83% specificity.

#### CONCLUSION

s This study demonstrates that radiomics-based signatures can predict brain-specific molecular alterations including KRAS, EGFR and MET mutations.

#### CLINICAL RELEVANCE/APPLICATION

While further validation is warranted in a larger cohort, the proposed predictive radiomics-based approach is cost-effective, non-invasive and will help identify NSCLC patients with BM that are likely to respond to targeted treatments.

Printed on: 02/07/23

## Abstract Archives of the RSNA, 2022

T5A-SPNR-10

### The Role of Susceptibility-Weighted Imaging as an Accessory Diagnostic Tool of Global Cerebral Anoxia in the Post Cardiac Arrest Setting

Tuesday, Nov. 29 12:15PM - 12:45PM Room: Learning Center - NR DPS

#### Participants

Alyssa Ionno, Syracuse, NY (*Presenter*) Nothing to Disclose

#### PURPOSE

To examine the utility of Susceptibility-Weighted Imaging (SWI) in patients with concern for acute hypoxic-ischemic injury (HII) to the brain in the post cardiac arrest setting. It is well known that Diffusion-Weighted Imaging is our most sensitive MR sequence to detect a hypoxic-ischemic event, however it is our goal to demonstrate SWI as an effective accessory tool that should be utilized to assist in qualifying the degree of ischemic injury.

#### METHODS AND MATERIALS

Retrospective chart review was conducted in our tertiary care center. A total of 50 adult patients were selected at random with a history of acute cardiac arrest and MRI evaluation with concern for anoxic brain injury. With an independent review from a board-certified Neuroradiologist, SWI sequences were evaluated with an emphasis on the appearance of the superficial cortical veins. The great cerebral vein along with visualized arterial vasculature was also evaluated. The appearance of these vessels was quantified using a scale of 0 - 3, 0 for absent or not seen, 1 for diminished appearance, 2 for present and normal, 3 for dilated. These findings were correlated with DWI results.

#### RESULTS

Of the 50 patients initially chart reviewed 37 demonstrated MR findings consistent with anoxic brain injury on either T2-weighted or DWI imaging. Within those 37 cases 26 had DWI findings consistent with acute anoxic brain injury (70%). SWI was unavailable or suboptimal in 6 cases leaving a total of 44 cases for complete analysis. Within the SWI subset, 34 of the 44 available cases demonstrated absent (0) or diminished (1) superficial cortical veins (77%). Importantly, only 5 of the 37 patients (14%) with any MRI findings characteristic of anoxic brain injury did not show any form of diminished superficial venous vasculature on SWI. Additionally, the great cerebral vein was absent or diminished in 30 of the 44 available cases (68%). In comparison to DWI, only 5 of the 26 (19%) cases with DWI findings consistent with HII did not show any form of diminished superficial or great venous vasculature on SWI. Interestingly, of the 13 available cases with no additional MR findings to suggest anoxic brain injury 4 demonstrated diminished or absent superficial cortical veins.

#### CONCLUSION

s In SWI, the amount of deoxy-hemoglobin content within the cortical veins directly correlates with their prominence. This can therefore be applied to episodes HII, which is secondary to a decrease in overall cerebral oxygen metabolism. Our data demonstrates a significant correlation with decreased vascular prominence on SWI in this setting.

#### CLINICAL RELEVANCE/APPLICATION

To further reinforce the use and addition of susceptibility weighted imaging in protocols for acute anoxic brain injury.

Printed on: 02/07/23

## Abstract Archives of the RSNA, 2022

T5A-SPNR-11

### Predictors of Intracranial Aneurysm Wall Enhancement on High Resolution MR Vessel Wall Imaging

Tuesday, Nov. 29 12:15PM - 12:45PM Room: Learning Center - NR DPS

#### Participants

Abhinav Patel, MBBS, Chicago, IL (*Presenter*) Nothing to Disclose

#### PURPOSE

MR Vessel Wall Imaging (VWI) is an increasingly utilized modality for evaluation of neurovascular pathologies like Intracranial aneurysms (IAs) and atherosclerotic plaques. Multiple studies have evaluated the associations between intracranial aneurysm wall enhancement (AWE), risk of rupture, and aneurysm growth on follow-up. In our study, we aim to identify predictors for AWE.

#### METHODS AND MATERIALS

IRB approval was obtained for a retrospective study. Patients with IAs greater or equal to 2mm and VWI imaging were included. AWE was evaluated qualitatively, and a quantitative assessment of the percentage increase in signal intensity (SI) was also performed using means of three point ROIs placed on aneurysm wall on pre and post-contrast axial T1-SPACE sequences. The increase in SI was normalized to white matter SI on pre and post-contrast images. Patient demographics, risk factors and IA size and morphology were recorded. IAs were grouped into small (<3.9mm), medium (4-7mm), and large (>7.1mm) sizes. Spearman rank test, linear regression, and one way ANOVA were used to assess statistical associations between an increase in signal intensity, size, and other variables using SPSS v28.

#### RESULTS

A total of 174 patients (Mean age = 62.5 (24-87), 74% females) with 214 IAs (Mean size = 5.149 mm (2-30 mm) were assessed. 18/174 (10.34%) patients presented with subarachnoid hemorrhage. On qualitative evaluation, AWE was observed in 112/214 ICAs (52.3%). IA size demonstrated a moderate correlation ( $r = 0.5$ ,  $p < 0.001$ , 95% CI, 0.372-0.609) to percentage increase in SI. There was a statistically significant ( $p < 0.001$ ) increase in percentage SI, 24.75%, 46.35%, and 79.69%, in small ( $n = 78$ ), medium ( $n = 96$ ), and large ( $n = 40$ ) aneurysm groups. Thrombosis of the aneurysm sac ( $r = 0.238$ ,  $p = 0.002$ , 95% CI, 0.085-0.381) and SAH demonstrated a statistically significant albeit weak correlation ( $r = 0.188$ ,  $p = 0.015$ , 95% CI, 0.032-0.0335) with AWE. There was no correlation between demographics, risk factors (HTN, HLD, family history, smoking) and AWE.

#### CONCLUSION

Destabilizing IA factors that may increase permeability appear to be associated with AWE or uptake, including large size, mural thrombus, and rupture.

#### CLINICAL RELEVANCE/APPLICATION

VWI holds an advantage over traditional vascular imaging techniques that are restricted to visualizing the vessel lumen. This study supports the hypothesis that AWE on MR VWI could be an indicator of aneurysm wall instability while lack of enhancement could correlate to wall stability.

Printed on: 02/07/23

## Abstract Archives of the RSNA, 2022

T5A-SPNR-12

### Characterization of Normal-Appearing White Matter Over 1-2 Years in Small Vessel Disease Using Quantitative Susceptibility Mapping and Free-Water Mapping

Tuesday, Nov. 29 12:15PM - 12:45PM Room: Learning Center - NR DPS

#### Participants

Yawen Sun, Shanghai, China (*Presenter*) Nothing to Disclose

#### PURPOSE

The aim of this study was to investigate alterations in the normal-appearing white matter (NAWM) with small vessel disease (SVD) over 1-2 years using quantitative susceptibility mapping and free-water (FW) mapping.

#### METHODS AND MATERIALS

Fifty-one SVD patients were included in this prospective study. Clinical testing and brain MRI scans were performed both at baseline and follow-up. Quantitative susceptibility (QS), fractional anisotropy (FA), mean diffusivity (MD), FW, FW-corrected FA (FAT), and FW-corrected MD (MDT) maps within white matter lesions (WMLs) and NAWM were generated for comparison. We also used the Johns Hopkins University Inventory of Cognitive Bias in Medicine (ICBM)-DTI-81 white matter (WM) label atlas as an anatomic guide and calculated the NAWM part in each of the WM tracts. The average regional values were extracted and paired t-test was used to analyze the longitudinal change. Partial correlations were used to assess the relationship between the MRI indices changes (e.g.  $QS_{followup-baseline}/QS_{baseline}$ ) and Montreal Cognitive Assessment (MoCA) scores changes ( $MoCA_{followup-baseline}/MoCA_{baseline}$ ) which represent the cognitive function.

#### RESULTS

Over 1-2 years, no significant difference was found in these MRI indices between baseline and follow-up in the WMLs region. In contrast, the QS values (index of demyelination) increased significantly in the NAWM at follow-up. Among WM tracts, we found the QS values in the NAWM part of the left superior frontal blade (SF), left occipital blade, right uncinate fasciculus, and right corticospinal tract (CST) were higher at follow-up than those at baseline. Results of FW (index of neuroinflammation/edema) analysis revealed that SVD patients at follow-up had increased FW in the NAWM part of the right CST and decreased FW in the NAWM part of the right inferior frontal blade (IF). The right SF and the right IF demonstrated significantly decreased FAT (indices of axonal loss) at follow-up compared to baseline. The degree of FAT changes in the NAWM part of the right IF were positively correlated with MoCA scores changes.

#### CONCLUSION

Our study revealed how WMLs and NAWM may change over the years. The results supported that SVD is a dynamic chronic disease and the NAWM in SVD is still in the progressive injury process. Distinguishing among demyelination, neuronal degeneration, and neuroinflammation in the NAWM in vivo may provide a better understanding of the progression of SVD.

#### CLINICAL RELEVANCE/APPLICATION

QSM and FW mapping can provide complementary information in the NAWM of SVD patients.

Printed on: 02/07/23

## Abstract Archives of the RSNA, 2022

T5A-SPNR-13

### Structural Disconnection Is Associated With Disease Severity in Neuromyelitis Optica Spectrum Disorder

Tuesday, Nov. 29 12:15PM - 12:45PM Room: Learning Center - NR DPS

#### Participants

Ji Young Woo, Seoul, Korea, Republic Of (*Presenter*) Nothing to Disclose

#### PURPOSE

Neuromyelitis optica spectrum disorder (NMOSD) is an autoimmune inflammatory and demyelinating disorder of the central nervous system (CNS). Accumulating evidence suggest that distinct pattern of MRI lesions characteristic of NMOSD exists and the brain MRI have potential prognostic implications. However, we do not fully understand how this brain lesions in NMOSD is associated to its rather severe and distinct clinical course. Here, we tried to investigate the association via brain structural disconnection.

#### METHODS AND MATERIALS

20 patients diagnosed with NMOSD with AQP4-IgG according to the 2015 International Panel for NMO Diagnosis (IPND) criteria. The white matter lesion ROIs were manually drawn section by section on the 3D FLAIR sequence. Structural disconnection was estimated using the Lesion Quantification Toolkit. Connectome-based predictive modeling (CPM) was used to predict patient's EDSS (Expanded Disability Status Scale) from their disconnection severity matrix. In addition, correlational tractography using 32 direction diffusion weighted image was conducted to reveal local connection associated with disease severity.

#### RESULTS

CPM successfully predicted the EDSS using the disconnection severity matrix ( $r = 0.506$ ,  $p = 0.028$ ;  $q2 = 0.274$ ). Among important edges in the prediction process, 19 edges were connecting the Motor - frontoparietal network, followed by 16 edges connecting the nodes within motor network and 15 edges connecting within frontoparietal network. Correlational tractography revealed local connectome in the peripendymal area is associated with EDSS score.

#### CONCLUSION

s The structural disconnection within and between the motor and frontoparietal networks emerged as being most informative in predictions. In other words, the more severe disconnections involving these networks is predictive of severe EDSS score. Also, local disconnectome in the peripendymal region is associated with EDSS score

#### CLINICAL RELEVANCE/APPLICATION

Using state-of the art imaging techniques and multivariate machine learning approach, we show that structural disconnection due to brain lesions, especially motor and fronto-parietal network, is predictive of disease severity in NMOSD.

Printed on: 02/07/23

## Abstract Archives of the RSNA, 2022

T5A-SPNR-14

### Spatial Similarity of MRI-Visible Perivascular Spaces in Healthy Young Adult Twins

Tuesday, Nov. 29 12:15PM - 12:45PM Room: Learning Center - NR DPS

#### Participants

Boeun Lee, (*Presenter*) Nothing to Disclose

#### PURPOSE

This study aims to determine whether genetic factors affect the location of dilated perivascular spaces (dPVS) by comparing healthy young twins and non-twin (NT) siblings.

#### METHODS AND MATERIALS

A total of 700 healthy young adult twins and NT siblings (138 monozygotic (MZ) twin pairs, 79 dizygotic (DZ) twin pairs, and 133 NT sibling pairs) were collected from the Human Connectome Project dataset. dPVS was automatically segmented and normalized to standard space. Then, spatial similarity indices (mean squared error [MSE], structural similarity [SSIM], and dice similarity [DS]) were calculated for dPVS in the basal ganglia (BGdPVS) and white matter (WMdPVS) between paired subjects before and after propensity score matching of dPVS volumes between groups. Within-pair correlations for the regional volumes of dPVS were also assessed using the intraclass correlation coefficient (ICC).

#### RESULTS

The spatial similarity of dPVS was significantly higher in MZ twins (higher DS [median, 0.382 and 0.310] and SSIM [0.963 and 0.887] and lower MSE [0.005 and 0.005] for BGdPVS and WMdPVS, respectively) than DZ twins (DS [0.121 and 0.119], SSIM [0.941 and 0.868], and MSE [0.010 and 0.011]) and NT siblings (DS [0.106 and 0.097], SSIM [0.924 and 0.848], and MSE [0.016 and 0.017]). No significant difference was found between DZ twins and NT siblings. Similar results were found even after subjects were matched according to dPVS volume. Regional dPVS volumes were also more correlated within pairs in MZ twins than DZ twins and NT siblings.

#### CONCLUSION

Our results suggest that genetic factors affect the location of dPVS.

#### CLINICAL RELEVANCE/APPLICATION

We demonstrated that location of dPVS as well as its overall burden might be genetically determined to some extent using high quality images of healthy young twins and NT siblings from a large dataset.

Printed on: 02/07/23

## Abstract Archives of the RSNA, 2022

T5A-SPNR-15

### Characterization of White Matter Microstructural Abnormalities Associated With Cognitive Dysfunction in Cerebral Small Vessel Disease With Cerebral Microbleeds

Tuesday, Nov. 29 12:15PM - 12:45PM Room: Learning Center - NR DPS

#### Participants

Haotian Xin, Jinan, China (*Presenter*) Nothing to Disclose

#### PURPOSE

To characterize white matter (WM) microstructural abnormalities with diffusion tensor imaging (DTI) and their relationship with cognitive dysfunction in cerebral small vessel disease (CSVD) patients with cerebral microbleeds (CMBs) at the group and individual levels.

#### METHODS AND MATERIALS

Fractional anisotropy (FA), mean diffusivity (MD), axial diffusivity (AD) and radial diffusivity (RD) images from 49 CSVD patients with CMBs (CSVD-c), 114 CSVD patients without CMBs (CSVD-n), and 83 controls were analyzed using DTI-derived tract-based spatial statistics (TBSS) to detect WM diffusion changes among groups. Pearson's correlations between regional diffusion changes and cognitive performance were investigated for all groups. Furthermore, machine learning and multivariate pattern analysis (MVPA) were applied for group classification and identifying the discriminative WM diffusion features for predicting CSVD patients with CMBs.

#### RESULTS

The CSVD-c group showed significant FA decrease, AD, RD and MD increases mainly in the bilateral superior longitudinal fasciculus (SLF), inferior fronto-occipital fasciculus (IFOF), anterior thalamic radiation (ATR), inferior longitudinal fasciculus (ILF), corticospinal tract (CST), corpus callosum, external capsule and right anterior limb of internal capsule (ALIC) compared with the CSVD-n and control groups. There was no significant difference in any diffusion metric between the CSVD-n and control groups. In addition, the widespread regional diffusion alterations among groups were significantly correlated with cognitive parameters in both the CSVD-c and CSVD-n groups. Notably, we applied the multiple kernel learning (MKL) technique in MVPA to combine regional diffusion features, yielding an average of >77% accuracy for three binary classifications, which shows a considerable improvement over the individual modality approach.

#### CONCLUSION

Our findings revealed that CSVD patients with CMBs have extensive WM microstructural deterioration and suggested a key role of CMBs in causing vascular cognitive impairment involved in auditory verbal, symbol digit and executive control. Combining DTI-derived diffusivity and anisotropy metrics can provide complementary information for assessing WM alterations associated with cognitive dysfunction and serve as a potential discriminative pattern to detect CSVD at the individual level.

#### CLINICAL RELEVANCE/APPLICATION

Our study may help to understand the pathology of CSVD and develop new objective neuroimaging biomarkers for diagnosis, monitoring the progression of disease or evaluating treatment efficacy.

Printed on: 02/07/23

## Abstract Archives of the RSNA, 2022

T5A-SPNR-16

### Quantitative Evaluation of White Matter Injury after Acute Carbon Monoxide Poisoning by Diffusion Tensor Imaging

Tuesday, Nov. 29 12:15PM - 12:45PM Room: Learning Center - NR DPS

#### Participants

Wenxuan Han, XI'AN, China (*Presenter*) Nothing to Disclose

#### PURPOSE

Carbon monoxide (CO) poisoning is one of the leading causes of poisoning death worldwide. At present, the brain injury mechanism of CO poisoning is still unclear, which may be related to ischemic brain tissue injury and white matter (WM) demyelination. Still, there is no consistent conclusion in existing studies. Therefore, DTI was used in this study to evaluate the microstructural integrity of white matter in patients with acute CO poisoning, and to provide evidence for the characteristics of early DTI in patients with acute CO poisoning.

#### METHODS AND MATERIALS

Twenty-four patients with acute CO poisoning were received MRI within 7 days after CO poisoning. Meanwhile, 25 age- and sex-matched healthy subjects were enrolled as controls for the study. MRI was performed using a 3.0-T scanner with a 24 channels head coil. MRI sequences included T1-weighted image (T1WI), T2WI and DTI were acquired. DTI data were processed using the FMRI Software Library (FSL) Diffusion Toolkit. Tract-Based Spatial Statistics (TBSS) was used to perform voxel-wise analysis. The differences between the two groups of demographic data were analyzed. Statistical analysis of DTI data was implemented using the permutation-based (non-parametric) randomize tool within FSL. A restrictive statistical threshold was used (Threshold-Free Cluster Enhancement threshold,  $p < 0.05$ , corrected for multiple comparisons).

#### RESULTS

Of the 24 analyzed patients, the median age was  $53.4 \pm 16.2$  years, and there were 5 male patients (20.8%). The median age of healthy controls was  $53.4 \pm 14.2$  years and there were 9 males (36.0%). There were no significant differences in sex or age between patients and controls ( $p=0.24$ ,  $p=0.99$ ). Fractional anisotropy (FA) value of genu, body and splenium of corpus callosum, bilateral frontal corona radiata and bilateral posterior WM in acute CO poisoning patients was significantly lower than that in the control group, while mean diffusivity (MD), axial diffusivity (AD), radial diffusivity (RD) was significantly higher than that in the control group. The spatial extents were relatively similar in all 4 DTI statistical maps.

#### CONCLUSION

s This study suggests that DTI can provide a basis for quantitative assessment of brain injury after acute CO poisoning.

#### CLINICAL RELEVANCE/APPLICATION

DTI may be a biomarker for varying injury severity in acute CO poisoning.

Printed on: 02/07/23

## Abstract Archives of the RSNA, 2022

T5A-SPNR-17

### Interaction Effect Between White Matter Hyperintensity Burden and Cognitive Status on the Grey Matter Volume: A Large Scale Cross-Sectional T1 and T2 Multi-Modal Study Using Automated Segmentation Tool

Tuesday, Nov. 29 12:15PM - 12:45PM Room: Learning Center - NR DPS

#### Participants

Regina Ey Kim, (*Presenter*) Researcher, NEUROPHET, Inc

#### PURPOSE

The correlation between the white matter hyperintensity (WMH) and brain atrophy has been increasingly recognized as the biomarker of conversion from mild cognitive impairment (MCI) to Alzheimer's disease (AD). However, due to the studies with limited subject ( $n < 100$ ), the related findings are debatable. In addition, the detailed WMH analysis, such as periventricular hyperintensity (PWMH) and deep white matter hyperintensity (DWMH), has not been investigated previously. To better understand the association between WM burden and grey matter (GM) atrophy, the interaction effect between WMH burden (both PWMH and DWMH) and cognitive status on the GM volume was investigated.

#### METHODS AND MATERIALS

A total of 3060 paired images of T1-weighted (T1w) MRI and T2- Fluid Attenuated Inversion Recovery (T2-FLAIR) MRI were utilized from seven research or clinical sites in Korea. Participants were categorized into cognitively normal ( $N=1540$ ), mild cognitive impairment (MCI,  $N=1099$ ), and dementia ( $N=421$ ) group based on their clinical assessments. T1w and T2-FLAIR images were processed and extracted their outcomes (seven GM volumes and three WMH ratio to WM) using previously developed tools. Multivariate linear regression analysis was then performed to identify interaction effect between WMH ratio to WM and cognitive status after adjusting for corresponding WMH ratio, GM volume, age, and sex.

#### RESULTS

Our results indicated the higher WMH burden was associated with the lower cingulate volume in MCI ( $-9.5\text{mL}$ ,  $p=0.022$ ) when compared to the control groups. This interaction effect was mainly driven by the PWMH ( $-9.6\text{mL}$ ,  $p=0.039$ ) rather than the DWMH ( $-0.1\text{mL}$ ,  $p=0.248$ ). For the dementia group, the larger GMV with increased WMH was observed for frontal ( $+69.9\text{mL}$ ,  $p=0.022$ ) and parietal GM ( $+55.7\text{mL}$ ,  $p=0.018$ ). The parietal result was mostly driven by the PWMH ( $80.2\text{mL}$ ,  $p=0.018$ ) too.

#### CONCLUSION

Our research demonstrated the significant interaction effect between the WMH burden and the cognitive type, highlighting the importance of observing WMH burden in details (e.g., PWMH vs. DWMH) for cognitive decline status.

#### CLINICAL RELEVANCE/APPLICATION

The WMH burden in association with cognitive decline, including MCI and dementia, should be closely monitored for their effect on brain atrophy.

Printed on: 02/07/23

## Abstract Archives of the RSNA, 2022

T5A-SPNR-18

### What Causes Us to Fail and What Happens Afterwards? A Retrospective Analysis of Failed Fluoroscopic Guided Lumbar Punctures at a Large Tertiary Medical Center

Tuesday, Nov. 29 12:15PM - 12:45PM Room: Learning Center - NR DPS

#### Participants

Myroslav Gerasymchuk, MD, (*Presenter*) Nothing to Disclose

#### PURPOSE

Fluoroscopic guided lumbar punctures (FGLP) is an image guided procedure performed to obtain cerebrospinal fluid (CSF). Rarely, FGLPs can be unsuccessful for variety of reasons including inability to enter the spinal canal or inability to collect CSF, even though the needle tip is seen in the spinal canal on fluoroscopy. To our knowledge, no published data on FGLP failure rates, causes of failures, and immediate outcomes of patients with failed FGLPs exists. We hypothesize that FGLPs have a high success rate, majority of failed FGLPs are due to inadequate egress of CSF through the needle, and majority of patients with failed FGLPs return and undergo a successful FGLP.

#### METHODS AND MATERIALS

We retrospectively reviewed charts of patients with failed FGLPs from 6/1/2018-3/31/2022 to collect demographic data and determine cause of FGLP failure (inability to collect CSF), if patient had a successful repeat FGLP, and if no further FGLP attempt was made, if the patient was successfully discharged.

#### RESULTS

From 6/1/2018-3/31/2022, n=922 FGLPs were performed on inpatient/ER patients. 46/922 (5.0%) of patients had failed initial attempts by 30 trainees at obtaining CSF. 23/46 (50%) of failures were due to lack of egress of CSF through the LP needle, though the needle tip was within the spinal canal. 10/23 patients (43%) returned to undergo FGLP on another date (mean 6.3 days (range 1-28 days) after 1st attempt) of which 70% underwent documented IV hydration prior to the FGLP and 90% were successful. 14/46 (30%) of failures were due to inability to access the spinal canal either due to degenerative changes (n=10), high BMI (>35) (n=3), or postsurgical scarring (n=1). 3/14 of patients returned to undergo another FGLP of which 2 were successful and 1 failed again. 17/46 (35%) of patients did not undergo further FGLP attempt as they improved clinically or other reasons for symptomatology were revealed and 100% of these patients were successfully discharged.

#### CONCLUSION

In our large sample, FGLPs had a success rate of 95%. Majority of the FGLPs failures were due to inability to collect CSF presumably due to low CSF pressure. Majority of these patients subsequently underwent a successful FGLP after hydration. Of patients who returned for a repeat FGLP after an initial FGLP failure due to degenerative bony changes or high BMI, 66% were successful. Few patients did not return for a repeat FGLP and were successfully discharged.

#### CLINICAL RELEVANCE/APPLICATION

FGLPs have a high success rate in obtaining CSF and majority of the FGLP failures are due to presumed low CSF pressure. Assurance of proper hydration may obviate a need for repeat FGLP. Physicians should also be aware that FGLPs can still fail and some patients will eventually be discharged without requiring CSF sampling.

Printed on: 02/07/23

## Abstract Archives of the RSNA, 2022

T5A-SPNR-19

### In Vitro and In Vivo Evaluation of US-Triggered Release from Novel Spinal Device

Tuesday, Nov. 29 12:15PM - 12:45PM Room: Learning Center - NR DPS

#### Participants

Flemming Forsberg, PhD, Philadelphia, PA (*Presenter*) Research Grant, Canon Medical Systems Corporation; Research support, Canon Medical Systems Corporation; Research support, General Electric Company; Speaker, General Electric Company; Research support, Siemens AG; Research Grant, Butterfly Network, Inc; Research support, Lantheus Medical Imaging, Inc; Research support, Bracco Group

#### PURPOSE

Bacterial infection following spinal fusion is a major clinical concern, with up to 15% incidence, despite aggressive peri-operative antibiotic treatments. To serve this need, we have designed and evaluated an US-activated bulk release system to combat post-surgical bacterial survival.

#### METHODS AND MATERIALS

Poly(lactic acid) (PLA) clips with a 0.79 cm<sup>3</sup> drug-loading reservoir were 3D printed, loaded with the appropriate payload, and sealed with a PLA film (0.05 ± 0.01 mm thick). Clips evaluated in vitro were loaded with 150 µL vancomycin (VAN, 400 mg/mL, Athenex) and 50 µL Sonazoid (GE Healthcare), and those tested in vivo with 150 µL methylene blue (MeB) solution and 50 µL Sonazoid. Long-term stability of Sonazoid in distilled water and VAN was determined over a 14-day incubation at 4°C. Microbubble counts were obtained via flow cytometry. Contrast enhancement was visualized with a Logiq E10 scanner (GE). VAN-loaded clips were submerged in 37°C water and insonated for 10 minutes using a curvilinear C6 probe. Power Doppler imaging (1.8 MHz, 6.5 kHz PRF, ISPTA 146.2 ± 1.4 mW/cm<sup>2</sup>) induced VAN release, quantified using spectrophotometry. MeB-loaded clips were implanted into a rabbit along the spinal midline at L2 and L5, as well as a pig at L1 and L3, then insonated in Doppler mode at 1.7 MHz for 20 minutes using the C6 probe (5.4 kHz PRF, ISPTA < 146 mW/cm<sup>2</sup>). Animals were sacrificed 2 hours post-insonation for evaluation.

#### RESULTS

VAN had a conservatory effect on Sonazoid ( $p = 0.007$ ) over the 14 days, since the number of Sonazoid microbubbles in distilled water had reduced by ~90% (from  $7.3 \pm 1.4 \times 10^7/\text{mL}$  to  $7.3 \pm 1.6 \times 10^6/\text{mL}$ ), while those incubated in the VAN solution reduced by ~60% (from  $8.9 \pm 6.7 \times 10^6/\text{mL}$  to  $3.3 \pm 9.3 \times 10^6/\text{mL}$ ). Contrast enhancement was observed from both solutions at 14 days, indicating retained cavitation ability. Insonated clips had an average cumulative VAN release of  $81.4 \pm 2.8$  mg at 72 hours. Uninsonated clips had only  $0.3 \pm 0.1$  mg average cumulative VAN release ( $p < 0.0001$ ). Clips retrieved from the rabbit showed no signs of PLA film rupture nor MeB staining on surrounding tissues. Following physical puncture of the PLA film, release of MeB solution was visible. The pig clip PLA film was visibly ruptured, and demonstrated some MeB staining of the overlying tissues.

#### CONCLUSION

These results demonstrate the ability to produce US-triggered release of an encapsulated prophylactic solution, and an important proof of concept for continuing large animal model in vivo evaluations.

#### CLINICAL RELEVANCE/APPLICATION

Existing methods are only partially successful in preventing infection after spinal fusion surgery. We designed an US-activated system for release of prophylactics to combat post-surgical infection.

Printed on: 02/07/23

## Abstract Archives of the RSNA, 2022

T5A-SPNR-2

### Intraorbital Findings in Giant Cell Arteritis on Black Blood MRI

Tuesday, Nov. 29 12:15PM - 12:45PM Room: Learning Center - NR DPS

#### Participants

Konstanze Guggenberger, MD, Wuerzburg, Germany (*Presenter*) Nothing to Disclose

#### PURPOSE

An expedient and accurate diagnosis of giant cell arteritis (GCA) is critical as blindness is an irreversible complication. Little is known about the spectrum of orbital imaging findings in GCA. We determined the prevalence of inflammatory changes of the intraorbital structures using high-resolution black blood MRI (BB-MRI) in patients with GCA compared to age-matched controls.

#### METHODS AND MATERIALS

A retrospective multicenter case-control study was performed screening for patients who underwent a BB-MRI on a 3 Tesla MR scanner, a clinical or histologic diagnosis of GCA, as well as age-matched controls. The BB-MRI pulse sequence was a post-contrast compressed-sensing (CS) T1-weighted sampling perfection with application-optimized contrasts using different flip angle evolution sequence. Two radiologists, blinded to clinical history, independently assessed for enhancement of the optic nerve, optic nerve sheath, ophthalmic artery vessel wall, optic chiasm, intraconal fat and extraocular muscle. Descriptive statistics were used to report percentages. Association of intraorbital BB-MRI findings with orbital symptoms was tested by Chi-Square analysis

#### RESULTS

56 patients (N=41 females; mean age 74 years) with GCA and 50 age-matched controls (17 female; mean age 70) met inclusion criteria. At the time of BB-MRI, 20 patients were steroid-naïve and 36 patients received a mean of 70 days (SD 133 days) of steroids. 32% of GCA patients showed inflammatory changes of at least one intraorbital structure. In GCA patients, optic nerve sheath enhancement (23%) was the most common BB-MRI finding, followed by ophthalmic artery vessel wall enhancement (OA-VWE) (14%). OA-VWE was unilateral in 9% and bilateral in 5%. Optic nerve enhancement was observed in one GCA patient. There was no significant correlation between patient reported orbital symptoms and pathologic enhancement of an intraorbital structure ( $p=0.10$ ). None of the age-matched control patients showed any inflammatory changes of intraorbital structures.

#### CONCLUSION

s BB-MRI revealed inflammatory findings in the orbits in up to 32% of patients with GCA independent of patient reported orbital symptoms. Optic nerve sheath enhancement was the most common intraorbital inflammatory change.

#### CLINICAL RELEVANCE/APPLICATION

BB-MRI is a promising imaging technique to assess early inflammatory orbital changes in patients with GCA and may have a diagnostic and prognostic role for ophthalmologic complications.

Printed on: 02/07/23

## Abstract Archives of the RSNA, 2022

T5A-SPNR-3

### Multimodal Imaging of Lateral Branch Circulation and Cerebral Hemodynamic Correlation in Moyamoya Disease

Tuesday, Nov. 29 12:15PM - 12:45PM Room: Learning Center - NR DPS

#### Participants

Yao Lu, Beijing, China (*Presenter*) Nothing to Disclose

#### PURPOSE

To investigate the relationship between collateral circulation and cerebral hemodynamics in patients with moyamoya disease and moyamoya syndrome using 4D CTA-CTP imaging.

#### METHODS AND MATERIALS

The clinical and imaging data of 32 patients with moyamoya disease and moyamoya syndrome in Beijing Hospital from January 2017 to January 2022 were retrospectively analyzed. 4D-CTA images were scored by ASPECTS multi-phases scoring system, and DSA images were scored by ASITN/SIR score. The patients were divided into good collateral circulation group, medium collateral circulation group and poor collateral circulation group based on collateral circulation score. The consistency and correlation of the two collateral scores were compared. The perfusion parameters including cerebral blood volume (CBV), cerebral blood flow (CBF), mean transit time (MTT), mean transit time (TTP) and delay time (DLT) were obtained at basal ganglia level. The regions of interest (ROI) were plotted in the frontal, temporal and occipital lobes of both hemispheres respectively. Total of 192 measurements were obtained for each perfusion parameter. The differences of perfusion parameters among the three groups were compared.

#### RESULTS

1. The consistency of the two collateral circulation scores was moderate ( $\text{Kappa}=0.693$ ,  $P<0.001$ ). Spearman correlation analysis showed the correlation was good ( $r=0.805$ ,  $P<0.001$ ). 2. There were statistically significant differences in CBF, MTT and TTP among the three groups [CBF (38.2 ml /100g/min vs 40.6 ml /100g/min vs 42.1 ml /100g/min,  $P=0.019$ ), MTT (4.9s vs 4.9s vs 4.5s), TTP (20.0s vs 18.3s vs 16.4s,  $P=0.012$ )]. The CBF value of the poor collateral circulation group was lower than that of the good collateral circulation group ( $P=0.015$  after Bonferroni correction). The MTT value of the moderate collateral circulation group was higher than that of the good collateral circulation group ( $P=0.005$  after Bonferroni correction). The TTP value of the poor collateral circulation group was higher than that of the good collateral circulation group ( $P=0.015$  after Bonferroni correction).

#### CONCLUSION

4D CTA-CTP is equivalent to DSA in evaluating collateral circulation in patients with moyamoya disease and moyamoya syndrome, and the cerebral hemodynamics can be assessed simultaneously, which has high clinical significance for disease monitoring.

#### CLINICAL RELEVANCE/APPLICATION

Multi-modal imaging can be used to monitor the cerebral hemodynamics of patients with moyamoya disease in a non-invasive manner, provide effective guidance for treatment, and observe the disease progression in real time.

Printed on: 02/07/23

## Abstract Archives of the RSNA, 2022

T5A-SPNR-5

### To Achieve Dramatic Radiation Dose and Contrast Dose Reduction with 70kVp Tube Voltage and Iterative Reconstruction for Head and Neck CT Angiography on Wide-detector CT: Comparison with Conventional CT Using 120kVp

Tuesday, Nov. 29 12:15PM - 12:45PM Room: Learning Center - NR DPS

#### Participants

Yanan Zhu, Ankang, China (*Presenter*) Nothing to Disclose

#### PURPOSE

To evaluate the clinical value of using 70kVp and new generation adaptive statistical iterative reconstruction (ASIR-V) for reducing radiation dose and contrast dose in head and neck computed tomographic angiography (CTA) on a 16cm wide-detector CT.

#### METHODS AND MATERIALS

Sixteen patients (Group A) were prospectively enrolled to undergo low radiation and contrast dose head and neck CTA using 70 kVp tube voltage and 25 mL contrast medium (CM) on a 16cm wide-detector CT system. Images were reconstructed using ASIR-V at 80% level. These images were compared with the historic data of 16 consecutive patients (Group B) who were scanned on a 64 slices CT scanner using conventional doses with 120 kVp and 50 mL CM. CT values and noise of the internal carotid artery (ICA), basilar artery (BA), middle cerebral artery (MCA), left thalamus, left centrum ovale and left cerebellar hemisphere were measured. The signal-to-noise ratio (SNR) and the contrast-to-noise ratio (CNR) for targeted arteries and brain parenchyma were calculated. Subjective image quality in terms of bone-brain interface, beam hardening artifact and gray matter and white matter contrast was evaluated. The volumetric CT dose index (CTDIvol) was recorded. Measurements from the two groups were statistically compared.

#### RESULTS

Group A reduced radiation dose by 94% ( $1.94 \pm 0.0 \text{mGy}$  vs.  $33.16 \pm 4.92 \text{mGy}$ ,  $p < 0.001$ ) and used half the contrast medium dose (25mL vs. 50mL) compared with Group B. There was no difference in the mean CT values of ICA, BA and MCA between Group A ( $507.95 \pm 171.06 \text{HU}$ ,  $430.43 \pm 169.20 \text{HU}$ ,  $431.06 \pm 152.85 \text{HU}$ , respectively) and Group B ( $427.09 \pm 97.01 \text{HU}$ ,  $341.88 \pm 79.17 \text{HU}$ ,  $328.40 \pm 84.74 \text{HU}$ , respectively) There were no differences in SNR and the CNR for the targeted arteries and brain parenchyma and no difference in subjective image quality between the two groups (all  $P > 0.05$ ).

#### CONCLUSION

The use of 70kVp and ASIR-V in head and neck CTA on a wide-detector CT system significantly reduces both radiation dose and contrast dose while providing excellent image quality, compared to the use of conventional protocols.

#### CLINICAL RELEVANCE/APPLICATION

Image quality of the head and neck CTA were not impaired at the low dose of 70kVp and 25ml iodinated contrast agent on wide-detector CT, allowing for radiation and contrast medium reduction.

Printed on: 02/07/23

## Abstract Archives of the RSNA, 2022

T5A-SPNR-6

### **Positive Correlation Between Cerebral Amyloid Angiopathy (CAA) And Transverse Relaxation Rate (R2): An Analysis of Ex-vivo MRI and Neuropathology**

Tuesday, Nov. 29 12:15PM - 12:45PM Room: Learning Center - NR DPS

#### **Participants**

Md Tahmid Yasar, (*Presenter*) Nothing to Disclose

#### **PURPOSE**

Cerebral amyloid angiopathy (CAA) is identified by deposition of amyloid in the cortical and meningeal vessel walls. In this work, the association of CAA with the transverse relaxation rate R2 values in a large community-based cohort of older adults was investigated.

#### **METHODS AND MATERIALS**

Cerebral hemispheres from 797 older adult participants of three cohort studies, the Rush Memory and Aging Project, the Minority Aging Research Study, and the Religious Orders Study were utilized in this work. All hemispheres were imaged ex-vivo at approximately 30 days postmortem using 3T clinical MRI scanners. Each scan included a multi-echo spin-echo sequence. The signals from different echoes were used to fit a mono-exponential T2 decay function (R2 is the reciprocal of T2) in each voxel. The obtained R2 maps were registered to an ex-vivo hemisphere template using ANTS. Following the MRI scan, each hemisphere underwent thorough neuropathologic evaluation. The assessed pathologies were: CAA, Alzheimer's pathology, LATE-NC, hippocampal sclerosis, Lewy bodies, arteriolosclerosis, atherosclerosis, gross and microscopic infarcts. Voxel-wise linear regression was carried out to determine the association of CAA with R2, controlling for all other pathologies listed above, demographics (age at death, sex, education), postmortem interval to fixation and imaging and scanner covariates. Statistical analysis was done using PALM with tail-accelerated 1000 permutations, threshold-free cluster enhancement, and family-wise error rate correction. Statistical significance was set at  $p < 0.05$ .

#### **RESULTS**

The analysis showed a spatial pattern of higher R2 values for elevated CAA scores. The pattern comprised of structures such as the caudate, putamen, nucleus accumbens, hippocampus, insula, anterior cingulate cortex, orbitofrontal cortex, and superior frontal cortex. Negative association between R2 values and CAA scores were not found.

#### **CONCLUSION**

Our work showed that CAA is associated with higher R2 among older adults, independent of demographic covariates and other neuropathologies. The spatial pattern included basal ganglia and frontal lobe structures.

#### **CLINICAL RELEVANCE/APPLICATION**

Our work demonstrates the association of CAA with relaxation rate R2 in older adults. The findings can be used to generate features for MRI-based classifier that can detect the CAA pathology.

Printed on: 02/07/23

## Abstract Archives of the RSNA, 2022

T5A-SPNR-7

### Migraine-Associated Vascular Changes on Structural 7T-MRI

Tuesday, Nov. 29 12:15PM - 12:45PM Room: Learning Center - NR DPS

#### Awards

**Trainee Research Prize - Medical Student**

#### Participants

Wilson Xu, Los Angeles, CA (*Presenter*) Nothing to Disclose

#### PURPOSE

Migraine is a complex medical disorder which might be associated with vascular-related changes in the brain, such as white matter hyperintensities (WMH), and in some cases cerebral microbleeds (CMB). The association between migraine and enlarged perivascular spaces (EPVS) has not been thoroughly investigated. Our study utilizes ultra-high field 7T MRI to compare structural microvascular changes in different types of migraine, comparing them for the first time to headache-free healthy controls (HC).

#### METHODS AND MATERIALS

Participants included 10 chronic migraine (CM), 10 episodic migraine without aura (EMWoA), and 5 age-matched HC. Inclusion criteria were ages 25-60 years and ongoing CM/EMWoA. Exclusion criteria were overt cognitive impairment, brain tumor, prior intracranial surgery, contraindications to MRI, and claustrophobia. Neuroimaging data were collected using 7T MRI scans utilizing T1, T2, FLAIR, and SWI/QSM sequences. We calculated EPVS in centrum semiovale (CSO) and basal ganglia (BG), WMH using the Fazekas scale, and CMB using the microbleed anatomical rating scale. We also collected clinical data such as disease duration and severity, symptoms at time of scan, presence of aura, and side of headache. Regression analysis compared neuroimaging data among CM, EMWoA, and HC.

#### RESULTS

Preliminary statistical analysis reveals that the number of EPVS in the CSO, but not in the BG, was significantly higher with migraine compared to HC ( $p=0.04$ ). Frequency of WMH and CMB in migraine did not differ significantly from that of HC. However, migraine patients showed a significant correlation between EPVS quantity in CSO and deep WMH severity ( $p=0.04$ ).

#### CONCLUSION

Significant differences in the EPVS in migraine compared to HC might be suggestive of glymphatic disruption within the brain, but whether such changes affect migraine development or result from migraine is unknown. EPVS may influence other vascular-related changes in migraine, suggesting a pathophysiological mechanism or possible use as an early imaging biomarker. Continued study with larger case populations and longitudinal follow-up will better establish the relationship between structural changes and migraine development and type.

#### CLINICAL RELEVANCE/APPLICATION

7T MRI allows us to measure EPVS in migraine more accurately, advancing our knowledge on the effect of vascular/glymphatic changes on various types of migraine for future disease-specific therapy.

Printed on: 02/07/23

## Abstract Archives of the RSNA, 2022

T5A-SPNR-8

### Migraine-Associated Perfusion Changes on 7T MRI

Tuesday, Nov. 29 12:15PM - 12:45PM Room: Learning Center - NR DPS

#### Participants

Brendon Chou, Arcadia, CA (*Presenter*) Nothing to Disclose

#### PURPOSE

Perfusion studies using Arterial Spin Labeling (ASL) in migraines have had conflicting results. However, these studies were limited by image resolution of 1.5 and 3T MRI scanners. Our study utilizes ultra-high field 7T MRI to investigate perfusion changes in different types of migraine with comparison to healthy controls (HC) for the first time to improve our understanding of migraine pathophysiology and guide diagnosis and treatment.

#### METHODS AND MATERIALS

Participants were recruited as 10 chronic migraine (CM), 10 episodic migraine without aura (EMWoA), and 5 age-matched HC. Inclusion criteria were ages 25-60 years and ongoing CM/EMWoA. Exclusion criteria were overt cognitive impairment, brain tumor, prior intracranial surgery, contraindications to MRI, and claustrophobia. Neuroimaging data were acquired using the Human Connectome Project protocol implemented on a 7T MRI scanner. For the quantification of cerebral blood flow, we adopted a 3D gradient and spin-echo (GRASE) pseudo-continuous ASL (pCASL) sequence with background suppression. We also collected clinical data such as disease duration and severity, symptoms at time of scan, presence of aura, and side of headache. Cerebral blood flow (CBF) maps were generated by performing pairwise subtraction of motion-corrected label and control images from pCASL data, which were subsequently averaged across the time series.

#### RESULTS

We observed a trend for higher cerebral blood flow (CBF) in the cortex and white matter of CM patients compared with HC or EMWoA patients ( $p=0.07$ ).

#### CONCLUSION

This study is novel in its usage of 7T MRI pCASL to assess perfusion changes in migraine patients. CBF increase within the cortex and white matter may reflect the lasting effects of cerebral hyperperfusion in chronic migraine or can be secondary to repetitive and frequent cortical hyperactivity. In order to understand the underlying mechanism of these changes, further studies are required to investigate the relationship between CBF and functional connectivity changes in different migraine types and phases.

#### CLINICAL RELEVANCE/APPLICATION

Increase in CBF in CM migraine compared to EMWoA or HC can be suggestive of more extensive vascular dysregulation in this group, which may help us understand the underlying mechanism, differentiate specific types of migraine and guide further treatment.

Printed on: 02/07/23

## Abstract Archives of the RSNA, 2022

T5A-SPOB

### OB/Gynecology Tuesday Poster Discussions - A

Tuesday, Nov. 29 12:15PM - 12:45PM Room: Learning Center - OB DPS

#### Participants

Tara A. Morgan, MD, San Francisco, CA (*Moderator*) Nothing to Disclose

#### Sub-Events

### T5A-SPOB-1 Role of Shear Wave Elastography of Placenta in Prediction of IUGR

#### Participants

Tulika Singh, MBBS, MD, (*Presenter*) Nothing to Disclose

#### PURPOSE

To compare placental elasticity values between normal pregnancy and pregnancies with IUGR and evaluate utility of shear wave elastography of placenta as a predictor for IUGR in average risk pregnancies.

#### METHODS AND MATERIALS

A prospective study was performed with 105 singleton pregnant women. Shear wave elastography of placenta was performed in all patients at 18-22wks and at 28-32wks. 5 measurements were obtained separately each along the fetal edge and the maternal edge of the placenta. The mean of 5 measurements was accepted as the mean placental elasticity value. During follow-up between 28th to 32nd weeks, fetal biometry and placental SWE were also measured. Fetus with EFBW <10th percentile, taken as IUGR. The patients were divided into two groups - normal pregnancies (group A) and pregnancy who developed IUGR (group B). Group comparisons were done using the Chi-Square test or Fisher's exact test. Receiver Operating Characteristic (ROC) curves were calculated to find maximal cut-off values for Developed IUGR / Did not develop IUGR.

#### RESULTS

Shear wave elasticity values at 18th to 22nd weeks for IUGR pregnancies along fetal edge of placenta ( 11.75 kPa vs 9.7 kPa) and along maternal edge of placenta ( 11.5 kPa vs 9.6 kPa) were significantly as compared to the normal pregnancies ( $p < 0.05$ ). Similarly, Mean elasticity values along fetal edge of placenta (14.54 kPa vs 10.7 kPa) and along maternal edge of placenta (14.07 kPa vs 10.82 kPa) were significantly higher in IUGR pregnancies compared to the control group ( $p < 0.001$ ) during 28th to 32nd weeks Using cut-off of 12.5kpa, we attained sensitivity of 73.7%, specificity of 86% and diagnostic accuracy of 83.8% for predicting preeclampsia.

#### CONCLUSION

s Placental elasticity values are significantly higher in pregnancies with IUGR than the normal pregnancies. Also, pregnancies with a stiffer placenta in the second trimester were associated with an increased likelihood of developing IUGR. Elastography can be used as a supplementary tool for prediction of IUGR.

#### CLINICAL RELEVANCE/APPLICATION

Placental elastography can evaluate the stiffness of placenta which is shown higher in pregnancy with IUGR. With more such validation study it will a supplementary tool for prediction of IUGR in addition to grey scale ultrasound and doppler study.

Printed on: 02/07/23

## Abstract Archives of the RSNA, 2022

T5A-SPOB-1

### Role of Shear Wave Elastography of Placenta in Prediction of IUGR

Tuesday, Nov. 29 12:15PM - 12:45PM Room: Learning Center - OB DPS

#### Participants

Tulika Singh, MBBS, MD, (*Presenter*) Nothing to Disclose

#### PURPOSE

To compare placental elasticity values between normal pregnancy and pregnancies with IUGR and evaluate utility of shear wave elastography of placenta as a predictor for IUGR in average risk pregnancies.

#### METHODS AND MATERIALS

A prospective study was performed with 105 singleton pregnant women. Shear wave elastography of placenta was performed in all patients at 18-22wks and at 28-32wks. 5 measurements were obtained separately each along the fetal edge and the maternal edge of the placenta. The mean of 5 measurements was accepted as the mean placental elasticity value. During follow-up between 28th to 32nd weeks, fetal biometry and placental SWE were also measured. Fetus with EFWW <10th percentile, taken as IUGR. The patients were divided into two groups - normal pregnancies (group A) and pregnancy who developed IUGR (group B). Group comparisons were done using the Chi-Square test or Fisher's exact test. Receiver Operating Characteristic (ROC) curves were calculated to find maximal cut-off values for Developed IUGR / Did not develop IUGR.

#### RESULTS

Shear wave elasticity values at 18th to 22nd weeks for IUGR pregnancies along fetal edge of placenta ( 11.75 kPa vs 9.7 kPa) and along maternal edge of placenta ( 11.5 kPa vs 9.6 kPa) were significantly as compared to the normal pregnancies ( $p < 0.05$ ). Similarly, Mean elasticity values along fetal edge of placenta (14.54 kPa vs 10.7 kPa) and along maternal edge of placenta (14.07 kPa vs 10.82 kPa) were significantly higher in IUGR pregnancies compared to the control group ( $p < 0.001$ ) during 28th to 32nd weeks Using cut-off of 12.5kpa, we attained sensitivity of 73.7%, specificity of 86% and diagnostic accuracy of 83.8% for predicting preeclampsia.

#### CONCLUSION

s Placental elasticity values are significantly higher in pregnancies with IUGR than the normal pregnancies. Also, pregnancies with a stiffer placenta in the second trimester were associated with an increased likelihood of developing IUGR. Elastography can be used as a supplementary tool for prediction of IUGR.

#### CLINICAL RELEVANCE/APPLICATION

Placental elastography can evaluate the stiffness of placenta which is shown higher in pregnancy with IUGR. With more such validation study it will a supplementary tool for prediction of IUGR in addition to grey scale ultrasound and doppler study.

Printed on: 02/07/23

## Abstract Archives of the RSNA, 2022

T5A-SPPD

### Pediatric Tuesday Poster Discussions - A

Tuesday, Nov. 29 12:15PM - 12:45PM Room: Learning Center - PD DPS

#### Participants

Adina L. Alazraki, MD, Atlanta, GA (*Moderator*) Nothing to Disclose  
Adina L. Alazraki, MD, Atlanta, GA (*Moderator*) Nothing to Disclose  
Sarah S. Milla, MD, Aurora, CO (*Moderator*) Nothing to Disclose  
Sarah S. Milla, MD, Aurora, CO (*Moderator*) Nothing to Disclose

#### Sub-Events

### T5A-SPPD-1 Subpial Hemorrhage: An Unknown but Relevant Form of Neonatal Stroke

#### Participants

Maria Parra Hernandez, MD, Valencia, Spain (*Presenter*) Nothing to Disclose

#### PURPOSE

Subpial hemorrhage is a rare subtype of intracranial hemorrhage typically seen in neonates. Because of its infrequency, it has been often misdiagnosed and underreported. The distinctive neuroimaging characteristics of MRI, sometimes appreciated in US, enables an accurate diagnosis. Our goal with this case series is to analyze the demographic, clinical, and neuroimaging characteristics and contribute to the knowledge of this entity.

#### METHODS AND MATERIALS

Retrospective identified cases of subpial hemorrhage in neonates who were admitted to our hospital between 2014 and 2022. All the cases had available clinical and neuroimaging records. Cranial US was the first imaging test performed. MRI sequences included T2WI, T1WI, DWI, and GRET2\*WI.

#### RESULTS

Ten patients were included, most of the neonates were male and full-term born (80% each). Pregnancy complications occurred in 60%. Most deliveries were vaginal (80%) and just two of them were instrumentalized. Signs of fetal distress during birth and coagulation abnormalities were present in 70% and 40% of cases, respectively. All patients eventually presented with apnea and/or clinical seizures within 48 hours of delivery. Subpial hemorrhages were mainly unifocal (80%) with heterogeneity in localization. On T2WI most cases presented a characteristic "yin-yang pattern", with two differentiated components: the "yin side" was the hypointense acute focal subpial collection, and the "yang side" was the hyperintense underlying compressed brain parenchyma (also hyperintense on DWI). 30% of the cases didn't present this sign and showed chronic phase characteristics instead. Medullary vein congestion and underlying parenchyma bleeding were observed in 70%, the lack of this finding was due to small collections with little mass effect. Concomitant intraventricular hemorrhage was seen in 60%. Cranial US detected an extra-axial hemorrhage in 70% of cases and parenchymal injury in 90%. Before 2022 all cases were misdiagnosed as subdural hemorrhage, some of them with subarachnoid or intraparenchymal bleeding, or as isolated cortical bleeding. Within the cases with more than a year of follow-up data, two had developmental delay and three had epilepsy.

#### CONCLUSION

Neonatal subpial hemorrhage is an entity with a distinctive neuroimaging pattern, whose knowledge allows a clear differentiation from other forms of intracranial hemorrhage. Despite MRI being fundamental in the diagnosis cranial US is an excellent screening tool.

#### CLINICAL RELEVANCE/APPLICATION

The importance of this pathology relies on its association with injury of adjacent cerebral parenchyma with potential long-term consequences. An accurate diagnosis allows an early intervention.

Printed on: 02/07/23

## Abstract Archives of the RSNA, 2022

T5A-SPPD-1

### Subpial Hemorrhage: An Unknown but Relevant Form of Neonatal Stroke

Tuesday, Nov. 29 12:15PM - 12:45PM Room: Learning Center - PD DPS

#### Participants

Maria Parra Hernandez, MD, Valencia, Spain (*Presenter*) Nothing to Disclose

#### PURPOSE

Subpial hemorrhage is a rare subtype of intracranial hemorrhage typically seen in neonates. Because of its infrequency, it has been often misdiagnosed and underreported. The distinctive neuroimaging characteristics of MRI, sometimes appreciated in US, enables an accurate diagnosis. Our goal with this case series is to analyze the demographic, clinical, and neuroimaging characteristics and contribute to the knowledge of this entity.

#### METHODS AND MATERIALS

Retrospective identified cases of subpial hemorrhage in neonates who were admitted to our hospital between 2014 and 2022. All the cases had available clinical and neuroimaging records. Cranial US was the first imaging test performed. MRI sequences included T2WI, T1WI, DWI, and GRET2\*WI.

#### RESULTS

Ten patients were included, most of the neonates were male and full-term born (80% each). Pregnancy complications occurred in 60%. Most deliveries were vaginal (80%) and just two of them were instrumentalized. Signs of fetal distress during birth and coagulation abnormalities were present in 70% and 40% of cases, respectively. All patients eventually presented with apnea and/or clinical seizures within 48 hours of delivery. Subpial hemorrhages were mainly unifocal (80%) with heterogeneity in localization. On T2WI most cases presented a characteristic "yin-yang pattern", with two differentiated components: the "yin side" was the hypointense acute focal subpial collection, and the "yang side" was the hyperintense underlying compressed brain parenchyma (also hyperintense on DWI). 30% of the cases didn't present this sign and showed chronic phase characteristics instead. Medullary vein congestion and underlying parenchyma bleeding were observed in 70%, the lack of this finding was due to small collections with little mass effect. Concomitant intraventricular hemorrhage was seen in 60%. Cranial US detected an extra-axial hemorrhage in 70% of cases and parenchymal injury in 90%. Before 2022 all cases were misdiagnosed as subdural hemorrhage, some of them with subarachnoid or intraparenchymal bleeding, or as isolated cortical bleeding. Within the cases with more than a year of follow-up data, two had developmental delay and three had epilepsy.

#### CONCLUSION

Neonatal subpial hemorrhage is an entity with a distinctive neuroimaging pattern, whose knowledge allows a clear differentiation from other forms of intracranial hemorrhage. Despite MRI being fundamental in the diagnosis cranial US is an excellent screening tool.

#### CLINICAL RELEVANCE/APPLICATION

The importance of this pathology relies on its association with injury of adjacent cerebral parenchyma with potential long-term consequences. An accurate diagnosis allows an early intervention.

Printed on: 02/07/23

## Abstract Archives of the RSNA, 2022

T5A-SPPH

### Physics Tuesday Poster Discussions - A

Tuesday, Nov. 29 12:15PM - 12:45PM Room: Learning Center - PH DPS

#### Participants

Fang Liu, PhD, Boston, MA (*Moderator*) Nothing to Disclose

#### Sub-Events

### T5A-SPPH-1 Investigating Clinical and Technical Image Quality in Chest CT: Ultra-Fast Scans vs Standard Speed Scans

#### Participants

Vera Tormodsrud, MSc, (*Presenter*) Nothing to Disclose

#### PURPOSE

New techniques for CT imaging need to be qualified. It is also important to see how they affect other aspects of image quality. In this study, clinical image quality was compared between ultra-fast and standard speed chest CT. Subjective assessment of motion artefacts and quality criteria in chest CT was rated by radiologists. In addition, an advanced image quality phantom with 3D resolution measurements was used to measure the non-motion image quality between the ultra-fast and standard speed imaging.

#### METHODS AND MATERIALS

Clinical observer study: Over a 2-year period (2019-2021), 33 patients were, on separate occasions, scanned with low dose chest CT using both standard speed protocol (exposure time 500ms, pitch 1) and an ultra-fast protocol (exposure time 280ms, pitch 1.5) (HyperDrive, GE Healthcare). CTDIvol was kept close to constant between the scan techniques, varying from 3 mGy to 6 mGy between patients depending on patient size. Three readers scored general image quality and motion artefacts using a Likert scale from 1-4. In addition, ultra-fast and standard speed scans were compared on different image quality criteria. Phantom study: A Catphan® 700 (The Phantom Laboratory, Salem NY) phantom, equipped with a 3D resolution wave module was scanned on a GE Revolution CT with ultra-fast and standard scan. Images were analyzed using the SMARI software (The Phantom Laboratory).

#### RESULTS

Clinical observer study: Analysis of data from one reader showed significantly higher image quality score ( $p=0,007$ ) and reduced motion artefacts (cardiac wall:  $p=0,001$  and lung tissue:  $p<0,001$ ) for the ultra-fast scan protocol. Visual score of structures in the lung were also improved with ultra-fast scans. Results pending from the remaining readers. Phantom study: Ultra-fast scans showed a slight reduction in volumetric resolution compared to the standard speed protocol. However, the counteracting blurring from motion in the standard speed scans cannot be detected by the phantom test.

#### CONCLUSION

Although ultra-fast scans may show reduced resolution in a non-motion phantom, the benefit of reduced motion artefacts, mainly from heart beats, improve overall image quality.

#### CLINICAL RELEVANCE/APPLICATION

Fast scanning may affect image quality but reduces motion artefacts. When motion artefacts are sufficiently reduced the resulting diagnostic quality is superior to that of the standard speed scans.

### T5A-SPPH-2 A Metal Artifact Reduction Algorithm for Computed Tomography Utilizing a Raw Data Level Noise Recovery Technique

#### Participants

Taisei Nakagawa, MSc, Kanazawa-Shi, Japan (*Presenter*) Nothing to Disclose

#### PURPOSE

The metal artifact reduction (MAR) algorithm has been clinically used for patients with metal implants; however, streak artifacts often remain and become obstacles for viewing soft tissues around the metal. The remained streaks tend to be due to the frequency split method (FS) that blends high-passed information in the uncorrected image to preserve anatomical details close to metal implants and improve unnatural image textures by high-frequency noise included in the high-passed information. The purpose of this study is to propose a MAR technique using a combination of the FS method and a low data level noise recovery that prevents the remaining of streak artifacts and improves unnatural image appearances that generally occur without the FS.

#### METHODS AND MATERIALS

The proposed method performs the sinogram inpainting with a noise recovery applied during the inpainting process. The noise levels were determined by the levels of projection data adjacent to portions for inpainting, using a simple calculation based on the Poisson distribution and the dose level (effective mAs) for acquiring each target raw data. In our method, the FS method was applied to restricted regions just around the metal; thereby, the streak artifacts generally occur over a wide area were suppressed. The noise

recovery was adopted to improve unnatural image textures caused by the restrictive FS. CT images of clinical cases of dental implant and hip prostheses (two cases each) were reconstructed by the FS method and our proposed method. The normalized artifact index (nAI) was measured with five consecutive images for each reconstruction.

## RESULTS

The proposed method improved nAI values from the FS method by 52.9% and 55.9% for the dental implant cases; 54.2% and 25.6% for the hip prostheses ( $p < 0.05$ ). The edge information around the metal was maintained by the FS method restrictively applied and unnatural image appearances were improved by the noise recovery.

## CONCLUSION

It was indicated that the proposed MAR method would improve the CT image quality for patients with metal implants, by suppressing the remaining of streak artifacts that frequently occurs in images reconstructed by the existing FS method.

## CLINICAL RELEVANCE/APPLICATION

The FS method for the MAR is useful; however, the remaining of streak artifacts is a drawback. Our proposed method can improve the drawback and achieve natural image appearances.

## 75A-SPPH-3 In Vivo Determination of Potential Iodine Contrast Agent Dose Reduction for Photon-Counting CT in Comparison to Conventional CTS for Venous Phase Abdominal Scans

Participants

Rashel De Stefanis, (*Presenter*) Nothing to Disclose

## PURPOSE

To calculate the possible contrast agent dose reduction based on clinical image quality criteria on photon-counting CT (PCCT) for venous phase abdominal CT scans using conventional CT-systems as a reference.

## METHODS AND MATERIALS

Scans were collected from 56 patients who had undergone a contrast-enhanced abdominal CT examination on both a photon-counting CT (NAEOTOM Alpha, Siemens), and a conventional CT within a time frame of 2 years. Conventional CT used tube current modulation and kVp modulation (80kVp - 120kVp); PCCT used tube current modulation and a standard kVp of 120. The PCCT images were reconstructed at 70 keV. Contrast injections used patient BMI and heart rate to achieve a global HU target. The iodine weight for examinations on the PCCT was lower than on conventional CT due to an immediate contrast dose reduction request by radiologists at commissioning. Contrast measurements were performed in all paired image sets, in 7 venous phase ROIs located in left iliac vein, vena cava, vena porta, liver segment 2 and 7, spleen and the right renal pyramid. We report averaged HU-values. Assuming that a given percentage reduction in the administered contrast weight ( $m$ ) yields the same percentage reduction in average HU, the weight of contrast agent on the PCCT to achieve the reference HU on conventional CT is  $m_{new} = m_{PCCT} \text{ measured} * HU_{reference} / HU_{PCCT}$ .

## RESULTS

No significant difference in HU values was found between the various conventional CT systems (single factor ANOVA,  $p = 0.30$ ); the data were pooled for further analysis. The PCCT scans yielded a mean HU of  $155 \pm 34$  at a mean administered iodine weight of  $27 \pm 4$  g. Conventional CT scans yielded a significantly different value of  $113 \pm 24$  HU at  $32 \pm 3$  g iodine (two-tailed paired t-test, HU:  $p \ll 0.01$ , weight iodine:  $p \ll 0.01$ ). From the measurements it follows that the reference enhancement of 113 HU in going from conventional CT to PCCT would be achieved with a 38% reduction in iodine (20 g). The proposed 38% reduction would change the average administered weight iodine from  $27 \text{ g} \pm 4$ , to an average weight of  $20 \text{ g} \pm 3$ . The HU enhancement would remain body weight independent and have reduced variance. In order to keep the timing identical, dilution rather than a shorter bolus should be applied.

## CONCLUSION

In venous phase abdominal photon-counting CT a contrast dose reduction of 38% on PCCT versus conventional scanners would lead to similar contrast intensities in the images. This target could be put in gradual optimization studies.

## CLINICAL RELEVANCE/APPLICATION

Several parameters have an impact on the enhancement after contrast agent administration; not all factors are incorporated in phantom studies. Our in vivo study suggests a 38% contrast agent reduction.

## 75A-SPPH-4 Impact on Image Quality and Liver Lesion Detection of an Artificial Intelligence Deep-Learning Reconstruction Algorithm

Participants

Quentin DURAND, Montpellier, France (*Presenter*) Nothing to Disclose

## PURPOSE

To assess the impact of an artificial intelligence deep-learning reconstruction (Precise Image; AI-DLR) algorithm on image quality and liver lesion detection compared to a hybrid iterative reconstruction (iDose4, IR) algorithm.

## METHODS AND MATERIALS

This retrospective study included 30 consecutive patients with at least one liver lesion diagnosed between December 2021 and February 2022. Images were reconstructed using the level 4 of IR algorithm (i4) and the levels Standard/Smooth/Smoothing of AI-DLR algorithm. A radiologist measured the mean attenuation and standard deviation placing ROIs in the fat, muscle, healthy liver and liver tumor areas. Two radiologists assessed subjectively and in consensus, the image noise, the image smoothness, the diagnostic and overall image quality and the confidence level using Likert scales.

## RESULTS

Of the 30 patients included, 17 were men and 13 women, of mean age  $70.4 \pm 9.8$  years. The mean CTDIvol was  $6.3 \pm 2.1$  mGy and

the mean dose-length product  $446.7 \pm 178.8$  mGy.cm. Compared to i4, HU values were similar with AI-DLR at all levels for all tissues studied. For each tissue, the image noise decreased with AI-DLR compared to i4 and decreased from Standard to Smooth ( $-28\% \pm 3\%$ ) and from Smooth to Smoother ( $-34\% \pm 8\%$ ). The subjective image assessment confirmed that the image noise decreased between i4 and AI-DLR and from Standard to Smoother levels but the opposite for the image smoothing. The highest scores of diagnostic and overall image quality were found for the Smooth and Smoother levels. The confidence level was rated "certain" for all patients for the three AI-DLR levels.

## CONCLUSION

The use of AI-DLR compared to i4 reduces the image noise and improves diagnostic and overall image quality. However, from Standard to Smoother levels, image smoothing is increased. The use of the Smooth and Smoother levels therefore seems suitable for the detection of liver lesions, but the radiologist's choice of level will depend on his/her appreciation of the image smoothness.

## CLINICAL RELEVANCE/APPLICATION

For the first time, we evaluated the impact on image quality and liver lesion detection of a new AI deep learning reconstruction algorithm developed by Philips Healthcare (Precise Image) compared to an iterative hybrid reconstruction.

## T5A-SPPH-5 Photon-counting Computer Tomography of Small Vessel Stents: A Phantom Study

### Participants

Thomas Stein, Freiburg, Germany (*Presenter*) Nothing to Disclose

## PURPOSE

Accurate assessment of intravascular stents is of crucial importance to proof patency or detect complications such as in-stent stenosis, thrombosis or fracture. Non-invasive imaging of small vessel stents using CT remains still a challenge. Photon-counting CT (PCD-CT) with a novel detector technology presents the potential to overcome current drawbacks by improving image quality and reducing image artifacts. Here, we use a small vessel stent phantom to investigate the value of PCD-CT with different reconstruction kernels in comparison to a conventional energy-integrating (EID) CT serving as reference standard.

## METHODS AND MATERIALS

For phantom measurements, 12 different stents comprising various sizes (2.25mm - 8 mm), designs (covered vs. non-covered) and vendors were used. Prior to image acquisition, the stents were filled with a water-contrast agent mixed diluted to 300 HU. All scans were performed on a clinical PCD-CT and a 3rd generation dual-source EID-CT serving as reference standard. First, PCD-CT images were reconstructed using dedicated vascular kernels (Bv40, Bv44, Bv48, Bv56, Bv60). For EID-CT, the established clinical acquisition and reconstruction settings were used. Subsequently, images were assessed quantitatively by calculating multi-row intensity profiles (increasing edge rise slope [ERS]=lower blooming artifacts). In addition, subjective image quality (overall, sharpness, noise, blooming, diagnostic confidence) was evaluated by three radiologists independently (5-point Likert-scale; 5=excellent) in a random fashion and blinded to the type of reconstruction and CT system. P-values are Bonferroni-corrected for multiple testing.

## RESULTS

Best objective image quality was observed in the Bv60 kernel reconstruction ( $ERS=1611.1 \pm 608.3$ ;  $p < 0.05$ ). Highest reading scores for overall image quality were found for Bv56/Bv60 images (3.3 [2.9-3.4] and 3.8 [3.6-3.8]), which were significantly superior to the EID-CT images (2 [2.0-2.4];  $p < 0.05$  for both comparisons). Similar results were found for sharpness, blooming and diagnostic confidence ( $p < 0.05$  for all comparisons). Most severe subjective image noise was found in Bv60 reconstructions ( $p < 0.05$  compared to Bv40).

## CONCLUSION

PCD-CT facilitates a significantly improved assessment of small vessel stents compared to a 3rd generation dual-source EID-CT. Confirmatory studies translating our findings into clinical routine are needed to investigate whether PCD-CT has the potential to reduce the number of invasive angiographies in the future.

## CLINICAL RELEVANCE/APPLICATION

PCD-CT significantly improves non-invasive imaging of small vessel stents in a phantom study. Prospective patient studies are necessary to confirm the clinical value in daily care.

## T5A-SPPH-6 Low Contrast Detectability Comparison between a Prototype Photon-Counting Computed Tomography System and a Conventional CT system across a range of attenuation levels

### Participants

Kirsten Lee Boedeker, PHD, Los Angeles, CA (*Presenter*) Employee, Canon Medical Systems Corporation

## PURPOSE

The goal of this work is to compare the Low Contrast Detectability (LCD) of a prototype photon-counting computed tomography (PCCT) system to a traditional Energy-Integrated Detector (EID) CT using comparable scan protocols across a range of attenuations, including low dose, large attenuation scenarios representative of bariatric patients.

## METHODS AND MATERIALS

The 20cm Catphan as well as a set of water phantoms 24cm, 32cm, and 40cm in diameter were scanned on a prototype PCCT, as well as on an EID-CT, with 120kVp and tube current ranging from 50 to 400mA, i.e., 5.7mGy to 40mGy. Counting images were generated based on total counts registered over five energy bins. For both systems, images were reconstructed using Filtered Backprojection (FBP) with a body kernel and reconstructed to a 500mm FOV. The prototype PCCT was based on a Canon Aquilion ONE VISION™ system. The smallest detector pixel size was 342μm, and each pixel can output measurements up to 6 energy bins starting from 20keV. The readout can be configured into various macro-pixel schemes to reconstruct images at different spatial resolutions. The 3x3 macro-pixel mode generates a similar detection pitch as the typical EID-CT, and the resulting images were evaluated here. Low Contrast Detectability was estimated by using a Fourier domain implementation of a Non-Prewhitening Model Observer (NPW MO) using the measured Modulation Transfer Function (MTF), Noise Power Spectrum (NPS) and a variety of task functions.

## RESULTS

The PCCT images had both higher MTF and lower noise compared to EID CT for all conditions. LCD was improved for all conditions. Compared to EID-CT, for a 5mm, 1% contrast object the PCCT counting images demonstrated increased LCD ranging from 5 to 47% for the 40cm phantom, 10 to 20% for the 32cm and 4 to 9% for the 24cm phantom.

## CONCLUSION

s The PCCT offers a considerable increase in low contrast performance, particularly in low dose/large size scenarios

## CLINICAL RELEVANCE/APPLICATION

The PCCT counting images offer better general low contrast detectability than the EID system and demonstrates the potential to achieve better performance in low dose scenarios, such as lung cancer screening or with bariatric patients.

## T5A-SPPH-7 Cardiac-Induced Motion of the Abdominal Organs and Its Effect on Ultra-High-Resolution CT

Participants

Amir Pourmorteza, PhD, Bethesda, MD (*Presenter*) Nothing to Disclose

## PURPOSE

The recent significant leap in spatial resolution of diagnostic CT scanners have made voxel sizes as small as 150 microns also called ultra-high-resolution (UHR) possible. With such spatial acuity, effects of biological motions such as the pulsatile motion of heart, the aorta, and systolic pressure wave in the abdominal organs, can no longer be neglected. Here, we measured the cardiac-induced motion of the abdominal organs such as the pancreas and the kidneys, and used the results to simulate its impact on the spatial resolution of a UHR CT scanner.

## METHODS AND MATERIALS

We acquired Displacement Encoding with Stimulated Echoes (DENSE) magnetic resonance images (MRI) in three volunteers. orthogonal 2D scans of the pancreas were acquired in the three main anatomical planes, all centered in one location in the body of the pancreas. Additional 2D axial images were acquired at the mid-level of the left kidney. The measured displacements were then used to guide a computer simulation of a UHR CT scanner. We simulated a disk of 200 HU the diameter of which pulsed with the biological displacements measured from DENSE-MRI. The resting diameter of the disk was set at 2 cm. CT images were reconstructed from the analytically calculated projections of the pulsating disk at standard resolution, and UHR, with CT detector pixel sizes of 0.5mm and 0.25 mm at the isocenter. Radial modulation transfer function (MTF) of the images were calculated and used for analysis.

## RESULTS

The range of pancreatic motion in 3D was 0.8-1.8 mm during a cardiac cycle (Fig 1). The analytical CT simulations showed that motion with amplitude of up to 1-mm did not significantly affect the MTF of the standard resolution system. However, the 1-mm motion reduced the MTF of the UHR system by approximately 38%. We simulated different CT acquisition windows and the MTF results showed significant correlation to the acquisition window. The best cardiac phase for pancreas imaging was different for the 3 participants.

## CONCLUSION

s The spatial resolution of UHR CT can easily be impacted by cardiac-induced motion in the abdominal organs. Here we established that motion-correction or abdominal CT gating strategies may be necessary to fully take advantage of this new technology.

## CLINICAL RELEVANCE/APPLICATION

With the new advances in the spatial resolution of CT, the old sub-pixel biological motions now amount to up 10 pixels with the new resolution. Therefore, if left uncorrected these motions will blur the UHR images. Here we present our measurements of the pancreatic displacement during a cardiac cycle, and recommend ways to correct it.

## T5A-SPPH-8 Reduction of Blooming Artifact using a Clinical Photon Counting Detector CT System and Novel Bioresorbable Flow Diverters

Participants

Emily Koons, Rochester, MN (*Presenter*) Nothing to Disclose

## PURPOSE

Metallic implants for aneurysm treatment require surveillance imaging to monitor both aneurysm closure and parent artery patency. Invasive catheter angiography remains the standard technique owing to substantial metallic blooming with CT. Our aim was to quantify blooming artifact reduction from novel bioresorbable flow diverters (BRFD) using a high-resolution photon-counting-detector (PCD) CT (NAEOTOM Alpha, Siemens) in comparison with a standard clinical device and an energy-integrating-detector (EID) CT (Force, Siemens).

## METHODS AND MATERIALS

Two BRFD composed of proprietary bioresorbable materials (primarily Mg and Fe alloys) and one standard clinical device were deployed in anatomical aneurysm models and perfused with 21mg/cc iodine solution mimicking contrast-enhanced vessels in the brain. Models were placed in a 20cm water tank and scanned on both EID and PCD. EID scans were performed using routine CTA Circle of Willis (COW) protocol in our institute: 120kV, 280 quality reference mAs. PCD scans were performed using an ultra-high-resolution (UHR) mode with 120x0.2mm collimation and 120kV. Tube current was adjusted such that CTDIvol between was matched (CTDIvol 43 mGy) between scanners. EID images were reconstructed using the routine clinical protocol (Hr40 kernel, 0.75mm slice thickness), while PCD images were reconstructed using 0.6mm slice thickness and a dedicated UHR kernel Hr89 that is only available on PCD. The aneurysm models were scanned on micro-CT which served as the reference standard. Radial line profiles were drawn across the flow diverter images over 4 angles and averaged across 3 slices. Inner lumen diameter of each diverter was measured based on semi-automated full width half maximum thresholding. Results were compared with measurements from microCT (reference standard).

## RESULTS

EID images showed substantial blooming artifacts, especially for the standard clinical device, which obstructed views of the neighboring aneurysms. Blooming artifacts were substantially reduced on PCD-UHR images, with sharper delineation of the flow diverters and better visualization of the aneurysms. Overall, EID underestimated inner lumen diameter (p<0.05) by 46 percent ( $1.95\pm 0.29\text{mm}$ ) compared to microCT ( $3.84\text{mm}$ ), which was reduced to 13 percent for PCD ( $3.42\pm 0.04\text{mm}$ ).

## CONCLUSION

s Decreased blooming artifacts using PCD UHR mode improved lumen visibility in all three devices compared to EID images. Novel BRFD materials decreased blooming artifacts, allowing better visualization of vessels and aneurysms.

## CLINICAL RELEVANCE/APPLICATION

Use of PCD UHR mode accompanied by novel BRFD allows for improved visualization of neuroanatomy following device deployment, leading to potential prevention of unnecessary interventions.

## T5A-SPPH-9 Renal Imaging at 5T Versus 3T: A Comparison Study

Participants

Liyun Zheng, Shanghai, China (*Presenter*) Nothing to Disclose

## PURPOSE

This study aimed to investigate the performance of renal MRI at 5T, and compare it with 3T.

## METHODS AND MATERIALS

Fifteen healthy volunteers were included in this study. All the participants were examined on a 3T MR scanner and a 5T MR scanner by using optimal coil setups for both field strengths, respectively. The MRI sequences included coronal T1-weighted 3D volume-interpolated breath-hold gradient-echo (GRE) sequence (QUICK 3D), axial T2-weighted fast spin-echo (FSE) with fat saturation and respiratory trigger, and diffusion weighted imaging (DWI). T2\* mapping was performed based on multi-echo GRE sequence. Qualitative and quantitative analysis were performed in consensus by two experienced radiologists. The image quality for each sequence type was evaluated by using a three-point scale (score 1 = poor quality, score 2 = moderate [diagnostic] quality, score 3 = good quality). The evaluation criteria were based on: 1) the cortico-medullary differentiation and 2) the delineation of adrenal glands, proximal ureter, renal arteries, and renal veins. Considering the chemical shift, B1 inhomogeneity, susceptibility, motion artifacts and the overall image impairment, the presence of artifacts was assessed by using a three-point scale (score 1 = strong impairment, score 2 = moderate impairment, score 3 = no artifact present or insignificant). For the quantitative analysis, SNR (cortex) = Signal (cortex)/noise, SNR (medulla) = Signal (medulla)/noise, and CNR = [Signal(cortex)-Signal(medulla)]/noise were measured for images of all the sequences. For functional imaging, mean apparent diffusion coefficient (ADC) and T2\* relaxation time were calculated from cortex and medulla for each subject, respectively. Wilcoxon signed rank-sum test was used to compare the visual evaluation scores and quantitative measurements between 3T and 5T images.

## RESULTS

For all the sequences, the image quality, SNR and CNR of 5T images were significantly higher than 3T images while there is no significant difference between the presence of artifacts. For the functional maps, ADC of the cortex is significantly higher than that of the medulla at both 3T and 5T. There were no significant differences for the ADCs between 3T and 5T. Further, T2\* value of the cortex is also significantly higher than that of the medulla at both 3T and 5T. Compared to 3T, renal MRI at 5T resulted in significantly shorter T2\* values in both cortex (66.14 ms in 3T and 44.62 ms in 5T) and medulla (30.39 ms in 3T and 16.67 ms in 5T).

## CONCLUSION

s Both anatomical images and functional maps of renal MRI were feasible at 5T.

## CLINICAL RELEVANCE/APPLICATION

In vivo 5T renal MRI may better elucidate the renal diseases with both anatomical and functional imaging, compared to conventional clinical MRI scanners.

Printed on: 02/07/23

## Abstract Archives of the RSNA, 2022

T5A-SPPH-1

### Investigating Clinical and Technical Image Quality in Chest CT: Ultra-Fast Scans vs Standard Speed Scans

Tuesday, Nov. 29 12:15PM - 12:45PM Room: Learning Center - PH DPS

#### Participants

Vera Tormodsrud, MSc, (*Presenter*) Nothing to Disclose

#### PURPOSE

New techniques for CT imaging need to be qualified. It is also important to see how they affect other aspects of image quality. In this study, clinical image quality was compared between ultra-fast and standard speed chest CT. Subjective assessment of motion artefacts and quality criteria in chest CT was rated by radiologists. In addition, an advanced image quality phantom with 3D resolution measurements was used to measure the non-motion image quality between the ultra-fast and standard speed imaging.

#### METHODS AND MATERIALS

Clinical observer study: Over a 2-year period (2019-2021), 33 patients were, on separate occasions, scanned with low dose chest CT using both standard speed protocol (exposure time 500ms, pitch 1) and an ultra-fast protocol (exposure time 280ms, pitch 1.5) (HyperDrive, GE Healthcare). CT DIvol was kept close to constant between the scan techniques, varying from 3 mGy to 6 mGy between patients depending on patient size. Three readers scored general image quality and motion artefacts using a Likert scale from 1-4. In addition, ultra-fast and standard speed scans were compared on different image quality criteria. Phantom study: A Catphan® 700 (The Phantom Laboratory, Salem NY) phantom, equipped with a 3D resolution wave module was scanned on a GE Revolution CT with ultra-fast and standard scan. Images were analyzed using the SMARI software (The Phantom Laboratory).

#### RESULTS

Clinical observer study: Analysis of data from one reader showed significantly higher image quality score ( $p=0,007$ ) and reduced motion artefacts (cardiac wall:  $p=0,001$  and lung tissue:  $p<0,001$ ) for the ultra-fast scan protocol. Visual score of structures in the lung were also improved with ultra-fast scans. Results pending from the remaining readers. Phantom study: Ultra-fast scans showed a slight reduction in volumetric resolution compared to the standard speed protocol. However, the counteracting blurring from motion in the standard speed scans cannot be detected by the phantom test.

#### CONCLUSION

s Although ultra-fast scans may show reduced resolution in a non-motion phantom, the benefit of reduced motion artefacts, mainly from heart beats, improve overall image quality.

#### CLINICAL RELEVANCE/APPLICATION

Fast scanning may affect image quality but reduces motion artefacts. When motion artefacts are sufficiently reduced the resulting diagnostic quality is superior to that of the standard speed scans.

Printed on: 02/07/23

## Abstract Archives of the RSNA, 2022

T5A-SPPH-2

### A Metal Artifact Reduction Algorithm for Computed Tomography Utilizing a Raw Data Level Noise Recovery Technique

Tuesday, Nov. 29 12:15PM - 12:45PM Room: Learning Center - PH DPS

#### Participants

Taisei Nakagawa, MSc, Kanazawa-Shi, Japan (*Presenter*) Nothing to Disclose

#### PURPOSE

The metal artifact reduction (MAR) algorithm has been clinically used for patients with metal implants; however, streak artifacts often remain and become obstacles for viewing soft tissues around the metal. The remained streaks tend to be due to the frequency split method (FS) that blends high-passed information in the uncorrected image to preserve anatomical details close to metal implants and improve unnatural image textures by high-frequency noise included in the high-passed information. The purpose of this study is to propose a MAR technique using a combination of the FS method and a low data level noise recovery that prevents the remaining of streak artifacts and improves unnatural image appearances that generally occur without the FS.

#### METHODS AND MATERIALS

The proposed method performs the sinogram inpainting with a noise recovery applied during the inpainting process. The noise levels were determined by the levels of projection data adjacent to portions for inpainting, using a simple calculation based on the Poisson distribution and the dose level (effective mAs) for acquiring each target raw data. In our method, the FS method was applied to restricted regions just around the metal; thereby, the streak artifacts generally occur over a wide area were suppressed. The noise recovery was adopted to improve unnatural image textures caused by the restrictive FS. CT images of clinical cases of dental implant and hip prostheses (two cases each) were reconstructed by the FS method and our proposed method. The normalized artifact index (nAI) was measured with five consecutive images for each reconstruction.

#### RESULTS

The proposed method improved nAI values from the FS method by 52.9% and 55.9% for the dental implant cases; 54.2% and 25.6% for the hip prostheses ( $p < 0.05$ ). The edge information around the metal was maintained by the FS method restrictively applied and unnatural image appearances were improved by the noise recovery.

#### CONCLUSION

It was indicated that the proposed MAR method would improve the CT image quality for patients with metal implants, by suppressing the remaining of streak artifacts that frequently occurs in images reconstructed by the existing FS method.

#### CLINICAL RELEVANCE/APPLICATION

The FS method for the MAR is useful; however, the remaining of streak artifacts is a drawback. Our proposed method can improve the drawback and achieve natural image appearances.

Printed on: 02/07/23

## Abstract Archives of the RSNA, 2022

T5A-SPPH-3

### **In Vivo Determination of Potential Iodine Contrast Agent Dose Reduction for Photon-Counting CT in Comparison to Conventional CTS for Venous Phase Abdominal Scans**

Tuesday, Nov. 29 12:15PM - 12:45PM Room: Learning Center - PH DPS

#### **Participants**

Rashel De Stefanis, (*Presenter*) Nothing to Disclose

#### **PURPOSE**

To calculate the possible contrast agent dose reduction based on clinical image quality criteria on photon-counting CT (PCCT) for venous phase abdominal CT scans using conventional CT-systems as a reference.

#### **METHODS AND MATERIALS**

Scans were collected from 56 patients who had undergone a contrast-enhanced abdominal CT examination on both a photon-counting CT (NAEOTOM Alpha, Siemens), and a conventional CT within a time frame of 2 years. Conventional CT used tube current modulation and kVp modulation (80kVp - 120kVp); PCCT used tube current modulation and a standard kVp of 120. The PCCT images were reconstructed at 70 keV. Contrast injections used patient BMI and heart rate to achieve a global HU target. The iodine weight for examinations on the PCCT was lower than on conventional CT due to an immediate contrast dose reduction request by radiologists at commissioning. Contrast measurements were performed in all paired image sets, in 7 venous phase ROIs located in left iliac vein, vena cava, vena porta, liver segment 2 and 7, spleen and the right renal pyramid. We report averaged HU-values. Assuming that a given percentage reduction in the administered contrast weight (m) yields the same percentage reduction in average HU, the weight of contrast agent on the PCCT to achieve the reference HU on conventional CT is  $m_{new} = m_{PCCT} \cdot \frac{HU_{reference}}{HU_{PCCT}}$ .

#### **RESULTS**

No significant difference in HU values was found between the various conventional CT systems (single factor ANOVA,  $p = 0.30$ ); the data were pooled for further analysis. The PCCT scans yielded a mean HU of  $155 \pm 34$  at a mean administered iodine weight of  $27 \pm 4$  g. Conventional CT scans yielded a significantly different value of  $113 \pm 24$  HU at  $32 \pm 3$  g iodine (two-tailed paired t-test, HU:  $p \ll 0.01$ , weight iodine:  $p \ll 0.01$ ). From the measurements it follows that the reference enhancement of 113 HU in going from conventional CT to PCCT would be achieved with a 38% reduction in iodine (20 g). The proposed 38% reduction would change the average administered weight iodine from  $27 \text{ g} \pm 4$ , to an average weight of  $20 \text{ g} \pm 3$ . The HU enhancement would remain body weight independent and have reduced variance. In order to keep the timing identical, dilution rather than a shorter bolus should be applied.

#### **CONCLUSION**

In venous phase abdominal photon-counting CT a contrast dose reduction of 38% on PCCT versus conventional scanners would lead to similar contrast intensities in the images. This target could be put in gradual optimization studies.

#### **CLINICAL RELEVANCE/APPLICATION**

Several parameters have an impact on the enhancement after contrast agent administration; not all factors are incorporated in phantom studies. Our in vivo study suggests a 38% contrast agent reduction.

Printed on: 02/07/23

## Abstract Archives of the RSNA, 2022

T5A-SPPH-4

### Impact on Image Quality and Liver Lesion Detection of an Artificial Intelligence Deep-Learning Reconstruction Algorithm

Tuesday, Nov. 29 12:15PM - 12:45PM Room: Learning Center - PH DPS

#### Participants

Quentin DURAND, Montpellier, France (*Presenter*) Nothing to Disclose

#### PURPOSE

To assess the impact of an artificial intelligence deep-learning reconstruction (Precise Image; AI-DLR) algorithm on image quality and liver lesion detection compared to a hybrid iterative reconstruction (iDose4, IR) algorithm.

#### METHODS AND MATERIALS

This retrospective study included 30 consecutive patients with at least one liver lesion diagnosed between December 2021 and February 2022. Images were reconstructed using the level 4 of IR algorithm (i4) and the levels Standard/Smooth/Smother of AI-DLR algorithm. A radiologist measured the mean attenuation and standard deviation placing ROIs in the fat, muscle, healthy liver and liver tumor areas. Two radiologists assessed subjectively and in consensus, the image noise, the image smoothness, the diagnostic and overall image quality and the confidence level using Likert scales.

#### RESULTS

Of the 30 patients included, 17 were men and 13 women, of mean age  $70.4 \pm 9.8$  years. The mean CT DIvol was  $6.3 \pm 2.1$  mGy and the mean dose-length product  $446.7 \pm 178.8$  mGy.cm. Compared to i4, HU values were similar with AI-DLR at all levels for all tissues studied. For each tissue, the image noise decreased with AI-DLR compared to i4 and decreased from Standard to Smooth ( $-28\% \pm 3\%$ ) and from Smooth to Smother ( $-34\% \pm 8\%$ ). The subjective image assessment confirmed that the image noise decreased between i4 and AI-DLR and from Standard to Smother levels but the opposite for the image smoothing. The highest scores of diagnostic and overall image quality were found for the Smooth and Smother levels. The confidence level was rated "certain" for all patients for the three AI-DLR levels.

#### CONCLUSION

The use of AI-DLR compared to i4 reduces the image noise and improves diagnostic and overall image quality. However, from Standard to Smother levels, image smoothing is increased. The use of the Smooth and Smother levels therefore seems suitable for the detection of liver lesions, but the radiologist's choice of level will depend on his/her appreciation of the image smoothness.

#### CLINICAL RELEVANCE/APPLICATION

For the first time, we evaluated the impact on image quality and liver lesion detection of a new AI deep learning reconstruction algorithm developed by Philips Healthcare (Precise Image) compared to an iterative hybrid reconstruction.

Printed on: 02/07/23

## Abstract Archives of the RSNA, 2022

T5A-SPPH-5

### Photon-counting Computer Tomography of Small Vessel Stents: A Phantom Study

Tuesday, Nov. 29 12:15PM - 12:45PM Room: Learning Center - PH DPS

#### Participants

Thomas Stein, Freiburg, Germany (*Presenter*) Nothing to Disclose

#### PURPOSE

Accurate assessment of intravascular stents is of crucial importance to proof patency or detect complications such as in-stent stenosis, thrombosis or fracture. Non-invasive imaging of small vessel stents using CT remains still a challenge. Photon-counting CT (PCD-CT) with a novel detector technology presents the potential to overcome current drawbacks by improving image quality and reducing image artifacts. Here, we use a small vessel stent phantom to investigate the value of PCD-CT with different reconstruction kernels in comparison to a conventional energy-integrating (EID) CT serving as reference standard.

#### METHODS AND MATERIALS

For phantom measurements, 12 different stents comprising various sizes (2.25mm - 8 mm), designs (covered vs. non-covered) and vendors were used. Prior to image acquisition, the stents were filled with a water-contrast agent mixed diluted to 300 HU. All scans were performed on a clinical PCD-CT and a 3rd generation dual-source EID-CT serving as reference standard. First, PCD-CT images were reconstructed using dedicated vascular kernels (Bv40, Bv44, Bv48, Bv56, Bv60). For EID-CT, the established clinical acquisition and reconstruction settings were used. Subsequently, images were assessed quantitatively by calculating multi-row intensity profiles (increasing edge rise slope [ERS]=lower blooming artifacts). In addition, subjective image quality (overall, sharpness, noise, blooming, diagnostic confidence) was evaluated by three radiologists independently (5-point Likert-scale; 5=excellent) in a random fashion and blinded to the type of reconstruction and CT system. P-values are Bonferroni-corrected for multiple testing.

#### RESULTS

Best objective image quality was observed in the Bv60 kernel reconstruction ( $ERS=1611.1\pm608.3$ ;  $p<0.05$ ). Highest reading scores for overall image quality were found for Bv56/Bv60 images (3.3 [2.9-3.4] and 3.8 [3.6-3.8]), which were significantly superior to the EID-CT images (2 [2.0-2.4];  $p<0.05$  for both comparisons). Similar results were found for sharpness, blooming and diagnostic confidence ( $p<0.05$  for all comparisons). Most severe subjective image noise was found in Bv60 reconstructions ( $p<0.05$  compared to Bv40).

#### CONCLUSION

s PCD-CT facilitates a significantly improved assessment of small vessel stents compared to a 3rd generation dual-source EID-CT. Confirmatory studies translating our findings into clinical routine are needed to investigate whether PCD-CT has the potential to reduce the number of invasive angiographies in the future.

#### CLINICAL RELEVANCE/APPLICATION

PCT-CT significantly improves non-invasive imaging of small vessel stents in a phantom study. Prospective patient studies are necessary to confirm the clinical value in daily care.

Printed on: 02/07/23

## Abstract Archives of the RSNA, 2022

T5A-SPPH-6

### Low Contrast Detectability Comparison between a Prototype Photon-Counting Computed Tomography System and a Conventional CT system across a range of attenuation levels

Tuesday, Nov. 29 12:15PM - 12:45PM Room: Learning Center - PH DPS

#### Participants

Kirsten Lee Boedeker, PHD, Los Angeles, CA (*Presenter*) Employee, Canon Medical Systems Corporation

#### PURPOSE

The goal of this work is to compare the Low Contrast Detectability (LCD) of a prototype photon-counting computed tomography (PCCT) system to a traditional Energy-Integrated Detector (EID) CT using comparable scan protocols across a range of attenuations, including low dose, large attenuation scenarios representative of bariatric patients.

#### METHODS AND MATERIALS

The 20cm Catphan as well as a set of water phantoms 24cm, 32cm, and 40cm in diameter were scanned on a prototype PCCT, as well as on an EID-CT, with 120kVp and tube current ranging from 50 to 400mA, i.e., 5.7mGy to 40mGy. Counting images were generated based on total counts registered over five energy bins. For both systems, images were reconstructed using Filtered Backprojection (FBP) with a body kernel and reconstructed to a 500mm FOV. The prototype PCCT was based on a Canon Aquilion ONE VISION™ system. The smallest detector pixel size was 342μm, and each pixel can output measurements up to 6 energy bins starting from 20keV. The readout can be configured into various macro-pixel schemes to reconstruct images at different spatial resolutions. The 3x3 macro-pixel mode generates a similar detection pitch as the typical EID-CT, and the resulting images were evaluated here. Low Contrast Detectability was estimated by using a Fourier domain implementation of a Non-Prewhitening Model Observer (NPW MO) using the measured Modulation Transfer Function (MTF), Noise Power Spectrum (NPS) and a variety of task functions.

#### RESULTS

The PCCT images had both higher MTF and lower noise compared to EID CT for all conditions. LCD was improved for all conditions. Compared to EID-CT, for a 5mm, 1% contrast object the PCCT counting images demonstrated increased LCD ranging from 5 to 47% for the 40cm phantom, 10 to 20% for the 32cm and 4 to 9% for the 24cm phantom.

#### CONCLUSION

s The PCCT offers a considerable increase in low contrast performance, particularly in low dose/large size scenarios

#### CLINICAL RELEVANCE/APPLICATION

The PCCT counting images offer better general low contrast detectability than the EID system and demonstrates the potential to achieve better performance in low dose scenarios, such as lung cancer screening or with bariatric patients.

Printed on: 02/07/23

## Abstract Archives of the RSNA, 2022

T5A-SPPH-7

### Cardiac-Induced Motion of the Abdominal Organs and Its Effect on Ultra-High-Resolution CT

Tuesday, Nov. 29 12:15PM - 12:45PM Room: Learning Center - PH DPS

#### Participants

Amir Pourmorteza, PhD, Bethesda, MD (*Presenter*) Nothing to Disclose

#### PURPOSE

The recent significant leap in spatial resolution of diagnostic CT scanners have made voxel sizes as small as 150 microns also called ultra-high-resolution (UHR) possible. With such spatial acuity, effects of biological motions such as the pulsatile motion of heart, the aorta, and systolic pressure wave in the abdominal organs, can no longer be neglected. Here, we measured the cardiac-induced motion of the abdominal organs such as the pancreas and the kidneys, and used the results to simulate its impact on the spatial resolution of a UHR CT scanner.

#### METHODS AND MATERIALS

We acquired Displacement Encoding with Stimulated Echoes (DENSE) magnetic resonance images (MRI) in three volunteers. orthogonal 2D scans of the pancreas were acquired in the three main anatomical planes, all centered in one location in the body of the pancreas. Additional 2D axial images were acquired at the mid-level of the left kidney. The measured displacements were then used to guide a computer simulation of a UHR CT scanner. We simulated a disk of 200 HU the diameter of which pulsated with the biological displacements measured from DENSE-MRI. The resting diameter of the disk was set at 2 cm. CT images were reconstructed from the analytically calculated projections of the pulsating disk at standard resolution, and UHR, with CT detector pixel sizes of 0.5mm and 0.25 mm at the isocenter. Radial modulation transfer function (MTF) of the images were calculated and used for analysis.

#### RESULTS

The range of pancreatic motion in 3D was 0.8-1.8 mm during a cardiac cycle (Fig 1). The analytical CT simulations showed that motion with amplitude of up to 1-mm did not significantly affect the MTF of the standard resolution system. However, the 1-mm motion reduced the MTF of the UHR system by approximately 38%. We simulated different CT acquisition windows and the MTF results showed significant correlation to the acquisition window. The best cardiac phase for pancreas imaging was different for the 3 participants.

#### CONCLUSION

The spatial resolution of UHR CT can easily be impacted by cardiac-induced motion in the abdominal organs. Here we established that motion-correction or abdominal CT gating strategies may be necessary to fully take advantage of this new technology.

#### CLINICAL RELEVANCE/APPLICATION

With the new advances in the spatial resolution of CT, the old sub-pixel biological motions now amount to up 10 pixels with the new resolution. Therefore, if left uncorrected these motions will blur the UHR images. Here we present our measurements of the pancreatic displacement during a cardiac cycle, and recommend ways to correct it.

Printed on: 02/07/23

## Abstract Archives of the RSNA, 2022

T5A-SPPH-8

### Reduction of Blooming Artifact using a Clinical Photon Counting Detector CT System and Novel Bioresorbable Flow Diverters

Tuesday, Nov. 29 12:15PM - 12:45PM Room: Learning Center - PH DPS

#### Participants

Emily Koons, Rochester, MN (*Presenter*) Nothing to Disclose

#### PURPOSE

Metallic implants for aneurysm treatment require surveillance imaging to monitor both aneurysm closure and parent artery patency. Invasive catheter angiography remains the standard technique owing to substantial metallic blooming with CT. Our aim was to quantify blooming artifact reduction from novel bioresorbable flow diverters (BRFD) using a high-resolution photon-counting-detector (PCD) CT (NAEOTOM Alpha, Siemens) in comparison with a standard clinical device and an energy-integrating-detector (EID) CT (Force, Siemens).

#### METHODS AND MATERIALS

Two BRFD composed of proprietary bioresorbable materials (primarily Mg and Fe alloys) and one standard clinical device were deployed in anatomical aneurysm models and perfused with 21mg/cc iodine solution mimicking contrast-enhanced vessels in the brain. Models were placed in a 20cm water tank and scanned on both EID and PCD. EID scans were performed using routine CTA Circle of Willis (COW) protocol in our institute: 120kV, 280 quality reference mAs. PCD scans were performed using an ultra-high-resolution (UHR) mode with 120x0.2mm collimation and 120kV. Tube current was adjusted such that CTDIvol between was matched (CTDIvol 43 mGy) between scanners. EID images were reconstructed using the routine clinical protocol (Hr40 kernel, 0.75mm slice thickness), while PCD images were reconstructed using 0.6mm slice thickness and a dedicated UHR kernel Hr89 that is only available on PCD. The aneurysm models were scanned on micro-CT which served as the reference standard. Radial line profiles were drawn across the flow diverter images over 4 angles and averaged across 3 slices. Inner lumen diameter of each diverter was measured based on semi-automated full width half maximum thresholding. Results were compared with measurements from microCT (reference standard).

#### RESULTS

EID images showed substantial blooming artifacts, especially for the standard clinical device, which obstructed views of the neighboring aneurysms. Blooming artifacts were substantially reduced on PCD-UHR images, with sharper delineation of the flow diverters and better visualization of the aneurysms. Overall, EID underestimated inner lumen diameter (p<0.05) by 46 percent ( $1.95\pm 0.29$ mm) compared to microCT (3.84mm), which was reduced to 13 percent for PCD ( $3.42\pm 0.04$ mm).

#### CONCLUSION

Decreased blooming artifacts using PCD UHR mode improved lumen visibility in all three devices compared to EID images. Novel BRFD materials decreased blooming artifacts, allowing better visualization of vessels and aneurysms.

#### CLINICAL RELEVANCE/APPLICATION

Use of PCD UHR mode accompanied by novel BRFD allows for improved visualization of neuroanatomy following device deployment, leading to potential prevention of unnecessary interventions.

Printed on: 02/07/23

## Abstract Archives of the RSNA, 2022

T5A-SPPH-9

### Renal Imaging at 5T Versus 3T: A Comparison Study

Tuesday, Nov. 29 12:15PM - 12:45PM Room: Learning Center - PH DPS

#### Participants

Liyun Zheng, Shanghai, China (*Presenter*) Nothing to Disclose

#### PURPOSE

This study aimed to investigate the performance of renal MRI at 5T, and compare it with 3T.

#### METHODS AND MATERIALS

Fifteen healthy volunteers were included in this study. All the participants were examined on a 3T MR scanner and a 5T MR scanner by using optimal coil setups for both field strengths, respectively. The MRI sequences included coronal T1-weighted 3D volume-interpolated breath-hold gradient-echo (GRE) sequence (QUICK 3D), axial T2-weighted fast spin-echo (FSE) with fat saturation and respiratory trigger, and diffusion weighted imaging (DWI). T2\* mapping was performed based on multi-echo GRE sequence. Qualitative and quantitative analysis were performed in consensus by two experienced radiologists. The image quality for each sequence type was evaluated by using a three-point scale (score 1 = poor quality, score 2 = moderate [diagnostic] quality, score 3 = good quality). The evaluation criteria were based on: 1) the cortico-medullary differentiation and 2) the delineation of adrenal glands, proximal ureter, renal arteries, and renal veins. Considering the chemical shift, B1 inhomogeneity, susceptibility, motion artifacts and the overall image impairment, the presence of artifacts was assessed by using a three-point scale (score 1 = strong impairment, score 2 = moderate impairment, score 3 = no artifact present or insignificant). For the quantitative analysis, SNR (cortex) = Signal (cortex)/noise, SNR (medulla) = Signal (medulla)/noise, and CNR = [Signal(cortex)-Signal(medulla)]/noise were measured for images of all the sequences. For functional imaging, mean apparent diffusion coefficient (ADC) and T2\* relaxation time were calculated from cortex and medulla for each subject, respectively. Wilcoxon signed rank-sum test was used to compare the visual evaluation scores and quantitative measurements between 3T and 5T images.

#### RESULTS

For all the sequences, the image quality, SNR and CNR of 5T images were significantly higher than 3T images while there is no significant difference between the presence of artifacts. For the functional maps, ADC of the cortex is significantly higher than that of the medulla at both 3T and 5T. There were no significant differences for the ADCs between 3T and 5T. Further, T2\* value of the cortex is also significantly higher than that of the medulla at both 3T and 5T. Compared to 3T, renal MRI at 5T resulted in significantly shorter T2\* values in both cortex (66.14 ms in 3T and 44.62 ms in 5T) and medulla (30.39 ms in 3T and 16.67 ms in 5T).

#### CONCLUSION

Both anatomical images and functional maps of renal MRI were feasible at 5T.

#### CLINICAL RELEVANCE/APPLICATION

In vivo 5T renal MRI may better elucidate the renal diseases with both anatomical and functional imaging, compared to conventional clinical MRI scanners.

Printed on: 02/07/23

## Abstract Archives of the RSNA, 2022

T5A-SPRO

### Radiation Oncology Tuesday Poster Discussions - A

Tuesday, Nov. 29 12:15PM - 12:45PM Room: Learning Center - RO DPS

#### Participants

Tarita Thomas, MD, PhD, Chicago, IL (*Moderator*) Nothing to Disclose

#### Sub-Events

### **T5A-SPRO-1 Comparison Between CT Texture Data, Resection Margin Status And Clinical Outcomes In Pancreatic Adenocarcinoma Resected After Induction Chemotherapy And Neoadjuvant Stereotactic Body Radiation Therapy**

#### Participants

Luca Geraci, MD, Verona, Italy (*Presenter*) Nothing to Disclose

#### PURPOSE

The aim of this study is to compare computed tomography (CT) texture analysis parameters with the resection margin status, the recurrence-free survival (RFS) and the overall survival (OS) in patients with pancreatic ductal adenocarcinoma (PDAC) resected after induction chemotherapy and neoadjuvant stereotactic body radiotherapy (SBRT). Preoperative prediction of patients who are likely to have positive resection margins and worse clinical outcome is beneficial to avoid early disease recurrence after surgery.

#### METHODS AND MATERIALS

Between January 2017 and May 2019, 134 patients with histologically proven unresectable PDAC underwent induction chemotherapy (FOLFIRINOX or Gemcitabine + Nab-Paclitaxel), followed by radiotherapy. Patients who received surgery after neoadjuvant SBRT were included. 47 texture features were extracted from 3D regions of interest (ROIs) based on unenhanced, arterial- and portal-phase CT images performed for SBRT planning. Clinical features and texture-derived parameters were compared; receiver operating characteristic (ROC) curves were constructed for the features that showed a significant difference between groups. Cox regression analysis and Kaplan-Meier curves were used to determine the association of clinical-pathological variables and texture parameters with RFS and OS.

#### RESULTS

43 patients (27 males, 16 females; mean age, 65 years; age range, 48-81 years) were included in this retrospective study. 14 patients (32.6%) had vascular resection. Patients with higher arterial HU\_Q1 had significantly shorter RFS than patients who didn't meet this criteria ( $p=.032$  and  $.005$ ; mean RFS 9.6 vs 14.8 months and 8 vs 14.3 months, respectively); no significant predictors were found for OS.

#### CONCLUSION

CT texture analysis could predict RFS in patients with PDAC resected after induction chemotherapy and neoadjuvant SBRT.

#### CLINICAL RELEVANCE/APPLICATION

Prediction of prognosis by adding texture analysis. Change in follow up and patients management.

Printed on: 02/07/23

## Abstract Archives of the RSNA, 2022

T5A-SPRO-1

### Comparison Between CT Texture Data, Resection Margin Status And Clinical Outcomes In Pancreatic Adenocarcinoma Resected After Induction Chemotherapy And Neoadjuvant Stereotactic Body Radiation Therapy

Tuesday, Nov. 29 12:15PM - 12:45PM Room: Learning Center - RO DPS

#### Participants

Luca Geraci, MD, Verona, Italy (*Presenter*) Nothing to Disclose

#### PURPOSE

The aim of this study is to compare computed tomography (CT) texture analysis parameters with the resection margin status, the recurrence-free survival (RFS) and the overall survival (OS) in patients with pancreatic ductal adenocarcinoma (PDAC) resected after induction chemotherapy and neoadjuvant stereotactic body radiotherapy (SBRT). Preoperative prediction of patients who are likely to have positive resection margins and worse clinical outcome is beneficial to avoid early disease recurrence after surgery.

#### METHODS AND MATERIALS

Between January 2017 and May 2019, 134 patients with histologically proven unresectable PDAC underwent induction chemotherapy (FOLFIRINOX or Gemcitabine + Nab-Paclitaxel), followed by radiotherapy. Patients who received surgery after neoadjuvant SBRT were included. 47 texture features were extracted from 3D regions of interest (ROIs) based on unenhanced, arterial- and portal-phase CT images performed for SBRT planning. Clinical features and texture-derived parameters were compared; receiver operating characteristic (ROC) curves were constructed for the features that showed a significant difference between groups. Cox regression analysis and Kaplan-Meier curves were used to determine the association of clinical-pathological variables and texture parameters with RFS and OS.

#### RESULTS

43 patients (27 males, 16 females; mean age, 65 years; age range, 48-81 years) were included in this retrospective study. 14 patients (32.6%) had vascular resection. Patients with higher arterial HU\_Q1 had significantly shorter RFS than patients who didn't meet this criteria ( $p=.032$  and  $.005$ ; mean RFS 9.6 vs 14.8 months and 8 vs 14.3 months, respectively); no significant predictors were found for OS.

#### CONCLUSION

s CT texture analysis could predict RFS in patients with PDAC resected after induction chemotherapy and neoadjuvant SBRT.

#### CLINICAL RELEVANCE/APPLICATION

Prediction of prognosis by adding texture analysis. Change in follow up and patients management.

Printed on: 02/07/23



## Abstract Archives of the RSNA, 2022

T5A-SPVA

### Vascular Tuesday Poster Discussions - A

Tuesday, Nov. 29 12:15PM - 12:45PM Room: Learning Center - VA DPS

#### Sub-Events

#### T5A-SPVA-1 Incidence of IVC Filter Thrombosis During the COVID-19 Pandemic at a Single Tertiary Referral Center

##### Participants

Bennett Ahearn, San Antonio, TX (*Presenter*) Nothing to Disclose

##### PURPOSE

Thrombotic complications in patients with COVID-19 have been well documented, however, data regarding the rate of inferior vena cava (IVC) filter thrombosis among patients diagnosed with COVID-19 is limited. We aim to compare the rate of IVC filter thrombosis in patients with and without a diagnosis of COVID-19.

##### METHODS AND MATERIALS

An IRB approved single institution retrospective chart review was conducted on IVC filters placed between January 1, 2020 to September 22, 2021. Patients with existing IVC thrombus (n=4) or no COVID-19 test on file (n=7) were excluded. The review included 111 patients (66 males, 45 females; mean age, 54 years; range, 15-94 years). Indications for IVC filter placement were DVT (n=59), Pulmonary Embolism (n=28), and prophylactic placement (n=24). The most common filter placed was the Denali filter (n=110). The remaining filter was an Option Elite. Patients were grouped by COVID-19 status and the rates of IVC thrombosis were compared using a chi-squared test.

##### RESULTS

Seventeen patients tested positive for COVID-19 while the remaining 94 patients were COVID negative. The average length of time between IVC filter placement and a positive COVID-19 test before or after filter placement was 43 days (range, 0-181 days). Three COVID-19 negative patients developed IVC thrombus (3.2%) at 3, 35, and 37 days after placement. Two COVID-19 positive patients developed IVC thrombus (11.7%) at 7 and 71 days post filter placement. The rates of IVC thrombosis were not statistically significant between cohorts (p=0.11).

##### CONCLUSION

Despite an increase in the risk of thrombotic complications in patients with COVID-19, there may not be a significant increase in the risk of IVC filter thrombosis. Larger datasets are needed to investigate the true risk of developing COVID-19 associated IVC filter thrombosis.

##### CLINICAL RELEVANCE/APPLICATION

Thrombotic complications in patients with COVID-19 have been well documented. This review compares the rate of IVC filter thrombosis in patients with and without a diagnosis of COVID-19.

Printed on: 02/07/23

## Abstract Archives of the RSNA, 2022

T5A-SPVA-1

### Incidence of IVC Filter Thrombosis During the COVID-19 Pandemic at a Single Tertiary Referral Center

Tuesday, Nov. 29 12:15PM - 12:45PM Room: Learning Center - VA DPS

#### Participants

Bennett Ahearn, San Antonio, TX (*Presenter*) Nothing to Disclose

#### PURPOSE

Thrombotic complications in patients with COVID-19 have been well documented, however, data regarding the rate of inferior vena cava (IVC) filter thrombosis among patients diagnosed with COVID-19 is limited. We aim to compare the rate of IVC filter thrombosis in patients with and without a diagnosis of COVID-19.

#### METHODS AND MATERIALS

An IRB approved single institution retrospective chart review was conducted on IVC filters placed between January 1, 2020 to September 22, 2021. Patients with existing IVC thrombus (n=4) or no COVID-19 test on file (n=7) were excluded. The review included 111 patients (66 males, 45 females; mean age, 54 years; range, 15-94 years). Indications for IVC filter placement were DVT (n=59), Pulmonary Embolism (n=28), and prophylactic placement (n=24) The most common filter placed was the Denali filter (n=110). The remaining filter was an Option Elite. Patients were grouped by COVID-19 status and the rates of IVC thrombosis were compared using a chi-squared test.

#### RESULTS

Seventeen patients tested positive for COVID-19 while the remaining 94 patients were COVID negative. The average length of time between IVC filter placement and a positive COVID-19 test before or after filter placement was 43 days (range, 0-181 days). Three COVID-19 negative patients developed IVC thrombus (3.2%) at 3, 35, and 37 days after placement. Two COVID-19 positive patients developed IVC thrombus (11.7%) at 7 and 71 days post filter placement. The rates of IVC thrombosis were not statistically significant between cohorts (p=0.11).

#### CONCLUSION

Despite an increase in the risk of thrombotic complications in patients with COVID-19, there may not be a significant increase in the risk of IVC filter thrombosis. Larger datasets are needed to investigate the true risk of developing COVID-19 associated IVC filter thrombosis.

#### CLINICAL RELEVANCE/APPLICATION

Thrombotic complications in patients with COVID-19 have been well documented. This review compares the rate of IVC filter thrombosis in patients with and without a diagnosis of COVID-19.

Printed on: 02/07/23

## Abstract Archives of the RSNA, 2022

T5B-SPBR

### Breast Tuesday Poster Discussions - B

Tuesday, Nov. 29 12:45PM - 1:15PM Room: Learning Center - BR DPS

#### Participants

Fredrik Strand, MD, PhD, Stockholm, Sweden (*Moderator*) Speaker, Lunit Inc  
Fredrik Strand, MD, PhD, Stockholm, Sweden (*Moderator*) Speaker, Lunit Inc  
Sophia Zackrisson, Malmo, Sweden (*Moderator*) Speaker, Siemens AG; Speaker, Bayer AG; Speaker, Pfizer Inc; Patent holder, PCT/EP2014/057372;  
Sophia Zackrisson, Malmo, Sweden (*Moderator*) Speaker, Siemens AG; Speaker, Bayer AG; Speaker, Pfizer Inc; Patent holder, PCT/EP2014/057372;

#### Sub-Events

### T5B-SPBR-1 A Three-sequence Abbreviated MRI Protocol to Evaluate Response to Breast Cancer Neoadjuvant Chemotherapy

#### Participants

Eduardo Dornelas, MD, PhD, (*Presenter*) Nothing to Disclose

#### PURPOSE

To develop an abbreviated MRI protocol (ABP-MRI) to evaluate response to neoadjuvant chemotherapy (NAC) for invasive breast cancer carcinoma with diagnostic performance equivalent to that of the full protocol (FP-MRI) and with reduction of the examination time.

#### METHODS AND MATERIALS

This was a retrospective, single-center, cross-sectional study. It comprised 210 consecutive women diagnosed with invasive breast carcinoma of no special type who underwent breast MRI after NAC between 2016 and 2020. Breast MRI scans were independently reevaluated by two radiologists, with a level of agreement of 96.2% (202/210), first with access only to axial 3D SPAIR without contrast and then to the first (two-sequences ABP-MRI), second (three-sequences ABP-MRI), and third (four-sequences ABP-MRI) post-contrast times and finally, to the FP-MRI. The diagnostic performance (sensitivity, specificity, positive predictive value, negative predictive value, and accuracy) of the three ABP-MRIs and the FP-MRI were analyzed comparing to the pathological results of the surgical specimen. The Wilcoxon non-parametric test ( $p$ -value  $< .050$ ) was used to compare the accuracy of ABP-MRIs and the FP-MRI in the measurement of the longest axis in the most extensive residual lesion.

#### RESULTS

The median age of the study population was 47 (24-80) years. The two-sequences ABP-MRI showed higher specificity (84.6%; 77/91), but a higher probability of false-negative (16.8%) and a lower sensitivity (83.2%; 99/119) than the three and four-sequences ABP-MRIs and the FP-MRI, which were identical in specificity (81.3%; 74/91), probability of false-negative (8.4%), and sensitivity (91.6%; 109/119). The three-sequences ABP-MRI showed an average underestimation of only 0.03 cm in the measurement of the longest axis of the residual lesion ( $p=0.008$ ) and with an average reduction in the acquisition time of 75% (20 minutes to 5 minutes), compared with FP-MRI.

#### CONCLUSION

The three-sequence ABP-MRI showed diagnostic performance equivalent to the FP-MRI, with a 75% reduction in the acquisition time.

#### CLINICAL RELEVANCE/APPLICATION

Using the three-sequence ABP-MRI to evaluate the response to NAC, patient discomfort and examination costs can be reduced without sacrificing diagnostic performance.

### T5B-SPBR-2 Changes in Kinetic Heterogeneity of Breast Cancer via Computer-aided Diagnosis of Magnetic Resonance Imaging Predict the Pathological Response to Neoadjuvant Systemic Therapy

#### Participants

Jin Joo Kim, MD, Busan, Korea, Republic Of (*Presenter*) Nothing to Disclose

#### PURPOSE

To evaluate whether the "computer-aided diagnosis (CAD)-extracted" kinetic heterogeneity of breast cancer on MRI, and changes therein during treatment, were associated with the pathological response to neoadjuvant systemic therapy (NST).

#### METHODS AND MATERIALS

Consecutive patients with invasive breast cancer, who underwent NST followed by surgery between 2014 and 2020, were retrospectively evaluated. Using a commercial CAD system, kinetic features (angiovolume, peak enhancement, delayed

enhancement profiles, and kinetic heterogeneity) of breast cancer were assessed with pre- and mid-treatment MRI. Multivariate logistic regression was used to identify the associations between CAD-extracted kinetic features and pathological complete response (pCR).

## RESULTS

A total of 130 patients (mean age, 55 years) were included, 37 (28.5%) of whom achieved a pCR. When the pre- and mid-treatment MRI data were compared, the pCR group exhibited greater changes in kinetic heterogeneity ( $86.14 \pm 32.05\%$  vs.  $8.50 \pm 141.01\%$ ,  $P < 0.001$ ) and angiovolume ( $95.20 \pm 14.29\%$  vs.  $19.89 \pm 320.16\%$ ;  $P < 0.001$ ) than the non-pCR group. Multivariate regression analysis showed that a large change in kinetic heterogeneity [odds ratio (OR) = 1.030,  $P < 0.001$ ], age (OR = 0.931,  $P = 0.005$ ), progesterone receptor negativity (OR = 7.831,  $P = 0.001$ ), and HER2 positivity (OR = 3.455,  $P = 0.017$ ) were associated with pCR.

## CONCLUSION

A greater change in the CAD-extracted kinetic heterogeneity of breast cancer between pre- and mid-treatment MRI was associated with a pCR in patients on NST.

## CLINICAL RELEVANCE/APPLICATION

CAD-extracted kinetic heterogeneity can be used as a quantitative imaging biomarker of tumor response to therapy to identify patients who are unlikely to respond well. This represents personalized medicine at its best, where the chemotherapy is tailored according to biological changes in breast cancer heterogeneity.

### T5B-SPBR-3 Diagnostic Value of the Ultrafast Technique When Added to The Standard Protocol in Breast MRI Screening for High-risk Patients: Multi-reader Study

Participants

Joya Hadchiti, MD, MD, Paris, France (*Presenter*) Nothing to Disclose

## PURPOSE

This study aims to show the diagnostic value of Ultrafast sequence when added to a classic MRI protocol in the screening of patients with a high risk of breast cancer. We compared the diagnostic accuracy of the two approaches using the BIRADS classification in correspondence with 4 readers and 3 levels of expertise.

## METHODS AND MATERIALS

We conducted a retrospective observational study on 181 women (mean age=48years, range 26-71 years) at high risk who underwent annual screening breast MRI between March 2018 and March 2019. Eligible women had at least a biopsy (n=35 including 3 malignant and 32 benign lesions) or 2 years of breast MRI follow-up. Four readers with different levels of experience (R1: 10 years, R2 and 3: 3 years, and R4: <6 months) classified lesions according to the BIRADS classification. They all made two reading sessions performed blindly with 2 month wash-out period. The first MRI reading session included the classic protocol consisting of T1, T2, DWI, and Vibrant sequences and the second reading included the full protocol consisting of T1, T2, DWI, Ultrafast DISCO, and vibrant sequences. The reference standard was defined as a combination of histological diagnosis for BIRADS IV and V classification and 2 years of imaging follow-up for BIRADS I, II, and III patients.

## RESULTS

All lesions were detected using both protocols. There were 3 malignant lesions. The accuracy of the reader BIRADS classification with the reference standard was higher when adding the Ultrafast sequence to the classic protocol for all readers (R1=87%/99%; R2=82%/89% R3=81%/85% R4=61%/84% for the classic and full protocol respectively). With the Ultrafast sequence, the beginner radiologist (R4) can catch up with the diagnostic performance of a more experienced radiologist. Compared to the classic protocol, we observed lower rates of false BIRADS III classified in the full protocol including the Ultrafast sequence decreasing the close follow up with cost and time-saving in the daily practices. Lower rates of false BIRADS IV are also noted avoiding unnecessary biopsy.

## CONCLUSION

The Ultrafast sequence presented an additive diagnostic value to the classic protocol for all readers. Due to its high performance, the Ultrafast sequence could be part of the standard breast MRI protocol.

## CLINICAL RELEVANCE/APPLICATION

By using the Ultrafast sequence, BIRADS classification performance is close to the real nature of the breast lesions. The shorter acquisition time of the Ultrafast sequence can make breast MRI screening more readily available beyond those at high risk for breast cancer however validation studies using data from a different population are warranted.

### T5B-SPBR-4 Abbreviated Breast MR: Our 2-Year Initial Experience

Participants

Lauren Burkard-Mandel, MD, PhD, (*Presenter*) Nothing to Disclose

## PURPOSE

The aim of this study was to retrospectively evaluate and present our two-year experience with AB-MR at our academic institution.

## METHODS AND MATERIALS

Employing eight specialty trained breast imagers, studies were interpreted via the ACR BI-RADS MR lexicon. The protocol utilized T1-weighted fat saturated pre- and post-contrast, Short T1 Inversion Recovery images, and was completed within 10 minutes. AB-MR was offered to asymptomatic women, whose ages ranged from 24 to 90 years.

## RESULTS

Out of 1338 patients included in the cohort for this study, 1111 (83.0%) were BI-RADS 1 or 2, 121 (9.0%) were a BI-RADS 3, and 106 (8%) were categorized as either BI-RADS 4 or 5 with recommended biopsy. Biopsy of BI-RADS 4 and 5 categorized patients

yielded 15 cancers for a PPV2 of 14.2% and a PPV3 of 18.5% with 81 of 106 patients undergoing the recommended biopsy. Overall, 16 cancers were detected, yielding a cancer detection rate of 12.0/1000. Over the next 12-24 months, no interval cancers were detected in these patients.

## CONCLUSION

s AB-MR demonstrates a notable cancer detection rate and may provide an alternative screening method to detecting breast cancers in high-risk patients.

## CLINICAL RELEVANCE/APPLICATION

Abbreviated MR screening may offer an alternative option, especially to high risk patients, which is both more affordable and less time consuming than full protocol MR.

## T5B-SPBR-5 Breast MRI Screening Results: Comparison Between Patients with Personal History of Breast Cancer and Other High-risk Patients

Participants

Karina Zoghbi, MD, Sao Paulo, Brazil (*Presenter*) Nothing to Disclose

## PURPOSE

Breast magnetic resonance imaging (MRI) is recommended for breast cancer screening in high-risk patients, however personal history of breast cancer is not considered an unequivocal recommendation for MRI surveillance. The aim of this study was to compare the results of breast cancer screening with magnetic resonance imaging (MRI) in patients with personal history of breast cancer and other high-risk patients.

## METHODS AND MATERIALS

Retrospective single-center IRB-approved study that included 597 patients (mean age: 48.8 years; range: 19-82 years) who performed screening breast MRI from January to December 2020.

## RESULTS

Most included patients had a prior history of breast cancer (n=354; 59.8%). MRI results were benign (BIRADS 1/2) in 425 (71.2%), probably benign (BIRADS 3) in 143 (24.0%) and suspicious (BIRADS 4/5) in 29 (4.9%). Eleven breast carcinomas were identified on screening MRI (cancer detection rate of 18.4/1000 exams; minimal cancer percentage: 54.5%; node-negative percentage: 90.9%). Abnormal interpretation rate was lower in patients with prior breast cancer compared with other high-risk factors (20.9% vs. 40.3%;  $p < 0.001$ ), however, there was no statistically significant difference on the rates of recommendation for tissue diagnosis (3.7% vs. 6.6%;  $p = 0.104$ ). The cancer detection rate was 20.5/1000 exams in patients with personal history of breast cancer and 14.1/1000 in other high-risk patients. PPV1 (abnormal interpretation) and PPV2 (recommendation for tissue diagnosis) were respectively 8.1% and 46.2% for patients with personal history, and 5.1% and 31.3% for other high-risk patients. During the 1-year follow-up after MRI, five other patients were diagnosed with malignancy (one patient with personal history of breast cancer and 4 patients with other high-risk factors), including three with ductal carcinoma in situ (DCIS) identified through calcifications on mammography and two with invasive carcinomas diagnosed 10 months after MRI.

## CONCLUSION

s Patients with personal history of breast cancer showed similar screening results to other high-risk patients, suggesting that MRI surveillance should be considered in this population.

## CLINICAL RELEVANCE/APPLICATION

Patients with personal history of breast cancer have higher than average risk to develop new malignant breast tumors and MRI surveillance should be considered in this population.

## T5B-SPBR-6 High Temporal/High Spatial Resolution Breast MRI Outperforms Standard Protocol in Patients with High Background Parenchymal Enhancement (BPE)

Participants

Sarah Eskreis-Winkler, MD, New York, NY (*Presenter*) Nothing to Disclose

## PURPOSE

Breast MRI is the most sensitive test for breast cancer detection, but high background parenchymal enhancement (BPE) can impact lesion conspicuity, leading to decreased positive predictive value (PPV) and specificity. With a high temporal/high spatial (HTHS) resolution MRI protocol, the breast is imaged within 1 minute after contrast injection, before BPE washes in, potentially improving diagnostic accuracy. The purpose of this study was to compare diagnostic performance of a HTHS protocol to a standard breast MR protocol in women with high BPE.

## METHODS AND MATERIALS

Breast MRI is the most sensitive test for breast cancer detection, but high background parenchymal enhancement (BPE) can impact lesion conspicuity, leading to decreased positive predictive value (PPV) and specificity. With a high temporal/high spatial (HTHS) resolution MRI protocol, the breast is imaged within 1 minute after contrast injection, before BPE washes in, potentially improving diagnostic accuracy. The purpose of this study was to compare diagnostic performance of a HTHS protocol to a standard breast MR protocol in women with high BPE.

## RESULTS

Our study cohort included 6,880 breast MRIs from 5,231 patients (mean age 53yrs), of which 1,342 exams (19.5%) had high BPE. Among these, CDR (37 per 1000 (25/676) v. 12 per 1000 (8/666);  $p = 0.002$ ) and PPV (24.3% (25/103) v. 9.3% (8/86);  $p = 0.004$ ) were increased with the HTHS protocol compared to the standard protocol. There was no significant difference in ICR (5.9/1000 v. 6.0/1000,  $p = 0.51$ ). For women with priors, CDR was increased with the HTHS protocol (2.6 per 1000 (12/463) v. 6.0 per 1000 (3/464);  $p = 0.001$ ). For those without priors, CDR trended higher with HTHS but was not statistically significant after applying Bonferonni correction (6.1 per 1000 (13/213) v. 2.5 per 1000 (5/202);  $p = 0.035$ ).

## CONCLUSION

s The HTHS protocol significantly improves diagnostic breast MRI performance in women with high BPE, with an additional cancer yield of 25 cancers per 1000 compared to the standard protocol, and with a concomitant decrease in unnecessary biopsies.

## CLINICAL RELEVANCE/APPLICATION

Our study shows that a high temporal/high spatial resolution breast MRI protocol detects more cancers and decreases unnecessary biopsies in patients with high background parenchymal enhancement compared to a standard breast MRI protocol. It should therefore be considered the protocol-of-choice for screening MRI in the future.

## T5B-SPBR-7 Potential of Stimulated Echo Acquisition Mode Diffusion Weighted Imaging (STEAM-DWI) in Breast MRI: First Experiences

Participants

Sabine Ohlmeyer, PhD, MD, Erlangen, Germany (*Presenter*) Nothing to Disclose

## PURPOSE

The spin echo diffusion weighted imaging (SE-DWI) technique is most commonly used for lesion characterisation in breast MRI, which does not allow the measurement of the diffusivity at diffusion times much longer than the T2 time. At these long diffusion times, the long-range structural tissue order could be assessed, which is potentially beneficial for the diagnostic performance. Furthermore, suppression of olefinic fat signal is sometimes insufficient. STEAM-DWI might overcome these limitations by using long mixing times, and therewith long diffusion times. The aim of this study was to assess image quality and diagnostic performance of STEAM-DWI in breast MRI compared to SE-DWI.

## METHODS AND MATERIALS

Prototypical STEAM-DWI and SE-DWI were performed in addition to the standard MRI protocol on a 3T MAGNETOM Vida scanner (Siemens Healthcare, Erlangen, Germany). Image quality was compared in 91 datasets, with respect to the presence of artifacts, signal voids, quality of fat suppression, and lesion and lymph node conspicuity. These parameters were rated using a 5-point Likert scale (1 = worst to 5 = best). The apparent diffusion coefficient (ADC) was measured in 27 mass lesions (16 breast carcinomas, 11 benign lesions), and the diagnostic value of both DWIs was statistically evaluated and compared.

## RESULTS

Artifacts and signal voids were almost negligible in both DWI datasets (STEAM 4.40 vs SE 4.02, and 4.88 vs 4.81, respectively). Fat suppression was significantly better in STEAM (4.32 vs 3.87,  $P < 0.001$ ,  $r = 0.27$ ). The conspicuity of mass lesions was quite similar with STEAM and SE (2.19 vs 1.91). No significant difference was observed for the AUC (STEAM, 0.50; SE, 0.52). The cut-off for differentiation of benign and malignant lesions was at  $ADC = 0.93 \cdot 10^{-3} \text{ mm}^2/\text{s}$  for STEAM and at  $1.05 \cdot 10^{-3} \text{ mm}^2/\text{s}$  for SE (both sensitivity, 1; specificity, 0.45). The conspicuity of axillary lymph nodes was better with SE than with STEAM (3.38 vs 1.50,  $P < 0.001$ ,  $r = 0.44$ ).

## CONCLUSION

s Our data indicate that STEAM-DWI might be a robust technique for diffusion-weighted breast imaging with better fat-suppression and equal diagnostic accuracy compared to SE-DWI. The conspicuity of axillary lymph nodes seems to be inferior in STEAM-DWI compared to SE-DWI, here T1 and T2 weighted sequences from the standard protocol may have to be taken also into account.

## CLINICAL RELEVANCE/APPLICATION

STEAM-DWI could represent a robust technique in breast MRI with stable fat saturation and same diagnostic accuracy compared to standard SE-DWI with regard to detection and characterization of mass lesions in breast tissue.

## T5B-SPBR-8 Breast Ultrasound Volume Sweep Imaging: A New Horizon in Breast Cancer Detection

Participants

Yu Zhao, MD, Rochester, NY (*Presenter*) Nothing to Disclose

## PURPOSE

Most of the world lacks access to basic breast imaging which presumably results in delays to detection of breast cancer. In low- and middle-income countries this delay can be on the scale of months. While ultrasound is an ideal imaging modality to screen for breast abnormalities, its deployment is limited by a lack of trained sonographers. In this study, we tested a simple volume sweep imaging (VSI) ultrasound protocol for the evaluation of palpable breast masses. This protocol can be performed by individuals without prior ultrasound training removing a major barrier to ultrasound deployment.

## METHODS AND MATERIALS

Medical students without prior ultrasound experience were trained to perform the VSI protocol with less than 2 hours of training. The VSI protocol involves placing an "X" over the patient's palpable lump and scanning in transverse, sagittal, and radial/antiradial orientations over the lump. The operator uses a preset obviating the need for technical adjustments. The scanner only performs the standardized sweeps of the probe which are saved as video clips for later interpretation by a specialist. The operator does not interpret the ultrasound images. Patients over 18 of either sex were enrolled in this study if they had a palpable breast mass. The trained medical student performed the VSI protocol with a handheld Butterfly iQ ultrasound probe. A standard of care (SOC) ultrasound was performed the same day by an experienced sonographer using a high-end ultrasound machine. Agreement was assessed for mass visualization, size, orientation, shape, margins, echogenicity, posterior acoustic features, and BI-RADS assessment. All interpretations were performed by an attending breast imager.

## RESULTS

Students scanned 170 palpable lumps with the VSI protocol. VSI showed 97% sensitivity and 100% specificity for breast mass detection. There was 97.6% agreement with standard of care (Cohen's  $\kappa=0.95$ ,  $p<0.0001$ ). All cancer presenting as a sonographic mass ( $n=20$ ) were detected. There was substantial agreement for mass characteristics between VSI and SOC, including 87% agreement on BI-RADS assessments (Cohen's  $\kappa=0.82$ ,  $p<0.0001$ ). The average largest mass diameter on SOC was  $23.1\pm 16.9 \text{ mm}$  and  $22.5\pm 15.6 \text{ mm}$  on VSI (ICC=0.98 (0.96-0.98),  $p<0.0001$ ). The Bland-Altman Bias for these measurements was  $-1.02$  ( $-7.8$ - $5.77$ ,

p=0.002)

#### **CONCLUSION**

s There was substantial agreement between VSI ultrasound and standard of care breast imaging for palpable lumps with VSI acquiring images of diagnostic quality.

#### **CLINICAL RELEVANCE/APPLICATION**

VSI breast ultrasound is a potential way to increase access to breast imaging in areas without other access to breast imaging. Access to VSI exams could potentially help decrease delays to diagnosis of breast cancer improving outcomes.

Printed on: 02/07/23

## Abstract Archives of the RSNA, 2022

T5B-SPBR-1

### A Three-sequence Abbreviated MRI Protocol to Evaluate Response to Breast Cancer Neoadjuvant Chemotherapy

Tuesday, Nov. 29 12:45PM - 1:15PM Room: Learning Center - BR DPS

#### Participants

Eduardo Dormelas, MD, PhD, (*Presenter*) Nothing to Disclose

#### PURPOSE

To develop an abbreviated MRI protocol (ABP-MRI) to evaluate response to neoadjuvant chemotherapy (NAC) for invasive breast cancer carcinoma with diagnostic performance equivalent to that of the full protocol (FP-MRI) and with reduction of the examination time.

#### METHODS AND MATERIALS

This was a retrospective, single-center, cross-sectional study. It comprised 210 consecutive women diagnosed with invasive breast carcinoma of no special type who underwent breast MRI after NAC between 2016 and 2020. Breast MRI scans were independently reevaluated by two radiologists, with a level of agreement of 96,2% (202/210), first with access only to axial 3D SPAIR without contrast and then to the first (two-sequences ABP-MRI), second (three-sequences ABP-MRI), and third (four-sequences ABP-MRI) post-contrast times and finally, to the FP-MRI. The diagnostic performance (sensitivity, specificity, positive predictive value, negative predictive value, and accuracy) of the three ABP-MRIs and the FP-MRI were analyzed comparing to the pathological results of the surgical specimen. The Wilcoxon non-parametric test ( $p$ -value  $< .050$ ) was used to compare the accuracy of ABP-MRIs and the FP-MRI in the measurement of the longest axis in the most extensive residual lesion.

#### RESULTS

The median age of the study population was 47 (24-80) years. The two-sequences ABP-MRI showed higher specificity (84.6%; 77/91), but a higher probability of false-negative (16.8%) and a lower sensitivity (83.2%; 99/119) than the three and four-sequences ABP-MRIs and the FP-MRI, which were identical in specificity (81.3%; 74/91), probability of false-negative (8.4%), and sensitivity (91.6%; 109/119). The three-sequences ABP-MRI showed an average underestimation of only 0.03 cm in the measurement of the longest axis of the residual lesion ( $p=0.008$ ) and with an average reduction in the acquisition time of 75% (20 minutes to 5 minutes), compared with FP-MRI.

#### CONCLUSION

s The three-sequence ABP-MRI showed diagnostic performance equivalent to the FP-MRI, with a 75% reduction in the acquisition time.

#### CLINICAL RELEVANCE/APPLICATION

Using the three-sequence ABP-MRI to evaluate the response to NAC, patient discomfort and examination costs can be reduced without sacrificing diagnostic performance.

Printed on: 02/07/23

## Abstract Archives of the RSNA, 2022

T5B-SPBR-2

### Changes in Kinetic Heterogeneity of Breast Cancer via Computer-aided Diagnosis of Magnetic Resonance Imaging Predict the Pathological Response to Neoadjuvant Systemic Therapy

Tuesday, Nov. 29 12:45PM - 1:15PM Room: Learning Center - BR DPS

#### Participants

Jin Joo Kim, MD, Busan, Korea, Republic Of (*Presenter*) Nothing to Disclose

#### PURPOSE

To evaluate whether the "computer-aided diagnosis (CAD)-extracted" kinetic heterogeneity of breast cancer on MRI, and changes therein during treatment, were associated with the pathological response to neoadjuvant systemic therapy (NST).

#### METHODS AND MATERIALS

Consecutive patients with invasive breast cancer, who underwent NST followed by surgery between 2014 and 2020, were retrospectively evaluated. Using a commercial CAD system, kinetic features (angiovolume, peak enhancement, delayed enhancement profiles, and kinetic heterogeneity) of breast cancer were assessed with pre- and mid-treatment MRI. Multivariate logistic regression was used to identify the associations between CAD-extracted kinetic features and pathological complete response (pCR).

#### RESULTS

A total of 130 patients (mean age, 55 years) were included, 37 (28.5%) of whom achieved a pCR. When the pre- and mid-treatment MRI data were compared, the pCR group exhibited greater changes in kinetic heterogeneity ( $86.14 \pm 32.05\%$  vs.  $8.50 \pm 141.01\%$ ,  $P < 0.001$ ) and angiovolume ( $95.20 \pm 14.29\%$  vs.  $19.89 \pm 320.16\%$ ;  $P < 0.001$ ) than the non-pCR group. Multivariate regression analysis showed that a large change in kinetic heterogeneity [odds ratio (OR) = 1.030,  $P < 0.001$ ], age (OR = 0.931,  $P = 0.005$ ), progesterone receptor negativity (OR = 7.831,  $P = 0.001$ ), and HER2 positivity (OR = 3.455,  $P = 0.017$ ) were associated with pCR.

#### CONCLUSION

A greater change in the CAD-extracted kinetic heterogeneity of breast cancer between pre- and mid-treatment MRI was associated with a pCR in patients on NST.

#### CLINICAL RELEVANCE/APPLICATION

CAD-extracted kinetic heterogeneity can be used as a quantitative imaging biomarker of tumor response to therapy to identify patients who are unlikely to respond well. This represents personalized medicine at its best, where the chemotherapy is tailored according to biological changes in breast cancer heterogeneity.

Printed on: 02/07/23

## Abstract Archives of the RSNA, 2022

T5B-SPBR-3

### Diagnostic Value of the Ultrafast Technique When Added to The Standard Protocol in Breast MRI Screening for High-risk Patients: Multi-reader Study

Tuesday, Nov. 29 12:45PM - 1:15PM Room: Learning Center - BR DPS

#### Participants

Joya Hadchiti, MD, MD, Paris, France (*Presenter*) Nothing to Disclose

#### PURPOSE

This study aims to show the diagnostic value of Ultrafast sequence when added to a classic MRI protocol in the screening of patients with a high risk of breast cancer. We compared the diagnostic accuracy of the two approaches using the BIRADS classification in correspondence with 4 readers and 3 levels of expertise.

#### METHODS AND MATERIALS

We conducted a retrospective observational study on 181 women (mean age=48years, range 26-71 years) at high risk who underwent annual screening breast MRI between March 2018 and March 2019. Eligible women had at least a biopsy (n=35 including 3 malignant and 32 benign lesions) or 2 years of breast MRI follow-up. Four readers with different levels of experience (R1: 10 years, R2 and 3: 3 years, and R4: <6 months) classified lesions according to the BIRADS classification. They all made two reading sessions performed blindly with 2 month wash-out period. The first MRI reading session included the classic protocol consisting of T1, T2, DWI, and Vibrant sequences and the second reading included the full protocol consisting of T1, T2, DWI, Ultrafast DISCO, and vibrant sequences. The reference standard was defined as a combination of histological diagnosis for BIRADS IV and V classification and 2 years of imaging follow-up for BIRADS I, II, and III patients.

#### RESULTS

All lesions were detected using both protocols. There were 3 malignant lesions. The accuracy of the reader BIRADS classification with the reference standard was higher when adding the Ultrafast sequence to the classic protocol for all readers ( R1=87%/99%; R2=82%/89% R3=81%/85% R4=61%/84% for the classic and full protocol respectively ). With the Ultrafast sequence, the beginner radiologist(R4) can catch up with the diagnostic performance of a more experienced radiologist. Compared to the classic protocol, we observed lower rates of false BIRADS III classified in the full protocol including the Ultrafast sequence decreasing the close follow up with cost and time-saving in the daily practices. Lower rates of false BIRADS IV are also noted avoiding unnecessary biopsy.

#### CONCLUSION

s The Ultrafast sequence presented an additive diagnostic value to the classic protocol for all readers. Due to its high performance, the Ultrafast sequence could be part of the standard breast MRI protocol.

#### CLINICAL RELEVANCE/APPLICATION

By using the Ultrafast sequence, BIRADS classification performance is close to the real nature of the breast lesions. The shorter acquisition time of the Ultrafast sequence can make breast MRI screening more readily available beyond those at high risk for breast cancer however validation studies using data from a different population are warranted.

Printed on: 02/07/23



## Abstract Archives of the RSNA, 2022

T5B-SPBR-4

### Abbreviated Breast MR: Our 2-Year Initial Experience

Tuesday, Nov. 29 12:45PM - 1:15PM Room: Learning Center - BR DPS

#### Participants

Lauren Burkard-Mandel, MD, PhD, (*Presenter*) Nothing to Disclose

#### PURPOSE

The aim of this study was to retrospectively evaluate and present our two-year experience with AB-MR at our academic institution.

#### METHODS AND MATERIALS

Employing eight specialty trained breast imagers, studies were interpreted via the ACR BI-RADS MR lexicon. The protocol utilized T1-weighted fat saturated pre- and post-contrast, Short T1 Inversion Recovery images, and was completed within 10 minutes. AB-MR was offered to asymptomatic women, whose ages ranged from 24 to 90 years.

#### RESULTS

Out of 1338 patients included in the cohort for this study, 1111 (83.0%) were BI-RADS 1 or 2, 121 (9.0%) were a BI-RADS 3, and 106 (8%) were categorized as either BI-RADS 4 or 5 with recommended biopsy. Biopsy of BI-RADS 4 and 5 categorized patients yielded 15 cancers for a PPV2 of 14.2% and a PPV3 of 18.5% with 81 of 106 patients undergoing the recommended biopsy. Overall, 16 cancers were detected, yielding a cancer detection rate of 12.0/1000. Over the next 12-24 months, no interval cancers were detected in these patients.

#### CONCLUSION

s AB-MR demonstrates a notable cancer detection rate and may provide an alternative screening method to detecting breast cancers in high-risk patients.

#### CLINICAL RELEVANCE/APPLICATION

Abbreviated MR screening may offer an alternative option, especially to high risk patients, which is both more affordable and less time consuming than full protocol MR.

Printed on: 02/07/23

## Abstract Archives of the RSNA, 2022

T5B-SPBR-5

### Breast MRI Screening Results: Comparison Between Patients with Personal History of Breast Cancer and Other High-risk Patients

Tuesday, Nov. 29 12:45PM - 1:15PM Room: Learning Center - BR DPS

#### Participants

Karina Zoghbi, MD, Sao Paulo, Brazil (*Presenter*) Nothing to Disclose

#### PURPOSE

Breast magnetic resonance imaging (MRI) is recommended for breast cancer screening in high-risk patients, however personal history of breast cancer is not considered an unequivocal recommendation for MRI surveillance. The aim of this study was to compare the results of breast cancer screening with magnetic resonance imaging (MRI) in patients with personal history of breast cancer and other high-risk patients.

#### METHODS AND MATERIALS

Retrospective single-center IRB-approved study that included 597 patients (mean age: 48.8 years; range: 19-82 years) who performed screening breast MRI from January to December 2020.

#### RESULTS

Most included patients had a prior history of breast cancer (n=354; 59.8%). MRI results were benign (BIRADS 1/2) in 425 (71.2%), probably benign (BIRADS 3) in 143 (24.0%) and suspicious (BIRADS 4/5) in 29 (4.9%). Eleven breast carcinomas were identified on screening MRI (cancer detection rate of 18.4/1000 exams; minimal cancer percentage: 54.5%; node-negative percentage: 90.9%). Abnormal interpretation rate was lower in patients with prior breast cancer compared with other high-risk factors (20.9% vs. 40.3%;  $p < 0.001$ ), however, there was no statistically significant difference on the rates of recommendation for tissue diagnosis (3.7% vs. 6.6%;  $p = 0.104$ ). The cancer detection rate was 20.5/1000 exams in patients with personal history of breast cancer and 14.1/1000 in other high-risk patients. PPV1 (abnormal interpretation) and PPV2 (recommendation for tissue diagnosis) were respectively 8.1% and 46.2% for patients with personal history, and 5.1% and 31.3% for other high-risk patients. During the 1-year follow-up after MRI, five other patients were diagnosed with malignancy (one patient with personal history of breast cancer and 4 patients with other high-risk factors), including three with ductal carcinoma in situ (DCIS) identified through calcifications on mammography and two with invasive carcinomas diagnosed 10 months after MRI.

#### CONCLUSION

Patients with personal history of breast cancer showed similar screening results to other high-risk patients, suggesting that MRI surveillance should be considered in this population.

#### CLINICAL RELEVANCE/APPLICATION

Patients with personal history of breast cancer have higher than average risk to develop new malignant breast tumors and MRI surveillance should be considered in this population.

Printed on: 02/07/23

## Abstract Archives of the RSNA, 2022

T5B-SPBR-6

### High Temporal/High Spatial Resolution Breast MRI Outperforms Standard Protocol in Patients with High Background Parenchymal Enhancement (BPE)

Tuesday, Nov. 29 12:45PM - 1:15PM Room: Learning Center - BR DPS

#### Participants

Sarah Eskreis-Winkler, MD, New York, NY (*Presenter*) Nothing to Disclose

#### PURPOSE

Breast MRI is the most sensitive test for breast cancer detection, but high background parenchymal enhancement (BPE) can impact lesion conspicuity, leading to decreased positive predictive value (PPV) and specificity. With a high temporal/high spatial (HTHS) resolution MRI protocol, the breast is imaged within 1 minute after contrast injection, before BPE washes in, potentially improving diagnostic accuracy. The purpose of this study was to compare diagnostic performance of a HTHS protocol to a standard breast MR protocol in women with high BPE.

#### METHODS AND MATERIALS

Breast MRI is the most sensitive test for breast cancer detection, but high background parenchymal enhancement (BPE) can impact lesion conspicuity, leading to decreased positive predictive value (PPV) and specificity. With a high temporal/high spatial (HTHS) resolution MRI protocol, the breast is imaged within 1 minute after contrast injection, before BPE washes in, potentially improving diagnostic accuracy. The purpose of this study was to compare diagnostic performance of a HTHS protocol to a standard breast MR protocol in women with high BPE.

#### RESULTS

Our study cohort included 6,880 breast MRIs from 5,231 patients (mean age 53yrs), of which 1,342 exams (19.5%) had high BPE. Among these, CDR (37 per 1000 (25/676) v. 12 per 1000 (8/666);  $p = 0.002$ ) and PPV (24.3% (25/103) v. 9.3% (8/86);  $p = 0.004$ ) were increased with the HTHS protocol compared to the standard protocol. There was no significant difference in ICR (5.9/1000 v. 6.0/1000,  $p = 0.51$ ). For women with priors, CDR was increased with the HTHS protocol (2.6 per 1000 (12/463) v. 6.0 per 1000 (3/464);  $p = 0.001$ ). For those without priors, CDR trended higher with HTHS but was not statistically significant after applying Bonferonni correction (6.1 per 1000 (13/213) v. 2.5 per 1000 (5/202);  $p = 0.035$ ).

#### CONCLUSION

s The HTHS protocol significantly improves diagnostic breast MRI performance in women with high BPE, with an additional cancer yield of 25 cancers per 1000 compared to the standard protocol, and with a concomitant decrease in unnecessary biopsies.

#### CLINICAL RELEVANCE/APPLICATION

Our study shows that a high temporal/high spatial resolution breast MRI protocol detects more cancers and decreases unnecessary biopsies in patients with high background parenchymal enhancement compared to a standard breast MRI protocol. It should therefore be considered the protocol-of-choice for screening MRI in the future.

Printed on: 02/07/23

## Abstract Archives of the RSNA, 2022

T5B-SPBR-7

### Potential of Stimulated Echo Acquisition Mode Diffusion Weighted Imaging (STEAM-DWI) in Breast MRI: First Experiences

Tuesday, Nov. 29 12:45PM - 1:15PM Room: Learning Center - BR DPS

#### Participants

Sabine Ohlmeyer, PhD, MD, Erlangen, Germany (*Presenter*) Nothing to Disclose

#### PURPOSE

The spin echo diffusion weighted imaging (SE-DWI) technique is most commonly used for lesion characterisation in breast MRI, which does not allow the measurement of the diffusivity at diffusion times much longer than the T2 time. At these long diffusion times, the long-range structural tissue order could be assessed, which is potentially beneficial for the diagnostic performance. Furthermore, suppression of olefinic fat signal is sometimes insufficient. STEAM-DWI might overcome these limitations by using long mixing times, and therewith long diffusion times. The aim of this study was to assess image quality and diagnostic performance of STEAM-DWI in breast MRI compared to SE-DWI.

#### METHODS AND MATERIALS

Prototypical STEAM-DWI and SE-DWI were performed in addition to the standard MRI protocol on a 3T MAGNETOM Vida scanner (Siemens Healthcare, Erlangen, Germany). Image quality was compared in 91 datasets, with respect to the presence of artifacts, signal voids, quality of fat suppression, and lesion and lymph node conspicuity. These parameters were rated using a 5-point Likert scale (1 = worst to 5 = best). The apparent diffusion coefficient (ADC) was measured in 27 mass lesions (16 breast carcinomas, 11 benign lesions), and the diagnostic value of both DWIs was statistically evaluated and compared.

#### RESULTS

Artifacts and signal voids were almost negligible in both DWI datasets (STEAM 4.40 vs SE 4.02, and 4.88 vs 4.81, respectively). Fat suppression was significantly better in STEAM (4.32 vs 3.87,  $P < 0.001$ ,  $r = 0.27$ ). The conspicuity of mass lesions was quite similar with STEAM and SE (2.19 vs 1.91). No significant difference was observed for the AUC (STEAM, 0.50; SE, 0.52). The cut-off for differentiation of benign and malignant lesions was at  $ADC = 0.93 \cdot 10^{-3} \text{ mm}^2/\text{s}$  for STEAM and at  $1.05 \cdot 10^{-3} \text{ mm}^2/\text{s}$  for SE (both sensitivity, 1; specificity, 0.45). The conspicuity of axillary lymph nodes was better with SE than with STEAM (3.38 vs 1.50,  $P < 0.001$ ,  $r = 0.44$ ).

#### CONCLUSION

s Our data indicate that STEAM-DWI might be a robust technique for diffusion-weighted breast imaging with better fat-suppression and equal diagnostic accuracy compared to SE-DWI. The conspicuity of axillary lymph nodes seems to be inferior in STEAM-DWI compared to SE-DWI, here T1 and T2 weighted sequences from the standard protocol may have to be taken also into account.

#### CLINICAL RELEVANCE/APPLICATION

STEAM-DWI could represent a robust technique in breast MRI with stable fat saturation and same diagnostic accuracy compared to standard SE-DWI with regard to detection and characterization of mass lesions in breast tissue.

Printed on: 02/07/23

## Abstract Archives of the RSNA, 2022

T5B-SPBR-8

### Breast Ultrasound Volume Sweep Imaging: A New Horizon in Breast Cancer Detection

Tuesday, Nov. 29 12:45PM - 1:15PM Room: Learning Center - BR DPS

#### Participants

Yu Zhao, MD, Rochester, NY (*Presenter*) Nothing to Disclose

#### PURPOSE

Most of the world lacks access to basic breast imaging which presumably results in delays to detection of breast cancer. In low- and middle-income countries this delay can be on the scale of months. While ultrasound is an ideal imaging modality to screen for breast abnormalities, its deployment is limited by a lack of trained sonographers. In this study, we tested a simple volume sweep imaging (VSI) ultrasound protocol for the evaluation of palpable breast masses. This protocol can be performed by individuals without prior ultrasound training removing a major barrier to ultrasound deployment.

#### METHODS AND MATERIALS

Medical students without prior ultrasound experience were trained to perform the VSI protocol with less than 2 hours of training. The VSI protocol involves placing an "X" over the patient's palpable lump and scanning in transverse, sagittal, and radial/antiradial orientations over the lump. The operator uses a preset obviating the need for technical adjustments. The scanner only performs the standardized sweeps of the probe which are saved as video clips for later interpretation by a specialist. The operator does not interpret the ultrasound images. Patients over 18 of either sex were enrolled in this study if they had a palpable breast mass. The trained medical student performed the VSI protocol with a handheld Butterfly iQ ultrasound probe. A standard of care (SOC) ultrasound was performed the same day by an experienced sonographer using a high-end ultrasound machine. Agreement was assessed for mass visualization, size, orientation, shape, margins, echogenicity, posterior acoustic features, and BI-RADS assessment. All interpretations were performed by an attending breast imager.

#### RESULTS

Students scanned 170 palpable lumps with the VSI protocol. VSI showed 97% sensitivity and 100% specificity for breast mass detection. There was 97.6% agreement with standard of care (Cohen's  $\kappa=0.95$ ,  $p<0.0001$ ). All cancer presenting as a sonographic mass ( $n=20$ ) were detected. There was substantial agreement for mass characteristics between VSI and SOC, including 87% agreement on BI-RADS assessments (Cohen's  $\kappa=0.82$ ,  $p<0.0001$ ). The average largest mass diameter on SOC was  $23.1\pm 16.9$  mm and  $22.5\pm 15.6$  mm on VSI (ICC= $0.98$  ( $0.96-0.98$ ,  $p<0.0001$ )). The Bland-Altman Bias for these measurements was  $-1.02$  ( $-7.8-5.77$ ,  $p=0.002$ )

#### CONCLUSION

s There was substantial agreement between VSI ultrasound and standard of care breast imaging for palpable lumps with VSI acquiring images of diagnostic quality.

#### CLINICAL RELEVANCE/APPLICATION

VSI breast ultrasound is a potential way to increase access to breast imaging in areas without other access to breast imaging. Access to VSI exams could potentially help decrease delays to diagnosis of breast cancer improving outcomes.

Printed on: 02/07/23

## Abstract Archives of the RSNA, 2022

T5B-SPCA

### Cardiac Tuesday Poster Discussions - B

Tuesday, Nov. 29 12:45PM - 1:15PM Room: Learning Center - CA DPS

#### Sub-Events

#### **T5B-SPCA-1 Prediction of Pericardial Adhesion and Diagnostic Performance of Hemodynamically Significant Constrictive Pericarditis by using Feature Tracking Cine MR**

##### Participants

Yasutoshi Ohta, MD, PhD, Suita, Japan (*Presenter*) Nothing to Disclose

##### PURPOSE

To investigate the diagnostic performances of pericardial adhesion and hemodynamically significant constrictive pericarditis using cine MR feature tracking

##### METHODS AND MATERIALS

Eligible cases were extracted from patients who underwent cardiac MRI between 2011 and 2021. From patients with suspected CP who underwent CMR and catheter-based hemodynamic evaluation, 24 patients (70±8 years) with cine imaging and tagging were selected (cath group). As an age-matched control group (control group), CMR images were extracted from 24 patients with no history of cardiac surgery or ischemic heart disease. 10 healthy-volunteer were also analyzed for comparison. Displacement and strain of fibrous pericardium and epicardium covering the entire ventricle were analyzed using the feature tracking (FT) method for cine short-axis images and evaluated on a global displacement graph of the pericardium surrounding the left and right ventricle, and the presence of dip or plateau was assessed from the graph. The presence of pericardial adhesions was evaluated on a 5-point scale by assessing the trajectory of myocardium points using cine images and the FT method. The ventricular septum was tracked using the FT method, and septal displacement was evaluated semiquantitatively utilizing a graph. In the cath group, the presence of adhesions was defined by tagging cine. In the combined control and cath CP group (n=48), the diagnosis of clinical CP was based on the presence of hemodynamic CP or pericardial adhesions proved by pericardiectomy. In catheterized patients (n=24), the diagnostic performance of each index for CP was evaluated based on the presence of hemodynamic CP by catheterization. The area under the receiver-operating characteristic curve (AUROC) was calculated for the diagnosis of pericardial adhesion based on pericardial adhesion in tagging cine.

##### RESULTS

For detecting hemodynamically significant CP, the sensitivity and specificity of each finding were: Septal bounce, 84.6% and 81.8%; Adhesion, 100% and 9.1%; Dip, 76.9% and 36.4%; Plateau, 69.2% and 45.5%, respectively. For clinical diagnosis of CP, sensitivity and specificity of each findings were: Septal bounce, 80.0% and 97.0%; Adhesion, 83.3% and 75.8%; Dip, 80.0% and 81.8%; Plateau, 73.3% and 78.8%, respectively. In healthy volunteers, septal bounce, adhesion, dip, and plateau were not observed. The AUROC of diagnosing pericardial adhesion by the FT method was 0.846.

##### CONCLUSION

s Feature-tracking cine MRI yields high diagnostic performance for hemodynamically significant CP.

##### CLINICAL RELEVANCE/APPLICATION

Although the tagging method has so far been considered beneficial for the diagnosis of pericardial adhesions, the FT method can also be used to evaluate the presence of adhesions.

#### **T5B-SPCA-2 Cardiovascular Magnetic Resonance Pulmonary Transit Time for Assessment of Global Diastolic Dysfunction and Mitral Regurgitation**

##### Participants

Martin Segeroth, Basel, Switzerland (*Presenter*) Nothing to Disclose

##### PURPOSE

Pulmonary transit time (PTT) is the time it takes blood to pass from the right ventricle to the left ventricle and as such is a surrogate marker of heart failure, pulmonary arterial hypertension and lung disease. We aim to associate PTT with global diastolic dysfunction and mitral regurgitation, which cannot be easily quantified in routine CMR scans.

##### METHODS AND MATERIALS

All patients referred for routine stress perfusion cardiac magnetic resonance (CMR) imaging to University Hospital Basel (Switzerland) with simultaneously available digital electrocardiograms and in-house echocardiographic assessment between January 2014 and August 2020 were included (n=83). Reporting of echocardiographies was done according to American Society of Echocardiography guidelines. Global diastolic dysfunction (GDD) was defined as more than a Grade I (impaired relaxation). Mitral regurgitation (MR) was defined as more than mild regurgitation. PTT was determined from CMR rest perfusion scans as the time in seconds between peak signal intensities of the time signal curves of the right and left ventricle. PTT normalized for heart rate

(nPTT) was calculated by multiplying PTT with the heart rate. The diagnostic accuracy was assessed by receiver operating characteristics curves.

## RESULTS

Median time between CMR and echocardiography was 6 days (IQR: 2 to 30 d). Higher PTT and nPTT values were associated with increasing GDD and MR. Echocardiographic parameters of diastolic dysfunction such as E/A ratio, E/e' ratio and tricuspid regurgitation (TR) velocity also correlated with CMR PTT and nPTT values. The diagnostic accuracy of PTT and nPTT for prediction of GDD as quantified by the area under the ROC curve (AUC) was 0.73 (CI 0.61 to 0.85;  $p = 0.001$ ) for PTT and 0.76 (CI 0.64 to 0.86;  $p < 0.001$ ) for nPTT. A PTT  $< 5.9$  s resulted in a specificity of 94%, a sensitivity of 46% and a negative predictive value of 77%. An nPTT  $< 567$  resulted in a specificity of 66%, a sensitivity of 76% and a NPV of 73% for GDD. For MR the diagnostic performance of PTT and nPTT amounted to an AUC of 0.80 (CI 0.68 to 0.92;  $p < 0.001$ ) for PTT and 0.79 (CI 0.65 to 0.90;  $p < 0.001$ ) for nPTT.

## CONCLUSION

s PTT as an easily obtainable hemodynamic parameter is elevated in patients with global diastolic dysfunction and moderate to severe mitral regurgitation.

## CLINICAL RELEVANCE/APPLICATION

In the assessment of patients with dyspnea, otherwise unexplained elevated values of PTT in perfusion CMR scans might be signs of relevant GDD or MVI and may trigger afresh echocardiographic assessment.

## T5B-SPCA-3 Noninvasive Prediction of Short-term Therapy Effect of Pulmonary Arterial Hypertension by Using Base-line Cardiac Magnetic Resonance Native T1 Mapping

Participants

Yue Wang, MD, (*Presenter*) Nothing to Disclose

## PURPOSE

To investigate the role of base-line Cardiac Magnetic Resonance (CMR) native T1 mapping for predicting the short-term therapy effect in pulmonary arterial hypertension (PAH) patients.

## METHODS AND MATERIALS

Thirty-four PAH patients who referred to our institution and received target therapy were retrospectively included. All patients underwent CMR examination prior to the beginning of the therapy. Patients were subdivided into effective group and ineffective group. Twenty-five healthy individuals were included as controls. Anterior right ventricular insertion point (ARVIP) native T1 times of all patients and controls were manually measured. The diameters of main pulmonary arterial (dMPA) and ascending aorta (dAA) were measured and ratio of dMPA/dAA was calculated. Receiver operating characteristics (ROC) curves and area under curve (AUC) were calculated.

## RESULTS

PAH patients showed higher mid ventricle ARVIP native T1 as compared with controls. Base-line ARVIP native T1 were significantly higher in ineffective group as compared with effective group. The AUC of base-line ARVIP native T1 for predicting the therapy effect was 0.788. The dMPA/dAA ratio was significantly lower in effective group. The combining model integrated dMPA/dAA and ARVIP native T1 for predicting therapy effect was 0.846.

## CONCLUSION

s The combining model integrated base-line ARVIP native T1 and dMPA/dAA ratio shows promise for prediction of the therapy effect of PAH patients

## CLINICAL RELEVANCE/APPLICATION

Base-line cardiac magnetic resonance native T1 mapping hold promise for predicting the therapy effect of PAH patients and may assist the selection of the tailored treatment strategy to improve prognosis.

Printed on: 02/07/23

## Abstract Archives of the RSNA, 2022

T5B-SPCA-1

### Prediction of Pericardial Adhesion and Diagnostic Performance of Hemodynamically Significant Constrictive Pericarditis by using Feature Tracking Cine MR

Tuesday, Nov. 29 12:45PM - 1:15PM Room: Learning Center - CA DPS

#### Participants

Yasutoshi Ohta, MD, PhD, Suita, Japan (*Presenter*) Nothing to Disclose

#### PURPOSE

To investigate the diagnostic performances of pericardial adhesion and hemodynamically significant constrictive pericarditis using cine MR feature tracking

#### METHODS AND MATERIALS

Eligible cases were extracted from patients who underwent cardiac MRI between 2011 and 2021. From patients with suspected CP who underwent CMR and catheter-based hemodynamic evaluation, 24 patients (70±8 years) with cine imaging and tagging were selected (cath group). As an age-matched control group (control group), CMR images were extracted from 24 patients with no history of cardiac surgery or ischemic heart disease. 10 healthy-volunteer were also analyzed for comparison. Displacement and strain of fibrous pericardium and epicardium covering the entire ventricle were analyzed using the feature tracking (FT) method for cine short-axis images and evaluated on a global displacement graph of the pericardium surrounding the left and right ventricle, and the presence of dip or plateau was assessed from the graph. The presence of pericardial adhesions was evaluated on a 5-point scale by assessing the trajectory of myocardium points using cine images and the FT method. The ventricular septum was tracked using the FT method, and septal displacement was evaluated semiquantitatively utilizing a graph. In the cath group, the presence of adhesions was defined by tagging cine. In the combined control and cath CP group (n=48), the diagnosis of clinical CP was based on the presence of hemodynamic CP or pericardial adhesions proved by pericardiectomy. In catheterized patients (n=24), the diagnostic performance of each index for CP was evaluated based on the presence of hemodynamic CP by catheterization. The area under the receiver-operating characteristic curve (AUROC) was calculated for the diagnosis of pericardial adhesion based on pericardial adhesion in tagging cine.

#### RESULTS

For detecting hemodynamically significant CP, the sensitivity and specificity of each finding were: Septal bounce, 84.6% and 81.8%; Adhesion, 100% and 9.1%; Dip, 76.9% and 36.4%; Plateau, 69.2% and 45.5%, respectively. For clinical diagnosis of CP, sensitivity and specificity of each findings were: Septal bounce, 80.0% and 97.0%; Adhesion, 83.3% and 75.8%; Dip, 80.0% and 81.8%; Plateau, 73.3% and 78.8%, respectively. In healthy volunteers, septal bounce, adhesion, dip, and plateau were not observed. The AUROC of diagnosing pericardial adhesion by the FT method was 0.846.

#### CONCLUSION

s Feature-tracking cine MRI yields high diagnostic performance for hemodynamically significant CP.

#### CLINICAL RELEVANCE/APPLICATION

Although the tagging method has so far been considered beneficial for the diagnosis of pericardial adhesions, the FT method can also be used to evaluate the presence of adhesions.

Printed on: 02/07/23

## Abstract Archives of the RSNA, 2022

T5B-SPCA-2

### Cardiovascular Magnetic Resonance Pulmonary Transit Time for Assessment of Global Diastolic Dysfunction and Mitral Regurgitation

Tuesday, Nov. 29 12:45PM - 1:15PM Room: Learning Center - CA DPS

#### Participants

Martin Segeroth, Basel, Switzerland (*Presenter*) Nothing to Disclose

#### PURPOSE

Pulmonary transit time (PTT) is the time it takes blood to pass from the right ventricle to the left ventricle and as such is a surrogate marker of heart failure, pulmonary arterial hypertension and lung disease. We aim to associate PTT with global diastolic dysfunction and mitral regurgitation, which cannot be easily quantified in routine CMR scans.

#### METHODS AND MATERIALS

All patients referred for routine stress perfusion cardiac magnetic resonance (CMR) imaging to University Hospital Basel (Switzerland) with simultaneously available digital electrocardiograms and in-house echocardiographic assessment between January 2014 and August 2020 were included (n=83). Reporting of echocardiographies was done according to American Society of Echocardiography guidelines. Global diastolic dysfunction (GDD) was defined as more than a Grade I (impaired relaxation). Mitral regurgitation (MR) was defined as more than mild regurgitation. PTT was determined from CMR rest perfusion scans as the time in seconds between peak signal intensities of the time signal curves of the right and left ventricle. PTT normalized for heart rate (nPTT) was calculated by multiplying PTT with the heart rate. The diagnostic accuracy was assessed by receiver operating characteristics curves.

#### RESULTS

Median time between CMR and echocardiography was 6 days (IQR: 2 to 30 d). Higher PTT and nPTT values were associated with increasing GDD and MR. Echocardiographic parameters of diastolic dysfunction such as E/A ratio, E/e' ratio and tricuspid regurgitation (TR) velocity also correlated with CMR PTT and nPTT values. The diagnostic accuracy of PTT and nPTT for prediction of GDD as quantified by the area under the ROC curve (AUC) was 0.73 (CI 0.61 to 0.85; p = 0.001) for PTT and 0.76 (CI 0.64 to 0.86; p < 0.001) for nPTT. A PTT < 5.9 s resulted in a specificity of 94%, a sensitivity of 46% and a negative predictive value of 77%. An nPTT < 567 resulted in a specificity of 66%, a sensitivity of 76% and a NPV of 73% for GDD. For MR the diagnostic performance of PTT and nPTT amounted to an AUC of 0.80 (CI 0.68 to 0.92; p < 0.001) for PTT and 0.79 (CI 0.65 to 0.90; p < 0.001) for nPTT.

#### CONCLUSION

s PTT as an easily obtainable hemodynamic parameter is elevated in patients with global diastolic dysfunction and moderate to severe mitral regurgitation.

#### CLINICAL RELEVANCE/APPLICATION

In the assessment of patients with dyspnea, otherwise unexplained elevated values of PTT in perfusion CMR scans might be signs of relevant GDD or MVI and may trigger afresh echocardiographic assessment.

Printed on: 02/07/23



## Abstract Archives of the RSNA, 2022

T5B-SPCA-3

### Noninvasive Prediction of Short-term Therapy Effect of Pulmonary Arterial Hypertension by Using Base-line Cardiac Magnetic Resonance Native T1 Mapping

Tuesday, Nov. 29 12:45PM - 1:15PM Room: Learning Center - CA DPS

#### Participants

Yue Wang, MD, (*Presenter*) Nothing to Disclose

#### PURPOSE

To investigate the role of base-line Cardiac Magnetic Resonance (CMR) native T1 mapping for predicting the short-term therapy effect in pulmonary arterial hypertension (PAH) patients.

#### METHODS AND MATERIALS

Thirty-four PAH patients who referred to our institution and received target therapy were retrospectively included. All patients underwent CMR examination prior to the beginning of the therapy. Patients were subdivided into effective group and ineffective group. Twenty-five healthy individuals were included as controls. Anterior right ventricular insertion point (ARVIP) native T1 times of all patients and controls were manually measured. The diameters of main pulmonary arterial (dMPA) and ascending aorta (dAA) were measured and ratio of dMPA/dAA was calculated. Receiver operating characteristics (ROC) curves and area under curve (AUC) were calculated.

#### RESULTS

PAH patients showed higher mid ventricle ARVIP native T1 as compared with controls. Base-line ARVIP native T1 were significantly higher in ineffective group as compared with effective group. The AUC of base-line ARVIP native T1 for predicting the therapy effect was 0.788. The dMPA/dAA ratio was significantly lower in effective group. The combining model integrated dMPA/dAA and ARVIP native T1 for predicting therapy effect was 0.846.

#### CONCLUSION

The combining model integrated base-line ARVIP native T1 and dMPA/dAA ratio shows promise for prediction of the therapy effect of PAH patients

#### CLINICAL RELEVANCE/APPLICATION

Base-line cardiac magnetic resonance native T1 mapping hold promise for predicting the therapy effect of PAH patients and may assist the selection of the tailored treatment strategy to improve prognosis.

Printed on: 02/07/23



## Abstract Archives of the RSNA, 2022

T5B-SPCH

### Chest Tuesday Poster Discussions - B

Wednesday, Nov. 30 12:45PM - 1:15PM Room: Learning Center - CH DPS

#### Participants

Joon Beom Seo, MD, PhD, Seoul, (*Moderator*) Stockholder, Promedius Inc; Stockholder, Coreline Soft, Co Ltd; Stockholder, Anymedi Inc

#### Sub-Events

### T5B-SPCH-1 Value of Computer Aided Diagnosis on Radiologists' Workflow and Recommendation for Reporting Lung Cancer Screening LDCT

#### Participants

Ren Yuan, MD, PhD, Vancouver, BC (*Presenter*) Nothing to Disclose

#### PURPOSE

In lung cancer screening, the utility of a Computer Aided Diagnostic (CAD) has not been tested in a prospective randomized clinical study. We aim to evaluate whether CAD would change the next step recommendation and how the use of CAD would influence the radiologist's reporting time.

#### METHODS AND MATERIALS

In the Vancouver site of the International Lung Screening Trial, the baseline CT scans were randomized to Radiologist or CAD reading-first arm (i.e. RAD-1st vs. CAD-1st). In Rad-1st arm, a chest radiologist read the CT alone, manually measured and recorded nodules (i.e., manual reading), and then turned on CAD annotations to accept, reject or add nodule(s) for the final "combined reading". In the CAD-1st arm, the CAD annotations were displayed first for the radiologist to accept, reject or add nodule(s) and to generate the report. In the RAD-1st arm, the PanCan nodule malignancy risk score (NEJM 2013) was automatically generated by the CAD based on the "combined reading" result and this score was also calculated for nodules found during "manual reading". Differences in triaging participants into biennial/annual follow-up. FU CT (Group 1), early recall CT in 3 months (Group 2) or diagnostic work-up referral (Group 3) were compared between the manual reading versus the combined reading. The radiologist's reading time was also compared between CAD-1st and Rad-1st arms.

#### RESULTS

Between 2016 and 2019, a total of 2053 ever smokers (age: 55~ 80 yo) who met the USPSTF 2013 screening criteria or those with a PLCOm2012 6-years lung cancer risk >1.5% were enrolled in the study. Seventy (3.4%) cancers were diagnosed after a minimum of 2-years of FU; 48/70 cancers were in Rad-1st arm. All cancers were successfully detected by both radiologist and CAD. In 42/48 cancers, the management recommendation using the PanCan nodule malignancy risk score was consistent between manual and combined reading. In 6/48 cancer cases, using CAD after manual reading prompted a shorter FU interval in 5 cancers (FU changed from 12 to 3 months in 3, and from 3 months to diagnostic workup in 2). In one 11.5mm GGN that was later found to be an adenocarcinoma, adding CAD changed the management from diagnostic work-up to a 3-month FU CT, which retrospectively seemed more appropriate. Radiologist's reading time was significantly shortened by using CAD concurrently in all 3 Groups (for CAD-1st versus Rad-1st arm: in Group1: 4.3±2.4 vs. 5.5±2.9 min; in Group2: 7.6±4.6 vs. 9.3± 4.6 min; in Group3: 7.9±3.9 vs. 12.3± 7.7 min, all p<0.05).

#### CONCLUSION

Using CAD improved accuracy of reporting and management recommendation. Reading concurrently with CAD saved the radiologist's reading time.

#### CLINICAL RELEVANCE/APPLICATION

These features are important regarding the clinical implementation of CAD in a screening program.

### T5B-SPCH-10 Role of Quantitative CT in evaluation of Chronic Obstructive Pulmonary Disease

#### Participants

Shuchi Bhatt, MD, MBBS, Delhi, India (*Presenter*) Nothing to Disclose

#### PURPOSE

COPD is diagnosed when post bronchodilator FEV1/FVC<0.70. Quantitative CT [QCT] can determine airway remodeling, air trapping emphysema in COPD. Aim: To determine compare QCT in cases controls, calculate inter-observer agreement and correlate with spirometry.

#### METHODS AND MATERIALS

After due ethical approval cross-sectional study was done over 18 months on 70 COPD patients using spirometry non-contrast chest CT (inspiration expiration) with 64 slice MDCT. 35 normal inspiratory chest CTs were controls. 1 mm sharp reconstructions

were used to calculate QCT parameters Parenchymal: • Emphysema: Mean lung density [MLD], % low attenuation areas %LAA(-950 HU) • Air trapping: %LAA(-850 HU), %LAA(-850 HU to -950 HU), • Inspiratory/Expiratory [I/E]-I/Evol, I/Eatt Airway: Segmental sub-segmental bronchi (1 each for upper, middle lower lobe for R L lung) • Inner luminal area (Ai) • Wall thickness [WT], wall area [WA], (WA%), Watt • Functional small airway disease: E(-850 HU) /I (-950 HU) Compared mean + SD QCT of cases controls (Unpaired student t test); QCT PFT of cases with Pearson correlation coefficient, ROC determined cut off values for QCT. ICC for Inter-observer agreement

## RESULTS

GOLD Stage III- 61.4%, stage II- 38.5% were present; 85.71% were males, mean age 59.74 yrs, 87% were smokers. Significant difference existed in cases controls for MLD, %LAA-950HU, Ai, WT, WA, WA % ( $p=0.00$ , and  $p=0.003$  for Ai seg) Cases: Excellent ICC  $>0.990$  existed for all except I/Eatt [ICC= 0.815], poor for bronchial Watt ICC= 0.358. Controls: ICC of 0.908 except for Watt [ICC=0.5]. Positive correlation: MLD with FEV1 [ $p=0.017$ ]; I/E lung density with FEV1 [ $p=0.019$ ] FVC [ $p=0.034$ ] existed. Negative correlation seen for %LAA(-950 HU) with FEV1 ( $p$ -value 0.000), FVC ( $p=0.001$ ) FEV1/FVC ( $p=0.023$ ); %LAA(-850 HU) with FEV1 [ $p=0.002$ ] FVC [ $p=0.009$ ]. WA % (seg, sub-seg) correlated negatively with FEV1 ( $p=0.013$ ) FVC [ $p=0.027$  for segmental]. Aiseg with FEV1 [ $p=0.008$ ] FVC [ $p=0.029$ ] correlated positively. MLD[HU] WTsubseg; %LAA(950HU), WTseg WA%subseg WAseg with sensitivity =90%. WAsubseg, %LAA(-950HU) WTsubseg had good specificity (80-89%). Cut off values are - MLD (-853.00 HU, 98.60%, 74.30%), %LAA(-950 HU) (13.24%, 91.50 %, 80.00%), WTseg (0.095cm, 91.40%, 74.30%), WTsubseg (0.065cm, 98.60% and 80%), WAseg(14.00mm<sup>2</sup>, 98.60%, 80%), WAsubseg(8.20mm<sup>2</sup>, 77.10%, 88.60%), WA%[sub-seg] (56.03%, 91.40%, 65.70%), WA%seg (60.65%, 84.305, 68.60%). Mean effective dose is 2.87 mSv (cases) 1.52 mSv (controls)

## CONCLUSION

s QCT detects cases of COPD correlated with spirometry.

## CLINICAL RELEVANCE/APPLICATION

QCT can selectively differentiate air flow limitation due to airway luminal compromise, emphysema, functional airway obstruction and optimize treatment.

## T5B-SPCH-2 Natural History of Persistent Pulmonary Subsolid Nodules at multidetector CT: Analysis of Predictors of Growth

Participants  
Yifan He, Dalian, China (*Presenter*) Nothing to Disclose

## PURPOSE

Long-term follow-up strategies for subsolid nodules (SSNs), risk factors influencing the appearance of subsequent growth of SSNs need to be clarified.

## METHODS AND MATERIALS

A total of 149 SSNs from 132 patients between June 2007 and October 2021 were retrospectively included in this study. All 149 SSNs on initial and final LDCT scans were manually segmented in three-dimensions to obtain SSNs diameter, density, volume and mass, thus to calculate volume doubling time (VDT) and mass doubling time (MDT). Kaplan-Meier analysis was performed using log-rank test, and independent risk factors affecting GGNs growth were analyzed using multivariate Cox proportional risk regression.

## RESULTS

The median follow-up time for 149 SSNs (135 non-solid nodules (NSNs) and 14 part-solid nodules (PSNs)) was 1313 (376-4703) days. The median VDT and MDT of 88 SSNs having grown were 1093.7 (range, 156.3-6799.0) days and 1003.9 (range, 142.3-7264.5) days respectively, the median MDT was significantly shorter than VDT ( $p < 0.001$ ). The cumulative percentages of SSN growth were significantly differed among the initial mean CT attenuation (m-CTA), diameter, volume, mass, age and vacuole subgroups (all  $p < 0.05$ ). The multivariate Cox risk regression analysis showed that vacuole (HR = 1.646,  $p = 0.048$ ), initial volume (HR = 0.999,  $p = 0.041$ ), and initial mass (HR = 1.002,  $p = 0.022$ ) were independent risk factors for SSN growth.

## CONCLUSION

s In patients with vacuole sign, larger initial volume and mass, a more rational follow-up period is necessary to observe the presence or absence of interval growth of the SSNs.

## CLINICAL RELEVANCE/APPLICATION

Persistent SSNs, especially showing interval growth, often indicate precursor glandular lesions or invasive adenocarcinomas (IACs). The diagnosis of SSN is challenging because there exists an apparent paradox, displaying indolent biological behavior with slow growth but a high rate of being malignant. There existed a large heterogeneity in the growth pattern of SSN, and the natural growth course of nodules and follow-up strategies need to be elucidated. Volume and mass are three-dimensional quantitative parameters that can reflect the actual growth of SSNs more accurately and earlier. In our study, vacuole, initial volume and mass were independent risk factors for the appearance of progression of SSN. Therefore, the observation of changes in these characteristics during follow-up is of value to assisting clinical practice and rational management of pulmonary nodules.

## T5B-SPCH-3 Volumetric Analysis: Effect on Pulmonary Nodule Diagnosis and Management in Clinical Practice

Participants  
Robert Lim, MD, (*Presenter*) Nothing to Disclose

## PURPOSE

To evaluate the effect of volumetric analysis on the diagnosis and management of indeterminate solid nodules on computed tomography (CT).

## METHODS AND MATERIALS

One hundred and seven CT cases of solid pulmonary nodules (size range, 6-15 mm) were selected, including 57 proven malignancies (lung cancer,  $n=34$ ; metastasis,  $n=23$ ) and 50 benign nodules. CT scans were from multiple institutions and of variable technique. Nine radiologists (attending,  $n=3$ ; fellows,  $n=3$ ; residents,  $n=3$ ) were asked their level of suspicion for malignancy (low/moderate or

high) and management recommendation (no follow-up; CT follow up; or care escalation) for baseline and follow-up studies first without and then with volumetric analysis. The effect of volumetric analysis on diagnosis and management of cases was assessed by logistic regression; its effect on timepoint when malignant nodules were first identified was tested by a test of symmetry. Differences in inter-observer kappa coefficients between assessments performed without and with volume analysis were tested by Gwet's linearized t-test for kappa.

## RESULTS

Improved sensitivity ( $p=0.011$ ) and earlier recognition ( $p<0.001$ ) of malignant nodules occurred with use of volumetric analysis. Attending radiologists showed higher sensitivity in recognition of malignant nodules ( $p=0.03$ ) and then to recommend care escalation ( $p<0.001$ ) as compared to trainees. Use of volumetric analysis altered management of nodules assessed to be of high suspicion for malignancy only in the fellow group ( $p=0.008$ ). Kappa statistics for suspicion for malignancy and recommended management were in the fair to substantial (0.38-0.66) and fair to good (0.33-0.50) ranges, respectively. Use of volumetric analysis improved inter-observer variability ( $p=0.004$ ) only for assessment of nodule malignancy on the second follow-up study from 0.52 to 0.66.

## CONCLUSION

s Volumetric analysis of solid indeterminate pulmonary nodules in routine clinical practice can result in improved sensitivity and earlier identification of malignant nodules. Its effect on recommendations for management of suspected malignant nodules is variable and may be influenced by reader experience.

## CLINICAL RELEVANCE/APPLICATION

Adoption of volumetric analysis of solid indeterminate pulmonary nodules in routine CT clinical practice may allow more sensitive and earlier detection of cancers.

### **T5B-SPCH-4 Will I Change Nodule Management Recommendations If I Change My CAD System: Volumetry of Artificial Pulmonary Nodules by Different CAD Systems**

Participants

Alan Peters, MD, Bern, Switzerland (*Presenter*) Nothing to Disclose

## PURPOSE

To evaluate and compare the measurement accuracy of two different CAD systems regarding artificial pulmonary nodules and assess the clinical impact of volumetric inaccuracies in a phantom study.

## METHODS AND MATERIALS

In this phantom study, 59 different phantom arrangements with 326 artificial nodules (178 solid, 148 ground-glass) were scanned at 80 kV, 100 kV and 120 kV. Four different nodule diameters were used: 5 mm, 8 mm, 10 mm and 12 mm. Scans were analyzed by a DL-based CAD and a standard CAD system. Relative volumetric errors (RVE) of each system vs. ground truth and the relative volume difference (RVD) DL-based vs. standard CAD were calculated. The Bland-Altman method was used to define the limits of agreement (LOA). The hypothetical impact on LungRADS classification was assessed for both systems.

## RESULTS

There was no difference between the three voltage groups regarding nodule volumetry. Regarding the solid nodules, the RVE of the 5 mm, 8 mm, 10 mm and 12 mm size group for the DL-CAD/standard CAD were 12.2/2.8% 1.3/-2.8%, -3.6/1.5% and -12.2/-0.3%, respectively. The corresponding values for the GGN were 25.6%/81.0%, 9.0%/28.0%, 7.6/20.6% and 6.8/21.2%. The mean RVD for solid nodules/GGN was 1.3/-15.2%. Regarding the LungRADS classification, 88.5% and 79.8% of all solid nodules were correctly assigned by the DL-CAD and the standard CAD, respectively. 14.9% of the nodules were assigned differently between the systems.

## CONCLUSION

s Patient management may be affected by volumetric inaccuracy of the CAD systems.

## CLINICAL RELEVANCE/APPLICATION

The results of this study highlight that supervision and / or manual correction by a radiologist is pertinent when using a CAD system in daily clinical routine.

### **T5B-SPCH-5 A General Approach for Automatic Segmentation of Pneumonia Pulmonary Nodule and Tuberculosis on CT Images**

Participants

Jiangdian Song, PhD, (*Presenter*) Nothing to Disclose

## PURPOSE

Accurate segmentation of lung lesions on CT images will inform clinical diagnosis of multiple lung diseases including COVID-19 pneumonia. As a common framework for image segmentation, generative adversarial network (GAN) is hampered by the limited annotated samples available and the catastrophic forgetting of the discriminator when used to segment diverse lung lesions on computed tomography (CT) images. Therefore, a general self-supervised adversarial learning architecture that does not require large amounts of labeled data and mitigates discriminator forgetting is proposed to segment lung lesions including pneumonia, lung nodules, and tuberculosis precisely and automatically on CT images.

## METHODS AND MATERIALS

For the generator network of the proposed model, a cascaded dual attention network with a context-aware pyramid feature extraction module is designed to model multi-scale semantic interdependencies of lung lesions in both spatial and channel dimensions. Then, a self-supervised rotation loss is introduced into the model to avoid discriminator forgetting and to achieve more efficient lung lesion feature representation. Multi-center pneumonia, lung nodule, and tuberculosis CT images were used to test the proposed model. A state-of-the-art nnU-Net is employed to compare with the proposed model on lung lesion segmentation.

## RESULTS

A total of 14,260, 14,266, and 3,361 images of pneumonia, lung nodule, and tuberculosis were used in this study, and the lesions were randomly divided into training, validation, and test datasets (8:1:1), respectively. Average dice coefficients (DCs) of 75.05%, 74.22%, and 71.58% for the three lesion types were obtained on the test dataset when using all the images. When the training dataset was reduced to 10%, DCs of 71.10%, 72.80%, and 69.43% were obtained on test datasets, respectively, and no significant decrease in DC was found ( $P > 0.10$ ). In addition, no significant difference was found between the nnU-Net and the proposed model for segmentation ( $P > 0.05$ ).

## CONCLUSION

Our study provided a self-supervised adversarial learning architecture to enable the use of limited training samples for accurately segmenting multiple types of lung lesions without the need for massive annotation sample. The proposed model achieved competitive segmentation result compared with the state-of-the-art segmentation network.

## CLINICAL RELEVANCE/APPLICATION

A general automatic segmentation approach for COVID-19 pneumonia, lung nodule, and tuberculosis enables to reduce the redundant work of repeatedly model training. Our model enables the reduction of GAN's dependence on massive manually annotated training data and thus relieves radiologists from tedious manual delineation labor.

## T5B-SPCH-6 CT Radiomics-based Clustering in Lung Cancer: A Comparison with Comprehensive Genomic Profiling

Participants

Motohiko Yamazaki, MD, PhD, (*Presenter*) Nothing to Disclose

## PURPOSE

Comprehensive genomic profiling (CGP) is a new technology that can analyze hundreds of cancer genes at one assay and enables to determine the total number of gene mutations called tumor mutation burden (TMB). In lung cancer, driver gene mutations can be candidates for molecular targeted therapies, while a high TMB suggests good response to immune checkpoint inhibitors. This study aimed to compare CT radiomics-based clustering with CGP data and patient prognosis in lung cancer.

## METHODS AND MATERIALS

This retrospective study comprised 93 patients with non-small cell lung cancer (66 adenocarcinomas and 27 squamous cell carcinomas) who underwent surgery. TMB and 415 cancer gene expression patterns were investigated in each surgical specimen by CGP using next-generation sequencing. All patients were classified into two clusters according to their radiomic features extracted from preoperative CT images using unsupervised k-means clustering. Differences between these two clusters were investigated with respect to gene mutations, TMB (low or high), recurrence-free survival, and visual CT features.

## RESULTS

Unsupervised clustering classified 55 patients into Cluster 1 and 38 patients into Cluster 2 according to their radiomic features. Cluster 1 exhibited a significantly higher proportion of TP53 and CDKN2B gene mutations but a lower proportion of EGFR gene mutations compared with Cluster 2 (TP53 mutations, 34/55 [61.8%] vs 12/38 [31.6%]; CDKN2B mutations, 26/55 [47.3%] vs 10/38 [26.3%]; EGFR mutations, 13/55 [23.6%] vs 17/38 [44.7%]; all  $P < 0.05$ ). A high TMB (= 20 mutations/megabase) was more frequently observed in Cluster 1 than in Cluster 2 (23/55 [41.8%] vs. 2/38 [5.3%];  $P < 0.01$ ). Recurrence-free survival at 5 years was significantly lower in Cluster 1 than in Cluster 2 (40.4% vs. 51.0%;  $P = 0.038$ ). For visual CT features, Cluster 1 was more likely to indicate a lobulated margin but was less frequently accompanied by ground-glass opacity, air-bronchogram, cavity, and vacuole sign compared to Cluster 2 (all  $P < 0.05$ ).

## CONCLUSION

CT radiomics-based clustering has significant association with CGP data as well as patient prognosis and may help predict genomic information in non-small cell lung cancer.

## CLINICAL RELEVANCE/APPLICATION

CGP provides valuable information to determine therapeutic agents for lung cancer, leading to precision medicine. However, CGP is very expensive and requires invasive tissue sampling. Therefore, CT examination, which is non-invasive and relatively low costs, plays an important role in predicting genomic information. CT radiomics-based clustering created in this study could help predict CGP data.

## T5B-SPCH-7 Correlation Between Intra-nodular Vessel and Tumor Invasiveness of Lung Adenocarcinoma Presenting as Ground-glass Nodules: A Deep Learning 3D Reconstruction Algorithm-based Quantitative Analysis on Non-contrast CT Images

Participants

Baolian Zhao, (*Presenter*) Nothing to Disclose

## PURPOSE

To quantitatively analyze the pulmonary vessels inside ground-glass nodules (GGNs) on non-contrast CT (NCCT) images using fully automated deep learning (DL) approach and investigate the relationship between intra-nodular vessel and tumor invasiveness.

## METHODS AND MATERIALS

A total of 741 pathologically confirmed GGNs from 719 patients were retrospectively collected, comprising 121 atypical adenomatous hyperplasia (AAH), 150 adenocarcinoma in situ (AIS), 154 minimally invasive adenocarcinoma (MIA) and 316 invasive adenocarcinoma (IAC). The pulmonary blood vessels were reconstructed on NCCT images using DL-based region segmentation and region growth technology (InferVisual Surgery Planning Research version). The presence of pulmonary vessels inside GGNs was quantitatively evaluated with respect to intra-nodular vessel prevalence and the automatically calculated vessel volume percentage, which were further compared across different invasiveness categories by the Chi-square test, analysis of variance (ANOVA) and Mann-Whitney U test.

## RESULTS

The automated DL algorithm showed high accuracy in vessels detection and reconstruction. There were significant differences in

The occurrence of internal vessels across different tumor invasiveness GGNs ( $p < 0.001$ ). The prevalence of intra-nodular vessels in IAC (66.5%) was significantly higher than that of AAH (35.5%,  $p < 0.001$ ), AIS (33.3%,  $p < 0.001$ ) and MIA (50.6%,  $p = 0.001$ ), while the vascular categories were similar (all  $p > 0.05$ ). Vascular changes were more common in invasive lesions (MIA and IAC) than pre-invasive lesions (AAH and AIS), which mainly manifested as increased vessel volume percentage (10.23% vs 3.85%,  $p < 0.001$ ). The average vessel volume percentage of IAC (12.01%) was also higher compared with that of AAH (3.85%), AIS (3.86%) and MIA (6.57%) with statistically significance (all  $p < 0.001$ ).

## CONCLUSION

The quantitative analysis of intra-nodular vessels on NCCT images demonstrated that the incidence of internal vessels in GGNs was related to their pathological invasiveness. GGNs with increased internal vessel percentages had higher possibility of tumor invasiveness.

## CLINICAL RELEVANCE/APPLICATION

Our deep learning-based quantitative analysis on NCCT images reveals that the incidence and volume percentage of intra-tumoral vessels in GGNs are correlated with pathological invasiveness.

### **T5B-SPCH-8 Cascade-network to Reduce False Positives for Pulmonary Nodule Detection on Chest X-ray Radiographs**

Participants  
Taehee Kim, Seoul, Korea, Republic Of (*Presenter*) Nothing to Disclose

## PURPOSE

Recently, many deep learning-based nodule detection algorithms for chest X-ray radiographs (CXRs) have reported promising results. In real clinical environment, however, those algorithms have been reported to produce many false positives (FPs) caused by the similarity between hard negatives (e.g., nipple shadow, bone island, superimposed pulmonary vessels, etc.) and real nodules. Here, we propose a cascade-network to reduce these FPs in nodule detection.

## METHODS AND MATERIALS

NODE21 challenge dataset (node21.grand-challenge.org) was utilized (training: 934/2404; validation: 100/300; testing: 100/300 for nodule/non-nodule CXRs). For each CXR in the training dataset, a set of multi-resolution patches (resolution: 112x112, 280x280, and 448x448) were generated. Three multi-resolution patches were resized to 112x112 and concatenated along the channel for training. Patches were classified as positive (i.e., nodule patches) when a nodule locates on the center of the patch. For nodule detection, two neural networks were used sequentially where first network was to detect nodule candidates on an input CXR, and the second network was to further screen out hard negatives. Both networks had same architecture (EfficientNet-B0) and trained based on multi-resolution patches. The output of the two networks was the probability of nodule for the input patch. The difference between the networks was the composition of training dataset. For first network, all negative patches for training were the patches with no nodule (i.e., non-nodule patches). In second network, half of negative patches for training were carefully selected among the false positive outputs in the training data of first network to design second network more sensitive to the hard negatives. The detection performances were measured based on the area under the Free-Response Receiver Operating Characteristics (FAUC) and Refined Competition Performance Metric (R-CPM). Comparison was performed before and after ablating second network.

## RESULTS

The nodule detection performances of the cascade-network (FAUC:0.6033(95% CI: 0.5848-0.6217), R-CPM:0.5995(0.5778-0.6211)) outperformed those of the first network only (FAUC:0.4987(0.4667-0.5308),  $p < 0.001$ , R-CPM:0.4967(0.4649-0.5285),  $p < 0.001$ ). When visually investigated, the outputs from the cascade-network showed a much smaller number of FPs.

## CONCLUSION

In this study, we proposed a cascade-network for nodule detection to reduce FPs, dramatically improving nodule detection performance.

## CLINICAL RELEVANCE/APPLICATION

The proposed cascade-network with sequential training scheme would enable development of a nodule detection algorithm with high positive predictive value efficiently by using network-driven hard negatives.

### **T5B-SPCH-9 Implications of Radiologist-interpreted Subjective Standards for Evaluating the Diagnostic Performance of a Deep Learning Model: A Malignant Lung Nodule Detection Task on Chest Radiographs**

Participants  
Jung Eun Huh, BA, Oxford, United Kingdom (*Presenter*) Nothing to Disclose

## PURPOSE

Little is known regarding the impact of radiologist-interpreted subjective standards as ground truth when evaluating the performance of deep learning (DL) models and their added value to radiologists. We assessed the adherence of the subjective standards to the reference standard, and the difference in diagnostic performance measurements of radiologists with and without a DL-based automatic detection (DLAD) model according to the standard used to detect malignant pulmonary nodules on chest radiographs.

## METHODS AND MATERIALS

This study included 50 patients with pathology- and CT-proven lung cancers (reference standards) with 50 chest radiographs between December 2015 and February 2021, and 50 control individuals with normal chest radiographs. Five subjective standards were constructed using 10 radiologists' interpretations and compared: individual judgment by the most experienced radiologist, majority vote, consensus judgments of 2 and 3 radiologists, and a latent class analysis (LCA) model. In separate reader tests, 10 other radiologists (who did not participate in constructing the subjective standards) interpreted the radiographs with and without the DLAD model, and their diagnostic performance was compared between the reference standard and the five subjective

standards. The t-test with the Bonferroni correction was used to compare adherence and diagnostic performance.

## **RESULTS**

The LCA model, which showed a sensitivity of 72.6% and a specificity of 100%, adhered more closely to the reference standard than any of the other subjective standards. In the reader tests, both the radiologists and the DLAD model tended to show overestimated sensitivity but underestimated specificity when the subjective standards were applied as the ground truths. However, these radiologists' tendencies were diminished by DLAD assistance (all P-values <0.001). Although using the DLAD improved the sensitivity and specificity (in some cases) when the subjective standards were used, the corresponding effects were estimated to be significantly smaller than when the reference standard was used (all P-values <0.001), except for sensitivity with the LCA model (P=0.094).

## **CONCLUSION**

s The LCA model showed the closest adherence to the reference standard for detecting malignant pulmonary nodules on chest radiographs. Radiologists' sensitivity and specificity values were overestimated and underestimated, respectively, and the DLAD added less value with the subjective standards than with the reference standard.

## **CLINICAL RELEVANCE/APPLICATION**

Since using only subjective standards can lead to bias in the diagnostic performance of DL models, evaluating DL models with a reference standard is necessary even in underserved settings.

Printed on: 02/07/23



## Abstract Archives of the RSNA, 2022

T5B-SPCH-1

### Value of Computer Aided Diagnosis on Radiologists' Workflow and Recommendation for Reporting Lung Cancer Screening LDCT

Wednesday, Nov. 30 12:45PM - 1:15PM Room: Learning Center - CH DPS

#### Participants

Ren Yuan, MD, PhD, Vancouver, BC (*Presenter*) Nothing to Disclose

#### PURPOSE

In lung cancer screening, the utility of a Computer Aided Diagnostic (CAD) has not been tested in a prospective randomized clinical study. We aim to evaluate whether CAD would change the next step recommendation and how the use of CAD would influence the radiologist's reporting time.

#### METHODS AND MATERIALS

In the Vancouver site of the International Lung Screening Trial, the baseline CT scans were randomized to Radiologist or CAD reading-first arm (i.e. RAD-1st vs. CAD-1st). In Rad-1st arm, a chest radiologist read the CT alone, manually measured and recorded nodules (i.e., manual reading), and then turned on CAD annotations to accept, reject or add nodule(s) for the final "combined reading". In the CAD-1st arm, the CAD annotations were displayed first for the radiologist to accept, reject or add nodule(s) and to generate the report. In the RAD-1st arm, the PanCan nodule malignancy risk score (NEJM 2013) was automatically generated by the CAD based on the "combined reading" result and this score was also calculated for nodules found during "manual reading". Differences in triaging participants into biennial/annual follow-up. FU CT (Group 1), early recall CT in 3 months (Group 2) or diagnostic work-up referral (Group 3) were compared between the manual reading versus the combined reading. The radiologist's reading time was also compared between CAD-1st and Rad-1st arms.

#### RESULTS

Between 2016 and 2019, a total of 2053 ever smokers (age: 55~ 80 yo) who met the USPSTF 2013 screening criteria or those with a PLCom2012 6-years lung cancer risk >1.5% were enrolled in the study. Seventy (3.4%) cancers were diagnosed after a minimum of 2-years of FU; 48/70 cancers were in Rad-1st arm. All cancers were successfully detected by both radiologist and CAD. In 42/48 cancers, the management recommendation using the PanCan nodule malignancy risk score was consistent between manual and combined reading. In 6/48 cancer cases, using CAD after manual reading prompted a shorter FU interval in 5 cancers (FU changed from 12 to 3 months in 3, and from 3 months to diagnostic workup in 2). In one 11.5mm GGN that was later found to be an adenocarcinoma, adding CAD changed the management from diagnostic work-up to a 3-month FU CT, which retrospectively seemed more appropriate. Radiologist's reading time was significantly shortened by using CAD concurrently in all 3 Groups (for CAD-1st versus Rad-1st arm: in Group1: 4.3±2.4 vs. 5.5±2.9 min; in Group2: 7.6±4.6 vs. 9.3± 4.6 min; in Group3: 7.9±3.9 vs. 12.3± 7.7 min, all p<0.05).

#### CONCLUSION

Using CAD improved accuracy of reporting and management recommendation. Reading concurrently with CAD saved the radiologist's reading time.

#### CLINICAL RELEVANCE/APPLICATION

These features are important regarding the clinical implementation of CAD in a screening program.

Printed on: 02/07/23

## Abstract Archives of the RSNA, 2022

T5B-SPCH-10

### Role of Quantitative CT in evaluation of Chronic Obstructive Pulmonary Disease

Wednesday, Nov. 30 12:45PM - 1:15PM Room: Learning Center - CH DPS

#### Participants

Shuchi Bhatt, MD, MBBS, Delhi, India (*Presenter*) Nothing to Disclose

#### PURPOSE

COPD is diagnosed when post bronchodilator FEV1/FVC<0.70. Quantitative CT [QCT] can determine airway remodeling, air trapping emphysema in COPD. Aim: To determine compare QCT in cases controls, calculate inter-observer agreement and correlate with spirometry.

#### METHODS AND MATERIALS

After due ethical approval cross-sectional study was done over 18 months on 70 COPD patients using spirometry non-contrast chest CT (inspiration expiration) with 64 slice MDCT. 35 normal inspiratory chest CTs were controls. 1 mm sharp reconstructions were used to calculate QCT parameters Parenchymal: • Emphysema: Mean lung density [MLD], % low attenuation areas %LAA(-950 HU) • Air trapping: %LAA(-850 HU), %LAA(-850 HU to -950 HU), • Inspiratory/Expiratory [I/E]-I/Evol, I/Eatt Airway: Segmental sub-segmental bronchi (1 each for upper, middle lower lobe for R L lung) • Inner luminal area (Ai) • Wall thickness [WT], wall area [WA], (WA%), Watt • Functional small airway disease: E(-850 HU) /I (-950 HU) Compared mean + SD QCT of cases controls (Unpaired student t test); QCT PFT of cases with Pearson correlation coefficient, ROC determined cut off values for QCT. ICC for Inter-observer agreement

#### RESULTS

GOLD Stage III- 61.4%, stage II- 38.5% were present; 85.71% were males, mean age 59.74 yrs, 87% were smokers. Significant difference existed in cases controls for MLD, %LAA-950HU, Ai, WT, WA, WA % (p=0.00, and p= 0.003 for Ai seg) Cases: Excellent ICC >0.990 existed for all except I/Eatt[ICC= 0.815], poor for bronchial Watt ICC= 0.358. Controls: ICC of 0.908 except for Watt [ICC=0.5]. Positive correlation: MLD with FEV1 [p =0.017]; I/E lung density with FEV1 [p =0.019] FVC [p=0.034] existed. Negative correlation seen for %LAA(-950 HU) with FEV1 (p-value 0.000), FVC (p= 0.001) FEV1/FVC (p= 0.023); %LAA(-850 HU) with FEV1 [p=0.002] FVC [p= 0.009]. WA % (seg, sub-seg) correlated negatively with FEV1 (p =0.013) FVC [p=0.027 for segmental]. Aiseg with FEV1 [p=0.008] FVC [p=0.029] correlated positively. MLD[HU] WTsubseg; %LAA(950HU), WTseg WA%subseg WAsseg with sensitivity =90%. WAsubseg, %LAA(-950HU) WTsubseg had good specificity (80-89%). Cut off values are - MLD (-853.00 HU,98.60%,74.30%), %LAA(-950 HU) (13.24%, 91.50 %, 80.00%), WTseg (0.095cm, 91.40%, 74.30%), WTsubseg (0.065cm,98.60% and 80%), WAsseg(14.00mm<sup>2</sup>, 98.60%. 80%), WAsubseg(8.20mm<sup>2</sup>,77.10%, 88.60%),WA%[sub-seg] (56.03%, 91.40%, 65.70%), WA%seg (60.65%, 84.305, 68.60%). Mean effective dose is 2.87 mSv (cases) 1.52 mSv (controls)

#### CONCLUSION

s QCT detects cases of COPD correlated with spirometry.

#### CLINICAL RELEVANCE/APPLICATION

QCT can selectively differentiate air flow limitation due to airway luminal compromise, emphysema, functional airway obstruction and optimize treatment.

Printed on: 02/07/23

## Abstract Archives of the RSNA, 2022

T5B-SPCH-2

### Natural History of Persistent Pulmonary Subsolid Nodules at multidetector CT: Analysis of Predictors of Growth

Wednesday, Nov. 30 12:45PM - 1:15PM Room: Learning Center - CH DPS

#### Participants

Yifan He, Dalian, China (*Presenter*) Nothing to Disclose

#### PURPOSE

Long-term follow-up strategies for subsolid nodules (SSNs), risk factors influencing the appearance of subsequent growth of SSNs need to be clarified.

#### METHODS AND MATERIALS

A total of 149 SSNs from 132 patients between June 2007 and October 2021 were retrospectively included in this study. All 149 SSNs on initial and final LDCT scans were manually segmented in three-dimensions to obtain SSNs diameter, density, volume and mass, thus to calculate volume doubling time (VDT) and mass doubling time (MDT). Kaplan-Meier analysis was performed using log-rank test, and independent risk factors affecting GGNs growth were analyzed using multivariate Cox proportional risk regression.

#### RESULTS

The median follow-up time for 149 SSNs (135 non-solid nodules (NSNs) and 14 part-solid nodules (PSNs)) was 1313 (376-4703) days. The median VDT and MDT of 88 SSNs having grown were 1093.7 (range, 156.3-6799.0) days and 1003.9 (range, 142.3-7264.5) days respectively, the median MDT was significantly shorter than VDT ( $p < 0.001$ ). The cumulative percentages of SSN growth were significantly differed among the initial mean CT attenuation (m-CTA), diameter, volume, mass, age and vacuole subgroups (all  $p < 0.05$ ). The multivariate Cox risk regression analysis showed that vacuole (HR = 1.646,  $p = 0.048$ ), initial volume (HR = 0.999,  $p = 0.041$ ), and initial mass (HR = 1.002,  $p = 0.022$ ) were independent risk factors for SSN growth.

#### CONCLUSION

s In patients with vacuole sign, larger initial volume and mass, a more rational follow-up period is necessary to observe the presence or absence of interval growth of the SSNs.

#### CLINICAL RELEVANCE/APPLICATION

Persistent SSNs, especially showing interval growth, often indicate precursor glandular lesions or invasive adenocarcinomas (IACs). The diagnosis of SSN is challenging because there exists an apparent paradox, displaying indolent biological behavior with slow growth but a high rate of being malignant. There existed a large heterogeneity in the growth pattern of SSN, and the natural growth course of nodules and follow-up strategies need to be elucidated. Volume and mass are three-dimensional quantitative parameters that can reflect the actual growth of SSNs more accurately and earlier. In our study, vacuole, initial volume and mass were independent risk factors for the appearance of progression of SSN. Therefore, the observation of changes in these characteristics during follow-up is of value to assisting clinical practice and rational management of pulmonary nodules.

Printed on: 02/07/23

## Abstract Archives of the RSNA, 2022

T5B-SPCH-3

### Volumetric Analysis: Effect on Pulmonary Nodule Diagnosis and Management in Clinical Practice

Wednesday, Nov. 30 12:45PM - 1:15PM Room: Learning Center - CH DPS

#### Participants

Robert Lim, MD, (*Presenter*) Nothing to Disclose

#### PURPOSE

To evaluate the effect of volumetric analysis on the diagnosis and management of indeterminate solid nodules on computed tomography (CT).

#### METHODS AND MATERIALS

One hundred and seven CT cases of solid pulmonary nodules (size range, 6-15 mm) were selected, including 57 proven malignancies (lung cancer, n=34; metastasis, n=23) and 50 benign nodules. CT scans were from multiple institutions and of variable technique. Nine radiologists (attending, n=3; fellows, n=3; residents, n=3) were asked their level of suspicion for malignancy (low/moderate or high) and management recommendation (no follow-up; CT follow up; or care escalation) for baseline and follow-up studies first without and then with volumetric analysis. The effect of volumetric analysis on diagnosis and management of cases was assessed by logistic regression; its effect on timepoint when malignant nodules were first identified was tested by a test of symmetry. Differences in inter-observer kappa coefficients between assessments performed without and with volume analysis were tested by Gwet's linearized t-test for kappa.

#### RESULTS

Improved sensitivity ( $p=0.011$ ) and earlier recognition ( $p<0.001$ ) of malignant nodules occurred with use of volumetric analysis. Attending radiologists showed higher sensitivity in recognition of malignant nodules ( $p=0.03$ ) and then to recommend care escalation ( $p<0.001$ ) as compared to trainees. Use of volumetric analysis altered management of nodules assessed to be of high suspicion for malignancy only in the fellow group ( $p=0.008$ ). Kappa statistics for suspicion for malignancy and recommended management were in the fair to substantial (0.38-0.66) and fair to good (0.33-0.50) ranges, respectively. Use of volumetric analysis improved inter-observer variability ( $p=0.004$ ) only for assessment of nodule malignancy on the second follow-up study from 0.52 to 0.66.

#### CONCLUSION

s Volumetric analysis of solid indeterminate pulmonary nodules in routine clinical practice can result in improved sensitivity and earlier identification of malignant nodules. Its effect on recommendations for management of suspected malignant nodules is variable and may be influenced by reader experience.

#### CLINICAL RELEVANCE/APPLICATION

Adoption of volumetric analysis of solid indeterminate pulmonary nodules in routine CT clinical practice may allow more sensitive and earlier detection of cancers.

Printed on: 02/07/23

## Abstract Archives of the RSNA, 2022

T5B-SPCH-4

### Will I Change Nodule Management Recommendations If I Change My CAD System: Volumetry of Artificial Pulmonary Nodules by Different CAD Systems

Wednesday, Nov. 30 12:45PM - 1:15PM Room: Learning Center - CH DPS

#### Participants

Alan Peters, MD, Bern, Switzerland (*Presenter*) Nothing to Disclose

#### PURPOSE

To evaluate and compare the measurement accuracy of two different CAD systems regarding artificial pulmonary nodules and assess the clinical impact of volumetric inaccuracies in a phantom study.

#### METHODS AND MATERIALS

In this phantom study, 59 different phantom arrangements with 326 artificial nodules (178 solid, 148 ground-glass) were scanned at 80 kV, 100 kV and 120 kV. Four different nodule diameters were used: 5 mm, 8 mm, 10 mm and 12 mm. Scans were analyzed by a DL-based CAD and a standard CAD system. Relative volumetric errors (RVE) of each system vs. ground truth and the relative volume difference (RVD) DL-based vs. standard CAD were calculated. The Bland-Altman method was used to define the limits of agreement (LOA). The hypothetical impact on LungRADS classification was assessed for both systems.

#### RESULTS

There was no difference between the three voltage groups regarding nodule volumetry. Regarding the solid nodules, the RVE of the 5 mm, 8 mm, 10 mm and 12 mm size group for the DL-CAD/standard CAD were 12.2/2.8%, 1.3/-2.8%, -3.6/1.5% and -12.2/-0.3%, respectively. The corresponding values for the GGN were 25.6%/81.0%, 9.0%/28.0%, 7.6/20.6% and 6.8/21.2%. The mean RVD for solid nodules/GGN was 1.3/-15.2%. Regarding the LungRADS classification, 88.5% and 79.8% of all solid nodules were correctly assigned by the DL-CAD and the standard CAD, respectively. 14.9% of the nodules were assigned differently between the systems.

#### CONCLUSION

s Patient management may be affected by volumetric inaccuracy of the CAD systems.

#### CLINICAL RELEVANCE/APPLICATION

The results of this study highlight that supervision and / or manual correction by a radiologist is pertinent when using a CAD system in daily clinical routine.

Printed on: 02/07/23

## Abstract Archives of the RSNA, 2022

T5B-SPCH-5

### A General Approach for Automatic Segmentation of Pneumonia Pulmonary Nodule and Tuberculosis on CT Images

Wednesday, Nov. 30 12:45PM - 1:15PM Room: Learning Center - CH DPS

#### Participants

Jiangdian Song, PhD, (*Presenter*) Nothing to Disclose

#### PURPOSE

Accurate segmentation of lung lesions on CT images will inform clinical diagnosis of multiple lung diseases including COVID-19 pneumonia. As a common framework for image segmentation, generative adversarial network (GAN) is hampered by the limited annotated samples available and the catastrophic forgetting of the discriminator when used to segment diverse lung lesions on computed tomography (CT) images. Therefore, a general self-supervised adversarial learning architecture that does not require large amounts of labeled data and mitigates discriminator forgetting is proposed to segment lung lesions including pneumonia, lung nodules, and tuberculosis precisely and automatically on CT images.

#### METHODS AND MATERIALS

For the generator network of the proposed model, a cascaded dual attention network with a context-aware pyramid feature extraction module is designed to model multi-scale semantic interdependencies of lung lesions in both spatial and channel dimensions. Then, a self-supervised rotation loss is introduced into the model to avoid discriminator forgetting and to achieve more efficient lung lesion feature representation. Multi-center pneumonia, lung nodule, and tuberculosis CT images were used to test the proposed model. A state-of-the-art nnU-Net is employed to compare with the proposed model on lung lesion segmentation.

#### RESULTS

A total of 14,260, 14,266, and 3,361 images of pneumonia, lung nodule, and tuberculosis were used in this study, and the lesions was randomly divided into training, validation, and test datasets (8:1:1), respectively. Average dice coefficients (DCs) of 75.05%, 74.22%, and 71.58% for the three lesion types were obtained on the test dataset when using all the images. When the training dataset was reduced to 10%, DCs of 71.10%, 72.80%, and 69.43% were obtained on test datasets, respectively, and no significant decrease in DC was found ( $P > 0.10$ ). In addition, no significant difference was found between the nnU-Net and the proposed model for segmentation ( $P > 0.05$ ).

#### CONCLUSION

s Our study provided a self-supervised adversarial learning architecture to enable the use of limited training samples for accurately segmenting multiple types of lung lesions without the need for massive annotation sample. The proposed model achieved competitive segmentation result compared with the state-of-the-art segmentation network.

#### CLINICAL RELEVANCE/APPLICATION

A general automatic segmentation approach for COVID-19 pneumonia, lung nodule, and tuberculosis enables to reduce the redundant work of repeatedly model training. Our model enables the reduction of GAN's dependence on massive manually annotated training data and thus relieves radiologists from tedious manual delineation labor.

Printed on: 02/07/23

## Abstract Archives of the RSNA, 2022

T5B-SPCH-6

### CT Radiomics-based Clustering in Lung Cancer: A Comparison with Comprehensive Genomic Profiling

Wednesday, Nov. 30 12:45PM - 1:15PM Room: Learning Center - CH DPS

#### Participants

Motohiko Yamazaki, MD, PhD, (*Presenter*) Nothing to Disclose

#### PURPOSE

Comprehensive genomic profiling (CGP) is a new technology that can analyze hundreds of cancer genes at one assay and enables to determine the total number of gene mutations called tumor mutation burden (TMB). In lung cancer, driver gene mutations can be candidates for molecular targeted therapies, while a high TMB suggests good response to immune checkpoint inhibitors. This study aimed to compare CT radiomics-based clustering with CGP data and patient prognosis in lung cancer.

#### METHODS AND MATERIALS

This retrospective study comprised 93 patients with non-small cell lung cancer (66 adenocarcinomas and 27 squamous cell carcinomas) who underwent surgery. TMB and 415 cancer gene expression patterns were investigated in each surgical specimen by CGP using next-generation sequencing. All patients were classified into two clusters according to their radiomic features extracted from preoperative CT images using unsupervised k-means clustering. Differences between these two clusters were investigated with respect to gene mutations, TMB (low or high), recurrence-free survival, and visual CT features.

#### RESULTS

Unsupervised clustering classified 55 patients into Cluster 1 and 38 patients into Cluster 2 according to their radiomic features. Cluster 1 exhibited a significantly higher proportion of TP53 and CDKN2B gene mutations but a lower proportion of EGFR gene mutations compared with Cluster 2 (TP53 mutations, 34/55 [61.8%] vs 12/38 [31.6%]; CDKN2B mutations, 26/55 [47.3%] vs 10/38 [26.3%]; EGFR mutations, 13/55 [23.6%] vs 17/38 [44.7%]; all  $P < 0.05$ ). A high TMB (= 20 mutations/megabase) was more frequently observed in Cluster 1 than in Cluster 2 (23/55 [41.8%] vs. 2/38 [5.3%];  $P < 0.01$ ). Recurrence-free survival at 5 years was significantly lower in Cluster 1 than in Cluster 2 (40.4% vs. 51.0%;  $P = 0.038$ ). For visual CT features, Cluster 1 was more likely to indicate a lobulated margin but was less frequently accompanied by ground-glass opacity, air-bronchogram, cavity, and vacuole sign compared to Cluster 2 (all  $P < 0.05$ ).

#### CONCLUSION

s CT radiomics-based clustering has significant association with CGP data as well as patient prognosis and may help predict genomic information in non-small cell lung cancer.

#### CLINICAL RELEVANCE/APPLICATION

CGP provides valuable information to determine therapeutic agents for lung cancer, leading to precision medicine. However, CGP is very expensive and requires invasive tissue sampling. Therefore, CT examination, which is non-invasive and relatively low costs, plays an important role in predicting genomic information. CT radiomics-based clustering created in this study could help predict CGP data.

Printed on: 02/07/23

## Abstract Archives of the RSNA, 2022

T5B-SPCH-7

### **Correlation Between Intra-nodular Vessel and Tumor Invasiveness of Lung Adenocarcinoma Presenting as Ground-glass Nodules: A Deep Learning 3D Reconstruction Algorithm-based Quantitative Analysis on Non-contrast CT Images**

Wednesday, Nov. 30 12:45PM - 1:15PM Room: Learning Center - CH DPS

#### **Participants**

Baolian Zhao, (*Presenter*) Nothing to Disclose

#### **PURPOSE**

To quantitatively analyze the pulmonary vessels inside ground-glass nodules (GGNs) on non-contrast CT (NCCT) images using fully automated deep learning (DL) approach and investigate the relationship between intra-nodular vessel and tumor invasiveness.

#### **METHODS AND MATERIALS**

A total of 741 pathologically confirmed GGNs from 719 patients were retrospectively collected, comprising 121 atypical adenomatous hyperplasia (AAH), 150 adenocarcinoma in situ (AIS), 154 minimally invasive adenocarcinoma (MIA) and 316 invasive adenocarcinoma (IAC). The pulmonary blood vessels were reconstructed on NCCT images using DL-based region segmentation and region growth technology (InferVisual Surgery Planning Research version). The presence of pulmonary vessels inside GGNs was quantitatively evaluated with respect to intra-nodular vessel prevalence and the automatically calculated vessel volume percentage, which were further compared across different invasiveness categories by the Chi-square test, analysis of variance (ANOVA) and Mann-Whitney U test.

#### **RESULTS**

The automated DL algorithm showed high accuracy in vessels detection and reconstruction. There were significant differences in the occurrences of internal vessels across different tumor invasiveness GGNs ( $p < 0.001$ ). The prevalence of intra-nodular vessels in IAC (66.5%) was significantly higher than that of AAH (35.5%,  $p < 0.001$ ), AIS (33.3%,  $p < 0.001$ ) and MIA (50.6%,  $p = 0.001$ ), while the vascular categories were similar (all  $p > 0.05$ ). Vascular changes were more common in invasive lesions (MIA and IAC) than pre-invasive lesions (AAH and AIS), which mainly manifested as increased vessel volume percentage (10.23% vs 3.85%,  $p < 0.001$ ). The average vessel volume percentage of IAC (12.01%) was also higher compared with that of AAH (3.85%), AIS (3.86%) and MIA (6.57%) with statistically significance (all  $p < 0.001$ ).

#### **CONCLUSION**

The quantitative analysis of intra-nodular vessels on NCCT images demonstrated that the incidence of internal vessels in GGNs was related to their pathological invasiveness. GGNs with increased internal vessel percentages had higher possibility of tumor invasiveness.

#### **CLINICAL RELEVANCE/APPLICATION**

Our deep learning-based quantitative analysis on NCCT images reveals that the incidence and volume percentage of intra-tumoral vessels in GGNs are correlated with pathological invasiveness.

Printed on: 02/07/23

## Abstract Archives of the RSNA, 2022

T5B-SPCH-8

### Cascade-network to Reduce False Positives for Pulmonary Nodule Detection on Chest X-ray Radiographs

Wednesday, Nov. 30 12:45PM - 1:15PM Room: Learning Center - CH DPS

#### Participants

Taehee Kim, Seoul, Korea, Republic Of (*Presenter*) Nothing to Disclose

#### PURPOSE

Recently, many deep learning-based nodule detection algorithms for chest X-ray radiographs (CXRs) have reported promising results. In real clinical environment, however, those algorithms have been reported to produce many false positives (FPs) caused by the similarity between hard negatives (e.g., nipple shadow, bone island, superimposed pulmonary vessels, etc.) and real nodules. Here, we propose a cascade-network to reduce these FPs in nodule detection.

#### METHODS AND MATERIALS

NODE21 challenge dataset (node21.grand-challenge.org) was utilized (training: 934/2404; validation: 100/300; testing: 100/300 for nodule/non-nodule CXRs). For each CXR in the training dataset, a set of multi-resolution patches (resolution: 112x112, 280x280, and 448x448) were generated. Three multi-resolution patches were resized to 112x112 and concatenated along the channel for training. Patches were classified as positive (i.e., nodule patches) when a nodule locates on the center of the patch. For nodule detection, two neural networks were used sequentially where first network was to detect nodule candidates on an input CXR, and the second network was to further screen out hard negatives. Both networks had same architecture (EfficientNet-B0) and trained based on multi-resolution patches. The output of the two networks was the probability of nodule for the input patch. The difference between the networks was the composition of training dataset. For first network, all negative patches for training were the patches with no nodule (i.e., non-nodule patches). In second network, half of negative patches for training were carefully selected among the false positive outputs in the training data of first network to design second network more sensitive to the hard negatives. The detection performances were measured based on the area under the Free-Response Receiver Operating Characteristics (FAUC) and Refined Competition Performance Metric (R-CPM). Comparison was performed before and after ablating second network.

#### RESULTS

The nodule detection performances of the cascade-network (FAUC:0.6033(95% CI: 0.5848-0.6217), R-CPM:0.5995(0.5778-0.6211)) outperformed those of the first network only (FAUC:0.4987(0.4667-0.5308),  $p < 0.001$ , R-CPM:0.4967(0.4649-0.5285),  $p < 0.001$ ). When visually investigated, the outputs from the cascade-network showed a much smaller number of FPs.

#### CONCLUSION

s In this study, we proposed a cascade-network for nodule detection to reduce FPs, dramatically improving nodule detection performance.

#### CLINICAL RELEVANCE/APPLICATION

The proposed cascade-network with sequential training scheme would enable development of a nodule detection algorithm with high positive predictive value efficiently by using network-driven hard negatives.

Printed on: 02/07/23

## Abstract Archives of the RSNA, 2022

T5B-SPCH-9

### Implications of Radiologist-interpreted Subjective Standards for Evaluating the Diagnostic Performance of a Deep Learning Model: A Malignant Lung Nodule Detection Task on Chest Radiographs

Wednesday, Nov. 30 12:45PM - 1:15PM Room: Learning Center - CH DPS

#### Participants

Jung Eun Huh, BA, Oxford, United Kingdom (*Presenter*) Nothing to Disclose

#### PURPOSE

Little is known regarding the impact of radiologist-interpreted subjective standards as ground truth when evaluating the performance of deep learning (DL) models and their added value to radiologists. We assessed the adherence of the subjective standards to the reference standard, and the difference in diagnostic performance measurements of radiologists with and without a DL-based automatic detection (DLAD) model according to the standard used to detect malignant pulmonary nodules on chest radiographs.

#### METHODS AND MATERIALS

This study included 50 patients with pathology- and CT-proven lung cancers (reference standards) with 50 chest radiographs between December 2015 and February 2021, and 50 control individuals with normal chest radiographs. Five subjective standards were constructed using 10 radiologists' interpretations and compared: individual judgment by the most experienced radiologist, majority vote, consensus judgments of 2 and 3 radiologists, and a latent class analysis (LCA) model. In separate reader tests, 10 other radiologists (who did not participate in constructing the subjective standards) interpreted the radiographs with and without the DLAD model, and their diagnostic performance was compared between the reference standard and the five subjective standards. The t-test with the Bonferroni correction was used to compare adherence and diagnostic performance.

#### RESULTS

The LCA model, which showed a sensitivity of 72.6% and a specificity of 100%, adhered more closely to the reference standard than any of the other subjective standards. In the reader tests, both the radiologists and the DLAD model tended to show overestimated sensitivity but underestimated specificity when the subjective standards were applied as the ground truths. However, these radiologists' tendencies were diminished by DLAD assistance (all P-values <0.001). Although using the DLAD improved the sensitivity and specificity (in some cases) when the subjective standards were used, the corresponding effects were estimated to be significantly smaller than when the reference standard was used (all P-values <0.001), except for sensitivity with the LCA model (P=0.094).

#### CONCLUSION

The LCA model showed the closest adherence to the reference standard for detecting malignant pulmonary nodules on chest radiographs. Radiologists' sensitivity and specificity values were overestimated and underestimated, respectively, and the DLAD added less value with the subjective standards than with the reference standard.

#### CLINICAL RELEVANCE/APPLICATION

Since using only subjective standards can lead to bias in the diagnostic performance of DL models, evaluating DL models with a reference standard is necessary even in underserved settings.

Printed on: 02/07/23

## Abstract Archives of the RSNA, 2022

T5B-SPER

### Emergency Tuesday Poster Discussions - B

Tuesday, Nov. 29 12:45PM - 1:15PM Room: Learning Center - ER DPS

#### Participants

Waleed Abdellatif, MD, MSc, Richardson, TX (*Moderator*) Nothing to Disclose

#### Sub-Events

### T5B-SPER-1 Brain Hemorrhage and ECMO therapy in Patients with Severe COVID-19-Disease: A Systematic Multicenter Review (First Insights into the COVID-ECMO trial)

#### Participants

Philipp Josef Kuhl, MD, Wuerzburg, Germany (*Presenter*) Nothing to Disclose

#### PURPOSE

To systematically evaluate the incidence of intracranial hemorrhage (ICH) associated with ECMO therapy in patients with COVID-19.

#### METHODS AND MATERIALS

Every COVID-19 patient admitted to intensive care unit (ICU) at 4 major German university hospitals throughout the course of the pandemic (03/2020 to 03/2022) who received a CT scan of the brain during hospitalization was retrospectively analyzed. Each scan was assessed for the presence of ICH. The most significant scan per patient was included for further analysis, usually at first occurrence of ICH. Patients with recent head trauma or preexisting ICH were excluded. On site, cerebral bleeding was rated for severity and predominant distribution type using a standardized set of specifications. Outcome, demographics, clinical data and time points of different events (e.g. admission to ICU, start of ECMO therapy) were obtained from patient records. The anonymized data sets were sent to the study center for statistical analysis.

#### RESULTS

In the university hospitals surveyed, 831 patients on ICU with COVID-19 underwent at least one CT scan of the brain (f=292, m=539, mean age 57.4±10.1 years). Nearly half of these patients (46,7%) received ECMO therapy (f=106, m=282; age 53.3±6,3 y). During or after ECMO, 89 patients (22,9%) sustained ICH, the vast majority of which was fatal (84,3%, n=75). Intraparenchymal hemorrhage was the most frequent predominant distribution type (41,6%), followed by subarachnoidal bleeding (38,2%). In patients who did not receive ECMO therapy, the occurrence of ICH was significantly lower (12.9% vs. 22.9%; p<0.01). Additionally, bleeding events showed a significantly lower mortality rate (45,6% vs. 84,3%; p<0.001).

#### CONCLUSION

In non-COVID patients, brain hemorrhage is the most severe complication of ECMO therapy, associated with high mortality rates of up to 73%. COVID-19 associated coagulopathy combined with therapeutic anticoagulation required for ECMO therapy predispose patients to an increased risk of bleeding, yet recent studies reported a wide range of ECMO-associated ICH rates varying from 3.5% to 35.4%, leaving the true risk rates further unknown. This study provides strong evidence for the incidence of intracranial hemorrhage associated to ECMO therapy being near 22% due to its systematic and multicentric approach. In addition, the assessed mortality rates demonstrate the severity of ICH as a side effect of ECMO therapy. With proceeding data collection by additional participating centers in Germany, we expect these results to further consolidate, allowing the calculation of various risk models that will support clinical decision making.

#### CLINICAL RELEVANCE/APPLICATION

These first study results can already support clinical decision making regarding ECMO therapy.

Printed on: 02/07/23

## Abstract Archives of the RSNA, 2022

T5B-SPER-1

### Brain Hemorrhage and ECMO therapy in Patients with Severe COVID-19-Disease: A Systematic Multicenter Review (First Insights into the COVID-ECMO trial)

Tuesday, Nov. 29 12:45PM - 1:15PM Room: Learning Center - ER DPS

#### Participants

Philipp Josef Kuhl, MD, Wuerzburg, Germany (*Presenter*) Nothing to Disclose

#### PURPOSE

To systematically evaluate the incidence of intracranial hemorrhage (ICH) associated with ECMO therapy in patients with COVID-19.

#### METHODS AND MATERIALS

Every COVID-19 patient admitted to intensive care unit (ICU) at 4 major German university hospitals throughout the course of the pandemic (03/2020 to 03/2022) who received a CT scan of the brain during hospitalization was retrospectively analyzed. Each scan was assessed for the presence of ICH. The most significant scan per patient was included for further analysis, usually at first occurrence of ICH. Patients with recent head trauma or preexisting ICH were excluded. On site, cerebral bleeding was rated for severity and predominant distribution type using a standardized set of specifications. Outcome, demographics, clinical data and time points of different events (e.g. admission to ICU, start of ECMO therapy) were obtained from patient records. The anonymized data sets were sent to the study center for statistical analysis.

#### RESULTS

In the university hospitals surveyed, 831 patients on ICU with COVID-19 underwent at least one CT scan of the brain (f=292, m=539, mean age 57.4±10.1 years). Nearly half of these patients (46,7%) received ECMO therapy (f=106, m=282; age 53.3±6,3 y). During or after ECMO, 89 patients (22,9%) sustained ICH, the vast majority of which was fatal (84,3%, n=75). Intraparenchymal hemorrhage was the most frequent predominant distribution type (41,6%), followed by subarachnoidal bleeding (38,2%). In patients who did not receive ECMO therapy, the occurrence of ICH was significantly lower (12.9% vs. 22.9%; p<0.01). Additionally, bleeding events showed a significantly lower mortality rate (45,6% vs. 84,3%; p<0.001).

#### CONCLUSION

In non-COVID patients, brain hemorrhage is the most severe complication of ECMO therapy, associated with high mortality rates of up to 73%. COVID-19 associated coagulopathy combined with therapeutic anticoagulation required for ECMO therapy predispose patients to an increased risk of bleeding, yet recent studies reported a wide range of ECMO-associated ICH rates varying from 3.5% to 35.4%, leaving the true risk rates further unknown. This study provides strong evidence for the incidence of intracranial hemorrhage associated to ECMO therapy being near 22% due to its systematic and multicentric approach. In addition, the assessed mortality rates demonstrate the severity of ICH as a side effect of ECMO therapy. With proceeding data collection by additional participating centers in Germany, we expect these results to further consolidate, allowing the calculation of various risk models that will support clinical decision making.

#### CLINICAL RELEVANCE/APPLICATION

These first study results can already support clinical decision making regarding ECMO therapy.

Printed on: 02/07/23

## Abstract Archives of the RSNA, 2022

T5B-SPGI

### Gastrointestinal Tuesday Poster Discussions - B

Tuesday, Nov. 29 12:45PM - 1:15PM Room: Learning Center - GI DPS

#### Participants

Leo Tsai, MD, PhD, Boston, MA (*Moderator*) Stockholder, Agile Devices Inc; Consultant, Agile Devices Inc

#### Sub-Events

### T5B-SPGI-1 **LI-RADS Treatment Response versus Modified RECIST for Diagnosing Viable Hepatocellular Carcinoma after Locoregional Therapy: A Systematic Review and Meta-Analysis of Comparative Studies**

#### Participants

Sungmok Kim, Suwon-Si, Korea, Republic Of (*Presenter*) Nothing to Disclose

#### PURPOSE

We aimed to systematically compare the performance of Liver Imaging Reporting and Data Systems Treatment Response (LR-TR) with the modified Response Evaluation Criteria in Solid Tumors (mRECIST) for diagnosing viable hepatocellular carcinoma (HCC) treated with locoregional therapy (LRT).

#### METHODS AND MATERIALS

Original studies of intra-individual comparisons between the diagnostic performance of LR-TR and mRECIST using dynamic contrast-enhanced CT or MRI were searched in MEDLINE and EMBASE up to August 25, 2021. The reference standard for tumor viability was surgical pathology. The meta-analytic pooled sensitivity and specificity of the viable category using each criterion were calculated using a bivariate random-effects model and compared using bivariate meta-regression. Heterogeneity was evaluated using Higgins inconsistency index (I<sup>2</sup>) test or Cochran Q test. Subgroup meta-regression analysis was performed to investigate the causes of heterogeneity between studies. Publication bias was evaluated by visual assessment of funnel plot and Deeks' asymmetry test.

#### RESULTS

For five eligible studies (430 patients with 631 treated observations), the pooled per-lesion sensitivities and specificities were 58% (95% confidence interval [CI], 45-70%; I<sup>2</sup>, 77%; Cochran Q test, P<0.1) and 93% (95% CI, 88-96%; I<sup>2</sup>, 0%; Cochran Q test, P=0.51) for the LR-TR viable category and 56% (95% CI, 42-69%; I<sup>2</sup>, 74%; Cochran Q test, P<0.1) and 86% (95% CI, 72-94%; I<sup>2</sup>, 82%; Cochran Q test, P<0.1) for the mRECIST viable category. The LR-TR viable category provided significantly higher pooled specificity (P<0.01) than mRECIST but comparable pooled sensitivity (P=0.53). Meta-regression analysis revealed that type of LRT and the most common etiology of liver disease were significantly associated with the study heterogeneity for the mRECIST viable category (P=0.01). There was no significant publication bias across the studies for both criteria (P=0.35).

#### CONCLUSION

s LR-TR algorithm demonstrated better specificity than mRECIST without significant difference in sensitivity for the diagnosis of pathologically viable HCC after LRT.

#### CLINICAL RELEVANCE/APPLICATION

The specificity of the viable category for the diagnosis of pathologically viable HCC was significantly higher when applying LR-TR than mRECIST, but the sensitivity was comparable.

### T5B-SPGI-10 **MRI Correlation with Liver Explant Pathology: Routine Clinical Care vs. Expert Reader Using the LIRADS Treatment Response Algorithm in Assessing Residual HCC After Y-90 Therapy**

#### Participants

Matthew Harwood, MD, Phoenix, AZ (*Presenter*) Nothing to Disclose

#### PURPOSE

The Liver Imaging Reporting and Data System treatment response algorithm (LIRADS-TRA) criteria can be used to predict HCC response to locoregional therapy, however, radiation-based methods such as transarterial radioembolization (TARE) with yttrium-90 have unique post-treatment features that can confound assessment. Prior studies used survival and/or time to progression as the primary endpoints after Y90. Few studies use pathology as the reference standard. This study compares an expert reader's blinded MRI or CT interpretation applying the LIRADS-TRA against interpretations obtained during routine clinical care.

#### METHODS AND MATERIALS

An IRB exemption was obtained. We identified adult patients (age range 37-72 years) who underwent liver explant after Y90 treatment for HCC (pre-treatment LR-5, OPTN5a/b, or biopsy proven HCC) then subsequently underwent liver transplant (dates of transplant between 10/2015 and 10/2021). Of the 96 patients identified, 27 were excluded because at least 90 days had not elapsed between treatment and MRI/CT, or because multiple treatments were employed. Ultimately, 25 patients with at least 1

treated HCC comprised the cohort. Most patients had MRIs before transplant (23/25), the rest multiphase CTs (2/25). Mean MELD scores at transplant for this cohort was  $13 \pm 5$  (mean  $\pm$ SD). The most common etiologies of cirrhosis were hepatitis C (40%), alcohol (24%), and NASH (20%). Mean time between treatment and MRI or CT was  $164 \pm 89$  days (mean  $\pm$ SD). A fellowship-trained, board-certified abdominal radiologist with >20 years of experience blinded to the presence or absence of residual viable tumor in liver explant specimens independently reviewed the pre- and post-treatment exams. When two or more tumors were present or treated, the dominant treated lesion was evaluated. The LIRADS-TRA was strictly adhered to, wherein only 6 of 25 (24%) clinical reports explicitly used the LIRADS-TRA. LR-TR viable and LR-TR equivocal were considered positive. LR-TR nonviable was considered negative.

## RESULTS

The clinical assessment and expert reader had fair agreement ( $\kappa=0.29$ ). Both "readers" had an accuracy of 60%. +LR for TRA: 2.3 (95%CI 0.55-9.7). -LR: 0.74 (0.45-1.2). In a separate analysis, successful tumor debulking (90% or greater tumor necrosis) was also considered as a binary outcome.

## CONCLUSION

Adherence to the LIRADS-TRA did not improve accuracy or test performance as expected. Previous authors evaluating liver resection pathology after Y90 showed higher accuracy. However, their post-treatment imaging time frame was not defined, whereas this study focused on the 6-month post-treatment exam.

## CLINICAL RELEVANCE/APPLICATION

To know the accuracy of our major CT and MRI criteria for assessing HCC treatment response, the LIRADS-TRA.

### **T5B-SPGI-3 Diagnostic Performance of LI-RADS v2018 Versus KLCA-NCC 2018 Criteria for Hepatocellular Carcinoma Using Magnetic Resonance Imaging: A Systematic Review and Meta-Analysis of Comparative Studies**

Participants

Jaeseung Shin, Seoul, Korea, Republic Of (*Presenter*) Nothing to Disclose

## PURPOSE

We performed a meta-analysis to compare the performance of the Liver Imaging Reporting and Data System (LI-RADS) v2018 and Korean Liver Cancer Association-National Cancer Center (KLCA-NCC) 2018 criteria for diagnosing hepatocellular carcinoma (HCC) using magnetic resonance imaging (MRI).

## METHODS AND MATERIALS

We searched the MEDLINE and EMBASE databases for studies published from January 1, 2018, to October 20, 2021, that compared the diagnostic performance of LR-5 of LI-RADS v2018 and definite HCC category of KLCA-NCC 2018 on MRI. Bivariate random-effects model was fitted to calculate the pooled per-observation sensitivity and specificity of both imaging criteria and compared the pooled estimates of paired data. Subgroup analysis was performed based on the observation size. Meta-regression analysis was performed to identify factors for study heterogeneity.

## RESULTS

Of the six studies included (2,109 observations and 1,471 HCCs), the pooled sensitivity of the definite HCC category of KLCA-NCC criteria (81%; 95% confidence interval [CI], 73-90%;  $I^2=86\%$ ) was higher than that of LR-5 of LI-RADS v2018 (65%; 95% CI, 53-78%;  $I^2=96\%$ ) for diagnosing HCC ( $P<0.001$ ), while the specificity was lower for KLCA-NCC 2018 (88%; 95% CI, 84-91%;  $I^2=13\%$ ) than for LI-RADS v2018 (93%; 95% CI, 91-96%;  $I^2=0\%$ ) ( $P=0.018$ ). For observations sized  $\geq 20$  mm, sensitivity was higher for KLCA-NCC 2018 than for LI-RADS v2018 (83% versus 75%;  $P=0.017$ ), with no significant difference in specificity (82% versus 86%;  $P=0.463$ ). Meta-regression analyses revealed reference standard as a significant factor contributing to the heterogeneity of sensitivities.

## CONCLUSION

The definite HCC category of KLCA-NCC 2018 provided a higher pooled sensitivity and lower pooled specificity than the LR-5 of LI-RADS v2018 for diagnosing HCC using MRI.

## CLINICAL RELEVANCE/APPLICATION

Compared with LI-RADS v2018, KLCA-NCC 2018 criteria might be preferred where sensitive diagnosis is demanded for earlier locoregional treatment (i.e. East Asia).

### **T5B-SPGI-4 Preoperative prediction of microvascular invasion in hepatocellular carcinoma based on three-phase contrast-enhanced CT images of the tumor and peritumoral regions**

Participants

Xiaofei Yue, (*Presenter*) Nothing to Disclose

## PURPOSE

To establish a clinical-radiomics nomogram for preoperative prediction of microvascular invasion (MVI) of hepatocellular carcinoma (HCC) and compare the diagnostic value of different tumor regions and phases for the MVI status in a non-invasive way.

## METHODS AND MATERIALS

335 HCC patients (161 MVI-negative and 174 MVI-positive) who underwent three-phase contrast-enhanced CT before surgery were enrolled from May 2017 to July 2020. Regions of interest (ROI) of the tumor, peritumor(10mm), and tumor-peritumor(10mm) were manually segmented in the arterial phase (AP) and portal venous phase (PVP), and delayed phase (DP) images. A total of nine groups of ROIs were obtained, and 1218 radiomics features were extracted, respectively. Patients were randomly assigned to the training and inter-validation cohorts in a ratio of 7:3. The Analysis of Variance and least absolute shrinkage and selection operator (LASSO) algorithms with ten-fold cross validation were used to select radiomics features. Nine radiomics scores (Rad-Score) were established using multivariate logistic regression analysis. In addition, we combined the nine Rad-Scores with 18 clinical factors and

23 radiographic scores to construct a clinical-radiomics nomogram with multivariate logistic regression. Furthermore, all radiomics models and the combined clinical-radiomics model were independently validated with the data of the hospital's sub-campus (40 patients). ROC curves were used to compare the predictive power of the multiple models. Decision curve analysis (DCA) was used to compare the clinical benefit of the models.

## RESULTS

Among the nine Rad-Scores, the tumor-peritumor in the AP cohort had the best predictive ability (AUCs of 0.912, 0.848, and 0.880 for the training cohort, inter-validation cohort, and independent validation cohort, respectively). The predicted values of the clinical model of AUCs were 0.775, 0.742, and 0.696 in the training cohort, inter-validation cohort, and independent validation cohort, respectively. The combined clinical-radiomics model performs well (AUCs for the training, inter-validation and independent validation cohorts are 0.938, 0.883, and 0.829). DCA demonstrated the highest clinical benefit in the combined clinical-radiomics model.

## CONCLUSION

The clinical-radiomics model has satisfactory results in preoperative prediction of MVI in patients with HCC and has potential value in guiding clinicians to individualize treatment.

## CLINICAL RELEVANCE/APPLICATION

MVI of HCC usually indicates an increased risk of recurrence and a poor prognosis. The clinical-radiomics model can predict MVI preoperatively and has potential value in guiding clinicians to individualize treatment.

### **T5B-SPGI-5 Abbreviated MRI for secondary surveillance of recurrent hepatocellular carcinoma after curative treatment**

Participants

Dong Ho Lee, MD, Seoul, Korea, Republic Of (*Presenter*) Nothing to Disclose

## PURPOSE

There is no consensus regarding the ideal imaging modality of secondary surveillance of hepatocellular carcinoma (HCC). This study aimed to evaluate the detection performance of abbreviated MRI (AMRI) for secondary surveillance for HCC after curative treatment including surgical resection or radiofrequency ablation (RFA).

## METHODS AND MATERIALS

This retrospective study analyzed 243 patients who received secondary surveillance for HCC using gadoxetic acid-enhanced MRI after more than two-year of disease-free period from curative treatment including surgical resection or RFA. Non-contrast AMRI (NC-AMRI) (T2-weighted and diffusion-weighted images), hepatobiliary phase AMRI (HBP-AMRI) (T2-weighted, diffusion-weighted and HBP images), and full-sequence MRI sets were independently reviewed by two abdominal radiologists. The confirmation of HCC was based either on histopathological confirmation or imaging-based diagnosis. HCC detection rate of each set was compared.

## RESULTS

A total of 42 recurred HCCs were confirmed in 39 patients. Per-lesion and per-patient sensitivities didn't show significant difference among three image sets in both reviewers ( $P=0.681$ ): Per-lesion sensitivity: 81.1%83.3%, 76.2%85.7%, and 81.0%83.3% for NC-AMRI, HBP-AMRI, and full-sequence MRI, respectively; and per-patient sensitivity: 79.5%83.3%, 79.5%85.7%, and 79.5%83.3% for NC-AMRI, HBP-AMRI, and full-sequence MRI. Per-patient specificity didn't show significant difference among three image set in both reviewers (95.6%97.1%, 96.1%97.1%, and 97.6%98.5% for NC-AMRI, HBP-AMRI, respectively;  $P=0.307$ ).

## CONCLUSION

NC-AMRI and HBP-AMRI had comparable detection performance to that of full-sequence gadoxetic acid-enhanced MRI during secondary surveillance for HCC after more than 2-year disease free interval following curative treatment. Based on its good detection performance, short scan times, and the lack of contrast agent-associated risks, NC-AMRI would be a promising option for secondary surveillance of HCC.

## CLINICAL RELEVANCE/APPLICATION

NC-AMRI would be a promising option for secondary surveillance for HCC after 2-year disease free interval following curative treatment including surgical resection and RFA.

### **T5B-SPGI-6 Preoperative prediction of microvascular invasion in hepatocellular carcinoma using computation modeling of interstitial fluid pressure and velocity**

Participants

Liyun Zheng, Shanghai, China (*Presenter*) Nothing to Disclose

## PURPOSE

The purpose of present study was to develop and validate a new method for the interstitial fluid pressure (IFP) measurement in hepatocellular carcinoma (HCC) patients. We also aimed to depict the microenvironment of the tumor of HCC and predict the microvascular invasion (MVI) status preoperatively and noninvasively by this IFP model.

## METHODS AND MATERIALS

A cohort of 27 patients were finally included in this study (mean age  $57.6 \pm 10.9$  years, 77.8% males). There were 15 patients in the MVI-positive group and 12 patients in the MVI-negative group. MRI examinations were performed using a 3T scanner (uMR790, United Imaging Healthcare). DCE-MRI scan sequence utilized a transverse T1-weighted spoiled GRE sequence to obtain acquisition, and 60 time points were acquired with mean temporal resolution of 3.1 s and a total acquisition time of ~3 min. Patients were allowed to breathe freely. The extended tofts model (ETM) was used to estimate the permeability parameters. Volume of Interest (VOI) for K<sub>trans</sub> estimation were manually delineated on the tumor lesion present in all slices in the late phases of T1-weighted DCE-MRI images. The tumor volume was calculated from the T1w dynamic images. The continuity partial differential equation (PDE) was implemented and the estimation of IFP and interstitial fluid velocity (IFV) were acquired. Mann-Whitney U test was performed to compare the mean IFP and mean IFV between MVI-positive group and MVI-negative group. The receiver operating characteristic (ROC) analysis was performed for differentiation between MVI-positive group and MVI-negative group. The Youden

index were exploited to determine the cutoff value, along with the area under the curve (AUC), sensitivity and specificity.  $P < 0.05$  was considered statistically significant.

## RESULTS

Significant difference was found in mean IFP between the MVI-positive group and MVI-negative group ( $P = 0.001$ ), while there was no statistically differences in mean IFV between the two groups ( $P = 0.626$ ). For the ROC analysis, mean IFP value proved to be the significant predictor with the best cut-off value 1854.22 Pa (AUC = 0.883, 95% confidence interval 0.701 to 0.974; sensitivity = 80.0%, specificity = 91.7%).

## CONCLUSION

The non-invasive interstitial fluid pressure (IFP) measurement model in liver tumors was developed. Significant difference was found in mean IFP between the MVI-positive group and MVI-negative group. IFP could be the significant predictor in the prediction of MVI status.

## CLINICAL RELEVANCE/APPLICATION

This study developed a new method for the noninvasive IFP measurement in HCC patients. Our results revealed that MVI status can be predicted by this IFP model preoperatively.

## T5B-SPGI-8 LI-RADS Category 4 Observations on Gadoxetic Acid-Enhanced MRI: Can Imaging Features Indicate High Risk of Early Progression (<6 Months) To LI-RADS Category 5?

Participants

Ijin Joo, MD, Seoul, (Presenter) Nothing to Disclose

## PURPOSE

To investigate the value of gadoxetic acid-enhanced MRI (Gd-EOB-MRI) features of LI-RADS category 4 (LR-4: probably hepatocellular carcinoma [HCC]) observations for predicting early progression to LR-5 (definitely HCC)

## METHODS AND MATERIALS

This retrospective study included liver observations in patients at high risk for HCC, assigned as LR-4 on index Gd-EOB-MRI and had available short-term (<6 months) follow-up Gd-EOB-MRI. For each observation, LI-RADS major and ancillary features on index MRI and final LI-RADS category on follow-up MRI were assessed by a consensus of three radiologists. Multivariate logistic regression analysis was performed to identify imaging predictors for early (<6 months) progression to LR-5. Diagnostic performances of each significant imaging feature and their combinations for identifying LR-4 observations with higher risk of early category progression were evaluated.

## RESULTS

Among 101 index LR-4 observations in 101 patients, 57 progressed to LR-5, while the other 44 remained stable as LR-4 within 6 months. Multivariate logistic regression analysis revealed that nonrim arterial phase hyperenhancement (APHE), nonperipheral "washout", restricted diffusion, and fat in mass at index MRI were independent predictors for early category progression (odds ratio = 3.75, 3.17, 5.36, 12.2;  $P = 0.037, 0.036, 0.003, 0.030$ , respectively). For predicting the early category progression, nonrim APHE showed the highest sensitivity (47/57, 82.5%) followed by restricted diffusion (39/57, 68.4%), nonperipheral "washout" (27/57, 47.4%), and fat in mass (8/57, 14.0%); while the highest specificity was found in fat in mass (43/44, 97.7%) followed by restricted diffusion (33/44, 75.0%), nonperipheral "washout" (31/44, 70.5%), and nonrim APHE (17/44, 38.6%). When two or more of four imaging features listed above were present, the sensitivity was 82.5% (47/57) and the specificity was 61.4% (27/44).

## CONCLUSION

LI-RADS major and ancillary features on Gd-EOB-MRI can help identify LR-4 observations with higher risk of early category progression to LR-5.

## CLINICAL RELEVANCE/APPLICATION

In LI-RADS category 4 observations, MRI-based risk stratification according to the probability of early category progression could potentially facilitate appropriate and timely management.

## T5B-SPGI-9 Diagnostic Performance of CT versus MRI Liver Imaging Reporting and Data System Category 5 for Hepatocellular Carcinoma: A Systematic Review and Meta-Analysis of Comparative Studies

Participants

Sunyoung Lee, Seoul, Korea, Republic Of (Presenter) Nothing to Disclose

## PURPOSE

To compare the performance of Liver Imaging Reporting and Data System category 5 (LR-5) for diagnosing HCC between CT and MRI using comparative studies.

## METHODS AND MATERIALS

The MEDLINE and EMBASE databases were searched from inception to April 21, 2021, to identify studies that directly compare the diagnostic performance of LR-5 for HCC between CT and MRI. Bivariate random-effects model was fitted to calculate the pooled per-observation sensitivity and specificity of LR-5 of each modality, and compare the pooled estimates of paired data. Subgroup analysis was performed according to MRI contrast agent.

## RESULTS

Seven studies with 1,145 observations (725 HCCs) were included in the final analysis. The pooled per-observation sensitivity of LR-5 for diagnosing HCC was higher using MRI (61%; 95% confidence interval [CI], 43-76%;  $I^2 = 95%$ ) than CT (48%; 95% CI, 31-65%;  $I^2 = 97%$ ) ( $P < 0.001$ ). The pooled per-observation specificities of LR-5 did not show statistically significant difference between CT (96%; 95% CI, 92-98%;  $I^2 = 0%$ ) and MRI (93%; 95% CI, 88-96%;  $I^2 = 16%$ ) ( $P = 0.054$ ). In the subgroup analysis, extracellular contrast agent-enhanced MRI showed significantly higher pooled per-observation sensitivity than gadoxetic acid-

enhanced MRI for diagnosing HCC (73% [95% CI, 55%-85%] vs. 55% [95% CI, 39%-70%]; P = 0.007), without a significant difference in specificity (93% [95% CI, 80%-98%] vs. 94% [95% CI, 87%-97%]; P = 0.884).

#### **CONCLUSION**

s The LR-5 of MRI showed significantly higher pooled per-observation sensitivity than CT for diagnosing HCC. The pooled per-observation specificities of LR-5 were comparable between the two modalities.

#### **CLINICAL RELEVANCE/APPLICATION**

Although LI-RADS provides a common diagnostic algorithm for CT or MRI, the per-observation performance of LR-5 can be affected by the imaging modality as well as the MRI contrast agent.

Printed on: 02/07/23

## Abstract Archives of the RSNA, 2022

T5B-SPGI-1

### **LI-RADS Treatment Response versus Modified RECIST for Diagnosing Viable Hepatocellular Carcinoma after Locoregional Therapy: A Systematic Review and Meta-Analysis of Comparative Studies**

Tuesday, Nov. 29 12:45PM - 1:15PM Room: Learning Center - GI DPS

#### **Participants**

Sungmok Kim, Suwon-Si, Korea, Republic Of (*Presenter*) Nothing to Disclose

#### **PURPOSE**

We aimed to systematically compare the performance of Liver Imaging Reporting and Data Systems Treatment Response (LR-TR) with the modified Response Evaluation Criteria in Solid Tumors (mRECIST) for diagnosing viable hepatocellular carcinoma (HCC) treated with locoregional therapy (LRT).

#### **METHODS AND MATERIALS**

Original studies of intra-individual comparisons between the diagnostic performance of LR-TR and mRECIST using dynamic contrast-enhanced CT or MRI were searched in MEDLINE and EMBASE up to August 25, 2021. The reference standard for tumor viability was surgical pathology. The meta-analytic pooled sensitivity and specificity of the viable category using each criterion were calculated using a bivariate random-effects model and compared using bivariate meta-regression. Heterogeneity was evaluated using Higgins inconsistency index (I<sup>2</sup>) test or Cochran Q test. Subgroup meta-regression analysis was performed to investigate the causes of heterogeneity between studies. Publication bias was evaluated by visual assessment of funnel plot and Deeks' asymmetry test.

#### **RESULTS**

For five eligible studies (430 patients with 631 treated observations), the pooled per-lesion sensitivities and specificities were 58% (95% confidence interval [CI], 45-70%; I<sup>2</sup>, 77%; Cochran Q test, P<0.1) and 93% (95% CI, 88-96%; I<sup>2</sup>, 0%; Cochran Q test, P=0.51) for the LR-TR viable category and 56% (95% CI, 42-69%; I<sup>2</sup>, 74%; Cochran Q test, P<0.1) and 86% (95% CI, 72-94%; I<sup>2</sup>, 82%; Cochran Q test, P<0.1) for the mRECIST viable category. The LR-TR viable category provided significantly higher pooled specificity (P<0.01) than mRECIST but comparable pooled sensitivity (P=0.53). Meta-regression analysis revealed that type of LRT and the most common etiology of liver disease were significantly associated with the study heterogeneity for the mRECIST viable category (P=0.01). There was no significant publication bias across the studies for both criteria (P=0.35).

#### **CONCLUSION**

s LR-TR algorithm demonstrated better specificity than mRECIST without significant difference in sensitivity for the diagnosis of pathologically viable HCC after LRT.

#### **CLINICAL RELEVANCE/APPLICATION**

The specificity of the viable category for the diagnosis of pathologically viable HCC was significantly higher when applying LR-TR than mRECIST, but the sensitivity was comparable.

Printed on: 02/07/23

## Abstract Archives of the RSNA, 2022

T5B-SPGI-10

### **MRI Correlation with Liver Explant Pathology: Routine Clinical Care vs. Expert Reader Using the LIRADS Treatment Response Algorithm in Assessing Residual HCC After Y-90 Therapy**

Tuesday, Nov. 29 12:45PM - 1:15PM Room: Learning Center - GI DPS

#### **Participants**

Matthew Harwood, MD, Phoenix, AZ (*Presenter*) Nothing to Disclose

#### **PURPOSE**

The Liver Imaging Reporting and Data System treatment response algorithm (LIRADS-TRA) criteria can be used to predict HCC response to locoregional therapy, however, radiation-based methods such as transarterial radioembolization (TARE) with yttrium-90 have unique post-treatment features that can confound assessment. Prior studies used survival and/or time to progression as the primary endpoints after Y90. Few studies use pathology as the reference standard. This study compares an expert reader's blinded MRI or CT interpretation applying the LIRADS-TRA against interpretations obtained during routine clinical care.

#### **METHODS AND MATERIALS**

An IRB exemption was obtained. We identified adult patients (age range 37-72 years) who underwent liver explant after Y90 treatment for HCC (pre-treatment LR-5, OPTN5a/b, or biopsy proven HCC) then subsequently underwent liver transplant (dates of transplant between 10/2015 and 10/2021). Of the 96 patients identified, 27 were excluded because at least 90 days had not elapsed between treatment and MRI/CT, or because multiple treatments were employed. Ultimately, 25 patients with at least 1 treated HCC comprised the cohort. Most patients had MRIs before transplant (23/25), the rest multiphase CTs (2/25). Mean MELD scores at transplant for this cohort was  $13 \pm 5$  (mean  $\pm$ SD). The most common etiologies of cirrhosis were hepatitis C (40%), alcohol (24%), and NASH (20%). Mean time between treatment and MRI or CT was  $164 \pm 89$  days (mean  $\pm$ SD). A fellowship-trained, board-certified abdominal radiologist with >20 years of experience blinded to the presence or absence of residual viable tumor in liver explant specimens independently reviewed the pre- and post-treatment exams. When two or more tumors were present or treated, the dominant treated lesion was evaluated. The LIRADS-TRA was strictly adhered to, wherein only 6 of 25 (24%) clinical reports explicitly used the LIRADS-TRA. LR-TR viable and LR-TR equivocal were considered positive. LR-TR nonviable was considered negative.

#### **RESULTS**

The clinical assessment and expert reader had fair agreement ( $\kappa=0.29$ ). Both "readers" had an accuracy of 60%. +LR for TRA: 2.3 (95%CI 0.55-9.7). -LR: 0.74 (0.45-1.2). In a separate analysis, successful tumor debulking (90% or greater tumor necrosis) was also considered as a binary outcome.

#### **CONCLUSION**

Adherence to the LIRADS-TRA did not improve accuracy or test performance as expected. Previous authors evaluating liver resection pathology after Y90 showed higher accuracy. However, their post-treatment imaging time frame was not defined, whereas this study focused on the 6-month post-treatment exam.

#### **CLINICAL RELEVANCE/APPLICATION**

To know the accuracy of our major CT and MRI criteria for assessing HCC treatment response, the LIRADS-TRA.

Printed on: 02/07/23

## Abstract Archives of the RSNA, 2022

T5B-SPGI-3

### Diagnostic Performance of LI-RADS v2018 Versus KLCA-NCC 2018 Criteria for Hepatocellular Carcinoma Using Magnetic Resonance Imaging: A Systematic Review and Meta-Analysis of Comparative Studies

Tuesday, Nov. 29 12:45PM - 1:15PM Room: Learning Center - GI DPS

#### Participants

Jaeseung Shin, Seoul, Korea, Republic Of (*Presenter*) Nothing to Disclose

#### PURPOSE

We performed a meta-analysis to compare the performance of the Liver Imaging Reporting and Data System (LI-RADS) v2018 and Korean Liver Cancer Association-National Cancer Center (KLCA-NCC) 2018 criteria for diagnosing hepatocellular carcinoma (HCC) using magnetic resonance imaging (MRI).

#### METHODS AND MATERIALS

We searched the MEDLINE and EMBASE databases for studies published from January 1, 2018, to October 20, 2021, that compared the diagnostic performance of LR-5 of LI-RADS v2018 and definite HCC category of KLCA-NCC 2018 on MRI. Bivariate random-effects model was fitted to calculate the pooled per-observation sensitivity and specificity of both imaging criteria and compared the pooled estimates of paired data. Subgroup analysis was performed based on the observation size. Meta-regression analysis was performed to identify factors for study heterogeneity.

#### RESULTS

Of the six studies included (2,109 observations and 1,471 HCCs), the pooled sensitivity of the definite HCC category of KLCA-NCC criteria (81%; 95% confidence interval [CI], 73-90%; I<sup>2</sup>=86%) was higher than that of LR-5 of LI-RADS v2018 (65%; 95% CI, 53-78%; I<sup>2</sup>=96%) for diagnosing HCC ( $P<0.001$ ), while the specificity was lower for KLCA-NCC 2018 (88%; 95% CI, 84-91%; I<sup>2</sup>=13%) than for LI-RADS v2018 (93%; 95% CI, 91-96%; I<sup>2</sup>=0%) ( $P=0.018$ ). For observations sized  $\geq 20$  mm, sensitivity was higher for KLCA-NCC 2018 than for LI-RADS v2018 (83% versus 75%;  $P=0.017$ ), with no significant difference in specificity (82% versus 86%;  $P=0.463$ ). Meta-regression analyses revealed reference standard as a significant factor contributing to the heterogeneity of sensitivities.

#### CONCLUSION

s The definite HCC category of KLCA-NCC 2018 provided a higher pooled sensitivity and lower pooled specificity than the LR-5 of LI-RADS v2018 for diagnosing HCC using MRI.

#### CLINICAL RELEVANCE/APPLICATION

Compared with LI-RADS v2018, KLCA-NCC 2018 criteria might be preferred where sensitive diagnosis is demanded for earlier locoregional treatment (i.e. East Asia).

Printed on: 02/07/23

## Abstract Archives of the RSNA, 2022

T5B-SPGI-4

### Preoperative prediction of microvascular invasion in hepatocellular carcinoma based on three-phase contrast-enhanced CT images of the tumor and peritumoral regions

Tuesday, Nov. 29 12:45PM - 1:15PM Room: Learning Center - GI DPS

#### Participants

Xiaofei Yue, (*Presenter*) Nothing to Disclose

#### PURPOSE

To establish a clinical-radiomics nomogram for preoperative prediction of microvascular invasion (MVI) of hepatocellular carcinoma (HCC) and compare the diagnostic value of different tumor regions and phases for the MVI status in a non-invasive way.

#### METHODS AND MATERIALS

335 HCC patients (161 MVI-negative and 174 MVI-positive) who underwent three-phase contrast-enhanced CT before surgery were enrolled from May 2017 to July 2020. Regions of interest (ROI) of the tumor, peritumor(10mm), and tumor-peritumor(10mm) were manually segmented in the arterial phase (AP) and portal venous phase (PVP), and delayed phase (DP) images. A total of nine groups of ROIs were obtained, and 1218 radiomics features were extracted, respectively. Patients were randomly assigned to the training and inter-validation cohorts in a ratio of 7:3. The Analysis of Variance and least absolute shrinkage and selection operator (LASSO) algorithms with ten-fold cross validation were used to select radiomics features. Nine radiomics scores (Rad-Score) were established using multivariate logistic regression analysis. In addition, we combined the nine Rad-Scores with 18 clinical factors and 23 radiographic scores to construct a clinical-radiomics nomogram with multivariate logistic regression. Furthermore, all radiomics models and the combined clinical-radiomics model were independently validated with the data of the hospital's sub-campus (40 patients). ROC curves were used to compare the predictive power of the multiple models. Decision curve analysis (DCA) was used to compare the clinical benefit of the models.

#### RESULTS

Among the nine Rad-Scores, the tumor-peritumor in the AP cohort had the best predictive ability (AUCs of 0.912, 0.848, and 0.880 for the training cohort, inter-validation cohort, and independent validation cohort, respectively). The predicted values of the clinical model of AUCs were 0.775, 0.742, and 0.696 in the training cohort, inter-validation cohort, and independent validation cohort, respectively. The combined clinical-radiomics model performs well (AUCs for the training, inter-validation and independent validation cohorts are 0.938, 0.883, and 0.829). DCA demonstrated the highest clinical benefit in the combined clinical-radiomics model.

#### CONCLUSION

The clinical-radiomics model has satisfactory results in preoperative prediction of MVI in patients with HCC and has potential value in guiding clinicians to individualize treatment.

#### CLINICAL RELEVANCE/APPLICATION

MVI of HCC usually indicates an increased risk of recurrence and a poor prognosis. The clinical-radiomics model can predict MVI preoperatively and has potential value in guiding clinicians to individualize treatment.

Printed on: 02/07/23

## Abstract Archives of the RSNA, 2022

T5B-SPGI-5

### Abbreviated MRI for secondary surveillance of recurrent hepatocellular carcinoma after curative treatment

Tuesday, Nov. 29 12:45PM - 1:15PM Room: Learning Center - GI DPS

#### Participants

Dong Ho Lee, MD, Seoul, Korea, Republic Of (*Presenter*) Nothing to Disclose

#### PURPOSE

There is no consensus regarding the ideal imaging modality of secondary surveillance of hepatocellular carcinoma (HCC). This study aimed to evaluate the detection performance of abbreviated MRI (AMRI) for secondary surveillance for HCC after curative treatment including surgical resection or radiofrequency ablation (RFA).

#### METHODS AND MATERIALS

This retrospective study analyzed 243 patients who received secondary surveillance for HCC using gadoxetic acid-enhanced MRI after more than two-year of disease-free period from curative treatment including surgical resection or RFA. Non-contrast AMRI (NC-AMRI) (T2-weighted and diffusion-weighted images), hepatobiliary phase AMRI (HBP-AMRI) (T2-weighted, diffusion-weighted and HBP images), and full-sequence MRI sets were independently reviewed by two abdominal radiologists. The confirmation of HCC was based either on histopathological confirmation or imaging-based diagnosis. HCC detection rate of each set was compared.

#### RESULTS

A total of 42 recurrent HCCs were confirmed in 39 patients. Per-lesion and per-patient sensitivities didn't show significant difference among three image sets in both reviewers ( $P=0.681$ ): Per-lesion sensitivity: 81.1%83.3%, 76.2%85.7%, and 81.0%83.3% for NC-AMRI, HBP-AMRI, and full-sequence MRI, respectively; and per-patient sensitivity: 79.5%83.3%, 79.5%85.7%, and 79.5%83.3% for NC-AMRI, HBP-AMRI, and full-sequence MRI. Per-patient specificity didn't show significant difference among three image set in both reviewers (95.6%97.1%, 96.1%97.1%, and 97.6%98.5% for NC-AMRI, HBP-AMRI, respectively;  $P=0.307$ ).

#### CONCLUSION

s NC-AMRI and HBP-AMRI had comparable detection performance to that of full-sequence gadoxetic acid-enhanced MRI during secondary surveillance for HCC after more than 2-year disease free interval following curative treatment. Based on its good detection performance, short scan times, and the lack of contrast agent-associated risks, NC-AMRI would be a promising option for secondary surveillance of HCC.

#### CLINICAL RELEVANCE/APPLICATION

NC-AMRI would be a promising option for secondary surveillance for HCC after 2-year disease free interval following curative treatment including surgical resection and RFA.

Printed on: 02/07/23

## Abstract Archives of the RSNA, 2022

T5B-SPGI-6

### Preoperative prediction of microvascular invasion in hepatocellular carcinoma using computation modeling of interstitial fluid pressure and velocity

Tuesday, Nov. 29 12:45PM - 1:15PM Room: Learning Center - GI DPS

#### Participants

Liyun Zheng, Shanghai, China (*Presenter*) Nothing to Disclose

#### PURPOSE

The purpose of present study was to develop and validate a new method for the interstitial fluid pressure (IFP) measurement in hepatocellular carcinoma (HCC) patients. We also aimed to depict the microenvironment of the tumor of HCC and predict the microvascular invasion (MVI) status preoperatively and noninvasively by this IFP model.

#### METHODS AND MATERIALS

A cohort of 27 patients were finally included in this study (mean age  $57.6 \pm 10.9$  years, 77.8% males). There were 15 patients in the MVI-positive group and 12 patients in the MVI-negative group. MRI examinations were performed using a 3T scanner (uMR790, United Imaging Healthcare). DCE-MRI scan sequence utilized a transverse T1-weighted spoiled GRE sequence to obtain acquisition, and 60 time points were acquired with mean temporal resolution of 3.1 s and a total acquisition time of  $\sim 3$  min. Patients were allowed to breathe freely. The extended tofts model (ETM) was used to estimate the permeability parameters. Volume of Interest (VOI) for Ktrans estimation were manually delineated on the tumor lesion present in all slices in the late phases of T1-weighted DCE-MRI images. The tumor volume was calculated from the T1w dynamic images. The continuity partial differential equation (PDE) was implemented and the estimation of IFP and interstitial fluid velocity (IFV) were acquired. Mann-Whitney U test was performed to compare the mean IFP and mean IFV between MVI-positive group and MVI-negative group. The receiver operating characteristic (ROC) analysis was performed for differentiation between MVI-positive group and MVI-negative group. The Youden index were exploited to determine the cutoff value, along with the area under the curve (AUC), sensitivity and specificity.  $P < 0.05$  was considered statistically significant.

#### RESULTS

Significant difference was found in mean IFP between the MVI-positive group and MVI-negative group ( $P = 0.001$ ), while there was no statistically differences in mean IFV between the two groups ( $P = 0.626$ ). For the ROC analysis, mean IFP value proved to be the significant predictor with the best cut-off value 1854.22 Pa (AUC = 0.883, 95% confidence interval 0.701 to 0.974; sensitivity = 80.0%, specificity = 91.7%).

#### CONCLUSION

The non-invasive interstitial fluid pressure (IFP) measurement model in liver tumors was developed. Significant difference was found in mean IFP between the MVI-positive group and MVI-negative group. IFP could be the significant predictor in the prediction of MVI status.

#### CLINICAL RELEVANCE/APPLICATION

This study developed a new method for the noninvasive IFP measurement in HCC patients. Our results revealed that MVI status can be predicted by this IFP model preoperatively.

Printed on: 02/07/23

## Abstract Archives of the RSNA, 2022

T5B-SPGI-8

### LI-RADS Category 4 Observations on Gadoteric Acid-Enhanced MRI: Can Imaging Features Indicate High Risk of Early Progression (<6 Months) To LI-RADS Category 5?

Tuesday, Nov. 29 12:45PM - 1:15PM Room: Learning Center - GI DPS

#### Participants

Ijin Joo, MD, Seoul, (*Presenter*) Nothing to Disclose

#### PURPOSE

To investigate the value of gadoteric acid-enhanced MRI (Gd-EOB-MRI) features of LI-RADS category 4 (LR-4: probably hepatocellular carcinoma [HCC]) observations for predicting early progression to LR-5 (definitely HCC)

#### METHODS AND MATERIALS

This retrospective study included liver observations in patients at high risk for HCC, assigned as LR-4 on index Gd-EOB-MRI and had available short-term (<6 months) follow-up Gd-EOB-MRI. For each observation, LI-RADS major and ancillary features on index MRI and final LI-RADS category on follow-up MRI were assessed by a consensus of three radiologists. Multivariate logistic regression analysis was performed to identify imaging predictors for early (<6 months) progression to LR-5. Diagnostic performances of each significant imaging feature and their combinations for identifying LR-4 observations with higher risk of early category progression were evaluated.

#### RESULTS

Among 101 index LR-4 observations in 101 patients, 57 progressed to LR-5, while the other 44 remained stable as LR-4 within 6 months. Multivariate logistic regression analysis revealed that nonrim arterial phase hyperenhancement (APHE), nonperipheral "washout", restricted diffusion, and fat in mass at index MRI were independent predictors for early category progression (odds ratio = 3.75, 3.17, 5.36, 12.2; P = 0.037, 0.036, 0.003, 0.030, respectively). For predicting the early category progression, nonrim APHE showed the highest sensitivity (47/57, 82.5%) followed by restricted diffusion (39/57, 68.4%), nonperipheral "washout" (27/57, 47.4%), and fat in mass (8/57, 14.0%); while the highest specificity was found in fat in mass (43/44, 97.7%) followed by restricted diffusion (33/44, 75.0%), nonperipheral "washout" (31/44, 70.5%), and nonrim APHE (17/44, 38.6%). When two or more of four imaging features listed above were present, the sensitivity was 82.5% (47/57) and the specificity was 61.4% (27/44).

#### CONCLUSION

s LI-RADS major and ancillary features on Gd-EOB-MRI can help identify LR-4 observations with higher risk of early category progression to LR-5.

#### CLINICAL RELEVANCE/APPLICATION

In LI-RADS category 4 observations, MRI-based risk stratification according to the probability of early category progression could potentially facilitate appropriate and timely management.

Printed on: 02/07/23

## Abstract Archives of the RSNA, 2022

T5B-SPGI-9

### Diagnostic Performance of CT versus MRI Liver Imaging Reporting and Data System Category 5 for Hepatocellular Carcinoma: A Systematic Review and Meta-Analysis of Comparative Studies

Tuesday, Nov. 29 12:45PM - 1:15PM Room: Learning Center - GI DPS

#### Participants

Sunyoung Lee, Seoul, Korea, Republic Of (*Presenter*) Nothing to Disclose

#### PURPOSE

To compare the performance of Liver Imaging Reporting and Data System category 5 (LR-5) for diagnosing HCC between CT and MRI using comparative studies.

#### METHODS AND MATERIALS

The MEDLINE and EMBASE databases were searched from inception to April 21, 2021, to identify studies that directly compare the diagnostic performance of LR-5 for HCC between CT and MRI. Bivariate random-effects model was fitted to calculate the pooled per-observation sensitivity and specificity of LR-5 of each modality, and compare the pooled estimates of paired data. Subgroup analysis was performed according to MRI contrast agent.

#### RESULTS

Seven studies with 1,145 observations (725 HCCs) were included in the final analysis. The pooled per-observation sensitivity of LR-5 for diagnosing HCC was higher using MRI (61%; 95% confidence interval [CI], 43-76%; I<sup>2</sup> = 95%) than CT (48%; 95% CI, 31-65%; I<sup>2</sup> = 97%) ( $P < 0.001$ ). The pooled per-observation specificities of LR-5 did not show statistically significant difference between CT (96%; 95% CI, 92-98%; I<sup>2</sup> = 0%) and MRI (93%; 95% CI, 88-96%; I<sup>2</sup> = 16%) ( $P = 0.054$ ). In the subgroup analysis, extracellular contrast agent-enhanced MRI showed significantly higher pooled per-observation sensitivity than gadoxetic acid-enhanced MRI for diagnosing HCC (73% [95% CI, 55%-85%] vs. 55% [95% CI, 39%-70%];  $P = 0.007$ ), without a significant difference in specificity (93% [95% CI, 80%-98%] vs. 94% [95% CI, 87%-97%];  $P = 0.884$ ).

#### CONCLUSION

The LR-5 of MRI showed significantly higher pooled per-observation sensitivity than CT for diagnosing HCC. The pooled per-observation specificities of LR-5 were comparable between the two modalities.

#### CLINICAL RELEVANCE/APPLICATION

Although LI-RADS provides a common diagnostic algorithm for CT or MRI, the per-observation performance of LR-5 can be affected by the imaging modality as well as the MRI contrast agent.

Printed on: 02/07/23

## Abstract Archives of the RSNA, 2022

T5B-SPGU

### Genitourinary Tuesday Poster Discussions - B

Tuesday, Nov. 29 12:45PM - 1:15PM Room: Learning Center - GU DPS

#### Sub-Events

#### **T5B-SPGU-1 Does The Mid-urethral Sling Surgery Changes The Pelvic Floor MRI Parameters In Females With Stress Urinary Incontinence?: An initial experience**

##### Participants

Mona Eldeeb, MBCh, PhD, (*Presenter*) Nothing to Disclose

##### PURPOSE

This study aimed to use pre and post-operative static and dynamic pelvic floor MRI to find out the parameters changed after the mid-urethral sling surgery. Also, we tried to compare post-operative quantitative and morphologic MRI pelvic floor parameters between the success and failure groups.

##### METHODS AND MATERIALS

This prospective study was conducted upon 42 female patients with stress urinary incontinence, the mean age was  $47.33 \pm 7.32$  years. 3T pelvic MRI examination was carried on at rest and during straining. Paired t-test was performed to compare preoperative and post-operative data, and to compare the post-operative MRI findings between success and failure groups.

##### RESULTS

Of the 42 case included in our study, 33 patient (78.57%) had successful surgery versus 9 patients (21.43%) had failed surgery. H line at rest decreased to  $5.46 \pm 0.89$  cm postoperatively from  $5.98 \pm 0.58$  cm preoperatively ( $p = 0.015$ ), Posterior vesicourethral angle (PUVA) decreased to  $121.94 \pm 9.13$  degree postoperatively from  $128.26 \pm 9.57$  degree preoperatively ( $p = 0.000$ ) at rest, and from  $152.34 \pm 9.2$  degree preoperatively to  $138.78 \pm 10.6$  degree postoperatively ( $p = 0.011$ ) during straining, difference in the vesical neck movement between rest and straining decreased from  $2.02 \pm 0.16$  cm preoperatively to  $1.162 \pm 0.817$  cm postoperatively ( $p = 0.000$ ). As regard comparison between pre and post-operative static parameters, the length of the suprapubic part of the urethra, the retropubic space and the pubovaginal space showed significant difference. Postoperatively, PUVA during straining and difference in vesicourethral angle between rest and straining showed significant difference between success and failure groups ( $p = 0.000$ ). The mean distance of the pubovaginal space in successful cases was  $2.354 \pm 0.425$  cm versus  $2.688 \pm 0.513$  cm in failed cases with a statistical significance noted in between ( $p$  value = 0.05).

##### CONCLUSION

s Quantitative dynamic and static pelvic floor MRI is a promising tool in the evaluation of urethral and bladder neck parameters successfully corrected after mid-urethral sling surgery.

##### CLINICAL RELEVANCE/APPLICATION

As limited data are available about the role of dynamic pelvic floor MRI in stress urinary incontinence before and after mid-urethral sling surgery, this might help in better selection of the patients who will benefit from the surgery depending on the assessed preoperative parameters

#### **T5B-SPGU-2 An AI and human reader study on recognition of ureter stone in non-contrast CT images**

##### Participants

Sang Wouk Cho, MS, Seoul, Korea, Republic Of (*Presenter*) Nothing to Disclose

##### PURPOSE

Diagnoses of ureter stones are required for interpretation of medical images in patients with severe pain and renal obstruction. Non-contrast computed tomography (NCCT) is the gold standard for diagnosis of ureter stones. We developed the diagnostic programed using Artificial Intelligence (AI) and compared the diagnostic performance between AI and physicians.

##### METHODS AND MATERIALS

Of 450 NCCT data set with and without ureter stone (50%, stone positive), each of 200 cases regarding of presence of ureter stone was randomly selected to question for 7 physicians (3 professors, 2 senior residents and 2 junior residents) and AI for identifying stones. TASK1 is drawing the location for stones by identifying at a single NCCT image, and TASK2 at whole series images. A Modified U-net-based segmentation model was trained using a cohort of 1,440 patients with urinary stones, and performance of AI was evaluated as a result of generating masks. Both the answer sheet and stone masks for training were annotated by a urologist and double-checked by two uro-radiologists.

##### RESULTS

In Task 1, the professors showed the highest diagnostic performances (accuracy/sensitivity/specificity: 0.815/0.692/0.938),

following junior residents and senior residents (0.811/0.748/0.875 and 0.749/0.607/0.890). The tendency of diagnostic performances in Task2 was similar to the results in Task1 (0.848/0.765/0.930, 0.659/0.452/0.865 and 0.660/0.388/0.933). In the Task1 of recognizing stones by a single slide, diagnostic performances of AI (0.850/0.720/0.980) revealed significantly higher than those of all physicians ( $p < 0.005$ ). In Task2, AI (0.725/0.775/0.675) showed less diagnostic performance than professors, but it revealed the superior to each of senior and junior residents ( $p < 0.001$ ). There were significant differences of positive predictive values (PPV: AI 0.973, senior 0.840, junior 0.858,  $p < 0.0001$ ) in Task1 and negative predictive values (NPV: AI 0.750, senior 0.617, junior 0.612,  $p < 0.0001$ ) in Task2. In comparison of diagnostic performance for Task 1 and Task 2 according to the AI and human reader, professors showed the higher accuracy, sensitivity and NPV in Task 2, but AI showed the higher sensitivity.

## CONCLUSION

s Although individual differences of diagnostic performances among physicians were associated with medical experiences, the diagnostic performances in AI were higher than those of senior and junior residents. Identifying ureter stone in whole series images was higher accuracy than that of Task 1 with recognizing stones by a single slide.

## CLINICAL RELEVANCE/APPLICATION

It is important to encounter many cases of ureter stone for physicians to recognize stones in NCCT. By providing guidance, AI could help residents reach better decisions to identify stones.

## T5B-SPGU-3 Improving Prostate Cancer Detection on MRI Using Prostate-Specific Antigen Density: Additional Benefit from Zone-Specific Analyses?

Participants

Charlie Hamm, MD, Berlin, Germany (*Presenter*) Nothing to Disclose

## PURPOSE

To evaluate the diagnostic value of ultrasound- and MRI-based prostate-specific antigen density (PSAD) to detect prostate cancer (PCa) and to compare PSAD based on whole organ volumetry against a transition zone-specific approach.

## METHODS AND MATERIALS

This study included 1716 consecutive patients, who underwent transrectal ultrasound (TRUS), prostate MRI, and consecutive transrectal ultrasound-guided biopsy. After exclusion of 27 cases due to bad image quality, PCa was confirmed in 1185/1689 patients (348 Gleason Score (GS)=6; 837 GS=7) and the mean PSA was  $11 \pm 23$ . Prostates of 1300 patients were manually segmented to train and test a deep learning (DL) nnUnet using cross-validation for automated prostate and prostate zone volumetry. Conventional whole organ-PSAD and transition zone-specific (TZ-s)PSAD were calculated. The results were compared to TRUS-based whole organ-PSAD and receiver operating characteristic area under the curve (AUC) of the models were determined using a hold-out test set comprising 389 patients, 55 of which were rated as PI-RADS 3.

## RESULTS

The DL system reliably segmented the peripheral and transition zone on axial T2W-MRI with a dice coefficient of 0.87 and 0.81, respectively. In the test group, the mean TZ-sPSAD was  $0.5 \pm 0.65$  and the cut-off value of 0.27 showed the highest diagnostic accuracy in detecting PCa with an accuracy, sensitivity, and specificity of 0.71, 0.72, and 0.69, respectively. When compared to the established PSAD cut-off value of 0.15, the TZ-sPSAD (AUC: 0.74) detected significantly more PCa than the conventional MRI- (AUC: 0.72,  $p = 0.04$ ) and TRUS-based PSAD (0.65,  $p < 0.001$ ), respectively. Furthermore, the number of correctly identified clinically significant (cs)PCa (GS=7) was increased by 9% (18 vs. 23/55) in the PI-RADS 3 group, while the number of cases detected in the PI-RADS 1/2 and 4/5 groups was comparable.

## CONCLUSION

s This study demonstrates a significantly improved PCa detection rate using MRI- compared to TRUS-based PSAD. Moreover, zone segmentation using a DL system to calculate TZ-sPSAD further improved PCa detection and can reduce the number of missed cases of csPCa in the PI-RADS 3 group.

## CLINICAL RELEVANCE/APPLICATION

DL systems enabling automated zone-specific prostate volumetry may improve prostate MRI analysis suggesting the TZ-sPSAD as a potential biomarker for the detection of PCa.

## T5B-SPGU-4 Performance of Clear Cell Likelihood Scores (ccLS) in Evaluating Solid Renal Masses at Multiparametric MRI: Single Center Cohort Study

Awards

Trainee Research Prize - Resident

Participants

Aisin Ibrahim, MD, (*Presenter*) Nothing to Disclose

## PURPOSE

The purpose of this study is to evaluate the accuracy and interobserver agreement of clear cell Likelihood scores (ccLS) in diagnosing clear cell renal cell carcinoma (ccRCC).

## METHODS AND MATERIALS

This retrospective single-center study evaluated consecutive patients with solid renal masses who underwent mpMRI followed by percutaneous biopsy and/or surgical excision between January 2010 and December 2020. Predominantly (>75%) cystic masses, masses with macroscopic fat and infiltrative masses were excluded. Two abdominal radiologists independently scored each renal mass according to the proposed ccLS algorithm. The diagnostic performance of ccLS categories for ccRCC was calculated using logistic regression modeling. Diagnostic accuracy for predicting ccRCC was calculated using 2x2 contingency tables. Interobserver agreement for ccLS was evaluated with Cohen's k statistic.

## RESULTS

A total of 79 patients (mean age, 63 years  $\pm$  12 [SD], 50 men) with 81 renal masses were evaluated. The mean size was 36 mm  $\pm$  28 (range, 10-160). Of the renal masses included, 44% (36/81) were ccRCC. The area under the receiver operating characteristic curve for the pooled results was 0.87 (95% CI: 0.79-0.95). Using ccLS = 4 to diagnose ccRCC, the sensitivity, specificity, and positive predictive value were 93% (95% CI: 79, 99), 63% (95% CI: 48, 77), and 67% (95% CI: 58, 75), respectively. The negative predictive value of ccLS = 2 was 93% (95% CI: 64, 99). The pooled proportion of ccRCC by ccLS category 1 to 5 were 10%, 0%, 10%, 57%, and 84% respectively. Interobserver agreement was moderate ( $k=0.47$ ).

#### **CONCLUSION**

s In this study, ccLS had moderate interobserver agreement and resulted in 67% positive predictive value in diagnosing ccRCC and 93% negative predictive value in excluding ccRCC.

#### **CLINICAL RELEVANCE/APPLICATION**

The ccLS system could be a clinically efficient non-invasive tool in the assessment of solid renal masses in clinical practice. This could aid active surveillance and potentially limit the use of renal biopsy mainly for indeterminate renal lesions.

Printed on: 02/07/23

## Abstract Archives of the RSNA, 2022

T5B-SPGU-1

### Does The Mid-urethral Sling Surgery Changes The Pelvic Floor MRI Parameters In Females With Stress Urinary Incontinence?: An initial experience

Tuesday, Nov. 29 12:45PM - 1:15PM Room: Learning Center - GU DPS

#### Participants

Mona Eldeeb, MBBCh, PhD, (*Presenter*) Nothing to Disclose

#### PURPOSE

This study aimed to use pre and post-operative static and dynamic pelvic floor MRI to find out the parameters changed after the mid-urethral sling surgery. Also, we tried to compare post-operative quantitative and morphologic MRI pelvic floor parameters between the success and failure groups.

#### METHODS AND MATERIALS

This prospective study was conducted upon 42 female patients with stress urinary incontinence, the mean age was 47.33 ±7.32 years. 3T pelvic MRI examination was carried on at rest and during straining. Paired t-test was performed to compare preoperative and post-operative data, and to compare the post-operative MRI findings between success and failure groups.

#### RESULTS

Of the 42 case included in our study, 33 patient (78.57%) had successful surgery versus 9 patients (21.43%) had failed surgery. H line at rest decreased to 5.46+ 0.89 cm postoperatively from 5.98+0.58 cm preoperatively ( $p = 0.015$ ), Posterior vesicourethral angle (PUVA) decreased to 121.94 + 9.13 degree postoperatively from 128.26+9.57 degree preoperatively ( $p= 0.000$ ) at rest, and from 152.34+9.2 degree preoperatively to 138.78+10.6 degree postoperatively ( $p= 0.011$ ) during straining, difference in the vesical neck movement between rest and straining decreased from 2.02+ 0.16 cm preoperatively to 1.162+ 0.817 cm postoperatively ( $p= 0.000$ ). As regard comparison between pre and post-operative static parameters, the length of the suprapubic part of the urethra, the retropubic space and the pubovaginal space showed significant difference. Postoperatively, PUVA during straining and difference in vesicourethral angle between rest and straining showed significant difference between success and failure groups ( $p = 0.000$ ). The mean distance of the pubovaginal space in successful cases was 2.354+ 0.425 cm versus 2.688+ 0.513 cm in failed cases with a statistical significance noted in between ( $p$  value =0.05).

#### CONCLUSION

s Quantitative dynamic and static pelvic floor MRI is a promising tool in the evaluation of urethral and bladder neck parameters successfully corrected after mid-urethral sling surgery.

#### CLINICAL RELEVANCE/APPLICATION

As limited data are available about the role of dynamic pelvic floor MRI in stress urinary incontinence before and after mid-urethral sling surgery, this might help in better selection of the patients who will benefit from the surgery depending on the assessed preoperative parameters

Printed on: 02/07/23



## Abstract Archives of the RSNA, 2022

T5B-SPGU-2

### An AI and human reader study on recognition of ureter stone in non-contrast CT images

Tuesday, Nov. 29 12:45PM - 1:15PM Room: Learning Center - GU DPS

#### Participants

Sang Wouk Cho, MS, Seoul, Korea, Republic Of (*Presenter*) Nothing to Disclose

#### PURPOSE

Diagnoses of ureter stones are required for interpretation of medical images in patients with severe pain and renal obstruction. Non-contrast computed tomography (NCCT) is the gold standard for diagnosis of ureter stones. We developed the diagnostic programed using Artificial Intelligence (AI) and compared the diagnostic performance between AI and physicians.

#### METHODS AND MATERIALS

Of 450 NCCT data set with and without ureter stone (50%, stone positive), each of 200 cases regarding of presence of ureter stone was randomly selected to question for 7 physicians (3 professors, 2 senior residents and 2 junior residents) and AI for identifying stones. TASK1 is drawing the location for stones by identifying at a single NCCT image, and TASK2 at whole series images. A Modified U-net-based segmentation model was trained using a cohort of 1,440 patients with urinary stones, and performance of AI was evaluated as a result of generating masks. Both the answer sheet and stone masks for training were annotated by a urologist and double-checked by two uro-radiologists.

#### RESULTS

In Task 1, the professors showed the highest diagnostic performances (accuracy/sensitivity/specificity: 0.815/0.692/0.938), following junior residents and senior residents (0.811/0.748/0.875 and 0.749/0.607/0.890). The tendency of diagnostic performances in Task2 was similar to the results in Task1 (0.848/0.765/0.930, 0.659/0.452/0.865 and 0.660/0.388/0.933). In the Task1 of recognizing stones by a single slide, diagnostic performances of AI (0.850/0.720/0.980) revealed significantly higher than those of all physicians ( $p < 0.005$ ). In Task2, AI (0.725/0.775/0.675) showed less diagnostic performance than professors, but it revealed the superior to each of senior and junior residents ( $p < 0.001$ ). There were significant differences of positive predictive values (PPV: AI 0.973, senior 0.840, junior 0.858,  $p < 0.0001$ ) in Task1 and negative predictive values (NPV: AI 0.750, senior 0.617, junior 0.612,  $p < 0.0001$ ) in Task2. In comparison of diagnostic performance for Task 1 and Task 2 according to the AI and human reader, professors showed the higher accuracy, sensitivity and NPV in Task 2, but AI showed the higher sensitivity.

#### CONCLUSION

s Although individual differences of diagnostic performances among physicians were associated with medical experiences, the diagnostic performances in AI were higher than those of senior and junior residents. Identifying ureter stone in whole series images was higher accuracy than that of Task 1 with recognizing stones by a single slide.

#### CLINICAL RELEVANCE/APPLICATION

It is important to encounter many cases of ureter stone for physicians to recognize stones in NCCT. By providing guidance, AI could help residents reach better decisions to indentify stones.

Printed on: 02/07/23

## Abstract Archives of the RSNA, 2022

T5B-SPGU-3

### Improving Prostate Cancer Detection on MRI Using Prostate-Specific Antigen Density: Additional Benefit from Zone-Specific Analyses?

Tuesday, Nov. 29 12:45PM - 1:15PM Room: Learning Center - GU DPS

#### Participants

Charlie Hamm, MD, Berlin, Germany (*Presenter*) Nothing to Disclose

#### PURPOSE

To evaluate the diagnostic value of ultrasound- and MRI-based prostate-specific antigen density (PSAD) to detect prostate cancer (PCa) and to compare PSAD based on whole organ volumetry against a transition zone-specific approach.

#### METHODS AND MATERIALS

This study included 1716 consecutive patients, who underwent transrectal ultrasound (TRUS), prostate MRI, and consecutive transrectal ultrasound-guided biopsy. After exclusion of 27 cases due to bad image quality, PCa was confirmed in 1185/1689 patients (348 Gleason Score (GS)=6; 837 GS=7) and the mean PSA was  $11\pm 23$ . Prostates of 1300 patients were manually segmented to train and test a deep learning (DL) nnUnet using cross-validation for automated prostate and prostate zone volumetry. Conventional whole organ-PSAD and transition zone-specific (TZ-s)PSAD were calculated. The results were compared to TRUS-based whole organ-PSAD and receiver operating characteristic area under the curve (AUC) of the models were determined using a hold-out test set comprising 389 patients, 55 of which were rated as PI-RADS 3.

#### RESULTS

The DL system reliably segmented the peripheral and transition zone on axial T2W-MRI with a dice coefficient of 0.87 and 0.81, respectively. In the test group, the mean TZ-sPSAD was  $0.5\pm 0.65$  and the cut-off value of 0.27 showed the highest diagnostic accuracy in detecting PCa with an accuracy, sensitivity, and specificity of 0.71, 0.72, and 0.69, respectively. When compared to the established PSAD cut-off value of 0.15, the TZ-sPSAD (AUC: 0.74) detected significantly more PCa than the conventional MRI- (AUC: 0.72,  $p=0.04$ ) and TRUS-based PSAD (0.65,  $p<0.001$ ), respectively. Furthermore, the number of correctly identified clinically significant (cs)PCa (GS=7) was increased by 9% (18 vs. 23/55) in the PI-RADS 3 group, while the number of cases detected in the PI-RADS 1/2 and 4/5 groups was comparable.

#### CONCLUSION

s This study demonstrates a significantly improved PCa detection rate using MRI- compared to TRUS-based PSAD. Moreover, zone segmentation using a DL system to calculate TZ-sPSAD further improved PCa detection and can reduce the number of missed cases of csPCa in the PI-RADS 3 group.

#### CLINICAL RELEVANCE/APPLICATION

DL systems enabling automated zone-specific prostate volumetry may improve prostate MRI analysis suggesting the TZ-sPSAD as a potential biomarker for the detection of PCa.

Printed on: 02/07/23

## Abstract Archives of the RSNA, 2022

T5B-SPGU-4

### Performance of Clear Cell Likelihood Scores (ccLS) in Evaluating Solid Renal Masses at Multi-parametric MRI: Single Center Cohort Study

Tuesday, Nov. 29 12:45PM - 1:15PM Room: Learning Center - GU DPS

#### Awards

**Trainee Research Prize - Resident**

#### Participants

Aisin Ibrahim, MD, (*Presenter*) Nothing to Disclose

#### PURPOSE

The purpose of this study is to evaluate the accuracy and interobserver agreement of clear cell Likelihood scores (ccLS) in diagnosing clear cell renal cell carcinoma (ccRCC).

#### METHODS AND MATERIALS

This retrospective single-center study evaluated consecutive patients with solid renal masses who underwent mpMRI followed by percutaneous biopsy and/or surgical excision between January 2010 and December 2020. Predominantly (>75%) cystic masses, masses with macroscopic fat and infiltrative masses were excluded. Two abdominal radiologists independently scored each renal mass according to the proposed ccLS algorithm. The diagnostic performance of ccLS categories for ccRCC was calculated using logistic regression modeling. Diagnostic accuracy for predicting ccRCC was calculated using 2x2 contingency tables. Interobserver agreement for ccLS was evaluated with Cohen's k statistic.

#### RESULTS

A total of 79 patients (mean age, 63 years  $\pm$  12 [SD], 50 men) with 81 renal masses were evaluated. The mean size was 36 mm  $\pm$  28 (range, 10-160). Of the renal masses included, 44% (36/81) were ccRCC. The area under the receiver operating characteristic curve for the pooled results was 0.87 (95% CI: 0.79-0.95). Using ccLS = 4 to diagnose ccRCC, the sensitivity, specificity, and positive predictive value were 93% (95% CI: 79, 99), 63% (95% CI: 48, 77), and 67% (95% CI: 58, 75), respectively. The negative predictive value of ccLS = 2 was 93% (95% CI: 64, 99). The pooled proportion of ccRCC by ccLS category 1 to 5 were 10%, 0%, 10%, 57%, and 84% respectively. Interobserver agreement was moderate (k=0.47).

#### CONCLUSION

In this study, ccLS had moderate interobserver agreement and resulted in 67% positive predictive value in diagnosing ccRCC and 93% negative predictive value in excluding ccRCC.

#### CLINICAL RELEVANCE/APPLICATION

The ccLS system could be a clinically efficient non-invasive tool in the assessment of solid renal masses in clinical practice. This could aid active surveillance and potentially limit the use of renal biopsy mainly for indeterminate renal lesions.

Printed on: 02/07/23

## Abstract Archives of the RSNA, 2022

T5B-SPHN

### Head and Neck Tuesday Poster Discussions - B

Tuesday, Nov. 29 12:45PM - 1:15PM Room: Learning Center - HN DPS

#### Sub-Events

#### T5B-SPHN-1 Magnetic Resonance Imaging of Giant Cell Arteritis with Ocular Involvement: A Systematic Review

##### Participants

Jae Song, MD, MS, Philadelphia, PA (*Presenter*) Nothing to Disclose

##### PURPOSE

A systematic review of the literature was performed to examine orbital MRI findings in patients diagnosed with giant cell arteritis (GCA) and presenting with ophthalmic symptoms.

##### METHODS AND MATERIALS

PubMed was searched from inception to August 14, 2020 with an updated search on January 16, 2022. The review was registered with PROSPERO (CRD42021254494). Publications were included if a patient diagnosed with biopsy-proven GCA with ocular symptoms underwent an orbital MRI. Data on demographics, clinical symptoms, ophthalmologic exam, MRI, and follow-up data were extracted. Counts are presented as percentages. Correlation between imaging findings and symptoms/outcomes are examined by Spearman's rank-order correlation.

##### RESULTS

From 1302 publications, 42 met inclusion criteria. Data were extracted from 44 patients (females=20; males=24; mean age 74.7 [60-86] years) presenting with ocular symptoms, imaged with an orbital MRI and diagnosed with GCA. A diagnosis of GCA was confirmed by temporal artery (81%) or extraocular muscle biopsy (2%). Vision loss (45%) and pain (23%) were the most common ophthalmologic symptoms reported. Treatment was delayed in 14 cases due to misdiagnosis. At presentation, visual symptoms were reported to be unilateral (44%), bilateral (35%), or sequential (8%). On orbital MRI, abnormal enhancement suggestive of ischemia or inflammation of the optic nerve sheath (51%), intraconal fat (35%), optic nerve/chiasm (9%), extraocular muscle (5%), and lacrimal gland (1%) were reported. Three cohort/cross-sectional studies used vessel wall MRI and reported ophthalmic artery vessel wall enhancement (44%). Among patients presenting with monocular visual symptoms (n=18), abnormal orbital MR findings ipsilateral to the symptomatic eye were concordant in 94% of cases and most frequently showed optic nerve sheath (59%) and/or intraconal fat (41%) enhancement. The asymptomatic contralateral eye also showed optic nerve sheath enhancement in 28% of the cases. Vision loss at initial presentation significantly correlated with optic nerve sheath (?=0.25, p=0.03) and optic nerve/chiasm (?=0.37, p=0.001) enhancement. Among 26 cases reporting outcomes, poor visual recovery at follow-up correlated with optic nerve/chiasm enhancement (?=0.44, p=0.002).

##### CONCLUSION

Nearly half of the patients diagnosed with GCA and ocular symptoms presented with vision loss, a symptom that significantly correlated with abnormal enhancement of the optic nerve and optic nerve sheath on MRI. Abnormal enhancement of orbital structures in both the symptomatic eye as well as the asymptomatic eye was reported in 28% of cases.

##### CLINICAL RELEVANCE/APPLICATION

Orbital MRI may have diagnostic and prognostic roles in patients with GCA and ocular symptoms.

#### T5B-SPHN-2 Skull-base Pseudotumor vs Nasopharyngeal Carcinoma: A Diagnostic Dilemma

##### Participants

Keivan Shifteh, MD, Brooklyn, NY (*Presenter*) Nothing to Disclose

##### PURPOSE

Nasopharyngeal Carcinoma (NPCa) is a primary mucosal malignancy arising in the nasopharynx, and is the most common nasopharyngeal malignancy in adults worldwide. However, multiple different pathologies can present in this region, and can be difficult to diagnose clinically. Many of them have similar appearances and can mimic NPCa on imaging, creating a diagnostic dilemma for radiologists. The purpose of this study is to describe common radiologic manifestations of NPCa, and to help establish a focused and clinically meaningful method of differentiating it from other pathologies in the Head Neck.

##### METHODS AND MATERIALS

Retrospective review of several cases of suspected nasopharyngeal carcinoma referred to radiology by ENT department.

##### RESULTS

A total of 18 cases of suspected nasopharyngeal carcinoma were referred to our department by ENT providers. These cases were comprised of 15 men and 3 women, with a male:female ratio of 5:1. Ages ranged from 19 to 87 years old. A total of 8/18 cases

(44%) were positive for NPCa, while 10/18 cases (56%) were negative. While all 18 of these cases demonstrated abnormal enhancement, only the biopsy-proven cases of NPCa involved the nasopharyngeal mucosa (8/8, 100%). Biopsy-negative cases were more likely to involve the prevertebral, carotid, parapharyngeal, and masticator spaces. Additionally, all 8 NPCa-positive cases demonstrated cervical adenopathy (100%), while only 2/10 negative cases did (20%). Biopsy-negative cases were more likely to result in osseous erosion/bone marrow signal abnormalities (90% vs 38% in positive-NPCa cases), more likely to demonstrate soft tissue necrosis (90% vs 0% in positive-NPCa cases), and more likely to demonstrate intracranial extension (50% vs 25% in positive-NPCa cases). Mastoid effusions were seen in 63% of positive-NPCa cases vs 90% in negative cases.

## CONCLUSION

s In our practice, ENT referrals for imaging of suspected Nasopharyngeal carcinoma are relatively common. Although tissue biopsy is the gold standard for diagnosis, radiologic assessment prior to biopsy can narrow down differential considerations and help guide referring physician's next steps. Our research demonstrates several key imaging features of biopsy-proven cases of NPCa that can help differentiate it from alternate diagnoses, such as NHL or IgG4-RD. Among them, involvement of the nasopharyngeal mucosa (ie. abnormal enhancement), positive cervical adenopathy, and a lack of soft tissue necrosis were the most relevant findings.

## CLINICAL RELEVANCE/APPLICATION

Tissue biopsy is the gold standard for the diagnosis of Nasopharyngeal Carcinoma. However, by focusing on specific imaging characteristics, a radiologist can help narrow differential considerations and guide the referring physician's next steps.

## T5B-SPHN-3 Prognostic Value of PET/CT and MR-base Baseline Radiomics Among Patients with Nasopharyngeal Carcinoma

### Participants

Roshini Kulanthaivelu, MBBS, FRCR, Toronto, ON (*Presenter*) Nothing to Disclose

## PURPOSE

Radiomics is an emerging imaging assessment technique, which has shown promise predicting survival among nasopharyngeal carcinoma (NPC) patients. Studies so far have focused on MR-based radiomic analysis. The aim of our study was to evaluate the prognostic value of clinical and radiomic parameters derived from both PET/CT and MR.

## METHODS AND MATERIALS

Retrospective evaluation of 124 NPC patients with PET/CT and radiotherapy planning MR (RP-MR). Primary tumors were segmented using dedicated software (LIFEx version 6.1) from PET, CT, contrast enhanced T1-weighted (T1-w), and T2-weighted (T2-w) MR sequences with 376 radiomic features extracted. Summary statistics described patient, disease and treatment characteristics. Kaplan Meier (KM) method estimated overall survival (OS) and progression free survival (PFS). Clinical factors selected based on univariate analysis and multivariate Cox model were subsequently constructed with radiomic features added.

## RESULTS

The final models comparing clinical, clinical + RP-MR, clinical + PET/CT and clinical + RP-MR + PET/CT for OS and PFS demonstrated that combined radiomics signatures were significantly associated with improved survival prognostication (AUC 0.62 vs 0.81 vs 0.75 vs 0.86 at 21 months for PFS and 0.56 vs 0.85 vs 0.79 vs 0.96 at 24 months for OS). Clinical + RP-MR features initially outperform clinical + PET/CT for both OS and PFS (<18 months), and later in the clinical course for PFS (>42 months).

## CONCLUSION

s Our study demonstrated that PET/CT-based radiomic features may improve survival prognostication among NPC patients when combined with baseline clinical and MR-based radiomic features.

## CLINICAL RELEVANCE/APPLICATION

Our study demonstrated the improved prognostic value of combined clinical + PET/CT + MR features compared with clinical, PET/CT or MR features individually for both OS and PFS (AUC 0.96 at 24 months in OS and 0.86 at 21 months in PFS). This could potentially have implications on future imaging. Since PET and MR radiomic features appear to have prognostic value, combined PET/MR may have a clinical role in staging, prognostication and potentially future surveillance of patients with NPC.

Printed on: 02/07/23

## Abstract Archives of the RSNA, 2022

T5B-SPHN-1

### Magnetic Resonance Imaging of Giant Cell Arteritis with Ocular Involvement: A Systematic Review

Tuesday, Nov. 29 12:45PM - 1:15PM Room: Learning Center - HN DPS

#### Participants

Jae Song, MD, MS, Philadelphia, PA (*Presenter*) Nothing to Disclose

#### PURPOSE

A systematic review of the literature was performed to examine orbital MRI findings in patients diagnosed with giant cell arteritis (GCA) and presenting with ophthalmic symptoms.

#### METHODS AND MATERIALS

PubMed was searched from inception to August 14, 2020 with an updated search on January 16, 2022. The review was registered with PROSPERO (CRD42021254494). Publications were included if a patient diagnosed with biopsy-proven GCA with ocular symptoms underwent an orbital MRI. Data on demographics, clinical symptoms, ophthalmologic exam, MRI, and follow-up data were extracted. Counts are presented as percentages. Correlation between imaging findings and symptoms/outcomes are examined by Spearman's rank-order correlation.

#### RESULTS

From 1302 publications, 42 met inclusion criteria. Data were extracted from 44 patients (females=20; males=24; mean age 74.7 [60-86] years) presenting with ocular symptoms, imaged with an orbital MRI and diagnosed with GCA. A diagnosis of GCA was confirmed by temporal artery (81%) or extraocular muscle biopsy (2%). Vision loss (45%) and pain (23%) were the most common ophthalmologic symptoms reported. Treatment was delayed in 14 cases due to misdiagnosis. At presentation, visual symptoms were reported to be unilateral (44%), bilateral (35%), or sequential (8%). On orbital MRI, abnormal enhancement suggestive of ischemia or inflammation of the optic nerve sheath (51%), intraconal fat (35%), optic nerve/chiasm (9%), extraocular muscle (5%), and lacrimal gland (1%) were reported. Three cohort/cross-sectional studies used vessel wall MRI and reported ophthalmic artery vessel wall enhancement (44%). Among patients presenting with monocular visual symptoms (n=18), abnormal orbital MR findings ipsilateral to the symptomatic eye were concordant in 94% of cases and most frequently showed optic nerve sheath (59%) and/or intraconal fat (41%) enhancement. The asymptomatic contralateral eye also showed optic nerve sheath enhancement in 28% of the cases. Vision loss at initial presentation significantly correlated with optic nerve sheath ( $r=0.25$ ,  $p=0.03$ ) and optic nerve/chiasm ( $r=0.37$ ,  $p=0.001$ ) enhancement. Among 26 cases reporting outcomes, poor visual recovery at follow-up correlated with optic nerve/chiasm enhancement ( $r=0.44$ ,  $p=0.002$ ).

#### CONCLUSION

Nearly half of the patients diagnosed with GCA and ocular symptoms presented with vision loss, a symptom that significantly correlated with abnormal enhancement of the optic nerve and optic nerve sheath on MRI. Abnormal enhancement of orbital structures in both the symptomatic eye as well as the asymptomatic eye was reported in 28% of cases.

#### CLINICAL RELEVANCE/APPLICATION

Orbital MRI may have diagnostic and prognostic roles in patients with GCA and ocular symptoms.

Printed on: 02/07/23

## Abstract Archives of the RSNA, 2022

T5B-SPHN-2

### Skull-base Pseudotumor vs Nasopharyngeal Carcinoma: A Diagnostic Dilemma

Tuesday, Nov. 29 12:45PM - 1:15PM Room: Learning Center - HN DPS

#### Participants

Keivan Shifteh, MD, Brooklyn, NY (*Presenter*) Nothing to Disclose

#### PURPOSE

Nasopharyngeal Carcinoma (NPCa) is a primary mucosal malignancy arising in the nasopharynx, and is the most common nasopharyngeal malignancy in adults worldwide. However, multiple different pathologies can present in this region, and can be difficult to diagnose clinically. Many of them have similar appearances and can mimic NPCa on imaging, creating a diagnostic dilemma for radiologists. The purpose of this study is to describe common radiologic manifestations of NPCa, and to help establish a focused and clinically meaningful method of differentiating it from other pathologies in the Head Neck.

#### METHODS AND MATERIALS

Retrospective review of several cases of suspected nasopharyngeal carcinoma referred to radiology by ENT department.

#### RESULTS

A total of 18 cases of suspected nasopharyngeal carcinoma were referred to our department by ENT providers. These cases were comprised of 15 men and 3 women, with a male:female ratio of 5:1. Ages ranged from 19 to 87 years old. A total of 8/18 cases (44%) were positive for NPCa, while 10/18 cases (56%) were negative. While all 18 of these cases demonstrated abnormal enhancement, only the biopsy-proven cases of NPCa involved the nasopharyngeal mucosa (8/8, 100%). Biopsy-negative cases were more likely to involve the prevertebral, carotid, parapharyngeal, and masticator spaces. Additionally, all 8 NPCa-positive cases demonstrated cervical adenopathy (100%), while only 2/10 negative cases did (20%). Biopsy-negative cases were more likely to result in osseous erosion/bone marrow signal abnormalities (90% vs 38% in positive-NPCa cases), more likely to demonstrate soft tissue necrosis (90% vs 0% in positive-NPCa cases), and more likely to demonstrate intracranial extension (50% vs 25% in positive-NPCa cases). Mastoid effusions were seen in 63% of positive-NPCa cases vs 90% in negative cases.

#### CONCLUSION

s In our practice, ENT referrals for imaging of suspected Nasopharyngeal carcinoma are relatively common. Although tissue biopsy is the gold standard for diagnosis, radiologic assessment prior to biopsy can narrow down differential considerations and help guide referring physician's next steps. Our research demonstrates several key imaging features of biopsy-proven cases of NPCa that can help differentiate it from alternate diagnoses, such as NHL or IgG4-RD. Among them, involvement of the nasopharyngeal mucosa (ie. abnormal enhancement), positive cervical adenopathy, and a lack of soft tissue necrosis were the most relevant findings.

#### CLINICAL RELEVANCE/APPLICATION

Tissue biopsy is the gold standard for the diagnosis of Nasopharyngeal Carcinoma. However, by focusing on specific imaging characteristics, a radiologist can help narrow differential considerations and guide the referring physician's next steps.

Printed on: 02/07/23

## Abstract Archives of the RSNA, 2022

T5B-SPHN-3

### Prognostic Value of PET/CT and MR-base Baseline Radiomics Among Patients with Nasopharyngeal Carcinoma

Tuesday, Nov. 29 12:45PM - 1:15PM Room: Learning Center - HN DPS

#### Participants

Roshini Kulanthaivelu, MBBS, FRCR, Toronto, ON (*Presenter*) Nothing to Disclose

#### PURPOSE

Radiomics is an emerging imaging assessment technique, which has shown promise predicting survival among nasopharyngeal carcinoma (NPC) patients. Studies so far have focused on MR-based radiomic analysis. The aim of our study was to evaluate the prognostic value of clinical and radiomic parameters derived from both PET/CT and MR.

#### METHODS AND MATERIALS

Retrospective evaluation of 124 NPC patients with PET/CT and radiotherapy planning MR (RP-MR). Primary tumors were segmented using dedicated software (LIFEx version 6.1) from PET, CT, contrast enhanced T1-weighted (T1-w), and T2-weighted (T2-w) MR sequences with 376 radiomic features extracted. Summary statistics described patient, disease and treatment characteristics. Kaplan Meier (KM) method estimated overall survival (OS) and progression free survival (PFS). Clinical factors selected based on univariate analysis and multivariate Cox model were subsequently constructed with radiomic features added.

#### RESULTS

The final models comparing clinical, clinical + RP-MR, clinical + PET/CT and clinical + RP-MR + PET/CT for OS and PFS demonstrated that combined radiomics signatures were significantly associated with improved survival prognostication (AUC 0.62 vs 0.81 vs 0.75 vs 0.86 at 21 months for PFS and 0.56 vs 0.85 vs 0.79 vs 0.96 at 24 months for OS). Clinical + RP-MR features initially outperform clinical + PET/CT for both OS and PFS (<18 months), and later in the clinical course for PFS (>42 months).

#### CONCLUSION

Our study demonstrated that PET/CT-based radiomic features may improve survival prognostication among NPC patients when combined with baseline clinical and MR-based radiomic features.

#### CLINICAL RELEVANCE/APPLICATION

Our study demonstrated the improved prognostic value of combined clinical + PET/CT + MR features compared with clinical, PET/CT or MR features individually for both OS and PFS (AUC 0.96 at 24 months in OS and 0.86 at 21 months in PFS). This could potentially have implications on future imaging. Since PET and MR radiomic features appear to have prognostic value, combined PET/MR may have a clinical role in staging, prognostication and potentially future surveillance of patients with NPC.

Printed on: 02/07/23

## Abstract Archives of the RSNA, 2022

T5B-SPIN

### Informatics Tuesday Poster Discussions - B

Tuesday, Nov. 29 12:45PM - 1:15PM Room: Learning Center - IN DPS

#### Sub-Events

#### T5B-SPIN-1 Artificial Intelligence in Detection of Submassive and Massive Pulmonary Embolism

##### Participants

Alexander Anavim, MD, (*Presenter*) Nothing to Disclose

##### PURPOSE

Pulmonary embolism (PE) is a medical emergency representing the third most common cause of death worldwide, responsible for 100,000 deaths annually within the United States alone. PE has high mortality rates within the first few hours of presentation, thus, accurate and timely diagnosis is essential for initiating potentially lifesaving interventions. Management of PE has dramatically improved with recent advances in device technology, allowing improved percutaneous thrombectomy early on in management of select submassive and massive pulmonary emboli. Artificial Intelligence (AI) powered algorithms are becoming more integrated within diagnostic radiology. The use of AI across multiple modalities and specialties within radiology is gradually changing clinical practice by enhancing accuracy and efficiency, interrater reliability, and overall workflow for more timely recommendations. AI algorithms have been shown to have a high sensitivity in detection of PE on CT pulmonary angiograms. Algorithms have also been developed to estimate right heart strain associated with PE. The purpose of our study was to determine accuracy of AI in detecting right heart strain in patients with PE.

##### METHODS AND MATERIALS

This is a single center, retrospective study. CT pulmonary angiograms (CTPA) of patients presenting to an urban center emergency department between July 25, 2021 and October 16, 2021, were reviewed. A total of 74 patients with acute PE shown in CTPA were included. An AI algorithm was used to calculate right to left ventricular ratio. The calculated results of right ventricular strain by AI algorithm, the radiology reports, and echocardiogram results were collected. A right ventricle to left ventricle ratio of 1.2 was set as a trigger for the AI algorithm to detect right heart strain.

##### RESULTS

The result of right ventricular strain calculated by AI algorithm and radiology reports was concordant in 64 cases (20 positive, 44 negative cases) and discordant in 10 cases (6 positive and 4 negative cases by AI). More than half of the patients (38/74 patients) had subsequent echocardiograms. Compared to the results of echocardiogram, the AI algorithm had a higher sensitivity (80% vs 73%) than the radiology reports with equivalent specificity (74%).

##### CONCLUSION

AI algorithms are non-inferior to radiology reports in detecting right heart strain in patients with PE.

##### CLINICAL RELEVANCE/APPLICATION

Machine learning has the potential to play a key role in clinical management of PE and expedite thrombectomy and other treatments of submassive and massive PE.

#### T5B-SPIN-2 Self-Supervised Learning with MoCo v2 for Publicly Accessible Chest X-ray Pretrained Model and Its Evaluation

##### Participants

Kyungjin Cho, MSc, BS, Seoul, Korea, Republic Of (*Presenter*) Nothing to Disclose

##### PURPOSE

To propose the self-supervised learning with contrastive learning for publicly accessible pretrained model (SSAP) of chest X-rays (CXRs), which has been trained using a considerable amount of CXR images, and evaluate its performances.

##### METHODS AND MATERIALS

For training an upstream method, 4.8M CXR images were obtained retrospectively from a tertiary hospital in South Korea. We trained the self-supervised contrastive pretraining method with unlabeled images using MoCo v2 to learn visual representations of CXR. The upstream method maximizes the similarity between two views of the same CXR images and minimizes the similarity between different CXR images. In downstream tasks, CXR images with 6 class diseases (normal, nodule, consolidation, pneumothorax, interstitial opacity, and pleural effusion) which were confirmed with near computed tomography scans within one month were collected from the same hospital but independently of the upstream dataset for the multi-class classification. Second, we used the CheXpert dataset for the external validation test. Third, adult posterior-anterior CXR pairs of rib-preserved and rib-suppressed images, generated using the Bone Suppression™ software (Samsung Electronics Co., Ltd.) for the bone suppression were collected. Finally, we evaluated SSAP and ImageNet pretrained models with three downstream tasks.

## RESULTS

In classification of 6 class diseases, accuracies of pretrained ImageNet and SSAP models, were 0.345, and 0.631, respectively. In external validation with CheXpert dataset, mean AUCs of pretrained ImageNet and SSAP models with 1%, 10%, 50%, and full datasets were 0.616, 0.700, 0.774, 0.795, and 0.638, 0.746, 0.790, 0.807, respectively. In bone suppression, PSNR, SSIM, RMSE of pretrained ImageNet and SSAP models were 34.99, 0.976, 4.410, and 37.77, 0.977, 3.301, respectively.

## CONCLUSION

The SSAP model showed the better performance and decent transferability in multiple datasets and data settings in multi-class and multi-label classification. SSAP can also be used for perceptual loss in image-to-image translation. This public model can help researchers overcome data imbalance, data shortage, and inaccessibility of medical image datasets.

## CLINICAL RELEVANCE/APPLICATION

The SSAP model can help researchers develop a CXR related model with better performance and robustness to overcome data imbalance, data shortage, and inaccessibility of medical image datasets.

## T5B-SPIN-3 Learning 2D Image-Level Annotations from 3D Exam-Level Annotations

### Participants

Ian Pan, MD, Brookline, MA (*Presenter*) Consultant, MD.ai, Inc; Consultant, Centaur Labs Inc; Consultant, Diagnosticos da America SA; Consultant, CoRead AI

### PURPOSE

Develop a deep learning-based approach to infer 2D image-level annotations from 3D exam-level annotations to reduce the annotation burden of developing image-level classification models.

### METHODS AND MATERIALS

21,744 head CT scans (18,938 patients) from the RSNA Intracranial Hemorrhage (ICH) Detection Challenge and 7,279 CT pulmonary angiograms from the RSNA-STR Pulmonary Embolism (PE) Detection Challenge were used for this study. Datasets were divided into training/validation (80%) and test (20%) sets, by patient (if available) or exam. 3D CNN models based on the X3D architecture were trained, for ICH, to predict 6 ICH classes (epidural, subdural, subarachnoid, intraparenchymal, intraventricular, any), and, for PE, the binary class of PE (vs. no PE). The final linear classification layer of the X3D model was removed after training. Inference was then performed on the whole dataset, producing a 3D class activation map for each exam and class. The 3D map was converted to a 1D sequence, with dimension corresponding to the z-axis, by taking the max of each 2D axial map. The sequence was then resampled to the number of images in the original exam and rescaled to a max of 1. Image-level pseudolabels were generated by applying a threshold of 0.2 to the sequence values. 2D CNNs based on the EfficientNet-B4 architecture were then trained on the pseudolabels and original image-level ground truth ("gold standard") to predict the above labels at the image level. A "naive" approach, where all images in an exam were assigned the exam-level label, served as a baseline. Performance was compared using the area under the receiver operating characteristic curve (AUC) and classification (multi- and single-label binary cross-entropy) loss.

## RESULTS

All values are calculated at the image level. For ICH, the naive approach achieved mean AUC 0.939, ranging from 0.911 for epidural hematoma to 0.962 for intraventricular hemorrhage, and a classification loss of 0.270. The pseudolabel approach achieved mean AUC 0.968, ranging from 0.949 to 0.989, and classification loss 0.075. The gold standard approach achieved mean AUC 0.977, ranging from 0.953 to 0.994, and a loss of 0.064. For PE, the naive approach achieved AUC 0.681 and loss 0.793, compared with AUC 0.895, loss 0.143 and AUC 0.929, loss 0.112 for the pseudolabel and gold standard approaches, respectively. All pairwise differences between approaches were statistically significant ( $p < 0.0001$ ).

## CONCLUSION

3D CNN models can generate 2D image-level labels suitable for training accurate 2D classification models.

## CLINICAL RELEVANCE/APPLICATION

Image-level pseudolabeling with 3D CNNs can considerably reduce the annotation effort required to develop deep learning models with 2D granularity.

## T5B-SPIN-4 Multi-head Deep Learning Model for The Detection of Prostate Cancer Lesions in Bi-parametric MRI

### Participants

Kourosh Jafari-Khouzani, Cambridge, MA (*Presenter*) Employee, IBM Corporation

### PURPOSE

Prostate cancer is the second leading cause of cancer death in men in the United States. Bi-parametric MRI (bp-MRI), comprising T2-weighted (T2W) and diffusion-weighted imaging (DWI), plays an essential role in the assessment of prostate cancer. Prostate Imaging Reporting and Data System (PI-RADS) serves as a standardized scoring system to assess the risk of clinically significant prostate cancer using bp-MRI, but it suffers from high intra- and inter-reader variability. We have proposed a multi-head deep learning model to automatically detect clinically significant cancers as determined by PI-RADS guidelines.

### METHODS AND MATERIALS

We collected a dataset of bp-MRI from 9 different providers and various scanners and imaging protocols in multiple sites in the United States, Europe, South America, and Asia. We selected a subset of 3076 studies for this project. A group of radiologists outlined and scored lesions in T2W and DWI volumes. In addition, they outlined the prostate gland and zones including the transitional zone (TZ), peripheral zone (PZ), central zone (CZ), and Anterior Fibromuscular Stroma (AFMS). We only included lesion masks that had PI-RADS scores 3, 4, and 5 in the training. Similarly, we annotated 341 studies from the publicly available dataset ProstateX for testing. A multi-head model was trained to simultaneously predict segmentation masks for lesions outlined in the T2W image and DWI, prostate, and zones, given the T2W image, apparent diffusion coefficient (ADC) map, and high b-value DWI. The model leveraged information from the prostate and zones by predicting their mask. In addition, we added convolutional LSTM blocks

to leverage information from the neighboring slices. We evaluated the network by 5-fold cross-validation and separately by the held-out test set. To evaluate performance, we report sensitivity and 3D Dice coefficients for the validation set as well as the test set.

## RESULTS

For the validation and test sets, we obtained average 3D Dice coefficients of 0.35 and 0.42 for lesions outlined in T2W, 0.41 and 0.44 for lesions outlined in DWI, 0.94 and 0.94 for prostate, 0.88 and 0.86 for TZ, 0.76 and 0.70 for PZ, 0.51 and 0.45 for CZ, and 0.57 and 0.44 for AFMS, respectively. The average sensitivity at one false positive per case was 91%.

## CONCLUSION

The proposed model simultaneously detects clinically significant lesions in T2W and DWI volumes and segments the prostate gland and its zones. This is an important step toward fully automating prostate cancer assessment and subsequently reducing its subjectivity.

## CLINICAL RELEVANCE/APPLICATION

PI-RADS assessment is subjective and time-consuming. Automatic detection of prostate cancer lesions is an important step toward making PI-RADS classification fully automated and more objective.

## T5B-SPIN-5 Fully Automated, Fast, and Accurate Intracranial Arterial Narrowing Detection: A Deep Learning Approach

Participants

Maxime Chagnon, BEng, MSc, (*Presenter*) Nothing to Disclose

## PURPOSE

Intracranial narrowing of the artery (INA) is a well-established cause of stroke worldwide. Radiologists routinely use computed tomography angiography (CTA) to manually analyze INA, yet this process is tedious and prone to inter-observer variability. We here present a novel approach using artificial intelligence (AI) and convolutional neural network (CNN) that rapidly locates INA on CTA without the need of user intervention. We believe that it was never done on CTA images before.

## METHODS AND MATERIALS

192 consecutive patients (mean age  $58 \pm 16$ , 111 females) with CTA ( $0.3 \times 0.3 \times 0.5$ mm) were retrospectively analyzed for INA by a neuroradiologist (author JC) and a resident (author SG). 96 were identified as having at least one INA (1-18 per patient, average  $4 \pm 4$ ), and 96 had no INA. To reduce computation complexity and to avoid training on unnecessary information, each image was divided into coarse patches ( $14.4 \times 14.4 \times 24$ mm) and each patch was labelled as INA positive or negative. We used 158 CTA to obtain a subset of patches with data augmentation (total patches = 3700, 50% positive) used to train a model (3d SE-RESNET). We used 12 new CTA images (90 patches, 50% positive) for testing and 16 new CTA (76 patches, 50% positive) for validation.

## RESULTS

Across all validation set patches, the detection rate was 83%, the false negative rate was 16% and precision was 92%. Our model correctly found 32 of all 38 INA. In general, our model underestimated the true number of INA sites by  $13\% \pm 17\%$ , but the average detection score was still relatively high ( $85\% \pm 17\%$ ).

## CONCLUSION

We successfully developed and validated an AI model capable of quickly ( $\sim 2$  min compute time per CTA) and accurately locating brain patches with INA. We believe this method may be helpful for providing a quick, but coarse analysis of INA topography without the need of user intervention. We are currently assessing the impact this method has in clinical evaluations.

## CLINICAL RELEVANCE/APPLICATION

Preliminary results indicate that the model presented can accurately and automatically locate INA on CTA. It is expected to reduce the burden of manual INA detection and improve reliability.

## T5B-SPIN-6 Transformer-Based Semi-Supervised Adversarial Learning for Liver Tumor Segmentation in Contrast-Enhanced MRI Images

Participants

Han Wen, Chengdu, China (*Presenter*) Nothing to Disclose

## PURPOSE

This study aims to construct a semi-supervised segmentation model for contrast-enhanced MRI of liver tumors using a deep learning approach on a small amount of labeled data and a large amount of unlabeled data to assist physicians in annotating liver tumors and reduce physician workload.

## METHODS AND MATERIALS

We retrospectively collected contrast-enhanced MRI of 126 patients with liver tumors. We randomly selected 20 MRI from the dataset as the test set. Our image preprocessing procedure was as follows. All MRI were resampled to  $1 \times 1 \times 1$ mm. The dataset was normalized by subtracting the mean divided by the standard deviation. Each MRI was centrally cropped and the size of the cropped patch was  $256 \times 256 \times 32$ mm. As shown in Figure 1, our semi-supervised segmentation model consists of a segmentation sub-network and an evaluation sub-network. The segmentation sub-network is a variant structure of Unet, where the encoder is a transformer and the decoder is a CNN, and features from multiple resolutions of the encoder are combined with the decoder to generate segmentation masks. The evaluation sub-network is a 5-layer CNN, each convolutional layer contains convolution, leaky\_relu and dropout. During the training process, the segmentation sub-network generates segmentation masks for unlabeled images and labeled images, and the evaluation sub-network learns by distinguishing between the two. The loss function of our semi-supervised segmentation model is  $L=L_{seg}+L_{adv}$ , where  $L_{seg}$  is used for labeled data, which consists of cross-entropy loss, dice loss and signed distance map loss.  $L_{adv}$  is used for both labeled data and unlabeled data, it is cross entropy loss.

## RESULTS

As shown in Table 1, on the 40% labeled data set, our method achieves the best performance compared to other methods on Dice, Jaccard, ASD, and 95HD, reaching 74.09%,60.36%, 3.26,15.92, respectively. Even the segmentation results of 100% labeled data are almost the same. As can be seen in Figure 2, the segmentation results of our method are significantly better than other models and comparable to the manual descriptions of physicians.

#### **CONCLUSION**

s In this study, we present a Transformer-based semi-supervised segmentation model for contrast-enhanced MRI of liver tumors. The model was trained using an adversarial learning approach and achieved very excellent results on a small amount of labeled data and a large amount of unlabeled data, and was comparable to manual annotation by physicians.

#### **CLINICAL RELEVANCE/APPLICATION**

For medical images, it is an expensive and time-consuming process for clinical experts to perform pixel-by-pixel annotation of a large number of segmentation masks. If our method is used it can reduce the physician's annotation time significantly.

Printed on: 02/07/23



## Abstract Archives of the RSNA, 2022

T5B-SPIN-1

### Artificial Intelligence in Detection of Submassive and Massive Pulmonary Embolism

Tuesday, Nov. 29 12:45PM - 1:15PM Room: Learning Center - IN DPS

#### Participants

Alexander Anavim, MD, (*Presenter*) Nothing to Disclose

#### PURPOSE

Pulmonary embolism (PE) is a medical emergency representing the third most common cause of death worldwide, responsible for 100,000 deaths annually within the United States alone. PE has high mortality rates within the first few hours of presentation, thus, accurate and timely diagnosis is essential for initiating potentially lifesaving interventions. Management of PE has dramatically improved with recent advances in device technology, allowing improved percutaneous thrombectomy early on in management of select submassive and massive pulmonary emboli. Artificial Intelligence (AI) powered algorithms are becoming more integrated within diagnostic radiology. The use of AI across multiple modalities and specialties within radiology is gradually changing clinical practice by enhancing accuracy and efficiency, interrater reliability, and overall workflow for more timely recommendations. AI algorithms have been shown to have a high sensitivity in detection of PE on CT pulmonary angiograms. Algorithms have also been developed to estimate right heart strain associated with PE. The purpose of our study was to determine accuracy of AI in detecting right heart strain in patients with PE.

#### METHODS AND MATERIALS

This is a single center, retrospective study. CT pulmonary angiograms (CTPA) of patients presenting to an urban center emergency department between July 25, 2021 and October 16, 2021, were reviewed. A total of 74 patients with acute PE shown in CTPA were included. An AI algorithm was used to calculate right to left ventricular ratio. The calculated results of right ventricular strain by AI algorithm, the radiology reports, and echocardiogram results were collected. A right ventricle to left ventricle ratio of 1.2 was set as a trigger for the AI algorithm to detect right heart strain.

#### RESULTS

The result of right ventricular strain calculated by AI algorithm and radiology reports was concordant in 64 cases (20 positive, 44 negative cases) and discordant in 10 cases (6 positive and 4 negative cases by AI). More than half of the patients (38/74 patients) had subsequent echocardiograms. Compared to the results of echocardiogram, the AI algorithm had a higher sensitivity (80% vs 73%) than the radiology reports with equivalent specificity (74%).

#### CONCLUSION

s AI algorithms are non-inferior to radiology reports in detecting right heart strain in patients with PE.

#### CLINICAL RELEVANCE/APPLICATION

Machine learning has the potential to play a key role in clinical management of PE and expedite thrombectomy and other treatments of submassive and massive PE.

Printed on: 02/07/23

## Abstract Archives of the RSNA, 2022

T5B-SPIN-2

### Self-Supervised Learning with MoCo v2 for Publicly Accessible Chest X-ray Pretrained Model and Its Evaluation

Tuesday, Nov. 29 12:45PM - 1:15PM Room: Learning Center - IN DPS

#### Participants

Kyungjin Cho, MSc, BS, Seoul, Korea, Republic Of (*Presenter*) Nothing to Disclose

#### PURPOSE

To propose the self-supervised learning with contrastive learning for publicly accessible pretrained model (SSAP) of chest X-rays (CXRs), which has been trained using a considerable amount of CXR images, and evaluate its performances.

#### METHODS AND MATERIALS

For training an upstream method, 4.8M CXR images were obtained retrospectively from a tertiary hospital in South Korea. We trained the self-supervised contrastive pretraining method with unlabeled images using MoCo v2 to learn visual representations of CXR. The upstream method maximizes the similarity between two views of the same CXR images and minimizes the similarity between different CXR images. In downstream tasks, CXR images with 6 class diseases (normal, nodule, consolidation, pneumothorax, interstitial opacity, and pleural effusion) which were confirmed with near computed tomography scans within one month were collected from the same hospital but independently of the upstream dataset for the multi-class classification. Second, we used the CheXpert dataset for the external validation test. Third, adult posterior-anterior CXR pairs of rib-preserved and rib-suppressed images, generated using the Bone Suppression™ software (Samsung Electronics Co., Ltd.) for the bone suppression were collected. Finally, we evaluated SSAP and ImageNet pretrained models with three downstream tasks.

#### RESULTS

In classification of 6 class diseases, accuracies of pretrained ImageNet and SSAP models, were 0.345, and 0.631, respectively. In external validation with CheXpert dataset, mean AUCs of pretrained ImageNet and SSAP models with 1%, 10%, 50%, and full datasets were 0.616, 0.700, 0.774, 0.795, and 0.638, 0.746, 0.790, 0.807, respectively. In bone suppression, PSNR, SSIM, RMSE of pretrained ImageNet and SSAP models were 34.99, 0.976, 4.410, and 37.77, 0.977, 3.301, respectively.

#### CONCLUSION

s The SSAP model showed the better performance and decent transferability in multiple datasets and data settings in multi-class and multi-label classification. SSAP can also be used for perceptual loss in image-to-image translation. This public model can help researchers overcome data imbalance, data shortage, and inaccessibility of medical image datasets.

#### CLINICAL RELEVANCE/APPLICATION

The SSAP model can help researchers develop a CXR related model with better performance and robustness to overcome data imbalance, data shortage, and inaccessibility of medical image datasets.

Printed on: 02/07/23



## Abstract Archives of the RSNA, 2022

T5B-SPIN-3

### Learning 2D Image-Level Annotations from 3D Exam-Level Annotations

Tuesday, Nov. 29 12:45PM - 1:15PM Room: Learning Center - IN DPS

#### Participants

Ian Pan, MD, Brookline, MA (*Presenter*) Consultant, MD.ai, Inc; Consultant, Centaur Labs Inc; Consultant, Diagnosticos da America SA; Consultant, CoRead AI

#### PURPOSE

Develop a deep learning-based approach to infer 2D image-level annotations from 3D exam-level annotations to reduce the annotation burden of developing image-level classification models.

#### METHODS AND MATERIALS

21,744 head CT scans (18,938 patients) from the RSNA Intracranial Hemorrhage (ICH) Detection Challenge and 7,279 CT pulmonary angiograms from the RSNA-STR Pulmonary Embolism (PE) Detection Challenge were used for this study. Datasets were divided into training/validation (80%) and test (20%) sets, by patient (if available) or exam. 3D CNN models based on the X3D architecture were trained, for ICH, to predict 6 ICH classes (epidural, subdural, subarachnoid, intraparenchymal, intraventricular, any), and, for PE, the binary class of PE (vs. no PE). The final linear classification layer of the X3D model was removed after training. Inference was then performed on the whole dataset, producing a 3D class activation map for each exam and class. The 3D map was converted to a 1D sequence, with dimension corresponding to the z-axis, by taking the max of each 2D axial map. The sequence was then resampled to the number of images in the original exam and rescaled to a max of 1. Image-level pseudolabels were generated by applying a threshold of 0.2 to the sequence values. 2D CNNs based on the EfficientNet-B4 architecture were then trained on the pseudolabels and original image-level ground truth ("gold standard") to predict the above labels at the image level. A "naive" approach, where all images in an exam were assigned the exam-level label, served as a baseline. Performance was compared using the area under the receiver operating characteristic curve (AUC) and classification (multi- and single-label binary cross-entropy) loss.

#### RESULTS

All values are calculated at the image level. For ICH, the naive approach achieved mean AUC 0.939, ranging from 0.911 for epidural hematoma to 0.962 for intraventricular hemorrhage, and a classification loss of 0.270. The pseudolabel approach achieved mean AUC 0.968, ranging from 0.949 to 0.989, and classification loss 0.075. The gold standard approach achieved mean AUC 0.977, ranging from 0.953 to 0.994, and a loss of 0.064. For PE, the naive approach achieved AUC 0.681 and loss 0.793, compared with AUC 0.895, loss 0.143 and AUC 0.929, loss 0.112 for the pseudolabel and gold standard approaches, respectively. All pairwise differences between approaches were statistically significant ( $p < 0.0001$ ).

#### CONCLUSION

3D CNN models can generate 2D image-level labels suitable for training accurate 2D classification models.

#### CLINICAL RELEVANCE/APPLICATION

Image-level pseudolabeling with 3D CNNs can considerably reduce the annotation effort required to develop deep learning models with 2D granularity.

Printed on: 02/07/23



## Abstract Archives of the RSNA, 2022

T5B-SPIN-4

### Multi-head Deep Learning Model for The Detection of Prostate Cancer Lesions in Bi-parametric MRI

Tuesday, Nov. 29 12:45PM - 1:15PM Room: Learning Center - IN DPS

#### Participants

Kourosh Jafari-Khouzani, Cambridge, MA (*Presenter*) Employee, IBM Corporation

#### PURPOSE

Prostate cancer is the second leading cause of cancer death in men in the United States. Bi-parametric MRI (bp-MRI), comprising T2-weighted (T2W) and diffusion-weighted imaging (DWI), plays an essential role in the assessment of prostate cancer. Prostate Imaging Reporting and Data System (PI-RADS) serves as a standardized scoring system to assess the risk of clinically significant prostate cancer using bp-MRI, but it suffers from high intra- and inter-reader variability. We have proposed a multi-head deep learning model to automatically detect clinically significant cancers as determined by PI-RADS guidelines.

#### METHODS AND MATERIALS

We collected a dataset of bp-MRI from 9 different providers and various scanners and imaging protocols in multiple sites in the United States, Europe, South America, and Asia. We selected a subset of 3076 studies for this project. A group of radiologists outlined and scored lesions in T2W and DWI volumes. In addition, they outlined the prostate gland and zones including the transitional zone (TZ), peripheral zone (PZ), central zone (CZ), and Anterior Fibromuscular Stroma (AFMS). We only included lesion masks that had PI-RADS scores 3, 4, and 5 in the training. Similarly, we annotated 341 studies from the publicly available dataset ProstateX for testing. A multi-head model was trained to simultaneously predict segmentation masks for lesions outlined in the T2W image and DWI, prostate, and zones, given the T2W image, apparent diffusion coefficient (ADC) map, and high b-value DWI. The model leveraged information from the prostate and zones by predicting their mask. In addition, we added convolutional LSTM blocks to leverage information from the neighboring slices. We evaluated the network by 5-fold cross-validation and separately by the held-out test set. To evaluate performance, we report sensitivity and 3D Dice coefficients for the validation set as well as the test set.

#### RESULTS

For the validation and test sets, we obtained average 3D Dice coefficients of 0.35 and 0.42 for lesions outlined in T2W, 0.41 and 0.44 for lesions outlined in DWI, 0.94 and 0.94 for prostate, 0.88 and 0.86 for TZ, 0.76 and 0.70 for PZ, 0.51 and 0.45 for CZ, and 0.57 and 0.44 for AFMS, respectively. The average sensitivity at one false positive per case was 91%.

#### CONCLUSION

The proposed model simultaneously detects clinically significant lesions in T2W and DWI volumes and segments the prostate gland and its zones. This is an important step toward fully automating prostate cancer assessment and subsequently reducing its subjectivity.

#### CLINICAL RELEVANCE/APPLICATION

PI-RADS assessment is subjective and time-consuming. Automatic detection of prostate cancer lesions is an important step toward making PI-RADS classification fully automated and more objective.

Printed on: 02/07/23

## Abstract Archives of the RSNA, 2022

T5B-SPIN-5

### Fully Automated, Fast, and Accurate Intracranial Arterial Narrowing Detection: A Deep Learning Approach

Tuesday, Nov. 29 12:45PM - 1:15PM Room: Learning Center - IN DPS

#### Participants

Maxime Chagnon, BEng, MSc, (*Presenter*) Nothing to Disclose

#### PURPOSE

Intracranial narrowing of the artery (INA) is a well-established cause of stroke worldwide. Radiologists routinely use computed tomography angiography (CTA) to manually analyze INA, yet this process is tedious and prone to inter-observer variability. We here present a novel approach using artificial intelligence (AI) and convolutional neural network (CNN) that rapidly locates INA on CTA without the need of user intervention. We believe that it was never done on CTA images before.

#### METHODS AND MATERIALS

192 consecutive patients (mean age  $58 \pm 16$ , 111 females) with CTA ( $0.3 \times 0.3 \times 0.5$ mm) were retrospectively analyzed for INA by a neuroradiologist (author JC) and a resident (author SG). 96 were identified as having at least one INA (1-18 per patient, average  $4 \pm 4$ ), and 96 had no INA. To reduce computation complexity and to avoid training on unnecessary information, each image was divided into coarse patches ( $14.4 \times 14.4 \times 24$ mm) and each patch was labelled as INA positive or negative. We used 158 CTA to obtain a subset of patches with data augmentation (total patches = 3700, 50% positive) used to train a model (3d SE-RESNET). We used 12 new CTA images (90 patches, 50% positive) for testing and 16 new CTA (76 patches, 50% positive) for validation.

#### RESULTS

Across all validation set patches, the detection rate was 83%, the false negative rate was 16% and precision was 92%. Our model correctly found 32 of all 38 INA. In general, our model underestimated the true number of INA sites by  $13\% \pm 17\%$ , but the average detection score was still relatively high ( $85\% \pm 17\%$ ).

#### CONCLUSION

We successfully developed and validated an AI model capable of quickly ( $\sim 2$  min compute time per CTA) and accurately locating brain patches with INA. We believe this method may be helpful for providing a quick, but coarse analysis of INA topography without the need of user intervention. We are currently assessing the impact this method has in clinical evaluations.

#### CLINICAL RELEVANCE/APPLICATION

Preliminary results indicate that the model presented can accurately and automatically locate INA on CTA. It is expected to reduce the burden of manual INA detection and improve reliability.

Printed on: 02/07/23

## Abstract Archives of the RSNA, 2022

T5B-SPIN-6

### Transformer-Based Semi-Supervised Adversarial Learning for Liver Tumor Segmentation in Contrast-Enhanced MRI Images

Tuesday, Nov. 29 12:45PM - 1:15PM Room: Learning Center - IN DPS

#### Participants

Han Wen, Chengdu, China (*Presenter*) Nothing to Disclose

#### PURPOSE

This study aims to construct a semi-supervised segmentation model for contrast-enhanced MRI of liver tumors using a deep learning approach on a small amount of labeled data and a large amount of unlabeled data to assist physicians in annotating liver tumors and reduce physician workload.

#### METHODS AND MATERIALS

We retrospectively collected contrast-enhanced MRI of 126 patients with liver tumors. We randomly selected 20 MRI from the dataset as the test set. Our image preprocessing procedure was as follows. All MRI were resampled to  $1 \times 1 \times 1$ mm. The dataset was normalized by subtracting the mean divided by the standard deviation. Each MRI was centrally cropped and the size of the cropped patch was  $256 \times 256 \times 32$ mm. As shown in Figure 1, our semi-supervised segmentation model consists of a segmentation sub-network and an evaluation sub-network. The segmentation sub-network is a variant structure of Unet, where the encoder is a transformer and the decoder is a CNN, and features from multiple resolutions of the encoder are combined with the decoder to generate segmentation masks. The evaluation sub-network is a 5-layer CNN, each convolutional layer contains convolution, leaky\_relu and dropout. During the training process, the segmentation sub-network generates segmentation masks for unlabeled images and labeled images, and the evaluation sub-network learns by distinguishing between the two. The loss function of our semi-supervised segmentation model is  $L=L_{seg}+L_{adv}$ , where  $L_{seg}$  is used for labeled data, which consists of cross-entropy loss, dice loss and signed distance map loss.  $L_{adv}$  is used for both labeled data and unlabeled data, it is cross entropy loss.

#### RESULTS

As shown in Table 1, on the 40% labeled data set, our method achieves the best performance compared to other methods on Dice, Jaccard, ASD, and 95HD, reaching 74.09%, 60.36%, 3.26, 15.92, respectively. Even the segmentation results of 100% labeled data are almost the same. As can be seen in Figure 2, the segmentation results of our method are significantly better than other models and comparable to the manual descriptions of physicians.

#### CONCLUSION

In this study, we present a Transformer-based semi-supervised segmentation model for contrast-enhanced MRI of liver tumors. The model was trained using an adversarial learning approach and achieved very excellent results on a small amount of labeled data and a large amount of unlabeled data, and was comparable to manual annotation by physicians.

#### CLINICAL RELEVANCE/APPLICATION

For medical images, it is an expensive and time-consuming process for clinical experts to perform pixel-by-pixel annotation of a large number of segmentation masks. If our method is used it can reduce the physician's annotation time significantly.

Printed on: 02/07/23

## Abstract Archives of the RSNA, 2022

T5B-SPIR

### Interventional Tuesday Poster Discussions - B

Tuesday, Nov. 29 12:45PM - 1:15PM Room: Learning Center - IR DPS

#### Sub-Events

#### **T5B-SPIR-1 Bare Metallic Stent as Salvage Treatment for Refractory Benign Biliary Strictures After Pediatric Liver Transplantation: Preliminary Experience in A Single-center Cohort**

Participants

Ludovico Dulcetta, MD, Bergamo, Italy (*Presenter*) Nothing to Disclose

#### **PURPOSE**

Liver transplant (LT) is the standard of care for pediatric patients with end-stage liver disease or congenital metabolic disorders. Biliary complications, in particular benign strictures, are a common cause of morbidity and graft dysfunction. Anastomotic and intrahepatic strictures frequently relapse after the standard percutaneous management with bilioplasty and surgical revision. The aim is to describe preliminary experience with metallic stent as salvage treatment in selected patients before relisting for retransplantation.

#### **METHODS AND MATERIALS**

Eight pediatric patients (3 female; mean age 20 months) after split left LT with refractory biliary strictures were treated with percutaneous transhepatic implantation of vascular balloon-expandable or biliary self-expandable bare metallic stents. Indications for stenting were signs of mechanical cholestasis and fibrosis at liver biopsy and failure of standard management with percutaneous transhepatic bilioplasty and/or surgical revision.

#### **RESULTS**

A total of 18 stents (3 biliary, 15 vascular) were implanted. Technical success was 100% without adverse events. A single anastomotic stent was used in 3 patients. Two parallel stents with the kissing-balloon technique to cover the confluence between segments 2 and 3 were implanted in 6 patients. In 1 patient 3 stents were imbricated due to incomplete coverage of the stenosis. Before stents implantation a mean of 3.6 PTC per patient was performed (7.8 months follow-up); after stents implantation a mean of 0.6 PTC (13.1 months follow-up). In one case stent patency was observed after 9 years.

#### **CONCLUSION**

s Preliminary data suggest that after pediatric LT, relapsing biliary strictures could be safely treated with metallic stents to reduce numbers of interventional procedures before surgical anastomosis revision or retransplantation.

#### **CLINICAL RELEVANCE/APPLICATION**

Although metal stents are intended for palliation in malignant biliary pathology, they could be considered to improve cholestatic symptoms in retransplantation waitlist.

#### **T5B-SPIR-2 Combined Microwave Ablation plus Osteosynthesis for Long Bone Metastases**

Participants

Claudio Pusceddu, MD, (*Presenter*) Nothing to Disclose

#### **PURPOSE**

to evaluate the feasibility, safety and efficacy of microwave ablation (MWA) in combination with open surgery nail positioning for the treatment of fractures or impending fractures of long bone metastases.

#### **METHODS AND MATERIALS**

Eleven patients (four men, seven women) with painful bone metastases of the humerus, femur or tibia with non-displaced fractures (one case) or impending fractures (10 cases) underwent open MWA in combination with osteosynthesis by locked nail positioning. Pain intensity was measured using a VAS score before and after treatment. CT or MRI were acquired at one month before and 1, 3, 6, 12 and 18 months after treatment.

#### **RESULTS**

All procedures were successfully completed without major complications. The level of pain was significantly reduced one month after treatment. For the patients with humerus metastases, the complete recovery of arm use took 8 weeks, while for the patients with femoral metastases the complete recovery of walking capacity took 11 weeks. The VAS score ranged from 7 (4-9) before treatment to 1.5 (0-2.5) after treatment. During a mid-term follow-up of 18 months (range 4-29 months), none of the patients showed tumor relapse or new fractures in the treated site. Two patients died due to tumor disease progression.

#### **CONCLUSION**

s Results of this preliminary study suggest that combined MWA and surgical osteosynthesis with locked nails is a safe and effective treatment for pathological fractures or malignant impending fractures of long bone metastases of the humerus, femur and tibia. Further analyses with larger cohorts are warranted to confirm these findings.

#### **CLINICAL RELEVANCE/APPLICATION**

Combined ablation and osteosynthesis treatment of long bone metastases may improve survival in patients with cancer

#### **T5B-SPIR-3 CT-based Radiomics Models May Predict the Early Efficacy of Microwave Ablation in Malignant Lung Tumors**

Participants

Fandong Zhu, Shaoxing, China (*Presenter*) Nothing to Disclose

#### **PURPOSE**

To establish and validate a radiomics model for predicting the early efficacy of microwave ablation (MWA) in malignant lung tumors.

#### **METHODS AND MATERIALS**

The study enrolled 104 malignant lung tumor patients (72 in the training cohort and 32 in the validation cohort) treated with MWA. Post-operation CT images were analyzed. To evaluate the therapeutic effect of ablation, three models were constructed by least absolute shrinkage and selection operator and logistic regression: the tumoral radiomics (T-RO), peritumoral radiomics (P-RO), and tumoral-peritumoral radiomics (TP-RO) models. Univariate and multivariate analyses were performed to identify clinical variables and radiomics features associated with early efficacy, which were incorporated into the combined nomogram (C-RO). The performance of the C-RO model was evaluated by the area under the receiver operating characteristic curve (AUC), calibration curve, and decision curve analysis. The efficacy of the C-RO model was quantified using the Cox regression model.

#### **RESULTS**

Four radiomics features were selected from the region of interest of tumor and peritumor CT images, which showed good performance for evaluating prognosis and early efficacy in two cohorts. The C-RO model was better than the T-RO model (AUC in training, 0.913 vs. 0.784;  $P = 0.055$ ), P-RO model (AUC in training, 0.913 vs. 0.740;  $P = 0.027$ ) and the TP-RO model (AUC in training, 0.913 vs. 0.814;  $P=0.130$ ). Decision curve analysis (DCA) confirmed the clinical benefit of the radiomics nomogram. Survival analysis revealed that in the C-RO model, the low-risk groups defined by best cutoff value had significantly better progression-free survival than the high-risk groups ( $P<0.05$ ).

#### **CONCLUSION**

s CT-based radiomics in malignant lung tumor patients after MWA could be useful for individualized risk classification and treatment.

#### **CLINICAL RELEVANCE/APPLICATION**

Traditional imaging methods lack sensitivity and specificity to evaluate the early efficacy of microwave ablation. The aim of this study was to evaluate tumor and peritumor radiomics-based models and their potential to predict the early efficacy of MWA in malignant lung tumors. The model constructed by integrating radiomics features extracted from the ROI in tumoral and peritumoral areas and clinical risk factors showed a stable and excellent predictive performance, providing a non-invasive and repeatable method to evaluate the outcomes of MWA.

#### **T5B-SPIR-4 Ability of the Renal Ablation-Specific (MC)2 Risk Scoring System to Predict Major Complications from Percutaneous Renal Microwave Ablation**

Participants

Cody Savage, BS, Tuscaloosa, AL (*Presenter*) Nothing to Disclose

#### **PURPOSE**

The (MC)2 score is a renal-ablation specific risk scoring system originally developed to predict major complications from percutaneous renal cryoablation. However, this scoring system has not been applied to patients undergoing percutaneous renal microwave ablation (MWA). The aim of this study is to assess the ability of the (MC)2 scoring system to identify patients at risk for major complications of percutaneous renal MWA.

#### **METHODS AND MATERIALS**

Retrospective review of all adult patients who underwent percutaneous renal MWA at two centers from 2009-2018. Patient demographics, medical histories, laboratory work, technical details of the procedure, tumor characteristics, and clinical outcomes were collected. The (MC)2 score was calculated for each patients. Patients were assigned to low-risk (<5), moderate-risk (5-8) and high-risk (>8) groups. Complications were graded according to CIRSE guidelines.

#### **RESULTS**

A total of 116 patients (M=66; F=50; median age=63 (range: 34-81)) were included. 11 (9.5%) and 23 (19.8%) experienced major or minor complications, respectively. Patients who developed major complications had a mean tumor diameter of 3.0 mm ( $\pm 1.4$ ). In this group, 21 patients (18.1%) had a central tumor, 20 patients (17.2%) had complicated diabetes, and 14 patient (12.1%) had a prior myocardial infarction. Among the low-risk, moderate-risk, and high-risk groups, the major complication rate was 7.8%, 13.2%, and 0%, respectively. The mean (MC)2 score for patients with major complications (4.8 ( $\pm 1.8$ )) was not higher than those with either minor complications (4.1 ( $\pm 1.6$ )) ( $p = 0.49$ ) or no complications (3.7 ( $\pm 1.5$ )) ( $p = 0.10$ ). The area under the ROC curve to predict major complications was 0.64, indicating a poor ability to predict major complications in this cohort. However, mean tumor size was greater in patients with major complications than those with minor complications ( $p=0.01$ ).

#### **CONCLUSION**

s The (MC)2 risk scoring system does not accurately identify patients at risk for major complications from percutaneous renal MWA. The mean tumor size alone may serve as a better indicator for risk assessment of major complications.

#### **CLINICAL RELEVANCE/APPLICATION**

Unlike in percutaneous renal cryoablation, the (MC)<sup>2</sup> scoring system is not effective at predicting which patients will develop major complications following percutaneous renal MWA. As such, risk stratification systems specific to the treatment modality need to be developed to accurately predict a patient's risk of major complications.

### **T5B-SPiR-5 Preliminary Results Developing a Novel Ex Vivo Human Liver Model to Investigate Microwave Ablation**

Participants

Carlos Ortiz, MD, San Antonio, TX (*Presenter*) Consultant, Argon Medical Devices, Inc

#### **PURPOSE**

We aim to develop a novel dual-perfused ex vivo model using explanted human research livers to investigate microwave ablation (MWA).

#### **METHODS AND MATERIALS**

Five explanted research livers (3 cirrhotic and 2 > 50% steatosis) were obtained under research consent. Each organ was recovered from a brain-dead human deceased donor by a transplant surgeon using standard surgical and preservation techniques. This study consists of three components: 1) develop a physiologic ex vivo model to perfuse human research livers, 2) use the model to assess the impact of perfusion mediated tissue cooling on MWA ablation measurements in a human model, and 3) compare observed ex vivo results to manufacturer reference data from nonperfused animal organs. A total of 27 ablations (12 perfused and 15 nonperfused) were performed at 140W for 6 minutes using a MWA system (Angiodynamics Solero). Pre- and post-ablation arteriogram, portal venogram, and cholangiogram were obtained. Ablations were sectioned along the probe trajectory to obtain maximal long axis diameter (LAD) and short axis diameter (SAD) for the zone of coagulation. Ellipsoid volume and sphericity were calculated. Standard statistical analysis was performed.

#### **RESULTS**

Continuous bile production was observed in three viable livers (60%), including one cirrhotic liver. Perfused ablations resulted in significantly smaller ablation dimensions than nonperfused ablations with average gross specimen MWA comparisons as follows (12 perfused ablations vs 15 nonperfused ablations, two-tailed t-test): SAD,  $3.2 \pm 0.4$  cm vs  $4.1 \pm 0.5$  cm ( $p < 0.001$ ); LAD,  $5.1 \pm 0.3$  cm vs  $6.1 \pm 0.4$  cm ( $p < 0.001$ ); volume,  $27.3 \pm 8.6$  mL vs  $54.3 \pm 12.7$  mL ( $p < 0.001$ ); sphericity,  $0.40 \pm 0.10$  vs  $0.45 \pm 0.10$  ( $p = 0.19$ ). No significant differences were observed in organ temperature and maximal probe wattage for perfused and nonperfused ablations. Comparing nonperfused ablations to manufacturer data, there were significant differences in LAD, SAD, and sphericity (one sample t-test,  $p < 0.05$ ). Comparing perfused ablations to manufacturer data, there were significant differences in LAD, SAD, volume, and sphericity (one sample t-test, all  $p < 0.001$ ). Post-ablation arteriograms demonstrated no contrast extravasation and a new arteriovenous fistula in a single organ.

#### **CONCLUSION**

The presence of perfusion significantly decreases MWA measurements in human livers. At a single device setting, significant differences in MWA measurements are seen in human livers compared to nonperfused manufacturer data.

#### **CLINICAL RELEVANCE/APPLICATION**

This ex vivo model allows for improved characterization of ablation measurements utilizing organs donated for medical research. An ex vivo human model could decrease variability between MWA reference data and clinical results.

### **T5B-SPiR-6 Specific Inhibitor of MMP Decrease Tumor Invasiveness After Radiofrequency Ablation in Liver Tumor Animal Model**

Participants

Bing Wang, (*Presenter*) Nothing to Disclose

#### **PURPOSE**

To determine whether matrix metalloproteinase (MMP) inhibitor batimastat (BB-94) could inhibit the progression of liver tumor after radiofrequency ablation (RFA) and achieve better therapeutic efficacy in an animal model.

#### **METHODS AND MATERIALS**

In vitro experiments, the proliferation of H22 cells was detected by CCK8 method and cell migration was detected by Transwell method. Next, H22 murine liver tumors were used for in vivo experiments. First, 32 mice with one tumor were randomized into four groups (n=8 each group): control (PBS only), RFA alone (65?, 5min), BB-94 (30 mg/kg), RFA+BB-94. The growth rate of the residual tumor and the end point survival were estimated and the pathologic changes were compared. Secondly, a total of 48 tumors in 24 animals were randomized into three groups (n= 8 each group): control (PBS only), RFA alone, RFA+BB-94. Each mouse was implanted two tumors subcutaneously, one tumor was ablated and the other was evaluated for distant metastasis after applying BB-94.

#### **RESULTS**

In vitro, the proliferation assay demonstrated that the H22 cells had significantly higher proliferation rate in the heat group than the control group ( $1.27 \pm 0.08$  vs  $0.82 \pm 0.07$ ,  $P=0.008$ ), and it could be inhibited by BB-94 ( $0.67 \pm 0.06$  vs  $0.37 \pm 0.01$ ,  $P=0.015$ ). In the cell migration assay, the H22 cells demonstrated enhanced invasive ability after heat experiment ( $33.7 \pm 2.1$  vs  $19.7 \pm 4.9$ ,  $P=0.011$ ). And it could be significantly suppressed after treated with BB-94 ( $32.3 \pm 3.5$  vs  $23.0 \pm 4.6$ ,  $P=0.009$ ). With one tumor animal, the growth rate of the residual tumor in the BB-94+RFA group was slower than that in the RFA alone group ( $P=0.003$ ). And combination of BB-94 could significantly prolong the survival of the mice ( $40.3 \pm 1.4$ d vs  $47.1 \pm 1.3$ d,  $P=0.002$ ). The expression of MMP9, Collagen I and VEGF at the coagulation margin were decreased after combined with BB-94. With two tumors animal, the tumor growth rate of metastasis tumor in the BB-94+RFA group was lower than that in the RFA group ( $P<0.001$ ).

#### **CONCLUSION**

BB-94 combined with RFA reduced the invasiveness of the tumor and improved the endpoint survival. It also helped to suppress the growth rate of metastasis tumor after RFA.

#### **CLINICAL RELEVANCE/APPLICATION**

Our data suggested that targeting the MMP process with the specific inhibition could increase overall ablation efficacy.

### **T5B-SPiR-7 Can Two-step Ablation Combined with Chemotherapeutic Liposomes Achieve Better Outcome Than Traditional RF Ablation? A Solid Tumor Animal Study**

Participants

Kun Zhao, (*Presenter*) Nothing to Disclose

#### **PURPOSE**

To determine whether two-step ablation using sequential low and high temperature heating can achieve improved outcomes in animal tumor models when combined with chemotherapeutic liposomes (LP).

#### **METHODS AND MATERIALS**

Balb/c mice bearing 4T1 tumor received paclitaxel-loaded liposomes followed 24hr later by either traditional RFA (70°C, 5min) or a low temperature RFA (45°C, 5min), or two-step RFA (45°C 2min+70°C 3min). Intratumoral drug accumulation and bio-distribution in major organs were evaluated. Periablational drug penetration was evaluated by pathologic staining and intratumoral interstitial fluid pressure (IFP) measured directly. For long-term outcomes, mice bearing 4T1 or H22 tumors were randomized into five groups (n = 8/group): control (no treatment), RFA alone, LP+RFA (45°C), LP+RFA (70°C) and LP+RFA (45+70°C). End-point survivals were compared among the different groups.

#### **RESULTS**

The greater intratumoral drug accumulation ( $3.35 \pm 0.32$  vs  $3.79 \pm 0.29 \times 10^8$ phot/cm<sup>2</sup>/s at 24hr,  $p=0.09$ ), deeper periablational drug penetration ( $45.7 \pm 5.0$  vs  $1.6 \pm 0.5$ ,  $p<0.001$ ), and reduced off-target drug deposition in major organs (liver  $96.1 \pm 31.6$  vs  $47.4 \pm 1.5 \times 10^6$ phot/cm<sup>2</sup>/s,  $p<0.001$ ) were found when combined with RFA (45°C) compared to drug alone. For long-term outcomes, 4T1 tumor growth rates for LP+ two-step RFA (45+70°C) were significantly slower than LP+RFA (70°C), LP+RFA (45°C), and RFA alone ( $P<0.01$  for all comparisons). End point survival for LP+ RFA (45+70°C) was also longer than for LP+RFA (70°C) (median 16 vs 10 days,  $p=0.003$ ) or LP+RFA 45°C (11 days,  $p=0.009$ ), RFA alone (8.3 days,  $p<0.001$ ) in H22 tumor models. The intratumoral IFP after RFA (45°C) was significantly lower than baseline RFA ( $5.4 \pm 3.6$  vs  $23.0 \pm 8.0$  mmHg,  $p<0.001$ ), but was not measurable after RFA (70°C).

#### **CONCLUSION**

s A two-step ablation combined with chemotherapeutic liposomes can achieve better survival benefit compared to traditional RFA in animal models.

#### **CLINICAL RELEVANCE/APPLICATION**

Two-step ablation of initial moderate hyperthermia followed by coagulative ablation temperatures combined with intravenous administration of chemotherapeutic liposomes can achieve a better outcome over single dose traditional high temperature ablation based upon the premise of greater drug accumulation and penetration. These results may provide a useful method for improving therapy outcome in clinical practice.

### **T5B-SPiR-8 Visualizing Recovery: Feasibility of Accelerometer-based Biometric Data Collection Among Interventional Oncology Patients**

Participants

Nicole Kim, BS, (*Presenter*) Nothing to Disclose

#### **PURPOSE**

The use of image-guided locoregional therapies (LRT) for the treatment of cancer holds several advantages over surgical interventions, including fewer hospitalizations and low complication rates. While shorter time to recovery is another theoretical benefit, recovery following LRT often takes place in the outpatient setting and patient health trajectories during this period are not well understood. This pilot study tested the feasibility of measuring post-LRT patient recovery using wearable accelerometer technology (WAT).

#### **METHODS AND MATERIALS**

Adult cancer patients referred to undergo LRT procedures were enrolled during their pre-procedural consultation visits in a dedicated interventional oncology clinic. All patients were provided with a Fitbit® Inspire 2 device to wear for 7-14 days prior to their interventional oncology procedure (baseline phase) and for 30 days thereafter (recovery phase). WAT-derived step count was continuously recorded throughout the study period. Post-procedure "recovery" was defined as a return to the baseline daily step count during the recovery phase after LRT. Patient responses to the RAND 36-Item Short Form (SF-36) Health Survey were also collected at enrollment, on the procedure day, and at 30-day follow-up to assess for changes over time. An interrupted time series design was used wherein pre- and post-LRT step count and SF-36 metrics were compared using cubic spline mixed modeling. Significance was set at  $p<0.05$ .

#### **RESULTS**

Twenty adult cancer patients were enrolled, and 18 completed the study (14 ablation, 4 embolization). Median age was 73 years (range 59-89 years; 67% male). Most patients wore the Fitbit devices without significant interruptions for the duration of the study period, and all completed the SF-36 surveys. Analysis of WAT-derived biometric data demonstrated a mean of 4850 (95% CI [4080, 5621]) steps taken during the baseline phase across all patients. Step count decreased to 2000 immediately following LRT, then steadily increased to 4568 (95% CI [3715, 5421]) steps, achieving a "recovery" plateau after an average of 10 days ( $p<0.001$ ). The SF-36 survey did not reliably capture patient recovery data; no significant change was observed between initial and follow-up assessments ( $p>0.10$ ).

#### **CONCLUSION**

s WAT effectively captures dynamic peri-procedural biophysical parameters not reflected in standard survey-based monitoring and can be reliably implemented to monitor patient recovery following interventional oncology procedures.

#### **CLINICAL RELEVANCE/APPLICATION**

Characterization of recovery following various interventional oncology procedures could facilitate appropriate intervention in patients with poor post-procedural progression and better inform treatment recommendations.

## **T5B-SPIR-9 MR-guided High Intensity Focused Ultrasound (MRgHIFU) in The treatment of Bone Metastases: Safety of Sensitive Structures Within 1 cm from Target Lesion**

### **Awards**

**Trainee Research Prize - Resident**

Participants

Valerio D'Agostino, MD, (*Presenter*) Nothing to Disclose

### **PURPOSE**

A distance greater than 1 cm between the target lesion and sensitive structures is highly recommended in MRgHIFU treatments of bone lesions. The aim of this work was to evaluate the safety of MRgHIFU treatment for pain palliation of bone metastases involving regions close to (<1cm) sensitive structures.

### **METHODS AND MATERIALS**

101 patients (56% female, 44% male; mean age 55±15,4) with 141 bone metastases were treated by MRgHIFU. Close proximity between the target lesion and sensitive structures (skin, nerves, vessels, sensitive organs) was measured on pre-treatment MR images, and metastases were divided in two groups according to this (> 1 cm distance - group A, < 1 cm - group B). VAS score at baseline, and at 3 and 6 months after treatment was assessed in all patients. MR/CT imaging was performed before and 3-6 months after treatment, in order to assess local tumour control according to MD Anderson criteria. Primary endpoint was the rate of major and minor complications on sensitive structures, according to the common terminology criteria for adverse events, version 5.0. Secondary endpoints included the assessment of the impact of such proximity (lesion to sensitive structures) on response to treatment - treatment efficacy.

### **RESULTS**

141 metastases were submitted to MRgHIFU (primary tumors: 33,5% breast, 13% prostate, 12,7% kidney, 40,8% others). 85 metastases were included in group A. Close proximity between the target lesion and sensitive structures was recorded for 56 metastases (6 skin, 22 nerves, 17 vessels, 6 sensitive organs - 11 with combined conditions) - group B. 1 case of Grade 1 Burn (group A) and 1 case of Grade 1 Prostatic Pain (group B) were observed. VAS at baseline was 5.9±2,7, with a significant reduction at 3 months (2,57±2.5, p lt0.0001) and at 6 months (2,82±2,83, p lt0.0001). Complete follow-up at 3 and 6 months after treatment was available for 61 patients. Complete response was observed in 16 cases, partial response in 18, stability in 23 and progression in 4 patients. Location in proximity of sensitive structures did not affect the outcome of treatments, as there was no statistically significant difference in both safety and efficacy between the two groups of patients.

### **CONCLUSION**

s MRgHIFU can be safely and effectively performed even on lesions located at <1 cm from sensitive structures.

### **CLINICAL RELEVANCE/APPLICATION**

A distance <1 cm from sensitive structures of the target lesion is considered an exclusion criterion for MRgHIFU treatment. The results of this study suggest the need for revision of MRgHIFU's exclusion criteria, in clinical practice and research.

Printed on: 02/07/23

## Abstract Archives of the RSNA, 2022

T5B-SPIR-1

### **Bare Metallic Stent as Salvage Treatment for Refractory Benign Biliary Strictures After Pediatric Liver Transplantation: Preliminary Experience in A Single-center Cohort**

Tuesday, Nov. 29 12:45PM - 1:15PM Room: Learning Center - IR DPS

#### **Participants**

Ludovico Dulcetta, MD, Bergamo, Italy (*Presenter*) Nothing to Disclose

#### **PURPOSE**

Liver transplant (LT) is the standard of care for pediatric patients with end-stage liver disease or congenital metabolic disorders. Biliary complications, in particular benign strictures, are a common cause of morbidity and graft dysfunction. Anastomotic and intrahepatic strictures frequently relapse after the standard percutaneous management with bilioplasty and surgical revision. The aim is to describe preliminary experience with metallic stent as salvage treatment in selected patients before relisting for retransplantation.

#### **METHODS AND MATERIALS**

Eight pediatric patients (3 female; mean age 20 months) after split left LT with refractory biliary strictures were treated with percutaneous transhepatic implantation of vascular balloon-expandable or biliary self-expandable bare metallic stents. Indications for stenting were signs of mechanical cholestasis and fibrosis at liver biopsy and failure of standard management with percutaneous transhepatic bilioplasty and/or surgical revision.

#### **RESULTS**

A total of 18 stents (3 biliary, 15 vascular) were implanted. Technical success was 100% without adverse events. A single anastomotic stent was used in 3 patients. Two parallel stents with the kissing-balloon technique to cover the confluence between segments 2 and 3 were implanted in 6 patients. In 1 patient 3 stents were imbricated due to incomplete coverage of the stenosis. Before stents implantation a mean of 3.6 PTC per patient was performed (7.8 months follow-up); after stents implantation a mean of 0.6 PTC (13.1 months follow-up). In one case stent patency was observed after 9 years.

#### **CONCLUSION**

s Preliminary data suggest that after pediatric LT, relapsing biliary strictures could be safely treated with metallic stents to reduce numbers of interventional procedures before surgical anastomosis revision or retransplantation.

#### **CLINICAL RELEVANCE/APPLICATION**

Although metal stents are intended for palliation in malignant biliary pathology, they could be considered to improve cholestatic symptoms in retransplantation waitlist.

Printed on: 02/07/23

## Abstract Archives of the RSNA, 2022

T5B-SPIR-2

### Combined Microwave Ablation plus Osteosynthesis for Long Bone Metastases

Tuesday, Nov. 29 12:45PM - 1:15PM Room: Learning Center - IR DPS

#### Participants

Claudio Pusceddu, MD, (*Presenter*) Nothing to Disclose

#### PURPOSE

to evaluate the feasibility, safety and efficacy of microwave ablation (MWA) in combination with open surgery nail positioning for the treatment of fractures or impending fractures of long bone metastases.

#### METHODS AND MATERIALS

Eleven patients (four men, seven women) with painful bone metastases of the humerus, femur or tibia with non-displaced fractures (one case) or impending fractures (10 cases) underwent open MWA in combination with osteosynthesis by locked nail positioning. Pain intensity was measured using a VAS score before and after treatment. CT or MRI were acquired at one month before and 1, 3, 6, 12 and 18 months after treatment.

#### RESULTS

All procedures were successfully completed without major complications. The level of pain was significantly reduced one month after treatment. For the patients with humerus metastases, the complete recovery of arm use took 8 weeks, while for the patients with femoral metastases the complete recovery of walking capacity took 11 weeks. The VAS score ranged from 7 (4-9) before treatment to 1.5 (0-2.5) after treatment. During a mid-term follow-up of 18 months (range 4-29 months), none of the patients showed tumor relapse or new fractures in the treated site. Two patients died due to tumor disease progression.

#### CONCLUSION

Results of this preliminary study suggest that combined MWA and surgical osteosynthesis with locked nails is a safe and effective treatment for pathological fractures or malignant impending fractures of long bone metastases of the humerus, femur and tibia. Further analyses with larger cohorts are warranted to confirm these findings.

#### CLINICAL RELEVANCE/APPLICATION

Combined ablation and osteosynthesis treatment of long bone metastases may improve survival in patients with cancer

Printed on: 02/07/23

## Abstract Archives of the RSNA, 2022

T5B-SPIR-3

### CT-based Radiomics Models May Predict the Early Efficacy of Microwave Ablation in Malignant Lung Tumors

Tuesday, Nov. 29 12:45PM - 1:15PM Room: Learning Center - IR DPS

#### Participants

Fandong Zhu, Shaoxing, China (*Presenter*) Nothing to Disclose

#### PURPOSE

To establish and validate a radiomics model for predicting the early efficacy of microwave ablation (MWA) in malignant lung tumors.

#### METHODS AND MATERIALS

The study enrolled 104 malignant lung tumor patients (72 in the training cohort and 32 in the validation cohort) treated with MWA. Post-operation CT images were analyzed. To evaluate the therapeutic effect of ablation, three models were constructed by least absolute shrinkage and selection operator and logistic regression: the tumoral radiomics (T-RO), peritumoral radiomics (P-RO), and tumoral-peritumoral radiomics (TP-RO) models. Univariate and multivariate analyses were performed to identify clinical variables and radiomics features associated with early efficacy, which were incorporated into the combined nomogram (C-RO). The performance of the C-RO model was evaluated by the area under the receiver operating characteristic curve (AUC), calibration curve, and decision curve analysis. The efficacy of the C-RO model was quantified using the Cox regression model.

#### RESULTS

Four radiomics features were selected from the region of interest of tumor and peritumor CT images, which showed good performance for evaluating prognosis and early efficacy in two cohorts. The C-RO model was better than the T-RO model (AUC in training, 0.913 vs. 0.784;  $P = 0.055$ ), P-RO model (AUC in training, 0.913 vs. 0.740;  $P = 0.027$ ) and the TP-RO model (AUC in training, 0.913 vs. 0.814;  $P=0.130$ ). Decision curve analysis (DCA) confirmed the clinical benefit of the radiomics nomogram. Survival analysis revealed that in the C-RO model, the low-risk groups defined by best cutoff value had significantly better progression-free survival than the high-risk groups ( $P<0.05$ ).

#### CONCLUSION

s CT-based radiomics in malignant lung tumor patients after MWA could be useful for individualized risk classification and treatment.

#### CLINICAL RELEVANCE/APPLICATION

Traditional imaging methods lack sensitivity and specificity to evaluate the early efficacy of microwave ablation. The aim of this study was to evaluate tumor and peritumor radiomics-based models and their potential to predict the early efficacy of MWA in malignant lung tumors. The model constructed by integrating radiomics features extracted from the ROI in tumoral and peritumoral areas and clinical risk factors showed a stable and excellent predictive performance, providing a non-invasive and repeatable method to evaluate the outcomes of MWA.

Printed on: 02/07/23

## Abstract Archives of the RSNA, 2022

T5B-SPIR-4

### Ability of the Renal Ablation-Specific (MC)2 Risk Scoring System to Predict Major Complications from Percutaneous Renal Microwave Ablation

Tuesday, Nov. 29 12:45PM - 1:15PM Room: Learning Center - IR DPS

#### Participants

Cody Savage, BS, Tuscaloosa, AL (*Presenter*) Nothing to Disclose

#### PURPOSE

The (MC)2 score is a renal-ablation specific risk scoring system originally developed to predict major complications from percutaneous renal cryoablation. However, this scoring system has not been applied to patients undergoing percutaneous renal microwave ablation (MWA). The aim of this study is to assess the ability of the (MC)2 scoring system to identify patients at risk for major complications of percutaneous renal MWA.

#### METHODS AND MATERIALS

Retrospective review of all adult patients who underwent percutaneous renal MWA at two centers from 2009-2018. Patient demographics, medical histories, laboratory work, technical details of the procedure, tumor characteristics, and clinical outcomes were collected. The (MC)2 score was calculated for each patient. Patients were assigned to low-risk (<5), moderate-risk (5-8) and high-risk (>8) groups. Complications were graded according to CIRSE guidelines.

#### RESULTS

A total of 116 patients (M=66; F=50; median age=63 (range: 34-81)) were included. 11 (9.5%) and 23 (19.8%) experienced major or minor complications, respectively. Patients who developed major complications had a mean tumor diameter of 3.0 mm ( $\pm 1.4$ ). In this group, 21 patients (18.1%) had a central tumor, 20 patients (17.2%) had complicated diabetes, and 14 patients (12.1%) had a prior myocardial infarction. Among the low-risk, moderate-risk, and high-risk groups, the major complication rate was 7.8%, 13.2%, and 0%, respectively. The mean (MC)2 score for patients with major complications (4.8 ( $\pm 1.8$ )) was not higher than those with either minor complications (4.1 ( $\pm 1.6$ )) ( $p=0.49$ ) or no complications (3.7 ( $\pm 1.5$ )) ( $p=0.10$ ). The area under the ROC curve to predict major complications was 0.64, indicating a poor ability to predict major complications in this cohort. However, mean tumor size was greater in patients with major complications than those with minor complications ( $p=0.01$ ).

#### CONCLUSION

The (MC)2 risk scoring system does not accurately identify patients at risk for major complications from percutaneous renal MWA. The mean tumor size alone may serve as a better indicator for risk assessment of major complications.

#### CLINICAL RELEVANCE/APPLICATION

Unlike in percutaneous renal cryoablation, the (MC)2 scoring system is not effective at predicting which patients will develop major complications following percutaneous renal MWA. As such, risk stratification systems specific to the treatment modality need to be developed to accurately predict a patient's risk of major complications.

Printed on: 02/07/23

## Abstract Archives of the RSNA, 2022

T5B-SPIR-5

### Preliminary Results Developing a Novel Ex Vivo Human Liver Model to Investigate Microwave Ablation

Tuesday, Nov. 29 12:45PM - 1:15PM Room: Learning Center - IR DPS

#### Participants

Carlos Ortiz, MD, San Antonio, TX (*Presenter*) Consultant, Argon Medical Devices, Inc

#### PURPOSE

We aim to develop a novel dual-perfused ex vivo model using explanted human research livers to investigate microwave ablation (MWA).

#### METHODS AND MATERIALS

Five explanted research livers (3 cirrhotic and 2 > 50% steatosis) were obtained under research consent. Each organ was recovered from a brain-dead human deceased donor by a transplant surgeon using standard surgical and preservation techniques. This study consists of three components: 1) develop a physiologic ex vivo model to perfuse human research livers, 2) use the model to assess the impact of perfusion mediated tissue cooling on MWA ablation measurements in a human model, and 3) compare observed ex vivo results to manufacturer reference data from nonperfused animal organs. A total of 27 ablations (12 perfused and 15 nonperfused) were performed at 140W for 6 minutes using a MWA system (Angiodynamics Solero). Pre- and post-ablation arteriogram, portal venogram, and cholangiogram were obtained. Ablations were sectioned along the probe trajectory to obtain maximal long axis diameter (LAD) and short axis diameter (SAD) for the zone of coagulation. Ellipsoid volume and sphericity were calculated. Standard statistical analysis was performed.

#### RESULTS

Continuous bile production was observed in three viable livers (60%), including one cirrhotic liver. Perfused ablations resulted in significantly smaller ablation dimensions than nonperfused ablations with average gross specimen MWA comparisons as follows (12 perfused ablations vs 15 nonperfused ablations, two-tailed t-test): SAD,  $3.2 \pm 0.4$  cm vs  $4.1 \pm 0.5$  cm ( $p < 0.001$ ); LAD,  $5.1 \pm 0.3$  cm vs  $6.1 \pm 0.4$  cm ( $p < 0.001$ ); volume,  $27.3 \pm 8.6$  mL vs  $54.3 \pm 12.7$  mL ( $p < 0.001$ ); sphericity,  $0.40 \pm 0.10$  vs  $0.45 \pm 0.10$  ( $p = 0.19$ ). No significant differences were observed in organ temperature and maximal probe wattage for perfused and nonperfused ablations. Comparing nonperfused ablations to manufacturer data, there were significant differences in LAD, SAD, and sphericity (one sample t-test,  $p < 0.05$ ). Comparing perfused ablations to manufacturer data, there were significant differences in LAD, SAD, volume, and sphericity (one sample t-test, all  $p < 0.001$ ). Post-ablation arteriograms demonstrated no contrast extravasation and a new arteriovenous fistula in a single organ.

#### CONCLUSION

The presence of perfusion significantly decreases MWA measurements in human livers. At a single device setting, significant differences in MWA measurements are seen in human livers compared to nonperfused manufacturer data.

#### CLINICAL RELEVANCE/APPLICATION

This ex vivo model allows for improved characterization of ablation measurements utilizing organs donated for medical research. An ex vivo human model could decrease variability between MWA reference data and clinical results.

Printed on: 02/07/23

## Abstract Archives of the RSNA, 2022

T5B-SPIR-6

### Specific Inhibitor of MMP Decrease Tumor Invasiveness After Radiofrequency Ablation in Liver Tumor Animal Model

Tuesday, Nov. 29 12:45PM - 1:15PM Room: Learning Center - IR DPS

#### Participants

Bing Wang, (*Presenter*) Nothing to Disclose

#### PURPOSE

To determine whether matrix metalloproteinase (MMP) inhibitor batimastat (BB-94) could inhibit the progression of liver tumor after radiofrequency ablation (RFA) and achieve better therapeutic efficacy in an animal model.

#### METHODS AND MATERIALS

In vitro experiments, the proliferation of H22 cells was detected by CCK8 method and cell migration was detected by Transwell method. Next, H22 murine liver tumors were used for in vivo experiments. First, 32 mice with one tumor were randomized into four groups (n=8 each group): control (PBS only), RFA alone (65°C, 5min), BB-94 (30 mg/kg), RFA+BB-94. The growth rate of the residual tumor and the end point survival were estimated and the pathologic changes were compared. Secondly, a total of 48 tumors in 24 animals were randomized into three groups (n= 8 each group): control (PBS only), RFA alone, RFA+BB-94. Each mouse was implanted two tumors subcutaneously, one tumor was ablated and the other was evaluated for distant metastasis after applying BB-94.

#### RESULTS

In vitro, the proliferation assay demonstrated that the H22 cells had significantly higher proliferation rate in the heat group than the control group ( $1.27\pm 0.08$  vs  $0.82\pm 0.07$ ,  $P=0.008$ ), and it could be inhibited by BB-94 ( $0.67\pm 0.06$  vs  $0.37\pm 0.01$ ,  $P=0.015$ ). In the cell migration assay, the H22 cells demonstrated enhanced invasive ability after heat experiment ( $33.7\pm 2.1$  vs  $19.7\pm 4.9$ ,  $P=0.011$ ). And it could be significantly suppressed after treated with BB-94 ( $32.3\pm 3.5$  vs  $23.0\pm 4.6$ ,  $P=0.009$ ). With one tumor animal, the growth rate of the residual tumor in the BB-94+RFA group was slower than that in the RFA alone group ( $P=0.003$ ). And combination of BB-94 could significantly prolong the survival of the mice ( $40.3\pm 1.4d$  vs  $47.1\pm 1.3d$ ,  $P=0.002$ ). The expression of MMP9, Collagen I and VEGF at the coagulation margin were decreased after combined with BB-94. With two tumors animal, the tumor growth rate of metastasis tumor in the BB-94+RFA group was lower than that in the RFA group ( $P<0.001$ ).

#### CONCLUSION

BB-94 combined with RFA reduced the invasiveness of the tumor and improved the endpoint survival. It also helped to suppress the growth rate of metastasis tumor after RFA.

#### CLINICAL RELEVANCE/APPLICATION

Our data suggested that targeting the MMP process with the specific inhibition could increase overall ablation efficacy.

Printed on: 02/07/23

## Abstract Archives of the RSNA, 2022

T5B-SPIR-7

### Can Two-step Ablation Combined with Chemotherapeutic Liposomes Achieve Better Outcome Than Traditional RF Ablation? A Solid Tumor Animal Study

Tuesday, Nov. 29 12:45PM - 1:15PM Room: Learning Center - IR DPS

#### Participants

Kun Zhao, (*Presenter*) Nothing to Disclose

#### PURPOSE

To determine whether two-step ablation using sequential low and high temperature heating can achieve improved outcomes in animal tumor models when combined with chemotherapeutic liposomes (LP).

#### METHODS AND MATERIALS

Balb/c mice bearing 4T1 tumor received paclitaxel-loaded liposomes followed 24hr later by either traditional RFA (70°C, 5min) or a low temperature RFA (45°C, 5min), or two-step RFA (45°C 2min+70°C 3min). Intratumoral drug accumulation and bio-distribution in major organs were evaluated. Periablational drug penetration was evaluated by pathologic staining and intratumoral interstitial fluid pressure (IFP) measured directly. For long-term outcomes, mice bearing 4T1 or H22 tumors were randomized into five groups (n = 8/group): control (no treatment), RFA alone, LP+RFA (45°C), LP+RFA (70°C) and LP+RFA (45+70°C). End-point survivals were compared among the different groups.

#### RESULTS

The greater intratumoral drug accumulation ( $3.35\pm 0.32$  vs  $3.79\pm 0.29$   $\times 10^8$ phot/cm<sup>2</sup>/s at 24hr,  $p=0.09$ ), deeper periablational drug penetration ( $45.7\pm 5.0$  vs  $1.6\pm 0.5$ ,  $p<0.001$ ), and reduced off-target drug deposition in major organs (liver  $96.1\pm 31.6$  vs  $47.4\pm 1.5$   $\times 10^6$ phot/cm<sup>2</sup>/s,  $p<0.001$ ) were found when combined with RFA (45°C) compared to drug alone. For long-term outcomes, 4T1 tumor growth rates for LP+ two-step RFA (45+70°C) were significantly slower than LP+RFA (70°C), LP+RFA (45°C), and RFA alone ( $P<0.01$  for all comparisons). End point survival for LP+ RFA (45+70°C) was also longer than for LP+RFA (70°C) (median 16 vs 10 days,  $p=0.003$ ) or LP+RFA 45°C (11 days,  $p=0.009$ ), RFA alone (8.3 days,  $p<0.001$ ) in H22 tumor models. The intratumoral IFP after RFA (45°C) was significantly lower than baseline RFA ( $5.4\pm 3.6$  vs  $23.0\pm 8.0$  mmHg,  $p<0.001$ ), but was not measurable after RFA (70°C).

#### CONCLUSION

A two-step ablation combined with chemotherapeutic liposomes can achieve better survival benefit compared to traditional RFA in animal models.

#### CLINICAL RELEVANCE/APPLICATION

Two-step ablation of initial moderate hyperthermia followed by coagulative ablation temperatures combined with intravenous administration of chemotherapeutic liposomes can achieve a better outcome over single dose traditional high temperature ablation based upon the premise of greater drug accumulation and penetration. These results may provide a useful method for improving therapy outcome in clinical practice.

Printed on: 02/07/23

## Abstract Archives of the RSNA, 2022

T5B-SPIR-8

### Visualizing Recovery: Feasibility of Accelerometer-based Biometric Data Collection Among Interventional Oncology Patients

Tuesday, Nov. 29 12:45PM - 1:15PM Room: Learning Center - IR DPS

#### Participants

Nicole Kim, BS, (*Presenter*) Nothing to Disclose

#### PURPOSE

The use of image-guided locoregional therapies (LRT) for the treatment of cancer holds several advantages over surgical interventions, including fewer hospitalizations and low complication rates. While shorter time to recovery is another theoretical benefit, recovery following LRT often takes place in the outpatient setting and patient health trajectories during this period are not well understood. This pilot study tested the feasibility of measuring post-LRT patient recovery using wearable accelerometer technology (WAT).

#### METHODS AND MATERIALS

Adult cancer patients referred to undergo LRT procedures were enrolled during their pre-procedural consultation visits in a dedicated interventional oncology clinic. All patients were provided with a Fitbit® Inspire 2 device to wear for 7-14 days prior to their interventional oncology procedure (baseline phase) and for 30 days thereafter (recovery phase). WAT-derived step count was continuously recorded throughout the study period. Post-procedure "recovery" was defined as a return to the baseline daily step count during the recovery phase after LRT. Patient responses to the RAND 36-Item Short Form (SF-36) Health Survey were also collected at enrollment, on the procedure day, and at 30-day follow-up to assess for changes over time. An interrupted time series design was used wherein pre- and post-LRT step count and SF-36 metrics were compared using cubic spline mixed modeling. Significance was set at  $p < 0.05$ .

#### RESULTS

Twenty adult cancer patients were enrolled, and 18 completed the study (14 ablation, 4 embolization). Median age was 73 years (range 59-89 years; 67% male). Most patients wore the Fitbit devices without significant interruptions for the duration of the study period, and all completed the SF-36 surveys. Analysis of WAT-derived biometric data demonstrated a mean of 4850 (95% CI [4080, 5621]) steps taken during the baseline phase across all patients. Step count decreased to 2000 immediately following LRT, then steadily increased to 4568 (95% CI [3715, 5421]) steps, achieving a "recovery" plateau after an average of 10 days ( $p < 0.001$ ). The SF-36 survey did not reliably capture patient recovery data; no significant change was observed between initial and follow-up assessments ( $p > 0.10$ ).

#### CONCLUSION

s WAT effectively captures dynamic peri-procedural biophysical parameters not reflected in standard survey-based monitoring and can be reliably implemented to monitor patient recovery following interventional oncology procedures.

#### CLINICAL RELEVANCE/APPLICATION

Characterization of recovery following various interventional oncology procedures could facilitate appropriate intervention in patients with poor post-procedural progression and better inform treatment recommendations.

Printed on: 02/07/23

## Abstract Archives of the RSNA, 2022

T5B-SPIR-9

### MR-guided High Intensity Focused Ultrasound (MRgHIFU) in The treatment of Bone Metastases: Safety of Sensitive Structures Within 1 cm from Target Lesion

Tuesday, Nov. 29 12:45PM - 1:15PM Room: Learning Center - IR DPS

#### Awards

Trainee Research Prize - Resident

#### Participants

Valerio D'Agostino, MD, (*Presenter*) Nothing to Disclose

#### PURPOSE

A distance greater than 1 cm between the target lesion and sensitive structures is highly recommended in MRgHIFU treatments of bone lesions. The aim of this work was to evaluate the safety of MRgHIFU treatment for pain palliation of bone metastases involving regions close to (lt1cm) sensitive structures.

#### METHODS AND MATERIALS

101 patients (56% female, 44% male; mean age 55±15,4) with 141 bone metastases were treated by MRgHIFU. Close proximity between the target lesion and sensitive structures (skin, nerves, vessels, sensitive organs) was measured on pre-treatment MR images, and metastases were divided in two groups according to this (> 1 cm distance - group A, < 1 cm - group B). VAS score at baseline, and at 3 and 6 months after treatment was assessed in all patients. MR/CT imaging was performed before and 3-6 months after treatment, in order to assess local tumour control according to MD Anderson criteria. Primary endpoint was the rate of major and minor complications on sensitive structures, according to the common terminology criteria for adverse events, version 5.0. Secondary endpoints included the assessment of the impact of such proximity (lesion to sensitive structures) on response to treatment - treatment efficacy.

#### RESULTS

141 metastases were submitted to MRgHIFU (primary tumors: 33,5% breast, 13% prostate, 12,7% kidney, 40,8% others). 85 metastases were included in group A. Close proximity between the target lesion and sensitive structures was recorded for 56 metastases (6 skin, 22 nerves, 17 vessels, 6 sensitive organs - 11 with combined conditions) - group B. 1 case of Grade 1 Burn (group A) and 1 case of Grade 1 Prostatic Pain (group B) were observed. VAS at baseline was 5.9±2,7, with a significant reduction at 3 months (2,57±2,5, p lt0.0001) and at 6 months (2,82±2,83, p lt0.0001). Complete follow-up at 3 and 6 months after treatment was available for 61 patients. Complete response was observed in 16 cases, partial response in 18, stability in 23 and progression in 4 patients. Location in proximity of sensitive structures did not affect the outcome of treatments, as there was no statistically significant difference in both safety and efficacy between the two groups of patients.

#### CONCLUSION

s MRgHIFU can be safely and effectively performed even on lesions located at lt1 cm from sensitive structures.

#### CLINICAL RELEVANCE/APPLICATION

A distance lt1 cm from sensitive structures of the target lesion is considered an exclusion criterion for MRgHIFU treatment. The results of this study suggest the need for revision of MRgHIFU's exclusion criteria, in clinical practice and research.

Printed on: 02/07/23

## Abstract Archives of the RSNA, 2022

T5B-SPMK

### Musculoskeletal Tuesday Poster Discussions - B

Tuesday, Nov. 29 12:45PM - 1:15PM Room: Learning Center - MK DPS

#### Sub-Events

#### T5B-SPMK-2 Voriconazole-induced Periostitis: Clinical, Laboratory and Imaging Features

##### Participants

Alwalid Ashmeik, MD, San Francisco, CA (*Presenter*) Nothing to Disclose

##### PURPOSE

There are several case reports of voriconazole-induced periostitis (VIP) developing in patients on chronic voriconazole therapy. However, studies have been limited by small sample sizes and variable radiological findings between cases. The goal of this study is to better characterize the clinical, laboratory and radiologic findings of VIP.

##### METHODS AND MATERIALS

100 participants with voriconazole use were identified using a PACS search tool. Health record data including age, gender, alkaline phosphatase (ALP) and voriconazole dose and treatment duration were collected. All imaging studies during the duration of treatment were reviewed by two radiology trainees and imaging features of VIP were confirmed by a board-certified musculoskeletal radiologist. Size, location and morphology of VIP lesions were recorded. Incident VIP was defined as new periostitis or enthesitis on imaging after 28 days or more of voriconazole treatment in the absence of an alternative diagnosis. Cumulative dose was calculated as the summation of daily dose from the date of initiation until the date of incident VIP. Differences in group characteristics were assessed using independent t-tests for continuous variables or chi-square tests for categorical variables. Firth's logistic regression models were performed using standardized values for cumulative voriconazole dose, treatment duration and ALP as predictors and incident VIP as the outcome.

##### RESULTS

Compared to participants without VIP (N = 91), participants with VIP (N = 9) had higher age (61.2 vs 42.0 years, P = 0.02), cumulative voriconazole dose (356.5 vs 136.4 g, P = 0.005), treatment duration (884.6 vs 322.6 days, P = 0.002) and ALP (300.8 vs 159.1 U/L, P = 0.003). There were 97 lesions with a mean length of 33.8 (SD 26.2) mm. The most common lesion location in the body was the hand (28.9%) and morphology was solid (37%). A one standard deviation increase in cumulative voriconazole dose (225.2 g) was associated with 80% higher odds of VIP (P = 0.01). A one standard deviation increase in treatment duration (537 days) was associated with 82% higher odds of VIP (P = 0.008). A one standard deviation increase in ALP (214.4 U/L) was associated with 88% higher odds of VIP (P = 0.01).

##### CONCLUSION

s Participants with VIP were older and had higher cumulative voriconazole dose, treatment duration and ALP compared with those that did not have VIP. Furthermore, increased cumulative voriconazole dose, treatment duration and ALP were associated with higher odds of VIP.

##### CLINICAL RELEVANCE/APPLICATION

VIP is an important entity for radiologists to recognize. A greater understanding of the clinical, laboratory and imaging features of this condition is essential given that voriconazole discontinuation is effective at reversing the disease course.

#### T5B-SPMK-3 Automated Deep Learning Tool for Volumetric Assessment of Abdominal Muscle Mass on CT

##### Participants

Phuong Vu, Philadelphia, PA (*Presenter*) Nothing to Disclose

##### PURPOSE

The purpose of this study was to develop a convolutional neural network (CNN) to automatically determine lean abdominal muscle volume for individual muscle groups using computed tomography (CT) for the diagnosis and assessment of sarcopenia.

##### METHODS AND MATERIALS

This retrospective study was conducted using the Penn Medicine BioBank (PMBB), a single-institutional research protocol that recruits adult participants during outpatient visits, including 34,150 patients for whom 186,721 CTs and years of detailed electronic health record, genomic, and laboratory data were collected. We developed a deep residual U-Net (ResUNet) using Pytorch to segment 12 abdominal muscle groups and determine lean muscle volume from CT scans. 105 CT studies were randomly selected to train the network; of these, 10 were used to teach Penn undergraduate students to label muscle groups. This dataset was enriched with 20 sets of 3 studies specific to different intra-abdominal pathologies (ventral hernia, abdominal abscess, etc.). Students labeled all 165 studies, encompassing 3300 axial CT slices and 980 labels, later verified and revised by a board-certified abdominal radiologist and physicist (H.S. and W.R.W.). The 165 accessions were divided into non-overlapping training (70%), validation (20%) and testing (10%) sets. Model performance was evaluated using the Sørensen-Dice coefficient.

## RESULTS

The model's performance (Dice scores) on the test data was (P, psoas):  $0.85 \pm 0.12$ , (QL, quadratus lumborum):  $0.72 \pm 0.14$ , (ES, erector spinae):  $0.91 \pm 0.07$ , (GM, gluteus medius):  $0.90 \pm 0.08$ , (RA, rectus abdominus):  $0.85 \pm 0.08$ , (LA, lateral abdominals):  $0.85 \pm 0.09$ . The average Dice score across all muscle groups was  $0.86 \pm 0.05$ . The addition of residual units to the CNN significantly reduced the time to model convergence and increased the validation Dice scores.

## CONCLUSION

These preliminary findings show that our CNN can automate detailed abdominal muscle volume measurement. Unlike prior efforts which only provided 2D information and did not distinguish between muscle groups, this technique provides 3D muscle segmentations of individual muscles

## CLINICAL RELEVANCE/APPLICATION

Sarcopenia is a prevalent but challenging diagnosis with far-reaching clinical and public health implications. There are currently no tools for direct 3D volumetric assessment of individual abdominal muscle mass. The CNN model we developed will dramatically impact sarcopenia diagnosis and research, elucidating its clinical and public health implications. Our overarching goal is to investigate genetic variants for sarcopenia and malnutrition, while describing genotype—phenotype associations of muscle mass in healthy humans using imaging-derived phenotypes

## T5B-SPMK-4 Femoral Version: Reliable and Reproducible MRI Measurement Compared to CT Using Fast 3D T1 Images Without Leg Holder

### Awards

Trainee Research Prize - Resident

### Participants

Till Lerch, MD, PhD, Bern, Switzerland (*Presenter*) Nothing to Disclose

## PURPOSE

Femoroacetabular Impingement (FAI) is a known cause for hip pain in young patients. Abnormal femoral version (FV) has been associated with extraarticular hip impingement. Variations in acquisition technique were subject of controversy for MRI-based measurement of FV. Knee bolstering is commonly used for MRI but could introduce bias to FV measurement. MRI- and CT-based measurements of FV were compared. Purposes (1) What is the reliability in terms of mean difference and correlation with and without bolstering? (2) What is the mean difference and correlation between two readers?

## METHODS AND MATERIALS

A retrospective IRB approved comparative radiologic study involving a total of 100 hips was performed. Of them, 52 hips (46 patients) underwent standard MRI with a knee bolstering, while 48 hips had no knee bolstering and additional MRI sequence. All patients (100 hips) had symptomatic FAI (mean age of  $28 \pm 10$  years). All patients underwent pelvic CT scan and MRI of the same hip joint (2016-2019). Mean interval time between CT and MRI was 20 days. In addition to the routine unilateral, multiplanar protocol for chondrolabral lesions, bilateral fast T1 VIBE Dixon of the pelvis and of the knee was acquired (acquisition time less than 1 minute) for 48 hips without bolstering to measure FV. Two readers independently measured FV on both CT and MRI scans on two separate sessions (Murphy method). Correlation between CT and MRI was assessed using Pearson correlation coefficient.

## RESULTS

(1) Mean absolute difference between MRI with bolstering and CT-based measurements of FV of 52 hips was  $6.0^\circ \pm 3$  ( $-10$ - $7$ ) for Reader 1 and  $8.4^\circ \pm 5$  ( $-21$ - $12$ ) for Reader 2. Mean absolute difference between MRI without bolstering and CT-based measurements of FV of 48 hips decreased to  $1.3^\circ \pm 0.8$  ( $0.2$ - $3.0$ ) for Reader 1 and  $2.3^\circ \pm 1.9$  ( $0$ - $10$ ) for Reader 2. Correlation of FV between MRI without bolstering and CT-based measurements was  $r=0.993$  ( $p<0.001$ ) for reader 1 and was  $r=0.975$  ( $p<0.001$ ) for reader 2. (2) Mean absolute difference of CT-based measurements of FV between two readers was  $2.9^\circ \pm 2$  ( $-0$ - $8$ ) and correlation was  $r=0.969$  ( $p<0.001$ ). Mean difference of MRI-based measurements without bolstering of FV between two readers was  $3.3^\circ \pm 3$  ( $0$ - $10$ ) and correlation was  $r=0.943$  ( $p<0.001$ ).

## CONCLUSION

MRI-based measurement of FV is as accurate and reliable as CT-based measurements when using T1 VIBE DIXON and in patients with FAI. Shorter MRI acquisition time and no bolstering during MRI decreased measurement errors in FV, leading to less misdiagnosis of FV.

## CLINICAL RELEVANCE/APPLICATION

We changed our clinical practice and use MRI with VIBE Dixon without knee bolstering for preoperative measurement of FV. This could reduce radiation dose for typically young patients of childbearing age compared to CT scans.

Printed on: 02/07/23

## Abstract Archives of the RSNA, 2022

T5B-SPMK-2

### Voriconazole-induced Periostitis: Clinical, Laboratory and Imaging Features

Tuesday, Nov. 29 12:45PM - 1:15PM Room: Learning Center - MK DPS

#### Participants

Alwalid Ashmeik, MD, San Francisco, CA (*Presenter*) Nothing to Disclose

#### PURPOSE

There are several case reports of voriconazole-induced periostitis (VIP) developing in patients on chronic voriconazole therapy. However, studies have been limited by small sample sizes and variable radiological findings between cases. The goal of this study is to better characterize the clinical, laboratory and radiologic findings of VIP.

#### METHODS AND MATERIALS

100 participants with voriconazole use were identified using a PACS search tool. Health record data including age, gender, alkaline phosphatase (ALP) and voriconazole dose and treatment duration were collected. All imaging studies during the duration of treatment were reviewed by two radiology trainees and imaging features of VIP were confirmed by a board-certified musculoskeletal radiologist. Size, location and morphology of VIP lesions were recorded. Incident VIP was defined as new periostitis or enthesitis on imaging after 28 days or more of voriconazole treatment in the absence of an alternative diagnosis. Cumulative dose was calculated as the summation of daily dose from the date of initiation until the date of incident VIP. Differences in group characteristics were assessed using independent t-tests for continuous variables or chi-square tests for categorical variables. Firth's logistic regression models were performed using standardized values for cumulative voriconazole dose, treatment duration and ALP as predictors and incident VIP as the outcome.

#### RESULTS

Compared to participants without VIP (N = 91), participants with VIP (N = 9) had higher age (61.2 vs 42.0 years, P = 0.02), cumulative voriconazole dose (356.5 vs 136.4 g, P = 0.005), treatment duration (884.6 vs 322.6 days, P = 0.002) and ALP (300.8 vs 159.1 U/L, P = 0.003). There were 97 lesions with a mean length of 33.8 (SD 26.2) mm. The most common lesion location in the body was the hand (28.9%) and morphology was solid (37%). A one standard deviation increase in cumulative voriconazole dose (225.2 g) was associated with 80% higher odds of VIP (P = 0.01). A one standard deviation increase in treatment duration (537 days) was associated with 82% higher odds of VIP (P = 0.008). A one standard deviation increase in ALP (214.4 U/L) was associated with 88% higher odds of VIP (P = 0.01).

#### CONCLUSION

s Participants with VIP were older and had higher cumulative voriconazole dose, treatment duration and ALP compared with those that did not have VIP. Furthermore, increased cumulative voriconazole dose, treatment duration and ALP were associated with higher odds of VIP.

#### CLINICAL RELEVANCE/APPLICATION

VIP is an important entity for radiologists to recognize. A greater understanding of the clinical, laboratory and imaging features of this condition is essential given that voriconazole discontinuation is effective at reversing the disease course.

Printed on: 02/07/23

## Abstract Archives of the RSNA, 2022

T5B-SPMK-3

### Automated Deep Learning Tool for Volumetric Assessment of Abdominal Muscle Mass on CT

Tuesday, Nov. 29 12:45PM - 1:15PM Room: Learning Center - MK DPS

#### Participants

Phuong Vu, Philadelphia, PA (*Presenter*) Nothing to Disclose

#### PURPOSE

The purpose of this study was to develop a convolutional neural network (CNN) to automatically determine lean abdominal muscle volume for individual muscle groups using computed tomography (CT) for the diagnosis and assessment of sarcopenia.

#### METHODS AND MATERIALS

This retrospective study was conducted using the Penn Medicine BioBank (PMBB), a single-institutional research protocol that recruits adult participants during outpatient visits, including 34,150 patients for whom 186,721 CTs and years of detailed electronic health record, genomic, and laboratory data were collected. We developed a deep residual U-Net (ResUNet) using Pytorch to segment 12 abdominal muscle groups and determine lean muscle volume from CT scans. 105 CT studies were randomly selected to train the network; of these, 10 were used to teach Penn undergraduate students to label muscle groups. This dataset was enriched with 20 sets of 3 studies specific to different intra-abdominal pathologies (ventral hernia, abdominal abscess, etc.). Students labeled all 165 studies, encompassing 3300 axial CT slices and 980 labels, later verified and revised by a board-certified abdominal radiologist and physicist (H.S. and W.R.W.). The 165 accessions were divided into non-overlapping training (70%), validation (20%) and testing (10%) sets. Model performance was evaluated using the Sørensen-Dice coefficient.

#### RESULTS

The model's performance (Dice scores) on the test data was (P, psoas):  $0.85 \pm 0.12$ , (QL, quadratus lumborum):  $0.72 \pm 0.14$ , (ES, erector spinae):  $0.91 \pm 0.07$ , (GM, gluteus medius):  $0.90 \pm 0.08$ , (RA, rectus abdominus):  $0.85 \pm 0.08$ , (LA, lateral abdominals):  $0.85 \pm 0.09$ . The average Dice score across all muscle groups was  $0.86 \pm 0.05$ . The addition of residual units to the CNN significantly reduced the time to model convergence and increased the validation Dice scores.

#### CONCLUSION

These preliminary findings show that our CNN can automate detailed abdominal muscle volume measurement. Unlike prior efforts which only provided 2D information and did not distinguish between muscle groups, this technique provides 3D muscle segmentations of individual muscles

#### CLINICAL RELEVANCE/APPLICATION

Sarcopenia is a prevalent but challenging diagnosis with far-reaching clinical and public health implications. There are currently no tools for direct 3D volumetric assessment of individual abdominal muscle mass. The CNN model we developed will dramatically impact sarcopenia diagnosis and research, elucidating its clinical and public health implications. Our overarching goal is to investigate genetic variants for sarcopenia and malnutrition, while describing genotype—phenotype associations of muscle mass in healthy humans using imaging-derived phenotypes

Printed on: 02/07/23

## Abstract Archives of the RSNA, 2022

T5B-SPMK-4

### Femoral Version: Reliable and Reproducible MRI Measurement Compared to CT Using Fast 3D T1 Images Without Leg Holder

Tuesday, Nov. 29 12:45PM - 1:15PM Room: Learning Center - MK DPS

#### Awards

Trainee Research Prize - Resident

#### Participants

Till Lerch, MD, PhD, Bern, Switzerland (*Presenter*) Nothing to Disclose

#### PURPOSE

Femoroacetabular Impingement (FAI) is a known cause for hip pain in young patients. Abnormal femoral version (FV) has been associated with extraarticular hip impingement. Variations in acquisition technique were subject of controversy for MRI-based measurement of FV. Knee bolstering is commonly used for MRI but could introduce bias to FV measurement. MRI- and CT-based measurements of FV were compared. Purposes (1) What is the reliability in terms of mean difference and correlation with and without bolstering? (2) What is the mean difference and correlation between two readers?

#### METHODS AND MATERIALS

A retrospective IRB approved comparative radiologic study involving a total of 100 hips was performed. Of them, 52 hips (46 patients) underwent standard MRI with a knee bolstering, while 48 hips had no knee bolstering and additional MRI sequence. All patients (100 hips) had symptomatic FAI (mean age of  $28 \pm 10$  years). All patients underwent pelvic CT scan and MRI of the same hip joint (2016-2019). Mean interval time between CT and MRI was 20 days. In addition to the routine unilateral, multiplanar protocol for chondrolabral lesions, bilateral fast T1 VIBE Dixon of the pelvis and of the knee was acquired (acquisition time less than 1 minute) for 48 hips without bolstering to measure FV. Two readers independently measured FV on both CT and MRI scans on two separate sessions (Murphy method). Correlation between CT and MRI was assessed using Pearson correlation coefficient.

#### RESULTS

(1) Mean absolute difference between MRI with bolstering and CT-based measurements of FV of 52 hips was  $6.0^\circ \pm 3$  (-10-7) for Reader 1 and  $8.4^\circ \pm 5$  (-21-12) for Reader 2. Mean absolute difference between MRI without bolstering and CT-based measurements of FV of 48 hips decreased to  $1.3^\circ \pm 0.8$  (0.2-3.0) for Reader 1 and  $2.3^\circ \pm 1.9$  (0-10) for Reader 2. Correlation of FV between MRI without bolstering and CT-based measurements was  $r=0.993$  ( $p<0.001$ ) for reader 1 and was  $r=0.975$  ( $p<0.001$ ) for reader 2. (2) Mean absolute difference of CT-based measurements of FV between two readers was  $2.9^\circ \pm 2$  (-0-8) and correlation was  $r=0.969$  ( $p<0.001$ ). Mean difference of MRI-based measurements without bolstering of FV between two readers was  $3.3^\circ \pm 3$  (0-10) and correlation was  $r=0.943$  ( $p<0.001$ ).

#### CONCLUSION

s MRI-based measurement of FV is as accurate and reliable as CT-based measurements when using T1 VIBE DIXON and in patients with FAI. Shorter MRI acquisition time and no bolstering during MRI decreased measurement errors in FV, leading to less misdiagnosis of FV.

#### CLINICAL RELEVANCE/APPLICATION

We changed our clinical practice and use MRI with VIBE Dixon without knee bolstering for preoperative measurement of FV. This could reduce radiation dose for typically young patients of childbearing age compared to CT scans.

Printed on: 02/07/23

## Abstract Archives of the RSNA, 2022

T5B-SPNMMI

### Nuclear Medicine/Molecular Imaging Tuesday Poster Discussion - B

Tuesday, Nov. 29 12:45PM - 1:15PM Room: Learning Center - NMMI DPS

#### Participants

Georges El Fakhri, PhD, Boston, MA (*Moderator*) Nothing to Disclose

#### Sub-Events

#### **T5B-SPNMMI-1 Additional Value of 18F-DCFPyL PET/MRI Radiomic Features for Nodal and Distant Metastases Detection of Prostate Cancer**

#### Participants

Adriano Basso Dias, MD, MSc, Toronto, ON (*Presenter*) Nothing to Disclose

#### PURPOSE

To evaluate the performance of combined PET and multiparametric MRI (mpMRI) radiomics for the prediction of nodal and distant metastases in patients with suspicion of prostate cancer (PCa), or patients being considered for focal ablative therapies (FT), or patients with unfavorable intermediate/high-risk PCa.

#### METHODS AND MATERIALS

This ethics review board-approved, retrospective analysis of two prospective clinical trials, included 103 men, with suspicion of PCa and negative systematic biopsies or clinically discordant low-risk PCa (n=20), those being considered for FT (n=31) and those with unfavorable intermediate or high-risk prostate cancer (n=52). All patients received 18F-DCFPyL PET/MRI. All suspicious lesions underwent biopsy. Whole-prostate segmentations were performed on each modality separately, including the whole-gland T2-weighted sequence, whole-gland apparent diffusion coefficient (ADC) map, and whole-gland PET images. Then, image biomarker standardization initiative (IBSI)-compliant radiomic features were extracted. A total of 307 features based on the PET and MRI images were calculated. Univariate Logistic Regression was done to find the predictive value of the extracted features.

#### RESULTS

A total of 103 patients (mean age= 65; mean PSA level= 23.4) were studied. Based on the PET/MRI findings, 22 (21%) patients had metastatic disease, including 14 patients with only nodal metastasis and 8 patients with both nodal and distant metastases. PCa was confirmed in 93 (90%) patients after the histopathologic evaluation, and 10 patients were negative for malignancy according to biopsy. Among the proven PCa patients, 37 (36%) patients were grouped in ISUP 1 and 2, and 56 (64%) patients were in ISUP 3,4 and 5. The calculated radiomic features extracted from the segmented prostate glands were associated with the metastatic status (nodal and/or distant metastases). DISCRETIZED, GLCM, and GLZLM were the most significant variables in the prediction, with odds ratios ranging from 3.49 (95% CI: 1.86-6.55) to 5.15 (95% CI: 2.42-10.95).

#### CONCLUSION

A whole-gland feature extraction could possibly predict the extraprostatic status of the PCa patients, showing the potential in prediction of metastatic disease (nodal and/or distant metastases). These findings indicate that by assessing the prostate gland as a whole could be potentially used for further treatment approach personalization in PCa patients.

#### CLINICAL RELEVANCE/APPLICATION

Detection of metastatic disease (nodal and/or distant metastases) is crucial for management of men with prostate cancer. 18F-DCFPyL PET/MRI Radiomics showed promising results as a predictor of metastases in patients with prostate cancer.

#### **T5B-SPNMMI-2 Preliminary Investigation on Adenovirus-Mediated Transferrin Receptor Reporter Gene in Colorectal Cell MRI Imaging**

#### Participants

Hua He, MMedSc, MMedSc, Yinchuan, China (*Presenter*) Nothing to Disclose

#### PURPOSE

To explore the best multiplicities of infection (MOI), the expression of the target gene and in vitro MRI imaging of adenovirus vector-mediated transferrin receptor (TFRC) reporter gene transfer of human colorectal Lovo cells.

#### METHODS AND MATERIALS

Lovo cells were transfected with recombinant adenovirus (Ad-TFRC) at 5, 10, 50, 100 MOI to determine the best MOI, and quantitative real-time PCR was performed to detect the cDNA of TFRC. The transfected cells were incubated in the culture medium including Tf-USPIO of variance concepts, and were observed by Prussian blue staining, then the cell viability was evaluated via Trypan blue staining. The labeled cells were scanned with 7.0T MR T2W, T2 map, T2\* map sequences, and the signatures were analyzed.

## RESULTS

Ad-TFRC were successfully transfected into Lovo cells. The best MOI was 50, and the efficiency of innovation was more than 90%. The relative expression amount of TFRC in transfected cells was higher than that in control Lovo cells by real-time quantitative PCR ( $P < 0.01$ ). Prussian blue staining numerous blue iron parts in transfected cells when the best labelling concentration was 1.5  $\mu\text{g/ml}$ . Trypan blue staining results of transfected Lovo cells and control Lovo cells was  $(93.80 \pm 1.60)\%$  and  $(95.10 \pm 2.30)\%$ , respectively ( $P > 0.05$ ). MRI Imaging in vitro shown that compared with control Lovo cells, the signal intensity decreased on T2WI, T2map and T2\*map sequences in transfected Lovo cells ( $P < 0.05$ ).

## CONCLUSION

s TFRC reporter gene can be efficiently mediated by adenovirus for expression in Lovo cells. After magnetization labeling, 7.0T MRI Imaging of Lovo cells can be successfully achieved in vitro.

## CLINICAL RELEVANCE/APPLICATION

Provide basic research basis for the occurrence and development mechanism of colorectal cancer.

## T5B-SPNMMI-3 Accurate PET Quantification Using 3D Recovery Coefficient for Small or Irregular Shaped Objects

Participants

Matthew Smith, MD, PhD, Nashville, TN (*Presenter*) Nothing to Disclose

## PURPOSE

Quantitation using SUV<sub>max</sub> is an approximation with known limitations in small objects. The purpose of this work is to investigate a method to accurately calculate the 3D recovery coefficient (3D-RC) in an object of any shape or size to provide accurate PET quantification.

## METHODS AND MATERIALS

The FWHMs of the PET/CT scanner (Philips Vereos) were measured in the radial (R), tangential (T), and axial (A) dimensions at isocenter and at 8 cm from the scanner centerline using point sources to determine the 3D point-spread function (3D-PSF) using a typical clinical reconstruction algorithm. Using Matlab, cylinders and spheres with diameters ranging from 1 mm to 40 mm and length of 400 mm were simulated with 0.625 mm pixel resolution. Each object was convolved with the measured 3D-PSF using a 3D-FFT to produce a 3D recovery coefficient (3D-RC) map. For each 3D-RC map, the max and mean recovery coefficients were recorded within the bounds of the object and plotted against object size.

## RESULTS

Measured FWHMs in water for R, A, and T directions were 4.5, 4.5, and 4.5 mm, respectively. Radial FWHM did not vary for objects up to 8 cm from the centerline. Simulated 3D-RC values were lower for spheres compared to cylinders and decreased with smaller object size, consistent with prior published data for cylinders and spheres.

## CONCLUSION

s A new approach to calculating an accurate 3D recovery coefficient for PET is presented and validated with prior published results. Unlike prior methods using lookup tables to estimate 3D-RC's for clinical PET, this method can easily be extended to irregularly shaped objects by simple 3D convolution. Future work includes phantom validation and application to clinical data.

## CLINICAL RELEVANCE/APPLICATION

Improved PET ROI quantification is needed for assessing tumor SUV response for small lesions as well as providing accurate measurements for quantitative PET. This method utilizes a new approach to accurately measure PET activity in small or irregularly-shaped objects (e.g. F-18 DOPA imaging of the putamen, lymph node conglomerates, or lung masses). For objects adjacent to high activity structures, this method can also generate spillover factors. This method can be easily incorporated into clinical practice using existing technology.

Printed on: 02/07/23

## Abstract Archives of the RSNA, 2022

T5B-SPNMMI-1

### Additional Value of 18F-DCFPyL PET/MRI Radiomic Features for Nodal and Distant Metastases Detection of Prostate Cancer

Tuesday, Nov. 29 12:45PM - 1:15PM Room: Learning Center - NMMI DPS

#### Participants

Adriano Basso Dias, MD, MSc, Toronto, ON (*Presenter*) Nothing to Disclose

#### PURPOSE

To evaluate the performance of combined PET and multiparametric MRI (mpMRI) radiomics for the prediction of nodal and distant metastases in patients with suspicion of prostate cancer (PCa), or patients being considered for focal ablative therapies (FT), or patients with unfavorable intermediate/high-risk PCa.

#### METHODS AND MATERIALS

This ethics review board-approved, retrospective analysis of two prospective clinical trials, included 103 men, with suspicion of PCa and negative systematic biopsies or clinically discordant low-risk PCa (n=20), those being considered for FT (n=31) and those with unfavorable intermediate or high-risk prostate cancer (n=52). All patients received 18F-DCFPyL PET/MRI. All suspicious lesions underwent biopsy. Whole-prostate segmentations were performed on each modality separately, including the whole-gland T2-weighted sequence, whole-gland apparent diffusion coefficient (ADC) map, and whole-gland PET images. Then, image biomarker standardization initiative (IBSI)-compliant radiomic features were extracted. A total of 307 features based on the PET and MRI images were calculated. Univariate Logistic Regression was done to find the predictive value of the extracted features.

#### RESULTS

A total of 103 patients (mean age= 65; mean PSA level= 23.4) were studied. Based on the PET/MRI findings, 22 (21%) patients had metastatic disease, including 14 patients with only nodal metastasis and 8 patients with both nodal and distant metastases. PCa was confirmed in 93 (90%) patients after the histopathologic evaluation, and 10 patients were negative for malignancy according to biopsy. Among the proven PCa patients, 37 (36%) patients were grouped in ISUP 1 and 2, and 56 (64%) patients were in ISUP 3,4 and 5. The calculated radiomic features extracted from the segmented prostate glands were associated with the metastatic status (nodal and/or distant metastases). DISCRETIZED, GLCM, and GLZLM were the most significant variables in the prediction, with odds ratios ranging from 3.49 (95% CI: 1.86-6.55) to 5.15 (95% CI: 2.42-10.95).

#### CONCLUSION

A whole-gland feature extraction could possibly predict the extraprostatic status of the PCa patients, showing the potential in prediction of metastatic disease (nodal and/or distant metastases). These findings indicate that by assessing the prostate gland as a whole could be potentially used for further treatment approach personalization in PCa patients.

#### CLINICAL RELEVANCE/APPLICATION

Detection of metastatic disease (nodal and/or distant metastases) is crucial for management of men with prostate cancer. 18F-DCFPyL PET/MRI Radiomics showed promising results as a predictor of metastases in patients with prostate cancer.

Printed on: 02/07/23

## Abstract Archives of the RSNA, 2022

T5B-SPNMMI-2

### Preliminary Investigation on Adenovirus-Mediated Transferrin Receptor Reporter Gene in Colorectal Cell MRI Imaging

Tuesday, Nov. 29 12:45PM - 1:15PM Room: Learning Center - NMMI DPS

#### Participants

Hua He, MMedSc, MMedSc, Yinchuan, China (*Presenter*) Nothing to Disclose

#### PURPOSE

To explore the best multiplicities of infection (MOI), the expression of the target gene and in vitro MRI imaging of adenovirus vector-mediated transferrin receptor (TFRC) reporter gene transfer of human colorectal Lovo cells.

#### METHODS AND MATERIALS

Lovo cells were transfected with recombinant adenovirus (Ad-TFRC) at 5, 10, 50, 100 MOI to determine the best MOI, and quantitative real-time PCR was performed to detect the cDNA of TFRC. The transfected cells were incubated in the culture medium including Tf-USPIO of various concentrations, and were observed by Prussian blue staining, then the cell viability was evaluated via Trypan blue staining. The labeled cells were scanned with 7.0T MR T2W, T2 map, T2\* map sequences, and the signatures were analyzed.

#### RESULTS

Ad-TFRC were successfully transfected into Lovo cells. The best MOI was 50, and the efficiency of infection was more than 90%. The relative expression amount of TFRC in transfected cells was higher than that in control Lovo cells by real-time quantitative PCR ( $P < 0.01$ ). Prussian blue staining showed numerous blue iron particles in transfected cells when the best labeling concentration was 1.5  $\mu\text{g}/\text{ml}$ . Trypan blue staining results of transfected Lovo cells and control Lovo cells were  $(93.80 \pm 1.60)\%$  and  $(95.10 \pm 2.30)\%$ , respectively ( $P > 0.05$ ). MRI imaging in vitro showed that compared with control Lovo cells, the signal intensity decreased on T2WI, T2 map and T2\* map sequences in transfected Lovo cells ( $P < 0.05$ ).

#### CONCLUSION

s TFRC reporter gene can be efficiently mediated by adenovirus for expression in Lovo cells. After magnetization labeling, 7.0T MRI imaging of Lovo cells can be successfully achieved in vitro.

#### CLINICAL RELEVANCE/APPLICATION

Provide basic research basis for the occurrence and development mechanism of colorectal cancer.

Printed on: 02/07/23

## Abstract Archives of the RSNA, 2022

T5B-SPNMMI-3

### Accurate PET Quantification Using 3D Recovery Coefficient for Small or Irregular Shaped Objects

Tuesday, Nov. 29 12:45PM - 1:15PM Room: Learning Center - NMMI DPS

#### Participants

Matthew Smith, MD, PhD, Nashville, TN (*Presenter*) Nothing to Disclose

#### PURPOSE

Quantitation using SUVmax is an approximation with known limitations in small objects. The purpose of this work is to investigate a method to accurately calculate the 3D recovery coefficient (3D-RC) in an object of any shape or size to provide accurate PET quantification.

#### METHODS AND MATERIALS

The FWHMs of the PET/CT scanner (Philips Vereos) were measured in the radial (R), tangential (T), and axial (A) dimensions at isocenter and at 8 cm from the scanner centerline using point sources to determine the 3D point-spread function (3D-PSF) using a typical clinical reconstruction algorithm. Using Matlab, cylinders and spheres with diameters ranging from 1 mm to 40 mm and length of 400 mm were simulated with 0.625 mm pixel resolution. Each object was convolved with the measured 3D-PSF using a 3D-FFT to produce a 3D recovery coefficient (3D-RC) map. For each 3D-RC map, the max and mean recovery coefficients were recorded within the bounds of the object and plotted against object size.

#### RESULTS

Measured FWHMs in water for R, A, and T directions were 4.5, 4.5, and 4.5 mm, respectively. Radial FWHM did not vary for objects up to 8 cm from the centerline. Simulated 3D-RC values were lower for spheres compared to cylinders and decreased with smaller object size, consistent with prior published data for cylinders and spheres.

#### CONCLUSION

A new approach to calculating an accurate 3D recovery coefficient for PET is presented and validated with prior published results. Unlike prior methods using lookup tables to estimate 3D-RC's for clinical PET, this method can easily be extended to irregularly shaped objects by simple 3D convolution. Future work includes phantom validation and application to clinical data.

#### CLINICAL RELEVANCE/APPLICATION

Improved PET ROI quantification is needed for assessing tumor SUV response for small lesions as well as providing accurate measurements for quantitative PET. This method utilizes a new approach to accurately measure PET activity in small or irregularly-shaped objects (e.g. F-18 DOPA imaging of the putamen, lymph node conglomerates, or lung masses). For objects adjacent to high activity structures, this method can also generate spillover factors. This method can be easily incorporated into clinical practice using existing technology.

Printed on: 02/07/23



## Abstract Archives of the RSNA, 2022

T5B-SPNPM

### Noninterpretive Skills/Quality Improvement/Practice Management Tuesday Poster Discussions - B

Tuesday, Nov. 29 12:45PM - 1:15PM Room: Learning Center - NPM DPS

#### Participants

Shaun A. Wahab, MD, Mason, OH (*Moderator*) Consultant, GlaxoSmithKline plc; Consultant, BioClinica, Inc; Consultant, Mersana Therapeutics, Inc

#### Sub-Events

#### T5B-SPNPM- Evaluating Faculty Teaching Skills in Diagnostic Imaging: Can We Ask Better Questions to Get More Useful Answers?

#### Participants

Daria Manos, FRCPC, Halifax, NS (*Presenter*) Speakers Bureau, Boehringer Ingelheim GmbH; Advisory Board, AstraZeneca PLC

#### PURPOSE

Faculty evaluation by residents is an important component of resident responsibility and professionalism. Unfortunately, many programs note difficulty obtaining quality feedback. Teaching evaluations in our department suffered from low response rates and poor utility. We sought to explore the limitations of the current process and to redesign it recognizing teaching activity specific to Diagnostic Imaging.

#### METHODS AND MATERIALS

The current evaluation process was assessed through feedback obtained from two focus groups (residents and members of the department education council) and interviews with the department chair. Several themes emerged. Residents noted evaluation-fatigue, insufficient time to complete evaluations, and concern evaluation was ineffectual. The department chair noted the number and quality of evaluations was insufficient to provide faculty support or to recognize excellence. Faculty expressed underappreciation related to low scores and/or low response rate, and noted poor utility of feedback. The evaluation form was redesigned based on focus group discussion and literature review of best practices. A department council including resident and faculty representatives reiteratively revised the form. The new process was trialed with 22 residents evaluating 47 faculty. Mixed methods were used to assess the intervention including quantity of responses and qualitative review of changes from the perspective of the residents, faculty, and departmental leadership.

#### RESULTS

The new form included DI-specific teaching activity, narrative scales, and an explanatory preamble. Residents were provided protected time to complete evaluations. Quality and quantity of faculty teaching evaluations improved with discipline-specific assessment, narrative scales, and protected time for evaluation. Overall response rate increased from 69% to 91% with individual faculty receiving up to 3.6 times the number of responses. Faculty felt better appreciated, particularly related to free-form resident comments. Initial feedback suggested small changes that will be incorporated in the future.

#### CONCLUSION

Developing a specific and practical faculty teaching evaluation form in DI allowed a more effective, efficient and supportive feedback process. The form was designed for use in any diagnostic imaging program, but further study is needed to confirm generalizability.

#### CLINICAL RELEVANCE/APPLICATION

Faculty teaching evaluations in Diagnostic Imaging were optimized by providing a form specific to Diagnostic Imaging, by using narrative anchored scores, and by better explaining the process to the residents.

#### T5B-SPNPM- The Association Between Radiology Research Funding and Community Inclusion and Investment

#### Participants

Antonio Lopez, BA, Philadelphia, PA (*Presenter*) Nothing to Disclose

#### PURPOSE

The recent COVID-19 pandemic highlighted substantial health inequities that will require a multifaceted approach to address. One component necessitates appropriate representation of underserved populations in imaging research. The purpose of this study was to determine the relationship between NIH research funding for radiology departments/hospital systems and their contribution toward health equity.

#### METHODS AND MATERIALS

This study used publicly available de-identified data and was deemed exempt by the institutional review board. The dependent variable was aggregate radiology research funding from 2017 - 2021 by Radiology Department, derived from the NIH Reporter. Independent variables were outcomes focused on equity measures captured in the 2021 Lown Institute Hospitals Index, which

evaluates hospital social responsibility by examining performance across health outcomes, value, and equity. The community benefit metric measures hospital spending on community health initiatives, including charity care, and their service of Medicaid patients. The inclusivity metric evaluates how a hospital's patient population reflects the demographics of their local community based on race, income, and education levels. Bivariable linear regression and Pearson's correlation coefficients (CC) were used to evaluate the association between Radiology research funding and measures of hospital community benefit and inclusivity.

## RESULTS

78 radiology departments received NIH funding between 2017-2021 ranging from \$195,000 to \$216,879,079 (median \$12,603,918). On measures of inclusivity, Radiology departments that received more funding were less likely to serve low-income patients (CC -0.442,  $p = 0.000$ ), racial/ethnic minority patients (CC -0.340,  $p = 0.003$ ), and patients with less education (CC -0.455,  $p = 0.000$ ). Radiology departments receiving more funding were ranked lower on the summary weighted measure of hospital inclusivity (CC 0.493,  $p = 0.000$ ). On measures of community benefit, there were no statistically significant associations between research funding and charity care spending (CC -0.192,  $p = 0.099$ ), community investment (CC -0.043,  $p = 0.773$ ), and Medicaid as a share of patient revenue (CC -0.098,  $p = 0.404$ ).

## CONCLUSION

s Radiology departments that received more NIH research dollars were less likely to serve racial/ethnic minority and low-income patients, and patients with lower education levels.

## CLINICAL RELEVANCE/APPLICATION

To improve health outcomes of vulnerable populations, efforts should focus on narrowing this research funding gap. Options might include redistributing funds to safety net facilities or fostering collaborations among well-funded institutions with those serving primarily underserved populations.

## T5B-SPNPM- Patient, Provider, and Practice Characteristics Predicting Use of Imaging in Primary Care

3

Participants

Sue Yi, PhD,BS, Madison, WI (*Presenter*) Nothing to Disclose

## PURPOSE

To evaluate differences in imaging utilization during primary care visits based on patient medical and sociodemographic variables; provider characteristics; and practice setting using nationally representative survey data.

## METHODS AND MATERIALS

Retrospective analysis of the National Ambulatory Medical Care Survey (NAMCS) for the years 2013-2018 was conducted. All patient visits coded as primary care were included in the sample. The major outcome variable was the use of diagnostic imaging also further subdivided by modality: MRI, CT, X-ray, ultrasound, mammography, and DXA. Multiple variable logistic regression analyses were performed to evaluate the influence of patient, provider, and practice level characteristics on imaging utilization. Stata survey procedures were used with NAMCS provided sampling weights to account for the complex survey sampling design and provide valid national-level estimates of imaging utilization.

## RESULTS

A total of 2,820,381,627 primary care visits were included in the five-year study period. (Data from 2017 is not available). Patient demographics included mean age of 41, 60% female, 64% White, 11% Black, 18% Hispanic, 7% Asian or other race/ethnicity. Overall, 13% of visits resulted in imaging use which did not vary significantly by year ( $p=0.18$ ). Increased rates of imaging were seen with Black (OR 1.30, 95% CI 1.08-1.56) and Hispanic (OR 1.35, 95% CI 1.12-1.62) patients; female patients (OR 1.87, 95% CI 1.65-2.11); in patients with serious comorbidities such as cancer (OR 1.44, 95% CI 1.17-1.79); and associated with advancing patient age ( $p<0.001$ ). Imaging use was higher when the provider was not the patient's PCP (OR 1.52, 95% CI 1.27-1.82) but did not vary by MD versus DO credential ( $p=0.08$ ). Imaging utilization did not vary significantly by region ( $p=0.95$ ) or rural versus urban location ( $p=0.79$ ).

## CONCLUSION

s Imaging utilization is lower in the primary care setting than what has been reported in the Emergency Department and the disparities in imaging use by patient race seen in that environment are not observed in primary care. This suggests that increasing patient access to primary care may promote health equity. Understanding other factors associated with increased imaging use including patient age, sex, and co-morbidities may help predict health system imaging utilization and guide resource allocation.

## CLINICAL RELEVANCE/APPLICATION

Promoting policies to increase patient access to primary care may promote more equitable access to diagnostic imaging.

Printed on: 02/07/23



## Abstract Archives of the RSNA, 2022

T5B-SPNPM-1

### Evaluating Faculty Teaching Skills in Diagnostic Imaging: Can We Ask Better Questions to Get More Useful Answers?

Tuesday, Nov. 29 12:45PM - 1:15PM Room: Learning Center - NPM DPS

#### Participants

Daria Manos, FRCPC, Halifax, NS (*Presenter*) Speakers Bureau, Boehringer Ingelheim GmbH; Advisory Board, AstraZeneca PLC

#### PURPOSE

Faculty evaluation by residents is an important component of resident responsibility and professionalism. Unfortunately, many programs note difficulty obtaining quality feedback. Teaching evaluations in our department suffered from low response rates and poor utility. We sought to explore the limitations of the current process and to redesign it recognizing teaching activity specific to Diagnostic Imaging.

#### METHODS AND MATERIALS

The current evaluation process was assessed through feedback obtained from two focus groups (residents and members of the department education council) and interviews with the department chair. Several themes emerged. Residents noted evaluation-fatigue, insufficient time to complete evaluations, and concern evaluation was ineffectual. The department chair noted the number and quality of evaluations was insufficient to provide faculty support or to recognize excellence. Faculty expressed underappreciation related to low scores and/or low response rate, and noted poor utility of feedback. The evaluation form was redesigned based on focus group discussion and literature review of best practices. A department council including resident and faculty representatives reiteratively revised the form. The new process was trialed with 22 residents evaluating 47 faculty. Mixed methods were used to assess the intervention including quantity of responses and qualitative review of changes from the perspective of the residents, faculty, and departmental leadership.

#### RESULTS

The new form included DI-specific teaching activity, narrative scales, and an explanatory preamble. Residents were provided protected time to complete evaluations. Quality and quantity of faculty teaching evaluations improved with discipline-specific assessment, narrative scales, and protected time for evaluation. Overall response rate increased from 69% to 91% with individual faculty receiving up to 3.6 times the number of responses. Faculty felt better appreciated, particularly related to free-form resident comments. Initial feedback suggested small changes that will be incorporated in the future.

#### CONCLUSION

Developing a specific and practical faculty teaching evaluation form in DI allowed a more effective, efficient and supportive feedback process. The form was designed for use in any diagnostic imaging program, but further study is needed to confirm generalizability.

#### CLINICAL RELEVANCE/APPLICATION

Faculty teaching evaluations in Diagnostic Imaging were optimized by providing a form specific to Diagnostic Imaging, by using narrative anchored scores, and by better explaining the process to the residents.

Printed on: 02/07/23



## Abstract Archives of the RSNA, 2022

T5B-SPNPM-2

### The Association Between Radiology Research Funding and Community Inclusion and Investment

Tuesday, Nov. 29 12:45PM - 1:15PM Room: Learning Center - NPM DPS

#### Participants

Antonio Lopez, BA, Philadelphia, PA (*Presenter*) Nothing to Disclose

#### PURPOSE

The recent COVID-19 pandemic highlighted substantial health inequities that will require a multifaceted approach to address. One component necessitates appropriate representation of underserved populations in imaging research. The purpose of this study was to determine the relationship between NIH research funding for radiology departments/hospital systems and their contribution toward health equity.

#### METHODS AND MATERIALS

This study used publicly available de-identified data and was deemed exempt by the institutional review board. The dependent variable was aggregate radiology research funding from 2017 - 2021 by Radiology Department, derived from the NIH Reporter. Independent variables were outcomes focused on equity measures captured in the 2021 Lown Institute Hospitals Index, which evaluates hospital social responsibility by examining performance across health outcomes, value, and equity. The community benefit metric measures hospital spending on community health initiatives, including charity care, and their service of Medicaid patients. The inclusivity metric evaluates how a hospital's patient population reflects the demographics of their local community based on race, income, and education levels. Bivariable linear regression and Pearson's correlation coefficients (CC) were used to evaluate the association between Radiology research funding and measures of hospital community benefit and inclusivity.

#### RESULTS

78 radiology departments received NIH funding between 2017-2021 ranging from \$195,000 to \$216,879,079 (median \$12,603,918). On measures of inclusivity, Radiology departments that received more funding were less likely to serve low-income patients (CC -0.442,  $p = 0.000$ ), racial/ethnic minority patients (CC -0.340,  $p = 0.003$ ), and patients with less education (CC -0.455,  $p = 0.000$ ). Radiology departments receiving more funding were ranked lower on the summary weighted measure of hospital inclusivity (CC 0.493,  $p = 0.000$ ). On measures of community benefit, there were no statistically significant associations between research funding and charity care spending (CC -0.192,  $p = 0.099$ ), community investment (CC -0.043,  $p = 0.773$ ), and Medicaid as a share of patient revenue (CC -0.098,  $p = 0.404$ ).

#### CONCLUSION

s Radiology departments that received more NIH research dollars were less likely to serve racial/ethnic minority and low-income patients, and patients with lower education levels.

#### CLINICAL RELEVANCE/APPLICATION

To improve health outcomes of vulnerable populations, efforts should focus on narrowing this research funding gap. Options might include redistributing funds to safety net facilities or fostering collaborations among well-funded institutions with those serving primarily underserved populations.

Printed on: 02/07/23



## Abstract Archives of the RSNA, 2022

T5B-SPNPM-3

### Patient, Provider, and Practice Characteristics Predicting Use of Imaging in Primary Care

Tuesday, Nov. 29 12:45PM - 1:15PM Room: Learning Center - NPM DPS

#### Participants

Sue Yi, PhD,BS, Madison, WI (*Presenter*) Nothing to Disclose

#### PURPOSE

To evaluate differences in imaging utilization during primary care visits based on patient medical and sociodemographic variables; provider characteristics; and practice setting using nationally representative survey data.

#### METHODS AND MATERIALS

Retrospective analysis of the National Ambulatory Medical Care Survey (NAMCS) for the years 2013-2018 was conducted. All patient visits coded as primary care were included in the sample. The major outcome variable was the use of diagnostic imaging also further subdivided by modality: MRI, CT, X-ray, ultrasound, mammography, and DXA. Multiple variable logistic regression analyses were performed to evaluate the influence of patient, provider, and practice level characteristics on imaging utilization. Stata survey procedures were used with NAMCS provided sampling weights to account for the complex survey sampling design and provide valid national-level estimates of imaging utilization.

#### RESULTS

A total of 2,820,381,627 primary care visits were included in the five-year study period. (Data from 2017 is not available). Patient demographics included mean age of 41, 60% female, 64% White, 11% Black, 18% Hispanic, 7% Asian or other race/ethnicity. Overall, 13% of visits resulted in imaging use which did not vary significantly by year ( $p=0.18$ ). Increased rates of imaging were seen with Black (OR 1.30, 95% CI 1.08-1.56) and Hispanic (OR 1.35, 95% CI 1.12-1.62) patients; female patients (OR 1.87, 95% CI 1.65-2.11); in patients with serious comorbidities such as cancer (OR 1.44, 95% CI 1.17-1.79); and associated with advancing patient age ( $p<0.001$ ). Imaging use was higher when the provider was not the patient's PCP (OR 1.52, 95% CI 1.27-1.82) but did not vary by MD versus DO credential ( $p=0.08$ ). Imaging utilization did not vary significantly by region ( $p=0.95$ ) or rural versus urban location ( $p=0.79$ ).

#### CONCLUSION

s Imaging utilization is lower in the primary care setting than what has been reported in the Emergency Department and the disparities in imaging use by patient race seen in that environment are not observed in primary care. This suggests that increasing patient access to primary care may promote health equity. Understanding other factors associated with increased imaging use including patient age, sex, and co-morbidities may help predict health system imaging utilization and guide resource allocation.

#### CLINICAL RELEVANCE/APPLICATION

Promoting policies to increase patient access to primary care may promote more equitable access to diagnostic imaging.

Printed on: 02/07/23

## Abstract Archives of the RSNA, 2022

T5B-SPNR

### Neuroradiology Tuesday Poster Discussions - B

Tuesday, Nov. 29 12:45PM - 1:15PM Room: Learning Center - NR DPS

#### Participants

Andrew Schweitzer, MD, Scarsdale, NY (*Moderator*) Nothing to Disclose

#### Sub-Events

### T5B-SPNR-1 Utility of Vertebral Volumetry in Predicting Early Adjacent Compression Fractures After Kyphoplasty

#### Participants

Ashwin Deshmukh, MBBS, FRCR, Milford, CT (*Presenter*) Nothing to Disclose

#### PURPOSE

Several studies have assessed factors associated with development of early adjacent compression fractures (eACF) in patients undergoing kyphoplasty. This first of its kind study explored whether metrics derived from vertebral volume measurements were associated with development of eACF.

#### METHODS AND MATERIALS

This retrospective study included patients aged 60 and above without spinal metastases who underwent thoracic and/or lumbar kyphoplasty for vertebral compression fractures. Patients who had pre and post procedural cross-sectional imaging, and follow-up imaging at a minimum of 3 months post procedure were included. Vertebral body volumes of the fractured vertebra before and after kyphoplasty were measured. Additionally, volumes of the immediately adjacent vertebrae on pre-procedural scans were also measured. Two metrics derived from vertebral body volume measurements were used to test for statistical significance among those who developed eACF (within three months of kyphoplasty) and those who did not: ratio of post-kyphoplasty volume to pre-kyphoplasty volume of the index vertebra; ratio of post-kyphoplasty volume of the index vertebra to average of volumes of the immediately adjacent vertebrae on pre-procedural imaging.

#### RESULTS

21 consecutive patients were included. Of these, eight patients developed eACF. The mean age and standard deviation (SD) of eACF and non-eACF groups were 80.5±7.99 years and 76.38±10.99 years, respectively. All but one patients in each group underwent bipedicular kyphoplasty. Four patients (4/8) in eACF group and seven patients (7/13) in non-eACF group had chronic fractures in the thoracolumbar spine on pre-procedural imaging. There was a significant difference among the ratios of post-kyphoplasty volume to pre-kyphoplasty volume of index vertebra in eACF and non-eACF groups, with higher ratios in the eACF group (mean±SD: 1.389±0.353 and 1.077±0.107 respectively; p=0.0072). There was no significant difference among the ratios of post-kyphoplasty volume of the index vertebra to the average of adjacent vertebral body volumes in eACF and non-eACF groups (mean±SD: 0.960±0.139 and 0.907±0.100 respectively; p=0.052).

#### CONCLUSION

Results from this pilot study are encouraging, with a significant difference in one of the two assessed metrics. A larger multi-institutional retrospective study assessing these metrics (including assessment of inter-observer variability), and comparison with previously published metrics is currently underway.

#### CLINICAL RELEVANCE/APPLICATION

If validated and standardized, these ratios could guide operators in injecting optimal volume of cement to avoid development of eACF, and also help inform an active surveillance protocol for those who might be at risk for eACF.

### T5B-SPNR-11 Ultrafast Cervical Spine MRI Using Deep Learning-Based Reconstruction: Diagnostic Equivalence to a Conventional Protocol

#### Participants

Atsushi Nakamoto, MD, PhD, Suita, Japan (*Presenter*) Nothing to Disclose

#### PURPOSE

To evaluate the diagnostic equivalency between an ultrafast MRI protocol (2 min 57 s) of the cervical spine using deep learning-based reconstruction (DLR) and a conventional MRI protocol (12 min 54 s).

#### METHODS AND MATERIALS

This study included 50 patients who underwent cervical spinal MRI of both conventional and ultrafast protocols, including sagittal T1-weighted, T2-weighted, short-TI inversion recovery, and axial T2\*-weighted images. Compared with the conventional protocol, the ultrafast protocol shortened the scanning time to about one fourth by using a lower number of excitations, a higher acceleration factor in compressed sensing, and a lower spatial resolution. To compensate for the decreased signal-to-noise ratio caused by shortened scanning time, noise reduction was performed using the Advanced Intelligent Clear-IQ Engine, a recently

commercially available DLR. Three neuroradiologists analysed all images for grading of degenerative changes using a four- or five-point scale and the presence of other spinal abnormalities. For the degenerative changes, inter-protocol intra-reader agreement was assessed by weighted kappa statistics. We also examined interchangeability between the two protocols by calculating the individual equivalence index as the estimated difference between the intra-protocol (conventional) inter-reader and inter-protocol inter-reader agreement. Regarding other abnormalities, the concordance rates of the three readers were calculated.

## RESULTS

The kappa values for canal stenosis, disc degeneration, foraminal stenosis, disc hernia, and endplate degeneration, ranged from 0.76 to 0.94, 0.54 to 0.66, 0.54 to 0.87, 0.67 to 0.91, and 0.51 to 0.79, respectively, indicating moderate to almost perfect agreement. Except for endplate degeneration, the 95% confidence interval of the individual equivalence index did not exceed 5%, indicating interchangeability between the two protocols. Six cord lesions and one vertebral lesion were detected as other spinal pathologies. The concordance rates of their detection between the two protocols were 100% in all three readers.

## CONCLUSION

s Our proposed ultrafast MRI protocol and the conventional protocol showed approximate diagnostic equivalence.

## CLINICAL RELEVANCE/APPLICATION

Our proposed ultrafast spine MRI protocol using DLR showed approximate diagnostic equivalence to a conventional protocol, suggesting its practicality for patients requiring a short examination time.

## T5B-SPNR- 12 Clinical and Imaging Features of Spinal Extradural Arachnoid Cysts: A Retrospective Study of 50 Cases

Participants

Ahmed Ahmed, MBBS, MSc, (*Presenter*) Nothing to Disclose

## PURPOSE

Spinal extradural arachnoid cysts (SEDAC) are rare pockets of CSF or CSF-like fluid that form next to thecal sac in the spine. They are thought to arise from CSF leaking through a dural defect forming an extradural cyst. Prior limited case series have described that they are often found incidentally and rarely cause spinal cord or nerve root compression. This study investigates the demographics and imaging spectrum of SEDACs at our academic institution and compares them with those reported in the literature.

## METHODS AND MATERIALS

We reviewed all imaging reports in our institution. Fifty cases with documented MRI diagnosis of SEDAC, Nabors criteria type I meningeal cyst (MC), were identified. We then studied patient demographics, presenting symptoms, cyst characteristics, and management outcomes. We also tested the association between cysts' largest diameter and their location, septation, thecal mass effect, myelopathy, bone remodeling, and extraforaminal extension.

## RESULTS

In all 50 subjects, SEDACs were solitary (single) and sporadic (non-familial). The majority were incidental (62%), located posteriorly (92%) and laterally (80%) in the thoracic and thoracolumbar regions (34%, 30%). They were associated with mild thecal mass effect (50%) and bone remodeling (92%). Among symptomatic SEDACs, back pain and radiculopathy were the most reported (68%). Larger cysts were seen caudally in the spinal canal and were associated with greater thecal mass effect, bone remodeling, and septations. All 25 cases (out of 50) that had follow-up MRIs showed stability. 4 out of the six subjects who underwent surgical management had complete or partial remission. One had cyst recurrence.

## CONCLUSION

s In this largest series of SEDACs, we found that most were discovered incidentally, stable over time, and most located in the thoracic spine dorsal to the thecal sac. Back pain and radiculopathy constituted most of the presenting symptoms. Treatment with complete surgical excision may yield the best results for symptomatic lesions.

## CLINICAL RELEVANCE/APPLICATION

It will help radiologists and clinicians be aware of SEDAC's different clinical presentations, imaging findings, and treatment outcomes.

## T5B-SPNR- 13 Quiet and Fast MR Imaging of Cervical Spine: A Preliminary Study with AI-assisted Compressed Sensing Quiet Sequences

Participants

Zhang Yukun, (*Presenter*) Nothing to Disclose

## PURPOSE

Acoustic noise was one of the major complaints for patients underwent MR examination, which may affect successful scan rates. The purpose of this study was to investigate the clinical feasibility and performance of quiet sequences with AI-assisted compressed sensing (ACS) on cervical spine imaging, compared to quiet sequences with Parallel Imaging (PI) using different acceleration factors (AFs), as well as conventional cervical spine sequences.

## METHODS AND MATERIALS

10 participants (6male, mean age: 47.57±17.25 years) were imaged at a 3T scanner (uMR Omega, Imaging Healthcare, Shanghai, China) using four different T1-weighted (T1WI) and T2-weighted (T2WI) sequences: conventional protocol, quiet protocol with PI (AF = 2,3) and quiet protocol with ACS (AF = 4)(Table 1). All of the quiet sequences were acquired with a noise reduction factor of 0.6. Noise sound level and acquisition time were recorded. Image quality was subjectively evaluated by two radiologists, using 4-point scores (Table 2). The mean signal to noise ratio (SNR) and mean contrast to noise ratio (CNR) estimation were performed by ROI analysis of the vertebra and the intervertebral disk (IVD) on T1WI and T2WI sequences (figure 1). The differences of qualitative and quantitative parameters between four protocols (conventional sequences, quiet sequences with PI AF = 2, quiet sequences with PI AF = 3 and quiet sequence with ACS AF = 4) were evaluated by Friedman test. SNR = SI vertebra, IVD /SD muscle, CNR = (SI vertebra, IVD - SI muscle)/SD muscle.

## RESULTS

There were no statistical differences in SNR, CNR of vertebra and IVD and subjective evaluation between routine sequences and different quiet sequences with acceleration methods ( $p > 0.05$ , Tables 3 and 4). Significant acoustic noise and acquisition time reduction was measured for quiet T1WI (36% reduction) and quiet T2WI (6% reduction) with ACS compared to conventional sequences (figure 2).

## CONCLUSION

This study demonstrated that both effective acoustic noise reduction and improved acceleration efficiency can be achieved for cervical spine in quiet sequences with ACS (AF = 4), without degrade image quality and quantitative SNR as well as CNR reduction.

## CLINICAL RELEVANCE/APPLICATION

Quiet T1WI and T2WI sequences with ACS may be promising methods for cervical spine imaging, which may increase patient comfort and benefit successful scan rates as well as clinical applications.

## T5B-SPNR- 14 **Deep-Learning Image Reconstruction on Low KEV Virtual Monochromatic Image of Dual-Energy CT Improves Image Quality of Adamkiewicz Artery**

Participants

Fuminari Tatsugami, MD, Hiroshima, Japan (*Presenter*) Nothing to Disclose

## PURPOSE

The detection of the artery of Adamkiewicz (AKA) and the anterior spinal artery (ASA) on CT can be challenging because of their small vascular diameter and the fact that they are surrounded by the spinal canal. Dual-energy CT can increase the iodine contrast by generating low-energy (keV) virtual monochromatic images (VMIs), but the image noise increases as the energy level decrease. Recently introduced deep learning image reconstruction (DLIR) algorithm reduces image noise drastically without degrading image texture compared to iterative reconstruction (IR) algorithms. We investigated whether the use of DLIR on low-keV VMIs can improve the image quality of AKA, using 70 keV VMIs reconstructed with IR algorithms as a reference standard.

## METHODS AND MATERIALS

We enrolled 20 patients who underwent CT aortography on a 256-slice CT scanner with dual-energy scan before aortic repair. We prepared the following images; VMI at 70 keV reconstructed with hybrid-IR (HIR), VMI at 40 keV reconstructed with HIR, and VMI at 40 keV reconstructed with DLIR. On axial images, CT attenuation profiles were generated crossing through the center of the ASA lumen, and the maximum value was recorded. The contrast-to-noise ratio (CNR) of ASA was calculated by using the following formula:  $CNR \text{ of ASA} = (\text{maximum CT number of the ASA} - \text{CT number of the spinal cord}) / \text{image noise of the spinal cord}$ . The overall image quality of AKA was visually evaluated by two radiologists using a four-point scale (1 = poor, 4 = excellent). Also, its continuity was visually evaluated using a four-point scale (1 = not visible, 4 = vascular continuity is fully recognized).

## RESULTS

The mean image noise in the aorta on 40 keV-DLIR images was slightly lower than on 40 keV-HIR images (43.0 vs. 44.4;  $p > 0.05$ ); they were higher than on 70 keV-HIR images (18.0;  $p < 0.01$ ). CNR of ASA was higher on 40 keV-DLIR images than on 40 keV-HIR and 70 keV-HIR images (11.1, 8.8, and 7.9, respectively;  $p < 0.05$ ). The mean image quality score for 40 keV-DLIR was the highest among the three reconstructions (3.3, 2.7, and 2.3, respectively). The mean score for delineation of AKA on 40 keV-DLIR images was comparable to 40 keV-HIR, but it was higher than on 70 keV-HIR images (3.6, 3.5, and 2.9, respectively).

## CONCLUSION

The use of DLIR on the low keV VMI significantly improves the image quality of AKA compared to conventional methods.

## CLINICAL RELEVANCE/APPLICATION

The use of DLIR on the low keV VMI significantly improves the image quality of AKA compared to conventional methods. It can be expected to improve diagnostic performance for the detection of AKA before aortic repair.

## T5B-SPNR- 15 **Blind Spot: Radiologic Reporting of Epidural Metastasis on Body CT in a 12-Year Retrospective Cohort Study**

Participants

Lauren M. Kim, MD, (*Presenter*) Nothing to Disclose

## PURPOSE

To determine whether imaging features of epidural tumor on CT imaging influenced radiologic reporting.

## METHODS AND MATERIALS

293 body CT examinations of 166 patients performed within 30 days of a spine MRI which diagnosed an epidural metastasis were identified. These 293 CT examinations were performed over a 12-year time period at a single institution, with each examination reported by 1 of 17 total radiologists. Majority vote decision among 3 radiologists determined consensus as to whether an epidural metastasis reported on spine MRI was plainly visible on body CT. Epidural metastases deemed plainly visible on body CT were manually segmented by one radiologist for quantitative image analysis. Weighted univariate  $\chi^2$ - and two-tailed t-test analyses were performed to identify statistically significant trends between epidural tumor imaging features and radiologic reporting of epidural metastasis on body CT.

## RESULTS

Epidural metastases reported on spine MRI were deemed plainly visible in 80.5% (236/293) of body CTs performed within 30 days, however 65.3% (154/236) of the body CT reports omitted their presence. 432 epidural tumors and which were deemed plainly visible on CT were manually segmented for quantitative image analysis. These epidural tumors were small, on average 1-2 cm<sup>3</sup>, and low contrast, with average relative contrast (Crel) values less than 1 and average contrast-to-noise (CNR) values between 1-2, representing the lower limit of what the human eye can perceive. The only imaging feature which positively impacted reporting was lesion volume ( $p=0.03$ ) on noncontrast CT, and lesion volume ( $p=0.006$ ) and percentage of spinal canal stenosis ( $p=0.001$ ) on

contrast CT. Mean HU epidural tumor=92 and mean SDHU spinal canal=48, suggesting that the optimal window settings by which to visualize epidural tumor on CT is WL 92/ WW 223.

## CONCLUSION

While body CT is moderately capable of displaying epidural tumor, the majority of these lesions go unreported and therefore likely undetected. Adequate magnification and customized windowing will likely improve the detection of epidural metastasis on CT.

## CLINICAL RELEVANCE/APPLICATION

Cognitive bias may preclude a radiologist's search for epidural tumor on body CT; and even when intentionally sought after, this lesion is difficult to see. Directed attention and optimized radiological searching technique may therefore be required, specifically adequate magnification and customized windowing will likely improve the detection of epidural metastasis on CT.

## T5B-SPNR- Association Between Ligamentous Injuries and Cranio-cervical Junction Malalignment 16

Participants  
David Timaran Montenegro, MD, Houston, TX (*Presenter*) Nothing to Disclose

## PURPOSE

To assess the association between cranio-cervical junction (CCJ) ligamentous injuries and atlantooccipital disassociation and/or atlantoaxial dislocation

## METHODS AND MATERIALS

Over a 3-year period, an observational, single center study was performed. In total, 443 subjects with CCJ trauma were reviewed. Only patients that were evaluated with cervical spine CT and MRI (171 subjects [39%]) were included in this study. Among them, 107 patients were male (62.5%) with a median age of 36 years (interquartile range [IQR] 24-57 years). Fisher exact test was performed for univariate analysis. Simple logistic regression analysis was used to determine odds ratios (OR) and confidence intervals (95% CI)

## RESULTS

In total, 15 patients (8.7%) were diagnosed with either atlantooccipital disassociation (8 patients [53%] or atlantoaxial dislocation (7 patients [47%]). Among patients with either type of CCJ disassociation, 7 (47%) were found to have ligamentous injuries ( $p=0.006$ ) (OR, 5.06 [95% CI, 1.79-14.71]). Injury of the apical ligament was seen in 3 patients (20%) ( $p=0.01$ ) (OR, 9.5 [95% CI, 2.13-37.78]). Additionally, left occipital condyle fracture was observed in 7 patients (47%) ( $p=0.01$ ) (OR, 4 [95% CI, 1.4-12.59]). Among patients with atlantoaxial dislocation only, epidural hematoma was seen in 4 (57%) subjects ( $p=0.04$ ). Among patients with atlantooccipital disassociation, 3 (37%) had disruption of the alar ligament ( $p=0.019$ ). Injuries of the other CCJ ligaments failed to demonstrate statistically significant associations with either type of CCJ disassociation

## CONCLUSION

Incidence of atlantooccipital and/or atlantoaxial malalignment reached 8.7%. CCJ ligamentous injuries were found in up to 47% of the cases. Disruption of the apical ligament was seen in 20% of the patients with either type of CCJ disassociation. Among patients with atlantooccipital disassociation only, 37% had alar ligament injuries. Injury to other CCJ ligaments was not associated with either type of CCJ disassociation

## CLINICAL RELEVANCE/APPLICATION

Literature about acute cranio-cervical junction trauma is limited due to the high mortality rate of patients with CCJ trauma at the scene of injury. Our study will help to understand the association of cervical structural injuries with severe cranio-cervical malalignment.

## T5B-SPNR- Application of synthetic MRI in Quantitative Diagnosis in Cervical Spondylotic Myelopathy 18

Participants  
Xiangyu Tang, Wuhan, China (*Presenter*) Nothing to Disclose

## PURPOSE

Cervical spondylotic myelopathy (CSM) is a chronic compressive spinal cord lesion. It is important to identify early symptoms and provide effective treatment. To date, previous studies have shown the feasibility of synthetic MRI (MAGIC) in spinal cord imaging on healthy volunteers. The objective of this work was to investigate the feasibility and diagnostic value of the quantitative PD, T1 and T2 values obtained by synthetic MRI in addressing the severity of CSM.

## METHODS AND MATERIALS

From August 2021 to March 2022, a total of 63 subjects were enrolled including 36 CSM patients and 27 healthy subjects (23 males and 40 females). A 3.0T MR scanner (GE, SIGNATM Architect) was used to perform MAGIC imaging sequence on each subject. Patients and controls were evaluated using the Japanese Orthopaedic Association (JOA) scale, a Visual Analogue Scale (VAS) and Neck Disability Index (NDI). The MAGIC images were post-processed using the GE workstation, and ROIs were manually drawn to measure the axial intervertebral discs and the spinal cord at the C2 vertebral level to generate T1, T2, and PD values. The cervical canal stenosis of subjects were graded according to the method of Kang, Y. After that, LSD-t test was used to compare the differences of each parameter value between each grade and C2 vertebral level, and Spearman correlation analysis was used to test the correlation between C2 vertebral body level and the maximum degree of intervertebral disc herniation and clinical mJOA score, VSA score, NDI score.

## RESULTS

The T1 mapping, T2 mapping and PD mapping were generated by MAGIC data (Figure 1). The PD value had a decreasing trend from grade 0 to grade 2. The PD value of C2 is bigger than the value of grade 0, grade 1 and grade 2, with statistically significant ( $P<0.01$ ), except for the difference between grade 3, showing the PD value had a potential for early diagnosis for CSM (Figure 2a). The T1 value had statistically difference between grade 3 and the other grade ( $P<0.05$ ). (Figure 2b) The T2 value had statistically difference between C2 and the other grade ( $P<0.05$ ), showing the CSM patients had the change of T2 values (Figure 2c).

## CONCLUSION

s MAGIC was shown to be a reliable and effective method in assessing CSM. The values of PD, T1 and T2 open up a new dimension on quantitative measures in assessing CSM

## CLINICAL RELEVANCE/APPLICATION

MAGIC has the potential for clinical diagnosis for CSM

## T5B-SPNR- Utility and National Trend of Use of Spine MRI in the Setting of Suspected Nonaccidental Trauma (NAT) 19

Participants

Jeffers Nguyen, MD, Centereach, NY (*Presenter*) Nothing to Disclose

## PURPOSE

Abusive head trauma (AHT) is the leading cause of morbidity and mortality in patients below the age of 2 with traumatic brain injury. Given the recently growing awareness of spinal injury in the setting of AHT, the current ACR guidelines now strongly recommend performing MRI of the cervical spine at the time of brain MRI, and that MRI of the total spine be considered. In this study, we aim to examine the MRI spine findings in patients hospitalized for suspected non-accidental trauma (NAT). In addition, we examined the national trend of use of spine MRI in the setting of suspected NAT using the Pediatric Health Information System (PHIS).

## METHODS AND MATERIALS

After obtaining approval of the institutional review board, a retrospective study was performed evaluating the spine MRI findings of children aged 0 to 2 years admitted for suspected NAT between January 2017 and December 2021. Using our radiology database (Nuance mPower) and the pediatric child abuse database at our institution, infants and young children aged <24 months who had whole spine MRI for suspected NAT were included. Clinical data, including patient demographics, clinical presentation, interventions, and clinical outcomes, were collected, and analyzed. Additionally, the PHIS database was used to identify hospitalizations for AHT from 1/1/17 to 12/31/21 in children < 2 years of age.

## RESULTS

A total of 24 patients with MRI of the spine for suspected NAT were identified. The median age at presentation was 5 months, and approximately two-thirds of patients were male. Although nearly all patients (96%) had findings compatible with AHT on brain MRI, only 9 patients (38%) had positive findings on MRI of the spine. Of those, the vast majority (89%) had thoracolumbar subdural hemorrhage, necessitating surgical evacuation in only one of them. Two patients had evidence of ligamentous injury in the cervical spine, one of which subsequently had a cervical collar placed. The national trend of use of spine MRI for suspected NAT is presented in Figure 1

## CONCLUSION

s Thoracolumbar subdural hemorrhage is the most common abnormality seen in patients with suspected NAT who underwent whole spine MRI at our institution. Follow up study with larger samples is needed to validate our data and guide future efforts to improve patient selection and study protocols.

## CLINICAL RELEVANCE/APPLICATION

There is increasing use of MRI Spine in patients suspected nonaccidental trauma. Severe spinal injury necessitating clinical intervention remains rare despite increased utilization of MRI of the spine.

## T5B-SPNR-2 Dural Branches Supplying the Anterior Fossa Dura Matter From the Anterior Cerebral Artery

Participants

Hiro Kiyosue, MD, (*Presenter*) Research Grant, Koninklijke Philips NV

## PURPOSE

It is known that a dural branch to the anterior cranial fossa occasionally originates from the anterior cerebral artery (ACA) which can supply dural hypervascular lesions such as meningioma and anterior fossa dural arteriovenous fistulas. Those dural branches are small but important in interventional procedures because embolic materials injected from the dural branch of the external carotid artery or the ophthalmic artery potentially migrate into the ACA via duro-pial anastomosis. However, no anatomical or angiographical studies regarding dural branches from the ACA have been reported yet. Herein, we evaluate dural branch to the anterior cranial fossa from the proximal portion of the ACA.

## METHODS AND MATERIALS

We retrospectively evaluated collateral pathways via the dural arterial anastomoses between the ethmoidal arteries of the ophthalmic artery or the sphenopalatine artery and the anterior cerebral artery in patients with severe stenosis or occlusion of the internal carotid artery. Biplane angiography and 3D angiography images including MPR images in 25 patients (50 sides) were reviewed by two neuroradiologists with a special interest in the origin of the dural branch of ACA.

## RESULTS

Duro-pial collaterals via the ethmoidal - ACA dural anastomoses were observed in 18 patients (72%) and 28 sides (56%). Detailed angioarchitecture could be evaluated in 19 sides. In 19 sides, 31 dural branches of the ACA were identified on 3D angiography, which originated from the olfactory artery at the distal portion (n=13) and at the proximal portion (n=7), the orbitofrontal artery (medial frontal artery) (n=2), and directly from ACA(A1 or A2) (n=9).

## CONCLUSION

s Dural branches from the proximal portion of the ACA or its branches frequently exists, which often originate at the distal portion of the olfactory artery. Careful attention for the duro-pial anastomosis via the dural branch of the ACA during embolization of the lesion on the anterior cranial fossa

## CLINICAL RELEVANCE/APPLICATION

Knowledge of the duro-pial anastomoses between the extracranial dural arteries (e.g. sphenopalatine artery) and the dural branch from the anterior cerebral artery is very important to avoid complications in neurointerventional procedures. This study clarifies the frequency and course/origin of the dural branches from the anterior cerebral artery.

## T5B-SPNR- Clinical Feasibility of Compressed Sensing for Three-dimensional MR Imaging of Cranial Nerves

20

Participants

HEDAN LUO, DALIAN, China (*Presenter*) Nothing to Disclose

## PURPOSE

This study aims to investigate the quality of three-dimensional MR images of cranial nerves based on united compressed sensing (uCS) with different acceleration factors (AFs) and compare with that of images using sensitivity encoding (SENSE), optimized imaging sequence and choose the most appropriate acceleration factor.

## METHODS AND MATERIALS

We prospectively recruited 14 volunteers (mean age, 40.86±3.60 years) who were scanned using a 3T MRI system (uMR Omega, United Imaging Healthcare, Shanghai, China). The T2-weighted images were acquired using a combination of 3D-MATRIX sequence and uCS with different AFs (3, 4, 5 and 6) and SENSE with AF of 2. Detailed parameters were listed in Table 1. The olfactory nerve(I), optic nerve(II) and trigeminal nerve(V) of cranial nerves were manually located and displayed in Fig.1. Signal to noise ratio (SNR) and contrast to noise ratio (CNR) were calculated from the signal intensity(SI) in cranial nerves.  $SNR = \frac{S_{II,II,V}}{SD_{CSF}}$ ,  $CNR = \frac{(S_{ICSF} - S_{II,II,V})}{SD_{CSF}}$ . SI of the small blood vessels close to the auditory nerve was measured and the corresponding Contrast Ratio (CR) was calculated.  $CR = \frac{(S_{ICSF} - S_{IVessel})}{(S_{ICSF} + S_{IVessel})}$  Image quality, including cranial nerve detail visibility, image noise and artifact and diagnostic value, was scored by two observers using a quartet-scale method for oculomotor nerve(III), facial nerve(VII) and glossopharyngeal nerve (IX). Friedman test was conducted to evaluate the differences of SNR, CNR, CR and score under different accelerating settings.

## RESULTS

Image quality scores were consistent between two observers (Cohen's kappa coefficient =0.864). There were significant differences in the SNR of cranial nerve II, CR of vascular, and image quality scores of cranial nerves III, VII, and IX under different accelerating settings (all P values < 0.05 for multiple comparisons). For post-hoc analysis, the CR of vascular when using uCS with AF of 5 was significantly larger than that when using SENSE (P value < 0.05). And the scores when using uCS with AF of 6 were significantly lower than those when using SENSE (all P values < 0.05). (Fig.2)

## CONCLUSION

uCS-based MR imaging of cranial nerves could save scanning time without loss of SNR and CNR, compared with conventional MRI using SENSE method. Taking into account both satisfactory image quality and tight clinical time-constraint, we recommended to select AF of 5 for uCS in routine MR scanning.

## CLINICAL RELEVANCE/APPLICATION

uCS-based MR imaging of cranial nerves showed high feasibility and clinical applicability: reducing scanning time and meanwhile ensuring image quality.

## T5B-SPNR-4 Visualization of Lenticulostriate Artery by Compressed Sensing Imaging

Participants

Huang Fuling, MBChB, (*Presenter*) Nothing to Disclose

## PURPOSE

Lenticulostriate artery (LSA) is a vital perforating artery in the brain, and its occlusion often leads to lacunar infarction. At present, digital subtraction angiography (DSA) is mainly used to realize the imaging of lenticulostriate artery in clinic, but the invasiveness of DSA is an important limiting factor. Some studies have shown that TOF (Time-Of-Flight) sequence has been able to obtain better images of lenticulostriate artery under high-field magnetic resonance system (7T). However, the diameter of the LSA is so small (about 0.3 - 0.7 mm) and the blood flow velocity is relatively slow, the imaging of the LSA is still a challenge with 3T MRI scanner. The study aims to visualize the LSA using 3D-TOF sequence and compressed sensing imaging on 3T system.

## METHODS AND MATERIALS

Thirty-two patients and twenty-two volunteers underwent brain MRI scanning with routine 3D-TOF sequence and compressed sensing imaging on 3T system. Lenticulostriate artery were reconstructed and visualized by volume rendering (VR) technique, the length and number of lenticulostriate artery were analyzed.

## RESULTS

The scanning time of 3D-TOF with and without compressed sensing sequence were 7 minutes and 8 minutes and 44 seconds, respectively, the LSAs were displayed clearly by VR technique on both condition. A total of one hundred and eight hemispheres were analyzed. The total number ( $p > 0.05$ ) and length ( $p > 0.05$ ) of LSAs were non-statistically different between 3D-TOF with and without compressed sensing imaging. There was a significant reduction ( $p < 0.05$ ) in length of visualized LSA in infarction patients compared with the normal people.

## CONCLUSION

We concluded that the compressed sensing technique is of clinical value in the analysis of morphological characteristics of lenticulostriate artery, and it shortens the imaging time to 7 minutes. In summary, using compressed sensing technique to visualize lenticulostriate artery can basically meet the requirements of clinical in scanning time.

## CLINICAL RELEVANCE/APPLICATION

Using compressed sensing technique to visualize lenticulostriate artery can basically meet the requirements of clinical in scanning time on 3T system.

## **T5B-SPNR-5 In Vitro US-Triggered Drug Release from Polymer Film Pocket**

Participants

Selin Isguven, Philadelphia, PA (*Presenter*) Nothing to Disclose

### **PURPOSE**

Infection after spinal fusion occurs in up to 16% of cases, with increased hospital stays and healthcare costs. To augment current therapies, we have designed a rupturable antibiotic reservoir that is stable for 3-5 days followed by US-triggered drug delivery (UTDD). We tested rupture as a function of cavitation nuclei, material properties, and acoustics.

### **METHODS AND MATERIALS**

Poly(lactic acid) (PLA) pockets (~3 mL volume; n = 24) comprised of one rupturable (0.5-1.2 g PLA) and one foundational (3 g PLA) film were assembled. Pockets were loaded with methylene blue (MeB) solution as a model drug and cavitation nuclei 1-1.5 mL Sonazoid microbubbles (GE Healthcare) or 2-2.8 mL nanodroplets derived from Definity microbubbles (Lantheus Medical Imaging). Pockets were submerged in water with and irradiated with clinical US or High Intensity Focused US (HIFU). Clinical US used a S50 scanner (SonoScape) with a curvilinear C1-6 probe for 20 min of Power Doppler imaging (2.2 MHz, highest line density, 100% power) followed by 10 min of flash replenishment imaging (3.0 MHz harmonic imaging at 100% power every 4 seconds). HIFU involved 20 min insonation (2.0 MHz at 4V with 50% duty cycle) using an SU-101 probe (Sonic Concepts) run by a 8116A pulse generator (Hewlett Packard) with 50 dB amplification. Three groups were compared using Fisher's exact test (Stata 15; StataCorp): film thickness (0.5 g PLA for rupturable film vs > 0.5 g), type of US (clinical vs HIFU), and cavitation agent (microbubbles vs nanodroplets).

### **RESULTS**

PLA film thickness was  $23 \pm 5 \mu\text{m}$  (0.5 g films) and  $61 \pm 10 \mu\text{m}$  (1.0 g films). Six out of 24 sealed and insonated pockets ruptured with insonation. Three of 8 pockets containing nanodroplets and three of 16 containing Sonazoid ruptured ( $p > 0.35$ ). 8 pockets were insonated with HIFU and 16 with clinical US; again, three ruptured in each group ( $p > 0.35$ ). The thickness of the rupturable film appeared to not make a difference as four of 16 thin and two of 8 thick films were ruptured.

### **CONCLUSION**

The feasibility of assembling a drug-loaded pocket using a biodegradable polymer film and achieving UTDD with internal cavitation nuclei was established. Using nanodroplets and applying HIFU were more successful for UTDD, even though the results did not reach statistical significance in this small sample size.

### **CLINICAL RELEVANCE/APPLICATION**

Triggered antibiotic release would increase infection control in spinal surgery. A UTDD system was developed that would be applicable to surgical implant placement and allow targeted, noninvasive, local drug delivery.

## **T5B-SPNR-6 Standardized Reporting Increases Sensitivity for Brain MRI Findings in Spontaneous Intracranial Hypotension**

Participants

Ryan Turner, (*Presenter*) Nothing to Disclose

### **PURPOSE**

MRI findings of spontaneous intracranial hypotension (SIH) can be subtle. This study sought to determine whether implementation of a standardized reporting template for brain MRI performed to evaluate for imaging features of SIH resulted in increased sensitivity for these findings, using a validated probabilistic scoring system as a gold standard.

### **METHODS AND MATERIALS**

A report template which includes a checklist of brain MRI features of SIH (dural enhancement, subdural collections, slumping of the brainstem, decreased mamillo-pontine interval, pituitary/venous engorgement, and hemosiderosis) was introduced at a tertiary academic center for voluntary use by reading neuroradiologists. 3 months of imaging reports were retrospectively reviewed by searching for indications of "SIH", "orthostatic headache", or "CSF leak". A neuroradiologist with subspecialty expertise in SIH blinded to the original reports assessed each exam for features of SIH and assigned a quantitative SIH Bern score corresponding to low, intermediate, or high probability of SIH. The original reports for those exams were scrutinized for whether the original reader utilized the standardized reporting template and whether the report impression accurately reflected the probability of SIH in a given patient compared with the gold standard retrospective review. Secondary analysis assessed which imaging features were most commonly missed by the original reader.

### **RESULTS**

Of 57 reports, 27/57 (47%) of cases utilized the standardized template and 30/57 (53%) of cases did not. In reports where the template was not used, 13 of 30 (43%) were discordant from the gold standard reader, whereas in the group that did use the template, 4 of 27 (15%) were discordant. This difference was statistically significant ( $p = .019$ ). Of discordant cases that did not use the template, the most commonly missed findings were prepontine cistern effacement (77%), suprasellar cistern effacement (69%), engorgement of venous sinus (54%) and reduced mamillo-pontine interval (46%).

### **CONCLUSION**

Standardized reporting of brain MRIs to evaluate for SIH improves the sensitivity of relevant imaging findings.

### **CLINICAL RELEVANCE/APPLICATION**

SIH is a challenging diagnosis; this work suggests that the use of a standardized reporting template when assessing for SIH imaging features can increase the sensitivity for subtle findings that may otherwise be missed.

## **T5B-SPNR-8 The Accessory Diagnostic Role of Diffusion-Weighted Imaging in the Assessment of Advanced MRI Spine Evaluation in the Setting of Multiple Myeloma and Metastatic Disease.**

Participants

Leen Alkukhun, MD, Syracuse, NY (*Presenter*) Nothing to Disclose

### **PURPOSE**

To assess the utility of diffusion-weighted images (DWI) in patients with history of metastatic disease and/or multiple myeloma to evaluate the degree of response of disease, in comparison to other MRI characteristics such as size and enhancement. Our goal is to illustrate the utility of DWI and the correlating ADC values as a diagnostic tool in differentiating progression of disease versus stable, post-therapy related restricted diffusion.

### **METHODS AND MATERIALS**

A retrospective chart review was conducted in our tertiary care center. A total of 20 patients with a history of metastasis and/or multiple myeloma with multiple spinal magnetic resonance imaging (MRI) with DWI sequences were collected. With additional independent review from a board-certified Neuroradiologist, DWI sequences and the correlating ADC values were obtained on both initial and follow-up spinal MRI post-therapy with an emphasis on the most diffusion restricting spinal lesions. Additional factors such as size and number of lesions and degree of enhancement were used to determine disease stage, this was quantified using a scale of 1 - 3, 1 for improving disease, 2 for disease progression, and 3 for stable disease. These findings were then correlated with the associated ADC values and degree of restricted diffusion.

### **RESULTS**

Of the 20 reviewed patients, three demonstrated disease improvement with the additional factors of degree of enhancement, size, and number of lesions, with corresponding increasing ADC values demonstrating decreasing restricted diffusion. Interestingly, 6 out of 7 patients with stable disease based on additional quantifying factors also demonstrated increasing ADC values suggesting a component of disease response and hypothetical improvement with continued follow-up. Patients that demonstrated deteriorating disease with increasing size or number of lesions also demonstrated decreasing ADC values (increasing restricted diffusion) in 3 of 5 cases. Additionally, two patients with MRI follow-up suggesting disease progression also demonstrated improving ADC values, this is of uncertain significance.

### **CONCLUSION**

s In applying this method in patients with either multiple myeloma or metastatic disease of the spine we believe there is a strong correlation between decreasing degree of restriction in the patient's spine lesions and a positive therapeutic response, even in the setting of otherwise stable disease.

### **CLINICAL RELEVANCE/APPLICATION**

In DWI, correlating ADC values can be used as a quantitative value of restriction degree. Although limited by our small cohort we believe continued retrospective analysis will further strengthen this correlation and further reinforce the argument for the addition of DWI imaging in routine spinal malignancy surveillance.

## **T5B-SPNR-9 Characterization of Radiopaque Microspheres with Dual-Energy CT and Interventional X-ray Imaging**

Participants

Ethan Nikolau, MS, Madison, WI (*Presenter*) Nothing to Disclose

### **PURPOSE**

To characterize the radiopacity of a novel barium-loaded microsphere and demonstrate visibility of the microspheres in an in vivo porcine splenic embolization model using different interventional imaging techniques.

### **METHODS AND MATERIALS**

Batches of 900-micron radiopaque microspheres were created by precipitation of barium sulfate into microsphere beads using sodium sulfate and barium chloride. Varying barium strengths (x1 to x10) were obtained through repetition of the barium loading steps. Syringes containing microspheres suspended in saline were placed within a 16 cm acrylic phantom. Dual-energy CT (DECT) scans were performed using a clinical CT scanner. Iodine (Water) basis images reconstructed from DECT scans were used to measure equivalent iodine density for each barium loading strength. Conventional CT scans were acquired at 80, 120, and 140 kV to determine CT number for each strength. A porcine study of splenic artery embolization was performed on an interventional x-ray system using the x5 strength microspheres to demonstrate in vivo microsphere visibility in C-arm cone beam CT (CBCT) images and 2D dual-energy (DE) images. 2D DE images with tissue subtraction were formed from successively acquired low and high energy image sequences.

### **RESULTS**

DECT scans demonstrated a close to linear relationship ( $R^2=0.978$ ) between equivalent iodine density and barium loading, ranging from 2.99 mg/mL to 36.5 mg/mL iodine equivalent for x1 to x10 strength microspheres. Conventional CT images of the x10 microspheres had CT numbers of 1767, 1144, and 971 HU at 80, 120 and 140 kV, respectively. Imaging of the x5 microspheres (22.0 mg/mL iodine equivalent) in vivo demonstrated a global distribution with visualization of the microspheres throughout the spleen in a post-embolization CBCT acquired without injected contrast agent. The microspheres were visible in the 2D DE images.

### **CONCLUSION**

s Radiopaque barium-loaded microspheres were prepared with up to 36.5 mg/mL iodine equivalent density. In an in vivo porcine model, the distribution of injected 22.0 mg/mL iodine equivalent microspheres was visualized in 3D CBCT images and tissue-subtracted 2D dual-energy images.

### **CLINICAL RELEVANCE/APPLICATION**

Barium loaded radiopaque microspheres visible on interventional imaging may provide direct intra- and post-procedural monitoring of both on- and off-target microsphere distribution and embolization.



## Abstract Archives of the RSNA, 2022

T5B-SPNR-1

### Utility of Vertebral Volumetry in Predicting Early Adjacent Compression Fractures After Kyphoplasty

Tuesday, Nov. 29 12:45PM - 1:15PM Room: Learning Center - NR DPS

#### Participants

Ashwin Deshmukh, MBBS, FRCR, Milford, CT (*Presenter*) Nothing to Disclose

#### PURPOSE

Several studies have assessed factors associated with development of early adjacent compression fractures (eACF) in patients undergoing kyphoplasty. This first of its kind study explored whether metrics derived from vertebral volume measurements were associated with development of eACF.

#### METHODS AND MATERIALS

This retrospective study included patients aged 60 and above without spinal metastases who underwent thoracic and/or lumbar kyphoplasty for vertebral compression fractures. Patients who had pre and post procedural cross-sectional imaging, and follow-up imaging at a minimum of 3 months post procedure were included. Vertebral body volumes of the fractured vertebra before and after kyphoplasty were measured. Additionally, volumes of the immediately adjacent vertebrae on pre-procedural scans were also measured. Two metrics derived from vertebral body volume measurements were used to test for statistical significance among those who developed eACF (within three months of kyphoplasty) and those who did not: ratio of post-kyphoplasty volume to pre-kyphoplasty volume of the index vertebra; ratio of post-kyphoplasty volume of the index vertebra to average of volumes of the immediately adjacent vertebrae on pre-procedural imaging.

#### RESULTS

21 consecutive patients were included. Of these, eight patients developed eACF. The mean age and standard deviation (SD) of eACF and non-eACF groups were  $80.5 \pm 7.99$  years and  $76.38 \pm 10.99$  years, respectively. All but one patients in each group underwent bipedicular kyphoplasty. Four patients (4/8) in eACF group and seven patients (7/13) in non-eACF group had chronic fractures in the thoracolumbar spine on pre-procedural imaging. There was a significant difference among the ratios of post-kyphoplasty volume to pre-kyphoplasty volume of index vertebra in eACF and non-eACF groups, with higher ratios in the eACF group (mean $\pm$ SD:  $1.389 \pm 0.353$  and  $1.077 \pm 0.107$  respectively;  $p=0.0072$ ). There was no significant difference among the ratios of post-kyphoplasty volume of the index vertebra to the average of adjacent vertebral body volumes in eACF and non-eACF groups (mean $\pm$ SD:  $0.960 \pm 0.139$  and  $0.907 \pm 0.100$  respectively;  $p=0.052$ ).

#### CONCLUSION

Results from this pilot study are encouraging, with a significant difference in one of the two assessed metrics. A larger multi-institutional retrospective study assessing these metrics (including assessment of inter-observer variability), and comparison with previously published metrics is currently underway.

#### CLINICAL RELEVANCE/APPLICATION

If validated and standardized, these ratios could guide operators in injecting optimal volume of cement to avoid development of eACF, and also help inform an active surveillance protocol for those who might be at risk for eACF.

Printed on: 02/07/23

## Abstract Archives of the RSNA, 2022

T5B-SPNR-11

### Ultrafast Cervical Spine MRI Using Deep Learning-Based Reconstruction: Diagnostic Equivalence to a Conventional Protocol

Tuesday, Nov. 29 12:45PM - 1:15PM Room: Learning Center - NR DPS

#### Participants

Atsushi Nakamoto, MD, PhD, Suita, Japan (*Presenter*) Nothing to Disclose

#### PURPOSE

To evaluate the diagnostic equivalency between an ultrafast MRI protocol (2 min 57 s) of the cervical spine using deep learning-based reconstruction (DLR) and a conventional MRI protocol (12 min 54 s).

#### METHODS AND MATERIALS

This study included 50 patients who underwent cervical spinal MRI of both conventional and ultrafast protocols, including sagittal T1-weighted, T2-weighted, short-TI inversion recovery, and axial T2\*-weighted images. Compared with the conventional protocol, the ultrafast protocol shortened the scanning time to about one fourth by using a lower number of excitations, a higher acceleration factor in compressed sensing, and a lower spatial resolution. To compensate for the decreased signal-to-noise ratio caused by shortened scanning time, noise reduction was performed using the Advanced Intelligent Clear-IQ Engine, a recently commercially available DLR. Three neuroradiologists analysed all images for grading of degenerative changes using a four- or five-point scale and the presence of other spinal abnormalities. For the degenerative changes, inter-protocol intra-reader agreement was assessed by weighted kappa statistics. We also examined interchangeability between the two protocols by calculating the individual equivalence index as the estimated difference between the intra-protocol (conventional) inter-reader and inter-protocol inter-reader agreement. Regarding other abnormalities, the concordance rates of the three readers were calculated.

#### RESULTS

The kappa values for canal stenosis, disc degeneration, foraminal stenosis, disc hernia, and endplate degeneration, ranged from 0.76 to 0.94, 0.54 to 0.66, 0.54 to 0.87, 0.67 to 0.91, and 0.51 to 0.79, respectively, indicating moderate to almost perfect agreement. Except for endplate degeneration, the 95% confidence interval of the individual equivalence index did not exceed 5%, indicating interchangeability between the two protocols. Six cord lesions and one vertebral lesion were detected as other spinal pathologies. The concordance rates of their detection between the two protocols were 100% in all three readers.

#### CONCLUSION

Our proposed ultrafast MRI protocol and the conventional protocol showed approximate diagnostic equivalence.

#### CLINICAL RELEVANCE/APPLICATION

Our proposed ultrafast spine MRI protocol using DLR showed approximate diagnostic equivalence to a conventional protocol, suggesting its practicality for patients requiring a short examination time.

Printed on: 02/07/23

## Abstract Archives of the RSNA, 2022

T5B-SPNR-12

### Clinical and Imaging Features of Spinal Extradural Arachnoid Cysts: A Retrospective Study of 50 Cases

Tuesday, Nov. 29 12:45PM - 1:15PM Room: Learning Center - NR DPS

#### Participants

Ahmed Ahmed, MBBS, MSc, (*Presenter*) Nothing to Disclose

#### PURPOSE

Spinal extradural arachnoid cysts (SEDAC) are rare pockets of CSF or CSF-like fluid that form next to thecal sac in the spine. They are thought to arise from CSF leaking through a dural defect forming an extradural cyst. Prior limited case series have described that they are often found incidentally and rarely cause spinal cord or nerve root compression. This study investigates the demographics and imaging spectrum of SEDACs at our academic institution and compares them with those reported in the literature.

#### METHODS AND MATERIALS

We reviewed all imaging reports in our institution. Fifty cases with documented MRI diagnosis of SEDAC, Nabors criteria type I meningeal cyst (MC), were identified. We then studied patient demographics, presenting symptoms, cyst characteristics, and management outcomes. We also tested the association between cysts' largest diameter and their location, septation, thecal mass effect, myelopathy, bone remodeling, and extraforaminal extension.

#### RESULTS

In all 50 subjects, SEDACs were solitary (single) and sporadic (non-familial). The majority were incidental (62%), located posteriorly (92%) and laterally (80%) in the thoracic and thoracolumbar regions (34%, 30%). They were associated with mild thecal mass effect (50%) and bone remodeling (92%). Among symptomatic SEDACs, back pain and radiculopathy were the most reported (68%). Larger cysts were seen caudally in the spinal canal and were associated with greater thecal mass effect, bone remodeling, and septations. All 25 cases (out of 50) that had follow-up MRIs showed stability. 4 out of the six subjects who underwent surgical management had complete or partial remission. One had cyst recurrence.

#### CONCLUSION

s In this largest series of SEDACs, we found that most were discovered incidentally, stable over time, and most located in the thoracic spine dorsal to the thecal sac. Back pain and radiculopathy constituted most of the presenting symptoms. Treatment with complete surgical excision may yield the best results for symptomatic lesions.

#### CLINICAL RELEVANCE/APPLICATION

It will help radiologists and clinicians be aware of SEDAC's different clinical presentations, imaging findings, and treatment outcomes.

Printed on: 02/07/23

## Abstract Archives of the RSNA, 2022

T5B-SPNR-13

### Quiet and Fast MR Imaging of Cervical Spine: A Preliminary Study with AI-assisted Compressed Sensing Quiet Sequences

Tuesday, Nov. 29 12:45PM - 1:15PM Room: Learning Center - NR DPS

#### Participants

Zhang Yukun, (*Presenter*) Nothing to Disclose

#### PURPOSE

Acoustic noise was one of the major complaints for patients underwent MR examination, which may affect successful scan rates. The purpose of this study was to investigate the clinical feasibility and performance of quiet sequences with AI-assisted compressed sensing (ACS) on cervical spine imaging, compared to quiet sequences with Parallel Imaging (PI) using different acceleration factors (AFs), as well as conventional cervical spine sequences.

#### METHODS AND MATERIALS

10 participants (6male, mean age:  $47.57 \pm 17.25$  years) were imaged at a 3T scanner (uMR Omega, Imaging Healthcare, Shanghai, China) using four different T1-weighted (T1WI) and T2-weighted (T2WI) sequences: conventional protocol, quiet protocol with PI (AF = 2,3) and quiet protocol with ACS (AF = 4)(Table 1). All of the quiet sequences were acquired with a noise reduction factor of 0.6. Noise sound level and acquisition time were recorded. Image quality was subjectively evaluated by two radiologists, using 4-point scores (Table 2). The mean signal to noise ratio (SNR) and mean contrast to noise ratio (CNR) estimation were performed by ROI analysis of the vertebra and the intervertebral disk (IVD) on T1WI and T2WI sequences (figure 1). The differences of qualitative and quantitative parameters between four protocols (conventional sequences, quiet sequences with PI AF = 2, quiet sequences with PI AF = 3 and quiet sequence with ACS AF = 4) were evaluated by Friedman test.  $SNR = SI \text{ vertebra, IVD} / SD \text{ muscle}$ ,  $CNR = (SI \text{ vertebra, IVD} - SI \text{ muscle}) / SD \text{ muscle}$ .

#### RESULTS

There were no statistical differences in SNR, CNR of vertebra and IVD and subjective evaluation between routine sequences and different quiet sequences with acceleration methods ( $p > 0.05$ , Tables 3 and 4). Significant acoustic noise and acquisition time reduction was measured for quiet T1WI (36% reduction) and quite T2WI (6% reduction) with ACS compared to conventional sequences (figure 2).

#### CONCLUSION

s This study demonstrated that both effective acoustic noise reduction and improved acceleration efficiency can be achieved for cervical spine in quiet sequences with ACS (AF = 4), without degrade image quality and quantitative SNR as well as CNR reduction.

#### CLINICAL RELEVANCE/APPLICATION

Quiet T1WI and T2WI sequences with ACS may be promising methods for cervical spine imaging, which may increase patient comfort and benefit successful scan rates as well as clinical applications.

Printed on: 02/07/23

## Abstract Archives of the RSNA, 2022

T5B-SPNR-14

### Deep-Learning Image Reconstruction on Low KEV Virtual Monochromatic Image of Dual-Energy CT Improves Image Quality of Adamkiewicz Artery

Tuesday, Nov. 29 12:45PM - 1:15PM Room: Learning Center - NR DPS

#### Participants

Fuminari Tatsugami, MD, Hiroshima, Japan (*Presenter*) Nothing to Disclose

#### PURPOSE

The detection of the artery of Adamkiewicz (AKA) and the anterior spinal artery (ASA) on CT can be challenging because of their small vascular diameter and the fact that they are surrounded by the spinal canal. Dual-energy CT can increase the iodine contrast by generating low-energy (keV) virtual monochromatic images (VMIs), but the image noise increases as the energy level decrease. Recently introduced deep learning image reconstruction (DLIR) algorithm reduces image noise drastically without degrading image texture compared to iterative reconstruction (IR) algorithms. We investigated whether the use of DLIR on low-keV VMIs can improve the image quality of AKA, using 70 keV VMIs reconstructed with IR algorithms as a reference standard.

#### METHODS AND MATERIALS

We enrolled 20 patients who underwent CT aortography on a 256-slice CT scanner with dual-energy scan before aortic repair. We prepared the following images; VMI at 70 keV reconstructed with hybrid-IR (HIR), VMI at 40 keV reconstructed with HIR, and VMI at 40 keV reconstructed with DLIR. On axial images, CT attenuation profiles were generated crossing through the center of the ASA lumen, and the maximum value was recorded. The contrast-to-noise ratio (CNR) of ASA was calculated by using the following formula:  $CNR\ of\ ASA = \frac{\text{maximum CT number of the ASA} - \text{CT number of the spinal cord}}{\text{image noise of the spinal cord}}$ . The overall image quality of AKA was visually evaluated by two radiologists using a four-point scale (1 = poor, 4 = excellent). Also, its continuity was visually evaluated using a four-point scale (1 = not visible, 4 = vascular continuity is fully recognized).

#### RESULTS

The mean image noise in the aorta on 40 keV-DLIR images was slightly lower than on 40 keV-HIR images (43.0 vs. 44.4;  $p > 0.05$ ); they were higher than on 70 keV-HIR images (18.0;  $p < 0.01$ ). CNR of ASA was higher on 40 keV-DLIR images than on 40 keV-HIR and 70 keV-HIR images (11.1, 8.8, and 7.9, respectively;  $p < 0.05$ ). The mean image quality score for 40 keV-DLIR was the highest among the three reconstructions (3.3, 2.7, and 2.3, respectively). The mean score for delineation of AKA on 40 keV-DLIR images was comparable to 40 keV-HIR, but it was higher than on 70 keV-HIR images (3.6, 3.5, and 2.9, respectively).

#### CONCLUSION

The use of DLIR on the low keV VMI significantly improves the image quality of AKA compared to conventional methods.

#### CLINICAL RELEVANCE/APPLICATION

The use of DLIR on the low keV VMI significantly improves the image quality of AKA compared to conventional methods. It can be expected to improve diagnostic performance for the detection of AKA before aortic repair.

Printed on: 02/07/23

## Abstract Archives of the RSNA, 2022

T5B-SPNR-15

### Blind Spot: Radiologic Reporting of Epidural Metastasis on Body CT in a 12-Year Retrospective Cohort Study

Tuesday, Nov. 29 12:45PM - 1:15PM Room: Learning Center - NR DPS

#### Participants

Lauren M. Kim, MD, (*Presenter*) Nothing to Disclose

#### PURPOSE

To determine whether imaging features of epidural tumor on CT imaging influenced radiologic reporting.

#### METHODS AND MATERIALS

293 body CT examinations of 166 patients performed within 30 days of a spine MRI which diagnosed an epidural metastasis were identified. These 293 CT examinations were performed over a 12-year time period at a single institution, with each examination reported by 1 of 17 total radiologists. Majority vote decision among 3 radiologists determined consensus as to whether an epidural metastasis reported on spine MRI was plainly visible on body CT. Epidural metastases deemed plainly visible on body CT were manually segmented by one radiologist for quantitative image analysis. Weighted univariate  $\chi^2$ - and two-tailed t-test analyses were performed to identify statistically significant trends between epidural tumor imaging features and radiologic reporting of epidural metastasis on body CT.

#### RESULTS

Epidural metastases reported on spine MRI were deemed plainly visible in 80.5% (236/293) of body CTs performed within 30 days, however 65.3% (154/236) of the body CT reports omitted their presence. 432 epidural tumors and which were deemed plainly visible on CT were manually segmented for quantitative image analysis. These epidural tumors were small, on average 1-2 cm<sup>3</sup>, and low contrast, with average relative contrast (Crel) values less than 1 and average contrast-to-noise (CNR) values between 1-2, representing the lower limit of what the human eye can perceive. The only imaging feature which positively impacted reporting was lesion volume ( $p=0.03$ ) on noncontrast CT, and lesion volume ( $p=0.006$ ) and percentage of spinal canal stenosis ( $p=0.001$ ) on contrast CT. Mean HU<sub>epidural tumor</sub>=92 and mean SDHU<sub>spinal canal</sub>=48, suggesting that the optimal window settings by which to visualize epidural tumor on CT is WL 92/ WW 223.

#### CONCLUSION

While body CT is moderately capable of displaying epidural tumor, the majority of these lesions go unreported and therefore likely undetected. Adequate magnification and customized windowing will likely improve the detection of epidural metastasis on CT.

#### CLINICAL RELEVANCE/APPLICATION

Cognitive bias may preclude a radiologist's search for epidural tumor on body CT; and even when intentionally sought after, this lesion is difficult to see. Directed attention and optimized radiological searching technique may therefore be required, specifically adequate magnification and customized windowing will likely improve the detection of epidural metastasis on CT.

Printed on: 02/07/23

## Abstract Archives of the RSNA, 2022

T5B-SPNR-16

### Association Between Ligamentous Injuries and Cranio-cervical Junction Malalignment

Tuesday, Nov. 29 12:45PM - 1:15PM Room: Learning Center - NR DPS

#### Participants

David Timaran Montenegro, MD, Houston, TX (*Presenter*) Nothing to Disclose

#### PURPOSE

To assess the association between cranio-cervical junction (CCJ) ligamentous injuries and atlantooccipital disassociation and/or atlantoaxial dislocation

#### METHODS AND MATERIALS

Over a 3-year period, an observational, single center study was performed. In total, 443 subjects with CCJ trauma were reviewed. Only patients that were evaluated with cervical spine CT and MRI (171 subjects [39%]) were included in this study. Among them, 107 patients were male (62.5%) with a median age of 36 years (interquartile range [IQR] 24-57 years). Fisher exact test was performed for univariate analysis. Simple logistic regression analysis was used to determine odds ratios (OR) and confidence intervals (95% CI)

#### RESULTS

In total, 15 patients (8.7%) were diagnosed with either atlantooccipital disassociation (8 patients [53%] or atlantoaxial dislocation (7 patients [47%]). Among patients with either type of CCJ disassociation, 7 (47%) were found to have ligamentous injuries ( $p=0.006$ ) (OR, 5.06 [95% CI, 1.79-14.71]). Injury of the apical ligament was seen in 3 patients (20%) ( $p=0.01$ ) (OR, 9.5 [95% CI, 2.13-37.78]). Additionally, left occipital condyle fracture was observed in 7 patients (47%) ( $p=0.01$ ) (OR, 4 [95% CI, 1.4-12.59]). Among patients with atlantoaxial dislocation only, epidural hematoma was seen in 4 (57%) subjects ( $p=0.04$ ). Among patients with atlantooccipital disassociation, 3 (37%) had disruption of the alar ligament ( $p=0.019$ ). Injuries of the other CCJ ligaments failed to demonstrate statistically significant associations with either type of CCJ disassociation

#### CONCLUSION

s Incidence of atlantooccipital and/or atlantoaxial malalignment reached 8.7%. CCJ ligamentous injuries were found in up to 47% of the cases. Disruption of the apical ligament was seen in 20% of the patients with either type pf CCJ disassociation. Among patients with atlantooccipital disassociation only, 37% had alar ligament injuries. Injury to other CCJ ligaments was not associated with either type of CCJ disassociation

#### CLINICAL RELEVANCE/APPLICATION

Literature about acute cranio-cervical junction trauma is limited due to the high mortality rate of patients with CCJ trauma at the scene of injury. Our study will help to understand the association of cervical structural injuries with severe cranio-cervical malalignment.

Printed on: 02/07/23

## Abstract Archives of the RSNA, 2022

T5B-SPNR-18

### Application of synthetic MRI in Quantitative Diagnosis in Cervical Spondylotic Myelopathy

Tuesday, Nov. 29 12:45PM - 1:15PM Room: Learning Center - NR DPS

#### Participants

Xiangyu Tang, Wuhan, China (*Presenter*) Nothing to Disclose

#### PURPOSE

Cervical spondylotic myelopathy (CSM) is a chronic compressive spinal cord lesion. It is important to identify early symptoms and provide effective treatment. To date, previous studies have shown the feasibility of synthetic MRI (MAGIC) in spinal cord imaging on healthy volunteers. The objective of this work was to investigate the feasibility and diagnostic value of the quantitative PD, T1 and T2 values obtained by synthetic MRI in addressing the severity of CSM.

#### METHODS AND MATERIALS

From August 2021 to March 2022, a total of 63 subjects were enrolled including 36 CSM patients and 27 healthy subjects (23 males and 40 females). A 3.0T MR scanner (GE, SIGNATM Architect) was used to perform MAGIC imaging sequence on each subject. Patients and controls were evaluated using the Japanese Orthopaedic Association (JOA) scale, a Visual Analogue Scale (VAS) and Neck Disability Index (NDI). The MAGIC images were post-processed using the GE workstation, and ROIs were manually drawn to measure the axial intervertebral discs and the spinal cord at the C2 vertebral level to generate T1, T2, and PD values. The cervical canal stenosis of subjects were graded according to the method of Kang, Y. After that, LSD-t test was used to compare the differences of each parameter value between each grade and C2 vertebral level, and Spearman correlation analysis was used to test the correlation between C2 vertebral body level and the maximum degree of intervertebral disc herniation and clinical mJOA score, VSA score, NDI score.

#### RESULTS

The T1 mapping, T2 mapping and PD mapping were generated by MAGIC data (Figure 1). The PD value had a decreasing trend from grade 0 to grade 2. The PD value of C2 is bigger than the value of grade 0, grade 1 and grade 2, with statistically significant ( $P < 0.01$ ), except for the difference between grade 3, showing the PD value had a potential for early diagnosis for CSM (Figure 2a). The T1 value had statistically difference between grade 3 and the other grade ( $P < 0.05$ ). (Figure 2b) The T2 value had statistically difference between C2 and the other grade ( $P < 0.05$ ), showing the CSM patients had the change of T2 values (Figure 2c).

#### CONCLUSION

MAGIC was shown to be a reliable and effective method in assessing CSM. The values of PD, T1 and T2 open up a new dimension on quantitative measures in assessing CSM

#### CLINICAL RELEVANCE/APPLICATION

MAGIC has the potential for clinical diagnosis for CSM

Printed on: 02/07/23



## Abstract Archives of the RSNA, 2022

T5B-SPNR-19

### Utility and National Trend of Use of Spine MRI in the Setting of Suspected Nonaccidental Trauma (NAT)

Tuesday, Nov. 29 12:45PM - 1:15PM Room: Learning Center - NR DPS

#### Participants

Jeffers Nguyen, MD, Centereach, NY (*Presenter*) Nothing to Disclose

#### PURPOSE

Abusive head trauma (AHT) is the leading cause of morbidity and mortality in patients below the age of 2 with traumatic brain injury. Given the recently growing awareness of spinal injury in the setting of AHT, the current ACR guidelines now strongly recommend performing MRI of the cervical spine at the time of brain MRI, and that MRI of the total spine be considered. In this study, we aim to examine the MRI spine findings in patients hospitalized for suspected non-accidental trauma (NAT). In addition, we examined the national trend of use of spine MRI in the setting of suspected NAT using the Pediatric Health Information System (PHIS).

#### METHODS AND MATERIALS

After obtaining approval of the institutional review board, a retrospective study was performed evaluating the spine MRI findings of children aged 0 to 2 years admitted for suspected NAT between January 2017 and December 2021. Using our radiology database (Nuance mPower) and the pediatric child abuse database at our institution, infants and young children aged <24 months who had whole spine MRI for suspected NAT were included. Clinical data, including patient demographics, clinical presentation, interventions, and clinical outcomes, were collected, and analyzed. Additionally, the PHIS database was used to identify hospitalizations for AHT from 1/1/17 to 12/31/21 in children < 2 years of age.

#### RESULTS

A total of 24 patients with MRI of the spine for suspected NAT were identified. The median age at presentation was 5 months, and approximately two-thirds of patients were male. Although nearly all patients (96%) had findings compatible with AHT on brain MRI, only 9 patients (38%) had positive findings on MRI of the spine. Of those, the vast majority (89%) had thoracolumbar subdural hemorrhage, necessitating surgical evacuation in only one of them. Two patients had evidence of ligamentous injury in the cervical spine, one of which subsequently had a cervical collar placed. The national trend of use of spine MRI for suspected NAT is presented in Figure 1

#### CONCLUSION

s Thoracolumbar subdural hemorrhage is the most common abnormality seen in patients with suspected NAT who underwent whole spine MRI at our institution. Follow up study with larger samples is needed to validate our data and guide future efforts to improve patient selection and study protocols.

#### CLINICAL RELEVANCE/APPLICATION

There is increasing use of MRI Spine in patients suspected nonaccidental trauma. Severe spinal injury necessitating clinical intervention remains rare despite increased utilization of MRI of the spine.

Printed on: 02/07/23

## Abstract Archives of the RSNA, 2022

T5B-SPNR-2

### Dural Branches Supplying the Anterior Fossa Dura Matter From the Anterior Cerebral Artery

Tuesday, Nov. 29 12:45PM - 1:15PM Room: Learning Center - NR DPS

#### Participants

Hiro Kiyosue, MD, (*Presenter*) Research Grant, Koninklijke Philips NV

#### PURPOSE

It is known that a dural branch to the anterior cranial fossa occasionally originates from the anterior cerebral artery (ACA) which can supply dural hypervascular lesions such as meningioma and anterior fossa dural arteriovenous fistulas. Those dural branches are small but important in interventional procedures because embolic materials injected from the dural branch of the external carotid artery or the ophthalmic artery potentially migrate into the ACA via duro-pial anastomosis. However, no anatomical or angiographical studies regarding dural branches from the ACA have been reported yet. Herein, we evaluate dural branch to the anterior cranial fossa from the proximal portion of the ACA.

#### METHODS AND MATERIALS

We retrospectively evaluated collateral pathways via the dural arterial anastomoses between the ethmoidal arteries of the ophthalmic artery or the sphenopalatine artery and the anterior cerebral artery in patients with severe stenosis or occlusion of the internal carotid artery. Biplane angiography and 3D angiography images including MPR images in 25 patients (50 sides) were reviewed by two neuroradiologists with a special interest in the origin of the dural branch of ACA.

#### RESULTS

Duro-pial collaterals via the ethmoidal - ACA dural anastomoses were observed in 18 patients (72%) and 28 sides (56%). Detailed angioarchitecture could be evaluated in 19 sides. In 19 sides, 31 dural branches of the ACA were identified on 3D angiography, which originated from the olfactory artery at the distal portion (n=13) and at the proximal portion (n=7), the orbitofrontal artery (medial frontal artery) (n=2), and directly from ACA(A1 or A2) (n=9).

#### CONCLUSION

s Dural branches from the proximal portion of the ACA or its branches frequently exists, which often originate at the distal portion of the olfactory artery. Careful attention for the duro-pial anastomosis via the dural branch of the ACA during embolization of the lesion on the anterior cranial fossa

#### CLINICAL RELEVANCE/APPLICATION

Knowledge of the duro-pial anastomoses between the extracranial dural arteries (e.g. sphenopalatine artery) and the dural branch from the anterior cerebral artery is very important to avoid complications in neurointerventional procedures. This study clarify the frequency and course/origin of the dural branches from the anterior cerebral artery.

Printed on: 02/07/23

## Abstract Archives of the RSNA, 2022

T5B-SPNR-20

### Clinical Feasibility of Compressed Sensing for Three-dimensional MR Imaging of Cranial Nerves

Tuesday, Nov. 29 12:45PM - 1:15PM Room: Learning Center - NR DPS

#### Participants

HEDAN LUO, DALIAN, China (*Presenter*) Nothing to Disclose

#### PURPOSE

This study aims to investigate the quality of three-dimensional MR images of cranial nerves based on united compressed sensing (uCS) with different acceleration factors (AFs) and compare with that of images using sensitivity encoding (SENSE), optimized Imaging sequence and choosed the most appropriate acceleration factor.

#### METHODS AND MATERIALS

We prospectively recruited 14 volunteers (mean age, 40.86±3.60 years) who were scanned using a 3T MRI system (uMR Omega, United Imaging Healthcare, Shanghai, China). The T2-weighted images were acquired using a combination of 3D-MATRIX sequence and uCS with different AFs (3, 4, 5 and 6) and SENSE with AF of 2. Detailed parameters were listed in Table 1. The olfactory nerve(I), optic nerve(II) and trigeminal nerve(V) of cranial nerves were manually located and displayed in Fig.1. Signal to noise ratio (SNR) and contrast to noise ratio (CNR) were calculated from the signal intensity(SI) in cranial nerves.  $SNR = \frac{SI_{II,II,V}}{SDCSF}$ ,  $CNR = \frac{(SICSF - SI_{vessel})}{(SICSF + SI_{vessel})}$ . SI of the small blood vessels close to the auditory nerve was measured and the corresponding Contrast Ratio (CR) was calculated.  $CR = \frac{(SICSF - SI_{vessel})}{(SICSF + SI_{vessel})}$ . Image quality, including cranial nerve detail visibility, image noise and artifact and diagnostic value, was scored by two observers using a quartet-scale method for oculomotor nerve(III), facial nerve(VII) and glossopharyngeal nerve (IX). Friedman test was conducted to evaluate the differences of SNR, CNR, CR and score under different accelerating settings.

#### RESULTS

Image quality scores were consistent between two observers (Cohen's kappa coefficient =0.864). There were significant differences in the SNR of cranial nerve II, CR of vascular, and image quality scores of cranial nerves III, VII, and IX under different accelerating settings (all P values < 0.05 for multiple comparisons). For post-hoc analysis, the CR of vascular when using uCS with AF of 5 was significantly larger than that when using SENSE (P value < 0.05). And the scores when using uCS with AF of 6 were significantly lower than those when using SENSE (all P values < 0.05). (Fig.2)

#### CONCLUSION

uCS-based MR imaging of cranial nerves could save scanning time without loss of SNR and CNR, compared with conventional MRI using SENSE method. Taking into account both satisfactory image quality and tight clinical time-constraint, we recommended to select AF of 5 for uCS in routine MR scanning.

#### CLINICAL RELEVANCE/APPLICATION

uCS-based MR imaging of cranial nerves showed high feasibility and clinical applicability: reducing scanning time and meanwhile ensuring image quality.

Printed on: 02/07/23

## Abstract Archives of the RSNA, 2022

T5B-SPNR-4

### Visualization of Lenticulostriate Artery by Compressed Sensing Imaging

Tuesday, Nov. 29 12:45PM - 1:15PM Room: Learning Center - NR DPS

#### Participants

Huang Fuling, MBChB, (*Presenter*) Nothing to Disclose

#### PURPOSE

Lenticulostriate artery (LSA) is a vital perforating artery in the brain, and its occlusion often leads to lacunar infarction. At present, digital subtraction angiography (DSA) is mainly used to realize the imaging of lenticulostriate artery in clinic, but the invasiveness of DSA is an important limiting factor. Some studies have shown that TOF (Time-Of-Flight) sequence has been able to obtain better images of lenticulostriate artery under high-field magnetic resonance system (7T). However, the diameter of the LSA is so small (about 0.3 - 0.7 mm) and the blood flow velocity is relatively slow, the imaging of the LSA is still a challenge with 3T MRI scanner. The study aims to visualize the LSA using 3D-TOF sequence and compressed sensing imaging on 3T system.

#### METHODS AND MATERIALS

Thirty-two patients and twenty-two volunteers underwent brain MRI scanning with routine 3D-TOF sequence and compressed sensing imaging on 3T system. Lenticulostriate artery were reconstructed and visualized by volume rendering (VR) technique, the length and number of lenticulostriate artery were analyzed.

#### RESULTS

The scanning time of 3D-TOF with and without compressed sensing sequence were 7 minutes and 8 minutes and 44 seconds, respectively, the LSAs were displayed clearly by VR technique on both condition. A total of one hundred and eight hemispheres were analyzed. The total number ( $p > 0.05$ ) and length ( $p > 0.05$ ) of LSAs were non-statistically different between 3D-TOF with and without compressed sensing imaging. There was a significant reduction ( $p < 0.05$ ) in length of visualized LSA in infarction patients compared with the normal people.

#### CONCLUSION

We concluded that the compressed sensing technique is of clinical value in the analysis of morphological characteristics of lenticulostriate artery, and it shortens the imaging time to 7 minutes. In summary, using compressed sensing technique to visualize lenticulostriate artery can basically meet the requirements of clinical in scanning time.

#### CLINICAL RELEVANCE/APPLICATION

Using compressed sensing technique to visualize lenticulostriate artery can basically meet the requirements of clinical in scanning time on 3T system.

Printed on: 02/07/23

## Abstract Archives of the RSNA, 2022

T5B-SPNR-5

### In Vitro US-Triggered Drug Release from Polymer Film Pocket

Tuesday, Nov. 29 12:45PM - 1:15PM Room: Learning Center - NR DPS

#### Participants

Selin Isguven, Philadelphia, PA (*Presenter*) Nothing to Disclose

#### PURPOSE

Infection after spinal fusion occurs in up to 16% of cases, with increased hospital stays and healthcare costs. To augment current therapies, we have designed a rupturable antibiotic reservoir that is stable for 3-5 days followed by US-triggered drug delivery (UTDD). We tested rupture as a function of cavitation nuclei, material properties, and acoustics.

#### METHODS AND MATERIALS

Poly(lactic acid) (PLA) pockets (~3 mL volume; n = 24) comprised of one rupturable (0.5-1.2 g PLA) and one foundational (3 g PLA) film were assembled. Pockets were loaded with methylene blue (MeB) solution as a model drug and cavitation nuclei 1-1.5 mL Sonazoid microbubbles (GE Healthcare) or 2-2.8 mL nanodroplets derived from Definity microbubbles (Lantheus Medical Imaging). Pockets were submerged in water with and irradiated with clinical US or High Intensity Focused US (HIFU). Clinical US used a S50 scanner (SonoScape) with a curvilinear C1-6 probe for 20 min of Power Doppler imaging (2.2 MHz, highest line density, 100% power) followed by 10 min of flash replenishment imaging (3.0 MHz harmonic imaging at 100% power every 4 seconds). HIFU involved 20 min insonation (2.0 MHz at 4V with 50% duty cycle) using an SU-101 probe (Sonic Concepts) run by a 8116A pulse generator (Hewlett Packard) with 50 dB amplification. Three groups were compared using Fisher's exact test (Stata 15; StataCorp): film thickness (0.5 g PLA for rupturable film vs > 0.5 g), type of US (clinical vs HIFU), and cavitation agent (microbubbles vs nanodroplets).

#### RESULTS

PLA film thickness was  $23 \pm 5 \mu\text{m}$  (0.5 g films) and  $61 \pm 10 \mu\text{m}$  (1.0 g films). Six out of 24 sealed and insonated pockets ruptured with insonation. Three of 8 pockets containing nanodroplets and three of 16 containing Sonazoid ruptured ( $p > 0.35$ ). 8 pockets were insonated with HIFU and 16 with clinical US; again, three ruptured in each group ( $p > 0.35$ ). The thickness of the rupturable film appeared to not make a difference as four of 16 thin and two of 8 thick films were ruptured.

#### CONCLUSION

The feasibility of assembling a drug-loaded pocket using a biodegradable polymer film and achieving UTDD with internal cavitation nuclei was established. Using nanodroplets and applying HIFU were more successful for UTDD, even though the results did not reach statistical significance in this small sample size.

#### CLINICAL RELEVANCE/APPLICATION

Triggered antibiotic release would increase infection control in spinal surgery. A UTDD system was developed that would be applicable to surgical implant placement and allow targeted, noninvasive, local drug delivery.

Printed on: 02/07/23



## Abstract Archives of the RSNA, 2022

T5B-SPNR-6

### Standardized Reporting Increases Sensitivity for Brain MRI Findings in Spontaneous Intracranial Hypotension

Tuesday, Nov. 29 12:45PM - 1:15PM Room: Learning Center - NR DPS

#### Participants

Ryan Turner, (*Presenter*) Nothing to Disclose

#### PURPOSE

MRI findings of spontaneous intracranial hypotension (SIH) can be subtle. This study sought to determine whether implementation of a standardized reporting template for brain MRI performed to evaluate for imaging features of SIH resulted in increased sensitivity for these findings, using a validated probabilistic scoring system as a gold standard.

#### METHODS AND MATERIALS

A report template which includes a checklist of brain MRI features of SIH (dural enhancement, subdural collections, slumping of the brainstem, decreased mamillo-pontine interval, pituitary/venous engorgement, and hemosiderosis) was introduced at a tertiary academic center for voluntary use by reading neuroradiologists. 3 months of imaging reports were retrospectively reviewed by searching for indications of "SIH", "orthostatic headache", or "CSF leak". A neuroradiologist with subspecialty expertise in SIH blinded to the original reports assessed each exam for features of SIH and assigned a quantitative SIH Bern score corresponding to low, intermediate, or high probability of SIH. The original reports for those exams were scrutinized for whether the original reader utilized the standardized reporting template and whether the report impression accurately reflected the probability of SIH in a given patient compared with the gold standard retrospective review. Secondary analysis assessed which imaging features were most commonly missed by the original reader.

#### RESULTS

Of 57 reports, 27/57 (47%) of cases utilized the standardized template and 30/57 (53%) of cases did not. In reports where the template was not used, 13 of 30 (43%) were discordant from the gold standard reader, whereas in the group that did use the template, 4 of 27 (15%) were discordant. This difference was statistically significant ( $p = .019$ ). Of discordant cases that did not use the template, the most commonly missed findings were prepontine cistern effacement (77%), suprasellar cistern effacement (69%), engorgement of venous sinus (54%) and reduced mamillo-pontine interval (46%).

#### CONCLUSION

s Standardized reporting of brain MRIs to evaluate for SIH improves the sensitivity of relevant imaging findings.

#### CLINICAL RELEVANCE/APPLICATION

SIH is a challenging diagnosis; this work suggests that the use of a standardized reporting template when assessing for SIH imaging features can increase the sensitivity for subtle findings that may otherwise be missed.

Printed on: 02/07/23

## Abstract Archives of the RSNA, 2022

T5B-SPNR-8

### **The Accessory Diagnostic Role of Diffusion-Weighted Imaging in the Assessment of Advanced MRI Spine Evaluation in the Setting of Multiple Myeloma and Metastatic Disease.**

Tuesday, Nov. 29 12:45PM - 1:15PM Room: Learning Center - NR DPS

#### **Participants**

Leen Alkukhun, MD, Syracuse, NY (*Presenter*) Nothing to Disclose

#### **PURPOSE**

To assess the utility of diffusion-weighted images (DWI) in patients with history of metastatic disease and/or multiple myeloma to evaluate the degree of response of disease, in comparison to other MRI characteristics such as size and enhancement. Our goal is to illustrate the utility of DWI and the correlating ADC values as a diagnostic tool in differentiating progression of disease versus stable, post-therapy related restricted diffusion.

#### **METHODS AND MATERIALS**

A retrospective chart review was conducted in our tertiary care center. A total of 20 patients with a history of metastasis and/or multiple myeloma with multiple spinal magnetic resonance imaging (MRI) with DWI sequences were collected. With additional independent review from a board-certified Neuroradiologist, DWI sequences and the correlating ADC values were obtained on both initial and follow-up spinal MRI post-therapy with an emphasis on the most diffusion restricting spinal lesions. Additional factors such as size and number of lesions and degree of enhancement were used to determine disease stage, this was quantified using a scale of 1 - 3, 1 for improving disease, 2 for disease progression, and 3 for stable disease. These findings were then correlated with the associated ADC values and degree of restricted diffusion.

#### **RESULTS**

Of the 20 reviewed patients, three demonstrated disease improvement with the additional factors of degree of enhancement, size, and number of lesions, with corresponding increasing ADC values demonstrating decreasing restricted diffusion. Interestingly, 6 out of 7 patients with stable disease based on additional quantifying factors also demonstrated increasing ADC values suggesting a component of disease response and hypothetical improvement with continued follow-up. Patients that demonstrated deteriorating disease with increasing size or number of lesions also demonstrated decreasing ADC values (increasing restricted diffusion) in 3 of 5 cases. Additionally, two patients with MRI follow-up suggesting disease progression also demonstrated improving ADC values, this is of uncertain significance.

#### **CONCLUSION**

In applying this method in patients with either multiple myeloma or metastatic disease of the spine we believe there is a strong correlation between decreasing degree of restriction in the patient's spine lesions and a positive therapeutic response, even in the setting of otherwise stable disease.

#### **CLINICAL RELEVANCE/APPLICATION**

In DWI, correlating ADC values can be used as a quantitative value of restriction degree. Although limited by our small cohort we believe continued retrospective analysis will further strengthen this correlation and further reinforce the argument for the addition of DWI imaging in routine spinal malignancy surveillance.

Printed on: 02/07/23

## Abstract Archives of the RSNA, 2022

T5B-SPNR-9

### Characterization of Radiopaque Microspheres with Dual-Energy CT and Interventional X-ray Imaging

Tuesday, Nov. 29 12:45PM - 1:15PM Room: Learning Center - NR DPS

#### Participants

Ethan Nikolau, MS, Madison, WI (*Presenter*) Nothing to Disclose

#### PURPOSE

To characterize the radiopacity of a novel barium-loaded microsphere and demonstrate visibility of the microspheres in an in vivo porcine splenic embolization model using different interventional imaging techniques.

#### METHODS AND MATERIALS

Batches of 900-micron radiopaque microspheres were created by precipitation of barium sulfate into microsphere beads using sodium sulfate and barium chloride. Varying barium strengths (x1 to x10) were obtained through repetition of the barium loading steps. Syringes containing microspheres suspended in saline were placed within a 16 cm acrylic phantom. Dual-energy CT (DECT) scans were performed using a clinical CT scanner. Iodine (Water) basis images reconstructed from DECT scans were used to measure equivalent iodine density for each barium loading strength. Conventional CT scans were acquired at 80, 120, and 140 kV to determine CT number for each strength. A porcine study of splenic artery embolization was performed on an interventional x-ray system using the x5 strength microspheres to demonstrate in vivo microsphere visibility in C-arm cone beam CT (CBCT) images and 2D dual-energy (DE) images. 2D DE images with tissue subtraction were formed from successively acquired low and high energy image sequences.

#### RESULTS

DECT scans demonstrated a close to linear relationship ( $R^2=0.978$ ) between equivalent iodine density and barium loading, ranging from 2.99 mg/mL to 36.5 mg/mL iodine equivalent for x1 to x10 strength microspheres. Conventional CT images of the x10 microspheres had CT numbers of 1767, 1144, and 971 HU at 80, 120 and 140 kV, respectively. Imaging of the x5 microspheres (22.0 mg/mL iodine equivalent) in vivo demonstrated a global distribution with visualization of the microspheres throughout the spleen in a post-embolization CBCT acquired without injected contrast agent. The microspheres were visible in the 2D DE images.

#### CONCLUSION

Radiopaque barium-loaded microspheres were prepared with up to 36.5 mg/mL iodine equivalent density. In an in vivo porcine model, the distribution of injected 22.0 mg/mL iodine equivalent microspheres was visualized in 3D CBCT images and tissue-subtracted 2D dual-energy images.

#### CLINICAL RELEVANCE/APPLICATION

Barium loaded radiopaque microspheres visible on interventional imaging may provide direct intra- and post-procedural monitoring of both on- and off-target microsphere distribution and embolization.

Printed on: 02/07/23

## Abstract Archives of the RSNA, 2022

T5B-SPOB

### OB/Gynecology Tuesday Poster Discussions - B

Tuesday, Nov. 29 12:45PM - 1:15PM Room: Learning Center - OB DPS

#### Participants

Tara A. Morgan, MD, San Francisco, CA (*Moderator*) Nothing to Disclose

#### Sub-Events

### T5B-SPOB-1 Multimodal Deep Learning Models Reach High Prediction Accuracy in the Diagnosis of Ovarian Cancer

#### Participants

Zimo Wang, MD, PhD, (*Presenter*) Nothing to Disclose

#### PURPOSE

The purpose of this study is to analyze the diagnostic performance of a deep multimodal representation model based on the integration of tumor ultrasound images, serum tumor markers, and patient menopausal status for the identification of benign and malignant ovarian tumors.

#### METHODS AND MATERIALS

A total of 1054 patients with ovarian tumors diagnosed from January 2015 to March 2022 by pathology (including 699 patients with benign ovarian tumors and 355 patients with malignant ovarian tumors) were retrospectively analyzed, and 4552 gray-scale and CDFI ultrasound images were collected. (including 2611 ultrasound images of benign ovarian tumors and 1941 ultrasound images of ovarian malignant tumors). In our research, a single-modality CNN model based on ultrasound images, a dual-modality CNN model based on ultrasound images and menopausal status, and a multi-modality CNN model based on ultrasound images, menopausal status, serum CA-125 and serum HE4 were constructed. The performance of these three models in differentiating benign and malignant ovarian tumors was compared.

#### RESULTS

The diagnostic accuracy and area under the curve (AUC) values for single-modality ultrasound images were 90.95% and 0.957. The dual-modality accuracy and area under the curve (AUC) values after combining menopausal status were 92.38% and 0.968. With the integration of ultrasound images, serum tumor markers and menopausal status, the diagnostic performance has gradually improved, and the diagnostic accuracy and AUC value of the multimodal model reached 93.80% and 0.983, achieving satisfactory predictive performance.

#### CONCLUSION

The multimodal representation learning model constructed by integrating ultrasound images, serum tumor markers and patient menopausal status outperforms the CNN model based on ultrasound images alone and the bimodal CNN model combined with menopausal status. We expect that the deep multimodal representation model can become a more efficient and accurate diagnostic tool, and improve the performance of ultrasound in the identification of benign and malignant ovarian tumors in clinical practice.

#### CLINICAL RELEVANCE/APPLICATION

The multimodal representation learning model constructed by integrating ultrasound images, serum tumor markers and patients' menopausal status can improve the accuracy of distinguishing benign and malignant ovarian tumors and provide more reliable reference information for clinicians.

### T5B-SPOB-2 Diffusion and Perfusion Properties of Placenta in Women with COVID19 Pregnancy Infection: A Preliminary IVIM MRI Study

#### Participants

Roberta Ninkova, MD, Rome, Italy (*Presenter*) Nothing to Disclose

#### PURPOSE

The aim of our research was to investigate the potential use of Intravoxel Incoherent Motion (IVIM) MRI in the study of microvascular and microstructural characteristics of the placenta in women with previous COVID-19 infection occurred during gestation.

#### METHODS AND MATERIALS

15 pregnant women with previous Covid-19 infection occurred during pregnancy were enrolled. Placental MRI was performed on 1.5T scanner, using a Diffusion-Weighted Echo-Planar Imaging sequence with 10 different b values (0,10,30,50,75,100,150,400,700,1000 s/mm<sup>2</sup>). For each placenta, 6 ROIs were manually placed on different areas of both Fetal and Maternal side. The mean values of fraction of perfusion f, Pseudo-Diffusion Coefficient D\* and Diffusion Coefficient D were obtained. Differences between f, D, D\* mean values of ex-Covid placentae and those of the uninfected control group (31 placentae) were assessed with Analysis of Variance (ANOVA) test with Bonferroni correction. Pearson test with Bonferroni correction was performed

to investigate the correlation between IVIM parameters and Gestational Age (GA) in both groups.

## **RESULTS**

We found a statistically significant difference in D between the Ex-Covid19 placentae and those of the uninfected control group, in both fetal ( $p=0,017$ ) and maternal side ( $p=0,012$ ). No significant differences were found in  $f$ ,  $D^*$  between two groups. In Ex-Covid 19 placentae, D has a negative correlation with GA in both maternal ( $p<0.02$ ) and fetal ( $p<0.04$ ) ROIs, depicting a decreased diffusivity trend with placental aging. No correlation between D and GA was found in normal placentae.

## **CONCLUSION**

s Placenta is a potential target organ for Covid19 infection via the ACE2 receptor expressed at the maternal-fetal interface, potentially leaving signs of placental injury. The cumulative published data on placenta with COVID-19 infection showed common histological features, with a higher rate of perfusion anomalies. SARS-CoV-2 placental infection is also associated with chronic inflammatory pathologies which include villitis and intervillitis. We think that quantification of the IVIM parameters shows a potential in improving knowledge of the in vivo microstructural changes occurring in these placentae.

## **CLINICAL RELEVANCE/APPLICATION**

In literature there are no MRI studies yet on Covid-19 and Placenta. In our experience, the quantitative detection of subtle microstructural changes in dysfunctional placentae using IVIM model may add useful information about the pathophysiology of pregnancy complications (IUGR, stillbirth...) that could potentially occur in COVID-19 patients.

Printed on: 02/07/23

## Abstract Archives of the RSNA, 2022

T5B-SPOB-1

### Multimodal Deep Learning Models Reach High Prediction Accuracy in the Diagnosis of Ovarian Cancer

Tuesday, Nov. 29 12:45PM - 1:15PM Room: Learning Center - OB DPS

#### Participants

Zimo Wang, MD, PhD, (*Presenter*) Nothing to Disclose

#### PURPOSE

The purpose of this study is to analyze the diagnostic performance of a deep multimodal representation model based on the integration of tumor ultrasound images, serum tumor markers, and patient menopausal status for the identification of benign and malignant ovarian tumors.

#### METHODS AND MATERIALS

A total of 1054 patients with ovarian tumors diagnosed from January 2015 to March 2022 by pathology (including 699 patients with benign ovarian tumors and 355 patients with malignant ovarian tumors) were retrospectively analyzed, and 4552 gray-scale and CDFI ultrasound images were collected. (including 2611 ultrasound images of benign ovarian tumors and 1941 ultrasound images of ovarian malignant tumors). In our research, a single-modality CNN model based on ultrasound images, a dual-modality CNN model based on ultrasound images and menopausal status, and a multi-modality CNN model based on ultrasound images, menopausal status, serum CA-125 and serum HE4 were constructed. The performance of these three models in differentiating benign and malignant ovarian tumors was compared.

#### RESULTS

The diagnostic accuracy and area under the curve (AUC) values for single-modality ultrasound images were 90.95% and 0.957. The dual-modality accuracy and area under the curve (AUC) values after combining menopausal status were 92.38% and 0.968. With the integration of ultrasound images, serum tumor markers and menopausal status, the diagnostic performance has gradually improved, and the diagnostic accuracy and AUC value of the multimodal model reached 93.80% and 0.983, achieving satisfactory predictive performance.

#### CONCLUSION

The multimodal representation learning model constructed by integrating ultrasound images, serum tumor markers and patient menopausal status outperforms the CNN model based on ultrasound images alone and the bimodal CNN model combined with menopausal status. We expect that the deep multimodal representation model can become a more efficient and accurate diagnostic tool, and improve the performance of ultrasound in the identification of benign and malignant ovarian tumors in clinical practice.

#### CLINICAL RELEVANCE/APPLICATION

The multimodal representation learning model constructed by integrating ultrasound images, serum tumor markers and patients' menopausal status can improve the accuracy of distinguishing benign and malignant ovarian tumors and provide more reliable reference information for clinicians.

Printed on: 02/07/23

## Abstract Archives of the RSNA, 2022

T5B-SPOB-2

### Diffusion and Perfusion Properties of Placenta in Women with COVID19 Pregnancy Infection: A Preliminary IVIM MRI Study

Tuesday, Nov. 29 12:45PM - 1:15PM Room: Learning Center - OB DPS

#### Participants

Roberta Ninkova, MD, Rome, Italy (*Presenter*) Nothing to Disclose

#### PURPOSE

The aim of our research was to investigate the potential use of Intravoxel Incoherent Motion (IVIM) MRI in the study of microvascular and microstructural characteristics of the placenta in women with previous COVID-19 infection occurred during gestation.

#### METHODS AND MATERIALS

15 pregnant women with previous Covid-19 infection occurred during pregnancy were enrolled. Placental MRI was performed on 1.5T scanner, using a Diffusion-Weighted Echo-Planar Imaging sequence with 10 different b values (0,10,30,50,75,100,150,400,700,1000 s/mm<sup>2</sup>). For each placenta, 6 ROIs were manually placed on different areas of both Fetal and Maternal side. The mean values of fraction of perfusion f, Pseudo-Diffusion Coefficient D\* and Diffusion Coefficient D were obtained. Differences between f, D, D\* mean values of ex-Covid placentae and those of the uninfected control group (31 placentae) were assessed with Analysis of Variance (ANOVA) test with Bonferroni correction. Pearson test with Bonferroni correction was performed to investigate the correlation between IVIM parameters and Gestational Age (GA) in both groups.

#### RESULTS

We found a statistically significant difference in D between the Ex-Covid19 placentae and those of the uninfected control group, in both fetal (p=0,017) and maternal side (p=0,012). No significant differences were found in f, D\* between two groups. In Ex-Covid 19 placentae, D has a negative correlation with GA in both maternal (p<0.02) and fetal (p<0.04) ROIs, depicting a decreased diffusivity trend with placental aging. No correlation between D and GA was found in normal placentae.

#### CONCLUSION

s Placenta is a potential target organ for Covid19 infection via the ACE2 receptor expressed at the maternal-fetal interface, potentially leaving signs of placental injury. The cumulative published data on placenta with COVID-19 infection showed common histological features, with a higher rate of perfusion anomalies. SARS-CoV-2 placental infection is also associated with chronic inflammatory pathologies which include villitis and intervillitis. We think that quantification of the IVIM parameters shows a potential in improving knowledge of the in vivo microstructural changes occurring in these placentae.

#### CLINICAL RELEVANCE/APPLICATION

In literature there are no MRI studies yet on Covid-19 and Placenta. In our experience, the quantitative detection of subtle microstructural changes in dysfunctional placentae using IVIM model may add useful information about the pathophysiology of pregnancy complications (IUGR, stillbirth...) that could potentially occur in COVID-19 patients.

Printed on: 02/07/23

## Abstract Archives of the RSNA, 2022

T5B-SPPD

### Pediatric Tuesday Poster Discussions - B

Tuesday, Nov. 29 12:45PM - 1:15PM Room: Learning Center - PD DPS

#### Participants

Brooke Lampl, DO, Pepper Pike, OH (*Moderator*) Nothing to Disclose

#### Sub-Events

### T5B-SPPD-1 Parkinsonism Syndrome in Primary Mitochondrial Disorders in Children: Imaging and Clinical Findings

#### Participants

Luis Tierradentro-Garcia, MD, Philadelphia, PA (*Presenter*) Nothing to Disclose

#### PURPOSE

Movement disorders may be observed in some patients with primary mitochondrial disorders (PMD). However, the frequency of the involvement of associated anatomic structures such as the substantia nigra (SN), the particular associated genetic mutations, and the specific clinical motor symptoms have not been reported. This study aims to analyze MRI abnormalities and follow-up changes of SN involvement in children with Parkinsonian movement disorder, in the context of genetically confirmed PMD to find the possible imaging and clinical correlation.

#### METHODS AND MATERIALS

In this retrospective analysis, we included patients younger than 18 years old with genetically confirmed PMD and brain MRI. We assessed the presence of various forms of movement disorder symptomatology in the clinical record and reported associated imaging abnormalities. MRI findings that were associated with symptoms of movement disorders or those with significant effect sizes ( $p=0.05-0.1$  and Cramer  $V > 1.5$ ) were tested through univariate logistic regression.

#### RESULTS

One hundred and seven patients with genetically confirmed PMD were included. The SN was involved in 32 (29.9%) patients, and among them, 28 (26.1%) had lesions on the baseline MRI. Follow-up studies were available for 22 subjects, in which four (18.2 %) had improvement of the lesions by MRI. Leigh syndrome (LS) was the most frequent PMD diagnosis in patients with SN involvement ( $n=26/32$ , 81%). LS was associated with SN involvement both at baseline MRI ( $p < 0.001$ ,  $V = 0.5$ ) and at all time-point pooled MRIs ( $p < 0.001$ ,  $V = 0.53$ ). Univariate model showed that mutation of genes encoding OXPHOS were strongly predictive (OR= 6.6, CI95% 2.6-17) of SN involvement at baseline (model  $\text{Chi}^2 = 16.5$ ,  $p < 0.001$ ,  $R^2 = 0.21$ ). SN involvement at baseline was also strongly predictive (OR= 26, CI95% 3.0-223) of Parkinsonism symptoms at baseline (model  $\text{Chi}^2 = 42.2$ ,  $p < 0.001$ ,  $R^2 = 0.31$ ).

#### CONCLUSION

SN involvement is a common MRI finding in PMD patients, especially for those with mutations in genes encoding OXPHOS and clinical LS. Early involvement of the SN in the disease course increases the likelihood of exhibiting Parkinsonism symptoms, strongly suggesting SN as the biological substrate of movement disorder symptoms in this population.

#### CLINICAL RELEVANCE/APPLICATION

Delineation of the prevalent types and anatomic substrate of movement disorders in patients with primary mitochondrial disorders can inform treatment regimens for these patients.

Printed on: 02/07/23

## Abstract Archives of the RSNA, 2022

T5B-SPPD-1

### Parkinsonism Syndrome in Primary Mitochondrial Disorders in Children: Imaging and Clinical Findings

Tuesday, Nov. 29 12:45PM - 1:15PM Room: Learning Center - PD DPS

#### Participants

Luis Tierradentro-Garcia, MD, Philadelphia, PA (*Presenter*) Nothing to Disclose

#### PURPOSE

Movement disorders may be observed in some patients with primary mitochondrial disorders (PMD). However, the frequency of the involvement of associated anatomic structures such as the substantia nigra (SN), the particular associated genetic mutations, and the specific clinical motor symptoms have not been reported. This study aims to analyze MRI abnormalities and follow-up changes of SN involvement in children with Parkinsonian movement disorder, in the context of genetically confirmed PMD to find the possible imaging and clinical correlation.

#### METHODS AND MATERIALS

In this retrospective analysis, we included patients younger than 18 years old with genetically confirmed PMD and brain MRI. We assessed the presence of various forms of movement disorder symptomatology in the clinical record and reported associated imaging abnormalities. MRI findings that were associated with symptoms of movement disorders or those with significant effect sizes ( $p=0.05-0.1$  and Cramer  $V > 1.5$ ) were tested through univariate logistic regression.

#### RESULTS

One hundred and seven patients with genetically confirmed PMD were included. The SN was involved in 32 (29.9%) patients, and among them, 28 (26.1%) had lesions on the baseline MRI. Follow-up studies were available for 22 subjects, in which four (18.2 %) had improvement of the lesions by MRI. Leigh syndrome (LS) was the most frequent PMD diagnosis in patients with SN involvement ( $n=26/32$ , 81%). LS was associated with SN involvement both at baseline MRI ( $p < 0.001$ ,  $V = 0.5$ ) and at all time-point pooled MRIs ( $p < 0.001$ ,  $V = 0.53$ ). Univariate model showed that mutation of genes encoding OXPHOS were strongly predictive (OR= 6.6, CI95% 2.6-17) of SN involvement at baseline (model  $\text{Chi}^2 = 16.5$ ,  $p < 0.001$ ,  $R^2 = 0.21$ ). SN involvement at baseline was also strongly predictive (OR= 26, CI95% 3.0-223) of Parkinsonism symptoms at baseline (model  $\text{Chi}^2 = 42.2$ ,  $p < 0.001$ ,  $R^2 = 0.31$ ).

#### CONCLUSION

SN involvement is a common MRI finding in PMD patients, especially for those with mutations in genes encoding OXPHOS and clinical LS. Early involvement of the SN in the disease course increases the likelihood of exhibiting Parkinsonism symptoms, strongly suggesting SN as the biological substrate of movement disorder symptoms in this population.

#### CLINICAL RELEVANCE/APPLICATION

Delineation of the prevalent types and anatomic substrate of movement disorders in patients with primary mitochondrial disorders can inform treatment regimens for these patients.

Printed on: 02/07/23

## Abstract Archives of the RSNA, 2022

T5B-SPPH

### Physics Tuesday Poster Discussions - B

Monday, Nov. 28 12:45PM - 1:15PM Room: Learning Center - PH DPS

#### Participants

Jian-Feng Chen, PhD, Naperville, IL (*Moderator*) Nothing to Disclose

#### Sub-Events

### **T5B-SPPH-2 Impact of the Automatic Patient Centering Proposed by a 3D Camera on Dose and Image Quality for Chest Abdomen and Pelvis CT Examination**

#### Participants

Joel Greffier, PhD, Nimes, France (*Presenter*) Nothing to Disclose

#### PURPOSE

To assess the impact of automatic patient centering proposed by a 3D camera on dose and image quality for chest-abdomen and pelvis CT examination

#### METHODS AND MATERIALS

A CT Torso CTU-41 anthropomorphic phantom (Kyoto Kagaku) with internal anatomical structures including head, thorax, abdomen and pelvis regions was used. All acquisitions were performed on the Incisive CT system (Philips Healthcare Systems) using the same acquisition and reconstruction parameters than those used for chest-abdomen-pelvic (CAP) CT examination in clinical practice. An experienced medical physicist first centered the phantom manually at the CT isocenter and performed 5 repeated acquisitions to assess the reproducibility of the automatic tube-current modulation system (reference values). Then, five experienced technologists manually and consecutively centered the phantom and one acquisition was made for each centering. Last, 5 acquisitions were performed using the automatic centering proposed by the 3D camera (Precise position system). The table height and the mean volume CT dose index (CTDI<sub>vol</sub>) were recorded. The image noise values were calculated with regions of interest (ROI, 1cm<sup>2</sup>) placed on lung (chest): 391 slices; liver (abdomen):155 slices; soft tissue (pelvis): 382 slices. The Wilcoxon test for paired samples was used to compare manual and automatic centering acquisitions to reference values

#### RESULTS

Considering whole scanned CAP area, the reference mean CTDI<sub>vol</sub> was 4.03 ± 0.02 mGy. The mean offset values from the table height reference position were of 23.0 ± 9.1 mm for manual centering and 8.5 ± 1.5 mm for automatic centering. The mean CTDI<sub>vol</sub> was similar for the manual centering compared to the reference acquisition (-4.5 ± 2.8%; p>0.05) and also for the automatic centering (4.2 ± 1.6%; p>0.05). For the lung tissue, the difference of mean noise was not significant for the manual centering and the reference acquisition (-2.5 ± 2.1%; p>0.05) and for the automatic centering (3.5%±0.8%; p>0.05). Similar results were observed for liver (-4.5 ± 4.0%; p>0.05 and 5.8 ± 1.9%; p>0.05, respectively) and pelvis soft tissue but with higher differences (9.0 ± 6.1%; p>0.05 and 5.5 ± 1.7%; p>0.05, respectively).

#### CONCLUSION

The new automatic patient centering system using a 3D camera allows reducing the table height offset from the isocenter. It increases the reproducibility of the centering compared with manual centering without significantly affecting the radiation dose and the image noise.

#### CLINICAL RELEVANCE/APPLICATION

The 3D camera allows rapid and reproducible patient positioning at the isocenter during CT examinations. It makes it possible to homogenize and standardize patient centering among technologists to improve practices in terms of dose and image quality.

### **T5B-SPPH-3 Assessing the Ability of a Deep-Silicon Photon Counting CT to Accurately Image a Realistic Patient-Specific 3-D Printed Lung Phantom**

#### Participants

Dominic Crotty, PhD, (*Presenter*) Employee, General Electric Company

#### PURPOSE

The objective of this study was to demonstrate the ability of an investigational edge-on silicon photon-counting computed tomography (PCCT) to accurately image a lifelike patient-specific three-dimensional (3-D) lung phantom.

#### METHODS AND MATERIALS

In this institutional review board-approved retrospective study, a patient with COVID-19 was identified who had undergone a routine thorax CT performed on a conventional CT system (Revolution EVO, GE Healthcare). On the basis of these data, a patient-specific lung phantom was 3-D printed (PixelPrint, University of Pennsylvania) with accurate attenuation profiles and textures. The printed phantom was placed inside a 20 cm bore of a technical phantom (Gammex multi-energy CT phantom, Sun Nuclear

Corporation) to match attenuations profiles of a typical patient (300 × 400 mm<sup>2</sup>). The setup was imaged using an investigational whole-body PCCT device (GE Healthcare) in axial mode with a 5 cm coverage at 120 kVp and 255 mAs. Reconstruction was performed utilizing a standard reconstruction algorithm with a STD kernel on a 1024x1024 matrix. Measurements of density accuracy and the similarity in the texture of images of the phantom were evaluated for both the PCCT and conventional CT.

## RESULTS

Identical regions were chosen for density measurements. Region of interest (ROI) measurements resulted in ROI-1 34.79HU / 32.10, ROI-2 -175.42HU / -169.96, and ROI-3 -854.05HU / -864.86HU for PCCT and conventional CT, respectively. The relative average error of less than 4% is reported when comparing PCCT and conventional CT. Subjective image texture appearances of parenchymal tissue in the phantom are like those in the original CT data set.

## CONCLUSION

The spatial resolution of the edge-on Si-based PCCT system can accurately represent the lung phantom derived from images acquired by a conventional commercial CT system. Further studies will be conducted with PixelPrint phantoms that include high spatial resolution features suitable for ultra-high-resolution PCCT scanners.

## CLINICAL RELEVANCE/APPLICATION

In order to evaluate next-generation CT systems, including ultra-high-resolution PCCTs, highly precise and lifelike phantoms are required to ensure a smooth transition into clinical practice.

### **T5B-SPPH-4 Evaluation of Task-based Automatic keV Selection for Photon Counting Detector CT in Comparison to Automatic kV Selection on Conventional CT**

Participants

Kishore Rajendran, PhD, Rochester, MN (*Presenter*) Nothing to Disclose

## PURPOSE

A new task-based virtual mono-energy image (VMI) keV selection tool (CARE keV, Siemens) has been introduced for clinical photon-counting detector (PCD) CT. The aim of this study was to assess performance of this auto-keV selection tool and compare with auto-kV selection (CARE kV, Siemens) on energy-integrating detector (EID) CT for different imaging tasks.

## METHODS AND MATERIALS

Two phantoms (18 x 24 cm and 25 x 32 cm, CIRS Sun Nuclear) containing iodine (2, 5, 10 mg/cc) and calcium (100 mg/cc) inserts were scanned on a clinical PCD-CT system (NAEOTOM Alpha, Siemens) and an EID-CT system (SOMATOM Force, Siemens). Four tasks were evaluated: non-contrast, bone, soft tissue with contrast, and vascular imaging. Tube current modulation and kV-keV configuration on PCD-CT were auto-set using CARE keV for an image quality level of 180. Similarly, tube current modulation and kV selection on EID-CT was enabled using CARE kV for a quality reference mAs of 180 at reference kV of 120. For all tasks, images were reconstructed using iterative reconstruction algorithm (strength 3), Br40 kernel, and 3 mm slice thickness on both systems. Mean and standard deviation of CT numbers were measured using circular regions-of-interests and contrast-to-noise ratio (CNR) calculated. Percent dose reduction for each task, relative to the non-contrast task were calculated.

## RESULTS

The auto-keV selection on PCD-CT enabled a task-based dose reduction (9%, 21%, 38% for bone, soft tissue, and vascular tasks relative to non-contrast task) irrespective of phantom size whereas the auto-kV selection on EID-CT showed size-dependent dose reduction with more dose reduction for smaller size phantom (12-61% on small phantom and 9-50% on large phantom). VMIs at 70, 65, 60 and 55 keV were auto-selected for non-contrast, bone, soft tissue with contrast and vascular tasks irrespective of phantom size on PCD-CT, while EID-CT CARE kV selected 70 to 90 kV for small phantom size and 70 to 100 kV for the large phantom size, for the four tasks. Mean percent changes in image contrast across phantom sizes and tasks were 13% for PCD-CT and 31% for EID-CT.

## CONCLUSION

A new task-dependent auto-keV selection tool on a clinical PCD-CT system provided similar contrast, noise, and CNR compared with an auto-kV selection tool available on a commercial EID-CT system.

## CLINICAL RELEVANCE/APPLICATION

Characterization of the auto-keV selection allows appropriate use of this new tool in clinical practice for optimizing image quality and radiation dose. The comparison between auto-keV and auto-kV selections tools can help translation of imaging protocols from one system to the other.

### **T5B-SPPH-5 Beam Hardening in Multi-Contrast Photon-Counting CT Imaging: A Phantom Study**

Participants

Amir Pourmorteza, PhD, Bethesda, MD (*Presenter*) Nothing to Disclose

## PURPOSE

Beam hardening artifacts can negatively influence myocardial CT measurements. Dense materials or materials with high effective atomic number cause more beam hardening. Photon-counting detectors (PCD) are inherently more susceptible to beam hardening due to equal weighting of detected photons regardless of their energies. The problem is further confounded by the introduction of new contrast agents such as gadolinium, with a prominent k-edge in the diagnostic CT energy range. The purpose of this study is to quantify the beam hardening effect of different materials in energy-integrating detectors (EID) and PCD at various tube voltage settings.

## METHODS AND MATERIALS

Pairs of test tubes were filled with dense contrast agents (iodine, gadolinium, and bismuth) and placed inside water phantom to cause beam hardening. The phantoms were scanned on EID (Somatom Force, Siemens Healthcare) and PCD (Naeotom Alpha, Siemens Healthcare) CT scanners at all available tube voltage settings for the PCD scanner (90, 120, 100 with Sn, and 140 with Sn pre-filtration). Images were reconstructed with standard water beam hardening correction but without any iodine/bone beam

hardening corrections. Virtual monoenergetic images (VMI) were calculated from PCD data.

## RESULTS

PCD images showed more beam hardening artifacts in all tube voltages compared to EID. PCD VMI could completely remove iodine beam hardening artifacts. Iodine BH artifacts decreased as we increased the tube voltage. However, gadolinium-based beam hardening artifacts had a different trend due to and increased at 120 kVp.

## CONCLUSION

s Energy-integrating detectors had less beam hardening artifacts compared to photon-counting detectors for x-ray tube voltages 120 kVp and higher. The inherent spectral information of PCDs can be used to effectively eliminate beam-hardening artifacts. However, special care is needed to correct beam hardening artifacts when k-edge contrast agents such as gadolinium and bismuth are present.

## CLINICAL RELEVANCE/APPLICATION

While PCDs are more susceptible to beam hardening, we could use the spectral information provided by PCDs to correct the beam hardening artifact. It is clear that BH correction algorithms, which are all tuned for iodine, need to be improved to account for the spectral effects of k-edge contrast agents such as gadolinium.

## T5B-SPPH-6 A Clinical Prototype CZT-Based Photon-Counting CT Scanner: First Experience in Low-Dose Lung Cancer Screening

Participants

Amir Pourmorteza, PhD, Bethesda, MD (*Presenter*) Nothing to Disclose

## PURPOSE

Here we report our initial assessment of the image quality of a whole-body prototype cadmium-zinc-telluride (CZT) photon-counting detector (PCD) CT scanner. The improved tissue contrast and lower radiation noise of PCDs make them suitable for scans such as low-dose lung cancer screening. In this work we focused on the non-spectral image reconstructed from all the detected photons above a low energy threshold set at 25 keV.

## METHODS AND MATERIALS

We used the COPDGENE2 phantom to simulate different types of healthy and pathological lung tissues under CT. All scans were performed at 120 kVp and at three different photon fluxes (50, 100, 200 mAs). Images were reconstructed with a filtered backprojection with a soft body kernel (FC13). For comparison, the phantom was also scanned on a state-of-the-art energy-integrating detector (EID) scanner (Aquilion One Genesis, Canon Medical Systems) at similar settings. We investigated CT number stability, contrast, and contrast-to-noise ratio of the two scanners.

## RESULTS

The PCD-CT images had CT numbers for all simulated types of lung tissue which were more robust to radiation dose, with maximum deviation of 0.8 vs 2.5 HU for PCD and EID images, respectively. Contrast and CNR of ground-glass opacifications and emphysema was higher for PCD images compared to the clinical EID measurements, indicating better detectability of these lesions with PCD at dose-matched settings.

## CONCLUSION

s The preliminary investigation of the new CZT PCD-CT prototype scanner showed improvements in CT number stability and CNR low-dose lung cancer screening tasks. This may lead to better detection and characterization of lung pathologies at reduced radiation doses or with better CNR. Further studies are warranted to assess the clinical performance of the prototype scanner.

## CLINICAL RELEVANCE/APPLICATION

Our initial investigation of the new CZT PCD-CT prototype showed improved performance in CT number stability and CNR specifically in low-dose lung CT scans which may lead to better detection and assessment of ground-glass nodules. The improved CNR may be used to lower the radiation dose of screening CT scans which will help include younger patients or patients with less packs per year in lung cancer screening.

## T5B-SPPH-7 Diagnostic Value of CT Lymphangiography in Primary Chyluria: A Retrospective Study

Participants

Qi Hao, Beijing, China (*Presenter*) Nothing to Disclose

## PURPOSE

To investigate the diagnostic value of CT lymphangiography (CTL) in primary chyluria.

## METHODS AND MATERIALS

Thirty-seven patients diagnosed as primary chyluria were recruited in this retrospective study. All patients were examined by DLG and CTL. The DLG was performed with a GE Innova 2000-IQ DSA machine, and a combined CT scan of the chest, abdomen and pelvis was performed with Siemens Sensation 16, Philips Brilliance spiral CT or GE revolution CT after 20min~2h. For CTL, the indexes were?Distribution of abnormal lymphatic vessels in the urinary system;?Lymphatic morphology and lymphatic reflux of bilateral iliac lymphatic, lumbar trunk and thoracic duct..The CTL signs of primary chyluria patients were statistically described by composition ratio of classification variables.

## RESULTS

CTL showed that lipiodol reflux was seen in 34 patients (91.9%) along the renal vasculature to the renal pelvis and calyces of unilateral or bilateral kidneys, of which 16 cases (43.2%) had lipiodol extending from the calyces into the renal parenchyma; 11 cases (29.7%) had reflux to the renal capsule area outside, 6 cases (16.2%) to the adrenal region, 7 cases (18.9%) to extraperitoneal and peri-intestinal, 12 cases (32.4%) to the bladder, and 4 cases (10.8%) to the peribladder region. And, CTL showed ipsilateral iliac lymphatic tortuosity and dilatation in 33 cases (89.2%), contralateral iliac lymphatic reflux in 26 cases (70.3%), ipsilateral lumbar

trunk tortuosity, dilatation and reflux in 23 cases (62.2%), contralateral lumbar trunk reflux in 29 cases (78.4%), ipsilateral renal reflux in 19 cases (51.4%), contralateral renal reflux in 24 cases (64.9%), thoracic duct reflux obstruction in 32 cases (86.5%), bronchomediastinal trunk reflux in 14 cases (37.8%), cervical trunk and subclavian trunk reflux in 11 cases (29.7%), 14 cases of bronchial mediastinal trunk reflux (37.8%), 11 cases of cervical trunk and subclavian trunk reflux (29.7%).

## CONCLUSION

s CTL can show the distribution, extent and severity of abnormal dilated lymphatic vessels in primary chyluria, in particular, it can clearly show the distribution of abnormal lymphatic vessels around the kidney and clarify the relationship with the surrounding tissue structure.

## CLINICAL RELEVANCE/APPLICATION

The CTL can provide an important imaging basis for the diagnosis and preoperative evaluation of primary chyluria, it is important for the preoperative evaluation and the development of the surgical plan.

## T5B-SPPH-8 On the Optimal Dose Modulation for Coronary Artery Calcium Scoring CT at Standard kVp

Participants

Jimmy Zhou, PhD, (*Presenter*) Nothing to Disclose

## PURPOSE

Coronary artery calcium scoring (CACs) CT is performed at 120 kVp in patients with borderline risk. As such, population dose has been a concern. The current dose modulation schemes use general approaches without considering the CACs image quality specifics. We aimed to find the optimal dose modulation based on the SCCT recommended CACs noise thresholds and new experimental data.

## METHODS AND MATERIALS

The study consisted of three parts. First, the noise measurements were performed on the images acquired from the Mercury phantom of tapered diameters (16 cm - 36 cm) with a dual-source Siemens Force CT, using gated CACS scans and a simulated ECG of 60 beats/min. The volume dose index (CTDI<sub>vol</sub>) was manually adjusted from 0.71 - 18.7 mGy at 120 kVp. The images were reconstructed to 3 mm thickness. The noise was correlated to the phantom diameter and CTDI<sub>vol</sub> (n = 264). The SCCT's recommended noise thresholds of 20 HU and 23 HU were used for the medium and large patient sizes, respectively. For the noise thresholds at the other diameters, an exponential function was used to obtain the size dependent thresholds. The corresponding CTDI<sub>vol</sub> was derived as a function of the phantom diameter. In the second part, the diameter (dp) of the Mercury phantom made of polyethylene was converted to the water equivalent diameter (dw). Lastly, the dw was converted to effective diameter (de) of the chest in the heart region using the retrospectively gathered clinical data (n = 21).

## RESULTS

The least-square surface fitting showed that the threshold noise is inversely proportional to the CTDI<sub>vol</sub> to a power of 0.405, and proportional to an exponential function of de multiplied by a parameter 0.061 (n = 264, R<sup>2</sup> = 0.968). The relations of dw, dp, and de were found to be: dw = 0.813de, and dw = 0.953dp.

## CONCLUSION

s An optimal dose modulation based on patient-size adjusted noise thresholds was established for coronary artery calcium scans.

## CLINICAL RELEVANCE/APPLICATION

Coronary artery calcium scoring CT dose optimization

## T5B-SPPH-9 Assessment of COVID-19 Pneumonia Using Darkfield Chest Radiography Compared to CT Imaging

Participants

Henriette Bast, Garching, Germany (*Presenter*) Nothing to Disclose

## PURPOSE

Dark-field chest radiography can detect microstructural changes of the lung parenchyma. Here, we compare dark-field chest radiography with CT imaging for the assessment of COVID-19 pneumonia.

## METHODS AND MATERIALS

Patients with a COVID-19 infection who underwent a chest CT were included if they had a category of 4, 5 or 6 according to the COVID-19 Reporting and Data System (CO-RADS) assessment scheme. Subjects with a medically indicated chest CT without any pathologic lung changes formed the control group. All participants were imaged at a CT scanner and at a clinical prototype for dark-field chest radiography. Four independent blinded readers rated the dark-field images in random order for the presence of COVID-19 in different lung zones. In the CT images, each of the five lung lobes was rated on a scale from 0 to 5 for the involvement of COVID-19 pneumonia by three independent blinded readers in random order and the sum of CT ratings for each patient was calculated. For quantitative analysis, each subject's COVID-19 CT index was calculated as the percentage of lung tissue above a threshold individually set for each patient. With Spearman's correlation coefficient, this COVID-19 CT index was tested for correlation with a subject's mean dark-field signal per lung volume (dark-field coefficient) and with the sum of CT ratings (total CT score).

## RESULTS

A total of 100 patients (59 males, 60 with COVID-19) were included with a mean age of 58 ± 14 years. The dark-field signal of COVID-19 patients is lower and less homogeneous compared to the one of healthy subjects. The dark-field coefficient was negatively correlated with both the CT-based COVID-19 index (r = -.24, p = .02) and the total CT score (r = -.36, p < .001).

## CONCLUSION

s The detection and visualization of COVID-19 pneumonia in dark-field images is consistent with the localization in CT images. Hence, dark-field imaging provides capability for the assessment of COVID-19.

**CLINICAL RELEVANCE/APPLICATION**

COVID-19 pneumonia can be assessed with dark-field chest radiography with less radiation dose than conventional CT imaging.

Printed on: 02/07/23

## Abstract Archives of the RSNA, 2022

T5B-SPPH-2

### Impact of the Automatic Patient Centering Proposed by a 3D Camera on Dose and Image Quality for Chest Abdomen and Pelvis CT Examination

Monday, Nov. 28 12:45PM - 1:15PM Room: Learning Center - PH DPS

#### Participants

Joel Greffier, PhD, Nimes, France (*Presenter*) Nothing to Disclose

#### PURPOSE

To assess the impact of automatic patient centering proposed by a 3D camera on dose and image quality for chest-abdomen and pelvis CT examination

#### METHODS AND MATERIALS

A CT Torso CTU-41 anthropomorphic phantom (Kyoto Kagaku) with internal anatomical structures including head, thorax, abdomen and pelvis regions was used. All acquisitions were performed on the Incisive CT system (Philips Healthcare Systems) using the same acquisition and reconstruction parameters than those used for chest-abdomen-pelvic (CAP) CT examination in clinical practice. An experienced medical physicist first centered the phantom manually at the CT isocenter and performed 5 repeated acquisitions to assess the reproducibility of the automatic tube-current modulation system (reference values). Then, five experienced technologists manually and consecutively centered the phantom and one acquisition was made for each centering. Last, 5 acquisitions were performed using the automatic centering proposed by the 3D camera (Precise position system). The table height and the mean volume CT dose index (CTDI<sub>vol</sub>) were recorded. The image noise values were calculated with regions of interest (ROI, 1cm<sup>2</sup>) placed on lung (chest): 391 slices; liver (abdomen):155 slices; soft tissue (pelvis): 382 slices. The Wilcoxon test for paired samples was used to compare manual and automatic centering acquisitions to reference values

#### RESULTS

Considering whole scanned CAP area, the reference mean CTDI<sub>vol</sub> was  $4.03 \pm 0.02$  mGy. The mean offset values from the table height reference position were of  $23.0 \pm 9.1$  mm for manual centering and  $8.5 \pm 1.5$  mm for automatic centering. The mean CTDI<sub>vol</sub> was similar for the manual centering compared to the reference acquisition ( $-4.5 \pm 2.8\%$ ;  $p>0.05$ ) and also for the automatic centering ( $4.2 \pm 1.6\%$ ;  $p>0.05$ ). For the lung tissue, the difference of mean noise was not significant for the manual centering and the reference acquisition ( $-2.5 \pm 2.1\%$ ;  $p>0.05$ ) and for the automatic centering ( $3.5\% \pm 0.8\%$ ;  $p>0.05$ ). Similar results were observed for liver ( $-4.5 \pm 4.0\%$ ;  $p>0.05$  and  $5.8 \pm 1.9\%$ ;  $p>0.05$ , respectively) and pelvis soft tissue but with higher differences ( $9.0 \pm 6.1\%$ ;  $p>0.05$  and  $5.5 \pm 1.7\%$ ;  $p>0.05$ , respectively).

#### CONCLUSION

The new automatic patient centering system using a 3D camera allows reducing the table height offset from the isocenter. It increases the reproducibility of the centering compared with manual centering without significantly affecting the radiation dose and the image noise.

#### CLINICAL RELEVANCE/APPLICATION

The 3D camera allows rapid and reproducible patient positioning at the isocenter during CT examinations. It makes it possible to homogenize and standardize patient centering among technologists to improve practices in terms of dose and image quality.

Printed on: 02/07/23

## Abstract Archives of the RSNA, 2022

T5B-SPPH-3

### Assessing the Ability of a Deep-Silicon Photon Counting CT to Accurately Image a Realistic Patient-Specific 3-D Printed Lung Phantom

Monday, Nov. 28 12:45PM - 1:15PM Room: Learning Center - PH DPS

#### Participants

Dominic Crotty, PhD, (*Presenter*) Employee, General Electric Company

#### PURPOSE

The objective of this study was to demonstrate the ability of an investigational edge-on silicon photon-counting computed tomography (PCCT) to accurately image a lifelike patient-specific three-dimensional (3-D) lung phantom.

#### METHODS AND MATERIALS

In this institutional review board-approved retrospective study, a patient with COVID-19 was identified who had undergone a routine thorax CT performed on a conventional CT system (Revolution EVO, GE Healthcare). On the basis of these data, a patient-specific lung phantom was 3-D printed (PixelPrint, University of Pennsylvania) with accurate attenuation profiles and textures. The printed phantom was placed inside a 20 cm bore of a technical phantom (Gammex multi-energy CT phantom, Sun Nuclear Corporation) to match attenuations profiles of a typical patient (300 × 400 mm<sup>2</sup>). The setup was imaged using an investigational whole-body PCCT device (GE Healthcare) in axial mode with a 5 cm coverage at 120 kVp and 255 mAs. Reconstruction was performed utilizing a standard reconstruction algorithm with a STD kernel on a 1024x1024 matrix. Measurements of density accuracy and the similarity in the texture of images of the phantom were evaluated for both the PCCT and conventional CT.

#### RESULTS

Identical regions were chosen for density measurements. Region of interest (ROI) measurements resulted in ROI-1 34.79HU / 32.10, ROI-2 -175.42HU / -169.96, and ROI-3 -854.05HU / -864.86HU for PCCT and conventional CT, respectively. The relative average error of less than 4% is reported when comparing PCCT and conventional CT. Subjective image texture appearances of parenchymal tissue in the phantom are like those in the original CT data set.

#### CONCLUSION

The spatial resolution of the edge-on Si-based PCCT system can accurately represent the lung phantom derived from images acquired by a conventional commercial CT system. Further studies will be conducted with PixelPrint phantoms that include high spatial resolution features suitable for ultra-high-resolution PCCT scanners.

#### CLINICAL RELEVANCE/APPLICATION

In order to evaluate next-generation CT systems, including ultra-high-resolution PCCTs, highly precise and lifelike phantoms are required to ensure a smooth transition into clinical practice.

Printed on: 02/07/23



## Abstract Archives of the RSNA, 2022

T5B-SPPH-4

### Evaluation of Task-based Automatic keV Selection for Photon Counting Detector CT in Comparison to Automatic kV Selection on Conventional CT

Monday, Nov. 28 12:45PM - 1:15PM Room: Learning Center - PH DPS

#### Participants

Kishore Rajendran, PhD, Rochester, MN (*Presenter*) Nothing to Disclose

#### PURPOSE

A new task-based virtual mono-energy image (VMI) keV selection tool (CARE keV, Siemens) has been introduced for clinical photon-counting detector (PCD) CT. The aim of this study was to assess performance of this auto-keV selection tool and compare with auto-kV selection (CARE kV, Siemens) on energy-integrating detector (EID) CT for different imaging tasks.

#### METHODS AND MATERIALS

Two phantoms (18 x 24 cm and 25 x 32 cm, CIRS Sun Nuclear) containing iodine (2, 5, 10 mg/cc) and calcium (100 mg/cc) inserts were scanned on a clinical PCD-CT system (NAEOTOM Alpha, Siemens) and an EID-CT system (SOMATOM Force, Siemens). Four tasks were evaluated: non-contrast, bone, soft tissue with contrast, and vascular imaging. Tube current modulation and kV-keV configuration on PCD-CT were auto-set using CARE keV for an image quality level of 180. Similarly, tube current modulation and kV selection on EID-CT was enabled using CARE kV for a quality reference mAs of 180 at reference kV of 120. For all tasks, images were reconstructed using iterative reconstruction algorithm (strength 3), Br40 kernel, and 3 mm slice thickness on both systems. Mean and standard deviation of CT numbers were measured using circular regions-of-interests and contrast-to-noise ratio (CNR) calculated. Percent dose reduction for each task, relative to the non-contrast task were calculated.

#### RESULTS

The auto-keV selection on PCD-CT enabled a task-based dose reduction (9%, 21%, 38% for bone, soft tissue, and vascular tasks relative to non-contrast task) irrespective of phantom size whereas the auto-kV selection on EID-CT showed size-dependent dose reduction with more dose reduction for smaller size phantom (12-61% on small phantom and 9-50% on large phantom). VMIs at 70, 65, 60 and 55 keV were auto-selected for non-contrast, bone, soft tissue with contrast and vascular tasks irrespective of phantom size on PCD-CT, while EID-CT CARE kV selected 70 to 90 kV for small phantom size and 70 to 100 kV for the large phantom size, for the four tasks. Mean percent changes in image contrast across phantom sizes and tasks were 13% for PCD-CT and 31% for EID-CT.

#### CONCLUSION

A new task-dependent auto-keV selection tool on a clinical PCD-CT system provided similar contrast, noise, and CNR compared with an auto-kV selection tool available on a commercial EID-CT system.

#### CLINICAL RELEVANCE/APPLICATION

Characterization of the auto-keV selection allows appropriate use of this new tool in clinical practice for optimizing image quality and radiation dose. The comparison between auto-keV and auto-kV selections tools can help translation of imaging protocols from one system to the other.

Printed on: 02/07/23

## Abstract Archives of the RSNA, 2022

T5B-SPPH-5

### Beam Hardening in Multi-Contrast Photon-Counting CT Imaging: A Phantom Study

Monday, Nov. 28 12:45PM - 1:15PM Room: Learning Center - PH DPS

#### Participants

Amir Pourmorteza, PhD, Bethesda, MD (*Presenter*) Nothing to Disclose

#### PURPOSE

Beam hardening artifacts can negatively influence myocardial CT measurements. Dense materials or materials with high effective atomic number cause more beam hardening. Photon-counting detectors (PCD) are inherently more susceptible to beam hardening due to equal weighting of detected photons regardless of their energies. The problem is further confounded by the introduction of new contrast agents such as gadolinium, with a prominent k-edge in the diagnostic CT energy range. The purpose of this study is to quantify the beam hardening effect of different materials in energy-integrating detectors (EID) and PCD at various tube voltage settings.

#### METHODS AND MATERIALS

Pairs of test tubes were filled with dense contrast agents (iodine, gadolinium, and bismuth) and placed inside water phantom to cause beam hardening. The phantoms were scanned on EID (Somatom Force, Siemens Healthcare) and PCD (Naeotom Alpha, Siemens Healthcare) CT scanners at all available tube voltage settings for the PCD scanner (90, 120, 100 with Sn, and 140 with Sn pre-filtration). Images were reconstructed with standard water beam hardening correction but without any iodine/bone beam hardening corrections. Virtual monoenergetic images (VMI) were calculated from PCD data.

#### RESULTS

PCD images showed more beam hardening artifacts in all tube voltages compared to EID. PCD VMI could completely remove iodine beam hardening artifacts. Iodine BH artifacts decreased as we increased the tube voltage. However, gadolinium-based beam hardening artifacts had a different trend due to and increased at 120 kVp.

#### CONCLUSION

s Energy-integrating detectors had less beam hardening artifacts compared to photon-counting detectors for x-ray tube voltages 120 kVp and higher. The inherent spectral information of PCDs can be used to effectively eliminate beam-hardening artifacts. However, special care is needed to correct beam hardening artifacts when k-edge contrast agents such as gadolinium and bismuth are present.

#### CLINICAL RELEVANCE/APPLICATION

While PCDs are more susceptible to beam hardening, we could use the spectral information provided by PCDs to correct the beam hardening artifact. It is clear that BH correction algorithms, which are all tuned for iodine, need to be improved to account for the spectral effects of k-edge contrast agents such as gadolinium.

Printed on: 02/07/23

## Abstract Archives of the RSNA, 2022

T5B-SPPH-6

### A Clinical Prototype CZT-Based Photon-Counting CT Scanner: First Experience in Low-Dose Lung Cancer Screening

Monday, Nov. 28 12:45PM - 1:15PM Room: Learning Center - PH DPS

#### Participants

Amir Pourmorteza, PhD, Bethesda, MD (*Presenter*) Nothing to Disclose

#### PURPOSE

Here we report our initial assessment of the image quality of a whole-body prototype cadmium-zinc-telluride (CZT) photon-counting detector (PCD) CT scanner. The improved tissue contrast and lower radiation noise of PCDs make them suitable for scans such as low-dose lung cancer screening. In this work we focused on the non-spectral image reconstructed from all the detected photons above a low energy threshold set at 25 keV.

#### METHODS AND MATERIALS

We used the COPDGENE2 phantom to simulate different types of healthy and pathological lung tissues under CT. All scans were performed at 120 kVp and at three different photon fluxes (50, 100, 200 mAs). Images were reconstructed with a filtered backprojection with a soft body kernel (FC13). For comparison, the phantom was also scanned on a state-of-the-art energy-integrating detector (EID) scanner (Aquilion One Genesis, Canon Medical Systems) at similar settings. We investigated CT number stability, contrast, and contrast-to-noise ratio of the two scanners.

#### RESULTS

The PCD-CT images had CT numbers for all simulated types of lung tissue which were more robust to radiation dose, with maximum deviation of 0.8 vs 2.5 HU for PCD and EID images, respectively. Contrast and CNR of ground-glass opacifications and emphysema was higher for PCD images compared to the clinical EID measurements, indicating better detectability of these lesions with PCD at dose-matched settings.

#### CONCLUSION

The preliminary investigation of the new CZT PCD-CT prototype scanner showed improvements in CT number stability and CNR in low-dose lung cancer screening tasks. This may lead to better detection and characterization of lung pathologies at reduced radiation doses or with better CNR. Further studies are warranted to assess the clinical performance of the prototype scanner.

#### CLINICAL RELEVANCE/APPLICATION

Our initial investigation of the new CZT PCD-CT prototype showed improved performance in CT number stability and CNR specifically in low-dose lung CT scans which may lead to better detection and assessment of ground-glass nodules. The improved CNR may be used to lower the radiation dose of screening CT scans which will help include younger patients or patients with less packs per year in lung cancer screening.

Printed on: 02/07/23

## Abstract Archives of the RSNA, 2022

T5B-SPPH-7

### Diagnostic Value of CT Lymphangiography in Primary Chyluria: A Retrospective Study

Monday, Nov. 28 12:45PM - 1:15PM Room: Learning Center - PH DPS

#### Participants

Qi Hao, Beijing, China (*Presenter*) Nothing to Disclose

#### PURPOSE

To investigate the diagnostic value of CT lymphangiography (CTL) in primary chyluria.

#### METHODS AND MATERIALS

Thirty-seven patients diagnosed as primary chyluria were recruited in this retrospective study. All patients were examined by DLG and CTL. The DLG was performed with a GE Innova 2000-IQ DSA machine, and a combined CT scan of the chest, abdomen and pelvis was performed with Siemens Sensation 16, Philips Brilliance spiral CT or GE revolution CT after 20min~2h. For CTL, the indexes were: Distribution of abnormal lymphatic vessels in the urinary system; Lymphatic morphology and lymphatic reflux of bilateral iliac lymphatic, lumbar trunk and thoracic duct. The CTL signs of primary chyluria patients were statistically described by composition ratio of classification variables.

#### RESULTS

CTL showed that lipiodol reflux was seen in 34 patients (91.9%) along the renal vasculature to the renal pelvis and calyces of unilateral or bilateral kidneys, of which 16 cases (43.2%) had lipiodol extending from the calyces into the renal parenchyma; 11 cases (29.7%) had reflux to the renal capsule area outside, 6 cases (16.2%) to the adrenal region, 7 cases (18.9%) to extrafascial and peri-intestinal, 12 cases (32.4%) to the bladder, and 4 cases (10.8%) to the peribladder region. And, CTL showed ipsilateral iliac lymphatic tortuosity and dilatation in 33 cases (89.2%), contralateral iliac lymphatic reflux in 26 cases (70.3%), ipsilateral lumbar trunk tortuosity, dilatation and reflux in 23 cases (62.2%), contralateral lumbar trunk reflux in 29 cases (78.4%), ipsilateral renal reflux in 19 cases (51.4%), contralateral renal reflux in 24 cases (64.9%), thoracic duct reflux obstruction in 32 cases (86.5%), bronchomediastinal trunk reflux in 14 cases (37.8%), cervical trunk and subclavian trunk reflux in 11 cases (29.7%), 14 cases of bronchial mediastinal trunk reflux (37.8%), 11 cases of cervical trunk and subclavian trunk reflux (29.7%).

#### CONCLUSION

CTL can show the distribution, extent and severity of abnormal dilated lymphatic vessels in primary chyluria, in particular, it can clearly show the distribution of abnormal lymphatic vessels around the kidney and clarify the relationship with the surrounding tissue structure.

#### CLINICAL RELEVANCE/APPLICATION

The CTL can provide an important imaging basis for the diagnosis and preoperative evaluation of primary chyluria, it is important for the preoperative evaluation and the development of the surgical plan.

Printed on: 02/07/23

## Abstract Archives of the RSNA, 2022

T5B-SPPH-8

### On the Optimal Dose Modulation for Coronary Artery Calcium Scoring CT at Standard kVp

Monday, Nov. 28 12:45PM - 1:15PM Room: Learning Center - PH DPS

#### Participants

Jimmy Zhou, PhD, (*Presenter*) Nothing to Disclose

#### PURPOSE

Coronary artery calcium scoring (CACs) CT is performed at 120 kVp in patients with borderline risk. As such, population dose has been a concern. The current dose modulation schemes use general approaches without considering the CACs image quality specifics. We aimed to find the optimal dose modulation based on the SCCT recommended CACs noise thresholds and new experimental data.

#### METHODS AND MATERIALS

The study consisted of three parts. First, the noise measurements were performed on the images acquired from the Mercury phantom of tapered diameters (16 cm - 36 cm) with a dual-source Siemens Force CT, using gated CAs scans and a simulated ECG of 60 beats/min. The volume dose index (CTDI<sub>vol</sub>) was manually adjusted from 0.71 - 18.7 mGy at 120 kVp. The images were reconstructed to 3 mm thickness. The noise was correlated to the phantom diameter and CTDI<sub>vol</sub> (n = 264). The SCCT's recommended noise thresholds of 20 HU and 23 HU were used for the medium and large patient sizes, respectively. For the noise thresholds at the other diameters, an exponential function was used to obtain the size dependent thresholds. The corresponding CTDI<sub>vol</sub> was derived as a function of the phantom diameter. In the second part, the diameter (dp) of the Mercury phantom made of polyethylene was converted to the water equivalent diameter (dw). Lastly, the dw was converted to effective diameter (de) of the chest in the heart region using the retrospectively gathered clinical data (n = 21).

#### RESULTS

The least-square surface fitting showed that the threshold noise is inversely proportional to the CTDI<sub>vol</sub> to a power of 0.405, and proportional to an exponential function of de multiplied by a parameter 0.061 (n = 264, R<sup>2</sup> = 0.968). The relations of dw, dp, and de were found to be:  $dw = 0.813de$ , and  $dw = 0.953dp$ .

#### CONCLUSION

An optimal dose modulation based on patient-size adjusted noise thresholds was established for coronary artery calcium scans.

#### CLINICAL RELEVANCE/APPLICATION

Coronary artery calcium scoring CT dose optimization

Printed on: 02/07/23

## Abstract Archives of the RSNA, 2022

T5B-SPPH-9

### Assessment of COVID-19 Pneumonia Using Darkfield Chest Radiography Compared to CT Imaging

Monday, Nov. 28 12:45PM - 1:15PM Room: Learning Center - PH DPS

#### Participants

Henriette Bast, Garching, Germany (*Presenter*) Nothing to Disclose

#### PURPOSE

Dark-field chest radiography can detect microstructural changes of the lung parenchyma. Here, we compare dark-field chest radiography with CT imaging for the assessment of COVID-19 pneumonia.

#### METHODS AND MATERIALS

Patients with a COVID-19 infection who underwent a chest CT were included if they had a category of 4, 5 or 6 according to the COVID-19 Reporting and Data System (CO-RADS) assessment scheme. Subjects with a medically indicated chest CT without any pathologic lung changes formed the control group. All participants were imaged at a CT scanner and at a clinical prototype for dark-field chest radiography. Four independent blinded readers rated the dark-field images in random order for the presence of COVID-19 in different lung zones. In the CT images, each of the five lung lobes was rated on a scale from 0 to 5 for the involvement of COVID-19 pneumonia by three independent blinded readers in random order and the sum of CT ratings for each patient was calculated. For quantitative analysis, each subject's COVID-19 CT index was calculated as the percentage of lung tissue above a threshold individually set for each patient. With Spearman's correlation coefficient, this COVID-19 CT index was tested for correlation with a subject's mean dark-field signal per lung volume (dark-field coefficient) and with the sum of CT ratings (total CT score).

#### RESULTS

A total of 100 patients (59 males, 60 with COVID-19) were included with a mean age of  $58 \pm 14$  years. The dark-field signal of COVID-19 patients is lower and less homogeneous compared to the one of healthy subjects. The dark-field coefficient was negatively correlated with both the CT-based COVID-19 index ( $r = -.24$ ,  $p = .02$ ) and the total CT score ( $r = -.36$ ,  $p < .001$ ).

#### CONCLUSION

The detection and visualization of COVID-19 pneumonia in dark-field images is consistent with the localization in CT images. Hence, dark-field imaging provides capability for the assessment of COVID-19.

#### CLINICAL RELEVANCE/APPLICATION

COVID-19 pneumonia can be assessed with dark-field chest radiography with less radiation dose than conventional CT imaging.

Printed on: 02/07/23

## Abstract Archives of the RSNA, 2022

W2-SPBR

### Breast Wednesday Poster Discussions

Wednesday, Nov. 30 9:00AM - 9:30AM Room: Learning Center - BR DPS

#### Participants

Brian S. Englander, MD, Philadelphia, PA (*Moderator*) Nothing to Disclose

#### Sub-Events

### W2-SPBR-1 Difference in US Visibility of Tissue Marker in Metastatic Lymph Nodes After Neoadjuvant Chemotherapy in The Breast Cancer Patients

#### Participants

Ka Eun Kim, MD, Seoul, Korea, Republic Of (*Presenter*) Nothing to Disclose

#### PURPOSE

This study is aimed to investigate the differences in ultrasound (US) visibility for localization of clipped metastatic lymph nodes after neoadjuvant chemotherapy (NAC) according to the type of tissue markers.

#### METHODS AND MATERIALS

In this single-center retrospective study, 59 consecutive breast cancer patients who underwent tissue marker insertion for histologically proven metastatic axillary lymph node between March 2020 and August 2021 were included. We inserted two different types of breast tissue markers; UltraClip™ (n=29) and UltraCor™ Twirl™ (n=30), within the metastatic axillary lymph node before NAC. After completion of NAC, the patients underwent sentinel lymph node biopsy or axillary dissection with (n=44) or without (n=15) localization of the clipped node. Medical records and imaging findings were retrospectively reviewed. We compared the US visibility and successful excision rate of clipped lymph node between the two types of tissue markers. Fisher's exact test were used for statistical analysis.

#### RESULTS

The overall US visibility of tissue markers after NAC was better in UltraCor™ Twirl™ than in UltraClip™ (86.7% vs 72.4%), but statistically not significant ( $p = 0.209$ ). However, UltraCor™ Twirl™ showed significantly better US visibility (83.3%, 15/18) than UltraClip™ (42.9%, 6/14) in the cases with no residual metastatic lymph node on US (n=32) ( $p = 0.027$ ). Meanwhile, type of tissue markers was not associated with successful excision of clipped lymph node ( $p = 1.000$ ). The patients who underwent preoperative US-guided localization for clipped lymph node showed higher successful excision rate than the patients without localization ( $p = 0.010$ ).

#### CONCLUSION

s UltraCor™ Twirl™ showed better US visibility than UltraClip™ in the metastatic axillary lymph node after NAC, especially when there was no residual suspicious lymph node on US.

#### CLINICAL RELEVANCE/APPLICATION

The visibility of tissue marker is important for localization. Comparing the US visibility of tissue marker for axillary lymph node would be helpful for successful targeted axillary dissection.

### W2-SPBR-2 Role of Hemastix As A Tool to Determine Pre-test Probability of Abnormal Pathology in Patients with Nipple Discharge

#### Participants

Ramapriya Ganti, MD, PhD, Charlottesville, VA (*Presenter*) Nothing to Disclose

#### PURPOSE

Nipple discharge accounts for approximately 5% of breast surgical evaluations and may be associated with malignancy in 2.7%-24.2% of cases. Visually, discharge for evidence of blood, a malignancy indicator, is subjective and can be inaccurate. The association of hemocult test results with abnormal pathology was analyzed to determine the utility of including hemocult testing during initial workup for nipple discharge.

#### METHODS AND MATERIALS

An IRB-approved retrospective cohort study was done of women who underwent breast imaging at our institution for nipple discharge from January 2008 to December 2018. Only patients who had tissue sampling or two years of imaging follow-up were included in the study. The results of all breast imaging and histopathology for workup of nipple discharge were extracted from each patient's medical record. Descriptors of the nipple discharge, including color, number of ducts involved, laterality, spontaneity, and results of hemocult testing were obtained from the radiology reports. Univariate and multivariate logistic regression analyses were conducted to determine whether hemocult results, imaging results, and/or discharge descriptors were associated with abnormal pathology, defined as papilloma or malignancy. Sensitivity, specificity, and other performance characteristics were calculated for

hemocult testing and imaging modalities.

## RESULTS

Of a total of 326 women who met inclusion criteria, 247/75.8% had reproducible discharge at time of imaging and 204/62.6% received a hemocult test. As part of the workup, 307/94.2% had a mammogram, 187/57.4% an ultrasound, 58/17.8% an MRI, and 131/40.4% a galactogram. Tissue sampling revealed non-malignant abnormal pathology in 118/32.6% and malignancy in 19/5.8%. Multivariate analysis showed that abnormal pathology was independently associated with positive hemocult results (adjusted odds ratio (AOR) 2.68;  $p=0.026$ ), single-duct (AOR 6.95;  $p<0.001$ ), spontaneous (AOR 3.84;  $p=0.013$ ), and suspicious colored discharge (AOR 4.37;  $p=0.041$ ). Positive hemocult test was also a predictor of abnormal pathology if all factor characteristics were unknown (OR 5.16;  $p<0.001$ ). Hemocult testing showed a sensitivity of 73.7% (95% CI: [63.6%-82.2%]) for abnormal pathology, similar to galactography (87.7%; 95% CI: [77.9%-94.2%]) and MRI (83.3%; 95% CI: [62.6%-95.3%]).

## CONCLUSION

s Hemocult testing is sensitive and independently associated with abnormal histopathology in patients with nipple discharge.

## CLINICAL RELEVANCE/APPLICATION

Hemocult testing may be a useful diagnostic tool in patients with nipple discharge prior to diagnostic imaging to help establish the pre-test probability of abnormal histopathology based on discharge characteristics.

## W2-SPBR-3 Contrast-enhanced Spectral Mammography-guided Breast Biopsy: Technique Feasibility and Comparison with MR-guided Vacuum-Assisted Breast Biopsy

Participants

Romy Heriteau, MD, (*Presenter*) Nothing to Disclose

## PURPOSE

Contrast-enhanced spectral mammography (CESM) is a recent imaging technique based on the association of spectral mammography and iodinated contrast agent to detect tumor enhancement, linked to neoangiogenesis. CESM is known to have same sensitivity as MRI with a higher specificity, higher Predictive Positive Value (PPV), and better conditions of accessibility and cost. The purpose of this study is to show the comparison of diagnostic performances of biopsies under CESM compared to biopsies under MRI in terms of availability, procedure duration and failure, side effects and cost

## METHODS AND MATERIALS

Retrospective evaluation of our 3 years' experience with CESM procedure and comparison with MR-biopsy procedure in our institution. All consecutive patient referred for an MRI or CESM-guided breast biopsy were included in our study. 25 patients for CESM biopsy and 107 patients for MRI biopsy were included. We analyzed two reliability parameters for each technique, the concordance between radiological BI-RADS classification and histological results of the biopsy. Then, the concordance between histological biopsy results and histological results after surgery. Procedure time, side effects and cost were also collected.

## RESULTS

athology results were categorized as benign (38 lesions in MRI and 13 in CESM), high-risk (22/5), or malignant (17/2 ductal carcinoma in situ (DCIS), 21/3 invasive ductal carcinoma, 6/2 invasive lobular carcinoma). Subsequent surgery for high-risk and malignant lesions revealed a 21% discordance rate and 15% underestimation rate for MRI and one discordance and underestimation for CESM ( $p>0.5$ ). Comparison between BI-RADS classification and pathology results revealed one discordance for MRI and none for CESM ( $p>0.5$ ). Duration was significantly shorter for CESM (median duration : 28 minutes) in comparison with MRI (median : 53 minutes) ( $p<0.05$ ). 15 side effects for MRI versus 2 for CESM have been registered ( $p = 0.53$ ). Economical study estimated the cost for a biopsy under MR-guided biopsy at 1213€ and a CESM- at 574€

## CONCLUSION

s CESM guided-biopsy may be an interesting alternative technique to MR-guided breast biopsy, with time and cost saving, without reducing accuracy.

## CLINICAL RELEVANCE/APPLICATION

CESM guided-biopsy is a simpler and more accessible alternative technique to MRI biopsies. This biopsy could be performed in more and more centers in the future.

## W2-SPBR-4 Should I Stay, or Should I Go? A Workforce Movement Survey of Breast Radiologists.

Participants

Grayson Baird, PhD, Providence, RI (*Presenter*) Nothing to Disclose

## PURPOSE

To evaluate factors associated with whether breast radiologists have left, or are considering leaving, their current job.

## METHODS AND MATERIALS

Practicing members of the Society of Breast Imaging were emailed a weblink to an IRB-approved surveys in February 2022. The survey included 32 questions about attitudes towards work and whether they had left their last position within the last two years, were thinking of leaving, or were not thinking of leaving their current position. Exploratory factor analysis (EFA) was used to evaluate construct validity. Internal consistency was evaluated with Cronbach's Alpha. Concurrent validity was examined using discriminant function analysis (DFA). All psychometric analyses were conducted using SAS.

## RESULTS

Response rate was 14% (230/1670), with 2 being dropped as they retired over 2 years ago. 82% (182/288) identified as being white, with 77% (173) identifying as female. 5% (11) were 35 years or younger, 33% (75) were between 36-45, 29% (66) were between 46-55, 25% (57) were between 56-65, and 7.5% (17) were 65 or older. The majority (73.6%, 167) reported 76-100% of their practice was focused on breast imaging. Of the 228, 23.3% (53) responded that they had left a practice within the last two

years, 21.9% (50) were thinking of leaving, and 54.8% (125) were not thinking of leaving--45% of respondents were either thinking of leaving or had recently left their practice. Factor analysis identified 5 latent variables (factors) from the 32 questions: 1. "Quality of Life" issues, 2. "Physician Socio-Cultural" issues, 3. "Workplace Condition" issues, 4. "Non-Physician Socio-Cultural" issues, and 5. "Career" issues. Cronbach's Alpha was .89, showing high internal consistency. DFA examined how well the 32 questions classified the groups (Figure 1). Those "staying" (red) clustered positively with the first function (x-axis), while those who "left" (blue) cluster negatively with the first function, and those who were thinking of "leaving" (green) clustered in between but negatively on the first function. Only the first function was significant,  $p < .01$ , which was highly related with questions concerning Quality of Life.

## CONCLUSION

s Quality of life is the factor most associated with workforce movement of breast radiologists. Almost one-half of breast radiologists had recently left or were considering leaving their positions. The survey showed good psychometric properties.

## CLINICAL RELEVANCE/APPLICATION

Almost one-half of breast radiologists had left or were considering leaving their positions. It may be important to measure attitudes towards workplace movement to understand why radiologists are staying and leaving.

## W2-SPBR-5 A Novel Anthropomorphic Model Observer for Micro-calcification Cluster Detection in Digital Mammography and Digital Breast Tomosynthesis Images for The VICTRE Pipeline

Participants

Katrien Houbrechts, Leuven, Belgium (*Presenter*) Siemens AG

## PURPOSE

Develop an anthropomorphic model observer for calcification cluster detection in digital mammography (DM) and digital breast tomosynthesis (DBT) for a clinical range of lesion sizes and dose levels, and illustrate its applicability to predict the impact of blurring.

## METHODS AND MATERIALS

Clusters with 5 round calcifications of 100  $\mu\text{m}$ , 150  $\mu\text{m}$  and 200  $\mu\text{m}$  diameter were randomly inserted in heterogeneous VICTRE breast phantoms. DM and DBT images were created using the VICTRE pipeline with a clinical Automatic Exposure Control (AEC) dose, AEC/2 and 2AEC. For both DM and DBT, 20 lesion-present and 120 lesion-absent samples were used for each condition to tune a two-layer Channelized Hotelling Observer (CHO) to four-alternative forced choice reading results of 6 human readers. The CHO performance in the presence of system blurring was investigated for 150  $\mu\text{m}$  clusters. For DM, the focus size and lesion height above the table was changed. For DBT, source motion was varied.

## RESULTS

The CHO (localization: 2 Laguerre-Gauss channels; classification: 8 Gabor channels) agreed closely with human results (mean error [-4.12;0.14], linear regression slope [0.98;1.07]) over the studied range of lesion sizes and dose levels for both modalities. CHO readout was more reproducible than human reading, with average standard deviation of 3% compared to 5-6%. The CHO was sensitive to microcalcification blurring. The DM CHO percent correctly detected targets (PC) for clusters located 5 mm above the table was 70 $\pm$ 4% and 64 $\pm$ 5% for focus sizes of 0.3 mm and 0.5 mm, respectively ( $p < 0.0001$ ). When located 40 mm above the table, the PC was 58 $\pm$ 4% and 46 $\pm$ 5%, respectively ( $p < 0.0001$ ). The DBT CHO showed a monotonic decrease in lesion detection performance as source motion blur increased; e.g. for 21 s scan time, the PC was 77 $\pm$ 4% and 57 $\pm$ 4% for a 90 ms and 150 ms exposure time, respectively ( $p < 0.0001$ ).

## CONCLUSION

s A two-layer CHO was shown to approximate human observer detection results for microcalcifications in DM and DBT images generated with the VICTRE pipeline and can be used to evaluate the influence of system settings on detection performance for in-silico studies.

## CLINICAL RELEVANCE/APPLICATION

The anthropomorphic CHO enables the accurate modelling of microcalcification detection performance for in-silico clinical studies.

Printed on: 02/07/23

## Abstract Archives of the RSNA, 2022

W2-SPBR-1

### Difference in US Visibility of Tissue Marker in Metastatic Lymph Nodes After Neoadjuvant Chemotherapy in The Breast Cancer Patients

Wednesday, Nov. 30 9:00AM - 9:30AM Room: Learning Center - BR DPS

#### Participants

Ka Eun Kim, MD, Seoul, Korea, Republic Of (*Presenter*) Nothing to Disclose

#### PURPOSE

This study is aimed to investigate the differences in ultrasound (US) visibility for localization of clipped metastatic lymph nodes after neoadjuvant chemotherapy (NAC) according to the type of tissue markers.

#### METHODS AND MATERIALS

In this single-center retrospective study, 59 consecutive breast cancer patients who underwent tissue marker insertion for histologically proven metastatic axillary lymph node between March 2020 and August 2021 were included. We inserted two different types of breast tissue markers; UltraClip™ (n=29) and UltraCor™ Twirl™ (n=30), within the metastatic axillary lymph node before NAC. After completion of NAC, the patients underwent sentinel lymph node biopsy or axillary dissection with (n=44) or without (n=15) localization of the clipped node. Medical records and imaging findings were retrospectively reviewed. We compared the US visibility and successful excision rate of clipped lymph node between the two types of tissue markers. Fisher's exact test were used for statistical analysis.

#### RESULTS

The overall US visibility of tissue markers after NAC was better in UltraCor™ Twirl™ than in UltraClip™ (86.7% vs 72.4%), but statistically not significant ( $p = 0.209$ ). However, UltraCor™ Twirl™ showed significantly better US visibility (83.3%, 15/18) than UltraClip™ (42.9%, 6/14) in the cases with no residual metastatic lymph node on US (n=32) ( $p = 0.027$ ). Meanwhile, type of tissue markers was not associated with successful excision of clipped lymph node ( $p = 1.000$ ). The patients who underwent preoperative US-guided localization for clipped lymph node showed higher successful excision rate than the patients without localization ( $p = 0.010$ ).

#### CONCLUSION

s UltraCor™ Twirl™ showed better US visibility than UltraClip™ in the metastatic axillary lymph node after NAC, especially when there was no residual suspicious lymph node on US.

#### CLINICAL RELEVANCE/APPLICATION

The visibility of tissue marker is important for localization. Comparing the US visibility of tissue marker for axillary lymph node would be helpful for successful targeted axillary dissection.

Printed on: 02/07/23

## Abstract Archives of the RSNA, 2022

W2-SPBR-2

### Role of Hemastix As A Tool to Determine Pre-test Probability of Abnormal Pathology in Patients with Nipple Discharge

Wednesday, Nov. 30 9:00AM - 9:30AM Room: Learning Center - BR DPS

#### Participants

Ramapriya Ganti, MD, PhD, Charlottesville, VA (*Presenter*) Nothing to Disclose

#### PURPOSE

Nipple discharge accounts for approximately 5% of breast surgical evaluations and may be associated with malignancy in 2.7%-24.2% of cases. Visually, discharge for evidence of blood, a malignancy indicator, is subjective and can be inaccurate. The association of hemocult test results with abnormal pathology was analyzed to determine the utility of including hemocult testing during initial workup for nipple discharge.

#### METHODS AND MATERIALS

An IRB-approved retrospective cohort study was done of women who underwent breast imaging at our institution for nipple discharge from January 2008 to December 2018. Only patients who had tissue sampling or two years of imaging follow-up were included in the study. The results of all breast imaging and histopathology for workup of nipple discharge were extracted from each patient's medical record. Descriptors of the nipple discharge, including color, number of ducts involved, laterality, spontaneity, and results of hemocult testing were obtained from the radiology reports. Univariate and multivariate logistic regression analyses were conducted to determine whether hemocult results, imaging results, and/or discharge descriptors were associated with abnormal pathology, defined as papilloma or malignancy. Sensitivity, specificity, and other performance characteristics were calculated for hemocult testing and imaging modalities.

#### RESULTS

Of a total of 326 women who met inclusion criteria, 247/75.8% had reproducible discharge at time of imaging and 204/62.6% received a hemocult test. As part of the workup, 307/94.2% had a mammogram, 187/57.4% an ultrasound, 58/17.8% an MRI, and 131/40.4% a galactogram. Tissue sampling revealed non-malignant abnormal pathology in 118/32.6% and malignancy in 19/5.8%. Multivariate analysis showed that abnormal pathology was independently associated with positive hemocult results (adjusted odds ratio (AOR) 2.68;  $p=0.026$ ), single-duct (AOR 6.95;  $p<0.001$ ), spontaneous (AOR 3.84;  $p=0.013$ ), and suspicious colored discharge (AOR 4.37;  $p=0.041$ ). Positive hemocult test was also a predictor of abnormal pathology if all factor characteristics were unknown (OR 5.16;  $p<0.001$ ). Hemocult testing showed a sensitivity of 73.7% (95% CI: [63.6%-82.2%]) for abnormal pathology, similar to galactography (87.7%; 95% CI: [77.9%-94.2%]) and MRI (83.3%; 95% CI: [62.6%-95.3%]).

#### CONCLUSION

Hemocult testing is sensitive and independently associated with abnormal histopathology in patients with nipple discharge.

#### CLINICAL RELEVANCE/APPLICATION

Hemocult testing may be a useful diagnostic tool in patients with nipple discharge prior to diagnostic imaging to help establish the pre-test probability of abnormal histopathology based on discharge characteristics.

Printed on: 02/07/23

## Abstract Archives of the RSNA, 2022

W2-SPBR-3

### Contrast-enhanced Spectral Mammography-guided Breast Biopsy: Technique Feasibility and Comparison with MR-guided Vacuum-Assisted Breast Biopsy

Wednesday, Nov. 30 9:00AM - 9:30AM Room: Learning Center - BR DPS

#### Participants

Romy Heriteau, MD, (*Presenter*) Nothing to Disclose

#### PURPOSE

Contrast-enhanced spectral mammography (CESM) is a recent imaging technique based on the association of spectral mammography and iodinated contrast agent to detect tumor enhancement, linked to neoangiogenesis. CESM is known to have same sensitivity as MRI with a higher specificity, higher Predictive Positive Value (PPV), and better conditions of accessibility and cost. The purpose of this study is to show the comparison of diagnostic performances of biopsies under CESM compared to biopsies under MRI in terms of availability, procedure duration and failure, side effects and cost

#### METHODS AND MATERIALS

Retrospective evaluation of our 3 years' experience with CESM procedure and comparison with MR-biopsy procedure in our institution. All consecutive patient referred for an MRI or CESM-guided breast biopsy were included in our study. 25 patients for CESM biopsy and 107 patients for MRI biopsy were included. We analyzed two reliability parameters for each technique, the concordance between radiological BI-RADS classification and histological results of the biopsy. Then, the concordance between histological biopsy results and histological results after surgery. Procedure time, side effects and cost were also collected.

#### RESULTS

athology results were categorized as benign (38 lesions in MRI and 13 in CESM), high-risk (22/5), or malignant (17/2 ductal carcinoma in situ (DCIS), 21/3 invasive ductal carcinoma, 6/2 invasive lobular carcinoma). Subsequent surgery for high-risk and malignant lesions revealed a 21% discordance rate and 15% underestimation rate for MRI and one discordance and underestimation for CESM ( $p > 0.5$ ). Comparison between BI-RADS classification and pathology results revealed one discordance for MRI and none for CESM ( $p > 0.5$ ). Duration was significantly shorter for CESM (median duration : 28 minutes) in comparison with MRI (median : 53 minutes) ( $p < 0.05$ ). 15 side effects for MRI versus 2 for CESM have been registered ( $p = 0.53$ ). Economical study estimated the cost for a biopsy under MR-guided biopsy at 1213€ and a CESM- at 574€

#### CONCLUSION

s CESM guided-biopsy may be an interesting alternative technique to MR-guided breast biopsy, with time and cost saving, without reducing accuracy.

#### CLINICAL RELEVANCE/APPLICATION

CESM guided-biopsy is a simpler and more accessible alternative technique to MRI biopsies. This biopsy could be performed in more and more centers in the future.

Printed on: 02/07/23

## Abstract Archives of the RSNA, 2022

W2-SPBR-4

### Should I Stay, or Should I Go? A Workforce Movement Survey of Breast Radiologists.

Wednesday, Nov. 30 9:00AM - 9:30AM Room: Learning Center - BR DPS

#### Participants

Grayson Baird, PhD, Providence, RI (*Presenter*) Nothing to Disclose

#### PURPOSE

To evaluate factors associated with whether breast radiologists have left, or are considering leaving, their current job.

#### METHODS AND MATERIALS

Practicing members of the Society of Breast Imaging were emailed a weblink to an IRB-approved surveys in February 2022. The survey included 32 questions about attitudes towards work and whether they had left their last position within the last two years, were thinking of leaving, or were not thinking of leaving their current position. Exploratory factor analysis (EFA) was used to evaluate construct validity. Internal consistency was evaluated with Cronbach's Alpha. Concurrent validity was examined using discriminant function analysis (DFA). All psychometric analyses were conducted using SAS.

#### RESULTS

Response rate was 14% (230/1670), with 2 being dropped as they retired over 2 years ago. 82% (182/288) identified as being white, with 77% (173) identifying as female. 5% (11) were 35 years or younger, 33% (75) were between 36-45, 29% (66) were between 46-55, 25% (57) were between 56-65, and 7.5% (17) were 65 or older. The majority (73.6%, 167) reported 76-100% of their practice was focused on breast imaging. Of the 228, 23.3% (53) responded that they had left a practice within the last two years, 21.9% (50) were thinking of leaving, and 54.8% (125) were not thinking of leaving--45% of respondents were either thinking of leaving or had recently left their practice. Factor analysis identified 5 latent variables (factors) from the 32 questions: 1. "Quality of Life" issues, 2. "Physician Socio-Cultural" issues, 3. "Workplace Condition" issues, 4. "Non-Physician Socio-Cultural" issues, and 5. "Career" issues. Cronbach's Alpha was .89, showing high internal consistency. DFA examined how well the 32 questions classified the groups (Figure 1). Those "staying" (red) clustered positively with the first function (x-axis), while those who "left" (blue) cluster negatively with the first function, and those who were thinking of "leaving" (green) clustered in between but negatively on the first function. Only the first function was significant,  $p < .01$ , which was highly related with questions concerning Quality of Life.

#### CONCLUSION

Quality of life is the factor most associated with workforce movement of breast radiologists. Almost one-half of breast radiologists had recently left or were considering leaving their positions. The survey showed good psychometric properties.

#### CLINICAL RELEVANCE/APPLICATION

Almost one-half of breast radiologists had left or were considering leaving their positions. It may be important to measure attitudes towards workplace movement to understand why radiologists are staying and leaving.

Printed on: 02/07/23

## Abstract Archives of the RSNA, 2022

W2-SPBR-5

### A Novel Anthropomorphic Model Observer for Micro-calcification Cluster Detection in Digital Mammography and Digital Breast Tomosynthesis Images for The VICTRE Pipeline

Wednesday, Nov. 30 9:00AM - 9:30AM Room: Learning Center - BR DPS

#### Participants

Katrien Houbrechts, Leuven, Belgium (*Presenter*) Siemens AG

#### PURPOSE

Develop an anthropomorphic model observer for calcification cluster detection in digital mammography (DM) and digital breast tomosynthesis (DBT) for a clinical range of lesion sizes and dose levels, and illustrate its applicability to predict the impact of blurring.

#### METHODS AND MATERIALS

Clusters with 5 round calcifications of 100  $\mu\text{m}$ , 150  $\mu\text{m}$  and 200  $\mu\text{m}$  diameter were randomly inserted in heterogeneous VICTRE breast phantoms. DM and DBT images were created using the VICTRE pipeline with a clinical Automatic Exposure Control (AEC) dose, AEC/2 and 2AEC. For both DM and DBT, 20 lesion-present and 120 lesion-absent samples were used for each condition to tune a two-layer Channelized Hotelling Observer (CHO) to four-alternative forced choice reading results of 6 human readers. The CHO performance in the presence of system blurring was investigated for 150  $\mu\text{m}$  clusters. For DM, the focus size and lesion height above the table was changed. For DBT, source motion was varied.

#### RESULTS

The CHO (localization: 2 Laguerre-Gauss channels; classification: 8 Gabor channels) agreed closely with human results (mean error [-4.12;0.14], linear regression slope [0.98;1.07]) over the studied range of lesion sizes and dose levels for both modalities. CHO readout was more reproducible than human reading, with average standard deviation of 3% compared to 5-6%. The CHO was sensitive to microcalcification blurring. The DM CHO percent correctly detected targets (PC) for clusters located 5 mm above the table was 70 $\pm$ 4% and 64 $\pm$ 5% for focus sizes of 0.3 mm and 0.5 mm, respectively ( $p < 0.0001$ ). When located 40 mm above the table, the PC was 58 $\pm$ 4% and 46 $\pm$ 5%, respectively ( $p < 0.0001$ ). The DBT CHO showed a monotonic decrease in lesion detection performance as source motion blur increased; e.g. for 21 s scan time, the PC was 77 $\pm$ 4% and 57 $\pm$ 4% for a 90 ms and 150 ms exposure time, respectively ( $p < 0.0001$ ).

#### CONCLUSION

A two-layer CHO was shown to approximate human observer detection results for microcalcifications in DM and DBT images generated with the VICTRE pipeline and can be used to evaluate the influence of system settings on detection performance for in-silico studies.

#### CLINICAL RELEVANCE/APPLICATION

The anthropomorphic CHO enables the accurate modelling of microcalcification detection performance for in-silico clinical studies.

Printed on: 02/07/23

## Abstract Archives of the RSNA, 2022

W2-SPCA

### Cardiac Wednesday Poster Discussion

Wednesday, Nov. 30 9:00AM - 9:30AM Room: Learning Center - CA DPS

#### Sub-Events

#### W2-SPCA-1 Myocardial Iron Imaging in Post-reperfusion Injury with Free-breathing, High-dynamic-range Cardiac Quantitative Susceptibility Mapping (HDR-QSM)

Participants

Yuheng Huang, MS, (*Presenter*) Nothing to Disclose

#### PURPOSE

The detection and quantification of intramyocardial hemorrhage (IMH) have been established as an essential biomarker for managing myocardial infarction (MI) patients. Quantitative susceptibility mapping (QSM) is the standard method for iron imaging in the brain. However, its application in the heart has been challenging because of major technical limitations, such as cardiac and respiratory motion during acquisition, strong B0 inhomogeneity in the heart, and the streaking artifacts caused by the highly concentrated iron in the hemorrhagic lesion. In this study, we developed a free-breathing, motion resolved, whole heart QSM technique with a High Dynamic Range QSM (HDR-QSM) reconstruction to overcome key confounders for iron imaging in hemorrhagic hearts.

#### METHODS AND MATERIALS

The study was approved by the IACUC at CSMC. Canines with hemorrhagic MIs were created (n=3) by coronary occlusion and reperfusion. Animals were scanned 7 Days post-MI in a clinical 3T scanner using a 3D, non-ECG gated, free-breathing multi-echo GRE sequence. To achieve reliable in-vivo cardiac QSM, a high-dynamic-range reconstruction algorithm was developed (panel A). In brief, phase images of the mGRE sequence were derived with an HDR, SNR optimized algorithm to ensure the fidelity of phase maps. Following, a two-step QSM reconstruction was adopted to minimize streaking artifacts from the extended iron concentration in IMH lesions.

#### RESULTS

Representative results from an IMH dog are presented in panel B. In the conventional iron-sensitive images ( $R2^*(1/T2^*)$  and standard QSM), strong off-resonance artifacts were observed at the heart-lung interfaces (red boxes) but were eliminated by the HDR-QSM. In addition, HDR-QSM corrected the strong streaking artifacts around the hemorrhagic zone compared to the standard QSM images (green boxes) and provides a more homogeneous susceptibility measure in the lesions. ROC analysis was conducted to compare the diagnosability between  $R2^*(1/T2^*)$  maps, standard QSM and HDR-QSM (panel C). By eliminating the off-resonance artifact at the inferolateral walls, the AUC of HDR-QSM is significantly higher than the other approaches and provides reliable IMH detection (AUC:  $R2^*(1/T2^*)=0.72$ ; standard QSM=0.74; HDR-QSM=0.85).

#### CONCLUSION

In this study, we developed a free-breathing cardiac QSM technique to quantify iron deposition in IMH. HDR-QSM opens up a reliable way for iron quantification in hearts and can potentially facilitate iron-guided precise patient management.

#### CLINICAL RELEVANCE/APPLICATION

HDR-QSM enables reliable in-vivo QSM imaging in the heart, it is helpful for various applications, particularly for quantifying IMH and iron concentration in patients with reperfusion injury.

#### W2-SPCA-2 Global and Regional Strain to Predict Ischemic LGE in Acute and Chronic ST-elevation Myocardial Infarction

Participants

Jennifer Erley, MD, Hamburg, Germany (*Presenter*) Nothing to Disclose

#### PURPOSE

To monitor left ventricular (LV) myocardial strain in ST-elevation myocardial infarction (STEMI) from acute to chronic stage and determine its ability to predict late gadolinium enhancement (LGE).

#### METHODS AND MATERIALS

Patients underwent cardiac magnetic resonance imaging (CMR) at a 1.5T scanner (Achieva, Philips) directly ( $8\pm 5$  days) after STEMI at baseline (BL) and at 6 ( $\pm 1.4$ )- month follow-up (FU). The imaging protocol included steady-state free precession (SSFP) sequences in long- and short-axis and LGE imaging. Feature-tracking (FT) (Segment, Medviso) analysis was conducted to determine myocardial strain. Myocardial segments were grouped in three categories according to the LGE pattern at BL: negative (LGE-), non-transmural (LGE+) and transmural (LGE++). Data are described using mean (standard deviation) or median (interquartile range). Wilcoxon test, receiver operating characteristic- and binary logistic regression analyses were conducted.

#### RESULTS

32 patients participated in this prospective study (81% male; age 59±10 years). Global and segmental longitudinal (GLS/SLS), radial (GLS/SRS) and circumferential (GCS/SCS) strain improved from BL to FU: GLS from -14±4% to -16±4%, p<0.001; GCS from -15±4% to -16±4%, p=0.023; GRS from 38±11% to 42±13%, p=0.006. However, regional strain was impaired at baseline and FU in LGE+ and ++ segments (SLS: -15% (-22 to 10) in LGE- vs. -9% (-16 to -5) in LGE+/++ segments at BL and -16% (-23 to -12) vs. -12% (-19 to -6) at FU; SRS: 34% (22 to 48) in LGE- vs. 17% (8 to 29) in LGE +/++ segments at BL and 36% (26 to 48) vs. 22% (11 to 38) at FU; SCS: -16% (-21 to -12) in LGE- vs. -9% (-14 to -3) in LGE+/++ segments at BL and -17% (-21 to -12) vs. -11% (-16 to -5) at FU; all p<0.001). Especially SCS distinguished LGE- from LGE +/++ segments (SLS: area under the curve (AUC)=0.66 [95% confidence interval (CI) 0.61-0.71], p<0.001; SRS: AUC=0.75 [0.70-0.79], p<0.001; SCS: AUC=0.77 [0.73-0.82], p<0.001). The odds of predicting LGE were not significant for SLS; 0.97 for SRS [0.951-0.981], p<0.001 and 1.1 for SCS [1.077-1.145], p<0.001.

## CONCLUSION

s Strain improved from acute to chronic STEMI, but regional strain was persistently impaired in LGE-positive myocardial segments. Circumferential strain was able to predict LGE.

## CLINICAL RELEVANCE/APPLICATION

Functional recovery and impairment after STEMI can be reliably determined with global and regional strain. Circumferential strain is able to predict focal LGE following STEMI.

## W2-SPCA-3 Regionalized Wall Strain is a Predictor of LV Systolic Function in a Swine Model

Participants

Jacob Ref, (Presenter) Nothing to Disclose

## PURPOSE

Global longitudinal strain (GLS) is utilized to assess early stage myocardial functional loss. Myocardial strain quantitatively provides regional and global areas of left ventricular (LV) dysfunction using GLS, circumferential (GCS) and radial strain (GRS). GRS and GCS are predictive of late-stage heart failure because these functions are preserved until advanced stages of heart disease. To our knowledge, this is the first analysis of regional cardiac wall strain in a swine model.

## METHODS AND MATERIALS

Male Yucatan mini swine underwent left anterior descending (LAD) balloon occlusion/reperfusion to simulate LAD myocardial infarction (MI). Cardiac MRI is performed with a 3T scanner (Skyra, Siemens Healthineers) prior to MI and 1 month post MI. Wall strain analysis was done in short axis (SAX) and long axis (LAX) planes. LV contours were drawn (CVI42, Calgary, Canada) using SAX and LAX images. Global strain values were collected for GLS, GCS and GRS. Median values were calculated to reflect myocardial health in vascular territories - LAD, circumflex (LCX) and right coronary (RCA) arteries.

## RESULTS

14 swine were evaluated at both baseline and 1-month post-MI. Average infarct size was 25±4%, GLS increased (P<0.01) from -15±2% to -11±2%. GCS increased (P<0.01) from -16±2% to -12±2%. GRS decreased (P<0.01) from 53±8% to 35±6%. LAD GLS increased (P<0.05) from -15±3% to -10±1%. LAD GCS increased (P<0.01) from -18±3% to -8±2%. LAD GRS decreased (P<0.01) from 52±9% to 27±4%. LCX GLS increased (P<0.05) from -15±3% to -8±2%. LCX GCS increased (P<0.05) from -21±2% to -18±2%. LCX GRS decreased (P<0.01) from 56±9% to 35±5%. RCA GLS increased (P<0.01) from -14±2% to -8±1%. RCA GCS increased from -17±2% to -11±3%. RCA GRS decreased from 55±10% to 43±8%.

## CONCLUSION

s Regional analysis of coronary vascular territories provided expected changes in LAD and LCX territories following LAD occlusion. LCX territory showed 8.5% less change than LAD territory. Strain values in RCA territory showed significant change in GLS but no significant change in GCS and GRS. We attribute adverse RCA GLS values to a compensatory phenomenon with RCA territory making up for the lack of involvement from LAD myocardial fibers.

## CLINICAL RELEVANCE/APPLICATION

Preclinical measurements of regional myocardial strain can be performed in a swine model as a predictor of heart failure outcomes.

## W2-SPCA-4 Myocardial Remodeling and Intracardiac Flow in the Acute Myocardial Infarction: From Coronary Occlusion to Eleven Weeks of Follow-Up in a Swine Model

Participants

Yura Ahn, MD, Seoul, Korea, Republic Of (Presenter) Nothing to Disclose

## PURPOSE

The goal of this study was to describe a chronological change in the left ventricular (LV) myocardium during a reperfused myocardial infarction (MI) using cutting-edge cardiac MRI (CMR) techniques.

## METHODS AND MATERIALS

The reperfused MI model was set to two swines, and serial CMR was performed at baseline, 0 day, 3 days, 1-, 2-, 3-, 4-, 5-, 6-, and 11-week after coronary artery balloon occlusion. A comprehensive CMR protocol included ventricular function, LV strain analysis, T1- and T2-mapping, stress- and rest-perfusion, late gadolinium-enhanced (LGE) images, and intracardiac 4D flow MRI. The LV myocardium was classified as infarcted-, adjacent-, and remote-area, and all CMR parameters were described accordingly.

## RESULTS

The %infarct and infarcted wall thickness decreased over time (baseline 30.9%, 11-week 17.4%; baseline 11.7mm, 11 weeks 2.9mm), whether LV volume and myocardial mass increased. Myocardial edema defined by T2 value was highest at 1 week (96.8 msec; baseline ). Both global and regional myocardial strains have gradually decreased. Notably, the adjacent area showed the greatest reduction in peak radial strain as compared to the remote and even infarcted area (11-week: adjacent 14.7%, remote 32.9%, infarct 23.8%). Flow stasis, as demonstrated by intracardiac 4D flow MRI, seems to be linked to lower myocardial strain.

## CONCLUSION

s In the reperfused MI model, CMR revealed changes in myocardial shape, tissue character, mechanics, and intracardiac flow over time.

#### **CLINICAL RELEVANCE/APPLICATION**

CMR helped researchers better understand the natural history and pathophysiology of MI in this animal study, with a focus on LV myocardial remodeling and intracardiac flow.

Printed on: 02/07/23

## Abstract Archives of the RSNA, 2022

W2-SPCA-1

### Myocardial Iron Imaging in Post-reperfusion Injury with Free-breathing, High-dynamic-range Cardiac Quantitative Susceptibility Mapping (HDR-QSM)

Wednesday, Nov. 30 9:00AM - 9:30AM Room: Learning Center - CA DPS

#### Participants

Yuheng Huang, MS, (*Presenter*) Nothing to Disclose

#### PURPOSE

The detection and quantification of intramyocardial hemorrhage (IMH) have been established as an essential biomarker for managing myocardial infarction (MI) patients. Quantitative susceptibility mapping (QSM) is the standard method for iron imaging in the brain. However, its application in the heart has been challenging because of major technical limitations, such as cardiac and respiratory motion during acquisition, strong  $B_0$  inhomogeneity in the heart, and the streaking artifacts caused by the highly concentrated iron in the hemorrhagic lesion. In this study, we developed a free-breathing, motion resolved, whole heart QSM technique with a High Dynamic Range QSM (HDR-QSM) reconstruction to overcome key confounders for iron imaging in hemorrhagic hearts.

#### METHODS AND MATERIALS

The study was approved by the IACUC at CSMC. Canines with hemorrhagic MIs were created ( $n=3$ ) by coronary occlusion and reperfusion. Animals were scanned 7 Days post-MI in a clinical 3T scanner using a 3D, non-ECG gated, free-breathing multi-echo GRE sequence. To achieve reliable in-vivo cardiac QSM, a high-dynamic-range reconstruction algorithm was developed (panel A). In brief, phase images of the mGRE sequence were derived with an HDR, SNR optimized algorithm to ensure the fidelity of phase maps. Following, a two-step QSM reconstruction was adopted to minimize streaking artifacts from the extended iron concentration in IMH lesions.

#### RESULTS

Representative results from an IMH dog are presented in panel B. In the conventional iron-sensitive images ( $R2^*(1/T2^*)$  and standard QSM), strong off-resonance artifacts were observed at the heart-lung interfaces (red boxes) but were eliminated by the HDR-QSM. In addition, HDR-QSM corrected the strong streaking artifacts around the hemorrhagic zone compared to the standard QSM images (green boxes) and provides a more homogeneous susceptibility measure in the lesions. ROC analysis was conducted to compare the diagnosability between  $R2^*(1/T2^*)$  maps, standard QSM and HDR-QSM (panel C). By eliminating the off-resonance artifact at the inferolateral walls, the AUC of HDR-QSM is significantly higher than the other approaches and provides reliable IMH detection (AUC:  $R2^*(1/T2^*)=0.72$ ; standard QSM=0.74; HDR-QSM=0.85).

#### CONCLUSION

s In this study, we developed a free-breathing cardiac QSM technique to quantify iron deposition in IMH. HDR-QSM opens up a reliable way for iron quantification in hearts and can potentially facilitate iron-guided precise patient management.

#### CLINICAL RELEVANCE/APPLICATION

HDR-QSM enables reliable in-vivo QSM imaging in the heart, it is helpful for various applications, particularly for quantifying IHM and iron concentration in patients with reperfusion injury.

Printed on: 02/07/23

## Abstract Archives of the RSNA, 2022

W2-SPCA-2

### Global and Regional Strain to Predict Ischemic LGE in Acute and Chronic ST-elevation Myocardial Infarction

Wednesday, Nov. 30 9:00AM - 9:30AM Room: Learning Center - CA DPS

#### Participants

Jennifer Erley, MD, Hamburg, Germany (*Presenter*) Nothing to Disclose

#### PURPOSE

To monitor left ventricular (LV) myocardial strain in ST-elevation myocardial infarction (STEMI) from acute to chronic stage and determine its ability to predict late gadolinium enhancement (LGE).

#### METHODS AND MATERIALS

Patients underwent cardiac magnetic resonance imaging (CMR) at a 1.5T scanner (Achieva, Philips) directly (8±5 days) after STEMI at baseline (BL) and at 6 (±1.4)- month follow-up (FU). The imaging protocol included steady-state free precession (SSFP) sequences in long- and short-axis and LGE imaging. Feature-tracking (FT) (Segment, Medviso) analysis was conducted to determine myocardial strain. Myocardial segments were grouped in three categories according to the LGE pattern at BL: negative (LGE-), non-transmural (LGE+) and transmural (LGE++). Data are described using mean (standard deviation) or median (interquartile range). Wilcoxon test, receiver operating characteristic- and binary logistic regression analyses were conducted.

#### RESULTS

32 patients participated in this prospective study (81% male; age 59±10 years). Global and segmental longitudinal (GLS/SLS), radial (GLS/SRS) and circumferential (GCS/SCS) strain improved from BL to FU: GLS from -14±4% to -16±4%,  $p<0.001$ ; GCS from -15±4% to -16±4%,  $p=0.023$ ; GRS from 38±11% to 42±13%,  $p=0.006$ . However, regional strain was impaired at baseline and FU in LGE+ and ++ segments (SLS: -15% (-22 to 10) in LGE- vs. -9% (-16 to -5) in LGE+/++ segments at BL and -16% (-23 to -12) vs. -12% (-19 to -6) at FU; SRS: 34% (22 to 48) in LGE- vs. 17% (8 to 29) in LGE +/++ segments at BL and 36% (26 to 48) vs. 22% (11 to 38) at FU; SCS: -16% (-21 to -12) in LGE- vs. -9% (-14 to -3) in LGE+/++ segments at BL and -17% (-21 to -12) vs. -11% (-16 to -5) at FU; all  $p<0.001$ ). Especially SCS distinguished LGE- from LGE +/++ segments (SLS: area under the curve (AUC)=0.66 [95% confidence interval (CI) 0.61-0.71],  $p<0.001$ ; SRS: AUC=0.75 [0.70-0.79],  $p<0.001$ ; SCS: AUC=0.77 [0.73-0.82],  $p<0.001$ ). The odds of predicting LGE were not significant for SLS; 0.97 for SRS [0.951-0.981],  $p<0.001$  and 1.1 for SCS [1.077-1.145],  $p<0.001$ .

#### CONCLUSION

s Strain improved from acute to chronic STEMI, but regional strain was persistently impaired in LGE-positive myocardial segments. Circumferential strain was able to predict LGE.

#### CLINICAL RELEVANCE/APPLICATION

Functional recovery and impairment after STEMI can be reliably determined with global and regional strain. Circumferential strain is able to predict focal LGE following STEMI.

Printed on: 02/07/23

## Abstract Archives of the RSNA, 2022

W2-SPCA-3

### Regionalized Wall Strain is a Predictor of LV Systolic Function in a Swine Model

Wednesday, Nov. 30 9:00AM - 9:30AM Room: Learning Center - CA DPS

#### Participants

Jacob Ref, (*Presenter*) Nothing to Disclose

#### PURPOSE

Global longitudinal strain (GLS) is utilized to assess early stage myocardial functional loss. Myocardial strain quantitatively provides regional and global areas of left ventricular (LV) dysfunction using GLS, circumferential (GCS) and radial strain (GRS). GRS and GCS are predictive of late-stage heart failure because these functions are preserved until advanced stages of heart disease. To our knowledge, this is the first analysis of regional cardiac wall strain in a swine model.

#### METHODS AND MATERIALS

Male Yucatan mini swine underwent left anterior descending (LAD) balloon occlusion/reperfusion to simulate LAD myocardial infarction (MI). Cardiac MRI is performed with a 3T scanner (Skyra, Siemens Healthineers) prior to MI and 1 month post MI. Wall strain analysis was done in short axis (SAX) and long axis (LAX) cines. LV contours were drawn (CVI42, Calgary, Canada) using SAX and LAX images. Global strain values were collected for GLS, GCS and GRS. Median values were calculated to reflect myocardial health in vascular territories - LAD, circumflex (LCX) and right coronary (RCA) arteries.

#### RESULTS

14 swine were evaluated at both baseline and 1-month post-MI. Average infarct size was 25±4%, GLS increased (P<0.01) from -15±2% to -11±2%. GCS increased (P<0.01) from -16±2% to -12±2%. GRS decreased (P<0.01) from 53±8% to 35±6%. LAD GLS increased (P<0.05) from -15±3% to -10±1%. LAD GCS increased (P<0.01) from -18±3% to -8±2%. LAD GRS decreased (P<0.01) from 52±9% to 27±4%. LCX GLS increased (P<0.05) from -15±3% to -8±2%. LCX GCS increased (P<0.05) from -21±2% to -18±2%. LCX GRS decreased (P<0.01) from 56±9% to 35±5%. RCA GLS increased (P<0.01) from -14±2% to -8±1%. RCA GCS increased from -17±2% to -11±3%. RCA GRS decreased from 55±10% to 43±8%.

#### CONCLUSION

s Regional analysis of coronary vascular territories provided expected changes in LAD and LCX territories following LAD occlusion. LCX territory showed 8.5% less change than LAD territory. Strain values in RCA territory showed significant change in GLS but no significant change in GCS and GRS. We attribute adverse RCA GLS values to a compensatory phenomenon with RCA territory making up for the lack of involvement from LAD myocardial fibers.

#### CLINICAL RELEVANCE/APPLICATION

Preclinical measurements of regional myocardial strain can be performed in a swine model as a predictor of heart failure outcomes.

Printed on: 02/07/23

## Abstract Archives of the RSNA, 2022

W2-SPCA-4

### **Myocardial Remodeling and Intracardiac Flow in the Acute Myocardial Infarction: From Coronary Occlusion to Eleven Weeks of Follow-Up in a Swine Model**

Wednesday, Nov. 30 9:00AM - 9:30AM Room: Learning Center - CA DPS

#### **Participants**

Yura Ahn, MD, Seoul, Korea, Republic Of (*Presenter*) Nothing to Disclose

#### **PURPOSE**

The goal of this study was to describe a chronological change in the left ventricular (LV) myocardium during a reperfused myocardial infarction (MI) using cutting-edge cardiac MRI (CMR) techniques.

#### **METHODS AND MATERIALS**

The reperfused MI model was set to two swines, and serial CMR was performed at baseline, 0 day, 3 days, 1-,2-,3-,4-,5-,6-, and 11-week after coronary artery balloon occlusion. A comprehensive CMR protocol included ventricular function, LV strain analysis, T1- and T2-mapping, stress- and rest-perfusion, late gadolinium-enhanced (LGE) images, and intracardiac 4D flow MRI. The LV myocardium was classified as infarcted-, adjacent-, and remote-area, and all CMR parameters were described accordingly.

#### **RESULTS**

The %infarct and infarcted wall thickness decreased over time (baseline 30.9%, 11-week 17.4%; baseline 11.7mm, 11 weeks 2.9mm), whether LV volume and myocardial mass increased. Myocardial edema defined by T2 value was highest at 1 week (96.8 msec; baseline ). Both global and regional myocardial strains have gradually decreased. Notably, the adjacent area showed the greatest reduction in peak radial strain as compared to the remote and even infarcted area (11-week: adjacent 14.7%, remote 32.9%, infarct 23.8%). Flow stasis, as demonstrated by intracardiac 4D flow MRI, seems to be linked to lower myocardial strain.

#### **CONCLUSION**

s In the reperfused MI model, CMR revealed changes in myocardial shape, tissue character, mechanics, and intracardiac flow over time.

#### **CLINICAL RELEVANCE/APPLICATION**

CMR helped researchers better understand the natural history and pathophysiology of MI in this animal study, with a focus on LV myocardial remodeling and intracardiac flow.

Printed on: 02/07/23

## Abstract Archives of the RSNA, 2022

W2-SPCH

### Chest Wednesday Poster Discussions

Wednesday, Nov. 30 9:00AM - 9:30AM Room: Learning Center - CH DPS

#### Participants

Anastasia Oikonomou, MD, PhD, Toronto, ON (*Moderator*) Nothing to Disclose

#### Sub-Events

### W2-SPCH-1 Value-added Opportunistic Screening: Prediction Model of Hypertension Based on Clinical and Thoracic Aorta Imaging Risk Factors

#### Participants

Jinrong Yang, (*Presenter*) Nothing to Disclose

#### PURPOSE

This study is to establish and verify a nomogram model based on clinical and thoracic aorta imaging risk factors for predicting the risk of hypertension.

#### METHODS AND MATERIALS

This is a cross-sectional study. A total of 804 patients were enrolled and the baseline clinical data, biochemical indicators, concomitant diseases and AI data (the diameter, area at 9 levels and volume, length at two adjacent levels of thoracic aorta recommended by AHA Guidelines (2010)) of them were collected. They were randomly divided into the training set of 562 cases (70%) and the validation set of 242 cases (30%). Both two sets, the blood pressure status was monitored and diagnosed according to 2018 ESC/ESH Guidelines for the management of arterial hypertension. In the training set, variance, t-test (for normal distribution) /Mann-Whitney U-test (for non-normal distribution), least absolute shrinkage and selection operator (LASSO) were used for selecting thoracic aorta imaging risk factors to construct AI measurement score and multivariate logistic backward stepwise regression were used to analyze the influencing factors of hypertension. According to the clinical application for different data conditions, five nomogram prediction models were constructed, named AIMeasure model, BasicClinical model, TotalClinical model, AIBasicClinical model, AITotalClinical model. Moreover, receiver operating characteristic (ROC) curve, calibration curve and decision curve analyses (DCA) were used to test the distinction, accuracy and clinical applicability of the model both in training set and validation set.

#### RESULTS

The results showed age, height, weight, creatinine, hyperlipidemia, atherosclerosis and thoracic aortic dilatation were all related to the occurrence of hypertension. The area under the ROC curve of the above five models was 0.73, 0.77, 0.83, 0.78, 0.84 in the training set and was 0.77, 0.78, 0.81, 0.78, 0.82 in the verification set, respectively. Moreover, the calibration curves and DCAs of the two sets performed well on accuracy and clinical practicality.

#### CONCLUSION

The risk prediction nomogram models have good predictive ability and clinical value, which could be used as an effective tool for the risk prediction of hypertension. Furthermore, they would facilitate earlier non-pharmacological intervention to prevent the future development of hypertension.

#### CLINICAL RELEVANCE/APPLICATION

To construct different hypertension prediction models using clinical and chest CT-based thoracic aorta diameters, which can be used in different clinical scenarios.

### W2-SPCH-2 Age and Gender Variations in Normal Bronchial Dimensions on Low-dose Chest CT: Assessment with An Automatic Airway Segmentation and Quantitative Analysis Prototype

#### Participants

Parisa Kaviani, MD, Boston, MA (*Presenter*) Nothing to Disclose

#### PURPOSE

We assessed if a machine learning (ML) prototype for airway segmentation and quantitative analysis (AI Rad Companion, Siemens Healthineers) can assess age and gender variations in normal bronchial dimensions on low-dose CT of the chest.

#### METHODS AND MATERIALS

The retrospective IRB-approved study included 201 adult patients (mean age  $46 \pm 14$  years; male: female 90:111) who underwent low-dose chest CT for lung nodule follow-up. Radiology report and images of all chest CT exams to exclude patients with any airway abnormalities including bronchial wall thickening, dilatation, plugging, nodularity or distortion. We processed thin-section CT images of all 201 patients with the ML prototype for airway segmentation and quantitation to extract following metric parameters: lumen diameter, lumen area, bronchial lumen volume, wall thickness, wall tapering, wall area, and wall area ratio for total lung

volumes and for each lung and lung lobes separately. Mann-Whitney test, Kruskal-Wallis test, and receiver operating characteristics analysis were performed for statistical analysis.

## RESULTS

The prototype could not process CT datasets of 7 patients due to issues related to image format. These were excluded from the statistical analysis. In the remaining patients, the prototype demonstrated substantial variations in bronchial dimensions (lumen and wall area ratios) based on patient gender with AUCs of 1.0 for the whole lung and 0.68-0.81 for lobe-based bronchial dimensions. Male had significantly larger 20.95% dimensions than female patients ( $p < 0.001$ ). There was a significant difference between different age groups (18-30 years, 31-40 years, 41-50 years, 51-60 years, and 61-70 years) for all parameters based on the whole lung volumes, and each lobe ( $p < 0.001$ ). There were variations in generations of segmented bronchial airways based on the lung lobes [LUL (median, M:F 5:4), LLL (M:F 7:5), RUL (M:F 8:6), RML (M:F 7:6), and RLL (M:F 7:9)].

## CONCLUSION

s Automatic airway segmentation and quantitative analysis prototype demonstrates substantial variations in age- and gender-based bronchial luminal, wall thickness, tapering, and wall area ratios on low-dose chest CT.

## CLINICAL RELEVANCE/APPLICATION

Understanding trends and dimensions of normal bronchial airway can help differentiate normal and abnormal airway dimensions in different patient age and gender groups.

### W2-SPCH-3 Challenges in Improving Measurement Variability Using Deep Learning-based Kernel Conversion for Airway Quantification on Chest CT

Participants

Jooae Choe, MD, PhD, Seoul, Korea, Republic Of (*Presenter*) Nothing to Disclose

## PURPOSE

This study aimed to assess the feasibility of deep learning-based kernel conversion for normalization of reconstruction kernel effects in airway quantification on chest CT.

## METHODS AND MATERIALS

This retrospective study included 30 patients who underwent nonenhanced volumetric chest CT with slice thickness of 1 or 1.25 mm in two centers from June 2021 to July 2021. For each subjects, chest CT reconstructed with five different kernels (soft-very sharp) using one of three vendors (Siemens,  $n = 10$ ; GE,  $n = 10$ ; and Toshiba,  $n = 10$ ). Deep learning-based kernel conversion of chest CT targeted for B30f kernel were performed in chest CT scans with different kernels other than soft kernels of each vendor. Automated quantification for airway was performed before and after normalization. The influence of different kernels and applying image conversion on airway quantification was assessed using ANOVA, paired t-test and concordance correlation coefficient (CCC).

## RESULTS

Bronchial wall thickness (Pi10, mean wall thickness, wall area%) and lumen diameter decreased when using a sharper reconstruction kernel (ANOVA, for all,  $P < .001$ ). Applying kernel conversion improved measurement variability between soft and other medium or sharp kernels for all quantitative airway measures (pooled CCC: original vs. converted images, 0.84 vs. 0.93) but significantly increased branch count (paired t-test,  $P < .001$ ). Applying only the segmentation mask from soft kernel (reference standard) on original images with medium to sharp kernels did not improve measurement variability of airway quantification (pooled CCC: original image vs. soft kernel mask over original image, 0.84 vs. 0.85), and the measurement variability was improved when both the soft kernel mask and kernel converted images were used for airway quantification (pooled CCC: original image vs. soft kernel mask converted image, 0.84 vs. 0.95).

## CONCLUSION

s While the use of kernel conversion for CT normalization improved the overall measurement variability of airway quantification, the segmentation of airways became less robust and precise. Further improvement in the algorithm regarding airway segmentation in converted images may be needed.

## CLINICAL RELEVANCE/APPLICATION

Deep learning-based kernel conversion can be applied for improving measurement variability of airway quantification but further improvement in the algorithm regarding airway segmentation in converted images should be preceded.

### W2-SPCH-4 Interstitial Lung Abnormalities in Patients with Locally Advanced Esophageal Cancer: Prevalence- Risk factors and Clinical Implications

Participants

Shu Chi Tseng, MD, Boston, MA (*Presenter*) Nothing to Disclose

## PURPOSE

Interstitial lung abnormalities (ILA) represent nondependent abnormalities on chest CT indicating lung parenchymal damages due to inflammation and fibrosis, and are associated with older age and smoking. The prevalence of ILA and its impact on clinical outcome have been studied in lung cancer, but not in other thoracic malignancies. Esophageal cancer is the 8th most common cancer and 6th in mortality worldwide, and is associated with smoking. The purpose of the study was to determine the prevalence of ILA on pre-treatment chest CT in patients with esophageal cancer undergoing chemoradiotherapy, and to identify the association between ILA versus clinical characteristics and overall survival (OS).

## METHODS AND MATERIALS

The study included 208 patients with locally advanced esophageal cancer (166 males, 42 females; median age, 65.6 years) who were considered surgical candidates and were treated with chemoradiotherapy as a part of planned tri-modality therapy, who had pre-treatment chest CT prior to the initiation of chemoradiotherapy. ILA was scored on pre-treatment chest CT using a sequential reading method by 3 readers, with a 3-point scale (0=no evidence of ILA, 1=equivocal for ILA, 2=ILA). Clinical characteristics and OS were compared in patients with ILA (score 2) and others.

## RESULTS

ILA was present in 14 out of 208 patients (7%) with esophageal cancer on pre-treatment chest CT. Patients with ILA were significantly older (median age: 69 vs. 65;  $p=0.011$ ), had a higher number of pack-years of smoking ( $p=0.02$ ), and more commonly had T4 stage disease ( $p=0.026$ ) than patients with ILA score of 1 or 0. The presence of ILA was associated with a lack of surgery after chemoradiotherapy; surgical resection was not performed in 50% (7/14) of patients with ILA, compared to in 20% (39/194) of patients without ILA on baseline CT ( $p=0.016$ ). The presence of baseline ILA was not associated with OS (log-rank  $p=0.75$ , Cox  $p=0.613$ ).

## CONCLUSION

s ILA was present in 7% of locally advanced esophageal cancer patients, with risk factors including older age, higher number of pack-year of smoking, and T4 disease. ILA on pre-treatment CT was associated with a lack of surgical resection after chemoradiotherapy, indicating an implication of ILA for treatment selection in these patients.

## CLINICAL RELEVANCE/APPLICATION

ILA on pre-treatment chest CT was noted in 7% of locally advanced esophageal cancer patients and associated with older age, smoking, and T4 disease. Patients with ILA were significantly less likely to undergo surgical resection after chemoradiotherapy, and thus ILA may have implications for treatment selection in esophageal cancer patients, which can be studied in a larger prospective cohort for validation.

## W2-SPCH-5 Interstitial Lung Abnormality (ILA) Progression in the Four-Year Follow-up of Patients with Esophageal Cancer

Participants

Akinori Hata, MD, PhD, Suita, Japan (*Presenter*) Nothing to Disclose

## PURPOSE

There is a growing awareness of the clinical significance of interstitial lung abnormality (ILA). Patients with esophageal cancer receive multidisciplinary treatment including surgery, chemotherapy, and radiation therapy. In particular, aspiration pneumonia is frequently experienced after surgery. These therapies and complications may affect the ILA progression. The purpose of our study was to investigate the prevalence of ILA progression in the four-year follow-up of patients with esophageal cancer.

## METHODS AND MATERIALS

This retrospective study investigated patients who were diagnosed with esophageal cancer from January 2011 to December 2015 and survived four years or more. The follow-up chest CT four years after diagnosis was evaluated for the prevalence of ILA with a 3-point visual scale (0=non-ILA, 1=indeterminate for ILA, and 2=ILA). In addition, ILA progression was assessed by comparing the follow-up CT at four years with the pretreatment baseline CT with a 5-point visual scale (1=definite regression, 2=probable regression, 3=no change, 4=probable progression, and 5=definite progression). Logistic regression was used to assess factors associated with ILA progression.

## RESULTS

Overall, 178 patients (median age, 67 years at diagnosis; interquartile range, 61-67 years; 155 men [87%]) were included. We identified 97 non-ILA patients (score 0, 54%), 55 patients indeterminate for ILA (score 1, 31%), and 26 patients with ILA (score 2, 15%) on the follow-up CTs. Of the 178 patients, 128 showed improvement or no change of ILA (score 1-3, 72%) and 50 showed ILA progression (score 4 or 5, 28%), including indeterminate for ILA. In the univariate logistic regression analysis, age was the significant factor associated with ILA progression (odds ratio 1.07 [95% confidence interval: 1.02, 1.12],  $P=.004$ ). However, surgery, chemotherapy, radiation therapy, sex, body mass index, smoking history, advanced stage, and pulmonary function test results at baseline (forced expiratory volume in 1 second [FEV1], forced vital capacity [FVC], and FEV1/FVC) were not significant ( $P>0.05$ ).

## CONCLUSION

s ILA progression was seen in 28% of four-year survivors with esophageal cancer. Although age was significantly associated with ILA progression, treatment options were not.

## CLINICAL RELEVANCE/APPLICATION

Postoperative esophageal cancer patients often suffer from aspiration, but our results suggest that aspiration due to esophageal cancer surgery may not be related to ILA progression.

## W2-SPCH-6 Imaging the Thymus and Anterior Mediastinum with Subtraction Imaging in CT: An Initial Clinical Experience

Participants

Vruti Dattani, MBBS, MA, (*Presenter*) Nothing to Disclose

## PURPOSE

Thymic and other anterior mediastinal lesions comprise a range of benign and malignant pathologies but contrast enhanced CT can fail to discriminate between these. Our study explores if iodine concentration obtained from image subtraction CT differs between benign and malignant anterior mediastinal lesions.

## METHODS AND MATERIALS

Consecutive adult patients planned for imaging of the anterior mediastinum underwent contrast enhanced CT thorax (120 kV, 40-300 mA) preceded by a low-dose CT thorax (135 kV, 10-20 mA). Scan parameters were slice thickness 3.0 mm, slice interval 2.4 mm, collimation 80 x 0.5 mm, pitch factor 0.814 and tube rotation time 0.5 seconds. Image subtraction software (Canon SURESubtraction) incorporating an elastic registration algorithm was used to generate iodine maps. The mean iodine concentration from 3 regions of interest per lesion was calculated relative to iodine concentration within the IVC. A diagnosis of benign or malignant was obtained from patient records based on a combination of histological, clinical and imaging features. Data was analysed using a machine learning algorithm (C-Support Vector Machine, SVM) using the 'sklearn' Python package. The classifier

was trained both without additional pre-processing and on a Principal Component Analysis (PCA) of the data.

## RESULTS

Anterior mediastinal lesions have been assessed in 50 patients (M= 22, F= 28, age range 18-87 years) of which 21 are benign and 29 malignant. Malignant lesions include high risk thymoma, thymic carcinoma and lymphoma. Mean iodine concentration in the benign lesions is 0.956 mg/ml (SD  $\pm$  0.628 mg/ml) and in the malignant lesions 0.903 mg/ml (SD  $\pm$  0.731 mg/ml). The SVM could classify the iodine concentration data with only 64% accuracy, this was not improved with PCA.

## CONCLUSION

s Hence we demonstrate no difference in iodine concentration between benign and malignant anterior mediastinal lesions. However further work is required to explore if iodine concentration from image subtraction CT could contribute to diagnosis when in concert with other imaging features seen on conventional CT imaging.

## CLINICAL RELEVANCE/APPLICATION

The addition of subtraction imaging to CT assessment of anterior mediastinal mass is of questionable value as we show iodine concentration cannot discriminate between benign and malignant lesions.

## W2-SPCH-7 Performance of Chest MRI for The Detection of Pulmonary Nodules: A Meta-analysis

Participants

Stephan Altmayer, MD, PhD, Framingham, MA (*Presenter*) Nothing to Disclose

## PURPOSE

To perform a meta-analysis of the diagnostic performance of chest MRI in the detection of pulmonary nodules.

## METHODS AND MATERIALS

MEDLINE, EMBASE, and Cochrane databases were searched through April 2022 for published English language studies. Studies were eligible if they evaluated the diagnostic performance of MRI for the detection of pulmonary nodules in patients with suspected thoracic malignancy (primary or metastatic) or undergoing lung cancer screening, which used chest CT as the reference standard for comparison of performance. Nodules with diameter <4mm, masses (>30 mm), or studies that did not specify the size of the nodules were excluded from the analysis. Other exclusion criteria included studies with less than 10 subjects, pediatric population, and nodules from known infectious or inflammatory etiology. Pooled per-lesion and per-patient sensitivity and specificity, respectively, were calculated with 95% confidence intervals (95% CI) using random-effects model in R.

## RESULTS

Eleven studies met the inclusion criteria with a total of 963 patients and 1149 nodules identified. The pooled per-lesion sensitivity of MRI was 88% (95% CI: 80-93%) for the detection of pulmonary nodules of size 4-30 mm. In the subgroup analysis by size, the pooled sensitivity of MRI for nodules <10 mm was 85% (95% CI: 77-91%), while the sensitivity for nodules 10-30 mm was 99% (95% CI: 89-99%). Only 4 studies reported per-patient data with true negatives and false positives for analysis of specificity (total of 90 true negatives). The pooled specificity of MRI in these studies was 94% (95% CI: 84-98%).

## CONCLUSION

s The diagnostic performance of MRI for detection of pulmonary nodules  $\geq$ 4 mm in the oncology setting is high with detection rates of 99% for nodules  $\geq$ 10 mm. Per-patient specificity of MRI was 94%.

## CLINICAL RELEVANCE/APPLICATION

Chest MRI can be a reasonable alternative to CT in the detection and follow-up of pulmonary nodules  $\geq$ 4 mm in patients with a high radiation burden. This modality also showed limited false-positive cases in a per-patient analysis.

Printed on: 02/07/23

## Abstract Archives of the RSNA, 2022

W2-SPCH-1

### Value-added Opportunistic Screening: Prediction Model of Hypertension Based on Clinical and Thoracic Aorta Imaging Risk Factors

Wednesday, Nov. 30 9:00AM - 9:30AM Room: Learning Center - CH DPS

#### Participants

Jinrong Yang, (*Presenter*) Nothing to Disclose

#### PURPOSE

This study is to establish and verify a nomogram model based on clinical and thoracic aorta imaging risk factors for predicting the risk of hypertension.

#### METHODS AND MATERIALS

This is a cross-sectional study. A total of 804 patients were enrolled and the baseline clinical data, biochemical indicators, concomitant diseases and AI data (the diameter, area at 9 levels and volume, length at two adjacent levels of thoracic aorta recommended by AHA Guidelines (2010)) of them were collected. They were randomly divided into the training set of 562 cases (70%) and the validation set of 242 cases (30%). Both two sets, the blood pressure status was monitored and diagnosed according to 2018 ESC/ESH Guidelines for the management of arterial hypertension. In the training set, variance, t-test (for normal distribution) /Mann-Whitney U-test (for non-normal distribution), least absolute shrinkage and selection operator (LASSO) were used for selecting thoracic aorta imaging risk factors to construct AI measurement score and multivariate logistic backward stepwise regression were used to analyze the influencing factors of hypertension. According to the clinical application for different data conditions, five nomogram prediction models were constructed, named AIMeasure model, BasicClinical model, TotalClinical model, AIBasicClinical model, AITotalClinical model. Moreover, receiver operating characteristic (ROC) curve, calibration curve and decision curve analyses (DCA) were used to test the distinction, accuracy and clinical applicability of the model both in training set and validation set.

#### RESULTS

The results showed age, height, weight, creatinine, hyperlipidemia, atherosclerosis and thoracic aortic dilatation were all related to the occurrence of hypertension. The area under the ROC curve of the above five models was 0.73, 0.77, 0.83, 0.78, 0.84 in the training set and was 0.77, 0.78, 0.81, 0.78, 0.82 in the verification set, respectively. Moreover, the calibration curves and DCAs of the two sets performed well on accuracy and clinical practicality.

#### CONCLUSION

The risk prediction nomogram models have good predictive ability and clinical value, which could be used as an effective tool for the risk prediction of hypertension. Furthermore, they would facilitate earlier non-pharmacological intervention to prevent the future development of hypertension.

#### CLINICAL RELEVANCE/APPLICATION

To construct different hypertension prediction models using clinical and chest CT-based thoracic aorta diameters, which can be used in different clinical scenarios.

Printed on: 02/07/23

## Abstract Archives of the RSNA, 2022

W2-SPCH-2

### Age and Gender Variations in Normal Bronchial Dimensions on Low-dose Chest CT: Assessment with An Automatic Airway Segmentation and Quantitative Analysis Prototype

Wednesday, Nov. 30 9:00AM - 9:30AM Room: Learning Center - CH DPS

#### Participants

Parisa Kaviani, MD, Boston, MA (*Presenter*) Nothing to Disclose

#### PURPOSE

We assessed if a machine learning (ML) prototype for airway segmentation and quantitative analysis (AI Rad Companion, Siemens Healthineers) can assess age and gender variations in normal bronchial dimensions on low-dose CT of the chest.

#### METHODS AND MATERIALS

The retrospective IRB-approved study included 201 adult patients (mean age  $46 \pm 14$  years; male: female 90:111) who underwent low-dose chest CT for lung nodule follow-up. Radiology report and images of all chest CT exams to exclude patients with any airway abnormalities including bronchial wall thickening, dilatation, plugging, nodularity or distortion. We processed thin-section CT images of all 201 patients with the ML prototype for airway segmentation and quantitation to extract following metric parameters: lumen diameter, lumen area, bronchial lumen volume, wall thickness, wall tapering, wall area, and wall area ratio for total lung volumes and for each lung and lung lobes separately. Mann-Whitney test, Kruskal-Wallis test, and receiver operating characteristics analysis were performed for statistical analysis.

#### RESULTS

The prototype could not process CT datasets of 7 patients due to issues related to image format. These were excluded from the statistical analysis. In the remaining patients, the prototype demonstrated substantial variations in bronchial dimensions (lumen and wall area ratios) based on patient gender with AUCs of 1.0 for the whole lung and 0.68-0.81 for lobe-based bronchial dimensions. Male had significantly larger 20.95% dimensions than female patients ( $p < 0.001$ ). There was a significant difference between different age groups (18-30 years, 31-40 years, 41-50 years, 51-60 years, and 61-70 years) for all parameters based on the whole lung volumes, and each lobe ( $p < 0.001$ ). There were variations in generations of segmented bronchial airways based on the lung lobes [LUL (median, M:F 5:4), LLL (M:F 7:5), RUL (M:F 8:6), RML (M:F 7:6), and RLL (M:F 7:9)].

#### CONCLUSION

s Automatic airway segmentation and quantitative analysis prototype demonstrates substantial variations in age- and gender-based bronchial luminal, wall thickness, tapering, and wall area ratios on low-dose chest CT.

#### CLINICAL RELEVANCE/APPLICATION

Understanding trends and dimensions of normal bronchial airway can help differentiate normal and abnormal airway dimensions in different patient age and gender groups.

Printed on: 02/07/23

## Abstract Archives of the RSNA, 2022

W2-SPCH-3

### Challenges in Improving Measurement Variability Using Deep Learning-based Kernel Conversion for Airway Quantification on Chest CT

Wednesday, Nov. 30 9:00AM - 9:30AM Room: Learning Center - CH DPS

#### Participants

Jooae Choe, MD, PhD, Seoul, Korea, Republic Of (*Presenter*) Nothing to Disclose

#### PURPOSE

This study aimed to assess the feasibility of deep learning-based kernel conversion for normalization of reconstruction kernel effects in airway quantification on chest CT.

#### METHODS AND MATERIALS

This retrospective study included 30 patients who underwent nonenhanced volumetric chest CT with slice thickness of 1 or 1.25 mm in two centers from June 2021 to July 2021. For each subjects, chest CT reconstructed with five different kernels (soft-very sharp) using one of three vendors (Siemens, n = 10; GE, n = 10; and Toshiba, n = 10). Deep learning-based kernel conversion of chest CT targeted for B30f kernel were performed in chest CT scans with different kernels other than soft kernels of each vendor. Automated quantification for airway was performed before and after normalization. The influence of different kernels and applying image conversion on airway quantification was assessed using ANOVA, paired t-test and concordance correlation coefficient (CCC).

#### RESULTS

Bronchial wall thickness (Pi10, mean wall thickness, wall area%) and lumen diameter decreased when using a sharper reconstruction kernel (ANOVA, for all,  $P < .001$ ). Applying kernel conversion improved measurement variability between soft and other medium or sharp kernels for all quantitative airway measures (pooled CCC: original vs. converted images, 0.84 vs. 0.93) but significantly increased branch count (paired t-test,  $P < .001$ ). Applying only the segmentation mask from soft kernel (reference standard) on original images with medium to sharp kernels did not improve measurement variability of airway quantification (pooled CCC: original image vs. soft kernel mask over original image, 0.84 vs. 0.85), and the measurement variability was improved when both the soft kernel mask and kernel converted images were used for airway quantification (pooled CCC: original image vs. soft kernel mask converted image, 0.84 vs. 0.95).

#### CONCLUSION

While the use of kernel conversion for CT normalization improved the overall measurement variability of airway quantification, the segmentation of airways became less robust and precise. Further improvement in the algorithm regarding airway segmentation in converted images may be needed.

#### CLINICAL RELEVANCE/APPLICATION

Deep learning-based kernel conversion can be applied for improving measurement variability of airway quantification but further improvement in the algorithm regarding airway segmentation in converted images should be preceded.

Printed on: 02/07/23

## Abstract Archives of the RSNA, 2022

W2-SPCH-4

### Interstitial Lung Abnormalities in Patients with Locally Advanced Esophageal Cancer: Prevalence- Risk factors and Clinical Implications

Wednesday, Nov. 30 9:00AM - 9:30AM Room: Learning Center - CH DPS

#### Participants

Shu Chi Tseng, MD, Boston, MA (*Presenter*) Nothing to Disclose

#### PURPOSE

Interstitial lung abnormalities (ILA) represent nondependent abnormalities on chest CT indicating lung parenchymal damages due to inflammation and fibrosis, and are associated with older age and smoking. The prevalence of ILA and its impact on clinical outcome have been studied in lung cancer, but not in other thoracic malignancies. Esophageal cancer is the 8th most common cancer and 6th in mortality worldwide, and is associated with smoking. The purpose of the study was to determine the prevalence of ILA on pre-treatment chest CT in patients with esophageal cancer undergoing chemoradiotherapy, and to identify the association between ILA versus clinical characteristics and overall survival (OS).

#### METHODS AND MATERIALS

The study included 208 patients with locally advanced esophageal cancer (166 males, 42 females; median age, 65.6 years) who were considered surgical candidates and were treated with chemoradiotherapy as a part of planned tri-modality therapy, who had pre-treatment chest CT prior to the initiation of chemoradiotherapy. ILA was scored on pre-treatment chest CT using a sequential reading method by 3 readers, with a 3-point scale (0=no evidence of ILA, 1=equivocal for ILA, 2=ILA). Clinical characteristics and OS were compared in patients with ILA (score 2) and others.

#### RESULTS

ILA was present in 14 out of 208 patients (7%) with esophageal cancer on pre-treatment chest CT. Patients with ILA were significantly older (median age: 69 vs. 65;  $p=0.011$ ), had a higher number of pack-years of smoking ( $p=0.02$ ), and more commonly had T4 stage disease ( $p=0.026$ ) than patients with ILA score of 1 or 0. The presence of ILA was associated with a lack of surgery after chemoradiotherapy; surgical resection was not performed in 50% (7/14) of patients with ILA, compared to in 20% (39/194) of patients without ILA on baseline CT ( $p=0.016$ ). The presence of baseline ILA was not associated with OS (log-rank  $p=0.75$ , Cox  $p=0.613$ ).

#### CONCLUSION

s ILA was present in 7% of locally advanced esophageal cancer patients, with risk factors including older age, higher number of pack-year of smoking, and T4 disease. ILA on pre-treatment CT was associated with a lack of surgical resection after chemoradiotherapy, indicating an implication of ILA for treatment selection in these patients.

#### CLINICAL RELEVANCE/APPLICATION

ILA on pre-treatment chest CT was noted in 7% of locally advanced esophageal cancer patients and associated with older age, smoking, and T4 disease. Patients with ILA were significantly less likely to undergo surgical resection after chemoradiotherapy, and thus ILA may have implications for treatment selection in esophageal cancer patients, which can be studied in a larger prospective cohort for validation.

Printed on: 02/07/23

## Abstract Archives of the RSNA, 2022

W2-SPCH-5

### Interstitial Lung Abnormality (ILA) Progression in the Four-Year Follow-up of Patients with Esophageal Cancer

Wednesday, Nov. 30 9:00AM - 9:30AM Room: Learning Center - CH DPS

#### Participants

Akinori Hata, MD, PhD, Suita, Japan (*Presenter*) Nothing to Disclose

#### PURPOSE

There is a growing awareness of the clinical significance of interstitial lung abnormality (ILA). Patients with esophageal cancer receive multidisciplinary treatment including surgery, chemotherapy, and radiation therapy. In particular, aspiration pneumonia is frequently experienced after surgery. These therapies and complications may affect the ILA progression. The purpose of our study was to investigate the prevalence of ILA progression in the four-year follow-up of patients with esophageal cancer.

#### METHODS AND MATERIALS

This retrospective study investigated patients who were diagnosed with esophageal cancer from January 2011 to December 2015 and survived four years or more. The follow-up chest CT four years after diagnosis was evaluated for the prevalence of ILA with a 3-point visual scale (0=non-ILA, 1=indeterminate for ILA, and 2=ILA). In addition, ILA progression was assessed by comparing the follow-up CT at four years with the pretreatment baseline CT with a 5-point visual scale (1=definite regression, 2=probable regression, 3=no change, 4=probable progression, and 5=definite progression). Logistic regression was used to assess factors associated with ILA progression.

#### RESULTS

Overall, 178 patients (median age, 67 years at diagnosis; interquartile range, 61-67 years; 155 men [87%]) were included. We identified 97 non-ILA patients (score 0, 54%), 55 patients indeterminate for ILA (score 1, 31%), and 26 patients with ILA (score 2, 15%) on the follow-up CTs. Of the 178 patients, 128 showed improvement or no change of ILA (score 1-3, 72%) and 50 showed ILA progression (score 4 or 5, 28%), including indeterminate for ILA. In the univariate logistic regression analysis, age was the significant factor associated with ILA progression (odds ratio 1.07 [95% confidence interval: 1.02, 1.12],  $P=.004$ ). However, surgery, chemotherapy, radiation therapy, sex, body mass index, smoking history, advanced stage, and pulmonary function test results at baseline (forced expiratory volume in 1 second [FEV1], forced vital capacity [FVC], and FEV1/FVC) were not significant ( $P>0.05$ ).

#### CONCLUSION

s ILA progression was seen in 28% of four-year survivors with esophageal cancer. Although age was significantly associated with ILA progression, treatment options were not.

#### CLINICAL RELEVANCE/APPLICATION

Postoperative esophageal cancer patients often suffer from aspiration, but our results suggest that aspiration due to esophageal cancer surgery may not be related to ILA progression.

Printed on: 02/07/23

## Abstract Archives of the RSNA, 2022

W2-SPCH-6

### Imaging the Thymus and Anterior Mediastinum with Subtraction Imaging in CT: An Initial Clinical Experience

Wednesday, Nov. 30 9:00AM - 9:30AM Room: Learning Center - CH DPS

#### Participants

Vruti Dattani, MBBS, MA, (*Presenter*) Nothing to Disclose

#### PURPOSE

Thymic and other anterior mediastinal lesions comprise a range of benign and malignant pathologies but contrast enhanced CT can fail to discriminate between these. Our study explores if iodine concentration obtained from image subtraction CT differs between benign and malignant anterior mediastinal lesions.

#### METHODS AND MATERIALS

Consecutive adult patients planned for imaging of the anterior mediastinum underwent contrast enhanced CT thorax (120 kV, 40-300 mA) preceded by a low-dose CT thorax (135 kV, 10-20 mA). Scan parameters were slice thickness 3.0 mm, slice interval 2.4 mm, collimation 80 x 0.5 mm, pitch factor 0.814 and tube rotation time 0.5 seconds. Image subtraction software (Canon SURESubtraction) incorporating an elastic registration algorithm was used to generate iodine maps. The mean iodine concentration from 3 regions of interest per lesion was calculated relative to iodine concentration within the IVC. A diagnosis of benign or malignant was obtained from patient records based on a combination of histological, clinical and imaging features. Data was analysed using a machine learning algorithm (C-Support Vector Machine, SVM) using the 'sklearn' Python package. The classifier was trained both without additional pre-processing and on a Principal Component Analysis (PCA) of the data.

#### RESULTS

Anterior mediastinal lesions have been assessed in 50 patients (M= 22, F= 28, age range 18-87 years) of which 21 are benign and 29 malignant. Malignant lesions include high risk thymoma, thymic carcinoma and lymphoma. Mean iodine concentration in the benign lesions is 0.956 mg/ml (SD ± 0.628 mg/ml) and in the malignant lesions 0.903 mg/ml (SD ± 0.731 mg/ml). The SVM could classify the iodine concentration data with only 64% accuracy, this was not improved with PCA.

#### CONCLUSION

s Hence we demonstrate no difference in iodine concentration between benign and malignant anterior mediastinal lesions. However further work is required to explore if iodine concentration from image subtraction CT could contribute to diagnosis when in concert with other imaging features seen on conventional CT imaging.

#### CLINICAL RELEVANCE/APPLICATION

The addition of subtraction imaging to CT assessment of anterior mediastinal mass is of questionable value as we show iodine concentration cannot discriminate between benign and malignant lesions.

Printed on: 02/07/23

## Abstract Archives of the RSNA, 2022

W2-SPCH-7

### Performance of Chest MRI for The Detection of Pulmonary Nodules: A Meta-analysis

Wednesday, Nov. 30 9:00AM - 9:30AM Room: Learning Center - CH DPS

#### Participants

Stephan Altmayer, MD, PhD, Framingham, MA (*Presenter*) Nothing to Disclose

#### PURPOSE

To perform a meta-analysis of the diagnostic performance of chest MRI in the detection of pulmonary nodules.

#### METHODS AND MATERIALS

MEDLINE, EMBASE, and Cochrane databases were searched through April 2022 for published English language studies. Studies were eligible if they evaluated the diagnostic performance of MRI for the detection of pulmonary nodules in patients with suspected thoracic malignancy (primary or metastatic) or undergoing lung cancer screening, which used chest CT as the reference standard for comparison of performance. Nodules with diameter <4mm, masses (>30 mm), or studies that did not specify the size of the nodules were excluded from the analysis. Other exclusion criteria included studies with less than 10 subjects, pediatric population, and nodules from known infectious or inflammatory etiology. Pooled per-lesion and per-patient sensitivity and specificity, respectively, were calculated with 95% confidence intervals (95% CI) using random-effects model in R.

#### RESULTS

Eleven studies met the inclusion criteria with a total of 963 patients and 1149 nodules identified. The pooled per-lesion sensitivity of MRI was 88% (95% CI: 80-93%) for the detection of pulmonary nodules of size 4-30 mm. In the subgroup analysis by size, the pooled sensitivity of MRI for nodules <10 mm was 85% (95% CI: 77-91%), while the sensitivity for nodules 10-30 mm was 99% (95% CI: 89-99%). Only 4 studies reported per-patient data with true negatives and false positives for analysis of specificity (total of 90 true negatives). The pooled specificity of MRI in these studies was 94% (95% CI: 84-98%).

#### CONCLUSION

The diagnostic performance of MRI for detection of pulmonary nodules  $\geq 4$  mm in the oncology setting is high with detection rates of 99% for nodules  $\geq 10$  mm. Per-patient specificity of MRI was 94%.

#### CLINICAL RELEVANCE/APPLICATION

Chest MRI can be a reasonable alternative to CT in the detection and follow-up of pulmonary nodules  $\geq 4$  mm in patients with a high radiation burden. This modality also showed limited false-positive cases in a per-patient analysis.

Printed on: 02/07/23



## Abstract Archives of the RSNA, 2022

W2-SPER

### Emergency Wednesday Poster Discussions

Wednesday, Nov. 30 9:00AM - 9:30AM Room: Learning Center - ER DPS

#### Participants

Christopher Potter, MD, Boston, MA (*Moderator*) Nothing to Disclose

#### Sub-Events

### W2-SPER-1 The Impact of Clinical Decision Support System on the Yield of Pulmonary Emboli on CT Pulmonary Angiography

#### Participants

Abdullah Khan, MD, Sacramento, CA (*Presenter*) Nothing to Disclose

#### PURPOSE

CT pulmonary angiography (CTPA) is generally considered to be overutilized and has low diagnostic yield for suspected acute pulmonary embolism (PE), prompting CMS to require consultation of Clinical Decision Support (CDS) at the time of order entry for suspected PE. We assess the effect of CDS on CTPA diagnostic yield by measuring test positivity pre and post implementation.

#### METHODS AND MATERIALS

CDS data and final radiology report impressions for all CTPA orders from the Emergency Department of our quaternary care hospital between July 2016 and April 2022 were obtained prior to and following our CDS go-live date in December 2019. Primary outcome was the percentage of reports positive for PE, determined by manual classification. Secondary outcomes were stratified by CDS appropriateness score and data elements captured at order entry: degree of clinical suspicion for PE, D-dimer status, and signs or symptoms of DVT. Pearson's Chi-squared test and logistic regression statistical tests were applied.

#### RESULTS

976 of 6953 CTPA exams were positive for PE (14.1%), including 546 of 3824 pre-CDS (14.3%) and 430 of 3129 post-CDS (13.7%;  $p=0.545$ ). 292 of 2036 exams deemed 'Appropriate' by CDS were positive (14.4%), while 40 of 382 'Inappropriate' exams were positive (10.5%;  $p=0.053$ ). 102 of the remaining 711 exams were positive (14.3%) - these had 'Moderate' appropriateness ( $n=4$ ), an indication that was out of scope for CDS ( $n=125$ ), or the score was not readily available for technical reasons ( $n=582$ ). Availability of stratified data elements was limited due to variable input by ordering providers when interfacing with the CDS. Stratification demonstrated no statistically significant differences in positivity rate between the High (16.8%), Moderate (10.5%), and Low (14.7%) clinical suspicion groups, between positive (6.3%) or negative (11.9%) signs/symptoms of DVT, or between elevated (12.2%) and normal (0%,  $n=8$ ) D-dimer stratifications.

#### CONCLUSION

There was no significant change in diagnostic yield following implementation of CDS for CTPA orders from the Emergency Department at a quaternary care hospital. Exams with 'High' clinical suspicion for PE had slightly higher and those with 'Inappropriate' CDS determinations slightly lower positivity rates, but none of the detected differences was statistically significant.

#### CLINICAL RELEVANCE/APPLICATION

CDS tools require tremendous effort and cost to design, implement, use, and maintain, and may not improve utilization. We found no difference in CTPA PE positivity pre and post CDS implementation.

Printed on: 02/07/23

## Abstract Archives of the RSNA, 2022

W2-SPER-1

### The Impact of Clinical Decision Support System on the Yield of Pulmonary Emboli on CT Pulmonary Angiography

Wednesday, Nov. 30 9:00AM - 9:30AM Room: Learning Center - ER DPS

#### Participants

Abdullah Khan, MD, Sacramento, CA (*Presenter*) Nothing to Disclose

#### PURPOSE

CT pulmonary angiography (CTPA) is generally considered to be overutilized and has low diagnostic yield for suspected acute pulmonary embolism (PE), prompting CMS to require consultation of Clinical Decision Support (CDS) at the time of order entry for suspected PE. We assess the effect of CDS on CTPA diagnostic yield by measuring test positivity pre and post implementation.

#### METHODS AND MATERIALS

CDS data and final radiology report impressions for all CTPA orders from the Emergency Department of our quaternary care hospital between July 2016 and April 2022 were obtained prior to and following our CDS go-live date in December 2019. Primary outcome was the percentage of reports positive for PE, determined by manual classification. Secondary outcomes were stratified by CDS appropriateness score and data elements captured at order entry: degree of clinical suspicion for PE, D-dimer status, and signs or symptoms of DVT. Pearson's Chi-squared test and logistic regression statistical tests were applied.

#### RESULTS

976 of 6953 CTPA exams were positive for PE (14.1%), including 546 of 3824 pre-CDS (14.3%) and 430 of 3129 post-CDS (13.7%;  $p=0.545$ ). 292 of 2036 exams deemed 'Appropriate' by CDS were positive (14.4%), while 40 of 382 'Inappropriate' exams were positive (10.5%;  $p=0.053$ ). 102 of the remaining 711 exams were positive (14.3%) - these had 'Moderate' appropriateness ( $n=4$ ), an indication that was out of scope for CDS ( $n=125$ ), or the score was not readily available for technical reasons ( $n=582$ ). Availability of stratified data elements was limited due to variable input by ordering providers when interfacing with the CDS. Stratification demonstrated no statistically significant differences in positivity rate between the High (16.8%), Moderate (10.5%), and Low (14.7%) clinical suspicion groups, between positive (6.3%) or negative (11.9%) signs/symptoms of DVT, or between elevated (12.2%) and normal (0%,  $n=8$ ) D-dimer stratifications.

#### CONCLUSION

There was no significant change in diagnostic yield following implementation of CDS for CTPA orders from the Emergency Department at a quaternary care hospital. Exams with 'High' clinical suspicion for PE had slightly higher and those with 'Inappropriate' CDS determinations slightly lower positivity rates, but none of the detected differences was statistically significant.

#### CLINICAL RELEVANCE/APPLICATION

CDS tools require tremendous effort and cost to design, implement, use, and maintain, and may not improve utilization. We found no difference in CTPA PE positivity pre and post CDS implementation.

Printed on: 02/07/23

## Abstract Archives of the RSNA, 2022

W2-SPGI

### Gastrointestinal Wednesday Poster Discussions

Wednesday, Nov. 30 9:00AM - 9:30AM Room: Learning Center - GI DPS

#### Participants

Lyndon Luk, MD, New York, NY (*Moderator*) Nothing to Disclose

#### Sub-Events

### W2-SPGI-10 Accelerated liver diffusion-weighted imaging with a deep learning-based reconstruction: Evaluation of image quality and performance for focal lesion detection in comparison with conventional diffusion-weighted imaging

#### Participants

Bohyun Kim, MD, Seoul, Korea, Republic Of (*Presenter*) Nothing to Disclose

#### PURPOSE

To assess image quality and performance for focal liver lesion (FLL) detection of an accelerated liver diffusion-weighted image with deep learning-based image reconstruction (DL-DWI) compared with conventional DWI (C-DWI) at 3T.

#### METHODS AND MATERIALS

This retrospective study assessed 102 patients who underwent respiratory-triggered DL-DWI and C-DWI using matched b-values (100, 800, 1000 s/mm<sup>2</sup>) and resolution (2.7 x 2.7 x 5 mm<sup>3</sup>) at 3T (MAGNETOM Vida; Siemens Healthcare). DL-DWI used the number of average of 1/1/1 for each b-value and a parallel imaging factor of 4, while those for C-DWI were 1/2/2 and 3, respectively. Two radiologists scored image qualities and measured apparent diffusion coefficient (ADC) values, signal intensity (SI), and signal-to-noise ratio (SI/SD) of two DWI (b = 1000 s/mm<sup>2</sup>) sets. For FLLs, conspicuity and margin sharpness scores, numbers, SI, and lesion-to-liver contrast [(SI<sub>lesion</sub>-SI<sub>liver</sub>)/(SI<sub>lesion</sub>+SI<sub>liver</sub>)] were assessed. Wilcoxon signed-rank test, Student t-test, and ? statistics evaluated differences and agreements.

#### RESULTS

DL-DWI reduced median acquisition time by 20% to C-DWI (391 s vs. 482 s; p < 0.001). DL-DWI received significantly higher scores for image noise and respiratory motion artifact (ps < 0.001), comparable scores for overall image quality, but lower scores for cardiac motion artifact (p < 0.001) in both readers (? , 0.35-0.63). ADC values were more homogeneous in DL-DWI, indicated by lesser variance in measurements and smaller SD across liver segments (p < 0.021). DL-DWI showed significantly higher SI (110.1 vs. 80.6; p < 0.001) and SNR (15.07 vs. 9.21; p < 0.001). FLLs were more conspicuous on DL-DWI (p < 0.019), with significantly higher SI (245 vs. 193.7; p < 0.001) and comparable lesion-to-liver contrast (0.41 vs. 0.39; p = 0.137). Lesser number of FLLs was detected in DL-DWI (130 vs. 148 and 138 vs. 147), though both readers identified a similar number of malignant FLLs (74/86 vs. 80/86 and 76/86 vs. 82/86, ps < 0.099). The mean size of the FLL missed or invisible on DL-DWI was 0.6 cm (range, 0.3-2.3) and frequently located near the capsule (9/15; 60%), with the largest lesion at S2.

#### CONCLUSION

s DL-DWI provided lower image noise, reduced motion artifact, homogeneous ADC values, and higher liver parenchymal SI within a significantly shorter time. Despite superior conspicuity and higher SI for FLL with DL-DWI, small lesions near the capsule or S2 tended to be missed/invisible, underlined by the lower score for cardiac motion artifact. This might attribute to protocol setting and suggests a corresponding refinement as future work.

#### CLINICAL RELEVANCE/APPLICATION

DL-DWI showed reduced image noise, better FLL conspicuity, and substantially higher liver parenchymal SI acquired within a 20% shorter scan time than C-DWI.

### W2-SPGI-2 Diagnostic performance of two kinds of abbreviated gadoxetic acid-enhanced MR protocols for the detection of colorectal liver metastases

#### Participants

Kumi Ozaki, MD, PhD, Fukui, Japan (*Presenter*) Nothing to Disclose

#### PURPOSE

To compare the diagnostic performance of two kinds of abbreviated enhanced magnetic resonance imaging (Ab-MRI) protocols with the standard MRI protocol for the detection of colorectal liver metastases.

#### METHODS AND MATERIALS

The study participants were 87 patients (51 males, 36 females; mean age, 67.2 ± 10.8 years) who had undergone gadoxetic acid-enhanced MRI during the initial work-up for colorectal cancer from 2010 to 2021. All exams were independently reviewed by two readers in three reading sessions: (1) only single-shot fast spin echo (FSE) T2-weighted or fat-suppressed-FSE-T2-weighted,

diffusion-weighted, and hepatobiliary phase images (Ab-MRI protocol 1 or 2), and (2) all acquired MRI sequences (standard protocol). The diagnostic performance was then statistically analyzed.

## RESULTS

A total of 380 lesions, including 195 metastases (51.4%), were analyzed. The results of the two Ab-MRI protocols were similar. The sensitivity, specificity, and positive and negative predictive values of Ab-MRI were non-inferior to those of standard MRI ( $p > 0.05$ ), while those of the combination of Ab-MRI protocol and CE-CT were higher than those of Ab-MRI alone, although not significantly different ( $p > 0.05$ ), and were quite similar to those of standard MRI ( $p > 0.05$ ).

## CONCLUSION

The diagnostic performance of both two kinds of Ab-MRI protocols was non-inferior to that of the standard protocol.

## CLINICAL RELEVANCE/APPLICATION

The diagnostic performance of both two kinds of abbreviated MRI protocols was non-inferior to that of the standard protocol for the detection of colorectal liver metastases.

### W2-SPGI-3 Study on biological activity of hepatic alveolar echinococcus by multimodal MR imaging combined with serum circulating free DNA .

Participants

Hai Hua Bao, Xining, China (*Presenter*) Nothing to Disclose

## PURPOSE

Hepatic alveolar echinococcosis (HAE) grows aggressively in the liver, and its growth characteristics are important for diagnosis and treatment. In this study, the biological activity of hepatic alveolar echinococcosis was studied by multi-mode MR imaging combined with circulating free DNA(cfDNA) in serum.

## METHODS AND MATERIALS

Seventy-two patients with HAE diagnosed clinically from August 2018 to January 2019 were included in the study. Serum cfDNA was detected before MRI. The examination equipment is a 3.0 T MRI scanner. The scanning sequence includes MRI plain scan and dynamic contrast examination, DWI and MRCP water imaging sequence; MRI evaluation first defines the location, size and imaging type of the lesion; The evaluation indexes of activity include the range of high signal band of DWI images(marginal band), microbubbles and enhancement characteristics. The marginal zone, microbubbles and ADC values were measured by T2WI, MRCP and DWI sequences ( $b = 800 \text{ mm/s}$ ) to further evaluate the biological activity of the lesions. The correlation between the size, imaging type of lesions and serum cfDNA was analyzed.

## RESULTS

1. Lesions characteristics: there were 92 lesions in 72 patients with HAE, including 16 lesions  $< 5 \text{ cm}$ , 36 lesions  $>5-10 \text{ cm}$  and 40 lesions  $>10\text{cm}$ . Imaging types of lesions: solid type 51 cases, liquefied type 7 cases, multiple nodular type 4 cases, mixed type 4 cases and calcified type 6 cases. 2. Evaluation of lesion activity: 49 lesions (53.3%) showed mild annular enhancement in portal vein phase after dynamic contrast-enhanced scanning; On DWI images, 87 lesions had high signal intensity (marginal zone) with limited diffusion, while 5 calcified lesions had no obvious marginal zone. The width of the band is between  $(0.28 \sim 0.98) \text{ cm}$ ; The average ADC value is about  $(1.10 \pm 0.17) \times 10^{-3} \text{ mm}^2/\text{s}$  measured at  $0.5\text{cm}$  in the marginal zone. Average ADC value of microbubbles is about  $(0.79 \pm 0.16) \times 10^{-3} \text{ mm}^2/\text{s}$ ; Compared with ADC, the difference was statistically significant ( $P < 0.05$ ). 3. Correlation between the size and classification of lesions and cfDNA: The cfDNA range of lesions with HAE=10cm is  $(98 \sim 11770) \text{ ng/ml}$ , which is higher than that of small lesions  $(0 \sim 98 \text{ ng/ml})$ , and the correlation between them is statistically different ( $r=0.482$ ,  $P = 0.000$ ); cfDNA was found in all types, with calcified DNA being the lowest  $(0 \sim 2 \text{ ng/ml})$  and solid's DNA being the highest  $(0 \sim 11770 \text{ ng/ml})$ .

## CONCLUSION

cfDNA is related to the size, imaging type and activity of HAE lesions, and MRI combined with cfDNA can better evaluate the biological activity of HAE lesions.

## CLINICAL RELEVANCE/APPLICATION

MRI combined with cfDNA can better evaluate the biological activity of HAE lesions.

### W2-SPGI-4 Detection of Lymph Node Metastases in Intrahepatic Cholangiocarcinoma - an Ongoing Challenge

Participants

Johannes Kolck, MD, (*Presenter*) Nothing to Disclose

## PURPOSE

Objectives of the present study were to investigate the predictive value of the short lymph node (LN) axis, a widely recognised discriminator for lymph node metastases (LNM) in tumor imaging, and to develop a predictive model for LNM in iCC based on multiple CT imaging features.

## METHODS AND MATERIALS

Retrospectively enrolled were 102 patients with pathologically proven mass-forming iCC, who underwent multiphase CT imaging prior to and standardised lymph node dissection during resection from 2005 to 2021. Two blinded radiologists assessed various quantitative and qualitative imaging characteristics. These were implemented to develop a prediction model for lymph node metastasis.

## RESULTS

Lymph node dissection (LND) was performed in all patients. In 3 cases pathology reports on LN status were missing or inconclusive. Survival estimates were almost significantly diminished ( $p = 0.07$ ) for LN positive patients and the prevalence of LNM was high at 42.4 %. Even after adjusting the short axis threshold to 5 mm, resulting in high sensitivity but low specificity for LNM, the LN

diameter proved to be a relevant but not reliable predictor. The detailed analysis of CT exams revealed four statistically significant imaging features: Presence of intrahepatic metastasis (CI 1.206 - 9.368;  $p = 0.020$ ), hilar infiltration (CI 1.507 - 14.650;  $p = 0.008$ ) and tumour outgrowth along the liver capsule (CI 1.665 - 27.984;  $p = 0.008$ ). Of which the latter two might indicate direct tumor involvement with lymphatic liver structures. These four were integrated into a prediction model, which substantially outperformed the sole consideration of LN axis in ROC analysis (AUC 0.8 vs 0.657).

## CONCLUSION

s LNM rates among patients suffering from ICC are high and worsen their prognosis. Predicting tumor positive LN in presurgical imaging remains a challenge, as evaluation of LN short axis alone appears insufficient. Based on four imaging features, we build a prediction model that proved enhanced discriminatory ability in LNM detection.

## CLINICAL RELEVANCE/APPLICATION

LN short axis alone is an unreliable imaging marker for LNM in ICC. Our data emphasise the need for standardized LND, in patients with LN diameters greater than 5 mm.

## W2-SPGI-5 Improving survival prediction with volumetric functional MRI and modified Fudan prognostic grading system for unresectable intrahepatic cholangiocarcinoma treated with systemic chemotherapy.

Participants

Alireza Mohseni, MD, Baltimore, MD (*Presenter*) Nothing to Disclose

## PURPOSE

This study aimed to compare the incremental value of volumetric functional MRI-derived parameters to the Fudan clinical prognostic scoring system in patients with intrahepatic cholangiocarcinoma (ICCA) treated with systemic chemotherapy.

## METHODS AND MATERIALS

This retrospective study included 114 patients with unresectable ICCA (age,  $65 \pm 11$  yrs; 53 men [47%]). Following baseline MRI, all patients received systemic chemotherapy. The single largest tumor was evaluated for anatomic (total tumor volume and maximum axial tumor diameter) and functional parameters (viable tumor volume, percentage viable tumor volume [ $100 \times$  viable tumor volume/whole tumor volume], viable tumor burden [ $100 \times$  viable tumor volume/whole liver volume], and apparent diffusion coefficient (ADC)). Based on previous research for the threshold of the venous enhancement parameter value, 40 was set as the lower limit of viability. For ADC, we used the cohort-derived median values as the threshold ( $1350 \times 10^{-6}$  mm<sup>2</sup>/sec). The strongest functional predictor of overall survival (OS) was identified using Cox regression. Fudan Score (using serum alkaline phosphatase, carbohydrate antigen 19-9, tumor margin type, tumor size, and the number of intrahepatic tumors) and a modified Fudan Score (with functional MRI parameters replacing subjective tumor characteristics) were used to calculate prognostic scores for each patient. The performance of both scores was measured and compared by the C-index and Kaplan-Meier survival estimates in different risk groups.

## RESULTS

Tumor ADC had the strongest association with OS among the volumetric functional MRI parameters. Both Fudan and modified Fudan scores (replacing tumor margin and diameter with ADC and percentage viable tumor volume) provided prognostic prediction, with differences in OS between low, intermediate, high, and very high-risk groups (Fudan,  $P = .041$ ; modified Fudan,  $P = 0.007$ ). The modified Fudan score had a c-index of 0.75 (95% CI, 0.65-0.84) for predicting survival, which was higher than the C-index of the original Fudan score (0.63 [95% CI, 0.52-0.73]).

## CONCLUSION

s The Fudan model was supplemented with ADC and percentage viable tumor volume to provide a more accurate prognosis for ICCA patients undergoing systemic chemotherapy, improving survival prediction performance by 12%.

## CLINICAL RELEVANCE/APPLICATION

Results of this study suggest the prognostic role of functional MRI in assessing outcome of patients with ICCA. Supplementing Fudan score with ADC and percentage viable tumor volume could better predict survival of ICCA patients.

## W2-SPGI-7 Demystifying the misty mesentery: when should we follow up?

Participants

Madusha Chandratilleke, MBBS, (*Presenter*) Nothing to Disclose

## PURPOSE

"Misty mesentery" is a common incidental radiological finding. The benign spectrum of mesenteric panniculitis is well described, but currently no guidelines exist to guide the radiological management or follow up. The purpose of this retrospective study, was to ascertain which features, if any, are concerning about this common incidental finding and if/when this should be followed up with further imaging.

## METHODS AND MATERIALS

Retrospective analysis was performed on 52 patients (derived from 500) who had findings of misty mesentery incidentally detected on a contrast enhanced CT scan. Any cases of mesenteric misting which had a clear cause such as trauma, infection or known malignancy were excluded. The incident study of each patient was read by two specialist abdominal Radiologists, who reached a consensus on each case and documented their findings according to an imaging checklist provided to them.

## RESULTS

Of the 52 cases, 41 were reported as benign, 8 reported as indeterminate and 3 reported as concerning. The 41 benign cases and 8 indeterminate cases either resolved, improved, remained stable or progressively calcified over an average time period of 5 years. 2 of the 'concerning' cases were later diagnosed as biopsy proven low grade follicular lymphoma, with an average time of disease progression being 2 years. The third 'concerning' case was biopsy proven sclerosing mesenteritis and had a unique radiological feature - calcification. Common features identified in both lymphoma cases: Mesenteric nodes 20 mm or larger, peritoneal nodes or mesenteric nodes outside the root of mesentery 20 mm or larger, retroperitoneal lymphadenopathy 10mm to gt 20 mm, obliteration

of 'fat ring sign'. Follow up recommendations in the original reports were varied included 'no follow up', 'a few months', '3 months', '3-6 months', '6 months', '6-9 months', and '6-12 months'.

## CONCLUSION

If a contrast enhanced CT abdomen is reported by an abdominal imaging specialist, the sensitivity of detecting concerning 'misty mesentery' should be close to 100%. Features of benignity are established in the literature, however based on this particular study, we can now confidently state that in the absence of concerning imaging features, follow up of incidental 'misty mesentery' is not recommended. Conversely, if some or all of the radiographic features of concern are present, appearances may reflect low grade lymphoma, in which case a follow up scan could be performed in 12 months, or biopsy may be considered.

## CLINICAL RELEVANCE/APPLICATION

These outcomes may alleviate patient and doctor anxiety regarding follow up recommendations and disease progression of mesenteric panniculitis and obviate unnecessary follow up imaging.

## W2-SPGI-8 Towards structured reporting of universally detected and labeled lesions in CT volumes

### Participants

Tejas Sudharshan Mathai, PhD, MS, (*Presenter*) Nothing to Disclose

### PURPOSE

To use an automated deep learning-based model to universally detect and label lesions in CT volumes, and create a structured "Lesions" subsection for entry into the "Findings" section of radiology reports.

### METHODS AND MATERIALS

The publicly available DeepLesion dataset containing 32,735 lesions identified on 32,120 CT slices was used. An annotated 30% subset of this dataset (9816 lesions from 9624 slices) consisting of lesion bounding box coordinates and anatomical labels (e.g. liver, pelvis etc.) were used in this study. Subsequently, a deep learning model (VFNet) trained on this data yielded the bounding box coordinates, confidence scores, and anatomical labels of predicted lesions. Following this, a structured "Lesions" subsection was created for inclusion in the "Findings" section of a radiology report, and contained the following: 1) Lesion location coordinates (denoted by a hyperlink, which when clicked on, displayed the lesion coordinates on a CT slice), 2) anatomical label, 3) prediction confidence, 4) study and series names, and 5) slice index of volume.

### RESULTS

The deep learning model detected and classified lesions with a sensitivities of 73.2%, 80%, and 83.3% at 2, 4, and 6 false positives (FP) per slice respectively. The model showed a recall (at 4 FP per slice) of 80% with the following class-wise breakdown: lung nodule (89%), mediastinal LN (85%), liver mass (81%), kidney (80%), soft tissue (77%), pelvic mass (76%), abdomen (70%), and bone (56%). As seen in Figs. 1A and 1B, classes with fewer samples (e.g. 'Bone') fared poorly compared with over-represented classes (e.g. 'Lung'). When lesions were divided by their size (= 1cm, clinically suspicious), the sensitivity at 4FP improved for classes with large data quantities (abdomen, mediastinum, liver). Qualitative evaluation revealed that many FP detections were true positives that were not labeled in the dataset, which reduced the overall sensitivity. A structured "Lesions" subsection was created for entry into the "Findings" section of a radiology report (see Fig. 1C-E).

### CONCLUSION

The presented approach universally detected and labeled lesions with 80% sensitivity at 4FP, while identifying important missed lesions in the original DeepLesion dataset. A structured "Lesion" subsection was created for entry into the "Findings" section of a radiology report.

### CLINICAL RELEVANCE/APPLICATION

Radiologists assessing cancer burden and managing patient therapy will benefit from a "second reader" AI model that reports a structured list of suspicious lesions in the "Findings" section.

## W2-SPGI-9 Diffusion tensor imaging and diffusion kurtosis imaging of the pancreas at 3 Tesla MRI - reproducibility and normal findings

### Participants

Carlos Bildeiro, MD, Lisbon, Portugal (*Presenter*) Nothing to Disclose

### PURPOSE

To assess the reproducibility of diffusion tensor imaging (DTI) and diffusion kurtosis imaging (DKI) of the pancreas at 3T MRI, and to describe the normal findings in a healthy population.

### METHODS AND MATERIALS

In this Institutional Review Board-approved prospective pilot study, healthy volunteers underwent two repeated sessions of abdominal MRI in a clinical 3T scanner, performing both DTI and DKI of the pancreas in each session. In each imaging session, a single acquisition of spin-echo echo-planar imaging (EPI) was performed, with 6 slices encompassing the entire pancreas, using 16 evenly distributed diffusion directions for b values of 0, 200, 1000 and 1700 s/mm<sup>2</sup>. The acquired data were pre-processed with denoising (Marchenko-Pastur principal component analysis) and Gibbs unringing algorithms. DTI analysis was performed for producing fractional anisotropy (FA) maps. DKI using the mean signal from all directions was used to calculate mean diffusivity (MD) and mean kurtosis (MK) maps. Standard apparent diffusion coefficient (ADC) maps were also produced. Two dedicated abdominal radiologists delineated the entire pancreas in each image, and the values measured for the pancreatic parenchyma were registered and compared.

### RESULTS

Ten volunteers (aged 30-60 years, 6 females and 4 males) underwent both imaging sessions. For all volunteers, the measurements performed on the pancreatic parenchyma revealed: median MK = 1.01 (IQR: 0.52); median MD = 2.44x10<sup>-3</sup> (IQR: 1.61x10<sup>-3</sup>) mm<sup>2</sup>/s; median FA = 0.21 (IQR: 0.11); median ADC = 1.12x10<sup>-3</sup> (IQR: 0.27x10<sup>-3</sup>) mm<sup>2</sup>/s. There was no significant variability in FA, MD, MK and ADC measurements within different sessions for each volunteer, determining intra-patient reproducibility. Values

obtained between different volunteers were also not significantly different, suggesting inter-patient reproducibility. Regarding inter-reader reliability, there was good agreement between both radiologists.

#### **CONCLUSION**

s DTI and DKI of the pancreas can be performed reliably with a single acquisition at clinical 3T MRI scanners, with adequate intra-patient and inter-patient reproducibility.

#### **CLINICAL RELEVANCE/APPLICATION**

This study describes the findings in healthy subjects when performing DTI and DKI of the pancreas and determines their reproducibility, both critical steps for its implementation in clinical practice

Printed on: 02/07/23

## Abstract Archives of the RSNA, 2022

W2-SPGI-10

### Accelerated liver diffusion-weighted imaging with a deep learning-based reconstruction: Evaluation of image quality and performance for focal lesion detection in comparison with conventional diffusion-weighted imaging

Wednesday, Nov. 30 9:00AM - 9:30AM Room: Learning Center - GI DPS

#### Participants

Bohyun Kim, MD, Seoul, Korea, Republic Of (*Presenter*) Nothing to Disclose

#### PURPOSE

To assess image quality and performance for focal liver lesion (FLL) detection of an accelerated liver diffusion-weighted image with deep learning-based image reconstruction (DL-DWI) compared with conventional DWI (C-DWI) at 3T.

#### METHODS AND MATERIALS

This retrospective study assessed 102 patients who underwent respiratory-triggered DL-DWI and C-DWI using matched b-values (100, 800, 1000 s/mm<sup>2</sup>) and resolution (2.7 x 2.7 x 5 mm<sup>3</sup>) at 3T (MAGNETOM Vida; Siemens Healthcare). DL-DWI used the number of average of 1/1/1 for each b-value and a parallel imaging factor of 4, while those for C-DWI were 1/2/2 and 3, respectively. Two radiologists scored image qualities and measured apparent diffusion coefficient (ADC) values, signal intensity (SI), and signal-to-noise ratio (SI/SD) of two DWI (b = 1000 s/mm<sup>2</sup>) sets. For FLLs, conspicuity and margin sharpness scores, numbers, SI, and lesion-to-liver contrast [(SI<sub>lesion</sub>-SI<sub>liver</sub>)/(SI<sub>lesion</sub>+SI<sub>liver</sub>)] were assessed. Wilcoxon signed-rank test, Student t-test, and  $\chi^2$  statistics evaluated differences and agreements.

#### RESULTS

DL-DWI reduced median acquisition time by 20% to C-DWI (391 s vs. 482 s; p < 0.001). DL-DWI received significantly higher scores for image noise and respiratory motion artifact (ps < 0.001), comparable scores for overall image quality, but lower scores for cardiac motion artifact (p < 0.001) in both readers (? , 0.35-0.63). ADC values were more homogeneous in DL-DWI, indicated by lesser variance in measurements and smaller SD across liver segments (p < 0.021). DL-DWI showed significantly higher SI (110.1 vs. 80.6; p < 0.001) and SNR (15.07 vs. 9.21; p < 0.001). FLLs were more conspicuous on DL-DWI (p < 0.019), with significantly higher SI (245 vs. 193.7; p < 0.001) and comparable lesion-to-liver contrast (0.41 vs. 0.39; p = 0.137). Lesser number of FLLs was detected in DL-DWI (130 vs. 148 and 138 vs. 147), though both readers identified a similar number of malignant FLLs (74/86 vs. 80/86 and 76/86 vs. 82/86, ps < 0.099). The mean size of the FLL missed or invisible on DL-DWI was 0.6 cm (range, 0.3-2.3) and frequently located near the capsule (9/15; 60%), with the largest lesion at S2.

#### CONCLUSION

s DL-DWI provided lower image noise, reduced motion artifact, homogeneous ADC values, and higher liver parenchymal SI within a significantly shorter time. Despite superior conspicuity and higher SI for FLL with DL-DWI, small lesions near the capsule or S2 tended to be missed/invisible, underlined by the lower score for cardiac motion artifact. This might attribute to protocol setting and suggests a corresponding refinement as future work.

#### CLINICAL RELEVANCE/APPLICATION

DL-DWI showed reduced image noise, better FLL conspicuity, and substantially higher liver parenchymal SI acquired within a 20% shorter scan time than C-DWI.

Printed on: 02/07/23

## Abstract Archives of the RSNA, 2022

W2-SPGI-2

### Diagnostic performance of two kinds of abbreviated gadoxetic acid-enhanced MR protocols for the detection of colorectal liver metastases

Wednesday, Nov. 30 9:00AM - 9:30AM Room: Learning Center - GI DPS

#### Participants

Kumi Ozaki, MD, PhD, Fukui, Japan (*Presenter*) Nothing to Disclose

#### PURPOSE

To compare the diagnostic performance of two kinds of abbreviated enhanced magnetic resonance imaging (Ab-MRI) protocols with the standard MRI protocol for the detection of colorectal liver metastases.

#### METHODS AND MATERIALS

The study participants were 87 patients (51 males, 36 females; mean age,  $67.2 \pm 10.8$  years) who had undergone gadoxetic acid-enhanced MRI during the initial work-up for colorectal cancer from 2010 to 2021. All exams were independently reviewed by two readers in three reading sessions: (1) only single-shot fast spin echo (FSE) T2-weighted or fat-suppressed-FSE-T2-weighted, diffusion-weighted, and hepatobiliary phase images (Ab-MRI protocol 1 or 2), and (2) all acquired MRI sequences (standard protocol). The diagnostic performance was then statistically analyzed.

#### RESULTS

A total of 380 lesions, including 195 metastases (51.4%), were analyzed. The results of the two Ab-MRI protocols were similar. The sensitivity, specificity, and positive and negative predictive values of Ab-MRI were non-inferior to those of standard MRI ( $p > 0.05$ ), while those of the combination of Ab-MRI protocol and CE-CT were higher than those of Ab-MRI alone, although not significantly different ( $p > 0.05$ ), and were quite similar to those of standard MRI ( $p > 0.05$ ).

#### CONCLUSION

s The diagnostic performance of both two kinds of Ab-MRI protocols was non-inferior to that of the standard protocol.

#### CLINICAL RELEVANCE/APPLICATION

The diagnostic performance of both two kinds of abbreviated MRI protocols was non-inferior to that of the standard protocol for the detection of colorectal liver metastases.

Printed on: 02/07/23

## Abstract Archives of the RSNA, 2022

W2-SPGI-3

### Study on biological activity of hepatic alveolar echinococcus by multimodal MR imaging combined with serum circulating free DNA .

Wednesday, Nov. 30 9:00AM - 9:30AM Room: Learning Center - GI DPS

#### Participants

Hai Hua Bao, Xining, China (*Presenter*) Nothing to Disclose

#### PURPOSE

Hepatic alveolar echinococcosis (HAE) grows aggressively in the liver, and its growth characteristics are important for diagnosis and treatment. In this study, the biological activity of hepatic alveolar echinococcosis was studied by multi-mode MR imaging combined with circulating free DNA(cfDNA) in serum.

#### METHODS AND MATERIALS

Seventy-two patients with HAE diagnosed clinically from August 2018 to January 2019 were included in the study. Serum cfDNA was detected before MRI. The examination equipment is a 3.0 T MRI scanner. The scanning sequence includes MRI plain scan and dynamic contrast examination, DWI and MRCP water imaging sequence; MRI evaluation first defines the location, size and imaging type of the lesion; The evaluation indexes of activity include the range of high signal band of DWI images(marginal band), microbubbles and enhancement characteristics. The marginal zone, microbubbles and ADC values were measured by T2WI, MRCP and DWI sequences ( $b = 800 \text{ mm/s}$ ) to further evaluate the biological activity of the lesions. The correlation between the size, imaging type of lesions and serum cfDNA was analyzed.

#### RESULTS

1. Lesions characteristics: there were 92 lesions in 72 patients with HAE, including 16 lesions  $< 5 \text{ cm}$ , 36 lesions  $>5-10 \text{ cm}$  and 40 lesions  $>10 \text{ cm}$ . Imaging types of lesions: solid type 51 cases, liquefied type 7 cases, multiple nodular type 4 cases, mixed type 4 cases and calcified type 6 cases. 2. Evaluation of lesion activity: 49 lesions (53.3%) showed mild annular enhancement in portal vein phase after dynamic contrast-enhanced scanning; On DWI images, 87 lesions had high signal intensity (marginal zone) with limited diffusion, while 5 calcified lesions had no obvious marginal zone. The width of the band is between  $(0.28 \sim 0.98) \text{ cm}$ ; The average ADC value is about  $(1.10 \pm 0.17) \times 10^{-3} \text{ mm}^2/\text{s}$  measured at  $0.5 \text{ cm}$  in the marginal zone. Average ADC value of microbubbles is about  $(0.79 \pm 0.16) \times 10^{-3} \text{ mm}^2/\text{s}$ ; Compared with ADC, the difference was statistically significant ( $P < 0.05$ ). 3. Correlation between the size and classification of lesions and cfDNA: The cfDNA range of lesions with HAE=10cm is  $(98 \sim 11770) \text{ ng/ml}$ , which is higher than that of small lesions  $(0 \sim 98 \text{ ng/ml})$ , and the correlation between them is statistically different ( $r=0.482, P = 0.000$ ); cfDNA was found in all types, with calcified DNA being the lowest  $(0 \sim 2 \text{ ng/ml})$  and solid's DNA being the highest  $(0 \sim 11770 \text{ ng/ml})$ .

#### CONCLUSION

cfDNA is related to the size, imaging type and activity of HAE lesions, and MRI combined with cfDNA can better evaluate the biological activity of HAE lesions.

#### CLINICAL RELEVANCE/APPLICATION

MRI combined with cfDNA can better evaluate the biological activity of HAE lesions.

Printed on: 02/07/23

## Abstract Archives of the RSNA, 2022

W2-SPGI-4

### Detection of Lymph Node Metastases in Intrahepatic Cholangiocarcinoma - an Ongoing Challenge

Wednesday, Nov. 30 9:00AM - 9:30AM Room: Learning Center - GI DPS

#### Participants

Johannes Kolck, MD, (*Presenter*) Nothing to Disclose

#### PURPOSE

Objectives of the present study were to investigate the predictive value of the short lymph node (LN) axis, a widely recognised discriminator for lymph node metastases (LNM) in tumor imaging, and to develop a predictive model for LNM in iCC based on multiple CT imaging features.

#### METHODS AND MATERIALS

Retrospectively enrolled were 102 patients with pathologically proven mass-forming iCC, who underwent multiphase CT imaging prior to and standardised lymph node dissection during resection from 2005 to 2021. Two blinded radiologists assessed various quantitative and qualitative imaging characteristics. These were implemented to develop a prediction model for lymph node metastasis.

#### RESULTS

Lymph node dissection (LND) was performed in all patients. In 3 cases pathology reports on LN status were missing or inconclusive. Survival estimates were almost significantly diminished ( $p = 0.07$ ) for LN positive patients and the prevalence of LNM was high at 42.4 %. Even after adjusting the short axis threshold to 5 mm, resulting in high sensitivity but low specificity for LNM, the LN diameter proved to be a relevant but not reliable predictor. The detailed analysis of CT exams revealed four statistically significant imaging features: Presence of intrahepatic metastasis (CI 1.206 - 9.368;  $p = 0.020$ ), hilar infiltration (CI 1.507 - 14.650;  $p = 0.008$ ) and tumour outgrowth along the liver capsule (CI 1.665 - 27.984;  $p = 0.008$ ). Of which the latter two might indicate direct tumor involvement with lymphatic liver structures. These four were integrated into a prediction model, which substantially outperformed the sole consideration of LN axis in ROC analysis (AUC 0.8 vs 0.657).

#### CONCLUSION

s LNM rates among patients suffering from iCC are high and worsen their prognosis. Predicting tumor positive LN in presurgical imaging remains a challenge, as evaluation of LN short axis alone appears insufficient. Based on four imaging features, we build a prediction model that proved enhanced discriminatory ability in LNM detection.

#### CLINICAL RELEVANCE/APPLICATION

LN short axis alone is an unreliable imaging marker for LNM in iCC. Our data emphasise the need for standardized LND, in patients with LN diameters greater than 5 mm.

Printed on: 02/07/23

## Abstract Archives of the RSNA, 2022

W2-SPGI-5

### Improving survival prediction with volumetric functional MRI and modified Fudan prognostic grading system for unresectable intrahepatic cholangiocarcinoma treated with systemic chemotherapy.

Wednesday, Nov. 30 9:00AM - 9:30AM Room: Learning Center - GI DPS

#### Participants

Alireza Mohseni, MD, Baltimore, MD (*Presenter*) Nothing to Disclose

#### PURPOSE

This study aimed to compare the incremental value of volumetric functional MRI-derived parameters to the Fudan clinical prognostic scoring system in patients with intrahepatic cholangiocarcinoma (ICCA) treated with systemic chemotherapy.

#### METHODS AND MATERIALS

This retrospective study included 114 patients with unresectable ICCA (age, 65±11 yrs; 53 men [47%]). Following baseline MRI, all patients received systemic chemotherapy. The single largest tumor was evaluated for anatomic (total tumor volume and maximum axial tumor diameter) and functional parameters (viable tumor volume, percentage viable tumor volume [ $100 \times$  viable tumor volume/whole tumor volume], viable tumor burden [ $100 \times$  viable tumor volume/whole liver volume], and apparent diffusion coefficient (ADC)). Based on previous research for the threshold of the venous enhancement parameter value, 40 was set as the lower limit of viability. For ADC, we used the cohort-derived median values as the threshold ( $1350 \times 10^{-6}$  mm<sup>2</sup>/sec). The strongest functional predictor of overall survival (OS) was identified using Cox regression. Fudan Score (using serum alkaline phosphatase, carbohydrate antigen 19-9, tumor margin type, tumor size, and the number of intrahepatic tumors) and a modified Fudan Score (with functional MRI parameters replacing subjective tumor characteristics) were used to calculate prognostic scores for each patient. The performance of both scores was measured and compared by the C-index and Kaplan-Meier survival estimates in different risk groups.

#### RESULTS

Tumor ADC had the strongest association with OS among the volumetric functional MRI parameters. Both Fudan and modified Fudan scores (replacing tumor margin and diameter with ADC and percentage viable tumor volume) provided prognostic prediction, with differences in OS between low, intermediate, high, and very high-risk groups (Fudan,  $P=.041$ ; modified Fudan,  $P=0.007$ ). The modified Fudan score had a c-index of 0.75 (95% CI, 0.65-0.84) for predicting survival, which was higher than the C-index of the original Fudan score (0.63 [95% CI, 0.52-0.73]).

#### CONCLUSION

The Fudan model was supplemented with ADC and percentage viable tumor volume to provide a more accurate prognosis for ICCA patients undergoing systemic chemotherapy, improving survival prediction performance by 12%.

#### CLINICAL RELEVANCE/APPLICATION

Results of this study suggest the prognostic role of functional MRI in assessing outcome of patients with ICCA. Supplementing Fudan score with ADC and percentage viable tumor volume could better predict survival of ICCA patients.

Printed on: 02/07/23

## Abstract Archives of the RSNA, 2022

W2-SPGI-7

### Demystifying the misty mesentery: when should we follow up?

Wednesday, Nov. 30 9:00AM - 9:30AM Room: Learning Center - GI DPS

#### Participants

Madusha Chandratilleke, MBBS, (*Presenter*) Nothing to Disclose

#### PURPOSE

"Misty mesentery" is a common incidental radiological finding. The benign spectrum of mesenteric panniculitis is well described, but currently no guidelines exist to guide the radiological management or follow up. The purpose of this retrospective study, was to ascertain which features, if any, are concerning about this common incidental finding and if/when this should be followed up with further imaging.

#### METHODS AND MATERIALS

Retrospective analysis was performed on 52 patients (derived from 500) who had findings of misty mesentery incidentally detected on a contrast enhanced CT scan. Any cases of mesenteric misting which had a clear cause such as trauma, infection or known malignancy were excluded. The incident study of each patient was read by two specialist abdominal Radiologists, who reached a consensus on each case and documented their findings according to an imaging checklist provided to them.

#### RESULTS

Of the 52 cases, 41 were reported as benign, 8 reported as indeterminate and 3 reported as concerning. The 41 benign cases and 8 indeterminate cases either resolved, improved, remained stable or progressively calcified over an average time period of 5 years. 2 of the 'concerning' cases were later diagnosed as biopsy proven low grade follicular lymphoma, with an average time of disease progression being 2 years. The third 'concerning' case was biopsy proven sclerosing mesenteritis and had a unique radiological feature - calcification. Common features identified in both lymphoma cases: Mesenteric nodes 20 mm or larger, peritoneal nodes or mesenteric nodes outside the root of mesentery 20 mm or larger, retroperitoneal lymphadenopathy 10mm to gt 20 mm, obliteration of 'fat ring sign'. Follow up recommendations in the original reports were varied included 'no follow up', 'a few months', '3 months', '3-6 months', '6 months', '6-9 months', and '6-12 months'.

#### CONCLUSION

If a contrast enhanced CT abdomen is reported by an abdominal imaging specialist, the sensitivity of detecting concerning 'misty mesentery' should be close to 100%. Features of benignity are established in the literature, however based on this particular study, we can now confidently state that in the absence of concerning imaging features, follow up of incidental 'misty mesentery' is not recommended. Conversely, if some or all of the radiographic features of concern are present, appearances may reflect low grade lymphoma, in which case a follow up scan could be performed in 12 months, or biopsy may be considered.

#### CLINICAL RELEVANCE/APPLICATION

These outcomes may alleviate patient and doctor anxiety regarding follow up recommendations and disease progression of mesenteric panniculitis and obviate unnecessary follow up imaging.

Printed on: 02/07/23

## Abstract Archives of the RSNA, 2022

W2-SPGI-8

### Towards structured reporting of universally detected and labeled lesions in CT volumes

Wednesday, Nov. 30 9:00AM - 9:30AM Room: Learning Center - GI DPS

#### Participants

Tejas Sudharshan Mathai, PhD, MS, (*Presenter*) Nothing to Disclose

#### PURPOSE

To use an automated deep learning-based model to universally detect and label lesions in CT volumes, and create a structured "Lesions" subsection for entry into the 'Findings' section of radiology reports.

#### METHODS AND MATERIALS

The publicly available DeepLesion dataset containing 32,735 lesions identified on 32,120 CT slices was used. An annotated 30% subset of this dataset (9816 lesions from 9624 slices) consisting of lesion bounding box coordinates and anatomical labels (e.g. liver, pelvis etc.) were used in this study. Subsequently, a deep learning model (VFNet) trained on this data yielded the bounding box coordinates, confidence scores, and anatomical labels of predicted lesions. Following this, a structured "Lesions" subsection was created for inclusion in the "Findings" section of a radiology report, and contained the following: 1) Lesion location coordinates (denoted by a hyperlink, which when clicked on, displayed the lesion coordinates on a CT slice), 2) anatomical label, 3) prediction confidence, 4) study and series names, and 5) slice index of volume.

#### RESULTS

The deep learning model detected and classified lesions with a sensitivities of 73.2%, 80%, and 83.3% at 2, 4, and 6 false positives (FP) per slice respectively. The model showed a recall (at 4 FP per slice) of 80% with the following class-wise breakdown: lung nodule (89%), mediastinal LN (85%), liver mass (81%), kidney (80%), soft tissue (77%), pelvic mass (76%), abdomen (70%), and bone (56%). As seen in Figs. 1A and 1B, classes with fewer samples (e.g. `Bone`) fared poorly compared with over-represented classes (e.g. `Lung`). When lesions were divided by their size (= 1cm, clinically suspicious), the sensitivity at 4FP improved for classes with large data quantities (abdomen, mediastinum, liver). Qualitative evaluation revealed that many FP detections were true positives that were not labeled in the dataset, which reduced the overall sensitivity. A structured "Lesions" subsection was created for entry into the "Findings" section of a radiology report (see Fig. 1C-E).

#### CONCLUSION

The presented approach universally detected and labeled lesions with 80% sensitivity at 4FP, while identifying important missed lesions in the original DeepLesion dataset. A structured "Lesion" subsection was created for entry into the "Findings" section of a radiology report.

#### CLINICAL RELEVANCE/APPLICATION

Radiologists assessing cancer burden and managing patient therapy will benefit from a "second reader" AI model that reports a structured list of suspicious lesions in the "Findings" section.

Printed on: 02/07/23

## Abstract Archives of the RSNA, 2022

W2-SPGI-9

### Diffusion tensor imaging and diffusion kurtosis imaging of the pancreas at 3 Tesla MRI - reproducibility and normal findings

Wednesday, Nov. 30 9:00AM - 9:30AM Room: Learning Center - GI DPS

#### Participants

Carlos Bilreiro, MD, Lisbon, Portugal (*Presenter*) Nothing to Disclose

#### PURPOSE

To assess the reproducibility of diffusion tensor imaging (DTI) and diffusion kurtosis imaging (DKI) of the pancreas at 3T MRI, and to describe the normal findings in a healthy population.

#### METHODS AND MATERIALS

In this Institutional Review Board-approved prospective pilot study, healthy volunteers underwent two repeated sessions of abdominal MRI in a clinical 3T scanner, performing both DTI and DKI of the pancreas in each session. In each imaging session, a single acquisition of spin-echo echo-planar imaging (EPI) was performed, with 6 slices encompassing the entire pancreas, using 16 evenly distributed diffusion directions for b values of 0, 200, 1000 and 1700 s/mm<sup>2</sup>. The acquired data were pre-processed with denoising (Marchenko-Pastur principal component analysis) and Gibbs unringing algorithms. DTI analysis was performed for producing fractional anisotropy (FA) maps. DKI using the mean signal from all directions was used to calculate mean diffusivity (MD) and mean kurtosis (MK) maps. Standard apparent diffusion coefficient (ADC) maps were also produced. Two dedicated abdominal radiologists delineated the entire pancreas in each image, and the values measured for the pancreatic parenchyma were registered and compared.

#### RESULTS

Ten volunteers (aged 30-60 years, 6 females and 4 males) underwent both imaging sessions. For all volunteers, the measurements performed on the pancreatic parenchyma revealed: median MK = 1.01 (IQR: 0.52); median MD = 2.44x10<sup>-3</sup> (IQR: 1.61x10<sup>-3</sup>) mm<sup>2</sup>/s; median FA = 0.21 (IQR: 0.11); median ADC = 1.12x10<sup>-3</sup> (IQR: 0.27x10<sup>-3</sup>) mm<sup>2</sup>/s. There was no significant variability in FA, MD, MK and ADC measurements within different sessions for each volunteer, determining intra-patient reproducibility. Values obtained between different volunteers were also not significantly different, suggesting inter-patient reproducibility. Regarding inter-reader reliability, there was good agreement between both radiologists.

#### CONCLUSION

s DTI and DKI of the pancreas can be performed reliably with a single acquisition at clinical 3T MRI scanners, with adequate intra-patient and inter-patient reproducibility.

#### CLINICAL RELEVANCE/APPLICATION

This study describes the findings in healthy subjects when performing DTI and DKI of the pancreas and determines their reproducibility, both critical steps for its implementation in clinical practice

Printed on: 02/07/23

## Abstract Archives of the RSNA, 2022

W2-SPGU

### Genitourinary Wednesday Poster Discussions

Wednesday, Nov. 30 9:00AM - 9:30AM Room: Learning Center - GU DPS

#### Sub-Events

#### W2-SPGU-1 The Role of Magnetic Resonance Imaging in Prostate Cancer Screening: Does it Perform Better than the Prostate-specific Antigen Test?

Participants

Taekmin Kim, MD, Seoul, Korea, Republic Of (*Presenter*) Nothing to Disclose

#### PURPOSE

To compare the performance of biparametric prostate magnetic resonance imaging (bpMRI) and prostate-specific antigen (PSA) testing as screening tests in a large paired-cohort study.

#### METHODS AND MATERIALS

We retrospectively reviewed 1,793 men who underwent both bpMRI and PSA testing for prostate cancer screening from January 2018 to June 2021. If PSA level was  $\geq 3$  ng/mL, or prostate cancer was suspected based on bpMRI, urology consultation was requested. We compared the proportion of men with positive MRI (PI-RADS 3-5 or 4-5) or PSA tests ( $\geq 3$  ng/mL). The cancer detection rates, false positive rates, and positive predictive values (calculated from all screening-positive cases [PPV1] or biopsied cases [PPV2]) were compared between two screening tests.

#### RESULTS

The proportion of the positive PSA test (150/1793, 8.4%; 95% CI 7.1-9.8%) was significantly higher than that of positive MRI results (PI-RADS 3-5, 62/1793, 3.5%; 2.7-4.5% and PI-RADS 4-5, 41/1793, 2.3%; 1.7-3.2%,  $P < 0.001$ ). The cancer detection rates were similar between two tests (1.1% in PI-RADS 3-5, PI-RADS 4-5, and PSA). The false positive rate was significantly higher in PSA test (7.4%) than those of PI-RADS 3-5 and 4-5 (2.4% and 1.2%, respectively,  $P < 0.05$ ). The positive predictive values (PPVs) were significantly lower in PSA test (PPV1, 12.7%; PPV2, 36.5%) than that in PI-RADS 3-5 (PPV1 32.3%, PPV2 58.8%) or PI-RADS 4-5 (PPV1, 46.3%; PPV2, 87.5%,  $P < 0.001$  for all).

#### CONCLUSION

s MRI-based screening may reduce the number of patients recommended for biopsy without increasing the risk of underdiagnosis than PSA-base screening.

#### CLINICAL RELEVANCE/APPLICATION

PSA-based screening has been used for prostate cancer screening, but the evidence of the benefits and harms is still controversial. MRI-based screening showed lower proportions of screening-positive cases, lower false positive rates, and higher PPVs than those of PSA-based screening.

#### W2-SPGU-2 Differentiation Clear Cell Renal Cell Carcinoma from Other Common Malignant and Benign Renal Masses on Multiphasic MRI: A Likert Based Multireader Analysis

Participants

Ali Bassir, MD, Los Angeles, CA (*Presenter*) Nothing to Disclose

#### PURPOSE

To determine the diagnostic performance and the interreader agreement of the Kidney MR score (KMRS) in differentiating benign and malignant lesions and clear cell renal cell carcinoma (ccRCC) from other common lesions on multiphasic magnetic resonance imaging (MRI).

#### METHODS AND MATERIALS

With IRB approval and HIPAA compliance, the study cohort comprised 178 patients with 191 pathologically proven and 11 stable, fatty renal masses (142 malignant, 54 benign, and 6 uncertain malignant potential). After training on 5 non study cases, four abdominal radiologists and four abdominal radiology fellows independently interpreted the study cohort and assigned a KMRS to each lesion on a 5-point scale to indicate the probability of benignity, malignancy, and ccRCC, blinded to clinical data. The MRS included both quantitative and qualitative features and ancillary findings to adjust the final score.

#### RESULTS

In distinguishing malignant from benign lesions, a KMRS = 4 had a median sensitivity, specificity, and AUC of 87.5% (83.8-94.6%), 69.5% (64.8-77.8%), and 0.79 (0.77-0.89), respectively. The median sensitivity and specificity of the KMRS = 2 in diagnosing benignity were 33.4% (31.5-40.7%) and 95.6% (93.9-99.3%), respectively. A KMRS of 5 had a median sensitivity, specificity, and AUC of 72.3% (65.4-78.3%), 87.0% (84.9-91.6%) and 0.82 (0.77-0.88), respectively for diagnosing ccRCC. The interreader

agreement (kappa (?) score) was 0.59-0.82.

## CONCLUSION

s The KMRS had relatively high performance for diagnosing malignant from benign T1 lesions and ccRCC from all other T1 lesions with good to excellent interreader agreement.

## CLINICAL RELEVANCE/APPLICATION

With further validation and refinement, it may become useful in routine clinical practice especially if augmented by artificial intelligence techniques to confidently diagnose renal lesions, with judicious use of alternative imaging techniques and renal mass biopsy to accurately triage patients to no further intervention, active surveillance, ablation, radiation or surgery.

## W2-SPGU-3 Artifact severity due to total hip replacement in 1.5T and 3T MRI of the prostate

Participants

Matthias Boschheidgen, Dusseldorf, Germany (*Presenter*) Nothing to Disclose

## PURPOSE

To evaluate image quality and diagnostic value of multiparametric MRI (mpMRI) of the prostate in patients with total hip replacement (THR) at 1.5 and 3 Tesla.

## METHODS AND MATERIALS

In this retrospective multicenter cohort study patients with uni- or bilateral THR and 1.5T or 3T mpMRI were included. Seventy consecutive, standard-of-care examinations per field strength were evaluated regarding their diagnostic value. The overall diagnostic value and prostate imaging quality score (PI-Qual) were assessed. Artifact severity in the localizer and mpMRI sequences (T2w, DWI, DCE) was scored on a 3-point-scale. Correlation between diagnostic value and artifacts was analysed. Moreover, a subgroup analysis focussed on image quality at different 3T scanner generations.

## RESULTS

140 consecutive patients (mean age 72, median PSA value 8.3 ng/ml) were included. When comparing 1.5T to 3T examinations, no significant differences were observed regarding the artifact severity of DWI and the localizer and the overall diagnostic value of the images. There was a strong correlation between the diagnostic value, PI-Qual score, and artifact severity in the localizer and DWI ( $t > 0.85$ ). T2 und DCE sequences showed overall low artifacts. Significant improvement in image quality for 3T at the latest scanner generation was observed, especially for DWI ( $p < 0.03$ ).

## CONCLUSION

s MpMRI of patients with THR can be conducted at both field strengths without significant differences in artifacts. The localizer is useful as an early forecasting feature for diagnostic value and particularly might be useful for contrast medium application decision. Patients with THR benefited from latest scanner generation and new DWI sequences.

## CLINICAL RELEVANCE/APPLICATION

Patients with hip replacements showed similar artifact severity at 1,5T and 3T scanners for prostate MRI examinations. Technicians can predict the extent of artifacts in the localizer already allowing an adjustment of the MRI parameters to receive the highest quality level achievable and DCE sequences should not be omitted in any cases with expected artifacts. For 3T latest scanner generations and newest DWI sequences showed reduced artifacts related to total hip replacement.

Printed on: 02/07/23

## Abstract Archives of the RSNA, 2022

W2-SPGU-1

### The Role of Magnetic Resonance Imaging in Prostate Cancer Screening: Does it Perform Better than the Prostate-specific Antigen Test?

Wednesday, Nov. 30 9:00AM - 9:30AM Room: Learning Center - GU DPS

#### Participants

Taekmin Kim, MD, Seoul, Korea, Republic Of (*Presenter*) Nothing to Disclose

#### PURPOSE

To compare the performance of biparametric prostate magnetic resonance imaging (bpMRI) and prostate-specific antigen (PSA) testing as screening tests in a large paired-cohort study.

#### METHODS AND MATERIALS

We retrospectively reviewed 1,793 men who underwent both bpMRI and PSA testing for prostate cancer screening from January 2018 to June 2021. If PSA level was  $\geq 3$  ng/mL, or prostate cancer was suspected based on bpMRI, urology consultation was requested. We compared the proportion of men with positive MRI (PI-RADS 3-5 or 4-5) or PSA tests ( $\geq 3$  ng/mL). The cancer detection rates, false positive rates, and positive predictive values (calculated from all screening-positive cases [PPV1] or biopsied cases [PPV2]) were compared between two screening tests.

#### RESULTS

The proportion of the positive PSA test (150/1793, 8.4%; 95% CI 7.1-9.8%) was significantly higher than that of positive MRI results (PI-RADS 3-5, 62/1793, 3.5%; 2.7-4.5% and PI-RADS 4-5, 41/1793, 2.3%; 1.7-3.2%,  $P < 0.001$ ). The cancer detection rates were similar between two tests (1.1% in PI-RADS 3-5, PI-RADS 4-5, and PSA). The false positive rate was significantly higher in PSA test (7.4%) than those of PI-RADS 3-5 and 4-5 (2.4% and 1.2%, respectively,  $P < 0.05$ ). The positive predictive values (PPVs) were significantly lower in PSA test (PPV1, 12.7%; PPV2, 36.5%) than that in PI-RADS 3-5 (PPV1 32.3%, PPV2 58.8%) or PI-RADS 4-5 (PPV1, 46.3%; PPV2, 87.5%,  $P < 0.001$  for all).

#### CONCLUSION

s MRI-based screening may reduce the number of patients recommended for biopsy without increasing the risk of underdiagnosis than PSA-base screening.

#### CLINICAL RELEVANCE/APPLICATION

PSA-based screening has been used for prostate cancer screening, but the evidence of the benefits and harms is still controversial. MRI-based screening showed lower proportions of screening-positive cases, lower false positive rates, and higher PPVs than those of PSA-based screening.

Printed on: 02/07/23



## Abstract Archives of the RSNA, 2022

W2-SPGU-2

### Differentiation Clear Cell Renal Cell Carcinoma from Other Common Malignant and Benign Renal Masses on Multiphasic MRI: A Likert Based Multireader Analysis

Wednesday, Nov. 30 9:00AM - 9:30AM Room: Learning Center - GU DPS

#### Participants

Ali Bassir, MD, Los Angeles, CA (*Presenter*) Nothing to Disclose

#### PURPOSE

To determine the diagnostic performance and the interreader agreement of the Kidney MR score (KMRS) in differentiating benign and malignant lesions and clear cell renal cell carcinoma (ccRCC) from other common lesions on multiphasic magnetic resonance imaging (MRI).

#### METHODS AND MATERIALS

With IRB approval and HIPAA compliance, the study cohort comprised 178 patients with 191 pathologically proven and 11 stable, fatty renal masses (142 malignant, 54 benign, and 6 uncertain malignant potential). After training on 5 non study cases, four abdominal radiologists and four abdominal radiology fellows independently interpreted the study cohort and assigned a KMRS to each lesion on a 5-point scale to indicate the probability of benignity, malignancy, and ccRCC, blinded to clinical data. The MRS included both quantitative and qualitative features and ancillary findings to adjust the final score.

#### RESULTS

In distinguishing malignant from benign lesions, a KMRS = 4 had a median sensitivity, specificity, and AUC of 87.5% (83.8-94.6%), 69.5% (64.8-77.8%), and 0.79 (0.77-0.89), respectively. The median sensitivity and specificity of the KMRS = 2 in diagnosing benignity were 33.4% (31.5-40.7%) and 95.6% (93.9-99.3%), respectively. A KMRS of 5 had a median sensitivity, specificity, and AUC of 72.3% (65.4-78.3%), 87.0% (84.9-91.6%) and 0.82 (0.77-0.88), respectively for diagnosing ccRCC. The interreader agreement (kappa (?) score) was 0.59-0.82.

#### CONCLUSION

s The KMRS had relatively high performance for diagnosing malignant from benign T1 lesions and ccRCC from all other T1 lesions with good to excellent interreader agreement.

#### CLINICAL RELEVANCE/APPLICATION

With further validation and refinement, it may become useful in routine clinical practice especially if augmented by artificial intelligence techniques to confidently diagnose renal lesions, with judicious use of alternative imaging techniques and renal mass biopsy to accurately triage patients to no further intervention, active surveillance, ablation, radiation or surgery.

Printed on: 02/07/23

## Abstract Archives of the RSNA, 2022

W2-SPGU-3

### Artifact severity due to total hip replacement in 1.5T and 3T MRI of the prostate

Wednesday, Nov. 30 9:00AM - 9:30AM Room: Learning Center - GU DPS

#### Participants

Matthias Boschheidgen, Dusseldorf, Germany (*Presenter*) Nothing to Disclose

#### PURPOSE

To evaluate image quality and diagnostic value of multiparametric MRI (mpMRI) of the prostate in patients with total hip replacement (THR) at 1.5 and 3 Tesla.

#### METHODS AND MATERIALS

In this retrospective multicenter cohort study patients with uni- or bilateral THR and 1.5T or 3T mpMRI were included. Seventy consecutive, standard-of-care examinations per field strength were evaluated regarding their diagnostic value. The overall diagnostic value and prostate imaging quality score (PI-Qual) were assessed. Artifact severity in the localizer and mpMRI sequences (T2w, DWI, DCE) was scored on a 3-point-scale. Correlation between diagnostic value and artifacts was analysed. Moreover, a subgroup analysis focussed on image quality at different 3T scanner generations.

#### RESULTS

140 consecutive patients (mean age 72, median PSA value 8.3 ng/ml) were included. When comparing 1.5T to 3T examinations, no significant differences were observed regarding the artifact severity of DWI and the localizer and the overall diagnostic value of the images. There was a strong correlation between the diagnostic value, PI-Qual score, and artifact severity in the localizer and DWI ( $t > 0.85$ ). T2 und DCE sequences showed overall low artifacts. Significant improvement in image quality for 3T at the latest scanner generation was observed, especially for DWI ( $p < 0.03$ ).

#### CONCLUSION

s MpMRI of patients with THR can be conducted at both field strengths without significant differences in artifacts. The localizer is useful as an early forecasting feature for diagnostic value and particularly might be useful for contrast medium application decision. Patients with THR benefited from latest scanner generation and new DWI sequences.

#### CLINICAL RELEVANCE/APPLICATION

Patients with hip replacements showed similar artifact severity at 1,5T and 3T scanners for prostate MRI examinations. Technicians can predict the extent of artifacts in the localizer already allowing an adjustment of the MRI parameters to receive the highest quality level achievable and DCE sequences should not be omitted in any cases with expected artifacts. For 3T latest scanner generations and newest DWI sequences showed reduced artifacts related to total hip replacement.

Printed on: 02/07/23

## Abstract Archives of the RSNA, 2022

W2-SPHN

### Head and Neck Wednesday Poster Discussions

Wednesday, Nov. 30 9:00AM - 9:30AM Room: Learning Center - HN DPS

#### Sub-Events

#### W2-SPHN-2 Is Qualitative Ultrasound Elastography Useful for Predicting Tumor Resectability in Locally Advanced Head and Neck Cancer?

##### Participants

Paul B. DiDomenico, MD, (*Presenter*) Nothing to Disclose

##### PURPOSE

Assessment of tumor involvement of the carotid sheath is important for surgical planning in head and neck cancer. Invasion of the carotid artery is a contraindication to surgery while invasion of other components of the carotid sheath is not. We investigated whether ultrasound elastography of the tumor and peri-tumoral tissues provides useful information for staging and prediction of tumor resectability.

##### METHODS AND MATERIALS

We conducted an IRB-approved prospective study of 27 patients with head and neck cancers to determine if tumor resectability could be accurately predicted by qualitative Ultrasound elastography of the tumor and through visualization of a separating fat plane between the tumor and structures within carotid sheath, in particular the carotid artery. Patients' elastogram images were independently interpreted by two board-certified Radiologists. We evaluated the images using a risk-stratification scoring system that combined evaluation of the qualitative elastogram with measured distance between the tumor and carotid artery. Inter-observer agreement was evaluated using the weighted Kappa statistic. Imaging findings were compared to either surgical or clinical staging information using Receiver Operating Characteristic (ROC)-Area Under the Curve (AUC) analysis.

##### RESULTS

The weighted Kappa statistic for the combined qualitative and ordinal distance stratification scores was 0.49. The highest agreement of 0.68 was found for evaluation of the qualitative elastography images. Fifteen of 27 patients had neck dissection surgery which provided information on local tumor invasion, and the remaining 12 patients were staged through a combination of clinical and other imaging information such as neck CT. One of two readers attained a statistically significant AUC of 0.77 (95% CI 0.59-0.95,  $p=0.04$ ) for the elastogram only. The best-performing model combined the elastogram findings with the binary observation of a fat plane separating the tumor from the carotid artery (AUC of 0.84, 95% CI 0.69-0.99,  $p=0.006$ ), which was equal or superior to visualization of a fat plane alone for both readers.

##### CONCLUSION

We evaluated the utility of ultrasound elastography for determining carotid artery invasion in head and neck cancer. There was good agreement between two Radiologists with general ultrasound skills, and one attained a statistically significant result with ROC-AUC analysis indicating good accuracy. Ultrasound elastography may serve as a useful adjunct for tumor staging and pre-surgical planning in head and neck cancer.

##### CLINICAL RELEVANCE/APPLICATION

Qualitative Ultrasound elastography may be a useful for pre-surgical planning in head and neck cancer, as an adjunct to clinical and other imaging findings.

#### W2-SPHN-3 Assessment of Tumor Burden and Response by RECIST vs Volume Change in HPV+ Oropharyngeal Cancer: An Exploratory Analysis of Prospective Trials

##### Participants

Muzamil Arshad, MD, PhD, Romeoville, IL (*Presenter*) Nothing to Disclose

##### PURPOSE

Using HPV+ oropharyngeal carcinoma as a tumor model, we report a comparison of RECIST and volumetric measurements from 2 consecutive prospective trials of response-adaptive de-escalation of therapy.

##### METHODS AND MATERIALS

Patients enrolled on 2 prospective phase II response adapted de-escalation trials for HPV+ oropharynx cancer were included in the analysis. Target lesions were initially assessed using RECIST 1.1 at baseline and post-induction therapy; patients with > 50% response by RECIST received de-escalated treatment. Primary tumors and nodes were retrospectively delineated on diagnostic scans before and after induction therapy to ascertain volumetric tumor burden and response. Mean differences in RECIST and volume were evaluated with paired t-tests. Linear regression and chi-squared analysis were used to evaluate the correlation between percent change in tumor burden as well as de-escalation-concordance. Analysis was thus done to identify proportion that responded 50% by volume.

## **RESULTS**

104 patients were evaluable. The mean post-induction therapy reduction in RECIST and volumetry was 3.13 cm and 25.18 cm<sup>3</sup> respectively. Primary tumor response to induction was greater than nodal response for both RECIST and volumetry. The mean percent difference in size post induction was 27.3% and 14.8% for RECIST and volumetry. Percent change in RECIST was correlated with volume change,  $r = 0.687$  ( $p < 0.001$ ). An increased proportion ( $p = 0.008$ ) of patients would be eligible for de-escalation based on response assessment (72% de-escalated by RECIST vs 89% by volumetry), and 4% ( $N = 4$ ) of patients who were de-escalated by RECIST would not meet criteria for de-escalation by volumetry. 2 of these 4 patients developed a local failure.

## **CONCLUSION**

While volumetry was correlated with RECIST, a large proportion of variance in volume-based measurements was not accounted for by RECIST. Patients that responded by RECIST but not volume had higher rates of local failure. A higher proportion of patients met response criteria by volume and could have been considered for de-escalation.

## **CLINICAL RELEVANCE/APPLICATION**

A volume based approach was found to have less variance and greater sensitivity to identify responders as compared with traditional RECIST response measurements

Printed on: 02/07/23

## Abstract Archives of the RSNA, 2022

W2-SPHN-2

### Is Qualitative Ultrasound Elastography Useful for Predicting Tumor Resectability in Locally Advanced Head and Neck Cancer?

Wednesday, Nov. 30 9:00AM - 9:30AM Room: Learning Center - HN DPS

#### Participants

Paul B. DiDomenico, MD, (*Presenter*) Nothing to Disclose

#### PURPOSE

Assessment of tumor involvement of the carotid sheath is important for surgical planning in head and neck cancer. Invasion of the carotid artery is a contraindication to surgery while invasion of other components of the carotid sheath is not. We investigated whether ultrasound elastography of the tumor and peri-tumoral tissues provides useful information for staging and prediction of tumor resectability.

#### METHODS AND MATERIALS

We conducted an IRB-approved prospective study of 27 patients with head and neck cancers to determine if tumor resectability could be accurately predicted by qualitative Ultrasound elastography of the tumor and through visualization of a separating fat plane between the tumor and structures within carotid sheath, in particular the carotid artery. Patients' elastogram images were independently interpreted by two board-certified Radiologists. We evaluated the images using a risk-stratification scoring system that combined evaluation of the qualitative elastogram with measured distance between the tumor and carotid artery. Inter-observer agreement was evaluated using the weighted Kappa statistic. Imaging findings were compared to either surgical or clinical staging information using Receiver Operating Characteristic (ROC)-Area Under the Curve (AUC) analysis.

#### RESULTS

The weighted Kappa statistic for the combined qualitative and ordinal distance stratification scores was 0.49. The highest agreement of 0.68 was found for evaluation of the qualitative elastography images. Fifteen of 27 patients had neck dissection surgery which provided information on local tumor invasion, and the remaining 12 patients were staged through a combination of clinical and other imaging information such as neck CT. One of two readers attained a statistically significant AUC of 0.77 (95% CI 0.59-0.95,  $p=0.04$ ) for the elastogram only. The best-performing model combined the elastogram findings with the binary observation of a fat plane separating the tumor from the carotid artery (AUC of 0.84, 95% CI 0.69-0.99,  $p=0.006$ ), which was equal or superior to visualization of a fat plane alone for both readers.

#### CONCLUSION

s We evaluated the utility of ultrasound elastography for determining carotid artery invasion in head and neck cancer. There was good agreement between two Radiologists with general ultrasound skills, and one attained a statistically significant result with ROC-AUC analysis indicating good accuracy. Ultrasound elastography may serve as a useful adjunct for tumor staging and pre-surgical planning in head and neck cancer.

#### CLINICAL RELEVANCE/APPLICATION

Qualitative Ultrasound elastography may be a useful for pre-surgical planning in head and neck cancer, as an adjunct to clinical and other imaging findings.

Printed on: 02/07/23

## Abstract Archives of the RSNA, 2022

W2-SPHN-3

### Assessment of Tumor Burden and Response by RECIST vs Volume Change in HPV+ Oropharyngeal Cancer: An Exploratory Analysis of Prospective Trials

Wednesday, Nov. 30 9:00AM - 9:30AM Room: Learning Center - HN DPS

#### Participants

Muzamil Arshad, MD, PhD, Romeoville, IL (*Presenter*) Nothing to Disclose

#### PURPOSE

Using HPV+ oropharyngeal carcinoma as a tumor model, we report a comparison of RECIST and volumetric measurements from 2 consecutive prospective trials of response-adaptive de-escalation of therapy.

#### METHODS AND MATERIALS

Patients enrolled on 2 prospective phase II response adapted de-escalation trials for HPV+ oropharynx cancer were included in the analysis. Target lesions were initially assessed using RECIST 1.1 at baseline and post-induction therapy; patients with > 50% response by RECIST received de-escalated treatment. Primary tumors and nodes were retrospectively delineated on diagnostic scans before and after induction therapy to ascertain volumetric tumor burden and response. Mean differences in RECIST and volume were evaluated with paired t-tests. Linear regression and chi-squared analysis were used to evaluate the correlation between percent change in tumor burden as well as de-escalation-concordance. Analysis was thus done to identify proportion that responded 50% by volume.

#### RESULTS

104 patients were evaluable. The mean post-induction therapy reduction in RECIST and volumetry was 3.13 cm and 25.18 cm<sup>3</sup> respectively. Primary tumor response to induction was greater than nodal response for both RECIST and volumetry. The mean percent difference in size post induction was 27.3% and 14.8% for RECIST and volumetry. Percent change in RECIST was correlated with volume change,  $r = 0.687$  ( $p < 0.001$ ). An increased proportion ( $p = 0.008$ ) of patients would be eligible for de-escalation based on response assessment (72% de-escalated by RECIST vs 89% by volumetry), and 4% ( $N = 4$ ) of patients who were de-escalated by RECIST would not meet criteria for de-escalation by volumetry. 2 of these 4 patients developed a local failure.

#### CONCLUSION

While volumetry was correlated with RECIST, a large proportion of variance in volume-based measurements was not accounted for by RECIST. Patients that responded by RECIST but not volume had higher rates of local failure. A higher proportion of patients met response criteria by volume and could have been considered for de-escalation.

#### CLINICAL RELEVANCE/APPLICATION

A volume based approach was found to have less variance and greater sensitivity to identify responders as compared with traditional RECIST response measurements

Printed on: 02/07/23



## Abstract Archives of the RSNA, 2022

W2-SPIN

### Informatics Wednesday Poster Discussions

Wednesday, Nov. 30 9:00AM - 9:30AM Room: Learning Center - IN DPS

#### Sub-Events

#### W2-SPIN-2 Segmentation of Post-Treatment Glioblastoma Tissue Types and Resection Cavities

##### Participants

Saif Baig, MD, (*Presenter*) Nothing to Disclose

##### PURPOSE

Adjuvant radiation therapy is critical to the management of glioblastoma, yet contouring post-surgical residual tumor and resection cavities is a laborious and time-intensive manual process. Fully automated segmentation of glioma volumes could reduce inter-rater variability and increase workflow efficiency for both radiation planning and routine longitudinal radiographic assessment. We sought to evaluate whether a 3D neural network would be comparable to expert manual contouring of post-operative glioblastoma tissue types and resection cavities.

##### METHODS AND MATERIALS

A retrospective cohort of 251 MRIs of patients with glioblastoma (average 56.8 years, 56% female) from several publicly available datasets at The Cancer Imaging Archive (TCIA), were randomly selected into training (176) and testing (75) samples. All patients had undergone surgery with a median 237 days from surgery (range 0-1368) and most had undergone adjuvant chemoradiation. T1, T1-post contrast, T2 and FLAIR images were registered, skull stripped and interpolated to 1x1x1. Four post-treatment tissue classes, consisting of edema/infiltrative tissue (ED), enhancing tissue (ET), necrotic core (NCR) and resection cavities (RC) were manually segmented by an expert neuroradiologist. The nnU-Net, a state-of-the-art 3D U-Net convolutional neural network was trained to predict the multiclass predictions using the four modalities as multichannel input.

##### RESULTS

Segmentation performance in the test set for the ED, ET and RC classes were at the level of inter-rater expert human reliability, as measured by Dice scores, which ranged from 0.79 to 0.89; volume similarities that ranged from 0.90 to 0.95; and Hausdorff distance metrics, which ranged from 4 to 6 mm. There was a near perfect correlation between manually segmented total lesion volumes (Pearson  $r = 0.99$ ).

##### CONCLUSION

3D convolutional neural networks were able to segment and quantify post treatment glioma tissue volumes, consisting of edema/infiltrative tissue, enhancing tissue, necrotic core, and resection cavities, with high accuracy.

##### CLINICAL RELEVANCE/APPLICATION

The results of this study support the potential clinical value of artificial-intelligence-based automated volumetric quantification of post-treatment diffuse glioma tissue volumes.

#### W2-SPIN-3 Measuring FEV1 from Preoperative Chest Computed Tomography Scans using Deep Learning

##### Participants

Ji-eun Oh, PhD, Goyang-si, Korea, Republic Of (*Presenter*) Nothing to Disclose

##### PURPOSE

To evaluate the feasibility of generating deep learning-based FEV1 measurements from preoperative chest computed tomography (CT) scans.

##### METHODS AND MATERIALS

We collected 565 preoperative chest CT scans and FEV1 values performed on subjects undergoing lung cancer surgery between 2009 and 2015. FEV1 values were between 0.81 and 4.86 with mean 2.52 and standard deviation 0.63. All scans were resized to the median voxel size of our entire dataset (2.5x0.668x0.668 mm) and all axial slices were padded to 672x672 pixels with the lowest pixel intensity of each slice. Each scan was then windowed twice and saved separately, with the first scaled between 0 and 1000 Hounsfield units and the second between -1000 and -250 HU. All axial slices were then resized to 224x224 pixels. We generate predictions using a feature extractor and a recurrent neural network (RNN). The feature extractor is a ResNet50 model pretrained on ImageNet with global average pooling and outputs embeddings with length 2048. Each pair of windowed axial slices is used as input for the ResNet model and the outputted embeddings are concatenated to make arrays with length 4096. The embeddings for each study was padded with arrays of zeros with length 4096 to create uniform 220x4096 inputs for the regressor. The RNN architecture comprised of the following layers: two successive gated recurrent units layers with hyperbolic tangent activation and sigmoid recurrent activation with 32 and 16 units respectively, dropout with rate 0.25, three successive blocks of dense layers, ReLU activation, and dropout with rate 0.25, followed by an output layer with one unit. The dense layers had had 256, 64, 32 units each. The regressor was trained with an Adam optimizer using default hyperparameters and mean absolute error loss for 1000

epochs.

## RESULTS

The model generated FEV1 predictions with mean absolute error of 0.301 L, root mean squared error of 0.381 L, mean absolute percentage error of 13.298 %. The Pearson correlation coefficient between the predicted and observed values was 0.816 ( $p < 0.001$ ).

## CONCLUSION

A recurrent neural network trained on embeddings from two different Hounsfield unit windows can measure FEV1 values from preoperative chest CT scans.

## CLINICAL RELEVANCE/APPLICATION

Chest CT scans may be sufficient in determining pulmonary function without spirometry. This system can enable repeatable FEV1 measurements.

## W2-SPIN-4 In Vivo Measurement of Abdominal Muscle Mass on CT using a Machine Learning Tool.

Participants

Chantal Chahine, MD, Philadelphia, PA (*Presenter*) Nothing to Disclose

## PURPOSE

Muscle mass is a chief determinant of health and disease, playing a key role in bone health, as well as whole-body protein metabolism, which has been implicated in various illnesses. There continues to be an unmet need for a reference standard for assessing muscle mass. The purpose of this study was to determine the distribution of lean abdominal muscle mass of different muscle groups and establish an association between sex, age and lean muscle mass using a machine learning tool applied to computed tomography (CT) images.

## METHODS AND MATERIALS

This retrospective study was conducted using a medical biobank (MBB), a single-institutional IRB-approved research protocol that recruits adult participants during outpatient visits, including 34,150 patients for whom 186,721 CTs and years of detailed electronic health record, genomic, and laboratory data were collected. Using a convenience cohort of 313 patients with abdominal CTs, we deployed a deep residual U-Net (ResUNet) to segment 12 abdominal muscle groups and determine lean muscle volume from non-contrast CTs. Inferencing was performed using software (Python 3.9.5 and Tensorflow) equipped with an Nvidia GTX 970 GPU. Associations between sex, age and lean muscle mass were determined using linear regression in R (R Foundation, Vienna). Descriptive statistics were reported as mean $\pm$ std. Statistical significance was assessed using  $p < 0.05$ . Volumes of individual muscle groups were plotted to distribution curves.

## RESULTS

Abdominal muscle mass and distribution for each muscle group was obtained. We found abdominal muscle mass of the L Psoas: 146.1 $\pm$ 55.4 g, R Psoas: 142.0 $\pm$ 52.8 g, L Quad. Lumb.: 55.6 $\pm$ 21.8 g, R Quad. Lumb.: 52.4 $\pm$ 20.7 g, L. Erec. Spinae: 409.5 $\pm$ 125.8 g, R. Erec. Spinae: 407.9 $\pm$ 121.2 g, L. Glut. Med.: 51.7 $\pm$ 38.1 g, R. Glut. Med.: 51.3 $\pm$ 38.9 g, L. Rect. Abd.: 124.8 $\pm$ 51.3 g, R. Rect. Abd.: 123.7 $\pm$ 55.9 g, L. Lat. Abd.: 464.8 $\pm$ 182.7 g, R. Lat. Abd.: 468.8 $\pm$ 186.9 g. There was strong negative correlation between abdominal muscle mass and age ( $\beta = -1.12$ ,  $p < 0.001$ ) after adjusting by sex ( $\beta$  [male sex] = 73.1,  $p < 0.001$ ).

## CONCLUSION

We were able to generate normative data about masses of different muscle groups and demonstrate a statistically significant negative association between muscle mass and age. Unlike prior efforts, these results are based on direct in-vivo measurement of abdominal muscle mass. We will apply this technique to a larger cohort to generate normative data of muscle mass distribution and lifetime variation in MBB patients grouped by illness, adjusting for age and sex.

## CLINICAL RELEVANCE/APPLICATION

This work will allow researchers to better include muscle mass data as a measurable variable in future investigations, elucidating its clinical and public health implications.

## W2-SPIN-5 Automatic Lesion Changes Detection and Classification by Bipartite Graph Lesions Matching

Participants

Leo Joskowicz, PhD, Jerusalem, Israel (*Presenter*) Officer, HighRAD Ltd

## PURPOSE

To evaluate the performance of a novel method that automatically identifies and classifies lesion changes in longitudinal CT scans based on individual lesion segmentations.

## METHODS AND MATERIALS

We have developed a method for the automatic detection and classification of lesion changes in longitudinal CT studies. The method is based on the analysis of pairs of consecutive pairs (prior and current) scans. It inputs the lesion segmentations in each scan (performed manually or obtained automatically) and outputs the lesion matching and the lesion changes in the same region of the evaluated organ. The method performs automatic prior and current scan deformable registration and matches the corresponding lesions in the scans based on their spatial location and their relative proximity. The matching is performed with a model-based bipartite graph technique in which lesions are represented by graph nodes and lesion matchings are represented by edges between the corresponding nodes. Once the matching is computed, three types of lesion changes are identified: existing lesions (appear in both scans), new lesions (appear in the current scan only), and disappeared lesions (appear in the prior scan only). We evaluated our method on two datasets: lung metastases in chest CT and liver metastases in CECT longitudinal studies. The lungs metastases dataset consists of 30 pairs of scans from 14 patients with a total of 266 lesions (mean of 7.79 $\pm$ 6.34 lesions per scan). The liver metastases dataset consists of 199 pairs of scans from 49 patients with a total of 4,046 lesions (mean of 10.16 $\pm$ 8.64 lesions per scan). Lesion segmentations were obtained by manual delineation of an expert radiologist, as well as ground truth lesion matching and lesion changes classification. The quality of the lesions pairing and the lesion changes classification was evaluated by

comparing the ground truth and computed lesions bipartite graphs.

## RESULTS

The lungs metastases matching and classification is perfect: all lesion pairings and lesion changes are correct. The liver metastases matching Precision is  $0.96\pm 0.04$  and the Recall is  $0.97\pm 0.03$ . The lesion classification specificity is  $0.97\pm 0.07$ , the precision is  $0.95\pm 0.03$ , and the recall is  $0.96\pm 0.03$ . Most of the errors were due to a few liver lesion clusters (conglomerates) and slight liver deformable registration inaccuracies.

## CONCLUSION

s Automatic lesion pairings and lesion changes analysis achieves high performance on consecutive pairs of liver and lung metastases on retrospective clinical studies.

## CLINICAL RELEVANCE/APPLICATION

Computer-aided lesion matching and lesion changes analysis may improve quantitative follow-up and evaluation of disease status, assessment of treatment efficacy and response to therapy.

## W2-SPIN-6 Reproducibility Crisis in Medical Image Radiomic Studies: Contribution of Dynamic Histogram Binning

Participants

Timothy L. Kline, PhD, Rochester, MN (*Presenter*) Nothing to Disclose

## PURPOSE

In the field of computer vision, extraction of image texture features is a fundamental process facilitating the development of AI algorithms to perform a wide range of tasks - from object detection and segmentation to region-of-interest classification. The purpose of this abstract is to educate the radiology AI/ML community regarding a foundational component of the radiomic feature pipeline involving dynamic histogram binning (DHB) which likely has contributed to poor generalization of machine learning models.

## METHODS AND MATERIALS

Screening mammograms were queried from our institution's imaging archive ranging from January 2009 to December 2019. Lesions were annotated as bounding boxes highlighting areas that had been subsequently biopsied. Images and masks were resampled to the median pixel dimensions and normalized. Radiomic features were extracted from the preprocessed images in Python using either PyRadiomics (where DHB is performed in accordance with the IBSI standard), or a modified code where static histogram binning (SHB) is performed. To investigate feature robustness, the original bounding boxes were eroded or dilated until the percent change in area exceeded either 10% or 20% (to simulate inter-observer variability). Simulation experiments and investigation of the underlying mathematical formulation of the features were used to explain the hyper-sensitivity of DHB to even modest changes in ROI definition.

## RESULTS

Use of DHB (i.e. binning based on ROI voxel intensities) caused a subset of radiomic features to be hyper-sensitive to ROI definition compared with SHB (i.e. binning based on standardized whole image voxel intensities). Comparing feature values pre and post morphological operations highlights artifactual variation attributable to DHB that is remedied by SHB. This DHB- induced feature hyper-sensitivity was observed in real-world data, and explainable by both simulation and the mathematical formulations of the individual features.

## CONCLUSION

s Here we show that a foundational component of the feature extraction procedure is flawed, relatively unknown to users and may have unintended downstream consequences on model performance. The de facto standard of dynamic histogram binning leads to an elevated sensitivity to even minor changes in the annotated regions. This finding may widely impact the majority of radiomic studies published in recent years and may contribute to well-known issues regarding poor reproducibility of developed machine learning models utilizing radiomics data.

## CLINICAL RELEVANCE/APPLICATION

Whole image binning and/or study specific ranges for calibrated images (as recommended in IBSI standard) should become standard practice for models built on top of image texture/radiomics features.

Printed on: 02/07/23

## Abstract Archives of the RSNA, 2022

W2-SPIN-2

### Segmentation of Post-Treatment Glioblastoma Tissue Types and Resection Cavities

Wednesday, Nov. 30 9:00AM - 9:30AM Room: Learning Center - IN DPS

#### Participants

Saif Baig, MD, (*Presenter*) Nothing to Disclose

#### PURPOSE

Adjuvant radiation therapy is critical to the management of glioblastoma, yet contouring post-surgical residual tumor and resection cavities is a laborious and time-intensive manual process. Fully automated segmentation of glioma volumes could reduce inter-rater variability and increase workflow efficiency for both radiation planning and routine longitudinal radiographic assessment. We sought to evaluate whether a 3D neural network would be comparable to expert manual contouring of post-operative glioblastoma tissue types and resection cavities.

#### METHODS AND MATERIALS

A retrospective cohort of 251 MRIs of patients with glioblastoma (average 56.8 years, 56% female) from several publicly available datasets at The Cancer Imaging Archive (TCIA), were randomly selected into training (176) and testing (75) samples. All patients had undergone surgery with a median 237 days from surgery (range 0-1368) and most had undergone adjuvant chemoradiation. T1, T1-post contrast, T2 and FLAIR images were registered, skull stripped and interpolated to 1x1x1. Four post-treatment tissue classes, consisting of edema/infiltrative tissue (ED), enhancing tissue (ET), necrotic core (NCR) and resection cavities (RC) were manually segmented by an expert neuroradiologist. The nnU-Net, a state-of-the-art 3D U-Net convolutional neural network was trained to predict the multiclass predictions using the four modalities as multichannel input.

#### RESULTS

Segmentation performance in the test set for the ED, ET and RC classes were at the level of inter-rater expert human reliability, as measured by Dice scores, which ranged from 0.79 to 0.89; volume similarities that ranged from 0.90 to 0.95; and Hausdorff distance metrics, which ranged from 4 to 6 mm. There was a near perfect correlation between manually segmented total lesion volumes (Pearson  $r = 0.99$ ).

#### CONCLUSION

3D convolutional neural networks were able to segment and quantify post treatment glioma tissue volumes, consisting of edema/infiltrative tissue, enhancing tissue, necrotic core, and resection cavities, with high accuracy.

#### CLINICAL RELEVANCE/APPLICATION

The results of this study support the potential clinical value of artificial-intelligence-based automated volumetric quantification of post-treatment diffuse glioma tissue volumes.

Printed on: 02/07/23



## Abstract Archives of the RSNA, 2022

W2-SPIN-3

### Measuring FEV1 from Preoperative Chest Computed Tomography Scans using Deep Learning

Wednesday, Nov. 30 9:00AM - 9:30AM Room: Learning Center - IN DPS

#### Participants

Ji-eun Oh, PhD, Goyang-si, Korea, Republic Of (*Presenter*) Nothing to Disclose

#### PURPOSE

To evaluate the feasibility of generating deep learning-based FEV1 measurements from preoperative chest computed tomography (CT) scans.

#### METHODS AND MATERIALS

We collected 565 preoperative chest CT scans and FEV1 values performed on subjects undergoing lung cancer surgery between 2009 and 2015. FEV1 values were between 0.81 and 4.86 with mean 2.52 and standard deviation 0.63. All scans were resized to the median voxel size of our entire dataset (2.5x0.668x0.668 mm) and all axial slices were padded to 672x672 pixels with the lowest pixel intensity of each slice. Each scan was then windowed twice and saved separately, with the first scaled between 0 and 1000 Hounsfield units and the second between -1000 and -250 HU. All axial slices were then resized to 224x224 pixels. We generate predictions using a feature extractor and a recurrent neural network (RNN). The feature extractor is a ResNet50 model pretrained on ImageNet with global average pooling and outputs embeddings with length 2048. Each pair of windowed axial slices is used as input for the ResNet model and the outputted embeddings are concatenated to make arrays with length 4096. The embeddings for each study was padded with arrays of zeros with length 4096 to create uniform 220x4096 inputs for the regressor. The RNN architecture comprised of the following layers: two successive gated recurrent units layers with hyperbolic tangent activation and sigmoid recurrent activation with 32 and 16 units respectively, dropout with rate 0.25, three successive blocks of dense layers, ReLU activation, and dropout with rate 0.25, followed by an output layer with one unit. The dense layers had had 256, 64, 32 units each. The regressor was trained with an Adam optimizer using default hyperparameters and mean absolute error loss for 1000 epochs.

#### RESULTS

The model generated FEV1 predictions with mean absolute error of 0.301 L, root mean squared error of 0.381 L, mean absolute percentage error of 13.298 %. The Pearson correlation coefficient between the predicted and observed values was 0.816 ( $p < 0.001$ ).

#### CONCLUSION

A recurrent neural network trained on embeddings from two different Hounsfield unit windows can measure FEV1 values from preoperative chest CT scans.

#### CLINICAL RELEVANCE/APPLICATION

Chest CT scans may be sufficient in determining pulmonary function without spirometry. This system can enable repeatable FEV1 measurements.

Printed on: 02/07/23

## Abstract Archives of the RSNA, 2022

W2-SPIN-4

### In Vivo Measurement of Abdominal Muscle Mass on CT using a Machine Learning Tool.

Wednesday, Nov. 30 9:00AM - 9:30AM Room: Learning Center - IN DPS

#### Participants

Chantal Chahine, MD, Philadelphia, PA (*Presenter*) Nothing to Disclose

#### PURPOSE

Muscle mass is a chief determinant of health and disease, playing a key role in bone health, as well as whole-body protein metabolism, which has been implicated in various illnesses. There continues to be an unmet need for a reference standard for assessing muscle mass. The purpose of this study was to determine the distribution of lean abdominal muscle mass of different muscle groups and establish an association between sex, age and lean muscle mass using a machine learning tool applied to computed tomography (CT) images.

#### METHODS AND MATERIALS

This retrospective study was conducted using a medical biobank (MBB), a single-institutional IRB-approved research protocol that recruits adult participants during outpatient visits, including 34,150 patients for whom 186,721 CTs and years of detailed electronic health record, genomic, and laboratory data were collected. Using a convenience cohort of 313 patients with abdominal CTs, we deployed a deep residual U-Net (ResUNet) to segment 12 abdominal muscle groups and determine lean muscle volume from non-contrast CTs. Inferencing was performed using software (Python 3.9.5 and Tensorflow) equipped with an Nvidia GTX 970 GPU. Associations between sex, age and lean muscle mass were determined using linear regression in R (R Foundation, Vienna). Descriptive statistics were reported as mean±std. Statistical significance was assessed using  $p < 0.05$ . Volumes of individual muscle groups were plotted to distribution curves.

#### RESULTS

Abdominal muscle mass and distribution for each muscle group was obtained. We found abdominal muscle mass of the L Psoas: 146.1±55.4 g, R Psoas: 142.0±52.8 g, L Quad. Lumb.: 55.6±21.8 g, R Quad. Lumb.: 52.4±20.7 g, L. Erec. Spinae: 409.5±125.8 g, R. Erec. Spinae: 407.9±121.2 g, L. Glut. Med.: 51.7±38.1 g, R. Glut. Med.: 51.3±38.9 g, L. Rect. Abd.: 124.8±51.3 g, R. Rect. Abd.: 123.7±55.9 g, L. Lat. Abd.: 464.8±182.7 g, R. Lat. Abd.: 468.8±186.9 g. There was strong negative correlation between abdominal muscle mass and age ( $\beta = -1.12$ ,  $p < 0.001$ ) after adjusting by sex ( $\beta$  [male sex] = 73.1,  $p < 0.001$ ).

#### CONCLUSION

s We were able to generate normative data about masses of different muscle groups and demonstrate a statistically significant negative association between muscle mass and age. Unlike prior efforts, these results are based on direct in-vivo measurement of abdominal muscle mass. We will apply this technique to a larger cohort to generate normative data of muscle mass distribution and lifetime variation in MBB patients grouped by illness, adjusting for age and sex.

#### CLINICAL RELEVANCE/APPLICATION

This work will allow researchers to better include muscle mass data as a measurable variable in future investigations, elucidating its clinical and public health implications.

Printed on: 02/07/23

## Abstract Archives of the RSNA, 2022

W2-SPIN-5

### Automatic Lesion Changes Detection and Classification by Bipartite Graph Lesions Matching

Wednesday, Nov. 30 9:00AM - 9:30AM Room: Learning Center - IN DPS

#### Participants

Leo Joskowicz, PhD, Jerusalem, Israel (*Presenter*) Officer, HighRAD Ltd

#### PURPOSE

To evaluate the performance of a novel method that automatically identifies and classifies lesion changes in longitudinal CT scans based on individual lesion segmentations.

#### METHODS AND MATERIALS

We have developed a method for the automatic detection and classification of lesion changes in longitudinal CT studies. The method is based on the analysis of pairs of consecutive pairs (prior and current) scans. It inputs the lesion segmentations in each scan (performed manually or obtained automatically) and outputs the lesion matching and the lesion changes in the same region of the evaluated organ. The method performs automatic prior and current scan deformable registration and matches the corresponding lesions in the scans based on their spatial location and their relative proximity. The matching is performed with a model-based bipartite graph technique in which lesions are represented by graph nodes and lesion matchings are represented by edges between the corresponding nodes. Once the matching is computed, three types of lesion changes are identified: existing lesions (appear in both scans), new lesions (appear in the current scan only), and disappeared lesions (appear in the prior scan only). We evaluated our method on two datasets: lung metastases in chest CT and liver metastases in CECT longitudinal studies. The lungs metastases dataset consists of 30 pairs of scans from 14 patients with a total of 266 lesions (mean of  $7.79 \pm 6.34$  lesions per scan). The liver metastases dataset consists of 199 pairs of scans from 49 patients with a total of 4,046 lesions (mean of  $10.16 \pm 8.64$  lesions per scan). Lesion segmentations were obtained by manual delineation of an expert radiologist, as well as ground truth lesion matching and lesion changes classification. The quality of the lesions pairing and the lesion changes classification was evaluated by comparing the ground truth and computed lesions bipartite graphs.

#### RESULTS

The lungs metastases matching and classification is perfect: all lesion pairings and lesion changes are correct. The liver metastases matching Precision is  $0.96 \pm 0.04$  and the Recall is  $0.97 \pm 0.03$ . The lesion classification specificity is  $0.97 \pm 0.07$ , the precision is  $0.95 \pm 0.03$ , and the recall is  $0.96 \pm 0.03$ . Most of the errors were due to a few liver lesion clusters (conglomerates) and slight liver deformable registration inaccuracies.

#### CONCLUSION

s Automatic lesion pairings and lesion changes analysis achieves high performance on consecutive pairs of liver and lung metastases on retrospective clinical studies.

#### CLINICAL RELEVANCE/APPLICATION

Computer-aided lesion matching and lesion changes analysis may improve quantitative follow-up and evaluation of disease status, assessment of treatment efficacy and response to therapy.

Printed on: 02/07/23

## Abstract Archives of the RSNA, 2022

W2-SPIN-6

### Reproducibility Crisis in Medical Image Radiomic Studies: Contribution of Dynamic Histogram Binning

Wednesday, Nov. 30 9:00AM - 9:30AM Room: Learning Center - IN DPS

#### Participants

Timothy L. Kline, PhD, Rochester, MN (*Presenter*) Nothing to Disclose

#### PURPOSE

In the field of computer vision, extraction of image texture features is a fundamental process facilitating the development of AI algorithms to perform a wide range of tasks - from object detection and segmentation to region-of-interest classification. The purpose of this abstract is to educate the radiology AI/ML community regarding a foundational component of the radiomic feature pipeline involving dynamic histogram binning (DHB) which likely has contributed to poor generalization of machine learning models.

#### METHODS AND MATERIALS

Screening mammograms were queried from our institution's imaging archive ranging from January 2009 to December 2019. Lesions were annotated as bounding boxes highlighting areas that had been subsequently biopsied. Images and masks were resampled to the median pixel dimensions and normalized. Radiomic features were extracted from the preprocessed images in Python using either PyRadiomics (where DHB is performed in accordance with the IBSI standard), or a modified code where static histogram binning (SHB) is performed. To investigate feature robustness, the original bounding boxes were eroded or dilated until the percent change in area exceeded either 10% or 20% (to simulate inter-observer variability). Simulation experiments and investigation of the underlying mathematical formulation of the features were used to explain the hyper-sensitivity of DHB to even modest changes in ROI definition.

#### RESULTS

Use of DHB (i.e. binning based on ROI voxel intensities) caused a subset of radiomic features to be hyper-sensitive to ROI definition compared with SHB (i.e. binning based on standardized whole image voxel intensities). Comparing feature values pre and post morphological operations highlights artifactual variation attributable to DHB that is remedied by SHB. This DHB-induced feature hyper-sensitivity was observed in real-world data, and explainable by both simulation and the mathematical formulations of the individual features.

#### CONCLUSION

Here we show that a foundational component of the feature extraction procedure is flawed, relatively unknown to users and may have unintended downstream consequences on model performance. The de facto standard of dynamic histogram binning leads to an elevated sensitivity to even minor changes in the annotated regions. This finding may widely impact the majority of radiomic studies published in recent years and may contribute to well-known issues regarding poor reproducibility of developed machine learning models utilizing radiomics data.

#### CLINICAL RELEVANCE/APPLICATION

Whole image binning and/or study specific ranges for calibrated images (as recommended in IBSI standard) should become standard practice for models built on top of image texture/radiomics features.

Printed on: 02/07/23

## Abstract Archives of the RSNA, 2022

W2-SPIR

### Interventional Wednesday Poster Discussions

Wednesday, Nov. 30 9:00AM - 9:30AM Room: Learning Center - IR DPS

#### Sub-Events

#### W2-SPIR-1 Radiogenomic Biomarkers for Microvascular Invasion predict the Clinical Outcome in Patients with Hepatocellular Carcinoma after Locoregional Therapies

Participants

Robin Schmidt, (*Presenter*) Nothing to Disclose

#### PURPOSE

Microvascular invasion (MVI) in hepatocellular carcinoma (HCC) represents an independent risk factor for early recurrence and poor survival outcome. MVI can only be determined invasively after operative treatments by histopathology. However, its clinical utility for minimally invasive locoregional therapies (LRT) as guideline-approved standard of care for many unresectable HCC patients remains limited. Radiogenomic venous invasion (RVI) and two-trait predictor of MVI (TTPVI) are two imaging biomarkers derived from linking imaging features to HCC-specific gene profile analyses to predict the presence of MVI. This study aims to compare their predictive value for the outcome of patients with HCC receiving LRT.

#### METHODS AND MATERIALS

This study included 95 HCC patients, who received either CT-guided brachytherapy alone (n=48) or combined with transarterial chemoembolization (TACE, n=47) between 01/2016-12/2017. Patients were stratified according to RVI and TTPVI being assessed on baseline contrast-enhanced MRI using decision-tree-models: Presence of internal vessels in arterial (TTPVI) or portalvenous phase (RVI), followed by absence of an hypointense halo (TTPVI/RVI) and a sharp tumor-liver-transition in portalvenous phase (RVI). Primary endpoints were overall survival (OS), progression-free survival (PFS), time to progression (TTP). Statistics included Fisher's exact test and Kaplan-Meier analysis.

#### RESULTS

Median OS (26.7 vs 23.7 months), median PFS (9.3 vs 7.3 months) and median TTP (9.8 vs 9.3 months) did not significantly differ between patients receiving brachytherapy and TACE/brachytherapy, respectively (Figure 1). While TTPVI was frequently observed in TACE/brachytherapy treated patients (60.9% vs 40.4%, p=0.063) than after brachytherapy alone, the presence of RVI occurred equally in both groups (32.6% vs 29.8%, p=0.825). As for brachytherapy, TTPVI achieved significant separation of OS (p<0.001) and PFS (p=0.029) but not TTP (p=0.142), while RVI was predictive of TTP (p=0.032), PFS (p=0.004) but not OS (p=0.078). Both biomarkers revealed poorer outcome after brachytherapy for positively scored patients at baseline. On the contrary, they did not achieve significant separation for any endpoint in patients following TACE/brachytherapy (Figure 2).

#### CONCLUSION

The findings underscore the potential of TTPVI/RVI to predict early recurrence and poor survival in HCC patients receiving brachytherapy. Those patients could potentially benefit from a prior TACE.

#### CLINICAL RELEVANCE/APPLICATION

RVI/TTPVI represent non-invasive prognostic biomarkers, that could be implemented into treatment allocation and monitoring strategies for unresectable HCC.

#### W2-SPIR-2 Ultrasound-guided Radiofrequency Ablation Treatment in Early Stage Breast Cancer: Efficacy of Ablation with Vacuum Assisted Biopsy and Magnetic Resonance

Participants

Jaime Jimenez, MD, Barcelona, Spain (*Presenter*) Nothing to Disclose

#### PURPOSE

To clinically validate the efficacy and safety of the cool-tip ablation method in breast tumors smaller than 2 cm.

#### METHODS AND MATERIALS

Eleven patients aged more than 70 years-old with luminal infiltrating ductal carcinoma of the breast were treated with ultrasonography (US)-guided percutaneous RFA between 2020-2022. Tumors measured less than 2 cm and were located more than 1 cm from the chest wall and skin. Effectiveness of the treatment was assessed with breast MRI and vacuum assisted biopsy (BAB) one month after RFA. Tumor viability was assessed with Nicotinamide adenine dinucleotide (NADH)-diaphorase.

#### RESULTS

MRI evaluation demonstrated round ablation area without tumor enhancement in all cases. Ten cases showed no evidence of viable tumor after BAB. One tumor with inconclusive pathological changes after BAB was surgically removed, nevertheless final analysis

showed no residual viable tumor. No recurrences have occurred after MRI follow-up for less than 6 months (5 cases), 6 months (1 case) and one year (3 cases). Breast cosmesis is excellent in all patients.

## CONCLUSION

s Preliminary results show that, in early stage tumors smaller than 2cm, cool-tip RFA ablation achieves complete tumor ablation with so far no signs of tumor recurrence in the patients included.

## CLINICAL RELEVANCE/APPLICATION

Preliminary studies on treatment of breast tumors with radiofrequency ablation (RFA) followed by surgical resection have demonstrated its feasibility, effectiveness, and safety in tumors smaller than 2 cm, with percentage of complete tumor ablation between 76-100%.

## W2-SPIR-4 Evaluation of Chemotherapy-free Interval Overall Survival and Progression-free Survival of Patients Undergoing Ablation of Pulmonary Sarcoma Metastases

Participants

Jose Maluf, MD, MD, Sao Paulo, Brazil (*Presenter*) Nothing to Disclose

## PURPOSE

To assess the chemotherapy-free interval, overall survival and progression-free survival of patients undergoing ablation of pulmonary sarcoma metastasis.

## METHODS AND MATERIALS

Retrospective study, carried out from the analysis of data from electronic medical record. Patients submitted to radiofrequency ablation of sarcoma pulmonary metastasis between 2013 and 2020 were included. Were excluded patients: with other primary tumors than sarcoma; with extrapulmonary metastases; who discontinued chemotherapy after ablation of lung metastases; as well as those who lost follow-up to the institution after ablative treatment. The data obtained were entered into Excel and later exported to the IBM SPSS version 20.0 program for statistical analysis. The Kaplan Meier curve was used to estimate the mean and median of overall survival and disease-free survival. It was considered a significance level of 5%.

## RESULTS

A total of 30 patients were included, with the majority (56.7%) being under 50 years old at the first ablation. The absolute majority (93.3%) of the tumors had high histological grade. Synovial sarcoma and fibrosarcoma were the most frequent histological subtypes (prevalences of 23.3% and 13.3%). Most patients (63.3%) had undergone previous chemotherapy treatment, while only 30% underwent previous surgical resection of lung metastases. Almost all underwent single lung ablations, with only 20% undergoing more than one metastasis ablation session. The median of treated nodules was 2 nodules per patient and only 6 patients died by the end of the study. The mean chemotherapy-free interval after lung metastases ablation treatment in the study population was 23.2 months, with a mean overall survival time of 69.3 months (95% confidence interval: 51.1 - 87.6 months) and median progression-free survival of 13 months (95% confidence interval: 9.2 to 16.8 months).

## CONCLUSION

s The results of this study show a significant chemotherapy-free interval in patients undergoing ablation of pulmonary sarcoma metastases, with relevant results for overall survival and progression-free survival.

## CLINICAL RELEVANCE/APPLICATION

Strategies that can promote a chemotherapy-free interval for patients with metastatic sarcomas are increasingly valued, aiming to reduce side effects and increase quality of life during cancer follow-up. The ablation of pulmonary metastases, used in other scenarios as curative therapy, emerged as a possible candidate for palliative measures, aiming to stop the natural course of the disease and promote a period without from chemotherapy to the patient.

## W2-SPIR-5 Percutaneous Cryoablation vs Microwave Ablation of Renal Cell Carcinoma: A Comparative Study of Effectiveness and Safety

Participants

Lilit Aslanyan, DO, MS, Atlanta, GA (*Presenter*) Nothing to Disclose

## PURPOSE

To evaluate differences in efficacy and safety between percutaneous cryoablation (CRA) and microwave ablation (MWA) of renal cell carcinoma (RCC).

## METHODS AND MATERIALS

From 2013-2017, consecutive RCC patients treated with CRA and MWA were retrospectively included. Baseline characteristics (age, gender, race, BMI, tumor size, RENAL-nephrometry score) were evaluated. Peri- and post-procedural variables (number of probes utilized, total CT dose, procedural time, incidence of hematoma and creatinine adverse-event (AE) grade =1, critical structure involvement, post-op hospitalization, Clavien-Dindo Class =1, complete response) were also evaluated. Overall-survival from initial treatment was calculated using Kaplan-Meier estimation and compared using log-rank analysis. Differences in variables were assessed with chi-square and student's t-test using JMP statistical software.

## RESULTS

176 patients were evaluated (130 CRA; 46 MWA). Overall mean age and gender was 68 years and 56% male. No significant differences in baseline characteristics (age, gender, race, BMI, tumor size, RENAL-nephrometry score) were noted. Compared to MWA, CRA was associated with more probes ( $2.1 \pm 1.2$  vs  $1.4 \pm 0.2$  probes;  $p < 0.0001$ ) and longer procedural time ( $94 \pm 3.4$  vs  $79 \pm 6.3$  min;  $p = 0.03$ ), but did not exhibit a significant difference in other peri- or post-procedural variables (total CT dose ( $2.9 \pm 0.2$  vs  $2.6 \pm 0.3$  Gy\*cm;  $p = 0.4$ ), hematoma incidence (30% vs 22%;  $p = 0.4$ ), Grade =1 creatinine AE (5% vs 12%,  $p = 0.3$ ), critical structure involvement (30% vs 22%;  $p = 0.4$ ), post-op hospitalization (24% vs 14%;  $p = 0.2$ ), Clavien-Dindo Class =1 (25% vs 14%;  $p = 0.2$ ), complete response (93% vs 90%;  $p = 0.4$ ), and overall-survival (4.1 vs 4.7 yrs;  $p = 0.8$ )).

## CONCLUSION

s For patients with RCC, CRA and MWA offer similar effectiveness and safety profiles despite CRA being associated with more ablation probes and procedural time.

## CLINICAL RELEVANCE/APPLICATION

For patients with renal cell carcinoma, percutaneous microwave and cryoablation offer similar effectiveness and safety profiles despite cryoablation being associated with more ablation probes and procedural time.

## W2-SPIR-6 Customized MR-guided Transurethral Ultrasound Ablation (TULSA) for Treatment of Localized Prostate Cancer and Concurrent Benign Prostate Hyperplasia: A Single Centre Retrospective Analysis of One Hundred Patients

Participants

Leonhard Steinmeister, MD, (*Presenter*) Nothing to Disclose

## PURPOSE

MR-guided transurethral ultrasound ablation (TULSA) has primarily been investigated for whole-gland prostate ablation, but is also well-suited for partial gland treatment. The purpose was to perform a clinical service evaluation of partial to whole-gland TULSA for patients with localized prostate cancer (CaP). TULSA was also evaluated as a combined therapy for a subset of patients presenting with both cancer and concurrent benign prostate hyperplasia (BPH).

## METHODS AND MATERIALS

This retrospective, consecutive clinical service evaluation included men with histopathologically-confirmed CaP who underwent TULSA either as primary or salvage treatment. The planned ablation was dependent on the individual tumor characteristics, concurrent BPH and patient preferences. The Clavien-Dindo classification was used to record complications. Surgeon-assessed functional outcomes were reported. Early treatment success was defined by negative multiparametric MRI (mpMRI) and lack of prostate specific antigen (PSA) recurrence.

## RESULTS

One hundred consecutive patients (95 treatment-naïve and 5 salvage) were included, with median follow-up of 14 months and a max of 36 months. Baseline median (IQR) age and PSA were 65 years (51-90) and 8.1 ng/ml (2.3-21), respectively. Three Grade IIIa adverse events were observed, with no bowel-related complications. For urinary continence outcomes, 1 patient worsened to 1 pad per day. All patients who were previously potent maintained erectile potency. Of the patient subgroup also seeking treatment for BPH, 85% reported symptom improvement. Median (IQR) PSA nadir after primary treatment was 1.3 ng/ml (0.4-2.5). Early treatment success when including all repeat treatments was 92%.

## CONCLUSION

s Customized prostate ablation with TULSA offers flexible ablation according to patients' disease characteristics and treatment expectations, providing favorable safety and promising early MRI and PSA results. TULSA is a feasible combination therapy for patients with both cancer and concurrent BPH. Local recurrence after initial treatment failure can be successfully retreated with TULSA.

## CLINICAL RELEVANCE/APPLICATION

Customized prostate ablation with MR-guided transurethral ultrasound ablation (TULSA) is a feasible combination therapy for patients with localized prostate cancer and concurrent benign prostate hyperplasia (BPH).

## W2-SPIR-7 Quantitative Image-Guided Intervention for Hepatocellular Carcinoma: DECT for In Vivo Application of Thermochemical Ablation

Participants

Emily Thompson, PhD, (*Presenter*) Nothing to Disclose

## PURPOSE

Thermochemical ablation (TCA) is a minimally invasive therapy under development for hepatocellular carcinoma. TCA delivers acid (AcOH) and base (NaOH) into tumors simultaneously, which react to completion in a mixing catheter at the time of injection, producing acetate salt, water, and releasing heat ( $>50^{\circ}\text{C}$ ) to induce lethal osmotic and thermal stress. However, these reagents are not distinguishable from tissues on computed tomography (CT), which makes imaging the delivery of TCA difficult. We address this issue by incorporating radiopaque cesium hydroxide (CsOH) as a novel theranostic reagent in TCA that is detectable with CT.

## METHODS AND MATERIALS

VX2 tumor fragments (0.3mL) were inoculated into New Zealand white rabbits' right and left flanks (n=16 rabbits). When tumor diameter reached 1-2cm, TCA was delivered as one of three treatment groups: untreated control, 5M TCA, or 10M TCA. The TCA base reagent was doped with 250mM CsOH. Catheters were placed under ultrasound guidance, and TCA was delivered. Dual-energy CT (DECT) was acquired pre- and post-TCA (Definition Edge, Siemens Healthineers). Material-specific images (Cs) were post-processed (Siemens Syngo Via) based on previous phantom calibrations to determine Cs concentration. Line profiles were drawn through the ablation center (ImageJ, NIH). 24-hours after TCA, subjects were euthanized, and the resulting damage was evaluated with histopathology.

## RESULTS

Cs was detected on CT following delivery of TCA in all tumors (n=21). Line profiles indicated the highest concentrations at the injection site and decreased concentrations at the tumor margins. Beyond the ablation zone, no Cs was detected. A dose-dependent trend in tissue necrosis was demonstrated between the 10M TCA treatment group and 5M TCA treatment group (p=0.0005) and untreated controls (p=0.0089).

## CONCLUSION

s CsOH is a viable theranostic reagent for the interventional application of TCA. With the inclusion of CsOH, DECT can provide

image guidance for the delivery, localization, and quantification of ablation agent.

#### **CLINICAL RELEVANCE/APPLICATION**

Quantitative assessment of CsOH distribution enables the use of DECT as a viable technique to track injectable image-guided ablations, such as TCA, and ensure therapeutic delivery.

#### **W2-SPIR-8 Assessing the Impact of Perfusion on Microwave Ablation Measurements in an Ex Vivo Bovine Kidney Model**

Participants

Annie Dang, BS, MS, San Antonio, TX (*Presenter*) Nothing to Disclose

#### **PURPOSE**

The use of microwave ablation (MWA) for treating early-stage renal cell cancer is on the rise. Currently, manufacturers provide guidance on anticipated treatment margins based on data from nonperfused organs. Organ perfusion has been shown to impact ablation size and understanding this impact is critical to maximize treatment outcomes. We aim to assess the impact of perfusion on MWA volumes using a perfused ex vivo bovine kidney model.

#### **METHODS AND MATERIALS**

Nine bovine kidneys were harvested and kept on ice following transplant protocol. An ex vivo perfusion system consisting of membrane oxygenator, warmer, and blood pressure monitor was used to perfuse the organ using defibrinated bovine blood. Perfusion was initiated within 8 hours of procurement. A MWA system (AngioDynamics Solero) was used to perform 72 ablations (36 perfused, 36 nonperfused) at 9 different power and time device settings (60 W, 100 W, and 140 W for 2, 4, and 6 minutes). Perfused and nonperfused ablations for each kidney were performed at the same device setting to limit variability between kidneys. Each ablation was sectioned along the trajectory of the probe for long axis diameter (LAD) and short axis diameter (SAD) measurements of the zone of coagulation. Two-tailed t-tests were used to compare perfused and non-perfused conditions and linear regression was used to determine the association between ablation volume and device setting.

#### **RESULTS**

Collapsed across time settings, there were the following differences in coagulation zone volume by power: 60 W) perfused  $2.3 \pm 1.0$  mL versus nonperfused  $7.2 \pm 2.7$  mL, p-value  $< 0.001$ ; 100 W) perfused  $5.4 \pm 2.1$  mL versus nonperfused  $11.5 \pm 5.6$  mL, p-value  $< 0.01$ ; and 140 W) perfused  $11.2 \pm 3.7$  mL versus nonperfused  $18.7 \pm 6.3$  mL,  $p < 0.01$ . For all ablation conditions, LAD, SAD, and volume were smaller in perfused groups compared to nonperfused groups. There was a statistically significant difference in ablation volume for 6 of the 9 device settings ( $p < 0.05$ ). Ablation volume positively correlated with applied power for both perfused and non-perfused ablations, with the following association: perfused,  $0.021 \text{ cm}^3/\text{W}$ ,  $R = 0.462$ ,  $p = 0.004$ ; nonperfused,  $0.029 \text{ cm}^3/\text{W}$ ,  $R = 0.565$ ,  $p < 0.001$ . No observed association was identified for applied time and ablation volume ( $R = 0.001$ ,  $p = 0.32$ ).

#### **CONCLUSION**

Observed ablation volumes were restricted to the size of the renal lobule, limiting translation of measurements to the clinical setting. This study demonstrates kidneys are highly vascular structures susceptible to the effects of perfusion mediated tissue cooling during MWA.

#### **CLINICAL RELEVANCE/APPLICATION**

These findings support clinical anticipation of significantly smaller renal MWA volumes compared to manufacturer data from nonperfused organs.

#### **W2-SPIR-9 Future Liver Remnant Hypertrophy Following Y-90 Radioembolization Lobectomy with Resin Microspheres**

Participants

Muhammad Malik, MD, Boston, MA (*Presenter*) Nothing to Disclose

#### **PURPOSE**

To evaluate the hypertrophy and kinetic growth rate of the future liver remnant (FLR) following Y-90 radioembolization lobectomy with resin microspheres in primary liver cancer.

#### **METHODS AND MATERIALS**

A HIPAA compliant, IRB-approved, retrospective review of patients treated with radioembolization lobectomy (RL) using resin microspheres for primary liver cancer from March 2016 to October 2021. Imaging studies were reviewed at three different time points; pre Y90-TARE (T0),  $< 4$  months post Y90-TARE (T1) and  $> 4$  months post Y90-TARE (T2). Exclusion criteria included prior portal vein embolization, Y-90 treatment to contralateral lobe  $< 6$ -months apart, and tumor in both hepatic lobes. Total liver volume (TLV), treated area volume (TAV), untreated area volume (UAV), and future liver remnant (FLR) at T0, T1 and T2 were manually calculated by a radiology fellow on TeraRecon software. Percentage of hypertrophy of treated lobe was calculated at T1 and T2, and kinetic growth rate (KGR) was calculated by the degree of hypertrophy at T1 over the number of weeks elapsed from the treatment date. Procedure characteristics and patient demographics were recorded. Statistical analysis was performed with paired t-test.

#### **RESULTS**

A total of 20 patients (Age:  $69 \pm 10$  years, 40% females) with primary liver cancer (40% cholangiocarcinoma, 60% hepatocellular carcinoma) underwent Y-90 radioembolization lobectomy (Table 1). Average Tumor size was  $9 \text{ cm} \pm 4$  (2-16). 6/15 (40%) tumors were multifocal and 5/15 (33%) were unifocal. The FLR at T0, T1 and T2 was 853 cc (IQR: 597-1291), 1117 cc (IQR: 631-1526) and 1424 cc (IQR: 594-1768), respectively. At T1, the average KGR/week was 2.3% and hypertrophy of 21.4% ( $p < 0.001$ ) and at T2 average KGR/week of 1.3%, with hypertrophy of 30% compared to T0 ( $P < 0.001$ ). Complete response was found in 13/20 (65%) and partial response in 5/20 (25%) patients. 2/20 (10%) patients progressed in their liver disease. Only 4 (20%) of patients underwent surgical resection.

#### **CONCLUSION**

s There is significant difference in hypertrophy of the future liver remnant volume following Y-90 radiation lobectomy with resin microspheres. A 65% of patients had complete treatment response, and only 20% of patients undergoing surgical resection.

**CLINICAL RELEVANCE/APPLICATION**

Future liver remnant hypertrophy following Y-90 radiation lobectomy is a potential indicator for future liver resection.

Printed on: 02/07/23

## Abstract Archives of the RSNA, 2022

W2-SPIR-1

### Radiogenomic Biomarkers for Microvascular Invasion predict the Clinical Outcome in Patients with Hepatocellular Carcinoma after Locoregional Therapies

Wednesday, Nov. 30 9:00AM - 9:30AM Room: Learning Center - IR DPS

#### Participants

Robin Schmidt, (*Presenter*) Nothing to Disclose

#### PURPOSE

Microvascular invasion (MVI) in hepatocellular carcinoma (HCC) represents an independent risk factor for early recurrence and poor survival outcome. MVI can only be determined invasively after operative treatments by histopathology. However, its clinical utility for minimally invasive locoregional therapies (LRT) as guideline-approved standard of care for many unresectable HCC patients remains limited. Radiogenomic venous invasion (RVI) and two-trait predictor of MVI (TTPVI) are two imaging biomarkers derived from linking imaging features to HCC-specific gene profile analyses to predict the presence of MVI. This study aims to compare their predictive value for the outcome of patients with HCC receiving LRT.

#### METHODS AND MATERIALS

This study included 95 HCC patients, who received either CT-guided brachytherapy alone (n=48) or combined with transarterial chemoembolization (TACE, n=47) between 01/2016-12/2017. Patients were stratified according to RVI and TTPVI being assessed on baseline contrast-enhanced MRI using decision-tree-models: Presence of internal vessels in arterial (TTPVI) or portalvenous phase (RVI), followed by absence of an hypointense halo (TTPVI/RVI) and a sharp tumor-liver-transition in portalvenous phase (RVI). Primary endpoints were overall survival (OS), progression-free survival (PFS), time to progression (TTP). Statistics included Fisher's exact test and Kaplan-Meier analysis.

#### RESULTS

Median OS (26.7 vs 23.7 months), median PFS (9.3 vs 7.3 months) and median TTP (9.8 vs 9.3 months) did not significantly differ between patients receiving brachytherapy and TACE/brachytherapy, respectively (Figure 1). While TTPVI was frequently observed in TACE/brachytherapy treated patients (60.9% vs 40.4%, p=0.063) than after brachytherapy alone, the presence of RVI occurred equally in both groups (32.6% vs 29.8%, p=0.825). As for brachytherapy, TTPVI achieved significant separation of OS (p<0.001) and PFS (p=0.029) but not TTP (p=0.142), while RVI was predictive of TTP (p=0.032), PFS (p=0.004) but not OS (p=0.078). Both biomarkers revealed poorer outcome after brachytherapy for positively scored patients at baseline. On the contrary, they did not achieve significant separation for any endpoint in patients following TACE/brachytherapy (Figure 2).

#### CONCLUSION

The findings underscore the potential of TTPVI/RVI to predict early recurrence and poor survival in HCC patients receiving brachytherapy. Those patients could potentially benefit from a prior TACE.

#### CLINICAL RELEVANCE/APPLICATION

RVI/TTPVI represent non-invasive prognostic biomarkers, that could be implemented into treatment allocation and monitoring strategies for unresectable HCC.

Printed on: 02/07/23



## Abstract Archives of the RSNA, 2022

W2-SPIR-2

### Ultrasound-guided Radiofrequency Ablation Treatment in Early Stage Breast Cancer: Efficacy of Ablation with Vacuum Assisted Biopsy and Magnetic Resonance

Wednesday, Nov. 30 9:00AM - 9:30AM Room: Learning Center - IR DPS

#### Participants

Jaime Jimenez, MD, Barcelona, Spain (*Presenter*) Nothing to Disclose

#### PURPOSE

To clinically validate the efficacy and safety of the cool-tip ablation method in breast tumors smaller than 2 cm.

#### METHODS AND MATERIALS

Eleven patients aged more than 70 years-old with luminal infiltrating ductal carcinoma of the breast were treated with ultrasonography (US)-guided percutaneous RFA between 2020-2022. Tumors measured less than 2 cm and were located more than 1 cm from the chest wall and skin. Effectiveness of the treatment was assessed with breast MRI and vacuum assisted biopsy (BAB) one month after RFA. Tumor viability was assessed with Nicotinamide adenine dinucleotide (NADH)-diaphorase.

#### RESULTS

MRI evaluation demonstrated round ablation area without tumor enhancement in all cases. Ten cases showed no evidence of viable tumor after BAB. One tumor with inconclusive pathological changes after BAB was surgically removed, nevertheless final analysis showed no residual viable tumor. No recurrences have occurred after MRI follow-up for less than 6 months (5 cases), 6 months (1 case) and one year (3 cases). Breast cosmesis is excellent in all patients.

#### CONCLUSION

s Preliminary results show that, in early stage tumors smaller than 2cm, cool-tip RFA ablation achieves complete tumor ablation with so far no signs of tumor recurrence in the patients included.

#### CLINICAL RELEVANCE/APPLICATION

Preliminary studies on treatment of breast tumors with radiofrequency ablation (RFA) followed by surgical resection have demonstrated its feasibility, effectiveness, and safety in tumors smaller than 2 cm, with percentage of complete tumor ablation between 76-100%.

Printed on: 02/07/23

## Abstract Archives of the RSNA, 2022

W2-SPIR-4

### Evaluation of Chemotherapy-free Interval Overall Survival and Progression-free Survival of Patients Undergoing Ablation of Pulmonary Sarcoma Metastases

Wednesday, Nov. 30 9:00AM - 9:30AM Room: Learning Center - IR DPS

#### Participants

Jose Maluf, MD, MD, Sao Paulo, Brazil (*Presenter*) Nothing to Disclose

#### PURPOSE

To assess the chemotherapy-free interval, overall survival and progression-free survival of patients undergoing ablation of pulmonary sarcoma metastasis.

#### METHODS AND MATERIALS

Retrospective study, carried out from the analysis of data from electronic medical record. Patients submitted to radiofrequency ablation of sarcoma pulmonary metastasis between 2013 and 2020 were included. Were excluded patients: with other primary tumors than sarcoma; with extrapulmonary metastases; who discontinued chemotherapy after ablation of lung metastases; as well as those who lost follow-up to the institution after ablative treatment. The data obtained were entered into Excel and later exported to the IBM SPSS version 20.0 program for statistical analysis. The Kaplan Meier curve was used to estimate the mean and median of overall survival and disease-free survival. It was considered a significance level of 5%.

#### RESULTS

A total of 30 patients were included, with the majority (56.7%) being under 50 years old at the first ablation. The absolute majority (93.3%) of the tumors had high histological grade. Synovial sarcoma and fibrosarcoma were the most frequent histological subtypes (prevalences of 23.3% and 13.3%). Most patients (63.3%) had undergone previous chemotherapy treatment, while only 30% underwent previous surgical resection of lung metastases. Almost all underwent single lung ablations, with only 20% undergoing more than one metastasis ablation session. The median of treated nodules was 2 nodules per patient and only 6 patients died by the end of the study. The mean chemotherapy-free interval after lung metastases ablation treatment in the study population was 23.2 months, with a mean overall survival time of 69.3 months (95% confidence interval: 51.1 - 87.6 months) and median progression-free survival of 13 months (95% confidence interval: 9.2 to 16.8 months).

#### CONCLUSION

The results of this study show a significant chemotherapy-free interval in patients undergoing ablation of pulmonary sarcoma metastases, with relevant results for overall survival and progression-free survival.

#### CLINICAL RELEVANCE/APPLICATION

Strategies that can promote a chemotherapy-free interval for patients with metastatic sarcomas are increasingly valued, aiming to reduce side effects and increase quality of life during cancer follow-up. The ablation of pulmonary metastases, used in other scenarios as curative therapy, emerged as a possible candidate for palliative measures, aiming to stop the natural course of the disease and promote a period without from chemotherapy to the patient.

Printed on: 02/07/23

## Abstract Archives of the RSNA, 2022

W2-SPIR-5

### **Percutaneous Cryoablation vs Microwave Ablation of Renal Cell Carcinoma: A Comparative Study of Effectiveness and Safety**

Wednesday, Nov. 30 9:00AM - 9:30AM Room: Learning Center - IR DPS

#### **Participants**

Lilit Aslanyan, DO, MS, Atlanta, GA (*Presenter*) Nothing to Disclose

#### **PURPOSE**

To evaluate differences in efficacy and safety between percutaneous cryoablation (CRA) and microwave ablation (MWA) of renal cell carcinoma (RCC).

#### **METHODS AND MATERIALS**

From 2013-2017, consecutive RCC patients treated with CRA and MWA were retrospectively included. Baseline characteristics (age, gender, race, BMI, tumor size, RENAL-nephrometry score) were evaluated. Peri- and post-procedural variables (number of probes utilized, total CT dose, procedural time, incidence of hematoma and creatinine adverse-event (AE) grade =1, critical structure involvement, post-op hospitalization, Clavien-Dindo Class =1, complete response) were also evaluated. Overall-survival from initial treatment was calculated using Kaplan-Meier estimation and compared using log-rank analysis. Differences in variables were assessed with chi-square and student's t-test using JMP statistical software.

#### **RESULTS**

176 patients were evaluated (130 CRA; 46 MWA). Overall mean age and gender was 68 years and 56% male. No significant differences in baseline characteristics (age, gender, race, BMI, tumor size, RENAL-nephrometry score) were noted. Compared to MWA, CRA was associated with more probes ( $2.1 \pm 1.2$  vs  $1.4 \pm 0.2$  probes;  $p < 0.0001$ ) and longer procedural time ( $94 \pm 3.4$  vs  $79 \pm 6.3$  min;  $p = 0.03$ ), but did not exhibit a significant difference in other peri- or post-procedural variables (total CT dose ( $2.9 \pm 0.2$  vs  $2.6 \pm 0.3$  Gy\*cm;  $p = 0.4$ ), hematoma incidence (30% vs 22%;  $p = 0.4$ ), Grade =1 creatinine AE (5% vs 12%,  $p = 0.3$ ), critical structure involvement (30% vs 22%;  $p = 0.4$ ), post-op hospitalization (24% vs 14%;  $p = 0.2$ ), Clavien-Dindo Class =1 (25% vs 14%;  $p = 0.2$ ), complete response (93% vs 90%;  $p = 0.4$ ), and overall-survival (4.1 vs 4.7 yrs;  $p = 0.8$ ))

#### **CONCLUSION**

s For patients with RCC, CRA and MWA offer similar effectiveness and safety profiles despite CRA being associated with more ablation probes and procedural time.

#### **CLINICAL RELEVANCE/APPLICATION**

For patients with renal cell carcinoma, percutaneous microwave and cryoablation offer similar effectiveness and safety profiles despite cryoablation being associated with more ablation probes and procedural time.

Printed on: 02/07/23

## Abstract Archives of the RSNA, 2022

W2-SPIR-6

### Customized MR-guided Transurethral Ultrasound Ablation (TULSA) for Treatment of Localized Prostate Cancer and Concurrent Benign Prostate Hyperplasia: A Single Centre Retrospective Analysis of One Hundred Patients

Wednesday, Nov. 30 9:00AM - 9:30AM Room: Learning Center - IR DPS

#### Participants

Leonhard Steinmeister, MD, (*Presenter*) Nothing to Disclose

#### PURPOSE

MR-guided transurethral ultrasound ablation (TULSA) has primarily been investigated for whole-gland prostate ablation, but is also well-suited for partial gland treatment. The purpose was to perform a clinical service evaluation of partial to whole-gland TULSA for patients with localized prostate cancer (CaP). TULSA was also evaluated as a combined therapy for a subset of patients presenting with both cancer and concurrent benign prostate hyperplasia (BPH).

#### METHODS AND MATERIALS

This retrospective, consecutive clinical service evaluation included men with histopathologically-confirmed CaP who underwent TULSA either as primary or salvage treatment. The planned ablation was dependent on the individual tumor characteristics, concurrent BPH and patient preferences. The Clavien-Dindo classification was used to record complications. Surgeon-assessed functional outcomes were reported. Early treatment success was defined by negative multiparametric MRI (mpMRI) and lack of prostate specific antigen (PSA) recurrence.

#### RESULTS

One hundred consecutive patients (95 treatment-naïve and 5 salvage) were included, with median follow-up of 14 months and a max of 36 months. Baseline median (IQR) age and PSA were 65 years (51-90) and 8.1 ng/ml (2.3-21), respectively. Three Grade IIIa adverse events were observed, with no bowel-related complications. For urinary continence outcomes, 1 patient worsened to 1 pad per day. All patients who were previously potent maintained erectile potency. Of the patient subgroup also seeking treatment for BPH, 85% reported symptom improvement. Median (IQR) PSA nadir after primary treatment was 1.3 ng/ml (0.4-2.5). Early treatment success when including all repeat treatments was 92%.

#### CONCLUSION

Customized prostate ablation with TULSA offers flexible ablation according to patients' disease characteristics and treatment expectations, providing favorable safety and promising early MRI and PSA results. TULSA is a feasible combination therapy for patients with both cancer and concurrent BPH. Local recurrence after initial treatment failure can be successfully retreated with TULSA.

#### CLINICAL RELEVANCE/APPLICATION

Customized prostate ablation with MR-guided transurethral ultrasound ablation (TULSA) is a feasible combination therapy for patients with localized prostate cancer and concurrent benign prostate hyperplasia (BPH).

Printed on: 02/07/23

## Abstract Archives of the RSNA, 2022

W2-SPIR-7

### Quantitative Image-Guided Intervention for Hepatocellular Carcinoma: DECT for In Vivo Application of Thermochemical Ablation

Wednesday, Nov. 30 9:00AM - 9:30AM Room: Learning Center - IR DPS

#### Participants

Emily Thompson, PhD, (*Presenter*) Nothing to Disclose

#### PURPOSE

Thermochemical ablation (TCA) is a minimally invasive therapy under development for hepatocellular carcinoma. TCA delivers acid (AcOH) and base (NaOH) into tumors simultaneously, which react to completion in a mixing catheter at the time of injection, producing acetate salt, water, and releasing heat ( $>50^{\circ}\text{C}$ ) to induce lethal osmotic and thermal stress. However, these reagents are not distinguishable from tissues on computed tomography (CT), which makes imaging the delivery of TCA difficult. We address this issue by incorporating radiopaque cesium hydroxide (CsOH) as a novel theranostic reagent in TCA that is detectable with CT.

#### METHODS AND MATERIALS

VX2 tumor fragments (0.3mL) were inoculated into New Zealand white rabbits' right and left flanks (n=16 rabbits). When tumor diameter reached 1-2cm, TCA was delivered as one of three treatment groups: untreated control, 5M TCA, or 10M TCA. The TCA base reagent was doped with 250mM CsOH. Catheters were placed under ultrasound guidance, and TCA was delivered. Dual-energy CT (DECT) was acquired pre-and post-TCA (Definition Edge, Siemens Healthineers). Material-specific images (Cs) were post-processed (Siemens Syngo Via) based on previous phantom calibrations to determine Cs concentration. Line profiles were drawn through the ablation center (ImageJ, NIH). 24-hours after TCA, subjects were euthanized, and the resulting damage was evaluated with histopathology.

#### RESULTS

Cs was detected on CT following delivery of TCA in all tumors (n=21). Line profiles indicated the highest concentrations at the injection site and decreased concentrations at the tumor margins. Beyond the ablation zone, no Cs was detected. A dose-dependent trend in tissue necrosis was demonstrated between the 10M TCA treatment group and 5M TCA treatment group ( $p=0.0005$ ) and untreated controls ( $p=0.0089$ ).

#### CONCLUSION

CsOH is a viable theranostic reagent for the interventional application of TCA. With the inclusion of CsOH, DECT can provide image guidance for the delivery, localization, and quantification of ablation agent.

#### CLINICAL RELEVANCE/APPLICATION

Quantitative assessment of CsOH distribution enables the use of DECT as a viable technique to track injectable image-guided ablations, such as TCA, and ensure therapeutic delivery.

Printed on: 02/07/23

## Abstract Archives of the RSNA, 2022

W2-SPIR-8

### Assessing the Impact of Perfusion on Microwave Ablation Measurements in an Ex Vivo Bovine Kidney Model

Wednesday, Nov. 30 9:00AM - 9:30AM Room: Learning Center - IR DPS

#### Participants

Annie Dang, BS, MS, San Antonio, TX (*Presenter*) Nothing to Disclose

#### PURPOSE

The use of microwave ablation (MWA) for treating early-stage renal cell cancer is on the rise. Currently, manufacturers provide guidance on anticipated treatment margins based on data from nonperfused organs. Organ perfusion has been shown to impact ablation size and understanding this impact is critical to maximize treatment outcomes. We aim to assess the impact of perfusion on MWA volumes using a perfused ex vivo bovine kidney model.

#### METHODS AND MATERIALS

Nine bovine kidneys were harvested and kept on ice following transplant protocol. An ex vivo perfusion system consisting of membrane oxygenator, warmer, and blood pressure monitor was used to perfuse the organ using defibrinated bovine blood. Perfusion was initiated within 8 hours of procurement. A MWA system (AngioDynamics Solero) was used to perform 72 ablations (36 perfused, 36 nonperfused) at 9 different power and time device settings (60 W, 100 W, and 140 W for 2, 4, and 6 minutes). Perfused and nonperfused ablations for each kidney were performed at the same device setting to limit variability between kidneys. Each ablation was sectioned along the trajectory of the probe for long axis diameter (LAD) and short axis diameter (SAD) measurements of the zone of coagulation. Two-tailed t-tests were used to compare perfused and non-perfused conditions and linear regression was used to determine the association between ablation volume and device setting.

#### RESULTS

Collapsed across time settings, there were the following differences in coagulation zone volume by power: 60 W) perfused  $2.3 \pm 1.0$  mL versus nonperfused  $7.2 \pm 2.7$  mL,  $p$ -value  $< 0.001$ ; 100 W) perfused  $5.4 \pm 2.1$  mL versus nonperfused  $11.5 \pm 5.6$  mL,  $p$ -value  $< 0.01$ ; and 140 W) perfused  $11.2 \pm 3.7$  mL versus nonperfused  $18.7 \pm 6.3$  mL,  $p < 0.01$ . For all ablation conditions, LAD, SAD, and volume were smaller in perfused groups compared to nonperfused groups. There was a statistically significant difference in ablation volume for 6 of the 9 device settings ( $p < 0.05$ ). Ablation volume positively correlated with applied power for both perfused and non-perfused ablations, with the following association: perfused,  $0.021 \text{ cm}^3/\text{W}$ ,  $R = 0.462$ ,  $p = 0.004$ ; nonperfused,  $0.029 \text{ cm}^3/\text{W}$ ,  $R = 0.565$ ,  $p < 0.001$ . No observed association was identified for applied time and ablation volume ( $R = 0.001$ ,  $p = 0.32$ ).

#### CONCLUSION

Observed ablation volumes were restricted to the size of the renal lobule, limiting translation of measurements to the clinical setting. This study demonstrates kidneys are highly vascular structures susceptible to the effects of perfusion mediated tissue cooling during MWA.

#### CLINICAL RELEVANCE/APPLICATION

These findings support clinical anticipation of significantly smaller renal MWA volumes compared to manufacturer data from nonperfused organs.

Printed on: 02/07/23

## Abstract Archives of the RSNA, 2022

W2-SPIR-9

### Future Liver Remnant Hypertrophy Following Y-90 Radioembolization Lobectomy with Resin Microspheres

Wednesday, Nov. 30 9:00AM - 9:30AM Room: Learning Center - IR DPS

#### Participants

Muhammad Malik, MD, Boston, MA (*Presenter*) Nothing to Disclose

#### PURPOSE

To evaluate the hypertrophy and kinetic growth rate of the future liver remnant (FLR) following Y-90 radioembolization lobectomy with resin microspheres in primary liver cancer.

#### METHODS AND MATERIALS

A HIPAA compliant, IRB-approved, retrospective review of patients treated with radioembolization lobectomy (RL) using resin microspheres for primary liver cancer from March 2016 to October 2021. Imaging studies were reviewed at three different time points; pre Y90-TARE (T0), < 4 months post Y90-TARE (T1) and > 4 months post Y90-TARE (T2). Exclusion criteria included prior portal vein embolization, Y-90 treatment to contralateral lobe <6-months apart, and tumor in both hepatic lobes. Total liver volume (TLV), treated area volume (TAV), untreated area volume (UAV), and future liver remnant (FLR) at T0, T1 and T2 were manually calculated by a radiology fellow on TeraRecon software. Percentage of hypertrophy of treated lobe was calculated at T1 and T2, and kinetic growth rate (KGR) was calculated by the degree of hypertrophy at T1 over the number of weeks elapsed from the treatment date. Procedure characteristics and patient demographics were recorded. Statistical analysis was performed with paired t-test.

#### RESULTS

A total of 20 patients (Age: 69+/-10 years, 40% females) with primary liver cancer (40% cholangiocarcinoma, 60% hepatocellular carcinoma) underwent Y-90 radioembolization lobectomy (Table 1). Average Tumor size was 9 cm ± 4 (2-16). 6/15 (40%) tumors were multifocal and 5/15 (33%) were unifocal. The FLR at T0, T1 and T2 was 853 cc (IQR: 597-1291), 1117 cc (IQR: 631-1526) and 1424 cc (IQR: 594-1768), respectively. At T1, the average KGR/week was 2.3% and hypertrophy of 21.4% (p<0.001) and at T2 average KGR/week of 1.3%, with hypertrophy of 30% compared to T0 (P<0.001). Complete response was found in 13/20 (65%) and partial response in 5/20 (25%) patients. 2/20 (10%) patients progressed in their liver disease. Only 4 (20%) of patients underwent surgical resection.

#### CONCLUSION

There is significant difference in hypertrophy of the future liver remnant volume following Y-90 radiation lobectomy with resin microspheres. A 65% of patients had complete treatment response, and only 20% of patients undergoing surgical resection.

#### CLINICAL RELEVANCE/APPLICATION

Future liver remnant hypertrophy following Y-90 radiation lobectomy is a potential indicator for future liver resection.

Printed on: 02/07/23

## Abstract Archives of the RSNA, 2022

W2-SPMK

### Musculoskeletal Wednesday Poster Discussions

Wednesday, Nov. 30 9:00AM - 9:30AM Room: Learning Center - MK DPS

#### Participants

Sarah Kamel, MD, Philadelphia, PA (*Moderator*) Nothing to Disclose  
Sarah Kamel, MD, Philadelphia, PA (*Moderator*) Nothing to Disclose  
Vishal Desai, MD, Philadelphia, PA (*Moderator*) Nothing to Disclose  
Vishal Desai, MD, Philadelphia, PA (*Moderator*) Nothing to Disclose

#### Sub-Events

### W2-SPMK-1 Transient Osteoporosis of the Hip: A Fleeting Diagnosis?

#### Participants

Aishwarya Gulati, MD, Philadelphia, PA (*Presenter*) Nothing to Disclose

#### PURPOSE

Transient osteoporosis of the hip (TOH) is a rare, self-limiting clinical diagnosis with unclear etiology. We hypothesize that TOH represents an underlying subchondral insufficiency fracture, and in nearly all cases a discrete fracture is visible on MRI.

#### METHODS AND MATERIALS

Retrospective PACS query identified patients with intense bone marrow edema (BME) in the femoral head on a hip MRI including small field of view (FOV) sequences, meeting imaging criteria for TOH. Those with avascular necrosis, marrow replacing processes, or history of antecedent trauma were excluded. Demographics and pre-MRI patient questionnaires were reviewed. Three musculoskeletal radiologists independently reviewed each case for presence of a definite subchondral fracture line on small FOV images. Extent of BME, reciprocal BME in the acetabulum, and size of joint effusion were also recorded.

#### RESULTS

50 patients meeting inclusion criteria were identified (29 females). Mean age was 62±12 years (range 35-84). Average symptom duration before MRI was 102±135 days. 10 patients had DEXA performed within 2 years of MRI, 6 demonstrating osteopenia/osteoporosis. Subchondral fractures were unanimously identified by readers in 44/50 (88%) cases. Interclass correlations coefficient with absolute agreement was 0.73 with 95% CI (0.57-0.84), indicating near-excellent agreement. Most cases demonstrated large joint effusion (24/50, 48%) and acetabular edema (32/50, 64%). Binomial logistic regression assessing impact of age, gender, pain duration, extent of BME and joint effusion identified increasing size of joint effusion as a statistically significant predictor of subchondral fracture ( $p=0.05$ ), with 6.9 higher odds of fracture. There was a strong correlation between osteopenia/osteoporosis on DEXA and presence of subchondral fracture ( $p<.001$ ).

#### CONCLUSION

A subchondral fracture line was identified on small FOV imaging in most cases identified as TOH. Findings such as a joint effusion and osteopenia/osteoporosis have a higher association with subchondral fractures.

#### CLINICAL RELEVANCE/APPLICATION

The diagnosis of TOH remains pervasive throughout medical literature and radiology reports. We argue that this term is misleading, as the underlying pathology likely reflects underlying subchondral insufficiency fracture. Accurate reporting of this finding is essential for ensuring appropriate conservative treatment.

### W2-SPMK-2 The Effect of Pre-Operative MRI Coracoid Dimensions on Latarjet Surgical Outcomes

#### Participants

Sarah Kamel, MD, Philadelphia, PA (*Presenter*) Nothing to Disclose

#### PURPOSE

To determine if pre-operative coracoid dimensions correspond with post-operative outcomes in patients treated for recurrent anterior shoulder dislocation by Latarjet coracoid transfer.

#### METHODS AND MATERIALS

Patients who underwent primary Latarjet surgery between 2009-2019 were identified. Included patients had pre-operative shoulder MRI and minimum of 2-year post-operative follow-up. Coracoid length was measured on axial MRI sequences as the distance from the coracoclavicular (CC) ligament insertion to the distal tip. Width measurements were obtained perpendicular to length at three locations (base, midpoint, tip) and averaged. Comparisons were made between shorter vs. longer coracoid length and width. Outcomes were recurrent instability, re-operation, complications, rate of and time until return-to-sport (RTS), and American Shoulder and Elbow Surgeons (ASES) score.

## RESULTS

56 patients were included, 16% female and with a mean age of 28.4 years. Patients with a shorter coracoid length (<22 mm, n=30) had similar rate of recurrent instability (shorter length 6.7% vs. longer length 3.8%; p=0.640), complication (10.0% vs. 15.4%; p=0.543), re-operation (3.3% vs. 7.7%; p=0.592), rate of RTS (76.5% vs. 58.8%; p=0.298), and post-operative ASES scores (85.0 vs. 81.6; p=0.612), relative to patients with a longer coracoid length (>22 mm, n=26). Likewise, patients with a narrower coracoid width (<10 mm, n=29) had similar prevalence of recurrent instability (narrower width 6.9% vs. wider width 3.7%; p=0.596), complication (17.2% vs. 7.4%; p=0.266), re-operation (3.5% vs. 7.4%; p=0.605), rate of RTS (66.7% vs. 68.4%; p=1.000), and post-operative ASES scores (87.1 vs. 80.0; p=0.286), relative to patients with a wider coracoid length (>10 mm, n=27).

## CONCLUSION

s Patients undergoing Latarjet coracoid transfer had similar rates of recurrent instability and post-operative outcomes regardless of pre-operative coracoid dimensions.

## CLINICAL RELEVANCE/APPLICATION

This MRI protocol for measuring coracoid dimensions closely accounts for the specific landmarks utilized during the Latarjet osteotomy by focusing on identification of the CC ligament insertion.

## W2-SPMK-3 Combined Femoral and Acetabular Version is Sex Related in Symptomatic Patients with Hip Dysplasia and Acetabular Retroversion

Participants

Till Lerch, MD, PhD, Bern, Switzerland (*Presenter*) Nothing to Disclose

## PURPOSE

Frequency of abnormal femoral and acetabular version(AV) and combined version is unclear in patients with developmental dysplasia of the hip(DDH). This study aimed to investigate mean femoral version(FV), the prevalence of increased FV and femoral retroversion, and combined version (combination of FV and AV) in patients with DDH and acetabular retroversion.

## METHODS AND MATERIALS

A retrospective IRB-approved observational study was performed with 78 symptomatic patients(90 hips) with hip pain due to DDH and with 65 patients with femoroacetabular impingement(FAI) due to acetabular retroversion (77 hips). Diagnosis was based on reference values calculated on AP radiographs. CT/MRI-based measurement of FV(Murphy method) and central AV were compared. Frequency of increased FV(FV>25°), severely increased FV(FV>35°) and excessive FV(FV>45°) and of femoral retroversion (FV<10°) was analysed. Combined version is the sum of FV and AV, equal to McKibbin index or COTAV index.

## RESULTS

Mean FV and combined version was significantly(p<0.001) increased of patients with DDH (mean±SD of 25±11° and 47±18°) compared to patients with acetabular retroversion (16±11° and 28±13°). Mean FV of female patients with DDH (27±16°) and acetabular retroversion (19±12°) was significantly(p<0.001) increased compared to male patients with DDH(18±13°) and acetabular retroversion (13±8°). Frequency of increased FV(FV>25°) was 47%, of severely increased FV(FV>35°) was 23% and excessive FV (FV>45°) was 8% for patients with DDH. Prevalence of femoral retroversion(FV<10°) was significantly(p<0.001) higher in patients acetabular retroversion(31%) compared to patients with DDH(17%). Combined version of female patients with DDH (51±17°) was significantly(p<0.001) increased compared to male patients with DDH(37±14°). Of patients with DDH, 18% had AV>25° combined with FV>25°. Of patients with acetabular retroversion, 12% had FV<10° combined with AV<10°.

## CONCLUSION

s Patients with DDH have remarkable sex differences of FV(9°) and combined version(14°). Patients with acetabular retroversion can be combined with femoral retroversion. Frequency of severely increased FV>35° (23%) is considerable for patients with DDH, but 17% had femoral retroversion.

## CLINICAL RELEVANCE/APPLICATION

Patients with DDH can be combined with increased FV but also with femoral retroversion. This underlines the importance of patient-specific evaluation and could influence internal rotation and postoperative outcome after hip preservation surgery.

## W2-SPMK-4 Automatic Segmentation of Pelvic Bones and Measurement of Center Edge Angle on Plain Radiographs Using Deep-Learning Network Trained With Digitally Reconstructed Radiography From CT

Participants

Yisak Kim, Seoul, Korea, Republic Of (*Presenter*) Nothing to Disclose

## PURPOSE

For the automatic measurement of many orthopedic parameters, accurate bone segmentation is necessary. However, it is often difficult to determine the exact boundary of bone structures on a 2D projection image such as a plain radiograph due to the overlap of bone with other tissues. The digitally reconstructed radiography (DRR) is a synthetic X-ray generated from the CT by projecting the 3D volumetric data onto the 2D plane. We trained a deep-learning model with DRRs to automatically segment pelvic bones and measure lateral center edge angle (CEA) on the actual pelvis anteroposterior (AP).

## METHODS AND MATERIALS

A total of 90 pelvis CT scans were used to generate 90 DRRs, and five bone segmentation masks (left and right pelvis, proximal femurs, and sacrum) were also generated for each DRR using the CT segmentation mask. DeepLab v3+ with EfficientNet-B0 encoder was used to develop the segmentation model. The model was validated in the external data of 173 pelvis AP with manually segmented femur masks. The model's performance was evaluated using the Dice similarity score (DSC) and intersection-over-union (IoU). We further developed an automated measurement algorithm of lateral CEA on pelvis AP. First, we found the best fit circle to the femur head using Hough transform. Then, CEA was measured using two lines passing through the center of the circle: a vertical line through the center of the femoral head and a line passing through the lateral acetabular rim.

## RESULTS

On DRRs, the deep-learning model showed good performance for the segmentation of five pelvic bones (DSC range, 0.95-0.99; IoU range, 0.91-0.97). On real pelvis AP, the model achieved DSC of 0.97 and IoU of 0.94 for segmenting proximal femur. The medians of manually measured right and left CEA were 41.1 (37.1-45.7) and 37.9 (34.4-43.2), respectively. The predicted CEA had significant correlations with manually measured CEA (right CEA: Pearson's  $r=0.54$ ,  $P<.001$ ; left CEA: Pearson's  $r=0.45$ ,  $P<.001$ ). The mean absolute errors of predicted right and left CEA were  $4.8^\circ$  and  $6.1^\circ$ , respectively (mean absolute percentage errors, 11.9% and 14.4%).

## CONCLUSION

s We developed a deep-learning based bone segmentation model on pelvis AP using DRRs with high accuracy. This segmentation model can be used as a core module for fully automatic radiographic measurement algorithms such as CEA measurements.

## CLINICAL RELEVANCE/APPLICATION

Automatic measurements of various orthopedic parameters can overcome the shortcomings of manual measurement, which is time-consuming and suffers from high inter- and intraobserver variability.

Printed on: 02/07/23



## Abstract Archives of the RSNA, 2022

W2-SPMK-1

### Transient Osteoporosis of the Hip: A Fleeting Diagnosis?

Wednesday, Nov. 30 9:00AM - 9:30AM Room: Learning Center - MK DPS

#### Participants

Aishwarya Gulati, MD, Philadelphia, PA (*Presenter*) Nothing to Disclose

#### PURPOSE

Transient osteoporosis of the hip (TOH) is a rare, self-limiting clinical diagnosis with unclear etiology. We hypothesize that TOH represents an underlying subchondral insufficiency fracture, and in nearly all cases a discrete fracture is visible on MRI.

#### METHODS AND MATERIALS

Retrospective PACS query identified patients with intense bone marrow edema (BME) in the femoral head on a hip MRI including small field of view (FOV) sequences, meeting imaging criteria for TOH. Those with avascular necrosis, marrow replacing processes, or history of antecedent trauma were excluded. Demographics and pre-MRI patient questionnaires were reviewed. Three musculoskeletal radiologists independently reviewed each case for presence of a definite subchondral fracture line on small FOV images. Extent of BME, reciprocal BME in the acetabulum, and size of joint effusion were also recorded.

#### RESULTS

50 patients meeting inclusion criteria were identified (29 females). Mean age was  $62 \pm 12$  years (range 35-84). Average symptom duration before MRI was  $102 \pm 135$  days. 10 patients had DEXA performed within 2 years of MRI, 6 demonstrating osteopenia/osteoporosis. Subchondral fractures were unanimously identified by readers in 44/50 (88%) cases. Interclass correlations coefficient with absolute agreement was 0.73 with 95% CI (0.57-0.84), indicating near-excellent agreement. Most cases demonstrated large joint effusion (24/50, 48%) and acetabular edema (32/50, 64%). Binomial logistic regression assessing impact of age, gender, pain duration, extent of BME and joint effusion identified increasing size of joint effusion as a statistically significant predictor of subchondral fracture ( $p=0.05$ ), with 6.9 higher odds of fracture. There was a strong correlation between osteopenia/osteoporosis on DEXA and presence of subchondral fracture ( $p<.001$ ).

#### CONCLUSION

A subchondral fracture line was identified on small FOV imaging in most cases identified as TOH. Findings such as a joint effusion and osteopenia/osteoporosis have a higher association with subchondral fractures.

#### CLINICAL RELEVANCE/APPLICATION

The diagnosis of TOH remains pervasive throughout medical literature and radiology reports. We argue that this term is misleading, as the underlying pathology likely reflects underlying subchondral insufficiency fracture. Accurate reporting of this finding is essential for ensuring appropriate conservative treatment.

Printed on: 02/07/23

## Abstract Archives of the RSNA, 2022

W2-SPMK-2

### The Effect of Pre-Operative MRI Coracoid Dimensions on Latarjet Surgical Outcomes

Wednesday, Nov. 30 9:00AM - 9:30AM Room: Learning Center - MK DPS

#### Participants

Sarah Kamel, MD, Philadelphia, PA (*Presenter*) Nothing to Disclose

#### PURPOSE

To determine if pre-operative coracoid dimensions correspond with post-operative outcomes in patients treated for recurrent anterior shoulder dislocation by Latarjet coracoid transfer.

#### METHODS AND MATERIALS

Patients who underwent primary Latarjet surgery between 2009-2019 were identified. Included patients had pre-operative shoulder MRI and minimum of 2-year post-operative follow-up. Coracoid length was measured on axial MRI sequences as the distance from the coracoclavicular (CC) ligament insertion to the distal tip. Width measurements were obtained perpendicular to length at three locations (base, midpoint, tip) and averaged. Comparisons were made between shorter vs. longer coracoid length and width. Outcomes were recurrent instability, re-operation, complications, rate of and time until return-to-sport (RTS), and American Shoulder and Elbow Surgeons (ASES) score.

#### RESULTS

56 patients were included, 16% female and with a mean age of 28.4 years. Patients with a shorter coracoid length (<22 mm, n=30) had similar rate of recurrent instability (shorter length 6.7% vs. longer length 3.8%; p=0.640), complication (10.0% vs. 15.4%; p=0.543), re-operation (3.3% vs. 7.7%; p=0.592), rate of RTS (76.5% vs. 58.8%; p=0.298), and post-operative ASES scores (85.0 vs. 81.6; p=0.612), relative to patients with a longer coracoid length (>22 mm, n=26). Likewise, patients with a narrower coracoid width (<10 mm, n=29) had similar prevalence of recurrent instability (narrower width 6.9% vs. wider width 3.7%; p=0.596), complication (17.2% vs. 7.4%; p=0.266), re-operation (3.5% vs. 7.4%; p=0.605), rate of RTS (66.7% vs. 68.4%; p=1.000), and post-operative ASES scores (87.1 vs. 80.0; p=0.286), relative to patients with a wider coracoid length (>10 mm, n=27).

#### CONCLUSION

s Patients undergoing Latarjet coracoid transfer had similar rates of recurrent instability and post-operative outcomes regardless of pre-operative coracoid dimensions.

#### CLINICAL RELEVANCE/APPLICATION

This MRI protocol for measuring coracoid dimensions closely accounts for the specific landmarks utilized during the Latarjet osteotomy by focusing on identification of the CC ligament insertion.

Printed on: 02/07/23

## Abstract Archives of the RSNA, 2022

W2-SPMK-3

### Combined Femoral and Acetabular Version is Sex Related in Symptomatic Patients with Hip Dysplasia and Acetabular Retroversion

Wednesday, Nov. 30 9:00AM - 9:30AM Room: Learning Center - MK DPS

#### Participants

Till Lerch, MD, PhD, Bern, Switzerland (*Presenter*) Nothing to Disclose

#### PURPOSE

Frequency of abnormal femoral and acetabular version (AV) and combined version is unclear in patients with developmental dysplasia of the hip (DDH). This study aimed to investigate mean femoral version (FV), the prevalence of increased FV and femoral retroversion, and combined version (combination of FV and AV) in patients with DDH and acetabular retroversion.

#### METHODS AND MATERIALS

A retrospective IRB-approved observational study was performed with 78 symptomatic patients (90 hips) with hip pain due to DDH and with 65 patients with femoroacetabular impingement (FAI) due to acetabular retroversion (77 hips). Diagnosis was based on reference values calculated on AP radiographs. CT/MRI-based measurement of FV (Murphy method) and central AV were compared. Frequency of increased FV (FV > 25°), severely increased FV (FV > 35°) and excessive FV (FV > 45°) and of femoral retroversion (FV < 10°) was analysed. Combined version is the sum of FV and AV, equal to McKibbin index or COTAV index.

#### RESULTS

Mean FV and combined version was significantly ( $p < 0.001$ ) increased of patients with DDH (mean  $\pm$  SD of  $25 \pm 11^\circ$  and  $47 \pm 18^\circ$ ) compared to patients with acetabular retroversion ( $16 \pm 11^\circ$  and  $28 \pm 13^\circ$ ). Mean FV of female patients with DDH ( $27 \pm 16^\circ$ ) and acetabular retroversion ( $19 \pm 12^\circ$ ) was significantly ( $p < 0.001$ ) increased compared to male patients with DDH ( $18 \pm 13^\circ$ ) and acetabular retroversion ( $13 \pm 8^\circ$ ). Frequency of increased FV (FV > 25°) was 47%, of severely increased FV (FV > 35°) was 23% and excessive FV (FV > 45°) was 8% for patients with DDH. Prevalence of femoral retroversion (FV < 10°) was significantly ( $p < 0.001$ ) higher in patients acetabular retroversion (31%) compared to patients with DDH (17%). Combined version of female patients with DDH ( $51 \pm 17^\circ$ ) was significantly ( $p < 0.001$ ) increased compared to male patients with DDH ( $37 \pm 14^\circ$ ). Of patients with DDH, 18% had AV > 25° combined with FV > 25°. Of patients with acetabular retroversion, 12% had FV < 10° combined with AV < 10°.

#### CONCLUSION

Patients with DDH have remarkable sex differences of FV (9°) and combined version (14°). Patients with acetabular retroversion can be combined with femoral retroversion. Frequency of severely increased FV > 35° (23%) is considerable for patients with DDH, but 17% had femoral retroversion.

#### CLINICAL RELEVANCE/APPLICATION

Patients with DDH can be combined with increased FV but also with femoral retroversion. This underlines the importance of patient-specific evaluation and could influence internal rotation and postoperative outcome after hip preservation surgery.

Printed on: 02/07/23

## Abstract Archives of the RSNA, 2022

W2-SPMK-4

### Automatic Segmentation of Pelvic Bones and Measurement of Center Edge Angle on Plain Radiographs Using Deep-Learning Network Trained With Digitally Reconstructed Radiography From CT

Wednesday, Nov. 30 9:00AM - 9:30AM Room: Learning Center - MK DPS

#### Participants

Yisak Kim, Seoul, Korea, Republic Of (*Presenter*) Nothing to Disclose

#### PURPOSE

For the automatic measurement of many orthopedic parameters, accurate bone segmentation is necessary. However, it is often difficult to determine the exact boundary of bone structures on a 2D projection image such as a plain radiograph due to the overlap of bone with other tissues. The digitally reconstructed radiography (DRR) is a synthetic X-ray generated from the CT by projecting the 3D volumetric data onto the 2D plane. We trained a deep-learning model with DRRs to automatically segment pelvic bones and measure lateral center edge angle (CEA) on the actual pelvis anteroposterior (AP).

#### METHODS AND MATERIALS

A total of 90 pelvis CT scans were used to generate 90 DRRs, and five bone segmentation masks (left and right pelvis, proximal femurs, and sacrum) were also generated for each DRR using the CT segmentation mask. DeepLab v3+ with EfficientNet-B0 encoder was used to develop the segmentation model. The model was validated in the external data of 173 pelvis AP with manually segmented femur masks. The model's performance was evaluated using the Dice similarity score (DSC) and intersection-over-union (IoU). We further developed an automated measurement algorithm of lateral CEA on pelvis AP. First, we found the best fit circle to the femur head using Hough transform. Then, CEA was measured using two lines passing through the center of the circle: a vertical line through the center of the femoral head and a line passing through the lateral acetabular rim.

#### RESULTS

On DRRs, the deep-learning model showed good performance for the segmentation of five pelvic bones (DSC range, 0.95-0.99; IoU range, 0.91-0.97). On real pelvis AP, the model achieved DSC of 0.97 and IoU of 0.94 for segmenting proximal femur. The medians of manually measured right and left CEA were 41.1 (37.1-45.7) and 37.9 (34.4-43.2), respectively. The predicted CEA had significant correlations with manually measured CEA (right CEA: Pearson's  $r=0.54$ ,  $P<.001$ ; left CEA: Pearson's  $r=0.45$ ,  $P<.001$ ). The mean absolute errors of predicted right and left CEA were 4.8° and 6.1°, respectively (mean absolute percentage errors, 11.9% and 14.4%).

#### CONCLUSION

s We developed a deep-learning based bone segmentation model on pelvis AP using DRRs with high accuracy. This segmentation model can be used as a core module for fully automatic radiographic measurement algorithms such as CEA measurements.

#### CLINICAL RELEVANCE/APPLICATION

Automatic measurements of various orthopedic parameters can overcome the shortcomings of manual measurement, which is time-consuming and suffers from high inter- and intraobserver variability.

Printed on: 02/07/23

## Abstract Archives of the RSNA, 2022

W2-SPMS

### Multisystem Wednesday Poster Discussion

Wednesday, Nov. 30 9:00AM - 9:30AM Room: Learning Center - MS DPS

#### Sub-Events

#### W2-SPMS-1 Splenic Size and Volume Measurements in Patients with Chronic Lymphocytic Leukemia

##### Participants

Olanrewaju Ogunleye, MBBS, Bethesda, MD (*Presenter*) Nothing to Disclose

##### PURPOSE

To determine which methods of assessment of splenic size most accurately represent the actual spleen volume in patients with Chronic Lymphocytic Leukemia (CLL).

##### METHODS AND MATERIALS

The Abdominal Computed Tomography images of 48 patients with CLL enrolled on a phase 2 clinical trial at two time-points before and after 2-months of continuous acalabrutinib treatment were analyzed. Linear one-dimensional measurements of the spleen were taken in different planes. Two-dimensional and three-dimensional measurements were calculated from the linear measurements using mathematical formulae. The spleen volume was determined by manual segmentation as the ground truth. Data derived were analyzed using the Pearson correlation and statistical significance was set at  $p < 0.05$ .

##### RESULTS

Among the single-dimensional measurements, the strongest correlation with the segmented splenic volume was the sagittal long axis diameter (LAD) ( $r=0.89$ ,  $p < 0.05$ ), followed closely by Coronal LAD ( $r=0.87$ ,  $p < 0.05$ ) and craniocaudal length (iwCLL) ( $r=0.84$ ,  $p < 0.05$ ). For the two-dimensional indices, the sum of LAD and short axis diameter (SAD) of the spleen in axial plane showed good correlation with the splenic volume ( $r=0.77$ ,  $p < 0.05$ ). Among the three-dimensional indices, the splenic index ( $0.523 \times \text{axial LAD} \times \text{axial SAD} \times \text{coronal height}$ ) and a formula for volume ( $30 + 0.58 \times \text{axial LAD} \times \text{axial SAD} \times \text{coronal height}$ ) had the strongest correlation (both  $r=0.92$ ,  $p < 0.05$ ) with the spleen volume.

##### CONCLUSION

Three-dimensional formulae showed the strongest correlation with volumetric reference spleen measurement in patients with CLL. Among unidimensional measurements, the sagittal LAD had the best correlation with the actual splenic volume. The two-dimensional calculation methods were less reliable.

##### CLINICAL RELEVANCE/APPLICATION

In patients with CLL, when volumetric measurement is not available, the three-dimensional formulae is the best estimate of absolute splenic volume. Among the various types of unidirectional measurements, the sagittal LAD most accurately estimates absolute splenic volume.

Printed on: 02/07/23

## Abstract Archives of the RSNA, 2022

W2-SPMS-1

### Splenic Size and Volume Measurements in Patients with Chronic Lymphocytic Leukemia

Wednesday, Nov. 30 9:00AM - 9:30AM Room: Learning Center - MS DPS

#### Participants

Olanrewaju Ogunleye, MBBS, Bethesda, MD (*Presenter*) Nothing to Disclose

#### PURPOSE

To determine which methods of assessment of splenic size most accurately represent the actual spleen volume in patients with Chronic Lymphocytic Leukemia (CLL).

#### METHODS AND MATERIALS

The Abdominal Computed Tomography images of 48 patients with CLL enrolled on a phase 2 clinical trial at two time-points before and after 2-months of continuous acalabrutinib treatment were analyzed. Linear one-dimensional measurements of the spleen were taken in different planes. Two-dimensional and three-dimensional measurements were calculated from the linear measurements using mathematical formulae. The spleen volume was determined by manual segmentation as the ground truth. Data derived were analyzed using the Pearson correlation and statistical significance was set at  $p < 0.05$ .

#### RESULTS

Among the single-dimensional measurements, the strongest correlation with the segmented splenic volume was the sagittal long axis diameter (LAD) ( $r=0.89$ ,  $p < 0.05$ ), followed closely by Coronal LAD ( $r=0.87$ ,  $p < 0.05$ ) and craniocaudal length (iwCLL) ( $r=0.84$ ,  $p < 0.05$ ). For the two-dimensional indices, the sum of LAD and short axis diameter (SAD) of the spleen in axial plane showed good correlation with the splenic volume ( $r=0.77$ ,  $p < 0.05$ ). Among the three-dimensional indices, the splenic index ( $0.523 \times \text{axial LAD} \times \text{axial SAD} \times \text{coronal height}$ ) and a formula for volume ( $30 + 0.58 \times \text{axial LAD} \times \text{axial SAD} \times \text{coronal height}$ ) had the strongest correlation (both  $r=0.92$ ,  $p < 0.05$ ) with the spleen volume.

#### CONCLUSION

Three-dimensional formulae showed the strongest correlation with volumetric reference spleen measurement in patients with CLL. Among unidimensional measurements, the sagittal LAD had the best correlation with the actual splenic volume. The two-dimensional calculation methods were less reliable.

#### CLINICAL RELEVANCE/APPLICATION

In patients with CLL, when volumetric measurement is not available, the three-dimensional formulae is the best estimate of absolute splenic volume. Among the various types of unidirectional measurements, the sagittal LAD most accurately estimates absolute splenic volume.

Printed on: 02/07/23



## Abstract Archives of the RSNA, 2022

W2-SPNMMI

### Nuclear Medicine/Molecular Imaging Wednesday Poster Discussion

Wednesday, Nov. 30 9:00AM - 9:30AM Room: Learning Center - NMMI DPS

#### Participants

Nadine Mallak, MD, Portland, OR (*Moderator*) Nothing to Disclose  
Nadine Mallak, MD, Portland, OR (*Moderator*) Nothing to Disclose  
Kevin P. Banks, MD, San Antonio, TX (*Moderator*) Nothing to Disclose  
Kevin P. Banks, MD, San Antonio, TX (*Moderator*) Nothing to Disclose

#### Sub-Events

#### W2-SPNMMI-1 Standardization of Quantitative Imaging Biomarkers of Lung Cancer Using Simulated 18F-FDG PET/CT Studies

Participants  
Pablo Aguiar, (*Presenter*) Research Consultant, Qubitech Health Intelligence

#### PURPOSE

To develop and validate a new methodology for the standardization of PET biomarkers in lung cancer based on simulated 18F-FDG PET/CT studies.

#### METHODS AND MATERIALS

Our methodology is based on the generation of simulated 18F-FDG PET/CT studies using a large database of lung tumour maps cropped from patient images. All lung tumour maps were randomly positioned into whole-body physiological 18F-FDG activity and attenuation maps. These activity/attenuation maps (which defines our ground-truth values) were entered as inputs for Monte Carlo simulation models of PET scanners from the SimPET platform (sim-pet.org), leading to the generation of simulated 18F-FDG PET/CT studies. This simulated database was used for the standardization of PET biomarkers in terms of tumour segmentation methods, both CT-based volumes (VOICT) and PET-based volumes with different thresholds (VOIPET25, VOIPET35 and VOIPET45). The standardization procedure was carried out through comparison between commonly used PET biomarkers in lung cancer and their corresponding ground-truth values.

#### RESULTS

We generated a large database of simulated 18F-FDG PET/CT images from 70 lung cancer patients [age: 47-87 years; stages I (11), II (2), III (23) and IV(25)]. It was characterized by the following ground-truth PET biomarkers (range): SUVr (0.7-8.9), MTV (0.94-140.9), Entropy (6.6-7.7), Dissimilarity (5.0-16.6), Homogeneity (0.12-0.28), Contrast (44.7-407.5), ZP (788-22408) and HILAE (0.04-0.6). The standardization analysis showed SUVr was strongly underestimated when using VOICT (-30%), but not when using VOIPET45 (2%) or VOIPET35(5%). Instead, MTV was strongly underestimated using VOIPET45 (-48%) but not using VOICT. Regarding texture features, Entropy, Dissimilarity and ZP were accurately estimated using VOIPET35 (8%) and Homogeneity, Contrast and HILAE using VOIPET45 (7%), while VOICT and VOICPET25 showed larger biases.

#### CONCLUSION

A new methodology was developed and validated for the standardization of PET biomarkers commonly used in lung cancer diagnosis using simulated 18F-FDG PET/CT studies. Our standardization study was carried out in terms of tumour delineation methods but our methodology can be used for the standardization of many others quantification methods or PET biomarkers.

#### CLINICAL RELEVANCE/APPLICATION

This is the first study proposing the standardization of quantitative PET biomarkers based on ground-truth measurements from patient 18F-FDG PET studies (other standardization procedures are commonly based on phantom measurements). All databases will be made available for the scientific community through the SimPET platform (sim-pet.org) for the further standardization of quantification methods or additional PET biomarkers.

#### W2-SPNMMI-2 Cartilage-targeting MnOx Nanoparticles Enhance Magnetic Resonance Detection and Cartilage Repair in Early Osteoarthritis

Participants  
Ting Lin, Guangzhou, China (*Presenter*) Nothing to Disclose

#### PURPOSE

Osteoarthritis (OA) is one of the leading causes of adult morbidity and disability worldwide. While the early detection and repair of cartilage lesions are crucial in the treatment of OA, they remain challenging because neither clinically used medicines nor magnetic resonance (MR) contrast agents can achieve detection and repair simultaneously. The purpose of this study was to develop theragnostic nanomaterials with optimal sizes, good biocompatibility, MR imaging and cartilage repair capability for OA therapy.

## **METHODS AND MATERIALS**

We conjugated carboxymethyl chitosan (CMC) with a cartilage-targeting peptide (WY) and then synthesized CMC-assisted manganese oxide (MnOx) NPs. The in vitro T1 relaxivity values of the NPs were quantified using a 3T MR scanner (Ingenia, Philip Healthcare, Best, Netherlands). The r1 relaxivity was calculated by linearly fitting the inverse T1 relaxation time against the Mn<sup>2+</sup> concentration of the NPs. WY-CMC-MnOx, non-cartilage-targeting LR-CMC-MnOx, or CMC-MnOx NPs were intraarticularly injected into the right knee joints of OA rats (destabilization of the medial meniscus model). The MR scans were conducted using a 7.0T animal MR imaging scanner (PharmaScan70/16 US, Bruker BioSpin MRI GmbH, Germany) equipped with a volumetric transmitter coil with an 86-mm inner diameter and a rat head surface receiver coil. The sagittal fat-saturated T1-weighted images were acquired with the following parameters: TR = 867.5 ms, TE = 6.5 ms, field of view = 22 × 32 mm, slice thickness = 0.7 mm, matrix dimensions = 184 × 266 × 16 slices, pixel bandwidth = 1050, and acquisition time = 3 min, 59 s. All rats underwent MR scans before the injections of the NPs (baseline images) and at 24 h after injection. The T1-weighted MR signal intensities within the regions of interest (ROIs; ~0.002 cm<sup>2</sup>) were acquired. The trend of signal changes was determined by plotting  $\rho$ SNR versus time. In vivo therapeutic effects of the NPs in DMM rat models were studied.

## **RESULTS**

WY-CMC-MnOx NPs demonstrated an excellent biocompatibility and a good T1 relaxivity of 1.72 Mm<sup>-1</sup>s<sup>-1</sup>. Owing to their ultrasmall size and cartilage-targeting ability, the WY-CMC-MnOx NPs considerably increased the MR imaging quality of cartilage lesions compared to non-cartilage-targeting LR-CMC-MnOx and CMC-MnOx NPs. In contrast, clinically used Gd-DPTA failed to detect the cartilage lesions. Furthermore, WY-CMC-MnOx enhanced OA therapy through efficient cartilage regeneration after intraarticularly injection in rats with early OA .

## **CONCLUSION**

s WY-CMC-MnOx NPs were successfully developed as new theranostic agents for OA therapy.

## **CLINICAL RELEVANCE/APPLICATION**

WY-CMC-MnOx NPs are promising for use in the diagnosis and treatment of early OA.

Printed on: 02/07/23

## Abstract Archives of the RSNA, 2022

W2-SPNMMI-1

### Standardization of Quantitative Imaging Biomarkers of Lung Cancer Using Simulated 18F-FDG PET/CT Studies

Wednesday, Nov. 30 9:00AM - 9:30AM Room: Learning Center - NMMI DPS

#### Participants

Pablo Aguiar, (*Presenter*) Research Consultant, Qubitech Health Intelligence

#### PURPOSE

To develop and validate a new methodology for the standardization of PET biomarkers in lung cancer based on simulated 18F-FDG PET/CT studies.

#### METHODS AND MATERIALS

Our methodology is based on the generation of simulated 18F-FDG PET/CT studies using a large database of lung tumour maps cropped from patient images. All lung tumour maps were randomly positioned into whole-body physiological 18F-FDG activity and attenuation maps. These activity/attenuation maps (which defines our ground-truth values) were entered as inputs for Monte Carlo simulation models of PET scanners from the SimPET platform (sim-pet.org), leading to the generation of simulated 18F-FDG PET/CT studies. This simulated database was used for the standardization of PET biomarkers in terms of tumour segmentation methods, both CT-based volumes (VOICT) and PET-based volumes with different thresholds (VOIPET25, VOIPET35 and VOIPET45). The standardization procedure was carried out through comparison between commonly used PET biomarkers in lung cancer and their corresponding ground-truth values.

#### RESULTS

We generated a large database of simulated 18F-FDG PET/CT images from 70 lung cancer patients [age: 47-87 years; stages I (11), II (2), III (23) and IV(25)]. It was characterized by the following ground-truth PET biomarkers (range): SUVr (0.7-8.9), MTV (0.94-140.9), Entropy (6.6-7.7), Dissimilarity (5.0-16.6), Homogeneity (0.12-0.28), Contrast (44.7-407.5), ZP (788-22408) and HILAE (0.04-0.6). The standardization analysis showed SUVr was strongly underestimated when using VOICT (-30%), but not when using VOIPET45 (2%) or VOIPET35(5%). Instead, MTV was strongly underestimated using VOIPET45 (-48%) but not using VOICT. Regarding texture features, Entropy, Dissimilarity and ZP were accurately estimated using VOIPET35 (8%) and Homogeneity, Contrast and HILAE using VOIPET45 (7%), while VOICT and VOICPET25 showed larger biases.

#### CONCLUSION

A new methodology was developed and validated for the standardization of PET biomarkers commonly used in lung cancer diagnosis using simulated 18F-FDG PET/CT studies. Our standardization study was carried out in terms of tumour delineation methods but our methodology can be used for the standardization of many others quantification methods or PET biomarkers.

#### CLINICAL RELEVANCE/APPLICATION

This is the first study proposing the standardization of quantitative PET biomarkers based on ground-truth measurements from patient 18F-FDG PET studies (other standardization procedures are commonly based on phantom measurements). All databases will be made available for the scientific community through the SimPET platform (sim-pet.org) for the further standardization of quantification methods or additional PET biomarkers.

Printed on: 02/07/23

## Abstract Archives of the RSNA, 2022

W2-SPNMMI-2

### Cartilage-targeting MnOx Nanoparticles Enhance Magnetic Resonance Detection and Cartilage Repair in Early Osteoarthritis

Wednesday, Nov. 30 9:00AM - 9:30AM Room: Learning Center - NMMI DPS

#### Participants

Ting Lin, Guangzhou, China (*Presenter*) Nothing to Disclose

#### PURPOSE

Osteoarthritis (OA) is one of the leading causes of adult morbidity and disability worldwide. While the early detection and repair of cartilage lesions are crucial in the treatment of OA, they remain challenging because neither clinically used medicines nor magnetic resonance (MR) contrast agents can achieve detection and repair simultaneously. The purpose of this study was to develop theragnostic nanomaterials with optimal sizes, good biocompatibility, MR imaging and cartilage repair capability for OA therapy.

#### METHODS AND MATERIALS

We conjugated carboxymethyl chitosan (CMC) with a cartilage-targeting peptide (WY) and then synthesized CMC-assisted manganese oxide (MnOx) NPs. The *in vitro* T1 relaxivity values of the NPs were quantified using a 3T MR scanner (Ingenia, Philip Healthcare, Best, Netherlands). The  $r_1$  relaxivity was calculated by linearly fitting the inverse T1 relaxation time against the Mn<sup>2+</sup> concentration of the NPs. WY-CMC-MnOx, non-cartilage-targeting LR-CMC-MnOx, or CMC-MnOx NPs were intraarticularly injected into the right knee joints of OA rats (destabilization of the medial meniscus model). The MR scans were conducted using a 7.0T animal MR imaging scanner (PharmaScan70/16 US, Bruker BioSpin MRI GmbH, Germany) equipped with a volumetric transmitter coil with an 86-mm inner diameter and a rat head surface receiver coil. The sagittal fat-saturated T1-weighted images were acquired with the following parameters: TR = 867.5 ms, TE = 6.5 ms, field of view = 22 × 32 mm, slice thickness = 0.7 mm, matrix dimensions = 184 × 266 × 16 slices, pixel bandwidth = 1050, and acquisition time = 3 min, 59 s. All rats underwent MR scans before the injections of the NPs (baseline images) and at 24 h after injection. The T1-weighted MR signal intensities within the regions of interest (ROIs; ~0.002 cm<sup>2</sup>) were acquired. The trend of signal changes was determined by plotting  $\rho$ SNR versus time. *In vivo* therapeutic effects of the NPs in DMM rat models were studied.

#### RESULTS

WY-CMC-MnOx NPs demonstrated an excellent biocompatibility and a good T1 relaxivity of 1.72 Mm<sup>-1</sup>s<sup>-1</sup>. Owing to their ultrasmall size and cartilage-targeting ability, the WY-CMC-MnOx NPs considerably increased the MR imaging quality of cartilage lesions compared to non-cartilage-targeting LR-CMC-MnOx and CMC-MnOx NPs. In contrast, clinically used Gd-DPTA failed to detect the cartilage lesions. Furthermore, WY-CMC-MnOx enhanced OA therapy through efficient cartilage regeneration after intraarticularly injection in rats with early OA.

#### CONCLUSION

WY-CMC-MnOx NPs were successfully developed as new theragnostic agents for OA therapy.

#### CLINICAL RELEVANCE/APPLICATION

WY-CMC-MnOx NPs are promising for use in the diagnosis and treatment of early OA.

Printed on: 02/07/23



## Abstract Archives of the RSNA, 2022

W2-SPNPM

### Noninterpretive Skills/Quality Improvement/Practice Management Wednesday Poster Discussions

Wednesday, Nov. 30 9:00AM - 9:30AM Room: Learning Center - NPM DPS

#### Participants

Rifat Wahab, DO, Cincinnati, OH (*Moderator*) Nothing to Disclose

#### Sub-Events

### W2-SPNPM- Impact of Neighborhood Socioeconomic Deprivation on Access to ACR Accredited Cross Sectional Imaging Facilities 1

#### Participants

Anand Narayan, MD, PhD, Verona, WI (*Presenter*) Nothing to Disclose

#### PURPOSE

Evaluate the effects of neighborhood deprivation at the zip code level on access to ACR accredited cross sectional imaging facilities.

#### METHODS AND MATERIALS

Area deprivation index (ADI) values were obtained from the University of Wisconsin Neighborhood Atlas, based on a validated HRSA measure that allows for national rankings of zip code level socioeconomic disadvantage. Disadvantage was dichotomized (high  $\geq$ 97th ADI percentile, low  $\leq$ 3rd ADI percentile). Urban/rural status was defined from US Department of Agriculture rural-urban commuting area (RUCA) codes. Outcomes included the presence or absence of ACR accredited cross sectional imaging facilities (yes/no). Chi square tests were used to evaluate the association between access and geographic disadvantage, stratified by urban/rural status.

#### RESULTS

Among 41,683 zip codes across the US, 2,796 were disadvantaged (1,160 rural, 1,636 urban) and 1,028 were advantaged (39 rural, 989 urban). Disadvantaged zip codes were more likely to be located in rural areas ( $p < 0.001$ ). Disadvantaged zip codes were less likely to have access to ACR accredited CT facilities (21 vs 32%,  $p < 0.001$ ), MRI (19 vs 32%,  $p < 0.001$ ), nuclear medicine (11 vs 18%,  $p < 0.001$ ), PET (7 vs 13%,  $p < 0.001$ ), ultrasound (14 vs 29%,  $p < 0.001$ ), lung cancer screening centers of excellence (5 vs 12%,  $p < 0.001$ ), diagnostic centers of excellence (1 vs 4%,  $p < 0.001$ ), and accredited radiation oncology facilities (3 vs 8%,  $p < 0.001$ ). Among urban areas, disadvantaged zip codes were less likely to have access to ACR accredited CT facilities (26 vs 33%,  $p < 0.001$ ), MRI (25 vs 33%,  $p < 0.001$ ), nuclear medicine (15 vs 19%,  $p = 0.007$ ), PET (9 vs 13%,  $p = 0.003$ ), ultrasound (20 vs 30%,  $p < 0.001$ ), lung cancer screening centers of excellence (7 vs 13%,  $p < 0.001$ ), diagnostic centers of excellence (2 vs 4%,  $p < 0.001$ ), and accredited radiation oncology facilities (5 vs 8%,  $p = 0.001$ ). Analyses for rural areas were limited by small numbers of advantaged zip codes.

#### CONCLUSION

Zip codes with high levels of socioeconomic disadvantage were less likely to have ACR accredited cross sectional imaging facilities, ACR centers of excellence and accredited radiation oncology facilities.

#### CLINICAL RELEVANCE/APPLICATION

Reducing disparities in access to quality imaging services will require radiology leaders to expand services in high disadvantage areas.

### W2-SPNPM- Usability of Hospital Price Estimators for Lumbar Spine MRI 2

#### Participants

Meagan Bechel, MD, PhD, (*Presenter*) Nothing to Disclose

#### PURPOSE

Evaluate usability of online hospital price estimators for a common imaging examination using surrogate patients

#### METHODS AND MATERIALS

Using the Amazon MTurk platform, we recruited adult English-speaking US-residents as surrogate patients to find the cash price for a non-contrast lumbar spine MRI examination for a self-pay patient using price estimator tools at four hospitals. All were asked to view a 3-minute tutorial video and report their experiences with the task, including the System Usability Scale (SUS) for the estimator, through a paid survey. We queried participants about demographics, insurance, prior imaging exposure, and assessed health literacy and health insurance literacy (HIL) using validated measures. Multivariable analysis for correct price identification and price estimator SUS were performed.

#### RESULTS

Of 660 respondents, 397 met eligibility criteria (70.8% <45 years; 43.8% female; 83.8% White). 84% found all four estimators; 1.5% were unable to locate any. Only 32% found the correct price at all four hospitals; 20.6% did not find any correct prices. Average SUS for the hospitals' estimators ranged between 63.0 and 78.8. The hospital with a similar estimator to that used in the tutorial video had highest SUS. Accuracy of price identification improved with later tasks. Higher HIL was associated with higher identification of at least one correct price (B,3.0;95%CI,0.6-5.4,  $p<0.01$ ) and higher SUS (B,14.7; 95%CI, 9.4-20.1,  $p<0.001$ ).

#### **CONCLUSION**

s Surrogate patients were able to locate hospital price estimators, but unable to effectively use them to obtain correct prices. Tutorial videos improved SUS, but correct price identification improved with practice.

#### **CLINICAL RELEVANCE/APPLICATION**

Hospital price estimators score average or below average on usability and cannot be successfully utilized by the majority of educated paid surrogate patients. Though usability improves with a tutorial video, both increased usability and health insurance literacy are necessary for price estimator tools to be accessible and beneficial. Therefore, they may represent an additional, but mitigatable barrier to equitable and timely evidence-based care.

Printed on: 02/07/23

## Abstract Archives of the RSNA, 2022

W2-SPNPM-1

### Impact of Neighborhood Socioeconomic Deprivation on Access to ACR Accredited Cross Sectional Imaging Facilities

Wednesday, Nov. 30 9:00AM - 9:30AM Room: Learning Center - NPM DPS

#### Participants

Anand Narayan, MD, PhD, Verona, WI (*Presenter*) Nothing to Disclose

#### PURPOSE

Evaluate the effects of neighborhood deprivation at the zip code level on access to ACR accredited cross sectional imaging facilities.

#### METHODS AND MATERIALS

Area deprivation index (ADI) values were obtained from the University of Wisconsin Neighborhood Atlas, based on a validated HRSA measure that allows for national rankings of zip code level socioeconomic disadvantage. Disadvantage was dichotomized (high  $\geq$ 97th ADI percentile, low  $\leq$ 3rd ADI percentile). Urban/rural status was defined from US Department of Agriculture rural-urban commuting area (RUCA) codes. Outcomes included the presence or absence of ACR accredited cross sectional imaging facilities (yes/no). Chi square tests were used to evaluate the association between access and geographic disadvantage, stratified by urban/rural status.

#### RESULTS

Among 41,683 zip codes across the US, 2,796 were disadvantaged (1,160 rural, 1,636 urban) and 1,028 were advantaged (39 rural, 989 urban). Disadvantaged zip codes were more likely to be located in rural areas ( $p < 0.001$ ). Disadvantaged zip codes were less likely to have access to ACR accredited CT facilities (21 vs 32%,  $p < 0.001$ ), MRI (19 vs 32%,  $p < 0.001$ ), nuclear medicine (11 vs 18%,  $p < 0.001$ ), PET (7 vs 13%,  $p < 0.001$ ), ultrasound (14 vs 29%,  $p < 0.001$ ), lung cancer screening centers of excellence (5 vs 12%,  $p < 0.001$ ), diagnostic centers of excellence (1 vs 4%,  $p < 0.001$ ), and accredited radiation oncology facilities (3 vs 8%,  $p < 0.001$ ). Among urban areas, disadvantaged zip codes were less likely to have access to ACR accredited CT facilities (26 vs 33%,  $p < 0.001$ ), MRI (25 vs 33%,  $p < 0.001$ ), nuclear medicine (15 vs 19%,  $p = 0.007$ ), PET (9 vs 13%,  $p = 0.003$ ), ultrasound (20 vs 30%,  $p < 0.001$ ), lung cancer screening centers of excellence (7 vs 13%,  $p < 0.001$ ), diagnostic centers of excellence (2 vs 4%,  $p < 0.001$ ), and accredited radiation oncology facilities (5 vs 8%,  $p = 0.001$ ). Analyses for rural areas were limited by small numbers of advantaged zip codes.

#### CONCLUSION

Zip codes with high levels of socioeconomic disadvantage were less likely to have ACR accredited cross sectional imaging facilities, ACR centers of excellence and accredited radiation oncology facilities.

#### CLINICAL RELEVANCE/APPLICATION

Reducing disparities in access to quality imaging services will require radiology leaders to expand services in high disadvantage areas.

Printed on: 02/07/23

## Abstract Archives of the RSNA, 2022

W2-SPNPM-2

### Usability of Hospital Price Estimators for Lumbar Spine MRI

Wednesday, Nov. 30 9:00AM - 9:30AM Room: Learning Center - NPM DPS

#### Participants

Meagan Bechel, MD, PhD, (*Presenter*) Nothing to Disclose

#### PURPOSE

Evaluate usability of online hospital price estimators for a common imaging examination using surrogate patients

#### METHODS AND MATERIALS

Using the Amazon MTurk platform, we recruited adult English-speaking US-residents as surrogate patients to find the cash price for a non-contrast lumbar spine MRI examination for a self-pay patient using price estimator tools at four hospitals. All were asked to view a 3-minute tutorial video and report their experiences with the task, including the System Usability Scale (SUS) for the estimator, through a paid survey. We queried participants about demographics, insurance, prior imaging exposure, and assessed health literacy and health insurance literacy (HIL) using validated measures. Multivariable analysis for correct price identification and price estimator SUS were performed.

#### RESULTS

Of 660 respondents, 397 met eligibility criteria (70.8% <45 years; 43.8% female; 83.8% White). 84% found all four estimators; 1.5% were unable to locate any. Only 32% found the correct price at all four hospitals; 20.6% did not find any correct prices. Average SUS for the hospitals' estimators ranged between 63.0 and 78.8. The hospital with a similar estimator to that used in the tutorial video had highest SUS. Accuracy of price identification improved with later tasks. Higher HIL was associated with higher identification of at least one correct price (B,3.0;95%CI,0.6-5.4,  $p<0.01$ ) and higher SUS (B,14.7; 95%CI, 9.4-20.1,  $p<0.001$ ).

#### CONCLUSION

Surrogate patients were able to locate hospital price estimators, but unable to effectively use them to obtain correct prices. Tutorial videos improved SUS, but correct price identification improved with practice.

#### CLINICAL RELEVANCE/APPLICATION

Hospital price estimators score average or below average on usability and cannot be successfully utilized by the majority of educated paid surrogate patients. Though usability improves with a tutorial video, both increased usability and health insurance literacy are necessary for price estimator tools to be accessible and beneficial. Therefore, they may represent an additional, but mitigatable barrier to equitable and timely evidence-based care.

Printed on: 02/07/23

## Abstract Archives of the RSNA, 2022

W2-SPNR

### Neuroradiology Wednesday Poster Discussions

Wednesday, Nov. 30 9:00AM - 9:30AM Room: Learning Center - NR DPS

#### Participants

Arsany Hakim, MBBCh, Aarau, (*Moderator*) Nothing to Disclose

#### Sub-Events

#### W2-SPNR-1 **Quantitative Analysis of Ischemic Infarct Lesion Distribution in Term Neonates With Increasing Severity of Hypoxic Ischemic Encephalopathy**

#### Participants

Pratheek Bobba, BS, New Haven, CT (*Presenter*) Nothing to Disclose

#### PURPOSE

Hypoxic ischemic encephalopathy (HIE) is a serious cause of long-term disability and mortality in neonates. The topographic pattern of HIE parenchymal injury as seen on DWI helps with differentiation of hypoxic brain injury from other potential mechanisms and prognostic categorization of HIE severity. Thus far, topographic patterns of HIE distribution and their relationship with HIE severity have been described subjectively. In this study, we use quantitative methodologies to characterize the location of ischemic lesions in term neonates with varying severity of HIE.

#### METHODS AND MATERIALS

We analyzed the imaging and health records of term neonates (>36 postmenstrual gestational week) who had MRI/DWI at our center (01/2013 to 03/2021) with radiological and clinical findings of HIE. Neonates were then categorized into mild, moderate, and severe HIE based on Samat classification (Arch Neurol 1976;33:695-705), inferred from medical records. We manually segmented ischemic lesions from DWI scans and co-registered them to a standard brain space. We mapped all lesions to one hemisphere for generation of lesion summation maps; and used voxel wise general linear models (GLM) to identify regions of the brain more likely to be infarcted in neonates with increasing severity of HIE.

#### RESULTS

We included 33 neonates; 20 with mild, 7 with moderate, and 6 with severe HIE. Median gestational ages at scan (interquartile) were 40.18 (37.81 - 41.77), 40.14 (38.77 - 41.25), and 41.33 (39.69 - 41.79) weeks respectively for the mild, moderate, and severe groups ( $p=0.31$ ). Median infarct volumes (interquartile) were 2.32 (0.71 - 15.42), 115.24 (65.14 - 124.16), and 28.56 (18.62 - 52.24) mL respectively for the mild, moderate, and severe groups ( $p=0.15$ ). In summation maps, ischemic lesions in neonates with mild and moderate HIE were predominantly in subcortical and deep white matter along the border zone of arterial supply territories, while ischemic lesions in neonates with severe HIE involved basal ganglia, hippocampus, and thalamus in addition to white matter (Figure 1A). In voxel wise GLM analysis, higher severity of HIE was significantly associated with the presence of ischemic lesions in hippocampus, medial thalamus, and posterior putamen, after correction for infant volume as a covariate (Figure 1B).

#### CONCLUSION

In quantitative analysis of term neonates, mild and moderate HIE infarct lesions were mostly localized to arterial territory border zone white matter, while severe HIE was significantly associated with infarction of basal ganglia and hippocampi.

#### CLINICAL RELEVANCE/APPLICATION

Objective and quantitative assessment of ischemic lesion topography helps with diagnostic differentiation of mechanisms of brain injury and prognostication of HIE in term neonates.

#### W2-SPNR-10 **Achieving Human-Level Performance for Artificial Intelligence-Based Brain Metastasis Detection by Combining Black-Blood Contrast-Enhanced MRI**

#### Participants

Ji Eun Park, MD, PhD, Seoul, Korea, Republic Of (*Presenter*) Nothing to Disclose

#### PURPOSE

To validate updated AI adding black-blood imaging for detection of brain metastasis by comparing its performance with AI based on GRE-T1WI alone and human readers.

#### METHODS AND MATERIALS

In this retrospective study, AI was developed with GRE-T1WI (GRE AI) and adding black-blood imaging (combined AI) using 503 brain metastasis dataset. The AI was validated in 62 consecutive patients who underwent both black-blood imaging and GRE-T1WI for diagnostic purposes and subsequent GRE-T1WI for planning of stereotactic radiosurgery between September 2021 and January 2022. Per-lesion detection sensitivity and positive predictive value (PPV) were measured. Two human readers independently performed lesion detection on both exams. The relative difference (RD) from the reference standard numbers of metastases was

compared between human readers and AI.

## RESULTS

Sixty-two patients were included for clinical validation (mean age 63.3 years, 53% male). Sensitivity was similar between GRE AI (93%, 95% confidence interval [CI]: 90-96%) and combined AI (92%, 95% CI: 89-94%,  $p=0.506$ ). The positive predictive value of the combined AI was significantly higher (89%, 95% CI: 86-92%,  $p<0.001$ ) than that of GRE AI (76%, 95% CI: 72-80%). GRE AI significantly overestimated metastases (RD: 0.05, 95% CI: 0.00-0.58) compared with human readers (RD: 0.00, 95% CI: -0.28, 0.15,  $p<0.001$ ), whereas the combined AI (RD: 0.00, 95% CI: 0.00-0.15) did not show a significant difference from human readers (RD: 0.00, 95% CI: -0.20-0.10,  $p=0.913$ ).

## CONCLUSION

The brain metastasis detection AI combined with black-blood imaging showed improved detection of true positive metastases and reduced overestimation, achieving similar performance to human readers.

## CLINICAL RELEVANCE/APPLICATION

Artificial intelligence-based brain metastasis detection algorithm that incorporates black-blood imaging can help to increase true positive detections and reduce overestimation, achieving similar performance to a human reader.

## W2-SPNR-11 Comparing Machine Learning Techniques to Recognize Parathyroid Adenomas from 4D CT Data

Participants  
Cynthia Greene, MD, PhD, (*Presenter*) Nothing to Disclose

## PURPOSE

Support vector machine (SVM) analysis is a linear learning approach using measurements on images to make predictions. Convolutional neural network (CNN) analysis is a sophisticated technique for machine learning that uses images to make predictions. Both of these methods use known data to build a model for predictions. Parathyroid adenomas are tumors with an early enhancement pattern that is used to help identify them to aid in detection and surgical planning. This study aims to compare SVM and CNN analyses on the accuracy of identifying parathyroid adenomas.

## METHODS AND MATERIALS

This is a HIPPA compliant retrospective study with IRB approval. Informed consent was waived. Ninety-three 4D-CTs of patients with pathology-proven parathyroid adenomas were reviewed; 94 parathyroid adenomas (1 case had 2 adenomas) and 112 lymph nodes. The mean attenuation of the lesion of interest in HU of each acquired phase (0, 25, 50, 75 sec) is used to build a model in the SVM analysis. A 2D slice through the lesions in each phase is used to perform sequence classification with ResNet50 as the pre-trained network to construct the CNN model in MatLab. The data is split randomly between a model and validation data set in a 2:1 ratio. The area under the curve (AUC) and accuracy are calculated for the model and validation data sets.

## RESULTS

The plot of the enhancement curves of parathyroid adenomas demonstrates early enhancement with washout, while lymph nodes have persistent enhancement. On the model data, the AUC of the CNN is 0.99 while the SVM is 0.95. The overall accuracy of the CNN on the validation data set is 92%, while the SVM is 88%. The accuracy for parathyroid adenomas specifically is 93% for the CNN and 83% for the SVM model.

## CONCLUSION

Both SVM and CNN models discriminate between parathyroid adenomas and lymph nodes well (88% vs. 92%), showing that lesion enhancement alone plays a significant role in distinguishing tissue types. The CNN more accurately identifies parathyroid adenomas in the validation data set than the SVM analysis, showing that using both spatial and enhancement information helps distinguish between features of parathyroid adenomas and lymph nodes better than enhancement alone. One of the limitations of this study is the limited number of lesions; more lesions would help clarify the statistics for these models, especially with variation in lesion shape and size. Comparing techniques like the SVM and CNN models can help identify imaging features to differentiate between lesions.

## CLINICAL RELEVANCE/APPLICATION

Machine learning algorithms will enhance detection and provide insight into imaging features identifiable with parathyroid adenomas using 4D CT data.

## W2-SPNR-12 NeuroScreener: Quantized Vector Embedded Autoencoder-based Abnormality Classifier from Brain MRI

Participants  
Jimin Kang, (*Presenter*) Employee, NEUROPHET, Inc

## PURPOSE

In this work, we propose a novel framework that is the first of its kind to detect identifiable abnormalities that may be present in the images to reduce time and effort in the clinical practice by assisting clinicians' brain image reading.

## METHODS AND MATERIALS

A dataset for this study was a T1-weighted brain MRI dataset with normal and anomalous images collected from the multicenter including ADNI, SNUH, CMCH, and YUHS. The anomalous images were categorized into three. First was defined as MR images with a severe artifact such as insufficient field of view (FOV), external foreign body (EFB), motion, and a spike which may not be proper for further interpretation of the image. We further included de-faced or skull-stripped images, which are preprocessed unintentionally and/or improperly for further processing or interpretation. Lastly, we also included MR images with large infarction, which may produce inferior results for the routine segmentation process. The normal MR image has no aforementioned abnormality. In this study, we utilized a residual block-based variational autoencoder (VAE) as a backbone network. The vector quantization (VQ) module performs that the continuous feature of the latent space was mapped to a trainable discrete embedding vector by a predetermined number. The output value of the discrete embedding space is then connected to the fully connected layer to classify the input T1 MR image. We trained our VQ-based network using the weighted summation of VQ loss, reconstruction loss,

and Binary Cross Entropy (BCE) loss. The VQ loss was then used to calculate the loss for the VQ module. The Mean Squared Error (MSE) loss was calculated between the generated output image from the decoder and the input image. Additionally, we empirically adjusted the parameters for the loss function by histogram analysis of the distribution of the output loss.

## RESULTS

Our results presented the accuracy as high as 95%, and Area Under Receiver Operating Characteristic (AUROC) showed as high as 0.9778. The mean accuracy of seven types of anomalies we investigated showed 89%.

## CONCLUSION

In this study, an image generator-based classifier was proposed to detect abnormality present in MR images using VAE, which is applied to the VQ module adaptively. The proposed framework has shown high performance in all matrices.

## CLINICAL RELEVANCE/APPLICATION

We hope this study could assist the radiologists by replacing the time-consuming image reading process with a faster and more efficient image reading, which could provide the anomaly information that MRI may have.

## W2-SPNR-13 Value Proposition of Food and Drug Administration (FDA)-Approved Artificial Intelligence (AI) Algorithms for Neuroimaging

### Awards

**Trainee Research Prize - Resident**

Participants

Suryansh Bajaj, MD, New Haven, CT (*Presenter*) Nothing to Disclose

### PURPOSE

The number of FDA-approved artificial intelligence (AI) algorithms for neuroimaging has grown in the last decade. The adoption of these algorithms into clinical practice depends largely on whether this technology provides significant value to radiologists in the clinical setting. The objective of this study is to understand current trends in FDA-cleared AI algorithms for neuroimaging and understand the value proposition of these algorithms as advertised by the developer.

### METHODS AND MATERIALS

We extracted a list of FDA-approved neuroimaging AI algorithms from the American College of Radiology (ACR) Data Science Institute AI Central database from May 2008 to January 2022. Product information of each device was collected from the database. For each device, we collected information of advertised value as presented on the developer's website.

### RESULTS

The database includes a total of 54 AI neuroimaging algorithms that were cleared by the FDA between May 2008 and January 2022. A majority of the algorithms (28/54, 51.9%) were compatible with CT images with 22 (40.7%) compatible with MR and 4 compatible with CTP and CTA (7.4%). Nine algorithms (16.7%) were compatible with multiple imaging modalities. Of these algorithms, 53 (98.1%) were approved with a 510(k) clearance and 1 (1.9%) received de novo clearance. Out of the 54 algorithms, we found websites that discussed the product for 51 algorithms. The most widely advertised value proposition was improved quality of care (34/51, 66.7%). A total of 19 algorithms (37.3%) argued they saved the user time, 8 (15.7%) decreased costs, and 6 (11.8%) increased revenue. Product websites for 24 algorithms (47.1%) showed testimonials advertising the value of the technology. Subgroup analysis was performed to compare algorithms compatible with CT to those with MRI and the algorithms involved in ICH to those in LVO.

### CONCLUSION

Our results indicate a wide range of value propositions advertised by developers to indicate the value of their product. Most developers argued that their product would improve patient care. Further research is necessary to determine whether the value advertised by the developer is actually demonstrated in clinical practice.

### CLINICAL RELEVANCE/APPLICATION

Given the rapid growth in the number, availability, and clinical application of AI algorithms across the US, it is important to understand different uses and value propositions provided by these software in current practice.

## W2-SPNR-14 Exploring Functional Connectivity in Chronic SCI Patients with Neuropathic Pain versus without Neuropathic Pain

Participants

Adam Flanders, MD, Philadelphia, PA (*Presenter*) Nothing to Disclose

### PURPOSE

Spinal cord injury (SCI) causes debilitating chronic pain. Despite decades of research, the pain pathway of neuropathic pain (NP) is unknown. Several lines of evidence show abnormal functioning of the brain in patients with SCI. We hypothesize that in patients with SCI and neuropathic pain the pain matrix is altered compared to patients with SCI without neuropathic pain.

### METHODS AND MATERIALS

This study examines the functional connectivity (FC) in SCI patients with moderate-severe chronic neuropathic pain compared to SCI patients with mild-no neuropathic pain. These groups were compared to control subjects. Subjects completed the Neuropathic Pain questionnaire and completed a neurological evaluation based on the International Standard Neurological Classification of SCI to define severity and level of injury. Of the 8 participants with SCI, 5 (44.8±17.56 y.o, 4M and 1F) indicated they had NP and 3 did not have NP (37.33±9.24 y.o, 2M and 1F). We also included 10 uninjured neurologically intact controls (24.8±4.61 y.o, 5M and 5F). FC metrics were obtained from the comparisons of resting state functional magnetic resonance imaging amongst our various groups (uninjured controls, SCI with NP and SCI without NP). For each comparison, an ROI-to-ROI connectivity analysis was pursued, encompassing a total of 170 ROIs based on a customized atlas derived from AAL3 atlas. The analysis accounted for covariates such as age and gender. To correct for multiple comparisons, a strict Bonferroni correction was applied with a significance level of

p<0.05/NROIs.

## RESULTS

When comparing the SCI cohort with uninjured subjects our results show statistically significant decreased FC in various thalamic nuclei including: medial and lateral pulvinar, lateral geniculate nucleus, and mediodorsal magnocellular. We postulate these findings are associated with suppressed inhibitory inputs from the zona incerta (ZI) and the anterior pretectal nucleus (APT) in those with NP following SCI. The suppressed inhibitory input causes enhanced activity at the posterior nucleus of the thalamus, S1 and thalamic nuclei regulated by ZI/APT. There were no significant differences of FC in patients with SCI without NP pain compared to controls.

## CONCLUSION

s Manipulations that enhance the activity of ZI/APT can improve the treatment in SCI pain. Additionally, the loss of inhibition within the thalamus and abnormal thalamocortical interactions can predispose patients for the development of chronic pain.

## CLINICAL RELEVANCE/APPLICATION

Our findings complement results from other neuroimaging studies and provide multi-modal evidence for identifying novel regions of the brain specific to the SCI cohort. These regions can serve as therapeutic targets to improve SCI neuropathic pain patients.

## W2-SPNR-15 **A Deep Learning Algorithm Trained with Multiphase CTA Images Could Improve Collateral Circulation Assessment in Acute Ischemic Stroke**

Participants  
Jingjie Wang, (*Presenter*) Nothing to Disclose

### PURPOSE

We tried to build a deep learning-based, objective, fast, and accurate collateral circulation assessment model.

### METHODS AND MATERIALS

We collected 92 acute ischemic stroke (AIS) patients with large vessel occlusion in the anterior circulation in our hospital from June 2020 to August 2021. We analyzed their baseline one-stop whole-brain four-dimensional computed tomography angiography (4D-CTA)/CT perfusion. The images of the arterial, arteriovenous, venous, and late venous phases were extracted from 4D-CTA according to the perfusion time density curve. The subtraction images of each phase were created by subtracting the non-contrast CT scan. Each patient was marked with good or poor collateral circulation.

### RESULTS

Based on the ResNet34 classification network, we developed a single-image input and a multi-image input network for binary classification of collateral circulation. The training and test sets were 65 and 27 patients, respectively, and Monte Carlo cross-validation was employed for five iterations. The network performance was evaluated by precision, accuracy, recall, F1 score, and AUC. All the five performance indicators of the single-image input model were higher than those of the other.

### CONCLUSION

s The single-image input processing network, combining multiphase CTA images, can better classify the AIS collateral circulation. This automated collateral assessment tool can help streamline clinical workflows, and screen patients for reperfusion therapy.

### CLINICAL RELEVANCE/APPLICATION

Collateral circulation is important for the treatment plan and prognosis of patients with acute ischemic stroke (AIS). However, due to the complexity and difficulty of quantifying the neurological vessels' structure, the evaluation of collateral circulation is challenging. Although scholars have tried and reported various methods for assessing collateral circulation, there is no unified standard for assessing collateral circulation. Even when the same assessment method is used, physicians have significant subjective differences. The development of computerized deep learning algorithms has brought new solutions to this difficulty. This study uses deep learning methods to achieve a rapid, objective, and accurate collateral circulation evaluation of the AIS patients.

## W2-SPNR-16 **Brain MRI Automated Volumetry vs Non-automated Planimetric Assessment for Differentiating Progressive Supranuclear Palsy From Parkinson's Disease and Healthy Subjects: Can Machine Learning Help the Radiologist Choice?**

Participants  
Francisco Mendoza, MD, (*Presenter*) Nothing to Disclose

### PURPOSE

Develop a machine learning model to determine the more accurate tool, between automated volumetry and non-automated planimetric assessment in differentiating Progressive Supranuclear Palsy (PSP) from Parkinson's disease (PD) and healthy subjects (HS).

### METHODS AND MATERIALS

We retrospectively assessed 141 patients with a clinical diagnosis of Parkinsonism paired by age and sex and with a group of HS (PSP n = 47, PE n = 68, HS=26) between January 2003 and April 2021. Patients without T1-MPRAGE were excluded, leaving 83 subjects (PSP n = 29, PD n = 54, HS n=26). We included different clinical subtypes of PSP: PSP-RS (n= 19), PSP-P (n= 5), PSP-PGF (n= 4), and PSP-F (n= 1). Using automatized SyngoviaBrainMorphometry software (Siemens), we obtained 109 volumes of interest (VOIs) for each brain MRI study, including absolute and normalized values. Two independent radiologists blind to diagnosis performed a planimetric assessment (Massey ratio, Oba ratio, MPRI 1.0, and MRP 2.0). The intraclass correlation coefficient (ICC) was used to assess interobserver agreement. We developed a machine-learning model based on multivariate feature selection and an extreme gradient boosting (XGB) vs. univariate feature selection and random forest (RF) with automated volumetric data and planimetric assessment to differentiate PSP from PD and HS. All subjects were randomly divided into training (85%) and validation (15%) data sets with the same proportions for each clinical group. The most relevant data obtained from each model were ordered by importance score (F-score: where 1.0 represents perfect precision and recall). Additionally, we assessed the diagnostic

accuracy of each tool using ROC curves.

## RESULTS

The global diagnostic performance of the volumetric model to differentiate between the three groups was 70.6% and 70.5% for the planimetric assessment. The most relevant automated brain volumetry was the mesencephalic-normalized volume (0.068), with an area under the curve (AUC) of 0.87. For planimetric assessment, the most important measurements were the mesencephalic width (0.33) with an AUC of 0.99, followed by the mesencephalic area (0.19) with an AUC of 0.94. The planimetric measurements presented very good reproducibility with interobserver intraclass correlation coefficients (ICC) of  $> 0.75$ .

## CONCLUSION

There is no significant difference between automatized volumetric volumes or planimetric assessment models in predicting the diagnosis of PSP or PD. The classic measurements of mesencephalic width or mesencephalic area have better diagnostic accuracy than volumetric values.

## CLINICAL RELEVANCE/APPLICATION

Automatized volumetric assessment of brain MRI is a helpful tool for differentiating Progressive Supranuclear Palsy from Parkinson's disease.

## W2-SPNR-18 Accurate Cerebellar Cortex Segmentation: A Deep-Learning-Based Approach

Participants

Fabiano Reis, Campinas, Brazil (*Presenter*) Nothing to Disclose

## PURPOSE

Cerebellum segmentation is a challenging task due to the intricately folded cortex and proximity with the cerebral cortex. Several tools reach excellent results in healthy controls, but in patients with cerebellar damage the segmentation might be catastrophic. Hence, we propose to develop an MRI tool to segment with accuracy abnormal and non-abnormal cerebellums using deep-learning algorithms.

## METHODS AND MATERIALS

We used T1-weighted MRI sequences acquired in a 3 T Philips Achieva at the University of Campinas. The dataset is composed of healthy controls, SCA1 (spinocerebellar ataxia), SCA3, and FRDA (Friedreich's Ataxia) subjects' acquisitions, 15 images of each group. A group of expert neuroradiologists labeled the images following a protocol to ensure quality and correctly identify the cerebellar fissures. We chose the 3D U-net architecture with a few modifications which is a consolidated model for segmentation tasks in the medical imaging domain. In order to assess the gains of our specialist segmented data, a segmentation model was trained. After that, we compared it along with ACAPULCO and CERES models to evaluate differences in segmentation performance.

## RESULTS

Our initial U-Net model was trained on Google Colab and achieved 0.921 for Dice score (DS) on the validation set. We randomly selected 14 images from the training set to assess the main segmentation tools (Our model, ACAPULCO and CERES). We found a mean DS of  $0.928 \pm 0.030$  for our model,  $DS = 0.909 \pm 0.043$  for ACAPULCO and  $DS = 0.918 \pm 0.039$  for Ceres. When we compared patients with the highest level of cerebellar damage, this difference of performance increases a lot (our model:  $DS = 0.904 \pm 0.041$ ; ACAPULCO:  $DS = 0.870 \pm 0.052$ ; CERES:  $DS = 0.888 \pm 0.052$ ). In addition, comparing the segmentation volume of our model against ACAPULCO and CERES outputs of 71 and 72 images from FRDA (subtle damage) and SCA3 (severe damage) patients, respectively, we found volumetric difference between our model and ACAPULCO for both group of patients ( $p < 0.001$ ). For CERES, we only identify volumetric differences for the SCA3 patients ( $p < 0.001$ ).

## CONCLUSION

Initial results show a promising methodology, whereas we are still working on gathering more expert-segmented images, in order to obtain sensitive variables to measure the impact of modifier agents of new therapies for several neurodegenerative disorders.

## CLINICAL RELEVANCE/APPLICATION

Cerebellum segmentation is a challenging task due to the intricately folded cortex and proximity with the cerebral cortex. Our initial results show a promising methodology, whereas we are still working on gathering more expert-segmented images, in order to obtain sensitive variables to measure the impact of modifier agents of new therapies for several neurodegenerative disorders.

## W2-SPNR-19 A Large-scale Granger Causality Approach for Functional MRI Data Analysis - Identification of Schizophrenia Patients

Participants

Ali Vosoughi, Rochester, NY (*Presenter*) Nothing to Disclose

## PURPOSE

To develop and evaluate a novel machine learning method for identifying patients with schizophrenia using large-scale Granger Causality (lsGC) by capturing connectivity differences in resting-state functional MRI (rsfMRI).

## METHODS AND MATERIALS

From the publicly available Centers of Biomedical Research Excellence (COBRE) fMRI data repository on 146 subjects (72 schizophrenia patients, 62 controls), we included the subsample of all 62 subjects under the age of 32 years (29 schizophrenia patients, 33 controls) using standard preprocessing by the Nilearn Python library and the NIAK resting-state pipeline, with functional parcellation into 122 brain regions [Bellec, NIAK, 2016]. For calculating directed functional connectivity between brain regions, we have recently developed the large-scale Granger Causality (lsGC) algorithm [Citation blinded for review] that combines dimension reduction with multivariate predictive causal modeling in high-dimensional fMRI time series. A 100-iteration cross-validation approach with 80%/20% train/test ratio was applied, where feature selection was performed on each training set using Kendall's tau rank correlation, followed by support vector machine classification. To quantitatively evaluate diagnostic accuracy of lsGC for correctly classifying schizophrenia patients and normal controls, we compare its performance with both a recent state-of-the-art causal discovery method (PCMC, [Runge et al., Science, 2019]), and the current clinical fMRI analysis standard of cross-

correlation (CC), reporting accuracy, area under ROC curve (AUC), and f1-score.

## RESULTS

The IsGC rsfMRI analysis method significantly outperformed both PCMRI and the clinical standard CC techniques at classifying schizophrenia patients from healthy subjects, with accuracy/AUC/f1 score of 100%/1.0/100% for IsGC, 86.4%/0.81/78.4% for PCMRI, and 65.8%/0.62/60.4% for CC, respectively.

## CONCLUSION

Our results suggest that IsGC significantly improves the diagnostic accuracy of correctly identifying patients with schizophrenia from rsfMRI neuroimaging. We conclude that, when compared to both conventional CC analysis and state-of-the-art PCMRI, IsGC is better suited to capture disease-related brain network connectivity changes in schizophrenia patients.

## CLINICAL RELEVANCE/APPLICATION

The IsGC method classifies schizophrenia subjects and controls by identifying relevant changes in fMRI connectivity, suggesting its potential use as a diagnostic imaging biomarker for neurologic disease.

## W2-SPNR-2 Accelerating Susceptibility Weighted Imaging With Deep Learning Validated in Acute Ischemic Stroke

Participants

Qi Duan, Beijing, China (*Presenter*) Nothing to Disclose

## PURPOSE

Susceptibility weighted imaging (SWI) can display low-flow rapid vessels and arterial thrombosis and provide cerebral hemodynamic information without the use of contrast media by its strong detection ability for the paramagnetic properties of deoxyhemoglobin, which is helpful for acute ischemic stroke (AIS) clinical diagnostic and treat strategy made. However, SWI imaging requires a long acquisition time, which increases the possibility of motion artifacts, and limits the spatial resolution and slice thickness. We aimed to evaluate the clinical feasibility of the accelerating SWI generated by a deep learning model in patients with AIS.

## METHODS AND MATERIALS

SWI data were collected from 45 AIS patients who underwent 3.0T MR examination in our hospital from January 2019 to January 2020. Using a sampling pattern library consisting of 3000 different two-dimensional variable-density random undersampling masks by referencing the k-space data retrospectively generated the undersampled SWI data, then using the complex-valued convolutional neural network (ComplexNet) to develop reconstruct high-quality SWI from highly accelerated k-space data. The data set was split into training (36 patients) and test (9 patients) sets (80% training and 20% test). The presence of susceptibility vessel sign (SVS) of each patient was assessed by two experienced radiologists.

## RESULTS

A total of 45 patients (mean age, 66.67 years  $\pm$ 14.05, 30 men). ComplexNet achieved high image quality with acceleration rates of 5, and there was no significant diagnostic performance difference between fully sampled and ComplexNet in image quality ( $p > 0.05$ ). The intraclass correlation coefficient (ICC) was excellent for the results of the assessment using ComplexNet SWI images between two readers (ICC = 0.750,  $p=0.006$ ).

## CONCLUSION

ComplexNet can accelerate SWI effectively and generate the image of high quality while showing superior ability in detecting SVS in AIS. Further use of the accelerating SWI, such as cerebral microbleeds detection, needs to be proven in large cohorts.

## CLINICAL RELEVANCE/APPLICATION

Susceptibility weighted imaging (SWI) can display low-flow rapid vessels and arterial thrombosis and provide cerebral hemodynamic information without the use of contrast media by its detection ability for paramagnetic properties of deoxyhemoglobin, which is of great value in acute ischemic stroke (AIS) patients' arterial thrombosis and cerebral microbleeds detection. However, SWI imaging requires a long acquisition time. We used a deep learning model to accelerate SWI, and evaluated the clinical feasibility of the accelerated SWI in patients with AIS.

## W2-SPNR-20 Comparison of Volume Measurements and Reliability of Two Commercial Software for Automatic Brain Volumetry

Participants

Jimin Kim, MD, Seoul, Korea, Republic Of (*Presenter*) Nothing to Disclose

## PURPOSE

Brain atrophy has close correlations with various neurodegenerative diseases. However visual assessment of brain atrophy tend to show high interobserver variability and low sensitivity. We aimed to evaluate the inter-method reliability and volumetric differences between NeuroQuant (NQ) and AQUA (AQ) using T1 sagittal sequence.

## METHODS AND MATERIALS

This retrospective study enrolled 202 patients without focal brain lesion. NQ and AQ were used for volumetric analysis of sagittal T1-weighted images with slice thickness of 1 mm. To analyze the inter-method difference, correlation, and reliability, we used the paired t-test, Pearson's correlation coefficient, intraclass correlation coefficient (ICC), and effect size (ES) using the SPSS software.

## RESULTS

The paired t-test showed significant volume differences in most regions except for the total and left side of parietal volume, white matter of right cerebral hemisphere, right frontal volume and right cingulate between the two methods. Volume measures by NQ and AQ showed good-to-excellent reliability ( $r= 0.634-0.892$ ,  $ICC=0.766-0.940$ ), except for caudate, nucleus accumbens, cingulate and pallidum which showed average to fair reliability ( $r= 0.371-0.448$ ,  $ICC= 0.470-0.617$ ). For the measurements of ES, volume differences were large in most regions ( $r= 0.01-9.52$ ). ES was the largest in the right pallidum and smallest in the right frontal lobe.

## CONCLUSION

s In most brain regions, AQ showed significantly larger volume measurements with large ES than NQ. However, NQ and AQ showed good to excellent inter-method reliability in volumetric measurements for most brain regions, with the exception of relative smaller region.

## CLINICAL RELEVANCE/APPLICATION

Therefore, clinicians should be aware that the volume measurements may vary by software and by region.

## W2-SPNR- Automatic Large Vessel Occlusion Detection via a Thrombus Segmentation Approach 21

Participants

Rotem Golan, PhD, (*Presenter*) Software developer, Circle Cardiovascular Imaging Inc

## PURPOSE

To introduce an explainable machine learning (ML) approach for large vessel occlusion (LVO) detection via thrombus segmentation, namely StrokeSENS LVO, and validate its performance on a large heterogeneous dataset of single-phase computed tomography angiography (CTA) scans of the head.

## METHODS AND MATERIALS

An explainable approach for LVO detection is proposed which is composed of two main components: (1) thrombus segmentation, and (2) segmentation of the large vessels of the anterior circulation of the brain; both of which are performed in three dimensions. Predicted thrombi of any size are flagged and their distance from the large vessels is measured to perform a final yes/no LVO decision. For validation, a total of 400 studies (217 LVO, 183 non-LVO) were used. The LVO group includes internal carotid artery (ICA) and m1 segment of the middle cerebral artery (M1-MCA) occlusions; and the non-LVO group includes more distal or posterior cerebral artery occlusions, no occlusions, and hemorrhagic stroke cases. Expert consensus reads were used as reference standard. Performance was evaluated using sensitivity and specificity and corresponding 95% confidence intervals (CI). Additional analysis was performed on several subgroups of interest.

## RESULTS

For detecting LVO, StrokeSENS LVO achieved a sensitivity of 90.3% [86.4%, 94.3%] and specificity of 95.1% [91.9%, 98.2%]. Furthermore, sensitivities of 88.5% [81.4%, 95.6%] on ICA cases (N=78) and 91.4% [86.7%, 96.0%] on M1-MCA cases (N=139) were noted; similarly, specificities of 98.2% [93.6%, 99.5%] on hemorrhagic stroke cases (N=110) and 90.4% [83.7%, 97.2%] on non-LVO-non-hemorrhage cases (N=73) were noted. Similar performances were observed across stratified datasets based on age, sex, scanner manufacturer and slice thickness when compared to the full cohort.

## CONCLUSION

s StrokeSENS LVO has demonstrated high sensitivity and specificity in detecting LVOs on a large heterogeneous dataset. The output of its components, i.e., predicted thrombus and vessels, can provide users with valuable information as to why certain predictions are made, and build clinicians' trust in using the tool in clinical practice.

## CLINICAL RELEVANCE/APPLICATION

Patients with acute ischemic stroke due to LVO are candidates to receive lifesaving endovascular treatment. Timely and reliable detection of LVO on CTA is challenging in many centers and therefore automating the process and providing an explainable tool to clinicians is of great importance.

## W2-SPNR-4 Ultra Low-iodine-load and Low-radiation 70 kVp Cerebral CT Angiography: Application of Deep learning-based Augmented Contrast Enhancement and Denoising Algorithms

Participants

Eun-Suk Cho, MD, PhD, Seoul, Korea, Republic Of (*Presenter*) Nothing to Disclose

## PURPOSE

To determine the feasibility of ultra low-iodine-load and low-radiation 70 kVp cerebral CT angiography (CTA) using deep learning-based augmented contrast enhancement (DL-ACE) and deep learning-based denoising (DL-DN) algorithms.

## METHODS AND MATERIALS

Forty-seven volunteers were randomly assigned to one of three CTA protocols: group A (100 kVp and 40 mL of 350 mg I/mL iodine contrast media (CM)), group B (70 kVp and 40 mL of 270 mg I/mL CM), or group C (70 kVp and 28 mL of 270 mg I/mL CM). Images of groups B and C were reconstructed using DL-ACE and DL-DN algorithms. DL-ACE (ClariACE, ClariPi) was developed based on the U-net architecture to predict vascular and parenchymal contrast enhancement by being trained with high-energy (150 kVp) and low-energy (80 kVp) datasets of dual-energy CT images. Augmented contrast-enhanced images were obtained by boosting the degree of enhancement in contrast-enhanced organs. DL-DN (ClariCT.AI, ClariPi) was designed to predict possible image noise by low radiation from standard-dose images, and denoised images were acquired by subtracting predicted noise from the originals. The vascular attenuation value and contrast-to-noise ratio (CNR) of cerebral arteries, subjective image quality, and radiation dose were compared among the groups.

## RESULTS

The vascular attenuations of groups B ( $405.0 \pm 43.3$  HU) and C ( $393.9 \pm 54.1$  HU) were significantly higher than that of group A ( $323.9 \pm 50.2$  HU). However, the CNR of group A ( $18.9 \pm 4.9$ ) was significantly higher than those of groups B ( $15.4 \pm 2.5$ ) and C ( $14.9 \pm 2.4$ ) because the image noise of groups B and C ( $23.3 \pm 2.2$ ) were significantly higher than that of group A ( $15.4 \pm 2.2$ ). After the application of DL-ACE and DL-DN, the image noise was significantly decreased in groups B and C ( $14.9 \pm 1.8$ ). The vascular attenuation and CNR were significantly increased in group B ( $768.7 \pm 87.5$  HU and  $49.1 \pm 9.3$ ) and group C ( $748.0 \pm 108.5$  HU and  $46.8 \pm 10.1$ ). CTDI of groups B and C ( $15.4$  mGy) was 23.5% lower than that of group A ( $20.13$  mGy).

## CONCLUSION

s Application of DL-ACE and DL-DN increased arterial attenuation by 89.8% and decreased image noise by 35.9% in cerebral CTA,

respectively. 70 kVp cerebral CTA using DL-ACE and DL-DE improved significantly higher arterial attenuation and CNR and lower image noise and provided better subjective image quality, although with 46.0% lower iodine load and 23.5% lower radiation dose, compared to 100 kVp CTA protocol.

#### **CLINICAL RELEVANCE/APPLICATION**

Deep learning-based augmented contrast enhancement and denoising algorithms produce high arterial enhancement and CNR and good image quality in cerebral CTA, even with ultra low-iodine-load and low-radiation.

#### **W2-SPNR-5 Could High kVp Non-Contrast Brain CT Improve Image Quality without Dose Increase?: Combined Use of Deep Learning Image Reconstruction and Automatic Current Modulation**

Participants  
Younghen Lee, MD, (*Presenter*) Nothing to Disclose

#### **PURPOSE**

To evaluate the impact of combined use of a new deep learning image reconstruction (DLIR) algorithm and automatic current modulation on image quality and dose reduction of non-contrast brain CT

#### **METHODS AND MATERIALS**

After the recent DLIR (TrueFidelity™, GE) launching, we obtained non-contrast brain CT images with different scanning condition during the recent ten-months (Dec,2019~Sep,2020), to optimize image quality and radiation dose (120kVp with ASIR-V 20%, 120/140kVp with DILR-mid, 140kVp with DILR-mid adding smart mA (noise index 7 and 8). For a comparison between those five different conditions, we retrospectively identified the normal brain CT cases of 151 young adults (mean age: 26.2 years). Region of interest based attenuation and noise measurements was done for supra-/infra-tentorial structure to compare SNR (signal to noise ratio), CNR (contrast to noise ratio) and CTDI and DLP

#### **RESULTS**

DLIR provided the better CNR and SNR than 20% ASIR-V by significant noise reduction. Compared to 120kVp with ASIR-V 20%, DLIR improved CNR and SNR of non-contrast 140kVp brain CT by mean 53.1% and 66.3% (noise index 7), 22.8%, and 41.5% (noise index 8) at the mean 8%, and 27% reduced doses by adding automatic current modulation

#### **CONCLUSION**

s Combined use of DLIR algorithm and automatic current modulation could be the potentially powerful tool for brain CT dose optimization

#### **CLINICAL RELEVANCE/APPLICATION**

Combined use of DLIR algorithm and automatic current modulation could be the potentially powerful tool for brain CT dose optimization

#### **W2-SPNR-8 Automatic Tumor Segmentation and Survival Prediction for Children with Diffuse Midline Gliomas**

Participants  
Zhifan Jiang, PhD, Washington, DC (*Presenter*) Nothing to Disclose

#### **PURPOSE**

Diffuse midline glioma (DMG) is a rare but fatal pediatric central nervous system (CNS) tumor with a median overall survival (OS) of 11 months from diagnosis. Tumor volume and appearance on MRI may be important indicators of progression, response to treatment and survival outcomes. However, there is no quantitative imaging tool available to help improve clinical management of DMG. The purpose of this work is to develop a machine learning-based automatic framework to quantitatively analyze DMG from a small dataset and predict patient OS one year after diagnosis.

#### **METHODS AND MATERIALS**

We retrospectively collected contrast-enhanced T1 and T2 (mostly FLAIR) weighted MRIs from DMG patients at diagnosis (n=42) and within 1 month after completion of radiation therapy (RT) (n=35). Contrast enhancing tumor region (ET) and the whole tumor (WT) were manually labeled. We first adapted the SegResNet deep learning model developed to automatically segment ET and WT of more common adult CNS tumors (i.e., glioblastoma multiforme [GBM]). The model was pre-trained on 1,000 GBM cases and was fine-tuned using the DMG dataset (n=77 images for 2 timepoints) with a 5-fold cross-validation. DMG cases with data at both timepoints (n=34) were used for survival prediction. We extracted the following MRI features based on automatic segmentations: ET and WT volumes (and relative to the brain volumes), ET relative to WT volumes, changes between the 2 timepoints of these volumes, tumor heterogeneity (i.e., intensity skewness and kurtosis), and voxel percentage for each cluster when applying Gaussian Mixture Model (GMM) clustering algorithm to classify the segmented WT volume into 3 clusters based on T1 and T2 image intensities. A support vector machine was used to predict 1-year survival from combinations of these features with leave-one-out validation.

#### **RESULTS**

Our automatic segmentation method resulted in Dice scores of  $0.841 \pm 0.072$  and  $0.831 \pm 0.073$ , and relative volume error of  $13.1\% \pm 11.4\%$  and  $16.3\% \pm 15.8\%$  for ET and WT, respectively. The 1-year survival prediction accuracy was 73.5% (sensitivity=70.6%, specificity=76.5%), achieved using 3 features: voxel percentage for the 2nd cluster of GMM clustering of WT volume on post-RT T1 images, skewness of WT volume on post-RT T2 images, and ET relative to WT volumes for post-RT images.

#### **CONCLUSION**

s Rare pediatric CNS tumor analysis can be efficiently performed from small datasets using transfer learning from comparable adult datasets to yield accurate automatic quantification of tumors and acceptable survival prediction.

#### **CLINICAL RELEVANCE/APPLICATION**

The prediction of OS from diagnosis and early post-treatment MR images has the potential to guide and improve the clinical

management of DMG and other rare pediatric conditions.

## **W2-SPNR-9 Novel Deep Learning Super-Resolution Algorithm Allows Substantial Improvement of Brain MRI Image Quality and Scan Time in a Multi-Site Study**

Participants

Tal Aharoni, MSc, Haifa, Israel (*Presenter*) Employee, RadNet, Inc;

### **PURPOSE**

To evaluate image quality, image resolution, and overall diagnostic sufficiency of low-resolution brain MRI images processed by a novel deep-learning (DL) resolution enhancement algorithm, compared to images acquired with higher resolution from multiple sites and MRI scanners.

### **METHODS AND MATERIALS**

73 sequences of 27 subjects (19-88 years) were obtained on 11 different clinical MRI scanners (1.2T, 1.5T and 3T) from different vendors (Philips, Hitachi, Siemens and GE) under multi-site IRB-approval (in USA, Israel and Brazil). Each patient was imaged using the site's routine high-resolution (HR) protocol and with 25-33% faster variants, solely compromising resolution in phase encoding direction. The low-resolution (LR) scans were processed by a novel convolutional-neural network (CNN) based super-resolution algorithm, trained on a vast amount of brain MRI images from scanners of multiple vendors with a variety of clinical indications, to produce enhanced resolution (ER) images. Independent, blinded, side-by-side comparisons of diagnostic quality, spatial resolution, noise level, artifacts appearance and contrast resolution were performed by 6 experienced neuroradiologists, using a 7-point Likert-scale (1=unacceptable, 7=excellent). An additional non-blind review by a highly experienced neuroradiologist (>15 years' experience) was performed comparing image details between the HR and ER scans. Statistical analysis was performed (using JASP 0.15) comparing (i) HR to ER scans and (ii) LR to ER scans. Statistical significance was determined by paired samples t-test testing for either superiority or non-inferiority of ER scans.

### **RESULTS**

Results (n=362 reads) exhibited superiority of the ER images over both the LR and HR images for diagnostic quality, spatial resolution, noise levels and contrast resolution ( $p<0.001$ ) and demonstrated non-inferiority for artifacts appearance ( $\beta=0.2$ ,  $p<0.001$ ). 21 out of the 73 reviewed series showed pathologies. Statistical results were reinforced by the nonblinded review, demonstrating equality for image details and diagnostic confidence between the ER and HR images.

### **CONCLUSION**

Results demonstrate superior overall image quality of low-resolution scans processed by a DL resolution enhancement algorithm compared to the routine HR scans across multiple sites and vendors, enabling MRI image resolution reduction and scan time shortening without adversely affecting image and diagnostic quality.

### **CLINICAL RELEVANCE/APPLICATION**

Substantial improvement of brain MRI Image quality and scan time can be achieved using a robust DL-algorithm, resolving the trade-off between resolution and acquisition time on a variety of scanners.

Printed on: 02/07/23

## Abstract Archives of the RSNA, 2022

W2-SPNR-1

### Quantitative Analysis of Ischemic Infarct Lesion Distribution in Term Neonates With Increasing Severity of Hypoxic Ischemic Encephalopathy

Wednesday, Nov. 30 9:00AM - 9:30AM Room: Learning Center - NR DPS

#### Participants

Pratheek Bobba, BS, New Haven, CT (*Presenter*) Nothing to Disclose

#### PURPOSE

Hypoxic ischemic encephalopathy (HIE) is a serious cause of long-term disability and mortality in neonates. The topographic pattern of HIE parenchymal injury as seen on DWI helps with differentiation of hypoxic brain injury from other potential mechanisms and prognostic categorization of HIE severity. Thus far, topographic patterns of HIE distribution and their relationship with HIE severity have been described subjectively. In this study, we use quantitative methodologies to characterize the location of ischemic lesions in term neonates with varying severity of HIE.

#### METHODS AND MATERIALS

We analyzed the imaging and health records of term neonates (>36 postmenstrual gestational week) who had MRI/DWI at our center (01/2013 to 03/2021) with radiological and clinical findings of HIE. Neonates were then categorized into mild, moderate, and severe HIE based on Sarnat classification (Arch Neurol 1976;33:695-705), inferred from medical records. We manually segmented ischemic lesions from DWI scans and co-registered them to a standard brain space. We mapped all lesions to one hemisphere for generation of lesion summation maps; and used voxel wise general linear models (GLM) to identify regions of the brain more likely to be infarcted in neonates with increasing severity of HIE.

#### RESULTS

We included 33 neonates; 20 with mild, 7 with moderate, and 6 with severe HIE. Median gestational ages at scan (interquartile) were 40.18 (37.81 - 41.77), 40.14 (38.77 - 41.25), and 41.33 (39.69 - 41.79) weeks respectively for the mild, moderate, and severe groups ( $p=0.31$ ). Median infarct volumes (interquartile) were 2.32 (0.71 - 15.42), 115.24 (65.14 - 124.16), and 28.56 (18.62 - 52.24) mL respectively for the mild, moderate, and severe groups ( $p=0.15$ ). In summation maps, ischemic lesions in neonates with mild and moderate HIE were predominantly in subcortical and deep white matter along the border zone of arterial supply territories, while ischemic lesions in neonates with severe HIE involved basal ganglia, hippocampus, and thalamus in addition to white matter (Figure 1A). In voxel wise GLM analysis, higher severity of HIE was significantly associated with the presence of ischemic lesions in hippocampus, medial thalamus, and posterior putamen, after correction for infant volume as a covariate (Figure 1B).

#### CONCLUSION

In quantitative analysis of term neonates, mild and moderate HIE infarct lesions were mostly localized to arterial territory border zone white matter, while severe HIE was significantly associated with infarction of basal ganglia and hippocampi.

#### CLINICAL RELEVANCE/APPLICATION

Objective and quantitative assessment of ischemic lesion topography helps with diagnostic differentiation of mechanisms of brain injury and prognostication of HIE in term neonates.

Printed on: 02/07/23

## Abstract Archives of the RSNA, 2022

W2-SPNR-10

### Achieving Human-Level Performance for Artificial Intelligence-Based Brain Metastasis Detection by Combining Black-Blood Contrast-Enhanced MRI

Wednesday, Nov. 30 9:00AM - 9:30AM Room: Learning Center - NR DPS

#### Participants

Ji Eun Park, MD, PhD, Seoul, Korea, Republic Of (*Presenter*) Nothing to Disclose

#### PURPOSE

To validate updated AI adding black-blood imaging for detection of brain metastasis by comparing its performance with AI based on GRE-T1WI alone and human readers.

#### METHODS AND MATERIALS

In this retrospective study, AI was developed with GRE-T1WI (GRE AI) and adding black-blood imaging (combined AI) using 503 brain metastasis dataset. The AI was validated in 62 consecutive patients who underwent both black-blood imaging and GRE-T1WI for diagnostic purposes and subsequent GRE-T1WI for planning of stereotactic radiosurgery between September 2021 and January 2022. Per-lesion detection sensitivity and positive predictive value (PPV) were measured. Two human readers independently performed lesion detection on both exams. The relative difference (RD) from the reference standard numbers of metastases was compared between human readers and AI.

#### RESULTS

Sixty-two patients were included for clinical validation (mean age 63.3 years, 53% male). Sensitivity was similar between GRE AI (93%, 95% confidence interval [CI]: 90-96%) and combined AI (92%, 95% CI: 89-94%,  $p=.506$ ). The positive predictive value of the combined AI was significantly higher (89%, 95% CI: 86-92%,  $p<.001$ ) than that of GRE AI (76%, 95% CI: 72-80%). GRE AI significantly overestimated metastases (RD: 0.05, 95% CI: 0.00-0.58) compared with human readers (RD: 0.00, 95% CI: -0.28, 0.15,  $p<.001$ ), whereas the combined AI (RD: 0.00, 95% CI: 0.00-0.15) did not show a significant difference from human readers (RD: 0.00, 95% CI: -0.20-0.10,  $p=.913$ ).

#### CONCLUSION

s The brain metastasis detection AI combined with black-blood imaging showed improved detection of true positive metastases and reduced overestimation, achieving similar performance to human readers.

#### CLINICAL RELEVANCE/APPLICATION

Artificial intelligence-based brain metastasis detection algorithm that incorporates black-blood imaging can help to increase true positive detections and reduce overestimation, achieving similar performance to a human reader.

Printed on: 02/07/23



## Abstract Archives of the RSNA, 2022

W2-SPNR-11

### Comparing Machine Learning Techniques to Recognize Parathyroid Adenomas from 4D CT Data

Wednesday, Nov. 30 9:00AM - 9:30AM Room: Learning Center - NR DPS

#### Participants

Cynthia Greene, MD, PhD, (Presenter) Nothing to Disclose

#### PURPOSE

Support vector machine (SVM) analysis is a linear learning approach using measurements on images to make predictions. Convolutional neural network (CNN) analysis is a sophisticated technique for machine learning that uses images to make predictions. Both of these methods use known data to build a model for predictions. Parathyroid adenomas are tumors with an early enhancement pattern that is used to help identify them to aid in detection and surgical planning. This study aims to compare SVM and CNN analyses on the accuracy of identifying parathyroid adenomas.

#### METHODS AND MATERIALS

This is a HIPPA compliant retrospective study with IRB approval. Informed consent was waived. Ninety-three 4D-CTs of patients with pathology-proven parathyroid adenomas were reviewed; 94 parathyroid adenomas (1 case had 2 adenomas) and 112 lymph nodes. The mean attenuation of the lesion of interest in HU of each acquired phase (0, 25, 50, 75 sec) is used to build a model in the SVM analysis. A 2D slice through the lesions in each phase is used to perform sequence classification with ResNet50 as the pre-trained network to construct the CNN model in MatLab. The data is split randomly between a model and validation data set in a 2:1 ratio. The area under the curve (AUC) and accuracy are calculated for the model and validation data sets.

#### RESULTS

The plot of the enhancement curves of parathyroid adenomas demonstrates early enhancement with washout, while lymph nodes have persistent enhancement. On the model data, the AUC of the CNN is 0.99 while the SVM is 0.95. The overall accuracy of the CNN on the validation data set is 92%, while the SVM is 88%. The accuracy for parathyroid adenomas specifically is 93% for the CNN and 83% for the SVM model.

#### CONCLUSION

Both SVM and CNN models discriminate between parathyroid adenomas and lymph nodes well (88% vs. 92%), showing that lesion enhancement alone plays a significant role in distinguishing tissue types. The CNN more accurately identifies parathyroid adenomas in the validation data set than the SVM analysis, showing that using both spatial and enhancement information helps distinguish between features of parathyroid adenomas and lymph nodes better than enhancement alone. One of the limitations of this study is the limited number of lesions; more lesions would help clarify the statistics for these models, especially with variation in lesion shape and size. Comparing techniques like the SVM and CNN models can help identify imaging features to differentiate between lesions.

#### CLINICAL RELEVANCE/APPLICATION

Machine learning algorithms will enhance detection and provide insight into imaging features identifiable with parathyroid adenomas using 4D CT data.

Printed on: 02/07/23



## Abstract Archives of the RSNA, 2022

W2-SPNR-12

### NeuroScreener: Quantized Vector Embedded Autoencoder-based Abnormality Classifier from Brain MRI

Wednesday, Nov. 30 9:00AM - 9:30AM Room: Learning Center - NR DPS

#### Participants

Jimin Kang, (*Presenter*) Employee, NEUROPHET, Inc

#### PURPOSE

In this work, we propose a novel framework that is the first of its kind to detect identifiable abnormalities that may be present in the images to reduce time and effort in the clinical practice by assisting clinicians' brain image reading.

#### METHODS AND MATERIALS

A dataset for this study was a T1-weighted brain MRI dataset with normal and anomalous images collected from the multicenter including ADNI, SNUH, CMCH, and YUHS. The anomalous images were categorized into three. First was defined as MR images with a severe artifact such as insufficient field of view (FOV), external foreign body (EFB), motion, and a spike which may not be proper for further interpretation of the image. We further included de-faced or skull-stripped images, which are preprocessed unintentionally and/or improperly for further processing or interpretation. Lastly, we also included MR images with large infarction, which may produce inferior results for the routine segmentation process. The normal MR image has no aforementioned abnormality. In this study, we utilized a residual block-based variational autoencoder (VAE) as a backbone network. The vector quantization (VQ) module performs that the continuous feature of the latent space was mapped to a trainable discrete embedding vector by a predetermined number. The output value of the discrete embedding space is then connected to the fully connected layer to classify the input T1 MR image. We trained our VQ-based network using the weighted summation of VQ loss, reconstruction loss, and Binary Cross Entropy (BCE) loss. The VQ loss was then used to calculate the loss for the VQ module. The Mean Squared Error (MSE) loss was calculated between the generated output image from the decoder and the input image. Additionally, we empirically adjusted the parameters for the loss function by histogram analysis of the distribution of the output loss.

#### RESULTS

Our results presented the accuracy as high as 95%, and Area Under Receiver Operating Characteristic (AUROC) showed as high as 0.9778. The mean accuracy of seven types of anomalies we investigated showed 89%.

#### CONCLUSION

In this study, an image generator-based classifier was proposed to detect abnormality present in MR images using VAE, which is applied to the VQ module adaptively. The proposed framework has shown high performance in all matrices.

#### CLINICAL RELEVANCE/APPLICATION

We hope this study could assist the radiologists by replacing the time-consuming image reading process with a faster and more efficient image reading, which could provide the anomaly information that MRI may have.

Printed on: 02/07/23



## Abstract Archives of the RSNA, 2022

W2-SPNR-13

### Value Proposition of Food and Drug Administration (FDA)-Approved Artificial Intelligence (AI) Algorithms for Neuroimaging

Wednesday, Nov. 30 9:00AM - 9:30AM Room: Learning Center - NR DPS

#### Awards

**Trainee Research Prize - Resident**

#### Participants

Suryansh Bajaj, MD, New Haven, CT (*Presenter*) Nothing to Disclose

#### PURPOSE

The number of FDA-approved artificial intelligence (AI) algorithms for neuroimaging has grown in the last decade. The adoption of these algorithms into clinical practice depends largely on whether this technology provides significant value to radiologists in the clinical setting. The objective of this study is to understand current trends in FDA-cleared AI algorithms for neuroimaging and understand the value proposition of these algorithms as advertised by the developer.

#### METHODS AND MATERIALS

We extracted a list of FDA-approved neuroimaging AI algorithms from the American College of Radiology (ACR) Data Science Institute AI Central database from May 2008 to January 2022. Product information of each device was collected from the database. For each device, we collected information of advertised value as presented on the developer's website.

#### RESULTS

The database includes a total of 54 AI neuroimaging algorithms that were cleared by the FDA between May 2008 and January 2022. A majority of the algorithms (28/54, 51.9%) were compatible with CT images with 22 (40.7%) compatible with MR and 4 compatible with CTP and CTA (7.4%). Nine algorithms (16.7%) were compatible with multiple imaging modalities. Of these algorithms, 53 (98.1%) were approved with a 510(k) clearance and 1 (1.9%) received de novo clearance. Out of the 54 algorithms, we found websites that discussed the product for 51 algorithms. The most widely advertised value proposition was improved quality of care (34/51, 66.7%). A total of 19 algorithms (37.3%) argued they saved the user time, 8 (15.7%) decreased costs, and 6 (11.8%) increased revenue. Product websites for 24 algorithms (47.1%) showed testimonials advertising the value of the technology. Subgroup analysis was performed to compare algorithms compatible with CT to those with MRI and the algorithms involved in ICH to those in LVO.

#### CONCLUSION

Our results indicate a wide range of value propositions advertised by developers to indicate the value of their product. Most developers argued that their product would improve patient care. Further research is necessary to determine whether the value advertised by the developer is actually demonstrated in clinical practice.

#### CLINICAL RELEVANCE/APPLICATION

Given the rapid growth in the number, availability, and clinical application of AI algorithms across the US, it is important to understand different uses and value propositions provided by these software in current practice.

Printed on: 02/07/23

## Abstract Archives of the RSNA, 2022

W2-SPNR-14

### Exploring Functional Connectivity in Chronic SCI Patients with Neuropathic Pain versus without Neuropathic Pain

Wednesday, Nov. 30 9:00AM - 9:30AM Room: Learning Center - NR DPS

#### Participants

Adam Flanders, MD, Philadelphia, PA (*Presenter*) Nothing to Disclose

#### PURPOSE

Spinal cord injury (SCI) causes debilitating chronic pain. Despite decades of research, the pain pathway of neuropathic pain (NP) is unknown. Several lines of evidence show abnormal functioning of the brain in patients with SCI. We hypothesize that in patients with SCI and neuropathic pain the pain matrix is altered compared to patients with SCI without neuropathic pain.

#### METHODS AND MATERIALS

This study examines the functional connectivity (FC) in SCI patients with moderate-severe chronic neuropathic pain compared to SCI patients with mild-no neuropathic pain. These groups were compared to control subjects. Subjects completed the Neuropathic Pain questionnaire and completed a neurological evaluation based on the International Standard Neurological Classification of SCI to define severity and level of injury. Of the 8 participants with SCI, 5 (44.8±17.56 y.o, 4M and 1F) indicated they had NP and 3 did not have NP (37.33±9.24 y.o, 2M and 1F). We also included 10 uninjured neurologically intact controls (24.8±4.61 y.o, 5M and 5F). FC metrics were obtained from the comparisons of resting state functional magnetic resonance imaging amongst our various groups (uninjured controls, SCI with NP and SCI without NP). For each comparison, an ROI-to-ROI connectivity analysis was pursued, encompassing a total of 170 ROIs based on a customized atlas derived from AAL3 atlas. The analysis accounted for covariates such as age and gender. To correct for multiple comparisons, a strict Bonferroni correction was applied with a significance level of  $p < 0.05/NROIs$ .

#### RESULTS

When comparing the SCI cohort with uninjured subjects our results show statistically significant decreased FC in various thalamic nuclei including: medial and lateral pulvinar, lateral geniculate nucleus, and mediodorsal magnocellular. We postulate these findings are associated with suppressed inhibitory inputs from the zona incerta (ZI) and the anterior pretectal nucleus (APT) in those with NP following SCI. The suppressed inhibitory input causes enhanced activity at the posterior nucleus of the thalamus, S1 and thalamic nuclei regulated by ZI/APT. There were no significant differences of FC in patients with SCI without NP pain compared to controls.

#### CONCLUSION

s Manipulations that enhance the activity of ZI/APT can improve the treatment in SCI pain. Additionally, the loss of inhibition within the thalamus and abnormal thalamocortical interactions can predispose patients for the development of chronic pain.

#### CLINICAL RELEVANCE/APPLICATION

Our findings complement results from other neuroimaging studies and provide multi-modal evidence for identifying novel regions of the brain specific to the SCI cohort. These regions can serve as therapeutic targets to improve SCI neuropathic pain patients.

Printed on: 02/07/23

## Abstract Archives of the RSNA, 2022

W2-SPNR-15

### **A Deep Learning Algorithm Trained with Multiphase CTA Images Could Improve Collateral Circulation Assessment in Acute Ischemic Stroke**

Wednesday, Nov. 30 9:00AM - 9:30AM Room: Learning Center - NR DPS

#### **Participants**

Jingjie Wang, (*Presenter*) Nothing to Disclose

#### **PURPOSE**

We tried to build a deep learning-based, objective, fast, and accurate collateral circulation assessment model.

#### **METHODS AND MATERIALS**

We collected 92 acute ischemic stroke (AIS) patients with large vessel occlusion in the anterior circulation in our hospital from June 2020 to August 2021. We analyzed their baseline one-stop whole-brain four-dimensional computed tomography angiography (4D-CTA)/CT perfusion. The images of the arterial, arteriovenous, venous, and late venous phases were extracted from 4D-CTA according to the perfusion time density curve. The subtraction images of each phase were created by subtracting the non-contrast CT scan. Each patient was marked with good or poor collateral circulation.

#### **RESULTS**

Based on the ResNet34 classification network, we developed a single-image input and a multi-image input network for binary classification of collateral circulation. The training and test sets were 65 and 27 patients, respectively, and Monte Carlo cross-validation was employed for five iterations. The network performance was evaluated by precision, accuracy, recall, F1 score, and AUC. All the five performance indicators of the single-image input model were higher than those of the other.

#### **CONCLUSION**

The single-image input processing network, combining multiphase CTA images, can better classify the AIS collateral circulation. This automated collateral assessment tool can help streamline clinical workflows, and screen patients for reperfusion therapy.

#### **CLINICAL RELEVANCE/APPLICATION**

Collateral circulation is important for the treatment plan and prognosis of patients with acute ischemic stroke (AIS). However, due to the complexity and difficulty of quantifying the neurological vessels' structure, the evaluation of collateral circulation is challenging. Although scholars have tried and reported various methods for assessing collateral circulation, there is no unified standard for assessing collateral circulation. Even when the same assessment method is used, physicians have significant subjective differences. The development of computerized deep learning algorithms has brought new solutions to this difficulty. This study uses deep learning methods to achieve a rapid, objective, and accurate collateral circulation evaluation of the AIS patients.

Printed on: 02/07/23

## Abstract Archives of the RSNA, 2022

W2-SPNR-16

### Brain MRI Automated Volumetry vs Non-automated Planimetric Assessment for Differentiating Progressive Supranuclear Palsy From Parkinson's Disease and Healthy Subjects: Can Machine Learning Help the Radiologist Choice?

Wednesday, Nov. 30 9:00AM - 9:30AM Room: Learning Center - NR DPS

#### Participants

Francisco Mendoza, MD, (Presenter) Nothing to Disclose

#### PURPOSE

Develop a machine learning model to determine the more accurate tool, between automated volumetry and non-automated planimetric assessment in differentiating Progressive Supranuclear Palsy (PSP) from Parkinson's disease (PD) and healthy subjects (HS).

#### METHODS AND MATERIALS

We retrospectively assessed 141 patients with a clinical diagnosis of Parkinsonism paired by age and sex and with a group of HS (PSP n = 47, PE n = 68, HS=26) between January 2003 and April 2021. Patients without T1-MPRAGE were excluded, leaving 83 subjects (PSP n = 29, PD n = 54, HS n=26). We included different clinical subtypes of PSP: PSP-RS (n= 19), PSP-P (n= 5), PSP-PGF (n= 4), and PSP-F (n= 1). Using automatized SyngoviaBrainMorphometry software (Siemens), we obtained 109 volumes of interest (VOIs) for each brain MRI study, including absolute and normalized values. Two independent radiologists blind to diagnosis performed a planimetric assessment (Massey ratio, Oba ratio, MPRI 1.0, and MRP 2.0). The intraclass correlation coefficient (ICC) was used to assess interobserver agreement. We developed a machine-learning model based on multivariate feature selection and an extreme gradient boosting (XGB) vs. univariate feature selection and random forest (RF) with automated volumetric data and planimetric assessment to differentiate PSP from PD and HS. All subjects were randomly divided into training (85%) and validation (15%) data sets with the same proportions for each clinical group. The most relevant data obtained from each model were ordered by importance score (F-score: where 1.0 represents perfect precision and recall). Additionally, we assessed the diagnostic accuracy of each tool using ROC curves.

#### RESULTS

The global diagnostic performance of the volumetric model to differentiate between the three groups was 70.6% and 70.5% for the planimetric assessment. The most relevant automated brain volumetry was the mesencephalic-normalized volume (0.068), with an area under de curve (AUC) of 0.87. For planimetric assessment, the most important measurements were the mesencephalic width (0.33 ) with an AUC of 0.99, followed by the mesencephalic area (0.19) with an AUC of 0.94. The planimetric measurements presented very good reproducibility with interobserver intraclass correlation coefficients (ICC) of > 0.75.

#### CONCLUSION

s There is no significant difference between automatized volumetric volumes or planimetric assessment models in predicting the diagnosis of PSP or PD. The classic measurements of mesencephalic width or mesencephalic have better diagnostic accuracy than volumetric values.

#### CLINICAL RELEVANCE/APPLICATION

Automatized volumetric assessment of brain MRI is a helpful tool for differentiating Progressive Supranuclear Palsy from Parkinson's disease.

Printed on: 02/07/23

## Abstract Archives of the RSNA, 2022

W2-SPNR-18

### Accurate Cerebellar Cortex Segmentation: A Deep-Learning-Based Approach

Wednesday, Nov. 30 9:00AM - 9:30AM Room: Learning Center - NR DPS

#### Participants

Fabiano Reis, Campinas, Brazil (*Presenter*) Nothing to Disclose

#### PURPOSE

Cerebellum segmentation is a challenging task due to the intricately folded cortex and proximity with the cerebral cortex. Several tools reach excellent results in healthy controls, but in patients with cerebellar damage the segmentation might be catastrophic. Hence, we propose to develop an MRI tool to segment with accuracy abnormal and non-abnormal cerebellums using deep-learning algorithms.

#### METHODS AND MATERIALS

We used T1-weighted MRI sequences acquired in a 3 T Philips Achieva at the University of Campinas. The dataset is composed of healthy controls, SCA1 (spinocerebellar ataxia), SCA3, and FRDA (Friedreich's Ataxia) subjects' acquisitions, 15 images of each group. A group of expert neuroradiologists labeled the images following a protocol to ensure quality and correctly identify the cerebellar fissures. We chose the 3D U-net architecture with a few modifications which is a consolidated model for segmentation tasks in the medical imaging domain. In order to assess the gains of our specialist segmented data, a segmentation model was trained. After that, we compared it along with ACAPULCO and CERES models to evaluate differences in segmentation performance.

#### RESULTS

Our initial U-Net model was trained on Google Colab and achieved 0.921 for Dice score (DS) on the validation set. We randomly selected 14 images from the training set to assess the main segmentation tools (Our model, ACAPULCO and CERES). We found a mean DS of  $0.928 \pm 0.030$  for our model,  $DS=0.909 \pm 0.043$  for ACAPULCO and  $DS=0.918 \pm 0.039$  for Ceres. When we compared patients with the highest level of cerebellar damage, this difference of performance increases a lot (our model:  $DS=0.904 \pm 0.041$ ; ACAPULCO:  $DS=0.870 \pm 0.052$ ; CERES:  $DS=0.888 \pm 0.052$ ). In addition, comparing the segmentation volume of our model against ACAPULCO and CERES outputs of 71 and 72 images from FRDA (subtle damage) and SCA3 (severe damage) patients, respectively, we found volumetric difference between our model and ACAPULCO for both group of patients ( $p < 0.001$ ). For CERES, we only identify volumetric differences for the SCA3 patients ( $p < 0.001$ ).

#### CONCLUSION

Initial results show a promising methodology, whereas we are still working on gathering more expert-segmented images, in order to obtain sensitive variables to measure the impact of modifier agents of new therapies for several neurodegenerative disorders.

#### CLINICAL RELEVANCE/APPLICATION

Cerebellum segmentation is a challenging task due to the intricately folded cortex and proximity with the cerebral cortex. Our initial results show a promising methodology, whereas we are still working on gathering more expert-segmented images, in order to obtain sensitive variables to measure the impact of modifier agents of new therapies for several neurodegenerative disorders.

Printed on: 02/07/23

## Abstract Archives of the RSNA, 2022

W2-SPNR-19

### A Large-scale Granger Causality Approach for Functional MRI Data Analysis - Identification of Schizophrenia Patients

Wednesday, Nov. 30 9:00AM - 9:30AM Room: Learning Center - NR DPS

#### Participants

Ali Vosoughi, Rochester, NY (*Presenter*) Nothing to Disclose

#### PURPOSE

To develop and evaluate a novel machine learning method for identifying patients with schizophrenia using large-scale Granger Causality (IsGC) by capturing connectivity differences in resting-state functional MRI (rsfMRI).

#### METHODS AND MATERIALS

From the publicly available Centers of Biomedical Research Excellence (COBRE) fMRI data repository on 146 subjects (72 schizophrenia patients, 62 controls), we included the subsample of all 62 subjects under the age of 32 years (29 schizophrenia patients, 33 controls) using standard preprocessing by the Nilearn Python library and the NIAK resting-state pipeline, with functional parcellation into 122 brain regions [Bellec, NIAK, 2016]. For calculating directed functional connectivity between brain regions, we have recently developed the large-scale Granger Causality (IsGC) algorithm [Citation blinded for review] that combines dimension reduction with multivariate predictive causal modeling in high-dimensional fMRI time series. A 100-iteration cross-validation approach with 80%/20% train/test ratio was applied, where feature selection was performed on each training set using Kendall's tau rank correlation, followed by support vector machine classification. To quantitatively evaluate diagnostic accuracy of IsGC for correctly classifying schizophrenia patients and normal controls, we compare its performance with both a recent state-of-the-art causal discovery method (PCMCI, [Runge et al., Science, 2019]), and the current clinical fMRI analysis standard of cross-correlation (CC), reporting accuracy, area under ROC curve (AUC), and f1-score.

#### RESULTS

The IsGC rsfMRI analysis method significantly outperformed both PCMCI and the clinical standard CC techniques at classifying schizophrenia patients from healthy subjects, with accuracy/AUC/f1 score of 100%/1.0/100% for IsGC, 86.4%/0.81/78.4% for PCMCI, and 65.8%/0.62/60.4% for CC, respectively.

#### CONCLUSION

Our results suggest that IsGC significantly improves the diagnostic accuracy of correctly identifying patients with schizophrenia from rsfMRI neuroimaging. We conclude that, when compared to both conventional CC analysis and state-of-the-art PCMCI, IsGC is better suited to capture disease-related brain network connectivity changes in schizophrenia patients.

#### CLINICAL RELEVANCE/APPLICATION

The IsGC method classifies schizophrenia subjects and controls by identifying relevant changes in fMRI connectivity, suggesting its potential use as a diagnostic imaging biomarker for neurologic disease.

Printed on: 02/07/23



## Abstract Archives of the RSNA, 2022

W2-SPNR-2

### Accelerating Susceptibility Weighted Imaging With Deep Learning Validated in Acute Ischemic Stroke

Wednesday, Nov. 30 9:00AM - 9:30AM Room: Learning Center - NR DPS

#### Participants

Qi Duan, Beijing, China (*Presenter*) Nothing to Disclose

#### PURPOSE

Susceptibility weighted imaging (SWI) can display low-flow rapid vessels and arterial thrombosis and provide cerebral hemodynamic information without the use of contrast media by its strong detection ability for the paramagnetic properties of deoxyhemoglobin, which is helpful for acute ischemic stroke (AIS) clinical diagnostic and treat strategy made. However, SWI imaging requires a long acquisition time, which increases the possibility of motion artifacts, and limits the spatial resolution and slice thickness. We aimed to evaluate the clinical feasibility of the accelerating SWI generated by a deep learning model in patients with AIS.

#### METHODS AND MATERIALS

SWI data were collected from 45 AIS patients who underwent 3.0T MR examination in our hospital from January 2019 to January 2020. Using a sampling pattern library consisting of 3000 different two-dimensional variable-density random undersampling masks by referencing the k-space data retrospectively generated the undersampled SWI data, then using the complex-valued convolutional neural network (ComplexNet) to develop reconstruct high-quality SWI from highly accelerated k-space data. The data set was split into training (36 patients) and test (9 patients) sets (80% training and 20% test). The presence of susceptibility vessel sign (SVS) of each patient was assessed by two experienced radiologists.

#### RESULTS

A total of 45 patients (mean age, 66.67 years  $\pm$ 14.05, 30 men). ComplexNet achieved high image quality with acceleration rates of 5, and there was no significant diagnostic performance difference between fully sampled and ComplexNet in image quality ( $p > 0.05$ ). The intraclass correlation coefficient (ICC) was excellent for the results of the assessment using ComplexNet SWI images between two readers (ICC = 0.750,  $p=0.006$ ).

#### CONCLUSION

s ComplexNet can accelerate SWI effectively and generate the image of high quality while showing superior ability in detecting SVS in AIS. Further use of the accelerating SWI, such as cerebral microbleeds detection, needs to be proven in large cohorts.

#### CLINICAL RELEVANCE/APPLICATION

Susceptibility weighted imaging (SWI) can display low-flow rapid vessels and arterial thrombosis and provide cerebral hemodynamic information without the use of contrast media by its detection ability for paramagnetic properties of deoxyhemoglobin, which is of great value in acute ischemic stroke (AIS) patients' arterial thrombosis and cerebral microbleeds detection. However, SWI imaging requires a long acquisition time. We used a deep learning model to accelerate SWI, and evaluated the clinical feasibility of the accelerated SWI in patients with AIS.

Printed on: 02/07/23

## Abstract Archives of the RSNA, 2022

W2-SPNR-20

### Comparison of Volume Measurements and Reliability of Two Commercial Software for Automatic Brain Volumetry

Wednesday, Nov. 30 9:00AM - 9:30AM Room: Learning Center - NR DPS

#### Participants

Jimin Kim, MD, Seoul, Korea, Republic Of (*Presenter*) Nothing to Disclose

#### PURPOSE

Brain atrophy has close correlations with various neurodegenerative diseases. However visual assessment of brain atrophy tend to show high interobserver variability and low sensitivity. We aimed to evaluate the inter-method reliability and volumetric differences between NeuroQuant (NQ) and AQUA (AQ) using T1 sagittal sequence.

#### METHODS AND MATERIALS

This retrospective study enrolled 202 patients without focal brain lesion. NQ and AQ were used for volumetric analysis of sagittal T1-weighted images with slice thickness of 1 mm. To analyze the inter-method difference, correlation, and reliability, we used the paired t-test, Pearson's correlation coefficient, intraclass correlation coefficient (ICC), and effect size (ES) using the SPSS software.

#### RESULTS

The paired t-test showed significant volume differences in most regions except for the total and left side of parietal volume, white matter of right cerebral hemisphere, right frontal volume and right cingulate between the two methods. Volume measures by NQ and AQ showed good-to-excellent reliability ( $r=0.634-0.892$ ,  $ICC=0.766-0.940$ ), except for caudate, nucleus accumbens, cingulate and pallidum which showed average to fair reliability ( $r=0.371-0.448$ ,  $ICC=0.470-0.617$ ). For the measurements of ES, volume differences were large in most regions ( $r=0.01-9.52$ ). ES was the largest in the right pallidum and smallest in the right frontal lobe.

#### CONCLUSION

s In most brain regions, AQ showed significantly larger volume measurements with large ES than NQ. However, NQ and AQ showed good to excellent inter-method reliability in volumetric measurements for most brain regions, with the exception of relative smaller region.

#### CLINICAL RELEVANCE/APPLICATION

Therefore, clinicians should be aware that the volume measurements may vary by software and by region.

Printed on: 02/07/23

## Abstract Archives of the RSNA, 2022

W2-SPNR-21

### Automatic Large Vessel Occlusion Detection via a Thrombus Segmentation Approach

Wednesday, Nov. 30 9:00AM - 9:30AM Room: Learning Center - NR DPS

#### Participants

Rotem Golan, PhD, (*Presenter*) Software developer, Circle Cardiovascular Imaging Inc

#### PURPOSE

To introduce an explainable machine learning (ML) approach for large vessel occlusion (LVO) detection via thrombus segmentation, namely StrokeSENS LVO, and validate its performance on a large heterogeneous dataset of single-phase computed tomography angiography (CTA) scans of the head.

#### METHODS AND MATERIALS

An explainable approach for LVO detection is proposed which is composed of two main components: (1) thrombus segmentation, and (2) segmentation of the large vessels of the anterior circulation of the brain; both of which are performed in three dimensions. Predicted thrombi of any size are flagged and their distance from the large vessels is measured to perform a final yes/no LVO decision. For validation, a total of 400 studies (217 LVO, 183 non-LVO) were used. The LVO group includes internal carotid artery (ICA) and m1 segment of the middle cerebral artery (M1-MCA) occlusions; and the non-LVO group includes more distal or posterior cerebral artery occlusions, no occlusions, and hemorrhagic stroke cases. Expert consensus reads were used as reference standard. Performance was evaluated using sensitivity and specificity and corresponding 95% confidence intervals (CI). Additional analysis was performed on several subgroups of interest.

#### RESULTS

For detecting LVO, StrokeSENS LVO achieved a sensitivity of 90.3% [86.4%, 94.3%] and specificity of 95.1% [91.9%, 98.2%]. Furthermore, sensitivities of 88.5% [81.4%, 95.6%] on ICA cases (N=78) and 91.4% [86.7%, 96.0%] on M1-MCA cases (N=139) were noted; similarly, specificities of 98.2% [93.6%, 99.5%] on hemorrhagic stroke cases (N=110) and 90.4% [83.7%, 97.2%] on non-LVO-non-hemorrhage cases (N=73) were noted. Similar performances were observed across stratified datasets based on age, sex, scanner manufacturer and slice thickness when compared to the full cohort.

#### CONCLUSION

StrokeSENS LVO has demonstrated high sensitivity and specificity in detecting LVOs on a large heterogeneous dataset. The output of its components, i.e., predicted thrombus and vessels, can provide users with valuable information as to why certain predictions are made, and build clinicians' trust in using the tool in clinical practice.

#### CLINICAL RELEVANCE/APPLICATION

Patients with acute ischemic stroke due to LVO are candidates to receive lifesaving endovascular treatment. Timely and reliable detection of LVO on CTA is challenging in many centers and therefore automating the process and providing an explainable tool to clinicians is of great importance.

Printed on: 02/07/23

## Abstract Archives of the RSNA, 2022

W2-SPNR-4

### Ultra Low-iodine-load and Low-radiation 70 kVp Cerebral CT Angiography: Application of Deep learning-based Augmented Contrast Enhancement and Denoising Algorithms

Wednesday, Nov. 30 9:00AM - 9:30AM Room: Learning Center - NR DPS

#### Participants

Eun-Suk Cho, MD, PhD, Seoul, Korea, Republic Of (*Presenter*) Nothing to Disclose

#### PURPOSE

To determine the feasibility of ultra low-iodine-load and low-radiation 70 kVp cerebral CT angiography (CTA) using deep learning-based augmented contrast enhancement (DL-ACE) and deep learning-based denoising (DL-DN) algorithms.

#### METHODS AND MATERIALS

Forty-seven volunteers were randomly assigned to one of three CTA protocols: group A (100 kVp and 40 mL of 350 mg I/mL iodine contrast media (CM)), group B (70 kVp and 40 mL of 270 mg I/mL CM), or group C (70 kVp and 28 mL of 270 mg I/mL CM). Images of groups B and C were reconstructed using DL-ACE and DL-DN algorithms. DL-ACE (ClariACE, ClariPi) was developed based on the U-net architecture to predict vascular and parenchymal contrast enhancement by being trained with high-energy (150 kVp) and low-energy (80 kVp) datasets of dual-energy CT images. Augmented contrast-enhanced images were obtained by boosting the degree of enhancement in contrast-enhanced organs. DL-DN (ClariCT.AI, ClariPi) was designed to predict possible image noise by low radiation from standard-dose images, and denoised images were acquired by subtracting predicted noise from the originals. The vascular attenuation value and contrast-to-noise ratio (CNR) of cerebral arteries, subjective image quality, and radiation dose were compared among the groups.

#### RESULTS

The vascular attenuations of groups B ( $405.0 \pm 43.3$  HU) and C ( $393.9 \pm 54.1$  HU) were significantly higher than that of group A ( $323.9 \pm 50.2$  HU). However, the CNR of group A ( $18.9 \pm 4.9$ ) was significantly higher than those of groups B ( $15.4 \pm 2.5$ ) and C ( $14.9 \pm 2.4$ ) because the image noise of groups B and C ( $23.3 \pm 2.2$ ) were significantly higher than that of group A ( $15.4 \pm 2.2$ ). After the application of DL-ACE and DL-DN, the image noise was significantly decreased in groups B and C ( $14.9 \pm 1.8$ ). The vascular attenuation and CNR were significantly increased in group B ( $768.7 \pm 87.5$  HU and  $49.1 \pm 9.3$ ) and group C ( $748.0 \pm 108.5$  HU and  $46.8 \pm 10.1$ ). CTDI of groups B and C (15.4 mGy) was 23.5% lower than that of group A (20.13 mGy).

#### CONCLUSION

s Application of DL-ACE and DL-DN increased arterial attenuation by 89.8% and decreased image noise by 35.9% in cerebral CTA, respectively. 70 kVp cerebral CTA using DL-ACE and DL-DE improved significantly higher arterial attenuation and CNR and lower image noise and provided better subjective image quality, although with 46.0% lower iodine load and 23.5% lower radiation dose, compared to 100 kVp CTA protocol.

#### CLINICAL RELEVANCE/APPLICATION

Deep learning-based augmented contrast enhancement and denoising algorithms produce high arterial enhancement and CNR and good image quality in cerebral CTA, even with ultra low-iodine-load and low-radiation.

Printed on: 02/07/23



## Abstract Archives of the RSNA, 2022

W2-SPNR-5

### Could High kVp Non-Contrast Brain CT Improve Image Quality without Dose Increase?: Combined Use of Deep Learning Image Reconstruction and Automatic Current Modulation

Wednesday, Nov. 30 9:00AM - 9:30AM Room: Learning Center - NR DPS

#### Participants

Younghen Lee, MD, (*Presenter*) Nothing to Disclose

#### PURPOSE

To evaluate the impact of combined use of a new deep learning image reconstruction (DLIR) algorithm and automatic current modulation on image quality and dose reduction of non-contrast brain CT

#### METHODS AND MATERIALS

After the recent DLIR (TrueFidelity™, GE) launching, we obtained non-contrast brain CT images with different scanning condition during the recent ten-months (Dec,2019~Sep,2020), to optimize image quality and radiation dose (120kVp with ASIR-V 20%, 120/140kVp with DLIR-mid, 140kVp with DLIR-mid adding smart mA (noise index 7 and 8). For a comparison between those five different conditions, we retrospectively identified the normal brain CT cases of 151 young adults (mean age: 26.2 years). Region of interest based attenuation and noise measurements was done for supra-/infra-tentorial structure to compare SNR (signal to noise ratio), CNR (contrast to noise ratio) and CTDI and DLP

#### RESULTS

DLIR provided the better CNR and SNR than 20% ASIR-V by significant noise reduction. Compared to 120kVp with ASIR-V 20%, DLIR improved CNR and SNR of non-contrast 140kVp brain CT by mean 53.1% and 66.3% (noise index 7), 22.8%, and 41.5% (noise index 8) at the mean 8%, and 27% reduced doses by adding automatic current modulation

#### CONCLUSION

s Combined use of DLIR algorithm and automatic current modulation could be the potentially powerful tool for brain CT dose optimization

#### CLINICAL RELEVANCE/APPLICATION

Combined use of DLIR algorithm and automatic current modulation could be the potentially powerful tool for brain CT dose optimization

Printed on: 02/07/23

## Abstract Archives of the RSNA, 2022

W2-SPNR-8

### Automatic Tumor Segmentation and Survival Prediction for Children with Diffuse Midline Gliomas

Wednesday, Nov. 30 9:00AM - 9:30AM Room: Learning Center - NR DPS

#### Participants

Zhifan Jiang, PhD, Washington, DC (*Presenter*) Nothing to Disclose

#### PURPOSE

Diffuse midline glioma (DMG) is a rare but fatal pediatric central nervous system (CNS) tumor with a median overall survival (OS) of 11 months from diagnosis. Tumor volume and appearance on MRI may be important indicators of progression, response to treatment and survival outcomes. However, there is no quantitative imaging tool available to help improve clinical management of DMG. The purpose of this work is to develop a machine learning-based automatic framework to quantitatively analyze DMG from a small dataset and predict patient OS one year after diagnosis.

#### METHODS AND MATERIALS

We retrospectively collected contrast-enhanced T1 and T2 (mostly FLAIR) weighted MRIs from DMG patients at diagnosis (n=42) and within 1 month after completion of radiation therapy (RT) (n=35). Contrast enhancing tumor region (ET) and the whole tumor (WT) were manually labeled. We first adapted the SegResNet deep learning model developed to automatically segment ET and WT of more common adult CNS tumors (i.e., glioblastoma multiforme [GBM]). The model was pre-trained on 1,000 GBM cases and was fine-tuned using the DMG dataset (n=77 images for 2 timepoints) with a 5-fold cross-validation. DMG cases with data at both timepoints (n=34) were used for survival prediction. We extracted the following MRI features based on automatic segmentations: ET and WT volumes (and relative to the brain volumes), ET relative to WT volumes, changes between the 2 timepoints of these volumes, tumor heterogeneity (i.e., intensity skewness and kurtosis), and voxel percentage for each cluster when applying Gaussian Mixture Model (GMM) clustering algorithm to classify the segmented WT volume into 3 clusters based on T1 and T2 image intensities. A support vector machine was used to predict 1-year survival from combinations of these features with leave-one-out validation.

#### RESULTS

Our automatic segmentation method resulted in Dice scores of  $0.841 \pm 0.072$  and  $0.831 \pm 0.073$ , and relative volume error of  $13.1\% \pm 11.4\%$  and  $16.3\% \pm 15.8\%$  for ET and WT, respectively. The 1-year survival prediction accuracy was 73.5% (sensitivity=70.6%, specificity=76.5%), achieved using 3 features: voxel percentage for the 2nd cluster of GMM clustering of WT volume on post-RT T1 images, skewness of WT volume on post-RT T2 images, and ET relative to WT volumes for post-RT images.

#### CONCLUSION

s Rare pediatric CNS tumor analysis can be efficiently performed from small datasets using transfer learning from comparable adult datasets to yield accurate automatic quantification of tumors and acceptable survival prediction.

#### CLINICAL RELEVANCE/APPLICATION

The prediction of OS from diagnosis and early post-treatment MR images has the potential to guide and improve the clinical management of DMG and other rare pediatric conditions.

Printed on: 02/07/23

## Abstract Archives of the RSNA, 2022

W2-SPNR-9

### Novel Deep Learning Super-Resolution Algorithm Allows Substantial Improvement of Brain MRI Image Quality and Scan Time in a Multi-Site Study

Wednesday, Nov. 30 9:00AM - 9:30AM Room: Learning Center - NR DPS

#### Participants

Tal Aharoni, MSc, Haifa, Israel (*Presenter*) Employee, RadNet, Inc;

#### PURPOSE

To evaluate image quality, image resolution, and overall diagnostic sufficiency of low-resolution brain MRI images processed by a novel deep-learning (DL) resolution enhancement algorithm, compared to images acquired with higher resolution from multiple sites and MRI scanners.

#### METHODS AND MATERIALS

73 sequences of 27 subjects (19-88 years) were obtained on 11 different clinical MRI scanners (1.2T, 1.5T and 3T) from different vendors (Philips, Hitachi, Siemens and GE) under multi-site IRB-approval (in USA, Israel and Brazil). Each patient was imaged using the site's routine high-resolution (HR) protocol and with 25-33% faster variants, solely compromising resolution in phase encoding direction. The low-resolution (LR) scans were processed by a novel convolutional-neural network (CNN) based super-resolution algorithm, trained on a vast amount of brain MRI images from scanners of multiple vendors with a variety of clinical indications, to produce enhanced resolution (ER) images. Independent, blinded, side-by-side comparisons of diagnostic quality, spatial resolution, noise level, artifacts appearance and contrast resolution were performed by 6 experienced neuroradiologists, using a 7-point Likert-scale (1=unacceptable, 7=excellent). An additional non-blind review by a highly experienced neuroradiologist (>15 years' experience) was performed comparing image details between the HR and ER scans. Statistical analysis was performed (using JASP 0.15) comparing (i) HR to ER scans and (ii) LR to ER scans. Statistical significance was determined by paired samples t-test testing for either superiority or non-inferiority of ER scans.

#### RESULTS

Results (n=362 reads) exhibited superiority of the ER images over both the LR and HR images for diagnostic quality, spatial resolution, noise levels and contrast resolution ( $p<0.001$ ) and demonstrated non-inferiority for artifacts appearance ( $\alpha=0.2$ ,  $p<0.001$ ). 21 out of the 73 reviewed series showed pathologies. Statistical results were reinforced by the nonblinded review, demonstrating equality for image details and diagnostic confidence between the ER and HR images.

#### CONCLUSION

Results demonstrate superior overall image quality of low-resolution scans processed by a DL resolution enhancement algorithm compared to the routine HR scans across multiple sites and vendors, enabling MRI image resolution reduction and scan time shortening without adversely affecting image and diagnostic quality.

#### CLINICAL RELEVANCE/APPLICATION

Substantial improvement of brain MRI Image quality and scan time can be achieved using a robust DL-algorithm, resolving the trade-off between resolution and acquisition time on a variety of scanners.

Printed on: 02/07/23



## Abstract Archives of the RSNA, 2022

W2-SPOB

### OB/Gynecology Wednesday Poster Discussions

Wednesday, Nov. 30 9:00AM - 9:30AM Room: Learning Center - OB DPS

#### Participants

Luyao Shen, MD, Sunnyvale, CA (*Moderator*) Nothing to Disclose

Printed on: 02/07/23



## Abstract Archives of the RSNA, 2022

W2-SPPD

### Pediatric Wednesday Poster Discussions

Wednesday, Nov. 30 9:00AM - 9:30AM Room: Learning Center - PD DPS

#### Participants

Rama Ayyala, MD, Cincinnati, OH (*Moderator*) Nothing to Disclose

Printed on: 02/07/23

## Abstract Archives of the RSNA, 2022

W2-SPPH

### Physics Wednesday Poster Discussions

Wednesday, Nov. 30 9:00AM - 9:30AM Room: Learning Center - PH DPS

#### Participants

Junguo Bian, PhD, Hinsdale, IL (*Moderator*) Nothing to Disclose

#### Sub-Events

### W2-SPPH-1 Analysis of Noise for the Structural Difference Between Healthy and Destroyed Liver Tissue in CT Images During Microwave Ablation Therapy

#### Participants

Naghmeh Mahmoodian, PhD, (*Presenter*) Nothing to Disclose

#### PURPOSE

Microwave ablation (MWA) is a minimally invasive therapy used for ablating the liver tumor in its location. Computed tomography (CT) as an interventional imaging modality is employed to visualize the therapy process. However, because of overlaying macroscopically visible changes in CT images during MWA therapy, it is difficult to distinguish between the lesion, healthy, and ablated tissue. Therefore, we propose a method for distinguishing among different tissue structures to determine the stopping point for ablating tumors using CT images acquired during MWA liver therapy.

#### METHODS AND MATERIALS

For all patients, CT scans were performed before and after the liver MWA therapy with a tube voltage of 120 KeV. The CT images were acquired before starting and after finishing the therapy, respectively, without and with a contrast agent. The ground truth was prepared manually based on the ablated tissue. The pre- and post-ablated images and corresponding ground truth images were aligned using non-rigid registration. This was then followed by automatic segmentation of the pre- and post-ablated CT images based on the ground truth. The region of interest (ROI) has been selected manually and converted into small patches with the size of 32 x 32 pixels. Different values of Gaussian noise have been added to the pre-ablated images, using two methods of noise power spectrum (NPS) measurement: -Fourier and task-based approaches- for analyzing the effects of noise on different tissue structures.

#### RESULTS

25 patients with a total of 650 pre-ablated images and a total of 1950 patches were included in the study. Six different Gaussian noise values of 0.005, 0.006, 0.007, 0.008, 0.009, and 0.01 were added on the pre-ablated images. The NPS was measured based on the Fourier- and Noise distributions were evaluated based on task-based methods. Then the best image and corresponding noise value was chosen based on the maximum distance between the NPS of healthy and ablated tissue that leads to the distinction between different tissue structures.

#### CONCLUSION

Distinguishing tissue characterization of the healthy, tumor, and ablated liver tissue in CT images has been achieved by analyzing the noise effects on different tissues. The difference appears in healthy and tumor tissue NPS results and increases by adding more noise to the CT images. The results show the possibility of determining the stopping point during an MWA therapy by measuring the change in the anatomical noise of different tissue structures.

#### CLINICAL RELEVANCE/APPLICATION

An essential issue of tumor ablation therapy is to detect when the entire tumor tissue has completely been destroyed. However, current methods can't present the changes in the CT images during MWA therapy, we provide a solution for that.

### W2-SPPH-2 Artifact Reduction Using Silver Beam Filtration in Interventional CT

#### Participants

Timothy Szczykutowicz, PhD, Madison, WI (*Presenter*) Consultant, Aidoc Medical Ltd; Consultant, Flowhow.ai; Consultant, medInt Holdings, LLC; Consultant, Alara, Inc; Consultant, AstoCT, Inc; Research Grant, General Electric Company; Research Grant, Canon Medical Systems Corporation

#### PURPOSE

Intraoperative visualization of devices such as ablation probes, drainage needles, and biopsy probes is important for avoiding critical structures and ensuring the intervention is accurately reaching the target structure. However, these devices produce strong metal artifacts in CT due to beam hardening and photon starvation which makes accurate visualization of tip and trajectory challenging. This study evaluates the use of silver filtration (SilverBeam, Canon Medical USA) to a biopsy procedure task and quantifies metal artifact as a function of beam energy and the presence of a silver filter.

#### METHODS AND MATERIALS

An anthropomorphic phantom (Lungman, Kyoto Kagaku) simulating a patient was scanned with a biopsy needle and its sheath (14

gauge) aligned in the axial plane inside the lung field. Images of the phantom and needle were acquired using an MDCT scanner (Aquilion One Prism Edition, Canon Medical USA) at beam energies of 100, 120, 135 kV, and at 120 kV with silver filtration. For each measurement, the CTDIvol (i.e., a surrogate for patient dose) was kept constant at 1 mGy. Metal artifacts from the biopsy probe were quantified by measuring the absolute error in CT numbers directly in front of the needle tip. Errors in CT number were normalized relative to the 120 kV scan with silver filtration. All measurements were repeated 3 times.

## RESULTS

Artifacts relative to using silver beam increased for all beam energies not using silver beam. Median artifact increases were 95% (i.e., a near doubling of CT number error) ( $p = 0.014$ ), 79% ( $p = 0.009$ ), and 34% ( $p = 0.015$ ) for 100, 120, and 135 kV respectively. Visually, the biopsy probe exhibited the smallest blooming artifact for 120 kV with silver filtration relative to all other scan conditions.

## CONCLUSION

Use of silver filtration for interventional CT procedures reduces metal artifacts at the device tip.

## CLINICAL RELEVANCE/APPLICATION

Device tip localization is essential for physician confidence their device has reached the intended target. This study demonstrated that the use of silver filtration decreases metal artifacts at device tips.

## W2-SPPH-3 Investigation of Thermal Injury Risks From High-Pressure Gas Supply Line (HPGSL) During MR Guided Cryoablation

Participants

Liqiang Ren, PhD, Rochester, MN (*Presenter*) Nothing to Disclose

## PURPOSE

To investigate the potential RF heating and frostbite risks from the high-pressure gas supply line (HPGSL) during MR guided cryoablation.

## METHODS AND MATERIALS

Ex vivo experiments were performed using an MRI-conditional Boston Scientific cryoablation system. An 8ft long HPGSL with a metallic inner tube delivers high pressure gases to the cryoneedle when plugged into the mobile connection panel (MCP). To investigate the potential RF heating risks, three experiments were performed with a cryoneedle inserted into porcine tissue on a 1.5T MRI scanner. The tissue was placed ~10 cm off the patient table center and covered by a single layer of dry operating room (OR) towel (thickness: ~1mm) serving as a thermal insulation layer between tissue and HPGSL. A segment of interest (SOI, ~3 cm) of HPGSL was in contact with the towel. A temperature monitoring system was used to record the temperature during executions of a T2-weighted sequence (~2.3 minutes; specific absorption rate: 2.3 W/kg) via four thermal sensors: three attached to HPGSL and one placed on tissue surface under SOI. Two experiments were performed with HPGSL unplugged and plugged into MCP, respectively. A third one was performed with HPGSL plugged into MCP and a 2.5 cm thick insulation pad inserted between HPGSL and towel. To investigate the frostbite risk, cryoablation experiments were performed with the cryoneedle inserted into a container filled with saline. Temperature changes during a 5-minute and a 7-minute freezing procedure were measured with three thermal sensors attached to HPGSL and one insulated from HPGSL by either a single layer OR towel or both the towel and the pad at ~15 cm away from the cryoneedle shaft, respectively.

## RESULTS

For RF heating risk investigations, temperature rises on HPGSL were much lower at the segment close to the tissue compared to other locations along HPGSL. With HPGSL disconnected and connected to MCP, the maximum tissue temperature rises were about 4.9 and 40° when only the towel was used for insulation, respectively. For frostbite risk investigations, the temperature drops along HPGSL reduced with increased distances from the cryoneedle shaft. With only a single layer of OR towel, the maximum temperature drop was about 20° at 15 cm from the shaft end. No temperature rises or drops were observed at the porcine tissue surface when the thick pad was inserted between thermal sensor and HPGSL.

## CONCLUSION

Skin injury could occur during MR guided cryoablation due to HPGSL induced RF heating and/or frostbite. To mitigate these risks, sufficient insulation between HPGSL and patient skin should be applied.

## CLINICAL RELEVANCE/APPLICATION

Sufficient insulation between HPGSL and patient should be applied to effectively improve patient safety undergoing MR guided cryoablation procedures.

## W2-SPPH-4 Technical Evaluation of Motor Evoked Potential Monitoring During MR-Guided Cryoablation of the Shoulder

Participants

Christopher Favazza, PhD, Rochester, MN (*Presenter*) Nothing to Disclose

## PURPOSE

Pre-procedural testing to evaluate potential RF heating risks and image quality penalties associated with motor evoked potential (MEP) monitoring during MR-guided cryoablation of the shoulder.

## METHODS AND MATERIALS

Using a porcine tissue phantom, a series of ex vivo experiments were conducted mimicking the clinical configuration for MEP monitoring during MR-guided cryoablation near the brachial plexus. Two needle electrodes were placed on the sides of the phantom "head" to simulate transcranial stimulation. Two needle electrode pairs and a ground electrode were placed in the "arm" to mimic muscle recording. Fluoroptic temperature sensors were inserted near the tips of all 7 electrodes. The phantom was placed "head" first into the scanner. To minimize heating risks, stimulation and recording/ground wires were routed along the center of the bore and exited the back and front of the scanner, respectively. Stimulation and recording wires were routed through a waveguide and

connected to the nerve monitoring system outside the scan room. Along with a single high specific absorption rate (SAR) T2-weighted sequence (2.5 W/kg), a series of proton-density (PD)-weighted sequences used to monitor cryoablations were executed with different combinations of experimental variables that influence heating—wire path, position relative to bore wall, and SAR. Heating was measured with thermal sensors and recorded. Image quality was assessed qualitatively by calculating the average contrast-to-noise ratio (CNR) on the PD images. Clinical workflow of interleaving MEP and image acquisitions was evaluated.

## RESULTS

Maximum temperatures rises of 0.6, 0.8 2.8 and 0.4°C were respectively measured for high SAR T2, PD monitoring sequence at 14 minutes (SAR= 1.9 W/kg), PD with phantom shifted to touch the bore wall, and low SAR PD (0.7 W/kg) with phantom touching bore wall. Image quality was adequate with an average CNR=117. Stimulation was successfully interleaved between successive PD monitoring acquisitions with low noise signal reception in absence of active MRI.

## CONCLUSION

s RF heating risks can be sufficiently minimized to allow for intraprocedural nerve monitoring during MR-guided cryoablation, especially when a low SAR sequence is used. Image quality is not significantly degraded. MEP monitoring is feasible and can be operated in between MR image acquisitions.

## CLINICAL RELEVANCE/APPLICATION

This work demonstrates that intraprocedural MEP monitoring can be safely performed during MR-guided cryoablation procedures without significantly compromising MRI imaging quality. A successful cryoablation treatment using MEP monitoring has been carried out based on these findings.

## W2-SPPH-6 Deep Learning Ring Artifact Correction in Photon-Counting Spectral CT

Participants

Dennis Hein, Stockholm, Sweden (*Presenter*) Research Collaborator, General Electric Company

## PURPOSE

To develop an image-domain ring artifact correction algorithm for photon-counting spectral CT using deep learning.

## METHODS AND MATERIALS

Numerical basis phantoms (soft tissue and bone) were generated by thresholding CT images from the KITS19 dataset. Imaging was simulated using a fan beam acquisition and a spectral response model of a photon-counting silicon detector with 0.5x0.5 mm<sup>2</sup> pixels. The simulation was performed for 120 kVp and 200 mAs with 2000 detectors and 2000 view angles. Detector inhomogeneity was simulated by independently applying a random threshold shift to each of the eight thresholds and each of the detector pixels. Two material decompositions were performed: one with the bin thresholds used in the simulation and one with the nominal bin thresholds—yielding images with ring artifacts. Images were reconstructed on a 1024x1024 grid using FBP. A version of the Unet (2D convolutional neural network), with bilinear upsampling to avoid checkerboard artifacts, was trained using ADAM to map a pair of ring corrupted basis images (observed) to their ring artifact free counterparts (truth). The loss function is the weighted sum of two terms: a L1-penalty for the basis images and a perceptual loss for the virtual monoenergetic images at 70 keV. The perceptual loss utilizes VGG16 as feature extractor.

## RESULTS

The degree of ring artifact correction is proxied by the change in the loss function between the ring corrupted and processed images (predicted). This metric yields an 83% reduction in the validation set. To measure the change in noise, six 24x24 ROIs are defined in a monoenergetic image at 70 keV. A two-sample F-test for equal variances is conducted against the alternative hypothesis that the variance in predicted is greater than in truth. The p-value for this test is 0.24 (1.8% increase in standard deviation) and hence the null cannot be rejected at any reasonable significance level.

## CONCLUSION

s This work proposes a deep learning-based image processing technique for ring artifact correction in photon-counting spectral CT and demonstrates its ability to produce ring corrected virtual monoenergetic images at a range of energy levels.

## CLINICAL RELEVANCE/APPLICATION

This work proposes a deep learning-based image processing technique for ring artifact correction in photon-counting spectral CT and demonstrates its ability to produce ring corrected virtual monoenergetic images at a range of energy levels.

## W2-SPPH-7 Deep Learning for Automatic Contrast Enhancement Phase Detection on Abdominal Computed Tomography

Participants

Natália Alves, MSc, Nijmegen, Netherlands (*Presenter*) Nothing to Disclose

## PURPOSE

Develop and validate a probabilistic convolutional neural network (CNN) for automatic classification of intravenous contrast enhancement (CE) phase on abdominal computed tomography (CT) scans.

## METHODS AND MATERIALS

This retrospective study included 2000 abdominal CE-CT scans from our centre, which had information about the CE phase on the DICOM header. In addition to the baseline non-contrast scan (non-CE), three contrast phases were considered at different time intervals after contrast agent administration: the arterial phase (AP) at 40-50 seconds, the portal-venous phase (PVP) at 60-70 seconds and the delayed phase (DP) at 150-240 seconds. The distribution of CE phases on the training/validation dataset was 25.3% non-CE, 25.3% AP, 27.7% PVP and 21.7% DP. Half of the scans were used for model training/validation and a half for independent model testing. A 3-dimensional Inception CNN was trained to perform this multiclass classification task using stratified 4-fold cross-validation for 100 epochs. The model predictions from the 4 folds were ensemble to generate a final likelihood score for each contrast phase in the independent test set. The phase with the highest score was then chosen as the final model output.

## RESULTS

The overall accuracy for the multiclass CNN was 92.4%, with only 76 out of the 1000 scans in the independent test set being incorrectly classified. The individual accuracies for each phase were 97.6% (244 out of 250) for non-CE, 95.6% (239 out of 250) for AP, 85.6% (214 out of 250) for PVP and 90.8% (227 out of 250) for DP. The most frequent mistake was in differentiating between the portal venous and delayed phases. This can be explained by the reduced amount of contrast agent in the abdomen and the high patient-specific and varied appearance of these two phases within the same protocol. Increasing the size and variety of the training data may improve performance for these two phases.

## CONCLUSION

Deep learning can accurately determine intravenous CE phase on multi-phase CE abdominal CT scans.

## CLINICAL RELEVANCE/APPLICATION

CE information is critical to diagnosis but often lacks from the image metadata. DL can accurately classify CE phases, important for AI automation and the curation of high-quality training datasets.

## W2-SPPH-8 Training to Improve Radiologist Performance for Liver Metastasis Detection at Contrast Enhanced CT

Participants

Scott Hsieh, Rochester, MN (*Presenter*) Nothing to Disclose

## PURPOSE

The value of a radiology exam depends on the interpreting radiologist. We hypothesized that targeted training would improve liver metastasis detection at contrast enhanced CT.

## METHODS AND MATERIALS

After IRB approval, readers (radiology residents, board-certified abdominal or non-abdominal radiologists) attended four sessions, each lasting 4 hours. (Session 1) Pre-training test: readers circumscribed all suspected metastases and rated confidence of malignancy in 40 portal phase abdominal CT exams (91 metastases total) with no feedback provided. (2) Search training: while interpreting 30 exams, readers were told to increase interpretation time to at least 3 min/exam, use liver windows at least 1.5 min/exam, and use coronal stack at least 25% of total time; and received concurrent eye tracker feedback highlighting gaze patterns. (3) Discrimination training: while interpreting 100 additional cropped liver images including 0-3 benign or malignant lesions, readers rated confidence of malignancy of the lesions, with truth revealed immediately. (4) Post-training test (identical to the pre-training test). Ground truth for liver metastases was determined using histopathology or progression. Performance was measured using per-lesion sensitivity and area under the jackknife free ROC curve (AUC), a measure of accuracy that also incorporates confidence ratings.

## RESULTS

We recruited 31 readers (8 subspecialized abdominal radiologists, 8 non-abdominal radiologists, 15 residents). Between pre- and post-training tests, mean [SD] sensitivity increased from 82 [8]% to 85 [5]% (paired t-test,  $p = 0.009$ ), but AUC did not significantly change (from 0.72 [0.08] to 0.71 [0.07],  $p = 0.36$ ). Mean changes in sensitivity for subspecialized abdominal radiologists, non-abdominal specialists, and trainees were -0.6%, 4.6%, and 3.5%, respectively; only trainees' change was significant ( $p = 0.02$ ). In the post-training test, use of liver windows ( $p < 0.001$ ) and coronal stack ( $p < 0.001$ ) both increased, but interpretation time did not change ( $p = 0.62$ ). Despite improved use of liver windows and coronal images, sensitivity improvements were modest. Small, peripheral metastases seemed to benefit the most from training.

## CONCLUSION

Targeted training resulted in improvements in sensitivity but not AUC for liver metastasis detection in CT.

## CLINICAL RELEVANCE/APPLICATION

Missed hepatic metastases could be reduced by training to improve readers' search behaviors.

## W2-SPPH-9 Utility of Variable-Rate Contrast Medium Injection at Computed Tomography: A Simulation Study

Participants

Toru Higaki, PhD, Minami-ku, Hiroshima, Japan (*Presenter*) Nothing to Disclose

## PURPOSE

For contrast-enhanced computed tomography (CT), the contrast medium (CM) volume is generally injected at a constant rate and is based on the study's purpose and the patient's body weight. We used computer simulation to evaluate the clinical benefit of a variable-rate CM injection.

## METHODS AND MATERIALS

We developed a contrast simulator using the circulation model proposed in 1998 by Bae et al. By inputting the contrast protocol and the patient's body indices, the time density curve (TDC) of any organ can be calculated. Besides the conventional constant-rate CM injection, a variable-rate injection comprised of up to 4 phases can be delivered. By specifying the target TDC shape, an injection protocol can be automatically calculated to obtain the TDC shape closest to the target. We compared the TDC of constant-rate- and variable-rate (4 phases) injections for hepatic dynamic CT (HDCT) and coronary CT angiography (CCTA). The target TDC shape for HDCT was 280 Hounsfield units (HU) and the injection time was 20 seconds at the abdominal aorta, for CCTA it was 300 HU delivered in 5 seconds at the ascending aorta. The CM and the saline were injected simultaneously so that the total injection rate was always 5.0 ml/sec.

## RESULTS

The rectangles present our findings. At HDCT, the TDC produced by the constant-rate injection of 96.0 ml CM into the abdominal aorta ascended beyond the target (upper left); the 4-phase injection of 89.9 ml (lower left) yielded a flat TDC almost in line with the target. The CM injection rate was lower in the later phases. At CCTA (upper and lower right), we observed a similar trend. However, the injected CM dose was lower and similar under both injection protocols (40.0 ml and 39.8 ml).

## **CONCLUSION**

s The variable-rate CM injection rate may result in more precise control of the TDC. In protocols with greater CM injection volumes, e.g. for HDCT, it may be possible to obtain the target TDC at a smaller CM dose.

## **CLINICAL RELEVANCE/APPLICATION**

CT contrast studies are less invasive with the variable 4-phase CM injection protocol because the target TDC can be obtained despite the lower CM dose.

Printed on: 02/07/23

## Abstract Archives of the RSNA, 2022

W2-SPPH-1

### **Analysis of Noise for the Structural Difference Between Healthy and Destroyed Liver Tissue in CT Images During Microwave Ablation Therapy**

Wednesday, Nov. 30 9:00AM - 9:30AM Room: Learning Center - PH DPS

#### **Participants**

Naghmeh Mahmoodian, PhD, (*Presenter*) Nothing to Disclose

#### **PURPOSE**

Microwave ablation (MWA) is a minimally invasive therapy used for ablating the liver tumor in its location. Computed tomography (CT) as an interventional imaging modality is employed to visualize the therapy process. However, because of overlaying macroscopically visible changes in CT images during MWA therapy, it is difficult to distinguish between the lesion, healthy, and ablated tissue. Therefore, we propose a method for distinguishing among different tissue structures to determine the stopping point for ablating tumors using CT images acquired during MWA liver therapy.

#### **METHODS AND MATERIALS**

For all patients, CT scans were performed before and after the liver MWA therapy with a tube voltage of 120 KeV. The CT images were acquired before starting and after finishing the therapy, respectively, without and with a contrast agent. The ground truth was prepared manually based on the ablated tissue. The pre- and post-ablated images and corresponding ground truth images were aligned using non-rigid registration. This was then followed by automatic segmentation of the pre- and post-ablated CT images based on the ground truth. The region of interest (ROI) has been selected manually and converted into small patches with the size of 32 x 32 pixels. Different values of Gaussian noise have been added to the pre-ablated images, using two methods of noise power spectrum (NPS) measurement: -Fourier and task-based approaches- for analyzing the effects of noise on different tissue structures.

#### **RESULTS**

25 patients with a total of 650 pre-ablated images and a total of 1950 patches were included in the study. Six different Gaussian noise values of 0.005, 0.006, 0.007, 0.008, 0.009, and 0.01 were added on the pre-ablated images. The NPS was measured based on the Fourier- and Noise distributions were evaluated based on task-based methods. Then the best image and corresponding noise value was chosen based on the maximum distance between the NPS of healthy and ablated tissue that leads to the distinction between different tissue structures.

#### **CONCLUSION**

Distinguishing tissue characterization of the healthy, tumor, and ablated liver tissue in CT images has been achieved by analyzing the noise effects on different tissues. The difference appears in healthy and tumor tissue NPS results and increases by adding more noise to the CT images. The results show the possibility of determining the stopping point during an MWA therapy by measuring the change in the anatomical noise of different tissue structures.

#### **CLINICAL RELEVANCE/APPLICATION**

An essential issue of tumor ablation therapy is to detect when the entire tumor tissue has completely been destroyed. However, current methods can't present the changes in the CT images during MWA therapy, we provide a solution for that.

Printed on: 02/07/23



## Abstract Archives of the RSNA, 2022

W2-SPPH-2

### Artifact Reduction Using Silver Beam Filtration in Interventional CT

Wednesday, Nov. 30 9:00AM - 9:30AM Room: Learning Center - PH DPS

#### Participants

Timothy Szczykutowicz, PhD, Madison, WI (*Presenter*) Consultant, Aidoc Medical Ltd; Consultant, Flowhow.ai; Consultant, medInt Holdings, LLC; Consultant, Alara, Inc; Consultant, AstoCT, Inc; Research Grant, General Electric Company; Research Grant, Canon Medical Systems Corporation

#### PURPOSE

Intraoperative visualization of devices such as ablation probes, drainage needles, and biopsy probes is important for avoiding critical structures and ensuring the intervention is accurately reaching the target structure. However, these devices produce strong metal artifacts in CT due to beam hardening and photon starvation which makes accurate visualization of tip and trajectory challenging. This study evaluates the use of silver filtration (SilverBeam, Canon Medical USA) to a biopsy procedure task and quantifies metal artifact as a function of beam energy and the presence of a silver filter.

#### METHODS AND MATERIALS

An anthropomorphic phantom (Lungman, Kyoto Kagaku) simulating a patient was scanned with a biopsy needle and its sheath (14 gauge) aligned in the axial plane inside the lung field. Images of the phantom and needle were acquired using an MDCT scanner (Aquilion One Prism Edition, Canon Medical USA) at beam energies of 100, 120, 135 kV, and at 120 kV with silver filtration. For each measurement, the CTDIvol (i.e., a surrogate for patient dose) was kept constant at 1 mGy. Metal artifacts from the biopsy probe were quantified by measuring the absolute error in CT numbers directly in front of the needle tip. Errors in CT number were normalized relative to the 120 kV scan with silver filtration. All measurements were repeated 3 times.

#### RESULTS

Artifacts relative to using silver beam increased for all beam energies not using silver beam. Median artifact increases were 95% (i.e., a near doubling of CT number error) ( $p = 0.014$ ), 79% ( $p = 0.009$ ), and 34% ( $p = 0.015$ ) for 100, 120, and 135 kV respectively. Visually, the biopsy probe exhibited the smallest blooming artifact for 120 kV with silver filtration relative to all other scan conditions.

#### CONCLUSION

Use of silver filtration for interventional CT procedures reduces metal artifacts at the device tip.

#### CLINICAL RELEVANCE/APPLICATION

Device tip localization is essential for physician confidence their device has reached the intended target. This study demonstrated that the use of silver filtration decreases metal artifacts at device tips.

Printed on: 02/07/23

## Abstract Archives of the RSNA, 2022

W2-SPPH-3

### Investigation of Thermal Injury Risks From High-Pressure Gas Supply Line (HPGSL) During MR Guided Cryoablation

Wednesday, Nov. 30 9:00AM - 9:30AM Room: Learning Center - PH DPS

#### Participants

Liqiang Ren, PhD, Rochester, MN (*Presenter*) Nothing to Disclose

#### PURPOSE

To investigate the potential RF heating and frostbite risks from the high-pressure gas supply line (HPGSL) during MR guided cryoablation.

#### METHODS AND MATERIALS

Ex vivo experiments were performed using an MRI-conditional Boston Scientific cryoablation system. An 8ft long HPGSL with a metallic inner tube delivers high pressure gases to the cryoneedle when plugged into the mobile connection panel (MCP). To investigate the potential RF heating risks, three experiments were performed with a cryoneedle inserted into porcine tissue on a 1.5T MRI scanner. The tissue was placed ~10 cm off the patient table center and covered by a single layer of dry operating room (OR) towel (thickness: ~1mm) serving as a thermal insulation layer between tissue and HPGSL. A segment of interest (SOI, ~3 cm) of HPGSL was in contact with the towel. A temperature monitoring system was used to record the temperature during executions of a T2-weighted sequence (~2.3 minutes; specific absorption rate: 2.3 W/kg) via four thermal sensors: three attached to HPGSL and one placed on tissue surface under SOI. Two experiments were performed with HPGSL unplugged and plugged into MCP, respectively. A third one was performed with HPGSL plugged into MCP and a 2.5 cm thick insulation pad inserted between HPGSL and towel. To investigate the frostbite risk, cryoablation experiments were performed with the cryoneedle inserted into a container filled with saline. Temperature changes during a 5-minute and a 7-minute freezing procedure were measured with three thermal sensors attached to HPGSL and one insulated from HPGSL by either a single layer OR towel or both the towel and the pad at ~15 cm away from the cryoneedle shaft, respectively.

#### RESULTS

For RF heating risk investigations, temperature rises on HPGSL were much lower at the segment close to the tissue compared to other locations along HPGSL. With HPGSL disconnected and connected to MCP, the maximum tissue temperature rises were about 4.9 and 40° when only the towel was used for insulation, respectively. For frostbite risk investigations, the temperature drops along HPGSL reduced with increased distances from the cryoneedle shaft. With only a single layer of OR towel, the maximum temperature drop was about 20° at 15 cm from the shaft end. No temperature rises or drops were observed at the porcine tissue surface when the thick pad was inserted between thermal sensor and HPGSL.

#### CONCLUSION

s Skin injury could occur during MR guided cryoablation due to HPGSL induced RF heating and/or frostbite. To mitigate these risks, sufficient insulation between HPGSL and patient skin should be applied.

#### CLINICAL RELEVANCE/APPLICATION

Sufficient insulation between HPGSL and patient should be applied to effectively improve patient safety undergoing MR guided cryoablation procedures.

Printed on: 02/07/23

## Abstract Archives of the RSNA, 2022

W2-SPPH-4

### Technical Evaluation of Motor Evoked Potential Monitoring During MR-Guided Cryoablation of the Shoulder

Wednesday, Nov. 30 9:00AM - 9:30AM Room: Learning Center - PH DPS

#### Participants

Christopher Favazza, PhD, Rochester, MN (*Presenter*) Nothing to Disclose

#### PURPOSE

Pre-procedural testing to evaluate potential RF heating risks and image quality penalties associated with motor evoked potential (MEP) monitoring during MR-guided cryoablation of the shoulder.

#### METHODS AND MATERIALS

Using a porcine tissue phantom, a series of ex vivo experiments were conducted mimicking the clinical configuration for MEP monitoring during MR-guided cryoablation near the brachial plexus. Two needle electrodes were placed on the sides of the phantom "head" to simulate transcranial stimulation. Two needle electrode pairs and a ground electrode were placed in the "arm" to mimic muscle recording. Fluoroptic temperature sensors were inserted near the tips of all 7 electrodes. The phantom was placed "head" first into the scanner. To minimize heating risks, stimulation and recording/ground wires were routed along the center of the bore and exited the back and front of the scanner, respectively. Stimulation and recording wires were routed through a waveguide and connected to the nerve monitoring system outside the scan room. Along with a single high specific absorption rate (SAR) T2-weighted sequence (2.5 W/kg), a series of proton-density (PD)-weighted sequences used to monitor cryoablations were executed with different combinations of experimental variables that influence heating—wire path, position relative to bore wall, and SAR. Heating was measured with thermal sensors and recorded. Image quality was assessed qualitatively by calculating the average contrast-to-noise ratio (CNR) on the PD images. Clinical workflow of interleaving MEP and image acquisitions was evaluated.

#### RESULTS

Maximum temperatures rises of 0.6, 0.8 2.8 and 0.4°C were respectively measured for high SAR T2, PD monitoring sequence at 14 minutes (SAR= 1.9 W/kg), PD with phantom shifted to touch the bore wall, and low SAR PD (0.7 W/kg) with phantom touching bore wall. Image quality was adequate with an average CNR=117. Stimulation was successfully interleaved between successive PD monitoring acquisitions with low noise signal reception in absence of active MRI.

#### CONCLUSION

s RF heating risks can be sufficiently minimized to allow for intraprocedural nerve monitoring during MR-guided cryoablation, especially when a low SAR sequence is used. Image quality is not significantly degraded. MEP monitoring is feasible and can be operated in between MR image acquisitions.

#### CLINICAL RELEVANCE/APPLICATION

This work demonstrates that intraprocedural MEP monitoring can be safely performed during MR-guided cryoablation procedures without significantly compromising MRI imaging quality. A successful cryoablation treatment using MEP monitoring has been carried out based on these findings.

Printed on: 02/07/23



## Abstract Archives of the RSNA, 2022

W2-SPPH-6

### Deep Learning Ring Artifact Correction in Photon-Counting Spectral CT

Wednesday, Nov. 30 9:00AM - 9:30AM Room: Learning Center - PH DPS

#### Participants

Dennis Hein, Stockholm, Sweden (*Presenter*) Research Collaborator, General Electric Company

#### PURPOSE

To develop an image-domain ring artifact correction algorithm for photon-counting spectral CT using deep learning.

#### METHODS AND MATERIALS

Numerical basis phantoms (soft tissue and bone) were generated by thresholding CT images from the KITS19 dataset. Imaging was simulated using a fan beam acquisition and a spectral response model of a photon-counting silicon detector with 0.5x0.5 mm<sup>2</sup> pixels. The simulation was performed for 120 kVp and 200 mAs with 2000 detectors and 2000 view angles. Detector inhomogeneity was simulated by independently applying a random threshold shift to each of the eight thresholds and each of the detector pixels. Two material decompositions were performed: one with the bin thresholds used in the simulation and one with the nominal bin thresholds—yielding images with ring artifacts. Images were reconstructed on a 1024x1024 grid using FBP. A version of the Unet (2D convolutional neural network), with bilinear upsampling to avoid checkerboard artifacts, was trained using ADAM to map a pair of ring corrupted basis images (observed) to their ring artifact free counterparts (truth). The loss function is the weighted sum of two terms: a L1-penalty for the basis images and a perceptual loss for the virtual monogenetic images at 70 keV. The perceptual loss utilizes VGG16 as feature extractor.

#### RESULTS

The degree of ring artifact correction is proxied by the change in the loss function between the ring corrupted and processed images (predicted). This metric yields an 83% reduction in the validation set. To measure the change in noise, six 24x24 ROIs are defined in a monoenergetic image at 70 keV. A two-sample F-test for equal variances is conducted against the alternative hypothesis that the variance in predicted is greater than in truth. The p-value for this test is 0.24 (1.8% increase in standard deviation) and hence the null cannot be rejected at any reasonable significance level.

#### CONCLUSION

This work proposes a deep learning-based image processing technique for ring artifact correction in photon-counting spectral CT and demonstrates its ability to produce ring corrected virtual monoenergetic images at a range of energy levels.

#### CLINICAL RELEVANCE/APPLICATION

This work proposes a deep learning-based image processing technique for ring artifact correction in photon-counting spectral CT and demonstrates its ability to produce ring corrected virtual monoenergetic images at a range of energy levels.

Printed on: 02/07/23

## Abstract Archives of the RSNA, 2022

W2-SPPH-7

### Deep Learning for Automatic Contrast Enhancement Phase Detection on Abdominal Computed Tomography

Wednesday, Nov. 30 9:00AM - 9:30AM Room: Learning Center - PH DPS

#### Participants

Natália Alves, MSc, Nijmegen, Netherlands (*Presenter*) Nothing to Disclose

#### PURPOSE

Develop and validate a probabilistic convolutional neural network (CNN) for automatic classification of intravenous contrast enhancement (CE) phase on abdominal computed tomography (CT) scans.

#### METHODS AND MATERIALS

This retrospective study included 2000 abdominal CE-CT scans from our centre, which had information about the CE phase on the DICOM header. In addition to the baseline non-contrast scan (non-CE), three contrast phases were considered at different time intervals after contrast agent administration: the arterial phase (AP) at 40-50 seconds, the portal-venous phase (PVP) at 60-70 seconds and the delayed phase (DP) at 150-240 seconds. The distribution of CE phases on the training/validation dataset was 25.3% non-CE, 25.3% AP, 27.7% PVP and 21.7% DP. Half of the scans were used for model training/validation and a half for independent model testing. A 3-dimensional Inception CNN was trained to perform this multiclass classification task using stratified 4-fold cross-validation for 100 epochs. The model predictions from the 4 folds were ensemble to generate a final likelihood score for each contrast phase in the independent test set. The phase with the highest score was then chosen as the final model output.

#### RESULTS

The overall accuracy for the multiclass CNN was 92.4%, with only 76 out of the 1000 scans in the independent test set being incorrectly classified. The individual accuracies for each phase were 97.6% (244 out of 250) for non-CE, 95.6% (239 out of 250) for AP, 85.6% (214 out of 250) for PVP and 90.8% (227 out of 250) for DP. The most frequent mistake was in differentiating between the portal venous and delayed phases. This can be explained by the reduced amount of contrast agent in the abdomen and the high patient-specific and varied appearance of these two phases within the same protocol. Increasing the size and variety of the training data may improve performance for these two phases.

#### CONCLUSION

Deep learning can accurately determine intravenous CE phase on multi-phase CE abdominal CT scans.

#### CLINICAL RELEVANCE/APPLICATION

CE information is critical to diagnosis but often lacks from the image metadata. DL can accurately classify CE phases, important for AI automation and the curation of high-quality training datasets.

Printed on: 02/07/23

## Abstract Archives of the RSNA, 2022

W2-SPPH-8

### Training to Improve Radiologist Performance for Liver Metastasis Detection at Contrast Enhanced CT

Wednesday, Nov. 30 9:00AM - 9:30AM Room: Learning Center - PH DPS

#### Participants

Scott Hsieh, Rochester, MN (*Presenter*) Nothing to Disclose

#### PURPOSE

The value of a radiology exam depends on the interpreting radiologist. We hypothesized that targeted training would improve liver metastasis detection at contrast enhanced CT.

#### METHODS AND MATERIALS

After IRB approval, readers (radiology residents, board-certified abdominal or non-abdominal radiologists) attended four sessions, each lasting 4 hours. (Session 1) Pre-training test: readers circumscribed all suspected metastases and rated confidence of malignancy in 40 portal phase abdominal CT exams (91 metastases total) with no feedback provided. (2) Search training: while interpreting 30 exams, readers were told to increase interpretation time to at least 3 min/exam, use liver windows at least 1.5 min/exam, and use coronal stack at least 25% of total time; and received concurrent eye tracker feedback highlighting gaze patterns. (3) Discrimination training: while interpreting 100 additional cropped liver images including 0-3 benign or malignant lesions, readers rated confidence of malignancy of the lesions, with truth revealed immediately. (4) Post-training test (identical to the pre-training test). Ground truth for liver metastases was determined using histopathology or progression. Performance was measured using per-lesion sensitivity and area under the jackknife free ROC curve (AUC), a measure of accuracy that also incorporates confidence ratings.

#### RESULTS

We recruited 31 readers (8 subspecialized abdominal radiologists, 8 non-abdominal radiologists, 15 residents). Between pre- and post-training tests, mean [SD] sensitivity increased from 82 [8]% to 85 [5]% (paired t-test,  $p = 0.009$ ), but AUC did not significantly change (from 0.72 [0.08] to 0.71 [0.07],  $p = 0.36$ ). Mean changes in sensitivity for subspecialized abdominal radiologists, non-abdominal specialists, and trainees were -0.6%, 4.6%, and 3.5%, respectively; only trainees' change was significant ( $p = 0.02$ ). In the post-training test, use of liver windows ( $p < 0.001$ ) and coronal stack ( $p < 0.001$ ) both increased, but interpretation time did not change ( $p = 0.62$ ). Despite improved use of liver windows and coronal images, sensitivity improvements were modest. Small, peripheral metastases seemed to benefit the most from training.

#### CONCLUSION

s Targeted training resulted in improvements in sensitivity but not AUC for liver metastasis detection in CT.

#### CLINICAL RELEVANCE/APPLICATION

Missed hepatic metastases could be reduced by training to improve readers' search behaviors.

Printed on: 02/07/23

## Abstract Archives of the RSNA, 2022

W2-SPPH-9

### Utility of Variable-Rate Contrast Medium Injection at Computed Tomography: A Simulation Study

Wednesday, Nov. 30 9:00AM - 9:30AM Room: Learning Center - PH DPS

#### Participants

Toru Higaki, PhD, Minami-ku, Hiroshima, Japan (*Presenter*) Nothing to Disclose

#### PURPOSE

For contrast-enhanced computed tomography (CT), the contrast medium (CM) volume is generally injected at a constant rate and is based on the study's purpose and the patient's body weight. We used computer simulation to evaluate the clinical benefit of a variable-rate CM injection.

#### METHODS AND MATERIALS

We developed a contrast simulator using the circulation model proposed in 1998 by Bae et al. By inputting the contrast protocol and the patient's body indices, the time density curve (TDC) of any organ can be calculated. Besides the conventional constant-rate CM injection, a variable-rate injection comprised of up to 4 phases can be delivered. By specifying the target TDC shape, an injection protocol can be automatically calculated to obtain the TDC shape closest to the target. We compared the TDC of constant-rate- and variable-rate (4 phases) injections for hepatic dynamic CT (HDCT) and coronary CT angiography (CCTA). The target TDC shape for HDCT was 280 Hounsfield units (HU) and the injection time was 20 seconds at the abdominal aorta, for CCTA it was 300 HU delivered in 5 seconds at the ascending aorta. The CM and the saline were injected simultaneously so that the total injection rate was always 5.0 ml/sec.

#### RESULTS

The rectangles present our findings. At HDCT, the TDC produced by the constant-rate injection of 96.0 ml CM into the abdominal aorta ascended beyond the target (upper left); the 4-phase injection of 89.9 ml (lower left) yielded a flat TDC almost in line with the target. The CM injection rate was lower in the later phases. At CCTA (upper and lower right), we observed a similar trend. However, the injected CM dose was lower and similar under both injection protocols (40.0 ml and 39.8 ml).

#### CONCLUSION

The variable-rate CM injection rate may result in more precise control of the TDC. In protocols with greater CM injection volumes, e.g. for HDCT, it may be possible to obtain the target TDC at a smaller CM dose.

#### CLINICAL RELEVANCE/APPLICATION

CT contrast studies are less invasive with the variable 4-phase CM injection protocol because the target TDC can be obtained despite the lower CM dose.

Printed on: 02/07/23



## Abstract Archives of the RSNA, 2022

W2-SPRO

### Radiation Oncology Wednesday Poster Discussions

Wednesday, Nov. 30 9:00AM - 9:30AM Room: Learning Center - RO DPS

#### Participants

Mary U. Feng, MD, Hillsborough, CA (*Moderator*) Royalties, Wolters Kluwer nv; Research Grant, Siemens AG; Research Grant, AstraZeneca PLC

#### Sub-Events

### W2-SPRO-1 Establishing Contouring Protocols for Local Organs at Risk for MRI-Guided Radiation Therapy of Adenocarcinoma of the Prostate

#### Participants

Sarah Dyke, BS, (*Presenter*) Nothing to Disclose

#### PURPOSE

To establish guidelines for contouring the urethra, penile bulb (PB), corpus cavernosum (CC), corpus spongiosum (CS), and the neurovascular bundle (NVB) for the purpose of consistent definition of regional organs at risk (OAR) for MRI-guided radiation treatment (RT) using a 1.5 Tesla MRI equipped linear accelerator (MR-Linac).

#### METHODS AND MATERIALS

Patients undergoing RT for prostate cancer on a 1.5 Tesla MRI Linac were enrolled in a prospective clinical trial (NCT04075305). Daily MR images from 10 patients were collected and the urethra, PB, CC, CS, and the NVB were contoured in MIM (MIM Software Inc, Beachwood, OH). Detailed contouring guidelines for identifying each structure were generated and presented to a diagnostic radiologist and four board certified radiation oncologists to test their reproducibility. Recommendations include using T2-weighted images and specific window levels for each structure. In order to show concordance between reference and observer contours, mean Hausdorff distances (HD) (mean distance between contours) and Jaccard coefficients (JC) (contouring area overlap) were obtained.

#### RESULTS

The mean HD for the CC was 0.2 (SD 0.06), and the mean JC was 0.54 (SD 0.11). The mean HD for the CS was 0.29 (SD 0.22), and the mean JC was 0.47 (SD 0.15). The mean HD for the PB was 0.17 (SD 0.08), and the mean JC was 0.58 (SD 0.12). The mean HD for the NVB was 0.32 (SD 0.18), and the mean JC was 0.32 (SD 0.10). The mean HD for the urethra was 0.19 (SD 0.11), and the mean JC was 0.25 (SD 0.13).

#### CONCLUSION

s Contouring guidelines were designed for the urethra, PB, CC, CS, and NVB using images from 1.5 Tesla MR-Linac. These OARs are challenging to contour and agreement across observers was modest/poor; additional methods to improve inter-observer variability are needed. Consistent contouring of these OARs is important for prospective evaluation of dosimetric criteria and clinical outcomes related to their exposure.

#### CLINICAL RELEVANCE/APPLICATION

Erectile dysfunction following RT is thought to be related to damage to structures involved in sexual function located near the prostate. Similarly, a mechanism of urinary toxicity may be related to RT dose to urinary structures. A reliable method for identifying these structures could better inform RT treatment plans and potentially improve erectile and urinary functional outcomes.

Printed on: 02/07/23



## Abstract Archives of the RSNA, 2022

W2-SPRO-1

### Establishing Contouring Protocols for Local Organs at Risk for MRI-Guided Radiation Therapy of Adenocarcinoma of the Prostate

Wednesday, Nov. 30 9:00AM - 9:30AM Room: Learning Center - RO DPS

#### Participants

Sarah Dyke, BS, (Presenter) Nothing to Disclose

#### PURPOSE

To establish guidelines for contouring the urethra, penile bulb (PB), corpus cavernosum (CC), corpus spongiosum (CS), and the neurovascular bundle (NVB) for the purpose of consistent definition of regional organs at risk (OAR) for MRI-guided radiation treatment (RT) using a 1.5 Tesla MRI equipped linear accelerator (MR-Linac).

#### METHODS AND MATERIALS

Patients undergoing RT for prostate cancer on a 1.5 Tesla MRI Linac were enrolled in a prospective clinical trial (NCT04075305). Daily MR images from 10 patients were collected and the urethra, PB, CC, CS, and the NVB were contoured in MIM (MIM Software Inc, Beachwood, OH). Detailed contouring guidelines for identifying each structure were generated and presented to a diagnostic radiologist and four board certified radiation oncologists to test their reproducibility. Recommendations include using T2-weighted images and specific window levels for each structure. In order to show concordance between reference and observer contours, mean Hausdorff distances (HD) (mean distance between contours) and Jaccard coefficients (JC) (contouring area overlap) were obtained.

#### RESULTS

The mean HD for the CC was 0.2 (SD 0.06), and the mean JC was 0.54 (SD 0.11). The mean HD for the CS was 0.29 (SD 0.22), and the mean JC was 0.47 (SD 0.15). The mean HD for the PB was 0.17 (SD 0.08), and the mean JC was 0.58 (SD 0.12). The mean HD for the NVB was 0.32 (SD 0.18), and the mean JC was 0.32 (SD 0.10). The mean HD for the urethra was 0.19 (SD 0.11), and the mean JC was 0.25 (SD 0.13).

#### CONCLUSION

s Contouring guidelines were designed for the urethra, PB, CC, CS, and NVB using images from 1.5 Tesla MR-Linac. These OARs are challenging to contour and agreement across observers was modest/poor; additional methods to improve inter-observer variability are needed. Consistent contouring of these OARs is important for prospective evaluation of dosimetric criteria and clinical outcomes related to their exposure.

#### CLINICAL RELEVANCE/APPLICATION

Erectile dysfunction following RT is thought to be related to damage to structures involved in sexual function located near the prostate. Similarly, a mechanism of urinary toxicity may be related to RT dose to urinary structures. A reliable method for identifying these structures could better inform RT treatment plans and potentially improve erectile and urinary functional outcomes.

Printed on: 02/07/23

## Abstract Archives of the RSNA, 2022

W2-SPVA

### Vascular Wednesday Poster Discussions

Wednesday, Nov. 30 9:00AM - 9:30AM Room: Learning Center - VA DPS

#### Sub-Events

#### W2-SPVA-1 Comparison of the Quality of Lymphatic Vessel Images Obtained Using Two Photoacoustic Imaging Systems

##### Participants

Yushi Suzuki, MD, PhD, (*Presenter*) Nothing to Disclose

##### PURPOSE

Photoacoustic imaging (PAI) has a resolution of 0.2 mm and can evaluate lymphatic vessels in greater detail than existing methods. A new device, the LUBO, has been introduced; this is smaller than the PAI-05 (both from Luxonus inc., Kawasaki, Japan), which was the device used until 2020. We aimed to determine the imaging capability of LUBO by comparing it head-to-head with the PAI-05.

##### METHODS AND MATERIALS

Two healthy individuals and two lymphedema patients underwent PAI of the area of interest using both the PAI-05 and LUBO. Each participant was injected with indocyanine green subcutaneously to visualize the lymphatic vessels. After confirming with a near-infrared camera that lymphatic flow had moved to the central part of the body, PAI was performed. A physician was requested to select the method with superior image clarity.

##### RESULTS

The LUBO produced sharper images of lymphatic vessels and veins than the PAI-05. In addition, the dermal backflow image obtained from a patient with lymphedema delineated the pre-collector lymphatic vessels more clearly.

##### CONCLUSION

s PAI can visualize detailed lymphatic flow and can be used for preoperative planning of lymphaticovenular anastomosis (LVA). The LUBO is smaller, occupying about 1/7th of the PAI-05 footprint, and requires a shorter imaging time of 5 minutes instead of the 10 minutes taken previously. Its preview function has also made it easier to capture movement in the target area. Further, observing lymphatic pumps has become easier.

##### CLINICAL RELEVANCE/APPLICATION

Improved visualization of lymphatic vessels and veins with the new model allows detection and evaluation of lymphatic vessels suitable for anastomosis, which will lead to improved LVA outcomes. Acknowledgment: This research was funded by a grant from The Japan Agency for Medical Research and Development (AMED) 19he2302002h0501.

Printed on: 02/07/23

## Abstract Archives of the RSNA, 2022

W2-SPVA-1

### Comparison of the Quality of Lymphatic Vessel Images Obtained Using Two Photoacoustic Imaging Systems

Wednesday, Nov. 30 9:00AM - 9:30AM Room: Learning Center - VA DPS

#### Participants

Yushi Suzuki, MD, PhD, (*Presenter*) Nothing to Disclose

#### PURPOSE

Photoacoustic imaging (PAI) has a resolution of 0.2 mm and can evaluate lymphatic vessels in greater detail than existing methods. A new device, the LUBO, has been introduced; this is smaller than the PAI-05 (both from Luxonus inc., Kawasaki, Japan), which was the device used until 2020. We aimed to determine the imaging capability of LUBO by comparing it head-to-head with the PAI-05.

#### METHODS AND MATERIALS

Two healthy individuals and two lymphedema patients underwent PAI of the area of interest using both the PAI-05 and LUBO. Each participant was injected with indocyanine green subcutaneously to visualize the lymphatic vessels. After confirming with a near-infrared camera that lymphatic flow had moved to the central part of the body, PAI was performed. A physician was requested to select the method with superior image clarity.

#### RESULTS

The LUBO produced sharper images of lymphatic vessels and veins than the PAI-05. In addition, the dermal backflow image obtained from a patient with lymphedema delineated the pre-collector lymphatic vessels more clearly.

#### CONCLUSION

s PAI can visualize detailed lymphatic flow and can be used for preoperative planning of lymphaticovenular anastomosis (LVA). The LUBO is smaller, occupying about 1/7th of the PAI-05 footprint, and requires a shorter imaging time of 5 minutes instead of the 10 minutes taken previously. Its preview function has also made it easier to capture movement in the target area. Further, observing lymphatic pumps has become easier.

#### CLINICAL RELEVANCE/APPLICATION

Improved visualization of lymphatic vessels and veins with the new model allows detection and evaluation of lymphatic vessels suitable for anastomosis, which will lead to improved LVA outcomes. Acknowledgment: This research was funded by a grant from The Japan Agency for Medical Research and Development (AMED) 19he2302002h0501.

Printed on: 02/07/23



## Abstract Archives of the RSNA, 2022

W5A-SPBR

### Breast Wednesday Poster Discussions - A

Wednesday, Nov. 30 12:15PM - 12:45PM Room: Learning Center - BR DPS

#### Participants

Georgia Spear, MD, Park Ridge, IL (*Moderator*) Research Grant, General Electric Company; Speakers Bureau, General Electric Company; Scientific Advisory Board, Hologic, Inc

#### Sub-Events

### W5A-SPBR- Discrepancy and Clinical Impact of Second Opinion Interpretation in Breast Imaging: A Single Institution Retrospective Analysis<sup>1</sup>

#### Participants

Lilian Wang, MD, Chicago, IL (*Presenter*) Nothing to Disclose

#### PURPOSE

The demand for second opinion (SO) interpretations in breast imaging has progressively increased, which may relate to increasing patient education/awareness, increasing complexity of breast cancer treatments, and the desire for subspecialized image interpretation. While this service is often provided at tertiary care centers to facilitate care in breast surgery, the impact of these interpretations on patient care is unclear. The purpose is to examine the impact of SO interpretations in breast imaging by assessing discrepancies between initial and second opinion review and their subsequent impact on clinical management for patients presenting to a tertiary care breast center.

#### METHODS AND MATERIALS

A retrospective database review was conducted of the SO interpretations rendered at our institution from December 1, 2020 to December 31, 2020. Interpretations were performed by 14 sub-specialized breast radiologists with a range of 1 - 20 years of experience. Outside facility interpretations were compared to second opinion interpretations in terms of BI-RADS assessment and recommendations. The results of additional imaging, biopsies, and surgical treatment were recorded.

#### RESULTS

All of the patients were adult females (n=85). 8 patients were lost to follow up after the second opinion interpretation was performed, resulting in 77 remaining patients, with an average age of 51 at the time of referral (range 18-79). When comparing the initial BIRADS and SO BIRADS, there was a change in BIRADS in 57%, with a decrease in 13.3%, an increase in 86.7%, and no change in 41.6%. 61.0% underwent additional imaging and 41.6% underwent subsequent imaging guided biopsy, one which was deferred. Of the 31 biopsies, 7 pathology results were malignant (22.6%), 9 were high risk (29.0%), and 15 were benign (48.4%). After additional imaging and biopsy, there was a major change in the surgical management in 22.1% of the cases, the large majority of whom underwent increased extent of disease resection and one whom averted surgical excision. The cancer detection rate was 11.7%. The overall PPV2 based on the recommendation for tissue diagnosis was 21.9%. The overall PPV3 based on the results of the biopsies actually performed was 22.6%.

#### CONCLUSION

Second opinion interpretations in breast imaging significantly impact diagnostic assessment and surgical management. The minor discrepancy rate between the initial and second opinion review was 57%. 51.6% of the biopsies yielded high risk or malignant pathology which led to a major change in the final surgical plan in 22% of the patients.

#### CLINICAL RELEVANCE/APPLICATION

Not only does the second opinion review increase the cancer detection rate, it can also have a substantial impact on the final surgical plan.

### W5A-SPBR- Disparities Associated with Patient Adherence to BI-RADS 3 Assessment Follow-up Recommendations<sup>2</sup>

#### Participants

Benjamin Wilson, MD, Lutherville Timonium, MD (*Presenter*) Nothing to Disclose

#### PURPOSE

To assess the relationship between sociodemographic factors and adherence rates in patients with a Breast Imaging Reporting and Data System (BI-RADS) 3 assessment.

#### METHODS AND MATERIALS

This retrospective cohort study reviewed data from all patients with a BI-RADS 3 assessment on mammography and ultrasound examinations at a single, multisite academic institution from January 1, 2015 to December 31, 2017. Appropriate follow-up was defined as returning for the first follow-up BI-RADS 3 examination between 3 and 9 months from the index examination. Delayed follow-up was defined as returning after 9 months from the index examination. Associations between BI-RADS 3 adherence rates

and patient sociodemographic characteristics were evaluated using univariate and multivariate logistic regression.

## RESULTS

There were 4038 unique patients in our study period, of which 2437 patients (60.4%) had appropriate follow-up, 765 (18.9%) patients had delayed follow-up and 836 patients (20.7%) were lost to follow-up. Univariate analysis demonstrated Black race, single relationship status, Medicaid and self-pay insurance status, and patients whose National Area Deprivation Index (ADI) is in the most disadvantaged 15% of neighborhoods were all sociodemographic factors associated with decreased likelihood adhering to BI-RADS 3 follow-up recommendations in a timely manner. In addition, on multivariate analysis, Medicaid insurance status remained significant for decreased likelihood of having appropriate BI-RADS 3 follow-up. Malignancy rate for all patients who returned for a BI-RADS 3 assessment follow-up in our cohort was 1.7% (55/3202) of which 27 (49%) were diagnosed at the 6-month follow-up, 20 (36%) at the 12-month follow-up, and 8 (15%) at the 24 or 36-month follow-up.

## CONCLUSION

Multiple sociodemographic disparities exist as barriers for appropriate adherence to follow-up recommendations in patients with a BI-RADS 3 assessment.

## CLINICAL RELEVANCE/APPLICATION

Adherence to follow-up recommendations and timely follow-up of abnormalities detected on breast imaging are important and could help to avoid a delayed breast cancer diagnosis. This is particularly important for racial minority patients and patients of low socioeconomic status, who are already at risk of having a more aggressive breast cancer course and have been shown to have higher breast cancer mortality rates.

## W5A-SPBR- Factors Associated with Decision to Undergo Mastectomy among Women with Ductal Carcinoma In Situ

### Participants

Manisha Bahl, MD, MPH, Cambridge, MA (*Presenter*) Consultant, Lunit Inc;Expert Advisory Committee, 2nd.MD

## PURPOSE

Mastectomy rates among women with ductal carcinoma in situ (DCIS) have dramatically increased over the last 20 years. The purpose of this study is to identify factors associated with the decision to undergo mastectomy among women with DCIS.

## METHODS AND MATERIALS

A retrospective study was conducted of women diagnosed with DCIS at an academic center from 2007 to 2016. Study subjects were diagnosed with unilateral DCIS by core needle biopsy and had subsequent surgery. Medical records were reviewed for year of surgery and type of surgical treatment, in addition to patient features, imaging features, and pathological features of DCIS at biopsy. Temporal trends in mastectomy rate by year were graphically visualized, and corresponding incidence rate ratios (IRRs) and 95% confidence intervals (CIs) of mastectomy rate by year were estimated using multivariable Poisson regression. Multivariable logistic regression models were also estimated to assess features associated with mastectomy. Adjusted odds ratios (aORs), 95% CIs, and Wald P values were calculated for each model.

## RESULTS

Over a ten-year period, 1313 women underwent surgical treatment for DCIS, of whom 1016 (77.4%) had breast-conserving surgery (BCS), 144 (11.0%) unilateral mastectomy, and 153 (11.7%) bilateral mastectomy. The rate of mastectomy increased over time (IRR 1.08, 95% CI: 1.04-1.13,  $P < 0.001$ ), which was largely attributed to women with dense rather than nondense breasts, but the rate of contralateral prophylactic mastectomy (CPM) did not increase over time (IRR 1.03, 95% CI: 0.97-1.10,  $P = 0.30$ ). With multivariable analysis, features associated with mastectomy were younger patient age, risk factors for breast cancer (such as BRCA1/2 mutations), a personal history of breast cancer, dense breast tissue, and pre-operative evaluation with MRI (all  $P < 0.05$ ). Features associated with CPM were younger patient age, White race, a personal history of breast cancer, a family history of breast cancer in a first-degree relative, and dense breast tissue (all  $P < 0.05$ ). There were no pathological features of DCIS at biopsy associated with mastectomy.

## CONCLUSION

Among women with DCIS, features associated with mastectomy are younger patient age, risk factors for breast cancer, a personal history of breast cancer, dense breast tissue, and pre-operative evaluation with MRI. Features associated with CPM are younger patient age, White race, a personal history of breast cancer, a family history of breast cancer, and dense breast tissue.

## CLINICAL RELEVANCE/APPLICATION

Understanding factors associated with the decision to undergo mastectomy rather than BCS will help clinicians improve patient education and better guide women with DCIS through the decision-making process.

## W5A-SPBR- Granulomatous Mastitis: A Retrospective Cohort Study in a Large County Hospital System

4

### Participants

Ahsan Khan, MD, (*Presenter*) Nothing to Disclose

## PURPOSE

Granulomatous mastitis (GM) is a chronic inflammatory breast disease of unclear etiology. We performed this study evaluate the clinical courses of women from our large Northern California county hospital.

## METHODS AND MATERIALS

With IRB approval, we retrospectively reviewed our Electronic Medical Records for biopsy-proven GM from 8/27/2015 to 4/2/2021, recording patient demographics, medical history, clinical presentation, imaging findings, microbiology, treatment, and follow-up.

## RESULTS

Of 73 women with GM (mean 36.9 years old; range 19 - 64 y), 58 (79.5%) were Hispanic/Latina ethnicity (institutional percentage:

25% Hispanic/Latina ethnicity) and 12 (16.4%) had history of tuberculosis. Presentations were tenderness (61/73, 83.6%), mass (50/73, 68.4%), erythema (25/73, 34.2%), induration (14/73, 19.2%), nipple discharge (11/73, 14.7%), and inverted nipple (5/73, 6.7%). Mammography showed mass (18/73, 24.7%) or asymmetry (14/73, 19.2%); ultrasound showed mass (43/73, 58.9%) and/or abscess (17/72, 23.3%). MRI (4) showed non-mass enhancement (2), rim-enhancing (2) or heterogeneously enhancing (1) lesions, and skin thickening (2). Patients had core biopsy (66/73, 90.4%), FNA (4/73, 5.5%), or surgery (3/73, 4.1%), isolating *Corynebacterium* (7/73, 9.6%), *Propionibacterium* (5/73, 6.8%), and *Mycobacterium tuberculosis* (2/73, 2.7%). Treatments were antibiotics (56/73, 74.7%), steroids (26/73, 34.7%) or immunosuppression (9.3%) for an average of 4.6 months. 21 (28%) patients had drainages; 2 (2.7%) had surgical excision. On follow-up, patients were lost (7) or followed clinically (66) (avg. 16.9 months, range 1-63), reporting no symptoms (43/65.2%, avg. 4.5 months), mild residual symptoms not requiring treatment (19/28.8%), or ongoing symptoms requiring treatment (4/6.0%). 10/43 patients with resolved symptoms recurred (avg. 8.9 months). Of 43 patients with follow-up imaging, 35 (81.4%) improved, 4 (9.3%) were stable, and 4 (9.3%) progressed.

## CONCLUSION

In our county hospital, GM most commonly affects young women of Hispanic/Latina descent. Clinical presentation, imaging characteristics, and treatments are variable which may pose clinical dilemmas.

## CLINICAL RELEVANCE/APPLICATION

Providers must be aware of risk factors, suspicious features, and potential pitfalls of granulomatous mastitis which requires a multidisciplinary algorithmic approach to treatment.

## W5A-SPBR- Surgical Outcomes of Lobular Neoplasia Found at MRI Guided Breast Biopsy

5

Participants

Jonathan Nguyen, MD, Charlottesville, VA (*Presenter*) Nothing to Disclose

## PURPOSE

To evaluate the upgrade rate of lobular neoplasia found at breast MRI guided core needle biopsy to malignancy on surgical excision.

## METHODS AND MATERIALS

A HIPAA compliant, IRB-approved retrospective review was performed at a single institution. Our breast biopsy database was reviewed from 7/1/2010-1/1/2022. Biopsies that demonstrated atypical lobular hyperplasia (ALH) or lobular carcinoma in situ (LCIS) as the most concerning pathology were included in the analysis. Lobular neoplasia associated with malignancy or any other high risk pathology (such as atypical ductal hyperplasia, papilloma or radial scar) were excluded. At our institution, all lobular neoplasia found on biopsy are recommended for surgical excision. The imaging findings and subsequent surgical pathology on excision of each case were reviewed. Statistical analysis was performed with Pearson exact tests to determine if an upgrade to malignancy was significantly associated with any imaging characteristics, including lesion morphology, lesion size, enhancement pattern, enhancement kinetics, T2 intensity, and study indication.

## RESULTS

The database yielded 534 MRI guided breast biopsies performed during the study timeframe. Lobular neoplasia was reported as the highest risk pathologic lesion in 29/534 (5.4%) cases. The morphologic characterization of these lesions demonstrated 11 masses (37.9%), 14 areas of non-mass enhancement (48.3%), and 4 foci (13.8%). Two out of the 29 (6.9%) cases of lobular neoplasia were upgraded to malignancy on surgical excision. None of the tested imaging characteristics was significantly associated with an upgrade to malignancy.

## CONCLUSION

The incidence of pure lobular neoplasia at MRI guided core needle biopsy is low, as is the upgrade rate of these lesions to malignancy on surgical excision. None of the tested imaging features are significant predictors of upgrade to malignancy on surgical excision.

## CLINICAL RELEVANCE/APPLICATION

Clinicians should be aware of the low upgrade rate of lobular neoplasia so they can better manage and discuss the pathology with patients after MRI guided core needle biopsy.

## W5A-SPBR- Diagnostic Accuracy in Male Breast Symptomatic Disease: A Single Centre Experience

6

Participants

Caterina Cazzella, MD, Modena, Italy (*Presenter*) Nothing to Disclose

## PURPOSE

To assess the diagnostic imaging accuracy in males with breast disease. To propose a diagnostic algorithm to evaluate the male patients with breast symptoms.

## METHODS AND MATERIALS

All men patients who underwent a breast biopsy between 2014 and 2021 were retrospectively enrolled. Mammography (MX) and breast ultrasound (US) results were classified according to BI-RADS (Breast Imaging Reporting and Data System) score from 0 to 6, and Appelbaum's classification (nodular, dendritic or diffuse pattern). Furthermore, all clinical-anamnesic data were reported. To define the diagnostic accuracy, breast imaging classifications were compared with the final histological diagnosis, considered as gold standard.

## RESULTS

A total of 223 patients were enrolled. All the patients performed US and, due to clinical conditions and radioprotection, only 52.9% (n=118) underwent MX. The majority (74.9%, n=167) demonstrated benign pathology (gynecomastia). Breast cancer was detected in 13.9% (n=31). Other nonneoplastic breast conditions were 11.2% (n=25). Breast imaging (MX and/or US) demonstrated 89% sensitivity and 91% specificity for gynecomastia and 80% sensitivity and 99% specificity for breast cancer, respectively. Most important malignancy predictors were: age (18 years), skin/nipple retraction, bloody nipple discharge and "nodular pattern" at imaging. Finally, a diagnostic algorithm was proposed. A combined final pattern assessment was assigned based on findings of both

US and MX imaging. Clinical and imaging results were afterwards recorded on a standard three-point classification scale, based on BI-RADS 5th Edition categories: 1 gynecomastia (BI-RADS 1 and 2); 2 undefined entity (BI-RADS 3); 3 malignant (BI-RADS 4 and 5).

## **CONCLUSION**

s Male breast cancer is rare. Integration of imaging and clinical-anamnestic data is useful to confirm the benign pathology, avoiding unnecessary surgery/invasive procedures.

## **CLINICAL RELEVANCE/APPLICATION**

Imaging is recommended for evaluation of male's indeterminate palpable breast mass. Protocols are not yet validated in literature; therefore we proposed an algorithm based on clinical-radiological integration.

## **W5A-SPBR- Incidence and Outcomes of COVID-19 Vaccine Related Lymphadenopathy on Screening Mammography across Vaccine Manufacturers**

Participants

Alexander Leyva, MD, Boston, MA (*Presenter*) Nothing to Disclose

## **PURPOSE**

To determine the incidence and outcomes of unilateral axillary lymphadenopathy related to COVID-19 vaccination across vaccine manufacturers at screening mammography.

## **METHODS AND MATERIALS**

This retrospective, multisite study included consecutive patients undergoing screening mammography from 02/8/2021-01/31/2022 with at least 3 months of follow-up. In the setting of documented recent (<6 weeks) vaccination, isolated ipsilateral axillary lymphadenopathy was considered a benign finding (BI-RADS 2). When administered >6 weeks previous, or if accompanied by a breast finding, axillary ultrasound was recommended (BI-RADS 0). Patient demographics and outcomes were retrieved from electronic medical records, COVID-19 vaccination status and manufacturer from a regional vaccine registry, and cancer outcomes from a regional tumor registry. A logistic regression was fit to estimate the association with days since prior COVID-19 vaccination and odds of an ipsilateral axillary finding, adjusted for age.

## **RESULTS**

44,473 patients (mean age 60.4 years +/- 11.4 years) underwent screening mammography at 5 sites. 39,067 (87.8%) underwent at least 1 COVID-19 vaccine dose. Median days since prior vaccine was 99.0 (IQR 40.0-179.0 days). 108 (0.3%) patients presented with unilateral lymphadenopathy in the setting of ipsilateral vaccination that did not vary across manufacturer (p=0.159). 80 (74.1%) presented <6 weeks from vaccination and deemed benign. 3 (3.8%) subsequently returned with a clinical concern in the same axilla and all were attributed BI-RADS 1/2. Of the 28 (25.9%) with ipsilateral lymphadenopathy >6 weeks from vaccination +/- ipsilateral breast finding, 9 (32.1%) were called back for additional evaluation. At diagnostic workup 4 were BI-RADS 1/2, 1 was BI-RADS 3, 4 were BI-RADS 4. Of those biopsied, 2 were malignant (both with ipsilateral breast malignancies) and 2 were benign. 19 (67.9%) were not called back due to a known non-breast malignancy or systemic illness or due to close proximity to the 6-week cutoff. Of the 19, 2 (10.5%) re-presented with a clinical concern in the same axilla and both were attributed BI-RADS 1/2. The odds of having an ipsilateral axillary finding significantly decreased for every 7 days since the prior COVID-19 vaccination dose (aOR 0.86, 95% CI 0.83-0.89, p<0.001).

## **CONCLUSION**

s The incidence of unilateral axillary lymphadenopathy post COVID-19 vaccination on screening mammography is low at 0.3% and does not vary across vaccine manufacturer. Isolated ipsilateral lymphadenopathy <6 weeks from vaccination had a 0% rate of malignancy.

## **CLINICAL RELEVANCE/APPLICATION**

Utilizing a pragmatic approach in managing unilateral lymphadenopathy in the setting of recent ipsilateral COVID-19 vaccination is both safe and effective.

Printed on: 02/07/23



## Abstract Archives of the RSNA, 2022

W5A-SPBR-1

### Discrepancy and Clinical Impact of Second Opinion Interpretation in Breast Imaging: A Single Institution Retrospective Analysis

Wednesday, Nov. 30 12:15PM - 12:45PM Room: Learning Center - BR DPS

#### Participants

Lilian Wang, MD, Chicago, IL (*Presenter*) Nothing to Disclose

#### PURPOSE

The demand for second opinion (SO) interpretations in breast imaging has progressively increased, which may relate to increasing patient education/awareness, increasing complexity of breast cancer treatments, and the desire for subspecialized image interpretation. While this service is often provided at tertiary care centers to facilitate care in breast surgery, the impact of these interpretations on patient care is unclear. The purpose is to examine the impact of SO interpretations in breast imaging by assessing discrepancies between initial and second opinion review and their subsequent impact on clinical management for patients presenting to a tertiary care breast center.

#### METHODS AND MATERIALS

A retrospective database review was conducted of the SO interpretations rendered at our institution from December 1, 2020 to December 31, 2020. Interpretations were performed by 14 sub-specialized breast radiologists with a range of 1 - 20 years of experience. Outside facility interpretations were compared to second opinion interpretations in terms of BI-RADS assessment and recommendations. The results of additional imaging, biopsies, and surgical treatment were recorded.

#### RESULTS

All of the patients were adult females (n=85). 8 patients were lost to follow up after the second opinion interpretation was performed, resulting in 77 remaining patients, with an average age of 51 at the time of referral (range 18-79). When comparing the initial BIRADS and SO BIRADS, there was a change in BIRADS in 57%, with a decrease in 13.3%, an increase in 86.7%, and no change in 41.6%. 61.0% underwent additional imaging and 41.6% underwent subsequent imaging guided biopsy, one which was deferred. Of the 31 biopsies, 7 pathology results were malignant (22.6%), 9 were high risk (29.0%), and 15 were benign (48.4%). After additional imaging and biopsy, there was a major change in the surgical management in 22.1% of the cases, the large majority of whom underwent increased extent of disease resection and one whom averted surgical excision. The cancer detection rate was 11.7%. The overall PPV2 based on the recommendation for tissue diagnosis was 21.9%. The overall PPV3 based on the results of the biopsies actually performed was 22.6%.

#### CONCLUSION

Second opinion interpretations in breast imaging significantly impact diagnostic assessment and surgical management. The minor discrepancy rate between the initial and second opinion review was 57%. 51.6% of the biopsies yielded high risk or malignant pathology which led to a major change in the final surgical plan in 22% of the patients.

#### CLINICAL RELEVANCE/APPLICATION

Not only does the second opinion review increase the cancer detection rate, it can also have a substantial impact on the final surgical plan.

Printed on: 02/07/23



## Abstract Archives of the RSNA, 2022

W5A-SPBR-2

### Disparities Associated with Patient Adherence to BI-RADS 3 Assessment Follow-up Recommendations

Wednesday, Nov. 30 12:15PM - 12:45PM Room: Learning Center - BR DPS

#### Participants

Benjamin Wilson, MD, Lutherville Timonium, MD (*Presenter*) Nothing to Disclose

#### PURPOSE

To assess the relationship between sociodemographic factors and adherence rates in patients with a Breast Imaging Reporting and Data System (BI-RADS) 3 assessment.

#### METHODS AND MATERIALS

This retrospective cohort study reviewed data from all patients with a BI-RADS 3 assessment on mammography and ultrasound examinations at a single, multisite academic institution from January 1, 2015 to December 31, 2017. Appropriate follow-up was defined as returning for the first follow-up BI-RADS 3 examination between 3 and 9 months from the index examination. Delayed follow-up was defined as returning after 9 months from the index examination. Associations between BI-RADS 3 adherence rates and patient sociodemographic characteristics were evaluated using univariate and multivariate logistic regression.

#### RESULTS

There were 4038 unique patients in our study period, of which 2437 patients (60.4%) had appropriate follow-up, 765 (18.9%) patients had delayed follow-up and 836 patients (20.7%) were lost to follow-up. Univariate analysis demonstrated Black race, single relationship status, Medicaid and self-pay insurance status, and patients whose National Area Deprivation Index (ADI) is in the most disadvantaged 15% of neighborhoods were all sociodemographic factors associated with decreased likelihood adhering to BI-RADS 3 follow-up recommendations in a timely manner. In addition, on multivariate analysis, Medicaid insurance status remained significant for decreased likelihood of having appropriate BI-RADS 3 follow-up. Malignancy rate for all patients who returned for a BI-RADS 3 assessment follow-up in our cohort was 1.7% (55/3202) of which 27 (49%) were diagnosed at the 6-month follow-up, 20 (36%) at the 12-month follow-up, and 8 (15%) at the 24 or 36-month follow-up.

#### CONCLUSION

Multiple sociodemographic disparities exist as barriers for appropriate adherence to follow-up recommendations in patients with a BI-RADS 3 assessment.

#### CLINICAL RELEVANCE/APPLICATION

Adherence to follow-up recommendations and timely follow-up of abnormalities detected on breast imaging are important and could help to avoid a delayed breast cancer diagnosis. This is particularly important for racial minority patients and patients of low socioeconomic status, who are already at risk of having a more aggressive breast cancer course and have been shown to have higher breast cancer mortality rates.

Printed on: 02/07/23

## Abstract Archives of the RSNA, 2022

W5A-SPBR-3

### Factors Associated with Decision to Undergo Mastectomy among Women with Ductal Carcinoma In Situ

Wednesday, Nov. 30 12:15PM - 12:45PM Room: Learning Center - BR DPS

#### Participants

Manisha Bahl, MD, MPH, Cambridge, MA (*Presenter*) Consultant, Lunit Inc;Expert Advisory Committee, 2nd.MD

#### PURPOSE

Mastectomy rates among women with ductal carcinoma in situ (DCIS) have dramatically increased over the last 20 years. The purpose of this study is to identify factors associated with the decision to undergo mastectomy among women with DCIS.

#### METHODS AND MATERIALS

A retrospective study was conducted of women diagnosed with DCIS at an academic center from 2007 to 2016. Study subjects were diagnosed with unilateral DCIS by core needle biopsy and had subsequent surgery. Medical records were reviewed for year of surgery and type of surgical treatment, in addition to patient features, imaging features, and pathological features of DCIS at biopsy. Temporal trends in mastectomy rate by year were graphically visualized, and corresponding incidence rate ratios (IRRs) and 95% confidence intervals (CIs) of mastectomy rate by year were estimated using multivariable Poisson regression. Multivariable logistic regression models were also estimated to assess features associated with mastectomy. Adjusted odds ratios (aORs), 95% CIs, and Wald P values were calculated for each model.

#### RESULTS

Over a ten-year period, 1313 women underwent surgical treatment for DCIS, of whom 1016 (77.4%) had breast-conserving surgery (BCS), 144 (11.0%) unilateral mastectomy, and 153 (11.7%) bilateral mastectomy. The rate of mastectomy increased over time (IRR 1.08, 95% CI: 1.04-1.13,  $P<0.001$ ), which was largely attributed to women with dense rather than nondense breasts, but the rate of contralateral prophylactic mastectomy (CPM) did not increase over time (IRR 1.03, 95% CI: 0.97-1.10,  $P=0.30$ ). With multivariable analysis, features associated with mastectomy were younger patient age, risk factors for breast cancer (such as BRCA1/2 mutations), a personal history of breast cancer, dense breast tissue, and pre-operative evaluation with MRI (all  $P<0.05$ ). Features associated with CPM were younger patient age, White race, a personal history of breast cancer, a family history of breast cancer in a first-degree relative, and dense breast tissue (all  $P<0.05$ ). There were no pathological features of DCIS at biopsy associated with mastectomy.

#### CONCLUSION

Among women with DCIS, features associated with mastectomy are younger patient age, risk factors for breast cancer, a personal history of breast cancer, dense breast tissue, and pre-operative evaluation with MRI. Features associated with CPM are younger patient age, White race, a personal history of breast cancer, a family history of breast cancer, and dense breast tissue.

#### CLINICAL RELEVANCE/APPLICATION

Understanding factors associated with the decision to undergo mastectomy rather than BCS will help clinicians improve patient education and better guide women with DCIS through the decision-making process.

Printed on: 02/07/23

## Abstract Archives of the RSNA, 2022

W5A-SPBR-4

### Granulomatous Mastitis: A Retrospective Cohort Study in a Large County Hospital System

Wednesday, Nov. 30 12:15PM - 12:45PM Room: Learning Center - BR DPS

#### Participants

Ahsan Khan, MD, (*Presenter*) Nothing to Disclose

#### PURPOSE

Granulomatous mastitis (GM) is a chronic inflammatory breast disease of unclear etiology. We performed this study evaluate the clinical courses of women from our large Northern California county hospital.

#### METHODS AND MATERIALS

With IRB approval, we retrospectively reviewed our Electronic Medical Records for biopsy-proven GM from 8/27/2015 to 4/2/2021, recording patient demographics, medical history, clinical presentation, imaging findings, microbiology, treatment, and follow-up.

#### RESULTS

Of 73 women with GM (mean 36.9 years old; range 19 - 64 y), 58 (79.5%) were Hispanic/Latina ethnicity (institutional percentage: 25% Hispanic/Latina ethnicity) and 12 (16.4%) had history of tuberculosis. Presentations were tenderness (61/73, 83.6%), mass (50/73, 68.4%), erythema (25/73, 34.2%), induration (14/73, 19.2%), nipple discharge (11/73, 14.7%), and inverted nipple (5/73, 6.7%). Mammography showed mass (18/73, 24.7%) or asymmetry (14/73, 19.2%); ultrasound showed mass (43/73, 58.9%) and/or abscess (17/72, 23.3%). MRI (4) showed non-mass enhancement (2), rim-enhancing (2) or heterogeneously enhancing (1) lesions, and skin thickening (2). Patients had core biopsy (66/73, 90.4%), FNA (4/73, 5.5%), or surgery (3/73, 4.1%), isolating *Corynebacterium* (7/73, 9.6%), *Propionibacterium* (5/73, 6.8%), and *Mycobacterium tuberculosis* (2/73, 2.7%). Treatments were antibiotics (56/73, 74.7%), steroids (26/73, 34.7%) or immunosuppression (9.3%) for an average of 4.6 months. 21 (28%) patients had drainages; 2 (2.7%) had surgical excision. On follow-up, patients were lost (7) or followed clinically (66) (avg. 16.9 months, range 1-63), reporting no symptoms (43/65.2%, avg. 4.5 months), mild residual symptoms not requiring treatment (19/28.8%), or ongoing symptoms requiring treatment (4/6.0%). 10/43 patients with resolved symptoms recurred (avg. 8.9 months). Of 43 patients with follow-up imaging, 35 (81.4%) improved, 4 (9.3%) were stable, and 4 (9.3%) progressed.

#### CONCLUSION

In our county hospital, GM most commonly affects young women of Hispanic/Latina descent. Clinical presentation, imaging characteristics, and treatments are variable which may pose clinical dilemmas.

#### CLINICAL RELEVANCE/APPLICATION

Providers must be aware of risk factors, suspicious features, and potential pitfalls of granulomatous mastitis which requires a multidisciplinary algorithmic approach to treatment.

Printed on: 02/07/23



## Abstract Archives of the RSNA, 2022

W5A-SPBR-5

### Surgical Outcomes of Lobular Neoplasia Found at MRI Guided Breast Biopsy

Wednesday, Nov. 30 12:15PM - 12:45PM Room: Learning Center - BR DPS

#### Participants

Jonathan Nguyen, MD, Charlottesville, VA (*Presenter*) Nothing to Disclose

#### PURPOSE

To evaluate the upgrade rate of lobular neoplasia found at breast MRI guided core needle biopsy to malignancy on surgical excision.

#### METHODS AND MATERIALS

A HIPAA compliant, IRB-approved retrospective review was performed at a single institution. Our breast biopsy database was reviewed from 7/1/2010-1/1/2022. Biopsies that demonstrated atypical lobular hyperplasia (ALH) or lobular carcinoma in situ (LCIS) as the most concerning pathology were included in the analysis. Lobular neoplasia associated with malignancy or any other high risk pathology (such as atypical ductal hyperplasia, papilloma or radial scar) were excluded. At our institution, all lobular neoplasia found on biopsy are recommended for surgical excision. The imaging findings and subsequent surgical pathology on excision of each case were reviewed. Statistical analysis was performed with Pearson exact tests to determine if an upgrade to malignancy was significantly associated with any imaging characteristics, including lesion morphology, lesion size, enhancement pattern, enhancement kinetics, T2 intensity, and study indication.

#### RESULTS

The database yielded 534 MRI guided breast biopsies performed during the study timeframe. Lobular neoplasia was reported as the highest risk pathologic lesion in 29/534 (5.4%) cases. The morphologic characterization of these lesions demonstrated 11 masses (37.9%), 14 areas of non-mass enhancement (48.3%), and 4 foci (13.8%). Two out of the 29 (6.9%) cases of lobular neoplasia were upgraded to malignancy on surgical excision. None of the tested imaging characteristics was significantly associated with an upgrade to malignancy.

#### CONCLUSION

The incidence of pure lobular neoplasia at MRI guided core needle biopsy is low, as is the upgrade rate of these lesions to malignancy on surgical excision. None of the tested imaging features are significant predictors of upgrade to malignancy on surgical excision.

#### CLINICAL RELEVANCE/APPLICATION

Clinicians should be aware of the low upgrade rate of lobular neoplasia so they can better manage and discuss the pathology with patients after MRI guided core needle biopsy.

Printed on: 02/07/23

## Abstract Archives of the RSNA, 2022

W5A-SPBR-6

### Diagnostic Accuracy in Male Breast Symptomatic Disease: A Single Centre Experience

Wednesday, Nov. 30 12:15PM - 12:45PM Room: Learning Center - BR DPS

#### Participants

Caterina Cazzella, MD, Modena, Italy (*Presenter*) Nothing to Disclose

#### PURPOSE

To assess the diagnostic imaging accuracy in males with breast disease. To propose a diagnostic algorithm to evaluate the male patients with breast symptoms.

#### METHODS AND MATERIALS

All men patients who underwent a breast biopsy between 2014 and 2021 were retrospectively enrolled. Mammography (MX) and breast ultrasound (US) results were classified according to BI-RADS (Breast Imaging Reporting and Data System) score from 0 to 6, and Appelbaum's classification (nodular, dendritic or diffuse pattern). Furthermore, all clinical-anamnestic data were reported. To define the diagnostic accuracy, breast imaging classifications were compared with the final histological diagnosis, considered as gold standard.

#### RESULTS

A total of 223 patients were enrolled. All the patients performed US and, due to clinical conditions and radioprotection, only 52.9% (n=118) underwent MX. The majority (74.9%, n=167) demonstrated benign pathology (gynecomastia). Breast cancer was detected in 13.9% (n=31). Other nonneoplastic breast conditions were 11.2% (n=25). Breast imaging (MX and/or US) demonstrated 89% sensitivity and 91% specificity for gynecomastia and 80% sensitivity and 99% specificity for breast cancer, respectively. Most important malignancy predictors were: age (18 years), skin/nipple retraction, bloody nipple discharge and "nodular pattern" at imaging. Finally, a diagnostic algorithm was proposed. A combined final pattern assessment was assigned based on findings of both US and MX imaging. Clinical and imaging results were afterwards recorded on a standard three-point classification scale, based on BI-RADS 5th Edition categories: 1 gynecomastia (BI-RADS 1 and 2); 2 undefined entity (BI-RADS 3); 3 malignant (BI-RADS 4 and 5).

#### CONCLUSION

Male breast cancer is rare. Integration of imaging and clinical-anamnestic data is useful to confirm the benign pathology, avoiding unnecessary surgery/invasive procedures.

#### CLINICAL RELEVANCE/APPLICATION

Imaging is recommended for evaluation of male's indeterminate palpable breast mass. Protocols are not yet validated in literature; therefore we proposed an algorithm based on clinical-radiological integration.

Printed on: 02/07/23

## Abstract Archives of the RSNA, 2022

W5A-SPBR-7

### Incidence and Outcomes of COVID-19 Vaccine Related Lymphadenopathy on Screening Mammography across Vaccine Manufacturers

Wednesday, Nov. 30 12:15PM - 12:45PM Room: Learning Center - BR DPS

#### Participants

Alexander Leyva, MD, Boston, MA (*Presenter*) Nothing to Disclose

#### PURPOSE

To determine the incidence and outcomes of unilateral axillary lymphadenopathy related to COVID-19 vaccination across vaccine manufacturers at screening mammography.

#### METHODS AND MATERIALS

This retrospective, multisite study included consecutive patients undergoing screening mammography from 02/8/2021-01/31/2022 with at least 3 months of follow-up. In the setting of documented recent (<6 weeks) vaccination, isolated ipsilateral axillary lymphadenopathy was considered a benign finding (BI-RADS 2). When administered >6 weeks previous, or if accompanied by a breast finding, axillary ultrasound was recommended (BI-RADS 0). Patient demographics and outcomes were retrieved from electronic medical records, COVID-19 vaccination status and manufacturer from a regional vaccine registry, and cancer outcomes from a regional tumor registry. A logistic regression was fit to estimate the association with days since prior COVID-19 vaccination and odds of an ipsilateral axillary finding, adjusted for age.

#### RESULTS

44,473 patients (mean age 60.4 years +/- 11.4 years) underwent screening mammography at 5 sites. 39,067 (87.8%) underwent at least 1 COVID-19 vaccine dose. Median days since prior vaccine was 99.0 (IQR 40.0-179.0 days). 108 (0.3%) patients presented with unilateral lymphadenopathy in the setting of ipsilateral vaccination that did not vary across manufacturer ( $p=0.159$ ). 80 (74.1%) presented <6 weeks from vaccination and deemed benign. 3 (3.8%) subsequently returned with a clinical concern in the same axilla and all were attributed BI-RADS 1/2. Of the 28 (25.9%) with ipsilateral lymphadenopathy >6 weeks from vaccination +/- ipsilateral breast finding, 9 (32.1%) were called back for additional evaluation. At diagnostic workup 4 were BI-RADS 1/2, 1 was BI-RADS 3, 4 were BI-RADS 4. Of those biopsied, 2 were malignant (both with ipsilateral breast malignancies) and 2 were benign. 19 (67.9%) were not called back due to a known non-breast malignancy or systemic illness or due to close proximity to the 6-week cutoff. Of the 19, 2 (10.5%) re-presented with a clinical concern in the same axilla and both were attributed BI-RADS 1/2. The odds of having an ipsilateral axillary finding significantly decreased for every 7 days since the prior COVID-19 vaccination dose (aOR 0.86, 95% CI 0.83-0.89,  $p<0.001$ ).

#### CONCLUSION

The incidence of unilateral axillary lymphadenopathy post COVID-19 vaccination on screening mammography is low at 0.3% and does not vary across vaccine manufacturer. Isolated ipsilateral lymphadenopathy <6 weeks from vaccination had a 0% rate of malignancy.

#### CLINICAL RELEVANCE/APPLICATION

Utilizing a pragmatic approach in managing unilateral lymphadenopathy in the setting of recent ipsilateral COVID-19 vaccination is both safe and effective.

Printed on: 02/07/23

## Abstract Archives of the RSNA, 2022

W5A-SPCA

### Cardiac Wednesday Poster Discussions - A

Wednesday, Nov. 30 12:15PM - 12:45PM Room: Learning Center - CA DPS

#### Sub-Events

#### **W5A-SPCA- Correlation between Quantitative Assessment of Epicardial Adipose Tissue and Atrial Fibrillation in Hypertrophic Cardiomyopathy by Cardiac Magnetic Resonance**

Participants

Xiaohu Li, MD, PhD, (Presenter) Nothing to Disclose

#### PURPOSE

To find out the relationship between EAT and atrial fibrillation (AF) in Chinese patients with hypertrophic cardiomyopathy (HCM).

#### METHODS AND MATERIALS

The study included 79 HCM patients (51 males and 28 females; mean age:53.7± 14.8 years; including 19 patients with AF and 60 patients without AF) and 20 healthy controls (11 males and 9 females; mean age:51.8± 19.8years). All participants underwent Laboratory examination, ECG, and cardiovascular magnetic resonance (CMR) examination. Function, volumes, the presence of late gadolinium enhancement (LGE), and the amount of EAT were assessed.

#### RESULTS

The epicardial adipose tissue volume index (EATVI) in HCM patients (60.5±18.4 ml/m<sup>2</sup>) was significantly higher than in healthy controls (47.9±4.5 ml/m<sup>2</sup>, P< 0.05). And HCM group had significantly bigger EATV and thicker EAT thickness than the healthy controls. Furthermore, EATV and EATVI were significantly greater between AF and without AF in HCM (143.4±32.6 ml vs 95.0±25.4 ml, P<0.001, and 81.9±17.1 ml vs 53.7±12.8 ml P< 0.001). The EATVI was associated with left ventricle wall thickness (LVWT), right atrioventricular groove (RAVG), and AF in multivariable linear regression analysis among HCM patients. Applying univariable logistic regression analysis, left ventricle ejection fractions (LVEF, OR, 0.921, P= 0.015), left atrium diameter (LAD, OR, 1.149, P= 0.007), left atrium diameter index (LAVI, OR, 1.028, P= 0.035), EATV (OR, 1.053, P< 0.001), EATVI (OR, 1.129, P< 0.001), RAVG (OR, 1.158, P= 0.029), superior interventricular groove (SIVG, OR, 1.443, P= 0.002) and inferior interventricular groove (IIVG, OR, 1.790, P= 0.001) remained independent predictor of the presence of AF in HCM patients (OR: 5.518, P= 0.038, OR: 1.397, P= 0.004, OR: 0.634, P= 0.022, respectively)

#### CONCLUSION

s HCM patients exhibited an increased EATVI in comparison to healthy controls, especially in HCM with AF. The EATVI was associated with LVWT, RAVG, and AF in HCM patients. LVEF, LAD, LAVI, EATV, EATVI, RAVG, SIVG, and IIVG is independent predictor of AF occurrence, and EA TV and EA TVI provide better performance.

#### CLINICAL RELEVANCE/APPLICATION

Increased epicardial adipose tissue (EAT) is a cardiometabolic tissue that is associated with poor cardiovascular outcomes. While the underlying magnetic resonance imaging features of this link are not well understood in hypertrophic cardiomyopathy.

#### **W5A-SPCA- Incipient Myocardial Dysfunction and Cardiopulmonary Structural Alterations are Associated with Persistent Symptoms after Infection by SARS-CoV2 Delta Strain**

Participants

Yoko Kato, MD, PhD, (Presenter) Speaker, Canon Medical Systems Corporation

#### PURPOSE

To define cardio-pulmonary alterations of structure and function associated with symptoms of Long Covid 3-19 months after infection with Delta Sars-CoV2.

#### METHODS AND MATERIALS

Patients at least 3 months post-COVID infection were recruited. COVID- related clinical information and demographics were collected from medical records. Comorbidities were obtained through a questionnaire. Ultra-high resolution CT (UHCT) was used to image lungs and perform coronary angiography within 3 weeks of cardiac MRI using CINE, T1/T2 map, and late gadolinium enhancement (LGE) on a 3.0T scanner (Canon Galan 3T). The association of the persistent post-COVID symptom with individual cardiac MRI index of function, deformation, and tissue characteristics in the worst tertile group was investigated with adjustments for the demographics, comorbidities, and other COVID-related information. The association between other COVID-related information with cardiac indices were also investigated.

#### RESULTS

(A) Forty-two participants at the median of 325 days post COVID diagnosis with the majority of SARS-CoV2 Delta infection

(diagnosis date between 4/7/2020 and 11/27/2021) were enrolled. The cardiac function and tissue characteristics were generally well maintained. (B) Persistent post-COVID symptoms were associated with reduced LVEF and LV strain and marginally associated with RVEF. History of pulmonary disease, 75% of which was asthma (a known risk factor of long COVID), was also associated with persistent post-COVID symptoms. (C) Hospitalization was marginally associated with reduced LVEF. Lung abnormality on UHCT was associated with reduced LAEF total, LA strain, and RVEF. All the 3 cases with LGE were within the worst tertile of LVEF. None of the COVID-related information was associated with native T1 (nT1)/ ECV/ T2 except association of hospitalization with elevated nT1.

## CONCLUSION

s In patients with SARS-CoV2 Delta infection, persistent COVID-related symptoms (Long Covid) were associated with LV, LA and RV dysfunction. Patients with cardiac dysfunction were more likely to have UHCT defined lung abnormalities and LGE myocardial fibrosis. There were no associations of Long Covid with changes in ECV or native T1 as well as T2 mapping.

## CLINICAL RELEVANCE/APPLICATION

In patients with SARS-CoV2 Delta infection, LV, LA and RV dysfunction were associated with persistent symptoms. Patients with LV dysfunction revealed pulmonary alterations and myocardial scar by cardio-pulmonary phenotyping.

## W5A-SPCA- Novel Metabolic Imaging Biomarker Using Disease-specific Peak in Single Breath-hold 1H-MR Spectroscopy for Assessment of Myocardial Involvement in Patients with Fabry Disease

Participants

Masaru Shiotani, RT, Suita, Japan (*Presenter*) Nothing to Disclose

## PURPOSE

Fabry disease is characterized by deposition of sphingolipids caused by a deficiency of the enzyme alpha-galactosidase A and cardiac involvement is crucial for morbidity and mortality. Therefore, measurement of myocardial sphingolipid deposition is an important for evaluation of the early cardiac involvement and the indication of enzyme replacement therapy. Metabolic imaging by 1H-MR Spectroscopy (MRS) has a potential as disease-specific biomarker to directly measure the abnormal accumulation. However, feasibility of for Fabry disease is still uncertain. This study aimed to assess the specific MRS peak of sphingolipids using simulated phantom and evaluate the feasibility of MRS for detection of myocardial metabolic abnormality in patients with Fabry disease.

## METHODS AND MATERIALS

Simulated phantom containing the Lyso-GB3 (one of the sphingolipids that is abnormal accumulation in Fabry disease) which were dissolved in methanol underwent MRS. We measured the spectral peak of simulated phantom and pure methanol. Seven patients with genetically proven Fabry disease involving the myocardium diagnosed by standard cardiac MRI and 7 healthy volunteers underwent cardiac MRS. MRS was obtained using single voxel PRESS sequence positioned within the ventricular septum with single breath-hold. The peak of sphingolipids (based on phantom study), lipid (0.9+1.3 ppm) and water (4.7 ppm) were used as metabolic indicators. Each peak ratio was compared between Fabry disease patients and volunteers.

## RESULTS

In phantom study, MRS showed specific spectra of Lyso-GB3 with intense resonance from 3.5 ppm compared with only methanol. Compared with the volunteer group, the 3.5ppm/water peak ratio in Fabry group was significantly higher, and there was no significant difference in the 3.5ppm+lipid/water and lipid/water peak ratio. The cut-off value for 3.5ppm/water peak ratio to differentiate between Fabry disease and volunteer was 0.031 (sensitivity 86 %, specificity 57%, AUC 0.78).

## CONCLUSION

s In phantom study, the peak of 3.5ppm in MRS was associated with Lyso-GB3 (one of the sphingolipids). This peak ratio showed the higher values in Fabry disease with cardiac involvement and enabled the detection of abnormal sphingolipids deposition with moderate diagnostic accuracy. To our knowledge, this is the first study to assess the myocardial abnormal content in Fabry disease using 3.5ppm peak of MRS.

## CLINICAL RELEVANCE/APPLICATION

3.5 ppm peak of MRS could be disease-specific imaging biomarker for direct quantification of myocardial sphingolipid accumulation of Fabry disease beyond the conventional MRI sequences. This metabolic imaging has a potential for evaluation of the early cardiac involvement, disease severity and indication of enzyme replacement therapy.

Printed on: 02/07/23

## Abstract Archives of the RSNA, 2022

W5A-SPCA-2

### Correlation between Quantitative Assessment of Epicardial Adipose Tissue and Atrial Fibrillation in Hypertrophic Cardiomyopathy by Cardiac Magnetic Resonance

Wednesday, Nov. 30 12:15PM - 12:45PM Room: Learning Center - CA DPS

#### Participants

Xiaohu Li, MD, PhD, (Presenter) Nothing to Disclose

#### PURPOSE

To find out the relationship between EAT and atrial fibrillation (AF) in Chinese patients with hypertrophic cardiomyopathy (HCM).

#### METHODS AND MATERIALS

The study included 79 HCM patients (51 males and 28 females; mean age:53.7± 14.8 years; including 19 patients with AF and 60 patients without AF) and 20 healthy controls (11 males and 9 females; mean age:51.8± 19.8years). All participants underwent Laboratory examination, ECG, and cardiovascular magnetic resonance (CMR) examination. Function, volumes, the presence of late gadolinium enhancement (LGE), and the amount of EAT were assessed.

#### RESULTS

The epicardial adipose tissue volume index (EATVI) in HCM patients (60.5±18.4 ml/m<sup>2</sup>) was significantly higher than in healthy controls (47.9±4.5 ml/m<sup>2</sup>, P< 0.05). And HCM group had significantly bigger EATV and thicker EAT thickness than the healthy controls. Furthermore, EATV and EATVI were significant greater between AF and without AF in HCM (143.4±32.6 ml vs 95.0±25.4 ml, P<0.001, and 81.9±17.1 ml vs 53.7±12.8 ml P< 0.001). The EATVI was associated with left ventricle wall thickness (LVWT), right atrioventricular groove (RAVG), and AF in multivariable linear regression analysis among HCM patients. Applying univariable logistic regression analysis, left ventricle ejection fractions (LVEF, OR, 0.921, P= 0.015), left atrium diameter (LAD, OR, 1.149, P= 0.007), left atrium diameter index (LAVI, OR, 1.028, P= 0.035), EATV (OR, 1.053, P< 0.001), EATVI (OR, 1.129, P< 0.001), RAVG (OR, 1.158, P= 0.029), superior interventricular groove (SIVG, OR, 1.443, P= 0.002) and inferior interventricular groove (IIVG, OR, 1.790, P= 0.001) remained independent predictor of the presence of AF in HCM patients (OR: 5.518, P= 0.038, OR: 1.397, P= 0.004, OR: 0.634, P= 0.022, respectively)

#### CONCLUSION

s HCM patients exhibited an increased EATVI in comparison to healthy controls, especially in HCM with AF. The EATVI was associated with LVWT, RAVG, and AF in HCM patients. LVEF, LAD, LAVI, EATV, EATVI, RAVG, SIVG, and IIVG is independent predictor of AF occurrence, and EA TV and EA TVI provide better performance.

#### CLINICAL RELEVANCE/APPLICATION

Increased epicardial adipose tissue (EAT) is a cardiometabolic tissue that is associated with poor cardiovascular outcomes. While the underlying magnetic resonance imaging features of this link are not well understood in hypertrophic cardiomyopathy.

Printed on: 02/07/23

## Abstract Archives of the RSNA, 2022

W5A-SPCA-3

### **Incipient Myocardial Dysfunction and Cardiopulmonary Structural Alterations are Associated with Persistent Symptoms after Infection by SARS-CoV2 Delta Strain**

Wednesday, Nov. 30 12:15PM - 12:45PM Room: Learning Center - CA DPS

#### **Participants**

Yoko Kato, MD, PhD, (*Presenter*) Speaker, Canon Medical Systems Corporation

#### **PURPOSE**

To define cardio-pulmonary alterations of structure and function associated with symptoms of Long Covid 3-19 months after infection with Delta Sars-CoV2.

#### **METHODS AND MATERIALS**

Patients at least 3 months post-COVID infection were recruited. COVID- related clinical information and demographics were collected from medical records. Comorbidities were obtained through a questionnaire. Ultra-high resolution CT (UHCT) was used to image lungs and perform coronary angiography within 3 weeks of cardiac MRI using CINE, T1/T2 map, and late gadolinium enhancement (LGE) on a 3.0T scanner (Canon Galan 3T). The association of the persistent post-COVID symptom with individual cardiac MRI index of function, deformation, and tissue characteristics in the worst tertile group was investigated with adjustments for the demographics, comorbidities, and other COVID-related information. The association between other COVID-related information with cardiac indices were also investigated.

#### **RESULTS**

(A) Forty-two participants at the median of 325 days post COVID diagnosis with the majority of SARS-CoV2 Delta infection (diagnosis date between 4/7/2020 and 11/27/2021) were enrolled. The cardiac function and tissue characteristics were generally well maintained. (B) Persistent post-COVID symptoms were associated with reduced LVEF and LV strain and marginally associated with RVEF. History of pulmonary disease, 75% of which was asthma (a known risk factor of long COVID), was also associated with persistent post-COVID symptoms. (C) Hospitalization was marginally associated with reduced LVEF. Lung abnormality on UHCT was associated with reduced LAEF total, LA strain, and RVEF. All the 3 cases with LGE were within the worst tertile of LVEF. None of the COVID-related information was associated with native T1 (nT1)/ ECV/ T2 except association of hospitalization with elevated nT1.

#### **CONCLUSION**

s In patients with SARS-CoV2 Delta infection, persistent COVID-related symptoms (Long Covid) were associated with LV, LA and RV dysfunction. Patients with cardiac dysfunction were more likely to have UHCT defined lung abnormalities and LGE myocardial fibrosis. There were no associations of Long Covid with changes in ECV or native T1 as well as T2 mapping.

#### **CLINICAL RELEVANCE/APPLICATION**

In patients with SARS-CoV2 Delta infection, LV, LA and RV dysfunction were associated with persistent symptoms. Patients with LV dysfunction revealed pulmonary alterations and myocardial scar by cardio-pulmonary phenotyping.

Printed on: 02/07/23

## Abstract Archives of the RSNA, 2022

W5A-SPCA-4

### Novel Metabolic Imaging Biomarker Using Disease-specific Peak in Single Breath-hold $^1\text{H}$ -MR Spectroscopy for Assessment of Myocardial Involvement in Patients with Fabry Disease

Wednesday, Nov. 30 12:15PM - 12:45PM Room: Learning Center - CA DPS

#### Participants

Masaru Shiotani, RT, Suita, Japan (*Presenter*) Nothing to Disclose

#### PURPOSE

Fabry disease is characterized by deposition of sphingolipids caused by a deficiency of the enzyme alpha-galactosidase A and cardiac involvement is crucial for morbidity and mortality. Therefore, measurement of myocardial sphingolipid deposition is an important for evaluation of the early cardiac involvement and the indication of enzyme replacement therapy. Metabolic imaging by  $^1\text{H}$ -MR Spectroscopy (MRS) has a potential as disease-specific biomarker to directly measure the abnormal accumulation. However, feasibility of for Fabry disease is still uncertain. This study aimed to assess the specific MRS peak of sphingolipids using simulated phantom and evaluate the feasibility of MRS for detection of myocardial metabolic abnormality in patients with Fabry disease.

#### METHODS AND MATERIALS

Simulated phantom containing the Lyso-GB3 (one of the sphingolipids that is abnormal accumulation in Fabry disease) which were dissolved in methanol underwent MRS. We measured the spectral peak of simulated phantom and pure methanol. Seven patients with genetically proven Fabry disease involving the myocardium diagnosed by standard cardiac MRI and 7 healthy volunteers underwent cardiac MRS. MRS was obtained using single voxel PRESS sequence positioned within the ventricular septum with single breath-hold. The peak of sphingolipids (based on phantom study), lipid (0.9+1.3 ppm) and water (4.7 ppm) were used as metabolic indicators. Each peak ratio was compared between Fabry disease patients and volunteers.

#### RESULTS

In phantom study, MRS showed specific spectra of Lyso-GB3 with intense resonance from 3.5 ppm compared with only methanol. Compared with the volunteer group, the 3.5ppm/water peak ratio in Fabry group was significantly higher, and there was no significant difference in the 3.5ppm+lipid/water and lipid/water peak ratio. The cut-off value for 3.5ppm/water peak ratio to differentiate between Fabry disease and volunteer was 0.031 (sensitivity 86 %, specificity 57%, AUC 0.78).

#### CONCLUSION

In phantom study, the peak of 3.5ppm in MRS was associated with Lyso-GB3 (one of the sphingolipids). This peak ratio showed the higher values in Fabry disease with cardiac involvement and enabled the detection of abnormal sphingolipids deposition with moderate diagnostic accuracy. To our knowledge, this is the first study to assess the myocardial abnormal content in Fabry disease using 3.5ppm peak of MRS.

#### CLINICAL RELEVANCE/APPLICATION

3.5 ppm peak of MRS could be disease-specific imaging biomarker for direct quantification of myocardial sphingolipid accumulation of Fabry disease beyond the conventional MRI sequences. This metabolic imaging has a potential for evaluation of the early cardiac involvement, disease severity and indication of enzyme replacement therapy.

Printed on: 02/07/23

## Abstract Archives of the RSNA, 2022

W5A-SPCH

### Chest Wednesday Poster Discussions - A

Wednesday, Nov. 30 12:15PM - 12:45PM Room: Learning Center - CH DPS

#### Participants

Elsie Nguyen, MD, Toronto, ON (*Moderator*) Nothing to Disclose

#### Sub-Events

### W5A-SPCH- Ultrashort Echo Time (UTE) MRI of The Lung In Term and Pre-term Infants 2

#### Participants

Yujie Chen, Chengdu, China (*Presenter*) Nothing to Disclose

#### PURPOSE

Postnatal lung development is important in infants, especially in preterm births while relevant imaging data is scarce. Ultrashort echo-time (UTE) MRI provides a non-invasive approach to explore the lung tissue architecture in term and preterm infants. The purpose of this study was to explore lung tissue architecture in term and preterm infants using three-dimensional (3D) UTE MRI.

#### METHODS AND MATERIALS

A total of sixty infants born term or preterm with morphologically normal lungs (26 preterm, 34 full-term, range 2 day to 1 year and 2 months) underwent 3D UTE MRI at a 3T pediatric MR scanner (Alpha, United Imaging Healthcare, Shanghai, China). Average lung parenchymal signal intensity was evaluated by two experienced radiologists. The whole lung signal intensity was calculated as the average signal intensity of both lungs. Paired t-test was used to test the differences of average lung signal intensities between term and preterm infants. Spearman rank correlation was performed to test the correlation of the lung parenchymal signal intensity to age. Interrater agreement was assessed using intraclass correlation coefficients (ICCs).

#### RESULTS

Interobserver reliability analysis revealed almost perfect agreement (ICC = 0.964). Average lung parenchymal signal intensity was significantly different ( $p=0.038$ ) in preterm (mean 282.4, SD 87.1) and full-term infants (mean 341.8, SD 128.8) (Figure 1). Lung signal intensity is positively correlated to age in infant period ( $r=0.319$ ,  $p=0.013$ ), and positively correlated to age in preterm group ( $r=0.408$ ,  $p=0.039$ ).

#### CONCLUSION

The UTE MRI technique for lung imaging has potential value in infants, especially in preterm births. This radiation-free technique shows lung structures clearly and is potentially valuable for the detection of disease.

#### CLINICAL RELEVANCE/APPLICATION

UTE MRI is a promising radiation-free approach for evaluation of lung structure of infants and is potentially valuable for the detection of disease.

### W5A-SPCH- Imaging of Central Lymphatic Abnormalities in Patients with Trisomy 21 3

#### Participants

Karen Ramirez Suarez, MD, Philadelphia, PA (*Presenter*) Nothing to Disclose

#### PURPOSE

To describe the clinical importance of lymphatic imaging in patients with Trisomy 21 and congenital heart disease and depict the most common imaging findings of the central lymphatic abnormalities in these patients.

#### METHODS AND MATERIALS

We conducted a single-center retrospective review of all patients with a confirmed history of Trisomy 21 who presented for lymphatic imaging over a 7-year period. Dynamic contrast-enhanced MR lymphangiography evaluation was performed which included unenhanced T2 weighted (T2-W) imaging and T1-weighted dynamic-contrast MR lymphangiography. A pediatric radiologist evaluated the images. The distribution of fluid on T2-W imaging and lymphatic flow of contrast agent are reported. Electronic medical records were reviewed for clinical history and outcomes.

#### RESULTS

We identified a total of 17 patients (13 male), including 8 infants, 7 children, and 2 adults. Congenital heart disease was present in all patients. Diagnosis included single ventricle physiology ( $n=9$ ), Tetralogy of Fallot ( $n=2$ ), atrial septal defect ( $n=2$ ), and ventricular septal defect ( $n=4$ ). Presenting symptoms included chylothorax ( $n=9$ ), plastic bronchitis ( $n=3$ ), chylous ascites ( $n=3$ ), protein-losing enteropathy ( $n=1$ ), and pericardial effusion ( $n=1$ ). 14 patients had surgical interventions including Fontan in 47% of cases ( $n=8$ ). Two patients died (12%) by the time the data was collected. In imaging evaluation, abnormal lymphatic flow with

pulmonary and/or mesenteric perfusion was seen in 15 patients (88%) and abnormalities in the thoracic duct were present in 11 patients (65%).

## CONCLUSION

s Patients with Trisomy 21 and clinical evidence of lymphatic dysfunction need lymphatic imaging evaluation to diagnose and treat central lymphatic abnormalities. Common imaging findings in these patients include retrograde lymphatic flow, pulmonary and mesenteric lymphatic perfusion, and thoracic duct abnormalities.

## CLINICAL RELEVANCE/APPLICATION

Patients with trisomy 21 have an increased risk for the development of lymphatic disorders, and the extent and nature of these abnormalities are poorly understood. Literature regarding lymphatic imaging evaluation and treatment in these patients is scarce. Understanding and recognizing characteristic lymphatic abnormalities in patients with Trisomy 21 may help with the diagnosis and treatment of these patients.

## W5A-SPCH- Reference Value of Cardiovascular Borders on Frontal Chest X-ray from Echocardiographically Confirmed Normal Subjects.

Participants

Dong Hyun Yang, MD, Seoul, Korea, Republic Of (*Presenter*) Nothing to Disclose

## PURPOSE

The purpose of this study was to determine the normal reference value of cardiovascular borders (CB) on frontal chest radiography (CXR) from normal cohorts confirmed by transthoracic echocardiography.

## METHODS AND MATERIALS

91,736 subjects with normal echocardiography and frontal CXR from a single center were enrolled in this study (study period, 2000 - 2016; mean age 53.7 years; 64.3% of male). Previously validated deep learning-based CB analysis system calculated cardiothoracic ratio (CTR), the width of each CB (right upper/lower, aortic knob, pulmonary artery, left atrial appendage [LAA], left lower, descending aorta), and carinal angle. Reference CB values in each age group and gender were determined. Correlation between CB values and echocardiography-driven measurements was demonstrated. CB values were compared with those of the external datasets (MIMIC-CXR CheXpert)

## RESULTS

Normal CTR is 0.44 (<40 years 0.42, >70 years 0.46; external datasets MIMIC-CXR 0.47, ChXpert 0.44). The normal carinal angle was 72 degrees (75 in MIMIC-CXR, 74 in CheXpert). The width (mm) of each CB is as follows: right upper 29.5, right lower 40.3, aortic knob 38.1, pulmonary artery 38.6, LAA 46.2, left lower 84.5, and descending aorta 34.1. The CTR, aortic knob, right upper CB, descending aorta, and left lower CB are increased with age. Ascending aortic diameter on echocardiography was correlated with the width of the right upper CB ( $r=0.23$ ), aortic knob ( $r=0.27$ ), descending aorta ( $r=0.28$ ), and left lower CB ( $r=0.25$ ).

## CONCLUSION

s The normal reference values for CB on frontal chest radiographs were determined using CB analysis software powered by deep learning.

## CLINICAL RELEVANCE/APPLICATION

The CB reference values obtained in this study may be used in conjunction with CXR analysis software for the purpose of identifying or classifying cardiovascular disease.

## W5A-SPCH- Image Quality and Radiation Dose of Contrast-Enhanced Chest CT acquired on a Clinical Photon-Counting Detector CT vs 2nd Generation Dual-Source CT in An Oncologic Cohort

Participants

Lukas Walder, Tuebingen, Germany (*Presenter*) Nothing to Disclose

## PURPOSE

Our aim was to compare image quality and patient dose of contrast-enhanced oncologic chest CT of 1st generation photon-counting detector (PCD-CT) and 2nd generation dual-source dual-energy CT (DSCT).

## METHODS AND MATERIALS

For this reason one hundred oncologic patients (63 male, 65±11 years, BMI: 16-42 kg/m<sup>2</sup>) were prospectively enrolled. Clinically indicated contrast-enhanced chest CT were obtained with PCD-CT and compared to previously obtained chest DSCT in the same individuals. The median time interval between the scans was three months. The same contrast media protocol was used for both scans. PCD-CT was performed in QuantumPlus mode (obtaining full spectral information) at 120kVp. DSCT was performed using 100 kV for Tube A and 140 kV for Tube B. "T3D" PCD-CT images were evaluated, which emulate conventional 120 keV polychromatic images. For DSCT, the convolution algorithm was set at I31f with class 1 iterative reconstruction, whereas comparable Br40 kernel and iterative reconstruction (Q1 and Q3) were applied for PCD-CT. Two radiologists assessed image quality using a 5-point Likert scale and performed measurements of vessels and lung parenchyma for signal-to-noise ratio (SNR) and contrast-to-noise ratio (CNR) measurements.

## RESULTS

PCD-CT CNR<sub>vessel</sub> was significantly higher than DSCT CNR<sub>vessel</sub> (all,  $p<0.05$ ). Readers rated image contrast of mediastinum, vessels, and lung parenchyma significantly higher on PCD-CT than DSCT images ( $p<0.001$ ). Q3 PCD-CT CNR<sub>lung\_parenchyma</sub> was significantly higher than DSCT CNR<sub>lung\_parenchyma</sub> and Q1 PCD-CT CNR<sub>lung\_parenchyma</sub> ( $p<0.01$ ). CTDI, DLP, SSDE mean values for PCD-CT and DSCT were 4.17±1.29 mGy vs. 7.21±0.49 mGy, 151.01±48.56 mGy\*cm vs. 288.64±31.17 mGy\*cm and 4.23±0.97 vs. 7.48±1.09, respectively.

## CONCLUSION

s PCD-CT enables oncologic chest CT with a significantly reduced dose while retaining image quality similar to a 2nd generation

s PCD-CT enables oncologic chest CT with a significantly reduced dose while retaining image quality similar to a 2nd generation DSCT for comparable protocol settings.

#### CLINICAL RELEVANCE/APPLICATION

The mean SSDE for the PCD-CT could be reduced by 43% compared to the previous DSCT examination

### W5A-SPCH- Lung Cancer Screening Using Clinical Photon-Counting-Detector CT and Energy-Integrating-Detector CT: A Prospective Patient Study

Participants  
Akitoshi Inoue, MD, PhD, Rochester, MN (*Presenter*) Nothing to Disclose

#### PURPOSE

To evaluate the image quality of photon-counting detector (PCD) CT in patients undergoing lung cancer screening compared with energy-integrating detector (EID) CT in a prospective multi-reader study.

#### METHODS AND MATERIALS

Patients undergoing clinically-indicated lung cancer screening at EID CT (SOMATOM Force, Siemens Healthineers GmbH) were prospectively recruited to undergo same-day research CT on an FDA-approved PCD-CT system (NAEOTOM Alpha, Siemens Healthineers GmbH) using Qr56 kernel, 0.8 mm slice thickness, 512x 512 matrix. Both systems used matched radiation dose (CTDIvol=0.9 mGy) using automatic exposure control. Three thoracic radiologists blinded to the image type compared PCD-CT and EID-CT images in a side-by-side fashion, using a 5-point Likert comparison score (-2 [left image is worse] to +2 [left image is better]) for artifact, sharpness, image noise, diagnostic image quality, emphysema visualization, and lung nodule evaluation. A post hoc correction of scores was performed (-2 [PCD-CT image is worse than EID-CT] to +2 [PCD-CT image is better than EID-CT]). A non-reader radiologist measured image noise as the standard deviation of CT number (HU).

#### RESULTS

Thirty-three patients (66.9 ± 5.6 years, 11 female,) were enrolled. 45% (15/33) patients had BMI over 30. Pulmonary nodules (3 ground-glass nodules; 1 part-solid nodule; 7 solid nodules, median diameter 6 mm [range: 4–11 mm]) were identified in 11 of 33 patients. Comparison scores were significantly higher (positive score = PCD-CT better) in sharpness (0.8 ± 0.6, p<0.001), image noise (0.3 ± 0.8, p<0.001), diagnostic image quality (0.4 ± 0.6, p<0.001), emphysema visualization (0.3 ± 0.6, p<0.001), and lung nodule borders (0.8 ± 0.9 p<0.001), but significantly lower for artifact (-0.4 ± 0.6; P<0.001). PCD-CT had significantly lower objective image noise (74.4 ± 10.5 vs. 80.1 ± 8.6; P=0.048) despite slightly lower dose CTDIvol (0.61 ± 0.21 vs. 0.73 ± 0.22; P<0.001).

#### CONCLUSION

s PCD-CT demonstrated better image quality in the evaluation of pulmonary emphysema and lung nodules compared to EID-CT in the setting of low-dose lung cancer screening CT.

#### CLINICAL RELEVANCE/APPLICATION

PCD-CT provides improved image quality in low-dose lung cancer screening to evaluate nodule and emphysema.

### W5A-SPCH- MRI-derived Ventilation Inhomogeneity from 3D-UTE MRI in Patients with Cystic Fibrosis on Therapy with CFTR Modulators

Participants  
Julius Heidenreich, MD, Wurzburg, Germany (*Presenter*) Nothing to Disclose

#### PURPOSE

To investigate the image-derived ventilation inhomogeneity of functional 3D UTE MRI compared with lung clearance index in patients under treatment with the new CFTR modulator combination therapy Trikafta.

#### METHODS AND MATERIALS

3D-UTE MRI imaging of the lungs was performed on a 3T MR-scanner (MAGNETOM Prisma, Siemens Healthcare GmbH, Erlangen, Germany). A prototypical 3D UTE VIBE sequence with a stack of spirals trajectory was used with the following parameters: TE = 0.05 ms; TR = 2.35 ms; flip angle = 4°, non-selective hard pulse duration = 60 µs; FOV = 600 mm x 600 mm; spiral interleaves = 264; readouts per spiral = 265; resolution = 2.3 mm isotrope; number of partitions = 102 ± 10; acquisition time per measurement = 12.3 ± 1.5 s. Sixteen patients with CF underwent MR imaging in 2019 and a follow-up examination in 2021. Images from in- and expiration were co-registered and segmented using a deep-learning approach. Signal intensities were analyzed per voxel. Voxelwise fractional ventilation, expansion rate and interquartile range (IQR) of ventilation as a measurement of ventilation inhomogeneity were obtained. The IQR of MRI ventilation was correlated with the results of pulmonary function tests and lung clearance index (LCI).

#### RESULTS

8 patients received a new therapy with the triple combination Trikafta (ivacaftor/elixacaftor/tezacaftor) between 2019 and 2021. 8 patients did not receive drug therapy between both examinations. The ventilation inhomogeneity (IQR) correlated almost perfectly with the LCI 2.5% in the initial and follow-up examination (Spearman's rho = 0.90, p < 0.01). Between initial and follow-up, LCI and MRI-derived ventilation inhomogeneity changed proportionally. MRI-derived ventilation inhomogeneity decreased significantly in patients on therapy (Wilcoxon p = 0.02). Color-coded ventilation maps could be used for visual and regional functional assessment as well as evaluation of morphology.

#### CONCLUSION

s Functional lung imaging with single breath-hold 3D-UTE MRI can be used for calculation of an MRI-derived ventilation inhomogeneity, which correlates almost perfectly with the lung clearance index, a sensitive measure for lung function. Using functional lung MRI, the clinical improvement of patients on therapy with the recently approved drug-combination ivacaftor/elixacaftor/tezacaftor can be evaluated based on image analysis.

## **CLINICAL RELEVANCE/APPLICATION**

For CF patients who need recurrent imaging of the lungs a radiation free approach which can be used for simultaneous morphologic and functional imaging is favourable.

## **W5A-SPCH- Quantitative CT in Chronic Lung Diseases: A Real-life Study of Changes in Physician's Decision Making**

Participants

Matheus Zanon, MD, MSc, Porto Alegre, Brazil (*Presenter*) Nothing to Disclose

## **PURPOSE**

To determine how physicians' diagnoses, diagnostic certainty, and management decisions are affected by the results of quantitative computed tomography (QCT) in the real-life management of chronic lung diseases.

## **METHODS AND MATERIALS**

Data was collected prospectively during 12 months from 5 different centers. Physicians were surveyed before and after QCT to determine the possible new diagnosis, diagnostic confidence, and management decisions. The doctors have access to all patients' functional and laboratory tests previously to QCT results. The QCT analysis comprised the following parameters: 1) total lung volume; 2) normal lung density volume; 3) normal lung index; 4) emphysema index; 5) percentage of high-attenuation areas; and 6) air trapping index.

## **RESULTS**

QTC analysis was done in 92 patients (men, 54; mean age 67+/- 21 years), and surveys were completed by 11 doctors (senior pulmonologists). The most common new diagnoses were chronic interstitial lung disease (15.2%) and emphysema (9.7%). Patient management was changed in 11 cases (11.9%) as follows: new specialized care by an ILD multidisciplinary team (n=7, 7.6%) and new targeted treatment of small airway disease (n=4, 4.3%). Pre-CT diagnostic confidence was inversely associated with the likelihood of a diagnostic change (p<.001). Diagnosis confidence increased 52.7% in COPD and 45.1% in ILD (both, p<.001). Median confidence post-QCT was high (75%).

## **CONCLUSION**

s After the QTC analysis, physicians frequently changed the final diagnoses, enhancing the diagnostic confidence. Up to 12% of patients with chronic lung diseases had their management changed due to QTC.

## **CLINICAL RELEVANCE/APPLICATION**

QCT substantially influence key attributes of physician decision making. Physicians performed new diagnoses in one-sixth of patients after QCT results became available. In most cases, physicians reported CT to be helpful in addressing certain diagnoses and rule-out diagnoses of concern.

Printed on: 02/07/23

## Abstract Archives of the RSNA, 2022

W5A-SPCH-2

### Ultrashort Echo Time (UTE) MRI of The Lung In Term and Pre-term Infants

Wednesday, Nov. 30 12:15PM - 12:45PM Room: Learning Center - CH DPS

#### Participants

Yujie Chen, Chengdu, China (*Presenter*) Nothing to Disclose

#### PURPOSE

Postnatal lung development is important in infants, especially in preterm births while relevant imaging data is scarce. Ultrashort echo-time (UTE) MRI provides a non-invasive approach to explore the lung tissue architecture in term and preterm infants. The purpose of this study was to explore lung tissue architecture in term and preterm infants using three-dimensional (3D) UTE MRI.

#### METHODS AND MATERIALS

A total of sixty infants born term or preterm with morphologically normal lungs (26 preterm, 34 full-term, range 2 day to 1 year and 2 months) underwent 3D UTE MRI at a 3T pediatric MR scanner (Alpha, United Imaging Healthcare, Shanghai, China). Average lung parenchymal signal intensity was evaluated by two experienced radiologists. The whole lung signal intensity was calculated as the average signal intensity of both lungs. Paired t-test was used to test the differences of average lung signal intensities between term and preterm infants. Spearman rank correlation was performed to test the correlation of the lung parenchymal signal intensity to age. Interrater agreement was assessed using intraclass correlation coefficients (ICCs).

#### RESULTS

Interobserver reliability analysis revealed almost perfect agreement (ICC = 0.964). Average lung parenchymal signal intensity was significantly different ( $p=0.038$ ) in preterm (mean 282.4, SD 87.1) and full-term infants (mean 341.8, SD 128.8) (Figure 1). Lung signal intensity is positively correlated to age in infant period ( $r=0.319$ ,  $p=0.013$ ), and positively correlated to age in preterm group ( $r=0.408$ ,  $p=0.039$ ).

#### CONCLUSION

The UTE MRI technique for lung imaging has potential value in infants, especially in preterm births. This radiation-free technique shows lung structures clearly and is potentially valuable for the detection of disease.

#### CLINICAL RELEVANCE/APPLICATION

UTE MRI is a promising radiation-free approach for evaluation of lung structure of infants and is potentially valuable for the detection of disease.

Printed on: 02/07/23

## Abstract Archives of the RSNA, 2022

W5A-SPCH-3

### Imaging of Central Lymphatic Abnormalities in Patients with Trisomy 21

Wednesday, Nov. 30 12:15PM - 12:45PM Room: Learning Center - CH DPS

#### Participants

Karen Ramirez Suarez, MD, Philadelphia, PA (*Presenter*) Nothing to Disclose

#### PURPOSE

To describe the clinical importance of lymphatic imaging in patients with Trisomy 21 and congenital heart disease and depict the most common imaging findings of the central lymphatic abnormalities in these patients.

#### METHODS AND MATERIALS

We conducted a single-center retrospective review of all patients with a confirmed history of Trisomy 21 who presented for lymphatic imaging over a 7-year period. Dynamic contrast-enhanced MR lymphangiography evaluation was performed which included unenhanced T2 weighted (T2-W) imaging and T1-weighted dynamic-contrast MR lymphangiography. A pediatric radiologist evaluated the images. The distribution of fluid on T2-W imaging and lymphatic flow of contrast agent are reported. Electronic medical records were reviewed for clinical history and outcomes.

#### RESULTS

We identified a total of 17 patients (13 male), including 8 infants, 7 children, and 2 adults. Congenital heart disease was present in all patients. Diagnosis included single ventricle physiology (n=9), Tetralogy of Fallot (n=2), atrial septal defect (n=2), and ventricular septal defect (n=4). Presenting symptoms included chylothorax (n=9), plastic bronchitis (n=3), chylous ascites (n=3), protein-losing enteropathy (n=1), and pericardial effusion (n=1). 14 patients had surgical interventions including Fontan in 47% of cases (n=8). Two patients died (12%) by the time the data was collected. In imaging evaluation, abnormal lymphatic flow with pulmonary and/or mesenteric perfusion was seen in 15 patients (88%) and abnormalities in the thoracic duct were present in 11 patients (65%).

#### CONCLUSION

Patients with Trisomy 21 and clinical evidence of lymphatic dysfunction need lymphatic imaging evaluation to diagnose and treat central lymphatic abnormalities. Common imaging findings in these patients include retrograde lymphatic flow, pulmonary and mesenteric lymphatic perfusion, and thoracic duct abnormalities.

#### CLINICAL RELEVANCE/APPLICATION

Patients with trisomy 21 have an increased risk for the development of lymphatic disorders, and the extent and nature of these abnormalities are poorly understood. Literature regarding lymphatic imaging evaluation and treatment in these patients is scarce. Understanding and recognizing characteristic lymphatic abnormalities in patients with Trisomy 21 may help with the diagnosis and treatment of these patients.

Printed on: 02/07/23

## Abstract Archives of the RSNA, 2022

W5A-SPCH-4

### Reference Value of Cardiovascular Borders on Frontal Chest X-ray from Echocardiographically Confirmed Normal Subjects.

Wednesday, Nov. 30 12:15PM - 12:45PM Room: Learning Center - CH DPS

#### Participants

Dong Hyun Yang, MD, Seoul, Korea, Republic Of (*Presenter*) Nothing to Disclose

#### PURPOSE

The purpose of this study was to determine the normal reference value of cardiovascular borders (CB) on frontal chest radiography (CXR) from normal cohorts confirmed by transthoracic echocardiography.

#### METHODS AND MATERIALS

91,736 subjects with normal echocardiography and frontal CXR from a single center were enrolled in this study (study period, 2000 - 2016; mean age 53.7 years; 64.3% of male). Previously validated deep learning-based CB analysis system calculated cardiothoracic ratio (CTR), the width of each CB (right upper/lower, aortic knob, pulmonary artery, left atrial appendage [LAA], left lower, descending aorta), and carinal angle. Reference CB values in each age group and gender were determined. Correlation between CB values and echocardiography-driven measurements was demonstrated. CB values were compared with those of the external datasets (MIMIC-CXR CheXpert)

#### RESULTS

Normal CTR is 0.44 (<40 years 0.42, >70 years 0.46; external datasets MIMIC-CXR 0.47, ChXpert 0.44). The normal carinal angle was 72 degrees (75 in MIMIC-CXR, 74 in CheXpert). The width (mm) of each CB is as follows: right upper 29.5, right lower 40.3, aortic knob 38.1, pulmonary artery 38.6, LAA 46.2, left lower 84.5, and descending aorta 34.1. The CTR, aortic knob, right upper CB, descending aorta, and left lower CB are increased with age. Ascending aortic diameter on echocardiography was correlated with the width of the right upper CB ( $r=0.23$ ), aortic knob ( $r=0.27$ ), descending aorta ( $r=0.28$ ), and left lower CB ( $r=0.25$ ).

#### CONCLUSION

The normal reference values for CB on frontal chest radiographs were determined using CB analysis software powered by deep learning.

#### CLINICAL RELEVANCE/APPLICATION

The CB reference values obtained in this study may be used in conjunction with CXR analysis software for the purpose of identifying or classifying cardiovascular disease.

Printed on: 02/07/23

## Abstract Archives of the RSNA, 2022

W5A-SPCH-5

### Image Quality and Radiation Dose of Contrast-Enhanced Chest CT acquired on a Clinical Photon-Counting Detector CT vs 2nd Generation Dual-Source CT in An Oncologic Cohort

Wednesday, Nov. 30 12:15PM - 12:45PM Room: Learning Center - CH DPS

#### Participants

Lukas Walder, Tuebingen, Germany (*Presenter*) Nothing to Disclose

#### PURPOSE

Our aim was to compare image quality and patient dose of contrast-enhanced oncologic chest CT of 1st generation photon-counting detector (PCD-CT) and 2nd generation dual-source dual-energy CT (DSCT).

#### METHODS AND MATERIALS

For this reason one hundred oncologic patients (63 male, 65±11 years, BMI: 16-42 kg/m<sup>2</sup>) were prospectively enrolled. Clinically indicated contrast-enhanced chest CT were obtained with PCD-CT and compared to previously obtained chest DSCT in the same individuals. The median time interval between the scans was three months. The same contrast media protocol was used for both scans. PCD-CT was performed in QuantumPlus mode (obtaining full spectral information) at 120kVp. DSCT was performed using 100 kV for Tube A and 140 kV for Tube B. "T3D" PCD-CT images were evaluated, which emulate conventional 120 keV polychromatic images. For DSCT, the convolution algorithm was set at I31f with class 1 iterative reconstruction, whereas comparable Br40 kernel and iterative reconstruction (Q1 and Q3) were applied for PCD-CT. Two radiologists assessed image quality using a 5-point Likert scale and performed measurements of vessels and lung parenchyma for signal-to-noise ratio (SNR) and contrast-to-noise ratio (CNR) measurements.

#### RESULTS

PCD-CT CNR<sub>vessel</sub> was significantly higher than DSCT CNR<sub>vessel</sub> (all, p<0.05). Readers rated image contrast of mediastinum, vessels, and lung parenchyma significantly higher on PCD-CT than DSCT images (p<0.001). Q3 PCD-CT CNR<sub>lung\_parenchyma</sub> was significantly higher than DSCT CNR<sub>lung\_parenchyma</sub> and Q1 PCD-CT CNR<sub>lung\_parenchyma</sub> (p<0.01). CTDI, DLP, SSDE mean values for PCD-CT and DSCT were 4.17±1.29 mGy vs. 7.21±0.49 mGy, 151.01±48.56 mGy\*cm vs. 288.64±31.17 mGy\*cm and 4.23±0.97 vs. 7.48±1.09, respectively.

#### CONCLUSION

s PCD-CT enables oncologic chest CT with a significantly reduced dose while retaining image quality similar to a 2nd generation DSCT for comparable protocol settings.

#### CLINICAL RELEVANCE/APPLICATION

The mean SSDE for the PCD-CT could be reduced by 43% compared to the previous DSCT examination

Printed on: 02/07/23

## Abstract Archives of the RSNA, 2022

W5A-SPCH-6

### Lung Cancer Screening Using Clinical Photon-Counting-Detector CT and Energy-Integrating-Detector CT: A Prospective Patient Study

Wednesday, Nov. 30 12:15PM - 12:45PM Room: Learning Center - CH DPS

#### Participants

Akitoshi Inoue, MD, PhD, Rochester, MN (*Presenter*) Nothing to Disclose

#### PURPOSE

To evaluate the image quality of photon-counting detector (PCD) CT in patients undergoing lung cancer screening compared with energy-integrating detector (EID) CT in a prospective multi-reader study.

#### METHODS AND MATERIALS

Patients undergoing clinically-indicated lung cancer screening at EID CT (SOMATOM Force, Siemens Healthineers GmbH) were prospectively recruited to undergo same-day research CT on an FDA-approved PCD-CT system (NAEOTOM Alpha, Siemens Healthineers GmbH) using Qr56 kernel, 0.8 mm slice thickness, 512x 512 matrix. Both systems used matched radiation dose (CTDIvol=0.9 mGy) using automatic exposure control. Three thoracic radiologists blinded to the image type compared PCD-CT and EID-CT images in a side-by-side fashion, using a 5-point Likert comparison score (-2 [left image is worse] to +2 [left image is better]) for artifact, sharpness, image noise, diagnostic image quality, emphysema visualization, and lung nodule evaluation. A post hoc correction of scores was performed (-2 [PCD-CT image is worse than EID-CT] to +2 [PCD-CT image is better than EID-CT]). A non-reader radiologist measured image noise as the standard deviation of CT number (HU).

#### RESULTS

Thirty-three patients (66.9 ± 5.6 years, 11 female,) were enrolled. 45% (15/33) patients had BMI over 30. Pulmonary nodules (3 ground-glass nodules; 1 part-solid nodule; 7 solid nodules, median diameter 6 mm [range: 4–11 mm]) were identified in 11 of 33 patients. Comparison scores were significantly higher (positive score = PCD-CT better) in sharpness (0.8 ± 0.6, p<0.001), image noise (0.3 ± 0.8, p<0.001), diagnostic image quality (0.4 ± 0.6, p<0.001), emphysema visualization (0.3 ± 0.6, p<0.001), and lung nodule borders (0.8 ± 0.9 p<0.001), but significantly lower for artifact (-0.4 ± 0.6; P<0.001). PCD-CT had significantly lower objective image noise (74.4 ± 10.5 vs. 80.1 ± 8.6; P=0.048) despite slightly lower dose CTDIvol (0.61 ± 0.21 vs. 0.73 ± 0.22; P<0.001).

#### CONCLUSION

s PCD-CT demonstrated better image quality in the evaluation of pulmonary emphysema and lung nodules compared to EID-CT in the setting of low-dose lung cancer screening CT.

#### CLINICAL RELEVANCE/APPLICATION

PCD-CT provides improved image quality in low-dose lung cancer screening to evaluate nodule and emphysema.

Printed on: 02/07/23

## Abstract Archives of the RSNA, 2022

W5A-SPCH-7

### MRI-derived Ventilation Inhomogeneity from 3D-UTE MRI in Patients with Cystic Fibrosis on Therapy with CFTR Modulators

Wednesday, Nov. 30 12:15PM - 12:45PM Room: Learning Center - CH DPS

#### Participants

Julius Heidenreich, MD, Wurzburg, Germany (*Presenter*) Nothing to Disclose

#### PURPOSE

To investigate the image-derived ventilation inhomogeneity of functional 3D UTE MRI compared with lung clearance index in patients under treatment with the new CFTR modulator combination therapy Trikafta.

#### METHODS AND MATERIALS

3D-UTE MRI imaging of the lungs was performed on a 3T MR-scanner (MAGNETOM Prisma, Siemens Healthcare GmbH, Erlangen, Germany). A prototypical 3D UTE VIBE sequence with a stack of spirals trajectory was used with the following parameters: TE = 0.05 ms; TR = 2.35 ms; flip angle = 4°, non-selective hard pulse duration = 60 μs; FOV = 600 mm x 600 mm; spiral interleaves = 264; readouts per spiral = 265; resolution = 2.3 mm isotrope; number of partitions = 102 ± 10; acquisition time per measurement = 12.3 ± 1.5 s. Sixteen patients with CF underwent MR imaging in 2019 and a follow-up examination in 2021. Images from in- and expiration were co-registered and segmented using a deep-learning approach. Signal intensities were analyzed per voxel. Voxelwise fractional ventilation, expansion rate and interquartile range (IQR) of ventilation as a measurement of ventilation inhomogeneity were obtained. The IQR of MRI ventilation was correlated with the results of pulmonary function tests and lung clearance index (LCI).

#### RESULTS

8 patients received a new therapy with the triple combination Trikafta (ivacaftor/elexacaftor/tezacaftor) between 2019 and 2021. 8 patients did not receive drug therapy between both examinations. The ventilation inhomogeneity (IQR) correlated almost perfectly with the LCI 2.5% in the initial and follow-up examination (Spearman's rho = 0.90, p < 0.01). Between initial and follow-up, LCI and MRI-derived ventilation inhomogeneity changed proportionally. MRI-derived ventilation inhomogeneity decreased significantly in patients on therapy (Wilcoxon p = 0.02). Color-coded ventilation maps could be used for visual and regional functional assessment as well as evaluation of morphology.

#### CONCLUSION

Functional lung imaging with single breath-hold 3D-UTE MRI can be used for calculation of an MRI-derived ventilation inhomogeneity, which correlates almost perfectly with the lung clearance index, a sensitive measure for lung function. Using functional lung MRI, the clinical improvement of patients on therapy with the recently approved drug-combination ivacaftor/elexacaftor/tezacaftor can be evaluated based on image analysis.

#### CLINICAL RELEVANCE/APPLICATION

For CF patients who need recurrent imaging of the lungs a radiation free approach which can be used for simultaneous morphologic and functional imaging is favourable.

Printed on: 02/07/23

## Abstract Archives of the RSNA, 2022

W5A-SPCH-8

### Quantitative CT in Chronic Lung Diseases: A Real-life Study of Changes in Physician's Decision Making

Wednesday, Nov. 30 12:15PM - 12:45PM Room: Learning Center - CH DPS

#### Participants

Matheus Zanon, MD, MSc, Porto Alegre, Brazil (*Presenter*) Nothing to Disclose

#### PURPOSE

To determine how physicians' diagnoses, diagnostic certainty, and management decisions are affected by the results of quantitative computed tomography (QCT) in the real-life management of chronic lung diseases.

#### METHODS AND MATERIALS

Data was collected prospectively during 12 months from 5 different centers. Physicians were surveyed before and after QCT to determine the possible new diagnosis, diagnostic confidence, and management decisions. The doctors have access to all patients' functional and laboratory tests previously to QCT results. The QCT analysis comprised the following parameters: 1) total lung volume; 2) normal lung density volume; 3) normal lung index; 4) emphysema index; 5) percentage of high-attenuation areas; and 6) air trapping index.

#### RESULTS

QTC analysis was done in 92 patients (men, 54; mean age 67+/- 21 years), and surveys were completed by 11 doctors (senior pulmonologists). The most common new diagnoses were chronic interstitial lung disease (15.2%) and emphysema (9.7%). Patient management was changed in 11 cases (11.9%) as follows: new specialized care by an ILD multidisciplinary team (n=7, 7.6%) and new targeted treatment of small airway disease (n=4, 4.3%). Pre-CT diagnostic confidence was inversely associated with the likelihood of a diagnostic change ( $p < .001$ ). Diagnosis confidence increased 52.7% in COPD and 45.1% in ILD (both,  $p < .001$ ). Median confidence post-QCT was high (75%).

#### CONCLUSION

s After the QTC analysis, physicians frequently changed the final diagnoses, enhancing the diagnostic confidence. Up to 12% of patients with chronic lung diseases had their management changed due to QTC.

#### CLINICAL RELEVANCE/APPLICATION

QCT substantially influence key attributes of physician decision making. Physicians performed new diagnoses in one-sixth of patients after QCT results became available. In most cases, physicians reported CT to be helpful in addressing certain diagnoses and rule-out diagnoses of concern.

Printed on: 02/07/23



## Abstract Archives of the RSNA, 2022

W5A-SPER

### Emergency Wednesday Poster Discussions - A

Wednesday, Nov. 30 12:15PM - 12:45PM Room: Learning Center - ER DPS

#### Participants

Refky Nicola, DO, Pittsford, NY (*Moderator*) Royalties, RELX

Printed on: 02/07/23

## Abstract Archives of the RSNA, 2022

W5A-SPGI

### Gastrointestinal Wednesday Poster Discussions - A

Wednesday, Nov. 30 12:15PM - 12:45PM Room: Learning Center - GI DPS

#### Participants

Alex Chan, DO, Rochester, MN (*Moderator*) Nothing to Disclose

#### Sub-Events

### W5A-SPGI-1 Usefulness of the combination of Fast3D Technique and Deep Learning Based Reconstruction for Magnetic Resonance Cholangiography

#### Participants

Kaori Shiraishi, Kumamoto, Japan (*Presenter*) Nothing to Disclose

#### PURPOSE

To evaluate the usefulness of the Fast3D technique and deep-learning-based reconstruction (DLR) at 3D-MRCP within a single breath-hold (BH).

#### METHODS AND MATERIALS

This retrospective study included 70 consecutive patients who underwent a respiratory gating MRCP and a single BH-MRCP with Fast3D between August and September 2021. BH images were reconstructed with and without DLR. The signal-to-noise ratio (SNR), contrast, contrast-to-noise ratio (CNR) between the common bile duct (CBD) and periductal tissues, and full width at half maximum (FWHM) of CBD on 3D-MRCP were evaluated quantitatively. Two board-certified radiologists scored image noise, contrast, artifacts, blur, and overall image quality of the three image types using a 4-point scale. Quantitative and qualitative scores were compared with using Friedman test and post hoc Nemenyi test.

#### RESULTS

This study consisted of 32 patients with biliary and pancreatic disorders (17 men and 15 women; age range, 26-92 years; mean age, 66.1 years). The SNR and CNR of MRCP were no significant differences between under respiratory gating and under BH without DLR. However, these were significantly higher under BH with DLR than under respiratory gating ( $P < 0.05$ ). The contrast and FWHM of MRCP under BH with and without DLR were lower than under respiratory gating (Contrast:  $P < 0.01$ , FWHM:  $P < 0.05$ ). Qualitative scores for noise, blur and overall image quality were higher under BH with DLR than those under respiratory gating ( $p < 0.05$ ). Contrast and Artifact were no significant differences between under BH with DLR and under respiratory gating ( $p < 0.05$ ).

#### CONCLUSION

The combination of the Fast3D technique and DLR is a useful technique for MRCP within a single BH without deterioration of image quality.

#### CLINICAL RELEVANCE/APPLICATION

The combination of the Fast3D technique and DLR is a useful technique for BH MRCP and can offer the comparable image quality with respiratory gating MRCP in a short scan time.

### W5A-SPGI-10 Explore the potential of diffusion-relaxation correlation spectroscopic imaging for evaluating response to neoadjuvant chemoradiotherapy in locally advanced rectal cancer

#### Participants

Xixi Zhao, Guangzhou, China (*Presenter*) Nothing to Disclose

#### PURPOSE

To determine the diagnostic performance of diffusion-relaxation correlation spectroscopic imaging (DR-CSI) in discriminating the pathological complete response (pCR) to neoadjuvant chemoradiotherapy (nCRT) in locally advanced rectal cancer (LARC).

#### METHODS AND MATERIALS

Nineteen patients with LARC underwent examination by a 3.0T MRI scanner (uMR780, United Imaging Healthcare, Shanghai, China) after nCRT. DR-CSI data were acquired for each patient using 24 DWI images with 6 b-values (0, 200, 500, 800, 1500, 2000 s/mm<sup>2</sup>) combining 4 TEs (102, 128, 154, 180 ms). Region of interests (ROI) were decided in rectum on 5 slices. DR-CSI spectra (range: D 0~5×10<sup>-3</sup> mm<sup>2</sup>/s, T2 0~150 ms) were constructed for each voxel, and a total spectrum summing all voxels was given. All spectra were segmented into 4 compartments, A (low D, short T2), B (high D, long T2), C (high D, long T2) and D (low D, long T2). Segmentation boundaries D 3×10<sup>-3</sup> mm<sup>2</sup>/s and T2 60 ms were chosen according to foreknowledge of rectum. Volume fraction V<sub>m</sub> for each compartment m was acquired in each voxel by spectral integration, and then averaged in the whole ROI.

#### RESULTS

Two main peaks separately with high and low diffusivity were observed in spectra of all patients. Compared to non-nCRT group

Two main peaks, separately, with high and low diffusivity, were observed in spectra of all patients. Compared to non-pCR group, pCR group showed decreased average VD ( $5.6 \pm 1.7\%$  vs  $7.2 \pm 2.0\%$ ), although not statistically significant ( $p=0.118$ ). ROC curve analysis indicated that the VD (AUC 0.756) has good diagnostic performance in distinguishing pCR from non-pCR patients, better than traditional ADC (0.500) and T2 value (0.539).

## CONCLUSION

In-vivo DR-CSI, disentangling tissue diffusivity and relaxometry at sub-voxel level, demonstrates its potential to evaluate response to nCRT in patients with LARC. VD was decreased in pCR group, although not significant, which may be due to small sampling number. The compartment D with slow diffusivity and high T2 should related with water concentration and may correlates with residual tumor, requiring confirmation by further research. Moreover, the V maps may assist recognizing areas of possible residual tumor, demonstrating potential in personalized subsequent treatment.

## CLINICAL RELEVANCE/APPLICATION

Although nCRT has become the standard treatment for LARC, current tumor response evaluation is still lack of accuracy. Radiologic indicator containing compositional information is of great value.

## W5A-SPGI-2 Liver T2-Weighted Imaging and Diffusion-weighted Imaging: Comparison of Respiratory-Frequency Modulated Continuous Wave Radar-trigger, Respiratory Belt-trigger and Navigator-trigger Acquisition

Participants

Xinyue Liang, Shanghai, China (*Presenter*) Nothing to Disclose

## PURPOSE

For abdominal MRI, respiratory motion artifacts could significantly degrade image quality. Respiratory belt-trigger (BT) and navigator-trigger (NT) acquisition have been widely used to mitigate motion artifacts. However, belt required external device and extra patient preparation time. Accuracy of NT depends on the quality and position of the navigator. Additionally, efficiency of NT was limited by the fixed acceptance window. Novel contactless respiratory-frequency modulated continuous wave radar trigger (FT) acquisition was developed recently without any additional setup steps. The aim of this study is to compare the performance of novel FT acquisition with traditional respiratory trigger acquisitions (BT and NT) for T2-weighted imaging (T2WI) and diffusion-weighted Imaging (DWI) of liver.

## METHODS AND MATERIALS

Seventeen volunteers were prospectively imaged on a 1.5T MR scanner (uMR 680; United Imaging Healthcare; Shanghai; China) using T2WI and DWI with FT, BT and NT acquisitions. Overall image quality, blurring, motion artifacts, and liver edge delineations were assessed on a 4-point scale by two radiologists. Signal-to-noise ratio (SNR) and apparent diffusion coefficient (ADC) value of liver parenchyma were calculated. Differences between three acquisitions were evaluated using Wilcoxon signed-ranks test. Inter-observer agreements between two radiologists were measured by intraclass correlation coefficients (ICCs).

## RESULTS

All acquisitions provided acceptable overall image quality (score  $> 2.8$ ) in all subjects on T2WI and DWI. There were no significant differences between three respiratory trigger acquisitions in qualitative scores (all  $p > 0.05$ ) on both sequences. The acquisition time of 179.2 sec for NT was significantly longer than that of 141.3 sec for BT and 142.8 sec for FT on T2WI ( $p < 0.05$ ). Quantitative parameters were comparable among FT, BT and NT, with mirror or no significant differences. Agreement between each reviewer was excellent (ICC  $> 0.9$ ).

## CONCLUSION

This study indicates that the novel FT acquisition provides comparable image quality and simplifies subject preparation steps compared to the use of traditional BT and NT acquisitions.

## CLINICAL RELEVANCE/APPLICATION

FT can be used as an effective respiratory trigger acquisition in T2WI and DWI of the liver, with high potential for improving MR workflow efficiency and patient comfort.

## W5A-SPGI-3 Image Quality Evolution of Diffusion-weighted imaging Sequences for the Assessment of Rectal Cancer

Participants

Maria El Homsy, MD, New York, NY (*Presenter*) Nothing to Disclose

## PURPOSE

To compare and evaluate image quality of 3 different diffusion-weighted imaging (DWI) sequences with low and high b values for the assessment of rectal cancer and to provide quantitative estimates of signal-to-noise ratio (SNR) and contrast-to-noise ratio (CNR).

## METHODS AND MATERIALS

This retrospective study included 30 consecutive patients who underwent 3.0 T MRI exams between January and June 2020. DWI was performed in each subject with 1) single-shot echo planar imaging (ssEPI) ( $b=800$  s/mm<sup>2</sup>), multiplexed sensitivity encoding (MUSE) ( $b=800$  s/mm<sup>2</sup>), MUSE ( $b=1500$  s/mm<sup>2</sup>), and FOV optimized and constrained undistorted single-shot (FOCUS) ( $b=1500$  s/mm<sup>2</sup>). Two radiologists independently subjectively scored the image quality, contour, and lesion conspicuity of the DW images based on a 5-point Likert scale. One radiologist drew ROI on rectal wall on the 4 sequences and ADC map. Inter-reader agreement was assessed by applying the procedure of weighted Cohens' kappa (?). Image scores were evaluated by using the Wilcoxon signed rank test with Bonferroni adjustment. The SNR, CNR, and ADC measurements between sequences were compared using the paired t-test.

## RESULTS

Both readers found image quality, contour, and conspicuity to be significantly superior with MUSE ( $b=800$  s/mm<sup>2</sup>) as compared to

ssEPI. MUSE (b=800 s/mm<sup>2</sup>) had the highest score for image quality and contour which was statistically significant for both readers as compared to all other acquisitions. Conspicuity was equally superior for both MUSE sequences. One reader had improved lesion conspicuity on MUSE (b=800 s/mm<sup>2</sup>) as compared to FOCUS. There was no significant difference between MUSE at different b-values for the assessment of conspicuity. There was good to excellent interreader agreement for all qualitative features (κ, 0.72-0.88). MUSE (b=800 s/mm<sup>2</sup>) had the highest SNR, and MUSE (b=1500 s/mm<sup>2</sup>) had the highest CNR. Significant difference in ADC were observed in comparing ssEPI to the other sequences (p<0.001), and between MUSE (b=800 s/mm<sup>2</sup>) and FOCUS.

## CONCLUSION

s MUSE has improved image quality and tumor conspicuity as compared to ssEPI. The choice of b value significantly affects ADC estimates in MUSE.

## CLINICAL RELEVANCE/APPLICATION

The use of MUSE can improve image quality and tumor conspicuity compared to the traditional DWI in rectal MRI. This can be in part related to better CNR, SNR, and reduced geometric distortion.

## W5A-SPGI-4 Artificial intelligence (AI) augmented reconstruction provides improved image quality and enables shorter breath-holds in contrast-enhanced liver MRI.

Participants  
Francesca Castagnoli, MD, (*Presenter*) Nothing to Disclose

## PURPOSE

To compare image quality and lesion detection using an AI-augmented contrast enhanced (CE) T1w MRI sequence in the liver [derived from applying a neural network (NN) trained on high-resolution images to conduct interpolation and partial Fourier reconstruction, in addition to iterative denoising (ID)] with a conventional CE T1w sequence.

## METHODS AND MATERIALS

50 consecutive patients who underwent clinical liver MRI with Gd-EOB-DTPA on a 1.5T scanner were prospectively enrolled. The protocol included a hepatobiliary phase conventional 17s CE-T1w sequence, a 17s T1w with NN reconstruction and ID and a 12s accelerated T1w with prototypical NN reconstruction and ID. The 3 image sets were analyzed independently by 2 blinded radiologists. Image assessment was made by evaluating the overall image quality, contrast-to-noise ratio (CNR), lesion edge sharpness, vessel edge sharpness and respiratory motion artefacts. Kruskal-Wallis test was used to compare image quality scores. Clinical lesion detection was assessed by identifying and counting focal liver lesions and measuring the diameter of the smallest lesion on the 12s NN+ID acquisition and 17s standard reconstruction. A 4-week break was granted between the reading sessions. Student's t-test was used to compare the number of lesions recorded and the diameter of smallest lesion.

## RESULTS

There were significantly higher scores for image quality, CNR, vessel edge sharpness and lesion edge sharpness for the 17s and 12s acquisitions using NN+ID compared with standard reconstruction (p<0.0001), but with no significant difference between 17s and 12s NN+ID acquisitions. No significant difference was found for respiratory motion artefacts (p>0.05) between all three image sets. For clinical lesion detection, there was no significant difference between the number of lesions and diameter of smallest lesion identified using 12s NN+ID compared with conventional 17s acquisition for either reader (p>0.05).

## CONCLUSION

s Advanced reconstruction methods using a trained neural network for data interpolation combined with iterative denoising can improve image quality while reducing the duration of breath-hold on T1w CE liver imaging, without compromising clinical lesion detection.

## CLINICAL RELEVANCE/APPLICATION

AI augmented T1-weighted imaging can improve image quality, reduce image acquisition time without compromising diagnostic performance. Reduction in breath-hold time can improve patient compliance for MRI liver examinations.

## W5A-SPGI-5 Title Usefulness of breath-hold fat-suppressed T2-weighted image (FS-T2WI) with deep learning-based reconstruction compared to free-breathing turbo spin echo FS-T2WI

Participants  
Fumihito Ichinohe, (*Presenter*) Nothing to Disclose

## PURPOSE

To show the usefulness of fat-suppressed T2-weighted images (FS-T2WI) with deep learning (DL)-based reconstruction by comparing acquisition time and image quality between respiratory-gated turbo spin echo (RG-TSE), breath-hold TSE with DL (BH-DL-TSE), and half Fourier single shot turbo spin echo with DL (BH-DL-HASTE).

## METHODS AND MATERIALS

Sixty-two consecutive patients who were suspected of having liver disease and underwent 3 T MRI were enrolled in this study. Forty-eight focal liver lesions > 10 mm were also enrolled. Three sets of FS-T2WI were acquired using RG-TSE, prototypical BH-DL-TSE, and prototypical BH-DL-HASTE, respectively. In the qualitative analysis, two radiologists independently evaluated the images quality (liver parenchyma, edge sharpness of the left and right lobes of the liver, intra-hepatic vessels clarity, and lesion conspicuity) using a five-point scale, and consensus was reached. In the quantitative analysis, we calculated the signal intensity ratio of the lesion and the liver (LLR) and the lesion and the muscle (LMR). Differences of each variable between the three groups were statistically analyzed using Friedman test and Dunn's multiple comparisons test.

## RESULTS

The mean acquisition time was 279 (95%CI 258-300 ) s in RG-TSE, 20 s × 2 in BH-DL-TSE, 20 s in BH-DL-HASTE. In the qualitative analysis, the score for intrahepatic vessels clarity was significantly higher in RG-TSE and BH-DL-TSE than in BH-DL-HASTE (P < 0.001). The score for edge sharpness of the left lobe was the highest in BH-DL-HASTE (P < 0.001), and it was significantly higher in BH-DL-TSE than in RG-TSE (P = 0.004). There was no significant difference in the score for liver parenchyma, edge sharpness of

the right lobe, and lesion conspicuity ( $P = 0.191, 0.570, 0.330$ , respectively). In the quantitative analysis, there was no statistically significant difference in LLR ( $P = 0.174$ ). LMR was significantly higher in BH-DL-TSE than in BH-DL-HASTE ( $P < 0.001$ ).

## CONCLUSION

s RG-TSE could be replaced by BH-DL-TSE in acquiring FS-T2WI, because BH-DL-TSE has comparable or better performance compared with RG-TSE. However, BH-DL-HASTE should be used complementarily with BH-DL-TSE, because BH-DL-HASTE has an advantage of motion resistant and disadvantage of vessel clarity over BH-DL-TSE.

## CLINICAL RELEVANCE/APPLICATION

Although RG-TSE is often used as a routine protocol for acquiring liver T2WI, BH-DL-TSE can be an alternative to it and may improve the image quality and efficiency of MRI of the liver.

## W5A-SPGI-6 Amide Proton Transfer Imaging of Rectal Cancer: Baseline values and Feasibility for Predicting neoadjuvant CRT-resistant

Participants

Lan Zhang, PhD, (*Presenter*) Nothing to Disclose

## PURPOSE

To determine whether APTw imaging is repeatable in rectal cancer and whether APTw imaging can predict neoadjuvant CRT-resistant for LARC.

## METHODS AND MATERIALS

Twenty-three patients with histological diagnostic rectal cancer and clinical T3-4 or N+ were prospectively recruited into this institutional review board-approved study. All participants were scanned at 3.0T using standard rectal protocols (T1WI, T2WI, DWI, contrast-enhanced) and APTw-imaging (acquired with 3D turbo-spin-echo sequence). Total mesorectal excision was performed on 21 patients (2 patient refusing operation after neoadjuvant CRT were finally excluded) and the relevant pathological features were evaluated. APT values were measured by two radiologists independently drawing ROIs on a commercially available post-processing workstation. Polygonal ROIs were placed in the solid component of a tumor on the T2WI image, avoiding cystic, large necrotic, or hemorrhagic components, and copied onto the APTw image by each radiologist. The size of ROIs were draw  $\approx 260 \text{ mm}^2$  ( $\approx 80$  pixels) and as large as possible. Pathological features including tumor grade and Tumor regression stage (TRG) were evaluated. Inter-observer agreement on APT values was analyzed using intraclass correlation coefficient (ICC). APT values were compared between the two groups classified by pathological grade using independent sample t-test, while the correlation between APT values and TRG was evaluated using Pearson correlation analysis.

## RESULTS

APT value of all tumors was  $3.55 \pm 1.78$  (%), range from 1.09 to 7.80). The ICC of APT values was 0.963 ( $p < 0.05$ ) between the 2 radiologists. 13 rectal tumors TRG graded as 0 or 1 were classified in CRT-response group, while 8 rectal tumors graded as 2 or 3 were classified in CRT-resistant group. APT values between the group of TRG0-1 and TRG2-3 were significantly different ( $p < 0.05$ ). The TRG was significantly associated with APT value ( $R = 0.796, p < 0.05$ ).

## CONCLUSION

s Rectal cancer is usually very proliferative and possesses high considerable potential in long-distance metastases, which likely lead to an abundant pool of mobile cellular proteins and peptides. We have established a baseline for the APT values in rectal cancer, which was shown significantly correlated with TRG after neoadjuvant CRT. We speculate that APT value may be a useful biomarker for assessing rectal pathological characteristics and predicting neoadjuvant CRT-resistant.

## CLINICAL RELEVANCE/APPLICATION

APTw imaging has a potential impact on the clinical therapeutic strategies for patients, and this needs to be validated in a further study with larger sample size.

## W5A-SPGI-7 3D Single Breath-Hold MRE for the Simultaneous Assessment of Liver Fibrosis and Inflammation.

Participants

Omar Darwish, BEng, London, United Kingdom (*Presenter*) Nothing to Disclose

## PURPOSE

3D MRE compared to 2D MRE sequences have the advantage of measuring both liver inflammation and fibrosis, however, require several 16-20 sec breath-holds with associated slice position misregistration. The purpose is to develop and validate a 3D multi-slice SMS accelerated GRE-MRE acquisition (Intenso MRE) done in a single 17 sec breath-hold.

## METHODS AND MATERIALS

A total of 19 subjects were included in this prospective study, 10 were healthy subject and 9 were patients with steatohepatitis. All subjects were imaged using Intenso MRE at 60Hz mechanical excitation. For the healthy subjects, a 3D multi breath-hold acquisition (eXpresso MRE) was performed for comparison. Patients had a single breath-hold 2D SE-EPI acquisition and liver biopsies (ISHAK scores) for validation. The viscoelastic parameters were measured for all subjects to include the magnitude of the shear modulus  $|G^*|$  [kPa], and Intenso MRE measured additionally the shear wave speed  $C_s$  [m/s] and the loss modulus  $G''$  [kPa].

## RESULTS

The average age and BMI for all subjects were  $38.5 \pm 14.7$  years, and  $28.0 \pm 6.6 \text{ kg/m}^2$ . A Bland-Altman plot of  $|G^*|$  (Figure 1 (A)) for all healthy subjects shows a bias of 0.035 kPa in Intenso relative to eXpresso and a maximum difference of 0.42 kPa, demonstrating excellent agreement between the two methods. There was a statistically significant linear relationship ( $R^2 = 0.97$  and  $p < 0.001$ ) for the estimated  $|G^*|$  in patients between Intenso and the 2D SE-EPI sequence (Figure 1(B)). A clear differentiation between the different ISHAK fibrosis scores in patients is visible using  $C_s$  (Figure 1 (C)). A generic power-law model is fitted to  $C_s$  versus ISHAK fibrosis score, i.e.,  $C_s(F) \propto F^d$ , with  $d = 0.88 \pm 0.12$  which suggests a nearly linear increase of  $C_s$  with respect to the ISHAK fibrosis score ( $R^2 = 0.96$  and  $p < 0.001$ ). Furthermore,  $G''$  increases with the ISHAK inflammation scores (Figure 1 (D)), allowing Intenso to quantify hepatic inflammation. A generic power-law is fitted to  $G''$  versus ISHAK inflammation score, i.e.,  $G''(I) \propto I^d$ , with

$d = 0.29 \pm 0.08$  ( $R^2=0.74$  and  $p < 0.001$ )

## CONCLUSION

s Intenso MRE is effective in measuring both liver fibrosis and inflammation simultaneously within a single breath-hold.

## CLINICAL RELEVANCE/APPLICATION

Multi-slice single breath-hold 3D MRE is a patient friendly method measuring both liver fibrosis and inflammation without the slice misregistration encountered in multi breath-hold 3D MRE techniques.

## W5A-SPGI-8 Comparison of Abdominal MRI at 0.55 T and 1.5 T: Initial evaluation in healthy subjects

Participants

Anupama Ramachandran, MD, (*Presenter*) Siemens AG

## PURPOSE

To compare the quality of abdominal MRI images acquired at 0.55T with images acquired at 1.5T in the same cohort of healthy subjects.

## METHODS AND MATERIALS

In this prospective IRB approved study, unenhanced MR imaging of the upper abdomen was performed in 12 healthy subjects on both 0.55T (Magnetom Free.Max) and a 1.5T (Magnetom Sola) MR system (Siemens Healthineers, Erlangen, Germany). The protocol comprised the following sequences: single-shot T2w TSE, fat sat T2w BLADE, DWI, 2D IP-OP dual-echo GRE, 3D FS T1w GRE, and respiratory triggered coronal 3D T2w TSE MRCP. The images were rated by 2 radiologists with 22 and 17 years' experience in body MRI on a 4-point scale (1: extremely poor, 2: poor, 3: good, 4: excellent) for the following features: signal-to-noise ratio, edge definition of organs (liver, spleen, pancreas, adrenals, kidneys), delineation of hepatic veins, artifacts, and overall image quality. MRCP images were rated for delineation of biliary and pancreatic ducts, and overall image quality. The Mann-Whitney U test was used to determine any statistically significant difference in image quality between the different field strengths for all sequences, where a p-value  $< 0.05$  was considered to be statistically significant

## RESULTS

Abdominal MRI with acceptable image quality (overall image quality score =3) was achieved in all 12 cases at 0.55T at an average acquisition time of  $22 \pm 4$  min. 3D MRCPs acquired at 0.55T had higher overall image quality scores than 1.5T ( $p = 0.04$  by reader 1). The overall image quality scores were significantly higher at 1.5T for coronal and axial single shot T2w TSE by both readers (reader 1:  $p=0.02$  and  $p=0.01$ , reader 2:  $p=0.003$  and  $p=0.0001$ , respectively). SNR scores were higher at 1.5T images for all sequences except DWI b50, for which the score was equal to (reader 1) or less than (reader2) that at 0.55T. The SNR ratings of coronal and axial single shot T2w TSE and were significantly higher at 1.5 T by both readers (reader 1:  $p=0.04$  and  $p=0.04$ , reader 2:  $p=0.0022$  and  $p=0.00008$ , respectively).

## CONCLUSION

s Diagnostically acceptable quality abdominal MR images can be obtained at 0.55T. While the image quality in some sequences including coronal and axial single shot T2w TSE and DWI at 0.55T may be improved, some sequences such as 3D MRCPs were rated higher at 0.55T than at 1.5T. Further work is needed to assess ratings from multiple radiologists, reader experience, and effect of various sequence settings on diagnostic accuracy.

## CLINICAL RELEVANCE/APPLICATION

A commercial 0.55T MRI system has the potential to provide acceptable quality abdominal MR images collected in healthy subjects. Further studies are needed to assess continued protocol and sequence refinement, as well as clinical performance.

## W5A-SPGI-9 Arterial Enhancement Fraction in Evaluating the Therapeutic Effect and Survival for Hepatocellular Carcinoma Patients Treated with DEB-TACE

Participants

Bin Chai, (*Presenter*) Nothing to Disclose

## PURPOSE

To retrospectively investigate relationships between arterial enhancement fraction (AEF) and treatment response and survival in hepatocellular carcinoma (HCC) patients treated with drug-eluting bead (DEB) TACE.

## METHODS AND MATERIALS

AEF of the primary HCC lesion (AEFpre) and residual tumor (AEFpost) were obtained from triphasic liver CT scans before and after DEB-TACE in 158 HCC patients. Wilcoxon-signed rank test was used to compare the AEFpre and AEFpost for different response groups. Cox regression analyses were used to determine the association between AEF and overall survival.

## RESULTS

There was no correlation between AEFpre and treatment response. The AEFpost was significantly lower than AEFpre in the partial response group (38.9% vs. 52.7%,  $p < 0.001$ ) and stable disease group (49.3% vs. 52.1%,  $p = 0.029$ ). In patients with disease progression, AEFpost was numerically higher than AEFpre (55.5% vs. 53.0%,  $p = 0.604$ ). Cox regression analyses showed that risk of death increased in patients with AEFpre  $> 57.95\%$  (HR = 1.66,  $p = 0.019$ ) and with AEFpost  $> 54.85\%$  (HR = 2.47,  $p < 0.001$ ), and the risk reduced in patients with decrease ratio  $> -0.102$  (HR = 0.32,  $p < 0.001$ ).

## CONCLUSION

s No prediction of response was possible before DEB-TACE based on AEF. The change in AEF of viable tumor is correlated with the response of HCC to DEB-TACE. In addition, the AEF could be a helpful predictor in future prospective studies on the embolization treatment for HCC.

## CLINICAL RELEVANCE/APPLICATION

Computed tomography perfusion imaging (CTPI), providing information about the hemodynamics properties of tissue at a microscopic level, has shown promising results for monitoring HCC and assessing treatment response more accurately than traditional morphologic imaging. However, Liver CTPI typically involves scanning the liver at numerous (>20) time points after IV contrast injection, thus requiring dedicated scanning protocols and the large radiation dose. Arterial enhancement fraction (AEF) derived from routine triphasic liver CT examinations is an ideal surrogate biomarker to estimate the perfusion information without extra exposure concern. Our findings showed that AEF could be an easily accessible parameters for monitoring the response of HCC to DEB-TACE, and be a useful prognostic factor for survival.

Printed on: 02/07/23



## Abstract Archives of the RSNA, 2022

W5A-SPGI-1

### Usefulness of the combination of Fast3D Technique and Deep Learning Based Reconstruction for Magnetic Resonance Cholangiography

Wednesday, Nov. 30 12:15PM - 12:45PM Room: Learning Center - GI DPS

#### Participants

Kaori Shiraishi, Kumamoto, Japan (*Presenter*) Nothing to Disclose

#### PURPOSE

To evaluate the usefulness of the Fast3D technique and deep-learning-based reconstruction (DLR) at 3D-MRCP within a single breath-hold (BH).

#### METHODS AND MATERIALS

This retrospective study included 70 consecutive patients who underwent a respiratory gating MRCP and a single BH-MRCP with Fast3D between August and September 2021. BH images were reconstructed with and without DLR. The signal-to-noise ratio (SNR), contrast, contrast-to-noise ratio (CNR) between the common bile duct (CBD) and periductal tissues, and full width at half maximum (FWHM) of CBD on 3D-MRCP were evaluated quantitatively. Two board-certified radiologists scored image noise, contrast, artifacts, blur, and overall image quality of the three image types using a 4-point scale. Quantitative and qualitative scores were compared with using Friedman test and post hoc Nemenyi test.

#### RESULTS

This study consisted of 32 patients with biliary and pancreatic disorders (17 men and 15 women; age range, 26-92 years; mean age, 66.1 years). The SNR and CNR of MRCP were no significant differences between under respiratory gating and under BH without DLR. However, these were significantly higher under BH with DLR than under respiratory gating ( $P < 0.05$ ). The contrast and FWHM of MRCP under BH with and without DLR were lower than under respiratory gating (Contrast:  $P < 0.01$ , FWHM:  $P < 0.05$ ). Qualitative scores for noise, blur and overall image quality were higher under BH with DLR than those under respiratory gating ( $p < 0.05$ ). Contrast and Artifact were no significant differences between under BH with DLR and under respiratory gating ( $p < 0.05$ ).

#### CONCLUSION

The combination of the Fast3D technique and DLR is a useful technique for MRCP within a single BH without deterioration of image quality.

#### CLINICAL RELEVANCE/APPLICATION

The combination of the Fast3D technique and DLR is a useful technique for BH MRCP and can offer the comparable image quality with respiratory gating MRCP in a short scan time.

Printed on: 02/07/23

## Abstract Archives of the RSNA, 2022

W5A-SPGI-10

### Explore the potential of diffusion-relaxation correlation spectroscopic imaging for evaluating response to neoadjuvant chemoradiotherapy in locally advanced rectal cancer

Wednesday, Nov. 30 12:15PM - 12:45PM Room: Learning Center - GI DPS

#### Participants

Xixi Zhao, Guangzhou, China (*Presenter*) Nothing to Disclose

#### PURPOSE

To determine the diagnostic performance of diffusion-relaxation correlation spectroscopic imaging (DR-CSI) in discriminating the pathological complete response (pCR) to neoadjuvant chemoradiotherapy (nCRT) in locally advanced rectal cancer (LARC).

#### METHODS AND MATERIALS

Nineteen patients with LARC underwent examination by a 3.0T MRI scanner (uMR780, United Imaging Healthcare, Shanghai, China) after nCRT. DR-CSI data were acquired for each patient using 24 DWI images with 6 b-values (0, 200, 500, 800, 1500, 2000 s/mm<sup>2</sup>) combining 4 TEs (102, 128, 154, 180 ms). Region of interests (ROI) were decided in rectum on 5 slices. DR-CSI spectra (range: D 0~5×10<sup>-3</sup> mm<sup>2</sup>/s, T2 0~150 ms) were constructed for each voxel, and a total spectrum summing all voxels was given. All spectra were segmented into 4 compartments, A (low D, short T2), B (high D, long T2), C (high D, long T2) and D (low D, long T2). Segmentation boundaries D 3×10<sup>-3</sup> mm<sup>2</sup>/s and T2 60 ms were chosen according to foreknowledge of rectum. Volume fraction V<sub>m</sub> for each compartment m was acquired in each voxel by spectral integration, and then averaged in the whole ROI.

#### RESULTS

Two main peaks, separately with high and low diffusivity, were observed in spectra of all patients. Compared to non-pCR group, pCR group showed decreased average VD (5.6±1.7% vs 7.2±2.0%), although not statistically significant (p=0.118). ROC curve analysis indicated that the VD (AUC 0.756) has good diagnostic performance in distinguishing pCR from non-pCR patients, better than traditional ADC (0.500) and T2 value (0.539).

#### CONCLUSION

s In-vivo DR-CSI, disentangling tissue diffusivity and relaxometry at sub-voxel level, demonstrates its potential to evaluate response to nCRT in patients with LARC. VD was decreased in pCR group, although not significant, which may be due to small sampling number. The compartment D with slow diffusivity and high T2 should related with water concentration and may correlates with residual tumor, requiring confirmation by further research. Moreover, the V maps may assist recognizing areas of possible residual tumor, demonstrating potential in personalized subsequent treatment.

#### CLINICAL RELEVANCE/APPLICATION

Although nCRT has become the standard treatment for LARC, current tumor response evaluation is still lack of accuracy. Radiologic indicator containing compositional information is of great value.

Printed on: 02/07/23

## Abstract Archives of the RSNA, 2022

W5A-SPGI-2

### Liver T2-Weighted Imaging and Diffusion-weighted Imaging: Comparison of Respiratory-Frequency Modulated Continuous Wave Radar-trigger, Respiratory Belt-trigger and Navigator-trigger Acquisition

Wednesday, Nov. 30 12:15PM - 12:45PM Room: Learning Center - GI DPS

#### Participants

Xinyue Liang, Shanghai, China (*Presenter*) Nothing to Disclose

#### PURPOSE

For abdominal MRI, respiratory motion artifacts could significantly degrade image quality. Respiratory belt-trigger (BT) and navigator-trigger (NT) acquisition have been widely used to mitigate motion artifacts. However, belt required external device and extra patient preparation time. Accuracy of NT depends on the quality and position of the navigator. Additionally, efficiency of NT was limited by the fixed acceptance window. Novel contactless respiratory-frequency modulated continuous wave radar trigger (FT) acquisition was developed recently without any additional setup steps. The aim of this study is to compare the performance of novel FT acquisition with traditional respiratory trigger acquisitions (BT and NT) for T2-weighted imaging (T2WI) and diffusion-weighted Imaging (DWI) of liver.

#### METHODS AND MATERIALS

Seventeen volunteers were prospectively imaged on a 1.5T MR scanner (uMR 680; United Imaging Healthcare; Shanghai; China) using T2WI and DWI with FT, BT and NT acquisitions. Overall image quality, blurring, motion artifacts, and liver edge delineations were assessed on a 4-point scale by two radiologists. Signal-to-noise ratio (SNR) and apparent diffusion coefficient (ADC) value of liver parenchyma were calculated. Differences between three acquisitions were evaluated using Wilcoxon signed-ranks test. Inter-observer agreements between two radiologists were measured by intraclass correlation coefficients (ICCs).

#### RESULTS

All acquisitions provided acceptable overall image quality (score > 2.8) in all subjects on T2WI and DWI. There were no significant differences between three respiratory trigger acquisitions in qualitative scores (all  $p > 0.05$ ) on both sequences. The acquisition time of 179.2 sec for NT was significantly longer than that of 141.3 sec for BT and 142.8 sec for FT on T2WI ( $p < 0.05$ ). Quantitative parameters were comparable among FT, BT and NT, with mirror or no significant differences. Agreement between each reviewer was excellent (ICC > 0.9).

#### CONCLUSION

s This study indicates that the novel FT acquisition provides comparable image quality and simplifies subject preparation steps compared to the use of traditional BT and NT acquisitions.

#### CLINICAL RELEVANCE/APPLICATION

FT can be used as an effective respiratory trigger acquisition in T2WI and DWI of the liver, with high potential for improving MR workflow efficiency and patient comfort.

Printed on: 02/07/23

## Abstract Archives of the RSNA, 2022

W5A-SPGI-3

### Image Quality Evolution of Diffusion-weighted imaging Sequences for the Assessment of Rectal Cancer

Wednesday, Nov. 30 12:15PM - 12:45PM Room: Learning Center - GI DPS

#### Participants

Maria El Homsy, MD, New York, NY (*Presenter*) Nothing to Disclose

#### PURPOSE

To compare and evaluate image quality of 3 different diffusion-weighted imaging (DWI) sequences with low and high b values for the assessment of rectal cancer and to provide quantitative estimates of signal-to-noise ratio (SNR) and contrast-to-noise ratio (CNR).

#### METHODS AND MATERIALS

This retrospective study included 30 consecutive patients who underwent 3.0 T MRI exams between January and June 2020. DWI was performed in each subject with 1) single-shot echo planar imaging (ssEPI) (b=800 s/mm<sup>2</sup>), multiplexed sensitivity encoding (MUSE) (b=800 s/mm<sup>2</sup>), MUSE (b=1500 s/mm<sup>2</sup>), and FOV optimized and constrained undistorted single-shot (FOCUS) (b=1500 s/mm<sup>2</sup>). Two radiologists independently subjectively scored the image quality, contour, and lesion conspicuity of the DW images based on a 5-point Likert scale. One radiologist drew ROI on rectal wall on the 4 sequences and ADC map. Inter-reader agreement was assessed by applying the procedure of weighted Cohens' kappa (?). Image scores were evaluated by using the Wilcoxon signed rank test with Bonferroni adjustment. The SNR, CNR, and ADC measurements between sequences were compared using the paired t-test.

#### RESULTS

Both readers found image quality, contour, and conspicuity to be significantly superior with MUSE (b=800 s/mm<sup>2</sup>) as compared to ssEPI. MUSE (b=800 s/mm<sup>2</sup>) had the highest score for image quality and contour which was statistically significant for both readers as compared to all other acquisitions. Conspicuity was equally superior for both MUSE sequences. One reader had improved lesion conspicuity on MUSE (b=800 s/mm<sup>2</sup>) as compared to FOCUS. There was no significant difference between MUSE at different b-values for the assessment of conspicuity. There was good to excellent interreader agreement for all qualitative features (?), 0.72-0.88). MUSE (b=800 s/mm<sup>2</sup>) had the highest SNR, and MUSE (b=1500 s/mm<sup>2</sup>) had the highest CNR. Significant difference in ADC were observed in comparing ssEPI to the other sequences (p<0.001), and between MUSE (b=800 s/mm<sup>2</sup>) and FOCUS.

#### CONCLUSION

s MUSE has improved image quality and tumor conspicuity as compared to ssEPI. The choice of b value significantly affects ADC estimates in MUSE.

#### CLINICAL RELEVANCE/APPLICATION

The use of MUSE can improve image quality and tumor conspicuity compared to the traditional DWI in rectal MRI. This can be in part related to better CNR, SNR, and reduced geometric distortion.

Printed on: 02/07/23

## Abstract Archives of the RSNA, 2022

W5A-SPGI-4

### Artificial intelligence (AI) augmented reconstruction provides improved image quality and enables shorter breath-holds in contrast-enhanced liver MRI.

Wednesday, Nov. 30 12:15PM - 12:45PM Room: Learning Center - GI DPS

#### Participants

Francesca Castagnoli, MD, (*Presenter*) Nothing to Disclose

#### PURPOSE

To compare image quality and lesion detection using an AI-augmented contrast enhanced (CE) T1w MRI sequence in the liver [derived from applying a neural network (NN) trained on high-resolution images to conduct interpolation and partial Fourier reconstruction, in addition to iterative denoising (ID)] with a conventional CE T1w sequence.

#### METHODS AND MATERIALS

50 consecutive patients who underwent clinical liver MRI with Gd-EOB-DTPA on a 1.5T scanner were prospectively enrolled. The protocol included a hepatobiliary phase conventional 17s CE-T1w sequence, a 17s T1w with NN reconstruction and ID and a 12s accelerated T1w with prototypical NN reconstruction and ID. The 3 image sets were analyzed independently by 2 blinded radiologists. Image assessment was made by evaluating the overall image quality, contrast-to-noise ratio (CNR), lesion edge sharpness, vessel edge sharpness and respiratory motion artefacts. Kruskal-Wallis test was used to compare image quality scores. Clinical lesion detection was assessed by identifying and counting focal liver lesions and measuring the diameter of the smallest lesion on the 12s NN+ID acquisition and 17s standard reconstruction. A 4-week break was granted between the reading sessions. Student's t-test was used to compare the number of lesions recorded and the diameter of smallest lesion.

#### RESULTS

There were significantly higher scores for image quality, CNR, vessel edge sharpness and lesion edge sharpness for the 17s and 12s acquisitions using NN+ID compared with standard reconstruction ( $p < 0.0001$ ), but with no significant difference between 17s and 12s NN+ID acquisitions. No significant difference was found for respiratory motion artefacts ( $p > 0.05$ ) between all three image sets. For clinical lesion detection, there was no significant difference between the number of lesions and diameter of smallest lesion identified using 12s NN+ID compared with conventional 17s acquisition for either reader ( $p > 0.05$ ).

#### CONCLUSION

s Advanced reconstruction methods using a trained neural network for data interpolation combined with iterative denoising can improve image quality while reducing the duration of breath-hold on T1w CE liver imaging, without compromising clinical lesion detection.

#### CLINICAL RELEVANCE/APPLICATION

AI augmented T1-weighted imaging can improve image quality, reduce image acquisition time without compromising diagnostic performance. Reduction in breath-hold time can improve patient compliance for MRI liver examinations.

Printed on: 02/07/23

## Abstract Archives of the RSNA, 2022

W5A-SPGI-5

### Title Usefulness of breath-hold fat-suppressed T2-weighted image (FS-T2WI) with deep learning-based reconstruction compared to free-breathing turbo spin echo FS-T2WI

Wednesday, Nov. 30 12:15PM - 12:45PM Room: Learning Center - GI DPS

#### Participants

Fumihito Ichinohe, (*Presenter*) Nothing to Disclose

#### PURPOSE

To show the usefulness of fat-suppressed T2-weighted images (FS-T2WI) with deep learning (DL)-based reconstruction by comparing acquisition time and image quality between respiratory-gated turbo spin echo (RG-TSE), breath-hold TSE with DL (BH-DL-TSE), and half Fourier single shot turbo spin echo with DL (BH-DL-HASTE).

#### METHODS AND MATERIALS

Sixty-two consecutive patients who were suspected of having liver disease and underwent 3 T MRI were enrolled in this study. Forty-eight focal liver lesions > 10 mm were also enrolled. Three sets of FS-T2WI were acquired using RG-TSE, prototypical BH-DL-TSE, and prototypical BH-DL-HASTE, respectively. In the qualitative analysis, two radiologists independently evaluated the images quality (liver parenchyma, edge sharpness of the left and right lobes of the liver, intra-hepatic vessels clarity, and lesion conspicuity) using a five-point scale, and consensus was reached. In the quantitative analysis, we calculated the signal intensity ratio of the lesion and the liver (LLR) and the lesion and the muscle (LMR). Differences of each variable between the three groups were statistically analyzed using Friedman test and Dunn's multiple comparisons test.

#### RESULTS

The mean acquisition time was 279 (95%CI 258-300 ) s in RG-TSE, 20 s × 2 in BH-DL-TSE, 20 s in BH-DL-HASTE. In the qualitative analysis, the score for intrahepatic vessels clarity was significantly higher in RG-TSE and BH-DL-TSE than in BH-DL-HASTE (P < 0.001). The score for edge sharpness of the left lobe was the highest in BH-DL-HASTE (P < 0.001), and it was significantly higher in BH-DL-TSE than in RG-TSE (P = 0.004). There was no significant difference in the score for liver parenchyma, edge sharpness of the right lobe, and lesion conspicuity (P = 0.191, 0.570, 0.330, respectively). In the quantitative analysis, there was no statistically significant difference in LLR (P = 0.174). LMR was significantly higher in BH-DL-TSE than in BH-DL-HASTE (P < 0.001).

#### CONCLUSION

RG-TSE could be replaced by BH-DL-TSE in acquiring FS-T2WI, because BH-DL-TSE has comparable or better performance compared with RG-TSE. However, BH-DL-HASTE should be used complementarily with BH-DL-TSE, because BH-DL-HASTE has an advantage of motion resistant and disadvantage of vessel clarity over BH-DL-TSE.

#### CLINICAL RELEVANCE/APPLICATION

Although RG-TSE is often used as a routine protocol for acquiring liver T2WI, BH-DL-TSE can be an alternative to it and may improve the image quality and efficiency of MRI of the liver.

Printed on: 02/07/23

## Abstract Archives of the RSNA, 2022

W5A-SPGI-6

### Amide Proton Transfer Imaging of Rectal Cancer: Baseline values and Feasibility for Predicting neoadjuvant CRT-resistant

Wednesday, Nov. 30 12:15PM - 12:45PM Room: Learning Center - GI DPS

#### Participants

Lan Zhang, PhD, (Presenter) Nothing to Disclose

#### PURPOSE

To determine whether APTw imaging is repeatable in rectal cancer and whether APTw imaging can predict neoadjuvant CRT-resistant for LARC.

#### METHODS AND MATERIALS

Twenty-three patients with histological diagnostic rectal cancer and clinical T3-4 or N+ were prospectively recruited into this institutional review board-approved study. All participants were scanned at 3.0T using standard rectal protocols (T1WI, T2WI, DWI, contrast-enhanced) and APTw-imaging (acquired with 3D turbo-spin-echo sequence). Total mesorectal excision was performed on 21 patients (2 patient refusing operation after neoadjuvant CRT were finally excluded) and the relevant pathological features were evaluated. APT values were measured by two radiologists independently drawing ROIs on a commercially available post-processing workstation. Polygonal ROIs were placed in the solid component of a tumor on the T2WI image, avoiding cystic, large necrotic, or hemorrhagic components, and copied onto the APTw image by each radiologist. The size of ROIs were draw =260 mm<sup>2</sup> (=80 pixels) and as large as possible. Pathological features including tumor grade and Tumor regression stage(TRG) were evaluated. Inter-observer agreement on APT values was analyzed using intraclass correlation coefficient (ICC). APT values were compared between the two groups classified by pathological grade using independent sample t-test, while the correlation between APT values and TRG was evaluated using Pearson correlation analysis.

#### RESULTS

APT value of all tumors was 3.55±1.78(% , range from 1.09 to 7.80). The ICC of APT values was 0.963(p<0.05) between the 2 radiologists. 13 rectal tumors TRG graded as 0 or 1 were classified in CRT-response group, while 8 rectal tumors graded as 2 or 3 were classified in CRT-resistant group. APT values between the group of TRG0-1 and TRG2-3 were significantly different(p<0.05). The TRG was significantly associated with APT value (R=0.796,p<0.05).

#### CONCLUSION

s Rectal cancer is usually very proliferative and possesses high considerable potential in long-distance metastases, which likely lead to an abundant pool of mobile cellular proteins and peptides. We have established a baseline for the APT values in rectal cancer, which was shown significantly correlated with TRG after neoadjuvant CRT. We speculate that APT value may be a useful biomarker for assessing rectal pathological characteristics and predicting neoadjuvant CRT-resistant.

#### CLINICAL RELEVANCE/APPLICATION

APTw imaging has a potential impact on the clinical therapeutic strategies for patients, and this needs to be validated in a further study with larger sample size.

Printed on: 02/07/23

## Abstract Archives of the RSNA, 2022

W5A-SPGI-7

### 3D Single Breath-Hold MRE for the Simultaneous Assessment of Liver Fibrosis and Inflammation.

Wednesday, Nov. 30 12:15PM - 12:45PM Room: Learning Center - GI DPS

#### Participants

Omar Darwish, BEng, London, United Kingdom (*Presenter*) Nothing to Disclose

#### PURPOSE

3D MRE compared to 2D MRE sequences have the advantage of measuring both liver inflammation and fibrosis, however, require several 16-20 sec breath-holds with associated slice position misregistration. The purpose is to develop and validate a 3D multi-slice SMS accelerated GRE-MRE acquisition (Intenso MRE) done in a single 17 sec breath-hold.

#### METHODS AND MATERIALS

A total of 19 subjects were included in this prospective study, 10 were healthy subject and 9 were patients with steatohepatitis. All subjects were imaged using Intenso MRE at 60Hz mechanical excitation. For the healthy subjects, a 3D multi breath-hold acquisition (eXpresso MRE) was performed for comparison. Patients had a single breath-hold 2D SE-EPI acquisition and liver biopsies (ISHAK scores) for validation. The viscoelastic parameters were measured for all subjects to include the magnitude of the shear modulus  $|G^*|$  [kPa], and Intenso MRE measured additionally the shear wave speed  $C_s$  [m/s] and the loss modulus  $G''$  [kPa].

#### RESULTS

The average age and BMI for all subjects were  $38.5 \pm 14.7$  years, and  $28.0 \pm 6.6$  kg/m<sup>2</sup>. A Bland-Altman plot of  $|G^*|$  (Figure 1 (A)) for all healthy subjects shows a bias of 0.035 kPa in Intenso relative to eXpresso and a maximum difference of 0.42 kPa, demonstrating excellent agreement between the two methods. There was a statistically significant linear relationship ( $R^2=0.97$  and  $p < 0.001$ ) for the estimated  $|G^*|$  in patients between Intenso and the 2D SE-EPI sequence (Figure 1(B)). A clear differentiation between the different ISHAK fibrosis scores in patients is visible using  $C_s$  (Figure 1 (C)). A generic power-law model is fitted to  $C_s$  versus ISHAK fibrosis score, i.e.,  $C_s(F) \propto F^d$ , with  $d = 0.88 \pm 0.12$  which suggests a nearly linear increase of  $C_s$  with respect to the ISHAK fibrosis score ( $R^2=0.96$  and  $p < 0.001$ ) Furthermore,  $G''$  increases with the ISHAK inflammation scores (Figure 1 (D)), allowing Intenso to quantify hepatic inflammation. A generic power-law is fitted to  $G''$  versus ISHAK inflammation score, i.e.,  $G''(I) \propto I^d$ , with  $d = 0.29 \pm 0.08$  ( $R^2=0.74$  and  $p < 0.001$ )

#### CONCLUSION

Intenso MRE is effective in measuring both liver fibrosis and inflammation simultaneously within a single breath-hold.

#### CLINICAL RELEVANCE/APPLICATION

Multi-slice single breath-hold 3D MRE is a patient friendly method measuring both liver fibrosis and inflammation without the slice misregistration encountered in multi breath-hold 3D MRE techniques.

Printed on: 02/07/23

## Abstract Archives of the RSNA, 2022

W5A-SPGI-8

### Comparison of Abdominal MRI at 0.55 T and 1.5 T: Initial evaluation in healthy subjects

Wednesday, Nov. 30 12:15PM - 12:45PM Room: Learning Center - GI DPS

#### Participants

Anupama Ramachandran, MD, (*Presenter*) Siemens AG

#### PURPOSE

To compare the quality of abdominal MRI images acquired at 0.55T with images acquired at 1.5T in the same cohort of healthy subjects.

#### METHODS AND MATERIALS

In this prospective IRB approved study, unenhanced MR imaging of the upper abdomen was performed in 12 healthy subjects on both 0.55T (Magnetom Free.Max) and a 1.5T (Magnetom Sola) MR system (Siemens Healthineers, Erlangen, Germany). The protocol comprised the following sequences: single-shot T2w TSE, fat sat T2w BLADE, DWI, 2D IP-OP dual-echo GRE, 3D FS T1w GRE, and respiratory triggered coronal 3D T2w TSE MRCP. The images were rated by 2 radiologists with 22 and 17 years' experience in body MRI on a 4-point scale (1: extremely poor, 2: poor, 3: good, 4: excellent) for the following features: signal-to-noise ratio, edge definition of organs (liver, spleen, pancreas, adrenals, kidneys), delineation of hepatic veins, artifacts, and overall image quality. MRCP images were rated for delineation of biliary and pancreatic ducts, and overall image quality. The Mann-Whitney U test was used to determine any statistically significant difference in image quality between the different field strengths for all sequences, where a p-value <0.05 was considered to be statistically significant

#### RESULTS

Abdominal MRI with acceptable image quality (overall image quality score =3) was achieved in all 12 cases at 0.55T at an average acquisition time of  $22 \pm 4$  min. 3D MRCPs acquired at 0.55T had higher overall image quality scores than 1.5T ( $p = 0.04$  by reader 1). The overall image quality scores were significantly higher at 1.5T for coronal and axial single shot T2w TSE by both readers (reader 1:  $p=0.02$  and  $p=0.01$ , reader 2:  $p=0.003$  and  $p=0.0001$ , respectively). SNR scores were higher at 1.5T images for all sequences except DWI b50, for which the score was equal to (reader 1) or less than (reader2) that at 0.55T. The SNR ratings of coronal and axial single shot T2w TSE and were significantly higher at 1.5 T by both readers (reader 1:  $p=0.04$  and  $p=0.04$ , reader 2:  $p=0.0022$  and  $p=0.00008$ , respectively).

#### CONCLUSION

Diagnostically acceptable quality abdominal MR images can be obtained at 0.55T. While the image quality in some sequences including coronal and axial single shot T2w TSE and DWI at 0.55T may be improved, some sequences such as 3D MRCPs were rated higher at 0.55T than at 1.5T. Further work is needed to assess ratings from multiple radiologists, reader experience, and effect of various sequence settings on diagnostic accuracy.

#### CLINICAL RELEVANCE/APPLICATION

A commercial 0.55T MRI system has the potential to provide acceptable quality abdominal MR images collected in healthy subjects. Further studies are needed to assess continued protocol and sequence refinement, as well as clinical performance.

Printed on: 02/07/23

## Abstract Archives of the RSNA, 2022

W5A-SPGI-9

### Arterial Enhancement Fraction in Evaluating the Therapeutic Effect and Survival for Hepatocellular Carcinoma Patients Treated with DEB-TACE

Wednesday, Nov. 30 12:15PM - 12:45PM Room: Learning Center - GI DPS

#### Participants

Bin Chai, (*Presenter*) Nothing to Disclose

#### PURPOSE

To retrospectively investigate relationships between arterial enhancement fraction (AEF) and treatment response and survival in hepatocellular carcinoma (HCC) patients treated with drug-eluting bead (DEB) TACE.

#### METHODS AND MATERIALS

AEF of the primary HCC lesion (AEFpre) and residual tumor (AEFpost) were obtained from triphasic liver CT scans before and after DEB-TACE in 158 HCC patients. Wilcoxon-signed rank test was used to compare the AEFpre and AEFpost for different response groups. Cox regression analyses were used to determine the association between AEF and overall survival.

#### RESULTS

There was no correlation between AEFpre and treatment response. The AEFpost was significantly lower than AEFpre in the partial response group (38.9% vs. 52.7%,  $p < 0.001$ ) and stable disease group (49.3% vs. 52.1%,  $p = 0.029$ ). In patients with disease progression, AEFpost was numerically higher than AEFpre (55.5% vs. 53.0%,  $p = 0.604$ ). Cox regression analyses showed that risk of death increased in patients with AEFpre  $> 57.95\%$  (HR = 1.66,  $p = 0.019$ ) and with AEFpost  $> 54.85\%$  (HR = 2.47,  $p < 0.001$ ), and the risk reduced in patients with decrease ratio  $> -0.102$  (HR = 0.32,  $p < 0.001$ ).

#### CONCLUSION

No prediction of response was possible before DEB-TACE based on AEF. The change in AEF of viable tumor is correlated with the response of HCC to DEB-TACE. In addition, the AEF could be a helpful predictor in future prospective studies on the embolization treatment for HCC.

#### CLINICAL RELEVANCE/APPLICATION

Computed tomography perfusion imaging (CTPI), providing information about the hemodynamics properties of tissue at a microscopic level, has shown promising results for monitoring HCC and assessing treatment response more accurately than traditional morphologic imaging. However, Liver CTPI typically involves scanning the liver at numerous ( $>20$ ) time points after IV contrast injection, thus requiring dedicated scanning protocols and the large radiation dose. Arterial enhancement fraction (AEF) derived from routine triphasic liver CT examinations is an ideal surrogate biomarker to estimate the perfusion information without extra exposure concern. Our findings showed that AEF could be an easily accessible parameters for monitoring the response of HCC to DEB-TACE, and be a useful prognostic factor for survival.

Printed on: 02/07/23

## Abstract Archives of the RSNA, 2022

W5A-SPGU

### Genitourinary Wednesday Poster Discussions - A

Wednesday, Nov. 30 12:15PM - 12:45PM Room: Learning Center - GU DPS

#### Sub-Events

#### **W5A-SPGU- Challenging early contrast-enhancement of malignant renal tumor after cryoablation therapy** 2

Participants

Sylvain Bodard, (*Presenter*) Nothing to Disclose

#### **PURPOSE**

Most of the early contrast enhancement (CE) of renal tumor following cryoablation therapy described in literature are related to residual tumor due to incomplete treatment. However, we've experienced an uncommon precocious benign contrast enhancement of the cryoablation zone during post-therapeutic follow-up. The aim of our study was to assess the initial follow-up contrast enhancement on MRI that could be challenging to distinguish from a persistent residual lesion.

#### **METHODS AND MATERIALS**

In this retrospective study, patients who underwent percutaneous cryotherapy for malignant renal tumors from January 2013 to December 2017 and exhibit early contrast enhancement of the ablation zone on MRI were included. A minimum 3-year follow-up in MRI was necessary for inclusion. Exclusion criteria were the diagnostic of benign renal tumor or with insufficient follow-up after cryoablation. The characteristics of the CE were systematically assessed by two independent investigators.

#### **RESULTS**

82 patients were included. Median age was 70 years  $\pm$  8 (range 20- 89 years). Tumor type included 76 RCC (93%), 2 chromophobe renal carcinomas (2%) and 2 clear cell tubulopapillary renal cell carcinomas (2%). All of the first follow-up MRI were performed at 24 hours. 8 patients had incomplete treatment, all of them showing CE in the ablation zone, the growing size of the CE at next follow-up. Residual tumor CE pattern include either early arterial wash-in at the endorenal side of the peripheric ablation zone, 5/9 were nodular shaped, with a mean size of 18mm (range: 12-27mm). 8 All were located on the peripheric endorenal side of the ablation zone. 7 of 8 (88%) incomplete treatment CE featured a significant wash-out (WO). Benign CE were spotted in 74 patients, all presenting a wash-in at the arterial phase, with a predominant non-nodular shape (51/74), a median length of 13mm (range 2-30mm). They were located either in the central zone (5/74), covering the whole ablation zone (4/74), peripheric on the endorenal side (30/74) or exorenal side (24/74). Every each of those CE regressed completely at the 6 weeks control MRI. Moreover, the majority of the benign findings presented a significant increase of the signal size (69/74) and intensity of the CE throughout the time, and a reverse WO (69/74).

#### **CONCLUSION**

We described in our study an early benign contrast enhancement of the cryoablation zone that is very similar to a residual tumoral lesion except for a significant increase of the signal size, a reverse WO the absence of wash-out and the spontaneous and complete regression at 1 month after treatment.

#### **CLINICAL RELEVANCE/APPLICATION**

These features can help differentiate between tumor remnant and physiological contrast uptake when a retreatment decision is necessary.

#### **W5A-SPGU- Evaluation of a T2-weighted Adrenal MRI Calculator to Differentiate Adrenal Pheochromocytoma from Lipid Poor Adrenal Adenoma** 3

Participants

Rosalind Gerson, MD, MSc, Cumberland, ON (*Presenter*) Nothing to Disclose

#### **PURPOSE**

To assess the sensitivity, specificity, and diagnostic accuracy of a quantitative and quantitative T2 MRI calculator in differentiating pheochromocytomas from lipid-poor adenomas.

#### **METHODS AND MATERIALS**

In this retrospective case-control study, three blinded radiologists assessed T2 weighted (T2W) MRI of 29 pathology confirmed pheochromocytomas and 23 lipid-poor adrenal adenomas. Nodule heterogeneity and signal intensity relative to renal cortex were subjectively rated on 5 point Likert scales. T2W signal intensity ratio (SIR) was calculated relative to ipsilateral skeletal muscle and entropy was calculated using histogram analysis following manual segmentation. Values were entered into qualitative and quantitative MR calculators previously developed using logistic regression models. Sensitivity, specificity, and diagnostic accuracy were determined using 2x2 table analysis.

#### **RESULTS**

For all three readers, subjective ratings for T2W SI and heterogeneity, as well as quantitative T2W SI ratio and entropy were significantly higher in pheochromocytoma compared to adenoma. Inter-observer agreement was fair to moderate ( $k=0.37-0.46$ ) for subjective T2W SI and fair ( $k=0.24-0.32$ ) for subjective heterogeneity. Sensitivity, specificity, and accuracy for pheochromocytoma diagnosis using the qualitative MR calculator ranged from 45-59%, 100%, and 72-79% respectively. Sensitivity, specificity, and accuracy for pheochromocytoma diagnosis using the quantitative MR calculator ranged from 93-100%, 87-96%, and 94-96% respectively.

#### **CONCLUSION**

A quantitative MR calculator using T2W SI and entropy can differentiate pheochromocytoma from lipid-poor adenoma with high sensitivity, specificity, and accuracy, and demonstrated higher sensitivity and accuracy than a qualitative MR calculator.

#### **CLINICAL RELEVANCE/APPLICATION**

Lipid-poor adrenal adenomas and pheochromocytomas have overlapping imaging features, but are differentiated with a high degree of sensitivity and specificity using a quantitative T2 MRI calculator.

Printed on: 02/07/23

## Abstract Archives of the RSNA, 2022

W5A-SPGU-2

### Challenging early contrast-enhancement of malignant renal tumor after cryoablation therapy

Wednesday, Nov. 30 12:15PM - 12:45PM Room: Learning Center - GU DPS

#### Participants

Sylvain Bodard, (*Presenter*) Nothing to Disclose

#### PURPOSE

Most of the early contrast enhancement (CE) of renal tumor following cryoablation therapy described in literature are related to residual tumor due to incomplete treatment. However, we've experienced an uncommon precocious benign contrast enhancement of the cryoablation zone during post-therapeutic follow-up. The aim of our study was to assess the initial follow-up contrast enhancement on MRI that could be challenging to distinguish from a persistent residual lesion.

#### METHODS AND MATERIALS

In this retrospective study, patients who underwent percutaneous cryotherapy for malignant renal tumors from January 2013 to December 2017 and exhibit early contrast enhancement of the ablation zone on MRI were included. A minimum 3-year follow-up in MRI was necessary for inclusion. Exclusion criteria were the diagnosis of benign renal tumor or with insufficient follow-up after cryoablation. The characteristics of the CE were systematically assessed by two independent investigators.

#### RESULTS

82 patients were included. Median age was 70 years  $\pm$  8 (range 20- 89 years). Tumor type included 76 RCC (93%), 2 chromophobe renal carcinomas (2%) and 2 clear cell tubulopapillary renal cell carcinomas (2%). All of the first follow-up MRI were performed at 24 hours. 8 patients had incomplete treatment, all of them showing CE in the ablation zone, the growing size of the CE at next follow-up. Residual tumor CE pattern include either early arterial wash-in at the endorenal side of the peripheral ablation zone, 5/9 were nodular shaped, with a mean size of 18mm (range: 12-27mm). 8 All were located on the peripheral endorenal side of the ablation zone. 7 of 8 (88%) incomplete treatment CE featured a significant wash-out (WO). Benign CE were spotted in 74 patients, all presenting a wash-in at the arterial phase, with a predominant non-nodular shape (51/74), a median length of 13mm (range 2-30mm). They were located either in the central zone (5/74), covering the whole ablation zone (4/74), peripheral on the endorenal side (30/74) or exorenal side (24/74). Every each of those CE regressed completely at the 6 weeks control MRI. Moreover, the majority of the benign findings presented a significant increase of the signal size (69/74) and intensity of the CE throughout the time, and a reverse WO (69/74).

#### CONCLUSION

We described in our study an early benign contrast enhancement of the cryoablation zone that is very similar to a residual tumoral lesion except for a significant increase of the signal size, a reverse WO the absence of wash-out and the spontaneous and complete regression at 1 month after treatment.

#### CLINICAL RELEVANCE/APPLICATION

These features can help differentiate between tumor remnant and physiological contrast uptake when a retreatment decision is necessary.

Printed on: 02/07/23

## Abstract Archives of the RSNA, 2022

W5A-SPGU-3

### Evaluation of a T2-weighted Adrenal MRI Calculator to Differentiate Adrenal Pheochromocytoma from Lipid Poor Adrenal Adenoma

Wednesday, Nov. 30 12:15PM - 12:45PM Room: Learning Center - GU DPS

#### Participants

Rosalind Gerson, MD, MSc, Cumberland, ON (*Presenter*) Nothing to Disclose

#### PURPOSE

To assess the sensitivity, specificity, and diagnostic accuracy of a quantitative and quantitative T2 MRI calculator in differentiating pheochromocytomas from lipid-poor adenomas.

#### METHODS AND MATERIALS

In this retrospective case-control study, three blinded radiologists assessed T2 weighted (T2W) MRI of 29 pathology confirmed pheochromocytomas and 23 lipid-poor adrenal adenomas. Nodule heterogeneity and signal intensity relative to renal cortex were subjectively rated on 5 point Likert scales. T2W signal intensity ratio (SIR) was calculated relative to ipsilateral skeletal muscle and entropy was calculated using histogram analysis following manual segmentation. Values were entered into qualitative and quantitative MR calculators previously developed using logistic regression models. Sensitivity, specificity, and diagnostic accuracy were determined using 2x2 table analysis.

#### RESULTS

For all three readers, subjective ratings for T2W SI and heterogeneity, as well as quantitative T2W SI ratio and entropy were significantly higher in pheochromocytoma compared to adenoma. Inter-observer agreement was fair to moderate ( $k=0.37-0.46$ ) for subjective T2W SI and fair ( $k=0.24-0.32$ ) for subjective heterogeneity. Sensitivity, specificity, and accuracy for pheochromocytoma diagnosis using the qualitative MR calculator ranged from 45-59%, 100%, and 72-79% respectively. Sensitivity, specificity, and accuracy for pheochromocytoma diagnosis using the quantitative MR calculator ranged from 93-100%, 87-96%, and 94-96% respectively.

#### CONCLUSION

A quantitative MR calculator using T2W SIR and entropy can differentiate pheochromocytoma from lipid-poor adenoma with high sensitivity, specificity, and accuracy, and demonstrated higher sensitivity and accuracy than a qualitative MR calculator.

#### CLINICAL RELEVANCE/APPLICATION

Lipid-poor adrenal adenomas and pheochromocytomas have overlapping imaging features, but are differentiated with a high degree of sensitivity and specificity using a quantitative T2 MRI calculator.

Printed on: 02/07/23

## Abstract Archives of the RSNA, 2022

W5A-SPHN

### Head and Neck Wednesday Poster Discussions - A

Wednesday, Nov. 30 12:15PM - 12:45PM Room: Learning Center - HN DPS

#### Sub-Events

#### **W5A-SPHN- Radiologic Depth of Invasion and Its Correlation with Pathologic Depth of Invasion in Tongue Squamous Cell Carcinoma: A Systematic Review and Meta-Analysis** 1

Participants

Min Kyoung Lee, MD, Seoul, Korea, Republic Of (*Presenter*) Nothing to Disclose

#### **PURPOSE**

To comprehensively assess the radiologic depth of invasion (rDOI) and its correlation with pathologic depth of invasion (pDOI) in tongue squamous cell carcinoma (SqCC) via a systematic review and meta-analysis.

#### **METHODS AND MATERIALS**

PubMed and EMBASE databases were searched to find pertinent original studies reporting rDOI of tongue SqCC published up until September 17, 2021. Studies that evaluated the correlations and mean differences (MD) between the rDOI and pDOI were included. We defined rDOI as the measurement based on any of the radiologic imaging modalities including US, CT, and MRI. The correlation coefficients and MD between rDOI and pDOI were meta-analytically pooled using a random-effects model. Subgroup analyses were performed according to the imaging modality. Pooled sensitivity and specificity were calculated using the bivariate model for studies investigating prediction of cervical lymph node (LN) metastasis based on rDOI. Between-study heterogeneity was assessed via Higgin's inconsistency index (I<sup>2</sup>). The quality assessment was based on the Newcastle-Ottawa scale for cohort and case-control studies.

#### **RESULTS**

Twenty-three studies including 1946 patients were eligible for analysis. All studies received good (n=9) to very good (n=14) quality ratings. The overall pooled correlation coefficient was 0.86 (95% CI, 0.82-0.90) and the pooled MD was 1.84 mm (95% CI, 1.02-2.67 mm). There were moderate to substantial heterogeneities among studies for MD (I<sup>2</sup>=68.6 %) and correlations (I<sup>2</sup>=88.6 %). Among the four studies predicting cervical LN, the pooled AUC, sensitivity, and specificity were 0.84 (95% CI, 0.80-0.87), 79% (95% CI, 58-91%) and 75% (95% CI, 44-92%), respectively. In subgroup analysis, MRI showed the largest MD (n=11; 2.62 mm, 95% CI, 2.02-3.22 mm) followed by US (n=2; -0.41 mm, 95% CI, -1.30-0.46 mm) and CT (n=2; 0.12 mm, 95% CI, -2.18-2.41 mm). The correlation coefficient was the highest in US (n=3; 0.91, 95% CI, 0.85-0.97) followed by MRI (n=12; 0.85, 95% CI, 0.81-0.90) and CT (n=2; 0.84, 95% CI, 0.61-1.07).

#### **CONCLUSION**

The rDOI measured by the three imaging modalities (US, CT, and MRI) demonstrated excellent correlations with pDOI. The rDOI was also useful in predicting cervical LN metastasis.

#### **CLINICAL RELEVANCE/APPLICATION**

The recent AJCC 8th edition included the depth of invasion (DOI) into T-classification of oral cavity cancers. Since pathologic DOI can only be acquired after surgical resection, preoperative non-invasive assessment of radiologic DOI would help clinicians in early assessment of patients' prognosis.

#### **W5A-SPHN- Radiomics Nomogram for the Preoperative Differential Diagnosis of Benign and Malignant Tumors in the Parotid Gland** 3

#### **Awards**

#### **Trainee Research Prize - Medical Student**

Participants

Sijing Feng, MBChB, BMedSc, Mosgiel, New Zealand (*Presenter*) Nothing to Disclose

#### **PURPOSE**

We aimed to develop and validate radiomic nomograms to allow preoperative differentiation between benign- and malignant parotid gland tumors (BPGT and MPGT, respectively), as well as between pleomorphic adenomas (PAs) and Warthin tumors (WTs).

#### **METHODS AND MATERIALS**

This retrospective study enrolled 183 parotid gland tumors (68 PAs, 62 WTs, and 53 MPGTs) and divided them into training (n = 128) and testing (n = 55) cohorts. In total, 2553 radiomics features were extracted from fat-saturated T2-weighted images, apparent diffusion coefficient maps, and contrast-enhanced T1-weighted images to construct single-, double-, and multi-sequence combined radiomics models, respectively. The radiomics score (Rad-score) was calculated using the best radiomics model and clinical features to develop the radiomics nomogram. The receiver operating characteristic curve and area under the curve (AUC)

were used to assess these models, and their performances were compared using DeLong's test. Calibration curves and decision curve analysis were used to assess the clinical usefulness of these models.

## **RESULTS**

The multi-sequence combined radiomics model exhibited better differentiation performance (BPGT vs. MPGT, AUC=0.863; PA vs. MPGT, AUC=0.929; WT vs. MPGT, AUC=0.825; PA vs. WT, AUC=0.927) than the single- and double sequence radiomic models. Nomogram based on the multi-sequence combined radiomics model and clinical features attained an improved classification performance (BPGT vs. MPGT, AUC=0.907; PA vs. MPGT, AUC=0.961; WT vs. MPGT, AUC=0.879; PA vs. WT, AUC=0.967).

## **CONCLUSION**

s Radiomics nomogram yielded excellent diagnostic performance in distinguishing BPGT from MPGT, PA from MPGT, and PA from WT, respectively.

## **CLINICAL RELEVANCE/APPLICATION**

Preoperative diagnosis of parotid gland tumors is of great significance, since in comparison to BPGT, MPGT often require much more aggressive approach, such as total parotidectomy with or without radiotherapy. MRI has the characteristics of noninvasive and high soft-tissue resolution, which is important when evaluating parotid gland tumors, but it is often subject to the subjective influence of the radiologist. In this study, we extracted 2553 radiomics features from FS-T2WI, ADC maps, and CE-T1WI to construct single-, double-, and multi-sequence combined radiomics models, respectively, and compared the diagnostic performance of these models. Then the Rad-score was calculated using the best radiomics model and incorporate clinical features to develop the radiomics nomogram to further improve differential diagnostic performance for parotid gland tumors.

Printed on: 02/07/23

## Abstract Archives of the RSNA, 2022

W5A-SPHN-1

### Radiologic Depth of Invasion and Its Correlation with Pathologic Depth of Invasion in Tongue Squamous Cell Carcinoma: A Systematic Review and Meta-Analysis

Wednesday, Nov. 30 12:15PM - 12:45PM Room: Learning Center - HN DPS

#### Participants

Min Kyoung Lee, MD, Seoul, Korea, Republic Of (*Presenter*) Nothing to Disclose

#### PURPOSE

To comprehensively assess the radiologic depth of invasion (rDOI) and its correlation with pathologic depth of invasion (pDOI) in tongue squamous cell carcinoma (SqCC) via a systematic review and meta-analysis.

#### METHODS AND MATERIALS

PubMed and EMBASE databases were searched to find pertinent original studies reporting rDOI of tongue SqCC published up until September 17, 2021. Studies that evaluated the correlations and mean differences (MD) between the rDOI and pDOI were included. We defined rDOI as the measurement based on any of the radiologic imaging modalities including US, CT, and MRI. The correlation coefficients and MD between rDOI and pDOI were meta-analytically pooled using a random-effects model. Subgroup analyses were performed according to the imaging modality. Pooled sensitivity and specificity were calculated using the bivariate model for studies investigating prediction of cervical lymph node (LN) metastasis based on rDOI. Between-study heterogeneity was assessed via Higgin's inconsistency index (I<sup>2</sup>). The quality assessment was based on the Newcastle-Ottawa scale for cohort and case-control studies.

#### RESULTS

Twenty-three studies including 1946 patients were eligible for analysis. All studies received good (n=9) to very good (n=14) quality ratings. The overall pooled correlation coefficient was 0.86 (95% CI, 0.82-0.90) and the pooled MD was 1.84 mm (95% CI, 1.02-2.67 mm). There were moderate to substantial heterogeneities among studies for MD (I<sup>2</sup>=68.6 %) and correlations (I<sup>2</sup>=88.6 %). Among the four studies predicting cervical LN, the pooled AUC, sensitivity, and specificity were 0.84 (95% CI, 0.80-0.87), 79% (95% CI, 58-91%) and 75% (95% CI, 44-92%), respectively. In subgroup analysis, MRI showed the largest MD (n=11; 2.62 mm, 95% CI, 2.02-3.22 mm) followed by US (n=2; -0.41 mm, 95% CI, -1.30-0.46 mm) and CT (n=2; 0.12 mm, 95% CI, -2.18-2.41 mm). The correlation coefficient was the highest in US (n=3; 0.91, 95% CI, 0.85-0.97) followed by MRI (n=12; 0.85, 95% CI, 0.81-0.90) and CT (n=2; 0.84, 95% CI, 0.61-1.07).

#### CONCLUSION

The rDOI measured by the three imaging modalities (US, CT, and MRI) demonstrated excellent correlations with pDOI. The rDOI was also useful in predicting cervical LN metastasis.

#### CLINICAL RELEVANCE/APPLICATION

The recent AJCC 8th edition included the depth of invasion (DOI) into T-classification of oral cavity cancers. Since pathologic DOI can only be acquired after surgical resection, preoperative non-invasive assessment of radiologic DOI would help clinicians in early assessment of patients' prognosis.

Printed on: 02/07/23

## Abstract Archives of the RSNA, 2022

W5A-SPHN-3

### Radiomics Nomogram for the Preoperative Differential Diagnosis of Benign and Malignant Tumors in the Parotid Gland

Wednesday, Nov. 30 12:15PM - 12:45PM Room: Learning Center - HN DPS

#### Awards

**Trainee Research Prize - Medical Student**

#### Participants

Sijing Feng, MBChB, BMedSc, Mosgiel, New Zealand (*Presenter*) Nothing to Disclose

#### PURPOSE

We aimed to develop and validate radiomic nomograms to allow preoperative differentiation between benign- and malignant parotid gland tumors (BPGT and MPGT, respectively), as well as between pleomorphic adenomas (PAs) and Warthin tumors (WTs).

#### METHODS AND MATERIALS

This retrospective study enrolled 183 parotid gland tumors (68 PAs, 62 WT, and 53 MPGTs) and divided them into training ( $n = 128$ ) and testing ( $n = 55$ ) cohorts. In total, 2553 radiomics features were extracted from fat-saturated T2-weighted images, apparent diffusion coefficient maps, and contrast-enhanced T1-weighted images to construct single-, double-, and multi-sequence combined radiomics models, respectively. The radiomics score (Rad-score) was calculated using the best radiomics model and clinical features to develop the radiomics nomogram. The receiver operating characteristic curve and area under the curve (AUC) were used to assess these models, and their performances were compared using DeLong's test. Calibration curves and decision curve analysis were used to assess the clinical usefulness of these models.

#### RESULTS

The multi-sequence combined radiomics model exhibited better differentiation performance (BPGT vs. MPGT,  $AUC=0.863$ ; PA vs. MPGT,  $AUC=0.929$ ; WT vs. MPGT,  $AUC=0.825$ ; PA vs. WT,  $AUC=0.927$ ) than the single- and double sequence radiomic models. Nomogram based on the multi-sequence combined radiomics model and clinical features attained an improved classification performance (BPGT vs. MPGT,  $AUC=0.907$ ; PA vs. MPGT,  $AUC=0.961$ ; WT vs. MPGT,  $AUC=0.879$ ; PA vs. WT,  $AUC=0.967$ ).

#### CONCLUSION

s Radiomics nomogram yielded excellent diagnostic performance in distinguishing BPGT from MPGT, PA from MPGT, and PA from WT, respectively.

#### CLINICAL RELEVANCE/APPLICATION

Preoperative diagnosis of parotid gland tumors is of great significance, since in comparison to BPGT, MPGT often require much more aggressive approach, such as total parotidectomy with or without radiotherapy. MRI has the characteristics of noninvasive and high soft-tissue resolution, which is important when evaluating parotid gland tumors, but it is often subject to the subjective influence of the radiologist. In this study, we extracted 2553 radiomics features from FS-T2WI, ADC maps, and CE-T1WI to construct single-, double-, and multi-sequence combined radiomics models, respectively, and compared the diagnostic performance of these models. Then the Rad-score was calculated using the best radiomics model and incorporate clinical features to develop the radiomics nomogram to further improve differential diagnostic performance for parotid gland tumors.

Printed on: 02/07/23

## Abstract Archives of the RSNA, 2022

W5A-SPIN

### Informatics Wednesday Poster Discussions - A

Wednesday, Nov. 30 12:15PM - 12:45PM Room: Learning Center - IN DPS

#### Sub-Events

#### W5A-SPIN-1 Deep Learning Image Reconstruction of Diffusion Weighted Imaging in Pelvic MRI at 1.5 Tesla

##### Participants

Sebastian Gassenmaier, MD, Tuebingen, Germany (*Presenter*) Nothing to Disclose

##### PURPOSE

The aim of this study was to investigate the impact of a novel deep learning image reconstruction algorithm for diffusion weighted imaging (DWI) including acquisition time reduction in 1.5T pelvic MRI on image quality parameters and diagnostic confidence.

##### METHODS AND MATERIALS

Thirty patients who were examined in February and March 2022 were retrospectively included in this monocentric study. All patients underwent a clinically indicated 1.5T pelvic MRI including DWI with two different b-values (b=50 s/mm<sup>2</sup> and b=800 s/mm<sup>2</sup>). Apparent diffusion coefficient maps were calculated. Afterwards, the raw data of standard DWI (DWISD) was processed using a novel deep learning image reconstruction algorithm resulting in datasets of DWIDL. This algorithm simulated a reduced acquisition time via reduction of averages in the high b-value. Standard acquisition applied one average for b=50 s/mm<sup>2</sup> and 12 averages for b=800 s/mm<sup>2</sup> resulting in an acquisition time of 2:58 min. DWIDL applied also one average for b=50 s/mm<sup>2</sup> but omitted 6 averages for b=800 s/mm<sup>2</sup> of the original data resulting in a reduced acquisition time of 1:42 min. Both datasets were independently evaluated by two radiologists in a blinded random order reading using a Likert scale ranging from 1 - 4 with 4 being the best. The following criteria were assessed: noise levels, extent of artifacts, sharpness, contrast, lesion detectability, overall image quality, and diagnostic confidence.

##### RESULTS

Mean patient age was 57 ± 15 years. Noise levels as well as the image contrast was evaluated to be significantly superior in DWIDL with a median of 4 in comparison to a median of 3 in DWISD (p<0.001 for both readers). The sharpness of images was also assessed to be better in DWIDL with a median of 4 versus a median of 4 in DWISD (p=0.020 for reader 1 and p=0.011 for reader 2). No significant differences were found regarding extent of artifacts, lesion detectability, overall image quality, and diagnostic confidence (p>0.05 for both readers).

##### CONCLUSION

Deep learning image reconstruction of DWI in pelvic MRI provides the opportunity of acquisition time reduction without loss of image quality.

##### CLINICAL RELEVANCE/APPLICATION

Deep learning image reconstruction offers a great opportunity for further acquisition time reduction of time-consuming DWI in combination with diagnostic image quality. These results demonstrate the potential of novel deep learning image reconstruction algorithms.

#### W5A-SPIN-2A multi-view Deep Learning-based Architecture for Thyroid Nodules Detection and Characterization

##### Participants

Sanaz Vahdati, MD, Rochester, MN (*Presenter*) Nothing to Disclose

##### PURPOSE

Thyroid cancer is regarded as one of the most rapidly growing malignancies in the general population, with an incidence rate of 14.6 per 100,000 in the United States. Thyroid Ultrasound (US) is the primary method to screen thyroid nodules and determine whether a nodule requires Fine Needle Aspiration (FNA). While the US is a safe and cheap method, FNA is an invasive and costly procedure for evaluating thyroid nodules. In recent years, deep learning (DL) has played a significant role in detecting and classifying different types of malignancies. Likewise, we propose a DL-based pipeline to detect and classify thyroid nodules into benign or malignant groups relying on two views of US imaging.

##### METHODS AND MATERIALS

Transverse and longitudinal views from B-mode US images of single thyroid nodules from 1003 patients were collected retrospectively. A total of 101 cases were held out as a testing set, and the rest of the data was used in five-fold cross-validation (CV). Two You Look Only Once (YOLO) v5 models, one for each view, were trained to detect nodules and classify them as benign or malignant. For each view, five models developed during the CV, one for each fold, were ensembled by using non-max suppression (NMS) to boost their collective generalizability. Finally, an extreme gradient boosting machine (XGBoost) model was trained on outputs of the ensembled models for both transverse and longitudinal views to yield a final prediction of malignancy for a single nodule. Mean average precision at 50% overlap (mAP0.5) was used to evaluate the YOLO models. The whole pipeline's performance

was evaluated using Area under receiving operating curve (AUROC). All the metrics were reported on the holdout test set.

## RESULTS

The total number of malignant nodules was 518 (of 1003 nodules: 51%), with 50 malignant nodules in the test set. The averaged mAP<sub>0.5</sub> of the five cross-validation folds for transverse, and longitudinal YOLO models were 0.70 (SD: 0.033) and 0.72 (SD: 0.039), respectively. The ensembled models for each view achieved a mAP<sub>0.5</sub> of 0.797 (for the transverse view) and 0.716 (for the longitudinal view). The whole pipeline, created by the XGBoost ensemble, reached an AUROC of 0.84 (CI 95%: 0.75-0.91) with sensitivity and specificity of 0.84 and 0.627, respectively. The negative predictive value of the pipeline was 0.799, with F1 score of 0.756.

## CONCLUSION

s We demonstrate the robustness of an ensemble of DL models receiving multiple views of thyroid US images to detect and characterize thyroid nodules.

## CLINICAL RELEVANCE/APPLICATION

This study proposes a DL-based pipeline to assist radiologists with diagnosing malignant thyroid nodules from multiple views of US images, which can eventually reduce unnecessary FNA for cases that are highly suggestive of being benign.

## W5A-SPIN-4 Automated Triage System to Screen No Change Follow-up Chest Radiographs Using Multi-task Deep Learning With Vision Transformer

Participants

Jeeyoung Kim, Seoul, Korea, Republic Of (*Presenter*) Nothing to Disclose

## PURPOSE

To propose a novel method to classify change/no-change in follow-up chest radiographs (CXR) using multi-task learning which performs three tasks at once including classifying normal/abnormal, matching similar regions, and classifying change/no-change.

## METHODS AND MATERIALS

A total of 404K baseline and follow-up CXR pairs were acquired from a tertiary hospital in South Korea, which contained 174K change and 230K no-change pairs. All CXRs were labeled based on radiologic reports with in-house natural language processing. Visual validation of labels was conducted by an expert thoracic radiologist with more than 20 years' experience, which showed approximately 80% accuracy in sampled dataset. For internal validation dataset, 1620 change/no-change pairs were enrolled. For two external datasets, one is 533 pairs collected from the same center, and the other is 430 pairs from the CheXpert dataset. All validation datasets were labeled with 100% accuracy by the radiologist. To overcome patient's posture, breath-hold level, aging, and other changes not related to disease progression, our network consists of four parts including Siamese network architecture, pretrained A DenseNet backbone U-Net with strong labels of diseases, Attend-and-Compare Module (ACM), a self-attention method to match the similar anatomical structure, and multi-task learning containing three loss functions to classify normal/abnormal, match each pair, and classify change/no-change. The baseline model is ResNet-152 and the full model contains CMT with all of the above mentioned. The AUC, accuracy, sensitivity, and specificity were evaluated in internal and external validations. In addition, saliency maps acquired by using Grad-CAM were used to compare the qualitative results. Hanley McNeil test is used for the statistical analysis.

## RESULTS

In internal validation, AUC, accuracy, sensitivity, and specificity of the full model were 0.77, 0.70, 0.57, and 0.83, respectively. In external validation dataset from same center, those were 0.85, 0.71, 0.51, and 0.91, and in CheXpert dataset, those were 0.76, 0.64, 0.34, and 0.93, respectively. Those of the baseline model were 0.72, 0.67, 0.56, and 0.78 for a same center validation dataset, and 0.66, 0.60, 0.40, and 0.71 for CheXpert dataset. For external validation dataset, all ROCs of full model show significantly better than those of the baseline model. (P-values < 0.01)

## CONCLUSION

s Our multi-task learning model can assist classifying change/no-change in follow-up CXRs which is one of the main tasks of radiologists.

## CLINICAL RELEVANCE/APPLICATION

This model could be used to develop fully automated triage system to screen no change follow-up CXRs in actual clinical practice which could reduce heavy burden of radiologists' reading.

## W5A-SPIN-5 Detection of Active Inflammatory Changes and Structural Damage to Sacroiliac Joints in Patients with Axial Spondyloarthritis Using Deep Learning

Participants

Keno Bressemer, MD, Berlin, Germany (*Presenter*) Nothing to Disclose

## PURPOSE

Develop an artificial neural network for detecting axial spondyloarthritis (axSpA)-induced inflammatory or structural changes of sacroiliac joints in MRI.

## METHODS AND MATERIALS

This multicenter retrospective study included MRI examinations from five cohorts of patients in whom axSpA was clinically suspected. The examinations were collected between 01/2006 and 09/2020 at university and community hospitals. Four of the cohorts were used for artificial neural network development and training, and one cohort was withheld for testing. Six experts in the field of rheumatologic imaging specializing in axSpA evaluated the MRIs of the training group for the presence of inflammatory changes or structural lesions. Seven additional experts evaluated the MRIs of the test cohort. Majority consensus among the experts was chosen as the final diagnosis. In case of a tie, another expert was consulted as a tiebreaker. To enable the training of a classification network, a homogenization of the data had to be performed first. This could be achieved by applying a U-Net autoencoder. Subsequently, a ResNet101-3d was trained for the detection of inflammatory and structural lesions. Area under the

receiver operating characteristic curve (AUC), sensitivity, and specificity were used to evaluate the performance of the classification network. A p-value of <.05 was considered significant.

## RESULTS

The five cohorts included 593 patients (302 women) with a mean age of  $37 \pm 11$  years. 477 patients were assigned to the training cohort and 116 patients to the test cohort. The prevalence of inflammatory changes in the exercise group was 41% and the prevalence of structural changes was 51%. In the test group, the prevalence of changes was significantly lower, with 21.6% inflammatory and 22.4 structural changes. On the test data set, the classification network achieved an AUC of 0.94 (95% CI 0.84-0.97) for the detection of inflammatory changes, 0.88 (0.80-0.95) for inflammatory changes meeting the ASAS definition, and 0.89 (0.81-0.96) for the detection of structural changes.

## CONCLUSION

Artificial neural networks can detect inflammatory or structural changes in sacroiliac joints even in heterogeneous multicenter MRI data.

## CLINICAL RELEVANCE/APPLICATION

The developed neural networks could help clinicians detect signs of axSpA in MRI earlier and thus help direct patients to appropriate treatment. In addition, it could serve as decision support tool in clinical trials.

## W5A-SPIN-6 Age Is More Than a Number: Estimating Biologic Age from Chest X-rays

Participants

Kaesha Thomas, MBBS, (Presenter) Nothing to Disclose

## PURPOSE

Chronological age, the time elapsed since birth, is the defacto measure of aging in clinical pathways such as medical formulas and screening guidelines. However, given the impact of biological and socioenvironmental factors on disease trajectory, chronological age may be an imprecise measure of the effects of aging versus biological age. Given the ability of AI to detect patterns not obvious to the human eye, we explore if AI can be used to determine biological age. We hypothesize that CXR-Age is a better predictor of observed, all-cause mortality than chronological age.

## METHODS AND MATERIALS

CXR-Age is an open-source, convolutional neural network (CNN) model trained using CXRs from 116,035 individuals from the Prostate, Lung, Colorectal and Ovarian Cancer National Lung Screening trials. Using a CXR dataset from Emory University Healthcare, we validated the performance of this CNN on 30,806 unique patient CXR images with an output of biological age (CXR-age). CXR-Age, chronological age and risk factors were compared to observed mortality. Gradient-weighted Class Activation Mapping (Grad-CAM) localized areas contributing to the highest probability for the prediction. Data analyses were conducted in Python and OpenAI. A p-value < 0.05 was statistically significant.

## RESULTS

Our cohort of 30,806 patients had a mean age of 64.5 (5.8) years and was 49% male. Most had a CXR-Age within 5 years their chronological age (57.4%, [17,694 of 30,806]). For patients with observed mortality (n=2,774), the AUC for CXR-Age was significantly greater than chronological age (0.523 and 0.595, respectively;  $p < 0.05$ ). Observed mortality in chronological age strata was found to be statistically different among CXR-Age strata ( $p < 0.01$ ). Patients with a CXR-Age  $\geq 70$  years had the highest mortality among the strata ([569 of 4,156], 13.7%). Patients with a CXR-Age greater than 5 years their original age had higher risk of observed mortality than those with a CXR-Age within 5 years their original age (RR=1.4,  $p < 0.01$ ). No significant association was found for those with a CXR-Age at least five years younger than their original age likely due to a lack of observed death within this stratum (RR=1.1,  $p=0.1$ ). The upper and lower mediastinum were common activation areas that contributed to the CXR-Age age estimate.

## CONCLUSION

In this cohort, patients with a CXR-Age more than 5 years their original age were at increased risk of observed mortality. Determining biological age from medical images like CXR may improve risk stratification of patients.

## CLINICAL RELEVANCE/APPLICATION

Chronological age is an imperfect measure of aging. In contrast, biological age extracted from chest radiographs using deep learning can improve risk stratification of patients and clinical assessment.

Printed on: 02/07/23

## Abstract Archives of the RSNA, 2022

W5A-SPIN-1

### Deep Learning Image Reconstruction of Diffusion Weighted Imaging in Pelvic MRI at 1.5 Tesla

Wednesday, Nov. 30 12:15PM - 12:45PM Room: Learning Center - IN DPS

#### Participants

Sebastian Gassenmaier, MD, Tuebingen, Germany (*Presenter*) Nothing to Disclose

#### PURPOSE

The aim of this study was to investigate the impact of a novel deep learning image reconstruction algorithm for diffusion weighted imaging (DWI) including acquisition time reduction in 1.5T pelvic MRI on image quality parameters and diagnostic confidence.

#### METHODS AND MATERIALS

Thirty patients who were examined in February and March 2022 were retrospectively included in this monocentric study. All patients underwent a clinically indicated 1.5T pelvic MRI including DWI with two different b-values ( $b=50$  s/mm<sup>2</sup> and  $b=800$  s/mm<sup>2</sup>). Apparent diffusion coefficient maps were calculated. Afterwards, the raw data of standard DWI (DWISD) was processed using a novel deep learning image reconstruction algorithm resulting in datasets of DWIDL. This algorithm simulated a reduced acquisition time via reduction of averages in the high b-value. Standard acquisition applied one average for  $b=50$  s/mm<sup>2</sup> and 12 averages for  $b=800$  s/mm<sup>2</sup> resulting in an acquisition time of 2:58 min. DWIDL applied also one average for  $b=50$  s/mm<sup>2</sup> but omitted 6 averages for  $b=800$  s/mm<sup>2</sup> of the original data resulting in a reduced acquisition time of 1:42 min. Both datasets were independently evaluated by two radiologists in a blinded random order reading using a Likert scale ranging from 1 - 4 with 4 being the best. The following criteria were assessed: noise levels, extent of artifacts, sharpness, contrast, lesion detectability, overall image quality, and diagnostic confidence.

#### RESULTS

Mean patient age was  $57 \pm 15$  years. Noise levels as well as the image contrast was evaluated to be significantly superior in DWIDL with a median of 4 in comparison to a median of 3 in DWISD ( $p < 0.001$  for both readers). The sharpness of images was also assessed to be better in DWIDL with a median of 4 versus a median of 4 in DWISD ( $p=0.020$  for reader 1 and  $p=0.011$  for reader 2). No significant differences were found regarding extent of artifacts, lesion detectability, overall image quality, and diagnostic confidence ( $p > 0.05$  for both readers).

#### CONCLUSION

Deep learning image reconstruction of DWI in pelvic MRI provides the opportunity of acquisition time reduction without loss of image quality.

#### CLINICAL RELEVANCE/APPLICATION

Deep learning image reconstruction offers a great opportunity for further acquisition time reduction of time-consuming DWI in combination with diagnostic image quality. These results demonstrate the potential of novel deep learning image reconstruction algorithms.

Printed on: 02/07/23

## Abstract Archives of the RSNA, 2022

W5A-SPIN-2

### A multi-view Deep Learning-based Architecture for Thyroid Nodules Detection and Characterization

Wednesday, Nov. 30 12:15PM - 12:45PM Room: Learning Center - IN DPS

#### Participants

Sanaz Vahdati, MD, Rochester, MN (*Presenter*) Nothing to Disclose

#### PURPOSE

Thyroid cancer is regarded as one of the most rapidly growing malignancies in the general population, with an incidence rate of 14.6 per 100,000 in the United States. Thyroid Ultrasound (US) is the primary method to screen thyroid nodules and determine whether a nodule requires Fine Needle Aspiration (FNA). While the US is a safe and cheap method, FNA is an invasive and costly procedure for evaluating thyroid nodules. In recent years, deep learning (DL) has played a significant role in detecting and classifying different types of malignancies. Likewise, we propose a DL-based pipeline to detect and classify thyroid nodules into benign or malignant groups relying on two views of US imaging.

#### METHODS AND MATERIALS

Transverse and longitudinal views from B-mode US images of single thyroid nodules from 1003 patients were collected retrospectively. A total of 101 cases were held out as a testing set, and the rest of the data was used in five-fold cross-validation (CV). Two You Look Only Once (YOLO) v5 models, one for each view, were trained to detect nodules and classify them as benign or malignant. For each view, five models developed during the CV, one for each fold, were ensembled by using non-max suppression (NMS) to boost their collective generalizability. Finally, an extreme gradient boosting machine (XGBoost) model was trained on outputs of the ensembled models for both transverse and longitudinal views to yield a final prediction of malignancy for a single nodule. Mean average precision at 50% overlap (mAP<sub>0.5</sub>) was used to evaluate the YOLO models. The whole pipeline's performance was evaluated using Area under receiving operating curve (AUROC). All the metrics were reported on the holdout test set.

#### RESULTS

The total number of malignant nodules was 518 (of 1003 nodules: 51%), with 50 malignant nodules in the test set. The averaged mAP<sub>0.5</sub> of the five cross-validation folds for transverse, and longitudinal YOLO models were 0.70 (SD: 0.033) and 0.72 (SD: 0.039), respectively. The ensembled models for each view achieved a mAP<sub>0.5</sub> of 0.797 (for the transverse view) and 0.716 (for the longitudinal view). The whole pipeline, created by the XGBoost ensemble, reached an AUROC of 0.84 (CI 95%: 0.75-0.91) with sensitivity and specificity of 0.84 and 0.627, respectively. The negative predictive value of the pipeline was 0.799, with F1 score of 0.756.

#### CONCLUSION

s We demonstrate the robustness of an ensemble of DL models receiving multiple views of thyroid US images to detect and characterize thyroid nodules.

#### CLINICAL RELEVANCE/APPLICATION

This study proposes a DL-based pipeline to assist radiologists with diagnosing malignant thyroid nodules from multiple views of US images, which can eventually reduce unnecessary FNA for cases that are highly suggestive of being benign.

Printed on: 02/07/23



## Abstract Archives of the RSNA, 2022

W5A-SPIN-4

### Automated Triage System to Screen No Change Follow-up Chest Radiographs Using Multi-task Deep Learning With Vision Transformer

Wednesday, Nov. 30 12:15PM - 12:45PM Room: Learning Center - IN DPS

#### Participants

Jeeyoung Kim, Seoul, Korea, Republic Of (*Presenter*) Nothing to Disclose

#### PURPOSE

To propose a novel method to classify change/no-change in follow-up chest radiographs (CXR) using multi-task learning which performs three tasks at once including classifying normal/abnormal, matching similar regions, and classifying change/no-change.

#### METHODS AND MATERIALS

A total of 404K baseline and follow-up CXR pairs were acquired from a tertiary hospital in South Korea, which contained 174K change and 230K no-change pairs. All CXRs were labeled based on radiologic reports with in-house natural language processing. Visual validation of labels was conducted by an expert thoracic radiologist with more than 20 years' experience, which showed approximately 80% accuracy in sampled dataset. For internal validation dataset, 1620 change/no-change pairs were enrolled. For two external datasets, one is 533 pairs collected from the same center, and the other is 430 pairs from the CheXpert dataset. All validation datasets were labeled with 100% accuracy by the radiologist. To overcome patient's posture, breath-hold level, aging, and other changes not related to disease progression, our network consists of four parts including Siamese network architecture, pretrained A DenseNet backbone U-Net with strong labels of diseases, Attend-and-Compare Module (ACM), a self-attention method to match the similar anatomical structure, and multi-task learning containing three loss functions to classify normal/abnormal, match each pair, and classify change/no-change. The baseline model is ResNet-152 and the full model contains CMT with all of the above mentioned. The AUC, accuracy, sensitivity, and specificity were evaluated in internal and external validations. In addition, saliency maps acquired by using Grad-CAM were used to compare the qualitative results. Hanley McNeil test is used for the statistical analysis.

#### RESULTS

In internal validation, AUC, accuracy, sensitivity, and specificity of the full model were 0.77, 0.70, 0.57, and 0.83, respectively. In external validation dataset from same center, those were 0.85, 0.71, 0.51, and 0.91, and in CheXpert dataset, those were 0.76, 0.64, 0.34, and 0.93, respectively. Those of the baseline model were 0.72, 0.67, 0.56, and 0.78 for a same center validation dataset, and 0.66, 0.60, 0.40, and 0.71 for CheXpert dataset. For external validation dataset, all ROCs of full model show significantly better than those of the baseline model. (P-values < 0.01)

#### CONCLUSION

Our multi-task learning model can assist classifying change/no-change in follow-up CXRs which is one of the main tasks of radiologists.

#### CLINICAL RELEVANCE/APPLICATION

This model could be used to develop fully automated triage system to screen no change follow-up CXRs in actual clinical practice which could reduce heavy burden of radiologists' reading.

Printed on: 02/07/23

## Abstract Archives of the RSNA, 2022

W5A-SPIN-5

### Detection of Active Inflammatory Changes and Structural Damage to Sacroiliac Joints in Patients with Axial Spondyloarthritis Using Deep Learning

Wednesday, Nov. 30 12:15PM - 12:45PM Room: Learning Center - IN DPS

#### Participants

Keno Bressemer, MD, Berlin, Germany (*Presenter*) Nothing to Disclose

#### PURPOSE

Develop an artificial neural network for detecting axial spondyloarthritis (axSpA)-induced inflammatory or structural changes of sacroiliac joints in MRI.

#### METHODS AND MATERIALS

This multicenter retrospective study included MRI examinations from five cohorts of patients in whom axSpA was clinically suspected. The examinations were collected between 01/2006 and 09/2020 at university and community hospitals. Four of the cohorts were used for artificial neural network development and training, and one cohort was withheld for testing. Six experts in the field of rheumatologic imaging specializing in axSpA evaluated the MRIs of the training group for the presence of inflammatory changes or structural lesions. Seven additional experts evaluated the MRIs of the test cohort. Majority consensus among the experts was chosen as the final diagnosis. In case of a tie, another expert was consulted as a tiebreaker. To enable the training of a classification network, a homogenization of the data had to be performed first. This could be achieved by applying a U-Net autoencoder. Subsequently, a ResNet101-3d was trained for the detection of inflammatory and structural lesions. Area under the receiver operating characteristic curve (AUC), sensitivity, and specificity were used to evaluate the performance of the classification network. A p-value of <.05 was considered significant.

#### RESULTS

The five cohorts included 593 patients (302 women) with a mean age of  $37 \pm 11$  years. 477 patients were assigned to the training cohort and 116 patients to the test cohort. The prevalence of inflammatory changes in the exercise group was 41% and the prevalence of structural changes was 51%. In the test group, the prevalence of changes was significantly lower, with 21.6% inflammatory and 22.4 structural changes. On the test data set, the classification network achieved an AUC of 0.94 (95% CI 0.84-0.97) for the detection of inflammatory changes, 0.88 (0.80-0.95) for inflammatory changes meeting the ASAS definition, and 0.89 (0.81-0.96) for the detection of structural changes.

#### CONCLUSION

Artificial neural networks can detect inflammatory or structural changes in sacroiliac joints even in heterogeneous multicenter MRI data.

#### CLINICAL RELEVANCE/APPLICATION

The developed neural networks could help clinicians detect signs of axSpA in MRI earlier and thus help direct patients to appropriate treatment. In addition, it could serve as decision support tool in clinical trials.

Printed on: 02/07/23

## Abstract Archives of the RSNA, 2022

W5A-SPIN-6

### Age Is More Than a Number: Estimating Biologic Age from Chest X-rays

Wednesday, Nov. 30 12:15PM - 12:45PM Room: Learning Center - IN DPS

#### Participants

Kaesha Thomas, MBBS, (Presenter) Nothing to Disclose

#### PURPOSE

Chronological age, the time elapsed since birth, is the defacto measure of aging in clinical pathways such as medical formulas and screening guidelines. However, given the impact of biological and socioenvironmental factors on disease trajectory, chronological age may be an imprecise measure of the effects of aging versus biological age. Given the ability of AI to detect patterns not obvious to the human eye, we explore if AI can be used to determine biological age. We hypothesize that CXR-Age is a better predictor of observed, all-cause mortality than chronological age.

#### METHODS AND MATERIALS

CXR-Age is an open-source, convolutional neural network (CNN) model trained using CXRs from 116,035 individuals from the Prostate, Lung, Colorectal and Ovarian Cancer National Lung Screening trials. Using a CXR dataset from Emory University Healthcare, we validated the performance of this CNN on 30,806 unique patient CXR images with an output of biological age (CXR-age). CXR-Age, chronological age and risk factors were compared to observed mortality. Gradient-weighted Class Activation Mapping (Grad-CAM) localized areas contributing to the highest probability for the prediction. Data analyses were conducted in Python and OpenAI. A p-value < 0.05 was statistically significant.

#### RESULTS

Our cohort of 30,806 patients had a mean age of 64.5 (5.8) years and was 49% male. Most had a CXR-Age within 5 years their chronological age (57.4%, [17,694 of 30,806]). For patients with observed mortality (n=2,774), the AUC for CXR-Age was significantly greater than chronological age (0.523 and 0.595, respectively;  $p < 0.05$ ). Observed mortality in chronological age strata was found to be statistically different among CXR-Age strata ( $p < 0.01$ ). Patients with a CXR-Age =70 years had the highest mortality among the strata ([569 of 4,156], 13.7%). Patients with a CXR-Age greater than 5 years their original age had higher risk of observed mortality than those with a CXR-Age within 5 years their original age (RR=1.4,  $p < 0.01$ ). No significant association was found for those with a CXR-Age at least five years younger than their original age likely due to a lack of observed death within this stratum (RR=1.1,  $p=0.1$ ). The upper and lower mediastinum were common activation areas that contributed to the CXR-Age age estimate.

#### CONCLUSION

s In this cohort, patients with a CXR-Age more than 5 years their original age were at increased risk of observed mortality. Determining biological age from medical images like CXR may improve risk stratification of patients.

#### CLINICAL RELEVANCE/APPLICATION

Chronological age is an imperfect measure of aging. In contrast, biological age extracted from chest radiographs using using deep learning can improve risk stratification of patients and clinical assessment.

Printed on: 02/07/23

## Abstract Archives of the RSNA, 2022

W5A-SP1R

### Interventional Wednesday Poster Discussions - A

Wednesday, Nov. 30 12:15PM - 12:45PM Room: Learning Center - IR DPS

#### Sub-Events

#### W5A-SP1R-1 Feasibility, Safety and Outcomes of Thermal Ablation of Kidney Cancer in the Elderly

Participants

Wenhui Zhou, MD, PhD, Menlo Park, CA (*Presenter*) Nothing to Disclose

#### PURPOSE

When renal cell carcinoma is diagnosed in patients of advanced age, patient co-morbidities may limit treatment options active surveillance only. This study assessed the technical results, procedural complications and survival outcome of thermal ablation in patients greater than 80 years of age diagnosed with stage T1 RCC.

#### METHODS AND MATERIALS

A retrospective analysis was performed of 113 patients greater than 80 years of age who underwent computed tomography-guided thermal ablations for 126 biopsy-proven T1N0M0 renal cell carcinoma (mean size = 3.2 cm, size SD = 1.3 cm) between October 2008 and March 2020. The rates of technical success, peri- and post-procedural complications, residual disease and local recurrence were examined. The Kaplan-Meier method was used to compute overall and cancer-specific survival.

#### RESULTS

Of the 103 elderly patients treated, the median age = 85 yrs, (range = 80 to 95 yrs) were treated and mean Charlson comorbidity index score was 3.8 (SD = 1.3). Technical success was achieved in all of the patients. Asymptomatic perinephric hematoma (Clavien-Dindo Grade I) was the most common complication, occurring in 23% of patients. Ureteral stricture requiring stent placement was the only major complication, and occurred in 2% of patients. Primary technique efficacy was achieved in 89% of cases. At 1, 3 and 5 years post-ablation, the overall survival rates were 98%, 85%, and 80%, RCC-specific survival rates were 100%, 100% and 98%, and local progression-free survival rates were 100%, 95%, and 92%, respectively.

#### CONCLUSION

Renal ablation appears technically feasible, well-tolerated and effective in treating stage T1 renal cell carcinoma in elderly patients. Small asymptomatic perinephric hematomas are a common complication following this procedure in this population.

#### CLINICAL RELEVANCE/APPLICATION

Thermal ablation may be an effective non-surgical alternative to nephrectomy or active surveillance for elderly patients diagnosed with renal cell carcinomas. For elderly patients motivated to pursue minimally invasive treatment for renal cell carcinoma, thermal ablation should be considered.

#### W5A-SP1R-3 Ablation Margin and Tumor Morphology Metrics from a Randomized Controlled Drug + Device Trial in 3-7 cm Hepatocellular Carcinoma

Participants

Katerina Lee, BS, Cedar Park, TX (*Presenter*) Nothing to Disclose

#### PURPOSE

We studied the factors associated with differences in local recurrence and survival in a clinical trial of patients with hepatocellular carcinoma (HCC) who underwent radiofrequency ablation (RFA).

#### METHODS AND MATERIALS

550 patients from the OPTIMA Trial (with solitary HCC lesions  $\leq 3$  but  $\geq 7$ cm, randomized to RFA or RFA+LTLD) were screened for well-defined tumor imaging on pre-RFA CT. 242 pre-ablation tumors and 338 post-ablation (28 days) de-vascularized volumes were manually segmented (3D Slicer). 187 pairs of corresponding pre-ablation and post-ablation CT scans were registered with General Registration (Elastix), and structural similarity was calculated in MatLab to assess registration quality (average 99.3% similarity) (Fig 1). Dice similarity metrics were recorded from the Radiotherapy Segment Comparison module. Segmented tumor and ablation zone overlap were used to define undertreated tumor and treated tumor (percent and absolute volume) (Fig 2). Multiple tumor morphology metrics were determined (3DSlicer MatLab). Relationships between these variables were analyzed using R. "Disease progression classes" were initially: complete response/no evidence of disease progression, distant hepatic recurrence, extrahepatic recurrence, incomplete response, local recurrence. These were further split into 2 final classes: Local recurrence (Yes or No). Survival data was analyzed for 122.

#### RESULTS

Univariate multinomial logistic regression showed significance between "local recurrence" and volume ( $p=.004$ ) and surface area

( $p=0.002$ ). Multivariate analysis revealed a significant relationship between "local recurrence" and age ( $p=0.0478$ ). Univariate analysis had significance with age ( $p=0.01$ ) and absolute overlap volume ( $p=0.02$ ). For survival (deceased vs alive at end of trial), there was a significant trend/relationship with age ( $p=0.0098$ ), percent overlap ( $p=0.05$ ), and absolute undertreated volume ( $p=0.055$ ) from univariate logistic regression.

## CONCLUSION

The correlations between tumor-ablation zone overlap and survival/local recurrence support the use of pre- and post-ablation image registration to verify coverage or predict recurrence.

## CLINICAL RELEVANCE/APPLICATION

Image assessment and registration with ablation may support standardization, quality control, and outcome prediction. Understanding the factors contributing to outcome would help tailor treatment approaches.

### W5A-SPiR-4 Percutaneous CT/MRI-US Fusion System Guided Radiofrequency Ablation of Hepatocellular Carcinoma in Difficult Locations: The Feasibility Rate and Mid-term Outcome

Participants

Jae Hyun Kim, MD, Seoul, Korea, Republic Of (*Presenter*) Nothing to Disclose

## PURPOSE

To investigate the feasibility rate and the mid-term outcomes of CT/MRI-US fusion system guided radiofrequency ablation (RFA) of hepatocellular carcinomas (HCCs) in difficult locations and to compare the results with non-difficult HCCs.

## METHODS AND MATERIALS

For this single-center retrospective study, from April 2019 to April 2020, a total of 533 patients with 572 HCCs were referred for CT/MRI-US fusion system guided RFA. The radiologic reports of 533 RFA planning US were reviewed in terms of the feasibility rate. The difficult locations were defined as follows: tumors located 1) = 5 mm from major vessels or bile ducts; 2) = 5 mm from diaphragm, colon, stomach, or right kidney; 3) = 1cm from pericardium. We calculated cumulative incidences of local tumor progression (LTP) by using Kaplan-Meier method between patients with HCCs in difficult locations and patients with non-difficult HCCs. LTP rates between two groups were compared by the chi-squared test. The patients with less than three months follow-up were excluded from these analyses.

## RESULTS

In 499 of 533 (93.6%) RFA planning US, percutaneous RFA of HCC was feasible. Among 499 HCC patients (mean tumor size=15.8 mm  $\pm$  0.60) who were feasible for RFA, 261 patients (52.3%) had at least one HCC with difficult location. Of the 499 patients, 10 patients had less than three months follow-up. During the median follow-up period of 28.5 months (range, 3.7-37.3 months), there was no significant difference in LTP rates between patients with difficult HCCs ( $n=251$ ) and patients with non-difficult HCCs ( $n=238$ ) (6.0% [15/251] vs. 6.3% [15/238];  $P=0.881$ ). The 1- and 2-year estimated cumulative incidences of LTP were 3.7% and 5.9% in patients with difficult HCCs; and 2.6% and 5.9% in patients with non-difficult HCCs.

## CONCLUSION

HCCs in difficult locations for RFA could be treated effectively with CT/MRI-US fusion system guided RFA, and there was no significant difference in LTP rates between patients with difficult HCCs and patients with non-difficult HCCs.

## CLINICAL RELEVANCE/APPLICATION

CT/MRI-US fusion system guided RFA could increase the feasibility rate and clinical outcomes of HCCs in difficult locations.

### W5A-SPiR-5 Percutaneous Cryoablation for Extra-Abdominal Desmoid Tumors: A Systematic Review

Participants

Tushar Garg, MD, Baltimore, MD (*Presenter*) Conference Travel, Siemens Healthineers

## PURPOSE

To systematically review the literature published on percutaneous cryoablation for the treatment of extra-abdominal desmoid (EAD) tumor and assess its safety and efficacy.

## METHODS AND MATERIALS

Using three databases, a systematic review was performed following Preferred Reporting Items for Systematic Reviews and Meta-analyses (PRISMA) guidelines. The search strategy used was "cryo\*" [All Fields] AND ("fibromatosis, aggressive" [MeSH Terms] OR ("fibromatosis" [All Fields] AND "aggressive" [All Fields]) OR "aggressive fibromatosis" [All Fields] OR "desmoid" [All Fields] OR "desmoids" [All Fields]). From all the articles the type of study, mean age of patients, number of patients, number of EAD tumor, EAD tumor size before cryoablation, follow-up characteristics, treatment results, and complications were recorded in Microsoft Excel and analyzed using IBM SPSS software (Armonk, NY).

## RESULTS

A total of ten studies with eight retrospective chart reviews and two prospective studies were included in the final analysis. A total of 219 patients were enrolled between ten studies and included 247 EAD tumors. The mean age of patients in the studies ranged from 24.2 to 41 years and the tumour volume ranged from 38.6 cm<sup>3</sup> to 258.6 cm<sup>3</sup>. A total of 284 procedures were performed with 79 (36.07%) patients undergoing cryoablation as the primary procedure. The mean imaging follow-up ranged from 11.3 to 53.7 months and was done with either CT or MRI. Complete response was seen in 74 (35.9%) tumors, partial response in 60 (32.25%) tumors, and disease progression or recurrence in 47 (21.86%) tumors. 91.3% (138) patients had symptoms prior to cryoablation due to EAD tumor and 88.4% (122) patients showed improvement in symptoms after the procedure. Only 17.82% of procedures were associated with complications with an even lower incidence of serious complications.

## CONCLUSION

Current data from the studies show that cryoablation is safe and well-tolerated in select patients with EAD tumors. Combining

open surgery with an image-guided approach can reduce adverse events, but further evaluation of the effect of this approach on treatment outcomes is needed. .

#### **CLINICAL RELEVANCE/APPLICATION**

Prospective investigations with long-term follow-up are required to further clarify the efficacy and safety profile of cryoablation and further establish its place in the treatment of EAD tumors

#### **W5A-SP1R-7 An Investigation on Clinical Usefulness of Motion Compensation of Cone-beam Computed Tomography for Trans-arterial Chemoembolization**

Participants

JANG SOON HWANG, (*Presenter*) Nothing to Disclose

#### **PURPOSE**

To evaluate the effect of a motion artifact correction algorithm (MACA) on C-arm computed tomography (CT) during transarterial chemoembolization (TACE) for hepatic malignancies.

#### **METHODS AND MATERIALS**

Among 769 patients who underwent TACE in a dedicated angiroom from June 2020 to March 2021, 42 patients with identifiable motion artifacts on their single C-arm CT scans were retrospectively evaluated. The image qualities of the native and motion-corrected data were compared using both qualitative and quantitative methods. The maximum intensity, sharpness, and diameter of the five segmental hepatic arteries were measured quantitatively using software. The overall quality of maximum intensity projection (MIP) images and conspicuity of tumor-supplying arteries were qualitatively graded by two independent readers. Paired t-tests and Wilcoxon signed-rank tests were used to compare the quantitative and qualitative parameters of native and motion corrected image sets. Inter-reader agreements of the qualitative measurements were addressed using a quadratic weighted kappa test.

#### **RESULTS**

The mean maximum intensity and sharpness of the hepatic arteries increased from  $2792.01 \pm 451.36$  HU to  $3148.40 \pm 594.46$  HU and from  $0.31 \pm 0.02$  /mm to  $0.34 \pm 0.02$  /mm, respectively, using MACA ( $p < 0.001$  and  $p < 0.001$ , respectively). In the same line, MACA decreased the mean diameter from  $2.02 \pm 0.27$  mm to  $1.78 \pm 0.26$  mm ( $p < 0.001$ ), suggesting improved vessel conspicuity with less blurred contours by motion compensation. With a regard to the qualitative analyses, inter-reader agreement was substantially beyond chance in both MIP images (weighted  $\kappa$ , 0.818; 95% confidence interval, 0.771-0.866) and tumor-supplying artery (weighted  $\kappa$ , .810; 95% confidence interval, 0.759 - 0.861) evaluation. The overall quality of the MIP images and conspicuity of the tumor-supplying artery were enhanced from 2.5-point to 3.0-point and the from 3.0-point to 4.0-point by MACA ( $p < 0.001$  and  $p < 0.001$ , respectively).

#### **CONCLUSION**

s MACA significantly improved both quantitative and qualitative image quality in patients with hepatic malignancies treated with TACE.

#### **CLINICAL RELEVANCE/APPLICATION**

A motion artifact correction algorithm can improve the quality of C-arm CT images degraded by motion artifact in patients treated with TACE, suggesting potential improvement of procedural outcomes.

#### **W5A-SP1R-8 Efficacy and Safety of DEB-TACE Plus Idarubicin Versus Epirubicin for Unresectable Hepatocellular Carcinoma**

Participants

Jiaping Li, Guangzhou, China (*Presenter*) Nothing to Disclose

#### **PURPOSE**

Drug-eluting beads transarterial chemoembolization (DEB-TACE) is one of the standard treatments for unresectable hepatocellular carcinoma (HCC), while the efficacy of epirubicin-loaded DEB-TACE remains unsatisfactory. Recent studies indicated idarubicin's remarkable effect on HCC. This study aimed to compare effectiveness and safety between idarubicin and epirubicin as the chemotherapeutic agent in DEB-TACE for unresectable HCC.

#### **METHODS AND MATERIALS**

This study included patients with unresectable HCC from January 2019 to May 2020 who received idarubicin-loaded DEB-TACE (IT group, n=111) or epirubicin-loaded DEB-TACE (ET group, n=117). Overall survival (OS), progression-free survival (PFS), local response and adverse events (AEs) were compared between the two groups.

#### **RESULTS**

Altogether 228 (55±12 years old, 203 men) consecutive cases were recruited. OS rates at 6 months were 91.6% and 60.8% in IT and ET groups; at 12 months, 68.4% and 42.8%. Median PFS rates were 7.9 and 2.6 months in IT and ET groups ( $P < 0.001$ ). Platelet count (OS: HR=0.45, PFS: HR=0.60), portal vein tumor thrombus (OS: HR=1.68, PFS: HR=1.91), and idarubicin treatment (OS: HR=3.60, PFS: HR=2.66) were independent predictors of OS and PFS (all  $P < 0.05$ ). Subgroup analysis suggested that ET group was superior to IT group in the subgroup with tumor size  $> 10$  cm (OS: HR=5.33,  $P=0.002$ ; PFS: HR=2.60,  $P=0.004$ ). AEs were consistent in both groups, and there were no Grade 3 or 4 adverse events.

#### **CONCLUSION**

s Idarubicin is a more effective and safer chemotherapeutic agent in DEB-TACE for the treatment of unresectable HCC.

#### **CLINICAL RELEVANCE/APPLICATION**

1.Idarubicin-loaded DEB-TACE is well-tolerated and safe for unresectable HCC.2.Idarubicin-loaded DEB-TACE is superior to doxorubicin-loaded DEB-TACE in survival improvement.3.Idarubicin-loaded DEB-TACE might be a new therapeutic option for

unresectable HCC.

Printed on: 02/07/23

## Abstract Archives of the RSNA, 2022

W5A-SP1R-1

### Feasibility, Safety and Outcomes of Thermal Ablation of Kidney Cancer in the Elderly

Wednesday, Nov. 30 12:15PM - 12:45PM Room: Learning Center - IR DPS

#### Participants

Wenhui Zhou, MD, PhD, Menlo Park, CA (*Presenter*) Nothing to Disclose

#### PURPOSE

When renal cell carcinoma is diagnosed in patients of advanced age, patient co-morbidities may limit treatment options active surveillance only. This study assessed the technical results, procedural complications and survival outcome of thermal ablation in patients greater than 80 years of age diagnosed with stage T1 RCC.

#### METHODS AND MATERIALS

A retrospective analysis was performed of 113 patients greater than 80 years of age who underwent computed tomography-guided thermal ablations for 126 biopsy-proven T1N0M0 renal cell carcinoma (mean size = 3.2 cm, size SD = 1.3 cm) between October 2008 and March 2020. The rates of technical success, peri- and post-procedural complications, residual disease and local recurrence were examined. The Kaplan-Meier method was used to compute overall and cancer-specific survival.

#### RESULTS

Of the 103 elderly patients treated, the median age = 85 yrs, (range = 80 to 95 yrs) were treated and mean Charlson comorbidity index score was 3.8 (SD = 1.3). Technical success was achieved in all of the patients. Asymptomatic perinephric hematoma (Clavien-Dindo Grade I) was the most common complication, occurring in 23% of patients. Ureteral stricture requiring stent placement was the only major complication, and occurred in 2% of patients. Primary technique efficacy was achieved in 89% of cases. At 1, 3 and 5 years post-ablation, the overall survival rates were 98%, 85%, and 80%, RCC-specific survival rates were 100%, 100% and 98%, and local progression-free survival rates were 100%, 95%, and 92%, respectively.

#### CONCLUSION

Renal ablation appears technically feasible, well-tolerated and effective in treating stage T1 renal cell carcinoma in elderly patients. Small asymptomatic perinephric hematomas are a common complication following this procedure in this population.

#### CLINICAL RELEVANCE/APPLICATION

Thermal ablation may be an effective non-surgical alternative to nephrectomy or active surveillance for elderly patients diagnosed with renal cell carcinomas. For elderly patients motivated to pursue minimally invasive treatment for renal cell carcinoma, thermal ablation should be considered.

Printed on: 02/07/23

## Abstract Archives of the RSNA, 2022

W5A-SP1R-3

### Ablation Margin and Tumor Morphology Metrics from a Randomized Controlled Drug + Device Trial in 3-7 cm Hepatocellular Carcinoma

Wednesday, Nov. 30 12:15PM - 12:45PM Room: Learning Center - IR DPS

#### Participants

Katerina Lee, BS, Cedar Park, TX (*Presenter*) Nothing to Disclose

#### PURPOSE

We studied the factors associated with differences in local recurrence and survival in a clinical trial of patients with hepatocellular carcinoma (HCC) who underwent radiofrequency ablation (RFA).

#### METHODS AND MATERIALS

550 patients from the OPTIMA Trial (with solitary HCC lesions  $\leq 3$  but  $\geq 7$ cm, randomized to RFA or RFA+LTLD) were screened for well-defined tumor imaging on pre-RFA CT. 242 pre-ablation tumors and 338 post-ablation (28 days) de-vascularized volumes were manually segmented (3D Slicer). 187 pairs of corresponding pre-ablation and post-ablation CT scans were registered with General Registration (Elastix), and structural similarity was calculated in MatLab to assess registration quality (average 99.3% similarity) (Fig 1). Dice similarity metrics were recorded from the Radiotherapy Segment Comparison module. Segmented tumor and ablation zone overlap were used to define undertreated tumor and treated tumor (percent and absolute volume) (Fig 2). Multiple tumor morphology metrics were determined (3DSlicer MatLab). Relationships between these variables were analyzed using R. "Disease progression classes" were initially: complete response/no evidence of disease progression, distant hepatic recurrence, extrahepatic recurrence, incomplete response, local recurrence. These were further split into 2 final classes: Local recurrence (Yes or No). Survival data was analyzed for 122.

#### RESULTS

Univariate multinomial logistic regression showed significance between "local recurrence" and volume ( $p=.004$ ) and surface area ( $p=.002$ ). Multivariate analysis revealed a significant relationship between "local recurrence" and age ( $p=0.0478$ ). Univariate analysis had significance with age ( $p=0.01$ ) and absolute overlap volume ( $p=0.02$ ). For survival (deceased vs alive at end of trial), there was a significant trend/relationship with age ( $p=0.0098$ ), percent overlap ( $p=.05$ ), and absolute undertreated volume ( $p=0.055$ ) from univariate logistic regression.

#### CONCLUSION

The correlations between tumor-ablation zone overlap and survival/local recurrence support the use of pre- and post-ablation image registration to verify coverage or predict recurrence.

#### CLINICAL RELEVANCE/APPLICATION

Image assessment and registration with ablation may support standardization, quality control, and outcome prediction. Understanding the factors contributing to outcome would help tailor treatment approaches.

Printed on: 02/07/23

## Abstract Archives of the RSNA, 2022

W5A-SP1R-4

### **Percutaneous CT/MRI-US Fusion System Guided Radiofrequency Ablation of Hepatocellular Carcinoma in Difficult Locations: The Feasibility Rate and Mid-term Outcome**

Wednesday, Nov. 30 12:15PM - 12:45PM Room: Learning Center - IR DPS

#### **Participants**

Jae Hyun Kim, MD, Seoul, Korea, Republic Of (*Presenter*) Nothing to Disclose

#### **PURPOSE**

To investigate the feasibility rate and the mid-term outcomes of CT/MRI-US fusion system guided radiofrequency ablation (RFA) of hepatocellular carcinomas (HCCs) in difficult locations and to compare the results with non-difficult HCCs.

#### **METHODS AND MATERIALS**

For this single-center retrospective study, from April 2019 to April 2020, a total of 533 patients with 572 HCCs were referred for CT/MRI-US fusion system guided RFA. The radiologic reports of 533 RFA planning US were reviewed in terms of the feasibility rate. The difficult locations were defined as follows: tumors located 1) = 5 mm from major vessels or bile ducts; 2) = 5 mm from diaphragm, colon, stomach, or right kidney; 3) = 1cm from pericardium. We calculated cumulative incidences of local tumor progression (LTP) by using Kaplan-Meier method between patients with HCCs in difficult locations and patients with non-difficult HCCs. LTP rates between two groups were compared by the chi-squared test. The patients with less than three months follow-up were excluded from these analyses.

#### **RESULTS**

In 499 of 533 (93.6%) RFA planning US, percutaneous RFA of HCC was feasible. Among 499 HCC patients (mean tumor size=15.8 mm  $\pm$  0.60) who were feasible for RFA, 261 patients (52.3%) had at least one HCC with difficult location. Of the 499 patients, 10 patients had less than three months follow-up. During the median follow-up period of 28.5 months (range, 3.7-37.3 months), there was no significant difference in LTP rates between patients with difficult HCCs (n=251) and patients with non-difficult HCCs (n=238) (6.0% [15/251] vs. 6.3% [15/238]; P=0.881). The 1- and 2-year estimated cumulative incidences of LTP were 3.7% and 5.9% in patients with difficult HCCs; and 2.6% and 5.9% in patients with non-difficult HCCs.

#### **CONCLUSION**

s HCCs in difficult locations for RFA could be treated effectively with CT/MRI-US fusion system guided RFA, and there was no significant difference in LTP rates between patients with difficult HCCs and patients with non-difficult HCCs.

#### **CLINICAL RELEVANCE/APPLICATION**

CT/MRI-US fusion system guided RFA could increase the feasibility rate and clinical outcomes of HCCs in difficult locations.

Printed on: 02/07/23

## Abstract Archives of the RSNA, 2022

W5A-SP1R-5

### Percutaneous Cryoablation for Extra-Abdominal Desmoid Tumors: A Systematic Review

Wednesday, Nov. 30 12:15PM - 12:45PM Room: Learning Center - IR DPS

#### Participants

Tushar Garg, MD, Baltimore, MD (*Presenter*) Conference Travel, Siemens Healthineers

#### PURPOSE

To systematically review the literature published on percutaneous cryoablation for the treatment of extra-abdominal desmoid (EAD) tumor and assess its safety and efficacy.

#### METHODS AND MATERIALS

Using three databases, a systematic review was performed following Preferred Reporting Items for Systematic Reviews and Meta-analyses (PRISMA) guidelines. The search strategy used was "cryo\*" [All Fields] AND ("fibromatosis, aggressive" [MeSH Terms] OR ("fibromatosis" [All Fields] AND "aggressive" [All Fields])) OR "aggressive fibromatosis" [All Fields] OR "desmoid" [All Fields] OR "desmoids" [All Fields]. From all the articles the type of study, mean age of patients, number of patients, number of EAD tumor, EAD tumor size before cryoablation, follow-up characteristics, treatment results, and complications were recorded in Microsoft Excel and analyzed using IBM SPSS software (Armonk, NY).

#### RESULTS

A total of ten studies with eight retrospective chart reviews and two prospective studies were included in the final analysis. A total of 219 patients were enrolled between ten studies and included 247 EAD tumors. The mean age of patients in the studies ranged from 24.2 to 41 years and the tumour volume ranged from 38.6 cm<sup>3</sup> to 258.6 cm<sup>3</sup>. A total of 284 procedures were performed with 79 (36.07%) patients undergoing cryoablation as the primary procedure. The mean imaging follow-up ranged from 11.3 to 53.7 months and was done with either CT or MRI. Complete response was seen in 74 (35.9%) tumors, partial response in 60 (32.25%) tumors, and disease progression or recurrence in 47 (21.86%) tumors. 91.3% (138) patients had symptoms prior to cryoablation due to EAD tumor and 88.4% (122) patients showed improvement in symptoms after the procedure. Only 17.82% of procedures were associated with complications with an even lower incidence of serious complications.

#### CONCLUSION

Current data from the studies show that cryoablation is safe and well-tolerated in select patients with EAD tumors. Combining open surgery with an image-guided approach can reduce adverse events, but further evaluation of the effect of this approach on treatment outcomes is needed.

#### CLINICAL RELEVANCE/APPLICATION

Prospective investigations with long-term follow-up are required to further clarify the efficacy and safety profile of cryoablation and further establish its place in the treatment of EAD tumors

Printed on: 02/07/23

## Abstract Archives of the RSNA, 2022

W5A-SP1R-7

### An Investigation on Clinical Usefulness of Motion Compensation of Cone-beam Computed Tomography for Trans-arterial Chemoembolization

Wednesday, Nov. 30 12:15PM - 12:45PM Room: Learning Center - IR DPS

#### Participants

JANG SOON HWANG, (*Presenter*) Nothing to Disclose

#### PURPOSE

To evaluate the effect of a motion artifact correction algorithm (MACA) on C-arm computed tomography (CT) during transarterial chemoembolization (TACE) for hepatic malignancies.

#### METHODS AND MATERIALS

Among 769 patients who underwent TACE in a dedicated angiroom from June 2020 to March 2021, 42 patients with identifiable motion artifacts on their single C-arm CT scans were retrospectively evaluated. The image qualities of the native and motion-corrected data were compared using both qualitative and quantitative methods. The maximum intensity, sharpness, and diameter of the five segmental hepatic arteries were measured quantitatively using software. The overall quality of maximum intensity projection (MIP) images and conspicuity of tumor-supplying arteries were qualitatively graded by two independent readers. Paired t-tests and Wilcoxon signed-rank tests were used to compare the quantitative and qualitative parameters of native and motion corrected image sets. Inter-reader agreements of the qualitative measurements were addressed using a quadratic weighted kappa test.

#### RESULTS

The mean maximum intensity and sharpness of the hepatic arteries increased from  $2792.01 \pm 451.36$  HU to  $3148.40 \pm 594.46$  HU and from  $0.31 \pm 0.02$  /mm to  $0.34 \pm 0.02$  /mm, respectively, using MACA ( $p < 0.001$  and  $p < 0.001$ , respectively). In the same line, MACA decreased the mean diameter from  $2.02 \pm 0.27$  mm to  $1.78 \pm 0.26$  mm ( $p < 0.001$ ), suggesting improved vessel conspicuity with less blurred contours by motion compensation. With a regard to the qualitative analyses, inter-reader agreement was substantially beyond chance in both MIP images (weighted  $\kappa$ , 0.818; 95% confidence interval, 0.771-0.866) and tumor-supplying artery (weighted  $\kappa$ , .810; 95% confidence interval, 0.759 - 0.861) evaluation. The overall quality of the MIP images and conspicuity of the tumor-supplying artery were enhanced from 2.5-point to 3.0-point and the from 3.0-point to 4.0-point by MACA ( $p < 0.001$  and  $p < 0.001$ , respectively).

#### CONCLUSION

s MACA significantly improved both quantitative and qualitative image quality in patients with hepatic malignancies treated with TACE.

#### CLINICAL RELEVANCE/APPLICATION

A motion artifact correction algorithm can improve the quality of C-arm CT images degraded by motion artifact in patients treated with TACE, suggesting potential improvement of procedural outcomes.

Printed on: 02/07/23

## Abstract Archives of the RSNA, 2022

W5A-SP1R-8

### Efficacy and Safety of DEB-TACE Plus Idarubicin Versus Epirubicin for Unresectable Hepatocellular Carcinoma

Wednesday, Nov. 30 12:15PM - 12:45PM Room: Learning Center - IR DPS

#### Participants

Jiaping Li, Guangzhou, China (*Presenter*) Nothing to Disclose

#### PURPOSE

Drug-eluting beads transarterial chemoembolization (DEB-TACE) is one of the standard treatments for unresectable hepatocellular carcinoma (HCC), while the efficacy of epirubicin-loaded DEB-TACE remains unsatisfactory. Recent studies indicated idarubicin's remarkable effect on HCC. This study aimed to compare effectiveness and safety between idarubicin and epirubicin as the chemotherapeutic agent in DEB-TACE for unresectable HCC.

#### METHODS AND MATERIALS

This study included patients with unresectable HCC from January 2019 to May 2020 who received idarubicin-loaded DEB-TACE (IT group, n=111) or epirubicin-loaded DEB-TACE (ET group, n=117). Overall survival (OS), progression-free survival (PFS), local response and adverse events (AEs) were compared between the two groups.

#### RESULTS

Altogether 228 (55±12 years old, 203 men) consecutive cases were recruited. OS rates at 6 months were 91.6% and 60.8% in IT and ET groups; at 12 months, 68.4% and 42.8%. Median PFS rates were 7.9 and 2.6 months in IT and ET groups ( $P<0.001$ ). Platelet count (OS: HR=0.45, PFS: HR=0.60), portal vein tumor thrombus (OS: HR=1.68, PFS: HR=1.91), and idarubicin treatment (OS: HR=3.60, PFS: HR=2.66) were independent predictors of OS and PFS (all  $P<0.05$ ). Subgroup analysis suggested that ET group was superior to IT group in the subgroup with tumor size >10 cm (OS: HR=5.33,  $P=0.002$ ; PFS: HR=2.60,  $P=0.004$ ). AEs were consistent in both groups, and there were no Grade 3 or 4 adverse events.

#### CONCLUSION

s Idarubicin is a more effective and safer chemotherapeutic agent in DEB-TACE for the treatment of unresectable HCC.

#### CLINICAL RELEVANCE/APPLICATION

1. Idarubicin-loaded DEB-TACE is well-tolerated and safe for unresectable HCC. 2. Idarubicin-loaded DEB-TACE is superior to doxorubicin-loaded DEB-TACE in survival improvement. 3. Idarubicin-loaded DEB-TACE might be a new therapeutic option for unresectable HCC.

Printed on: 02/07/23

## Abstract Archives of the RSNA, 2022

W5A-SPMK

### Musculoskeletal Wednesday Poster Discussions - A

Wednesday, Nov. 30 12:15PM - 12:45PM Room: Learning Center - MK DPS

#### Sub-Events

#### W5A-SPMK- Natural History of Progression of Gluteal Tendon Tears Using MRI

1

Participants

Zachary Pryor, MD, (*Presenter*) Nothing to Disclose

#### PURPOSE

To identify imaging features predictive of progression of gluteal tendinopathy to guide clinicians on optimal period of intervention.

#### METHODS AND MATERIALS

Noncontrast MRI hip/bony pelvis exams at 1.5T were retrospectively reviewed between 2003-2021 on patients >40 years old. Patients meeting inclusion criteria had two MRIs performed >6 months and <10 years apart. Patients were excluded for prior surgery, trauma, osteonecrosis, malignancy, or complete gluteal tear on initial imaging. Axial T2 FS and coronal T1 and STIR sequences were used to grade gluteus medius pathology as follows: tendinosis, low-grade partial thickness (PT) tear, high-grade PT tear, complete tear. Greater trochanteric bursitis was graded as none, mild, moderate, severe. Muscle atrophy on coronal T1 weighted sequence was categorized by Goutallier classification. Tensor fasciae latae angle (TFLA) was calculated between the anterior superior iliac spine, greater trochanter and TFL. Progression of tendon pathology on subsequent exam was assessed and statistical analysis performed.

#### RESULTS

45 hips met inclusion criteria for the study, 27% of which were male and with a mean age of  $67.8 \pm 10.8$ . The mean interval between the two MRI exams was  $32.3 \pm 20.7$  months. 19/45 patients presented with low-grade PT tears, of which 10 progressed to high-grade on subsequent exam. The proportion of progression in patients presenting with low-grade PT tearing was greater than those with either tendinosis or high-grade tearing ( $p=0.02$ ). Degree of bursitis on initial MRI was associated with tendinopathy progression ( $p=0.036$ ). Patients with TFLA <162° had higher rate of tendinopathy progression ( $p=0.0224$ ).

#### CONCLUSION

Gluteus medius tendinopathy is more likely to progress when initially present with concomitant greater trochanteric bursitis and narrowed TFLA, which may contribute to extrinsic compressive force.

#### CLINICAL RELEVANCE/APPLICATION

Special attention recommended to the presence of low-grade PT tears and hips experiencing greater extrinsic compressive forces as these were more likely to progress on subsequent exam.

#### W5A-SPMK- Impact of Photon-counting-detector CT on Radiation Dose Reduction for Femoroacetabular Impingement Evaluation

3

Participants

Dennis Adaaquah, MD, Rochester, MN (*Presenter*) Nothing to Disclose

#### PURPOSE

To demonstrate feasibility of ultra-high-resolution (UHR) low-dose photon-counting detector (PCD) CT imaging of the pelvis for radiologic evaluation and surgical planning for femoroacetabular impingement (FAI).

#### METHODS AND MATERIALS

Patients who underwent a standard dose energy-integrating detector (EID) CT (SOMATOM Edge or Force, Siemens Healthcare) of the pelvis for FAI evaluation were recruited to undergo the same exam on a PCD-CT system (NAEOTOM Alpha, Siemens) in UHR mode. PCD-CT exams were acquired at either the same dose as the EID-CT or 50% dose. Simulated 50% dose EID-CT images were generated with noise insertion algorithms, for a total of 3 image sets per patient. Matched multiplanar reconstructions (Br62/64, 1 mm thickness) were generated for both the EID-CT and the PCD-CT exams. Two fellowship-trained musculoskeletal radiologists independently evaluated randomized EID-CT and PCD-CT images, blinded to CT system and radiation dose. Alpha angle and acetabular version measurements were computed for each image. Radiologist perception of image quality based on image noise, artifacts, and bone cortex visualization as well as confidence in non-FAI pathology was rated on 4-point scale (3 = adequate for diagnostic task). Preference tests of (1) PCD-CT at standard dose, (2) PCD-CT at 50% dose, and (3) EID-CT at 50% dose relative to standard dose EID-CT were performed using Wilcoxon Rank test.

#### RESULTS

20 patients underwent pelvis CTs (mean CT DIvol = 4.5 mGy (standard dose EID-CT, N=20); 4.0 mGy (standard dose PCD-CT,

N=10); and 2.6 mGy (half-dose PCD-CT, N=10)). Three patients had bilateral exams that were independently reviewed, for a total of 69 unique image sets. Standard dose EID-CT images were consistently scored as adequate for diagnostic task in all categories (range 2.8-2.9). Simulated half-dose EID-CT images received significantly lower average scores in all categories (range 1.8-2.3,  $p<0.001$ ). Conversely, PCD-CT images at standard dose were scored significantly higher than the reference EID-CT (range 3.4-4,  $p<0.05$ ). Finally, half-dose PCD-CT images were scored significantly higher than the standard EID-CT for noise and cortex visualization ( $p<0.05$ ), and equivalent for artifact and visualization of non-FAI pathology ( $p>0.05$ ).

#### **CONCLUSION**

s UHR-PCD-CT at matched radiation dose is superior to EID-CT for FAI evaluation. PCD-CT enables 50% radiation dose reduction compared to EID while still being diagnostically adequate for FAI evaluation.

#### **CLINICAL RELEVANCE/APPLICATION**

Evaluation of FAI tends to involve young patients. The lower noise intrinsic of UHR-PCD-CT compared to EID-CT can be leveraged for 50% radiation dose reduction for FAI imaging, without compromising image quality and diagnostic certainty.

Printed on: 02/07/23

## Abstract Archives of the RSNA, 2022

W5A-SPMK-1

### Natural History of Progression of Gluteal Tendon Tears Using MRI

Wednesday, Nov. 30 12:15PM - 12:45PM Room: Learning Center - MK DPS

#### Participants

Zachary Pryor, MD, (*Presenter*) Nothing to Disclose

#### PURPOSE

To identify imaging features predictive of progression of gluteal tendinopathy to guide clinicians on optimal period of intervention.

#### METHODS AND MATERIALS

Noncontrast MRI hip/bony pelvis exams at 1.5T were retrospectively reviewed between 2003-2021 on patients >40 years old. Patients meeting inclusion criteria had two MRIs performed >6 months and <10 years apart. Patients were excluded for prior surgery, trauma, osteonecrosis, malignancy, or complete gluteal tear on initial imaging. Axial T2 FS and coronal T1 and STIR sequences were used to grade gluteus medius pathology as follows: tendinosis, low-grade partial thickness (PT) tear, high-grade PT tear, complete tear. Greater trochanteric bursitis was graded as none, mild, moderate, severe. Muscle atrophy on coronal T1 weighted sequence was categorized by Goutallier classification. Tensor fasciae latae angle (TFLA) was calculated between the anterior superior iliac spine, greater trochanter and TFL. Progression of tendon pathology on subsequent exam was assessed and statistical analysis performed.

#### RESULTS

45 hips met inclusion criteria for the study, 27% of which were male and with a mean age of  $67.8 \pm 10.8$ . The mean interval between the two MRI exams was  $32.3 \pm 20.7$  months. 19/45 patients presented with low-grade PT tears, of which 10 progressed to high-grade on subsequent exam. The proportion of progression in patients presenting with low-grade PT tearing was greater than those with either tendinosis or high-grade tearing ( $p=0.02$ ). Degree of bursitis on initial MRI was associated with tendinopathy progression ( $p=0.036$ ). Patients with TFLA <162° had higher rate of tendinopathy progression ( $p=0.0224$ ).

#### CONCLUSION

s Gluteus medius tendinopathy is more likely to progress when initially present with concomitant greater trochanteric bursitis and narrowed TFLA, which may contribute to extrinsic compressive force.

#### CLINICAL RELEVANCE/APPLICATION

Special attention recommended to the presence of low-grade PT tears and hips experiencing greater extrinsic compressive forces as these were more likely to progress on subsequent exam.

Printed on: 02/07/23

## Abstract Archives of the RSNA, 2022

W5A-SPMK-3

### Impact of Photon-counting-detector CT on Radiation Dose Reduction for Femoroacetabular Impingement Evaluation

Wednesday, Nov. 30 12:15PM - 12:45PM Room: Learning Center - MK DPS

#### Participants

Dennis Adaaquah, MD, Rochester, MN (*Presenter*) Nothing to Disclose

#### PURPOSE

To demonstrate feasibility of ultra-high-resolution (UHR) low-dose photon-counting detector (PCD) CT imaging of the pelvis for radiologic evaluation and surgical planning for femoroacetabular impingement (FAI).

#### METHODS AND MATERIALS

Patients who underwent a standard dose energy-integrating detector (EID) CT (SOMATOM Edge or Force, Siemens Healthcare) of the pelvis for FAI evaluation were recruited to undergo the same exam on a PCD-CT system (NAEOTOM Alpha, Siemens) in UHR mode. PCD-CT exams were acquired at either the same dose as the EID-CT or 50% dose. Simulated 50% dose EID-CT images were generated with noise insertion algorithms, for a total of 3 image sets per patient. Matched multiplanar reconstructions (Br62/64, 1 mm thickness) were generated for both the EID-CT and the PCD-CT exams. Two fellowship-trained musculoskeletal radiologists independently evaluated randomized EID-CT and PCD-CT images, blinded to CT system and radiation dose. Alpha angle and acetabular version measurements were computed for each image. Radiologist perception of image quality based on image noise, artifacts, and bone cortex visualization as well as confidence in non-FAI pathology was rated on 4-point scale (3 = adequate for diagnostic task). Preference tests of (1) PCD-CT at standard dose, (2) PCD-CT at 50% dose, and (3) EID-CT at 50% dose relative to standard dose EID-CT were performed using Wilcoxon Rank test.

#### RESULTS

20 patients underwent pelvis CTs (mean CTDIvol = 4.5 mGy (standard dose EID-CT, N=20); 4.0 mGy (standard dose PCD-CT, N=10); and 2.6 mGy (half-dose PCD-CT, N=10)). Three patients had bilateral exams that were independently reviewed, for a total of 69 unique image sets. Standard dose EID-CT images were consistently scored as adequate for diagnostic task in all categories (range 2.8-2.9). Simulated half-dose EID-CT images received significantly lower average scores in all categories (range 1.8-2.3,  $p < 0.001$ ). Conversely, PCD-CT images at standard dose were scored significantly higher than the reference EID-CT (range 3.4-4,  $p < 0.05$ ). Finally, half-dose PCD-CT images were scored significantly higher than the standard EID-CT for noise and cortex visualization ( $p < 0.05$ ), and equivalent for artifact and visualization of non-FAI pathology ( $p > 0.05$ ).

#### CONCLUSION

s UHR-PCD-CT at matched radiation dose is superior to EID-CT for FAI evaluation. PCD-CT enables 50% radiation dose reduction compared to EID while still being diagnostically adequate for FAI evaluation.

#### CLINICAL RELEVANCE/APPLICATION

Evaluation of FAI tends to involve young patients. The lower noise intrinsic of UHR-PCD-CT compared to EID-CT can be leveraged for 50% radiation dose reduction for FAI imaging, without compromising image quality and diagnostic certainty.

Printed on: 02/07/23

## Abstract Archives of the RSNA, 2022

W5A-SPMS

### Multisystem Wednesday Poster Discussion - A

Wednesday, Nov. 30 12:15PM - 12:45PM Room: Learning Center - MS DPS

#### Sub-Events

#### **W5A-SPMS- Development and Validation of CTbased Radiomics Model of PET-negative Residual CT Masses for The Prediction of Relapsefree Survival in Lymphoma Patients Showing Complete Metabolic Response**

#### Participants

Hyun Jin Kim, MD, Seoul, Korea, Republic Of (*Presenter*) Nothing to Disclose

#### PURPOSE

PET-negative residual CT masses (PnRCMs) are usually dismissed as nonviable post-treatment lesions in lymphoma patients showing complete metabolic response (CMR). We aimed to develop and validate CT-based radiomics score of PnRCM for predicting relapse-free survival (RFS) in lymphoma patients showing CMR after first line chemotherapy.

#### METHODS AND MATERIALS

A total 247 patients who showed CMR after completion of first line chemotherapy for PET-avid lymphomas were recruited for model development. Patients with PnRCM were selected in accordance with the Lugano criteria, and 3-D segmentation was done on contrast-enhanced CT. Radiomics features for masses were extracted and radiomics scores were constructed using the Least absolute shrinkage and selection operator analysis. Cox regression analysis was performed with radiomics and clinical parameters (IPI score, age, aggressiveness of lymphoma, and treatment including rituximab). The efficiency of the model was evaluated using area under the curve (AUC). For validation of the model, 154 patients with PnRCM from an outside hospital were recruited and analyzed in the same way.

#### RESULTS

Among the included patients, 76 patients (30.1%) had PnRCM in the development cohort. Kaplan-Meier analysis showed that patients with PnRCM had significantly shorter RFS ( $p=0.009$ ) than those without PnRCM. In Kaplan-Meier analysis using the cutoff value generated by maximally selected rank statistics, high radiomics score group showed significantly shorter RFS ( $p=0.0016$ ). Multivariate Cox regression analysis also showed that IPI score (hazard ratio [HR]=0.249;  $p=0.006$ ), treatment including rituximab (HR=3.517, 5.193;  $p=0.007$ , 0.006) and radiomics score (HR=3.047;  $p=0.002$ ) were related factors for RFS. In estimating RFS, the radiomics model and combined model showed an AUC of 0.74 and 0.80, respectively. In the validation cohort, the radiomics model and the combined model showed an AUC of 0.73 and 0.82 respectively.

#### CONCLUSION

The combined model that incorporated both clinical parameters and CT based radiomics score showed good performance in predicting recurrence in lymphoma patients with PnRCM.

#### CLINICAL RELEVANCE/APPLICATION

If the CT-based radiomics model can sensitively detect PnRCM with a high probability of relapse, it will be helpful in determining a patient's treatment strategy.

Printed on: 02/07/23

## Abstract Archives of the RSNA, 2022

W5A-SPMS-1

### Development and Validation of CTbased Radiomics Model of PET-negative Residual CT Masses for The Prediction of Relapsefree Survival in Lymphoma Patients Showing Complete Metabolic Response

Wednesday, Nov. 30 12:15PM - 12:45PM Room: Learning Center - MS DPS

#### Participants

Hyun Jin Kim, MD, Seoul, Korea, Republic Of (*Presenter*) Nothing to Disclose

#### PURPOSE

PET-negative residual CT masses (PnRCMs) are usually dismissed as nonviable post-treatment lesions in lymphoma patients showing complete metabolic response (CMR). We aimed to develop and validate CT-based radiomics score of PnRCM for predicting relapse-free survival (RFS) in lymphoma patients showing CMR after first line chemotherapy.

#### METHODS AND MATERIALS

A total 247 patients who showed CMR after completion of first line chemotherapy for PET-avid lymphomas were recruited for model development. Patients with PnRCM were selected in accordance with the Lugano criteria, and 3-D segmentation was done on contrast-enhanced CT. Radiomics features for masses were extracted and radiomics scores were constructed using the Least absolute shrinkage and selection operator analysis. Cox regression analysis was performed with radiomics and clinical parameters (IPI score, age, aggressiveness of lymphoma, and treatment including rituximab). The efficiency of the model was evaluated using area under the curve (AUC). For validation of the model, 154 patients with PnRCM from an outside hospital were recruited and analyzed in the same way.

#### RESULTS

Among the included patients, 76 patients (30.1%) had PnRCM in the development cohort. Kaplan-Meier analysis showed that patients with PnRCM had significantly shorter RFS ( $p=0.009$ ) than those without PnRCM. In Kaplan-Meier analysis using the cutoff value generated by maximally selected rank statistics, high radiomics score group showed significantly shorter RFS ( $p=0.0016$ ). Multivariate Cox regression analysis also showed that IPI score (hazard ratio [HR]=0.249;  $p=0.006$ ), treatment including rituximab (HR=3.517, 5.193;  $p=0.007, 0.006$ ) and radiomics score (HR=3.047;  $p=0.002$ ) were related factors for RFS. In estimating RFS, the radiomics model and combined model showed an AUC of 0.74 and 0.80, respectively. In the validation cohort, the radiomics model and the combined model showed an AUC of 0.73 and 0.82 respectively.

#### CONCLUSION

s The combined model that incorporated both clinical parameters and CT based radiomics score showed good performance in predicting recurrence in lymphoma patients with PnRCM.

#### CLINICAL RELEVANCE/APPLICATION

If the CT-based radiomics model can sensitively detect PnRCM with a high probability of relapse, it will be helpful in determining a patient's treatment strategy.

Printed on: 02/07/23

## Abstract Archives of the RSNA, 2022

W5A-SPNMMI

### Nuclear Medicine/Molecular Imaging Wednesday Poster Discussion - A

Wednesday, Nov. 30 12:15PM - 12:45PM Room: Learning Center - NMMI DPS

#### Participants

Mary Ellen Koran, MD, PhD, Nashville, TN (*Moderator*) Nothing to Disclose

Mary Ellen Koran, MD, PhD, Nashville, TN (*Moderator*) Nothing to Disclose

Kevin P. Banks, MD, San Antonio, TX (*Moderator*) Nothing to Disclose

Kevin P. Banks, MD, San Antonio, TX (*Moderator*) Nothing to Disclose

#### Sub-Events

#### W5A-SPNMMI-1 Application of Machine Learning Approach Using Clinical and 18F-FDG-PET-based Radiomic Features to Predict Prognosis in Patients with Laryngeal Cancer

#### Participants

Masatoyo Nakajo, MD, PhD, Kagoshima, Japan (*Presenter*) Nothing to Disclose

#### PURPOSE

Laryngeal cancer is one of the most common head and neck cancer. Even with careful treatment, advanced stage disease (T-stage 3-4 tumors) has a significantly worse survival with 3-yr disease specific survival around 50%. Thus, accurate diagnostic methods to predict tumor aggressiveness are needed for pretreatment risk stratification. The purpose of this study was to examine whether the machine learning (ML) approach using 18F-FDG-PET-based radiomic features is useful for predicting prognosis in patients with laryngeal cancer.

#### METHODS AND MATERIALS

This retrospective study included 49 patients with laryngeal cancer who underwent 18F-FDG-PET/CT before treatment. Seven clinical (age, sex, T-stage, N-stage, M-stage, UICC stage, and treatment) and 40 PET-based radiomic features were used to predict disease progression using six different ML algorithms (random forest, neural network, k-nearest neighbors, naïve Bayes, logistic regression, and support vector machine) with a ten-fold cross-validation and stratified sampling method. Each ML algorithm calculated the probability for disease progression. The AUCs were calculated to compare the predictive performances between the conventional SUV-related parameters (SUVmax, MTV, TLG) and the ML algorithms. Survival curves were drawn using the Kaplan-Meier method, and the significance of difference between survival curves was tested using the log-rank test.

#### RESULTS

Of 49 patients, 17 had disease progression. On the ROC analysis for conventional SUV-related parameters, the AUC for predicting progression was 0.64 for SUVmax, 0.65 for MTV and 0.72 for TLG, respectively. Among 6 ML algorithms, the naïve Bayes model was the best performing classifier with highest AUC of 0.83. The AUC of this naïve Bayes model was significantly higher than that of each conventional SUV-related parameter ( $p < 0.05$ , each). In the naïve Bayes model, 5-year PFS was significantly higher in predicted non-progression than predicted progression (83.7% vs. 33.5%,  $p < 0.001$ ).

#### CONCLUSION

The ML approach using clinical and pretreatment 18F-FDG-PET-based radiomic features may be useful for predicting tumor progression in patients with laryngeal cancer.

#### CLINICAL RELEVANCE/APPLICATION

The ML approach using clinical and 18F-FDG-PET-based radiomic features may be more useful than SUV-related parameters for predicting tumor progression in patients with laryngeal cancer.

#### W5A-SPNMMI-2 Fibrin-Targeting Molecular MRI in Inflammatory CNS Disorders

#### Participants

Johannes Lohmeier, MD, (*Presenter*) Nothing to Disclose

#### PURPOSE

Fibrin deposition is a fundamental pathophysiological event in the inflammatory component of various CNS disorders, such as multiple sclerosis (MS) or Alzheimer's disease. Beyond its traditional role in coagulation, fibrin elicits immunoinflammatory changes with oxidative-stress response and activation of CNS-resident/peripheral immune-cells contributing to CNS injury. To investigate if CNS-fibrin deposition can be determined using molecular MRI.

#### METHODS AND MATERIALS

Specificity and efficacy of a peptide-conjugated Gd-based molecular MRI probe (EP2104-R) to visualise and quantify CNS-fibrin deposition were evaluated. Probe efficacy to specifically target CNS-fibrin deposition in murine adoptive-transfer experimental autoimmune encephalomyelitis (EAE), a preclinical model for MS ( $n = 12$ ), was assessed. Findings were validated using IHC and LA-

ICP MS. Deposition of fibrin in neuroinflammatory conditions was investigated and its diagnostic capacity for disease staging and monitoring as well as quantification of immunoinflammatory response was determined. Results were compared using t-tests (two groups) or one-way ANOVA with multiple comparisons test. Linear regression was used to model the relationship between variables.

## **RESULTS**

For the first time (to our knowledge), CNS-fibrin deposition was visualised and quantified in vivo using molecular imaging. Signal enhancement was apparent in EAE lesions even 12 h after administration of EP2104-R due to targeted binding ( $M \pm SD$ ,  $1.07 \pm 0.10$  (baseline) vs.  $0.73 \pm 0.09$  (EP2104-R),  $p = .008$ ), which could be inhibited with an MRI-silent analogue ( $M \pm SD$ ,  $0.60 \pm 0.14$  (EP2104-R) vs.  $0.96 \pm 0.13$  (EP2104-La),  $p = .006$ ). CNS fibrin deposition corresponded to immunoinflammatory activity ( $R^2 = 0.85$ ,  $p < .001$ ) and disability ( $R^2 = 0.81$ ,  $p < .001$ ) in a model for MS, which suggests a clinical role for staging and monitoring. Additionally, EP2104-R showed substantially higher SNR ( $M \pm SD$ ,  $6.6 \pm 1$  (EP2104-R) vs.  $2.7 \pm 0.4$  (gadobutrol),  $p = .004$ ) than clinically used contrast media, which increases sensitivity for lesion detection.

## **CONCLUSION**

s Molecular imaging of CNS-fibrin deposition provides an imaging biomarker for inflammatory CNS pathology, which corresponds to pathophysiological ECM remodelling and disease activity, and yields high signal-to-noise ratio, which can improve diagnostic neuroimaging across several neurological diseases with variable degrees of barrier impairment.

## **CLINICAL RELEVANCE/APPLICATION**

We proposed CNS-fibrin deposition as a non-invasive imaging biomarker for CNS pathology, which is sensitive to disease activity and acts as a surrogate for neuroinflammation and barrier impairment.

Printed on: 02/07/23

## Abstract Archives of the RSNA, 2022

W5A-SPNMMI-1

### Application of Machine Learning Approach Using Clinical and 18F-FDG-PET-based Radiomic Features to Predict Prognosis in Patients with Laryngeal Cancer

Wednesday, Nov. 30 12:15PM - 12:45PM Room: Learning Center - NMMI DPS

#### Participants

Masatoyo Nakajo, MD, PhD, Kagoshima, Japan (*Presenter*) Nothing to Disclose

#### PURPOSE

Laryngeal cancer is one of the most common head and neck cancer. Even with careful treatment, advanced stage disease (T-stage 3-4 tumors) has a significantly worse survival with 3-yr disease specific survival around 50%. Thus, accurate diagnostic methods to predict tumor aggressiveness are needed for pretreatment risk stratification. The purpose of this study was to examine whether the machine learning (ML) approach using 18F-FDG-PET-based radiomic features is useful for predicting prognosis in patients with laryngeal cancer.

#### METHODS AND MATERIALS

This retrospective study included 49 patients with laryngeal cancer who underwent 18F-FDG-PET/CT before treatment. Seven clinical (age, sex, T-stage, N-stage, M-stage, UICC stage, and treatment) and 40 PET-based radiomic features were used to predict disease progression using six different ML algorithms (random forest, neural network, k-nearest neighbors, naïve Bayes, logistic regression, and support vector machine) with a ten-fold cross-validation and stratified sampling method. Each ML algorithm calculated the probability for disease progression. The AUCs were calculated to compare the predictive performances between the conventional SUV-related parameters (SUVmax, MTV, TLG) and the ML algorithms. Survival curves were drawn using the Kaplan-Meier method, and the significance of difference between survival curves was tested using the log-rank test.

#### RESULTS

Of 49 patients, 17 had disease progression. On the ROC analysis for conventional SUV-related parameters, the AUC for predicting progression was 0.64 for SUVmax, 0.65 for MTV and 0.72 for TLG, respectively. Among 6 ML algorithms, the naïve Bayes model was the best performing classifier with highest AUC of 0.83. The AUC of this naïve Bayes model was significantly higher than that of each conventional SUV-related parameter ( $p < 0.05$ , each). In the naïve Bayes model, 5-year PFS was significantly higher in predicted non-progression than predicted progression (83.7% vs. 33.5%,  $p < 0.001$ ).

#### CONCLUSION

The ML approach using clinical and pretreatment 18F-FDG-PET-based radiomic features may be useful for predicting tumor progression in patients with laryngeal cancer.

#### CLINICAL RELEVANCE/APPLICATION

The ML approach using clinical and 18F-FDG-PET-based radiomic features may be more useful than SUV-related parameters for predicting tumor progression in patients with laryngeal cancer.

Printed on: 02/07/23

## Abstract Archives of the RSNA, 2022

W5A-SPNMMI-2

### Fibrin-Targeting Molecular MRI in Inflammatory CNS Disorders

Wednesday, Nov. 30 12:15PM - 12:45PM Room: Learning Center - NMMI DPS

#### Participants

Johannes Lohmeier, MD, (*Presenter*) Nothing to Disclose

#### PURPOSE

Fibrin deposition is a fundamental pathophysiological event in the inflammatory component of various CNS disorders, such as multiple sclerosis (MS) or Alzheimer's disease. Beyond its traditional role in coagulation, fibrin elicits immunoinflammatory changes with oxidative-stress response and activation of CNS-resident/peripheral immune-cells contributing to CNS injury. To investigate if CNS-fibrin deposition can be determined using molecular MRI.

#### METHODS AND MATERIALS

Specificity and efficacy of a peptide-conjugated Gd-based molecular MRI probe (EP2104-R) to visualise and quantify CNS-fibrin deposition were evaluated. Probe efficacy to specifically target CNS-fibrin deposition in murine adoptive-transfer experimental autoimmune encephalomyelitis (EAE), a preclinical model for MS (n = 12), was assessed. Findings were validated using IHC and LA-ICP MS. Deposition of fibrin in neuroinflammatory conditions was investigated and its diagnostic capacity for disease staging and monitoring as well as quantification of immunoinflammatory response was determined. Results were compared using t-tests (two groups) or one-way ANOVA with multiple comparisons test. Linear regression was used to model the relationship between variables.

#### RESULTS

For the first time (to our knowledge), CNS-fibrin deposition was visualised and quantified in vivo using molecular imaging. Signal enhancement was apparent in EAE lesions even 12 h after administration of EP2104-R due to targeted binding ( $M \pm SD$ ,  $1.07 \pm 0.10$  (baseline) vs.  $0.73 \pm 0.09$  (EP2104-R),  $p = .008$ ), which could be inhibited with an MRI-silent analogue ( $M \pm SD$ ,  $0.60 \pm 0.14$  (EP2104-R) vs.  $0.96 \pm 0.13$  (EP2104-La),  $p = .006$ ). CNS fibrin deposition corresponded to immunoinflammatory activity ( $R^2 = 0.85$ ,  $p < .001$ ) and disability ( $R^2 = 0.81$ ,  $p < .001$ ) in a model for MS, which suggests a clinical role for staging and monitoring. Additionally, EP2104-R showed substantially higher SNR ( $M \pm SD$ ,  $6.6 \pm 1$  (EP2104-R) vs.  $2.7 \pm 0.4$  (gadobutrol),  $p = .004$ ) than clinically used contrast media, which increases sensitivity for lesion detection.

#### CONCLUSION

s Molecular imaging of CNS-fibrin deposition provides an imaging biomarker for inflammatory CNS pathology, which corresponds to pathophysiological ECM remodelling and disease activity, and yields high signal-to-noise ratio, which can improve diagnostic neuroimaging across several neurological diseases with variable degrees of barrier impairment.

#### CLINICAL RELEVANCE/APPLICATION

We proposed CNS-fibrin deposition as a non-invasive imaging biomarker for CNS pathology, which is sensitive to disease activity and acts as a surrogate for neuroinflammation and barrier impairment.

Printed on: 02/07/23



## Abstract Archives of the RSNA, 2022

W5A-SPNPM

### Noninterpretive Skills/Quality Improvement/Practice Management Wednesday Poster Discussions - A

Wednesday, Nov. 30 12:15PM - 12:45PM Room: Learning Center - NPM DPS

#### Participants

Tharakeswara Bathala, MD, Houston, TX (*Moderator*) Nothing to Disclose

#### Sub-Events

#### **W5A-SPNPM-2 Impact of COVID-19 Pandemic on Imaging Workload in Radiology; A Case Study of MRI Service in an UK District General Hospital Trust With 1200 Bed Capacity**

#### Participants

Chao Jin Ho, MBChB, BSc, (*Presenter*) Nothing to Disclose

#### PURPOSE

The 2019 coronavirus disease (COVID-19) pandemic has been a global health issue with vast social-economical and human mortality impact. The first UK national lockdown was implemented in 23 March 2020 to curb the spread of COVID-19. This study aims to evaluate the impact of the COVID-19 pandemic on MRI volumes and reporting time by comparing MRI imaging volumes and reporting time before and during the COVID-19 pandemic.

#### METHODS AND MATERIALS

The scan volumes and reporting time of MRI scans performed in four different MRI sites in the Durham and Darlington hospital trust were retrospectively reviewed at three different time periods: 1) pre-pandemic (March to June 2019 or P1) 2) start of the COVID-19 pandemic (March to June 2020 or P2) 3) second year of the COVID-19 pandemic (March to June 2021 or P3) Statistical differences in average monthly MRI scans and average MRI reporting time were compared with t test.

#### RESULTS

In P1, total MRI scans= 5628, average monthly scans= 1407, average reporting time= 4.56 days. In P2, total MRI scans= 4484, average monthly scans= 1121, average reporting time= 3.22 days. In P3, total MRI scans= 8412, average monthly scans= 2103, average reporting time= 3.69 days. MRI scans in P2 is 20.3% lower ( $p < 0.05$ ) than P1 and 46.7% lower ( $p < 0.01$ ) than P3. The average reporting time in P2 is 29.4% lower ( $p < 0.01$ ) than P1 and 12.7% lower ( $p < 0.02$ ) than P3.

#### CONCLUSION

The COVID-19 Pandemic accounted for 20.3% decrease in MRI volumes and 29.4% decrease in MRI reporting time. MRI volumes in P3 has recovered with MRI scans 149% of the pre-pandemic volumes. Analysing MRI referral locations found 40.4% and 40.9% of P3 scans are from primary care and outpatients respectively.

#### CLINICAL RELEVANCE/APPLICATION

The trend in MRI volumes during the COVID-19 pandemic may be a reflection across radiology sites within and possibly outside of UK. The staggering increase in MRI referrals and imaging workload may have been a result of virtual clinical consultations, putting emphasis on imaging, accelerating throughput in Radiology. As 40.4% of MRI volumes in March to June 2021 were generated in primary care, we recommend educating primary care physicians to request appropriate imaging for sustainable delivery of high-quality imaging services. As the pandemic settles, it is important to monitor imaging workload and reporting time so as to plan and optimise future imaging services in Radiology.

#### **W5A-SPNPM-3 Fallout and Benefits of the 21ST Century Cures Act: A Survey of Referring Providers**

#### Participants

Shravan Sridhar, MD, MS, (*Presenter*) Nothing to Disclose

#### PURPOSE

The 21st Century Cures Act prohibits information blocking practices and mandates the timely release of radiology reports to patients. This study aims to investigate the impact of these practices on patients, clinicians, and clinical workflows.

#### METHODS AND MATERIALS

A prospective single-center quality improvement survey was administered by email to 313 providers from October 26, 2021 to November 17, 2021. Respondents who spend at least 20% clinical time at our healthcare system and 10% time on outpatient services were given the opportunity to complete an additional survey encompassing positive and negative effects of prohibition of information blocking practices following implementation. The survey questions were vetted by leadership with experience in survey design. Descriptive statistics were calculated.

#### RESULTS

Of 313 people offered the survey, 290 responded (93% response rate) across 40 different specialties and subspecialties. Following

Of the people entered the survey, 239 responses (59% response rate) across 10 different specialties and subspecialties following implementation of the Cures Act, 172 respondents (59%) reported spending somewhat more or significantly more time discussing results with patients overall while only 7 respondents (2%) reported spending somewhat less or significantly less time. 232 (80%) of respondents reported somewhat more or significantly more time spent discussing results with patients outside of clinic visits but during regular work hours, and 227 (78%) reported spending more time outside of regular work hours. As a result of patients having access to radiology reports before meeting with their medical provider, 108 (42%), 121 (46%), 136 (52%), and 135 (52%) providers reported patients were sometimes or often better emotionally prepared to discuss results, more knowledgeable about their medical condition, better at asking questions, and better engaged in their medical decision making, respectively. 233 (86%), 239 (88%), 189 (72%), 89 (37%), and 16 (7%) providers indicated patients sometimes or often experienced anxiety, confusion, online research with incorrect interpretations, disruption to other life activities, and physical injury, respectively.

## **CONCLUSION**

s The immediate release of radiology reports directly to patients has both positive and negative effects on patients and increases the time clinicians spend discussing results with patients outside regular working hours.

## **CLINICAL RELEVANCE/APPLICATION**

Providers agree the release of radiology reports benefits patient knowledge and engagement during their clinical appointments. However, optimized institutional policies and processes/communication pathways are needed to emotionally support patients accessing their results immediately and providers who are subjected to increased patient communications beyond regular work hours.

Printed on: 02/07/23

## Abstract Archives of the RSNA, 2022

W5A-SPNPM-2

### Impact of COVID-19 Pandemic on Imaging Workload in Radiology; A Case Study of MRI Service in an UK District General Hospital Trust With 1200 Bed Capacity

Wednesday, Nov. 30 12:15PM - 12:45PM Room: Learning Center - NPM DPS

#### Participants

Chao Jin Ho, MBCh, BSc, (*Presenter*) Nothing to Disclose

#### PURPOSE

The 2019 coronavirus disease (COVID-19) pandemic has been a global health issue with vast social-economical and human mortality impact. The first UK national lockdown was implemented in 23 March 2020 to curb the spread of COVID-19. This study aims to evaluate the impact of the COVID-19 pandemic on MRI volumes and reporting time by comparing MRI imaging volumes and reporting time before and during the COVID-19 pandemic.

#### METHODS AND MATERIALS

The scan volumes and reporting time of MRI scans performed in four different MRI sites in the Durham and Darlington hospital trust were retrospectively reviewed at three different time periods: 1) pre-pandemic (March to June 2019 or P1) 2) start of the COVID-19 pandemic (March to June 2020 or P2) 3) second year of the COVID-19 pandemic (March to June 2021 or P3). Statistical differences in average monthly MRI scans and average MRI reporting time were compared with t test.

#### RESULTS

In P1, total MRI scans= 5628, average monthly scans= 1407, average reporting time= 4.56 days. In P2, total MRI scans= 4484, average monthly scans= 1121, average reporting time= 3.22 days. In P3, total MRI scans= 8412, average monthly scans= 2103, average reporting time= 3.69 days. MRI scans in P2 is 20.3% lower ( $p<0.05$ ) than P1 and 46.7% lower ( $p<0.01$ ) than P3. The average reporting time in P2 is 29.4% lower ( $p<0.01$ ) than P1 and 12.7% lower ( $p<0.02$ ) than P3.

#### CONCLUSION

The COVID-19 Pandemic accounted for 20.3% decrease in MRI volumes and 29.4% decrease in MRI reporting time. MRI volumes in P3 has recovered with MRI scans 149% of the pre-pandemic volumes. Analysing MRI referral locations found 40.4% and 40.9% of P3 scans are from primary care and outpatients respectively.

#### CLINICAL RELEVANCE/APPLICATION

The trend in MRI volumes during the COVID-19 pandemic may be a reflection across radiology sites within and possibly outside of UK. The staggering increase in MRI referrals and imaging workload may have been a result of virtual clinical consultations, putting emphasis on imaging, accelerating throughput in Radiology. As 40.4% of MRI volumes in March to June 2021 were generated in primary care, we recommend educating primary care physicians to request appropriate imaging for sustainable delivery of high-quality imaging services. As the pandemic settles, it is important to monitor imaging workload and reporting time so as to plan and optimise future imaging services in Radiology.

Printed on: 02/07/23



## Abstract Archives of the RSNA, 2022

W5A-SPNPM-3

### Fallout and Benefits of the 21ST Century Cures Act: A Survey of Referring Providers

Wednesday, Nov. 30 12:15PM - 12:45PM Room: Learning Center - NPM DPS

#### Participants

Shravan Sridhar, MD, MS, (*Presenter*) Nothing to Disclose

#### PURPOSE

The 21st Century Cures Act prohibits information blocking practices and mandates the timely release of radiology reports to patients. This study aims to investigate the impact of these practices on patients, clinicians, and clinical workflows.

#### METHODS AND MATERIALS

A prospective single-center quality improvement survey was administered by email to 313 providers from October 26, 2021 to November 17, 2021. Respondents who spend at least 20% clinical time at our healthcare system and 10% time on outpatient services were given the opportunity to complete an additional survey encompassing positive and negative effects of prohibition of information blocking practices following implementation. The survey questions were vetted by leadership with experience in survey design. Descriptive statistics were calculated.

#### RESULTS

Of 313 people offered the survey, 290 responded (93% response rate) across 40 different specialties and subspecialties. Following implementation of the Cures Act, 172 respondents (59%) reported spending somewhat more or significantly more time discussing results with patients overall while only 7 respondents (2%) reported spending somewhat less or significantly less time. 232 (80%) of respondents reported somewhat more or significantly more time spent discussing results with patients outside of clinic visits but during regular work hours, and 227 (78%) reported spending more time outside of regular work hours. As a result of patients having access to radiology reports before meeting with their medical provider, 108 (42%), 121 (46%), 136 (52%), and 135 (52%) providers reported patients were sometimes or often better emotionally prepared to discuss results, more knowledgeable about their medical condition, better at asking questions, and better engaged in their medical decision making, respectively. 233 (86%), 239 (88%), 189 (72%), 89 (37%), and 16 (7%) providers indicated patients sometimes or often experienced anxiety, confusion, online research with incorrect interpretations, disruption to other life activities, and physical injury, respectively.

#### CONCLUSION

The immediate release of radiology reports directly to patients has both positive and negative effects on patients and increases the time clinicians spend discussing results with patients outside regular working hours.

#### CLINICAL RELEVANCE/APPLICATION

Providers agree the release of radiology reports benefits patient knowledge and engagement during their clinical appointments. However, optimized institutional policies and processes/communication pathways are needed to emotionally support patients accessing their results immediately and providers who are subjected to increased patient communications beyond regular work hours.

Printed on: 02/07/23

## Abstract Archives of the RSNA, 2022

W5A-SPNR

### Neuroradiology Wednesday Poster Discussions - A

Wednesday, Nov. 30 12:15PM - 12:45PM Room: Learning Center - NR DPS

#### Participants

Hediyeh Baradaran, MD, MS, Salt Lake City, UT (*Moderator*) Nothing to Disclose

#### Sub-Events

#### W5A-SPNR- Enhancing Segmentation of Infarct and Penumbra Tissue on CT Perfusion Using Deep Learning 1

Participants

Mohammad Mahdi Shiraz Bhurwani, PhD, (*Presenter*) Stockholder, qas.ai

#### PURPOSE

An important imaging component used to triage patients with acute ischemic stroke (AIS) is the size and location of infarct and penumbra tissue. CT perfusion (CTP) software is typically employed and uses contralateral hemisphere relative thresholding to determine infarct and penumbra. This approach is not robust and is widely contested by the scientific community. Providing a more accurate segmentation of infarct and penumbra tissue would allow neuroradiologists to make the best decision regarding optimal clinical workflow. In this study we investigate if the use of a deep learning-based algorithm can improve the segmentation of infarct and penumbra tissue on CTP hemodynamic maps when compared with commercially available software.

#### METHODS AND MATERIALS

CTP and follow-up diffusion weighted imaging (DWI) scans were retrospectively collected for patients presenting with AIS. Patients in the infarct only sub-study received successful mechanical thrombectomy (mTICI 2b,2c,3) and the DWI within 48 hours of treatment to ensure halting of conversion of penumbra to infarct from time of CTP to DWI imaging. Patients in the infarct and penumbra sub-study received no treatment and the DWI imaging more than 48 hours after presentation to ensure conversion of all penumbra to infarct from time of CTP to DWI imaging. This resulted in 1920 and 1888 axial CTP map slices in the infarct, and infarct and penumbra sub-studies. Commercial CTP software (Olea Sphere 3.0 SP28) was used to generate cerebral blood flow, cerebral blood volume, mean transit time, time to peak, and delay time maps for each case. Deep learning-based algorithms were trained to segment infarct or infarct and penumbra using preprocessed CTP maps. Segmentation performance was evaluated using Dice coefficients (DC), and mean absolute volume errors (ml) (MAVE).

#### RESULTS

The trained algorithm segmented infarct tissue with a DC of  $0.64 \pm 0.03$  (0.63,0.65), and MAVE of  $4.91 \pm 0.94$  (4.5,5.32) ml. In comparison, the commercial software predicted infarct with a DC of  $0.31 \pm 0.17$  (0.26,0.36) and MAVE of  $9.77 \pm 8.35$  (7.12,12.42) ml. The algorithm was able to segment infarct and penumbra with a DC of  $0.61 \pm 0.04$  (0.6,0.63), and MAVE of  $6.51 \pm 1.37$  (5.91,7.11) ml. In comparison, the commercial software predicted infarct and penumbra with a DC of  $0.3 \pm 0.19$  (0.25,0.35) and MAVE of  $9.18 \pm 7.55$  (7.25,11.11) ml.

#### CONCLUSION

Use of deep learning algorithms to segment infarct and penumbra volume is proven to be accurate and outperforms current contralateral hemisphere relative threshold methods. Such an algorithm can enhance the treatment selection for AIS patients.

#### CLINICAL RELEVANCE/APPLICATION

The enhanced identification of infarct and penumbra tissue would improve triaging of patients with AIS and could thus enhance patient outcome.

#### W5A-SPNR- Deep Learning-Based Differentiation of Atypical Parkinsonian Syndromes Using Susceptibility 10 Weighted Images

Participants

Wonjune Choi, Pusan, Korea, Republic Of (*Presenter*) Nothing to Disclose

#### PURPOSE

Atypical parkinsonian syndromes (APs) such as progressive supranuclear palsy (PSP) and a parkinsonian variant of multiple system atrophy (MSA-P) show similar symptoms and signs as Parkinson's disease (PD), but additional symptoms with different rates of functional deterioration. Each parkinsonian syndrome has unique topographic pattern of iron accumulation, and susceptibility weighted imaging (SWI) is widely used to detect these specific patterns of localized iron concentration in the deep brain nuclei regions. In this work, therefore, we propose a novel framework for differentiating APS from PD in SWI using a deep learning (DL)-based approach with explainable AI.

#### METHODS AND MATERIALS

We obtained the T1-weighted (T1w) and SWI MRI scans of 33 MSA-P, 21 PSP, and 66 PD patients using protocols approved by the

IRB. First, bias-field correction and intensity normalization were applied. Second, the SWI volume was registered in the MNI space using the hybrid contrast (HC) images generated as a linear combination of T1w and SWI. To select the deep brain nuclei regions, we extracted 15 slices from 70 to 85 of the MNI space axial axis, and cropped each slice to the size of 120x100 with the center of the slice. Then, we used the pretrained ResNet152 model to classify each image into subtypes of APS. The model was implemented by minimizing the Binary-Cross-Entropy loss using Adam optimizer for a learning rate of  $1e-4$ . Convergence was achieved using batch size of 16 for each 100 epochs. The model was evaluated with a 5-fold cross validation test by measuring the balanced accuracy (bAcc), sensitivity (Sen) and specificity (Spe). We also compared with the conventional machine learning (ML) methods such as quadratic discriminant analysis (QDA) and support vector machine (SVM). Finally, we used Gradient-weighted Class Activation Mapping (Grad-CAM) to highlight important regions (heatmap) used for differentiation of APS.

## RESULTS

The proposed DL-based method achieved the performance with bACC of 0.9399, Sen of 0.9360 and Spe of 0.9439 for differentiation of MSA-P and PD; while QDA (SVM) achieved 0.8804 (0.8981), 0.8501 (0.9046), 0.9107 (0.8917). For MSA-P vs. PSP, the DL-based method achieved bAcc of 0.8522, Sen of 0.8483 and Spe of 0.8562 than QDA (SVM): 0.8380 (0.7862), 0.8561 (0.8802) and 0.8201 (0.6922). Heatmap from Grad-CAM shows that the prediction of the DL model was highly influenced by the putamen and globus pallidus regions.

## CONCLUSION

The proposed DL-based method differentiates APSs significantly better than the ML-based methods, and also holds promise for identifying regions impacted by APSs.

## CLINICAL RELEVANCE/APPLICATION

The high classification accuracy of our explainable DL model may contribute to a reliable clinical diagnosis of PD and APS.

## W5A-SPNR- 11 Effect of different pre ASiR-V on image quality and radiation dose of energy spectrum CT: A Phantom Study

Participants

Yaoming Ma, (Presenter) Nothing to Disclose

## PURPOSE

To investigate the impact of different pre adaptive statistical iterative reconstruction - Veo (ASiR-V) level on image quality and radiation dose of spectral CT.

## METHODS AND MATERIALS

A polypropylene cylindrical phantom(QSP Phantom dimension) with nine tubes containing different concentrations of iodine (0, 2.5, 5, 10, 20 mgI/ml) was scanned in gemstone spectral imaging (GSI) mode using fast kV switch (80/140 kV), the tube current is 485mA, the layer thickness is 1.25mm, the collimation width is 80mm, noise index (NI)5HU, pitch 0.992:1, dual energy CT (Revolution CT, GE Healthcare). Three groups of pre-ASiR-V weight (30%,40%,50% increments) was used for spectral CT scanning. Eleven groups of images were selected from the scan center and five layers above and below. The area of ROI was 1 / 2-1 / 3 of the cross-sectional area of the phantom tube, and the CT value and SD value of 20% and 10% iodine and water membrane tube were measured. The CT dose index (CTDI) of ASiR-V spectral scan with different weights was recorded. The dose length product (DLP), CT value and noise (SD) of the tube were recorded. The DLP across three groups were analyzed by simple linear regression analysis CT value and noise (SD), across three groups were analyzed by one-way ANOVA.

## RESULTS

With the increase of pre-selected ASiR-V level, noise (SD) showed the SD value remains unchanged. There was significant difference in DLP among groups (7.95mSv, 6.87mSv,4.73mSv for 30%,40%,50%pre-ASiR-V, respectively.  $P < 0.05$ ). There were no significant differences in SD among groups ( $9.92 \pm 0.55$ (I20),  $10.51 \pm 0.56$ (I10),  $9.80 \pm 0.61$ (H20), for 30% pre-ASiR-V,  $10.04 \pm 0.44$ (I20),  $10.04 \pm 0.44$ (I10),  $10.01 \pm 0.37$ (H20)40% pre-ASiR-V,  $10.52 \pm 0.64$ (I20),  $10.12 \pm 0.34$ (I10),  $10.52 \pm 0.50$ (H20),50% pre-ASiR-V,  $F = 2.130$ ,  $p > 0.05$ ).

## CONCLUSION

Conclusion: ASiR-V does not affect the image quality of energy spectrum scanning (SD), and can significantly reduce the radiation dose (CTDI) while maintaining the image quality of energy spectrum scanning (SD).

## CLINICAL RELEVANCE/APPLICATION

ASiR-V does not affect the image quality (SD) of energy spectrum scanning, and can significantly reduce the radiation dose (CTDI) while keeping the image quality (SD) of energy spectrum scanning unchanged. Correlation of clinical application: through the basic research of phantom, spectral CT scanning can provide the same image quality, increase the proportion of ASiR-V iterative algorithm and reduce the radiation dose. This study has guiding significance for the application of spectral CT scanning in different clinical scenes.

## W5A-SPNR- 12 Brain MRI volumetric machine learning model: A potential tool to differentiate Progressive Supranuclear Palsy from Parkinson's disease patients and healthy subjects.

Participants

Francisco Mendoza, MD, (Presenter) Nothing to Disclose

## PURPOSE

To develop a machine learning model to differentiate Progressive Supranuclear Palsy (PSP) from Parkinson's disease (PD) and healthy subjects (HS) using an automated volumetry of brain MRI, validate its performance, and determine the most relevant Volumes of Interest (VOIs).

## METHODS AND MATERIALS

We retrospectively assessed a total of 141 patients with a clinical diagnosis of Parkinsonism paired by age and sex and with a group of HS (PSP n = 47, PD n = 68, HS=26) between January 2003 and April 2021 and analyzed their brain MRI. Patients without T1 high

resolution sequences (T1-MPRAGE) were excluded, leaving 83 patients (PSP n = 29, PD n = 54, HS n=26). We included different clinical subtypes of PSP: PSP-RS (n= 19), PSP-P (n= 5), PSP-PGF (n= 4), and PSP-F (n= 1). Using automatized SyngoviaBrainMorphometry software (Siemens), we obtained 109 VOIs for each subject, including absolute and normalized values. We developed a machine learning model based on multivariate feature selection and an extreme gradient boosting (XGB) vs. univariate feature selection and random forest (RF) to differentiate PSP from PD and HS. All subjects were randomly divided into training (85%) and validation (15%) data sets with the same proportions for each clinical group. The most relevant VOIs were obtained from the model, order by importance score (F-score; where 1.0 represents perfect precision and recall). Additionally, we assessed the diagnostic accuracy of each VOI using ROC curves.

## RESULTS

The global diagnostic performance of the model to differentiate between the three groups was 70.6%. The diagnostic accuracy of the model to differentiate each group from the other was: PSP (88.2%), PD (70.6%), and HS (76.5%). The VOIs that presented higher importance scores were the mesencephalic normalized volume (0.068), frontal right white matter volume normalized and absolute (0.053), left hippocampus absolute volume (0.040), left globus pallidum absolute volume (0.036), right hippocampus normalized volume (0.035), right thalamus absolute volume (0.032), frontal right gray matter normalized volume (0.032), left deep white matter normalized volume (0.030) and right hippocampus absolute volume (0.028). The AUC to differentiate PSP from PD and/or HS was: for the mesencephalic normalized volume =0.87, the left globus pallidum absolute volume =0.72, for the left hippocampus absolute volume = 0.59, and the right hippocampus normalized volume= 0.57.

## CONCLUSION

The developed machine learning model using an automated volumetry of brain MRI showed accurate discrimination between PSP, PD, and HS.

## CLINICAL RELEVANCE/APPLICATION

Automatized volumetric assessment of brain MRI is a helpful tool for differentiating Progressive Supranuclear Palsy from Parkinson's disease.

## W5A-SPNR- Multimodal Brain Tumor Segmentation using Deep Convolutional Neural Networks 13

Participants

Rimjhim Agrawal, PhD, Bangalore, India (*Presenter*) Nothing to Disclose

## PURPOSE

Brain tumours are one of the leading causes of death worldwide. As a result, it is critical to discover it as soon as possible. Numerous ways have been developed to forecast and segment the tumour. They do, however, have a number of drawbacks, including the requirement for specialised assistance, the lengthy run-time, and the selection of an appropriate feature extractor. To overcome these difficulties, we suggest a convolutional neural network-based technique for concurrently predicting and segmenting a cerebral tumour using multimodal structural magnetic resonance images (T1w, FLAIR and Post contrast T1w).

## METHODS AND MATERIALS

We used mpMRI Brain Tumor Segmentation (BRATS 2021) dataset. For each scan annotation consists of 3 classes - Enhancing Tumor (ET) , Peritumoral Edematous Tissue (ED) and necrotic tumour core (NCR). Our Method was developed by training deep neural networks (DNN) using only 3 Modalities - T1w, FLAIR and Post contrast T1w for generating tumour segmentation masks.

## RESULTS

In this study, training and validation was performed on 1251 mpMRI scans and we were able to achieve a mean dice score coefficient (DSC) of 0.89. Also, validation was performed for 50 scans with annotations obtained from an expert radiologist achieving a mean DSC of 0.86 and tumor core DSC of 0.89.

## CONCLUSION

The fully automated brain tumor segmentation method developed on a well-established benchmark (BraTS 2021) dataset demonstrated that it can provide both efficient and robust segmentation compared to manually obtained ground truth. Additionally, our method with only three modalities as input can achieve comparable results to the state-of-the-art methods with four modalities. The proposed method enables objective assessment for clinical tasks such as surgery pre-planning, tumor grade detection and post surgery monitoring.

## CLINICAL RELEVANCE/APPLICATION

This research suggests accurate and quick segmentation using deep convolutional neural networks of different subregions of a tumour, and has crucial clinical implications in brain tumour diagnosis, prognosis, treatment and presurgical planning.

## W5A-SPNR- A light-weight deep learning web app for rapid identification of poor-quality structural MRI scans: A 16 multi-institutional study

Participants

Thomas Desilvio, Cleveland, OH (*Presenter*) Nothing to Disclose

## PURPOSE

Screening and diagnosis of neurological disorders largely relies on T1-weighted (T1w) MRI. Presence of one or more artifacts can degrade MR image quality to the extent they are unusable for disease diagnosis, whether by machines or radiologists. Visual inspection and quality assessment of MRI scans to identify cases requiring exclusion or rescanning is often time-consuming and laborious. We present multi-institutional validation of a scalable, light-weight deep learning-based (DL) web-app for rapid identification of poor quality T1w brain MRI scans.

## METHODS AND MATERIALS

We utilized publicly available cohorts from ABIDE-I (17 institutes, 1102 T1w MRIs, including 3 expert-reader quality ratings) and TCGA-GBM (5 institutes, 152 T1-POST MRIs). TCGA-GBM was internally evaluated by 3 radiologists to assign quality labels similar to ABIDE-I. Training cohort was curated from ABIDE-I (n=454, 15 institutions), where every scan was assigned "good quality

(GQ)/poor quality (PQ)" based on rating agreement between 2+ readers. Remaining ABIDE-I datasets were split into internal validation (V1, n=400) and external validation (V2, n=248, 2 institutions). TCGA-GBM was additionally used for external validation (V3). For V1-V3, "ground truth" labeling of scans as GQ/PQ was based on mean opinion score of raters. A mid-brain 3D sub-volume (with foreground identification) from each scan used as input to a 3D ResNet18 model, optimized to predict PQ scans via training cohort. Additionally, 64 quality measurements (QMs) from the publicly available MRIQC tool (quantifying SNR, intensity contrast, motion, entropy artifacts) were used to train a random forest classifier for identifying PQ scans. Hold-out evaluation of ResNet and QM models was performed in terms of accuracy of identifying PQ scans on V1-V3.

## RESULTS

The ResNet DL model achieved accuracies of 0.89, 0.83, and 0.89 in V1, V2, and V3, respectively for identifying PQ scans. MRIQC-based QM models performed significantly worse with accuracies of 0.77 (V1;  $p < 0.001$ ), 0.75 (V2;  $p < 0.001$ ), and 0.76 (V3;  $p < 0.001$ ) in identifying PQ scans. The DL web-app took  $< 1$  min/MRI volume for classifying each scan as PQ or GQ.

## CONCLUSION

Our light-weight deep learning based web interface can enable rapid identification of poor-quality brain MRI scans, and offers improved performance compared to standard image quality measures.

## CLINICAL RELEVANCE/APPLICATION

Rapid automated identification of poor-quality MRI scans could have significant implications for downstream machine learning analysis as well as radiology interpretation and disease diagnosis.

### W5A-SPNR-18 Post-processing to improve accuracy of Deep Learning Algorithm for Intracranial Hemorrhage Detection: Our experience of introducing an analytical approach simulating Radiologist Reasoning

Participants

Anjali Agrawal, MD, Delhi, PA (*Presenter*) Nothing to Disclose

## PURPOSE

Deep learning tools are being increasingly used to optimize radiologist efficiency in the emergency setting, however, overprediction and false positive (FP) results may be counterproductive. We investigated the value of additional post-processing refinements into the deep learning algorithm developed in our lab for the detection of intracranial hemorrhage (ICH) with the intention of introducing specific reasoning and logic similar to that applied by radiologists.

## METHODS AND MATERIALS

A deep learning algorithm for ICH detection was developed using a fully convolutional neural network, U-NET with image segmentation and hemorrhage classification properties. Upon validation, several recurring FPs at specific locations posed a challenge in increasing overall accuracy to acceptable levels. Various new approaches were then developed to specifically address each type of FP. Deep learning models were used to decrease FPs instance-wise and slice-wise in calcification and artifact models respectively. Image processing and coding logic were used to decrease FPs in the region of basal ganglia, falx, dural sinus, volume averaging from dense calvaria, and FPs due to accentuated appearance of grey-white matter junction in older patients.

## RESULTS

We analyzed 4512 studies of which 2036 were negative and 2476 were positive for intracranial hemorrhage sequentially using the ICH detection deep learning model, without and with post-processing algorithms. The results achieved without and with post-processing were sensitivity (recall) of 96.77% and 90.47%, specificity of 41.99% and 90.28%, precision of 66.98, 91.88%, F1 score of 79.17% and 91.17%, and Area Under Curve of 0.694 and 0.904 respectively.

## CONCLUSION

Postprocessing techniques brought about significant improvement in the model performance by reducing the number of false-positive results.

## CLINICAL RELEVANCE/APPLICATION

Our research explores ways to improve the analytical capabilities of deep learning tools by using postprocessing techniques with the goal to develop a more optimal triage workflow in the emergency setting.

### W5A-SPNR-19 Radiomics Analysis Distinguish Between Primary Central Nervous System Lymphoma, Glioblastoma, and Brain Metastasis

Participants

Murat AK, MD, Pittsburgh, PA (*Presenter*) Nothing to Disclose

## PURPOSE

To investigate the diagnostic performance of radiomics-based machine learning in differentiating glioblastoma (GBM), primary central nervous system lymphoma (PCNSL) and brain metastasis (BM).

## METHODS AND MATERIALS

We retrospectively identified 1075 patients from three institutions with untreated solitary, pathologically proven cases of PCNSL (133), GBM (433), and breast or lung BM (509). For each tumor, we segmented edema, contrast enhancement, necrosis, and contralateral white matter (cWM) volume of interest (VOI) for T2 FLAIR and T1 post-contrast sequences. A total of 205 texture features were extracted from each sequence's VOI including 10 histogram based first-order features and 195 second-order features using gray-level co-occurrence matrices. After feature normalization using cWM, we divided the 195 second level features by the volumes of each VOI to generate another 195 volume-independent features per VOI and 2,400 features per MRI. We performed feature selection with Least Absolute Shrinkage and Selection Operator (LASSO). We split the cohort into 70% training and 30% testing sets. We used XGBoost (eXtreme Gradient Boosting) algorithm to perform three-way classification and generate the radiomics model. The predictive performance of the models for classifying each tumor type against all others (i.e., BM versus PCNSL and GBM) was estimated using the receiver operating characteristic (ROC) curve, summarized as the area under the curve (AUC).

## RESULTS

LASSO identified 216 independent features, of which 20 most relevant used for model building. Our three-classification model robustly differentiated ( $p < 0.001$ ) between PCNSL (AUC 0.95), GBM (AUC 0.97), and BM (AUC 0.96) and achieved 88% accuracy. The model obtained 76.9% sensitivity and 98.2% specificity for PCNS prediction, 86% sensitivity and 94.7% specificity for the GBM prediction and 92.7% sensitivity 86.3% specificity for the BM prediction.

## CONCLUSION

This study presents radiomics-based signature that can successfully differentiate between PCNSL, GBM, and BM. Although further independent validation is warranted the proposed predictive radiomics-based signature is cost-effective, non-invasive and enable better patient stratification, management, and clinical decision-making

## CLINICAL RELEVANCE/APPLICATION

A major challenge in the management of brain tumor is distinguishing tumor type as there are currently no reliable non-invasive biomarkers to predict them. Our data suggests that radiomics using MRI is an cost-effective and non-invasive approach to identify brain tumor type.

## W5A-SPNR- Automated Lumbar Disc Herniation Grading Through AP-Diameter Measurement in MR Imaging 2

Participants

Li Zhang, PhD, Princeton, NJ (*Presenter*) Employee, Covera Health

## PURPOSE

Lumbar disc herniation (LDH) is often diagnosed using MR, and automated AI pipelines are used to reduce variation in grading severity. A fully automated AI-powered pipeline was used to detect, localize, and segment LDH at each Functional Spinal Unit (FSU) level (L1-2 through L5-S1) and use the anterior-posterior diameter (APD) of the segmented LDH to grade severity.

## METHODS AND MATERIALS

Sagittal T2 sequences of MR lumbar spine were collected from 589 studies. 2,872 FSU manually segmented voxel-wise as background - 0 (No segmentation), disc - 1, and herniated disc region - 2. The studies were randomly split into train-validation-test sets in a 75:10:15 ratio. A deep reinforcement model was trained to identify the L1-2 through L5-S1 disc centers. Associated FSUs were cropped to 8 x 8 x 5 cm then fed to a convolutional neural network. An Attention U-Net was trained to segment the images on a 2D slice with 2 adjacent slices provided to the left and right of the target slice. The APD was estimated by summing the voxels' resolution at the apex of the estimated LDH region. A severity is assigned based on this measurement (Normal: 0mm; Small: APD = 3mm; Moderate: 3mm < APD = 6mm; Large: 6mm < APD). If an APD measurement error misassigns the severity by 1-degree, we call it 1-degree error, 1-degree error includes misassignment between Normal and Small, Small and Moderate, Moderate and Large. Similarly, 2-degree error is defined as severity misassignment between Normal and Moderate, Small and Large.

## RESULTS

The model achieves an RMSE in APD of  $1.33 \pm 1.33$ mm and an average ratio of predicted to ground truth APD of  $1.14 \pm 0.89$  for the true positive predictions. The model accuracy is further evaluated by the assigned severities based on APD. The 1-degree misassignment is 34% where 47% of these are between normal and small and 37% are between small and moderate both with an RMSE of 1.8mm. These, however, are in general inconsequential, the clinical significant 2-degree severity classification error is only 4%.

## CONCLUSION

Segmentation of Lumbar MR has the advantage of providing visualization and location and automated measurement of LDH which can assist diagnosis and reduce interobserver variation.

## CLINICAL RELEVANCE/APPLICATION

Automated detection, localization and measurement of LDH pipeline can provide precise, reproducible analysis of pathology which can be useful for quality analysis, enhancing efficiency of utilizing experts.

## W5A-SPNR- Deep learning for classification of Cranial Ultrasound in Preterm Babies 3

Participants

Tahani Ahmad, MD, (*Presenter*) Nothing to Disclose

## PURPOSE

Cranial ultrasound (CUS) is widely used as a screening tool to assess brain injury in preterm infants. Severe abnormalities on CUS are known to be associated with Neurodevelopmental impairment (NDI). This study investigates the feasibility of using deep learning to identify abnormalities in CUS images collected from a preborn preterm cohort that are routinely clinically assessed for NDI. The objective is to train a model that can classify normal vs. abnormal imaging findings and assess its usability for computer-aided diagnosis that can have merit in daily practice as a complementary decision aid.

## METHODS AND MATERIALS

This is a retrospective study of a cohort of very preterm infants born between January 2004 and Dec 2016 and admitted to the Neonatal Intensive Care Unit at IWK Health, Canada. The sample size includes images from 619 patients (4180 images) collected during 3-time points (first week, 6th week of age, and a term-equivalent age). At each point, 3 coronal images were selected at specific landmarks. Each image was anonymized. CUS pixels intensities are normalized and resized to a standard 224x224 pixel. Regions outside of the brain were masked and set to pixel intensity zero. A trained radiologist manually labeled each image as either normal or abnormal. The dataset is split into training/test sets (90:10 percent split). Due to the class imbalance in the dataset, the Area Under the Curve (AUC) was chosen as the metric of reference. The abnormal cases where the model very confidently predicted the image as abnormal were selected, then an approach called Gradcam was applied. In this approach, the saliency of each individual pixel is visualized. The original image has a heatmap overlaid on it, the areas with more red are what lead the model to make its prediction.

## RESULTS

We tested different CNN architectures. The total number of normal images is 3531/4180, and the total number of images with abnormal findings is 649/4180. Preliminary results indicate an average of 0.794 AUC (0.757-0.83) using 10 bootstraps stratified sampling strategies using DensNet169

## CONCLUSION

This is a preliminary work to provide a tool to assist clinicians during early NDI assessment by classifying CUS into normal scans and scans with abnormal imaging features that can have merit in daily practice as a complimentary decision aid. Although the dataset is currently limited, early results are positive and likely to improve as more images are going to be included.

## CLINICAL RELEVANCE/APPLICATION

Cranial ultrasounds to assess neurodevelopmental impairment is a challenging task subject to high variability. Computer-aided diagnosis tool might help reduce false positive and false negative rates.

## W5A-SPNR- Prediction of Primary Tumor Entity of Brain Metastases Using Machine Learning based on Radiomic Features Derived from Routine MRI

Participants  
Quirin Strotzer, MD, Regensburg, Germany (*Presenter*) Nothing to Disclose

## PURPOSE

This study aims to determine the primary tumor entity of brain metastases using machine learning based on radiomic features obtained from routine MRI sequences.

## METHODS AND MATERIALS

This multicenter project included 251 patients for whom non-standardized routine MRI sequences T1, T1CE, T2, and FLAIR (from various scanners, 1.5T and 3T) and histologic determination of the primary tumor were available. A preprocessing pipeline was set up using Python libraries, including co-registration, normalization, and automated tumor segmentation using a Convolutional Neural Network with U-shaped architecture. Radiomic features were extracted and selected with a LASSO regression. Metastases were grouped into five classes: the four most frequently occurring primary entities (adenocarcinoma of the lung, melanoma, breast cancer, colorectal cancer) and a fifth group including all less common primaries. Using a five-fold cross-validation scheme, machine learning classifiers were tested on the train/validation partition of the dataset (80%) to predict the primary tumor based on the radiomic features. The performance was evaluated using a holdout test set (20%).

## RESULTS

A total of 728 brain metastases were individually segmented. For each metastasis, 3852 radiomic features were extracted. The LASSO regression identified 60 variables with the greatest impact on classification. An AdaBoost classifier yielded the best results for this five-class classification task on the holdout test set (accuracy: 0.601; area under the receiver operating characteristic curve: 0.854). A feature importance analysis showed that the most essential variables for the classifier were second-order statistics features derived from the contrast-enhanced T1-weighted sequences.

## CONCLUSION

Primary tumor entity prediction might be feasible via radiomic feature analysis of non-standardized routine MRI sequences. Further relevant read-outs such as oncogenic driver mutations could be within reach.

## CLINICAL RELEVANCE/APPLICATION

Predicting the primary tumor of brain metastases using radiomic features derived from non-standardized routine MRI sequences would significantly enhance the diagnostic value of routine MRI scans and reduce morbidity from invasive biopsies.

## W5A-SPNR- Accelerated Creation of a Glioma Database for Machine Learning Prediction Model Development using PACS-Integrated Tools

Participants  
Victor Becerra, MD, Albany, NY (*Presenter*) Nothing to Disclose

## PURPOSE

The creation of well-annotated imaging datasets is crucial for the development of accurate and reproducible machine learning (ML) algorithms. Although an increasing number of ML algorithms are being developed in the academic setting, many of them are created in research-specific software incompatible with the routine clinical workflow. Our purpose was to facilitate the creation of a large, annotated glioma database by implementing clinical PACS-integrated tools for image segmentation and radiomic feature extraction.

## METHODS AND MATERIALS

Data from our institution's radiation oncology registry from 2012 to 2019 was used. Glioma images from these patients and the BRaTS 2021 challenge were segmented using a home-grown PACS-integrated (Visage Imaging, Inc) U-net algorithm. These were subsequently validated by a board-certified neuroradiologist. A home-grown PACS-integrated PyRadiomics feature extraction tool was then deployed on the annotated dataset.

## RESULTS

Over the course of only 5 months, segmentations and annotations were completed in 595 patients (236 females, 359 males, with a mean age of 50.92 years). Grade distribution was as follows: 245 Grade 4, 52 Grade 3; 97 Grade 2; 26 Grade 1; 175 unknown. Molecular subtypes included IDH (87 mutated, 355 wild-type, 153 unknown), 1p/19q (65 deleted or co-deleted, 87 intact, 443 unknown), MGMT promotor (162 methylated, 70 partially methylated, 207 unmethylated, 156 unknown), EGFR (55 amplified, 121 not amplified, 419 unknown), ATRX (28 mutated, 130 retained, 437 unknown), Ki-67 (433 known, 162 unknown) and p53 (395 known, 200 unknown). To generate a geographically distinct validation set, metadata labels were created for imaging acquired outside our institution.

## CONCLUSION

Our PACS-integrated image segmentation tool has allowed us to create a large number of images in an accelerated manner that is

s Our PACS-integrated image annotation tools have allowed us to curate a large number of images in an accelerated manner that is compatible with the clinical workflow. On average, over 100 gliomas were annotated per month, thus establishing that these tools may be game-changing in the development of annotated imaging databases.

#### CLINICAL RELEVANCE/APPLICATION

The development of clinical PACS-integrated tools for data curation has the potential to facilitate and accelerate the development of large-scale well-annotated imaging datasets which can be used for algorithm development, radiomic feature extraction, among others.

#### W5A-SPNR- Multi-Scale Fusion 3D Convolutional Neural Networks Based on Attention Mechanism for Survival Prediction of Glioma Patients

Participants

Xuan Yu, (*Presenter*) Nothing to Disclose

#### PURPOSE

Due to the individual differences of different patients with glioma and individualized precision treatment, the survival time performance of different patients is quite different. Constructing a reliable survival prediction model and analyzing the MRIs of patients with glioma, further mining objective features from the images have extremely important clinical value for the prognosis of patients. We develop a multi-scale fusion 3D convolutional neural networks deep learning model based on attention mechanism to predict the survival time of glioma patients.

#### METHODS AND MATERIALS

MRIs from 270 cases were included, of which 207 from BraTS 2019 datasets and 63 from the private datasets of the hospital. Firstly, MRIs are preprocessed and a saliency-aware method is adopted to enhance the tumor region. Next we present a 3D convolutional structure to refine multiple scale characteristics of enhanced T1 Weighted imaging. Two crucial designs are shown in the model, one of which is fusing multi-scale features to explore level information in MRIs, and another is the attention gate make the model automatically focus on the crucial area in the images. Finally through the full connection layer to achieve the survival time analysis. The model includes prediction of short, medium, and long-term survival risk classification.

#### RESULTS

The cases were divided into low-risk group( $SD \geq 450$ ), medium-risk group( $300 \leq SD < 450$ ) and high-risk group( $SD \leq 300$ ) according to the Survival Days(SD). The ROC results show low-risk group AUC is always higher than medium- and high-risk group AUC in training, verification and test sets, which indicates low-risk group is easier to classify. The classification performance of medium-risk group and high-risk group are close. And the medium or high survival risk of patients is relative difficult to study due to the survival time is affected by more complex factors including the degree of tumor necrosis, the individual differences, whether has other disease and so on. By comparing with the popular 3D Unet model, sensitivity, specificity and AUC in our model displays relatively better performance.

#### CONCLUSION

s Our research demonstrates that appropriate MRIs data preprocessing and saliency-aware enhancement could better show the lesion characteristics of images. 3D convolutional structure preserves the important spatial features. Fusing different scale features is helpful to achieve higher classification accuracy, and the attention gate focuses more on the key areas in the MRIs. Our method is effective to mine MRIs deep features thus to achieve the goal of glioma patients' survival time prediction.

#### CLINICAL RELEVANCE/APPLICATION

This work provides some support for the operation, treatment and survival evaluation of patients with gliomas.

#### W5A-SPNR- Deep Learning of Dynamic Susceptibility Contrast Perfusion-weighted Imaging to Predict the Local Recurrence in Glioblastoma Patients

Participants

Roh-Eul Yoo, MD, PhD, Seoul, Korea, Republic Of (*Presenter*) Nothing to Disclose

#### PURPOSE

To develop a deep learning model based on multiparametric MR imaging including dynamic susceptibility contrast perfusion-weighted imaging (DSC-PWI) that predict the local recurrence in patients with glioblastoma (GBM).

#### METHODS AND MATERIALS

This retrospective study included 213 consecutive GBM patients who underwent standard treatment between May 2010 and April 2021 and had both preoperative MR including DSC-PWI and 1 year follow-up 3T MRI. Patients were divided into the training set (172 patients [58 ± 14 years; 90 men] from 2010 to 2019) and test set (41 patients [56 ± 14 years; 23 men] from 2020 to 2021). Each patient was categorized as local recurrence or non-recurrence group with respect to the presence of local recurrence at 1 year after the diagnosis. Using the follow-up contrast-enhanced T1-weighted image (CE-T1WI) as the reference standard, the sites of local recurrence were annotated in a non-enhancing T2 hyperintense lesion on preoperative T2 FLAIR images. A deep learning model based on conventional MR and DSC-PWI was developed using nnU-Net. The deep learning model performance was validated on the test set. Diagnostic performance of the two models were compared using the McNemar test.

#### RESULTS

Training set and test set included 73 and 17 recurrence cases, respectively. In the test set, the multiparametric deep learning model using the combination of conventional MR and DSC-PWI showed a significantly higher sensitivity than the model based on conventional MRI alone in predicting the risk of recurrence (71% [12 of 17] vs. 29% [5 of 17],  $P = .031$ ). The specificity of the model based on the combination of conventional MR and DSC-PWI did not significantly differ from that based on the conventional MRI alone (42% [10 of 24] vs. 58% [14 of 24],  $P = .34$ ).

#### CONCLUSION

s A deep learning model based on multiparametric MR imaging including DSC-PWI can be used to predict the risk of local recurrence

in GBM patients.

#### **CLINICAL RELEVANCE/APPLICATION**

A deep learning model based on the combination of conventional and DSC-MRI could be used to stratify the risk of local recurrence in GBM patients and potentially to guide radiation treatment planning.

#### **W5A-SPNR- From Accuracy to Consensus: Towards a New Paradigm for Assessing Model Performance**

8

Participants

Simas Glinskis, Ithaca, NY (*Presenter*) Employee, Covera Health, Inc

#### **PURPOSE**

Machine learning model performance is typically analyzed through accuracy and other statistical measures contingent on consistent ground truth labels. This assumption falls apart with medical applications where considerable inter-reader variability is present due to variation in clinical interpretation. We designed a new statistical mechanism to assess model performance which incorporates multiple sources of truth.

#### **METHODS AND MATERIALS**

MRI lumbar spine studies from 207 patients, 1035 functional spine units, were collected and multi-annotated by 10 subspecialty radiologists. The data was partitioned into a ground truth set using labels from the most experienced radiologist available and a secondary set from the remaining experts. Deep learning based models for classification of disc herniation (DH), central canal stenosis (CCS), and nerve root compression (NRC) were used to generate severity predictions. Those predictions were split into two groups, where they agreed with ground truth (agree) and where they did not (disagree). Distributions of label consensus (LC) were generated for both groups by computing the average agreement between ground truth and external annotations for each prediction.

#### **RESULTS**

Accuracy of normal, mean agree LC and mean disagree LC are 87%, 97%, and 41% for NRC, 91%, 98% and 37% for CCS, and 74%, 92%, and 47% for DH, respectively. While accuracy is sensitive to the annotation that is selected as the gold standard, LC distributions generate a better measure of model performance which incorporates information from all of the experts. For the disagree set, there is low consensus which unfairly lowers accuracy and for the agree set we see very high consensus which the models are able to capture. Agree LC consistently outperforms accuracy and better represents the predictive power of the model when measured against a group of labels.

#### **CONCLUSION**

s We designed label consensus to analyze the performance of machine learning models by incorporating multi-annotated data. When there is inter-reader variability among experts conventional accuracy fails to incorporate information from the corpus of annotators and is sensitive to the choice of gold standard label while consensus is not.

#### **CLINICAL RELEVANCE/APPLICATION**

Our proposed label consensus evaluation provides a more effective way of assessing AI model performance in applications with significant inter-reader variability.

Printed on: 02/07/23

## Abstract Archives of the RSNA, 2022

W5A-SPNR-1

### Enhancing Segmentation of Infarct and Penumbra Tissue on CT Perfusion Using Deep Learning

Wednesday, Nov. 30 12:15PM - 12:45PM Room: Learning Center - NR DPS

#### Participants

Mohammad Mahdi Shiraz Bhurwani, PhD, (*Presenter*) Stockholder, qas.ai

#### PURPOSE

An important imaging component used to triage patients with acute ischemic stroke (AIS) is the size and location of infarct and penumbra tissue. CT perfusion (CTP) software is typically employed and uses contralateral hemisphere relative thresholding to determine infarct and penumbra. This approach is not robust and is widely contested by the scientific community. Providing a more accurate segmentation of infarct and penumbra tissue would allow neuroradiologists to make the best decision regarding optimal clinical workflow. In this study we investigate if the use of a deep learning-based algorithm can improve the segmentation of infarct and penumbra tissue on CTP hemodynamic maps when compared with commercially available software.

#### METHODS AND MATERIALS

CTP and follow-up diffusion weighted imaging (DWI) scans were retrospectively collected for patients presenting with AIS. Patients in the infarct only sub-study received successful mechanical thrombectomy (mTICI 2b,2c,3) and the DWI within 48 hours of treatment to ensure halting of conversion of penumbra to infarct from time of CTP to DWI imaging. Patients in the infarct and penumbra sub-study received no treatment and the DWI imaging more than 48 hours after presentation to ensure conversion of all penumbra to infarct from time of CTP to DWI imaging. This resulted in 1920 and 1888 axial CTP map slices in the infarct, and infarct and penumbra sub-studies. Commercial CTP software (Olea Sphere 3.0 SP28) was used to generate cerebral blood flow, cerebral blood volume, mean transit time, time to peak, and delay time maps for each case. Deep learning-based algorithms were trained to segment infarct or infarct and penumbra using preprocessed CTP maps. Segmentation performance was evaluated using Dice coefficients (DC), and mean absolute volume errors (ml) (MAVE).

#### RESULTS

The trained algorithm segmented infarct tissue with a DC of  $0.64 \pm 0.03$  (0.63,0.65), and MAVE of  $4.91 \pm 0.94$  (4.5,5.32) ml. In comparison, the commercial software predicted infarct with a DC of  $0.31 \pm 0.17$  (0.26,0.36) and MAVE of  $9.77 \pm 8.35$  (7.12,12.42) ml. The algorithm was able to segment infarct and penumbra with a DC of  $0.61 \pm 0.04$  (0.6,0.63), and MAVE of  $6.51 \pm 1.37$  (5.91,7.11) ml. In comparison, the commercial software predicted infarct and penumbra with a DC of  $0.3 \pm 0.19$  (0.25,0.35) and MAVE of  $9.18 \pm 7.55$  (7.25,11.11) ml.

#### CONCLUSION

Use of deep learning algorithms to segment infarct and penumbra volume is proven to be accurate and outperforms current contralateral hemisphere relative threshold methods. Such an algorithm can enhance the treatment selection for AIS patients.

#### CLINICAL RELEVANCE/APPLICATION

The enhanced identification of infarct and penumbra tissue would improve triaging of patients with AIS and could thus enhance patient outcome.

Printed on: 02/07/23

## Abstract Archives of the RSNA, 2022

W5A-SPNR-10

### Deep Learning-Based Differentiation of Atypical Parkinsonian Syndromes Using Susceptibility Weighted Images

Wednesday, Nov. 30 12:15PM - 12:45PM Room: Learning Center - NR DPS

#### Participants

Wonjune Choi, Pusan, Korea, Republic Of (*Presenter*) Nothing to Disclose

#### PURPOSE

Atypical parkinsonian syndromes (APs) such as progressive supranuclear palsy (PSP) and a parkinsonian variant of multiple system atrophy (MSA-P) show similar symptoms and signs as Parkinson's disease (PD), but additional symptoms with different rates of functional deterioration. Each parkinsonian syndrome has unique topographic pattern of iron accumulation, and susceptibility weighted imaging (SWI) is widely used to detect these specific patterns of localized iron concentration in the deep brain nuclei regions. In this work, therefore, we propose a novel framework for differentiating APS from PD in SWI using a deep learning (DL)-based approach with explainable AI.

#### METHODS AND MATERIALS

We obtained the T1-weighted (T1w) and SWI MRI scans of 33 MSA-P, 21 PSP, and 66 PD patients using protocols approved by the IRB. First, bias-field correction and intensity normalization were applied. Second, the SWI volume was registered in the MNI space using the hybrid contrast (HC) images generated as a linear combination of T1w and SWI. To select the deep brain nuclei regions, we extracted 15 slices from 70 to 85 of the MNI space axial axis, and cropped each slice to the size of 120x100 with the center of the slice. Then, we used the pretrained ResNet152 model to classify each image into subtypes of APS. The model was implemented by minimizing the Binary-Cross-Entropy loss using Adam optimizer for a learning rate of  $1e-4$ . Convergence was achieved using batch size of 16 for each 100 epochs. The model was evaluated with a 5-fold cross validation test by measuring the balanced accuracy (bAcc), sensitivity (Sen) and specificity (Spe). We also compared with the conventional machine learning (ML) methods such as quadratic discriminant analysis (QDA) and support vector machine (SVM). Finally, we used Gradient-weighted Class Activation Mapping (Grad-CAM) to highlight important regions (heatmap) used for differentiation of APS.

#### RESULTS

The proposed DL-based method achieved the performance with bACC of 0.9399, Sen of 0.9360 and Spe of 0.9439 for differentiation of MSA-P and PD; while QDA (SVM) achieved 0.8804 (0.8981), 0.8501 (0.9046), 0.9107 (0.8917). For MSA-P vs. PSP, the DL-based method achieved bAcc of 0.8522, Sen of 0.8483 and Spe of 0.8562 than QDA (SVM): 0.8380 (0.7862), 0.8561 (0.8802) and 0.8201 (0.6922). Heatmap from Grad-CAM shows that the prediction of the DL model was highly influenced by the putamen and globus pallidus regions.

#### CONCLUSION

The proposed DL-based method differentiates APSs significantly better than the ML-based methods, and also holds promise for identifying regions impacted by APSs.

#### CLINICAL RELEVANCE/APPLICATION

The high classification accuracy of our explainable DL model may contribute to a reliable clinical diagnosis of PD and APS.

Printed on: 02/07/23

## Abstract Archives of the RSNA, 2022

W5A-SPNR-11

### Effect of different pre ASiR-V on image quality and radiation dose of energy spectrum CT: A Phantom Study

Wednesday, Nov. 30 12:15PM - 12:45PM Room: Learning Center - NR DPS

#### Participants

Yaoming Ma, (*Presenter*) Nothing to Disclose

#### PURPOSE

To investigate the impact of different pre adaptive statistical iterative reconstruction - Veo (ASiR-V) level on image quality and radiation dose of spectral CT.

#### METHODS AND MATERIALS

A polypropylene cylindrical phantom(QSP Phantom dimension) with nine tubes containing different concentrations of iodine (0, 2.5, 5, 10, 20 mgI/ml) was scanned in gemstone spectral imaging (GSI) mode using fast kV switch (80/140 kV), the tube current is 485mA, the layer thickness is 1.25mm, the collimation width is 80mm, noise index (NI)5HU, pitch 0.992:1, dual energy CT (Revolution CT, GE Healthcare). Three groups of pre-ASiR-V weight (30%,40%,50% increments) was used for spectral CT scanning. Eleven groups of images were selected from the scan center and five layers above and below. The area of ROI was 1 / 2-1 / 3 of the cross-sectional area of the phantom tube, and the CT value and SD value of 20% and 10% iodine and water membrane tube were measured. The CT dose index (CTDI) of ASiR-V spectral scan with different weights was recorded. The dose length product (DLP), CT value and noise (SD) of the tube were recorded. The DLP across three groups were analyzed by simple linear regression analysis CT value and noise (SD), across three groups were analyzed by one-way ANOVA.

#### RESULTS

With the increase of pre-selected ASiR-V level, noise (SD) showed the SD value remains unchanged. There was significant difference in DLP among groups (7.95mSv, 6.87mSv, 4.73mSv for 30%,40%,50%pre-ASiR-V, respectively.  $P < 0.05$ ). There were no significant differences in SD among groups ( $9.92 \pm 0.55$ (I20),  $10.51 \pm 0.56$ (I10),  $9.80 \pm 0.61$ (H2O), for 30% pre-ASiR-V,  $10.04 \pm 0.44$ (I20),  $10.04 \pm 0.44$ (I10),  $10.01 \pm 0.37$ (H2O)40% pre-ASiR-V,  $10.52 \pm 0.64$ (I20),  $10.12 \pm 0.34$ (I10),  $10.52 \pm 0.50$ (H2O), 50% pre-ASiR-V,  $F = 2.130$ ,  $p > 0.05$ ).

#### CONCLUSION

Conclusion: ASiR-V does not affect the image quality of energy spectrum scanning (SD), and can significantly reduce the radiation dose (CTDI) while maintaining the image quality of energy spectrum scanning (SD).

#### CLINICAL RELEVANCE/APPLICATION

ASiR-V does not affect the image quality (SD) of energy spectrum scanning, and can significantly reduce the radiation dose (CTDI) while keeping the image quality (SD) of energy spectrum scanning unchanged. Correlation of clinical application: through the basic research of phantom, spectral CT scanning can provide the same image quality, increase the proportion of ASiR-V iterative algorithm and reduce the radiation dose. This study has guiding significance for the application of spectral CT scanning in different clinical scenes.

Printed on: 02/07/23

## Abstract Archives of the RSNA, 2022

W5A-SPNR-12

### Brain MRI volumetric machine learning model: A potential tool to differentiate Progressive Supranuclear Palsy from Parkinson's disease patients and healthy subjects.

Wednesday, Nov. 30 12:15PM - 12:45PM Room: Learning Center - NR DPS

#### Participants

Francisco Mendoza, MD, (Presenter) Nothing to Disclose

#### PURPOSE

To develop a machine learning model to differentiate Progressive Supranuclear Palsy (PSP) from Parkinson's disease (PD) and healthy subjects (HS) using an automated volumetry of brain MRI, validate its performance, and determine the most relevant Volumes of Interest (VOIs).

#### METHODS AND MATERIALS

We retrospectively assessed a total of 141 patients with a clinical diagnosis of Parkinsonism paired by age and sex and with a group of HS (PSP n = 47, PD n = 68, HS=26) between January 2003 and April 2021 and analyzed their brain MRI. Patients without T1 high resolution sequences (T1-MPRAGE) were excluded, leaving 83 patients (PSP n = 29, PD n = 54, HS n=26). We included different clinical subtypes of PSP: PSP-RS (n= 19), PSP-P (n= 5), PSP-PGF (n= 4), and PSP-F (n= 1). Using automatized SyngoviaBrainMorphometry software (Siemens), we obtained 109 VOIs for each subject, including absolute and normalized values. We developed a machine learning model based on multivariate feature selection and an extreme gradient boosting (XGB) vs. univariate feature selection and random forest (RF) to differentiate PSP from PD and HS. All subjects were randomly divided into training (85%) and validation (15%) data sets with the same proportions for each clinical group. The most relevant VOIs were obtained from the model, order by importance score (F-score; where 1.0 represents perfect precision and recall). Additionally, we assessed the diagnostic accuracy of each VOI using ROC curves.

#### RESULTS

The global diagnostic performance of the model to differentiate between the three groups was 70.6%. The diagnostic accuracy of the model to differentiate each group from the other was: PSP (88.2%), PD (70.6%), and HS (76.5%). The VOIs that presented higher importance scores were the mesencephalic normalized volume (0.068), frontal right white matter volume normalized and absolute (0.053), left hippocampus absolute volume (0.040), left globus pallidum absolute volume (0.036), right hippocampus normalized volume (0.035), right thalamus absolute volume (0.032), frontal right gray matter normalized volume (0.032), left deep white matter normalized volume (0.030) and right hippocampus absolute volume (0.028). The AUC to differentiate PSP from PD and/or HS was: for the mesencephalic normalized volume =0.87, the left globus pallidum absolute volume =0.72, for the left hippocampus absolute volume = 0.59, and the right hippocampus normalized volume= 0.57.

#### CONCLUSION

The developed machine learning model using an automated volumetry of brain MRI showed accurate discrimination between PSP, PD, and HS.

#### CLINICAL RELEVANCE/APPLICATION

Automatized volumetric assessment of brain MRI is a helpful tool for differentiating Progressive Supranuclear Palsy from Parkinson's disease.

Printed on: 02/07/23

## Abstract Archives of the RSNA, 2022

W5A-SPNR-13

### Multimodal Brain Tumor Segmentation using Deep Convolutional Neural Networks

Wednesday, Nov. 30 12:15PM - 12:45PM Room: Learning Center - NR DPS

#### Participants

Rimjhim Agrawal, PhD, Bangalore, India (*Presenter*) Nothing to Disclose

#### PURPOSE

Brain tumours are one of the leading causes of death worldwide. As a result, it is critical to discover it as soon as possible. Numerous ways have been developed to forecast and segment the tumour. They do, however, have a number of drawbacks, including the requirement for specialised assistance, the lengthy run-time, and the selection of an appropriate feature extractor. To overcome these difficulties, we suggest a convolutional neural network-based technique for concurrently predicting and segmenting a cerebral tumour using multimodal structural magnetic resonance images (T1w, FLAIR and Post contrast T1w).

#### METHODS AND MATERIALS

We used mpMRI Brain Tumor Segmentation (BRATS 2021) dataset. For each scan annotation consists of 3 classes - Enhancing Tumor (ET) , Peritumoral Edematous Tissue (ED) and necrotic tumour core (NCR). Our Method was developed by training deep neural networks (DNN) using only 3 Modalities - T1w, FLAIR and Post contrast T1w for generating tumour segmentation masks.

#### RESULTS

In this study, training and validation was performed on 1251 mpMRI scans and we were able to achieve a mean dice score coefficient (DSC) of 0.89. Also, validation was performed for 50 scans with annotations obtained from an expert radiologist achieving a mean DSC of 0.86 and tumor core DSC of 0.89.

#### CONCLUSION

The fully automated brain tumor segmentation method developed on a well-established benchmark (BraTS 2021) dataset demonstrated that it can provide both efficient and robust segmentation compared to manually obtained ground truth. Additionally, our method with only three modalities as input can achieve comparable results to the state-of-the-art methods with four modalities. The proposed method enables objective assessment for clinical tasks such as surgery pre-planning, tumor grade detection and post surgery monitoring.

#### CLINICAL RELEVANCE/APPLICATION

This research suggests accurate and quick segmentation using deep convolutional neural networks of different subregions of a tumour, and has crucial clinical implications in brain tumour diagnosis, prognosis, treatment and presurgical planning.

Printed on: 02/07/23

## Abstract Archives of the RSNA, 2022

W5A-SPNR-16

### A light-weight deep learning web app for rapid identification of poor-quality structural MRI scans: A multi-institutional study

Wednesday, Nov. 30 12:15PM - 12:45PM Room: Learning Center - NR DPS

#### Participants

Thomas Desilvio, Cleveland, OH (*Presenter*) Nothing to Disclose

#### PURPOSE

Screening and diagnosis of neurological disorders largely relies on T1-weighted (T1w) MRI. Presence of one or more artifacts can degrade MR image quality to the extent they are unusable for disease diagnosis, whether by machines or radiologists. Visual inspection and quality assessment of MRI scans to identify cases requiring exclusion or rescanning is often time-consuming and laborious. We present multi-institutional validation of a scalable, light-weight deep learning-based (DL) web-app for rapid identification of poor quality T1w brain MRI scans.

#### METHODS AND MATERIALS

We utilized publicly available cohorts from ABIDE-I (17 institutes, 1102 T1w MRIs, including 3 expert-reader quality ratings) and TCGA-GBM (5 institutes, 152 T1-POST MRIs). TCGA-GBM was internally evaluated by 3 radiologists to assign quality labels similar to ABIDE-I. Training cohort was curated from ABIDE-I (n=454, 15 institutions), where every scan was assigned "good quality (GQ)/poor quality (PQ)" based on rating agreement between 2+ readers. Remaining ABIDE-I datasets were split into internal validation (V1, n=400) and external validation (V2, n=248, 2 institutions). TCGA-GBM was additionally used for external validation (V3). For V1-V3, "ground truth" labeling of scans as GQ/PQ was based on mean opinion score of raters. A mid-brain 3D sub-volume (with foreground identification) from each scan used as input to a 3D ResNet18 model, optimized to predict PQ scans via training cohort. Additionally, 64 quality measurements (QMs) from the publicly available MRIQC tool (quantifying SNR, intensity contrast, motion, entropy artifacts) were used to train a random forest classifier for identifying PQ scans. Hold-out evaluation of ResNet and QM models was performed in terms of accuracy of identifying PQ scans on V1-V3.

#### RESULTS

The ResNet DL model achieved accuracies of 0.89, 0.83, and 0.89 in V1, V2, and V3, respectively for identifying PQ scans. MRIQC-based QM models performed significantly worse with accuracies of 0.77 (V1;  $p < 0.001$ ), 0.75 (V2;  $p < 0.001$ ), and 0.76 (V3;  $p < 0.001$ ) in identifying PQ scans. The DL web-app took  $< 1$  min/MRI volume for classifying each scan as PQ or GQ.

#### CONCLUSION

Our light-weight deep learning based web interface can enable rapid identification of poor-quality brain MRI scans, and offers improved performance compared to standard image quality measures.

#### CLINICAL RELEVANCE/APPLICATION

Rapid automated identification of poor-quality MRI scans could have significant implications for downstream machine learning analysis as well as radiology interpretation and disease diagnosis.

Printed on: 02/07/23



## Abstract Archives of the RSNA, 2022

W5A-SPNR-18

### Post-processing to improve accuracy of Deep Learning Algorithm for Intracranial Hemorrhage Detection: Our experience of introducing an analytical approach simulating Radiologist Reasoning

Wednesday, Nov. 30 12:15PM - 12:45PM Room: Learning Center - NR DPS

#### Participants

Anjali Agrawal, MD, Delhi, PA (*Presenter*) Nothing to Disclose

#### PURPOSE

Deep learning tools are being increasingly used to optimize radiologist efficiency in the emergency setting, however, overprediction and false positive (FP) results may be counterproductive. We investigated the value of additional post-processing refinements into the deep learning algorithm developed in our lab for the detection of intracranial hemorrhage (ICH) with the intention of introducing specific reasoning and logic similar to that applied by radiologists.

#### METHODS AND MATERIALS

A deep learning algorithm for ICH detection was developed using a fully convolutional neural network, U-NET with image segmentation and hemorrhage classification properties. Upon validation, several recurring FPs at specific locations posed a challenge in increasing overall accuracy to acceptable levels. Various new approaches were then developed to specifically address each type of FP. Deep learning models were used to decrease FPs instance-wise and slice-wise in calcification and artifact models respectively. Image processing and coding logic were used to decrease FPs in the region of basal ganglia, falx, dural sinus, volume averaging from dense calvaria, and FPs due to accentuated appearance of grey-white matter junction in older patients.

#### RESULTS

We analyzed 4512 studies of which 2036 were negative and 2476 were positive for intracranial hemorrhage sequentially using the ICH detection deep learning model, without and with post-processing algorithms. The results achieved without and with post-processing were sensitivity (recall) of 96.77% and 90.47%, specificity of 41.99% and 90.28%, precision of 66.98, 91.88%, F1 score of 79.17% and 91.17%, and Area Under Curve of 0.694 and 0.904 respectively.

#### CONCLUSION

s Postprocessing techniques brought about significant improvement in the model performance by reducing the number of false-positive results.

#### CLINICAL RELEVANCE/APPLICATION

Our research explores ways to improve the analytical capabilities of deep learning tools by using postprocessing techniques with the goal to develop a more optimal triage workflow in the emergency setting.

Printed on: 02/07/23

## Abstract Archives of the RSNA, 2022

W5A-SPNR-19

### Radiomics Analysis Distinguish Between Primary Central Nervous System Lymphoma, Glioblastoma, and Brain Metastasis

Wednesday, Nov. 30 12:15PM - 12:45PM Room: Learning Center - NR DPS

#### Participants

Murat AK, MD, Pittsburgh, PA (*Presenter*) Nothing to Disclose

#### PURPOSE

To investigate the diagnostic performance of radiomics-based machine learning in differentiating glioblastoma (GBM), primary central nervous system lymphoma (PCNSL) and brain metastasis (BM).

#### METHODS AND MATERIALS

We retrospectively identified 1075 patients from three institutions with untreated solitary, pathologically proven cases of PCNSL (133), GBM (433), and breast or lung BM (509). For each tumor, we segmented edema, contrast enhancement, necrosis, and contralateral white matter (cWM) volume of interest (VOI) for T2 FLAIR and T1 post-contrast sequences. A total of 205 texture features were extracted from each sequence's VOI including 10 histogram based first-order features and 195 second-order features using gray-level co-occurrence matrices. After feature normalization using cWM, we divided the 195 second level features by the volumes of each VOI to generate another 195 volume-independent features per VOI and 2,400 features per MRI. We performed feature selection with Least Absolute Shrinkage and Selection Operator (LASSO). We split the cohort into 70% training and 30% testing sets. We used XGBoost (eXtreme Gradient Boosting) algorithm to perform three-way classification and generate the radiomics model. The predictive performance of the models for classifying each tumor type against all others (i.e., BM versus PCNSL and GBM) was estimated using the receiver operating characteristic (ROC) curve, summarized as the area under the curve (AUC).

#### RESULTS

LASSO identified 216 independent features, of which 20 most relevant used for model building. Our three-classification model robustly differentiated ( $p < 0.001$ ) between PCNSL (AUC 0.95), GBM (AUC 0.97), and BM (AUC 0.96) and achieved 88% accuracy. The model obtained 76.9% sensitivity and 98.2% specificity for PCNS prediction, 86% sensitivity and 94.7% specificity for the GBM prediction and 92.7% sensitivity 86.3% specificity for the BM prediction.

#### CONCLUSION

s This study presents radiomics-based signature that can successfully differentiate between PCNSL, GBM, and BM. Although further independent validation is warranted the proposed predictive radiomics-based signature is cost-effective, non-invasive and enable better patient stratification, management, and clinical decision-making

#### CLINICAL RELEVANCE/APPLICATION

A major challenge in the management of brain tumor is distinguishing tumor type as there are currently no reliable non-invasive biomarkers to predict them. Our data suggests that radiomics using MRI is an cost-effective and non-invasive approach to identify brain tumor type.

Printed on: 02/07/23

## Abstract Archives of the RSNA, 2022

W5A-SPNR-2

### Automated Lumbar Disc Herniation Grading Through AP-Diameter Measurement in MR Imaging

Wednesday, Nov. 30 12:15PM - 12:45PM Room: Learning Center - NR DPS

#### Participants

Li Zhang, PhD, Princeton, NJ (*Presenter*) Employee, Covera Health

#### PURPOSE

Lumbar disc herniation (LDH) is often diagnosed using MR, and automated AI pipelines are used to reduce variation in grading severity. A fully automated AI-powered pipeline was used to detect, localize, and segment LDH at each Functional Spinal Unit (FSU) level (L1-2 through L5-S1) and use the anterior-posterior diameter (APD) of the segmented LDH to grade severity.

#### METHODS AND MATERIALS

Sagittal T2 sequences of MR lumbar spine were collected from 589 studies. 2,872 FSU manually segmented voxel-wise as background - 0 (No segmentation), disc - 1, and herniated disc region - 2. The studies were randomly split into train-validation-test sets in a 75:10:15 ratio. A deep reinforcement model was trained to identify the L1-2 through L5-S1 disc centers. Associated FSUs were cropped to 8 x 8 x 5 cm then fed to a convolutional neural network. An Attention U-Net was trained to segment the images on a 2D slice with 2 adjacent slices provided to the left and right of the target slice. The APD was estimated by summing the voxels' resolution at the apex of the estimated LDH region. A severity is assigned based on this measurement (Normal: 0mm; Small: APD = 3mm; Moderate: 3mm < APD = 6mm; Large: 6mm < APD). If an APD measurement error misassigns the severity by 1-degree, we call it 1-degree error, 1-degree error includes misassignment between Normal and Small, Small and Moderate, Moderate and Large. Similarly, 2-degree error is defined as severity misassignment between Normal and Moderate, Small and Large.

#### RESULTS

The model achieves an RMSE in APD of  $1.33 \pm 1.33$ mm and an average ratio of predicted to ground truth APD of  $1.14 \pm 0.89$  for the true positive predictions. The model accuracy is further evaluated by the assigned severities based on APD. The 1-degree misassignment is 34% where 47% of these are between normal and small and 37% are between small and moderate both with an RMSE of 1.8mm. These, however, are in general inconsequential, the clinical significant 2-degree severity classification error is only 4%.

#### CONCLUSION

s Segmentation of Lumbar MR has the advantage of providing visualization and location and automated measurement of LDH which can assist diagnosis and reduce interobserver variation.

#### CLINICAL RELEVANCE/APPLICATION

Automated detection, localization and measurement of LDH pipeline can provide precise, reproducible analysis of pathology which can be useful for quality analysis, enhancing efficiency of utilizing experts.

Printed on: 02/07/23

## Abstract Archives of the RSNA, 2022

W5A-SPNR-3

### Deep learning for classification of Cranial Ultrasound in Preterm Babies

Wednesday, Nov. 30 12:15PM - 12:45PM Room: Learning Center - NR DPS

#### Participants

Tahani Ahmad, MD, (*Presenter*) Nothing to Disclose

#### PURPOSE

Cranial ultrasound (CUS) is widely used as a screening tool to assess brain injury in preterm infants. Severe abnormalities on CUS are known to be associated with Neurodevelopmental impairment (NDI). This study investigates the feasibility of using deep learning to identify abnormalities in CUS images collected from a preborn preterm cohort that are routinely clinically assessed for NDI. The objective is to train a model that can classify normal vs. abnormal imaging findings and assess its usability for computer-aided diagnosis that can have merit in daily practice as a complementary decision aid.

#### METHODS AND MATERIALS

This is a retrospective study of a cohort of very preterm infants born between January 2004 and Dec 2016 and admitted to the Neonatal Intensive Care Unit at IWK Health, Canada. The sample size includes images from 619 patients (4180 images) collected during 3-time points (first week, 6th week of age, and a term-equivalent age). At each point, 3 coronal images were selected at specific landmarks. Each image was anonymized. CUS pixels intensities are normalized and resized to a standard 224x224 pixel. Regions outside of the brain were masked and set to pixel intensity zero. A trained radiologist manually labeled each image as either normal or abnormal. The dataset is split into training/test sets (90:10 percent split). Due to the class imbalance in the dataset, the Area Under the Curve (AUC) was chosen as the metric of reference. The abnormal cases where the model very confidently predicted the image as abnormal were selected, then an approach called Gradcam was applied. In this approach, the saliency of each individual pixel is visualized. The original image has a heatmap overlaid on it, the areas with more red are what lead the model to make its prediction.

#### RESULTS

We tested different CNN architectures. The total number of normal images is 3531/4180, and the total number of images with abnormal findings is 649/4180. Preliminary results indicate an average of 0.794 AUC (0.757-0.83) using 10 bootstraps stratified sampling strategies using DensNet169

#### CONCLUSION

s This is a preliminary work to provide a tool to assist clinicians during early NDI assessment by classifying CUS into normal scans and scans with abnormal imaging features that can have merit in daily practice as a complimentary decision aid. Although the dataset is currently limited, early results are positive and likely to improve as more images are going to be included.

#### CLINICAL RELEVANCE/APPLICATION

Cranial ultrasounds to assess neurodevelopmental impairment is a challenging task subject to high variability. Computer-aided diagnosis tool might help reduce false positive and false negative rates.

Printed on: 02/07/23

## Abstract Archives of the RSNA, 2022

W5A-SPNR-4

### Prediction of Primary Tumor Entity of Brain Metastases Using Machine Learning based on Radiomic Features Derived from Routine MRI

Wednesday, Nov. 30 12:15PM - 12:45PM Room: Learning Center - NR DPS

#### Participants

Quirin Strotzer, MD, Regensburg, Germany (*Presenter*) Nothing to Disclose

#### PURPOSE

This study aims to determine the primary tumor entity of brain metastases using machine learning based on radiomic features obtained from routine MRI sequences.

#### METHODS AND MATERIALS

This multicenter project included 251 patients for whom non-standardized routine MRI sequences T1, T1CE, T2, and FLAIR (from various scanners, 1.5T and 3T) and histologic determination of the primary tumor were available. A preprocessing pipeline was set up using Python libraries, including co-registration, normalization, and automated tumor segmentation using a Convolutional Neural Network with U-shaped architecture. Radiomic features were extracted and selected with a LASSO regression. Metastases were grouped into five classes: the four most frequently occurring primary entities (adenocarcinoma of the lung, melanoma, breast cancer, colorectal cancer) and a fifth group including all less common primaries. Using a five-fold cross-validation scheme, machine learning classifiers were tested on the train/validation partition of the dataset (80%) to predict the primary tumor based on the radiomic features. The performance was evaluated using a holdout test set (20%).

#### RESULTS

A total of 728 brain metastases were individually segmented. For each metastasis, 3852 radiomic features were extracted. The LASSO regression identified 60 variables with the greatest impact on classification. An AdaBoost classifier yielded the best results for this five-class classification task on the holdout test set (accuracy: 0.601; area under the receiver operating characteristic curve: 0.854). A feature importance analysis showed that the most essential variables for the classifier were second-order statistics features derived from the contrast-enhanced T1-weighted sequences.

#### CONCLUSION

s Primary tumor entity prediction might be feasible via radiomic feature analysis of non-standardized routine MRI sequences. Further relevant read-outs such as oncogenic driver mutations could be within reach.

#### CLINICAL RELEVANCE/APPLICATION

Predicting the primary tumor of brain metastases using radiomic features derived from non-standardized routine MRI sequences would significantly enhance the diagnostic value of routine MRI scans and reduce morbidity from invasive biopsies.

Printed on: 02/07/23

## Abstract Archives of the RSNA, 2022

W5A-SPNR-5

### Accelerated Creation of a Glioma Database for Machine Learning Prediction Model Development using PACS-Integrated Tools

Wednesday, Nov. 30 12:15PM - 12:45PM Room: Learning Center - NR DPS

#### Participants

Victor Becerra, MD, Albany, NY (*Presenter*) Nothing to Disclose

#### PURPOSE

The creation of well-annotated imaging datasets is crucial for the development of accurate and reproducible machine learning (ML) algorithms. Although an increasing number of ML algorithms are being developed in the academic setting, many of them are created in research-specific software incompatible with the routine clinical workflow. Our purpose was to facilitate the creation of a large, annotated glioma database by implementing clinical PACS-integrated tools for image segmentation and radiomic feature extraction.

#### METHODS AND MATERIALS

Data from our institution's radiation oncology registry from 2012 to 2019 was used. Glioma images from these patients and the BRaTS 2021 challenge were segmented using a home-grown PACS-integrated (Visage Imaging, Inc) U-net algorithm. These were subsequently validated by a board-certified neuroradiologist. A home-grown PACS-integrated PyRadiomics feature extraction tool was then deployed on the annotated dataset.

#### RESULTS

Over the course of only 5 months, segmentations and annotations were completed in 595 patients (236 females, 359 males, with a mean age of 50.92 years). Grade distribution was as follows: 245 Grade 4, 52 Grade 3; 97 Grade 2; 26 Grade 1; 175 unknown. Molecular subtypes included IDH (87 mutated, 355 wild-type, 153 unknown), 1p/19q (65 deleted or co-deleted, 87 intact, 443 unknown), MGMT promotor (162 methylated, 70 partially methylated, 207 unmethylated, 156 unknown), EGFR (55 amplified, 121 not amplified, 419 unknown), ATRX (28 mutated, 130 retained, 437 unknown), Ki-67 (433 known, 162 unknown) and p53 (395 known, 200 unknown). To generate a geographically distinct validation set, metadata labels were created for imaging acquired outside our institution.

#### CONCLUSION

Our PACS-integrated image annotation tools have allowed us to curate a large number of images in an accelerated manner that is compatible with the clinical workflow. On average, over 100 gliomas were annotated per month, thus establishing that these tools may be game-changing in the development of annotated imaging databases.

#### CLINICAL RELEVANCE/APPLICATION

The development of clinical PACS-integrated tools for data curation has the potential to facilitate and accelerate the development of large-scale well-annotated imaging datasets which can be used for algorithm development, radiomic feature extraction, among others.

Printed on: 02/07/23

## Abstract Archives of the RSNA, 2022

W5A-SPNR-6

### Multi-Scale Fusion 3D Convolutional Neural Networks Based on Attention Mechanism for Survival Prediction of Glioma Patients

Wednesday, Nov. 30 12:15PM - 12:45PM Room: Learning Center - NR DPS

#### Participants

Xuan Yu, (*Presenter*) Nothing to Disclose

#### PURPOSE

Due to the individual differences of different patients with glioma and individualized precision treatment, the survival time performance of different patients is quite different. Constructing a reliable survival prediction model and analyzing the MRIs of patients with glioma, further mining objective features from the images have extremely important clinical value for the prognosis of patients. We develop a multi-scale fusion 3D convolutional neural networks deep learning model based on attention mechanism to predict the survival time of glioma patients.

#### METHODS AND MATERIALS

MRIs from 270 cases were included, of which 207 from BraTS 2019 datasets and 63 from the private datasets of the hospital. Firstly, MRIs are preprocessed and a saliency-aware method is adopted to enhance the tumor region. Next we present a 3D convolutional structure to refine multiple scale characteristics of enhanced T1 Weighted imaging. Two crucial designs are shown in the model, one of which is fusing multi-scale features to explore level information in MRIs, and another is the attention gate make the model automatically focus on the crucial area in the images. Finally through the full connection layer to achieve the survival time analysis. The model includes prediction of short, medium, and long-term survival risk classification.

#### RESULTS

The cases were divided into low-risk group( $SD \geq 450$ ), medium-risk group( $300 \leq SD < 450$ ) and high-risk group( $SD \leq 300$ ) according to the Survival Days(SD). The ROC results show low-risk group AUC is always higher than medium- and high-risk group AUC in training, verification and test sets, which indicates low-risk group is easier to classify. The classification performance of medium-risk group and high-risk group are close. And the medium or high survival risk of patients is relative difficult to study due to the survival time is affected by more complex factors including the degree of tumor necrosis, the individual differences, whether has other disease and so on. By comparing with the popular 3D Unet model, sensitivity, specificity and AUC in our model displays relatively better performance.

#### CONCLUSION

Our research demonstrates that appropriate MRIs data preprocessing and saliency-aware enhancement could better show the lesion characteristics of images. 3D convolutional structure preserves the important spatial features. Fusing different scale features is helpful to achieve higher classification accuracy, and the attention gate focuses more on the key areas in the MRIs. Our method is effective to mine MRIs deep features thus to achieve the goal of glioma patients' survival time prediction.

#### CLINICAL RELEVANCE/APPLICATION

This work provides some support for the operation, treatment and survival evaluation of patients with gliomas.

Printed on: 02/07/23

## Abstract Archives of the RSNA, 2022

W5A-SPNR-7

### Deep Learning of Dynamic Susceptibility Contrast Perfusion-weighted Imaging to Predict the Local Recurrence in Glioblastoma Patients

Wednesday, Nov. 30 12:15PM - 12:45PM Room: Learning Center - NR DPS

#### Participants

Roh-Eul Yoo, MD, PhD, Seoul, Korea, Republic Of (*Presenter*) Nothing to Disclose

#### PURPOSE

To develop a deep learning model based on multiparametric MR imaging including dynamic susceptibility contrast perfusion-weighted imaging (DSC-PWI) that predict the local recurrence in patients with glioblastoma (GBM).

#### METHODS AND MATERIALS

This retrospective study included 213 consecutive GBM patients who underwent standard treatment between May 2010 and April 2021 and had both preoperative MR including DSC-PWI and 1 year follow-up 3T MRI. Patients were divided into the training set (172 patients [58 ± 14 years; 90 men] from 2010 to 2019) and test set (41 patients [56 ± 14 years; 23 men] from 2020 to 2021). Each patient was categorized as local recurrence or non-recurrence group with respect to the presence of local recurrence at 1 year after the diagnosis. Using the follow-up contrast-enhanced T1-weighted image (CE-T1WI) as the reference standard, the sites of local recurrence were annotated in a non-enhancing T2 hyperintense lesion on preoperative T2 FLAIR images. A deep learning model based on conventional MR and DSC-PWI was developed using nnU-Net. The deep learning model performance was validated on the test set. Diagnostic performance of the two models were compared using the McNemar test.

#### RESULTS

Training set and test set included 73 and 17 recurrence cases, respectively. In the test set, the multiparametric deep learning model using the combination of conventional MR and DSC-PWI showed a significantly higher sensitivity than the model based on conventional MRI alone in predicting the risk of recurrence (71% [12 of 17] vs. 29% [5 of 17],  $P = .031$ ). The specificity of the model based on the combination of conventional MR and DSC-PWI did not significantly differ from that based on the conventional MRI alone (42% [10 of 24] vs. 58% [14 of 24],  $P = .34$ ).

#### CONCLUSION

A deep learning model based on multiparametric MR imaging including DSC-PWI can be used to predict the risk of local recurrence in GBM patients.

#### CLINICAL RELEVANCE/APPLICATION

A deep learning model based on the combination of conventional and DSC-MRI could be used to stratify the risk of local recurrence in GBM patients and potentially to guide radiation treatment planning.

Printed on: 02/07/23



## Abstract Archives of the RSNA, 2022

W5A-SPNR-8

### From Accuracy to Consensus: Towards a New Paradigm for Assessing Model Performance

Wednesday, Nov. 30 12:15PM - 12:45PM Room: Learning Center - NR DPS

#### Participants

Simas Glinskis, Ithaca, NY (*Presenter*) Employee, Covera Health, Inc

#### PURPOSE

Machine learning model performance is typically analyzed through accuracy and other statistical measures contingent on consistent ground truth labels. This assumption falls apart with medical applications where considerable inter-reader variability is present due to variation in clinical interpretation. We designed a new statistical mechanism to assess model performance which incorporates multiple sources of truth.

#### METHODS AND MATERIALS

MRI lumbar spine studies from 207 patients, 1035 functional spine units, were collected and multi-annotated by 10 subspecialty radiologists. The data was partitioned into a ground truth set using labels from the most experienced radiologist available and a secondary set from the remaining experts. Deep learning based models for classification of disc herniation (DH), central canal stenosis (CCS), and nerve root compression (NRC) were used to generate severity predictions. Those predictions were split into two groups, where they agreed with ground truth (agree) and where they did not (disagree). Distributions of label consensus (LC) were generated for both groups by computing the average agreement between ground truth and external annotations for each prediction.

#### RESULTS

Accuracy of normal, mean agree LC and mean disagree LC are 87%, 97%, and 41% for NRC, 91%, 98% and 37% for CCS, and 74%, 92%, and 47% for DH, respectively. While accuracy is sensitive to the annotation that is selected as the gold standard, LC distributions generate a better measure of model performance which incorporates information from all of the experts. For the disagree set, there is low consensus which unfairly lowers accuracy and for the agree set we see very high consensus which the models are able to capture. Agree LC consistently outperforms accuracy and better represents the predictive power of the model when measured against a group of labels.

#### CONCLUSION

s We designed label consensus to analyze the performance of machine learning models by incorporating multi-annotated data. When there is inter-reader variability among experts conventional accuracy fails to incorporate information from the corpus of annotators and is sensitive to the choice of gold standard label while consensus is not.

#### CLINICAL RELEVANCE/APPLICATION

Our proposed label consensus evaluation provides a more effective way of assessing AI model performance in applications with significant inter-reader variability.

Printed on: 02/07/23



## Abstract Archives of the RSNA, 2022

W5A-SPOB

### OB/Gynecology Wednesday Poster Discussions - A

Wednesday, Nov. 30 12:15PM - 12:45PM Room: Learning Center - OB DPS

#### Participants

Priyanka Jha, MBBS, San Francisco, CA (*Moderator*) Nothing to Disclose

Printed on: 02/07/23

## Abstract Archives of the RSNA, 2022

W5A-SPPD

### Pediatric Wednesday Poster Discussions - A

Wednesday, Nov. 30 12:15PM - 12:45PM Room: Learning Center - PD DPS

#### Participants

Sudha A. Anupindi, MD, Philadelphia, PA (*Moderator*) Nothing to Disclose

#### Sub-Events

### W5A-SPPD- A Clinical-Radiomics of Pituitary MRI to Differentiate the Growth Hormone Deficiency from Idiopathic Short Stature<sup>1</sup>

#### Participants

Shiyun Tian, MD, (*Presenter*) Nothing to Disclose

#### PURPOSE

Growth retardation can be caused by Growth Hormone Deficiency (GHD) and Idiopathic Short Stature (ISS). Radiomics recognizes complex patterns in imaging data by extracting high-throughput features of Anterior pituitary heterogeneity in a non-invasive manner. Based on non-contrast-enhanced (NCE)/contrast-enhanced (CE) Magnetic Resonance (MR) T1WI images, we try to develop a clinical-radiomics model and validate its predictive capacity to identify GHD and ISS presented as no visual abnormality in pituitary on MRI.

#### METHODS AND MATERIALS

The clinical and MRI data of 102 patients first diagnosed as growth retardation in pediatrics and scanned with pituitary MRI from May 2011 to August 2021 were collected retrospectively. According to the clinical findings and hormone examination, the patients were divided into GHD ((n = 74) and ISS ((n = 28). It is randomly divided into training set (n = 71) and verification set (n = 31) by random number table method. In total, 851 radiomics features were extracted from the 3D region of anterior pituitary (ROI), we performed a clinical-radiomics analysis based on pretreatment NCE-MRI (NCE-radiomics) and CE-MRI images (CE-radiomics), respectively. Meanwhile, a combined-radiomics model based on NCE-MRI and CE-MRI images was constructed. Finally, we developed their corresponding nomograms incorporating clinical factors. ROC was used to evaluate models' predictive performance in the training and testing set, and a DeLong test was employed to compare the differences between different models.

#### RESULTS

In total, 851 features were extracted from the T1WI-MRI and CET1WI images, respectively. The ICC was used to screen out 140 and 154 related features. Subsequently, to prevent model overfitting, the 8 and 11 features with optimal correlation coefficients were retained, respectively. The AUCs of the Clinical-T1WI, Clinical-CE-T1WI and Combine radiomics models were 0.7267 (95% CI: 0.5856, 0.8679), 0.8421 (95% CI: 0.7422, 0.9420), and 0.8462 (95% CI: 0.7465, 0.9458) in the training set, respectively, which were confirmed in the test set by AUCs of 0.5960 (95% CI: 0.3715, 0.8204), 0.6162 (95% CI: 0.4037, 0.8286), and 0.6515 (95% CI: 0.4351, 0.8679), respectively.

#### CONCLUSION

The MRI-based radiomics model can be helpful to distinguish GHD and ISS, and combined with clinical features, which can improve diagnostic accuracy on MRI provides histological information for pituitary without abnormality.

#### CLINICAL RELEVANCE/APPLICATION

The MRI-based radiomics of the pituitary is helpful in the diagnosis of patients with growth retardation.

Printed on: 02/07/23

## Abstract Archives of the RSNA, 2022

W5A-SPPD-1

### A Clinical-Radiomics of Pituitary MRI to Differentiate the Growth Hormone Deficiency from Idiopathic Short Stature

Wednesday, Nov. 30 12:15PM - 12:45PM Room: Learning Center - PD DPS

#### Participants

Shiyun Tian, MD, (*Presenter*) Nothing to Disclose

#### PURPOSE

Growth retardation can be caused by Growth Hormone Deficiency (GHD) and Idiopathic Short Stature (ISS). Radiomics recognizes complex patterns in imaging data by extracting high-throughput features of Anterior pituitary heterogeneity in a non-invasive manner. Based on non-contrast-enhanced (NCE)/contrast-enhanced (CE) Magnetic Resonance (MR) T1WI images, we try to develop a clinical-radiomics model and validate its predictive capacity to identify GHD and ISS presented as no visual abnormality in pituitary on MRI.

#### METHODS AND MATERIALS

The clinical and MRI data of 102 patients first diagnosed as growth retardation in pediatrics and scanned with pituitary MRI from May 2011 to August 2021 were collected retrospectively. According to the clinical findings and hormone examination, the patients were divided into GHD ((n = 74) and ISS ((n = 28). It is randomly divided into training set (n = 71) and verification set (n = 31) by random number table method. In total, 851 radiomics features were extracted from the 3D region of anterior pituitary (ROI), we performed a clinical-radiomics analysis based on pretreatment NCE-MRI (NCE-radiomics) and CE-MRI images (CE-radiomics), respectively. Meanwhile, a combined-radiomics model based on NCE-MRI and CE-MRI images was constructed. Finally, we developed their corresponding nomograms incorporating clinical factors. ROC was used to evaluate models' predictive performance in the training and testing set, and a DeLong test was employed to compare the differences between different models.

#### RESULTS

In total, 851 features were extracted from the T1WI-MRI and CET1WI images, respectively. The ICC was used to screen out 140 and 154 related features. Subsequently, to prevent model overfitting, the 8 and 11 features with optimal correlation coefficients were retained, respectively. The AUCs of the Clinical-T1WI, Clinical-CE-T1WI and Combine radiomics models were 0.7267 (95% CI: 0.5856, 0.8679), 0.8421 (95% CI: 0.7422, 0.9420), and 0.8462 (95% CI: 0.7465, 0.9458) in the training set, respectively, which were confirmed in the test set by AUCs of 0.5960 (95% CI: 0.3715, 0.8204), 0.6162 (95% CI: 0.4037, 0.8286), and 0.6515 (95% CI: 0.4351, 0.8679), respectively.

#### CONCLUSION

s The MRI-based radiomics model can be helpful to distinguish GHD and ISS, and combined with clinical features, which can improve diagnostic accuracy on MRI provides histological information for pituitary without abnormality.

#### CLINICAL RELEVANCE/APPLICATION

The MRI-based radiomics of the pituitary is helpful in the diagnosis of patients with growth retardation.

Printed on: 02/07/23

## Abstract Archives of the RSNA, 2022

W5A-SPPH

### Physics Wednesday Poster Discussions - A

Wednesday, Nov. 30 12:15PM - 12:45PM Room: Learning Center - PH DPS

#### Participants

Kevin Little, PhD, Chicago, IL (*Moderator*) Nothing to Disclose

#### Sub-Events

### **W5A-SPPH- Evaluation of Residual Disease after Neoadjuvant Chemotherapy Using Manganese-Enhanced Magnetic Resonance Imaging in an Orthotopic Mouse Model** 1

#### Participants

Myoung Kyoung Kim, Seoul, Korea, Republic Of (*Presenter*) Nothing to Disclose

#### PURPOSE

Manganese-enhanced magnetic resonance imaging using hollow manganese silicate (HMS-MRI) predicts a pathologic complete response (pCR) more accurately than does gadolinium-enhanced MRI (Gd-MRI) because manganese-enhanced MRI reflects not only vascularity but also viable tumor cellularity after chemotherapy. This study aimed to compare the accuracy of HMS-MRI and Gd-MRI in predicting lesion size and viable tumor burden after chemotherapy using in vivo and in vitro experiments.

#### METHODS AND MATERIALS

BT474 cells and orthotopic xenograft mouse models of human breast cancer, based on BT474 cell inoculation, were used for the in vivo and in vitro experiments, respectively. In vivo, 18 female mice underwent Gd-MRI and HMS-MRI before and after chemotherapy. Two sets of BT474 cell pellets, treated with or without chemotherapy, were imaged by adding MnCl<sub>2</sub> or gadolinium. Tumor size and residual tumor cellularity after treatment obtained from Gd-MRI and HMS-MRI were compared with pathological findings.

#### RESULTS

Differences in residual tumor size and cellularity measured by MRIs were also correlated with pathological findings. Agreements in both tumor size and residual tumor cellularity between HMS-MRI and pathology were stronger than those between Gd-MRI and pathology. The lower the tumor/stroma ratio in pathological specimens, the larger was the difference in residual tumor cellularity between Gd-MRI and HMS-MRI ( $R = -0.62$ ,  $P = 0.018$ ). BT474 cell pellets showed signal enhancement after exposure to MnCl<sub>2</sub>, and the degree of enhancement decreased when cell pellets were exposed to chemotherapeutic agents.

#### CONCLUSION

Our results suggested that HMS-MRI can predict pCR more accurately than Gd-MRI when a pCR is suspected.

#### CLINICAL RELEVANCE/APPLICATION

Considering the active clinical trend for omitting surgery if pCR is highly suspected, our study suggested that HMS-MRI is a promising method for patient selection. In particular, HMS can be used to image breast cancer, which would be the first step in the wider use of HMS.

### **W5A-SPPH- When Will PROPELLER Technique Improve Quality in Acquisition of T2W-FRFSE Images of Abdomen MRI? Comparative Analysis According to Patient's Respiratory Patterns** 2

#### Participants

Kyungmin Lee, Gyeonggi-Do, Korea, Republic Of (*Presenter*) Nothing to Disclose

#### PURPOSE

To evaluate the value of periodically rotated overlapping parallel lines with enhanced reconstruction (PROPELLER) technique to reduce respiratory artifacts and improve image quality in acquisition of T2-weighted (T2W) respiratory triggering fast recovery fast spin echo (FRFSE) images according to patient's respiratory pattern.

#### METHODS AND MATERIALS

In 200 consecutive patients who underwent abdominal MRI, T2W-FRFSE images were obtained with and without PROPELLER. Patients were divided into four groups according to respiratory patterns and rates (Group A: regular, =14 times/min; B: regular, 15-17 times/min; C: regular, =18 times/min; D: irregular, any rate). Qualitative image quality was assessed independently by two radiologists for ghost artifacts, edge sharpness, image noise, and overall image quality. Quantitative indices of signal-to-noise-ratio (SNR) and contrast-to-noise-ratio (CNR) were also analyzed by two radiologists. These indices were compared between two techniques in each group using Wilcoxon signed-rank test. Inter-observer agreement was assessed using Cohen's Kappa test and intraclass correlation coefficient.

#### RESULTS

In group A and B, T2W-FRFSE images without PROPELLER showed better image quality than those with PROPELLER in all qualitative and quantitative indices ( $p < 0.05$ ), except for ghost artifact in group A ( $p = 0.404$ ). In contrast, in group C and D, T2W-FRFSE images with PROPELLER showed better image quality than those without PROPELLER in all qualitative and quantitative indices ( $p < 0.05$ ) except for SNR in group C ( $p = 0.339$ ). Inter-observer agreements between two radiologists were excellent in all qualitative indices (kappa values  $> 0.8$ ) and quantitative indices (ICCs  $> 0.8$ ).

## CONCLUSION

s Acquisition of T2W-FRFSE with PROPELLER yielded better image quality in patients with fast or inconsistent respiration than T2W-FRFSE without PROPELLER, and vice versa in patients with slow and steady respiration.

## CLINICAL RELEVANCE/APPLICATION

Whether or not to utilize PROPELLER in acquisition of T2W-FRFSE should be determined according to the patient's respiratory pattern and rate.

## W5A-SPPH- Toward a Simple Surrogate for Abdominopelvic Adipose Tissue Volume - Systematic MRI Assessment 3 in Patients With Different BMI Classes

Participants

Nicolas Linder, MD, Leipzig, Germany (*Presenter*) Nothing to Disclose

## PURPOSE

Obesity is a leading health problem worldwide with numerous comorbidities, such as cardiovascular disease, with the amount of visceral fat often regarded as an important factor for prognosis. In routine practice, many have used the sagittal abdominal diameter (SAD) as a simple clinical marker of visceral fat. The aim of this work was to systematically correlate (MRI-derived) SADMR with the abdominopelvic visceral and subcutaneous adipose tissue (VAT/SAT) volume in patients with obesity.

## METHODS AND MATERIALS

Full abdominopelvic MR datasets were available from 266 patients (196 females and 70 males) with obesity. SADMR was determined on axial images by the respective distance of a line through the center of the vertebral body at different levels (lumbar disc compartments L1-L2 to L5-S1 and umbilicus). VAT and SAT volumes were determined with a semiautomatic segmentation software. Agreement between SADMR and AT volumes was evaluated by correlation coefficients R.

## RESULTS

SADMR ranged from 21.7 cm to 39.0 cm and total volume of VAT (SAT) ranged from 0.9 to 14.0 L (4.8 to 39.4 L). Over all patients, R values between SADMR and VAT ranged from 0.66 at L5-S1 to 0.71 at L2-L3 (mean R of 0.69). Between sexes, the highest R value was larger for women (0.74 at L2-L3 vs. 0.69 at L3-L4). Similarly strong correlations were also seen between SADMR and SAT with R values between 0.67 (L2-L3) and 0.73 (L5-S1) overall, and higher values for each sex. Strong correlations of SADMR were also maintained within BMI subgroups for each sex with VAT but not with SAT

## CONCLUSION

s A gender-specific sagittal abdominal diameter has been shown to be a reliable measure for simple and rapid estimation of visceral fat volume in patients with different degrees of obesity.

## CLINICAL RELEVANCE/APPLICATION

The presented parameter MRI-derived sagittal abdominal diameter (SADMR) promises to be a simple but reliable imaging marker of visceral obesity.

## W5A-SPPH- Novel Free-Breathing Day-Optimizing-Throughput Sequences in Comparison with Conventional 4 Breath-Hold Examinations During Whole-Body MRI

Participants

Vitali Koch, MD, Frankfurt am Main, Germany (*Presenter*) Nothing to Disclose

## PURPOSE

To assess and compare novel free-breathing DOT sequences (Day Optimizing Throughput) with conventional breath-hold examinations in whole-body magnetic resonance imaging (MRI).

## METHODS AND MATERIALS

This prospective study included 26 subjects with a variety of pathologies who had undergone whole body 1.5-Tesla MRI. Image quality, diagnostic confidence, and image noise were evaluated by two experienced radiologists. Diagnostic performance for the overall detection of pathologies in both sequences was assessed using the area under the receiver operating characteristics curve (AUC). Additionally, study participants were asked to rate their examination experience in a satisfaction survey using a 10-point Likert scale.

## RESULTS

MR free-breathing scans were rated as at least equivalent to conventional MR scans in more than 90% of cases, showing high overall diagnostic accuracy (95% [95% CI 92-100]) and performance (AUC 0.971, 95% CI 0.942 to 0.988;  $P < 0.0001$ ) for the assessment of pathologies at simultaneously reduced examination time ( $50 \pm 4$  vs.  $59 \pm 5$  minutes;  $P < 0.0001$ ). Interrater agreement was excellent for both, free-breathing ( $\kappa = 0.96$  [95% CI, 0.88-1.00]) and conventional scans ( $\kappa = 0.93$  [95% CI, 0.84-1.00]). Ratings for image quality, image noise, and diagnostic confidence differed not significantly between the two types of MR image acquisition (all  $P > 0.05$ ).

## CONCLUSION

s MR images generated with free-breathing DOT sequences yielded similar diagnostic performance at equivalent image quality and noise levels compared to conventional breath-hold algorithms. Moreover, the long examination time of whole-body MRI could be considerably shortened for a more tolerable whole-body MRI experience.

## CLINICAL RELEVANCE/APPLICATION

Free-breathing Day-Optimizing-Throughput (DOT) MRI yields comparable diagnostic accuracy compared to breath-hold MRI. Free-breathing DOT sequences provide high diagnostic confidence at low image noise levels. Free-breathing DOT whole-body MRI may represent a viable alternative to conventional MRI.

## W5A-SPPH- Technical and Clinical Considerations of a Physical Phantom for CT Radiomics Analysis

5

Participants

Bino A. Varghese, PhD, Los Angeles, CA (*Presenter*) Nothing to Disclose

## PURPOSE

Radiomic measurements can be impacted by differences in protocol and equipment. Statistical approaches such as ComBat reduces this impact, however, they ignore the variable relationship, between different radiomic metrics and imaging parameters, leading to suboptimal harmonization for some metrics. We identify key phantom characteristics to help build a physical phantom for CT-radiomics harmonization, particularly, the higher-order texture metrics.

## METHODS AND MATERIALS

CT scans of a radiomics phantom comprising of 18 novel 3D printed inserts with varying size, shape, and material combinations were acquired on a 64-slice CT scanner (Brilliance 64, Philips Healthcare). The images were acquired at 120 kV, 250mAs, CTDIvol of 16.36 mGy, 2mm slice thickness and reconstructed using iDose1. Radiomics analysis was performed using the Cancer Imaging Phenomics Toolkit (CaPTk), following automated segmentation of volumes of interests (VOIs) of the 18 inserts. To add perspective to our findings we compared them to 3 additional VOIs obtained of an anthropomorphic liver phantom, a patient liver CT scan, and a water phantom, at comparable imaging settings. Percent difference in Hounsfield units (HU) between phantom and tissue was used to assess the biological equivalency and <10% was used to claim equivalent.

## RESULTS

The HU for all 18 VOIs from the phantom ranged from -30 to 120 compared with a range of 0-118 for liver tissue. One of our novel phantom inserts, T3-6B, had >50% radiomic features that have <10% difference from liver tissue (patient). Second-order texture metrics, particularly, those of Neighborhood Gray Tone Difference Matrix (NGTDM), which are also representatives of the signal to noise ratio of CT scans, mostly show extreme values in the water phantom VOI compared to the VOIs from the phantom.

## CONCLUSION

The practice of using water phantom values which represent a structureless entity, will help identify limits of threshold for radiomic metrics, particularly texture. The practice of comparing the values to those from patient scans will help establish clinical relevance. By adopting some of the patterns from the radiomics phantom within the liver phantom, we will be able to selectively harmonize texture metrics, depending on its order and explore its association with imaging variables.

## CLINICAL RELEVANCE/APPLICATION

Development of phantoms untangling the relationship between radiomic metrics and imaging variables will help establish quality assurance and control standards which are warranted for the clinical translation of radiomics.

## W5A-SPPH- Postural Effect on Renal Volume: Evaluation Using Multi-Posture MRI

6

Participants

Seiya Nakagawa, BA, (*Presenter*) Nothing to Disclose

## PURPOSE

Measurement of renal volume is vital for the early identification and monitoring of renal diseases. Nevertheless, it is unclear how postural changes, i.e., differences in the effects of gravity, alter renal volume. In this study, we evaluated the postural effect on renal volume in the supine and upright positions using an original magnetic resonance imaging (MRI) system that can image in any posture (multiposture MRI).

## METHODS AND MATERIALS

Renal volume was evaluated in seven healthy volunteers (mean age,  $22.7 \pm 1.0$  years; body mass index,  $20.5 \pm 1.0$  kg/m<sup>2</sup>) in the supine and upright positions using multiposture MRI (0.4 T). A breath-hold 3D gradient-echo sequence was used to acquire coronal T1-weighted images of the right and left kidneys in the supine and upright positions. Then, the right and left renal volumes (whole kidney, renal cortex, medulla, and pelvis) were measured and compared across positions.

## RESULTS

The whole kidney volume in the upright position (right kidney,  $122.3 \pm 20.1$  mL; left kidney,  $120.0 \pm 14.5$  mL) was significantly lower than that in the supine position (right kidney,  $139.9 \pm 21.0$  mL; left kidney,  $133.8 \pm 18.9$  mL) for both the right and left kidneys ( $P < 0.05$  for both). The renal cortex volume in the upright position (right kidney,  $77.0 \pm 12.2$  mL; left kidney,  $75.3 \pm 6.3$  mL) was significantly lower than that in the supine position (right kidney,  $89.3 \pm 12.9$  mL; left kidney,  $85.0 \pm 10.1$  mL) for both the right and left kidneys ( $P < 0.05$  for both). The renal medulla volume in the upright position (right kidney,  $40.6 \pm 7.3$  mL; left kidney,  $38.5 \pm 7.1$  mL) was significantly lower than that in the supine position (right kidney,  $45.5 \pm 8.7$  mL; left kidney,  $42.7 \pm 7.7$  mL) for both the right and left kidneys ( $P < 0.05$  for both). These findings revealed a decrease in blood volume and urine volume owing to the fluid shift effect when standing. Moreover, in comparison with the standard MRI examination of the kidney, multiposture MRI provided additional diagnostic information on the regulatory function to the gravity. However, no significant difference was observed in the renal pelvis volume between the supine and upright positions for both the right and left kidneys. Furthermore, no significant differences were observed in the volume change ratio from the supine to upright between the right and left kidneys.

## CONCLUSION

An upright position reduces renal volume. Multiposture MRI enables the assessment of the postural effect on renal volume.

## CLINICAL RELEVANCE/APPLICATION

An upright position reduces renal volume. Multiposture MRI revealed differences in the renal volume between the upright and supine

positions, thereby providing new diagnostic information on the regulatory function to the gravity as compared with the standard MRI examination of the kidney.

## **W5A-SPPH- Comparison of Image Quality Metrics Between Solid-State Digital-BGO PET/CT and Time-of-Flight LSO Systems**

Participants

Tala Palchan Hazan, PhD, (*Presenter*) Nothing to Disclose

### **PURPOSE**

A recently designed digital solid-state positron emission tomography/x-ray CT system (PET/CT) scanner with bismuth germanate (BGO) scintillators coupled to silicon photomultipliers provides for a 32 cm axial field of view. Image quality metrics from this ultra-high sensitivity digital-BGO system without time-of-flight (TOF) were compared to a lutetium oxyorthosilicate (LSO) based TOF PET/CT scanner.

### **METHODS AND MATERIALS**

A national electrical manufacturers association (NEMA) image quality (IQ) phantom was prepared as per NEMA NU 2-2018 with a fluorine-18 radiotracer. The 6 hot spheres (10 to 37 mm in diameter) were scanned on the LSO and digital-BGO systems. List mode data were binned to 12 decay-corrected 2-minute equivalent acquisitions, each with approximately the same number of incident counts. In both systems, images were reconstructed using an ordered subset expectation maximization (OSEM) algorithm and compared (Kruskal-Wallis test) to TOF-OSEM from the LSO system. Additional LSO OSEM reconstructions relisted scans to 1.4, 2.25 and 3.6 times the number of incident counts. The IQ metric was the contrast to noise ratio (CNR), calculated by dividing the contrast of hot sphere activity with respect to the background by the coefficient of variation of the background.

### **RESULTS**

All CNRs of the digital-BGO system were the same or greater compared to LSO TOF-OSEM. For the smallest feature, there was no statistically significant difference ( $p < 0.001$ ) in the CNR of the 10 mm sphere (CNR<sub>10</sub>) between LSO TOF-OSEM ( $25.8 \pm 2.1$ , mean  $\pm$  std. dev.) and the digital-BGO ( $24.8 \pm 1.4$ ). There was also no significant difference ( $p < 0.001$ ) in CNR<sub>10</sub> between LSO TOF-OSEM and LSO OSEM using 2.25 times the number of incident counts ( $26.8 \pm 1.9$ ). Using 1.0 or 1.4 times the number of incident counts were insufficient to match LSO TOF-OSEM ( $19.0 \pm 1.8$ , and  $21.5 \pm 1.8$ , respectively). Using 3.6 times the number of incident counts significantly improved CNR<sub>10</sub> ( $35.0 \pm 0.9$ ,  $p < 0.001$ ) compared to LSO TOF-OSEM.

### **CONCLUSION**

The ultra-high sensitivity of a solid-state 32 cm axial FOV digital-BGO PET/CT system provides for image quality similar to TOF systems, as measured by CNR in NEMA phantoms.

### **CLINICAL RELEVANCE/APPLICATION**

The ultra-high sensitivity of a novel solid-state digital-BGO PET/CT system provides for high quality imaging of small features, enabling the diagnosis of pathology through functional imaging.

## **W5A-SPPH- Multiparametric MRI Method Development for Clinical Prostate Imaging Using 5T MR Imaging**

Participants

Liyun Zheng, Shanghai, China (*Presenter*) Nothing to Disclose

### **PURPOSE**

The purpose of this study was to evaluate the development of prostate MRI at 5T by providing assessment of image quality on clinical sequences, including T1-weighted (T1W), T2-weighted (T2W) and diffusion-weighted imaging (DWI) sequences.

### **METHODS AND MATERIALS**

Ten healthy subjects (mean age,  $55.5 \pm 7.5$ ) were measured on a 5T MR scanner (uMR Jupiter, United Imaging Healthcare, Shanghai, China), using a 24-channel transmit/receive body array coil. SAR-monitoring and B0 and B1+ shimming were performed. Imaging sequences including: (1) axial T1W quick3D gradient echo (GRE) sequence (TR/TE = 3.34/1.42 ms, FA = 15°, Bandwidth = 850 Hz, 60 slices, Slice thickness = 3 mm, FOV = 300 × 400 mm, Matrix = 410 × 608, Number of averages = 2, Acquisition time = 16.9s); (2) axial T2W fat-saturated fast spin echo (FSE) sequence (TR/TE = 2600/128.24 ms, FA = 90°, Bandwidth = 200 Hz, 30 slices, Slice thickness = 5mm, FOV = 380 × 300 mm, Matrix = 639 × 504, Number of averages = 2, Acquisition time = 2min10s); and (3) echo-planar imaging (EPI) - DWI (TR/TE = 3650/53 ms, FA = 90°, Bandwidth = 2100 Hz, 30 slices, Slice thickness = 5 mm, FOV = 180 × 380 mm, Matrix = 410 × 608, b = 50, 800 s/mm<sup>2</sup>, Number of averages = 2, 4). Image analysis was performed by two experienced radiologists in consensus. For all the sequences, overall image quality (5 = excellent, 1 = non-diagnostic) and presence of artifacts (5 = pronounced, 1 = none) were assessed on a 5-point scale. Visibility of anatomical structures, defined as distinction between peripheral and transition zone, seminal vesicles, and delineation of the prostate, was graded on T2W images utilizing a five-point scale (5 = excellent, 1 = unacceptable). For DWI, geometric distortion (defined as modification in size, profile, and/or orientation due to inhomogeneities of the magnetic field in relation to T2W images) was evaluated on a 5-point scale (5 = very high distortion, 1 = no distortion).

### **RESULTS**

Overall image quality of T1W image was scored as moderate to good ( $3.9 \pm 0.5$ ), T2W image was scored as good to excellent ( $4.1 \pm 0.8$ ), while DWI was scored as moderate ( $3.0 \pm 0.6$ ). Presence of artifacts of T1W, T2W and DWI images were scored as none to minimal ( $1.5 \pm 0.5$  for T1W,  $1.4 \pm 0.5$  for T2W,  $1.8 \pm 0.5$  for DWI). Visibility of anatomical structures for T2W at 5T was graded as good to excellent ( $4.2 \pm 0.7$ ). Upon DWI at 5T, the geometric distortion was graded as no distortion to low distortion ( $1.5 \pm 0.9$ ).

### **CONCLUSION**

This study proved that prostate MRI, including T1W, T2W and DWI sequences at 5T can achieve diagnostic image quality.

### **CLINICAL RELEVANCE/APPLICATION**

According to current results about image quality, presence of artifacts, visibility of anatomical structures of T2W images, and geometric distortion of DWI, clinical prostate imaging is feasible at 5T MRI.

## W5A-SPPH- How to Handle Zero Counts in Low Dose Photon Counting CT Imaging? 9

Participants

Dan Bushe, MSc, BSc, Madison, WI (*Presenter*) Nothing to Disclose

### PURPOSE

The probability of registering a count of zero for a given pixel is significantly higher for photon counting detectors (PCDs) when compared with energy integrating detectors (EIDs). This is a result of the general one-to-one correspondence between the digital output of the PCD with the absorbed x-ray photons and the higher spatial resolution of PCD detectors (0.15-0.3 mm). In contrast, a single x-ray photon can generate tens to hundreds of digital counts in EID elements with a size of 1 mm or larger. This problem becomes further exacerbated when considering low dose PCD-CT applications, large patient imaging, and the allocation of counts to various energy bins for spectral imaging. Zero counts must be corrected before the nonlinear log transform is taken to generate the sinograms for CT image reconstruction. However, replacing zeros by any positive number alters the statistical distribution of counts and introduces biases that can manifest as severe shading or blooming artifacts. The purpose of this work was to develop a novel PCD-CT zero-count correction method that not only corrects zero-counts but also minimizes CT number biases.

### METHODS AND MATERIALS

In this work, a novel Laurent expansion was introduced to approximate the log-transformed projection data. The coefficients of the truncated Laurent expansion were calibrated using the correspondence between low dose scans with zero counts and high-dose scans without zero counts. This method was experimentally validated using a CdTe-based PCD-CT system with 4 test objects and under 4 different dose levels. The severity of the zero counts problem ranged from less than 0.1% to 22%.

### RESULTS

With a conventional zero-count replacement correction, images demonstrated severe blooming and shading artifacts due to sinogram biases. The proposed method eliminated those artifacts and reduced CT number biases from -930 HU (95% CI: -1267, -592HU ) to -0.8 HU (95% CI: -1.5, -0.2 HU) for a Teflon insert and from 790 HU (95% CI: 552, 1028 HU) to 3.4 HU (95% CI: 3.0, 3.9 HU) for an air insert. For both conventional and proposed corrections, the limiting spatial resolution of the CT images was matched at 9 lp/cm.

### CONCLUSION

s The proposed PCD-CT zero-count correction strategy not only corrects for zero-count pixels but also removes the associated biases. The method takes only a single pass and is computationally efficient. Furthermore, the method does not use any spatial filtering and thus does not introduce any spatial resolution loss.

### CLINICAL RELEVANCE/APPLICATION

Zero detector counts are common in PCD-CT and severely degrade clinical diagnostic performance. This work addresses the long-standing zero-count correction problem and further elevates the clinical trustworthiness of PCD-CT.

Printed on: 02/07/23

## Abstract Archives of the RSNA, 2022

W5A-SPPH-1

### Evaluation of Residual Disease after Neoadjuvant Chemotherapy Using Manganese-Enhanced Magnetic Resonance Imaging in an Orthotopic Mouse Model

Wednesday, Nov. 30 12:15PM - 12:45PM Room: Learning Center - PH DPS

#### Participants

Myoung Kyoung Kim, Seoul, Korea, Republic Of (*Presenter*) Nothing to Disclose

#### PURPOSE

Manganese-enhanced magnetic resonance imaging using hollow manganese silicate (HMS-MRI) predicts a pathologic complete response (pCR) more accurately than does gadolinium-enhanced MRI (Gd-MRI) because manganese-enhanced MRI reflects not only vascularity but also viable tumor cellularity after chemotherapy. This study aimed to compare the accuracy of HMS-MRI and Gd-MRI in predicting lesion size and viable tumor burden after chemotherapy using *in vivo* and *in vitro* experiments.

#### METHODS AND MATERIALS

BT474 cells and orthotopic xenograft mouse models of human breast cancer, based on BT474 cell inoculation, were used for the *in vivo* and *in vitro* experiments, respectively. *In vivo*, 18 female mice underwent Gd-MRI and HMS-MRI before and after chemotherapy. Two sets of BT474 cell pellets, treated with or without chemotherapy, were imaged by adding MnCl<sub>2</sub> or gadolinium. Tumor size and residual tumor cellularity after treatment obtained from Gd-MRI and HMS-MRI were compared with pathological findings.

#### RESULTS

Differences in residual tumor size and cellularity measured by MRIs were also correlated with pathological findings. Agreements in both tumor size and residual tumor cellularity between HMS-MRI and pathology were stronger than those between Gd-MRI and pathology. The lower the tumor:stroma ratio in pathological specimens, the larger was the difference in residual tumor cellularity between Gd-MRI and HMS-MRI ( $R = -0.62$ ,  $P = 0.018$ ). BT474 cell pellets showed signal enhancement after exposure to MnCl<sub>2</sub>, and the degree of enhancement decreased when cell pellets were exposed to chemotherapeutic agents.

#### CONCLUSION

Our results suggested that HMS-MRI can predict pCR more accurately than Gd-MRI when a pCR is suspected.

#### CLINICAL RELEVANCE/APPLICATION

Considering the active clinical trend for omitting surgery if pCR is highly suspected, our study suggested that HMS-MRI is a promising method for patient selection. In particular, HMS can be used to image breast cancer, which would be the first step in the wider use of HMS.

Printed on: 02/07/23

## Abstract Archives of the RSNA, 2022

W5A-SPPH-2

### When Will PROPELLER Technique Improve Quality in Acquisition of T2W-FRFSE Images of Abdomen MRI? Comparative Analysis According to Patient's Respiratory Patterns

Wednesday, Nov. 30 12:15PM - 12:45PM Room: Learning Center - PH DPS

#### Participants

Kyungmin Lee, Gyeonggi-Do, Korea, Republic Of (*Presenter*) Nothing to Disclose

#### PURPOSE

To evaluate the value of periodically rotated overlapping parallel lines with enhanced reconstruction (PROPELLER) technique to reduce respiratory artifacts and improve image quality in acquisition of T2-weighted (T2W) respiratory triggering fast recovery fast spin echo (FRFSE) images according to patient's respiratory pattern.

#### METHODS AND MATERIALS

In 200 consecutive patients who underwent abdominal MRI, T2W-FRFSE images were obtained with and without PROPELLER. Patients were divided into four groups according to respiratory patterns and rates (Group A: regular, =14 times/min; B: regular, 15-17 times/min; C: regular, =18 times/min; D: irregular, any rate). Qualitative image quality was assessed independently by two radiologists for ghost artifacts, edge sharpness, image noise, and overall image quality. Quantitative indices of signal-to-noise-ratio (SNR) and contrast-to-noise-ratio (CNR) were also analyzed by two radiologists. These indices were compared between two techniques in each group using Wilcoxon signed-rank test. Inter-observer agreement was assessed using Cohen's Kappa test and intraclass correlation coefficient.

#### RESULTS

In group A and B, T2W-FRFSE images without PROPELLER showed better image quality than those with PROPELLER in all qualitative and quantitative indices ( $p < 0.05$ ), except for ghost artifact in group A ( $p = 0.404$ ). In contrast, in group C and D, T2W-FRFSE images with PROPELLER showed better image quality than those without PROPELLER in all qualitative and quantitative indices ( $p < 0.05$ ) except for SNR in group C ( $p = 0.339$ ). Inter-observer agreements between two radiologists were excellent in all qualitative indices (kappa values  $> 0.8$ ) and quantitative indices (ICCs  $> 0.8$ ).

#### CONCLUSION

s Acquisition of T2W-FRFSE with PROPELLER yielded better image quality in patients with fast or inconsistent respiration than T2W-FRFSE without PROPELLER, and vice versa in patients with slow and steady respiration.

#### CLINICAL RELEVANCE/APPLICATION

Whether or not to utilize PROPELLER in acquisition of T2W-FRFSE should be determined according to the patient's respiratory pattern and rate.

Printed on: 02/07/23

## Abstract Archives of the RSNA, 2022

W5A-SPPH-3

### Toward a Simple Surrogate for Abdominopelvic Adipose Tissue Volume - Systematic MRI Assessment in Patients With Different BMI Classes

Wednesday, Nov. 30 12:15PM - 12:45PM Room: Learning Center - PH DPS

#### Participants

Nicolas Linder, MD, Leipzig, Germany (*Presenter*) Nothing to Disclose

#### PURPOSE

Obesity is a leading health problem worldwide with numerous comorbidities, such as cardiovascular disease, with the amount of visceral fat often regarded as an important factor for prognosis. In routine practice, many have used the sagittal abdominal diameter (SAD) as a simple clinical marker of visceral fat. The aim of this work was to systematically correlate (MRI-derived) SADMR with the abdominopelvic visceral and subcutaneous adipose tissue (VAT/SAT) volume in patients with obesity.

#### METHODS AND MATERIALS

Full abdominopelvic MR datasets were available from 266 patients (196 females and 70 males) with obesity. SADMR was determined on axial images by the respective distance of a line through the center of the vertebral body at different levels (lumbar disc compartments L1-L2 to L5-S1 and umbilicus). VAT and SAT volumes were determined with a semiautomatic segmentation software. Agreement between SADMR and AT volumes was evaluated by correlation coefficients R.

#### RESULTS

SADMR ranged from 21.7 cm to 39.0 cm and total volume of VAT (SAT) ranged from 0.9 to 14.0 L (4.8 to 39.4 L). Over all patients, R values between SADMR and VAT ranged from 0.66 at L5-S1 to 0.71 at L2-L3 (mean R of 0.69). Between sexes, the highest R value was larger for women (0.74 at L2-L3 vs. 0.69 at L3-L4). Similarly strong correlations were also seen between SADMR and SAT with R values between 0.67 (L2-L3) and 0.73 (L5-S1) overall, and higher values for each sex. Strong correlations of SADMR were also maintained within BMI subgroups for each sex with VAT but not with SAT

#### CONCLUSION

A gender-specific sagittal abdominal diameter has been shown to be a reliable measure for simple and rapid estimation of visceral fat volume in patients with different degrees of obesity.

#### CLINICAL RELEVANCE/APPLICATION

The presented parameter MRI-derived sagittal abdominal diameter (SADMR) promises to be a simple but reliable imaging marker of visceral obesity.

Printed on: 02/07/23

## Abstract Archives of the RSNA, 2022

W5A-SPPH-4

### **Novel Free-Breathing Day-Optimizing-Throughput Sequences in Comparison with Conventional Breath-Hold Examinations During Whole-Body MRI**

Wednesday, Nov. 30 12:15PM - 12:45PM Room: Learning Center - PH DPS

#### **Participants**

Vitali Koch, MD, Frankfurt am Main, Germany (*Presenter*) Nothing to Disclose

#### **PURPOSE**

To assess and compare novel free-breathing DOT sequences (Day Optimizing Throughput) with conventional breath-hold examinations in whole-body magnetic resonance imaging (MRI).

#### **METHODS AND MATERIALS**

This prospective study included 26 subjects with a variety of pathologies who had undergone whole body 1.5-Tesla MRI. Image quality, diagnostic confidence, and image noise were evaluated by two experienced radiologists. Diagnostic performance for the overall detection of pathologies in both sequences was assessed using the area under the receiver operating characteristics curve (AUC). Additionally, study participants were asked to rate their examination experience in a satisfaction survey using a 10-point Likert scale.

#### **RESULTS**

MR free-breathing scans were rated as at least equivalent to conventional MR scans in more than 90% of cases, showing high overall diagnostic accuracy (95% [95% CI 92-100]) and performance (AUC 0.971, 95% CI 0.942 to 0.988;  $P < 0.0001$ ) for the assessment of pathologies at simultaneously reduced examination time ( $50 \pm 4$  vs.  $59 \pm 5$  minutes;  $P < 0.0001$ ). Interrater agreement was excellent for both, free-breathing ( $\kappa = 0.96$  [95% CI, 0.88-1.00]) and conventional scans ( $\kappa = 0.93$  [95% CI, 0.84-1.00]). Ratings for image quality, image noise, and diagnostic confidence differed not significantly between the two types of MR image acquisition (all  $P > 0.05$ ).

#### **CONCLUSION**

s MR images generated with free-breathing DOT sequences yielded similar diagnostic performance at equivalent image quality and noise levels compared to conventional breath-hold algorithms. Moreover, the long examination time of whole-body MRI could be considerably shortened for a more tolerable whole-body MRI experience.

#### **CLINICAL RELEVANCE/APPLICATION**

Free-breathing Day-Optimizing-Throughput (DOT) MRI yields comparable diagnostic accuracy compared to breath-hold MRI. Free-breathing DOT sequences provide high diagnostic confidence at low image noise levels. Free-breathing DOT whole-body MRI may represent a viable alternative to conventional MRI.

Printed on: 02/07/23

## Abstract Archives of the RSNA, 2022

W5A-SPPH-5

### Technical and Clinical Considerations of a Physical Phantom for CT Radiomics Analysis

Wednesday, Nov. 30 12:15PM - 12:45PM Room: Learning Center - PH DPS

#### Participants

Bino A. Varghese, PhD, Los Angeles, CA (*Presenter*) Nothing to Disclose

#### PURPOSE

Radiomic measurements can be impacted by differences in protocol and equipment. Statistical approaches such as ComBat reduces this impact, however, they ignore the variable relationship, between different radiomic metrics and imaging parameters, leading to suboptimal harmonization for some metrics. We identify key phantom characteristics to help build a physical phantom for CT-radiomics harmonization, particularly, the higher-order texture metrics.

#### METHODS AND MATERIALS

CT scans of a radiomics phantom comprising of 18 novel 3D printed inserts with varying size, shape, and material combinations were acquired on a 64-slice CT scanner (Brilliance 64, Philips Healthcare). The images were acquired at 120 kV, 250mAs, CTDIvol of 16.36 mGy, 2mm slice thickness and reconstructed using iDose1. Radiomics analysis was performed using the Cancer Imaging Phenomics Toolkit (CaPTk), following automated segmentation of volumes of interests (VOIs) of the 18 inserts. To add perspective to our findings we compared them to 3 additional VOIs obtained of an anthropomorphic liver phantom, a patient liver CT scan, and a water phantom, at comparable imaging settings. Percent difference in Hounsfield units (HU) between phantom and tissue was used to assess the biological equivalency and <10% was used to claim equivalent.

#### RESULTS

The HU for all 18 VOIs from the phantom ranged from -30 to 120 compared with a range of 0-118 for liver tissue. One of our novel phantom inserts, T3-6B, had >50% radiomic features that have <10% difference from liver tissue (patient). Second-order texture metrics, particularly, those of Neighborhood Gray Tone Difference Matrix (NGTDM), which are also representatives of the signal to noise ratio of CT scans, mostly show extreme values in the water phantom VOI compared to the VOIs from the phantom.

#### CONCLUSION

The practice of using water phantom values which represent a structureless entity, will help identify limits of threshold for radiomic metrics, particularly texture. The practice of comparing the values to those from patient scans will help establish clinical relevance. By adopting some of the patterns from the radiomics phantom within the liver phantom, we will be able to selectively harmonize texture metrics, depending on its order and explore its association with imaging variables.

#### CLINICAL RELEVANCE/APPLICATION

Development of phantoms untangling the relationship between radiomic metrics and imaging variables will help establish quality assurance and control standards which are warranted for the clinical translation of radiomics.

Printed on: 02/07/23

## Abstract Archives of the RSNA, 2022

W5A-SPPH-6

### Postural Effect on Renal Volume: Evaluation Using Multi-Posture MRI

Wednesday, Nov. 30 12:15PM - 12:45PM Room: Learning Center - PH DPS

#### Participants

Seiya Nakagawa, BA, (*Presenter*) Nothing to Disclose

#### PURPOSE

Measurement of renal volume is vital for the early identification and monitoring of renal diseases. Nevertheless, it is unclear how postural changes, i.e., differences in the effects of gravity, alter renal volume. In this study, we evaluated the postural effect on renal volume in the supine and upright positions using an original magnetic resonance imaging (MRI) system that can image in any posture (multiposture MRI).

#### METHODS AND MATERIALS

Renal volume was evaluated in seven healthy volunteers (mean age,  $22.7 \pm 1.0$  years; body mass index,  $20.5 \pm 1.0$  kg/m<sup>2</sup>) in the supine and upright positions using multiposture MRI (0.4 T). A breath-hold 3D gradient-echo sequence was used to acquire coronal T1-weighted images of the right and left kidneys in the supine and upright positions. Then, the right and left renal volumes (whole kidney, renal cortex, medulla, and pelvis) were measured and compared across positions.

#### RESULTS

The whole kidney volume in the upright position (right kidney,  $122.3 \pm 20.1$  mL; left kidney,  $120.0 \pm 14.5$  mL) was significantly lower than that in the supine position (right kidney,  $139.9 \pm 21.0$  mL; left kidney,  $133.8 \pm 18.9$  mL) for both the right and left kidneys ( $P < 0.05$  for both). The renal cortex volume in the upright position (right kidney,  $77.0 \pm 12.2$  mL; left kidney,  $75.3 \pm 6.3$  mL) was significantly lower than that in the supine position (right kidney,  $89.3 \pm 12.9$  mL; left kidney,  $85.0 \pm 10.1$  mL) for both the right and left kidneys ( $P < 0.05$  for both). The renal medulla volume in the upright position (right kidney,  $40.6 \pm 7.3$  mL; left kidney,  $38.5 \pm 7.1$  mL) was significantly lower than that in the supine position (right kidney,  $45.5 \pm 8.7$  mL; left kidney,  $42.7 \pm 7.7$  mL) for both the right and left kidneys ( $P < 0.05$  for both). These findings revealed a decrease in blood volume and urine volume owing to the fluid shift effect when standing. Moreover, in comparison with the standard MRI examination of the kidney, multiposture MRI provided additional diagnostic information on the regulatory function to the gravity. However, no significant difference was observed in the renal pelvis volume between the supine and upright positions for both the right and left kidneys. Furthermore, no significant differences were observed in the volume change ratio from the supine to upright between the right and left kidneys.

#### CONCLUSION

An upright position reduces renal volume. Multiposture MRI enables the assessment of the postural effect on renal volume.

#### CLINICAL RELEVANCE/APPLICATION

An upright position reduces renal volume. Multiposture MRI revealed differences in the renal volume between the upright and supine positions, thereby providing new diagnostic information on the regulatory function to the gravity as compared with the standard MRI examination of the kidney.

Printed on: 02/07/23

## Abstract Archives of the RSNA, 2022

W5A-SPPH-7

### Comparison of Image Quality Metrics Between Solid-State Digital-BGO PET/CT and Time-of-Flight LSO Systems

Wednesday, Nov. 30 12:15PM - 12:45PM Room: Learning Center - PH DPS

#### Participants

Tala Palchan Hazan, PhD, (*Presenter*) Nothing to Disclose

#### PURPOSE

A recently designed digital solid-state positron emission tomography/x-ray CT system (PET/CT) scanner with bismuth germanate (BGO) scintillators coupled to silicon photomultipliers provides for a 32 cm axial field of view. Image quality metrics from this ultra-high sensitivity digital-BGO system without time-of-flight (TOF) were compared to a lutetium oxyorthosilicate (LSO) based TOF PET/CT scanner.

#### METHODS AND MATERIALS

A national electrical manufacturers association (NEMA) image quality (IQ) phantom was prepared as per NEMA NU 2-2018 with a fluorine-18 radiotracer. The 6 hot spheres (10 to 37 mm in diameter) were scanned on the LSO and digital-BGO systems. List mode data were binned to 12 decay-corrected 2-minute equivalent acquisitions, each with approximately the same number of incident counts. In both systems, images were reconstructed using an ordered subset expectation maximization (OSEM) algorithm and compared (Kruskal-Wallis test) to TOF-OSEM from the LSO system. Additional LSO OSEM reconstructions relisted scans to 1.4, 2.25 and 3.6 times the number of incident counts. The IQ metric was the contrast to noise ratio (CNR), calculated by dividing the contrast of hot sphere activity with respect to the background by the coefficient of variation of the background.

#### RESULTS

All CNRs of the digital-BGO system were the same or greater compared to LSO TOF-OSEM. For the smallest feature, there was no statistically significant difference ( $p < 0.001$ ) in the CNR of the 10 mm sphere (CNR<sub>10</sub>) between LSO TOF-OSEM ( $25.8 \pm 2.1$ , mean  $\pm$  std. dev.) and the digital-BGO ( $24.8 \pm 1.4$ ). There was also no significant difference ( $p < 0.001$ ) in CNR<sub>10</sub> between LSO TOF-OSEM and LSO OSEM using 2.25 times the number of incident counts ( $26.8 \pm 1.9$ ). Using 1.0 or 1.4 times the number of incident counts were insufficient to match LSO TOF-OSEM ( $19.0 \pm 1.8$ , and  $21.5 \pm 1.8$ , respectively). Using 3.6 times the number of incident counts significantly improved CNR<sub>10</sub> ( $35.0 \pm 0.9$ ,  $p < 0.001$ ) compared to LSO TOF-OSEM.

#### CONCLUSION

The ultra-high sensitivity of a solid-state 32 cm axial FOV digital-BGO PET/CT system provides for image quality similar to TOF systems, as measured by CNR in NEMA phantoms.

#### CLINICAL RELEVANCE/APPLICATION

The ultra-high sensitivity of a novel solid-state digital-BGO PET/CT system provides for high quality imaging of small features, enabling the diagnosis of pathology through functional imaging.

Printed on: 02/07/23

## Abstract Archives of the RSNA, 2022

W5A-SPPH-8

### Multiparametric MRI Method Development for Clinical Prostate Imaging Using 5T MR Imaging

Wednesday, Nov. 30 12:15PM - 12:45PM Room: Learning Center - PH DPS

#### Participants

Liyun Zheng, Shanghai, China (*Presenter*) Nothing to Disclose

#### PURPOSE

The purpose of this study was to evaluate the development of prostate MRI at 5T by providing assessment of image quality on clinical sequences, including T1-weighted (T1W), T2-weighted (T2W) and diffusion-weighted imaging (DWI) sequences.

#### METHODS AND MATERIALS

Ten healthy subjects (mean age,  $55.5 \pm 7.5$ ) were measured on a 5T MR scanner (uMR Jupiter, United Imaging Healthcare, Shanghai, China), using a 24-channel transmit/receive body array coil. SAR-monitoring and B0 and B1+ shimming were performed. Imaging sequences including: (1) axial T1W quick3d gradient echo (GRE) sequence (TR/TE = 3.34/1.42 ms, FA = 15°, Bandwidth = 850 Hz, 60 slices, Slice thickness = 3 mm, FOV = 300 × 400 mm, Matrix = 410 × 608, Number of averages = 2, Acquisition time = 16.9s); (2) axial T2W fat-saturated fast spin echo (FSE) sequence (TR/TE = 2600/128.24 ms, FA = 90°, Bandwidth = 200 Hz, 30 slices, Slice thickness = 5mm, FOV = 380 × 300 mm, Matrix = 639 × 504, Number of averages = 2, Acquisition time = 2min10s); and (3) echo-planar imaging (EPI) - DWI (TR/TE = 3650/53 ms, FA = 90°, Bandwidth = 2100 Hz, 30 slices, Slice thickness = 5 mm, FOV = 180 × 380 mm, Matrix = 410 × 608, b = 50, 800 s/mm<sup>2</sup>, Number of averages = 2, 4). Image analysis was performed by two experienced radiologists in consensus. For all the sequences, overall image quality (5 = excellent, 1 = non-diagnostic) and presence of artifacts (5 = pronounced, 1 = none) were assessed on a 5-point scale. Visibility of anatomical structures, defined as distinction between peripheral and transition zone, seminal vesicles, and delineation of the prostate, was graded on T2W images utilizing a five-point scale (5 = excellent, 1 = unacceptable). For DWI, geometric distortion (defined as modification in size, profile, and/or orientation due to inhomogeneities of the magnetic field in relation to T2W images) was evaluated on a 5-point scale (5 = very high distortion, 1 = no distortion).

#### RESULTS

Overall image quality of T1W image was scored as moderate to good ( $3.9 \pm 0.5$ ), T2W image was scored as good to excellent ( $4.1 \pm 0.8$ ), while DWI was scored as moderate ( $3.0 \pm 0.6$ ). Presence of artifacts of T1W, T2W and DWI images were scored as none to minimal ( $1.5 \pm 0.5$  for T1W,  $1.4 \pm 0.5$  for T2W,  $1.8 \pm 0.5$  for DWI). Visibility of anatomical structures for T2W at 5T was graded as good to excellent ( $4.2 \pm 0.7$ ). Upon DWI at 5T, the geometric distortion was graded as no distortion to low distortion ( $1.5 \pm 0.9$ ).

#### CONCLUSION

This study proved that prostate MRI, including T1W, T2W and DWI sequences at 5T can achieve diagnostic image quality.

#### CLINICAL RELEVANCE/APPLICATION

According to current results about image quality, presence of artifacts, visibility of anatomical structures of T2W images, and geometric distortion of DWI, clinical prostate imaging is feasible at 5T MRI.

Printed on: 02/07/23

## Abstract Archives of the RSNA, 2022

W5A-SPPH-9

### How to Handle Zero Counts in Low Dose Photon Counting CT Imaging?

Wednesday, Nov. 30 12:15PM - 12:45PM Room: Learning Center - PH DPS

#### Participants

Dan Bushe, MSc, BSc, Madison, WI (*Presenter*) Nothing to Disclose

#### PURPOSE

The probability of registering a count of zero for a given pixel is significantly higher for photon counting detectors (PCDs) when compared with energy integrating detectors (EIDs). This is a result of the general one-to-one correspondence between the digital output of the PCD with the absorbed x-ray photons and the higher spatial resolution of PCD detectors (0.15-0.3 mm). In contrast, a single x-ray photon can generate tens to hundreds of digital counts in EID elements with a size of 1 mm or larger. This problem becomes further exacerbated when considering low dose PCD-CT applications, large patient imaging, and the allocation of counts to various energy bins for spectral imaging. Zero counts must be corrected before the nonlinear log transform is taken to generate the sinograms for CT image reconstruction. However, replacing zeros by any positive number alters the statistical distribution of counts and introduces biases that can manifest as severe shading or blooming artifacts. The purpose of this work was to develop a novel PCD-CT zero-count correction method that not only corrects zero-counts but also minimizes CT number biases.

#### METHODS AND MATERIALS

In this work, a novel Laurent expansion was introduced to approximate the log-transformed projection data. The coefficients of the truncated Laurent expansion were calibrated using the correspondence between low dose scans with zero counts and high-dose scans without zero counts. This method was experimentally validated using a CdTe-based PCD-CT system with 4 test objects and under 4 different dose levels. The severity of the zero counts problem ranged from less than 0.1% to 22%.

#### RESULTS

With a conventional zero-count replacement correction, images demonstrated severe blooming and shading artifacts due to sinogram biases. The proposed method eliminated those artifacts and reduced CT number biases from -930 HU (95% CI: -1267, -592HU) to -0.8 HU (95% CI: -1.5, -0.2 HU) for a Teflon insert and from 790 HU (95% CI: 552, 1028 HU) to 3.4 HU (95% CI: 3.0, 3.9 HU) for an air insert. For both conventional and proposed corrections, the limiting spatial resolution of the CT images was matched at 9 lp/cm.

#### CONCLUSION

The proposed PCD-CT zero-count correction strategy not only corrects for zero-count pixels but also removes the associated biases. The method takes only a single pass and is computationally efficient. Furthermore, the method does not use any spatial filtering and thus does not introduce any spatial resolution loss.

#### CLINICAL RELEVANCE/APPLICATION

Zero detector counts are common in PCD-CT and severely degrade clinical diagnostic performance. This work addresses the long-standing zero-count correction problem and further elevates the clinical trustworthiness of PCD-CT.

Printed on: 02/07/23

## Abstract Archives of the RSNA, 2022

W5A-SPRO

### Radiation Oncology Wednesday Poster Discussions - A

Wednesday, Nov. 30 12:15PM - 12:45PM Room: Learning Center - RO DPS

#### Participants

Tracy M. Sherertz, MD, Seattle, WA (*Moderator*) Nothing to Disclose

#### Sub-Events

### W5A-SPRO- Performance of Conventional and Machine Learning Approaches for the Diagnosis of Tumor Recurrence on MRI After Radiation Therapy of Brain Metastases<sup>1</sup>

#### Participants

Samy Ammari, MD, PhD, Villejuif, France (*Presenter*) Nothing to Disclose

#### PURPOSE

Objective of this study : To compare the performance of conventional and machine-learning approaches for the diagnosis of tumor recurrence after radiation therapy of brain metastases

#### METHODS AND MATERIALS

184 symptomatic patients with solitary metastatic brain lesions treated with radiation therapy were enrolled in a monocentric retrospective study from June 2013 to May 2018. The diagnosis was tumor recurrence (n=71) and radiation necrosis (n=113) using as reference standard expert-consensus derived from pathology and long-term follow-up. 37 potential predictors were recorded at the time of radiological progression (7-15 months after therapy): 6 clinical features and 31 imaging features including 20 radiomics features derived from standard of care 3D T1-gadolinium sequences. We compared four approaches (A, B, C, D): expert report using MRI sequences without (A) and with delayed-contrast MRI (TRAM) sequences (B), 11 non-Radiomics imaging features alone (C) and a signature combining variables selected using unsupervised machine-learning algorithms (D, training:validation sets: n=144:40 pts).

#### RESULTS

Overall (n=184), approaches B and C (using TRAM sequence alone) reached comparable performances with respective AUCs[95CI] of 78.7%[72.3%-85.1%] and 76.8%[70.3%-83.3%]. Both significantly outperformed approach A with AUC[95CI] of 57.4%[50.7%-64.1%] (DeLong's test, p-value=10-7). In the validation set (n=40), the signature reached an AUC[95CI] of 92%[87%-97%]

#### CONCLUSION

s A quantitative analysis of TRAM sequence seems the best approach for the diagnosis of recurrent tumor after radiation therapy. It is parsimonious, objective and less time-consuming than interpreting all sequences. A signature derived from the analysis of standard of care 3D T1-gadolinium sequence showed promising results that warrant prospective validation.

#### CLINICAL RELEVANCE/APPLICATION

radiomics in combination with clinical data have successfully predicted the survival of recurrent GBM patients treated with bevacizumab. Three different binary models for survival prediction at 9, 12, and 15 months with high performances were built, which could lead to the creation of a convenient tool for decision making and the orientation to a more patient-specific treatment in the era of personalized medicine. Larger trials are needed for better identification and adaptation of these models in GBM patients.

Printed on: 02/07/23

## Abstract Archives of the RSNA, 2022

W5A-SPRO-1

### Performance of Conventional and Machine Learning Approaches for the Diagnosis of Tumor Recurrence on MRI After Radiation Therapy of Brain Metastases

Wednesday, Nov. 30 12:15PM - 12:45PM Room: Learning Center - RO DPS

#### Participants

Samy Ammari, MD, PhD, Villejuif, France (*Presenter*) Nothing to Disclose

#### PURPOSE

Objective of this study : To compare the performance of conventional and machine-learning approaches for the diagnosis of tumor recurrence after radiation therapy of brain metastases

#### METHODS AND MATERIALS

184 symptomatic patients with solitary metastatic brain lesions treated with radiation therapy were enrolled in a monocentric retrospective study from June 2013 to May 2018. The diagnosis was tumor recurrence (n=71) and radiation necrosis (n=113) using as reference standard expert-consensus derived from pathology and long-term follow-up. 37 potential predictors were recorded at the time of radiological progression (7-15 months after therapy): 6 clinical features and 31 imaging features including 20 radiomics features derived from standard of care 3D T1-gadolinium sequences. We compared four approaches (A, B, C, D): expert report using MRI sequences without (A) and with delayed-contrast MRI (TRAM) sequences (B), 11 non-Radiomics imaging features alone (C) and a signature combining variables selected using unsupervised machine-learning algorithms (D, training:validation sets: n=144:40 pts).

#### RESULTS

Overall (n=184), approaches B and C (using TRAM sequence alone) reached comparable performances with respective AUCs[95CI] of 78.7%[72.3%-85.1%] and 76.8%[70.3%-83.3%]. Both significantly outperformed approach A with AUC[95CI] of 57.4%[50.7%-64.1%] (DeLong's test, p-value=10<sup>-7</sup>). In the validation set (n=40), the signature reached an AUC[95CI] of 92%[87%-97%]

#### CONCLUSION

s A quantitative analysis of TRAM sequence seems the best approach for the diagnosis of recurrent tumor after radiation therapy. It is parsimonious, objective and less time-consuming than interpreting all sequences. A signature derived from the analysis of standard of care 3D T1-gadolinium sequence showed promising results that warrant prospective validation.

#### CLINICAL RELEVANCE/APPLICATION

radiomics in combination with clinical data have successfully predicted the survival of recurrent GBM patients treated with bevacizumab. Three different binary models for survival prediction at 9, 12, and 15 months with high performances were built, which could lead to the creation of a convenient tool for decision making and the orientation to a more patient-specific treatment in the era of personalized medicine. Larger trials are needed for better identification and adaptation of these models in GBM patients.

Printed on: 02/07/23

## Abstract Archives of the RSNA, 2022

W5A-SPVA

### Vascular Wednesday Poster Discussions - A

Wednesday, Nov. 30 12:15PM - 12:45PM Room: Learning Center - VA DPS

#### Sub-Events

#### **W5A-SPVA-1 The Role of Dual-Energy CT Spectral Parameters in the Differentiation Between Thrombosis and Intravenous Bolus Injection Caused Superior Vena Cava Artifacts**

##### Participants

Qingle Wang, PhD, (*Presenter*) Nothing to Disclose

##### PURPOSE

To explore the value of dual-energy CT spectral parameters in distinguishing right upper pulmonary artery (PA) artifact (caused by intravenous bolus injection) and thrombus.

##### METHODS AND MATERIALS

18 patients with thrombosis (verified by two experienced radiologists) underwent pulmonary artery computed tomography angiography (CTPA)(Revolution,GE healthcare) were included. Virtual monochromatic images at 70, 90 keV, iodine-based decomposition images and effective atomic number (Eff-Z) images were obtained. ROIs were placed on the low-density area of the right upper PA (artifacts, AF), the corresponding normal area of left upper PA (NOM), and embolism area (PE, if left upper PA embolism, change the nearby normal right middle PA). Then, slopes of spectral curves from 40 to 90 keV (?40-90 keV) and 50 to 100 keV (?50-100 keV), CT values of monochromatic images at 70, 90 keV (HU70keV, 90keV), Eff-Z, iodine concentration (IC), were measured and calculated. Eff-Z and IC were normalized by the values on PA trunk to derive a normalized Eff-Z (Neff-Z) and normalized IC (NIC). One-way ANOVA, Kruskal Wallis U, LSD and Mann-Whitney U were used for comparison, and receiver operation curve (ROC) was utilized for evaluating the differentiation performance of spectral parameters, and sensitivity, specificity and area under curve (AUC) were calculated.

##### RESULTS

On NOM, AF and PE, HU70keV were (362.12±83.59, 292.55±71.83, 164.32±85.31, p<0.05), HU90keV were (211.37±51.84, 161.30±47.21, 66.03±66.22,p<0.05), NIC were (1.49±1.99, 0.88±0.13, 0.69±0.26,,), NEff-Z were (1.00±0.03, 0.98±0.03, 0.92±0.10),?40-90 keV were (0.81±0.01, 0.83±0.03, 0.91±0.08), ?50-100 keV were (0.77±0.02, 0.80±0.05, 0.93±0.15), with statistical differences between AF and PE (p<0.05), NOM and PE (p<0.05). For the differentiation between AF and PE, HU70keV (threshold of 228.51), HU90keV (threshold of 78.89), NEff-Z (0.92), NIC (0.72),?40-90 keV (0.89),?50-100 keV (0.89) showed sensitivities of (0.88, 0.94, 1.00, 0.94, 0.67, 0.67), specificities of (0.78, 0.72, 0.44, 0.50, 0.94, 0.94), AUC of (0.87, 0.89, 0.67, 0.73, 0.85, 0.85). The diagnostic efficiency of HU90 keV is the highest.

##### CONCLUSION

s CT spectral parameters played an important role in differentiating the right upper PA artifact interference of contrast medium in superior vena cava from PE, therein HU90 keV had highest diagnostic efficiency.

##### CLINICAL RELEVANCE/APPLICATION

When CTPA, contrast accumulation in superior vena cava results in focal artifacts, which is similar to small emboli. Spectral CT quantitative parameters are helpful for the differentiation and increasing diagnostic confidence.

Printed on: 02/07/23

## Abstract Archives of the RSNA, 2022

W5A-SPVA-1

### The Role of Dual-Energy CT Spectral Parameters in the Differentiation Between Thrombosis and Intravenous Bolus Injection Caused Superior Vena Cava Artifacts

Wednesday, Nov. 30 12:15PM - 12:45PM Room: Learning Center - VA DPS

#### Participants

Qingle Wang, PhD, (Presenter) Nothing to Disclose

#### PURPOSE

To explore the value of dual-energy CT spectral parameters in distinguishing right upper pulmonary artery (PA) artifact (caused by intravenous bolus injection) and thrombus.

#### METHODS AND MATERIALS

18 patients with thrombosis (verified by two experienced radiologists) underwent pulmonary artery computed tomography angiography (CTPA)(Revolution,GE healthcare) were included. Virtual monochromatic images at 70, 90 keV, iodine-based decomposition images and effective atomic number (Eff-Z) images were obtained. ROIs were placed on the low-density area of the right upper PA (artifacts, AF), the corresponding normal area of left upper PA (NOM), and embolism area (PE, if left upper PA embolism, change the nearby normal right middle PA). Then, slopes of spectral curves from 40 to 90 keV (?40-90 keV) and 50 to 100 keV (?50-100 keV), CT values of monochromatic images at 70, 90 keV (HU70keV, 90keV), Eff-Z, iodine concentration (IC), were measured and calculated. Eff-Z and IC were normalized by the values on PA trunk to derive a normalized Eff-Z (Neff-Z) and normalized IC (NIC). One-way ANOVA, Kruskal Wallis U, LSD and Mann-Whitney U were used for comparison, and receiver operation curve (ROC) was utilized for evaluating the differentiation performance of spectral parameters, and sensitivity, specificity and area under curve (AUC) were calculated.

#### RESULTS

On NOM, AF and PE, HU70keV were (362.12±83.59, 292.55±71.83, 164.32±85.31, p<0.05), HU90keV were (211.37±51.84, 161.30±47.21, 66.03±66.22,p<0.05), NIC were (1.49±1.99, 0.88±0.13, 0.69±0.26,), NEff-Z were (1.00±0.03, 0.98±0.03, 0.92±0.10),?40-90 keV were (0.81±0.01, 0.83±0.03, 0.91±0.08), ?50-100 keV were (0.77±0.02, 0.80±0.05, 0.93±0.15), with statistical differences between AF and PE (p<0.05), NOM and PE (p<0.05). For the differentiation between AF and PE, HU70keV (threshold of 228.51), HU90keV (threshold of 78.89), NEff-Z (0.92), NIC (0.72),?40-90 keV (0.89),?50-100 keV (0.89) showed sensitivities of (0.88, 0.94, 1.00, 0.94, 0.67, 0.67), specificities of (0.78, 0.72, 0.44, 0.50, 0.94, 0.94), AUC of (0.87, 0.89, 0.67, 0.73, 0.85, 0.85). The diagnostic efficiency of HU90 keV is the highest.

#### CONCLUSION

s CT spectral parameters played an important role in differentiating the right upper PA artifact interference of contrast medium in superior vena cava from PE, therein HU90 keV had highest diagnostic efficiency.

#### CLINICAL RELEVANCE/APPLICATION

When CTPA, contrast accumulation in superior vena cava results in focal artifacts, which is similar to small emboli. Spectral CT quantitative parameters are helpful for the differentiation and increasing diagnostic confidence.

Printed on: 02/07/23

## Abstract Archives of the RSNA, 2022

W5B-SPBR

### Breast Wednesday Poster Discussions - B

Wednesday, Nov. 30 12:45PM - 1:15PM Room: Learning Center - BR DPS

#### Participants

Panagiotis Kapetas, MD, PhD, Vienna, Austria (*Moderator*) Nothing to Disclose

#### Sub-Events

#### W5B-SPBR- Automated Breast Arterial Calcification Detection is Improved with Digital Breast Tomosynthesis 1

Participants

Tara Retson, MD, PhD, San Diego, CA (*Presenter*) Research Consultant, CureMetrix, Inc; Stock options, CureMetrix, Inc

#### PURPOSE

Breast arterial calcification (BAC) represents a risk marker for cardiovascular disease (CVD) but is widely underreported by radiologists. Automated detection software may improve BAC reporting by radiologists and also provide a consistent scale for characterizing BAC extent. We demonstrate the accuracy of an artificial intelligence (AI) model for breast arterial calcification (BAC) detection and localization on full field digital (FFDM) and digital breast tomosynthesis (DBT) mammograms.

#### METHODS AND MATERIALS

A total of 1204 images from 473 patients from 3 different institutions in the United States were studied. Of these, 256 patients underwent FFDM exams and 217 patients had DBT exams. The AI model, cmAngio™ (CureMetrix, Inc, La Jolla, CA) is a deep convolutional neural network for BAC segmentation and quantification which can provide both binary (BAC presence vs absence) results and the Bradley score™ (which ranges from 0-100). The Bradley score quantitates characteristics of BAC at the case level, including extent. The area under the receiver operating characteristic curve (AUROC) for presence or absence of BAC was calculated, with 95% bootstrap confidence intervals (CI). For BAC segmentation, average precision (AP) of BAC positive pixels is used as the primary performance metric. Precision, sensitivity, specificity of cmAngio from FFDM vs. DBT was obtained.

#### RESULTS

For BAC detection, cmAngio achieved an image-level area under the curve (AUROC) of 0.966 [CI:0.956, 0.984] and a case level AUROC of 0.945 [CI:0.894, 0.973] for FFDM. The image-level AUROC of 0.977 [CI:0.961, 0.988] and a case level AUROC of 0.966 [CI:0.939, 0.988] was achieved with cmAngio for DBT. For BAC segmentation, cmAngio achieved an AP of 0.614 [CI:0.599, 0.629] and 0.752 [CI:0.731, 0.773] for FFDM and DBT respectively. At the threshold level of 0.5, cmAngio achieved a precision, sensitivity, specificity of 0.629, 0.512, 1.000 for FFDM and on DBT achieved a precision, sensitivity and specificity of 0.733, 0.557, 1.000.

#### CONCLUSION

BAC detection with cmAngio is excellent, and noted to be slightly superior for DBT compared to FFDM. This is partially due to the fact that the masking effect of dense tissue on BAC, as occurs with other types of lesions on FFDM, is reduced in DBT.

#### CLINICAL RELEVANCE/APPLICATION

Reporting of breast arterial calcifications may be enhanced through the use of this highly accurate automated artificial intelligence model for both full field digital and digital breast tomosynthesis mammography.

#### W5B-SPBR- Radiomic Features at Breast MRI Predict Non-Upgrade of DCIS Lesions to Invasive Malignancy 2

Participants

Dana Ataya, MD, Tampa, FL (*Presenter*) Nothing to Disclose

#### PURPOSE

Identification of ductal carcinoma in-situ (DCIS) lesions diagnosed on core biopsy which will not be upgraded to invasive breast cancer on excision could guide clinical management in cases where de-escalation of therapy is preferred. We investigated whether radiomic features extracted from DCIS lesions on dynamic contrast enhanced (DCE)-MRI predicted non-upgrade to invasive malignancy.

#### METHODS AND MATERIALS

113 DCIS lesions diagnosed on core biopsy were divided into training (80) and testing (33) cohorts. DCIS lesions were identified by a sub-specialized breast radiologist and segmented on pre-operative DCE-MRI. Four perfusion parameters were used to generate voxel multi-parametric maps: wash-in (WIS) and washout (WOS) slopes, percentage enhancement (PE), and signal enhancement ratio (SER). Consensus clustering and superpixel maps divided each tumor into three perfusional subregions (habitats). Following z-score normalization of total signal intensity on T1 weighted post-gadolinium acquisition, 306 radiomics features were extracted from the three habitat subregions (Model 1) and from the whole DCIS lesion (Model 2). Using a minimum redundancy maximum relevance (MRMR) algorithm, correlation of features to outcome was rank ordered with the top 10% of features selected for further analysis. The selected radiomic features were used to train a binary (upgrade vs. no upgrade) decision tree classification system for each

model. The final trained models were used to classify each core biopsy DCIS lesion in the testing cohort into the binary outcome of upgrade to invasive malignancy on surgical pathology.

## RESULTS

The frequency of upgrade from DCIS on core biopsy to invasive malignancy on excision was similar in both cohorts (22.5% training; 22.2% testing). Radiomic features extracted from each subregion and from the whole lesion within both cohorts were examined. Of 306 extracted radiomic features, the MRMR algorithm identified an optimal set of 4 features from the three subregions (habitats) and 4 features from the whole lesion that were most informative. Model 1 predicted non-upgrade to invasive malignancy with 78% accuracy (66.7% true positives (TP), 81.5% true negatives (TN)). Model 2 predicted non-upgrade to invasive malignancy with 87.9% accuracy (83.3% TP, 88.9% TN).

## CONCLUSION

s Radiomic features on dynamic contrast enhanced breast MRI can assist at identifying DCIS lesions at low risk of upgrade to invasive malignancy.

## CLINICAL RELEVANCE/APPLICATION

Identification of DCIS lesions at low-risk of upgrade to invasive malignancy can help guide clinical management of patients, particularly if de-escalation of therapy is desired.

## W5B-SPBR- Multi-Parametric MRI-Based Radiomics Models for Early Neoadjuvant Systemic Treatment Response Prediction in Triple Negative Breast Cancer (TNBC)

Participants  
Bikash Panthi, Houston, TX (*Presenter*) Nothing to Disclose

## PURPOSE

TNBC accounts for 10-20 % of all breast cancers and is often treated with neoadjuvant systemic therapy (NAST). Early prediction of the treatment response can potentially triage the patients without pathological complete response (pCR) to alternative treatments to improve outcomes. In this study, we investigated if the radiomic models based on the dynamic contrast-enhanced (DCE) and diffusion-weighted imaging (DWI) MRI images obtained early during NAST can be a noninvasive biomarker for pCR prediction.

## METHODS AND MATERIALS

Our analysis included 182 stage I-III TNBC patients who were enrolled in an IRB-approved prospective clinical trial (NCT02276433) and who had multiparametric MRIs at baseline (BL), post 2 cycles (C2), and post 4 cycles (C4) of NAST before surgery. Tumors were segmented on the 2.5 minutes DCE subtraction images and on the b=800 DWI images. Whole-tumor histogram-based first-order texture features (p=10) and radiomic features were extracted (p=300 radiomic Grey Level Co-occurrence matrix (GLCM) features) with an in-house Matlab toolbox. Treatment response at surgery (pCR vs non-pCR) was assessed. The samples were split into training and testing data sets by a 2:1 ratio. Area under the receiver operating characteristics curve (AUC ROC) was performed for univariate analysis in predicting pCR status. Logistic regression with elastic net regularization was performed for texture feature selection. Parameter optimization was performed by using 5-fold cross-validation based on mean cross-validated AUC in the training set.

## RESULTS

Of the total 182 patients, 94 (52%) had pCR and 88 (48%) had non-pCR. Thirty-six multivariate models combining radiomic features from both DCE and DWI had AUC > 0.7 (p<0.003), two of which showed AUC > 0.8 (p<0.001) in both training and testing data. The first model combined 4 radiomic features from C2 (1 GLCM feature), C4 (percentile 5, 1 GLCM feature) and their changes in C4/C2 (mean) with AUC=0.808, and the second model combined 13 radiomic features at BL (kurtosis, 2 GLCM features), C2 (1 GLCM feature), C4 (3 GLCM features) and their changes in C2/BL (1 GLCM feature), C4/BL (percentile 99, minimum, mean) and C4/C2 (mean, 1 GLCM feature) with AUC=0.816.

## CONCLUSION

s Multi-parametric MRI-based radiomics models showed high accuracy for early prediction of NAST response in TNBC patients.

## CLINICAL RELEVANCE/APPLICATION

Radiomic models based on multi-parametric MRI can potentially be helpful for the selection of the appropriate treatment strategy for TNBC patients undergoing NAST.

## W5B-SPBR- The Impact of Social Determinants of Health on the Time Between Diagnostic Breast Imaging and Biopsy at a Safety Net Hospital

Participants  
Kevin Dao, Boston, MA (*Presenter*) Nothing to Disclose

## PURPOSE

There is limited literature on the direct impact of social determinants of health (SDH) on delays in breast cancer diagnosis via breast imaging. Identifying SDH associated with longer lapses between imaging and biopsy is essential to early-stage detection of breast cancer. Previous work demonstrated associations between both housing and food insecurity with longer lapses between diagnostic imaging and biopsy. With this study, we aim to expand upon this retrospective analysis with a longer study period, more participants, and improved data cleaning techniques to better understand how SDH may affect the lapse between imaging and biopsy.

## METHODS AND MATERIALS

This retrospective study was IRB approved and HIPAA compliant. Informed consent was waived. Patients who underwent screening mammography between January 1 2015 and January 1 2020 were assessed for timing of recommended biopsy due to a BIRADS 4 or 5. SDH were assessed with the unique Tool for Health Resilience in Vulnerable Environments (THRIVE) screening questionnaire developed at Boston Medical Center. Associations between imaging-biopsy timing and 8 explanatory SDH variables were assessed

with multivariate Cox proportional hazard modeling, as well as demographic data.

## RESULTS

2885 unique patients who underwent 3142 unique diagnostic imaging studies were included in the multivariate analysis. Of those 3142 studies, 196 (6.2%) had not yet been followed by the recommended biopsy by the end of the study period. 2159 patients (74.8%) had SDH data in at least one domain, and the individual domains ranged from 875 patients (30.3%) with complete data for education to 2073 patients (71.8%) with complete data for food insecurity. A positive screen for at least one SDH was associated with a longer lapse between diagnostic imaging and biopsy ( $p=0.048$ ). Further, housing insecurity alone was nearly associated with longer lapses between diagnostic imaging and biopsy ( $p=0.059$ ). Paradoxically, those who desired more education were found to have shorter lapses between diagnostic imaging and biopsy ( $p=0.037$ ).

## CONCLUSION

Of the eight SDH screened, housing insecurity was most close to association with longer lapses between diagnostic imaging and biopsy. However, only the aggregate of all SDH was associated with a statistically significant lengthening of this lapse. Patients who desired more education were found to have shorter lapses, but this survey domain had the lowest completion rate.

## CLINICAL RELEVANCE/APPLICATION

Identification of SDH that may affect the time from imaging to biopsy can potentially inform targeted programs to intervene. Government and health system interventions addressing SDH, notably housing insecurity, could allow for shorter time to breast cancer diagnosis and treatment.

## W5B-SPBR- BI-RADS-0 Screening Mammography: Risk Factors Associated with Prolonged Follow-up Time to Diagnostic Evaluation

Participants  
Samantha Platt, MD, New York, NY (*Presenter*) Nothing to Disclose

## PURPOSE

BI-RADS-0 screening mammograms require follow-up diagnostic imaging, optimally within 60 days. Our study aims to identify risk factors for prolonged follow-up.

## METHODS AND MATERIALS

We conducted a retrospective, observational, case-control study of women aged 40-91 from breast centers in the Mount Sinai System who had nondiagnostic BI-RADS-0 screening mammogram between 3/19/18-3/19/20. Sociodemographic information was collected from a self-reported screening questionnaire. Patients who underwent screening in the mobile mammography van or had incorrect follow-up dates were excluded. Analysis 1: Goal was to identify risk factors associated with the following outcomes categories: <60d follow-up, >60d follow-up or no follow-up. Chi-squared tests and univariate logistic regressions were performed. Significant variables were included in multinomial logistic regression model with <60d follow-up as the reference group. Analysis 2: Goal was to identify risk factors that lead to prolonged follow-up times among women with follow-up. Shapiro-Wilk test determined a non-normal distribution of the dependent variable (0.61,  $p < 0.0001$ ). Spearman's rank coefficient of correlation, Mann Whitney Wilcoxon Test, and Kruskal-Wallis Tests were used.

## RESULTS

Our review returned 5,034 screening mammograms. Of 4,552 patients included in the study, 904 (19.9%) had no follow-up. Of the 3,648 (80.1%) with follow-up, 2,797 (76.7%) had a follow-up examination <60d (avg. 22.1 days) and 851 (23.3%) had follow-up >60d (avg. 190.4 days). Multinomial log regression found that Asian women, black women, and those who identified as "other" were independently more likely to have no or >60d follow-up ( $p<0.05$ ). Women who did not report their race were more likely to have no or >60d follow-up ( $p<0.05$ ). Women who completed the questionnaire in Spanish were more likely to have no or >60d follow-up ( $p<0.05$ ). Amongst women with follow-up, black women, those who identified as "other", LatinX women, and those completed the questionnaire in Spanish had significant follow-up delays ( $p<0.05$ ). BRCA+ patients had shorter follow-up times ( $p<0.05$ ).

## CONCLUSION

Follow-up time is affected by patient-specific breast cancer risk factors such as BRCA status as well as disparities in health care access by race, primary language and Latinx heritage.

## CLINICAL RELEVANCE/APPLICATION

There are risk factors associated with prolonged follow-up time to diagnostic evaluation that need to be targeted in order to improve patient outcomes.

## W5B-SPBR- Frequency and outcome of probably benign findings (BI-RADS 3) in patients with a personal history of breast cancer (PHBC) imaged with digital mammography (DM) vs. digital breast tomosynthesis (DBT)

Participants  
Lily Offit, Boston, MA (*Presenter*) Nothing to Disclose

## PURPOSE

Probably benign (BI-RADS 3) findings are those with <2% malignancy rate, and are followed with imaging at 6, 12, and 24 months. Few studies have reported probably benign outcomes in patients with a personal history of breast cancer (PHBC) and have shown >2% malignancy rates. The purpose of this study is to determine the frequency, findings, and outcomes of probably benign findings in patients with PHBC imaged with digital mammography (DM) versus digital breast tomosynthesis (DBT).

## METHODS AND MATERIALS

This is a retrospective review of 14,845 mammogram reports in patients with PHBC (mastectomy and/or lumpectomy). Of these, 8,422 exams (56.7%) were DM between 10/2014-9/16 and 6,423 exams (43.3%) were DBT between 2/2017-12/2018. Frequency and indication of BI-RADS 3 assignment, mammographic finding (calcifications, architectural distortions, asymmetries, or mass), and

biopsy or follow-up imaging outcomes were compared between DM and DBT.

## RESULTS

In the study periods, there were 901/14,845 (6.1%) examinations coded as BI-RADS 3, with 717 unique BI-RADS 3 findings. DBT led to a reduced use of probably benign assignments when compared to DM (6.4% for DM vs. 5.6% for DBT,  $p=0.04$ ). DM had a higher rate of malignancy of subsequently biopsied BI-RADS findings when compared to DBT [(4.8% (21/442) DM vs. 1.8% (5/275) DBT ( $p=0.04$ )). DBT showed a 10.1% increase in percent of masses detected compared to DM ( $p=0.004$ ). There was a trend towards more probably benign calcifications detected in DM ( $p=0.06$ ).

## CONCLUSION

Use of DBT in individuals with a prior history of breast cancer led to a decrease in rate of BI-RADS 3 assignment. DM BI-RADS 3 rate of malignancy was 4.8%, higher than the accepted 2% malignancy rate, and decreased to 1.8% with use of DBT.

## CLINICAL RELEVANCE/APPLICATION

Insight into BI-RADS 3 usage and malignancy rates between imaging modalities will help establish whether probably benign assessments in patients with PHBC are being utilized appropriately to identify cancers early and reduce unnecessary biopsies.

## W5B-SPBR- Interval Breast Cancers Compared to Screen Detected Breast Cancers: A Retrospective Cohort Study 7

Participants

Emily Ambinder, MD, MSc, Ellicott City, MD (*Presenter*) Nothing to Disclose

## PURPOSE

Mammographic screening improves mortality from breast cancer through early detection. We aim to identify clinical and imaging features that differentiate screen detected breast cancers from interval breast cancers in order to inform and improve breast cancer screening for all women in the era of precision medicine.

## METHODS AND MATERIALS

All screening mammograms ( $n=211,514$ ) performed between 7/1/2013 and 6/30/2020 at our institution were reviewed. Patients with breast cancer diagnosed within one year of screening were included in this study. Patient, imaging, and cancer characteristics of screen detected breast cancers and interval breast cancers were compared using the Chi square test, Fisher test, and Wilcoxon Rank Sum Test. Interval cancers were defined as breast cancers diagnosed within one year of a negative screening mammogram.

## RESULTS

During the study period, 1,232 women were diagnosed with breast cancer and included in this study (mean age 64 years, standard deviation 11 years). Overall sensitivity of screening mammography was 91% (1,121 screen detected breast cancers and 111 interval cancers). Interval cancers were most often palpable (62/111=56%) or identified on a high-risk screening breast MRI (20/111=18%). Patient age, race, and screening exam modality (FFDM versus DBT) were similar for patients with screen detected cancers and interval cancers (all  $p>0.05$ ). Breast density was higher for patients with interval cancers (heterogeneously dense or extremely dense: 86/111=77% versus 683/1121=61%,  $p<.001$ ). Compared to screen detected cancers, interval cancers were less often ductal carcinoma in situ or primary tumor stage 1 (69/111=62% versus 981/1121=88%,  $p<0.001$ ) and less often regional lymph node stage 0 (89/111=80% versus 990/1121=88%,  $p<0.001$ ). Interval cancers were less often hormone receptor positive (ER+: 73/94=78% versus 746/824=91%,  $p<0.001$ ), and less often had low proliferative indices (Ki67 <20%: 21/52=40% versus 301/488=62%,  $p=0.005$ ). HER2 positivity was similar for the two groups (8/91=9% versus 84/804=10%,  $p=0.76$ ).

## CONCLUSION

We found that mammographic screening has a high sensitivity for detection of breast cancer (91%). Interval cancers were often palpable or identified on a screening breast MRI and were associated with dense breast tissue but did not differ by age and race compared to screen detected cancers. Interval cancers were higher stage with less favorable molecular features compared to screen detected cancers.

## CLINICAL RELEVANCE/APPLICATION

While screening mammography has a high sensitivity for detecting breast cancer, novel approaches are needed to identify interval cancers earlier as these are often higher stage with unfavorable molecular features compared to screen detected cancers.

Printed on: 02/07/23

## Abstract Archives of the RSNA, 2022

W5B-SPBR-1

### Automated Breast Arterial Calcification Detection is Improved with Digital Breast Tomosynthesis

Wednesday, Nov. 30 12:45PM - 1:15PM Room: Learning Center - BR DPS

#### Participants

Tara Retson, MD, PhD, San Diego, CA (*Presenter*) Research Consultant, CureMetrix, Inc; Stock options, CureMetrix, Inc

#### PURPOSE

Breast arterial calcification (BAC) represents a risk marker for cardiovascular disease (CVD) but is widely underreported by radiologists. Automated detection software may improve BAC reporting by radiologists and also provide a consistent scale for characterizing BAC extent. We demonstrate the accuracy of an artificial intelligence (AI) model for breast arterial calcification (BAC) detection and localization on full field digital (FFDM) and digital breast tomosynthesis (DBT) mammograms.

#### METHODS AND MATERIALS

A total of 1204 images from 473 patients from 3 different institutions in the United States were studied. Of these, 256 patients underwent FFDM exams and 217 patients had DBT exams. The AI model, cmAngio™ (CureMetrix, Inc, La Jolla, CA) is a deep convolutional neural network for BAC segmentation and quantification which can provide both binary (BAC presence vs absence) results and the Bradley score™ (which ranges from 0-100). The Bradley score quantitates characteristics of BAC at the case level, including extent. The area under the receiver operating characteristic curve (AUROC) for presence or absence of BAC was calculated, with 95% bootstrap confidence intervals (CI). For BAC segmentation, average precision (AP) of BAC positive pixels is used as the primary performance metric. Precision, sensitivity, specificity of cmAngio form FFDM vs. DBT was obtained.

#### RESULTS

For BAC detection, cmAngio achieved an image-level area under the curve (AUROC) of 0.966 [CI:0.956, 0.984] and a case level AUROC of 0.945 [CI:0.894, 0.973] for FFDM. The image-level AUROC of 0.977 [CI:0.961, 0.988] and a case level AUROC of 0.966 [CI:0.939, 0.988] was achieved with cmAngio for DBT. For BAC segmentation, cmAngio achieved an AP of 0.614 [CI:0.599, 0.629] and 0.752 [CI:0.731, 0.773] for FFDM and DBT respectively. At the threshold level of 0.5, cmAngio achieved a precision, sensitivity, specificity of 0.629, 0.512, 1.000 for FFDM and on DBT achieved a precision, sensitivity and specificity of 0.733, 0.557, 1.000.

#### CONCLUSION

s BAC detection with cmAngio is excellent, and noted to be slightly superior for DBT compared to FFDM. This is partially due to the fact that the masking effect of dense tissue on BAC, as occurs with other types of lesions on FFDM, is reduced in DBT.

#### CLINICAL RELEVANCE/APPLICATION

Reporting of breast arterial calcifications may be enhanced through the use of this highly accurate automated artificial intelligence model for both full field digital and digital breast tomosynthesis mammography.

Printed on: 02/07/23

## Abstract Archives of the RSNA, 2022

W5B-SPBR-2

### Radiomic Features at Breast MRI Predict Non-Upgrade of DCIS Lesions to Invasive Malignancy

Wednesday, Nov. 30 12:45PM - 1:15PM Room: Learning Center - BR DPS

#### Participants

Dana Ataya, MD, Tampa, FL (*Presenter*) Nothing to Disclose

#### PURPOSE

Identification of ductal carcinoma in-situ (DCIS) lesions diagnosed on core biopsy which will not be upgraded to invasive breast cancer on excision could guide clinical management in cases where de-escalation of therapy is preferred. We investigated whether radiomic features extracted from DCIS lesions on dynamic contrast enhanced (DCE)-MRI predicted non-upgrade to invasive malignancy.

#### METHODS AND MATERIALS

113 DCIS lesions diagnosed on core biopsy were divided into training (80) and testing (33) cohorts. DCIS lesions were identified by a sub-specialized breast radiologist and segmented on pre-operative DCE-MRI. Four perfusion parameters were used to generate voxel multi-parametric maps: wash-in (WIS) and washout (WOS) slopes, percentage enhancement (PE), and signal enhancement ratio (SER). Consensus clustering and superpixel maps divided each tumor into three perfusional subregions (habitats). Following z-score normalization of total signal intensity on T1 weighted post-gadolinium acquisition, 306 radiomics features were extracted from the three habitat subregions (Model 1) and from the whole DCIS lesion (Model 2). Using a minimum redundancy maximum relevance (MRMR) algorithm, correlation of features to outcome was rank ordered with the top 10% of features selected for further analysis. The selected radiomic features were used to train a binary (upgrade vs. no upgrade) decision tree classification system for each model. The final trained models were used to classify each core biopsy DCIS lesion in the testing cohort into the binary outcome of upgrade to invasive malignancy on surgical pathology.

#### RESULTS

The frequency of upgrade from DCIS on core biopsy to invasive malignancy on excision was similar in both cohorts (22.5% training; 22.2% testing). Radiomic features extracted from each subregion and from the whole lesion within both cohorts were examined. Of 306 extracted radiomic features, the MRMR algorithm identified an optimal set of 4 features from the three subregions (habitats) and 4 features from the whole lesion that were most informative. Model 1 predicted non-upgrade to invasive malignancy with 78% accuracy (66.7% true positives (TP), 81.5% true negatives (TN)). Model 2 predicted non-upgrade to invasive malignancy with 87.9% accuracy (83.3% TP, 88.9% TN).

#### CONCLUSION

s Radiomic features on dynamic contrast enhanced breast MRI can assist at identifying DCIS lesions at low risk of upgrade to invasive malignancy.

#### CLINICAL RELEVANCE/APPLICATION

Identification of DCIS lesions at low-risk of upgrade to invasive malignancy can help guide clinical management of patients, particularly if de-escalation of therapy is desired.

Printed on: 02/07/23

## Abstract Archives of the RSNA, 2022

W5B-SPBR-3

### Multi-Parametric MRI-Based Radiomics Models for Early Neoadjuvant Systemic Treatment Response Prediction in Triple Negative Breast Cancer (TNBC)

Wednesday, Nov. 30 12:45PM - 1:15PM Room: Learning Center - BR DPS

#### Participants

Bikash Panthi, Houston, TX (*Presenter*) Nothing to Disclose

#### PURPOSE

TNBC accounts for 10-20 % of all breast cancers and is often treated with neoadjuvant systemic therapy (NAST). Early prediction of the treatment response can potentially triage the patients without pathological complete response (pCR) to alternative treatments to improve outcomes. In this study, we investigated if the radiomic models based on the dynamic contrast-enhanced (DCE) and diffusion-weighted imaging (DWI) MRI images obtained early during NAST can be a noninvasive biomarker for pCR prediction.

#### METHODS AND MATERIALS

Our analysis included 182 stage I-III TNBC patients who were enrolled in an IRB-approved prospective clinical trial (NCT02276433) and who had multiparametric MRIs at baseline (BL), post 2 cycles (C2), and post 4 cycles (C4) of NAST before surgery. Tumors were segmented on the 2.5 minutes DCE subtraction images and on the b=800 DWI images. Whole-tumor histogram-based first-order texture features ( $p=10$ ) and radiomic features were extracted ( $p=300$  radiomic Grey Level Co-occurrence matrix (GLCM) features) with an in-house Matlab toolbox. Treatment response at surgery (pCR vs non-pCR) was assessed. The samples were split into training and testing data sets by a 2:1 ratio. Area under the receiver operating characteristics curve (AUC ROC) was performed for univariate analysis in predicting pCR status. Logistic regression with elastic net regularization was performed for texture feature selection. Parameter optimization was performed by using 5-fold cross-validation based on mean cross-validated AUC in the training set.

#### RESULTS

Of the total 182 patients, 94 (52%) had pCR and 88 (48%) had non-pCR. Thirty-six multivariate models combining radiomic features from both DCE and DWI had AUC > 0.7 ( $p<0.003$ ), two of which showed AUC > 0.8 ( $p<0.001$ ) in both training and testing data. The first model combined 4 radiomic features from C2 (1 GLCM feature), C4 (percentile 5, 1 GLCM feature) and their changes in C4/C2 (mean) with AUC=0.808, and the second model combined 13 radiomic features at BL (kurtosis, 2 GLCM features), C2 (1 GLCM feature), C4 (3 GLCM features) and their changes in C2/BL (1 GLCM feature), C4/BL (percentile 99, minimum, mean) and C4/C2 (mean, 1 GLCM feature) with AUC=0.816.

#### CONCLUSION

s Multi-parametric MRI-based radiomics models showed high accuracy for early prediction of NAST response in TNBC patients.

#### CLINICAL RELEVANCE/APPLICATION

Radiomic models based on multi-parametric MRI can potentially be helpful for the selection of the appropriate treatment strategy for TNBC patients undergoing NAST.

Printed on: 02/07/23



## Abstract Archives of the RSNA, 2022

W5B-SPBR-4

### The Impact of Social Determinants of Health on the Time Between Diagnostic Breast Imaging and Biopsy at a Safety Net Hospital

Wednesday, Nov. 30 12:45PM - 1:15PM Room: Learning Center - BR DPS

#### Participants

Kevin Dao, Boston, MA (*Presenter*) Nothing to Disclose

#### PURPOSE

There is limited literature on the direct impact of social determinants of health (SDH) on delays in breast cancer diagnosis via breast imaging. Identifying SDH associated with longer lapses between imaging and biopsy is essential to early-stage detection of breast cancer. Previous work demonstrated associations between both housing and food insecurity with longer lapses between diagnostic imaging and biopsy. With this study, we aim to expand upon this retrospective analysis with a longer study period, more participants, and improved data cleaning techniques to better understand how SDH may affect the lapse between imaging and biopsy.

#### METHODS AND MATERIALS

This retrospective study was IRB approved and HIPAA compliant. Informed consent was waived. Patients who underwent screening mammography between January 1 2015 and January 1 2020 were assessed for timing of recommended biopsy due to a BIRADS 4 or 5. SDH were assessed with the unique Tool for Health Resilience in Vulnerable Environments (THRIVE) screening questionnaire developed at Boston Medical Center. Associations between imaging-biopsy timing and 8 explanatory SDH variables were assessed with multivariate Cox proportional hazard modeling, as well as demographic data.

#### RESULTS

2885 unique patients who underwent 3142 unique diagnostic imaging studies were included in the multivariate analysis. Of those 3142 studies, 196 (6.2%) had not yet been followed by the recommended biopsy by the end of the study period. 2159 patients (74.8%) had SDH data in at least one domain, and the individual domains ranged from 875 patients (30.3%) with complete data for education to 2073 patients (71.8%) with complete data for food insecurity. A positive screen for at least one SDH was associated with a longer lapse between diagnostic imaging and biopsy ( $p=0.048$ ). Further, housing insecurity alone was nearly associated with longer lapses between diagnostic imaging and biopsy ( $p=0.059$ ). Paradoxically, those who desired more education were found to have shorter lapses between diagnostic imaging and biopsy ( $p=0.037$ ).

#### CONCLUSION

Of the eight SDH screened, housing insecurity was most close to association with longer lapses between diagnostic imaging and biopsy. However, only the aggregate of all SDH was associated with a statistically significant lengthening of this lapse. Patients who desired more education were found to have shorter lapses, but this survey domain had the lowest completion rate.

#### CLINICAL RELEVANCE/APPLICATION

Identification of SDH that may affect the time from imaging to biopsy can potentially inform targeted programs to intervene. Government and health system interventions addressing SDH, notably housing insecurity, could allow for shorter time to breast cancer diagnosis and treatment.

Printed on: 02/07/23

## Abstract Archives of the RSNA, 2022

W5B-SPBR-5

### **BI-RADS-0 Screening Mammography: Risk Factors Associated with Prolonged Follow-up Time to Diagnostic Evaluation**

Wednesday, Nov. 30 12:45PM - 1:15PM Room: Learning Center - BR DPS

#### **Participants**

Samantha Platt, MD, New York, NY (*Presenter*) Nothing to Disclose

#### **PURPOSE**

BI-RADS-0 screening mammograms require follow-up diagnostic imaging, optimally within 60 days. Our study aims to identify risk factors for prolonged follow-up.

#### **METHODS AND MATERIALS**

We conducted a retrospective, observational, case-control study of women aged 40-91 from breast centers in the Mount Sinai System who had nondiagnostic BI-RADS-0 screening mammogram between 3/19/18-3/19/20. Sociodemographic information was collected from a self-reported screening questionnaire. Patients who underwent screening in the mobile mammography van or had incorrect follow-up dates were excluded. Analysis 1: Goal was to identify risk factors associated with the following outcomes categories: <60d follow-up, >60d follow-up or no follow-up. Chi-squared tests and univariate logistic regressions were performed. Significant variables were included in multinomial logistic regression model with <60d follow-up as the reference group. Analysis 2: Goal was to identify risk factors that lead to prolonged follow-up times among women with follow-up. Shapiro-Wilk test determined a non-normal distribution of the dependent variable (0.61,  $p < 0.0001$ ). Spearman's rank coefficient of correlation, Mann Whitney Wilcoxon Test, and Kruskal-Wallis Tests were used.

#### **RESULTS**

Our review returned 5,034 screening mammograms. Of 4,552 patients included in the study, 904 (19.9%) had no follow-up. Of the 3,648 (80.1%) with follow-up, 2,797 (76.7%) had a follow-up examination <60d (avg. 22.1 days) and 851 (23.3%) had follow-up >60d (avg. 190.4 days). Multinomial log regression found that Asian women, black women, and those who identified as "other" were independently more likely to have no or >60d follow-up ( $p < 0.05$ ). Women who did not report their race were more likely to have no or >60d follow-up ( $p < 0.05$ ). Women who completed the questionnaire in Spanish were more likely to have no or >60d follow-up ( $p < 0.05$ ). Amongst women with follow-up, black women, those who identified as "other", LatinX women, and those completed the questionnaire in Spanish had significant follow-up delays ( $p < 0.05$ ). BRCA+ patients had shorter follow-up times ( $p < 0.05$ ).

#### **CONCLUSION**

Follow-up time is affected by patient-specific breast cancer risk factors such as BRCA status as well as disparities in health care access by race, primary language and Latinx heritage.

#### **CLINICAL RELEVANCE/APPLICATION**

There are risk factors associated with prolonged follow-up time to diagnostic evaluation that need to be targeted in order to improve patient outcomes.

Printed on: 02/07/23

## Abstract Archives of the RSNA, 2022

W5B-SPBR-6

### Frequency and outcome of probably benign findings (BI-RADS 3) in patients with a personal history of breast cancer (PHBC) imaged with digital mammography (DM) vs. digital breast tomosynthesis (DBT)

Wednesday, Nov. 30 12:45PM - 1:15PM Room: Learning Center - BR DPS

#### Participants

Lily Offit, Boston, MA (*Presenter*) Nothing to Disclose

#### PURPOSE

Probably benign (BI-RADS 3) findings are those with <2% malignancy rate, and are followed with imaging at 6, 12, and 24 months. Few studies have reported probably benign outcomes in patients with a personal history of breast cancer (PHBC) and have shown >2% malignancy rates. The purpose of this study is to determine the frequency, findings, and outcomes of probably benign findings in patients with PHBC imaged with digital mammography (DM) versus digital breast tomosynthesis (DBT).

#### METHODS AND MATERIALS

This is a retrospective review of 14,845 mammogram reports in patients with PHBC (mastectomy and/or lumpectomy). Of these, 8,422 exams (56.7%) were DM between 10/2014-9/16 and 6,423 exams (43.3%) were DBT between 2/2017-12/2018. Frequency and indication of BI-RADS 3 assignment, mammographic finding (calcifications, architectural distortions, asymmetries, or mass), and biopsy or follow-up imaging outcomes were compared between DM and DBT.

#### RESULTS

In the study periods, there were 901/14,845 (6.1%) examinations coded as BI-RADS 3, with 717 unique BI-RADS 3 findings. DBT led to a reduced use of probably benign assignments when compared to DM (6.4% for DM vs. 5.6% for DBT,  $p=0.04$ ). DM had a higher rate of malignancy of subsequently biopsied BI-RADS findings when compared to DBT [(4.8% (21/442) DM vs. 1.8% (5/275) DBT ( $p=0.04$ )). DBT showed a 10.1% increase in percent of masses detected compared to DM ( $p=0.004$ ). There was a trend towards more probably benign calcifications detected in DM ( $p=0.06$ ).

#### CONCLUSION

Use of DBT in individuals with a prior history of breast cancer led to a decrease in rate of BI-RADS 3 assignment. DM BI-RADS 3 rate of malignancy was 4.8%, higher than the accepted 2% malignancy rate, and decreased to 1.8% with use of DBT.

#### CLINICAL RELEVANCE/APPLICATION

Insight into BI-RADS 3 usage and malignancy rates between imaging modalities will help establish whether probably benign assessments in patients with PHBC are being utilized appropriately to identify cancers early and reduce unnecessary biopsies.

Printed on: 02/07/23

## Abstract Archives of the RSNA, 2022

W5B-SPBR-7

### Interval Breast Cancers Compared to Screen Detected Breast Cancers: A Retrospective Cohort Study

Wednesday, Nov. 30 12:45PM - 1:15PM Room: Learning Center - BR DPS

#### Participants

Emily Ambinder, MD, MSc, Ellicott City, MD (*Presenter*) Nothing to Disclose

#### PURPOSE

Mammographic screening improves mortality from breast cancer through early detection. We aim to identify clinical and imaging features that differentiate screen detected breast cancers from interval breast cancers in order to inform and improve breast cancer screening for all women in the era of precision medicine.

#### METHODS AND MATERIALS

All screening mammograms (n= 211,514) performed between 7/1/2013 and 6/30/2020 at our institution were reviewed. Patients with breast cancer diagnosed within one year of screening were included in this study. Patient, imaging, and cancer characteristics of screen detected breast cancers and interval breast cancers were compared using the Chi square test, Fisher test, and Wilcoxon Rank Sum Test. Interval cancers were defined as breast cancers diagnosed within one year of a negative screening mammogram.

#### RESULTS

During the study period, 1,232 women were diagnosed with breast cancer and included in this study (mean age 64 years, standard deviation 11 years). Overall sensitivity of screening mammography was 91% (1,121 screen detected breast cancers and 111 interval cancers). Interval cancers were most often palpable (62/111=56%) or identified on a high-risk screening breast MRI (20/111=18%). Patient age, race, and screening exam modality (FFDM versus DBT) were similar for patients with screen detected cancers and interval cancers (all  $p > 0.05$ ). Breast density was higher for patients with interval cancers (heterogeneously dense or extremely dense: 86/111=77% versus 683/1121=61%,  $p < .001$ ). Compared to screen detected cancers, interval cancers were less often ductal carcinoma in situ or primary tumor stage 1 (69/111=62% versus 981/1121=88%,  $p < 0.001$ ) and less often regional lymph node stage 0 (89/111=80% versus 990/1121=88%,  $p < 0.001$ ). Interval cancers were less often hormone receptor positive (ER+: 73/94=78% versus 746/824=91%,  $p < 0.001$ ), and less often had low proliferative indices (Ki67 <20%: 21/52=40% versus 301/488=62%,  $p = 0.005$ ). HER2 positivity was similar for the two groups (8/91=9% versus 84/804=10%,  $p = 0.76$ ).

#### CONCLUSION

s We found that mammographic screening has a high sensitivity for detection of breast cancer (91%). Interval cancers were often palpable or identified on a screening breast MRI and were associated with dense breast tissue but did not differ by age and race compared to screen detected cancers. Interval cancers were higher stage with less favorable molecular features compared to screen detected cancers.

#### CLINICAL RELEVANCE/APPLICATION

While screening mammography has a high sensitivity for detecting breast cancer, novel approaches are needed to identify interval cancers earlier as these are often higher stage with unfavorable molecular features compared to screen detected cancers.

Printed on: 02/07/23

## Abstract Archives of the RSNA, 2022

W5B-SPCA

### Cardiac Wednesday Poster Discussions - B

Wednesday, Nov. 30 12:45PM - 1:15PM Room: Learning Center - CA DPS

#### Sub-Events

#### W5B-SPCA- Changes of Cardiac Function in Diabetic Pigs: A Pilot Study Using Cardiac MRI<sup>1</sup>

Participants

Wei-Feng Yan, MD, Chengdu, China (*Presenter*) Nothing to Disclose

#### PURPOSE

To investigate the feasibility of cardiac MRI in the evaluation of cardiac dysfunction in diabetic pigs.

#### METHODS AND MATERIALS

The diabetic pig model induced by streptozotocin (STZ) was established in 16 adult Bama mini-pigs. The porcine heart was scanned by 3.0T MRI at different times, and the left ventricular (LV) myocardial strain was analyzed by tissue tracking technique. The changes of left ventricular (LV) structure, function and myocardial strain over time were compared in diabetic pigs.

#### RESULTS

13 pigs were successfully modeled (fasting blood glucose was higher than 7.0mmol/L for three consecutive weeks). Cardiac MRI scans were performed in pigs before modeling (n = 13), one month after modeling (n = 13), 6 months after modeling (n = 13), 10 months after modeling (n = 11) and 16 months after modeling (n = 6). As the disease progresses, there were no significant changes in LV remodeling index (1.27±0.34 vs. 1.14±0.55 vs. 0.96±0.2 vs. 1.16±0.22 vs. 1.16±0.37) and ejection fraction (57.93±9.81 vs. 50.82±11.21 vs. 54.58±15.29 vs. 60.23±10.88 vs. 63.75±14.65), but the longitudinal peak strain of LV decreased gradually (-10.37±2.92 vs. -9.89±2.92 vs. -9.49±3.53 vs. -8.72±2.59 vs. -6.97±3.55).

#### CONCLUSION

The decrease of LV longitudinal peak strain could be the early manifestation of cardiac dysfunction in diabetic pigs.

#### CLINICAL RELEVANCE/APPLICATION

Cardiac MRI tissue tracking technique may reflect the early changes of the heart in diabetic cardiomyopathy.

#### W5B-SPCA- Identification of Fibrosis in Hypertrophic Cardiomyopathy: A Radiomic Study on Cardiac Magnetic Resonance Cine Imaging<sup>2</sup>

Participants

Cailing Pu, (*Presenter*) Nothing to Disclose

#### PURPOSE

Hypertrophic cardiomyopathy (HCM) patients often need to undergo repeated enhanced cardiac magnetic resonance (CMR) to detect fibrosis during their lifetime follow-up. We aimed to develop a practical model based on cine imaging to help identify patients with a high risk of fibrosis and screen patients without fibrosis to avoid unnecessary injection of contrast.

#### METHODS AND MATERIALS

273 HCM patients were divided into training set and test set at the ratio of 7:3. Logistic regression analysis was used to find predictive image features to construct CMR model. Radiomic features were derived from the maximal wall thickness (MWT) slice and entire left ventricular (LV) myocardium, and extreme gradient boosting was used to build radiomic models. Integrated models were established by fusing image features and radiomic model. Model performance was validated in the test set and was presented by receiver operating characteristic curve, calibration curve and decision curve analysis (DCA).

#### RESULTS

We established five prediction models, including CMR model, R1 and R2 model (constructed based on the MWT layer and entire LV myocardium respectively) and two integrated models (ICMR+R1 and ICMR+R2). In the test set, ICMR+R2 model had excellent AUC value, diagnostic accuracy, sensitivity and F1 score in identifying positive late gadolinium enhancement patients, performance values were 0.898, 89.02%, 92.54%, 93.23% respectively. The calibration plot and DCA indicated that ICMR+R2 model was well calibrated and had better net benefit than other models.

#### CONCLUSION

The predictive model fusing image features and radiomics from entire LV myocardium had good diagnostic performance, robustness and clinic utility.

#### CLINICAL RELEVANCE/APPLICATION

1. HCM is prone to fibrosis. Patients with HCM need to undergo repeated enhanced cardiac magnetic resonance to detect fibrosis during their lifetime follow-up. 2. The predictive model constructed based on entire left ventricular myocardium outperformed than that by maximal wall thickness slice. 3. The predictive model fusing image features and radiomics from entire left ventricular myocardium had excellent diagnostic performance, robustness and clinic utility.

### **W5B-SPCA-3 Utility of Dual-energy CT Radiomics in The Detection of Left Atrial Appendage Thrombi in Patients with Atrial Fibrillation**

Participants

Wenhuan Li, MD, (*Presenter*) Nothing to Disclose

#### **PURPOSE**

This study aimed to investigate whether radiomics from dual-energy computed tomography (CT)-derived iodine overlay maps performed better than that from routine contrast-enhanced CT images in the detection of left atrial appendage (LAA) thrombus in patients with atrial fibrillation.

#### **METHODS AND MATERIALS**

One hundred and ten consecutive patients were prospectively recruited and scanned in the early contrast-enhanced phase using third-generation dual-source CT in dual-energy mode. Radiomic features were extracted from three-dimensional segmentation of the filling defect. The ratios of iodine concentration and Hounsfield units (HU) in the filling defects to those in the ascending aorta (AA) were calculated. The diagnostic performances of radiomics from iodine overlay maps and routine contrast-enhanced CT images in the detection of LAA thrombus were assessed and compared with the ratios of iodine concentration and HU, respectively.

#### **RESULTS**

Transesophageal echocardiography (TEE) demonstrated thrombus in 16 (15%), spontaneous echo contrast in 24 (22%), and no abnormality in 70 (64%) patients. With TEE findings as the reference standard in LAA thrombus detection, radiomics from iodine overlay maps performed better than that from routine contrast-enhanced CT images (area under the receiver operating characteristic curve, 0.96 vs. 0.89;  $P < 0.05$ ). Radiomics from iodine overlay maps performed better than LAA/AA iodine concentration ratio (0.96 vs. 0.93;  $P < 0.05$ ) and radiomics from routine contrast-enhanced CT images performed better than LAA/AA HU ratio (0.89 vs. 0.85;  $P < 0.05$ ).

#### **CONCLUSION**

s Radiomics from iodine overlay maps performed better than radiomics from routine contrast-enhanced CT images in LAA thrombus detection.

#### **CLINICAL RELEVANCE/APPLICATION**

Accurate detection of LAA thrombus is extremely important. Radiomics from iodine overlay maps performed better than radiomics from routine contrast-enhanced CT images in LAA thrombus detection.

Printed on: 02/07/23

## Abstract Archives of the RSNA, 2022

W5B-SPCA-1

### Changes of Cardiac Function in Diabetic Pigs: A Pilot Study Using Cardiac MRI

Wednesday, Nov. 30 12:45PM - 1:15PM Room: Learning Center - CA DPS

#### Participants

Wei-Feng Yan, MD, Chengdu, China (*Presenter*) Nothing to Disclose

#### PURPOSE

To investigate the feasibility of cardiac MRI in the evaluation of cardiac dysfunction in diabetic pigs.

#### METHODS AND MATERIALS

The diabetic pig model induced by streptozotocin (STZ) was established in 16 adult Bama mini-pigs. The porcine heart was scanned by 3.0T MRI at different times, and the left ventricular (LV) myocardial strain was analyzed by tissue tracking technique. The changes of left ventricular (LV) structure, function and myocardial strain over time were compared in diabetic pigs.

#### RESULTS

13 pigs were successfully modeled (fasting blood glucose was higher than 7.0mmol/L for three consecutive weeks). Cardiac MRI scans were performed in pigs before modeling (n = 13), one month after modeling (n = 13), 6 months after modeling (n = 13), 10 months after modeling (n = 11) and 16 months after modeling (n = 6). As the disease progresses,, there were no significant changes in LV remodeling index (1.27±0.34 vs. 1.14±0.55 vs. 0.96±0.2 vs. 1.16±0.22 vs. 1.16±0.37) and ejection fraction (57.93±9.81 vs. 50.82±11.21 vs. 54.58±15.29 vs. 60.23±10.88 vs. 63.75±14.65), but the longitudinal peak strain of LV decreased gradually (-10.37±2.92 vs. -9.89±2.92 vs. -9.49±3.53 vs. -8.72±2.59 vs. -6.97±3.55).

#### CONCLUSION

s The decrease of LV longitudinal peak strain could be the early manifestation of cardiac dysfunction in diabetic pigs.

#### CLINICAL RELEVANCE/APPLICATION

Cardiac MRI tissue tracking technique may reflect the early changes of the heart in diabetic cardiomyopathy.

Printed on: 02/07/23

## Abstract Archives of the RSNA, 2022

W5B-SPCA-2

### Identification of Fibrosis in Hypertrophic Cardiomyopathy: A Radiomic Study on Cardiac Magnetic Resonance Cine Imaging

Wednesday, Nov. 30 12:45PM - 1:15PM Room: Learning Center - CA DPS

#### Participants

Cailing Pu, (*Presenter*) Nothing to Disclose

#### PURPOSE

Hypertrophic cardiomyopathy (HCM) patients often need to undergo repeated enhanced cardiac magnetic resonance (CMR) to detect fibrosis during their lifetime follow-up. We aimed to develop a practical model based on cine imaging to help identify patients with a high risk of fibrosis and screen patients without fibrosis to avoid unnecessary injection of contrast.

#### METHODS AND MATERIALS

273 HCM patients were divided into training set and test set at the ratio of 7:3. Logistic regression analysis was used to find predictive image features to construct CMR model. Radiomic features were derived from the maximal wall thickness (MWT) slice and entire left ventricular (LV) myocardium, and extreme gradient boosting was used to build radiomic models. Integrated models were established by fusing image features and radiomic model. Model performance was validated in the test set and was presented by receiver operating characteristic curve, calibration curve and decision curve analysis (DCA).

#### RESULTS

We established five prediction models, including CMR model, R1 and R2 model (constructed based on the MWT layer and entire LV myocardium respectively) and two integrated models (ICMR+R1 and ICMR+R2). In the test set, ICMR+R2 model had excellent AUC value, diagnostic accuracy, sensitivity and F1 score in identifying positive late gadolinium enhancement patients, performance values were 0.898, 89.02%, 92.54%, 93.23% respectively. The calibration plot and DCA indicated that ICMR+R2 model was well calibrated and had better net benefit than other models.

#### CONCLUSION

The predictive model fusing image features and radiomics from entire LV myocardium had good diagnostic performance, robustness and clinic utility.

#### CLINICAL RELEVANCE/APPLICATION

1. HCM is prone to fibrosis. Patients with HCM need to undergo repeated enhanced cardiac magnetic resonance to detect fibrosis during their lifetime follow-up. 2. The predictive model constructed based on entire left ventricular myocardium outperformed than that by maximal wall thickness slice. 3. The predictive model fusing image features and radiomics from entire left ventricular myocardium had excellent diagnostic performance, robustness and clinic utility.

Printed on: 02/07/23



## Abstract Archives of the RSNA, 2022

W5B-SPCA-3

### Utility of Dual-energy CT Radiomics in The Detection of Left Atrial Appendage Thrombi in Patients with Atrial Fibrillation

Wednesday, Nov. 30 12:45PM - 1:15PM Room: Learning Center - CA DPS

#### Participants

Wenhuan Li, MD, (*Presenter*) Nothing to Disclose

#### PURPOSE

This study aimed to investigate whether radiomics from dual-energy computed tomography (CT)-derived iodine overlay maps performed better than that from routine contrast-enhanced CT images in the detection of left atrial appendage (LAA) thrombus in patients with atrial fibrillation.

#### METHODS AND MATERIALS

One hundred and ten consecutive patients were prospectively recruited and scanned in the early contrast-enhanced phase using third-generation dual-source CT in dual-energy mode. Radiomic features were extracted from three-dimensional segmentation of the filling defect. The ratios of iodine concentration and Hounsfield units (HU) in the filling defects to those in the ascending aorta (AA) were calculated. The diagnostic performances of radiomics from iodine overlay maps and routine contrast-enhanced CT images in the detection of LAA thrombus were assessed and compared with the ratios of iodine concentration and HU, respectively.

#### RESULTS

Transesophageal echocardiography (TEE) demonstrated thrombus in 16 (15%), spontaneous echo contrast in 24 (22%), and no abnormality in 70 (64%) patients. With TEE findings as the reference standard in LAA thrombus detection, radiomics from iodine overlay maps performed better than that from routine contrast-enhanced CT images (area under the receiver operating characteristic curve, 0.96 vs. 0.89;  $P < 0.05$ ). Radiomics from iodine overlay maps performed better than LAA/AA iodine concentration ratio (0.96 vs. 0.93;  $P < 0.05$ ) and radiomics from routine contrast-enhanced CT images performed better than LAA/AA HU ratio (0.89 vs. 0.85;  $P < 0.05$ ).

#### CONCLUSION

s Radiomics from iodine overlay maps performed better than radiomics from routine contrast-enhanced CT images in LAA thrombus detection.

#### CLINICAL RELEVANCE/APPLICATION

Accurate detection of LAA thrombus is extremely important. Radiomics from iodine overlay maps performed better than radiomics from routine contrast-enhanced CT images in LAA thrombus detection.

Printed on: 02/07/23

## Abstract Archives of the RSNA, 2022

W5B-SPCH

### Chest Wednesday Poster Discussions - B

Wednesday, Nov. 30 12:45PM - 1:15PM Room: Learning Center - CH DPS

#### Participants

Elsie Nguyen, MD, Toronto, ON (*Moderator*) Nothing to Disclose

#### Sub-Events

### W5B-SPCH- **Comparing UTE1H-MRI Derived Ventilation Measurement and 19F-MRI Ventilation Parameters in Patients with Cystic Fibrosis**

#### Participants

Maria Mihailescu, BS, Chapel Hill, NC (*Presenter*) Nothing to Disclose

#### PURPOSE

UTE 1H-MRI could allow for non-invasive ventilation measurements in the lungs by examining changes in structure during ventilatory cycles. 19F-MRI with inhaled perfluoropropane (PFP) gas has been established as a reliable assessment of lung ventilation. Our goal is to better understand the potential of 1H-MRI derived ventilation parameters by comparing values to 19F-MRI derived ventilation parameters.

#### METHODS AND MATERIALS

15 19F-MRI and 1H-MRI scans from patients with cystic fibrosis before and after treatment with elexacaftor/tezacaftor/ivacaftor were used for method development. To analyze ventilation from 19F-MRI, signal intensity-time curves during PFP wash-in and wash-out for each voxel were fitted to a bi-exponential model to find the time constant that characterizes gas wash-out ( $t_2$ ). To determine ventilation maps for 1H-MRI images, a 3D Jacobian was computed on a voxel-by-voxel basis between maximum inhalation and maximum exhalation. Heat maps of ventilation parameters from each imaging modality were created. Ventilation defect percentages (VDP) were calculated to compare the two ventilation parameters.

#### RESULTS

When comparing 19F-MRI and 1H-MRI VDP for 15 scans, there was no significant correlation coefficient. If scans with minimum lung disease are excluded (Defined as 19F-MRI determined VDP <3%), the remaining 11 scans had a correlation coefficient of 0.77 when comparing VDPs.

#### CONCLUSION

For moderate to severe lung disease VDP determined from 19F-MRI and 1H-MRI have a high correlation coefficient, suggesting that 1H-MRI determined VDP may be a useful functional assessment marker in these patients. For mild lung disease, ventilation parameters are not significantly related. One explanation for this is that severe lung disease has drastic effects on the lung parenchyma altering its normal movement and allowing for detection as the magnitude of the Jacobian between inspiration and expiration. For mild lung disease, factors that impact air movement such as inflammation or minimal mucus plugging may not register at the level of structural movement. With higher resolution 1H-MRI scans, the Jacobian magnitude could be calculated at the alveolar level to allow for measurement of ventilation in mild lung disease.

#### CLINICAL RELEVANCE/APPLICATION

The 1H-MRI Jacobian magnitude may be useful in characterizing VDP for moderate to severe lung disease without the need for 19F-MRI imaging, a potentially financially prohibitive modality that is not suitable for all patient populations.

### W5B-SPCH- **How Normal Is a Normal Chest X-Ray: Does a Comprehensive Artificial Intelligence Model Identify Significant Findings in Chest Radiographs Interpreted as Normal in Clinical Practice?**

#### Participants

Arpit Talwar, MBBS, MMed, (*Presenter*) Nothing to Disclose

#### PURPOSE

Chest x-ray (CXR) interpretation is one of the most subjective and complex of radiology tasks. Accuracy depends on the radiologists' level of experience and training with the potential of human error related to workload, fatigue and interruptions impacting on patient care. Validated comprehensive deep-learning models may assist in improving diagnostic accuracy and departmental workflow. We therefore aimed to evaluate the performance of radiologist reported normal chest x-rays within the hospital setting against a comprehensive deep-learning model.

#### METHODS AND MATERIALS

A retrospective analysis of CXRs that had been reported as normal in adults ( $\geq 18$  years) was performed on consecutive patients at St. Vincent's Hospital Melbourne from Jan-May 2016. A validated deep-learning model with a total dataset of 60 significant findings was applied on the included studies. Significant findings were adjudicated by two chest radiologists with over 10 years-experience.

Disagreements were re-reviewed to reach a consensus. Level of agreement between radiologists and the model was also assessed.

## RESULTS

Of the 490 studies included in this preliminary analysis, 444 (90.6%) showed no significant finding predictions by the model (specificity 93.3%). 64 significant findings were identified by the model across 46 studies (9.4%). 50% were rejected by the adjudicators (model PPV 0.5) with 32 findings (6.3%) across 22 studies deemed to be missed by the reporting radiologist. The most common missed finding was distended bowel (18.8%) with a single case of solitary pulmonary nodule (3.1%) and superior mediastinal mass (3.1%) identified. Within our cohort, a total of 4 studies (0.8%) had findings that were of particular concern. Substantial inter-rater agreement was achieved between the model and radiologists (weighted  $\kappa$  value of 0.64 (95% CI 0.52 - 0.75)).

## CONCLUSION

Our preliminary results demonstrate that an AI model provided a useful tool in auditing CXRs reported as normal in a public hospital setting, where radiology trainees report the majority of these studies. The AI model demonstrated that a significant percentage (6.3%) of CXRs had findings deemed significant, missed in the initial report.

## CLINICAL RELEVANCE/APPLICATION

Integration of a highly specific AI model in a real-world reporting environment has the potential to improve departmental workflow and reduce human error, ultimately improving patient care.

## W5B-SPCH- Predicting Outcomes of Lung Transplants Based on Pre-operative Chest CT Scans in Patients with Scleroderma

Participants  
Jiantao Pu, PhD, (*Presenter*) Nothing to Disclose

## PURPOSE

To investigate the feasibility of predicting the outcomes of lung transplants in patients with scleroderma based on pre-treatment chest CT scans.

## METHODS AND MATERIALS

We created a cohort consisting of 104 subjects who were diagnosed with scleroderma and underwent lung transplants from 2005 to 2020. Based on the pre-treatment chest CT scans, we quantified: (1) lung volume, (2) heart volume, (3) chest cavity volume, (4) distances between sternum and spines, (5) artery and vein volumes, and (6) the volume and density of five body tissues (i.e., skeleton muscle, subcutaneous fat, visceral fat, intramuscular fat, and bone). The backward stepwise logistic/linear regression was used to predict chest open, postoperative mechanical support, AKI requiring dialysis, primary graft dysfunction (PGD), and ICU stay (days). For PGD, we dichotomized these patients on whether they were Grade 3 or not on postoperative day 3. The prediction models were evaluated using the area under the receiver-operating characteristic (ROC) curve (AUC). The R-squared (R<sup>2</sup>) was used to assess the performance of the model for predicting ICU stay.

## RESULTS

The prediction models showed an AUC of 0.899 (95% CI: 0.837-0.960) for assessing chest open, an AUC of 0.930 (95% CI: 0.880-0.980) for assessing AKI requiring dialysis demonstrated, an AUC of 0.953 (95% CI: 0.917-0.989) for predicting postoperative mechanical support. When assessing PGD Grade 3, the prediction model had an AUC of 0.988 (95% CI: 0.965-1.0) with variables formed primarily by the body tissues and the geometric characteristics of the chest cavity. When predicting the total ICU stay, the computer model demonstrated an R<sup>2</sup> of 0.37, indicating that 37% of the variance in the outcome was explained by the model.

## CONCLUSION

The outcomes of lung transplants in patients with scleroderma are significantly associated with the geometric characteristics of the lungs and the body compositions of the recipients.

## CLINICAL RELEVANCE/APPLICATION

Patients with scleroderma have an increased risk of complications after lung transplantation. Awareness of the factors contributing to the complications will maximize the benefit of lung transplants.

## W5B-SPCH- Artificial Intelligence-assisted Analysis to Facilitate Effective Detection of Humeral Lesions in the Simple Chest Radiograph

Participants  
Harim Kim, MD, (*Presenter*) Nothing to Disclose

## PURPOSE

While chest radiograph (CR) is a basic modality for patient assessment, the humerus remains an easily negligible spot. Thus, it can be of great aid to the reader if an artificial intelligence (AI) system automatically diagnoses and visualizes tumors of humerus in CR, particularly with high sensitivity. However, as there is no prior AI study on this subject, we newly proposed an advanced AI system for detecting humerus tumors, with better sensitivity and tumor visualization, and compared its usefulness with radiologists.

## METHODS AND MATERIALS

Our AI system differs from existing ones in that it uses a new training objective named false-positive activation area reduction (FPAR), which improves both the tumor detection sensitivity and tumor visualization ability of AI by learning not to activate the class activation map in areas unrelated to the region of interest (i.e., outside humerus or tumor). A total of 2994 CRs for 1500 normal and 1494 CT-proven humeral tumor CRs were provided as an AI training set. The AI program and two trainee radiologists (R1 and R2) were commonly tested with holdout test data, not used for AI training, of 119 normal and 102 tumor patients. The radiologists were tested twice with the same test set, and the second time, they were provided with AI test results.

## RESULTS

Technically, the proposed AI system improved the sensitivity (92.4%) by 2.2% compared to the baseline (90.2%) and it also

Technically, the proposed AI system improved the sensitivity (63.4%) by 3.2% compared to the baseline (60.2%) and it also improved the tumor localization accuracy (82%) by 13% compared to the baseline (69%), demonstrating the effectiveness of FPAR. In comparison with radiologists, trainee radiologists showed different sensitivity and accuracy in detecting humerus lesions. Overall sensitivity, specificity, and accuracy of radiologists were 54.4%, 94.9%, and 82.3% and when compared with AI, AI showed a significantly higher sensitivity of 68.6% ( $p=0.0025$ ). Also, AI showed higher sensitivity and accuracy ( $p=0.0007$  and  $0.0339$  respectively) but did not outperform in specificity ( $p=0.1298$ ). When assisted by AI, the performance of two trainee radiologists did not differ significantly. And compared with results not assisted by AI, sensitivity and accuracy showed improvement, most notably in the trainee with lower sensitivity.

## CONCLUSION

The utilization of FPAR effectively enhances true-positives in humeral tumor detection and reduces false-positives in humeral tumor visualization. This advanced AI is proven to make radiologists detect humerus lesions better, especially for trainee radiologists with less experience and lower sensitivity.

## CLINICAL RELEVANCE/APPLICATION

Our AI system may help radiologists pay better attention to possible humeral lesions, as humerus can be easily overlooked in CR.

## W5B-SPCH- Pulmonary Alveolar Echinococcosis: CT Findings and Classification

4

Participants

Hai Hua Bao, Xining, China (*Presenter*) Nothing to Disclose

## PURPOSE

Alveolar echinococcosis, which is prevalent on the Tibetan plateau, is a multisystemic infectious parasitic disease that poses a serious health risk to humans. Pulmonary alveolar echinococcosis (PAE) is a lesion secondarily induced by direct infiltration and hematogenous dissemination from hepatic AE lesions and mostly in the middle-late stages. Currently, studies on the CT-morphological classification of PAE are scarce. The study aims to clarify the CT imaging findings and classification of PAE.

## METHODS AND MATERIALS

The study analysed the CT manifestations of patients with AE diagnosed by clinical and imaging examinations at the Affiliated Hospital of Qinghai University from 2014 to 2021. One hundred and eighty-nine patients (age, 43 years  $\pm$  13 [standard deviation]; gender, 93 men and 96 women) were evaluated. All patients living at a high altitude of 2500 - 3500m. A GE 256-layer CT scanner was used for plain and enhanced scan to observe the distribution, morphology and typing characteristics of the lesions. Statistics were performed using SPSS software.

## RESULTS

The CT manifestations of PAE are mostly multiple nodules, which were mainly peripheral distribution and mostly in the lower lobes. The diameter of the lesions ranged from 2mm to 9cm. 189 cases of AE in patients with primary lesions are from the liver. CT imaging characteristics were categorized into four types: I. small solid nodules ( $\leq 1$  cm) (37/189, 19.6%); II. large solid nodules ( $> 1$  cm) (158/189, 83.6%); III. solid nodules with cavity (70/189, 37.0%); IV. calcified nodules (32/189, 16.9%). Different types of nodules can be shown on CT images of the same patient. The probability of the primary foci in the liver invading blood vessels and diaphragm are hepatic vein (62.4%), inferior vena cava (52.5%), portal vein (69.3%), hepatic artery (53.5%) and diaphragm (86.1%) respectively. Approximately 54.5% of patients had operation history.

## CONCLUSION

The CT findings of PAE, which is secondarily induced from primary foci in the liver, are mostly peripheral distribution and mainly in the lower lobes. The CT classification of PAE is more common in types II and III.

## CLINICAL RELEVANCE/APPLICATION

The CT-morphological classification of PAE could help to clarify the progression of the disease and provide a basis for the early interference and the choice of treatment schedule.

## W5B-SPCH- Chest X-Ray at Emergency Admission, SOFA Score and NIV: Potential Value in Predicting Barotrauma in Ventilated COVID-19 Patients during the First Pandemic Peak

5

Participants

Francesco Stanco, (*Presenter*) Nothing to Disclose

## PURPOSE

To assess the value of chest X-ray (CXR), SOFA (Sequential Organ Failure Assessment) score and NIV (non-invasive ventilation) at emergency admission to predict barotrauma in mechanically ventilated COVID-19 patients. To report the distribution of barotrauma at chest CT.

## METHODS AND MATERIALS

SARS-CoV-2 positive patients, first admitted to the emergency department and then to the intensive care unit (ICU), between February 20th and April 15th, 2020, were retrospectively evaluated. All patients were divided into two groups, according to the occurrence/absence of barotrauma. CXR were assessed by 1 experienced radiologist using Brixia score (BS). SOFA score was calculated by the referring physicians at ICU admittance and NIV days prior intubation were collected. Distribution of barotrauma (pneumomediastinum/pneumothorax/subcutaneous emphysema) were annotated from unenhanced chest CT scan during ICU hospitalization.

## RESULTS

A total of 117 SARS-CoV-2 patients (24 females, mean age 59.95 years) were included. Thirty-seven (37/117; 31.6%) mechanically ventilated patients developed barotrauma (25 pneumomediastinum, 23 pneumothorax, 24 subcutaneous emphysema). Compared to the non-barotrauma group, barotrauma patients demonstrated higher BS values (mean value 12.05 vs 9.38,  $p$ -value 0.0041), and underwent longer NIV (mean value 4.20 vs 2.75 days,  $p$ -value 0.0075). No significant correlation with SOFA score was found. A model using these three tested predictors (BS, SOFA score, NIV days) resulted as the best model to predict development of

barotrauma.

## CONCLUSION

s Barotrauma occurred in a non-negligible percentage of mechanically ventilated patients with COVID-19 pneumonia. The best predicting model for barotrauma was obtained by the simultaneous employment of three independent variables selected with simple logistic regression: BS, SOFA score, and NIV days.

## CLINICAL RELEVANCE/APPLICATION

Integrated clinical-radiological assessment may predict the risk of barotrauma in mechanically ventilated COVID-19 patients, a complication potentially impacting proper management of these cases.

## W5B-SPCH- Second-Opinion Subspecialty Consultations in Chest Radiology

6

Participants

Mohammad Jalili, MD, Los Angeles, CA (*Presenter*) Nothing to Disclose

## PURPOSE

The purpose of this study is twofold. The primary aim is to assess the significance of subspecialty second-opinion consultations for CT examinations in thoracic imaging. The secondary aim is to assess the prevalence and reimbursement rates of over-read interpretations across academic cardiothoracic sections.

## METHODS AND MATERIALS

Reports from 100 random chest CTs referred to a single academic institution for second-opinion consultation were reviewed by two radiologists by consensus. Outside and inside reports were compared using a previously published 5-point scale. Clinically important differences were defined as those likely to change patient management. Additionally, a 6-question survey was sent to the section head of every academic cardiothoracic radiology department in the U.S.A. asking how their department handles over-read requests.

## RESULTS

Of all the second-opinion examinations, 69% (69/100) had an outside report available for comparison and inclusion in the study. There were no discrepancies in 70% of cases (48/69). In the remaining 30% (21 cases), 6 cases had nonsignificant discrepancies (Type 2 or 3) and 15 cases had clinically significant discrepancies (Type 4 and 5). 19 out of 56 (33%) survey recipients responded to the survey. All 19 (100%) respondents stated that their institution does provide second opinion consultations for outside studies. Out of the 19 respondents, 10 departments over-read greater than 20 studies per week, 5 departments over-read 10-20 per week and 4 over-read less than 10 per week. 9 out of 19 respondents stated that they were reimbursed less for over-reads than home institution studies while 3/19 stated that reimbursement is higher than home institution studies. The remainder are unsure of reimbursement rates.

## CONCLUSION

s Subspecialty second-opinion review by a cardiothoracic fellowship trained radiologist was more meticulous than outside reports in 30% of studies when clinical/pathologic confirmation was made. Of the 21 cases with a discrepancy, 71% (15/21) had clinically significant discrepancies (Type 4 and 5). Of these clinically significant discrepancies, there is almost equal numbers of interpreting vs detecting abnormalities (6 vs 7). All survey respondents (33% of total surveys) provided second-opinion interpretations in some capacity. Approximately 52% of the departments which provided second-opinion interpretations over-read over 20 studies per week.

## CLINICAL RELEVANCE/APPLICATION

Formal second opinion interpretations provide added value to referring providers and ultimately the patients. However, given the increasing number of second-opinion interpretation requests, an organized workflow is necessary for proper handling and appropriate billing.

## W5B-SPCH- Relationships between Right and Left Ventricle Function and Lung Volumes in Subjects free of Cardiovascular Diseases

7

Participants

Ricarda von Kruchten, MD, (*Presenter*) Nothing to Disclose

## PURPOSE

The volumetric assessment of MRI-derived global cardiac function includes right (RV) and left ventricular (LV) systolic and diastolic function, but the degree to which MRI-derived lung volumes impact and/or modify parameters of RV and LV function remains unclear. The aim of our study was to investigate the relationship between lung volumes, and parameters of RV and LV function in the KORA-MRI study.

## METHODS AND MATERIALS

From the KORA-MRI cohort study, 361 subjects (mean age 56.1±9.1 years; 43% women) underwent a whole-body 3T MRI scan. Cardiac function parameters were measured using a cine-steady-state free precession sequence using cvi42. Lung volumes were derived semi-automatically using an in-house algorithm. Linear regression analyses were performed to assess the relationships between lung volumes and RV and LV function parameters adjusted for age, sex, and cardiovascular risk factors.

## RESULTS

RV end-diastolic volume was positively associated with LV end-diastolic volume ( $\beta=28.1$ ,  $p<0.001$ ), LV end-systolic volume ( $\beta=11.0$ ,  $p<0.001$ ), LV stroke volume ( $\beta=17.0$ ,  $p<0.001$ ), and inversely with LV ejection fraction ( $\beta=-1.4$ ,  $p=0.001$ ). RV end-systolic volume was positively associated with LV end-diastolic volume ( $\beta=21.2$ ,  $p<0.001$ ), LV end-systolic volume ( $\beta=11.5$ ,  $p<0.001$ ), LV stroke volume ( $\beta=9.7$ ,  $p<0.001$ ), and inversely with LV ejection fraction ( $\beta=-3.3$ ,  $p<0.001$ ). When adjusting for lung volumes, the association between RV and LV did not attenuate, and no effect modification was observed. Despite the differences in lung volumes in both men and women, we did not observe any gender differences with respect to the association between RV and LV parameters.

## CONCLUSION

s In subjects free of cardiovascular diseases, MRI-derived RV and LV function parameters were strongly associated, consistent with the notion that RV function is crucial for LV function, and independent of lung volumes.

#### CLINICAL RELEVANCE/APPLICATION

Cardio-pulmonary relationships in health and disease are well known. Therefore, parameters of cardiac function and pulmonary function can be useful clinical tools used for diagnosis, risk-stratification, and prognosis. MRI is an excellent tool for the assessment of both lung volumes and volumetric parameters of both right (RV) and left ventricular (LV) function. Our study aimed to examine the fundamental relationships between right and left ventricular function and lung volumes in subjects free of cardiovascular diseases.

#### W5B-SPCH-8 Localization-adjusted Diagnostic Performance and Diagnostic Impact of A Commercialized Computer-aided Detection System for Pneumothorax and Consolidation

Participants  
Hongjun Yoon, Seoul, Korea, Republic Of (*Presenter*) Nothing to Disclose

#### PURPOSE

To develop a deep learning algorithm for automated diagnosis of chest abnormalities (consolidation and pneumothorax) and evaluate its diagnostic performance with various dice scores.?

#### METHODS AND MATERIALS

We, retrospectively, collected 22,338 chest radiographs from two hospitals. All radiographs are confirmed by the corresponding CT or radiological report. These are 12,065 consolidation (CON) cases and 6,783 of them are labeled by radiologist. For pneumothorax (PNX), 3,707 cases are selected (2,379 with segmentation mask and 1,328 without). Since manual pixel-level annotation is time-consuming and cumbersome, we exploited the semi-supervised approach. We designed a U-net based deep learning model which was trained with both segmentation and classification labels, when available. On the other hand, when not available, classification label was only used. Considering the importance of lesion localization and interpretability of algorithm, we introduced a dice-adjusted sensitivity evaluation method, which only predictions that exceeded each dice threshold were considered accurate predictions. Unlike sensitivities, specificities could not be considered because dice calculation requires a reference standard lesion annotation (i.e., radiographs without abnormalities do not have lesions to annotate).

#### RESULTS

We used the 1,050 examination images to test our model with external dataset (300 CON, 250 PNX, 500 normal). The model has been evaluated with dice score, dice-adjusted sensitivity, specificity, and AUROC. For CON, our model achieved 0.691 (95% CI: 0.664-0.718), 0.933 (95% CI: 0.945-0.975), 0.948 (95% CI: 0.930-0.963), 0.960 (95% CI: 0.945-0.975) for dice score, dice-adjusted sensitivity, specificity, and AUROC, respectively. For PNX, our model achieved 0.798 (95% CI: 0.770-0.826), 0.956 (95% CI: 0.923-0.978), 0.996 (95% CI: 0.989-0.999), 0.978 (95% CI: 0.965-0.991) for dice, dice-adjusted sensitivity, specificity, and AUROC, respectively.

#### CONCLUSION

s Our deep learning model detected chest X-ray abnormalities (consolidation and pneumothorax) with high diagnostic performance and pixel-level segmentation score.??

#### CLINICAL RELEVANCE/APPLICATION

To apply deep learning based automated analysis algorithm into actual practice, we propose a semi-supervised learning model to detect abnormal findings (CON and PNX) with outperformed localization.

#### W5B-SPCH-9 Opportunistic Detection of Diabetes from Frontal Chest Radiography in 104,473 Patients

Participants  
Ayis T. Pyrros, MD, (*Presenter*) Nothing to Disclose

#### PURPOSE

Chest radiographs (CXRs) are one of the most frequently ordered radiological exams and can potentially be utilized as a biomarker. Our aim was to explore the use of a multitask deep learning (DL) model to detect diabetes from ambulatory frontal radiographs in a large clinical dataset.

#### METHODS AND MATERIALS

Material and Methods: A multitask DL model was trained and tested on 303,604 (55% female; mean age, 58) frontal CXRs from 2010 to 2021 at a single institution, using PyTorch and ResNet34, with 5-fold cross-validation. Patient age, BMI, HbA1c, diabetes, and select comorbidities (CHF, cardiac arrhythmias, morbid obesity, COPD, and vascular disease) from the electronic health record (EHR) were then validated on CXRs from ambulatory patients on out-of-fold predictions. Ground truth labels for diabetes were based on current ICD10 codes and HbA1c  $\geq 6.5\%$ . Days between diagnosis of diabetes and initial CXR were calculated. Patients with a diagnosis of diabetes predating the CXR were excluded, as well as patients with less than a year of follow-up. The discriminatory ability of the DL model was assessed using area under receiver operating characteristic curve (ROC AUC) compared with the ground truth labels and with other predictors (BMI, Social Deprivation Index). An optimal threshold was calculated using Youden's index from the DL predictor. CXR saliency maps were generated.

#### RESULTS

A total of 104,473 CXRs in unique patient (mean age, 53;  $\pm 17$  [SD]; 56% women) were evaluated in the final validation set, of whom 9,319 (8.9%) had a diagnosis of diabetes. The model's overall discriminatory ability for diabetes was an ROC AUC of 0.819 (95% CI: 0.815-0.823), versus ROC AUC of 0.542 (95% CI: 0.536-0.548) using SDI as a predictor, and AUC 0.686 (95% CI: 0.681-0.692) using BMI, with all curves demonstrating comparative p-values  $< 0.001$ . The mean number of days from CXR to diabetes diagnosis was 1,009 ( $\pm 953$  [SD]). At an optimal threshold of 0.11 for the DL predictor, the sensitivity, specificity, negative predictive value, and positive predictive value was 79%, 69%, 97%, and 20%, respectively. Of the 37,625 patients above the threshold, 29,800 (79%) patients did not have a diagnosis of diabetes, and of those, 13,804 (46%) did not have a HbA1c value and 8,109 (27%) had a HbA1c between 5.7-6.4%.

**CONCLUSION**

s Chest radiography can be utilized opportunistically to aid in detecting patients with diabetes and prediabetes.

**CLINICAL RELEVANCE/APPLICATION**

Earlier detection of diabetes may allow for improved screening and intervention, potentially reducing the time to diagnosis and treatment.

Printed on: 02/07/23

## Abstract Archives of the RSNA, 2022

W5B-SPCH-1

### Comparing UTE1H-MRI Derived Ventilation Measurement and 19F-MRI Ventilation Parameters in Patients with Cystic Fibrosis

Wednesday, Nov. 30 12:45PM - 1:15PM Room: Learning Center - CH DPS

#### Participants

Maria Mihailescu, BS, Chapel Hill, NC (*Presenter*) Nothing to Disclose

#### PURPOSE

UTE 1H-MRI could allow for non-invasive ventilation measurements in the lungs by examining changes in structure during ventilatory cycles. 19F-MRI with inhaled perfluoropropane (PFP) gas has been established as a reliable assessment of lung ventilation. Our goal is to better understand the potential of 1H-MRI derived ventilation parameters by comparing values to 19F-MRI derived ventilation parameters.

#### METHODS AND MATERIALS

15 19F-MRI and 1H-MRI scans from patients with cystic fibrosis before and after treatment with elexacaftor/tezacaftor/ivacaftor were used for method development. To analyze ventilation from 19F-MRI, signal intensity-time curves during PFP wash-in and wash-out for each voxel were fitted to a bi-exponential model to find the time constant that characterizes gas wash-out ( $t_2$ ). To determine ventilation maps for 1H-MRI images, a 3D Jacobian was computed on a voxel-by-voxel basis between maximum inhalation and maximum exhalation. Heat maps of ventilation parameters from each imaging modality were created. Ventilation defect percentages (VDP) were calculated to compare the two ventilation parameters.

#### RESULTS

When comparing 19F-MRI and 1H-MRI VDP for 15 scans, there was no significant correlation coefficient. If scans with minimum lung disease are excluded (Defined as 19F-MRI determined VDP <3%), the remaining 11 scans had a correlation coefficient of 0.77 when comparing VDPs.

#### CONCLUSION

For moderate to severe lung disease VDP determined from 19F-MRI and 1H-MRI have a high correlation coefficient, suggesting that 1H-MRI determined VDP may be a useful functional assessment marker in these patients. For mild lung disease, ventilation parameters are not significantly related. One explanation for this is that severe lung disease has drastic effects on the lung parenchyma altering its normal movement and allowing for detection as the magnitude of the Jacobian between inspiration and expiration. For mild lung disease, factors that impact air movement such as inflammation or minimal mucus plugging may not register at the level of structural movement. With higher resolution 1H-MRI scans, the Jacobian magnitude could be calculated at the alveolar level to allow for measurement of ventilation in mild lung disease.

#### CLINICAL RELEVANCE/APPLICATION

The 1H-MRI Jacobian magnitude may be useful in characterizing VDP for moderate to severe lung disease without the need for 19F-MRI imaging, a potentially financially prohibitive modality that is not suitable for all patient populations.

Printed on: 02/07/23

## Abstract Archives of the RSNA, 2022

W5B-SPCH-10

### How Normal Is a Normal Chest X-Ray: Does a Comprehensive Artificial Intelligence Model Identify Significant Findings in Chest Radiographs Interpreted as Normal in Clinical Practice?

Wednesday, Nov. 30 12:45PM - 1:15PM Room: Learning Center - CH DPS

#### Participants

Arpit Talwar, MBBS, MEd, (*Presenter*) Nothing to Disclose

#### PURPOSE

Chest x-ray (CXR) interpretation is one of the most subjective and complex of radiology tasks. Accuracy depends on the radiologists' level of experience and training with the potential of human error related to workload, fatigue and interruptions impacting on patient care. Validated comprehensive deep-learning models may assist in improving diagnostic accuracy and departmental workflow. We therefore aimed to evaluate the performance of radiologist reported normal chest x-rays within the hospital setting against a comprehensive deep-learning model.

#### METHODS AND MATERIALS

A retrospective analysis of CXRs that had been reported as normal in adults (= 18 years) was performed on consecutive patients at St. Vincent's Hospital Melbourne from Jan-May 2016. A validated deep-learning model with a total dataset of 60 significant findings was applied on the included studies. Significant findings were adjudicated by two chest radiologists with over 10 years-experience. Disagreements were re-reviewed to reach a consensus. Level of agreement between radiologists and the model was also assessed.

#### RESULTS

Of the 490 studies included in this preliminary analysis, 444 (90.6%) showed no significant finding predictions by the model (specificity 93.3%). 64 significant findings were identified by the model across 46 studies (9.4%). 50% were rejected by the adjudicators (model PPV 0.5) with 32 findings (6.3%) across 22 studies deemed to be missed by the reporting radiologist. The most common missed finding was distended bowel (18.8%) with a single case of solitary pulmonary nodule (3.1%) and superior mediastinal mass (3.1%) identified. Within our cohort, a total of 4 studies (0.8%) had findings that were of particular concern. Substantial inter-rater agreement was achieved between the model and radiologists (weighted  $\kappa$  value of 0.64 (95% CI 0.52 - 0.75)).

#### CONCLUSION

Our preliminary results demonstrate that an AI model provided a useful tool in auditing CXRs reported as normal in a public hospital setting, where radiology trainees report the majority of these studies. The AI model demonstrated that a significant percentage (6.3%) of CXRs had findings deemed significant, missed in the initial report.

#### CLINICAL RELEVANCE/APPLICATION

Integration of a highly specific AI model in a real-world reporting environment has the potential to improve departmental workflow and reduce human error, ultimately improving patient care.

Printed on: 02/07/23

## Abstract Archives of the RSNA, 2022

W5B-SPCH-2

### Predicting Outcomes of Lung Transplants Based on Pre-operative Chest CT Scans in Patients with Scleroderma

Wednesday, Nov. 30 12:45PM - 1:15PM Room: Learning Center - CH DPS

#### Participants

Jiantao Pu, PhD, (*Presenter*) Nothing to Disclose

#### PURPOSE

To investigate the feasibility of predicting the outcomes of lung transplants in patients with scleroderma based on pre-treatment chest CT scans.

#### METHODS AND MATERIALS

We created a cohort consisting of 104 subjects who were diagnosed with scleroderma and underwent lung transplants from 2005 to 2020. Based on the pre-treatment chest CT scans, we quantified: (1) lung volume, (2) heart volume, (3) chest cavity volume, (4) distances between sternum and spines, (5) artery and vein volumes, and (6) the volume and density of five body tissues (i.e., skeleton muscle, subcutaneous fat, visceral fat, intramuscular fat, and bone). The backward stepwise logistic/linear regression was used to predict chest open, postoperative mechanical support, AKI requiring dialysis, primary graft dysfunction (PGD), and ICU stay (days). For PGD, we dichotomized these patients on whether they were Grade 3 or not on postoperative day 3. The prediction models were evaluated using the area under the receiver-operating characteristic (ROC) curve (AUC). The R-squared (R<sup>2</sup>) was used to assess the performance of the model for predicting ICU stay.

#### RESULTS

The prediction models showed an AUC of 0.899 (95% CI: 0.837-0.960) for assessing chest open, an AUC of 0.930 (95% CI: 0.880-0.980) for assessing AKI requiring dialysis demonstrated, an AUC of 0.953 (95% CI: 0.917-0.989) for predicting postoperative mechanical support. When assessing PGD Grade 3, the prediction model had an AUC of 0.988 (95% CI: 0.965-1.0) with variables formed primarily by the body tissues and the geometric characteristics of the chest cavity. When predicting the total ICU stay, the computer model demonstrated an R<sup>2</sup> of 0.37, indicating that 37% of the variance in the outcome was explained by the model.

#### CONCLUSION

s The outcomes of lung transplants in patients with scleroderma are significantly associated with the geometric characteristics of the lungs and the body compositions of the recipients.

#### CLINICAL RELEVANCE/APPLICATION

Patients with scleroderma have an increased risk of complications after lung transplantation. Awareness of the factors contributing to the complications will maximize the benefit of lung transplants.

Printed on: 02/07/23

## Abstract Archives of the RSNA, 2022

W5B-SPCH-3

### Artificial Intelligence-assisted Analysis to Facilitate Effective Detection of Humeral Lesions in the Simple Chest Radiograph

Wednesday, Nov. 30 12:45PM - 1:15PM Room: Learning Center - CH DPS

#### Participants

Harim Kim, MD, (*Presenter*) Nothing to Disclose

#### PURPOSE

While chest radiograph (CR) is a basic modality for patient assessment, the humerus remains an easily negligible spot. Thus, it can be of great aid to the reader if an artificial intelligence (AI) system automatically diagnoses and visualizes tumors of humerus in CR, particularly with high sensitivity. However, as there is no prior AI study on this subject, we newly proposed an advanced AI system for detecting humerus tumors, with better sensitivity and tumor visualization, and compared its usefulness with radiologists.

#### METHODS AND MATERIALS

Our AI system differs from existing ones in that it uses a new training objective named false-positive activation area reduction (FPAR), which improves both the tumor detection sensitivity and tumor visualization ability of AI by learning not to activate the class activation map in areas unrelated to the region of interest (i.e., outside humerus or tumor). A total of 2994 CRs for 1500 normal and 1494 CT-proven humeral tumor CRs were provided as an AI training set. The AI program and two trainee radiologists (R1 and R2) were commonly tested with holdout test data, not used for AI training, of 119 normal and 102 tumor patients. The radiologists were tested twice with the same test set, and the second time, they were provided with AI test results.

#### RESULTS

Technically, the proposed AI system improved the sensitivity (83.4%) by 3.2% compared to the baseline (80.2%) and it also improved the tumor localization accuracy (82%) by 13% compared to the baseline (69%), demonstrating the effectiveness of FPAR. In comparison with radiologists, trainee radiologists showed different sensitivity and accuracy in detecting humerus lesions. Overall sensitivity, specificity, and accuracy of radiologists were 54.4%, 94.9%, and 82.3% and when compared with AI, AI showed a significantly higher sensitivity of 68.6% ( $p=0.0025$ ). Also, AI showed higher sensitivity and accuracy ( $p=0.0007$  and  $0.0339$  respectively) but did not outperform in specificity ( $p=0.1298$ ). When assisted by AI, the performance of two trainee radiologists did not differ significantly. And compared with results not assisted by AI, sensitivity and accuracy showed improvement, most notably in the trainee with lower sensitivity.

#### CONCLUSION

The utilization of FPAR effectively enhances true-positives in humeral tumor detection and reduces false-positives in humeral tumor visualization. This advanced AI is proven to make radiologists detect humerus lesions better, especially for trainee radiologists with less experience and lower sensitivity.

#### CLINICAL RELEVANCE/APPLICATION

Our AI system may help radiologists pay better attention to possible humeral lesions, as humerus can be easily overlooked in CR.

Printed on: 02/07/23

## Abstract Archives of the RSNA, 2022

W5B-SPCH-4

### Pulmonary Alveolar Echinococcosis: CT Findings and Classification

Wednesday, Nov. 30 12:45PM - 1:15PM Room: Learning Center - CH DPS

#### Participants

Hai Hua Bao, Xining, China (*Presenter*) Nothing to Disclose

#### PURPOSE

Alveolar echinococcosis, which is prevalent on the Tibetan plateau, is a multisystemic infectious parasitic disease that poses a serious health risk to humans. Pulmonary alveolar echinococcosis (PAE) is a lesion secondarily induced by direct infiltration and hematogenous dissemination from hepatic AE lesions and mostly in the middle-late stages. Currently, studies on the CT-morphological classification of PAE are scarce. The study aims to clarify the CT imaging findings and classification of PAE.

#### METHODS AND MATERIALS

The study analysed the CT manifestations of patients with AE diagnosed by clinical and imaging examinations at the Affiliated Hospital of Qinghai University from 2014 to 2021. One hundred and eighty-nine patients (age, 43 years  $\pm$  13 [standard deviation]; gender, 93 men and 96 women) were evaluated. All patients living at a high altitude of 2500 - 3500m. A GE 256-layer CT scanner was used for plain and enhanced scan to observe the distribution, morphology and typing characteristics of the lesions. Statistics were performed using SPSS software.

#### RESULTS

The CT manifestations of PAE are mostly multiple nodules, which were mainly peripheral distribution and mostly in the lower lobes. The diameter of the lesions ranged from 2mm to 9cm. 189 cases of AE in patients with primary lesions are from the liver. CT imaging characteristics were categorized into four types: I. small solid nodules ( $\leq$  1 cm) (37/189, 19.6%); II. large solid nodules ( $>$  1 cm) (158/189, 83.6%); III. solid nodules with cavity (70/189, 37.0%); IV. calcified nodules (32/189, 16.9%). Different types of nodules can be shown on CT images of the same patient. The probability of the primary foci in the liver invading blood vessels and diaphragm are hepatic vein (62.4%), inferior vena cava (52.5%), portal vein (69.3%), hepatic artery (53.5%) and diaphragm (86.1%) respectively. Approximately 54.5% of patients had operation history.

#### CONCLUSION

The CT findings of PAE, which is secondarily induced from primary foci in the liver, are mostly peripheral distribution and mainly in the lower lobes. The CT classification of PAE is more common in types II and III.

#### CLINICAL RELEVANCE/APPLICATION

The CT-morphological classification of PAE could help to clarify the progression of the disease and provide a basis for the early interference and the choice of treatment schedule.

Printed on: 02/07/23

## Abstract Archives of the RSNA, 2022

W5B-SPCH-5

### **Chest X-Ray at Emergency Admission, SOFA Score and NIV: Potential Value in Predicting Barotrauma in Ventilated COVID-19 Patients during the First Pandemic Peak**

Wednesday, Nov. 30 12:45PM - 1:15PM Room: Learning Center - CH DPS

#### **Participants**

Francesco Stanco, (*Presenter*) Nothing to Disclose

#### **PURPOSE**

To assess the value of chest X-ray (CXR), SOFA (Sequential Organ Failure Assessment) score and NIV (non-invasive ventilation) at emergency admission to predict barotrauma in mechanically ventilated COVID-19 patients. To report the distribution of barotrauma at chest CT.

#### **METHODS AND MATERIALS**

SARS-CoV-2 positive patients, first admitted to the emergency department and then to the intensive care unit (ICU), between February 20th and April 15th, 2020, were retrospectively evaluated. All patients were divided into two groups, according to the occurrence/absence of barotrauma. CXR were assessed by 1 experienced radiologist using Brixia score (BS). SOFA score was calculated by the referring physicians at ICU admittance and NIV days prior intubation were collected. Distribution of barotrauma (pneumomediastinum/pneumothorax/subcutaneous emphysema) were annotated from unenhanced chest CT scan during ICU hospitalization.

#### **RESULTS**

A total of 117 SARS-CoV-2 patients (24 females, mean age 59.95 years) were included. Thirty-seven (37/117; 31.6%) mechanically ventilated patients developed barotrauma (25 pneumomediastinum, 23 pneumothorax, 24 subcutaneous emphysema). Compared to the non-barotrauma group, barotrauma patients demonstrated higher BS values (mean value 12.05 vs 9.38, p-value 0.0041), and underwent longer NIV (mean value 4.20 vs 2.75 days, p-value 0.0075). No significant correlation with SOFA score was found. A model using these three tested predictors (BS, SOFA score, NIV days) resulted as the best model to predict development of barotrauma.

#### **CONCLUSION**

Barotrauma occurred in a non-negligible percentage of mechanically ventilated patients with COVID-19 pneumonia. The best predicting model for barotrauma was obtained by the simultaneous employment of three independent variables selected with simple logistic regression: BS, SOFA score, and NIV days.

#### **CLINICAL RELEVANCE/APPLICATION**

Integrated clinical-radiological assessment may predict the risk of barotrauma in mechanically ventilated COVID-19 patients, a complication potentially impacting proper management of these cases.

Printed on: 02/07/23



## Abstract Archives of the RSNA, 2022

W5B-SPCH-6

### Second-Opinion Subspecialty Consultations in Chest Radiology

Wednesday, Nov. 30 12:45PM - 1:15PM Room: Learning Center - CH DPS

#### Participants

Mohammad Jalili, MD, Los Angeles, CA (*Presenter*) Nothing to Disclose

#### PURPOSE

The purpose of this study is twofold. The primary aim is to assess the significance of subspecialty second-opinion consultations for CT examinations in thoracic imaging. The secondary aim is to assess the prevalence and reimbursement rates of over-read interpretations across academic cardiothoracic sections.

#### METHODS AND MATERIALS

Reports from 100 random chest CTs referred to a single academic institution for second-opinion consultation were reviewed by two radiologists by consensus. Outside and inside reports were compared using a previously published 5-point scale. Clinically important differences were defined as those likely to change patient management. Additionally, a 6-question survey was sent to the section head of every academic cardiothoracic radiology department in the U.S.A. asking how their department handles over-read requests.

#### RESULTS

Of all the second-opinion examinations, 69% (69/100) had an outside report available for comparison and inclusion in the study. There were no discrepancies in 70% of cases (48/69). In the remaining 30% (21 cases), 6 cases had nonsignificant discrepancies (Type 2 or 3) and 15 cases had clinically significant discrepancies (Type 4 and 5). 19 out of 56 (33%) survey recipients responded to the survey. All 19 (100%) respondents stated that their institution does provide second opinion consultations for outside studies. Out of the 19 respondents, 10 departments over-read greater than 20 studies per week, 5 departments over-read 10-20 per week and 4 over-read less than 10 per week. 9 out of 19 respondents stated that they were reimbursed less for over-reads than home institution studies while 3/19 stated that reimbursement is higher than home institution studies. The remainder are unsure of reimbursement rates.

#### CONCLUSION

Subspecialty second-opinion review by a cardiothoracic fellowship trained radiologist was more meticulous than outside reports in 30% of studies when clinical/pathologic confirmation was made. Of the 21 cases with a discrepancy, 71% (15/21) had clinically significant discrepancies (Type 4 and 5). Of these clinically significant discrepancies, there is almost equal numbers of interpreting vs detecting abnormalities (6 vs 7). All survey respondents (33% of total surveys) provided second-opinion interpretations in some capacity. Approximately 52% of the departments which provided second-opinion interpretations over-read over 20 studies per week.

#### CLINICAL RELEVANCE/APPLICATION

Formal second opinion interpretations provide added value to referring providers and ultimately the patients. However, given the increasing number of second-opinion interpretation requests, an organized workflow is necessary for proper handling and appropriate billing.

Printed on: 02/07/23

## Abstract Archives of the RSNA, 2022

W5B-SPCH-7

### Relationships between Right and Left Ventricle Function and Lung Volumes in Subjects free of Cardiovascular Diseases

Wednesday, Nov. 30 12:45PM - 1:15PM Room: Learning Center - CH DPS

#### Participants

Ricarda von Kruchten, MD, (*Presenter*) Nothing to Disclose

#### PURPOSE

The volumetric assessment of MRI-derived global cardiac function includes right (RV) and left ventricular (LV) systolic and diastolic function, but the degree to which MRI-derived lung volumes impact and/or modify parameters of RV and LV function remains unclear. The aim of our study was to investigate the relationship between lung volumes, and parameters of RV and LV function in the KORA-MRI study.

#### METHODS AND MATERIALS

From the KORA-MRI cohort study, 361 subjects (mean age 56.1±9.1 years; 43% women) underwent a whole-body 3T MRI scan. Cardiac function parameters were measured using a cine-steady-state free precession sequence using cvi42. Lung volumes were derived semi-automatically using an in-house algorithm. Linear regression analyses were performed to assess the relationships between lung volumes and RV and LV function parameters adjusted for age, sex, and cardiovascular risk factors.

#### RESULTS

RV end-diastolic volume was positively associated with LV end-diastolic volume ( $\beta=28.1$ ,  $p<0.001$ ), LV end-systolic volume ( $\beta=11.0$ ,  $p<0.001$ ), LV stroke volume ( $\beta=17.0$ ,  $p<0.001$ ), and inversely with LV ejection fraction ( $\beta=-1.4$ ,  $p=0.001$ ). RV end-systolic volume was positively associated with LV end-diastolic volume ( $\beta=21.2$ ,  $p<0.001$ ), LV end-systolic volume ( $\beta=11.5$ ,  $p<0.001$ ), LV stroke volume ( $\beta=9.7$ ,  $p<0.001$ ), and inversely with LV ejection fraction ( $\beta=-3.3$ ,  $p<0.001$ ). When adjusting for lung volumes, the association between RV and LV did not attenuate, and no effect modification was observed. Despite the differences in lung volumes in both men and women, we did not observe any gender differences with respect to the association between RV and LV parameters.

#### CONCLUSION

In subjects free of cardiovascular diseases, MRI-derived RV and LV function parameters were strongly associated, consistent with the notion that RV function is crucial for LV function, and independent of lung volumes.

#### CLINICAL RELEVANCE/APPLICATION

Cardio-pulmonary relationships in health and disease are well known. Therefore, parameters of cardiac function and pulmonary function can be useful clinical tools used for diagnosis, risk-stratification, and prognosis. MRI is an excellent tool for the assessment of both lung volumes and volumetric parameters of both right (RV) and left ventricular (LV) function. Our study aimed to examine the fundamental relationships between right and left ventricular function and lung volumes in subjects free of cardiovascular diseases.

Printed on: 02/07/23

## Abstract Archives of the RSNA, 2022

W5B-SPCH-8

### Localization-adjusted Diagnostic Performance and Diagnostic Impact of A Commercialized Computer-aided Detection System for Pneumothorax and Consolidation

Wednesday, Nov. 30 12:45PM - 1:15PM Room: Learning Center - CH DPS

#### Participants

Hongjun Yoon, Seoul, Korea, Republic Of (*Presenter*) Nothing to Disclose

#### PURPOSE

To develop a deep learning algorithm for automated diagnosis of chest abnormalities (consolidation and pneumothorax) and evaluate its diagnostic performance with various dice scores.?

#### METHODS AND MATERIALS

We, retrospectively, collected 22,338 chest radiographs from two hospitals. All radiographs are confirmed by the corresponding CT or radiological report. These are 12,065 consolidation (CON) cases and 6,783 of them are labeled by radiologist. For pneumothorax (PNX), 3,707 cases are selected (2,379 with segmentation mask and 1,328 without). Since manual pixel-level annotation is time-consuming and cumbersome, we exploited the semi-supervised approach. We designed a U-net based deep learning model which was trained with both segmentation and classification labels, when available. On the other hand, when not available, classification label was only used. Considering the importance of lesion localization and interpretability of algorithm, we introduced a dice-adjusted sensitivity evaluation method, which only predictions that exceeded each dice threshold were considered accurate predictions. Unlike sensitivities, specificities could not be considered because dice calculation requires a reference standard lesion annotation (i.e., radiographs without abnormalities do not have lesions to annotate).

#### RESULTS

We used the 1,050 examination images to test our model with external dataset (300 CON, 250 PNX, 500 normal). The model has been evaluated with dice score, dice-adjusted sensitivity, specificity, and AUROC. For CON, our model achieved 0.691 (95% CI: 0.664 = p=0.718), 0.933 (95% CI: 0.945 = p=0.975), 0.948 (95% CI: 0.930 = p=0.963), 0.960 (95% CI: 0.945 = p=0.975) for dice score, dice-adjusted sensitivity, specificity, and AUROC, respectively. For PNX, our model achieved 0.798 (95% CI: 0.770 = p=0.826), 0.956 (95% CI: 0.923 = p=0.978), 0.996 (95% CI: 0.989 = p=0.999), 0.978 (95% CI: 0.965 = p=0.991) for dice, dice-adjusted sensitivity, specificity, and AUROC, respectively.

#### CONCLUSION

Our deep learning model detected chest X-ray abnormalities (consolidation and pneumothorax) with high diagnostic performance and pixel-level segmentation score.?

#### CLINICAL RELEVANCE/APPLICATION

To apply deep learning based automated analysis algorithm into actual practice, we propose a semi-supervised learning model to detect abnormal findings (CON and PNX) with outperformed localization.

Printed on: 02/07/23

## Abstract Archives of the RSNA, 2022

W5B-SPCH-9

### Opportunistic Detection of Diabetes from Frontal Chest Radiography in 104,473 Patients

Wednesday, Nov. 30 12:45PM - 1:15PM Room: Learning Center - CH DPS

#### Participants

Ayis T. Pyrros, MD, (Presenter) Nothing to Disclose

#### PURPOSE

Chest radiographs (CXR) are one of the most frequently ordered radiological exams and can potentially be utilized as a biomarker. Our aim was to explore the use of a multitask deep learning (DL) model to detect diabetes from ambulatory frontal radiographs in a large clinical dataset.

#### METHODS AND MATERIALS

Material and Methods: A multitask DL model was trained and tested on 303,604 (55% female; mean age, 58) frontal CXRs from 2010 to 2021 at a single institution, using PyTorch and ResNet34, with 5-fold cross-validation. Patient age, BMI, HbA1c, diabetes, and select comorbidities (CHF, cardiac arrhythmias, morbid obesity, COPD, and vascular disease) from the electronic health record (EHR) were then validated on CXRs from ambulatory patients on out-of-fold predictions. Ground truth labels for diabetes were based on current ICD10 codes and HbA1c  $\geq 6.5\%$ . Days between diagnosis of diabetes and initial CXR were calculated. Patients with a diagnosis of diabetes predating the CXR were excluded, as well as patients with less than a year of follow-up. The discriminatory ability of the DL model was assessed using area under receiver operating characteristic curve (ROC AUC) compared with the ground truth labels and with other predictors (BMI, Social Deprivation Index). An optimal threshold was calculated using Youden's index from the DL predictor. CXR saliency maps were generated.

#### RESULTS

A total of 104,473 CXRs in unique patient (mean age, 53;  $\pm 17$  [SD]; 56% women) were evaluated in the final validation set, of whom 9,319 (8.9%) had a diagnosis of diabetes. The model's overall discriminatory ability for diabetes was an ROC AUC of 0.819 (95% CI: 0.815-0.823), versus ROC AUC of 0.542 (95% CI: 0.536-0.548) using SDI as a predictor, and AUC 0.686 (95% CI: 0.681-0.692) using BMI, with all curves demonstrating comparative p-values  $< 0.001$ . The mean number of days from CXR to diabetes diagnosis was 1,009 ( $\pm 953$  [SD]). At an optimal threshold of 0.11 for the DL predictor, the sensitivity, specificity, negative predictive value, and positive predictive value was 79%, 69%, 97%, and 20%, respectively. Of the 37,625 patients above the threshold, 29,800 (79%) patients did not have a diagnosis of diabetes, and of those, 13,804 (46%) did not have a HbA1c value and 8,109 (27%) had a HbA1c between 5.7-6.4%.

#### CONCLUSION

Chest radiography can be utilized opportunistically to aid in detecting patients with diabetes and prediabetes.

#### CLINICAL RELEVANCE/APPLICATION

Earlier detection of diabetes may allow for improved screening and intervention, potentially reducing the time to diagnosis and treatment.

Printed on: 02/07/23



## Abstract Archives of the RSNA, 2022

W5B-SPER

### Emergency Wednesday Poster Discussions - B

Wednesday, Nov. 30 12:45PM - 1:15PM Room: Learning Center - ER DPS

#### Participants

Refky Nicola, DO, Pittsford, NY (*Moderator*) Royalties, RELX

#### Sub-Events

### W5B-SPER-1 Advantages of Spectral CT Relative to Conventional CT for Detection and Characterization of Foreign Bodies in an In-Vitro Musculoskeletal and a Sinus Cavity Model

#### Participants

Jason Matakas, MD, MS, (*Presenter*) Nothing to Disclose

#### PURPOSE

The purpose of this study is to determine whether spectral CT demonstrates improved performance compared to conventional CT for detecting and characterizing foreign bodies (FBs) in in-vitro models. This study focuses on materials that are typically not well visualized on conventional CT.

#### METHODS AND MATERIALS

Seven commonly encountered FB materials including glass, graphite, wood (woodchip, toothpick, plant stem) and plastic (fork, tough plastic) were cut into cylinders of five designated sizes (20x3, 10x3, 5x3, 2.5x2.5, 1x1mm). These 35 FBs were randomly arranged in a plastic cassette (sinus cavity model) and imaged in a spectral CT scanner (Philips IQon, 256-slice scanner). Subsequently, 45 vertical tracks were made in three fresh chicken breasts using a 17-gauge non-coring needle, and all 35 FBs were randomly inserted, leaving some tracks empty. These musculoskeletal models were imaged immediately after preparation. Two fellowship-trained musculoskeletal attending radiologists, who were blinded to FB location, size, and number, independently reviewed the conventional CT and spectral CT images (effective atomic number [Z<sub>eff</sub>] and electron density maps obtained using Philips IntelliSpace Portal 9.0), assigning subjective visibility ratings to all visualized FBs based on a four-point Likert scale.

#### RESULTS

Within the musculoskeletal model, spectral CT demonstrated superior sensitivity and has a lower size detection limit for plant stem, tough plastic, toothpick and woodchip, compared to conventional CT ( $p < .05$ ). For radiopaque materials (glass, graphite) and plastic fork, spectral CT did not appreciably increase detectability, but demonstrated comparable sensitivity. Within the sinus cavity model, spectral CT demonstrated superior sensitivity and had a lower size detection limit for all FBs ( $p < .05$ ), except for glass, which had comparable sensitivity. Of note, spectral CT characteristics varied for different types of wood (processed versus natural).

#### CONCLUSION

Spectral CT improves visibility and lowers size detection limits of most of the trialed materials of relatively low radiodensity that are poorly visualized or non-visualized on conventional CT. This holds true for FBs in both muscle and air.

#### CLINICAL RELEVANCE/APPLICATION

Utilization of spectral CT can augment the viewer's ability to detect FBs that may otherwise be missed on conventional CT. Furthermore, spectral data may assist in foreign body characterization.

Printed on: 02/07/23

## Abstract Archives of the RSNA, 2022

W5B-SPER-1

### Advantages of Spectral CT Relative to Conventional CT for Detection and Characterization of Foreign Bodies in an In-Vitro Musculoskeletal and a Sinus Cavity Model

Wednesday, Nov. 30 12:45PM - 1:15PM Room: Learning Center - ER DPS

#### Participants

Jason Matakas, MD, MS, (Presenter) Nothing to Disclose

#### PURPOSE

The purpose of this study is to determine whether spectral CT demonstrates improved performance compared to conventional CT for detecting and characterizing foreign bodies (FBs) in in-vitro models. This study focuses on materials that are typically not well visualized on conventional CT.

#### METHODS AND MATERIALS

Seven commonly encountered FB materials including glass, graphite, wood (woodchip, toothpick, plant stem) and plastic (fork, tough plastic) were cut into cylinders of five designated sizes (20x3, 10x3, 5x3, 2.5x2.5, 1x1mm). These 35 FBs were randomly arranged in a plastic cassette (sinus cavity model) and imaged in a spectral CT scanner (Philips IQon, 256-slice scanner). Subsequently, 45 vertical tracks were made in three fresh chicken breasts using a 17-gauge non-coring needle, and all 35 FBs were randomly inserted, leaving some tracks empty. These musculoskeletal models were imaged immediately after preparation. Two fellowship-trained musculoskeletal attending radiologists, who were blinded to FB location, size, and number, independently reviewed the conventional CT and spectral CT images (effective atomic number [Z<sub>eff</sub>] and electron density maps obtained using Philips IntelliSpace Portal 9.0), assigning subjective visibility ratings to all visualized FBs based on a four-point Likert scale.

#### RESULTS

Within the musculoskeletal model, spectral CT demonstrated superior sensitivity and has a lower size detection limit for plant stem, tough plastic, toothpick and woodchip, compared to conventional CT ( $p < .05$ ). For radiopaque materials (glass, graphite) and plastic fork, spectral CT did not appreciably increase detectability, but demonstrated comparable sensitivity. Within the sinus cavity model, spectral CT demonstrated superior sensitivity and had a lower size detection limit for all FBs ( $p < .05$ ), except for glass, which had comparable sensitivity. Of note, spectral CT characteristics varied for different types of wood (processed versus natural).

#### CONCLUSION

Spectral CT improves visibility and lowers size detection limits of most of the trialed materials of relatively low radiodensity that are poorly visualized or non-visualized on conventional CT. This holds true for FBs in both muscle and air.

#### CLINICAL RELEVANCE/APPLICATION

Utilization of spectral CT can augment the viewer's ability to detect FBs that may otherwise be missed on conventional CT. Furthermore, spectral data may assist in foreign body characterization.

Printed on: 02/07/23

## Abstract Archives of the RSNA, 2022

W5B-SPGI

### Gastrointestinal Wednesday Poster Discussions - B

Wednesday, Nov. 30 12:45PM - 1:15PM Room: Learning Center - GI DPS

#### Participants

Daniela Pfeiffer, MD, Munich, (*Moderator*) Nothing to Disclose

#### Sub-Events

### W5B-SPGI-1 Interobserver Concordance in Predicting Complete Response on MRI in Rectal Cancer Patients Post Neoadjuvant Chemo-radiotherapy

#### Participants

Aashna Karbhari, MD, (*Presenter*) Nothing to Disclose

#### PURPOSE

To identify the accuracy of MRI in identifying complete pathologic response (pCR) in rectal cancer patients post NACRT, to allow better patient selection for watch and wait (WW) protocol.

#### METHODS AND MATERIALS

This was an IRB approved retrospective review of MRIs of 80 cases of lower and mid rectal cancer patients from January 2018 to March 2022. Study cohort consisted of 40 patients on the WW protocol post NACRT, and another 40 whose post NACRT MRI suggested complete / near complete response but subsequently underwent surgery. Baseline MRIs (available in 58/80 patients) were evaluated for tumor morphology, location, craniocaudal length and circumferential involvement. Post-treatment MRIs (80 patients) were additionally evaluated for pattern of response on T2 and DWI. Overall primary tumor bed response was classified as complete (CR- only T2 dark fibrosis, no restricted diffusion), near complete (nCR- predominantly T2 dark fibrosis with patchy T2 intermediate signal/ restricted diffusion/mucinous change) or as residual disease (predominant intermediate signal / frank restricted diffusion). Patients with pCR on pathology or who had a disease free interval of 12 months post NACRT on WW protocol were regarded as complete response. Cohen's Kappa statistic was used to evaluate inter-observer concordance in prediction of pCR as well as in interpretation of individual MRI parameters like T2 and DWI.

#### RESULTS

Median patient age was 47 years (range = 15 - 73 years) with 47 males and 33 females. A combination of T2 and DWI in evaluating rectal MRIs post NACRT was found to have good inter-observer agreement (Cohen's Kappa=0.6). For categorising residual disease, sensitivity, specificity, negative and positive predictive values of Observer 1 were 81.5%, 58.4%, 86.1%, 50% and for Observer 2 were 70.4%, 71.7%, 82.6% and 55.9% respectively. Statistically significant association of complete response was found with <25% circumferential wall involvement (p=0.03) and polypoidal pattern of growth (0.004) at baseline.

#### CONCLUSION

s Combined evaluation of T2 and DWI on MRI has moderate specificity and sensitivity for characterising residual disease and a good negative predictive value. Despite good inter-observer agreement in interpreting post NACRT rectal MRIs, MRI was not found to significantly identify pCR.

#### CLINICAL RELEVANCE/APPLICATION

Identification of pCR on MRI can enable appropriate selection of patients to be managed under the watch and wait protocol.

### W5B-SPGI- 10 Inferior Vena Cava Reflux: Does it Mean There is a Right Heart Dysfunction?

#### Participants

Ahmad Alhamshari, MBBS, (*Presenter*) Nothing to Disclose

#### PURPOSE

Retrograde flow into the inferior vena cava and/or hepatic veins have been associated with right heart dysfunction such as tricuspid valve regurgitation. However, much of the studies in the literature were conducted on patients' with other medical illnesses which may affect the finding. So, we are conducting a study on population of healthy liver donors to assess the association. Also, we are reporting the frequency of each reflux grade which may range from grade I "no reflux is present" to grade VI "severe reflux that reaches peripheral hepatic veins".

#### METHODS AND MATERIALS

Computed tomography (CT) scan of the abdomen with contrast enhancement and transthoracic echocardiography are some of the essential investigation for evaluation of liver donors. We retrospectively reviewed all the CT scans and echocardiographic reports of potential liver donors. CT scans were used to assess the reflux on contrast material into the inferior vena cava and/or hepatic veins during the venous phase. Reflux severity were graded from grade I to grade VI. Echocardiographic reports were reviewed for the presence of the tricuspid regurgitation. Tricuspid regurgitations were reported as normal, trace or mild regurgitation.

## RESULTS

We had 246 donors, with mean age of 34 and range from 23-59. There was a male predominance 180 cases (73.2%). The severity of the reflux were reported as normal or mild reflux (grade I-III), or moderate to severe reflux (grade IV-VI). We had 149 (60.6%) cases of normal to mild reflux and 97 (39.4%) of moderate to severe reflux. There was no significant correlation between the reflux severity and the presence of right heart dysfunction.

## CONCLUSION

s The presence of inferior vena cava and or hepatic veins reflux is a relatively common finding in CT scans. Its presence does not correlate with right heart dysfunction.

## CLINICAL RELEVANCE/APPLICATION

Since there is no correlation with right heart dysfunction, it is not warranted to perform any cardiac investigation in case of presence of reflux.

## W5B-SPGI-2A Nomogram Combining Clinicopathology, IVIM-DWI, MRI Radiomics Parameters to Predict Postoperative DFS in Patients with Rectal Adenocarcinoma

Participants

Rixin Su, (*Presenter*) Nothing to Disclose

## PURPOSE

This study aimed to establish an effective prognostic nomogram to predict postoperative disease-free survival (DFS) in patients with rectal adenocarcinoma.

## METHODS AND MATERIALS

A total of 156 rectal adenocarcinoma patients admitted to our hospital were retrospectively collected. The patients were divided into training and verification cohort. Clinicopathological data of the patients were collected and IVIM-DWI parameters of the primary rectal adenocarcinoma were measured. Radiomic parameters were extracted on DWI and T2-weighted images. Radiomic features were screened and radiomic scores (Rads-score) were calculated. Correlation analysis, Kaplan-Meier analysis, univariate and multivariate analysis were used in the training group to identify factors associated with disease-free survival (DFS) and to screen independent predictors. Prognostic nomograms were constructed, and the model predictive efficacy and net benefit were evaluated. Validation was performed in the validation cohort.

## RESULTS

Kaplan-Meier analysis showed that patients in the poor differentiation group had worse DFS than those in the well/moderate differentiation group ( $P < 0.001$ ), patients in the T4 stage group had worse DFS than those in the T1-3 stage group ( $P < 0.001$ ), patients in the CEA = 5 group had worse DFS than those in the CEA < 5 group ( $P < 0.001$ ), patients in the f value = 46.6 group had worse DFS than those in the f-value < 46.6 group ( $P < 0.001$ ), and patients in the Radsscore = -1 group had better DFS than those in the Radsscore < -1 group. Univariate analysis revealed pretreatment the differentiation, T stage, CEA, f-value, and Rads-score were significantly correlated with DFS. Multivariate analysis showed that the differentiation, T stage, CEA, f value, and Rads-score were independent prognostic factors affecting DFS. A prognostic nomogram model combining clinicopathology, IVIM-DWI and radiomics parameters was developed. The concordance index (C-index) of the nomogram in the training and validation cohort were 0.816 and 0.861, respectively. The model showed good predictive efficacy in both training and validation groups. Decision curve analysis (DCA) in the training and validation cohort demonstrated that the prognostic nomogram was clinically useful.

## CONCLUSION

s The prognostic nomogram with a combination of the differentiation, T stage, CEA, f value and Rads-score can be applied in the individualized prediction of postoperative DFS in patients with rectal adenocarcinoma.

## CLINICAL RELEVANCE/APPLICATION

The prognostic nomogram with a combination of the differentiation, T stage, CEA, f value and Rads-score can be applied in the individualized prediction of postoperative DFS in patients with rectal adenocarcinoma. It is beneficial to the recovery of patients.

## W5B-SPGI-3 Spectral Parameters Measured by Fast kVp Switching Dual-Energy CT: Association with Ki-67 Expression in Hepatocellular Carcinoma complicated with hepatitis

Participants

Caiyun Li, BMedSc, BS, Xiamen, China (*Presenter*) Nothing to Disclose

## PURPOSE

To investigate the correlation between spectral parameters obtained from contrast-enhanced spectral CT scanning and Ki-67 expression in hepatocellular carcinoma (HCC).

## METHODS AND MATERIALS

29 HCC patients with hepatitis complicated underwent both pathological examination and two-phase contrast-enhanced CT scanning with spectral imaging mode were included in this study. Then iodine-, water- and fat-based material decomposition images as well as virtual monochromatic images acquired at energies ranging from 90 to 140 keV were reconstructed. Region of interest (ROI) was placed on the lesion, and water and fat density, iodine concentration, CT values at monochromatic energy images (HU90-140keV), as well as effective atomic number were measured. The effective atomic number and iodine concentration for lesions were normalized by those for aorta to derive normalized atomic number (Neff-Z) and normalized iodine concentration (NIC). Ki-67 expression level was determined by Ki-67 positivity rate according to immunohistochemistry analysis. Pearson coefficient was used to analyze the correlation between spectral parameters and Ki-67 positivity.

## RESULTS

The Neff-Z, NIC, HU90-140keV, water and fat density were positively and fairly correlated with the Ki-67 expression, and correlation coefficient  $r$  (95% confidence interval,  $P$  value), were 0.476 (0.133-0.718,  $P = 0.009$ ), 0.402 (0.041-0.670,  $P = 0.031$ ),

0.381-0.459 (0.016-0.707,  $P = 0.042-0.012$ ), 0.422 (0.066-0.683,  $P = 0.023$ ) and 0.465 (0.119-0.710,  $P = 0.011$ ), respectively. Particularly, Neff-Z showed strongest correlation with Ki-67 expression. Additionally, the correlation between CT value and Ki-67 was enhanced gradually with the increase of monochromatic energy (90keV to 140keV).

## CONCLUSION

s The Neff-Z, NIC, HU90-140keV, water and fat density obtained from spectral scanning on dual-energy CT exhibited positive and fair correlation with Ki-67 expression.

## CLINICAL RELEVANCE/APPLICATION

Spectral scanning on Dual energy CT provides a new noninvasive method and various parameters to evaluate Ki-67 (indicative of proliferative activity) expression in HCC, which is valuable for clinical diagnosis and treatment.

## W5B-SPGI-4 Discordance rates on primary tumor assessment between Blinded Independent Central Review (BICR) readers in advanced or metastatic esophageal cancer applying RECIST 1.1 criteria

Participants

Yan Liu, MD, PhD, Forest, Belgium (*Presenter*) Nothing to Disclose

## PURPOSE

The aim of this study is to assess the inter-reader variability between paired readers in the baseline lesion selection on esophagus and its impact on the response evaluation applying RECIST 1.1.

## METHODS AND MATERIALS

We included 426 esophageal cancer subjects with 1506 timepoints included in the BICR process and assessed by 8 independent radiologists. We investigated TL distribution in different organs at baseline. Subsequently, we analyzed the discordance rates of baseline assessment of esophagus, categorized as no lesion, target lesion (TL), and non-target lesion (NTL) and its impact on the overall response discordance as well.

## RESULTS

Two hundred forty-nine (58.5%) subjects had evidence of disease, with either TL or NTL selected on esophagus by at least one reader at baseline. When both readers considered evidence of disease on esophagus ( $n=125$ ), the discordance of TL vs NTL selection was 46.4%. The most common sites of TL selected by the readers were lymph nodes. The baseline TL distribution in different organs is listed in Figure 1. Two readers considered esophageal lesions as TLs regularly. Considering overall response assessment, 13 subjects with baseline esophageal NTL had progressive disease (PD) due to the progression of the specified esophageal lesions by at least one reader, while both readers assigned PD on 6 subjects.

## CONCLUSION

s This study demonstrated high discrepancies on assessing presence or measurability of primary esophageal tumor selection applying RECIST 1.1 with potential impact on local progression discrepancy. Therefore, reader training at the study initiation could be helpful to reach more consensus among readers through the group discussion on challenging cases.

## CLINICAL RELEVANCE/APPLICATION

It is challenging to use RECIST 1.1 for the response assessment in esophageal cancer, because primary lesions could infiltrate the cavity organ and appear with unclear margins, the presence of scar tissue due to the prior local treatment may cause ambiguity in the evaluation, and certain examines such as the use of barium meal and endoscopy are omitted from the evaluation. Therefore, the primary lesion assessment could be classified with high discrepancy.

## W5B-SPGI-6 Deep Learning for Detection of Iso-attenuating Pancreatic Adenocarcinoma in Computer Tomography

Participants

Megan Schuurmans, (*Presenter*) Nothing to Disclose

## PURPOSE

Investigate the ability of deep learning to localize iso-attenuating pancreatic adenocarcinoma (pCa) in computed tomography (CT) images and assess the effect of including prior anatomy information on localization performance.

## METHODS AND MATERIALS

This retrospective study included contrast-enhanced CT scans in the portal-venous phase of 44 patients from the public Medical Segmentation Decathlon dataset, who had a visually iso-attenuating tumour. Two previously developed deep learning (DL) algorithms based on the 3D nnUnet framework were applied to the set of iso-attenuating lesions: one considering only tumour information (nnUnet\_T) and one considering both tumour and surrounding anatomical structures, namely pancreas parenchyma, common bile duct, pancreatic duct, arteries and veins (nnUNet\_MS). Each model created 10 different outputs, based on 2 random initialisations and 5-fold cross validation. The performance of the two models at pCa localization was evaluated with average precision. A permutation test was performed to show statistical significance.

## RESULTS

The average precision for the nnUNet\_MS was  $80.0\% \pm 8.6\%$ , while for the nnUnet\_T model it was  $72.9\% \pm 7.1\%$  ( $p < 0.05$ ). This indicates that surrounding anatomy aids in localization of iso-attenuating pCa lesions. By having prior anatomy information available for training the localization network, the nnUNet\_MS network is able to better focus on regions of image where tumour is located, avoiding most confusion with other anatomical structures. The nnUNet\_MS failed in 8 cases to localize the tumour, in which 4/8 cases the tumour was localized without high confidence but partially overlapping with the ground truth location, 3/8 cases the tumour was detected next to the ground truth location, and 1/8 cases the tumour was detected outside the pancreas.

## CONCLUSION

s In current clinical workup the detection of iso-attenuating pCa lesions on CT is very challenging, as the attenuation is similar to the pancreas parenchyma. The proposed 3D nnUnet\_MS model can be used to detect and localize iso-attenuating lesions.

## CLINICAL RELEVANCE/APPLICATION

Iso-attenuating pCa is linked to earlier stages of disease and better outcome, but is challenging to detect on CT. When taking surrounding anatomic information into account DL can accurately detect iso-attenuating lesions.

### W5B-SPGI-7 Tumor diversity features across pre- and post-chemoradiation MRI are associated with degree of pathologic response to chemoradiation in rectal cancers: a multi-institution study

Participants

Thomas Desilvio, Cleveland, OH (*Presenter*) Nothing to Disclose

## PURPOSE

Locally advanced rectal cancers (LARC) are routinely treated with neoadjuvant therapy (chemoradiation and/or chemotherapy, nCRT), but evaluating tumor response in vivo is limited even with high-resolution MRI. Accurately categorizing LARC patients as complete, partial, poor, or incomplete/non-response could enable more personalized interventions. We evaluated a novel suite of radiomic tumor diversity features across pre- and post-chemoradiation MRI for characterizing the pathologic grade of tumor response in LARC.

## METHODS AND MATERIALS

IRB-approved, retrospective study. We utilized a discovery cohort of T2-weighted (T2w) MRI scans from 3 institutions: (i) C1: 156 pre-nCRT baseline MRI scans, (ii) C2: 80 post-nCRT follow-up MRI scans. The hold-out validation cohort C3 comprised 39 patients with both pre- and post-nCRT MRI scans. LARC response to nCRT was categorized via pathologic AJCC tumor regression grade (ypTRG): ypTRG0 implying pCR (no residual tumor cells), and ypTRG1-3 corresponding to non/poor/partial response. 38 radiomic tumor diversity features were extracted from annotated tumor (on pre-nCRT) or rectal wall (on post-nCRT), to quantify fractal dimensions, surface topology, and persistent homology. Top 5 tumor diversity features associated with pCR were identified via cross-validated machine learning analysis, separately within C1 and C2. Features identified in common between C1 C2 were used to cluster unseen patients in C3 via unsupervised consensus clustering (Pearson correlation, 1000 iterations). Cluster overlap accuracies were calculated by first identifying which cluster corresponded to which ypTRG (based on precision/recall values) and then calculating what fraction of the datasets from each ypTRG group were correctly clustered together

## RESULTS

3 tumor diversity measurements (capturing fractal dimensions and shape topology) were commonly associated with pCR across pre-nCRT and post-nCRT MRI. Combining pre- and post- tumor diversity features yielded excellent cluster overlap accuracies for all ypTRG groups: 0.67 for ypTRG0, 0.93 for ypTRG1, 1.00 for ypTRG2, 0.5 for ypTRG3 and 1.0 for metastatic ypTRG0

## CONCLUSION

s Novel tumor diversity features across pre- and post-treatment MRI may effectively characterize the continuum for pathologic degree of tumor response (complete, partial, poor, none) after chemoradiation in LARC.

## CLINICAL RELEVANCE/APPLICATION

Non-invasive, quantitative characterization of the degree of tumor response after chemoradiation via novel tumor diversity features on MRI could enable personalized risk profiling and targeted intervention in rectal cancers.

### W5B-SPGI-8 Prognostic significance of Magnetic resonance imaging-detected Tumor Deposits in T3 and T4 Rectal Cancer

Participants

Yutao Que, (*Presenter*) Nothing to Disclose

## PURPOSE

Tumor deposits (TD) have shown to be a marker of poor prognostic feather in colorectal cancer. However, there are limited number of studies on the relationship between Magnetic resonance imaging-detected tumor deposits (mrTDs) and their clinical outcome following neoadjuvant therapy. The aims of the study are to evaluate the incidence and clinical significance of mrTDs in T3 and T4 patients with rectal cancer, including those underwent neoadjuvant treatment.

## METHODS AND MATERIALS

This retrospective study included patients with T3/T4 rectal cancer without synchronous metastasis who underwent surgery between 2015 and 2021 in a tertiary referral hospital. MRI evaluates tumor features (tumor location, T stage, N stage, mesorectal fascia [MRF], extramural venous invasion [EMVI] and mrTDs) before any treatment is performed.

## RESULTS

208 patients with a median follow up of 3.3 (range 0.2 - 7.0) years were reviewed. Patients with mrTDs had higher rate of lymph node involvement (OR: 7.812; P = 0.001) and extramural venous invasion (OR: 6.952; P = 0.000). Among 95 patients underwent neoadjuvant therapy, 3-year disease free survival (DFS) was significant higher in mrTD-negative group compared mr-TD positive group (48.5% vs 78.3%; P = 0.002). Of 66 mrTD-positive patients, there was not statistically difference in 3-year disease-free survival between patients with and without neoadjuvant treatment (48.6% vs 71.0%; P = 0.069). Positive mr-EMVI and mrTDs were associated with less tumor regression.

## CONCLUSION

s mrTDs are a poor prognostic marker in T3/T4 rectal cancer patients. The oncological results of tumor deposit in T3/T4 patients with and without neoadjuvant treatment are similar, which indicate that patients may benefit from more aggressive treatments.

## CLINICAL RELEVANCE/APPLICATION

The oncological results of tumor deposit in T3/T4 patients with and without neoadjuvant treatment are similar, which indicate that patients may benefit from more aggressive treatments, such as induction chemotherapy followed by chemoradiation therapy.

### W5B-SPGI-9 Feasibility of PCASL in noninvasive pancreatic blood perfusion

Participants

Yuling Zhang, (*Presenter*) Nothing to Disclose

## **PURPOSE**

This study aimed to investigate the feasibility of the pseudo-continuous arterial spin labeling (PCASL) technique for evaluating pancreatic blood perfusion noninvasively in healthy volunteers.

## **METHODS AND MATERIALS**

Forty-one healthy volunteers underwent a prototypic PCASL protocol at different time points before and after glucose stimulation (5, 10, 15, 20, and 25 minutes) on a 3T MR system (MAGNETOM Prisma, Siemens Healthcare, Erlangen, Germany). The parameters of the PCASL was performed using a 3D single-shot Turbo Gradient Spin Echo sequence with following parameters: repetition time = 7000 ms; echo time = 20.8 ms; field of view = 320 × 160 mm<sup>2</sup>; voxel size = 5 × 5 × 6 mm<sup>3</sup>; spin labeling duration = 1500 ms; post-labeling delay = 1500 ms; and acquisition time = 2 min 27 s. PCASL images were acquired in a free breathing manner with retrospective motion correction. The pancreatic blood flow (PBF) map was generated inline after data acquisition. The PBF values of the pancreatic body, tail, and pancreas (the mean value of body and tail) were recorded and analyzed.

## **RESULTS**

The PBF values showed good reproducibility (all ICC > 0.75). Statistically significant differences in PBF were found in different parts of the pancreas before and after glucose stimulation at different time points (all P < .05). A similar time trend was observed; PBF reached a maximum at 5 minutes, then gradually decreased, returned to baseline levels at about 15 minutes, and thereafter decreased significantly with time (all P < .05). Statistically significant differences in PBF were found between the body and the tail at 0 and 5 minutes (all P < .05). The PBF of volunteers of different sex or age were significantly different in the same part of the pancreas at different time points, but not in the same part at the same time point (all P > .05).

## **CONCLUSION**

s ASL can noninvasively evaluate the changes in PBF before and after glucose stimulation.

## **CLINICAL RELEVANCE/APPLICATION**

PCASL, which is used to evaluate and monitor the changes in PBF, serves as a new method for revealing the changes in blood flow when islet β cells secrete insulin.

Printed on: 02/07/23

## Abstract Archives of the RSNA, 2022

W5B-SPGI-1

### Interobserver Concordance in Predicting Complete Response on MRI in Rectal Cancer Patients Post Neoadjuvant Chemo-radiotherapy

Wednesday, Nov. 30 12:45PM - 1:15PM Room: Learning Center - GI DPS

#### Participants

Aashna Karbhari, MD, (Presenter) Nothing to Disclose

#### PURPOSE

To identify the accuracy of MRI in identifying complete pathologic response (pCR) in rectal cancer patients post NACRT, to allow better patient selection for watch and wait (WW) protocol.

#### METHODS AND MATERIALS

This was an IRB approved retrospective review of MRIs of 80 cases of lower and mid rectal cancer patients from January 2018 to March 2022. Study cohort consisted of 40 patients on the WW protocol post NACRT, and another 40 whose post NACRT MRI suggested complete / near complete response but subsequently underwent surgery. Baseline MRIs (available in 58/80 patients) were evaluated for tumor morphology, location, craniocaudal length and circumferential involvement. Post-treatment MRIs (80 patients) were additionally evaluated for pattern of response on T2 and DWI. Overall primary tumor bed response was classified as complete (CR- only T2 dark fibrosis, no restricted diffusion), near complete (nCR- predominantly T2 dark fibrosis with patchy T2 intermediate signal/ restricted diffusion/mucinous change) or as residual disease (predominant intermediate signal / frank restricted diffusion). Patients with pCR on pathology or who had a disease free interval of 12 months post NACRT on WW protocol were regarded as complete response. Cohen's Kappa statistic was used to evaluate inter-observer concordance in prediction of pCR as well as in interpretation of individual MRI parameters like T2 and DWI.

#### RESULTS

Median patient age was 47 years (range = 15 - 73 years) with 47 males and 33 females. A combination of T2 and DWI in evaluating rectal MRIs post NACRT was found to have good inter-observer agreement (Cohen's Kappa=0.6). For categorising residual disease, sensitivity, specificity, negative and positive predictive values of Observer 1 were 81.5%, 58.4%, 86.1%, 50% and for Observer 2 were 70.4%, 71.7%, 82.6% and 55.9% respectively. Statistically significant association of complete response was found with <25% circumferential wall involvement (p=0.03) and polypoidal pattern of growth (0.004) at baseline.

#### CONCLUSION

s Combined evaluation of T2 and DWI on MRI has moderate specificity and sensitivity for characterising residual disease and a good negative predictive value. Despite good inter-observer agreement in interpreting post NACRT rectal MRIs, MRI was not found to significantly identify pCR.

#### CLINICAL RELEVANCE/APPLICATION

Identification of pCR on MRI can enable appropriate selection of patients to be managed under the watch and wait protocol.

Printed on: 02/07/23

## Abstract Archives of the RSNA, 2022

W5B-SPGI-10

### Inferior Vena Cava Reflux: Does it Mean There is a Right Heart Dysfunction?

Wednesday, Nov. 30 12:45PM - 1:15PM Room: Learning Center - GI DPS

#### Participants

Ahmad Alhamshari, MBBS, (*Presenter*) Nothing to Disclose

#### PURPOSE

Retrograde flow into the inferior vena cava and/or hepatic veins have been associated with right heart dysfunction such as tricuspid valve regurgitation. However, much of the studies in the literature were conducted on patients' with other medical illnesses which may affect the finding. So, we are conducting a study on population of healthy liver donors to assess the association. Also, we are reporting the frequency of each reflux grade which may range from grade I "no reflux is present" to grade VI "severe reflux that reaches peripheral hepatic veins".

#### METHODS AND MATERIALS

Computed tomography (CT) scan of the abdomen with contrast enhancement and transthoracic echocardiography are some of the essential investigation for evaluation of liver donors. We retrospectively reviewed all the CT scans and echocardiographic reports of potential liver donors. CT scans were used to assess the reflux on contrast material into the inferior vena cava and/or hepatic veins during the venous phase. Reflux severity were graded from grade I to grade VI. Echocardiographic reports were reviewed for the presence of the tricuspid regurgitation. Tricuspid regurgitations were reported as normal, trace or mild regurgitation.

#### RESULTS

We had 246 donors, with mean age of 34 and range from 23-59. There was a male predominance 180 cases (73.2%). The severity of the reflux were reported as normal or mild reflux (grade I-III), or moderate to severe reflux (grade IV-VI). We had 149 (60.6%) cases of normal to mild reflux and 97 (39.4%) of moderate to severe reflux. There was no significant correlation between the reflux severity and the presence of right heart dysfunction.

#### CONCLUSION

The presence of inferior vena cava and or hepatic veins reflux is a relatively common finding in CT scans. Its presence does not correlate with right heart dysfunction.

#### CLINICAL RELEVANCE/APPLICATION

Since there is no correlation with right heart dysfunction, it is not warranted to perform any cardiac investigation in case of presence of reflux.

Printed on: 02/07/23

## Abstract Archives of the RSNA, 2022

W5B-SPGI-2

### **A Nomogram Combining Clinicopathology, IVIM-DWI, MRI Radiomics Parameters to Predict Postoperative DFS in Patients with Rectal Adenocarcinoma**

Wednesday, Nov. 30 12:45PM - 1:15PM Room: Learning Center - GI DPS

#### **Participants**

Rixin Su, (*Presenter*) Nothing to Disclose

#### **PURPOSE**

This study aimed to establish an effective prognostic nomogram to predict postoperative disease-free survival (DFS) in patients with rectal adenocarcinoma.

#### **METHODS AND MATERIALS**

A total of 156 rectal adenocarcinoma patients admitted to our hospital were retrospectively collected. The patients were divided into training and verification cohort. Clinicopathological data of the patients were collected and IVIM-DWI parameters of the primary rectal adenocarcinoma were measured. Radiomic parameters were extracted on DWI and T2-weighted images. Radiomic features were screened and radiomic scores (Rads-score) were calculated. Correlation analysis, Kaplan-Meier analysis, univariate and multivariate analysis were used in the training group to identify factors associated with disease-free survival (DFS) and to screen independent predictors. Prognostic nomograms were constructed, and the model predictive efficacy and net benefit were evaluated. Validation was performed in the validation cohort.

#### **RESULTS**

Kaplan-Meier analysis showed that patients in the poor differentiation group had worse DFS than those in the well/moderate differentiation group ( $P < 0.001$ ), patients in the T4 stage group had worse DFS than those in the T1-3 stage group ( $P < 0.001$ ), patients in the CEA = 5 group had worse DFS than those in the CEA < 5 group ( $P < 0.001$ ), patients in the f value = 46.6 group had worse DFS than those in the f-value < 46.6 group ( $P < 0.001$ ), and patients in the Radsscore = -1 group had better DFS than those in the Radsscore < -1 group. Univariate analysis revealed pretreatment the differentiation, T stage, CEA, f-value, and Rads-score were significantly correlated with DFS. Multivariate analysis showed that the differentiation, T stage, CEA, f value, and Rads-score were independent prognostic factors affecting DFS. A prognostic nomogram model combining clinicopathology, IVIM-DWI and radiomics parameters was developed. The concordance index (C-index) of the nomogram in the training and validation cohort were 0.816 and 0.861, respectively. The model showed good predictive efficacy in both training and validation groups. Decision curve analysis (DCA) in the training and validation cohort demonstrated that the prognostic nomogram was clinically useful.

#### **CONCLUSION**

The prognostic nomogram with a combination of the differentiation, T stage, CEA, f value and Rads-score can be applied in the individualized prediction of postoperative DFS in patients with rectal adenocarcinoma.

#### **CLINICAL RELEVANCE/APPLICATION**

The prognostic nomogram with a combination of the differentiation, T stage, CEA, f value and Rads-score can be applied in the individualized prediction of postoperative DFS in patients with rectal adenocarcinoma. It is beneficial to the recovery of patients.

Printed on: 02/07/23

## Abstract Archives of the RSNA, 2022

W5B-SPGI-3

### Spectral Parameters Measured by Fast kVp Switching Dual-Energy CT: Association with Ki-67 Expression in Hepatocellular Carcinoma complicated with hepatitis

Wednesday, Nov. 30 12:45PM - 1:15PM Room: Learning Center - GI DPS

#### Participants

Caiyun Li, BMedSc, BS, Xiamen, China (*Presenter*) Nothing to Disclose

#### PURPOSE

To investigate the correlation between spectral parameters obtained from contrast-enhanced spectral CT scanning and Ki-67 expression in hepatocellular carcinoma (HCC).

#### METHODS AND MATERIALS

29 HCC patients with hepatitis complicated underwent both pathological examination and two-phase contrast-enhanced CT scanning with spectral imaging mode were included in this study. Then iodine-, water- and fat-based material decomposition images as well as virtual monochromatic images acquired at energies ranging from 90 to 140 keV were reconstructed. Region of interest (ROI) was placed on the lesion, and water and fat density, iodine concentration, CT values at monochromatic energy images (HU90-140keV), as well as effective atomic number were measured. The effective atomic number and iodine concentration for lesions were normalized by those for aorta to derive normalized atomic number (Neff-Z) and normalized iodine concentration (NIC). Ki-67 expression level was determined by Ki-67 positivity rate according to immunohistochemistry analysis. Pearson coefficient was used to analyze the correlation between spectral parameters and Ki-67 positivity.

#### RESULTS

The Neff-Z, NIC, HU90-140keV, water and fat density were positively and fairly correlated with the Ki-67 expression, and correlation coefficient  $r$  (95% confidence interval, P value), were 0.476 (0.133-0.718,  $P = 0.009$ ), 0.402 (0.041-0.670,  $P = 0.031$ ), 0.381-0.459 (0.016-0.707,  $P = 0.042$ -0.012), 0.422 (0.066-0.683,  $P = 0.023$ ) and 0.465 (0.119-0.710,  $P = 0.011$ ), respectively. Particularly, Neff-Z showed strongest correlation with Ki-67 expression. Additionally, the correlation between CT value and Ki-67 was enhanced gradually with the increase of monochromatic energy (90keV to 140keV).

#### CONCLUSION

s The Neff-Z, NIC, HU90-140keV, water and fat density obtained from spectral scanning on dual-energy CT exhibited positive and fair correlation with Ki-67 expression.

#### CLINICAL RELEVANCE/APPLICATION

Spectral scanning on Dual energy CT provides a new noninvasive method and various parameters to evaluate Ki-67 (indicative of proliferative activity) expression in HCC, which is valuable for clinical diagnosis and treatment.

Printed on: 02/07/23



## Abstract Archives of the RSNA, 2022

W5B-SPGI-4

### Discordance rates on primary tumor assessment between Blinded Independent Central Review (BICR) readers in advanced or metastatic esophageal cancer applying RECIST 1.1 criteria

Wednesday, Nov. 30 12:45PM - 1:15PM Room: Learning Center - GI DPS

#### Participants

Yan Liu, MD, PhD, Forest, Belgium (*Presenter*) Nothing to Disclose

#### PURPOSE

The aim of this study is to assess the inter-reader variability between paired readers in the baseline lesion selection on esophagus and its impact on the response evaluation applying RECIST 1.1.

#### METHODS AND MATERIALS

We included 426 esophageal cancer subjects with 1506 timepoints included in the BICR process and assessed by 8 independent radiologists. We investigated TL distribution in different organs at baseline. Subsequently, we analyzed the discordance rates of baseline assessment of esophagus, categorized as no lesion, target lesion (TL), and non-target lesion (NTL) and its impact on the overall response discordance as well.

#### RESULTS

Two hundred forty-nine (58.5%) subjects had evidence of disease, with either TL or NTL selected on esophagus by at least one reader at baseline. When both readers considered evidence of disease on esophagus (n=125), the discordance of TL vs NTL selection was 46.4%. The most common sites of TL selected by the readers were lymph nodes. The baseline TL distribution in different organs is listed in Figure 1. Two readers considered esophageal lesions as TLs regularly. Considering overall response assessment, 13 subjects with baseline esophageal NTL had progressive disease (PD) due to the progression of the specified esophageal lesions by at least one reader, while both readers assigned PD on 6 subjects.

#### CONCLUSION

s This study demonstrated high discrepancies on assessing presence or measurability of primary esophageal tumor selection applying RECIST 1.1 with potential impact on local progression discrepancy. Therefore, reader training at the study initiation could be helpful to reach more consensus among readers through the group discussion on challenging cases.

#### CLINICAL RELEVANCE/APPLICATION

It is challenging to use RECIST 1.1 for the response assessment in esophageal cancer, because primary lesions could infiltrate the cavity organ and appear with unclear margins, the presence of scar tissue due to the prior local treatment may cause ambiguity in the evaluation, and certain examines such as the use of barium meal and endoscopy are omitted from the evaluation. Therefore, the primary lesion assessment could be classified with high discrepancy.

Printed on: 02/07/23

## Abstract Archives of the RSNA, 2022

W5B-SPGI-6

### Deep Learning for Detection of Iso-attenuating Pancreatic Adenocarcinoma in Computer Tomography

Wednesday, Nov. 30 12:45PM - 1:15PM Room: Learning Center - GI DPS

#### Participants

Megan Schuurmans, (*Presenter*) Nothing to Disclose

#### PURPOSE

Investigate the ability of deep learning to localize iso-attenuating pancreatic adenocarcinoma (pCa) in computed tomography (CT) images and assess the effect of including prior anatomy information on localization performance.

#### METHODS AND MATERIALS

This retrospective study included contrast-enhanced CT scans in the portal-venous phase of 44 patients from the public Medical Segmentation Decathlon dataset, who had a visually iso-attenuating tumour. Two previously developed deep learning (DL) algorithms based on the 3D nnUnet framework were applied to the set of iso-attenuating lesions: one considering only tumour information (nnUnet\_T) and one considering both tumour and surrounding anatomical structures, namely pancreas parenchyma, common bile duct, pancreatic duct, arteries and veins (nnUnet\_MS). Each model created 10 different outputs, based on 2 random initialisations and 5-fold cross validation. The performance of the two models at pCa localization was evaluated with average precision. A permutation test was performed to show statistical significance.

#### RESULTS

The average precision for the nnUnet\_MS was  $80.0\% \pm 8.6\%$ , while for the nnUnet\_T model it was  $72.9\% \pm 7.1\%$  ( $p < 0.05$ ). This indicates that surrounding anatomy aids in localization of iso-attenuating pCa lesions. By having prior anatomy information available for training the localization network, the nnUnet\_MS network is able to better focus on regions of image where tumour is located, avoiding most confusion with other anatomical structures. The nnUnet\_MS failed in 8 cases to localize the tumour, in which 4/8 cases the tumour was localized without high confidence but partially overlapping with the ground truth location, 3/8 cases the tumour was detected next to the ground truth location, and 1/8 cases the tumour was detected outside the pancreas.

#### CONCLUSION

In current clinical workup the detection of iso-attenuating pCa lesions on CT is very challenging, as the attenuation is similar to the pancreas parenchyma. The proposed 3D nnUnet\_MS model can be used to detect and localize iso-attenuating lesions.

#### CLINICAL RELEVANCE/APPLICATION

Iso-attenuating pCa is linked to earlier stages of disease and better outcome, but is challenging to detect on CT. When taking surrounding anatomic information into account DL can accurately detect iso-attenuating lesions.

Printed on: 02/07/23

## Abstract Archives of the RSNA, 2022

W5B-SPGI-7

### Tumor diversity features across pre- and post-chemoradiation MRI are associated with degree of pathologic response to chemoradiation in rectal cancers: a multi-institution study

Wednesday, Nov. 30 12:45PM - 1:15PM Room: Learning Center - GI DPS

#### Participants

Thomas Desilvio, Cleveland, OH (*Presenter*) Nothing to Disclose

#### PURPOSE

Locally advanced rectal cancers (LARC) are routinely treated with neoadjuvant therapy (chemoradiation and/or chemotherapy, nCRT), but evaluating tumor response in vivo is limited even with high-resolution MRI. Accurately categorizing LARC patients as complete, partial, poor, or incomplete/non-response could enable more personalized interventions. We evaluated a novel suite of radiomic tumor diversity features across pre- and post-chemoradiation MRI for characterizing the pathologic grade of tumor response in LARC.

#### METHODS AND MATERIALS

IRB-approved, retrospective study. We utilized a discovery cohort of T2-weighted (T2w) MRI scans from 3 institutions: (i) C1: 156 pre-nCRT baseline MRI scans, (ii) C2: 80 post-nCRT follow-up MRI scans. The hold-out validation cohort C3 comprised 39 patients with both pre- and post-nCRT MRI scans. LARC response to nCRT was categorized via pathologic AJCC tumor regression grade (ypTRG): ypTRG0 implying pCR (no residual tumor cells), and ypTRG1-3 corresponding to non/poor/partial response. 38 radiomic tumor diversity features were extracted from annotated tumor (on pre-nCRT) or rectal wall (on post-nCRT), to quantify fractal dimensions, surface topology, and persistent homology. Top 5 tumor diversity features associated with pCR were identified via cross-validated machine learning analysis, separately within C1 and C2. Features identified in common between C1 C2 were used to cluster unseen patients in C3 via unsupervised consensus clustering (Pearson correlation, 1000 iterations). Cluster overlap accuracies were calculated by first identifying which cluster corresponded to which ypTRG (based on precision/recall values) and then calculating what fraction of the datasets from each ypTRG group were correctly clustered together

#### RESULTS

3 tumor diversity measurements (capturing fractal dimensions and shape topology) were commonly associated with pCR across pre-nCRT and post-nCRT MRI. Combining pre- and post- tumor diversity features yielded excellent cluster overlap accuracies for all ypTRG groups: 0.67 for ypTRG0, 0.93 for ypTRG1, 1.00 for ypTRG2, 0.5 for ypTRG3 and 1.0 for metastatic ypTRG0

#### CONCLUSION

Novel tumor diversity features across pre- and post-treatment MRI may effectively characterize the continuum for pathologic degree of tumor response (complete, partial, poor, none) after chemoradiation in LARC.

#### CLINICAL RELEVANCE/APPLICATION

Non-invasive, quantitative characterization of the degree of tumor response after chemoradiation via novel tumor diversity features on MRI could enable personalized risk profiling and targeted intervention in rectal cancers.

Printed on: 02/07/23

## Abstract Archives of the RSNA, 2022

W5B-SPGI-8

### Prognostic significance of Magnetic resonance imaging-detected Tumor Deposits in T3 and T4 Rectal Cancer

Wednesday, Nov. 30 12:45PM - 1:15PM Room: Learning Center - GI DPS

#### Participants

Yutao Que, (*Presenter*) Nothing to Disclose

#### PURPOSE

Tumor deposits (TD) have shown to be a marker of poor prognostic feather in colorectal cancer. However, there are limited number of studies on the relationship between Magnetic resonance imaging-detected tumor deposits (mrTDs) and their clinical outcome following neoadjuvant therapy. The aims of the study are to evaluate the incidence and clinical significance of mrTDs in T3 and T4 patients with rectal cancer, including those underwent neoadjuvant treatment.

#### METHODS AND MATERIALS

This retrospective study included patients with T3/T4 rectal cancer without synchronous metastasis who underwent surgery between 2015 and 2021 in a tertiary referral hospital. MRI evaluates tumor features (tumor location, T stage, N stage, mesorectal fascia [MRF], extramural venous invasion [EMVI] and mrTDs) before any treatment is performed.

#### RESULTS

208 patients with a median follow up of 3.3 (range 0.2 - 7.0) years were reviewed. Patients with mrTDs had higher rate of lymph node involvement (OR: 7.812; P = 0.001) and extramural venous invasion (OR: 6.952; P = 0.000). Among 95 patients underwent neoadjuvant therapy, 3-year disease free survival (DFS) was significant higher in mrTD-negative group compared mr-TD positive group (48.5% vs 78.3%; P = 0.002). Of 66 mrTD-positive patients, there was not statistically difference in 3-year disease-free survival between patients with and without neoadjuvant treatment (48.6% vs 71.0%; P = 0.069). Positive mr-EMVI and mrTDs were associated with less tumor regression.

#### CONCLUSION

s mrTDs are a poor prognostic marker in T3/T4 rectal cancer patients. The oncological results of tumor deposit in T3/T4 patients with and without neoadjuvant treatment are similar, which indicate that patients may benefit from more aggressive treatments.

#### CLINICAL RELEVANCE/APPLICATION

The oncological results of tumor deposit in T3/T4 patients with and without neoadjuvant treatment are similar, which indicate that patients may benefit from more aggressive treatments, such as induction chemotherapy followed by chemoradiation therapy.

Printed on: 02/07/23

## Abstract Archives of the RSNA, 2022

W5B-SPGI-9

### Feasibility of PCASL in noninvasive pancreatic blood perfusion

Wednesday, Nov. 30 12:45PM - 1:15PM Room: Learning Center - GI DPS

#### Participants

Yuling Zhang, (*Presenter*) Nothing to Disclose

#### PURPOSE

This study aimed to investigate the feasibility of the pseudo-continuous arterial spin labeling (PCASL) technique for evaluating pancreatic blood perfusion noninvasively in healthy volunteers.

#### METHODS AND MATERIALS

Forty-one healthy volunteers underwent a prototypic PCASL protocol at different time points before and after glucose stimulation (5, 10, 15, 20, and 25 minutes) on a 3T MR system (MAGNETOM Prisma, Siemens Healthcare, Erlangen, Germany). The parameters of the PCASL was performed using a 3D single-shot Turbo Gradient Spin Echo sequence with following parameters: repetition time = 7000 ms; echo time = 20.8 ms; field of view = 320 × 160 mm<sup>2</sup>; voxel size = 5 × 5 × 6 mm<sup>3</sup>; spin labeling duration = 1500 ms; post-labeling delay = 1500 ms; and acquisition time = 2 min 27 s. PCASL images were acquired in a free breathing manner with retrospective motion correction. The pancreatic blood flow (PBF) map was generated inline after data acquisition. The PBF values of the pancreatic body, tail, and pancreas (the mean value of body and tail) were recorded and analyzed.

#### RESULTS

The PBF values showed good reproducibility (all ICC > 0.75). Statistically significant differences in PBF were found in different parts of the pancreas before and after glucose stimulation at different time points (all P < .05). A similar time trend was observed; PBF reached a maximum at 5 minutes, then gradually decreased, returned to baseline levels at about 15 minutes, and thereafter decreased significantly with time (all P < .05). Statistically significant differences in PBF were found between the body and the tail at 0 and 5 minutes (all P < .05). The PBF of volunteers of different sex or age were significantly different in the same part of the pancreas at different time points, but not in the same part at the same time point (all P > .05).

#### CONCLUSION

s ASL can noninvasively evaluate the changes in PBF before and after glucose stimulation.

#### CLINICAL RELEVANCE/APPLICATION

PCASL, which is used to evaluate and monitor the changes in PBF, serves as a new method for revealing the changes in blood flow when islet β cells secrete insulin.

Printed on: 02/07/23

## Abstract Archives of the RSNA, 2022

W5B-SPGU

### Genitourinary Wednesday Poster Discussions - B

Wednesday, Nov. 30 12:45PM - 1:15PM Room: Learning Center - GU DPS

#### Sub-Events

#### W5B-SPGU- Spatial Distribution of Prostate Cancer Detection using Multiparametric MRI

1

Participants

Fatemeh Zabihollahy, Los Angeles, CA (*Presenter*) Nothing to Disclose

#### PURPOSE

Multiparametric MRI (mpMRI) has significantly improved prostate cancer (PCa) diagnosis, but its spatial characteristic of tumor detection has not been fully understood. We aim to investigate the spatial correlations of the mpMRI performance in detecting clinically significant (cs)PCa with PI-RADS= 3 across different subjects.

#### METHODS AND MATERIALS

In this IRB approved, HIPAA compliant study cohort, 704 consecutive men underwent mpMRI prior to radical prostatectomy with thin-section whole-mount histopathology (WMHP) correlation at a single tertiary institution between 2010 and 2020 with annotation of true positive (TP), false negative (FN), and false-positive (FP) lesions. All WMHP and MRI-based findings were cognitively registered to the PI-RADS v2.1 based prostate sector map and the TP, FN, and FP lesions in each sector were assigned. Sector-based cancer prevalence (CP) and detection rate (DR) of mpMRI were then calculated as the number of csPCa divided by the whole number of csPCa lesions and TP/(TP+FN) in each sector, respectively. The correlation between DR and various locations of csPCa (GS= 7) tumors across the prostate sector map was evaluated using a chi-square test.

#### RESULTS

As shown in Figure 1 the CP and DR maps for csPCa lesions varied across sectors. csPCa lesions were most prevalent in the left and right posterior-lateral mid-gland peripheral zone (PZ), and the DR in the corresponding locations was significantly higher than the overall DR (70.2%; p-value<0.01). The most compromised DR in the right posterior basal transitional zone (TZ) and the left anterior apical PZ. The csPCa lesions in TZ were missed more than in the PZ (DR 63.3% vs. 69.3%; (p<0.01)) while the prevalence of csPCa was higher in PZ over TZ (CP of 64.5% vs. 23.2%). There was no significant difference in the laterality of CP and DR in the PZ. The csPCa lesions in the anterior PZ were also most likely to be missed by mpMRI (p-value<0.001).

#### CONCLUSION

s In a 704-patient cohort with mpMRI and WMHP with per lesion sector-based detection mpMRI was best in the PZ and least in the anterior TZ and PZ; attention to these sectors may further improve PCa diagnosis.

#### CLINICAL RELEVANCE/APPLICATION

The results may reduce the need for systematic prostate biopsy as it helps obtain samples from areas with the highest CP instead of removing samples from random areas of the prostate gland.

#### W5B-SPGU- MR-US fusion biopsy of the prostate assisted by artificial intelligence segmentation based on deep learning

2

Participants

Sung Il Hwang, MD, PhD, Seongnam-si, Korea, Republic Of (*Presenter*) Nothing to Disclose

#### PURPOSE

Performing target biopsies at the lesions suspected by a radiologist and by artificial intelligence (AI) segmented, to compare the cancer detection rates from these target lesions.

#### METHODS AND MATERIALS

This is a prospective, explorative study performed in a single institution with IRB approval. From Oct 2021 to Feb 2022, a total of 100 patients who requested for the fusion biopsy of the prostate were enrolled. Multiparametric MRI including diffusion weighted image and dynamic contrast enhancement was performed with 3.0T machine. Under Prostate Imaging Reporting and Data System (PI-RADS) 2.1, a human index lesion with score over three was annotated by a urologist. Automatic cancer detection and segmentation were done using PROMISE-I software, based on deep learning. The largest segmented lesion was marked as an AI Index lesion. If more than two lesions were segmented, a lesion with higher PI-RADS scoring or larger volume was chosen. Two core targeted biopsy was done for each index lesion by another urologist. If human and AI index lesions are identical, only target biopsy with two cores was done, and marked as both human and AI index lesions. Twelve core systemic randomized biopsy was followed after target biopsy. Clinically significant cancer detection rates (CSCDR) per patient and per core were calculated and compared.

#### RESULTS

Overall CDR by the patient was 51% and CSCDR was 39%, respectively. In 52 out of 100 patients, the human and AI index lesion was identical and underwent fourteen cores of biopsy. In another 44 patients, either the index lesions from human and AI were different from each other (N=14), or only one index lesion by human (N=3)/ AI (N=27) was present. In the remaining four patients, neither human nor AI could detect lesion, resulting in systemic biopsy only. Core-based CSCDR from human index lesion was 44.9% (31/69) and CSCDR from AI was 33.3% (31/93) ( $p < 0.05$ ). In a subgroup analysis of excluding PI-RADS score 2 lesions (N=27) from AI index lesions, CSCDR rose to 47.0% (31/66).

## CONCLUSION

s Core-based CSCDR from the human index lesion was higher than from the AI index. False positive detection from AI was the main problem, necessitating expert PI-RADS scoring after automatic segmentation.

## CLINICAL RELEVANCE/APPLICATION

Review by the expert is essential to decide target lesion from the segmented lesions by AI.

### W5B-SPGU- Integration of MRI biomarkers with molecular profiling for prostate cancer early detection: a prospective cohort validation study

3

Participants

Martina Pecoraro, MD, Roma, Italy (*Presenter*) Nothing to Disclose

## PURPOSE

(i) to comprehensively integrate MRI biomarkers, validated microRNAs, and clinical data to implement PCa early detection; (ii) to test different proposed diagnostic pathways to compare performance and patients' outcomes in terms of biopsy avoidance, accurate diagnosis of clinically significant cancer (csPCa), and reduction in overdiagnosis of clinically insignificant cancer (cisPCa); (iii) to build a risk-based diagnostic algorithm using the identified biomarkers.

## METHODS AND MATERIALS

We prospectively enrolled 123 consecutive naïve patients with the suspicion of PCa. All patients underwent MRI and, according to PI-RADS categorization, target biopsy and blood sampling for molecular profiling. The exclusion criteria included a lack of high-quality MR images, and of an adequate sample for microRNAs extraction. Network analysis was applied to identify the biomarkers drivers of csPCa.

## RESULTS

We have identified among the MRI biomarkers (i.e., PI-RADS score, ADC/normalized ADC, perfusion markers) those correlating with disease status (csPCa), tumor aggressiveness (ISUP category) and expression of miRNAs. Preliminary results have shown that ADC ( $r=-0.51$ ,  $p=0.02$ ), normalized ADC values ( $r=-0.64$ ,  $p=0.002$ ), and PI-RADS assessment score ( $r=0.73$ ;  $p=0.02$ ) strongly correlate with csPCa and specific miRNAs expression (i.e., miR-302a-5p, miR-520d-3p/miR-548a-3p). Once the driver biomarkers will be further validated, we are going to perform the analysis for the secondary objectives of the study.

## CONCLUSION

s This approach will allow for accurate patient allocation to biopsy, and for stratification into risk group categories, reducing overdiagnosis and overtreatment.

## CLINICAL RELEVANCE/APPLICATION

The study will provide evidence for a diagnostic paradigm shift that sees MRI biomarkers and molecular data as the prebiopsy triage of patients at risk.

### W5B-SPGU- Utility of Diffusion Weighted Imaging-Based Radiomics Nomogram to Predict Pelvic Lymph Nodes Metastasis in Prostate Cancer

4

Participants

Xiang Liu, (*Presenter*) Nothing to Disclose

## PURPOSE

To explore the feasibility of DWI-based radiomics for preoperative PLNM prediction in PCa patients at the nodal level

## METHODS AND MATERIALS

The preoperative MR images of 1116 pathologically confirmed lymph nodes (LNs) from 84 PCa patients were enrolled. The subjects were divided into a primary cohort (67 patients with 192 positive and 716 negative LNs) and a held-out cohort (17 patients with 43 positive and 165 negative LNs) at a 4:1 ratio. Two PLNM prediction models were constructed based on automatic LN segmentation with quantitative radiological LN features alone (Model 1) and combining radiological and radiomics features (Model 2) via multiple logistic regression. The visual assessments of junior (Model 3) and senior (Model 4) radiologists were compared.

## RESULTS

No significant difference was found between the area under curve (AUCs) of Models 1 and 2 (0.89 vs.0.90;  $P = 0.573$ ) in held-out cohort. Model 2 showed the highest AUC (0.83) for PLNM prediction in the LN subgroup with a short diameter = 10 mm compared with Model 1 (0.78), Model 3 (0.66), and Model 4 (0.74). The C-index of the nomogram analysis (0.91) and decision curve analysis (DCA) curves confirmed the clinical usefulness and benefit of Model 2.

## CONCLUSION

s A DWI-based radiomics nomogram incorporating the LN radiomics signature with quantitative radiological features is feasible for PLNM prediction in PCa patients, particularly for normal-sized LNM.

## CLINICAL RELEVANCE/APPLICATION

A key advantage of this study is indicated by the result that the combined radiomics model has more predictive efficacy than senior

radiologists for differentiating malignant and benign normal-sized PLNM, a finding that could be helpful for patients with PCa to optimize decision-making and adjust adjuvant treatments.

Printed on: 02/07/23

## Abstract Archives of the RSNA, 2022

W5B-SPGU-1

### Spatial Distribution of Prostate Cancer Detection using Multiparametric MRI

Wednesday, Nov. 30 12:45PM - 1:15PM Room: Learning Center - GU DPS

#### Participants

Fatemeh Zabihollahy, Los Angeles, CA (*Presenter*) Nothing to Disclose

#### PURPOSE

Multiparametric MRI (mpMRI) has significantly improved prostate cancer (PCa) diagnosis, but its spatial characteristic of tumor detection has not been fully understood. We aim to investigate the spatial correlations of the mpMRI performance in detecting clinically significant (cs)PCa with PI-RADS= 3 across different subjects.

#### METHODS AND MATERIALS

In this IRB approved, HIPAA compliant study cohort, 704 consecutive men underwent mpMRI prior to radical prostatectomy with thin-section whole-mount histopathology (WMHP) correlation at a single tertiary institution between 2010 and 2020 with annotation of true positive (TP), false negative (FN), and false-positive (FP) lesions. All WMHP and MRI-based findings were cognitively registered to the PI-RADS v2.1 based prostate sector map and the TP, FN, and FP lesions in each sector were assigned. Sector-based cancer prevalence (CP) and detection rate (DR) of mpMRI were then calculated as the number of csPCa divided by the whole number of csPCa lesions and TP/(TP+FN) in each sector, respectively. The correlation between DR and various locations of csPCa (GS= 7) tumors across the prostate sector map was evaluated using a chi-square test.

#### RESULTS

As shown in Figure 1 the CP and DR maps for csPCa lesions varied across sectors. csPCa lesions were most prevalent in the left and right posterior-lateral mid-gland peripheral zone (PZ), and the DR in the corresponding locations was significantly higher than the overall DR (70.2%;  $p$ -value<0.01). The most compromised DR in the right posterior basal transitional zone (TZ) and the left anterior apical PZ. The csPCa lesions in TZ were missed more than in the PZ (DR 63.3% vs. 69.3%; ( $p$ <0.01)) while the prevalence of csPCa was higher in PZ over TZ (CP of 64.5% vs. 23.2%). There was no significant difference in the laterality of CP and DR in the PZ. The csPCa lesions in the anterior PZ were also most likely to be missed by mpMRI ( $p$ -value<0.001).

#### CONCLUSION

In a 704-patient cohort with mpMRI and WMHP with per lesion sector-based detection mpMRI was best in the PZ and least in the anterior TZ and PZ; attention to these sectors may further improve PCa diagnosis.

#### CLINICAL RELEVANCE/APPLICATION

The results may reduce the need for systematic prostate biopsy as it helps obtain samples from areas with the highest CP instead of removing samples from random areas of the prostate gland.

Printed on: 02/07/23

## Abstract Archives of the RSNA, 2022

W5B-SPGU-2

### MR-US fusion biopsy of the prostate assisted by artificial intelligence segmentation based on deep learning

Wednesday, Nov. 30 12:45PM - 1:15PM Room: Learning Center - GU DPS

#### Participants

Sung Il Hwang, MD, PhD, Seongnam-si, Korea, Republic Of (*Presenter*) Nothing to Disclose

#### PURPOSE

Performing target biopsies at the lesions suspected by a radiologist and by artificial intelligence (AI) segmented, to compare the cancer detection rates from these target lesions.

#### METHODS AND MATERIALS

This is a prospective, explorative study performed in a single institution with IRB approval. From Oct 2021 to Feb 2022, a total of 100 patients who requested for the fusion biopsy of the prostate were enrolled. Multiparametric MRI including diffusion weighted image and dynamic contrast enhancement was performed with 3.0T machine. Under Prostate Imaging Reporting and Data System (PI-RADS) 2.1, a human index lesion with score over three was annotated by a urologist. Automatic cancer detection and segmentation were done using PROMISE-I software, based on deep learning. The largest segmented lesion was marked as an AI Index lesion. If more than two lesions were segmented, a lesion with higher PI-RADS scoring or larger volume was chosen. Two core targeted biopsy was done for each index lesion by another urologist. If human and AI index lesions are identical, only target biopsy with two cores was done, and marked as both human and AI index lesions. Twelve core systemic randomized biopsy was followed after target biopsy. Clinically significant cancer detection rates (CSCDR) per patient and per core were calculated and compared.

#### RESULTS

Overall CDR by the patient was 51% and CSCDR was 39%, respectively. In 52 out of 100 patients, the human and AI index lesion was identical and underwent fourteen cores of biopsy. In another 44 patients, either the index lesions from human and AI were different from each other (N=14), or only one index lesion by human (N=3)/ AI (N=27) was present. In the remaining four patients, neither human nor AI could detect lesion, resulting in systemic biopsy only. Core-based CSCDR from human index lesion was 44.9% (31/69) and CSCDR from AI was 33.3% (31/93) ( $p < 0.05$ ). In a subgroup analysis of excluding PI-RADS score 2 lesions (N=27) from AI index lesions, CSCDR rose to 47.0% (31/66).

#### CONCLUSION

s Core-based CSCDR from the human index lesion was higher than from the AI index. False positive detection from AI was the main problem, necessitating expert PI-RADS scoring after automatic segmentation.

#### CLINICAL RELEVANCE/APPLICATION

Review by the expert is essential to decide target lesion from the segmented lesions by AI.

Printed on: 02/07/23

## Abstract Archives of the RSNA, 2022

W5B-SPGU-3

### Integration of MRI biomarkers with molecular profiling for prostate cancer early detection: a prospective cohort validation study

Wednesday, Nov. 30 12:45PM - 1:15PM Room: Learning Center - GU DPS

#### Participants

Martina Pecoraro, MD, Roma, Italy (*Presenter*) Nothing to Disclose

#### PURPOSE

(i) to comprehensively integrate MRI biomarkers, validated microRNAs, and clinical data to implement PCa early detection; (ii) to test different proposed diagnostic pathways to compare performance and patients' outcomes in terms of biopsy avoidance, accurate diagnosis of clinically significant cancer (csPCa), and reduction in overdiagnosis of clinically insignificant cancer (cisPCa); (iii) to build a risk-based diagnostic algorithm using the identified biomarkers.

#### METHODS AND MATERIALS

We prospectively enrolled 123 consecutive naïve patients with the suspicion of PCa. All patients underwent MRI and, according to PI-RADS categorization, target biopsy and blood sampling for molecular profiling. The exclusion criteria included a lack of high-quality MR images, and of an adequate sample for microRNAs extraction. Network analysis was applied to identify the biomarkers drivers of csPCa.

#### RESULTS

We have identified among the MRI biomarkers (i.e., PI-RADS score, ADC/normalized ADC, perfusion markers) those correlating with disease status (csPCa), tumor aggressiveness (ISUP category) and expression of miRNAs. Preliminary results have shown that ADC ( $r=-0.51$ ,  $p=0.02$ ), normalized ADC values ( $r=-0.64$ ,  $p=0.002$ ), and PI-RADS assessment score ( $r=0.73$ ;  $p=0.02$ ) strongly correlate with csPCa and specific miRNAs expression (i.e., miR-302a-5p, miR-520d-3p/miR-548a-3p). Once the driver biomarkers will be further validated, we are going to perform the analysis for the secondary objectives of the study.

#### CONCLUSION

This approach will allow for accurate patient allocation to biopsy, and for stratification into risk group categories, reducing overdiagnosis and overtreatment.

#### CLINICAL RELEVANCE/APPLICATION

The study will provide evidence for a diagnostic paradigm shift that sees MRI biomarkers and molecular data as the prebiopsy triage of patients at risk.

Printed on: 02/07/23



## Abstract Archives of the RSNA, 2022

W5B-SPGU-4

### Utility of Diffusion Weighted Imaging-Based Radiomics Nomogram to Predict Pelvic Lymph Nodes Metastasis in Prostate Cancer

Wednesday, Nov. 30 12:45PM - 1:15PM Room: Learning Center - GU DPS

#### Participants

Xiang Liu, (Presenter) Nothing to Disclose

#### PURPOSE

To explore the feasibility of DWI-based radiomics for preoperative PLNM prediction in PCa patients at the nodal level

#### METHODS AND MATERIALS

The preoperative MR images of 1116 pathologically confirmed lymph nodes (LNs) from 84 PCa patients were enrolled. The subjects were divided into a primary cohort (67 patients with 192 positive and 716 negative LNs) and a held-out cohort (17 patients with 43 positive and 165 negative LNs) at a 4:1 ratio. Two PLNM prediction models were constructed based on automatic LN segmentation with quantitative radiological LN features alone (Model 1) and combining radiological and radiomics features (Model 2) via multiple logistic regression. The visual assessments of junior (Model 3) and senior (Model 4) radiologists were compared.

#### RESULTS

No significant difference was found between the area under curve (AUCs) of Models 1 and 2 (0.89 vs.0.90;  $P = 0.573$ ) in held-out cohort. Model 2 showed the highest AUC (0.83) for PLNM prediction in the LN subgroup with a short diameter = 10 mm compared with Model 1 (0.78), Model 3 (0.66), and Model 4 (0.74). The C-index of the nomogram analysis (0.91) and decision curve analysis (DCA) curves confirmed the clinical usefulness and benefit of Model 2.

#### CONCLUSION

A DWI-based radiomics nomogram incorporating the LN radiomics signature with quantitative radiological features is feasible for PLNM prediction in PCa patients, particularly for normal-sized LNM.

#### CLINICAL RELEVANCE/APPLICATION

A key advantage of this study is indicated by the result that the combined radiomics model has more predictive efficacy than senior radiologists for differentiating malignant and benign normal-sized PLNM, a finding that could be helpful for patients with PCa to optimize decision-making and adjust adjuvant treatments.

Printed on: 02/07/23

## Abstract Archives of the RSNA, 2022

W5B-SPHN

### Head and Neck Wednesday Poster Discussions - B

Wednesday, Nov. 30 12:45PM - 1:15PM Room: Learning Center - HN DPS

#### Sub-Events

#### **W5B-SPHN- Lateralization of Cerebral Blood Flow In the Auditory Pathway of Patients with Idiopathic Tinnitus: An Arterial Spin Labeling Study** 1

##### Participants

Xiaoshuai Li, (*Presenter*) Nothing to Disclose

##### PURPOSE

To assess the lateralization of cerebral blood flow (CBF) in the entire auditory pathway of patients with idiopathic tinnitus and healthy controls (HCs) using 3D pseudocontinuous arterial spin labeling (pcASL).

##### METHODS AND MATERIALS

Thirty-six patients with idiopathic tinnitus and 43 age- and gender-matched HCs underwent 3D-pcASL scanning using 3.0T MRI system. Region of interest (ROI) analysis was performed on the auditory pathway of both groups. The clinical data of all subjects were analyzed.

##### RESULTS

In patients with idiopathic tinnitus and HCs, the CBF in the left primary auditory cortex (PAC) was significantly higher than that in the right, while the CBF in the right secondary auditory cortex, auditory associative cortex, and medial geniculate body was significantly higher than that in the left. In HCs, the CBF in the right inferior colliculus (IC) was significantly higher than that in the left, while no significant difference in CBF between the bilateral IC was found in tinnitus patients. Compared with HCs, tinnitus patients exhibited significantly higher CBF in the bilateral PAC (right:  $P = 0.005$ ; left:  $P = 0.01$ ) and lower CBF in the right IC ( $P = 0.013$ ). The reduced CBF in the right IC was positively correlated with tinnitus severity ( $r = 0.506$ ,  $P = 0.002$ ).

##### CONCLUSION

This study confirms the asymmetry of the entire auditory pathway and investigates the underlying neuropathology of idiopathic tinnitus from in terms of CBF.

##### CLINICAL RELEVANCE/APPLICATION

This study not only investigated the underlying neuropathology of tinnitus in terms of CBF but also may have implications for the rationale of tinnitus treatment protocols based on lateralized hyperactivity.

#### **W5B-SPHN- Static And Dynamic Evaluation with MRI of Larynx and Oro-Pharyngeal Cavity in Professional Opera Singers** 2

##### Participants

Marco Di Girolamo, MD, (*Presenter*) Nothing to Disclose

##### PURPOSE

To assess the anatomical configuration of phonetic organs by MRI in professional opera singers with different vocal range.

##### METHODS AND MATERIALS

26 professional opera singers (12 men (7 tenors and 5 basses) and 14 women (8 sopranos and 6 mezzosopranos) were evaluated with MRI. We performed both static and dynamic study with MRI. The static study was performed with TSE T2-weighted axial scans at the level of larynx (TR:2000 ms; TE:120ms; slice thick:3mm) in order to evaluate the area of superior surface of vocal cord. In the dynamic study, the singers were asked to perform a prolonged vocalization at a comfortable tonality of the fundamental vowel [a]. We performed a midsagittal Turbo Field Echo scan (TR:12ms; TE:6ms; fa:30°; acq.time:6s) at the level of the oro-pharyngeal cavity measuring the area of the mouth and pharyngeal lumen. These data underwent statistical evaluation using the Mann-Whitney U-test (non-parametric test) considering: 1) vocal tessitura; 2) size of the vocal cord; 3) area of the mouth and pharyngeal lumen during the utterance of the vowel [a].

##### RESULTS

The average size of the vocal cord was: 0.71 cm<sup>2</sup> for sopranos; 1.20 cm<sup>2</sup> for mezzosopranos; 1.58 cm<sup>2</sup> for tenors; 2.88 cm<sup>2</sup> for basses. The average area of mouth and pharyngeal lumen on midsagittal scan during the utterance of the vowel a was: 15.8 cm<sup>2</sup> for sopranos; 14.6 cm<sup>2</sup> for mezzosopranos; 23.6 cm<sup>2</sup> for tenors; 32.2 cm<sup>2</sup> for basses. We found that the differences in vocal cord size between sopranos and mezzosopranos ( $P: 0.0641$ ) and between tenors and basses ( $P: 0.0833$ ) are tendentially statistically significant. The variation in vocal tract size during the utterance of the vowel a between tenors and basses is considered tendentially statistically significant ( $P: 0.0833$ ) while the difference between sopranos and mezzosopranos is not considered

statistically significant (P: 0.6434). The difference in the vocal register between soprano and mezzosoprano is less considerable in comparison with tenor and bass or with soprano and contralto.

## CONCLUSION

Our results demonstrate a correlation between the surface of the vocal cord and the configuration of vocal tract and the vocal tessitura of a singer.

## CLINICAL RELEVANCE/APPLICATION

Long vocal cord and wide vocal tract are characteristic of singers with low-pitched voice types (bass, baritone, contralto) while short vocal cord and narrow vocal tract are characteristic of singers with high-pitched voice types (tenor, soprano).

## W5B-SPHN- Clinoradiological Characteristics in The Differential Diagnosis of Follicular-patterned Lesions of the Thyroid: A Multicenter Cohort Study

Participants

Haerin Lee, Suwon, Korea, Republic Of (*Presenter*) Nothing to Disclose

## PURPOSE

The preoperative differential diagnosis of follicular-patterned lesions is often challenging. This multicenter cohort study investigated the clinicoradiological characteristics relevant to the differential diagnosis of such lesions.

## METHODS AND MATERIALS

From June to September 2015, 4,787 thyroid nodules (= 1.0 cm) with a final diagnosis of benign follicular nodule (BN, n=4461), follicular adenoma (FA, n=136), follicular carcinoma (FC, n=62), and follicular-variant of papillary thyroid carcinoma (FVPTC, n=128) were included from 26 institutions. The clinicoradiological characteristics of these groups were compared using logistic regression analyses, and the relative importance of those characteristics was determined using a random forest algorithm.

## RESULTS

Compared to BN, distinguishing features of FA, FC, and FVPTC were patient age (odds ratio [OR], 0.969), lesion diameter (OR: 1.054), solid composition (OR: 2.262), hypoechogenicity (OR: 2.183), and halo (OR, 1.763) (all P < 0.05). Compared to FA, FC differed with respect to lesion diameter (OR: 1.039) and rim calcifications (OR: 16.692), while FVPTC differed with respect to patient age (OR: 0.966), lesion diameter (OR: 0.973), macrocalcifications (OR: 3.590), and non-smooth margin (OR: 2.477) (all P < 0.05). The five relative feature importance for differential diagnosis of FA, FC, and FVPTC from BN were lesion diameter, composition, echogenicity, orientation, and patient age. The most important relative features of FC and FVPTC from FA were rim calcifications and macrocalcifications, respectively.

## CONCLUSION

Although follicular-patterned lesions have overlapping clinical, radiological, and cytological features, the relative importance of those features as assessed in a large clinical cohort may provide information valuable to preoperative decision-making.

## CLINICAL RELEVANCE/APPLICATION

1. Our multicenter cohort study showed that follicular-patterned neoplasms could be distinguished from BN based on their larger diameter, solid composition, hypoechogenicity, halo, and the younger age of patients associated with them. 2. Compared to FA, FC tumors were of larger diameter and characterized by rim calcifications whereas FVPTC were of smaller diameter and differed by their macrocalcifications, non-smooth margin, and the younger age of patients. 3. On the basis of our findings, the new risk stratification system for follicular-patterned lesions should be considered for a preoperative decision-making.

Printed on: 02/07/23

## Abstract Archives of the RSNA, 2022

W5B-SPHN-1

### Lateralization of Cerebral Blood Flow In the Auditory Pathway of Patients with Idiopathic Tinnitus: An Arterial Spin Labeling Study

Wednesday, Nov. 30 12:45PM - 1:15PM Room: Learning Center - HN DPS

#### Participants

Xiaoshuai Li, (*Presenter*) Nothing to Disclose

#### PURPOSE

To assess the lateralization of cerebral blood flow (CBF) in the entire auditory pathway of patients with idiopathic tinnitus and healthy controls (HCs) using 3D pseudocontinuous arterial spin labeling (pcASL).

#### METHODS AND MATERIALS

Thirty-six patients with idiopathic tinnitus and 43 age- and gender-matched HCs underwent 3D-pcASL scanning using 3.0T MRI system. Region of interest (ROI) analysis was performed on the auditory pathway of both groups. The clinical data of all subjects were analyzed.

#### RESULTS

In patients with idiopathic tinnitus and HCs, the CBF in the left primary auditory cortex (PAC) was significantly higher than that in the right, while the CBF in the right secondary auditory cortex, auditory associative cortex, and medial geniculate body was significantly higher than that in the left. In HCs, the CBF in the right inferior colliculus (IC) was significantly higher than that in the left, while no significant difference in CBF between the bilateral IC was found in tinnitus patients. Compared with HCs, tinnitus patients exhibited significantly higher CBF in the bilateral PAC (right:  $P = 0.005$ ; left:  $P = 0.01$ ) and lower CBF in the right IC ( $P = 0.013$ ). The reduced CBF in the right IC was positively correlated with tinnitus severity ( $r = 0.506$ ,  $P = 0.002$ ).

#### CONCLUSION

s This study confirms the asymmetry of the entire auditory pathway and investigates the underlying neuropathology of idiopathic tinnitus from in terms of CBF.

#### CLINICAL RELEVANCE/APPLICATION

This study not only investigated the underlying neuropathology of tinnitus in terms of CBF but also may have implications for the rationale of tinnitus treatment protocols based on lateralized hyperactivity.

Printed on: 02/07/23

## Abstract Archives of the RSNA, 2022

W5B-SPHN-2

### Static And Dynamic Evaluation with MRI of Larynx and Oro-Pharyngeal Cavity in Professional Opera Singers

Wednesday, Nov. 30 12:45PM - 1:15PM Room: Learning Center - HN DPS

#### Participants

Marco Di Girolamo, MD, (*Presenter*) Nothing to Disclose

#### PURPOSE

To assess the anatomical configuration of phonetic organs by MRI in professional opera singers with different vocal range.

#### METHODS AND MATERIALS

26 professional opera singers (12 men (7 tenors and 5 basses) and 14 women (8 sopranos and 6 mezzosopranos) were evaluated with MRI. We performed both static and dynamic study with MRI. The static study was performed with TSE T2-weighted axial scans at the level of larynx (TR:2000 ms; TE:120ms; slice thick:3mm) in order to evaluate the area of superior surface of vocal cord. In the dynamic study, the singers were asked to perform a prolonged vocalization at a comfortable tonality of the fundamental vowel [a]. We performed a midsagittal Turbo Field Echo scan (TR:12ms; TE:6ms; fa:30°; acq.time:6s) at the level of the oro-pharyngeal cavity measuring the area of the mouth and pharyngeal lumen. These data underwent statistical evaluation using the Mann-Whitney U-test (non-parametric test) considering: 1) vocal tessitura; 2) size of the vocal cord; 3) area of the mouth and pharyngeal lumen during the utterance of the vowel [a].

#### RESULTS

The average size of the vocal cord was: 0.71 cm<sup>2</sup> for sopranos; 1.20 cm<sup>2</sup> for mezzosopranos; 1.58 cm<sup>2</sup> for tenors; 2.88 cm<sup>2</sup> for basses. The average area of mouth and pharyngeal lumen on midsagittal scan during the utterance of the vowel a was: 15.8 cm<sup>2</sup> for sopranos; 14.6 cm<sup>2</sup> for mezzosopranos; 23.6 cm<sup>2</sup> for tenors; 32.2 cm<sup>2</sup> for basses. We found that the differences in vocal cord size between sopranos and mezzosopranos (P: 0.0641) and between tenors and basses (P: 0.0833) are tendentially statistically significant. The variation in vocal tract size during the utterance of the vowel a between tenors and basses is considered tendentially statistically significant (P: 0.0833) while the difference between sopranos and mezzosopranos is not considered statistically significant (P: 0.6434). The difference in the vocal register between soprano and mezzosoprano is less considerable in comparison with tenor and bass or with soprano and contralto.

#### CONCLUSION

Our results demonstrate a correlation between the surface of the vocal cord and the configuration of vocal tract and the vocal tessitura of a singer.

#### CLINICAL RELEVANCE/APPLICATION

Long vocal cord and wide vocal tract are characteristic of singers with low-pitched voice types (bass, baritone, contralto) while short vocal cord and narrow vocal tract are characteristic of singers with high-pitched voice types (tenor, soprano).

Printed on: 02/07/23

## Abstract Archives of the RSNA, 2022

W5B-SPHN-3

### Clinicoradiological Characteristics in The Differential Diagnosis of Follicular-patterned Lesions of the Thyroid: A Multicenter Cohort Study

Wednesday, Nov. 30 12:45PM - 1:15PM Room: Learning Center - HN DPS

#### Participants

Haerin Lee, Suwon, Korea, Republic Of (*Presenter*) Nothing to Disclose

#### PURPOSE

The preoperative differential diagnosis of follicular-patterned lesions is often challenging. This multicenter cohort study investigated the clinicoradiological characteristics relevant to the differential diagnosis of such lesions.

#### METHODS AND MATERIALS

From June to September 2015, 4,787 thyroid nodules (= 1.0 cm) with a final diagnosis of benign follicular nodule (BN, n=4461), follicular adenoma (FA, n=136), follicular carcinoma (FC, n=62), and follicular-variant of papillary thyroid carcinoma (FVPTC, n=128) were included from 26 institutions. The clinicoradiological characteristics of these groups were compared using logistic regression analyses, and the relative importance of those characteristics was determined using a random forest algorithm.

#### RESULTS

Compared to BN, distinguishing features of FA, FC, and FVPTC were patient age (odds ratio [OR], 0.969), lesion diameter (OR: 1.054), solid composition (OR: 2.262), hypoechogenicity (OR: 2.183), and halo (OR, 1.763) (all  $P < 0.05$ ). Compared to FA, FC differed with respect to lesion diameter (OR: 1.039) and rim calcifications (OR: 16.692), while FVPTC differed with respect to patient age (OR: 0.966), lesion diameter (OR: 0.973), macrocalcifications (OR: 3.590), and non-smooth margin (OR: 2.477) (all  $P < 0.05$ ). The five relative feature importance for differential diagnosis of FA, FC, and FVPTC from BN were lesion diameter, composition, echogenicity, orientation, and patient age. The most important relative features of FC and FVPTC from FA were rim calcifications and macrocalcifications, respectively.

#### CONCLUSION

Although follicular-patterned lesions have overlapping clinical, radiological, and cytological features, the relative importance of those features as assessed in a large clinical cohort may provide information valuable to preoperative decision-making.

#### CLINICAL RELEVANCE/APPLICATION

1. Our multicenter cohort study showed that follicular-patterned neoplasms could be distinguished from BN based on their larger diameter, solid composition, hypoechogenicity, halo, and the younger age of patients associated with them. 2. Compared to FA, FC tumors were of larger diameter and characterized by rim calcifications whereas FVPTC were of smaller diameter and differed by their macrocalcifications, non-smooth margin, and the younger age of patients. 3. On the basis of our findings, the new risk stratification system for follicular-patterned lesions should be considered for a preoperative decision-making.

Printed on: 02/07/23

## Abstract Archives of the RSNA, 2022

W5B-SPIN

### Informatics Wednesday Poster Discussions - B

Wednesday, Nov. 30 12:45PM - 1:15PM Room: Learning Center - IN DPS

#### Sub-Events

#### W5B-SPIN-1 GAN-based Contrast Media Reduction in MRI in A Large Animal Experiment

##### Participants

Johannes Haubold, MD, Essen, Germany (*Presenter*) Speaker, Siemens AG

##### PURPOSE

The aim was to establish virtual contrast enhancement in MRI with generative adversarial network (GAN) to reduce the amount of hepatobiliary contrast agent(CA) in a large animal model.

##### METHODS AND MATERIALS

120 exams were performed on a clinical 1.5 T MRI on six different occasions with 20 healthy Goettingen minipigs, 50% low-dose(ICM)(0.005mmol/kg, gadoxetate) and 50% with normal-dose(nCM)(0.025mmol/kg). These included arterial, portal venous, venous, and hepatobiliary contrast phases(20 and 30 minutes). One animal had to be excluded due to incomplete examinations. Three of the 19 animals were chosen at random and withheld for validation (18 examinations). The remaining 16 animals (96 examinations) were used to train a GAN for image-to-image conversion from ICM to nCM (vCM).Following that, ROI measurements in the abdominal aorta, inferior vena cava, portal vein, liver parenchyma, and autochthonous back muscles were obtained, and the vascular and parenchymal CNR was determined. In addition, the nCM and vCM data were shown in a visual-Turing-test(VTT) to three consultant radiologists, who had to assess whether they would have reported both sequences identical(pathologically consistent) and which sequence was the nCM sequence.

##### RESULTS

Pooled vascular ( $p<0.0001$ ) and parenchymal ( $p<0.0001$ ) CNR increased significantly from ICM to vCM and were not significantly different between vCM and nCM exams (vascular CNR (mean $\pm$ SD): ICM 17.6 $\pm$ 6.0, vCM 41.8 $\pm$ 9.7 and nCM 48.4 $\pm$ 12.2; parenchymal CNR (mean $\pm$ SD): ICM 21.6 $\pm$ 6.1, vCM 30.2 $\pm$ 7.0, nCM 32.4 $\pm$ 8.7). On median, the consultant radiologist indicated that the nCM and vCM sequences are pathologically consistent in 100 percent of the studies and correctly identified the normal-dose series in 59.5 percent of the instances.

##### CONCLUSION

This feasibility study on healthy minipigs demonstrates that, GAN-based contrast enhancement can lower the amount of hepatobiliary CA on MRI by up to 80% while retaining equivalent image quality.

##### CLINICAL RELEVANCE/APPLICATION

GAN-based contrast enhancement can reduce costs and exposure of patients to gadolinium-based CA.

#### W5B-SPIN-2 Impact of AI for Pathology Detection From Knee MRI

##### Participants

Gaspard d'Assignies, MD, Paris, France (*Presenter*) Founder, Incepto Medical SAS;Employee, Incepto Medical SAS;Stockholder, Incepto Medical SAS

##### PURPOSE

To evaluate the impact of artificial intelligence (AI) models on diagnostic performances of a panel of readers for detecting meniscal and ligament tears from knee MRI.

##### METHODS AND MATERIALS

An evaluation dataset consisted of 200 knee MRI (mean age 52.4, 52% male), for which gold standard diagnosis for Medial and Lateral Menisci (MM and LM), Anterior Cruciate Ligament (ACL), and Medial Collateral Ligament (MCL) was established via expert consensus of 3 musculoskeletal radiologists. Six experienced readers were asked to each review 100 exams (stratified for pathology prevalence) without the help of the AI, and the remaining 100 assisted by the AI. The AI model was a CE marked product (keros 1.0 - Incepto medical (c)). Readers' performances were evaluated using sensitivity/specificity, while Receiver Operating Characteristic curves were used for the AI performances. Chi-square testing was used for statistical significance of performance comparisons.

##### RESULTS

Pathology prevalence for MM, LM, ACL and MCL were 40%, 18.5%, 40% and 20%, respectively. Readers' sensitivity (without / with AI) values for MM, LM, ACL and MCL were 0.858/0.908 (95% CI [0.799, 0.875]/[0.879, 0.927],  $p=0.088$ ), 0.685/0.712 (95% CI [0.665, 0.747]/[0.641, 0.783],  $p=0.661$ ), 0.783/0.917 (95% CI [0.734, 0.809]/[0.858, 0.95],  $p<1e-4$ ), and 0.592/0.742 (95% CI [0.506, 0.684]/[0.686, 0.791],  $p=0.014$ ), respectively. Readers' specificity (without / with AI) values for MM, LM, ACL and MCL were

0.836/0.906 (95% CI [0.801, 0.872]/[0.858, 0.95],  $p=0.005$ ), 0.969/0.947 (95% CI [0.965, 0.981]/[0.932, 0.96],  $p=0.079$ ), 0.972/0.894 (95% CI [0.959, 0.978]/[0.866, 0.915],  $p<1e-4$ ), and 0.962/0.954 (95% CI [0.957, 0.972]/[0.947, 0.965],  $p=0.518$ ), respectively.

## CONCLUSION

s AI assistance led to an increased specificity for MM and an increased sensitivity for MCL. For ACL, it led to an increased sensitivity and a decreased specificity.

## CLINICAL RELEVANCE/APPLICATION

AI algorithms appear to bring an overall positive impact on radiological performances. Additional care must be paid to balance sensitivity vs. specificity of the AI assistance according to the clinical relevance for the considered structure.

## W5B-SPIN-3 Ultrasonic Texture Features as Radiomic Biomarkers for Screening Cardiac Remodeling and Dysfunction

Participants  
Quincy Hathaway, PhD, (*Presenter*) Nothing to Disclose

## PURPOSE

Point-of-care ultrasound (POCUS) workflows allow for rapid screening of cardiac abnormalities for guiding appropriate early triage and management. Morphometry and textural features (radiomics) in POCUS images could aid in the rapid automated expert-level screening of left ventricular (LV) myocardial remodeling and dysfunction without requiring any quantitative measurements.

## METHODS AND MATERIALS

We developed Machine-learning (ML) models using three clinical cohorts that included 1,915 subjects: 1) an expert-annotated registry of POCUS ( $n=943$ , 80% training and 20% internal validation), 2) a prospective institutional POCUS cohort for external validation ( $n=275$ ), and 3) a prospective external validation ML model on high-end ultrasound systems ( $n=484$ ) for a head-to-head comparison of radiomics-based prediction with standardized quantitative measurements obtained during comprehensive echocardiography. With radiomic features from the parasternal long axis, we developed an explainable ML model and a direct image-derived black-box convolutional neural network (CNN) model. Echocardiography of wildtype ( $n=10$ ) and *Leptr-/-* ( $n=8$ ) mice were assessed longitudinally at 3 and 25 weeks, and radiomic features of importance were correlated with histopathological features of myocyte disarray and hypertrophy.

## RESULTS

The receiver operating characteristic (ROC) area under the curve (AUC) for predicting expert annotated LV myocardial remodeling and dysfunction was higher for texture-based interpretable ML than the black-box, deep learning model (0.84, 0.73 and 0.75 vs. 0.53, 0.59, and 0.58;  $P=0.0001$  for internal and external POCUS and high-end ultrasound validation studies, respectively). Furthermore, the radiomics model predicted time-to-event outcomes in the external POCUS (100% vs. 82% survival,  $P=0.0001$ ) and high-end ultrasound studies (93% vs. 85% survival,  $P=0.0031$ ). *Leptr-/-* obese mice revealed LV remodeling through increased cardiomyocyte diameter ( $>20\%$  increase, compared to controls) that positively correlated with two radiomics biomarkers of importance extracted from the interventricular septum ( $r = 0.79$  and  $0.90$ ,  $P=0.0001$ ), respectively.

## CONCLUSION

s Texture-based ML models can be applied to cardiac POCUS to mirror an expert physician's ability to screen for the presence of LV myocardial remodeling and dysfunction without quantitative measurements.

## CLINICAL RELEVANCE/APPLICATION

Traditional cardiac point-of-care ultrasound requires expert-level interpretation to assess clinical findings; our model can automate the interpretation of left ventricular structural and functional changes without quantitative measurements.

## W5B-SPIN-4 Is It Time for Radiologists to Build AI? International Validation of Radiologist-trained AI Models to Identify Causes of Suboptimal Chest Radiographs

Participants  
Giridhar Dasegowda, MBBS, Boston, MA (*Presenter*) Nothing to Disclose

## PURPOSE

Generalizability of artificial intelligence (AI) models is a critical step towards its use in diverse clinical practices. Such efforts are hampered due to lack of data diversity in single study or country studies. Therefore, we assessed the performance of radiologist-trained AI models to differentiate suboptimal (sCXR) and optimal (oCXR) chest radiographs on a diverse multicenter data from 7 countries.

## METHODS AND MATERIALS

Our IRB-approved study included 10,687 CXRs from adult patients (age  $> 18$  years) from 7 countries (US, Brazil, Lebanon, India, Italy, Croatia, Iran: 14 imaging sites). The CXRs represented consecutive portable radiographs from each site. All de-identified CXRs were reviewed and annotated for the presence and causes of suboptimality on an AI server-based platform (CARPL AI). After annotation, all CXRs were uploaded into an AI building platform (Cognex Inc.) that allows non-programmers to build, train and test AI model for clinical applications. The platform allowed training (7508 CXRs: 3048 oCXR, 7508 sCXR from 7 sites, 2 country) and testing (3179 CXRs: 2490 sCXR, 689 oCXR from 7 other international sites) of 8 AI models for identifying various causes of sCXR. Receiver operating characteristics analyses were performed.

## RESULTS

The AI models classified sCXR with missing apices, right CP angle and left CP angle lung with 98%, 96%, 98% accuracies, and AUCs (95% CI) of 0.84 (0.80-0.88), 0.92(0.89-0.95) and 0.93 (0.90-0.95), respectively. AI identified under- and over-exposure with 93% and 94% accuracy, with 0.93 AUC (95% CI 0.90-0.95) and 0.86 AUC (95% CI 0.82-0.90). The presence of low lung volume was identified with 92% accuracy, and 0.94 AUC (95% CI 0.91-0.96). Lungs obscured by overlying chin was identified with 95% accuracy and AUC of 0.94 (95% CI 0.91-0.96). The AI accuracy and AUC for patient rotation were 95% and 0.92 (95% CI 0.89-

0.95), respectively.

## CONCLUSION

The eight AI models had high accuracy and generalizable performance for identifying suboptimal CXRs across 14 sites from 7 countries across four continents.

## CLINICAL RELEVANCE/APPLICATION

International generalizability evaluation of AI models can help overcome lack of data diversity and representations from single country or site studies, which helps prove model trustworthiness.

## W5B-SPIN-5 DeepLiverNet 2.0: A Deep Transformer Model for Liver Stiffness Classification Using T2-Weighted MRI Data

Participants

Redha Ali, PhD, Cincinnati, OH (*Presenter*) Nothing to Disclose

## PURPOSE

To develop an improved version of DeepLiverNet 1.0 for categorically classifying the degree of liver stiffening using anatomic T2-weighted MRI in children and young adults with known or suspected pediatric chronic liver disease.

## METHODS AND MATERIALS

Clinical axial T2-weighted fast spin-echo fat-saturated MRI images and 2D MR elastography liver stiffness measurements were clinically acquired from 1236 children and young adult patients with known or suspected pediatric chronic liver disease. We propose DeepLiverNet 2.0 in order to improve upon our prior work DeepLiverNet 1.0, that classified patients into one of two groups, no/mild liver stiffening <3 kPa or moderate/severe liver stiffening =3 kPa, which derived from MR elastography (Fig. 1). Specifically, we replaced the prior model's transfer learning block with the state-of-art Swin Transformer for latent imaging feature extraction. Swin Transformer is a hierarchical transformer implemented by shifting window partitions between consecutive self-attention layers. Such sliding window schema enhances efficiency by limiting self-attention computation to non-overlapping local windows while allowing for cross-window connection. Model performance was assessed using ten-fold cross-validation.

## RESULTS

The proposed DeepLiverNet 2.0 model was able to categorically classify the severity of liver stiffening with an accuracy [mean  $\pm$  standard deviation]  $82.7 \pm 0.02\%$ , sensitivity  $73.3 \pm 4.0\%$ , specificity  $87.7 \pm 4.0\%$ , and AUC  $0.84 \pm 0.04$ . It outperformed the DeepLiverNet 1.0 model by a significant margin of 0.08 on AUC ( $0.76 \pm 0.01$ ;  $P < 0.0001$ ), as well as on accuracy ( $77.8 \pm 1.0\%$ ;  $P < 0.0001$ ), sensitivity ( $67.2 \pm 4.0\%$ ;  $P = 0.004$ ), and specificity ( $83.4 \pm 4.0\%$   $P = 0.03$ ).

## CONCLUSION

By updating our previously developed feature extraction module using a state-of-the-art Swin Transformer, we have demonstrated that the proposed DeepLiverNet 2.0 model has better capability than DeepLiverNet 1.0 to stratify the severity of liver stiffening using anatomic T2-weighted MRI data in children and young adults with known or suspected pediatric chronic liver disease. Extensive model optimization is likely to further improve performance.

## CLINICAL RELEVANCE/APPLICATION

Our DeepLiverNet 2.0 AI model can categorically classify the severity of liver stiffening using anatomic T2-weighted MRI in children and young adults. Model refinements and incorporation of clinical features may soon decrease the need for MR elastography.

Printed on: 02/07/23

## Abstract Archives of the RSNA, 2022

W5B-SPIN-1

### GAN-based Contrast Media Reduction in MRI in A Large Animal Experiment

Wednesday, Nov. 30 12:45PM - 1:15PM Room: Learning Center - IN DPS

#### Participants

Johannes Haubold, MD, Essen, Germany (*Presenter*) Speaker, Siemens AG

#### PURPOSE

The aim was to establish virtual contrast enhancement in MRI with generative adversarial network (GAN) to reduce the amount of hepatobiliary contrast agent(CA) in a large animal model.

#### METHODS AND MATERIALS

120 exams were performed on a clinical 1.5 T MRI on six different occasions with 20 healthy Goettingen minipigs, 50% low-dose(ICM)(0.005mmol/kg, gadoxetate) and 50% with normal-dose(nCM)(0.025mmol/kg). These included arterial, portal venous, venous, and hepatobiliary contrast phases(20 and 30 minutes). One animal had to be excluded due to incomplete examinations. Three of the 19 animals were chosen at random and withheld for validation (18 examinations). The remaining 16 animals (96 examinations) were used to train a GAN for image-to-image conversion from ICM to nCM (vCM).Following that, ROI measurements in the abdominal aorta, inferior vena cava, portal vein, liver parenchyma, and autochthonous back muscles were obtained, and the vascular and parenchymal CNR was determined. In addition, the nCM and vCM data were shown in a visual-Turing-test(VTT) to three consultant radiologists, who had to assess whether they would have reported both sequences identical(pathologically consistent) and which sequence was the nCM sequence.

#### RESULTS

Pooled vascular ( $p<0.0001$ ) and parenchymal ( $p<0.0001$ ) CNR increased significantly from ICM to vCM and were not significantly different between vCM and nCM exams (vascular CNR (mean $\pm$ SD): ICM 17.6 $\pm$ 6.0, vCM 41.8 $\pm$ 9.7 and nCM 48.4 $\pm$ 12.2; parenchymal CNR (mean $\pm$ SD): ICM 21.6 $\pm$ 6.1, vCM 30.2 $\pm$ 7.0, nCM 32.4 $\pm$ 8.7). On median, the consultant radiologist indicated that the nCM and vCM sequences are pathologically consistent in 100 percent of the studies and correctly identified the normal-dose series in 59.5 percent of the instances.

#### CONCLUSION

s This feasibility study on healthy minipigs demonstrates that, GAN-based contrast enhancement can lower the amount of hepatobiliary CA on MRI by up to 80% while retaining equivalent image quality.

#### CLINICAL RELEVANCE/APPLICATION

GAN-based contrast enhancement can reduce costs and exposure of patients to gadolinium-based CA.

Printed on: 02/07/23



## Abstract Archives of the RSNA, 2022

W5B-SPIN-3

### Ultrasonic Texture Features as Radiomic Biomarkers for Screening Cardiac Remodeling and Dysfunction

Wednesday, Nov. 30 12:45PM - 1:15PM Room: Learning Center - IN DPS

#### Participants

Quincy Hathaway, PhD, (*Presenter*) Nothing to Disclose

#### PURPOSE

Point-of-care ultrasound (POCUS) workflows allow for rapid screening of cardiac abnormalities for guiding appropriate early triage and management. Morphometry and textural features (radiomics) in POCUS images could aid in the rapid automated expert-level screening of left ventricular (LV) myocardial remodeling and dysfunction without requiring any quantitative measurements.

#### METHODS AND MATERIALS

We developed Machine-learning (ML) models using three clinical cohorts that included 1,915 subjects: 1) an expert-annotated registry of POCUS (n=943, 80% training and 20% internal validation), 2) a prospective institutional POCUS cohort for external validation (n=275), and 3) a prospective external validation ML model on high-end ultrasound systems (n=484) for a head-to-head comparison of radiomics-based prediction with standardized quantitative measurements obtained during comprehensive echocardiography. With radiomic features from the parasternal long axis, we developed an explainable ML model and a direct image-derived black-box convolutional neural network (CNN) model. Echocardiography of wildtype (n=10) and *Lepr<sup>-/-</sup>* (n=8) mice were assessed longitudinally at 3 and 25 weeks, and radiomic features of importance were correlated with histopathological features of myocyte disarray and hypertrophy.

#### RESULTS

The receiver operating characteristic (ROC) area under the curve (AUC) for predicting expert annotated LV myocardial remodeling and dysfunction was higher for texture-based interpretable ML than the black-box, deep learning model (0.84, 0.73 and 0.75 vs. 0.53, 0.59, and 0.58;  $P=0.0001$  for internal and external POCUS and high-end ultrasound validation studies, respectively). Furthermore, the radiomics model predicted time-to-event outcomes in the external POCUS (100% vs. 82% survival,  $P=0.0001$ ) and high-end ultrasound studies (93% vs. 85% survival,  $P=0.0031$ ). *Lepr<sup>-/-</sup>* obese mice revealed LV remodeling through increased cardiomyocyte diameter (>20% increase, compared to controls) that positively correlated with two radiomics biomarkers of importance extracted from the interventricular septum ( $r = 0.79$  and  $0.90$ ,  $P=0.0001$ ), respectively.

#### CONCLUSION

s Texture-based ML models can be applied to cardiac POCUS to mirror an expert physician's ability to screen for the presence of LV myocardial remodeling and dysfunction without quantitative measurements.

#### CLINICAL RELEVANCE/APPLICATION

Traditional cardiac point-of-care ultrasound requires expert-level interpretation to assess clinical findings; our model can automate the interpretation of left ventricular structural and functional changes without quantitative measurements.

Printed on: 02/07/23



## Abstract Archives of the RSNA, 2022

W5B-SPIN-4

### Is It Time for Radiologists to Build AI? International Validation of Radiologist-trained AI Models to Identify Causes of Suboptimal Chest Radiographs

Wednesday, Nov. 30 12:45PM - 1:15PM Room: Learning Center - IN DPS

#### Participants

Giridhar Dasegowda, MBBS, Boston, MA (*Presenter*) Nothing to Disclose

#### PURPOSE

Generalizability of artificial intelligence (AI) models is a critical step towards its use in diverse clinical practices. Such efforts are hampered due to lack of data diversity in single study or country studies. Therefore, we assessed the performance of radiologist-trained AI models to differentiate suboptimal (sCXR) and optimal (oCXR) chest radiographs on a diverse multicenter data from 7 countries.

#### METHODS AND MATERIALS

Our IRB-approved study included 10,687 CXRs from adult patients (age > 18 years) from 7 countries (US, Brazil, Lebanon, India, Italy, Croatia, Iran: 14 imaging sites). The CXRs represented consecutive portable radiographs from each site. All de-identified CXRs were reviewed and annotated for the presence and causes of suboptimality on an AI server-based platform (CARPL AI). After annotation, all CXRs were uploaded into an AI building platform (Cognex Inc.) that allows non-programmers to build, train and test AI model for clinical applications. The platform allowed training (7508 CXRs: 3048 oCXR, 7508 sCXR from 7 sites, 2 country) and testing (3179 CXRs: 2490 sCXR, 689 oCXR from 7 other international sites) of 8 AI models for identifying various causes of sCXR. Receiver operating characteristics analyses were performed.

#### RESULTS

The AI models classified sCXR with missing apices, right CP angle and left CP angle lung with 98%, 96%, 98% accuracies, and AUCs (95% CI) of 0.84 (0.80-0.88), 0.92(0.89-0.95) and 0.93 (0.90-0.95), respectively. AI identified under- and over-exposure with 93% and 94% accuracy, with 0.93 AUC (95% CI 0.90-0.95) and 0.86 AUC (95% CI 0.82-0.90). The presence of low lung volume was identified with 92% accuracy, and 0.94 AUC (95% CI 0.91-0.96). Lungs obscured by overlying chin was identified with 95% accuracy and AUC of 0.94 (95% CI 0.91-0.96). The AI accuracy and AUC for patient rotation were 95% and 0.92 (95% CI 0.89-0.95), respectively.

#### CONCLUSION

s The eight AI models had high accuracy and generalizable performance for identifying suboptimal CXRs across 14 sites from 7 countries across four continents.

#### CLINICAL RELEVANCE/APPLICATION

International generalizability evaluation of AI models can help overcome lack of data diversity and representations from single country or site studies, which helps prove model trustworthiness.

Printed on: 02/07/23

## Abstract Archives of the RSNA, 2022

W5B-SPIN-5

### DeepLiverNet 2.0: A Deep Transformer Model for Liver Stiffness Classification Using T2-Weighted MRI Data

Wednesday, Nov. 30 12:45PM - 1:15PM Room: Learning Center - IN DPS

#### Participants

Redha Ali, PhD, Cincinnati, OH (*Presenter*) Nothing to Disclose

#### PURPOSE

To develop an improved version of DeepLiverNet 1.0 for categorically classifying the degree of liver stiffening using anatomic T2-weighted MRI in children and young adults with known or suspected pediatric chronic liver disease.

#### METHODS AND MATERIALS

Clinical axial T2-weighted fast spin-echo fat-saturated MRI images and 2D MR elastography liver stiffness measurements were clinically acquired from 1236 children and young adult patients with known or suspected pediatric chronic liver disease. We propose DeepLiverNet 2.0 in order to improve upon our prior work DeepLiverNet 1.0, that classified patients into one of two groups, no/mild liver stiffening <3 kPa or moderate/severe liver stiffening =3 kPa, which derived from MR elastography (Fig. 1). Specifically, we replaced the prior model's transfer learning block with the state-of-art Swin Transformer for latent imaging feature extraction. Swin Transformer is a hierarchical transformer implemented by shifting window partitions between consecutive self-attention layers. Such sliding window schema enhances efficiency by limiting self-attention computation to non-overlapping local windows while allowing for cross-window connection. Model performance was assessed using ten-fold cross-validation.

#### RESULTS

The proposed DeepLiverNet 2.0 model was able to categorically classify the severity of liver stiffening with an accuracy [mean  $\pm$  standard deviation]  $82.7 \pm 0.02\%$ , sensitivity  $73.3 \pm 4.0\%$ , specificity  $87.7 \pm 4.0\%$ , and AUC  $0.84 \pm 0.04$ . It outperformed the DeepLiverNet 1.0 model by a significant margin of 0.08 on AUC ( $0.76 \pm 0.01$ ;  $P < 0.0001$ ), as well as on accuracy ( $77.8 \pm 1.0\%$ ;  $P < 0.0001$ ), sensitivity ( $67.2 \pm 4.0\%$ ;  $P = 0.004$ ), and specificity ( $83.4 \pm 4.0\%$   $P = 0.03$ ).

#### CONCLUSION

By updating our previously developed feature extraction module using a state-of-the-art Swin Transformer, we have demonstrated that the proposed DeepLiverNet 2.0 model has better capability than DeepLiverNet 1.0 to stratify the severity of liver stiffening using anatomic T2-weighted MRI data in children and young adults with known or suspected pediatric chronic liver disease. Extensive model optimization is likely to further improve performance.

#### CLINICAL RELEVANCE/APPLICATION

Our DeepLiverNet 2.0 AI model can categorically classify the severity of liver stiffening using anatomic T2-weighted MRI in children and young adults. Model refinements and incorporation of clinical features may soon decrease the need for MR elastography.

Printed on: 02/07/23

## Abstract Archives of the RSNA, 2022

W5B-SP1R

### Interventional Wednesday Poster Discussions - B

Wednesday, Nov. 30 12:45PM - 1:15PM Room: Learning Center - IR DPS

#### Sub-Events

#### W5B-SP1R-1 Super-selective Trans-arterial Embolization of Intractable Hematuria

##### Participants

Jong Hyouk Yun, MD, PhD, Busan, Korea, Republic Of (*Presenter*) Nothing to Disclose

##### PURPOSE

To evaluate the effectiveness and clinical outcomes of super-selective transarterial embolization (TAE) for the management of intractable hematuria.

##### METHODS AND MATERIALS

20 patients with intractable hematuria who underwent super-selective TAE from April 2014 to July 2021 were included in this retrospective study. Embolization of vesical arteries was performed in all 20 patients using gelfoam particle. The patients were divided into two groups based on the cause of hematuria; radiation cystitis group and cancer bleeding group. Retrospective evaluation of technical and clinical success rates, hematuria grade, serum hemoglobin level (g/dL), complications and mortality rate was performed. The hematuria was graded as follows: grade I, no hematuria; grade II, microscopic hematuria; grade III, macroscopic hematuria without transfusion; grade IV, macroscopic hematuria with intermittent transfusion; and grade V, macroscopic hematuria with daily transfusion. The Wilcoxon signed-rank test for continuous variables was performed to compare the pre- and post-embolization hematuria grade and serum hemoglobin level within each group.

##### RESULTS

The technical success rate was 100% (20/20 patients). Overall clinical success rate was 85% (17/20 patients), 90% (10/11 patients) in radiation cystitis group and 77% (7/9 patients) in cancer bleeding group. On follow-up, overall mean serum hemoglobin level significantly improved ( $p < 0.001$ ), and also in radiation cystitis group ( $p < 0.001$ ) and cancer bleeding group ( $p < 0.004$ ). Hematuria grade also showed significant improvement in general ( $p < 0.001$ ), and also in radiation cystitis group ( $p < 0.004$ ) and cancer bleeding group ( $p < 0.017$ ). Minor complications were noted in 8/20 (40%) of the cases notably post embolization syndrome, which was well managed conservatively with analgesics and antipyretics. There was no major complication in both groups. Seven deaths occurred during the mean follow up period of  $9.6 \pm 31$  months, however none of the deaths were procedure-related.

##### CONCLUSION

Super-selective TAE seems to be a technically feasible and clinically effective treatment for intractable hematuria, both in radiation cystitis patients and cancer bleeding patients.

##### CLINICAL RELEVANCE/APPLICATION

There are several treatment options in intractable hematuria including peroral medication, intravesical agents endoscopic management and embolization. Super-selective TAE is a safe and effective treatment option to improve intractable hematuria, both in radiation cystitis patients and cancer bleeding patients.

#### W5B-SP1R-2 Radiomic Analysis of Post-treatment SPECT Imaging for Predicting Treatment Response Following Liver Radioembolization.

##### Participants

Kamil Bahit, (*Presenter*) Nothing to Disclose

##### PURPOSE

The distribution of yttrium-90 (Y90) microsphere deposition may predict outcomes following transarterial radioembolization (TARE) for the treatment of hepatocellular carcinoma (HCC). The purpose of this study was to quantify particle distribution on post-Y90 bremsstrahlung SPECT/CT scans using radiomic feature analysis and correlate findings with treatment response.

##### METHODS AND MATERIALS

Adult patients with HCC who underwent Y90 TARE were retrospectively enrolled from a single academic medical center. Overall survival and recurrence data were obtained following electronic medical record review. Pre-treatment contrast-enhanced CT or MR imaging was used to manually segment tumor volumes, which were fused with raw SPECT data from corresponding post-Y90 bremsstrahlung scans to generate a volume of interest (VOI). Radiomic features were then extracted from this VOI in 3D Slicer using the Radiomics module and modeled with tumor recurrence accounting for patient death using unsupervised (principal component analysis) and supervised (classification function analysis) parsimony modeling, along with a competing risk hazard regression analysis. Statistical significance was set at  $p < 0.05$ .

##### RESULTS

34 patients with HCC treated using Y90 TARE (mean age 73.6 +/- 10.4 years; 85.3% male; mean single largest dimension of tumor 5.9 cm) were enrolled between April 2017 and December 2020. Unsupervised principal component analysis of 96 unique radiomic features yielded a 3-component model wherein a single component best predicted post-Y90 recurrence (HR: 0.61, 95% CI [0.38, 0.96]). Subsequent classification functional analysis demonstrated that the radiomic feature "Large Area Emphasis," a measure of image heterogeneity, yielded the single strongest association with patient outcomes. For every 1 unit increase in Large Area Emphasis on post-Y90 SPECT/CT images, the hazard of tumor recurrence increased by 68% (HR:1.680, 95% CI [1.31, 2.16],  $p < 0.0001$ ).

## CONCLUSION

s Radiomic features derived from post-treatment bremsstrahlung SPECT/CT scans can predict outcomes following TARE for treatment of HCC, with greater heterogeneity in the distribution of Y90 activity associated with increased risk of tumor recurrence.

## CLINICAL RELEVANCE/APPLICATION

Radiomic analysis of post-treatment SPECT imaging can aid in identifying patients with a high risk for tumor recurrence.

## W5B-SPiR-6 Bronchial and Pulmonary Arteries Embolization in Patients with Lung Cancer: Long Term Results

### Participants

Antoine Khalil, MD, PhD, Paris, France (*Presenter*) Spouse, Employee, sanofi-aventis Group; Research Consultant, Becton, Dickinson and Company; Research Consultant, GEMS; Research Consultant, Medtronic plc

### PURPOSE

To analyze the bronchial (BAE) and pulmonary (PAE) arteries embolization outcomes in patients with lung cancer admitted to control or to prevent hemoptysis.

### METHODS AND MATERIALS

All consecutive patients with primary lung cancer (44 adenocarcinoma, 30 squamous cell carcinoma, 18 other non-small cell, and 7 small cell lung cancer) and referred in our center for BAE or PAE between 21st September 2015 and 31st December 2021 were included in this observational retrospective review. Inclusion criteria were lung cancer histologically proved with a TNM classification (9 Stage I,II; 33 stage III; 57 stage IV) and bronchial and/or pulmonary arteriography performed. Arteriography outcomes were reported after the first-line treatment of hemoptysis along with management of early (< 1 month) and late (> 1 month) recurrences of hemoptysis. Overall and hemoptysis-free survival were also reported.

### RESULTS

In the 99 (83 males, median age 64 y "Q1: 56.4; Q4:71.6) patients included in this cohort, 98 were treated to control hemoptysis and 3 to prevent massive hemoptysis in necrosis tumor before starting chemotherapy, immunotherapy or both. Two patients who were initially treated to prevent hemoptysis, later underwent embolization to treat non-massive hemoptysis. In 98 patients with hemoptysis, BAE alone was performed in first intention in 81 patients, PAE alone in 9 patients and both BAE PAE were performed in 8 patients. Immediate control of bleeding was achieved in 69/98 patients (70.4 %) in first-line treatment (57 with one session, 10 with two sessions and 2 with three sessions). A recurrence of hemoptysis was observed after the first month in 16/98 patients (16.3 %). The mean recurrence time after the first embolization was 284 days in these patients, with a median time of 169 days. The management of these late recurrences consisted in embolization in 7 patients (6 of them died due to the progression of disease) and exclusive medical treatment in 9 patients (2 died of massive hemoptysis and 2 due to the progression of the disease). Overall survival was 78.9 % at 1 month, 60.6 % at 6 months and 51 % at 12 months. Hemoptysis-free survival was 75.5 % at 1 month, 60.3 % at 6 months and 58.3 % at 12 months.

### CONCLUSION

s Thoracic arteries embolization (systemic and pulmonary arteries) is effective and safe for hemoptysis support in patients with broncho-pulmonary cancer. Hemoptysis control was reached for 69 patients (70.4%) in first line treatment.

### CLINICAL RELEVANCE/APPLICATION

Endovascular management of hemoptysis is safe and effective. The use of CT-angiography leads us to manage up to 10% of our patients with pulmonary artery embolization or stenting. In case of recurrence the re-embolisation could stop hemoptysis and prevent the death with massive hemoptysis

## W5B-SPiR-7 Racial and Ethnic Disparities Among Participants in Hepatocellular Carcinoma Clinical Studies Evaluating Transarterial Therapies

### Participants

Tushar Garg, MD, Baltimore, MD (*Presenter*) Conference Travel, Siemens Healthineers

### PURPOSE

Over the past two decades, there has been rapid development in the use of transarterial therapies (TA) for the management of hepatocellular carcinoma (HCC). The race and ethnic representation of participants in these clinical trials are poorly understood. To look at the current status of racial and ethnic representation in TA therapies trials for HCC, we evaluated completed studies for their reporting of race and ethnicity and compared it to the current United States HCC population.

### METHODS AND MATERIALS

The clinicaltrials.gov registry was queried in this cross-sectional study for completed US-based clinical studies evaluating the use of TA therapies for HCC in January 2022. The number of people affected with HCC by race and ethnicity was identified using the US population data from the US censuses and then combining it with the data collected from the SEER database. The underrepresentation (<1) and overrepresentation (>1) as the ratio of actual number of enrolled cases and the expected number of cases for each trial with 95% confidence intervals was estimated. Logistic regression and Pearson chi-square test were used for statistical analysis.

### RESULTS

27 (34 %) of the 79 eligible studies had appropriate data about the ethnic and racial composition of participants. There was no

27 (91.2%) of the 73 eligible studies had appropriate data about the ethnic and racial composition of participants. There was no statistical association between source of funding (NIH vs. other) and reporting of race and ethnicity ( $p=0.48$ ). White and Non-Hispanic or Latino participants were overrepresented with a ratio of 1.15 (95% CI, 1.08-1.30; 1591 observed vs. 1307 expected) and 1.35 (95% CI, 1.27-1.43; 937 observed vs. 703 expected), respectively. All the other racial and ethnic groups were underrepresented: Black participants with a ratio of 0.79 (95% CI, 0.53-1.06; 188 observed vs. 311 expected), Asian participants with a ratio of 0.55 (95% CI, 0.19-0.91; 73 observed vs. 172 expected), and Hispanic or Latino with a ratio of 0.30 (95% CI, 0.15-0.46; 71 observed vs. 291 expected).

## CONCLUSION

s In this cross-sectional study, racial and ethnic minorities were found to be underrepresented and poor reporting of these categories was seen in clinical trials.

## CLINICAL RELEVANCE/APPLICATION

When designing future studies appropriate representation of different racial and ethnic groups should be considered and detailed reporting of participants in different racial and ethnic groups should be provided.

## W5B-SP1R-8 Validation of an Ex vivo Renal Perfusion Model for Quantifying Microvascular Distribution of Embolic Microspheres

### Participants

Daniel Derrick, BS, San Antonio, TX (*Presenter*) Nothing to Disclose

## PURPOSE

An ex vivo model for preclinical characterization of microembolic agents and their microvascular distribution would be beneficial for guiding future in vivo studies. This study uses MicroCT analysis to evaluate the utility of an ex vivo perfusion model to assess the vascular distribution of LC beads (Boston Scientific) as a function of their diameter.

## METHODS AND MATERIALS

Porcine left kidneys were harvested from a local butcher, flushed with heparinized saline, and transported to the laboratory on ice. The renal artery was cannulated and pulsatile perfusion with normal saline was initiated. A subsegmental artery was selected using a microwire and the tissue was dyed using Evan's blue to visually identify the embolization zone for sample submission. LC beads (40-90  $\mu\text{m}$ ) suspended in Visipaque contrast solution were delivered to the target zone until stasis was observed under fluoroscopy. Pre- and post-embolic digital subtraction angiography (DSA) images were collected. In the same kidney, a second subsegmental arterial zone was embolized with LC beads (70-150  $\mu\text{m}$ ) via the methods described. Tissue segments of each embolization zone were submitted for MicroCT analysis. Percent opacification profile at various vessel diameters was collected to assess microembolic distribution pattern. Additional tissue segments were analyzed by pathology to assess tissue integrity and embolization pattern.

## RESULTS

Pre-embolization DSA demonstrated adequate arterial flow of contrast, cortical blushing, and venous return. Post-embolization DSA demonstrated no visualization of contrast flow to the embolized zone. MicroCT analysis of tissue samples embolized by 40-90  $\mu\text{m}$  beads demonstrated the highest percentage of opacified tissue in vessels 60-90  $\mu\text{m}$  in diameter (32.7%). Tissue embolized with beads 70-150  $\mu\text{m}$  demonstrated the highest percentage of opacified tissue in vessels 298-338  $\mu\text{m}$  (16.0%). Histology demonstrated well-preserved cortical and medullary tissue with 40-90  $\mu\text{m}$  beads embolizing up to 80% of arterial vessels and 70-150  $\mu\text{m}$  beads embolizing up to 70% of arterial vessels. Sphere edges marginated along the surface of the endothelium.

## CONCLUSION

s By demonstrating the difference in vascular distribution between two microsphere sizes, this study demonstrates the utility of an ex vivo perfusion model to assess the vascular distribution of microembolic agents based on sphere diameter.

## CLINICAL RELEVANCE/APPLICATION

This system provides an informative preclinical model which may provide benefits such as preserving resources and decreasing cost for interventional translational research. This model assesses the vascular distribution of microembolics and has the potential to contribute to additional innovations in future intravascular interventions.

Printed on: 02/07/23

## Abstract Archives of the RSNA, 2022

W5B-SP1R-1

### Super-selective Trans-arterial Embolization of Intractable Hematuria

Wednesday, Nov. 30 12:45PM - 1:15PM Room: Learning Center - IR DPS

#### Participants

Jong Hyouk Yun, MD, PhD, Busan, Korea, Republic Of (*Presenter*) Nothing to Disclose

#### PURPOSE

To evaluate the effectiveness and clinical outcomes of super-selective transarterial embolization (TAE) for the management of intractable hematuria.

#### METHODS AND MATERIALS

20 patients with intractable hematuria who underwent super-selective TAE from April 2014 to July 2021 were included in this retrospective study. Embolization of vesical arteries was performed in all 20 patients using gelfoam particle. The patients were divided into two groups based on the cause of hematuria; radiation cystitis group and cancer bleeding group. Retrospective evaluation of technical and clinical success rates, hematuria grade, serum hemoglobin level (g/dL), complications and mortality rate was performed. The hematuria was graded as follows: grade I, no hematuria; grade II, microscopic hematuria; grade III, macroscopic hematuria without transfusion; grade IV, macroscopic hematuria with intermittent transfusion; and grade V, macroscopic hematuria with daily transfusion. The Wilcoxon signed-rank test for continuous variables was performed to compare the pre- and post-embolization hematuria grade and serum hemoglobin level within each group.

#### RESULTS

The technical success rate was 100% (20/20 patients). Overall clinical success rate was 85% (17/20 patients), 90% (10/11 patients) in radiation cystitis group and 77% (7/9 patients) in cancer bleeding group. On follow-up, overall mean serum hemoglobin level significantly improved ( $p < 0.001$ ), and also in radiation cystitis group ( $p < 0.001$ ) and cancer bleeding group ( $p < 0.004$ ). Hematuria grade also showed significant improvement in general ( $p < 0.001$ ), and also in radiation cystitis group ( $p < 0.004$ ) and cancer bleeding group ( $p < 0.017$ ). Minor complications were noted in 8/20 (40%) of the cases notably post embolization syndrome, which was well managed conservatively with analgesics and antipyretics. There was no major complication in both groups. Seven deaths occurred during the mean follow up period of  $9.6 \pm 31$  months, however none of the deaths were procedure-related.

#### CONCLUSION

Super-selective TAE seems to be a technically feasible and clinically effective treatment for intractable hematuria, both in radiation cystitis patients and cancer bleeding patients.

#### CLINICAL RELEVANCE/APPLICATION

There are several treatment options in intractable hematuria including peroral medication, intravesical agents endoscopic management and embolization. Super-selective TAE is a safe and effective treatment option to improve intractable hematuria, both in radiation cystitis patients and cancer bleeding patients.

Printed on: 02/07/23

## Abstract Archives of the RSNA, 2022

W5B-SP1R-2

### **Radiomic Analysis of Post-treatment SPECT Imaging for Predicting Treatment Response Following Liver Radioembolization.**

Wednesday, Nov. 30 12:45PM - 1:15PM Room: Learning Center - IR DPS

#### **Participants**

Kamil Bahit, (*Presenter*) Nothing to Disclose

#### **PURPOSE**

The distribution of yttrium-90 (Y90) microsphere deposition may predict outcomes following transarterial radioembolization (TARE) for the treatment of hepatocellular carcinoma (HCC). The purpose of this study was to quantify particle distribution on post-Y90 bremsstrahlung SPECT/CT scans using radiomic feature analysis and correlate findings with treatment response.

#### **METHODS AND MATERIALS**

Adult patients with HCC who underwent Y90 TARE were retrospectively enrolled from a single academic medical center. Overall survival and recurrence data were obtained following electronic medical record review. Pre-treatment contrast-enhanced CT or MR imaging was used to manually segment tumor volumes, which were fused with raw SPECT data from corresponding post-Y90 bremsstrahlung scans to generate a volume of interest (VOI). Radiomic features were then extracted from this VOI in 3D Slicer using the Radiomics module and modeled with tumor recurrence accounting for patient death using unsupervised (principal component analysis) and supervised (classification function analysis) parsimony modeling, along with a competing risk hazard regression analysis. Statistical significance was set at  $p < 0.05$ .

#### **RESULTS**

34 patients with HCC treated using Y90 TARE (mean age 73.6 +/- 10.4 years; 85.3% male; mean single largest dimension of tumor 5.9 cm) were enrolled between April 2017 and December 2020. Unsupervised principal component analysis of 96 unique radiomic features yielded a 3-component model wherein a single component best predicted post-Y90 recurrence (HR: 0.61, 95% CI [0.38, 0.96]). Subsequent classification functional analysis demonstrated that the radiomic feature "Large Area Emphasis," a measure of image heterogeneity, yielded the single strongest association with patient outcomes. For every 1 unit increase in Large Area Emphasis on post-Y90 SPECT/CT images, the hazard of tumor recurrence increased by 68% (HR:1.680, 95% CI [1.31, 2.16],  $p < 0.0001$ ).

#### **CONCLUSION**

s Radiomic features derived from post-treatment bremsstrahlung SPECT/CT scans can predict outcomes following TARE for treatment of HCC, with greater heterogeneity in the distribution of Y90 activity associated with increased risk of tumor recurrence.

#### **CLINICAL RELEVANCE/APPLICATION**

Radiomic analysis of post-treatment SPECT imaging can aid in identifying patients with a high risk for tumor recurrence.

Printed on: 02/07/23

## Abstract Archives of the RSNA, 2022

W5B-SP1R-6

### Bronchial and Pulmonary Arteries Embolization in Patients with Lung Cancer: Long Term Results

Wednesday, Nov. 30 12:45PM - 1:15PM Room: Learning Center - IR DPS

#### Participants

Antoine Khalil, MD, PhD, Paris, France (*Presenter*) Spouse, Employee, sanofi-aventis Group; Research Consultant, Becton, Dickinson and Company; Research Consultant, GEMS; Research Consultant, Medtronic plc

#### PURPOSE

To analyze the bronchial (BAE) and pulmonary (PAE) arteries embolization outcomes in patients with lung cancer admitted to control or to prevent hemoptysis.

#### METHODS AND MATERIALS

All consecutive patients with primary lung cancer (44 adenocarcinoma, 30 squamous cell carcinoma, 18 other non-small cell, and 7 small cell lung cancer) and referred in our center for BAE or PAE between 21st September 2015 and 31st December 2021 were included in this observational retrospective review. Inclusion criteria were lung cancer histologically proved with a TNM classification (9 Stage I,II; 33 stage III; 57 stage IV) and bronchial and/or pulmonary arteriography performed. Arteriography outcomes were reported after the first-line treatment of hemoptysis along with management of early (< 1 month) and late (> 1 month) recurrences of hemoptysis. Overall and hemoptysis-free survival were also reported.

#### RESULTS

In the 99 (83 males, median age 64 y "Q1: 56.4; Q4:71.6) patients included in this cohort, 98 were treated to control hemoptysis and 3 to prevent massive hemoptysis in necrosis tumor before starting chemotherapy, immunotherapy or both. Two patients who were initially treated to prevent hemoptysis, later underwent embolization to treat non-massive hemoptysis. In 98 patients with hemoptysis, BAE alone was performed in first intention in 81 patients, PAE alone in 9 patients and both BAE PAE were performed in 8 patients. Immediate control of bleeding was achieved in 69/98 patients (70.4 %) in first-line treatment (57 with one session, 10 with two sessions and 2 with three sessions). A recurrence of hemoptysis was observed after the first month in 16/98 patients (16.3 %). The mean recurrence time after the first embolization was 284 days in these patients, with a median time of 169 days. The management of these late recurrences consisted in embolization in 7 patients (6 of them died due to the progression of disease) and exclusive medical treatment in 9 patients (2 died of massive hemoptysis and 2 due to the progression of the disease). Overall survival was 78.9 % at 1 month, 60.6 % at 6 months and 51 % at 12 months. Hemoptysis-free survival was 75.5 % at 1 month, 60.3 % at 6 months and 58.3 % at 12 months.

#### CONCLUSION

s Thoracic arteries embolization (systemic and pulmonary arteries) is effective and safe for hemoptysis support in patients with broncho-pulmonary cancer. Hemoptysis control was reached for 69 patients (70.4%) in first line treatment.

#### CLINICAL RELEVANCE/APPLICATION

Endovascular management of hemoptysis is safe and effective. The use of CT-angiography leads us to manage up to 10% of our patients with pulmonary artery embolization or stenting. In case of recurrence the re-embolisation could stop hemoptysis and prevent the death with massive hemoptysis

Printed on: 02/07/23

## Abstract Archives of the RSNA, 2022

W5B-SP1R-7

### Racial and Ethnic Disparities Among Participants in Hepatocellular Carcinoma Clinical Studies Evaluating Transarterial Therapies

Wednesday, Nov. 30 12:45PM - 1:15PM Room: Learning Center - IR DPS

#### Participants

Tushar Garg, MD, Baltimore, MD (*Presenter*) Conference Travel, Siemens Healthineers

#### PURPOSE

Over the past two decades, there has been rapid development in the use of transarterial therapies (TA) for the management of hepatocellular carcinoma (HCC). The race and ethnic representation of participants in these clinical trials are poorly understood. To look at the current status of racial and ethnic representation in TA therapies trials for HCC, we evaluated completed studies for their reporting of race and ethnicity and compared it to the current United States HCC population.

#### METHODS AND MATERIALS

The clinicaltrials.gov registry was queried in this cross-sectional study for completed US-based clinical studies evaluating the use of TA therapies for HCC in January 2022. The number of people affected with HCC by race and ethnicity was identified using the US population data from the US censuses and then combining it with the data collected from the SEER database. The underrepresentation (<1) and overrepresentation (>1) as the ratio of actual number of enrolled cases and the expected number of cases for each trial with 95% confidence intervals was estimated. Logistic regression and Pearson chi-square test were used for statistical analysis.

#### RESULTS

27 (34.2%) of the 79 eligible studies had appropriate data about the ethnic and racial composition of participants. There was no statistical association between source of funding (NIH vs. other) and reporting of race and ethnicity ( $p=0.48$ ). White and Non-Hispanic or Latino participants were overrepresented with a ratio of 1.15 (95% CI, 1.08-1.30; 1591 observed vs. 1307 expected) and 1.35 (95% CI, 1.27-1.43; 937 observed vs. 703 expected), respectively. All the other racial and ethnic groups were underrepresented: Black participants with a ratio of 0.79 (95% CI, 0.53-1.06; 188 observed vs. 311 expected), Asian participants with a ratio of 0.55 (95% CI, 0.19-0.91; 73 observed vs. 172 expected), and Hispanic or Latino with a ratio of 0.30 (95% CI, 0.15-0.46; 71 observed vs. 291 expected).

#### CONCLUSION

s In this cross-sectional study, racial and ethnic minorities were found to be underrepresented and poor reporting of these categories was seen in clinical trials.

#### CLINICAL RELEVANCE/APPLICATION

When designing future studies appropriate representation of different racial and ethnic groups should be considered and detailed reporting of participants in different racial and ethnic groups should be provided.

Printed on: 02/07/23

## Abstract Archives of the RSNA, 2022

W5B-SP1R-8

### Validation of an Ex vivo Renal Perfusion Model for Quantifying Microvascular Distribution of Embolic Microspheres

Wednesday, Nov. 30 12:45PM - 1:15PM Room: Learning Center - IR DPS

#### Participants

Daniel Derrick, BS, San Antonio, TX (*Presenter*) Nothing to Disclose

#### PURPOSE

An ex vivo model for preclinical characterization of microembolic agents and their microvascular distribution would be beneficial for guiding future in vivo studies. This study uses MicroCT analysis to evaluate the utility of an ex vivo perfusion model to assess the vascular distribution of LC beads (Boston Scientific) as a function of their diameter.

#### METHODS AND MATERIALS

Porcine left kidneys were harvested from a local butcher, flushed with heparinized saline, and transported to the laboratory on ice. The renal artery was cannulated and pulsatile perfusion with normal saline was initiated. A subsegmental artery was selected using a microwire and the tissue was dyed using Evan's blue to visually identify the embolization zone for sample submission. LC beads (40-90  $\mu\text{m}$ ) suspended in Visipaque contrast solution were delivered to the target zone until stasis was observed under fluoroscopy. Pre- and post-embolic digital subtraction angiography (DSA) images were collected. In the same kidney, a second subsegmental arterial zone was embolized with LC beads (70-150  $\mu\text{m}$ ) via the methods described. Tissue segments of each embolization zone were submitted for MicroCT analysis. Percent opacification profile at various vessel diameters was collected to assess microembolic distribution pattern. Additional tissue segments were analyzed by pathology to assess tissue integrity and embolization pattern.

#### RESULTS

Pre-embolization DSA demonstrated adequate arterial flow of contrast, cortical blushing, and venous return. Post-embolization DSA demonstrated no visualization of contrast flow to the embolized zone. MicroCT analysis of tissue samples embolized by 40-90  $\mu\text{m}$  beads demonstrated the highest percentage of opacified tissue in vessels 60-90  $\mu\text{m}$  in diameter (32.7%). Tissue embolized with beads 70-150  $\mu\text{m}$  demonstrated the highest percentage of opacified tissue in vessels 298-338  $\mu\text{m}$  (16.0%). Histology demonstrated well-preserved cortical and medullary tissue with 40-90  $\mu\text{m}$  beads embolizing up to 80% of arterial vessels and 70-150  $\mu\text{m}$  beads embolizing up to 70% of arterial vessels. Sphere edges marginated along the surface of the endothelium.

#### CONCLUSION

By demonstrating the difference in vascular distribution between two microsphere sizes, this study demonstrates the utility of an ex vivo perfusion model to assess the vascular distribution of microembolic agents based on sphere diameter.

#### CLINICAL RELEVANCE/APPLICATION

This system provides an informative preclinical model which may provide benefits such as preserving resources and decreasing cost for interventional translational research. This model assesses the vascular distribution of microembolics and has the potential to contribute to additional innovations in future intravascular interventions.

Printed on: 02/07/23

## Abstract Archives of the RSNA, 2022

W5B-SPMK

### Musculoskeletal Wednesday Poster Discussions - B

Wednesday, Nov. 30 12:45PM - 1:15PM Room: Learning Center - MK DPS

#### Sub-Events

#### **W5B-SPMK- Clinical Assessment Of Iterative Metal Artifact Reduction (imar) Technique in Reducing Metal Artifacts In Ct Examination Of Patients With Femoral Fracture After Metal Internal Fixation.**

##### Participants

Liu Xing, (*Presenter*) Nothing to Disclose

##### PURPOSE

To explore the clinical value of iMAR technique in reducing metal artifacts in CT examination of patients with femoral fracture after metal internal fixation.

##### METHODS AND MATERIALS

Thirty patients with femoral fracture after metal internal fixation were prospectively collected and examined by Siemens single-source dual-energy CT (SOMATOM Definition Edge CT). The original data were reconstructed respectively in iMAR iterative reconstruction group (Group A) and conventional iterative reconstruction group (Group B). The CT and SD values of the high density artifacts, low density artifacts, the surrounding soft tissue areas and the same layer of contralateral artifact-free affected areas in the two groups of images were measured respectively, and the difference between the two groups was compared by paired t-test. Two senior radiologists used the 5-component table (1~5 points, non-assessable ~ excellent) method to score the metal artifacts removal ability of the two groups. Mann-Whitney U test was used to compare the subjective scores and the consistency of the scores was analyzed by Kappa test.

##### RESULTS

There was no significant difference in CT values at the opposite side of the same layer without artifacts ( $P > 0.05$ ). The CT values in Group A were significantly reduced in the high density artifact area ( $p < 0.05$ ), while significantly increased in the low density artifact area ( $p < 0.05$ ) and were more closer to the CT values in the corresponding anatomical areas at the opposite side of the same layer. In terms of image noise, SD values in each measurement area of group A's images are lower than those of group B, and are significantly lower in high density areas and low density areas ( $p < 0.05$ ). In terms of subjective score, the results of two groups of image evaluation are excellent consistent (Kappa=0.906,  $p < 0.05$ ). The subjective score of group A is significantly higher than that of the control group, and the subjective score is increased by 1.6 (Group A:  $4.18 \pm 0.12$ , Group B:  $2.56 \pm 0.33$ ;  $P < 0.05$ ).

##### CONCLUSION

iMAR technique can significantly reduce metal artifacts around dental implants, correct CT values of surrounding tissues, help to accurately observe tissue structures around implants, improve image quality, which has great clinical application value.

##### CLINICAL RELEVANCE/APPLICATION

It is preferable to use iMAR technique in femoral fracture examinations as it allows better image quality and help to accurately observe tissue structures around implants.

#### **W5B-SPMK- Feasibility Study of Synthetic MRI in Shoulder Imaging**

3

##### Participants

Yabo Ni, Yinchuan, China (*Presenter*) Nothing to Disclose

##### PURPOSE

To investigate the feasibility of magnetic resonance image compilation in volunteers shoulder scanning.

##### METHODS AND MATERIALS

67 healthy volunteers were recruited and scanned on a GE Architect 3.0T scanner using conventional anatomical imaging sequences (T2W-FSE in oblique coronal view and PDW imaging in oblique sagittal view) and magnetic resonance image compilation (Magic) sequence (in both oblique coronal and sagittal view). Two researchers scored the image quality of conventional and Magic sequence. The signal intensity of humeral cephalomedullary cavity and deltoid muscle, standard deviation of air was measured on conventional T2WI images and PDW images. The T2 and PD values of the humerus head medullary cavity and deltoid muscle were measured by Magic T2 mapping and PD mapping image. At the same time, region of interest (ROI) was drawn at the air of the conventional sequence image, and the ROI signal intensity was taken as the noise intensity of the conventional sequence and corresponding Magic sequence. Signal noise ratio (SNR) and carrier to noise ratio (CNR) were calculated according to the formula  $SNR = SI_{\text{Humeral head pulp cavity}} / 0.66 / X_{\text{Humeral head pulp cavity}}$ ,  $CNR = (SI_{\text{deltoid muscle}} - SI_{\text{humeral head medullary cavity}}) / 0.66 / X_{\text{air}}$ . One-way ANOVA was used to compare the CNR and SNR, rank test was used to compare subjective scores of images, and Kappa test was used to evaluate the consistency of subjective scores between the two physicians.

## RESULTS

The image quality score of conventional sequence and Magic sequence was significantly different, the image quality score of conventional sequence at oblique coronal position  $4.08 \pm 0.32$  and oblique sagittal position  $4.03 \pm 0.34$  was higher than that of Magic sequence at oblique coronal position  $3.21 \pm 0.38$  and oblique sagittal position  $3.19 \pm 0.13$ , the difference was statistically significant ( $P < 0.05$ ), and Kappa values were 0.733 and 0.753 respectively. On oblique coronal T2WI images, SNR  $17.81 \pm 6.91$  and CNR  $-3.20 \pm 1.03$  of Magic sequence images were higher than those of conventional sequence SNR  $7.69 \pm 3.09$  and CNR  $-628.73 \pm 348.78$ , and the differences were statistically significant ( $P < 0.05$ ). In oblique sagittal PDW images, SNR  $27.11 \pm 1.54$  and CNR  $112.14 \pm 69.25$  of Magic sequence images were higher than those of conventional sequence SNR  $8.42 \pm 6.46$  and CNR  $-876.13 \pm 461.51$ , and the difference was statistically significant ( $P < 0.05$ ).

## CONCLUSION

The quality of the shoulder image obtained by Magic sequence is similar to that obtained by conventional sequence scan, which can be used for MRI shoulder scanning.

## CLINICAL RELEVANCE/APPLICATION

Synthetic MRI applied to the shoulder can obtain more quantitative parameters for quantitative diagnosis of the disease.

## W5B-SPMK- An Investigation of 2D Magnetic Resonance Shoulder Imaging Using Deep Learning (DL) based Algorithm

Participants

Jing Liu, (*Presenter*) Nothing to Disclose

## PURPOSE

To investigate the feasibility of deep learning-based MRI (DL-MRI) in the application of 2D shoulder imaging and compare its performance with conventional MR imaging (Non-DL MRI).

## METHODS AND MATERIALS

Non-DL MRI and DL-MRI of 2D shoulder imaging (including Axial and Coronal Proton density (PD) weighted imaging (WI), Axial and Coronal T1WI and Sagittal T2WI) were performed for 51 patients (21M30F, mean age:  $54 \pm 16$ ). Three radiologists assessed image quality according to a five-point scale. And the lesions assessment was conducted by two radiologists independently. A Kendall W test was performed to assess interobserver agreement of the image quality scores. A nonparametric test (Wilcoxon test) was performed to compare the image quality. For lesion diagnosis, the interobserver and interstudy agreement were evaluated by kappa analysis. Paired t-tests were conducted for SNR and |CNR| comparison. A survey was conducted in 400 patients with DL-MRI among 20 radiologists.

## RESULTS

The mean scan time for shoulder DL-MRI (6min1s) was nearly 50% decrease compared with that for Non-DL MRI (11min25sec). The image quality was higher in both PDWI and T2WI of DL-MRI compared with those of Non-DL MRI, and the image quality showed comparable in T1WI between DL-MRI and Non-DL MRI. Good interobserver agreement was found for image quality of all the MR sequences on both DL-MRI (Kendall W values range from 0.588 to 0.902,  $P < 0.001$ ) and Non-DL MRI (Kendall W values range from 0.751 to 0.865,  $P < 0.001$ ). Both the SNRs and |CNR| were significantly higher in Ax PDWI, Cor PDWI, and Sag T2WI of DL-MRI by the paired t-test. The SNRs and |CNR| were slightly higher in Ax T1WI of DL-MRI, and comparable in Cor T1WI of DL-MRI with comparison of Non-DL MRI. High interobserver agreements for all the lesions in Non-DL MRI and DL-MRI (Table 4, kappa value = 0.913 to 1.000,  $P < 0.001$ ) and interstudy agreements of all lesions' assessment were observed (kappa value = 1.000, with  $P < 0.001$  in all cases). The results of satisfaction survey obtained 5 scores for both image quality and the diagnostic demands meets among all the radiologists.

## CONCLUSION

DL-MRI shoulder imaging can greatly reduce the scan time, while improve imaging quality of PDWI and T2WI compared to Non-DL MRI. It could be a clinical routine with greatly improved work efficiency in future.

## CLINICAL RELEVANCE/APPLICATION

DL-MRI shoulder imaging can greatly reduce the scan time, while improve imaging quality of PDWI and T2WI compared to Non-DL MRI.

Printed on: 02/07/23

## Abstract Archives of the RSNA, 2022

W5B-SPMK-1

### Clinical Assessment Of Iterative Metal Artifact Reduction (imar) Technique in Reducing Metal Artifacts In Ct Examination Of Patients With Femoral Fracture After Metal Internal Fixation.

Wednesday, Nov. 30 12:45PM - 1:15PM Room: Learning Center - MK DPS

#### Participants

Liu Xing, (*Presenter*) Nothing to Disclose

#### PURPOSE

To explore the clinical value of iMAR technique in reducing metal artifacts in CT examination of patients with femoral fracture after metal internal fixation.

#### METHODS AND MATERIALS

Thirty patients with femoral fracture after metal internal fixation were prospectively collected and examined by Siemens single-source dual-energy CT (SOMATOM Definition Edge CT). The original data were reconstructed respectively in iMAR iterative reconstruction group (Group A) and conventional iterative reconstruction group (Group B). The CT and SD values of the high density artifacts, low density artifacts, the surrounding soft tissue areas and the same layer of contralateral artifact-free affected areas in the two groups of images were measured respectively, and the difference between the two groups was compared by paired t-test. Two senior radiologists used the 5-component table (1~5 points, non-assessable ~ excellent) method to score the metal artifacts removal ability of the two groups. Mann-Whitney U test was used to compare the subjective scores and the consistency of the scores was analyzed by Kappa test.

#### RESULTS

There was no significant difference in CT values at the opposite side of the same layer without artifacts ( $P > 0.05$ ). The CT values in Group A were significantly reduced in the high density artifact area ( $p < 0.05$ ), while significantly increased in the low density artifact area ( $p < 0.05$ ) and were more closer to the CT values in the corresponding anatomical areas at the opposite side of the same layer. In terms of image noise, SD values in each measurement area of group A's images are lower than those of group B, and are significantly lower in high density areas and low density areas ( $p < 0.05$ ). In terms of subjective score, the results of two groups of image evaluation are excellent consistent (Kappa=0.906,  $p < 0.05$ ). The subjective score of group A is significantly higher than that of the control group, and the subjective score is increased by 1.6 (Group A:  $4.18 \pm 0.12$ , Group B:  $2.56 \pm 0.33$ ;  $P < 0.05$ ).

#### CONCLUSION

iMAR technique can significantly reduce metal artifacts around dental implants, correct CT values of surrounding tissues, help to accurately observe tissue structures around implants, improve image quality, which has great clinical application value.

#### CLINICAL RELEVANCE/APPLICATION

It is preferable to use iMAR technique in femoral fracture examinations as it allows better image quality and help to accurately observe tissue structures around implants.

Printed on: 02/07/23

## Abstract Archives of the RSNA, 2022

W5B-SPMK-3

### Feasibility Study of Synthetic MRI in Shoulder Imaging

Wednesday, Nov. 30 12:45PM - 1:15PM Room: Learning Center - MK DPS

#### Participants

Yabo Ni, Yinchuan, China (*Presenter*) Nothing to Disclose

#### PURPOSE

To investigate the feasibility of magnetic resonance image compilation in volunteers shoulder scanning.

#### METHODS AND MATERIALS

67 healthy volunteers were recruited and scanned on a GE Architect 3.0T scanner using conventional anatomical imaging sequences (T2W-FSE in oblique coronal view and PDW imaging in oblique sagittal view) and magnetic resonance image compilation (Magic) sequence (in both oblique coronal and sagittal view). Two researchers scored the image quality of conventional and Magic sequence. The signal intensity of humeral cephalomedullary cavity and deltoid muscle, standard deviation of air was measured on conventional T2WI images and PDW images. The T2 and PD values of the humerus head medullary cavity and deltoid muscle were measured by Magic T2 mapping and PD mapping image. At the same time, region of interest(ROI) was drawn at the air of the conventional sequence image, and the ROI signal intensity was taken as the noise intensity of the conventional sequence and corresponding Magic sequence. Signal noise ratio (SNR) and carrier to noise ratio (CNR) were calculated according to the formula  $SNR = SI_{\text{Humeral head pulp cavity}} / 0.66 / X_{\text{Humeral head pulp cavity}}$ ,  $CNR = (SI_{\text{deltoid muscle}} - SI_{\text{humeral head medullary cavity}}) / 0.66 / X_{\text{air}}$ . One-way ANOVA was used to compare the CNR and SNR, rank test was used to compare subjective scores of images, and Kappa test was used to evaluate the consistency of subjective scores between the two physicians.

#### RESULTS

The image quality score of conventional sequence and Magic sequence was significantly different, the image quality score of conventional sequence at oblique coronal position  $4.08 \pm 0.32$  and oblique sagittal position  $4.03 \pm 0.34$  was higher than that of Magic sequence at oblique coronal position  $3.21 \pm 0.38$  and oblique sagittal position  $3.19 \pm 0.13$ , the difference was statistically significant ( $P < 0.05$ ), and Kappa values were 0.733 and 0.753 respectively. On oblique coronal T2WI images, SNR  $17.81 \pm 6.91$  and CNR  $-3.20 \pm 1.03$  of Magic sequence images were higher than those of conventional sequence SNR  $7.69 \pm 3.09$  and CNR  $-628.73 \pm 348.78$ , and the differences were statistically significant ( $P < 0.05$ ). In oblique sagittal PDW images, SNR  $27.11 \pm 1.54$  and CNR  $112.14 \pm 69.25$  of Magic sequence images were higher than those of conventional sequence SNR  $8.42 \pm 6.46$  and CNR  $-876.13 \pm 461.51$ , and the difference was statistically significant ( $P < 0.05$ ).

#### CONCLUSION

s The quality of the shoulder image obtained by Magic sequence is similar to that obtained by conventional sequence scan, which can be used for MRI shoulder scanning.

#### CLINICAL RELEVANCE/APPLICATION

Synthetic MRI applied to the shoulder can obtain more quantitative parameters for quantitative diagnosis of the disease.

Printed on: 02/07/23

## Abstract Archives of the RSNA, 2022

W5B-SPMK-4

### An Investigation of 2D Magnetic Resonance Shoulder Imaging Using Deep Learning (DL) based Algorithm

Wednesday, Nov. 30 12:45PM - 1:15PM Room: Learning Center - MK DPS

#### Participants

Jing Liu, (*Presenter*) Nothing to Disclose

#### PURPOSE

To investigate the feasibility of deep learning-based MRI (DL-MRI) in the application of 2D shoulder imaging and compare its performance with conventional MR imaging (Non-DL MRI).

#### METHODS AND MATERIALS

Non-DL MRI and DL-MRI of 2D shoulder imaging (including Axial and Coronal Proton density (PD) weighted imaging (WI), Axial and Coronal T1WI and Sagittal T2WI) were performed for 51 patients (21M30F, mean age: 54±16). Three radiologists assessed image quality according to a five-point scale. And the lesions assessment was conducted by two radiologists independently. A Kendall W test was performed to assess interobserver agreement of the image quality scores. A nonparametric test (Wilcoxon test) was performed to compare the image quality. For lesion diagnosis, the interobserver and interstudy agreement were evaluated by kappa analysis. Paired t-tests were conducted for SNR and |CNR| comparison. A survey was conducted in 400 patients with DL-MRI among 20 radiologists.

#### RESULTS

The mean scan time for shoulder DL-MRI (6min1s) was nearly 50% decrease compared with that for Non-DL MRI (11min25sec). The image quality was higher in both PDWI and T2WI of DL-MRI compared with those of Non-DL MRI, and the image quality showed comparable in T1WI between DL-MRI and Non-DL MRI. Good interobserver agreement was found for image quality of all the MR sequences on both DL-MRI (Kendall W values range from 0.588 to 0.902,  $P < 0.001$ ) and Non-DL MRI (Kendall W values range from 0.751 to 0.865,  $P < 0.001$ ). Both the SNRs and |CNR| were significantly higher in Ax PDWI, Cor PDWI, and Sag T2WI of DL-MRI by the paired t-test. The SNRs and |CNR| were slightly higher in Ax T1WI of DL-MRI, and comparable in Cor T1WI of DL-MRI with comparison of Non-DL MRI. High interobserver agreements for all the lesions in Non-DL MRI and DL-MRI (Table 4, kappa value = 0.913 to 1.000,  $P < 0.001$ ) and interstudy agreements of all lesions' assessment were observed (kappa value = 1.000, with  $P < 0.001$  in all cases). The results of satisfaction survey obtained 5 scores for both image quality and the diagnostic demands meets among all the radiologists.

#### CONCLUSION

s DL-MRI shoulder imaging can greatly reduce the scan time, while improve imaging quality of PDWI and T2WI compared to Non-DL MRI. It could be a clinical routine with greatly improved work efficiency in future.

#### CLINICAL RELEVANCE/APPLICATION

DL-MRI shoulder imaging can greatly reduce the scan time, while improve imaging quality of PDWI and T2WI compared to Non-DL MRI.

Printed on: 02/07/23



## Abstract Archives of the RSNA, 2022

W5B-SPMS

### Multisystem Wednesday Poster Discussion - B

Wednesday, Nov. 30 12:45PM - 1:15PM Room: Learning Center - MS DPS

#### Sub-Events

#### W5B-SPMS- Learning the Assessment of Tumor Response Categories from Structured Radiology Reports<sup>1</sup>

Participants

Matthias Fink, MD, BSc, Heidelberg, Germany (*Presenter*) Nothing to Disclose

#### PURPOSE

To use the data mining advantages of structured oncology reports (SOR) to train a deep NLP model aimed at rapid tumor response category (TRC) classification of patients from free-text oncology reports (FTOR), and to compare its performance against three conventional NLP algorithms and a human baseline.

#### METHODS AND MATERIALS

In this retrospective study, databases of three independent radiology departments were queried for SOR and FTOR from 03/2018-08/2021. An automated data mining and curation pipeline was developed to extract RECIST-related TRCs from SOR for ground truth definition. We trained Google's deep learning NLP algorithm BERT and three feature-rich NLP algorithms on automatically extracted and labelled SOR to predict the TRCs progressive disease (PD), stable disease (SD), partial response (PR), and complete response (CR) in FTOR. Models' F1 scores were compared against seven human annotators (two radiologists, two medical students, and three radiology technologist students) with a different level of radiological expertise. Lexical and semantic analyses of the reports were conducted to investigate human and model performance on FTOR.

#### RESULTS

Oncologic findings and TRCs were accurately mined from 9653/12833 (75.2%) queried SOR, yielding oncologic reports from 10455 patients (mean age, 60 years  $\pm$  14; 5303 women) that met inclusion criteria. On 802 FTOR, BERT achieved better TRC classification results (F1, 0.70; 95% CI: 0.68, 0.73) than the best-performing NLP reference Linear-SVC (F1, 0.63; 95% CI: 0.61, 0.66) and radiology technologist students (F1, 0.65; 95% CI: 0.63, 0.67), had similar performance to medical students (F1, 0.73; 95% CI: 0.72, 0.75), but was inferior to radiologists (F1, 0.79; 95% CI: 0.78, 0.81). Lexical complexity and semantic ambiguities in FTOR influenced human and model performance, revealing maximum F1-drops of -0.17 and -0.19, respectively.

#### CONCLUSION

Data mining of SOR enabled an automated and accurate labeling approach to train a deep learning NLP model for ascertaining tumor response categories in free-text reports. The trained NLP model reached novice medical but not radiologists' performance in curating oncologic outcomes from radiology FTOR.

#### CLINICAL RELEVANCE/APPLICATION

Using structured radiology reports as a "science-ready" data resource for machine learning purposes without prior manual annotation effort by expert readers appears to be feasible. The developed NLP model may be able to extract clinically relevant oncologic end points from large volumes of longitudinal free text reports and offers a potential advantage as an automated clinical decision-support tool for patients referred for multidisciplinary tumor board assessment.

Printed on: 02/07/23

## Abstract Archives of the RSNA, 2022

W5B-SPMS-1

### Learning the Assessment of Tumor Response Categories from Structured Radiology Reports

Wednesday, Nov. 30 12:45PM - 1:15PM Room: Learning Center - MS DPS

#### Participants

Matthias Fink, MD, BSc, Heidelberg, Germany (*Presenter*) Nothing to Disclose

#### PURPOSE

To use the data mining advantages of structured oncology reports (SOR) to train a deep NLP model aimed at rapid tumor response category (TRC) classification of patients from free-text oncology reports (FTOR), and to compare its performance against three conventional NLP algorithms and a human baseline.

#### METHODS AND MATERIALS

In this retrospective study, databases of three independent radiology departments were queried for SOR and FTOR from 03/2018-08/2021. An automated data mining and curation pipeline was developed to extract RECIST-related TRCs from SOR for ground truth definition. We trained Google's deep learning NLP algorithm BERT and three feature-rich NLP algorithms on automatically extracted and labelled SOR to predict the TRCs progressive disease (PD), stable disease (SD), partial response (PR), and complete response (CR) in FTOR. Models' F1 scores were compared against seven human annotators (two radiologists, two medical students, and three radiology technologist students) with a different level of radiological expertise. Lexical and semantic analyses of the reports were conducted to investigate human and model performance on FTOR.

#### RESULTS

Oncologic findings and TRCs were accurately mined from 9653/12833 (75.2%) queried SOR, yielding oncologic reports from 10455 patients (mean age, 60 years  $\pm$  14; 5303 women) that met inclusion criteria. On 802 FTOR, BERT achieved better TRC classification results (F1, 0.70; 95% CI: 0.68, 0.73) than the best-performing NLP reference Linear-SVC (F1, 0.63; 95% CI: 0.61, 0.66) and radiology technologist students (F1, 0.65; 95% CI: 0.63, 0.67), had similar performance to medical students (F1, 0.73; 95% CI: 0.72, 0.75), but was inferior to radiologists (F1, 0.79; 95% CI: 0.78, 0.81). Lexical complexity and semantic ambiguities in FTOR influenced human and model performance, revealing maximum F1-drops of -0.17 and -0.19, respectively.

#### CONCLUSION

Data mining of SOR enabled an automated and accurate labeling approach to train a deep learning NLP model for ascertaining tumor response categories in free-text reports. The trained NLP model reached novice medical but not radiologists' performance in curating oncologic outcomes from radiology FTOR.

#### CLINICAL RELEVANCE/APPLICATION

Using structured radiology reports as a "science-ready" data resource for machine learning purposes without prior manual annotation effort by expert readers appears to be feasible. The developed NLP model may be able to extract clinically relevant oncologic end points from large volumes of longitudinal free text reports and offers a potential advantage as an automated clinical decision-support tool for patients referred for multidisciplinary tumor board assessment.

Printed on: 02/07/23

## Abstract Archives of the RSNA, 2022

W5B-SPNMMI

### Nuclear Medicine/Molecular Imaging Wednesday Poster Discussion - B

Wednesday, Nov. 30 12:45PM - 1:15PM Room: Learning Center - NMMI DPS

#### Participants

Mary Ellen Koran, MD, PhD, Nashville, TN (*Moderator*) Nothing to Disclose  
Mary Ellen Koran, MD, PhD, Nashville, TN (*Moderator*) Nothing to Disclose  
Kevin P. Banks, MD, San Antonio, TX (*Moderator*) Nothing to Disclose  
Kevin P. Banks, MD, San Antonio, TX (*Moderator*) Nothing to Disclose

#### Sub-Events

#### W5B-SPNMMI-1 Utility of PET/MR Imaging for Therapy Response Assessment of Patients With Ewing Sarcoma: Preliminary Results

#### Participants

Johannes Grueneisen, Essen, Germany (*Presenter*) Nothing to Disclose

#### PURPOSE

To evaluate the clinical applicability of integrated PET/MR imaging for staging and monitoring the effectiveness of primary systemic treatment in Ewing sarcoma patients.

#### METHODS AND MATERIALS

A total of 11 juvenile patients ( $17.9 \pm 3.3$  years) with confirmed Ewing sarcoma, scheduled for induction polychemotherapy according to the VIDE-regimen, were prospectively enrolled for a PET/MR examination before, during and after the end of neoadjuvant therapy. Two experienced physicians analysed the imaging datasets. They were asked to identify all tumor lesions and to define treatment response according to the RECIST 1.1 and PERCIST criteria in all three examinations of each patient. Histopathological analysis after biopsy/surgery and follow-up imaging served as the reference standard.

#### RESULTS

In 7 of the 11 patients the primary tumor arose in the bone and in the remaining 4 patients in soft tissue. In 8 patients lymph node and/or distant metastases were detected at initial diagnosis. For RECIST analysis, the mean sum of the longest diameters was  $97.2 \pm 35.2$  mm at the baseline examination,  $85.4 \pm 28.1$  mm (-12.1%) at the first follow-up and  $68.1 \pm 26.9$  mm (-29.9%) at the second follow-up scan. Mean activity (SUV<sub>peak</sub>) of the hottest tumor lesions amounted to:  $6.6 \pm 2.5$  at baseline,  $3.6 \pm 2.3$  (-45.5%) at the first follow-up and to  $2.8 \pm 1.9$  (-57.6%) at the second follow-up examination. According to the reference standard, a total of 3 patients achieved complete response (CR), 6 patients partial response (PR), whereas one patient showed stable disease (SD) and another patient progressive disease (PD). RECIST 1.1 categorized the response to treatment in 5/11 patients correctly and showed a tendency to underestimate the response to treatment in the remaining 6 patients. PERCIST defined response to treatment in 9/11 patients correctly, and misclassified 2 patients with a PR as CR.

#### CONCLUSION

These preliminary results demonstrate a good diagnostic performance of integrated 18F-FDG PET/MRI for primary staging of patients with Ewing sarcoma and underline potential advantages of PERCIST over RECIST for assessing treatment effects of induction chemotherapy.

#### CLINICAL RELEVANCE/APPLICATION

PET/MRI may serve as a valuable imaging tool for initial evaluation and response assessment of juvenile patients with Ewing sarcoma, combining morphological and metabolic information, accompanied by a reasonable radiation dose for the patient.

#### W5B-SPNMMI-2 Development and External Validation of a Nomogram Based on 18F-FDG to Identify the Cancer-associated Cachexia

#### Participants

Yang Jiang, PhD, MD, (*Presenter*) Nothing to Disclose

#### PURPOSE

This study attempted to develop and validate a combined nomogram incorporating clinical information and PET features for identifying the risk of cancer-associated cachexia.

#### METHODS AND MATERIALS

FDG PET/CT data from 676 cancer patients were analyzed retrospectively. Patients were divided into a development cohort ( $n = 390$ ) and an external validation cohort ( $n = 286$ ) according to different medical centers. Results of the clinical laboratory tests for metabolic levels and organ and tissue-specific FDG uptake obtained from the cachexia and non-cachexia groups were compared statistically. Logistic regression analysis was performed to identify independent variables associated with cachexia in the

development cohort for generating the nomogram. The performance of the nomogram was tested using the data from an external validation cohort and evaluated by area under the receiver operating characteristic curve (AUC), calibration curve, and decision curves.

## RESULTS

Based on the data from the development cohort of 390 patients (mean age, 61 years  $\pm$  12 [standard deviation]; 221 men) and a validation cohort of 286 patients (54  $\pm$  14; 135 men), it is found that age (odds ratio [OR], 2.285; 95% confidence interval [CI]: 1.387, 3.765;  $P = 0.001$ ), BMI (OR, 3.486; 95% CI: 1.718, 7.072;  $P = 0.001$ ), hemoglobin (OR, 1.871; 95% CI: 1.120, 3.126;  $P = 0.02$ ), maximum SUV of the liver (OR, 2.316; 95% CI: 1.422, 3.770;  $P = 0.001$ ), and minimum SUV of the subcutaneous fat (OR, 2.991; 95% CI: 1.702, 5.259;  $P = 0.001$ ) were independently associated with cachexia. The nomogram incorporating these variables showed great discrimination (AUC = 0.763, 95% CI: 0.706-0.821), calibration and clinical net benefit in the external validation cohort.

## CONCLUSION

This study developed and externally validated a PET-based nomogram incorporating age, BMI, hemoglobin, maximum SUV of the liver, and average SUV of subcutaneous fat.

## CLINICAL RELEVANCE/APPLICATION

Nuclear medicine physicians can help identify patients with high-risk cancer-related cachexia using the nomogram described in this study when reading patients' PET/CT images.

## W5B-SPNMMI-3 A Novel Self-Assembling High Performance Organic Nanofluorophore for Intraoperative NIR-II Image-Guided Tumor Resection

Participants

Eric Tanifum, PhD, Houston, TX (*Presenter*) Consultant, Alzeca Biosciences, LLC; Stockholder, Alzeca Biosciences, LLC

## PURPOSE

Oral cavity cancers are in the top 10 most common solid tumors worldwide. Surgery with adequate resection margins lead to higher survival and a reduction in local recurrence, but adequate resections are only achieved in 15-26% of cases due to the complex anatomy of the oral cavity and the lack of intraoperative guidance. Success with indocyanine green (ICG) have established the value of NIR imaging in precision tumor resection. NIR-II dyes which can selectively target solid tumors are highly desirable due to greater tissue penetration depth in the NIR-II window. We present a novel organic NIR-II dye XW-03-66 which self-assembles into nanoclusters in solution and selectively accumulates in mouse tumor models of oral cancer following intravenous administration, via the enhanced permeation and retention (EPR) effect

## METHODS AND MATERIALS

XW-03-66 was synthesized from commercially available materials and the structure confirmed by NMR and MALDI. Spectroscopic data were collected using a UV-1600PC spectrophotometer and a NS3 NanoSpectralyzer. Cluster size was determined by Oblique Illumination Microscopy (OIM) and Atomic Force Microscopy (AFM). NIR-II imaging was conducted on a purpose-built instrument. MOC2 and MEER tumor models were used to assess intraoperative tumor resection procedures. Mice were administered a dose of 1 mg/Kg of the agent and surgery was performed 72 h post-injection. Imaging parameters: 470 mA, 500 ms/frame. Images processed and analyzed using ImageJ software.

## RESULTS

XW-03-66 has an absorption maximum at 796 nm and a NIR-II fluorescence maximum 1018 nm. OIM and AFM analyses show that it self-assembles into nanoscale mesoscopic solute-rich clusters with a mean hydrodynamic diameter of 80 nm. Pharmacokinetic studies in nude mice ( $n = 4$ ), show that it has a long systemic circulation half-life (6.5 h), and is cleared via the mononuclear phagocytic system (MPS). Long circulation allows the agent to traverse leaky vasculature and accumulate in solid tumors, enabling NIR-II image-guided tumor resection with adequate margins.

## CONCLUSION

XW-03-66 self assembles into mesoscopic solute-rich clusters in aqueous media. Following intravenous administration, it passively accumulates in two different mouse tumor model of oral cancer by the EPR effect, enabling intraoperative NIR-II image-guided tumor resection.

## CLINICAL RELEVANCE/APPLICATION

Reports show significant advances in clinical instrumentation for fluorescence image-guided surgeries. NIR-II dyes such as XW-03-66 which specifically label solid tumors will find broad applications in intraoperative image-guided tumor surgeries

Printed on: 02/07/23

## Abstract Archives of the RSNA, 2022

W5B-SPNMMI-1

### Utility of PET/MR Imaging for Therapy Response Assessment of Patients With Ewing Sarcoma: Preliminary Results

Wednesday, Nov. 30 12:45PM - 1:15PM Room: Learning Center - NMMI DPS

#### Participants

Johannes Grueneisen, Essen, Germany (*Presenter*) Nothing to Disclose

#### PURPOSE

To evaluate the clinical applicability of integrated PET/MR imaging for staging and monitoring the effectiveness of primary systemic treatment in Ewing sarcoma patients.

#### METHODS AND MATERIALS

A total of 11 juvenile patients ( $17.9 \pm 3.3$  years) with confirmed Ewing sarcoma, scheduled for induction polychemotherapy according to the VIDE-regimen, were prospectively enrolled for a PET/MR examination before, during and after the end of neoadjuvant therapy. Two experienced physicians analysed the imaging datasets. They were asked to identify all tumor lesions and to define treatment response according to the RECIST 1.1 and PERCIST criteria in all three examinations of each patient. Histopathological analysis after biopsy/surgery and follow-up imaging served as the reference standard.

#### RESULTS

In 7 of the 11 patients the primary tumor arose in the bone and in the remaining 4 patients in soft tissue. In 8 patients lymph node and/or distant metastases were detected at initial diagnosis. For RECIST analysis, the mean sum of the longest diameters was  $97.2 \pm 35.2$  mm at the baseline examination,  $85.4 \pm 28.1$  mm (-12.1%) at the first follow-up and  $68.1 \pm 26.9$  mm (-29.9%) at the second follow-up scan. Mean activity (SUV<sub>peak</sub>) of the hottest tumor lesions amounted to:  $6.6 \pm 2.5$  at baseline,  $3.6 \pm 2.3$  (-45.5%) at the first follow-up and to  $2.8 \pm 1.9$  (-57.6%) at the second follow-up examination. According to the reference standard, a total of 3 patients achieved complete response (CR), 6 patients partial response (PR), whereas one patient showed stable disease (SD) and another patient progressive disease (PD). RECIST 1.1 categorized the response to treatment in 5/11 patients correctly and showed a tendency to underestimate the response to treatment in the remaining 6 patients. PERCIST defined response to treatment in 9/11 patients correctly, and misclassified 2 patients with a PR as CR.

#### CONCLUSION

These preliminary results demonstrate a good diagnostic performance of integrated 18F-FDG PET/MRI for primary staging of patients with Ewing sarcoma and underline potential advantages of PERCIST over RECIST for assessing treatment effects of induction chemotherapy.

#### CLINICAL RELEVANCE/APPLICATION

PET/MRI may serve as a valuable imaging tool for initial evaluation and response assessment of juvenile patients with Ewing sarcoma, combining morphological and metabolic information, accompanied by a reasonable radiation dose for the patient.

Printed on: 02/07/23

## Abstract Archives of the RSNA, 2022

W5B-SPNMMI-2

### Development and External Validation of a Nomogram Based on 18F-FDG to Identify the Cancer-associated Cachexia

Wednesday, Nov. 30 12:45PM - 1:15PM Room: Learning Center - NMMI DPS

#### Participants

Yang Jiang, PhD, MD, (Presenter) Nothing to Disclose

#### PURPOSE

This study attempted to develop and validate a combined nomogram incorporating clinical information and PET features for identifying the risk of cancer-associated cachexia.

#### METHODS AND MATERIALS

FDG PET/CT data from 676 cancer patients were analyzed retrospectively. Patients were divided into a development cohort (n = 390) and an external validation cohort (n = 286) according to different medical centers. Results of the clinical laboratory tests for metabolic levels and organ and tissue-specific FDG uptake obtained from the cachexia and non-cachexia groups were compared statistically. Logistic regression analysis was performed to identify independent variables associated with cachexia in the development cohort for generating the nomogram. The performance of the nomogram was tested using the data from an external validation cohort and evaluated by area under the receiver operating characteristic curve (AUC), calibration curve, and decision curves.

#### RESULTS

Based on the data from the development cohort of 390 patients (mean age, 61 years  $\pm$  12 [standard deviation]; 221 men) and a validation cohort of 286 patients (54  $\pm$  14; 135 men), it is found that age (odds ratio [OR], 2.285; 95% confidence interval [CI]: 1.387, 3.765; P = 0.001), BMI (OR, 3.486; 95% CI: 1.718, 7.072; P = 0.001), hemoglobin (OR, 1.871; 95% CI: 1.120, 3.126; P = 0.02), maximum SUV of the liver (OR, 2.316; 95% CI: 1.422, 3.770; P = 0.001), and minimum SUV of the subcutaneous fat (OR, 2.991; 95% CI: 1.702, 5.259; P = 0.001) were independently associated with cachexia. The nomogram incorporating these variables showed great discrimination (AUC = 0.763, 95% CI: 0.706-0.821), calibration and clinical net benefit in the external validation cohort.

#### CONCLUSION

This study developed and externally validated a PET-based nomogram incorporating age, BMI, hemoglobin, maximum SUV of the liver, and average SUV of subcutaneous fat.

#### CLINICAL RELEVANCE/APPLICATION

Nuclear medicine physicians can help identify patients with high-risk cancer-related cachexia using the nomogram described in this study when reading patients' PET/CT images.

Printed on: 02/07/23

## Abstract Archives of the RSNA, 2022

W5B-SPNMMI-3

### A Novel Self-Assembling High Performance Organic Nanofluorophore for Intraoperative NIR-II Image-Guided Tumor Resection

Wednesday, Nov. 30 12:45PM - 1:15PM Room: Learning Center - NMMI DPS

#### Participants

Eric Tanifum, PhD, Houston, TX (*Presenter*) Consultant, Alzeca Biosciences, LLC; Stockholder, Alzeca Biosciences, LLC

#### PURPOSE

Oral cavity cancers are in the top 10 most common solid tumors worldwide. Surgery with adequate resection margins lead to higher survival and a reduction in local recurrence, but adequate resections are only achieved in 15-26% of cases due to the complex anatomy of the oral cavity and the lack of intraoperative guidance. Success with indocyanine green (ICG) have established the value of NIR imaging in precision tumor resection. NIR-II dyes which can selectively target solid tumors are highly desirable due to greater tissue penetration depth in the NIR-II window. We present a novel organic NIR-II dye XW-03-66 which self-assembles into nanoclusters in solution and selectively accumulates in mouse tumor models of oral cancer following intravenous administration, via the enhanced permeation and retention (EPR) effect

#### METHODS AND MATERIALS

XW-03-66 was synthesized from commercially available materials and the structure confirmed by NMR and MALDI. Spectroscopic data were collected using a UV-1600PC spectrophotometer and a NS3 NanoSpectralyzer. Cluster size was determined by Oblique Illumination Microscopy (OIM) and Atomic Force Microscopy (AFM). NIR-II imaging was conducted on a purpose-built instrument. MOC2 and MEER tumor models were used to assess intraoperative tumor resection procedures. Mice were administered a dose of 1 mg/Kg of the agent and surgery was performed 72 h post-injection. Imaging parameters: 470 mA, 500 ms/frame. Images processed and analyzed using ImageJ software.

#### RESULTS

XW-03-66 has an absorption maximum at 796 nm and a NIR-II fluorescence maximum 1018 nm. OIM and AFM analyses show that it self-assembles into nanoscale mesoscopic solute-rich clusters with a mean hydrodynamic diameter of 80 nm. Pharmacokinetic studies in nude mice (n = 4), show that it has a long systemic circulation half-life (6.5 h), and is cleared via the mononuclear phagocytic system (MPS). Long circulation allows the agent to traverse leaky vasculature and accumulate in solid tumors, enabling NIR-II image-guided tumor resection with adequate margins.

#### CONCLUSION

s XW-03-66 self assembles into mesoscopic solute-rich clusters in aqueous media. Following intravenous administration, it passively accumulates in two different mouse tumor model of oral cancer by the EPR effect, enabling intraoperative NIR-II image-guided tumor resection.

#### CLINICAL RELEVANCE/APPLICATION

Reports show significant advances in clinical instrumentation for fluorescence image-guided surgeries. NIR-II dyes such as XW-03-66 which specifically label solid tumors will find broad applications in intraoperative image-guided tumor surgeries

Printed on: 02/07/23

## Abstract Archives of the RSNA, 2022

W5B-SPNPM

### Noninterpretive Skills/Quality Improvement/Practice Management Wednesday Poster Discussions - B

Wednesday, Nov. 30 12:45PM - 1:15PM Room: Learning Center - NPM DPS

#### Participants

Tharakeswara Bathala, MD, Houston, TX (*Moderator*) Nothing to Disclose

#### Sub-Events

#### **W5B-SPNPM-1 Assessing Patient Comfort During MR Imaging at 0.55T and 1.5T - How Much Do Bore Size and Noise Matter?**

#### Participants

Hanns-Christian Breit, MD, Basel, Switzerland (*Presenter*) Nothing to Disclose

#### PURPOSE

To assess patient comfort perception when imaged on a newly introduced 0.55T low-field MR scanner system with a wide bore opening compared to a traditional 1.5T MR scanner system.

#### METHODS AND MATERIALS

50 patients (mean age: 66.2±17.0 years, 28 men) undergoing MR examinations with an equivalent imaging protocol both at a 0.55T (MAGENTOM Free.Max, Siemens Shenzhen Magnetic Resonance Ltd.) and a 1.5T scanner system (MAGNETOM Avanto Fit, Siemens Healthcare GmbH) within a timeframe of three hours between 05/2021-06/2021 were included into the analysis. The 0.55T MR system provides a bore opening of 80 cm, while the diameter of the 1.5T scanner system's bore is 60 cm. Four patient groups were defined: (1) cranial or cervical spine MRI using a head/neck coil (n=27), (2) lumbar or thoracic spine MRI using only the in-table spine coils (n=10), (3) hip MRI using a large flex coil (n=8), (4) upper or lower extremity MRI using small flex coils (n=5). Maximum noise levels of all performed imaging protocols were measured in decibels (dB) during separate scans by a volume meter placed in the center of the bores. Following the 0.55T MR examination, patients evaluated (1) sense of space, (2) noise level, and (3) overall sensation on a 5-point Likert scale (range: 1 = "much worse" to 5 = "much better") using a questionnaire.

#### RESULTS

Sense of space was perceived as "better" or "much better" by 84% of patients for imaging examinations performed on the 0.55T MR scanner system with the larger bore opening of 80 cm (mean score: 4.34±0.75). Similarly, 84% of patients rated noise levels as "better" or "much better" when imaged on the low-field scanner system (3.90±0.61). The overall sensation during the imaging examination at 0.55T was rated as "better" or "much better" by 78% of patients (3.96±0.70). Quantitative loudness assessment confirmed significantly reduced maximum noise levels for all MR imaging protocols performed on the 0.55T MR scanner system, compared to imaging at 1.5T, i.e. brain MRI (83.8±3.6 dB vs. 89.3±5.4 dB; p=.04), spine MRI (83.7±3.7 dB vs. 89.4±2.6 dB; p=.004) and hip MRI (86.3±5.0 dB vs. 89.1±1.4 dB; p=.04).

#### CONCLUSION

Patients perceive MR imaging on the investigated 0.55T low-field MR scanner system as more comfortable given its larger bore opening and reduced noise levels during image acquisition.

#### CLINICAL RELEVANCE/APPLICATION

New concepts regarding bore design and noise level reduction of MR scanner systems may help to further reduce patient anxiety and improve well-being when undergoing MR imaging.

#### **W5B-SPNPM-2 Emergency Department Brain MRI Utilization Patterns: With Prior Specialty Consultation vs. Without Prior Specialty Consultation**

#### Participants

Zachary Mosher, BS, MEng, Minneapolis, MN (*Presenter*) Stockholder, Johnson & Johnson; Employee, Center for Diagnostic Imaging

#### PURPOSE

Although brain MRI is frequently used in management of patients in an Emergency Department (ED) and ED Observation Unit (EDOU)<sup>1</sup>, there is limited data on clinical pathways driving utilization. The purpose of this study is to characterize association of specialty consultation with MRI results and patient disposition.

#### METHODS AND MATERIALS

Brain MRI exams performed on ED patients at our institution between January 1, 2021, and June 30, 2021, were retrospectively reviewed to determine association of specialty consultation with imaging findings and patient admission. Findings in MRI reports were categorized as: 1. No intracranial abnormality 2. Chronic intracranial abnormality 3. Acute, non-vascular intracranial abnormality 4. Acute, vascular intracranial abnormality Chi square test was performed to compare subspecialty consultation prior to ordering brain MRI (neurology, other subspecialty, or none) with rates of acute MRI findings (score 3 or 4) and admission.

## RESULTS

In the 6 month sample period 638 brain MRI studies were ordered on ED patients, with 370 (58.0%) following neurological consult, 67 (10.5%) following a specialty consult other than neurology, and 201 (31.5%) without a consult. A total of 137/638 (21.4%) brain MRI's demonstrated acute findings of, and 247/638 (38.7%) patients were admitted. There was no significant association between consultation and acute findings on MRI ( $\chi^2$  (df = 2, N=638) = 4.05, p = 0.13), but there was a strong association between consultation and admission ( $\chi^2$  (df = 2, N=638) = 21.65, p = 0.0002). Over half of the patients admitted had no acute findings on brain MRI 131/247 (53%), and this varied by consult status: 41.7% for non-neurological consultation, 30.1% neurological consult, and 14.5% of patients without prior consultation.

## CONCLUSION

For ED patients with specialty consultation prior to Brain MRI, the lack of association with acute findings and high rate of admission of patients with no acute findings suggests clinical rather than imaging factors drive decisions on disposition. In cases without specialty consultation, patients with a negative brain MRI were less likely to be admitted suggesting it may be used to triage patients amenable for discharge.

## CLINICAL RELEVANCE/APPLICATION

For ED patients with specialty consult prior to Brain MRI, the lack of association with acute findings and high rate of admission of patients with no acute findings suggests clinical rather than imaging factors drive decisions on disposition.

## W5B-SPNPM-3 Financial Value of a System Model for Managing Incidental Imaging Findings in Emergency Department Patients

Participants

Tianyuan Fu, MD, Cleveland, OH (*Presenter*) Nothing to Disclose

## PURPOSE

To estimate the rate of actionable incidental findings (IF) in emergency department (ED) patients and evaluate the downstream revenue from a health system model for improving patient follow-up of radiologist recommendations.

## METHODS AND MATERIALS

A pilot study was conducted at 11 community hospital EDs in a large health system between July 2021 and October 2021. 5,246 imaging exams, predominantly CT and MRI of the chest and abdomen, were reviewed. Using the ACR appropriateness criteria for IF identification and follow-up, 134 exams were flagged for review by a nurse navigator. After a chart review, 95 were deemed actionable cases (e.g. new diagnosis, clinically relevant, patient in system). We developed a range of estimates for downstream revenues within 3 months of IFs: (1) Expected Revenue: revenue expected from recommended diagnostic workflows standardized for each IF category; (2) Actual Revenue: revenue actually received by the system for diagnostic procedures related to each patient's IF; and (3) Actual Cancer-related Revenue: revenue received by the system for any encounter with a cancer diagnosis related to each patient's IF, where applicable. Data from the pilot study was used to estimate volumes and revenues associated with IFs across our entire health system by applying rates of IFs in the pilot to system imaging volumes.

## RESULTS

Most frequently encountered IF's were lung nodules (39%), pancreatic (12%), and renal (12%) lesions. Of the 95 actionable cases, 9 new cancers were identified in the 3-month follow-up period. The annual estimated volume (rate) of actionable IFs system-wide is 2,018 (1.8%). The estimated Expected Revenue from IF enterprise-wide was estimated to be \$1.2 million whereas the net Actual Revenue was \$1.6 million.

## CONCLUSION

Actionable IFs were present in nearly 2% of body CT and MR exams in our community EDs. Extrapolation of downstream volumes and revenue from follow-up care to the entire health system provides valuable information to support a program infrastructure to improve patient-centered care of IF.

## CLINICAL RELEVANCE/APPLICATION

Incidental findings may represent early malignancy or treatable conditions. A robust program for IF follow-up care can not only improve patient outcomes but also provide resources to scale closed-loop care across a large health system.

Printed on: 02/07/23

## Abstract Archives of the RSNA, 2022

W5B-SPNPM-1

### Assessing Patient Comfort During MR Imaging at 0.55T and 1.5T - How Much Do Bore Size and Noise Matter?

Wednesday, Nov. 30 12:45PM - 1:15PM Room: Learning Center - NPM DPS

#### Participants

Hanns-Christian Breit, MD, Basel, Switzerland (*Presenter*) Nothing to Disclose

#### PURPOSE

To assess patient comfort perception when imaged on a newly introduced 0.55T low-field MR scanner system with a wide bore opening compared to a traditional 1.5T MR scanner system.

#### METHODS AND MATERIALS

50 patients (mean age: 66.2±17.0 years, 28 men) undergoing MR examinations with an equivalent imaging protocol both at a 0.55T (MAGENTOM Free.Max, Siemens Shenzhen Magnetic Resonance Ltd.) and a 1.5T scanner system (MAGNETOM Avanto Fit, Siemens Healthcare GmbH) within a timeframe of three hours between 05/2021-06/2021 were included into the analysis. The 0.55T MR system provides a bore opening of 80 cm, while the diameter of the 1.5T scanner system's bore is 60 cm. Four patient groups were defined: (1) cranial or cervical spine MRI using a head/neck coil (n=27), (2) lumbar or thoracic spine MRI using only the in-table spine coils (n=10), (3) hip MRI using a large flex coil (n=8), (4) upper or lower extremity MRI using small flex coils (n=5). Maximum noise levels of all performed imaging protocols were measured in decibels (dB) during separate scans by a volume meter placed in the center of the bores. Following the 0.55T MR examination, patients evaluated (1) sense of space, (2) noise level, and (3) overall sensation on a 5-point Likert scale (range: 1= "much worse" to 5 = "much better") using a questionnaire.

#### RESULTS

Sense of space was perceived as "better" or "much better" by 84% of patients for imaging examinations performed on the 0.55T MR scanner system with the larger bore opening of 80 cm (mean score: 4.34±0.75). Similarly, 84% of patients rated noise levels as "better" or "much better" when imaged on the low-field scanner system (3.90±0.61). The overall sensation during the imaging examination at 0.55T was rated as "better" or "much better" by 78% of patients (3.96±0.70). Quantitative loudness assessment confirmed significantly reduced maximum noise levels for all MR imaging protocols performed on the 0.55T MR scanner system, compared to imaging at 1.5T, i.e. brain MRI (83.8±3.6 dB vs. 89.3±5.4 dB; p=.04), spine MRI (83.7±3.7 dB vs. 89.4±2.6 dB; p=.004) and hip MRI (86.3±5.0 dB vs. 89.1±1.4 dB; p=.04)

#### CONCLUSION

Patients perceive MR imaging on the investigated 0.55T low-field MR scanner system as more comfortable given its larger bore opening and reduced noise levels during image acquisition.

#### CLINICAL RELEVANCE/APPLICATION

New concepts regarding bore design and noise level reduction of MR scanner systems may help to further reduce patient anxiety and improve well-being when undergoing MR imaging.

Printed on: 02/07/23

## Abstract Archives of the RSNA, 2022

W5B-SPNPM-2

### Emergency Department Brain MRI Utilization Patterns: With Prior Specialty Consultation vs. Without Prior Specialty Consultation

Wednesday, Nov. 30 12:45PM - 1:15PM Room: Learning Center - NPM DPS

#### Participants

Zachary Mosher, BS, MEng, Minneapolis, MN (*Presenter*) Stockholder, Johnson & Johnson; Employee, Center for Diagnostic Imaging

#### PURPOSE

Although brain MRI is frequently used in management of patients in an Emergency Department (ED) and ED Observation Unit (EDOU)<sup>1</sup>, there is limited data on clinical pathways driving utilization. The purpose of this study is to characterize association of specialty consultation with MRI results and patient disposition.

#### METHODS AND MATERIALS

Brain MRI exams performed on ED patients at our institution between January 1, 2021, and June 30, 2021, were retrospectively reviewed to determine association of specialty consultation with imaging findings and patient admission. Findings in MRI reports were categorized as: 1. No intracranial abnormality 2. Chronic intracranial abnormality 3. Acute, non-vascular intracranial abnormality 4. Acute, vascular intracranial abnormality Chi square test was performed to compare subspecialty consultation prior to ordering brain MRI (neurology, other subspecialty, or none) with rates of acute MRI findings (score 3 or 4) and admission.

#### RESULTS

In the 6 month sample period 638 brain MRI studies were ordered on ED patients, with 370 (58.0%) following neurological consult, 67 (10.5%) following a specialty consult other than neurology, and 201 (31.5%) without a consult. A total of 137/638 (21.4%) brain MRI's demonstrated acute findings of, and 247/638 (38.7%) patients were admitted. There was no significant association between consultation and acute findings on MRI ( $\chi^2$  (df = 2, N=638) = 4.05, p = 0.13), but there was a strong association between consultation and admission ( $\chi^2$  (df = 2, N=638) = 21.65, p = 0.0002). Over half of the patients admitted had no acute findings on brain MRI 131/247 (53%), and this varied by consult status: 41.7% for non-neurological consultation, 30.1% neurological consult, and 14.5% of patients without prior consultation.

#### CONCLUSION

For ED patients with specialty consultation prior to Brain MRI, the lack of association with acute findings and high rate of admission of patients with no acute findings suggests clinical rather than imaging factors drive decisions on disposition. In cases without specialty consultation, patients with a negative brain MRI were less likely to be admitted suggesting it may be used to triage patients amenable for discharge.

#### CLINICAL RELEVANCE/APPLICATION

For ED patients with specialty consult prior to Brain MRI, the lack of association with acute findings and high rate of admission of patients with no acute findings suggests clinical rather than imaging factors drive decisions on disposition.

Printed on: 02/07/23



## Abstract Archives of the RSNA, 2022

W5B-SPNPM-3

### Financial Value of a System Model for Managing Incidental Imaging Findings in Emergency Department Patients

Wednesday, Nov. 30 12:45PM - 1:15PM Room: Learning Center - NPM DPS

#### Participants

Tianyuan Fu, MD, Cleveland, OH (*Presenter*) Nothing to Disclose

#### PURPOSE

To estimate the rate of actionable incidental findings (IF) in emergency department (ED) patients and evaluate the downstream revenue from a health system model for improving patient follow-up of radiologist recommendations.

#### METHODS AND MATERIALS

A pilot study was conducted at 11 community hospital EDs in a large health system between July 2021 and October 2021. 5,246 imaging exams, predominantly CT and MRI of the chest and abdomen, were reviewed. Using the ACR appropriateness criteria for IF identification and follow-up, 134 exams were flagged for review by a nurse navigator. After a chart review, 95 were deemed actionable cases (e.g. new diagnosis, clinically relevant, patient in system). We developed a range of estimates for downstream revenues within 3 months of IFs: (1) Expected Revenue: revenue expected from recommended diagnostic workflows standardized for each IF category; (2) Actual Revenue: revenue actually received by the system for diagnostic procedures related to each patient's IF; and (3) Actual Cancer-related Revenue: revenue received by the system for any encounter with a cancer diagnosis related to each patient's IF, where applicable. Data from the pilot study was used to estimate volumes and revenues associated with IFs across our entire health system by applying rates of IFs in the pilot to system imaging volumes.

#### RESULTS

Most frequently encountered IFs were lung nodules (39%), pancreatic (12%), and renal (12%) lesions. Of the 95 actionable cases, 9 new cancers were identified in the 3-month follow-up period. The annual estimated volume (rate) of actionable IFs system-wide is 2,018 (1.8%). The estimated Expected Revenue from IF enterprise-wide was estimated to be \$1.2 million whereas the net Actual Revenue was \$1.6 million.

#### CONCLUSION

s Actionable IFs were present in nearly 2% of body CT and MR exams in our community EDs. Extrapolation of downstream volumes and revenue from follow-up care to the entire health system provides valuable information to support a program infrastructure to improve patient-centered care of IF.

#### CLINICAL RELEVANCE/APPLICATION

Incidental findings may represent early malignancy or treatable conditions. A robust program for IF follow-up care can not only improve patient outcomes but also provide resources to scale closed-loop care across a large health system.

Printed on: 02/07/23

## Abstract Archives of the RSNA, 2022

W5B-SPNR

### Neuroradiology Wednesday Poster Discussions - B

Wednesday, Nov. 30 12:45PM - 1:15PM Room: Learning Center - NR DPS

#### Participants

Gelareh Sadigh, MD, Irvine, GA (*Moderator*) Research Grant, TailorMed Medical Ltd

#### Sub-Events

### W5B-SPNR- Minimum Number of Segmentations Required to Develop a Glioma Volumetric Auto-Segmentation Algorithm 1

#### Participants

Irene Dixe de Oliveira Santo, MD, New Haven, CT (*Presenter*) Nothing to Disclose

#### PURPOSE

Volumetric segmentation of gliomas provides valuable information on tumor morphology compared to the standard linear or two-dimensional measurements. However, it has yet to be implemented into routine clinical practice. Some of the major barriers include the amount of time required for manual segmentation and the high intra- and inter-reader variability. One possible solution may involve the use of fully automatic machine learning volumetric segmentation algorithms trained and validated on clinical imaging data.

#### METHODS AND MATERIALS

A U-Net-based segmentation algorithm was trained on 1251 gliomas from the multi-institutional BraTS 2021 dataset, and tested on our institution's internal database, consisting of images from 285 gliomas. Testing was divided into six batches, the first being comprised of 35 cases, and the remaining five containing 50 cases per batch. The algorithm's output consisted of "Whole" (FLAIR, hyperintensity), "Core" (PGSE or PGGE, T1c + hyperintensity), and "Necrotic" segmentations (PSGE or PGGE, central non-enhancement). DICE scores were calculated as a measure of overlap between the algorithm's segmentations and the manual segmentations by a board-certified neuroradiologist.

#### RESULTS

The DICE scores mean for whole tumor segmentation of the BraTS 2021-trained U-Net-based algorithm was 0.82 in the initial batch (n = 35). Gradual training using the subsequent five internal batches improved the DICE scores mean to approximately 0.84 for "Whole" segmentations. After completion of gradual training, DICE scores for the "Core" and "Necrotic" segmentations were found to be approximately 0.63, and 0.32, respectively.

#### CONCLUSION

Our results have shown that the segmentation algorithm performance can be improved with batches as small as 50 cases. DICE scores were highest for "Whole" segmentations, followed by "Core," with substantially lower performance for "Necrotic" segmentations.

#### CLINICAL RELEVANCE/APPLICATION

The creation of fully automated volumetric segmentation algorithms from small datasets may allow this data to be incorporated into routine clinical practice facilitating treatment-response estimation or early recurrence prediction.

### W5B-SPNR- Validating AI Model's Accuracy to Detect Intracranial Hemorrhage 10

#### Participants

Seema Al-Shaikhli, BS, (*Presenter*) Nothing to Disclose

#### PURPOSE

Timely detection of intracranial hemorrhage (ICH) is crucial to providing prompt life-saving measures. The application of artificial intelligence (AI) in detecting ICH has become increasingly prevalent as imaging utilization continues to rise. We aim to validate Viz.ai ICH, an AI application which identifies suspected ICH.

#### METHODS AND MATERIALS

A retrospective review of patients' radiology reports who received a non-contrast brain CT within a single institution between September 2021 and December 2021 was performed. Each report was reviewed for the presence of ICH and positive cases were categorized based on subtype, timing, and size/volume via imaging review by a neuroradiologist. The Viz.ai ICH output was reviewed for positive cases. Diagnostic performance was calculated by utilizing Viz.ai ICH as the index test and the radiologists' interpretation as the reference standard test.

#### RESULTS

A total of 4,203 non-contrast brain CTs were retrieved. of which 387 were positive per the radiology impression. Overall sensitivity

of Viz.ai ICH was 68%, specificity was 99%, positive predictive value was 90%, and negative predictive value was 97%. Subgroup analysis was performed based on hemorrhage subtypes intraparenchymal, subarachnoid, subdural, and intraventricular, of which the sensitivities were calculated to be 86%, 57%, 56%, and 42% respectively. Further stratification revealed sensitivity improves with higher acuity and volume/size across all ICH subtypes. Meningioma was found to be a common false-positive finding (3 of 22, 14%).

## CONCLUSION

s Overall diagnostic performance of the considered AI model was very promising, particularly for large volume/size ICH. As the AI algorithm continues to improve, the positive impact on patient care will be substantial.

## CLINICAL RELEVANCE/APPLICATION

Accurate detection of ICH is essential for providing prompt treatment. AI alerts the radiologist to the presence of hemorrhage within 1-2 minutes from scan completion leading to faster diagnosis.

## W5B-SPNR- Super-dose: a deep learning method to increase the sensitivity of MRI in neuro-oncology via virtual contrast dose amplification 11

Participants

Samy Ammari, MD, PhD, Villejuif, France (*Presenter*) Nothing to Disclose

## PURPOSE

Intravenous gadolinium-based contrast agents (GBCA) are particularly powerful to increase MRI sensitivity. However, the recent evidence of gadolinium deposition in various tissues prevents from simply increasing GBCA doses to further improve MRI diagnosis performance. In this study, we evaluate a deep learning method that amplifies the effects of GBCA injection on routine gradient echo brain T1 MRI.

## METHODS AND MATERIALS

T1, T2-Flair, diffusion, quarter-dose T1ce (low-T1ce), standard-dose T1ce (T1ce) and T1ce with variable flip angles (vfa-T1ce) sequences were acquired during 250 MRI exams of patients with mixed conditions. A deep learning model was trained, using data from 150 exams, to virtually enhance low-T1ce into routine T1ce, using zero-dose sequences as complementary information. The trained model was then evaluated with the 100 remaining exams for its capacity to enhance the routine T1ce into relevant "super-dose" images (sup-T1ce). Tumor regions on synthetic sup-T1ce, routine T1ce and reference vfa-T1ce were analyzed in sub-regions by two experienced radiologists. Endpoints were to evaluate if sup-T1ce outperformed routine T1ce in terms of sensitivity (SE) and false detection rates (FDR).

## RESULTS

Out of 187 masses diagnosed on vfa-T1ce, a significantly higher proportion was correctly identified on sup-T1ce than on T1ce (75% versus 59%,  $p < 0.001$ ). The FDR was slightly higher for sup-T1ce than for T1ce (0.14/case versus 0.05/case), but this difference was not significant. For both sup-T1ce and T1ce, no significant differences were found between examiners in terms of SE or FDR. Detection metrics improved when only larger lesions were considered, with SE reaching up to 96% for sup-T1ce and 88% for T1ce ( $p = 0.008$ ) at the 10 millimeters threshold. For all lesion sizes, the SE of sup-T1ce remained significantly higher than T1ce, and no statistical difference was found in terms of FDR.

## CONCLUSION

s Our deep learning model significantly improved the sensitivity of routine contrast-enhanced brain T1 MRI sequences without degrading its specificity.

## CLINICAL RELEVANCE/APPLICATION

A higher sensitivity of brain MRI may allow the detection of smaller tumors and thus earlier treatment onsets, ultimately improving patient survival.

## W5B-SPNR- Direct Comparison of Traditional Machine Learning and Deep Learning Commercial Artificial Intelligence Solutions for Detection of Large Vessel Occlusion 13

Participants

Jacob Schlossman, (*Presenter*) Nothing to Disclose

## PURPOSE

Despite the availability of commercial artificial intelligence tools for large vessel occlusion (LVO) detection, there is a lack of data comparing traditional machine learning and deep learning solutions in a real-world setting. The purpose of this study is to compare and validate the performance of two AI-based tools for LVO detection in anterior circulation stroke.

## METHODS AND MATERIALS

This was a retrospective, single center study performed at a comprehensive stroke center using anonymized data from December 2020 to June 2021. A total of 263 CTA cases for suspected stroke were included. RAPID LVO is a traditional machine learning model which primarily relies on vessel density threshold assessment, while CINA LVO is an end-to-end deep learning tool implemented with multiple neural networks for detection and localization tasks. Ground truth was based off interpretation of the raw data from the CTA by radiology reports and confirmed by a board-certified neuroradiologist (9 years experience). Performance metrics were analyzed by location of LVO: ICA, M1 MCA, or both. Patients with isolated M2 middle cerebral artery (MCA) occlusions were analyzed separately.

## RESULTS

There were 29 positive and 224 negative LVO cases. RAPID LVO demonstrated an accuracy of 0.86, sensitivity of 0.90, specificity of 0.86, PPV of 0.45, and NPV of 0.98, while CINA demonstrated an accuracy of 0.96, sensitivity of 0.76, specificity of 0.98, PPV of 0.85, and NPV of 0.97. Of the 29 positive LVO cases, there were 11 ICA LVOs and 23 M1 LVOs based on the ground truth. There were 5 patients who were observed as having both an ICA and M1 LVO. For ICA LVOs, RAPID demonstrated a sensitivity of .63, while CINA demonstrated a sensitivity of .22. For M1 LVOs, RAPID demonstrated a sensitivity of 0.80, while CINA demonstrated a

sensitivity of .70. Of the 10 M2 LVOs analyzed separately, there were 8 positive and 2 negative cases. CINA and RAPID both recognized the two negative cases as such. CINA successfully detected 3/8 positive M2 LVOs, while RAPID successfully detected 8/8.

## CONCLUSION

s Both tools successfully detected the majority of ICA and M1 MCA occlusions. RAPID had overall higher sensitivity while CINA had higher accuracy and specificity. Interestingly, both tools were able to detect some, but not all M2 MCA occlusions.

## CLINICAL RELEVANCE/APPLICATION

This is the first study to compare the performance of traditional and deep learning LVO tools in the clinical setting. Future research could assess how the tools impact radiology turnaround times and door-to-treatment times. As more automated LVO tools become commercially available, it will be paramount to conduct comparison studies to validate their performance and understand their limitations.

## W5B-SPNR- 14 Artificial Intelligence-based Evaluation of Brain Metastasis Enables Clinical Referral Suggestion: A Clinical Cohort Study

### Participants

Hana Jeong, MD, Seoul, Korea, Republic Of (*Presenter*) Nothing to Disclose

### PURPOSE

Artificial intelligence (AI) enables detection, lesion counts, and volumetry of brain metastasis. AI metastasis detection that incorporates black-blood imaging with reduced false positives may provide therapeutic guidance. We aimed to test clinical referral suggestions for patients with brain metastasis based on AI evaluation.

### METHODS AND MATERIALS

In this retrospective study, we applied AI for brain metastasis on black-blood imaging for consecutive 131 patients who had been diagnosed and treated for newly developed brain metastases in solid tumors between October 2020 and April 2021. The algorithm detects, counts, and segments brain metastasis. Based on the number and volume of metastases detected by AI, initial clinical referrals were suggested as one of following 4 categories: short-term imaging follow-up without treatment (group A), surgery (B), stereotactic radiosurgery (C), and whole brain radiotherapy or systematic chemotherapy (D). Performance was validated by comparing with the actual clinical decisions according to the European Association of Neuro-Oncology (EANO)-European Society for Medical Oncology (ESMO) guidelines.

### RESULTS

Total 131 patients were included (mean age 64.2 years, 59% male). The mean number and volume of AI detected metastases were significantly different among groups (Kruskal-Wallis test,  $P = .001$  and  $.001$ , respectively), with the largest number and volume in group D (mean number and volume, 27.8 and 5256.0mL), followed by group C (4.2 and 1141.1 mL), B (1.0 and 800.0 mL), and A (1.4 and 21.8 mL). AI system proposed the referral suggestions same as the actual clinical decisions with an accuracy of 84.0% (110/131) of the patients in the validation set.

### CONCLUSION

s AI based evaluation of metastasis detection and volumetry can suggest clinical referrals, showing great accuracy compared to actual clinical decisions. It may be used in clinical settings where prompt and accurate treatment decisions are required.

## CLINICAL RELEVANCE/APPLICATION

For patients with newly diagnosed brain metastasis, AI algorithm of detection and segmentation can aid in evaluation by providing prompt and consistent clinical referrals to clinicians, which can lead to better patient outcomes.

## W5B-SPNR- 15 Retrospective Study for Automated Detection of Critical Findings in Multiparametric Brain MRI Using 3D Neural Networks in Emergency Room According to Infarction Size

### Participants

Jimin Kim, MD, Seoul, Korea, Republic Of (*Presenter*) Nothing to Disclose

### PURPOSE

The early diagnosis of acute ischemic lesion is very crucial because the prognosis is highly dependent on time. The infarction size is one of the most important prognosis factors. In this paper, we validate a deep learning based research application according to clinical importance such as infarction size.

### METHODS AND MATERIALS

833 MRI exams performed in emergency department were retrospectively reviewed by two neuroradiologists. Two were excluded due to severe metallic artifacts and cervical cord infarction. Reviewers were blinded to patient's information and each other's results. We categorized infarction into 5 visual classes according to size; Class 1 = lacunar infarction (n=80), Class 2 = smaller than one-half lobar infarction (n=48), Class 3 = larger than one-half lobar and up to one lobar infarction (n=19), Class 4 = multilobar infarction (n=21) and Class 5 = embolic infarction (n=43). Especially, lacunar infarctions were reviewed by three neuroradiologists because of their ambiguity. All 831 cases were also processed by an AI-based research application (NeuroTriage, Siemens Healthcare, Germany)

### RESULTS

The research application showed sensitivity/specificity/area under the receiver operating characteristic curve (AUC) of 79.1%/92.3%/0.888 for overall infarction. For Class 1, the performance was 62.5%/92.3%/0.727. For Class 2, performance was 85.4%/92.3%/0.855. For Class 3, performance was 100%/92.3%/0.919. For Class 4, performance was 95.2%/92.3%/0.905. For Class 5, performance was 86%/92.3%/0.844. Mean diagnosis time was 64hr 47min 19sec for readers and 60.8sec for research application, with 99.9% time reduction.

### CONCLUSION

s The diagnostic performance for acute infarction of research application was good to excellent except for Class 1 infarction, which was fair. It tends to show better performance in the infarction of higher clinical importance. This study shows how the performance is based on its clinical significance and it is very novel way in evaluating infarction through deep learning algorithm. The processing time of the application was significantly faster than of radiologists.

#### CLINICAL RELEVANCE/APPLICATION

Therefore, the application could aid the fast diagnosis and decision making of acute infarction in general situations and reduce time duration for stroke patients to receive appropriate treatment.

#### W5B-SPNR- 16 **Deep Learning Reconstruction vs. Hybrid-Type Iterative Reconstruction: Capability for Image Quality Improvements of Peritumoral Vessels and Predicting Surgical Risks for Intracranial Meningiomas on Contrast-Enhanced CT Angiography**

Participants

Kazuhiro Murayama, MD, Toyoake, Japan (*Presenter*) Research Grant, Canon Medical Systems Corporation

#### PURPOSE

To determine the capability of deep learning reconstruction (DLR) for image quality improvements of peritumoral vessels and determine the relationship between peritumoral vessel number and surgical risk for intracranial meningiomas on contrast-enhanced ultra-high resolution CT angiography (CE-UHR-CTA) as compared with hybrid-type iterative reconstruction (IR).

#### METHODS AND MATERIALS

29 patients with intracranial meningiomas underwent brain CE-UHR-CTA and were reconstructed by DLR and hybrid-type IR and surgical resection. To assess surgical risk in each patient, surgical time and intraoperative bleeding volume were recorded. To determine the utility of DLR for CE-UHR-CTA, CT value of peritumoral vessels and SD of normal appearance white matter (NAWM) were assessed by ROI measurements at arterial and venous phases. Image J software was used to analyze particles to define the number of peritumoral vessels with the threshold. For quantitative image quality assessment, the number of vessels, SNR in peritumoral area and CNR between peritumoral vessel and NAWM were determined at each phase. To compare the quantitative indexes between two methods, CT values, SD, SNR, CNR and the number of peritumoral vessels on CE-UHR-CTA at each phase were compared between DLR and hybrid-type IR by Wilcoxon signed rank test. Then, number of peritumoral vessel on each CE-UHR-CTA were correlated with surgical risk by Pearson's correlation was performed.

#### RESULTS

CT values, SNR and CNR of DLR at each phase were significantly higher than those of hybrid-type IR ( $p < 0.05$ ). The number of peritumoral vessel on CE-UHR-CTA reconstructed with DLR was significantly higher than that with hybrid-type IR ( $p < 0.05$ ). There was significant correlation between the number of peritumoral vessel on CE-UHR-CTA with DLR and surgical time (artery phase;  $r = 0.43$ ,  $p < 0.05$ , venous phase;  $r = 0.40$ ,  $p < 0.05$ ), although there were no significant correlations between that on CE-UHR-CTA with hybrid-type IR at each phase and surgical time or between each CE-UHR-CTA and intraoperative bleeding volume ( $p > 0.05$ ).

#### CONCLUSION

s DLR has a potential for improving the depiction of peritumoral vessels and capability for predicting surgical risk for intracranial meningiomas on CE-UHR-CTA.

#### CLINICAL RELEVANCE/APPLICATION

DLR has a potential for improving the depiction of peritumoral vessels and capability for predicting surgical risk for intracranial meningiomas on CE-UHR-CTA.

#### W5B-SPNR- 17 **Unsupervised identification of MRI artifacts via integration of deep learning and image quality measures**

Participants

Thomas Desilvio, Cleveland, OH (*Presenter*) Nothing to Disclose

#### PURPOSE

Brain MRI scans are widely used for neurological evaluation, but often can be compromised by artifacts (e.g., ringing, ghosting, motion). Identifying specific MRI artifacts is critical for refining imaging protocols and guiding post-processing and downstream analysis that can enhance clinical and research interpretation; but requires time intensive and often subjective effort. We present results for unsupervised identification of brain MRI artifacts via automated integration of deep learning with MR quality measures (QMs).

#### METHODS AND MATERIALS

Using cohorts from ABIDE-I (17 institutes, 1102 T1w MRIs, 3 reader quality ratings) a ResNet18 model was trained ( $n = 454$ , 15 institutions) with labels of good quality (GQ) / poor quality (PQ), assigned based on rating agreement by 2+ readers. TCGA-GBM (5 institutes, 152 T1-POST MRIs) were then evaluated by three radiologists who labeled each scan as harboring each artifact type (ghosting, banding, motion, ringing) or otherwise; which was used as ground truth. Model inference was performed on the unseen TCGA-GBM cohort to yield 64 final-layer DL features per scan. 15 QMs (e.g., SNR, intensity-based contrast, variation, entropy measurements) via the MRQy tool were also extracted from each TCGA-GBM scan. 3 sets of features underwent unsupervised consensus clustering (see figure 1). Each clustering result was evaluated by identifying cluster correspondence with artifact type, and then calculating fraction of datasets per artifact group correctly clustered together to yield cluster overlap accuracy.

#### RESULTS

Combining DL and QMs achieved the best overall cluster overlap accuracies across all artifact types: 0.82 (banding), 0.78 (motion), 0.77 (ringing), and 0.84 (ghosting). QMs clustering achieved lower cluster overlap accuracies of 0.71 (banding), 0.75 (motion), 0.79 (ringing), and 0.80 (ghosting). DL features alone performed significantly worse with accuracies of 0.52 (banding), 0.63 (motion), 0.68 (ringing), and 0.66 (ghosting).

#### CONCLUSION

s Combined DL quality evaluation and image quality measures can enable unsupervised detection of brain MRI image artifacts.

#### **CLINICAL RELEVANCE/APPLICATION**

Detection of specific MRI image artifacts aids downstream image analysis and imaging protocol improvement. Deep learning and standard image quality measures appear complementary for this task.

#### **W5B-SPNR- Tailoring radiologist behaviour by individualising F beta levels for predictions of an AI model**

18

Participants

Peter R. Brotchie, MBBS, PhD, Fitzroy, Australia (*Presenter*) Consultant, Annalise-AI Pty Ltd

#### **PURPOSE**

When interpreting diagnostic imaging studies, radiologists rate of false negatives tends to higher than false positives on average, resulting in higher precision than recall. This is not desirable for critical findings where the cost of a false negative (eg. missed bleed) is greater than the cost of a false positive (eg. unnecessary MRI scan). The relative importance of recall and precision can be chosen for AI model predictions by choosing F-beta values for model thresholds. Our study assessed whether differences in F-beta values for the model findings influenced the radiologist precision and recall balance.

#### **METHODS AND MATERIALS**

A comprehensive CT brain convoluted neural network algorithm was used to investigate the effect of F-beta values of thresholds across a number of clinical findings, when comparing radiologist performance with and without the AI model assistance. F-beta values were chosen based on the criticality of the finding. The change in precision and recall for radiologists unassisted vs assisted was compared between groups of findings with F-beta values greater than 1, equal to 1 and lower than 1.

#### **RESULTS**

When unaided, radiologists' precision was higher than recall across all three groups of findings. When aided by the AI, radiologists' precision remained higher than recall for findings with an F-beta value of less than 1. However, for findings with F-beta values greater than 1 (critical findings), the recall significantly increased without a decrement in precision, resulting in higher recall than precision (Fig 1).

#### **CONCLUSION**

s Altering the F-beta levels for finding predictions by a CT brain AI model markedly changed the behaviour of radiologists when using the model, influencing them to significantly increase recall over precision for critical findings.

#### **CLINICAL RELEVANCE/APPLICATION**

This is a desirable result as the ratio of false positives to false negatives should be based on the criticality of a finding given that the cost of a false negative will be higher than a false positive for critical findings.

#### **W5B-SPNR- Clinical evaluation of deep-learning model for an automatic scoring of Alberta Stroke Program Early CT Score (ASPECTS) on non-contrast CT: A comparison study to the consensus of experts**

2

Participants

Jin Soo Lee, Suwon, Korea, Republic Of (*Presenter*) Nothing to Disclose

#### **PURPOSE**

Since the ASPECTS has been used in clinical practice for over 20 years, the most prominent problem is the inter-rater difference. It may result from the rater's experience, or it may be according to the infarction around the borderline. Due to these differences, there have been required to consistent ASPECTS calculation, and recently, software has been reported to produce coherent ASPECTS using deep-learning technique. Therefore, in this study, the clinical applicability of deep learning-based software will be evaluated by comparing to the consensus of two experienced experts.

#### **METHODS AND MATERIALS**

The non-contrast CT (NCCT) of 487 AIS patients were used for learning the model, and it was included only cases in which MRI were taken within an hour after NCCT scanning. For the model learning, one experienced stroke expert evaluated whether the occurrences of early ischemic change (EIC) and old infarction (OI) in NCCT images by referring to MRI, such as DWI, ADC, and FLAIR. 326 patients were registered in the clinical evaluation. The results of the model were compared with the consensus generated by two stroke experts. A comparison between the deep-learning model and the experts' consensus was conducted by the Bland and Altman (BA) agreement. Finally, with the consensus as the ground truth, the sensitivity and specificity of the model for 10 regions of interest (ROIs) were calculated.

#### **RESULTS**

The BA agreement had a mean difference of 0.032 [95% confidence interval (CI): -0.076 ~ 0.141], and the upper and lower limit of agreement (LOA) were 2.8 [95% CI: 2.615 ~ 2.986] and -2.736 [95% CI: -2.914 ~ -2.55], respectively. For ASPECTS calculation, sensitivity and specificity to detect the EIC for 10 ROIs were 0.628 [95% CI: 0.585 ~ 0.671] and 0.966 [95% CI: 0.961 ~ 0.97], respectively. Also, in the dichotomized analysis based on 4 points ( $\leq 4$  vs.  $>4$ ), the sensitivity and specificity were 0.972 [95% CI: 0.959 ~ 0.985] and 0.619 [95% CI: 0.472 ~ 0.766], respectively.

#### **CONCLUSION**

s The deep-learning model proposed for automatic ASPECT scoring confirmed reasonable agreement and accuracy compared with expert consensus; therefore, it is highly recommended to use for assisting clinicians in clinical environment.

#### **CLINICAL RELEVANCE/APPLICATION**

This deep-learning model has been integrated into the commercial Heuron-cASPECTS software. It will be a useful tool for clinicians to make fast decision of diagnosis and treatment, especially, it will be valuable in remote regions where neuro-radiology expert may be limited.

Participants  
20 **Multi-Center Radiomics Analysis Predict Pseudo-Progression vs. True Progression in Glioblastoma Patients**

Murat AK, MD, Pittsburgh, PA (*Presenter*) Nothing to Disclose

**PURPOSE**

To discriminate progressive disease (PD) vs. pseudoprogression (PsP) utilizing the radiomics analysis in glioblastoma (GBM).

**METHODS AND MATERIALS**

We evaluated 686 patients from three institutions of which 487 were TP, and 199 were PsP. We segmented edema, contrast enhancement, necrosis, and hemorrhage for each patient. Their respective contralateral white matter (cWM) regions of interest (ROI). 205 texture features were extracted from each sequence's volume of interest (VOI), including 10 histogram-based first-order features and 195 second-order gray-level co-occurrence matrices features. After normalization, the 195 second-order features were divided by their volume to produce 195 volume-independent—a total of 400 features extracted per VOI and 1600 features per patients. We removed features that are highly correlated (Pearson's correlation coefficient >0.80) and performed feature selection on the remaining features using the SHapley Additive exPlanations (SHAP) package that measures the feature importance. We split the cohort into 90% training and 10% testing. We used XGBoost algorithm to generate the radiomics model. The predictive performance of the models for classifying each lesion (PD versus PSP) was estimated using the receiver operating characteristic curve, summarized as the area under the curve.

**RESULTS**

Out of the 1600 total features, 1491 features correlated greater than 0.80. These highly correlated features were removed from the total set, leaving 109 features. Feature selection with SHAP method on 109 features identified 86 that contribute highly to the outcome prediction. 30 of the 86 were most relevant and were used for model building. Our model's training set accuracy with 10-fold cross-validation was 80%, and the testing set accuracy was 81%, with sensitivity and specificity of 79% and 84%, respectively.

**CONCLUSION**

Our study presents a radiomics model that can successfully differentiate between PD vs. PsP in GBM patients.

**CLINICAL RELEVANCE/APPLICATION**

PsP can mimic PD radiographically; our study presents a radiomics model for noninvasive, individualized prediction of PsP in GBM at the time of the clinical question.

**W5B-SPNR-4 Investigation on the image quality of head and neck CTA using energy spectrum combined with adaptive iterative scanning and deep learning algorithm**

Participants  
Deng Jie, (*Presenter*) Nothing to Disclose

**PURPOSE**

To investigate the influence and application value of spectral CT single-energy imaging combined with adaptive iterative reconstruction (ASIR) technology and deep learning algorithm on head and neck CT angiography (CTA).

**METHODS AND MATERIALS**

Comparison of energy spectrum (40kev, 60kev, 80kev) scanning, adaptive statistical iterative reconstruction algorithm (Adaptive Statistical Iterative Reconstruction-Veo, ASIR-V) and deep learning algorithm (DLIR-L, DLIR-M, DLIR-H) in 88 patients undergoing head and neck CTA examination image quality, volume projection and maximum density projection processing were performed on a total of five sets of images. The effects of different reconstruction methods on the image quality of head and neck CTA were evaluated from the two aspects of objective measurement and subjective score.

**RESULTS**

Objective evaluation: The CT value, SD value, SNR, and CNR of images with different reconstruction methods in each blood vessel in the seven groups were statistically different in each part ( $P < 0.05$ ). Partial analysis of the aortic arch DLIR-H > DLIR-L > ASIR-40% > 60kev > 80kev > 40kev ( $24.72 \pm 5.72$ ,  $P < 0.005$ ) was statistically significant, In the SNR comparison, the aortic arch part DLIR-H > DLIR-L > ASIR-40% > 60kev > 80kev > 40kev ( $28.41 \pm 35.06$ ,  $P < 0.05$ ), Comparing the CNR part again, DLIR-H has the highest CNR in the aortic arch, middle cerebral artery, vertebral artery and basilar artery, respectively ( $80.71 \pm 112.93$ ) and ( $76.57 \pm 84.33$ ) ( $63.84 \pm 32.94$ ) ( $59.51 \pm 29.48$ ) ( $P < 0.05$ ), with statistical difference. Subjective evaluation: Between each group, the Kappa value of the subjective score of the two diagnostic group physicians for the image reconstruction quality was 0.72. The scores of VR reconstructed images showed no statistical difference between the groups ( $P = 0.668$ ). There was no statistical difference in the scores of MIP reconstruction images among the groups ( $P = 0.467$ ). CPR reconstruction image score DLIR-H group > DLIR-M group > DLIR-L group > ASIR-40% group > A3 group > A2 group > A1 group, there were significant differences in the scores among the groups ( $P < 0.05$ ).

**CONCLUSION**

In terms of image quality of head and neck CTA examination, DLIR can reduce image noise, improve image SNR, and lower radiation dose than ASIR reconstruction technology and energy spectrum scanning. be applied in.

**CLINICAL RELEVANCE/APPLICATION**

Different reconstruction methods applied to head and neck CTA scanning, DLIR has more advantages than ASIR reconstruction and energy spectrum scanning technology.

**W5B-SPNR-5 Faster, Lighter, Scalable: Harnessing data-mined line annotations for automated tumor segmentation on brain MRI**

Participants

Vivek Yadav, MS, BEng, (*Presenter*) Stockholder, Moderna, Inc

## PURPOSE

Tumor segmentation provides more accurate quantification of tumor burden versus linear measurement and is the major prerequisite step for radiomic analysis. While fully-supervised learning can yield high-performing segmentation models, the time and effort required to manually label large training sets limits clinical utility. We investigate whether datamined tumor line annotations can be utilized to develop a brain MRI tumor segmentation model without the need for manually segmented training data.

## METHODS AND MATERIALS

In this retrospective study, a previously described tumor detection model trained using clinical line annotations mined from PACS was leveraged with unsupervised segmentation (Otsu thresholding) to generate pseudo-masks of enhancing tumors on T1-weighted post-contrast images. Pseudo-masks were used to train baseline segmentation models using Mask R-CNN and HRNet architectures, which were employed within a semi-supervised learning (SSL) framework to automatically refine the pseudo-masks. Following each self-refinement cycle, a new model was trained and tested on a held-out set consisting of 319 manually segmented images from 93 adult patients (278 intra-axial and 88 extra-axial tumors) and performance evaluated using Dice score (DSC). The SSL cycles continued until performance peaked or plateaued. Two deployment methods were compared: (1) conventional end-to-end segmentation, and (2) a hybrid pipeline combining end-to-end segmentation with detection plus patch-wise segmentation.

## RESULTS

Baseline segmentation models achieved DSC of 0.838 (Mask R-CNN) and 0.841 (HRNet), which improved with self-refinement to 0.871 (after 8 cycles) and 0.873 (after 7 cycles), respectively. The hybrid pipeline (maximum DSC 0.884, Mask R-CNN) outperformed end-to-end segmentation (maximum DSC 0.873, HRNet).

## CONCLUSION

s Line annotations mined from PACS can be harnessed in concert with unsupervised and semi-supervised techniques to achieve high-performing brain MRI tumor segmentation models, avoiding the need for manually segmented training data. This development pipeline provides a potential mechanism to rapidly establish tumor segmentation capabilities across imaging modalities.

## CLINICAL RELEVANCE/APPLICATION

Accurate segmentation of tumors on brain MRI is achieved by leveraging clinical line annotations from PACS within an automated pipeline, avoiding the need for any manually segmented training data.

## W5B-SPNR- Investigation on iodine suppression effect of virtual non-contrast images in different concentrations of iodine: A Phantom Study

6

Participants

Yaoming Ma, (*Presenter*) Nothing to Disclose

## PURPOSE

To investigate the value of virtual non-contrast images in suppressing iodine in different concentrations of iodine.

## METHODS AND MATERIALS

A polypropylene cylindrical phantom (QSP Phantom dimension) with nine tubes containing different concentrations of iodine (0, 2.5, 5, 10, 20 mgI/ml) was scanned using a spectral CT (Revolution, GE Healthcare) in gemstone spectral imaging (GSI) mode using fast kV switch (80/140 kV), the tube current is 485mA, the layer thickness is 1.25mm, the collimation width is 80mm, noise index (NI) 5HU, pitch 0.992:1. pre-ASiR-V 30% weight was used for gemstone spectral CT scanning. The CT and SD values of the images before and after iodine suppression of 20%, 10%, 5% and 2.5% iodine were measured. The area of region of interest (ROI) was 1 / 2-1 / 3 of the cross-sectional area of the somatosensory canal, and the size was consistent. The iodine suppression rate of different concentrations of iodine was calculated (iodine suppression rate =  $\{(CT \text{ value } 1 - CT \text{ value } 2) / CT \text{ value } 1\} * 100\%$ , CT value 1 was the CT value of the image before iodine suppression, CT value 2 was the CT value of the image after iodine suppression). The difference between the two groups was compared by one-way ANOVA, and the difference was statistically significant ( $P < 0.05$ ).

## RESULTS

The CT value of iodine 20 before iodine suppression was  $431.5 \pm 67\text{Hu}$ , iodine 10, CT value was  $211.89 \pm 57\text{Hu}$ , iodine 5 CT value was  $107.09 \pm 82\text{Hu}$ , iodine 2.5, CT value was  $53.93 \pm 68\text{Hu}$ , the difference between the two groups was statistically significant ( $P < 0.05$ ); The CT value of iodine 20 after iodine suppression was  $14.34 \pm 42\text{Hu}$ , iodine 10, CT value was  $13.84 \pm 80\text{Hu}$ , iodine 5 CT value was  $15.2 \pm 62\text{Hu}$ , iodine 2.5, CT value was  $13.99 \pm 46\text{Hu}$ , there was no significant difference between the two groups ( $P > 0.05$ ). The iodine inhibition rates of iodine 20, 10, 5 and 2.5 were 96.67%, 93.45%, 85.77%, 74.02% respectively, and the iodine inhibition rates gradually decreased, and the difference between the groups was statistically significant ( $P < 0.05$ ).

## CONCLUSION

s From the evaluation of iodine suppression rate and CT value of virtual plain scan (VNC) images with different concentrations of iodine, the virtual plain scan (VNC) iodine suppression technology has a good effect on different concentrations of blood vessels.

## W5B-SPNR- Can Machine Learning Be Better Than Biased Readers?

7

Participants

Rui Zhu, BSc, Toronto, ON (*Presenter*) Nothing to Disclose

## PURPOSE

The purpose is to determine if machine learning algorithms can overcome reader biases and more closely match multiple reader consensus than individual readers' diagnostic accuracy when training a binary convolutional neural network (CNN) classifier. Training deep learning models in medical imaging requires large amounts of labeled data. It is common to divide the training data amongst multiple readers with varying levels of expertise to minimize the effort. Alternatively, multiple small datasets labeled by different readers are combined for training. In both scenarios the readers' consensus is not obtained leading to a biased dataset.

## METHODS AND MATERIALS

This study used a binary-class chest X-ray dataset and corresponding labels of pediatric pneumonia obtained from Guangzhou Women and Children's Medical Center. Wrong labels are generated for biased readers by sampling from the probability distribution of their biases defined by Bernoulli distributions of producing an observed label given the true label. The true labels were assumed to be the consensus of the readers. The readers' performances were evaluated based on their annotations on the test set. The models' testing performances were compared to readers' performances. Resnet18 without transfer learning was used as baseline model. A variation of Resnet18 with modified loss function was used as an improvement on the baseline model.

## RESULTS

The baseline model's test accuracy was higher than the average accuracy of the biased readers (59%-69%) by 2%-9% when the average accuracy of all readers was 73%-79%. The improved model with the modified loss function trained on a dataset containing 30% biased labels achieved 86% test accuracy, being higher than the average of all readers (69%), when readers' labels can compensate each other's errors. The improved model with the modified loss function produced more robust accuracies (79%-86%) than the baseline model (70%-83%) while varying the strengths and the types of the biases held by the readers.

## CONCLUSION

This study demonstrated that it is possible for machine learning algorithms to overcome individual readers' biases in training a binary CNN classifier. It is recommended to use robust loss functions as they are easy to implement and effective in mitigating biased labels.

## CLINICAL RELEVANCE/APPLICATION

AI technology assists medical practitioners to analyze radiological images efficiently to inform patients of their condition timely. Our study focuses on training AI on datasets with biased labels.

## W5B-SPNR- Effectiveness of a Convolutional Neural Network Artificial Intelligence Algorithm in the Detection of Intracranial Hemorrhage on Noncontrast CT Imaging

Participants  
Ayden Jacob, Boca Raton, FL (*Presenter*) Consultant, Aidoc Medical Ltd

## PURPOSE

Radiologic misdiagnosis of intracranial hemorrhage (ICH) may result in poor patient outcomes. This study aimed to assess the accuracy and clinical viability of an AI-based algorithm in the detection of ICH on noncontrast CT (NCCT) imaging.

## METHODS AND MATERIALS

An FDA approved AI solution based on a convolutional neural network was used to assess 8468 NCCTs. Data was collected from 29 different facilities. Slice thickness ranged from 0.625 mm to 5mm. NCCTs were retrospectively processed through the AI solution and assigned a positive or negative for ICH allocation. Each report was analyzed by a natural language processing software and assigned a positive or negative for ICH allocation per the radiologist's interpretation. Cases were stratified as concordant, wherein the radiologist and AI interpretation agreed, and discordant, in which interpretations differed. NLP results for discordant cases were externally validated. 2 board certified neuroradiologists and 1 general radiologist assessed discordant NCCTs for ICH to determine ground truth by majority opinion.

## RESULTS

98 AI positives were engaged with by the radiologist at the time of data collection and were excluded from the cohort. Concordant cases included 288 double positives (AI+/Rad+) and 7950 double negatives (AI-/Rad-). 132 discordant cases included 100 scans positive by AI and negative per radiologist's report (AI+/Rad-), and 32 scans negative by AI and positive by report (AI-/Rad+). Following consensus review by 3 radiologists, individual and combined accuracy metrics were acquired for both entities. Radiologist metrics included an accuracy of 99.1%, sensitivity of 94.5%, and a specificity of 99.9%. AI demonstrated an accuracy of 98.8%, sensitivity of 93.6%, and a specificity of 99.1%. Differences in accuracy and specificity were statistically significant ( $p < .00001$ ) whereas sensitivity was not ( $p = .61708$ ). Combined accuracy was 99.6% with minimal loss of specificity (99%). The radiologists detected 309 positive cases, and an additional 18 ICHs were detected by the AI solution, providing an added detection rate of 5.8%.

## CONCLUSION

This study demonstrates that an AI-solution can assist radiologists in the diagnosis of ICH. Radiologists leveraging AI-solutions have an increased sensitivity in the detection of ICH.

## CLINICAL RELEVANCE/APPLICATION

The combined precision and accuracy of the AI-radiologist combination highlights the value of coupling a high sensitivity screening test (AI) with a higher specificity validation test (radiologist). Synergy between radiologists and AI solutions in the detection of ICH may improve patient outcomes through minimizing false negative rates.

Printed on: 02/07/23

## Abstract Archives of the RSNA, 2022

W5B-SPNR-1

### Minimum Number of Segmentations Required to Develop a Glioma Volumetric Auto-Segmentation Algorithm

Wednesday, Nov. 30 12:45PM - 1:15PM Room: Learning Center - NR DPS

#### Participants

Irene Dixe de Oliveira Santo, MD, New Haven, CT (*Presenter*) Nothing to Disclose

#### PURPOSE

Volumetric segmentation of gliomas provides valuable information on tumor morphology compared to the standard linear or two-dimensional measurements. However, it has yet to be implemented into routine clinical practice. Some of the major barriers include the amount of time required for manual segmentation and the high intra- and inter-reader variability. One possible solution may involve the use of fully automatic machine learning volumetric segmentation algorithms trained and validated on clinical imaging data.

#### METHODS AND MATERIALS

A U-Net-based segmentation algorithm was trained on 1251 gliomas from the multi-institutional BraTS 2021 dataset, and tested on our institution's internal database, consisting of images from 285 gliomas. Testing was divided into six batches, the first being comprised of 35 cases, and the remaining five containing 50 cases per batch. The algorithm's output consisted of "Whole" (FLAIR, hyperintensity), "Core" (PGSE or PGGE, T1c + hyperintensity), and "Necrotic" segmentations (PSGE or PGGE, central non-enhancement). DICE scores were calculated as a measure of overlap between the algorithm's segmentations and the manual segmentations by a board-certified neuroradiologist.

#### RESULTS

The DICE scores mean for whole tumor segmentation of the BraTS 2021-trained U-Net-based algorithm was 0.82 in the initial batch (n = 35). Gradual training using the subsequent five internal batches improved the DICE scores mean to approximately 0.84 for "Whole" segmentations. After completion of gradual training, DICE scores for the "Core" and "Necrotic" segmentations were found to be approximately 0.63, and 0.32, respectively.

#### CONCLUSION

Our results have shown that the segmentation algorithm performance can be improved with batches as small as 50 cases. DICE scores were highest for "Whole" segmentations, followed by "Core," with substantially lower performance for "Necrotic" segmentations.

#### CLINICAL RELEVANCE/APPLICATION

The creation of fully automated volumetric segmentation algorithms from small datasets may allow this data to be incorporated into routine clinical practice facilitating treatment-response estimation or early recurrence prediction.

Printed on: 02/07/23



## Abstract Archives of the RSNA, 2022

W5B-SPNR-10

### Validating AI Model's Accuracy to Detect Intracranial Hemorrhage

Wednesday, Nov. 30 12:45PM - 1:15PM Room: Learning Center - NR DPS

#### Participants

Seema Al-Shaikhli, BS, (*Presenter*) Nothing to Disclose

#### PURPOSE

Timely detection of intracranial hemorrhage (ICH) is crucial to providing prompt life-saving measures. The application of artificial intelligence (AI) in detecting ICH has become increasingly prevalent as imaging utilization continues to rise. We aim to validate Viz.ai ICH, an AI application which identifies suspected ICH.

#### METHODS AND MATERIALS

A retrospective review of patients' radiology reports who received a non-contrast brain CT within a single institution between September 2021 and December 2021 was performed. Each report was reviewed for the presence of ICH and positive cases were categorized based on subtype, timing, and size/volume via imaging review by a neuroradiologist. The Viz.ai ICH output was reviewed for positive cases. Diagnostic performance was calculated by utilizing Viz.ai ICH as the index test and the radiologists' interpretation as the reference standard test.

#### RESULTS

A total of 4,203 non-contrast brain CTs were retrieved, of which 387 were positive per the radiology impression. Overall sensitivity of Viz.ai ICH was 68%, specificity was 99%, positive predictive value was 90%, and negative predictive value was 97%. Subgroup analysis was performed based on hemorrhage subtypes intraparenchymal, subarachnoid, subdural, and intraventricular, of which the sensitivities were calculated to be 86%, 57%, 56%, and 42% respectively. Further stratification revealed sensitivity improves with higher acuity and volume/size across all ICH subtypes. Meningioma was found to be a common false-positive finding (3 of 22, 14%).

#### CONCLUSION

s Overall diagnostic performance of the considered AI model was very promising, particularly for large volume/size ICH. As the AI algorithm continues to improve, the positive impact on patient care will be substantial.

#### CLINICAL RELEVANCE/APPLICATION

Accurate detection of ICH is essential for providing prompt treatment. AI alerts the radiologist to the presence of hemorrhage within 1-2 minutes from scan completion leading to faster diagnosis.

Printed on: 02/07/23

## Abstract Archives of the RSNA, 2022

W5B-SPNR-11

### Super-dose: a deep learning method to increase the sensitivity of MRI in neuro-oncology via virtual contrast dose amplification

Wednesday, Nov. 30 12:45PM - 1:15PM Room: Learning Center - NR DPS

#### Participants

Samy Ammari, MD, PhD, Villejuif, France (*Presenter*) Nothing to Disclose

#### PURPOSE

Intravenous gadolinium-based contrast agents (GBCA) are particularly powerful to increase MRI sensitivity. However, the recent evidence of gadolinium deposition in various tissues prevents from simply increasing GBCA doses to further improve MRI diagnosis performance. In this study, we evaluate a deep learning method that amplifies the effects of GBCA injection on routine gradient echo brain T1 MRI.

#### METHODS AND MATERIALS

T1, T2-Flair, diffusion, quarter-dose T1ce (low-T1ce), standard-dose T1ce (T1ce) and T1ce with variable flip angles (vfa-T1ce) sequences were acquired during 250 MRI exams of patients with mixed conditions. A deep learning model was trained, using data from 150 exams, to virtually enhance low-T1ce into routine T1ce, using zero-dose sequences as complementary information. The trained model was then evaluated with the 100 remaining exams for its capacity to enhance the routine T1ce into relevant "super-dose" images (sup-T1ce). Tumor regions on synthetic sup-T1ce, routine T1ce and reference vfa-T1ce were analyzed in sub-regions by two experienced radiologists. Endpoints were to evaluate if sup-T1ce outperformed routine T1ce in terms of sensitivity (SE) and false detection rates (FDR).

#### RESULTS

Out of 187 masses diagnosed on vfa-T1ce, a significantly higher proportion was correctly identified on sup-T1ce than on T1ce (75% versus 59%,  $p < 0.001$ ). The FDR was slightly higher for sup-T1ce than for T1ce (0.14/case versus 0.05/case), but this difference was not significant. For both sup-T1ce and T1ce, no significant differences were found between examiners in terms of SE or FDR. Detection metrics improved when only larger lesions were considered, with SE reaching up to 96% for sup-T1ce and 88% for T1ce ( $p = 0.008$ ) at the 10 millimeters threshold. For all lesion sizes, the SE of sup-T1ce remained significantly higher than T1ce, and no statistical difference was found in terms of FDR.

#### CONCLUSION

Our deep learning model significantly improved the sensitivity of routine contrast-enhanced brain T1 MRI sequences without degrading its specificity.

#### CLINICAL RELEVANCE/APPLICATION

A higher sensitivity of brain MRI may allow the detection of smaller tumors and thus earlier treatment onsets, ultimately improving patient survival.

Printed on: 02/07/23



## Abstract Archives of the RSNA, 2022

W5B-SPNR-13

### Direct Comparison of Traditional Machine Learning and Deep Learning Commercial Artificial Intelligence Solutions for Detection of Large Vessel Occlusion

Wednesday, Nov. 30 12:45PM - 1:15PM Room: Learning Center - NR DPS

#### Participants

Jacob Schlossman, (*Presenter*) Nothing to Disclose

#### PURPOSE

Despite the availability of commercial artificial intelligence tools for large vessel occlusion (LVO) detection, there is a lack of data comparing traditional machine learning and deep learning solutions in a real-world setting. The purpose of this study is to compare and validate the performance of two AI-based tools for LVO detection in anterior circulation stroke.

#### METHODS AND MATERIALS

This was a retrospective, single center study performed at a comprehensive stroke center using anonymized data from December 2020 to June 2021. A total of 263 CTA cases for suspected stroke were included. RAPID LVO is a traditional machine learning model which primarily relies on vessel density threshold assessment, while CINA LVO is an end-to-end deep learning tool implemented with multiple neural networks for detection and localization tasks. Ground truth was based off interpretation of the raw data from the CTA by radiology reports and confirmed by a board-certified neuroradiologist (9 years experience). Performance metrics were analyzed by location of LVO: ICA, M1 MCA, or both. Patients with isolated M2 middle cerebral artery (MCA) occlusions were analyzed separately.

#### RESULTS

There were 29 positive and 224 negative LVO cases. RAPID LVO demonstrated an accuracy of 0.86, sensitivity of 0.90, specificity of 0.86, PPV of 0.45, and NPV of 0.98, while CINA demonstrated an accuracy of 0.96, sensitivity of 0.76, specificity of 0.98, PPV of 0.85, and NPV of 0.97. Of the 29 positive LVO cases, there were 11 ICA LVOs and 23 M1 LVOs based on the ground truth. There were 5 patients who were observed as having both an ICA and M1 LVO. For ICA LVOs, RAPID demonstrated a sensitivity of .63, while CINA demonstrated a sensitivity of .22. For M1 LVOs, RAPID demonstrated a sensitivity of 0.80, while CINA demonstrated a sensitivity of .70. Of the 10 M2 LVOs analyzed separately, there were 8 positive and 2 negative cases. CINA and RAPID both recognized the two negative cases as such. CINA successfully detected 3/8 positive M2 LVOs, while RAPID successfully detected 8/8.

#### CONCLUSION

Both tools successfully detected the majority of ICA and M1 MCA occlusions. RAPID had overall higher sensitivity while CINA had higher accuracy and specificity. Interestingly, both tools were able to detect some, but not all M2 MCA occlusions.

#### CLINICAL RELEVANCE/APPLICATION

This is the first study to compare the performance of traditional and deep learning LVO tools in the clinical setting. Future research could assess how the tools impact radiology turnaround times and door-to-treatment times. As more automated LVO tools become commercially available, it will be paramount to conduct comparison studies to validate their performance and understand their limitations.

Printed on: 02/07/23

## Abstract Archives of the RSNA, 2022

W5B-SPNR-14

### Artificial Interlligence-based Evaluation of Brain Metastasis Enables Clinical Referral Suggestion: A Clinical Cohort Study

Wednesday, Nov. 30 12:45PM - 1:15PM Room: Learning Center - NR DPS

#### Participants

Hana Jeong, MD, Seoul, Korea, Republic Of (*Presenter*) Nothing to Disclose

#### PURPOSE

Artificial intelligence (AI) enables detection, lesion counts, and volumetry of brain metastasis. AI metastasis detection that incorporates black-blood imaging with reduced false positives may provide therapeutic guidance. We aimed to test clinical referral suggestions for patients with brain metastasis based on AI evaluation.

#### METHODS AND MATERIALS

In this retrospective study, we applied AI for brain metastasis on black-blood imaging for consecutive 131 patients who had been diagnosed and treated for newly developed brain metastases in solid tumors between October 2020 and April 2021. The algorithm detects, counts, and segments brain metastasis. Based on the number and volume of metastases detected by AI, initial clinical referrals were suggested as one of following 4 categories: short-term imaging follow-up without treatment (group A), surgery (B), stereotactic radiosurgery (C), and whole brain radiotherapy or systematic chemotherapy (D). Performance was validated by comparing with the actual clinical decisions according to the European Association of Neuro-Oncology (EANO)-European Society for Medical Oncology (ESMO) guidelines.

#### RESULTS

Total 131 patients were included (mean age 64.2 years, 59% male). The mean number and volume of AI detected metastases were significantly different among groups (Kruskal-Wallis test,  $P = .001$  and  $.001$ , respectively), with the largest number and volume in group D (mean number and volume, 27.8 and 5256.0mL), followed by group C (4.2 and 1141.1 mL), B (1.0 and 800.0 mL), and A (1.4 and 21.8 mL). AI system proposed the referral suggestions same as the actual clinical decisions with an accuracy of 84.0% (110/131) of the patients in the validation set.

#### CONCLUSION

s AI based evaluation of metastasis detection and volumetry can suggest clinical referrals, showing great accuracy compared to actual clinical decisions. It may be used in clinical settings where prompt and accurate treatment decisions are required.

#### CLINICAL RELEVANCE/APPLICATION

For patients with newly diagnosed brain metastasis, AI algorithm of detection and segmentation can aid in evaluation by providing prompt and consistent clinical referrals to clinicians, which can lead to better patient outcomes.

Printed on: 02/07/23

## Abstract Archives of the RSNA, 2022

W5B-SPNR-15

### Retrospective Study for Automated Detection of Critical Findings in Multiparametric Brain MRI Using 3D Neural Networks in Emergency Room According to Infarction Size

Wednesday, Nov. 30 12:45PM - 1:15PM Room: Learning Center - NR DPS

#### Participants

Jimin Kim, MD, Seoul, Korea, Republic Of (*Presenter*) Nothing to Disclose

#### PURPOSE

The early diagnosis of acute ischemic lesion is very crucial because the prognosis is highly dependent on time. The infarction size is one of the most important prognosis factors. In this paper, we validate a deep learning based research application according to clinical importance such as infarction size.

#### METHODS AND MATERIALS

833 MRI exams performed in emergency department were retrospectively reviewed by two neuroradiologists. Two were excluded due to severe metallic artifacts and cervical cord infarction. Reviewers were blinded to patient's information and each other's results. We categorized infarction into 5 visual classes according to size; Class 1 = lacunar infarction (n=80), Class 2 = smaller than one-half lobar infarction (n=48), Class 3 = larger than one-half lobar and up to one lobar infarction (n=19), Class 4 = multilobar infarction (n=21) and Class 5 = embolic infarction (n=43). Especially, lacunar infarctions were reviewed by three neuroradiologists because of their ambiguity. All 831 cases were also processed by an AI-based research application (NeuroTriage, Siemens Healthcare, Germany)

#### RESULTS

The research application showed sensitivity/specificity/area under the receiver operating characteristic curve (AUC) of 79.1%/92.3%/0.888 for overall infarction. For Class 1, the performance was 62.5%/92.3%/0.727. For Class 2, performance was 85.4%/92.3%/0.855. For Class 3, performance was 100%/92.3%/0.919. For Class 4, performance was 95.2%/92.3%/0.905. For Class 5, performance was 86%/92.3%/0.844. Mean diagnosis time was 64hr 47min 19sec for readers and 60.8sec for research application, with 99.9% time reduction.

#### CONCLUSION

The diagnostic performance for acute infarction of research application was good to excellent except for Class 1 infarction, which was fair. It tends to show better performance in the infarction of higher clinical importance. This study shows how the performance is based on its clinical significance and it is very novel way in evaluating infarction through deep learning algorithm. The processing time of the application was significantly faster than of radiologists.

#### CLINICAL RELEVANCE/APPLICATION

Therefore, the application could aid the fast diagnosis and decision making of acute infarction in general situations and reduce time duration for stroke patients to receive appropriate treatment.

Printed on: 02/07/23

## Abstract Archives of the RSNA, 2022

W5B-SPNR-16

### Deep Learning Reconstruction vs. Hybrid-Type Iterative Reconstruction: Capability for Image Quality Improvements of Peritumoral Vessels and Predicting Surgical Risks for Intracranial Meningiomas on Contrast-Enhanced CT Angiography

Wednesday, Nov. 30 12:45PM - 1:15PM Room: Learning Center - NR DPS

#### Participants

Kazuhiro Murayama, MD, Toyoake, Japan (*Presenter*) Research Grant, Canon Medical Systems Corporation

#### PURPOSE

To determine the capability of deep learning reconstruction (DLR) for image quality improvements of peritumoral vessels and determine the relationship between peritumoral vessel number and surgical risk for intracranial meningiomas on contrast-enhanced ultra-high resolution CT angiography (CE-UHR-CTA) as compared with hybrid-type iterative reconstruction (IR).

#### METHODS AND MATERIALS

29 patients with intracranial meningiomas underwent brain CE-UHR-CTA and were reconstructed by DLR and hybrid-type IR and surgical resection. To assess surgical risk in each patient, surgical time and intraoperative bleeding volume were recorded. To determine the utility of DLR for CE-UHR-CTA, CT value of peritumoral vessels and SD of normal appearance white matter (NAWM) were assessed by ROI measurements at arterial and venous phases. Image J software was used to analyze particles to define the number of peritumoral vessels with the threshold. For quantitative image quality assessment, the number of vessels, SNR in peritumoral area and CNR between peritumoral vessel and NAWM were determined at each phase. To compare the quantitative indexes between two methods, CT values, SD, SNR, CNR and the number of peritumoral vessels on CE-UHR-CTA at each phase were compared between DLR and hybrid-type IR by Wilcoxon signed rank test. Then, number of peritumoral vessel on each CE-UHR-CTA were correlated with surgical risk by Pearson's correlation was performed.

#### RESULTS

CT values, SNR and CNR of DLR at each phase were significantly higher than those of hybrid-type IR ( $p < 0.05$ ). The number of peritumoral vessel on CE-UHR-CTA reconstructed with DLR was significantly higher than that with hybrid-type IR ( $p < 0.05$ ). There was significant correlation between the number of peritumoral vessel on CE-UHR-CTA with DLR and surgical time (artery phase;  $r = 0.43$ ,  $p < 0.05$ , venous phase;  $r = 0.40$ ,  $p < 0.05$ ), although there were no significant correlations between that on CE-UHR-CTA with hybrid-type IR at each phase and surgical time or between each CE-UHR-CTA and intraoperative bleeding volume ( $p > 0.05$ ).

#### CONCLUSION

s DLR has a potential for improving the depiction of peritumoral vessels and capability for predicting surgical risk for intracranial meningiomas on CE-UHR-CTA.

#### CLINICAL RELEVANCE/APPLICATION

DLR has a potential for improving the depiction of peritumoral vessels and capability for predicting surgical risk for intracranial meningiomas on CE-UHR-CTA.

Printed on: 02/07/23

## Abstract Archives of the RSNA, 2022

W5B-SPNR-17

### Unsupervised identification of MRI artifacts via integration of deep learning and image quality measures

Wednesday, Nov. 30 12:45PM - 1:15PM Room: Learning Center - NR DPS

#### Participants

Thomas Desilvio, Cleveland, OH (*Presenter*) Nothing to Disclose

#### PURPOSE

Brain MRI scans are widely used for neurological evaluation, but often can be compromised by artifacts (e.g., ringing, ghosting, motion). Identifying specific MRI artifacts is critical for refining imaging protocols and guiding post-processing and downstream analysis that can enhance clinical and research interpretation; but requires time intensive and often subjective effort. We present results for unsupervised identification of brain MRI artifacts via automated integration of deep learning with MR quality measures (QMs).

#### METHODS AND MATERIALS

Using cohorts from ABIDE-I (17 institutes, 1102 T1w MRIs, 3 reader quality ratings) a ResNet18 model was trained (n=454, 15 institutes) with labels of good quality (GQ) / poor quality (PQ), assigned based on rating agreement by 2+ readers. TCGA-GBM (5 institutes, 152 T1-POST MRIs) were then evaluated by three radiologists who labeled each scan as harboring each artifact type (ghosting, banding, motion, ringing) or otherwise; which was used as ground truth. Model inference was performed on the unseen TCGA-GBM cohort to yield 64 final-layer DL features per scan. 15 QMs (e.g., SNR, intensity-based contrast, variation, entropy measurements) via the MRQy tool were also extracted from each TCGA-GBM scan. 3 sets of features underwent unsupervised consensus clustering (see figure 1). Each clustering result was evaluated by identifying cluster correspondence with artifact type, and then calculating fraction of datasets per artifact group correctly clustered together to yield cluster overlap accuracy.

#### RESULTS

Combining DL and QMs achieved the best overall cluster overlap accuracies across all artifact types: 0.82 (banding), 0.78 (motion), 0.77 (ringing), and 0.84 (ghosting). QMs clustering achieved lower cluster overlap accuracies of 0.71 (banding), 0.75 (motion), 0.79 (ringing), and 0.80 (ghosting). DL features alone performed significantly worse with accuracies of 0.52 (banding), 0.63 (motion), 0.68 (ringing), and 0.66 (ghosting).

#### CONCLUSION

s Combined DL quality evaluation and image quality measures can enable unsupervised detection of brain MRI image artifacts.

#### CLINICAL RELEVANCE/APPLICATION

Detection of specific MRI image artifacts aids downstream image analysis and imaging protocol improvement. Deep learning and standard image quality measures appear complementary for this task.

Printed on: 02/07/23

## Abstract Archives of the RSNA, 2022

W5B-SPNR-18

### Tailoring radiologist behaviour by individualising F beta levels for predictions of an AI model

Wednesday, Nov. 30 12:45PM - 1:15PM Room: Learning Center - NR DPS

#### Participants

Peter R. Brotchie, MBBS, PhD, Fitzroy, Australia (*Presenter*) Consultant, Annalise-AI Pty Ltd

#### PURPOSE

When interpreting diagnostic imaging studies, radiologists rate of false negatives tends to higher than false positives on average, resulting in higher precision than recall. This is not desirable for critical findings where the cost of a false negative (eg. missed bleed) is greater than the cost of a false positive (eg. unnecessary MRI scan). The relative importance of recall and precision can be chosen for AI model predictions by choosing F-beta values for model thresholds. Our study assessed whether differences in F-beta values for the model findings influenced the radiologist precision and recall balance.

#### METHODS AND MATERIALS

A comprehensive CT brain convoluted neural network algorithm was used to investigate the effect of F-beta values of thresholds across a number of clinical findings, when comparing radiologist performance with and without the AI model assistance. F-beta values were chosen based on the criticality of the finding. The change in precision and recall for radiologists unassisted vs assisted was compared between groups of findings with F-beta values greater than 1, equal to 1 and lower than 1.

#### RESULTS

When unaided, radiologists' precision was higher than recall across all three groups of findings. When aided by the AI, radiologists' precision remained higher than recall for findings with an F-beta value of less than 1. However, for findings with F-beta values greater than 1 (critical findings), the recall significantly increased without a decrement in precision, resulting in higher recall than precision (Fig 1).

#### CONCLUSION

Altering the F-beta levels for finding predictions by a CT brain AI model markedly changed the behaviour of radiologists when using the model, influencing them to significantly increase recall over precision for critical findings.

#### CLINICAL RELEVANCE/APPLICATION

This is a desirable result as the ratio of false positives to false negatives should be based on the criticality of a finding given that the cost of a false negative will be higher than a false positive for critical findings.

Printed on: 02/07/23

## Abstract Archives of the RSNA, 2022

W5B-SPNR-2

### Clinical evaluation of deep-learning model for an automatic scoring of Alberta Stroke Program Early CT Score (ASPECTS) on non-contrast CT: A comparison study to the consensus of experts

Wednesday, Nov. 30 12:45PM - 1:15PM Room: Learning Center - NR DPS

#### Participants

Jin Soo Lee, Suwon, Korea, Republic Of (*Presenter*) Nothing to Disclose

#### PURPOSE

Since the ASPECTS has been used in clinical practice for over 20 years, the most prominent problem is the inter-rater difference. It may result from the rater's experience, or it may be according to the infarction around the borderline. Due to these differences, there have been required to consistent ASPECTS calculation, and recently, software has been reported to produce coherent ASPECTS using deep-learning technique. Therefore, in this study, the clinical applicability of deep learning-based software will be evaluated by comparing to the consensus of two experienced experts.

#### METHODS AND MATERIALS

The non-contrast CT (NCCT) of 487 AIS patients were used for learning the model, and it was included only cases in which MRI were taken within an hour after NCCT scanning. For the model learning, one experienced stroke expert evaluated whether the occurrences of early ischemic change (EIC) and old infarction (OI) in NCCT images by referring to MRI, such as DWI, ADC, and FLAIR. 326 patients were registered in the clinical evaluation. The results of the model were compared with the consensus generated by two stroke experts. A comparison between the deep-learning model and the experts' consensus was conducted by the Bland and Altman (BA) agreement. Finally, with the consensus as the ground truth, the sensitivity and specificity of the model for 10 regions of interest (ROIs) were calculated.

#### RESULTS

The BA agreement had a mean difference of 0.032 [95% confidence interval (CI): -0.076 ~ 0.141], and the upper and lower limit of agreement (LOA) were 2.8 [95% CI: 2.615 ~ 2.986] and -2.736 [95% CI: -2.914 ~ -2.55], respectively. For ASPECTS calculation, sensitivity and specificity to detect the EIC for 10 ROIs were 0.628 [95% CI: 0.585 ~ 0.671] and 0.966 [95% CI: 0.961 ~ 0.97], respectively. Also, in the dichotomized analysis based on 4 points ( $\leq 4$  vs.  $>4$ ), the sensitivity and specificity were 0.972 [95% CI: 0.959 ~ 0.985] and 0.619 [95% CI: 0.472 ~ 0.766], respectively.

#### CONCLUSION

The deep-learning model proposed for automatic ASPECT scoring confirmed reasonable agreement and accuracy compared with expert consensus; therefore, it is highly recommended to use for assisting clinicians in clinical environment.

#### CLINICAL RELEVANCE/APPLICATION

This deep-learning model has been integrated into the commercial Heuron-cASPECTS software. It will be a useful tool for clinicians to make fast decision of diagnosis and treatment, especially, it will be valuable in remote regions where neuro-radiology expert may be limited.

Printed on: 02/07/23



## Abstract Archives of the RSNA, 2022

W5B-SPNR-20

### Multi-Center Radiomics Analysis Predict Pseudo-Progression vs. True Progression in Glioblastoma Patients

Wednesday, Nov. 30 12:45PM - 1:15PM Room: Learning Center - NR DPS

#### Participants

Murat AK, MD, Pittsburgh, PA (*Presenter*) Nothing to Disclose

#### PURPOSE

To discriminate progressive disease (PD) vs. pseudoprogression (PsP) utilizing the radiomics analysis in glioblastoma (GBM).

#### METHODS AND MATERIALS

We evaluated 686 patients from three institutions of which 487 were TP, and 199 were PsP. We segmented edema, contrast enhancement, necrosis, and hemorrhage for each patient. Their respective contralateral white matter (cWM) regions of interest (ROI). 205 texture features were extracted from each sequence's volume of interest (VOI), including 10 histogram-based first-order features and 195 second-order gray-level co-occurrence matrices features. After normalization, the 195 second-order features were divided by their volume to produce 195 volume-independent—a total of 400 features extracted per VOI and 1600 features per patients. We removed features that are highly correlated (Pearson's correlation coefficient  $>0.80$ ) and performed feature selection on the remaining features using the SHapley Additive exPlanations (SHAP) package that measures the feature importance. We split the cohort into 90% training and 10% testing. We used XGBoost algorithm to generate the radiomics model. The predictive performance of the models for classifying each lesion (PD versus PSP) was estimated using the receiver operating characteristic curve, summarized as the area under the curve.

#### RESULTS

Out of the 1600 total features, 1491 features correlated greater than 0.80. These highly correlated features were removed from the total set, leaving 109 features. Feature selection with SHAP method on 109 features identified 86 that contribute highly to the outcome prediction. 30 of the 86 were most relevant and were used for model building. Our model's training set accuracy with 10-fold cross-validation was 80%, and the testing set accuracy was 81%, with sensitivity and specificity of 79% and 84%, respectively.

#### CONCLUSION

Our study presents a radiomics model that can successfully differentiate between PD vs. PsP in GBM patients.

#### CLINICAL RELEVANCE/APPLICATION

PsP can mimic PD radiographically; our study presents a radiomics model for noninvasive, individualized prediction of PsP in GBM at the time of the clinical question.

Printed on: 02/07/23

## Abstract Archives of the RSNA, 2022

W5B-SPNR-4

### Investigation on the image quality of head and neck CTA using energy spectrum combined with adaptive iterative scanning and deep learning algorithm

Wednesday, Nov. 30 12:45PM - 1:15PM Room: Learning Center - NR DPS

#### Participants

Deng Jie, (*Presenter*) Nothing to Disclose

#### PURPOSE

To investigate the influence and application value of spectral CT single-energy imaging combined with adaptive iterative reconstruction (ASIR) technology and deep learning algorithm on head and neck CT angiography (CTA).

#### METHODS AND MATERIALS

Comparison of energy spectrum (40keV, 60keV, 80keV) scanning, adaptive statistical iterative reconstruction algorithm (Adaptive Statistical Iterative Reconstruction-Veo, ASIR-V) and deep learning algorithm (DLIR-L, DLIR-M, DLIR-H) in 88 patients undergoing head and neck CTA examination. Image quality, volume projection and maximum density projection processing were performed on a total of five sets of images. The effects of different reconstruction methods on the image quality of head and neck CTA were evaluated from the two aspects of objective measurement and subjective score.

#### RESULTS

Objective evaluation: The CT value, SD value, SNR, and CNR of images with different reconstruction methods in each blood vessel in the seven groups were statistically different in each part ( $P < 0.05$ ). Partial analysis of the aortic arch DLIR-H > DLIR-L > ASIR-40% > 60keV > 80keV > 40keV ( $24.72 \pm 5.72$ ,  $P < 0.005$ ) was statistically significant. In the SNR comparison, the aortic arch part DLIR-H > DLIR-L > ASIR-40% > 60keV > 80keV > 40keV ( $28.41 \pm 35.06$ ,  $P < 0.05$ ). Comparing the CNR part again, DLIR-H has the highest CNR in the aortic arch, middle cerebral artery, vertebral artery and basilar artery, respectively ( $80.71 \pm 112.93$ ) and ( $76.57 \pm 84.33$ ) ( $63.84 \pm 32.94$ ) ( $59.51 \pm 29.48$ ) ( $P < 0.05$ ), with statistical difference. Subjective evaluation: Between each group, the Kappa value of the subjective score of the two diagnostic group physicians for the image reconstruction quality was 0.72. The scores of VR reconstructed images showed no statistical difference between the groups ( $P = 0.668$ ). There was no statistical difference in the scores of MIP reconstruction images among the groups ( $P = 0.467$ ). CPR reconstruction image score DLIR-H group > DLIR-M group > DLIR-L group > ASIR-40% group > A3 group > A2 group > A1 group, there were significant differences in the scores among the groups ( $P < 0.05$ ).

#### CONCLUSION

In terms of image quality of head and neck CTA examination, DLIR can reduce image noise, improve image SNR, and lower radiation dose than ASIR reconstruction technology and energy spectrum scanning. be applied in.

#### CLINICAL RELEVANCE/APPLICATION

Different reconstruction methods applied to head and neck CTA scanning, DLIR has more advantages than ASIR reconstruction and energy spectrum scanning technology.

Printed on: 02/07/23

## Abstract Archives of the RSNA, 2022

W5B-SPNR-5

### Faster, Lighter, Scalable: Harnessing data-mined line annotations for automated tumor segmentation on brain MRI

Wednesday, Nov. 30 12:45PM - 1:15PM Room: Learning Center - NR DPS

#### Participants

Vivek Yadav, MS, BEng, (*Presenter*) Stockholder, Moderna, Inc

#### PURPOSE

Tumor segmentation provides more accurate quantification of tumor burden versus linear measurement and is the major prerequisite step for radiomic analysis. While fully-supervised learning can yield high-performing segmentation models, the time and effort required to manually label large training sets limits clinical utility. We investigate whether data-mined tumor line annotations can be utilized to develop a brain MRI tumor segmentation model without the need for manually segmented training data.

#### METHODS AND MATERIALS

In this retrospective study, a previously described tumor detection model trained using clinical line annotations mined from PACS was leveraged with unsupervised segmentation (Otsu thresholding) to generate pseudo-masks of enhancing tumors on T1-weighted post-contrast images. Pseudo-masks were used to train baseline segmentation models using Mask R-CNN and HRNet architectures, which were employed within a semi-supervised learning (SSL) framework to automatically refine the pseudo-masks. Following each self-refinement cycle, a new model was trained and tested on a held-out set consisting of 319 manually segmented images from 93 adult patients (278 intra-axial and 88 extra-axial tumors) and performance evaluated using Dice score (DSC). The SSL cycles continued until performance peaked or plateaued. Two deployment methods were compared: (1) conventional end-to-end segmentation, and (2) a hybrid pipeline combining end-to-end segmentation with detection plus patch-wise segmentation.

#### RESULTS

Baseline segmentation models achieved DSC of 0.838 (Mask R-CNN) and 0.841 (HRNet), which improved with self-refinement to 0.871 (after 8 cycles) and 0.873 (after 7 cycles), respectively. The hybrid pipeline (maximum DSC 0.884, Mask R-CNN) outperformed end-to-end segmentation (maximum DSC 0.873, HRNet).

#### CONCLUSION

Line annotations mined from PACS can be harnessed in concert with unsupervised and semi-supervised techniques to achieve high-performing brain MRI tumor segmentation models, avoiding the need for manually segmented training data. This development pipeline provides a potential mechanism to rapidly establish tumor segmentation capabilities across imaging modalities.

#### CLINICAL RELEVANCE/APPLICATION

Accurate segmentation of tumors on brain MRI is achieved by leveraging clinical line annotations from PACS within an automated pipeline, avoiding the need for any manually segmented training data.

Printed on: 02/07/23

## Abstract Archives of the RSNA, 2022

W5B-SPNR-6

### Investigation on iodine suppression effect of virtual non-contrast images in different concentrations of iodine: A Phantom Study

Wednesday, Nov. 30 12:45PM - 1:15PM Room: Learning Center - NR DPS

#### Participants

Yaoming Ma, (*Presenter*) Nothing to Disclose

#### PURPOSE

To investigate the value of virtual non-contrast images in suppressing iodine in different concentrations of iodine.

#### METHODS AND MATERIALS

A polypropylene cylindrical phantom (QSP Phantom dimension) with nine tubes containing different concentrations of iodine (0, 2.5, 5, 10, 20 mgI/ml) was scanned using a spectral CT (Revolution, GE Healthcare) in gemstone spectral imaging (GSI) mode using fast kV switch (80/140 kV), the tube current is 485mA, the layer thickness is 1.25mm, the collimation width is 80mm, noise index (NI) 5HU, pitch 0.992:1. pre-ASiR-V 30% weight was used for gemstone spectral CT scanning. The CT and SD values of the images before and after iodine suppression of 20%, 10%, 5% and 2.5% iodine were measured. The area of region of interest (ROI) was 1 / 2-1 / 3 of the cross-sectional area of the somatosensory canal, and the size was consistent. The iodine suppression rate of different concentrations of iodine was calculated (iodine suppression rate =  $\{(CT \text{ value } 1 - CT \text{ value } 2) / CT \text{ value } 1\} * 100\%$ , CT value 1 was the CT value of the image before iodine suppression, CT value 2 was the CT value of the image after iodine suppression). The difference between the two groups was compared by one-way ANOVA, and the difference was statistically significant ( $P < 0.05$ ).

#### RESULTS

The CT value of iodine 20 before iodine suppression was  $431.5 \pm 67\text{Hu}$ , iodine 10, CT value was  $211.89 \pm 57\text{Hu}$ , iodine 5 CT value was  $107.09 \pm 82\text{Hu}$ , iodine 2.5, CT value was  $53.93 \pm 68\text{Hu}$ , the difference between the two groups was statistically significant ( $P < 0.05$ ); The CT value of iodine 20 after iodine suppression was  $14.34 \pm 42\text{Hu}$ , iodine 10, CT value was  $13.84 \pm 80\text{Hu}$ , iodine 5 CT value was  $15.2 \pm 62\text{Hu}$ , iodine 2.5, CT value was  $13.99 \pm 46\text{Hu}$ , there was no significant difference between the two groups ( $P > 0.05$ ). The iodine inhibition rates of iodine 20, 10, 5 and 2.5 were 96.67%, 93.45%, 85.77%, 74.02% respectively, and the iodine inhibition rates gradually decreased, and the difference between the groups was statistically significant ( $P < 0.05$ ).

#### CONCLUSION

From the evaluation of iodine suppression rate and CT value of virtual plain scan (VNC) images with different concentrations of iodine, the virtual plain scan (VNC) iodine suppression technology has a good effect on different concentrations of blood vessels.

Printed on: 02/07/23

## Abstract Archives of the RSNA, 2022

W5B-SPNR-7

### Can Machine Learning Be Better Than Biased Readers?

Wednesday, Nov. 30 12:45PM - 1:15PM Room: Learning Center - NR DPS

#### Participants

Rui Zhu, BSc, Toronto, ON (*Presenter*) Nothing to Disclose

#### PURPOSE

The purpose is to determine if machine learning algorithms can overcome reader biases and more closely match multiple reader consensus than individual readers' diagnostic accuracy when training a binary convolutional neural network (CNN) classifier. Training deep learning models in medical imaging requires large amounts of labeled data. It is common to divide the training data amongst multiple readers with varying levels of expertise to minimize the effort. Alternatively, multiple small datasets labeled by different readers are combined for training. In both scenarios the readers' consensus is not obtained leading to a biased dataset.

#### METHODS AND MATERIALS

This study used a binary-class chest X-ray dataset and corresponding labels of pediatric pneumonia obtained from Guangzhou Women and Children's Medical Center. Wrong labels are generated for biased readers by sampling from the probability distribution of their biases defined by Bernoulli distributions of producing an observed label given the true label. The true labels were assumed to be the consensus of the readers. The readers' performances were evaluated based on their annotations on the test set. The models' testing performances were compared to readers' performances. Resnet18 without transfer learning was used as baseline model. A variation of Resnet18 with modified loss function was used as an improvement on the baseline model.

#### RESULTS

The baseline model's test accuracy was higher than the average accuracy of the biased readers (59%-69%) by 2%-9% when the average accuracy of all readers was 73%-79%. The improved model with the modified loss function trained on a dataset containing 30% biased labels achieved 86% test accuracy, being higher than the average of all readers (69%), when readers' labels can compensate each other's errors. The improved model with the modified loss function produced more robust accuracies (79%-86%) than the baseline model (70%-83%) while varying the strengths and the types of the biases held by the readers.

#### CONCLUSION

s This study demonstrated that it is possible for machine learning algorithms to overcome individual readers' biases in training a binary CNN classifier. It is recommended to use robust loss functions as they are easy to implement and effective in mitigating biased labels.

#### CLINICAL RELEVANCE/APPLICATION

AI technology assists medical practitioners to analyze radiological images efficiently to inform patients of their condition timely. Our study focuses on training AI on datasets with biased labels.

Printed on: 02/07/23

## Abstract Archives of the RSNA, 2022

W5B-SPNR-9

### Effectiveness of a Convolutional Neural Network Artificial Intelligence Algorithm in the Detection of Intracranial Hemorrhage on Noncontrast CT Imaging

Wednesday, Nov. 30 12:45PM - 1:15PM Room: Learning Center - NR DPS

#### Participants

Ayden Jacob, Boca Raton, FL (*Presenter*) Consultant, Aidoc Medical Ltd

#### PURPOSE

Radiologic misdiagnosis of intracranial hemorrhage (ICH) may result in poor patient outcomes. This study aimed to assess the accuracy and clinical viability of an AI-based algorithm in the detection of ICH on noncontrast CT (NCCT) imaging.

#### METHODS AND MATERIALS

An FDA approved AI solution based on a convolutional neural network was used to assess 8468 NCCTs. Data was collected from 29 different facilities. Slice thickness ranged from 0.625 mm to 5mm. NCCTs were retrospectively processed through the AI solution and assigned a positive or negative for ICH allocation. Each report was analyzed by a natural language processing software and assigned a positive or negative for ICH allocation per the radiologist's interpretation. Cases were stratified as concordant, wherein the radiologist and AI interpretation agreed, and discordant, in which interpretations differed. NLP results for discordant cases were externally validated. 2 board certified neuroradiologists and 1 general radiologist assessed discordant NCCTs for ICH to determine ground truth by majority opinion.

#### RESULTS

98 AI positives were engaged with by the radiologist at the time of data collection and were excluded from the cohort. Concordant cases included 288 double positives (AI+/Rad+) and 7950 double negatives (AI-/Rad-). 132 discordant cases included 100 scans positive by AI and negative per radiologist's report (AI+/Rad-), and 32 scans negative by AI and positive by report (AI-/Rad+). Following consensus review by 3 radiologists, individual and combined accuracy metrics were acquired for both entities. Radiologist metrics included an accuracy of 99.1%, sensitivity of 94.5%, and a specificity of 99.9%. AI demonstrated an accuracy of 98.8%, sensitivity of 93.6%, and a specificity of 99.1%. Differences in accuracy and specificity were statistically significant ( $p < .00001$ ) whereas sensitivity was not ( $p = .61708$ ). Combined accuracy was 99.6% with minimal loss of specificity (99%). The radiologists detected 309 positive cases, and an additional 18 ICHs were detected by the AI solution, providing an added detection rate of 5.8%.

#### CONCLUSION

This study demonstrates that an AI-solution can assist radiologists in the diagnosis of ICH. Radiologists leveraging AI-solutions have an increased sensitivity in the detection of ICH.

#### CLINICAL RELEVANCE/APPLICATION

The combined precision and accuracy of the AI-radiologist combination highlights the value of coupling a high sensitivity screening test (AI) with a higher specificity validation test (radiologist). Synergy between radiologists and AI solutions in the detection of ICH may improve patient outcomes through minimizing false negative rates.

Printed on: 02/07/23

## Abstract Archives of the RSNA, 2022

W5B-SPOB

### OB/Gynecology Wednesday Poster Discussions - B

Wednesday, Nov. 30 12:45PM - 1:15PM Room: Learning Center - OB DPS

#### Participants

Priyanka Jha, MBBS, San Francisco, CA (*Moderator*) Nothing to Disclose

#### Sub-Events

#### W5B-SPOB- Cervical Cancer Heterogeneity: Spatial Habitats from Multiparametric MRI in Predicting Tumor Stages 1

Participants

Xinyue Liang, Shanghai, China (*Presenter*) Nothing to Disclose

#### PURPOSE

Tumors are commonly heterogeneous, which is informative for characterization, staging classification and outcome prediction. It is of great value to study noninvasive method for assessing intratumor heterogeneity in cervical cancer. This study aimed to assess the clinic feasibility and performance of the tumor heterogeneity characterized by spatial habitats from multiparametric MRI to predict FIGO stages of cervical cancer patients.

#### METHODS AND MATERIALS

Ninety-seven patients at different stages (FIGO IA-IIIC2) cervical cancer were involved in this study. All the MRI examinations were performed on a 3.0T MR scanner (uMR 780; United Imaging Healthcare, Shanghai, China) using T1-weighted (T1W), T2-weighted (T2W) and diffusion weighted imaging (DWI) ( $b = 0$  and  $1500 \text{ s/mm}^2$ ). K-means clustering method was used for classifying different habitats, of which deriving the volume size and fraction. Clusters amounts 3, 4, 5 and 6 were initially set, and three spatial habitats were adopted for an explainable biological meaning. The performance of habitats analysis and mean ADC of the tumor between low FIGO stages (IA and IB) with high FIGO stages (II and III) of cervical cancer were assessed using the Mann-Whitney U test.

#### RESULTS

Three MRI habitats (hyperemia tissue, lipid tissue, and solid tissue habitat) were identified within the tumor, among which hyperemia tissue (high DW, high T2W, and low T1W values) was highly correlated with tumor stages ( $p < 0.001$ ). The volume size and fraction of hyperemia habitat in high FIGO stage were significantly higher than those in low FIGO stage (AUC = 0.78 and AUC = 0.77,  $p < 0.001$ ), outperforming mean ADC values (AUC = 0.59,  $p > 0.05$ ). In addition, solid tissue and lipid tissue were insignificant in differentiating tumor stages ( $p > 0.05$ ).

#### CONCLUSION

Hyperemia tissue habitats from multiparametric MRI performed excellent discrimination of the tumor staging in cervical cancer.

#### CLINICAL RELEVANCE/APPLICATION

Habitat analysis from multiparametric MRI can provide a non-invasive and innovative approach towards intratumor heterogeneity, which is promising in differentiating cervical cancer stages.

#### W5B-SPOB- Multi-Plane Segmentation of Uterus, Endometrium and Uterine Fibroids From MR Images Using Self-Configuring nNU-Net 2

Participants

Xinyu Liu, MD, Beijing, China (*Presenter*) Nothing to Disclose

#### PURPOSE

Uterine fibroids are the most common gynecologic benign tumors and contribute to significant morbidity. MRI provides an accurate assessment of the number, location, and type of fibroids. However, the segmentation of uterus and uterine fibroids from MR images is difficult to achieve. We proposed a self-configuring MR imaging segmentation method based on the nNU-Net deep learning network.

#### METHODS AND MATERIALS

Two multi-plane (T2 sagittal and T2 axial images of the female pelvis MR images) datasets are used to validate the performance of the proposed uterus, endometrium, and uterine fibroids segmentation algorithm in this research. nNU-Net systematically addresses the configuration of entire segmentation pipelines and provides visualization and description of the most relevant design choices.

#### RESULTS

The dataset enrolls 199 patients with 5mm slice thickness MR volumes. They are randomly divided into 159 for training, and 40 for testing. The Dice similarity coefficient (DSC) of the uterus, endometrium, and uterine fibroids are 91.3%, 80.8%, and 77.0% in T2 sagittal MR images using the nNU-Net deep learning network; the hausdorff\_95 (95HD) of these three are 7.426, 6.654 and

10.926mm. The DSC of the uterus, endometrium, and uterine fibroids are 92.0%, 73.4%, 79.6% in T2 axial MR images, the 95HD are 7.324, 11.057, and 9.716mm.

#### **CONCLUSION**

s We have proposed a self-configuring nnU-Net deep learning network method to segment uterus, endometrium, and uterine fibroids automatically.

#### **CLINICAL RELEVANCE/APPLICATION**

Correctly classifying and recognizing fibroids is essential for treatment planning and the prevention of complications.

Printed on: 02/07/23

## Abstract Archives of the RSNA, 2022

W5B-SPOB-1

### Cervical Cancer Heterogeneity: Spatial Habitats from Multiparametric MRI in Predicting Tumor Stages

Wednesday, Nov. 30 12:45PM - 1:15PM Room: Learning Center - OB DPS

#### Participants

Xinyue Liang, Shanghai, China (*Presenter*) Nothing to Disclose

#### PURPOSE

Tumors are commonly heterogeneous, which is informative for characterization, staging classification and outcome prediction. It is of great value to study noninvasive method for assessing intratumor heterogeneity in cervical cancer. This study aimed to assess the clinic feasibility and performance of the tumor heterogeneity characterized by spatial habitats from multiparametric MRI to predict FIGO stages of cervical cancer patients.

#### METHODS AND MATERIALS

Ninety-seven patients at different stages (FIGO IA-IIIC2) cervical cancer were involved in this study. All the MRI examinations were performed on a 3.0T MR scanner (uMR 780; United Imaging Healthcare, Shanghai, China) using T1-weighted (T1W), T2-weighted (T2W) and diffusion weighted imaging (DWI) ( $b = 0$  and  $1500 \text{ s/mm}^2$ ). K-means clustering method was used for classifying different habitats, of which deriving the volume size and fraction. Clusters amounts 3, 4, 5 and 6 were initially set, and three spatial habitats were adopted for an explainable biological meaning. The performance of habitats analysis and mean ADC of the tumor between low FIGO stages (IA and IB) with high FIGO stages (II and III) of cervical cancer were assessed using the Mann-Whitney U test.

#### RESULTS

Three MRI habitats (hyperemia tissue, lipid tissue, and solid tissue habitat) were identified within the tumor, among which hyperemia tissue (high DW, high T2W, and low T1W values) was highly correlated with tumor stages ( $p < 0.001$ ). The volume size and fraction of hyperemia habitat in high FIGO stage were significantly higher than those in low FIGO stage (AUC = 0.78 and AUC = 0.77,  $p < 0.001$ ), outperforming mean ADC values (AUC = 0.59,  $p > 0.05$ ). In addition, solid tissue and lipid tissue were insignificant in differentiating tumor stages ( $p > 0.05$ ).

#### CONCLUSION

Hyperemia tissue habitats from multiparametric MRI performed excellent discrimination of the tumor staging in cervical cancer.

#### CLINICAL RELEVANCE/APPLICATION

Habitat analysis from multiparametric MRI can provide a non-invasive and innovative approach towards intratumor heterogeneity, which is promising in differentiating cervical cancer stages.

Printed on: 02/07/23

## Abstract Archives of the RSNA, 2022

W5B-SPOB-2

### Multi-Plane Segmentation of Uterus, Endometrium and Uterine Fibroids From MR Images Using Self-Configuring nnU-Net

Wednesday, Nov. 30 12:45PM - 1:15PM Room: Learning Center - OB DPS

#### Participants

Xinyu Liu, MD, Beijing, China (*Presenter*) Nothing to Disclose

#### PURPOSE

Uterine fibroids are the most common gynecologic benign tumors and contribute to significant morbidity. MRI provides an accurate assessment of the number, location, and type of fibroids. However, the segmentation of uterus and uterine fibroids from MR images is difficult to achieve. We proposed a self-configuring MR imaging segmentation method based on the nnU-Net deep learning network.

#### METHODS AND MATERIALS

Two multi-plane (T2 sagittal and T2 axial images of the female pelvis MR images) datasets are used to validate the performance of the proposed uterus, endometrium, and uterine fibroids segmentation algorithm in this research. nnU-Net systematically addresses the configuration of entire segmentation pipelines and provides visualization and description of the most relevant design choices.

#### RESULTS

The dataset enrolls 199 patients with 5mm slice thickness MR volumes. They are randomly divided into 159 for training, and 40 for testing. The Dice similarity coefficient (DSC) of the uterus, endometrium, and uterine fibroids are 91.3%, 80.8%, and 77.0% in T2 sagittal MR images using the nnU-Net deep learning network; the hausdorff\_95 (95HD) of these three are 7.426, 6.654 and 10.926mm. The DSC of the uterus, endometrium, and uterine fibroids are 92.0%, 73.4%, 79.6% in T2 axial MR images, the 95HD are 7.324, 11.057, and 9.716mm.

#### CONCLUSION

s We have proposed a self-configuring nnU-Net deep learning network method to segment uterus, endometrium, and uterine fibroids automatically.

#### CLINICAL RELEVANCE/APPLICATION

Correctly classifying and recognizing fibroids is essential for treatment planning and the prevention of complications.

Printed on: 02/07/23

## Abstract Archives of the RSNA, 2022

W5B-SPPD

### Pediatric Wednesday Poster Discussions - B

Wednesday, Nov. 30 12:45PM - 1:15PM Room: Learning Center - PD DPS

#### Participants

Adina L. Alazraki, MD, Atlanta, GA (*Moderator*) Nothing to Disclose

#### Sub-Events

### W5B-SPPD- A Comparative Study of Different Machine Learning Classifiers for Differentiating Pediatric Cerebellar Tumors: Medulloblastomas, Ependymomas and Pilocytic Astrocytomas<sup>1</sup>

#### Participants

Bilgin Keserci, PhD, (*Presenter*) Nothing to Disclose

#### PURPOSE

The aim of this study is to comparatively investigate the role of machine learning (ML) classifiers in distinguishing pediatric cerebellar tumors.

#### METHODS AND MATERIALS

This retrospective study included preoperative magnetic resonance imaging (MRI) of 63 patients with pediatric posterior fossa tumors, including medulloblastomas (n=40), ependymomas (n=9), and pilocytic astrocytomas (n=14). Eighteen MRI features were extracted from T2-weighted (T2W) images, contrast-enhanced T1-weighted (CE-T1) images, fluid-attenuated inversion recovery (FLAIR) images and diffusion weighted images (DWIs). We compared five different machine learning classifiers (i.e., Logistic Regression (LR), Support Vector Machine (SVM), K-nearest Neighbors (KNN), Random Forest (RF) and Gradient Boosting (GBM) for differentiation of the 3 most common pediatric posterior fossa tumors. The diagnostic ability of ML classifiers was performed by means of standard performance metrics, including the area under the receiver operating characteristic curve (AUROC), accuracy, sensitivity, specificity, F1-score and average cross validation score in five folds cross-validation.

#### RESULTS

The KNN algorithm showed the best predictive performance with an AUROC of 0.96 and accuracy of 0.95, followed by the GBM, RF, LR and SVC classifiers, which yielded an AUROC of 0.93, 0.89, 0.86 and 0.82, and accuracy of 0.95, 0.9, 0.86 and 0.86, respectively. For all five different machine learning classifiers, specificity ranged from 0.71 to 1.0, sensitivity ranged from 0.86 to 1.0, F1-score ranged from 0.89 to 0.96, and average cross validation score ranged from 0.83 to 0.9. Medulloblastomas showed iso-intensity on T2W and FLAIR images meanwhile ependymomas and pilocytic astrocytomas appeared hyper-intensity on T2W and FLAIR images. Medulloblastomas and ependymomas were mostly high intensity on DWI, whereas pilocytic astrocytomas were usually low intensity on DWI.

#### CONCLUSION

We have compared different ML classifiers for prediction of the most common posterior fossa tumors, and found that KNN algorithm achieved greater accuracy in tumor differentiation.

#### CLINICAL RELEVANCE/APPLICATION

It is crucial to develop a novel artificial intelligence-based noninvasive diagnostic tool to be implemented in a clinical setting. Such a tool would not only help in differentiating the tumor type and grade of the tumor but also assist in planning the treatment. It will also reduce the need for biopsy for diagnosis.

Printed on: 02/07/23

## Abstract Archives of the RSNA, 2022

W5B-SPPD-1

### **A Comparative Study of Different Machine Learning Classifiers for Differentiating Pediatric Cerebellar Tumors: Medulloblastomas, Ependymomas and Pilocytic Astrocytomas**

Wednesday, Nov. 30 12:45PM - 1:15PM Room: Learning Center - PD DPS

#### **Participants**

Bilgin Keserci, PhD, (*Presenter*) Nothing to Disclose

#### **PURPOSE**

The aim of this study is to comparatively investigate the role of machine learning (ML) classifiers in distinguishing pediatric cerebellar tumors.

#### **METHODS AND MATERIALS**

This retrospective study included preoperative magnetic resonance imaging (MRI) of 63 patients with pediatric posterior fossa tumors, including medulloblastomas (n=40), ependymomas (n=9), and pilocytic astrocytomas (n=14). Eighteen MRI features were extracted from T2-weighted (T2W) images, contrast-enhanced T1-weighted (CE-T1) images, fluid-attenuated inversion recovery (FLAIR) images and diffusion weighted images (DWIs). We compared five different machine learning classifiers (i.e., Logistic Regression (LR), Support Vector Machine (SVM), K-nearest Neighbors (KNN), Random Forest (RF) and Gradient Boosting (GBM) for differentiation of the 3 most common pediatric posterior fossa tumors. The diagnostic ability of ML classifiers was performed by means of standard performance metrics, including the area under the receiver operating characteristic curve (AUROC), accuracy, sensitivity, specificity, F1-score and average cross validation score in five folds cross-validation.

#### **RESULTS**

The KNN algorithm showed the best predictive performance with an AUROC of 0.96 and accuracy of 0.95, followed by the GBM, RF, LR and SVC classifiers, which yielded an AUROC of 0.93, 0.89, 0.86 and 0.82, and accuracy of 0.95, 0.9, 0.86 and 0.86, respectively. For all five different machine learning classifiers, specificity ranged from 0.71 to 1.0, sensitivity ranged from 0.86 to 1.0, F1-score ranged from 0.89 to 0.96, and average cross validation score ranged from 0.83 to 0.9. Medulloblastomas showed iso-intensity on T2W and FLAIR images meanwhile ependymomas and pilocytic astrocytomas appeared hyper-intensity on T2W and FLAIR images. Medulloblastomas and ependymomas were mostly high intensity on DWI, whereas pilocytic astrocytomas were usually low intensity on DWI.

#### **CONCLUSION**

s We have compared different ML classifiers for prediction of the most common posterior fossa tumors, and found that KNN algorithm achieved greater accuracy in tumor differentiation.

#### **CLINICAL RELEVANCE/APPLICATION**

It is crucial to develop a novel artificial intelligence-based noninvasive diagnostic tool to be implemented in a clinical setting. Such a tool would not only help in differentiating the tumor type and grade of the tumor but also assist in planning the treatment. It will also reduce the need for biopsy for diagnosis.

Printed on: 02/07/23



## Abstract Archives of the RSNA, 2022

W5B-SPPH

### Physics Wednesday Poster Discussions - B

Wednesday, Nov. 30 12:45PM - 1:15PM Room: Learning Center - PH DPS

#### Sub-Events

#### W5B-SPPH- Image Reconstruction for Dedicated TOF PET Brain Systems Without Transmission Data 1

Participants

Chien-Min Kao, PhD, Chicago, IL (*Presenter*) Stockholder, Walgreens Boots Alliance, Inc

#### PURPOSE

For PET imaging of the brain, dedicated systems of high resolution and sensitivity are necessary. For hybrid PET/MR imaging, integrated and insert systems are developed. These systems often lack a CT system to produce attenuation images needed for accurate reconstruction while quantification is important for staging brain disorders. It has been shown that TOF PET data alone may allow simultaneous activity and attenuation (SAA) image reconstruction. However, the standard maximum-likelihood attenuation-activity (MLAA) algorithm can be unstable. This work develops a constrained MLAA method to improve reconstruction.

#### METHODS AND MATERIALS

We apply the alternating direction method of multipliers (ADMM) to optimize the nonconvex cost function of the TOF PET data in SAA incorporating constraints on the total variations (TVs) on the attenuation (AT) and activity (AC) maps and also on the total level of the latter. Numerical AT and AC maps for the adult brain are created, the former includes a skull enclosing uniform water attenuation, whereas the latter contains the gray matter (GM), the white matter (WM), and a 1cm-diameter lesion (L) in the WM, using a 5:1:3 activity ratio (GM:WM:L). Two TOF resolutions, 200 and 600 ps, are examined. Data containing approximately 1-million events are generated. AT and AC maps obtained with our proposed (TV-MLAA) and the existing MLAA algorithms are compared with the known truths.

#### RESULTS

The AT and AC maps produced by MLAA grow increasingly noisier as iteration increases. In contrast, the AT and CT maps of the TV-MLAA remain stable and appear convergent. Visually, the AC maps of TV-MLAA show decreased noise but well-preserved boundary and contrast between the GM and WM with lesion readily identified, in comparison to those of MLAA. We also evaluate the contrast-to-noise ratio (CNR) of the lesion. For TV-MLAA, the CNRs are 1.01 for both TOFs, whereas for 100-iteration MLAA, the CNR is 0.55 at 200 ps but degrades to 0.36 at 600 ps.

#### CONCLUSION

We develop the TV-MLAA algorithm for SAA reconstruction from TOF PET data, and consider 200 and 600 ps TOFs that bracket the present resolution range. At both resolutions, we show that the TV-MLAA algorithm stably yields qualitatively and quantitatively accurate AC maps. Based on our preliminary results, the lesion CNR achieved with TV-MLAA is two to three times that of MLAA.

#### CLINICAL RELEVANCE/APPLICATION

Quantitative PET imaging is important for brain disorders but unlike PET/CT systems attenuation maps of the brain may not be readily available when using the hybrid PET/MR and dedicated PET brain imaging systems. The TV-MLAA algorithm developed may be useful for these emerging imaging technologies by allowing accurate image reconstruction from TOF PET data alone.

#### W5B-SPPH- High-Resolution MRI and Diffusion-Weighted Imaging of the Human Pancreas at 5 Tesla 2

Participants

Liyun Zheng, Shanghai, China (*Presenter*) Nothing to Disclose

#### PURPOSE

The purpose of this study was to explore the feasibility of imaging the pancreas at 5T and evaluate the practical improvement of high-resolution magnetic resonance imaging (MRI) and diffusion-weighted imaging (DWI) at 5T as compared with 3T.

#### METHODS AND MATERIALS

Eighteen healthy subjects were recruited for this prospective study. MRI examinations were performed on both 3T and 5T scanners. The MRI sequences included T2-weighted fast spin-echo (FSE) and DWI with reduced field-of-view (FOV). Subjective image analysis with a 4-point Likert scale was performed by two experienced radiologists. Signal-to-noise ratio (SNR) and apparent diffusion coefficient (ADC) value were measured in the head, body, and tail of the pancreas. Coefficient of variation (CV) of ADC was calculated as  $CV(ADC) = SD(ADC) / \text{mean}(ADC)$ . A series of paired Wilcoxon tests was used to compare the subjective image quality, mean ADC value, and CV of ADC between 3T and 5T measurements.  $P < 0.05$  was considered statistically significant.

#### RESULTS

For T2-weighted images, there was no significant difference in image quality ratings between 3T and 5T ( $P = 0.593$ ). At lower b-

value images ( $b = 0 \text{ s/mm}^2$ ), the image quality ratings had no significant difference between different magnetic field strengths, while at higher b-value images ( $b = 800 \text{ s/mm}^2$ ), the ratings were significantly higher at 5T ( $P = 0.046$ ). The mean ratios of SNR at 5 T to 3 T of the T2 images for the pancreatic head, body, and tail were 1.16, 1.33, and 1.39, respectively. For the DWI images ( $b = 800 \text{ s/mm}^2$ ), the corresponding ratios were 1.29, 1.40, and 1.24, respectively. The SNRs of both T2-weighted and DWI images were significantly higher at 5T than at 3T ( $P$  ranging from 0.0002 to 0.0095 for all comparisons). For both 3T and 5T, mean ADC values on pancreatic head were significantly higher than those of tail ( $P = 0.016$  for 3T, and  $P = 0.018$  for 5T), while no significant difference was observed between pancreatic head and body ( $P = 0.679$  for 3T, and  $P = 0.445$  for 5T). There was no significant difference in mean ADC values and CV of ADC between 3T and 5T ( $P > 0.05$  for all comparisons).

## CONCLUSION

This initial study proved that 5T MRI can be used to acquire high-resolution pancreatic imaging with higher SNR and sufficient image quality.

## CLINICAL RELEVANCE/APPLICATION

This initial study proved that 5T MRI can be used to acquire high-resolution pancreas imaging with higher SNR and sufficient image quality. Consequently, pancreas MRI at 5T may be useful for the diagnosis and management of pancreatic diseases.

## W5B-SPPH- Clinical Evaluation of Rubidium-82 Generator for Cardiac PET Imaging

3

Participants

Rameshwar Prasad, PHD, Chicago, IL (*Presenter*) Nothing to Disclose

## PURPOSE

Positron emission tomography (PET) using Rubidium-82 allows myocardial perfusion imaging and absolute functional assessment of ventricular function due to its higher diagnostic accuracy and its onsite generator-based availability in clinics. Precise and consistent production and infusion of contaminants-free Rubidium-82 is required for accurate myocardial estimates and radiation safety. In this study, we evaluated the performance of Rubidium-82 generator for high-throughput, high-volume cardiac PET imaging using constant flow and constant activity delivery techniques.

## METHODS AND MATERIALS

Daily performance metrics of 10 strontium-82/rubidium-82 ( $^{82}\text{Sr}/^{82}\text{Rb}$ ) generators (RUBY-FILL, Canada) were studied for over 20 months infusing over 5000 patients. An automated daily quality control (QC) procedure was performed on each day of clinical use and the eluted Rb-82 was measured by the onboard dose calibrator of the elution system. On-board dose calibrator constancy, Sr82/Rb82 and Sr85/Rb82 breakthrough were assessed. Percent deviation in delivered activity and duration are assessed for each patient (rest and stress) using constant activity (CA) and constant flow (CF) infusion methods.

## RESULTS

Percent constancy deviation was  $0.73 \pm 0.4$ . Sr82/Rb82 and Sr85/Rb82 breakthrough (% USP) were  $5.1 \pm 1.4$  and  $0.87 \pm 0.6$  respectively. Net delivered activity deviation (%) was higher for rest studies than stress whereas delivery duration (%) was higher for stress studies. Delivered activity deviation (%) for CF and CA were  $0.01 \pm 0.18$  and  $0.03 \pm 0.54$ , respectively. Sr-82/Rb-82 and Sr-85/Rb-82 breakthrough was found higher than limits for 3 patients due to incorrect use of proscribed elution saline.

## CONCLUSION

s RUBY-FILL™ Rb-82 generator provided consistent Rb-82 activities for high throughput clinical cardiac PET imaging. Sr-82/Rb-82 and Sr-85/Rb-82 breakthrough were within the radiation safety limits during the studied period of 20 months except a day. Constant flow is preferred infusion method based on our institutional experience.

## CLINICAL RELEVANCE/APPLICATION

Generator based Rb-82 provides readily availability of radiotracer and weight-based quantitation of myocardial blood flow and perfusion with optimal radiation safety.

## W5B-SPPH- Validation of a Deep Learning Model for COVID-19 Diagnosis from Portable and Stationary Dual-Energy Chest Radiography Units

4

Participants

Mena Shenouda, BS, (*Presenter*) Nothing to Disclose

## PURPOSE

To validate a deep learning model for COVID-19 diagnosis from chest radiographs (CXR) and to compare performance on images from portable units vs. stationary dual-energy subtraction units.

## METHODS AND MATERIALS

A deep learning model trained on CXRs from a single institution was previously published. To validate this trained model, a large cohort of cases from the same institution was retrospectively collected as an independent test set. The data comprised the first CXR acquired <2 days after the patients' reverse transcription polymerase chain reaction (PCR) tests for the SARS-CoV-2 virus. Among the 12,251 patients, 2,464 (20.1%) had tested positive, and 9,787 (79.9%) had tested negative for the virus. CXRs of 9,471 (77.3%) patients were acquired using portable units, and CXRs of 2,780 (22.7%) patients were acquired using stationary units with COVID prevalences of 20.5% and 18.8%, respectively. The COVID diagnosis classification task was performed using standard images alone, soft-tissue images alone, and a combination of the two via feature fusion. Portable soft-tissue images were generated post-acquisition with commercial software. No model training or fine-tuning was performed. Classification between the radiographs of COVID-positive and COVID-negative patients was evaluated using the area under the receiver operating characteristic curve (AUC) as the performance metric.

## RESULTS

Performance of the model on images from both modalities yielded AUC values [95% CI] of 0.69 [0.68, 0.70] for standard images, 0.67 [0.66, 0.69] for soft-tissue images, and 0.66 [0.65, 0.68] for their combination. For CXRs acquired from portable units, AUCs for standard images, soft-tissue images, and their combination were 0.70 [0.69, 0.72], 0.68 [0.67, 0.70], and 0.67 [0.66, 0.69],

respectively. For CXRs acquired from stationary units, AUCs for standard images, soft-tissue images, and their combination were 0.66 [0.64, 0.69], 0.64 [0.61, 0.67], and 0.64 [0.61, 0.67], respectively. AUCs were significantly higher for CXRs acquired from portable vs. stationary units ( $p=0.007$ , 0.004, and 0.04 for standard images, soft-tissue images, and their combination, respectively). Within both modalities, the highest AUC was achieved for standard CXRs.

## CONCLUSION

This study tested a previously trained model for radiography-based COVID-19 diagnosis on a large, independent in-house dataset with promising results.

## CLINICAL RELEVANCE/APPLICATION

AI generalizability in the differentiation of COVID-positive and COVID-negative patients based on chest radiography was demonstrated on a large dataset from a single institution as a precursor to using the Medical Imaging and Data Resource Center (MIDRC) multi-institution initiative, which will further validate this model.

## W5B-SPPH- Modified Diffusion Imaging With Phase-Contrast Using Motion-Compensated Diffusion Encoding (MDIP) For Quantification of Regional Cerebral Blood Flow

Participants

Genki Nambu, BA, (Presenter) Nothing to Disclose

## PURPOSE

We recently developed a method of diffusion imaging with phase-contrast (DIP) for quantification of regional cerebral blood flow (rCBF), in which the total CBF (tCBF) from phase-contrast magnetic resonance imaging (PC-MRI) was used to convert the perfusion-related diffusion parameters ( $D^*$ ) in the brain. However, DIP is sensitive to brain pulsation and takes up to 10 min. To tackle these issues, we developed a modified DIP (mDIP) in which a motion-compensated diffusion gradient was applied, and the number of b-values were minimized.

## METHODS AND MATERIALS

Eleven healthy volunteers (nine men and two women; mean age, 23.9 years) participated in this study. On a 3.0-T MRI, diffusion-weighted images of the whole brain were acquired using single-shot diffusion echo-planar imaging with the first-order motion-compensated diffusion gradient to reduce the brain pulsation effect. Further, the number of b-values was minimized (0, 10, 100, and 800 s/mm<sup>2</sup>) to shorten the scan time (1 min 55 sec). Next, we performed voxel-wise estimations of the  $D^*$ , perfusion fraction (F), multiplication of  $D^*$  and F ( $FD^*$ ), and restricted diffusion coefficient using biexponential function. Furthermore, PC-MRI was performed to obtain the tCBF from the volumetric flow rate at the main feeding arteries into the cranium (1 min 32 sec). By using the tCBF obtained from PC-MRI, we converted the  $FD^*$  in the brain into absolute rCBF. We determined rCBF using mDIP and arterial spin labeling (ASL) and their correlations in gray and white matter (GM and WM, respectively) in healthy volunteers and assessed the relationship between the two methods.

## RESULTS

The rCBF images obtained using mDIP and ASL provided good contrast between the GM and WM as well as general resemblance. A highly significant positive correlation between the mDIP and ASL in terms of rCBF was observed in GM ( $R = 0.88$ ,  $P < 0.05$ ), which was higher than that of DIP without motion-compensated diffusion gradient, whereas the correlation between the methods was still poor in WM ( $P > 0.05$ ). The rCBF values in GM ( $41.5 \pm 14.8$  mL/100 g/min) and WM ( $16.6 \pm 10.9$  mL/100 g/min) obtained using mDIP were consistent with the values assessed using [15O]-water positron emission tomography reported in literature.

## CONCLUSION

mDIP makes it possible to quantitatively evaluate rCBF as well as standard diffusion parameters within 3 min 30 sec.

## CLINICAL RELEVANCE/APPLICATION

mDIP makes it possible to quantitatively evaluate rCBF as well as standard diffusion parameters within 3 min 30 sec.

## W5B-SPPH- Automatic Evaluation of Appropriateness for Abdominal Dynamic Contrast-Enhanced CT Phases Using Deep Convolutional Neural Network Trained by Quantitative Index for Dynamic Contrast-Enhanced CT Phases

Participants

Akira Yamada, MD, PhD, Matsumoto, Japan (Presenter) Nothing to Disclose

## PURPOSE

To develop automated model for evaluating appropriateness of abdominal dynamic contrast-enhanced CT (DCE-CT) phases using convolutional neural network (CNN) and quantitative index for DCE-CT phases (Dynamic Phase Index, DPI).

## METHODS AND MATERIALS

Sixty patients who underwent abdominal DCE-CT with 7 arterial phases (scan time = 22, 28, 34, 40, 46, 52, and 58 s after 100 mL of intravenous contrast media injection at 3 mL/s) for pre-operative evaluation were included in this study. Patients were randomly divided into training (38 patients) and validation (22 patients) cohorts. The appropriateness of each DCE-CT phase as arterial phase was evaluated by a board-certified radiologist qualitatively and classified into 3 labels, "too early", "adequate", and "too late". DPI as a quantitative index for DCE-CT phase was determined from combination of scan time and contrast enhancement in target vessels (left ventricle, abdominal aorta, right renal vein, supra mesenteric vein, and inferior vena cava) on DCE-CT. Three DCE-CT images at the level of left ventricle, right renal vein, and inferior vena cava were imported into pre-trained CNN (VGG-16) and image features were extracted for the random forest classifier. The classifier was trained according to two strategies that are qualitative and quantitative-qualitative models. In qualitative model, the imported DCE-CT images were classified into qualitative labels directly. In quantitative-qualitative model, DPI was first determined from imported DCE-CT images and then classified into qualitative labels according to optimized thresholds. The classification accuracy was compared between automated models and blinded visual assessment by a radiologist.

## RESULTS

The classification accuracy for appropriateness of DCE-CT phase in a validation cohort was 0.90 (95%CI: 0.89-0.91) for quantitative-qualitative model, 0.84 (0.83-0.84) for qualitative model, and 0.79 (0.78-0.80) for visual assessment by a radiologist, respectively.

## CONCLUSION

The appropriateness of DCE-CT phases can be determined automatically using CNN with the better accuracy than a visual assessment by radiologist. The classification accuracy improves when the CNN was trained with use of quantitative index for DCE-CT phase compared to use of qualitative labels. In other words, DPI can be used as reliable quantitative index for DCE-CT phase.

## CLINICAL RELEVANCE/APPLICATION

The proposed model enables accurate and automated selection of appropriate DCE-CT images from big data. This is important for building high quality image database for machine learning models. Furthermore, DPI as a quantitative index for DCE-CT phases can be used as one of reliable imaging features to develop machine learning based diagnostic models in future.

## W5B-SPPH- Preliminary Report on Harmonization of First-Order Texture Metrics Using the Combat Tool in Water Phantom Data 7

Participants  
Bino A. Varghese, PhD, Los Angeles, CA (*Presenter*) Nothing to Disclose

## PURPOSE

Statistical harmonization approaches like ComBat have been shown to improve radiomics reproducibility, however its performance under varying noise scenarios have not been studied. We evaluate this capacity in CT radiomic features extracted from imaging a large water phantom acquired under varying dose and slice thickness conditions.

## METHODS AND MATERIALS

CT scans were acquired on a 16 cm detector GE Revolution CT scanner with variations across 3 different slice thicknesses: 0.625mm, 1.25mm and 2.5mm and 5 different dose levels: CTDIvol of 13,86 mGy (standard dose) and 40, 50, 60 and 70% reductions of the standard dose varying one at a time. Water phantom images were reconstructed using filtered back projection. The texture panel of 70 features belonging to first-order CT texture analysis metrics was extracted using the Cancer Imaging Phenomics Toolkit, following automated segmentation of 4 volumes of interest. The Python version of neuroCombat was used.

## RESULTS

Our results confirm that the ComBat algorithm effectively removes variations of all first-order statistical radiomic features from different dose levels and across the 3 slice thickness conditions. ComBat harmonized data exhibited lower dispersion around the mean compared to non-harmonized data. Furthermore, reduction in mean dispersion was larger in data from thicker slices.

## CONCLUSION

Despite evidence for Combat harmonization from clinical scan, our experiment using phantom demonstrated the capacity of Combat in removing variation from different dose and scan thickness levels. ComBat harmonization eliminates more variations from thicker slices.

## CLINICAL RELEVANCE/APPLICATION

Factors affecting radiomics performance also affect radiomics harmonization efforts. Therefore, the impact of these factors on radiomic performance and harmonization should be considered in future radiomics studies.

## W5B-SPPH- Robustness of Texture Biomarkers of Bone to Spatially Variant Blur in Ultra High Resolution CT 8

Participants  
Gengxin Shi, (*Presenter*) Nothing to Disclose

## PURPOSE

Compared to current conventional CT, the recently introduced Ultra-High Resolution CT (UHR CT) utilizes a new generation of detectors with ~2x finer pixels. In this setting, spatial resolution is dominated by factors other than pixel aperture, for example the spatially variant projection integration and view sampling blurs at fast scan speeds. We investigate the impact of these non-stationarities on texture biomarkers of bone obtained from UHR CT.

## METHODS AND MATERIALS

Data was acquired with Canon Aquilion Precision CT operated in an UHR mode (0.25 mm pixels/slice thickness, 0.4x0.5 focal spot) and in a Normal Resolution (NR) mode (0.5 mm pixels/slice thickness, 0.8x1.2 mm focal spot). Scans were obtained at 0.35 sec/rotation and 1.5 sec/rotation. For texture analysis, human femur was imaged at 0 - 20 cm from the isocenter. Gray Level Concordance and Run Length Matrix (GLCM and GLRM) texture features were obtained in 42 volumes of interest (5 mm<sup>3</sup>) placed at homologous locations in the femoral head. For each radial distance, reproducibility of each texture feature was quantified as the Concordance Correlation Coefficient (CCC) against the feature value at the isocenter, where the view sampling blur is minimal

## RESULTS

The visualization of trabecular bone is generally superior in UHR than NR, but the relative loss of spatial resolution at 150 mm from the isocenter and 0.35 sec rotation compared to 1.5 sec rotation is more pronounced in UHR. When texture features are used to quantify cancellous structures, the CCCs between the isocenter and 150 mm radial shift are generally  $>0.7$  for the UHR mode and 1.5 sec scan, deteriorating by typically  $>20\%$  for the 0.35 sec scan. The difference in CCC at 150 mm between the slow and fast acquisitions is less substantial in the NR mode (generally  $<10\%$ ).

## CONCLUSION

Due to the non-stationary spatial resolution associated with view sampling, texture features of bone derived from UHR CT exhibit substantial dependence on spatial location, especially for fast acquisitions. Ongoing work investigates the impact of this inter-scan

variability on radiomic models of bone health based on assays of texture biomarkers.

#### **CLINICAL RELEVANCE/APPLICATION**

Development of radiomic models of bone health from Ultra-High Resolution CT (UHR CT) data requires consideration of inter-scan texture variability due to spatially variant view sampling blur.

#### **W5B-SPPH- Retrospective Review of Doses Delivered to the Uterus of Pregnant Women During CT Examinations**

Participants

Joel Greffier, PhD, Nimes, France (*Presenter*) Nothing to Disclose

#### **PURPOSE**

To review the uterine doses (UD) calculated for pregnant women per CT acquisition and per CT examination in our Institution in the last 8 years.

#### **METHODS AND MATERIALS**

Consecutive pregnant women who underwent CT examination and for whom a UD calculation was performed by a medical physicist were retrospectively included from June 2014 to February 2022. UDs were computed per CT acquisition using the CT Expo 2.4 software and were summed up to obtain the total UD per CT examination. The CTDIvol and dose-length product (DLP) values were retrieved from the dose report and compared with those calculated by the software.

#### **RESULTS**

256 pregnant women were included, of mean age of  $29.4 \pm 5.5$  [18-48] years, at  $24.5 \pm 10.4$  week of amenorrhea [1-40]. UDs were computed for 339 CT acquisitions. The CTDIvol and DLP computed in the software were significantly higher than those retrieved on the dose reports ( $P < 0.05$ ). The highest UDs were reported for the abdomen-pelvis ( $10.93 \pm 5.74$  [1.2- 24.1] mGy), chest-abdomen-pelvis ( $9.79 \pm 7.09$  [3.9- 22.1] mGy), pelvis ( $18.50 \pm 17.96$  [5.8- 31.2] mGy) and lumbar spine ( $10.24 \pm 11.38$  [2.3- 29.6] mGy) examinations. The total UDs per CT examination were higher than 20 mGy for 10 pregnant women and the maximum total UD was 52.3 mGy

#### **CONCLUSION**

s The highest UDs were found for examinations directly exposing the pelvis. With current dose levels and in optimized practices, UDs per CT acquisition and CT examination were always below 100mGy. UD calculations could not be performed for CT examinations that did not directly expose the pelvis ( $UD < 1mGy$ ).

#### **CLINICAL RELEVANCE/APPLICATION**

Based on the results presented in this study and on our experience, we have also made recommendations for the management of pregnant women in CT.

Printed on: 02/07/23



## Abstract Archives of the RSNA, 2022

W5B-SPPH-1

### Image Reconstruction for Dedicated TOF PET Brain Systems Without Transmission Data

Wednesday, Nov. 30 12:45PM - 1:15PM Room: Learning Center - PH DPS

#### Participants

Chien-Min Kao, PhD, Chicago, IL (*Presenter*) Stockholder, Walgreens Boots Alliance, Inc

#### PURPOSE

For PET imaging of the brain, dedicated systems of high resolution and sensitivity are necessary. For hybrid PET/MR imaging, integrated and insert systems are developed. These systems often lack a CT system to produce attenuation images needed for accurate reconstruction while quantification is important for staging brain disorders. It has been shown that TOF PET data alone may allow simultaneous activity and attenuation (SAA) image reconstruction. However, the standard maximum-likelihood attenuation-activity (MLAA) algorithm can be unstable. This work develops a constrained MLAA method to improve reconstruction.

#### METHODS AND MATERIALS

We apply the alternating direction method of multipliers (ADMM) to optimize the nonconvex cost function of the TOF PET data in SAA incorporating constraints on the total variations (TVs) on the attenuation (AT) and activity (AC) maps and also on the total level of the latter. Numerical AT and AC maps for the adult brain are created, the former includes a skull enclosing uniform water attenuation, whereas the latter contains the gray matter (GM), the white matter (WM), and a 1cm-diameter lesion (L) in the WM, using a 5:1:3 activity ratio (GM:WM:L). Two TOF resolutions, 200 and 600 ps, are examined. Data containing approximately 1-million events are generated. AT and AC maps obtained with our proposed (TV-MLAA) and the existing MLAA algorithms are compared with the known truths.

#### RESULTS

The AT and AC maps produced by MLAA grow increasingly noisier as iteration increases. In contrast, the AT and CT maps of the TV-MLAA remain stable and appear convergent. Visually, the AC maps of TV-MLAA show decreased noise but well-preserved boundary and contrast between the GM and WM with lesion readily identified, in comparison to those of MLAA. We also evaluate the contrast-to-noise ratio (CNR) of the lesion. For TV-MLAA, the CNRs are 1.01 for both TOFs, whereas for 100-iteration MLAA, the CNR is 0.55 at 200 ps but degrades to 0.36 at 600 ps.

#### CONCLUSION

s We develop the TV-MLAA algorithm for SAA reconstruction from TOF PET data, and consider 200 and 600 ps TOFs that bracket the present resolution range. At both resolutions, we show that the TV-MLAA algorithm stably yields qualitatively and quantitatively accurate AC maps. Based on our preliminary results, the lesion CNR achieved with TV-MLAA is two to three times that of MLAA.

#### CLINICAL RELEVANCE/APPLICATION

Quantitative PET imaging is important for brain disorders but unlike PET/CT systems attenuation maps of the brain may not be readily available when using the hybrid PET/MR and dedicated PET brain imaging systems. The TV-MLAA algorithm developed may be useful for these emerging imaging technologies by allowing accurate image reconstruction from TOF PET data alone.

Printed on: 02/07/23

## Abstract Archives of the RSNA, 2022

W5B-SPPH-2

### High-Resolution MRI and Diffusion-Weighted Imaging of the Human Pancreas at 5 Tesla

Wednesday, Nov. 30 12:45PM - 1:15PM Room: Learning Center - PH DPS

#### Participants

Liyun Zheng, Shanghai, China (*Presenter*) Nothing to Disclose

#### PURPOSE

The purpose of this study was to explore the feasibility of imaging the pancreas at 5T and evaluate the practical improvement of high-resolution magnetic resonance imaging (MRI) and diffusion-weighted imaging (DWI) at 5T as compared with 3T.

#### METHODS AND MATERIALS

Eighteen healthy subjects were recruited for this prospective study. MRI examinations were performed on both 3T and 5T scanners. The MRI sequences included T2-weighted fast spin-echo (FSE) and DWI with reduced field-of-view (FOV). Subjective image analysis with a 4-point Likert scale was performed by two experienced radiologists. Signal-to-noise ratio (SNR) and apparent diffusion coefficient (ADC) value were measured in the head, body, and tail of the pancreas. Coefficient of variation (CV) of ADC was calculated as  $CV(ADC)=SD(ADC)/mean(ADC)$ . A series of paired Wilcoxon tests was used to compare the subjective image quality, mean ADC value, and CV of ADC between 3T and 5T measurements.  $P < 0.05$  was considered statistically significant.

#### RESULTS

For T2-weighted images, there was no significant difference in image quality ratings between 3T and 5T ( $P = 0.593$ ). At lower b-value images ( $b = 0 \text{ s/mm}^2$ ), the image quality ratings had no significant difference between different magnetic field strengths, while at higher b-value images ( $b = 800 \text{ s/mm}^2$ ), the ratings were significantly higher at 5T ( $P = 0.046$ ). The mean ratios of SNR at 5 T to 3 T of the T2 images for the pancreatic head, body, and tail were 1.16, 1.33, and 1.39, respectively. For the DWI images ( $b = 800 \text{ s/mm}^2$ ), the corresponding ratios were 1.29, 1.40, and 1.24, respectively. The SNRs of both T2-weighted and DWI images were significantly higher at 5T than at 3T ( $P$  ranging from 0.0002 to 0.0095 for all comparisons). For both 3T and 5T, mean ADC values on pancreatic head were significantly higher than those of tail ( $P = 0.016$  for 3T, and  $P = 0.018$  for 5T), while no significant difference was observed between pancreatic head and body ( $P = 0.679$  for 3T, and  $P = 0.445$  for 5T). There was no significant difference in mean ADC values and CV of ADC between 3T and 5T ( $P > 0.05$  for all comparisons).

#### CONCLUSION

This initial study proved that 5T MRI can be used to acquire high-resolution pancreatic imaging with higher SNR and sufficient image quality.

#### CLINICAL RELEVANCE/APPLICATION

This initial study proved that 5T MRI can be used to acquire high-resolution pancreas imaging with higher SNR and sufficient image quality. Consequently, pancreas MRI at 5T may be useful for the diagnosis and management of pancreatic diseases.

Printed on: 02/07/23

## Abstract Archives of the RSNA, 2022

W5B-SPPH-3

### Clinical Evaluation of Rubidium-82 Generator for Cardiac PET Imaging

Wednesday, Nov. 30 12:45PM - 1:15PM Room: Learning Center - PH DPS

#### Participants

Rameshwar Prasad, PHD, Chicago, IL (*Presenter*) Nothing to Disclose

#### PURPOSE

Positron emission tomography (PET) using Rubidium-82 allows myocardial perfusion imaging and absolute functional assessment of ventricular function due to its higher diagnostic accuracy and its onsite generator-based availability in clinics. Precise and consistent production and infusion of contaminants-free Rubidium-82 is required for accurate myocardial estimates and radiation safety. In this study, we evaluated the performance of Rubidium-82 generator for high-throughput, high-volume cardiac PET imaging using constant flow and constant activity delivery techniques.

#### METHODS AND MATERIALS

Daily performance metrics of 10 strontium-82/rubidium-82 ( $^{82}\text{Sr}/^{82}\text{Rb}$ ) generators (RUBY-FILL, Canada) were studied for over 20 months infusing over 5000 patients. An automated daily quality control (QC) procedure was performed on each day of clinical use and the eluted Rb-82 was measured by the onboard dose calibrator of the elution system. On-board dose calibrator constancy, Sr82/Rb82 and Sr85/Rb82 breakthrough were assessed. Percent deviation in delivered activity and duration are assessed for each patient (rest and stress) using constant activity (CA) and constant flow (CF) infusion methods.

#### RESULTS

Percent constancy deviation was  $0.73 \pm 0.4$ . Sr82/Rb82 and Sr85/Rb82 breakthrough (% USP) were  $5.1 \pm 1.4$  and  $0.87 \pm 0.6$  respectively. Net delivered activity deviation (%) was higher for rest studies than stress whereas delivery duration (%) was higher for stress studies. Delivered activity deviation (%) for CF and CA were  $0.01 \pm 0.18$  and  $0.03 \pm 0.54$ , respectively. Sr-82/Rb-82 and Sr-85/Rb-82 breakthrough was found higher than limits for 3 patients due to incorrect use of proscribed elution saline.

#### CONCLUSION

s RUBY-FILL™ Rb-82 generator provided consistent Rb-82 activities for high throughput clinical cardiac PET imaging. Sr-82/Rb-82 and Sr-85/Rb-82 breakthrough were within the radiation safety limits during the studied period of 20 months except a day. Constant flow is preferred infusion method based on our institutional experience.

#### CLINICAL RELEVANCE/APPLICATION

Generator based Rb-82 provides readily availability of radiotracer and weight-based quantitation of myocardial blood flow and perfusion with optimal radiation safety.

Printed on: 02/07/23

## Abstract Archives of the RSNA, 2022

W5B-SPPH-4

### Validation of a Deep Learning Model for COVID-19 Diagnosis from Portable and Stationary Dual-Energy Chest Radiography Units

Wednesday, Nov. 30 12:45PM - 1:15PM Room: Learning Center - PH DPS

#### Participants

Mena Shenouda, BS, (*Presenter*) Nothing to Disclose

#### PURPOSE

To validate a deep learning model for COVID-19 diagnosis from chest radiographs (CXR) and to compare performance on images from portable units vs. stationary dual-energy subtraction units.

#### METHODS AND MATERIALS

A deep learning model trained on CXRs from a single institution was previously published. To validate this trained model, a large cohort of cases from the same institution was retrospectively collected as an independent test set. The data comprised the first CXR acquired <2 days after the patients' reverse transcription polymerase chain reaction (PCR) tests for the SARS-CoV-2 virus. Among the 12,251 patients, 2,464 (20.1%) had tested positive, and 9,787 (79.9%) had tested negative for the virus. CXRs of 9,471 (77.3%) patients were acquired using portable units, and CXRs of 2,780 (22.7%) patients were acquired using stationary units with COVID prevalences of 20.5% and 18.8%, respectively. The COVID diagnosis classification task was performed using standard images alone, soft-tissue images alone, and a combination of the two via feature fusion. Portable soft-tissue images were generated post-acquisition with commercial software. No model training or fine-tuning was performed. Classification between the radiographs of COVID-positive and COVID-negative patients was evaluated using the area under the receiver operating characteristic curve (AUC) as the performance metric.

#### RESULTS

Performance of the model on images from both modalities yielded AUC values [95% CI] of 0.69 [0.68, 0.70] for standard images, 0.67 [0.66, 0.69] for soft-tissue images, and 0.66 [0.65, 0.68] for their combination. For CXRs acquired from portable units, AUCs for standard images, soft-tissue images, and their combination were 0.70 [0.69, 0.72], 0.68 [0.67, 0.70], and 0.67 [0.66, 0.69], respectively. For CXRs acquired from stationary units, AUCs for standard images, soft-tissue images, and their combination were 0.66 [0.64, 0.69], 0.64 [0.61, 0.67], and 0.64 [0.61, 0.67], respectively. AUCs were significantly higher for CXRs acquired from portable vs. stationary units ( $p=0.007$ ,  $0.004$ , and  $0.04$  for standard images, soft-tissue images, and their combination, respectively). Within both modalities, the highest AUC was achieved for standard CXRs.

#### CONCLUSION

This study tested a previously trained model for radiography-based COVID-19 diagnosis on a large, independent in-house dataset with promising results.

#### CLINICAL RELEVANCE/APPLICATION

AI generalizability in the differentiation of COVID-positive and COVID-negative patients based on chest radiography was demonstrated on a large dataset from a single institution as a precursor to using the Medical Imaging and Data Resource Center (MIDRC) multi-institution initiative, which will further validate this model.

Printed on: 02/07/23

## Abstract Archives of the RSNA, 2022

W5B-SPPH-5

### Modified Diffusion Imaging With Phase-Contrast Using Motion-Compensated Diffusion Encoding (mDIP) For Quantification of Regional Cerebral Blood Flow

Wednesday, Nov. 30 12:45PM - 1:15PM Room: Learning Center - PH DPS

#### Participants

Genki Nambu, BA, (*Presenter*) Nothing to Disclose

#### PURPOSE

We recently developed a method of diffusion imaging with phase-contrast (DIP) for quantification of regional cerebral blood flow (rCBF), in which the total CBF (tCBF) from phase-contrast magnetic resonance imaging (PC-MRI) was used to convert the perfusion-related diffusion parameters ( $D^*$ ) in the brain. However, DIP is sensitive to brain pulsation and takes up to 10 min. To tackle these issues, we developed a modified DIP (mDIP) in which a motion-compensated diffusion gradient was applied, and the number of b-values were minimized.

#### METHODS AND MATERIALS

Eleven healthy volunteers (nine men and two women; mean age, 23.9 years) participated in this study. On a 3.0-T MRI, diffusion-weighted images of the whole brain were acquired using single-shot diffusion echo-planar imaging with the first-order motion-compensated diffusion gradient to reduce the brain pulsation effect. Further, the number of b-values was minimized (0, 10, 100, and 800 s/mm<sup>2</sup>) to shorten the scan time (1 min 55 sec). Next, we performed voxel-wise estimations of the  $D^*$ , perfusion fraction (F), multiplication of  $D^*$  and F ( $FD^*$ ), and restricted diffusion coefficient using biexponential function. Furthermore, PC-MRI was performed to obtain the tCBF from the volumetric flow rate at the main feeding arteries into the cranium (1 min 32 sec). By using the tCBF obtained from PC-MRI, we converted the  $FD^*$  in the brain into absolute rCBF. We determined rCBF using mDIP and arterial spin labeling (ASL) and their correlations in gray and white matter (GM and WM, respectively) in healthy volunteers and assessed the relationship between the two methods.

#### RESULTS

The rCBF images obtained using mDIP and ASL provided good contrast between the GM and WM as well as general resemblance. A highly significant positive correlation between the mDIP and ASL in terms of rCBF was observed in GM ( $R = 0.88$ ,  $P < 0.05$ ), which was higher than that of DIP without motion-compensated diffusion gradient, whereas the correlation between the methods was still poor in WM ( $P > 0.05$ ). The rCBF values in GM ( $41.5 \pm 14.8$  mL/100 g/min) and WM ( $16.6 \pm 10.9$  mL/100 g/min) obtained using mDIP were consistent with the values assessed using [15O]-water positron emission tomography reported in literature.

#### CONCLUSION

mDIP makes it possible to quantitatively evaluate rCBF as well as standard diffusion parameters within 3 min 30 sec.

#### CLINICAL RELEVANCE/APPLICATION

mDIP makes it possible to quantitatively evaluate rCBF as well as standard diffusion parameters within 3 min 30 sec.

Printed on: 02/07/23

## Abstract Archives of the RSNA, 2022

W5B-SPPH-6

### Automatic Evaluation of Appropriateness for Abdominal Dynamic Contrast-Enhanced CT Phases Using Deep Convolutional Neural Network Trained by Quantitative Index for Dynamic Contrast-Enhanced CT Phases

Wednesday, Nov. 30 12:45PM - 1:15PM Room: Learning Center - PH DPS

#### Participants

Akira Yamada, MD, PhD, Matsumoto, Japan (*Presenter*) Nothing to Disclose

#### PURPOSE

To develop automated model for evaluating appropriateness of abdominal dynamic contrast-enhanced CT (DCE-CT) phases using convolutional neural network (CNN) and quantitative index for DCE-CT phases (Dynamic Phase Index, DPI).

#### METHODS AND MATERIALS

Sixty patients who underwent abdominal DCE-CT with 7 arterial phases (scan time = 22, 28, 34, 40, 46, 52, and 58 s after 100 mL of intravenous contrast media injection at 3 mL/s) for pre-operative evaluation were included in this study. Patients were randomly divided into training (38 patients) and validation (22 patients) cohorts. The appropriateness of each DCE-CT phase as arterial phase was evaluated by a board-certified radiologist qualitatively and classified into 3 labels, "too early", "adequate", and "too late". DPI as a quantitative index for DCE-CT phase was determined from combination of scan time and contrast enhancement in target vessels (left ventricle, abdominal aorta, right renal vein, supra mesenteric vein, and inferior vena cava) on DCE-CT. Three DCE-CT images at the level of left ventricle, right renal vein, and inferior vena cava were imported into pre-trained CNN (VGG-16) and image features were extracted for the random forest classifier. The classifier was trained according to two strategies that are qualitative and quantitative-qualitative models. In qualitative model, the imported DCE-CT images were classified into qualitative labels directly. In quantitative-qualitative model, DPI was first determined from imported DCE-CT images and then classified into qualitative labels according to optimized thresholds. The classification accuracy was compared between automated models and blinded visual assessment by a radiologist.

#### RESULTS

The classification accuracy for appropriateness of DCE-CT phase in a validation cohort was 0.90 (95%CI: 0.89-0.91) for quantitative-qualitative model, 0.84 (0.83-0.84) for qualitative model, and 0.79 (0.78-0.80) for visual assessment by a radiologist, respectively.

#### CONCLUSION

The appropriateness of DCE-CT phases can be determined automatically using CNN with the better accuracy than a visual assessment by radiologist. The classification accuracy improves when the CNN was trained with use of quantitative index for DCE-CT phase compared to use of qualitative labels. In other words, DPI can be used as reliable quantitative index for DCE-CT phase.

#### CLINICAL RELEVANCE/APPLICATION

The proposed model enables accurate and automated selection of appropriate DCE-CT images from big data. This is important for building high quality image database for machine learning models. Furthermore, DPI as a quantitative index for DCE-CT phases can be used as one of reliable imaging features to develop machine learning based diagnostic models in future.

Printed on: 02/07/23

## Abstract Archives of the RSNA, 2022

W5B-SPPH-7

### Preliminary Report on Harmonization of First-Order Texture Metrics Using the Combat Tool in Water Phantom Data

Wednesday, Nov. 30 12:45PM - 1:15PM Room: Learning Center - PH DPS

#### Participants

Bino A. Varghese, PhD, Los Angeles, CA (*Presenter*) Nothing to Disclose

#### PURPOSE

Statistical harmonization approaches like ComBat have been shown to improve radiomics reproducibility, however its performance under varying noise scenarios have not been studied. We evaluate this capacity in CT radiomic features extracted from imaging a large water phantom acquired under varying dose and slice thickness conditions.

#### METHODS AND MATERIALS

CT scans were acquired on a 16 cm detector GE Revolution CT scanner with variations across 3 different slice thicknesses: 0.625mm, 1.25mm and 2.5mm and 5 different dose levels: CTDIvol of 13,86 mGy (standard dose) and 40, 50, 60 and 70% reductions of the standard dose varying one at a time. Water phantom images were reconstructed using filtered back projection. The texture panel of 70 features belonging to first-order CT texture analysis metrics was extracted using the Cancer Imaging Phenomics Toolkit, following automated segmentation of 4 volumes of interest. The Python version of neuroCombat was used.

#### RESULTS

Our results confirm that the ComBat algorithm effectively removes variations of all first-order statistical radiomic features from different dose levels and across the 3 slice thickness conditions. ComBat harmonized data exhibited lower dispersion around the mean compared to non-harmonized data. Furthermore, reduction in mean dispersion was larger in data from thicker slices.

#### CONCLUSION

Despite evidence for Combat harmonization from clinical scan, our experiment using phantom demonstrated the capacity of Combat in removing variation from different dose and scan thickness levels. ComBat harmonization eliminates more variations from thicker slices.

#### CLINICAL RELEVANCE/APPLICATION

Factors affecting radiomics performance also affect radiomics harmonization efforts. Therefore, the impact of these factors on radiomic performance and harmonization should be considered in future radiomics studies.

Printed on: 02/07/23

## Abstract Archives of the RSNA, 2022

W5B-SPPH-8

### Robustness of Texture Biomarkers of Bone to Spatially Variant Blur in Ultra High Resolution CT

Wednesday, Nov. 30 12:45PM - 1:15PM Room: Learning Center - PH DPS

#### Participants

Gengxin Shi, (*Presenter*) Nothing to Disclose

#### PURPOSE

Compared to current conventional CT, the recently introduced Ultra-High Resolution CT (UHR CT) utilizes a new generation of detectors with  $\sim 2x$  finer pixels. In this setting, spatial resolution is dominated by factors other than pixel aperture, for example the spatially variant projection integration and view sampling blurs at fast scan speeds. We investigate the impact of these non-stationarities on texture biomarkers of bone obtained from UHR CT.

#### METHODS AND MATERIALS

Data was acquired with Canon Aquilion Precision CT operated in an UHR mode (0.25 mm pixels/slice thickness, 0.4x0.5 focal spot) and in a Normal Resolution (NR) mode (0.5 mm pixels/slice thickness, 0.8x1.2 mm focal spot). Scans were obtained at 0.35 sec/rotation and 1.5 sec/rotation. For texture analysis, human femur was imaged at 0 - 20 cm from the isocenter. Gray Level Concordance and Run Length Matrix (GLCM and GLRM) texture features were obtained in 42 volumes of interest (5 mm<sup>3</sup>) placed at homologous locations in the femoral head. For each radial distance, reproducibility of each texture feature was quantified as the Concordance Correlation Coefficient (CCC) against the feature value at the isocenter, where the view sampling blur is minimal

#### RESULTS

The visualization of trabecular bone is generally superior in UHR than NR, but the relative loss of spatial resolution at 150 mm from the isocenter and 0.35 sec rotation compared to 1.5 sec rotation is more pronounced in UHR. When texture features are used to quantify cancellous structures, the CCCs between the isocenter and 150 mm radial shift are generally  $>0.7$  for the UHR mode and 1.5 sec scan, deteriorating by typically  $>20\%$  for the 0.35 sec scan. The difference in CCC at 150 mm between the slow and fast acquisitions is less substantial in the NR mode (generally  $<10\%$ ).

#### CONCLUSION

Due to the non-stationary spatial resolution associated with view sampling, texture features of bone derived from UHR CT exhibit substantial dependence on spatial location, especially for fast acquisitions. Ongoing work investigates the impact of this inter-scan variability on radiomic models of bone health based on assays of texture biomarkers.

#### CLINICAL RELEVANCE/APPLICATION

Development of radiomic models of bone health from Ultra-High Resolution CT (UHR CT) data requires consideration of inter-scan texture variability due to spatially variant view sampling blur.

Printed on: 02/07/23

## Abstract Archives of the RSNA, 2022

W5B-SPPH-9

### Retrospective Review of Doses Delivered to the Uterus of Pregnant Women During CT Examinations

Wednesday, Nov. 30 12:45PM - 1:15PM Room: Learning Center - PH DPS

#### Participants

Joel Greffier, PhD, Nimes, France (*Presenter*) Nothing to Disclose

#### PURPOSE

To review the uterine doses (UD) calculated for pregnant women per CT acquisition and per CT examination in our Institution in the last 8 years.

#### METHODS AND MATERIALS

Consecutive pregnant women who underwent CT examination and for whom a UD calculation was performed by a medical physicist were retrospectively included from June 2014 to February 2022. UDs were computed per CT acquisition using the CT Expo 2.4 software and were summed up to obtain the total UD per CT examination. The CTDIvol and dose-length product (DLP) values were retrieved from the dose report and compared with those calculated by the software.

#### RESULTS

256 pregnant women were included, of mean age of  $29.4 \pm 5.5$  [18-48] years, at  $24.5 \pm 10.4$  week of amenorrhea [1-40]. UDs were computed for 339 CT acquisitions. The CTDIvol and DLP computed in the software were significantly higher than those retrieved on the dose reports ( $P < 0.05$ ). The highest UDs were reported for the abdomen-pelvis ( $10.93 \pm 5.74$  [1.2-24.1] mGy), chest-abdomen-pelvis ( $9.79 \pm 7.09$  [3.9- 22.1] mGy), pelvis ( $18.50 \pm 17.96$  [5.8-31.2] mGy) and lumbar spine ( $10.24 \pm 11.38$  [2.3- 29.6] mGy) examinations. The total UDs per CT examination were higher than 20 mGy for 10 pregnant women and the maximum total UD was 52.3 mGy

#### CONCLUSION

The highest UDs were found for examinations directly exposing the pelvis. With current dose levels and in optimized practices, UDs per CT acquisition and CT examination were always below 100mGy. UD calculations could not be performed for CT examinations that did not directly expose the pelvis ( $UD < 1mGy$ ).

#### CLINICAL RELEVANCE/APPLICATION

Based on the results presented in this study and on our experience, we have also made recommendations for the management of pregnant women in CT.

Printed on: 02/07/23

## Abstract Archives of the RSNA, 2022

W5B-SPRO

### Radiation Oncology Wednesday Poster Discussions - B

Wednesday, Nov. 30 12:45PM - 1:15PM Room: Learning Center - RO DPS

#### Participants

Anna Shapiro, MD, Syracuse, NY (*Moderator*) Nothing to Disclose

#### Sub-Events

### W5B-SPRO- Application of Energy-Spectrum CT to Assess Sensitivity to Heavy Ion Irradiation in RAT C6 Glioma<sup>1</sup>

#### Participants

Yu feng Li, MMedSc, (*Presenter*) Nothing to Disclose

#### PURPOSE

To study the value of multi-parameter quantification of energy-spectral CT in assessing the efficacy and response of C6 glioma in rats irradiated with different doses of heavy ion beam (12C6+).

#### METHODS AND MATERIALS

C6 cells at logarithmic growth stage were implanted into the right basal ganglia region of Wistar rat brain with a small animal stereotactic apparatus to establish a rat C6 glioma model; energy-spectrum CT scans were performed before and on days 7 and 14 after irradiation with different doses (1.0Gy and 2.0Gy) of 12C6+ ion beam, and the best single-energy CT values, iodine concentration values and slope of energy-spectrum curves were detected in the solid tumor area, liquefied necrotic area and tumor peripheral area. The tumor-bearing rats were marked as dying when they refused to eat and drink or had severe physical impairment.

#### RESULTS

Compared with the sham-irradiated rats in the 0 Gy group, the tumors in the 1.0 Gy and 2.0 Gy irradiated rats showed an increase in tumor volume in the early stage (7 d), a slight increase in blood perfusion in the solid tumor area, a slight increase in iodine concentration and single-energy CT values, and an expansion of liquefied necrosis inside the tumor; in the later stage (14 d), the solid tumor area shrank, and multiple liquefied areas around the tumor occurred, and the single-energy CT values at 65 keV, iodine concentration and the slope of the energy spectrum in the solid tumor area decreased. The tumor volume in the 2.0 Gy irradiated rats (7d and 14d) was smaller than that in the 1.0 Gy irradiated group, and the iodine concentration and CT value in the solid tumor area were lower than those in the 1.0 Gy irradiated group. The 35-d survival rate of the irradiated rats (1.0 Gy=40% 2.0 Gy=55%) was significantly higher than that of the 0 Gy sham-irradiated group (0 Gy=29%).

#### CONCLUSION

s Quantitative parameters of energy-spectrum CT, including 65 keV single-energy CT values, slope of the energy-spectrum curve and iodine concentration, can respond to the inhibitory effect of 12C6+ ion beam on the growth and invasion of rat C6 gliomas. Therefore, energy spectrum CT can be used as a non-invasive and dynamic assay to assess the response of glioma after heavy ion irradiation.

#### CLINICAL RELEVANCE/APPLICATION

Radiation therapy is one of the important treatments for refractory or recurrent glioma. However, due to the high irradiation dose, the tendency to damage normal brain tissue, and the difficulties in precise irradiation dose fractionation and radiosensitivity assessment, it is essential to explore more optimal radiotherapy strategies and detection modes. 12C6+ has the advantages of inverted deep dose distribution and high relative biological effects, and may provide an effective treatment for malignant and recurrent brain tumors.

Printed on: 02/07/23

## Abstract Archives of the RSNA, 2022

W5B-SPRO-1

### Application of Energy-Spectrum CT to Assess Sensitivity to Heavy Ion Irradiation in RAT C6 Glioma

Wednesday, Nov. 30 12:45PM - 1:15PM Room: Learning Center - RO DPS

#### Participants

Yu feng Li, MMedSc, (*Presenter*) Nothing to Disclose

#### PURPOSE

To study the value of multi-parameter quantification of energy-spectral CT in assessing the efficacy and response of C6 glioma in rats irradiated with different doses of heavy ion beam (12C6+).

#### METHODS AND MATERIALS

C6 cells at logarithmic growth stage were implanted into the right basal ganglia region of Wistar rat brain with a small animal stereotactic apparatus to establish a rat C6 glioma model; energy-spectrum CT scans were performed before and on days 7 and 14 after irradiation with different doses (1.0Gy and 2.0Gy) of 12C6+ ion beam, and the best single-energy CT values, iodine concentration values and slope of energy-spectrum curves were detected in the solid tumor area, liquefied necrotic area and tumor peripheral area. The tumor-bearing rats were marked as dying when they refused to eat and drink or had severe physical impairment.

#### RESULTS

Compared with the sham-irradiated rats in the 0 Gy group, the tumors in the 1.0 Gy and 2.0 Gy irradiated rats showed an increase in tumor volume in the early stage (7 d), a slight increase in blood perfusion in the solid tumor area, a slight increase in iodine concentration and single-energy CT values, and an expansion of liquefied necrosis inside the tumor; in the later stage (14 d), the solid tumor area shrank, and multiple liquefied areas around the tumor occurred, and the single-energy CT values at 65 keV, iodine concentration and the slope of the energy spectrum in the solid tumor area decreased. The tumor volume in the 2.0 Gy irradiated rats (7d and 14d) was smaller than that in the 1.0 Gy irradiated group, and the iodine concentration and CT value in the solid tumor area were lower than those in the 1.0 Gy irradiated group. The 35-d survival rate of the irradiated rats (1.0 Gy=40% 2.0 Gy=55%) was significantly higher than that of the 0 Gy sham-irradiated group (0 Gy=29%).

#### CONCLUSION

s Quantitative parameters of energy-spectrum CT, including 65 keV single-energy CT values, slope of the energy-spectrum curve and iodine concentration, can respond to the inhibitory effect of 12C6+ ion beam on the growth and invasion of rat C6 gliomas. Therefore, energy spectrum CT can be used as a non-invasive and dynamic assay to assess the response of glioma after heavy ion irradiation.

#### CLINICAL RELEVANCE/APPLICATION

Radiation therapy is one of the important treatments for refractory or recurrent glioma. However, due to the high irradiation dose, the tendency to damage normal brain tissue, and the difficulties in precise irradiation dose fractionation and radiosensitivity assessment, it is essential to explore more optimal radiotherapy strategies and detection modes. 12C6+ has the advantages of inverted deep dose distribution and high relative biological effects, and may provide an effective treatment for malignant and recurrent brain tumors.

Printed on: 02/07/23



## Abstract Archives of the RSNA, 2022

BREE

### Breast Education Exhibits

Sunday, Nov. 27 8:00AM - 9:00AM Room: Learning Center - BR

#### Sub-Events

#### **BREE-1 Imaging and Management of High-Risk Breast Lesions: An Update of Current Evidence**

##### Awards

##### Cum Laude

##### Participants

Richard E. Sharpe JR, MD, MBA, Scottsdale, AZ (*Presenter*) Nothing to Disclose

##### TEACHING POINTS

High-risk breast lesions (HRL) are a group of specific heterogeneous lesions that can be associated with a synchronous or adjacent breast cancer and that confer an increased lifetime risk of breast cancer. Providing high quality care for patients with HRLs requires careful correlation of specific patient history and imaging characteristics with histopathologic or cytopathologic results for concordance by the physician performing the biopsy. High-risk and malignant diagnoses should routinely prompt multidisciplinary discussion to determine optimal management. Excise specific HRLs because of the risk of upgrading the diagnosis to ductal carcinoma in situ or invasive cancer. Excise ALL HRL lesions demonstrating radiology pathology discordance. For patients with >1 HRL diagnosis after core needle biopsy, management should be based on the HRL with the highest risk of upgrade.

##### TABLE OF CONTENTS/OUTLINE

Overview of image guided biopsy process. Explanation of types of high-risk breast lesions, imaging and pathological findings, and associated risks of upgrade to malignancy for each, including: atypical ductal hyperplasia, flat epithelial atypia, lobular hyperplasia (ALH, LCIS), papillary lesions, radial scars/complex sclerosing lesions, fibroepithelial lesions, and phyllodes. Update of the current evidence regarding imaging and pathological correlation and management of each lesion type. Presentation of high yield point of care summary practice resources to support efficient management of patients with high-risk lesions.

#### **BREE-10 Breast Malignancy Subtypes with Hybrid Use of Accelerated and Abbreviated Breast MRI in Screening Higher-Than-Average Risk Patients**

##### Participants

Ashley Huppe, MD, Kansas City, KS (*Presenter*) Nothing to Disclose

##### TEACHING POINTS

Breast cancer screening guidelines for higher-than-average risk patients are expanding. Therefore, a supplemental screening exam is needed that is both cost-effective and accurate for detection of malignancy. The widespread use of full protocol screening MRI has limitations, and novel techniques have been developed to address these drawbacks. While abbreviated MRI addresses the cost, patient discomfort and time constraints of full-protocol exams, accelerated techniques can improve specificity of abbreviated MRI by providing a temporal analysis of contrast enhancement. Given their recent emergence, many are unfamiliar with the distinctions between these techniques and associated imaging appearance of various malignancy subtypes. After this presentation, participants will be able to:-Review breast cancer screening guidelines for higher-than-average risk patients-Understand the differences between acquisition of accelerated and abbreviated MRI-Describe the applications and benefits of accelerated and abbreviated MRI-Appreciate appearance of malignancy subtypes on accelerated and abbreviated MRI

##### TABLE OF CONTENTS/OUTLINE

1) Introductiona) Summarize current guidelines for breast cancer screening in higher-than-average risk patientsb) Discuss benefits and limitations of full protocol screening MRIc) Review accelerated and abbreviated MRIi) Define terminologyii) Discuss differences, clinical applications and benefits2) Case-based review of appearance of malignancy subtypes on accelerated and abbreviated MRI used in the screening settinga) Ductal carcinoma in-situb) Invasive ductal carcinomac) Invasive lobular carcinomad) Multifocal disease3) Conclusion

#### **BREE-100 The Various Faces of a Fibroadenoma**

##### Participants

Natalia Orthmann, MD, Sao Paulo, Brazil (*Presenter*) Nothing to Disclose

##### TEACHING POINTS

The purpose of this exhibit is: 1. To emphasize the importance of fibroadenoma findings in the different methods, as it is a common finding of benign breast lesions. 2. To show the epidemiology, histological origin, imaging, anatomopathological correlation when possible, association with medication use, and differential diagnoses of the fibroadenoma. 3. To present fibroepithelial tumors, with emphasis on fibroadenoma and its types. 4. To review imaging findings of breast lesions suggestive of fibroadenomas. 5. To illustrate the different imaging methods to assess the fibroadenoma, such as Ultrasound (US), Mammography (MG), tomosynthesis

(TS) and Magnetic Resonance (MR)

#### TABLE OF CONTENTS/OUTLINE

1. Literature review focusing on fibroadenoma and its differential diagnoses. 2. To illustrate and discuss the pathology of fibroadenoma, highlighting epidemiology; subtypes; progression in different imaging methods. 3. Review of the pathological development of fibroadenomas and its differential diagnoses through illustrative cases. 4. Example cases with mammographic, ultrasonographic and pathologic correlation when available. 5. Summary and conclusion.

#### **BREE-101 Breast and Beyond! Breast Manifestations of Systemic Diseases**

Participants

Ayla Yamamoto Mota, MD, Sao Paulo, Brazil (*Presenter*) Nothing to Disclose

#### TEACHING POINTS

-To describe breast manifestations of ordinary and rare systemic diseases in different modalities (ultrasound, mammography and MR)- To demonstrate the importance to know patient's comorbidity and background

#### TABLE OF CONTENTS/OUTLINE

-Introduction - Ultrasound, mammography and MR images: clinical cases of breast manifestations of systemic diseases- Conclusion

#### **BREE-102 A-Z of Triple Negative Breast Cancer**

Participants

Tatiana Tucunduva, MD, (*Presenter*) Nothing to Disclose

#### TEACHING POINTS

-Define Triple negative breast cancer (TNBC)-Review the histopathological aspects -Review the molecular aspects -Review the spectrum of findings (mammography, US and MRI) -Pitfalls -Worse prognostic factors -News in treatment

#### TABLE OF CONTENTS/OUTLINE

1. TNBC definition 2. Histological and molecular aspects of TNBC 3. the spectrum of findings:On mammography, the mass more often appears irregular in shape and spiculated margins and may even contain benign aspects. Most show no calcification and are rarely associated with DCIS, as rapid carcinogenesis bypasses this stage.On ultrasound, TNBC often appears as a hypoechoic mass with uncircumscribed margins.Magnetic resonance imaging (MRI) is the most sensitive method to evaluate TNBC and shows some typical features such as annular enhancement and an intralesional T2 hyperintense signal, factors suggestive of malignancy.4. PitfallsBecause some lesions do not show desmoplastic reactions due to the aggressiveness of most triple-negative breast cancers, some radiologic features may resemble benign (cysts) or probably benign (B3) lesions.5. Worse prognostic factor.Compared with other breast cancer subtypes, TNBC has a worse prognosis because it is highly invasive. About 45% have distant metastases and the mortality rate is about 40% within the first 5 years.6. News in treatmentDue to its molecular subtype, TNBC does not respond to the usual specific hormonal therapies. Therefore, even for smaller lesions, chemotherapy is the main systemic treatment.However, different subgroups within TNBC share some molecular features that allow targeted, individualized therapeutic intervention.

#### **BREE-103 One View, What To Do? A Review of the Imaging Appearance and Management of the Breast Asymmetry**

Participants

Cara Connolly, MD, Nashville, TN (*Presenter*) Nothing to Disclose

#### TEACHING POINTS

The breast asymmetry seen in one mammographic view has long been the subject of diagnostic dilemmas for mammographers. Retrospective reviews have reported up to one third of breast cancers may have been seen as asymmetries. However, most screening callbacks for asymmetries are attributed to summation artifact, the overlapping of normal breast tissue. With incorporation of tomosynthesis, the recall rate for asymmetries has decreased but continues to present screening and diagnostic challenges. This exhibit will incorporate examples of asymmetries on both standard 2D imaging and tomosynthesis with both benign and malignant results, as well as review the diagnostic algorithm for management.

#### TABLE OF CONTENTS/OUTLINE

Benign cases of asymmetries will include summation artifact, PASH, fibrocystic change, fat necrosis, fibroadenomatoid change and abscess. Biopsy-proven malignancies will be highlighted, including invasive ductal carcinoma, invasive lobular carcinoma, ductal carcinoma in situ, lymphoma, and angiosarcoma.

#### **BREE-104 The Myriad of High Risk Breast Lesions: Review of Radiographic and Histologic Features and their Challenging Management**

**Awards**

**Certificate of Merit**

Participants

Saba Naamo, MD, Danville, PA (*Presenter*) Nothing to Disclose

#### TEACHING POINTS

High risk lesions (HRLs) are pathologically diverse lesions with an uncertain malignant potential that attribute an elevated lifetime risk for breast cancer. With a wide spectrum of clinical and radiological features, core needle biopsy is required to diagnose HRLs and tailor their management. We review the clinical, radiographic and histologic features of each of the HRLs and their potential for malignant transformation. We will also dive into the controversy and complexity of the current management as well as recent literature to delineate a guide for appropriate clinical management and the fine balance of risk/benefit. Teaching points: Recognize the clinical presentation, multimodality imaging findings and histologic manifestation of the HRLs Describe radiographic features of

HRLs that are commonly associated with malignancy Management and guidelines based on current evidence Imaging surveillance for patients with HRLs

## TABLE OF CONTENTS/OUTLINE

Table of contents: ? Introduction and overview of HRLs ? Describe individual HRLs including: ? Definition ? Common clinical and radiological multimodality presentation ? Radiographic/Histologic concordance ? Spectrum of current management and guidelines ? Surveillance of non-surgically/surgically excised lesions

### **BREE-105 Implementation of Synthetic Mammography: Benefits, Drawbacks, and Pitfalls**

#### **Awards**

**Identified for RadioGraphics  
Certificate of Merit**

Participants

Sona Chikarmane, MD, Newtonville, MA (*Presenter*) Nothing to Disclose

#### **TEACHING POINTS**

- Synthetic mammography (SM) is a 2D reconstruction from digital breast tomosynthesis (DBT) developed to replace full-field digital mammography (DM) obtained after the DBT acquisition.
- SM reduces radiation dose and shortens acquisition time for screening mammography.
- Studies have shown that DBT+SM significantly reduced recall rates and had equal cancer detection rates compared to DBT+DM.
- SM increases conspicuity of calcifications and architectural distortion; SM has demonstrated decreased conspicuity of asymmetries, with no change in detection of masses.
- SM may lead to artifacts such as "pseudo-calcifications", blurring of skin edge, artifact from metallic foreign bodies, and may underestimate breast density.
- Despite widespread availability, breast radiologists are slow to adopt SM due to concern about artifacts and dislike of contrast/appearance of findings on SM compared to DM.

## TABLE OF CONTENTS/OUTLINE

1. Introduction to SM: definition, reason for development, and hesitation over utilization
2. Screening performance metrics: recall rates, cancer detection rates, positive predictive value
3. Findings on mammography: conspicuity of calcifications, masses, asymmetries and architectural distortion in DBT+SM vs. DBT+DM
4. Breast density assessment on SM and DM and discussion of clinical implications
5. Review of artifacts on SM
6. Remaining challenges of implementation and potential to improve performance through artificial intelligence

### **BREE-106 The Male Breast - A Review of Clinical, Imaging Findings and Diagnostic Work-up**

Participants

Josefa Galobardes Monge, MD, Parla, Spain (*Presenter*) Nothing to Disclose

#### **TEACHING POINTS**

To review clinical presentation, imaging features and pathologic findings in male breast pathology. • To illustrate imaging findings (mammogram, contrast enhanced mammography, US, CT) of cases from our series of breast lesions in males with pathologic correlation. • To analyze and discuss the specific management of breast lesions in men including imaging and interventional procedures. • To emphasize pitfalls, diagnostic difficulties and differential diagnosis.

## TABLE OF CONTENTS/OUTLINE

We present: Clinical signs and symptoms. Techniques in evaluation of male breasts. Mammograms, contrast enhanced mammography, US, MR, CT. Differential diagnosis. Imaging appearances (spiculated mass, circumscribed mass, microcalcifications). Diagnostic work-up and recommendations for management. Specific considerations in male patients different from women. Different entities illustrated include. Benign: gynecomastia (diffuse, nodular and dendritic), epidermal inclusion cyst, lipoma, hematoma, foreign body granuloma, papilloma, fibromatosis; Malignant: ductal carcinoma in situ (DCIS), invasive ductal carcinomas uni and bilateral, metastasis to the breast (lung cancer), lymphoma

### **BREE-107 High-risk Lesions Breast: A Diagnostic Dilemma for the Radiologist and Pathologist**

Participants

Jacobo Emmanuel Garcia, MD, (*Presenter*) Nothing to Disclose

#### **TEACHING POINTS**

To expose the relative risk associated with breast cancer in women biopsied with ultrasound or stereotaxic guidance with results of proliferative lesions. Know the high-risk lesions according to the Ellis classification. Identify the main radiological characteristics of high-risk lesions in mammography and ultrasound. Exhibit the pathological characteristics to identify proliferative lesions. Suggest adequate and individualized management in response to the pathology of high-risk lesions of the breast.

## TABLE OF CONTENTS/OUTLINE

1. Definition of high-risk lesions of the breast.
  - 1.1. Ellis classification of lesions B3.
  - 1.2. Epidemiology and associated risk of proliferative lesions of the breast.
  - 1.3. Radiological findings of high-risk lesions of the breast.
2. Breast intervention techniques
  - 2.1. Image-guided interventional techniques for obtaining samples of suspicious lesions.
  - 2.2. Pathological features that facilitate differentiation.
3. The handling of the surgeon and the radiologist before the result of the pathologist, in B3 lesions.

### **BREE-108 Implementing AI CAD for Mammography - Learnings After Having Screened 55,000 Women**

Participants

Karin Dembrower, MD, PhD, Stockholm, Sweden (*Presenter*) Nothing to Disclose

#### **TEACHING POINTS**

How to prepare radiologists and AI for implementation in mammography screening  
What to expect as a radiologist when starting to use AI  
What are the results of combined radiologist and AI CAD mammography reading  
Case review highlighting important teaching

points

#### TABLE OF CONTENTS/OUTLINE

AI CAD in practice  
Preparing radiologists and AI for implementation  
Radiologist impressions, change over time  
Preliminary results of our study with AI as third reader  
Review of cases with important teaching points

#### **BREE-109 Breast Cancer Disparities that Affect Black Women**

Participants

Hillary Bui, DO, (*Presenter*) Nothing to Disclose

#### TEACHING POINTS

Become familiar with breast cancer disparities that affect Black women  
Become familiar with screening guidelines' impact on Black women  
Understand the importance of risk assessment by age 30  
Learn about social determinants of health

#### TABLE OF CONTENTS/OUTLINE

Case-based and interactive exhibit with answers and explanations appearing on mouse clicks.  
Case #1: Barriers to accessing care  
Social Determinants of Health  
Economic factors (e.g., income, insurance, childcare, transportation)  
Education level, literacy  
Language  
Medical mistrust  
Case #2: Black woman at average risk diagnosed with Stage II breast cancer (BC) at 44  
Black women more likely to be diagnosed with BC <50 versus Non-Hispanic White Women (NHW)  
Black women more likely to be diagnosed with triple-negative BC  
Black women more likely to be diagnosed at later stages of BC  
Black women have higher mortality associated with BC  
Importance of risk assessment by the age of 30, particularly in Black women  
Screening guidelines for average-risk women  
Case #3: Black woman at elevated risk diagnosed with multicentric DCIS at 31  
Black women more likely to be diagnosed with BC <35 versus NHW  
When to refer women for genetic counseling  
Black women less likely to undergo genetic testing  
Screening guidelines for high-risk women  
Conclusions  
Initiating screening mammography after age 40 disproportionately impacts Black women  
Omitting risk assessment by age 30 disproportionately impacts Black women  
Breast radiologists should be aware of disparities in BC to provide optimal care

#### **BREE-11 Community Outreach in Breast Imaging: What Radiologists Can Do to Close the Gap for the Underserved and Uninsured Population**

**Awards**

**Identified for RadioGraphics**

Participants

Angel Su, MD, CYPRESS, TX (*Presenter*) Nothing to Disclose

#### TEACHING POINTS

After the Affordable Care Act was implemented, the uninsured population in the United States of America decreased significantly. However, since 2017, a steady increase has been noticed, reaching up to 28.9 million in 2019. Unfortunately, the largest increases continue to affect minorities disproportionately and the COVID-19 pandemic, which resulted in lockdowns that delayed screening mammograms, further highlighted these disparities. Radiologists, and more specifically, breast imagers, must recognize this situation as this population is disproportionately diagnosed at later stages, has a higher mortality rate, less continuity of care, and overall lower survival. The purpose of this abstract is to familiarize the radiologist with the uninsured and underserved population and how these patients are affected by breast cancer, demonstrate current statistics, and propose strategies that breast imagers can pursue individually or as a group to close the disproportional gap for the underserved.

#### TABLE OF CONTENTS/OUTLINE

1. Introduction. 2. Who are these patients: Analyzing the data. 3. Breast cancer in the uninsured and underserved population: approach, navigating the options and obstacles, disparities 4. What else can the breast imager do? A) Radiologist-Patient interaction B) Radiologist-Referring physician interaction C) Radiologist-Community interaction D) Radiologist and the Media E) Radiologist and Legislature. 5. Conclusion

#### **BREE-110 AI for Mammography: What Radiologists Need to Know**

Participants

Sieun Lee, MD, Yongin, Korea, Republic Of (*Presenter*) Nothing to Disclose

#### TEACHING POINTS

Teaching points - AI-CAD can improve the diagnostic performance of radiologists, and help close the learning gap for inexperienced readers.- Stand-alone AI-CAD has shown variable performance in previous studies, suggesting a cautious approach is needed to implement its use for triaging or workload reduction.- Future AI will predict the possibility of cancers beyond the current diagnosis of present abnormalities in combination with the clinical model, which will allow more stratified and personalized screening to take place.

#### TABLE OF CONTENTS/OUTLINE

Improving the accuracy of breast cancer diagnosis - How AI-CAD differs from conventional CAD in terms of false-positive results- Retrospective, but large-scale evidence for AI-CAD - Cancers missed by AI-CAD  
Improving efficiency for radiologists - Triaging screening mammography - Recommendations for the best use of AI-CAD  
Personalized predictions of cancer risk- Better way to estimate breast density- New model that includes additional clinical risk factors- Suggestions for personalized screening

#### **BREE-112 Looking Through BI-RADS Terminology for Contrast-Enhanced Mammography - An Updated Guide to Understand CEM Supplement**

**Awards**

**Certificate of Merit**

Participants

Diana Galvis Zambrano, BSc, MD, Mexico City, Mexico (*Presenter*) Nothing to Disclose

## TEACHING POINTS

1. To describe Contrast-enhanced mammography (CEM) technique and image acquisition. 2. To outline contrast enhanced mammography - breast imaging lexicon - from ACR BI-RADS supplement. 3. To illustrate different imaging findings, the correlation with other imaging techniques and the appropriate form to report based in the new CEM BI-RADS supplement. 4. To review and compare the advantages and drawbacks of each image model. 5. To understand how and what should be in the report of a CEM study.

## TABLE OF CONTENTS/OUTLINE

1. Background and history of CEM. 2. Description of protocol and imaging acquisition in contrast-enhanced mammography and associated technical details. 3. Review the CEM breast imaging lexicon from BI-RADS supplement. 4. Case-based CEM BI-RADS lexicon supplement interpretation in multiple scenarios and pathologies. 5. Correlation of radiological findings between CEM and other techniques. 6. Discuss actual indications, limitations and the future of CEM. 7. Take home points

## BREE-113 To Freeze Or Not To Freeze? That Is The Question: Cryoablation For The Treatment Of Breast Cancer

Participants

Kenneth Tomkovich, MD, Freehold, NJ (*Presenter*) Consultant, IceCure Medical, Inc; Speakers Bureau, IceCure Medical, Inc

## TEACHING POINTS

The purpose of this exhibit is: 1. Discuss the historical perspective of breast cancer treatment from radical mastectomy in the late 1800's to current practice. 2. To discuss the use of image guided cryoablation in the treatment of cancer in organs other than the breast. 3. To demonstrate the optimal technique to perform successful ultrasound guided cryoablation of primary breast cancer. 4. To illustrate important "new normal" imaging findings commonly seen following breast cancer cryoablation. 5. Review recent publications and abstracts on the topic of breast cancer cryoablation as an alternative to surgical lumpectomy.

## TABLE OF CONTENTS/OUTLINE

History of surgical treatment for breast cancer. Cryoablation therapy application in organs other than the breast. Technique of ultrasound guided breast cancer cryoablation. Present the imaging findings post breast cancer cryoablation: Mammography, Ultrasound, MRI. Future implications based on a review of recent publications and abstracts.

## BREE-114 The Horizontal Approach for Tomosynthesis and Stereotactic Guided Breast Biopsy: Review of Technique and Advantages

Participants

Janice Thai, MD, (*Presenter*) Nothing to Disclose

## TEACHING POINTS

1. To expand the proceduralist's armamentarium by introducing a different approach to performing stereotactic breast biopsy. 2. To demonstrate the horizontal approach technique, and highlight the technical advantages inherent to a needle trajectory that is parallel to the image detector. 3. To inform the appropriate use of the horizontal approach in technically challenging anatomy/lesion location, including thin breast, superficial/retroareolar lesion, and posterior chest wall/inferior lesion.

## TABLE OF CONTENTS/OUTLINE

- Review of patient positioning, targeting approach, procedural technique, and device set up based on the two most popular commercially available systems
- Review of the advantages of the horizontal approach over the vertical approach, with real life case examples
- Review of needle targeting error and problem solving for optimal efficiency
- Review of tips and tricks to maximize technical success and patient comfort

## BREE-115 Breast Radiofrequency Identification Marker Localization: Technique, Tips, and Troubleshooting

Participants

Jared Vearrier, MD, (*Presenter*) Nothing to Disclose

## TEACHING POINTS

1. Understand technology behind radiofrequency identification (RFID) markers  
2. Pros/cons of using RFID markers compared to other localization methods  
3. Understand optimal technique for US and Stereotactic marker placement  
4. Learn tips and suggestions for troubleshooting challenging cases

## TABLE OF CONTENTS/OUTLINE

Introduction-Utilization of wireless localization-Technology  
US guided RFID Placement-Pros/Cons-Technique of US guided placement-  
Challenges and tip/tricks for RFID placement  
\*\*Larger biopsy makers can obstruct the deployment path of the RFID marker and result in posterior migration\*\*  
\*\*Forward migration of the RFID marker along the biopsy track of large gauge biopsy needles  
Stereotactic/Tomosynthesis-Pros/Cons-Technique of Stereotactic placement\*\*  
\*\*Two view stereotactic technique can be employed or a single view tomosynthesis guided technique.\*\*  
\*\*Challenges:\*\*  
\*\*Unrecognized motion during placement\*\*  
\*\*Marker migration: 1) Accordion effect; 2) Migration along the biopsy track; 3) Floating in hematoma/displacement by a hematoma; 4) Resorption of air at the biopsy cavity/Changes to biopsy marker site after neoadjuvant chemotherapy; 5) RFID Marker displacement by biopsy marker\*\*  
\*\*Difficulty seeing target on Tomosynthesis slice after applicator placement  
Post-Procedure Imaging-Utilization of post-procedure imaging  
Conclusion-Breast RFID markers have various frequencies to aid in surgical excision and is a great alternative to other wireless localization devices-Awareness of the challenges that a radiologist can encounter during placement is important to avoid migration and misplacement during deployment

## BREE-116HC Imaging Features Following Breast Explant Surgery: A Pictorial Essay

Participants

Yusuf Akpolat, MD, Houston, TX (*Presenter*) Nothing to Disclose

## TEACHING POINTS

1. Breast implants can be removed with breast explantation surgery (BFS) for various reasons, including patient dissatisfaction

1. Breast implants can be removed with breast explantation surgery (BES) for various reasons, including patient dissatisfaction, capsular contracture, implant infection or rupture, breast implant-associated anaplastic large cell lymphoma, and a recently emerging phenomenon called breast implant illness. 2. BES techniques include capsulotomy, partial, total, or en bloc capsulectomy. Adjunctive aesthetic or reconstructive procedures after BES include fat grafting, mastopexy, augmentation, and reconstruction with flaps. 3. The majority of the post-BES breast imaging findings are related to the surgical scar/bed, thus, confirming the type of explantation surgery is important. 4. Imaging findings after BES include focal and global asymmetries, architectural distortions, calcifications, calcified and non-calcified fat necrosis, masses, hematomas, seromas, capsular calcifications, and silicone granulomas. 5. Most importantly, since these patients have residual breast tissue, paying attention to suspicious imaging features is necessary.

#### TABLE OF CONTENTS/OUTLINE

1. Breast Explant Surgery Techniques  
2. Findings  
a. Global Asymmetry  
b. Architectural Distortion  
c. Calcifications/Fat Necrosis  
d. Asymmetries and Masses Anterior to the Pectoralis Major Muscle  
e. Implant Capsule/Calcifications  
f. Silicone Granulomas/Free Silicone  
g. Suspicious Findings  
Please visit the Learning Center to also view this presentation in hardcopy format.

#### BREE-117 Pregnancy-associated Breast Cancer: The Perfect Storm

Participants

Julia Colombo, MD, Buenos Aires, Argentina (*Presenter*) Nothing to Disclose

#### TEACHING POINTS

- There is clinical and imaging difficulty in making an accurate diagnosis of breast cancer due to typical changes occurring during pregnancy and lactation.
- The vast majority of mammary alterations in pregnancy correspond to benign pathology.
- The differential imaging diagnosis is complex due to the similar appearance in many cases to benign pathology
- Any palpable area that remains for more than 2 weeks during pregnancy should be investigated.
- Ultrasound is the first choice in the evaluation of masses.
- Mammography is essential for its complementary contribution.
- MRI during pregnancy should be used if the benefits outweigh the risks and the information cannot be obtained by any other method.
- Core needle biopsy is of choice for final diagnosis.
- Pregnancy-associated breast cancer tends to have a worse prognosis due to delayed diagnosis
- The incidence is increasing in developed countries due to the postponement of motherhood.

#### TABLE OF CONTENTS/OUTLINE

- Definition of pregnancy-associated breast cancer (PABC)
- Some peculiarities of pregnancy-associated breast cancer.
- Imaging methods for the diagnosis of breast cancer during pregnancy and lactation. Safety and effectiveness.
- Some cases of our daily practice.
- Conclusion.

#### BREE-118HC Fast-Growing Fibroepithelial Breast Tumors: Tips for Proper Radio-Pathologic Correlation

Participants

Amanda Tavares, MD, Sao Paulo, Brazil (*Presenter*) Nothing to Disclose

#### TEACHING POINTS

Fibroepithelial neoplasms are the most common breast tumors in clinical practice, especially in younger women. Despite most of these lesions are benign, they can present significant growth. Due to the overlapping histopathologic features, the differential diagnosis between Fibroadenoma (FA) and Phyllodes Tumor (PT) may be difficult on core-needle biopsies and radiopathologic correlation may contribute to the management of those lesions. FA are the most common lesions and usually have slow growth pattern; however, they can increase due to hormonal changes, especially during pregnancy and lactation. FA variants (eg. complex, giant and juvenile FA) may also present as fast-growing tumors. At imaging, FA usually present as oval and circumscribed masses, with high-signal on T2-weighted images, homogeneous enhancement or dark internal septations, and persistent kinetics on magnetic resonance imaging (MRI). PT usually present as fast-growing tumors and may be benign, borderline or malignant. They usually have image characteristics similar to those of FA, but may show cysts or necrosis related to the tumor's rapid growth. There is higher risk of malignancy if the tumor presents non-circumscribed margins, irregular cystic walls, peritumoral edema, low signal on T2 sequences and low apparent diffusion coefficient.

#### TABLE OF CONTENTS/OUTLINE

Fibroepithelial neoplasms of the breast  
Clinical and histopathologic features  
Imaging and Differential Diagnosis Summary  
Please visit the Learning Center to also view this presentation in hardcopy format.

#### BREE-119 Nipple-Areolar Complex, What the Radiologist Should Know

Participants

Natalia Orthmann, MD, Sao Paulo, Brazil (*Presenter*) Nothing to Disclose

#### TEACHING POINTS

The purpose of this exhibit is: 1. To show the epidemiology, histological origin, imaging aspects in the different methods, anatomopathological and clinical correlation, when possible. 2. To review the imaging findings of the suggestive nipple-areolar complex and its differential diagnoses. 3. To illustrate the different imaging methods to assess the nipple-areolar complex, such as Ultrasound (US), Mammography (MG), tomosynthesis (TS) and Magnetic Resonance (MR). 4. To suggest techniques for better assessment of the nipple-areolar complex.

#### TABLE OF CONTENTS/OUTLINE

1. Literature review focusing on nipple-areolar complex diseases and its differential diagnoses. 2. To illustrate and discuss the pathology of nipple-areolar complex diseases, highlighting epidemiology; anatomy; progression in different imaging methods. 3. Review of the pathological development of nipple-areolar complex diseases through illustrative cases. 4. Example cases with mammographic, ultrasonographic, clinical and pathological correlation when available. 5. Examples of cases with suggestions of techniques for better evaluation of the nipple-areolar complex. 6. Summary and conclusion.

#### BREE-12 Second look and Targeted Ultrasound Made Very Very Easy, a Case-Based Review

Participants

Sepideh Sefidbakht, MD, Powel, OH (*Presenter*) Nothing to Disclose

#### TEACHING POINTS

Understanding the relationship between location of lesions in ultrasound and mammogram and MRI is not always intuitive. This makes targeted and second look ultrasounds challenging to learn. Following a few simple rules and being aware of the pitfalls and peculiarities associated with each modality can accelerate the learning curve and enhance the accuracy of performing second look and targeted ultrasounds. Using simplified rules, 3D schematics and simple animations we will review the basic concepts of second-look and targeted ultrasound. Then using a case-based approach we will practice the basic concepts of second look and targeted US. The purpose of this exhibit is to:1-Review the basic concepts of correlating lesions between modalities (clockwise location, depth, shape size)2-Review the basic characteristics of the CC view in mammogram (depicting medial, lateral, superior inferior lesions and the role of rolled-over views)3\_Review the basic characteristics and peculiarities of the of the MLO view in mammogram and how it affects where we see lesions; the concept of clockwise and counterclockwise rotation of the breast and how it affects lesion perception.4-Review the basic characteristics of the lesions seen in MRI (location, depth, concordance and discordance between extent of enhancement and US appearance)

#### TABLE OF CONTENTS/OUTLINE

- Looking for a nonpalpable lesion seen in MG or MRI; The Four Golden Rules
- 3D depiction of lesions in CC view; The Four Golden Rules of the CC view
- 3D depiction of lesions in MLO view; The Four Golden Rules of the MLO view
- Second look ultrasound, The Four Golden Rules
- Case-based practice of second look and targeted ultrasound

#### BREE-120 Are You Sure It's Cancer? Desmoid Tumors Mimicking Malignant Lesions

Participants

Natalia Lima, Sao Paulo, Brazil (*Presenter*) Nothing to Disclose

#### TEACHING POINTS

The purposes of this exhibit are:To review the main aspects of desmoid tumors and its ability to mimic malignant lesions;To exemplify, by using interesting cases from our breast radiology group, different types of presentation of desmoid tumors;To show the main conclusion for each clinical case;To emphasize the importance of knowing this kind of tumors and differential diagnoses in order to help in daily clinical practice.

#### TABLE OF CONTENTS/OUTLINE

Teaching cases showing the challenging aspects based on imaging findings and correlate with clinical and pathological findings in different scenarios, mimicking solid-cystic complex, increasing palpable mass, posterior masses and spiculated masses, as well as in gardner syndrome; Explanations about the behaviour of desmoid tumors, as a benign neoplasm but with aggressive characteristics.

#### BREE-121 Lactation Education: Breast MRI Pathology, Pearls, and Pitfalls

##### Awards

##### Identified for RadioGraphics

Participants

Kali Xu, MD, (*Presenter*) Nothing to Disclose

#### TEACHING POINTS

- The lactating breast undergoes marked physiologic changes that can make conventional imaging evaluation with mammography and ultrasound challenging.- MRI is increasingly recognized as a safe and effective supplemental tool for both diagnostic evaluation and screening of lactating patients in the appropriate clinical setting.- Learning to recognize normal physiologic findings, common benign entities, and signs of malignancy in the lactating breast on MRI will improve diagnostic accuracy and facilitate proper clinical management.

#### TABLE OF CONTENTS/OUTLINE

I. Review clinical indications for breast MRI during lactation.II. Illustrate characteristic features of the lactating breast on MRI, including atypical scenarios (post-breast conservation, unilateral breastfeeding).III. Provide case examples of benign entities encountered during lactation (galactocele, lactating adenoma, fibroadenoma).IV. Review MRI features of pregnancy-associated breast cancer (PABC) using case examples illustrating a spectrum of pathology and clinical scenarios. Correlative mammography and ultrasound images will be incorporated where appropriate. Emphasis will be placed on demonstrating how breast MRI may depict more extensive disease than conventional imaging, leading to changes in clinical management.V. Discuss risks and benefits of FNA vs. core biopsy for sampling of suspicious imaging findings in lactating patients, with emphasis on careful correlation of radiologic, pathologic, and clinical findings to avoid delays in cancer diagnosis.

#### BREE-122 Breast Parenchymal Changes After Breast Conservative Treatment - What the Radiologist Must Know How to Differentiate

Participants

Almudena Gil Boronat, MD, Madrid, Spain (*Presenter*) Nothing to Disclose

#### TEACHING POINTS

- To briefly review the breast cancer conservative treatment, whose current protocols include the use of adjuvant breast radiotherapy. - To explain the different breast parenchymal findings expected after conservative treatment, depending on the time elapsed after it. - To emphasize that although most of them are benign in nature, they can present suspicious radiological semiology, and it is important to know them in order to differentiate them from a local recurrence.

#### TABLE OF CONTENTS/OUTLINE

1. Quick review of adjuvant radiotherapy after breast-conserving surgery. 2. Explain the different types of glandular changes expected after conservative treatment depending on the time of evolution, classified as early changes, intermediate changes and late changes. 3. We focus on explaining the situations that generate the greatest difficulties to differentiate them from a local recurrence. 4. Conclusions. 5. Take home points. 6. Bibliography.

## **BREE-123 Pregnancy-associated Breast Cancer and the Role of Imaging in the Pregnant and Lactating Patient**

Participants

Julia Kirsten, MD, Fenton, MO (*Presenter*) Nothing to Disclose

### **TEACHING POINTS**

1. Describe the background, etiology, biomarker status and most common histological types behind pregnancy-associated breast cancer. 2. Discuss screening and diagnostic guidelines and review current updates regarding the role of imaging for pregnant and lactating women. 3. Review common benign pregnancy-related lesions, potential complications, radiation safety, and treatment of pregnancy-associated breast cancer.

### **TABLE OF CONTENTS/OUTLINE**

1. Introduction to pregnancy-associated breast cancer and challenges in diagnosis 2. Etiology, histological type, and biomarker status of pregnancy-associated breast cancer 3. Clinical manifestations of pregnancy-associated breast cancer (palpable breast mass, unilateral milk rejection, etc) 4. Initial imaging of breast cancer screening during pregnancy (high and elevated risk patients, 39 and under, summary of recommendations from ACR, ACOG, AJR) 5. Initial imaging of breast cancer screening during pregnancy (40 years and older, summary of recommendations from ACR, ACOG, AJR) 6. Initial imaging of breast cancer screening during lactation 7. Initial imaging of pregnant women with a palpable breast mass 8. Use of MRI in the pregnant/lactating patient (concerns regarding heat deposition into the fetus, damage to auditory nerves, gadolinium-induced fetal toxicity) 9. Common benign pregnancy-related breast lesions 10. Complications of biopsies in pregnant and lactating women (milk fistulas, increased risk of bleeding and infection, breast pseudoaneurysm) 11. Radiation safety and recommendations 12. Treatment of pregnancy-associated breast cancer 13. Conclusion

## **BREE-124 Common Questions and Challenging Scenarios of the Daily Practice Using the BI-RADS® Atlas**

Participants

Karina Pesce, MD, Capital Federal, Argentina (*Presenter*) Nothing to Disclose

### **TEACHING POINTS**

1-Review the management recommendations suggested by the ACR for clinical cases that generate different inquiries during daily practice. 2-Describe the different clinical scenarios that constitute the exception to the rule in the management of categorization recommendations.

### **TABLE OF CONTENTS/OUTLINE**

The American College of Radiology (ACR) has established the Breast Imaging Reporting and Data System (BI-RADS) to guide the breast cancer screening and diagnostic routine. This educational poster is aimed at doctors who are new to breast diagnosis and is intended to be a practical guide to solve the most frequent doubts following the recommendations of experts from the American College of Radiology. Frequently asked questions will be reviewed through clinical cases.

## **BREE-125 False Negatives in Breast Screening and How to Avoid Them**

Participants

Agustina Graziani, MD, (*Presenter*) Nothing to Disclose

### **TEACHING POINTS**

1. Identify the factors that influence false negative results in all diagnostic modalities. 2. Analyze the causes of false negatives. 3. Discuss possible strategies to avoid false negatives.

### **TABLE OF CONTENTS/OUTLINE**

Breast cancer is a common disease among women and it is the second leading cause of death from cancer. Timely diagnosis allows detection in early stages, with better outcome, better prognosis and with fewer comorbidities in the instituted treatments. Diagnosis can be made with breast imaging either by mammography, ultrasound and magnetic resonance imaging. The percentage of false negatives on imaging studies in the literature varies between 8-10%, between 9 and 22% and 4.4% respectively. The most common causes that lead to a misdiagnosis can be classified as related to: 1. The technical aspect of the imaging modality. 2. The Patient. 3. The Reporting physician. 4. The lesion. Early detection of breast cancer is one of the most important prognostic indicators, and diagnostic errors in breast imaging represent missed opportunities for timely treatment. Improving diagnostic accuracy requires a multidimensional approach, however recognizing causes of false negatives allows us to adopt useful strategies to avoid them and thus favorably impact the reduction of morbidity and mortality.

## **BREE-126 Pseudoangiomatous Stromal Hyperplasia of the Breast (PASH) - Tips and Tricks for Diagnosis**

Participants

Rosa M. Lorente-Ramos, MD, PhD, Madrid, Spain (*Presenter*) Nothing to Disclose

### **TEACHING POINTS**

To review pseudoangiomatous stromal hyperplasia of the breast, highlighting clinical presentation, pathological and imaging findings as well as differences from breast cancer To illustrate common and uncommon imaging findings in mammogram and contrast enhanced mammography (CEM), US, MR, of cases from our series with pathological correlation. To analyze and discuss the specific management of those lesions, including diagnostic difficulties and imaging work-up. To emphasize pitfalls and clues to differential diagnosis.

### **TABLE OF CONTENTS/OUTLINE**

Pseudoangiomatous stromal hyperplasia (PASH) is a benign mesenchymal proliferating lesion. It is frequently found as an incidental histological finding in breast biopsies performed for other lesion but it can present as a mass (also called nodular PASH) or breast enlargement, which may mimic malignant lesions. Keys for differential diagnosis should be recognized. We present: - Definition. - Clinical presentation. - Pathological findings. - Imaging findings: Mammograms/CEM, US, MR. - Differential diagnosis. - Management and outcomes.

## **BREE-127 High-risk Breast Lesions - What the Radiologist Should Know About the Diagnostic and Therapeutic Implications**

Participants

Ladys Camargo, MD, Ciudad Autonoma de Buenos Aires, Argentina (*Presenter*) Nothing to Disclose

### **TEACHING POINTS**

Describe the lesions included in the histopathological B3 category of the Ellis classification. Correlate imaging and histopathological findings. Discuss the diagnostic algorithm and management of B3 lesions.

### **TABLE OF CONTENTS/OUTLINE**

One of the main challenges of breast pathology is the diagnosis of lesions with indeterminate radiological characteristics and their proper management. The same occurs with the diagnosis of histological lesions considered to be of uncertain malignant potential, framed according to the Ellis histological classification as B3 lesions. Over time, personalized management has been favored to reduce overtreatment and thus lower the high healthcare costs associated with surgical excision. The main objective of this work is to provide a precise approach to high-risk lesions, correlating their imaging and pathology findings and discussing their proper management. 1. Introduction. 2- Classification of B3 lesions according to Ellis histological classification. 3- Imaging characteristics of B3 lesions (mammography, US, MRI). 4- Radio-Pathological correlation. 5- Clinical cases. 6- Diagnostic Algorithm. 7- Discussion of the Management of B3 Lesions. 8- Conclusions. 9- Bibliography.

## **BREE-128 Male - Malignant or Mimic? A Seven-Year Institutional Review of Male Breast Biopsies with Radiology-Pathology Correlation**

Participants

Esraa Hazim Hasan Al-Jabbari, MBCHB, Galveston, TX (*Presenter*) Nothing to Disclose

### **TEACHING POINTS**

1. An overview of male breast findings which were biopsied and/or resected over the last seven-years (April 1st, 2015 - March 31st, 2022) within our institution. 2. Discuss imaging and pathologic features of some pertinent benign and malignant lesions of the male breast. 3. Highlight imaging features suggestive of a benign etiology to limit false negative biopsies. 4. Highlight the risk factors for male breast cancer. 5. Discuss potential breast cancer screening programs in at-risk male populations including trans-gender patients.

### **TABLE OF CONTENTS/OUTLINE**

Introduction; Embryologic and anatomic overview of the male breast; Institutional experience with male breast findings; Malignant breast findings in males; Benign mimics of breast malignancies in males; Risk factors for male breast cancer; Potential screening guidelines in at-risk male population; Conclusion.

## **BREE-129 Dermatofibrosarcoma Protuberans: A rare Differential Diagnosis in Superficial Breast Lesions - Imaging Findings and Histopathological Correlation**

Participants

Camila Acras, MD, Sao Paulo, Brazil (*Presenter*) Nothing to Disclose

### **TEACHING POINTS**

- To present the features of dermatofibrosarcoma protuberans (DFSP) in the breast through imaging findings on mammography (MG), ultrasonography (US), and magnetic resonance imaging (MRI) - To review the DFSP imaging signs, and discuss the differential diagnosis

### **TABLE OF CONTENTS/OUTLINE**

- Introduction. - Identify and describe differential imaging findings, including the ones that can suggest the diagnosis of DFSP - Report the survey of institutional data from the analysis of the results of breast biopsies performed in recent years that confirmed histological diagnostic of DFSP - Report the institutional data from the analysis of the breast biopsies performed in recent years that confirmed histological diagnostic of DFSP - Conclusion.

## **BREE-13 Echogenic Breast Lesions: A Road Map for the Breast Radiologist**

Participants

Luciano Fabrizio, Buenos Aires, Argentina (*Presenter*) Nothing to Disclose

### **TEACHING POINTS**

1- Identify benign and malignant breast pathology that manifest as echogenic ultrasound lesions. 2- Correlate ultrasonographic and mammographic findings. 3- Correlate imaging findings with histopathological study. 4- Discuss the diagnostic algorithm for echogenic breast lesions. 5- Identify imaging key-points for each echogenic lesions.

### **TABLE OF CONTENTS/OUTLINE**

- Introduction: echogenic images and their epidemiology. - Ultrasound key-points for characterizing benign and malignant entities. - Diagnostic algorithm. - Conclusions. - Annex I: characteristics table of benign and malignant echogenic lesions. - Annex II: diagnostic algorithm (categorization and biopsy indications).

## **BREE-130 Prone Tomosynthesis-guided Breast Biopsy: A Guide for Trainees and Experts Alike**

**Awards**

**Identified for RadioGraphics**

Participants

Luciano Chala, MD, Sao Paulo, Brazil (*Presenter*) Nothing to Disclose

## TEACHING POINTS

1. Step-by-step review of tomosynthesis-guided breast biopsy technique. 2. Discuss all indications, complications, and contraindications of the method. 3. Share our experience with cases illustrating situations where tomosynthesis has helped improve our biopsy results.

## TABLE OF CONTENTS/OUTLINE

- To obtain more accurate and reliable results, it is important to be familiar with the steps of tomosynthesis-guided biopsy. We demonstrate the technique step-by-step with actual photos from our daily practice so that residents can learn the procedure comprehensively. - In recent years, tomosynthesis-guided biopsy has gained popularity. We discuss all indications for this method and compare its limitations and complications with supine tomosynthesis-guided and stereotactic biopsies. - Tomosynthesis-guided breast biopsy in the prone position can sometimes offer advantages over other methods and even shorten the overall duration of the biopsy. We illustrate the following advantages with some cases: identification of lesions visible only on tomosynthesis, the possibility of lateral access in thin breast thickness, improved calcifications conspicuity, and identification of intravascular calcifications, which helps to distinguish them from linear calcifications and also allows better planning by avoiding blood vessels to reduce hemorrhage-related complications.

## BREE-131 SOS Within the Breast: The Must-Knows of Handling Emergent Breast Cases

Participants

Kristina Michaudet, MD, Stanford, CA (*Presenter*) Nothing to Disclose

## TEACHING POINTS

Breast emergencies are infrequent but can be diagnostically challenging especially during off hour nights and weekends. Very few experienced breast imagers nor specialized sonographers may be available during acute breast situations. Breast emergencies may present as complications of interventional procedures such as pseudoaneurysms or post biopsy hematomas. Numerous patients also return to the emergency department setting following mastectomy and reconstruction. Additionally, acute situations may be related to infection and inflammation in both cancer and non-cancer patients. Most importantly, a seemingly infectious process can masquerade an underlying mass and malignancy. The importance of follow up imaging for ED breast complaints is imperative.

## TABLE OF CONTENTS/OUTLINE

The poster will be organized to include a review of both common and uncommon emergently presenting breast conditions. Examples of emergency breast cases including infection in puerperal and non puerperal cases will be showcased as well as first time presentation of malignancy through acute settings. Breast ultrasound utilization will be discussed along with the patient factors and characteristics which may be most pertinent for suspected infection and abscess. Management and knowledge of appropriate follow-up-protocols is key particularly for the non- breast imager encountering these unique cases on call. Emergency procedures and treatments such as embolization will be highlighted in cases of post biopsy complications such as bleeding and pseudoaneurysm formation.

## BREE-132 Non-mass Lesion on Ultrasound - The New Finding to Incorporate

### Awards

#### Certificate of Merit

Participants

Karen Mena Moreno, MD, Buenos Aires City, Argentina (*Presenter*) Nothing to Disclose

## TEACHING POINTS

1. Analyze the correlations between histopathologic findings and non-mass breast lesions on ultrasound. 2. Discuss the management of non-mass findings on ultrasound. 3. Demonstrate the importance of recognizing non-mass lesions.

## TABLE OF CONTENTS/OUTLINE

Introduction. Review of the definition and sonographic characteristics of non-mass findings. Description and correlation of breast imaging findings on mammography and MR. Clinical cases with histological correlation. Diagnostic algorithm. Treatment and management considerations. Discuss controversial cases. Take-home points. Conclusions.

## BREE-14 Next Top Model: An Overview of Breast Cancer Risk Assessment Models

Participants

Pooja Agrawal, Houston, TX (*Presenter*) Nothing to Disclose

## TEACHING POINTS

1. Introduce breast cancer risk assessment models available for estimating an individual's risk of developing breast cancer or risk for carrying a gene mutation that may predispose to developing breast cancer. 2. Review the strengths and limitations of each model and the model's applicability to underrepresented populations. 3. Provide example cases and narratives that demonstrate the use of breast cancer risk assessment models for different women.

## TABLE OF CONTENTS/OUTLINE

1. Introduction: Review breast cancer statistics including morbidity and mortality disparities amongst patient populations, define breast cancer risk assessment, review guidelines and recommendations for breast cancer risk assessment (American College of Radiology, Society of Breast Imaging, American Society of Breast Surgeons, American College of Obstetricians and Gynecologists), and discuss current utilization (or lack of utilization) of breast cancer risk assessment. 2. Review available risk models, including risk factors assessed, strengths, and limitations: Gail Model, Claus Model, BRCAPRO Model, IBIS aka Tyrer-Cuzick Model, Jonker Model, BOADICEA Model. 3. Demonstrate breast cancer risk assessment performance: Provide examples of how risk assessment is performed, review recommendations for patients found to be at high risk. 4. Show case examples of breast cancer risk assessment for women belonging to minority groups or underrepresented populations. 5. Conclusion and application of breast cancer risk assessment models to clinical practice

## BREE-15 Problem-Solving Breast MRI

## Awards

### Identified for RadioGraphics Certificate of Merit

#### Participants

Beatriu Reig, MD, MPH, New York, NY (*Presenter*) Nothing to Disclose

#### TEACHING POINTS

1. MRI does not replace careful diagnostic workup with mammogram and ultrasound 2. Negative MRI should not obviate the need for biopsy for a suspicious finding detected on mammography/tomosynthesis or ultrasound 3. A negative MRI is reassuring in low-suspicion mammo/tomosynthesis findings such as asymmetries, focal asymmetries, and post-surgical change

#### TABLE OF CONTENTS/OUTLINE

1. Brief introduction a. Indications for MRI b. MRI Sensitivity/specificity 2. Indications for problem-solving MRI a. Equivocal or uncertain imaging i. Lesion visible on some but not all views ii. Change over time: true change versus technical difference iii. Change at surgical site iv. Sternalis muscle b. Negative imaging with clinical concern i. Suspicious nipple discharge c. BIRADS 4 lesions i. Difficult biopsy due to technical issues ii. Discordant biopsy iii. Tomosynthesis-only finding without tomo-guided biopsy capability 3. Inappropriate use of problem-solving MRI a. Preceding or replacing diagnostic mammo and US b. In lieu of biopsy of a suspicious finding identifiable by mammo, US, or clinical exam c. Evaluation of mammographic calcifications 4. Future directions a. Increasing use of tomosynthesis decreases need for problem-solving MRI i. Better evaluate equivocal findings ii. Biopsy one-view findings b. Triaging tool for active surveillance vs surgical excision for high risk lesions detected on percutaneous biopsy i. Low grade DCIS ii. ADH, atypia iii. Radial scar c. Improving accuracy leads to improved utility of problem solving MRI i. Diffusion weighted imaging ii. Artificial intelligence in MRI d. Problem solving MRI more feasible as MRI becomes faster and cheaper i. Abbreviated MRI impact ii. Increased MRI screening

### BREE-16 The Use of Diffusion-weighted Sequence in the Evaluation of Breast Lesions: What the Radiologist Needs to Know

#### Participants

Giselle Mello, PhD, Sao Paulo, Brazil (*Presenter*) Nothing to Disclose

#### TEACHING POINTS

- Review the fundamental principles of diffusion-weighted imaging (DWI).- Review the concepts of breast lesions cellularity.- Review the concepts of ADC mapping.- Illustrate with cases how to differentiate benign from malignant lesions and correlate the histopathologic findings with their ADC values to allow for earlier and more accurate diagnosis and individualized patient care.- Create a pictorial essay to illustrate the use of DWI to differentiate complex breast lesions with peripheral enhancement that, when combined with clinical and histopathologic findings, can provide valuable information for therapy.

#### TABLE OF CONTENTS/OUTLINE

1) Principles of diffusion-weighted imaging (DWI).2) The concept of apparent diffusion coefficient (ADC).3) Lesion cellularity.4) Benign and malignant DWI findings and their corresponding ADC values.5) Differentiation of complex peripheral enhancing breast lesions.6) DWI findings for predicting pathologic response in neoadjuvant treatment of breast cancer.7) A series of cases using DWI sequences and correlation of their ADC values with histopathological findings.

### BREE-17 Anatomical Approach for the Imaging and Diagnosis of Nipple Areolar Complex Abnormalities

## Awards

### Certificate of Merit

#### Participants

Claudia Cotes, MD, Houston, TX (*Presenter*) Nothing to Disclose

#### TEACHING POINTS

The nipple areolar complex is a region of the the breast with a complex anatomy from which several benign and malignant pathology may arise. It is important to understand anatomic features of this region for an appropriate differential diagnosis when abnormalities in this area are encountered. The imaging evaluation of this region can be technically difficult due to superimposition of tissues in mammography and artifacts and/or technical limitations on ultrasound which can limit the appropriate diagnosis of these abnormalities. This exhibit will provide a review of the clinical and imaging findings of interesting pathologic processes in the nipple areolar complex utilizing an anatomical approach, as well as interactive examples of imaging technique for proper evaluation of this region. Workup algorithms based on the ACR appropriateness criteria for clinical findings related to the nipple areolar complex will also be provided.

#### TABLE OF CONTENTS/OUTLINE

1. Introduction 2. Imaging Anatomy of the Nipple Areolar Complex 3. Imaging of the Nipple Areolar Complex: Tips and Tricks for optimal evaluation4. Anatomy based Pathology Review: a. Skin and Subcutaneous Soft Tissue: Sebaceous Cyst, Epidermal Inclusion Cyst, Montgomery Gland Cyst, Cellulitis/Abscess, Eczema, Paget Disease b. Breast Parenchyma and Connective Tissue: Adenoma, Fibroadenoma, Lipoma, Fibroadenolipoma, Abscess c. Ductal system: Ductal Ectasia, Intraductal Papilloma, Ductal Carcinoma In-Situ, Invasive Ductal Carcinoma 5. Workup Algorithms 6.Conclusion

### BREE-19 Green is the New Pink- Reducing the Carbon Footprint of Breast Imaging Practices

#### Participants

Tom Soker, DO, Cleveland, OH (*Presenter*) Nothing to Disclose

#### TEACHING POINTS

Recognized as one of the greatest global health challenges of the 21st century, climate change poses substantial risks to the health and well-being of the world's population. With healthcare overall contributing up to 10% of greenhouse emissions in the United States, imaging has been identified as one of the major contributors. Therefore, breast radiologists should embrace

environmentally friendly strategies to mitigate future health effects. Specific learning objectives for this exhibit include: 1) Understand the current state of climate change and how it relates to medicine. 2) Review how breast imaging practices currently contribute to climate change. 3) Describe steps that breast imaging practices can take now to reduce their carbon footprint. 4) Describe initiatives that breast imaging can embrace to further accelerate adoption of "greener" practices and engage the broader community.

#### TABLE OF CONTENTS/OUTLINE

Using text, schematics and cases, we will discuss the current challenges that breast imaging practices face and focus on specific steps that practices can take to reduce their carbon footprint and become "greener". 1) Reduce waste -- Decrease glove use; incorporate biodegradable disinfectant wipes; adopt electronic data entry; temperature off-hour modulation; off-hour power down of equipment, lights and computers. 2) Reuse/Recycle - sterilization of equipment rather than disposal; recycle packaging 3) Greener workflow - routine same day interpretations and biopsies; adoption of telehealth; electronic transfer of imaging to outside facilities

#### **BREE-2      Serving the Underserved: A Safety-net Framework to Provide High-quality, Comprehensive and Culturally Competent Breast Imaging Care**

##### **Awards**

**Identified for RadioGraphics  
Magna Cum Laude**

##### Participants

Berat Bersu Ozcan, MD, (*Presenter*) Nothing to Disclose

#### TEACHING POINTS

1. Groups that may experience breast cancer (BC) disparities include those defined by race/ethnicity, national origin, cultural beliefs, age, education, socioeconomic status, geographic location, disability, gender identity and sexual orientation. 2. BC screening increases early detection. Improving access supported through radiology-community partnerships using educational programs and community outreach can reduce disparities in BC mortality. 3. Women in safety-net systems who receive a BC diagnosis experience significant access related delays. Delays as short as 30 days affect BC outcomes. 4. Genetic factors contribute to higher mortality in Black and Hispanic women including significantly younger age at diagnosis and a higher incidence of aggressive hormone receptor-negative BC than White women. Black women with hormone-positive cancer have worse 21-gene assay scores and higher BC-specific mortality compared to Whites in all risk groups. 5. With the complexity of breast imaging, cancer care and safety-net systems, formal care coordination programs are essential to help women navigate through screening and diagnosis to treatment.

#### TABLE OF CONTENTS/OUTLINE

Define at-risk or vulnerable patient populations and the role of safety-net hospitals. Summarize population-based breast cancer screening programs and efforts in the United States. Review outcomes and health disparities for underrepresented minorities and underserved women in the United States. Discuss barriers to care and strategies to improve screening uptake and reduce breast cancer disparities.

#### **BREE-20      A Comprehensive Look at Disparities in Breast Cancer in the Non-Hispanic Black, Hispanic, and Transgender Community and What Policy Changes Should be Considered**

##### Participants

Frances Perez, MD, Houston, TX (*Presenter*) Nothing to Disclose

#### TEACHING POINTS

The incidence of breast cancer are higher for non-Hispanic Blacks (NHB) younger than 45 years of age than for non-Hispanic Whites (NHW) in that same age group. Approximately 30% of all breast cancer diagnosed in NHB and Hispanic woman are diagnosed in woman under the age of 50. According to the Surveillance, Epidemiology, and End Results (SEER) data, minority women are 72% more likely to present to with invasive disease at time of diagnostic when compared to NHW. Minority women as 58% more likely to be diagnosed with advanced-stage breast cancer under the age of 50. Currently, the World Professional Association of Transgender Health lack guidelines on breast cancer screening. Furthermore, large databases in the U.S, like the SEER and National Cancer Database (NCDB) do not capture non-binary genders.

#### TABLE OF CONTENTS/OUTLINE

Through a case based multimodality approach we will exhibit several clinical cases that demonstrate the degree of advance invasive disease that minority women present with under the age of 50. We will discuss the breast cancer screening barriers that transgender individuals face, and the implications that this lack of resource has in this patient population. Throughout this exhibit, we will identify the most salient contributing factors including social determinants of health, breast cancer incidences within different ethnic and cultural groups, the difference in tumor biology and genomic that contribute to a higher mortality, as well as disparities in breast cancer treatments. To conclude, we will discuss strategies that may be implemented in order to mitigate these diversity related disparities.

#### **BREE-21      Imaging Approach and Challenges to Breast Cancer in Young Patients**

##### Participants

Cara Connolly, MD, Nashville, TN (*Presenter*) Nothing to Disclose

#### TEACHING POINTS

1. Review the diagnostic algorithm and appropriateness criteria for imaging studies in women less than age 40 and pregnant and lactating patients 2. Review genetic syndromes that increase the risk of breast cancer in this age group 3. Review the imaging appearance of pregnancy associated breast cancer and its mimics 4. Present examples of malignancy highlighting the diagnostic dilemmas unique to this patient population.

#### TABLE OF CONTENTS/OUTLINE

Up to 7% of invasive breast cancers are diagnosed in patients less than 40 years old, with lower survival rates compared to older

age groups, and poorer outcomes disproportionately affecting young black women. Because routine screening does not typically include women in this age group, most cancers (up to 80%) are diagnosed when patients self-present with a breast complaint or lump, often at advanced stage. Further, breast cancers in this age group tend to be hormone-receptor negative with aggressive features. Breast cancer in pregnant and lactating patients in this age group presents an additional diagnostic dilemma due to the physiologic changes occurring in the perinatal period, often leading to misdiagnosis and delay in treatment. Example topics to be covered, including but not limited to, the following: -Diagnostic Imaging Workflow - Patients Under 40 - Pregnant/Lactating Patients - Predisposing Genetic Syndromes and Germline Mutations - Pregnancy Associated Breast Cancer and Mimics - DCIS - Invasive Mammary Carcinoma

#### **BREE-22 Delayed Diagnosis in Medically Underserved Individuals: Identifying Granulomatous Mastitis**

Participants

Molly Downey, MD, (*Presenter*) Nothing to Disclose

##### **TEACHING POINTS**

1. Idiopathic granulomatous mastitis (IGM) is an uncommon inflammatory disease of the breast with nonspecific imaging findings which requires core needle biopsy for pathologic diagnosis. 2. Though there is incomplete evidence on prevalence among racial or ethnic groups, many published studies suggest a Hispanic or non-Caucasian predominance. Premenopausal women with a history of lactation are most affected. 3. Diagnosis of IGM is by histopathology findings of lobulocentric granulomatous inflammation, with the additional findings of suppurative lipogranulomas and *Corynebacterium* infection characteristic for cystic neutrophilic granulomatous mastitis (CNGM). 4. Enhanced understanding by the radiologist of the symptoms, imaging appearance, and histopathologic features of IGM is essential to avoid late diagnosis or misdiagnosis, especially in medically underserved individuals.

##### **TABLE OF CONTENTS/OUTLINE**

1. Background of IGM a) Prevalence and demographics b) Proposed pathophysiology of IGM and subtype CNGM c) Clinical presentation d) Diagnostic workup e) Histopathologic appearance of IGM and CNGM 2. Case-based imaging review of IGM and mimics a) IGM and CNGM b) Chronic abscess c) Infectious mastitis d) Diabetic mastopathy e) Inflammatory breast cancer 3. Treatment, disease course and prognosis 4. Team-based approach for diagnosis a) Clinical presentation and referral to radiology b) Communication with Pathologists

#### **BREE-23 How to Reduce Missed Breast Cancer on Automated Breast Ultrasound**

Participants

Sung Kim, MD, (*Presenter*) Nothing to Disclose

##### **TEACHING POINTS**

Ultrasound (US) is more commonly used for adjunctive screening for dense breast. Automated breast ultrasound (ABUS) is also commonly employed with advantage of its production of reproducible, high-resolution images and its reduced dependency on human operators. Supplementing mammography with ABUS screening resulted in positive outcomes that were similar to those associated with handheld US (HHUS) screening, including increased detections of invasive cancer and reduced rates of interval cancer. However, due to the large number of images in the scan, reading a full ABUS examination can be lengthy and cancers may be easily overlooked. Possible causes for missing breast lesions on US include perception errors of isoechoic and heterogeneous echoic lesions, deep lesions, subareolar lesions, poor positioning or technique, misinterpretation, and subtle features of malignancy. Also ABUS encountered artifacts. Here, we review possible causes of missed cancers on ABUS and discuss methods to reduce them.

##### **TABLE OF CONTENTS/OUTLINE**

1. Pros and cons of automated breast ultrasound (ABUS) 2. ABUS as a supplemental screening tool 3. Causes of missed cancers on ABUS 1) Technique and artifacts 2) Errors in detection 3) Errors in interpretation 4) Tumor morphology 5) True negative cases 4. Solutions to reduce missed cancer

#### **BREE-24 Breast Fibromatosis in Very Young Women - As Ugly and Benign as Ever, but with a Different Presentation: A Series of 6 Cases**

Participants

Andres Vicentela, MD, (*Presenter*) Nothing to Disclose

##### **TEACHING POINTS**

1. Present our experience with breast fibromatosis (BF) in women younger than 25 years old which shows a different clinical and radiological pattern compared to the classic BF in older women (findings not yet described in actual literature). 2. Give details of the imaging signs that characterize BF in mammography, ultrasound and MRI at this age range. 3. Understand the natural history, prognosis and treatment options available

##### **TABLE OF CONTENTS/OUTLINE**

1. Introduction a. Definition of breast fibromatosis, demographics and typical clinical presentation b. Imaging findings on mammography, ultrasound and MRI c. Histopathology characteristics, natural history, prognosis and treatment options 2. Our experience in breast fibromatosis in women younger than 25 years old. a. Clinical presentation b. Imaging characteristics on different modalities c. Histopathologic findings d. Surgical resolution e. Follow up 3. Highlight the difference between classic BF and the pattern of this pathology in very young women.

#### **BREE-25 From the Breast to the Bone: Multimodality Imaging Review of Osseous Metastases from Breast Cancer**

Participants

Daniel Morgan, DO, (*Presenter*) Nothing to Disclose

##### **TEACHING POINTS**

1. Understand the epidemiology of osseous metastatic disease in breast cancer and the imaging modalities that evaluate for osseous metastases 2. Discuss mimics, pitfalls, and pearls when assessing for osseous metastatic disease in breast cancer 3. Know

the imaging features of osseous metastases and their mimics to accurately diagnose metastatic disease and recognize when it is appropriate to biopsy an osseous lesion in question<sup>4</sup>. Examine current treatment options for osseous metastatic disease, the biology of the primary and metastatic lesions, and their treatment-related imaging features

#### TABLE OF CONTENTS/OUTLINE

Introduction: • Epidemiologic factors • Appropriate imaging evaluation to assess for osseous metastases • Most common locations for osseous metastases • Osseous Metastatic Disease as Initial Presentation: • Hip • Ribs • Spine compression fracture • Skull/skull base • Differential Diagnosis: • Sternal metastasis vs hemangioma • Multiple sclerotic osseous metastases vs osteopoikilosis • Sacral metastasis vs insufficiency fractures or sacroiliitis • Enchondroma • Fibrous dysplasia • Aneurysmal bone cyst • Metastases from non-breast primary malignancy • Treatment: • Local treatment • Systemic treatment • Treatment response/treatment related changes • Biology of breast cancer metastases

#### BREE-26 Rare Beauty in the Breast: Introduction to Unusual Breast Lesions

##### Awards

##### Certificate of Merit

Participants

Hee Jung Choi, MD, Mexico City, Mexico (*Presenter*) Nothing to Disclose

##### TEACHING POINTS

1. Review general features of unusual benign and malignant breast lesions. 2. Analyze multimodality imaging findings of each lesion and correlate the findings with the underlying histopathologic and clinical findings. 3. Recognize breast imaging abnormalities and describe key findings of each imaging method that lead to perform interventional procedures. 4. Discuss the imaging follow-up and management of uncommon breast lesions.

#### TABLE OF CONTENTS/OUTLINE

1. Analyze macroscopic and microscopic normal anatomy of the breast and identify the origins of unusual lesions. 2. Identification of uncommon breast lesions by category: a. Benign and malignant breast neoplasms: lymphomas, neuroendocrine tumors, sarcomas, mucinous, apocrine and inflammatory carcinomas, breast metastases, benign and malignant phyllodes tumor, hamartoma and tubular adenoma. b. Mastitis and complications: acute mastitis, chronic granulomatous mastitis and breast abscess formation. c. Miscellaneous: neurofibromatosis, arteriovenous malformation, silicone mastopathy and foreign modeling agent reactions. d. Breast pathology in men: primary breast cancers and metastases, gynecomastia and tricoepithelioma. 3. Review the key points of each disease: a. Epidemiology b. Clinical presentation c. Histopathologic characteristics d. Multimodality imaging findings e. Illustration of the examples 4. Discuss the management of atypical breast lesions including treatment and imaging-guided diagnostic biopsies with an assessment of proper technique in mammography, contrast-enhanced mammography, ultrasound and MRI.

#### BREE-27 I Am Not Who You Think I Am: Benign Mimics of Breast Malignancy with Multimodality and Pathologic Correlation

##### Awards

##### Certificate of Merit

Participants

Toma Omofoye, MD, Houston, TX (*Presenter*) Nothing to Disclose

##### TEACHING POINTS

To demonstrate: 1. Common and uncommon benign entities may have imaging features typically associated with breast malignancy. 2. Imaging workup of "malignant-appearing but benign" breast lesions with multimodality appearance (Mammography, DBT, Ultrasound, Contrast-Enhanced Mammography, MRI, and/or Molecular Breast Imaging). The histopathologic correlation will be included where possible. 3. Appropriate broadening of differential diagnoses can aid in radiologic-pathologic correlation after percutaneous core biopsy.

#### TABLE OF CONTENTS/OUTLINE

Based on cases at a tertiary oncologic referral center, we review breast imaging lesions with suspicious imaging features mimicking primary breast malignancy. • Introduction • Inflammatory/Infectious: Idiopathic granulomatous mastitis, Diabetic/lymphocytic mastopathy, Infectious mastitis, Mondor disease • Systemic conditions: Amyloidosis, Sarcoidosis • Tumors: Granular cell tumor, Tubular adenoma, Nipple adenoma, Pseudoangiomatous stromal hyperplasia (PASH), Phyllodes, Papilloma, Fibromatosis, Neurofibroma • Proliferative lesions: Sclerosing adenosis, Complex sclerosing lesions, Stromal fibrosis • Anatomic findings: Sternalis muscle, Coopers ligament • Male breast: Gynecomastia, Hemangioma • Posttraumatic conditions: Fat necrosis, Foreign body reaction, Postsurgical scar • Conclusion

#### BREE-28 Contrast-enhanced Mammography Artifacts and Pitfalls - Tips and Tricks to Understand Them and to Avoid Image Misinterpretation

##### Awards

##### Identified for RadioGraphics

Participants

Rosa M. Lorente-Ramos, MD, PhD, Madrid, Spain (*Presenter*) Nothing to Disclose

##### TEACHING POINTS

-To learn technique of contrast enhanced mammography (CEM). -To review CEM image artifacts and physical considerations causing artifacts related to digital mammography and specific to CEM. - To become familiar with pitfalls and diagnostic limitations in CEM and tips and tricks to avoid interference in image interpretation.

#### TABLE OF CONTENTS/OUTLINE

We review the basics of CEM highlighting artifacts and factors that may interfere with image interpretation. We present: 1. Basics of CEM. 2. Technique 3. Image artifacts. - Digital mammography artifacts: patient positioning, hair, antiperspirant, patient motion. -

Contrast-related: contrast splatter, timing of image acquisition after contrast administration, transient retention of contrast in vessels. -CEM specific: Air artifact. Improper positioning causing skin folds; Rim, halo or breast-within-a-breast artifact. Scattered radiation from differences in breast tissue thickness between chest wall and breast edge; Skin line artifact. Due to scattered radiation from non-uniform thickness of skin; Ripple artifact. Patient motion between HE and LE, sometimes respiratory movements or cardiac pulsations transmitted through the chest wall. 4. Pitfalls. Axillary tail and medial lesions near the chest wall not included in the imaging field- Background parenchymal enhancement. Negative Contrast Enhancement: imaging a cyst or coarse calcification. "Eclipse sign". Hematoma caused by biopsy obscuring contrast enhancement of breast cancer. "Crescent sign" enhancement of the wall of a simple cyst. False negative lesions. DCIS, low-grade infiltrating cancer (lobar, mucinous). False positive lesions. Skin lesions, lymph nodes, benign enhancing lesions.

### **BREE-29 (Nearly) Ouchless! Ultrasound-Guided Core Nipple Biopsy is within a Breast Imager's Wheelhouse**

Participants

Sophia O'Brien, MD, Philadelphia, PA (*Presenter*) Nothing to Disclose

#### **TEACHING POINTS**

The nipple-areolar complex (NAC) is comprised of numerous cell types and can thus demonstrate a variety of benign and malignant pathologies (1). Due to its superficial location, the NAC is not amenable to stereotactic- or MR-guidance. Historically, suspicious nipple symptoms and imaging abnormalities have been evaluated via surgical biopsy or skin punch biopsy. More recently, however, there have been reports of ultrasound-guided core nipple biopsies (US-CNB) of suspicious nipple calcifications and nipple masses (Omofoye 2015, Burk 2021). This educational exhibit will describe how to perform US-CNB step-by-step, highlighting the unique approach and considerations for this specialized percutaneous procedure. The educational material will be supplemented with numerous images from US-CNB performed at our institution. 1. Ultrasound-guided core nipple biopsy (US-CNB) can be performed safely for nearly all abnormalities seen on imaging. 2. Appropriate anesthesia eliminates patient discomfort during US-CNB. 3. US-CNB is adequate for diagnosis. 4. US-CNB is a feasible percutaneous sampling technique well within the breast imager's wheelhouse, thus avoiding surgery while maintaining nipple integrity and aesthetics.

#### **TABLE OF CONTENTS/OUTLINE**

1. Background: NAC physiology and pathology 2. Historical Nipple Sampling Techniques 3. US-CNB: Technique and special considerations 4. Cases to Highlight the technical teaching points

### **BREE-3 Breast Cancer Epidemiology and Imaging Patterns in Underserved Women**

Participants

Scott Kleinpeter, MD, (*Presenter*) Nothing to Disclose

#### **TEACHING POINTS**

African American women are 42% more likely to die from breast cancer, have a two-fold higher risk of triple negative breast cancer, and have a higher prevalence of BRCA1 and BRCA2 genetic mutations. African American women are 72% more likely to be diagnosed with invasive disease under age 50 and are 58% more likely to be diagnosed with advanced-stage disease under age 50. Factors affecting disparities in health outcomes include genetic risk factors, health literacy, income level, health insurance status, comorbidities, cultural beliefs, geographical location, and gender identity. Current screening recommendations for USPSTF are not race-based. Temporal differences in breast cancer peak diagnosis results in disproportionate effects of delayed screening on minority women due to younger average age at diagnosis (African American peak diagnosis in 40's vs. white peak diagnosis in 60's). Timely breast cancer risk assessment, genetic testing (if applicable), ACR recommended screening surveillance, and patient education are key components to improve breast cancer mortality. Increasing access to screening in vulnerable populations is a multidisciplinary task and radiologists play a key role in identifying imaging patterns and reaching patients at higher risk.

#### **TABLE OF CONTENTS/OUTLINE**

a. Review of published literature on disparities in breast cancer screening and mortality. b. Factors influencing breast cancer risk in vulnerable populations. c. Review of ACR screening recommendations for women at high risk. d. Case collection illustrating imaging patterns in our underserved population.

### **BREE-30 Challenging Scenarios in MRI Guided Procedures: Tips and Tricks to Maximize Technical Success**

Participants

Janice Thai, MD, (*Presenter*) Nothing to Disclose

#### **TEACHING POINTS**

1. To illustrate technically challenging anatomy and lesion location for MRI guided breast biopsy or localization. 2. To demonstrate useful approaches and techniques for overcoming technical challenges in MRI guided procedures. 3. To review the management options and alternatives following failed procedures.

#### **TABLE OF CONTENTS/OUTLINE**

• Illustrative review of equipment set up, device, and patient positioning • Challenging case potpourri • Critical review of real-life cases and lessons learned from failed procedures • Review of preprocedural planning and procedural techniques to maximize technical success

### **BREE-31 Breast Imaging and Intervention During Pregnancy and Lactation**

**Awards**

**Certificate of Merit**

**Identified for RadioGraphics**

Participants

Amy Fowler, MD, PhD, Madison, WI (*Presenter*) Author with royalties, RELX

#### **TEACHING POINTS**

Physiologic changes in the breast during pregnancy and lactation can pose diagnostic challenges on imaging and physical

examination. Recognition of expected physiologic changes and classically benign entities on imaging is important to avoid unnecessary intervention. Identification of suspicious imaging features prompting biopsy recommendation are critical to avoid delays in diagnosis of pregnancy-associated breast cancer, the most common invasive cancer diagnosed during pregnancy. This presentation will focus on the appropriate breast imaging evaluation and management during pregnancy and lactation. The exhibit will also highlight ACR guidelines for breast cancer screening based on age and risk profile during pregnancy and lactation.

#### TABLE OF CONTENTS/OUTLINE

I. Hormonal and histologic changes within the breast II. Expected physiologic changes on breast imaging a. Mammographic appearance (lactation) b. Sonographic appearance (pregnancy/lactation) c. MRI appearance (lactation) III. Breast cancer screening guidelines during pregnancy/lactation IV. Imaging workup for clinical symptoms during pregnancy/lactation a. Palpable mass, nipple discharge, focal pain V. Biopsy considerations for this patient population a. Techniques b. Complications including milk fistula VI. Imaging features and management of common benign and malignant entities a. Benign i. Galactocele ii. Lactational changes iii. Lactating adenoma iv. Fibroadenoma with lactational changes v. Mastitis, abscess vi. Granulomatous mastitis vii. Reactive lymph nodes viii. Accessory axillary breast tissue b. Malignant i. Pregnancy-associated breast cancer

#### BREE-32 The Many Faces of Triple Negative Breast Cancer

##### Awards

##### Cum Laude

##### Participants

Beatriz Adrada, MD, Houston, TX (*Presenter*) Nothing to Disclose

#### TEACHING POINTS

- Triple negative breast cancer (TNBC) is a heterogeneous group of tumors defined by the absence of estrogen/progesterone receptors and lack of HER2 overexpression that confer a poor prognosis.
- TNBCs are classified using six molecular subtypes according to their gene expression patterns: luminal androgen receptor, two mesenchymal-like subgroups (Mesenchymal M and MSL), immunomodulatory, and two basal-like subgroups (BL1, BL2).
- Chemotherapy is the primary established systemic treatment for patients with TNBC. The treatment response differs depending on the molecular subtype, as well as the imaging features.

#### TABLE OF CONTENTS/OUTLINE

This educational exhibit will present a practical, multi-modality guide on approaching triple negative breast cancer (TNBC). A multi-modality review of the characteristic imaging features of TNBC will be presented, including features that may indicate whether a patient will respond to neoadjuvant chemotherapy. Imaging assessment of TNBC response to neoadjuvant chemotherapy will be detailed, including response patterns and imaging features that could indicate pathologic complete response (pCR). A clinical update on the recommended treatment of TNBC will be presented.

#### BREE-33 Axillary Imaging in Breast Cancer: When, Who and How?

##### Participants

Dogan Polat, MD, Dallas, TX (*Presenter*) Nothing to Disclose

#### TEACHING POINTS

- To illustrate axillary anatomy and imaging findings of metastatic axillary lymph nodes with various imaging modalities
- To discuss role of axillary imaging to predict survival, tumor stage and recurrence in newly diagnosed breast cancer
- Recognizing and management of axillary adenopathy after COVID-19 vaccination
- To demonstrate importance of pre-operative axillary imaging in guiding treatment decisions regarding axillary lymph node dissection, sentinel lymph node biopsy, and neoadjuvant chemotherapy (NACT)
- To showcase uses of axillary imaging to determine response to NACT
- To demonstrate use of axillary imaging in identifying abnormal appearing lymph nodes for further sampling and biopsies
- To compare advantages of different imaging modalities in the evaluation of the axilla
- To explain possible pitfalls of axillary imaging in identifying lymph node metastasis and evaluation of response to neoadjuvant chemotherapy

#### TABLE OF CONTENTS/OUTLINE

- Overview of axillary imaging
- Role of radiology in assessment of axillary nodes
- Characteristic features of different axillary pathologies
- Differential diagnosis, prognosis, and biopsy approaches
- Challenging clinical cases with axillary imaging
- Recognizing COVID-19 vaccine induced LAPs
- Future directions and summary
- Future directions and summary

#### BREE-34 Performance Benchmarks and Management Guidelines for BI-RADS Category 3 Assessment on Breast MRI

##### Awards

##### Identified for RadioGraphics

##### Participants

Onalisa Winblad, MD, Leawood, KS (*Presenter*) Nothing to Disclose

#### TEACHING POINTS

There is significant variability in radiologist usage of BI-RADS Category 3 assessment on breast MRI due to lack of robust data to guide management. No combination of MRI BI-RADS descriptors has proven to meet the " $<2\%$  but greater than  $0\%$  likelihood of malignancy" historical definition of BI-RADS Category 3, which is well supported in the literature for both mammography and ultrasound. This likely accounts for the substantial confusion and misuse of BI-RADS Category 3 assessment on breast MRI. Recent reports demonstrate increased utilization of breast MRI, partially due to improved access made possible by modern abbreviated protocols. Given the increasing volume of breast MRI, it is imperative that radiologists understand acceptable performance benchmarks and appropriate use of BI-RADS Category 3 on MRI to avoid unnecessary follow-up or missed cancer diagnosis.

#### TABLE OF CONTENTS/OUTLINE

I. Performance benchmarks for breast MRI III. Summary of ACR BI-RADS Atlas 2013 recommendations for assigning BI-RADS Category 3 on breast MRI III. Review of scientific, peer-reviewed literature A. Characteristics and outcomes B. Patient compliance C. False negatives IV. Guidelines for assigning BI-RADS Category 3 assessment on breast MRI supported by ACR BI-RADS Atlas and scientific

### **BREE-35 Ductography in the era of Breast MRI: Technique and Approach**

#### Participants

Eduardo Cordero Castro, MD, Memphis, TN (*Presenter*) Nothing to Disclose

#### TEACHING POINTS

**SYNOPSIS:** Nipple discharge is the third most common complaint seen in breast centers. Spontaneous discharge causes patient anxiety. The incidence of nipple discharge in breast cancer is 5-12%. Characteristics of suspicious discharge include unilateral, single duct, spontaneous, bloody, or clear color. Imaging modalities used to evaluate patients include mammogram, US, MRI and ductography. **TEACHING POINTS:** The learner will: 1. Review the incidence, clinical presentation, and management of nipple discharge. 2. Know the imaging protocols used to evaluate nipple discharge based on ACR appropriateness criteria. 3. Identify intraductal lesions by imaging that warrant further evaluation.

#### TABLE OF CONTENTS/OUTLINE

Introduction, Clinical presentation, Causes of nipple discharge, Imaging assessment, Differential considerations of intraductal lesions, Role of mammogram and US, MRI findings, Challenges of localizing MRI findings in the subareolar region, Recommended management of nipple discharge without imaging correlation, Recommended management of positive ductogram findings, Pictorial review of ductogram findings, complications during ductogram (bubbles, duct perforation, extravasation, fissurization, lymphatic uptake, incomplete filling), and positive ductogram findings. Clinical management, Algorithm for imaging patients with nipple discharge, Conclusion

### **BREE-36 Histological Special Types of Breast Cancer - How Special Are They? A Pictorial Essay**

#### Awards

#### Certificate of Merit

#### Participants

Karina Pesce, MD, Capital Federal, Argentina (*Presenter*) Nothing to Disclose

#### TEACHING POINTS

Describe the imaging features histological special types of breast carcinoma. Identify the characteristics of each of these tumors that allow them to be differentiated from other breast carcinomas. Discuss the differential diagnosis and management.

#### TABLE OF CONTENTS/OUTLINE

Histological special types of breast cancer constitute a spectrum of lesions from low to high grade aggressiveness. They present different clinical, radiological, and pathological presentations, and although there are no pathognomonic characteristics, there are trends that every breast radiologist should be aware of. 1-Introduction. 2-Histological special types of breast cancer: The WHO spectrum. 3-Appearance mammography, ultrasound, and MRI. 4-Discuss diagnostic challenges and management dilemmas the histological special types of breast cancer. 5- Clinical cases with histological correlation. 6-Take-home points. 7-Conclusion.

### **BREE-37 Yikes, A Red Breast! - A Breast Imager's Approach to Diagnosis and Management**

#### Participants

Joshua Weinstein, MD, (*Presenter*) Nothing to Disclose

#### TEACHING POINTS

Breast erythema is a common clinical complaint that can often cause substantial anxiety for patients. The differential is broad, ranging from benign dermatologic conditions, infectious or inflammatory processes, or neoplasms. In this exhibit, we will review this differential and present several exemplary cases of patients who initially presented with breast redness and were ultimately diagnosed with a variety of conditions, including inflammatory breast cancer, angiosarcoma, granulomatous mastitis, breast cellulitis, mastitis related to lactation, mastitis related to an infected foreign body, chronic mastitis, and radiation changes. By reviewing these entities, radiologists can familiarize themselves with the varying clinical presentations of the "red breast" to appropriately image and guide management.

#### TABLE OF CONTENTS/OUTLINE

1. Review the varied clinical presentations and differential diagnoses of breast erythema. 2. Discuss the role of multimodality imaging to diagnose the cause of breast redness. 3. Describe approach to management based on a combination of clinical and radiologic findings.

### **BREE-38 Ain't No Mountain High Enough! Review of Imaging, Histologic and Management Considerations of High-risk Breast Lesions**

#### Participants

Hee Jung Choi, MD, Mexico City, Mexico (*Presenter*) Nothing to Disclose

#### TEACHING POINTS

1. Review general features of high risk lesions with illustrations of classic cases using multimodality imaging methods and correlation of the image findings with the underlying histopathologic and clinical findings. 2. Identify imaging and clinical risk factors for malignancy upgrades. 3. Discuss current imaging follow-up and management, as well as controversies in high-risk breast lesions management after the diagnosis.

#### TABLE OF CONTENTS/OUTLINE

1. Analyze macro and microscopic normal anatomy of the breast and identify origin of each of the high-risk breast lesions. 2. Identification of high-risk breast lesions by category: a. Atypical ductal hyperplasia b. Lobular breast neoplasia - Atypical lobular hyperplasia - Lobular carcinoma in situ (classic and pleomorphic) c. Papillary lesions - Benign papillary lesions - Intraductal papilloma with atypical hyperplasia d. Flat epithelial atypia e. Radial scar or complex sclerosis lesion 3. Review the key points of each lesion: a.

Epidemiologyb. Clinical presentationc. Histopathologic characteristicsd. Multimodality imaging findingse. Malignancy upgrades risk percentages and risk factorsf. Recent guidelines for management g. Illustration of the classic cases4. Discuss and analyze the recent management and imaging follow-up guidelines.

### **BREE-39 Current Status of Optoacoustic Breast Imaging and Future Trends in Clinical Application: Is It Ready for Prime Time?**

Participants

Berat Bersu Ozcan, MD, (*Presenter*) Nothing to Disclose

#### **TEACHING POINTS**

Optoacoustic imaging (OAI) uses non-ionizing, laser light to create thermoelastic expansion in tissues and detect resultant ultrasonic emission. Parametric maps of molecules (melanin, hemoglobin and lipids) that absorb light and scatter acoustic waves are fused with anatomic images, allowing scalable, relative real time molecular assessment in tissues. Since rapidly dividing cancer cells cause hypoxia and lead to tumor-driven angiogenesis, OAI can detect the presence and degree of relative hypoxia in cancers relative to normal tissue. This can increase the specificity of breast mass assessment without compromising the sensitivity compared to the grayscale US alone. Therefore, adjunctive use of OAI can decrease breast biopsies. Molecular subtypes of breast cancer show differing OAI features and levels of hypoxia. Luminal cancers have higher total external feature scores (9.3 vs 8.8;  $p < .05$ ) and lower total internal feature scores (6.8 vs 7.7;  $p < .001$ ) than triple negative and HER2+ cancers. OAI is a thriving field of research whose potential impact on the clinic can be high. However, larger multicenter cohort studies and clinical trials are needed to establish the trends observed and accelerate clinical translation.

#### **TABLE OF CONTENTS/OUTLINE**

1. Optoacoustic Imaging Principles 2. Why Optoacoustic Breast Imaging: Pros and Cons 3. Handheld versus Tomographic Optoacoustic Breast Imaging Technique 4. Current Clinical Applications and Future Directions 5. Pitfalls and Lessons Learned

### **BREE-4 Multimodality Imaging Review of Metastases to the Breast**

Participants

Jiewen Li, DO, (*Presenter*) Nothing to Disclose

#### **TEACHING POINTS**

1. Review normal breast anatomy allowing for metastases to the breast 2. Discuss common and uncommon metastases to the breast 3. Demonstrate imaging characteristics of metastases to the breast in a case-based approach

#### **TABLE OF CONTENTS/OUTLINE**

-Introduction-Definition of metastases to the breast-Typical patient population affected and prognosis-Anatomy of the breast to allow for metastases to the breast\*Vascular/Hematogenous\*Lymphatic\*Direct extension-Common and uncommon metastases to the breast-Typical imaging appearance reported in literature\*Mammogram\*Ultrasound\*MRI-Case-based approach to imaging appearance of extramammary metastases\*Lymphoma\*Leukemia\*Melanoma\*Lung\*Esophageal\*Ovarian\*Plasmacytoma\*Thyroid\*Renal\*Sarcoma-Conclusion\*Recognizing the most common imaging appearance of metastases to the breast can help guide appropriate management and further treatment\*Metastases to the breast generally carry a poor prognosis and any delay in diagnosis can have significant impact\*Metastases to the breast commonly manifest as an irregular mass and typically lack calcifications except for serous ovarian cancer

### **BREE-40 Ultrasound Computed Tomography of the Breast: Techniques, Tips and Tricks**

Participants

Ken Oba, MD, Chuoku, Japan (*Presenter*) Nothing to Disclose

#### **TEACHING POINTS**

1. To review the physics principles of ultrasound computed tomography (UCT). 2. To discuss the advantages of UCT compared to conventional clinical ultrasound imaging in breast imaging. 3. To become familiar with normal and abnormal imaging findings. 4. To understand the limitations of UCT in detection, diagnosis, local staging, and follow-up.

#### **TABLE OF CONTENTS/OUTLINE**

1. Basics of UCT. 2. Technique. 3. Anatomy and breast density in UCT. 4. Controversies. 5. Cases. Cases include: - Benign lesions Fibroadenoma Phyllodes tumor Hamartoma Breast lymphoma - Malignant lesions Invasive ductal carcinoma Ductal carcinoma in situ Invasive lobular carcinoma Mucinous carcinoma Breast lymphoma - Artifacts - Others Hematoma Postoperative change Breast reconstruction

### **BREE-41 Hiding in Plain Sight: Cancers in Dense Breasts**

**Awards**

**Identified for RadioGraphics**

Participants

Alexis De La Cruz, DO, (*Presenter*) Nothing to Disclose

#### **TEACHING POINTS**

1. Discuss dense breast tissue as it relates to cancer risk and value of supplemental screening in women 2. Summarize prior trials and studies that have made an impact on current breast density guidelines 3. Review current breast density legislation and future directions 4. Illustrate mammographic clues/hints for identifying breast cancer in dense breasts using a case-based format

#### **TABLE OF CONTENTS/OUTLINE**

Introduction-Definitions\*\* BI-RADS categories\*\* Quantitative measurements- Factors that contribute to breast density\*\* Age\*\* Pregnancy/breastfeeding\*\* Hormone replacement therapy\*\* Bodyweight- Why does it matter? \*\* Increased breast cancer risk\*\*

Decreased sensitivity and specificity with mammography\*\* Possible need for supplemental imaging-Breast density legislation\*\* Current status\*\*Future directionsAppropriateness Criteria/Screening Recommendations- Risk Stratification- Screening Modalities\*\* Mammography, Digital Breast Tomosynthesis (DBT), Contrast-Enhanced Mammography (CEM), Ultrasound, MRI, Abbreviated MRI, FDG-PET breast dedicated, and Molecular Breast Imaging (MBI)Identification of high risk patients\*\* Risk assessment toolsEvidence Based value of supplemental screening\*\*Breast MRI\*\* Breast UltrasoundRadiologic signs to look for in the evaluation of dense breasts using mammography- Subtle spiculation and distortion- Retroglandular fat findings- Nipple distortion and/or gradual retraction- Changes in mass density (increase inhomogeneity)- Halo effect (peripheral lucency)- Fat glandular interface density

#### **BREE-42 Architectural Distortion of the Breast: Imaging, Diagnostic Challenges and Treatment**

Participants

Israel Rodriguez Suarez, MD, Mexico City, Mexico (*Presenter*) Nothing to Disclose

##### **TEACHING POINTS**

With this educational exhibit the radiologist will be able to: a. Know the normal architecture of the breast in mammography. b. Differentiate between a spiculated mass, architectural distortion and pseudo distortion of the breast parenchyma in mammography. c. Use the imaging tools with an orderly approach to confirm an architectural distortion in mammography: spot compression views, tomosynthesis. d. Identify and characterize an architectural distortion by ultrasound and breast MRI. e. Choose the better imaging biopsy method according to each particular circumstance. f. Learn the differential diagnoses of architectural distortion to make an appropriate radiology pathology correlation. g. Know the current management proposals after percutaneous tissue diagnosis, including the usefulness of breast MRI and contrast enhanced mammography.

##### **TABLE OF CONTENTS/OUTLINE**

a. Introduction b. Definition c. Normal architecture of the breast d. Imaging of architectural distortion: Mammography, Tomosynthesis, Ultrasonography, Breast MRI. e. Image guided biopsy methods f. Differential diagnoses: Radial Scar or complex sclerosing lesion, Invasive ductal carcinoma, Tubular carcinoma, Invasive lobular carcinoma, Ductal carcinoma in situ, Postsurgical scar, Fat necrosis, Sclerosing adenosis, Focal fibrosis, Diabetic mastopathy. g. Management considerations: Follow up, surgical excision, vacuum assisted excision. Problem solving breast MRI and contrast enhanced mammography.

#### **BREE-43 Breast Cancer Recurrence: Multi-modality Imaging in Patients Undergoing Breast Conservation Treatment**

**Awards**

**Certificate of Merit**

Participants

Miral Patel, MD, Houston, TX (*Presenter*) Nothing to Disclose

##### **TEACHING POINTS**

Understanding the terminology and the different treatment options that are available for breast conservation can aid radiologists in detecting recurrence. The post treatment breast appearance will be reviewed as a baseline to understand what these changes look like. Furthermore, a review of the appearance of breast cancer recurrence in multiple cases amongst the various imaging modalities can aid radiologists in early detection.

##### **TABLE OF CONTENTS/OUTLINE**

This educational exhibit reviews: Breast conservation treatment (BCT): Definitions, surgical techniques and radiation treatmentExpected breast imaging findings after BCTMulti-modality case-based review of recurrence: Tips and tricks to distinguish expected post-operative and radiation changes from tumor recurrence on mammography, ultrasound, magnetic resonance imaging, molecular breast imaging, and contrast enhanced mammography

#### **BREE-44 Sheep in Wolf's Clothing: The Many Faces of Granulomatous Mastitis**

Participants

Tais Batista, MD, Sao Paulo, Brazil (*Presenter*) Nothing to Disclose

##### **TEACHING POINTS**

The purposes of this exhibit areTo review the epidemiology and risk factors for the development of granulomatous mastitis;To discuss the main clinical presentations of these mastitis and its subgroups;To review the main differential diagnoses, as well as overlapping and confounding imaging factors, mainly with carcinomas;To discuss the experience of our institution in a 20 years time period regarding clinical aspects and difficulties in its diagnosis;To describe its histopathological features;To discuss the importance of the multimodality imaging findings in association with histopathological aspects to achieve an accurate diagnosis;To discuss the role of imaging in monitoring the therapeutic response.

##### **TABLE OF CONTENTS/OUTLINE**

Epidemiology of granulomatous mastitis and factors related to its prevalence in underserved populations;Main clinical presentations;Typical multimodality imaging findings (MRI, ultrasound and mammography) from cases of our radiology department;Diagnostic challenges, main differentials, and key points for early suspicion of this pathology;Particularities of treatment and imaging response after therapy;Summary and Conclusion.

#### **BREE-45 Male Nipple Discharge: Beyond the Basics**

Participants

Javier Azcona Saenz, MD, (*Presenter*) Nothing to Disclose

##### **TEACHING POINTS**

1) To review the importance of male nipple discharge. 2) To expose the main causes of nipple discharge in men, both benign and malignant, together with their radiological manifestations. 3) To focus on the radiological findings of male breast carcinoma in all imaging techniques, including Digital Breast Tomosynthesis and Contrast-Enhanced Mammography.

## TABLE OF CONTENTS/OUTLINE

1) Introduction. 2) Causes of male nipple discharge. 2.1) Benign: Gynecomastia, Mammary duct ectasia, Dermatitis, Papilloma, Abscess. 2.2) Malignant: Ductal carcinoma in situ, Invasive carcinoma, Papillary carcinoma of the breast, Others. 3) Characteristic imaging findings: Mammography/Tomosynthesis, Ultrasound, MRI, Contrast-enhanced mammography. 4) Conclusion. 5) References.

### BREE-46 Pitfalls of Breast Imaging in the Emergency Room

Participants

Neha Khemani, MD, Boston, MA (*Presenter*) Nothing to Disclose

#### TEACHING POINTS

1. Clinical breast symptoms seen in the ED are most often related to infection and inflammation. 2. Breast abscess is typically treated as an urgent condition requiring intervention (ultrasound-guided drainage or incision and drainage). 3. Rarely, inflammatory symptoms can indicate malignancy, thus diagnostic accuracy and close follow-up are necessary to avoid a missed cancer diagnosis. 4. The purpose of this exhibit is to review common breast diagnoses seen in the ED and potential pitfalls of performing breast imaging after hours.

## TABLE OF CONTENTS/OUTLINE

1. Clinical breast symptoms encountered in the ED and indications for imaging. 2. US imaging features of mastitis and abscess. 3. Common diagnoses seen on after-hours breast ultrasound. 4. Pitfalls of after-hours breast imaging with case-based examples: a. Variable experience of ER radiologist and sonographer in breast imaging. b. Technically suboptimal exams. c. Unavailability of mammography to fully characterize a lesion if needed. d. Unavailability of breast imaging support staff to arrange for biopsy or follow-up care. e. High grade breast carcinomas mimicking abscess. 5. Strategies to ensure appropriate care and follow-up for patients with urgent breast complaints.

### BREE-47 There is More to the Breast than Cancer - A Pictorial Case-based Quiz and Review of Rare Benign Breast Lesions

Awards

Certificate of Merit

Participants

Ines Alonso Sanchez, MD, Bilbao, Spain (*Presenter*) Nothing to Disclose

#### TEACHING POINTS

- Unusual breast benign lesions can be a diagnostic challenge for radiologists, and we should be familiar with their imaging and clinical features. - We must be aware of the limitations of the available breast imaging modalities and know that, in many cases, we need a biopsy to make the diagnosis. - A multidisciplinary approach to these entities is essential to manage them correctly.

## TABLE OF CONTENTS/OUTLINE

Objective: This presentation aims to revise in quiz format a series of cases of unusual breast benign lesions and describe their imaging and clinical features to strengthen radiologists' skills to recognize and properly approach these conditions. Background: Most patients with breast pathology have concern that they have cancer. Therefore, in this area of practice, it is particularly important to be aware of potential diagnostic pitfalls to avoid emotional suffering to our patients. Findings: We present a series of cases of interesting benign breast lesions with different etiologies, such as inflammatory, vascular, tumors of neural origin, metabolic diseases, proliferative disorders and abnormal protein deposit diseases. Some of these lesions can mimic malignancies, and we should remember clinical features and patients' medical history may help lower the level of suspicion and the patients' emotional unease. Nevertheless, there are limitations of the imaging modalities, and in most cases, a biopsy is needed to make the diagnosis. Conclusions: Despite breast cancer being a common diagnosis; we may still face diagnostic challenges with unusual benign breast lesions which may sometimes mimic cancer.

### BREE-48 Pregnancy Associated Breast Cancer - What Is It and How Not to Miss It

Participants

Haydee Ojeda-Fournier, MD, San Diego, CA (*Presenter*) Research Consultant, View Point Medical, Inc; Stock options, CureMetrix, Inc

#### TEACHING POINTS

Pregnancy-associated breast cancer (PABC) is defined as breast cancer diagnosed during pregnancy, within one year post-partum, or during lactation. Although rare, this disease has a more aggressive course and is often associated with a poorer prognosis. Several studies have found evidence of a delayed diagnosis in pregnant women. But lack of awareness among women and physicians is also believed to play a crucial role in delayed diagnosis. However, the majority of breast lesions during pregnancy and lactation are benign. Still, approximately 20% of breast masses prove to be malignant. By the end of this educational exhibit, the learner will: 1. Review the incidence, clinical presentation, and management of pregnancy-associated breast cancer. 2. Know the imaging protocols recommended to evaluate the pregnant or nursing patient based on ACR appropriateness criteria. 3. Identify lesions that should be biopsied during pregnancy and lactation.

## TABLE OF CONTENTS/OUTLINE

Introduction; Define pregnancy-associated breast cancer; Clinical presentation of breast cancer during pregnancy or lactation; Review imaging recommendations for pregnant women vs. lactating women; Differential considerations of breast lesions during pregnancy; Mammogram and US findings of pregnant and lactating women; MRI considerations in the pregnant and lactating patient; Recommended management of breast masses without imaging correlation in pregnant and lactating patients; Recommended management of positive imaging findings; Pictorial review of PABC; Clinical management and outcomes of PABC; Algorithm for imaging pregnant and lactating patients so as not to miss a PABC; Conclusion.

### BREE-49 A Primer on Imaging of Molecular Subtypes of Breast Cancer

Participants

Sepideh Sefidbakht, MD, Powel, OH (*Presenter*) Nothing to Disclose

## TEACHING POINTS

\_To review the clinical relevance of Breast Cancer subtypes and the implications for patient management and imaging.\_To review the basic pathologic and clinical characteristics of each major molecular subtype along with their typical imaging appearance.\_To show how this knowledge affects decision making using a case-based approach

## TABLE OF CONTENTS/OUTLINE

\_Introduction: basic pathology of molecular subtypes of breast cancer; how to diagnose and implications for patient management\_Luminal A breast Cancer, Pathology, Prognosis, multimodality imaging characteristics\_Luminal B breast Cancer, Pathology, Prognosis, multimodality imaging characteristics\_HER2-enriched breast Cancer, Pathology, Prognosis, multimodality imaging characteristics\_Basal-like breast Cancer, Pathology, Prognosis, multimodality imaging characteristics\_Case-based review of typical and atypical presentations of various subtypes

### BREE-50 Unusual Infections of the Breast - A Pictorial Review

Participants  
Sabine Popp, MD, Vienna, Austria (*Presenter*) Nothing to Disclose

## TEACHING POINTS

- Unusual infectious diseases of the breast are uncommon but important for radiologists to be aware of, as they may be indistinguishable from breast cancer and are treatable.
- Consider Tuberculosis in patients with a persistent abscess or atypical mass, especially if from a high Tuberculosis incidence country.
- In patients with incidental breast calcification detected at screening from endemic countries, consider Schistosomiasis (amorphous, segmental distribution), Dracunculiasis (coarse linear, serpiginous) or chronic Filariasis (serpiginous, tubular and coiled).
- Recurrent breast abscesses can be caused by rare organisms such as Actinomyces and Corynebacterium, therefore it is important to send a fine needle aspirate for microbiology to direct treatment.
- In patients with nipple eczema, consider Lyme disease as a differential to Paget's disease, especially if regional lymphadenopathy is present.

## TABLE OF CONTENTS/OUTLINE

- Learning objectives
- Introduction
- Organisms - for each of the below: epidemiology, clinical presentation, imaging features (mammography, ultrasound, MRI), diagnosis and treatment
  - o Bacteria
  - Tuberculosis
  - Other mycobacteria
  - Actinomycosis
  - Lyme disease
  - Brucella
  - Cryptococcus
  - o Parasites
  - Schistosomiasis
  - Filariasis
  - Cysticercosis
  - Hydatid cyst
  - Dracunculiasis
  - Other rare organisms
- Differential diagnoses
- Summary table
- Conclusion

### BREE-51 You've Got a Friend in Me: How Radiologists Can Help Patients and Multidisciplinary Colleagues in the Diagnosis and Management of Fibroepithelial Lesions

**Awards**  
**Cum Laude**  
**Identified for RadioGraphics**

Participants  
Jody C. Hayes, BS, MD, Dallas, TX (*Presenter*) Nothing to Disclose

## TEACHING POINTS

1. When a fibroepithelial lesion (FEL) is suspected, biopsy specimens should include the margin of the mass for a more definitive diagnosis on histopathology.
2. For large masses, biopsy specimens should be taken from different areas to ensure adequate sampling as phyllodes tumors (PT) often demonstrate tumor heterogeneity with fibroadenoma-like regions.
3. Surgical resection is indicated for rapidly growing biopsy-proven benign FEL or borderline PT whose growth rate exceeds 20% in largest dimension in a six-month interval.
4. Staging chest CT should be performed for malignant PT due to their propensity for hematogenous spread with the lungs being the most common site.
5. Frequent follow-up imaging with breast ultrasound or chest CTs may be indicated for locally aggressive malignant PT to identify early recurrence.

## TABLE OF CONTENTS/OUTLINE

1. Define the spectrum of fibroepithelial lesions (FEL) with pertinent incidence and demographic information.
2. Review imaging and pathologic findings for the spectrum of FEL.
3. Discuss steps radiologists can take to help in the diagnosis and management of FEL with an emphasis on radiological, pathological, and clinical concordance.
4. Define the role of imaging for the post-biopsy or post-surgical FEL patient.

### BREE-52 Everything That Looks Like BI-RADS 5, But Is Not

Participants  
Maria Ares-Rego, MD, Santiago de Compostela, Spain (*Presenter*) Nothing to Disclose

## TEACHING POINTS

To review the imaging features used in a BI-RADS 5 assessment.To illustrate benign entities that can mimic malignancy ( the most common are chronic and inflammatory mastitis, fat necrosis, complex sclerosing lesions, granular cell tumors, lymphocytic mastopathy, infection...); to describe imaging findings, clinical history.To review the specific imaging features of these benign entities depicted at mammography, US, MRI.To relate radiologic-pathologic correlation and clinical history to decide the management of a discordant biopsy result.To familiarize radiologist with the knowlegde of the variety of benign entities may be categorized as BI-RADS 5 to include them within the differential diagnostic.

## TABLE OF CONTENTS/OUTLINE

Presentation of BI-RADS 5 clasification.Describe benign entities possibly classified as BI-RADS 5.Utility of imaging techniques.Imaging findings: specific features and clinical history.Management.Differential diagnostic

### BREE-53 Difficult MRI-Guided, Vacuum-Assisted Core Biopsies of the Breast: Tips and Tricks

Participants

Wenhui Zhou, MD, PhD, Menlo Park, CA (*Presenter*) Nothing to Disclose

#### TEACHING POINTS

Magnetic resonance imaging (MRI) is the most sensitive method to detect abnormalities of the breast. Due to its limited specificity, MRI-detected lesions often require tissue sampling to establish the diagnosis. Breast imagers should be cognizant of patient, anatomical, and technical factors that predispose to a potentially difficult MRI-guided breast biopsy. The purpose of this educational exhibit is to demonstrate techniques and tools to safely and successfully biopsy breast lesions. Completing this educational exhibit will allow participants to 1) Appreciate patient, anatomical and technical factors that predispose to difficult MRI-guided breast biopsies 2) Recognize pre-procedural planning, techniques and tools to optimize lesion visualization, targeting and sampling 3) Implement this knowledge during MRI-guided biopsies to minimize MR cancellations, unsafe procedures and nondiagnostic samples.

#### TABLE OF CONTENTS/OUTLINE

This case-based exhibit will demonstrate procedural planning and tips for successful difficult-to-perform MRI-guided breast biopsies including: 1) for bilateral lesions, perform simultaneous biopsy using lateral to medial approaches bilaterally 2) for posterolateral lesions, apply arm-down and arm-up maneuvers to facilitate safe access route 3) for lesions offset from the obturator tip, re-target with a second introducer and directionally sample if necessary 4) for posteromedial lesions, utilize a tangential, oblique approach to allow adequate access to the target 5) for vague or obscured lesions, consider the use of a T2-weight or DWI sequence to improve visualization. We will summarize take-home points to facilitate transfer of knowledge.

#### **BREE-54 How To Report a Contrast Enhanced Mammography (CEM) Study - An Illustrated and Practical Review of BIRADS 2022 Supplement for CEM**

##### Awards

##### Certificate of Merit

Participants

Rosa M. Lorente-Ramos, MD, PhD, Madrid, Spain (*Presenter*) Nothing to Disclose

#### TEACHING POINTS

-To review contrast enhanced mammography (CEM) basics and technique. -To analyze steps in interpretation of a CEM study. - To describe CEM lexicon and report structure. - To become familiar with normal and abnormal imaging findings in CEM providing correlation with imaging (mammogram, US, MR) and pathology.

#### TABLE OF CONTENTS/OUTLINE

We review the basics and state-of-the-art of CEM highlighting adequate interpretation of the exam according to the latest BIRADS recommendations for CEM reporting. 1. Basics of CEM. 2. Technique: Image acquisition: Low-energy images (LE) like a digital mammogram. Recombined images (subtraction of the low-energy from the high-energy images) (RC). Signal from background breast tissue is cancelled highlighting areas of iodine uptake. 3. Image interpretation steps. -LE. Morphological assessment -RC. Functional assessment. 4. BIRADS lexicon for CEM. - General overview: breast density (LE), Background parenchymal enhancement (RC). - LE findings. - RC findings: mass, non-mass enhancement, enhancing asymmetry, lesion conspicuity. - Lesion description on both: morphology, internal enhancement pattern, extent of enhancement, lesion conspicuity. 5. Report structure. Indication, technique, previous exams, breast composition, findings description, assessment, management.

#### **BREE-55 Staging Breast Cancer: A Case Based Review**

Participants

Aline Guimaraes, MD, (*Presenter*) Nothing to Disclose

#### TEACHING POINTS

Staging Breast Cancer nowadays is not only about defining the anatomic extent of disease. The most recent edition of the AJCC (American Joint Committee on Cancer), the eighth edition, now incorporate prognostic biomarkers to more accurately predict clinical outcomes and treatment response on an individual basis. In this didactic exhibit, we will discuss each aspect of Breast Cancer Staging in a case-based review. It is imperative to know the potential and limitations of each imaging modality (mammography, ultrasound and magnetic resonance imaging) and what to look for and describe on the exams. It is also important to comprehend other relevant aspects such as tumor grade, ER (estrogen receptor), PR (progesterone receptor) and HER2 (human epidermal growth factor receptor 2) status. Fundamentally understanding these aspects will provide more prognostic information than the anatomic stage alone and contribute to improve medical practice.

#### TABLE OF CONTENTS/OUTLINE

1. Mental Map with the following information 1. AJCC Staging System (application criteria) 2. Breast Cancer Stage 2.1. Clinical Staging 2.2. Pathologic Staging 2.3. Posttherapy staging after Neoadjuvant Chemotherapy, Radiation Therapy and Hormonal Therapy 2.4. Nodal staging 2.5. Clinical staging of metastasis 2.6. Stage migration 2. Relevant aspects to consider in breast imaging when staging breast cancer 3. Case based review of aspects mentioned above

#### **BREE-56 Review of Breast Anatomy - Normal Variants and Expected Physiologic Changes in the Breast**

Participants

Hubert Huang, MD, (*Presenter*) Nothing to Disclose

#### TEACHING POINTS

The female breast follows a predictable sequence of development. The mature adult breast is subject to a variety of physiologic effects during embryologic development, aging and hormonal changes. As a result, the female breast demonstrates a wide spectrum of normal appearance, some of which are congenital variants such as polythelia and polymastia, while others are acquired or physiologic but still considered normal, such as changes in density during pregnancy, lactation, and those typically seen with aging. Recognizing normal physiologic changes and anatomic variants can present a challenge to the radiologist. However, it is imperative to do so since the optimal modalities and views for evaluating these entities will differentiate them from potentially suspicious findings. We will present and discuss normal female breast development and anatomy, congenital and physiologic variants, and ways to avoid misdiagnoses.

## TABLE OF CONTENTS/OUTLINE

1. We will review normal anatomy of the breast. 2. We will discuss expected normal female breast developmental changes. 3. We will discuss variations in breast pattern and density in different physiologic conditions such as pregnancy and breastfeeding, as well as aging. 4. We will discuss normal and congenital breast anatomic variants. 5. We will review common and avoidable pitfalls of imaging variants that may mimic malignancy.

### **BREE-57HC Be Prepared - It's Not Because It's Rare that It Won't Happen! What the Radiologist Needs to Know About Angiosarcoma of the Breast**

Participants

Amanda Tavares, MD, Sao Paulo, Brazil (*Presenter*) Nothing to Disclose

#### TEACHING POINTS

Angiosarcoma represents less 1% of soft tissue sarcomas and is a very aggressive tumor with a poor prognosis. It depicts approximately 0.04% of malignant breast neoplasms and 8% of breast sarcomas, presenting with rapid and silent growth. The radiological findings are nonspecific, but the radiologist must be aware of the imaging features to avoid misdiagnosis. Primary breast angiosarcoma has an unknown etiology, affects younger patients (30-40 years) and usually presents as a palpable mass. Bilateral involvement is often associated with pregnancy or contralateral metastatic spread. There are no pathognomonic findings on conventional imaging. Nonetheless, on magnetic resonance imaging, the persistent enhancement in the dynamic study with late concentric filling may suggest this diagnosis. There may be areas of necrosis, hemorrhage and infarction within the tumor. Secondary breast angiosarcoma often occurs after local radiation therapy, with a mean latency period of 5-6 years. Besides that, chronic breast lymphedema and genetic predisposition are also risk factors. It commonly occurs in older patients (over 60 years) and may manifest as a palpable mass or just thickening and discoloration of the skin. Imaging findings are similar to the primary form.

## TABLE OF CONTENTS/OUTLINE

General aspects of angiosarcoma of the breast: Etiology, Prognosis, Diagnosis; Primary Breast Angiosarcoma; Secondary Breast Angiosarcoma; Summary Please visit the Learning Center to also view this presentation in hardcopy format.

### **BREE-58 Mimicking of an Abscess or Hematoma: Complex Mass Presentations of Triple Negative Breast Cancers**

Awards

Identified for RadioGraphics

Participants

Dogan Polat, MD, Dallas, TX (*Presenter*) Nothing to Disclose

#### TEACHING POINTS

Triple negative breast cancers are 16% of breast cancers in non African American women and 27% of breast cancers in African American women, often associated with BRCA 1 mutation and aggressive features, and poor prognostic outcome. Carefully assess margins of anechoic masses or complex masses which favor abscesses or hematoma, particularly if there is no overlying skin thickening or secondary signs of infection. Triple negative breast cancers can have posterior acoustic enhancement sonographically (therefore look for irregular margins, wall thickening, solid components). Triple negative breast cancers can present as a round hyperdense mass mammographically, therefore caution if one notes a round (not oval) mass, especially hyperdense (on attachment). Triple negative breast cancer can mimic other benign processes such as fibroadenoma, therefore careful margin assessment is important. Carefully review the axilla mammographically on patients with a history of breast cancer, using comparison to prior studies.

## TABLE OF CONTENTS/OUTLINE

1. Review mammographic and sonographic appearances of triple negative breast cancers and define triple negative breast cancer. 2. Recognize indistinct margins, thick walls, and lack of skin thickening in anechoic appearing irregular triple negative malignant masses and identify findings which raise concern for malignancy in these cases. 3. Review margin assessment of masses on ultrasound, particularly the sides of margins in a partially circumscribed mass. 4. Review metastatic patterns of triple negative breast cancer and mammographic assessment of the axilla in follow up of patients with history of breast cancer.

### **BREE-59 Fat-Containing Breast Masses: A Multi-Modality Review and Management Considerations**

Participants

Alison Gegios, MD, Whitefish Bay, WI (*Presenter*) Nothing to Disclose

#### TEACHING POINTS

Fat-containing entities in the breast constitute a variety of predominantly benign conditions and rarely malignant neoplasms. This presentation will focus on the recognition and diagnosis of fat-containing breast lesions to facilitate appropriate management and avoid unnecessary work-up and interventions. It will also discuss scenarios in which biopsy of fat-containing breast masses may be warranted.

## TABLE OF CONTENTS/OUTLINE

1. Imaging features consistent with fat on multiple modalities: • MRI • Ultrasound • Mammogram 2. Imaging features and management of common and uncommon benign fat-containing lesions • Lipoma • Hamartoma • Fat necrosis • Oil cyst • Intramammary lymph node • Galactocele • Steatocystoma multiplex • Angiolipoma • Hibernoma

### **BREE-6 Much More Than Lymph Nodes! A Practical Approach to Axillary Imaging**

Participants

Carolina Kiebert, Sao Paulo, Brazil (*Presenter*) Nothing to Disclose

#### TEACHING POINTS

The axilla will be reviewed by the different imaging modalities. The main aim is to describe the common axillary lesions. The present slides and

To show axillary anatomy in the different imaging modalities. To review the indications for axillary imaging. To present clinical and imaging findings of axillary masses according to the anatomical location of the lesion. To familiarize general radiologists with these findings in order to expedite accurate diagnosis. To discuss percutaneous interventions in axillary masses and the appropriate patient management depending on the diagnosis.

#### TABLE OF CONTENTS/OUTLINE

Radiologists are familiar with the evaluation of the axillary levels and staging of breast cancer, but we rarely discuss other pathologies that can be located in the axilla other than breast cancer lymph-node metastasis. Understanding the anatomy of the axilla can help radiologists to identify accurate diagnoses according to the anatomical location of the lesion once percutaneous biopsy may be inappropriate. This educational exhibit will compile anatomy and different findings with illustrative images from our radiology department. Knowledge of the clinical and imaging findings may improve detection of the differential diagnosis for such lesions, improving appropriate patient management.

#### BREE-60 Metaplastic Breast Carcinoma: Review of Imaging, Histopathology and Management Algorithm

Participants

Janice Thai, MD, (*Presenter*) Nothing to Disclose

#### TEACHING POINTS

1. To review the imaging spectrum of metaplastic carcinoma of the breast. 2. To review the histopathology and pathophysiology of this rare tumor subtype. 3. To review the treatment and management algorithm.

#### TABLE OF CONTENTS/OUTLINE

• Imaging review of common and uncommon features of metaplastic carcinoma • Review of unique histo and pathophysiology of metaplastic carcinoma. • Review of current evidence-based management algorithm

#### BREE-61 Spectrum of Mucinous and Mucocele-like Lesions: Imaging and Histopathologic Review

Participants

Janice Thai, MD, (*Presenter*) Nothing to Disclose

#### TEACHING POINTS

1. To review the imaging spectrum of mucinous and mucocele-like lesions. 2. To review the histopathology and distinct tumor/high risk lesion subtype. 3. To review the treatment and management algorithm.

#### TABLE OF CONTENTS/OUTLINE

• Imaging review of common and uncommon features of mucinous and mucocele-like lesions • Review of unique histo and pathophysiology of mucinous and mucocele-like lesions • Review of current evidence-based management algorithm

#### BREE-62 PET Mammography from Indications to Interpretation

Participants

Rasha M. Kamal, MD, Cairo, Egypt (*Presenter*) Nothing to Disclose

#### TEACHING POINTS

PEM is a specialized application of PET to visualize breast tissue metabolic changes with a much higher spatial resolution thus allowing the visualization of smaller tumor cells. In this educational exhibit the technique of PEM will be discussed in detail. The qualitative and quantitative (the PUV and Lesion to background activity) assessment of PEM images will be illustrated. The pattern of radiotracer uptake in the different histopathology and molecular subtype will be also discussed. The main indications of PEM include: - Enhanced lesion characterization. - Preoperative staging - Response to NAC therapy monitoring. - Post breast cancer surveillance. - Screening for women with dense breasts. - Metastases of unknown primary The advantages and disadvantages of PEM will be highlighted to allow the sound practice of this novel imaging modality.

#### TABLE OF CONTENTS/OUTLINE

1. Technique of PEM 2. Indications 3. Interpretation (quantitative and qualitative assessment 4. Advantages and disadvantages of PEM

#### BREE-63 Evolving Role of Nuclear Medicine and Molecular Imaging in Breast Cancer - A Case-based Multimodality Pictorial Review with Teaching Pearls

##### Awards

##### Certificate of Merit

Participants

Fatima Elahi, DO, Lincolnwood, IL (*Presenter*) Nothing to Disclose

#### TEACHING POINTS

Breast cancer continues to be the most common cause of malignancy for women in the United States with current imaging standards centered around mammography, CT, ultrasound, and MRI. Nuclear Medicine (NM) and molecular imaging (MI) including PET CT have now become essential tools in the diagnosis and management of patients with Breast cancer. Often times the findings have resulted in decisions that change the course of treatment in about 24-48% of patients. We provide a case-based multimodality pictorial review of the evolving role of Nuclear Medicine and Molecular Imaging in the management of patients with breast cancer.

#### TABLE OF CONTENTS/OUTLINE

Our educational exhibit aims to 1) Highlight the impact of various NM and MI tracers and modalities such as Lymphoscintigraphy including Mannose-binding Tc-99m Tilmamcept for targeted lymphatic mapping and Sentinel node localization, mammo-scintigraphy (Molecular breast imaging (MBI)), MDP Bone scan, F-18 Sodium Fluoride PET CT, F-18 FDG PET CT, Hormonal receptor imaging

(such as F18-Fluoroestradiol PET CT); Radionuclide ventriculogram (MUGA Scan); Palliative treatment of painful bone metastasis using strontium-89/samarium 153; PET CT guided interventions and biopsy; 2) Case-based discussions highlighting the indications, sensitivity, and specificity rates and limitations of these studies; 3) Discuss challenging cases including axillary lymphadenopathy secondary to COVID 19 vaccination, FLARE phenomenon, somatostatin receptor-expressing breast cancers on Ga-68 DOTATATE PET CT, evaluating Post-operative breast for local recurrence and male breast cancer; 4) utility of texture analysis.

#### **BREE-64 Overcoming Burnout Towards Brilliance in Breast Radiologists after COVID-19**

Participants

Jay R. Parikh, MD, West University Place, TX (*Presenter*) Nothing to Disclose

##### **TEACHING POINTS**

Burnout has been recognized by the World Health Organization as a syndrome conceptualized as resulting from chronic workplace stress that has not been successfully managed. A previous study showed that there is a high prevalence of burnout across practicing clinical breast radiologists. Physician wellness (well-being) is defined by quality of life, which includes the absence of ill-being and the presence of positive physical, mental, social and integrated well-being. The unprecedented COVID-19 pandemic has brought challenges to the practicing breast radiologist. Initially, there was a reduced workload volume early in the pandemic which then rebounded into high volumes of breast screening and diagnostic studies. Coupled with his volume were challenges of maintaining family work-life balance and regular social isolation, compounding the negative work environment. The COVID-related work environment has previously been described as unsustainable for radiologists. Surveys of clinically practicing radiologists during COVID-19 have demonstrated a high rate of burnout and increased subjective stress by breast radiologists. Strategies that may be deployed post COVID-19 to mitigate radiologist burnout include implementing a culture in the workplace that prioritizes and promotes wellness, addressing operational inefficiencies and increasing resiliency of practicing breast radiologist.

##### **TABLE OF CONTENTS/OUTLINE**

A. Burnout. B. Burnout in Breast Radiologists C. COVID-19 Impact on breast radiology D. Implementing a culture of wellness. E. Addressing operational inefficiencies F. Increasing radiologist resiliency

#### **BREE-65 Understanding Fibroepithelial Lesions of the Breast - A Primer for Residents and Fellows**

Participants

Tara Retson, MD, PhD, San Diego, CA (*Presenter*) Research Consultant, CureMetrix, Inc; Stock options, CureMetrix, Inc

##### **TEACHING POINTS**

**SYNOPSIS:** Fibroepithelial lesions (FEL) of the breast are biphasic neoplasms with variable amounts of stromal and epithelial proliferation. They range from benign fibroadenomas to malignant phyllodes tumors, fibroadenomas being the most diagnosed breast lesion on core needle biopsy. Other FEL includes cellular and juvenile fibroadenoma and benign, borderline, and malignant phyllodes. **TEACHING POINTS:** By the end of this educational exhibit, the learner will: 1. Review the incidence, clinical presentation, and management of FEL of the breast. 2. Know the imaging protocols used to evaluate FEL, including mammogram, US, and MRI, based on age and ACR appropriateness criteria. 3. Understand the classification of FEL based on the WHO classification. 4. Identify FEL that is locally aggressive and warrants further surgical management.

##### **TABLE OF CONTENTS/OUTLINE**

Introduction; Clinical presentation of FEL; Differential considerations of FEL include differentiation of malignant phyllodes from metaplastic breast cancer and sarcoma; Understanding the grading of phyllodes tumors; Imaging assessment of FEL; Role of mammogram and US in the evaluation of FEL; MRI findings of FELs; Recommended clinical management of FEL; A pictorial review of FEL; Algorithm for imaging patients with suspected FEL; Conclusion

#### **BREE-66 Superficial Lesions of the Breast - What Residents Need To Know?**

Participants

Karen Caro, PhD, La Plata, Argentina (*Presenter*) Nothing to Disclose

##### **TEACHING POINTS**

1. To illustrate imaging features of superficial lesions of the breast. 2. Characteristics of superficial lesions of the breast. 3. Distinguish superficial lesions of the breast versus parenchymal lesions.

##### **TABLE OF CONTENTS/OUTLINE**

The thin epidermis is composed of several cell layers and contains no blood or lymphatic vessels and may not be distinguished from the dermis at imaging. However, within the dermis reside hair follicles, sebaceous glands, sweat glands, nerve endings, and blood and lymph vessels. The hypodermis typically contains nerves, lymphatics, larger blood vessels, and fatty tissue. The importance of delimiting the layers of the skin and its components help us to identify the lesions that can originate at this level. For example, the presence of a tract—which represents extension of the hair follicle from the dermis up through the epidermis—that extends from the lesion to the epidermal skin surface also confirms a dermal origin and is indicative of a sebaceous or epidermal inclusion cyst. It is so that in the present work we will analyze different images and their characteristics that will help us to define their probable origin. **Conclusions** The importance of identifying skin lesions and differentiating them from those located in the mammary parenchyma helps us to define BI-RADS, since many times we can perform controls or even biopsies, which can be avoided, through an adequate study of their location through image and do not forget the importance of a physical examination and questioning

#### **BREE-67 What's Normal Anymore - Lymph Node Evaluation and the Changing Guidelines of COVID**

Participants

Anna Hollen, MD, (*Presenter*) Nothing to Disclose

##### **TEACHING POINTS**

- Review the impacts of COVID-19 vaccination on axillary lymphadenopathy.
- Understand the approach to lymph node evaluation in breast practice.
- Understand the differences between normal and abnormal lymph nodes.
- Through case examples, understand when lymphadenopathy is benign and when further workup is necessary.

## TABLE OF CONTENTS/OUTLINE

- Overview of COVID impacts, breast imaging society guidelines and institutional specific operational changes
- Review of lymph node evaluation in breast practice and use of ultrasound
- Normal vs. abnormal lymph node features
- Case-based illustration of lymph node pathology and appropriate assessment/management
- Benign reactive lymphadenopathy related to COVID vaccination
- Lymphoma
- Breast cancer unknown at time of workup
- Metastatic, known breast cancer
- Melanoma
- Unknown primary

### BREE-68 Radial Sclerosing Lesions: An Updated Approach to Multidisciplinary Management

Participants

Allison Aripoli, MD, Kansas City, KS (*Presenter*) Nothing to Disclose

#### TEACHING POINTS

1. Radial sclerosis lesions (RSL) are benign lesions that often present with suspicious imaging features such as mammographic architectural distortion.
2. RSL are often seen in association with other benign or high-risk proliferative lesions.
3. Newer literature demonstrates lower malignancy upgrade rates of RSL, especially RSL without associated atypia, resulting in shifting management paradigm toward de-escalation of routine surgical excision of RSL.
4. Upgrade of a "pure" RSL to atypia at surgical excision is an additional important consideration to provide relevant information for appropriate individual risk stratification and risk reduction.
5. Radiology-pathology concordance and multidisciplinary review are essential for treatment decisions. Institutional review of upgrade rates can help define management.

#### TABLE OF CONTENTS/OUTLINE

1. Introductiona. Imaging appearance of RSL and overlap with malignancyb. Pathology reviewc. Association with other benign or high-risk proliferative lesions
2. Historical shifts in understanding and managing RSLa. Older studies and upgrade ratesb. Newer studies and upgrade ratesc. American Society of Breast Surgeons Consensus Guidelines for management of RSLd. Factors related to risk of upgradee. Lack of consensus for management among contemporary studies
3. Radiology-pathology concordance and multidisciplinary conference reviewa. De-escalation of routine surgical excision of concordant RSL based on contemporary published and institutional datab. Long-term follow-up and management

### BREE-69 Pregnancy Associated Breast Cancer: Diagnostic Approach and Imaging Pitfalls

Participants

Charisma DeSai, MD, Dallas, TX (*Presenter*) Nothing to Disclose

#### TEACHING POINTS

1. Definition: Pregnancy associated breast cancer (PABC) is cancer that develops during pregnancy, breastfeeding, or in the first year postpartum.
2. Understand the epidemiology and pathophysiology of PABC.
3. Review the risk factors associated with PABC and reasons for diagnostic delay.
4. Review the expected breast imaging findings in the pregnant and lactating breast.
5. Review the imaging and clinical findings of PABC.
6. Review of ACR appropriateness criteria of breast screening and staging during pregnancy and lactation.
7. Create a diagnostic approach to symptomatic breast during pregnancy and lactation.
8. Explore the different surgical and systemic management options for PABC with respect to fetal and maternal safety.

#### TABLE OF CONTENTS/OUTLINE

1. Risk factors associated with PABC
2. Expected imaging findings of the breast during pregnancy and lactation
3. Review of ACR appropriateness criteria of breast imaging and staging during pregnancy and lactation based on patient age and lifetime risk for breast cancer
4. Diagnostic approach to symptomatic breast during pregnancy and lactation
5. Review of radiological findings in:- PABC.- Benign conditions associated with pregnancy and lactation: Breast abscess, lactational mastitis.- How to differentiate lactational mastitis and inflammatory breast cancer
6. Role of imaging guided biopsy
7. Treatment options for PABC including surgical management

### BREE-7 Abdominopelvic Manifestations of Metastatic Breast Cancer and Treatment-Related Complications

#### Awards

##### Certificate of Merit

Participants

Annie Rhee, MD, (*Presenter*) Nothing to Disclose

#### TEACHING POINTS

1. Common sites of breast cancer metastases on abdominal/pelvic imaging are the liver and bones. Less common sites are the peritoneum, gastrointestinal tract, ovary, and retroperitoneum.
2. Invasive lobular carcinoma metastases are often infiltrative, which can be difficult to evaluate in earlier stages of disease on imaging. Recognizing complications such as small bowel strictures or obstruction in patients with a history of breast cancer can prompt further investigation.
3. Treatment related complications such as pseudocirrhosis, endometrial hyperplasia, and post-surgical changes should also be recognized in these patients.

#### TABLE OF CONTENTS/OUTLINE

Background: IDC ILCLiver Metastases Focal mass Diffuse infiltration Treatment-related pseudocirrhosis Bile Ducts Biliary obstruction Pancreas MetastasesMass vs infiltrative lesions Adrenal MetastasesDiffuse/nodular thickeningMass GI tract Stomach Linitis plastica Focal ulcerations Small bowel Infiltration obstruction Colon rectum Linitis plastica Ovarian Metastases Primary ovarian cancer in BRCA positive patients Uterus endometrium Metastases Infiltrative Tamoxifen related pathologyEndometrial spectrum (hyperplasia to carcinoma)AdenomyosisLeiomyomaUterine sarcoma Peritoneum Nodular vs infiltrative Retroperitoneum MetastasesInfiltrative fibrotic with urinary tract complications Lymph nodesDistribution of lymphatic spreadAbdominal wall Metastases Postsurgical changesDIEP flap Bones Metastases Blastic, lytic, mixed Pathologic fracture Treatment changes Conclusions

### BREE-70 2022 New Trends in Breast Density - What Should We Know?

#### Awards

##### Identified for RadioGraphics

Participants

Flavia Sarquis, MD, Buenos Aires, Argentina (*Presenter*) Nothing to Disclose

#### TEACHING POINTS

Digital mammography (DM) is the most commonly utilized modality in asymptomatic women in the preventative setting, with continuous advancement in breast density measurement. Women with dense breasts have an increased risk of developing breast cancer. Breast density is the most common factor that may prompt women to seek additional screening beyond mammography to increase the likelihood of early cancer detection. After reading this educational exhibit the radiologist will know: Women with dense breasts have clear downsides of breast cancer screening facing an increased risk of late diagnosis. Early diagnosis and treatment are vital. The pandemic has taught us what needs to be done. The realistic limitations of mammography in dense breasts and the benefits of additional screening. Stratification of breast cancer prevention and screening requires mammographic density measures predictive of cancer. New recommendations of breast cancer screening in women with extremely dense breasts.

#### TABLE OF CONTENTS/OUTLINE

Breast density is a biomarker of objectively measurable characteristics that indicate an underlying physiological or pathological process. Current evidence on breast cancer screening in women with dense breasts. Added detection with supplemental screening. Principles of shared decision-making. Illustrative-based cases. Conclusions

#### BREE-71 T2 Hyperintense Breast Lesions on MRI - A Pictorial Guide for Residents

Participants

Maria Jose Chico, Buenos Aires, Argentina (*Presenter*) Nothing to Disclose

#### TEACHING POINTS

In this educational exhibit, through simple iconographic examples, we will teach residents how to identify and recognize the different benign and malignant lesions that may present with high signal intensity in T2 weighted images in breast magnetic resonance. Teaching points: 1) To describe benign and malignant lesions which are hyperintense in T2 weighted images in breast MRI. 2) To illustrate with several examples adding helpful suggestions that will enable residents to make the correct diagnosis.

#### TABLE OF CONTENTS/OUTLINE

1- Introduction 2- MRI technique 3- Benign lesions: Cysts, Seroma, Hematoma, Intramammary lymph nodes, Apocrine cystic metaplasia, Cavernous hemangioma, Myxoid fibroadenoma, Benign Phyllodes tumor 4- Malignant lesions: Mucinous/colloid carcinoma, Metaplastic carcinoma, Papillary carcinoma, Triple Negative Basal Like carcinoma, Necrotic/hemorrhagic invasive ductal carcinoma, Malignant Phyllodes, Metastases 5- Conclusions

#### BREE-72 Demystifying Lesions and Artifacts - A Pocket Guide for Automated Breast Ultrasound

Participants

Fernanda P. Pereira, MD, PhD, (*Presenter*) Nothing to Disclose

#### TEACHING POINTS

#Automated breast ultrasound (ABUS) is a valuable screening tool for breast cancer designed to overcome some of the issues regarding hand-held breast ultrasound (HHBUS), such as operator dependency, less experience with breast exams, low sensitivity and reproducibility. #ABUS main indication is to use as an adjunct method to mammography for screening asymptomatic women with dense breasts. #Correct identification of lesions and artifacts produced by ABUS is essential for the best evaluation, as acquisition is done by a technician and interpretation is performed by the specialist without knowing potential pitfalls during the exam.

#### TABLE OF CONTENTS/OUTLINE

1- Concept of automated breast ultrasound (ABUS); 2- ABUS: atlas of benign lesions; 3- ABUS: atlas of malignant lesions; 4- Main differences between ABUS and hand-held breast ultrasound (HHBUS); 5- ABUS: pitfalls and artifacts; 6- ABUS: other applications and final considerations.

#### BREE-73 Male Breast Cancer - Spectrum of Imaging Appearance and Current Imaging Recommendations

Participants

Soudabeh Fazeli Dehkordy, MD, MPH, San Diego, CA (*Presenter*) Nothing to Disclose

#### TEACHING POINTS

Synopsis: Imaging of the male breast is typical in routine radiology breast imaging. Most of the findings in male patients are benign, gynecomastia being by far the most common imaging diagnosis. Male breast cancer is uncommon, accounting for less than 1% of all breast cancers. The incidence of breast cancer in men is low, but it increases with age, and the 5-year survival rates are similar, stage by stage, between men and women. Men tend to present with more advanced stages of the disease. When axillary metastatic disease is present, the prognosis is worst and negatively affects the treatment. We reviewed 32 male breast cancer imaging studies from our teaching files, including mammograms, US, and MRI, to catalog the imaging presentations of breast cancer. TEACHING POINTS By the end of this educational exhibit, the learner will: 1. Review the incidence, clinical presentation, and management of male breast cancer. 2. Know the imaging protocols recommended to evaluate males based on ACR appropriateness criteria. 3. Identify the multimodality imaging appearance of malignant male breast lesions.

#### TABLE OF CONTENTS/OUTLINE

Introduction; Incidence and risk factor for male breast cancer; Clinical presentation of male breast cancer; Review of imaging recommendations for male breast; Differential considerations; Mammographic and US findings; MRI indications and appearance of male breast cancer; Recommended management of male breast cancers; Algorithm for imaging male patients with breast cancer and for follow up into survivorship; Conclusion.

#### BREE-74 The Imaging of Ductal Carcinoma in SITU - Where It Is and Where It's Going

Participants

Daniela Cunha, MD, Coralville, IA (*Presenter*) Nothing to Disclose

## TEACHING POINTS

Ductal carcinoma in situ (DCIS) is the most prevalent form of breast cancer. It can be pathologically classified via the nuclear grade (low, intermediate, high) or by the architectural subtype (comedo, cribriform, micropapillary, solid, or mixed) with increased preference for nuclear grading. Approximately 75% of DCIS present with calcifications and mammography remains its main detection modality; ultrasound (US) may show a mass within a dilated duct but is nonspecific. Magnetic resonance imaging (MRI) however, is proving to be a useful supplementary tool in evaluating the extent of DCIS for surgical planning as well as a prognostic tool for predicting potential for upgrade from DCIS to invasive ductal carcinoma (IDC). While DCIS most commonly presents as a non-mass enhancement, IDC more often presents as an enhancing mass. With advancements in MRI, there is the potential to confidently differentiate low-grade from high-grade DCIS in the future.

## TABLE OF CONTENTS/OUTLINE

DCIS - Pathology classification - Mammography findings - Ultrasound and MRI findings - Increasing importance of MRI in DCIS prognosis and treatment

### **BREE-75 Idiopathic Granulomatous Mastitis and Its Differential Diagnoses - A Practical Guide for Its Identification**

Participants

Jorge Hernandez Espinoza, MD, CABA, Argentina (*Presenter*) Nothing to Disclose

## TEACHING POINTS

Mention the main pathophysiological, demographic and clinical aspects of Idiopathic Granulomatous Mastitis (IGM). Recognize the most common findings of IGM in mammography, ultrasound and magnetic resonance imaging, and their main differential diagnoses.

## TABLE OF CONTENTS/OUTLINE

Idiopathic granulomatous mastitis is a rare chronic inflammatory condition of the breast of unknown aetiology. It is commonly seen in women of childbearing age, but also in perimenopausal women. The diagnostic challenge is that it can mimic many conditions, including malignancy. The most common clinical presentation is a breast lump in any quadrant, or diffuse involvement of the breast. It manifests with axillary pain, erythema, edema or lymphadenopathy. Other chronic inflammatory pathologies considered in the differential diagnosis include plasma cell mastitis, tuberculosis, histoplasmosis, inflammatory carcinoma and Wegener's granulomatosis. Histopathology provides a definitive diagnosis, thus avoiding unnecessary mastectomies. On mammography it is common to find focal asymmetry, a darkened or irregularly shaped mass. On ultrasound, a large irregular hypoechoic parallel mass with tubular extensions is prominent. A hypoechoic and parallel circumscribed mass, or a mass with angular, lobulated, or indistinct margins, associated or not with posterior acoustic shadowing, has been reported. With color Doppler we can visualize the hypervascularization of the tissue surrounding the lesion. IGM in magnetic resonance imaging can be observed as a non-regional or segmental mass enhancement, or a mass enhancement with heterogeneous enhancement, lesions with enhancement of their margins or the presence of microabscesses.

### **BREE-76 Don't Forget the Pec! A Case-based Review of Pectoral Muscle Abnormalities on Breast Imaging**

**Awards**

**Certificate of Merit**

Participants

Almir Bitencourt, MD, PhD, Sao Paulo, Brazil (*Presenter*) Nothing to Disclose

## TEACHING POINTS

- To show a multimodal review of the pectoral muscles in breast imaging. - To teach breast radiologists to evaluate the pectoral muscles, mainly in mammograms, MRI and ultrasound. - To illustrate some conditions focusing in abnormalities showed by interesting cases of our institutions. - To give hints on how not to obviate the evaluation of these muscles in breast exams.

## TABLE OF CONTENTS/OUTLINE

1. A description of pectoral muscles anatomy and functions. 2. An introduction of pectoral muscles imaging aspects in breast exams (mammograms, ultrasound and MRI). 3. To show the importance of pectoral evaluation to avoid misdiagnosis of lesions in this area. 4. Interesting cases of pectoral muscles conditions: - Normal variations (Pectoralis quartus muscle, sternalis muscle, Langer's axillary arch and Poland Syndrome); - Benign conditions (Subpectoral lipoma, pectoral muscle abscess, pectoral hemangioma and ossifying myositis); - Malignant conditions (sarcoma and lymphoma of the pectoral muscles). 5. Most common pitfalls in pectoral muscles evaluation.

### **BREE-77HC The Wave of Silicone Explanation: What To Expect in Breast Images?**

Participants

Amanda Tavares, MD, Sao Paulo, Brazil (*Presenter*) Nothing to Disclose

## TEACHING POINTS

In the past years, the term breast implant illness has becoming strong, especially with the power of social media, to describe physical and psychological symptoms possibly related to breast implants. The silicone is also discussed as a causal factor of ASIA syndrome (Autoimmune Syndrome Induced by Adjuvants). The exact mechanism whereby the implant can induce such diseases is uncertain, and there is still not enough scientific evidence to justify the diagnosis. Many patients report partial or complete resolution of symptoms after the silicone explant and plastic surgery societies already report an increase in the performance of such procedures. Regardless of the surgical technique used for implant removal and capsulectomy, steatonecrosis is a frequent complication. Volume restoration after explantation by autologous fat grafting will also present as oil cysts on imaging. Anterior capsulectomy is an alternative when the posterior capsule is adhered to the chest wall, increasing the risk of pneumothorax, in these cases the base of the capsule left intact can be seen in subsequent images. Breast and axillary residual free silicone may be a result of extracapsular rupture or even gel-bleeding of the removed implants, presenting as hyperdense nodules on mammography, dirty posterior acoustic shadowing on ultrasound, without significant enhancement on MRI. Correlation with previous exams and clinical history is essential to confirm the diagnosis and avoid unnecessary procedures.

## TABLE OF CONTENTS/OUTLINE

Breast implant illness ASIA syndrome Breast imaging after silicone explantation Please visit the Learning Center to also view this presentation in hardcopy format.

### **BREE-78 Multipictorial Review of Papillary Lesions: An Essential Guide for Residents!**

Participants

Antonio Jose Cueva Guerrero, MD, (*Presenter*) Nothing to Disclose

#### **TEACHING POINTS**

After the exhibit the reader will be able to: • Understand the ductal anatomy of the breast • Create a visual standard for the normal ductal pattern of the breast • Recognize papillary lesions from benign to malignant • Comprehend the use of each imaging modality for evaluating normality • Identify and be able to report pathology, using understandable parameters

#### **TABLE OF CONTENTS/OUTLINE**

- Introduction- Anatomy- Classification- Benign lesions- Malignant lesions- Imaging methods- Conclusions

### **BREE-79 Epithelial Lesions of The Breast: Solving Questions You Didn't Know You Have**

Participants

Sofia Maksoud, MD, Sao Paulo, Brazil (*Presenter*) Nothing to Disclose

#### **TEACHING POINTS**

Benign epithelial and fibroepithelial lesions of the breast are responsible for about 80% of palpable lesions. Histologically, they are classified as fibrocystic changes and associated conditions. Fibrocystic changes are classified as non-proliferative, including cysts, or proliferative, including papillomas, radial scar, sclerosing adenoma, and ductal or lobular hyperplasia. Associate conditions include fibroadenomas and their variants, sclerosing lesions, papilloma and proliferative disease. Mammography, ultrasound and magnetic resonance imaging of the breasts may be helpful in differentiating benign from suspicious lesions in the breast. The objective of this study is to review, through a case-based presentation, the imaging aspect in these lesions, and the role of imaging in differing these conditions from suspicious malign findings.

#### **TABLE OF CONTENTS/OUTLINE**

Evaluation of cases of benign epithelial and fibroepithelial lesions of the breast from the digital file of our institution, demonstrating their presentation in different imaging modalities, including ultrasonography, mammography and magnetic resonance imaging, correlating them with the histopathological findings. The work also includes discussion of the topic based on the literature, teaching points and the references.

### **BREE-8 Pearls and Pitfalls of Automated Breast Ultrasound Interpretation**

**Awards**

**Certificate of Merit**

**Identified for RadioGraphics**

Participants

Ashley Huppe, MD, Kansas City, KS (*Presenter*) Nothing to Disclose

#### **TEACHING POINTS**

There is increasing utilization of automated ultrasound (AUS) for breast cancer supplemental screening, in part due to increased breast density awareness and federal legislation requiring breast density notification. Given the unique nature of volumetric acquisition on AUS, many radiologists are unfamiliar with identification of breast cancer in the multiplanar format. Additionally, the wide format transducer can generate artifacts which can result in false positives. After this presentation, participants will be able to: • Discuss rationale and guidelines for supplemental screening and review currently available supplemental screening options • Describe benefits and limitations of AUS for breast cancer screening • Compare outcomes data between automated and handheld breast ultrasound screening • Learn the pearls of proper AUS interpretation including unique imaging features and knobology to increase cancer detection and avoid unnecessary callbacks • Review AUS challenges and pitfalls including recognition of artifacts and identification of benign findings

#### **TABLE OF CONTENTS/OUTLINE**

1. Introduction: supplemental screening a. Rationale b. Options 2. AUS for breast cancer screening a. Overview i. Indications and limitations ii. Compare and contrast with handheld screening iii. Technique b. Imaging interpretation i. Pearls 1. Correlation with current and prior mammography and ultrasound images 2. Visualization of lesions in at least two data sets 3. Use of unique AUS tools for lesion characterization, including coronal/sagittal planes and software rotation ii. Pitfalls 1. Acquisition challenges 2. Compression and shadowing artifact 3. Identification of benign findings 3. Conclusion

### **BREE-80 Axillary Region - Which Road? Beyond Lymph Node**

Participants

Isabela Ferracini, MD, Sao Paulo, Brazil (*Presenter*) Nothing to Disclose

#### **TEACHING POINTS**

The most common metastatic presentation of breast cancer is enlarged lymph nodes with atypical characteristics in the axillary region, which is why this location must be carefully examined in all breast imaging exams. However, due to the various anatomical structures in this region, many conditions may also present with pain and/or palpable nodulation and are not distinguishable in physical examination, including pathologies that involve neural and vascular structures, subcutaneous tissue, bone and muscular structures, among others. In this way, a thorough evaluation of the armpits through the various modalities of imaging exams is an important tool in elucidating the diagnosis and determining the best treatment. The aim of this study is to address lymph node and non-lymph node axillary radiological findings and their main characteristics.

#### **TABLE OF CONTENTS/OUTLINE**

Cases containing mammography, ultrasound, computed tomography and magnetic resonance images and 3D reconstruction.

cases concerning mammography, ultrasound, computer tomography, and magnetic resonance images and of reconstruction, obtained from the digital file of our institution, were used. We approach a didact review of some of the most common conditions involving the axillary region, their imaging aspects and how to differentiate them in imaging exams, including teaching points and references.

### **BREE-81 All That Glitters is Not Gold - Malignant Breast Lesions with Hyperintense Signal on T2**

#### **Awards**

#### **Certificate of Merit**

Participants

Marina Santos, Sao Paulo, Brazil (*Presenter*) Nothing to Disclose

#### **TEACHING POINTS**

The purposes of this exhibit are:1- To review our institution's cases of malignant lesions presenting with high signal intensity on MRI T2-weighted images;2- To describe the aspects of these lesions: morphology, T1 and T2 WI features, enhancement pattern and diagnostic clues;3- To evaluate the histological factors that could cause high signal intensity on T2 WI on each lesion such as cystic component, mucinous or loose myxoid stroma, edema, hemorrhagic or necrotic changes;4- To explore the imaging aspects differentiating malignant from benign lesions with high T2 signal such as inflammatory, cystic or infectious etiologies.

#### **TABLE OF CONTENTS/OUTLINE**

1- Review cases of malignant lesions presenting with hyperintense signal on T2 WI from our radiology department, documented in multiple methods (MRI, ultrasound and mammography), such as: mucinous carcinoma;metaplastic carcinoma;papillary carcinoma;invasive ductal carcinoma;fibroepithelial tumours.2- Correlation of these cases with histopathological findings justifying the high signal on T2: extensive necrosis; cystic content; mucinous stroma.3- Review some benign differential diagnosis such as inflammatory, cystic and infectious etiologies.

### **BREE-82HC An Overview of Breast Plasmacytoma With Radiologic-Pathologic Correlation: Key Considerations and Major Features**

Participants

Pooya Torkian, MD, Minneapolis, MN (*Presenter*) Nothing to Disclose

#### **TEACHING POINTS**

The purpose of this project is to describe radiological and pathological findings of breast plasmacytoma in patients with multiple myeloma. We explore multimodality imaging results of mammography, ultrasound, positron emission tomography/computed tomography (PET/CT), CT, magnetic resonance imaging, and tomosynthesis. We provide a pictorial review of the most notable imaging findings of breast plasmacytoma for the awareness of radiologists and clinicians to improve the standard of care.

#### **TABLE OF CONTENTS/OUTLINE**

1. Introduction 2. Overview of breast plasmacytoma in multiple myeloma 3. A pictorial review of imaging findings of breast plasmacytoma in mammography, ultrasound, PET/CT, CT, MRI, and tomosynthesis 4. Strengths and weaknesses of the different modalities 5. Discuss the future application of multimodality imaging in breast plasmacytoma Please visit the Learning Center to also view this presentation in hardcopy format.

### **BREE-83 Breast Masses in Children and Adolescents: What Do We Need To Know?**

Participants

Thais Kuwazuru, MD, Sao Paulo, Brazil (*Presenter*) Nothing to Disclose

#### **TEACHING POINTS**

The aim of this exhibition is to:1. Review the current concepts about breast disorders and normal breast development and its variations in children and adolescents.2. Discuss the differences between each imaging modality.3. Describe the rates of breast lesions in this age group in our hospital.4. Highlight the importance of this knowledge to guide the proper management of these patients

#### **TABLE OF CONTENTS/OUTLINE**

1. INTRODUCTIONa. Epidemiological profile of breast lesions in this population.b. Recommendations for screening, control and surveillance.2. IMAGING INTERPRETATIONa. Imaging techniques acquisition and protocols.b. Use of ACR BI-RADS and structured reporting of the findings on this population.3. STATISTICAL DATAa. Breast imaging data from in women under the age of 19 from our institution between January 2020 and April 2021.b. Correlation with literature data.4. INTERACTIVE CASE-BASED DIDACTICSa. Sample cases to illustrate and solidify the concepts about the main findings in this population.5. FUTURE DIRECTIONS AND TAKE HOME MESSAGES

### **BREE-84 WANTED: Complete Radiological Response to Neoadjuvant Chemotherapy**

Participants

Natalia Lima, Sao Paulo, Brazil (*Presenter*) Nothing to Disclose

#### **TEACHING POINTS**

The purposes of this exhibit are:1. To review the main aspects related to neoadjuvant chemotherapy response, including complete response, partial response, stable disease, and progressive disease.2. To evaluate the pathologic response (including pCR and residual cancer burden score - RCB) and correlate to radiologic response in some cases from our institution;3. To emphasize the importance of looking for residual lesions in all sequences of MRI, including T2, in order to avoid missing lesions;4. To show, based on interesting cases from our breast radiology group, different kinds of response to neoadjuvant chemotherapy in a variety of histological and immunohistochemical subtypes;

#### **TABLE OF CONTENTS/OUTLINE**

· Radiological response patterns to neoadjuvant chemotherapy:- Complete, partial (concentric and with peripheral lesions),

stability, progression of injury· Pathologic response using RCB and its parameters: - Primary tumor dimension - Cellularity - Size of the largest nodal metastasis - Number of positive lymphonodes· Concepts of radiologic and pathologic complete response· Teaching cases showing the challenging aspects based on imaging findings and correlate with clinical and pathological findings in different scenarios, such as: - Ductal carcinoma with tumoral seeding - Mucinous carcinoma mimicking a parical response - Inflammatory carcinoma with complete response - Complete response of calcifications on a lobular carcinoma

## **BREE-85 Challenges in the Interpretation of Breast Findings In The Emergency Setting: Recommendations for the Non-Breast Imager**

### **Awards**

#### **Identified for RadioGraphics**

Participants

Steven Lee, MD, Bellaire, TX (*Presenter*) Nothing to Disclose

#### **TEACHING POINTS**

Emergencies in Breast Imaging are uncommon. Although infectious conditions such as mastitis and breast abscess are commonly encountered in the emergency department, many additional entities may be recognized, including breast cancer. Most emergency departments do not have mammography units, making the evaluation of these patients incomplete and this emphasizes the importance of ultrasound technique and imaging interpretation in this setting. This is especially important when images are reviewed remotely by the Breast Imaging team. With this exhibit, the learner will be exposed to imaging examples of breast emergencies in the ER/inpatient setting, technique tips and tricks for the ultrasound evaluation of the breast in the ER, relevant patient and imaging information that breast imagers require for remote interpretation, and appropriate recommendation, treatment, and follow up for patients in the emergency setting.

#### **TABLE OF CONTENTS/OUTLINE**

Introduction. Breast imaging emergencies in the ED and Breast Imaging Department: Mastitis, Abscess, Trauma/Hematoma, Fluid Collection, Masses, Pseudoaneurysm, Vasovagal Reaction. Ultrasound technique tips and tricks for evaluation in the ED. Algorithm for recommendations and follow up of breast imaging emergencies. Conclusion and Summary

## **BREE-86 LCIS and It's Variants - Review of What We Know**

Participants

Joe Khoury, DO, MBA, Manhasset, NY (*Presenter*) Nothing to Disclose

#### **TEACHING POINTS**

Classic LCIS and atypical lobular hyperplasia (ALH) both demonstrate noninvasive proliferation of lobular cells within the TDLU. LCIS involves >50% of acini while ALH involves <50%. LCIS is a risk factor and non obligate precursor of invasive breast carcinoma. RR for development of breast cancer in those with LCIS is 9-10x the general population. Subsequent breast cancer can occur in either breast and includes DCIS and invasive cancers. Most often, LCIS is an incidental finding on pathology. However, there are known multimodality imaging findings associated with LCIS. Pure LCIS includes classic (cLCIS) and non classic types (including pLCIS). Management of LCIS continues to evolve. Upgrade rate to ILC ranges from 0-67% depending upon the study and histology Given low upgrade rates for cLCIS (0-5%), excision diagnosed on needle biopsy with concordant imaging and when no other lesions requiring excision are present is no longer routine. Cases are often recommended for follow up with PE, mammography and often MRI. Because of the higher upgrade rate of pLCIS and biologic behavior similar to DCIS, guidelines for pLCIS and LCIS with discordant imaging is surgical excision with negative margins, without RT. In studies, chemoprevention with Tamoxifen or an aromatase inhibitor in patients with LCIS resulted in a significant reduction in 10 year cancer risk. Bilateral prophylactic mastectomy has been considered an option by some but current guidelines prefer risk reducing endocrine agents.

#### **TABLE OF CONTENTS/OUTLINE**

BackgroundComparison of Classic and Pleomorphic LCISHistologyImaging CharacteristicsManagementCases

## **BREE-87 Rare But Mighty Breast Cancers: What the Future Holds**

Participants

William Hiatt, MS, BS, (*Presenter*) Nothing to Disclose

#### **TEACHING POINTS**

1. Review the current World Health Organization classification system of epithelial breast cancers 2. Introduce the recent expansion in molecular understandings of breast cancer, emphasizing six rarer epithelial tumor subtypes 3. Highlight the recent proposal of a new schema that unifies histological-molecular breast tumor analyses 4. Understand how these findings impact our patients' care via knowledge of known tumor behavior 5. Provide radiologic profiles of two tumor subtypes, metaplastic carcinoma and micropapillary carcinoma

#### **TABLE OF CONTENTS/OUTLINE**

1. How are we currently classifying tumors? 1a. Histological analysis vs. molecular classification 2. How are we expanding our molecular understanding of rarer breast tumors? 2a. Proposal of a novel schema that blends tumor histology biomarker data into a more unified classification system 3. Newly expanded molecular profiles of several rarer tumor types that further explain tumor morphology behavior 4. Imaging and Overview Profile: Metaplastic Carcinoma 5. Imaging and Overview Profile: Micropapillary Carcinoma 6. Future directions in rare breast radiology 7. References

## **BREE-88 Paradigms for Papilloma Management**

Participants

Sherwin Chiu, MD,MPH, (*Presenter*) Nothing to Disclose

#### **TEACHING POINTS**

(1) Understand the clinical significance of intraductal papillomas.(2) Recognize the imaging findings associated with intraductal papillomas.(3) Review the current paradigm for management of intraductal papillomas.

## TABLE OF CONTENTS/OUTLINE

(1) Significance: (a) Classically presents as unilateral nipple discharge. (b) Nipple discharge or dilated ducts warrant further evaluation. (c) Intraductal papillomas with atypia or discordance should be excised, however asymptomatic papillomas without suspicious imaging or atypia may be appropriate for surveillance.(2) Imaging Findings: (a) On mammography, papillomas may present as ductal dilatation and occasionally as a circumscribed mass with associated calcifications. (b) Ultrasound findings typically show a vascularized circumscribed mass with associated ductal dilatation. (c) On MRI, papillomas appear as an enhancing intraductal mass with associated ductal dilatation.(3) Management: (a) Historically, treatment required excisional biopsy or lumpectomy to exclude atypia or underlying malignancy. (b) Ultrasound guided vacuum removal of papillomas has shown promise in removing lesions without the need for surgery. (c) Clinical follow-up with ultrasound is becoming more favored for small, solitary papillomas without atypia due to low rates of malignancy upgrading.

### **BREE-89 Imaging the Male Breast: Gynecomastia, Male Breast Cancer, and Beyond**

#### **Awards**

#### **Identified for RadioGraphics**

#### **Magna Cum Laude**

#### Participants

Heather Duke, MD, Chicago, IL (*Presenter*) Nothing to Disclose

#### **TEACHING POINTS**

1. Male breast complaints have increased in recent years, and it is therefore increasingly important for radiologists to be knowledgeable about imaging features of pathology that can occur in the male breast.2. Male breast pathology most commonly includes gynecomastia, and the chief differential consideration is male breast cancer. However, there are a number of other entities that can occur in the male breast of which radiologists should be aware, in order to perform adequate concordance of biopsy results with imaging findings.3. Male breast pathology can involve structures of the subcutaneous tissues, including skin, fat, muscle, blood vessels, lymphatics, and nerves. Alternatively, pathology can originate from ductal and stromal breast tissue in males, with lobular pathology being extremely rare given lack of progesterone-dependent lobular proliferation in males.

## TABLE OF CONTENTS/OUTLINE

1. Male Breast Development and Important Differences from the Female Breast2. Gynecomastia (most common pathology) versus Male Breast Cancer3. Less Common But Important Male Breast Pathology and Imaging Findingsa. Skin - sebaceous/epidermal inclusion cystsb. Fat - lipoma and fat necrosisc. Muscle/Fascia - Desmoid tumord. Blood vessels/vascular tumors - vascular malformations, hemangioma, angioliipomae. Nerves - schwannomas, granular cell tumorsf. Lymphatics - intramammary lymph nodeg. Ductal tissue - intraductal papillomah. Stromal tissue - PASH, myofibrosarcomai. Other - subareolar abscess, diabetic mastopathy

### **BREE-9 Breast Implant Associated Anaplastic Large Cell Lymphoma (BIA-ALCL): A Multimodality Imaging Review**

#### Participants

Kanchan Phalak, MD, (*Presenter*) Nothing to Disclose

#### **TEACHING POINTS**

1) Breast Implant Associated Anaplastic Large Cell Lymphoma (BIA-ALCL) manifests as a late-onset effusion or mass in patients with exposure to textured implants. 2) Breast ultrasonography is an appropriate test for initial evaluation of presenting clinical symptoms such as swelling and pain. 3) Cytologic or histologic analysis is important to distinguish BIA-ALCL from other pathologies. 4) Imaging modalities such as MRI, CT and PET can help characterize BIA-ALCL.

## TABLE OF CONTENTS/OUTLINE

1) Clinical Issuesa. Etiology and Pathophysiology b. Presentation c. Demographics d. Natural History and Prognosis e. Treatment 2) Pathology a. General Features b. Staging, Grading, and Classification 3) Imaging Findings a. General Features b. Mammogram c. Ultrasound d. MRI e. PET-CT f. CT g. Image-Guided Biopsy 4) Differential Diagnosis 5) Pictorial review of cases

### **BREE-90 The ABC of PABC (Pregnancy Associated Breast Cancer): Playing Hide and Seek with the Radiologist**

#### Participants

Martha Espitia Lopez, MD, Mexico, Mexico (*Presenter*) Nothing to Disclose

#### **TEACHING POINTS**

Know the definition of breast cancer associated with pregnancy. Know the physiological changes during pregnancy and lactation. Recognize normal and suspicious breast images in pregnancy and lactation.

## TABLE OF CONTENTS/OUTLINE

Breast cancer is one of the most common cancers in pregnant and non-pregnant women. Pregnancy is considered a risk factor for the development of breast cancer. Breast cancer is now the most common malignancy diagnosed during pregnancy, with an estimated incidence of 1 in 3000 pregnancies in the United States. Gestational or pregnancy-associated breast cancer is defined as breast cancer that is diagnosed during pregnancy, in the first year postpartum, or at any time during lactation, but is often a late finding due to expected physiological changes in breast cancer. Ultrasound is the imaging study of choice due to its high sensitivity and in the absence of radiation. The tumors found in these patients are usually high grade with high cell proliferation, as well as negative hormone receptors. Histologically, the most frequent type is infiltrating ductal carcinoma, found in up to 80% of cases. The treatment for these patients should not be extended beyond the first trimester, after the twelfth week of gestation it is possible to start chemotherapy during the second and third trimesters, likewise mastectomy can be performed during this period. Radiotherapy is contraindicated during pregnancy, it can be performed after birth. Endocrine treatment begins after delivery.

### **BREE-91 Interesting Axillary Pathology in Breast Imaging**

#### Participants

Joseph Hoang, MD, (*Presenter*) Nothing to Disclose

## TEACHING POINTS

Axillary masses and lesions are occasionally discovered during routine screening and diagnostic breast imaging. In many instances, the masses are found to be lymph nodes, however, other uncommon pathologic entities exist in the axilla that are often overlooked. - Review axillary mass work up and clinical presentation of patients with palpable abnormality- Discuss abnormal, benign lymph node pathologies- Review primary breast malignancy in the axilla- Elucidate on several etiologies of axillary masses outside of breast tissue origin- Present interesting cases of axillary masses within each category as delineated above

## TABLE OF CONTENTS/OUTLINE

- Review typical patient presentation, pertinent imaging modalities and workup - Discuss criteria for benign lymph node morphology- Present and discuss abnormal lymph nodes with benign pathology- Present cases of primary breast cancers in the axilla not involved by a lymph node- Discuss and review etiologies of masses in the axilla outside of breast origin include: Vascular/Lymphatic origin, Dermal and fatty, Neurogenic origin, Musculoskeletal origin- Present cases of differing etiologies as included above.

### BREE-92 The Dark Star of the Breast: A Confusing Lesion

Participants

Magaly Henriquez Urrea, MD, MSc, Mexico City, Mexico (*Presenter*) Nothing to Disclose

## TEACHING POINTS

A radial scar (RS) is a pathologic process that consists of a central fibroelastic core with distorted and entrapped ducts, and peripherally, with ducts and lobules distributed in a radiating appearance. In addition, the fibroelastic core is contracted, with a "pulled inward" appearance. A specific pathologic characteristic of an RS is the intact myoepithelial cell layer. This is an important feature to differentiate it from an invasive carcinoma. The most typical appearance on digital mammography (DM) and on digital breast tomosynthesis (DBT) of a RS is the architectural distortion, with thin and long radiating spicules against a background of radiolucent fat, creating a "dark star" appearance. The most common ultrasound finding is a hypoechoic, irregular mass with indistinct margins. Posterior acoustic shadowing can also be seen.

## TABLE OF CONTENTS/OUTLINE

Definition. Causes. Epidemiology and Clinical Presentation. Pathology. Imaging Findings. Mammography and tomosynthesis. Mammographic criteria. Ultrasound. Contrast-enhanced Mammography. Conclusion. References.

### BREE-93 Redefining Needle Targeting Error in the Prone and Upright Stereotactic Breast Biopsy: Recognition and Problem Solving

Participants

Janice Thai, MD, (*Presenter*) Nothing to Disclose

## TEACHING POINTS

1. The traditional approach for the teaching of stereotactic breast biopsy regarding needle targeting error hinges on established convention that is largely based on the 2D prone stereotactic biopsy system (retired model). Recent advances in technology introduced an updated prone and upright systems, for which the convention of needle targeting error do not apply. This exhibit highlights the differences between the old and new prone models, as well as the upright model, pertaining to needle targeting error.
2. To illustrate the X, Y, and Z axes used to determine needle targeting error and approaches to overcome targeting errors.

## TABLE OF CONTENTS/OUTLINE

- Review of the prone and upright stereotactic systems, regarding the X, Y, and Z axes and their directionality used in defining needle targeting error
- Review of how needle error targeting is defined in both the prone and upright systems, and solutions to overcome needle targeting errors
- Case review of real-life scenarios and problem solving

### BREE-94 Male Breast Lesions - That We Need to Know

Participants

Samira Nader, MD, Buenos Aires, Argentina (*Presenter*) Nothing to Disclose

## TEACHING POINTS

- Recognize the radiological characteristics of the lesion that help to identify it as benign or malignant according to the BIRADS classification.- Describe the entities that most frequently affect the male breast, especially cancer and gynecomastia as its main simulator.

## TABLE OF CONTENTS/OUTLINE

TABLE OF CONTENTS. Normal characteristics of the breast in men and their differences with respect to women. Types of most common lesions in the male breast. Generalities, incidence and risk factors of male breast cancer. Ultrasound and mammographic findings of male breast lesions; types of tumors found and their histopathological correlation. RESUME. Male breast cancer represents 1% of all breast cancers, and less than 1% of all cancers in men. Screening in men is not justified, which partly explains the later diagnosis. 90% of breast cancers in men express estrogen receptors and 80%, progesterone receptors. Biomarkers such as HER2 and Ki67 are taken as a reference to characterize breast tumors as in women. On mammography, a lobulated, irregular, high-density retroareolar mass with poorly defined or spiculated margins can be observed. Calcifications are present in 13-30% of cases, the pleomorphic type being rarer. Ultrasound may reveal a solid, hypoechoic, retroareolar mass with angled, spiculated or microlobulated margins, or a complex cystic mass. Taking a sample for histopathological study is generally performed under ultrasound guidance. Histologically, the vast majority are invasive ductal carcinoma (85-90%) or ductal carcinoma in situ.

### BREE-95 Case-based Review of Contrast-enhanced Mammograms: False Positives and False Negatives with Strategies to Improve Cancer Detection and Staging

Awards

Identified for RadioGraphics

Cum Laude

Participants  
Molly Carnahan, MD, Phoenix, AZ (*Presenter*) Nothing to Disclose

#### TEACHING POINTS

Similar to contrast-enhanced-MRI, false-positive (FP) CEM can occur with benign processes False-negative (FN) can occur in marked BPE, minimal lesional enhancement or lesions off the field-of-view Prompt repositioning should be performed to overcome FNs with positioning or medically located lesions Low-grade cancers may not enhance. Decision to pursue imaging guided biopsy should be based on the most suspicious imaging feature

#### TABLE OF CONTENTS/OUTLINE

CEM background Principles behind cancer detection New BIRADS lexicon Defining breast imaging modalities' diagnostic performance: true positive, true negative, FP and FN Understand causes of CEM FP and FN to improve these measures FP on CEM FP pathology (benign lesions) on CEM: case-based review How CEM FP compare to CE-MRI and MBI FN on CEM FN CEM (missed cancers): case-based review of errors Inadequate visualization of lesion or extent of disease Poor patient positioning Lesion off the FOV (ex. medial or posterior lesions) or abuts breast implants BPE obscuring lesion Lack of lesion enhancement No IV contrast on imaging (ex. missed bolus or contrast extravasation) Negative enhancement artifact obscuring cancer (ex. hematoma) Cancers with no enhancement Errors of characterization: lesions with seemingly benign features How CEM FN compare to CE-MRI and MBI Pearls for the reader Real time interpretations: prompt re-positioning if needed Suspicious calcifications, architectural distortion or masses should be biopsied regardless of CEM enhancement Technical limitations of CEM for posterior lesions and evaluating lymphadenopathy should be considered when staging new cancers

#### BREE-96 Interactive Case-Based Review of new Contrast-Enhanced Mammography BI-RADS Lexicon

Participants  
Lyndia Moravia, MD, (*Presenter*) Nothing to Disclose

#### TEACHING POINTS

Teaching Points: CEM BI-RADS has recently been published to guide CEM interpretation. Including both low-energy (LE) and recombined imaging (RC) findings in exam interpretation is critical. The standard mammography lexicon is used to describe the LE findings. A new lexicon was developed to describe RC findings that is similar to the breast MRI but with changes specific to CEM. Key differences include the absence of the term 'focus', the addition of the term 'enhancing asymmetry', removal of the mass internal enhancement characteristic of dark internal septations, and removal of the non-mass enhancement internal enhancement pattern of clustered ring. In addition, when LE findings are seen with enhancement, internal enhancement pattern, lesion conspicuity compared to background parenchymal enhancement, and extent of enhancement relative to LE finding should be described.

#### TABLE OF CONTENTS/OUTLINE

1. Review the main elements of the new CEM BI-RADS. 2. Summarize the differences between MRI lexicon and CEM recombined imaging lexicon. 3. Emphasize the key points of the new CEM BI-RADS through an interactive case-based review.

#### BREE-97 How to Navigate Breast Tumor Board: A Resident and Fellow Primer

Participants  
Atharva Thakore, MD, (*Presenter*) Nothing to Disclose

#### TEACHING POINTS

1. Review the role of the radiologist in multidisciplinary breast tumor board. 2. Understand the oncologic and surgical management of breast cancer in the context of pretreatment imaging. 3. Identify imaging features important to clinical decision making.

#### TABLE OF CONTENTS/OUTLINE

Introduction? Getting to know the Interdisciplinary Team and their Role? Accreditation Standards and Quality Metrics? Breast Cancer Staging; Imaging vs Clinical? Imaging Presentation for Tumor Board? Elements to Include; Key Images--Tumor Size and Location; How to Take Measurements--Imaging Lymph Node Status Tumor Board Terminology and Concepts by Subspecialty? Medical Oncology--Tumor Markers/Receptors--Tumor Biology/Genetics--Indications for Neoadjuvant Chemotherapy--Reporting Response to Neoadjuvant Chemotherapy--Indications for Adjuvant Chemotherapy? Surgical Oncology--Surgical Axillary Management--SLNB vs ALND--Breast Conservation Surgery vs Mastectomy--Breast Conservation Surgery--Mastectomy/Nipple Sparing Mastectomy? Radiation Oncology--Whole Breast Radiation Therapy and Boost--Accelerated Partial Breast Irradiation--Chest Wall Irradiation--Regional Nodal Irradiation Recommendations? Preoperative Localization--Wire Localization--Virtual Navigation Clips--Bracketing? Further Evaluation--Second Look Ultrasound--MRI Biopsy--Axillary Biopsy Conclusions: 1. Understanding the principles of breast cancer oncologic management is valuable for the radiology trainee. 2. Clinically relevant imaging features should be highlighted and presented in multidisciplinary tumor board. 3. Make recommendations appropriate to a patient's specific tumor biology and treatment plan

#### BREE-98 All Roads Lead to Rome: Multi-modality Imaging of Benign and Malignant Pathologies of the Nipple Areolar Complex

##### Awards

Identified for RadioGraphics  
Certificate of Merit

Participants  
Mary Guirguis, MD, Houston, TX (*Presenter*) Nothing to Disclose

#### TEACHING POINTS

- \*The normal imaging appearance of the nipple and the nipple areolar complex can be variable.
- \*Understanding the normal spectrum of imaging appearance across different breast imaging modalities is essential for the radiologist.
- \*Meticulously assessing the nipple areolar complex across different modalities while understanding its spectrum of imaging appearance allows for accurate identification of pathology in this region.
- \*Different benign and malignant pathological entities can be seen within the nipple and nipple areolar complex.
- \*Correlation with the patient's symptoms is key to understanding the imaging findings and clinical

management.

#### **TABLE OF CONTENTS/OUTLINE**

This educational exhibit will present a practical guide on how to approach the nipple areolar complex across different imaging modalities. Through a multi-modality case-based approach, we will present the spectrum of the normal appearance of the nipple and the nipple areolar complex. Imaging of benign and malignant pathologies that affect the nipple and nipple areolar complex will be presented across the different breast imaging and cross-sectional modalities. Tips, pitfalls, and practical approaches will be highlighted through a case-based multi-modality approach.

#### **BREE-99 Multimodality Imaging of Postmastectomy Breast Reconstruction Techniques and Complications**

##### **Awards**

**Identified for RadioGraphics**

**Certificate of Merit**

Participants

Faezeh Sodagari, MD, (*Presenter*) Nothing to Disclose

#### **TEACHING POINTS**

Breast reconstruction is commonly performed to restore chest symmetry in women undergoing mastectomy as part of breast cancer treatment or prophylaxis. Various reconstruction techniques are currently available including implant-based reconstruction or microvascular autologous reconstruction using pedicled or free flap techniques. The goal of this exhibit is to review surgical techniques used in postmastectomy reconstruction, imaging appearance of postoperative changes and complications, and imaging guidelines for the evaluation of the reconstructed breast.

#### **TABLE OF CONTENTS/OUTLINE**

1) Introduction: a) Surgical techniques used in breast reconstruction methods, including implant placement, pedicled flaps, free flaps and preoperative planning; b) Indications, contraindications, advantages, and disadvantages of different postmastectomy breast reconstruction techniques; c) Techniques for the reconstruction of the nipple-areolar complex 2) Normal postsurgical findings and their evolution in time such as edema and soft tissue emphysema 3) Imaging findings of early and late complications such as hemorrhage, infection, flap ischemia, fat necrosis, implant rupture 4) Implications of reconstruction method for radiation treatment planning 5) Multimodality evaluation of reconstructed breast for new or recurrent cancer including guidelines and controversies of MRI surveillance of reconstructed breast 6) Clinical outcomes and summary

Printed on: 02/07/23



## Abstract Archives of the RSNA, 2022

BREE-1

### Imaging and Management of High-Risk Breast Lesions: An Update of Current Evidence

Sunday, Nov. 27 8:00AM - 9:00AM Room: Learning Center - BR

#### Awards

Cum Laude

#### Participants

Richard E. Sharpe JR, MD, MBA, Scottsdale, AZ (*Presenter*) Nothing to Disclose

#### TEACHING POINTS

High-risk breast lesions (HRL) are a group of specific heterogeneous lesions that can be associated with a synchronous or adjacent breast cancer and that confer an increased lifetime risk of breast cancer. Providing high quality care for patients with HRLs requires careful correlation of specific patient history and imaging characteristics with histopathologic or cytopathologic results for concordance by the physician performing the biopsy. High-risk and malignant diagnoses should routinely prompt multidisciplinary discussion to determine optimal management. Excise specific HRLs because of the risk of upgrading the diagnosis to ductal carcinoma in situ or invasive cancer. Excise ALL HRL lesions demonstrating radiology pathology discordance. For patients with >1 HRL diagnosis after core needle biopsy, management should be based on the HRL with the highest risk of upgrade.

#### TABLE OF CONTENTS/OUTLINE

Overview of image guided biopsy process. Explanation of types of high-risk breast lesions, imaging and pathological findings, and associated risks of upgrade to malignancy for each, including: atypical ductal hyperplasia, flat epithelial atypia, lobular hyperplasia (ALH, LCIS), papillary lesions, radial scars/complex sclerosing lesions, fibroepithelial lesions, and phyllodes. Update of the current evidence regarding imaging and pathological correlation and management of each lesion type. Presentation of high yield point of care summary practice resources to support efficient management of patients with high-risk lesions.

Printed on: 02/07/23



## Abstract Archives of the RSNA, 2022

BREE-10

### Breast Malignancy Subtypes with Hybrid Use of Accelerated and Abbreviated Breast MRI in Screening Higher-Than-Average Risk Patients

Sunday, Nov. 27 8:00AM - 9:00AM Room: Learning Center - BR

#### Participants

Ashley Huppe, MD, Kansas City, KS (*Presenter*) Nothing to Disclose

#### TEACHING POINTS

Breast cancer screening guidelines for higher-than-average risk patients are expanding. Therefore, a supplemental screening exam is needed that is both cost-effective and accurate for detection of malignancy. The widespread use of full protocol screening MRI has limitations, and novel techniques have been developed to address these drawbacks. While abbreviated MRI addresses the cost, patient discomfort and time constraints of full-protocol exams, accelerated techniques can improve specificity of abbreviated MRI by providing a temporal analysis of contrast enhancement. Given their recent emergence, many are unfamiliar with the distinctions between these techniques and associated imaging appearance of various malignancy subtypes. After this presentation, participants will be able to:-Review breast cancer screening guidelines for higher-than-average risk patients-Understand the differences between acquisition of accelerated and abbreviated MRI-Describe the applications and benefits of accelerated and abbreviated MRI-Appreciate appearance of malignancy subtypes on accelerated and abbreviated MRI

#### TABLE OF CONTENTS/OUTLINE

1) Introductiona) Summarize current guidelines for breast cancer screening in higher-than-average risk patientsb) Discuss benefits and limitations of full protocol screening MRIC) Review accelerated and abbreviated MRIi) Define terminologyii) Discuss differences, clinical applications and benefits2) Case-based review of appearance of malignancy subtypes on accelerated and abbreviated MRI used in the screening settinga) Ductal carcinoma in-situb) Invasive ductal carcinomac) Invasive lobular carcinomad) Multifocal disease3) Conclusion

Printed on: 02/07/23



## Abstract Archives of the RSNA, 2022

BREE-100

### The Various Faces of a Fibroadenoma

Sunday, Nov. 27 8:00AM - 9:00AM Room: Learning Center - BR

#### Participants

Natalia Orthmann, MD, Sao Paulo, Brazil (*Presenter*) Nothing to Disclose

#### TEACHING POINTS

The purpose of this exhibit is: 1. To emphasize the importance of fibroadenoma findings in the different methods, as it is a common finding of benign breast lesions. 2. To show the epidemiology, histological origin, imaging, anatomopathological correlation when possible, association with medication use, and differential diagnoses of the fibroadenoma. 3. To present fibroepithelial tumors, with emphasis on fibroadenoma and its types. 4. To review imaging findings of breast lesions suggestive of fibroadenomas. 5. To illustrate the different imaging methods to assess the fibroadenoma, such as Ultrasound (US), Mammography (MG), tomosynthesis (TS) and Magnetic Resonance (MR)

#### TABLE OF CONTENTS/OUTLINE

1. Literature review focusing on fibroadenoma and its differential diagnoses. 2. To illustrate and discuss the pathology of fibroadenoma, highlighting epidemiology; subtypes; progression in different imaging methods. 3. Review of the pathological development of fibroadenomas and its differential diagnoses through illustrative cases. 4. Example cases with mammographic, ultrasonographic and pathologic correlation when available. 5. Summary and conclusion.

Printed on: 02/07/23



## Abstract Archives of the RSNA, 2022

BREE-101

### Breast and Beyond! Breast Manifestations of Systemic Diseases

Sunday, Nov. 27 8:00AM - 9:00AM Room: Learning Center - BR

#### Participants

Ayla Yamamoto Mota, MD, Sao Paulo, Brazil (*Presenter*) Nothing to Disclose

#### TEACHING POINTS

-To describe breast manifestations of ordinary and rare systemic diseases in different modalities (ultrasound, mammography and MR)- To demonstrate the importance to know patient 's comorbidity and background

#### TABLE OF CONTENTS/OUTLINE

-Introduction - Ultrasound, mammography and MR images: clinical cases of breast manifestations of systemic diseases- Conclusion

Printed on: 02/07/23

## Abstract Archives of the RSNA, 2022

BREE-102

### A-Z of Triple Negative Breast Cancer

Sunday, Nov. 27 8:00AM - 9:00AM Room: Learning Center - BR

#### Participants

Tatiana Tucunduva, MD, (*Presenter*) Nothing to Disclose

#### TEACHING POINTS

-Define Triple negative breast cancer (TNBC)-Review the histopathological aspects -Review the molecular aspects -Review the spectrum of findings (mammography, US and MRI) -Pitfalls -Worse prognostic factors -News in treatment

#### TABLE OF CONTENTS/OUTLINE

1. TNBC definition 2. Histological and molecular aspects of TNBC 3. the spectrum of findings:On mammography, the mass more often appears irregular in shape and spiculated margins and may even contain benign aspects. Most show no calcification and are rarely associated with DCIS, as rapid carcinogenesis bypasses this stage.On ultrasound, TNBC often appears as a hypoechoic mass with uncircumscribed margins.Magnetic resonance imaging (MRI) is the most sensitive method to evaluate TNBC and shows some typical features such as annular enhancement and an intralesional T2 hyperintense signal, factors suggestive of malignancy.4. PiffallsBecause some lesions do not show desmoplastic reactions due to the aggressiveness of most triple-negative breast cancers, some radiologic features may resemble benign (cysts) or probably benign (B3) lesions.5. Worse prognostic factor.Compared with other breast cancer subtypes, TNBC has a worse prognosis because it is highly invasive. About 45% have distant metastases and the mortality rate is about 40% within the first 5 years.6. News in treatmentDue to its molecular subtype, TNBC does not respond to the usual specific hormonal therapies. Therefore, even for smaller lesions, chemotherapy is the main systemic treatment.However, different subgroups within TNBC share some molecular features that allow targeted, individualized therapeutic intervention.

Printed on: 02/07/23



## Abstract Archives of the RSNA, 2022

BREE-103

### One View, What To Do? A Review of the Imaging Appearance and Management of the Breast Asymmetry

Sunday, Nov. 27 8:00AM - 9:00AM Room: Learning Center - BR

#### Participants

Cara Connolly, MD, Nashville, TN (*Presenter*) Nothing to Disclose

#### TEACHING POINTS

The breast asymmetry seen in one mammographic view has long been the subject of diagnostic dilemmas for mammographers. Retrospective reviews have reported up to one third of breast cancers may have been seen as asymmetries. However, most screening callbacks for asymmetries are attributed to summation artifact, the overlapping of normal breast tissue. With incorporation of tomosynthesis, the recall rate for asymmetries has decreased but continues to present screening and diagnostic challenges. This exhibit will incorporate examples of asymmetries on both standard 2D imaging and tomosynthesis with both benign and malignant results, as well as review the diagnostic algorithm for management.

#### TABLE OF CONTENTS/OUTLINE

Benign cases of asymmetries will include summation artifact, PASH, fibrocystic change, fat necrosis, fibroadenomatoid change and abscess. Biopsy-proven malignancies will be highlighted, including invasive ductal carcinoma, invasive lobular carcinoma, ductal carcinoma in situ, lymphoma, and angiosarcoma.

Printed on: 02/07/23



## Abstract Archives of the RSNA, 2022

BREE-104

### The Myriad of High Risk Breast Lesions: Review of Radiographic and Histologic Features and their Challenging Management

Sunday, Nov. 27 8:00AM - 9:00AM Room: Learning Center - BR

#### Awards

**Certificate of Merit**

#### Participants

Saba Naamo, MD, Danville, PA (*Presenter*) Nothing to Disclose

#### TEACHING POINTS

High risk lesions (HRLs) are pathologically diverse lesions with an uncertain malignant potential that attribute an elevated lifetime risk for breast cancer. With a wide spectrum of clinical and radiological features, core needle biopsy is required to diagnose HRLs and tailor their management. We review the clinical, radiographic and histologic features of each of the HRLs and their potential for malignant transformation. We will also dive into the controversy and complexity of the current management as well as recent literature to delineate a guide for appropriate clinical management and the fine balance of risk/benefit. Teaching points: Recognize the clinical presentation, multimodality imaging findings and histologic manifestation of the HRLs Describe radiographic features of HRLs that are commonly associated with malignancy Management and guidelines based on current evidence Imaging surveillance for patients with HRLs

#### TABLE OF CONTENTS/OUTLINE

Table of contents: ? Introduction and overview of HRLs ? Describe individual HRLs including: ? Definition ? Common clinical and radiological multimodality presentation ? Radiographic/Histologic concordance ? Spectrum of current management and guidelines ? Surveillance of non-surgically/surgically excised lesions

Printed on: 02/07/23

## Abstract Archives of the RSNA, 2022

BREE-105

### Implementation of Synthetic Mammography: Benefits, Drawbacks, and Pitfalls

Sunday, Nov. 27 8:00AM - 9:00AM Room: Learning Center - BR

#### Awards

Identified for RadioGraphics  
Certificate of Merit

#### Participants

Sona Chikarmane, MD, Newtonville, MA (*Presenter*) Nothing to Disclose

#### TEACHING POINTS

- Synthetic mammography (SM) is a 2D reconstruction from digital breast tomosynthesis (DBT) developed to replace full-field digital mammography (DM) obtained after the DBT acquisition.
- SM reduces radiation dose and shortens acquisition time for screening mammography.
- Studies have shown that DBT+SM significantly reduced recall rates and had equal cancer detection rates compared to DBT+DM.
- SM increases conspicuity of calcifications and architectural distortion; SM has demonstrated decreased conspicuity of asymmetries, with no change in detection of masses.
- SM may lead to artifacts such as "pseudo-calcifications", blurring of skin edge, artifact from metallic foreign bodies, and may underestimate breast density.
- Despite widespread availability, breast radiologists are slow to adopt SM due to concern about artifacts and dislike of contrast/appearance of findings on SM compared to DM.

#### TABLE OF CONTENTS/OUTLINE

1. Introduction to SM: definition, reason for development, and hesitation over utilization
2. Screening performance metrics: recall rates, cancer detection rates, positive predictive value
3. Findings on mammography: conspicuity of calcifications, masses, asymmetries and architectural distortion in DBT+SM vs. DBT+DM
4. Breast density assessment on SM and DM and discussion of clinical implications
5. Review of artifacts on SM
6. Remaining challenges of implementation and potential to improve performance through artificial intelligence

Printed on: 02/07/23

## Abstract Archives of the RSNA, 2022

BREE-106

### The Male Breast - A Review of Clinical, Imaging Findings and Diagnostic Work-up

Sunday, Nov. 27 8:00AM - 9:00AM Room: Learning Center - BR

#### Participants

Josefa Galobardes Monge, MD, Parla, Spain (*Presenter*) Nothing to Disclose

#### TEACHING POINTS

To review clinical presentation, imaging features and pathologic findings in male breast pathology. • To illustrate imaging findings (mammogram, contrast enhanced mammography, US, CT) of cases from our series of breast lesions in males with pathologic correlation. • To analyze and discuss the specific management of breast lesions in men including imaging and interventional procedures. • To emphasize pitfalls, diagnostic difficulties and differential diagnosis.

#### TABLE OF CONTENTS/OUTLINE

We present: Clinical signs and symptoms. Techniques in evaluation of male breasts. Mammograms, contrast enhanced mammography, US, MR, CT. Differential diagnosis. Imaging appearances (spiculated mass, circumscribed mass, microcalcifications). Diagnostic work-up and recommendations for management. Specific considerations in male patients different from women. Different entities illustrated include. Benign: gynecomastia (diffuse, nodular and dendritic), epidermal inclusion cyst, lipoma, hematoma, foreign body granuloma, papilloma, fibromatosis; Malignant: ductal carcinoma in situ (DCIS), invasive ductal carcinomas uni and bilateral, metastasis to the breast (lung cancer), lymphoma

Printed on: 02/07/23



## Abstract Archives of the RSNA, 2022

BREE-107

### High-risk Lesions Breast: A Diagnostic Dilemma for the Radiologist and Pathologist

Sunday, Nov. 27 8:00AM - 9:00AM Room: Learning Center - BR

#### Participants

Jacobo Emmanuel Garcia, MD, (*Presenter*) Nothing to Disclose

#### TEACHING POINTS

To expose the relative risk associated with breast cancer in women biopsied with ultrasound or stereotaxic guidance with results of proliferative lesions. Know the high-risk lesions according to the Ellis classification. Identify the main radiological characteristics of high-risk lesions in mammography and ultrasound. Exhibit the pathological characteristics to identify proliferative lesions. Suggest adequate and individualized management in response to the pathology of high-risk lesions of the breast.

#### TABLE OF CONTENTS/OUTLINE

1. Definition of high-risk lesions of the breast. 1.1. Ellis classification of lesions B3. 1.2. Epidemiology and associated risk of proliferative lesions of the breast. 1.3. Radiological findings of high-risk lesions of the breast. 2. Breast intervention techniques. 2.1. Image-guided interventional techniques for obtaining samples of suspicious lesions. 2.2. Pathological features that facilitate differentiation. 2.3. The handling of the surgeon and the radiologist before the result of the pathologist, in B3 lesions. n lesions B3.

Printed on: 02/07/23



## Abstract Archives of the RSNA, 2022

BREE-108

### Implementing AI CAD for Mammography - Learnings After Having Screened 55,000 Women

Sunday, Nov. 27 8:00AM - 9:00AM Room: Learning Center - BR

#### Participants

Karin Dembrower, MD, PhD, Stockholm, Sweden (*Presenter*) Nothing to Disclose

#### TEACHING POINTS

How to prepare radiologists and AI for implementation in mammography screening  
What to expect as a radiologist when starting to use AI  
What are the results of combined radiologist and AI CAD mammography reading  
Case review highlighting important teaching points

#### TABLE OF CONTENTS/OUTLINE

AI CAD in practice  
Preparing radiologists and AI for implementation  
Radiologist impressions, change over time  
Preliminary results of our study with AI as third reader  
Review of cases with important teaching points

Printed on: 02/07/23



## Abstract Archives of the RSNA, 2022

BREE-109

### Breast Cancer Disparities that Affect Black Women

Sunday, Nov. 27 8:00AM - 9:00AM Room: Learning Center - BR

#### Participants

Hillary Bui, DO, (Presenter) Nothing to Disclose

#### TEACHING POINTS

Become familiar with breast cancer disparities that affect Black women  
Become familiar with screening guidelines' impact on Black women  
Understand the importance of risk assessment by age 30  
Learn about social determinants of health

#### TABLE OF CONTENTS/OUTLINE

Case-based and interactive exhibit with answers and explanations appearing on mouse clicks.  
Case #1: Barriers to accessing care  
Social Determinants of Health  
Economic factors (e.g., income, insurance, childcare, transportation)  
Education level, literacy  
Language  
Medical mistrust  
Case #2: Black woman at average risk diagnosed with Stage II breast cancer (BC) at 44  
Black women more likely to be diagnosed with BC <50 versus Non-Hispanic White Women (NHW)  
Black women more likely to be diagnosed with triple-negative BC  
Black women more likely to be diagnosed at later stages of BC  
Black women have higher mortality associated with BC  
Importance of risk assessment by the age of 30, particularly in Black women  
Screening guidelines for average-risk women  
Case #3: Black woman at elevated risk diagnosed with multicentric DCIS at 31  
Black women more likely to be diagnosed with BC <35 versus NHW  
When to refer women for genetic counseling  
Black women less likely to undergo genetic testing  
Screening guidelines for high-risk women  
Conclusions  
Initiating screening mammography after age 40 disproportionately impacts Black women  
Omitting risk assessment by age 30 disproportionately impacts Black women  
Breast radiologists should be aware of disparities in BC to provide optimal care

Printed on: 02/07/23



## Abstract Archives of the RSNA, 2022

BREE-11

### Community Outreach in Breast Imaging: What Radiologists Can Do to Close the Gap for the Underserved and Uninsured Population

Sunday, Nov. 27 8:00AM - 9:00AM Room: Learning Center - BR

#### Awards

Identified for RadioGraphics

#### Participants

Angel Su, MD, CYPRESS, TX (*Presenter*) Nothing to Disclose

#### TEACHING POINTS

After the Affordable Care Act was implemented, the uninsured population in the United States of America decreased significantly. However, since 2017, a steady increase has been noticed, reaching up to 28.9 million in 2019. Unfortunately, the largest increases continue to affect minorities disproportionately and the COVID-19 pandemic, which resulted in lockdowns that delayed screening mammograms, further highlighted these disparities. Radiologists, and more specifically, breast imagers, must recognize this situation as this population is disproportionately diagnosed at later stages, has a higher mortality rate, less continuity of care, and overall lower survival. The purpose of this abstract is to familiarize the radiologist with the uninsured and underserved population and how these patients are affected by breast cancer, demonstrate current statistics, and propose strategies that breast imagers can pursue individually or as a group to close the disproportional gap for the underserved.

#### TABLE OF CONTENTS/OUTLINE

1.Introduction. 2. Who are these patients: Analyzing the data. 3. Breast cancer in the uninsured and underserved population: approach, navigating the options and obstacles, disparities 4. What else can the breast imager do? A) Radiologist-Patient interaction B) Radiologist-Referring physician interaction C) Radiologist-Community interaction D) Radiologist and the Media E) Radiologist and Legislature. 5. Conclusion

Printed on: 02/07/23



## Abstract Archives of the RSNA, 2022

BREE-110

### AI for Mammography: What Radiologists Need to Know

Sunday, Nov. 27 8:00AM - 9:00AM Room: Learning Center - BR

#### Participants

Sieun Lee, MD, Yongin, Korea, Republic Of (*Presenter*) Nothing to Disclose

#### TEACHING POINTS

Teaching points - AI-CAD can improve the diagnostic performance of radiologists, and help close the learning gap for inexperienced readers.- Stand-alone AI-CAD has shown variable performance in previous studies, suggesting a cautious approach is needed to implement its use for triaging or workload reduction.- Future AI will predict the possibility of cancers beyond the current diagnosis of present abnormalities in combination with the clinical model, which will allow more stratified and personalized screening to take place.

#### TABLE OF CONTENTS/OUTLINE

Improving the accuracy of breast cancer diagnosis - How AI-CAD differs from conventional CAD in terms of false-positive results- Retrospective, but large-scale evidence for AI-CAD - Cancers missed by AI-CAD Improving efficiency for radiologists - Triaging screening mammography - Recommendations for the best use of AI-CAD Personalized predictions of cancer risk- Better way to estimate breast density- New model that includes additional clinical risk factors- Suggestions for personalized screening

Printed on: 02/07/23



## Abstract Archives of the RSNA, 2022

BREE-112

### Looking Through BI-RADS Terminology for Contrast-Enhanced Mammography - An Updated Guide to Understand CEM Supplement

Sunday, Nov. 27 8:00AM - 9:00AM Room: Learning Center - BR

#### Awards

Certificate of Merit

#### Participants

Diana Galvis Zambrano, BSc, MD, Mexico City, Mexico (*Presenter*) Nothing to Disclose

#### TEACHING POINTS

1. To describe Contrast-enhanced mammography (CEM) technique and image acquisition. 2. To outline contrast enhanced mammography - breast imaging lexicon - from ACR BI-RADS supplement. 3. To illustrate different imaging findings, the correlation with other imaging techniques and the appropriate form to report based in the new CEM BI-RADS supplement. 4. To review and compare the advantages and drawbacks of each image model. 5. To understand how and what should be in the report of a CEM study.

#### TABLE OF CONTENTS/OUTLINE

1. Background and history of CEM. 2. Description of protocol and imaging acquisition in contrast-enhanced mammography and associated technical details. 3. Review the CEM breast imaging lexicon from BI-RADS supplement. 4. Case-based CEM BI-RADS lexicon supplement interpretation in multiple scenarios and pathologies. 5. Correlation of radiological findings between CEM and other techniques. 6. Discuss actual indications, limitations and the future of CEM. 7. Take home points

Printed on: 02/07/23



## Abstract Archives of the RSNA, 2022

BREE-113

### To Freeze Or Not To Freeze? That Is The Question: Cryoablation For The Treatment Of Breast Cancer

Sunday, Nov. 27 8:00AM - 9:00AM Room: Learning Center - BR

#### Participants

Kenneth Tomkovich, MD, Freehold, NJ (*Presenter*) Consultant, IceCure Medical, Inc; Speakers Bureau, IceCure Medical, Inc

#### TEACHING POINTS

The purpose of this exhibit is: 1. Discuss the historical perspective of breast cancer treatment from radical mastectomy in the late 1800's to current practice. 2. To discuss the use of image guided cryoablation in the treatment of cancer in organs other than the breast. 3. To demonstrate the optimal technique to perform successful ultrasound guided cryoablation of primary breast cancer. 4. To illustrate important "new normal" imaging findings commonly seen following breast cancer cryoablation. 5. Review recent publications and abstracts on the topic of breast cancer cryoablation as an alternative to surgical lumpectomy.

#### TABLE OF CONTENTS/OUTLINE

History of surgical treatment for breast cancer. Cryoablation therapy application in organs other than the breast. Technique of ultrasound guided breast cancer cryoablation. Present the imaging findings post breast cancer cryoablation: Mammography, Ultrasound, MRI. Future implications based on a review of recent publications and abstracts.

Printed on: 02/07/23



## Abstract Archives of the RSNA, 2022

BREE-114

### **The Horizontal Approach for Tomosynthesis and Stereotactic Guided Breast Biopsy: Review of Technique and Advantages**

Sunday, Nov. 27 8:00AM - 9:00AM Room: Learning Center - BR

#### **Participants**

Janice Thai, MD, (*Presenter*) Nothing to Disclose

#### **TEACHING POINTS**

1. To expand the proceduralist's armamentarium by introducing a different approach to performing stereotactic breast biopsy. 2. To demonstrate the horizontal approach technique, and highlight the technical advantages inherent to a needle trajectory that is parallel to the image detector. 3. To inform the appropriate use of the horizontal approach in technically challenging anatomy/lesion location, including thin breast, superficial/retroareolar lesion, and posterior chest wall/inferior lesion.

#### **TABLE OF CONTENTS/OUTLINE**

- Review of patient positioning, targeting approach, procedural technique, and device set up based on the two most popular commercially available systems
- Review of the advantages of the horizontal approach over the vertical approach, with real life case examples
- Review of needle targeting error and problem solving for optimal efficiency
- Review of tips and tricks to maximize technical success and patient comfort

Printed on: 02/07/23



## Abstract Archives of the RSNA, 2022

BREE-115

### Breast Radiofrequency Identification Marker Localization: Technique, Tips, and Troubleshooting

Sunday, Nov. 27 8:00AM - 9:00AM Room: Learning Center - BR

#### Participants

Jared Vearrier, MD, (*Presenter*) Nothing to Disclose

#### TEACHING POINTS

1. Understand technology behind radiofrequency identification (RFID) markers  
2. Pros/cons of using RFID markers compared to other localization methods  
3. Understand optimal technique for US and Stereotactic marker placement  
4. Learn tips and suggestions for troubleshooting challenging cases

#### TABLE OF CONTENTS/OUTLINE

Introduction-Utilization of wireless localization-Technology  
US guided RFID Placement-Pros/Cons-Technique of US guided placement-  
Challenges and tip/tricks for RFID placement in a case base format  
\*\*Larger biopsy makers can obstruct the deployment path of the RFID marker and result in posterior migration  
\*\*Forward migration of the RFID marker along the biopsy track of large gauge biopsy needles  
Stereotactic/Tomosynthesis-Pros/Cons-Technique of Stereotactic placement  
\*\*Two view stereotactic technique can be employed or a single view tomosynthesis guided technique.  
\*\*Challenges:  
\*\*Unrecognized motion during placement  
\*\*Marker migration: 1) Accordion effect; 2) Migration along the biopsy track; 3) Floating in hematoma/displacement by a hematoma; 4) Resorption of air at the biopsy cavity/Changes to biopsy marker site after neoadjuvant chemotherapy; 5) RFID Marker displacement by biopsy marker  
\*\*Difficulty seeing target on Tomosynthesis slice after applicator placement  
Post-Procedure Imaging-Utilization of post-procedure imaging  
Conclusion-Breast RFID markers have various frequencies to aid in surgical excision and is a great alternative to other wireless localization devices-Awareness of the challenges that a radiologist can encounter during placement is important to avoid migration and misplacement during deployment

Printed on: 02/07/23

## Abstract Archives of the RSNA, 2022

BREE-116HC

### Imaging Features Following Breast Explant Surgery: A Pictorial Essay

Sunday, Nov. 27 8:00AM - 9:00AM Room: Learning Center - BR

#### Participants

Yusuf Akpolat, MD, Houston, TX (*Presenter*) Nothing to Disclose

#### TEACHING POINTS

1. Breast implants can be removed with breast explantation surgery (BES) for various reasons, including patient dissatisfaction, capsular contracture, implant infection or rupture, breast implant-associated anaplastic large cell lymphoma, and a recently emerging phenomenon called breast implant illness. 2. BES techniques include capsulotomy, partial, total, or en bloc capsulectomy. Adjunctive aesthetic or reconstructive procedures after BES include fat grafting, mastopexy, augmentation, and reconstruction with flaps. 3. The majority of the post-BES breast imaging findings are related to the surgical scar/bed, thus, confirming the type of explantation surgery is important. 4. Imaging findings after BES include focal and global asymmetries, architectural distortions, calcifications, calcified and non-calcified fat necrosis, masses, hematomas, seromas, capsular calcifications, and silicone granulomas. 5. Most importantly, since these patients have residual breast tissue, paying attention to suspicious imaging features is necessary.

#### TABLE OF CONTENTS/OUTLINE

1. Breast Explant Surgery Techniques  
2. Findings  
a. Global Asymmetry  
b. Architectural Distortion  
c. Calcifications/Fat Necrosis  
d. Asymmetries and Masses Anterior to the Pectoralis Major Muscle  
e. Implant Capsule/Calcifications  
f. Silicone Granulomas/Free Silicone  
g. Suspicious Findings  
Please visit the Learning Center to also view this presentation in hardcopy format.

Printed on: 02/07/23



## Abstract Archives of the RSNA, 2022

BREE-117

### Pregnancy-associated Breast Cancer: The Perfect Storm

Sunday, Nov. 27 8:00AM - 9:00AM Room: Learning Center - BR

#### Participants

Julia Colombo, MD, Buenos Aires, Argentina (*Presenter*) Nothing to Disclose

#### TEACHING POINTS

- There is clinical and imaging difficulty in making an accurate diagnosis of breast cancer due to typical changes occurring during pregnancy and lactation.
- The vast majority of mammary alterations in pregnancy correspond to benign pathology.
- The differential imaging diagnosis is complex due to the similar appearance in many cases to benign pathology.
- Any palpable area that remains for more than 2 weeks during pregnancy should be investigated.
- Ultrasound is the first choice in the evaluation of masses.
- Mammography is essential for its complementary contribution.
- MRI during pregnancy should be used if the benefits outweigh the risks and the information cannot be obtained by any other method.
- Core needle biopsy is of choice for final diagnosis.
- Pregnancy-associated breast cancer tends to have a worse prognosis due to delayed diagnosis.
- The incidence is increasing in developed countries due to the postponement of motherhood.

#### TABLE OF CONTENTS/OUTLINE

- Definition of pregnancy-associated breast cancer (PABC)
- Some peculiarities of pregnancy-associated breast cancer.
- Imaging methods for the diagnosis of breast cancer during pregnancy and lactation. Safety and effectiveness.
- Some cases of our daily practice.
- Conclusion.

Printed on: 02/07/23



## Abstract Archives of the RSNA, 2022

BREE-118HC

### Fast-Growing Fibroepithelial Breast Tumors: Tips for Proper Radio-Pathologic Correlation

Sunday, Nov. 27 8:00AM - 9:00AM Room: Learning Center - BR

#### Participants

Amanda Tavares, MD, Sao Paulo, Brazil (*Presenter*) Nothing to Disclose

#### TEACHING POINTS

Fibroepithelial neoplasms are the most common breast tumors in clinical practice, especially in younger women. Despite most of these lesions are benign, they can present significant growth. Due to the overlapping histopathologic features, the differential diagnosis between Fibroadenoma (FA) and Phyllodes Tumor (PT) may be difficult on core-needle biopsies and radiopathologic correlation may contribute to the management of those lesions. FA are the most common lesions and usually have slow growth pattern; however, they can increase due to hormonal changes, especially during pregnancy and lactation. FA variants (eg. complex, giant and juvenile FA) may also present as fast-growing tumors. At imaging, FA usually present as oval and circumscribed masses, with high-signal on T2-weighted images, homogeneous enhancement or dark internal septations, and persistent kinetics on magnetic resonance imaging (MRI). PT usually present as fast-growing tumors and may be benign, borderline or malignant. They usually have image characteristics similar to those of FA, but may show cysts or necrosis related to the tumor's rapid growth. There is higher risk of malignancy if the tumor presents non-circumscribed margins, irregular cystic walls, peritumoral edema, low signal on T2 sequences and low apparent diffusion coefficient.

#### TABLE OF CONTENTS/OUTLINE

Fibroepithelial neoplasms of the breast Clinical and histopathologic features Imaging and Differential Diagnosis Summary Please visit the Learning Center to also view this presentation in hardcopy format.

Printed on: 02/07/23



## Abstract Archives of the RSNA, 2022

BREE-119

### Nipple-Areolar Complex, What the Radiologist Should Know

Sunday, Nov. 27 8:00AM - 9:00AM Room: Learning Center - BR

#### Participants

Natalia Orthmann, MD, Sao Paulo, Brazil (*Presenter*) Nothing to Disclose

#### TEACHING POINTS

The purpose of this exhibit is: 1.To show the epidemiology, histological origin, imaging aspects in the different methods, anatomopathological and clinical correlation, when possible. 2.To review the imaging findings of the suggestive nipple-areolar complex and its differential diagnoses. 3.To illustrate the different imaging methods to assess the nipple-areolar complex, such as Ultrasound (US), Mammography (MG), tomosynthesis (TS) and Magnetic Resonance (MR). 4.To suggest techniques for better assessment of the nipple-areolar complex.

#### TABLE OF CONTENTS/OUTLINE

1.Literature review focusing on nipple-areolar complex diseases and its differential diagnoses. 2.To illustrate and discuss the pathology of nipple-areolar complex diseases, highlighting epidemiology; anatomy; progression in different imaging methods. 3. Review of the pathological development of nipple-areolar complex diseases through illustrative cases. 4. Example cases with mammographic, ultrasonographic, clinical and pathological correlation when available. 5. Examples of cases with suggestions of techniques for better evaluation of the nipple-areolar complex 6. Summary and conclusion.

Printed on: 02/07/23



## Abstract Archives of the RSNA, 2022

BREE-12

### Second look and Targeted Ultrasound Made Very Very Easy, a Case-Based Review

Sunday, Nov. 27 8:00AM - 9:00AM Room: Learning Center - BR

#### Participants

Sepideh Sefidbakht, MD, Powel, OH (*Presenter*) Nothing to Disclose

#### TEACHING POINTS

Understanding the relationship between location of lesions in ultrasound and mammogram and MRI is not always intuitive. This makes targeted and second look ultrasounds challenging to learn. Following a few simple rules and being aware of the pitfalls and peculiarities associated with each modality can accelerate the learning curve and enhance the accuracy of performing second look and targeted ultrasounds. Using simplified rules, 3D schematics and simple animations we will review the basic concepts of second-look and targeted ultrasound. Then using a case-based approach we will practice the basic concepts of second look and targeted US. The purpose of this exhibit is to: 1-Review the basic concepts of correlating lesions between modalities (clockwise location, depth, shape size) 2-Review the basic characteristics of the CC view in mammogram (depicting medial, lateral, superior inferior lesions and the role of rolled-over views) 3-Review the basic characteristics and peculiarities of the of the MLO view in mammogram and how it affects where we see lesions; the concept of clockwise and counterclockwise rotation of the breast and how it affects lesion perception. 4-Review the basic characteristics of the lesions seen in MRI (location, depth, concordance and discordance between extent of enhancement and US appearance)

#### TABLE OF CONTENTS/OUTLINE

- Looking for a nonpalpable lesion seen in MG or MRI; The Four Golden Rules
- 3D depiction of lesions in CC view; The Four Golden Rules of the CC view
- 3D depiction of lesions in MLO view; The Four Golden Rules of the MLO view
- Second look ultrasound, The Four Golden Rules
- Case-based practice of second look and targeted ultrasound

Printed on: 02/07/23

## Abstract Archives of the RSNA, 2022

BREE-120

### Are You Sure It's Cancer? Desmoid Tumors Mimicking Malignant Lesions

Sunday, Nov. 27 8:00AM - 9:00AM Room: Learning Center - BR

#### Participants

Natalia Lima, Sao Paulo, Brazil (*Presenter*) Nothing to Disclose

#### TEACHING POINTS

The purposes of this exhibit are: To review the main aspects of desmoid tumors and its ability to mimic malignant lesions; To exemplify, by using interesting cases from our breast radiology group, different types of presentation of desmoid tumors; To show the main conclusion for each clinical case; To emphasize the importance of knowing this kind of tumors and differential diagnoses in order to help in daily clinical practice.

#### TABLE OF CONTENTS/OUTLINE

Teaching cases showing the challenging aspects based on imaging findings and correlate with clinical and pathological findings in different scenarios, mimicking solid-cystic complex, increasing palpable mass, posterior masses and spiculated masses, as well as in Gardner syndrome; Explanations about the behaviour of desmoid tumors, as a benign neoplasm but with aggressive characteristics.

Printed on: 02/07/23



## Abstract Archives of the RSNA, 2022

BREE-121

### Lactation Education: Breast MRI Pathology, Pearls, and Pitfalls

Sunday, Nov. 27 8:00AM - 9:00AM Room: Learning Center - BR

#### Awards

Identified for RadioGraphics

#### Participants

Kali Xu, MD, (*Presenter*) Nothing to Disclose

#### TEACHING POINTS

- The lactating breast undergoes marked physiologic changes that can make conventional imaging evaluation with mammography and ultrasound challenging.- MRI is increasingly recognized as a safe and effective supplemental tool for both diagnostic evaluation and screening of lactating patients in the appropriate clinical setting.- Learning to recognize normal physiologic findings, common benign entities, and signs of malignancy in the lactating breast on MRI will improve diagnostic accuracy and facilitate proper clinical management.

#### TABLE OF CONTENTS/OUTLINE

I. Review clinical indications for breast MRI during lactation.II. Illustrate characteristic features of the lactating breast on MRI, including atypical scenarios (post-breast conservation, unilateral breastfeeding).III. Provide case examples of benign entities encountered during lactation (galactocele, lactating adenoma, fibroadenoma).IV. Review MRI features of pregnancy-associated breast cancer (PABC) using case examples illustrating a spectrum of pathology and clinical scenarios. Correlative mammography and ultrasound images will be incorporated where appropriate. Emphasis will be placed on demonstrating how breast MRI may depict more extensive disease than conventional imaging, leading to changes in clinical management.V. Discuss risks and benefits of FNA vs. core biopsy for sampling of suspicious imaging findings in lactating patients, with emphasis on careful correlation of radiologic, pathologic, and clinical findings to avoid delays in cancer diagnosis.

Printed on: 02/07/23



## Abstract Archives of the RSNA, 2022

BREE-122

### Breast Parenchymal Changes After Breast Conservative Treatment - What the Radiologist Must Know How to Differentiate

Sunday, Nov. 27 8:00AM - 9:00AM Room: Learning Center - BR

#### Participants

Almudena Gil Boronat, MD, Madrid, Spain (*Presenter*) Nothing to Disclose

#### TEACHING POINTS

- To briefly review the breast cancer conservative treatment, whose current protocols include the use of adjuvant breast radiotherapy. - To explain the different breast parenchymal findings expected after conservative treatment, depending on the time elapsed after it. - To emphasize that although most of them are benign in nature, they can present suspicious radiological semiology, and it is important to know them in order to differentiate them from a local recurrence.

#### TABLE OF CONTENTS/OUTLINE

1. Quick review of adjuvant radiotherapy after breast-conserving surgery. 2. Explain the different types of glandular changes expected after conservative treatment depending on the time of evolution, classified as early changes, intermediate changes and late changes. 3. We focus on explaining the situations that generate the greatest difficulties to differentiate them from a local recurrence. 4. Conclusions. 5. Take home points. 6. Bibliography.

Printed on: 02/07/23

## Abstract Archives of the RSNA, 2022

BREE-123

### Pregnancy-associated Breast Cancer and the Role of Imaging in the Pregnant and Lactating Patient

Sunday, Nov. 27 8:00AM - 9:00AM Room: Learning Center - BR

#### Participants

Julia Kirsten, MD, Fenton, MO (*Presenter*) Nothing to Disclose

#### TEACHING POINTS

1. Describe the background, etiology, biomarker status and most common histological types behind pregnancy-associated breast cancer. 2. Discuss screening and diagnostic guidelines and review current updates regarding the role of imaging for pregnant and lactating women. 3. Review common benign pregnancy-related lesions, potential complications, radiation safety, and treatment of pregnancy-associated breast cancer.

#### TABLE OF CONTENTS/OUTLINE

1. Introduction to pregnancy-associated breast cancer and challenges in diagnosis 2. Etiology, histological type, and biomarker status of pregnancy-associated breast cancer 3. Clinical manifestations of pregnancy-associated breast cancer (palpable breast mass, unilateral milk rejection, etc) 4. Initial imaging of breast cancer screening during pregnancy (high and elevated risk patients, 39 and under, summary of recommendations from ACR, ACOG, AJR) 5. Initial imaging of breast cancer screening during pregnancy (40 years and older, summary of recommendations from ACR, ACOG, AJR) 6. Initial imaging of breast cancer screening during lactation 7. Initial imaging of pregnant women with a palpable breast mass 8. Use of MRI in the pregnant/lactating patient (concerns regarding heat deposition into the fetus, damage to auditory nerves, gadolinium-induced fetal toxicity) 9. Common benign pregnancy-related breast lesions 10. Complications of biopsies in pregnant and lactating women (milk fistulas, increased risk of bleeding and infection, breast pseudoaneurysm) 11. Radiation safety and recommendations 12. Treatment of pregnancy-associated breast cancer 13. Conclusion

Printed on: 02/07/23



## Abstract Archives of the RSNA, 2022

BREE-124

### Common Questions and Challenging Scenarios of the Daily Practice Using the BI-RADS® Atlas

Sunday, Nov. 27 8:00AM - 9:00AM Room: Learning Center - BR

#### Participants

Karina Pesce, MD, Capital Federal, Argentina (*Presenter*) Nothing to Disclose

#### TEACHING POINTS

1-Review the management recommendations suggested by the ACR for clinical cases that generate different inquiries during daily practice. 2-Describe the different clinical scenarios that constitute the exception to the rule in the management of categorization recommendations.

#### TABLE OF CONTENTS/OUTLINE

The American College of Radiology (ACR) has established the Breast Imaging Reporting and Data System (BI-RADS) to guide the breast cancer screening and diagnostic routine. This educational poster is aimed at doctors who are new to breast diagnosis and is intended to be a practical guide to solve the most frequent doubts following the recommendations of experts from the American College of Radiology. Frequently asked questions will be reviewed through clinical cases.

Printed on: 02/07/23



## Abstract Archives of the RSNA, 2022

BREE-125

### False Negatives in Breast Screening and How to Avoid Them

Sunday, Nov. 27 8:00AM - 9:00AM Room: Learning Center - BR

#### Participants

Agustina Graziani, MD, (*Presenter*) Nothing to Disclose

#### TEACHING POINTS

1. Identify the factors that influence false negative results in all diagnostic modalities.2. Analyze the causes of false negatives.3. Discuss possible strategies to avoid false negatives.

#### TABLE OF CONTENTS/OUTLINE

Breast cancer is a common disease among women and it is the second leading cause of death from cancer. Timely diagnosis allows detection in early stages, with better outcome, better prognosis and with fewer comorbidities in the instituted treatments. Diagnosis can be made with breast imaging either by mammography, ultrasound and magnetic resonance imaging. The percentage of false negatives on imaging studies in the literature varies between 8-10%, between 9 and 22% and 4.4% respectively. The most common causes that lead to a misdiagnosis can be classified as related to:1. The technical aspect of the imaging modality.2. The Patient.3. The Reporting physician.4. The lesion. Early detection of breast cancer is one of the most important prognostic indicators, and diagnostic errors in breast imaging represent missed opportunities for timely treatment. Improving diagnostic accuracy requires a multidimensional approach, however recognizing causes of false negatives allows us to adopt useful strategies to avoid them and thus favorably impact the reduction of morbidity and mortality.

Printed on: 02/07/23

## Abstract Archives of the RSNA, 2022

BREE-126

### **Pseudoangiomatous Stromal Hyperplasia of the Breast (PASH) - Tips and Tricks for Diagnosis**

Sunday, Nov. 27 8:00AM - 9:00AM Room: Learning Center - BR

#### **Participants**

Rosa M. Lorente-Ramos, MD, PhD, Madrid, Spain (*Presenter*) Nothing to Disclose

#### **TEACHING POINTS**

To review pseudoangiomatous stromal hyperplasia of the breast, highlighting clinical presentation, pathological and imaging findings as well as differences from breast cancer To illustrate common and uncommon imaging findings in mammogram and contrast enhanced mammography (CEM), US, MR, of cases from our series with pathological correlation. To analyze and discuss the specific management of those lesions, including diagnostic difficulties and imaging work-up. To emphasize pitfalls and clues to differential diagnosis.

#### **TABLE OF CONTENTS/OUTLINE**

Pseudoangiomatous stromal hyperplasia (PASH) is a benign mesenchymal proliferating lesion. It is frequently found as an incidental histological finding in breast biopsies performed for other lesion but it can present as a mass (also called nodular PASH) or breast enlargement, which may mimic malignant lesions malignant lesions. Keys for differential diagnosis should be recognized. We present:  
- Definition. - Clinical presentation. - Pathological findings. - Imaging findings: Mammograms/CEM, US, MR. - Differential diagnosis. - Management and outcomes.

Printed on: 02/07/23



## Abstract Archives of the RSNA, 2022

BREE-127

### High-risk Breast Lesions - What the Radiologist Should Know About the Diagnostic and Therapeutic Implications

Sunday, Nov. 27 8:00AM - 9:00AM Room: Learning Center - BR

#### Participants

Ladys Camargo, MD, Ciudad Autonoma de Buenos Aires, Argentina (*Presenter*) Nothing to Disclose

#### TEACHING POINTS

Describe the lesions included in the histopathological B3 category of the Ellis classification. Correlate imaging and histopathological findings. Discuss the diagnostic algorithm and management of B3 lesions.

#### TABLE OF CONTENTS/OUTLINE

One of the main challenges of breast pathology is the diagnosis of lesions with indeterminate radiological characteristics and their proper management. The same occurs with the diagnosis of histological lesions considered to be of uncertain malignant potential, framed according to the Ellis histological classification as B3 lesions. Over time, personalized management has been favored to reduce overtreatment and thus lower the high healthcare costs associated with surgical excision. The main objective of this work is to provide a precise approach to high-risk lesions, correlating their imaging and pathology findings and discussing their proper management. 1. Introduction. 2- Classification of B3 lesions according to Ellis histological classification. 3- Imaging characteristics of B3 lesions (mammography, US, MRI). 4- Radio-Pathological correlation. 5- Clinical cases. 6- Diagnostic Algorithm. 7- Discussion of the Management of B3 Lesions. 8- Conclusions. 9- Bibliography.

Printed on: 02/07/23



## Abstract Archives of the RSNA, 2022

BREE-128

### Male - Malignant or Mimic? A Seven-Year Institutional Review of Male Breast Biopsies with Radiology-Pathology Correlation

Sunday, Nov. 27 8:00AM - 9:00AM Room: Learning Center - BR

#### Participants

Esraa Hazim Hasan Al-Jabbari, MBCHB, Galveston, TX (*Presenter*) Nothing to Disclose

#### TEACHING POINTS

1. An overview of male breast findings which were biopsied and/or resected over the last seven-years (April 1st, 2015 -March 31st, 2022) within our institution. 2. Discuss imaging and pathologic features of some pertinent benign and malignant lesions of the male breast. 3. Highlight imaging features suggestive of a benign etiology to limit false negative biopsies. 4. Highlight the risk factors for male breast cancer. 5. Discuss potential breast cancer screening programs in at- risk male populations including trans-gender patients.

#### TABLE OF CONTENTS/OUTLINE

Introduction; Embryologic and anatomic overview of the male breast; Institutional experience with male breast findings; Malignant breast findings in males; Benign mimics of breast malignancies in males; Risk factors for male breast cancer; Potential screening guidelines in at - risk male population; Conclusion.

Printed on: 02/07/23



## Abstract Archives of the RSNA, 2022

BREE-129

### **Dermatofibrosarcoma Protuberans: A rare Differential Diagnosis in Superficial Breast Lesions - Imaging Findings and Histopathological Correlation**

Sunday, Nov. 27 8:00AM - 9:00AM Room: Learning Center - BR

#### **Participants**

Camila Acras, MD, Sao Paulo, Brazil (*Presenter*) Nothing to Disclose

#### **TEACHING POINTS**

- To present the features of dermatofibrosarcoma protuberans (DFSP) in the breast through imaging findings on mammography (MG), ultrasonography (US), and magnetic resonance imaging (MRI) - To review the DFSP imaging signs, and discuss the differential diagnosis

#### **TABLE OF CONTENTS/OUTLINE**

- Introduction. - Identify and describe differential imaging findings, including the ones that can suggest the diagnosis of DFSP - Report the survey of institutional data from the analysis of the results of breast biopsies performed in recent years that confirmed histological diagnostic of DFSP - Report the institutional data from the analysis of the breast biopsies performed in recent years that confirmed histological diagnostic of DFSP - Conclusion.

Printed on: 02/07/23



## Abstract Archives of the RSNA, 2022

BREE-13

### Echogenic Breast Lesions: A Road Map for the Breast Radiologist

Sunday, Nov. 27 8:00AM - 9:00AM Room: Learning Center - BR

#### Participants

Luciano Fabrizio, Buenos Aires, Argentina (*Presenter*) Nothing to Disclose

#### TEACHING POINTS

1- Identify benign and malignant breast pathology that manifest as echogenic ultrasound lesions.2- Correlate ultrasonographic and mammographic findings.3- Correlate imaging findings with histopathological study.4- Discuss the diagnostic algorithm for echogenic breast lesions.5- Identify imaging key-points for each echogenic lesions.

#### TABLE OF CONTENTS/OUTLINE

-Introduction: echogenic images and their epidemiology.-Ultrasound key-points for characterizing benign and malignant entities.-Diagnostic algorithm.-Conclusions.-Annex I: characteristics table of benign and malignant echogenic lesions.-Annex II: diagnostic algorithm (categorization and biopsy indications).

Printed on: 02/07/23



## Abstract Archives of the RSNA, 2022

BREE-130

### Prone Tomosynthesis-guided Breast Biopsy: A Guide for Trainees and Experts Alike

Sunday, Nov. 27 8:00AM - 9:00AM Room: Learning Center - BR

#### Awards

Identified for RadioGraphics

#### Participants

Luciano Chala, MD, Sao Paulo, Brazil (*Presenter*) Nothing to Disclose

#### TEACHING POINTS

1. Step-by-step review of tomosynthesis-guided breast biopsy technique  
2. Discuss all indications, complications, and contraindications of the method.  
3. Share our experience with cases illustrating situations where tomosynthesis has helped improve our biopsies results.

#### TABLE OF CONTENTS/OUTLINE

- To obtain more accurate and reliable results, it is important to be familiar with the steps of tomosynthesis-guided biopsy. We demonstrate the technique step-by-step with actual photos from our daily practice so that residents can learn the procedure comprehensively.  
- In recent years, tomosynthesis-guided biopsy has gained popularity. We discuss all indications for this method and compare its limitations and complications with supine tomosynthesis-guided and stereotactic biopsies.  
- Tomosynthesis-guided breast biopsy in the prone position can sometimes offer advantages over other methods and even shorten the overall duration of the biopsy. We illustrate the following advantages with some cases: identification of lesions visible only on tomosynthesis, the possibility of lateral access in thin breast thickness, improved calcifications conspicuity, and identification of intravascular calcifications, which helps to distinguish them from linear calcifications and also allows better planning by avoiding blood vessels to reduce hemorrhage-related complications.

Printed on: 02/07/23



## Abstract Archives of the RSNA, 2022

BREE-131

### SOS Within the Breast: The Must-Knows of Handling Emergent Breast Cases

Sunday, Nov. 27 8:00AM - 9:00AM Room: Learning Center - BR

#### Participants

Kristina Michaudet, MD, Stanford, CA (*Presenter*) Nothing to Disclose

#### TEACHING POINTS

Breast emergencies are infrequent but can be diagnostically challenging especially during off hour nights and weekends. Very few experienced breast imagers nor specialized sonographers may be available during acute breast situations. Breast emergencies may present as complications of interventional procedures such as pseudoaneurysms or post biopsy hematomas. Numerous patients also return to the emergency department setting following mastectomy and reconstruction. Additionally, acute situations may be related to infection and inflammation in both cancer and non-cancer patients. Most importantly, a seemingly infectious process can masquerade an underlying mass and malignancy. The importance of follow up imaging for ED breast complaints is imperative.

#### TABLE OF CONTENTS/OUTLINE

The poster will be organized to include a review of both common and uncommon emergently presenting breast conditions. Examples of emergency breast cases including infection in puerperal and non puerperal cases will be showcased as well as first time presentation of malignancy through acute settings. Breast ultrasound utilization will be discussed along with the patient factors and characteristics which may be most pertinent for suspected infection and abscess. Management and knowledge of appropriate follow-up-protocols is key particularly for the non- breast imager encountering these unique cases on call. Emergency procedures and treatments such as embolization will be highlighted in cases of post biopsy complications such as bleeding and pseudoaneurysm formation.

Printed on: 02/07/23



## Abstract Archives of the RSNA, 2022

BREE-132

### Non-mass Lesion on Ultrasound - The New Finding to Incorporate

Sunday, Nov. 27 8:00AM - 9:00AM Room: Learning Center - BR

#### Awards

Certificate of Merit

#### Participants

Karen Mena Moreno, MD, Buenos Aires City, Argentina (*Presenter*) Nothing to Disclose

#### TEACHING POINTS

1. Analyze the correlations between histopathologic findings and non-mass breast lesions on ultrasound.2. Discuss the management of non-mass findings on ultrasound.3. Demonstrate the importance of recognizing non-mass lesions.

#### TABLE OF CONTENTS/OUTLINE

Introduction. Review of the definition and sonographic characteristics of non-mass findings. Description and correlation of breast imaging findings on mammography and MR. Clinical cases with histological correlation. Diagnostic algorithm. Treatment and management considerations. Discuss controversial cases. Take-home points. Conclusions.

Printed on: 02/07/23



## Abstract Archives of the RSNA, 2022

BREE-14

### Next Top Model: An Overview of Breast Cancer Risk Assessment Models

Sunday, Nov. 27 8:00AM - 9:00AM Room: Learning Center - BR

#### Participants

Pooja Agrawal, Houston, TX (*Presenter*) Nothing to Disclose

#### TEACHING POINTS

1. Introduce breast cancer risk assessment models available for estimating an individual's risk of developing breast cancer or risk for carrying a gene mutation that may predispose to developing breast cancer. 2. Review the strengths and limitations of each model and the model's applicability to underrepresented populations. 3. Provide example cases and narratives that demonstrate the use of breast cancer risk assessment models for different women.

#### TABLE OF CONTENTS/OUTLINE

1. Introduction: Review breast cancer statistics including morbidity and mortality disparities amongst patient populations, define breast cancer risk assessment, review guidelines and recommendations for breast cancer risk assessment (American College of Radiology, Society of Breast Imaging, American Society of Breast Surgeons, American College of Obstetricians and Gynecologists), and discuss current utilization (or lack of utilization) of breast cancer risk assessment. 2. Review available risk models, including risk factors assessed, strengths, and limitations: Gail Model, Claus Model, BRCAPRO Model, IBIS aka Tyrer-Cuzick Model, Jonker Model, BOADICEA Model. 3. Demonstrate breast cancer risk assessment performance: Provide examples of how risk assessment is performed, review recommendations for patients found to be at high risk. 4. Show case examples of breast cancer risk assessment for women belonging to minority groups or underrepresented populations. 5. Conclusion and application of breast cancer risk assessment models to clinical practice

Printed on: 02/07/23



## Abstract Archives of the RSNA, 2022

BREE-15

### Problem-Solving Breast MRI

Sunday, Nov. 27 8:00AM - 9:00AM Room: Learning Center - BR

#### Awards

Identified for RadioGraphics  
Certificate of Merit

#### Participants

Beatrui Reig, MD, MPH, New York, NY (*Presenter*) Nothing to Disclose

#### TEACHING POINTS

1. MRI does not replace careful diagnostic workup with mammogram and ultrasound 2. Negative MRI should not obviate the need for biopsy for a suspicious finding detected on mammography/tomosynthesis or ultrasound 3. A negative MRI is reassuring in low-suspicion mammo/tomosynthesis findings such as asymmetries, focal asymmetries, and post-surgical change

#### TABLE OF CONTENTS/OUTLINE

1. Brief introduction a. Indications for MRI b. MRI Sensitivity/specificity 2. Indications for problem-solving MRI a. Equivocal or uncertain imaging i. Lesion visible on some but not all views ii. Change over time: true change versus technical difference iii. Change at surgical site iv. Sternalis muscle b. Negative imaging with clinical concern i. Suspicious nipple discharge c. BIRADS 4 lesions i. Difficult biopsy due to technical issues ii. Discordant biopsy iii. Tomosynthesis-only finding without tomo-guided biopsy capability 3. Inappropriate use of problem-solving MRI a. Preceding or replacing diagnostic mammo and US b. In lieu of biopsy of a suspicious finding identifiable by mammo, US, or clinical exam c. Evaluation of mammographic calcifications 4. Future directions a. Increasing use of tomosynthesis decreases need for problem-solving MRI i. Better evaluate equivocal findings ii. Biopsy one-view findings b. Triaging tool for active surveillance vs surgical excision for high risk lesions detected on percutaneous biopsy i. Low grade DCIS ii. ADH, atypia iii. Radial scar c. Improving accuracy leads to improved utility of problem solving MRI i. Diffusion weighted imaging ii. Artificial intelligence in MRI d. Problem solving MRI more feasible as MRI becomes faster and cheaper i. Abbreviated MRI impact ii. Increased MRI screening

Printed on: 02/07/23



## Abstract Archives of the RSNA, 2022

BREE-16

### The Use of Diffusion-weighted Sequence in the Evaluation of Breast Lesions: What the Radiologist Needs to Know

Sunday, Nov. 27 8:00AM - 9:00AM Room: Learning Center - BR

#### Participants

Giselle Mello, PhD, Sao Paulo, Brazil (*Presenter*) Nothing to Disclose

#### TEACHING POINTS

- Review the fundamental principles of diffusion-weighted imaging (DWI).- Review the concepts of breast lesions cellularity.- Review the concepts of ADC mapping.- Illustrate with cases how to differentiate benign from malignant lesions and correlate the histopathologic findings with their ADC values to allow for earlier and more accurate diagnosis and individualized patient care.- Create a pictorial essay to illustrate the use of DWI to differentiate complex breast lesions with peripheral enhancement that, when combined with clinical and histopathologic findings, can provide valuable information for therapy.

#### TABLE OF CONTENTS/OUTLINE

1) Principles of diffusion-weighted imaging (DWI).2) The concept of apparent diffusion coefficient (ADC).3) Lesion cellularity.4) Benign and malignant DWI findings and their corresponding ADC values.5) Differentiation of complex peripheral enhancing breast lesions.6) DWI findings for predicting pathologic response in neoadjuvant treatment of breast cancer.7) A series of cases using DWI sequences and correlation of their ADC values with histopathological findings.

Printed on: 02/07/23



## Abstract Archives of the RSNA, 2022

BREE-17

### Anatomical Approach for the Imaging and Diagnosis of Nipple Areolar Complex Abnormalities

Sunday, Nov. 27 8:00AM - 9:00AM Room: Learning Center - BR

#### Awards

Certificate of Merit

#### Participants

Claudia Cotes, MD, Houston, TX (*Presenter*) Nothing to Disclose

#### TEACHING POINTS

The nipple areolar complex is a region of the the breast with a complex anatomy from which several benign and malignant pathology may arise. It is important to understand anatomic features of this region for an appropriate differential diagnosis when abnormalities in this area are encountered. The imaging evaluation of this region can be technically difficult due to superimposition of tissues in mammography and artifacts and/or technical limitations on ultrasound which can limit the appropriate diagnosis of these abnormalities. This exhibit will provide a review of the clinical and imaging findings of interesting pathologic processes in the nipple areolar complex utilizing an anatomical approach, as well as interactive examples of imaging technique for proper evaluation of this region. Workup algorithms based on the ACR appropriateness criteria for clinical findings related to the nipple areolar complex will also be provided.

#### TABLE OF CONTENTS/OUTLINE

1. Introduction 2. Imaging Anatomy of the Nipple Areolar Complex 3. Imaging of the Nipple Areolar Complex: Tips and Tricks for optimal evaluation 4. Anatomy based Pathology Review: a. Skin and Subcutaneous Soft Tissue: Sebaceous Cyst, Epidermal Inclusion Cyst, Montgomery Gland Cyst, Cellulitis/Abscess, Eczema, Paget Disease b. Breast Parenchyma and Connective Tissue: Adenoma, Fibroadenoma, Lipoma, Fibroadenolipoma, Abscess c. Ductal system: Ductal Ectasia, Intraductal Papilloma, Ductal Carcinoma In-Situ, Invasive Ductal Carcinoma 5. Workup Algorithms 6. Conclusion

Printed on: 02/07/23



## Abstract Archives of the RSNA, 2022

BREE-19

### Green is the New Pink- Reducing the Carbon Footprint of Breast Imaging Practices

Sunday, Nov. 27 8:00AM - 9:00AM Room: Learning Center - BR

#### Participants

Tom Soker, DO, Cleveland, OH (*Presenter*) Nothing to Disclose

#### TEACHING POINTS

Recognized as one of the greatest global health challenges of the 21st century, climate change poses substantial risks to the health and well-being of the world's population. With healthcare overall contributing up to 10% of greenhouse emissions in the United States, imaging has been identified as one of the major contributors. Therefore, breast radiologists should embrace environmentally friendly strategies to mitigate future health effects. Specific learning objectives for this exhibit include: 1) Understand the current state of climate change and how it relates to medicine. 2) Review how breast imaging practices currently contribute to climate change. 3) Describe steps that breast imaging practices can take now to reduce their carbon footprint. 4) Describe initiatives that breast imaging can embrace to further accelerate adoption of "greener" practices and engage the broader community.

#### TABLE OF CONTENTS/OUTLINE

Using text, schematics and cases, we will discuss the current challenges that breast imaging practices face and focus on specific steps that practices can take to reduce their carbon footprint and become "greener". 1) Reduce waste -- Decrease glove use; incorporate biodegradable disinfectant wipes; adopt electronic data entry; temperature off-hour modulation; off-hour power down of equipment, lights and computers. 2) Reuse/Recycle - sterilization of equipment rather than disposal; recycle packaging 3) Greener workflow - routine same day interpretations and biopsies; adoption of telehealth; electronic transfer of imaging to outside facilities

Printed on: 02/07/23



## Abstract Archives of the RSNA, 2022

BREE-2

### Serving the Underserved: A Safety-net Framework to Provide High-quality, Comprehensive and Culturally Competent Breast Imaging Care

Sunday, Nov. 27 8:00AM - 9:00AM Room: Learning Center - BR

#### Awards

Identified for RadioGraphics

Magna Cum Laude

#### Participants

Berat Bersu Ozcan, MD, (Presenter) Nothing to Disclose

#### TEACHING POINTS

1. Groups that may experience breast cancer (BC) disparities include those defined by race/ethnicity, national origin, cultural beliefs, age, education, socioeconomic status, geographic location, disability, gender identity and sexual orientation. 2. BC screening increases early detection. Improving access supported through radiology-community partnerships using educational programs and community outreach can reduce disparities in BC mortality. 3. Women in safety-net systems who receive a BC diagnosis experience significant access related delays. Delays as short as 30 days affect BC outcomes. 4. Genetic factors contribute to higher mortality in Black and Hispanic women including significantly younger age at diagnosis and a higher incidence of aggressive hormone receptor-negative BC than White women. Black women with hormone-positive cancer have worse 21-gene assay scores and higher BC-specific mortality compared to Whites in all risk groups. 5. With the complexity of breast imaging, cancer care and safety-net systems, formal care coordination programs are essential to help women navigate through screening and diagnosis to treatment.

#### TABLE OF CONTENTS/OUTLINE

Define at-risk or vulnerable patient populations and the role of safety-net hospitals. Summarize population-based breast cancer screening programs and efforts in the United States. Review outcomes and health disparities for underrepresented minorities and underserved women in the United States. Discuss barriers to care and strategies to improve screening uptake and reduce breast cancer disparities.

Printed on: 02/07/23



## Abstract Archives of the RSNA, 2022

BREE-20

### A Comprehensive Look at Disparities in Breast Cancer in the Non-Hispanic Black, Hispanic, and Transgender Community and What Policy Changes Should be Considered

Sunday, Nov. 27 8:00AM - 9:00AM Room: Learning Center - BR

#### Participants

Frances Perez, MD, Houston, TX (*Presenter*) Nothing to Disclose

#### TEACHING POINTS

The incidence of breast cancer are higher for non-Hispanic Blacks (NHB) younger than 45 years of age than for non-Hispanic Whites (NHW) in that same age group. Approximately 30% of all breast cancer diagnosed in NHB and Hispanic woman are diagnosed in woman under the age of 50. According to the Surveillance, Epidemiology, and End Results (SEER) data, minority women are 72% more likely to present to with invasive disease at time of diagnostic when compared to NHW. Minority women as 58% more likely to be diagnosed with advanced-stage breast cancer under the age of 50. Currently, the World Professional Association of Transgender Health lack guidelines on breast cancer screening. Furthermore, large databases in the U.S, like the SEER and National Cancer Database (NCDB) do not capture non-binary genders.

#### TABLE OF CONTENTS/OUTLINE

Through a case based multimodality approach we will exhibit several clinical cases that demonstrate the degree of advance invasive disease that minority women present with under the age of 50. We will discuss the breast cancer screening barriers that transgender individuals face, and the implications that this lack of resource has in this patient population. Throughout this exhibit, we will identify the most salient contributing factors including social determinants of health, breast cancer incidences within different ethnic and cultural groups, the difference in tumor biology and genomic that contribute to a higher mortality, as well as disparities in breast cancer treatments. To conclude, we will discuss strategies that may be implemented in order to mitigate these diversity related disparities.

Printed on: 02/07/23



## Abstract Archives of the RSNA, 2022

BREE-21

### Imaging Approach and Challenges to Breast Cancer in Young Patients

Sunday, Nov. 27 8:00AM - 9:00AM Room: Learning Center - BR

#### Participants

Cara Connolly, MD, Nashville, TN (*Presenter*) Nothing to Disclose

#### TEACHING POINTS

1. Review the diagnostic algorithm and appropriateness criteria for imaging studies in women less than age 40 and pregnant and lactating patients  
2. Review genetic syndromes that increase the risk of breast cancer in this age group  
3. Review the imaging appearance of pregnancy associated breast cancer and its mimics  
4. Present examples of malignancy highlighting the diagnostic dilemmas unique to this patient population.

#### TABLE OF CONTENTS/OUTLINE

Up to 7% of invasive breast cancers are diagnosed in patients less than 40 years old, with lower survival rates compared to older age groups, and poorer outcomes disproportionately affecting young black women. Because routine screening does not typically include women in this age group, most cancers (up to 80%) are diagnosed when patients self-present with a breast complaint or lump, often at advanced stage. Further, breast cancers in this age group tend to be hormone-receptor negative with aggressive features. Breast cancer in pregnant and lactating patients in this age group presents an additional diagnostic dilemma due to the physiologic changes occurring in the perinatal period, often leading to misdiagnosis and delay in treatment. Example topics to be covered, including but not limited to, the following: -Diagnostic Imaging Workflow -Patients Under 40 -Pregnant/Lactating Patients -Predisposing Genetic Syndromes and Germline Mutations -Pregnancy Associated Breast Cancer and Mimics -DCIS -Invasive Mammary Carcinoma

Printed on: 02/07/23



## Abstract Archives of the RSNA, 2022

BREE-22

### Delayed Diagnosis in Medically Underserved Individuals: Identifying Granulomatous Mastitis

Sunday, Nov. 27 8:00AM - 9:00AM Room: Learning Center - BR

#### Participants

Molly Downey, MD, (*Presenter*) Nothing to Disclose

#### TEACHING POINTS

1. Idiopathic granulomatous mastitis (IGM) is an uncommon inflammatory disease of the breast with nonspecific imaging findings which requires core needle biopsy for pathologic diagnosis. 2. Though there is incomplete evidence on prevalence among racial or ethnic groups, many published studies suggest a Hispanic or non-Caucasian predominance. Premenopausal women with a history of lactation are most affected. 3. Diagnosis of IGM is by histopathology findings of lobulocentric granulomatous inflammation, with the additional findings of suppurative lipogranulomas and *Corynebacterium* infection characteristic for cystic neutrophilic granulomatous mastitis (CNGM). 4. Enhanced understanding by the radiologist of the symptoms, imaging appearance, and histopathologic features of IGM is essential to avoid late diagnosis or misdiagnosis, especially in medically underserved individuals.

#### TABLE OF CONTENTS/OUTLINE

1. Background of IGMa) Prevalence and demographicsb) Proposed pathophysiology of IGM and subtype CNGMc) Clinical presentationd) Diagnostic workupe) Histopathologic appearance of IGM and CNGM2. Case-based imaging review of IGM and mimicsa) IGM and CNGMb) Chronic abscessc) Infectious mastitisd) Diabetic mastopathye) Inflammatory breast cancer3. Treatment, disease course and prognosis4. Team-based approach for diagnosisa) Clinical presentation and referral to radiologyb) Communication with Pathologists

Printed on: 02/07/23



## Abstract Archives of the RSNA, 2022

BREE-23

### How to Reduce Missed Breast Cancer on Automated Breast Ultrasound

Sunday, Nov. 27 8:00AM - 9:00AM Room: Learning Center - BR

#### Participants

Sung Kim, MD, (*Presenter*) Nothing to Disclose

#### TEACHING POINTS

Ultrasound (US) is more commonly used for adjunctive screening for dense breast. Automated breast ultrasound (ABUS) is also commonly employed with advantage of its production of reproducible, high-resolution images and its reduced dependency on human operators. Supplementing mammography with ABUS screening resulted in positive outcomes that were similar to those associated with handheld US (HHUS) screening, including increased detections of invasive cancer and reduced rates of interval cancer. However, due to the large number of images in the scan, reading a full ABUS examination can be lengthy and cancers may be easily overlooked. Possible causes for missing breast lesions on US include perception errors of isoechogenic and heterogeneous echogenic lesions, deep lesions, subareolar lesions, poor positioning or technique, misinterpretation, and subtle features of malignancy. Also ABUS encountered artifacts. Here, we review possible causes of missed cancers on ABUS and discuss methods to reduce them.

#### TABLE OF CONTENTS/OUTLINE

1. Pros and cons of automated breast ultrasound (ABUS) 2. ABUS as a supplemental screening tool 3. Causes of missed cancers on ABUS 1) Technique and artifacts 2) Errors in detection 3) Errors in interpretation 4) Tumor morphology 5) True negative cases 4. Solutions to reduce missed cancer

Printed on: 02/07/23



## Abstract Archives of the RSNA, 2022

BREE-24

### **Breast Fibromatosis in Very Young Women - As Ugly and Benign as Ever, but with a Different Presentation: A Series of 6 Cases**

Sunday, Nov. 27 8:00AM - 9:00AM Room: Learning Center - BR

#### **Participants**

Andres Vicentela, MD, (*Presenter*) Nothing to Disclose

#### **TEACHING POINTS**

1. Present our experience with breast fibromatosis (BF) in women younger than 25 years old which shows a different clinical and radiological pattern compared to the classic BF in older women (findings not yet described in actual literature).2. Give details of the imaging signs that characterize BF in mammography, ultrasound and MRI at this age range.3. Understand the natural history, prognosis and treatment options available

#### **TABLE OF CONTENTS/OUTLINE**

1. Introductiona. Definition of breast fibromatosis, demographics and typical clinical presentationb. Imaging findings on mammography, ultrasound and MRIC. Histopathology characteristics, natural history, prognosis and treatment options.2. Our experience in breast fibromatosis in women younger than 25 years old.a. Clinical presentationb. Imaging characteristics on different modalitiesc. Histopathologic findingsd. Surgical resolutione. Follow up3. Highlight the difference between classic BF and the pattern of this pathology in very young women.

Printed on: 02/07/23

## Abstract Archives of the RSNA, 2022

BREE-25

### From the Breast to the Bone: Multimodality Imaging Review of Osseous Metastases from Breast Cancer

Sunday, Nov. 27 8:00AM - 9:00AM Room: Learning Center - BR

#### Participants

Daniel Morgan, DO, (*Presenter*) Nothing to Disclose

#### TEACHING POINTS

1. Understand the epidemiology of osseous metastatic disease in breast cancer and the imaging modalities that evaluate for osseous metastases  
2. Discuss mimics, pitfalls, and pearls when assessing for osseous metastatic disease in breast cancer  
3. Know the imaging features of osseous metastases and their mimics to accurately diagnose metastatic disease and recognize when it is appropriate to biopsy an osseous lesion in question  
4. Examine current treatment options for osseous metastatic disease, the biology of the primary and metastatic lesions, and their treatment-related imaging features

#### TABLE OF CONTENTS/OUTLINE

Introduction:• Epidemiologic factors• Appropriate imaging evaluation to assess for osseous metastases• Most common locations for osseous metastases  
Osseous Metastatic Disease as Initial Presentation:• Hip• Ribs• Spine compression fracture• Skull/skull base  
Differential Diagnosis:• Sternal metastasis vs hemangioma• Multiple sclerotic osseous metastases vs osteopoikilosis• Sacral metastasis vs insufficiency fractures or sacroiliitis• Enchondroma• Fibrous dysplasia• Aneurysmal bone cyst• Metastases from non-breast primary malignancy  
Treatment:• Local treatment• Systemic treatment• Treatment response/treatment related changes  
Biology of breast cancer metastases

Printed on: 02/07/23



## Abstract Archives of the RSNA, 2022

BREE-26

### Rare Beauty in the Breast: Introduction to Unusual Breast Lesions

Sunday, Nov. 27 8:00AM - 9:00AM Room: Learning Center - BR

#### Awards

Certificate of Merit

#### Participants

Hee Jung Choi, MD, Mexico City, Mexico (*Presenter*) Nothing to Disclose

#### TEACHING POINTS

1. Review general features of unusual benign and malignant breast lesions.2. Analyze multimodality imaging findings of each lesion and correlate the findings with the underlying histopathologic and clinical findings.3. Recognize breast imaging abnormalities and describe key findings of each imaging method that lead to perform interventional procedures.4. Discuss the imaging follow-up and management of uncommon breast lesions.

#### TABLE OF CONTENTS/OUTLINE

1. Analyze macroscopic and microscopic normal anatomy of the breast and identify the origins of unusual lesions.2. Identification of uncommon breast lesions by category:a. Benign and malignant breast neoplasms: lymphomas, neuroendocrine tumors, sarcomas, mucinous, apocrine and inflammatory carcinomas, breast metastases, benign and malignant phyllodes tumor, hamartoma and tubular adenoma.b. Mastitis and complications: acute mastitis, chronic granulomatous mastitis and breast abscess formation.c. Miscellaneous: neurofibromatosis, arteriovenous malformation, silicone mastopathy and foreign modeling agent reactions.d. Breast pathology in men: primary breast cancers and metastases, gynecomastia and tricoepithelioma.3. Review the key points of each disease:a. Epidemiologyb. Clinical presentationc. Histopathologic characteristicsd. Multimodality imaging findingse. Illustration of the examples4. Discuss the management of atypical breast lesions including treatment and imaging-guided diagnostic biopsies with an assessment of proper technique in mammography, contrast-enhanced mammography, ultrasound and MRI.

Printed on: 02/07/23



## Abstract Archives of the RSNA, 2022

BREE-27

### I Am Not Who You Think I Am: Benign Mimics of Breast Malignancy with Multimodality and Pathologic Correlation

Sunday, Nov. 27 8:00AM - 9:00AM Room: Learning Center - BR

#### Awards

Certificate of Merit

#### Participants

Toma Omofoye, MD, Houston, TX (*Presenter*) Nothing to Disclose

#### TEACHING POINTS

To demonstrate: 1. Common and uncommon benign entities may have imaging features typically associated with breast malignancy. 2. Imaging workup of "malignant-appearing but benign" breast lesions with multimodality appearance (Mammography, DBT, Ultrasound, Contrast-Enhanced Mammography, MRI, and/or Molecular Breast Imaging). The histopathologic correlation will be included where possible. 3. Appropriate broadening of differential diagnoses can aid in radiologic-pathologic correlation after percutaneous core biopsy.

#### TABLE OF CONTENTS/OUTLINE

Based on cases at a tertiary oncologic referral center, we review breast imaging lesions with suspicious imaging features mimicking primary breast malignancy. • Introduction • Inflammatory/Infectious: Idiopathic granulomatous mastitis, Diabetic/lymphocytic mastopathy, Infectious mastitis, Mondor disease • Systemic conditions: Amyloidosis, Sarcoidosis • Tumors: Granular cell tumor, Tubular adenoma, Nipple adenoma, Pseudoangiomatous stromal hyperplasia (PASH), Phyllodes, Papilloma, Fibromatosis, Neurofibroma • Proliferative lesions: Sclerosing adenosis, Complex sclerosing lesions, Stromal fibrosis • Anatomic findings: Sternalis muscle, Coopers ligament • Male breast: Gynecomastia, Hemangioma • Posttraumatic conditions: Fat necrosis, Foreign body reaction, Postsurgical scar • Conclusion

Printed on: 02/07/23



## Abstract Archives of the RSNA, 2022

BREE-28

### Contrast-enhanced Mammography Artifacts and Pitfalls - Tips and Tricks to Understand Them and to Avoid Image Misinterpretation

Sunday, Nov. 27 8:00AM - 9:00AM Room: Learning Center - BR

#### Awards

Identified for RadioGraphics

#### Participants

Rosa M. Lorente-Ramos, MD, PhD, Madrid, Spain (*Presenter*) Nothing to Disclose

#### TEACHING POINTS

-To learn technique of contrast enhanced mammography (CEM). -To review CEM image artifacts and physical considerations causing artifacts related to digital mammography and specific to CEM.- To become familiar with pitfalls and diagnostic limitations in CEM and tips and tricks to avoid interference in image interpretation.

#### TABLE OF CONTENTS/OUTLINE

We review the basics of CEM highlighting artifacts and factors that may interfere with image interpretation. We present: 1. Basics of CEM. 2. Technique 3. Image artifacts. - Digital mammography artifacts: patient positioning, hair, antiperspirant, patient motion. - Contrast-related: contrast splatter, timing of image acquisition after contrast administration, transient retention of contrast in vessels. -CEM specific: Air artifact. Improper positioning causing skin folds; Rim, halo or breast-within-a-breast artifact. Scattered radiation from differences in breast tissue thickness between chest wall and breast edge; Skin line artifact. Due to scattered radiation from non-uniform thickness of skin; Ripple artifact. Patient motion between HE and LE, sometimes respiratory movements or cardiac pulsations transmitted through the chest wall. 4. Pitfalls. Axillary tail and medial lesions near the chest wall not included in the imaging field- Background parenchymal enhancement. Negative Contrast Enhancement: imaging a cyst or coarse calcification. "Eclipse sign". Hematoma caused by biopsy obscuring contrast enhancement of breast cancer. "Crescent sign" enhancement of the wall of a simple cyst. False negative lesions. DCIS, low-grade infiltrating cancer (lobar, mucinous). False positive lesions. Skin lesions, lymph nodes, benign enhancing lesions.

Printed on: 02/07/23



## Abstract Archives of the RSNA, 2022

BREE-29

### **(Nearly) Ouchless! Ultrasound-Guided Core Nipple Biopsy is within a Breast Imager's Wheelhouse**

Sunday, Nov. 27 8:00AM - 9:00AM Room: Learning Center - BR

#### **Participants**

Sophia O'Brien, MD, Philadelphia, PA (*Presenter*) Nothing to Disclose

#### **TEACHING POINTS**

The nipple-areolar complex (NAC) is comprised of numerous cell types and can thus demonstrate a variety of benign and malignant pathologies (1). Due to its superficial location, the NAC is not amenable to stereotactic- or MR-guidance. Historically, suspicious nipple symptoms and imaging abnormalities have been evaluated via surgical biopsy or skin punch biopsy. More recently, however, there have been reports of ultrasound-guided core nipple biopsies (US-CNB) of suspicious nipple calcifications and nipple masses (Omofoye 2015, Burk 2021). This educational exhibit will describe how to perform US-CNB step-by-step, highlighting the unique approach and considerations for this specialized percutaneous procedure. The educational material will be supplemented with numerous images from US-CNB performed at our institution. 1. Ultrasound-guided core nipple biopsy (US-CNB) can be performed safely for nearly all abnormalities seen on imaging 2. Appropriate anesthesia eliminates patient discomfort during US-CNB 3. US-CNB is adequate for diagnosis 4. US-CNB is a feasible percutaneous sampling technique well within the breast imager's wheelhouse, thus avoiding surgery while maintaining nipple integrity and aesthetics

#### **TABLE OF CONTENTS/OUTLINE**

1. Background: NAC physiology and pathology 2. Historical Nipple Sampling Techniques 3. US-CNB: Technique and special considerations 4. Cases to Highlight the technical teaching points

Printed on: 02/07/23



## Abstract Archives of the RSNA, 2022

BREE-3

### Breast Cancer Epidemiology and Imaging Patterns in Underserved Women

Sunday, Nov. 27 8:00AM - 9:00AM Room: Learning Center - BR

#### Participants

Scott Kleinpeter, MD, (*Presenter*) Nothing to Disclose

#### TEACHING POINTS

African American women are 42% more likely to die from breast cancer, have a two-fold higher risk of triple negative breast cancer, and have a higher prevalence of BRCA1 and BRCA2 genetic mutations. African American women are 72% more likely to be diagnosed with invasive disease under age 50 and are 58% more likely to be diagnosed with advanced-stage disease under age 50. Factors affecting disparities in health outcomes include genetic risk factors, health literacy, income level, health insurance status, comorbidities, cultural beliefs, geographical location, and gender identity. Current screening recommendations for USPSTF are not race-based. Temporal differences in breast cancer peak diagnosis results in disproportionate effects of delayed screening on minority women due to younger average age at diagnosis (African American peak diagnosis in 40's vs. white peak diagnosis in 60's). Timely breast cancer risk assessment, genetic testing (if applicable), ACR recommended screening surveillance, and patient education are key components to improve breast cancer mortality. Increasing access to screening in vulnerable populations is a multidisciplinary task and radiologists play a key role in identifying imaging patterns and reaching patients at higher risk.

#### TABLE OF CONTENTS/OUTLINE

a. Review of published literature on disparities in breast cancer screening and mortality. b. Factors influencing breast cancer risk in vulnerable populations. c. Review of ACR screening recommendations for women at high risk. d. Case collection illustrating imaging patterns in our underserved population.

Printed on: 02/07/23



## Abstract Archives of the RSNA, 2022

BREE-30

### Challenging Scenarios in MRI Guided Procedures: Tips and Tricks to Maximize Technical Success

Sunday, Nov. 27 8:00AM - 9:00AM Room: Learning Center - BR

#### Participants

Janice Thai, MD, (*Presenter*) Nothing to Disclose

#### TEACHING POINTS

1. To illustrate technically challenging anatomy and lesion location for MRI guided breast biopsy or localization. 2. To demonstrate useful approaches and techniques for overcoming technical challenges in MRI guided procedures. 3. To review the management options and alternatives following failed procedures.

#### TABLE OF CONTENTS/OUTLINE

- Illustrative review of equipment set up, device, and patient positioning
- Challenging case potpourri
- Critical review of real-life cases and lessons learned from failed procedures
- Review of preprocedural planning and procedural techniques to maximize technical success

Printed on: 02/07/23



## Abstract Archives of the RSNA, 2022

BREE-31

### Breast Imaging and Intervention During Pregnancy and Lactation

Sunday, Nov. 27 8:00AM - 9:00AM Room: Learning Center - BR

#### Awards

Certificate of Merit

Identified for RadioGraphics

#### Participants

Amy Fowler, MD, PhD, Madison, WI (*Presenter*) Author with royalties, RELX

#### TEACHING POINTS

Physiologic changes in the breast during pregnancy and lactation can pose diagnostic challenges on imaging and physical examination. Recognition of expected physiologic changes and classically benign entities on imaging is important to avoid unnecessary intervention. Identification of suspicious imaging features prompting biopsy recommendation are critical to avoid delays in diagnosis of pregnancy-associated breast cancer, the most common invasive cancer diagnosed during pregnancy. This presentation will focus on the appropriate breast imaging evaluation and management during pregnancy and lactation. The exhibit will also highlight ACR guidelines for breast cancer screening based on age and risk profile during pregnancy and lactation.

#### TABLE OF CONTENTS/OUTLINE

I. Hormonal and histologic changes within the breast II. Expected physiologic changes on breast imaging a. Mammographic appearance (lactation) b. Sonographic appearance (pregnancy/lactation) c. MRI appearance (lactation) III. Breast cancer screening guidelines during pregnancy/lactation IV. Imaging workup for clinical symptoms during pregnancy/lactation a. Palpable mass, nipple discharge, focal pain V. Biopsy considerations for this patient population a. Techniques b. Complications including milk fistula VI. Imaging features and management of common benign and malignant entities a. Benign i. Galactocele ii. Lactational changes iii. Lactating adenoma iv. Fibroadenoma with lactational changes v. Mastitis, abscess vi. Granulomatous mastitis vii. Reactive lymph nodes viii. Accessory axillary breast tissue b. Malignant i. Pregnancy-associated breast cancer

Printed on: 02/07/23



## Abstract Archives of the RSNA, 2022

BREE-32

### The Many Faces of Triple Negative Breast Cancer

Sunday, Nov. 27 8:00AM - 9:00AM Room: Learning Center - BR

#### Awards

Cum Laude

#### Participants

Beatriz Adrada, MD, Houston, TX (*Presenter*) Nothing to Disclose

#### TEACHING POINTS

- Triple negative breast cancer (TNBC) is a heterogeneous group of tumors defined by the absence of estrogen/progesterone receptors and lack of HER2 overexpression that confer a poor prognosis.
- TNBCs are classified using six molecular subtypes according to their gene expression patterns: luminal androgen receptor, two mesenchymal-like subgroups (Mesenchymal M and MSL), immunomodulatory, and two basal-like subgroups (BL1, BL2).
- Chemotherapy is the primary established systemic treatment for patients with TNBC. The treatment response differs depending on the molecular subtype, as well as the imaging features.

#### TABLE OF CONTENTS/OUTLINE

This educational exhibit will present a practical, multi-modality guide on approaching triple negative breast cancer (TNBC). A multi-modality review of the characteristic imaging features of TNBC will be presented, including features that may indicate whether a patient will respond to neoadjuvant chemotherapy. Imaging assessment of TNBC response to neoadjuvant chemotherapy will be detailed, including response patterns and imaging features that could indicate pathologic complete response (pCR). A clinical update on the recommended treatment of TNBC will be presented.

Printed on: 02/07/23



## Abstract Archives of the RSNA, 2022

BREE-33

### Axillary Imaging in Breast Cancer: When, Who and How?

Sunday, Nov. 27 8:00AM - 9:00AM Room: Learning Center - BR

#### Participants

Dogan Polat, MD, Dallas, TX (*Presenter*) Nothing to Disclose

#### TEACHING POINTS

- To illustrate axillary anatomy and imaging findings of metastatic axillary lymph nodes with various imaging modalities
- To discuss role of axillary imaging to predict survival, tumor stage and recurrence in newly diagnosed breast cancer
- Recognizing and management of axillary adenopathy after COVID-19 vaccination
- To demonstrate importance of pre-operative axillary imaging in guiding treatment decisions regarding axillary lymph node dissection, sentinel lymph node biopsy, and neoadjuvant chemotherapy (NACT)
- To showcase uses of axillary imaging to determine response to NACT
- To demonstrate use of axillary imaging in identifying abnormal appearing lymph nodes for further sampling and biopsies
- To compare advantages of different imaging modalities in the evaluation of the axilla
- To explain possible pitfalls of axillary imaging in identifying lymph node metastasis and evaluation of response to neoadjuvant chemotherapy

#### TABLE OF CONTENTS/OUTLINE

- Overview of axillary imaging
- Role of radiology in assessment of axillary nodes
- Characteristic features of different axillary pathologies
- Differential diagnosis, prognosis, and biopsy approaches
- Challenging clinical cases with axillary imaging
- Recognizing COVID-19 vaccine induced LAPs
- Future directions and summary

Printed on: 02/07/23



## Abstract Archives of the RSNA, 2022

BREE-34

### Performance Benchmarks and Management Guidelines for BI-RADS Category 3 Assessment on Breast MRI

Sunday, Nov. 27 8:00AM - 9:00AM Room: Learning Center - BR

#### Awards

Identified for RadioGraphics

#### Participants

Onalisa Winblad, MD, Leawood, KS (*Presenter*) Nothing to Disclose

#### TEACHING POINTS

There is significant variability in radiologist usage of BI-RADS Category 3 assessment on breast MRI due to lack of robust data to guide management. No combination of MRI BI-RADS descriptors has proven to meet the "<2% but greater than 0% likelihood of malignancy" historical definition of BI-RADS Category 3, which is well supported in the literature for both mammography and ultrasound. This likely accounts for the substantial confusion and misuse of BI-RADS Category 3 assessment on breast MRI. Recent reports demonstrate increased utilization of breast MRI, partially due to improved access made possible by modern abbreviated protocols. Given the increasing volume of breast MRI, it is imperative that radiologists understand acceptable performance benchmarks and appropriate use of BI-RADS Category 3 on MRI to avoid unnecessary follow-up or missed cancer diagnosis.

#### TABLE OF CONTENTS/OUTLINE

I. Performance benchmarks for breast MRI  
II. Summary of ACR BI-RADS Atlas 2013 recommendations for assigning BI-RADS Category 3 on breast MRI  
III. Review of scientific, peer-reviewed literature  
A. Characteristics and outcomes  
B. Patient compliance  
C. False negatives  
IV. Guidelines for assigning BI-RADS Category 3 assessment on breast MRI supported by ACR BI-RADS Atlas and scientific literature  
V. BI-RADS Category 3 imaging case review

Printed on: 02/07/23



## Abstract Archives of the RSNA, 2022

BREE-35

### Ductography in the era of Breast MRI: Technique and Approach

Sunday, Nov. 27 8:00AM - 9:00AM Room: Learning Center - BR

#### Participants

Eduardo Cordero Castro, MD, Memphis, TN (*Presenter*) Nothing to Disclose

#### TEACHING POINTS

**SYNOPSIS:** Nipple discharge is the third most common complaint seen in breast centers. Spontaneous discharge causes patient anxiety. The incidence of nipple discharge in breast cancer is 5-12%. Characteristics of suspicious discharge include unilateral, single duct, spontaneous, bloody, or clear color. Imaging modalities used to evaluate patients include mammogram, US, MRI and ductography. **TEACHING POINTS:** The learner will: 1. Review the incidence, clinical presentation, and management of nipple discharge. 2. Know the imaging protocols used to evaluate nipple discharge based on ACR appropriateness criteria. 3. Identify intraductal lesions by imaging that warrant further evaluation.

#### TABLE OF CONTENTS/OUTLINE

Introduction, Clinical presentation, Causes of nipple discharge, Imaging assessment, Differential considerations of intraductal lesions, Role of mammogram and US, MRI findings, Challenges of localizing MRI findings in the subareolar region, Recommended management of nipple discharge without imaging correlation, Recommended management of positive ductogram findings, Pictorial review of ductogram findings, complications during ductogram (bubbles, duct perforation, extravasation, fissurization, lymphatic uptake, incomplete filling), and positive ductogram findings. Clinical management, Algorithm for imaging patients with nipple discharge, Conclusion

Printed on: 02/07/23



## Abstract Archives of the RSNA, 2022

BREE-36

### Histological Special Types of Breast Cancer - How Special Are They? A Pictorial Essay

Sunday, Nov. 27 8:00AM - 9:00AM Room: Learning Center - BR

#### Awards

Certificate of Merit

#### Participants

Karina Pesce, MD, Capital Federal, Argentina (*Presenter*) Nothing to Disclose

#### TEACHING POINTS

Describe the imaging features histological special types of breast carcinoma. Identify the characteristics of each of these tumors that allow them to be differentiated from other breast carcinomas. Discuss the differential diagnosis and management.

#### TABLE OF CONTENTS/OUTLINE

Histological special types of breast cancer constitute a spectrum of lesions from low to high grade aggressiveness. They present different clinical, radiological, and pathological presentations, and although there are no pathognomonic characteristics, there are trends that every breast radiologist should be aware of. 1-Introduction. 2-Histological special types of breast cancer: The WHO spectrum. 3-Appearance mammography, ultrasound, and MRI. 4-Discuss diagnostic challenges and management dilemmas the histological special types of breast cancer. 5- Clinical cases with histological correlation. 6-Take-home points. 7-Conclusion.

Printed on: 02/07/23



## Abstract Archives of the RSNA, 2022

BREE-37

### Yikes, A Red Breast! - A Breast Imager's Approach to Diagnosis and Management

Sunday, Nov. 27 8:00AM - 9:00AM Room: Learning Center - BR

#### Participants

Joshua Weinstein, MD, (*Presenter*) Nothing to Disclose

#### TEACHING POINTS

Breast erythema is a common clinical complaint that can often cause substantial anxiety for patients. The differential is broad, ranging from benign dermatologic conditions, infectious or inflammatory processes, or neoplasms. In this exhibit, we will review this differential and present several exemplary cases of patients who initially presented with breast redness and were ultimately diagnosed with a variety of conditions, including inflammatory breast cancer, angiosarcoma, granulomatous mastitis, breast cellulitis, mastitis related to lactation, mastitis related to an infected foreign body, chronic mastitis, and radiation changes. By reviewing these entities, radiologists can familiarize themselves with the varying clinical presentations of the "red breast" to appropriately image and guide management.

#### TABLE OF CONTENTS/OUTLINE

1. Review the varied clinical presentations and differential diagnoses of breast erythema. 2. Discuss the role of multimodality imaging to diagnose the cause of breast redness. 3. Describe approach to management based on a combination of clinical and radiologic findings.

Printed on: 02/07/23

## Abstract Archives of the RSNA, 2022

BREE-38

### **Ain't No Mountain High Enough! Review of Imaging, Histologic and Management Considerations of High-risk Breast Lesions**

Sunday, Nov. 27 8:00AM - 9:00AM Room: Learning Center - BR

#### **Participants**

Hee Jung Choi, MD, Mexico City, Mexico (*Presenter*) Nothing to Disclose

#### **TEACHING POINTS**

1. Review general features of high risk lesions with illustrations of classic cases using multimodality imaging methods and correlation of the image findings with the underlying histopathologic and clinical findings. 2. Identify imaging and clinical risk factors for malignancy upgrades. 3. Discuss current imaging follow-up and management, as well as controversies in high-risk breast lesions management after the diagnosis.

#### **TABLE OF CONTENTS/OUTLINE**

1. Analyze macro and microscopic normal anatomy of the breast and identify origin of each of the high-risk breast lesions. 2. Identification of high-risk breast lesions by category: a. Atypical ductal hyperplasia b. Lobular breast neoplasia - Atypical lobular hyperplasia - Lobular carcinoma in situ (classic and pleomorphic) c. Papillary lesions - Benign papillary lesions - Intraductal papilloma with atypical hyperplasia d. Flat epithelial atypia e. Radial scar or complex sclerosis lesion 3. Review the key points of each lesion: a. Epidemiology b. Clinical presentation c. Histopathologic characteristics d. Multimodality imaging findings e. Malignancy upgrades risk percentages and risk factors f. Recent guidelines for management g. Illustration of the classic cases 4. Discuss and analyze the recent management and imaging follow-up guidelines.

Printed on: 02/07/23



## Abstract Archives of the RSNA, 2022

BREE-39

### Current Status of Optoacoustic Breast Imaging and Future Trends in Clinical Application: Is It Ready for Prime Time?

Sunday, Nov. 27 8:00AM - 9:00AM Room: Learning Center - BR

#### Participants

Berat Bersu Ozcan, MD, (*Presenter*) Nothing to Disclose

#### TEACHING POINTS

Optoacoustic imaging (OAI) uses non-ionizing, laser light to create thermoelastic expansion in tissues and detect resultant ultrasonic emission. Parametric maps of molecules (melanin, hemoglobin and lipids) that absorb light and scatter acoustic waves are fused with anatomic images, allowing scalable, relative real time molecular assessment in tissues. Since rapidly dividing cancer cells cause hypoxia and lead to tumor-driven angiogenesis, OAI can detect the presence and degree of relative hypoxia in cancers relative to normal tissue. This can increase the specificity of breast mass assessment without compromising the sensitivity compared to the grayscale US alone. Therefore, adjunctive use of OAI can decrease breast biopsies. Molecular subtypes of breast cancer show differing OAI features and levels of hypoxia. Luminal cancers have higher total external feature scores (9.3 vs 8.8;  $p < .05$ ) and lower total internal feature scores (6.8 vs 7.7;  $p < .001$ ) than triple negative and HER2+ cancers. OAI is a thriving field of research whose potential impact on the clinic can be high. However, larger multicenter cohort studies and clinical trials are needed to establish the trends observed and accelerate clinical translation.

#### TABLE OF CONTENTS/OUTLINE

1. Optoacoustic Imaging Principles 2. Why Optoacoustic Breast Imaging: Pros and Cons 3. Handheld versus Tomographic Optoacoustic Breast Imaging Technique 4. Current Clinical Applications and Future Directions 5. Pitfalls and Lessons Learned

Printed on: 02/07/23



## Abstract Archives of the RSNA, 2022

BREE-4

### Multimodality Imaging Review of Metastases to the Breast

Sunday, Nov. 27 8:00AM - 9:00AM Room: Learning Center - BR

#### Participants

Jiewen Li, DO, (*Presenter*) Nothing to Disclose

#### TEACHING POINTS

1. Review normal breast anatomy allowing for metastases to the breast  
2. Discuss common and uncommon metastases to the breast  
3. Demonstrate imaging characteristics of metastases to the breast in a case-based approach

#### TABLE OF CONTENTS/OUTLINE

-Introduction-Definition of metastases to the breast-Typical patient population affected and prognosis-Anatomy of the breast to allow for metastases to the breast\*Vascular/Hematogenous\*Lymphatic\*Direct extension-Common and uncommon metastases to the breast-Typical imaging appearance reported in literature\*Mammogram\*Ultrasound\*MRI-Case-based approach to imaging appearance of extramammary metastases\*Lymphoma\*Leukemia\*Melanoma\*Lung\*Esophageal\*Ovarian\*Plasmacytoma\*Thyroid\*Renal\*Sarcoma-Conclusion\*Recognizing the most common imaging appearance of metastases to the breast can help guide appropriate management and further treatment\*Metastases to the breast generally carry a poor prognosis and any delay in diagnosis can have significant impact\*Metastases to the breast commonly manifest as an irregular mass and typically lack calcifications except for serous ovarian cancer

Printed on: 02/07/23



## Abstract Archives of the RSNA, 2022

BREE-40

### Ultrasound Computed Tomography of the Breast: Techniques, Tips and Tricks

Sunday, Nov. 27 8:00AM - 9:00AM Room: Learning Center - BR

#### Participants

Ken Oba, MD, Chuoku, Japan (*Presenter*) Nothing to Disclose

#### TEACHING POINTS

1. To review the physics principles of ultrasound computed tomography (UCT).2. To discuss the advantages of UCT compared to conventional clinical ultrasound imaging in breast imaging.3. To become familiar with normal and abnormal imaging findings.4. To understand the limitations of UCT in detection, diagnosis, local staging, and follow-up.

#### TABLE OF CONTENTS/OUTLINE

1. Basics of UCT.2. Technique3. Anatomy and breast density in UCT4. Controversies5. CasesCases include:- Benign lesionsFibroadenomaPhyllodes tumorHamartomaBreast lymphoma-Malignant lesionsInvasive ductal carcinomaDuctal carcinoma in situInvasive lobular carcinomaMucinous carcinomaBreast lymphoma-Artifacts- OthersHematomaPostoperative changeBreast reconstruction

Printed on: 02/07/23

## Abstract Archives of the RSNA, 2022

BREE-41

### Hiding in Plain Sight: Cancers in Dense Breasts

Sunday, Nov. 27 8:00AM - 9:00AM Room: Learning Center - BR

#### Awards

Identified for RadioGraphics

#### Participants

Alexis De La Cruz, DO, (*Presenter*) Nothing to Disclose

#### TEACHING POINTS

1. Discuss dense breast tissue as it relates to cancer risk and value of supplemental screening in women  
2. Summarize prior trials and studies that have made an impact on current breast density guidelines  
3. Review current breast density legislation and future directions  
4. Illustrate mammographic clues/hints for identifying breast cancer in dense breasts using a case-based format

#### TABLE OF CONTENTS/OUTLINE

Introduction-Definitions\*\* BI-RADS categories\*\* Quantitative measurements- Factors that contribute to breast density\*\* Age\*\* Pregnancy/breastfeeding\*\* Hormone replacement therapy\*\* Bodyweight- Why does it matter? \*\* Increased breast cancer risk\*\* Decreased sensitivity and specificity with mammography\*\* Possible need for supplemental imaging-Breast density legislation\*\* Current status\*\*Future directionsAppropriateness Criteria/Screening Recommendations- Risk Stratification- Screening Modalities\*\* Mammography, Digital Breast Tomosynthesis (DBT), Contrast-Enhanced Mammography (CEM), Ultrasound, MRI, Abbreviated MRI, FDG-PET breast dedicated, and Molecular Breast Imaging (MBI)Identification of high risk patients\*\* Risk assessment toolsEvidence Based value of supplemental screening\*\*Breast MRI\*\* Breast UltrasoundRadiologic signs to look for in the evaluation of dense breasts using mammography- Subtle spiculation and distortion- Retroglandular fat findings- Nipple distortion and/or gradual retraction- Changes in mass density (increase inhomogeneity)- Halo effect (peripheral lucency)- Fat glandular interface density

Printed on: 02/07/23



## Abstract Archives of the RSNA, 2022

BREE-42

### Architectural Distortion of the Breast: Imaging, Diagnostic Challenges and Treatment

Sunday, Nov. 27 8:00AM - 9:00AM Room: Learning Center - BR

#### Participants

Israel Rodriguez Suarez, MD, Mexico City, Mexico (*Presenter*) Nothing to Disclose

#### TEACHING POINTS

With this educational exhibit the radiologist will be able to: a. Know the normal architecture of the breast in mammography. b. Differentiate between a spiculated mass, architectural distortion and pseudo distortion of the breast parenchyma in mammography. c. Use the imaging tools with an orderly approach to confirm an architectural distortion in mammography: spot compression views, tomosynthesis. d. Identify and characterize an architectural distortion by ultrasound and breast MRI. e. Choose the better imaging biopsy method according to each particular circumstance. f. Learn the differential diagnoses of architectural distortion to make an appropriate radiology pathology correlation. g. Know the current management proposals after percutaneous tissue diagnosis, including the usefulness of breast MRI and contrast enhanced mammography.

#### TABLE OF CONTENTS/OUTLINE

a. Introduction b. Definition c. Normal architecture of the breast d. Imaging of architectural distortion: Mammography, Tomosynthesis, Ultrasonography, Breast MRI. e. Image guided biopsy methods f. Differential diagnoses: Radial Scar or complex sclerosing lesion, Invasive ductal carcinoma, Tubular carcinoma, Invasive lobular carcinoma, Ductal carcinoma in situ, Postsurgical scar, Fat necrosis, Sclerosing adenosis, Focal fibrosis, Diabetic mastopathy. g. Management considerations: Follow up, surgical excision, vacuum assisted excision. Problem solving breast MRI and contrast enhanced mammography.

Printed on: 02/07/23



## Abstract Archives of the RSNA, 2022

BREE-43

### Breast Cancer Recurrence: Multi-modality Imaging in Patients Undergoing Breast Conservation Treatment

Sunday, Nov. 27 8:00AM - 9:00AM Room: Learning Center - BR

#### Awards

Certificate of Merit

#### Participants

Miral Patel, MD, Houston, TX (*Presenter*) Nothing to Disclose

#### TEACHING POINTS

Understanding the terminology and the different treatment options that are available for breast conservation can aid radiologists in detecting recurrence. The post treatment breast appearance will be reviewed as a baseline to understand what these changes look like. Furthermore, a review of the appearance of breast cancer recurrence in multiple cases amongst the various imaging modalities can aid radiologists in early detection.

#### TABLE OF CONTENTS/OUTLINE

This educational exhibit reviews: Breast conservation treatment (BCT): Definitions, surgical techniques and radiation treatment  
Expected breast imaging findings after BCT  
Multi-modality case-based review of recurrence: Tips and tricks to distinguish expected post-operative and radiation changes from tumor recurrence on mammography, ultrasound, magnetic resonance imaging, molecular breast imaging, and contrast enhanced mammography

Printed on: 02/07/23



## Abstract Archives of the RSNA, 2022

BREE-44

### Sheep in Wolf's Clothing: The Many Faces of Granulomatous Mastitis

Sunday, Nov. 27 8:00AM - 9:00AM Room: Learning Center - BR

#### Participants

Tais Batista, MD, Sao Paulo, Brazil (*Presenter*) Nothing to Disclose

#### TEACHING POINTS

The purposes of this exhibit are To review the epidemiology and risk factors for the development of granulomatous mastitis; To discuss the main clinical presentations of these mastitis and its subgroups; To review the main differential diagnoses, as well as overlapping and confounding imaging factors, mainly with carcinomas; To discuss the experience of our institution in a 20 years time period regarding clinical aspects and difficulties in its diagnosis; To describe its histopathological features; To discuss the importance of the multimodality imaging findings in association with histopathological aspects to achieve an accurate diagnosis; To discuss the role of imaging in monitoring the therapeutic response.

#### TABLE OF CONTENTS/OUTLINE

Epidemiology of granulomatous mastitis and factors related to its prevalence in underserved populations; Main clinical presentations; Typical multimodality imaging findings (MRI, ultrasound and mammography) from cases of our radiology department; Diagnostic challenges, main differentials, and key points for early suspicion of this pathology; Particularities of treatment and imaging response after therapy; Summary and Conclusion.

Printed on: 02/07/23



## Abstract Archives of the RSNA, 2022

BREE-45

### Male Nipple Discharge: Beyond the Basics

Sunday, Nov. 27 8:00AM - 9:00AM Room: Learning Center - BR

#### Participants

Javier Azcona Saenz, MD, (*Presenter*) Nothing to Disclose

#### TEACHING POINTS

1) To review the importance of male nipple discharge. 2) To expose the main causes of nipple discharge in men, both benign and malignant, together with their radiological manifestations. 3) To focus on the radiological findings of male breast carcinoma in all imaging techniques, including Digital Breast Tomosynthesis and Contrast-Enhanced Mammography.

#### TABLE OF CONTENTS/OUTLINE

1) Introduction. 2) Causes of male nipple discharge. 2.1) Benign: Gynecomastia, Mammary duct ectasia, Dermatitis, Papilloma, Abscess. 2.2) Malignant: Ductal carcinoma in situ, Invasive carcinoma, Papillary carcinoma of the breast, Others. 3) Characteristic imaging findings: Mammography/Tomosynthesis, Ultrasound, MRI, Contrast-enhanced mammography. 4) Conclusion. 5) References.

Printed on: 02/07/23



## Abstract Archives of the RSNA, 2022

BREE-46

### Pitfalls of Breast Imaging in the Emergency Room

Sunday, Nov. 27 8:00AM - 9:00AM Room: Learning Center - BR

#### Participants

Neha Khemani, MD, Boston, MA (*Presenter*) Nothing to Disclose

#### TEACHING POINTS

1. Clinical breast symptoms seen in the ED are most often related to infection and inflammation  
2. Breast abscess is typically treated as an urgent condition requiring intervention (ultrasound-guided drainage or incision and drainage)  
3. Rarely, inflammatory symptoms can indicate malignancy, thus diagnostic accuracy and close follow-up are necessary to avoid a missed cancer diagnosis  
4. The purpose of this exhibit is to review common breast diagnoses seen in the ED and potential pitfalls of performing breast imaging after hours

#### TABLE OF CONTENTS/OUTLINE

1. Clinical breast symptoms encountered in the ED and indications for imaging  
2. US imaging features of mastitis and abscess  
3. Common diagnoses seen on after-hours breast ultrasound  
4. Pitfalls of after-hours breast imaging with case-based examples:  
a. Variable experience of ER radiologist and sonographer in breast imaging  
b. Technically suboptimal exams  
c. Unavailability of mammography to fully characterize a lesion if needed  
d. Unavailability of breast imaging support staff to arrange for biopsy or follow-up care  
e. High grade breast carcinomas mimicking abscess  
5. Strategies to ensure appropriate care and follow-up for patients with urgent breast complaints

Printed on: 02/07/23



## Abstract Archives of the RSNA, 2022

BREE-47

### There is More to the Breast than Cancer - A Pictorial Case-based Quiz and Review of Rare Benign Breast Lesions

Sunday, Nov. 27 8:00AM - 9:00AM Room: Learning Center - BR

#### Awards

Certificate of Merit

#### Participants

Ines Alonso Sanchez, MD, Bilbao, Spain (*Presenter*) Nothing to Disclose

#### TEACHING POINTS

- Unusual breast benign lesions can be a diagnostic challenge for radiologists, and we should be familiar with their imaging and clinical features.- We must be aware of the limitations of the available breast imaging modalities and know that, in many cases, we need a biopsy to make the diagnosis. - A multidisciplinary approach to these entities is essential to manage them correctly.

#### TABLE OF CONTENTS/OUTLINE

Objective: This presentation aims to revise in quiz format a series of cases of unusual breast benign lesions and describe their imaging and clinical features to strengthen radiologists' skills to recognize and properly approach these conditions. Background: Most patients with breast pathology have concern that they have cancer. Therefore, in this area of practice, it is particularly important to be aware of potential diagnostic pitfalls to avoid emotional suffering to our patients. Findings: We present a series of cases of interesting benign breast lesions with different etiologies, such as inflammatory, vascular, tumors of neural origin, metabolic diseases, proliferative disorders and abnormal protein deposit diseases. Some of these lesions can mimic malignancies, and we should remember clinical features and patients' medical history may help lower the level of suspicion and the patients' emotional unease. Nevertheless, there are limitations of the imaging modalities, and in most cases, a biopsy is needed to make the diagnosis. Conclusions: Despite breast cancer being a common diagnosis; we may still face diagnostic challenges with unusual benign breast lesions which may sometimes mimic cancer.

Printed on: 02/07/23



## Abstract Archives of the RSNA, 2022

BREE-48

### Pregnancy Associated Breast Cancer - What Is It and How Not to Miss It

Sunday, Nov. 27 8:00AM - 9:00AM Room: Learning Center - BR

#### Participants

Haydee Ojeda-Fournier, MD, San Diego, CA (*Presenter*) Research Consultant, View Point Medical, Inc; Stock options, CureMetrix, Inc

#### TEACHING POINTS

Pregnancy-associated breast cancer (PABC) is defined as breast cancer diagnosed during pregnancy, within one year post-partum, or during lactation. Although rare, this disease has a more aggressive course and is often associated with a poorer prognosis. Several studies have found evidence of a delayed diagnosis in pregnant women. But lack of awareness among women and physicians is also believed to play a crucial role in delayed diagnosis. However, the majority of breast lesions during pregnancy and lactation are benign. Still, approximately 20% of breast masses prove to be malignant. By the end of this educational exhibit, the learner will: 1. Review the incidence, clinical presentation, and management of pregnancy-associated breast cancer. 2. Know the imaging protocols recommended to evaluate the pregnant or nursing patient based on ACR appropriateness criteria. 3. Identify lesions that should be biopsied during pregnancy and lactation.

#### TABLE OF CONTENTS/OUTLINE

Introduction; Define pregnancy-associated breast cancer; Clinical presentation of breast cancer during pregnancy or lactation; Review imaging recommendations for pregnant women vs. lactating women; Differential considerations of breast lesions during pregnancy; Mammogram and US findings of pregnant and lactating women; MRI considerations in the pregnant and lactating patient; Recommended management of breast masses without imaging correlation in pregnant and lactating patients; Recommended management of positive imaging findings; Pictorial review of PABC; Clinical management and outcomes of PABC; Algorithm for imaging pregnant and lactating patients so as not to miss a PABC; Conclusion.

Printed on: 02/07/23



## Abstract Archives of the RSNA, 2022

BREE-49

### A Primer on Imaging of Molecular Subtypes of Breast Cancer

Sunday, Nov. 27 8:00AM - 9:00AM Room: Learning Center - BR

#### Participants

Sepideh Sefidbakht, MD, Powel, OH (*Presenter*) Nothing to Disclose

#### TEACHING POINTS

\_To review the clinical relevance of Breast Cancer subtypes and the implications for patient management and imaging.\_To review the basic pathologic and clinical characteristics of each major molecular subtype along with their typical imaging appearance.\_To show how this knowledge affects decision making using a case-based approach

#### TABLE OF CONTENTS/OUTLINE

\_Introduction: basic pathology of molecular subtypes of breast cancer; how to diagnose and implications for patient management\_Luminal A breast Cancer, Pathology, Prognosis, multimodality imaging characteristics\_Luminal B breast Cancer, Pathology, Prognosis, multimodality imaging characteristics\_HER2-enriched breast Cancer, Pathology, Prognosis, multimodality imaging characteristics\_Basal-like breast Cancer, Pathology, Prognosis, multimodality imaging characteristics\_Case-based review of typical and atypical presentations of various subtypes

Printed on: 02/07/23

## Abstract Archives of the RSNA, 2022

BREE-50

### Unusual Infections of the Breast - A Pictorial Review

Sunday, Nov. 27 8:00AM - 9:00AM Room: Learning Center - BR

#### Participants

Sabine Popp, MD, Vienna, Austria (*Presenter*) Nothing to Disclose

#### TEACHING POINTS

• Unusual infectious diseases of the breast are uncommon but important for radiologists to be aware of, as they may be indistinguishable from breast cancer and are treatable. • Consider Tuberculosis in patients with a persistent abscess or atypical mass, especially if from a high Tuberculosis incidence country. • In patients with incidental breast calcification detected at screening from endemic countries, consider Schistosomiasis (amorphous, segmental distribution), Dracunculiasis (coarse linear, serpiginous) or chronic Filariasis (serpiginous, tubular and coiled). • Recurrent breast abscesses can be caused by rare organisms such as Actinomyces and Corynebacterium, therefore it is important to send a fine needle aspirate for microbiology to direct treatment. • In patients with nipple eczema, consider Lyme disease as a differential to Paget's disease, especially if regional lymphadenopathy is present.

#### TABLE OF CONTENTS/OUTLINE

• Learning objectives • Introduction • Organisms - for each of the below: epidemiology, clinical presentation, imaging features (mammography, ultrasound, MRI), diagnosis and treatment o Bacteria • Tuberculosis • Other mycobacteria • Actinomycosis • Lyme disease • Brucella • Cryptococcus o Parasites • Schistosomiasis • Filariasis • Cysticercosis • Hydatid cyst • Dracunculiasis • Other rare organisms • Differential diagnoses • Summary table • Conclusion

Printed on: 02/07/23



## Abstract Archives of the RSNA, 2022

BREE-51

### You've Got a Friend in Me: How Radiologists Can Help Patients and Multidisciplinary Colleagues in the Diagnosis and Management of Fibroepithelial Lesions

Sunday, Nov. 27 8:00AM - 9:00AM Room: Learning Center - BR

#### Awards

**Cum Laude**

**Identified for RadioGraphics**

#### Participants

Jody C. Hayes, BS, MD, Dallas, TX (*Presenter*) Nothing to Disclose

#### TEACHING POINTS

1. When a fibroepithelial lesion (FEL) is suspected, biopsy specimens should include the margin of the mass for a more definitive diagnosis on histopathology.2. For large masses, biopsy specimens should be taken from different areas to ensure adequate sampling as phyllodes tumors (PT) often demonstrate tumor heterogeneity with fibroadenoma-like regions.3. Surgical resection is indicated for rapidly growing biopsy-proven benign FEL or borderline PT whose growth rate exceeds 20% in largest dimension in a six-month interval.4. Staging chest CT should be performed for malignant PT due to their propensity for hematogenous spread with the lungs being the most common site.5. Frequent follow-up imaging with breast ultrasound or chest CTs may be indicated for locally aggressive malignant PT to identify early recurrence.

#### TABLE OF CONTENTS/OUTLINE

1. Define the spectrum of fibroepithelial lesions (FEL) with pertinent incidence and demographic information.2. Review imaging and pathologic findings for the spectrum of FEL.3. Discuss steps radiologists can take to help in the diagnosis and management of FEL with an emphasis on radiological, pathological, and clinical concordance.4. Define the role of imaging for the post-biopsy or post-surgical FEL patient.

Printed on: 02/07/23



## Abstract Archives of the RSNA, 2022

BREE-52

### Everything That Looks Like BI-RADS 5, But Is Not

Sunday, Nov. 27 8:00AM - 9:00AM Room: Learning Center - BR

#### Participants

Maria Ares-Rego, MD, Santiago de Compostela, Spain (*Presenter*) Nothing to Disclose

#### TEACHING POINTS

To review the imaging features used in a BI-RADS 5 assessment. To illustrate benign entities that can mimic malignancy (the most common are chronic and inflammatory mastitis, fat necrosis, complex sclerosing lesions, granular cell tumors, lymphocytic mastopathy, infection...); to describe imaging findings, clinical history. To review the specific imaging features of these benign entities depicted at mammography, US, MRI. To relate radiologic-pathologic correlation and clinical history to decide the management of a discordant biopsy result. To familiarize radiologist with the knowledge of the variety of benign entities may be categorized as BI-RADS 5 to include them within the differential diagnostic.

#### TABLE OF CONTENTS/OUTLINE

Presentation of BI-RADS 5 classification. Describe benign entities possibly classified as BI-RADS 5. Utility of imaging techniques. Imaging findings: specific features and clinical history. Management. Differential diagnostic

Printed on: 02/07/23



## Abstract Archives of the RSNA, 2022

BREE-53

### Difficult MRI-Guided, Vacuum-Assisted Core Biopsies of the Breast: Tips and Tricks

Sunday, Nov. 27 8:00AM - 9:00AM Room: Learning Center - BR

#### Participants

Wenhui Zhou, MD, PhD, Menlo Park, CA (*Presenter*) Nothing to Disclose

#### TEACHING POINTS

Magnetic resonance imaging (MRI) is the most sensitive method to detect abnormalities of the breast. Due to its limited specificity, MRI-detected lesions often require tissue sampling to establish the diagnosis. Breast imagers should be cognizant of patient, anatomical, and technical factors that predispose to a potentially difficult MRI-guided breast biopsy. The purpose of this educational exhibit is to demonstrate techniques and tools to safely and successfully biopsy breast lesions. Completing this educational exhibit will allow participants to 1) Appreciate patient, anatomical and technical factors that predispose to difficult MRI-guided breast biopsies 2) Recognize pre-procedural planning, techniques and tools to optimize lesion visualization, targeting and sampling 3) Implement this knowledge during MRI-guided biopsies to minimize MR cancellations, unsafe procedures and nondiagnostic samples.

#### TABLE OF CONTENTS/OUTLINE

This case-based exhibit will demonstrate procedural planning and tips for successful difficult-to-perform MRI-guided breast biopsies including: 1) for bilateral lesions, perform simultaneous biopsy using lateral to medial approaches bilaterally 2) for posterolateral lesions, apply arm-down and arm-up maneuvers to facilitate safe access route 3) for lesions offset from the obturator tip, re-target with a second introducer and directionally sample if necessary 4) for posteromedial lesions, utilize a tangential, oblique approach to allow adequate access to the target 5) for vague or obscured lesions, consider the use of a T2-weight or DWI sequence to improve visualization. We will summarize take-home points to facilitate transfer of knowledge.

Printed on: 02/07/23



## Abstract Archives of the RSNA, 2022

BREE-54

### How To Report a Contrast Enhanced Mammography (CEM) Study - An Illustrated and Practical Review of BIRADS 2022 Supplement for CEM

Sunday, Nov. 27 8:00AM - 9:00AM Room: Learning Center - BR

#### Awards

Certificate of Merit

#### Participants

Rosa M. Lorente-Ramos, MD, PhD, Madrid, Spain (*Presenter*) Nothing to Disclose

#### TEACHING POINTS

-To review contrast enhanced mammography (CEM) basics and technique. -To analyze steps in interpretation of a CEM study. - To describe CEM lexicon and report structure. - To become familiar with normal and abnormal imaging findings in CEM providing correlation with imaging (mammogram, US, MR) and pathology.

#### TABLE OF CONTENTS/OUTLINE

We review the basics and state-of-the-art of CEM highlighting adequate interpretation of the exam according to the latest BIRADS recommendations for CEM reporting. 1. Basics of CEM. 2. Technique: Image acquisition: Low-energy images (LE) like a digital mammogram. Recombined images (subtraction of the low-energy from the high-energy images) (RC). Signal from background breast tissue is cancelled highlighting areas of iodine uptake. 3. Image interpretation steps. -LE. Morphological assessment -RC. Functional assessment. 4. BIRADS lexicon for CEM. - General overview: breast density (LE), Background parenchymal enhancement (RC). - LE findings. - RC findings: mass, non-mass enhancement, enhancing asymmetry, lesion conspicuity. - Lesion description on both: morphology, internal enhancement pattern, extent of enhancement, lesion conspicuity. 5. Report structure. Indication, technique, previous exams, breast composition, findings description, assessment, management.

Printed on: 02/07/23



## Abstract Archives of the RSNA, 2022

BREE-55

### Staging Breast Cancer: A Case Based Review

Sunday, Nov. 27 8:00AM - 9:00AM Room: Learning Center - BR

#### Participants

Aline Guimaraes, MD, (*Presenter*) Nothing to Disclose

#### TEACHING POINTS

Staging Breast Cancer nowadays is not only about defining the anatomic extent of disease. The most recent edition of the AJCC (American Joint Committee on Cancer), the eighth edition, now incorporate prognostic biomarkers to more accurately predict clinical outcomes and treatment response on an individual basis. In this didactic exhibit, we will discuss each aspect of Breast Cancer Staging in a case-based review. It is imperative to know the potential and limitations of each imaging modality (mammography, ultrasound and magnetic resonance imaging) and what to look for and describe on the exams. It is also important to comprehend other relevant aspects such as tumor grade, ER (estrogen receptor), PR (progesterone receptor) and HER2 (human epidermal growth factor receptor 2) status. Fundamentally understanding these aspects will provide more prognostic information than the anatomic stage alone and contribute to improve medical practice.

#### TABLE OF CONTENTS/OUTLINE

1. Mental Map with the following information 1. AJCC Staging System (application criteria) 2. Breast Cancer Stage 2.1. Clinical Staging 2.2. Pathologic Staging 2.3. Posttherapy staging after Neoadjuvant Chemotherapy, Radiation Therapy and Hormonal Therapy 2.4. Nodal staging 2.5. Clinical staging of metastasis 2.6. Stage migration 2. Relevant aspects to consider in breast imaging when staging breast cancer 3. Case based review of aspects mentioned above

Printed on: 02/07/23



## Abstract Archives of the RSNA, 2022

BREE-56

### Review of Breast Anatomy - Normal Variants and Expected Physiologic Changes in the Breast

Sunday, Nov. 27 8:00AM - 9:00AM Room: Learning Center - BR

#### Participants

Hubert Huang, MD, (*Presenter*) Nothing to Disclose

#### TEACHING POINTS

The female breast follows a predictable sequence of development. The mature adult breast is subject to a variety of physiologic effects during embryologic development, aging and hormonal changes. As a result, the female breast demonstrates a wide spectrum of normal appearance, some of which are congenital variants such as polythelia and polymastia, while others are acquired or physiologic but still considered normal, such as changes in density during pregnancy, lactation, and those typically seen with aging. Recognizing normal physiologic changes and anatomic variants can present a challenge to the radiologist. However, it is imperative to do so since the optimal modalities and views for evaluating these entities will differentiate them from potentially suspicious findings. We will present and discuss normal female breast development and anatomy, congenital and physiologic variants, and ways to avoid misdiagnoses.

#### TABLE OF CONTENTS/OUTLINE

1. We will review normal anatomy of the breast. 2. We will discuss expected normal female breast developmental changes. 3. We will discuss variations in breast pattern and density in different physiologic conditions such as pregnancy and breastfeeding, as well as aging. 4. We will discuss normal and congenital breast anatomic variants. 5. We will review common and avoidable pitfalls of imaging variants that may mimic malignancy.

Printed on: 02/07/23



## Abstract Archives of the RSNA, 2022

BREE-57HC

### Be Prepared - It's Not Because It's Rare that It Won't Happen! What the Radiologist Needs to Know About Angiosarcoma of the Breast

Sunday, Nov. 27 8:00AM - 9:00AM Room: Learning Center - BR

#### Participants

Amanda Tavares, MD, Sao Paulo, Brazil (*Presenter*) Nothing to Disclose

#### TEACHING POINTS

Angiosarcoma represents less than 1% of soft tissue sarcomas and is a very aggressive tumor with a poor prognosis. It depicts approximately 0.04% of malignant breast neoplasms and 8% of breast sarcomas, presenting with rapid and silent growth. The radiological findings are nonspecific, but the radiologist must be aware of the imaging features to avoid misdiagnosis. Primary breast angiosarcoma has an unknown etiology, affects younger patients (30-40 years) and usually presents as a palpable mass. Bilateral involvement is often associated with pregnancy or contralateral metastatic spread. There are no pathognomonic findings on conventional imaging. Nonetheless, on magnetic resonance imaging, the persistent enhancement in the dynamic study with late concentric filling may suggest this diagnosis. There may be areas of necrosis, hemorrhage and infarction within the tumor. Secondary breast angiosarcoma often occurs after local radiation therapy, with a mean latency period of 5-6 years. Besides that, chronic breast lymphedema and genetic predisposition are also risk factors. It commonly occurs in older patients (over 60 years) and may manifest as a palpable mass or just thickening and discoloration of the skin. Imaging findings are similar to the primary form.

#### TABLE OF CONTENTS/OUTLINE

General aspects of angiosarcoma of the breast: Etiology, Prognosis, Diagnosis; Primary Breast Angiosarcoma; Secondary Breast Angiosarcoma; Summary Please visit the Learning Center to also view this presentation in hardcopy format.

Printed on: 02/07/23



## Abstract Archives of the RSNA, 2022

BREE-58

### Mimicking of an Abscess or Hematoma: Complex Mass Presentations of Triple Negative Breast Cancers

Sunday, Nov. 27 8:00AM - 9:00AM Room: Learning Center - BR

#### Awards

Identified for RadioGraphics

#### Participants

Dogan Polat, MD, Dallas, TX (*Presenter*) Nothing to Disclose

#### TEACHING POINTS

Triple negative breast cancers are 16% of breast cancers in non African American women and 27% of breast cancers in African American women, often associated with BRCA 1 mutation and aggressive features, and poor prognostic outcome. Carefully assess margins of anechoic masses or complex masses which favor abscesses or hematoma, particularly if there is no overlying skin thickening or secondary signs of infection. Triple negative breast cancers can have posterior acoustic enhancement sonographically (therefore look for irregular margins, wall thickening, solid components). Triple negative breast cancers can present as a round hyperdense mass mammographically, therefore caution if one notes a round (not oval) mass, especially hyperdense (on attachment). Triple negative breast cancer can mimic other benign processes such as fibroadenoma, therefore careful margin assessment is important. Carefully review the axilla mammographically on patients with a history of breast cancer, using comparison to prior studies.

#### TABLE OF CONTENTS/OUTLINE

1. Review mammographic and sonographic appearances of triple negative breast cancers and define triple negative breast cancer.
2. Recognize indistinct margins, thick walls, and lack of skin thickening in anechoic appearing irregular triple negative malignant masses and identify findings which raise concern for malignancy in these cases.
3. Review margin assessment of masses on ultrasound, particularly the sides of margins in a partially circumscribed mass.
4. Review metastatic patterns of triple negative breast cancer and mammographic assessment of the axilla in follow up of patients with history of breast cancer.

Printed on: 02/07/23



## Abstract Archives of the RSNA, 2022

BREE-59

### Fat-Containing Breast Masses: A Multi-Modality Review and Management Considerations

Sunday, Nov. 27 8:00AM - 9:00AM Room: Learning Center - BR

#### Participants

Alison Gegios, MD, Whitefish Bay, WI (*Presenter*) Nothing to Disclose

#### TEACHING POINTS

Fat-containing entities in the breast constitute a variety of predominantly benign conditions and rarely malignant neoplasms. This presentation will focus on the recognition and diagnosis of fat-containing breast lesions to facilitate appropriate management and avoid unnecessary work-up and interventions. It will also discuss scenarios in which biopsy of fat-containing breast masses may be warranted.

#### TABLE OF CONTENTS/OUTLINE

1. Imaging features consistent with fat on multiple modalities: • MRI • Ultrasound • Mammogram  
2. Imaging features and management of common and uncommon benign fat-containing lesions • Lipoma • Hamartoma • Fat necrosis • Oil cyst • Intramammary lymph node • Galactocele • Steatocystoma multiplex • Angiolipoma • Hibernoma

Printed on: 02/07/23



## Abstract Archives of the RSNA, 2022

BREE-6

### Much More Than Lymph Nodes! A Practical Approach to Axillary Imaging

Sunday, Nov. 27 8:00AM - 9:00AM Room: Learning Center - BR

#### Participants

Carolina Kiebert, Sao Paulo, Brazil (*Presenter*) Nothing to Disclose

#### TEACHING POINTS

To show axillary anatomy in the different imaging modalities. To review the indications for axillary imaging. To present clinical and imaging findings of axillary masses according to the anatomical location of the lesion. To familiarize general radiologists with these findings in order to expedite accurate diagnosis. To discuss percutaneous interventions in axillary masses and the appropriate patient management depending on the diagnosis.

#### TABLE OF CONTENTS/OUTLINE

Radiologists are familiar with the evaluation of the axillary levels and staging of breast cancer, but we rarely discuss other pathologies that can be located in the axilla other than breast cancer lymph-node metastasis. Understanding the anatomy of the axilla can help radiologists to identify accurate diagnoses according to the anatomical location of the lesion once percutaneous biopsy may be inappropriate. This educational exhibit will compile anatomy and different findings with illustrative images from our radiology department. Knowledge of the clinical and imaging findings may improve detection of the differential diagnosis for such lesions, improving appropriate patient management.

Printed on: 02/07/23



## Abstract Archives of the RSNA, 2022

BREE-60

### Metaplastic Breast Carcinoma: Review of Imaging, Histopathology and Management Algorithm

Sunday, Nov. 27 8:00AM - 9:00AM Room: Learning Center - BR

#### Participants

Janice Thai, MD, (*Presenter*) Nothing to Disclose

#### TEACHING POINTS

1. To review the imaging spectrum of metaplastic carcinoma of the breast. 2. To review the histopathology and pathophysiology of this rare tumor subtype. 3. To review the treatment and management algorithm.

#### TABLE OF CONTENTS/OUTLINE

- Imaging review of common and uncommon features of metaplastic carcinoma
- Review of unique histo and pathophysiology of metaplastic carcinoma.
- Review of current evidence-based management algorithm

Printed on: 02/07/23



## Abstract Archives of the RSNA, 2022

BREE-61

### Spectrum of Mucinous and Mucocele-like Lesions: Imaging and Histopathologic Review

Sunday, Nov. 27 8:00AM - 9:00AM Room: Learning Center - BR

#### Participants

Janice Thai, MD, (*Presenter*) Nothing to Disclose

#### TEACHING POINTS

1. To review the imaging spectrum of mucinous and mucocele-like lesions. 2. To review the histopathology and distinct tumor/high risk lesion subtype. 3. To review the treatment and management algorithm.

#### TABLE OF CONTENTS/OUTLINE

- Imaging review of common and uncommon features of mucinous and mucocele-like lesions
- Review of unique histo and pathophysiology of mucinous and mucocele-like lesions
- Review of current evidence-based management algorithm

Printed on: 02/07/23



## Abstract Archives of the RSNA, 2022

BREE-62

### PET Mammography from Indications to Interpretation

Sunday, Nov. 27 8:00AM - 9:00AM Room: Learning Center - BR

#### Participants

Rasha M. Kamal, MD, Cairo, Egypt (*Presenter*) Nothing to Disclose

#### TEACHING POINTS

PEM is a specialized application of PET to visualize breast tissue metabolic changes with a much higher spatial resolution thus allowing the visualization of smaller tumor cells. In this educational exhibit the technique of PEM will be discussed in detail. The qualitative and quantitative (the PUV and Lesion to background activity) assessment of PEM images will be illustrated. The pattern of radiotracer uptake in the different histopathology and molecular subtype will be also discussed. The main indications of PEM include: - Enhanced lesion characterization. - Preoperative staging - Response to NAC therapy monitoring. - Post breast cancer surveillance. - Screening for women with dense breasts. - Metastases of unknown primary The advantages and disadvantages of PEM will be highlighted to allow the sound practice of this novel imaging modality.

#### TABLE OF CONTENTS/OUTLINE

1. Technique of PEM 2. Indications 3. Interpretation (quantitative and qualitative assessment 4. Advantages and disadvantages of PEM

Printed on: 02/07/23



## Abstract Archives of the RSNA, 2022

BREE-63

### Evolving Role of Nuclear Medicine and Molecular Imaging in Breast Cancer - A Case-based Multi-modality Pictorial Review with Teaching Pearls

Sunday, Nov. 27 8:00AM - 9:00AM Room: Learning Center - BR

#### Awards

Certificate of Merit

#### Participants

Fatima Elahi, DO, Lincolnwood, IL (*Presenter*) Nothing to Disclose

#### TEACHING POINTS

Breast cancer continues to be the most common cause of malignancy for women in the United States with current imaging standards centered around mammography, CT, ultrasound, and MRI. Nuclear Medicine (NM) and molecular imaging (MI) including PET CT have now become essential tools in the diagnosis and management of patients with Breast cancer. Often times the findings have resulted in decisions that change the course of treatment in about 24-48% of patients. We provide a case-based multimodality pictorial review of the evolving role of Nuclear Medicine and Molecular Imaging in the management of patients with breast cancer.

#### TABLE OF CONTENTS/OUTLINE

Our educational exhibit aims to 1) Highlight the impact of various NM and MI tracers and modalities such as Lymphoscintigraphy including Mannose-binding Tc-99m Tilmanocept for targeted lymphatic mapping and Sentinel node localization, mammo-scintigraphy (Molecular breast imaging (MBI)), MDP Bone scan, F-18 Sodium Fluoride PET CT, F-18 FDG PET CT, Hormonal receptor imaging (such as F18-Fluoroestradiol PET CT); Radionuclide ventriculogram (MUGA Scan); Palliative treatment of painful bone metastasis using strontium-89/samarium 153; PET CT guided interventions and biopsy; 2) Case-based discussions highlighting the indications, sensitivity, and specificity rates and limitations of these studies; 3) Discuss challenging cases including axillary lymphadenopathy secondary to COVID 19 vaccination, FLARE phenomenon, somatostatin receptor-expressing breast cancers on Ga-68 DOTATATE PET CT, evaluating Post-operative breast for local recurrence and male breast cancer; 4) utility of texture analysis.

Printed on: 02/07/23



## Abstract Archives of the RSNA, 2022

BREE-64

### Overcoming Burnout Towards Brilliance in Breast Radiologists after COVID-19

Sunday, Nov. 27 8:00AM - 9:00AM Room: Learning Center - BR

#### Participants

Jay R. Parikh, MD, West University Place, TX (*Presenter*) Nothing to Disclose

#### TEACHING POINTS

Burnout has been recognized by the World Health Organization as a syndrome conceptualized as resulting from chronic workplace stress that has not been successfully managed. A previous study showed that there is a high prevalence of burnout across practicing clinical breast radiologists. Physician wellness (well-being) is defined by quality of life, which includes the absence of ill-being and the presence of positive physical, mental, social and integrated well-being. The unprecedented COVID-19 pandemic has brought challenges to the practicing breast radiologist. Initially, there was a reduced workload volume early in the pandemic which then rebounded into high volumes of breast screening and diagnostic studies. Coupled with this volume were challenges of maintaining family work-life balance and regular social isolation, compounding the negative work environment. The COVID-related work environment has previously been described as unsustainable for radiologists. Surveys of clinically practicing radiologists during COVID-19 have demonstrated a high rate of burnout and increased subjective stress by breast radiologists. Strategies that may be deployed post COVID-19 to mitigate radiologist burnout include implementing a culture in the workplace that prioritizes and promotes wellness, addressing operational inefficiencies and increasing resiliency of practicing breast radiologist.

#### TABLE OF CONTENTS/OUTLINE

A. Burnout. B. Burnout in Breast Radiologists C. COVID-19 Impact on breast radiology D. Implementing a culture of wellness. E. Addressing operational inefficiencies F. Increasing radiologist resiliency

Printed on: 02/07/23



## Abstract Archives of the RSNA, 2022

BREE-65

### Understanding Fibroepithelial Lesions of the Breast - A Primer for Residents and Fellows

Sunday, Nov. 27 8:00AM - 9:00AM Room: Learning Center - BR

#### Participants

Tara Retson, MD, PhD, San Diego, CA (*Presenter*) Research Consultant, CureMetrix, Inc; Stock options, CureMetrix, Inc

#### TEACHING POINTS

**SYNOPSIS:** Fibroepithelial lesions (FEL) of the breast are biphasic neoplasms with variable amounts of stromal and epithelial proliferation. They range from benign fibroadenomas to malignant phyllodes tumors, fibroadenomas being the most diagnosed breast lesion on core needle biopsy. Other FEL includes cellular and juvenile fibroadenoma and benign, borderline, and malignant phyllodes. **TEACHING POINTS:** By the end of this educational exhibit, the learner will: 1. Review the incidence, clinical presentation, and management of FEL of the breast. 2. Know the imaging protocols used to evaluate FEL, including mammogram, US, and MRI, based on age and ACR appropriateness criteria. 3. Understand the classification of FEL based on the WHO classification. 4. Identify FEL that is locally aggressive and warrants further surgical management.

#### TABLE OF CONTENTS/OUTLINE

Introduction; Clinical presentation of FEL; Differential considerations of FEL include differentiation of malignant phyllodes from metaplastic breast cancer and sarcoma; Understanding the grading of phyllodes tumors; Imaging assessment of FEL; Role of mammogram and US in the evaluation of FEL; MRI findings of FELs; Recommended clinical management of FEL; A pictorial review of FEL; Algorithm for imaging patients with suspected FEL; Conclusion

Printed on: 02/07/23

## Abstract Archives of the RSNA, 2022

BREE-66

### Superficial Lesions of the Breast - What Residents Need To Know?

Sunday, Nov. 27 8:00AM - 9:00AM Room: Learning Center - BR

#### Participants

Karen Caro, PhD, La Plata, Argentina (*Presenter*) Nothing to Disclose

#### TEACHING POINTS

1. To illustrate imaging features of superficial lesions of the breast. 2.Characteristics of superficial lesions of the breast. 3. Distinguish superficial lesions of the breast versus parenchymal lesions.

#### TABLE OF CONTENTS/OUTLINE

The thin epidermis is composed of several cell layers and contains no blood or lymphatic vessels and may not be distinguished from the dermis at imaging . However, within the dermis reside hair follicles, sebaceous glands, sweat glands, nerve endings, and blood and lymph vessels. The hypodermis typically contains nerves, lymphatics, larger blood vessels, and fatty tissue. The importance of delimiting the layers of the skin and its components help us to identify the lesions that can originate at this level For example, the presence of a tract—which represents extension of the hair follicle from the dermis up through the epidermis—that extends from the lesion to the epidermal skin surface also confirms a dermal origin and is indicative of a sebaceous or epidermal inclusion cyst. It is so that in the present work we will analyze different images and their characteristics that will help us to define their probable origin. Conclusions The importance of identifying skin lesions and differentiating them from those located in the mammary parenchyma helps us to define BI-RADS, since many times we can perform controls or even biopsies, which can be avoided, through an adequate study of their location through image and do not forget the importance of a physical examination and questioning

Printed on: 02/07/23

## Abstract Archives of the RSNA, 2022

BREE-67

### What's Normal Anymore - Lymph Node Evaluation and the Changing Guidelines of COVID

Sunday, Nov. 27 8:00AM - 9:00AM Room: Learning Center - BR

#### Participants

Anna Hollen, MD, (*Presenter*) Nothing to Disclose

#### TEACHING POINTS

- Review the impacts of COVID-19 vaccination on axillary lymphadenopathy.
- Understand the approach to lymph node evaluation in breast practice.
- Understand the differences between normal and abnormal lymph nodes.
- Through case examples, understand when lymphadenopathy is benign and when further workup is necessary.

#### TABLE OF CONTENTS/OUTLINE

- Overview of COVID impacts, breast imaging society guidelines and institutional specific operational changes
- Review of lymph node evaluation in breast practice and use of ultrasound
- Normal vs. abnormal lymph node features
- Case-based illustration of lymph node pathology and appropriate assessment/management
- Benign reactive lymphadenopathy related to COVID vaccination
- Lymphoma
- Breast cancer unknown at time of workup
- Metastatic, known breast cancer
- Melanoma
- Unknown primary

Printed on: 02/07/23



## Abstract Archives of the RSNA, 2022

BREE-68

### Radial Sclerosing Lesions: An Updated Approach to Multidisciplinary Management

Sunday, Nov. 27 8:00AM - 9:00AM Room: Learning Center - BR

#### Participants

Allison Aripoli, MD, Kansas City, KS (*Presenter*) Nothing to Disclose

#### TEACHING POINTS

1. Radial sclerosis lesions (RSL) are benign lesions that often present with suspicious imaging features such as mammographic architectural distortion. 2. RSL are often seen in association with other benign or high-risk proliferative lesions. 3. Newer literature demonstrates lower malignancy upgrade rates of RSL, especially RSL without associated atypia, resulting in shifting management paradigm toward de-escalation of routine surgical excision of RSL. 4. Upgrade of a "pure" RSL to atypia at surgical excision is an additional important consideration to provide relevant information for appropriate individual risk stratification and risk reduction. 5. Radiology-pathology concordance and multidisciplinary review are essential for treatment decisions. Institutional review of upgrade rates can help define management.

#### TABLE OF CONTENTS/OUTLINE

1. Introduction  
a. Imaging appearance of RSL and overlap with malignancy  
b. Pathology review  
c. Association with other benign or high-risk proliferative lesions  
2. Historical shifts in understanding and managing RSL  
a. Older studies and upgrade rates  
b. Newer studies and upgrade rates  
c. American Society of Breast Surgeons Consensus Guidelines for management of RSL  
d. Factors related to risk of upgrade  
e. Lack of consensus for management among contemporary studies  
3. Radiology-pathology concordance and multidisciplinary conference review  
a. De-escalation of routine surgical excision of concordant RSL based on contemporary published and institutional data  
b. Long-term follow-up and management

Printed on: 02/07/23

## Abstract Archives of the RSNA, 2022

BREE-69

### **Pregnancy Associated Breast Cancer: Diagnostic Approach and Imaging Pitfalls**

Sunday, Nov. 27 8:00AM - 9:00AM Room: Learning Center - BR

#### **Participants**

Charisma DeSai, MD, Dallas, TX (*Presenter*) Nothing to Disclose

#### **TEACHING POINTS**

1. Definition: Pregnancy associated breast cancer (PABC) is cancer that develops during pregnancy, breastfeeding, or in the first year postpartum.2. Understand the epidemiology and pathophysiology of PABC.3. Review the risk factors associated with PABC and reasons for diagnostic delay.4. Review the expected breast imaging findings in the pregnant and lactating breast.5. Review the imaging and clinical findings of PABC.6. Review of ACR appropriateness criteria of breast screening and staging during pregnancy and lactation.7. Create a diagnostic approach to symptomatic breast during pregnancy and lactation.8. Explore the different surgical and systemic management options for PABC with respect to fetal and maternal safety.

#### **TABLE OF CONTENTS/OUTLINE**

1. Risk factors associated with PABC2. Expected imaging findings of the breast during pregnancy and lactation.3. Review of ACR appropriateness criteria of breast imaging and staging during pregnancy and lactation based on patient age and lifetime risk for breast cancer.4. Diagnostic approach to symptomatic breast during pregnancy and lactation5. Review of radiological findings in:- PABC.- Benign conditions associated with pregnancy and lactation: Breast abscess, lactational mastitis.- How to differentiate lactational mastitis and inflammatory breast cancer.6. Role of imaging guided biopsy.7 Treatment options for PABC including surgical management

Printed on: 02/07/23



## Abstract Archives of the RSNA, 2022

BREE-7

### Abdominopelvic Manifestations of Metastatic Breast Cancer and Treatment-Related Complications

Sunday, Nov. 27 8:00AM - 9:00AM Room: Learning Center - BR

#### Awards

Certificate of Merit

#### Participants

Annie Rhee, MD, (*Presenter*) Nothing to Disclose

#### TEACHING POINTS

1. Common sites of breast cancer metastases on abdominal/pelvic imaging are the liver and bones. Less common sites are the peritoneum, gastrointestinal tract, ovary, and retroperitoneum. 2. Invasive lobular carcinoma metastases are often infiltrative, which can be difficult to evaluate in earlier stages of disease on imaging. Recognizing complications such as small bowel strictures or obstruction in patients with a history of breast cancer can prompt further investigation. 3. Treatment related complications such as pseudocirrhosis, endometrial hyperplasia, and post-surgical changes should also be recognized in these patients.

#### TABLE OF CONTENTS/OUTLINE

Background: IDC ILCLiver Metastases Focal mass Diffuse infiltration Treatment-related pseudocirrhosis Bile Ducts Biliary obstruction Pancreas MetastasesMass vs infiltrative lesions Adrenal MetastasesDiffuse/nodular thickeningMass GI tract Stomach Linitis plastica Focal ulcerations Small bowel Infiltration obstruction Colon rectum Linitis plastica Ovarian Metastases Primary ovarian cancer in BRCA positive patients Uterus endometrium Metastases Infiltrative Tamoxifen related pathologyEndometrial spectrum (hyperplasia to carcinoma)AdenomyosisLeiomyomaUterine sarcoma Peritoneum Nodular vs infiltrative Retroperitoneum MetastasesInfiltrative fibrotic with urinary tract complications Lymph nodesDistribution of lymphatic spreadAbdominal wall Metastases Postsurgical changesDIEP flap Bones Metastases Blastic, lytic, mixed Pathologic fracture Treatment changes Conclusions

Printed on: 02/07/23



## Abstract Archives of the RSNA, 2022

BREE-70

### 2022 New Trends in Breast Density - What Should We Know?

Sunday, Nov. 27 8:00AM - 9:00AM Room: Learning Center - BR

#### Awards

Identified for RadioGraphics

#### Participants

Flavia Sarquis, MD, Buenos Aires, Argentina (*Presenter*) Nothing to Disclose

#### TEACHING POINTS

Digital mammography (DM) is the most commonly utilized modality in asymptomatic women in the preventative setting, with continuous advancement in breast density measurement. Women with dense breasts have an increased risk of developing breast cancer. Breast density is the most common factor that may prompt women to seek additional screening beyond mammography to increase the likelihood of early cancer detection. After reading this educational exhibit the radiologist will know: Women with dense breasts have clear downsides of breast cancer screening facing an increased risk of late diagnosis. Early diagnosis and treatment are vital. The pandemic has taught us what needs to be done. The realistic limitations of mammography in dense breasts and the benefits of additional screening. Stratification of breast cancer prevention and screening requires mammographic density measures predictive of cancer. New recommendations of breast cancer screening in women with extremely dense breasts.

#### TABLE OF CONTENTS/OUTLINE

Breast density is a biomarker of objectively measurable characteristics that indicate an underlying physiological or pathological process. Current evidence on breast cancer screening in women with dense breasts. Added detection with supplemental screening. Principles of shared decision-making. Illustrative-based cases. Conclusions

Printed on: 02/07/23

## Abstract Archives of the RSNA, 2022

BREE-71

### T2 Hyperintense Breast Lesions on MRI - A Pictorial Guide for Residents

Sunday, Nov. 27 8:00AM - 9:00AM Room: Learning Center - BR

#### Participants

Maria Jose Chico, Buenos Aires, Argentina (*Presenter*) Nothing to Disclose

#### TEACHING POINTS

In this educational exhibit, through simple iconographic examples, we will teach residents how to identify and recognize the different benign and malignant lesions that may present with high signal intensity in T2 weighted images in breast magnetic resonance. Teaching points: 1) To describe benign and malignant lesions which are hyperintense in T2 weighted images in breast MRI. 2) To illustrate with several examples adding helpful suggestions that will enable residents to make the correct diagnosis.

#### TABLE OF CONTENTS/OUTLINE

1- Introduction  
2- MRI technique  
3- Benign lesions: Cysts, Seroma, Hematoma, Intramammary lymph nodes, Apocrine cystic metaplasia, Cavernous hemangioma, Myxoid fibroadenoma, Benign Phyllodes tumor  
4- Malignant lesions: Mucinous/colloid carcinoma, Metaplastic carcinoma, Papillary carcinoma, Triple Negative Basal Like carcinoma, Necrotic/hemorrhagic invasive ductal carcinoma, Malignant Phyllodes, Metastases  
5- Conclusions

Printed on: 02/07/23



## Abstract Archives of the RSNA, 2022

BREE-72

### Demystifying Lesions and Artifacts - A Pocket Guide for Automated Breast Ultrasound

Sunday, Nov. 27 8:00AM - 9:00AM Room: Learning Center - BR

#### Participants

Fernanda P. Pereira, MD, PhD, (*Presenter*) Nothing to Disclose

#### TEACHING POINTS

#Automated breast ultrasound (ABUS) is a valuable screening tool for breast cancer designed to overcome some of the issues regarding hand-held breast ultrasound (HHBUS), such as operator dependency, less experience with breast exams, low sensitivity and reproducibility. #ABUS main indication is to use as an adjunct method to mammography for screening asymptomatic women with dense breasts. #Correct identification of lesions and artifacts produced by ABUS is essential for the best evaluation, as acquisition is done by a technician and interpretation is performed by the specialist without knowing potential pitfalls during the exam.

#### TABLE OF CONTENTS/OUTLINE

1- Concept of automated breast ultrasound (ABUS); 2- ABUS: atlas of benign lesions; 3- ABUS: atlas of malignant lesions; 4- Main differences between ABUS and hand-held breast ultrasound (HHBUS); 5- ABUS: pitfalls and artifacts; 6- ABUS: other applications and final considerations.

Printed on: 02/07/23



## Abstract Archives of the RSNA, 2022

BREE-73

### Male Breast Cancer - Spectrum of Imaging Appearance and Current Imaging Recommendations

Sunday, Nov. 27 8:00AM - 9:00AM Room: Learning Center - BR

#### Participants

Soudabeh Fazeli Dehkordy, MD,MPH, San Diego, CA (*Presenter*) Nothing to Disclose

#### TEACHING POINTS

Synopsis: Imaging of the male breast is typical in routine radiology breast imaging. Most of the findings in male patients are benign, gynecomastia being by far the most common imaging diagnosis. Male breast cancer is uncommon, accounting for less than 1% of all breast cancers. The incidence of breast cancer in men is low, but it increases with age, and the 5-year survival rates are similar, stage by stage, between men and women. Men tend to present with more advanced stages of the disease. When axillary metastatic disease is present, the prognosis is worst and negatively affects the treatment. We reviewed 32 male breast cancer imaging studies from our teaching files, including mammograms, US, and MRI, to catalog the imaging presentations of breast cancer. TEACHING POINTS By the end of this educational exhibit, the learner will: 1. Review the incidence, clinical presentation, and management of male breast cancer. 2. Know the imaging protocols recommended to evaluate males based on ACR appropriateness criteria. 3. Identify the multimodality imaging appearance of malignant male breast lesions.

#### TABLE OF CONTENTS/OUTLINE

Introduction; Incidence and risk factor for male breast cancer; Clinical presentation of male breast cancer; Review of imaging recommendations for male breast; Differential considerations; Mammographic and US findings; MRI indications and appearance of male breast cancer; Recommended management of male breast cancers; Algorithm for imaging male patients with breast cancer and for follow up into survivorship; Conclusion.

Printed on: 02/07/23



## Abstract Archives of the RSNA, 2022

BREE-74

### The Imaging of Ductal Carcinoma in SITU - Where It Is and Where It's Going

Sunday, Nov. 27 8:00AM - 9:00AM Room: Learning Center - BR

#### Participants

Daniela Cunha, MD, Coralville, IA (*Presenter*) Nothing to Disclose

#### TEACHING POINTS

Ductal carcinoma in situ (DCIS) is the most prevalent form of breast cancer. It can be pathologically classified via the nuclear grade (low, intermediate, high) or by the architectural subtype (comedo, cribriform, micropapillary, solid, or mixed) with increased preference for nuclear grading. Approximately 75% of DCIS present with calcifications and mammography remains its main detection modality; ultrasound (US) may show a mass within a dilated duct but is nonspecific. Magnetic resonance imaging (MRI) however, is proving to be a useful supplementary tool in evaluating the extent of DCIS for surgical planning as well as a prognostic tool for predicting potential for upgrade from DCIS to invasive ductal carcinoma (IDC). While DCIS most commonly presents as a non-mass enhancement, IDC more often presents as an enhancing mass. With advancements in MRI, there is the potential to confidently differentiate low-grade from high-grade DCIS in the future.

#### TABLE OF CONTENTS/OUTLINE

DCIS - Pathology classification - Mammography findings - Ultrasound and MRI findings - Increasing importance of MRI in DCIS prognosis and treatment

Printed on: 02/07/23

## Abstract Archives of the RSNA, 2022

BREE-75

### Idiopathic Granulomatous Mastitis and Its Differential Diagnoses - A Practical Guide for Its Identification

Sunday, Nov. 27 8:00AM - 9:00AM Room: Learning Center - BR

#### Participants

Jorge Hernandez Espinoza, MD, CABA, Argentina (*Presenter*) Nothing to Disclose

#### TEACHING POINTS

Mention the main pathophysiological, demographic and clinical aspects of Idiopathic Granulomatous Mastitis (IGM). Recognize the most common findings of IGM in mammography, ultrasound and magnetic resonance imaging, and their main differential diagnoses.

#### TABLE OF CONTENTS/OUTLINE

Idiopathic granulomatous mastitis is a rare chronic inflammatory condition of the breast of unknown aetiology. It is commonly seen in women of childbearing age, but also in perimenopausal women. The diagnostic challenge is that it can mimic many conditions, including malignancy. The most common clinical presentation is a breast lump in any quadrant, or diffuse involvement of the breast. It manifests with axillary pain, erythema, edema or lymphadenopathy. Other chronic inflammatory pathologies considered in the differential diagnosis include plasma cell mastitis, tuberculosis, histoplasmosis, inflammatory carcinoma and Wegener's granulomatosis. Histopathology provides a definitive diagnosis, thus avoiding unnecessary mastectomies. On mammography it is common to find focal asymmetry, a darkened or irregularly shaped mass. On ultrasound, a large irregular hypoechoic parallel mass with tubular extensions is prominent. A hypoechoic and parallel circumscribed mass, or a mass with angular, lobulated, or indistinct margins, associated or not with posterior acoustic shadowing, has been reported. With color Doppler we can visualize the hypervascularization of the tissue surrounding the lesion. IGM in magnetic resonance imaging can be observed as a non-regional or segmental mass enhancement, or a mass enhancement with heterogeneous enhancement, lesions with enhancement of their margins or the presence of microabscesses.

Printed on: 02/07/23

## Abstract Archives of the RSNA, 2022

BREE-76

### Don't Forget the Pec! A Case-based Review of Pectoral Muscle Abnormalities on Breast Imaging

Sunday, Nov. 27 8:00AM - 9:00AM Room: Learning Center - BR

#### Awards

Certificate of Merit

#### Participants

Almir Bitencourt, MD, PhD, Sao Paulo, Brazil (*Presenter*) Nothing to Disclose

#### TEACHING POINTS

- To show a multimodal review of the pectoral muscles in breast imaging.- To teach breast radiologists to evaluate the pectoral muscles, mainly in mammograms, MRI and ultrasound. - To illustrate some conditions focusing in abnormalities showed by interesting cases of our institutions. - To give hints on how not to obliivate the evaluation of these muscles in breast exams.

#### TABLE OF CONTENTS/OUTLINE

1. A description of pectoral muscles anatomy and functions. 2. An introduction of pectoral muscles imaging aspects in breast exams (mammograms, ultrasound and MRI). 3. To show the importance of pectoral evaluation to avoid misdiagnosis of lesions in this area.4. Interesting cases of pectoral muscles conditions: - Normal variations (Pectoralis quartus muscle, sternalis muscle, Langer's axillary arch and Poland Syndrome); - Benign conditions (Subpectoral lipoma, pectoral muscle abscess, pectoral hemangioma and ossifying myositis); - Malignant conditions (sarcoma and lymphoma of the pectoral muscles).5. Most common pitfalls in pectoral muscles evaluation.

Printed on: 02/07/23



## Abstract Archives of the RSNA, 2022

BREE-77HC

### The Wave of Silicone Explanation: What To Expect in Breast Images?

Sunday, Nov. 27 8:00AM - 9:00AM Room: Learning Center - BR

#### Participants

Amanda Tavares, MD, Sao Paulo, Brazil (*Presenter*) Nothing to Disclose

#### TEACHING POINTS

In the past years, the term breast implant illness has becoming strong, especially with the power of social media, to describe physical and psychological symptoms possibly related to breast implants. The silicone is also discussed as a causal factor of ASIA syndrome (Autoimmune Syndrome Induced by Adjuvants). The exact mechanism whereby the implant can induce such diseases is uncertain, and there is still not enough scientific evidence to justify the diagnosis. Many patients report partial or complete resolution of symptoms after the silicone explant and plastic surgery societies already report an increase in the performance of such procedures. Regardless of the surgical technique used for implant removal and capsulectomy, steatonecrosis is a frequent complication. Volume restoration after explantation by autologous fat grafting will also present as oil cysts on imaging. Anterior capsulectomy is an alternative when the posterior capsule is adhered to the chest wall, increasing the risk of pneumothorax, in these cases the base of the capsule left intact can be seen in subsequent images. Breast and axillary residual free silicone may be a result of extracapsular rupture or even gel-bleeding of the removed implants, presenting as hyperdense nodules on mammography, dirty posterior acoustic shadowing on ultrasound, without significant enhancement on MRI. Correlation with previous exams and clinical history is essential to confirm the diagnosis and avoid unnecessary procedures.

#### TABLE OF CONTENTS/OUTLINE

Breast implant illness ASIA syndrome Breast imaging after silicone explantation Please visit the Learning Center to also view this presentation in hardcopy format.

Printed on: 02/07/23



## Abstract Archives of the RSNA, 2022

BREE-78

### Multipictorial Review of Papillary Lesions: An Essential Guide for Residents!

Sunday, Nov. 27 8:00AM - 9:00AM Room: Learning Center - BR

#### Participants

Antonio Jose Cueva Guerrero, MD, (*Presenter*) Nothing to Disclose

#### TEACHING POINTS

After the exhibit the reader will be able to: • Understand the ductal anatomy of the breast • Create a visual standard for the normal ductal pattern of the breast • Recognize papillary lesions from benign to malignant • Comprehend the use of each imaging modality for evaluating normality • Identify and be able to report pathology, using understandable parameters

#### TABLE OF CONTENTS/OUTLINE

- Introduction- Anatomy- Classification- Benign lesions- Malignant lesions- Imaging methods- Conclusions

Printed on: 02/07/23



## Abstract Archives of the RSNA, 2022

BREE-79

### Epithelial Lesions of The Breast: Solving Questions You Didn't Know You Have

Sunday, Nov. 27 8:00AM - 9:00AM Room: Learning Center - BR

#### Participants

Sofia Maksoud, MD, Sao Paulo, Brazil (*Presenter*) Nothing to Disclose

#### TEACHING POINTS

Benign epithelial and fibroepithelial lesions of the breast are responsible for about 80% of palpable lesions. Histologically, they are classified as fibrocystic changes and associated conditions. Fibrocystic changes are classified as non-proliferative, including cysts, or proliferative, including papillomas, radial scar, sclerosing adenoma, and ductal or lobular hyperplasia. Associate conditions include fibroadenomas and their variants, sclerosing lesions, papilloma and proliferative disease. Mammography, ultrasound and magnetic resonance imaging of the breasts may be helpful in differentiating benign from suspicious lesions in the breast. The objective of this study is to review, through a case-based presentation, the imaging aspect in these lesions, and the role of imaging in differing these conditions from suspicious malign findings.

#### TABLE OF CONTENTS/OUTLINE

Evaluation of cases of benign epithelial and fibroepithelial lesions of the breast from the digital file of our institution, demonstrating their presentation in different imaging modalities, including ultrasonography, mammography and magnetic resonance imaging, correlating them with the histopathological findings. The work also includes discussion of the topic based on the literature, teaching points and the references.

Printed on: 02/07/23



## Abstract Archives of the RSNA, 2022

BREE-8

### Pearls and Pitfalls of Automated Breast Ultrasound Interpretation

Sunday, Nov. 27 8:00AM - 9:00AM Room: Learning Center - BR

#### Awards

Certificate of Merit

Identified for RadioGraphics

#### Participants

Ashley Huppe, MD, Kansas City, KS (*Presenter*) Nothing to Disclose

#### TEACHING POINTS

There is increasing utilization of automated ultrasound (AUS) for breast cancer supplemental screening, in part due to increased breast density awareness and federal legislation requiring breast density notification. Given the unique nature of volumetric acquisition on AUS, many radiologists are unfamiliar with identification of breast cancer in the multiplanar format. Additionally, the wide format transducer can generate artifacts which can result in false positives. After this presentation, participants will be able to:

- Discuss rationale and guidelines for supplemental screening and review currently available supplemental screening options
- Describe benefits and limitations of AUS for breast cancer screening
- Compare outcomes data between automated and handheld breast ultrasound screening
- Learn the pearls of proper AUS interpretation including unique imaging features and knobology to increase cancer detection and avoid unnecessary callbacks
- Review AUS challenges and pitfalls including recognition of artifacts and identification of benign findings

#### TABLE OF CONTENTS/OUTLINE

1. Introduction: supplemental screening. Rationaleb. Options2. AUS for breast cancer screeninga. Overviewi. Indications and limitationsii. Compare and contrast with handheld screeningiii. Techniqueb. Imaging interpretationi. Pearls1. Correlation with current and prior mammography and ultrasound images2. Visualization of lesions in at least two data sets3. Use of unique AUS tools for lesion characterization, including coronal/sagittal planes and software rotationii. Pitfalls1. Acquisition challenges2. Compression and shadowing artifact3. Identification of benign findings3. Conclusion

Printed on: 02/07/23



## Abstract Archives of the RSNA, 2022

BREE-80

### Axillary Region - Which Road? Beyond Lymph Node

Sunday, Nov. 27 8:00AM - 9:00AM Room: Learning Center - BR

#### Participants

Isabela Ferracini, MD, Sao Paulo, Brazil (*Presenter*) Nothing to Disclose

#### TEACHING POINTS

The most common metastatic presentation of breast cancer is enlarged lymph nodes with atypical characteristics in the axillary region, which is why this location must be carefully examined in all breast imaging exams. However, due to the various anatomical structures in this region, many conditions may also present with pain and/or palpable nodulation and are not distinguishable in physical examination, including pathologies that involve neural and vascular structures, subcutaneous tissue, bone and muscular structures, among others. In this way, a thorough evaluation of the armpits through the various modalities of imaging exams is an important tool in elucidating the diagnosis and determining the best treatment. The aim of this study is to address lymph node and non-lymph node axillary radiological findings and their main characteristics.

#### TABLE OF CONTENTS/OUTLINE

Cases containing mammography, ultrasound, computed tomography and magnetic resonance images and 3D reconstruction, obtained from the digital file of our institution, were used. We approach a didact review of some of the most common conditions involving the axillary region, their imaging aspects and how to differentiate them in imaging exams, including teaching points and references.

Printed on: 02/07/23



## Abstract Archives of the RSNA, 2022

BREE-81

### All That Glitters is Not Gold - Malignant Breast Lesions with Hyperintense Signal on T2

Sunday, Nov. 27 8:00AM - 9:00AM Room: Learning Center - BR

#### Awards

Certificate of Merit

#### Participants

Marina Santos, Sao Paulo, Brazil (*Presenter*) Nothing to Disclose

#### TEACHING POINTS

The purposes of this exhibit are:1- To review our institution's cases of malignant lesions presenting with high signal intensity on MRI T2-weighted images;2- To describe the aspects of these lesions: morphology, T1 and T2 WI features, enhancement pattern and diagnostic clues;3- To evaluate the histological factors that could causes high signal intensity on T2 WI on each lesion such as cystic component, mucinous or loose myxoid stroma, edema, hemorrhagic or necrotic changes;4- To explore the imaging aspects differentiating malignant from benign lesions with high T2 signal such as inflammatory, cystic or infectious etiologies.

#### TABLE OF CONTENTS/OUTLINE

1- Review cases of malignant lesions presenting with hyperintense signal on T2 WI from our radiology department, documented in multiple methods (MRI, ultrasound and mammography), such as:mucinous carcinoma;metaplastic carcinoma;papillary carcinoma;invasive ductal carcinoma;fibroepithelial tumours.2- Correlation of these cases with histopathological findings justifying the high signal on T2: extensive necrosis; cystic content; mucinous stroma.3- Review some benign differential diagnosis such as inflammatory, cystic and infectious etiologies.

Printed on: 02/07/23



## Abstract Archives of the RSNA, 2022

BREE-82HC

### **An Overview of Breast Plasmacytoma With Radiologic-Pathologic Correlation: Key Considerations and Major Features**

Sunday, Nov. 27 8:00AM - 9:00AM Room: Learning Center - BR

#### **Participants**

Pooya Torkian, MD, Minneapolis, MN (*Presenter*) Nothing to Disclose

#### **TEACHING POINTS**

The purpose of this project is to describe radiological and pathological findings of breast plasmacytoma in patients with multiple myeloma. We explore multimodality imaging results of mammography, ultrasound, positron emission tomography/computed tomography (PET/CT), CT, magnetic resonance imaging, and tomosynthesis. We provide a pictorial review of the most notable imaging findings of breast plasmacytoma for the awareness of radiologists and clinicians to improve the standard of care.

#### **TABLE OF CONTENTS/OUTLINE**

1. Introduction 2. Overview of breast plasmacytoma in multiple myeloma 3. A pictorial review of imaging findings of breast plasmacytoma in mammography, ultrasound, PET/CT, CT, MRI, and tomosynthesis 4. Strengths and weaknesses of the different modalities 5. Discuss the future application of multimodality imaging in breast plasmacytoma Please visit the Learning Center to also view this presentation in hardcopy format.

Printed on: 02/07/23



## Abstract Archives of the RSNA, 2022

BREE-83

### Breast Masses in Children and Adolescents: What Do We Need To Know?

Sunday, Nov. 27 8:00AM - 9:00AM Room: Learning Center - BR

#### Participants

Thais Kuwazuru, MD, Sao Paulo, Brazil (*Presenter*) Nothing to Disclose

#### TEACHING POINTS

The aim of this exhibition is to:1. Review the current concepts about breast disorders and normal breast development and its variations in children and adolescents.2. Discuss the differences between each imaging modality.3. Describe the rates of breast lesions in this age group in our hospital.4. Highlight the importance of this knowledge to guide the proper management of these patients

#### TABLE OF CONTENTS/OUTLINE

1. INTRODUCTIONa. Epidemiological profile of breast lesions in this population.b. Recommendations for screening, control and surveillance.2. IMAGING INTERPRETATIONa. Imaging techniques acquisition and protocols.b. Use of ACR BI-RADS and structured reporting of the findings on this population.3. STATISTICAL DATAa. Breast imaging data from in women under the age of 19 from our institution between January 2020 and April 2021.b. Correlation with literature data.4. INTERACTIVE CASE-BASED DIDACTICSa. Sample cases to illustrate and solidify the concepts about the main findings in this population.5. FUTURE DIRECTIONS AND TAKE HOME MESSAGES

Printed on: 02/07/23



## Abstract Archives of the RSNA, 2022

BREE-84

### **WANTED: Complete Radiological Response to Neoadjuvant Chemotherapy**

Sunday, Nov. 27 8:00AM - 9:00AM Room: Learning Center - BR

#### **Participants**

Natalia Lima, Sao Paulo, Brazil (*Presenter*) Nothing to Disclose

#### **TEACHING POINTS**

The purposes of this exhibit are:1. To review the main aspects related to neoadjuvant chemotherapy response, including complete response, partial response, stable disease, and progressive disease.2. To evaluate the pathologic response (including pCR and residual cancer burden score - RCB) and correlate to radiologic response in some cases from our institution;3. To emphasize the importance of looking for residual lesions in all sequences of MRI, including T2, in order to avoid missing lesions;4. To show, based on interesting cases from our breast radiology group, different kinds of response to neoadjuvant chemotherapy in a variety of histological and immunohistochemical subtypes;

#### **TABLE OF CONTENTS/OUTLINE**

· Radiological response patterns to neoadjuvant chemotherapy:- Complete, partial (concentric and with peripheral lesions), stability, progression of injury· Pathologic response using RCB and its parameters: - Primary tumor dimension - Cellularity - Size of the largest nodal metastasis - Number of positive lymphonodes· Concepts of radiologic and pathologic complete response· Teaching cases showing the challenging aspects based on imaging findings and correlate with clinical and pathological findings in different scenarios, such as: - Ductal carcinoma with tumoral seeding - Mucinous carcinoma mimicking a partial response - Inflammatory carcinoma with complete response - Complete response of calcifications on a lobular carcinoma

Printed on: 02/07/23



## Abstract Archives of the RSNA, 2022

BREE-85

### Challenges in the Interpretation of Breast Findings In The Emergency Setting: Recommendations for the Non-Breast Imager

Sunday, Nov. 27 8:00AM - 9:00AM Room: Learning Center - BR

#### Awards

Identified for RadioGraphics

#### Participants

Steven Lee, MD, Bellaire, TX (*Presenter*) Nothing to Disclose

#### TEACHING POINTS

Emergencies in Breast Imaging are uncommon. Although infectious conditions such as mastitis and breast abscess are commonly encountered in the emergency department, many additional entities may be recognized, including breast cancer. Most emergency departments do not have mammography units, making the evaluation of these patients incomplete and this emphasizes the importance of ultrasound technique and imaging interpretation in this setting. This is especially important when images are reviewed remotely by the Breast Imaging team. With this exhibit, the learner will be exposed to imaging examples of breast emergencies in the ER/inpatient setting, technique tips and tricks for the ultrasound evaluation of the breast in the ER, relevant patient and imaging information that breast imagers require for remote interpretation, and appropriate recommendation, treatment, and follow up for patients in the emergency setting.

#### TABLE OF CONTENTS/OUTLINE

Introduction. Breast imaging emergencies in the ED and Breast Imaging Department: Mastitis, Abscess, Trauma/Hematoma, Fluid Collection, Masses, Pseudoaneurysm, Vasovagal Reaction. Ultrasound technique tips and tricks for evaluation in the ED. Algorithm for recommendations and follow up of breast imaging emergencies. Conclusion and Summary

Printed on: 02/07/23



## Abstract Archives of the RSNA, 2022

BREE-86

### LCIS and It's Variants - Review of What We Know

Sunday, Nov. 27 8:00AM - 9:00AM Room: Learning Center - BR

#### Participants

Joe Khoury, DO, MBA, Manhasset, NY (*Presenter*) Nothing to Disclose

#### TEACHING POINTS

Classic LCIS and atypical lobular hyperplasia (ALH) both demonstrate noninvasive proliferation of lobular cells within the TDLU. LCIS involves >50% of acini while ALH involves <50%. LCIS is a risk factor and non obligate precursor of invasive breast carcinoma. RR for development of breast cancer in those with LCIS is 9-10x the general population. Subsequent breast cancer can occur in either breast and includes DCIS and invasive cancers. Most often, LCIS is an incidental finding on pathology. However, there are known multimodality imaging findings associated with LCIS. Pure LCIS includes classic (cLCIS) and non classic types (including pLCIS). Management of LCIS continues to evolve. Upgrade rate to ILC ranges from 0-67% depending upon the study and histology Given low upgrade rates for cLCIS (0-5%), excision diagnosed on needle biopsy with concordant imaging and when no other lesions requiring excision are present is no longer routine. Cases are often recommended for follow up with PE, mammography and often MRI. Because of the higher upgrade rate of pLCIS and biologic behavior similar to DCIS, guidelines for pLCIS and LCIS with discordant imaging is surgical excision with negative margins, without RT. In studies, chemoprevention with Tamoxifen or an aromatase inhibitor in patients with LCIS resulted in a significant reduction in 10 year cancer risk. Bilateral prophylactic mastectomy has been considered an option by some but current guidelines prefer risk reducing endocrine agents.

#### TABLE OF CONTENTS/OUTLINE

Background Comparison of Classic and Pleomorphic LCIS Histology Imaging Characteristics Management Cases

Printed on: 02/07/23



## Abstract Archives of the RSNA, 2022

BREE-87

### Rare But Mighty Breast Cancers: What the Future Holds

Sunday, Nov. 27 8:00AM - 9:00AM Room: Learning Center - BR

#### Participants

William Hiatt, MS, BS, (Presenter) Nothing to Disclose

#### TEACHING POINTS

1. Review the current World Health Organization classification system of epithelial breast cancers 2. Introduce the recent expansion in molecular understandings of breast cancer, emphasizing six rarer epithelial tumor subtypes 3. Highlight the recent proposal of a new schema that unifies histological-molecular breast tumor analyses 4. Understand how these findings impact our patients' care via knowledge of known tumor behavior 5. Provide radiologic profiles of two tumor subtypes, metaplastic carcinoma and micropapillary carcinoma

#### TABLE OF CONTENTS/OUTLINE

1. How are we currently classifying tumors? 1a. Histological analysis vs. molecular classification 2. How are we expanding our molecular understanding of rarer breast tumors? 2a. Proposal of a novel schema that blends tumor histology biomarker data into a more unified classification system 3. Newly expanded molecular profiles of several rarer tumor types that further explain tumor morphology behavior 4. Imaging and Overview Profile: Metaplastic Carcinoma 5. Imaging and Overview Profile: Micropapillary Carcinoma 6. Future directions in rare breast radiology 7. References

Printed on: 02/07/23

## Abstract Archives of the RSNA, 2022

BREE-88

### Paradigms for Papilloma Management

Sunday, Nov. 27 8:00AM - 9:00AM Room: Learning Center - BR

#### Participants

Sherwin Chiu, MD,MPH, (*Presenter*) Nothing to Disclose

#### TEACHING POINTS

(1) Understand the clinical significance of intraductal papillomas.(2) Recognize the imaging findings associated with intraductal papillomas.(3) Review the current paradigm for management of intraductal papillomas.

#### TABLE OF CONTENTS/OUTLINE

(1) Significance: (a) Classically presents as unilateral nipple discharge. (b) Nipple discharge or dilated ducts warrant further evaluation. (c) Intraductal papillomas with atypia or discordance should be excised, however asymptomatic papillomas without suspicious imaging or atypia may be appropriate for surveillance.(2) Imaging Findings: (a) On mammography, papillomas may present as ductal dilatation and occasionally as a circumscribed mass with associated calcifications. (b) Ultrasound findings typically show a vascularized circumscribed mass with associated ductal dilatation. (c) On MRI, papillomas appear as an enhancing intraductal mass with associated ductal dilatation.(3) Management: (a) Historically, treatment required excisional biopsy or lumpectomy to exclude atypia or underlying malignancy. (b) Ultrasound guided vacuum removal of papillomas has shown promise in removing lesions without the need for surgery. (c) Clinical follow-up with ultrasound is becoming more favored for small, solitary papillomas without atypia due to low rates of malignancy upgrading.

Printed on: 02/07/23



## Abstract Archives of the RSNA, 2022

BREE-89

### Imaging the Male Breast: Gynecomastia, Male Breast Cancer, and Beyond

Sunday, Nov. 27 8:00AM - 9:00AM Room: Learning Center - BR

#### Awards

Identified for RadioGraphics  
Magna Cum Laude

#### Participants

Heather Duke, MD, Chicago, IL (*Presenter*) Nothing to Disclose

#### TEACHING POINTS

1. Male breast complaints have increased in recent years, and it is therefore increasingly important for radiologists to be knowledgeable about imaging features of pathology that can occur in the male breast. 2. Male breast pathology most commonly includes gynecomastia, and the chief differential consideration is male breast cancer. However, there are a number of other entities that can occur in the male breast of which radiologists should be aware, in order to perform adequate concordance of biopsy results with imaging findings. 3. Male breast pathology can involve structures of the subcutaneous tissues, including skin, fat, muscle, blood vessels, lymphatics, and nerves. Alternatively, pathology can originate from ductal and stromal breast tissue in males, with lobular pathology being extremely rare given lack of progesterone-dependent lobular proliferation in males.

#### TABLE OF CONTENTS/OUTLINE

1. Male Breast Development and Important Differences from the Female Breast 2. Gynecomastia (most common pathology) versus Male Breast Cancer 3. Less Common But Important Male Breast Pathology and Imaging Findings a. Skin - sebaceous/epidermal inclusion cysts b. Fat - lipoma and fat necrosis c. Muscle/Fascia - Desmoid tumor d. Blood vessels/vascular tumors - vascular malformations, hemangioma, angioliipomae. Nerves - schwannomas, granular cell tumors f. Lymphatics - intramammary lymph node g. Ductal tissue - intraductal papilloma h. Stromal tissue - PASH, myofibroblastoma i. Other - subareolar abscess, diabetic mastopathy

Printed on: 02/07/23



## Abstract Archives of the RSNA, 2022

BREE-9

### Breast Implant Associated Anaplastic Large Cell Lymphoma (BIA-ALCL): A Multimodality Imaging Review

Sunday, Nov. 27 8:00AM - 9:00AM Room: Learning Center - BR

#### Participants

Kanchan Phalak, MD, (*Presenter*) Nothing to Disclose

#### TEACHING POINTS

1) Breast Implant Associated Anaplastic Large Cell Lymphoma (BIA-ALCL) manifests as a late-onset effusion or mass in patients with exposure to textured implants. 2) Breast ultrasonography is an appropriate test for initial evaluation of presenting clinical symptoms such as swelling and pain. 3) Cytologic or histologic analysis is important to distinguish BIA-ALCL from other pathologies. 4) Imaging modalities such as MRI, CT and PET can help characterize BIA-ALCL.

#### TABLE OF CONTENTS/OUTLINE

1) Clinical Issues a. Etiology and Pathophysiology b. Presentation c. Demographics d. Natural History and Prognosis e. Treatment 2) Pathology a. General Features b. Staging, Grading, and Classification 3) Imaging Findings a. General Features b. Mammogram c. Ultrasound d. MRI e. PET-CT f. CT g. Image-Guided Biopsy 4) Differential Diagnosis 5) Pictorial review of cases

Printed on: 02/07/23



## Abstract Archives of the RSNA, 2022

BREE-90

### The ABC of PABC (Pregnancy Associated Breast Cancer): Playing Hide and Seek with the Radiologist

Sunday, Nov. 27 8:00AM - 9:00AM Room: Learning Center - BR

#### Participants

Martha Espitia Lopez, MD, Mexico, Mexico (*Presenter*) Nothing to Disclose

#### TEACHING POINTS

Know the definition of breast cancer associated with pregnancy. Know the physiological changes during pregnancy and lactation. Recognize normal and suspicious breast images in pregnancy and lactation.

#### TABLE OF CONTENTS/OUTLINE

Breast cancer is one of the most common cancers in pregnant and non-pregnant women. Pregnancy is considered a risk factor for the development of breast cancer. Breast cancer is now the most common malignancy diagnosed during pregnancy, with an estimated incidence of 1 in 3000 pregnancies in the United States. Gestational or pregnancy-associated breast cancer is defined as breast cancer that is diagnosed during pregnancy, in the first year postpartum, or at any time during lactation, but is often a late finding due to expected physiological changes in breast cancer. Ultrasound is the imaging study of choice due to its high sensitivity and in the absence of radiation. The tumors found in these patients are usually high grade with high cell proliferation, as well as negative hormone receptors. Histologically, the most frequent type is infiltrating ductal carcinoma, found in up to 80% of cases. The treatment for these patients should not be extended beyond the first trimester, after the twelfth week of gestation it is possible to start chemotherapy during the second and third trimesters, likewise mastectomy can be performed during this period. Radiotherapy is contraindicated during pregnancy, it can be performed after birth. Endocrine treatment begins after delivery.

Printed on: 02/07/23

## Abstract Archives of the RSNA, 2022

BREE-91

### Interesting Axillary Pathology in Breast Imaging

Sunday, Nov. 27 8:00AM - 9:00AM Room: Learning Center - BR

#### Participants

Joseph Hoang, MD, (*Presenter*) Nothing to Disclose

#### TEACHING POINTS

Axillary masses and lesions are occasionally discovered during routine screening and diagnostic breast imaging. In many instances, the masses are found to be lymph nodes, however, other uncommon pathologic entities exist in the axilla that are often overlooked. - Review axillary mass work up and clinical presentation of patients with palpable abnormality- Discuss abnormal, benign lymph node pathologies- Review primary breast malignancy in the axilla- Elucidate on several etiologies of axillary masses outside of breast tissue origin- Present interesting cases of axillary masses within the each category as delineated above

#### TABLE OF CONTENTS/OUTLINE

- Review typical patient presentation, pertinent imaging modalities and workup - Discuss criteria for benign lymph node morphology- Present and discuss abnormal lymph nodes with benign pathology- Present cases of primary breast cancers in the axilla not involved by a lymph node- Discuss and review etiologies of masses in the axilla outside of breast origin include: Vascular/Lymphatic origin, Dermal and fatty, Neurogenic origin, Musculoskeletal origin- Present cases of differing etiologies as included above.

Printed on: 02/07/23



## Abstract Archives of the RSNA, 2022

BREE-92

### The Dark Star of the Breast: A Confusing Lesion

Sunday, Nov. 27 8:00AM - 9:00AM Room: Learning Center - BR

#### Participants

Magaly Henriquez Urrea, MD, MSc, Mexico City, Mexico (*Presenter*) Nothing to Disclose

#### TEACHING POINTS

A radial scar (RS) is a pathologic process that consists of a central fibroelastic core with distorted and entrapped ducts, and peripherally, with ducts and lobules distributed in a radiating appearance. In addition, the fibroelastic core is contracted, with a "pulled inward" appearance. A specific pathologic characteristic of an RS is the intact myoepithelial cell layer. This is an important feature to differentiate it from an invasive carcinoma. The most typical appearance on digital mammography (DM) and on digital breast tomosynthesis (DBT) of a RS is the architectural distortion, with thin and long radiating spicules against a background of radiolucent fat, creating a "dark star" appearance. The most common ultrasound finding is a hypoechoic, irregular mass with indistinct margins. Posterior acoustic shadowing can also be seen.

#### TABLE OF CONTENTS/OUTLINE

Definition. Causes. Epidemiology and Clinical Presentation. Pathology. Imaging Findings. Mammography and tomosynthesis. Mammographic criteria. Ultrasound. Contrast-enhanced Mammography. Conclusion. References.

Printed on: 02/07/23



## Abstract Archives of the RSNA, 2022

BREE-93

### **Redefining Needle Targeting Error in the Prone and Upright Stereotactic Breast Biopsy: Recognition and Problem Solving**

Sunday, Nov. 27 8:00AM - 9:00AM Room: Learning Center - BR

#### **Participants**

Janice Thai, MD, (*Presenter*) Nothing to Disclose

#### **TEACHING POINTS**

1. The traditional approach for the teaching of stereotactic breast biopsy regarding needle targeting error hinges on established convention that is largely based on the 2D prone stereotactic biopsy system (retired model). Recent advances in technology introduced an updated prone and upright systems, for which the convention of needle targeting error do not apply. This exhibit highlights the differences between the old and new prone models, as well as the upright model, pertaining to needle targeting error.
2. To illustrate the X, Y, and Z axes used to determine needle targeting error and approaches to overcome targeting errors.

#### **TABLE OF CONTENTS/OUTLINE**

- Review of the prone and upright stereotactic systems, regarding the X, Y, and Z axes and their directionality used in defining needle targeting error
- Review of how needle error targeting is defined in both the prone and upright systems, and solutions to overcome needle targeting errors
- Case review of real-life scenarios and problem solving

Printed on: 02/07/23

## Abstract Archives of the RSNA, 2022

BREE-94

### Male Breast Lesions - That We Need to Know

Sunday, Nov. 27 8:00AM - 9:00AM Room: Learning Center - BR

#### Participants

Samira Nader, MD, Buenos Aires, Argentina (*Presenter*) Nothing to Disclose

#### TEACHING POINTS

- Recognize the radiological characteristics of the lesion that help to identify it as benign or malignant according to the BIRADS classification.- Describe the entities that most frequently affect the male breast, especially cancer and gynecomastia as its main simulator.

#### TABLE OF CONTENTS/OUTLINE

TABLE OF CONTENTS. Normal characteristics of the breast in men and their differences with respect to women. Types of most common lesions in the male breast. Generalities, incidence and risk factors of male breast cancer. Ultrasound and mammographic findings of male breast lesions; types of tumors found and their histopathological correlation. RESUME. Male breast cancer represents 1% of all breast cancers, and less than 1% of all cancers in men. Screening in men is not justified, which partly explains the later diagnosis. 90% of breast cancers in men express estrogen receptors and 80%, progesterone receptors. Biomarkers such as HER2 and Ki67 are taken as a reference to characterize breast tumors as in women. On mammography, a lobulated, irregular, high-density retroareolar mass with poorly defined or spiculated margins can be observed. Calcifications are present in 13-30% of cases, the pleomorphic type being rarer. Ultrasound may reveal a solid, hypoechoic, retroareolar mass with angled, spiculated or microlubulated margins, or a complex cystic mass. Taking a sample for histopathological study is generally performed under ultrasound guidance. Histologically, the vast majority are invasive ductal carcinoma (85-90%) or ductal carcinoma in situ.

Printed on: 02/07/23



## Abstract Archives of the RSNA, 2022

BREE-95

### Case-based Review of Contrast-enhanced Mammograms: False Positives and False Negatives with Strategies to Improve Cancer Detection and Staging

Sunday, Nov. 27 8:00AM - 9:00AM Room: Learning Center - BR

#### Awards

Identified for RadioGraphics

Cum Laude

#### Participants

Molly Carnahan, MD, Phoenix, AZ (*Presenter*) Nothing to Disclose

#### TEACHING POINTS

Similar to contrast-enhanced-MRI, false-positive (FP) CEM can occur with benign processes False-negative (FN) can occur in marked BPE, minimal lesional enhancement or lesions off the field-of-view Prompt repositioning should be performed to overcome FNs with positioning or medically located lesions Low-grade cancers may not enhance. Decision to pursue imaging guided biopsy should be based on the most suspicious imaging feature

#### TABLE OF CONTENTS/OUTLINE

CEM background Principles behind cancer detection New BIRADS lexicon Defining breast imaging modalities' diagnostic performance: true positive, true negative, FP and FN Understand causes of CEM FP and FN to improve these measures FP on CEM FP pathology (benign lesions) on CEM: case-based review How CEM FP compare to CE-MRI and MBI FN on CEM FN CEM (missed cancers): case-based review of errors Inadequate visualization of lesion or extent of disease Poor patient positioning Lesion off the FOV (ex. medial or posterior lesions) or abuts breast implants BPE obscuring lesion Lack of lesion enhancement No IV contrast on imaging (ex. missed bolus or contrast extravasation) Negative enhancement artifact obscuring cancer (ex. hematoma) Cancers with no enhancement Errors of characterization: lesions with seemingly benign features How CEM FN compare to CE-MRI and MBI Pearls for the reader Real time interpretations: prompt re-positioning if needed Suspicious calcifications, architectural distortion or masses should be biopsied regardless of CEM enhancement Technical limitations of CEM for posterior lesions and evaluating lymphadenopathy should be considered when staging new cancers

Printed on: 02/07/23



## Abstract Archives of the RSNA, 2022

BREE-96

### Interactive Case-Based Review of new Contrast-Enhanced Mammography BI-RADS Lexicon

Sunday, Nov. 27 8:00AM - 9:00AM Room: Learning Center - BR

#### Participants

Lyndia Moravia, MD, (*Presenter*) Nothing to Disclose

#### TEACHING POINTS

Teaching Points: CEM BI-RADS has recently been published to guide CEM interpretation. Including both low-energy (LE) and recombined imaging (RC) findings in exam interpretation is critical. The standard mammography lexicon is used to describe the LE findings. A new lexicon was developed to describe RC findings that is similar to the breast MRI but with changes specific to CEM. Key differences include the absence of the term 'focus', the addition of the term 'enhancing asymmetry', removal of the mass internal enhancement characteristic of dark internal septations, and removal of the non-mass enhancement internal enhancement pattern of clustered ring. In addition, when LE findings are seen with enhancement, internal enhancement pattern, lesion conspicuity compared to background parenchymal enhancement, and extent of enhancement relative to LE finding should be described.

#### TABLE OF CONTENTS/OUTLINE

1. Review the main elements of the new CEM BI-RADS. 2. Summarize the differences between MRI lexicon and CEM recombined imaging lexicon. 3. Emphasize the key points of the new CEM BI-RADS through an interactive case-based review.

Printed on: 02/07/23



## Abstract Archives of the RSNA, 2022

BREE-97

### How to Navigate Breast Tumor Board: A Resident and Fellow Primer

Sunday, Nov. 27 8:00AM - 9:00AM Room: Learning Center - BR

#### Participants

Atharva Thakore, MD, (*Presenter*) Nothing to Disclose

#### TEACHING POINTS

1. Review the role of the radiologist in multidisciplinary breast tumor board. 2. Understand the oncologic and surgical management of breast cancer in the context of pretreatment imaging. 3. Identify imaging features important to clinical decision making.

#### TABLE OF CONTENTS/OUTLINE

Introduction? Getting to know the Interdisciplinary Team and their Role? Accreditation Standards and Quality Metrics? Breast Cancer Staging; Imaging vs Clinical? Imaging Presentation for Tumor Board? Elements to Include; Key Images--Tumor Size and Location; How to Take Measurements--Imaging Lymph Node Status Tumor Board Terminology and Concepts by Subspecialty? Medical Oncology--Tumor Markers/Receptors--Tumor Biology/Genetics--Indications for Neoadjuvant Chemotherapy--Reporting Response to Neoadjuvant Chemotherapy--Indications for Adjuvant Chemotherapy? Surgical Oncology--Surgical Axillary Management--SLNB vs ALND--Breast Conservation Surgery vs Mastectomy--Breast Conservation Surgery--Mastectomy/Nipple Sparing Mastectomy? Radiation Oncology--Whole Breast Radiation Therapy and Boost--Accelerated Partial Breast Irradiation--Chest Wall Irradiation--Regional Nodal Irradiation Recommendations? Preoperative Localization--Wire Localization--Virtual Navigation Clips--Bracketing? Further Evaluation--Second Look Ultrasound--MRI Biopsy--Axillary Biopsy Conclusions: 1. Understanding the principles of breast cancer oncologic management is valuable for the radiology trainee. 2. Clinically relevant imaging features should be highlighted and presented in multidisciplinary tumor board. 3. Make recommendations appropriate to a patient's specific tumor biology and treatment plan

Printed on: 02/07/23



## Abstract Archives of the RSNA, 2022

BREE-98

### All Roads Lead to Rome: Multi-modality Imaging of Benign and Malignant Pathologies of the Nipple Areolar Complex

Sunday, Nov. 27 8:00AM - 9:00AM Room: Learning Center - BR

#### Awards

Identified for RadioGraphics  
Certificate of Merit

#### Participants

Mary Guirguis, MD, Houston, TX (*Presenter*) Nothing to Disclose

#### TEACHING POINTS

- \*The normal imaging appearance of the nipple and the nipple areolar complex can be variable.
- \*Understanding the normal spectrum of imaging appearance across different breast imaging modalities is essential for the radiologist.
- \*Meticulously assessing the nipple areolar complex across different modalities while understanding its spectrum of imaging appearance allows for accurate identification of pathology in this region.
- \*Different benign and malignant pathological entities can be seen within the nipple and nipple areolar complex.
- \*Correlation with the patient's symptoms is key to understanding the imaging findings and clinical management.

#### TABLE OF CONTENTS/OUTLINE

This educational exhibit will present a practical guide on how to approach the nipple areolar complex across different imaging modalities. Through a multi-modality case-based approach, we will present the spectrum of the normal appearance of the nipple and the nipple areolar complex. Imaging of benign and malignant pathologies that affect the nipple and nipple areolar complex will be presented across the different breast imaging and cross-sectional modalities. Tips, pitfalls, and practical approaches will be highlighted through a case-based multi-modality approach.

Printed on: 02/07/23



## Abstract Archives of the RSNA, 2022

BREE-99

### Multimodality Imaging of Postmastectomy Breast Reconstruction Techniques and Complications

Sunday, Nov. 27 8:00AM - 9:00AM Room: Learning Center - BR

#### Awards

Identified for RadioGraphics  
Certificate of Merit

#### Participants

Faezeh Sodagari, MD, (*Presenter*) Nothing to Disclose

#### TEACHING POINTS

Breast reconstruction is commonly performed to restore chest symmetry in women undergoing mastectomy as part of breast cancer treatment or prophylaxis. Various reconstruction techniques are currently available including implant-based reconstruction or microvascular autologous reconstruction using pedicled or free flap techniques. The goal of this exhibit is to review surgical techniques used in postmastectomy reconstruction, imaging appearance of postoperative changes and complications, and imaging guidelines for the evaluation of the reconstructed breast.

#### TABLE OF CONTENTS/OUTLINE

1) Introduction: a) Surgical techniques used in breast reconstruction methods, including implant placement, pedicled flaps, free flaps and preoperative planning; b) Indications, contraindications, advantages, and disadvantages of different postmastectomy breast reconstruction techniques; c) Techniques for the reconstruction of the nipple-areolar complex 2) Normal postsurgical findings and their evolution in time such as edema and soft tissue emphysema 3) Imaging findings of early and late complications such as hemorrhage, infection, flap ischemia, fat necrosis, implant rupture 4) Implications of reconstruction method for radiation treatment planning 5) Multimodality evaluation of reconstructed breast for new or recurrent cancer including guidelines and controversies of MRI surveillance of reconstructed breast 6) Clinical outcomes and summary

Printed on: 02/07/23

## Abstract Archives of the RSNA, 2022

CAEE

### Cardiac Education Exhibits

Sunday, Nov. 27 8:00AM - 9:00AM Room: Learning Center - CA

#### Sub-Events

#### CAEE-10 Mitral Annular Disjunction in Cardiac MR: What to Know and What to Look For

##### Awards

##### Identified for RadioGraphics

##### Participants

Jose Batista Araujo Filho, MD, Sao Paulo, Brazil (*Presenter*) Nothing to Disclose

##### TEACHING POINTS

1) Mitral Annular Disjunction (MAD) definition and its association with Mitral valve prolapse (MVP) and ventricular arrhythmic events  
2) The advantages of CMR in MAD diagnosis, stratification and prognosis  
3) Update on state-of-the-art CMR new sequences for evaluating MAD

##### TABLE OF CONTENTS/OUTLINE

1) INTRODUCTION 1.1) Definition and importance of MAD 1.2) Association with MVP, ventricular arrhythmias and sudden cardiac death 1.3) Presence of MAD in normal subjects  
2) CARDIAC MR (CMR) ROLE IN MAD 2.1) CMR advantages over echocardiography 2.2) How to measure the MAD distance properly 2.3) Other CMR findings useful for the diagnosis and prognosis 2.4) New CMR tools for MAD stratification (T1 mapping and Strain)  
3) CMR IN MAD DIAGNOSIS 3.1) Case example of a long MAD 3.2) MAD association with MVP and regurgitation 3.3) Myocardial Fibrosis presence - late gadolinium enhancement (LGE)  
4) CMR IN MAD STRATIFICATION 4.1) How to evaluate papillary muscle LGE 4.2) CMR T1 mapping importance  
5) CHALLENGES IN MAD/TAKE HOME MESSAGES 5.1) MAD diagnostic pitfalls and its clinical relevance 5.2) Strain CMR as a new tool to assess regional contractile dysfunction 5.3) Red flags on MVP

#### CAEE-11 The Essential Three Roles of Imaging in the Management of Chronic Thromboembolic Pulmonary Hypertension

##### Participants

Satoshi Higuchi, MD, PhD, (*Presenter*) Nothing to Disclose

##### TEACHING POINTS

Chronic thromboembolic pulmonary hypertension (CTEPH), caused by stenosis and obstruction of the pulmonary arteries by organized thrombi, is a major cause of chronic pulmonary hypertension and life-threatening disease if untreated. The prognosis is improving as a treatment strategy has been established. The role of imaging is classified into three categories: 1) detection of perfusion defects for diagnosis, 2) assessment of vascular lesions to establish a treatment strategy, and 3) evaluation of cardiac function for assessment of treatment efficacy or prognosis. Participants will learn the pathophysiologic processes of CTEPH, the essential three roles of imaging in the management of CTEPH, and future perspectives of imaging in CTEPH.

##### TABLE OF CONTENTS/OUTLINE

1. What is CTEPH? 2. The pathophysiologic processes of CTEPH 3. The essential three roles of imaging in CTEPH a. Diagnosis: lung perfusion defects b. Establishment of treatment strategy: assessment of vascular lesions c. Assessment of treatment efficacy and prognosis: evaluation of cardiac function 4. Future perspectives 5. Summary

#### CAEE-12 Pre- and Post-Operative Imaging Findings of Chronic Thromboembolic Pulmonary Hypertension (CTEPH)

##### Participants

Yogesh Gupta, DO, (*Presenter*) Nothing to Disclose

##### TEACHING POINTS

1. Illustrate the proposed pathophysiology of CTEPH. 2. Detail the role of pre-operative imaging with computed tomography angiography (CTA), dual energy CT (DECT), ventilation perfusion (V/Q) scintigraphy, magnetic resonance angiography (MRA), MR perfusion, and 4D phase contrast MR. 3. Provide radiological examples, practical tips for aiding in diagnosis and describing current diagnostic challenges. 4. Highlight key findings that the radiologist should convey to the interventionist to best help guide therapy. 5. Demonstrate clinical correlates from our Pulmonary Hypertension Center with post-procedural outcomes from pulmonary endarterectomy, percutaneous balloon pulmonary angioplasty, and percutaneous ultrasound accelerated thrombolysis (EKOS®) as well as outcomes from medical therapies including pulmonary vasodilators and anticoagulation. 6. Overview of emerging artificial intelligence technologies that may facilitate CTEPH diagnosis.

##### TABLE OF CONTENTS/OUTLINE

This pictorial review is designed for residents, fellows, general radiologists, thoracic radiologists, interventional radiologists, and non-radiology participants. The primary goals are to describe the pre- and post-operative imaging features of CTEPH with clinical correlation and post-surgical outcomes. This will be achieved by discussing: 1. CTEPH in the WHO classification scheme. 2. Clinical features of and risk factors for CTEPH 3. Pathophysiology of CTEPH 4. Diagnostic algorithm. 5. Multimodality imaging overview. 6. Overview of treatment options.

### **CAEE-13 3D Printing in Cardiovascular Diseases: State-of-the-Art**

#### **Awards**

#### **Cum Laude**

#### Participants

Prabhakar Rajiah, MD, FRCR, Rochester, MN (*Presenter*) Nothing to Disclose

#### **TEACHING POINTS**

1. To review the principles and techniques of 3D printing 2. To discuss the utility of 3D printing in cardiovascular diseases (CVD) 3. To illustrate the applications of 3D printing in CVD

#### **TABLE OF CONTENTS/OUTLINE**

1. INTRODUCTION 2. 3D PRINTING PROCESS- Image acquisition; segmentation; mesh, 3D printing; air drying; fixation 3. SOURCE DATA- CT, MRI, Hybrid 4. IMAGE ACQUISITION RECONSTRUCTION STRATEGIES CT- ECG-gating, High contrast, high isotropic spatial resolution; MRI- Volumetric acquisition, high CNR sequences, ECG-gating, less artifacts 5. 3D MESH FILE FORMATS- STL, VRML, novel 6. 3D PRINTING METHODS- Material jetting, binder jetting, Vat polymerization, material extrusion, powder bed fusion 7. APPLICATIONS OF 3D PRINTING Identification of anatomic landmarks; Involvement of adjacent structures, relationship; Planning surgeries/interventions; Device size; Printing interventional wires; Education of trainees, patients; Communication with clinicians; 8. APPLICATIONS OF 3D PRINTING IN CVD WITH CASE EXAMPLES Congenital heart diseases (septal defects, complex CHD)- Surgical planning, roadmap; Structural heart disease (Aortic, pulmonary, mitral, tricuspid valve interventions, LAA closure)- Preprocedural planning, device selection, bench testing; Neoplasms- relationship/involvement of adjacent structures; Hypertrophic cardiomyopathy- Outflow anatomy, relationship to adjacent structures; Cardiac aneurysms/ pseudoaneurysms- Anatomy, relationship; Vascular disease- Chronic dissection, aneurysms, Marfan syndrome 9. ACCURACY LIMITATIONS 10. UTILITY OF AI 11. PITFALLS 12. TIPS ON SETTING UP A 3D PRINTING SERVICE

### **CAEE-16 Multi-modality Cardiac Imaging in Myocarditis Following COVID-19 Vaccination**

#### Participants

Constantin Marschner, MD, Toronto, ON (*Presenter*) Nothing to Disclose

#### **TEACHING POINTS**

1. Myocarditis following COVID-19 vaccination is rare. However, adolescent and young adult males are at highest risk. Chest pain is the most common presenting symptom. 2. Cardiac imaging plays an important role in the diagnosis of acute myocarditis following vaccination, with typical findings on cardiac MRI including subepicardial late gadolinium enhancement and co-localizing edema at the basal to mid inferior lateral wall. 3. The disease course is typically transient and mild, with resolution of symptoms within 1-3 weeks in most patients. Limited follow-up data demonstrates resolution of myocardial edema but persistence of late gadolinium enhancement in some patients. 4. Longer term follow-up is needed to determine whether persistent imaging abnormalities are associated with adverse outcomes, including arrhythmias and heart failure.

#### **TABLE OF CONTENTS/OUTLINE**

The purpose of this educational exhibit is to: 1. Review the incidence, pathophysiology, risk factors, and clinical outcomes of myocarditis following COVID-19 vaccination 2. Demonstrate the role of cardiac imaging in establishing a diagnosis of myocarditis following vaccination including echocardiography, cardiac MRI, and PET 3. Illustrate multi-modality cardiac imaging findings in patients with myocarditis following vaccination, at the time of acute presentation and at follow-up

### **CAEE-17 Comprehensive Assessment of Cardiac Amyloidosis with Cardiac MRI: Morphology, Function and Tissue Characterization**

#### Participants

Filipe Carvalho, MD, (*Presenter*) Nothing to Disclose

#### **TEACHING POINTS**

Cardiac amyloidosis is a challenging diagnosis that usually requires increased clinical awareness and multimodality evaluation for timely diagnosis. In this presentation, the reader should learn how to identify the spectrum of morphologic features of cardiac amyloidosis and to address the role of cardiac MRI in the main differential diagnosis. We will demonstrate the main delayed enhancement patterns with potential imaging pitfalls and discuss the applicability of new mapping techniques (native T1 and Extracellular Volume Fraction [ECV]) on the diagnostic and prognostic assessment

#### **TABLE OF CONTENTS/OUTLINE**

(1) Introduction and Background. (2) Present the main morphological features of cardiac amyloidosis: enlarged atria, left ventricle hypertrophy, diastolic dysfunction. (3) Discuss the role of tissue characterization with native T1 mapping, ECV, TI-scout, magnitude and PSIR delayed enhancement techniques in the prognostic and diagnostic assessment. (4) Illustrate the main imaging pitfalls and possible differential diagnosis. (5) Take-Home messages and teaching points.

### **CAEE-18 Cardiac MRI 2D Phase Contrast Flow Imaging: Pearls and Pitfalls**

#### Participants

Claire Brookmeyer, MD, (*Presenter*) Nothing to Disclose

#### **TEACHING POINTS**

Review pearls and pitfalls in the application of phase contrast 2D flow imaging to cardiac MR. Emphasize important pitfalls in the

acquisition of phase contrast 2D flow sequences. Explain indications and utilization of 2D flow imaging to cardiac valvular stenosis and regurgitation, as well as intracardiac shunts.

#### TABLE OF CONTENTS/OUTLINE

Introduction: Background information on valvular stenosis and regurgitation, intracardiac shunt, Role of velocity and flow quantification in the detection and management of cardiac valvular pathologies and intracardiac shunts. Technical pearls and pitfalls: Basic physics concepts behind phase contrast imaging to determine flow, Imaging plane set up for aorta and main pulmonary artery, Slice location selection, VENC selection and aliasing, In-plane and Through-plane techniques, Temporal resolution. Imaging protocols and Post-Acquisition Processing: Steady state free precession cine sequences for Functional assessment, stroke volume quantification, Phase contrast sequences for velocity and flow assessment. Application: Regurgitation (Mitral, Aortic), Stenosis (Aortic, Mitral), Intracardiac shunt Qp/Qs

#### CAEE-19 Preprocedural Assessment of Left Atrial Appendage Closure Using Dedicated CT Image

Participants

Naoki Hosoda, (Presenter) Nothing to Disclose

#### TEACHING POINTS

To learn about the pre-procedural assessment for left atrial appendage treatment. To learn measurement method of LAA dimensions. To learn advantage of preoperative assessment for LAAC with CT. To learn about necessity of CT.

#### TABLE OF CONTENTS/OUTLINE

A. Pre-procedurally clarifies the intracardiac thrombus and LAA morphology. B. Usefulness of CT to measure in the same way as TEE. C. Risk assessment by morphology and simulation of optimal sheath selection using CT volume data. D. CT predicts not only the risk of the intervention based on anatomical features of the LAA but also the thrombus, device size, sheath type, optimal location for septal puncture and pre-procedurally clarifies LAA dimensions.

#### CAEE-2 Taking It to the Next Level - What's New with CAD-RADS 2022

Awards

Certificate of Merit

Participants

Arzu Canan, MD, Dallas, TX (Presenter) Nothing to Disclose

#### TEACHING POINTS

Purpose: The purpose of this educational exhibit is to review the update version of CAD-RADS (Coronary Artery Disease Reporting and Data System) and to highlight the changes compared to prior version with illustrative case examples. Major teaching point CAD-RADS not only provides a common and standardized lexicon for interpretation of coronary CT angiography findings but also provides specific recommendations for further management of patients. Although the main seven categories remain similar in the updated version, the new CAD-RADS scoring system allows for more comprehensive evaluation and description of coronary atherosclerosis with the addition of new features, such as plaque volume assessment and physiologic significance of stenosis.

#### TABLE OF CONTENTS/OUTLINE

This exhibit includes a systematic review of the CAD-RADS categories and modifiers, followed by case based examples. The systematic review includes 1. The rationale and the evidence for updated CAD-RADS will be reviewed 2. CAD-RADS Categories (0-5 and N): What is same and different with illustrative case examples 3. Modifiers: N, S, G, V, etc.: What is the same and what is new with illustrative case examples 4. New features 5. Recommendations: What is same and different with illustrative case examples Conclusion It is of importance to understand the differences between the original and the newest version of CAD-RADS and to implement those changes into the clinical practice in order to improve communication and to facilitate decision making process for further management of patients. This exhibit equips the learner with the required knowledge in a practical illustrated manner.

#### CAEE-20 Cardiac Electrophysiology 101 and the Role of Radiologist

Awards

Identified for RadioGraphics

Participants

Prabhakar Rajiah, MD, FRCR, Rochester, MN (Presenter) Nothing to Disclose

#### TEACHING POINTS

Electrophysiology (EP) deals with diagnosis and management of heart rhythm problems. It is important for a cardiac radiologist to know the basics of EP and roles where they can contribute 1. To review the basic techniques used in cardiac EP 2. To correlate EP findings with cardiac CT/MRI 3. To understand the role of CT/MRI in cardiac EP

#### TABLE OF CONTENTS/OUTLINE

1. INTRODUCTION - Cardiac action potential, arrhythmia mechanisms 2. CARDIAC EP- Role, advantages 3. STANDARD EP TESTS- Catheters, measurement of electric potentials 4. ATRIAL FIBRILLATION/FLUTTER - a. EP for diagnosis and ablation; b. Pre-procedural CT/MR -for anatomy, thrombus, scar; c. Procedural- Electroanatomic mapping, ablation types; d. Post-procedural CT/MR- Vein stenosis, thrombus, bleed, esophagoatrial fistula, perforation, pericardial effusion; e. Left atrial appendage closure- Pre-procedural planning, post procedural complications 5. VENTRICULAR ARRHYTHMIAS -a. EP techniques for characterization; b. EP ablation; c. Scar (substrate) evaluation- detection, mapping, heterogeneity in MRI/CT ; d. Ablation procedure- electroanatomic mapping, CARTO; e. MRI-guided ablation 6. LV DYSYNCHRONY - a. Evaluation with MRI/strain; b. CRT procedure; c. Venous anatomy CT/MRI ; d. MRI/CT- Scar 7. SUDDEN CARDIAC DEATH a. Identifying at-risk patients; b. MRI/CT for diagnosis 8. BRADYCARDIA- Sinus, heart blocks - MRI, PET/CT for sarcoidosis 9. SYNCOPE - Table tilt test 10. COMPLEX CONGENITAL/POST-SURGICAL ANATOMY- Imaging guidance for navigation to appropriate chamber. 11. IMAGE GUIDED RETRIEVAL OF RETAINED LEADS

#### CAEE-21 Coronary CT Angiography with Myocardial Late Enhancement Protocol in the Emergency Room: Tips and Tricks

Participants

Lucas Farias, MD, Sao Paulo, Brazil (*Presenter*) Nothing to Disclose

#### TEACHING POINTS

The purpose of this exhibit is:- To review coronary CT angiography with myocardial late enhancement protocols in the evaluation of patients with chest pain.- To review the pharmacokinetics of late iodine enhancement at CT as alternative to the gadolinium at MRI.- To assess the utility of the coronary CT angiography with myocardial late enhancement protocol in the emergency room to exclude coronary obstruction in patients with suspected acute myocarditis.- To correlate important findings with the anatomy and pathophysiology.- To discuss image findings according to the patterns of late enhancement to differentiate between ischemic and nonischemic myocardial damage, to enhance radiologists' skills.- To review usual and unusual patterns of acute myocardial infarction, myocarditis and others non-ischemic cardiomyopathies. - To highlight their characteristics to familiarize radiologists with these conditions, preventing unfavorable patient outcome.

#### TABLE OF CONTENTS/OUTLINE

Table of contents/outline - Applied myocardial anatomy and vascularization. - Pharmacokinetics of late iodine enhancement. - Patterns of myocardial late enhancement. - CT angiography with myocardial late enhancement protocol. - Case series diagnosed with CT angiography with myocardial late enhancement protocol. - Sample cases of pearls, pitfalls, diagnostic difficulties, and mimics. - Summary and take-home messages.

#### CAEE-22 Can Spectral Cardiac CT Find New Clinical Value in Ischemic Heart Disease?

Participants

Junji Mochizuki, MSc,RT, (*Presenter*) Nothing to Disclose

#### TEACHING POINTS

To learn about special characteristic of spectral imaging : Dual layer Spectral cardiac CT.To learn about the use of spectral imaging coronary and myocardium evaluation.To illustrate various clinical applications using these techniques by presenting clinical images.

#### TABLE OF CONTENTS/OUTLINE

A. The virtual monochromatic image (VMI) allows evaluation of energy-dependent changes in CT number of coronary artery plaques.B. The low-energy VMI reduces the CT number of epicardial fat and clearly depicts the thrombus and coronary artery plaques.C. The VMI reduces beam-hardening artifacts. In addition, low-energy images can clearly detect areas of abnormal perfusion because the CT number of normal myocardium are increased.D. The extracellular volume function with iodine density imaging can accurately assess myocardial viability.

#### CAEE-23 Chronic Thromboembolic Pulmonary Hypertension (CTEPH): A Multimodality Imaging Review

Participants

Scott Adams, MD,PhD, Saskatoon, SK (*Presenter*) Nothing to Disclose

#### TEACHING POINTS

1. Chronic thromboembolic pulmonary hypertension (CTEPH) is defined as pulmonary hypertension due to persistent obstruction of the pulmonary arteries from pulmonary embolism despite at least 3 months of anticoagulation.2. Ventilation-perfusion (V/Q) scintigraphy has high sensitivity for CTEPH and is a first-line imaging modality for ruling out CTEPH. In addition, SPECT-CT offers increased sensitivity and specificity.3. CT pulmonary angiography has higher specificity than V/Q scintigraphy for CTEPH, but lower sensitivity. CT features include partial or complete filling defects, bands, and webs within the pulmonary arteries; pulmonary artery dilation; right ventricular dilation and hypertrophy; bronchial artery dilation; and mosaic attenuation of the lung parenchyma.4. Dual-energy CT has been shown to improve detection of distal CTEPH and provide additional information on pulmonary vascular reserve and parenchymal arterial perfusion.5. In the future, 4D-flow MRI may play a role in treatment selection and assessment of treatment response.

#### TABLE OF CONTENTS/OUTLINE

DefinitionPathophysiologyClinical presentation and patient demographicsImaging features- Radiography- CT, including high-resolution CT, CT pulmonary angiography, and dual-energy CT- MRI, including MR angiography and 4D-flow- Echocardiography- Conventional angiography- Ventilation/perfusion (V/Q) scintigraphy and SPECT-CTDiagnostic approach, including the role of imaging in diagnosis, patient selection for treatment, and post-operative follow-upClinical management options

#### CAEE-24 Cardiovascular Manifestations of Connective Tissue Disease

Participants

Jospeh Mansour, MD, (*Presenter*) Nothing to Disclose

#### TEACHING POINTS

List the various cardiac and vascular entities that can occur with connective tissues diseasesDescribe the pathophysiology, risk factors, and management for each etiology.Illustrate the spectrum of imaging findings and differential diagnoses for each of these entities

#### TABLE OF CONTENTS/OUTLINE

Rheumatoid arthritisa. Pulmonary hypertensionb. Vasculitis and aortitisc. Aortic aneurysmd. CardiomyopathySystemic Lupus erythematosusa. Pericardial effusionb. Vasculitisc. Pulmonary embolismd. Lupus myocarditis and cardiomyopathye. Libman-Sacks endocarditisSclerodermaa. Pulmonary hypertensionb. Cardiomyopathyc. Infarcts and microvascular diseasePolymyositis and dermatomyositisa. Myocarditisc. Coronary artery diseaseSjogren syndromea. Pericardial effusionb. Cardiomyopathyc. Pulmonary hypertensionSUMMARY: Patients with connective tissue diseases can suffer from cardiovascular complications which may impact both morbidity and mortality. Diagnosing these entities can be challenging, both clinically and with imaging, and is often delayed. Familiarity with these conditions and their imaging features can help the radiologist recognize these entities and aid in diagnosis.

#### CAEE-25 State of the Art Cardiac MR Imaging of Ischemic Heart Disease

## Awards

### Certificate of Merit

#### Participants

Felipe Sanchez, MD, Toronto, Chile (*Presenter*) Nothing to Disclose

### TEACHING POINTS

-1. Ischemic heart disease (IHD) is the worldwide leading cause of death and disability.2. Cardiac MR allows for the evaluation of global and regional cardiac function and provides superb myocardial characterization in a same evaluation.3. Cardiac MR can accurately depict myocardial edema, infarction, hemorrhage, and microvascular obstruction.4. Current Cardiac MR imaging strategies have widely accepted diagnostic and prognostic value.5. Emerging techniques and applications aim to improve prognostic and diagnostic performance of Cardiac MR.

### TABLE OF CONTENTS/OUTLINE

-1. Significance of IHD.2. Basic physiopathology of IHD.3. Role of Cardiac MR in the workflow of IHD.4. Functional imaging.5. Edema imaging.6. Infarct characterization.a. Depicting myocardial infarct and "at risk" zones: classic and novel strategies.b. MVO and myocardial hemorrhage: role of T2\*7. Stress perfusion.8. Novel tools for viability assessment and risk stratification.a. Feature tracking: Patterns of impaired myocardial contraction.b. Post-reperfusion hemorrhage, persistent edema, and adverse remodeling.c. 4D-flow in IHD.9. Technical considerations.

## CAEE-26 Arrhythmogenic Cardiomyopathies: What the Imager Should Know

## Awards

### Identified for RadioGraphics

### Certificate of Merit

#### Participants

Mauricio S. Galizia, MD, , (*Presenter*) Nothing to Disclose

### TEACHING POINTS

- Arrhythmogenic Cardiomyopathies (AC) are a group of myocardial diseases that are associated with ventricular arrhythmias and sudden cardiac death
- Although arrhythmogenic right ventricular cardiomyopathy (ARVC) was the first disease described in which morphologic and structural ventricular abnormalities were associated with arrhythmias, AC can involve the right ventricle, the left ventricle, or both
- The main sub-phenotypes of AC include the classical ARVC, left-dominant AC, and arrhythmogenic dilated cardiomyopathy
- Many genetic mutations have been found to be associated with AC, most often genes that encode desmosome structural proteins
- AC can be associated with ventricular systolic dysfunction and/or ventricular dilation. However, symptoms of arrhythmia or history of arrhythmic cardiac arrest can occur in patient with no structural myocardial abnormalities and may represent early developing AC
- There are diagnostic criteria for ARVC; however, similar criteria for the other AC phenotypes is lacking

### TABLE OF CONTENTS/OUTLINE

1. Definition of arrhythmogenic cardiomyopathy (AC). 2. Description of the desmosome and its constituent proteins: Desmoglein, desmocollin, plakophilin, junctional plakoglobin, desmoplakin 3. Association between AC and genetic diseases of the desmosome: difference between disease and phenotype. 4. Typical clinical presentation and imaging findings (with a greater focus on CMR) of the following phenotypes: Arrhythmogenic right ventricular cardiomyopathy (ARVC), left-dominant arrhythmogenic cardiomyopathy, arrhythmogenic dilated cardiomyopathy 5. Differential diagnoses and mimics: Dilated Cardiomyopathy, sarcoidosis, myocarditis

## CAEE-27 Cutting the Edge of HCM: Tailored Planning of Surgical Myectomy in Obstructive Hypertrophic Cardiomyopathy

## Awards

### Magna Cum Laude

### Identified for RadioGraphics

#### Participants

Sunhyang Lee, MD, Seoul, Korea, Republic Of (*Presenter*) Nothing to Disclose

### TEACHING POINTS

1. To set the cardiac CT protocols and image analysis methods for simulation of successful surgical myectomy in patients with obstructive hypertrophic cardiomyopathy (HCM).2. To demonstrate tailored planning of surgical myectomy using multiphase cardiac CT images, especially volume rendering images and 3D printing

### TABLE OF CONTENTS/OUTLINE

1. Classification of HCM based on surgical approach- Septal HCM- Apical HCM- Mixed, or diffuse type HCM- Combined abnormal papillary muscles2. Multiphase Cardiac CT Protocol3. CT Image Analysis Methods1) Cardiac function analysis (esp. apical, mixed, and diffuse type HCM)2) Surgeon's views- Trans-aortic view- Trans-apical view3) Papillary muscle evaluation4) Simulation of potential myectomy extent5) Comparison between pre- and post- myectomy CT images4. Various Examples1) Simulation of myectomy in septal HCM and comparison with postoperative CT2) Simulation of myectomy in diffuse HCM and comparison with postoperative CT3) Simulation of myectomy in mixed type HCM and comparison with postoperative CT4) Simulation of myectomy in HCM with abnormal papillary muscle

## CAEE-28 Differential Diagnosis of Cardiac Amyloidosis: Pearls and Pitfalls

#### Participants

Patricia Oliveros Ordas, MD, Majadahonda, Spain (*Presenter*) Nothing to Disclose

### TEACHING POINTS

Cardiac amyloidosis (CA) is a rare disease caused by the extracellular deposition of insoluble fibrillar proteinaceous material in the

myocardium. Due to the complexity and multisystemic involvement of amyloidosis, a high index of suspicion for CA should be maintained. Typical MRI appearance of CA includes left ventricle myocardial thickening with preserved systolic function, increased atrial volume, and altered gadolinium kinetics with the presence of late enhancement with a subendocardial or transmural pattern. Other common causes of cardiomyopathy that may present as left ventricular hypertrophy should be excluded, such as depositional cardiomyopathies, hypertensive cardiomyopathy, hypertrophic cardiomyopathy, and cardiac sarcoidosis, among others. After reviewing our extensive casuistry and our sample of 80 patients with CA, we present the findings that will allow an easier differential diagnosis by imaging between these pathologies.

#### TABLE OF CONTENTS/OUTLINE

• Introduction: most frequent morphologic, functional and tissue characterization MRI findings in CA • Imaging differential diagnosis of CA that includes: \* Depositional cardiomyopathies (Fabry's disease, Danon's disease) \* Hypertensive cardiomyopathy \* Hereditary cardiomyopathies \* Cardiac sarcoidosis \* Others • Conclusions

#### CAEE-29 MRI Mapping in the study of Myocardial Disease

Participants

Susana Otero Muinelo, MD, (Presenter) Nothing to Disclose

#### TEACHING POINTS

1. To illustrate the role of T1, T2 and T2\* mapping MRI sequences and extracellular volume in myocardial diseases. 2. To recognize findings of most common myocardial diseases on T1, T2 and T2\* maps and correlate them with other findings on cardiac MRI.

#### TABLE OF CONTENTS/OUTLINE

Cardiac T1, T2 and T2\* mapping can provide information about myocardial disease that remains undetected using conventional techniques. The quantitative approach allows noninvasive characterization of myocardial properties such as extracellular volume expansion, edema, or other abnormalities in tissue composition. Thus, increased T1-native due to fibrosis in hypertrophic cardiomyopathy or to amyloid deposition or shortened T1-native due to glycosphingolipids in Anderson-Fabry disease could be evaluated. T2 mapping can detect myocardial edema in myocarditis, Takotsubo cardiomyopathy or myocardial infarction, whereas low T2\* can be useful in iron overload and hemorrhage. We present cases of hypertrophic, dilated and restricted cardiomyopathy, acute myocardial disease as myocarditis or Tako-Tsubo and infiltrative cardiomyopathies and review the advantages, limitations and applications of T1 and T2 mapping to characterize these ones and other myocardial diseases. Multiparametric cardiac MRI provides prognostic information of structural and functional characteristics and myocardial composition. Incorporation of myocardial mapping on clinical routine increases the usefulness of MRI for the diagnosis and characterization of myocardial diseases.

#### CAEE-3 Unraveling the Mysteries of Congenital Heart Disease: A Skills-based Approach

Awards

Cum Laude

Participants

Shravan Sridhar, MD, MS, (Presenter) Nothing to Disclose

#### TEACHING POINTS

1. Become familiar with common congenital heart diseases and morphologic features 2. Learn of important imaging features 3. Understand how management relies on imaging metrics 4. Gain skills to use in practice 5. Apply skills in the assessment of complex congenital heart diseases

#### TABLE OF CONTENTS/OUTLINE

1. Title 2. Table of common CHD and skill list 3. Bicuspid AV morphology (per 2021 consensus) 4. Understanding management 5. Skill 1: Peak speed quant with PC VENC (in-plane, through plane) 6. Common shunts (ASD, VSD, PDA) and features that determine treatment (2018 AHA guidelines) 7. Understanding management 8. Skill 2: Qp/Qs quant 9. Right-sided obstruction (pulmonic stenosis, tetralogy of Fallot, pulmonary atresia spectrum) 10. Understanding management 11. Skill 3: Valve regurgitation quantification with phase contrast velocity-encoded images, fractional pulmonary flow quantification 12. Left-sided obstruction (coarctation, aortic stenosis, Williams syndrome, Shone complex) 13. Understanding management 14. Skill 4: Flow quant for coarctation 15. TGA (D, L) 16. Understanding management 17. Skill 5: Anatomic mapping - situs, right, left, terms used in describing discordance (e.g. anatomic vs morphologic) 18. Other conotruncal anomalies (truncus, DORV, DOLV) 19. Understanding management 20. Skill 6: Rules to diff between Tetralogy, truncus, DORV, and DOLV 21. Single ventricle (HLHS, HRHS, Ebstein's, tricuspid atresia, DORV) 22. Understanding management 23. Skill 7: Flow mapping, "checks and balances" 24. PAPVR, TAPVR 25. Understanding management 26. Skill 8: Angiography 27. References

#### CAEE-30 Multi-modality Imaging of Cardiac Paragangliomas - A Review

Participants

Joao Carvalho, MD, (Presenter) Nothing to Disclose

#### TEACHING POINTS

? Paragangliomas are rare neuroendocrine tumors originating from autonomic paraganglia. Heart involvement is rare, accounting for <1% of primary cardiac tumors. Most cardiac paragangliomas are incidentally detected on echocardiography or CT, or during the work-up of symptomatic patients with elevated (nor)metanephrine levels or genetic predisposition. ? Most cardiac paragangliomas are located around the great vessels, coronary arteries (atrioventricular groove) or the atria, which can be explained by tumor origin from the paraganglia and the distribution of the cardiac plexus. ? On MRI cardiac paragangliomas typically have low to intermediate signal on T1, and high signal on T2. The tumors are strongly vascularized, with high uptake on first-pass perfusion, and heterogeneous on late gadolinium enhancement. ? Functional imaging with radiolabeled somatostatin analogues is indicated to screen for additional tumor locations or metastatic disease. ? Surgical excision is the only curative treatment. CT or invasive angiography should be performed pre-operatively to precisely delineate tumor vascularization and assess the need for revascularization. Paragangliomas can be vascularized by the left and/or right coronary artery, posing additional surgical challenges.

#### TABLE OF CONTENTS/OUTLINE

1. Background: epidemiology, clinical presentation. 2. Diagnosis: tumor location, tissue characteristics, vascularization. 3.

Management: metastatic/multiple disease, surgical planning, radionuclide therapy.

### **CAEE-31 Virtual Reality Imaging - Pre-operative Visualization Modality Equipped with Simultaneous Quantification for Valvular Disease**

Participants

Yukihiro Nagatani, MD, Otsu, Japan (*Presenter*) Nothing to Disclose

#### **TEACHING POINTS**

The purpose of this exhibit is: 1. To review general outline of image data display algorithm adopted for virtual reality imaging (VRI) based on advanced visualization software and actual clinical application of VRI 2. To learn crucial anatomical distances and/or dimensions to be accurately measured in pre-operative assessment for valvular disease 3. To introduce valuable experimental model by using ex-vivo swine heart reproducing physiological movements of valves and myocardium 4. To review specific sequences for valvular disease in cardiac magnetic resonance imaging (MRI) from conventional to updated ones

#### **TABLE OF CONTENTS/OUTLINE**

ž VRI using visualization toolkit with reproducible 3-dimensional measurement ž Detailed description of experimental system enabling endoscopic observation under physiological state and quantitative assessment of intramuscular vasculature by using ex-vivo swine heart. ž Clinical advantage with application of 3-dimensional or 4-dimensional VRI: realization of easy and reliable measurement supported with visual assessment ž Anatomy, dynamics and disease of aortic valve and root including our endoscopic observation result ž Various imaging sequences useful for valvular disease assessment: from conventional and high-speed cine images such as steady-state Free Processing and 4-dimensional flow MRI

### **CAEE-32 What Hides in the Epicardial Space? Differential Diagnosis of Epicardial Masses**

**Awards**

**Certificate of Merit**

**Identified for RadioGraphics**

Participants

Adria Roset Altadill, MD, (*Presenter*) Nothing to Disclose

#### **TEACHING POINTS**

- The epicardial space has a diversity of components that can be the origin of various types of masses. - The epicardial masses can be divided into tumoral, non-tumoral or pseudo-masses.

#### **TABLE OF CONTENTS/OUTLINE**

The location is a helpful feature in order to diagnose cardiac masses, but epicardial masses are usually dismissed. The epicardial space includes the epicardial fat and the visceral pericardium. It is composed of a lining of mesothelial cells and connective tissue, along with a variable amount of fat, containing coronary vessels, lymphatics and nerves. Due to its diversity of components, different kinds of masses can be found in the epicardial space. They can be divided into tumoral, non-tumoral or pseudo-masses. The epicardial tumoral masses include lipoma, lymphoma, angiosarcoma, mesothelioma and metastases. Regarding non-tumoral etiologies, IgG4-related coronary disease, Erdheim-Chester and hydatid infection can be encountered. Finally, there are epicardial pseudo-masses either secondary to lipomatosis, purulent pericarditis, coronary aneurysms or postsurgical changes. In this education exhibit we show examples of each case, emphasizing the distinguishing features and the clues for the differential diagnosis.

### **CAEE-33 To the Heart of the Matter: A Systematic Approach to Interpretation of Cardiac MR for Trainees**

**Awards**

**Identified for RadioGraphics**

Participants

Aeman Muneeb, MBBS, (*Presenter*) Nothing to Disclose

#### **TEACHING POINTS**

Approach to reading a conventional cardiac MR. 1. How to identify and learn the contribution of each sequences commonly used in Cardiac MR studies 2. To recognize the normal appearance of the heart in the common Cardiac MR sequences (cardiac chamber size, thickness, signal characteristics, normal function on visual analysis, interpretation of basic quantification parameters for function and flows) 3. Understand common appearances of diseases of the cardiac structure, myocardium, valves and pericardium. 4. Visual analysis of the Myomaps (native T1, T2, T2\*). 5. Basic principles of quantitative Myomaps analysis.

#### **TABLE OF CONTENTS/OUTLINE**

Step 1: Know your patient - review the clinical scenario and relevant prior imaging. Step 2: Anatomical assessment. Step 3: Visual assessment of function. Step 4 Hemodynamic Assessment - Function and Flow quantification parameters. Step 5: Tissue Characterization. Step 6: Differential diagnosis: Characteristic appearance of common diseases.

### **CAEE-34 Multimodality Imaging in Cardiac Masses**

Participants

Ayaz Aghayev, MD, Newton, MA (*Presenter*) Nothing to Disclose

#### **TEACHING POINTS**

- Cardiac masses are rare entities; however, they can be associated with high morbidity and mortality.- Cardiac masses broadly can be classified as non-neoplastic masses such as thrombus, normal/variant cardiac structures, and neoplastic masses (primary and secondary/metastatic tumors).- The educational exhibit will elucidate the diagnostic approach even before the imaging, based on the patient's demographics, and prior disease/comorbidities.- On imaging, differential diagnosis can be elaborated based on the location of the tumor; for example, the most common benign myxoma is usually located in the left atrium and attached to the interatrial septum; primary cardiac malignancy - angiosarcoma - is exclusively located along the right atrium/ventricle as an

infiltrative mass.- The next step will focus on available imaging modalities for cardiac masses such as echocardiography (TTE/TEE), cardiac CT, cardiac MRI, and PET/CT, and their specific imaging characteristics for certain masses. For example, fat density lesion on a CT is consistent with lipoma; avid LGE in intramyocardial mass is a feature of fibroma, or Dotatate uptake in cardiac mass is diagnostic of paraganglioma.- Lastly in this educational exhibit, we will provide a proposed algorithm for patients with suspected cardiac masses or incidentally detected on echo/chest CT.

#### TABLE OF CONTENTS/OUTLINE

1. Cardiac mass classification.2. Diagnostic approach to the patient with suspected or incidentally detected cardiac mass.3. Available imaging modalities that can be utilized in cardiac masses.4. Key imaging features of cardiac masses- Cardiac CT, Cardiac MRI, and PET-CT (including pitfalls).5. Proposed algorithm for suspected cardiac masses.

#### CAEE-35 Potential Applications of Radiomics Based Texture Analysis in Cardiac Magnetic Resonance (CMR)

Participants

Avanti Gulhane, MD, Seattle, WA (*Presenter*) Nothing to Disclose

#### TEACHING POINTS

We will discuss potential applications for radiomic analysis of CMR studies. 1.As a proof of concept, we will describe technique for texture analysis of LGE-PSIR to identify first, second and higher order features in patients with ischemic and non-ischemic myocardial diseases. 2.Potential advantages of using radiomics texture analysis for quantitative assessment of CMR images. 3.Several texture features such as first order entropy, kurtosis, grey level co-occurrence matrix non uniformity, grey level run length matrix non uniformity and wavelet transform can be obtained using Pyradiomics, an open-source software. 4.We will illustrate comparative analysis of radiomic features in LGE images of a normal volunteer and patients with ischemic and non-ischemic heart diseases

#### TABLE OF CONTENTS/OUTLINE

Specific areas where CMR radiomics analysis may aid on diagnostic characterization will be described. Example of radiomic analysis obtained from LGE-PSIR will be illustrated by showing specific texture parameters that can be obtained. We will illustrate the method by showing examples of radiomic features in several diseases on CMR including myocardial infarction, hypertrophic cardiomyopathy, myocarditis, dilated cardiomyopathy and normal heart. Images will be sampled to 1x1x1 mm using linear interpolation and discretized to a fixed bin width of 25 units for the basic preprocessing within the Pyradiomics software. Examples of feature types extracted and analyzed are • First Order Statistics • Shape-based (2D and 3D) • Gray Level Co-occurrence Matrix • Gray Level Run Length Matrix • Gray Level Size Zone Matrix • Neighbouring Gray Tone Difference Matrix • Gray Level Dependence Matrix • Wavelet-based features

#### CAEE-36 Mulmodality Imaging of Atrioventricular Groove Masses - Diagnostic Approach

Awards

Certificate of Merit

Participants

Prabhakar Rajiah, MD, FRCR, Rochester, MN (*Presenter*) Nothing to Disclose

#### TEACHING POINTS

The atrioventricular (AV) groove is the space that encircles the right and left AV valves. 1. To review the masses involving the atrioventricular (AV) groove. 2. To discuss the role of multimodality imaging in the diagnosis and characterization of these masses. 3. To illustrate the imaging appearances of several types of AV groove masses

#### TABLE OF CONTENTS/OUTLINE

• INTRODUCTION • ANATOMY OF AV GROOVE- Right coronary artery, left circumflex coronary artery, coronary sinus, fat, lymphatics, nerves. • MULTIMODALITY IMAGING- CT, MRI, Nuclear medicine, Echocardiography, cardiac catheterization • DISCUSSION AND ILLUSTRATION OF THE FOLLOWING MASSES IN THE AV GROOVE WITH CASE EXAMPLES AND PATHOLOGICAL CORRELATION A. VASCULAR LESIONS - Coronary artery aneurysm - Coronary bypass graft aneurysmpseudoaneurysm - Cardiac chamber aneurysm/pseudoaneurysm - Coronary fistula - Vascular malformation B. INFLAMMATORY - IgG4 disease - Erdheim Chester disease - Vasculitis - Sarcoidosis - Hematoma C. BENIGN NEOPLASMS - Paraganglioma - Schwannoma - Hemangioma - Thymoma D. MALIGNANT NEOPLASMS - Sarcoma - Lymphoma - Metastases E. MISCELLANEOUS - Calcification and pericardial constriction - Caseous mitral annular calcification - Fatty proliferation - Pericardial hematoma - Intracamerar RCA • DIAGNOSTIC APPROACH AND ALGORITHM - Infiltrative versus well-defined margins - Hypervascular versus hypovascular - Late gadolinium enhancement - High T2 signal

#### CAEE-37HC Pre- and Postoperative Imaging Evaluation of Ross Procedure Candidates: Anatomy, Complications, and What the Surgeon Wants to Know

Participants

Lisa Xuan, MD, BSc, Newmarket, ON (*Presenter*) Nothing to Disclose

#### TEACHING POINTS

1. The Ross procedure is a technically complex cardiac surgery which replaces a diseased aortic valve with a native pulmonic autograft.2. There is growing interest for the Ross procedure in young patients, due to improved longevity and the ability of the native autograft to grow and adapt overtime.3. Preoperative cardiac MR evaluation is integral for patient selection and surgical planning, while postoperative surveillance aids in diagnosing complications and quantifying myocardial remodeling as a measure of success.4. Relevant cardiac anatomy and MR imaging findings of the Ross procedure are reviewed.5. Example cardiac MR protocols and synoptic reporting frameworks are provided, with details tailored for the cardiac surgeon, and can be utilized to foster a strong multidisciplinary Ross program.

#### TABLE OF CONTENTS/OUTLINE

Overview of Ross procedure surgical technique:- Indications- Illustrations of the procedure and pertinent cardiac anatomy (generated by our medical illustrator)Cardiac MR protocol and reporting:- Pre/postoperative protocols and follow-up intervals-Synoptic reporting frameworkReview of imaging:- What the cardiac surgeon wants to know- Relevant radiologic findings in pre and

post-operative Ross patients- Postoperative cardiac remodeling as a measure of success (e.g. left ventricular mass regression on cardiac MR)- Potential complications (e.g. pulmonic autograft failure (autograft annular dilatation))Clinical ImplicationsSummaryPlease visit the Learning Center to also view this presentation in hardcopy format.

### **CAEE-38 Multimodality Imaging of Valvular Infections**

#### **Awards**

**Certificate of Merit  
Identified for RadioGraphics**

#### **Participants**

Jordi Broncano, MD, Cordoba, (*Presenter*) Nothing to Disclose

#### **TEACHING POINTS**

1. To analyze the role of advanced imaging in the diagnosis and management of patients with infective endocarditis (IE). 2. To describe the main imaging clues for accurate diagnosis of valvular and perivalvular features as well as extracardiac findings in IE. 3. To identify the potential pitfalls of IE and the main imaging tips for differentiating from IE.

#### **TABLE OF CONTENTS/OUTLINE**

1. Definition of IE: Modified Duke Criteria 2. Epidemiology in IE: Unveiling the high-risk patient 3. Role of Imaging in IE: Pros and Cons - Echocardiography: Transthoracic and transesophageal - Cardiac Computed Tomography - Positron Emission Tomography/Computed tomography (PET/CT) - Cardiac MRI: Is there a role for it? 4. Imaging Pearls in IE 4.1. Valvular disease - Vegetation - Leaflet perforation - Leaflet aneurysm 4.2. Perivalvular disease: - Dehiscence pseudoaneurysm - Perivalvular abscess - Perivalvular fistula 4.4. Extracardiac embolic events 5. Infective Endocarditis Masqueraders - Non-bacterial thrombotic endocarditis (Marantic Endocarditis) - Papillary fibroelastoma - Caseous Necrosis of the Mitral Valve (CNMV) - Lamb's Excrecences - Valvular thrombosis - Inflammatory pannus - Myxoma - HALT - Cusp prolapse 6. Diagnostic imaging algorithm 7. Take Home points

### **CAEE-39 Stress Cardiac Magnetic Resonance Imaging: Our Experience in a Community Hospital Setting**

#### **Participants**

Mahmoud Shalaby, MD, Lansdowne, PA (*Presenter*) Nothing to Disclose

#### **TEACHING POINTS**

1- Describe the basic principles of stress cardiac magnetic resonance (CMR) perfusion imaging, including technique and imaging protocol. 2- Discuss the clinical applications of stress CMR. 3- Illustrate stress CMR interpretation and data analysis. 4- Highlight stress CMR pitfalls and artifacts.

#### **TABLE OF CONTENTS/OUTLINE**

1- Stress CMR perfusion tracers; clinical applications and contraindications. 2- Pulse sequences and imaging protocols. 3- Stress CMR interpretation and data analysis; qualitative and quantitative interpretation. 4- Clinical applications of stress CMR in large-vessel and microangiopathy coronary artery disease. 6- Pitfalls and artifacts: - Dark rim artifact. - Susceptibility artifact. - Chemical shift artifact. 7- Limitations of stress CMR.

### **CAEE-4 Expanding Fractional Flow Reserve (FFR) CT: Challenges and Emerging Applications**

#### **Participants**

Fabio Trindade, MD, Curitiba, Brazil (*Presenter*) Nothing to Disclose

#### **TEACHING POINTS**

The aim of this exhibition is to review: 1) What is Fractional Flow Reserve (FFR) and its relevance in coronary artery disease (CAD). 2) Technical Aspects of Machine-learning-based FFRCT (ML FFRCT) calculation. 3) Current and potential contributions of FFRCT in CAD. 4) Advantages and challenges of Machine-learning-based FFRCT. 5) Emerging applications and future directions of FFRCT.

#### **TABLE OF CONTENTS/OUTLINE**

1. INTRODUCTION 1.1. FFR overview: definition, interpretation, invasive and non-invasive techniques 2. FFRCT: BRIEF REVIEW OF SUPPORTIVE EVIDENCE 3. ML-FFRCT : WHAT THE RADIOLOGIST NEEDS TO KNOW 3.1. Advantages and disadvantages 3.2. How to measure: a step-by-step approach 3.3. Limitations and pitfalls 4. ML-FFRCT IN REAL LIFE: INTERACTIVE CHALLENGING SCENARIOS 4.1. Myocardial bridging 4.2. Coronary stents 4.3. Coronary artery anomalies, including interarterial course 4.4. Coronary dissection 4.5. Other conditions 5. FUTURE DIRECTIONS AND EMERGING APPLICATIONS 6. TAKE HOME MESSAGES

### **CAEE-40 Indications and Imaging Findings of CMR in the Acutely Ill Patient**

#### **Participants**

Daniel Vargas, MD, Denver, CO (*Presenter*) Nothing to Disclose

#### **TEACHING POINTS**

Cardiac MR is quickly becoming a powerful and increasingly utilized tool in the evaluation of acutely ill patients. To this end, institutions, radiologists and cardiologists should strive to have the infrastructure and preparation to offer CMR to hospitalized patients. The purpose of this exhibit is: 1. Review CMR protocols for evaluation of acutely ill patients 2. Discuss CMR tools that may aid in shortening acquisition and/or improve image quality in this group of patients 3. Review the imaging findings and pitfalls of the most common conditions encountered in the inpatient setting

#### **TABLE OF CONTENTS/OUTLINE**

1. CMR protocol for acutely ill patients a. Basic and advanced sequences. b. Tools to shorten acquisition time. c. Tools to improve image quality. 2. Common indications and imaging findings in acutely ill patients. a. Elevated troponins (myocarditis, takotsubo, myocardial infarction, etc). b. Decreased ejection fraction / Heart failure (identifying cardiomyopathy, drug toxicity, etc). c. Arrhythmia and Heart-block. d. Intracardiac mass. e. Pericardial emergencies

## **CAEE-41 Congenital Coronary Artery Anomalies with Lethal Conditions or Sudden Death Risk; Coronary CT and Conventional Angiographic Evaluation**

Participants

Keizo Tanitame, MD, Hiroshima, Japan (*Presenter*) Nothing to Disclose

### **TEACHING POINTS**

Numerous variations of coronary artery anomalies exist. Some are benign, but others are hemodynamically significant and potentially lethal. The anomalous origin of the coronary artery from the pulmonary artery is a potentially lethal condition. In the patients with anomalous origin of the coronary artery from the contralateral sinus or single coronary artery, coronary artery compression between aorta and pulmonary trunk is a risk factor of sudden death during exercise. Coronary artery fistulae are the most common hemodynamically significant abnormalities, and to-and-fro flow is seen in the dilated coronary arteries. Myocardial bridge is generally benign, but occasionally associated with angina, myocardial infarction, and sudden death. We demonstrate congenital coronary anomalies with lethal conditions or sudden death risk and discuss the radiological evaluation of their severity and treatment outcome.

### **TABLE OF CONTENTS/OUTLINE**

1. Anomalous origin of the coronary artery from the pulmonary artery - Development of collaterals and retrograde blood flow from the anomalous coronary artery to the pulmonary artery on conventional coronary angiography 2. Multi-detector CT coronary angiography for evaluating anomalous origin of the coronary artery - Visualization of the anomalous origin and subsequent passage of the coronary artery 3. Anomalous origin of the coronary artery with a risk of sudden death - Coronary artery compression between aorta and right ventricular outflow tract 4. Congenital coronary artery fistulae - Evaluation of the size of the fistula and the degree of to-and-fro flow 5. Myocardial bridge - Cardiac CT evaluation of the depth and length of the bridge and the severity of systolic stenosis

## **CAEE-42 Out on the Road: Revisiting Coronary Artery Anomalies**

### **Awards**

**Identified for RadioGraphics  
Certificate of Merit**

Participants

Lucas Farias, MD, Sao Paulo, Brazil (*Presenter*) Nothing to Disclose

### **TEACHING POINTS**

The purpose of this exhibit is: 1) To review usual and unusual cases of congenital heart diseases. 2) To discuss the classification of coronary anomalies. 3) To understand coronary anomalies by associating schematic drawings with MPR and three-dimensional reconstructions, correlating them with coronary angiography (animated gif). 4) To correlate important findings with the anatomy, embryology, and pathophysiology. 5) To discuss image findings in order to enhance radiologists' skills. 6) To review CT protocols in the evaluation of patients with suspected coronary artery anomalies. 7) To highlight their characteristics in order to familiarize radiologists with these conditions, preventing unfavorable patient outcome.

### **TABLE OF CONTENTS/OUTLINE**

1) Applied embryology and anatomy of the coronary arteries. 2) CTA protocols in the evaluation of patients with suspected coronary artery anomalies. 3) Anomalies of origination and course of coronary artery. 4) Anomalies of intrinsic coronary arterial anatomy. 5) Anomalies of coronary termination. 6) Anomalous anastomotic vessels. 7) Sample cases of pearls, pitfalls, diagnostic difficulties, and mimics. 8) Summary and take-home messages.

## **CAEE-43 Spectrum presentation of Chagas Cardiomyopathy (Ch-CMP) by CMR**

Participants

Hector Manuel Medina, MD, Bogota, Colombia (*Presenter*) Nothing to Disclose

### **TEACHING POINTS**

-Cardiac magnetic resonance (CMR) is useful to determine ventricular function and fibrosis in patients with Chagas cardiomyopathy (Ch-CMP). - In ch-CMP patients, inflammation and vascular dysfunction causes severe vasodilation, which promotes tissue ischemia and fibrosis in water-shed segments. This can occur during the acute and chronic stages of the disease condition. In Ch-CMP, the most common scar locations are at the left ventricular apex and the basal inferolateral wall. These segments present with akinesis, and fibrosis noted in late gadolinium enhancement sequences (LGE), which can be transmural, sub-epicardial, mid-myocardial, and sub-endocardial. -CMR is also helpful in identifying ventricular thrombi in this population using perfusion, early gadolinium enhancement (EGE), and LGE. -The main differential diagnoses of Ch-CMP are Anderson-Fabry disease, ischemic cardiomyopathy, idiopathic cardiomyopathy, sarcoidosis disease and myocarditis.

### **TABLE OF CONTENTS/OUTLINE**

Distribution of scar in Ch-CMP Phases of Ch-CMP include ventricular microaneurysm, ventricular aneurysm, severe heart failure and intracavitary thrombi Frequently used sequences and technique-Functional evaluation with maps of T1 and T2-Steady-state free precession (SSFP) in short axis, 3 chamber Scar and fibrosis: Intravenous contrast (gadobutrol)- EGE- LGE

## **CAEE-45 Cardiac MRI Lessons Learned: Pearls and Pitfalls from Training to Remember as an Attending**

### **Awards**

**Identified for RadioGraphics**

Participants

Prabhakar Rajiah, MD, FRCR, Rochester, MN (*Presenter*) Nothing to Disclose

### **TEACHING POINTS**

1. To review the lessons learned in cardiac MRI on sequences, protocols, interpretation, pitfalls and problem-solving. 2. To illustrate these key lessons with representative case examples.

## TABLE OF CONTENTS/OUTLINE

1. PROTOCOLS Gadolinium versus Ferumoxytol, sequence adaptations; Cardiac devices- Adaptations (including wideband technique)  
2. ARTIFACTS AND SOLUTIONS MOTION- Prospective triggering, real-time, compressed sensing; Single-shot, resp. nav. and gating; STIR- Pseudolesion subendocardium, edema from coil sensitivity; PERFUSION- Gibbs artifact; MRA- T2 shortening pseudofilling defects, subtraction misregistration; LGE- T1 selection (esp. amyloidosis), Partial voluming; PSIR artifacts; Failed fat suppression (vs pericarditis), normal blood pool in recesses; 3D WHOLE HEART- Partial voluming; 2D/4D FLOW- Aliasing; resolution limitation, Noise without contrast; T1 MAP- Motion, imaging in other phases; STRAIN- Diastolic fading; 3. ARTIFACTS AS SOLUTIONS SUSCEPTIBILITY- Iron quant; CHEMICAL SHIFT- fat identification 4. INTERPRETATIVE PITFALLS Pseudomasses (Crista terminalis, Taenia sagittalis, Chiari network, Coumadin ridge, lipomatous hypertrophy, MAC, focal HCM, pseudothrombus, moderator band, pericardial recess); CABG aneurysm vs neoplasm; Prominent trabeculations vs LV non compaction; LV apical thinning vs aneurysm; MVO vs spared myocardium; Benign fat vs ARVD; Valve leaflets- Bicuspid vs tricuspid; Pseudo vs true Coarctation; Ductus diverticulum vs aneurysm; Vasculitis vs IMH 5. BLIND SPOTS 6. TIPS TRICKS Long T1 for LGE in cardiac masses; 3D T1w imaging for pericarditis; VENC higher than predicted; Dark blood-LGE for subtle scars

### CAEE-46 Getting to the Heart of Cardiac Masses: Pearls and Pitfalls

Participants

Andrea Cangiani Furlani, MD, (*Presenter*) Nothing to Disclose

#### TEACHING POINTS

1) Overview of cardiac masses (primary neoplasms - benign and malignant -, metastasis, infectious, thrombus). 2) 90% of primary cardiac tumors are benign. Metastases via various mechanisms are much more common than primary cardiac malignancies. Metastatic mechanisms determine imaging characteristics. 3) Discuss in detail with illustrative cases the typical MRI and CT characteristics of specific cardiac neoplasms and their common differential diagnostic considerations, including pearls and pitfalls.

## TABLE OF CONTENTS/OUTLINE

I. Overview. a) Locations of cardiac masses by chamber. b) Tips for distinguishing neoplasms from infection and thrombus. II. Benign cardiac neoplasms. a) Myxoma. b) Fibroelastoma. c) Fibroma, d) Lipoma. e) Cystic tumor of the AV node. f) Congenital cyst. III. Metastases. a) Hematogenous spread. b) Lymphangitic spread. c) Vascular invasion- IVC, SVC, pulmonary veins. d) Direct invasion. IV. Primary cardiac malignancies. a) Angiosarcoma. b) Other sarcomas. c) Lymphoma. The aims of this abstract are: 1. To review etiology, location, and typical clinical scenarios of different cardiac masses. 2. To review imaging findings of benign cardiac neoplasia (myxoma, fibroelastoma, fibroma, lipoma, hemangioma, cystic tumor, and differential diagnosis such as lipomatous hypertrophy of the interatrial septum). 3. To review the mechanisms of metastatic disease (hematogenous, lymphangitic, direct and vascular invasion).

### CAEE-47 Coronary Artery Fistulas: a Pictorial Essay

Participants

Desiree Louise Batista, MD, (*Presenter*) Nothing to Disclose

#### TEACHING POINTS

To describe classification and the main subtypes of coronary fistulas (CFs). To describe the hemodynamic implications on the cardiac structures/cavities of drainage. To describe the importance of coronary CT angiography (CCTA) for the diagnosis, course, path and drainage of CFs, as well as depiction of the relationship between the affected vessel and the nearby structures.

## TABLE OF CONTENTS/OUTLINE

CF is an anomalous direct connection between one or more coronary arteries (CA) and a cardiac chamber (coronary-cameral fistula) or a large vessel (arteriovenous fistula). CFs can be congenital or acquired, single or multiple, isolated or associated with other congenital cardiac malformations. CFs originating from the right coronary artery are the most frequent (50-70%) and 40% of CFs drain into the right ventricle. The degree of shunting is associated with its size and the pressure gradient between the coronary and the draining site. Drainage to the right heart is related to left-to-right shunt, causing variable degrees of volume overload and pulmonary hypertension. Drainage to the LV may cause hemodynamic changes similar to aortic regurgitation. Drainage to the pulmonary artery and left atrium generates volume overload to the LV. There may be reduced myocardial flow distal to the fistula (coronary steal phenomenon), myocardial ischemia and progression to heart failure. The main complications are rupture, infarction and infective endocarditis. CCTA is the gold-standard non-invasive method to explore the complex anatomy of CFs, allowing 3D reconstructions and assessment of vessel of origin, pathway and site of drainage, which may aid to treatment decisions.

### CAEE-48 1H-Magnetic Resonance Spectroscopy for Metabolic Imaging of Myocardial Triglyceride Content - How To Do It"

Participants

Bernhard Petritsch, MD, Wuerzburg, Germany (*Presenter*) Research Consultant, Siemens AG

#### TEACHING POINTS

To review the indications, contraindications, and limitations of 1H-Magnetic Resonance Spectroscopy (1H-MRS) of the myocardium. To highlight the potential benefit of a metabolic investigation embedded in a comprehensive examination of cardiac morphology and function. To learn about parameter settings for spectroscopic data acquisition, including voxel placement and positioning of a navigator for double (respiratory and ECG) triggered data acquisition. To interpret cardiac 1H-MR spectra of healthy subjects, patients suffering from congenital or acquired metabolic disorders, and to learn about potential pitfalls of spectroscopic imaging of the heart.

## TABLE OF CONTENTS/OUTLINE

A. How does 1H-Magnetic Resonance Spectroscopy (1H-MRS) of the myocardium work? B. Technical requirements C. Spectroscopic data acquisition; positioning of respiratory motion gating navigator; voxel placement in the septum D. Spectroscopic data postprocessing E. Image analysis in healthy subjects and patients; age dependency of myocardial triglyceride content; Metabolic syndrome, Morbus Fabry F. Pitfalls of cardiac 1H-MRS G. Limitations of cardiac 1H-MRS; alternative imaging modalities

### CAEE-49 Novel Assessment of Physiological Mitral Valve Morphology and Surgical Simulation for MICS MVP via

## 3D Printed Cardiac Models and Immersive 3D Virtual Reality System

Participants

Koichi Osuda, RT, (*Presenter*) Nothing to Disclose

### TEACHING POINTS

Minimally invasive cardiac surgery (MICS) mitral valve plasty (MVP) has a lower risk of associated complications including mediastinitis, and advantage of quick rehabilitation compared to median sternotomy approach. However, surgical procedures are technically demanding due to narrow operative field and deep working space. To understand the comprehensive mitral anatomy, we attempt to create patient-specific 3D printed left atrioventricular models and developed a novel approach for simulating MICS MVP procedures via immersive 3D virtual reality (VR) system.

### TABLE OF CONTENTS/OUTLINE

3D VR datasets were converted, using CT data which has submillimeter spatial resolution. 3D printed models and 3D VR systems were faithfully reproduced mitral complex structure consisting of mitral leaflets, chordae tendineae, papillary muscles, and prolapsing leaflet. 3D printed models and 3D VR systems enable surgeon to assess physiological morphology through cardiac cycle (systole to diastole), practically, though it is impossible to recognize that intraoperatively. Furthermore, this method allowed surgeon to simulate not only surgical procedures, but also appropriate intercostal thoracotomy approach position, and considering precise device size in advance. 3D printed models and 3D VR systems are clinically available and promising for facilitating the operation strategy optimization and assistant for MICS MVP procedures safely. There will be contributions to clinical practice for preoperative accurate assessment and simulation.

### CAEE-5 State of the Art Imaging in Surveillance of Repaired Tetralogy of Fallot: Imaging in Therapeutic Planning and Risk Assessment

Awards

Certificate of Merit

Participants

Yoshiaki Ota, MD, Ann Arbor, MI (*Presenter*) Nothing to Disclose

### TEACHING POINTS

The purpose of this exhibit is: 1. Understand the central role of cardiac MR (CMR) in post repair Tetralogy of Fallot (TOF) to assess anatomic and functional sequelae. 2. Learn the role of MR in clinical decision making and prognostication. 3. Illustrate the spectrum of new imaging techniques and their applications in repaired TOF. 4. To learn the utility of imaging prior to and following transcatheter pulmonary valve replacement (TPVR).

### TABLE OF CONTENTS/OUTLINE

Outline: 1. Background- Most common cyanotic congenital heart disease characterized by ventricular septal defect, pulmonary stenosis (right ventricular outflow obstruction), dextroposition of the aorta (overriding aorta), and right ventricular hypertrophy. 2. Pathophysiology of repaired TOF- Role of imaging in assessing sequelae of repair, clinical decision making, planning TPVR, outcomes and prognostication. a. Imaging protocols for surveillance emphasizing new techniques such as 4D flow, parametric mapping, strain imaging. b. MR derived parameters and their role in timing and planning of pulmonic valve intervention and risk assessment (ventricular size and function, presence and extent of Late Gadolinium Enhancement, regurgitation quantification, residual ventricular septal defect, and vascular anatomy). c. Indications for Pulmonary Valve Replacement. d. Procedural aspects of TPVR and available devices. e. Pre-intervention imaging for patients and device selection: protocols, imaging modalities, 3D printing. f. Post-TPVR imaging and complications. g. Future directions.

### CAEE-50 Three-dimensional (3D) Procedure Planning for Transcatheter Mitral Valve Replacement

Participants

Nicole Wake, PhD, Aurora, OH (*Presenter*) Employee, General Electric Company

### TEACHING POINTS

A. Transcatheter Mitral Valve Replacement (TMVR) is a minimally invasive procedure that replaces the valve using a device that clips onto the faulty valve. B. Multi-detector computed tomography (MDCT) of the mitral valve and aortic outflow tract is important for appropriate patient and device selection. C. A multidisciplinary approach is required for patient selection and procedure planning. D. Planning for TMVR is traditionally performed by visualizing medical imaging data and using two-dimensional (2D) measurements to determine appropriate valve sizing. E. Three-dimensional (3D) visualization can provide enhanced visualization and superior planning regarding device sizing and placement. F. For complicated cases, 3D printing can be performed to create a precise model of the anatomy and allow for enhanced surgical planning.

### TABLE OF CONTENTS/OUTLINE

1. Review of mitral valve disease. 2. Overview of multi-detector computed tomography (MDCT) for mitral valve disease evaluation. 3. Synopsis of currently available valves for TMVR procedures. 4. Outline of two-dimensional (2D) image analysis and valve sizing. 5. Description of three-dimensional (3D) visualization, image analysis, and device planning. 6. Summary of 3D printing and use for planning TMVR.

### CAEE-51 Spectrum of Imaging Findings in Takotsubo Cardiomyopathy

Participants

Camila V. Machado, MD, (*Presenter*) Nothing to Disclose

### TEACHING POINTS

After attending to this exhibit, the learner should be able: 1. To understand both clinical and laboratory features of Takotsubo Cardiomyopathy. 2. To recognize the major imaging findings of Takotsubo Cardiomyopathy on magnetic resonance imaging (MRI). 3. To correlate the imaging findings on MRI, echocardiography and ventriculography. 4. To understand the importance of cardiac MRI in the diagnosis of Takotsubo Cardiomyopathy and in the evaluation of differential diagnoses. 5. To analyze the role of MRI in the

detection of acute complications and in the follow-up of the patients.

#### TABLE OF CONTENTS/OUTLINE

? Diagnosis of Takotsubo Cardiomyopathy ? Epidemiology ? Clinical findings, stressful events ? MRI, echocardiogram and ventriculography? Importance of MRI for the diagnosis and characterization of Takotsubo Cardiomyopathy ? Assessment of segmental changes in contractility (cine, strain) ? Assessment of myocardial edema (T2 weighted images, T1 and T2 mapping) ? Assessment of myocardial necrosis / fibrosis (late gadolinium enhancement)? Atypical manifestations of Takotsubo Cardiomyopathy (different patterns of contractile change)? The role of MRI in excluding other causes of chest pain ? Myocarditis / pericarditis ? Acute myocardial infarction ? Extracardiac pathologies (pulmonary, pleural, musculoskeletal)? The role of MRI in the detection of acute complications and the follow-up of the patients ? Heart failure, pleural/pericardial effusion, intracavitary thrombus, ventricular wall rupture

#### CAEE-52 Three-Dimensional Fusion Technique with CT and LGE-MRI for Cardiac Resynchronization Therapy

Participants

Yoshihiro Haga, Sendai, Japan (*Presenter*) Nothing to Disclose

#### TEACHING POINTS

Cardiac resynchronization therapy (CRT) is an established treatment for patients with severe heart failure (HF). Factors influencing CRT response are Fig. 1. In particular, it is important to know the left ventricular (LV) lead location and the extent of myocardial scar. These can be assessed by the contrast computed tomography coronary venography (CTCV) or late gadolinium enhancement by cardiac magnetic resonance (LGE-CMR) imaging. However, these cannot be observed on the same three-dimensional image. Therefore, we devised a method that a three-dimensional fusion technique combined the two images derived from CTCV and LGE-CMR imaging.

#### TABLE OF CONTENTS/OUTLINE

1. Understanding the treatment of heart failure (HF) using cardiac resynchronization therapy (CRT). 2. Understanding the key points for a successful CRT. 3. Understanding the preoperative CT scan of CRT. 4. Understanding the importance of Fusion image with CT and LGE-CMR. 5. Features of CRT: International guidelines on CRT implantation 6. The key points for a successful CRT: QRS duration, LV scar tissue, LV lead position, etc. 7. Fusion image with CT and LGE-MRI: three-dimensional fusion technique

#### CAEE-53 A New Evaluation Method for Coronary Plaque by DECT

Participants

Takayoshi Yamaguchi, (*Presenter*) Nothing to Disclose

#### TEACHING POINTS

1. Review the current status of coronary plaque assessment and summarize its limitations 2. Summary of advantages and disadvantages of Dual energy CT compared to Single energy CT 3. Questions about spectral analysis of plaques from coronary CTA 4. Explains new image analysis methods to improve plaque identification accuracy 5. Presenting the correlation between a new plaque evaluation method by CT and intravascular imaging

#### TABLE OF CONTENTS/OUTLINE

1. Introduction 2. Explain the importance of assessing plaque characteristics using coronary CT 3. Comparison of plaque evaluation by coronary CT and IVUS or OCT 4. Explain the advantages of assessing plaque with dual energy CT 5. Limitations for assessing plaque in the arterial phase 6. Proposal of new imaging techniques and methods for improving the ability to characterize plaque tissue using dual energy CT 7. Explain the characteristics of the measured values in various types of plaque tissues and the changes in the spectral HU curve 8. Correlation between new tissue characterization method by DECT and evaluation by intravascular imaging

#### CAEE-54 Structured Pretransplant Cardiac CT Report in Adult Patients with Congenital Heart Disease: What the Radiologist Should Analyze

Participants

Rebeca Gil Vallano, Madrid, Spain (*Presenter*) Nothing to Disclose

#### TEACHING POINTS

- To analyze the radiological findings, which cardiac surgeons need for the surgical planning of heart transplant in adults with congenital heart disease (CHD).- To propose a structured report of pretransplant cardiac CT.

#### TABLE OF CONTENTS/OUTLINE

Our hospital is a referral center for heart transplantation in pediatric and adult patients with CHD. Imaging tests - echocardiogram, magnetic resonance, and computed tomography (CT) - show the cardiac abnormal anatomy. CT additionally demonstrates other findings in these patients with complex anatomies and, in some cases, multisystem disorders (lung anatomy, aorto-pulmonary collaterals, previous surgeries, vascular accesses, rib cage, abdominal anatomy). In our work we will focus on the CT examination performed preoperatively. We will revise the CT acquisition technique, and we will evaluate its benefits, since this technique acquires 3D data with a wide field of view that allow a comprehensive evaluation of the anatomy with good spatiotemporal resolution and multiplanar reconstruction capacity. In the interpretation of these studies, it is very important to carry out a systematic and practical assessment of the preoperative aspects. For this reason, we use a structured report, which we will develop in detail and illustrate with cases from our center. We will emphasize the information needed by surgeons and show the methodology we use to obtain it. Radiologists have a fundamental role through the radiological report in the pretransplant surgical planning of adult patients with CHD.

#### CAEE-56 Advanced Cardiovascular Computed Tomography Imaging in Children with Congenital Variants and Anomalies of the Aortic Arch: From Volume Rendering to 3D Models and 3D Printing

Participants

Flavio Zuccarino, MD, Barcelona, Spain (*Presenter*) Nothing to Disclose

## TEACHING POINTS

To discuss the main indications for cardiovascular CT in newborns and children with congenital anomalies of the aortic arch (CAAA). To outline the key imaging findings, advantages and limitations of CT in CAAA, enhancing the usefulness of volume rendering (VR) and 3D models in differential diagnosis and the design of an optimal therapeutic approach.

## TABLE OF CONTENTS/OUTLINE

We discuss, in a short background, the advantages and limitations of CT in CAAA diagnosis. We analyze different CT acquisition protocols depending on patient age and pathology. We organize CT findings of different CAAA as: Left-sided aortic arch anomalies. Right-sided aortic arch anomalies. Double aortic arch Cervical Aortic Arch Persistent Fifth Aortic Arch Interrupted Aortic Arch Aortic Arch Hypoplasia Coarctation Pseudocoarctation Gothic aortic arch We review key CT findings of different CAAA, focusing on 3D imaging reconstructions and 3D models. We define the relationship of the aorta to the airways, esophagus, and other cardiovascular and thoracic structures that play a pivotal role in CAAA diagnosis. We discuss potential differential diagnosis of CAAA. OUTLINE Radiologists should be familiar with CT key imaging findings and with the advantages and limitations of 3D advanced techniques to establish an optimal diagnostic approach and therapeutic management.

## CAEE-57 Arrhythmogenic Left Ventricular Cardiomyopathy (ALVC); Understanding Current Concepts

Participants

Daniel Ocazionez-Trujillo, MD, Houston, TX (*Presenter*) Nothing to Disclose

## TEACHING POINTS

- Genotype-phenotype correlation studies have demonstrated that mutations in Desmoplakin and Filament C genes are the most common gene defects causing ALVC. - Patients with ALVC usually complain of symptoms of both arrhythmia (palpitations, chest tightness, syncope) and LV heart failure. - Imaging modalities in ALVC usually reveal severe LV dysfunction with preserved to mildly impaired RV function. Often this entity has been misdiagnosed as dilated cardiomyopathy, chronic myocarditis, myocardial infarction, or double ventricular involvement type ARVC. - Reported Cardiac MRI findings in ALVC include dilated left ventricle, fatty infiltration, irregular lateral wall contour with a "serrated" shape and areas of mesocardial and epicardial delayed enhancement in a "ring like" distribution involving the septal and lateral walls.

## TABLE OF CONTENTS/OUTLINE

- Definition - Clinical presentation - Genetics - Imaging findings on Cardiac MRI - Differential diagnosis - Conclusion

## CAEE-58 The Multiple Facets of Cardiac Amyloidosis - Diagnostic Imaging Overview

Participants

Aarushi Gupta, MD, MBBS, (*Presenter*) Nothing to Disclose

## TEACHING POINTS

• Diagnosis of cardiac amyloidosis is challenging and can be misinterpreted for hypertensive heart disease or hypertrophic cardiomyopathy, particularly in older patients with heart failure with preserved ejection fraction (HFpEF). • Recent treatment advances such as Tafamidis for ATTR amyloidosis (Transthyretin amyloidosis) can delay disease progression. An understanding of imaging features can help in early diagnosis and appropriate management of patients. • Echocardiography, cardiac MRI and nuclear Tc-99 pyrophosphate scan are complementary and can help in establishing the diagnosis.

## TABLE OF CONTENTS/OUTLINE

1. Background on common types of cardiac amyloidosis: • AL (Light chain) and ATTR amyloid (hereditary and wild type) • Clinical manifestations of amyloidosis • How to differentiate ATTR from AL amyloidosis using clinical and biochemical parameters 2. Imaging in diagnosis of cardiac amyloidosis with focus on ATTR amyloidosis • Echocardiography, cardiac MRI and different LGE patterns (with discussion of QALE score) • Caveats in establishing diagnosis including technical challenges like determining the nulling time of myocardium • Recent advances in MR cardiac imaging including parametric tissue mapping (for diagnosis and prognosis) and myocardial strain (for early detection of LV dysfunction) 3. Discuss role of nuclear medicine techniques like Tc-99 pyrophosphate scan and recent American Society of Nuclear Cardiology (ASNC) guidelines for diagnosis • Correlative MR cardiac and Tc-99 pyrophosphate images will be provided 4. Discuss new disease modifying therapies for ATTR amyloidosis such as Tafamidis 5. Conclusion

## CAEE-59 Cardiac Amyloid - Correlation of Cardiac Magnetic Resonance and Pathology

Participants

Navpreet Khurana, MBBS, (*Presenter*) Nothing to Disclose

## TEACHING POINTS

1. Describe the classic imaging findings of cardiac amyloidosis (CA) on cardiac magnetic resonance (CMR). 2. Understand the conditions which can mimic CA on CMR - false positives. 3. Understand the incremental value of nuclear medicine.

## TABLE OF CONTENTS/OUTLINE

1. Findings of CA on CMR. 2. Role of Nuclear Medicine in diagnosing CA. 3. Review of cases - positive CMR and positive pathology. 4. Review of cases - positive CMR and negative pathology. 5. Review of cases - negative CMR and positive pathology.

## CAEE-6 Cardiac MRI in Congenital Heart Disease: Pearls and Pitfalls

Participants

Priyanka Garg, MBBS, MD, New Delhi, India (*Presenter*) Nothing to Disclose

## TEACHING POINTS

Cardiac MRI is a powerful tool giving relevant anatomical and physiological information of cardiovascular structures in congenital heart disease. The purpose of this exhibit is to: 1. Discuss the various pearls and pitfalls relevant to planning, acquisition and interpretation of cardiac MR images. 2. Enumerate specific points that need special consideration while imaging in paediatric

patients. 3. Describe the role of cardiac MR imaging in patients with congenital heart disease.

#### TABLE OF CONTENTS/OUTLINE

1. Introduction 2. Patient selection 3. Sedation requirement 4. ECG placement 5. Cardiac MR sequences 6. Cardiac MR planning 7. Phase contrast imaging 8. Angiographic imaging 9. Post processing including ventricular volumetry, flow assessment, shunt fraction and important formulae for regurgitant fraction 10. Role of cardiac MRI in congenital heart disease 11. Take home message

#### CAEE-60 Multimodal Imaging Characterization of Cardiac Tumors Emphasizing PET with Pathology Correlation Using the New 2021 WHO Classification

##### Awards

##### Identified for RadioGraphics

Participants

Maria Clara Lorca, MD, Pittsford, NY (*Presenter*) Nothing to Disclose

##### TEACHING POINTS

Due to their rarity and overlapping imaging characteristics, tumors and tumor-like conditions of the heart can be a radiological challenge. It's important to be familiar with their imaging presentation in order to improve diagnostic accuracy and avoid unnecessary invasive procedures. 1. New 2021 WHO Classification of Cardiac Tumors 2. Depict cardiac tumors and cardiac tumor-like radiological features 3. Describe the importance of PET-CT in the diagnosis and follow up of cardiac tumors 4. Discuss the cardiac tumor-like conditions including cardiac thrombus, mediastinal abscess, pericardial hematoma, pericardial cyst 5. Describe the pearls and pitfalls that some entities demonstrate in the cardiac imaging, including benign entities that can appear as a cardiac pseudotumor

#### TABLE OF CONTENTS/OUTLINE

This education exhibit reviews biopsy-proven cases of cardiac lesions and their mimics and depict their radiological features, including images pearls and pitfalls. Review with clinical pictures, illustrative case examples, and original illustrations the cardiac tumors in a systematic fashion. Incorporate the new 2021 WHO classification of the cardiac tumors. Depict the imaging appearances of various types of cardiac tumor-like conditions and how to accurately differentiate them from cardiac tumors.

#### CAEE-61 Imaging of Acute and Chronic Cardiac Complications of COVID-19

##### Awards

##### Identified for RadioGraphics

##### Certificate of Merit

Participants

Felipe Sanchez, MD, Toronto, Chile (*Presenter*) Nothing to Disclose

##### TEACHING POINTS

1. Acute cardiac complications in patients with COVID-19 are relatively rare but include myocarditis, thrombosis and ischemia 2. Cardiac imaging plays an important role in the diagnosis of acute myocardial injury in patients with COVID-19, with typical findings on cardiac MRI including edema, high native T1, and co-localizing late gadolinium enhancement 3. Patients who have recovered from COVID-19 are at increased risk of cardiovascular disease, including those with persistent symptoms and post-acute sequelae of SARS-CoV-2 infection (or long COVID) 4. Cardiac MRI can be useful in patients with persistent symptoms and functional impairment after COVID-19 to evaluate for the sequelae of myocarditis, left ventricular ejection fraction, strain, and parametric mapping

#### TABLE OF CONTENTS/OUTLINE

The purpose of this educational exhibit is to: 1. Review the acute and chronic cardiac complications related to COVID-19 including incidence, pathophysiology, risk factors, and clinical outcomes 2. Demonstrate the role of cardiac imaging in establishing a diagnosis of myocarditis following COVID-19 3. Illustrate multi-modality cardiac imaging findings in patients recovered from COVID-19 with persistent symptoms

#### CAEE-62 Pearls and Pitfalls in Cardiac Imaging

Participants

Furkan Ufuk, MD, Denizli, Turkey (*Presenter*) Nothing to Disclose

##### TEACHING POINTS

? To review the cardiac pseudotumors and challenging diagnoses ? To review the cardiac outpouchings and differential diagnoses ? To review the cardiac and coronary artery anatomic variations

#### TABLE OF CONTENTS/OUTLINE

1. Cardiac pseudotumors Right atrial pseudotumor due to prominent crista terminalis, lipomatous hypertrophy of the interatrial septum, caseous mitral annular calcification, focal hypertrophic cardiomyopathy, microvascular obstruction, left atrial appendage pseudothrombus, ventricular noncompaction. 2. Cardiac outpouchings: True and false left ventricular aneurysms, ventricular diverticula, ventricular clefts and crypts, atrial diverticula and aneurysms, interatrial septal aneurysm, sinus valsalva aneurysm, interventricular septal aneurysm, mitral-aortic intervalvular fibrosa pseudoaneurysm. 3. Cardiac and coronary artery anatomic variations and congenital lesions: Patent foramen ovale, interatrial septal pouch, coronary artery anomalies, coronary artery tortuosity, coronary artery fistulas. 4. Coronary artery lesions and pseudolesions: Coronary artery aneurysm, RCA pseudostenosis due to streak artifact, overestimation of stenosis due to calcified plaque, myocardial bridging. 5. Pulmonary vein abnormalities and anatomical variations: right top pulmonary vein, pulmonary venous varix, pulmonary vein thrombosis, partial anomalous pulmonary venous return, anomalous midline common ostium of the left and right inferior pulmonary veins

#### CAEE-63 Imaging of Left Ventricular Assist Device (LVAD) Driveline Infections and Other Common LVAD Complications

Participants

Mahati Mokkarala, MD, Saint Louis, MO (*Presenter*) Nothing to Disclose

#### TEACHING POINTS

Teaching Points: The purpose of this exhibit is to: 1. Illustrate the common LVAD devices and components of the left ventricular assist device on CT. 2. Imaging characteristics of LVAD infections that lead to operative management. 3. Understand imaging of additional LVAD complications.

#### TABLE OF CONTENTS/OUTLINE

Content Organization: 1. Basics on type and anatomy of drive line parts: - Description of multiple types of LVAD machines. Older models: Jarvik, Thoratec, Heartmate - Diagram of most recent LVAD machine, Heartmate III and components on CT. 2. CT imaging of LVAD infections that lead to operative management - Drive line soft tissue thickening that can involve adjacent musculature, peritoneum - Drive line and adjacent left ventricular assist device fluid collection/abscess 3. Nuclear medicine imaging of LVAD infections - Description of PET/CT findings including increased FDG uptake by the driveline and LVAD - Comparison of PET/CT and white blood scintigraphy scans 4. CT imaging of additional more local LVAD complications including the following: - Increased risk of LVAD structural, outflow and inflow cannula, pump systemic thrombosis - Increased risk of local hemorrhage - LVAD device and cannula mechanical breakage, device failure - Involvement of adjacent soft tissue and vascular structures 5. CT imaging of more systemic, LVAD related, complications - Increased risk of right ventricular dysfunction and aortic valve disease - Increased risk of systemic hemorrhage (GI bleeding), thrombosis (stroke, PE).

#### CAEE-64 Spectrum of Cardiothoracic Imaging Findings in Drug Abuse

Participants

Gaurav Watane, MBBS, MD, Pittsburgh, PA (*Presenter*) Nothing to Disclose

#### TEACHING POINTS

1. To recognize the emergent and non-emergent cardiothoracic imaging findings in the recreational drug abuse 2. To gain awareness through example cases of the associated complications 3. To discuss the complementary role of CT/MRI, PET/CT, and echocardiography in the management

#### TABLE OF CONTENTS/OUTLINE

1. Case-based review of the spectrum of cardiothoracic imaging findings in the recreational drug abuse; including infective endocarditis with or without vegetations, pulmonary embolism, septic emboli, thrombophlebitis, Spontaneous coronary artery dissection (SCAD), Vaping associated lung injury (EVALI) 2. Current status of various imaging modalities and their limitations in the imaging of Cardiothoracic complications

#### CAEE-65HC Characterization of Atrial Masses through Cardiac Magnetic Resonance Imaging

Participants

Hector Manuel Medina, MD, Bogota, Colombia (*Presenter*) Nothing to Disclose

#### TEACHING POINTS

Teaching Points- Cardiac magnetic resonance (CMR) provides a reliable and detailed evaluation of cardiac masses.- While biopsy remains the cornerstone of diagnosis, CMR has been proven safe and effective at assessing atrial masses and determining its extension, vascular involvement and providing differential diagnoses.- Based on this assessment, a multidisciplinary medical and/or surgical management plan can be established.- Follow-up based on CMR after treatment yields an equivalent comparison, thus optimizing treatment decisions.

#### TABLE OF CONTENTS/OUTLINE

\*?able of Contents/Outline: A Case-Based Approach- Epidemiology of the most common atrial masses.- Radiologic features and characterization (preliminary diagnosis through imaging) and correlation with biopsies.- CMR as an ideal tool for the diagnosis of atrial masses.- Use of steady-state free precession (SSFP), T1-weighted (T1W), short tau inversion recovery (STIR), early gadolinium enhancement (EGE), late gadolinium enhancement (LGE), and perfusion sequences.- Multidisciplinary medical and surgical management strategy formulation.- Useful tool for disease staging and follow-up. Please visit the Learning Center to also view this presentation in hardcopy format.

#### CAEE-66 Be Aware of the Heart in an Oncologic Scenario! Cardiac Metastases - A Pictorial Essay

Participants

Pedro Matta, Sao Paulo, Brazil (*Presenter*) Nothing to Disclose

#### TEACHING POINTS

Review the main radiologic features that differentiate primary and secondary cardiac masses and discuss the role of advanced cardiac imaging modalities in evaluating these lesions Describe anatomical landmarks involved in metastatic spread to the heart such as pericardium, epicardium, myocardium, valves and chambers. Understand the epidemiology, including prevalence, most common origins and histologic types of metastatic involvement of the heart. Propose a diagnostic workflow based on tumor features including size, borders, tissue invasion, site, pericardial involvement, single or multiple lesions and tissue characteristics, describing contrast enhancement, T1 and T2WI signal intensity. Identify the major red flags regarding imaging signs associated with cardiac involvement.

#### TABLE OF CONTENTS/OUTLINE

Major malignant secondary cardiac tumors, including epidemiology, pathophysiology and imaging findings: Poorly differentiated small cell type, Leukemic infiltrate and mass, Melanoma metastasis, Osteosarcoma metastasis and Angiosarcoma. The role of multimodality imaging techniques, such as US, CT, MRI, PETCT, in the evaluation of cardiac masses, listing advantages and disadvantages in diagnosis and surgical planning including Echocardiography, Computed tomography, Magnetic Resonance Imaging and PETCT. Differential diagnosis, potential pitfalls and artifacts to keep in mind when evaluating a potential cardiac mass.

## CAEE-67 Radiologic Evaluation of Transcatheter Valve Replacements

Participants

Demetrios Raptis, MD, Frontenac, MO (*Presenter*) Nothing to Disclose

### TEACHING POINTS

• Discuss indications and contraindications for transcatheter valve replacement with emphasis on pulmonic, mitral, and tricuspid valve replacements and brief discussion of transcatheter aortic valves. Review preprocedural imaging work-up for transcatheter valve replacements specific to each valve. Case based review of complications of transcatheter valve replacements

### TABLE OF CONTENTS/OUTLINE

Brief review of transcatheter aortic valve replacement Discuss indications for transcatheter valve replacements • Pulmonic • Mitral • Tricuspid Review preprocedural imaging of transcatheter valve replacements with emphasis on measurements and accesses routes both standard and alternative • Pulmonic • Mitral • Tricuspid Case based review of complications in transcatheter valve replacement including but not limited to: • Misplaced/malpositioned valves • Embolized valves • Outflow tract obstructions • Paravalvular prosthetic leaks • Hypo-attenuating leaflet thickening • Hypo-attenuation affecting motion • Coronary obstruction • Vascular complications/bleeding • Valve malfunction • Embolic phenomenon • Septic emboli

## CAEE-7 Heterotaxy: What the Radiologist Needs to Know to Get It Right

Participants

Maria Clara Lorca, MD, Pittsford, NY (*Presenter*) Nothing to Disclose

### TEACHING POINTS

Heterotaxy syndrome remains a diagnostic challenge, especially for radiology residents. While situs anomalies have a rare incidence, it is important to recognize them early in part due to their correlation with congenital heart disease. The aim of this project is to review the anatomic imaging appearance of heterotaxy syndrome on CT and MRI and how to incorporate heterotaxy findings into the segmental classification of congenital heart disease.

### TABLE OF CONTENTS/OUTLINE

Become familiar with the anatomic imaging appearance of heterotaxy syndrome on CT and MR. Briefly review of the embryology, epidemiology, and terminology of heterotaxy syndrome, also known as situs ambiguous. Become familiarized with anatomic and physiologic imaging appearance of the more common forms of heterotaxy syndrome in the chest and abdomen (CT and MR), with a focus on right versus left isomerism. How to incorporate heterotaxy findings into the segmental classification of congenital heart disease using the three-part segmental notation utilized in the Van Praagh classification system.

## CAEE-8 Cardiac Magnetic Resonance Imaging of Acute Myocarditis: A Review Focusing on Quantitative Evaluation Methods

Participants

Nobuko Tanitame, MD, Hiroshima, Japan (*Presenter*) Nothing to Disclose

### TEACHING POINTS

Acute myocarditis (AM) could result in arrhythmia, dilated cardiomyopathy or chronic heart failure. Although endomyocardial biopsy has been the gold standard in diagnosis of AM, it is invasive and has low diagnostic sensitivity. Cardiac magnetic resonance (CMR) imaging is currently considered to be the most comprehensive diagnostic tool in the evaluation of AM. Generally, T2- and T1-weighted imaging and late gadolinium enhancement (LGE) are used for diagnosing AM. Furthermore, novel quantitative techniques such as native T1, T2 mapping and extracellular volume (ECV) are recommended to allow more objective assessment of myocardial injury. We focus on quantitative methods, diagnostic strategy and pitfalls of CMR imaging in the patients with AM.

### TABLE OF CONTENTS/OUTLINE

1. Recent development of CMR imaging and processing techniques 2. Establishment of standard values for quantitative analysis of CMR imaging 3. Cine MR imaging (ejection fraction, flow analysis using phase-contrast method) - Cardiac function, left and right ventricular asynergy 4. Black blood T2-weighted STIR (T2 mapping using T2-prep SSFP) - Myocardial edema 5. Native T1 mapping using MOLLI - Myocardial edema, hyperemia, necrosis, fibrosis 6. Gadolinium-enhanced perfusion CMR - Hyperemia, capillary leak 7. LGE (ECV using analysis software) - Myocardial necrosis, fibrosis 8. Representative cases and diagnostic pitfalls of AM

## CAEE-9 2020: What Does the Radiologist Need to Know About Major Changes in the Diagnosis of Arrhythmogenic Cardiomyopathy?

Participants

Alan Hummel, Sao Paulo, Brazil (*Presenter*) Nothing to Disclose

### TEACHING POINTS

The goal of this exhibit is to: 1. Understand what arrhythmogenic cardiomyopathy is and what is its pathophysiology. 2. Describe the significant changes in the diagnostic criteria that occurred in 2020. 3. Outline the diagnostic criteria for the right ventricle. 4. Discuss the "new" types of involvement: biventricular and isolated from the left ventricle.

### TABLE OF CONTENTS/OUTLINE

1. Arrhythmogenic dysplasia of the right ventricle - the precursor; 2. Review the basic anatomy of the right ventricle and their relationships; 3. What is arrhythmogenic cardiomyopathy? 4. Is it possible to differentiate: myocardial fat vs fibrosis? 5. Padua Criteria - Major changes in 2020. 5.1. Padua Criteria - Exposing the Criteria 5.2. Padua Criteria - Image 5.3. Padua criteria - Other methods 5.4. Morphofunctional criteria 5.5. Structural criteria 6. Morphofunctional abnormalities of the right ventricle 6.1. Exposing the major and minor criteria 6.2. Examples 7. Morphofunctional abnormalities of the left ventricle 7.1. Exposing the minor criteria 7.2. Examples 8. Structural abnormalities of the right ventricle 8.1. Exposing the major criteria 8.2. Examples 9. Structural abnormalities of the left ventricle 9.1. Exposing the major criteria 9.2. Examples 10. Diagnostic algorithm 11. Summary in 1 slide





## Abstract Archives of the RSNA, 2022

CAEE-10

### Mitral Annular Disjunction in Cardiac MR: What to Know and What to Look For

Sunday, Nov. 27 8:00AM - 9:00AM Room: Learning Center - CA

#### Awards

Identified for RadioGraphics

#### Participants

Jose Batista Araujo Filho, MD, Sao Paulo, Brazil (*Presenter*) Nothing to Disclose

#### TEACHING POINTS

- 1) Mitral Annular Disjunction (MAD) definition and its association with Mitral valve prolapse (MVP) and ventricular arrhythmic events
- 2) The advantages of CMR in MAD diagnosis, stratification and prognosis
- 3) Update on state-of-the-art CMR new sequences for evaluating MAD

#### TABLE OF CONTENTS/OUTLINE

- 1) INTRODUCTION
  - 1.1) Definition and importance of MAD
  - 1.2) Association with MVP, ventricular arrhythmias and sudden cardiac death
  - 1.3) Presence of MAD in normal subjects
- 2) CARDIAC MR (CMR) ROLE IN MAD
  - 2.1) CMR advantages over echocardiography
  - 2.2) How to measure the MAD distance properly
  - 2.3) Other CMR findings useful for the diagnosis and prognosis
  - 2.4) New CMR tools for MAD stratification (T1 mapping and Strain)
- 3) CMR IN MAD DIAGNOSIS
  - 3.1) Case example of a long MAD
  - 3.2) MAD association with MVP and regurgitation
  - 3.3) Myocardial Fibrosis presence - late gadolinium enhancement (LGE)
- 4) CMR IN MAD STRATIFICATION
  - 4.1) How to evaluate papillary muscle LGE
  - 4.2) CMR T1 mapping importance
- 5) CHALLENGES IN MAD/TAKE HOME MESSAGES
  - 5.1) MAD diagnostic pitfalls and its clinical relevance
  - 5.2) Strain CMR as a new tool to assess regional contractile dysfunction
  - 5.3) Red flags on MVP

Printed on: 02/07/23



## Abstract Archives of the RSNA, 2022

CAEE-11

### The Essential Three Roles of Imaging in the Management of Chronic Thromboembolic Pulmonary Hypertension

Sunday, Nov. 27 8:00AM - 9:00AM Room: Learning Center - CA

#### Participants

Satoshi Higuchi, MD, PhD, (*Presenter*) Nothing to Disclose

#### TEACHING POINTS

Chronic thromboembolic pulmonary hypertension (CTEPH), caused by stenosis and obstruction of the pulmonary arteries by organized thrombi, is a major cause of chronic pulmonary hypertension and life-threatening disease if untreated. The prognosis is improving as a treatment strategy has been established. The role of imaging is classified into three categories: 1) detection of perfusion defects for diagnosis, 2) assessment of vascular lesions to establish a treatment strategy, and 3) evaluation of cardiac function for assessment of treatment efficacy or prognosis. Participants will learn the pathophysiologic processes of CTEPH, the essential three roles of imaging in the management of CTEPH, and future perspectives of imaging in CTEPH.

#### TABLE OF CONTENTS/OUTLINE

1. What is CTEPH? 2. The pathophysiologic processes of CTEPH 3. The essential three roles of imaging in CTEPH a. Diagnosis: lung perfusion defects b. Establishment of treatment strategy: assessment of vascular lesions c. Assessment of treatment efficacy and prognosis: evaluation of cardiac function 4. Future perspectives 5. Summary

Printed on: 02/07/23



## Abstract Archives of the RSNA, 2022

CAEE-12

### Pre- and Post-Operative Imaging Findings of Chronic Thromboembolic Pulmonary Hypertension (CTEPH)

Sunday, Nov. 27 8:00AM - 9:00AM Room: Learning Center - CA

#### Participants

Yogesh Gupta, DO, (Presenter) Nothing to Disclose

#### TEACHING POINTS

1. Illustrate the proposed pathophysiology of CTEPH. 2. Detail the role of pre-operative imaging with computed tomography angiography (CTA), dual energy CT (DECT), ventilation perfusion (V/Q) scintigraphy, magnetic resonance angiography (MRA), MR perfusion, and 4D phase contrast MR. 3. Provide radiological examples, practical tips for aiding in diagnosis and describing current diagnostic challenges. 4. Highlight key findings that the radiologist should convey to the interventionist to best help guide therapy. 5. Demonstrate clinical correlates from our Pulmonary Hypertension Center with post-procedural outcomes from pulmonary endarterectomy, percutaneous balloon pulmonary angioplasty, and percutaneous ultrasound accelerated thrombolysis (EKOS®) as well as outcomes from medical therapies including pulmonary vasodilators and anticoagulation. 6. Overview of emerging artificial intelligence technologies that may facilitate CTEPH diagnosis.

#### TABLE OF CONTENTS/OUTLINE

This pictorial review is designed for residents, fellows, general radiologists, thoracic radiologists, interventional radiologists, and non-radiology participants. The primary goals are to describe the pre- and post-operative imaging features of CTEPH with clinical correlation and post-surgical outcomes. This will be achieved by discussing: 1. CTEPH in the WHO classification scheme. 2. Clinical features of and risk factors for CTEPH 3. Pathophysiology of CTEPH 4. Diagnostic algorithm. 5. Multimodality imaging overview. 6. Overview of treatment options.

Printed on: 02/07/23



## Abstract Archives of the RSNA, 2022

CAEE-13

### 3D Printing in Cardiovascular Diseases: State-of-the-Art

Sunday, Nov. 27 8:00AM - 9:00AM Room: Learning Center - CA

#### Awards

Cum Laude

#### Participants

Prabhakar Rajiah, MD, FRCR, Rochester, MN (*Presenter*) Nothing to Disclose

#### TEACHING POINTS

1. To review the principles and techniques of 3D printing 2. To discuss the utility of 3D printing in cardiovascular diseases (CVD) 3. To illustrate the applications of 3D printing in CVD

#### TABLE OF CONTENTS/OUTLINE

1. INTRODUCTION 2. 3D PRINTING PROCESS- Image acquisition; segmentation; mesh, 3D printing; air drying; fixation 3. SOURCE DATA- CT, MRI, Hybrid 4. IMAGE ACQUISITION RECONSTRUCTION STRATEGIES CT- ECG-gating, High contrast, high isotropic spatial resolution; MRI- Volumetric acquisition, high CNR sequences, ECG-gating, less artifacts 5. 3D MESH FILE FORMATS- STL, VRML, novel 6. 3D PRINTING METHODS- Material jetting, binder jetting, Vat polymerization, material extrusion, powder bed fusion 7. APPLICATIONS OF 3D PRINTING Identification of anatomic landmarks; Involvement of adjacent structures, relationship; Planning surgeries/interventions; Device size; Printing interventional wires; Education of trainees, patients; Communication with clinicians; 8. APPLICATIONS OF 3D PRINTING IN CVD WITH CASE EXAMPLES Congenital heart diseases (septal defects, complex CHD)- Surgical planning, roadmap; Structural heart disease (Aortic, pulmonary, mitral, tricuspid valve interventions, LAA closure)- Preprocedural planning, device selection, bench testing; Neoplasms- relationship/involvement of adjacent structures; Hypertrophic cardiomyopathy- Outflow anatomy, relationship to adjacent structures; Cardiac aneurysms/ pseudoaneurysms- Anatomy, relationship; Vascular disease- Chronic dissection, aneurysms, Marfan syndrome 9. ACCURACY LIMITATIONS 10. UTILITY OF AI 11. PITFALLS 12. TIPS ON SETTING UP A 3D PRINTING SERVICE

Printed on: 02/07/23



## Abstract Archives of the RSNA, 2022

CAEE-16

### Multi-modality Cardiac Imaging in Myocarditis Following COVID-19 Vaccination

Sunday, Nov. 27 8:00AM - 9:00AM Room: Learning Center - CA

#### Participants

Constantin Marschner, MD, Toronto, ON (*Presenter*) Nothing to Disclose

#### TEACHING POINTS

1. Myocarditis following COVID-19 vaccination is rare. However, adolescent and young adult males are at highest risk. Chest pain is the most common presenting symptom. 2. Cardiac imaging plays an important role in the diagnosis of acute myocarditis following vaccination, with typical findings on cardiac MRI including subepicardial late gadolinium enhancement and co-localizing edema at the basal to mid inferior lateral wall. 3. The disease course is typically transient and mild, with resolution of symptoms within 1-3 weeks in most patients. Limited follow-up data demonstrates resolution of myocardial edema but persistence of late gadolinium enhancement in some patients. 4. Longer term follow-up is needed to determine whether persistent imaging abnormalities are associated with adverse outcomes, including arrhythmias and heart failure.

#### TABLE OF CONTENTS/OUTLINE

The purpose of this educational exhibit is to: 1. Review the incidence, pathophysiology, risk factors, and clinical outcomes of myocarditis following COVID-19 vaccination. 2. Demonstrate the role of cardiac imaging in establishing a diagnosis of myocarditis following vaccination including echocardiography, cardiac MRI, and PET. 3. Illustrate multi-modality cardiac imaging findings in patients with myocarditis following vaccination, at the time of acute presentation and at follow-up.

Printed on: 02/07/23



## Abstract Archives of the RSNA, 2022

CAEE-17

### Comprehensive Assessment of Cardiac Amyloidosis with Cardiac MRI: Morphology, Function and Tissue Characterization

Sunday, Nov. 27 8:00AM - 9:00AM Room: Learning Center - CA

#### Participants

Filipe Carvalho, MD, (*Presenter*) Nothing to Disclose

#### TEACHING POINTS

Cardiac amyloidosis is a challenging diagnosis that usually requires increased clinical awareness and multimodality evaluation for timely diagnosis. In this presentation, the reader should learn how to identify the spectrum of morphologic features of cardiac amyloidosis and to address the role of cardiac MRI in the main differential diagnosis. We will demonstrate the main delayed enhancement patterns with potential imaging pitfalls and discuss the applicability of new mapping techniques (native T1 and Extracellular Volume Fraction [ECV]) on the diagnostic and prognostic assessment

#### TABLE OF CONTENTS/OUTLINE

(1) Introduction and Background. (2) Present the main morphological features of cardiac amyloidosis: enlarged atria, left ventricle hypertrophy, diastolic dysfunction. (3) Discuss the role of tissue characterization with native T1 mapping, ECV, TI-scout, magnitude and PSIR delayed enhancement techniques in the prognostic and diagnostic assessment. (4) Illustrate the main imaging pitfalls and possible differential diagnosis. (5) Take-Home messages and teaching points.

Printed on: 02/07/23



## Abstract Archives of the RSNA, 2022

CAEE-18

### Cardiac MRI 2D Phase Contrast Flow Imaging: Pearls and Pitfalls

Sunday, Nov. 27 8:00AM - 9:00AM Room: Learning Center - CA

#### Participants

Claire Brookmeyer, MD, (*Presenter*) Nothing to Disclose

#### TEACHING POINTS

Review pearls and pitfalls in the application of phase contrast 2D flow imaging to cardiac MR. Emphasize important pitfalls in the acquisition of phase contrast 2D flow sequences. Explain indications and utilization of 2D flow imaging to cardiac valvular stenosis and regurgitation, as well as intracardiac shunts.

#### TABLE OF CONTENTS/OUTLINE

Introduction: Background information on valvular stenosis and regurgitation, intracardiac shunt, Role of velocity and flow quantification in the detection and management of cardiac valvular pathologies and intracardiac shunts. Technical pearls and pitfalls: Basic physics concepts behind phase contrast imaging to determine flow, Imaging plane set up for aorta and main pulmonary artery, Slice location selection, VENC selection and aliasing, In-plane and Through-plane techniques, Temporal resolution. Imaging protocols and Post-Acquisition Processing: Steady state free precession cine sequences for Functional assessment, stroke volume quantification, Phase contrast sequences for velocity and flow assessment. Application: Regurgitation (Mitral, Aortic), Stenosis (Aortic, Mitral), Intracardiac shunt Qp/Qs

Printed on: 02/07/23



## Abstract Archives of the RSNA, 2022

CAEE-19

### Preprocedural Assessment of Left Atrial Appendage Closure Using Dedicated CT Image

Sunday, Nov. 27 8:00AM - 9:00AM Room: Learning Center - CA

#### Participants

Naoki Hosoda, (*Presenter*) Nothing to Disclose

#### TEACHING POINTS

To learn about the pre-procedural assessment for left atrial appendage treatment. To learn measurement method of LAA dimensions. To learn advantage of preoperative assessment for LAAC with CT. To learn about necessity of CT.

#### TABLE OF CONTENTS/OUTLINE

A. Pre-procedurally clarifies the intracardiac thrombus and LAA morphology. B. Usefulness of CT to measure in the same way as TEE. C. Risk assessment by morphology and simulation of optimal sheath selection using CT volume data. D. CT predicts not only the risk of the intervention based on anatomical features of the LAA but also the thrombus, device size, sheath type, optimal location for septal puncture and pre-procedurally clarifies LAA dimensions.

Printed on: 02/07/23



## Abstract Archives of the RSNA, 2022

CAEE-2

### Taking It to the Next Level - What's New with CAD-RADS 2022

Sunday, Nov. 27 8:00AM - 9:00AM Room: Learning Center - CA

#### Awards

Certificate of Merit

#### Participants

Arzu Canan, MD, Dallas, TX (*Presenter*) Nothing to Disclose

#### TEACHING POINTS

Purpose: The purpose of this educational exhibit is to review the update version of CAD-RADS (Coronary Artery Disease Reporting and Data System) and to highlight the changes compared to prior version with illustrative case examples. Major teaching point CAD-RADS not only provides a common and standardized lexicon for interpretation of coronary CT angiography findings but also provides specific recommendations for further management of patients. Although the main seven categories remain similar in the updated version, the new CAD-RADS scoring system allows for more comprehensive evaluation and description of coronary atherosclerosis with the addition of new features, such as plaque volume assessment and physiologic significance of stenosis.

#### TABLE OF CONTENTS/OUTLINE

This exhibit includes a systematic review of the CAD-RADS categories and modifiers, followed by case based examples. The systematic review includes 1. The rationale and the evidence for updated CAD-RADS will be reviewed 2. CAD-RADS Categories (0-5 and N): What is same and different with illustrative case examples 3. Modifiers: N, S, G, V, etc.: What is the same and what is new with illustrative case examples 4. New features 5. Recommendations: What is same and different with illustrative case examples Conclusion It is of importance to understand the differences between the original and the newest version of CAD-RADS and to implement those changes into the clinical practice in order to improve communication and to facilitate decision making process for further management of patients. This exhibit equips the learner with the required knowledge in a practical illustrated manner.

Printed on: 02/07/23

## Abstract Archives of the RSNA, 2022

CAEE-20

### Cardiac Electrophysiology 101 and the Role of Radiologist

Sunday, Nov. 27 8:00AM - 9:00AM Room: Learning Center - CA

#### Awards

Identified for RadioGraphics

#### Participants

Prabhakar Rajiah, MD, FRCR, Rochester, MN (*Presenter*) Nothing to Disclose

#### TEACHING POINTS

Electrophysiology (EP) deals with diagnosis and management of heart rhythm problems. It is important for a cardiac radiologist to know the basics of EP and roles where they can contribute 1. To review the basic techniques used in cardiac EP 2. To correlate EP findings with cardiac CT/MRI 3. To understand the role of CT/MRI in cardiac EP

#### TABLE OF CONTENTS/OUTLINE

1. INTRODUCTION - Cardiac action potential, arrhythmia mechanisms 2. CARDIAC EP- Role, advantages 3. STANDARD EP TESTS- Catheters, measurement of electric potentials 4. ATRIAL FIBRILLATION/FLUTTER - a. EP for diagnosis and ablation; b. Pre-procedural CT/MR -for anatomy, thrombus, scar; c. Procedural- Electroanatomic mapping, ablation types; d. Post-procedural CT/MR- Vein stenosis, thrombus, bleed, esophagoatrial fistula, perforation, pericardial effusion; e. Left atrial appendage closure- Pre-procedural planning, post procedural complications 5. VENTRICULAR ARRHYTHMIAS -a. EP techniques for characterization; b. EP ablation; c. Scar (substrate) evaluation- detection, mapping, heterogeneity in MRI/CT ; d. Ablation procedure- electroanatomic mapping, CARTO; e. MRI-guided ablation 6. LV DYSYNCHRONY - a. Evaluation with MRI/strain; b. CRT procedure; c. Venous anatomy CT/MRI ; d. MRI/CT- Scar 7. SUDDEN CARDIAC DEATH a. Identifying at-risk patients; b. MRI/CT for diagnosis 8. BRADYCARDIA- Sinus, heart blocks - MRI, PET/CT for sarcoidosis 9. SYNCOPE - Table tilt test 10. COMPLEX CONGENITAL/POST-SURGICAL ANATOMY- Imaging guidance for navigation to appropriate chamber. 11. IMAGE GUIDED RETRIEVAL OF RETAINED LEADS

Printed on: 02/07/23



## Abstract Archives of the RSNA, 2022

CAEE-21

### Coronary CT Angiography with Myocardial Late Enhancement Protocol in the Emergency Room: Tips and Tricks

Sunday, Nov. 27 8:00AM - 9:00AM Room: Learning Center - CA

#### Participants

Lucas Farias, MD, Sao Paulo, Brazil (*Presenter*) Nothing to Disclose

#### TEACHING POINTS

The purpose of this exhibit is:- To review coronary CT angiography with myocardial late enhancement protocols in the evaluation of patients with chest pain.- To review the pharmacokinetics of late iodine enhancement at CT as alternative to the gadolinium at MRI.- To assess the utility of the coronary CT angiography with myocardial late enhancement protocol in the emergency room to exclude coronary obstruction in patients with suspected acute myocarditis.- To correlate important findings with the anatomy and pathophysiology.- To discuss image findings according to the patterns of late enhancement to differentiate between ischemic and nonischemic myocardial damage, to enhance radiologists' skills.- To review usual and unusual patterns of acute myocardial infarction, myocarditis and others non-ischemic cardiomyopathies. - To highlight their characteristics to familiarize radiologists with these conditions, preventing unfavorable patient outcome.

#### TABLE OF CONTENTS/OUTLINE

Table of contents/outline - Applied myocardial anatomy and vascularization. - Pharmacokinetics of late iodine enhancement. - Patterns of myocardial late enhancement. - CT angiography with myocardial late enhancement protocol. - Case series diagnosed with CT angiography with myocardial late enhancement protocol. - Sample cases of pearls, pitfalls, diagnostic difficulties, and mimics. - Summary and take-home messages.

Printed on: 02/07/23



## Abstract Archives of the RSNA, 2022

CAEE-22

### Can Spectral Cardiac CT Find New Clinical Value in Ischemic Heart Disease?

Sunday, Nov. 27 8:00AM - 9:00AM Room: Learning Center - CA

#### Participants

Junji Mochizuki, MSc,RT, (*Presenter*) Nothing to Disclose

#### TEACHING POINTS

To learn about special characteristic of spectral imaging : Dual layer Spectral cardiac CT.To learn about the use of spectral imaging coronary and myocardium evaluation.To illustrate various clinical applications using these techniques by presenting clinical images.

#### TABLE OF CONTENTS/OUTLINE

A. The virtual monochromatic image (VMI) allows evaluation of energy-dependent changes in CT number of coronary artery plaques.B. The low-energy VMI reduces the CT number of epicardial fat and clearly depicts the thrombus and coronary artery plaques.C. The VMI reduces beam-hardening artifacts. In addition, low-energy images can clearly detect areas of abnormal perfusion because the CT number of normal myocardium are increased.D. The extracellular volume function with iodine density imaging can accurately assess myocardial viability.

Printed on: 02/07/23



## Abstract Archives of the RSNA, 2022

CAEE-23

### Chronic Thromboembolic Pulmonary Hypertension (CTEPH): A Multimodality Imaging Review

Sunday, Nov. 27 8:00AM - 9:00AM Room: Learning Center - CA

#### Participants

Scott Adams, MD, PhD, Saskatoon, SK (*Presenter*) Nothing to Disclose

#### TEACHING POINTS

1. Chronic thromboembolic pulmonary hypertension (CTEPH) is defined as pulmonary hypertension due to persistent obstruction of the pulmonary arteries from pulmonary embolism despite at least 3 months of anticoagulation. 2. Ventilation-perfusion (V/Q) scintigraphy has high sensitivity for CTEPH and is a first-line imaging modality for ruling out CTEPH. In addition, SPECT-CT offers increased sensitivity and specificity. 3. CT pulmonary angiography has higher specificity than V/Q scintigraphy for CTEPH, but lower sensitivity. CT features include partial or complete filling defects, bands, and webs within the pulmonary arteries; pulmonary artery dilation; right ventricular dilation and hypertrophy; bronchial artery dilation; and mosaic attenuation of the lung parenchyma. 4. Dual-energy CT has been shown to improve detection of distal CTEPH and provide additional information on pulmonary vascular reserve and parenchymal arterial perfusion. 5. In the future, 4D-flow MRI may play a role in treatment selection and assessment of treatment response.

#### TABLE OF CONTENTS/OUTLINE

Definition  
Pathophysiology  
Clinical presentation and patient demographics  
Imaging features- Radiography- CT, including high-resolution CT, CT pulmonary angiography, and dual-energy CT- MRI, including MR angiography and 4D-flow- Echocardiography- Conventional angiography- Ventilation/perfusion (V/Q) scintigraphy and SPECT-CT  
Diagnostic approach, including the role of imaging in diagnosis, patient selection for treatment, and post-operative follow-up  
Clinical management options

Printed on: 02/07/23



## Abstract Archives of the RSNA, 2022

CAEE-24

### Cardiovascular Manifestations of Connective Tissue Disease

Sunday, Nov. 27 8:00AM - 9:00AM Room: Learning Center - CA

#### Participants

Jospeh Mansour, MD, (*Presenter*) Nothing to Disclose

#### TEACHING POINTS

List the various cardiac and vascular entities that can occur with connective tissues diseases. Describe the pathophysiology, risk factors, and management for each etiology. Illustrate the spectrum of imaging findings and differential diagnoses for each of these entities.

#### TABLE OF CONTENTS/OUTLINE

Rheumatoid arthritis. Pulmonary hypertension. Vasculitis and aortitis. Aortic aneurysm. Cardiomyopathy. Systemic Lupus erythematosus. Pericardial effusion. Vasculitis. Pulmonary embolism. Lupus myocarditis and cardiomyopathy. Libman-Sacks endocarditis. Scleroderma. Pulmonary hypertension. Cardiomyopathy. Infarcts and microvascular disease. Polymyositis and dermatomyositis. Myocarditis. Coronary artery disease. Sjogren syndrome. Pericardial effusion. Cardiomyopathy. Pulmonary hypertension. SUMMARY: Patients with connective tissue diseases can suffer from cardiovascular complications which may impact both morbidity and mortality. Diagnosing these entities can be challenging, both clinically and with imaging, and is often delayed. Familiarity with these conditions and their imaging features can help the radiologist recognize these entities and aid in diagnosis.

Printed on: 02/07/23



## Abstract Archives of the RSNA, 2022

CAEE-25

### State of the Art Cardiac MR Imaging of Ischemic Heart Disease

Sunday, Nov. 27 8:00AM - 9:00AM Room: Learning Center - CA

#### Awards

Certificate of Merit

#### Participants

Felipe Sanchez, MD, Toronto, Chile (*Presenter*) Nothing to Disclose

#### TEACHING POINTS

-1. Ischemic heart disease (IHD) is the worldwide leading cause of death and disability.2. Cardiac MR allows for the evaluation of global and regional cardiac function and provides superb myocardial characterization in a same evaluation.3. Cardiac MR can accurately depict myocardial edema, infarction, hemorrhage, and microvascular obstruction.4. Current Cardiac MR imaging strategies have widely accepted diagnostic and prognostic value.5. Emerging techniques and applications aim to improve prognostic and diagnostic performance of Cardiac MR.

#### TABLE OF CONTENTS/OUTLINE

-1. Significance of IHD.2. Basic physiopathology of IHD.3. Role of Cardiac MR in the workflow of IHD.4. Functional imaging.5. Edema imaging.6. Infarct characterization.a. Depicting myocardial infarct and "at risk" zones: classic and novel strategies.b. MVO and myocardial hemorrhage: role of T2\*.7. Stress perfusion.8. Novel tools for viability assessment and risk stratification.a. Feature tracking: Patterns of impaired myocardial contraction.b. Post-reperfusion hemorrhage, persistent edema, and adverse remodeling.c. 4D-flow in IHD.9. Technical considerations.

Printed on: 02/07/23



## Abstract Archives of the RSNA, 2022

CAEE-26

### Arrhythmogenic Cardiomyopathies: What the Imager Should Know

Sunday, Nov. 27 8:00AM - 9:00AM Room: Learning Center - CA

#### Awards

Identified for RadioGraphics  
Certificate of Merit

#### Participants

Mauricio S. Galizia, MD, , (Presenter) Nothing to Disclose

#### TEACHING POINTS

- Arrhythmogenic Cardiomyopathies (AC) are a group of myocardial diseases that are associated with ventricular arrhythmias and sudden cardiac death
- Although arrhythmogenic right ventricular cardiomyopathy (ARVC) was the first disease described in which morphologic and structural ventricular abnormalities were associated with arrhythmias, AC can involve the right ventricle, the left ventricle, or both
- The main sub-phenotypes of AC include the classical ARVC, left-dominant AC, and arrhythmogenic dilated cardiomyopathy
- Many genetic mutations have been found to be associated with AC, most often genes that encode desmosome structural proteins
- AC can be associated with ventricular systolic dysfunction and/or ventricular dilation. However, symptoms of arrhythmia or history of arrhythmic cardiac arrest can occur in patient with no structural myocardial abnormalities and may represent early developing AC
- There are diagnostic criteria for ARVC; however, similar criteria for the other AC phenotypes is lacking

#### TABLE OF CONTENTS/OUTLINE

1. Definition of arrhythmogenic cardiomyopathy (AC).
2. Description of the desmosome and its constituent proteins: Desmoglein, desmocollin, plakophilin, junctional plakoglobin, desmoplakin
3. Association between AC and genetic diseases of the desmosome: difference between disease and phenotype.
4. Typical clinical presentation and imaging findings (with a greater focus on CMR) of the following phenotypes: Arrhythmogenic right ventricular cardiomyopathy (ARVC), left-dominant arrhythmogenic cardiomyopathy, arrhythmogenic dilated cardiomyopathy
5. Differential diagnoses and mimics: Dilated Cardiomyopathy, sarcoidosis, myocarditis

Printed on: 02/07/23

## Abstract Archives of the RSNA, 2022

CAEE-27

### Cutting the Edge of HCM: Tailored Planning of Surgical Myectomy in Obstructive Hypertrophic Cardiomyopathy

Sunday, Nov. 27 8:00AM - 9:00AM Room: Learning Center - CA

#### Awards

**Magna Cum Laude**  
**Identified for RadioGraphics**

#### Participants

Sunhyang Lee, MD, Seoul, Korea, Republic Of (*Presenter*) Nothing to Disclose

#### TEACHING POINTS

1. To set the cardiac CT protocols and image analysis methods for simulation of successful surgical myectomy in patients with obstructive hypertrophic cardiomyopathy (HCM).2. To demonstrate tailored planning of surgical myectomy using multiphase cardiac CT images, especially volume rendering images and 3D printing

#### TABLE OF CONTENTS/OUTLINE

1. Classification of HCM based on surgical approach- Septal HCM- Apical HCM- Mixed, or diffuse type HCM- Combined abnormal papillary muscles2. Multiphase Cardiac CT Protocol3. CT Image Analysis Methods1) Cardiac function analysis (esp. apical, mixed, and diffuse type HCM)2) Surgeon's views- Trans-aortic view- Trans-apical view3) Papillary muscle evaluation4) Simulation of potential myectomy extent5) Comparison between pre- and post- myectomy CT images4. Various Examples1) Simulation of myectomy in septal HCM and comparison with postoperative CT2) Simulation of myectomy in diffuse HCM and comparison with postoperative CT3) Simulation of myectomy in mixed type HCM and comparison with postoperative CT4) Simulation of myectomy in HCM with abnormal papillary muscle

Printed on: 02/07/23



## Abstract Archives of the RSNA, 2022

CAEE-28

### Differential Diagnosis of Cardiac Amyloidosis: Pearls and Pitfalls

Sunday, Nov. 27 8:00AM - 9:00AM Room: Learning Center - CA

#### Participants

Patricia Oliveros Ordas, MD, Majadahonda, Spain (*Presenter*) Nothing to Disclose

#### TEACHING POINTS

Cardiac amyloidosis (CA) is a rare disease caused by the extracellular deposition of insoluble fibrillar proteinaceous material in the myocardium. Due to the complexity and multisystemic involvement of amyloidosis, a high index of suspicion for CA should be maintained. Typical MRI appearance of CA includes left ventricle myocardial thickening with preserved systolic function, increased atrial volume, and altered gadolinium kinetics with the presence of late enhancement with a subendocardial or transmural pattern. Other common causes of cardiomyopathy that may present as left ventricular hypertrophy should be excluded, such as depositional cardiomyopathies, hypertensive cardiomyopathy, hypertrophic cardiomyopathy, and cardiac sarcoidosis, among others. After reviewing our extensive casuistry and our sample of 80 patients with CA, we present the findings that will allow an easier differential diagnosis by imaging between these pathologies.

#### TABLE OF CONTENTS/OUTLINE

- Introduction: most frequent morphologic, functional and tissue characterization MRI findings in CA
- Imaging differential diagnosis of CA that includes:
  - \* Depositional cardiomyopathies (Fabry's disease, Danon's disease)
  - \* Hypertensive cardiomyopathy
  - \* Hereditary cardiomyopathies
  - \* Cardiac sarcoidosis
  - \* Others
- Conclusions

Printed on: 02/07/23



## Abstract Archives of the RSNA, 2022

CAEE-29

### MRI Mapping in the study of Myocardial Disease

Sunday, Nov. 27 8:00AM - 9:00AM Room: Learning Center - CA

#### Participants

Susana Otero Muinelo, MD, (*Presenter*) Nothing to Disclose

#### TEACHING POINTS

1. To illustrate the role of T1, T2 and T2\* mapping MRI sequences and extracellular volume in myocardial diseases. 2. To recognize findings of most common myocardial diseases on T1, T2 and T2\* maps and correlate them with other findings on cardiac MRI.

#### TABLE OF CONTENTS/OUTLINE

Cardiac T1, T2 and T2\* mapping can provide information about myocardial disease that remains undetected using conventional techniques. The quantitative approach allows noninvasive characterization of myocardial properties such as extracellular volume expansion, edema, or other abnormalities in tissue composition. Thus, increased T1-native due to fibrosis in hypertrophic cardiomyopathy or to amyloid deposition or shortened T1-native due to glycosphingolipids in Anderson-Fabry disease could be evaluated. T2 mapping can detect myocardial edema in myocarditis, Takotsubo cardiomyopathy or myocardial infarction, whereas low T2\* can be useful in iron overload and hemorrhage. We present cases of hypertrophic, dilated and restricted cardiomyopathy, acute myocardial disease as myocarditis or Tako-Tsubo and infiltrative cardiomyopathies and review the advantages, limitations and applications of T1 and T2 mapping to characterize these ones and other myocardial diseases. Multiparametric cardiac MRI provides prognostic information of structural and functional characteristics and myocardial composition. Incorporation of myocardial mapping on clinical routine increases the usefulness of MRI for the diagnosis and characterization of myocardial diseases.

Printed on: 02/07/23



## Abstract Archives of the RSNA, 2022

CAEE-3

### Unraveling the Mysteries of Congenital Heart Disease: A Skills-based Approach

Sunday, Nov. 27 8:00AM - 9:00AM Room: Learning Center - CA

#### Awards

Cum Laude

#### Participants

Shravan Sridhar, MD, MS, (*Presenter*) Nothing to Disclose

#### TEACHING POINTS

1. Become familiar with common congenital heart diseases and morphologic features  
2. Learn of important imaging features  
3. Understand how management relies on imaging metrics  
4. Gain skills to use in practice  
5. Apply skills in the assessment of complex congenital heart diseases

#### TABLE OF CONTENTS/OUTLINE

1. Title  
2. Table of common CHD and skill list  
3. Bicuspid AV morphology (per 2021 consensus)  
4. Understanding management  
5. Skill 1: Peak speed quant with PC VENC (in-plane, through plane)  
6. Common shunts (ASD, VSD, PDA) and features that determine treatment (2018 AHA guidelines)  
7. Understanding management  
8. Skill 2: Qp/Qs quant  
9. Right-sided obstruction (pulmonic stenosis, tetralogy of Fallot, pulmonary atresia spectrum)  
10. Understanding management  
11. Skill 3: Valve regurgitation quantification with phase contrast velocity-encoded images, fractional pulmonary flow quantification  
12. Left-sided obstruction (coarctation, aortic stenosis, Williams syndrome, Shone complex)  
13. Understanding management  
14. Skill 4: Flow quant for coarctation  
15. TGA (D, L)  
16. Understanding management  
17. Skill 5: Anatomic mapping - situs, right, left, terms used in describing discordance (e.g. anatomic vs morphologic)  
18. Other conotruncal anomalies (truncus, DORV, DOLV)  
19. Understanding management  
20. Skill 6: Rules to diff between Tetralogy, truncus, DORV, and DOLV  
21. Single ventricle (HLHS, HRHS, Ebstein's, tricuspid atresia, DORV)  
22. Understanding management  
23. Skill 7: Flow mapping, "checks and balances"  
24. PAPVR, TAPVR  
25. Understanding management  
26. Skill 8: Angiography  
27. References

Printed on: 02/07/23



## Abstract Archives of the RSNA, 2022

CAEE-30

### Multi-modality Imaging of Cardiac Paragangliomas - A Review

Sunday, Nov. 27 8:00AM - 9:00AM Room: Learning Center - CA

#### Participants

Joao Carvalho, MD, (*Presenter*) Nothing to Disclose

#### TEACHING POINTS

? Paragangliomas are rare neuroendocrine tumors originating from autonomic paraganglia. Heart involvement is rare, accounting for <1% of primary cardiac tumors. Most cardiac paragangliomas are incidentally detected on echocardiography or CT, or during the work-up of symptomatic patients with elevated (nor)metanephrine levels or genetic predisposition. ? Most cardiac paragangliomas are located around the great vessels, coronary arteries (atrioventricular groove) or the atria, which can be explained by tumor origin from the paraganglia and the distribution of the cardiac plexus. ? On MRI cardiac paragangliomas typically have low to intermediate signal on T1, and high signal on T2. The tumors are strongly vascularized, with high uptake on first-pass perfusion, and heterogeneous on late gadolinium enhancement. ? Functional imaging with radiolabeled somatostatin analogues is indicated to screen for additional tumor locations or metastatic disease. ? Surgical excision is the only curative treatment. CT or invasive angiography should be performed pre-operatively to precisely delineate tumor vascularization and assess the need for revascularization. Paragangliomas can be vascularized by the left and/or right coronary artery, posing additional surgical challenges.

#### TABLE OF CONTENTS/OUTLINE

1. Background: epidemiology, clinical presentation. 2. Diagnosis: tumor location, tissue characteristics, vascularization. 3. Management: metastatic/multiple disease, surgical planning, radionuclide therapy.

Printed on: 02/07/23



## Abstract Archives of the RSNA, 2022

CAEE-31

### Virtual Reality Imaging - Pre-operative Visualization Modality Equipped with Simultaneous Quantification for Valvular Disease

Sunday, Nov. 27 8:00AM - 9:00AM Room: Learning Center - CA

#### Participants

Yukihiro Nagatani, MD, Otsu, Japan (*Presenter*) Nothing to Disclose

#### TEACHING POINTS

The purpose of this exhibit is: 1. To review general outline of image data display algorithm adopted for virtual reality imaging (VRI) based on advanced visualization software and actual clinical application of VRI 2. To learn crucial anatomical distances and/or dimensions to be accurately measured in pre-operative assessment for valvular disease 3. To introduce valuable experimental model by using ex-vivo swine heart reproducing physiological movements of valves and myocardium 4. To review specific sequences for valvular disease in cardiac magnetic resonance imaging (MRI) from conventional to updated ones

#### TABLE OF CONTENTS/OUTLINE

ž VRI using visualization toolkit with reproducible 3-dimensional measurement ž Detailed description of experimental system enabling endoscopic observation under physiological state and quantitative assessment of intramuscular vasculature by using ex-vivo swine heart. ž Clinical advantage with application of 3-dimensional or 4-dimensional VRI: realization of easy and reliable measurement supported with visual assessment ž Anatomy, dynamics and disease of aortic valve and root including our endoscopic observation result ž Various imaging sequences useful for valvular disease assessment: from conventional and high-speed cine images such as steady-state Free Processing and 4-dimensional flow MRI

Printed on: 02/07/23



## Abstract Archives of the RSNA, 2022

CAEE-32

### What Hides in the Epicardial Space? Differential Diagnosis of Epicardial Masses

Sunday, Nov. 27 8:00AM - 9:00AM Room: Learning Center - CA

#### Awards

Certificate of Merit

Identified for RadioGraphics

#### Participants

Adria Roset Altadill, MD, (*Presenter*) Nothing to Disclose

#### TEACHING POINTS

- The epicardial space has a diversity of components that can be the origin of various types of masses. - The epicardial masses can be divided into tumoral, non-tumoral or pseudo-masses.

#### TABLE OF CONTENTS/OUTLINE

The location is a helpful feature in order to diagnose cardiac masses, but epicardial masses are usually dismissed. The epicardial space includes the epicardial fat and the visceral pericardium. It is composed of a lining of mesothelial cells and connective tissue, along with a variable amount of fat, containing coronary vessels, lymphatics and nerves. Due to its diversity of components, different kinds of masses can be found in the epicardial space. They can be divided into tumoral, non-tumoral or pseudo-masses. The epicardial tumoral masses include lipoma, lymphoma, angiosarcoma, mesothelioma and metastases. Regarding non-tumoral etiologies, IgG4-related coronary disease, Erdheim-Chester and hydatid infection can be encountered. Finally, there are epicardial pseudo-masses either secondary to lipomatosis, purulent pericarditis, coronary aneurysms or postsurgical changes. In this education exhibit we show examples of each case, emphasizing the distinguishing features and the clues for the differential diagnosis.

Printed on: 02/07/23



## Abstract Archives of the RSNA, 2022

CAEE-33

### To the Heart of the Matter: A Systematic Approach to Interpretation of Cardiac MR for Trainees

Sunday, Nov. 27 8:00AM - 9:00AM Room: Learning Center - CA

#### Awards

Identified for RadioGraphics

#### Participants

Aeman Muneeb, MBBS, (*Presenter*) Nothing to Disclose

#### TEACHING POINTS

Approach to reading a conventional cardiac MR. 1. How to identify and learn the contribution of each sequences commonly used in Cardiac MR studies 2. To recognize the normal appearance of the heart in the common Cardiac MR sequences (cardiac chamber size, thickness, signal characteristics, normal function on visual analysis, interpretation of basic quantification parameters for function and flows) 3. Understand common appearances of diseases of the cardiac structure, myocardium, valves and pericardium. 4. Visual analysis of the Myomaps (native T1, T2, T2\*). 5. Basic principles of quantitative Myomaps analysis.

#### TABLE OF CONTENTS/OUTLINE

Step 1: Know your patient - review the clinical scenario and relevant prior imaging. Step 2: Anatomical assessment. Step 3: Visual assessment of function. Step 4 Hemodynamic Assessment - Function and Flow quantification parameters. Step 5: Tissue Characterization. Step 6: Differential diagnosis: Characteristic appearance of common diseases.

Printed on: 02/07/23



## Abstract Archives of the RSNA, 2022

CAEE-34

### Multimodality Imaging in Cardiac Masses

Sunday, Nov. 27 8:00AM - 9:00AM Room: Learning Center - CA

#### Participants

Ayaz Aghayev, MD, Newton, MA (*Presenter*) Nothing to Disclose

#### TEACHING POINTS

- Cardiac masses are rare entities; however, they can be associated with high morbidity and mortality.- Cardiac masses broadly can be classified as non-neoplastic masses such as thrombus, normal/variant cardiac structures, and neoplastic masses (primary and secondary/metastatic tumors).- The educational exhibit will elucidate the diagnostic approach even before the imaging, based on the patient's demographics, and prior disease/comorbidities.- On imaging, differential diagnosis can be elaborated based on the location of the tumor; for example, the most common benign myxoma is usually located in the left atrium and attached to the interatrial septum; primary cardiac malignancy - angiosarcoma - is exclusively located along the right atrium/ventricle as an infiltrative mass.- The next step will focus on available imaging modalities for cardiac masses such as echocardiography (TTE/TEE), cardiac CT, cardiac MRI, and PET/CT, and their specific imaging characteristics for certain masses. For example, fat density lesion on a CT is consistent with lipoma; avid LGE in intramyocardial mass is a feature of fibroma, or Dotatate uptake in cardiac mass is diagnostic of paraganglioma.- Lastly in this educational exhibit, we will provide a proposed algorithm for patients with suspected cardiac masses or incidentally detected on echo/chest CT.

#### TABLE OF CONTENTS/OUTLINE

1. Cardiac mass classification.2. Diagnostic approach to the patient with suspected or incidentally detected cardiac mass.3. Available imaging modalities that can be utilized in cardiac masses.4. Key imaging features of cardiac masses- Cardiac CT, Cardiac MRI, and PET-CT (including pitfalls).5. Proposed algorithm for suspected cardiac masses.

Printed on: 02/07/23



## Abstract Archives of the RSNA, 2022

CAEE-35

### Potential Applications of Radiomics Based Texture Analysis in Cardiac Magnetic Resonance (CMR)

Sunday, Nov. 27 8:00AM - 9:00AM Room: Learning Center - CA

#### Participants

Avanti Gulhane, MD, Seattle, WA (*Presenter*) Nothing to Disclose

#### TEACHING POINTS

We will discuss potential applications for radiomic analysis of CMR studies. 1.As a proof of concept, we will describe technique for texture analysis of LGE-PSIR to identify first, second and higher order features in patients with ischemic and non-ischemic myocardial diseases. 2.Potential advantages of using radiomics texture analysis for quantitative assessment of CMR images. 3.Several texture features such as first order entropy, kurtosis, grey level co-occurrence matrix non uniformity, grey level run length matrix non uniformity and wavelet transform can be obtained using Pyradiomics, an open-source software. 4.We will illustrate comparative analysis of radiomic features in LGE images of a normal volunteer and patients with ischemic and non-ischemic heart diseases

#### TABLE OF CONTENTS/OUTLINE

Specific areas where CMR radiomics analysis may aid on diagnostic characterization will be described. Example of radiomic analysis obtained from LGE-PSIR will be illustrated by showing specific texture parameters that can be obtained. We will illustrate the method by showing examples of radiomic features in several diseases on CMR including myocardial infarction, hypertrophic cardiomyopathy, myocarditis, dilated cardiomyopathy and normal heart. Images will be sampled to 1x1x1 mm using linear interpolation and discretized to a fixed bin width of 25 units for the basic preprocessing within the Pyradiomics software. Examples of feature types extracted and analyzed are • First Order Statistics • Shape-based (2D and 3D) • Gray Level Co-occurrence Matrix • Gray Level Run Length Matrix • Gray Level Size Zone Matrix • Neighbouring Gray Tone Difference Matrix • Gray Level Dependence Matrix • Wavelet-based features

Printed on: 02/07/23



## Abstract Archives of the RSNA, 2022

CAEE-36

### Mulmodality Imaging of Atrioventricular Groove Masses - Diagnostic Approach

Sunday, Nov. 27 8:00AM - 9:00AM Room: Learning Center - CA

#### Awards

Certificate of Merit

#### Participants

Prabhakar Rajiah, MD, FRCR, Rochester, MN (*Presenter*) Nothing to Disclose

#### TEACHING POINTS

The atrioventricular (AV) groove is the space that encircles the right and left AV valves. 1. To review the masses involving the atrioventricular (AV) groove. 2. To discuss the role of multimodality imaging in the diagnosis and characterization of these masses. 3. To illustrate the imaging appearances of several types of AV groove masses

#### TABLE OF CONTENTS/OUTLINE

• INTRODUCTION • ANATOMY OF AV GROOVE- Right coronary artery, left circumflex coronary artery, coronary sinus, fat, lymphatics, nerves. • MULTIMODALITY IMAGING- CT, MRI, Nuclear medicine, Echocardiography, cardiac catheterization • DISCUSSION AND ILLUSTRATION OF THE FOLLOWING MASSES IN THE AV GROOVE WITH CASE EXAMPLES AND PATHOLOGICAL CORRELATION A. VASCULAR LESIONS - Coronary artery aneurysm - Coronary bypass graft aneurysm/pseudoaneurysm - Cardiac chamber aneurysm/pseudoaneurysm - Coronary fistula - Vascular malformation B. INFLAMMATORY - IgG4 disease - Erdheim Chester disease - Vasculitis - Sarcoidosis - Hematoma C. BENIGN NEOPLASMS - Paraganglioma - Schwannoma - Hemangioma - Thymoma D. MALIGNANT NEOPLASMS - Sarcoma - Lymphoma - Metastases E. MISCELLANEOUS - Calcification and pericardial constriction - Caseous mitral annular calcification - Fatty proliferation - Pericardial hematoma - Intracameral RCA • DIAGNOSTIC APPROACH AND ALGORITHM - Infiltrative versus well-defined margins - Hypervascular versus hypovascular - Late gadolinium enhancement - High T2 signal

Printed on: 02/07/23



## Abstract Archives of the RSNA, 2022

CAEE-37HC

### Pre- and Postoperative Imaging Evaluation of Ross Procedure Candidates: Anatomy, Complications, and What the Surgeon Wants to Know

Sunday, Nov. 27 8:00AM - 9:00AM Room: Learning Center - CA

#### Participants

Lisa Xuan, MD, BSc, Newmarket, ON (*Presenter*) Nothing to Disclose

#### TEACHING POINTS

1. The Ross procedure is a technically complex cardiac surgery which replaces a diseased aortic valve with a native pulmonic autograft. 2. There is growing interest for the Ross procedure in young patients, due to improved longevity and the ability of the native autograft to grow and adapt overtime. 3. Preoperative cardiac MR evaluation is integral for patient selection and surgical planning, while postoperative surveillance aids in diagnosing complications and quantifying myocardial remodeling as a measure of success. 4. Relevant cardiac anatomy and MR imaging findings of the Ross procedure are reviewed. 5. Example cardiac MR protocols and synoptic reporting frameworks are provided, with details tailored for the cardiac surgeon, and can be utilized to foster a strong multidisciplinary Ross program.

#### TABLE OF CONTENTS/OUTLINE

Overview of Ross procedure surgical technique:- Indications- Illustrations of the procedure and pertinent cardiac anatomy (generated by our medical illustrator) Cardiac MR protocol and reporting:- Pre/postoperative protocols and follow-up intervals- Synoptic reporting framework Review of imaging:- What the cardiac surgeon wants to know- Relevant radiologic findings in pre and post-operative Ross patients- Postoperative cardiac remodeling as a measure of success (e.g. left ventricular mass regression on cardiac MR)- Potential complications (e.g. pulmonic autograft failure (autograft annular dilatation)) Clinical Implications Summary Please visit the Learning Center to also view this presentation in hardcopy format.

Printed on: 02/07/23



## Abstract Archives of the RSNA, 2022

CAEE-38

### Multimodality Imaging of Valvular Infections

Sunday, Nov. 27 8:00AM - 9:00AM Room: Learning Center - CA

#### Awards

**Certificate of Merit**

**Identified for RadioGraphics**

#### Participants

Jordi Broncano, MD, Cordoba, (*Presenter*) Nothing to Disclose

#### TEACHING POINTS

1. To analyze the role of advanced imaging in the diagnosis and management of patients with infective endocarditis (IE). 2. To describe the main imaging clues for accurate diagnosis of valvular and perivalvular features as well as extracardiac findings in IE. 3. To identify the potential pitfalls of IE and the main imaging tips for differentiating from IE.

#### TABLE OF CONTENTS/OUTLINE

1. Definition of IE: Modified Duke Criteria 2. Epidemiology in IE: Unveiling the high-risk patient 3. Role of Imaging in IE: Pros and Cons - Echocardiography: Transthoracic and transesophageal - Cardiac Computed Tomography - Positron Emission Tomography/Computed tomography (PET/CT) - Cardiac MRI: Is there a role for it? 4. Imaging Pearls in IE 4.1. Valvular disease - Vegetation - Leaflet perforation - Leaflet aneurysm 4.2. Perivalvular disease: - Dehiscence pseudoaneurysm - Perivalvular abscess - Perivalvular fistula 4.4. Extracardiac embolic events 5. Infective Endocarditis Masqueraders - Non-bacterial thrombotic endocarditis (Marantic Endocarditis) - Papillary fibroelastoma - Caseous Necrosis of the Mitral Valve (CNMV) - Lamb's Exscrecences - Valvular thrombosis - Inflammatory pannus - Myxoma - HALT - Cusp prolapse 6. Diagnostic imaging algorithm 7. Take Home points

Printed on: 02/07/23



## Abstract Archives of the RSNA, 2022

CAEE-39

### Stress Cardiac Magnetic Resonance Imaging: Our Experience in a Community Hospital Setting

Sunday, Nov. 27 8:00AM - 9:00AM Room: Learning Center - CA

#### Participants

Mahmoud Shalaby, MD, Lansdowne, PA (*Presenter*) Nothing to Disclose

#### TEACHING POINTS

1- Describe the basic principles of stress cardiac magnetic resonance (CMR) perfusion imaging, including technique and imaging protocol. 2- Discuss the clinical applications of stress CMR. 3- Illustrate stress CMR interpretation and data analysis. 4- Highlight stress CMR pitfalls and artifacts.

#### TABLE OF CONTENTS/OUTLINE

1- Stress CMR perfusion tracers; clinical applications and contraindications. 2- Pulse sequences and imaging protocols. 3- Stress CMR interpretation and data analysis; qualitative and quantitative interpretation. 4- Clinical applications of stress CMR in large-vessel and microangiopathy coronary artery disease. 6- Pitfalls and artifacts: - Dark rim artifact. - Susceptibility artifact. - Chemical shift artifact. 7- Limitations of stress CMR.

Printed on: 02/07/23



## Abstract Archives of the RSNA, 2022

CAEE-4

### Expanding Fractional Flow Reserve (FFR) CT: Challenges and Emerging Applications

Sunday, Nov. 27 8:00AM - 9:00AM Room: Learning Center - CA

#### Participants

Fabio Trindade, MD, Curitiba, Brazil (*Presenter*) Nothing to Disclose

#### TEACHING POINTS

The aim of this exhibition is to review: 1) What is Fractional Flow Reserve (FFR) and its relevance in coronary artery disease (CAD). 2) Technical Aspects of Machine-learning-based FFRCT (ML FFRCT) calculation. 3) Current and potential contributions of FFRCT in CAD. 4) Advantages and challenges of Machine-learning-based FFRCT. 5) Emerging applications and future directions of FFRCT.

#### TABLE OF CONTENTS/OUTLINE

1. INTRODUCTION 1.1. FFR overview: definition, interpretation, invasive and non-invasive techniques 2. FFRCT: BRIEF REVIEW OF SUPPORTIVE EVIDENCE 3. ML-FFRCT : WHAT THE RADIOLOGIST NEEDS TO KNOW 3.1. Advantages and disadvantages 3.2. How to measure: a step-by-step approach 3.3. Limitations and pitfalls 4. ML-FFRCT IN REAL LIFE: INTERACTIVE CHALLENGING SCENARIOS 4.1. Myocardial bridging 4.2. Coronary stents 4.3. Coronary artery anomalies, including interarterial course 4.4. Coronary dissection 4.5. Other conditions 5. FUTURE DIRECTIONS AND EMERGING APPLICATIONS 6. TAKE HOME MESSAGES

Printed on: 02/07/23



## Abstract Archives of the RSNA, 2022

CAEE-40

### Indications and Imaging Findings of CMR in the Acutely Ill Patient

Sunday, Nov. 27 8:00AM - 9:00AM Room: Learning Center - CA

#### Participants

Daniel Vargas, MD, Denver, CO (*Presenter*) Nothing to Disclose

#### TEACHING POINTS

Cardiac MR is quickly becoming a powerful and increasingly utilized tool in the evaluation of acutely ill patients. To this end, institutions, radiologists and cardiologists should strive to have the infrastructure and preparation to offer CMR to hospitalized patients. The purpose of this exhibit is: 1. Review CMR protocols for evaluation of acutely ill patients 2. Discuss CMR tools that may aid in shortening acquisition and/or improve image quality in this group of patients 3. Review the imaging findings and pitfalls of the most common conditions encountered in the inpatient setting

#### TABLE OF CONTENTS/OUTLINE

1. CMR protocol for acutely ill patients a. Basic and advanced sequences. b. Tools to shorten acquisition time. c. Tools to improve image quality. 2. Common indications and imaging findings in acutely ill patients. a. Elevated troponins (myocarditis, takotsubo, myocardial infarction, etc). b. Decreased ejection fraction / Heart failure (identifying cardiomyopathy, drug toxicity, etc). c. Arrhythmia and Heart-block. d. Intracardiac mass. e. Pericardial emergencies

Printed on: 02/07/23



## Abstract Archives of the RSNA, 2022

CAEE-41

### **Congenital Coronary Artery Anomalies with Lethal Conditions or Sudden Death Risk; Coronary CT and Conventional Angiographic Evaluation**

Sunday, Nov. 27 8:00AM - 9:00AM Room: Learning Center - CA

#### **Participants**

Keizo Tanitame, MD, Hiroshima, Japan (*Presenter*) Nothing to Disclose

#### **TEACHING POINTS**

Numerous variations of coronary artery anomalies exist. Some are benign, but others are hemodynamically significant and potentially lethal. The anomalous origin of the coronary artery from the pulmonary artery is a potentially lethal condition. In the patients with anomalous origin of the coronary artery from the contralateral sinus or single coronary artery, coronary artery compression between aorta and pulmonary trunk is a risk factor of sudden death during exercise. Coronary artery fistulae are the most common hemodynamically significant abnormalities, and to-and-fro flow is seen in the dilated coronary arteries. Myocardial bridge is generally benign, but occasionally associated with angina, myocardial infarction, and sudden death. We demonstrate congenital coronary anomalies with lethal conditions or sudden death risk and discuss the radiological evaluation of their severity and treatment outcome.

#### **TABLE OF CONTENTS/OUTLINE**

1. Anomalous origin of the coronary artery from the pulmonary artery - Development of collaterals and retrograde blood flow from the anomalous coronary artery to the pulmonary artery on conventional coronary angiography 2. Multi-detector CT coronary angiography for evaluating anomalous origin of the coronary artery - Visualization of the anomalous origin and subsequent passage of the coronary artery 3. Anomalous origin of the coronary artery with a risk of sudden death - Coronary artery compression between aorta and right ventricular outflow tract 4. Congenital coronary artery fistulae - Evaluation of the size of the fistula and the degree of to-and-fro flow 5. Myocardial bridge - Cardiac CT evaluation of the depth and length of the bridge and the severity of systolic stenosis

Printed on: 02/07/23



## Abstract Archives of the RSNA, 2022

CAEE-42

### Out on the Road: Revisiting Coronary Artery Anomalies

Sunday, Nov. 27 8:00AM - 9:00AM Room: Learning Center - CA

#### Awards

Identified for RadioGraphics  
Certificate of Merit

#### Participants

Lucas Farias, MD, Sao Paulo, Brazil (*Presenter*) Nothing to Disclose

#### TEACHING POINTS

The purpose of this exhibit is: 1) To review usual and unusual cases of congenital heart diseases. 2) To discuss the classification of coronary anomalies. 3) To understand coronary anomalies by associating schematic drawings with MPR and three-dimensional reconstructions, correlating them with coronary angiography (animated gif). 4) To correlate important findings with the anatomy, embryology, and pathophysiology. 5) To discuss image findings in order to enhance radiologists' skills. 6) To review CT protocols in the evaluation of patients with suspected coronary artery anomalies. 7) To highlight their characteristics in order to familiarize radiologists with these conditions, preventing unfavorable patient outcome.

#### TABLE OF CONTENTS/OUTLINE

1) Applied embryology and anatomy of the coronary arteries. 2) CTA protocols in the evaluation of patients with suspected coronary artery anomalies. 3) Anomalies of origination and course of coronary artery. 4) Anomalies of intrinsic coronary arterial anatomy. 5) Anomalies of coronary termination. 6) Anomalous anastomotic vessels. 7) Sample cases of pearls, pitfalls, diagnostic difficulties, and mimics. 8) Summary and take-home messages.

Printed on: 02/07/23



## Abstract Archives of the RSNA, 2022

CAEE-43

### Spectrum presentation of Chagas Cardiomyopathy (Ch-CMP) by CMR

Sunday, Nov. 27 8:00AM - 9:00AM Room: Learning Center - CA

#### Participants

Hector Manuel Medina, MD, Bogota, Colombia (*Presenter*) Nothing to Disclose

#### TEACHING POINTS

-Cardiac magnetic resonance (CMR) is useful to determine ventricular function and fibrosis in patients with Chagas cardiomyopathy (Ch-CMP). - In ch-CMP patients, inflammation and vascular dysfunction causes severe vasodilation, which promotes tissue ischemia and fibrosis in water-shed segments. This can occur during the acute and chronic stages of the disease condition. In Ch-CMP, the most common scar locations are at the left ventricular apex and the basal inferolateral wall. These segments present with akinesis, and fibrosis noted in late gadolinium enhancement sequences (LGE), which can be transmural, sub-epicardial, mid-myocardial, and sub-endocardial.-CMR is also helpful in identifying ventricular thrombi in this population using perfusion, early gadolinium enhancement (EGE), and LGE.-The main differential diagnoses of Ch-CMP are Anderson-Fabry disease, ischemic cardiomyopathy, idiopathic cardiomyopathy, sarcoidosis disease and myocarditis.

#### TABLE OF CONTENTS/OUTLINE

Distribution of scar in Ch-CMP Phases of Ch-CMP include ventricular microaneurysm, ventricular aneurysm, severe heart failure and intracavitary thrombi Frequently used sequences and technique-Functional evaluation with maps of T1 and T2-Steady-state free precession (SSFP) in short axis, 3 chamber Scar and fibrosis: Intravenous contrast (gadobutrol)- EGE- LGE

Printed on: 02/07/23

## Abstract Archives of the RSNA, 2022

CAEE-45

### Cardiac MRI Lessons Learned: Pearls and Pitfalls from Training to Remember as an Attending

Sunday, Nov. 27 8:00AM - 9:00AM Room: Learning Center - CA

#### Awards

Identified for RadioGraphics

#### Participants

Prabhakar Rajiah, MD, FRCR, Rochester, MN (*Presenter*) Nothing to Disclose

#### TEACHING POINTS

1. To review the lessons learned in cardiac MRI on sequences, protocols, interpretation, pitfalls and problem-solving. 2. To illustrate these key lessons with representative case examples.

#### TABLE OF CONTENTS/OUTLINE

1. PROTOCOLS Gadolinium versus Ferumoxytol, sequence adaptations; Cardiac devices- Adaptations (including wideband technique)  
2. ARTIFACTS AND SOLUTIONS MOTION- Prospective triggering, real-time, compressed sensing; Single-shot, resp. nav. and gating; STIR- Pseudolesion subendocardium, edema from coil sensitivity; PERFUSION- Gibbs artifact; MRA- T2 shortening pseudofilling defects, subtraction misregistration; LGE- T1 selection (esp. amyloidosis), Partial voluming; PSIR artifacts; Failed fat suppression (vs pericarditis), normal blood pool in recesses; 3D WHOLE HEART- Partial voluming; 2D/4D FLOW- Aliasing; resolution limitation, Noise without contrast; T1 MAP- Motion, imaging in other phases; STRAIN- Diastolic fading; 3. ARTIFACTS AS SOLUTIONS  
SUSCEPTIBILITY- Iron quant; CHEMICAL SHIFT- fat identification 4. INTERPRETATIVE PITFALLS Pseudomasses (Crista terminalis, Taenia sagittalis, Chiari network, Coumadin ridge, lipomatous hypertrophy, MAC, focal HCM, pseudothrombus, moderator band, pericardial recess); CABG aneurysm vs neoplasm; Prominent trabeculations vs LV non compaction; LV apical thinning vs aneurysm; MVO vs spared myocardium; Benign fat vs ARVD; Valve leaflets- Bicuspid vs tricuspid; Pseudo vs true Coarctation; Ductus diverticulum vs aneurysm; Vasculitis vs IMH 5. BLIND SPOTS 6. TIPS TRICKS Long T1 for LGE in cardiac masses; 3D T1w imaging for pericarditis; VENC higher than predicted; Dark blood-LGE for subtle scars

Printed on: 02/07/23



## Abstract Archives of the RSNA, 2022

CAEE-46

### Getting to the Heart of Cardiac Masses: Pearls and Pitfalls

Sunday, Nov. 27 8:00AM - 9:00AM Room: Learning Center - CA

#### Participants

Andrea Cangiani Furlani, MD, (*Presenter*) Nothing to Disclose

#### TEACHING POINTS

1) Overview of cardiac masses (primary neoplasms - benign and malignant -, metastasis, infectious, thrombus). 2) 90% of primary cardiac tumors are benign. Metastases via various mechanisms are much more common than primary cardiac malignancies. Metastatic mechanisms determine imaging characteristics. 3) Discuss in detail with illustrative cases the typical MRI and CT characteristics of specific cardiac neoplasms and their common differential diagnostic considerations, including pearls and pitfalls.

#### TABLE OF CONTENTS/OUTLINE

I. Overview. a) Locations of cardiac masses by chamber. b) Tips for distinguishing neoplasms from infection and thrombus. II. Benign cardiac neoplasms. a) Myxoma. b) Fibroelastoma. c) Fibroma, d) Lipoma. e) Cystic tumor of the AV node. f) Congenital cyst. III. Metastases. a) Hematogenous spread. b) Lymphangitic spread. c) Vascular invasion- IVC, SVC, pulmonary veins. d) Direct invasion. IV. Primary cardiac malignancies. a) Angiosarcoma. b) Other sarcomas. c) Lymphoma. The aims of this abstract are: 1. To review etiology, location, and typical clinical scenarios of different cardiac masses. 2. To review imaging findings of benign cardiac neoplasia (myxoma, fibroelastoma, fibroma, lipoma, hemangioma, cystic tumor, and differential diagnosis such as lipomatous hypertrophy of the interatrial septum). 3. To review the mechanisms of metastatic disease (hematogenous, lymphangitic, direct and vascular invasion).

Printed on: 02/07/23

## Abstract Archives of the RSNA, 2022

CAEE-47

### Coronary Artery Fistulas: a Pictorial Essay

Sunday, Nov. 27 8:00AM - 9:00AM Room: Learning Center - CA

#### Participants

Desiree Louise Batista, MD, (*Presenter*) Nothing to Disclose

#### TEACHING POINTS

To describe classification and the main subtypes of coronary fistulas (CFs). To describe the hemodynamic implications on the cardiac structures/cavities of drainage. To describe the importance of coronary CT angiography (CCTA) for the diagnosis, course, path and drainage of CFs, as well as depiction of the relationship between the affected vessel and the nearby structures.

#### TABLE OF CONTENTS/OUTLINE

CF is an anomalous direct connection between one or more coronary arteries (CA) and a cardiac chamber (coronary-cameral fistula) or a large vessel (arteriovenous fistula). CFs can be congenital or acquired, single or multiple, isolated or associated with other congenital cardiac malformations. CFs originating from the right coronary artery are the most frequent (50-70%) and 40% of CFs drain into the right ventricle. The degree of shunting is associated with its size and the pressure gradient between the coronary and the draining site. Drainage to the right heart is related to left-to-right shunt, causing variable degrees of volume overload and pulmonary hypertension. Drainage to the LV may cause hemodynamic changes similar to aortic regurgitation. Drainage to the pulmonary artery and left atrium generates volume overload to the LV. There may be reduced myocardial flow distal to the fistula (coronary steal phenomenon), myocardial ischemia and progression to heart failure. The main complications are rupture, infarction and infective endocarditis. CCTA is the gold-standard non-invasive method to explore the complex anatomy of CFs, allowing 3D reconstructions and assessment of vessel of origin, pathway and site of drainage, which may aid to treatment decisions.

Printed on: 02/07/23



## Abstract Archives of the RSNA, 2022

CAEE-48

### 1H-Magnetic Resonance Spectroscopy for Metabolic Imaging of Myocardial Triglyceride Content - How To Do It"

Sunday, Nov. 27 8:00AM - 9:00AM Room: Learning Center - CA

#### Participants

Bernhard Petritsch, MD, Wuerzburg, Germany (*Presenter*) Research Consultant, Siemens AG

#### TEACHING POINTS

To review the indications, contraindications, and limitations of 1H-Magnetic Resonance Spectroscopy (1H-MRS) of the myocardium. To highlight the potential benefit of a metabolic investigation embedded in a comprehensive examination of cardiac morphology and function. To learn about parameter settings for spectroscopic data acquisition, including voxel placement and positioning of a navigator for double (respiratory and ECG) triggered data acquisition. To interpret cardiac 1H-MR spectra of healthy subjects, patients suffering from congenital or acquired metabolic disorders, and to learn about potential pitfalls of spectroscopic imaging of the heart.

#### TABLE OF CONTENTS/OUTLINE

A. How does 1H-Magnetic Resonance Spectroscopy (1H-MRS) of the myocardium work  
B. Technical requirements  
C. Spectroscopic data acquisition; positioning of respiratory motion gating navigator; voxel placement in the septum  
D. Spectroscopic data postprocessing  
E. Image analysis in healthy subjects and patients; age dependency of myocardial triglyceride content; Metabolic syndrome, Morbus Fabry  
F. Pitfalls of cardiac 1H-MRSG. Limitations of cardiac 1H-MRS; alternative imaging modalities

Printed on: 02/07/23



## Abstract Archives of the RSNA, 2022

CAEE-49

### Novel Assessment of Physiological Mitral Valve Morphology and Surgical Simulation for MICS MVP via 3D Printed Cardiac Models and Immersive 3D Virtual Reality System

Sunday, Nov. 27 8:00AM - 9:00AM Room: Learning Center - CA

#### Participants

Koichi Osuda, RT, (*Presenter*) Nothing to Disclose

#### TEACHING POINTS

Minimally invasive cardiac surgery (MICS) mitral valve plasty (MVP) has a lower risk of associated complications including mediastinitis, and advantage of quick rehabilitation compared to median sternotomy approach. However, surgical procedures are technically demanding due to narrow operative field and deep working space. To understand the comprehensive mitral anatomy, we attempt to create patient-specific 3D printed left atrioventricular models and developed a novel approach for simulating MICS MVP procedures via immersive 3D virtual reality (VR) system.

#### TABLE OF CONTENTS/OUTLINE

3D VR datasets were converted, using CT data which has submillimeter spatial resolution. 3D printed models and 3D VR systems were faithfully reproduced mitral complex structure consisting of mitral leaflets, chordae tendineae, papillary muscles, and prolapsing leaflet. 3D printed models and 3D VR systems enable surgeon to assess physiological morphology through cardiac cycle (systole to diastole), practically, though it is impossible to recognize that intraoperatively. Furthermore, this method allowed surgeon to simulate not only surgical procedures, but also appropriate intercostal thoracotomy approach position, and considering precise device size in advance. 3D printed models and 3D VR systems are clinically available and promising for facilitating the operation strategy optimization and assistant for MICS MVP procedures safely. There will be contributions to clinical practice for preoperative accurate assessment and simulation.

Printed on: 02/07/23

## Abstract Archives of the RSNA, 2022

CAEE-5

### State of the Art Imaging in Surveillance of Repaired Tetralogy of Fallot: Imaging in Therapeutic Planning and Risk Assessment

Sunday, Nov. 27 8:00AM - 9:00AM Room: Learning Center - CA

#### Awards

**Certificate of Merit**

#### Participants

Yoshiaki Ota, MD, Ann Arbor, MI (*Presenter*) Nothing to Disclose

#### TEACHING POINTS

The purpose of this exhibit is: 1. Understand the central role of cardiac MR (CMR) in post repair Tetralogy of Fallot (TOF) to assess anatomic and functional sequelae 2. Learn the role of MR in clinical decision making and prognostication 3. Illustrate the spectrum of new imaging techniques and their applications in repaired TOF. 4. To learn the utility of imaging prior to and following transcatheter pulmonary valve replacement (TPVR).

#### TABLE OF CONTENTS/OUTLINE

Outline 1. Background- Most common cyanotic congenital heart disease characterized by ventricular septal defect, pulmonary stenosis (right ventricular outflow obstruction), dextroposition of the aorta (overriding aorta), and right ventricular hypertrophy 2. Pathophysiology of repaired TOF- Role of imaging in assessing sequelae of repair, clinical decision making, planning TPVR, outcomes and prognostication a. Imaging protocols for surveillance emphasizing new techniques such as 4D flow, parametric mapping, strain imaging b. MR derived parameters and their role in timing and planning of pulmonic valve intervention and risk assessment (ventricular size and function, presence and extent of Late Gadolinium Enhancement, regurgitation quantification, residual ventricular septal defect, and vascular anatomy) c. Indications for Pulmonary Valve Replacement d. Procedural aspects of TPVR and available devices e. Pre-intervention imaging for patients and device selection: protocols, imaging modalities, 3D printing f. Post-TPVR imaging and complications g. Future directions

Printed on: 02/07/23



## Abstract Archives of the RSNA, 2022

CAEE-50

### Three-dimensional (3D) Procedure Planning for Transcatheter Mitral Valve Replacement

Sunday, Nov. 27 8:00AM - 9:00AM Room: Learning Center - CA

#### Participants

Nicole Wake, PhD, Aurora, OH (*Presenter*) Employee, General Electric Company

#### TEACHING POINTS

A. Transcatheter Mitral Valve Replacement (TMVR) is a minimally invasive procedure that replaces the valve using a device that clips onto the faulty valve. B. Multi-detector computed tomography (MDCT) of the mitral valve and aortic outflow tract is important for appropriate patient and device selection. C. A multidisciplinary approach is required for patient selection and procedure planning. D. Planning for TMVR is traditionally performed by visualizing medical imaging data and using two-dimensional (2D) measurements to determine appropriate valve sizing. E. Three-dimensional (3D) visualization can provide enhanced visualization and superior planning regarding device sizing and placement. F. For complicated cases, 3D printing can be performed to create a precise model of the anatomy and allow for enhanced surgical planning.

#### TABLE OF CONTENTS/OUTLINE

1. Review of mitral valve disease. 2. Overview of multi-detector computed tomography (MDCT) for mitral valve disease evaluation. 3. Synopsis of currently available valves for TMVR procedures. 4. Outline of two-dimensional (2D) image analysis and valve sizing. 5. Description of three-dimensional (3D) visualization, image analysis, and device planning. 6. Summary of 3D printing and use for planning TMVR.

Printed on: 02/07/23



## Abstract Archives of the RSNA, 2022

CAEE-51

### Spectrum of Imaging Findings in Takotsubo Cardiomyopathy

Sunday, Nov. 27 8:00AM - 9:00AM Room: Learning Center - CA

#### Participants

Camila V. Machado, MD, (*Presenter*) Nothing to Disclose

#### TEACHING POINTS

After attending to this exhibit, the learner should be able: 1. To understand both clinical and laboratory features of Takotsubo Cardiomyopathy. 2. To recognize the major imaging findings of Takotsubo Cardiomyopathy on magnetic resonance imaging (MRI). 3. To correlate the imaging findings on MRI, echocardiography and ventriculography. 4. To understand the importance of cardiac MRI in the diagnosis of Takotsubo Cardiomyopathy and in the evaluation of differential diagnoses. 5. To analyze the role of MRI in the detection of acute complications and in the follow-up of the patients.

#### TABLE OF CONTENTS/OUTLINE

? Diagnosis of Takotsubo Cardiomyopathy ? Epidemiology ? Clinical findings, stressful events ? MRI, echocardiogram and ventriculography? Importance of MRI for the diagnosis and characterization of Takotsubo Cardiomyopathy ? Assessment of segmental changes in contractility (cine, strain) ? Assessment of myocardial edema (T2 weighted images, T1 and T2 mapping) ? Assessment of myocardial necrosis / fibrosis (late gadolinium enhancement)? Atypical manifestations of Takotsubo Cardiomyopathy (different patterns of contractile change)? The role of MRI in excluding other causes of chest pain ? Myocarditis / pericarditis ? Acute myocardial infarction ? Extracardiac pathologies (pulmonary, pleural, musculoskeletal)? The role of MRI in the detection of acute complications and the follow-up of the patients ? Heart failure, pleural/pericardial effusion, intracavitary thrombus, ventricular wall rupture

Printed on: 02/07/23



## Abstract Archives of the RSNA, 2022

CAEE-52

### Three-Dimensional Fusion Technique with CT and LGE-MRI for Cardiac Resynchronization Therapy

Sunday, Nov. 27 8:00AM - 9:00AM Room: Learning Center - CA

#### Participants

Yoshihiro Haga, Sendai, Japan (*Presenter*) Nothing to Disclose

#### TEACHING POINTS

Cardiac resynchronization therapy (CRT) is an established treatment for patients with severe heart failure (HF). Factors influencing CRT response are Fig. 1. In particular, it is important to know the left ventricular (LV) lead location and the extent of myocardial scar. These can be assessed by the contrast computed tomography coronary venography (CTCV) or late gadolinium enhancement by cardiac magnetic resonance (LGE-CMR) imaging. However, these cannot be observed on the same three-dimensional image. Therefore, we devised a method that a three-dimensional fusion technique combined the two images derived from CTCV and LGE-CMR imaging.

#### TABLE OF CONTENTS/OUTLINE

1. Understanding the treatment of heart failure (HF) using cardiac resynchronization therapy (CRT). 2. Understanding the key points for a successful CRT. 3. Understanding the preoperative CT scan of CRT. 4. Understanding the importance of Fusion image with CT and LGE-CMR. 5. Features of CRT: International guidelines on CRT implantation 6. The key points for a successful CRT: QRS duration, LV scar tissue, LV lead position, etc. 7. Fusion image with CT and LGE-MRI: three-dimensional fusion technique

Printed on: 02/07/23



## Abstract Archives of the RSNA, 2022

CAEE-53

### A New Evaluation Method for Coronary Plaque by DECT

Sunday, Nov. 27 8:00AM - 9:00AM Room: Learning Center - CA

#### Participants

Takayoshi Yamaguchi, (*Presenter*) Nothing to Disclose

#### TEACHING POINTS

1. Review the current status of coronary plaque assessment and summarize its limitations 2. Summary of advantages and disadvantages of Dual energy CT compared to Single energy CT 3. Questions about spectral analysis of plaques from coronary CTA 4. Explains new image analysis methods to improve plaque identification accuracy 5. Presenting the correlation between a new plaque evaluation method by CT and intravascular imaging

#### TABLE OF CONTENTS/OUTLINE

1. Introduction 2. Explain the importance of assessing plaque characteristics using coronary CT 3. Comparison of plaque evaluation by coronary CT and IVUS or OCT 4. Explain the advantages of assessing plaque with dual energy CT 5. Limitations for assessing plaque in the arterial phase 6. Proposal of new imaging techniques and methods for improving the ability to characterize plaque tissue using dual energy CT 7. Explain the characteristics of the measured values in various types of plaque tissues and the changes in the spectral HU curve 8. Correlation between new tissue characterization method by DECT and evaluation by intravascular imaging

Printed on: 02/07/23



## Abstract Archives of the RSNA, 2022

CAEE-54

### Structured Pretransplant Cardiac CT Report in Adult Patients with Congenital Heart Disease: What the Radiologist Should Analyze

Sunday, Nov. 27 8:00AM - 9:00AM Room: Learning Center - CA

#### Participants

Rebeca Gil Vallano, Madrid, Spain (*Presenter*) Nothing to Disclose

#### TEACHING POINTS

- To analyze the radiological findings, which cardiac surgeons need for the surgical planning of heart transplant in adults with congenital heart disease (CHD).- To propose a structured report of pretransplant cardiac CT.

#### TABLE OF CONTENTS/OUTLINE

Our hospital is a referral center for heart transplantation in pediatric and adult patients with CHD. Imaging tests - echocardiogram, magnetic resonance, and computed tomography (CT) - show the cardiac abnormal anatomy. CT additionally demonstrates other findings in these patients with complex anatomies and, in some cases, multisystem disorders (lung anatomy, aorto-pulmonary collaterals, previous surgeries, vascular accesses, rib cage, abdominal anatomy). In our work we will focus on the CT examination performed preoperatively. We will revise the CT acquisition technique, and we will evaluate its benefits, since this technique acquires 3D data with a wide field of view that allow a comprehensive evaluation of the anatomy with good spatiotemporal resolution and multiplanar reconstruction capacity. In the interpretation of these studies, it is very important to carry out a systematic and practical assessment of the preoperative aspects. For this reason, we use a structured report, which we will develop in detail and illustrate with cases from our center. We will emphasize the information needed by surgeons and show the methodology we use to obtain it. Radiologists have a fundamental role through the radiological report in the pretransplant surgical planning of adult patients with CHD.

Printed on: 02/07/23



## Abstract Archives of the RSNA, 2022

CAEE-56

### Advanced Cardiovascular Computed Tomography Imaging in Children with Congenital Variants and Anomalies of the Aortic Arch: From Volume Rendering to 3D Models and 3D Printing

Sunday, Nov. 27 8:00AM - 9:00AM Room: Learning Center - CA

#### Participants

Flavio Zuccarino, MD, Barcelona, Spain (*Presenter*) Nothing to Disclose

#### TEACHING POINTS

To discuss the main indications for cardiovascular CT in newborns and children with congenital anomalies of the aortic arch (CAAA). To outline the key imaging findings, advantages and limitations of CT in CAAA, enhancing the usefulness of volume rendering (VR) and 3D models in differential diagnosis and the design of an optimal therapeutic approach.

#### TABLE OF CONTENTS/OUTLINE

We discuss, in a short background, the advantages and limitations of CT in CAAA diagnosis. We analyze different CT acquisition protocols depending on patient age and pathology. We organize CT findings of different CAAA as: Left-sided aortic arch anomalies. Right-sided aortic arch anomalies. Double aortic arch Cervical Aortic Arch Persistent Fifth Aortic Arch Interrupted Aortic Arch Aortic Arch Hypoplasia Coarctation Pseudocoarctation Gothic aortic arch We review key CT findings of different CAAA, focusing on 3D imaging reconstructions and 3D models. We define the relationship of the aorta to the airways, esophagus, and other cardiovascular and thoracic structures that play a pivotal role in CAAA diagnosis. We discuss potential differential diagnosis of CAAA. OUTLINE Radiologists should be familiar with CT key imaging findings and with the advantages and limitations of 3D advanced techniques to establish an optimal diagnostic approach and therapeutic management.

Printed on: 02/07/23



## Abstract Archives of the RSNA, 2022

CAEE-57

### Arrhythmogenic Left Ventricular Cardiomyopathy (ALVC); Understanding Current Concepts

Sunday, Nov. 27 8:00AM - 9:00AM Room: Learning Center - CA

#### Participants

Daniel Ocazonez-Trujillo, MD, Houston, TX (*Presenter*) Nothing to Disclose

#### TEACHING POINTS

- Genotype-phenotype correlation studies have demonstrated that mutations in Desmoplakin and Filament C genes are the most common gene defects causing ALVC.- Patients with ALVC usually complain of symptoms of both arrhythmia (palpitations, chest tightness, syncope) and LV heart failure.- Imaging modalities in ALVC usually reveal severe LV dysfunction with preserved to mildly impaired RV function. Often this entity has been misdiagnosed as dilated cardiomyopathy, chronic myocarditis, myocardial infarction, or double ventricular involvement type ARVC.- Reported Cardiac MRI findings in ALVC include dilated left ventricle, fatty infiltration, irregular lateral wall contour with a "serrated" shape and areas of mesocardial and epicardial delayed enhancement in a "ring like" distribution involving the septal and lateral walls.

#### TABLE OF CONTENTS/OUTLINE

-Definition-Clinical presentation-Genetics-Imaging findings on Cardiac MRI-Differential diagnosis-Conclusion

Printed on: 02/07/23



## Abstract Archives of the RSNA, 2022

CAEE-58

### The Multiple Facets of Cardiac Amyloidosis -Diagnostic Imaging Overview

Sunday, Nov. 27 8:00AM - 9:00AM Room: Learning Center - CA

#### Participants

Aarushi Gupta, MD, MBBS, (*Presenter*) Nothing to Disclose

#### TEACHING POINTS

- Diagnosis of cardiac amyloidosis is challenging and can be misinterpreted for hypertensive heart disease or hypertrophic cardiomyopathy, particularly in older patients with heart failure with preserved ejection fraction (HFpEF).
- Recent treatment advances such as Tafamidis for ATTR amyloidosis (Transthyretin amyloidosis) can delay disease progression. An understanding of imaging features can help in early diagnosis and appropriate management of patients.
- Echocardiography, cardiac MRI and nuclear Tc-99 pyrophosphate scan are complementary and can help in establishing the diagnosis.

#### TABLE OF CONTENTS/OUTLINE

1. Background on common types of cardiac amyloidosis:• AL (Light chain) and ATTR amyloid (hereditary and wild type)• Clinical manifestations of amyloidosis• How to differentiate ATTR from AL amyloidosis using clinical and biochemical parameters
2. Imaging in diagnosis of cardiac amyloidosis with focus on ATTR amyloidosis• Echocardiography, cardiac MRI and different LGE patterns (with discussion of QALE score)• Caveats in establishing diagnosis including technical challenges like determining the nulling time of myocardium• Recent advances in MR cardiac imaging including parametric tissue mapping (for diagnosis and prognosis) and myocardial strain (for early detection of LV dysfunction)
3. Discuss role of nuclear medicine techniques like Tc-99 pyrophosphate scan and recent American Society of Nuclear Cardiology (ASNC) guidelines for diagnosis •Correlative MR cardiac and Tc-99 pyrophosphate images will be provided
4. Discuss new disease modifying therapies for ATTR amyloidosis such as Tafamidis
5. Conclusion

Printed on: 02/07/23



## Abstract Archives of the RSNA, 2022

CAEE-59

### Cardiac Amyloid - Correlation of Cardiac Magnetic Resonance and Pathology

Sunday, Nov. 27 8:00AM - 9:00AM Room: Learning Center - CA

#### Participants

Navpreet Khurana, MBBS, (*Presenter*) Nothing to Disclose

#### TEACHING POINTS

1. Describe the classic imaging findings of cardiac amyloidosis (CA) on cardiac magnetic resonance (CMR). 2. Understand the conditions which can mimic CA on CMR - false positives. 3. Understand the incremental value of nuclear medicine.

#### TABLE OF CONTENTS/OUTLINE

1. Findings of CA on CMR. 2. Role of Nuclear Medicine in diagnosing CA. 3. Review of cases - positive CMR and positive pathology. 4. Review of cases - positive CMR and negative pathology. 5. Review of cases - negative CMR and positive pathology.

Printed on: 02/07/23



## Abstract Archives of the RSNA, 2022

CAEE-6

### Cardiac MRI in Congenital Heart Disease: Pearls and Pitfalls

Sunday, Nov. 27 8:00AM - 9:00AM Room: Learning Center - CA

#### Participants

Priyanka Garg, MBBS, MD, New Delhi, India (*Presenter*) Nothing to Disclose

#### TEACHING POINTS

Cardiac MRI is a powerful tool giving relevant anatomical and physiological information of cardiovascular structures in congenital heart disease. The purpose of this exhibit is to: 1. Discuss the various pearls and pitfalls relevant to planning, acquisition and interpretation of cardiac MR images. 2. Enumerate specific points that need special consideration while imaging in paediatric patients. 3. Describe the role of cardiac MR imaging in patients with congenital heart disease.

#### TABLE OF CONTENTS/OUTLINE

1. Introduction 2. Patient selection 3. Sedation requirement 4. ECG placement 5. Cardiac MR sequences 6. Cardiac MR planning 7. Phase contrast imaging 8. Angiographic imaging 9. Post processing including ventricular volumetry, flow assessment, shunt fraction and important formulae for regurgitant fraction 10. Role of cardiac MRI in congenital heart disease 11. Take home message

Printed on: 02/07/23



## Abstract Archives of the RSNA, 2022

CAEE-60

### Multimodal Imaging Characterization of Cardiac Tumors Emphasizing PET with Pathology Correlation Using the New 2021 WHO Classification

Sunday, Nov. 27 8:00AM - 9:00AM Room: Learning Center - CA

#### Awards

Identified for RadioGraphics

#### Participants

Maria Clara Lorca, MD, Pittsford, NY (*Presenter*) Nothing to Disclose

#### TEACHING POINTS

Due to their rarity and overlapping imaging characteristics, tumors and tumor-like conditions of the heart can be a radiological challenge. It's important to be familiar with their imaging presentation in order to improve diagnostic accuracy and avoid unnecessary invasive procedures.1. New 2021 WHO Classification of Cardiac Tumors2. Depict cardiac tumors and cardiac tumor-like radiological features3. Describe the importance of PET-CT in the diagnosis and follow up of cardiac tumors4. Discuss the cardiac tumor-like conditions including cardiac thrombus, mediastinal abscess, pericardial hematoma, pericardial cyst5. Describe the pearls and pitfalls that some entities demonstrate in the cardiac imaging, including benign entities that can appear as a cardiac pseudotumor

#### TABLE OF CONTENTS/OUTLINE

This education exhibit reviews biopsy-proven cases of cardiac lesions and their mimics and depict their radiological features, including images pearls and pitfalls. Review with clinical pictures, illustrative case examples, and original illustrations the cardiac tumors in a systematic fashion. Incorporate the new 2021 WHO classification of the cardiac tumors. Depict the imaging appearances of various types of cardiac tumor-like conditions and how to accurately differentiated them from cardiac tumors.

Printed on: 02/07/23



## Abstract Archives of the RSNA, 2022

CAEE-61

### Imaging of Acute and Chronic Cardiac Complications of COVID-19

Sunday, Nov. 27 8:00AM - 9:00AM Room: Learning Center - CA

#### Awards

Identified for RadioGraphics  
Certificate of Merit

#### Participants

Felipe Sanchez, MD, Toronto, Chile (*Presenter*) Nothing to Disclose

#### TEACHING POINTS

1. Acute cardiac complications in patients with COVID-19 are relatively rare but include myocarditis, thrombosis and ischemia<sup>2</sup>. Cardiac imaging plays an important role in the diagnosis of acute myocardial injury in patients with COVID-19, with typical findings on cardiac MRI including edema, high native T1, and co-localizing late gadolinium enhancement<sup>3</sup>. Patients who have recovered from COVID-19 are at increased risk of cardiovascular disease, including those with persistent symptoms and post-acute sequelae of SARS-CoV-2 infection (or long COVID)<sup>4</sup>. Cardiac MRI can be useful in patients with persistent symptoms and functional impairment after COVID-19 to evaluate for the sequelae of myocarditis, left ventricular ejection fraction, strain, and parametric mapping

#### TABLE OF CONTENTS/OUTLINE

The purpose of this educational exhibit is to: 1. Review the acute and chronic cardiac complications related to COVID-19 including incidence, pathophysiology, risk factors, and clinical outcomes<sup>2</sup>. Demonstrate the role of cardiac imaging in establishing a diagnosis of myocarditis following COVID-19<sup>3</sup>. Illustrate multi-modality cardiac imaging findings in patients recovered from COVID-19 with persistent symptoms

Printed on: 02/07/23

## Abstract Archives of the RSNA, 2022

CAEE-62

### Pearls and Pitfalls in Cardiac Imaging

Sunday, Nov. 27 8:00AM - 9:00AM Room: Learning Center - CA

#### Participants

Furkan Ufuk, MD, Denizli, Turkey (*Presenter*) Nothing to Disclose

#### TEACHING POINTS

? To review the cardiac pseudotumors and challenging diagnoses ? To review the cardiac outpouchings and differential diagnoses ?  
To review the cardiac and coronary artery anatomic variations

#### TABLE OF CONTENTS/OUTLINE

1. Cardiac pseudotumors Right atrial pseudotumor due to prominent crista terminalis, lipomatous hypertrophy of the interatrial septum, caseous mitral annular calcification, focal hypertrophic cardiomyopathy, microvascular obstruction, left atrial appendage pseudothrombus, ventricular noncompaction. 2. Cardiac outpouchings: True and false left ventricular aneurysms, ventricular diverticula, ventricular clefts and crypts, atrial diverticula and aneurysms, interatrial septal aneurysm, sinus valsalva aneurysm, interventricular septal aneurysm, mitral-aortic intervalvular fibrosa pseudoaneurysm. 3. Cardiac and coronary artery anatomic variations and congenital lesions: Patent foramen ovale, interatrial septal pouch, coronary artery anomalies, coronary artery tortuosity, coronary artery fistulas, 4. Coronary artery lesions and pseudolesions: Coronary artery aneurysm, RCA pseudostenosis due to streak artifact, overestimation of stenosis due to calcified plaque, myocardial bridging. 5. Pulmonary vein abnormalities and anatomical variations: right top pulmonary vein, pulmonary venous varix, pulmonary vein thrombosis, partial anomalous pulmonary venous return, anomalous midline common ostium of the left and right inferior pulmonary veins

Printed on: 02/07/23



## Abstract Archives of the RSNA, 2022

CAEE-63

### Imaging of Left Ventricular Assist Device (LVAD) Driveline Infections and Other Common LVAD Complications

Sunday, Nov. 27 8:00AM - 9:00AM Room: Learning Center - CA

#### Participants

Mahati Mokkarala, MD, Saint Louis, MO (*Presenter*) Nothing to Disclose

#### TEACHING POINTS

Teaching Points: The purpose of this exhibit is to: 1. Illustrate the common LVAD devices and components of the left ventricular assist device on CT. 2. Imaging characteristics of LVAD infections that lead to operative management. 3. Understand imaging of additional LVAD complications.

#### TABLE OF CONTENTS/OUTLINE

Content Organization: 1. Basics on type and anatomy of drive line parts: - Description of multiple types of LVAD machines. Older models: Jarvik, Thoratec, Heartmate - Diagram of most recent LVAD machine, Heartmate III and components on CT. 2. CT imaging of LVAD infections that lead to operative management - Drive line soft tissue thickening that can involve adjacent musculature, peritoneum - Drive line and adjacent left ventricular assist device fluid collection/abscess 3. Nuclear medicine imaging of LVAD infections - Description of PET/CT findings including increased FDG uptake by the driveline and LVAD - Comparison of PET/CT and white blood scintigraphy scans 4. CT imaging of additional more local LVAD complications including the following: - Increased risk of LVAD structural, outflow and inflow cannula, pump systemic thrombosis - Increased risk of local hemorrhage - LVAD device and cannula mechanical breakage, device failure - Involvement of adjacent soft tissue and vascular structures 5. CT imaging of more systemic, LVAD related, complications - Increased risk of right ventricular dysfunction and aortic valve disease - Increased risk of systemic hemorrhage (GI bleeding), thrombosis (stroke, PE).

Printed on: 02/07/23



## Abstract Archives of the RSNA, 2022

CAEE-64

### Spectrum of Cardiothoracic Imaging Findings in Drug Abuse

Sunday, Nov. 27 8:00AM - 9:00AM Room: Learning Center - CA

#### Participants

Gaurav Watane, MBBS, MD, Pittsburgh, PA (*Presenter*) Nothing to Disclose

#### TEACHING POINTS

1. To recognize the emergent and non-emergent cardiothoracic imaging findings in the recreational drug abuse 2. To gain awareness through example cases of the associated complications 3. To discuss the complementary role of CT/MRI, PET/CT, and echocardiography in the management

#### TABLE OF CONTENTS/OUTLINE

1. Case-based review of the spectrum of cardiothoracic imaging findings in the recreational drug abuse; including infective endocarditis with or without vegetations, pulmonary embolism, septic emboli, thrombophlebitis, Spontaneous coronary artery dissection (SCAD), Vaping associated lung injury (EVALI)2. Current status of various imaging modalities and their limitations in the imaging of Cardiothoracic complications

Printed on: 02/07/23



## Abstract Archives of the RSNA, 2022

CAEE-65HC

### Characterization of Atrial Masses through Cardiac Magnetic Resonance Imaging

Sunday, Nov. 27 8:00AM - 9:00AM Room: Learning Center - CA

#### Participants

Hector Manuel Medina, MD, Bogota, Colombia (*Presenter*) Nothing to Disclose

#### TEACHING POINTS

Teaching Points- Cardiac magnetic resonance (CMR) provides a reliable and detailed evaluation of cardiac masses.- While biopsy remains the cornerstone of diagnosis, CMR has been proven safe and effective at assessing atrial masses and determining its extension, vascular involvement and providing differential diagnoses.- Based on this assessment, a multidisciplinary medical and/or surgical management plan can be established.- Follow-up based on CMR after treatment yields an equivalent comparison, thus optimizing treatment decisions.

#### TABLE OF CONTENTS/OUTLINE

\*?able of Contents/Outline: A Case-Based Approach- Epidemiology of the most common atrial masses.- Radiologic features and characterization (preliminary diagnosis through imaging) and correlation with biopsies.- CMR as an ideal tool for the diagnosis of atrial masses.- Use of steady-state free precession (SSFP), T1-weighted (T1W), short tau inversion recovery (STIR), early gadolinium enhancement (EGE), late gadolinium enhancement (LGE), and perfusion sequences.- Multidisciplinary medical and surgical management strategy formulation.- Useful tool for disease staging and follow-up.Please visit the Learning Center to also view this presentation in hardcopy format.

Printed on: 02/07/23



## Abstract Archives of the RSNA, 2022

CAEE-66

### Be Aware of the Heart in an Oncologic Scenario! Cardiac Metastases - A Pictorial Essay

Sunday, Nov. 27 8:00AM - 9:00AM Room: Learning Center - CA

#### Participants

Pedro Matta, Sao Paulo, Brazil (*Presenter*) Nothing to Disclose

#### TEACHING POINTS

Review the main radiologic features that differentiate primary and secondary cardiac masses and discuss the role of advanced cardiac imaging modalities in evaluating these lesions. Describe anatomical landmarks involved in metastatic spread to the heart such as pericardium, epicardium, myocardium, valves and chambers. Understand the epidemiology, including prevalence, most common origins and histologic types of metastatic involvement of the heart. Propose a diagnostic workflow based on tumor features including size, borders, tissue invasion, site, pericardial involvement, single or multiple lesions and tissue characteristics, describing contrast enhancement, T1 and T2WI signal intensity. Identify the major red flags regarding imaging signs associated with cardiac involvement.

#### TABLE OF CONTENTS/OUTLINE

Major malignant secondary cardiac tumors, including epidemiology, pathophysiology and imaging findings: Poorly differentiated small cell type, Leukemic infiltrate and mass, Melanoma metastasis, Osteosarcoma metastasis and Angiosarcoma. The role of multimodality imaging techniques, such as US, CT, MRI, PETCT, in the evaluation of cardiac masses, listing advantages and disadvantages in diagnosis and surgical planning including Echocardiography, Computed tomography, Magnetic Resonance Imaging and PETCT. Differential diagnosis, potential pitfalls and artifacts to keep in mind when evaluating a potential cardiac mass.

Printed on: 02/07/23



## Abstract Archives of the RSNA, 2022

CAEE-67

### Radiologic Evaluation of Transcatheter Valve Replacements

Sunday, Nov. 27 8:00AM - 9:00AM Room: Learning Center - CA

#### Participants

Demetrios Raptis, MD, Frontenac, MO (*Presenter*) Nothing to Disclose

#### TEACHING POINTS

- Discuss indications and contraindications for transcatheter valve replacement with emphasis on pulmonic, mitral, and tricuspid valve replacements and brief discussion of transcatheter aortic valves. Review preprocedural imaging work-up for transcatheter valve replacements specific to each valve. Case based review of complications of transcatheter valve replacements

#### TABLE OF CONTENTS/OUTLINE

Brief review of transcatheter aortic valve replacement Discuss indications for transcatheter valve replacements • Pulmonic • Mitral • Tricuspid Review preprocedural imaging of transcatheter valve replacements with emphasis on measurements and accesses routes both standard and alternative • Pulmonic • Mitral • Tricuspid Case based review of complications in transcatheter valve replacement including but not limited to: • Misplaced/malpositioned valves • Embolized valves • Outflow tract obstructions • Paravalvular prosthetic leaks • Hypo-attenuating leaflet thickening • Hypo-attenuation affecting motion • Coronary obstruction • Vascular complications/bleeding • Valve malfunction • Embolic phenomenon • Septic emboli

Printed on: 02/07/23



## Abstract Archives of the RSNA, 2022

CAEE-7

### Heterotaxy: What the Radiologist Needs to Know to Get It Right

Sunday, Nov. 27 8:00AM - 9:00AM Room: Learning Center - CA

#### Participants

Maria Clara Lorca, MD, Pittsford, NY (*Presenter*) Nothing to Disclose

#### TEACHING POINTS

Heterotaxy syndrome remains a diagnostic challenge, especially for radiology residents. While situs anomalies have a rare incidence, it is important to recognize them early in part due to their correlation with congenital heart disease. The aim of this project is to review the anatomic imaging appearance of heterotaxy syndrome on CT and MRI and how to incorporate heterotaxy findings into the segmental classification of congenital heart disease.

#### TABLE OF CONTENTS/OUTLINE

Become familiar with the anatomic imaging appearance of heterotaxy syndrome on CT and MR. Briefly review of the embryology, epidemiology, and terminology of heterotaxy syndrome, also known as situs ambiguous. Become familiarized with anatomic and physiologic imaging appearance of the more common forms of heterotaxy syndrome in the chest and abdomen (CT and MR), with a focus on right versus left isomerism. How to incorporate heterotaxy findings into the segmental classification of congenital heart disease using the three-part segmental notation utilized in the Van Praagh classification system.

Printed on: 02/07/23



## Abstract Archives of the RSNA, 2022

CAEE-8

### Cardiac Magnetic Resonance Imaging of Acute Myocarditis: A Review Focusing on Quantitative Evaluation Methods

Sunday, Nov. 27 8:00AM - 9:00AM Room: Learning Center - CA

#### Participants

Nobuko Tanitame, MD, Hiroshima, Japan (*Presenter*) Nothing to Disclose

#### TEACHING POINTS

Acute myocarditis (AM) could result in arrhythmia, dilated cardiomyopathy or chronic heart failure. Although endomyocardial biopsy has been the gold standard in diagnosis of AM, it is invasive and has low diagnostic sensitivity. Cardiac magnetic resonance (CMR) imaging is currently considered to be the most comprehensive diagnostic tool in the evaluation of AM. Generally, T2- and T1-weighted imaging and late gadolinium enhancement (LGE) are used for diagnosing AM. Furthermore, novel quantitative techniques such as native T1, T2 mapping and extracellular volume (ECV) are recommended to allow more objective assessment of myocardial injury. We focus on quantitative methods, diagnostic strategy and pitfalls of CMR imaging in the patients with AM.

#### TABLE OF CONTENTS/OUTLINE

1. Recent development of CMR imaging and processing techniques 2. Establishment of standard values for quantitative analysis of CMR imaging 3. Cine MR imaging (ejection fraction, flow analysis using phase-contrast method) - Cardiac function, left and right ventricular asynergy 4. Black blood T2-weighted STIR (T2 mapping using T2-prep SSFP) - Myocardial edema 5. Native T1 mapping using MOLLI - Myocardial edema, hyperemia, necrosis, fibrosis 6. Gadolinium-enhanced perfusion CMR - Hyperemia, capillary leak 7. LGE (ECV using analysis software) - Myocardial necrosis, fibrosis 8. Representative cases and diagnostic pitfalls of AM

Printed on: 02/07/23



## Abstract Archives of the RSNA, 2022

CAEE-9

### 2020: What Does the Radiologist Need to Know About Major Changes in the Diagnosis of Arrhythmogenic Cardiomyopathy?

Sunday, Nov. 27 8:00AM - 9:00AM Room: Learning Center - CA

#### Participants

Alan Hummel, Sao Paulo, Brazil (*Presenter*) Nothing to Disclose

#### TEACHING POINTS

The goal of this exhibit is to: 1. Understand what arrhythmogenic cardiomyopathy is and what is its pathophysiology. 2. Describe the significant changes in the diagnostic criteria that occurred in 2020. 3. Outline the diagnostic criteria for the right ventricle. 4. Discuss the "new" types of involvement: biventricular and isolated from the left ventricle.

#### TABLE OF CONTENTS/OUTLINE

1. Arrhythmogenic dysplasia of the right ventricle - the precursor; 2. Review the basic anatomy of the right ventricle and their relationships; 3. What is arrhythmogenic cardiomyopathy? 4. Is it possible to differentiate: myocardial fat vs fibrosis? 5. Padua Criteria - Major changes in 2020. 5.1. Padua Criteria - Exposing the Criteria 5.2. Padua Criteria - Image 5.3. Padua criteria - Other methods 5.4. Morphofunctional criteria 5.5. Structural criteria 6. Morphofunctional abnormalities of the right ventricle 6.1. Exposing the major and minor criteria 6.2. Examples 7. Morphofunctional abnormalities of the left ventricle 7.1. Exposing the minor criteria 7.2. Examples 8. Structural abnormalities of the right ventricle 8.1. Exposing the major criteria 8.2. Examples 9. Structural abnormalities of the left ventricle 9.1. Exposing the major criteria 9.2. Examples 10. Diagnostic algorithm 11. Summary in 1 slide

Printed on: 02/07/23



## Abstract Archives of the RSNA, 2022

CHEE

### Chest Education Exhibits

Sunday, Nov. 27 8:00AM - 9:00AM Room: Learning Center - CH

#### Sub-Events

#### CHEE-1 Postoperative Chest Imaging Findings: Pearls and Pitfalls

##### Awards

##### Certificate of Merit

##### Participants

Sofía Ventura- Diaz, MD, Madrid, Spain (*Presenter*) Nothing to Disclose

##### TEACHING POINTS

To have an understanding of the different surgical techniques, including invasive and minimally invasive procedures  
To review the different types of lung resection  
To know the indications of thoracic surgery  
To recognize normal expected findings  
To identify potential complications in chest radiography and CT in order to optimize patient care in the postoperative period

##### TABLE OF CONTENTS/OUTLINE

Surgical techniques: minimally invasive techniques (video-assisted thoracoscopic surgery and robotic- assisted thoracic surgery) and open thoracotomies (Posterolateral, Shaw-Paulson, Anterolateral, axillary thoracotomy, thoracoabdominal incision, bilateral anterior transternal thoracotomy...) Types of lung resection and indications: sublobar resection (including wedge resection and segmentectomy), lobectomy, pneumonectomy (intrapleural, extrapleural, intrapericardial) Normal findings for each type of resection in Radiographs and Computed Tomography Complications: • Airway and lung complications: Atelectasis, Pneumonia, Pulmonary edema, Acute respiratory distress syndrome, Air leak/bronchopleural fistula, Post pneumonectomy syndrome, lobar torsion, lung herniation. • Mediastinal and cardiovascular complications: Mediastinal hematoma, Acute mediastinitis/mediastinal abscess, Pneumopericardium, Cardiac herniation, Stump thrombus, Pulmonar Pseudoaneurysm. • Pleural and esophageal complications: Empyema, Hemothorax, Chylothorax, Esophageal anastomotic leak and esophagopleural fistula.

#### CHEE-10 Hidden in Plain Sight: Applications of the Aorto-Esophageal Ligament

##### Participants

Nanditha Guruvaiah, BSc, Staten Island, NY (*Presenter*) Nothing to Disclose

##### TEACHING POINTS

While it is not uncommon to see central mediastinal pathology on cross-sectional imaging, it is important to understand the pathway influencing the spread of disease at a radiological point of view. Mediastinal facial planes can be visualized in cross sectional imaging such as CT and MRI. However, MRI is more successful in identifying the mediastinal visceral fascia and the aorto-esophageal (AE) ligament; which courses from the anterior aspect of the aorta to the left lateral aspect of the esophagus. This recently discovered unknown anatomy aids us in understanding the possible pathway of spread of disease processes such as infection, air, fluid, and soft tissue (lipomas) in the mediastinum. CT and MRI could also be useful in determining the lymph node metastasis and tumor in growth in relation to the AE ligament. In addition, the aorto-esophageal ligament can be utilized in the preoperative planning of minimally invasive thoracic surgeries.

##### TABLE OF CONTENTS/OUTLINE

- Introduction to anatomy of Aorto-Esophageal Ligament
- Classification of Mediastinal compartments on cross section imaging
- Role of Imaging in identifying AE ligament - benefits and limitations
- Application of AE ligament in imaging - Spread of disease (gas, fluid and soft tissue) in the mediastinum - Preoperative surgical planning - Oncology imaging, notably spread of lymph nodes
- Case based learning
- What Radiologists should know about AE ligament

#### CHEE-100 Interpreting the Unexpected: Diagnostic Imaging Findings in Mycobacterium Chimaera Infection

##### Participants

Andrew Moore, MD, (*Presenter*) Nothing to Disclose

##### TEACHING POINTS

1. Mycobacterium chimaera (MC) is an indolent infection that is often misdiagnosed or underrecognized. Having a high clinical suspicion and knowing its various imaging manifestations help avoid delay in diagnosis and allow for earlier treatment
2. Slowly developing or enlarging peri-sternotomy fluid collections, soft-tissue thickening or both, without other clinical findings to suggest acute infection may be seen with mycobacterium chimaera infection
3. PET/CT is a useful adjunct to suggest indolent infection in patients with unremarkable CT scans and in those with a high clinical suspicion of infection

##### TABLE OF CONTENTS/OUTLINE

1. Background/Epidemiology a. MC is a nontuberculous mycobacterium found in environment b. Disease manifestations include

disseminated, pulmonary and surgical site c. Water used in Heater-Cooler Devices (HCD) became contaminated by MC which is then aerosolized by HCD fans during cardiothoracic surgery d. Surgical site or disseminated disease occurs after cardiothoracic surgery where patient, implanted material or both become infected with aerosolized MC 2. Clinical Course of MC Infection 3. CT PET/CT Findings a. Sternotomy site b. Blurred vascular wall c. Insidious development of fluid collections and soft tissue thickening/tracts d. Persistent fluid collections despite treatment enhancement characteristics e. Disseminated disease 4. Conclusion

### **CHEE-101 Pulmonary Fungal Disease Patterns in CT: Recognizing and Differentiating**

Participants

Isabela Oliveira, MD, Campinas, Brazil (*Presenter*) Nothing to Disclose

#### **TEACHING POINTS**

Recognize the different radiologic patterns of fungal lung infections. Be familiar with the main fungal entities involved in certain radiologic patterns. Know the main differential diagnoses for the mentioned patterns. Differentiate between the entities involved in both immunocompetent and immunocompromised hosts.

#### **TABLE OF CONTENTS/OUTLINE**

1. Introduction. 2. Systematic approach - imaging patterns of thoracic fungal diseases: a. Ground glass opacities; b. Nodules; c. The halo and reversed halo signs; d. Miliary pattern; e. Mediastinal involvement; f. Airway disease; g. Cavitations. 3. Pattern-based differential diagnosis: Ground glass due to viral infection; Nodules related to lung metastasis; The halo and reversed halo sign related to organizing pneumonia; Miliary pattern related to neoplasia; Mediastinal involvement related to neoplasia; Airway disease related to viral respiratory tract infection; Cavitations related to vasculitis. 4. Major fungal pathogens according to imaging patterns and immunological status (immunocompetent vs. immunocompromised hosts). 5. Summary

### **CHEE-102 Emergency and Critical Care Chest Radiography: Pitfalls and Pearls with CT Correlation**

Participants

Sayed Mohammad Seyedsaadat, MD, (*Presenter*) Nothing to Disclose

#### **TEACHING POINTS**

1. Prompt diagnosis of many emergent conditions with chest radiography requires appreciation of subtle or easily misinterpreted radiographic findings; a systematic search pattern is essential for prompt detection. 2. Awareness of direct and indirect findings of pleural and parenchymal emergencies such as pneumothorax, hemothorax, bronchopleural fistula, empyema, laceration, and abscess can prevent treatment delays. 3. Early detection of abnormal mediastinal lines, stripes, and interfaces can be clues to life-threatening pathology such as aortic dissection, mediastinitis, and mediastinal hemorrhage. 4. Diaphragmatic injuries, fractures, and sternal dehiscence are frequently missed emergent radiographic findings, requiring a high level of suspicion and knowledge of common patterns of injury. 5. Attention to the position and the courses of the lines and tubes in their entirety on the chest radiograph can help to detect extrathoracic device misplacement or related complications.

#### **TABLE OF CONTENTS/OUTLINE**

Pitfalls and pearls of chest imaging in the emergency and critical care unit with CXR/CT correlation. Pleura (PTx on supine CXR, bronchopleural fistula, empyema) Lung Parenchyma (Cardiogenic vs noncardiogenic pulmonary edema, lung abscess) Heart and vessels (Traumatic aortic injury, mediastinal hematoma, mediastinitis) Diaphragm and chest wall (Diaphragmatic rupture, sternal dehiscence, fractures) Lines and tubes (Vascular, cardiac, pleural, airway devices) PDF Upload.

### **CHEE-103 Osseous Lesions in Oncologic Patients**

Participants

Alexander Sytov, (*Presenter*) Nothing to Disclose

#### **TEACHING POINTS**

The finding of an incidental focal osseous lesion in an oncologic patient poses a unique diagnostic challenge due to the heightened concern for metastasis. While the majority of osseous lesions are benign, many may closely resemble metastasis on imaging, prompting the need for clear methods of differentiation. By following an algorithm for categorizing osseous lesions, radiologists may confidently recommend follow-up imaging studies while avoiding unnecessary referrals. After reviewing this exhibit, the learner will be able to:- Employ a systematic method to characterize osseous lesions according to their density, composition, and cortical features- Identify imaging features that characterize osseous lesions as malignant or benign (such as: wide zone of transition, discontinuous cortex, soft tissue component replacing the medullary cavity, or extension beyond the margin of the bone)- Identify several frequently encountered benign osseous lesions that resemble metastasis- Establish an appropriate imaging algorithm to further characterize osseous lesions in these patients

#### **TABLE OF CONTENTS/OUTLINE**

- Introduction: imaging features of osseous lesions with special emphasis on features suggestive of malignancy- Pictorial review of several commonly encountered benign osseous lesions that resemble metastasis in oncologic patients- Imaging algorithm to further characterize osseous lesions

### **CHEE-104 Read Like A Pro: Tips and Tricks to Interpret Like a Cardiothoracic Radiologist**

**Awards**

**Certificate of Merit**

Participants

Melissa Carroll, MD, Kansas City, KS (*Presenter*) Nothing to Disclose

#### **TEACHING POINTS**

1. Misconceptions in chest imaging may lead to excessive imaging, missed diagnoses, or inappropriate therapies, such as missed detection of malignancy manifesting as cyst associated lung cancer. Other misconceptions may lead to unnecessary follow up of nodules identified on incomplete thoracic exams. 2. Knowledge of these misconceptions may lower costs, increase accuracy, and improve patient outcomes.

## TABLE OF CONTENTS/OUTLINE

1. Background  
2. Malignancy  
a. Lung cancer manifesting as cyst associated malignancy, persistent consolidation and subsolid nodule  
b. Incidental nodule on incomplete chest CT  
c. Intrapulmonary lymph node  
3. Diffuse Lung Disease  
a. Reverse halo sign with pulmonary infarct  
b. DIPNECH as underdiagnosed disease  
c. Patchy tree-in-bud opacities from infectious or aspiration bronchiolitis  
d. Differentiating airspace enlargement with fibrosis from honeycombing  
e. Dendriiform pulmonary ossification due to pulmonary fibrosis or aspiration  
4. Mediastinum  
a. Pericardial recesses misinterpreted as lymphadenopathy  
b. Distinguishing normal thymus from mass  
5. Vasculature  
a. Flow-related artifacts mimicking pulmonary embolism or dissection  
b. Diffuse tree-in-bud opacities with excipient lung disease  
c. Beaded vasculature with endovascular metastases  
6. Pleura/Chest Wall  
a. Extrapleural fat deposition mimicking cardiomegaly or pleural effusion  
b. Elastofibroma mimicking chest wall mass  
7. Conclusion

## CHEE-105 Unraveling the maze - Patterns of lung cancer lymphatic dissemination

Participants

Marcus Vinicius Silva Ferreira, MD, Sao Paulo, Brazil (*Presenter*) Nothing to Disclose

### TEACHING POINTS

This exhibition aims to review: • Anatomy of the lymphatic drainage of the lungs and mediastinal node stations. • Multimodality imaging staging of lung cancer, with focus on lymph node (LN) status and its importance to the appropriate lung cancer management. • Indications and impact of different types of lymphadenectomy: selective versus systematic node dissection. • A practical approach to lobe-specific nodal spread of lung cancer with imaging correlations.

## TABLE OF CONTENTS/OUTLINE

1. BACKGROUND  
1.1. Lung cancer overview  
2. 8TH LUNG CANCER STAGE CLASSIFICATION  
3. LYMPH NODE EVALUATION  
3.1. Invasive and non-invasive approach to mediastinal nodal evaluation  
3.2. Imaging characteristics of suspicious nodes  
4. LYMPHATIC ANATOMY  
4.1. Lungs and bronchial tree  
4.2. Mediastinal Lymph nodes stations  
5. LOBE-SPECIFIC PATTERNS OF LYMPHATIC SPREAD  
5.1. Right upper lobe  
5.2. Right middle lobe  
5.3. Right Lower Lobe  
5.4. Left Upper Lobe / Lingula  
5.5. Left Lower Lobe  
6. IS IT FEASIBLE TO ADOPT A SELECTIVE APPROACH? EVIDENCE SO FAR  
7. NOVEL IMAGING TECHNIQUES AND FUTURE DIRECTIONS  
8. TAKE-HOME MESSAGES

## CHEE-106 Basics of Lung Cancer Related to Cysts and Enlarged Cystic Air-spaces: Survival Guide for General Radiologist

Participants

Laima Tamkeviciute, MD, (*Presenter*) Nothing to Disclose

### TEACHING POINTS

1. Lung cancer can manifest as lung cysts or enlarged airspaces.  
2. This type of lung cancer represents significant number of missed diagnosis.  
3. The main concerning features of lung cysts and enlarged cystic air-spaces include: wall thickening or nodules, adjacent ground glass changes, multilocular cysts, increase in size or change of internal structure overtime.  
4. Knowledge of the various imaging presentations of lung cancer is essential for timely diagnosis and treatment thus preventing development of invasive disease.

## TABLE OF CONTENTS/OUTLINE

I. Introduction: 1. Why do we have to raise awareness about lung cysts and enlarged cystic air-spaces? 2. What is the mechanism and pathogenesis of lung cysts and enlarged cystic air-spaces? II. Imaging findings 1. How lung cysts and enlarged cystic air-spaces should be described? 2. What are the concerning features of lung cysts and enlarged cystic air-spaces? 3. How malignant cysts and enlarged air-spaces can change overtime? III. Conclusion and take home message

## CHEE-109 Ultrasound Guided-Procedures in the Lung - What, When and How

Participants

Ivan Vollmer, MD, Barcelona, Spain (*Presenter*) Nothing to Disclose

### TEACHING POINTS

-To describe the indications for interventional procedures in pulmonary pathology.  
-To review the interventional lung procedures that can be performed with ultrasound guidance.  
-To analyze the advantages and disadvantages of ultrasound guidance.  
-To describe how each procedure is carried out.

## TABLE OF CONTENTS/OUTLINE

The different interventional lung procedures that can be performed with ultrasound guidance will be reviewed:-Lung biopsy-Pneumonia puncture.-Lung abscess drainage.-Intraoperative localization of lung nodules.The specific indications for each lung procedure as well as its advantages of using ultrasound guidance over other techniques such as CT will be covered.Moreover, the technique that should be used in each procedure and the pre and post procedure recommendations will also be addressed.

## CHEE-11 From Gemcitabine, through Checkpoint Inhibitors to CAR T Cell - Evolution of Managing Treatment Related Pneumonitis in Cancer: Beyond Diagnosis

Awards

Certificate of Merit

Participants

Kaustav Bera, MD, Cleveland, OH (*Presenter*) Nothing to Disclose

### TEACHING POINTS

1. Review cancer drugs that are primarily responsible for causing pneumonitis as well as differentiating it from other treatment related findings  
2. Discuss the CT imaging patterns of drug-induced pneumonitis  
3. Discuss potential mimics of drug-induced pneumonitis patterns including cytokine release syndrome in CAR-T cell therapy  
4. Discuss the crucial role of the radiologist in monitoring/management of treatment-related pneumonitis with a focus on established guidelines  
5. Discuss use-cases of common

anti-neoplastic agents causing pneumonitis - from Gemcitabine, through ICI to CAR-T cells

#### TABLE OF CONTENTS/OUTLINE

1. Discuss common anti-neoplastic agents that cause pneumonitis  
2. Enumerate prevalently reported imaging patterns of pneumonitis, along with their typical imaging findings  
3. Discuss other potential complications of anti-cancer therapy (Pleural effusions, Pneumonia, Worsening tumor burden, airway obstruction)  
4. Common mimics of drug-induced pneumonitis (atypical pneumonia, COVID-19, Cytokine release syndrome)  
5. Discuss presenting clinical symptoms and grading system for drug-induced pneumonitis (CTCAE and ASCO)  
6. Management guidelines for drug-induced pneumonitis with special focus on checkpoint inhibitors (ICI), targeted therapy, Antimetabolites (Gemcitabine)  
7. How a Radiologist plays an important role in management  
8. Prognosis and clinical outcome of patients developing drug-induced pneumonitis  
9. Real-world cases showing management and clinical course of drug-induced pneumonitis in cancer therapies from Bleomycin, Gemcitabine to combination ICI and CAR-T cells

#### CHEE-110 Added Diagnostic Value of Portable Dual-energy Chest X-ray in a Non-radiological Reviewing Environment

Participants

Karim Karim, PhD, Waterloo, ON (*Presenter*) Officer, KA Imaging Inc

#### TEACHING POINTS

- Understand Dual-Energy Subtraction (DES) X-ray, the limitations of the old Dual-Exposure DES techniques, and how a Single Exposure portable detector can overcome these limitations.
- Understand the clinical benefits enabled by portable Single Exposure Dual-Energy for small nodules identification, pneumonia, pneumothorax, and finding line and tube tips.
- Learn about the added diagnostic value of dual-energy portable chest X-ray in a non-radiological reviewing environment for both regular and radiology trained clinicians.

#### TABLE OF CONTENTS/OUTLINE

This exhibit teaches the added diagnostic value of dual-energy X-rays (DEX) obtained using a novel portable multilayer detector in a reviewing environment simulating a non-radiological practice. A set of 28 AP images were obtained using a novel portable multilayer DEX detector. A team of five (5) readers was recruited that included two fellowship-trained chest radiologists and the rest non-specialists. The team was provided with the conventional X-ray images first, and subsequently were unblinded to the corresponding DEX images. For both sets of images, the readers were asked to assess the presence of pulmonary nodules > 5 mm, pneumothorax, pneumonia (left and right lung), bone fractures, and tips of central and GI lines using a five point scale. Readers were also asked whether the additional DEX images (soft tissue, bone) impacted their confidence. Initial results show that DEX images, taken alongside CR, helped improve diagnostic confidence.

#### CHEE-111 Bronchoscopic Lung Volume Reduction: Pre and Post Procedure Imaging Assessment

Awards

Certificate of Merit

Participants

Daniel Green, MD, (*Presenter*) Nothing to Disclose

#### TEACHING POINTS

1) Bronchosopic lung volume reduction is a non-pharmacologic treatment for severe COPD, 2) Less invasive alternative to lung volume reduction surgery, 3) Goal is complete collapse of the most emphysematous lobe, 4) Imaging is necessary for patient selection, and radiologists have an important role in multidisciplinary discussion, 5) The main role of pre-procedure CT is assessment of emphysema severity, emphysema distribution, and fissure integrity, 6) Sagittal and coronal reconstructions are helpful for fissure integrity, 7) Pneumothorax is the most common complication but does not typically affect clinical outcome

#### TABLE OF CONTENTS/OUTLINE

1) Description of procedure, 2) Patient selection, 3) Chest CT protocol, 4) Pre-procedure imaging assessment, 5) Expected post-procedure imaging findings, 6) Complications, 7) Other bronchosopic lung volume reduction techniques in development

#### CHEE-112 Postoperative Imaging After Surgery for Lung Cancer - From Relatively Common Complications to Rare Complications that Radiologists Need to Know

Participants

Makiko Murota, MD, Kitagun, Japan (*Presenter*) Nothing to Disclose

#### TEACHING POINTS

The purpose of the exhibit is: 1. To review surgical procedures and the postoperative changes for lung cancer. 2. To describe the imaging features of the complications after surgery. 3. To discuss how even rare complications can be radiologically significant.

#### TABLE OF CONTENTS/OUTLINE

1. The surgical procedures for lung cancer  
2. The imaging findings of the normal postoperative changes: CXR and CT  
3. The imaging features and the clinical manifestations of the complications after surgery: relatively common complications and rare complications  
4. Summary

#### CHEE-113 Imaging of Mechanical Circulatory Support Devices For Right Ventricular Failure

Participants

Gregory Jew, MD, Rochester, NY (*Presenter*) Nothing to Disclose

#### TEACHING POINTS

1. Review of options for acute mechanical right ventricular circulatory support including: The TandemHeart centrifugal flow pump (TandemLife, Pittsburgh, PA), the axial-flow Impella RP catheter (Abiomed Inc, Danvers, MA), the Protek Duo dual lumen cannula, and the veno-arterial extracorporeal membrane oxygenation (VA-ECMO).  
1a. Review of right ventricular bypass methods.  
1b. Review

of methods of oxygenation.2. Review of options for durable mechanical right ventricular circulatory support including: The CentriMag pump (St. Jude, Minneapolis, MN) RA-to-PA cannulation as well as commercially available LVADs, including the Jarvik and HeartWare devices.3. Review of common complications of RVADs including access site complications, pulmonary and other complications such as cannula malposition, and abandoned cannula.

#### TABLE OF CONTENTS/OUTLINE

1. Background/Indications for RVADs/RV Bypass and Oxygenation Methods.2. Imaging for percutaneous acute and durable mechanical circulatory support systems: Direct and indirect RV bypass systems: Protek Duo, VA-ECMO, Impella RP.Durable mechanical circulatory support systems: Jarvik, Centrimag.3. Access site complications of RVADs: access site hematoma, access vessel thrombosis, access site infection.4. Pulmonary complications of RVADs: pulmonary edema, organizing pneumonia, ARDS, septic emboli.5. Other complications of RVADs such as a malpositioned cannula, abandoned cannula, distal hemorrhage.

#### CHEE-114 Abnormal Gas on Chest X-Ray: A Primer with CT Correlation

##### Awards

##### Identified for RadioGraphics

Participants

Sameer Singhal, MD, Boston, MA (*Presenter*) Nothing to Disclose

##### TEACHING POINTS

1. Gas collections in the lung tend to be spherical, while gas collections in the pleura tend to be longer in one dimension.2. Pneumopericardium appears as "clean" gas that is bounded by the superior pericardial recess, while pneumomediastinum is "dirty" gas that can track superiorly into the neck.3. It is critically important to scan the upper abdomen for incidental abnormal gas, including pneumatosis and pneumoperitoneum.

#### TABLE OF CONTENTS/OUTLINE

1. Abnormal air in the lungsa. Bullaba. Cavitory consolidation2. Abnormal air in the pleuraa. Pneumothorax, including deep sulcusb. Hydropneumothorax - distinguish from intraparenchymal gas3. Abnormal air in the mediastinum. Pneumopericardiumb. Pneumomediastinumc. Signs: ring-around-the-artery, continuous diaphragmd. Herniae. Post-surgical4. Abnormal air in the abdomena. Pneumoperitoneumb. Pneumobiliac. Portal venous gas and pneumatosis

#### CHEE-115 Pulmonary Manifestations of IgG4 Related Disease

##### Awards

##### Certificate of Merit

Participants

Santiago Restrepo, MD, San Antonio, TX (*Presenter*) Nothing to Disclose

##### TEACHING POINTS

IgG4 is a systemic fibroinflammatory disease characterized by dense infiltration of IgG4 positive plasma cells in the affected tissues with or without elevated plasma levels of IgG4.The inflammatory infiltration can lead to the development of fibrotic tumefactive lesions that may affect any tissue often mimicking a neoplastic process.Thoracic involvement may affect the lung parenchyma, airways, the interstitium, pleura and the mediastinum.Most common manifestation include pulmonary nodules, interstitial lung disease, peribronchovascular infiltration, lymphadenopathy and fibrosing mediastinitis.

#### TABLE OF CONTENTS/OUTLINE

Definition, Pathophysiology, Histopathology, Associated or related conditions, Common clinical phenotypes, Pulmonary disease, Fibrosing mediastinitis, Cardiovascular involvement

#### CHEE-116 Interstitial Lung Disease in Rheumatoid Arthritis

Participants

Elisa Antolinos Macho, MD, Madrid, Spain (*Presenter*) Nothing to Disclose

##### TEACHING POINTS

- To know, identify and become familiar with the typical (and not so typical) radiological patterns of RA in lung involvement.- To suggest an early diagnosis in patients who have not shown any other RA manifestations and be able to offer a sooner treatment in these cases.

#### TABLE OF CONTENTS/OUTLINE

1. Introduction and generalities: rheumatoid arthritis is a multisystemic disease of uncertain etiology, with many factors involved (female sex, genetics, non genetic factors, biologic markers...).2. Extraarticular manifestations (EAM): although the typical manifestation is polyarthropaty, up to half of the patients who has RA, present extraarticular manifestations, more frequently in those who has positive analytic markers. Cardiovascular and respiratory EAM are the most important involvement in mobility and mortality terms.3. Pulmonary manifestations: An important group of the patients who undergoes this disease (60-80%) presents pulmonary involvement in the course of the disease, being interstitial involvement the second most important cause of mortality in these patients (after cardiovascular involvement). These manifestations can precede articular affection up to 15% of the cases, and only in 10% of those, has significant clinical manifestations.4. Review of the typical patterns:- Usual Interstitial Pneumonia (UIP).- Non-Specific Interstitial Pneumonia (NSIP).- Organizing Pneumonia (OP).- Lymphocytic Interstitial Pneumonitis (LIP).5. Summary.

#### CHEE-117 Four-dimensional Angiography of Pulmonary Arteriovenous Malformation: How Do We Detect the Hidden" Last Normal Branch for Endovascular Therapy?

Participants

Shota Yamamoto, MD, PhD, (*Presenter*) Nothing to Disclose

## TEACHING POINTS

Pulmonary arteriovenous malformations (PAVMs) are abnormal direct vascular communications between pulmonary arteries and veins which create high-flow right-to-left shunts. Even when asymptomatic, presence of PAVMs increases patients' risk of substantial morbidity and mortality mainly from the effects of paradoxical emboli. Potential complications include stroke, cerebral abscess, pulmonary hemorrhage and hypoxia. Transcatheter embolization eliminates the abnormal right-to-left-shunting. For more effective embolization, preventing recanalization after PAVMs embolization is the most important. Recently, the Japanese nationwide cohort study has revealed that embolization of the last normal branch was a key factor affected the prevention of recanalization. The last normal branch is generally identified on preoperative multi-detector CT, but the identification rate on the conventional angiography is low (39%). We performed dynamic imaging with Cone-beam CT utilizing two-step dilution and balloon catheter occlusion, which allows for precise assessment of vessel shape and number, the last normal branch and shunting points during the procedure. Its innovative four-dimensional angiography can detect the "hidden" normal last branch and smoothly execute the treatment straight away. This presentation reviews the updated imaging modalities regarding vascular structural understanding and planning the endovascular therapy of PAVMs.

## TABLE OF CONTENTS/OUTLINE

i. Anatomical categories of PAVMs ii. What is the last normal branch of PAVM? Why is it important? iii. Imaging modalities for planning for embolization (4D angiography) iv. Ideal embolization based on anatomical structure

### CHEE-118 Pulmonary Parenchymal Imaging Using Ultra-high Resolution CT - Estimating Lung Vascularity Using Radiologic Lung Weight

Participants

Hiroshi Moriya, MD, Fukushima, Japan (*Presenter*) Advisor, California Capital Equity, LLC; Research Grant, Canon Medical Systems Corporation

## TEACHING POINTS

In UHRCT, the reliability of CT values of small structures is improved by reducing the partial volume effect due to the miniaturization of voxels. In particular, the contrast effect of small vessels with a diameter of 1 mm or less is enhanced. And the entire peripheral lung parenchyma can be displayed by deleting the cardiovascular image. This technique can display blood vessel distribution and contrast effect distribution (Moriya et al, Peripheral Pulmonary Artery Imaging Using Ultra-high Resolution CT - A New Method Of Evaluating Vascularity In The Lung Field CHEE-37 RSNA2021). On the other hand, the contrast effect and vascularity of the lung can be calculated using the radiologic lung density measurement, which is a method of converting the lung weight from the CT value. We present this technique and typical cases.

## TABLE OF CONTENTS/OUTLINE

1. Method: UHRCT (SHR mode: 1024matrix 0.25mm), Workstation used: Ziostation2 (Segmentation of lung parenchyma, each lobe, lung + blood vessels of any thickness) 2. Typical cases Case1 (dynamic contrast CT before lung cancer surgery): Contrast-enhanced phase were well reflected in radiologic lung weight. Peripheral pulmonary vessel involvement was less than 10%. Case2 (Pulmonary artery thromboembolism): Lung vascularity before and after treatment was calculated for each lobe. The therapeutic effect of the thrombus lesion was reflected in the radiologic lung weight. 3. This method can be an easy pulmonary blood flow evaluation method.

### CHEE-119 Step by Step: Radiological Features of Pulmonary Vascular disease Made Simple

Participants

Sofia Gambetta I, MD, MD, Pilar, Argentina (*Presenter*) Nothing to Disclose

## TEACHING POINTS

Identifying pulmonary vascular disease and their causes. Providing methodological guidelines in order to approach the diagnosis of the pathologies that involve pulmonary vascularity. Presenting frequent and uncommon presentation of pulmonary vascular disease. Correlating the radiological features with clinical, histopathological and laboratory findings.

## TABLE OF CONTENTS/OUTLINE

Introduction. Pulmonary vascular disease explained: Pulmonary hypertension, acute and chronic pulmonary thromboembolism, congenital and acquired pulmonary venous return anomalies, diffuse alveolar hemorrhage and vasculitis. Case-based approach with radiologic correlation. Imaging findings with clinical, laboratory and histological correlations. Diagnostic and therapeutic algorithm. Conclusion.

### CHEE-12 Pulmonary Ablation: From Techniques to Complications

Awards

Certificate of Merit

Participants

Jose Maluf, MD, MD, Sao Paulo, Brazil (*Presenter*) Nothing to Disclose

## TEACHING POINTS

- Understand how pulmonary ablation works and its role in thoracic malignancies treatment
- Learn about the different techniques involved in pulmonary ablation
- Recognize expected imaging features of the post ablation zone
- Identify the main complications related to pulmonary ablation

## TABLE OF CONTENTS/OUTLINE

- Introduction - General concepts about pulmonary ablation: o Current context o The procedure o Indications and contraindications o Imaging surveillance
- Different techniques: o Radiofrequency ablation (RFA) o Microwaves ablation (MWA) o Cryoablation o Irreversible electroporation (IEP)
- Post-ablation zone features: What to expect?
- Case based review - Complications related to

pulmonary ablation: o Aseptical Pleuritis o Pneumothorax o Lung Hemorrhage o Aspergilloma o Bronchopleural Fistula o Air embolism o Rib fracture o Other complications • Future perspectives • Conclusions and key takeaways

## **CHEE-120 Vascular Complications of Infections: Beyond COVID-19**

Participants

Babina Gosangi, MD, MPH, New Haven, MA (*Presenter*) Nothing to Disclose

### **TEACHING POINTS**

1. Vascular complications of infection can be divided into thromboembolic disorders and non-thromboembolic disorders. 2. Thromboemboli from infections could be due to endothelial damage, hyperviscosity, embolization of vegetations containing infectious material or embolization of the culprit organism. Such conditions include COVID-19 infection, infectious endocarditis, Lemierre's syndrome and parasitic embolization into the pulmonary arteries (Echinococcus). 3. Vascular infections could also result from contiguous spread of infection from the adjacent organs causing inflammation of the vessels such as infectious aortitis associated with vertebral osteomyelitis, empyema or pneumonia. 4. Infections can damage the vessel wall and cause aneurysm such as Rasmussen's aneurysm or mycotic aneurysm.

### **TABLE OF CONTENTS/OUTLINE**

• Introduction • Pulmonary embolism- COVID-19 infection • Septic infarcts- Infective endocarditis • Internal jugular vein thrombus- Lemierre's syndrome • Infectious aortitis- Tuberculous aortitis, syphilitic aortitis, HIV aortitis, pyogenic aortitis • Mycotic aneurysm • Rasmussen's aneurysm- Tuberculosis • Conclusion

## **CHEE-121 Emboli or Else? Beware the Pitfalls in CTEPH Diagnosis - Chronic Thromboembolic Pulmonary Hypertension Lookalikes in CT Pulmonary Angiography**

Participants

Wagner Diniz de Paula, MD, PhD, Brasilia, Brazil (*Presenter*) Nothing to Disclose

### **TEACHING POINTS**

Recognize the signs of chronic pulmonary emboli and pulmonary hypertension on CT, review the pathophysiology of pulmonary hypertension in CTEPH, and learn clues to identify common and uncommon mimickers of CTEPH on CT.

### **TABLE OF CONTENTS/OUTLINE**

Chronic thromboembolic pulmonary hypertension (CTEPH) results from pulmonary artery obstruction due to non-resolving pulmonary embolism (PE). Among PE survivors, CTEPH is estimated to occur in 1% to 5% of cases. It is a potentially treatable cause of pulmonary arterial hypertension (PAH) and, if left untreated, may progress to right heart failure and death. CT signs of PE, PAH and CTEPH will be reviewed and clues to differential diagnosis will be provided. Some conditions may simulate CTEPH on imaging, encompassing intravascular, extravascular, and vascular (parietal) causes. Intravascular mimickers of CTEPH include pulmonary arterial malignancies (primary intimal sarcoma, metastatic tumoral thrombi) and in situ pulmonary thrombosis due to long-standing PAH (e.g., in cyanogenic congenital heart disease and schistosomiasis). Extravascular causes comprise IgG4-related and granulomatous fibrosing mediastinitis. Vascular abnormalities include congenital anomalies such as proximal interruption of the pulmonary artery and acquired physiological disturbances related to pulmonary hypoxic vasoconstriction.

## **CHEE-122 CT in Acute Pulmonary Embolism: Filling Defects and Beyond**

**Awards**

**Certificate of Merit**

Participants

Kaustav Bera, MD, Cleveland, OH (*Presenter*) Nothing to Disclose

### **TEACHING POINTS**

1. Review the clinical, laboratory and diagnostic work up of patients suspected with acute pulmonary embolism (PE) 2. Discuss the typical and atypical CT appearance of acute PE and its mimics using an algorithmic approach 3. Discuss the important acute and emergent pathology beyond PE, that can mimic acute PE symptoms, visualized on a CT PE study 4. Briefly review additional incidental findings on a CT PE study 5. Illustrate newer advances in CT technology (Dual energy and multi-energy CT) and artificial intelligence methods for improved diagnostic assessment

### **TABLE OF CONTENTS/OUTLINE**

1. When do you suspect an Acute PE - Risk factors, clinical history, symptoms, physical examination, laboratory findings 2. Clinical risk scores to determine whether imaging should be obtained in suspected Acute PE a. Wells score b. Pulmonary Embolism Rule-out criteria (PERC) c. Geneva score 3. Role of Bedside diagnostics in PE (Chest Radiograph, EKG, Ultrasound) and diagnostic signs. 4. Discuss the algorithmic approach to obtain diagnostic imaging in PE 5. Imaging modalities including gold standard and alternatives to evaluate for PE 6. Imaging technique and challenges to obtain a diagnostic CT exam 7. CT imaging in acute PE - primary and ancillary findings 8. Step wise approach to CT interpretation 9. Clinical examples showing conditions mimicking PE on CT imaging - Beyond filling defects a. Acute PE mimicking pathology (Acute aortic pathology, airway obstruction etc.) b. Other Urgent pathology (Pyelonephritis, abscess, arterial bleeds, DVT etc.) c. Incidental findings (Nodules, Nephrolithiasis, Cholelithiasis) 10. Newer imaging techniques for PE diagnosis 11. Future directions including role of Artificial Intelligence

## **CHEE-123 Spectrum of Pulmonary Aspergillosis**

**Awards**

**Certificate of Merit**

Participants

Gerald Hefferman, MD, Somerville, MA (*Presenter*) Nothing to Disclose

### **TEACHING POINTS**

1. The manifestations of pulmonary aspergillosis depend on the host immune state and underlying pulmonary disease. 2. Non-

invasive infections by aspergillus are airway-centered (e.g. APBA, mycetoma), while invasive infections often manifest by destruction of pulmonary vasculature (e.g. angioinvasive aspergillosis).

#### TABLE OF CONTENTS/OUTLINE

1. Allergic bronchopulmonary aspergillosis. High attenuation mucus. 2. Mycetoma. 3. Monod sign. 4. Angioinvasive aspergillosis. Halo sign. 5. Air crescent sign. 6. COVID-19 superinfection. 7. Tracheobronchial aspergillosis. 8. Airway-invasive aspergillosis. 9. Chronic necrotizing aspergillosis

#### CHEE-124 A Radiological Guide to Connective Tissue Disorders associated Interstitial Lung Diseases (CTD-ILDs)

Participants

Aarushi Gupta, MD, MBBS, (Presenter) Nothing to Disclose

#### TEACHING POINTS

- Describe high resolution CT (HRCT) patterns of various Connective Tissue Disorders associated Interstitial Lung Diseases (CTD-ILDs) with representative cases including usual interstitial pneumonia (UIP), non-specific interstitial pneumonia (NSIP), fibrosing organizing pneumonia (OP), lymphocytic interstitial pneumonia (LIP), follicular/obliterative bronchiolitis and other rare entities
- Review common radiological signs used for diagnosis of CTD-ILDs including exuberant honeycombing, anterior upper lobe and straight edge sign
- Brief overview of new concepts like Interstitial Pneumonia with Autoimmune Features (IPAF) and CTD associated Interstitial Lung abnormalities (CTD-ILAs), their radiological findings and management

#### TABLE OF CONTENTS/OUTLINE

1. Definition, epidemiology and clinical manifestations of CTD-ILDs 2. Radiological signs and patterns suggestive of CTD-ILDs on HRCT chest 3. Specific Imaging patterns seen in different CTD-ILDs (Rheumatoid arthritis, Systemic Sclerosis, Systemic Lupus Erythematosus, Polymyositis/Dermatomyositis, Sjogren syndrome) with representative cases 4. Overview of IPAF 5. Definition and management of CTD-ILAs 6. Conclusion-highlighting radiological pearls

#### CHEE-125 Pulmonary and Pleuropulmonary Blastomas

Participants

Santiago Restrepo, MD, San Antonio, TX (Presenter) Nothing to Disclose

#### TEACHING POINTS

Blastomas represent a group of primary malignancies with proliferation of immature element that look like fetal lung. They typically have a biphasic composition with malignant mesenchymal and epithelial immature component. Two types: Pleuropulmonary blastoma (PPB) seen in children and Pulmonary Blastoma (PB) seen in adults. PPB is the most common primary lung malignancy in children, and most present in patients less than 6 years old. DICER1 mutation is seen in 66% of patients with PPB. Other DICER1 related tumors are seen in 40% of affected patients. Imaging presentation is misleading and often confused with other entities like CCAM, sequestration, congenital lobar emphysema etc.

#### TABLE OF CONTENTS/OUTLINE

Definition. DICER1 mutation. DICER1 associated tumors. 2015 WHO classification. Histopathology. Pathologic-radiologic correlation. Phenotypes and prognosis. Imaging manifestation. Differential diagnosis

#### CHEE-126 Post CABG Chest Radiography: How to Make the Complicated Uncomplicated

Participants

Justin Little, MD, Winston-Salem, NC (Presenter) Nothing to Disclose

#### TEACHING POINTS

Complications after coronary artery bypass grafting (CABG) are common and can range from simple atelectasis or pleural effusions to misplaced lines and other support apparatus issues, to more serious issues such as a pulmonary edema, mediastinal hematoma, or pneumothorax. Portable chest radiography is the mainstay of initial evaluation. It is fast with low radiation and gives the radiologist information that allows for quick action. Overlapping anatomic structures and support apparatus devices in combination with the limitations of portable radiography makes the diagnosis of CABG complications a radiologist's dreaded dilemma. Being able to quickly identify the most common complications is essential to maintaining efficiency and accuracy and preventing morbidity and mortality in the postoperative state.

#### TABLE OF CONTENTS/OUTLINE

1. Introduction 2. Types of CABG (on-pump, off-pump, minimally invasive) 3. Postoperative CABG complications - Immediate (< 24 hours) v. Subacute (1-7 days) v. Chronic (> 7 days) - Complication Categories: 1. Lines and tubes 2. Parenchymal 3. Mediastinal 4. Soft tissue/musculoskeletal 4. Role of imaging: ICU plain chest radiography 5. How to report a postoperative CABG chest radiograph 6. Correlation with CT imaging for increased understanding 7. Algorithm for "next-step" recommendations for complications 8. Multidisciplinary approach and perspective of CT surgeons about the most clinically useful information from radiology

#### CHEE-127 Thinking Beyond Bronchogenic Carcinoma: A Primer of Rare Pulmonary and Pleural Pathologies

Participants

Ankush Jajodia, MD, MBBS, New Delhi, India (Presenter) Nothing to Disclose

#### TEACHING POINTS

LEARNING OBJECTIVES 1. To give an overview of some uncommon pulmonary and pleural pathologies. 2. To review the spectrum of imaging manifestations of uncommon entities in lung and pleura. 3. To highlight the importance of clinical history, immunohistochemistry and histopathology in arriving at the correct diagnosis. BACKGROUND: Due to their overlapping imaging appearance, imaging-based diagnosis of many rare neoplastic and non-neoplastic conditions affecting the lung and pleura can be challenging. Being familiar with some of the rare and unusual entities, along with relevant clinical history, can aid a radiologist in narrowing down the differential diagnosis. Thinking outside the box and looking for certain potential distinguishing features may help in making an early and accurate diagnosis. Key imaging features on CT and MRI for uncommon pulmonary and pleural pathologies will

be reviewed in this educational exhibit. These include spindle cell sarcoma of the lung, sclerosing pulmonary hemangioma, sclerosing pneumocytoma, pulmonary paraganglioma, pleural hemangioma, malignant peripheral nerve sheath tumor of the pleura and pleural epithelioid hemangioendothelioma. **CONCLUSION:** A wide range of pulmonary and pleural conditions exhibit imaging features that are similar to more common pathologies such as bronchogenic carcinoma and pleural metastasis. Awareness of additional less common conditions, as well as an understanding of their pathologic background, will aid in accurate diagnosis.

#### TABLE OF CONTENTS/OUTLINE

Pictorial depiction of rare cases

#### CHEE-128 Typical and Atypical Diseases involving the Pleura Radiologic-Pathologic Correlation

Participants

Patricia De Groot, MD, Houston, TX (*Presenter*) Nothing to Disclose

#### TEACHING POINTS

Primary benign lesions of the pleura are much less common than malignant diseases of the pleura. Distinguishing benign from malignant pleural diseases affects prognosis, treatment and outcomes. CT features suggesting malignancy are circumferential pleural thickening; nodular pleural thickening; parietal pleural thickening >1 cm; mediastinal pleural involvement. Malignant primary mesothelioma (MPM) is the most common primary malignancy of the pleura. However, pleural metastases are much more common than primary pleural tumors. The most common primaries metastasizing to pleura include lung, breast and GI carcinomas, particularly adenocarcinomas, and lymphoma. Some pleural tumors may manifest focally or be diffuse. Age, sex and clinical history play a part in both radiologic and pathologic diagnosis. We review helpful imaging findings in the differential diagnosis of pleural diseases and illustrate radiologic-pathologic correlation of benign and malignant pleural lesions.

#### TABLE OF CONTENTS/OUTLINE

Benign vs Malignant: Benign includes solitary fibrous tumor, lipoma, schwannoma, endometriosis, pleuritis. Primary malignant includes MPM, solitary fibrous tumor, liposarcoma, PNET, synovial sarcoma, vascular sarcoma. Secondary malignant includes metastatic disease from lung cancer, lymphoma, plasmacytoma. Focal versus Diffuse: Typical focal includes metastatic disease, solitary fibrous tumor, schwannoma, thymoma, lipoma. Atypical focal includes PNET, synovial sarcoma, liposarcoma, meningioma, endometriosis. Typical diffuse includes metastatic disease, MPM, fibrothorax, thymoma. Atypical diffuse includes lymphoma, synovial sarcoma, epithelioid hemangioendothelioma.

#### CHEE-13 Lung Ultrasound - Ugly Duckling into Swan: A Case-based Approach Demonstrating the Effectiveness of This Method in the Evaluation of Several Pediatric Lung and Pleural Pathologies

Participants

Marcos Brotto, , Brazil (*Presenter*) Nothing to Disclose

#### TEACHING POINTS

During the pandemic caused by the SARS-CoV-2, lung ultrasound (US) has become a promising diagnostic method at the bedside mostly due to its fundamental role in patients who develop infection with severe acute respiratory syndrome. Since then, many studies have proven its value, especially in the pediatric age group. The high demand caused by the viral pneumonia pandemic intensified its use and consequently expanded its applicability in several situations, including pathologies accidentally detected, showing the high accuracy of the method. In addition, lung US provides dynamic data, feature that only ultrasound allows when compared to other imaging methods. For many reasons the pediatric population benefits a great deal from the use of US as a first line method, including the assessment of thoracic and pleural pathologies. US may also provide useful information that eliminates the need for more invasive or expensive studies, especially in cases with mild clinical changes.

#### TABLE OF CONTENTS/OUTLINE

The intention of this presentation is to demonstrate, through a series of cases, the extensive scope of ultrasound in the evaluation of the pediatric thorax. Demonstrate the main ultrasound findings in several parenchymal and pleural pathologies such as pneumonia, abscess, pleural effusion, empyema, among others, proving that the US can be used in the serial evaluation of these conditions. Discuss US radiological findings and their correlations with chest radiograph and chest tomography, and how sonographers can reproduce them adequately in many cases.

#### CHEE-14 Uncommon Non-thromboembolic Conditions Affecting the Pulmonary Vasculature - Beyond Thromboembolism

##### Awards

##### Certificate of Merit

Participants

Helena Peris, MD, Sabadell, Spain (*Presenter*) Nothing to Disclose

#### TEACHING POINTS

- To review uncommon non-thromboembolic entities that change the morphology or density of the pulmonary arteries on CT or PET/CT.- To describe imaging features of rare conditions that mimic pulmonary thromboembolism and/or bronchial pathology or cause pulmonary hypertension.

#### TABLE OF CONTENTS/OUTLINE

I. Background: Some uncommon conditions unrelated to thromboembolism can affect the pulmonary arteries, changing the imaging appearance of vessels in the proximal and/or distal pulmonary vasculature. These entities show key CT or PET-CT findings; their knowledge allows us to make the proper diagnosis. II. Content: We classify the entities into four categories: - Neoplastic (benign or malignant): pulmonary artery sarcoma, intravascular metastases, pulmonary tumor thrombotic microangiopathy, and intravascular leiomyomatosis. - Inflammatory: vasculitis (Takayasu arteritis and Behçet's disease), thrombosis in situ. - Iatrogenic: embolization of non-biologic material or gas during invasive procedures such as vertebroplasty, embolization, or colonoscopy and 18 FDG embolism in a PET/CT. - Miscellaneous: expiratory lung disease and pulmonary artery sheath hematoma, as a complication of acute aortic dissection. III. Conclusions: Detailed observation of the proximal and distal pulmonary arteries can provide diagnostic clues to unusual

conditions causing pulmonary hypertension, simulating pulmonary thromboembolism or bronchial pathology.

### **CHEE-15 How Radiologists Can Help Surgeons on the Planning of a Lung Segmentectomy - Significant Pulmonary Veins Variations**

Participants

Vitor Bichuette, MD, Uberaba, Brazil (*Presenter*) Nothing to Disclose

#### **TEACHING POINTS**

To review pulmonary venous anatomy and the most common pattern of drainage. How a segmentectomy is performed, focusing on techniques to identify the intersegmental plane and the role of the pulmonary veins during the procedure. To explain anatomical variations of pulmonary veins, its significance in lung segmentectomies and how to identify them using computed tomography (CT). To present intraoperative complications related to pulmonary veins anomalies. Applications of CT with 3D reconstructions to reduce the risk of complications during the surgical procedure.

#### **TABLE OF CONTENTS/OUTLINE**

Introduction - General concepts of pulmonary venous anatomy Typical pattern of pulmonary venous drainage The use of CT to identify anatomical variations Lung segmentectomy's technique: • A step-by-step explanation of how to perform a lung segmentectomy. • Pitfalls and some anatomical variations to know during the surgical procedure. • The use of technologies to avoid intraoperative complications Case-Based Review: Sample cases explaining and demonstrating anatomical variations of the pulmonary veins and how CT can be used to identify and prevent intraoperative complications. This section will present illustrative cases of each: Separate veins draining the middle lobe Middle lobe vein emptying into the left atrium Direct drainage from segment 6R Vein draining the right superior lobe running posteriorly to the intermediate bronchus Lingular drainage emptying into the left inferior pulmonary vein Long common trunk of left pulmonary veins Future Directions: the role of CT with 3D reconstructions and 3D printing in lung segmentectomy planning Conclusion and key takeaways.

### **CHEE-16 Chronic Fibrous Interstitial Lung Diseases (CFILD) - Exploring Acute and Chronic Complications through an Imaging-based Approach**

Participants

Alan Hummel, Sao Paulo, Brazil (*Presenter*) Nothing to Disclose

#### **TEACHING POINTS**

The purpose of this exhibit is to: 1. Analyze the major complications of chronic interstitial lung disease, demonstrating both acute and chronic complications through didactic cases; 2. Discuss how an imaging-based approach can be used to differentiate between acute and chronic complications; 3. Distinguish between exacerbations and decompensations in chronic interstitial lung diseases, emphasizing the role of imaging in both characterization and etiologic investigation.

#### **TABLE OF CONTENTS/OUTLINE**

1.0. Chronic fibrosing interstitial pneumonia 1.1. Basic evaluation algorithm (CDEF mnemonic) 1.2. Imaging technical considerations 2.0 Acute and chronic complications (the basics to memorize - with mnemonics) 3.0 Acute complications 3.1. Decompensation vs exacerbation 3.2. Exacerbation 3.2.1. idiopathic 3.2.2. surgical procedures 3.2.3. infectious trigger 3.3. Acute decompensation 3.3.1. pneumomediastinum 3.3.2. pneumothorax 3.3.3. Pulmonary thromboembolism 3.3.4. infections 3.3.5. Aspiration 3.3.6. hydrostatic edema 4.0 chronic complications 4.1. aspergilloma 4.2. tuberculosis 4.3. Pulmonary hypertension 4.4. pulmonary ossification 4.5. neoplasms 5.0. Summary 6.0 References

### **CHEE-17 Fistulas of the Chest - An Unexpected Journey**

Participants

Kristie Yang, MD, (*Presenter*) Nothing to Disclose

#### **TEACHING POINTS**

This education exhibit will: 1) Review the types of fistulas that can occur within the chest, 2) Identify clinical and radiologic features of fistulas within the chest, and 3) Review complications and management of such fistulas.

#### **TABLE OF CONTENTS/OUTLINE**

1. Introduction 2. Etiologies of various fistulas within the chest 3. Clinical history and symptoms 4. Imaging features of a. Bronchopleural fistulas b. Esophageal-pleural fistulas c. Gastropleural fistulas d. Pancreaticopleural fistulas e. Vascular fistulas 5. Complications and management of fistulas 6. Summary and conclusion

### **CHEE-18 Imaging of the Diaphragm: Anatomy, Variations, and Pathologic Conditions**

Participants

Furkan Ufuk, MD, Denizli, Turkey (*Presenter*) Nothing to Disclose

#### **TEACHING POINTS**

? To review the radiological anatomy and function of the diaphragm. ? To review the anatomic variations of the diaphragm. ? To review the multimodality imaging findings in primary or secondary pathologic conditions of the diaphragm

#### **TABLE OF CONTENTS/OUTLINE**

1. Anatomy and function of the diaphragm: The diaphragm is the most important respiratory muscle and is the muscle structure that separates the abdominal and thoracic cavities. 2. Anatomic Variations: Common anatomic variations of the diaphragm include diaphragmatic slip, bundles (nodular crura), the extension of diaphragmatic muscle fibres onto the m. quadratus lumborum, and prominent or hypertrophic median and lateral arcuate ligaments. 3. Pathologic conditions of the diaphragm: A) Primary pathological conditions of the diaphragm: That includes eventration, diaphragmatic herniation, diaphragmatic injuries, diaphragmatic tumors and tumor-like lesions. B) Secondary pathological conditions of the diaphragm: That includes diaphragmatic paralysis, diaphragmatic weakness due to neuromuscular disorders or prolonged mechanical ventilation, and tumors that invade the diaphragm.



pulmonary amyloidosis, Erdheim Chester disease, Niemann- Picks disease), malignancies (lymphoma, leukemia, Kaposi's sarcoma), congenital (congenital lymphangiectasia, diffuse pulmonary lymphangiomatosis, Yellow nail syndrome), iatrogenic (cytotoxic agents, radiation, lipoid pneumonia, silicone injection, EVALI/Vaping). Clues to differentiating the interlobular septal thickening based on type, distribution and other associated pulmonary and extrapulmonary findings will be reviewed.

## **CHEE-22 Ex Vivo Lung Perfusion (EVLP) and the Radiologist's Role**

Participants

Zhao Zhang, DO, (*Presenter*) Nothing to Disclose

### **TEACHING POINTS**

1. EVLP is an advanced preservation tool for lung transplantation and has expanded the donor pool by perfusing the lungs ex vivo allowing for longer preservation time. 2. Radiologists may participate in the EVLP team to evaluate lung radiographs during EVLP. 3. Diagnostic tests and treatments can be performed on the lungs to optimize the quality of the transplant organ. 4. Radiologists may have an increasingly important role in the future of EVLP as more transplant centers adopt this strategy of lung preservation and distribution.

### **TABLE OF CONTENTS/OUTLINE**

1. Overview, Background, Terminology 2. Donor lung evaluation prior to EVLP 3. Radiologist's role in EVLP with case examples a. Radiographic donor screening for masses, infection, contusion. b. Discuss potential radiographic exclusion criteria. c. Assessment of radiographic changes of the post perfusion lungs; correlating with other diagnostic tests d. Correctly identify complications (atelectasis vs pulmonary edema) e. Discuss how EVLP may impact radiologist training 4. Conclusion

## **CHEE-23 A Practical Approach to Diaphragmatic Ultrasound: From Tricks to Tips**

Participants

Niels Vinicius Padua Carvalho, MD, Sao Paulo, Brazil (*Presenter*) Nothing to Disclose

### **TEACHING POINTS**

The aim of this exhibition is to review 1. Multimodality anatomic imaging of diaphragm, focusing on ultrasonography (US) 2. Technical and clinical aspects of diaphragmatic US, including a proposal for structured reporting 3. Tips and tricks to evaluate diaphragm function (mobility) and trophism (diaphragm thickness and thickness fraction) 4. Pathologic conditions detected through diaphragmatic US

### **TABLE OF CONTENTS/OUTLINE**

1. INTRODUCTION a. Anatomy of diaphragm with multimodality imaging b. Anatomic versus functional imaging 2. DIAPHRAGM US: TECHNICAL ASPECTS a. Probes, positioning and acoustic windows b. US modalities: B and M modes c. Step-by-step approach (videos and images) 3. DIAPHRAGM US: CLINICAL ASPECTS a. Diaphragm paralysis b. Critically ill patients on mechanical ventilation c. Other respiratory diseases, including asthma, chronic obstructive pulmonary disease, cystic fibrosis, interstitial lung disease and COVID-19 d. Neuromuscular disorder e. Pediatric patients 4. DIAPHRAGM US: A PRACTICAL APPROACH a. Tricks and tips b. Multimodality imaging correlations c. Structured reporting 5. DIAPHRAGM US IN THE REAL WORLD a. Challenges and limitations of diaphragm US 6. FUTURE DIRECTIONS AND TAKE HOME MESSAGES

## **CHEE-24 Spectral CT in Cardiothoracic Imaging: Potential Applications that Radiologists Should Know**

**Awards**

**Cum Laude**

Participants

Flavio Zuccarino, MD, Barcelona, Spain (*Presenter*) Nothing to Disclose

### **TEACHING POINTS**

To analyze spectral CT feasibility in cardiac and thoracic pathologies. To underline its advantages and limitations compared to conventional CT. To define the clinical scenarios in which spectral CT findings are key in patient's management.

### **TABLE OF CONTENTS/OUTLINE**

We make a short introduction about spectral CT imaging techniques. We focus on Spectral GSI CT imaging that we used in the different cases of this exhibit. We describe Spectral CT findings in different cardiac and thoracic pathologies organized as: Vascular diseases Acute Pulmonary embolism Chronic Pulmonary embolism Hemoptysis Congenital vascular diseases (Sequestration, MAV, others) Lung diseases Consolidations (pneumonia, atelectasis, infarcts, organizing processes) Interstitial diseases (fibrosis, emphysema, post-covid, mosaic perfusion) Neoplasm (Lung neoplasm, mediastinal neoplasm and masses) Cardiac Diseases Acute Myocardial Infarct, Myocarditis, Myocardial masses OUTLINE Spectral CT imaging is a relatively new technique which presents several advantages and may give functional data about different cardiac and thoracic diseases. Radiologists should be familiar with this technique that can play a pivotal role in patient management.

## **CHEE-25 Don't Touch the Animals: Chest Radiologists View- Zoonoses**

**Awards**

**Certificate of Merit**

**Identified for RadioGraphics**

Participants

Hannah Hodges, MD, Albuquerque, NM (*Presenter*) Nothing to Disclose

### **TEACHING POINTS**

Teaching points: 1. Identify zoonotic organisms and their animal vectors to which humans are susceptible. 2. Understand the cardiothoracic symptoms and clinical findings of infection. 3. Recognize the multimodality radiologic appearances of these diseases. 4. Learn laboratory and other testing that confirms the diagnosis.

## TABLE OF CONTENTS/OUTLINE

Content Organization:1- Introductiona Organisms and animal vectors2- Cardiothoracic findings of Zoonosesa. Tularemiab. Plaguec. Anthraxd. Leptospirosise. Monkeypoxf. Hantavirusg. Echinococcus3- Radiologic assessmenta. Identifying features, morphology, and distributionb. Multimodality radiologic appearances4- Pitfallsa. Potential mimics 5- Summary

### CHEE-26 Pitfalls in Thymic Imaging

#### Awards

Identified for RadioGraphics

Certificate of Merit

Participants

Maximiliano Klug, MD, Ramat Gan, Israel (*Presenter*) Nothing to Disclose

#### TEACHING POINTS

1- Thymic hyperplasia, thymic cysts and thymoma may be difficult to distinguish by CT imaging alone. MRI of the mediastinum helps in the differential diagnosis. 2- Chemical shift sequences can differentiate thymic hyperplasia from thymoma. Correct use of the Chemical-Shift-Ratio identifies cases of hyperplasia when the characteristic signal drop is not identified. Small lesions may not be measurable due to inaccurate ROI placement and calculation. DWI in small lesions may be challenging as well. 3- Thymic cysts are typically hyperintense on T2-weighted images (T2WI). Pitfalls in identifying cyst on T2WI include intermediate T2WI signal of some cysts due to proteinaceous content and pseudo-nodules due to cardiac motion. Careful inspection of T1 weighted images with and without intravenous contrast may overcome these limitations. 4- Newer thymic MRI protocols including delayed phases are important to distinguish malignant from benign thymic lesions. Nevertheless, longer MRI studies may be prone to additional artifacts due to breathing. Breathing correction and subtraction imaging may help. 5- Thymoma pleural metastases can be missed leading to erroneous staging. Typical overlooked locations are adjacent to atelectatic lung or the crux of the diaphragm.

## TABLE OF CONTENTS/OUTLINE

1- To describe thymic imaging techniques and radiologic appearance of thymic entities. 2- To discuss pitfalls in interpretation and possible imaging solutions. 3- To discuss blind-spots in thymoma pleural metastatic disease.

### CHEE-27 Unfamiliar Thoracic Anatomy: You Only Know What You Know

Participants

Mohamed Elboraey, MD, (*Presenter*) Nothing to Disclose

#### TEACHING POINTS

- Understanding of thoracic anatomy is essential for accurate interpretation of thoracic imaging.- Some unfamiliar/less frequently encountered thoracic anatomic and variant structures can simulate pathology.- Prospectively differentiating these structures from true pathology will prevent overcalling pathologic processes and unnecessary downstream investigations.

## TABLE OF CONTENTS/OUTLINE

- Review anatomic structures at CXR, CT, and MRI:a. Vasculature (inferior pulmonary vein confluence with left atrium; L SVC, cardiophrenic veins, azygos vein).b. Hilar anatomy (inferior pulmonary ligament vs sublobar septum).c. Pulmonary fissures (accessory or incomplete fissures, fissural lymph nodes).d. Pericardium (pericardial recesses simulating lymphadenopathy or mediastinal masses; mediastinal vs epicardial fat).e. Lymph nodes (unnamed stations, left supraclavicular lymph node vs vein confluence, extrapleural space nodes).f. Chest wall (axillary/breast variants, muscular arches).- Emphasize how radiologists can differentiate these entities from true pathology by imaging evaluation with case examples.

### CHEE-28 Going with the Flow: Understanding Flow Artifacts

#### Awards

Identified for RadioGraphics

Magna Cum Laude

Participants

Caroline Robb, MD, (*Presenter*) Nothing to Disclose

#### TEACHING POINTS

- Flow artifacts are commonly encountered in contrast-enhanced CT imaging studies and may be mistaken for important pathologic conditions, such as embolism or dissection.
- Radiologists must be familiar with the appearance of flow artifacts and comfortable distinguishing these artifacts from true pathologic conditions.
- By understanding the mechanics of flow artifacts, radiologists can better recognize the clinical settings that predispose to flow artifacts, such as pneumonia or altered cardiac output.
- Radiologists must know how to troubleshoot a suspected flow artifact, including how to adjust imaging protocols, when to recommend additional imaging studies, and which additional imaging studies are most helpful.
- Flow artifacts can be used as a tool when the radiologist encounters vascular pathology, such as when evaluating aortic dissection flaps.

## TABLE OF CONTENTS/OUTLINE

- Discuss the physical mechanics of vascular blood flow and how these mechanics can give rise to flow artifacts.
- Review how to distinguish flow artifact from true pathologic conditions, such as pulmonary embolism or aortic dissection.
- Examine the causes of flow artifacts and how these artifacts may present in various clinical settings, such as pneumonia or altered cardiac output.
- Discuss how to troubleshoot suspected flow artifact, including the utility of delayed image acquisition and MRI.
- Evaluate how flow artifacts can be used as a diagnostic tool, such as when assessing aortic dissection flaps.

### CHEE-29 Pericardial Recesses on Multidetector CT: Beyond Tips and Tricks Around the Heart

Participants

Alex Carvalho Monteiro, (*Presenter*) Nothing to Disclose

#### TEACHING POINTS

The purpose of this exhibition is: • Review common and uncommon cases related to the pericardial sinuses and recesses. • Correlate important findings with the anatomy of pericardial recesses. • Discuss imaging findings according to the classification of pericardial recesses to enhance radiologists' skills. • Highlight their characteristics for radiologists with these conditions, avoiding unfavorable patient outcome. • Despite its characteristic density, describe the importance of distinguishing them from pathologic process, as mediastinal lymphadenopathy, and mediastinal cystic mass. • Correlate with the impact on the onco-image.

#### TABLE OF CONTENTS/OUTLINE

• Applied anatomy of the pericardial recesses: superior pericardial recess, right lung recess, left lung recess, postcaval recess, right pulmonary venous recess, superior pericardial recess, transverse sinus, left pulmonary venous recess and oblique sinus. • Evaluation of cases of prominent recesses with variable extensions, which may be possible confounding mechanisms. • Examples of pearl cases, diagnostic difficulties, and mimicry. • Summary and take-home messages.

#### CHEE-30 **Developments in Lung Cancer - What Radiologists Should Know About the WHO Classification Updates and Developments in Molecular Biology Research**

##### Awards

Identified for RadioGraphics

Cum Laude

Participants

Tomoaki Sasaki, MD, (*Presenter*) Nothing to Disclose

#### TEACHING POINTS

Lung cancer is the leading cause of cancer death worldwide, and determination of the histological type is essential for management. Surgical resection is performed in the early stage, and the surgical specimen allows radiological-pathological investigation. In 2021, the WHO classification of thoracic tumors was updated. These revisions deal with lung cancer prognosis and recognize several new entities. Unfortunately, about 70% of lung cancers are unresectable when diagnosed. Histological diagnosis must therefore rely on molecular analysis of a small biopsy tissue. Accurate knowledge regarding the molecular biology and immunohistopathology of lung cancers has thus become crucial. Radiological imaging plays an important role in the management of both early and advanced stage lung cancers. Therefore, radiologists must be familiar with all updates made to the WHO classification and molecular biology. The aim of this presentation is 1) to understand the radiological-pathological correlations in surgical specimens according to the new WHO classification, 2) to update our knowledge of lung cancer molecular biology, and 3) to acknowledge the limitations of small biopsy samples.

#### TABLE OF CONTENTS/OUTLINE

1. Introduction: Revision of the WHO classification  
2. Radiological-Pathological correlations from surgical specimens: Adenocarcinomas, Squamous cell carcinomas, Sarcomatoid carcinomas, Neuroendocrine carcinomas, Salivary gland-type tumors, etc.  
3. Molecular biology: EGFR, ALK, ROS1, HER2, RET, BRAF V600F, KRAS, NTRK, METamp, NRG1 fusion, PD-L1, etc.  
4. Limitations of small biopsy samples  
5. Conclusion

#### CHEE-31 **MRI of Anterior Mediastinal Masses: When to Image and Approach to Interpretation**

Participants

Tetsuro Araki, MD, PhD, Philadelphia, PA (*Presenter*) Nothing to Disclose

#### TEACHING POINTS

1. To understand appropriate settings to recommend MRI for the evaluation of anterior mediastinal masses (AMM). 2. To understand the main roles of MRI in characterization of AMM. 3. To understand key features for the differential diagnoses of AMM.

#### TABLE OF CONTENTS/OUTLINE

1. Indication of MRI for AMM  
a. Incidentally found AMM on CT or chest radiograph  
b. Preoperative characterization and staging of AMM  
c. Screening for associated findings of AMM (lymph nodes or pleural lesions)  
d. MRI protocols for AMM  
e. Alternative imaging options to MRI.  
2. Main roles of MRI in characterization of AMM  
a. Cystic vs solid  
b. Benign vs malignant (Normal/hyperplastic thymus vs neoplasm)  
c. Risk stratification or staging  
3. Key MRI features for the differentiation of AMM  
a. T1 and T2 signal intensity  
b. Enhancement on post contrast images  
c. Demonstration of microscopic fat on out of phase T1-weighted images  
d. Diffusion weighted images/ADC map  
4. Case review of AMM  
a. Normal/hyperplastic thymus (fat saturated or non-saturated thymic hyperplasia)  
b. Thymic cyst/bronchogenic cyst  
c. Ectopic thyroid tissue/retrosternal thyroid goiter  
d. Thymic epithelial tumors (thymoma, thymic carcinoma, neuroendocrine tumors)  
e. Primary mediastinal large B-cell lymphoma (PMBCL)  
f. Thymolipoma/lipoma  
g. Metastasis  
5. Summary

#### CHEE-32 **Pitfalls and Tricks of Variants in Thoracic Imaging: Who Wants To Be... Normal?**

Participants

Mariana Peleja, MD, Sao Paulo, Brazil (*Presenter*) Nothing to Disclose

#### TEACHING POINTS

The purpose of this exhibit is:- To play an adapted game show ("Who wants to be a millionaire") related to normal variants in thoracic imaging.- To illustrate normal variants in thoracic imaging.- To differentiate between normal and pathological cases in CT and MRI imaging.- To demonstrate cases of physiological uptake on PET/CT.- To go through several typical and atypical findings in thoracic imaging to facilitate radiological understanding and diagnosis.

#### TABLE OF CONTENTS/OUTLINE

- Interactive game show.- Interactive cases related to normal variants in thoracic imaging.- Reporting language for imaging findings related to the variants in thoracic imaging.- Review of imaging findings according to illustrative cases of: 1. Chest wall; 2. Diaphragm; 3. Pleura; 4. Lungs; 5. Mediastinum: heart, great vessels, airways, esophagus, thymus, neural and lymphatic structures;- Summary and gained knowledge.

#### CHEE-33 **Photon-Counting CT in Chest Applications**

## Awards

### Certificate of Merit

Participants

Fides Schwartz, MD, Durham, NC (*Presenter*) Nothing to Disclose

### TEACHING POINTS

Photon-counting computed tomography (PCCT) is a new technology in CT imaging. PCCT uses energy-resolving detectors, instead of integrating the entire x-ray signal (energy integrating detectors: EID), enabling spectral acquisitions without the need of specialized acquisition strategies (e.g., dual-source). PCCT records photons in different energy bins, starting at a minimum energy threshold, so electronic noise can be avoided altogether. PCCT detectors used a two-step conversion (x-rays to electrical signal), rather than the 3-step conversion EID (x-rays to light to electrical signal), and inherently have higher spatial resolution as no septa (dead space to separate voxels) are needed. This project is geared toward introducing the emerging technology of PCCT to the RSNA chest imaging community. The details of this technology will be explained using diagrams and examples of standard EID patient scans in comparison to PCCT scans to demonstrate the performance of the new scanner system. These examples will include tumor monitoring, lung cancer screening and contrasted chest CT.

### TABLE OF CONTENTS/OUTLINE

1. PCCT - Detectors a. Comparison of energy-integrating vs photon-counting detectors b. How is higher spatial resolution of PCCT achieved? 2. PCCT - Photon Binning a. How does photon binning work? b. How are energy thresholds defined? c. How do thresholds help with electronic noise? 3. PCCT - Spectral Data a. How is it always available? b. What can it be used for?

### CHEE-34 Wait, You Can See Motion on Chest Radiographs?! Dynamic Digital Radiography (DDR)

Participants

Donald Benson JR, MD, PhD, Little Rock, AR (*Presenter*) Nothing to Disclose

### TEACHING POINTS

1. Dynamic digital radiography (DDR) is a newer technology enabling rapid acquisition of multiple sequential radiographs with field of view and spatial resolution similar to that of conventional radiography. 2. The simultaneous acquisition of detailed anatomical and functional imaging enables identification and evaluation of potential lung nodules, diaphragmatic motion, chest wall motion and restricted lung motion. 3. As a digital acquisition DDR enables computerized mathematical evaluation of lung areas, lung volumes, graphing diaphragmatic motion and potential pulmonary function parameters.

### TABLE OF CONTENTS/OUTLINE

After a brief introduction to this technology, the following potential applications will be discussed: 1. Improved evaluation of potential lung nodules. 2. Evaluation of diaphragm function. 3. Follow up evaluation of post-surgical chest patients. 4. Potential assessment of pulmonary ventilation and perfusion. 5. Comprehensive pre-operative lung transplant evaluation. 6. Correlation of measured lung areas and estimated volumes with pulmonary function testing. 7. Evaluation of diffuse lung disease, e.g., post-COVID patients, and patients with interstitial lung disease, chronic obstructive pulmonary disease, cystic fibrosis, among others.

### CHEE-35 Lung Contrast-enhanced Ultrasound (CEUS): How I Do It

## Awards

### Identified for RadioGraphics

Participants

Sergio Jimenez Serrano, Barcelona, Spain (*Presenter*) Nothing to Disclose

### TEACHING POINTS

The purpose of this educational exhibit is:- To explain how to correctly perform a lung contrast-enhanced ultrasound (CEUS).- To describe the basics of pulmonary vascularization, which are fundamental to interpreting a lung CEUS.- To review the clinical situations in which lung CEUS may be useful in diagnosing and treating pulmonary pathology.

### TABLE OF CONTENTS/OUTLINE

Pulmonary CEUS has experienced a constantly growing in the study of pulmonary pathology. In this educational exhibit we will focus on:- Explaining the exploration technique.- Reviewing the physiopathology of the pulmonary vasculature.- Reviewing the characteristic findings in CEUS in non-tumor entities such as:• Pulmonary atelectasis• Round atelectasis• Pulmonary infarction• Pneumonia• Lung abscess• Radiation pneumonitis- Describing the main findings that can help us differentiate between aggressive and non-aggressive pulmonary neoplasms (with examples).- Radiological findings in CEUS that can help us in the diagnosis of lymphoma or lung metastases.- The importance of CEUS in interventional procedures:• Evaluation of tumor necrosis.• Choice of puncture point.• Differentiate obstructive atelectasis from tumor lesion.• Avoid vascular structures.• Prevent the biopsy of benign lung lesions.

### CHEE-36 Stick To Your Rib - A Radiologist Guide for Rib Cartilage Evaluation before Reconstruction Surgeries

Participants

Felipe A. de Oliveira, MD, Sao Paulo, Brazil (*Presenter*) Nothing to Disclose

### TEACHING POINTS

? Provide an overview of the normal costal arch cartilage anatomy, and how its used as autogenous graft material for cartilage reconstruction surgeries; ? To explain how to evaluate the costal arch cartilages (degree of calcification, and calcification morphological patterns) on X-Ray, US and CT scan; ? Application of Artificial Intelligence assisting CT scan evaluation; ? To exemplify how to report the normal and abnormal crucial findings to the surgeon; ? To introduce the related surgical cartilage reconstructive techniques.

### TABLE OF CONTENTS/OUTLINE

1) Costal arch cartilae overview. A) Anatomy of costal arch cartilae. B) Costal arch cartilae and its adjacent structures

anatomical relations. C) Histology of costal arch cartilage. 2) Costal arch cartilage employment as an autologous donor site for cartilage reconstructions surgeries - pros and cons. 3) Costal arch cartilage calcifications as a complicating factor for surgical outcomes. 4) Imaging evaluation, epidemiology and examples of costal arch cartilage calcifications. A) X-Ray. B) US. C) CT scan. 5) How to report. 6) Rib (costal arch) cartilage harvesting surgical technique. 7) Examples of cartilage reconstructive surgical techniques in which costal arch cartilage is employed. A) Rhinoplasty. B) Microtia otoplasty. C) General face reconstructive surgeries. 8) Take-home messages.

### **CHEE-37 Between the Walls: Understanding the Extrapleural Space and the Extrapleural Fat Sign**

Participants

Guillem Dolz Alvarez De La Ballina, MD, Valldoreix, Spain (*Presenter*) Nothing to Disclose

#### **TEACHING POINTS**

To review the normal anatomy of the extrapleural space (EPS). To describe the extrapleural fat sign (internal displacement of the adipose tissue layer), a clue to locating different conditions in the EPS. To show the many entities that can involve the EPS, emphasizing the role of CT.

#### **TABLE OF CONTENTS/OUTLINE**

Background: The EPS lies between the parietal pleura, the chest wall and diaphragm. It is a poorly understood anatomical compartment which can lead to diagnostic errors. Anatomical scheme. Extrapleural fat can be displaced, enlarged, or affected by: - Blood (extrapleural hematoma): from trauma, iatrogenic lesion of a thoracic vessel, aortic dissection or aneurysm rupture, spontaneous bleeding. - Air (extrapleural emphysema): barotrauma. - Fat: non-pathologic (obesity or estrogens), lipoma, chronic pleural conditions. - Edema/Infection: acute pleural exudates, empyema necessitatis. - Soft tissue: extramedullary hematopoiesis, neurogenic lesions, primary or metastatic pleural tumors, infiltration of lung tumor, chest-wall malignancies. - Calcium: chronic hematoma/empyema, asbestos related pleural disease. Conclusions: The extrapleural fat sign helps differentiate between pleural and extrapleural lesions. Conditions involving the EPS may require different treatment approaches than pleural or lung diseases.

### **CHEE-38 Leukemia and the Thoracic Plethora- Perplexities, Patterns and Problem Solving**

Participants

Shubham Padashetty JR, MD, Mumbai, India (*Presenter*) Nothing to Disclose

#### **TEACHING POINTS**

Leukemia presents with multitude of disease related and various infective and noninfective presentations. Presentations include ground glass opacities, centrilobular nodules, interstitial septal thickening in various patterns. Mediastinal, pleural, nodal and bony involvement also need to be carefully looked for. Disease related manifestations include nodal, parenchymal, mediastinal and bony involvement, biopsy is necessitated in conditions when inflammatory and infective pathology is ruled out. Drugs and infection related injuries require both clinical and radiological approach based addressal with knowledge of specific pattern of presentations. For instance apical predominance with cystic changes are seen in PCP pneumonia, unsharp hazy ground glass changes with confluent centrilobular nodules seen in CMV pneumonia, tree-in-bud pattern in mycobacterial diseases. Non-contrast CT and HRCT thorax are a valuable tool in diagnosis, follow-up, serial correlation of presentations. They also aid in guiding image guided interventions when necessary. This educational exhibit aims to familiarize with various paradigms of presentations, pattern based understanding and clinico-biochemical correlation, henceforth providing apt differentials. Clinical radiology plays a key role in reducing morbidity and mortality in hematolymphoid malignancies when timely approach and diagnosis helps early treatment.

#### **TABLE OF CONTENTS/OUTLINE**

1. Flow chart of pulmonary manifestations in leukemia 2. Disease related manifestations 3. Non infectious pulmonary complications 4. Infections and their patterns of involvement.

### **CHEE-39 Breast Implants in Chest CT: What Can We See?**

**Awards**

**Certificate of Merit**

Participants

Vinicius Nobre, MD, (*Presenter*) Nothing to Disclose

#### **TEACHING POINTS**

The purpose of this exhibit is: To review the components of the most common breast implants and prostheses, as well the main pathological conditions involving them. To emphasize that chest computed tomography (CT), which is widely available and allows rapid image acquisition, can detect incidental findings involving breast implants. To discuss the pathophysiology of breast implant conditions and their imaging findings, especially on CT, correlating them with more specific studies for breast implant evaluation. To offer a didactic case-based review on the theme, proving teaching points and references, in order to allow radiologists to detect abnormalities involving breast implants in CT scans performed for different reasons.

#### **TABLE OF CONTENTS/OUTLINE**

Breast implants and their normal appearance in CT. Intracapsular breast implant rupture: Imaging findings, including signs such as the "keyhole", "subcapsular", "linguine" and "droplet", discontinuity of the elastomer, among others. Degrees of implant collapse: uncollapsed, minimal, partial and full collapse. Extracapsular breast implant rupture: Imaging findings, including extra capsular silicone and siliconomas. Diagnostic difficulties and mimics. Capsular contracture: Image findings. Breast implant rotation: Image findings. Other breast implants complications related to the theme. Summary and take-home messages.

### **CHEE-4 Extracorporeal Membrane Oxygenation [ECMO]: What the hECMO Am I Looking At?**

Participants

Nina L. Terry, MD, JD, Hoover, AL (*Presenter*) Stockholder, Johnson & Johnson; Spouse, Stockholder, Johnson & Johnson; Stockholder, Kimberly-Clark Corporation; Spouse, Stockholder, Kimberly-Clark Corporation; Stockholder, Microsoft Corporation; Spouse, Stockholder, Microsoft Corporation; Spouse, Stockholder, Amgen

## TEACHING POINTS

1. For adults two major ECMO types function to bypass the lungs [veno-venous (VV)] or the heart and lungs [veno-arterial (VA)] with variable catheter types and positions for both. 2. ECMO catheters are imaged with radiographs, echocardiography and CT both incidentally and intentionally. 3. Radiologists should recognize appropriate configuration/positioning of the various types and be aware of potential complications for each. 4. Radiologists need to know the indications for contrast and the indications and contraindications for stopping ECMO or clamping the ECMO catheters to optimize image quality.

## TABLE OF CONTENTS/OUTLINE

- Introduction o Overview of ECMO o Importance to the average radiologist
- Normal catheter placement for ECMO o Venovenous ECMO § Single lumen vs. dual lumen catheters o Venoarterial ECMO § Peripheral vs. central catheterization § Comparing points of entry o Effect of cannula sizing on correct placement (especially emergency settings)
- Comparing imaging modalities used to verify correct catheter placement o Echocardiography o Chest Radiograph [CXR] o Computed Tomography [CT]
- Visualizing complications during/post catheter placement o Contrast CT or Non-contrast CT: Indications o Safety and technical issues in giving contrast to a patient on ECMO
- Special cases to consider o ECMO during COVID-19
- Conclusion o Radiologists have an important role in diagnosis and patient safety with the growing use of ECMO technology

## CHEE-40 "Reduce Fat Fast": A Systematic Approach to Fat-containing Lesions in Adult Thoracic Imaging and Its Differential Diagnosis.

Participants  
Carlos Penaranda, MD, (*Presenter*) Nothing to Disclose

## TEACHING POINTS

1. Approach the differential diagnosis of fat-containing lesions in the chest. 2. Recognize the fat-containing lesions, using radiologic features as Hounsfield Units (HU) measurement at computed tomography (CT), or the signal intensity characteristics of fat at magnetic resonance imaging (MR). 3. Correlate lesion location with the fat imaging characteristics to narrow the differential diagnosis.

## TABLE OF CONTENTS/OUTLINE

1. Imaging characteristics of fat-containing lesions in the thorax employing ultrasound, computed tomography (CT) and magnetic resonance imaging (MR). 2. Schematic approach of various fat-containing lesions and their location in the chest. 3. Sample cases from our institution with their radiographic and epidemiological features.

## CHEE-41 Inhalational Injuries in Burn Patients: Is Chest Radiography Still Relevant?

Participants  
Jaime Fields, MD, Winston Salem, NC (*Presenter*) Nothing to Disclose

## TEACHING POINTS

Pulmonary complications are a common cause of morbidity and mortality in burn patients. It is important that radiologists are familiar with these complications so that early and specific diagnosis is made on chest imaging. While admission radiographs are often normal or underestimate findings, within just a few days pulmonary complications can be severe. While CT is a useful tool, many burn patients do not undergo CT imaging of the chest. Thus it is important for radiologist to be familiar with the radiographic features of these complications and utilize timing after injury as a diagnostic tool.

## TABLE OF CONTENTS/OUTLINE

- Pathophysiology of burns and radiographic correlation (what happens on alveolar level)
- Timeline of pulmonary complications
- Role of radiologist in utilizing this timeline when interpreting chest radiographs
- Algorithm demonstrating management of inhalational injury
- Findings suggestive of acute inhalational injury
- With what frequency should chest radiographs be obtained?
- Chest radiograph and CT correlation of varied imaging findings
- ARDS as a complication of direct alveolar injury or secondary complications
- Phases of ARDS
- Delayed pulmonary complications
- Long term complications: subglottic stenosis, bronchiectasis, bronchiolitis
- Multidisciplinary approach
- Role of imaging in follow up
- Role of other imaging modalities not previously discussed
- Bonus: Vaping associated lung injury chest radiograph and CT correlates

## CHEE-42 Distinguishing Fraternal Twins on Chest Radiograph: Primer for Residents

**Awards**  
**Magna Cum Laude**  
**Identified for RadioGraphics**

Participants  
Kaitlin Gibson, MD, (*Presenter*) Nothing to Disclose

## TEACHING POINTS

- Two distinct pathologies although similar in appearance on chest radiographs have nuanced differences (fraternal twins). Differentiating these may be challenging for residents.
- Accurate differentiation is important as this impacts management strategies.
- Case based review of radiographic "fraternal twins" with tips on differentiating two is presented.
- Example: Large apical bulla is differentiated from pneumothorax by the convex margin of the bulla as compared to the parallel margin to chest wall in pneumothorax.
- Length of air fluid levels is equal on frontal and lateral view in lung abscess and is unequal in empyema.
- Diaphragmatic eventration has preserved sharp posterior costophrenic angle on lateral radiograph whereas flattened in paralysis, etc.

## TABLE OF CONTENTS/OUTLINE

Case examples of fraternal twins with tips on differentiation

1. Pneumothorax / large bulla
2. Pneumothorax / pneumomediastinum
3. Pneumomediastinum / pneumopericardium
4. Lung abscess / empyema
5. Diaphragmatic eventration / paralysis
6. Hilar mass / enlarged pulmonary artery (Hilum convergence sign)
7. Hilar mass / anterior/ posterior mediastinal mass (Hilum overlay sign)
8. Anterior / posterior mediastinal mass (Cervicothoracic and thoracoabdominal signs)
9. Lung mass / pleural/extra pleural mass
10. Opaque hemithorax: atelectasis/ consolidation / pleural effusion
11. Cardiomegaly / pericardial effusion
12. Portal venous air / pneumobilia
- 13.

Basilar atelectasis / subpulmonic effusion

#### **CHEE-43 The Anomalies of Thoracic Vein in Adults**

Participants

Makiko Murota, MD, Kitagun, Japan (*Presenter*) Nothing to Disclose

##### **TEACHING POINTS**

1. To review the anomalies of the thoracic systemic veins and the pulmonary veins. 2. To describe characteristic imaging features on multiple modalities, including chest radiograph, CT, and MRI. 3. To discuss the importance of clinical implications and the pitfall.

##### **TABLE OF CONTENTS/OUTLINE**

1. Normal anatomy 2. Embryology 3. The anomalies of the thoracic systemic veins: persistent left superior vena cava (PLSVC), postaoortic left innominate vein (PALIV), azygous/hemiazygous continuation of inferior vena cava, azygous lobe, and others 4. The anomalies of the pulmonary veins: left common pulmonary vein, separate middle lobe vein, aberrant vein (right top pulmonary vein), partial anomalous pulmonary venous return, scimitar syndrome, meandering pulmonary vein and others

#### **CHEE-44 Extracardiac Congenital Thoracic Vascular Anomalies - A General Radiologist's Guide**

Participants

Sanjana Kamath, FRCR, MBBS, (*Presenter*) Nothing to Disclose

##### **TEACHING POINTS**

1. Congenital thoracic vascular anomalies can present in adulthood. 2. Assessment of thoracic vasculature in compartments can simplify complex vascular anatomy aiding understanding and communication of results. 3. CT is well placed to assess all vascular compartments within the thorax and provide datasets for 3D reconstructions to further communicate findings and plan surgical intervention.

##### **TABLE OF CONTENTS/OUTLINE**

Systemic venous pathology (including left SVC, anomalous drainage to left atrium and azygous continuation of the IVC). Pulmonary arteries (absence or disconnection of branch pulmonary artery, pulmonary stenosis e.g. in Edwards syndrome, patent ductus arteriosus, aortopulmonary window and arteriovenous malformations). Pulmonary veins (partial and total anomalous return, sinus venosus ASD and scimitar syndrome). Aortic (truncus arteriosus and hemitruncus, congenitally corrected transposition of the great arteries, right arch with anomalous left subclavian artery, left arch with anomalous right subclavian artery, double arch, coarctation, interruption of the arch, pulmonary sequestration).

#### **CHEE-45 Beyond Aortopathies- Vascular Conditions Of The Thorax Associated With Genetic Conditions**

Participants

Riddhi Borse, MD, New Haven, MA (*Presenter*) Nothing to Disclose

##### **TEACHING POINTS**

1. Introduction to the vascular structures of the thorax. 2. Enlisting various vascular conditions of the thorax associated with genetic conditions and discussing commonly associated imaging findings affecting the various vessels of the thorax. 3. Detailed case-based description of thoracic imaging findings associated with inherited vascular conditions, along with common differential diagnoses. 4. Developing a Checklist and Understanding the salient features to be reported when encountering these inherited vascular conditions of the thorax.

##### **TABLE OF CONTENTS/OUTLINE**

1. Description of various vascular conditions with genetic predisposition and their associated common thoracic imaging findings. 2. Brief discussion on Ehlers Danlos, Marfan's, Turners syndromes and associated constellation of imaging findings with a focus on related vascular thoracic imaging findings, case examples and common differential diagnoses. 3. Brief discussion on BMPR2 and Factor V Leiden Mutations, associated constellation of imaging findings with a focus on related vascular thoracic imaging findings, case examples and common differential diagnoses. 4. Brief discussion on Cystic Fibrosis, Hereditary hemorrhagic Telangiectasia's and associated constellation of imaging findings with a focus on related vascular thoracic imaging findings, case examples and common differential diagnoses. 5. Enlisting salient imaging features to be added in the report based on what the clinician needs to know for each of the above listed conditions.

#### **CHEE-46 Scimitar Syndrome - Taking a Sharper Look**

Participants

Melissa Carroll, MD, Kansas City, KS (*Presenter*) Nothing to Disclose

##### **TEACHING POINTS**

1. Review the definition and variations of scimitar syndrome with a focus on imaging findings. 2. Familiarize the reader with common and uncommon congenital anomalies associated with scimitar syndrome to improve radiology exam interpretation. 3. Discuss clinical presentation and complications of scimitar syndrome.

##### **TABLE OF CONTENTS/OUTLINE**

1. Background 2. Definition a. Scimitar syndrome (hypogenetic lung or congenital venolobar syndrome) refers to partial anomalous venous drainage of the right lung to the IVC with hypoplasia of the ipsilateral lung, systemic artery supply, and dextroposition of the heart b. Scimitar sign refers to the curved, tubular opacity adjacent to the right heart border on chest radiograph representing the anomalous vein and is considered pathognomonic for scimitar syndrome. Scimitar refers to a Turkish sword with a curved blade 3. Types a. Infantile type presents in infancy and associated with congenital heart disease b. Childhood/adult type, which can be asymptomatic or result in recurrent infection. 4. Imaging Findings a. Chest radiograph as a screening tool b. Contrast enhanced CT to define anatomy and identify other anomalies c. Phase contrast MRI to quantify shunt d. Pertinent radiology report findings for surgical planning 5. Associated congenital anomalies a. Lungs and airways b. Vascular c. Cardiac 6. Clinical considerations and complications a. Discuss range of clinical manifestations and presentation including congestive heart failure in infants and recurrent

infection in adults b. Cardiovascular complications c. Pulmonary complications d. Post surgical imaging 7. Conclusion

#### **CHEE-47 Pre- and Post-operative Evaluation of the Patient with Chronic Thromboembolic Pulmonary Hypertension**

Participants

Tami Bang, MD, Aurora, CO (*Presenter*) Nothing to Disclose

##### **TEACHING POINTS**

1. Define chronic thromboembolic pulmonary hypertension (CTEPH) and describe its development 2. Review the imaging findings in CTEPH 3. Discuss surgical management of CTEPH 4. Review the role of the radiologist in the diagnosis, evaluation, and management of CTEPH

##### **TABLE OF CONTENTS/OUTLINE**

1. Definition of Chronic Thromboembolic Pulmonary Hypertension (CTEPH) 2. Pathophysiology of CTEPH 3. Multimodality Diagnosis of CTEPH (CT, Echo, V/Q scan, CMR, Angiography) 4. Surgical Management of CTEPH 5. What does the referring team need to know? a. Is the case operable b. What is the likelihood of RV recovery c. Are there accessible targets for endarterectomy?

#### **CHEE-48 Chronic Pulmonary Embolism: What Radiologists Should Know**

Participants

Marcelo Carvalho, MD, Sao Paulo, Brazil (*Presenter*) Nothing to Disclose

##### **TEACHING POINTS**

- To review the major direct and indirect findings of both acute and chronic pulmonary embolism on CT angiography.- To discuss the role of iodine map in chronic pulmonary embolism.- To highlight other important differential diagnosis of chronic PE as well as potential pitfalls.

##### **TABLE OF CONTENTS/OUTLINE**

Introduction: basic concepts on chronic pulmonary embolism (epidemiology, pathophysiology, clinical findings and treatment goals) CTA protocol for pulmonary embolism Acute x chronic pulmonary embolism: a CTA-centered approach Current state of the iodine map in chronic pulmonary embolism Other differential diagnosis to keep in mind Idiopathic pulmonary hypertension and in situ thrombosis Pulmonary artery sarcoma Vasculitis Congenital anomalies Potential pitfalls and artifacts in chronic pulmonary embolism

#### **CHEE-49 Following the Contrast: How to Recognize Thoracic Flow Artifacts and Vascular Shunts on Thoracic Multidetector Computed Tomography**

Participants

Elisenda Foraster, MD, Sabadell, Spain (*Presenter*) Nothing to Disclose

##### **TEACHING POINTS**

To learn the causes of thoracic flow artifacts and provide clues to distinguish them from true filling defects. To be aware of persistent and anomalous cardiac communications that are relevant in clinical practice and its typical imaging findings.

##### **TABLE OF CONTENTS/OUTLINE**

I. Background Thoracic flow artifacts as well vascular and cardiac shunts can be challenging for radiologists to diagnose. We propose a practical approach to recognize the main causes and CT features in both situations. II. Content A) Thoracic flow artifacts ("smoke"): non-opacified blood in a contrast-filled chamber, indicative of incomplete opacification. 1. Pulmonary artery (mimicking pulmonary embolism): bilateral smoke (heart failure, early/fast scanning, transient interruption of contrast) or unilateral smoke (focal lung abnormality, collateral vessel inflow). 2. Aortic pseudo-dissection. 3. Left atrial appendage pseudo-thrombus. B) Congenital or acquired shunt (aberrant pathway): Abnormal passage of contrast between cardiac chambers or between vascular structures and cardiac chambers, indicative of an abnormal communication. 1. Congenital atrial septal defect, patent foramen ovale, ventricular septal defect. 2. Acquired: collateral venous pathway from stenosis or occlusion of the superior vena cava. III. Conclusions Recognizing smoke can help prevent misdiagnosis of important diseases like pulmonary embolism or aortic dissection, and detection of contrast aberrant-paths provide a diagnosis clue to the presence of shunts or vascular stenosis.

#### **CHEE-5 Vasculitides: Diagnostic Tips and Tricks through Thoracic Imaging**

Participants

Glenda Costa Feitosa, MD, Sao Paulo, Brazil (*Presenter*) Nothing to Disclose

##### **TEACHING POINTS**

Vasculitides are multi-systemic diseases that can lead to severe consequences if left untreated. There are several ways these disease processes can present on imaging. Thoracic imaging, for instance, has a lot to add when characterizing them, given the considerable importance of the great vessels of the mediastinum and the lung involvement commonly shown. Knowledge of typical findings that suggest a diagnosis of vasculitis is therefore a valuable asset for the radiologist and yields better outcomes.

##### **TABLE OF CONTENTS/OUTLINE**

Inflammatory diseases of the vessel walls can affect small, medium and large vessels in all segments of the body. These are often treatable diseases, bringing alleviation of the inflammatory activity and better overall outcomes. These diseases can be quite a challenge to diagnose, as they can present similarly to one another and have a nonspecific clinical course and laboratory features. The intention of this presentation is to demonstrate, through a series of cases, different vasculitides and diagnostic tips that helped suggesting these diagnoses through imaging, such as the vessels involved by parietal thickening and aneurysms, lung opacities and their temporal evolution, as well as some associations with patient characteristics and clinical features. Chest multidetector computerized tomography is the main method to be explored, an imaging modality that has a lot to offer in this task since the great mediastinal vessels and lungs are often involved.

#### **CHEE-50 Mimickers of Chronic Thromboembolic Pulmonary Hypertension: A Pictorial Review**

Participants

Albert Domingo Senan, MD, Madrid, Spain (*Presenter*) Nothing to Disclose

#### TEACHING POINTS

Highlight the role of imaging tests in chronic thromboembolic pulmonary hypertension (CTEPH) focused on the detection and characterization of those pathologies that can mimic this disease, because both therapeutic management and prognosis are substantially different.

#### TABLE OF CONTENTS/OUTLINE

CTEPH represents a special form of PH potentially curable by surgical treatment (thromboendarterectomy). Imaging tests play a fundamental role in this disease: they confirm the diagnosis, establish the location and extension of the lesions in order to plan the most appropriate treatment (surgery vs. angioplasty vs. medical treatment) and they detect other associated injuries that may condition the patient management. They also allow diagnosis of other pathologies that may have been erroneously labeled as CTEPH. For this reason, it is essential to know what the mimicking pathologies are and the radiological signs that allow them to be detected. The main pathologies that can mimic CTEPH are sarcomas of the pulmonary arteries, large vessel vasculitis (Takayasu's arteritis), fibrosing mediastinitis, in situ thrombosis, pulmonary intravascular hydatid disease, and congenital interruption of the pulmonary artery. These pathologies and the keys to their diagnosis are reviewed.

#### CHEE-51 News Pathways in Thoracic Imaging: A Roadmap to Congenital Vascular Anomalies

Participants

Alex Dias, MD, Sao Paulo, Brazil (*Presenter*) Nothing to Disclose

#### TEACHING POINTS

1. Review relevant anatomy, embryogenesis, and pathophysiology of congenital thoracic vascular anomalies. 2. Correlate clinical findings and complaints in childhood and adult life with imaging findings of vascular anomalies, according to subgroups and classifications. 3. Summarize imaging protocols and post-processing techniques. 4. Highlight the role of invasive and non-invasive imaging techniques for anomalies of the great thoracic vessels. 5. Discuss the relevance of multidisciplinary team meetings and the role of radiologists in patient care with case reviews.

#### TABLE OF CONTENTS/OUTLINE

1. Applied anatomy and embryogenesis of pulmonary arteries, pulmonary veins, aortic arch, and superior vena cava. 2. Congenital variants and anomalies: 2.1. Pulmonary arteries. 2.2. Pulmonary veins (total and partial anomalous pulmonary venous return). 2.3. Aortic arch. 2.4. Superior vena cava. 3. Sample cases and outcome review: 3.1. State-of-the-art imaging protocols and post-processing techniques. 3.2. Current and potential diagnostic methods, including invasive and non-invasive studies. 3.3. Follow-up, treatment, and prognosis. 4. Congenital vascular anomalies: practical approach and structure reporting. 5. Summary and take-home messages.

#### CHEE-52 Venous Anatomic Variants In The Thorax

Participants

Riddhi Borse, MD, New Haven, MA (*Presenter*) Nothing to Disclose

#### TEACHING POINTS

1. To understand normal vascular anatomy of the thorax, common and uncommon anatomic vascular variants. 2. To classify venous variant anatomy in the thorax based on draining veins. 3. To identify salient imaging features of described anatomic variants in a case based method, common differential diagnoses, and important points to be reported based on their clinical presentations.

#### TABLE OF CONTENTS/OUTLINE

1. Description of normal vascular anatomic structures within the thorax, common and uncommon anatomic variants. 2. Classification of venous anatomic variant anatomy in the thorax based on draining veins as follows: • Azygous Vein- Absent Azygous, Azygous Continuation of Inferior Vena Cava, Azygous Fissure variant in right upper lobe • Hemiazygos Vein- Left Superior Intercostal Vein, Hemiazygos continuation of the IVC, Accessory Hemiazygos Veins. • Superior Vena Cava- Persistent left SVC, Retroaortic Left Brachiocephalic Vein. • Pulmonary Vein- Partial and Total Anomalous Pulmonary Venous Return, Scimitar Syndrome, Accessory and Meandering Pulmonary veins 3. Brief description, salient imaging features, differential diagnoses and examples of anatomic variants draining into the azygous vein. 4. Important points to be included in reporting above listed anatomic variants from a clinical and interventional standpoint.

#### CHEE-53 Challenges and Pitfalls in Lung Cancer Screening

Participants

Hanna Ferreira Dalla Pria, MD, MD Anderson, Houston, TX (*Presenter*) Nothing to Disclose

#### TEACHING POINTS

• Updated USPSTF recommendations lung cancer screening (LCS). • LDCT Lung-RADS classification, reporting, and management recommendations with emphasis on challenging imaging findings and atypical patterns. • The spectrum of potential pitfalls in pulmonary nodule detection and characterization, including equivocal or atypical presentations, is important for avoiding misinterpretation that can alter patient management.

#### TABLE OF CONTENTS/OUTLINE

• Brief review of LCS history and impact, highlighting recently updated guidelines. • Interactive imaging-based approach with teaching points for diagnosis and/or work-up of equivocal cases with challenging imaging findings and atypical presentations on LDCT screening, chest CT and PET/CT imaging. • Discussion and Illustration of main LDCT screening pitfalls and causes of false positive and false negative screening results including, for example, artifacts related to CT technique, inflammatory and post-treatment changes mimicking neoplasm, cystic and cavitary lesions, pleural attached nodules, endobronchial lesions, temporary regression of malignant nodules. • Discussion and Illustration of main PET/CT pitfalls and false positive and false negative findings in the investigation of screen-detected nodules. • Limitations and new directions. • Take-home messages.

## **CHEE-54 COVID-19 Infection: Chest-CT of Complications During Acute Infection and Late Imaging Findings**

Participants

Leonardo Kenji Mitsutake, MD, Sao Paulo, Brazil (*Presenter*) Nothing to Disclose

### **TEACHING POINTS**

The purpose of this exhibit is:- Briefly review the epidemiology of COVID-19 infection and of post COVID-19 CT lungs abnormalities.- Describe and illustrate lung complications related to COVID-19 infection.- Describe post COVID-19 chest CT imaging protocols and technics.- Review the radiological management and follow-up protocols of post COVID-19 pneumonia.- Describe and illustrate the post COVID-19 CT lungs abnormalities, evolution patterns and complications.

### **TABLE OF CONTENTS/OUTLINE**

1. Introduction: COVID-19 epidemiology review. Post COVID-19 CT lungs abnormalities epidemiology and predictors.2. Lung complications related to COVID-19 infection: Pneumothorax / Pneumodiastinum / Bronchopleural fistula. Co-infection / superinfection. Vascular complications.3. Post COVID-19 Chest CT protocols.4. Post COVID-19 imaging follow-up: Review of societies recommendations and propositions.5. Key Imaging Findings: Main post COVID-19 CT findings. Imaging evolution patterns. Review of fibrotic-like changes. Post-treatment related complications.6. Take home messages.

## **CHEE-56 Systematic Approach of Congenital Chest Malformations**

Participants

Taila Moura Fe, Sao Paulo, Brazil (*Presenter*) Nothing to Disclose

### **TEACHING POINTS**

The purposes of this exhibit are:1. Make a multimodality-based didactic review of the various chest malformations. 2. Propose a didactic categorization of these conditions in: -Bronchopulmonary malformations. -Malformations of the pulmonary vessels. - Malformations of the thoracic wall and diaphragm 3. Illustrate those conditions based on cases from our chest radiology group.

### **TABLE OF CONTENTS/OUTLINE**

We will discuss the following congenital chest malformations and focus on their imaging features using a multimodality approach in this exhibit.1. Bronchopulmonary malformations: -Bronchial atresia. -Accessory bronchus. -Bronchogenic cyst. -Congenital lobar overinflation. -Congenital pulmonary airways malformation (CPAM). -Pulmonary sequestration. -Pulmonary aplasia, hypoplasia, and agenesis. 2. Malformations of the pulmonary vessels: -Unilateral absence of the pulmonary artery. -Pulmonary artery sling. - Congenital pulmonary venolobar syndrome.3. Thoracic wall and diaphragm malformations: -Bochdalek hernia. -Morgagni hernia.

## **CHEE-57 Breasts on Thorax CT's - Better Not Turn a Blind Eye**

Participants

Izabel Karam, MD, Sao Paulo, Brazil (*Presenter*) Nothing to Disclose

### **TEACHING POINTS**

The purposes of this exhibit are:To emphasize the importance of basic breast image knowledge for the general and thoracic specialized radiologist when reporting chest CTs;To review mammary anatomy;To illustrate several breast pathologies and its findings in chest CTs from our department in didactic sections to improve understanding.

### **TABLE OF CONTENTS/OUTLINE**

To review the mammary anatomy:Thoracic wall (ribs and muscles);Mammary lobules and ducts;Areola and nipple;Neoplasms and other tumors:Fibroadenoma;Ductal invasive carcinoma;Metastases to breasts;Breast cancer in male patient;Evaluating local extension and lymphatic spreading;Male breasts;Infections and organized collections:Mammary abscess;Organizing hematomas;Post mammoplasty intramammary hematoma;Industrial silicone injection;Implant-related changes:Intrathoracic migration of breast implant after thoracoscopic surgery;Flipped implant;Postoperative abscess;Intracapsular implant rupture;Implant contraction;Implant-related lymphoma.

## **CHEE-58 Imaging Diagnosis as Biomarkers for Lung Cancer with Driver Oncogene Mutation / Gene Translocation in the Era of Personalized Medicine**

Participants

Masahiro Yanagawa, MD, PhD, Suita, Japan (*Presenter*) Nothing to Disclose

### **TEACHING POINTS**

In the era of personalized medicine, imaging diagnosis plays an important part as biomarkers of the following items: prediction for pathological diagnosis, prediction for prognosis, prediction for driver oncogenes, evaluation of treatment response, and evaluation of side effects, etc. Imaging is not always perfect, but it can capture the whole image of lung cancer. This education exhibit focuses on CT imaging in lung cancer with driver oncogene mutation / gene translocation positive and quantitative analysis for predicting gene. It is much appreciated if our information would be useful in your clinical and research setting.

### **TABLE OF CONTENTS/OUTLINE**

1. CT imaging in lung cancer with driver oncogene mutation/gene translocation positive: EGFR (epidermal growth factor receptor) mutation, ALK (anaplastic lymphoma kinase) rearrangement, ROS1 (c-ros oncogene) rearrangement, BRAF (v-raf murine viral oncogene homolog B1) mutation, MET exon 14 skipping-mutation, NTRK fusion, and Others [rearranged during transfection proto-oncogene (RET) fusion, KRAS mutation, and human epidermal growth factor receptor 2 (HER-2) mutation]. 2. CT imaging for an immune checkpoint inhibitor in lung cancer with programmed death ligand 1 (PD-L1). 3. Quantitative analysis for predicting gene: Radiomics approach. 4. Tailor-made medicine: Molecular-targeted therapies for driver oncogene mutations / gene translocations.

## **CHEE-59 Myocardial Assessment on CT: Don't Miss a Beat**

Participants

Elizabeth Lee, MD, Ann Arbor, MI (*Presenter*) Nothing to Disclose

## TEACHING POINTS

1. Although myocardium is typically evaluated with cardiac CT there is an opportunity to identify abnormalities on routine CTs done for other reasons. 2. Attention to myocardial contour, attenuation and enhancement patterns on a routine chest CT can enable detection of previously unsuspected disease. 3. Recognition of myocardial abnormalities on routine chest CT will help in early detection of cardiac abnormalities and appropriate management.

## TABLE OF CONTENTS/OUTLINE

Given the widespread use of chest CT, cardiac abnormalities are increasingly being identified on chest CTs often done for other reasons. While several reports have shown the value of incidentally discovered abnormalities (such as coronary anomalies) there is scant literature on myocardial abnormalities. These are challenging to detect, however, attention to this can enable diagnosis of unsuspected disease. The following myocardial abnormalities will be discussed: Attenuation: Differential attenuation between blood pool and myocardium (anemia); Fat deposition (tuberous sclerosis, prior infarct, arrhythmogenic cardiomyopathy, benign); Focal low attenuation (acute myocardial infarction (MI), acute myocarditis); Calcification (old MI, calcified tumor, renal failure) Morphology and enhancement: Thickened with diffuse heterogeneous enhancement (infiltrative processes, Loeffler); Focal thickening with abnormal enhancement (acute MI, myocarditis); Normal thickness with focal heterogeneous enhancement (tumor, acute MI); Thinning (chronic MI, aneurysm/pseudoaneurysm) Future directions: Strain, role of artificial intelligence. Pitfalls: Artifacts can simulate myocardial pathology

## CHEE-60 Taming the Broncho: An Imaging Guide to Acute Bronchial Disorders

Participants

Christopher Song, BS, (*Presenter*) Nothing to Disclose

## TEACHING POINTS

1) Various diseases of the bronchi can cause acute symptoms and physiologic abnormalities. 2) We will apply a systematic approach to analyzing and characterizing bronchial disorders in the emergent setting. These disorders can be grouped into the following categories: endobronchial lesions, bronchiectasis, bronchial wall thickening, and bronchomalacia. 3) Post-processing reconstructions should be utilized to better visualize and highlight characteristic imaging features.

## TABLE OF CONTENTS/OUTLINE

Endobronchial lesions- Benign: Aspiration pneumonia, foreign body aspiration, broncholith, pulmonary hamartoma- Malignant: Carcinoid, adenoid cystic carcinoma, mucoepidermoid carcinoma, metastasis Bronchiectasis - Cystic fibrosis- Graft versus host disease- Primary ciliary dyskinesia- Infection (e.g., nontuberculous mycobacterium, *Pseudomonas aeruginosa*)- Allergic bronchopulmonary aspergillosis- Tracheobronchomegaly- Williams-Campbell syndrome- Bronchial atresia Bronchial wall thickening- Bronchial asthma- Relapsing polychondritis- Tracheobronchial amyloidosis- Sarcoidosis- Granulomatous with polyangiitis- Infection (e.g. tuberculosis, *Klebsiella*) Bronchomalacia Bronchial trauma- Bronchopleural fistula- Bronchomediastinal fistula- Bronchial disruption/rupture

## CHEE-61 Air trapping in Diffuse Lung Diseases: An Imaging Approach to the Differential Diagnosis with Pathologic Correlation (Mechanisms and Imaging Clues)

### Awards

#### Certificate of Merit

Participants

Tomas C. Franquet, MD, PhD, Barcelona, Spain (*Presenter*) Nothing to Disclose

## TEACHING POINTS

Air trapping is a manifestation of many diverse entities such as infections, aspiration or inhalation of foreign substances, immunologic and connective tissue disorders, and miscellaneous causes. The presence of air trapping is an excellent clue to the diagnosis of small airways disease. Air trapping consists of focal zones of decreased attenuation commonly seen at expiratory thin-section CT scans of the lungs obtained during suspended expiration following a forced exhalation. The goals of this exhibit are to help the learner: 1) To review a variety of diffuse lung diseases commonly associated with air trapping 2) To emphasize the diagnostic value of volumetric expiratory CT 3) Present radiology-pathology correlation 4) Provide an algorithmic approach to a differential diagnosis

## TABLE OF CONTENTS/OUTLINE

1. Introduction. Review Diffuse lung diseases associated with air trapping 2. Review the diagnostic value of volumetric expiratory HRCT scans in providing additional significant information in the evaluation of a variety of diffuse lung diseases with suspected airway abnormalities. 3. Recognize pathologic mechanisms for air trapping in diffuse lung diseases and their impact on radiologic appearance 4. Etiologies of air trapping related to diffuse lung diseases: Infectious Causes, Immunologically mediated, Drug-induced, Toxic/chemical fume inhalation, and miscellaneous causes/associations 5. Algorithm to approach air trapping in diffuse lung diseases. 6. Conclusion

## CHEE-62 Recognizing the Many Faces of Thoracic Tuberculosis

Participants

Makiko Murota, MD, Kitagun, Japan (*Presenter*) Nothing to Disclose

## TEACHING POINTS

*Mycobacterium tuberculosis* infects one third of the world's population and tuberculosis continues to be a major global public health problem. Imaging diagnosis of tuberculosis is sometimes challenging and complex. The purpose of the exhibit is: 1. To review the etiology of tuberculosis. 2. To describe the imaging features of tuberculosis, including the thoracic region other than the lungs. 3. To discuss the complications and sequelae.

## TABLE OF CONTENTS/OUTLINE

1. The etiology of tuberculosis 2. The imaging findings of pulmonary tuberculosis: primary tuberculosis, postprimary tuberculosis including typical and atypical pattern, bronchial tuberculosis, tuberculoma, and miliary tuberculosis 3. The imaging features and the

clinical manifestations of complications and sequelae: lung parenchyma, airways, blood vessels, mediastinum, pleura, chest wall 4. The differential diagnosis 5. Summary

## **CHEE-63 Tropical Diseases - A Comprehensive Review of Thoracic and Abdominal Imaging Manifestations**

Participants

Heli Rueda, MD, Bogota, Colombia (*Presenter*) Nothing to Disclose

### **TEACHING POINTS**

To review the pathophysiology, histopathology, and imaging manifestations of thoracic and abdominal tropical diseases. To mention the imaging patterns of parasitic tropical diseases with their histological correlation. To conceptualize the role of imaging in the diagnosis of tropical diseases.

### **TABLE OF CONTENTS/OUTLINE**

1. Introduction 2. Tropical diseases classification and physiopathology. 3. Epidemiology and Imaging findings of tropical diseases in computed tomography and its pathological correlation of: a. Parasites: i. Helminth Infections: 1. Ascariasis 2. Echinococcosis 3. Paragonimiasis 4. Strongyloidiasis ii. Protozoal Infections: 1. Amebiasis 2. Leishmaniasis 3. Chagas disease 4. Malaria b. Bacterial: i. Salmonellosis ii. Tuberculosis c. Fungal: i. Paracoccidiomycosis d. Viral: i. Dengue fever 4. Conclusions.

## **CHEE-64 High-attenuation Mediastinal Abnormalities - Beyond Lymph Nodes Benign Calcifications**

Participants

Lucimara Parajara, MD, Sao Bernardo Do Campo, Brazil (*Presenter*) Nothing to Disclose

### **TEACHING POINTS**

- To review the main causes of calcified mediastinal lymph nodes - To review conditions other than calcified lymph nodes that can cause high attenuation lesions in the mediastinum compartments

### **TABLE OF CONTENTS/OUTLINE**

All radiologists are used to describing calcified mediastinal lymph nodes. We will discuss several other conditions that may present with a high-attenuation pattern in the mediastinum: - Calcified lymph nodes: a) Healed granulomatous infection b) Sarcoidosis c) Chronic silicosis - Calcified masses a) Thyroid pathologies b) Germ cell neoplasm c) Calcified mediastinal cysts d) Healed lymphoma - Calcified tissue involving mediastinal structures: a) Inflammatory pseudotumor b) Fibrosing mediastinitis c) Tracheobronchial amyloidosis - Other conditions: a) Pitfalls: azygos vein contrast, contrast inside lymphatic ducts b) Foreign body: device embolism, aspiration

## **CHEE-65 Multidisciplinary Panel of Sarcoidosis Beyond the Basics: A Primer on Unusual Cases**

Participants

Jessica Marchi, Sao Paulo, Brazil (*Presenter*) Nothing to Disclose

### **TEACHING POINTS**

To provide a brief overview of the fundamental classic radiologic and histologic findings of sarcoidosis. To demonstrate and discuss the others presentations of thoracic sarcoidosis that are outside the usual. To illustrate the correlation between radiological and histological findings, focusing on atypical cases.

### **TABLE OF CONTENTS/OUTLINE**

Besides thoracic sarcoidosis's common findings (bilateral hilar lymph node enlargement, micronodules with a perilymphatic distribution, fibrotic changes, and bilateral perihilar opacities), one must remember its atypical manifestations and the possibility of concomitance with lung abnormalities of another nature. We will review the most common thoracic sarcoidosis presentations in this educational exhibit, as well as illustrate and describe atypical manifestations and complications. When pertinent, we will also include radiology-pathology correlation for the cases.

## **CHEE-66 Dynamic Chest Radiography for Pulmonary Vascular Diseases: Clinical Applications and Correlation with Other Imaging Modalities**

**Awards**

**Cum Laude**

Participants

Yuzo Yamasaki, MD, PhD, (*Presenter*) Research Grant, Konica Minolta, Inc

### **TEACHING POINTS**

1) To explain the basic principles of lung perfusion assessment using dynamic chest radiography (DCR) 2) To discuss the advantages of DCR compared to other imaging modalities 3) To review multiple, specific clinical applications of DCR for pulmonary vascular diseases and compare them with other imaging modalities

### **TABLE OF CONTENTS/OUTLINE**

1) Basic principles of DCR • System composition • Acquisition techniques 2) Different acquisitions of DCR imaging • Lung perfusion images • Lung ventilation images 3) Different methods of DCR lung perfusion imaging • Cross-correlation method • Reference frame-subtraction method 4) Advantages compared to other imaging modalities • Readily available • No need for contrast media or radionuclides • Non-invasive • Low radiation exposure • Cost-effective 5) Clinical applications and correlation with other imaging modalities • Pulmonary arterial diseases - Acute pulmonary thromboembolism - Chronic thromboembolic pulmonary hypertension - Pulmonary arteriovenous malformation - Pulmonary arterial stenosis/occlusion • Pulmonary venous diseases - Partial anomalous pulmonary venous return - Pulmonary venous stenosis/occlusion 6) Limitations

## **CHEE-67 Imaging Technologies to Guide the Interventional Pulmonologist: Dynamic Digital Tomography and Dual Source CT.**

Participants

Samuel McCollum, (*Presenter*) Nothing to Disclose

#### TEACHING POINTS

Dynamic low dose evaluation of the airway with Digital Tomosynthesis (DTS) and Dual Source Computed Tomography can be used to monitor complex airway pathologies and airway devices. Having an institution-specific DTS may reduce use of CT imaging, lowering cost and radiation exposure. Dynamic DSCT imaging decreases radiation dose to conventional CT acquisition

#### TABLE OF CONTENTS/OUTLINE

1. An introduction to Digital Tomosynthesis and dynamic DSCT: Acquisition and Current Uses  
2. Case 1: 37-year-old male with post-intubation stricture—we discuss how the stenotic airway is poorly visualized by conventional radiograph, yet can be readily visualized using DTS.  
3. Case 2: 28-year old female with post-intubation stricture. We demonstrate how can provide a functional assessment of the airways by imaging the trachea in both the inspiratory and expiratory phase post-dilation  
4. Case 3: 67-year-old male with NSCLC complicated by malignant tracheal stenosis. We will see that DTS allows for visualization of an intraluminal mass.  
5. Case 4: 57 year old female with malignant stricture s/p stent placement with recurrent airway obstruction. DTS enabled low dose evaluation and monitoring of therapeutic interventions.  
6. Case 5: 72-year-old male with left lung transplant for usual interstitial pneumonia status post endobronchial stent placement. We show how DTS enables visualization of the endobronchial stent in both inspiration and expiration, again enabling one to monitor stability of airways and associated devices while avoiding the cost and radiation of CT imaging.  
7. Discussion

#### CHEE-68 From Lines Stripes to Cubes Cylinders: A 3D Visual Guide to Conventional Chest Radiography

##### Awards

Cum Laude

Identified for RadioGraphics

Participants

Albert Jiao, MD, Boston, MA (*Presenter*) Nothing to Disclose

#### TEACHING POINTS

Purpose Identification of anatomic structures in the chest on 2D conventional chest radiography may be challenging for new trainees. Due to the subtlety of pleural lining on CT, the concepts of expanded, effaced, or obliterated pleural borders on interaction with the mediastinum may be difficult to understand with radiographic and cross-sectional imaging correlation. 3D cinematic rendering, which can accentuate the draping effects of pleural borders, may provide a novel way to understand classic chest radiography. Teaching Points

- Identify the anatomic structures in the chest that create the classic “lines and stripes” on chest radiography though the assist of 3D cinematic rendering (CR) depictions.
- Recognize the abnormal appearances of the borders on CXR, and the corresponding appropriate pathologies in the differential diagnosis through a case-based teaching series.

#### TABLE OF CONTENTS/OUTLINE

Outline  
1. Normal pleural anatomy and mediastinal borders. 2. Anterior Junction Line. a. Anterior mediastinal mass differential. 3. Posterior Junction Line. a. Posterior mediastinal mass differential. 4. Aorto-pulmonic relationships. a. AP stripe AP window differential. 5. Paraspinal Lines. a. Right left paraspinal line differentials. 6. Posterior tracheal stripe differentials. 7. Azygosoesophageal recess differentials

#### CHEE-69HC Practical Guide of US-guided Percutaneous Needle Biopsy (PCNB) for Thoracic Lesions

Participants

Hang Jun Cho, Daegu, Korea, Republic Of (*Presenter*) Nothing to Disclose

#### TEACHING POINTS

To guide clinical application of US-guided percutaneous needle biopsy (PCNB) for thoracic lesions.

#### TABLE OF CONTENTS/OUTLINE

1. Introduction of US-guided percutaneous needle biopsy (PCNB) - Indications - Advantages and limitations  
2. US images of thoracic lesions - Subpleural lung lesions - Pleural lesions- Bony thorax lesions- Anterior mediastinal lesions- Soft tissue lesions  
3. Procedure of US-guided PCNB - Localization of the lesion - Risk evaluation- Determination of the target - Acquisition of the tissue- Evaluation of immediate post-procedural complication  
4. Diagnostic performance and complication rate of US-guided PCNB - Diagnostic yield - Complication rate - CT guided vs. US guided PCNB  
Please visit the Learning Center to also view this presentation in hardcopy format.

#### CHEE-7 Let Us Find the Nodule in a Haystack: A Quick Look through Current Techniques for Image-guided Preoperative and Intraoperative Localization of Small Lung Nodules Prior to Video-assisted Thoracoscopic Surgery Resection

Participants

Igor Radalov, MD, Barcelona, Spain (*Presenter*) Nothing to Disclose

#### TEACHING POINTS

1) To define the characteristics of lung nodules amenable to image-guided localization before video-assisted thoracoscopic surgery (VATS) resection.  
2) To explain the advantages, disadvantages, and techniques of the different modalities available in the localization of lung nodules prior to VATS resection.  
3) To review the results of the different modalities available for the localization of lung nodules before VATS resection. Particular focus on new techniques: Radioactive tracer injection (ROLL) and radioactive seed placement.

#### TABLE OF CONTENTS/OUTLINE

1. Introduction.  
2. Lung nodules amenable for image-guided localization before VATS resection.  
3. Currently available modalities for lung nodule localization.  
3.1. Preoperative.  
3.1.1. Hookwire placement. 3.1.2. Microcoil placement. 3.1.3. Dye injection. 3.2.

Intraoperative.3.2.1. Ultrasound. 3.3. Mixed.3.3.1. Radioactive seed placement. 3.3.2. Radioactive tracer injection (ROLL). 4. Comparative results.4.1. Detection rate.4.2. Conversion to thoracotomy rate.4.3. Complications.5. Summarize.6. Conclusion.

## **CHEE-70 Thoracic Paragangliomas: Imaging Review and Considerations for Clinical Practice**

Participants

Fiona McCurdie, MBChB, BA, (*Presenter*) Nothing to Disclose

### **TEACHING POINTS**

1. Paragangliomas (PGL) within the thorax: where do they occur and in whom? Experience from a specialist centre  
2. Multimodality imaging features of thoracic PGLs: strengths and challenges of imaging modalities; lessons from missed lesions  
3. Considerations for management and recommendations for screening and surveillance

### **TABLE OF CONTENTS/OUTLINE**

1. Thoracic PGLs - what the general radiologist needs to know  
a. Overview of pathophysiology  
b. Succinate Dehydrogenase deficiency disorders  
c. Summary of literature - anatomical location and clinical presentation  
2. Our cohort of 17 thoracic PGL cases - two decades' experience in a specialist centre  
a. How the PGLs are identified: screening vs. surveillance vs symptomatic  
b. Locations of PGLs within the mediastinum: i. Superior ii. Anterior iii. Middle 1. Cardiac iv. Posterior v. Correlation symptoms and biochemistry  
c. Discussion of management: i. Surgical considerations ii. Medical including radionuclide therapy  
3. Radiological lessons:  
a. Common imaging findings i. CT - including cardiac CT ii. MRI - whole body, cardiac MRI iii. Functional imaging - Gallium Dotatate PET, FDG PET, MIBG SPECT, Octreotide iv. Plain radiograph  
b. Key differential diagnosis  
c. Learning from errors: which imaging modalities are PGLs most frequently missed on? What do we learn when we look back in retrospect?  
4. Recommendations for imaging screening and surveillance

## **CHEE-71 Disorders with Ocular and Thoracic Involvement**

**Awards**

**Identified for RadioGraphics**

Participants

Patrick Lang, MD, PhD, (*Presenter*) Nothing to Disclose

### **TEACHING POINTS**

Numerous medical conditions have multiorgan imaging findings. Here, we review specifically the ocular and cardiothoracic findings of selected infectious, inflammatory, autoimmune, neoplastic, and hereditary disorders. These correlations are meant to remind the astute clinician that certain ophthalmologic signs should trigger a careful radiologic evaluation that includes imaging of the head and chest.

### **TABLE OF CONTENTS/OUTLINE**

1. Introduction. 2. Examples of cases: a. Infectious conditions: aspergillosis, nocardiosis, COVID-19. b. Inflammatory conditions: sarcoidosis, IgG-4 sclerosing disease. c. Autoimmune conditions: Graves' disease, scleroderma, Sjogren's syndrome. d. Neoplastic conditions: uveal melanoma, lymphoma, lung cancer. e. Hereditary conditions: Marfan syndrome, Ehlers Danlos syndrome, tuberous sclerosis, neurofibromatosis type 1. 3. Conclusion.

## **CHEE-72 Tortuous Path: Congenital Anomalies of the Systemic Thoracic Veins**

Participants

Carlos Marin, MD, PhD, Madrid, Spain (*Presenter*) Nothing to Disclose

### **TEACHING POINTS**

1. To review the anatomy and embryology of the systemic thoracic veins. 2. To describe imaging findings in congenital anomalies of the systemic thoracic veins (CASTV). 3. To emphasize the physiologic consequences of these anomalies, and their impact in associated congenital heart diseases surgery.

### **TABLE OF CONTENTS/OUTLINE**

Congenital anomalies of the systemic thoracic veins are commonly underdiagnosed, in part because they are often asymptomatic or have little or no clinical consequences. They are frequently discovered as an incidental finding in a radiological examination for unrelated reasons, but sometimes are diagnosed because an anomalous course of a central venous line or during a systematic study for congenital heart disease. In certain cardiac or thoracic surgical procedures it is of prime importance to diagnose these anomalies to prevent surgical failure or complications. Pulmonary venous anomalous connections to the systemic thoracic veins and Raghb syndrome can be symptomatic and diagnosed at early age or be discovered in adulthood in patients with right heart dilatation or cardiac symptoms. Besides azygos lobe, a well-known normal variant, the most common CASTV include: 1. Persistent left superior vena cava (SVC) (with or without absent right SVC). 2. Left superior intercostal vein variants. 3. SVC aneurysm. 4. Pulmonary venous anomalous connections to the SVC. 5. Absent inferior vena cava with an enlarged azygos vein. 6. Persistence of the levoatriocardinal vein. 7. Persistent left SVC with absence of the coronary sinus (Raghb syndrome). 8. Subaortic innominate vein. We describe the embryology, anatomy, physiology, imaging findings, and potential complications of these anomalies.

## **CHEE-73 The Role of Cinematic Rendering in the Analysis of Complex Vascular and Mediastinal Pathology: How We Do It**

Participants

Elliot Fishman, MD, Owings Mills, MD (*Presenter*) Co-founder, HipGraphics, Inc; Stockholder, HipGraphics, Inc; Institutional Grant support, Siemens AG; Institutional Grant support, General Electric Company; Consultant, Exact Sciences Corporation; Consultant, Imaging Endpoints

### **TEACHING POINTS**

1. Cinematic Rendering provides unique 3D capabilities allowing for detailed analysis of complex soft tissue and vascular anatomy allowing for improved analysis of chest and mediastinal pathology  
2. Cinematic rendering is especially valuable for evaluation of complex vascular pathology ranging from aortic dissection to aneurysm as well as coarctation of the aorta and coronary artery

anomalies3. 3D mapping is an important tool for transmitting critical information to the referring physician and the patient care team4. complex anatomy defined with cinematic rendering is helpful in pre-operative planning and in analyzing complex structures for robotic surgery5. Cinematic Rendering is a helpful tool for teaching residents and fellows in complex cases of vascular anatomy and anomalies

#### TABLE OF CONTENTS/OUTLINE

1. CT protocols for optimizing data acquisition for 3D mapping2. protocols and techniques used for Cinematic Rendering including the use of presets to optimize workflow and throughput3. representative case studies are presented using axial, multiplanar, MIP and Cinematic Rendering to show how we use the technique in clinical practice. The advantages of Cinematic Rendering in select clinical applications will be discussed4. case studies will be divided into section including;a. vascular anatomy and anomaliesb. aortic aneurysm including dissection, intramural hematoma, ulcerations and active bleedingc. congenital anomalies including coarctation of the aorta and arch anomaliesd. cardiac pathology including cardiac tumors including atrial myxoma and angiosarcoma, and coronary artery fistulae e. mediastinal masses that involve or are in close proximity to key vascular structures

#### CHEE-74 Pulmonary Vascular Diseases: Spectrum of Manifestations in the Chest

Participants  
Juliana Sitta, MD, Jackson, MS (*Presenter*) Nothing to Disclose

#### TEACHING POINTS

Review of the pathophysiology and categorization of pulmonary vascular diseases. Describe imaging patterns on CT and traditional angiography. Analyze common and uncommon etiologies with a case-based review.

#### TABLE OF CONTENTS/OUTLINE

This presentation aims to discuss imaging findings in the diagnosis and categorization of pulmonary vascular diseases including acute pulmonary embolism, chronic thromboembolic pulmonary hypertension, pulmonary arteriovenous malformation, venous anomalies and mimics, hereditary hemorrhagic telangiectasia, granulomatous with polyangiitis, and microscopic polyangiitis. We will explore the spectrum of chest CT findings within the pulmonary vasculature, parenchyma, airways, mediastinum, and heart that help the radiologist narrow down the differential diagnosis. We will provide a review of the diagnostic criteria and key imaging findings, correlated with physiopathology and current categorization. We will also include a discussion of pros and cons of the currently available diagnostic tools and an update of the most recent imaging technical advancements. Additionally, a case-based review exemplifies common and uncommon pulmonary vascular pathologies.

#### CHEE-75 Pearls and Pitfalls in Pulmonary Vascular Disease

**Awards**  
**Certificate of Merit**

Participants  
Furkan Ufuk, MD, Denizli, Turkey (*Presenter*) Nothing to Disclose

#### TEACHING POINTS

? To review the spectrum of pulmonary vascular diseases and imaging features ? To review the clinical presentation associated with each pulmonary vascular disease

#### TABLE OF CONTENTS/OUTLINE

Pulmonary embolism, chronic thromboembolic pulmonary hypertension (CTEPH), pulmonary arterial hypertension (PAH), pulmonary arteriovenous malformations (PAVM), Portopulmonary hypertension, cavopulmonary pulmonary artery aneurysm/pseudoaneurysm, bronchial artery aneurysm/pseudoaneurysm, tumor thrombotic microangiopathy, in situ pulmonary artery thrombosis after receiving radiation therapy, pulmonary artery angiosarcoma, tumoral invasion of pulmonary artery or vein, pulmonary vein thrombosis, cement embolism, pulmonary vein varix, pulmonary veno-occlusive disease, pulmonary capillary hemangiomatosis, pulmonary sequestration, abnormal pulmonary venous return, pulmonary vasculitides.

#### CHEE-76 Multimodality Imaging of Pulmonary Embolism: A Guide for the Radiologist

**Awards**  
**Certificate of Merit**

Participants  
Flavio Zuccarino, MD, Barcelona, Spain (*Presenter*) Nothing to Disclose

#### TEACHING POINTS

To describe imaging findings in Pulmonary Embolism (PE) at different imaging modalities. To underline advantages and limitations of these techniques and to define the clinical scenarios in which they are key in patient management.

#### TABLE OF CONTENTS/OUTLINE

After a short introduction about PE etiology and incidence, we review PE imaging findings at different non-invasive techniques. We organize PE typical imaging findings as: Chest Radiography, Chest Ultrasound, CT Angiography, Spectral CT, Cardiac MR, V/Q (ventilation/perfusion) scan. We discuss advantages and limitations of these imaging modalities as the potential differential diagnosis. We analyze the differences between acute and chronic PE, focusing especially on Spectral CT findings. We evaluate the impact of these imaging techniques on patient prognosis, especially focusing on CT and cardiac MR. Conclusions  
OUTLINE PE represents a lifethreatening condition with a challenging diagnosis. Radiologists should be familiar with PE findings at all imaging modalities that may be key in patient management and treatment.

#### CHEE-77 New Imaging Modalities in the Diagnosis, Treatment, and Follow-up of Chronic Thromboembolic Pulmonary Hypertension: Correlation Between Dual Energy CT, Cone Beam CT and Digital Subtraction Angiography.

Participants

Alfredo Paez Carpio, MD, Barcelona, Spain (*Presenter*) Nothing to Disclose

#### TEACHING POINTS

To explain the basics and technique of dual-energy CT (DE-CT) and cone-beam CT (CB-CT), specifically during the management of patients with chronic thromboembolic pulmonary hypertension (CTEPH). To describe the imaging findings observed in the newly available imaging modalities: DE-CT and CB-CT in patients with CTEPH, with correlation with digital subtraction angiography (DSA). To explain the current role of DE-CTA and CB-CTA in the diagnosis, treatment and follow-up of patients with CTEPH.

#### TABLE OF CONTENTS/OUTLINE

1.- Introduction. 2.- Basic concepts of DE-CT and CB-CT. 2.1.- DE-CT basics and technique in the study of CTEPH. 2.2.- CB-CT basics and technique in the study of CTEPH. 3.- DE-CT and CB-CT in the diagnosis of suspected CTEPH. 3.1.- Added value compared to conventional CT and DSA. 3.2.- DE-CT imaging findings. 3.3.- CB-CT imaging findings. 3.4.- Correlation with DSA. 4.- DE-CT and CB-CT in the planning of invasive treatment for CTEPH. 4.1.- DE-CT and CB-CT in the planning of pulmonary endarterectomy. 4.2.- DE-CT and CB-CT in the planning of balloon pulmonary angioplasty. 4.3.- Added value of both techniques compared to conventional CT and DSA. 5.- Postprocedural CB-CT and DE-CT imaging findings. 5.1.- Normal spectrum of post-BPA and post-PEA imaging findings. 5.2.- Complications of BPA and PEA. 5.3.- Post-procedural imaging follow-up. 6.- Role of DE-CT and CB-CT in the long-term follow-up of patients with CTEPH. 7.- Current scientific evidence and status of both techniques in established diagnostic algorithms. 8.- Summarize. 9.- Conclusion.

#### CHEE-78 Bubbles in the Chest: A Pictorial Review of Cystic Lesions in the Paediatric Chest

Participants

Shrea Gulati, MBBS, MD, Delhi, India (*Presenter*) Nothing to Disclose

#### TEACHING POINTS

A wide spectrum of pathologies in the paediatric population can present as cystic lesions in the thorax. Imaging findings on chest radiography and computed tomography (CT) can provide diagnostic clues to the aetiology. Evolution of imaging findings on serial imaging can provide crucial diagnostic clues.

#### TABLE OF CONTENTS/OUTLINE

? Introduction ? Overview and classification of the cystic lesions in the paediatric chest  
Classification based on aetiology: Congenital cystic lesions - Congenital pulmonary airway malformation/ Hybrid lesion, Bronchogenic cyst, Cystic lung disease in neuro-cutaneous syndromes [Tuberous Sclerosis, Neurofibromatosis-1 (NF-1)], Syndromic cystic lung disease (Down's syndrome, Birt-Hogg-Dube syndrome)  
Acquired cystic lesions - Post infective- tuberculosis, pneumatocele, Diffuse lung disease- Lymphangioliomyomatosis and Langerhans cell histiocytosis, Broncho-pulmonary dysplasia (BPD), End-stage Interstitial lung disease (ILD)/Diffuse lung disease (DLD), Post traumatic pneumatocele  
Mimics - Bronchiectasis, Pulmonary interstitial emphysema, Emphysema (alpha 1 antitrypsin deficiency)  
Classification based on pattern: Single simple cyst - Bronchogenic cyst, Post traumatic pneumatocele  
Single complex/ conglomerated cysts - Congenital pulmonary airway malformation/ Hybrid lesion  
Multiple bilateral cysts - Post infective- tuberculosis, pneumatocele, Diffuse lung disease- Lymphangioliomyomatosis and Langerhans cell histiocytosis, BPD, End-stage ILD/DLD, Cystic lung disease in neuro-cutaneous syndromes (Tuberous Sclerosis, NF-1), Syndromic cystic lung disease (Down's syndrome, Birt-Hogg-Dube syndrome)

#### CHEE-79 Benign and Malignant Tumors of the Trachea

Participants

Daniel Vargas, MD, Denver, CO (*Presenter*) Nothing to Disclose

#### TEACHING POINTS

Tracheal neoplasms are rare, with less than 10% of these lesions considered benign. The radiologist is in a unique position of often being the first health team member to encounter these lesions. The objectives of this exhibit are: 1. Discuss epidemiology of tracheal neoplasms 2. Review the clinical and imaging presentation of some of the most common benign and malignant tracheal neoplasms. 3. Familiarize the radiologist with entities that act as mimics or pitfalls in the evaluation of the trachea

#### TABLE OF CONTENTS/OUTLINE

1. Benign Tracheal Neoplasms a. Tracheal Papilloma b. Hemangioma c. Paraganglioma d. Chondroma e. Hamartoma f. Neurogenic tumors 2. Malignant Tracheal Neoplasms a. Metastases b. Direct Invasion c. Squamous Cell Carcinoma d. Adenoid Cystic Carcinoma e. Mucoepidermoid Carcinoma f. Carcinoid Tumor g. Chondrosarcoma

#### CHEE-8 An Image is Worth a Thousand Words: Important Considerations about Connective Tissue Disease-Associated Interstitial Lung Disease

Participants

Bruna Alexandre, MD, Sao Paulo, Brazil (*Presenter*) Nothing to Disclose

#### TEACHING POINTS

Briefly review the main connective tissue disorders (CTD) typical clinical presentations and laboratory findings, and the expected pattern of interstitial lung disease (ILD) for each CTD; Introduce the readers to interstitial pneumonia with autoimmune features (IPAF); Recognize the most typical imaging features of ILDs and other thoracic manifestations of CTDs; Highlight the role of the radiologist in differential diagnosis and detecting complications.

#### TABLE OF CONTENTS/OUTLINE

INTRODUCTION: Connective tissue disorders (CTD) and their relation with interstitial lung diseases (ILD); CTD key points to diagnosis; Interstitial pneumonia with autoimmune features - when ILD takes the spotlight. IMAGING FINDINGS: Step by step approach and algorithm to evaluate connective tissue disease associated with interstitial lung disease (CTD-ILD); CTD-ILD: major patterns of involvement and suggestive signs at Chest CT; Other thoracic manifestations of connective tissue diseases. DIFFERENTIAL DIAGNOSIS AND COMPLICATIONS; TAKE-HOME MESSAGES

#### CHEE-80 Benign and Malignant Tracheobronchial Neoplasms: A Comprehensive Review with Radiologic,

## Bronchoscopic and Pathologic Correlation

### Awards

#### Identified for RadioGraphics

#### Participants

Alexander Phan, MD, New York, NY (*Presenter*) Nothing to Disclose

#### TEACHING POINTS

Tracheobronchial neoplasms are much less common than lung parenchymal neoplasms but can be associated with significant morbidity and mortality. They include a broad differential of both benign and malignant entities, extending far beyond more commonly known pathologies such as squamous cell carcinoma and carcinoid. Airway lesions may be incidental findings on imaging or present with symptoms related to airway narrowing or mucosal irritation, invasion of adjacent structures, or distant metastatic disease. While there is considerable overlap in clinical presentation, imaging, and bronchoscopic appearances, an awareness of potential distinguishing factors may help narrow the differential diagnosis. The authors review the epidemiology, imaging characteristics, typical anatomic distributions, bronchoscopic appearances, and histopathology of a wide range of neoplastic entities involving the tracheobronchial tree. Special attention is paid to any distinguishing features.

#### TABLE OF CONTENTS/OUTLINE

1. Primary malignant tumors: squamous cell carcinoma, malignant salivary gland tumors (adenoid cystic carcinoma and mucoepidermoid carcinoma), carcinoid, sarcomas, primary tracheobronchial lymphoma, and inflammatory myofibroblastic tumor. 2. Secondary malignant tumors (direct invasion or hematogenous spread). 3. Benign neoplasms: hamartoma, chondroma, lipoma, papilloma, amyloid, leiomyoma, neurogenic lesions, and benign salivary gland tumors (pleomorphic adenoma and mucous gland adenoma).

### CHEE-81 Usual Interstitial Pneumonia (UIP): A Primer for Radiologists

#### Participants

Katherine Cheng, MD, (*Presenter*) Nothing to Disclose

#### TEACHING POINTS

1. Usual Interstitial Pneumonia (UIP) is the most common histologic pattern of fibrosis and has typical imaging findings on HRCT. 2. UIP is an imaging/histologic diagnosis while Idiopathic Pulmonary Fibrosis (IPF) is a multidisciplinary diagnosis. 3. While most patients with UIP pattern of fibrosis are diagnosed with IPF, this imaging pattern can be seen in other settings such as connective tissue related disease, hypersensitivity pneumonitis, asbestosis, vasculitis, familial pulmonary fibrosis, and drug reaction

#### TABLE OF CONTENTS/OUTLINE

1. Distinguish UIP from IPF 2. Review histologic and imaging patterns of UIP; review updated 2022 ATS criteria diagnosis for IPF. 3. Explore the differential diagnosis for UIP and associated imaging findings including IPF, connective tissue disease, hypersensitivity pneumonitis, asbestosis, vasculitis, familial pulmonary fibrosis, and drug reaction. 4. Present multidisciplinary approach to UIP including the clinical presentations and serologic markers that can aid the radiologist.

### CHEE-82 Imaging Guide to Connective Tissue Disease Related Interstitial Lung Disease (CTD-ILD)

#### Participants

Yogesh Gupta, DO, (*Presenter*) Nothing to Disclose

#### TEACHING POINTS

1. Provide a foundation for the clinical diagnosis of CTDs that may present with ILD including symptomatology and serologic markers. 2. Describe the radiologic and pathologic patterns of CTD-ILD 3. Review helpful imaging signs in the diagnosis of CTD-ILD. 4. Discuss idiopathic pneumonia with autoimmune features (IPAF). 5. Review the specific prognosis and management of CTD-ILDs, with comparison to ILDs secondary to other causes.

#### TABLE OF CONTENTS/OUTLINE

CTD-ILD represents an underdiagnosed subset of ILDs. The imaging appearance of CTD-ILDs can often precede the rheumatic signs with interpretation of these cases difficult for even experienced radiologists. The literature on CTD-ILD has progressed over recent years, underscored by the emergence of new diagnostic criteria and characteristic imaging patterns. This presentation will provide the radiologist with a comprehensive framework to best facilitate diagnosis and guide management of these diseases. This exhibit is designed for residents, fellows, as well as general and thoracic radiologists. The primary goal is to achieve better understanding of clinical and imaging features of various CTD-ILDs, drawing from our large multicenter patient database. 1. Clinical features of CTDs manifesting with ILD. 2. Pathophysiology of CTD-ILDs. 3. CT imaging characteristics of CTD-ILDs, including imaging signs. 4. Prognosis and management of CTD-ILDs.

### CHEE-83 Breast Cancer in Women: Multidisciplinary Approach to the Kaleidoscopic Pulmonary Manifestations on CT

#### Participants

Cleoneice Isabela Silva Muller, MD, PhD, (*Presenter*) Author with royalties, RELX; Author with royalties, Wolters Kluwer nv; Speaker, AstraZeneca PLC; Speaker, General Electric Company

#### TEACHING POINTS

Introduction Pulmonary abnormalities on computed tomography (CT) in women with breast cancer may be secondary to pulmonary metastases, radiotherapy or systemic treatment of the primary tumor or metastases, increased prevalence of other cancers, or be due to an unrelated cause. In this exhibit we review the range of pulmonary abnormalities seen on CT and present representative cases illustrating the value of multidisciplinary discussion based on weekly oncology tumor board meetings at our institution and systematic follow-up of all patients. 1) To review the typical and atypical manifestations of pulmonary metastases at presentation and with progression or improvement. 2) To illustrate the CT findings of pulmonary complications related to treatment including radiation, chemotherapy, hormone therapy, targeted therapy and immunotherapy. 3) To discuss the differential diagnosis of

unrelated pulmonary abnormalities that may affect management. 4) To highlight the importance of multidisciplinary discussion in reaching a timely diagnosis.

#### **TABLE OF CONTENTS/OUTLINE**

1) Introduction; 2) Spectrum of manifestations and types of response of pulmonary metastases; 3) Pulmonary complications of radiotherapy; 4) Pulmonary complications of systemic therapy; 5) Unrelated pulmonary conditions; 6) Conclusions.

#### **CHEE-84 Chest Ultrasound: US Technique, Normal anatomy, Pearls and Pitfalls**

Participants

Heli Rueda, MD, Bogota, Colombia (*Presenter*) Nothing to Disclose

#### **TEACHING POINTS**

Review the appropriate technique and parameters to perform chest ultrasonography. Describe the normal anatomy of the chest wall, pleura, and lung parenchyma in ultrasound imaging, its pearls, and pitfalls. Illustrate the most common imaging findings in ultrasound of the pathologies involving the chest wall, diaphragm, pleura, and lung parenchyma.

#### **TABLE OF CONTENTS/OUTLINE**

Introduction  
Chest ultrasound technique  
Anatomy of the chest wall, pleura, and lung parenchyma in ultrasound  
Common imaging findings in the pathology of:  
Chest Wall and diaphragm  
Diaphragm paralysis  
Neoplastic involvement  
Pleura  
Pleural effusion  
Pneumothorax  
Pleural thickening  
Lung Parenchyma  
Atelectasis  
Consolidation  
Pulmonary edema  
Pulmonary nodules  
Conclusion

#### **CHEE-85HC Suboptimal Chest Radiography - Applying Art to the Science of Mitigating the Mammoth Issue**

Participants

Giridhar Dasegowda, MBBS, Boston, MA (*Presenter*) Nothing to Disclose

#### **TEACHING POINTS**

The audience will learn about the applied art and science in suboptimal chest radiographs (CXR): 1. Various causes of suboptimal CXRs with case-based illustration 2. Impact of suboptimal CXRs: The missed and misinterpreted findings 3. How parallel suboptimality affects the representation of art: Connecting CXR illusions with artistic allusions 4. Where and how artificial intelligence (AI) helps in mitigating suboptimal CXRs

#### **TABLE OF CONTENTS/OUTLINE**

The four-part exhibit will begin with case-based illustrations of what makes CXRs suboptimal and/or rejected for repeat acquisition. The second part will illustrate the impact of suboptimality on CXR findings including the missed and misinterpreted ones. In the third part, the presenting authors will use their own self-drawn, painted artwork to highlight how suboptimality affects the representation of art and interpretation of suboptimal CXRs. The final part informs about the role of AI in mitigating suboptimal CXRs. The free-to-share and display exhibit will help raise awareness about suboptimal CXRs and inspire a positive downward trend in suboptimal CXR frequency which according to some exist in as much as 90% of all CXRs. Please visit the Learning Center to also view this presentation in hardcopy format.

#### **CHEE-86 Perceptual Errors in Cardiothoracic Imaging**

Participants

Siddhi Hegde, MBBS, Mangalore, India (*Presenter*) Nothing to Disclose

#### **TEACHING POINTS**

-Studies have shown some areas of radiology have miss rates and (false negative) and false-positive rates as high as 30% of daily reads. -Errors have a significant impact on patient care and increase healthcare costs and burdens. -Perceptual errors can be due to errors in scanning, recognition, or decision. -Identifying and understanding the causes of perceptual errors, increasing awareness amongst trainees, and improving educational models can improve detection and localization accuracy. -Perceptual training algorithms geared toward the reduction of perceptual errors may be a useful adjunct to conventional radiology training.

#### **TABLE OF CONTENTS/OUTLINE**

-Different types of diagnostic errors in radiology and their frequency -What radiologists need to know about perceptual errors in the setting of cardiothoracic imaging. -Table demonstrating different types of perceptual errors in radiology, definitions, and potential means to overcome them.

#### **CHEE-87 "Down The Rabbit Hole": The Many Fistulous Pathways in the Thorax**

Participants

Murilo Peixoto, MD, Sao Paulo, Brazil (*Presenter*) Nothing to Disclose

#### **TEACHING POINTS**

Fistulous tracts in the thorax can involve a number of different spaces and have multiple causes. These unusual communications are hard to depict well, and when only standard imaging protocols are used they are often overlooked or misinterpreted. Imaging acquisition techniques and tips can be used to alter the common protocols and demonstrate these tracts more conspicuously.

#### **TABLE OF CONTENTS/OUTLINE**

Acquired and congenital fistulous tracts of the thoracic region often pose significant diagnostic difficulties to the radiologist. Multiple spaces can be involved, such as the tracheobronchial tree, pleural space, the digestive tract (such as the esophagus and stomach), the lymphatic and the circulatory systems; and many etiologies can be the culprit, such as infectious or inflammatory diseases, neoplasms, surgical and medical procedures, and so on. This presentation is a series of cases, by no means exhaustive, of the many fistulous tracts within the thoracic region, some of which with an unusual presentation. Tips and techniques of imaging acquisition are presented, in order to help better depicting these conditions.

#### **CHEE-88 Bronchial Morphology Changes after Lobectomy - Examination by Inspiratory and Expiratory**

## Imaging with Ultra-High-Resolution CT

### Participants

Hiroshi Moriya, MD, Fukushima, Japan (*Presenter*) Advisor, California Capital Equity, LLC; Research Grant, Canon Medical Systems Corporation

### TEACHING POINTS

Advances in CT technology and computer processing technology have made it easier to perform precise morphological disassembly and automatic extraction and volume measurement of anatomical structures. In the diagnosis after lobectomy, morphological changes such as thoracic deformity, pleural thickening, organizing pleural effusion, lung parenchyma, bronchi, and pulmonary arteries and veins can be analyzed. In particular, ultra-high-resolution CT (UHRCT) with improved spatial resolution can perform morphological measurement more precisely than conventional CT, so in addition to changes in the anatomical position of each lobe and the volume of the remaining lobe before and after excision.

### TABLE OF CONTENTS/OUTLINE

Equipment and method: UHRCT (Aquilion Precision, SHR mode), inspiratory / expiratory imaging. Workstation (Ziostation 1K). Results: It was possible to calculate the spatial position of the residual lobe and the ventilation volume for each lobe. By automatic extraction of the bronchial tree, it was possible to depict 3-dimensional expansion and flexion. Bronchial flexion case: Right upper lobectomy. There is an air trapping in the middle lobe. Decreased ventilation of the middle lobe located at the apex of the lung, and flexion and stenosis of the bronchus at the expiratory phase were confirmed. Adhesion case: Partial resection of the right upper lobe. Extensive adhesions due to pleural dissemination. Ventilation of the middle lobe is restricted. The bronchus was confirmed to be patency. Summary: UHRCT is excellent for bronchial morphological analysis. Inspiratory and expiratory CT can be used to analyze changes in bronchial morphology, movement and rotation of the lobes.

### CHEE-89 Cardiovascular Devices on Chest Radiographs

#### Participants

Taila Moura Fe, Sao Paulo, Brazil (*Presenter*) Nothing to Disclose

### TEACHING POINTS

The purposes of this exhibit are: Examine the most common cardiovascular devices seen on chest radiographs. Describe each cardiovascular device, including its proper location, components, types, and major complications. Illustrate those cardiovascular devices, using both usual and unusual cases from our chest radiology group.

### TABLE OF CONTENTS/OUTLINE

This exhibit will go over various cardiovascular devices that can be seen on a chest x-ray. The anticipated correct position, as well as the major complications associated with those devices, will be detailed and illustrated. Cardiac devices: - Pacemaker. - Ventricular assist device. - Occlusion devices. - Mitraclip. - Valve prosthesis. - Loop event recorder. Vascular devices: - Central venous catheter. - Port-a-cath. - Swan-Ganz catheter. - Intra-aortic balloon pump. - Extracorporeal membrane oxygenation (ECMO). - Exogenous material embolized.

### CHEE-9 When Chest MRI Plays the Big Role: a Guide for Useful Applications on Daily Practice

#### Participants

Murilo Peixoto, MD, Sao Paulo, Brazil (*Presenter*) Nothing to Disclose

### TEACHING POINTS

- Thoracic lesions can have a wide variety of differential diagnoses. - Chest magnetic resonance imaging (MRI) can be helpful for narrowing down the different etiologies when lesions detected in other imaging methods demonstrate nonspecific features. - Chest MRI is an increasingly available method that uses no ionizing radiation and has sufficient spatial resolution for a number of usages.

### TABLE OF CONTENTS/OUTLINE

Chest MRI is a widely underappreciated imaging modality, despite its large applicability in the evaluation of abnormalities of cardiovascular origin, of the mediastinum, the pleural space, the brachial plexus, the chest wall and even the lung parenchyma. It is thought that a broader usage of chest MRI is discouraged by the motion artifacts generated by cardiac and respiratory motions and the low signal-to-noise ratio yielded by the large amount of air in the lungs. However, there is great value in utilizing the multiple resources offered by MRI, such as T1, T2, diffusion, in-phase and out-of-phase sequences in order to narrow down the differential diagnoses of lesions found through other imaging methods such as computerized tomography (CT). MRI quality and availability is continuously increasing over the years, so radiologists are facing these diagnostic dilemmas more and more frequently, and knowledge of the behavior of thoracic lesions on MRI is also increasingly important. In this work, we intend to demonstrate how the resources offered by chest MRI can be used to narrow down the differential diagnoses of different thoracic lesions.

### CHEE-90 A Pictorial Review of Pleural Disease: Multimodality Imaging and Differential Diagnosis

#### Awards

Identified for RadioGraphics

Certificate of Merit

#### Participants

Aya Yamada, Kashihara, Japan (*Presenter*) Nothing to Disclose

### TEACHING POINTS

1) To review the spectrum of clinico-radiological features of pleural diseases 2) To discuss the clinico-radiological key findings in the differential diagnosis

### TABLE OF CONTENTS/OUTLINE

1) Clinical findings of pleural diseases 2) Illustrated findings of the following pleural anatomy and diseases I Normal variants (incomplete fissure, accessory fissure) II Asbestos pleural diseases (pleural plaque, pleural mesothelioma) III Inflammatory and infectious

diseases (fibrinous pleuritis, TB/actinomycotic empyema)| Pleural tumors (solitary fibrous tumors, neurogenic tumors, desmoid-type fibromatosis)| Lymphoproliferative diseases (pyothorax associated lymphoma, methotrexate-associated lymphoproliferative disorders)| Miscellaneous (thoracic endometriosis, talc pleurodesis)<sup>3</sup> Clinico-radiological key findings in the differential diagnosis

### **CHEE-91 Pulmonary Tuberculosis: Beyond The Typical Patterns**

Participants

Matheus Garcia Lago Machado, MD, Rio de Janeiro, Brazil (*Presenter*) Nothing to Disclose

#### **TEACHING POINTS**

Discuss the physiopathology, epidemiology, and clinical manifestations of pulmonary tuberculosis (PTB). Learn to recognize the atypical distribution of small nodules and uncommon patterns of PTB. Review and illustrate imaging findings. Discuss the main differential diagnosis.

#### **TABLE OF CONTENTS/OUTLINE**

Comprehensive review of pulmonary tuberculosis: pathogenesis; epidemiology; clinical manifestations. Atypical distribution of small nodules and uncommon patterns clusters of non-coalescent small nodules; coalescent small nodules - Galaxy sign; nodular reversed halo sign; subpleural nodules and fissural nodularity; halo sign; mass-like consolidation; pulmonary artery pseudoaneurysm - Rasmussen's aneurysm; tracheobronchial abnormalities; endogenous reactivation. Main differential diagnosis.

### **CHEE-92 The Nerve of Some Chest Diseases: Conditions affecting the Thorax and Nervous System**

**Awards**

**Certificate of Merit**

Participants

Girish S. Shroff, MD, Houston, TX (*Presenter*) Nothing to Disclose

#### **TEACHING POINTS**

A variety of systemic diseases may affect both the nervous system and the thorax, while other diseases primarily affecting the thorax may manifest with neurological abnormalities. Correlations of signs, symptoms, and imaging findings in the neurological system with those in the thorax can help guide further diagnostic work-up and treatment. We will illustrate the imaging appearance of several systemic/neurological diseases with thoracic manifestations as well as discuss conditions in the thorax that can lead to neurologic symptoms.

#### **TABLE OF CONTENTS/OUTLINE**

Inflammatory: Sarcoidosis Dermatomyositis/polymyositis IgG4 disease Infectious: COVID-19 Tuberculosis Invasive fungal infection Syphilis Malignancy: Myasthenia gravis and thymic abnormalities Meningioma with intrathoracic metastases Paraganglioma Vascular: Vasculitis (Giant Cell Arteritis and Takayasu Arteritis) Congenital: Tuberous sclerosis Hereditary hemorrhagic telangiectasia Neurofibromatosis type 1

### **CHEE-93 Something is Not Right in the Chest! Postoperative Thoracic Surgery Complications That Cannot be Overlooked in a CT Scan - A Pictorial Essay**

Participants

Yuri Neves, MD, Sao Paulo, Brazil (*Presenter*) Nothing to Disclose

#### **TEACHING POINTS**

1-Discuss the role of radiology in postoperative thoracic evaluation. 2-Review normal postoperative findings of most common thoracic surgeries, such as lung resections: segmentectomy, lobectomy, and pneumonectomy. 3-Recognize the imaging findings related to postoperative complications and what is important to report. 4-Highlight the radiologist role in decision-making within a multidisciplinary team when assessing thoracic surgery early and late outcomes.

#### **TABLE OF CONTENTS/OUTLINE**

1-Introduction: basic concepts on thoracic surgery (most common techniques and clinical scenarios, purpose / goals, highlights of operative technique). 2-CT protocols available and importance of x-ray analysis.3 - Normal postoperative findings (acute and chronic): Surgical threads; Band atelectasis and fibrotic streaks; Mediastinal and diaphragm shift; Compensatory remanent lung hyperinflation; Pneumothorax (small); Pleural effusion (small or non-loculated).4-Postoperative complications and its findings: Empyema; Bronchopleural fistula; Re-expansion pulmonary edema; Airway and / or vascular stenosis or compressions; Kinking of bronchial branch; Post bronchoplasty bronchial stenosis (telescoping); Pulmonary torsion; Postpneumonectomy syndrome; Inadvertent pulmonary vein clamping; Hilar hematoma; Pulmonary hernia.

### **CHEE-94 Beyond 5Ts: Pearls and Pitfalls in Diagnosis of Anterior Mediastinal Masses**

Participants

Tetsuro Araki, MD, PhD, Philadelphia, PA (*Presenter*) Nothing to Disclose

#### **TEACHING POINTS**

1. To understand appropriate image modalities for anterior mediastinal masses (AMM). 2. To understand common differential diagnosis of AMM. 3. To understand key image finding in differential diagnoses of AMM.

#### **TABLE OF CONTENTS/OUTLINE**

1. Appropriate selection of image modalities for AMM a. Role of chest radiograph, CT, and MRI b. Additional imaging options (Dual-energy CT, PET/CT, SPECT) 2. Anatomy of mediastinum a. Mediastinal compartment suggested by Felson b. Cross sectional mediastinal compartment suggested by ITMIG c. Common lesions in each compartment 3. Review of 5Ts a. Thymic epithelial tumors: Top of differential of AMM? b. Thyroid tumor: Is MRI helpful? c. Teratoma: Macroscopic fat, when it's malignant? d. Terrible lymphoma: Why terrible? e. Thoracic aorta: not neoplastic, though f. Are 5Ts common as AMM? 4. Beyond 5Ts: More practical DD of AMM than 5Ts a. Lymph nodes b. Benign mediastinal lesions (Thymic cyst/pericardial cyst) • Unilocular vs multilocular thymic

cyst • Morgagni hernia c. Normal/hyperplastic thymus • Normal morphology of thymus • What is "normal" thymus for age and sex • True vs lymphoid hyperplasia d. Ectopic thyroid lesion 5. Key image features useful in differential a. CT density and MRI signal density on T1 and T2WI b. Solid vs cystic c. Microscopic and macroscopic fat d. Detection of calcification e. Diffusion weighted images/ADC map f. FDG uptake on PET/CT g. Iodine and fat quantification on DE-CT 6. Summary

### **CHEE-95 "Pop Under Pressure" - Common and Uncommon Imaging Findings in Barotrauma**

Participants

Caleb Carroll, BS, (*Presenter*) Nothing to Disclose

#### **TEACHING POINTS**

1. Pulmonary barotrauma is typically diagnosed on imaging and can be associated with increased mortality therefore it is important to recognize and promptly manage barotrauma. Critical to diagnosis is a high suspicion especially in those at high risk. 2. In addition to common imaging findings (pneumomediastinum, pneumothorax, pneumoperitoneum, and subcutaneous emphysema), few uncommon findings (pneumopericardium, broncho-pleural fistula, tension lung cyst, subpleural air cyst and air embolism) may be present.

#### **TABLE OF CONTENTS/OUTLINE**

1. Discuss definition, possible mechanisms and etiologies associated with pulmonary barotrauma. 2. Epidemiology of barotrauma in different clinical scenarios. 3. Illustrative cases showing common and uncommon manifestations of barotrauma. 4. Briefly discuss clinical features, the prevention, diagnostic evaluation, and management of barotrauma.

### **CHEE-96 The Many Faces of Tracheal Pathology - CT Image-based Quiz and Review of Normal Variants and Main Tracheobronchial Diseases**

Participants

Carlota Garcia de Andoin Sojo, MD, Bilbao, Spain (*Presenter*) Nothing to Disclose

#### **TEACHING POINTS**

CT is the best non-invasive imaging modality to evaluate the trachea and its potential diseases. Most tracheal diseases cause stenosis and have different causes and treatments. The knowledge of their specific features in CT helps to approach the diagnosis.

#### **TABLE OF CONTENTS/OUTLINE**

Objectives To review tracheal diseases and their characteristic features on CT. To describe normal variants of the tracheobronchial tree. Findings: A CT image-based quiz will lead the review of: Normal Variants: The knowledge of the non-pathological variants of the tracheobronchial tree will avoid mistakes. The most frequent anatomical variants are tracheal bronchus and accessory cardiac bronchus. Tracheal pathology: Tracheal diseases are congenital or acquired and can be diffuse or focal. Most of them cause tracheal stenosis in asymptomatic patients. These pathologies can have iatrogenic, neoplastic, congenital origins or be related to systemic diseases. Neoplastic causes can be benign or malignant and include hamartomas, papillomas, lipomas, leiomyomas, epidermoid carcinomas, adenoid cystic carcinomas or metastases. Other origins are sheath trachea, tracheobronchomalacia, tracheobronchial amyloidosis, sarcoidosis, Wegener granulomatosis, relapsing polychondritis, tracheobronchopathia osteochondroplastica and inflammatory bowel disease with tracheobronchial involvement. The Mounier-Kuhn syndrome is a rare entity that causes tracheobronchomegalia. Conclusion Several tracheal diseases show slight symptoms and subtle CT findings. The knowledge of these entities enables radiologists to reduce the differential diagnosis and give information to plan future bronchoscopies and treatments.

### **CHEE-97 That Escalated Quickly: Etiology, Pathophysiology, and Imaging Findings of Rapidly Progressive Interstitial Lung Disease**

Participants

Andrew Simmerman, MD, (*Presenter*) Nothing to Disclose

#### **TEACHING POINTS**

1. The lungs' response to acute injury follows a predictable course even across disparate etiologies. Radiologists should recognize the typical imaging manifestations of RP-ILD along with their associated disorders. 2. Acute complications of RP-ILD include pneumomediastinum and pneumothorax. 3. RP-ILD may resolve or evolve into other chronic ILD patterns.

#### **TABLE OF CONTENTS/OUTLINE**

I. Overview of acute lung injury and healing process a. Acute/subacute i. Histology of diffuse alveolar damage (DAD) and organizing pneumonia (OP) ii. HRCT appearance of DAD and OP b. Chronic i. Resolution or fibrosis II. Defining RP-ILD a. Timeline b. Severity c. Alternative names in the literature III. Etiologies of RP-ILD, with example cases a. Connective tissue disease i. Various types: myositis, rheumatoid arthritis, scleroderma, lupus ii. Anti-melanoma differentiation-associated gene 5 dermatomyositis (high association with RP-ILD) b. Viral infection i. COVID-19/SARS/MERS ii. Influenza c. Acute Interstitial Pneumonia d. Acute Exacerbation of ILD e. Treatment-related pneumonitis i. Medications ii. Chemotherapy/immunotherapy iii. Radiation IV. Clinical significance of RP-ILD a. Treatment b. Prognosis: acute and chronic phases c. Follow-up

### **CHEE-98 Pulmonary Actinomycosis: CT Findings and Differential Diagnosis**

Participants

Yoshie Kunihiro, MD, Ube, Japan (*Presenter*) Nothing to Disclose

#### **TEACHING POINTS**

Pulmonary actinomycosis is a chronic suppurative infection caused by *Actinomyces* species and the infection occurs typically due to aspiration of endogenous organisms. There are a variety of CT findings of pulmonary actinomycosis, however, there are some key points for differential diagnosis. The purpose of this exhibit is: 1. To explain the clinical characteristics and the common CT findings of pulmonary actinomycosis. 2. To review the CT images of pulmonary actinomycosis with uncommon findings such as bronchiectatic form and endobronchial calcified nodule. 3. To discuss the differential diagnosis of pulmonary actinomycosis, including pulmonary tuberculosis, fungal infection, lung cancer and granulomatosis with polyangiitis.

## TABLE OF CONTENTS/OUTLINE

(1) Clinical characteristics of pulmonary actinomycosis (2) CT findings of pulmonary actinomycosis (3) Sample cases (4) Differential diagnosis

## CHEE-99 Thoracic Parasitic Disease: A Radiologic and Pathologic Review

Participants

Cecilia Davis-Hayes, MD, (*Presenter*) Nothing to Disclose

## TEACHING POINTS

Parasitic diseases affect immunocompetent and immunocompromised patients worldwide. To create an accurate differential diagnosis for thoracic infections, radiologists must utilize both patient travel history and characteristic imaging findings. Understanding both imaging patterns and the geographic distribution of these diseases will help to narrow the differential and can impact clinical testing and management. Although some parasitic infections result in nonspecific imaging findings, familiarity with their imaging features as well as their epidemiological, clinical, and pathologic features may be helpful in to ensure the appropriate diagnosis and treatment.

## TABLE OF CONTENTS/OUTLINE

1. Review endemic thoracic parasitic diseases A. Helminths i. Cestodes (tapeworm), e.g Echinococcus ii. Nematodes (roundworm), e.g Strongyloidiasis Ascariasis iii. Trematode (flake), e.g. Schistosomiasis B. Protozoa i. Amebiasis ii. Trypanosomiasis (Chagas Disease)2. Epidemiology 3. Modes of transmission/ lifecycle 4. Geographic distribution 5. Clinical presentation 6. Imaging/ pathology findings

Printed on: 02/07/23



## Abstract Archives of the RSNA, 2022

CHEE-1

### Postoperative Chest Imaging Findings: Pearls and Pitfalls

Sunday, Nov. 27 8:00AM - 9:00AM Room: Learning Center - CH

#### Awards

Certificate of Merit

#### Participants

Sofía Ventura- Diaz, MD, Madrid, Spain (*Presenter*) Nothing to Disclose

#### TEACHING POINTS

To have an understanding of the different surgical techniques, including invasive and minimally invasive procedures  
To review the different types of lung resection  
To know the indications of thoracic surgery  
To recognize normal expected findings  
To identify potential complications in chest radiography and CT in order to optimize patient care in the postoperative period

#### TABLE OF CONTENTS/OUTLINE

Surgical techniques: minimally invasive techniques (video-assisted thoracoscopic surgery and robotic- assisted thoracic surgery) and open thoracotomies (Posterolateral, Shaw-Paulson, Anterolateral, axillary thoracotomy, thoracoabdominal incision, bilateral anterior transternal thoracotomy...) Types of lung resection and indications: sublobar resection (including wedge resection and segmentectomy), lobectomy, pneumonectomy (intrapleural, extrapleural, intrapericardial) Normal findings for each type of resection in Radiographs and Computed Tomography Complications: • Airway and lung complications: Atelectasis, Pneumonia, Pulmonary edema, Acute respiratory distress syndrome, Air leak/bronchopleural fistula, Post pneumonectomy syndrome, lobar torsion, lung herniation. • Mediastinal and cardiovascular complications: Mediastinal hematoma, Acute mediastinitis/mediastinal abscess, Pneumopericardium, Cardiac herniation, Stump thrombus, Pulmonary Pseudoaneurysm. • Pleural and esophageal complications: Empyema, Hemothorax, Chylothorax, Esophageal anastomotic leak and esophagopleural fistula.

Printed on: 02/07/23

## Abstract Archives of the RSNA, 2022

CHEE-10

### Hidden in Plain Sight: Applications of the Aorto-Esophageal Ligament

Sunday, Nov. 27 8:00AM - 9:00AM Room: Learning Center - CH

#### Participants

Nanditha Guruvaiah, BSc, Staten Island, NY (*Presenter*) Nothing to Disclose

#### TEACHING POINTS

While it is not uncommon to see central mediastinal pathology on cross-sectional imaging, it is important to understand the pathway influencing the spread of disease at a radiological point of view. Mediastinal facial planes can be visualized in cross sectional imaging such as CT and MRI. However, MRI is more successful in identifying the mediastinal visceral fascia and the aorto-esophageal (AE) ligament; which courses from the anterior aspect of the aorta to the left lateral aspect of the esophagus. This recently discovered unknown anatomy aids us in understanding the possible pathway of spread of disease processes such as infection, air, fluid, and soft tissue (lipomas) in the mediastinum. CT and MRI could also be useful in determining the lymph node metastasis and tumor in growth in relation to the AE ligament. In addition, the aorto-esophageal ligament can be utilized in the preoperative planning of minimally invasive thoracic surgeries.

#### TABLE OF CONTENTS/OUTLINE

- Introduction to anatomy of Aorto-Esophageal Ligament
- Classification of Mediastinal compartments on cross section imaging
- Role of Imaging in identifying AE ligament - benefits and limitations
- Application of AE ligament in imaging - Spread of disease (gas, fluid and soft tissue) in the mediastinum - Preoperative surgical planning - Oncology imaging, notably spread of lymph nodes
- Case based learning
- What Radiologists should know about AE ligament

Printed on: 02/07/23



## Abstract Archives of the RSNA, 2022

CHEE-100

### Interpreting the Unexpected: Diagnostic Imaging Findings in Mycobacterium Chimaera Infection

Sunday, Nov. 27 8:00AM - 9:00AM Room: Learning Center - CH

#### Participants

Andrew Moore, MD, (*Presenter*) Nothing to Disclose

#### TEACHING POINTS

1. Mycobacterium chimaera (MC) is an indolent infection that is often misdiagnosed or underrecognized. Having a high clinical suspicion and knowing its various imaging manifestations help avoid delay in diagnosis and allow for earlier treatment 2. Slowly developing or enlarging peri-sternotomy fluid collections, soft-tissue thickening or both, without other clinical findings to suggest acute infection may be seen with mycobacterium chimaera infection 3. PET/CT is a useful adjunct to suggest indolent infection in patients with unremarkable CT scans and in those with a high clinical suspicion of infection

#### TABLE OF CONTENTS/OUTLINE

1. Background/Epidemiology a. MC is a nontuberculous mycobacterium found in environment b. Disease manifestations include disseminated, pulmonary and surgical site c. Water used in Heater-Cooler Devices (HCD) became contaminated by MC which is then aerosolized by HCD fans during cardiothoracic surgery d. Surgical site or disseminated disease occurs after cardiothoracic surgery where patient, implanted material or both become infected with aerosolized MC 2. Clinical Course of MC Infection 3. CT PET/CT Findings a. Sternotomy site b. Blurred vascular wall c. Insidious development of fluid collections and soft tissue thickening/tracts d. Persistent fluid collections despite treatment enhancement characteristics e. Disseminated disease 4. Conclusion

Printed on: 02/07/23

## Abstract Archives of the RSNA, 2022

CHEE-101

### **Pulmonary Fungal Disease Patterns in CT: Recognizing and Differentiating**

Sunday, Nov. 27 8:00AM - 9:00AM Room: Learning Center - CH

#### **Participants**

Isabela Oliveira, MD, Campinas, Brazil (*Presenter*) Nothing to Disclose

#### **TEACHING POINTS**

Recognize the different radiologic patterns of fungal lung infections. Be familiar with the main fungal entities involved in certain radiologic patterns. Know the main differential diagnoses for the mentioned patterns. Differentiate between the entities involved in both immunocompetent and immunocompromised hosts.

#### **TABLE OF CONTENTS/OUTLINE**

1. Introduction. 2. Systematic approach - imaging patterns of thoracic fungal diseases: a. Ground glass opacities; b. Nodules; c. The halo and reversed halo signs; d. Miliary pattern; e. Mediastinal involvement; f. Airway disease; g. Cavitations. 3. Pattern-based differential diagnosis: Ground glass due to viral infection; Nodules related to lung metastasis; The halo and reversed halo sign related to organizing pneumonia; Miliary pattern related to neoplasia; Mediastinal involvement related to neoplasia; Airway disease related to viral respiratory tract infection; Cavitations related to vasculitis. 4. Major fungal pathogens according to imaging patterns and immunological status (immunocompetent vs. immunocompromised hosts). 5. Summary

Printed on: 02/07/23



## Abstract Archives of the RSNA, 2022

CHEE-102

### Emergency and Critical Care Chest Radiography: Pitfalls and Pearls with CT Correlation

Sunday, Nov. 27 8:00AM - 9:00AM Room: Learning Center - CH

#### Participants

Sayed Mohammad Seyedsaadat, MD, (*Presenter*) Nothing to Disclose

#### TEACHING POINTS

1. Prompt diagnosis of many emergent conditions with chest radiography requires appreciation of subtle or easily misinterpreted radiographic findings; a systematic search pattern is essential for prompt detection. 2. Awareness of direct and indirect findings of pleural and parenchymal emergencies such as pneumothorax, hemothorax, bronchopleural fistula, empyema, laceration, and abscess can prevent treatment delays. 3. Early detection of abnormal mediastinal lines, stripes, and interfaces can be clues to life-threatening pathology such as aortic dissection, mediastinitis, and mediastinal hemorrhage. 4. Diaphragmatic injuries, fractures, and sternal dehiscence are frequently missed emergent radiographic findings, requiring a high level of suspicion and knowledge of common patterns of injury. 5. Attention to the position and the courses of the lines and tubes in their entirety on the chest radiograph can help to detect extrathoracic device misplacement or related complications.

#### TABLE OF CONTENTS/OUTLINE

Pitfalls and pearls of chest imaging in the emergency and critical care unit with CXR/CT correlation. Pleura (PTx on supine CXR, bronchopleural fistula, empyema) Lung Parenchyma (Cardiogenic vs noncardiogenic pulmonary edema, lung abscess) Heart and vessels (Traumatic aortic injury, mediastinal hematoma, mediastinitis) Diaphragm and chest wall (Diaphragmatic rupture, sternal dehiscence, fractures) Lines and tubes (Vascular, cardiac, pleural, airway devices) PDF Upload.

Printed on: 02/07/23



## Abstract Archives of the RSNA, 2022

CHEE-103

### Osseous Lesions in Oncologic Patients

Sunday, Nov. 27 8:00AM - 9:00AM Room: Learning Center - CH

#### Participants

Alexander Sytov, (*Presenter*) Nothing to Disclose

#### TEACHING POINTS

The finding of an incidental focal osseous lesion in an oncologic patient poses a unique diagnostic challenge due to the heightened concern for metastasis. While the majority of osseous lesions are benign, many may closely resemble metastasis on imaging, prompting the need for clear methods of differentiation. By following an algorithm for categorizing osseous lesions, radiologists may confidently recommend follow-up imaging studies while avoiding unnecessary referrals. After reviewing this exhibit, the learner will be able to:- Employ a systematic method to characterize osseous lesions according to their density, composition, and cortical features- Identify imaging features that characterize osseous lesions as malignant or benign (such as: wide zone of transition, discontinuous cortex, soft tissue component replacing the medullary cavity, or extension beyond the margin of the bone)- Identify several frequently encountered benign osseous lesions that resemble metastasis- Establish an appropriate imaging algorithm to further characterize osseous lesions in these patients

#### TABLE OF CONTENTS/OUTLINE

- Introduction: imaging features of osseous lesions with special emphasis on features suggestive of malignancy- Pictorial review of several commonly encountered benign osseous lesions that resemble metastasis in oncologic patients- Imaging algorithm to further characterize osseous lesions

Printed on: 02/07/23



## Abstract Archives of the RSNA, 2022

CHEE-104

### Read Like A Pro: Tips and Tricks to Interpret Like a Cardiothoracic Radiologist

Sunday, Nov. 27 8:00AM - 9:00AM Room: Learning Center - CH

#### Awards

Certificate of Merit

#### Participants

Melissa Carroll, MD, Kansas City, KS (*Presenter*) Nothing to Disclose

#### TEACHING POINTS

1. Misconceptions in chest imaging may lead to excessive imaging, missed diagnoses, or inappropriate therapies, such as missed detection of malignancy manifesting as cyst associated lung cancer. Other misconceptions may lead to unnecessary follow up of nodules identified on incomplete thoracic exams. 2. Knowledge of these misconceptions may lower costs, increase accuracy, and improve patient outcomes.

#### TABLE OF CONTENTS/OUTLINE

1. Background  
2. Malignancy  
a. Lung cancer manifesting as cyst associated malignancy, persistent consolidation and subsolid nodule  
b. Incidental nodule on incomplete chest CT  
c. Intrapulmonary lymph node  
3. Diffuse Lung Disease  
a. Reverse halo sign with pulmonary infarct  
b. DIPNECH as underdiagnosed disease  
c. Patchy tree-in-bud opacities from infectious or aspiration bronchiolitis  
d. Differentiating airspace enlargement with fibrosis from honeycombing  
e. Dendriform pulmonary ossification due to pulmonary fibrosis or aspiration  
4. Mediastinum  
a. Pericardial recesses misinterpreted as lymphadenopathy  
b. Distinguishing normal thymus from mass  
5. Vasculature  
a. Flow-related artifacts mimicking pulmonary embolism or dissection  
b. Diffuse tree-in-bud opacities with excipient lung disease  
c. Beaded vasculature with endovascular metastases  
6. Pleura/Chest Wall  
a. Extrapleural fat deposition mimicking cardiomegaly or pleural effusion  
b. Elastofibroma mimicking chest wall mass  
7. Conclusion

Printed on: 02/07/23



## Abstract Archives of the RSNA, 2022

CHEE-105

### Unraveling the maze - Patterns of lung cancer lymphatic dissemination

Sunday, Nov. 27 8:00AM - 9:00AM Room: Learning Center - CH

#### Participants

Marcus Vinicius Silva Ferreira, MD, Sao Paulo, Brazil (*Presenter*) Nothing to Disclose

#### TEACHING POINTS

This exhibition aims to review: • Anatomy of the lymphatic drainage of the lungs and mediastinal node stations. • Multimodality imaging staging of lung cancer, with focus on lymph node (LN) status and its importance to the appropriate lung cancer management. • Indications and impact of different types of lymphadenectomy: selective versus systematic node dissection. • A practical approach to lobe-specific nodal spread of lung cancer with imaging correlations.

#### TABLE OF CONTENTS/OUTLINE

1. BACKGROUND 1.1. Lung cancer overview 2. 8TH LUNG CANCER STAGE CLASSIFICATION 3. LYMPH NODE EVALUATION 3.1. Invasive and non-invasive approach to mediastinal nodal evaluation 3.2. Imaging characteristics of suspicious nodes 4. LYMPHATIC ANATOMY 4.1. Lungs and bronchial tree 4.2. Mediastinal Lymph nodes stations 5. LOBE-SPECIFIC PATTERNS OF LYMPHATIC SPREAD 5.1. Right upper lobe 5.2. Right middle lobe 5.3. Right Lower Lobe 5.4. Left Upper Lobe / Lingula 5.5. Left Lower Lobe 6. IS IT FEASIBLE TO ADOPT A SELECTIVE APPROACH? EVIDENCE SO FAR 7. NOVEL IMAGING TECHNIQUES AND FUTURE DIRECTIONS 8. TAKE-HOME MESSAGES

Printed on: 02/07/23



## Abstract Archives of the RSNA, 2022

CHEE-106

### Basics of Lung Cancer Related to Cysts and Enlarged Cystic Air-spaces: Survival Guide for General Radiologist

Sunday, Nov. 27 8:00AM - 9:00AM Room: Learning Center - CH

#### Participants

Laima Tamkeviciute, MD, (*Presenter*) Nothing to Disclose

#### TEACHING POINTS

1. Lung cancer can manifest as lung cysts or enlarged airspaces. 2. This type of lung cancer represents significant number of missed diagnosis. 3. The main concerning features of lung cysts and enlarged cystic air-spaces include: wall thickening or nodules, adjacent ground glass changes, multilocular cysts, increase in size or change of internal structure overtime. 4. Knowledge of the various imaging presentations of lung cancer is essential for timely diagnosis and treatment thus preventing development of invasive disease.

#### TABLE OF CONTENTS/OUTLINE

I. Introduction: 1. Why do we have to raise awareness about lung cysts and enlarged cystic air-spaces? 2. What is the mechanism and pathogenesis of lung cysts and enlarged cystic air-spaces? II. Imaging findings 1. How lung cysts and enlarged cystic air-spaces should be described? 2. What are the concerning features of lung cysts and enlarged cystic air-spaces? 3. How malignant cysts and enlarged air-spaces can change overtime? III. Conclusion and take home message

Printed on: 02/07/23

## Abstract Archives of the RSNA, 2022

CHEE-109

### Ultrasound Guided-Procedures in the Lung - What, When and How

Sunday, Nov. 27 8:00AM - 9:00AM Room: Learning Center - CH

#### Participants

Ivan Vollmer, MD, Barcelona, Spain (*Presenter*) Nothing to Disclose

#### TEACHING POINTS

-To describe the indications for interventional procedures in pulmonary pathology.-To review the interventional lung procedures that can be performed with ultrasound guidance.-To analyze the advantages and disadvantages of ultrasound guidance.-To describe how each procedure is carried out.

#### TABLE OF CONTENTS/OUTLINE

The different interventional lung procedures that can be performed with ultrasound guidance will be reviewed:-Lung biopsy-Pneumonia puncture.-Lung abscess drainage.-Intraoperative localization of lung nodules.The specific indications for each lung procedure as well as its advantages of using ultrasound guidance over other techniques such as CT will be covered.Moreover, the technique that should be used in each procedure and the pre and post procedure recommendations will also be addressed.

Printed on: 02/07/23



## Abstract Archives of the RSNA, 2022

CHEE-11

### From Gemcitabine, through Checkpoint Inhibitors to CAR T Cell - Evolution of Managing Treatment Related Pneumonitis in Cancer: Beyond Diagnosis

Sunday, Nov. 27 8:00AM - 9:00AM Room: Learning Center - CH

#### Awards

**Certificate of Merit**

#### Participants

Kaustav Bera, MD, Cleveland, OH (*Presenter*) Nothing to Disclose

#### TEACHING POINTS

1. Review cancer drugs that are primarily responsible for causing pneumonitis as well as differentiating it from other treatment related findings 2. Discuss the CT imaging patterns of drug-induced pneumonitis 3. Discuss potential mimics of drug-induced pneumonitis patterns including cytokine release syndrome in CAR-T cell therapy 4. Discuss the crucial role of the radiologist in monitoring/management of treatment-related pneumonitis with a focus on established guidelines 5. Discuss use-cases of common anti-neoplastic agents causing pneumonitis - from Gemcitabine, through ICI to CAR-T cells

#### TABLE OF CONTENTS/OUTLINE

1. Discuss common anti-neoplastic agents that cause pneumonitis 2. Enumerate prevalently reported imaging patterns of pneumonitis, along with their typical imaging findings 3. Discuss other potential complications of anti-cancer therapy (Pleural effusions, Pneumonia, Worsening tumor burden, airway obstruction) 4. Common mimics of drug-induced pneumonitis (atypical pneumonia, COVID-19, Cytokine release syndrome) 5. Discuss presenting clinical symptoms and grading system for drug-induced pneumonitis (CTCAE and ASCO) 6. Management guidelines for drug-induced pneumonitis with special focus on checkpoint inhibitors (ICI), targeted therapy, Antimetabolites (Gemcitabine) 7. How a Radiologist plays an important role in management 8. Prognosis and clinical outcome of patients developing drug-induced pneumonitis 9. Real-world cases showing management and clinical course of drug-induced pneumonitis in cancer therapies from Bleomycin, Gemcitabine to combination ICI and CAR-T cells

Printed on: 02/07/23



## Abstract Archives of the RSNA, 2022

CHEE-110

### Added Diagnostic Value of Portable Dual-energy Chest X-ray in a Non-radiological Reviewing Environment

Sunday, Nov. 27 8:00AM - 9:00AM Room: Learning Center - CH

#### Participants

Karim Karim, PhD, Waterloo, ON (*Presenter*) Officer, KA Imaging Inc

#### TEACHING POINTS

- Understand Dual-Energy Subtraction (DES) X-ray, the limitations of the old Dual-Exposure DES techniques, and how a Single Exposure portable detector can overcome these limitations.
- Understand the clinical benefits enabled by portable Single Exposure Dual-Energy for small nodules identification, pneumonia, pneumothorax, and finding line and tube tips.
- Learn about the added diagnostic value of dual-energy portable chest X-ray in a non-radiological reviewing environment for both regular and radiology trained clinicians.

#### TABLE OF CONTENTS/OUTLINE

This exhibit teaches the added diagnostic value of dual-energy X-rays (DEX) obtained using a novel portable multilayer detector in a reviewing environment simulating a non-radiological practice. A set of 28 AP images were obtained using a novel portable multilayer DEX detector. A team of five (5) readers was recruited that included two fellowship-trained chest radiologists and the rest non-specialists. The team was provided with the conventional X-ray images first, and subsequently were unblinded to the corresponding DEX images. For both sets of images, the readers were asked to assess the presence of pulmonary nodules > 5 mm, pneumothorax, pneumonia (left and right lung), bone fractures, and tips of central and GI lines using a five point scale. Readers were also asked whether the additional DEX images (soft tissue, bone) impacted their confidence. Initial results show that DEX images, taken alongside CR, helped improve diagnostic confidence.

Printed on: 02/07/23



## Abstract Archives of the RSNA, 2022

CHEE-111

### Bronchoscopic Lung Volume Reduction: Pre and Post Procedure Imaging Assessment

Sunday, Nov. 27 8:00AM - 9:00AM Room: Learning Center - CH

#### Awards

Certificate of Merit

#### Participants

Daniel Green, MD, (*Presenter*) Nothing to Disclose

#### TEACHING POINTS

1) Bronchoscopic lung volume reduction is a non-pharmacologic treatment for severe COPD, 2) Less invasive alternative to lung volume reduction surgery, 3) Goal is complete collapse of the most emphysematous lobe, 4) Imaging is necessary for patient selection, and radiologists have an important role in multidisciplinary discussion, 5) The main role of pre-procedure CT is assessment of emphysema severity, emphysema distribution, and fissure integrity, 6) Sagittal and coronal reconstructions are helpful for fissure integrity, 7) Pneumothorax is the most common complication but does not typically affect clinical outcome

#### TABLE OF CONTENTS/OUTLINE

1) Description of procedure, 2) Patient selection, 3) Chest CT protocol, 4) Pre-procedure imaging assessment, 5) Expected post-procedure imaging findings, 6) Complications, 7) Other bronchoscopic lung volume reduction techniques in development

Printed on: 02/07/23



## Abstract Archives of the RSNA, 2022

CHEE-112

### Postoperative Imaging After Surgery for Lung Cancer - From Relatively Common Complications to Rare Complications that Radiologists Need to Know

Sunday, Nov. 27 8:00AM - 9:00AM Room: Learning Center - CH

#### Participants

Makiko Murota, MD, Kitagun, Japan (*Presenter*) Nothing to Disclose

#### TEACHING POINTS

The purpose of the exhibit is: 1. To review surgical procedures and the postoperative changes for lung cancer. 2. To describe the imaging features of the complications after surgery. 3. To discuss how even rare complications can be radiologically significant.

#### TABLE OF CONTENTS/OUTLINE

1. The surgical procedures for lung cancer
2. The imaging findings of the normal postoperative changes: CXR and CT
3. The imaging features and the clinical manifestations of the complications after surgery: relatively common complications and rare complications
4. Summary

Printed on: 02/07/23



## Abstract Archives of the RSNA, 2022

CHEE-113

### Imaging of Mechanical Circulatory Support Devices For Right Ventricular Failure

Sunday, Nov. 27 8:00AM - 9:00AM Room: Learning Center - CH

#### Participants

Gregory Jew, MD, Rochester, NY (*Presenter*) Nothing to Disclose

#### TEACHING POINTS

1. Review of options for acute mechanical right ventricular circulatory support including: The TandemHeart centrifugal flow pump (TandemLife, Pittsburgh, PA), the axial-flow Impella RP catheter (Abiomed Inc, Danvers, MA), the Protek Duo dual lumen cannula, and the veno-arterial extracorporeal membrane oxygenation (VA-ECMO).1a. Review of right ventricular bypass methods.1b. Review of methods of oxygenation.2. Review of options for durable mechanical right ventricular circulatory support including: The CentriMag pump (St. Jude, Minneapolis, MN) RA-to-PA cannulation as well as commercially available LVADs, including the Jarvik and HeartWare devices.3. Review of common complications of RVADs including access site complications, pulmonary and other complications such as cannula malposition, and abandoned cannula.

#### TABLE OF CONTENTS/OUTLINE

1. Background/Indications for RVADs/RV Bypass and Oxygenation Methods.2. Imaging for percutaneous acute and durable mechanical circulatory support systems: Direct and indirect RV bypass systems: Protek Duo, VA-ECMO, Impella RP.Durable mechanical circulatory support systems: Jarvik, Centrimag.3. Access site complications of RVADs: access site hematoma, access vessel thrombosis, access site infection.4. Pulmonary complications of RVADs: pulmonary edema, organizing pneumonia, ARDS, septic emboli.5. Other complications of RVADs such as a malpositioned cannula, abandoned cannula, distal hemorrhage.

Printed on: 02/07/23

## Abstract Archives of the RSNA, 2022

CHEE-114

### Abnormal Gas on Chest X-Ray: A Primer with CT Correlation

Sunday, Nov. 27 8:00AM - 9:00AM Room: Learning Center - CH

#### Awards

Identified for RadioGraphics

#### Participants

Sameer Singhal, MD, Boston, MA (*Presenter*) Nothing to Disclose

#### TEACHING POINTS

1. Gas collections in the lung tend to be spherical, while gas collections in the pleura tend to be longer in one dimension.2. Pneumopericardium appears as "clean" gas that is bounded by the superior pericardial recess, while pneumomediastinum is "dirty" gas that can track superiorly into the neck.3. It is critically important to scan the upper abdomen for incidental abnormal gas, including pneumatosis and pneumoperitoneum.

#### TABLE OF CONTENTS/OUTLINE

1. Abnormal air in the lungs. Bullab. Cavitory consolidation2. Abnormal air in the pleuraa. Pneumothorax, including deep sulcusb. Hydropneumothorax - distinguish from intraparenchymal gas3. Abnormal air in the mediastinuma. Pneumopericardiumb. Pneumomediastinumd. Signs: ring-around-the-artery, continuous diaphragm. Herniae. Post-surgical4. Abnormal air in the abdomen. Pneumoperitoneumb. Pneumobiliac. Portal venous gas and pneumatosis

Printed on: 02/07/23



## Abstract Archives of the RSNA, 2022

CHEE-115

### Pulmonary Manifestations of IgG4 Related Disease

Sunday, Nov. 27 8:00AM - 9:00AM Room: Learning Center - CH

#### Awards

Certificate of Merit

#### Participants

Santiago Restrepo, MD, San Antonio, TX (*Presenter*) Nothing to Disclose

#### TEACHING POINTS

IgG4 is a systemic fibroinflammatory disease characterized by dense infiltration of IgG4 positive plasma cells in the affected tissues with or without elevated plasma levels of IgG4. The inflammatory infiltration can lead to the development of fibrotic tumefactive lesions that may affect any tissue often mimicking a neoplastic process. Thoracic involvement may affect the lung parenchyma, airways, the interstitium, pleura and the mediastinum. Most common manifestations include pulmonary nodules, interstitial lung disease, peribronchovascular infiltration, lymphadenopathy and fibrosing mediastinitis.

#### TABLE OF CONTENTS/OUTLINE

Definition, Pathophysiology, Histopathology, Associated or related conditions, Common clinical phenotypes, Pulmonary disease, Fibrosing mediastinitis, Cardiovascular involvement

Printed on: 02/07/23

## Abstract Archives of the RSNA, 2022

CHEE-116

### Interstitial Lung Disease in Rheumatoid Arthritis

Sunday, Nov. 27 8:00AM - 9:00AM Room: Learning Center - CH

#### Participants

Elisa Antolinos Macho, MD, Madrid, Spain (*Presenter*) Nothing to Disclose

#### TEACHING POINTS

- To know, identify and become familiar with the typical (and not so typical) radiological patterns of RA in lung involvement.- To suggest an early diagnosis in patients who have not shown any other RA manifestations and be able to offer a sooner treatment in these cases.

#### TABLE OF CONTENTS/OUTLINE

1. Introduction and generalities: rheumatoid arthritis is a multisystemic disease of uncertain etiology, with many factors involved (female sex, genetics, non genetic factors, biologic markers...).2. Extraarticular manifestations (EAM): although the typical manifestation is polyarthropaty, up to half of the patients who has RA, present extraarticular manifestations, more frequently in those who has positive analytic markers. Cardiovascular and respiratory EAM are the most important involvement in mobility and mortality terms.3. Pulmonary manifestations: An important group of the patients who undergoes this disease (60-80%) presents pulmonary involvement in the course of the disease, being interstitial involvement the second most important cause of mortality in these patients (after cardiovascular involvement). These manifestations can precede articular affectation up to 15% of the cases, and only in 10% of those, has significant clinical manifestations.4. Review of the typical patterns:- Usual Interstitial Pneumonia (UIP).- Non-Specific Interstitial Pneumonia (NSIP).- Organizing Pneumonia (OP).- Lymphocytic Interstitial Pneumonitis (LIP).5. Summary.

Printed on: 02/07/23



## Abstract Archives of the RSNA, 2022

CHEE-117

### Four-dimensional Angiography of Pulmonary Arteriovenous Malformation: How Do We Detect the Hidden Last Normal Branch for Endovascular Therapy?

Sunday, Nov. 27 8:00AM - 9:00AM Room: Learning Center - CH

#### Participants

Shota Yamamoto, MD, PhD, (Presenter) Nothing to Disclose

#### TEACHING POINTS

Pulmonary arteriovenous malformations (PAVMs) are abnormal direct vascular communications between pulmonary arteries and veins which create high-flow right-to-left shunts. Even when asymptomatic, presence of PAVMs increases patients' risk of substantial morbidity and mortality mainly from the effects of paradoxical emboli. Potential complications include stroke, cerebral abscess, pulmonary hemorrhage and hypoxia. Transcatheter embolization eliminates the abnormal right-to-left-shunting. For more effective embolization, preventing recanalization after PAVMs embolization is the most important. Recently, the Japanese nationwide cohort study has revealed that embolization of the last normal branch was a key factor affected the prevention of recanalization. The last normal branch is generally identified on preoperative multi-detector CT, but the identification rate on the conventional angiography is low (39%). We performed dynamic imaging with Cone-beam CT utilizing two-step dilution and balloon catheter occlusion, which allows for precise assessment of vessel shape and number, the last normal branch and shunting points during the procedure. Its innovative four-dimensional angiography can detect the "hidden" normal last branch and smoothly execute the treatment straight away. This presentation reviews the updated imaging modalities regarding vascular structural understanding and planning the endovascular therapy of PAVMs.

#### TABLE OF CONTENTS/OUTLINE

i. Anatomical categories of PAVMs ii. What is the last normal branch of PAVM? Why is it important? iii. Imaging modalities for planning for embolization (4D angiography) iv. Ideal embolization based on anatomical structure

Printed on: 02/07/23



## Abstract Archives of the RSNA, 2022

CHEE-118

### **Pulmonary Parenchymal Imaging Using Ultra-high Resolution CT - Estimating Lung Vascularity Using Radiologic Lung Weight**

Sunday, Nov. 27 8:00AM - 9:00AM Room: Learning Center - CH

#### **Participants**

Hiroshi Moriya, MD, Fukushima, Japan (*Presenter*) Advisor, California Capital Equity, LLC; Research Grant, Canon Medical Systems Corporation

#### **TEACHING POINTS**

In UHRCT, the reliability of CT values of small structures is improved by reducing the partial volume effect due to the miniaturization of voxels. In particular, the contrast effect of small vessels with a diameter of 1 mm or less is enhanced. And the entire peripheral lung parenchyma can be displayed by deleting the cardiovascular image. This technique can display blood vessel distribution and contrast effect distribution (Moriya et al, Peripheral Pulmonary Artery Imaging Using Ultra-high Resolution CT - A New Method Of Evaluating Vascularity In The Lung Field CHEE-37 RSNA2021). On the other hand, the contrast effect and vascularity of the lung can be calculated using the radiologic lung density measurement, which is a method of converting the lung weight from the CT value. We present this technique and typical cases.

#### **TABLE OF CONTENTS/OUTLINE**

1. Method: UHRCT (SHR mode: 1024matrix 0.25mm), Workstation used: Ziostation2 (Segmentation of lung parenchyma, each lobe, lung + blood vessels of any thickness) 2. Typical cases Case1 (dynamic contrast CT before lung cancer surgery): Contrast-enhanced phase were well reflected in radiologic lung weight. Peripheral pulmonary vessel involvement was less than 10%. Case2 (Pulmonary artery thromboembolism): Lung vascularity before and after treatment was calculated for each lobe. The therapeutic effect of the thrombus lesion was reflected in the radiologic lung weight. 3. This method can be an easy pulmonary blood flow evaluation method.

Printed on: 02/07/23



## Abstract Archives of the RSNA, 2022

CHEE-119

### Step by Step: Radiological Features of Pulmonary Vascular disease Made Simple

Sunday, Nov. 27 8:00AM - 9:00AM Room: Learning Center - CH

#### Participants

Sofia Gambetta I, MD, MD, Pilar, Argentina (*Presenter*) Nothing to Disclose

#### TEACHING POINTS

Identifying pulmonary vascular disease and their causes. Providing methodological guidelines in order to approach the diagnosis of the pathologies that involve pulmonary vascularity. Presenting frequent and uncommon presentation of pulmonary vascular disease. Correlating the radiological features with clinical, histopathological and laboratory findings.

#### TABLE OF CONTENTS/OUTLINE

Introduction. Pulmonary vascular disease explained: Pulmonary hypertension, acute and chronic pulmonary thromboembolism, congenital and acquired pulmonary venous return anomalies, diffuse alveolar hemorrhage and vasculitis. Case-based approach with radiologic correlation. Imaging findings with clinical, laboratory and histological correlations. Diagnostic and therapeutic algorithm. Conclusion.

Printed on: 02/07/23



## Abstract Archives of the RSNA, 2022

CHEE-12

### Pulmonary Ablation: From Techniques to Complications

Sunday, Nov. 27 8:00AM - 9:00AM Room: Learning Center - CH

#### Awards

Certificate of Merit

#### Participants

Jose Maluf, MD, MD, Sao Paulo, Brazil (*Presenter*) Nothing to Disclose

#### TEACHING POINTS

- Understand how pulmonary ablation works and its role in thoracic malignancies treatment
- Learn about the different techniques involved in pulmonary ablation
- Recognize expected imaging features of the post ablation zone
- Identify the main complications related to pulmonary ablation

#### TABLE OF CONTENTS/OUTLINE

- Introduction - General concepts about pulmonary ablation:
  - o Current context
  - o The procedure
  - o Indications and contraindications
  - o Imaging surveillance
- Different techniques:
  - o Radiofrequency ablation (RFA)
  - o Microwaves ablation (MWA)
  - o Cryoablation
  - o Irreversible electroporation (IEP)
- Post-ablation zone features: What to expect?
- Case based review - Complications related to pulmonary ablation:
  - o Aseptic Pleuritis
  - o Pneumothorax
  - o Lung Hemorrhage
  - o Aspergilloma
  - o Bronchopleural Fistula
  - o Air embolism
  - o Rib fracture
  - o Other complications
- Future perspectives
- Conclusions and key takeaways

Printed on: 02/07/23



## Abstract Archives of the RSNA, 2022

CHEE-120

### Vascular Complications of Infections: Beyond COVID-19

Sunday, Nov. 27 8:00AM - 9:00AM Room: Learning Center - CH

#### Participants

Babina Gosangi, MD, MPH, New Haven, MA (*Presenter*) Nothing to Disclose

#### TEACHING POINTS

1. Vascular complications of infection can be divided into thromboembolic disorders and non-thromboembolic disorders. 2. Thromboemboli from infections could be due to endothelial damage, hyperviscosity, embolization of vegetations containing infectious material or embolization of the culprit organism. Such conditions include COVID-19 infection, infectious endocarditis, Lemierre's syndrome and parasitic embolization into the pulmonary arteries (*Echinococcus*). 3. Vascular infections could also result from contiguous spread of infection from the adjacent organs causing inflammation of the vessels such as infectious aortitis associated with vertebral osteomyelitis, empyema or pneumonia. 4. Infections can damage the vessel wall and cause aneurysm such as Rasmussen's aneurysm or mycotic aneurysm.

#### TABLE OF CONTENTS/OUTLINE

• Introduction • Pulmonary embolism- COVID-19 infection • Septic infarcts- Infective endocarditis • Internal jugular vein thrombus- Lemierre's syndrome • Infectious aortitis- Tuberculous aortitis, syphilitic aortitis, HIV aortitis, pyogenic aortitis • Mycotic aneurysm • Rasmussen's aneurysm- Tuberculosis • Conclusion

Printed on: 02/07/23



## Abstract Archives of the RSNA, 2022

CHEE-121

### **Emboli or Else? Beware the Pitfalls in CTEPH Diagnosis - Chronic Thromboembolic Pulmonary Hypertension Lookalikes in CT Pulmonary Angiography**

Sunday, Nov. 27 8:00AM - 9:00AM Room: Learning Center - CH

#### **Participants**

Wagner Diniz de Paula, MD, PhD, Brasilia, Brazil (*Presenter*) Nothing to Disclose

#### **TEACHING POINTS**

Recognize the signs of chronic pulmonary emboli and pulmonary hypertension on CT, review the pathophysiology of pulmonary hypertension in CTEPH, and learn clues to identify common and uncommon mimickers of CTEPH on CT.

#### **TABLE OF CONTENTS/OUTLINE**

Chronic thromboembolic pulmonary hypertension (CTEPH) results from pulmonary artery obstruction due to non-resolving pulmonary embolism (PE). Among PE survivors, CTEPH is estimated to occur in 1% to 5% of cases. It is a potentially treatable cause of pulmonary arterial hypertension (PAH) and, if left untreated, may progress to right heart failure and death. CT signs of PE, PAH and CTEPH will be reviewed and clues to differential diagnosis will be provided. Some conditions may simulate CTEPH on imaging, encompassing intravascular, extravascular, and vascular (parietal) causes. Intravascular mimickers of CTEPH include pulmonary arterial malignancies (primary intimal sarcoma, metastatic tumoral thrombi) and in situ pulmonary thrombosis due to long-standing PAH (e.g., in cyanogenic congenital heart disease and schistosomiasis). Extravascular causes comprise IgG4-related and granulomatous fibrosing mediastinitis. Vascular abnormalities include congenital anomalies such as proximal interruption of the pulmonary artery and acquired physiological disturbances related to pulmonary hypoxic vasoconstriction.

Printed on: 02/07/23



## Abstract Archives of the RSNA, 2022

CHEE-122

### CT in Acute Pulmonary Embolism: Filling Defects and Beyond

Sunday, Nov. 27 8:00AM - 9:00AM Room: Learning Center - CH

#### Awards

Certificate of Merit

#### Participants

Kaustav Bera, MD, Cleveland, OH (*Presenter*) Nothing to Disclose

#### TEACHING POINTS

1. Review the clinical, laboratory and diagnostic work up of patients suspected with acute pulmonary embolism (PE) 2. Discuss the typical and atypical CT appearance of acute PE and its mimics using an algorithmic approach 3. Discuss the important acute and emergent pathology beyond PE, that can mimic acute PE symptoms, visualized on a CT PE study 4. Briefly review additional incidental findings on a CT PE study 5. Illustrate newer advances in CT technology (Dual energy and multi-energy CT) and artificial intelligence methods for improved diagnostic assessment

#### TABLE OF CONTENTS/OUTLINE

1. When do you suspect an Acute PE - Risk factors, clinical history, symptoms, physical examination, laboratory findings 2. Clinical risk scores to determine whether imaging should be obtained in suspected Acute PE a. Wells score b. Pulmonary Embolism Rule-out criteria (PERC) c. Geneva score 3. Role of Bedside diagnostics in PE (Chest Radiograph, EKG, Ultrasound) and diagnostic signs 4. Discuss the algorithmic approach to obtain diagnostic imaging in PE 5. Imaging modalities including gold standard and alternatives to evaluate for PE 6. Imaging technique and challenges to obtain a diagnostic CT exam 7. CT imaging in acute PE - primary and ancillary findings 8. Step wise approach to CT interpretation 9. Clinical examples showing conditions mimicking PE on CT imaging - Beyond filling defects a. Acute PE mimicking pathology (Acute aortic pathology, airway obstruction etc.) b. Other Urgent pathology (Pyelonephritis, abscess, arterial bleeds, DVT etc.) c. Incidental findings (Nodules, Nephrolithiasis, Cholelithiasis) 10. Newer imaging techniques for PE diagnosis 11. Future directions including role of Artificial Intelligence

Printed on: 02/07/23



## Abstract Archives of the RSNA, 2022

CHEE-123

### Spectrum of Pulmonary Aspergillosis

Sunday, Nov. 27 8:00AM - 9:00AM Room: Learning Center - CH

#### Awards

Certificate of Merit

#### Participants

Gerald Hefferman, MD, Somerville, MA (*Presenter*) Nothing to Disclose

#### TEACHING POINTS

1. The manifestations of pulmonary aspergillosis depend on the host immune state and underlying pulmonary disease. 2. Non-invasive infections by aspergillus are airway-centered (e.g. APBA, mycetoma), while invasive infections often manifest by destruction of pulmonary vasculature (e.g. angioinvasive aspergillosis).

#### TABLE OF CONTENTS/OUTLINE

1. Allergic bronchopulmonary aspergillosis. High attenuation mucus. 2. Mycetoma. Monod sign. 3. Angioinvasive aspergillosis. Halo sign. Air crescent sign. COVID-19 superinfection. 4. Tracheobronchial aspergillosis. 5. Airway-invasive aspergillosis. 6. Chronic necrotizing aspergillosis

Printed on: 02/07/23



## Abstract Archives of the RSNA, 2022

CHEE-124

### A Radiological Guide to Connective Tissue Disorders associated Interstitial Lung Diseases (CTD-ILDs)

Sunday, Nov. 27 8:00AM - 9:00AM Room: Learning Center - CH

#### Participants

Aarushi Gupta, MD, MBBS, (*Presenter*) Nothing to Disclose

#### TEACHING POINTS

- Describe high resolution CT (HRCT) patterns of various Connective Tissue Disorders associated Interstitial Lung Diseases (CTD-ILDs) with representative cases including usual interstitial pneumonia (UIP), non-specific interstitial pneumonia (NSIP), fibrosing organizing pneumonia (OP), lymphocytic interstitial pneumonia (LIP), follicular/obliterative bronchiolitis and other rare entities
- Review common radiological signs used for diagnosis of CTD-ILDs including exuberant honeycombing, anterior upper lobe and straight edge sign
- Brief overview of new concepts like Interstitial Pneumonia with Autoimmune Features (IPAF) and CTD associated Interstitial Lung abnormalities (CTD-ILAs), their radiological findings and management

#### TABLE OF CONTENTS/OUTLINE

1. Definition, epidemiology and clinical manifestations of CTD-ILDs
2. Radiological signs and patterns suggestive of CTD-ILDs on HRCT chest
3. Specific Imaging patterns seen in different CTD-ILDs (Rheumatoid arthritis, Systemic Sclerosis, Systemic Lupus Erythematosus, Polymyositis/Dermatomyositis, Sjogren syndrome) with representative cases
4. Overview of IPAF
5. Definition and management of CTD-ILAs
6. Conclusion-highlighting radiological pearls

Printed on: 02/07/23



## Abstract Archives of the RSNA, 2022

CHEE-125

### Pulmonary and Pleuropulmonary Blastomas

Sunday, Nov. 27 8:00AM - 9:00AM Room: Learning Center - CH

#### Participants

Santiago Restrepo, MD, San Antonio, TX (*Presenter*) Nothing to Disclose

#### TEACHING POINTS

Blastomas represent a group of primary malignancies with proliferation of immature element that look like fetal lung. They typically have a biphasic composition with malignant mesenchymal and epithelial immature component. Two types: Pleuropulmonary blastoma (PPB) seen in children and Pulmonary Blastoma (PB) seen in adults. PPPB is the most common primary lung malignancy in children, and most present in patients less than 6 years old. DICER1 mutation is seen in 66% of patients with PPB. Other DICER1 related tumors are seen in 40% of affected patients. Imaging presentation is misleading and often confused with other entities like CCAM, sequestration, congenital lobar emphysema etc.

#### TABLE OF CONTENTS/OUTLINE

Definition. DICER1 mutation. DICER1 associated tumors. 2015 WHO classification. Histopathology. Pathologic-radiologic correlation. Phenotypes and prognosis. Imaging manifestation. Differential diagnosis

Printed on: 02/07/23



## Abstract Archives of the RSNA, 2022

CHEE-126

### Post CABG Chest Radiography: How to Make the Complicated Uncomplicated

Sunday, Nov. 27 8:00AM - 9:00AM Room: Learning Center - CH

#### Participants

Justin Little, MD, Winston-Salem, NC (*Presenter*) Nothing to Disclose

#### TEACHING POINTS

Complications after coronary artery bypass grafting (CABG) are common and can range from simple atelectasis or pleural effusions to misplaced lines and other support apparatus issues, to more serious issues such as a pulmonary edema, mediastinal hematoma, or pneumothorax. Portable chest radiography is the mainstay of initial evaluation. It is fast with low radiation and gives the radiologist information that allows for quick action. Overlapping anatomic structures and support apparatus devices in combination with the limitations of portable radiography makes the diagnosis of CABG complications a radiologist's dreaded dilemma. Being able to quickly identify the most common complications is essential to maintaining efficiency and accuracy and preventing morbidity and mortality in the postoperative state.

#### TABLE OF CONTENTS/OUTLINE

1. Introduction 2. Types of CABG (on-pump, off-pump, minimally invasive) 3. Postoperative CABG complications - Immediate (< 24 hours) v. Subacute (1-7 days) v. Chronic (> 7 days) - Complication Categories: 1. Lines and tubes 2. Parenchymal 3. Mediastinal 4. Soft tissue/musculoskeletal 4. Role of imaging: ICU plain chest radiography 5. How to report a postoperative CABG chest radiograph 6. Correlation with CT imaging for increased understanding 7. Algorithm for "next-step" recommendations for complications 8. Multidisciplinary approach and perspective of CT surgeons about the most clinically useful information from radiology

Printed on: 02/07/23



## Abstract Archives of the RSNA, 2022

CHEE-127

### Thinking Beyond Bronchogenic Carcinoma: A Primer of Rare Pulmonary and Pleural Pathologies

Sunday, Nov. 27 8:00AM - 9:00AM Room: Learning Center - CH

#### Participants

Ankush Jajodia, MD, MBBS, New Delhi, India (*Presenter*) Nothing to Disclose

#### TEACHING POINTS

LEARNING OBJECTIVES 1. To give an overview of some uncommon pulmonary and pleural pathologies. 2. To review the spectrum of imaging manifestations of uncommon entities in lung and pleura. 3. To highlight the importance of clinical history, immunohistochemistry and histopathology in arriving at the correct diagnosis. BACKGROUND: Due to their overlapping imaging appearance, imaging-based diagnosis of many rare neoplastic and non-neoplastic conditions affecting the lung and pleura can be challenging. Being familiar with some of the rare and unusual entities, along with relevant clinical history, can aid a radiologist in narrowing down the differential diagnosis. Thinking outside the box and looking for certain potential distinguishing features may help in making an early and accurate diagnosis. Key imaging features on CT and MRI for uncommon pulmonary and pleural pathologies will be reviewed in this educational exhibit. These include spindle cell sarcoma of the lung, sclerosing pulmonary hemangioma, sclerosing pneumocytoma, pulmonary paraganglioma, pleural hemangioma, malignant peripheral nerve sheath tumor of the pleura and pleural epithelioid hemangioendothelioma. CONCLUSION: A wide range of pulmonary and pleural conditions exhibit imaging features that are similar to more common pathologies such as bronchogenic carcinoma and pleural metastasis. Awareness of additional less common conditions, as well as an understanding of their pathologic background, will aid in accurate diagnosis.

#### TABLE OF CONTENTS/OUTLINE

Pictorial depiction of rare cases

Printed on: 02/07/23

## Abstract Archives of the RSNA, 2022

CHEE-128

### Typical and Atypical Diseases involving the Pleura Radiologic-Pathologic Correlation

Sunday, Nov. 27 8:00AM - 9:00AM Room: Learning Center - CH

#### Participants

Patricia De Groot, MD, Houston, TX (*Presenter*) Nothing to Disclose

#### TEACHING POINTS

Primary benign lesions of the pleura are much less common than malignant diseases of the pleura. Distinguishing benign from malignant pleural diseases affects prognosis, treatment and outcomes. CT features suggesting malignancy are circumferential pleural thickening; nodular pleural thickening; parietal pleural thickening >1 cm; mediastinal pleural involvement. Malignant primary mesothelioma (MPM) is the most common primary malignancy of the pleura. However, pleural metastases are much more common than primary pleural tumors. The most common primaries metastasizing to pleura include lung, breast and GI carcinomas, particularly adenocarcinomas, and lymphoma. Some pleural tumors may manifest focally or be diffuse. Age, sex and clinical history play a part in both radiologic and pathologic diagnosis. We review helpful imaging findings in the differential diagnosis of pleural diseases and illustrate radiologic-pathologic correlation of benign and malignant pleural lesions.

#### TABLE OF CONTENTS/OUTLINE

Benign vs Malignant: Benign includes solitary fibrous tumor, lipoma, schwannoma, endometriosis, pleuritis. Primary malignant includes MPM, solitary fibrous tumor, liposarcoma, PNET, synovial sarcoma, vascular sarcoma. Secondary malignant includes metastatic disease from lung cancer, lymphoma, plasmacytoma. Focal versus Diffuse: Typical focal includes metastatic disease, solitary fibrous tumor, schwannoma, thymoma, lipoma. Atypical focal includes PNET, synovial sarcoma, liposarcoma, meningioma, endometriosis. Typical diffuse includes metastatic disease, MPM, fibrothorax, thymoma. Atypical diffuse includes lymphoma, synovial sarcoma, epithelioid hemangioendothelioma.

Printed on: 02/07/23



## Abstract Archives of the RSNA, 2022

CHEE-13

### Lung Ultrasound - Ugly Duckling into Swan: A Case-based Approach Demonstrating the Effectiveness of This Method in the Evaluation of Several Pediatric Lung and Pleural Pathologies

Sunday, Nov. 27 8:00AM - 9:00AM Room: Learning Center - CH

#### Participants

Marcos Brotto, , Brazil (*Presenter*) Nothing to Disclose

#### TEACHING POINTS

During the pandemic caused by the SARS-CoV-2, lung ultrasound (US) has become a promising diagnostic method at the bedside mostly due to its fundamental role in patients who develop infection with severe acute respiratory syndrome. Since then, many studies have proven its value, especially in the pediatric age group. The high demand caused by the viral pneumonia pandemic intensified its use and consequently expanded its applicability in several situations, including pathologies accidentally detected, showing the high accuracy of the method. In addition, lung US provides dynamic data, feature that only ultrasound allows when compared to other imaging methods. For many reasons the pediatric population benefits a great deal from the use of US as a first line method, including the assessment of thoracic and pleural pathologies. US may also provide useful information that eliminates the need for more invasive or expensive studies, especially in cases with mild clinical changes.

#### TABLE OF CONTENTS/OUTLINE

The intention of this presentation is to demonstrate, through a series of cases, the extensive scope of ultrasound in the evaluation of the pediatric thorax. Demonstrate the main ultrasound findings in several parenchymal and pleural pathologies such as pneumonia, abscess, pleural effusion, empyema, among others, proving that the US can be used in the serial evaluation of these conditions. Discuss US radiological findings and their correlations with chest radiograph and chest tomography, and how sonographers can reproduce them adequately in many cases.

Printed on: 02/07/23



## Abstract Archives of the RSNA, 2022

CHEE-14

### Uncommon Non-thromboembolic Conditions Affecting the Pulmonary Vasculature - Beyond Thromboembolism

Sunday, Nov. 27 8:00AM - 9:00AM Room: Learning Center - CH

#### Awards

Certificate of Merit

#### Participants

Helena Peris, MD, Sabadell, Spain (*Presenter*) Nothing to Disclose

#### TEACHING POINTS

- To review uncommon non-thromboembolic entities that change the morphology or density of the pulmonary arteries on CT or PET/CT.- To describe imaging features of rare conditions that mimic pulmonary thromboembolism and/or bronchial pathology or cause pulmonary hypertension.

#### TABLE OF CONTENTS/OUTLINE

I. Background:Some uncommon conditions unrelated to thromboembolism can affect the pulmonary arteries, changing the imaging appearance of vessels in the proximal and/or distal pulmonary vasculature. These entities show key CT or PET-CT findings; their knowledge allows us to make the proper diagnosis.II. Content:We classify the entities into four categories:- Neoplastic (benign or malignant): pulmonary artery sarcoma, intravascular metastases, pulmonary tumor thrombotic microangiopathy, and intravascular leiomyomatosis.- Inflammatory: vasculitis (Takayasu arteritis and Behçet's disease), thrombosis in situ.- Iatrogenic: embolization of non-biologic material or gas during invasive procedures such as vertebroplasty, embolization, or colonoscopy and 18 FDG embolism in a PET/CT.- Miscellaneous: excipient lung disease and pulmonary artery sheath hematoma, as a complication of acute aortic dissection.III. Conclusions:Detailed observation of the proximal and distal pulmonary arteries can provide diagnostic clues to unusual conditions causing pulmonary hypertension, simulating pulmonary thromboembolism or bronchial pathology.

Printed on: 02/07/23

## Abstract Archives of the RSNA, 2022

CHEE-15

### How Radiologists Can Help Surgeons on the Planning of a Lung Segmentectomy - Significant Pulmonary Veins Variations

Sunday, Nov. 27 8:00AM - 9:00AM Room: Learning Center - CH

#### Participants

Vitor Bichuette, MD, Uberaba, Brazil (*Presenter*) Nothing to Disclose

#### TEACHING POINTS

To review pulmonary venous anatomy and the most common pattern of drainage. How a segmentectomy is performed, focusing on techniques to identify the intersegmental plane and the role of the pulmonary veins during the procedure. To explain anatomical variations of pulmonary veins, its significance in lung segmentectomies and how to identify them using computed tomography (CT). To present intraoperative complications related to pulmonary veins anomalies. Applications of CT with 3D reconstructions to reduce the risk of complications during the surgical procedure.

#### TABLE OF CONTENTS/OUTLINE

Introduction - General concepts of pulmonary venous anatomy Typical pattern of pulmonary venous drainage The use of CT to identify anatomical variations Lung segmentectomy's technique: • A step-by-step explanation of how to perform a lung segmentectomy. • Pitfalls and some anatomical variations to know during the surgical procedure. • The use of technologies to avoid intraoperative complications Case-Based Review: Sample cases explaining and demonstrating anatomical variations of the pulmonary veins and how CT can be used to identify and prevent intraoperative complications. This section will present illustrative cases of each: Separate veins draining the middle lobe Middle lobe vein emptying into the left atrium Direct drainage from segment 6R Vein draining the right superior lobe running posteriorly to the intermediate bronchus Lingular drainage emptying into the left inferior pulmonary vein Long common trunk of left pulmonary veins Future Directions: the role of CT with 3D reconstructions and 3D printing in lung segmentectomy planning Conclusion and key takeaways.

Printed on: 02/07/23



## Abstract Archives of the RSNA, 2022

CHEE-16

### Chronic Fibrous Interstitial Lung Diseases (CFILD) - Exploring Acute and Chronic Complications through an Imaging-based Approach

Sunday, Nov. 27 8:00AM - 9:00AM Room: Learning Center - CH

#### Participants

Alan Hummel, Sao Paulo, Brazil (*Presenter*) Nothing to Disclose

#### TEACHING POINTS

The purpose of this exhibit is to: 1. Analyze the major complications of chronic interstitial lung disease, demonstrating both acute and chronic complications through didactic cases; 2. Discuss how an imaging-based approach can be used to differentiate between acute and chronic complications; 3. Distinguish between exacerbations and decompensations in chronic interstitial lung diseases, emphasizing the role of imaging in both characterization and etiologic investigation.

#### TABLE OF CONTENTS/OUTLINE

1.0. Chronic fibrosing interstitial pneumonia  
1.1. Basic evaluation algorithm (CDEF mnemonic)  
1.2. Imaging technical considerations  
2.0 Acute and chronic complications (the basics to memorize - with mnemonics)  
3.0 Acute complications  
3.1. Decompensation vs exacerbation  
3.2. Exacerbation  
3.2.1. idiopathic  
3.2.2. surgical procedures  
3.2.3. infectious trigger  
3.3. Acute decompensation  
3.3.1. pneumomediastinum  
3.3.2. pneumothorax  
3.3.3. Pulmonary thromboembolism  
3.3.4. infections  
3.3.5. Aspiration  
3.3.6. hydrostatic edema  
4.0 chronic complications  
4.1. aspergilloma  
4.2. tuberculosis  
4.3. Pulmonary hypertension  
4.4. pulmonary ossification  
4.5. neoplasms  
5.0. Summary  
6.0 References

Printed on: 02/07/23



## Abstract Archives of the RSNA, 2022

CHEE-17

### Fistulas of the Chest - An Unexpected Journey

Sunday, Nov. 27 8:00AM - 9:00AM Room: Learning Center - CH

#### Participants

Kristie Yang, MD, (*Presenter*) Nothing to Disclose

#### TEACHING POINTS

This education exhibit will: 1) Review the types of fistulas that can occur within the chest, 2) Identify clinical and radiologic features of fistulas within the chest, and 3) Review complications and management of such fistulas.

#### TABLE OF CONTENTS/OUTLINE

1. Introduction  
2. Etiologies of various fistulas within the chest  
3. Clinical history and symptoms  
4. Imaging features of a. Bronchopleural fistulas b. Esophageal-pleural fistulas c. Gastropleural fistulas d. Pancreaticopleural fistulas e. Vascular fistulas  
5. Complications and management of fistulas  
6. Summary and conclusion

Printed on: 02/07/23



## Abstract Archives of the RSNA, 2022

CHEE-18

### Imaging of the Diaphragm: Anatomy, Variations, and Pathologic Conditions

Sunday, Nov. 27 8:00AM - 9:00AM Room: Learning Center - CH

#### Participants

Furkan Ufuk, MD, Denizli, Turkey (*Presenter*) Nothing to Disclose

#### TEACHING POINTS

? To review the radiological anatomy and function of the diaphragm. ? To review the anatomic variations of the diaphragm. ? To review the multimodality imaging findings in primary or secondary pathologic conditions of the diaphragm

#### TABLE OF CONTENTS/OUTLINE

1. Anatomy and function of the diaphragm: The diaphragm is the most important respiratory muscle and is the muscle structure that separates the abdominal and thoracic cavities. 2. Anatomic Variations: Common anatomic variations of the diaphragm include diaphragmatic slip, bundles (nodular crura), the extension of diaphragmatic muscle fibres onto the m.quadratus lumborum, and prominent or hypertrophic median and lateral arcuate ligaments. 3. Pathologic conditions of the diaphragm: A) Primary pathological conditions of the diaphragm: That includes eventration, diaphragmatic herniation, diaphragmatic injuries, diaphragmatic tumors and tumor-like lesions. B) Secondary pathological conditions of the diaphragm: That includes diaphragmatic paralysis, diaphragmatic weakness due to neuromuscular disorders or prolonged mechanical ventilation, and tumors that invade the diaphragm.

Printed on: 02/07/23

## Abstract Archives of the RSNA, 2022

CHEE-19

### A Primer for Diagnostic Imaging of Thymus - From Age Related Changes to Thymic Tumors and Everything in Between

Sunday, Nov. 27 8:00AM - 9:00AM Room: Learning Center - CH

#### Awards

**Certificate of Merit**

#### Participants

Daisuke Yamada, MD, Tokyo, Japan (*Presenter*) Nothing to Disclose

#### TEACHING POINTS

The thymus is an organ that changes due to a variety of reasons, from aging to pathologic causes. Distinguish between benign and neoplastic changes can be challenging. Further, most thymic tumors are asymptomatic when detected, and histopathological diagnosis is not straightforward, so imaging plays an extremely important role in the evaluation of thymic lesions. In this presentation, we introduce the imaging spectrum of the thymus, from benign findings such as normal maturation and benign lesions to neoplasms.

#### TABLE OF CONTENTS/OUTLINE

Presentation goals: 1. To demonstrate age-specific changes in normal thymus 2. To demonstrate thymic hyperplasia depending on a variety of causes 3. To demonstrate multimodality imaging findings of various mediastinal tumors based on WHO classification  
Illustrative imaging/cases include: 1. Age-related changes in the thymus gland 1. Thymic hyperplasia of a variety of causes 1. Thymomas, including atypical variants 1. Thymic carcinoma 1. Thymic neuroendocrine tumor 1. Germ cell tumor of the mediastinum 1. Lymphoma of the mediastinum 1. Histiocytic and dendritic cell neoplasm of the mediastinum 1. Myeloid sarcoma and extramedullary acute myeloid leukemia 1. Soft tissue tumor of the mediastinum 1. Ectopic tumor of the thymus

Printed on: 02/07/23



## Abstract Archives of the RSNA, 2022

CHEE-2

### **Pulmonary Vein Stump Thrombus after Lobectomy: Radiological Approach and What Radiologists Need to Know**

Sunday, Nov. 27 8:00AM - 9:00AM Room: Learning Center - CH

#### **Participants**

Koji Takumi, MD, PhD, Kagoshima, Japan (*Presenter*) Nothing to Disclose

#### **TEACHING POINTS**

Recently, a frequent occurrence of pulmonary vein (PV) stump thrombus following surgical treatment for lung cancer, especially left upper lobectomy, has been reported. The incidence of PV stump thrombus after left upper lobectomy ranged from 3.4% to 17.9%. Moreover, there is increasing evidence that PV stump thrombus is associated with postoperative cerebral infarction. It is important for radiologists to understand the occurrence mechanism, complications, and radiological features of PV stump thrombus after lobectomy to avoid misdiagnosis and improper patient management. The purposes of this exhibit are as follows: 1. To illustrate the etiology and epidemiology of PV stump thrombus after lobectomy. 2. To discuss the mechanism of PV stump thrombus formation after lobectomy based on radiological findings. 3. To review the complications and radiological imaging features of clinical cases of PV stump thrombus after lobectomy

#### **TABLE OF CONTENTS/OUTLINE**

1. Overview of the PV stump thrombus after lobectomy. 2. Clinicopathological and imaging features of PV stump thrombus after lobectomy and the complications. 3. Radiological approach to PV stump thrombus after lobectomy using 4D flow MRI, cine MRI, and 3D CT images

Printed on: 02/07/23



## Abstract Archives of the RSNA, 2022

CHEE-20

### Adult Primary Mediastinal Germ Cell Tumors: Update from the WHO Blue Book, 5th Edition (2021)

Sunday, Nov. 27 8:00AM - 9:00AM Room: Learning Center - CH

#### Participants

Cody Thornburgh, MD, (*Presenter*) Nothing to Disclose

#### TEACHING POINTS

Primary mediastinal germ cell tumors (MGCT) are rare and generally affect young men. Imaging findings when used in conjunction with serological markers and patient demographics can often identify the specific type of MGCT and allows differentiation from other malignant and benign entities. Correlating surveillance imaging with serological markers allows for increased confidence in determining post-treatment response from tumor recurrence.

#### TABLE OF CONTENTS/OUTLINE

Background  
Definitions and classification of MGCT  
a. WHO classification  
b. Cell-line based classification  
Imaging and histochemical features of MGCT sub-types  
a. Classic imaging patterns at presentation including radiography, CT PET/CT  
b. Use of biomarkers in diagnosis and response  
Comparison to other mediastinal tumors  
a. Lymphoma  
b. Thymic epithelial neoplasms  
c. Thymic Hyperplasia, Normal Thymic tissue  
d. Metastatic Disease  
e. Ectopic thyroid  
Common pitfalls in diagnosis and determining recurrence  
a. Growing teratoma syndrome  
b. Misclassification of benign thymic tissue  
c. Identifying surgical scar tissue as residual tumor

Printed on: 02/07/23



## Abstract Archives of the RSNA, 2022

CHEE-21

### Uncommon Causes of Interlobular Septal Thickening: How to Tell Them Apart?

Sunday, Nov. 27 8:00AM - 9:00AM Room: Learning Center - CH

#### Participants

Achala Donuru, MD, Philadelphia, PA (*Presenter*) Nothing to Disclose

#### TEACHING POINTS

Interlobular septal thickening is a frequent finding in patients with diffuse lung disease. While pulmonary edema and lymphangitic spread of tumor are the commonly encountered causes of interlobular septal thickening, there are several less common causes. It is important to differentiate the various diagnoses by the contour, distribution of interlobular septal thickening, other pulmonary and extrapulmonary findings. This presentation gives clues to the chest radiologists and pulmonologists to arrive at the final diagnosis.

#### TABLE OF CONTENTS/OUTLINE

Various causes of interlobular septal thickening will be discussed including infections (COVID-19 pneumonia, viral pneumonia, Pneumocystis carinii pneumonia), interstitial pneumonias (lymphocytic Interstitial pneumonia, non-specific interstitial pneumonia, eosinophilic pneumonia, and idiopathic pulmonary fibrosis), depositional/infiltrative conditions (pulmonary alveolar proteinosis, pulmonary amyloidosis, Erdheim Chester disease, Niemann- Picks disease), malignancies (lymphoma, leukemia, Kaposi's sarcoma), congenital (congenital lymphangiectasia, diffuse pulmonary lymphangiomatosis, Yellow nail syndrome), iatrogenic (cytotoxic agents, radiation, lipoid pneumonia, silicone injection, EVALI/Vaping). Clues to differentiating the interlobular septal thickening based on type, distribution and other associated pulmonary and extrapulmonary findings will be reviewed.

Printed on: 02/07/23



## Abstract Archives of the RSNA, 2022

CHEE-22

### Ex Vivo Lung Perfusion (EVLP) and the Radiologist's Role

Sunday, Nov. 27 8:00AM - 9:00AM Room: Learning Center - CH

#### Participants

Zhao Zhang, DO, (*Presenter*) Nothing to Disclose

#### TEACHING POINTS

1. EVLP is an advanced preservation tool for lung transplantation and has expanded the donor pool by perfusing the lungs ex vivo allowing for longer preservation time. 2. Radiologists may participate in the EVLP team to evaluate lung radiographs during EVLP. 3. Diagnostic tests and treatments can be performed on the lungs to optimize the quality of the transplant organ. 4. Radiologists may have an increasingly important role in the future of EVLP as more transplant centers adopt this strategy of lung preservation and distribution.

#### TABLE OF CONTENTS/OUTLINE

1. Overview, Background, Terminology 2. Donor lung evaluation prior to EVLP 3. Radiologist's role in EVLP with case examples a. Radiographic donor screening for masses, infection, contusion. b. Discuss potential radiographic exclusion criteria. c. Assessment of radiographic changes of the post perfusion lungs; correlating with other diagnostic tests d. Correctly identify complications (atelectasis vs pulmonary edema) e. Discuss how EVLP may impact radiologist training 4. Conclusion

Printed on: 02/07/23



## Abstract Archives of the RSNA, 2022

CHEE-23

### A Practical Approach to Diaphragmatic Ultrasound: From Tricks to Tips

Sunday, Nov. 27 8:00AM - 9:00AM Room: Learning Center - CH

#### Participants

Niels Vinicius Padua Carvalho, MD, Sao Paulo, Brazil (*Presenter*) Nothing to Disclose

#### TEACHING POINTS

The aim of this exhibition is to review1. Multimodality anatomic imaging of diaphragm, focusing on ultrasonography (US)2. Technical and clinical aspects of diaphragmatic US, including a proposal for structured reporting3. Tips and tricks to evaluate diaphragm function (mobility) and trophism (diaphragm thickness and thickness fraction)4. Pathologic conditions detected through diaphragmatic US

#### TABLE OF CONTENTS/OUTLINE

1. INTRODUCTIONa. Anatomy of diaphragm with multimodality imagingb. Anatomic versus functional imaging2. DIAPHRAGM US: TECHNICAL ASPECTSa. Probes, positioning and acoustic windowsb. US modalities: B and M modesc. Step-by-step approach (videos and images)3. DIAPHRAGM US: CLINICAL ASPECTS a. Diaphragm paralysisb. Critically ill patients on mechanical ventilationc. Other respiratory diseases, including asthma, chronic obstructive pulmonary disease, cystic fibrosis, interstitial lung disease and COVID-19d. Neuromuscular disorderse. Pediatric patients4. DIAPHRAGM US: A PRACTICAL APPROACH a. Tricks and tips b. Multimodality imaging correlations c. Structured reporting5. DIAPHRAGM US IN THE REAL WORLD a. Challenges and limitations of diaphragm US 6. FUTURE DIRECTIONS AND TAKE HOME MESSAGES

Printed on: 02/07/23



## Abstract Archives of the RSNA, 2022

CHEE-24

### Spectral CT in Cardiothoracic Imaging: Potential Applications that Radiologists Should Know

Sunday, Nov. 27 8:00AM - 9:00AM Room: Learning Center - CH

#### Awards

Cum Laude

#### Participants

Flavio Zuccarino, MD, Barcelona, Spain (*Presenter*) Nothing to Disclose

#### TEACHING POINTS

To analyze spectral CT feasibility in cardiac and thoracic pathologies. To underline its advantages and limitations compared to conventional CT. To define the clinical scenarios in which spectral CT findings are key in patient's management.

#### TABLE OF CONTENTS/OUTLINE

We make a short introduction about spectral CT imaging techniques. We focus on Spectral GSI CT imaging that we used in the different cases of this exhibit. We describe Spectral CT findings in different cardiac and thoracic pathologies organized as: Vascular diseases Acute Pulmonary embolism Chronic Pulmonary embolism Hemoptysis Congenital vascular diseases (Sequestration, MAV, others) Lung diseases Consolidations (pneumonia, atelectasis, infarcts, organizing processes) Interstitial diseases (fibrosis, emphysema, post-covid, mosaic perfusion) Neoplasm (Lung neoplasm, mediastinal neoplasm and masses) Cardiac Diseases Acute Myocardial Infarct, Myocarditis, Myocardial masses

OUTLINE Spectral CT imaging is a relatively new technique which presents several advantages and may give functional data about different cardiac and thoracic diseases. Radiologists should be familiar with this technique that can play a pivotal role in patient management.

Printed on: 02/07/23



## Abstract Archives of the RSNA, 2022

CHEE-25

### Don't Touch the Animals: Chest Radiologists View- Zoonoses

Sunday, Nov. 27 8:00AM - 9:00AM Room: Learning Center - CH

#### Awards

Certificate of Merit

Identified for RadioGraphics

#### Participants

Hannah Hodges, MD, Albuquerque, NM (*Presenter*) Nothing to Disclose

#### TEACHING POINTS

Teaching points:1. Identify zoonotic organisms and their animal vectors to which humans are susceptible.2. Understand the cardiothoracic symptoms and clinical findings of infection.3. Recognize the multimodality radiologic appearances of these diseases.4. Learn laboratory and other testing that confirms the diagnosis.

#### TABLE OF CONTENTS/OUTLINE

Content Organization:1- Introductiona Organisms and animal vectors2- Cardiothoracic findings of Zoonosesa. Tularemiab. Plaguec. Anthraxd. Leptospirosise. Monkeypoxf. Hantavirusg. Echinococcus3- Radiologic assessmenta. Identifying features, morphology, and distributionb. Multimodality radiologic appearances4- Pitfallsa. Potential mimics 5- Summary

Printed on: 02/07/23

## Abstract Archives of the RSNA, 2022

CHEE-26

### Pitfalls in Thymic Imaging

Sunday, Nov. 27 8:00AM - 9:00AM Room: Learning Center - CH

#### Awards

Identified for RadioGraphics  
Certificate of Merit

#### Participants

Maximiliano Klug, MD, Ramat Gan, Israel (*Presenter*) Nothing to Disclose

#### TEACHING POINTS

1- Thymic hyperplasia, thymic cysts and thymoma may be difficult to distinguish by CT imaging alone. MRI of the mediastinum helps in the differential diagnosis. 2- Chemical shift sequences can differentiate thymic hyperplasia from thymoma. Correct use of the Chemical-Shift-Ratio identifies cases of hyperplasia when the characteristic signal drop is not identified. Small lesions may not be measurable due to inaccurate ROI placement and calculation. DWI in small lesions may be challenging as well. 3- Thymic cysts are typically hyperintense on T2-weighted images (T2WI). Pitfalls in identifying cyst on T2WI include intermediate T2WI signal of some cysts due to proteinaceous content and pseudo-nodules due to cardiac motion. Careful inspection of T1 weighted images with and without intravenous contrast may overcome these limitations. 4- Newer thymic MRI protocols including delayed phases are important to distinguish malignant from benign thymic lesions. Nevertheless, longer MRI studies may be prone to additional artifacts due to breathing. Breathing correction and subtraction imaging may help. 5- Thymoma pleural metastases can be missed leading to erroneous staging. Typical overlooked locations are adjacent to atelectatic lung or the crux of the diaphragm.

#### TABLE OF CONTENTS/OUTLINE

1- To describe thymic imaging techniques and radiologic appearance of thymic entities. 2- To discuss pitfalls in interpretation and possible imaging solutions. 3- To discuss blind-spots in thymoma pleural metastatic disease.

Printed on: 02/07/23



## Abstract Archives of the RSNA, 2022

CHEE-27

### Unfamiliar Thoracic Anatomy: You Only Know What You Know

Sunday, Nov. 27 8:00AM - 9:00AM Room: Learning Center - CH

#### Participants

Mohamed Elboraey, MD, (*Presenter*) Nothing to Disclose

#### TEACHING POINTS

- Understanding of thoracic anatomy is essential for accurate interpretation of thoracic imaging.- Some unfamiliar/less frequently encountered thoracic anatomic and variant structures can simulate pathology.- Prospectively differentiating these structures from true pathology will prevent overcalling pathologic processes and unnecessary downstream investigations.

#### TABLE OF CONTENTS/OUTLINE

- Review anatomic structures at CXR, CT, and MRI:a. Vasculature (inferior pulmonary vein confluence with left atrium; L SVC, cardiophrenic veins, azygos vein).b. Hilar anatomy (inferior pulmonary ligament vs sublobar septum).c. Pulmonary fissures (accessory or incomplete fissures, fissural lymph nodes).d. Pericardium (pericardial recesses simulating lymphadenopathy or mediastinal masses; mediastinal vs epicardial fat).e. Lymph nodes (unnamed stations, left supraclavicular lymph node vs vein confluence, extrapleural space nodes).f. Chest wall (axillary/breast variants, muscular arches).- Emphasize how radiologists can differentiate these entities from true pathology by imaging evaluation with case examples.

Printed on: 02/07/23



## Abstract Archives of the RSNA, 2022

CHEE-28

### Going with the Flow: Understanding Flow Artifacts

Sunday, Nov. 27 8:00AM - 9:00AM Room: Learning Center - CH

#### Awards

Identified for RadioGraphics

Magna Cum Laude

#### Participants

Caroline Robb, MD, (Presenter) Nothing to Disclose

#### TEACHING POINTS

- Flow artifacts are commonly encountered in contrast-enhanced CT imaging studies and may be mistaken for important pathologic conditions, such as embolism or dissection.
- Radiologists must be familiar with the appearance of flow artifacts and comfortable distinguishing these artifacts from true pathologic conditions.
- By understanding the mechanics of flow artifacts, radiologists can better recognize the clinical settings that predispose to flow artifacts, such as pneumonia or altered cardiac output.
- Radiologists must know how to troubleshoot a suspected flow artifact, including how to adjust imaging protocols, when to recommend additional imaging studies, and which additional imaging studies are most helpful.
- Flow artifacts can be used as a tool when the radiologist encounters vascular pathology, such as when evaluating aortic dissection flaps.

#### TABLE OF CONTENTS/OUTLINE

- Discuss the physical mechanics of vascular blood flow and how these mechanics can give rise to flow artifacts.
- Review how to distinguish flow artifact from true pathologic conditions, such as pulmonary embolism or aortic dissection.
- Examine the causes of flow artifacts and how these artifacts may present in various clinical settings, such as pneumonia or altered cardiac output.
- Discuss how to troubleshoot suspected flow artifact, including the utility of delayed image acquisition and MRI.
- Evaluate how flow artifacts can be used as a diagnostic tool, such as when assessing aortic dissection flaps.

Printed on: 02/07/23



## Abstract Archives of the RSNA, 2022

CHEE-29

### Pericardial Recesses on Multidetector CT: Beyond Tips and Tricks Around the Heart

Sunday, Nov. 27 8:00AM - 9:00AM Room: Learning Center - CH

#### Participants

Alex Carvalho Monteiro, (*Presenter*) Nothing to Disclose

#### TEACHING POINTS

The purpose of this exhibition is: • Review common and uncommon cases related to the pericardial sinuses and recesses. • Correlate important findings with the anatomy of pericardial recesses. • Discuss imaging findings according to the classification of pericardial recesses to enhance radiologists' skills. • Highlight their characteristics for radiologists with these conditions, avoiding unfavorable patient outcome. • Despite its characteristic density, describe the importance of distinguishing them from pathologic process, as mediastinal lymphadenopathy, and mediastinal cystic mass. • Correlate with the impact on the onco-image.

#### TABLE OF CONTENTS/OUTLINE

• Applied anatomy of the pericardial recesses: superior pericardial recess, right lung recess, left lung recess, postcaval recess, right pulmonary venous recess, superior pericardial recess, transverse sinus, left pulmonary venous recess and oblique sinus. • Evaluation of cases of prominent recesses with variable extensions, which may be possible confounding mechanisms. • Examples of pearl cases, diagnostic difficulties, and mimicry. • Summary and take-home messages.

Printed on: 02/07/23



## Abstract Archives of the RSNA, 2022

CHEE-30

### Developments in Lung Cancer - What Radiologists Should Know About the WHO Classification Updates and Developments in Molecular Biology Research

Sunday, Nov. 27 8:00AM - 9:00AM Room: Learning Center - CH

#### Awards

Identified for RadioGraphics

Cum Laude

#### Participants

Tomoaki Sasaki, MD, (*Presenter*) Nothing to Disclose

#### TEACHING POINTS

Lung cancer is the leading cause of cancer death worldwide, and determination of the histological type is essential for management. Surgical resection is performed in the early stage, and the surgical specimen allows radiological-pathological investigation. In 2021, the WHO classification of thoracic tumors was updated. These revisions deal with lung cancer prognosis and recognize several new entities. Unfortunately, about 70% of lung cancers are unresectable when diagnosed. Histological diagnosis must therefore rely on molecular analysis of a small biopsy tissue. Accurate knowledge regarding the molecular biology and immunohistopathology of lung cancers has thus become crucial. Radiological imaging plays an important role in the management of both early and advanced stage lung cancers. Therefore, radiologists must be familiar with all updates made to the WHO classification and molecular biology. The aim of this presentation is 1) to understand the radiological-pathological correlations in surgical specimens according to the new WHO classification, 2) to update our knowledge of lung cancer molecular biology, and 3) to acknowledge the limitations of small biopsy samples.

#### TABLE OF CONTENTS/OUTLINE

1. Introduction: Revision of the WHO classification  
2. Radiological-Pathological correlations from surgical specimens: Adenocarcinomas, Squamous cell carcinomas, Sarcomatoid carcinomas, Neuroendocrine carcinomas, Salivary gland-type tumors, etc  
3. Molecular biology: EGFR, ALK, ROS1, HER2, RET, BRAF V600F, KRAS, NTRK, METamp, NRG1 fusion, PD-L1, etc  
4. Limitations of small biopsy samples  
5. Conclusion

Printed on: 02/07/23

## Abstract Archives of the RSNA, 2022

CHEE-31

### **MRI of Anterior Mediastinal Masses: When to Image and Approach to Interpretation**

Sunday, Nov. 27 8:00AM - 9:00AM Room: Learning Center - CH

#### **Participants**

Tetsuro Araki, MD, PhD, Philadelphia, PA (*Presenter*) Nothing to Disclose

#### **TEACHING POINTS**

1. To understand appropriate settings to recommend MRI for the evaluation of anterior mediastinal masses (AMM). 2. To understand the main roles of MRI in characterization of AMM. 3. To understand key features for the differential diagnoses of AMM.

#### **TABLE OF CONTENTS/OUTLINE**

1. Indication of MRI for AMM a. Incidentally found AMM on CT or chest radiograph b. Preoperative characterization and staging of AMM c. Screening for associated findings of AMM (lymph nodes or pleural lesions) d. MRI protocols for AMM e. Alternative imaging options to MRI. 2. Main roles of MRI in characterization of AMM a. Cystic vs solid b. Benign vs malignant (Normal/hyperplastic thymus vs neoplasm) c. Risk stratification or staging 3. Key MRI features for the differentiation of AMM a. T1 and T2 signal intensity b. Enhancement on post contrast images c. Demonstration of microscopic fat on out of phase T1-weighted images d. Diffusion weighted images/ADC map 4. Case review of AMM a. Normal/hyperplastic thymus (fat saturated or non-saturated thymic hyperplasia) b. Thymic cyst/bronchogenic cyst c. Ectopic thyroid tissue/retrosternal thyroid goiter d. Thymic epithelial tumors (thymoma, thymic carcinoma, neuroendocrine tumors) e. Primary mediastinal large B-cell lymphoma (PMBCL) f. Thymolipoma/lipoma g. Metastasis 5. Summary

Printed on: 02/07/23



## Abstract Archives of the RSNA, 2022

CHEE-32

### Pitfalls and Tricks of Variants in Thoracic Imaging: Who Wants To Be... Normal?

Sunday, Nov. 27 8:00AM - 9:00AM Room: Learning Center - CH

#### Participants

Mariana Peleja, MD, Sao Paulo, Brazil (*Presenter*) Nothing to Disclose

#### TEACHING POINTS

The purpose of this exhibit is:- To play an adapted game show ("Who wants to be a millionaire") related to normal variants in thoracic imaging.- To illustrate normal variants in thoracic imaging.- To differentiate between normal and pathological cases in CT and MRI imaging.- To demonstrate cases of physiological uptake on PET/CT.- To go through several typical and atypical findings in thoracic imaging to facilitate radiological understanding and diagnosis.

#### TABLE OF CONTENTS/OUTLINE

- Interactive game show.- Interactive cases related to normal variants in thoracic imaging.- Reporting language for imaging findings related to the variants in thoracic imaging.- Review of imaging findings according to illustrative cases of:1.Chest wall;2.Diaphragm;3.Pleura;4.Lungs;5.Mediastinum: heart, great vessels, airways, esophagus, thymus, neural and lymphatic structures;- Summary and gained knowledge.

Printed on: 02/07/23



## Abstract Archives of the RSNA, 2022

CHEE-33

### Photon-Counting CT in Chest Applications

Sunday, Nov. 27 8:00AM - 9:00AM Room: Learning Center - CH

#### Awards

Certificate of Merit

#### Participants

Fides Schwartz, MD, Durham, NC (*Presenter*) Nothing to Disclose

#### TEACHING POINTS

Photon-counting computed tomography (PCCT) is a new technology in CT imaging. PCCT uses energy-resolving detectors, instead of integrating the entire x-ray signal (energy integrating detectors: EID), enabling spectral acquisitions without the need of specialized acquisition strategies (e.g., dual-source). PCCT records photons in different energy bins, starting at a minimum energy threshold, so electronic noise can be avoided altogether. PCCT detectors used a two-step conversion (x-rays to electrical signal), rather than the 3-step conversion EID (x-rays to light to electrical signal), and inherently have higher spatial resolution as no septa (dead space to separate voxels) are needed. This project is geared toward introducing the emerging technology of PCCT to the RSNA chest imaging community. The details of this technology will be explained using diagrams and examples of standard EID patient scans in comparison to PCCT scans to demonstrate the performance of the new scanner system. These examples will include tumor monitoring, lung cancer screening and contrasted chest CT.

#### TABLE OF CONTENTS/OUTLINE

1. PCCT - Detectors a. Comparison of energy-integrating vs photon-counting detectors b. How is higher spatial resolution of PCCT achieved? 2. PCCT - Photon Binning a. How does photon binning work? b. How are energy thresholds defined? c. How do thresholds help with electronic noise? 3. PCCT - Spectral Data a. How is it always available? b. What can it be used for?

Printed on: 02/07/23



## Abstract Archives of the RSNA, 2022

CHEE-34

### Wait, You Can See Motion on Chest Radiographs?! Dynamic Digital Radiography (DDR)

Sunday, Nov. 27 8:00AM - 9:00AM Room: Learning Center - CH

#### Participants

Donald Benson JR, MD, PhD, Little Rock, AR (*Presenter*) Nothing to Disclose

#### TEACHING POINTS

1. Dynamic digital radiography (DDR) is a newer technology enabling rapid acquisition of multiple sequential radiographs with field of view and spatial resolution similar to that of conventional radiography. 2. The simultaneous acquisition of detailed anatomical and functional imaging enables identification and evaluation of potential lung nodules, diaphragmatic motion, chest wall motion and restricted lung motion. 3. As a digital acquisition DDR enables computerized mathematical evaluation of lung areas, lung volumes, graphing diaphragmatic motion and potential pulmonary function parameters.

#### TABLE OF CONTENTS/OUTLINE

After a brief introduction to this technology, the following potential applications will be discussed: 1. Improved evaluation of potential lung nodules. 2. Evaluation of diaphragm function. 3. Follow up evaluation of post-surgical chest patients. 4. Potential assessment of pulmonary ventilation and perfusion. 5. Comprehensive pre-operative lung transplant evaluation. 6. Correlation of measured lung areas and estimated volumes with pulmonary function testing. 7. Evaluation of diffuse lung disease, e.g., post-COVID patients, and patients with interstitial lung disease, chronic obstructive pulmonary disease, cystic fibrosis, among others.

Printed on: 02/07/23



## Abstract Archives of the RSNA, 2022

CHEE-35

### Lung Contrast-enhanced Ultrasound (CEUS): How I Do It

Sunday, Nov. 27 8:00AM - 9:00AM Room: Learning Center - CH

#### Awards

Identified for RadioGraphics

#### Participants

Sergio Jimenez Serrano, Barcelona, Spain (*Presenter*) Nothing to Disclose

#### TEACHING POINTS

The purpose of this educational exhibit is:- To explain how to correctly perform a lung contrast-enhanced ultrasound (CEUS).- To describe the basics of pulmonary vascularization, which are fundamental to interpreting a lung CEUS.- To review the clinical situations in which lung CEUS may be useful in diagnosing and treating pulmonary pathology.

#### TABLE OF CONTENTS/OUTLINE

Pulmonary CEUS has experienced a constantly growing in the study of pulmonary pathology. In this educational exhibit we will focus on:- Explaining the exploration technique.- Reviewing the physiopathology of the pulmonary vasculature.- Reviewing the characteristic findings in CEUS in non-tumor entities such as:• Pulmonary atelectasis• Round atelectasis• Pulmonary infarction• Pneumonia• Lung abscess• Radiation pneumonitis- Describing the main findings that can help us differentiate between aggressive and non-aggressive pulmonary neoplasms (with examples).- Radiological findings in CEUS that can help us in the diagnosis of lymphoma or lung metastases.- The importance of CEUS in interventional procedures:• Evaluation of tumor necrosis.• Choice of puncture point.• Differentiate obstructive atelectasis from tumor lesion.• Avoid vascular structures.• Prevent the biopsy of benign lung lesions.

Printed on: 02/07/23

## Abstract Archives of the RSNA, 2022

CHEE-36

### Stick To Your Rib - A Radiologist Guide for Rib Cartilage Evaluation before Reconstruction Surgeries

Sunday, Nov. 27 8:00AM - 9:00AM Room: Learning Center - CH

#### Participants

Felipe A. de Oliveira, MD, Sao Paulo, Brazil (*Presenter*) Nothing to Disclose

#### TEACHING POINTS

? Provide an overview of the normal costal arch cartilage anatomy, and how its used as autogenous graft material for cartilage reconstruction surgeries;? To explain how to evaluate the costal arch cartilages (degree of calcification, and calcification morphological patterns) on X-Ray, US and CT scan; ?Application of Artificial Intelligence assisting CT scan evaluation; ?To exemplify how to report the normal and abnormal crucial findings to the surgeon; ? To introduce the related surgical cartilage reconstructive techniques.

#### TABLE OF CONTENTS/OUTLINE

1) Costal arch cartilage overview. A) Anatomy of costal arch cartilage. B) Costal arch cartilage and its adjacent structures anatomical relations. C) Histology of costal arch cartilage. 2) Costal arch cartilage employment as an autologous donor site for cartilage reconstructions surgeries - pros and cons. 3) Costal arch cartilage calcifications as a complicating factor for surgical outcomes. 4) Imaging evaluation, epidemiology and examples of costal arch cartilage calcifications. A) X-Ray. B) US. C) CT scan. 5) How to report. 6) Rib (costal arch) cartilage harvesting surgical technique. 7) Examples of cartilage reconstructive surgical techniques in which costal arch cartilage is employed. A) Rhinoplasty. B) Microtia otoplasty. C) General face reconstructive surgeries. 8) Take-home messages.

Printed on: 02/07/23

## Abstract Archives of the RSNA, 2022

CHEE-37

### Between the Walls: Understanding the Extrapleural Space and the Extrapleural Fat Sign

Sunday, Nov. 27 8:00AM - 9:00AM Room: Learning Center - CH

#### Participants

Guillem Dolz Alvarez De La Ballina, MD, Valldoreix, Spain (*Presenter*) Nothing to Disclose

#### TEACHING POINTS

To review the normal anatomy of the extrapleural space (EPS). To describe the extrapleural fat sign (internal displacement of the adipose tissue layer), a clue to locating different conditions in the EPS. To show the many entities that can involve the EPS, emphasizing the role of CT.

#### TABLE OF CONTENTS/OUTLINE

Background: The EPS lies between the parietal pleura, the chest wall and diaphragm. It is a poorly understood anatomical compartment which can lead to diagnostic errors. Anatomical scheme. Extrapleural fat can be displaced, enlarged, or affected by: - Blood (extrapleural hematoma): from trauma, iatrogenic lesion of a thoracic vessel, aortic dissection or aneurysm rupture, spontaneous bleeding. - Air (extrapleural emphysema): barotrauma. - Fat: non-pathologic (obesity or estrogens), lipoma, chronic pleural conditions. - Edema/Infection: acute pleural exudates, empyema necessitatis. - Soft tissue: extramedullary hematopoiesis, neurogenic lesions, primary or metastatic pleural tumors, infiltration of lung tumor, chest-wall malignancies. - Calcium: chronic hematoma/empyema, asbestos related pleural disease. Conclusions: The extrapleural fat sign helps differentiate between pleural and extrapleural lesions. Conditions involving the EPS may require different treatment approaches than pleural or lung diseases.

Printed on: 02/07/23



## Abstract Archives of the RSNA, 2022

CHEE-38

### Leukemia and the Thoracic Plethora- Perplexities, Patterns and Problem Solving

Sunday, Nov. 27 8:00AM - 9:00AM Room: Learning Center - CH

#### Participants

Shubham Padashetty JR, MD, Mumbai, India (*Presenter*) Nothing to Disclose

#### TEACHING POINTS

Leukemia presents with multitude of disease related and various infective and noninfective presentations. Presentations include ground glass opacities, centrilobular nodules, interstitial septal thickening in various patterns. Mediastinal, pleural, nodal and bony involvement also need to be carefully looked for. Disease related manifestations include nodal, parenchymal, mediastinal and bony involvement, biopsy is necessitated in conditions when inflammatory and infective pathology is ruled out. Drugs and infection related injuries require both clinical and radiological approach based addressal with knowledge of specific pattern of presentations. For instance apical predominance with cystic changes are seen in PCP pneumonia, unsharp hazy ground glass changes with confluent centrilobular nodules seen in CMV pneumonia, tree-in-bud pattern in mycobacterial diseases. Non-contrast CT and HRCT thorax are a valuable tool in diagnosis, follow-up, serial correlation of presentations. They also aid in guiding image guided interventions when necessary. This educational exhibit aims to familiarize with various paradigms of presentations, pattern based understanding and clinico-biochemical correlation, henceforth providing apt differentials. Clinical radiology plays a key role in reducing morbidity and mortality in hematolymphoid malignancies when timely approach and diagnosis helps early treatment.

#### TABLE OF CONTENTS/OUTLINE

1. Flow chart of pulmonary manifestations in leukemia
2. Disease related manifestations
3. Non infectious pulmonary complications
4. Infections and their patterns of involvement.

Printed on: 02/07/23



## Abstract Archives of the RSNA, 2022

CHEE-39

### Breast Implants in Chest CT: What Can We See?

Sunday, Nov. 27 8:00AM - 9:00AM Room: Learning Center - CH

#### Awards

Certificate of Merit

#### Participants

Vinicius Nobre, MD, (*Presenter*) Nothing to Disclose

#### TEACHING POINTS

The purpose of this exhibit is: To review the components of the most common breast implants and prostheses, as well the main pathological conditions involving them. To emphasize that chest computed tomography (CT), which is widely available and allows rapid image acquisition, can detect incidental findings involving breast implants. To discuss the pathophysiology of breast implants conditions and their imaging findings, especially on CT, correlating them with more specific studies for breast implant evaluation. To offer a didactic case-based review on the theme, proving teaching points and references, in order to allow radiologists to detect abnormalities involving breast implants in CT scans performed for different reasons.

#### TABLE OF CONTENTS/OUTLINE

Breast implants and their normal appearance in CT. Intracapsular breast implant rupture: Imaging findings, including signs such as the "keyhole", "subcapsular", "linguine" and "droplet", discontinuity of the elastomer, among others. Degrees of implant collapse: uncollapsed, minimal, partial and full collapse. Extracapsular breast implant rupture: Imaging findings, including extra capsular silicone and siliconomas. Diagnostic difficulties and mimics. Capsular contracture: Image findings. Breast implant rotation: Image findings. Other breast implants complications related to the theme. Summary and take-home messages.

Printed on: 02/07/23



## Abstract Archives of the RSNA, 2022

CHEE-4

### Extracorporeal Membrane Oxygenation [ECMO]: What the hECMO Am I Looking At?

Sunday, Nov. 27 8:00AM - 9:00AM Room: Learning Center - CH

#### Participants

Nina L. Terry, MD, JD, Hoover, AL (*Presenter*) Stockholder, Johnson & Johnson; Spouse, Stockholder, Johnson & Johnson; Stockholder, Kimberly-Clark Corporation; Spouse, Stockholder, Kimberly-Clark Corporation; Stockholder, Microsoft Corporation; Spouse, Stockholder, Microsoft Corporation; Spouse, Stockholder, Amgen

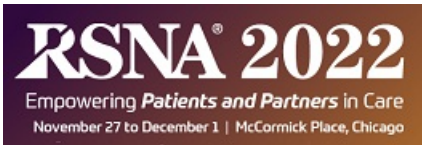
#### TEACHING POINTS

1. For adults two major ECMO types function to bypass the lungs [veno-venous (VV)] or the heart and lungs [veno-arterial (VA)] with variable catheter types and positions for both. 2. ECMO catheters are imaged with radiographs, echocardiography and CT both incidentally and intentionally. 3. Radiologists should recognize appropriate configuration/positioning of the various types and be aware of potential complications for each. 4. Radiologists need to know the indications for contrast and the indications and contraindications for stopping ECMO or clamping the ECMO catheters to optimize image quality.

#### TABLE OF CONTENTS/OUTLINE

- Introduction
- o Overview of ECMO
- o Importance to the average radiologist
- Normal catheter placement for ECMO
- o Venovenous ECMO
- § Single lumen vs. dual lumen catheters
- o Venoarterial ECMO
- § Peripheral vs. central catheterization
- § Comparing points of entry
- o Effect of cannula sizing on correct placement (especially emergency settings)
- Comparing imaging modalities used to verify correct catheter placement
- o Echocardiography
- o Chest Radiograph [CXR]
- o Computed Tomography [CT]
- Visualizing complications during/post catheter placement
- o Contrast CT or Non-contrast CT: Indications
- o Safety and technical issues in giving contrast to a patient on ECMO
- Special cases to consider
- o ECMO during COVID-19
- Conclusion
- o Radiologists have an important role in diagnosis and patient safety with the growing use of ECMO technology

Printed on: 02/07/23



## Abstract Archives of the RSNA, 2022

CHEE-40

### "Reduce Fat Fast": A Systematic Approach to Fat-containing Lesions in Adult Thoracic Imaging and Its Differential Diagnosis.

Sunday, Nov. 27 8:00AM - 9:00AM Room: Learning Center - CH

#### Participants

Carlos Penaranda, MD, (*Presenter*) Nothing to Disclose

#### TEACHING POINTS

1. Approach the differential diagnosis of fat-containing lesions in the chest. 2. Recognize the fat-containing lesions, using radiologic features as Hounsfield Units (HU) measurement at computed tomography (CT), or the signal intensity characteristics of fat at magnetic resonance imaging (MR). 3. Correlate lesion location with the fat imaging characteristics to narrow the differential diagnosis.

#### TABLE OF CONTENTS/OUTLINE

1. Imaging characteristics of fat-containing lesions in the thorax employing ultrasound, computed tomography (CT) and magnetic resonance imaging (MR). 2. Schematic approach of various fat-containing lesions and their location in the chest. 3. Sample cases from our institution with their radiographic and epidemiological features.

Printed on: 02/07/23



## Abstract Archives of the RSNA, 2022

CHEE-41

### Inhalational Injuries in Burn Patients: Is Chest Radiography Still Relevant?

Sunday, Nov. 27 8:00AM - 9:00AM Room: Learning Center - CH

#### Participants

Jaime Fields, MD, Winston Salem, NC (*Presenter*) Nothing to Disclose

#### TEACHING POINTS

Pulmonary complications are a common cause of morbidity and mortality in burn patients. It is important that radiologists are familiar with these complications so that early and specific diagnosis is made on chest imaging. While admission radiographs are often normal or underestimate findings, within just a few days pulmonary complications can be severe. While CT is a useful tool, many burn patients do not undergo CT imaging of the chest. Thus it is important for radiologist to be familiar with the radiographic features of these complications and utilize timing after injury as a diagnostic tool.

#### TABLE OF CONTENTS/OUTLINE

- Pathophysiology of burns and radiographic correlation (what happens on alveolar level)
- Timeline of pulmonary complications
- Role of radiologist in utilizing this timeline when interpreting chest radiographs
- Algorithm demonstrating management of inhalational injury
- Findings suggestive of acute inhalational injury
- With what frequency should chest radiographs be obtained?
- Chest radiograph and CT correlation of varied imaging findings
- ARDS as a complication of direct alveolar injury or secondary complications
- Phases of ARDS
- Delayed pulmonary complications
- Long term complications: subglottic stenosis, bronchiectasis, bronchiolitis
- Multidisciplinary approach
- Role of imaging in follow up
- Role of other imaging modalities not previously discussed
- Bonus: Vaping associated lung injury chest radiograph and CT correlates

Printed on: 02/07/23



## Abstract Archives of the RSNA, 2022

CHEE-42

### Distinguishing Fraternal Twins on Chest Radiograph: Primer for Residents

Sunday, Nov. 27 8:00AM - 9:00AM Room: Learning Center - CH

#### Awards

**Magna Cum Laude**

**Identified for RadioGraphics**

#### Participants

Kaitlin Gibson, MD, (*Presenter*) Nothing to Disclose

#### TEACHING POINTS

- Two distinct pathologies although similar in appearance on chest radiographs have nuanced differences (fraternal twins). Differentiating these may be challenging for residents.
- Accurate differentiation is important as this impacts management strategies.
- Case based review of radiographic "fraternal twins" with tips on differentiating two is presented.
- Example: Large apical bulla is differentiated from pneumothorax by the convex margin of the bulla as compared to the parallel margin to chest wall in pneumothorax.
- Length of air fluid levels is equal on frontal and lateral view in lung abscess and is unequal in empyema.
- Diaphragmatic eventration has preserved sharp posterior costophrenic angle on lateral radiograph whereas flattened in paralysis, etc.

#### TABLE OF CONTENTS/OUTLINE

Case examples of fraternal twins with tips on differentiation

1. Pneumothorax / large bulla
2. Pneumothorax / pneumomediastinum
3. Pneumomediastinum / pneumopericardium
4. Lung abscess / empyema
5. Diaphragmatic eventration / paralysis
6. Hilar mass / enlarged pulmonary artery (Hilum convergence sign)
7. Hilar mass / anterior/ posterior mediastinal mass (Hilum overlay sign)
8. Anterior / posterior mediastinal mass (Cervicothoracic and thoracoabdominal signs)
9. Lung mass / pleural/extra pleural mass
10. Opaque hemithorax: atelectasis/ consolidation / pleural effusion
11. Cardiomegaly / pericardial effusion
12. Portal venous air / pneumobilia
13. Basilar atelectasis / subpulmonic effusion

Printed on: 02/07/23



## Abstract Archives of the RSNA, 2022

CHEE-43

### The Anomalies of Thoracic Vein in Adults

Sunday, Nov. 27 8:00AM - 9:00AM Room: Learning Center - CH

#### Participants

Makiko Murota, MD, Kitagun, Japan (*Presenter*) Nothing to Disclose

#### TEACHING POINTS

1. To review the anomalies of the thoracic systemic veins and the pulmonary veins. 2. To describe characteristic imaging features on multiple modalities, including chest radiograph, CT, and MRI. 3. To discuss the importance of clinical implications and the pitfall.

#### TABLE OF CONTENTS/OUTLINE

1. Normal anatomy 2. Embryology 3. The anomalies of the thoracic systemic veins: persistent left superior vena cava (PLSVC), postaoctic left innominate vein (PALIV), azygous/hemiazygous continuation of inferior vena cava, azygous lobe, and others 4. The anomalies of the pulmonary veins: left common pulmonary vein, separate middle lobe vein, aberrant vein (right top pulmonary vein), partial anomalous pulmonary venous return, scimitar syndrome, meandering pulmonary vein and others

Printed on: 02/07/23



## Abstract Archives of the RSNA, 2022

CHEE-44

### Extracardiac Congenital Thoracic Vascular Anomalies - A General Radiologist's Guide

Sunday, Nov. 27 8:00AM - 9:00AM Room: Learning Center - CH

#### Participants

Sanjana Kamath, FRCR, MBBS, (*Presenter*) Nothing to Disclose

#### TEACHING POINTS

1. Congenital thoracic vascular anomalies can present in adulthood. 2. Assessment of thoracic vasculature in compartments can simplify complex vascular anatomy aiding understanding and communication of results. 3. CT is well placed to assess all vascular compartments within the thorax and provide datasets for 3D reconstructions to further communicate findings and plan surgical intervention.

#### TABLE OF CONTENTS/OUTLINE

Systemic venous pathology (including left SVC, anomalous drainage to left atrium and azygous continuation of the IVC). Pulmonary arteries (absence or disconnection of branch pulmonary artery, pulmonary stenosis e.g. in Edwards syndrome, patent ductus arteriosus, aortopulmonary window and arteriovenous malformations). Pulmonary veins (partial and total anomalous return, sinus venosus ASD and scimitar syndrome). Aortic (truncus arteriosus and hemitruncus, congenitally corrected transposition of the great arteries, right arch with anomalous left subclavian artery, left arch with anomalous right subclavian artery, double arch, coarctation, interruption of the arch, pulmonary sequestration).

Printed on: 02/07/23



## Abstract Archives of the RSNA, 2022

CHEE-45

### Beyond Aortopathies- Vascular Conditions Of The Thorax Associated With Genetic Conditions

Sunday, Nov. 27 8:00AM - 9:00AM Room: Learning Center - CH

#### Participants

Riddhi Borse, MD, New Haven, MA (*Presenter*) Nothing to Disclose

#### TEACHING POINTS

1. Introduction to the vascular structures of the thorax.2. Enlisting various vascular conditions of the thorax associated with genetic conditions and discussing commonly associated imaging findings affecting the various vessels of the thorax.3. Detailed case-based description of thoracic imaging findings associated with inherited vascular conditions, along with common differential diagnoses.4. Developing a Checklist and Understanding the salient features to be reported when encountering these inherited vascular conditions of the thorax.

#### TABLE OF CONTENTS/OUTLINE

1. Description of various vascular conditions with genetic predisposition and their associated common thoracic imaging findings.2. Brief discussion on Ehlers Danlos, Marfan's, Turners syndromes and associated constellation of imaging findings with a focus on related vascular thoracic imaging findings, case examples and common differential diagnoses.3. Brief discussion on BMP2 and Factor V Leiden Mutations, associated constellation of imaging findings with a focus on related vascular thoracic imaging findings, case examples and common differential diagnoses.4. Brief discussion on Cystic Fibrosis, Hereditary hemorrhagic Telangiectasia's and associated constellation of imaging findings with a focus on related vascular thoracic imaging findings, case examples and common differential diagnoses.5. Enlisting salient imaging features to be added in the report based on what the clinician needs to know for each of the above listed conditions.

Printed on: 02/07/23

## Abstract Archives of the RSNA, 2022

CHEE-46

### Scimitar Syndrome - Taking a Sharper Look

Sunday, Nov. 27 8:00AM - 9:00AM Room: Learning Center - CH

#### Participants

Melissa Carroll, MD, Kansas City, KS (*Presenter*) Nothing to Disclose

#### TEACHING POINTS

1. Review the definition and variations of scimitar syndrome with a focus on imaging findings. 2. Familiarize the reader with common and uncommon congenital anomalies associated with scimitar syndrome to improve radiology exam interpretation. 3. Discuss clinical presentation and complications of scimitar syndrome.

#### TABLE OF CONTENTS/OUTLINE

1. Background  
2. Definition  
a. Scimitar syndrome (hypogenetic lung or congenital venolobar syndrome) refers to partial anomalous venous drainage of the right lung to the IVC with hypoplasia of the ipsilateral lung, systemic artery supply, and dextroposition of the heart  
b. Scimitar sign refers to the curved, tubular opacity adjacent to the right heart border on chest radiograph representing the anomalous vein and is considered pathognomonic for scimitar syndrome. Scimitar refers to a Turkish sword with a curved blade  
3. Types  
a. Infantile type presents in infancy and associated with congenital heart disease  
b. Childhood/adult type, which can be asymptomatic or result in recurrent infection  
4. Imaging Findings  
a. Chest radiograph as a screening tool  
b. Contrast enhanced CT to define anatomy and identify other anomalies  
c. Phase contrast MRI to quantify shunt  
d. Pertinent radiology report findings for surgical planning  
5. Associated congenital anomalies  
a. Lungs and airways  
b. Vascular  
c. Cardiac  
6. Clinical considerations and complications  
a. Discuss range of clinical manifestations and presentation including congestive heart failure in infants and recurrent infection in adults  
b. Cardiovascular complications  
c. Pulmonary complications  
d. Post surgical imaging  
7. Conclusion

Printed on: 02/07/23



## Abstract Archives of the RSNA, 2022

CHEE-47

### Pre- and Post-operative Evaluation of the Patient with Chronic Thromboembolic Pulmonary Hypertension

Sunday, Nov. 27 8:00AM - 9:00AM Room: Learning Center - CH

#### Participants

Tami Bang, MD, Aurora, CO (*Presenter*) Nothing to Disclose

#### TEACHING POINTS

1. Define chronic thromboembolic pulmonary hypertension (CTEPH) and describe its development 2. Review the imaging findings in CTEPH 3. Discuss surgical management of CTEPH 4. Review the role of the radiologist in the diagnosis, evaluation, and management of CTEPH

#### TABLE OF CONTENTS/OUTLINE

1. Definition of Chronic Thromboembolic Pulmonary Hypertension (CTEPH) 2. Pathophysiology of CTEPH 3. Multimodality Diagnosis of CTEPH (CT, Echo, V/Q scan, CMR, Angiography) 4. Surgical Management of CTEPH 5. What does the referring team need to know?  
a. Is the case operable b. What is the likelihood of RV recovery c. Are there accessible targets for endarterectomy?

Printed on: 02/07/23



## Abstract Archives of the RSNA, 2022

CHEE-48

### Chronic Pulmonary Embolism: What Radiologists Should Know

Sunday, Nov. 27 8:00AM - 9:00AM Room: Learning Center - CH

#### Participants

Marcelo Carvalho, MD, Sao Paulo, Brazil (*Presenter*) Nothing to Disclose

#### TEACHING POINTS

- To review the major direct and indirect findings of both acute and chronic pulmonary embolism on CT angiography.- To discuss the role of iodine map in chronic pulmonary embolism.- To highlight other important differential diagnosis of chronic PE as well as potential pitfalls.

#### TABLE OF CONTENTS/OUTLINE

Introduction: basic concepts on chronic pulmonary embolism (epidemiology, pathophysiology, clinical findings and treatment goals)CTA protocol for pulmonary embolismAcute x chronic pulmonary embolism: a CTA-centered approachCurrent state of the iodine map in chronic pulmonary embolismOther differential diagnosis to keep in mindIdiopathic pulmonary hypertension and in situ thrombosisPulmonary artery sarcomaVasculitisCongenital anomaliesPotential pitfalls and artifacts in chronic pulmonary embolism

Printed on: 02/07/23



## Abstract Archives of the RSNA, 2022

CHEE-49

### Following the Contrast: How to Recognize Thoracic Flow Artifacts and Vascular Shunts on Thoracic Multidetector Computed Tomography

Sunday, Nov. 27 8:00AM - 9:00AM Room: Learning Center - CH

#### Participants

Elisenda Foraster, MD, Sabadell, Spain (*Presenter*) Nothing to Disclose

#### TEACHING POINTS

To learn the causes of thoracic flow artifacts and provide clues to distinguish them from true filling defects. To be aware of persistent and anomalous cardiac communications that are relevant in clinical practice and its typical imaging findings.

#### TABLE OF CONTENTS/OUTLINE

I. Background Thoracic flow artifacts as well vascular and cardiac shunts can be challenging for radiologists to diagnose. We propose a practical approach to recognize the main causes and CT features in both situations. II. Content A) Thoracic flow artifacts ("smoke"): non-opacified blood in a contrast-filled chamber, indicative of incomplete opacification. 1. Pulmonary artery (mimicking pulmonary embolism): bilateral smoke (heart failure, early/fast scanning, transient interruption of contrast) or unilateral smoke (focal lung abnormality, collateral vessel inflow). 2. Aortic pseudo-dissection. 3. Left atrial appendage pseudo-thrombus. B) Congenital or acquired shunt (aberrant pathway): Abnormal passage of contrast between cardiac chambers or between vascular structures and cardiac chambers, indicative of an abnormal communication. 1. Congenital atrial septal defect, patent foramen ovale, ventricular septal defect. 2. Acquired: collateral venous pathway from stenosis or occlusion of the superior vena cava. III. Conclusions Recognizing smoke can help prevent misdiagnosis of important diseases like pulmonary embolism or aortic dissection, and detection of contrast aberrant-paths provide a diagnosis clue to the presence of shunts or vascular stenosis.

Printed on: 02/07/23



## Abstract Archives of the RSNA, 2022

CHEE-5

### Vasculitides: Diagnostic Tips and Tricks through Thoracic Imaging

Sunday, Nov. 27 8:00AM - 9:00AM Room: Learning Center - CH

#### Participants

Glenda Costa Feitosa, MD, Sao Paulo, Brazil (*Presenter*) Nothing to Disclose

#### TEACHING POINTS

Vasculitides are multi-systemic diseases that can lead to severe consequences if left untreated. There are several ways these disease processes can present on imaging. Thoracic imaging, for instance, has a lot to add when characterizing them, given the considerable importance of the great vessels of the mediastinum and the lung involvement commonly shown. Knowledge of typical findings that suggest a diagnosis of vasculitis is therefore a valuable asset for the radiologist and yields better outcomes.

#### TABLE OF CONTENTS/OUTLINE

Inflammatory diseases of the vessel walls can affect small, medium and large vessels in all segments of the body. These are often treatable diseases, bringing alleviation of the inflammatory activity and better overall outcomes. These diseases can be quite a challenge to diagnose, as they can present similarly to one another and have a nonspecific clinical course and laboratory features. The intention of this presentation is to demonstrate, through a series of cases, different vasculitides and diagnostic tips that helped suggesting these diagnoses through imaging, such as the vessels involved by parietal thickening and aneurysms, lung opacities and their temporal evolution, as well as some associations with patient characteristics and clinical features. Chest multidetector computerized tomography is the main method to be explored, an imaging modality that has a lot to offer in this task since the great mediastinal vessels and lungs are often involved.

Printed on: 02/07/23



## Abstract Archives of the RSNA, 2022

CHEE-50

### Mimickers of Chronic Thromboembolic Pulmonary Hypertension: A Pictorial Review

Sunday, Nov. 27 8:00AM - 9:00AM Room: Learning Center - CH

#### Participants

Albert Domingo Senan, MD, Madrid, Spain (*Presenter*) Nothing to Disclose

#### TEACHING POINTS

Highlight the role of imaging tests in chronic thromboembolic pulmonary hypertension (CTEPH) focused on the detection and characterization of those pathologies that can mimic this disease, because both therapeutic management and prognosis are substantially different.

#### TABLE OF CONTENTS/OUTLINE

CTEPH represents a special form of PH potentially curable by surgical treatment (thromboendarterectomy). Imaging tests play a fundamental role in this disease: they confirm the diagnosis, establish the location and extension of the lesions in order to plan the most appropriate treatment (surgery vs. angioplasty vs. medical treatment) and they detect other associated injuries that may condition the patient management. They also allow diagnosis of other pathologies that may have been erroneously labeled as CTEPH. For this reason, it is essential to know what the mimicking pathologies are and the radiological signs that allow them to be detected. The main pathologies that can mimic CTEPH are sarcomas of the pulmonary arteries, large vessel vasculitis (Takayasu's arteritis), fibrosing mediastinitis, in situ thrombosis, pulmonary intravascular hydatid disease, and congenital interruption of the pulmonary artery. These pathologies and the keys to their diagnosis are reviewed.

Printed on: 02/07/23



## Abstract Archives of the RSNA, 2022

CHEE-51

### News Pathways in Thoracic Imaging: A Roadmap to Congenital Vascular Anomalies

Sunday, Nov. 27 8:00AM - 9:00AM Room: Learning Center - CH

#### Participants

Alex Dias, MD, Sao Paulo, Brazil (*Presenter*) Nothing to Disclose

#### TEACHING POINTS

1. Review relevant anatomy, embryogenesis, and pathophysiology of congenital thoracic vascular anomalies. 2. Correlate clinical findings and complaints in childhood and adult life with imaging findings of vascular anomalies, according to subgroups and classifications. 3. Summarize imaging protocols and post-processing techniques. 4. Highlight the role of invasive and non-invasive imaging techniques for anomalies of the great thoracic vessels. 5. Discuss the relevance of multidisciplinary team meetings and the role of radiologists in patient care with case reviews.

#### TABLE OF CONTENTS/OUTLINE

1. Applied anatomy and embryogenesis of pulmonary arteries, pulmonary veins, aortic arch, and superior vena cava. 2. Congenital variants and anomalies: 2.1. Pulmonary arteries. 2.2. Pulmonary veins (total and partial anomalous pulmonary venous return). 2.3. Aortic arch. 2.4. Superior vena cava. 3. Sample cases and outcome review: 3.1. State-of-the-art imaging protocols and post-processing techniques. 3.2. Current and potential diagnostic methods, including invasive and non-invasive studies. 3.3. Follow-up, treatment, and prognosis. 4. Congenital vascular anomalies: practical approach and structure reporting. 5. Summary and take-home messages.

Printed on: 02/07/23



## Abstract Archives of the RSNA, 2022

CHEE-52

### Venous Anatomic Variants In The Thorax

Sunday, Nov. 27 8:00AM - 9:00AM Room: Learning Center - CH

#### Participants

Riddhi Borse, MD, New Haven, MA (*Presenter*) Nothing to Disclose

#### TEACHING POINTS

1.To understand normal vascular anatomy of the thorax, common and uncommon anatomic vascular variants. 2. To classify venous variant anatomy in the thorax based on draining veins. 3.To identify salient imaging features of described anatomic variants in a case based method, common differential diagnoses, and important points to be reported based on their clinical presentations.

#### TABLE OF CONTENTS/OUTLINE

1. Description of normal vascular anatomic structures within the thorax, common and uncommon anatomic variants. 2. Classification of venous anatomic variant anatomy in the thorax based on draining veins as follows:• Azygous Vein- Absent Azygous, Azygous Continuation of Inferior Vena Cava, Azygous Fissure variant in right upper lobe • Hemiazygos Vein- Left Superior Intercostal Vein, Hemiazygos continuation of the IVC, Accessory Hemiazygos Veins. • Superior Vena Cava- Persistent left SVC, Retroaortic Left Brachiocephalic Vein. • Pulmonary Vein- Partial and Total Anomalous Pulmonary Venous Return, Scimitar Syndrome, Accessory and Meandering Pulmonary veins 3. Brief description, salient imaging features, differential diagnoses and examples of anatomic variants draining into the azygous vein. 4. Important points to be included in reporting above listed anatomic variants from a clinical and interventional standpoint.

Printed on: 02/07/23



## Abstract Archives of the RSNA, 2022

CHEE-53

### Challenges and Pitfalls in Lung Cancer Screening

Sunday, Nov. 27 8:00AM - 9:00AM Room: Learning Center - CH

#### Participants

Hanna Ferreira Dalla Pria, MD, MD Anderson, Houston, TX (*Presenter*) Nothing to Disclose

#### TEACHING POINTS

- Updated USPSTF recommendations lung cancer screening (LCS).
- LDCT Lung-RADS classification, reporting, and management recommendations with emphasis on challenging imaging findings and atypical patterns.
- The spectrum of potential pitfalls in pulmonary nodule detection and characterization, including equivocal or atypical presentations, is important for avoiding misinterpretation that can alter patient management.

#### TABLE OF CONTENTS/OUTLINE

- Brief review of LCS history and impact, highlighting recently updated guidelines.
- Interactive imaging-based approach with teaching points for diagnosis and/or work-up of equivocal cases with challenging imaging findings and atypical presentations on LDCT screening, chest CT and PET/CT imaging.
- Discussion and Illustration of main LDCT screening pitfalls and causes of false positive and false negative screening results including, for example, artifacts related to CT technique, inflammatory and post-treatment changes mimicking neoplasm, cystic and cavitary lesions, pleural attached nodules, endobronchial lesions, temporary regression of malignant nodules.
- Discussion and Illustration of main PET/CT pitfalls and false positive and false negative findings in the investigation of screen-detected nodules.
- Limitations and new directions.
- Take-home messages.

Printed on: 02/07/23



## Abstract Archives of the RSNA, 2022

CHEE-54

### COVID-19 Infection: Chest-CT of Complications During Acute Infection and Late Imaging Findings

Sunday, Nov. 27 8:00AM - 9:00AM Room: Learning Center - CH

#### Participants

Leonardo Kenji Mitsutake, MD, Sao Paulo, Brazil (*Presenter*) Nothing to Disclose

#### TEACHING POINTS

The purpose of this exhibit is:- Briefly review the epidemiology of COVID-19 infection and of post COVID-19 CT lungs abnormalities.- Describe and illustrate lung complications related to COVID-19 infection.- Describe post COVID-19 chest CT imaging protocols and technics.- Review the radiological management and follow-up protocols of post COVID-19 pneumonia.- Describe and illustrate the post COVID-19 CT lungs abnormalities, evolution patterns and complications.

#### TABLE OF CONTENTS/OUTLINE

1. Introduction: COVID-19 epidemiology review. Post COVID-19 CT lungs abnormalities epidemiology and predictors.2. Lung complications related to COVID-19 infection: Pneumothorax / Pneumodiastinum / Bronchopleural fistula. Co-infection / superinfection. Vascular complications.3. Post COVID-19 Chest CT protocols.4. Post COVID-19 imaging follow-up: Review of societies recommendations and propositions.5. Key Imaging Findings: Main post COVID-19 CT findings. Imaging evolution patterns. Review of fibrotic-like changes. Post-treatment related complications.6. Take home messages.

Printed on: 02/07/23



## Abstract Archives of the RSNA, 2022

CHEE-56

### Systematic Approach of Congenital Chest Malformations

Sunday, Nov. 27 8:00AM - 9:00AM Room: Learning Center - CH

#### Participants

Taila Moura Fe, Sao Paulo, Brazil (*Presenter*) Nothing to Disclose

#### TEACHING POINTS

The purposes of this exhibit are: 1. Make a multimodality-based didactic review of the various chest malformations. 2. Propose a didactic categorization of these conditions in: -Bronchopulmonary malformations. -Malformations of the pulmonary vessels. - Malformations of the thoracic wall and diaphragm 3. Illustrate those conditions based on cases from our chest radiology group.

#### TABLE OF CONTENTS/OUTLINE

We will discuss the following congenital chest malformations and focus on their imaging features using a multimodality approach in this exhibit. 1. Bronchopulmonary malformations: -Bronchial atresia. -Accessory bronchus. -Bronchogenic cyst. -Congenital lobar overinflation. -Congenital pulmonary airways malformation (CPAM). -Pulmonary sequestration. -Pulmonary aplasia, hypoplasia, and agenesis. 2. Malformations of the pulmonary vessels: -Unilateral absence of the pulmonary artery. -Pulmonary artery sling. - Congenital pulmonary venolobar syndrome. 3. Thoracic wall and diaphragm malformations: -Bochdalek hernia. -Morgagni hernia.

Printed on: 02/07/23



## Abstract Archives of the RSNA, 2022

CHEE-57

### Breasts on Thorax CT's - Better Not Turn a Blind Eye

Sunday, Nov. 27 8:00AM - 9:00AM Room: Learning Center - CH

#### Participants

Izabel Karam, MD, Sao Paulo, Brazil (*Presenter*) Nothing to Disclose

#### TEACHING POINTS

The purposes of this exhibit are: To emphasize the importance of basic breast image knowledge for the general and thoracic specialized radiologist when reporting chest CTs; To review mammary anatomy; To illustrate several breast pathologies and its findings in chest CTs from our department in didactic sections to improve understanding.

#### TABLE OF CONTENTS/OUTLINE

To review the mammary anatomy: Thoracic wall (ribs and muscles); Mammary lobules and ducts; Areola and nipple; Neoplasms and other tumors: Fibroadenoma; Ductal invasive carcinoma; Metastases to breasts; Breast cancer in male patient; Evaluating local extension and lymphatic spreading; Male breasts; Infections and organized collections: Mammary abscess; Organizing hematomas; Post mammoplasty intramammary hematoma; Industrial silicone injection; Implant-related changes: Intrathoracic migration of breast implant after thoracoscopic surgery; Flipped implant; Postoperative abscess; Intracapsular implant rupture; Implant contraction; Implant-related lymphoma.

Printed on: 02/07/23

## Abstract Archives of the RSNA, 2022

CHEE-58

### Imaging Diagnosis as Biomarkers for Lung Cancer with Driver Oncogene Mutation / Gene Translocation in the Era of Personalized Medicine

Sunday, Nov. 27 8:00AM - 9:00AM Room: Learning Center - CH

#### Participants

Masahiro Yanagawa, MD, PhD, Suita, Japan (*Presenter*) Nothing to Disclose

#### TEACHING POINTS

In the era of personalized medicine, imaging diagnosis plays an important part as biomarkers of the following items: prediction for pathological diagnosis, prediction for prognosis, prediction for driver oncogenes, evaluation of treatment response, and evaluation of side effects, etc. Imaging is not always perfect, but it can capture the whole image of lung cancer. This education exhibit focuses on CT imaging in lung cancer with driver oncogene mutation / gene translocation positive and quantitative analysis for predicting gene. It is much appreciated if our information would be useful in your clinical and research setting.

#### TABLE OF CONTENTS/OUTLINE

1. CT imaging in lung cancer with driver oncogene mutation/gene translocation positive: EGFR (epidermal growth factor receptor) mutation, ALK (anaplastic lymphoma kinase) rearrangement, ROS1 (c-ros oncogene) rearrangement, BRAF (v-raf murine viral oncogene homolog B1) mutation, MET exon 14 skipping-mutation, NTRK fusion, and Others [rearranged during transfection proto-oncogene (RET) fusion, KRAS mutation, and human epidermal growth factor receptor 2 (HER-2) mutation]. 2. CT imaging for an immune checkpoint inhibitor in lung cancer with programmed death ligand 1 (PD-L1). 3. Quantitative analysis for predicting gene: Radiomics approach. 4. Tailor-made medicine: Molecular-targeted therapies for driver oncogene mutations / gene translocations.

Printed on: 02/07/23



## Abstract Archives of the RSNA, 2022

CHEE-59

### Myocardial Assessment on CT: Don't Miss a Beat

Sunday, Nov. 27 8:00AM - 9:00AM Room: Learning Center - CH

#### Participants

Elizabeth Lee, MD, Ann Arbor, MI (*Presenter*) Nothing to Disclose

#### TEACHING POINTS

1. Although myocardium is typically evaluated with cardiac CT there is an opportunity to identify abnormalities on routine CTs done for other reasons. 2. Attention to myocardial contour, attenuation and enhancement patterns on a routine chest CT can enable detection of previously unsuspected disease. 3. Recognition of myocardial abnormalities on routine chest CT will help in early detection of cardiac abnormalities and appropriate management.

#### TABLE OF CONTENTS/OUTLINE

Given the widespread use of chest CT, cardiac abnormalities are increasingly being identified on chest CTs often done for other reasons. While several reports have shown the value of incidentally discovered abnormalities (such as coronary anomalies) there is scant literature on myocardial abnormalities. These are challenging to detect, however, attention to this can enable diagnosis of unsuspected disease. The following myocardial abnormalities will be discussed: Attenuation: Differential attenuation between blood pool and myocardium (anemia); Fat deposition (tuberous sclerosis, prior infarct, arrhythmogenic cardiomyopathy, benign); Focal low attenuation (acute myocardial infarction (MI), acute myocarditis); Calcification (old MI, calcified tumor, renal failure) Morphology and enhancement: Thickened with diffuse heterogeneous enhancement (infiltrative processes, Loeffler); Focal thickening with abnormal enhancement (acute MI, myocarditis); Normal thickness with focal heterogeneous enhancement (tumor, acute MI); Thinning (chronic MI, aneurysm/pseudoaneurysm) Future directions: Strain, role of artificial intelligence. Pitfalls: Artifacts can simulate myocardial pathology

Printed on: 02/07/23

## Abstract Archives of the RSNA, 2022

CHEE-60

### Taming the Broncho: An Imaging Guide to Acute Bronchial Disorders

Sunday, Nov. 27 8:00AM - 9:00AM Room: Learning Center - CH

#### Participants

Christopher Song, BS, (*Presenter*) Nothing to Disclose

#### TEACHING POINTS

1) Various diseases of the bronchi can cause acute symptoms and physiologic abnormalities. 2) We will apply a systematic approach to analyzing and characterizing bronchial disorders in the emergent setting. These disorders can be grouped into the following categories: endobronchial lesions, bronchiectasis, bronchial wall thickening, and bronchomalacia. 3) Post-processing reconstructions should be utilized to better visualize and highlight characteristic imaging features.

#### TABLE OF CONTENTS/OUTLINE

Endobronchial lesions- Benign: Aspiration pneumonia, foreign body aspiration, broncholith, pulmonary hamartoma- Malignant: Carcinoid, adenoid cystic carcinoma, mucoepidermoid carcinoma, metastasis- Bronchiectasis - Cystic fibrosis- Graft versus host disease- Primary ciliary dyskinesia- Infection (e.g., nontuberculous mycobacterium, *Pseudomonas aeruginosa*)- Allergic bronchopulmonary aspergillosis- Tracheobronchomegaly- Williams-Campbell syndrome- Bronchial atresia- Bronchial wall thickening- Bronchial asthma- Relapsing polychondritis- Tracheobronchial amyloidosis- Sarcoidosis- Granulomatous with polyangiitis- Infection (e.g. tuberculosis, *Klebsiella*)- Bronchomalacia- Bronchial trauma- Bronchopleural fistula- Bronchomediastinal fistula- Bronchial disruption/rupture

Printed on: 02/07/23



## Abstract Archives of the RSNA, 2022

CHEE-61

### Air trapping in Diffuse Lung Diseases: An Imaging Approach to the Differential Diagnosis with Pathologic Correlation (Mechanisms and Imaging Clues)

Sunday, Nov. 27 8:00AM - 9:00AM Room: Learning Center - CH

#### Awards

Certificate of Merit

#### Participants

Tomas C. Franquet, MD, PhD, Barcelona, Spain (*Presenter*) Nothing to Disclose

#### TEACHING POINTS

Air trapping is a manifestation of many diverse entities such as infections, aspiration or inhalation of foreign substances, immunologic and connective tissue disorders, and miscellaneous causes. The presence of air trapping is an excellent clue to the diagnosis of small airways disease. Air trapping consists of focal zones of decreased attenuation commonly seen at expiratory thin-section CT scans of the lungs obtained during suspended expiration following a forced exhalation. The goals of this exhibit are to help the learner: 1) To review a variety of diffuse lung diseases commonly associated with air trapping 2) To emphasize the diagnostic value of volumetric expiratory CT 3) Present radiology-pathology correlation 4) Provide an algorithmic approach to a differential diagnosis

#### TABLE OF CONTENTS/OUTLINE

1. Introduction. Review Diffuse lung diseases associated with air trapping
2. Review the diagnostic value of volumetric expiratory HRCT scans in providing additional significant information in the evaluation of a variety of diffuse lung diseases with suspected airway abnormalities.
3. Recognize pathologic mechanisms for air trapping in diffuse lung diseases and their impact on radiologic appearance
4. Etiologies of air trapping related to diffuse lung diseases: Infectious Causes, Immunologically mediated, Drug-induced, Toxic/chemical fume inhalation, and miscellaneous causes/associations
5. Algorithm to approach air trapping in diffuse lung diseases.
6. Conclusion

Printed on: 02/07/23



## Abstract Archives of the RSNA, 2022

CHEE-62

### Recognizing the Many Faces of Thoracic Tuberculosis

Sunday, Nov. 27 8:00AM - 9:00AM Room: Learning Center - CH

#### Participants

Makiko Murota, MD, Kitagun, Japan (*Presenter*) Nothing to Disclose

#### TEACHING POINTS

Mycobacterium tuberculosis infects one third of the world's population and tuberculosis continues to be a major global public health problem. Imaging diagnosis of tuberculosis is sometimes challenging and complex. The purpose of the exhibit is: 1. To review the etiology of tuberculosis. 2. To describe the imaging features of tuberculosis, including the thoracic region other than the lungs. 3. To discuss the complications and sequelae.

#### TABLE OF CONTENTS/OUTLINE

1. The etiology of tuberculosis 2. The imaging findings of pulmonary tuberculosis: primary tuberculosis, postprimary tuberculosis including typical and atypical pattern, bronchial tuberculosis, tuberculoma, and miliary tuberculosis 3. The imaging features and the clinical manifestations of complications and sequelae: lung parenchyma, airways, blood vessels, mediastinum, pleura, chest wall 4. The differential diagnosis 5. Summary

Printed on: 02/07/23

## Abstract Archives of the RSNA, 2022

CHEE-63

### Tropical Diseases - A Comprehensive Review of Thoracic and Abdominal Imaging Manifestations

Sunday, Nov. 27 8:00AM - 9:00AM Room: Learning Center - CH

#### Participants

Heli Rueda, MD, Bogota, Colombia (*Presenter*) Nothing to Disclose

#### TEACHING POINTS

To review the pathophysiology, histopathology, and imaging manifestations of thoracic and abdominal tropical diseases. To mention the imaging patterns of parasitic tropical diseases with their histological correlation. To conceptualize the role of imaging in the diagnosis of tropical diseases.

#### TABLE OF CONTENTS/OUTLINE

1. Introduction  
2. Tropical diseases classification and physiopathology.  
3. Epidemiology and Imaging findings of tropical diseases in computed tomography and its pathological correlation of:  
a. Parasites:  
I. Helminth Infections:  
1. Ascariasis  
2. Echinococcosis  
3. Paragonimiasis  
4. Strongyloidiasis  
ii. Protozoal Infections:  
1. Amebiasis  
2. Leishmaniasis  
3. Chagas disease  
4. Malaria  
b. Bacterial:  
i. Salmonellosis  
ii. Tuberculosis  
c. Fungal:  
i. Paracoccidiomycosis  
d. Viral:  
i. Dengue fever  
4. Conclusions.

Printed on: 02/07/23

## Abstract Archives of the RSNA, 2022

CHEE-64

### High-attenuation Mediastinal Abnormalities - Beyond Lymph Nodes Benign Calcifications

Sunday, Nov. 27 8:00AM - 9:00AM Room: Learning Center - CH

#### Participants

Lucimara Parajara, MD, Sao Bernardo Do Campo, Brazil (*Presenter*) Nothing to Disclose

#### TEACHING POINTS

- To review the main causes of calcified mediastinal lymph nodes- To review conditions other than calcified lymph nodes that can cause high attenuation lesions in the mediastinum compartments

#### TABLE OF CONTENTS/OUTLINE

All radiologists are used to describing calcified mediastinal lymph nodes. We will discuss several other conditions that may present with a high-attenuation pattern in the mediastinum: - Calcified lymph nodes: a)Healed granulomatous infection b)Sarcoidosis c)Chronic silicosis - Calcified masses a)Thyroid pathologies b)Germ cell neoplasm c)Calcified mediastinal cysts d)Healed lymphoma - Calcified tissue involving mediastinal structures: a)Inflammatory pseudotumor b)Fibrosing mediastinitis c)Tracheobronchial amyloidosis - Other conditions: a)Pitfalls: azygos vein contrast, contrast inside lymphatic ducts b)Foreign body: device embolism, aspiration

Printed on: 02/07/23



## Abstract Archives of the RSNA, 2022

CHEE-65

### Multidisciplinary Panel of Sarcoidosis Beyond the Basics: A Primer on Unusual Cases

Sunday, Nov. 27 8:00AM - 9:00AM Room: Learning Center - CH

#### Participants

Jessica Marchi, Sao Paulo, Brazil (*Presenter*) Nothing to Disclose

#### TEACHING POINTS

To provide a brief overview of the fundamental classic radiologic and histologic findings of sarcoidosis. To demonstrate and discuss the others presentations of thoracic sarcoidosis that are outside the usual. To illustrate the correlation between radiological and histological findings, focusing on atypical cases.

#### TABLE OF CONTENTS/OUTLINE

Besides thoracic sarcoidosis's common findings (bilateral hilar lymph node enlargement, micronodules with a perilymphatic distribution, fibrotic changes, and bilateral perihilar opacities), one must remember its atypical manifestations and the possibility of concomitance with lung abnormalities of another nature. We will review the most common thoracic sarcoidosis presentations in this educational exhibit, as well as illustrate and describe atypical manifestations and complications. When pertinent, we will also include radiology-pathology correlation for the cases.

Printed on: 02/07/23



## Abstract Archives of the RSNA, 2022

CHEE-66

### Dynamic Chest Radiography for Pulmonary Vascular Diseases: Clinical Applications and Correlation with Other Imaging Modalities

Sunday, Nov. 27 8:00AM - 9:00AM Room: Learning Center - CH

#### Awards

Cum Laude

#### Participants

Yuzo Yamasaki, MD, PhD, (*Presenter*) Research Grant, Konica Minolta, Inc

#### TEACHING POINTS

1) To explain the basic principles of lung perfusion assessment using dynamic chest radiography (DCR) 2) To discuss the advantages of DCR compared to other imaging modalities 3) To review multiple, specific clinical applications of DCR for pulmonary vascular diseases and compare them with other imaging modalities

#### TABLE OF CONTENTS/OUTLINE

1) Basic principles of DCR •System composition •Acquisition techniques 2) Different acquisitions of DCR imaging •Lung perfusion images •Lung ventilation images 3) Different methods of DCR lung perfusion imaging •Cross-correlation method •Reference frame-subtraction method 4) Advantages compared to other imaging modalities •Readily available •No need for contrast media or radionuclides •Non-invasive •Low radiation exposure •Cost-effective 5) Clinical applications and correlation with other imaging modalities •Pulmonary arterial diseases - Acute pulmonary thromboembolism - Chronic thromboembolic pulmonary hypertension - Pulmonary arteriovenous malformation - Pulmonary arterial stenosis/occlusion •Pulmonary venous diseases - Partial anomalous pulmonary venous return - Pulmonary venous stenosis/occlusion 6) Limitations

Printed on: 02/07/23



## Abstract Archives of the RSNA, 2022

CHEE-67

### Imaging Technologies to Guide the Interventional Pulmonologist: Dynamic Digital Tomography and Dual Source CT.

Sunday, Nov. 27 8:00AM - 9:00AM Room: Learning Center - CH

#### Participants

Samuel McCollum, (*Presenter*) Nothing to Disclose

#### TEACHING POINTS

Dynamic low dose evaluation of the airway with Digital Tomosynthesis (DTS) and Dual Source Computed Tomography can be used to monitor complex airway pathologies and airway devices. Having an institution-specific DTS may reduce use of CT imaging, lowering cost and radiation exposure. Dynamic DSCT imaging decreases radiation dose to conventional CT acquisition

#### TABLE OF CONTENTS/OUTLINE

1. An introduction to Digital Tomosynthesis and dynamic DSCT: Acquisition and Current Uses
2. Case 1: 37-year-old male with post-intubation stricture—we discuss how the stenotic airway is poorly visualized by conventional radiograph, yet can be readily visualized using DTS.
3. Case 2: 28-year old female with post-intubation stricture. We demonstrate how can provide a functional assessment of the airways by imaging the trachea in both the inspiratory and expiratory phase post-dilation
4. Case 3: 67-year-old male with NSCLC complicated by malignant tracheal stenosis. We will see that DTS allows for visualization of an intraluminal mass.
5. Case 4: 57 year old female with malignant stricture s/p stent placement with recurrent airway obstruction. DTS enabled low dose evaluation and monitoring of therapeutic interventions.
6. Case 5: 72-year-old male with left lung transplant for usual interstitial pneumonia status post endobronchial stent placement. We show how DTS enables visualization of the endobronchial stent in both inspiration and expiration, again enabling one to monitor stability of airways and associated devices while avoiding the cost and radiation of CT imaging.
7. Discussion

Printed on: 02/07/23



## Abstract Archives of the RSNA, 2022

CHEE-68

### From Lines Stripes to Cubes Cylinders: A 3D Visual Guide to Conventional Chest Radiography

Sunday, Nov. 27 8:00AM - 9:00AM Room: Learning Center - CH

#### Awards

Cum Laude

Identified for RadioGraphics

#### Participants

Albert Jiao, MD, Boston, MA (*Presenter*) Nothing to Disclose

#### TEACHING POINTS

Purpose Identification of anatomic structures in the chest on 2D conventional chest radiography may be challenging for new trainees. Due to the subtlety of pleural lining on CT, the concepts of expanded, effaced, or obliterated pleural borders on interaction with the mediastinum may be difficult to understand with radiographic and cross-sectional imaging correlation. 3D cinematic rendering, which can accentuate the draping effects of pleural borders, may provide a novel way to understand classic chest radiography. Teaching Points• Identify the anatomic structures in the chest that create the classic "lines and stripes" on chest radiography through the assist of 3D cinematic rendering (CR) depictions. • Recognize the abnormal appearances of the borders on CXR, and the corresponding appropriate pathologies in the differential diagnosis through a case-based teaching series.

#### TABLE OF CONTENTS/OUTLINE

Outline1. Normal pleural anatomy and mediastinal borders. 2. Anterior Junction Line. a. Anterior mediastinal mass differential. 3. Posterior Junction Line. a. Posterior mediastinal mass differential. 4. Aorto-pulmonic relationships. a. AP stripe AP window differential. 5. Paraspinal Lines. a. Right left paraspinal line differentials. 6. Posterior tracheal stripe differentials. 7. Azygosoesophageal recess differentials

Printed on: 02/07/23



## Abstract Archives of the RSNA, 2022

CHEE-69HC

### Practical Guide of US-guided Percutaneous Needle Biopsy (PCNB) for Thoracic Lesions

Sunday, Nov. 27 8:00AM - 9:00AM Room: Learning Center - CH

#### Participants

Hang Jun Cho, Daegu, Korea, Republic Of (*Presenter*) Nothing to Disclose

#### TEACHING POINTS

To guide clinical application of US-guided percutaneous needle biopsy (PCNB) for thoracic lesions.

#### TABLE OF CONTENTS/OUTLINE

1. Introduction of US-guided percutaneous needle biopsy (PCNB) - Indications - Advantages and limitations 2. US images of thoracic lesions - Subpleural lung lesions - Pleural lesions- Bony thorax lesions- Anterior mediastinal lesions- Soft tissue lesions 3. Procedure of US-guided PCNB - Localization of the lesion - Risk evaluation- Determination of the target - Acquisition of the tissue- Evaluation of immediate post-procedural complication4. Diagnostic performance and complication rate of US-guided PCNB - Diagnostic yield - Complication rate - CT guided vs. US guided PCNBPlease visit the Learning Center to also view this presentation in hardcopy format.

Printed on: 02/07/23



## Abstract Archives of the RSNA, 2022

CHEE-7

### Let Us Find the Nodule in a Haystack: A Quick Look through Current Techniques for Image-guided Preoperative and Intraoperative Localization of Small Lung Nodules Prior to Video-assisted Thoracoscopic Surgery Resection

Sunday, Nov. 27 8:00AM - 9:00AM Room: Learning Center - CH

#### Participants

Igor Radalov, MD, Barcelona, Spain (*Presenter*) Nothing to Disclose

#### TEACHING POINTS

1) To define the characteristics of lung nodules amenable to image-guided localization before video-assisted thoracoscopic surgery (VATS) resection. 2) To explain the advantages, disadvantages, and techniques of the different modalities available in the localization of lung nodules prior to VATS resection. 3) To review the results of the different modalities available for the localization of lung nodules before VATS resection. Particular focus on new techniques: Radioactive tracer injection (ROLL) and radioactive seed placement.

#### TABLE OF CONTENTS/OUTLINE

1. Introduction. 2. Lung nodules amenable for image-guided localization before VATS resection. 3. Currently available modalities for lung nodule localization. 3.1. Preoperative. 3.1.1. Hookwire placement. 3.1.2. Microcoil placement. 3.1.3. Dye injection. 3.2. Intraoperative. 3.2.1. Ultrasound. 3.3. Mixed. 3.3.1. Radioactive seed placement. 3.3.2. Radioactive tracer injection (ROLL). 4. Comparative results. 4.1. Detection rate. 4.2. Conversion to thoracotomy rate. 4.3. Complications. 5. Summarize. 6. Conclusion.

Printed on: 02/07/23

## Abstract Archives of the RSNA, 2022

CHEE-70

### Thoracic Paragangliomas: Imaging Review and Considerations for Clinical Practice

Sunday, Nov. 27 8:00AM - 9:00AM Room: Learning Center - CH

#### Participants

Fiona McCurdie, MBChB, BA, (*Presenter*) Nothing to Disclose

#### TEACHING POINTS

1. Paragangliomas (PGL) within the thorax: where do they occur and in whom? Experience from a specialist centre  
2. Multimodality imaging features of thoracic PGLs: strengths and challenges of imaging modalities; lessons from missed lesions  
3. Considerations for management and recommendations for screening and surveillance

#### TABLE OF CONTENTS/OUTLINE

1. Thoracic PGLs - what the general radiologist needs to know  
a. Overview of pathophysiology  
b. Succinate Dehydrogenase deficiency disorders  
c. Summary of literature - anatomical location and clinical presentation  
2. Our cohort of 17 thoracic PGL cases - two decades' experience in a specialist centre  
a. How the PGLs are identified: screening vs. surveillance vs symptomatic  
b. Locations of PGLs within the mediastinum: i. Superior ii. Anterior iii. Middle 1. Cardiac iv. Posterior v. Correlation symptoms and biochemistry  
c. Discussion of management: i. Surgical considerations ii. Medical including radionuclide therapy  
3. Radiological lessons:  
a. Common imaging findings  
i. CT - including cardiac CT  
ii. MRI - whole body, cardiac MRI  
iii. Functional imaging - Gallium Dotatate PET, FDG PET, MIBG SPECT, Octreotide  
iv. Plain radiograph  
b. Key differential diagnosis  
c. Learning from errors: which imaging modalities are PGLs most frequently missed on? What do we learn when we look back in retrospect?  
4. Recommendations for imaging screening and surveillance

Printed on: 02/07/23



## Abstract Archives of the RSNA, 2022

CHEE-71

### Disorders with Ocular and Thoracic Involvement

Sunday, Nov. 27 8:00AM - 9:00AM Room: Learning Center - CH

#### Awards

Identified for RadioGraphics

#### Participants

Patrick Lang, MD, PhD, (*Presenter*) Nothing to Disclose

#### TEACHING POINTS

Numerous medical conditions have multiorgan imaging findings. Here, we review specifically the ocular and cardiothoracic findings of selected infectious, inflammatory, autoimmune, neoplastic, and hereditary disorders. These correlations are meant to remind the astute clinician that certain ophthalmologic signs should trigger a careful radiologic evaluation that includes imaging of the head and chest.

#### TABLE OF CONTENTS/OUTLINE

1. Introduction. 2. Examples of cases: a. Infectious conditions: aspergillosis, nocardiosis, COVID-19. b. Inflammatory conditions: sarcoidosis, IgG-4 sclerosing disease. c. Autoimmune conditions: Graves' disease, scleroderma, Sjogren's syndrome. d. Neoplastic conditions: uveal melanoma, lymphoma, lung cancer. e. Hereditary conditions: Marfan syndrome, Ehlers Danlos syndrome, tuberous sclerosis, neurofibromatosis type 1. 3. Conclusion.

Printed on: 02/07/23



## Abstract Archives of the RSNA, 2022

CHEE-72

### Tortuous Path: Congenital Anomalies of the Systemic Thoracic Veins

Sunday, Nov. 27 8:00AM - 9:00AM Room: Learning Center - CH

#### Participants

Carlos Marin, MD, PhD, Madrid, Spain (*Presenter*) Nothing to Disclose

#### TEACHING POINTS

1. To review the anatomy and embryology of the systemic thoracic veins. 2. To describe imaging findings in congenital anomalies of the systemic thoracic veins (CASTV). 3. To emphasize the physiologic consequences of these anomalies, and their impact in associated congenital heart diseases surgery.

#### TABLE OF CONTENTS/OUTLINE

Congenital anomalies of the systemic thoracic veins are commonly underdiagnosed, in part because they are often asymptomatic or have little or no clinical consequences. They are frequently discovered as an incidental finding in a radiological examination for unrelated reasons, but sometimes are diagnosed because an anomalous course of a central venous line or during a systematic study for congenital heart disease. In certain cardiac or thoracic surgical procedures it is of prime importance to diagnose these anomalies to prevent surgical failure or complications. Pulmonary venous anomalous connections to the systemic thoracic veins and Raghb syndrome can be symptomatic and diagnosed at early age or be discovered in adulthood in patients with right heart dilatation or cardiac symptoms. Besides azygos lobe, a well-known normal variant, the most common CASTV include: 1. Persistent left superior vena cava (SVC) (with or without absent right SVC). 2. Left superior intercostal vein variants. 3. SVC aneurysm. 4. Pulmonary venous anomalous connections to the SVC. 5. Absent inferior vena cava with an enlarged azygous vein. 6. Persistence of the levoatriocardinal vein. 7. Persistent left SVC with absence of the coronary sinus (Raghb syndrome). 8. Subaortic innominate vein. We describe the embryology, anatomy, physiology, imaging findings, and potential complications of these anomalies.

Printed on: 02/07/23



## Abstract Archives of the RSNA, 2022

CHEE-73

### The Role of Cinematic Rendering in the Analysis of Complex Vascular and Mediastinal Pathology: How We Do It

Sunday, Nov. 27 8:00AM - 9:00AM Room: Learning Center - CH

#### Participants

Elliot Fishman, MD, Owings Mills, MD (*Presenter*) Co-founder, HipGraphics, Inc; Stockholder, HipGraphics, Inc; Institutional Grant support, Siemens AG; Institutional Grant support, General Electric Company; Consultant, Exact Sciences Corporation; Consultant, Imaging Endpoints

#### TEACHING POINTS

1. Cinematic Rendering provides unique 3D capabilities allowing for detailed analysis of complex soft tissue and vascular anatomy allowing for improved analysis of chest and mediastinal pathology  
2. Cinematic rendering is especially valuable for evaluation of complex vascular pathology ranging from aortic dissection to aneurysm as well as coarctation of the aorta and coronary artery anomalies  
3. 3D mapping is an important tool for transmitting critical information to the referring physician and the patient care team  
4. complex anatomy defined with cinematic rendering is helpful in pre-operative planning and in analyzing complex structures for robotic surgery  
5. Cinematic Rendering is a helpful tool for teaching residents and fellows in complex cases of vascular anatomy and anomalies

#### TABLE OF CONTENTS/OUTLINE

1. CT protocols for optimizing data acquisition for 3D mapping  
2. protocols and techniques used for Cinematic Rendering including the use of presets to optimize workflow and throughput  
3. representative case studies are presented using axial, multiplanar, MIP and Cinematic Rendering to show how we use the technique in clinical practice. The advantages of Cinematic Rendering in select clinical applications will be discussed  
4. case studies will be divided into section including;  
a. vascular anatomy and anomalies  
b. aortic aneurysm including dissection, intramural hematoma, ulcerations and active bleeding  
c. congenital anomalies including coarctation of the aorta and arch anomalies  
d. cardiac pathology including cardiac tumors including atrial myxoma and angiosarcoma, and coronary artery fistulae  
e. mediastinal masses that involve or are in close proximity to key vascular structures

Printed on: 02/07/23



## Abstract Archives of the RSNA, 2022

CHEE-74

### **Pulmonary Vascular Diseases: Spectrum of Manifestations in the Chest**

Sunday, Nov. 27 8:00AM - 9:00AM Room: Learning Center - CH

#### **Participants**

Juliana Sitta, MD, Jackson, MS (*Presenter*) Nothing to Disclose

#### **TEACHING POINTS**

Review of the pathophysiology and categorization of pulmonary vascular diseases. Describe imaging patterns on CT and traditional angiography. Analyze common and uncommon etiologies with a case-based review.

#### **TABLE OF CONTENTS/OUTLINE**

This presentation aims to discuss imaging findings in the diagnosis and categorization of pulmonary vascular diseases including acute pulmonary embolism, chronic thromboembolic pulmonary hypertension, pulmonary arteriovenous malformation, venous anomalies and mimics, hereditary hemorrhagic telangiectasia, granulomatous with polyangiitis, and microscopic polyangiitis. We will explore the spectrum of chest CT findings within the pulmonary vasculature, parenchyma, airways, mediastinum, and heart that help the radiologist narrow down the differential diagnosis. We will provide a review of the diagnostic criteria and key imaging findings, correlated with physiopathology and current categorization. We will also include a discussion of pros and cons of the currently available diagnostic tools and an update of the most recent imaging technical advancements. Additionally, a case-based review exemplifies common and uncommon pulmonary vascular pathologies.

Printed on: 02/07/23



## Abstract Archives of the RSNA, 2022

CHEE-75

### Pearls and Pitfalls in Pulmonary Vascular Disease

Sunday, Nov. 27 8:00AM - 9:00AM Room: Learning Center - CH

#### Awards

Certificate of Merit

#### Participants

Furkan Ufuk, MD, Denizli, Turkey (*Presenter*) Nothing to Disclose

#### TEACHING POINTS

? To review the spectrum of pulmonary vascular diseases and imaging features ? To review the clinical presentation associated with each pulmonary vascular disease

#### TABLE OF CONTENTS/OUTLINE

Pulmonary embolism, chronic thromboembolic pulmonary hypertension (CTEPH), pulmonary arterial hypertension (PAH), pulmonary arteriovenous malformations (PAVM), Portopulmonary hypertension, cavopulmonary pulmonary artery aneurysm/pseudoaneurysm, bronchial artery aneurysm/pseudoaneurysm, tumor thrombotic microangiopathy, in situ pulmonary artery thrombosis after receiving radiation therapy, pulmonary artery angiosarcoma, tumoral invasion of pulmonary artery or vein, pulmonary vein thrombosis, cement embolism, pulmonary vein varix, pulmonary veno-occlusive disease, pulmonary capillary hemangiomatosis, pulmonary sequestration, abnormal pulmonary venous return, pulmonary vasculitides.

Printed on: 02/07/23



## Abstract Archives of the RSNA, 2022

CHEE-76

### Multimodality Imaging of Pulmonary Embolism: A Guide for the Radiologist

Sunday, Nov. 27 8:00AM - 9:00AM Room: Learning Center - CH

#### Awards

Certificate of Merit

#### Participants

Flavio Zuccarino, MD, Barcelona, Spain (*Presenter*) Nothing to Disclose

#### TEACHING POINTS

To describe imaging findings in Pulmonary Embolism (PE) at different imaging modalities. To underline advantages and limitations of these techniques and to define the clinical scenarios in which they are key in patient management.

#### TABLE OF CONTENTS/OUTLINE

After a short introduction about PE etiology and incidence, we review PE imaging findings at different non-invasive techniques. We organize PE typical imaging findings as: Chest Radiography, Chest Ultrasound, CT Angiography, Spectral CT, Cardiac MR, V/Q (ventilation/perfusion) scan. We discuss advantages and limitations of these imaging modalities as the potential differential diagnosis. We analyze the differences between acute and chronic PE, focusing especially on Spectral CT findings. We evaluate the impact of these imaging techniques on patient prognosis, especially focusing on CT and cardiac MR. Conclusions OUTLINE PE represents a life-threatening condition with a challenging diagnosis. Radiologists should be familiar with PE findings at all imaging modalities that may be key in patient management and treatment.

Printed on: 02/07/23

## Abstract Archives of the RSNA, 2022

CHEE-77

### **New Imaging Modalities in the Diagnosis, Treatment, and Follow-up of Chronic Thromboembolic Pulmonary Hypertension: Correlation Between Dual Energy CT, Cone Beam CT and Digital Subtraction Angiography.**

Sunday, Nov. 27 8:00AM - 9:00AM Room: Learning Center - CH

#### **Participants**

Alfredo Paez Carpio, MD, Barcelona, Spain (*Presenter*) Nothing to Disclose

#### **TEACHING POINTS**

To explain the basics and technique of dual-energy CT (DE-CT) and cone-beam CT (CB-CT), specifically during the management of patients with chronic thromboembolic pulmonary hypertension (CTEPH). To describe the imaging findings observed in the newly available imaging modalities: DE-CT and CB-CT in patients with CTEPH, with correlation with digital subtraction angiography (DSA). To explain the current role of DE-CTA and CB-CTA in the diagnosis, treatment and follow-up of patients with CTEPH.

#### **TABLE OF CONTENTS/OUTLINE**

1.- Introduction. 2.- Basic concepts of DE-CT and CB-CT. 2.1.- DE-CT basics and technique in the study of CTEPH. 2.2.- CB-CT basics and technique in the study of CTEPH. 3.- DE-CT and CB-CT in the diagnosis of suspected CTEPH. 3.1.- Added value compared to conventional CT and DSA. 3.2.- DE-CT imaging findings. 3.3.- CB-CT imaging findings. 3.4.- Correlation with DSA. 4.- DE-CT and CB-CT in the planning of invasive treatment for CTEPH. 4.1.- DE-CT and CB-CT in the planning of pulmonary endarterectomy. 4.2.- DE-CT and CB-CT in the planning of balloon pulmonary angioplasty. 4.3.- Added value of both techniques compared to conventional CT and DSA. 5.- Postprocedural CB-CT and DE-CT imaging findings. 5.1.- Normal spectrum of post-BPA and post-PEA imaging findings. 5.2.- Complications of BPA and PEA. 5.3.- Post-procedural imaging follow-up. 6.- Role of DE-CT and CB-CT in the long-term follow-up of patients with CTEPH. 7.- Current scientific evidence and status of both techniques in established diagnostic algorithms. 8.- Summarize. 9.- Conclusion.

Printed on: 02/07/23

## Abstract Archives of the RSNA, 2022

CHEE-78

### Bubbles in the Chest: A Pictorial Review of Cystic Lesions in the Paediatric Chest

Sunday, Nov. 27 8:00AM - 9:00AM Room: Learning Center - CH

#### Participants

Shrea Gulati, MBBS, MD, Delhi, India (*Presenter*) Nothing to Disclose

#### TEACHING POINTS

A wide spectrum of pathologies in the paediatric population can present as cystic lesions in the thorax. Imaging findings on chest radiography and computed tomography (CT) can provide diagnostic clues to the aetiology. Evolution of imaging findings on serial imaging can provide crucial diagnostic clues.

#### TABLE OF CONTENTS/OUTLINE

? Introduction ? Overview and classification of the cystic lesions in the paediatric chest  
Classification based on aetiology: Congenital cystic lesions - Congenital pulmonary airway malformation/ Hybrid lesion, Bronchogenic cyst, Cystic lung disease in neuro-cutaneous syndromes [Tuberous Sclerosis, Neurofibromatosis-1 (NF-1)], Syndromic cystic lung disease (Down's syndrome, Birt-Hogg-Dube syndrome)  
Acquired cystic lesions - Post infective- tuberculosis, pneumatocele, Diffuse lung disease- Lymphangioliomyomatosis and Langerhans cell histiocytosis, Broncho-pulmonary dysplasia (BPD), End-stage Interstitial lung disease (ILD)/Diffuse lung disease (DLD), Post traumatic pneumatocele  
Mimics - Bronchiectasis, Pulmonary interstitial emphysema, Emphysema (alpha 1 antitrypsin deficiency)  
Classification based on pattern: Single simple cyst - Bronchogenic cyst, Post traumatic pneumatocele  
Single complex/ conglomerated cysts - Congenital pulmonary airway malformation/ Hybrid lesion  
Multiple bilateral cysts - Post infective- tuberculosis, pneumatocele, Diffuse lung disease- Lymphangioliomyomatosis and Langerhans cell histiocytosis, BPD, End-stage ILD/DLD, Cystic lung disease in neuro-cutaneous syndromes (Tuberous Sclerosis, NF-1), Syndromic cystic lung disease (Down's syndrome, Birt-Hogg-Dube syndrome)

Printed on: 02/07/23



## Abstract Archives of the RSNA, 2022

CHEE-79

### Benign and Malignant Tumors of the Trachea

Sunday, Nov. 27 8:00AM - 9:00AM Room: Learning Center - CH

#### Participants

Daniel Vargas, MD, Denver, CO (*Presenter*) Nothing to Disclose

#### TEACHING POINTS

Tracheal neoplasms are rare, with less than 10% of these lesions considered benign. The radiologist is in a unique position of often being the first health team member to encounter these lesions. The objectives of this exhibit are: 1. Discuss epidemiology of tracheal neoplasms. 2. Review the clinical and imaging presentation of some of the most common benign and malignant tracheal neoplasms. 3. Familiarize the radiologist with entities that act as mimics or pitfalls in the evaluation of the trachea

#### TABLE OF CONTENTS/OUTLINE

1. Benign Tracheal Neoplasms a. Tracheal Papilloma b. Hemangioma c. Paraganglioma d. Chondroma e. Hamartoma f. Neurogenic tumors  
2. Malignant Tracheal Neoplasms a. Metastases b. Direct Invasion c. Squamous Cell Carcinoma d. Adenoid Cystic Carcinoma  
e. Mucoepidermoid Carcinoma f. Carcinoid Tumor g. Chondrosarcoma

Printed on: 02/07/23



## Abstract Archives of the RSNA, 2022

CHEE-8

### An Image is Worth a Thousand Words: Important Considerations about Connective Tissue Disease-Associated Interstitial Lung Disease

Sunday, Nov. 27 8:00AM - 9:00AM Room: Learning Center - CH

#### Participants

Bruna Alexandre, MD, Sao Paulo, Brazil (*Presenter*) Nothing to Disclose

#### TEACHING POINTS

Briefly review the main connective tissue disorders (CTD) typical clinical presentations and laboratory findings, and the expected pattern of interstitial lung disease (ILD) for each CTD; Introduce the readers to interstitial pneumonia with autoimmune features (IPAF); Recognize the most typical imaging features of ILDs and other thoracic manifestations of CTDs; Highlight the role of the radiologist in differential diagnosis and detecting complications.

#### TABLE OF CONTENTS/OUTLINE

INTRODUCTION: Connective tissue disorders (CTD) and their relation with interstitial lung diseases (ILD); CTD key points to diagnosis; Interstitial pneumonia with autoimmune features - when ILD takes the spotlight. IMAGING FINDINGS: Step by step approach and algorithm to evaluate connective tissue disease associated with interstitial lung disease (CTD-ILD); CTD-ILD: major patterns of involvement and suggestive signs at Chest CT; Other thoracic manifestations of connective tissue diseases. DIFFERENTIAL DIAGNOSIS AND COMPLICATIONS; TAKE-HOME MESSAGES

Printed on: 02/07/23

## Abstract Archives of the RSNA, 2022

CHEE-80

### Benign and Malignant Tracheobronchial Neoplasms: A Comprehensive Review with Radiologic, Bronchoscopic and Pathologic Correlation

Sunday, Nov. 27 8:00AM - 9:00AM Room: Learning Center - CH

#### Awards

Identified for RadioGraphics

#### Participants

Alexander Phan, MD, New York, NY (*Presenter*) Nothing to Disclose

#### TEACHING POINTS

Tracheobronchial neoplasms are much less common than lung parenchymal neoplasms but can be associated with significant morbidity and mortality. They include a broad differential of both benign and malignant entities, extending far beyond more commonly known pathologies such as squamous cell carcinoma and carcinoid. Airway lesions may be incidental findings on imaging or present with symptoms related to airway narrowing or mucosal irritation, invasion of adjacent structures, or distant metastatic disease. While there is considerable overlap in clinical presentation, imaging, and bronchoscopic appearances, an awareness of potential distinguishing factors may help narrow the differential diagnosis. The authors review the epidemiology, imaging characteristics, typical anatomic distributions, bronchoscopic appearances, and histopathology of a wide range of neoplastic entities involving the tracheobronchial tree. Special attention is paid to any distinguishing features.

#### TABLE OF CONTENTS/OUTLINE

1. Primary malignant tumors: squamous cell carcinoma, malignant salivary gland tumors (adenoid cystic carcinoma and mucoepidermoid carcinoma), carcinoid, sarcomas, primary tracheobronchial lymphoma, and inflammatory myofibroblastic tumor. 2. Secondary malignant tumors (direct invasion or hematogenous spread). 3. Benign neoplasms: hamartoma, chondroma, lipoma, papilloma, amyloid, leiomyoma, neurogenic lesions, and benign salivary gland tumors (pleomorphic adenoma and mucous gland adenoma).

Printed on: 02/07/23



## Abstract Archives of the RSNA, 2022

CHEE-81

### Usual Interstitial Pneumonia (UIP): A Primer for Radiologists

Sunday, Nov. 27 8:00AM - 9:00AM Room: Learning Center - CH

#### Participants

Katherine Cheng, MD, (*Presenter*) Nothing to Disclose

#### TEACHING POINTS

1. Usual Interstitial Pneumonia (UIP) is the most common histologic pattern of fibrosis and has typical imaging findings on HRCT. 2. UIP is an imaging/histologic diagnosis while Idiopathic Pulmonary Fibrosis (IPF) is a multidisciplinary diagnosis. 3. While most patients with UIP pattern of fibrosis are diagnosed with IPF, this imaging pattern can be seen in other settings such as connective tissue related disease, hypersensitivity pneumonitis, asbestosis, vasculitis, familial pulmonary fibrosis, and drug reaction

#### TABLE OF CONTENTS/OUTLINE

1. Distinguish UIP from IPF 2. Review histologic and imaging patterns of UIP; review updated 2022 ATS criteria diagnosis for IPF. 3. Explore the differential diagnosis for UIP and associated imaging findings including IPF, connective tissue disease, hypersensitivity pneumonitis, asbestosis, vasculitis, familial pulmonary fibrosis, and drug reaction. 4. Present multidisciplinary approach to UIP including the clinical presentations and serologic markers that can aid the radiologist.

Printed on: 02/07/23



## Abstract Archives of the RSNA, 2022

CHEE-82

### Imaging Guide to Connective Tissue Disease Related Interstitial Lung Disease (CTD-ILD)

Sunday, Nov. 27 8:00AM - 9:00AM Room: Learning Center - CH

#### Participants

Yogesh Gupta, DO, (Presenter) Nothing to Disclose

#### TEACHING POINTS

1. Provide a foundation for the clinical diagnosis of CTDs that may present with ILD including symptomatology and serologic markers. 2. Describe the radiologic and pathologic patterns of CTD-ILD 3. Review helpful imaging signs in the diagnosis of CTD-ILD. 4. Discuss idiopathic pneumonia with autoimmune features (IPAF). 5. Review the specific prognosis and management of CTD-ILDs, with comparison to ILDs secondary to other causes.

#### TABLE OF CONTENTS/OUTLINE

CTD-ILD represents an underdiagnosed subset of ILDs. The imaging appearance of CTD-ILDs can often precede the rheumatic signs with interpretation of these cases difficult for even experienced radiologists. The literature on CTD-ILD has progressed over recent years, underscored by the emergence of new diagnostic criteria and characteristic imaging patterns. This presentation will provide the radiologist with a comprehensive framework to best facilitate diagnosis and guide management of these diseases. This exhibit is designed for residents, fellows, as well as general and thoracic radiologists. The primary goal is to achieve better understanding of clinical and imaging features of various CTD-ILDs, drawing from our large multicenter patient database. 1. Clinical features of CTDs manifesting with ILD. 2. Pathophysiology of CTD-ILDs. 3. CT imaging characteristics of CTD-ILDs, including imaging signs. 4. Prognosis and management of CTD-ILDs.

Printed on: 02/07/23



## Abstract Archives of the RSNA, 2022

CHEE-83

### Breast Cancer in Women: Multidisciplinary Approach to the Kaleidoscopic Pulmonary Manifestations on CT

Sunday, Nov. 27 8:00AM - 9:00AM Room: Learning Center - CH

#### Participants

Cleonice Isabela Silva Muller, MD, PhD, (*Presenter*) Author with royalties, RELX; Author with royalties, Wolters Kluwer nv; Speaker, AstraZeneca PLC; Speaker, General Electric Company

#### TEACHING POINTS

Introduction Pulmonary abnormalities on computed tomography (CT) in women with breast cancer may be secondary to pulmonary metastases, radiotherapy or systemic treatment of the primary tumor or metastases, increased prevalence of other cancers, or be due to an unrelated cause. In this exhibit we review the range of pulmonary abnormalities seen on CT and present representative cases illustrating the value of multidisciplinary discussion based on weekly oncology tumor board meetings at our institution and systematic follow-up of all patients. 1) To review the typical and atypical manifestations of pulmonary metastases at presentation and with progression or improvement. 2) To illustrate the CT findings of pulmonary complications related to treatment including radiation, chemotherapy, hormone therapy, targeted therapy and immunotherapy. 3) To discuss the differential diagnosis of unrelated pulmonary abnormalities that may affect management. 4) To highlight the importance of multidisciplinary discussion in reaching a timely diagnosis.

#### TABLE OF CONTENTS/OUTLINE

1) Introduction; 2) Spectrum of manifestations and types of response of pulmonary metastases; 3) Pulmonary complications of radiotherapy; 4) Pulmonary complications of systemic therapy; 5) Unrelated pulmonary conditions; 6) Conclusions.

Printed on: 02/07/23



## Abstract Archives of the RSNA, 2022

CHEE-84

### Chest Ultrasound: US Technique, Normal anatomy, Pearls and Pitfalls

Sunday, Nov. 27 8:00AM - 9:00AM Room: Learning Center - CH

#### Participants

Heli Rueda, MD, Bogota, Colombia (*Presenter*) Nothing to Disclose

#### TEACHING POINTS

Review the appropriate technique and parameters to perform chest ultrasonography. Describe the normal anatomy of the chest wall, pleura, and lung parenchyma in ultrasound imaging, its pearls, and pitfalls. Illustrate the most common imaging findings in ultrasound of the pathologies involving the chest wall, diaphragm, pleura, and lung parenchyma.

#### TABLE OF CONTENTS/OUTLINE

Introduction  
Chest ultrasound technique  
Anatomy of the chest wall, pleura, and lung parenchyma in ultrasound.  
Common imaging findings in the pathology of:  
Chest Wall and diaphragm  
Diaphragm paralysis  
Neoplastic involvement  
Pleura  
Pleural effusion  
Pneumothorax  
Pleural thickening  
Lung Parenchyma  
Atelectasis  
Consolidation  
Pulmonary edema  
Pulmonary nodules  
Conclusion

Printed on: 02/07/23



## Abstract Archives of the RSNA, 2022

CHEE-85HC

### Suboptimal Chest Radiography - Applying Art to the Science of Mitigating the Mammoth Issue

Sunday, Nov. 27 8:00AM - 9:00AM Room: Learning Center - CH

#### Participants

Giridhar Dasegowda, MBBS, Boston, MA (*Presenter*) Nothing to Disclose

#### TEACHING POINTS

The audience will learn about the applied art and science in suboptimal chest radiographs (CXR): 1. Various causes of suboptimal CXRs with case-based illustration 2. Impact of suboptimal CXRs: The missed and misinterpreted findings 3. How parallel suboptimality affects the representation of art: Connecting CXR illusions with artistic allusions 4. Where and how artificial intelligence (AI) helps in mitigating suboptimal CXRs

#### TABLE OF CONTENTS/OUTLINE

The four-part exhibit will begin with case-based illustrations of what makes CXRs suboptimal and/or rejected for repeat acquisition. The second part will illustrate the impact of suboptimality on CXR findings including the missed and misinterpreted ones. In the third part, the presenting authors will use their own self-drawn, painted artwork to highlight how suboptimality affects the representation of art and interpretation of suboptimal CXRs. The final part informs about the role of AI in mitigating suboptimal CXRs. The free-to-share and display exhibit will help raise awareness about suboptimal CXRs and inspire a positive downward trend in suboptimal CXR frequency which according to some exist in as much as 90% of all CXRs. Please visit the Learning Center to also view this presentation in hardcopy format.

Printed on: 02/07/23



## Abstract Archives of the RSNA, 2022

CHEE-86

### Perceptual Errors in Cardiothoracic Imaging

Sunday, Nov. 27 8:00AM - 9:00AM Room: Learning Center - CH

#### Participants

Siddhi Hegde, MBBS, Mangalore, India (*Presenter*) Nothing to Disclose

#### TEACHING POINTS

-Studies have shown some areas of radiology have miss rates and (false negative) and false-positive rates as high as 30% of daily reads. -Errors have a significant impact on patient care and increase healthcare costs and burdens. -Perceptual errors can be due to errors in scanning, recognition, or decision. -Identifying and understanding the causes of perceptual errors, increasing awareness amongst trainees, and improving educational models can improve detection and localization accuracy. -Perceptual training algorithms geared toward the reduction of perceptual errors may be a useful adjunct to conventional radiology training.

#### TABLE OF CONTENTS/OUTLINE

-Different types of diagnostic errors in radiology and their frequency -What radiologists need to know about perceptual errors in the setting of cardiothoracic imaging. -Table demonstrating different types of perceptual errors in radiology, definitions, and potential means to overcome them.

Printed on: 02/07/23



## Abstract Archives of the RSNA, 2022

CHEE-87

### "Down The Rabbit Hole": The Many Fistulous Pathways in the Thorax

Sunday, Nov. 27 8:00AM - 9:00AM Room: Learning Center - CH

#### Participants

Murilo Peixoto, MD, Sao Paulo, Brazil (*Presenter*) Nothing to Disclose

#### TEACHING POINTS

Fistulous tracts in the thorax can involve a number of different spaces and have multiple causes. These unusual communications are hard to depict well, and when only standard imaging protocols are used they are often overlooked or misinterpreted. Imaging acquisition techniques and tips can be used to alter the common protocols and demonstrate these tracts more conspicuously.

#### TABLE OF CONTENTS/OUTLINE

Acquired and congenital fistulous tracts of the thoracic region often pose significant diagnostic difficulties to the radiologist. Multiple spaces can be involved, such as the tracheobronchial tree, pleural space, the digestive tract (such as the esophagus and stomach), the lymphatic and the circulatory systems; and many etiologies can be the culprit, such as infectious or inflammatory diseases, neoplasms, surgical and medical procedures, and so on. This presentation is a series of cases, by no means exhaustive, of the many fistulous tracts within the thoracic region, some of which with an unusual presentation. Tips and techniques of imaging acquisition are presented, in order to help better depicting these conditions.

Printed on: 02/07/23



## Abstract Archives of the RSNA, 2022

CHEE-88

### Bronchial Morphology Changes after Lobectomy - Examination by Inspiratory and Expiratory Imaging with Ultra-High-Resolution CT

Sunday, Nov. 27 8:00AM - 9:00AM Room: Learning Center - CH

#### Participants

Hiroshi Moriya, MD, Fukushima, Japan (*Presenter*) Advisor, California Capital Equity, LLC; Research Grant, Canon Medical Systems Corporation

#### TEACHING POINTS

Advances in CT technology and computer processing technology have made it easier to perform precise morphological disassembly and automatic extraction and volume measurement of anatomical structures. In the diagnosis after lobectomy, morphological changes such as thoracic deformity, pleural thickening, organizing pleural effusion, lung parenchyma, bronchi, and pulmonary arteries and veins can be analyzed. In particular, ultra-high-resolution CT (UHRCT) with improved spatial resolution can perform morphological measurement more precisely than conventional CT, so in addition to changes in the anatomical position of each lobe and the volume of the remaining lobe before and after excision.

#### TABLE OF CONTENTS/OUTLINE

Equipment and method: UHRCT (Aquilion Precision, SHR mode), inspiratory / expiratory imaging. Workstation (Ziostation 1K). Results: It was possible to calculate the spatial position of the residual lobe and the ventilation volume for each lobe. By automatic extraction of the bronchial tree, it was possible to depict 3-dimensional expansion and flexion. Bronchial flexion case: Right upper lobectomy. There is an air trapping in the middle lobe. Decreased ventilation of the middle lobe located at the apex of the lung, and flexion and stenosis of the bronchus at the expiratory phase were confirmed. Adhesion case: Partial resection of the right upper lobe. Extensive adhesions due to pleural dissemination. Ventilation of the middle lobe is restricted. The bronchus was confirmed to be patency. Summary: UHRCT is excellent for bronchial morphological analysis. Inspiratory and expiratory CT can be used to analyze changes in bronchial morphology, movement and rotation of the lobes.

Printed on: 02/07/23



## Abstract Archives of the RSNA, 2022

CHEE-89

### Cardiovascular Devices on Chest Radiographs

Sunday, Nov. 27 8:00AM - 9:00AM Room: Learning Center - CH

#### Participants

Taila Moura Fe, Sao Paulo, Brazil (*Presenter*) Nothing to Disclose

#### TEACHING POINTS

The purposes of this exhibit are: Examine the most common cardiovascular devices seen on chest radiographs. Describe each cardiovascular device, including its proper location, components, types, and major complications. Illustrate those cardiovascular devices, using both usual and unusual cases from our chest radiology group.

#### TABLE OF CONTENTS/OUTLINE

This exhibit will go over various cardiovascular devices that can be seen on a chest x-ray. The anticipated correct position, as well as the major complications associated with those devices, will be detailed and illustrated. Cardiac devices: - Pacemaker. - Ventricular assist device. - Occlusion devices. - Mitraclip. - Valve prosthesis. - Loop event recorder. Vascular devices: - Central venous catheter. - Port-a-cath. - Swan-Ganz catheter. - Intra-aortic balloon pump. - Extracorporeal membrane oxygenation (ECMO). - Exogenous material embolized.

Printed on: 02/07/23



## Abstract Archives of the RSNA, 2022

CHEE-9

### When Chest MRI Plays the Big Role: a Guide for Useful Applications on Daily Practice

Sunday, Nov. 27 8:00AM - 9:00AM Room: Learning Center - CH

#### Participants

Murilo Peixoto, MD, Sao Paulo, Brazil (*Presenter*) Nothing to Disclose

#### TEACHING POINTS

- Thoracic lesions can have a wide variety of differential diagnoses. - Chest magnetic resonance imaging (MRI) can be helpful for narrowing down the different etiologies when lesions detected in other imaging methods demonstrate nonspecific features. - Chest MRI is an increasingly available method that uses no ionizing radiation and has sufficient spatial resolution for a number of usages.

#### TABLE OF CONTENTS/OUTLINE

Chest MRI is a widely underappreciated imaging modality, despite its large applicability in the evaluation of abnormalities of cardiovascular origin, of the mediastinum, the pleural space, the brachial plexus, the chest wall and even the lung parenchyma. It is thought that a broader usage of chest MRI is discouraged by the motion artifacts generated by cardiac and respiratory motions and the low signal-to-noise ratio yielded by the large amount of air in the lungs. However, there is great value in utilizing the multiple resources offered by MRI, such as T1, T2, diffusion, in-phase and out-of-phase sequences in order to narrow down the differential diagnoses of lesions found through other imaging methods such as computerized tomography (CT). MRI quality and availability is continuously increasing over the years, so radiologists are facing these diagnostic dilemmas more and more frequently, and knowledge of the behavior of thoracic lesions on MRI is also increasingly important. In this work, we intend to demonstrate how the resources offered by chest MRI can be used to narrow down the differential diagnoses of different thoracic lesions.

Printed on: 02/07/23

## Abstract Archives of the RSNA, 2022

CHEE-90

### A Pictorial Review of Pleural Disease: Multimodality Imaging and Differential Diagnosis

Sunday, Nov. 27 8:00AM - 9:00AM Room: Learning Center - CH

#### Awards

Identified for RadioGraphics  
Certificate of Merit

#### Participants

Aya Yamada, Kashihara, Japan (*Presenter*) Nothing to Disclose

#### TEACHING POINTS

1) To review the spectrum of clinico-radiological features of pleural diseases2) To discuss the clinico-radiological key findings in the differential diagnosis

#### TABLE OF CONTENTS/OUTLINE

1) Clinical findings of pleural diseases2) Illustrated findings of the following pleural anatomy and diseasesI Normal variants (incomplete fissure, accessory fissure)I Asbestos pleural diseases (pleural plaque, pleural mesothelioma)I Inflammatory and infectious diseases (fibrinous pleuritis, TB/actinomycotic empyema)I Pleural tumors (solitary fibrous tumors, neurogenic tumors, desmoid-type fibromatosis)I Lymphoproliferative diseases (pyothorax associated lymphoma, methotrexate-associated lymphoproliferative disorders)I Miscellaneous (thoracic endometriosis, talc pleurodesis)3) Clinico-radiological key findings in the differential diagnosis

Printed on: 02/07/23



## Abstract Archives of the RSNA, 2022

CHEE-91

### **Pulmonary Tuberculosis: Beyond The Typical Patterns**

Sunday, Nov. 27 8:00AM - 9:00AM Room: Learning Center - CH

#### **Participants**

Matheus Garcia Lago Machado, MD, Rio de Janeiro, Brazil (*Presenter*) Nothing to Disclose

#### **TEACHING POINTS**

Discuss the pathophysiology, epidemiology, and clinical manifestations of pulmonary tuberculosis (PTB). Learn to recognize the atypical distribution of small nodules and uncommon patterns of PTB. Review and illustrate imaging findings. Discuss the main differential diagnosis.

#### **TABLE OF CONTENTS/OUTLINE**

Comprehensive review of pulmonary tuberculosis: pathogenesis; epidemiology; clinical manifestations. Atypical distribution of small nodules and uncommon patterns clusters of non-coalescent small nodules; coalescent small nodules - Galaxy sign; nodular reversed halo sign; subpleural nodules and fissural nodularity; halo sign; mass-like consolidation; pulmonary artery pseudoaneurysm - Rasmussen's aneurysm; tracheobronchial abnormalities; endogenous reactivation. Main differential diagnosis.

Printed on: 02/07/23



## Abstract Archives of the RSNA, 2022

CHEE-92

### The Nerve of Some Chest Diseases: Conditions affecting the Thorax and Nervous System

Sunday, Nov. 27 8:00AM - 9:00AM Room: Learning Center - CH

#### Awards

Certificate of Merit

#### Participants

Girish S. Shroff, MD, Houston, TX (*Presenter*) Nothing to Disclose

#### TEACHING POINTS

A variety of systemic diseases may affect both the nervous system and the thorax, while other diseases primarily affecting the thorax may manifest with neurological abnormalities. Correlations of signs, symptoms, and imaging findings in the neurological system with those in the thorax can help guide further diagnostic work-up and treatment. We will illustrate the imaging appearance of several systemic/neurological diseases with thoracic manifestations as well as discuss conditions in the thorax that can lead to neurologic symptoms.

#### TABLE OF CONTENTS/OUTLINE

Inflammatory: Sarcoidosis Dermatomyositis/polymyositis IgG4 disease Infectious: COVID-19 Tuberculosis Invasive fungal infection Syphilis Malignancy: Myasthenia gravis and thymic abnormalities Meningioma with intrathoracic metastases Paraganglioma Vascular: Vasculitis (Giant Cell Arteritis and Takayasu Arteritis) Congenital: Tuberous sclerosis Hereditary hemorrhagic telangiectasia Neurofibromatosis type 1

Printed on: 02/07/23



## Abstract Archives of the RSNA, 2022

CHEE-93

### Something is Not Right in the Chest! Postoperative Thoracic Surgery Complications That Cannot be Overlooked in a CT Scan - A Pictorial Essay

Sunday, Nov. 27 8:00AM - 9:00AM Room: Learning Center - CH

#### Participants

Yuri Neves, MD, Sao Paulo, Brazil (*Presenter*) Nothing to Disclose

#### TEACHING POINTS

1-Discuss the role of radiology in postoperative thoracic evaluation. 2-Review normal postoperative findings of most common thoracic surgeries, such as lung resections: segmentectomy, lobectomy, and pneumonectomy. 3-Recognize the imaging findings related to postoperative complications and what is important to report. 4-Highlight the radiologist role in decision-making within a multidisciplinary team when assessing thoracic surgery early and late outcomes.

#### TABLE OF CONTENTS/OUTLINE

1-Introduction: basic concepts on thoracic surgery (most common techniques and clinical scenarios, purpose / goals, highlights of operative technique). 2-CT protocols available and importance of x-ray analysis.3 - Normal postoperative findings (acute and chronic): Surgical threads; Band atelectasis and fibrotic streaks; Mediastinal and diaphragm shift; Compensatory remanescant lung hyperinflation; Pneumothorax (small); Pleural effusion (small or non-loculated).4-Postoperative complications and its findings: Empyema; Bronchopleural fistula; Re-expansion pulmonary edema; Airway and / or vascular stenosis or compressions; Kinking of bronchial branch; Post bronchoplasty bronchial stenosis (telescoping); Pulmonary torsion; Postpneumonectomy syndrome; Inadvertent pulmonary vein clamping; Hilar hematoma; Pulmonary hernia.

Printed on: 02/07/23

## Abstract Archives of the RSNA, 2022

CHEE-94

### Beyond 5Ts: Pearls and Pitfalls in Diagnosis of Anterior Mediastinal Masses

Sunday, Nov. 27 8:00AM - 9:00AM Room: Learning Center - CH

#### Participants

Tetsuro Araki, MD, PhD, Philadelphia, PA (*Presenter*) Nothing to Disclose

#### TEACHING POINTS

1. To understand appropriate image modalities for anterior mediastinal masses (AMM). 2. To understand common differential diagnosis of AMM. 3. To understand key image finding in differential diagnoses of AMM.

#### TABLE OF CONTENTS/OUTLINE

1. Appropriate selection of image modalities for AMM a. Role of chest radiograph, CT, and MRI b. Additional imaging options (Dual-energy CT, PET/CT, SPECT) 2. Anatomy of mediastinum a. Mediastinal compartment suggested by Felson b. Cross sectional mediastinal compartment suggested by ITMIG c. Common lesions in each compartment 3. Review of 5Ts a. Thymic epithelial tumors: Top of differential of AMM? b. Thyroid tumor: Is MRI helpful? c. Teratoma: Macroscopic fat, when it's malignant? d. Terrible lymphoma: Why terrible? e. Thoracic aorta: not neoplastic, though f. Are 5Ts common as AMM? 4. Beyond 5Ts: More practical DD of AMM than 5Ts a. Lymph nodes b. Benign mediastinal lesions (Thymic cyst/pericardial cyst) • Unilocular vs multilocular thymic cyst • Morgagni hernia c. Normal/hyperplastic thymus • Normal morphology of thymus • What is "normal" thymus for age and sex • True vs lymphoid hyperplasia d. Ectopic thyroid lesion 5. Key image features useful in differential a. CT density and MRI signal density on T1 and T2WI b. Solid vs cystic c. Microscopic and macroscopic fat d. Detection of calcification e. Diffusion weighted images/ADC map f. FDG uptake on PET/CT g. Iodine and fat quantification on DE-CT 6. Summary

Printed on: 02/07/23



## Abstract Archives of the RSNA, 2022

CHEE-95

### "Pop Under Pressure" - Common and Uncommon Imaging Findings in Barotrauma

Sunday, Nov. 27 8:00AM - 9:00AM Room: Learning Center - CH

#### Participants

Caleb Carroll, BS, (*Presenter*) Nothing to Disclose

#### TEACHING POINTS

1. Pulmonary barotrauma is typically diagnosed on imaging and can be associated with increased mortality therefore it is important to recognize and promptly manage barotrauma. Critical to diagnosis is a high suspicion especially in those at high risk. 2. In addition to common imaging findings (pneumomediastinum, pneumothorax, pneumoperitoneum, and subcutaneous emphysema), few uncommon findings (pneumopericardium, broncho-pleural fistula, tension lung cyst, subpleural air cyst and air embolism) may be present.

#### TABLE OF CONTENTS/OUTLINE

1. Discuss definition, possible mechanisms and etiologies associated with pulmonary barotrauma. 2. Epidemiology of barotrauma in different clinical scenarios. 3. Illustrative cases showing common and uncommon manifestations of barotrauma. 4. Briefly discuss clinical features, the prevention, diagnostic evaluation, and management of barotrauma.

Printed on: 02/07/23

## Abstract Archives of the RSNA, 2022

CHEE-96

### The Many Faces of Tracheal Pathology - CT Image-based Quiz and Review of Normal Variants and Main Tracheobronchial Diseases

Sunday, Nov. 27 8:00AM - 9:00AM Room: Learning Center - CH

#### Participants

Carlota Garcia de Andoin Sojo, MD, Bilbao, Spain (*Presenter*) Nothing to Disclose

#### TEACHING POINTS

CT is the best non-invasive imaging modality to evaluate the trachea and its potential diseases. Most tracheal diseases cause stenosis and have different causes and treatments. The knowledge of their specific features in CT helps to approach the diagnosis.

#### TABLE OF CONTENTS/OUTLINE

**Objectives** To review tracheal diseases and their characteristic features on CT. To describe normal variants of the tracheobronchial tree.  
**Findings:** A CT image-based quiz will lead the review of:  
**Normal Variants:** The knowledge of the non-pathological variants of the tracheobronchial tree will avoid mistakes. The most frequent anatomical variants are tracheal bronchus and accessory cardiac bronchus.  
**Tracheal pathology:** Tracheal diseases are congenital or acquired and can be diffuse or focal. Most of them cause tracheal stenosis in asymptomatic patients. These pathologies can have iatrogenic, neoplastic, congenital origins or be related to systemic diseases. Neoplastic causes can be benign or malignant and include hamartomas, papillomas, lipomas, leiomyomas, epidermoid carcinomas, adenoid cystic carcinomas or metastases. Other origins are sabre-sheath trachea, tracheobronchomalacia, tracheobronchial amyloidosis, sarcoidosis, Wegener granulomatosis, relapsing polychondritis, tracheobronchopathia osteochondroplastica and inflammatory bowel disease with tracheobronchial involvement. The Mounier-Kuhn syndrome is a rare entity that causes tracheobronchomegaly.  
**Conclusion** Several tracheal diseases show slight symptoms and subtle CT findings. The knowledge of these entities enables radiologists to reduce the differential diagnosis and give information to plan future bronchoscopies and treatments.

Printed on: 02/07/23

## Abstract Archives of the RSNA, 2022

CHEE-97

### **That Escalated Quickly: Etiology, Pathophysiology, and Imaging Findings of Rapidly Progressive Interstitial Lung Disease**

Sunday, Nov. 27 8:00AM - 9:00AM Room: Learning Center - CH

#### **Participants**

Andrew Simmerman, MD, (*Presenter*) Nothing to Disclose

#### **TEACHING POINTS**

1. The lungs' response to acute injury follows a predictable course even across disparate etiologies. Radiologists should recognize the typical imaging manifestations of RP-ILD along with their associated disorders. 2. Acute complications of RP-ILD include pneumomediastinum and pneumothorax. 3. RP-ILD may resolve or evolve into other chronic ILD patterns.

#### **TABLE OF CONTENTS/OUTLINE**

I. Overview of acute lung injury and healing process  
a. Acute/subacute  
i. Histology of diffuse alveolar damage (DAD) and organizing pneumonia (OP)  
ii. HRCT appearance of DAD and OP  
b. Chronic  
i. Resolution or fibrosis  
II. Defining RP-ILD  
a. Timeline  
b. Severity  
c. Alternative names in the literature  
III. Etiologies of RP-ILD, with example cases  
a. Connective tissue disease  
i. Various types: myositis, rheumatoid arthritis, scleroderma, lupus  
ii. Anti-melanoma differentiation-associated gene 5 dermatomyositis (high association with RP-ILD)  
b. Viral infection  
i. COVID-19/SARS/MERS  
ii. Influenza  
c. Acute Interstitial Pneumonia  
d. Acute Exacerbation of ILD  
e. Treatment-related pneumonitis  
i. Medications  
ii. Chemotherapy/immunotherapy  
iii. Radiation  
IV. Clinical significance of RP-ILD  
a. Treatment  
b. Prognosis: acute and chronic phases  
c. Follow-up

Printed on: 02/07/23



## Abstract Archives of the RSNA, 2022

CHEE-98

### **Pulmonary Actinomycosis: CT Findings and Differential Diagnosis**

Sunday, Nov. 27 8:00AM - 9:00AM Room: Learning Center - CH

#### **Participants**

Yoshie Kunihiro, MD, Ube, Japan (*Presenter*) Nothing to Disclose

#### **TEACHING POINTS**

Pulmonary actinomycosis is a chronic suppurative infection caused by *Actinomyces* species and the infection occurs typically due to aspiration of endogenous organisms. There are a variety of CT findings of pulmonary actinomycosis, however, there are some key points for differential diagnosis. The purpose of this exhibit is: 1. To explain the clinical characteristics and the common CT findings of pulmonary actinomycosis. 2. To review the CT images of pulmonary actinomycosis with uncommon findings such as bronchiectatic form and endobronchial calcified nodule. 3. To discuss the differential diagnosis of pulmonary actinomycosis, including pulmonary tuberculosis, fungal infection, lung cancer and granulomatosis with polyangiitis.

#### **TABLE OF CONTENTS/OUTLINE**

(1) Clinical characteristics of pulmonary actinomycosis (2) CT findings of pulmonary actinomycosis (3) Sample cases (4) Differential diagnosis

Printed on: 02/07/23

## Abstract Archives of the RSNA, 2022

CHEE-99

### Thoracic Parasitic Disease: A Radiologic and Pathologic Review

Sunday, Nov. 27 8:00AM - 9:00AM Room: Learning Center - CH

#### Participants

Cecilia Davis-Hayes, MD, (*Presenter*) Nothing to Disclose

#### TEACHING POINTS

Parasitic diseases effect immunocompetent and immunocompromised patients worldwide. To create an accurate differential diagnosis for thoracic infections, radiologists must utilize both patient travel history and characteristic imaging findings. Understanding both imaging patterns and the geographic distribution of these diseases will help to narrow the differential and can impact clinical testing and management. Although some parasitic infections result in nonspecific imaging findings, familiarity with their imaging features as well as their epidemiological, clinical, and pathologic features may be helpful in to ensure the appropriate diagnosis and treatment.

#### TABLE OF CONTENTS/OUTLINE

1. Review endemic thoracic parasitic diseases A. Helminths i. Cestodes (tapeworm), e.g Echinococcus ii. Nematodes (roundworm), e.g Strongyloidiasis Ascariasis iii. Trematode (flake), e.g. Schistosomiasis B. Protozoa i. Amebiasis ii. Trypanosomiasis (Chagas Disease)2. Epidemiology 3. Modes of transmission/ lifecycle 4. Geographic distribution 5. Clinical presentation 6. Imaging/ pathology findings

Printed on: 02/07/23

## Abstract Archives of the RSNA, 2022

EREE

### Emergency Radiology Education Exhibits

Sunday, Nov. 27 8:00AM - 9:00AM Room: Learning Center - ER

#### Sub-Events

#### **EREE-1 Blunt Splenic Injury: What's New and Important - A Review by the ASER (American Society of Emergency Radiology) Expert Panel**

Participants

Aishwariya Vegunta, MD, Stratford, CT (*Presenter*) Nothing to Disclose

#### TEACHING POINTS

1. Severity grading of Blunt Splenic Injury (BSI) using American Association for the Surgery of Trauma (AAST) 2018 Organ Injury Scoring (OIS). 2. Importance of detecting vascular injury and its impact on management. 3. Types of vascular injury: Contained Vascular Injury (CVI) and Active Splenic Hemorrhage (ASH). 4. Key Role of CT protocol in Vascular Injury Detection. 5. Management options: Operative vs. Conservative and future advances.

#### TABLE OF CONTENTS/OUTLINE

Table of Contents/Outline: ? Background/scope of the problem: Spleen is the second most common injured abdominal organ? Examples of Blunt Splenic Injury and grading using 2018 AAST OIS? Types of Splenic Vascular Injuries: a. Contained Vascular Injury. Pseudoaneurysm. Arteriovenous fistula. Active Splenic Hemorrhage (ASH)? Optimizing CT protocols- Arterial phase imaging/ multiphase acquisition increases sensitivity and improves differentiation of splenic vascular injury ? Management of BSI and the impact of CT detection of splenic vascular injury: Trend toward Nonoperative management (NOM) and role of splenic artery embolization (SAE) ? When NOM fails: Potential factors and next steps? Follow up imaging for delayed splenic rupture: When to do it and what to look for

#### **EREE-10 A Pregnant Patient in Pain: What the ER Radiologist Needs to Know About the Findings, Reporting, and Significance**

Participants

Dana Galvan, MD, Albuquerque, NM (*Presenter*) Nothing to Disclose

#### TEACHING POINTS

1. Improve understanding of the radiologic evaluation of pregnant patients in emergency settings, including the reporting of first and second/third trimester fetal sonography. 2. Familiarize radiologists and in-training radiologists with the imaging appearance, incidence, and follow up recommendations of common emergent causes of maternal acute abdomen. 3. To review key traumatic pathologies and findings in pregnancy such as uterine rupture and the Traumatic Abruption Placenta Scale. 4. Highlight key findings of urgent special consideration cases of multiple gestations and emergent ectopic pregnancy findings.

#### TABLE OF CONTENTS/OUTLINE

-Introduction to emergency department visits during pregnancy including common presenting complaints, symptoms, and initial imaging modalities selected to investigate. -Review of maternal and fetal radiation exposure in the emergency setting, including effect on fetus and threshold doses. -Review of sonographic first trimester findings including SRU criteria, terminology, and findings for pregnancy failure. -Review of second trimester ultrasound findings including how to identify relevant findings, report findings, and their significance. -Sonographic placental and cervical pathologies of the second and third trimesters, with key imaging findings, clinical significance, and follow-up recommendations. -Common traumatic injuries including uterine rupture and review of the Traumatic Abruption Placenta Scale (TAPS). -Differential diagnosis, clinical significance, and follow-up recommendations of several maternal acute abdomen pathologies. -Imaging finding review of multiple gestation emergencies, ectopic and heterotopic pregnancies.

#### **EREE-11 Age Estimation of Unidentified Cadavers Using Postmortem CT Imaging**

Participants

Wataru Fukumoto, MD, PhD, Hiroshima, Japan (*Presenter*) Nothing to Disclose

#### TEACHING POINTS

For the identification of unknown cadavers, an accurate estimation of the age at the time of death is needed. Classical methods assess morphological changes of the pubic symphysis, its auricular surface, and cranial sutures and teeth. However, as these assessments rely on the experience and expertise of the evaluator, their accuracy is limited, especially in elderly cadavers. Because postmortem computed tomography (PMCT) using multiplanar reconstruction- and 3D images reveals the bone structure clearly, it is superior to the classical methods. We introduce and describe the utility of age estimation methods based on PMCT.

#### TABLE OF CONTENTS/OUTLINE

1. Importance of age estimation in forensic science 2. Classical age estimation methods 3. Age estimation using PMCT images

•Importance of age estimation in forensic science •Classical age estimation methods of age estimation using dental images  
•Measurement of the bone density of the pubic symphysis •CT value and volumetric analysis of the proximal femur •Maturity of the medial clavicular epiphysis •The ossification score of the sternum and ribs •Evaluation of osteophytes in the vertebrae 4. A new approach for age estimation using PMCT and deep learning

## **EREE-12 Automated CT Perfusion (CTP) interpretation in Acute Stroke: Primer for On-call Radiologist**

### **Awards**

#### **Certificate of Merit**

#### **Participants**

Ashlesha Udare, MBBS, MD, (*Presenter*) Nothing to Disclose

#### **TEACHING POINTS**

1. To understand the growing need of emergency automated CTP evaluation 2. The 3 questions approach for fast and accurate interpretation

#### **TABLE OF CONTENTS/OUTLINE**

Background: AHA2018 AIS guidelines recommend perfusion imaging for INR subject selection at 6-24 hours after insult. Automated CTP using AI technology has been used in several recent large LVO endovascular therapy trials. Using case-based approach with 2 FDA approved AI solutions from our institution, we aim to acquaint the on-call radiologist interpreting automated CTP data using a simplified 3 questions approach 1. Is the CTP diagnostic/non-diagnostic? Understanding the basics of CTP acquisition and processing by the AI software. technical pitfalls: motion, contrast bolus, AIF/VOF selection, erroneous calculation of perfusion abnormality near the skull base, truncation of dynamic curve, z-axis coverage.2. Is there infarct core volume measurement error?- Underestimated on CTP outputs in the extended time window if received IV tPA, leptomeningeal collaterals lead to partial reperfusion of completely infarcted: Noncontrast CT ASPECTS-Overestimated in cases of ghost infarct hyperacute stroke, early reperfusion: Stricter rCBF threshold for core infarct estimation.3. Is there ischemic penumbra measurement error?-Overestimated in proximal vessel stenosis, leukoariosis, fetal PCA: Evaluate CTA, MTT-Wrong inclusion of opposite hemisphere, beyond vascular territory by automated software-Stroke mimics, lacunar infarcts and posterior circulation strokes.Conclusion: Fast interpretation of the complex automated CTP data by a simplified 3 questions approach for the on-call radiologist and to optimize patient selection for reperfusion.

## **EREE-13 Emphysematous Osteomyelitis: A Review of Imaging Features and Pitfalls for the Emergency Radiologist to Avoid**

### **Awards**

#### **Certificate of Merit**

#### **Participants**

Kush Purohit, MD, MS, Pittsburgh, PA (*Presenter*) Nothing to Disclose

#### **TEACHING POINTS**

Discuss the pathogenesis and clinical presentation of emphysematous osteomyelitis (EO), a rare, lethal variant of osteomyelitis caused by infection from gas-forming organisms.Understand key x-ray features and limitations of radiography, including inconspicuous or radiographically occult intraosseous air.Describe the characteristic CT "pumice stone pattern" of irregularly irregular 2-5 mm intraosseous foci of gas.Discuss conventional MRI findings, including T1 hypointense and T2 hyperintense marrow signal abnormalities, and correlate with radiography and CT.Understand local susceptibility artifact from intraosseous air can obscure T1 and T2 signal abnormalities and may be misinterpreted as calcification or hemosiderin deposition, a potential pitfall for the emergency radiologist.Explore PET-MRI as a useful tool in diagnosing EO and localizing infection spread.

#### **TABLE OF CONTENTS/OUTLINE**

Emphysematous osteomyelitis background: Epidemiology, pathogenesis, clinical presentationRadiography: Typical features and pitfallsMRI: Review of imaging features. Susceptibility artifact as a major potential pitfall for the emergency radiologistCT: The most useful diagnostic study with characteristic "pumice stone pattern" of intraosseous gasPET-MRI: A useful emerging tool with review of typical imaging features

## **EREE-14HC Fistulas: From The Mouth To The Anus.CHAR(13) + CHAR(10)Our Experience Searching For An Accurate Diagnosis.**

#### **Participants**

Rodrigo Loto, MD, Rosario, Argentina (*Presenter*) Nothing to Disclose

#### **TEACHING POINTS**

List to appropriate diagnostic imaging studies.Describe the anatomic locations, causes and clinical features of uncommon fistulas.How to do it. Identify the radiologic finding in the various types of fistulas.A fistulogram/sinogram is used to diagnose and assess the size and shape of fistulas and sinuses and prepare a treatment plan.Fistulograms are used to assess many types of fistulas, including those that form between: two loops of intestine the anal canal and skin near the anus the vagina and another body part such as the colon, rectum, small intestine or bladder.

#### **TABLE OF CONTENTS/OUTLINE**

This pictorial review shares our initial experience with MDCT fistulography in evaluating fistulas, demonstrates various components of fistulas, and discusses the types of fistulas. MDCT is the most common modality used for assessment of fistulas, especially with the use of fistulography. The injection of positive contrast well-delineates the fistulous tract and its branching pattern and connections. CT also enables multiplanar reconstruction and thin cuts for good anatomical details. Orally administered Contrast Media opacification may be helpful. is relatively well tolerated but it can be painful when injecting the contrast material into the fistulous tract. Is important identify the anatomic locations and clinical features to proceed. Fistulas are diverse in their anatomy and clinical presentation. Radiologists must be familiar with the radiologic findings for both accurate diagnosis and, in many cases, guidance of management planning.Please visit the Learning Center to also view this presentation in hardcopy format.

## **EREE-15 Recreational Drug Abuse- the Spectrum of Imaging Findings**

Participants

Edward Choe, DO, (*Presenter*) Nothing to Disclose

#### TEACHING POINTS

1. The opioid epidemic coupled with the COVID-19 pandemic has drastically increased the prevalence of recreational drug abuse. 2. Increasing prevalence of substance use should prompt radiologists to familiarize themselves with common and uncommon imaging patterns, and different routes of self-administration. 3. Substance use will often have multisystem sequelae. 4. Additional factors to consider when evaluating a patient should include but are not limited to concomitant infections such as HIV and hepatitis, the imaging features of which may complicate image interpretation.

#### TABLE OF CONTENTS/OUTLINE

The primary goal of this exhibit is to review the imaging findings of recreational drug abuse. Patients with substance use often present with a spectrum of multisystem abnormalities beyond direct soft tissue or vascular injury. Vascular complications include pseudoaneurysm, thrombophlebitis, and mycotic aneurysm. In the musculoskeletal system, findings include cellulitis, abscess, fasciitis and septic arthritis, discitis/osteomyelitis, and findings related to ischemia or immobility. In the CNS, complications include dural venous thrombosis, hemorrhage, ischemia, and sequelae of cerebral vasospasm such as PRES. Cardiovascular complications include valvular vegetations, septic emboli, dissection and myocardial infarct. Intra-abdominal complications include septic emboli with infarction of the spleen, kidneys, or bowel, as well as pancreatitis. The imaging findings of these entities will be illustrated, along with potential pitfalls associated with concomitant HIV and viral hepatitis.

#### EREE-16 Imaging Atlas of the AAST Organ Injury Scaling: Spleen, Liver and Kidney

Participants

Bárbara Santos, Sao Paulo, Brazil (*Presenter*) Nothing to Disclose

#### TEACHING POINTS

- Non-operative management of blunt abdominal trauma, including endovascular treatment, is increasingly applied, therefore, recognizing and defining the key imaging features of trauma-related injury is crucial. - The CT-based organ injury scaling established by the American Association for the Surgery of Trauma (AAST) is the most used to assess injury severity and guide clinical decision-making, a useful tool to those caring for the injured patient. - The most significant change in the 2018 revision of AAST organ injury scale is the incorporation of CT diagnosed vascular injury. The presence of a vascular injury is associated with higher failure rates of nonoperative management, therefore higher grades are used in the presence of a vascular injury.

#### TABLE OF CONTENTS/OUTLINE

- Introduction - CT protocol for trauma assessment. - Changes made in the 2018 revision of the AAST Organ Injury Scaling for spleen, liver, and kidney and how its relate with clinical management. - Definition by CT imaging of all general types of traumatic injuries on solid organs. - Imaging atlas of the organ injury scaling established by AAST for spleen, liver, and kidney. - Pitfalls on trauma-related evaluation of spleen, liver, and kidney. - Take home messages.?

#### EREE-17 Pelvic Trauma for the Diagnostic and Interventional Radiologist: From Plain Film to Angioembolization

Participants

Javier Hernandez, BS, San Antonio, TX (*Presenter*) Nothing to Disclose

#### TEACHING POINTS

- Use cases to review significant diagnostic findings (plain film and CT) with corresponding angiographic findings for pelvic trauma. - Characterize the role of interventional radiology in the management of pelvic trauma. - Provide a clinical algorithm for initiating pelvic trauma angiography.

#### TABLE OF CONTENTS/OUTLINE

Introduction Pelvic Anatomy: Bony Landmarks with Vascular Associations, Iliac Artery Branch Patterns Variants of Interest: Corona mortis; Variable Origins of Inferior Gluteal, Internal Pudendal, Superior Gluteal and Obturator Artery. Pelvic Trauma Societal Guidelines WSES, ACR, EAST Plain film, CT and Angiographic findings Blush, Truncation, Pseudoaneurysm, Large Vessel Transection, Traumatic Arteriovenous Fistula Metrics of Interventional Radiology in Hemorrhagic Trauma Cumulative National Response Times, Frequency of Angiography in Pelvic Trauma Clinical Algorithm for Pelvic Angiography Case Presentations: Open Book Fracture, Superior Gluteal Artery Laceration, Bilateral Internal Iliac Transection, Multivessel Internal Iliac Artery Embolization Outcomes of Angioembolization: Mortality, Morbidity, Recurrence Conclusion Clinical Implications In the setting of pelvic trauma, angiography and embolization serve as critical interventions to mitigate deterioration in hemorrhagic shock. Knowledge of unique vascular injuries and their imaging aid diagnosticians and interventionalists in facilitating clinical management.

#### EREE-18 The Puzzle Never Solved: Imaging of Abdominal Emergencies in Pregnancy, Still a Dilemma

Participants

Teodorescu Andreea, MD, (*Presenter*) Nothing to Disclose

#### TEACHING POINTS

To illustrate the spectrum of different presentations of abdominal emergencies in pregnant patients. To review the imaging findings of acute emergencies that will help us to think beyond specific conclusion in an emergency setting. To discuss the risks to the fetus from diagnostic imaging modalities and contrast agents. To propose recommendations for emergency diagnostic imaging of pregnant patients. To summarize the role of imaging (including ultrasound, CT, and MR imaging) in diagnosing acute and emergent pregnancy-related conditions using a CASE-BASED APPROACH.

#### TABLE OF CONTENTS/OUTLINE

Acute abdomen in pregnancy remains one of the most challenging diagnostic and therapeutic dilemmas today. The differential diagnosis during pregnancy is extensive in that the abdominal pain may be obstetric in nature or may be caused by diseases of other intraabdominal or intrapelvic structures. Because of the anatomic and physiologic changes that occur with pregnancy, localization of disease can be difficult. Appendicitis and complicated biliary pathology are the most frequent causes of non-obstetric

acute abdomen in the pregnant patient. Pathological causes of obstetric emergencies which are life-threatening include ruptured ectopic pregnancy, abruption, HELLP syndrome, acute fatty liver of pregnancy, and uterine rupture. Imaging studies are essential adjuncts in the diagnostic evaluation of acute emergency conditions due to clinical and laboratory masking in this subgroup. However, confusion about the safety of these modalities for pregnant women and their infants often results in unnecessary avoidance of useful diagnostic tests.

### **EREE-19 Small Bowel Diverticulosis And Diverticulitis: A Pictorial Review**

Participants

Namita Bhagat, MD, Shelton, CT (*Presenter*) Nothing to Disclose

#### **TEACHING POINTS**

- Small bowel diverticulosis is uncommon and is usually a disease of 6th-7th decade. Diverticulitis occurs in 6.5-10% patients. Other complications include perforation, bleeding and bowel obstruction.
- Small bowel diverticulitis is a rare entity and is often overlooked as a cause of abdominal pain in the elderly because of resemblance of imaging features with other causes of acute abdominal pain and its anatomical location within the mesenteric border at surgery where these diverticuli are obscured by large penetrating blood vessels.
- It is imperative to be familiar with imaging features and to look for clues which may suggest small bowel diverticulitis, such as the presence of non-inflamed diverticuli in adjacent small bowel and presence of a normal appearing appendix in cases of ileal diverticulitis. Delayed diagnosis leads to complications and can be fatal with mortality rate of 25-50%.
- Accurate diagnosis on imaging aids in appropriate patient management, and may help reduce morbidity and mortality.

#### **TABLE OF CONTENTS/OUTLINE**

Describe etiology, pathophysiology and complications of small bowel diverticulosis and diverticulitis. To review the imaging findings of small bowel diverticulosis and diverticulitis on CT. Describe other differential diagnosis for causes of right lower quadrant pain which mimic imaging appearance: for example uncomplicated and complicated acute appendicitis, colonic diverticulitis, Crohn's disease, acute typhlitis, Meckel's diverticulitis, etc.

### **EREE-2 Paranasal Sinuses on Acute Head Imaging: What the Radiologist Needs to Know**

Participants

Veronika Majcher, MD, Cambridge, United Kingdom (*Presenter*) Nothing to Disclose

#### **TEACHING POINTS**

Incidental findings involving the paranasal sinuses are common on CT and MR head scans performed in the acute setting. In the majority of cases, opacification of sinuses is secondary to mild inflammation and can be safely dismissed. However, recognising patterns and imaging features of paranasal sinus findings on these scans can opportunistically pick up pathology benefiting from further investigation or even identify the cause of presenting symptoms. After reviewing this exhibit, the reader will be able to: 1) Revise the basic anatomy and drainage pathways of the paranasal sinuses in order to understand patterns of disease; 2) review common and rarer benign and invasive paranasal sinus pathology using case examples; 3) recognise worrisome features that necessitate further investigation and referral.

#### **TABLE OF CONTENTS/OUTLINE**

1. Anatomy and imaging of the paranasal sinuses 2. Drainage pathways and patterns of disease 3. Interpretation and significance of pathological changes within paranasal sinuses a. Mucosal thickening b. Soft tissue density and bone changes c. Specific signs of acute/chronic/fungal disease 4. Signs of invasive and infiltrative disease a. Review areas 5. Complications of sinusitis

### **EREE-20 Emergency Radiology Peer Learning Pearls: Focus on Appendix Cases**

Participants

Alyssa Sherwill, MD, (*Presenter*) Nothing to Disclose

#### **TEACHING POINTS**

- Discuss the use of peer learning in evaluating cases of misdiagnosed appendicitis on CT, MRI, and ultrasound
- Careful evaluation for defects in the appendiceal wall is crucial to assess for gangrenous appendicitis, particularly if there is an appendicolith
- Air in the appendix is not reliable marker of a normal appendix, and can be mistaken on MRI as an appendicolith
- Secondary ancillary findings of appendicitis may be subtle and should not be ignored
- Many appendicitis overcalls are related to adjacent inflammatory processes
- Appendiceal malignancy and mucoceles can simulate appendicitis

#### **TABLE OF CONTENTS/OUTLINE**

1. Introduction to Peer Learning 2. Complicated Appendicitis a. Gangrenous Appendicitis b. Perforated Appendicitis c. Remote Complications of Appendicitis 3. Missed Appendicitis a. Air in Appendix b. Subtle Ancillary Findings c. Appendiceal Location in Pregnancy d. Satisfaction of Search Bias 4. Appendicitis Overcalls a. Secondary Appendicitis i. Pelvic Inflammatory Disease ii. Cecal or Ascending Colonic Diverticulitis iii. Infectious or Inflammatory Enteritis iv. Bile Leak b. Endometriosis c. Cystic Fibrosis d. Chronic Appendicitis 5. Neoplastic Mimickers a. Appendiceal Mucinous Neoplasms b. Carcinoid c. Metastases

### **EREE-21 Stroke Alert!" ER Dilemma, What is Next? CT Perfusion (CTP) or Fast Brain MRI**

Participants

Ahmed Moawad, MD, Darby, PA (*Presenter*) Nothing to Disclose

#### **TEACHING POINTS**

- Reviewing the current imaging guidelines for acute stroke - Comparing the difference between fast MRI and CTP in diagnosis of different acute neurological deficit scenarios - Introducing the use of different imaging modalities in management decisions - Highlighting role of Fast MRI and CTP in follow up treated stroke.

#### **TABLE OF CONTENTS/OUTLINE**

# Introduction - Fast brain MRI protocol CTP protocol and parameters - - Current guidelines in stroke imaging - Limitation of fast brain MRI Drawbacks and pitfalls of CTP # Different scenarios of acute neurological deficit diagnosis - Accuracy of Fast MRI and

CTP in stroke diagnosis - Imaging in Ischemic stroke vs. Intra-cerebral hemorrhage - Stroke with unknown duration "Wake-up" - Transient ischemic attack - Stroke mimickers: Seizures, Hypoglycemia, Cerebral venous thrombosis, Acute multiple sclerosis flare, Migraine aura- Posterior fossa stroke - Lacunar infarct - Hyperacute infarcts - Hypoperfusion state: Cardiac failure, Shock, Chronic carotid artery occlusion# Management of ischemic stroke - Predicting outcome using imaging modalities and clinical scores Identification of final ischemic infarct core \* Mismatch between initial infarct core - final infarct \* Ghost infarct core - Identification of ischemic salvageable tissue (Penumbra) \* Role of perfusion imaging (CTP and MR perfusion) \* DWI in identification of penumbra\* MRI vs. CTP for Thrombectomy Selection - DEFUSE 3 and DAWN trial - Management of stroke by DWI-FLAIR mismatch vs. CTP - WAKE UP vs. EXTEND trial# Follow up stroke treatment - Follow up hemorrhagic transformation - Assessment of reperfusion state and infarct volume

## **EREE-22 Spinal Hematomas: Pearls and Pitfalls for MRI Evaluation in Emergency Radiology**

Participants

Maria Galante I, MD, Santander, Spain (*Presenter*) Nothing to Disclose

### **TEACHING POINTS**

1) To make a pictorial review of the main meningeal layers and the 4 spaces: epidural, subdural, subarachnoid and intramedullary space. 2) To identify in MRI technique the different types of spinal hematomas 3) To detail the most important imaging features of each type of hematoma, in order to differentiate one from another. 4) To describe the main alternative diagnosis 5) To highlight pitfalls that may be found during the imaging assessment. 6) To suggest an MRI protocol for the evaluation of spinal hematomas for non-subspecialized radiologists

### **TABLE OF CONTENTS/OUTLINE**

Etiology of spinal hematomas Symptoms Anatomical Review of the spine: layers and spaces MRI appearance of blood in routine sequences MRI protocol for the evaluation of spinal hematomas in emergency radiology Epidural hematomas Subdural hematomas Subarachnoid Hemorrhage Intramedullary Hematoma Pitfalls and differential diagnosis Treatment Conclusions

## **EREE-23 Confronting and Overcoming Emergency Radiology Biases**

**Awards**

**Identified for RadioGraphics**

**Magna Cum Laude**

Participants

Se-Young Yoon, MD, (*Presenter*) Nothing to Disclose

### **TEACHING POINTS**

- With the transition to peer learning review of cases, many diagnostic errors in radiology can be attributed to cognitive biases. Because of the high volume and rapid pace of emergency radiology, exam interpretations may be heavily reliant on biases and heuristics. Thus, a more focused evaluation of emergency radiology specific biases is needed to avoid diagnostic pitfalls.- We aim to review common biases in emergency radiology in this exhibit, organized by the expected stage of occurrence during the process of reading an imaging study.- Several cognitive biases that have not yet been defined in radiological publications, to the best of our knowledge, will be discussed. These include: triage cueing, contrast effect, provider bias, treater bias, and need for closure.- Emergency radiology peer learning case examples are provided to illustrate how and which biases may have occurred.- Strategies to recognize and overcome biases will be discussed, with an emphasis on those that may be more prevalent in the emergency setting.

### **TABLE OF CONTENTS/OUTLINE**

- Cognitive biases commonly seen in emergency radiology-- Definitions and brief examples (list on slide #1)- Peer learning case examples illustrating various cognitive biases- Strategies in recognizing and overcoming biases

## **EREE-24 An Approach to Acute Traumatic and Non-traumatic Diaphragmatic Abnormalities**

**Awards**

**Identified for RadioGraphics**

**Certificate of Merit**

Participants

Nicolas Murray, MD, FRCPC, Vancouver, BC (*Presenter*) Co-investigator, Siemens AG

### **TEACHING POINTS**

Acute traumatic and non-traumatic diaphragmatic abnormalities are a heterogeneous group of relatively uncommon pathologies affecting the normal structure and function of the diaphragm. These include diaphragmatic hernia, laceration, traumatic and spontaneous rupture, thoracoabdominal fistulae, infection, and endometriosis. Because the diaphragm is the primary inspiratory muscle, disruption to its integrity can cause clinically significant consequences. Imaging plays an essential role in investigation. However, these pathologies can be easily missed as findings are often subtle. Therefore, understanding the anatomy and radiologic findings allows for efficient and accurate diagnosis and management.

### **TABLE OF CONTENTS/OUTLINE**

Diaphragm anatomy and normal variation. Introduction and differential diagnosis of acute diaphragmatic abnormalities. Imaging modalities for the diaphragm. Pathogenesis, incidence, clinical presentation, diagnosis, radiologic findings, and general management of non-traumatic and traumatic diaphragmatic abnormalities including (1) diaphragmatic hernias, (2) spontaneous diaphragm rupture, (3) endometriosis-related diaphragmatic disease, (4) trans-diaphragmatic fistula, (5) infection of the diaphragm, (6) blunt injuries, (7) penetrating injuries, and (8) traumatic diaphragm rupture. Summary of take-home points.

## **EREE-25 CT of Blunt Acute Thoracic Aortic Injury: A Primer for Diagnostic Radiologists**

**Awards**

**Certificate of Merit**

Participants  
Alok Mittal, MBBS, MD, Muscat, Oman (*Presenter*) Nothing to Disclose

#### TEACHING POINTS

-To identify and differentiate blunt traumatic aortic injuries from various normal variants and injury mimics on CT.-To illustrate direct and ancillary CT features of blunt traumatic aortic injuries.-To differentiate minimal and severe aortic injuries using original illustrations and animations.-To correlate aortic injuries with the most commonly used classification schemes.-To summarize the management algorithm and the role of interventional radiologists in acute aortic injury.

#### TABLE OF CONTENTS/OUTLINE

-MDCT protocol to diagnose and characterize aortic injury patterns.-Review of the anatomical variation and mimics.-Spectrum of aortic injuries on CT and how to correctly characterize them?-Aortic injury classification systems and simplified approach.-Common pitfalls- how to identify and avoid them?-Management of Aortic injuries and the role of the interventional radiologist.

#### EREE-26 Penile Trauma: From Diagnosis to Treatment

Participants  
Victor Jabour, MD, Sao Paulo, Brazil (*Presenter*) Nothing to Disclose

#### TEACHING POINTS

The purposes of this exhibit are: 1. To review the main indications of penis ultrasound in the context of urgency 2. To show the technique of the penis ultrasound 3. To show based on cases from our ultrasound group important structures that must be evaluated in the ultrasound of the penis 4. To review based on cases from our ultrasound group the main penile injuries in the context of emergency and the respective treatments

#### TABLE OF CONTENTS/OUTLINE

Main indications for penile ultrasound in an emergency setting 2 Penile ultrasound technique and documentation protocol used in our ultrasound group 3 Illustrate with cases from our ultrasound group the main penile injuries in the context of emergency and the respective treatments

#### EREE-27 Artificial Intelligence (AI) Imaging Algorithms in the ICU: Augmenting the Radiologist

Participants  
Kaustav Bera, MD, Cleveland, OH (*Presenter*) Nothing to Disclose

#### TEACHING POINTS

1. Learn about the unmet needs when it comes to ICU imaging both from the point of view of the primary provider as well as the radiologist 2. How Artificial Intelligence (AI) algorithms can benefit both the ICU physician as well as the reading radiologist 3. Illustrate real-world use cases where AI-imaging algorithms are already in use in the ICU as well as potential high-yield use cases for AI 4. Challenges and limitations that AI enabled tools need to overcome before seamless integration in ICU

#### TABLE OF CONTENTS/OUTLINE

1. Fundamentals of imaging in the ICUa. What the primary team physician wantsb. What the reading radiologist wantsc. Unmet need in the ICU which AI can fulfill2. A Brief Primer on AIa. AI, Machine Learning, Deep Learning - A Brief Primer.b. Framework of AI in clinical use 3. Modalities and use cases for AI in ICU Imaginga. Imaging to determine ICU Admission/Transfer i. AI to predict which COVID-19 patients need urgent mechanical ventilation ii. AI to diagnose cholecystitis, ascending cholangitis from US imaging iii. AI to automatically detect cord compression/cauda equina from spinal MRI iv. AI to detect stroke v. AI to detect hemorrhageb. Imaging within the ICU for monitoring/change in status i. AI for urgent pathology on Chest radiograph (Pneumothorax) ii. AI for lines/tubes detection on Chest radiograph iii. AI to detect Pulmonary Embolism iv. AI to detect Acute aortic pathology 4. Real world use cases of seamlessly integrated AI tools 5. How AI can benefit ICU management both for the radiologist and the physician 6. Future directions

#### EREE-28 CT Evaluation of Abdominal Emergencies in Oncologic Patients

##### Awards Certificate of Merit

Participants  
Joon-Il Choi, MD, PhD, Seoul, Korea, Republic Of (*Presenter*) Research Grant, Guerbet SA; Research Grant, Samsung Electronics Co, Ltd

#### TEACHING POINTS

1. To suggest tailored MDCT protocols for evaluating oncologic abdominal emergencies based on symptoms and clinical impressions 2. To familiarize with various common and uncommon medical risk factors of abdominal emergencies in oncologic patients and pertinent MDCT findings 3. To systemically evaluate causes of acute abdomen in oncologic patients in an MDCT

#### TABLE OF CONTENTS/OUTLINE

1. Tailored MDCT protocols for oncologic abdominal emergencies evaluation 1) Recommended routine protocol for a general indication in the emergency room 2) Symptom and clinical impression-based optimal protocols - Clinical scenarios: solid organ bleeding, hollow viscus bleeding, bowel obstruction, bowel perforation, biliary obstruction, acute renal failure 2. Various medical risk factors of abdominal oncologic emergencies 1) Therapy-related risk factors - Chemotherapeutic agent - External radiation therapy - Locoregional treatments - Recent major surgery - Other invasive therapeutic procedure 2) Immunocompromised host 3) Bleeding tendency of the host 3. A systematic radiologic approach for abdominal oncologic emergencies 1) An organ-based assessment for the causes of the acute abdomen in oncologic patients 2) MDCT findings of common oncologic abdominal emergencies 3) Proposed structured report form to facilitate a thorough evaluation of the abdomen

#### EREE-29 Bone-induced Streak Artifact Reduction in Emergency Abdominal CT Using the Deep Learning-based Image Reconstruction

Participants

Tetsuya Hirairi, MS, (*Presenter*) Nothing to Disclose

#### TEACHING POINTS

The streak artifact, which is frequently observed in abdominal CT images obtained at the emergency trauma patients with arms-down positioning, is known to degrade diagnostic image quality. To solve this problem, deep learning-based image reconstruction is adapted to in emergency abdominal CT. Advanced intelligent Clear-IQ Engine (AiCE), is a type of deep learning-based image reconstruction, is compared with conventional hybrid Iterative reconstruction (HIR). Quantitative artifact estimation is evaluated by the normalize artifact index (nAI) with an abdominal phantom between two dense objects which is simulated arms down positioning. CT number inaccuracy is evaluated by abdominal CT images of 20 clinical patients with arms-down positioning by setting region of interest in the liver and the spleen. As a result, DLR method significantly decreased nAI and improved the CT number accuracy compared to HIR. It was suggested that DLR was useful for the bone-induced streak artifact reduction in emergency abdominal CT.

#### TABLE OF CONTENTS/OUTLINE

1. Clinical problems with conventional emergency CT. 2. Deep learning-based image reconstruction technology AiCE. 3. Normalize artifact index of the fantom simulated arms down positioning. 4. Improvement of the CT number accuracy. 5. Clinical performance in Emergency CT.

#### EREE-3 No Time to Dye: How to Diagnose and Manage Critical Diseases with Non-contrast Enhanced CT

Participants

Yukiko Michishita, MD, (*Presenter*) Nothing to Disclose

#### TEACHING POINTS

1) To share useful imaging findings of various critical diseases in non-contrast enhanced CT (NCECT), with emphasis on the significance of prompt response to treatment regardless of contrast enhanced CT (CECT). 2) To understand the settings where CECT is still required for appropriate treatment strategies as well as diagnosis.

#### TABLE OF CONTENTS/OUTLINE

To learn how to diagnose and manage critical diseases with NCECT, following topics are discussed; 1) Classical findings on CECT, 2) Useful findings on NCECT, 3) Clinical perspective, 4) Significance of prompt action according to findings on NCECT, 5) Diagnostic accuracy of NCECT, 6) Significance of CECT. Featured pathologies are as follows; A. Acute thromboembolisms: 1) Cerebral infarction, 2) Acute pulmonary embolism, 3) SMA embolism/thrombosis, 4) Cerebral venous sinus thrombosis. B. Vascular diseases: 1) Acute aortic dissection, 2) SMA dissection, 3) Impeding rupture of aortic aneurysm. C. Bleedings: 1) Trauma and other bleeders, 2) Gastrointestinal bleeding, 3) Intracranial hematoma. D. Ischemia: 1) Bowel strangulation, 2) Non-occlusive mesenteric ischemia. E. Inflammatory diseases and others: 1) Gangrenous appendicitis, 2) Severe acute cholecystitis, 3) Severe acute pancreatitis, 4) Hepatic abscess, 5) Mycotic aneurysm.

#### EREE-30 Cervical Catastrophe: Identifying Tracheal Injury Before It Is Too Late

Participants

Ethan Jiang, BSc, (*Presenter*) Nothing to Disclose

#### TEACHING POINTS

1. Early and accurate detection of tracheal trauma is crucial to reduce the significant morbidity and mortality associated with these injuries. 2. A low threshold of suspicion for tracheal injury facilitates timely decision-making and intervention in the setting of trauma. 3. Injuries to neighboring structures, such as the esophagus, are often concomitant to tracheal injury following blunt and penetrating neck trauma.

#### TABLE OF CONTENTS/OUTLINE

We outline an approach to suspected tracheal injury in the setting of trauma. The focus will be on using imaging to change clinical outcomes through early identification, especially when the clinical presentation is nonspecific. 1. Overview of relevant neck anatomy. 2. Epidemiology of tracheal trauma. 3. Etiology, mechanisms, and pathophysiology; a) Blunt, penetrating, and iatrogenic tracheal trauma; b) Different anatomical sites of injury. 4. Clinical presentation predictive of impending deterioration. 5. Approach to diagnosis in cases of suspected tracheal trauma; a) Role of X-ray; CT, fluoroscopy, and bronchoscopy; b) Pearls and pitfalls of diagnosis. 6. Key imaging findings to guide non-operative vs surgical management. 7. Short- and long-term complications of tracheal injuries; a) Identifying concomitant injuries, such as esophageal trauma.

#### EREE-31 Revisiting the Renal Trauma: An Illustrated Journey

Participants

Ali Baykan, MD, Adiyaman, Turkey (*Presenter*) Nothing to Disclose

#### TEACHING POINTS

1. To describe the mechanisms of the renal trauma 2. To discuss imaging features of renal trauma and CT technique 3. To discuss the grading systems (The American Association for the Surgery of Trauma) related to renal trauma 4. To highlight the importance of kidney injuries in patients with abdominal trauma

#### TABLE OF CONTENTS/OUTLINE

Introduction Incidence, mechanism of kidney injury, clinical features, and indications for imaging in renal trauma Description of current American Association for the Surgery of Trauma kidney injury grades Management of kidney injury Conclusion

#### EREE-32 The Liver Trauma: Imaging and Multidisciplinary Approach

Participants

Ali Baykan, MD, Adiyaman, Turkey (*Presenter*) Nothing to Disclose

## TEACHING POINTS

1. To describe the mechanisms of the liver trauma 2. To discuss imaging features of liver trauma and CT technique 3. To discuss the grading systems (The American Association for the Surgery of Trauma) related to liver trauma 4. To highlight the importance of liver injuries in patients with abdominal trauma

## TABLE OF CONTENTS/OUTLINE

Introduction Incidence, mechanism of liver injury, clinical features, and indications for imaging in liver trauma Description of American Association for the Surgery of Trauma's updated liver injury scoring scale Multidisciplinary management of liver injury Conclusion

### EREE-33 Pancreatic Trauma: Imaging and Illustrations of a Fragile Organ

#### Awards

##### Certificate of Merit

Participants

Ali Baykan, MD, Adiyaman, Turkey (*Presenter*) Nothing to Disclose

## TEACHING POINTS

1. To describe the mechanisms of the pancreatic trauma 2. To discuss imaging features of pancreatic trauma and imaging (CT, MRCP, etc.) techniques 3. To discuss the grading systems (The American Association for the Surgery of Trauma) related to pancreatic trauma 4. To highlight the importance of pancreatic injuries in patients with abdominal trauma

## TABLE OF CONTENTS/OUTLINE

Introduction Incidence, mechanism of pancreatic injury, clinical features, and indications for imaging in pancreatic trauma Description of American Association for the Surgery of Trauma's updated pancreatic injury scoring scale Multidisciplinary management of pancreatic injury Conclusion

### EREE-34 Limitations of AI-based Hemorrhage Detection: Where AI Can't Help You (Yet)

Participants

Stefan Niehues, MD, Berlin, Germany (*Presenter*) Speaker, Bracco Group; Speaker, Guerbet SA; Speaker, Canon Medical Systems Corporation; Speaker, Teleflex Incorporated

## TEACHING POINTS

Detection of intracranial hemorrhage is a reliable application of AI, but is susceptible to artifacts. False-positive findings are related to motion artifacts, beam hardening artifacts due to foreign material inside or outside the patient, calcifications i.e. after surgery or with patients with meningioma or metastasis. False-negative findings can occur in patients with subacute hemorrhage, very subtle subarachnoidal bleedings, intracranial contrast extravasation, and chronic subdural hematomas.

## TABLE OF CONTENTS/OUTLINE

1) AI-based intracranial hemorrhage detection - basics and numbers 2) Correct findings 3) False positives 4) False negatives 5) Approaches for future developments

### EREE-35 Delivering Clinical Impact in Emergency Departments: CXR xAI Pipeline for Comprehensive Clinical Risk Prediction

Participants

Michelle Chua, Brookline, MA (*Presenter*) Nothing to Disclose

## TEACHING POINTS

Integration of clinical information and radiological findings is required for clinical risk prediction Comprehensive risk prediction models may be developed using a fine-tuning approach, which is more efficient than a full training approach Our CXR xAI model was pre-trained to detect 20 radiographic features and subsequently used, in combination with clinical information, to predict oxygen requirement in ED patients with COVID-19 Calibrated classifier confidence is displayed and comparable CXRs are extracted from the Model-Derived Atlas Our CXR xAI model captures a broad scope of cardiorespiratory pathophysiological manifestations and cardiothoracic comorbidities and may also be used, for example, to predict unplanned return to ED in patients with acute heart failure and elderly patients with community acquired pneumonia As CXRs are inexpensive and routinely obtained, fully automated risk prediction using radiographic features may improve the safety and quality of clinical care in EDs

## TABLE OF CONTENTS/OUTLINE

Full training and fine-tuning approaches for comprehensive clinical risk prediction CXR xAI model architecture and case illustration for acute heart failure COVID-19 xAI pipeline for prediction of oxygen requirement and model performance metrics

### EREE-37 The Acute Abdomen: What the Surgeon Wants to Know - A Case-Based Survival Guide for the On-Call Resident

#### Awards

##### Identified for RadioGraphics

Participants

John Kirby, MD, Rochester, MN (*Presenter*) Nothing to Disclose

## TEACHING POINTS

Abdominal pain is a common presenting symptom in the Emergency Department. Many life-threatening conditions can present as an "acute abdomen," requiring surgical intervention. The radiologist may be the first person to suggest the need for surgical evaluation and can provide key information to the surgeon regarding potential complications and pertinent normal variants. Understanding the surgeon's perspective can lead to concise reports, faster turnaround time, and improved outcomes.

## TABLE OF CONTENTS/OUTLINE

Review common imaging modalities in the non-traumatic acute setting and preferred protocols for evaluating acute abdominal pain. Discussion of the five major categories of abdominal pain requiring surgical intervention; Ischemia, obstruction, infection, perforation, and active bleeding. Case-based review demonstrating examples of the most common etiologies from each of the major categories. Each case will include a discussion of significant findings to make the diagnosis, pertinent anatomical variants, and a summary table of relevant reporting findings to the surgeon. Many of our cases will contain a QR code that the viewer can scan with their mobile device to access an interactive PACS to review the case and more accurately simulate real-life scenarios. Conclusion: At the end of the exhibit, we hope that the reader will better understand findings relevant to the surgeon and can assist in identifying and reporting relevant potential complications.

### EREE-38 Acute Mechanical SBO: A Step-by-step Guide for Radiology Residents!

Participants

Abdul-Rahman Abualruz, MD, (*Presenter*) Nothing to Disclose

#### TEACHING POINTS

Acute mechanical small bowel obstruction (SBO) is a common surgical emergency with high mortality rates when complicated by bowel ischemia (up to 40%). Computed Tomography (CT) has an essential role in confirming the SBO diagnosis, identifying the cause of obstruction, detecting associated variations, and evaluating severity. CT outperforms physical exam and laboratory testing with high specificity in predicting bowel ischemia which is crucial for correct and timely management of SBO.

## TABLE OF CONTENTS/OUTLINE

Review clinical management guidelines of SBO. Critical imaging findings to look for and include in the radiology report that impacts clinical management presented via a suggested structured report for SBO. CT imaging evaluation of SBO (CT protocol, use of IV and PO contrast, added value of Dual Energy CT). Review CT imaging criteria for diagnosis of acute mechanical SBO. A pictorial review of causes of SBO (extrinsic vs. intrinsic etiologies) and pitfalls for correct interpretation with emphasis on: Adhesive vs. Non-adhesive SBO, Closed vs. Open loop obstruction, Partial vs. Complete obstruction, Specific CT findings that predict bowel ischemia. A step-by-step summary guide for SBO diagnosis.

### EREE-39 The Value of Ultrasound in Bowel Pathology in the Emergency Room

Participants

Maria P. Moncayo Hinojosa, MD, Madrid, Spain (*Presenter*) Nothing to Disclose

#### TEACHING POINTS

1) Highlight the diagnostic performance of ultrasound in acute bowel pathology.2) Review of the anatomy and histology of the bowel and its correlation with the ultrasound image.3) Exhibition of the technique and of the diagnostic keys for its correct interpretation.4) Ultrasound review of intestinal pathology and its correlation with computed tomography.

## TABLE OF CONTENTS/OUTLINE

1) Introduction, generalities and anatomy of the bowel.2) Anatomical correlation between ultrasound and the histology of the bowel.3) General considerations and ultrasound exploration technique.4) How to recognize pathological intestinal loops?5) Radiological cases and surprise diagnoses in the ultrasound emergency room of our health center.5)Conclusions.

### EREE-4 Revised American Association for the Surgery of Trauma (AAST) Scales

#### Awards

Identified for RadioGraphics

Cum Laude

Participants

Irene Dixe de Oliveira Santo, MD, New Haven, CT (*Presenter*) Nothing to Disclose

#### TEACHING POINTS

- Review the usefulness of the American Association for the Surgery of Trauma Organ Injury Severity (AAST OIS) scale
- Describe the main changes to the revised 2018 AAST OIS compared to the 1994 and 1989 AAST scales
- Discuss imaging specifications and protocoling considerations in suspected organ injury due to blunt abdominal trauma
- Provide an overview of the recommended management of solid injury organ trauma and how it is affected by grading

## TABLE OF CONTENTS/OUTLINE

History, usefulness, and implications of grading in traumaValidation of the liver, spleen, and kidneys scales and impact on mortality, operative rate, and hospitalization costStandard CT protocol and technique, the benefit of dual-phase imaging, and indications of the excretory phaseThe role of alternative imagingRevised AAST grading with multiple examples from our institutionCurrent management guidelines

### EREE-40HC Obstructive Hydrocephalus - Not So Simple After All

Participants

Michal Holesta, (*Presenter*) Nothing to Disclose

#### TEACHING POINTS

Obstructive hydrocephalus is a severe condition, that can manifest with acute symptoms or slowly developing signs of increased intracranial pressure. This usually depends on the type of underlying condition and the speed with which the hydrocephalus develops. We will overview common and rare causes of obstructive hydrocephalus, diagnostic algorithms and imaging findings on CT and MRI, including signs of transependymal edema, using cases from our clinical practice. We will also present several cases of rare causes of acute hydrocephalus, including colloid cyst, blood clot in aqueductus Sylvii (mimicking flow void on T2W) and neurosarcoidosis.

## TABLE OF CONTENTS/OUTLINE

1. Overview, etiology and pathophysiology of obstructive hydrocephalus. Typical clinical symptoms. 2. Diagnostic algorithms and imaging findings on CT and MRI. Imaging signs of transependymal edema. 3. Case series of rare causes of acute hydrocephalus. 4. Treatment and follow-up of obstructive hydrocephalus. 5. Conclusion and key imaging points. Please visit the Learning Center to also view this presentation in hardcopy format.

### EREE-41 Pearls and Pitfalls in postmortem imaging: Dead Men Do Tell Tales

#### Awards

#### Certificate of Merit

#### Participants

Yohei Ikebe, MD, PhD, Sapporo, Japan (*Presenter*) Nothing to Disclose

#### TEACHING POINTS

1. To summarize the typical and atypical postmortem changes 2. To review the diagnostic findings of postmortem imaging

## TABLE OF CONTENTS/OUTLINE

1. introduction 1-A. role of postmortem imaging 1-B. methods of postmortem CT and MRI scan 2. early postmortem changes 2-A. hypostasis 2-B. vessel wall and vessel cavity 2-C. air way and pleural fluid retention 2-D. brain 2-E. others 3. late postmortem changes 3-A. putrefaction 3-B. autolysis 3-C. gastromalacia, oesophagomalacia 4. pitfalls 4-A. changes of cardiopulmonary resuscitation 4-B. course of postmortem changes 5. diagnostic findings 5-A. Acute hemorrhage (aortic dissection, aortic aneurysm rupture, etc.) 5-B. trauma 5-C. hanging 5-D. hypothermia 5-E. burn death 5-F. drowning

### EREE-42 Making the Grade: A Pictorial Review of the Revised 2018 AAST Abdominal Solid Organ Injury Scales

#### Participants

Samuel Elias, MD, West Caldwell, NJ (*Presenter*) Nothing to Disclose

#### TEACHING POINTS

The goal of this exhibit is to provide a pictorial review of the revised 2018 AAST injury scoring scale for the liver, kidney, and spleen. Every injury grade for each organ is presented with an original diagram alongside the imaging criteria. Teaching points are presented in a clear manner and include descriptions of key radiologic terms, recognition of benign and pathologic mimics, protocoling technique, and clinical management considerations. Angiographic and intraoperative images from our interventional radiology and trauma surgeon colleagues are also included to help cultivate an appreciation of the multidisciplinary management of these injuries.

## TABLE OF CONTENTS/OUTLINE

1) Introduction. 2) Spleen -Grades 1-5 (diagrams, definitions, teaching points, imaging pearls) -Cases (CT, angiographic, and/or intraoperative images with description of findings, management, and teaching points). 3) Liver -Grades 1-5 (diagrams, definitions, teaching points, imaging pearls) -Cases (CT, angiographic, and/or intraoperative images with description of findings, management, and teaching points). 4) Kidney -Grades 1-5 (diagrams, definitions, teaching points, imaging pearls) -Cases (CT, angiographic, and/or intraoperative images with description of findings, management, and teaching points). 5) Conclusion

### EREE-43 Liver or Die Situation--Spleen better days: Reviewing the 2018 Updates of the AAST Liver and Spleen Injury Scoring Scales

#### Participants

Elias Gunnell, MD, Chapel Hill, NC (*Presenter*) Nothing to Disclose

#### TEACHING POINTS

1. Trauma is the most frequent cause of death in the first four decades of life, and the abdomen is the third most common site of injury. 2. The radiologist plays a crucial role in the evaluation and description of splenic and liver injury in abdominal trauma. 3. Accurate description of splenic and liver injury is a pivotal component of patient management and treatment selection. 4. Understanding the revised AAST Liver and Spleen Injury Scales is necessary for accurate description of abdominal trauma as operative rate and increased mortality are associated with increasing grades of injury.

## TABLE OF CONTENTS/OUTLINE

This educational exhibit will discuss the updated 2018 American Association for the Surgery of Trauma (AAST) guidelines for injury scoring, pertaining to the liver and spleen. The presentation will include the following: - Briefly overview the statistics for abdominal trauma and incidence of liver and spleen injury. - Discuss the updated AAST Injury Scoring Scale and compare it to the previous version. - Review and illustrate the multiple grades of liver injury, with important imaging findings. - Review and illustrate the multiple grades of splenic injury, with important imaging findings. - Explain how patient management changes based on the grade of injury.

### EREE-44 Imaging in Non-accidental Trauma - A Primer for Trainees

#### Participants

Surabhi Subramanian, MBBS,MD, (*Presenter*) Nothing to Disclose

#### TEACHING POINTS

• 1. Illustrate the mechanism and mode of presentation • 2. Outline the diagnostic imaging protocol • 3. Discuss the typical presentation and mimicker

## TABLE OF CONTENTS/OUTLINE

Nonaccidental trauma is one of the prominent causes of childhood injury and death in the pediatric population. This exhibit will serve as a primer for radiology trainees to diagnose NAT in an emergency setting. The most common mechanism of NAT is violent

shaking. Some highly specific lesions of child abuse are metaphyseal fractures, multiple rib fractures of different ages, scapular fractures, sternal fractures, and posterior vertebral element fractures. More than 60 % of child abuse cases present in emergency settings. Radiologists can be the first to suggest the possibility of child abuse. Infant's head is larger in comparison to the body making them more prone to CNS injury. CT head, 3D reconstruction is especially helpful in detecting skull fractures. MRI is very sensitive to look for blood products in the brain and spine. The skeletal survey must be ordered for patients suspected with child abuse. Nuclear imaging is performed if skeletal survey is equivocal. Radiologists must be aware of highly suspicious radiological findings and mimickers of nonaccidental trauma.

#### **EREE-45 Vascular Injury Following Trauma: A Pictorial Review of Findings on CT Angiography**

Participants

Navpreet Khurana, MBBS, (*Presenter*) Nothing to Disclose

##### **TEACHING POINTS**

1. Describe the range of findings of vascular injury following blunt and penetrating trauma on CT angiogram. 2. Correlate findings on physical examination, CT angiogram, and catheter angiogram. 3. Appreciate the pitfalls of CT angiography, which lead to false positives and false negatives. 4. Describe the interventions for vascular injury.

##### **TABLE OF CONTENTS/OUTLINE**

1. CT angiogram protocol - how to optimize the detection of traumatic vascular injury. 2. Range of appearance of active bleeding on CT angiogram. 3. The value of the non-contrast acquisition. 4. Arterial spasm vs. arterial transection - similarities and differences in appearance. 5. Correlation of findings on CT angiogram with catheter angiogram. 6. Surgical interventions for vascular injury.

#### **EREE-46 Trauma Drama: Breaking Down the 2018 AAST Scoring for Spleen and Liver**

Participants

Katherine Copely, MD, (*Presenter*) Nothing to Disclose

##### **TEACHING POINTS**

Review the updated 2018 AAST guidelines for Spleen and Liver Injuries? Discuss the importance of imaging protocols? Recognize key features on CT images and correlating diagrams to improve recall and recognition? Examine challenging cases and pertinent pitfalls

##### **TABLE OF CONTENTS/OUTLINE**

The purpose of this presentation is to discuss the rationale for updating the AAST grading systems and what updates occurred between 1994 and 2018 focusing on the spleen and liver, the implications for patient care, as well as to discuss importance of imaging protocols in detecting these injuries. An illustrated table of spleen and liver injuries will be included to highlight the similarities and differences in grading criteria for each organ. Image intensive examples of each grade of liver and spleen injuries will comprise the bulk of the presentation. Challenging cases and pitfalls will help cement and allow practice of these key imaging findings.

#### **EREE-47 Splenic Trauma: When the Neglected One Hurts**

Participants

Ali Baykan, MD, Adiyaman, Turkey (*Presenter*) Nothing to Disclose

##### **TEACHING POINTS**

1. To describe the mechanisms of the splenic trauma 2. To discuss imaging features of splenic trauma and CT technique 3. To discuss the grading systems (The American Association for the Surgery of Trauma) related to splenic trauma 4. To highlight the importance of splenic injuries in patients with abdominal trauma

##### **TABLE OF CONTENTS/OUTLINE**

Introduction Incidence, mechanism of splenic injury, clinical features, and indications for imaging in splenic trauma Description of American Association for the Surgery of Trauma's updated splenic injury scoring scale Multidisciplinary management of splenic injury Conclusion

#### **EREE-5 Nontraumatic Temporal Bone Emergencies: A Non-traumatizing Guide for Radiologists**

##### **Awards**

Identified for RadioGraphics

Participants

Rodrigo Carneiro, MD, Sao Paulo, Brazil (*Presenter*) Nothing to Disclose

##### **TEACHING POINTS**

- To identify important anatomic landmarks in the temporal bone.- To review the imaging technique and protocols for the evaluation of temporal bone emergencies.- To recognize the clinical presentations and imaging features of nontraumatic temporal bone emergencies

##### **TABLE OF CONTENTS/OUTLINE**

- Introduction- Temporal Bone Anatomy- Imaging Technique and Protocols - Clinical Presentations and Imaging Findings of Nontraumatic Temporal Bone Emergencies with Multiple Teaching Cases (External, Middle, and Inner Ear)- Conclusions- References

#### **EREE-6 Acute Temporal Bone Pathology**

Participants

Ashraf Abdulhalim, MD, (*Presenter*) Nothing to Disclose

##### **TEACHING POINTS**

1. A simplified anatomic checklist-based approach can enable an emergency radiologist to accurately and efficiently identify acute temporal bone pathology, and this approach will be reviewed in this exhibit. 2. The radiologist plays an important role by identifying key imaging findings and providing diagnoses that can direct treatment by prompting an emergency physician to admit a patient for inpatient management, order a surgical consult, or order further imaging to check for related complications. The absence of these findings are also pertinent negatives that enable clinicians to proceed with treatment in the ED or discharge a patient with outpatient follow-up. 3. This exhibit will review traumatic and acute non-traumatic pathology in a case-based format, with emphasis on key imaging findings that affect management and prognosis.

#### TABLE OF CONTENTS/OUTLINE

I. Relevant anatomic structures and landmarks in the temporal bone for the emergency radiologist  
II. Checklist for non-traumatic and traumatic pathology  
III. Non-traumatic Pathology  
a. Infection  
i. Acute otitis externa  
ii. Malignant otitis externa  
iii. Coalescent mastoiditis with Bezold abscess  
iv. Temporomandibular joint abscess  
b. Aggressive neoplasm that might present with acute symptoms  
i. Langerhans cell histiocytosis  
ii. Paraganglioma  
IV. Traumatic Pathology  
a. Otic capsule violating versus non-otic capsule violating fractures  
b. Horizontal versus longitudinal fractures  
c. Isolated tympanic plate fracture  
d. Sutures/fissures that mimic fractures

#### EREE-7 Cardiac Findings Detectable on Non-Gated CT: What the Emergency Radiologist Needs to Know

##### Awards

##### Cum Laude

##### Participants

Dana Galvan, MD, Albuquerque, NM (*Presenter*) Nothing to Disclose

##### TEACHING POINTS

1. After completing this educational exhibit, the learner will have an improved understanding of cardiac findings that can be identified on non-gated CT examinations, performed in the emergency setting.  
2. Be able to differentiate pathologic abnormalities based on key cardiac anatomic landmarks including the pericardium, myocardium, cardiac chambers, appendages, and coronary arteries.  
3. Recognize key device and procedural complications on non-gated CT emergency situations.

#### TABLE OF CONTENTS/OUTLINE

-Introduction to the use of non-gated chest CT as an imaging modality in the emergency setting  
-Anatomy review of normal cardiac anatomy as seen on non-gated CT with labeling of structures and normal size measurements  
-Pericardium radiologic abnormalities including differential diagnosis, clinical significance, and follow-up recommendations with case examples and imaging: Anemia, Congenital Absence, Effusions, Abnormal and Normal Enhancement, Defects, and Calcification  
-Myocardium radiologic abnormalities including differential diagnosis, clinical significance, and follow-up recommendations with case examples and imaging: Myocardial infarction, Abnormal and Normal Fat Deposition, Cardiomyopathies  
-Cardiac Masses radiologic abnormalities including differential diagnosis, clinical significance, and follow-up recommendations with case examples and imaging: Cardiac pseudo-masses, Cardiac Thrombus, Cardiac Neoplasms  
-Other Cardiac Anomalies Detected on Non-Gated CT including differential diagnosis, clinical significance, and follow-up recommendations with case examples and imaging: Engorged Coronary Arteries, Post-Procedural Complication, and Device Failures

#### EREE-8 Imaging Features of Torsion of Various Organs in the Whole Body

##### Awards

##### Identified for RadioGraphics

##### Participants

Akihiro Nakamata, (*Presenter*) Nothing to Disclose

##### TEACHING POINTS

Torsion can present in various organs in the whole body, which cause a decreased blood flow due to twisted blood vessels. Therefore, emergent surgical intervention is often necessary to improve the blood flow. Radiologists should recognize imaging features of torsion of various organs in the whole body for the management of treatment options. The purpose of this exhibit is:  
1. To review a torsion of various organs in the whole body.  
2. To discuss the clinical and imaging features of the torsion.  
3. To classify various torsions into subtypes based on imaging findings reflecting the background pathology.

#### TABLE OF CONTENTS/OUTLINE

1. Subtypes based on imaging findings reflecting the background pathology.  
2. Torsion of various organs in this presentation.  
Chest; Lung lobe, Extralobar sequestration, Solitary fibrous tumor of the pleura, Pericardial appendage, Pericardial fat pad.  
Abdomen; Accessory liver lobe, Spleen, Accessory spleen, Stomach, Small intestine, Cecum Transverse colon, Sigmoid colon, Gastrointestinal Stromal Tumor (GIST), Meckel's diverticulum, Epiploic appendage, Omentum.  
Pelvis; Ovary, Ovarian tumor, Paraovarian cyst, Fallopian tube, Uterus, Uterine leiomyoma, Parasitic leiomyoma, Testis, Testicular appendage.

#### EREE-9 Pictorial Review of Acute Appendicitis and Beyond

##### Participants

Claudia Gabriela Moldovanu, MD, (*Presenter*) Nothing to Disclose

##### TEACHING POINTS

At the end of this educational exhibit, the audience will be able to differentiate the alternative diagnoses for the purpose of directing appropriate patient management.

#### TABLE OF CONTENTS/OUTLINE

Acute appendicitis is the most common diagnosis suspected in patients presenting in emergency rooms with acute abdominal pain. Early diagnosis depends on recognition of characteristic signs and symptoms: right lower quadrant or periumbilical pain, localized tenderness, fever, and leukocytosis. The differential diagnosis for an abnormal appendix on imaging includes other inflammatory/non-neoplastic and neoplastic processes. In this pictorial essay, we review the normal anatomy of the appendix and outline the pathogenesis, clinical manifestations, and imaging findings that are characteristic of acute appendicitis and its

complications, common or less common abnormalities (areas of focus include abdominopelvic abscess, peritonitis, pyelephlebitis, pyelethrombosis, and hepatic abscess). Inflammatory/nonneoplastic processes including serosal appendicitis, stump appendicitis, and foreign body appendicitis are discussed. Neoplastic considerations include appendiceal neuroendocrine tumors, mucinous and non-mucinous epithelial neoplasms, and lymphoma. A brief discussion of important pearls in the imaging assessment and diagnosis for each pathological presentation is then provided. It is important for the radiologist to be familiar with common imaging features and to be familiar with the various anatomical locations and other less common appendiceal abnormalities that can mimic or present concomitantly with acute appendicitis for accurate diagnosis and appropriate management.

Printed on: 02/07/23



## Abstract Archives of the RSNA, 2022

EREE-1

### Blunt Splenic Injury: What's New and Important - A Review by the ASER (American Society of Emergency Radiology) Expert Panel

Sunday, Nov. 27 8:00AM - 9:00AM Room: Learning Center - ER

#### Participants

Aishwariya Vegunta, MD, Stratford, CT (*Presenter*) Nothing to Disclose

#### TEACHING POINTS

1. Severity grading of Blunt Splenic Injury (BSI) using American Association for the Surgery of Trauma (AAST) 2018 Organ Injury Scaling (OIS). 2. Importance of detecting vascular injury and its impact on management. 3. Types of vascular injury: Contained Vascular Injury (CVI) and Active Splenic Hemorrhage (ASH). 4. Key Role of CT protocol in Vascular Injury Detection. 5. Management options: Operative vs. Conservative and future advances.

#### TABLE OF CONTENTS/OUTLINE

Table of Contents/Outline: ? Background/scope of the problem: Spleen is the second most common injured abdominal organ? Examples of Blunt Splenic Injury and grading using 2018 AAST OIS? Types of Splenic Vascular Injuries: a. Contained Vascular Injury. Pseudoaneurysm. Arteriovenous fistula. Active Splenic Hemorrhage (ASH)? Optimizing CT protocols- Arterial phase imaging/ multiphase acquisition increases sensitivity and improves differentiation of splenic vascular injury ? Management of BSI and the impact of CT detection of splenic vascular injury: Trend toward Nonoperative management (NOM) and role of splenic artery embolization (SAE) ? When NOM fails: Potential factors and next steps? Follow up imaging for delayed splenic rupture: When to do it and what to look for

Printed on: 02/07/23



## Abstract Archives of the RSNA, 2022

EREE-10

### A Pregnant Patient in Pain: What the ER Radiologist Needs to Know About the Findings, Reporting, and Significance

Sunday, Nov. 27 8:00AM - 9:00AM Room: Learning Center - ER

#### Participants

Dana Galvan, MD, Albuquerque, NM (*Presenter*) Nothing to Disclose

#### TEACHING POINTS

1. Improve understanding of the radiologic evaluation of pregnant patients in emergency settings, including the reporting of first and second/third trimester fetal sonography. 2. Familiarize radiologists and in-training radiologists with the imaging appearance, incidence, and follow up recommendations of common emergent causes of maternal acute abdomen. 3. To review key traumatic pathologies and findings in pregnancy such as uterine rupture and the Traumatic abruptio placenta scale. 4. Highlight key findings of urgent special consideration cases of multiple gestations and emergent ectopic pregnancy findings.

#### TABLE OF CONTENTS/OUTLINE

-Introduction to emergency department visits during pregnancy including common presenting complaints, symptoms, and initial imaging modalities selected to investigate. -Review of maternal and fetal radiation exposure in the emergency setting, including effect on fetus and threshold doses. -Review of sonographic first trimester findings including SRU criteria, terminology, and findings for pregnancy failure. -Review of second trimester ultrasound findings including how to identify relevant findings, report findings, and their significance. -Sonographic placental and cervical pathologies of the second and third trimesters, with key imaging findings, clinical significance, and follow-up recommendations. -Common traumatic injuries including uterine rupture and review of the Traumatic Abruption Placenta Scale (TAPS). -Differential diagnosis, clinical significance, and follow-up recommendations of several maternal acute abdomen pathologies. -Imaging finding review of multiple gestation emergencies, ectopic and heterotopic pregnancies.

Printed on: 02/07/23



## Abstract Archives of the RSNA, 2022

EREE-11

### Age Estimation of Unidentified Cadavers Using Postmortem CT Imaging

Sunday, Nov. 27 8:00AM - 9:00AM Room: Learning Center - ER

#### Participants

Wataru Fukumoto, MD, PhD, Hiroshima, Japan (*Presenter*) Nothing to Disclose

#### TEACHING POINTS

For the identification of unknown cadavers, an accurate estimation of the age at the time of death is needed. Classical methods assess morphological changes of the pubic symphysis, its auricular surface, and cranial sutures and teeth. However, as these assessments rely on the experience and expertise of the evaluator, their accuracy is limited, especially in elderly cadavers. Because postmortem computed tomography (PMCT) using multiplanar reconstruction- and 3D images reveals the bone structure clearly, it is superior to the classical methods. We introduce and describe the utility of age estimation methods based on PMCT.

#### TABLE OF CONTENTS/OUTLINE

1. Importance of age estimation in forensic science 2. Classical age estimation methods 3. Age estimation using PMCT images  
•Measurement of the bone density of the pubic symphysis •CT value and volumetric analysis of the proximal femur •Maturity of the medial clavicular epiphysis •The ossification score of the sternum and ribs •Evaluation of osteophytes in the vertebrae 4. A new approach for age estimation using PMCT and deep learning

Printed on: 02/07/23



## Abstract Archives of the RSNA, 2022

EREE-12

### Automated CT Perfusion (CTP) interpretation in Acute Stroke: Primer for On-call Radiologist

Sunday, Nov. 27 8:00AM - 9:00AM Room: Learning Center - ER

#### Awards

Certificate of Merit

#### Participants

Ashlesha Udare, MBBS, MD, (*Presenter*) Nothing to Disclose

#### TEACHING POINTS

1. To understand the growing need of emergency automated CTP evaluation 2. The 3 questions approach for fast and accurate interpretation

#### TABLE OF CONTENTS/OUTLINE

Background: AHA2018 AIS guidelines recommend perfusion imaging for INR subject selection at 6-24 hours after insult. Automated CTP using AI technology has been used in several recent large LVO endovascular therapy trials. Using case-based approach with 2 FDA approved AI solutions from our institution, we aim to acquaint the on-call radiologist interpreting automated CTP data using a simplified 3 questions approach 1. Is the CTP diagnostic/non-diagnostic? Understanding the basics of CTP acquisition and processing by the AI software. technical pitfalls: motion, contrast bolus, AIF/VOF selection, erroneous calculation of perfusion abnormality near the skull base, truncation of dynamic curve, z-axis coverage. 2. Is there infarct core volume measurement error? Underestimated on CTP outputs in the extended time window if received IV tPA, leptomeningeal collaterals lead to partial reperfusion of completely infarcted: Noncontrast CT ASPECTS-Overestimated in cases of ghost infarct hyperacute stroke, early reperfusion: Stricter rCBF threshold for core infarct estimation. 3. Is there ischemic penumbra measurement error? Overestimated in proximal vessel stenosis, leukoriosis, fetal PCA: Evaluate CTA, MTT-Wrong inclusion of opposite hemisphere, beyond vascular territory by automated software-Stroke mimics, lacunar infarcts and posterior circulation strokes. Conclusion: Fast interpretation of the complex automated CTP data by a simplified 3 questions approach for the on-call radiologist and to optimize patient selection for reperfusion.

Printed on: 02/07/23



## Abstract Archives of the RSNA, 2022

EREE-13

### Emphysematous Osteomyelitis: A Review of Imaging Features and Pitfalls for the Emergency Radiologist to Avoid

Sunday, Nov. 27 8:00AM - 9:00AM Room: Learning Center - ER

#### Awards

Certificate of Merit

#### Participants

Kush Purohit, MD, MS, Pittsburgh, PA (*Presenter*) Nothing to Disclose

#### TEACHING POINTS

Discuss the pathogenesis and clinical presentation of emphysematous osteomyelitis (EO), a rare, lethal variant of osteomyelitis caused by infection from gas-forming organisms. Understand key x-ray features and limitations of radiography, including inconspicuous or radiographically occult intraosseous air. Describe the characteristic CT "pumice stone pattern" of irregularly irregular 2-5 mm intraosseous foci of gas. Discuss conventional MRI findings, including T1 hypointense and T2 hyperintense marrow signal abnormalities, and correlate with radiography and CT. Understand local susceptibility artifact from intraosseous air can obscure T1 and T2 signal abnormalities and may be misinterpreted as calcification or hemosiderin deposition, a potential pitfall for the emergency radiologist. Explore PET-MRI as a useful tool in diagnosing EO and localizing infection spread.

#### TABLE OF CONTENTS/OUTLINE

Emphysematous osteomyelitis background: Epidemiology, pathogenesis, clinical presentation  
Radiography: Typical features and pitfalls  
MRI: Review of imaging features. Susceptibility artifact as a major potential pitfall for the emergency radiologist  
CT: The most useful diagnostic study with characteristic "pumice stone pattern" of intraosseous gas  
PET-MRI: A useful emerging tool with review of typical imaging features

Printed on: 02/07/23



## Abstract Archives of the RSNA, 2022

EREE-14HC

### **Fistulas: From The Mouth To The Anus.CHAR(13) + CHAR(10)Our Experience Searching For An Accurate Diagnosis.**

Sunday, Nov. 27 8:00AM - 9:00AM Room: Learning Center - ER

#### **Participants**

Rodrigo Loto, MD, Rosario, Argentina (*Presenter*) Nothing to Disclose

#### **TEACHING POINTS**

List to appropriate diagnostic imaging studies. Describe the anatomic locations, causes and clinical features of uncommon fistulas. How to do it. Identify the radiologic finding in the various types of fistulas. A fistulogram/sinogram is used to diagnose and assess the size and shape of fistulas and sinuses and prepare a treatment plan. Fistulograms are used to assess many types of fistulas, including those that form between: two loops of intestine the anal canal and skin near the anus the vagina and another body part such as the colon, rectum, small intestine or bladder.

#### **TABLE OF CONTENTS/OUTLINE**

This pictorial review shares our initial experience with MDCT fistulography in evaluating fistulas, demonstrates various components of fistulas, and discusses the types of fistulas. MDCT is the most common modality used for assessment of fistulas, especially with the use of fistulography. The injection of positive contrast well-delineates the fistulous tract and its branching pattern and connections. CT also enables multiplanar reconstruction and thin cuts for good anatomical details. Orally administered Contrast Media opacification may be helpful. is relatively well tolerated but it can be painful when injecting the contrast material into the fistulous tract. Is important identify the anatomic locations and clinical features to proceed. Fistulas are diverse in their anatomy and clinical presentation. Radiologists must be familiar with the radiologic findings for both accurate diagnosis and, in many cases, guidance of management planning. Please visit the Learning Center to also view this presentation in hardcopy format.

Printed on: 02/07/23



## Abstract Archives of the RSNA, 2022

EREE-15

### Recreational Drug Abuse- the Spectrum of Imaging Findings

Sunday, Nov. 27 8:00AM - 9:00AM Room: Learning Center - ER

#### Participants

Edward Choe, DO, (*Presenter*) Nothing to Disclose

#### TEACHING POINTS

1. The opioid epidemic coupled with the COVID-19 pandemic has drastically increased the prevalence of recreational drug abuse. 2. Increasing prevalence of substance use should prompt radiologists to familiarize themselves with common and uncommon imaging patterns, and different routes of self-administration. 3. Substance use will often have multisystem sequelae. 4. Additional factors to consider when evaluating a patient should include but are not limited to concomitant infections such as HIV and hepatitis, the imaging features of which may complicate image interpretation.

#### TABLE OF CONTENTS/OUTLINE

The primary goal of this exhibit is to review the imaging findings of recreational drug abuse. Patients with substance use often present with a spectrum of multisystem abnormalities beyond direct soft tissue or vascular injury. Vascular complications include pseudoaneurysm, thrombophlebitis, and mycotic aneurysm. In the musculoskeletal system, findings include cellulitis, abscess, fasciitis and septic arthritis, discitis/osteomyelitis, and findings related to ischemia or immobility. In the CNS, complications include dural venous thrombosis, hemorrhage, ischemia, and sequelae of cerebral vasospasm such as PRES. Cardiovascular complications include valvular vegetations, septic emboli, dissection and myocardial infarct. Intra-abdominal complications include septic emboli with infarction of the spleen, kidneys, or bowel, as well as pancreatitis. The imaging findings of these entities will be illustrated, along with potential pitfalls associated with concomitant HIV and viral hepatitis.

Printed on: 02/07/23



## Abstract Archives of the RSNA, 2022

EREE-16

### Imaging Atlas of the AAST Organ Injury Scaling: Spleen, Liver and Kidney

Sunday, Nov. 27 8:00AM - 9:00AM Room: Learning Center - ER

#### Participants

Bárbara Santos, Sao Paulo, Brazil (*Presenter*) Nothing to Disclose

#### TEACHING POINTS

- Non-operative management of blunt abdominal trauma, including endovascular treatment, is increasingly applied, therefore, recognizing and defining the key imaging features of trauma-related injury is crucial. ?- The CT-based organ injury scaling established by the American Association for the Surgery of Trauma (AAST) is the most used to assess injury severity and guide clinical decision-making, a useful tool to those caring for the injured patient.?- The most significant change in the 2018 revision of AAST organ injury scale is the incorporation of CT diagnosed vascular injury. The presence of a vascular injury is associated with higher failure rates of nonoperative management, therefore higher grades are used in the presence of a vascular injury.

#### TABLE OF CONTENTS/OUTLINE

- Introduction?- CT protocol for trauma assessment.?- Changes made in the 2018 revision of the AAST Organ Injury Scaling for spleen, liver, and kidney and how its relate with clinical management.?- Definition by CT imaging of all general types of traumatic injuries on solid organs.?- Imaging atlas of the organ injury scaling established by AAST for spleen, liver, and kidney.?- Pitfalls on trauma-related evaluation of spleen, liver, and kidney.?- Take home messages.?

Printed on: 02/07/23



## Abstract Archives of the RSNA, 2022

EREE-17

### Pelvic Trauma for the Diagnostic and Interventional Radiologist: From Plain Film to Angioembolization

Sunday, Nov. 27 8:00AM - 9:00AM Room: Learning Center - ER

#### Participants

Javier Hernandez, BS, San Antonio, TX (*Presenter*) Nothing to Disclose

#### TEACHING POINTS

-Use cases to review significant diagnostic findings (plain film and CT) with corresponding angiographic findings for pelvic trauma.- Characterize the role of interventional radiology in the management of pelvic trauma.-Provide a clinical algorithm for initiating pelvic trauma angiography.

#### TABLE OF CONTENTS/OUTLINE

IntroductionPelvic Anatomy: Bony Landmarks with Vascular Associations, Iliac Artery Branch PatternsVariants of Interest: Corona mortis; Variable Origins of Inferior Gluteal, Internal Pudendal, Superior Gluteal and Obturator Artery.Pelvic Trauma Societal Guidelines WSES, ACR, EASTPlain film, CT and Angiographic findings Blush, Truncation, Pseudoaneurysm, Large Vessel Transection, Traumatic Arteriovenous FistulaMetrics of Intervention Radiology in Hemorrhagic Trauma Cumulative National Response Times, Frequency of Angiography in Pelvic TraumaClinical Algorithm for Pelvic AngiographyCase Presentations: Open Book Fracture, Superior Gluteal Artery Laceration, Bilateral Internal Iliac Transection, Multivessel Internal Iliac Artery EmbolizationOutcomes of Angioembolization: Mortality, Morbidity, RecurrenceConclusionClinical Implications In the setting of pelvic trauma, angiography and embolization serve as critical interventions to mitigate deterioration in hemorrhagic shock. Knowledge of unique vascular injuries and their imaging aid diagnosticians and interventionalists in facilitating clinical management.

Printed on: 02/07/23



## Abstract Archives of the RSNA, 2022

EREE-18

### The Puzzle Never Solved: Imaging of Abdominal Emergencies in Pregnancy, Still a Dilemma

Sunday, Nov. 27 8:00AM - 9:00AM Room: Learning Center - ER

#### Participants

Teodorescu Andreea, MD, (*Presenter*) Nothing to Disclose

#### TEACHING POINTS

To illustrate the spectrum of different presentations of abdominal emergencies in pregnant patients. To review the imaging findings of acute emergencies that will help us to think beyond specific conclusion in an emergency setting. To discuss the risks to the fetus from diagnostic imaging modalities and contrast agents. To propose recommendations for emergency diagnostic imaging of pregnant patients. To summarize the role of imaging (including ultrasound, CT, and MR imaging) in diagnosing acute and emergent pregnancy-related conditions using a CASE-BASED APPROACH.

#### TABLE OF CONTENTS/OUTLINE

Acute abdomen in pregnancy remains one of the most challenging diagnostic and therapeutic dilemmas today. The differential diagnosis during pregnancy is extensive in that the abdominal pain may be obstetric in nature or may be caused by diseases of other intraabdominal or intrapelvic structures. Because of the anatomic and physiologic changes that occur with pregnancy, localization of disease can be difficult. Appendicitis and complicated biliary pathology are the most frequent causes of non-obstetric acute abdomen in the pregnant patient. Pathological causes of obstetric emergencies which are life-threatening include ruptured ectopic pregnancy, abruption, HELLP syndrome, acute fatty liver of pregnancy, and uterine rupture. Imaging studies are essential adjuncts in the diagnostic evaluation of acute emergency conditions due to clinical and laboratory masking in this subgroup. However, confusion about the safety of these modalities for pregnant women and their infants often results in unnecessary avoidance of useful diagnostic tests.

Printed on: 02/07/23



## Abstract Archives of the RSNA, 2022

EREE-19

### Small Bowel Diverticulosis And Diverticulitis: A Pictorial Review

Sunday, Nov. 27 8:00AM - 9:00AM Room: Learning Center - ER

#### Participants

Namita Bhagat, MD, Shelton, CT (*Presenter*) Nothing to Disclose

#### TEACHING POINTS

- Small bowel diverticulosis is uncommon and is usually a disease of 6th-7th decade. Diverticulitis occurs in 6.5-10% patients. Other complications include perforation, bleeding and bowel obstruction.
- Small bowel diverticulitis is a rare entity and is often overlooked as a cause of abdominal pain in the elderly because of resemblance of imaging features with other causes of acute abdominal pain and its anatomical location within the mesenteric border at surgery where these diverticuli are obscured by large penetrating blood vessels.
- It is imperative to be familiar with imaging features and to look for clues which may suggest small bowel diverticulitis, such as the presence of non-inflamed diverticuli in adjacent small bowel and presence of a normal appearing appendix in cases of ileal diverticulitis. Delayed diagnosis leads to complications and can be fatal with mortality rate of 25-50%.
- Accurate diagnosis on imaging aids in appropriate patient management, and may help reduce morbidity and mortality.

#### TABLE OF CONTENTS/OUTLINE

Describe etiology, pathophysiology and complications of small bowel diverticulosis and diverticulitis. To review the imaging findings of small bowel diverticulosis and diverticulitis on CT. Describe other differential diagnosis for causes of right lower quadrant pain which mimic imaging appearance: for example uncomplicated and complicated acute appendicitis, colonic diverticulitis, Crohn's disease, acute typhlitis, Meckel's diverticulitis, etc.

Printed on: 02/07/23



## Abstract Archives of the RSNA, 2022

EREE-2

### Paranasal Sinuses on Acute Head Imaging: What the Radiologist Needs to Know

Sunday, Nov. 27 8:00AM - 9:00AM Room: Learning Center - ER

#### Participants

Veronika Majcher, MD, Cambridge, United Kingdom (*Presenter*) Nothing to Disclose

#### TEACHING POINTS

Incidental findings involving the paranasal sinuses are common on CT and MR head scans performed in the acute setting. In the majority of cases, opacification of sinuses is secondary to mild inflammation and can be safely dismissed. However, recognising patterns and imaging features of paranasal sinus findings on these scans can opportunistically pick up pathology benefiting from further investigation or even identify the cause of presenting symptoms. After reviewing this exhibit, the reader will be able to: 1) Revise the basic anatomy and drainage pathways of the paranasal sinuses in order to understand patterns of disease; 2) review common and rarer benign and invasive paranasal sinus pathology using case examples; 3) recognise worrisome features that necessitate further investigation and referral.

#### TABLE OF CONTENTS/OUTLINE

1. Anatomy and imaging of the paranasal sinuses 2. Drainage pathways and patterns of disease 3. Interpretation and significance of pathological changes within paranasal sinuses a. Mucosal thickening b. Soft tissue density and bone changes c. Specific signs of acute/chronic/fungal disease 4. Signs of invasive and infiltrative disease a. Review areas 5. Complications of sinusitis

Printed on: 02/07/23



## Abstract Archives of the RSNA, 2022

EREE-20

### Emergency Radiology Peer Learning Pearls: Focus on Appendix Cases

Sunday, Nov. 27 8:00AM - 9:00AM Room: Learning Center - ER

#### Participants

Alyssa Sherwill, MD, (*Presenter*) Nothing to Disclose

#### TEACHING POINTS

- Discuss the use of peer learning in evaluating cases of misdiagnosed appendicitis on CT, MRI, and ultrasound
- Careful evaluation for defects in the appendiceal wall is crucial to assess for gangrenous appendicitis, particularly if there is an appendicolith
- Air in the appendix is not reliable marker of a normal appendix, and can be mistaken on MRI as an appendicolith
- Secondary ancillary findings of appendicitis may be subtle and should not be ignored
- Many appendicitis overcalls are related to adjacent inflammatory processes
- Appendiceal malignancy and mucocoeles can simulate appendicitis

#### TABLE OF CONTENTS/OUTLINE

- 1.Introduction to Peer Learning
- 2.Complicated Appendicitis
  - a.Gangrenous Appendicitis
  - b.Perforated Appendicitis
  - c.Remote Complications of Appendicitis
- 3.Missed Appendicitis
  - a.Air in Appendix
  - b.Subtle Ancillary Findings
  - c.Appendiceal Location in Pregnancy
  - d.Satisfaction of Search Bias
- 4.Appendicitis Overcalls
  - a.Secondary Appendicitis
    - i.Pelvic Inflammatory Disease
    - ii.Cecal or Ascending Colonic Diverticulitis
    - iii.Infectious or Inflammatory Enteritis
  - iv.Bile Leak
  - b.Endometriosis
  - c.Cystic Fibrosis
  - d.Chronic Appendicitis
- 5.Neoplastic Mimickers
  - a.Appendiceal Mucinous Neoplasms
  - b.Carcinoid
  - c.Metastases

Printed on: 02/07/23



## Abstract Archives of the RSNA, 2022

EREE-21

### Stroke Alert!" ER Dilemma, What is Next? CT Perfusion (CTP) or Fast Brain MRI

Sunday, Nov. 27 8:00AM - 9:00AM Room: Learning Center - ER

#### Participants

Ahmed Moawad, MD, Darby, PA (*Presenter*) Nothing to Disclose

#### TEACHING POINTS

- Reviewing the current imaging guidelines for acute stroke - Comparing the difference between fast MRI and CTP in diagnosis of different acute neurological deficit scenarios - Introducing the use of different imaging modalities in management decisions - Highlighting role of Fast MRI and CTP in follow up treated stroke.

#### TABLE OF CONTENTS/OUTLINE

# Introduction - Fast brain MRI protocol CTP protocol and parameters - - Current guidelines in stroke imaging - Limitation of fast brain MRI Drawbacks and pitfalls of CTP # Different scenarios of acute neurological deficit diagnosis - Accuracy of Fast MRI and CTP in stroke diagnosis - Imaging in Ischemic stroke vs. Intra-cerebral hemorrhage - Stroke with unknown duration "Wake-up" - Transient ischemic attack - Stroke mimickers: Seizures, Hypoglycemia, Cerebral venous thrombosis, Acute multiple sclerosis flare, Migraine aura- Posterior fossa stroke - Lacunar infarct - Hyperacute infarcts - Hypoperfusion state: Cardiac failure, Shock, Chronic carotid artery occlusion# Management of ischemic stroke - Predicting outcome using imaging modalities and clinical scores Identification of final ischemic infarct core \* Mismatch between initial infarct core - final infarct \* Ghost infarct core - Identification of ischemic salvageable tissue (Penumbra) \* Role of perfusion imaging (CTP and MR perfusion) \* DWI in identification of penumbra\* MRI vs. CTP for Thrombectomy Selection - DEFUSE 3 and DAWN trial - Management of stroke by DWI-FLAIR mismatch vs. CTP - WAKE UP vs. EXTEND trial# Follow up stroke treatment - Follow up hemorrhagic transformation - Assessment of reperfusion state and infarct volume

Printed on: 02/07/23



## Abstract Archives of the RSNA, 2022

EREE-22

### Spinal Hematomas: Pearls and Pitfalls for MRI Evaluation in Emergency Radiology

Sunday, Nov. 27 8:00AM - 9:00AM Room: Learning Center - ER

#### Participants

Maria Galante I, MD, Santander, Spain (*Presenter*) Nothing to Disclose

#### TEACHING POINTS

1) To make a pictorial review of the main meningeal layers and the 4 spaces: epidural, subdural, subarachnoid and intramedullary space. 2) To identify in MRI technique the different types of spinal hematomas 3) To detail the most important imaging features of each type of hematoma, in order to differentiate one from another. 4) To describe the main alternative diagnosis 5) To highlight pitfalls that may be found during the imaging assessment. 6) To suggest an MRI protocol for the evaluation of spinal hematomas for non-subspecialized radiologists

#### TABLE OF CONTENTS/OUTLINE

Etiology of spinal hematomas Symptoms Anatomical Review of the spine: layers and spaces MRI appearance of blood in routine sequences MRI protocol for the evaluation of spinal hematomas in emergency radiology Epidural hematomas Subdural hematomas Subarachnoid Hemorrhage Intramedullary Hematoma Pitfalls and differential diagnosis Treatment Conclusions

Printed on: 02/07/23



## Abstract Archives of the RSNA, 2022

EREE-23

### Confronting and Overcoming Emergency Radiology Biases

Sunday, Nov. 27 8:00AM - 9:00AM Room: Learning Center - ER

#### Awards

Identified for RadioGraphics  
Magna Cum Laude

#### Participants

Se-Young Yoon, MD, (*Presenter*) Nothing to Disclose

#### TEACHING POINTS

- With the transition to peer learning review of cases, many diagnostic errors in radiology can be attributed to cognitive biases. Because of the high volume and rapid pace of emergency radiology, exam interpretations may be heavily reliant on biases and heuristics. Thus, a more focused evaluation of emergency radiology specific biases is needed to avoid diagnostic pitfalls.- We aim to review common biases in emergency radiology in this exhibit, organized by the expected stage of occurrence during the process of reading an imaging study.- Several cognitive biases that have not yet been defined in radiological publications, to the best of our knowledge, will be discussed. These include: triage cueing, contrast effect, provider bias, treater bias, and need for closure.- Emergency radiology peer learning case examples are provided to illustrate how and which biases may have occurred.- Strategies to recognize and overcome biases will be discussed, with an emphasis on those that may be more prevalent in the emergency setting.

#### TABLE OF CONTENTS/OUTLINE

- Cognitive biases commonly seen in emergency radiology-- Definitions and brief examples (list on slide #1)- Peer learning case examples illustrating various cognitive biases- Strategies in recognizing and overcoming biases

Printed on: 02/07/23



## Abstract Archives of the RSNA, 2022

EREE-24

### An Approach to Acute Traumatic and Non-traumatic Diaphragmatic Abnormalities

Sunday, Nov. 27 8:00AM - 9:00AM Room: Learning Center - ER

#### Awards

Identified for RadioGraphics  
Certificate of Merit

#### Participants

Nicolas Murray, MD, FRCPC, Vancouver, BC (*Presenter*) Co-investigator, Siemens AG

#### TEACHING POINTS

Acute traumatic and non-traumatic diaphragmatic abnormalities are a heterogeneous group of relatively uncommon pathologies affecting the normal structure and function of the diaphragm. These include diaphragmatic hernia, laceration, traumatic and spontaneous rupture, thoracoabdominal fistulae, infection, and endometriosis. Because the diaphragm is the primary inspiratory muscle, disruption to its integrity can cause clinically significant consequences. Imaging plays an essential role in investigation. However, these pathologies can be easily missed as findings are often subtle. Therefore, understanding the anatomy and radiologic findings allows for efficient and accurate diagnosis and management.

#### TABLE OF CONTENTS/OUTLINE

Diaphragm anatomy and normal variation. Introduction and differential diagnosis of acute diaphragmatic abnormalities. Imaging modalities for the diaphragm. Pathogenesis, incidence, clinical presentation, diagnosis, radiologic findings, and general management of non-traumatic and traumatic diaphragmatic abnormalities including (1) diaphragmatic hernias, (2) spontaneous diaphragm rupture, (3) endometriosis-related diaphragmatic disease, (4) trans-diaphragmatic fistula, (5) infection of the diaphragm, (6) blunt injuries, (7) penetrating injuries, and (8) traumatic diaphragm rupture. Summary of take-home points.

Printed on: 02/07/23



## Abstract Archives of the RSNA, 2022

EREE-25

### CT of Blunt Acute Thoracic Aortic Injury: A Primer for Diagnostic Radiologists

Sunday, Nov. 27 8:00AM - 9:00AM Room: Learning Center - ER

#### Awards

Certificate of Merit

#### Participants

Alok Mittal, MBBS, MD, Muscat, Oman (*Presenter*) Nothing to Disclose

#### TEACHING POINTS

-To identify and differentiate blunt traumatic aortic injuries from various normal variants and injury mimics on CT.-To illustrate direct and ancillary CT features of blunt traumatic aortic injuries.-To differentiate minimal and severe aortic injuries using original illustrations and animations.-To correlate aortic injuries with the most commonly used classification schemes.-To summarize the management algorithm and the role of interventional radiologists in acute aortic injury.

#### TABLE OF CONTENTS/OUTLINE

-MDCT protocol to diagnose and characterize aortic injury patterns.-Review of the anatomical variation and mimics.-Spectrum of aortic injuries on CT and how to correctly characterize them?-Aortic injury classification systems and simplified approach.-Common pitfalls- how to identify and avoid them?-Management of Aortic injuries and the role of the interventional radiologist.

Printed on: 02/07/23



## Abstract Archives of the RSNA, 2022

EREE-26

### Penile Trauma: From Diagnosis to Treatment

Sunday, Nov. 27 8:00AM - 9:00AM Room: Learning Center - ER

#### Participants

Victor Jabour, MD, Sao Paulo, Brazil (*Presenter*) Nothing to Disclose

#### TEACHING POINTS

The purposes of this exhibit are: 1. To review the main indications of penis ultrasound in the context of urgency 2. To show the technique of the penis ultrasound 3. To show based on cases from our ultrasound group important structures that must be evaluated in the ultrasound of the penis 4. To review based on cases from our ultrasound group the main penile injuries in the context of emergency and the respective treatments

#### TABLE OF CONTENTS/OUTLINE

Main indications for penile ultrasound in an emergency setting 2 Penile ultrasound technique and documentation protocol used in our ultrasound group 3 Illustrate with cases from our ultrasound group the main penile injuries in the context of emergency and the respective treatments

Printed on: 02/07/23



## Abstract Archives of the RSNA, 2022

EREE-27

### Artificial Intelligence (AI) Imaging Algorithms in the ICU: Augmenting the Radiologist

Sunday, Nov. 27 8:00AM - 9:00AM Room: Learning Center - ER

#### Participants

Kaustav Bera, MD, Cleveland, OH (*Presenter*) Nothing to Disclose

#### TEACHING POINTS

1. Learn about the unmet needs when it comes to ICU imaging both from the point of view of the primary provider as well as the radiologist 2. How Artificial Intelligence (AI) algorithms can benefit both the ICU physician as well as the reading radiologist 3. Illustrate real-world use cases where AI-imaging algorithms are already in use in the ICU as well as potential high-yield use cases for AI 4. Challenges and limitations that AI enabled tools need to overcome before seamless integration in ICU

#### TABLE OF CONTENTS/OUTLINE

1. Fundamentals of imaging in the ICUa. What the primary team physician wantsb. What the reading radiologist wantsc. Unmet need in the ICU which AI can fulfill2. A Brief Primer on AIa. AI, Machine Learning, Deep Learning - A Brief Primer.b. Framework of AI in clinical use 3. Modalities and use cases for AI in ICU Imaginga. Imaging to determine ICU Admission/Transfer i. AI to predict which COVID-19 patients need urgent mechanical ventilation ii. AI to diagnose cholecystitis, ascending cholangitis from US imaging iii. AI to automatically detect cord compression/cauda equina from spinal MRI iv. AI to detect stroke v. AI to detect hemorrhageb. Imaging within the ICU for monitoring/change in status i. AI for urgent pathology on Chest radiograph (Pneumothorax) ii. AI for lines/tubes detection on Chest radiograph iii. AI to detect Pulmonary Embolism iv. AI to detect Acute aortic pathology 4. Real world use cases of seamlessly integrated AI tools 5. How AI can benefit ICU management both for the radiologist and the physician 6. Future directions

Printed on: 02/07/23



## Abstract Archives of the RSNA, 2022

EREE-28

### CT Evaluation of Abdominal Emergencies in Oncologic Patients

Sunday, Nov. 27 8:00AM - 9:00AM Room: Learning Center - ER

#### Awards

Certificate of Merit

#### Participants

Joon-Il Choi, MD, PhD, Seoul, Korea, Republic Of (*Presenter*) Research Grant, Guerbet SA; Research Grant, Samsung Electronics Co, Ltd

#### TEACHING POINTS

1. To suggest tailored MDCT protocols for evaluating oncologic abdominal emergencies based on symptoms and clinical impressions
2. To familiarize with various common and uncommon medical risk factors of abdominal emergencies in oncologic patients and pertinent MDCT findings
3. To systemically evaluate causes of acute abdomen in oncologic patients in an MDCT

#### TABLE OF CONTENTS/OUTLINE

1. Tailored MDCT protocols for oncologic abdominal emergencies evaluation
  - 1) Recommended routine protocol for a general indication in the emergency room
  - 2) Symptom and clinical impression-based optimal protocols - Clinical scenarios: solid organ bleeding, hollow viscus bleeding, bowel obstruction, bowel perforation, biliary obstruction, acute renal failure
2. Various medical risk factors of abdominal oncologic emergencies
  - 1) Therapy-related risk factors - Chemotherapeutic agent - External radiation therapy - Locoregional treatments - Recent major surgery - Other invasive therapeutic procedure
  - 2) Immunocompromised host
  - 3) Bleeding tendency of the host
3. A systematic radiologic approach for abdominal oncologic emergencies
  - 1) An organ-based assessment for the causes of the acute abdomen in oncologic patients
  - 2) MDCT findings of common oncologic abdominal emergencies
  - 3) Proposed structured report form to facilitate a thorough evaluation of the abdomen

Printed on: 02/07/23



## Abstract Archives of the RSNA, 2022

EREE-29

### **Bone-induced Streak Artifact Reduction in Emergency Abdominal CT Using the Deep Learning-based Image Reconstruction**

Sunday, Nov. 27 8:00AM - 9:00AM Room: Learning Center - ER

#### **Participants**

Tetsuya Hirairi, MS, (*Presenter*) Nothing to Disclose

#### **TEACHING POINTS**

The streak artifact, which is frequently observed in abdominal CT images obtained at the emergency trauma patients with arms-down positioning, is known to degrade diagnostic image quality. To solve this problem, deep learning-based image reconstruction is adapted to in emergency abdominal CT. Advanced intelligent Clear-IQ Engine (AiCE), is a type of deep learning-based image reconstruction, is compared with conventional hybrid Iterative reconstruction (HIR). Quantitative artifact estimation is evaluated by the normalize artifact index (nAI) with an abdominal phantom between two dense objects which is simulated arms down positioning. CT number inaccuracy is evaluated by abdominal CT images of 20 clinical patients with arms-down positioning by setting region of interest in the liver and the spleen. As a result, DLR method significantly decreased nAI and improved the CT number accuracy compared to HIR. It was suggested that DLR was useful for the bone-induced streak artifact reduction in emergency abdominal CT.

#### **TABLE OF CONTENTS/OUTLINE**

1. Clinical problems with conventional emergency CT. 2. Deep learning-based image reconstruction technology AiCE. 3. Normalize artifact index of the phantom simulated arms down positioning. 4. Improvement of the CT number accuracy. 5. Clinical performance in Emergency CT.

Printed on: 02/07/23



## Abstract Archives of the RSNA, 2022

EREE-3

### No Time to Dye: How to Diagnose and Manage Critical Diseases with Non-contrast Enhanced CT

Sunday, Nov. 27 8:00AM - 9:00AM Room: Learning Center - ER

#### Participants

Yukiko Michishita, MD, (*Presenter*) Nothing to Disclose

#### TEACHING POINTS

1) To share useful imaging findings of various critical diseases in non-contrast enhanced CT (NCECT), with emphasis on the significance of prompt response to treatment regardless of contrast enhanced CT (CECT). 2) To understand the settings where CECT is still required for appropriate treatment strategies as well as diagnosis.

#### TABLE OF CONTENTS/OUTLINE

To learn how to diagnose and manage critical diseases with NCECT, following topics are discussed; 1) Classical findings on CECT, 2) Useful findings on NCECT, 3) Clinical perspective, 4) Significance of prompt action according to findings on NCECT, 5) Diagnostic accuracy of NCECT, 6) Significance of CECT. Featured pathologies are as follows; A. Acute thromboembolisms: 1) Cerebral infarction, 2) Acute pulmonary embolism, 3) SMA embolism/thrombosis, 4) Cerebral venous sinus thrombosis. B. Vascular diseases: 1) Acute aortic dissection, 2) SMA dissection, 3) Impeding rupture of aortic aneurysm. C. Bleedings: 1) Trauma and other bleeders, 2) Gastrointestinal bleeding, 3) Intracranial hematoma. D. Ischemia: 1) Bowel strangulation, 2) Non-occlusive mesenteric ischemia. E. Inflammatory diseases and others: 1) Gangrenous appendicitis, 2) Severe acute cholecystitis, 3) Severe acute pancreatitis, 4) Hepatic abscess, 5) Mycotic aneurysm.

Printed on: 02/07/23



## Abstract Archives of the RSNA, 2022

EREE-30

### Cervical Catastrophe: Identifying Tracheal Injury Before It Is Too Late

Sunday, Nov. 27 8:00AM - 9:00AM Room: Learning Center - ER

#### Participants

Ethan Jiang, BSc, (*Presenter*) Nothing to Disclose

#### TEACHING POINTS

1. Early and accurate detection of tracheal trauma is crucial to reduce the significant morbidity and mortality associated with these injuries. 2. A low threshold of suspicion for tracheal injury facilitates timely decision-making and intervention in the setting of trauma. 3. Injuries to neighboring structures, such as the esophagus, are often concomitant to tracheal injury following blunt and penetrating neck trauma.

#### TABLE OF CONTENTS/OUTLINE

We outline an approach to suspected tracheal injury in the setting of trauma. The focus will be on using imaging to change clinical outcomes through early identification, especially when the clinical presentation is nonspecific. 1. Overview of relevant neck anatomy. 2. Epidemiology of tracheal trauma. 3. Etiology, mechanisms, and pathophysiology; a) Blunt, penetrating, and iatrogenic tracheal trauma; b) Different anatomical sites of injury. 4. Clinical presentation predictive of impending deterioration. 5. Approach to diagnosis in cases of suspected tracheal trauma; a) Role of X-ray; CT, fluoroscopy, and bronchoscopy; b) Pearls and pitfalls of diagnosis. 6. Key imaging findings to guide non-operative vs surgical management. 7. Short- and long-term complications of tracheal injuries; a) Identifying concomitant injuries, such as esophageal trauma.

Printed on: 02/07/23



## Abstract Archives of the RSNA, 2022

EREE-31

### Revisiting the Renal Trauma: An Illustrated Journey

Sunday, Nov. 27 8:00AM - 9:00AM Room: Learning Center - ER

#### Participants

Ali Baykan, MD, Adiyaman, Turkey (*Presenter*) Nothing to Disclose

#### TEACHING POINTS

1. To describe the mechanisms of the renal trauma 2. To discuss imaging features of renal trauma and CT technique 3. To discuss the grading systems (The American Association for the Surgery of Trauma) related to renal trauma 4. To highlight the importance of kidney injuries in patients with abdominal trauma

#### TABLE OF CONTENTS/OUTLINE

Introduction Incidence, mechanism of kidney injury, clinical features, and indications for imaging in renal trauma Description of current American Association for the Surgery of Trauma kidney injury grades Management of kidney injury Conclusion

Printed on: 02/07/23



## Abstract Archives of the RSNA, 2022

EREE-32

### The Liver Trauma: Imaging and Multidisciplinary Approach

Sunday, Nov. 27 8:00AM - 9:00AM Room: Learning Center - ER

#### Participants

Ali Baykan, MD, Adiyaman, Turkey (*Presenter*) Nothing to Disclose

#### TEACHING POINTS

1. To describe the mechanisms of the liver trauma 2. To discuss imaging features of liver trauma and CT technique 3. To discuss the grading systems (The American Association for the Surgery of Trauma) related to liver trauma 4. To highlight the importance of liver injuries in patients with abdominal trauma

#### TABLE OF CONTENTS/OUTLINE

Introduction Incidence, mechanism of liver injury, clinical features, and indications for imaging in liver trauma Description of American Association for the Surgery of Trauma's updated liver injury scoring scale Multidisciplinary management of liver injury Conclusion

Printed on: 02/07/23



## Abstract Archives of the RSNA, 2022

EREE-33

### Pancreatic Trauma: Imaging and Illustrations of a Fragile Organ

Sunday, Nov. 27 8:00AM - 9:00AM Room: Learning Center - ER

#### Awards

Certificate of Merit

#### Participants

Ali Baykan, MD, Adiyaman, Turkey (*Presenter*) Nothing to Disclose

#### TEACHING POINTS

1. To describe the mechanisms of the pancreatic trauma 2. To discuss imaging features of pancreatic trauma and imaging (CT, MRCP, etc.) techniques 3. To discuss the grading systems (The American Association for the Surgery of Trauma) related to pancreatic trauma 4. To highlight the importance of pancreatic injuries in patients with abdominal trauma

#### TABLE OF CONTENTS/OUTLINE

Introduction Incidence, mechanism of pancreatic injury, clinical features, and indications for imaging in pancreatic trauma  
Description of American Association for the Surgery of Trauma's updated pancreatic injury scoring scale Multidisciplinary management of pancreatic injury Conclusion

Printed on: 02/07/23



## Abstract Archives of the RSNA, 2022

EREE-34

### Limitations of AI-based Hemorrhage Detection: Where AI Can't Help You (Yet)

Sunday, Nov. 27 8:00AM - 9:00AM Room: Learning Center - ER

#### Participants

Stefan Niehues, MD, Berlin, Germany (*Presenter*) Speaker, Bracco Group; Speaker, Guerbet SA; Speaker, Canon Medical Systems Corporation; Speaker, Teleflex Incorporated

#### TEACHING POINTS

Detection of intracranial hemorrhage is a reliable application of AI, but is susceptible to artifacts. False-positive findings are related to motion artifacts, beam hardening artifacts due to foreign material inside or outside the patient, calcifications i.e. after surgery or with patients with meningioma or metastasis. False-negative findings can occur in patients with subacute hemorrhage, very subtle subarachnoidal bleedings, intracranial contrast extravasation, and chronic subdural hematomas.

#### TABLE OF CONTENTS/OUTLINE

1) AI-based intracranial hemorrhage detection - basics and numbers 2) Correct findings 3) False positives 4) False negatives 5) Approaches for future developments

Printed on: 02/07/23



## Abstract Archives of the RSNA, 2022

EREE-35

### Delivering Clinical Impact in Emergency Departments: CXR xAI Pipeline for Comprehensive Clinical Risk Prediction

Sunday, Nov. 27 8:00AM - 9:00AM Room: Learning Center - ER

#### Participants

Michelle Chua, Brookline, MA (*Presenter*) Nothing to Disclose

#### TEACHING POINTS

Integration of clinical information and radiological findings is required for clinical risk prediction. Comprehensive risk prediction models may be developed using a fine-tuning approach, which is more efficient than a full training approach. Our CXR xAI model was pre-trained to detect 20 radiographic features and subsequently used, in combination with clinical information, to predict oxygen requirement in ED patients with COVID-19. Calibrated classifier confidence is displayed and comparable CXRs are extracted from the Model-Derived Atlas. Our CXR xAI model captures a broad scope of cardiorespiratory pathophysiological manifestations and cardiothoracic comorbidities and may also be used, for example, to predict unplanned return to ED in patients with acute heart failure and elderly patients with community acquired pneumonia. As CXRs are inexpensive and routinely obtained, fully automated risk prediction using radiographic features may improve the safety and quality of clinical care in EDs.

#### TABLE OF CONTENTS/OUTLINE

Full training and fine-tuning approaches for comprehensive clinical risk prediction. CXR xAI model architecture and case illustration for acute heart failure. COVID-19 xAI pipeline for prediction of oxygen requirement and model performance metrics.

Printed on: 02/07/23



## Abstract Archives of the RSNA, 2022

EREE-37

### The Acute Abdomen: What the Surgeon Wants to Know - A Case-Based Survival Guide for the On-Call Resident

Sunday, Nov. 27 8:00AM - 9:00AM Room: Learning Center - ER

#### Awards

Identified for RadioGraphics

#### Participants

John Kirby, MD, Rochester, MN (*Presenter*) Nothing to Disclose

#### TEACHING POINTS

Abdominal pain is a common presenting symptom in the Emergency Department. Many life-threatening conditions can present as an "acute abdomen," requiring surgical intervention. The radiologist may be the first person to suggest the need for surgical evaluation and can provide key information to the surgeon regarding potential complications and pertinent normal variants. Understanding the surgeon's perspective can lead to concise reports, faster turnaround time, and improved outcomes.

#### TABLE OF CONTENTS/OUTLINE

Review common imaging modalities in the non-traumatic acute setting and preferred protocols for evaluating acute abdominal pain. Discussion of the five major categories of abdominal pain requiring surgical intervention; Ischemia, obstruction, infection, perforation, and active bleeding. Case-based review demonstrating examples of the most common etiologies from each of the major categories. Each case will include a discussion of significant findings to make the diagnosis, pertinent anatomical variants, and a summary table of relevant reporting findings to the surgeon. Many of our cases will contain a QR code that the viewer can scan with their mobile device to access an interactive PACS to review the case and more accurately simulate real-life scenarios.

Conclusion: At the end of the exhibit, we hope that the reader will better understand findings relevant to the surgeon and can assist in identifying and reporting relevant potential complications.

Printed on: 02/07/23



## Abstract Archives of the RSNA, 2022

EREE-38

### Acute Mechanical SBO: A Step-by-step Guide for Radiology Residents!

Sunday, Nov. 27 8:00AM - 9:00AM Room: Learning Center - ER

#### Participants

Abdul-Rahman Abualruz, MD, (*Presenter*) Nothing to Disclose

#### TEACHING POINTS

Acute mechanical small bowel obstruction (SBO) is a common surgical emergency with high mortality rates when complicated by bowel ischemia (up to 40%). Computed Tomography (CT) has an essential role in confirming the SBO diagnosis, identifying the cause of obstruction, detecting associated variations, and evaluating severity. CT outperforms physical exam and laboratory testing with high specificity in predicting bowel ischemia which is crucial for correct and timely management of SBO.

#### TABLE OF CONTENTS/OUTLINE

Review clinical management guidelines of SBO. Critical imaging findings to look for and include in the radiology report that impacts clinical management presented via a suggested structured report for SBO. CT imaging evaluation of SBO (CT protocol, use of IV and PO contrast, added value of Dual Energy CT). Review CT imaging criteria for diagnosis of acute mechanical SBO. A pictorial review of causes of SBO (extrinsic vs. intrinsic etiologies) and pitfalls for correct interpretation with emphasis on: Adhesive vs. Non-adhesive SBO, Closed vs. Open loop obstruction, Partial vs. Complete obstruction, Specific CT findings that predict bowel ischemia. A step-by-step summary guide for SBO diagnosis.

Printed on: 02/07/23



## Abstract Archives of the RSNA, 2022

EREE-39

### The Value of Ultrasound in Bowel Pathology in the Emergency Room

Sunday, Nov. 27 8:00AM - 9:00AM Room: Learning Center - ER

#### Participants

Maria P. Moncayo Hinojosa, MD, Madrid, Spain (*Presenter*) Nothing to Disclose

#### TEACHING POINTS

1) Highlight the diagnostic performance of ultrasound in acute bowel pathology.2) Review of the anatomy and histology of the bowel and its correlation with the ultrasound image.3) Exhibition of the technique and of the diagnostic keys for its correct interpretation.4) Ultrasound review of intestinal pathology and its correlation with computed tomography.

#### TABLE OF CONTENTS/OUTLINE

1) Introduction, generalities and anatomy of the bowel.2) Anatomical correlation between ultrasound and the histology of the bowel.3) General considerations and ultrasound exploration technique.4) How to recognize pathological intestinal loops?5) Radiological cases and surprise diagnoses in the ultrasound emergency room of our health center.5)Conclusions.

Printed on: 02/07/23



## Abstract Archives of the RSNA, 2022

EREE-4

### Revised American Association for the Surgery of Trauma (AAST) Scales

Sunday, Nov. 27 8:00AM - 9:00AM Room: Learning Center - ER

#### Awards

Identified for RadioGraphics

Cum Laude

#### Participants

Irene Dixe de Oliveira Santo, MD, New Haven, CT (*Presenter*) Nothing to Disclose

#### TEACHING POINTS

- Review the usefulness of the American Association for the Surgery of Trauma Organ Injury Severity (AAST OIS) scale
- Describe the main changes to the revised 2018 AAST OIS compared to the 1994 and 1989 AAST scales
- Discuss imaging specifications and protocoling considerations in suspected organ injury due to blunt abdominal trauma
- Provide an overview of the recommended management of solid injury organ trauma and how it is affected by grading

#### TABLE OF CONTENTS/OUTLINE

History, usefulness, and implications of grading in trauma  
Validation of the liver, spleen, and kidneys scales and impact on mortality, operative rate, and hospitalization cost  
Standard CT protocol and technique, the benefit of dual-phase imaging, and indications of the excretory phase  
The role of alternative imaging  
Revised AAST grading with multiple examples from our institution  
Current management guidelines

Printed on: 02/07/23



## Abstract Archives of the RSNA, 2022

EREE-40HC

### Obstructive Hydrocephalus - Not So Simple After All

Sunday, Nov. 27 8:00AM - 9:00AM Room: Learning Center - ER

#### Participants

Michal Holesta, (*Presenter*) Nothing to Disclose

#### TEACHING POINTS

Obstructive hydrocephalus is a severe condition, that can manifest with acute symptoms or slowly developing signs of increased intracranial pressure. This usually depends on the type of underlying condition and the speed with which the hydrocephalus develops. We will overview common and rare causes of obstructive hydrocephalus, diagnostic algorithms and imaging findings on CT and MRI, including signs of transependymal edema, using cases from our clinical practice. We will also present several cases of rare causes of acute hydrocephalus, including colloid cyst, blood clot in aqueductus Sylvii (mimicking flow void on T2W) and neurosarcoidosis.

#### TABLE OF CONTENTS/OUTLINE

1. Overview, etiology and pathophysiology of obstructive hydrocephalus. Typical clinical symptoms. 2. Diagnostic algorithms and imaging findings on CT and MRI. Imaging signs of transependymal edema. 3. Case series of rare causes of acute hydrocephalus. 4. Treatment and follow-up of obstructive hydrocephalus. 5. Conclusion and key imaging points. Please visit the Learning Center to also view this presentation in hardcopy format.

Printed on: 02/07/23



## Abstract Archives of the RSNA, 2022

EREE-41

### Pearls and Pitfalls in postmortem imaging: Dead Men Do Tell Tales

Sunday, Nov. 27 8:00AM - 9:00AM Room: Learning Center - ER

#### Awards

Certificate of Merit

#### Participants

Yohei Ikebe, MD, PhD, Sapporo, Japan (*Presenter*) Nothing to Disclose

#### TEACHING POINTS

1. To summarize the typical and atypical postmortem changes 2. To review the diagnostic findings of postmortem imaging

#### TABLE OF CONTENTS/OUTLINE

1. introduction 1-A. role of postmortem imaging 1-B. methods of postmortem CT and MRI scan 2. early postmortem changes 2-A. hypostasis 2-B. vessel wall and vessel cavity 2-C. air way and pleural fluid retention 2-D. brain 2-E. others 3. late postmortem changes 3-A. putrefaction 3-B. autolysis 3-C. gastromalacia, oesophagomalacia 4. pitfalls 4-A. changes of cardiopulmonary resuscitation 4-B. course of postmortem changes 5. diagnostic findings 5-A. Acute hemorrhage (aortic dissection, aortic aneurysm rupture, etc.) 5-B. trauma 5-C. hanging 5-D. hypothermia 5-E. burn death 5-F. drowning

Printed on: 02/07/23



## Abstract Archives of the RSNA, 2022

EREE-42

### Making the Grade: A Pictorial Review of the Revised 2018 AAST Abdominal Solid Organ Injury Scales

Sunday, Nov. 27 8:00AM - 9:00AM Room: Learning Center - ER

#### Participants

Samuel Elias, MD, West Caldwell, NJ (*Presenter*) Nothing to Disclose

#### TEACHING POINTS

The goal of this exhibit is to provide a pictorial review of the revised 2018 AAST injury scoring scale for the liver, kidney, and spleen. Every injury grade for each organ is presented with an original diagram alongside the imaging criteria. Teaching points are presented in a clear manner and include descriptions of key radiologic terms, recognition of benign and pathologic mimics, protocoling technique, and clinical management considerations. Angiographic and intraoperative images from our interventional radiology and trauma surgeon colleagues are also included to help cultivate an appreciation of the multidisciplinary management of these injuries.

#### TABLE OF CONTENTS/OUTLINE

1) Introduction. 2) Spleen -Grades 1-5 (diagrams, definitions, teaching points, imaging pearls) -Cases (CT, angiographic, and/or intraoperative images with description of findings, management, and teaching points). 3) Liver -Grades 1-5 (diagrams, definitions, teaching points, imaging pearls) -Cases (CT, angiographic, and/or intraoperative images with description of findings, management, and teaching points). 4) Kidney -Grades 1-5 (diagrams, definitions, teaching points, imaging pearls) -Cases (CT, angiographic, and/or intraoperative images with description of findings, management, and teaching points). 5) Conclusion

Printed on: 02/07/23



## Abstract Archives of the RSNA, 2022

EREE-43

### Liver or Die Situation--Spleen better days: Reviewing the 2018 Updates of the AAST Liver and Spleen Injury Scoring Scales

Sunday, Nov. 27 8:00AM - 9:00AM Room: Learning Center - ER

#### Participants

Elias Gunnell, MD, Chapel Hill, NC (*Presenter*) Nothing to Disclose

#### TEACHING POINTS

1. Trauma is the most frequent cause of death in the first four decades of life, and the abdomen is the third most common site of injury. 2. The radiologist plays a crucial role in the evaluation and description of splenic and liver injury in abdominal trauma. 3. Accurate description of splenic and liver injury is a pivotal component of patient management and treatment selection. 4. Understanding the revised AAST Liver and Spleen Injury Scales is necessary for accurate description of abdominal trauma as operative rate and increased mortality are associated with increasing grades of injury.

#### TABLE OF CONTENTS/OUTLINE

This educational exhibit will discuss the updated 2018 American Association for the Surgery of Trauma (AAST) guidelines for injury scoring, pertaining to the liver and spleen. The presentation will include the following: - Briefly overview the statistics for abdominal trauma and incidence of liver and spleen injury. - Discuss the updated AAST Injury Scoring Scale and compare it to the previous version. - Review and illustrate the multiple grades of liver injury, with important imaging findings. - Review and illustrate the multiple grades of splenic injury, with important imaging findings. - Explain how patient management changes based on the grade of injury.

Printed on: 02/07/23



## Abstract Archives of the RSNA, 2022

EREE-44

### Imaging in Non-accidental Trauma - A Primer for Trainees

Sunday, Nov. 27 8:00AM - 9:00AM Room: Learning Center - ER

#### Participants

Surabhi Subramanian, MBBS,MD, (*Presenter*) Nothing to Disclose

#### TEACHING POINTS

- 1. Illustrate the mechanism and mode of presentation
- 2. Outline the diagnostic imaging protocol
- 3. Discuss the typical presentation and mimicker

#### TABLE OF CONTENTS/OUTLINE

Nonaccidental trauma is one of the prominent causes of childhood injury and death in the pediatric population. This exhibit will serve as a primer for radiology trainees to diagnose NAT in an emergency setting. The most common mechanism of NAT is violent shaking. Some highly specific lesions of child abuse are metaphyseal fractures, multiple rib fractures of different ages, scapular fractures, sternal fractures, and posterior vertebral element fractures. More than 60 % of child abuse cases present in emergency settings. Radiologists can be the first to suggest the possibility of child abuse. Infant's head is larger in comparison to the body making them more prone to CNS injury. CT head, 3D reconstruction is especially helpful in detecting skull fractures. MRI is very sensitive to look for blood products in the brain and spine. The skeletal survey must be ordered for patients suspected with child abuse. Nuclear imaging is performed if skeletal survey is equivocal. Radiologists must be aware of highly suspicious radiological findings and mimickers of nonaccidental trauma.

Printed on: 02/07/23



## Abstract Archives of the RSNA, 2022

EREE-45

### Vascular Injury Following Trauma: A Pictorial Review of Findings on CT Angiography

Sunday, Nov. 27 8:00AM - 9:00AM Room: Learning Center - ER

#### Participants

Navpreet Khurana, MBBS, (*Presenter*) Nothing to Disclose

#### TEACHING POINTS

1. Describe the range of findings of vascular injury following blunt and penetrating trauma on CT angiogram. 2. Correlate findings on physical examination, CT angiogram, and catheter angiogram. 3. Appreciate the pitfalls of CT angiography, which lead to false positives and false negatives. 4. Describe the interventions for vascular injury.

#### TABLE OF CONTENTS/OUTLINE

1. CT angiogram protocol - how to optimize the detection of traumatic vascular injury. 2. Range of appearance of active bleeding on CT angiogram. 3. The value of the non-contrast acquisition. 4. Arterial spasm vs. arterial transection - similarities and differences in appearance. 5. Correlation of findings on CT angiogram with catheter angiogram. 6. Surgical interventions for vascular injury.

Printed on: 02/07/23



## Abstract Archives of the RSNA, 2022

EREE-46

### Trauma Drama: Breaking Down the 2018 AAST Scoring for Spleen and Liver

Sunday, Nov. 27 8:00AM - 9:00AM Room: Learning Center - ER

#### Participants

Katherine Copely, MD, (*Presenter*) Nothing to Disclose

#### TEACHING POINTS

Review the updated 2018 AAST guidelines for Spleen and Liver Injuries? Discuss the importance of imaging protocols? Recognize key features on CT images and correlating diagrams to improve recall and recognition? Examine challenging cases and pertinent pitfalls

#### TABLE OF CONTENTS/OUTLINE

The purpose of this presentation is to discuss the rationale for updating the AAST grading systems and what updates occurred between 1994 and 2018 focusing on the spleen and liver, the implications for patient care, as well as to discuss importance of imaging protocols in detecting these injuries. An illustrated table of spleen and liver injuries will be included to highlight the similarities and differences in grading criteria for each organ. Image intensive examples of each grade of liver and spleen injuries will comprise the bulk of the presentation. Challenging cases and pitfalls will help cement and allow practice of these key imaging findings.

Printed on: 02/07/23



## Abstract Archives of the RSNA, 2022

EREE-47

### Splenic Trauma: When the Neglected One Hurts

Sunday, Nov. 27 8:00AM - 9:00AM Room: Learning Center - ER

#### Participants

Ali Baykan, MD, Adiyaman, Turkey (*Presenter*) Nothing to Disclose

#### TEACHING POINTS

1. To describe the mechanisms of the splenic trauma 2. To discuss imaging features of splenic trauma and CT technique 3. To discuss the grading systems (The American Association for the Surgery of Trauma) related to splenic trauma 4. To highlight the importance of splenic injuries in patients with abdominal trauma

#### TABLE OF CONTENTS/OUTLINE

Introduction Incidence, mechanism of splenic injury, clinical features, and indications for imaging in splenic trauma Description of American Association for the Surgery of Trauma's updated splenic injury scoring scale Multidisciplinary management of splenic injury Conclusion

Printed on: 02/07/23



## Abstract Archives of the RSNA, 2022

EREE-5

### Nontraumatic Temporal Bone Emergencies: A Non-traumatizing Guide for Radiologists

Sunday, Nov. 27 8:00AM - 9:00AM Room: Learning Center - ER

#### Awards

Identified for RadioGraphics

#### Participants

Rodrigo Carneiro, MD, Sao Paulo, Brazil (*Presenter*) Nothing to Disclose

#### TEACHING POINTS

- To identify important anatomic landmarks in the temporal bone.- To review the imaging technique and protocols for the evaluation of temporal bone emergencies.- To recognize the clinical presentations and imaging features of nontraumatic temporal bone emergencies

#### TABLE OF CONTENTS/OUTLINE

- Introduction- Temporal Bone Anatomy- Imaging Technique and Protocols - Clinical Presentations and Imaging Findings of Nontraumatic Temporal Bone Emergencies with Multiple Teaching Cases (External, Middle, and Inner Ear)- Conclusions- References

Printed on: 02/07/23



## Abstract Archives of the RSNA, 2022

EREE-6

### Acute Temporal Bone Pathology

Sunday, Nov. 27 8:00AM - 9:00AM Room: Learning Center - ER

#### Participants

Ashraf Abdulhalim, MD, (*Presenter*) Nothing to Disclose

#### TEACHING POINTS

1. A simplified anatomic checklist-based approach can enable an emergency radiologist to accurately and efficiently identify acute temporal bone pathology, and this approach will be reviewed in this exhibit. 2. The radiologist plays an important role by identifying key imaging findings and providing diagnoses that can direct treatment by prompting an emergency physician to admit a patient for inpatient management, order a surgical consult, or order further imaging to check for related complications. The absence of these findings are also pertinent negatives that enable clinicians to proceed with treatment in the ED or discharge a patient with outpatient follow-up. 3. This exhibit will review traumatic and acute non-traumatic pathology in a case-based format, with emphasis on key imaging findings that affect management and prognosis.

#### TABLE OF CONTENTS/OUTLINE

I. Relevant anatomic structures and landmarks in the temporal bone for the emergency radiologist  
II. Checklist for non-traumatic and traumatic pathology  
III. Non-traumatic Pathology  
a. Infection  
i. Acute otitis externa  
ii. Malignant otitis externa  
iii. Coalescent mastoiditis with Bezold abscess  
iv. Temporomandibular joint abscess  
b. Aggressive neoplasm that might present with acute symptoms  
i. Langerhans cell histiocytosis  
ii. Paraganglioma  
IV. Traumatic Pathology  
a. Otic capsule violating versus non-otic capsule violating fractures  
b. Horizontal versus longitudinal fractures  
c. Isolated tympanic plate fracture  
d. Sutures/fissures that mimic fractures

Printed on: 02/07/23



## Abstract Archives of the RSNA, 2022

EREE-7

### Cardiac Findings Detectable on Non-Gated CT: What the Emergency Radiologist Needs to Know

Sunday, Nov. 27 8:00AM - 9:00AM Room: Learning Center - ER

#### Awards

Cum Laude

#### Participants

Dana Galvan, MD, Albuquerque, NM (*Presenter*) Nothing to Disclose

#### TEACHING POINTS

1. After completing this educational exhibit, the learner will have an improved understanding of cardiac findings that can be identified on non-gated CT examinations, performed in the emergency setting. 2. Be able to differentiate pathologic abnormalities based on key cardiac anatomic landmarks including the pericardium, myocardium, cardiac chambers, appendages, and coronary arteries. 3. Recognize key device and procedural complications on non-gated CT emergency situations.

#### TABLE OF CONTENTS/OUTLINE

-Introduction to the use of non-gated chest CT as an imaging modality in the emergency setting -Anatomy review of normal cardiac anatomy as seen on non-gated CT with labeling of structures and normal size measurements -Pericardium radiologic abnormalities including differential diagnosis, clinical significance, and follow-up recommendations with case examples and imaging: Anemia, Congenital Absence, Effusions, Abnormal and Normal Enhancement, Defects, and Calcification -Myocardium radiologic abnormalities including differential diagnosis, clinical significance, and follow-up recommendations with case examples and imaging: Myocardial infarction, Abnormal and Normal Fat Deposition, Cardiomyopathies -Cardiac Masses radiologic abnormalities including differential diagnosis, clinical significance, and follow-up recommendations with case examples and imaging: Cardiac pseudo-masses, Cardiac Thrombus, Cardiac Neoplasms -Other Cardiac Anomalies Detected on Non-Gated CT including differential diagnosis, clinical significance, and follow-up recommendations with case examples and imaging: Engorged Coronary Arteries, Post-Procedural Complication, and Device Failures

Printed on: 02/07/23



## Abstract Archives of the RSNA, 2022

EREE-8

### Imaging Features of Torsion of Various Organs in the Whole Body

Sunday, Nov. 27 8:00AM - 9:00AM Room: Learning Center - ER

#### Awards

Identified for RadioGraphics

#### Participants

Akihiro Nakamata, (*Presenter*) Nothing to Disclose

#### TEACHING POINTS

Torsion can present in various organs in the whole body, which cause a decreased blood flow due to twisted blood vessels. Therefore, emergent surgical intervention is often necessary to improve the blood flow. Radiologists should recognize imaging features of torsion of various organs in the whole body for the management of treatment options. The purpose of this exhibit is: 1. To review a torsion of various organs in the whole body. 2. To discuss the clinical and imaging features of the torsion. 3. To classify various torsions into subtypes based on imaging findings reflecting the background pathology.

#### TABLE OF CONTENTS/OUTLINE

1. Subtypes based on imaging findings reflecting the background pathology. 2. Torsion of various organs in this presentation. Chest; Lung lobe, Extralobar sequestration, Solitary fibrous tumor of the pleura, Pericardial appendage, Pericardial fat pad. Abdomen; Accessory liver lobe, Spleen, Accessory spleen, Stomach, Small intestine, Cecum Transverse colon, Sigmoid colon, Gastrointestinal Stromal Tumor (GIST), Meckel's diverticulum, Epiploic appendage, Omentum. Pelvis; Ovary, Ovarian tumor, Paraovarian cyst, Fallopian tube, Uterus, Uterine leiomyoma, Parasitic leiomyoma, Testis, Testicular appendage.

Printed on: 02/07/23



## Abstract Archives of the RSNA, 2022

FREE-9

### Pictorial Review of Acute Appendicitis and Beyond

Sunday, Nov. 27 8:00AM - 9:00AM Room: Learning Center - ER

#### Participants

Claudia Gabriela Moldovanu, MD, (*Presenter*) Nothing to Disclose

#### TEACHING POINTS

At the end of this educational exhibit, the audience will be able to differentiate the alternative diagnoses for the purpose of directing appropriate patient management.

#### TABLE OF CONTENTS/OUTLINE

Acute appendicitis is the most common diagnosis suspected in patients presenting in emergency rooms with acute abdominal pain. Early diagnosis depends on recognition of characteristic signs and symptoms: right lower quadrant or periumbilical pain, localized tenderness, fever, and leukocytosis. The differential diagnosis for an abnormal appendix on imaging includes other inflammatory/non-neoplastic and neoplastic processes. In this pictorial essay, we review the normal anatomy of the appendix and outline the pathogenesis, clinical manifestations, and imaging findings that are characteristic of acute appendicitis and its complications, common or less common abnormalities (areas of focus include abdominopelvic abscess, peritonitis, pyelephlebitis, pyelethrombosis, and hepatic abscess). Inflammatory/nonneoplastic processes including serosal appendicitis, stump appendicitis, and foreign body appendicitis are discussed. Neoplastic considerations include appendiceal neuroendocrine tumors, mucinous and non-mucinous epithelial neoplasms, and lymphoma. A brief discussion of important pearls in the imaging assessment and diagnosis for each pathological presentation is then provided. It is important for the radiologist to be familiar with common imaging features and to be familiar with the various anatomical locations and other less common appendiceal abnormalities that can mimic or present concomitantly with acute appendicitis for accurate diagnosis and appropriate management.

Printed on: 02/07/23

## Abstract Archives of the RSNA, 2022

GIEE

### Gastrointestinal Education Exhibits

Sunday, Nov. 27 8:00AM - 9:00AM Room: Learning Center - GI

#### Sub-Events

#### **GIEE-1 Split Scar Sign (SSS): How to Interpret It In The Context of Response to Neoadjuvant Treatment in Rectal Cancer**

##### Participants

Ana Uski, MD, Sao Paulo, Brazil (*Presenter*) Nothing to Disclose

##### TEACHING POINTS

Describe the typical MRI imaging findings in cases of SSS+ and SSS-. Demonstrate the applicability of MRI in the context of neoadjuvant radiotherapy in rectal cancer and its potential limitations. Propose a structured report for local re-staging purposes.

##### TABLE OF CONTENTS/OUTLINE

Radical mesorectal excision surgery contributes substantially to patient morbidity in the context of rectal cancer. A number of clinical trials support the use of neoadjuvant radiation as a form of initial approach in an attempt at more conservative treatment, and responders to this modality have a favorable prognosis and similar outcomes to those who underwent radical surgery. In this context, MRI is the imaging modality of choice in response assessment to predict fibrosis or suspicious areas of viable neoplastic tissue. The split scar sign (SSS) is assessed on high-resolution T2-WI, positive or present when a thin regular 1-2 mm layer of hypointense "fibrosis" is well defined on the endoluminal aspect of the tumor site (corresponding to fibrous submucosa). Whenever the tumor site is not "organized" and this T2WI hypointensity layer is broken focally, the signal should be considered absent or negative. The positive or present SSS (+) has a very high specificity (97%) and positive predictive value (93/94%) for sustained complete response in case of neoadjuvant radiotherapy in rectal cancer. A good quality examination with the appropriate technique is necessary as well as the recognition of the imaging findings related to the presence or absence of this sign (SSS) and potential limitations of MRI.

#### **GIEE-10 Management of Incidentally Detected Gallbladder Polyps: Review of Clinical Scenarios Using the 2021 SRU Gallbladder Polyp Consensus Guideline**

##### Participants

Christopher Fung, MD, Edmonton, AB (*Presenter*) Stockholder, Mikata Health

##### TEACHING POINTS

Incidental gallbladder (GB) polyps are common, seen in 3-6% of the general population, often benign cholesterol polyps. Few GB polyps (6%) are neoplastic (intracholecystic papillary neoplasm, ICPN). While ICPNs have malignant potential, malignant transformation is believed rare. GB cancers also typically arise from flat dysplastic epithelium, not polyps. Yet the concern a small polyp may harbor a future or early neoplasm has led past guidelines to suggest relatively aggressive management; recent studies show significant overtreatment of predominantly benign GB lesions. In 2021 the Society of Radiologists in Ultrasound (SRU) convened a multidisciplinary committee to review current literature and construct updated guidelines for the management of incidentally detected GB polyps. The SRU Guidelines, to be published in 2022 (Radiology), stratify risk into three categories: Extremely Low, Low, and Indeterminate Risk. Clinical examples and common questions will be addressed.

##### TABLE OF CONTENTS/OUTLINE

1. Background and review of prior guidelines a. Overview of gallbladder polyps and underlying pathology b. Discussion of current literature and recommendations 2. 2021 SRU Gallbladder Polyp Consensus Recommendations a. Applicable and excluded patient populations b. Risk Categories: Extremely Low Risk, Low Risk, Indeterminate Risk 3. Common and uncommon clinical scenarios a. Polyp measurement b. Sessile versus pedunculated c. Determination of growth d. Doppler assessment e. Multiple versus single gallbladder polyps f. The role of alternative modalities such as contrast-enhanced ultrasound and MRI g. Other risk factors: primary sclerosing cholangitis, age, ethnicity, geographic location

#### **GIEE-100 Gastrointestinal Neuroendocrine Neoplasms on Multimodality Imaging With Emphasis on Dynamic CT: Case Review with Radiology Pathology Correlation**

##### Awards

##### Certificate of Merit

##### Participants

Nobuyuki Takeyama, MD, (*Presenter*) Nothing to Disclose

##### TEACHING POINTS

To describe the comprehensive categorization system between well-differentiated neuroendocrine tumors (NETs), poorly differentiated neuroendocrine carcinomas (NECs), and mixed neuroendocrine-non-neuroendocrine neoplasms (MiNENs) on the basis

of the WHO 2019 classification for gastrointestinal neuroendocrine neoplasms (GI-NENs). To review multimodality imaging of endoscopy, enteroscopy, endoscopic ultrasound, and cross-sectional images (CT, MRI, SPECT, and PET) in this case-based review presentation correlated with pathology.

#### TABLE OF CONTENTS/OUTLINE

1.Introduction including definition, epidemiology, genetic evidence, clinical features, and TNM staging in GI-NENs.2.Pathology of the WHO 2019 classification for grading and differentiation of GI-NENs to discuss differentiation, mitosis index, Ki-67 index and immunostaining. 3.Case-based review presentations with multimodality imaging for esophageal NEC, gastric NET, NEC and MiNEN, ampullary NET, duodenal NET, duodenal gastrinomas with MEN 1, small bowel NET, metastases of

#### GIEE-101 Anal Cancer Imaging: What We Know and What is On The Horizon

##### Awards

##### Certificate of Merit

##### Participants

Jessica Gomes, MD, Sao Paulo, Brazil (*Presenter*) Nothing to Disclose

##### TEACHING POINTS

Know the epidemiology, increasing number of cases, and risk factors of anal squamous cell carcinoma (SCC)Recognize the imaging differences between rectal adenocarcinoma and anal SCCBe familiar with future directions in anal SCC staging

#### TABLE OF CONTENTS/OUTLINE

INTRODUCTIONEpidemiologyRisk factorsRECTAL ADENOCARCINOMA X ANAL SQUAMOUS CELL CARCINOMA ANAL SCC  
TREATMENTChemoradiation therapy (CRT) and how to prevent sequelaeSurgeryTumor recurrence/persistenceAnal margin tumor approachROLE OF IMAGINGStaging scenarioRestaging scenarioTHE MOST RECENT CONSENSUSHow to stagingHow to restaging post CRTWHAT'S ON THE HORIZONINTERACTIVE CHALLENGING SCENARIOS

#### GIEE-102 Hepatobiliary and Pancreatic Tumor Board Primer for Radiologists: Review of AJCC Staging and NCCN Guidelines

##### Participants

Madiha Aslam, MD, Darby, PA (*Presenter*) Nothing to Disclose

##### TEACHING POINTS

Review of AJCC for radiological staging of hepatobiliary and pancreatic tumors. Review of NCCN guidelines for stage-based treatment planning of hepatobiliary and pancreatic tumors. Review of NCCN guidelines for follow up of post treatment hepato-bilio pancreatic tumors. Radiological implication of AJCC and NCCN guidelines in tumor boards for determining the further diagnostic steps and making decisions about the appropriate treatment. Pitfalls in imaging.

#### TABLE OF CONTENTS/OUTLINE

Tumor staging and stage-based treatment planning is a crucial step in appropriate cancer treatment and being a part of multidisciplinary team in tumor boards, radiologists play a critical role in diagnosing, characterizing, initial staging, determining resectability, and surveillance of cancer patients. This helps the rest of the team to choose the appropriate treatment therapies and determine the follow up interval for post treatment cases. We will provide a comprehensive review of the AJCC staging and NCCN guidelines for hepato bilio pancreatic tumors using multiple imaging modalities, which will help the radiologists in day-to-day tumor boards to solve the staging and decision dilemmas.

#### GIEE-103 Imaging Assessment of Small Gastrointestinal Lesions. How Can we Improve the Detection or Suspect of Early Tumors?

##### Participants

Tomas Lacerda, MD, Sao Paulo, Brazil (*Presenter*) Nothing to Disclose

##### TEACHING POINTS

TEACHING POINTS:Initial malignant lesions may be an incidental finding.We must pay special attention to small findings in patients with a background that favors malignancy, such as neoplastic syndromes and a known primary tumor.Understand how we can and should improve our imaging protocol according to each patients background.Review when we should consider complementation with different methods and how to choose the best protocol.Understand which characteristics of small lesions may favour malignancy.Protocol pearls for certain tumor types.

#### TABLE OF CONTENTS/OUTLINE

Epidemiological considerations that may change our interpretation and pretest probability of a disease when characterizing a small lesion.Imaging examples of small lesions that were confirmed as malignant on follow up, biopsy or surgery: Neuroendocrine tumors; Initial metastasis; Small cholangiocarcinoma; Early CHCImaging protocol and imaging methods discussion regarding small lesions: When to include additional phases in our protocol; When to consider MRI evaluation; Hepatocyte-specific contrast indications; PET scan evaluation considerations.

#### GIEE-104 Do Not Forget the Pipes: Inferior Vena Cava: Abnormal Finding and Their Imaging Appearance

##### Participants

Teresa Garcia, MD, Buenos Aires, Argentina (*Presenter*) Nothing to Disclose

##### TEACHING POINTS

To review the usual anatomy and the most common congenital variants of the inferior vena cava (IVC).To describe the most used IVC imaging techniques, its relevance and usefulness.To highlight the pathologies that may affect the IVC and the associated radiological findings.To describe the most frequent IVC pitfalls.

## TABLE OF CONTENTS/OUTLINE

Brief review of the anatomy and embryology of the inferior vena cava Imaging techniques and its relevance. Most common IVC congenital variants. Pathologies that can involve IVC ( primary and secondary involvement) Pitfalls at IVC imaging and miscellaneous imaging.

### GIEE-105 Acute Mesenteric Ischemia: A Primer

Participants  
Ken Nakanote, MD, Salt Lake City, UT (*Presenter*) Nothing to Disclose

#### TEACHING POINTS

Understand the different etiologies of acute mesenteric ischemia Recall the CT protocol used in the evaluation of acute mesenteric ischemia Evaluate for the radiological features associated with each etiology of acute mesenteric ischemia

## TABLE OF CONTENTS/OUTLINE

A. Background B. Etiology and pathophysiology C. Clinical presentation D. Evaluation Imaging- ACR appropriateness guidelines- CT protocol- Imaging findings for different etiologies 2. Non-imaging E. Treatment and management F. Summary

### GIEE-106 Demystifying the Mesentery: A Differential-Based Approach to Mesenteric Pathology

Participants  
Daniel Schneider, MD, Ann Arbor, MI (*Presenter*) Nothing to Disclose

#### TEACHING POINTS

- Review anatomy of the mesentery with illustrations - Review common and rare, focal and diffuse mesenteric pathologies with imaging examples - Present an imaging-based approach to various mesenteric pathology

## TABLE OF CONTENTS/OUTLINE

1. Mesenteric anatomy 2. Differential diagnoses for mesenteric infiltration a. Edema i. Hepatic failure, hypoproteinemia ii. Venous thrombosis iii. Angioedema (angiotensin converting enzyme inhibitor-associated angioedema) b. Hemorrhage i. Trauma c. Inflammation i. Pancreatitis ii. Crohn's disease iii. Post-operative iv. Sclerosing encapsulating peritonitis v. COVID-19 d. Neoplasm i. Peritoneal carcinomatosis ii. Lymphoma iii. Carcinoid iv. Mesothelioma v. Primary peritoneal serous neoplasm vi. Pseudomyxoma peritonei vii. Desmoid viii. Lymphangioma e. Sclerosing mesenteritis i. Mesenteric panniculitis ii. Retractable mesenteritis f. Idiopathic 3. Conclusion a. Mesenteric infiltration is often nonspecific and can pose diagnostic challenges to the radiologist. Knowledge of key imaging features associated with various mesenteric pathologies can help narrow the differential diagnosis in appropriate clinical setting.

### GIEE-107 Seeing Through the Mist: An Interactive Tour of Mesenteric Pathology

#### Awards

**Certificate of Merit**

**Identified for RadioGraphics**

Participants  
Amelia Kernizan, MD, (*Presenter*) Nothing to Disclose

#### TEACHING POINTS

Mesenteric lesions are frequently encountered incidentally on abdominal imaging. As many of the underlying etiologies appear similar on CT and/or MRI, they often pose a diagnostic dilemma. The broad differential diagnosis for these lesions ranges from benign etiologies including infection, inflammation, and benign neoplasia to malignant etiologies such as carcinoid, lymphoma and metastatic disease. Via a multiple-choice case-based approach, this presentation will provide a framework for approaching solid mesenteric lesions, while providing pathologic correlation to highlight their similarities and differences, as well as how the histology influences their imaging appearance.

## TABLE OF CONTENTS/OUTLINE

I. Review of normal peritoneal anatomy and histology. II. Quiz-style case-based review of solid mesenteric masses. IIa. Discussion of sclerosing mesenteritis with cases of mesenteric panniculitis and retractile mesenteritis showing radiologic-pathologic correlation. IIb. Case of multiple mesenteric masses highlighting the differential and pertinent imaging findings. IIc. Case of mesenteric mass with associated small bowel masses. IId. Case of a 68Ga-DOTATATE-avid mass with potential pitfalls to avoid with this imaging modality. III. Summary with our method for approaching and differentiating between commonly encountered incidental mesenteric lesions.

### GIEE-108 All Around the Liver: The Perihepatic Space and Why It Matters

Participants  
Helena de Souza, MD, Sao Paulo, Brazil (*Presenter*) Nothing to Disclose

#### TEACHING POINTS

- The perihepatic space is often involved in a spectrum of diseases, including intrahepatic lesions that extend into the capsule and conditions arising from adjacent or pelvic organs. It is covered by the peritoneum, and it includes the right subphrenic space, the subhepatic space, the lesser sac, and the left perihepatic space.- The distribution and dynamics of the peritoneal fluid influence the spread of inflammatory and tumor processes to the perihepatic space. The correct evaluation of this space is part of abdominal radiology workup and the knowledge of the main abnormalities is crucial for the best report.- The objectives of this exhibit are to highlight different etiologies of perihepatic involvement, from inflammatory/infectious diseases (stone-related abscesses, Fitz-Hugh-Curtis Syndrome, peritoneal tuberculosis, echinococcosis), endometriotic and metastatic lesions, to rare primary peritoneal tumors (peritoneal malignant mesothelioma, desmoplastic small round cell tumor, peritoneal serous papillary carcinoma, periportal plexiform neurofibroma, and hepatic hilum lymphoma), with illustrative cases (CT and MRI).

## TABLE OF CONTENTS/OUTLINE

Background of the perihepatic space. Evaluation of the anatomy and physiology of the perihepatic space and its peritoneal fluid dynamic. Case-based review of a range of cases including the main and rarer abnormalities of the perihepatic space with respective MRI and CT findings. Radiological correlation with the peritoneal fluid flow distribution.

### GIEE-109 GIST: What The Radiologist Should Know

Participants  
Cristina Cano Pardo, MD, Pontevedra, Spain (*Presenter*) Nothing to Disclose

#### TEACHING POINTS

To identify typical and atypical radiological findings of gastrointestinal stromal tumors (GIST). To know the radiological criteria used in GIST for the evaluation of tumor response. To review what factors have been proposed as relevant when predicting prognosis and response to treatment.

## TABLE OF CONTENTS/OUTLINE

Relevant information towards the diagnosis of GIST will be clearly exposed using examples of different cases seen in our center. We will review the main radiological characteristics of GIST in order to suggest a correct differential diagnosis and adequately suggest this pathology. GIST complications and their different responses to treatment are not rare, especially in the emergency room. That is why we will display some key points to identify those situations and ensure a rapid diagnosis and treatment. Likewise, it is interesting to know the different response criteria to treatment so as not to confuse a favorable evolution with a progression of the disease.

### GIEE-11 Vascular Ultrasound in the Setting of Post-kidney, Liver, and Pancreas Transplantation: The Ins and Outs of Post-surgical Anatomy and Need-to-know Pathology

Participants  
Harrison Lee, MD, MBA, (*Presenter*) Nothing to Disclose

#### TEACHING POINTS

1. Ultrasound is typically the first-line option for post-surgical evaluation in the setting of kidney, liver, and pancreas transplantation. A focused review of vascular complications across these organ transplantations can enable a comparative and more conceptual-based approach toward this topic. 2. Kidney, liver, and pancreas transplantation can be performed using different surgical techniques leading to variable post-surgical vascular configurations. 3. Post-transplant vascular complications differ across etiology, timing, and clinical presentations, largely falling into categories of thrombosis, stenosis, and post-biopsy complications, with early and accurate detection being essential to preventing graft failure.

## TABLE OF CONTENTS/OUTLINE

I. Kidney transplantation A. Post-transplant vascular anatomy and variations B. Common indications for ultrasound C. Vascular complications 1. Renal artery thrombosis, stenosis 2. Renal vein thrombosis, stenosis 3. Post-biopsy vascular complications (arteriovenous fistula, pseudoaneurysm) II. Liver transplantation A. Post-transplant vascular anatomy and variations B. Common indications for ultrasound C. Vascular complications 1. Hepatic artery thrombosis, stenosis 2. Portal vein thrombosis, stenosis 3. Hepatic vein stenosis 4. IVC thrombosis, stenosis III. Pancreas transplantation A. Post-transplant vascular anatomy and variations B. Common indications for ultrasound C. Vascular complications 1. Thrombosis, stenosis 2. Post-biopsy vascular complications

### GIEE-110 Up Your Game: A Masterclass on CT Contrast in Abdominal Imaging

Participants  
Alex Chan, DO, Rochester, MN (*Presenter*) Nothing to Disclose

#### TEACHING POINTS

-Review how contrast agent distribution reflects physiology and provides a foundation for diagnosis, problem-solving, and avoiding imaging pitfalls. -Discuss diagnostic advantages and pitfalls related to iodinated contrast distribution, altered hemodynamics, x-ray interaction, and contrast timing. -Collaborative use of gained knowledge to focus on problem solving complex post-surgical cases

## TABLE OF CONTENTS/OUTLINE

The goal of this education exhibit is to review how contrast agent distribution reflects physiology in normal and diseased states which provides the foundation for understanding how CT contrast agent enhancement patterns can be used for diagnosis, problem-solving, and avoiding imaging pitfalls. We will first discuss the physiologic redistribution effect of typical iodinated contrast agent from the intravascular to interstitial space. Next, we will discuss the effects of altered vascular hemodynamics, for example, in the setting of VA-ECMO and inhomogeneous venous return. Following, the physics of x-ray interaction with iodinated contrast will be discussed accompanied with its diagnostic challenges and exploitation with dual energy CT. Additionally, we will discuss the diagnostic sensitivity of various pathologies related to CT technique/contrast timing and explore the utility of bowel contrast agents. Throughout the presentation, we will use these main ideas to problem solve complex postsurgical patients. In conclusion, the audience will gain a higher level of understanding of CT contrast agents and apply these concepts to improve diagnostic confidence at daily practice.

### GIEE-111 Imaging in The Spectrum of Periportal Soft Tissue Pathologies

Participants  
Sinduja Sivaramalingam, DMRD, MBBS, (*Presenter*) Nothing to Disclose

#### TEACHING POINTS

1. Learning the anatomical structures involving the porta hepatis and their importance. 2. To classify various periportal pathologies based upon the structure of origin. 3. To study the radiological features of the individual pathologies, the unique patterns and differentiating points from other pathologies.

## TABLE OF CONTENTS/OUTLINE

BACKGROUND:ANATOMY OF THE PORTA HEPATIS: ROLE OF IMAGING MODALITIES:CLASSIFICATION OF PERIportal PATHOLOGIES BASED ON THE STRUCTURE OF ORIGIN1) DUCTAL AND PERI-DUCTAL PATHOLOGIES: • Cholangiocarcinoma (large duct carcinoma)-periductal and infiltrating, hilar types, advanced locally aggressive spread • Intraductal papillary neoplasm of the bile duct (IPNB)/ biliary papillomatosis • Primary neuroendocrine tumors of the bile ducts Cholangitis • IgG4 related sclerosing cholangitis • Langerhans cell histiocytosis - proliferative and fibrotic phase 2) LYMPH NODAL PATHOLOGIES: • Benign reactive hyperplasia of periportal nodes. • Infective nodes • Peritoneal carcinomatosis / Loco-regional spread of tumor 3) NERVES AND CONNECTIVE TISSUE:• Schwannoma, Neurofibroma • Sarcomas 4) POST SURGICAL OR POST TRANSPLANT CASES: • Periportal inflammatory soft tissue • Tumor recurrence • Post Transplant lymphoproliferative disorder.IMPORTANCE OF PREVIOUS IMAGES/ FOLLOW UP.ROLE OF TUMOUR MARKERS.CONCLUSION: Primary step in the diagnostic approach would be identification of the structure or epicenter of origin and then considering the relevant differentials.

### **GIEE-112 Test Your Knowledge: Reviewing Classic Hepatobiliary Radiologic Signs**

Participants

Larissa Lima, Sao Paulo, Brazil (*Presenter*) Nothing to Disclose

#### **TEACHING POINTS**

The purposes of this quiz are:1. Recognize some classic radiologic signs (a way that makes easier to achieve diferent diagnosis).2. To discuss the pathophysiologic characteristics associated with these radiologic findings.3. Improve the memorize process making associations, since many signs use metaphorical language, such as comparision with objects.4. At the end of the quiz, the reader must be able to recognize these signs and associated pathologies, consolidating the acquired knowledge.

#### **TABLE OF CONTENTS/OUTLINE**

1. The presentation describes classic signs associated with hepatobiliary diseases through Computed Tomography (CT) and Magnetic Resonance (MR) images, in a case-based quiz format.2. Illustrative key points: improve understanding of the correlation between the sign and pathophysiologic process involved.3. Pictorial review of most frequent hepatobiliary signs and associated disease, for example: adenomyomatosis (pearl necklace/rosary sign; hourglass gallbladder), inflammatory hepatic adenoma (atoll sign), hepatic hydatid disease (water-lily sign ) and more.4. Key images that the radiologist must actively look to recognize the sign.

### **GIEE-113 Imaging of Small Bowel Tumors: What Radiologists Should Know**

Participants

Kiyoka Maeba, MD, Kurashiki-City, Japan (*Presenter*) Nothing to Disclose

#### **TEACHING POINTS**

The purpose of this presentation is:1) To demonstrate epidemiology of small bowel tumors and the characteristic imaging findings of ultrasound, endoscopy, computed tomography and magnetic resonance imaging including the radiologic-pathologic correlation.2) To learn about the differentiation between benign and malignant small bowel tumors by imaging of various modalities.

#### **TABLE OF CONTENTS/OUTLINE**

CONTENTS ORGANIZATIONDECISION TREE FOR SMALL BOWEL TUMORS BENIGN BOWEL TUMORS - Polyp/Polyposis syndromes- Lipoma - Ectopic endometriosis- HemangiomaMALIGNANT SMALL BOWEL TUMORS- Adenocarcinoma- Neuroendocrine tumor: NET- Gastrointestinal stromal tumor: GIST- Malignant lymphoma - Metastatic disease- Sarcoma

### **GIEE-114 Simplified Approach to Lateral Pelvic Nodes in Rectal Cancer Addressing Controversies, Categorization and Involvement**

#### **Awards**

**Certificate of Merit**

Participants

Harmeet Kaur, MD, Houston, TX (*Presenter*) Stock options, Health Catalyst;Stock options, Nuance Communications, Inc

#### **TEACHING POINTS**

•What constitute LPLN compartments in the pelvisWhat are the boundaries of LPLN compartments on CT/MR •What are the pathways of lymphatic rectum and why are these important •What the most commonly involved LPLN compartments in rectal cancer What are the currently proposed size criteria for LPLN involvement?What are the circumstances in which these criteria should be applied?

#### **TABLE OF CONTENTS/OUTLINE**

Definition of LPLN compartments based on exisiting surgical literatureDefintion of boundaries of LPLN compartments on CT/MRSimplified imaging criteria to define LPLN on cross sectional imagingClarification of pathways of lymphatic spread in the pelvis and how this impacts nodal involmentSurvey of the current criteria of LPLN involment in the literature implication for radiologistsSize crtieria for LPLN what do these really mean?

### **GIEE-115 Clinical And Radiological Features Of Hepatocellular Carcinoma: An Update In The Era Of Systemic Therapy**

#### **Awards**

**Cum Laude**

Participants

Mariko Irizato, Kashihara, Japan (*Presenter*) Nothing to Disclose

#### **TEACHING POINTS**

The purpose of the exhibit is to update knowledge of hyperintense HCC on the hepatobiliary phase (HBP) of EOB-MRI, not only for diagnosis but also for early prediction of treatment effect, leading to personalized therapy in the future, and to recognize various cases of HCC with atypical imaging features on multimodality imaging.

## TABLE OF CONTENTS/OUTLINE

With recent advances in systemic therapy for HCC, treatment strategies for HCC are changing. Now radiologists are required not only to diagnose but also to predict early treatment effects and contribute to appropriate treatment selection. As an imaging finding linked to predicting treatment effects, the signal intensity of HCC on HBP of EOB-MRI has recently attracted attention. Hyperintense HCC on HBP of EOB-MRI showed a correlation with the therapeutic effects of various treatments, such as immunotherapy, TACE, and hepatic arterial infusion chemotherapy (HAIC). HCC is also a genetically and molecularly diverse group. Actually, approximately 40% of HCCs do not show typical imaging features, such as Li-RADS major imaging feature of HCC, including hyperenhancement (APHE), portal venous phase, delayed phase washout, and capsule appearance. The atypical imaging features of HCC are generally associated with pathological type and molecular phenotype. Understanding HCC with atypical imaging features can improve diagnostic accuracy and help clinicians plan strategies for better treatment.1) Hyperintense HCC on HBP of EOB-MRIa) Etiology and Imaging findingsb) Treatment prediction: TACE, HAIC, and systemic therapy c) Differential diagnosis: the hepatic tumor with hyperintensity on HBP 2) Multimodality imaging of HCC with atypical imaging features

### GIEE-116 MR of Anorectal Fistulas: Current and Evolving Concepts Simplified

Participants

Nabih Nakrou, MD, Boston, MA (*Presenter*) Nothing to Disclose

#### TEACHING POINTS

The purpose of this exhibit is to: Review anatomy of the anorectal region and MR imaging landmarks relative to anorectal fistula classification. Demonstrate the role of MR in presurgical planning for anorectal fistulas, including anatomic mapping, fistula track relation to the sphincters and pelvic organs, detecting internal and external fistula openings, assessing the degree of fistula complexity, and associate fluid collections. Discuss current and evolving concepts of anorectal fistula management and imaging features predicting prognosis. Validate with sample cases MR contribution to diagnosis and decision-making.

## TABLE OF CONTENTS/OUTLINE

The present role of MR in diagnosis and management of anorectal fistula:-Anatomy of the anorectal regions and anal sphincters. MR protocols and optimizing imaging techniques in detecting anorectal fistulas.-Anorectal fistula classifications. Imaging manifestation and diagnostic pearls for each fistula subtype. Surgical approach and treatment options. Radiologic appearance of postsurgical devices. Example cases and illustrations of the above contents.

### GIEE-117 Evaluating the Performance of Segmentation Models for Liver, Spleen, and Fat by Radiologists

Participants

Ari Borthakur, PhD, MBA, Philadelphia, PA (*Presenter*) Nothing to Disclose

#### TEACHING POINTS

Opportunistic screening (1) with abdominal CT examinations, capturing anatomic structures beyond the main clinical indication for performing the exam, may provide the opportunity for more comprehensive analyses of the entire abdomen and pelvis (2). It provides additional value to both patients, by uncovering incidental findings without additional scans, and providers, by improving both quality and service offerings, potentially mitigating risk and improving revenue without additional scan costs (3). The challenge, however, is that opportunistic screening has the potential to increase the burden of unnecessary work for providers. Artificial Intelligence (AI) based machine learning (ML) approaches can help reduce some of this burden particularly in the automation of tedious tasks like image segmentation (4). We present a comprehensive approach to evaluating the performance of an AI algorithm for fully automated CT-based body composition measurements (5) with automated reporting to PACS prior to deployment in routine clinical workflow. References Cited 1. P. J. Pickhardt, *Radiology*, 211561 (2022). 2. L. L. Berland et al., *J Am Coll Radiol* 7, 754-773 (2010). 3. P. J. Pickhardt et al., *Radiology* 249, 151-159 (2008). 4. J. Mongan, A. Vagal, C. C. Wu, *Radiol Artif Intell* 4, e220039 (2022). 5. M. T. MacLean et al., *J Am Med Inform Assoc* 28, 1178-1187 (2021).

## TABLE OF CONTENTS/OUTLINE

A. Clinical need for an AI solution a. Current approaches to body organ segmentation b. Our solution i. Automated phenotyping ii. Structured reporting c. Impact on patient care d. Cost implications B. Evaluating the value of the output for radiologists a. Reader studies b. Analyses of Concordance

### GIEE-118 Biliopancreatic Anatomic Variants: Radiologic Findings And Clinical Relevance

Participants

Kamila Albuquerque, Vila Velha, Brazil (*Presenter*) Nothing to Disclose

#### TEACHING POINTS

Biliopancreatic anatomic variants are common and they are more frequently diagnosed nowadays due to the increasing number of patients submitted to radiology exams. Recognizing these variants is essential to avoid misdiagnosis of pathologies and in the preoperative of biliopancreatic surgeries. The purpose of this exhibit is to make a brief review of pancreatic and biliary tract embryology and review the main biliopancreatic anatomic variants and their clinical relevance.

## TABLE OF CONTENTS/OUTLINE

Introduction with a schematic review of the embryology of the pancreas and biliary tract. Present with images from CT, MR, ERCP, and USG illustrative cases of biliopancreatic anatomic variants and anomalies including annular pancreas, pancreas divisum, ectopic pancreas, ansa pancreatica, pancreatic hypoplasia, circumportal pancreas, dorsal pancreatic agenesis, anomalous biliopancreatic junction, low cystic duct insertion, gallbladder duplication, Caroli disease, intrahepatic bile ducts variations, among others. Correlate each one of these cases with its clinical/surgical relevance. Summary and take-home notes.

### GIEE-119HC Radiologic Review of Small Bowel Malignancies with Their Mimicking Lesions

Participants

Jongsoo Lee, MD, Incheon, Korea, Republic Of (*Presenter*) Nothing to Disclose

#### TEACHING POINTS

When radiologists inspect computed tomography (CT) images, small bowel malignancies are often easy to miss because of the small size, which can lead to mistake for normal small bowel due to their similar enhancement to small bowel or non-specific enhancement. In addition, small bowel malignancies are sometimes mistaken for masses from other origins, such as the uterus, rectum, or omentum. In this article, we illustrate various small bowel malignancies and their mimicking lesions with typical and atypical features on CT imaging as well as their clinical manifestations.

#### TABLE OF CONTENTS/OUTLINE

1. Introduction 2. Small bowel gastrointestinal stromal tumor (GIST) 3. Small bowel adenocarcinoma 4. Small bowel lymphoma 5. Small bowel sarcoma 6. Small bowel plasmacytoma (Extramedullary plasmacytoma) 7. Small bowel neuroendocrine tumor (NET) 8. Mass-like small bowel lesions mimicking small bowel malignancies 9. Clinical history of small bowel malignancy: anemia, weight loss, vomiting, nonspecific abdominal pain Small bowel malignancies can be easily missed or misdiagnosed by radiologists because of their rarity, nonspecific symptoms, and overlapping imaging features, especially when manifesting with small sizes. However, if radiologists know some characteristic imaging features of small bowel malignancies and their mimicking lesions, and perform a careful inspection of the entire small bowel loops, especially when patients present with gastrointestinal bleeding symptoms, optimal detection and diagnosis of small bowel malignancies can be achieved. Please visit the Learning Center to also view this presentation in hardcopy format.

#### GIEE-12 High Frequency Imaging in Hepatobiliary Ultrasound: Zooming In

##### Awards

##### Identified for RadioGraphics

##### Participants

Michael Enea, DO, Philadelphia, PA (*Presenter*) Nothing to Disclose

##### TEACHING POINTS

1. Understand the benefits and limitations of using a high frequency linear transducer (= 12 MHz) for adult hepatobiliary imaging and how it can improve confidence in ultrasound interpretations. 2. Compare routine and high frequency imaging of liver parenchyma and surface contour in patients on a spectrum including normal, steatosis, fibrosis, and cirrhosis. 3. Demonstrate the usefulness of high frequency liver imaging for focal hepatic lesions. 4. Understand the advantage of high frequency imaging for biliary pathology including dilatation, sludge, and calculi. 5. Compare low and high frequency imaging for the evaluation of gallbladder wall thickening, integrity, focal lesions, and calculi.

#### TABLE OF CONTENTS/OUTLINE

1. General- how technique affects high frequency imaging a. Variable transducer frequencies b. Different machine settings c. Patient habitus 2. Liver a. Diffuse parenchymal liver disease i. Steatosis 1. Homogeneous increased echogenicity 2. Focal fat ii. Fibrosis 1. Coarse echotexture 2. Correlate with shear wave elastography iii. Cirrhosis 1. Nodular surface 2. Regenerative nodules 3. Parenchymal atrophy b. Focal liver lesions i. Hepatocellular carcinoma ii. Metastases iii. Cysts c. Other i. Fulminant liver failure ii. Periportal edema iii. Portal thrombosis- benign and malignant iv. Varices 3. Biliary Ducts a. Choledocholithiasis b. Biliary duct dilation c. Biliary cast d. Von Meyenburg Complexes 4. Gallbladder a. Wall thickening b. Integrity of wall a. Adenomyomatosis b. Focal lesions: polyps, masses

#### GIEE-120 Imaging of External Hernias of The Abdomen: Revisited

##### Participants

Manabu Minami, MD, PhD, (*Presenter*) Nothing to Disclose

##### TEACHING POINTS

External hernias of the abdomen are clinically common problems and frequently require imaging evaluation preoperatively. Various kinds of external hernias can occur in the abdominal wall. In the era of three-dimensional imaging using CT and MRI, a more precise evaluation of the structure of each hernia (hernia orifice, hernia sac, its content, and its covering) and complications such as inflammation, bowel obstruction/incarceration, and strangulation can be analyzed than before. In this presentation, we review various kinds of external hernias of the abdomen and show radiological anatomy using three-dimensional images with representative cases as well as their rare types. Understanding the membranous structures of the abdominal wall related to external hernias will be essential for GI radiologists to provide more critical information to surgeons in patient management and surgical planning.

#### TABLE OF CONTENTS/OUTLINE

1. General consideration of external hernias of the abdomen 2. Classification of external abdominal hernias and their imaging findings: case presentations a. groin (inguinal): indirect (external), direct (internal), femoral, b. umbilical/periumbilical: cf. omphalocele, c. ventral (anterior): epigastric/hypogastric (linea alba), suprapubic, Spigelian (linea semilunaris), d. lumbar (lateral): superior lumbar (Grynfeltt-Lesshaft), inferior lumbar (Petit), e. pelvic floor (inferior): obturator foramen, sciatic foramen, perineal, f. cicatricial: traumatic, incisional, parastomal, trocar site 3. Conclusions

#### GIEE-121 MR Enterography in Chron Disease: Detection of Complications

##### Participants

Maria Luisa Rosa, MD, (*Presenter*) Nothing to Disclose

##### TEACHING POINTS

MR Enterography is the gold-standard method for studying the small-bowel in patients with Chron's Disease, not only to depict active inflammatory disease, but to exclude complications, as the presence of fibrostenosing and/or penetrating disease alters medical treatment and may imply surgical intervention. The aim of this work is to depict the imaging findings of complicated Crohn's disease on MR Enterography and discuss the correct terminology and potential differential diagnoses of such findings.

#### TABLE OF CONTENTS/OUTLINE

Through pictorial review we illustrate the different aspects of penetrating disease such as such as sinuses, simple and complex fistulas, inflammatory masses and abscesses, concentrating on what defines and differentiates them from pseudo-sacculations or deep ulcers and from adhesions, that can be misinterpreted on imaging studies as sinuses and fistulas, respectively. In regards to stenosing disease, we explain the criteria for defining a stricture and provide examples of strictures with and without active inflammation as the distinction is important for determining the treatment plan. We will also clarify the circumstances in which you

can consider a probable stricture even when there is no upstream dilation. We will discuss how to potentially differentiate occlusion due to peritoneal adhesions from fibrotic strictures; and from functional abnormalities sometimes seen in these patients who demonstrate dilated small bowel loops without mechanical obstruction.

### **GIEE-122 Do You Remember The Meckel Diverticulum?**

Participants

Cristina Berastegi Santamaria, MD, Bilbao, Spain (*Presenter*) Nothing to Disclose

#### **TEACHING POINTS**

The purpose of this exhibit is: 1. To describe Meckel diverticulum's characteristics 2. To review imaging findings of Meckel's diverticulum on computer tomography 3. To describe the radiologic features of complications of Meckel diverticulum 4. To correlate the histological findings with the radiological perspective

#### **TABLE OF CONTENTS/OUTLINE**

1. Embryology of Meckel diverticulum 2. Pathology of Meckel diverticulum 3. Review of imaging findings on CT and pathological correlation (sample cases) - Non complicated Meckel diverticulum - Complicated Meckel diverticulum Hemorrhage Bezoar Intestinal obstruction Diverticulitis Neoplasms Volvulation Intussusception 4. Conclusions and taking-home messages

### **GIEE-123 Anisakiasis: What Radiologists Need to Know**

Participants

Ines Alonso Sanchez, MD, Bilbao, Spain (*Presenter*) Nothing to Disclose

#### **TEACHING POINTS**

- Become familiar with the radiological findings of anisakiasis, because it is an underdiagnosed parasitosis with an increasing incidence worldwide.- Initial clinical suspicion is sometimes difficult as the symptoms are non-specific, and a multidisciplinary approach is important to make an accurate diagnosis.

#### **TABLE OF CONTENTS/OUTLINE**

Objectives: Review and describe the main clinical, radiological and epidemiological features of the different forms of Anisakiasis. Background: Anisakiasis is a zoonosis caused by accidental infection by *Anisakis simplex* due to the ingestion of raw or undercooked fish that affects mainly the gastrointestinal tract. Although the highest prevalence of anisakiasis is found in Asia and it is rare in the United States and Europe, the incidence is expected to increase worldwide as cultural globalization of food habits increases opportunities to eat raw or undercooked seafood. Imaging findings: Severe submucosal edema, ascites, fluid collection and mesenteric fat infiltration. Diagnosis: Clinical suspicion is helpful but difficult in some cases, especially in intestinal anisakiasis, and CT findings may suggest the possibility of anisakiasis when characteristic imaging features are present. Laboratory tests or endoscopic direct visualization give a definite diagnosis. Treatment: Generally symptomatic and in some cases endoscopic larvae removal. Conclusions: Anisakiasis is a rare and underdiagnosed parasitosis that affects the gastrointestinal tract. As its incidence is increasing worldwide, it is important that we are familiar with the characteristic clinical and radiological manifestations.

### **GIEE-124 The Many Faces Of Colitis: An Imaging Review**

Participants

Gustavo Alonzo Correa I, MD, Mexico City, Mexico (*Presenter*) Nothing to Disclose

#### **TEACHING POINTS**

To describe the normal appearance of the colon in the different imaging modalities. To explain the appearances, pathogenesis and differential diagnosis of CT colonic enhancement patterns. To discuss the differential diagnosis of colitis based on imaging findings, epidemiology and clinical history.

#### **TABLE OF CONTENTS/OUTLINE**

Introduction Normal anatomy of the colon in the different imaging modalities Classification of CT colonic enhancement patterns Infectious colitis Pseudomembranous colitis Neutropenic colitis (Typhlitis) Radiation colitis Inflammatory bowel disease Ischemic colitis Take home points

### **GIEE-126 Post-operative Abdominal Complications Following Colorectal Surgery on CT: Pearls and Pitfalls**

#### **Awards**

#### **Certificate of Merit**

Participants

Deevia Kotecha, MBChB, BSc, Wilmslow, United Kingdom (*Presenter*) Nothing to Disclose

#### **TEACHING POINTS**

1) To illustrate the spectrum of early post-operative complications, emphasizing the importance of the timing of surgery. 2) To distinguish expected post-operative CT appearances versus a complication, highlighting useful tips and potential pitfalls. 3) To relate the type of surgery to key review areas on post operative imaging (including recent advances in endoluminal and robotic surgery). 4) To discuss the utility of positive luminal contrast in problem solving.

#### **TABLE OF CONTENTS/OUTLINE**

The post-operative abdomen is challenging. Knowledge of the potential complications is important to every radiologist so that life-threatening conditions can be quickly diagnosed and treated. Post-operative GI complications covered will be broadly categorised into the following headings. A range of examples with key learning points will be illustrated and where relevant correlate with any pre-operative imaging. • Abnormal gas patterns o Location and volume of free gas. o Retained surgical swabs o Haemostatic agents. • Fluid collectionso Anastomotic leakso Urinoma • Vascular complicationso Bowel ischaemiao Arterio-venous fistulao Pseudo-aneurysm

### **GIEE-127 Improving CT Colonography Standards**

Participants

Aishwariya Vegunta, MD, Stratford, CT (*Presenter*) Nothing to Disclose

#### TEACHING POINTS

Discuss various standards to maximize the quality of CT colonography.

#### TABLE OF CONTENTS/OUTLINE

Background: There is an increasing incidence of colorectal cancer which is a largely preventable disease if identified at precursor polyp stage and removed. CTC Performance standards: a. Patient Information and experience. b. Bowel Preparation: 1. Diet. 2. Catharsis: Dry versus wet agents and 3. Tagging of residual stool and fluid. Bowel preparation for same-day CTC after incomplete colonoscopy. c. Imaging: A. CT technique/ Scanning parameters and radiation risk. B. Colonic distension with carbon dioxide, using an automated insufflator. C. Scout to assess for adequate bowel distension. D. Dual-position scanning in Supine and prone positions versus decubitus position. d. Interpretation: A. Colonic and extracolonic findings are reported in a standard examination as per CT Colonography Reporting and Data System (C-RADS). B. Colonic interpretation involving primary 2-D and primary 3-D reviews. Flat lesions measuring 3 mm or less in height are better depicted with contrast tagging at 2D while 3D reviews are better at smaller polyp detection and greater conspicuity of polyps at or near the folds. C. CTC descriptors including polyp morphology, location and measurements. D. Pitfalls in CTC interpretation. e. Management decisions and interval surveillance: Follow-up recommendations on polyp management and role of surveillance CTC. f. CTC outcome measures: Audits and ACR's CTC registry.

#### GIEE-128 Roux-en-Y Gastric Bypass: Post-surgical Anatomy and Most Common Complications

Participants

Ines Alonso Sanchez, MD, Bilbao, Spain (*Presenter*) Nothing to Disclose

#### TEACHING POINTS

- Review the Roux-en-Y gastric bypass surgical technique and understand the normal post-surgical anatomy and radiological findings. - Describe and explain the most frequent complications and their imaging manifestations using a series of cases from our institution as examples.

#### TABLE OF CONTENTS/OUTLINE

Background Obesity is a disease of epidemic proportions. Non-surgical treatment fails in 95% of the patients, and therefore bariatric surgery is the most effective, yet invasive, treatment. There are two surgical approaches for achieving weight loss: bypass procedures and restrictive procedures. Roux-en-Y gastric bypass is the most popular technique and obtains greater sustained weight loss and higher sustained long-term success than other techniques. Findings: As radiologists, we should be familiar with the anatomic changes caused by this surgery, in order to be able to recognize them and identify possible complications. Complications In this presentation, we describe the most common complications of gastric bypass surgery (mainly post-operative leaks, small bowel obstruction, gastro-gastric fistula and ulceration) and their imaging features based on cases of our centre. We revise the imaging techniques recommended to examine each type of complication and key findings to identify them. Conclusions Bariatric surgery is increasing dramatically, especially Roux-en-Y gastric bypass and radiologists should be able to recognize the anatomic changes that this surgery involves and the most frequent complications it may have.

#### GIEE-129 Barium Swallow Radiological Technique to Evaluate Hiatal Hernias and Other Commonly Associated Findings

Participants

Tatiana J. Ludena Camacho I, MD, Mexico City, Mexico (*Presenter*) Nothing to Disclose

#### TEACHING POINTS

- Explain the anatomy thorough diagrams as well as the typical imaging findings.- Review the different types of hernia and much more frequently observed in radiological practice.- Simplify the correct technique for the execution of the esophagogram.- Present through real clinical cases usual findings during an esophagogram.

#### TABLE OF CONTENTS/OUTLINE

1. Introduction.2. Anatomy3. Technique4. Hiatal hernias- Definitions.- Pearls and pitfalls.- Key terms of the radiographic lexicon terms.- Categories.5. Other common findings in Barium Esophagogram.6. Conclusions.

#### GIEE-13 Anatomic Basis of Rectal Cancer Staging: Clarifying Controversies and Confusion

##### Awards

Identified for RadioGraphics  
Cum Laude

Participants

Muhammad Awiwi, MD, Houston, TX (*Presenter*) Nothing to Disclose

#### TEACHING POINTS

Despite the adoption of rectal MRI as a mandatory staging tool for rectal cancer, inconsistencies still exist in defining anatomic landmarks even among experts (Lambregts DMJ et al. 2022).

#### TABLE OF CONTENTS/OUTLINE

This exhibit aims to review controversies in anatomic issues, propose the best opinion based on the evolving literature, and discuss impact on management. Anatomic landmarks to be discussed include: Re-definition of the rectum and its upper/lower boundaries.- The anatomy of the anal sphincter and staging of tumors involving this structure.- The definition of circumferential resection margin (CRM) will vary depending on surgical procedure and does not equate to mesorectal fascia (MRF). - Clarify the difference between peritoneal involvement and mesorectal fascia involvement in the upper rectum.- Clarify the anatomic boundaries of lateral pelvic nodes and their clinical significance.

## **GIEE-130 Complications of Percutaneous Liver Procedures: Bleeding and Beyond**

Participants

James Palmer, MD, Tucson, AZ (*Presenter*) Nothing to Disclose

### **TEACHING POINTS**

1.) Percutaneous diagnostic and therapeutic liver procedures are commonly performed and range from biopsy to more invasive treatments such as ablation and biliary interventions. 2.) While these procedures are generally safe, major complications do occur usually at a rate of 0.1-5%. Bleeding is one of the most common complications and various manifestations of bleeding are important to recognize as they may require different treatment approaches. 3.) Non-hemorrhagic complications are diagnosed primarily by imaging and the radiologist should be aware of the range of complications so that timely treatment can be instituted.

### **TABLE OF CONTENTS/OUTLINE**

1.) Brief overview of literature regarding complications of percutaneous liver procedures a.) Definition of minor vs. major complications 2.) Multimodality case-based review of complications with teaching points and discussion of treatment implications. a.) Hemorrhagic and Vascular i.) Subcapsular hematoma, hemoperitoneum ii.) Pseudoaneurysm, active bleeding, AVF iii.) Arterial vs. Venous bleeding iv.) Thrombosis b.) Biliary i.) Bile leak/biloma ii.) Stricture iii.) Hemobilia c.) Infectious i.) Liver abscess ii.) Biliary sepsis d.) Local i.) Organ injury (diaphragm, GB, stomach, colon) ii.) Residual/recurrent tumor iii.) Liver infarction iv.) Tumor seeding e.) Thoracic i.) Pneumothorax, hemothorax Hemopericardium

## **GIEE-131 Multimodality Imaging of Tumor Thrombus in Hepatocellular Carcinoma**

Participants

Ulysses Torres, MD, PhD, Sao Paulo, Brazil (*Presenter*) Nothing to Disclose

### **TEACHING POINTS**

- To review and illustrate the vascular involvement in hepatocellular carcinoma (HCC) on ultrasound, computerized tomography (CT), and magnetic resonance imaging (MRI).
- To prepare abdominal radiologists to identify the most common hepatic venous thrombosis sites on imaging in HCC, with emphasis on portal vein.
- To present imaging features of tumor thrombosis according to LI-RADS v2018.
- To present clinical cases from our institution with a multidisciplinary approach, some correlated with pathology results and individualized treatment.
- To recognize potential pitfalls in image interpretation and differential diagnosis of tumor thrombus.

### **TABLE OF CONTENTS/OUTLINE**

- Background: the importance of a multimodality assessment of vascular involvement in HCC, which can be subtle.
- The impact of tumor thrombus on management in patient care.
- Categorization according to LI-RADS v2018.
- Illustrative cases of our institution with the main hepatic tumor thrombus sites with imaging features and interpretation on: o Ultrasound. o CT. o MRI.
- Challenging cases of tumor thrombosis in HCC (as infiltrative carcinoma).
- Differential diagnosis with hematic thrombosis.
- Tips and tricks.

## **GIEE-132 Advanced CT Techniques In the Evaluation of Hepatocellular Carcinoma: Roles of Ultra-high-resolution CT, Dual-energy CT, Contrast Enhancement Boost Technique, and Radiomics**

Participants

Masatoshi Hori, MD, Kobe, Japan (*Presenter*) Research Grant, Canon Medical Systems Corporation

### **TEACHING POINTS**

1. Understanding the characteristics of advanced techniques such as 1024-matrix ultra-high resolution (UHR) CT, dual-energy CT, contrast enhancement boost (CE boost) technique, and radiomics. 2. Understanding how radiologists can use advanced techniques to detect and characterize hepatocellular carcinoma (HCC). 3. Understanding the prospects for advanced techniques to improve the management of patients with HCC.

### **TABLE OF CONTENTS/OUTLINE**

A. Introduction B. Ultra-high-resolution (UHR) CT with a 1024 matrix B-1. Spatial resolution, image noise, and deep learning reconstruction B-2. Tumor margin can be better delineated, potentially resulting in improved assessment of microvascular invasion C. Dual-energy CT (DECT) C-1. Material decomposition C-2. Virtual monochromatic imaging (VMI) can enhance tumor-to-liver contrast C-3. Beyond the dual-energy CT: Hope for photon counting CT D. Contrast enhancement boost (CE boost) technique: a postprocessing technique for increasing the degree of contrast enhancement D-1. Principles: Roles of image subtraction, non-rigid registration, and denoising D-2. CE boost combined with multiphasic CT can improve the detection of small HCC D-3. CE boost can be combined with low-keV VMI in DECT to further increase the conspicuity of HCC E. Radiomics F. Clinical roles of the advanced techniques in evaluating HCC G. Conclusion

## **GIEE-133 Hepatic Hydatid Disease: Typical and Atypical Imaging Features with Clinical Correlation and Impact on Management**

**Awards**

**Certificate of Merit**

Participants

Mohamed Ibrahim, MBCh, Rochester, MN (*Presenter*) Nothing to Disclose

### **TEACHING POINTS**

1. Understand the etiopathogenesis of hydatid disease 2. Highlight hepatic and extrahepatic hydatidosis imaging features (cardiac, brain, spine, muscular, subcutaneous, and adrenal) 3. Highlight different IR management for hepatic hydatid cysts

### **TABLE OF CONTENTS/OUTLINE**

1. Etiopathogenesis of hydatid disease:• Historical overview• Echinococci types, lifecycle, infection sources, and clinical relevance• Hydatid cyst composition and imaging features 2. Imaging features of different stages:• WHO IWG 2001 management classification and radiological classification (Active vs transient vs inactive)• Extrahepatic lesions (brain, spleen, pulmonary, spine, pyriformis

muscle, subcutaneous and adrenal) • CT vs MRI, which is better? 3. Management; indications, contraindications, procedural steps, and imaging follow-up • Surgical: conservative (partial cystectomy, and deroofing) vs radical (pericystectomy vs hepatic resection) • IR options. Discussing PAIR cases and highlighting why it is better i. PAIR "Percutaneous puncture under sonographic guidance, Aspiration of a substantial amount, Injection of sclerosing agent, Re-aspiration) ii. D-PAI: Double puncture-aspiration-injection iii. PEVAC: Percutaneous evacuate on of cyst content

### **GIEE-134 Uncommon Primary Liver Tumors in Adults: An Image Review**

Participants

Guillem Dolz Alvarez De La Ballina, MD, Valldoreix, Spain (*Presenter*) Nothing to Disclose

#### **TEACHING POINTS**

To show the wide spectrum of unusual primary liver tumors that can arise from the different progenitor cells in the liver, and review the imaging findings of these uncommon lesions. To assess features that may help in the diagnosis of rare hepatic tumors.

#### **TABLE OF CONTENTS/OUTLINE**

Introduction to unusual hepatic tumors Description of hepatocellular tumors: - Fibrolamellar hepatocarcinoma- Hepatocarcinoma- Hepatoblastoma Review of epithelial/cholangiocellular tumors: - Intraductal papillary tumor of the bile ducts- Cystic mucinous tumor Mesenchymal tumors: - Angiomyolipoma- Angiosarcoma- Hepatic epithelioid hemangioendothelioma- Inflammatory myofibroblastic tumor- Solitary fibrous tumor Primary hepatic neuroendocrine carcinoma. Primary hepatic lymphoma. Others: - Necrotic nodule of the liver- Bruccellar liver abscess ( brucellosis). Conclusions

### **GIEE-135 In Between Peritoneal and Retroperitoneal Layers: The Spread of Disease in The Abdominal Cavity**

Participants

Marcela Santos Conde, MD, Sao Paulo, Brazil (*Presenter*) Nothing to Disclose

#### **TEACHING POINTS**

1. Recognizing the types of disease spread in the abdominal cavity (interfascial, intraperitoneal, subperitoneal and transperitoneal). 2. Understanding the anatomy of the peritoneum and retroperitoneum and its correlation with disease spread. 3. Expected findings on disease spread in the abdominal cavity, from tumoral dissemination to inflammatory disease and trauma.

#### **TABLE OF CONTENTS/OUTLINE**

Introduction: general aspects of the disease spread in the peritoneum and retroperitoneum. Anatomy of the retroperitoneum as it relates to interfascial spread of diseases. Peritoneal cavity and the circulation of ascitic fluid as it relates to intraperitoneal disease spread. Anatomy of peritoneal ligaments and omental sacs as it relates to subperitoneal spread of diseases. Understanding the relation of retroperitoneal and peritoneal organs with the peritoneal membrane as it relates to transperitoneal spread of disease. Take home messages.

### **GIEE-136 Peritoneal MRI: Dedicated Protocol, Tips and Tricks**

#### **Awards**

##### **Certificate of Merit**

Participants

Anais Delagnes, Angers, France (*Presenter*) Nothing to Disclose

#### **TEACHING POINTS**

-To know the MRI sequences to be performed and the order of execution -To understand usefulness of each sequence for the detection of peritoneal malignancies -To know how to adapt patient preparation and sequence parameters in case of MRI artifacts

#### **TABLE OF CONTENTS/OUTLINE**

Magnetic Resonance Imaging (MRI) has an emerging role in the exploration of peritoneal malignancy. The knowledge and the management of peritoneal pathologies have considerably evolved over the last decade, especially with the possibility of curative treatment of peritoneal metastatic disease. Peritoneal MRI is routinely performed in referral centers and play essential role at different stages of the management: for the selection of patients for curative surgery, in the preoperative phase to optimize mapping of lesions, and in surveillance for early detection of recurrence. A dedicated and detailed protocol is proposed to perform a peritoneal MRI. Each step are explained including the preparation of the patient, oral and intravenous contrast agent and drugs used. Then each sequences (recommended and optional) with their parameters and the optimized order of realization are detailed, as well as their usefulness to detect peritoneal lesions and their limits. Finally, tips and tricks to limit artifacts are given, in particular to reduce artifacts related to the MR technique like susceptibility artifact and related to the patient condition (for exemple the black hole artifact caused by the presence of ascites).

### **GIEE-137 Illustrative Cases of Acute Pancreatitis and Commonly Encountered Complications**

Participants

Klaudio Gjeluci, MD, MS, (*Presenter*) Nothing to Disclose

#### **TEACHING POINTS**

1. Demonstrate the wide array of acute pancreatitis encountered on imaging. 2. Discuss the utility of imaging. 3. Evolution of interstitial edematous pancreatitis and necrotizing pancreatitis. 4. Summarize the nomenclature of the 2012 Revised Atlanta Classification for acute pancreatitis. 5. Review of common complications of acute pancreatitis through illustrative cases.

#### **TABLE OF CONTENTS/OUTLINE**

Utility of imaging in acute pancreatitis and complications: Limited in the early phase of the disease process Clinical diagnosis: epigastric pain and elevated pancreatic enzymes three times the normal level Diagnostic in cases where elevated pancreatic enzymes do not meet the threshold criteria. Typically, in late presentation of acute pancreatitis Determining unclear etiology Gallstone pancreatitis Obstructive neoplastic process Predictor of mortality in the late phase of disease process Extent of

necrosisInfectionLocal complications: pseudoaneurysm/bleeding, venous thrombosis, CBD stricture, pancreatic duct strictureDiscuss  
Case Examples with Imaging Findings:Acute interstitial edematous pancreatitisAcute necrotizing pancreatitis Acute pancreatic fluid  
collectionAcute necrotic collectionPseudocystWalled-off necrosisInfected walled-off necrosisBleeding splenic artery  
pseudoaneurysmLarge gastroduodenal artery pseudoaneurysmInteresting case of splenic vein thrombosis

### **GIEE-138 What Radiologists Should Know for The Early Detection of Small Pancreatic Ductal Adenocarcinoma**

Participants

Yoshihiko Fukukura, MD, PhD, Kagoshima, Japan (*Presenter*) Nothing to Disclose

#### **TEACHING POINTS**

Pancreatic ductal adenocarcinoma (PDAC) still has a dismal prognosis because of the difficulty in early diagnosis, although small PDAC has a good prognosis with a 5-year survival rate of 68.7% for stage IA disease. CT and MR are the most frequent imaging modalities used for evaluating patients with clinically suspected PDAC. However, these modalities often fail to demonstrate small PDAC. The possibility of diagnosing precursor lesions of the pancreas (pancreatic intraepithelial neoplasia [PanIN-3]) and small PDAC may greatly improve the prognosis of PDAC. The purpose of this exhibit is 1. To illustrate CT and MR imaging findings of PanIN and small PDAC 2. To discuss how to improve the detection of PDAC.

#### **TABLE OF CONTENTS/OUTLINE**

1. Summarize the definition, etiology, and clinical and histological features of PanIN and small PDAC (<20 mm) 2. Describe the characteristic CT and MR imaging findings of PanIN and small PDAC (<20 mm) with histopathological correlation 3. Highlight how to improve the detection of PDAC (tumor delineation and important secondary signs) 4. Discuss the diagnostic approach to potentially achieve earlier detection of PDAC 5. Summary: Knowledge of characteristic CT and MRI features and how to improve tumor delineation is important to improve the prognosis of patients with PDAC.

### **GIEE-139 Bubbles and Marbles in the Pancreas: Demystifying Cystic and Solid Pancreatic Lesions with Emphasis on Management**

Participants

Katherine Chung, MD, Stony Brook, NY (*Presenter*) Nothing to Disclose

#### **TEACHING POINTS**

Imaging characteristics of cystic and solid lesions of the pancreas are well studied. However, with ongoing research in management and prognosis of these pancreatic lesions, it can be confusing for practicing radiologists and trainees to form recommendations for patients and clinicians. In this education exhibit, we will describe classic imaging findings of pancreatic lesions, review their clinical features, and discuss the latest recommendations on treatment options and management of these lesions. We present a pictorial review of cystic and solid lesions of the pancreas to guide radiologists on the management of these lesions.

#### **TABLE OF CONTENTS/OUTLINE**

Solid pancreatic lesions:? Ductal adenocarcinoma,? Neuroendocrine tumors, Metastasis, ? Lymphoma.Cystic pancreatic lesions:? Intrapancreatic Mucinous Neoplasms (IPMN), Serous Cystadenoma, Mucinous cystadenoma?, Solid Pseudopapillary Neoplasm?. Mimickers?: Pseudocyst,? Duodenal diverticulum?.

### **GIEE-14 CT and MR Enterography in Celiac Disease: What Should Residents Know?**

#### **Awards**

**Identified for RadioGraphics**

Participants

Andrea Penizzotto, DMRD, (*Presenter*) Nothing to Disclose

#### **TEACHING POINTS**

The role of small bowel imaging is most important in patients with nonresponsive celiac disease and to exclude celiac disease related complications.The most specific imaging finding of celiac disease is the jejunoileal fold reversal pattern, but other findings are those of a nonspecific malabsorptive pattern.Ulcerative jejunitis, small bowel wall thickening, and small bowel dilation are more commonly seen in patients with refractory celiac disease.Ascites, pleural effusion and/or subcutaneous edema are related to severe malnutrition secondary to refractory celiac disease.

#### **TABLE OF CONTENTS/OUTLINE**

1) Introduction 2) Imaging protocolsCT enterography MR enterography3) Imaging analysis: Systemic approach4) Intestinal findingsIleal jejunoizationJejunum fold flatteningFold pattern reversalIntestine wall thickeningBowel dilatationStrictureIntussusception5) Extra-intestinal findingsMesenteric adenopathyMesenteric vascular engorgementHyposplenismAscites6) ComplicationsUlcerative jejunoileitisMalignancyCavitary mesenteric lymph node syndrome7) Take home messages

### **GIEE-140 Mimickers of Pancreatic Adenocarcinoma: What to Watch for at Tumor Board and the Workstation**

Participants

Andrea Esquivel Mora, MD, San Jose, Costa Rica (*Presenter*) Nothing to Disclose

#### **TEACHING POINTS**

Neoplastic and non-neoplastic pancreatic conditions can mimic pancreatic ductal adenocarcinoma (PDAC) on cross-sectional imaging. Our purpose is to: • Highlight distinguishing clinical and radiologic features that provide a clue to the correct (non-PDAC) diagnosis • Understand treatment and outcome implications for these mimics

#### **TABLE OF CONTENTS/OUTLINE**

Around 90% of pancreatic cancers are pancreatic adenocarcinoma while other pancreatic tumors are infrequently seen. This exhibit will highlight distinguishing radiologic and clinical features of PDAC mimics. 1. Uncommon exocrine pancreatic neoplasms.\*Acinar cell carcinoma \*Pancreatoblastoma \*Squamous and Adenosquamous Ca \*Colloid Carcinoma \*Invasive IPMN \*Mucinous

cystadenocarcinoma 2. Non-exocrine pancreatic neoplasms that can mimic pancreatic cancer. \*Pancreatic neuroendocrine neoplasms \*Metastasis 3. Benign mimics of pancreatic cancer: "groove pancreatitis", focal autoimmune pancreatitis, mass forming chronic pancreatitis, obstructive chronic pancreatitis, and focal steatosis 4. Key imaging features that can distinguish these entities from PDAC: multifocality, multiple ductal strictures, hemorrhage, duct-penetrating sign, low duct-to-parenchyma ratio, collateral duct dilatation, "sandwich sign", hyperenhancement, calcifications, and capsule like rim or loss of lobulations. 5. Clinical features that can support the differential diagnosis are the history of a primary tumor, sex, age, predisposing genetic syndromes, and serum markers (IgG4, trypsin).

#### **GIEE-141 The Perceptual Problem in Pancreatic Imaging**

Participants

Abraham Fourie Bezuidenhout, MD, Boston, MA (*Presenter*) Nothing to Disclose

##### **TEACHING POINTS**

Diagnostic errors are common and can affect overall patient care, none more so than in the setting of pancreatic ductal adenocarcinoma (PDAC). In the absence of a PDAC screening program for the general population, the onus of early diagnosis is primarily placed on radiologists which largely determine patient outcomes and is an understandable source of anxiety to radiologists. Diagnostic errors can occur at any time in the process, from initial perception to final image interpretation. Cognitive errors include perceptual challenges and a myriad of cognitive biases which are particularly common and impactful in pancreatic imaging. Becoming aware of perceptual challenges specifically related to PDAC as well as understanding the various biases, related to internal and external pressures, can allow radiologists to minimize diagnostic errors and thereby help improve patient outcomes. In this exhibit we will provide explanations, insight and a framework for understanding the basis of these diagnostic errors and potential avenues to minimize them.

##### **TABLE OF CONTENTS/OUTLINE**

What contributes to diagnostic errors in the setting of PDAC? What's the unique perceptual challenges of PDAC? Direct vs indirect signs of PDAC. Which cognitive biases are in play in pancreatic imaging? Internal and external factors contributing to bias. Common vs newly described biases as it pertains to pancreatic imaging. How to overcome biases with guidelines to create an environment of peer learning which enables systematic improvement, rather than viewing it as individual failures.

#### **GIEE-142 Ultrasound: Lumps and Bumps in the Anterior Abdominal Wall**

Participants

Marie Vogel, MD, (*Presenter*) Nothing to Disclose

##### **TEACHING POINTS**

1. Ultrasound is a low cost, low risk, widely accessible imaging tool that can serve as a first line imaging modality in characterizing superficial lesions. 2. A thorough understanding of abdominal wall anatomy and scanning techniques will allow the radiologist to confidently identify common abdominal wall pathologies. 3. By combining scanning technique, anatomic knowledge and patient history, the radiologist can troubleshoot challenging cases and confidently arrive at the correct diagnosis.

##### **TABLE OF CONTENTS/OUTLINE**

1. A brief overview of the advantages and disadvantages of ultrasound in the assessment of superficial lumps and bumps in the abdominal wall. 2. Review the anatomy of the abdominal wall and its ultrasonographic appearance. 3. Review use and limitations of ultrasound and key ultrasound scanning techniques. 4. Case based presentation of common lumps and bumps, describing key ultrasound findings, scanning tips and tricks, common mimics and/or complications, clinical presentation and management of these pathologies including but not limited to: Subcutaneous lesions: lipoma and epidermal inclusion cyst; Hernias: direct versus indirect inguinal hernia, femoral hernia, incisional hernia; Sequelae of trauma and infection: hematoma, abscess, Morax-Lavallee lesion; Neoplasms: desmoid tumor, liposarcoma, melanoma; Miscellaneous lesions: adenopathy, endometriosis.

#### **GIEE-143 Ultrasound of the Portal Vein: ImPORTant Things to Know**

##### **Awards**

##### **Identified for RadioGraphics**

Participants

Matthew Simon, MD, Philadelphia, PA (*Presenter*) Nothing to Disclose

##### **TEACHING POINTS**

1. Understand normal ultrasound appearance of portal veins in grayscale, color and spectral Doppler 2. Recognize abnormalities of the portal vein including thrombus (bland and tumor), cavernous transformation and portal venous gas 3. Identify abnormal waveforms and abnormal direction of flow in the portal veins and formulate a differential diagnosis 4. Understand the normal ultrasound appearance of a TIPS and recognize complications

##### **TABLE OF CONTENTS/OUTLINE**

1. Normal ultrasound of portal vein a. Anatomy i. 3D rendering of portal venous system b. Grayscale c. Doppler i. Color ii. Waveforms iii. Velocities 2. Abnormalities of flow a. Slow flow b. Helical flow c. Abnormal flow due to portal hypertension i. Alterations of velocity and direction 1. Hepatofugal flow: partial and complete 2. Perihepatic varices: paraumbilical, coronary, gallbladder 3. Portal Vein Thrombosis a. Bland thrombus 1. Causes 2. Acute versus chronic 3. Differentiating occlusive from non-occlusive b. Tumor thrombus 1. Hepatocellular carcinoma and other tumors 2. Grayscale, cine clips 3. Doppler: arterial flow within thrombus c. Chronic occlusion/Cavernous Transformation 4. Portal venous gas a. Causes b. Differentiate from pneumobilia c. Gray scale and Doppler appearance 5. Other a. Effect of cardiac disease on portal system b. Portal fistula i. Portal-hepatic venous ii. Portal-hepatic arterial 6. TIPS a. Normal appearance on Grayscale and Doppler i. when to image a TIPS after insertion ii. protocol for imaging a TIPS iii. effect on other vessels b. Complications i. Thrombus ii. Stenosis

#### **GIEE-144 Big Kids with Tummy Pains: Classically Pediatric Acute Abdominal Presentations in Adults**

Participants

Neel Jain, MA, MBBS, (*Presenter*) Nothing to Disclose

## TEACHING POINTS

1. Review of the adult presentation of pediatric acute abdominal pathology with discussion of imaging findings. 2. Illustrated conditions include Meckel's diverticulum, intussusception, anatomical variants, intestinal malrotation, mesenteric adenitis. 3. Highlight important review areas and implications. 4. Insight into their clinical management.

## TABLE OF CONTENTS/OUTLINE

Pediatric pathology is often not a primary focus for adult GI radiologists and clinicians. Whilst uncommon, pediatric abdominal pathologies can also present later in life. It is therefore crucial that the radiologist on call considers pediatric illnesses and underlying congenital structural abnormalities within their differential diagnosis. We present a case-based educational exhibit to familiarize radiologists with the key imaging findings.

### **GIEE-145 Hidden Gem: Ultrasonography Detection Differentiation of Sclerosing Cholangitis**

Participants

Moran Drucker Iarovich, MD, (*Presenter*) Nothing to Disclose

## TEACHING POINTS

Teaching Points • Review different etiologies of sclerosing cholangitis • Discuss specific SC manifestations, including: background, clinical presentation, mechanism, treatment • Emphasize sonographic features of each, to allow an educated query of appropriate diagnosis

## TABLE OF CONTENTS/OUTLINE

Sclerosing cholangitis is a progressive cholestatic disease, characterized by inflammation, fibrosis strictures. It is divided into primary sclerosing cholangitis (PSC) secondary sclerosing cholangitis (SSC). PSC is idiopathic, often seen in young males with concomitant ulcerative colitis, while SSC denotes a spectrum of progressive cholestatic diseases which have an identifiable, even treatable cause. SSC etiologies are divided into five mechanistic categories: immune-mediated, drug-induced, infectious, obstructive, or ischemic. Differentiation between the various causes of sclerosing cholangitis is imperative for appropriate patient management. Ultrasound (U/S) is the primary imaging of choice for evaluation of the biliary tree, being accurate, available, cost-effective, impervious to motion, safe. U/S is underrecognized as a diagnostic and problem-solving tool in assessment of PSC SSC. U/S's high spatial resolution allows detection of fine ductal features not often seen by MRCP. Subcapular ducts are often only visible on U/S. As well, it has the highest sensitivity for detection of intrahepatic stones bile duct casts. However, lack of familiarity means that many diagnostic features of biliary diseases are often missed. In this review we will describe the typical U/S features of PSC SSC.

### **GIEE-146 Spectrum of Clinically Important Isolated and Concomitant Anatomical Variations of Biliary Ducts, Pancreatic Duct and Gall Bladder on MR Cholangiopancreatography (MRCP): What Not to Miss and What Radiologist Should Know to Help the Clinician in This Era of Advanced Hepato-Biliary Surgery!"**

Participants

Aruna Pallewatte, MD, FRCR, (*Presenter*) Nothing to Disclose

## TEACHING POINTS

1) Learn embryological basis of anomalies of hepatic, biliary and pancreatic ducts 2) Optimal MRCP protocol/Physics 3) Know classification of anatomical variants in configuration of intra/extrahepatic biliary ducts (BD) with clinical relevance 4) Appreciate classification of cystic duct pancreatic duct (PD) variations based on course insertion 5) Classification MRI features of Gall bladder (GB) variations such as duplication, intrahepatic GB. 6) Learn incidence of variations with literature comparison 7) Learn clinical significance (eg longterm effects, Surgeon's needs) of identified hepato-biliary-pancreatic duct variations and how to document them accurately on pre-op MRCP report to answer clinical needs 8) Learn to avoid diagnostic pitfalls and mimics causing misinterpretation on MRI/MRCP

## TABLE OF CONTENTS/OUTLINE

1) Introduction to spectrum of BD, PD, Cystic duct GB anatomical variants, aberrant anatomy embryological basis with illustrations 2) Optimised MRCP protocol 3) Huang classification of Right Left intra hepatic BD illustrated with our MRCP images - Demography incidence 4) Classification of extrahepatic BD, PD and cystic duct variants with our sample cases 5) MRCP of Intrahepatic GB, double GB and classification 6) Pictorial depiction of concomitant BD, PD, GB variants and choledochal cysts with sample MRI cases 7) Diagnostic Mimics pitfalls, clues to avoid them 8) Potential longterm complications of variants such as pancreatitis 9) Challenges to Hepatobiliary surgery and value of pre operative documenting of anatomical variants 10) Guidance for systematic MRI/MRCP reporting focused specially for hepatic transplantation, hepatic resection, ERCP, laparoscopic surgery etc.

### **GIEE-147 Gallbladder Malignancy and its Many Mimics**

Participants

Matthew Carr, MD, (*Presenter*) Nothing to Disclose

## TEACHING POINTS

Gallbladder Malignancy and its Many Mimics Teaching Points: 1. Gallbladder malignancy tends to predominantly present in several different ways on imaging as an: intraluminal mass lesion, asymmetric wall thickening, or polyp. 2: Many potential mimics of gallbladder malignancy exist. Use the clinical history, all available views, and all modalities to create a more informed differential. 3: How the lesion evolves (or doesn't evolve) over time can help narrow or change the differential. 4: Sometimes you don't know if it is malignancy or a benign process. When in doubt take it out! (Or biopsy).

## TABLE OF CONTENTS/OUTLINE

Table of Contents: - 1. Different gall bladder malignancies and their presentations (some with rad-path correlation). - 2. Metastatic diseases to the gallbladder (including lung and melanoma). - 3. The different potential mimics of gall bladder cancer (cholecystitis, adenomyomatosis, etc) - 4. Multiple case-based examples where specifics of the patient presentation help aid the differential diagnosis. - 5. Multiple case-based examples where the temporal course of the lesion changes the differential. - 6. Xanthogranulomatous cholecystitis cases (the great mimicker) with rad path correlation.

## **GIEE-148 What Went Wrong? Hepatobiliopancreatic Postoperative Complications: A Primer for Radiologists**

### **Awards**

#### **Certificate of Merit**

#### Participants

Lucas Roberto Leles Oliveira, MD, Sao Paulo, Brazil (*Presenter*) Nothing to Disclose

#### **TEACHING POINTS**

- Recognize hepatobiliopancreatic (HBP) anatomy and anatomical variations.
- Understand most common types of HBP surgeries.
- Know radiologists role in the pre- and postoperative settings.
- Recognize HBP postoperative complications through multimodality imagings.

#### **TABLE OF CONTENTS/OUTLINE**

INTRODUCTION: o Overview of frequency, relevance, and cost of HBP surgeries. o HBP anatomy including key anatomical variations as they relate to surgical complications. o Summary of most common types of HBP surgeries. 2. IMAGING ON THE PREOPERATIVE SETTING: o Presurgical roadmap to optimize the surgery and avoid complications. o Pros and cons of each imaging modality. 3. IMAGING ON THE POSTOPERATIVE SETTING: o Step by step didactic approach in assessing patients after HBP surgery: § Surgical notes; § What to ask to the multidisciplinary team; § Clinical notes and laboratory tests; § How to decide which imaging modality; § Best protocol; § Ultrasound approach; § CT approach; § MRI approach; § How to report and communicate; o Surgical complications: § Acute versus chronic; § Main groups: vascular, biliary, GI tract, infectious, other. 4. WHAT IS THE ROLE OF INTERVENTIONAL RADIOLOGY. 5. WHAT'S ON THE HORIZON. 6. INTERACTIVE CHALLENGING SCENARIOS.

## **GIEE-149 Back to the Basics: US Findings in Acute Cholecystitis-Tips for New Residents**

#### Participants

Mariana De Los Santos Carmona, MD, Ciudad de Mexico, Mexico (*Presenter*) Nothing to Disclose

#### **TEACHING POINTS**

To show normal anatomy, pathology and its variants.-To identify in a simpler way the ultrasonographic characteristics of acute cholecystitis, in special for new residents.-To recognize different clinical characteristics that help to recognize acute cholecystitis.-To give advice for new residents when performing an ultrasound, to help base the most accurate diagnosis and thus decide on interdisciplinary management.-To be familiar with the sonographic technique, tips, pitfalls, limitations and troubleshooting for the right upper quadrant pain.-This discussion will help residents to reinforce the radiological and clinical features of acute cholecystitis, keeping in mind that interdisciplinary consensus remains the gold standard for diagnosis

#### **TABLE OF CONTENTS/OUTLINE**

1.Objectives.2.Review the anatomy of the gallbladder and its variants. 3.Discuss the global panorama about the importance of acute cholecystitis. 4.Explain the clinical characteristics based on Tokyo's criteria for acute cholecystitis as a multidisciplinary approach. 5.Discuss the algorithm of the ultrasound technique used to evaluate the right upper quadrant pain. 6.Recognize and illustrate the main ultrasonographic findings in this pathology. 7.Present a series of cases to exemplify the most important ultrasonographic findings of acute cholecystitis, as well tips for the correct approach. 8.Recognize differential diagnoses of right upper quadrant pain. 9.Conclusions. 10.References

## **GIEE-15 Clinical Photon Counting Abdominopelvic CT: A Crash Course!**

### **Awards**

#### **Certificate of Merit**

#### Participants

Bari Dane, MD, New York, NY (*Presenter*) Nothing to Disclose

#### **TEACHING POINTS**

Conventional CT uses energy integrating detectors (EID), in which x-rays create visible light that is converted to electrical pulses to create images. Photon counting CT (PCCT) detectors directly convert photons into electrical pulses, allowing electronic noise elimination and leading to significant dose reduction. Unlike EID, PCCT counts the energy of each photon, including low energy photons. This improves image contrast, makes every CT multienergy, and permits electronic baseline noise removal. Downsides include K-escape and charge sharing in PCCT can reduce spectral separation.

#### **TABLE OF CONTENTS/OUTLINE**

1. PCCT versus EID physics2. Clinical benefits a. Improved spatial and contrast resolution, without dose penalty - Small vessel visualization - Small lesion visibility and characterization in low contrast areas (pancreas, liver, peritoneum) - Better iodine contrast to noise ratio, lower intravenous contrast dose b. Multienergy every scan - Simultaneous high pitch and multienergy - Incidental finding characterization c. Remove electronic noise - Better image quality in obese patients - Lower dose CT - Better virtual noncontrast (VNC) image quality3. Current Version Pitfalls a. Cross-scatter artifact with dual-source mode b. Urographic phase derived VNC artifact c. Slower reconstruction time

## **GIEE-150 MRI Anal Fistula: Anatomy of Anal Canal**

#### Participants

Christian Torres Ramirez, MD, (*Presenter*) Nothing to Disclose

#### **TEACHING POINTS**

Learning objectiveIdentify the anatomy of the anal canal by MRI to achieve an adequate classification of anal fistula.IntroductionThe anal fistula corresponds to an anomalous path that connects the anal canal with the skin. MRI is the imaging modality of choice due to its high resolution, allowing an adequate characterization of the anatomy and also greater precision in the classification of the anal fistula.Teaching pointsThe anal canal is limited between the dentate line and the anal verge. The layers of this wall are mucosa, submucosa and muscularis. The muscularis layer is composed from the innermost to the outermost layer, by the internal anal sphincter(IAS), the intersphincteric liner and the external anal sphincter(EAS). The IAS is a continuation of the

muscular layer of the rectum, and the EAS is composed of skeletal muscle. The MRI is the imaging modality recommended in ESGAR consensus. The protocol used in our institution is performed in 1.5 T and 3 T, the MRI sequences and the planes are axial, coronal and sagittal T2-weighted, and post-contrast T1-weighted sequences are performed. The axial acquisition performed align with respect to anal canal axis. By magnetic resonance imaging in axial T2-weighted sequences, the anal canal is a circumference of 5 layers: the innermost layer mucosa (hyperintense), submucosa (hypointense), IAS (hyperintense), intersphincteric liner (hyperintense) and the outermost layer EAS (hypointense). The Parks classification is used for anal fistula: intersphincteric, transsphincteric, suprasphincteric and extrasphincteric.

#### TABLE OF CONTENTS/OUTLINE

1. Learning objective  
2. Introduction  
3. Teaching points

#### **GIEE-152 The Anterior and Sub-peritoneal Compartments of The Extraperitoneal Space: Comprehensive Imaging Review of Anatomy and Pathologies**

Participants

Arvin Saremi, MS, (*Presenter*) Nothing to Disclose

#### TEACHING POINTS

Review the relevant anatomy of the structures participating in formation of the anterior extraperitoneal space  
Review characteristic imaging findings of common and uncommon pathologies involving this region

#### TABLE OF CONTENTS/OUTLINE

Normal embryology and anatomy of the anterior extraperitoneal space  
Development Transversalis fascia Umbilical prevesical fascia Umbilicovesical fascia Fascia around the round ligament  
Imaging characteristics with cadaveric correlation  
Abdominal above the umbilicus  
Retropubic or prevesical space of Retzius  
Prevesical, perivesical, and paravesical spaces  
The retroinguinal space of Bogros  
Connections to Subperitoneal pelvic space, presacral space and retroperitoneum  
Relationship to the vessels, median and medial umbilical ligaments  
Anatomical variations  
Abnormalities of the anterior extraperitoneal space  
Infection and abscess  
Post trauma changes  
Malignancies  
Relevance for extraperitoneal laparoscopic surgery  
Relevant considerations for percutaneous interventions

#### **GIEE-153 All of the Guts, None of the Glory: An Overview of the Abdominal Radiograph**

Participants

Elaine Smith, MD, Birmingham, AL (*Presenter*) Nothing to Disclose

#### TEACHING POINTS

1. Review the most common bowel pathology and gas appearances on abdominal radiographs and understand clinical relevance.  
2. Discuss common and uncommon calcifications that can be seen on the abdominal radiograph.  
3. Highlight most common "corner" pitfalls to increase sensitivity for these commonly missed pathologies.

#### TABLE OF CONTENTS/OUTLINE

Introduction  
Bowel- Small bowel obstruction- Large bowel obstruction- Ileus- Enteritis/colitis- Pneumatosis  
Air- Free intraperitoneal air- Portal venous gas- Retroperitoneal gas- Emphysematous cholecystitis- Emphysematous cystitis  
Calcifications- Renal stones- Gallstones- Calcified mass(es)- Vascular  
Corners- Lung bases- Cardiac- Proximal thighs  
Conclusion

#### **GIEE-154 The Spectrum of Interpretive and Perceptual Biases in Abdominal Radiology**

**Awards**

**Identified for RadioGraphics**

Participants

Jonathan Kruskal, MBChB, Boston, MA (*Presenter*) Nothing to Disclose

#### TEACHING POINTS

For abdominal radiologists, cognitive biases impact our interpretive and perceptual skills predisposing to diagnostic errors. Published data suggests that such biases are particularly common and impactful in abdominal radiology. A broad spectrum of recognized (common and less common) as well as newly emerging biases occur in abdominal radiology. Being aware of one's personal diagnostic biases, as well as strategies for mitigating their occurrence, is likely to improve our diagnostic performance. Familiarity with the spectrum of biases enables cases to be categorized in the peer learning and improvement meeting.

#### TABLE OF CONTENTS/OUTLINE

What are cognitive biases? How do biases impact abdominal radiologists? How to construct your Personal Bias Profile? Brief explanations, clinical examples and strategies for mitigating the following biases:  
Common biases: anchoring, confirmation, availability, automation, bandwagon, satisfaction of search and of report, premature closure, zebra retreat, representative, outcomes, framing, attribution, context, authority, premature closure, provider, hindsight, alliterative, blind spot, regret, scout neglect and inattention biases.  
Newly recognized biases: hanging protocol, risk averse, clinical trial, demographic, productivity, follow up, trainee assumption, provisional report, structured report and remote reader biases.

#### **GIEE-155 Drug-associated Hepatobiliary and Pancreatic Disorders: Pictorial Essay**

Participants

Shintaro Ichikawa, MD, PhD, Hamamatsu, Japan (*Presenter*) Nothing to Disclose

#### TEACHING POINTS

Various disorders of the hepatobiliary system and pancreas are caused by several drugs, and imaging diagnosis is often challenging. Familiarity with these conditions may improve diagnostic accuracy and patient management. The purpose of this presentation is to describe the imaging findings of drug-associated hepatobiliary and pancreatic disorders and to identify tips for correct diagnosis.

#### TABLE OF CONTENTS/OUTLINE

The following drug-associated hepatobiliary and pancreatic disorders are discussed along with their key imaging findings: 1. Drug-induced acute liver failure Imaging findings are non-specific and include hepatomegaly with heterogeneous parenchymal enhancement, periportal edema, gallbladder wall thickening, and ascites. 2. Sinusoidal obstruction syndrome (SOS) A diffuse hypointense reticular pattern in the hepatobiliary phase is a highly specific sign for the diagnosis. 3. Pseudocirrhosis Imaging manifestations may be identical to those of liver cirrhosis. 4. Immune-related adverse events (irAEs) Cholangitis and pancreatitis may develop after immune checkpoint inhibitors therapy. 5. Methotrexate-associated lymphoproliferative disorders It is visible as a periportal infiltrating hypodense mass on computed tomography and is weakly enhanced. 6. Amiodarone deposition in the liver 7. Ceftriaxone-associated gallbladder pseudolithiasis 8. Secondary iron overload

### **GIEE-156 "Don't Forget Me!" Said the Spleen: Multimodality Imaging of The Spleen and Its Pathology**

Participants

Adrian Xu, MD, Salt Lake City, UT (*Presenter*) Nothing to Disclose

#### **TEACHING POINTS**

Know the normal anatomy of the spleen Identify congenital anomalies of the spleen and their associated systemic pathologies Understand the multiple imaging modalities used in the assessment of splenic pathologies and the pitfalls Know and accurately diagnose focal and diffuse pathologies in the spleen on imaging

#### **TABLE OF CONTENTS/OUTLINE**

A. Anatomy B. Multimodality imaging of the spleen and associated pitfalls C. Splenic pathologies 1. Congenital including asplenia and polysplenia and their associated imaging findings in other systems 2. Focal masses i. Benign ii. Indeterminant iii. Malignant 3. Diffuse processes (Splenomegaly/granulomas) 4. Other i. Rupture ii. Infarct iii. Splenosis iv. Peliosis D. Summary

### **GIEE-158 Spectrum of Findings After Radiation-based Therapy In the Liver**

Participants

Emre Altinmakas, MD, New York, NY (*Presenter*) Nothing to Disclose

#### **TEACHING POINTS**

Stereotactic body radiotherapy (SBRT) and transarterial radioembolization (TARE) with Yttrium-90 are the two commonly used treatment options for primary liver cancer and liver metastasis in patients unsuitable for surgery. Patients receiving such treatments require to undergo imaging surveillance with CT or MRI as there is possibility of incomplete tumor response. Careful assessment of these follow-up studies is essential to proper patient management. It is also crucial for radiologist to be aware of expected treatment-specific changes within the treatment zone as well as non-treated liver parenchyma following each type of treatment. The purposes of this exhibit are 1. To discuss the concept of tumor response assessment after radiation-based therapies 2. Demonstrate expected posttreatment changes within the targeted as well as surrounding non-targeted liver parenchyma following SBRT and TARE 3. To review potential complications of radiation-based therapies

#### **TABLE OF CONTENTS/OUTLINE**

Table of contents/outline 1. What are the optimal imaging follow-up strategies after radiation-based therapies for liver cancer? 2. How should we assess response after SBRT? • Imaging features of non-viable tumor • Imaging features of viable tumor 3. How should we assess response after TARE? • Imaging features of non-viable tumor • Imaging features of viable tumor 4. What are the expected posttreatment findings within targeted region as well as surrounding off-target liver following TARE and SBRT? 5. Potential complications of radiation-based therapies 6. Summary

### **GIEE-159 Atypical Focal Nodular Hyperplasia: Don't Let It Fool You**

**Awards**

**Cum Laude**

Participants

Brendan O'Connor, MD, (*Presenter*) Nothing to Disclose

#### **TEACHING POINTS**

-Focal nodular hyperplasia (FNH) is a benign hepatic lesion with a typical imaging presentation at CT and MR imaging. -Rarely, FNH may show histological components that lead to an atypical imaging presentation mimicking other benign and malignant lesions. Atypical features include intralesional fat, iron, calcifications, sinusoidal dilatation, and significant growth. FNH occurring in an abnormal liver, defined as FNH-like lesions, may present a diagnostic challenge. -Illustrated overview of typical and atypical presentations of FNH and FNH-like lesions with representative rad-path correlation cases, along with key diagnostic clues for an accurate diagnosis of FNH and FNH-like lesions based on a constellation of multiple imaging features to include iso-to-hyperintensity on hepatobiliary phase imaging.

#### **TABLE OF CONTENTS/OUTLINE**

-Epidemiology, pathology of FNH -Typical features of FNH on CT and MR imaging (with extra-cellular and hepatobiliary Gd-based contrast agents). -Atypical imaging presentation of FNH to include steatotic and steatohepatic FNHs, calcification, intralesional sinusoidal dilatation, abnormal growth and intralesional iron-Definition and pathology of FNH-like lesions. -Imaging presentation of FNH-like lesions. -Key clues for accurate diagnosis of FNH and FNH-like lesions and differential diagnosis with other hepatic lesions (e.g hepatocellular adenoma).

### **GIEE-16 Hepatocellular Carcinoma: A Primer for Residents**

**Awards**

**Certificate of Merit**

Participants

Marika Pitot, MD, Rochester, MN (*Presenter*) Nothing to Disclose

#### **TEACHING POINTS**

1) Review the typical imaging appearance of HCC on CT and MRI 2) Learn about the various patterns of HCC presentation 3) Review the recognized histologic subtypes of HCC with an emphasis on characteristic differentiating imaging features 4) Understand HCC imaging features that correlate with favorable versus poor outcome 5) Review LIRADS categorization with some examples

#### TABLE OF CONTENTS/OUTLINE

1. HCC overview a. Typical HCC appearance on imaging b. Patterns of presentation on imaging i. Nodular (expansive) - single, dominant nodule, with or without satellite nodules ii. Multifocal nodules iii. Infiltrative (massive) iv. Cirrhotomimetic v. Pedunculated c. Histologic growth patterns of HCC 2. Histologic subtypes of HCC a. Frequency b. Characteristic and "buzzword" imaging features 3. Favorable and poor prognostic features of HCCs a. Favorable imaging signs include single, small nodule with smooth margins, no necrosis, and homogenous enhancement. Other favorable features include low tumor stiffness on elastography, uptake of hepatobiliary contrast suggestive of beta-catenin activation, and occurrence in a normal or non-cirrhotic liver b. Poor prognostic imaging signs include large size at presentation, multifocality, evidence of necrosis, heterogeneous enhancement, ill-defined margins, and macroscopic vascular invasion. 4. LIRADS characterization overview a. Explanation of LIRADS categorization with examples

#### **GIEE-160 This Is Not a Soap Bubble-What's Going on In The Liver?: A Surviving Guide for Radiological Workup of Cystic Liver Lesions**

Participants  
Gabriella Cagliari, Sao Paulo, Brazil (*Presenter*) Nothing to Disclose

#### TEACHING POINTS

Cystic hepatic lesions are very common in daily practice. The differential diagnosis ranges from benign lesions with no clinical significance to malignant neoplasms and potentially lethal conditions. Some cystic hepatic lesions have classical findings, allowing a correct diagnosis based on imaging findings only. On the other hand, some presentations may be challenging. In most cases, familiarity with the most relevant radiologic key features in combination with critical clinical and laboratory information is enough for adequate lesion characterization. The purpose of this presentation is to review the main cystic liver lesions, recalling imaging features from typical to challenging cases; a series of diagnostic tips will be presented, as well as a practical guide on how to develop objective reasoning in face of such cases.

#### TABLE OF CONTENTS/OUTLINE

1) Review the most common liver cystic lesions and their imaging features with didactical cases. 2) Provide a didactic approach to differential diagnoses. 3) Tips that can be helpful in face of challenging cases. 4) Surviving guide that can be useful for a quick consultation.

#### **GIEE-161 A to Z of Focal Nodular Hyperplasia (FNH)**

Participants  
Sophie Cheshire, MBChB, FRCR, (*Presenter*) Nothing to Disclose

#### TEACHING POINTS

1. Imaging features of FNH including typical findings and rarer features 2. Multiple imaging modalities presented 3. A unique method of presenting the findings using letters of the alphabet as an aide memoir

#### TABLE OF CONTENTS/OUTLINE

FNH is a common benign lesion, encountered on multiple imaging modalities. It is therefore important to recognise the key features of both typical and atypical lesions for accurate diagnosis in order to prevent unnecessary intervention. This display will include ultrasound examples, using both colour doppler and contrast enhanced techniques. All MRI sequences will be demonstrated with key learning points illustrated. The importance of liver specific contrast agents is highlighted, along with the pathology and aetiology of the lesion. The unique selling point for this presentation is the format which should be easy to remember and help in consolidating knowledge. The points to be covered using an A to Z format are as follows: Arterialisation, Biopsy, Contrast enhanced ultrasound, Doppler, Exophytic lesion, Fat, Glutamine synthetase, Hepatobiliary phase, Isointensity, Juicy orange, Kupffer cells, Lobulated, MRI, Nodules, OATP receptors, Pathology, Question, Ring on hepatobiliary phase, Scar, Telangiectatic, Ultrasound, Vascular malformation, Washout, Xtra fun fact, Young, Zero malignant.

#### **GIEE-162 Pumping Iron: Iron Overload Imaging**

Participants  
Timothy McMahon, MD, MS, New York, NY (*Presenter*) Nothing to Disclose

#### TEACHING POINTS

Iron is an essential mineral critical to oxygen transport but it can have a toxic effect at high concentration. Absorption is regulated, but primary hemochromatosis and hemosiderosis lead to toxicity. The liver stores and regulates iron. Primary hemochromatosis and hemosiderosis cause toxic buildup of iron in the liver which has characteristic imaging appearances. Primary hemochromatosis typically affects the liver and pancreas on MRI. Hemosiderosis, which is usually due to frequent blood transfusions secondary to various anemias, typically affects the liver, spleen, and bone marrow. Intravascular hemolysis can affect the kidneys. MRI can qualitatively and quantitatively assess iron overload and assists in diagnosing and managing hemochromatosis and hemosiderosis.

#### TABLE OF CONTENTS/OUTLINE

Intro Iron absorption, transport, and regulation Iron overload causes and clinical impact Diagnosis, treatment, and management of iron overload Imaging Noncontrast CT Typical appearance Confounding factors and differential with cases Dual energy CT Methodology and typical appearance Iron content quantification MRI Basic physics Qualitative assessment In/out of phase imaging analysis Imaging patterns with case examples Quantitative assessment Methodology - Benefits and drawbacks Signal Intensity ratios T2/R2 relaxometry (FerriScan) T2\* and R2\* relaxometry Quantitative Susceptibility Mapping Example cases with effects of treatment SQUID Biomagnetometry - Advantages, disadvantages, and relevance Conclusion

## **GIEE-163 A Multimodality Approach to Inflammatory Bowel Disease and Complications**

### **Awards**

#### **Certificate of Merit**

#### Participants

Weibo Fu, BS, Augusta, GA (*Presenter*) Nothing to Disclose

#### **TEACHING POINTS**

1) To review the pathophysiology of common imaging findings seen in inflammatory bowel disease. 2) To demonstrate barium enema, CT, and MRI findings of acute and chronic inflammatory bowel disease, associated findings, and diverse complications. 3) To discuss the advantages and disadvantages of currently available imaging modalities for inflammatory bowel disease.

#### **TABLE OF CONTENTS/OUTLINE**

Inflammatory bowel disease (IBD) most commonly occurs in North America and Europe, with an estimated combined patient population of 4-5 million in both regions. Incidence of IBD has been gradually rising since the mid-20th century, likely due to widespread changes in dietary patterns along with environmental factors. Cross-sectional imaging modalities such as computed tomography (CT) and magnetic resonance (MR) enterography are now more commonly utilized because of their ability to detect subtle changes in inflammation, high clinical sensitivity, and ability to detect complications such as a) fistulae, b) bowel obstruction, c) intussusception, and d) abscesses outside the bowel lumen. Though resolution for both CT and MR are comparable, MR has the added benefit of zero radiation exposure.

## **GIEE-164 Prediction of Cirrhosis-related Complications at Dual-energy CT and MRI**

#### Participants

Ra On Kang, MD, Jinju, Korea, Republic Of (*Presenter*) Nothing to Disclose

#### **TEACHING POINTS**

\* Describe the clinical states of cirrhosis according to the development of disease complications (varices and decompensation events) with the progression of pathophysiological mechanisms and hemodynamic. \* Discuss the clinical importance of noninvasive prediction of these complications in cirrhosis. \* Discuss how and whether routine dual-energy CT (DECT) and MRI can predict future complications in cirrhosis based on the recent quantitative studies.

#### **TABLE OF CONTENTS/OUTLINE**

Epidemiology  
Clinical states in cirrhosis  
Management implications of clinical states of cirrhosis  
DECT and MRI-based techniques for prediction of cirrhosis-related complications- DECT- T1 mapping- T2 mapping  
Future directions  
Summary

## **GIEE-165 Multiparametric MRI of The Liver: Practical Tips For Starters**

#### Participants

Marina Raze, MD, Sao Paulo, Brazil (*Presenter*) Nothing to Disclose

#### **TEACHING POINTS**

-MAFLD, aprendendo mais sobre a nova 'epidemia'- Learn and review basic protocol sequences for a complete liver assessment- Execution and preparation tips- Limitations for measures of steatosis and iron overload- Illustrate the findings and correlate them with clinic application- Learn how to make illustrative radiology reports- Attention to the most common pitfalls

#### **TABLE OF CONTENTS/OUTLINE**

- Imaging protocols- Imaging aspects that may be mistaken- Pitfalls- Practical examples- Impact the liver evaluation and clinical application in everyday life- Illustrated and structured report

## **GIEE-166 Evaluation of Hepatic Steatosis, Inflammation and Fibrosis in NAFLD by Imaging: An Overview**

#### Participants

Jong Yeong Kim, MD, Seoul, Korea, Republic Of (*Presenter*) Nothing to Disclose

#### **TEACHING POINTS**

Since significant differences are found in the prognosis of NAFLD depending on histological findings including fibrosis and steatosis, exact diagnosis of these conditions is clinically crucial. Many studies for non-invasive methods to estimate the histological severity of NAFLD instead of liver biopsy have been undertaken, mainly in the field of radiological and biochemical examinations. The purposes of this review are 1) to explain the principal, clinical application, pros/cons and limitations of imaging techniques for hepatic steatosis, fibrosis and hepatitis 2) to review the recently developed machine-learning based evaluations (computer aided diagnosis and radiomics) of conventional US, CT and MR images for the measurement of intrahepatic fat and fibrosis, 3) to discuss the future of these techniques, the possibility for wider clinical applications and roles in clinical trials for the treatment of diffuse liver disease

#### **TABLE OF CONTENTS/OUTLINE**

• Background  
• Hepatic steatosis  
1. US based techniques  
1) Gray scale imaging  
2) Controlled attenuation parameter  
3) Attenuation imaging  
2. Unenhanced CT  
3. MRI based techniques  
1) Two point DIXON  
2) MR spectroscopy  
3) MRI-PDFF  
• Differentiation of NASH from simple steatosis  
• Hepatic fibrosis  
1. US based techniques  
1) Transient elastography  
2) Shear wave-based elastography: Point SWE, ARFI, Supersonic shearwave  
2. MRI based techniques  
1) Diffusion weighted imaging  
2) Hepatocyte-specific contrast agent enhanced imaging  
3) MR elastography  
• Machine learning based evaluation of hepatic steatosis and fibrosis with US, CT, MR images  
• Can we replace liver biopsy by imaging studies for hepatic steatosis or fibrosis?  
• Conclusion

## **GIEE-167 Don't Be So thick! A Practical Approach to Common and Uncommon Causes of Gastric Wall Thickening**

#### Participants

Edward Lawrence, MD, PhD, (*Presenter*) Nothing to Disclose

#### TEACHING POINTS

Gastric wall thickening can present a diagnostic challenge due the overlapping features of normal rugal folds, inflammation, and neoplasm. Features that suggest true gastric wall thickening include altered wall enhancement, asymmetric thickening, adjacent stranding, or local adenopathy Lower attenuation (edema) or mural stratification favors a benign process related to infection or inflammation. Intermediate/soft tissue attenuation favors neoplastic processes such as lymphoma or adenocarcinoma. Additional diagnostic work-up will frequently include further evaluation with endoscopy and endoscopic biopsy

#### TABLE OF CONTENTS/OUTLINE

1. Basics of gastric wall evaluation 2. Tips and tricks a. Differentiating true versus pseudo-thickening b. Differentiating malignant versus benign thickening 3. Malignant causes (e.g., linitis plastica, lymphoma, gastric adenocarcinoma) 4. Benign causes - common (e.g., gastritis) and uncommon (e.g., Ménétrier's disease) a. Inflammatory/infiltrative b. Infectious

#### GIEE-168 Spaces and Places: A Radiologist's Roadmap to the Peritoneum and Retroperitoneum

Participants

Christopher Sears, MD, (*Presenter*) Nothing to Disclose

#### TEACHING POINTS

Teaching Points The peritoneum and retroperitoneum, with their myriad spaces, pouches, and ligaments, are difficult to comprehend, let alone identify on imaging. However, understanding how the peritoneal reflections limit, circulate, and react to disease can facilitate the correct diagnosis and proper care. After reviewing this education exhibit, the learner will be able to: Understand and identify structures and spaces of the peritoneum and retroperitoneum. Appreciate the significance of the peritoneum and retroperitoneum, with respect to the spread of and response to infection, the staging of cancers, and the severity and localization of traumatic injuries. Recognize how medical and surgical management changes when peritoneal borders are violated.

#### TABLE OF CONTENTS/OUTLINE

Outline 1.) Overview of the anatomy, spaces, and pouches of the peritoneum and retroperitoneum. 2.) Differences regarding the peritoneum of males and females. 3.) Case-based demonstration of the significance of the peritoneum, with regards to management and outcomes in cancer, trauma. and infection.

#### GIEE-169 Unraveling the Superficial, Internal and Complex Hernias: Case-based Guide for Accurate Diagnosis

Participants

Hunter Sellers, BS, MD, Houston, TX (*Presenter*) Nothing to Disclose

#### TEACHING POINTS

1. Hernias are a very common pathology found on imaging with a large variety of presentation types. We provide multiple examples of hernias, both superficial and internal. 2. Superficial hernias can occur anywhere along the anterior, lateral, or posterior abdominal wall and can be simple containing only fat, or complex containing organs. We have cases of these simple and complex hernias, and hernias which contain pathology in the hernia sac. 3. Internal hernias can be intimidating to radiologists who are unfamiliar with the specific imaging patterns, our goal is to provide examples of these hernias along with the etiologies to help improve diagnostic acumen and accuracy. 4. The important goal of reporting pertinent information of type of hernias to clinicians to ensure that patients receive the best treatment possible.

#### TABLE OF CONTENTS/OUTLINE

Discussion of superficial hernias, which include inguinal, umbilical, Spigelian, amyand, Richter, incisional and others. Elucidate internal hernias, which include paraduodenal, Foramen of Winslow, Petersen and others. Highlight features of complex hernias. Imaging tips on recognizing specific hernia types. Report pertinent information that the clinicians want to know. Conclusion.

#### GIEE-17 Imaging Diagnosis of Hepatocellular Carcinoma in the Era of Molecular Targeted Therapy and Immunotherapy

##### Awards

##### Certificate of Merit

Participants

Azusa Kitao, MD, PhD, Kanazawa, Japan (*Presenter*) Nothing to Disclose

#### TEACHING POINTS

1. To understand the mechanisms and application of molecular targeted therapy and immuno-therapy for HCC 2. To know the role of imaging in evaluation and prediction of treatment response of HCC 3. To learn the adverse events of these systemic therapies for HCC that can be assessed by imaging

#### TABLE OF CONTENTS/OUTLINE

1. History and treatment mechanisms-Molecular targeted therapy-Immunotherapy 2. Application-Clinical and imaging criteria-Roles in multidisciplinary therapy 3. Evaluation of treatment response-Guidelines, especially in modified response evaluation criteria in solid tumors (RECIST)-Imaging modalities and techniques: dynamic CT, dynamic MRI, contrast enhanced US and radiomics-Pitfalls 4. Prediction of treatment response based on molecular subclassification of HCC-Molecular targeted therapy: dynamic CT, intravoxel incoherent motion (IVIM) and 18F-FDG PET/CT-Immunotherapy: gadoxetate-enhanced MRI 5. Adverse reactions of molecular targeted therapy and immunotherapy-Tumor related reactions-Systemic reactions Summary The radiologists should know the imaging features related to molecular targeted therapy and immunotherapy for HCC in the era of personalized medicine.

#### GIEE-170 Imaging Postoperative Abdomen: What A Radiologist Should Know?

Participants

Smily Sharma, MD, MBBS, Jodhpur, India (*Presenter*) Nothing to Disclose

## TEACHING POINTS

1) To understand the anatomical basis of common and uncommon surgical procedures 2) To elaborate on the salient features of various pathologies encountered in cross-sectional imaging of the post-operative abdomen 3) To illustrate the distinguishing imaging features of complications of laparotomy 4) To propose an algorithmic approach to the differential diagnosis of various pathologies 5) To highlight red flag imaging biomarkers with implications on management strategies

## TABLE OF CONTENTS/OUTLINE

1) Introduction 2) Radiological anatomy of common and uncommon abdominal surgeries 3) Imaging of complications of Hepatobiliary surgeries including Whipple, Extended hepatectomy, Roux en Y jejunostomy, resection and anastomosis, rectal surgeries and Cholecystectomy 4) Imaging of complications of Genitourinary surgeries including nephrectomy, hysterectomy and caesarean section 5) Understanding the chronology and pathophysiology of early and late complications 6) Tailored regimens of cross sectional imaging to optimise image acquisition 7) Diagnostic challenges posed by sequelae of laparotomy including structures, adhesions and scar 8) Endovascular management of Vascular complications of Abdominal surgery 9) Conclusion

## GIEE-171 Basics of RUQ Ultrasound for Trainees: Anatomy, How to Scan and Diagnoses to Know for Call

### Awards

Identified for RadioGraphics  
Magna Cum Laude

Participants

Gail Stanton, MD, Milwaukie, OR (*Presenter*) Nothing to Disclose

## TEACHING POINTS

1.) Understand basic principles of ultrasound and how to acquire ultrasound images of the right upper quadrant. 2.) Review anatomy of the RUQ on cine ultrasound images including hepatobiliary, pancreatic and regional anatomy. 3.) Identify common pathology seen in the right upper quadrant, with a focus on high yield on-call ultrasound findings and diagnoses for trainees.

## TABLE OF CONTENTS/OUTLINE

1.) Basic principles of ultrasound imaging. a.) Ultrasound probe selection and sonographic windows to assess the liver, gallbladder, and pancreas illustrated with images/movies. b.) Knobology basics: Image optimization for best image quality. 2.) Imaging review of labelled cine images of right upper quadrant anatomy. a.) Hepatobiliary - hepatic segments, vasculature, biliary system. b.) Pancreas and upper abdominal vasculature. c.) Regional anatomy - Bowel, right kidney, thorax. 3.) Review imaging of RUQ pathology. a.) Hepatic - diffuse liver disease, mass, abscess, TIPS, portal vein thrombus, portal vein gas. b.) Biliary - Cholecystitis, cholelithiasis, obstruction, choledocholithiasis, adenomyomatosis, gallbladder cancer, pneumobilia. c.) Pancreatic - pancreatic mass, pancreatitis. d.) Peritoneum.

## GIEE-172 Fantastic 'Four': Imaging of Hepatic Segment 4 - Management and Surgical Implications

### Awards

Certificate of Merit

Participants

Bryce Carson, MD, San Antonio, TX (*Presenter*) Nothing to Disclose

## TEACHING POINTS

Discuss anatomy, embryology, arterial, portal venous supply hepatic venous drainage biliary drainage of segment 4 (S4) Review select pseudotumors, developmental, inflammatory, and neoplastic pathologies specific to S4 Discuss the clinical significance of S4 vasculature, bile ducts in living donor liver transplant viability complications

## TABLE OF CONTENTS/OUTLINE

Introduction Anatomy: Couinaud, International Hepato-Pancreatico-Biliary Association New World Terminology Classifications Embryology Hepatic arteries Portal veins Hepatic veins Bile ducts Imaging Modalities: US, CT MRI Implications of living donor transplant hepatic resection surgeries: Hepatic artery thrombosis, venous congestion post-operative bile leak Pseudotumors: Focal fat deposition, sparing perfusion abnormalities due to aberrant vessels Hot quadrant lobe sign in superior vena cava syndrome Target-like lesions in S4 Ciliary Hepatic Foregut cyst Ingested gastric foreign bodies perforating S4: Toothpicks, fish bones wires bristles from grill cleaning brush Mucinous cystic neoplasm of the liver (MCN) Direct tumor extension from stomach gastrohepatic ligament Conclusion Clinical Implications Knowledge of arterial, portal venous, hepatic venous, bile duct anatomy of S4 vascular variations is crucial in successful liver donor liver transplant other left lobe resections. Focal fat sparing, deposition are more common in S4 due to peculiar venous drainage. Given embryologic origin in close proximity to esophagus stomach, MCN ciliated foregut cyst develop exclusively in S4.

## GIEE-173 Utility and Limitations of 18F-FDG PET/CT For the Evaluation of Hepatic Lesions

Participants

Shota Kondo, Hiroshima, Japan (*Presenter*) Nothing to Disclose

## TEACHING POINTS

a. In well-to-moderately differentiated hepatocellular carcinoma (HCC), the 18F-fluorodeoxy-glucose (FDG) uptake tends to be poor. A high FDG uptake is associated with histologically poor differentiation, microvascular invasion, and a poor prognosis. Therefore, 18F-FDG-PET is useful for estimating the malignancy grade of HCC. b. Although most intrahepatic cholangiocellular carcinomas (ICC) show elevated FDG uptake, in some the uptake may be poor. c. A marked FDG uptake may identify rare malignant hepatic tumors such as malignant lymphoma and leiomyosarcoma. d. As it is difficult to differentiate malignant hepatic tumors from inflammation with only the degree of FDG uptake, findings of other imaging modalities should be considered.

## TABLE OF CONTENTS/OUTLINE

1. Molecular background of 18F-FDG 2. Technical and physiological pitfalls of 18F-FDG PET/CT 3. Imaging findings of various hepatic lesions on 18F-FDG-PET/CT scans 4. The advantages and limitations of 18F-FDG-PET/CT vis-à-vis other imaging modalities for the

diagnosis of hepatic lesions 5. The future prospects of nuclear imaging for the diagnosis of hepatic lesions

### **GIEE-174 Multimodality Comprehensive Imaging Review of Benign and Malignant Hepatic Vascular Abnormalities: Pearls and Pitfalls**

Participants

Mohd Zahid, MD, Birmingham, AL (*Presenter*) Nothing to Disclose

#### **TEACHING POINTS**

Hepatic vascular lesions have a wide spectrum of clinical presentations and varying degrees of malignancies. They range from benign tumors such as hepatic hemangiomas, benign/low-grade malignancies such as hepatic small vessel neoplasia, tumors with high malignant potential such as hepatic perivascular epithelioid cell tumors, and hepatic hemangiopericytomas, other tumors with intermediate degrees of malignancy such as hepatic epithelioid hemangioendothelioma, up to malignancies developed more often in the context of immunodeficiency syndrome-Kaposi sarcomas, and high-grade malignancies with a poor outcome such as hepatic angiosarcomas. On Imaging, differentiation of primary malignant vascular tumors of the liver from benign neoplasms or vascular abnormalities is often difficult. After reviewing this exhibit, the learner will be able to: 1. Understand the epidemiology, pathology, and imaging appearance of common and uncommon benign and malignant hepatic vascular lesions or neoplasms 2. Imaging tips to differentiate vascular lesions from other non-vascular abnormalities.

#### **TABLE OF CONTENTS/OUTLINE**

A. WHO Classification of hepatic vascular neoplasms B. Epidemiology and pathophysiology. C. Multimodality imaging of benign and vascular lesions with imaging tips and pitfalls

### **GIEE-175 Pearls in Imaging of Biliary and Vascular Complications of Orthotopic Liver Transplant**

Participants

Ana Gonzalez, Chicago, IL (*Presenter*) Nothing to Disclose

#### **TEACHING POINTS**

1) Orthotopic liver transplantation (OLT) is the definitive treatment for patients with end-stage liver disease accounting for 22.8% of all organ transplantations in the United States (OPTN). 2) Although the advances in OLT have led to reduced morbidity and mortality, the procedure continues to be associated with a high rate of complications occurring in 25-30% of cases (NG 2015). 3) We will highlight the surgical technique and anatomy of OLT with a brief overview of different anastomosis techniques. 4) We will review the imaging techniques for peri- and post-operative evaluation of transplanted grafts including normal imaging appearance post-transplantation. 5) We will summarize the most common post-operative complications following OLT with their associated radiologic findings and discuss possible interventional solutions.

#### **TABLE OF CONTENTS/OUTLINE**

Summary of OLT surgical approach Surgical anatomy with location of anastomoses for the hepatic artery, portal vein, inferior vena cava, and biliary duct system accompanied with illustrations. Imaging of transplanted grafts Grayscale and Doppler ultrasound for routine surveillance post-transplantation. Describe common waveform characteristics seen with specific complications. The use of CT and MRI to further explore suspected abnormalities followed by angiography. Common OLT complications with associated radiologic findings i. Biliary complications including biliary strictures and bilomas. ii. Vascular complications including arterial and venous stenosis, thrombosis, and pseudoaneurysm formation. Brief imaging review of OLT complications pre- and post- treatment with interventional radiology procedures.

### **GIEE-176 Imaging Findings of Post-chemotherapy Non-Metastatic Hepatic Parenchymal Changes**

Participants

San Yu Leung, MBBS, (*Presenter*) Nothing to Disclose

#### **TEACHING POINTS**

Use of chemotherapy has revolutionized management of cancer in past decades. Liver toxicity is commonly observed among different types of chemotherapy drugs. The aim of this exhibit is to illustrate radiological features of various chemotherapy-associated hepatic parenchymal changes, with examples in different imaging modalities, and to demonstrate potential complications of these liver injury patterns with representative cases. Early recognition of these liver conditions allow prompt clinical action to be taken, thus optimizing management and avoiding severe complications.

#### **TABLE OF CONTENTS/OUTLINE**

1. Introduction 2. To illustrate cases and radiological features of: a. Pseudocirrhosis in breast cancer and non breast cancer patients with liver metastasis, as well as its potential complications b. Chemotherapy-related hepatic steatosis c. Chemotherapy-related hepatitis d. Chemotherapy-related cholangiopathy 3. Summary of key teaching points

### **GIEE-177 Ultrasound Based Hepatic Fat Quantification**

Participants

Nuran Seneviratne, MA, MBBS, London, United Kingdom (*Presenter*) Nothing to Disclose

#### **TEACHING POINTS**

Non-alcoholic fatty liver disease (NAFLD) is a growing cause of cirrhosis, hepatocellular carcinoma and liver transplant. Currently, steatosis is graded by subjective assessment of liver echogenicity and attenuation, with significant interobserver variability and sub-optimal detection of mild or greater steatosis ( $S > 0$ ). Controlled Attenuation Parameter is widely used (found in the Fibroscan® system, Echosens). Different disease states and probes impact measurement and for  $S > 0$  steatosis, it has a high false negative rate and low sensitivity. Quantitative metrics are now offered by various vendors, relying on changes in backscatter, attenuation and the speed of sound found in steatotic livers. Attenuation Imaging (Canon) and Ultrasound Guided Attenuation Parameter (General Electric) show excellent  $S > 0$  performance in NAFLD and other aetiologies of hepatic steatosis compared to both MRI and histology. Fatty Liver Attenuation Index (Samsung) shows moderate performance at the  $S > 0$  task in 351 patients with mixed aetiologies of chronic liver disease at histology. Ultrasound Derived Fat Fraction (Siemens Healthineers) obtains 15 point shear wave

and a steatosis percentage from a single large region of interest, also showing excellent S>0 performance. These technologies are in their early stages. Larger clinical trials are needed to determine optimal steatosis grade cut-off values and compare results across vendors.

#### **TABLE OF CONTENTS/OUTLINE**

Introduction Qualitative Assessment Quantitative Assessment Conclusion

#### **GIEE-178 Diffuse Liver Disease and Its Quantification in MRI for Rookies**

Participants

Camilo Soler Becerra, PhD, Bogota, Colombia (*Presenter*) Nothing to Disclose

#### **TEACHING POINTS**

- NAFLD is the most common chronic liver disease worldwide. It has increasing prevalence among adults and children.
- Iron overload may lead to liver cirrhosis, hepatocellular carcinoma, and cardiac and endocrine complications.
- Fibrosis is the final stage of diffuse liver disease, with its complications and which we want to anticipate.
- Measurement of fat, iron overload and liver stiffness by MRI is a noninvasive and accurate approach.
- Knowledge of the protocol and the post-process will lead more hospitals worldwide to diagnose and quantify these pathologies, being of great help to the patient and other specialties. For example, we observe two similar liver parenchyma in images A and B. Still, we identify greater hardness in image B when quantifying liver stiffness, which alerts us about an inflammatory process.

#### **TABLE OF CONTENTS/OUTLINE**

1. Introduction. 2. FatFrac. 3. Iron quantification. 4. Elastography. 5. Conclusions.

#### **GIEE-179 The Falciform Ligament and Ligamentum Teres Hepatis Revisited**

Participants

Tomoya Nishiyama, MD, (*Presenter*) Nothing to Disclose

#### **TEACHING POINTS**

The falciform ligament and the ligamentum teres hepatis have been considered as insignificant embryological remnants that include umbilical artery and vein. The purpose of this educational exhibit is to spotlight the clinical importance of the falciform ligament and the ligamentum teres hepatis in the radiological perspective.

#### **TABLE OF CONTENTS/OUTLINE**

This education exhibit includes 4 categories; (i) clinical embryology; (ii) clinical anatomy; (iii) clinical use for packing material; (iv) pathological conditions and disease process. Schematic illustrations of the embryology and anatomy and case based-presentations using CT images, macroscopic specimens and operative findings will be presented.

#### **GIEE-18 It Looks Like Liver Cancer, But What Is It Really?: Pearls and Pitfalls for Diagnosis of Pathological Entities Mimicking Liver Malignancies**

**Awards**

**Certificate of Merit**

Participants

Hanna Ferreira Dalla Pria, MD, MD Anderson, Houston, TX (*Presenter*) Nothing to Disclose

#### **TEACHING POINTS**

- Recognize the most common mimickers of liver malignancies.
- Illustrate key clinical and imaging findings that may help distinguishing benign from malignant liver lesions.
- Discuss relevant tips including clinical information, and diagnostic workup which could help in making precise diagnosis
- Discuss appropriate management options including, tissue sampling or follow-up.

#### **TABLE OF CONTENTS/OUTLINE**

1. Overview of liver findings on imaging modalities -Prevalence, relevance, costs -Cancer facts and statistics 2022 -ACR white paper recommendations for management of incidental liver lesions 2. Clinical and Pathological Background -Symptoms -Key pathological and laboratorial findings 3. Imaging-based approach to assess mimickers of liver malignancies on imaging -Background liver -Pattern of the liver findings -Combined clinical and imaging algorithm 4. Illustrate a spectrum of imaging findings, differentiation with pathological correlation -Benign nodules: e.g. atypical hemangiomas, inflammatory pseudotumor, FNH-like lesions. -Inflammatory: IgG4-related disease, eosinophilic hepatitis, confluent fibrosis. -Infectious: ex. parasitic infections, pseudotumoral granulomatosis, abscess. -Precancerous: ex. dysplastic nodules, bile duct adenoma. -Miscellaneous: ex. vascular shunts, infarction. 5. Multidisciplinary liver tumor board -What do non-radiologist liver physicians and surgeons need to know -What do radiologists need to ask. 6. Interactive case examples -Sample cases to illustrate challenging scenarios and provide tips to reach a specific diagnoses

#### **GIEE-180 Ultrasound and Computed Tomography in The Evaluation of Mesenteric Lesions**

Participants

Snehal Kose, MBBS, MD, (*Presenter*) Nothing to Disclose

#### **TEACHING POINTS**

Explain the anatomy and contents of the mesentery Describe ultrasound (USG) and computed tomographic (CT) features of primary and secondary solid mesenteric lesions, mesenteric cystic lesions, secondary mesenteric involvement in inflammatory/ infectious conditions like tuberculosis and inflammatory bowel disease and vascular lesions affecting mesentery. Highlight the importance of cross sectional imaging in diagnosis, detection of complications and management of mesenteric lesions Discuss a stepwise algorithm to approach mesenteric lesions for providing thoughtful differentials

#### **TABLE OF CONTENTS/OUTLINE**

Anatomy and contents of the small bowel mesentery USG and computed tomographic (CT) features of - Primary mesenteric solid neoplasms Mesenteric cystic lesions Unilocular cysts Multilocular cysts Secondary mesenteric solid lesions and their routes of spread Deposits Lymphadenopathy Stellate mesentery Mesenteric involvement in tuberculosis and inflammatory bowel disease Vascular anomalies of mesentery SMA thrombosis with acute mesenteric ischemia SMA-SMV arteriovenous fistula Complications due to mesenteric lesions Bowel Urological Vascular Management of mesenteric lesions Image guided biopsy Planning surgical strategy Stepwise algorithm for imaging evaluation of mesenteric lesions

### **GIEE-181 Diagnostic Approach to Peritoneal Lesions**

Participants

Mihran Khdir, MBChB, (*Presenter*) Nothing to Disclose

#### **TEACHING POINTS**

A wide spectrum of abnormalities affect the peritoneum; including neoplastic, infectious, and inflammatory etiologies as well as spread of ectopic tissues. Anatomy of the peritoneal cavity and its ligaments determine the patterns of disease spread. In this educational exhibit, we provide a comprehensive radiologic diagnostic approach to peritoneal lesions based of the predominant composition (solid, cystic, hemorrhagic, calcific, lipomatous, and gas containing). Each entity will be discussed briefly along with illustrated images of various cases.

#### **TABLE OF CONTENTS/OUTLINE**

Peritoneal Anatomy; Outline of Diagnostic Approach to Peritoneal Lesions; Solid Lesions; Cystic Lesions; Hemorrhagic Lesions; Calcific Lesions; Lipomatous Lesions; Gas Containing Lesions

### **GIEE-182 Peritoneal Carcinomatosis on CT and MR: How Not to Miss A Single Case**

Participants

Ana Veron, MD, (*Presenter*) Nothing to Disclose

#### **TEACHING POINTS**

To depict the most frequent and the not so common sites and imaging features of peritoneal carcinomatosis on CT and MR. To propose how to systematically look for peritoneal implants on CT and MR, acknowledging the technical limitations. To describe the differential diagnosis and pitfalls

#### **TABLE OF CONTENTS/OUTLINE**

IntroductionThe peritoneum is the second most common metastatic localization for abdominal tumors, only surpassed by the liver. Peritoneal metastases in tumors of an extraabdominal origin occur less frequently. Early diagnosis of peritoneal carcinomatosis based on imaging findings is not always easy but it is essential in staging and managing primary tumors. CT is usually the first diagnostic tool but its performance is poor when it comes to detecting subcentimetric implants and those in anatomically difficult sites. MR has proved to have a better performance due to its better contrast resolution. Material and methodsThe revision of 300 peritoneal carcinomatosis cases from our database (comprising tumors of digestive origin, breast, gynecologic, testicular, renal, neuroendocrine, melanoma, lung, head and neck and soft tissue) has allowed us to establish a systematic diagnostic approach. Examples of the how and where to look for peritoneal implants, bearing in mind the anatomical sites and the major pathways of spread will be described, enhancing the added value of multiplanar reconstructions. Typical and less common presentations will be described using a case-based approach. Despite the non-specificity of the imaging findings, in some cases there are helpful hints to suggest the origin of the primary tumor. Examples of pitfalls and differential diagnosis will also be discussed.

### **GIEE-183HC MR Defecography For the Evaluation of Pelvic Floor Dysfunction**

Participants

EUNBYUL CHO, (*Presenter*) Nothing to Disclose

#### **TEACHING POINTS**

Among the worldwide women, pelvic floor disorder is common health problem which is hard to say other people. and it is significant problem lowering their quality of life and causing to morbidity. Pelvic floor disorder means overall pelvic floor functional disorders caused by impairment of the ligament, fascia, muscles supporting the pelvic organs. Conventional defecography is performed with fluoroscopy after injection of barium contrast to rectum. But it can evaluate pelvic floor disorder concentrating posterior compartment of pelvic floor and has risk of exposure to ionizing radiation to patient and doctor. MR defecography is dynamic study to evaluate pelvic floor disorder during defecation using US gel in real time and has been proven accurate and reliable for checking multiple compartments of pelvic floor. It is used to diagnosis of rectocele, intussusception, and anismus. we review normal female pelvic floor anatomy and MR defecography which can accurate diagnosis of pelvic floor disorder involving all three compartments of pelvic floor and improve the postoperative results. Our teaching points are as follows. To review normal anatomy of the pelvic floor, To compare MR defecography to fluor defecography, To introduce the concepts of the integral theory ; anatomically-based diagnostic methods locate damaged structure.

#### **TABLE OF CONTENTS/OUTLINE**

1) Subdivisions of female pelvic anatomy (three compartment) : anterior compartment -middle compartment -posterior compartment  
2) Defecation function evaluation 3) Comparison of fluoro defecography and MR defecography. 4) Introduce the concepts of the integral theory Please visit the Learning Center to also view this presentation in hardcopy format.

### **GIEE-184 MRCP Image Optimization**

Participants

Khyati Bidani, MBBS, New Delhi, India (*Presenter*) Nothing to Disclose

#### **TEACHING POINTS**

1. Using ultrafast technique (RARE< HASTE< SSFSE) reduces artifacts and improves acquisition time  
2. Use breathing independent sequences

## TABLE OF CONTENTS/OUTLINE

1. Applications of MRCP (Congenital anomalies, choledocholithiasis, biliary strictures, cystic pancreatic tumors, biliary injuries). 2. Common indications (Failed MRCP, contraindication to MRCP and post biliary-enteric anastomosis case). 3. Advantages and disadvantages of MRCP over ERCP. 4. Techniques (2D Vs. 3D). 5. Factors affecting image quality. 6. Artifacts (Susceptibility, motion and other artifacts). 7. Image optimization techniques.

### **GIEE-185 Gastric Cancer: Pearls, Pitfalls and Lessons Learned from The Multidisciplinary Tumor Board**

Participants

Stephen Kwak, MD, Rochester, NY (*Presenter*) Nothing to Disclose

#### **TEACHING POINTS**

Gastric carcinoma is one of the most common malignancies worldwide and is currently the fourth leading cause of cancer-related deaths. While early gastric cancers are limited to the mucosa and submucosa and usually manifest as focal wall thickening with possible ulceration, advanced cancers involve the muscularis propria or even deeper, manifesting as diffuse, infiltrative thickening with ulceration and possible linitis plastica. Upper gastrointestinal endoscopy is currently accepted as the gold standard for detection of gastric cancer, while Multidetector Computed Tomography (MDCT) is preferred for staging of the tumor. MDCT allows for assessment of tumor depth, lymph node involvement, and disease spread which may be through subperitoneal dissemination, direct invasion, transperitoneal dissemination, or hematogenous spread. Careful preoperative staging is essential for proper surgical treatment, as complete resection of the tumor and surrounding lymph nodes is the only cure. In this exhibit we will discuss the MDCT technique and imaging features of gastric cancer with treatment approaches and various pearls and pitfalls learned during our experience at gastric cancer tumor board.

#### **TABLE OF CONTENTS/OUTLINE**

Introduction; Staging of gastric cancer; Imaging modalities; Treatment algorithm; Medical management; Surgical management; Imaging; Pearls and Pitfalls

### **GIEE-186 Postoperative Upper Gastrointestinal Fluoroscopy: What the Radiologist Needs to Know**

Participants

Matheus Fritzen, MD, Sao Paulo, Brazil (*Presenter*) Nothing to Disclose

#### **TEACHING POINTS**

- Describe the surgical anatomy and normal imaging findings of the main upper gastrointestinal surgeries in fluoroscopy. - Evaluate the main imaging findings of the routine use of postoperative contrast swallow. - Illustrate the major complications of upper gastrointestinal surgeries.

#### **TABLE OF CONTENTS/OUTLINE**

- Describe major headings (e.g., anatomy, physiology, imaging techniques, etc.) - Describe the following surgeries and identify the major complications of these: Bariatric Surgery (Sleeve and Y-Roux), gastrectomy, Nissen fundoplication, hiatus hernia repair, Peroral endoscopic myotomy (POEM)- Imaging in postoperative barium or iodine contrast to diagnose the main postoperative complications.

### **GIEE-187HC Preoperative MRCP for Laparoscopic Cholecystectomy: What Radiologists Need to Know**

Participants

Young-Hwan Lee, MD, Iksan, Korea, Republic Of (*Presenter*) Nothing to Disclose

#### **TEACHING POINTS**

1. To clarify the role of MRCP in preoperative evaluation of acute or chronic cholecystitis. 2. To understand the normal variations of bile duct anatomy to avoid surgical injury in laparoscopic cholecystectomy. 3. To describe the useful MRCP findings for differential diagnosis of various wall thickening gallbladder lesions.

#### **TABLE OF CONTENTS/OUTLINE**

1. Review of various MRCP techniques 2. Classification of bile duct anatomy using MRCP of a total of 879 patients were examined before laparoscopic cholecystectomy. Cases of bile duct injury during cholecystectomy were added. 3. Representative cases of gallbladder diseases, such as acute cholecystitis, chronic cholecystitis, gallstones, adenomyomatosis, xanthogranulomatous cholecystitis, Mirizzi syndrome, cholangitis with common bile duct stones, and wall thickening type gallbladder carcinoma, were included, and their imaging findings with literature review were illustrated. Conclusion: MRCP is a useful method for preoperative evaluation of biliary anatomy to prevent surgical complications. In various cases such as inflammatory and malignant diseases, accurate diagnosis is possible through preoperative MRCP. Please visit the Learning Center to also view this presentation in hardcopy format.

### **GIEE-188 The Typical and Atypical Appearances of Pancreatic Neuroendocrine Tumors: The Role of CT Angiography and Cinematic Rendering**

Participants

Elliot Fishman, MD, Owings Mills, MD (*Presenter*) Co-founder, HipGraphics, Inc; Stockholder, HipGraphics, Inc; Institutional Grant support, Siemens AG; Institutional Grant support, General Electric Company; Consultant, Exact Sciences Corporation; Consultant, Imaging Endpoints

#### **TEACHING POINTS**

1. Understand how to use multiphase CT with CT angiography and 3D mapping with Cinematic Rendering to optimize detection of pancreatic neuroendocrine tumors 2. understand the range of appearance of pancreatic neuroendocrine tumors and how to distinguish them from other pancreatic tumors 3. learn how to optimize staging of pancreatic neuroendocrine tumors by creating vascular 3D maps for staging of vascular involvement and for pre-op surgical planning 4. understand the challenges and pitfalls in the diagnosis of pancreatic neuroendocrine tumors 5. understand how cinematic rendering can be valuable in small tumor detection and staging of larger tumors

## TABLE OF CONTENTS/OUTLINE

1. CT scan protocols and role of dual phase imaging and CTA2. role of Cinematic Rendering and how to optimize cinematic rendering for lesion detection and staging.3. learn how to generate and interpret the images created by Cinematic rendering4. case studies and examples showing typical and atypical appearances5. potential pitfalls and challenges6. role of CT and AI in the near time to help build on cinematic rendering over time.

### **GIEE-189 Covid-19- Associated Secondary Sclerosing Cholangitis: Imaging Features on Magnetic Resonance Imaging and Magnetic Resonance Cholangiopancreatography**

Participants

Manon Germann, Zurich, Switzerland (*Presenter*) Nothing to Disclose

#### TEACHING POINTS

- Prolonged cholestasis in critically ill patients after severe COVID-19 infection may indicate the presence of secondary sclerosing cholangitis (SSC).
- Affected patients are at high risk of progression to biliary cirrhosis requiring liver transplantation.
- Since differential diagnosis to other causes of cholestatic liver injury can be difficult based on clinical and laboratory findings alone, imaging with MRI and MRCP can be crucial to help confirm the diagnosis.
- COVID 19-associated SSC mostly affects intrahepatic bile ducts showing strictures with or without upstream dilatation, bile duct beading, vanishing ducts and periductal edema.
- The extrahepatic bile ducts are typically spared.
- Changes of the liver parenchyma are commonly observed including patchy arterial enhancement, reduced uptake of hepatobiliary contrast agent and signal changes on T2- and diffusion weighted-images.
- Hepatic macrovascular changes and periportal lymphadenopathy are not typically seen.

## TABLE OF CONTENTS/OUTLINE

1) Background a. Epidemiology b. Pathogenesis c. Clinical presentation d. Diagnosis 2) Imaging findings a. Biliary tree b. Liver parenchyma c. Hepatic vessels d. Other findings 3) Clinical implication and prognosis 4) Conclusion

### **GIEE-19 Response Evaluation Criteria in GI Cancers: What to Use and How to Measure: An Emerging Challenge in the Era of Novel Cancer Treatments**

**Awards**

**Identified for RadioGraphics**

Participants

Francesca Castagnoli, MD, (*Presenter*) Nothing to Disclose

#### TEACHING POINTS

- Therapeutic response is assessed by tumour diameter measurements (WHO, RECIST 1.1, and iRECIST), tumour enhancement (mRECIST, EASL, RECLIC) or CT density (CHOI). Metabolic response is measured on PET by the standardized uptake value (SUV) normalized to the lean body weight (PERCIST).
- Novel therapeutics and therapy-induced non-tumoral changes can lead to interpretation pitfalls.
- In rectal cancer, MRI-derived tumour regression grade (TRG) infers pathological response to guide treatment and disease prognosis.
- Functional imaging, radiomics, artificial intelligence and machine learning provide new and early biomarkers of response but require further qualification.

## TABLE OF CONTENTS/OUTLINE

- GI Cancer therapies: 1) FDA-approved chemotherapies, targeted therapies and immunotherapies 2) external/internal radiotherapy
- Imaging response criteria: when, where and how?
- Patterns of response, stable disease and progression.
- Atypical response patterns: pseudo-progression, hyper-progression, dissociated response, abscopal effect.
- Potential pitfalls from non-tumoral effects of treatment: Hepatic steatosis, Sinusoidal obstruction syndrome, Others.
- MRI-TRG [after Mandard/Rodel] applied to rectal cancer after neoadjuvant treatment.
- LI-RADS, a structured reporting system, for treatment response of hepatocellular carcinoma.
- Imaging response evaluation after neoadjuvant treatments of pancreatic cancer.
- Functional imaging: DCE-MRI, DWI and others; myth or reality?
- Radiomics: summary of current evidence.
- AI and machine learning: potential applications

### **GIEE-190 Hyperthermic Intraperitoneal Chemotherapy (HIPEC): A Radiological Primer**

Participants

Mary Renton, MBCh, (*Presenter*) Nothing to Disclose

#### TEACHING POINTS

- The treatment of peritoneal carcinomatosis has been revolutionised by cytoreductive surgery with hyperthermic intraperitoneal chemotherapy (HIPEC).- HIPEC is used in a combined approach immediately following surgery and involves heated chemotherapy agents being temporarily instilled into the abdominopelvic cavity.- The associated high morbidity means an optimised patient selection process is vital.- We review key patterns of peritoneal disease and their prognostic implications.- We summarise common and important HIPEC complications.

## TABLE OF CONTENTS/OUTLINE

- Background into the clinical indications and outcomes for HIPEC.- Review of common sites of peritoneal disease and types (nodular, mass or plaque-like).- Review of prognostic imaging features, including, gastrointestinal involvement, mesenteric and retroperitoneal lymphadenopathy, ureteric obstruction, psoas or pelvic sidewall involvement and gastrohepatic ligament disease.- Review of radiological contraindications to HIPEC, including extra-abdominal metastases and massive retroperitoneal lymphadenopathy.- Review of post-HIPEC complications, including ascites, splenic/ovarian venous thrombosis, pseudoaneurysm, haemoperitoneum, lymphocyte, perihepatic hematoma, pancreatic fistula and ureteric injury.- Importance of radiological assessment in the selection and management of HIPEC patients.

### **GIEE-191 Spleen Doppler and Elastography: What the Radiologist Needs to Know**

Participants

Mariana Del Rio Gonzalez, MD, Monterrey, Mexico (*Presenter*) Nothing to Disclose

#### TEACHING POINTS

1- To review splenic and vascular anatomy. 2- To discuss the differences in Strain and Shear Wave Elastography. 3- To identify the different techniques of Shear Wave Elastography. 4- To learn the indications and adequate protocol of splenic Doppler and Elastography. 5- To teach how to interpret and report findings.

#### TABLE OF CONTENTS/OUTLINE

1. Introduction 2. Splenic anatomy: A) Parenchyma B) Circulation 3. Elastography: A) Strain vs Shear Wave 4. Shear Wave Techniques: A) 1D Transient Elastography B) Point Shear Wave Elastography C) 2D Shear Wave Elastography 5. Indications 6. Protocol: A) Technique B) Errors C) Artifacts 7. Report: A) Interpretation B) Suggested Reporting

#### **GIEE-2 In Search of Harmony: Where Do We Still Disagree in the Radiological TNM Staging of Rectal Cancer?: A Pictorial Review Based on the Published Findings of a Recent International Survey and Multidisciplinary Expert Consensus**

Participants

Ulysses Torres, MD, PhD, Sao Paulo, Brazil (*Presenter*) Nothing to Disclose

#### TEACHING POINTS

- Recently, a global online survey was carried out among 321 experts from 32 countries to identify points of controversy in the applicability of the TNM system (8th ed.) for the radiological staging of rectal cancer. A total of 16 problem areas were identified, grouped in topics related to clinical tumor staging in low-rectal cancers, definitions for cT4b and cM1a disease, definitions for mesorectal fascia involvement, evaluation of lymph nodes versus tumor deposits, and staging of lateral lymph nodes.- These critical areas remain considerable points of dissensus even among experts in rectal cancer imaging, and their awareness by residents, general radiologists, and even abdominal radiologists is paramount for better and more consistent use of the TNM system in the everyday radiological practice.- An illustrated case-based review with schematic drawings may be a didactical and straightforward way of exhibiting such a range of controversies, facilitating their comprehension by a general audience. Secondly, it may also help make more understandable the points of consensus proposed and published by the international multidisciplinary panel of specialists.

#### TABLE OF CONTENTS/OUTLINE

1) Presentation of the 16 problem areas identified, illustrating them with schematical drawings. 2) Imaging-based review with didactical clinical cases exhibiting such critical points of controversies. 3) Tips on how to report the radiological findings in such cases in the light of the consensus proposed by the panel of experts.

#### **GIEE-20 Early Detection of Pancreas Adenocarcinoma: Time to Give Up or Time to Double Survival?**

Participants

Hala Khasawneh, MBBS, Rochester, MN (*Presenter*) Nothing to Disclose

#### TEACHING POINTS

Highlight the emerging concepts and recent advances in the domain of early detection of pancreas ductal adenocarcinoma (PDA):  
1. Dire prognosis of PDA: Early detection is the only intervention with the highest potential to improve outcomes  
2. Rationale for early detection: Substantial differences in the 5-year survival between stage I (26-months) versus stage IV disease (4.8-months)  
3. Challenges of early detection including inability of imaging to identify early PDA  
4. Emerging evidence supporting the role of Artificial Intelligence (AI) to augment imaging-based screening efforts for early detection of PDA in high-risk cohorts

#### TABLE OF CONTENTS/OUTLINE

1. PDA as an almost uniformly fatal disease  
2. Rationale for early PDA detection: What is "early" PDA and why is it critical to detect PDA at a stage when surgical cure is a possibility?  
3. Challenges and opportunities for population-based screening for PDA  
a) The Define (D)-Enrich (E)-Find (F) protocol as an emerging paradigm  
4. High-risk cohorts: a) Familial PDA and subjects with germline mutations b) New-onset diabetes (NOD) with high Enriching New-Onset Diabetes for Pancreas Cancer model (END-PAC) score c) Potential precursor lesions such as intraductal papillary mucinous neoplasms  
5. Limitations of imaging to detect early or incidental PDA: a) Imaging findings of early PDA b) Factors contributing to missed PDA on imaging  
6. AI tools being developed to augment screening efforts for PDA: a) Pancreas segmentation tools b) Imaging signature of pancreatic carcinogenesis at the prediagnostic stage c) AI-augmented detection of PDA on CTs  
7. Potential utility of molecular imaging for early detection of PDA

#### **GIEE-21 Imaging of Young-onset Colorectal Cancer**

Participants

James Fish, MBBS, London, United Kingdom (*Presenter*) Nothing to Disclose

#### TEACHING POINTS

Young onset colorectal cancer is defined as a colorectal tumour diagnosed at < 50 years. The incidence of young-onset colorectal cancer is on the rise, currently constituting approximately 10% of all cases. As such, reporting radiologists should have a good understanding of the imaging features and considerations associated with such patients including:  
• The risk factors and pre-disposing conditions associated with young-onset colorectal cancer.  
• The imaging manifestations frequently encountered on CT and MRI with correlation to histopathology and genetic markers.  
• Imaging appearances during the disease course including complex surgical management.

#### TABLE OF CONTENTS/OUTLINE

A case based educational exhibit including multiple examples of young-onset colorectal cancer with referenced teaching points. To include:  
• Demographics and epidemiology  
• Risk factors associated with young-onset colorectal cancer and associated imaging features. Including Hereditary syndromes (e.g. Lynch syndrome), genetic mutations and inflammatory bowel disease  
• Imaging presentations on MRI and CT with histopathological and genetic correlation, including synchronous or metachronous cancers.  
• Staging imaging and imaging during the disease course.  
• Post-treatment appearances, including complex surgical management e.g. exenteration, pelvic side wall clearance and peritoneal therapies.  
• Risk stratification and follow-up imaging surveillance.

## GIEE-22 Posttreatment Challenges in Rectal Cancer MRI: A Systematic Approach

### Awards

#### Cum Laude

#### Participants

Lucas Roberto Leles Oliveira, MD, Sao Paulo, Brazil (*Presenter*) Nothing to Disclose

#### TEACHING POINTS

• Understanding the critical role that MRI plays in rectal cancer staging and restaging. • Comprehend that several histopathologic changes may occur within rectal tumors after chemoradiation treatment, such as fibrosis or increased mucin production. • Radiologists play a crucial role in “watch-and-wait” programs for select patients with rectal cancer and should understand how to differentiate the several types of response, as well as how these posttreatment changes may be evaluated with high-spatial-resolution MRI.

#### TABLE OF CONTENTS/OUTLINE

• INTRODUCTION: o Rectal cancer treatment guidelines overview: § Selecting whether primary surgery or neoadjuvant treatment is an optimal approach; § Neoadjuvant treatment options: chemoradiotherapy versus total neoadjuvant therapy (TNT). o Primary tumor and nodal assessment with MRI. • ASSESSMENT OF TREATMENT RESPONSE: A SYSTEMATIC APPROACH. o Posttreatment changes in the primary tumor o Tumor Restaging: Histopathologic and MRI regression grades: § Identifying incomplete/poor responders, as well as “near-complete” and complete responders. o Patterns of tumor response: shrinking versus fragmentation; fibrosis and increased mucin production. • “WATCH-AND-WAIT”: PATIENT SELECTION AND CURRENT CONTROVERSIES. • FUTURE DIRECTIONS IN RECTAL CANCER TREATMENT AND IMAGING. • TAKE HOME MESSAGES.

## GIEE-23 #PRO TuMor# Becoming a PRO in Rectal TuMor: A Simple Way and Quiz Not to Miss the Tumoral Regression Grade After Neoadjuvant Therapy

#### Participants

Aaron Alarcon Novillo, Rio De Janeiro, Brazil (*Presenter*) Nothing to Disclose

#### TEACHING POINTS

> To demonstrate the importance of the radiologist in the context of rectal cancer, with a special interest in post-neoadjuvant evaluation.> To familiarize radiologists with the tumor regression grade (TRG) and its importance.> To demonstrate a simple way to minimize possible errors in the tumor regression grade (TRG).> To train the correct characterization of the tumor regression grade (TRG) based on recent cases using a simple way.

#### TABLE OF CONTENTS/OUTLINE

IntroductionRectal neoplasm is the third most common type of tumor in men and the second in women. Surgical treatment with total mesorectal excision is the gold standard, however, in cases of locally advanced tumors at diagnosis, neoadjuvant chemotherapy and radiotherapy are required. Magnetic resonance imaging is one of the mainstays in the management of patients with rectal tumors, providing primary staging and re-staging after neoadjuvant therapy. In the latter context, the response to treatment is evaluated by MRI, which provides the tumor regression grade (TRG) and re-staging, fundamental factors directly related to patient survival, which is again managed according to the imaging findings.We evaluated several MRI scans of post-neoadjuvant rectal tumors, with emphasis on the adequate qualification of the TRG, and we also developed a simple sequence of questions with a mnemonic (PRO TuMor) to assist in the proper characterization of the TRG, reducing possible errors.At the end of the presentation, we selected some MRI images in a quiz format for training purposes, using PRO TuMor.

## GIEE-24 Post Pancreatic Surgery Complications: Diagnostic Imaging Approach

### Awards

#### Identified for RadioGraphics Certificate of Merit

#### Participants

Ayman H. Gaballah, MD, FRCR, Columbia, MO (*Presenter*) Nothing to Disclose

#### TEACHING POINTS

• Review indications of pancreatic surgeries • Illustrate types of pancreatic surgeries • Discuss complications of pancreatic surgeries and their imaging features, including pancreas transplant • Highlight management options of these complications

#### TABLE OF CONTENTS/OUTLINE

1. Introduction a. Normal anatomy b. Indications for pancreatic surgery 2. Approaches to pancreatic surgeries: a. Endoscopic b. Minimally invasive- laparoscopic and robotic c. Open pancreatectomy 3. Types of pancreatic surgeries: a. Necrosectomy and abscess drainage b. Lateral pancreaticojejunostomy (Puestow) c. Beger procedure d. Frey procedure e. Pancreaticoduodenectomy (Whipple’s procedure) f. Distal/central pancreatectomy g. Total pancreatectomy h. Pancreatic transplant surgery 4. Normal postoperative imaging findings 5. Multimodality Imaging features of post-surgical complications: a. Pancreatico-biliary complications i. Transient fluid collection ii. Biliary leaks/bilomas iii. Pseudocysts iv. Pancreatitis v. Pancreatic fistulas 1. Pancreatic-enteric fistulas 2. Pancreatic-cutaneous fistulas vi. Anastomotic stenosis vii. Infections (abscess and peritonitis) viii. Local disease recurrence b. Vascular complications i. Arterial injuries ii. Hematomas iii. Arteriovenous fistulas iv. Vascular thrombosis c. Bowel complications i. Delayed gastric emptying ii. Bowel ischemia iii. Bowel injury iv. Anastomotic leak v. Anastomotic stenosis vi. Afferent loop syndrome d. Solid-organ complications: (e.g., liver infarction, splenic injury, etc.) e. Abdominal compartment syndrome f. Pancreatic transplantation i. Rejection ii. Vascular complications Inflammation, infection, necrosis

## GIEE-25 The Postoperative Pancreas

#### Participants

Ryan Clayton, MD, (*Presenter*) Nothing to Disclose

#### TEACHING POINTS

\* Review indications for various pancreatic surgeries and circumstances under which they are done.\* Understand the postoperative anatomy after common and uncommon pancreatic surgeries, as seen on radiologic studies including CT, MRI, Ultrasound, fluoroscopy and nuclear medicine.\* Be aware of the complications of the postoperative pancreas, and their imaging appearance. \* After reviewing this material, the radiologist will more easily and accurately identify normal postoperative anatomy after pancreatic surgeries (both common and uncommon), leading to improved diagnosis of potential complications and avoiding pitfalls such as misinterpreting postoperative anatomy as pathology.

#### **TABLE OF CONTENTS/OUTLINE**

\* Indications, anatomy and radiologic appearance of common pancreatic procedures: Whipple procedure (Classic, Pylorus-sparing), Distal pancreatectomy, Total pancreatectomy, Puestow procedure. Devices (CIVA sheet, Cystgastrostomy device). \* Complications of common pancreatic procedures and their radiologic appearance: Leaks (Anastomotic leak, Pancreatic fistula, Bile leak), Other collections (Abscess, Hematoma), Strictures (Gastrojejunal anastomotic stricture, Bile duct stricture, Pancreatic duct stricture), Delayed gastric emptying, Vascular complications (Portomesenteric venous thrombosis, Portomesenteric venous stenosis, Aneurysms and pseudoaneurysms), Tumor recurrence.

#### **GIEE-26 Out of Place: Ectopic and Accessory Tissues**

##### **Awards**

##### **Certificate of Merit**

Participants

Patricia Dantas I, MD, Sao Paulo, Brazil (*Presenter*) Nothing to Disclose

##### **TEACHING POINTS**

The purposes of this exhibit are:1) Review the most relevant imaging findings of ectopic and accessory tissue types, using a didactic approach by illustrations and cased-based imaging.2) Review the pathophysiology and embryology that are related to ectopic tissues, helping to understand the imaging findings in Computed Tomography (CT) and Magnetic Resonance (MR) imaging.3) Discuss the relevance of different ectopic tissue imaging presentations correlating with possible clinical complications.4) Improve knowledge about the main differential diagnoses and the main patterns of image appearance that are the key points to clarify diagnostic challenges.

#### **TABLE OF CONTENTS/OUTLINE**

1) Pictorial review of most frequent image findings of different ectopic and accessory tissue types.2) Cased-based review of ectopic tissue clinical presentation, frequent location, imaging findings, possible complications and differential diagnosis: pancreas, spleen, liver, gallbladder, leiomyomatosis, genitourinary system and endometriosis.3) Illustrative key points: improve understanding of the correlation between embryology and ectopic tissue imaging findings.4) Highlight the relevant imaging findings that aid surgical decisions.5) Conclusions and "take home messages": consolidate the acquired knowledge.

#### **GIEE-27 Postoperative Complications of Hepatobiliopancreatic Surgeries: Where To Look?**

Participants

Cristiane Costa, Sao Paulo, Brazil (*Presenter*) Nothing to Disclose

##### **TEACHING POINTS**

Revisit the surgical techniques involving the pancreas, liver, and bile ducts for the various pathologies that involve these organs. To review the most relevant complications of hepatobiliopancreatic surgeries and correlate with the imaging findings of computed tomography (CT), magnetic resonance imaging (MRI), and cholangiopancreatography (MRCP). Illustrate the cases of complications and demonstrate the therapeutical options.

#### **TABLE OF CONTENTS/OUTLINE**

Surgical techniques of hepatobiliopancreatic surgeries. Imaging protocols. Advantages and disadvantages of CT, MRI, and MRCP. Expected findings on postoperative imaging evaluation. Key sites where the radiologist should actively look for complications. Illustrate with cases the imaging findings of complications that must be described in the report. Demonstrate surgical and non-surgical treatment options.

#### **GIEE-28 Fixing The Edges: A Critical Analysis of Rectal Carcinoma After Neoadjuvant Therapy**

Participants

Paulo Antunes, MD, Niteroi, Brazil (*Presenter*) Nothing to Disclose

##### **TEACHING POINTS**

1. To recognize the MRI pitfalls in restaging rectal cancer after neoadjuvant treatment with chemotherapy and/or radiotherapy. 2. Test the limits of MRI rectal cancer re-staging emphasizing the difference between the misdiagnosis that is a limitation of the MRI and those that can be avoided thru a careful analysis by the radiologist

#### **TABLE OF CONTENTS/OUTLINE**

Introduction: Basic concepts of image analysis in rectal carcinoma after neoadjuvant treatment. Discussion- Correlation between MRI TRG scoring and histopathological TRG in selected cases. - Is that fibrosis or tumor cells? Follow-up results for patients eligible for watch and wait; - Mesorectal e pelvic nodes: the assessment of response comparing MRI and histopathologic or MRI follow-up;- Detecting complete clinical response after neoadjuvant therapy. Conclusion Summary with pearls and best tips of the analysis of MR rectal carcinoma after neoadjuvant treatment.

#### **GIEE-29 Cruisin' the Lumen: Fluoroscopic Evaluation of Normal and Abnormal Gastrointestinal Tract Luminal Anatomy in the Postoperative Setting**

##### **Awards**

##### **Cum Laude**

Participants  
Sonia Gaur, MD, (*Presenter*) Nothing to Disclose

#### TEACHING POINTS

1. Fluoroscopy is a cost-effective method of postoperatively distending the esophagus, stomach, and bowel to assess for postoperative anastomotic leak and other complications. Learning fluoroscopy requires exposure to high volume of cases including those performed in the postoperative setting. 2. Identify common postoperative settings in which fluoroscopy is performed for anatomic evaluation. 3. Review normal postoperative luminal anatomy and the fluoroscopic appearance of postoperative complications. 4. Review fluoroscopic techniques that are helpful in diagnosing postoperative complications.

#### TABLE OF CONTENTS/OUTLINE

1. Introduction - commonly encountered postprocedural scenarios in the fluoroscopy suite 2. Postoperative scenarios including explanation of surgery, expected postoperative appearance, possible complications, and corresponding normal and abnormal fluoroscopic cases. Technique and important views will be emphasized for each case. Case selection includes -- a) Zenker's diverticulotomy/diverticulectomy; b) evaluation for iatrogenic esophageal perforation; c) transhiatal esophagectomy; d) hiatal hernia repair; e) bariatric surgery (gastric sleeve surgery roux-en-y gastric bypass); f) percutaneous gastrostomy evaluation and g) colorectal surgeries (low anterior resection, ileoanal J-pouch creation, ileocolonic anastomosis).

#### GIEE-3 **Surgery or Follow-up? That is the Question: The Diagnostic Dilemma of Intraductal Papillary Mucinous Neoplasms**

**Awards**  
**Certificate of Merit**

Participants  
Akio Tamura, MD, (*Presenter*) Nothing to Disclose

#### TEACHING POINTS

The diagnosis of intraductal papillary mucinous neoplasms (IPMNs) is complex because adherence to the clinical guidelines depends on numerous imaging features and clinician opinions. The rate of accuracy of diagnostic guidelines for the presence of advanced dysplasia or cancer is 50-80%. Therefore, a small percentage of patients will be overtreated and some patients with IPMNs with high-grade dysplasia or cancer will be overlooked. This educational exhibit explains the key diagnostic imaging aspects of IPMNs and suggests methods to solve this dilemma in real-world clinical practice.

#### TABLE OF CONTENTS/OUTLINE

1. Why do IPMNs matter? 2. Algorithm for the management of suspected IPMNs 3. Solving the imaging dilemma of IPMN 4. Pancreatic cystic disease vs. IPMN

#### GIEE-30 **Diffuse Infiltrative Small Bowel Disease and Its Mimics**

**Awards**  
**Identified for RadioGraphics**

Participants  
Preet Dhillon, MD, Rochester, MN (*Presenter*) Nothing to Disclose

#### TEACHING POINTS

1. Review the differential for a diffuse infiltrative small bowel disease process. 2. Present the clinical presentation and imaging findings of several diffusely infiltrative diseases within the small bowel, in order to delineate the unique features of each entity. 3. Review entities that may mimic infiltrative bowel disease on imaging.

#### TABLE OF CONTENTS/OUTLINE

The presentation will present the following disease categories and examples of infiltrative bowel disease within them. A non-exhaustive list of example cases by category is provided. 1. Infectious: Mycobacterium avium intracellulare (MAI), Whipple disease, Histoplasmosis, Coccidiomycosis 2. Inflammatory: IgA vasculitis, graft-vs-host disease, radiation enteritis 3. Neoplastic: Metastatic lobular breast carcinoma, acute myelogenous leukemia, diffuse large B-cell lymphoma, post-transplant lymphoproliferative disorder 4. Other: Amyloidosis, endometriosis, hemorrhage, lymphangiectasia Summary: An infiltrative small bowel disease will manifest as a segmental or diffuse degree of small bowel wall thickening. Although these disease processes may share many characteristics, there are key clinical and imaging attributes of each that can be examined. This education exhibit aims to present several cases demonstrating disease processes in which the small bowel is diffusely infiltrated. The unique features of each disease entity will be examined in order to best differentiate them, with additional cases presented as potential mimics.

#### GIEE-31 **Postoperative Colon Tract: What's That Hookup and What Could Go Wrong?**

Participants  
Aman Khurana, MD, Lexington, KY (*Presenter*) Nothing to Disclose

#### TEACHING POINTS

Review indications and techniques of the common colonic surgical procedures with diagrammatic depiction. Multimodality imaging review of the normal post-surgical anatomy and associated complications with diagrammatic correlation. Summarize the appropriate imaging workup of patients suspected of postoperative gastrointestinal complications.

#### TABLE OF CONTENTS/OUTLINE

1. Review indications for colon surgeries and relevant variants that would alter surgical approach (robotic vs. other). 2. Review post-surgical anatomy of ileal-anal anastomosis, Hartmann pouch and its reversal, APR, colostomy complications and reversal, rectopexy, etc. 3. Imaging of post-operative complications such as anastomotic leaks, afferent loop syndrome, and parastomal hernias, lower abdominal resection, etc. 4. Review multimodality imaging evaluation including the role of barium studies, CT, MRI, and relevant endoscopic correlation. 5. Algorithmic approach in the setting of unknown surgical anatomy.

## **GIEE-32      Advanced CT Imaging Techniques for Characterization of Suspected Hepatocellular Carcinoma: Spectral CT, Low kVp Technique, Deep Learning, and Beyond**

Participants

Amir Borhani, MD, Chicago, IL (*Presenter*) Institutional research agreement, Siemens AG

### **TEACHING POINTS**

1. Advanced CT techniques and novel CT-based software are increasingly used in daily clinical practice. These new approaches can improve accuracy of CT in detection and characterization of focal liver lesions while ensuring optimized radiation dose and image quality. 2. The appropriate use of these new techniques can improve characterization of focal hepatic lesions in at-risk population.

### **TABLE OF CONTENTS/OUTLINE**

Current Status of CT in Liver Imaging • Overview of techniques and protocols • Dosage and timing of iodinated contrast • Effect on detection and conspicuity of hepatic lesions • ACR LI-RADS CT technical recommendations Spectral CT: Dual-energy and Multi-energy CT • Overview of basic principles of spectral CT • Review of current acquisition techniques • Advantages of spectral CT for LI-RADS classification • Suggested protocols and workflow Low kVp CT • Overview of physical principles of mass attenuation coefficient • Advantages and disadvantages of low kVp CT imaging • Added value of low kVp CT technique for LI-RADS classification Deep Learning (DL) Techniques • Background • Novel DL-based noise reduction and image reconstruction techniques • Role in detection and characterization of focal hepatic lesions • Computer-assisted detection (CAD) Novel Post-Processing Techniques • Background • Image subtraction • Value in assessment of focal hepatic lesions and classification

## **GIEE-33      Congestive Hepatopathy: Pathophysiology, Workup, and Typical and Atypical Imaging Findings with Pathological Correlation**

Participants

Marta Flory, MD, Redwood City, CA (*Presenter*) Nothing to Disclose

### **TEACHING POINTS**

Understand the pathophysiology of congestive hepatopathy and its effects on the liver parenchyma Recognize the imaging findings of congestive hepatopathy Know the benign and malignant lesions that develop in congested livers and how to use imaging features and techniques to distinguish them

### **TABLE OF CONTENTS/OUTLINE**

1. Liver vascular anatomy and sinusoidal architecture 2. Pathophysiology of congestive hepatopathy 3. Etiologies of congestive hepatopathy 4. Imaging findings of congestive hepatopathy a. Diffuse liver abnormalities b. Focal lesions associated with congestive hepatopathy 5. Challenges and pitfalls in imaging of congestive hepatopathy a. Assessment of hepatic fibrosis b. Differentiation of benign hypervascular lesions from hepatocellular carcinoma c. Proposed algorithm for workup of focal hepatic lesions in setting of congestive hepatopathy?

## **GIEE-34      Upset Stomach: CT and Fluoroscopic Imaging of the Stomach after Surgery, Endoscopic Interventions, and Unusual Devices**

### **Awards**

**Identified for RadioGraphics**

Participants

Preethi Raghu, MD, San Francisco, CA (*Presenter*) Nothing to Disclose

### **TEACHING POINTS**

1) Review normal postsurgical CT and fluoroscopic imaging appearance after gastric surgical interventions for weight loss, reflux management, and gastroparesis treatment. 2) Discuss normal postprocedural CT and fluoroscopic imaging appearance after endoscopic sleeve gastropasty, transoral incisionless fundoplication (TIF), gastric peroral endoscopic myotomy (G-POEM), and other specialized endoscopic procedures. 3) Recognize the normal CT and fluoroscopic appearance of various gastric devices, including those used for weight loss, reflux management, and pancreatitis. 4) Understand the CT and fluoroscopic imaging appearance of the complications associated with these gastric surgeries, procedures, and devices.

### **TABLE OF CONTENTS/OUTLINE**

1) Postsurgical Stomach: a) Roux-en-Y gastric bypass b) Laparoscopic sleeve gastrectomy c) Laparoscopic banding d) Nissen/complete fundoplication e) Toupet/partial fundoplication f) Gastric pacemaker placement. 2) Postprocedural Stomach: a) Endoscopic sleeve gastropasty b) Transoral incisionless fundoplication (TIF) c) Transgastric Rendezvous technique d) Endoscopic Ultrasound Directed Transgastric ERCP (EDGE) e) Gastric Peroral Endoscopic Myotomy (G-POEM). 3) Unusual Devices: a) LINX Reflux Management System b) Intra-gastric balloon c) Aspire Assist Device d) Axios stent and drainage e) Metallic gastric stent for cancer

## **GIEE-35      Choices, Choices, Choices: What Your Multidisciplinary HCC Treatment Team Wants to Know?**

Participants

Omar Kamal, MD, MSc, Portland, OR (*Presenter*) Nothing to Disclose

### **TEACHING POINTS**

1. Different treatment options exist for hepatocellular carcinoma (HCC) including surgical, locoregional and systemic therapies. Appropriate choice of therapy is crucial to improve clinical outcomes. 2. HCC treatment guidelines incorporate different clinical and imaging variables to guide treatment options. 3. Radiologists need to be familiar with how imaging findings can change treatment planning for HCC and what is the crucial information that the multidisciplinary liver team (MDLT) wants to know.

### **TABLE OF CONTENTS/OUTLINE**

1. Brief overview of HCC management: a. Surveillance. b. Overview of HCC staging and treatment options. i. Describe various treatment options. ii. Status of stereotactic body radiation therapy (SBRT). iii. Goals of noncurative treatments. c. HCC imaging features and role of biopsy in diagnosis and management. 2. Tumor burden and treatment considerations: a. Single vs. Multiple b.

Size. c. Location in relation to other structures. 3. Liver status and treatment considerations: a. Background liver disease. b. Liver volume. c. Signs and symptoms of Portal hypertension. d. Portal vein thrombosis. e. Arterial anatomy. f. Metastasis. g. Liver transplant candidacy. h. Performance status. 4. Treatment response: a. Size vs. viability. b. LI-RADS treatment response criteria. c. Specific challenges for TARE and SBRT. 5. Common questions for radiologists during MDLTs.

### **GIEE-36 Peritumoral Area of Focal Liver Lesions: Imaging-pathological Correlation and Clinical Significance**

#### **Awards**

#### **Certificate of Merit**

#### **Participants**

Kumi Ozaki, MD, PhD, Fukui, Japan (*Presenter*) Nothing to Disclose

#### **TEACHING POINTS**

Peritumoral area of focal liver lesions is the liver parenchyma adjacent to focal hepatic lesions, which is often altered due to compression of the tumors, drainage of blood flow of the lesion, vascular or bile duct invasion as well as due to malignant infiltration in some cases. These histological findings are plainly reflected in the imaging findings. In some tumors, the imaging findings of peritumoral area could be helpful for an accurate diagnosis and could be biomarkers of malignant grades or prognosis. The radiologist should pay attention to not only the tumor itself but also peritumoral area.

#### **TABLE OF CONTENTS/OUTLINE**

1. Introduction. 2. The definition of "peritumoral area," and several imaging findings of peritumoral area. 3. Imaging-pathological correlation of peritumoral area of each lesion as follows; peritumoral arterial enhancement (corona enhancement) of hepatocellular carcinoma, peritumoral hyper- or hypointensity on hepatobiliary phase of hepatocellular carcinoma, peritumoral arterial enhancement and peritumoral hypointensity on hepatobiliary phase of colorectal liver metastases, peritumoral hyperintensity on hepatobiliary phase of liver metastases from neuroendocrine tumor, and peritumoral arterial enhancement (arteriportal shunt) of cavernous hemangioma. 4. Non-existence of peritumoral changes of simple cysts or focal nodular hyperplasia 5. Clinical significance of peritumoral area of each lesions such as microvascular invasion, prognosis, the effect of chemotherapy, and the influence on the results of radiomics analyses. 6. Summary of the clinical significance of peritumoral area of focal liver lesions. 7. Conclusion.

### **GIEE-37 Why Do Mucin-producing Cystic Neoplasms of the Liver Confuse Us?: Top Tips To Get the Right Diagnosis**

#### **Awards**

#### **Certificate of Merit**

#### **Participants**

Sofia Santos, MD, Lisbon, Portugal (*Presenter*) Nothing to Disclose

#### **TEACHING POINTS**

This exhibit intends to: (1)To clarify and to compare the old and the new nomenclature of mucin-producing cystic neoplasms of the liver.(2)To summarize the characteristic features of hepatic mucinous cystic neoplasms (MCN) and intraductal papillary neoplasms of the bile duct (IPNB). (3)To highlight the key differences between MCN and IPNB and to present the main differential diagnoses. (4)To understand the impact of an adequate differential diagnosis.The main teaching points are: Mucinous cystic neoplasms of the liver are rare neoplasms that include hepatic mucinous cystic neoplasms (MCN), previously known as cystadenoma and cystadenocarcinoma, and intraductal papillary neoplasms of the bile duct (IPNB). The keys for distinguishing MCN and IPNB are based on the presence of bile ductal communication (only in the case of IPNB) and the presence of sub-epithelial ovarian stroma (only in the case of MCN). The differential diagnosis encompasses non-neoplastic cystic lesions and cystic metastases. The five top tips to the radiologist are: (1) to look for ductal communication, (2) to assess for bile duct dilation, (3) to look for thickened enhancing septa, mural solid nodules and calcifications, (4) to take into account location and number of lesion(s), and (5) to review the clinical data (namely primary extra-hepatic malignancy).

#### **TABLE OF CONTENTS/OUTLINE**

- Mucin-producing cystic neoplasms of the liver: the old and the new nomenclature- Hepatic mucinous cystic neoplasms (MCN) and intraductal papillary neoplasms of the bile duct (IPNB): epidemiologic, clinical, histological, and imaging features- MCN versus IPNB: top tips to the radiologist- Therapeutic insights- Diagnostic flowchart

### **GIEE-38 Imaging Assessment after Partial Hepatectomies: Surgical Technique and Type of Parenchymal Transection Performed: Normal Findings and Complications**

#### **Participants**

Juan C. Spina JR, MD, (*Presenter*) Nothing to Disclose

#### **TEACHING POINTS**

1- In the last two decades there has been an increase in the number of hepatic surgeries performed, together with an improvement in surgical techniques and new dissection devices. 2- Radiologists play a key role in the process of surgical planning and post surgical evaluation. Knowledge of types of resection is important to interpretate postsurgical liver appearance. 3- In the acute post surgical period, imaging helps to identify complications and contributes to define treatment.

#### **TABLE OF CONTENTS/OUTLINE**

1) Introduction. 2) Type of hepatectomies and technique- left hepatectomy, right hepatectomy, trisegmentectomy, segmentectomy, atypical segmentectomy, alpps, mini alpps.- liver hanging maneuver- Pringle Maneuver- liver transection methods: clamp crushing, electric scalpel, CUSA, water jet, tissue link. When and why?. 3)- Imaging findings after hepatectomies.- Normal findings: fluid collection, hypodense line, hepatic perfusion abnormalities, air bubbles, omentum adipose tissue, extraluminal gas.- Pathologic findings: biloma, hematoma, abscess, pulmonary complications. Tips for the correct diagnosis and differentiation. Example cases and evaluation test. Conclusion

## **GIEE-39 Liver MR Elastography: A Case-based Approach on Quality Control and Main Technical Failures**

Participants

Marcelo Mota, (*Presenter*) Nothing to Disclose

### **TEACHING POINTS**

- Review the basic principles of elastography, focusing on the liver
- Summarize the liver magnetic resonance elastography technique
- Describe the steps in the evaluation and quality control of elastography images
- Recognize the main causes of low-quality and nondiagnostic elastograms
- Illustrate with didactic cases some technical failures of liver MR elastography and how to potentially correct them

### **TABLE OF CONTENTS/OUTLINE**

? INTRODUCTION - Important concepts - Basic principles of elastography ? LIVER MR ELASTOGRAPHY TECHNIQUE - Typical liver MR elastography configuration - Raw data and post-processed images ? IMAGES QUALITY CONTROL - How to evaluate elastography images and ensure their quality ? LOW-QUALITY AND NONDIAGNOSTIC ELASTOGRAMS - Main causes of technical failures during the liver MR elastography ? INTERACTIVE CASE-BASED DIDACTICS - Sample cases to illustrate and solidify the concepts - How to potentially correct low-quality and nondiagnostic elastograms ? TAKE HOME MESSAGES

## **GIEE-4 Postoperative Complications of Hepatobiliary Surgery: An Imaging Review**

**Awards**

**Certificate of Merit**

Participants

John Kirby, MD, Rochester, MN (*Presenter*) Nothing to Disclose

### **TEACHING POINTS**

- Review normal liver segmentation, vascular, biliary anatomy, and variants
- Recognize the normal appearance of the postoperative liver
- Recognize early complications such as abscess, parenchymal necrosis, and bile leak
- Describe pertinent vascular findings such as active bleeding, pseudoaneurysm, stenoses, and thrombosis
- Understand the post ablation appearance of the liver and potential complications
- Many of our cases will contain a QR code that will allow the reader to open a fully functional PACS interface on their mobile device

### **TABLE OF CONTENTS/OUTLINE**

- Background: Liver surgery is a common procedure and complication rates can be as high as 50%. With the high-risk nature, radiologists can play an important role in the early detection and management of potential complications.
- Review normal hepatic anatomy including the conventional segmental divisions, vasculature, and biliary system.
- Terminology including wedge resections, segmentectomy, and hepatectomy to assist the radiologist in reviewing operative reports and accurately describing imaging findings.
- Normal/expected post operative appearances
- Case based examples illustrated utilizing multiple modalities to demonstrate common complications that radiologists may encounter:
  - o CT and MR examples of early complications requiring hospital admission
  - o Vascular and biliary complications and interventions
  - o Utility of nuclear medicine studies
  - o Evaluation of long-term complications.
  - o Post ablation appearance and potential complications.

## **GIEE-40 Colitis in Cancer: Going Beyond Immune Checkpoint Inhibitors: Diagnosis, Monitoring and Management**

Participants

Kaustav Bera, MD, Cleveland, OH (*Presenter*) Nothing to Disclose

### **TEACHING POINTS**

1. To review cancer drugs that are primarily responsible for causing colitis 2. Review the different etiologies of colitis and imaging findings that help differentiate them from cancer-therapy associated colitis 3. To discuss the CT imaging patterns of colitis of different etiologies 4. To discuss the crucial role of the radiologist in monitoring/management of treatment-related colitis. 5. Review established grading and management guidelines for treatment related colitis

### **TABLE OF CONTENTS/OUTLINE**

1. Discuss common anti-neoplastic agents that cause colitis 2. Enumerate etiologies of colitis, along with their typical imaging findingsi) Immune checkpoint inhibitor associated colitisii) Drug-induced colitisiii) Infectious colitis -a. Neutropenic colitisb. Pseudomembranous colitisiv) Radiation induced colitis v) Inflammatory - Ulcerative colitis/Crohn disease vi) Ischemic colitis 3. Discuss clinical findings, history and risk factors for developing colitis 4. Discuss mimics of colitis a. Diverticulitis b. Appendicitis c. Epiploic appendagitis 5. Discuss presenting clinical symptoms and grading system for drug-induced colitis6. Management guidelines for drug-induced colitis with special focus on checkpoint inhibitors (ICI), targeted therapy, Car-T cell therapy 7. How a Radiologist plays an important role in monitoring and management 8. Prognosis and clinical outcome of patients developing drug-induced colitis 9. Real-world cases showing management and clinical course of drug-induced colitis in cancer therapies from to combination ICI and CAR-T cells as well as additional causes of colitis in cancer patients

## **GIEE-41 Fundamentals of Response Evaluation for Abdominal Tumors**

Participants

Marcelo Cortes, MD, Petropolis, Brazil (*Presenter*) Nothing to Disclose

### **TEACHING POINTS**

? Overview of the application of tumor response criteria and quantitative imaging and its benefits for clinical trials and novel oncology therapeutics. ? The role of radiologists in the standardization of tumor evaluation for clinical trials. ? Basics on response assessment and quantitative analysis of the most prevalent abdominopelvic tumors. ? Updates in imaging management and surveillance strategies for abdominal tumors. ? The role of imaging and genetic/molecular evaluation

### **TABLE OF CONTENTS/OUTLINE**

Based on extensive imaging experience from a leading cancer center ? A brief review of abdominopelvic tumors, highlighting the

based on extensive imaging experience from a leading cancer center: ? A brief review of abdominopelvic tumors, highlighting the clinical and laboratory features that can be helpful in diagnosis and management. ? Review of the main criteria for clinical trials and clinical decision support employed to evaluate abdominopelvic tumors, for instance, RECIST 1.1, irRECIST, iRECIST, irRC, Lugano, Cheson, EASL, imRECIST, itRECIST, PERCIST, RECIL, and Choi. ? Tumor metrics criteria evaluation for abdominal tumors response compared to radiomics and imaging genomics role. ? Evaluation of immunotherapy: main concepts and practical application of tumor response evaluation. ? Interactive imaging-based approach with teaching points for response evaluation, work-up and recurrence of abdominopelvic tumors, challenges of immunotherapy evaluation, and equivocal cases on anatomic (CT/MRI) and functional (PET/CT and PET MRI) cross-sectional imaging. ? Current guidelines. ? Limitations of current imaging methods and new directions. ? Take-home messages.

#### **GIEE-42 Typical and Atypical Findings in Cirrhotic Liver: Pearls and Pitfalls for Diagnosis of Benign and Malignant Lesions**

Participants

Xiaoyang Liu, MD, PhD, (*Presenter*) Nothing to Disclose

##### **TEACHING POINTS**

1. Case-based review on imaging pitfalls and pearls of focal liver lesions in cirrhosis. 2. The distortion of normal liver parenchyma by fibrous and regenerative tissue can change the typical appearance of many benign lesions, causing misdiagnosis as malignancy. 3. As the most common primary malignancy arising from cirrhotic liver, hepatocellular carcinomas (HCC) can have atypical imaging appearance. 4. Contrast enhanced ultrasound (CEUS) can provide characterization of focal liver lesions in addition to CT and MRI to achieve accurate diagnosis.

##### **TABLE OF CONTENTS/OUTLINE**

Technical pitfalls in cirrhotic liver imaging: 1) HCC may be nearly isointense to background liver on heavily T2 weighted MR images. 2) CT and MRI can miss early enhancement pattern of HCC due to mistiming. 3) Replacement of liver parenchyma by fibrous and regenerative tissue in cirrhosis can lead to decreased penetration by ultrasound. Benign lesions mimicking malignancy: 1) Regenerative nodules. 2) Siderotic nodules. 3) Confluent fibrosis. 4) Hemangioma with pseudo washout. Atypical appearance of HCC 1) Hypovascular. 2) Cystic. 3) Fat containing HCC. 4) Nodule in nodule HCC. Other malignancies mimicking HCC 1) Intrahepatic cholangiocarcinoma. 2) Metastases. CEUS providing added value to CT and MRI, for differentiation of benign versus malignant lesions 1) HCC washout not shown on CT or MRI, but demonstrated by CEUS, due to the purely intravascular nature. 2) More sensitive detection of arterial hyperenhancement, due to its real-time nature.

#### **GIEE-43 2022 Update of the Barcelona Clinic Liver Cancer Recommendations: What the Radiologist Needs to Know**

**Awards**

**Certificate of Merit**

Participants

Vikrant Khare, MD, (*Presenter*) Nothing to Disclose

##### **TEACHING POINTS**

Teaching Points Although many hepatocellular carcinoma staging systems exist, the Barcelona Clinic Liver Cancer (BCLC) staging system is the most widely validated system which provides guidelines for therapy based on tumor stage and underlying liver function. Following the BCLC treatment guidelines has survival benefits for HCC patients, and the 2022 expanded upon its previous iteration for a more personalized and individualized approach, taking into consideration local technical and expertise availability in conjunction with the tumor profile. Knowledge of the imaging findings for each BCLC stage and understanding the updated treatment recommendations for each stage are required to ensure appropriate clinical decisions and management for each patient. This exhibit aims to highlight the imaging appearance of HCC for various BCLC stages while highlighting the key differences in the 2022 version.

##### **TABLE OF CONTENTS/OUTLINE**

Outline Brief background on HCC and the BCLC staging system Highlight key updates of the BCLC 2022 staging system Case based review illustrating the key imaging features of each stage BCLC-0, very early stage BCLC-A, early stage BCLC-B, intermediate stage BCLC-C, advanced stage BCLC-D, terminal stage Case-based review highlighting the various treatment options recommended by the updated BCLC system for each stage, with an emphasis on locoregional interventional treatments

#### **GIEE-44 Imaging Findings of Early Gastrointestinal and Hepatobiliary Cancers: Pitfalls and Pearls**

**Awards**

**Certificate of Merit**

Participants

Alecio Lombardi, MD, San Diego, CA (*Presenter*) Nothing to Disclose

##### **TEACHING POINTS**

Describe the imaging modalities of choice for the detection of early gastrointestinal and hepatobiliary cancers; Understand MRI technique and protocols, common challenges, and how to overcome them; Highlight imaging pearls and pitfalls for the characterization of early lesions on each modality; Underscore imaging characteristics that help in the differential diagnosis; Recognize key anatomical landmarks for surgical planning; Know what to include in the radiology report; Discuss future directions in the image analysis of early gastrointestinal and hepatobiliary cancers.

##### **TABLE OF CONTENTS/OUTLINE**

INTRODUCTION: General overview and definitions; Common gastrointestinal and hepatobiliary cancers. IMAGING TECHNIQUE: Modalities of choice; Sensitivity, specificity, and accuracy across methods; Protocols; Difficulties and how to overcome them to obtain high-quality images. IMAGING INTERPRETATION: Structured imaging analysis; Pitfalls and pearls; Anatomic Landmarks: What the Surgeon wants to know?; What should be included in the radiology report. STRATEGIES TO OVERCOME THE CHALLENGING CASES: Imaging characteristics that help in the differential diagnosis; WHAT'S ON THE HORIZON TO ASSESS EARLY GASTROINTESTINAL AND HEPATOBILIARY CANCER: Dual-energy CT; Digital Subtraction Angiography; DWI; Radiomics; Artificial

Intelligence applied to image acquisition, reconstruction; Quantitative Imaging Analysis; PET/MRI; New nuclear medicine radionuclides; Nanoparticles.

#### **GIEE-45 Renal Transplant Complications From A-Z: A Multimodality Case Based Review**

Participants

Meghan Stanton, MD, Syracuse, NY (*Presenter*) Nothing to Disclose

##### **TEACHING POINTS**

- The kidney is the most commonly transplanted solid organ and therefore it is imperative that the radiologist be familiar with the surgical procedure, as well as the post operative complications.
- Understanding the general timeline of specific complications in order to narrow the differential of imaging findings.
- Recognize the imaging findings of the most common and the rare postoperative complications related to renal transplantation.

##### **TABLE OF CONTENTS/OUTLINE**

- Review of the renal transplant surgical procedure and normal post-operative anatomy
- Imaging modalities used to assess the allograft
- Complication timeline
- Perinephric fluid collections
- Vascular complications
- Collecting system complications
- Parenchymal abnormalities
- Abdominopelvic complications
- Conclusion

#### **GIEE-46 Mimickers of Pancreatic Cancer: Lessons Learned**

**Awards**

**Identified for RadioGraphics**

**Magna Cum Laude**

Participants

Camila Vendrami, MD, Chicago, IL (*Presenter*) Nothing to Disclose

##### **TEACHING POINTS**

- Review of characteristic and atypical pancreatic ductal adenocarcinoma imaging and clinical findings
- Review of imaging and clinical features that allow differentiation between pancreatic ductal adenocarcinoma and its mimickers

##### **TABLE OF CONTENTS/OUTLINE**

Pancreatic ductal adenocarcinoma is the most common primary tumor of the pancreas. Several pancreatic conditions can mimic the appearance of pancreatic ductal adenocarcinoma, including inflammatory conditions, uncommon primary pancreatic tumors, and metastases to the pancreas. Imaging differentiation between these lesions and pancreatic ductal adenocarcinoma can be difficult because of overlapping features; however, knowledge of their typical imaging characteristics and clinical presentation may assist in their differentiation. 1. Introduction 2. What key imaging and clinical features of pancreatic ductal adenocarcinoma suggest this diagnosis and what are the atypical findings? 3. What clinical and imaging features differentiate mimickers (acute and chronic pancreatitis, groove pancreatitis, autoimmune pancreatitis, high-grade neuroendocrine tumors, metastases, other less common benign and malignant tumors) from pancreatic ductal adenocarcinoma? 4. Take home points

#### **GIEE-47 Liver MR Elastography: Practical Guidance for Interpretation and Reporting**

**Awards**

**Magna Cum Laude**

Participants

Guilherme M. Cunha, MD, Seattle, WA (*Presenter*) Nothing to Disclose

##### **TEACHING POINTS**

- 1) Review principles of MR elastography (MRE) for noninvasive assessment of liver fibrosis.
- 2) Summarize the literature on diagnostic accuracy of MRE in different liver disease etiologies.
- 3) Review pitfalls and confounders.
- 4) Provide guidance on liver MRE reporting and interpretation.
- 5) Discuss future directions.

##### **TABLE OF CONTENTS/OUTLINE**

- 1) Introduction: Stiffness as a biomarker of liver fibrosis and clinical significance.
- 2) Basic principles of MRE.
- 3) Clinical application detection and staging of liver fibrosis, liver stiffness and histology fibrosis stages, contexts of use and populations.
- 4) Diagnostic performance: overview of meta-analyses, MRE sequence, disease-specific MRE-determined liver stiffness thresholds.
- 5) Pitfalls and confounders a. Technical: improper hardware setup, left lobe vs right lobe, wave frequency dependencies, region of interest (ROI) placement. b. Biological: steatosis, iron overload, inflammation, cholestasis and venous congestion, expiration vs inspiration, fasting vs postprandial state.
- 6) Image interpretation Image analysis and interpretation (wave and elastograms), ROI approaches, stiffness thresholds and disease-specific interpretation.
- 7) Reporting: what to report, how to report it, QIBA recommendations.
- 8) Future directions: new contexts of use and applications, technical innovations.

#### **GIEE-48 A Beginners Guide to Liver Iron Quantification: What a Radiology Resident Ought to Know**

Participants

Archit Dikshit, MBBS, (*Presenter*) Nothing to Disclose

##### **TEACHING POINTS**

- (1) Iron overload could be due to primary hemochromatosis (hereditary) or secondary hemochromatosis (acquired by blood transfusions) and can cause serious complications including liver cirrhosis and heart failure.
- (2) MRI based iron quantification is increasingly being preferred to biopsy which is invasive, and not representative in inhomogenous distribution and serum ferritin which can be inaccurate in inflammatory states.
- (3) MRI based liver iron quantification is the recommended technique for estimating liver iron concentration in patients with increased serum Ferritin levels and assessing its trend in patients with repeated blood transfusions.
- (4) Superparamagnetic property of iron is the basis of quantification by MRI as it creates magnetic field inhomogeneity (estimated by QSM), which leads to signal drop of liver (measured by SIR method) and shortening of T2 and T2\* times (measured by relaxometry).
- (5) The choice of method of iron quantification is made according to the availability of resources, and level of iron

overload. (6) In cases with very high iron overload, R2\* based relaxometry mapping gives error and use of signal intensity ratio method is preferred.

#### TABLE OF CONTENTS/OUTLINE

(1) Iron metabolism (2) Iron Overload and its clinical implications (3) Monitoring of Iron Overload (4) Clinical Indication for liver iron quantification (5) Principle of MRI based Iron Quantification (a) Principles (b) Relaxometry: T2 and T2\* (c) Signal Intensity Ratio (SIR) Method (d) Quantum Susceptibility Mapping (QSM) Method (6) Merits and Demerits of MRI based Iron Quantification methods in practical usage (a) T2 Relaxometry (b) T2\* Relaxometry (c) SIR (d) QSM (7) How to practically use different tools and methods

#### GIEE-49 **Ultrasound of the Abdominal Wall: Pearls and Pitfalls**

Participants

Christian Burgos-Sanchez, MD, (*Presenter*) Nothing to Disclose

#### TEACHING POINTS

-Recognize normal anatomy of the abdominal wall-Know and identify the types of hernias that occur in the abdominal wall-Identify normal and pathologic conditions that may clinically mimic hernias

#### TABLE OF CONTENTS/OUTLINE

1. Introductiona. Hernia general terms and definitionsb. Hernia ultrasound protocolc. Normal abdominal wall anatomy2. Abdominal wall hernia casesa. Umbilical herniab. Indirect inguinal herniac. Direct inguinal herniad. Spigelian herniae. Lumbar herniaf. Incisional hernia3. Abdominal wall pathology mimicking herniaa. Lipomab. Cellulitisc. Post op fat necrosisd. Rectus sheath hematomae. Endometrioma in C-section scarf. Lung cancer metastasis4. Inguinal pathology mimicking herniaa. Metastatic lymph nodeb. Hydrocelec. Rhabdomyosarcomad. Spermatic cord lipomae. Encysted hydrocelef. Undescended testicle5. Vascular pathology mimicking herniaa. Varicose veinsb. Pseudoaneurysmc. Thrombosed veins6. Conclusion and summary

#### GIEE-5 **The Portal Vein: A Comprehensive Review**

##### Awards

Identified for RadioGraphics

Participants

Ben Layton, BMBS, FRCR, Blackburn, United Kingdom (*Presenter*) Nothing to Disclose

#### TEACHING POINTS

Combining radiological case examples with succinct explanation and illustrations this exhibit will provide a comprehensive summary of the portal vein (PV). This will:• Guide the radiologist in successful description of PV anatomy and branching patterns leading to optimal surgical approach. • Teach recognition and correct interpretation of rare topographic portal vein variations such as circumportal pancreas and preduodenal PV. • Provide an understanding of the appearances, associations and complications of PV shunts including congenital (E.g., Abernethy malformations, hereditary hemorrhagic telangiectasia) and acquired shunts (E.g., cirrhosis, traumatic). • Examine all pathology of the PV, including tips to differentiate between bland and tumour thrombus and explain sequelae with case examples (E.g., cavernous transformation, THAD/hepatic artery buffer response and portal biliopathy) • Deliver an overview of the newly described disease entity "porto-sinusoidal vascular disorder" clarifying the nomenclature associated with it and distinguishing it from cirrhosis and non-cirrhotic portal hypertension

#### TABLE OF CONTENTS/OUTLINE

Portal vein anatomy: branching pattern variations and extrahepatic topographyMalformations of the portal vein: associations and sequelaeDisease processes affecting the portal veinPortal vein interventionSummary and recommendations

#### GIEE-50 **Beyond the Images: A Simplified Approach for Rectal Cancer Mimics and Variants**

Participants

Katherine Wei, MD, Orange, CA (*Presenter*) Nothing to Disclose

#### TEACHING POINTS

This exhibit aims to provide an overview of the different benign and neoplastic mimickers of rectal cancer that can be encountered and provide an evidence-based framework for how to approach the differential diagnoses for rectal masses.

#### TABLE OF CONTENTS/OUTLINE

Different categories of rectal masses/rectal cancer mimickers to be discussed include: -Large rectal masses: In addition to advanced stage or poorly differentiated adenocarcinoma, high grade neoplasms such as poorly differentiated squamous cell carcinoma, high-grade neuroendocrine tumor, adenosquamous carcinoma, or lymphoma may be considered. If the tumor is eccentrically located, non-epithelial/mesenchymal tumors such as gastrointestinal stromal tumor or tumor of adjacent organ origin should be in the differential. -Anorectal junction masses of unknown histology: These lesions present a dilemma, as staging and treatment of anal cancer differ from rectal adenocarcinoma. -Precancerous/early-stage rectal cancer: These lesions have differing morphological and enhancement patterns compared to more locally advanced disease. -Benign rectal masses: Differentials include vascular malformations/hemangiomas, solitary rectal ulcer syndrome, and endometriosis implants. -Metastasis, including direct invasion of adjacent organs and commonly confused non-rectal cancer origin metastasis.

#### GIEE-51 **Beyond Infectious, Inflammatory, or Ischemic" Morphologic Approach to Bowel Wall Thickening**

Participants

Nabih Nakrou, MD, Boston, MA (*Presenter*) Nothing to Disclose

#### TEACHING POINTS

The purpose of this exhibit is to: Identify imaging patterns of wall thickening in the stomach, small bowel, and colon.Discuss the differential diagnosis of bowel wall thickening based on imaging characteristics, morphology, distribution, secondary signs, and clinical presentation. Present correlative endoscopic gross images when available.

## TABLE OF CONTENTS/OUTLINE

The presentation will include Anatomic layers of the bowel wall. Pathophysiology of bowel wall thickening including wall layers involvement with edema, hemorrhage, inflammatory and neoplastic cells, fatty deposits, and fibrotic replacement. Differential diagnosis, example cases, and concurrent endoscopic images of gastric wall thickening are classified into diffuse, segmental, focal, and multifocal wall thickening. Differential diagnosis, example cases, and concurrent capsule endoscopic images of bowel wall thickening are classified into diffuse, segmental, and nodular fold thickening. Differential diagnosis, example cases, and concurrent colonoscopy images of bowel wall thickening are classified into diffuse, segmental, and nodular fold thickening. Address secondary signs favoring one diagnosis over others.

### **GIEE-52 Periapillary Disorders: Running Away From the Obvious - A Pictorial Essay of Periapillary Lesions**

#### **Awards**

##### **Certificate of Merit**

#### Participants

Ulysses Torres, MD, PhD, Sao Paulo, Brazil (*Presenter*) Nothing to Disclose

#### **TEACHING POINTS**

- To review the general anatomy of the ampullary region and its variants with schematic drawings correlated with CT and MRI.
- Expose the possible periampullary disorders categorized into four large groups (anatomical variations, tumoral, inflammatory, and miscellaneous). To unravel the main differential diagnoses of periampullary involvement with didactic cases, literature review, and main imaging aspects.

## TABLE OF CONTENTS/OUTLINE

Diagram and educational schematic drawings for diagnostic of the ampullary and periampullary lesions, dividing them as:- Anatomical variations: including cases of pancreas divisum, annular pancreas, and independent drainage of the common bile duct and pancreatic duct. - Tumoral disorders: including cases of a duodenum GIST, a papilla tumor, and a Frantz Tumor - Inflammatory disorders: such as paraduodenal pancreatitis, bulging duodenal papilla, and HIV papillitis. - Miscellaneous disorders: presenting other kinds of periampullary involvement, including a case of collateral circulation mimicking a neoplastic pathology, ischemic cholangiopathy, and intradiverticular papilla.

### **GIEE-53 Body MRI Pulse Sequences: An Atlas and User Guide**

#### **Awards**

##### **Identified for RadioGraphics**

##### **Certificate of Merit**

#### Participants

Anup Shetty, MD, Saint Louis, MO (*Presenter*) Nothing to Disclose

#### **TEACHING POINTS**

Body MRI protocols can be daunting for the new trainee or novice reader, with a multitude of pulse sequences and a wide variety of acronyms. Understanding of basic MRI physics provides a framework for how to optimally use these sequences in clinical practice. Knowledge of the sequences as building blocks also informs efficient protocol design. This exhibit will: 1) Highlight basic MRI physics principles that underpin core body MRI sequences 2) Provide a framework of the families of sequences used in body MRI protocols, including individual vendors sequence names and key parameters 3) Illustrate technical considerations and clinical utility of each sequence through case examples 4) Describe how to build efficient protocols for indications such as liver masses, pancreaticobiliary imaging, renal/adrenal imaging, pelvic imaging, and imaging the moving patient

## TABLE OF CONTENTS/OUTLINE

- relevant body MRI physics: single-shot, free-breathing, respiratory navigation, chemical shift, hepatobiliary contrast- sequence families: single-shot fast-spin echo, balanced steady-state free-precession, diffusion-weighted, spoiled gradient echo (chemical shift, quantitative multi-echo imaging, dynamic imaging), high resolution/small field of view imaging- for each sequence: vendor names/acronyms, key sequence parameters (TR, TE, flip angle, acquisition time, breath-holding strategy), technical considerations (SNR, artifacts, sensitivity to motion and susceptibility, need for fat suppression), and clinical applications- body MRI protocols: what sequences to include and why, using examples such as liver mass, pancreaticobiliary, renal/adrenal, and pelvic imaging, and how to image the moving patient

### **GIEE-54 Success is Best When Shared: A Multidisciplinary Interpretation of Rectal Adenocarcinoma Regression**

#### Participants

Olivia Errecondo, MD, (*Presenter*) Nothing to Disclose

#### **TEACHING POINTS**

? To review the role of MRI in restaging rectal cancer, emphasizing the use of T2 weighted images and diffusion weighted images. ? To describe the basis of neoadjuvant treatment in rectal cancer, making a brief analysis of the Prodigy, Opra and Rapido Trial. ? To accomplish a description of the tumor regression grade system (TRG) using cases from our database as examples. ? To highlight the importance of multidisciplinary approach between imaging findings, endoscopy and histopathologic results.

## TABLE OF CONTENTS/OUTLINE

? Introduction. ? Rectal MRI basis. ? Neoadjuvant chemoradiotherapy in rectal cancer. ? TRG review. ? Conclusion.

### **GIEE-55 Hepatic Nodular Regenerative Hyperplasia: Radiologic-Pathologic Correlation**

#### Participants

Arpan Patel, MD, (*Presenter*) Nothing to Disclose

#### **TEACHING POINTS**

This educational exhibit will aim to: Describe and define Nodular Regenerative Hyperplasia (NRH) from a clinical, radiological and

This educational exhibit will discuss evidence and some research regarding non-cirrhotic portal hypertension (NRH) from a clinical, radiological and histopathological perspective with the use of CT and MRI imaging. Compare and contrast NRH from other liver pathology. Distinguish NRH from other adaptive liver reactions that precede non-cirrhotic portal hypertension. Describe the causes and associations of NRH.

#### TABLE OF CONTENTS/OUTLINE

- NRH Background
- NRH and other liver adaptive reactions causing non-cirrhotic intrahepatic portal hypertension
- Epidemiology
- Aetiology and pathogenesis
- Histopathological-Radiological correlation with CT and MRI Imaging
- Molecular background
- Imaging features
- Imaging pearls and pitfalls
- Mimics of NRH
- Appearance with hepatobiliary phase Gadoteric Acid- enhanced MR imaging
- Summary

#### GIEE-56 Imaging Techniques for Quantification of Liver Fat and Iron

Participants

Sarah Bastawrous, DO, Seattle, WA (*Presenter*) Nothing to Disclose

#### TEACHING POINTS

1. Review the importance of identifying liver fat and iron in the general population and in patients with liver disease. 2. Discuss ultrasound and MR imaging techniques for detection and quantification of liver fat and iron. 3. Illustrate these imaging techniques with clinical vignettes, including pearls and pitfalls.

#### TABLE OF CONTENTS/OUTLINE

1. Background and clinical importance of identifying abnormal accumulation of liver fat and iron. 2. Risks, clinical implications, impact on health care costs and mortality in patients with abnormal liver fat or iron. 3. Benefits of early detection and intervention in patients with abnormal fat and/or iron in the liver. 4. Ultrasound and MR imaging techniques for detection and quantification of liver fat and iron, including physical concepts, technique, interpretation, limitations, and future trends. 5. Multimodality case-based examples and appropriate clinical indications. 6. How to calculate and report fat and iron content.

#### GIEE-57 Back to our Origins: Abdominal Radiography and Its Uses

Participants

Elisa Antolinos Macho, MD, Madrid, Spain (*Presenter*) Nothing to Disclose

#### TEACHING POINTS

- Going over current abdominal X-ray purposes and indications. - Optimal technique review and basic projections. - Learning basic radiological anatomy. - Knowing most common abnormalities and underlying disease.

#### TABLE OF CONTENTS/OUTLINE

Indications Technique Basic projections 1) AP supine view 2) AP erect view 3) Lateral decubitus view 4) PA erect view Regional anatomy - Air (luminogram) - Organ silhouettes - Fat stripes - Bone Abdominal X-Ray semiology - Hepatobiliary Hepatomegaly, Splenomegaly, Cholelithiasis, Calcified cysts - Genitourinary Urolithiasis and other calcified structures - Gastrointestinal Bowel obstruction (Small bowel obstruction, large bowel obstruction and volvulus), and pneumoperitoneum - Foreign bodies - Medical devices

#### GIEE-58 MRI Findings of the Rectum and Anus: Beyond Tumor Staging

Awards

Certificate of Merit

Participants

Sergio Jimenez Serrano, Barcelona, Spain (*Presenter*) Nothing to Disclose

#### TEACHING POINTS

The purpose of this educational exhibit is:- To analyze the different pathological processes that can be found in the imaging modalities intended for the characterization and staging of rectoanal or perirectal pathology, beyond the adenocarcinoma and squamous neoplasia.- To illustrate the characteristic image features of these processes, especially on MRI, emphasizing those aspects that can be clues to orientate the diagnosis.

#### TABLE OF CONTENTS/OUTLINE

We have realized a retrospective review of patients in whom an imaging study, mostly MRI, has been requested to evaluate rectoanal or perirectal diseases in the last 12 years and whose definitive diagnosis has been other than primary neoplasia (adenocarcinoma or squamous neoplasia) or perianal fistula extension study. The final diagnosis was histologically confirmed. In this way, we present 44 patients and we have classified them into six groups:- Inflammatory/infectious pathology. - Endometriosis.- Neoplastic pathology Benign: schwannoma, leiomyoma, myelolipoma, hemangioma, diffuse rectal hemangiomas. Malign: neuroendocrine tumor, melanoma, plasmablastic lymphoma, undifferentiated pleomorphic sarcoma.- Secondary neoplastic involvement ? highlights a rare and specific form of involvement such as rectal proctitis.- Congenital and developmental lesions.- Other benign processes.

#### GIEE-59 Pancreas-kidney Transplant: Imaging Before, During and After Transplant

Participants

Carlos Felipe Reyna, MD, Sao Paulo, Brazil (*Presenter*) Nothing to Disclose

#### TEACHING POINTS

To better understand pancreas-kidney transplant, its technique and complications using a didactic approach using images and illustrations. To show the different imaging methods for evaluating transplant complications, such as Computed Tomography (CT) and Ultrasound (US). To highlight the surgical complications using cases from our database and the importance of their detection. To highlight the importance of a structured report.

## TABLE OF CONTENTS/OUTLINE

1. Review of the pancreas-kidney transplant and its technique through illustrations and images. 2. Explore pancreas-kidney complications supported by cross-sectional imaging cases, such as CT and US. 3. Preoperative and postoperative knowledge of pancreas-kidney transplant is mandatory for surgical planning and thus helping to identify postoperative complications. This information must be a part of the structured report. 4. Summary and take home messages.

### GIEE-6 Tough to Swallow: Adventures in Postoperative GI Fluoroscopy

Participants

Elainea Smith, MD, Birmingham, AL (*Presenter*) Nothing to Disclose

#### TEACHING POINTS

1. Review the most common gastrointestinal surgical procedures performed and common indications - from pharynx to anus. 2. Discuss case examples of the expected postoperative appearance of these procedures. 3. Highlight the most common post operative complications and their fluoroscopic appearance.

## TABLE OF CONTENTS/OUTLINE

Introduction  
Pharynx- Laryngectomy  
Esophagus- Zenker's diverticulectomy and diverticulectomy- Reflux management devices (such as Linx device)- POEM- Esophagectomy- Hiatal hernia repair- Heller myotomy  
Stomach- Fundoplication- Sleeve gastrectomy- Roux-en-Y gastric bypass- Total gastrectomy  
Small bowel - Gastrostomy or gastrojejunostomy catheters- Whipple procedure- Pylorus sparing whipple  
Large bowel- Partial colectomy- LAR versus APR  
Summary

### GIEE-60 Strictures in Crohn's Disease: What a Radiologist Needs to Know

Participants

Antonio Bevere, Rome, Italy (*Presenter*) Nothing to Disclose

#### TEACHING POINTS

- Illustrate how to recognize bowel stenosis in Patients with Crohn's disease (CD), show the differences between inflammatory and fibrotic strictures, and explain their implication on the treatment choice. - How to describe intestinal stenosis in CD patients and which information should be included in the report to guide the management. - Exclude other potential differential diagnosis, including adhesive disease and bowel cancer.

## TABLE OF CONTENTS/OUTLINE

Stricture is a frequent complication in CD. The precise definition of stricture has not been defined yet, and varies across studies, comprising either luminal stenosis with intestinal wall thickening with or without pre-stenotic dilatation, and lesion-causing stenosis lower than 1 cm. The site of strictures usually follows the distribution of inflammation, frequently involving the ileum. Even though CT- and MR-enterography offer great visualization of the intestinal tract, defining strictures remains challenging. Assessing strictures, the transition point should be carefully evaluated to establish the cause of bowel obstruction and exclude other potential differential diagnosis, including adhesive disease and bowel cancer. In addition, in CD inflammation and fibrosis are strictly connected mechanisms, which usually coexist in the same Patient and even in the same intestinal tract in varying degrees, making the diagnosis even more complex. MR exams can accurately differentiate between inflammatory and fibrotic strictures, guiding the correct treatment choice. Inflammatory strictures are treated with anti-inflammatory drugs; on the other hand, fibrotic strictures are treated mechanically with intestinal resection or endoscopic dilatation.

### GIEE-61 Clinical and Radiological Scores for Assessing Inflammation in Crohn's Disease

Participants

Jordi Rimola, MD, PhD, (*Presenter*) Consultant, Alimentiv Health Trust; Speaker, Takeda Pharmaceutical Company Limited; Consultant, Johnson & Johnson; Consultant, Boehringer Ingelheim GmbH; Research Grant, AbbVie Inc

#### TEACHING POINTS

1-To familiarize radiologists with activity indices of Crohn's disease (CD) used by gastroenterologists including clinical and endoscopic scores  
2-To describe the main validated activity scores and other imaging biomarkers for assessing inflammation in patients with CD  
3-To provide a practical guide on the correct use and interpretation of imaging biomarkers in CD  
4-To discuss the potential contribution of imaging biomarkers in assessing therapeutic efficacy and to applied as endpoints in clinical research

## TABLE OF CONTENTS/OUTLINE

1- Limitation of endoscopy as reference standard to assess inflammation and therapeutic response in patients with CD  
Cross-sectional imaging may overcome these limitations and offers additional advantages  
2- Description of Magnetic Resonance Enterography (MRE) and intestinal ultrasound (IUS) activity scores have been developed and validated  
Detailed list of MRE and IUS activity scores and other imaging biomarkers (e.g. motility) in CD  
Evidence supporting their satisfactory inter- and intra-reader reproducibility, and validity against a range of reference standards  
Optimal use and interpretation. Not forget ulcerative colitis  
3- Rational and limitations to consider activity scores as endpoints in clinical research in CD.

### GIEE-62 Rectal MR: A Refresher on Low Rectal Cancers at Initial Staging

**Awards**

**Identified for RadioGraphics**

**Certificate of Merit**

Participants

David Kim, MD, Madison, WI (*Presenter*) Shareholder, Elucent Medical

#### TEACHING POINTS

1. The 'anorectal junction to tumor' distance can estimate potential distal surgical margin and thus helps to determine the surgical approach. 2. MRF involvement at the pelvic floor can be inferred by the T category status for low cancers. 3. Cancer involvement of the anal sphincter in the context of T staging is remains undefined by AJCC. The recommendation is to be descriptive. It is

important to have a strong grasp of anal sphincter anatomy to accurately describe tumor involvement with particular emphasis regarding the tumor relationship to the intersphincteric space. 4. External iliac and inguinal lymph nodes are regional (N+) not M disease when there is cancer involvement of the anal sphincter. 5. The histology of the tumor must be confirmed as adenocarcinoma. If squamous in histology, a low cancer is staged and treated as an anal cancer.

#### TABLE OF CONTENTS/OUTLINE

Background • Rectal MR and clinical staging • Classification (high/mid/low) Low rectal cancers (special considerations) • Anatomy of the anal sphincter • Treatment approaches • Staging issues and areas of controversy • Histology Summary

#### GIEE-63 MR and CT Enterography: Expanding the Knowledge and Digesting the Information

Participants

Martin Horwarth, Sao Paulo, Brazil (*Presenter*) Nothing to Disclose

#### TEACHING POINTS

1 - Review the imaging findings for inflammatory bowel disease when using enterography protocols in CT and MR. 2 - Illustrate these findings and correlate them with the correct terms to use on radiology reports. 3 - Showcase the most common pitfalls that can be mistaken for active inflammatory disease and what to look for besides the bowel.

#### TABLE OF CONTENTS/OUTLINE

1 - Advantages and disadvantages of CT and MR. 2 - Exam protocols. 3 - Imaging findings in Crohn's disease and their descriptors. 4 - Imaging findings in non-specific intestinal inflammatory conditions. 5 - Pitfalls that may be mistaken for active inflammation. 6 - Other sites of interest for when analyzing a patient with Crohn's disease.

#### GIEE-64 When it is NOT Appendicitis: What to Look for in Appendiceal Disease Besides Inflammation

Participants

Joao Stern, MD, Rio de Janeiro, Brazil (*Presenter*) Nothing to Disclose

#### TEACHING POINTS

- Review literature in appendiceal malignancies and benign disease. - Demonstrate images patterns of the different diseases of the appendix. - Postulate a flowchart to investigate appendiceal disease

#### TABLE OF CONTENTS/OUTLINE

Appendicitis is one of the most common acute abdominal inflammatory disease and demands surgical treatment. Other appendix afflictions are rare in comparison and frequently overlooked. Radiologists must know the different diagnosis, to recognize when it's not appendicitis and impact the surgical or clinical management.

#### GIEE-65 Icing on the Cake: Added Value of Dual Energy CT (DECT) in Challenging Biliary Pathologies

Participants

Victoria Kim, MD, (*Presenter*) Nothing to Disclose

#### TEACHING POINTS

1. Understand basic technique of dual energy CT (DECT) imaging. 2. Describe the role of DECT in complex biliary pathologies. 3. Show how DECT aids appropriate management of challenging biliary cases.

#### TABLE OF CONTENTS/OUTLINE

1. Background: DECT has a variety of emerging clinical applications. By acquiring images at both high and low x-ray energies, computer software analysis can estimate chemical composition of materials. Images are reconstructed to enhance or suppress appearance of different materials. CT is often first choice of cross-sectional imaging in outpatient and acute care settings due its relative ease of acquisition and lower cost compared to MRI. DECT is a particularly useful tool in imaging biliary pathologies to add greater information and value from a single imaging encounter. 2. Gallstone disease: Noncalcified cholesterol stones are less apparent on single-energy contrast enhanced CT, but attenuate differently at various energies and are better visualized on monoenergetic images. 3. Postoperative cases: Iodine map and virtual non-contrast (VNC) images distinguish true postoperative abscesses. 4. Biliary malignancy: Iodine map and VNC images distinguish enhancing tissue versus biliary hematoma. 5. Other pathology: In unusual cases such as gallbladder volvulus, iodine map and VNC images identify gallbladder ischemia and expedite management. VI. Conclusions: DECT has an exciting range of applications for biliary pathology, aiding in appropriate management and minimizing additional studies and delayed care.

#### GIEE-66 Save Your Tears for Another Day: Unmasking Pancreatic Adenocarcinoma

Participants

Ahmed Elsakka, MD, Rutherford, NJ (*Presenter*) Nothing to Disclose

#### TEACHING POINTS

- Recognize early focal pancreatic abnormalities on CT associated with subsequent diagnosis of early-stage pancreatic ductal adenocarcinoma (PDAC).
- Understand the role and limitations of radiology on primary staging and restaging.
- Comprehend common imaging pitfalls and benign mimickers of PDAC.
- Recognize post-surgical complications.
- Recognize different patterns of recurrence on imaging.
- Understand imaging response to CRT and current limitations.
- Be familiar with future directions on PDAC.

#### TABLE OF CONTENTS/OUTLINE

1. INTRODUCTION oWorld prevalence and cancer Facts and statistics 2022. oRelevance, costs. 2. TREATMENT SUMMARY 3. ROLE OF IMAGING oEarly detection oInitial staging oCommon pitfalls •Vascular involvement from surgical perspective •Peritoneal carcinomatosis versus inflammatory changes or congestion. •Regional and extra-regional nodal metastasis. •Perineural invasion: myth or fact? oMimickers •Pancreatitis. •Duodenal diverticulitis. •Prominent pancreatic lobulations. •Uneven fat deposition oRestaging •Imaging criteria and limitations. oTumor recurrence •Common locations. •Imaging patterns. •Role of follow up comparison 4. RADIOSURGICAL CORRELATION oWhen we were wrong 5. POST-OPERATIVE COMPLICATIONS oPre-surgical red flags.

oConcerning imaging findings. 6.MULTIDISCIPLINARY TUMOR BOARD oWhat they need to know and what we need to ask 7.WHAT'S ON THE HORIZON

## **GIEE-67 NCCN Guideline Driven Gastrointestinal Tract Tumor Board: A Primer for Radiologists**

Participants

Basem Jaber, MD, Darby, PA (*Presenter*) Nothing to Disclose

### **TEACHING POINTS**

\* Demonstrating a radiologist's role in the clinical management of GI tumors.\* Reviewing NCCN guidelines for GI tumors.\* Highlighting the use of different imaging modalities in management decisions.\* Identifying possible pitfalls in multidisciplinary tumor board discussions from a radiology standpoint.

### **TABLE OF CONTENTS/OUTLINE**

GI tract cancers are one of the most common malignancies discussed during multidisciplinary tumor board meetings. The National Cancer Committee Network (NCCN) publishes guidelines that are considered the gold standard for management of malignancies. This exhibit is a pictorial review of cancers of the stomach, small bowel, colon and rectum with emphasis on the NCCN guidelines. Key points:\* Description of the role of imaging in cancer staging.\* Multimodality imaging for initial workup.\* Outline of impact of radiology on the surgical management and medical treatment of GI cancers.\* Highlight of potential conflicts and pitfalls in tumor boards discussions.\* Imaging principles for active surveillance.

## **GIEE-68 Multimodality Approach to Complications of Pancreatitis**

Participants

Kaustubh Shiralkar, MD, Houston, TX (*Presenter*) Nothing to Disclose

### **TEACHING POINTS**

Acute and chronic pancreatitis may lead to a wide array of complications which can be visualized on imaging. Our exhibit will focus on understanding the use and unique advantages of ultrasound, CT, and MRI including secretin enhanced MRI to better characterize complications of acute and chronic pancreatitis to aid in management decisions. Acute pancreatitis may lead to numerous local complications including acute peripancreatic fluid collections, necrosis with or without superimposed infection, fistula formation, and vascular complications such as hemorrhage from erosion of nearby vessels, pseudoaneurysm formation, and adjacent venous thrombosis. Chronic pancreatitis may lead to pseudocyst formation with possible dissection into the mediastinum or adjacent peritoneal compartments, parenchymal atrophy or enlargement with or without calcifications, and decreased exocrine reserve which may be evaluated on secretin enhanced MRI. This exhibit will also focus on effective reporting for management and clinical decision making.

### **TABLE OF CONTENTS/OUTLINE**

Peripancreatic fluid collections, pancreatic and peripancreatic necrosis, emphysematous pancreatitis, fistula formation, vascular complications, chronic pancreatitis pseudocyst formation, ductal stenosis

## **GIEE-69 Congenital Cystic Lesions of the Biliary Tract: A Pictorial Review**

Participants

Abel Gonzalez Huete, MD, Madrid, Spain (*Presenter*) Nothing to Disclose

### **TEACHING POINTS**

1. To explain congenital cystic lesions of the biliary tree: congenital hepatic fibrosis, biliary hamartomas (von Meyenburg complexes), autosomal dominant polycystic disease, Caroli disease and choledochal cysts. 2. To review the embryology, physiology and pathogenesis. 3. To illustrate the imaging findings. 4. To discuss their differential diagnosis illustrated by sample cases.

### **TABLE OF CONTENTS/OUTLINE**

1. Introduction. 2. Embryopathogenesis. 3. Anomalies of the intrahepatic bile ducts. - Congenital hepatic fibrosis: Etiopathogenesis, Imaging findings. - Biliary hamartomas (von Meyenburg complexes): Etiopathogenesis, Imaging findings (Ultrasound, CT, MR), Differential diagnosis. - Caroli disease: Etiopathogenesis, Types (Caroli disease proper, Caroli Syndrome), Imaging findings (Ultrasound, CT, MR), Complications, Differential diagnosis. - Autosomal dominant polycystic disease: Etiopathogenesis, Imaging findings (Ultrasound, CT, MR), Complications, Extrahepatic associations. 4. Anomalies of the extrahepatic bile ducts. - Choledochal cysts: Etiopathogenesis, Imaging findings, Classification, Complications. 5. Summary.

## **GIEE-7 Multimodality Imaging Evaluation of Gastroenteropancreatic Neuroendocrine Neoplasms: A Diagnostic Challenge**

Participants

Monica Munoz-Lopez, MD, Mexico City, Mexico (*Presenter*) Nothing to Disclose

### **TEACHING POINTS**

- To review the origin, pathophysiology and classification of gastroenteropancreatic neuroendocrine neoplasms.- To recognize the utility of anatomical and somatostatin receptor functional imaging in the diagnosis, staging, prognosis and selection of treatment.- To identify, in a case- based review, the main challenges and pitfalls of functional imaging in the diagnosis and follow- up of GEP NETs.- To understand the radiologists role in the selection of treatment with theranostic agents.

### **TABLE OF CONTENTS/OUTLINE**

- Introduction to gastroenteropancreatic neuroendocrine neoplasms (GEP NENs): origin, pathophysiology and clinical syndromes- The WHO 2019 classification of GEP NENs: well- differentiated neuroendocrine tumor versus poorly differentiated neuroendocrine carcinoma- Multimodality anatomical and somatostatin receptor imaging criteria in diagnosis and staging- Pitfalls in interpretation of somatostatin receptor imaging- Prognostic value of dual positron emission tomography imaging with 18F-FDG and 18F-OC for NENs- Overview of theranostic agents for treatment of NENs

## **GIEE-70      Multimodality Imaging of Biliary Tract Conditions: What Radiologists Should Know**

### **Awards**

#### **Identified for RadioGraphics**

#### **Participants**

Camila Vendrami, MD, Chicago, IL (*Presenter*) Nothing to Disclose

#### **TEACHING POINTS**

· Review of biliary tract imaging technique · Identify the multimodality imaging features of benign and malignant conditions of the biliary tract · Discuss pitfalls in the interpretation of MR imaging and CT findings in the biliary tract

#### **TABLE OF CONTENTS/OUTLINE**

The biliary tract may be affected by a wide variety of pathologic conditions, some with similar clinical presentations. Biliary tract imaging plays a key role in determining the etiology, location, and severity of the condition and any complications. Imaging also guides management of biliary tract diseases including the most appropriate intervention when required. 1. Introduction 2. Imaging technique: what are the uses and how are standard MR cholangiopancreatography, 3D isotropic MR cholangiopancreatography and contrast-enhanced MR cholangiography and DECT performed? 3. What features characterize, on multimodality imaging including but not malignant to benign biliary (choledochal cysts including Caroli disease, cholangitis, recurrent pyogenic cholangitis, primary sclerosing cholangitis, ischemic cholangiopathy) and pre-malignant and malignant conditions (intraductal papillary neoplasm of the bile duct-IPNB-, cholangiocarcinoma and metastases)? 4. Review imaging pitfalls in the biliary tract imaging: blooming artifact, physiologic variants of the biliary system and pulsation/compression artifact 5. Take home points

## **GIEE-71      Extramural Venous Invasion in Rectal Cancer Before and After Neoadjuvant Therapy Beyond Classic Findings: Recognition of Detailed Characteristics and Tumor Deposit**

#### **Participants**

Akitoshi Inoue, MD, PhD, Rochester, MN (*Presenter*) Nothing to Disclose

#### **TEACHING POINTS**

Extramural venous invasion (EMVI) is a well-investigated prognostic factor predicting poor survival in rectal cancer despite no statement in American Joint Committee on Cancer TNM staging system. EMVI was described as an expanded, irregular vessel with intermediate tumor-signal intensity; however, detailed characteristics such as the number, diameter, and location of the involved vessel, and treatment response are gathering attention, aiming to predict precise patient outcomes and stratify risk. Tumor deposits (TDs), defined as cancer nodules located in the mesorectum without evidence of underlying lymph node architecture on histopathology, are recently reported as irregular nodules in the mesorectum directly interrupting the course of the vein with tapering into the vein on MRI. MR-detected TDs are reported to be a prognostic factor as well as pathological TDs. The purposes of this exhibit are: 1. To review imaging findings of EMVI and TDs in rectal cancer 2. To discuss the clinical significance of EMVI and TDs in contemporary therapeutic strategy in rectal cancer.

#### **TABLE OF CONTENTS/OUTLINE**

1. Detection of EMVI and imaging pitfalls 2. What are TDs? Imaging findings and cutting-edge knowledge. 3. Detailed characteristics of EMVI and difference between EMVI and TDs 4. Assessing response of EMVI and TDs after neoadjuvant therapy 5. Summary

## **GIEE-72      Closing the Loop on Challenging and Complex Small Bowel Obstructions**

#### **Participants**

Michael Hartung, MD, Madison, WI (*Presenter*) Consultant, Innovenn, Inc; Consultant, Otsuka Holdings Co, Ltd

#### **TEACHING POINTS**

1. Complex small bowel obstructions often bring both diagnostic and management dilemmas to the radiology and surgical teams. 2. The radiologist plays a major role in providing a confident interpretation of the baseline CT exam that influences management and follow-up. 3. Complex small bowel obstructions can be divided up into mechanical, neoplastic, and closed-loop categories. The key findings that raise the concern of closed-loop physiology include the beak sign, asymmetric edema, clustered loops with radial vessels, dilated C or U-shaped loops, and swirling narrowed vasculature. 4. Important mimics and pitfalls to consider when evaluating a complex bowel case include ischemia, angioedema, inflammatory enteritides, and graft versus host disease.

#### **TABLE OF CONTENTS/OUTLINE**

A. Defining simple versus complex small bowel obstruction- Mechanical- Abdominal and pelvic external hernias- Gallstone ileus - Afferent loop syndrome- Endometriosis B. Neoplastic- Benign- Primary tumors- Secondary tumors C. Closed-loop- Key signs of CLO- Adhesive disease- Internal hernia- Gastric bypass related- Volvulus D. Mimics and pitfalls- Non-obstructive ischemia- Angioedema- Inflammatory enteritides (vasculitis, eosinophilic, IBD)- Radiation and GVHD E. A practical approach to reporting challenging cases

## **GIEE-73      Bariatric Surgery: Imaging of Normal Post Operative Appearance and Complications**

#### **Participants**

Adina Laufer, MD, New York, NY (*Presenter*) Nothing to Disclose

#### **TEACHING POINTS**

The goal of this exhibit is to familiarize the participants with the surgical anatomy of the most common forms of bariatric surgery. Participants can then use that knowledge as a basis to identify complications of bariatric surgery and corresponding CT and fluoroscopic imaging features. Upon completion of this educational exhibit, participants will be familiar with the normal CT and fluoroscopic imaging appearance as well as the CT and fluoroscopic appearance of postoperative complications for the most commonly performed bariatric procedures. Familiarity with this subject will allow for prompt diagnosis and management for bariatric patients.

#### **TABLE OF CONTENTS/OUTLINE**

CT and GI fluoroscopic appearance of: -Gastric bypass-Gastric band-Sleeve gastrectomy This exhibit will highlight the CT and

fluoroscopic appearance for the gamut of postoperative complications including but not limited to: -leaks-strictures-marginal ulcers-hernias-small bowel obstruction-intussusception-gastroesophageal reflux

## **GIEE-74 The Art of Letting It Flow: Small Bowel Follow-Through in the Age of Cross-Sectional Imaging**

### **Awards**

**Identified for RadioGraphics**

Participants

Shamus Moran, MD, Seattle, WA (*Presenter*) Nothing to Disclose

### **TEACHING POINTS**

1) Review the indications, contraindications, and technique for the small bowel follow-through 2) Review the normal fluoroscopic appearance of small bowel anatomy 3) Provide a practical algorithmic approach to small bowel pathologies on fluoroscopy with an emphasis on clinical significance 4) Discuss the role of the small bowel follow-through in small bowel motility assessment 5) Fluoroscopic - cross-sectional imaging correlation

### **TABLE OF CONTENTS/OUTLINE**

Introduction. Indications, contraindications, and technique. Discussion of the following entities with case examples and an approach for diagnosis and further management  
Motility Assessment: • Normal small bowel transit times • Bedside SBFT for assessment of small bowel obstruction.  
Congenital: • Duplication cyst communicating with ileum • Cystic fibrosis • Meckel's diverticulum • Malrotation.  
Infectious: • Ascariasis • Giardiasis • Mononucleosis • Strongyloides • Tuberculous enteritis • Typhoid ileitis • Whipple's disease.  
Inflammatory: • Crohn disease (stenosis, diffuse mucosal thickening, colonic fistulae, enteroenteric fistula, sacculation, polyp, cobble stone) • Eosinophilic enterocolitis • Radiation enteritis • Scleroderma • Celiac Sprue • Amyloidosis • Henoch-Schoenlein Purpura • GVHD • Sclerosing mesenteritis.  
Neoplastic: • Adenocarcinoma • Carcinoid • Gastrointestinal stromal tumors • Lymphoma • Zollinger-Ellison syndrome • Metastasis.  
Miscellaneous: • Ischemia • Intestinal neuropathy • Small bowel - small bowel intussusception • Diverticulosis • Hypoalbuminemia

## **GIEE-75 Ulcerative Colitis on MR Enterography: Beyond the Scope of Endoscope!**

### **Awards**

**Identified for RadioGraphics**

Participants

Mehmam Amouei, MD, (*Presenter*) Nothing to Disclose

### **TEACHING POINTS**

Ulcerative colitis (UC) is a chronic inflammatory disease that can present at various stages of disease activity. Ileocolonoscopy and biopsy are the tests of choice to diagnose ulcerative colitis and assess disease severity. The value of MR enterography (MRE) is its usefulness in transmural/extramural assessment and identification of disease complications and extraintestinal manifestations. On the other hand, a complete colonoscopy might be unachievable in some patients, even in the expert hands, due to anatomical limitations or disease severity. However, this role is less emphasized compared to Crohn's disease due to the gradual course of UC, which is confined to the mucosa/submucosal layers of the colon. Beyond describing UC extension and severity, after completing this educational material, the readers will be able to recognize the value of MRE in: 1. Assessment of GI tract abnormalities beyond the colon in UC. 2. Identifying acute complications related to UC. 3. Describing benign and malignant disorders superimposed on UC. 4. Diagnosis of post-surgical complications in UC.

### **TABLE OF CONTENTS/OUTLINE**

Ø Background Ø Technical considerations Ø Imaging features of UC variants in MRE Ø Acute complications Ø Extra-colonic manifestations Ø Benign disorders superimposed on UC Ø Malignant disorders superimposed on UC Ø Post-surgical findings and complications Ø Mimickers Ø A practical algorithm for interpretation of MRE in UC Ø Conclusion Ø References

## **GIEE-76 Liver Transplant Primer For Radiologists: A Question-Based and Case-Based Review**

### **Awards**

**Certificate of Merit**

Participants

Roberta Catania, MD, Chicago, IL (*Presenter*) Institutional Research Grant, Siemens AG

### **TEACHING POINTS**

1. Familiarity with surgical techniques for deceased-donor and living-donor liver transplantation and postoperative anatomy 2. Familiarity with pertinent variant anatomies affecting the future transplant and role of imaging for their pre-operative assessment 3. Familiarity with role of imaging in early post-operative assessment of liver allograft 4. Familiarity with the common post-transplant complications and their imaging findings

### **TABLE OF CONTENTS/OUTLINE**

[All information will be presented and highlighted in an interactive questions-based and case-based format.]  
Indications • Current and expanding indications for liver transplantation • The issues with organ availability and organ allocation  
Surgical Techniques • Surgical techniques for deceased liver transplant • Surgical techniques for living donor liver transplant • Postsurgical anatomy  
Pretransplant evaluation • Imaging assessment of recipient for surgical candidacy • Imaging assessment of living donor candidate  
Overview of different imaging techniques and protocols  
Pertinent variant biliary and vascular anatomy that may affect surgical planning  
Segmentation and calculation of liver volumes  
Postoperative complications • Early post-operative complications • Delayed post-operative complications  
Post-Transplant Lymphoproliferative Disorder (PTLD) and other malignancies

## **GIEE-77 Diffuse Bile Ducts Abnormalities: A Case Base Review with Histopathologic Correlation**

Participants

Francisco Manuel Moreno SR, (*Presenter*) Nothing to Disclose

## TEACHING POINTS

o To provide a comprehensive review of bile pathway anatomy and a basic approach to its histology  
o To be able to identify abnormal appearance of the biliary tree on radiologic images, image patterns and the most common causes of diffuse biliary tree diseases  
o To include anatomopathological correlation for the pathologies reviewed so the radiologic signs associated to each entity can be better understood.  
o Key signs to be considered to differentiate malignance from other diseases

## TABLE OF CONTENTS/OUTLINE

1. Overview 2. Possible etiologies 3. Case based - review with histopathologic correlation 4. Pearls 5. Conclusions

### GIEE-78 **Vascular Complications of Hepatopancreatobiliary Surgeries and Liver Transplant**

Participants

Dayhane De Souza, MD, Sao Paulo, Brazil (*Presenter*) Nothing to Disclose

## TEACHING POINTS

1 - To demonstrate the vascular reconstructions techniques in hepatopancreatobiliary surgeries, including the liver transplant scenario.  
2 - To recognize the vascular surgical complications and how to elaborate a structured report that may help the clinical management.  
3 - To illustrate the different imaging methods for evaluating vascular complications, such as Computed Tomography (CT) and ultrasonography (US).

## TABLE OF CONTENTS/OUTLINE

1 - Illustration of typical imaging features of vascular complications supported by the use of graphics and cross-sectional imaging cases, such as arterial and venous stenosis and thrombosis.  
2 - Knowledge of hepatic vascular reconstruction is mandatory for early recognition of postoperative complications.  
3 - Summary and take home messages.

### GIEE-79 **A Step-by-Step Approach to the Understanding of Dysphagia: What Not to Miss in a Swallow Mechanism!**

Participants

Yumi Kimura Sandoval, MD, Mexico City, Mexico (*Presenter*) Nothing to Disclose

## TEACHING POINTS

- Recognize the importance of swallow mechanism in the diagnostic algorithm of dysphagia- Learn the indications and technique used in the performance of a swallow mechanism- Review the normal anatomy of the oral cavity, oropharynx, hypopharynx, and esophagus- Understand the physiology and different phases involved in deglutition- Case-based review of the main radiologic signs and features observed in deglutition alterations leading to dysphagia

## TABLE OF CONTENTS/OUTLINE

1. Normal anatomy - Oral cavity - Oropharynx - Hypopharynx - Esophagus - Anatomic variants  
2. Indications and technique of swallow mechanism - Useful projections - Oral contrast consistencies  
3. Deglutition physiology - Oral phase - Pharyngeal phase - Esophageal phase  
4. Deglutition pathology a) Oral phase: - Lip incompetence - Leakage to the oropharynx - Nasopharyngeal reflux b) Pharyngeal phase: - Functional alterations: penetration, aspiration, asymmetry, stasis, cricopharyngeal dysfunction- Structural alterations: esophageal web, Killian Jamieson`s diverticulum, Zenker`s diverticulum c) Esophageal phase: - Functional: achalasia, diffuse esophageal spasm - Structural: epiphrenic diverticulum

### GIEE-8 **From A to Z(ebras): Vascular Findings and Complications After Liver Transplant**

Participants

Heba Albasha, MD, Cincinnati, OH (*Presenter*) Nothing to Disclose

## TEACHING POINTS

- Review surgical techniques of liver transplant with a focus on vascular anatomy.
- Discuss imaging findings of common vascular complications after liver transplant.
- Understand and recognize unique imaging findings of uncommon vascular findings and complications of liver transplant.

## TABLE OF CONTENTS/OUTLINE

1. Liver transplant surgical techniques a. Review of liver transplant anatomy, including that of conventional, piggyback, deceased donor, and split liver techniques  
2. Imaging work-up of liver transplant complications  
3. Hepatic artery complications a. Hepatic artery thrombosis b. Hepatic artery stenosis c. Hepatic artery kinking d. Reversal of hepatic arterial flow e. Hepatic arterial-portal venous fistula f. Hepatic artery pseudoaneurysm  
4. Portal vein complications a. Portal vein thrombosis b. Portal vein stenosis c. Portal vein compression d. Portal vein size discrepancy e. Portal steal f. Primary nonfunction  
5. Hepatic vein/IVC complications a. IVC thrombosis b. IVC stenosis c. Venocaval anastomotic stricture

### GIEE-80 **LR-M in LI-RADS v2018: Non-HCC Malignancies and Atypical HCC**

**Awards**

**Cum Laude**

Participants

Tatsuyuki Tonan, MD, Kurume, Japan (*Presenter*) Nothing to Disclose

## TEACHING POINTS

Illustrate the malignant tumor (non-HCC malignancies and atypical HCC), which are classified as LR-M in the LI-RADS v2018 as follows:  
1. The definition of LR-M criteria including "targetoid" and "nontargetoid" imaging appearance on EOB-enhanced MRI.  
2. The relationship between the targetoid/nontargetoid imaging appearances and pathological findings (i.e., fibrosis, peliotic change, mucin, cell density/ ischemia, necrosis).  
3. The relationship between delayed (or persistent) extracellular contrast enhancement effects and targetoid imaging appearances.  
4. Exhibit of non-HCC malignancies with targetoid or nontargetoid imaging appearance

(i.e., intrahepatic cholangiocarcinoma, cholangiolocellular carcinoma, sarcomatous HCC, neuroendocrine tumors, mucinous carcinoma, intraductal papillary neoplasm of the bile duct and primary hepatic lymphoma). 5. New knowledge about the atypical HCCs with targetoid or nontargetoid imaging appearance favoring non-HCC malignancies.

#### **TABLE OF CONTENTS/OUTLINE**

LI-RADS v2017 introduced an important update to the LI-RADS-M (LR-M; probably or definitely malignant but not HCC specific) category to clarify appropriate use. Specifically, LR-M was modified as follows: "targetoid mass" including peripheral hypercellularity and central stromal fibrosis or "nontargetoid mass" including an infiltrative appearance, marked diffusion restriction, necrosis or severe ischemia, in addition to features that suggest a non-HCC malignancy in radiologist's judgment. While these imaging findings are not specific finding, to understand these imaging findings are helpful in the diagnosis of hepatic tumors, and is important in assignment of the LI-RADS.

#### **GIEE-81 Post-Operative CT Findings After Whipple Procedure: Normal Findings and Complications**

Participants

Vamshi Mugu, MD, Rochester, MN (*Presenter*) Nothing to Disclose

#### **TEACHING POINTS**

1) Identify components of post-operative anatomy for a) Standard Whipple b) Pylorus-sparing Whipple 2) Identify normal post-operative findings and distinguish them from complications

#### **TABLE OF CONTENTS/OUTLINE**

1) Conventional Whipple consists of a) Partial pancreatectomy and pancreaticojejunostomy b) Duodenectomy c) Distal gastrectomy and gastrojejunostomy d) Cholecystectomy and hepaticojejunostomy 2) Pylorus-sparing Whipple consists of a) Partial pancreatectomy and pancreaticojejunostomy b) Partial duodenectomy and duodenojejunostomy c) Cholecystectomy and hepaticojejunostomy 3) Common normal post-operative findings a) Post-operative anatomy: 1) Hepaticojejunostomy 2) Pancreaticojejunostomy 3) Gastrojejunostomy b) Vascular reconstructions c) Jejunal limb edema 4) CT appearance of post-operative complications a) Delayed gastric emptying (a clinical diagnosis) b) Pancreatic fistula c) Biliary leak d) Hemorrhage e) Acute pancreatitis f) Vascular thrombus

#### **GIEE-82 Fat's All Folks: A Case-Based Tour of Benign and Malignant Abdominopelvic Lesions**

Participants

Alana Fruauff, MD, BS, New York, NY (*Presenter*) Nothing to Disclose

#### **TEACHING POINTS**

Intralesional fat within the abdominopelvic viscera narrows differential diagnosis for benign and malignant disease processes. Abdominal and pelvic fat distribution can help diagnose co-existent and unrecognized disease. The presence of fat within a lesion does not automatically suggest a benign diagnosis. It is critical for radiologists to identify when a fat-containing lesion is most likely malignant.

#### **TABLE OF CONTENTS/OUTLINE**

1. Introduction of fat-containing lesions and typical appearance on ultrasound, CT, and MRI. Case-based review of benign and malignant fatty lesions in the following locations: a. Right upper abdomen b. GI tract c. Renal and adrenal glands d. Reproductive system e. Retroperitoneum f. Mesentery/peritoneum

#### **GIEE-83 GISTS and the Limits of RECIST: State of the Art Imaging and Treatment of Gastrointestinal Stromal Tumors**

Participants

Xin Zhan, MD, (*Presenter*) Nothing to Disclose

#### **TEACHING POINTS**

GIST is the most common single type of sarcoma and the most common mesenchymal tumor in the GI tract. Teaching points include 1) Approximately 25% of GIST are discovered incidentally. GISTs have 3 morphologic patterns: spindle, epithelioid, and Wild-Type which can be associated with genetic syndromes and worse prognosis. 2) The diagnostic workup of GIST consists of the initial imaging with contrast-enhanced CT (CECT), detection of metastasis with CECT or PET/MRI, and definitive diagnosis by histopathology. Given its propensity for the stomach, CT protocols for GIST can be optimized with changes in patient position, use of oral water, CO<sub>2</sub> crystals or positive enteric contrast. Multiphase CECT is useful in differentiating enhancement patterns of GIST vs other tumors. 3) Surgery remains the standard of care for localized tumors, but systemic therapy may be indicated based off unfavorable tumor locations, metastases, and genetic mutations. New biologic treatments (Imatinib, Sunitinib) have changed the clinical management of GIST and radiomic response evaluation continues to evolve to better assess disease progression. RECIST focuses on unidimensional, anatomic measurements, CHOI evaluates both anatomic and functional measurements, while PERCIST measures the metabolic response of tumors. We will discuss the strengths and weaknesses of these different criteria and how they impact patient management.

#### **TABLE OF CONTENTS/OUTLINE**

GIST Outline: - Pathophysiology - Clinical manifestations - Diagnostic imaging modalities/imaging features - Optimizing imaging protocols - Differential diagnoses on imaging - Treatment options, new biologic drugs - Radiomics (RECIST, PERCIST, CHOI) strengths and weaknesses

#### **GIEE-84 What Do You Look at Plain Radiograph Abdomen?**

Participants

Axel Torres Monarrez, MD, Tlalpan, Mexico (*Presenter*) Nothing to Disclose

#### **TEACHING POINTS**

\* To review the indications, limitations, and benefits of plain abdominal radiographs. \* To discuss the basic projections in the

abdominal radiograph.\* To show normal anatomy and its variants.\* To analyze the systematic approach for interpretation of abdominal radiographs and provide a guide for residents.\* To recognize normal bowel from the abnormal small and large bowel. \* To be familiarize with descriptive terms for common bone and soft tissue abnormalities seen on abdominal radiographs.\* To review abnormal calcification on an abdominal radiograph. \* To review the lines, tubes, and other devices commonly seen on AXR including their purposes and proper positions.

#### TABLE OF CONTENTS/OUTLINE

1. Review of indications, advantages, and disadvantages of plain abdominal radiographs. 2. Discuss the basic projections in the abdominal radiograph. 3. Explain the normal anatomy and its variants. 4. Discuss the algorithm for the evaluation of abdominal x-ray. 5. Present a series of cases to exemplify the most important diseases presented in AXR: - Abnormal calcifications: solid organs, hollow organs, and others. - Classification of bowel gas patterns: intraluminal and extraluminal. - Fluid/Soft Tissue Density: intraluminal and extraluminal. - Displacement of Structures: splenomegaly and hepatomegaly. - Bone and soft tissue abnormalities: osteophytes, neoplasms, post traumatic, and metabolic. 6. Recognize and illustrate devices commonly seen on AXR, the lines, tubes, and drains with demonstrative cases. 7. Conclusions and a complete section of key points of what residents need to know of abdominal X-rays. 8. References.

#### GIEE-85 **Cosmetic Surgery in the Abdomen and Pelvis: Post-Operative Appearances and Complications**

Participants

Madeleine Sertic, MBBCh, Boston, MA (*Presenter*) Nothing to Disclose

#### TEACHING POINTS

Since the turn of the 21st century, there has been a significant increase in the number of Cosmetic Surgeries performed. In 2020 alone, there were more than 2 million cosmetic procedures in the United States, including over 200,000 liposuction procedures, over 90,000 abdominoplasties, and more than 20,000 gluteal augmentation surgeries. While most of these cases do not undergo routine pre- or post-operative imaging, the increased incidence of these surgeries has led to an increased number of post-op patients who are imaged for other reasons. It is important to understand the expected post-operative appearances of these procedures so as to not misdiagnose pathology, and to correctly identify complications, if present. The expected post-surgical appearances and possible complications vary depending on the specific surgery. Gluteal injections and implants can be complicated by silicone granuloma formation or implant rupture. Abdominoplasty with gluteal fat transfer (i.e. "Brazilian Butt Lift") can be complicated by fat embolism; the risk varies with the surgical technique used. Complications for most procedures include infection, hematoma, and dehiscence.

#### TABLE OF CONTENTS/OUTLINE

Background on Cosmetic Surgery  
Abdominal Wall Augmentation  
Liposuction  
Abdominoplasty  
Abdominoplasty with Gluteal Fat Transfer  
Gluteal Augmentation  
Implants  
Injections  
Pelvic Augmentation  
Cosmetic Phalloplasty  
Cosmetic Labiaplasty  
Complications  
Hematoma  
Infection  
Dehiscence  
Fat Embolism  
Granuloma Formation  
Implant Rupture

#### GIEE-86 **Utilization of Perfusion CT to Improve the Diagnostic Accuracy of Pancreatic Cancer**

Participants

Konno Yoshihiro, PhD, (*Presenter*) Nothing to Disclose

#### TEACHING POINTS

The accuracy improvement of diagnostic imaging of pancreatic cancer including the early lesion is necessary. Functional information obtained by perfusion CT (PCT) would be able to address unmet clinical needs in conventional diagnostic imaging based on morphological images. We have developed a novel protocol that incorporates volumetric PCT into multiphase contrast-enhanced CT, enabling broad clinical use. Besides reducing radiation exposure, this method provides high-resolution perfusion information through parametric map fused with morphological images. In general, pancreatic cancer is depicted as a decreased area of blood flow and blood volume and a prolonged area of mean transit time compared with the background pancreatic parenchyma. Imaging assessment using PCT increased the diagnostic accuracy of small pancreatic cancers and helped detect minute lesion that was not visible as a mass. Perfusion information is associated with histopathological features, and its detailed examination may be useful in the management of pancreatic cancer.

#### TABLE OF CONTENTS/OUTLINE

1. Clinical issues in imaging diagnosis of pancreatic cancer. 2. Development of PCT imaging protocol. 3. High-resolution perfusion imaging: Parametric map analysis. 4. Reduction of exposure dose. 5. Imaging evaluation of pancreatic cancer using PCT. 6. Clinical usefulness and research applications.

#### GIEE-88 **The Forgotten Organ: Role of Contrast Ultrasound in the Evaluation of Splenic Lesion**

Participants

Paula Garcia, MEd, PhD, (*Presenter*) Nothing to Disclose

#### TEACHING POINTS

- To assess the role of contrast enhanced ultrasound (CEUS) in the characterization of non-traumatic splenic focal lesions.
- To review the technique used and the main fundamentals of CEUS as well as the main indications.
- To analyze the different focal splenic lesions through representative cases with special emphasis on the semiology of the lesions and their behavior after the injection of ultrasound contrast material.

#### TABLE OF CONTENTS/OUTLINE

Focal splenic lesions (FSL) are rare compared to those of other organs such as the liver and are often discovered incidentally. Conventional ultrasound and Doppler ultrasound have a limited role in the characterization of FSL, many of them being non-specific due to the wide spectrum of radiological manifestations they may present. CEUS is an accessible, inexpensive and safe technique that can help in the characterization of FSL. We analyzed the main imaging findings supporting us in the anatomopathological diagnosis, through representative cases performed in our center of both benign (simple cyst, abscesses, cystic lymphangioma, hemangioma, hamartoma) and malignant (lymphoma, metastasis) lesions. CEUS has an added role in the characterization of FSL allowing to see the enhancement of lesions in real time. Therefore, the spleen presents a special appetite for contrast due to the unique histological characteristics of this organ. CEUS may become a good alternative when other diagnostic techniques such as

computed tomography (CT) and magnetic resonance imaging (MRI) are not available.

### **GIEE-89 Role of Ultrasound Contrast in the Evaluation of Gallbladder Pathology**

Participants

Kanupriya Vijay, MBBS, MD, Jacksonville, FL (*Presenter*) Nothing to Disclose

#### **TEACHING POINTS**

1. Conventional grayscale ultrasound (US) is useful in evaluating various gallbladder diseases; however, assessment of microvasculature is often needed for detailed wall assessment and to distinguish many benign from malignant processes. 2. Contrast-enhanced ultrasound (CEUS) is an easy and effective modality to differentiate conditions such as tumefactive sludge from gallbladder cancer. 3. CEUS may be useful in differentiating benign wall thickening from adenomyomatosis and chronic cholecystitis and gallbladder cancer. 4. CEUS can accurately demonstrate the microvasculature used to differentiate adherent biliary precipitate from polyps, and can help identify features of malignancy. 5. Cholecystectomy tube injection of ultrasound contrast can be used to determine cystic duct patency and identify leak.

#### **TABLE OF CONTENTS/OUTLINE**

1. Introduction:a. Briefly review microbubble formulation and pharmacokineticsb. Discuss imaging techniques with CEUS to optimize image quality 2. Case guided review of various gallbladder pathologies a. Benign i. Stones ii. Adenomyomatosis iii. Polyps iv. Chronic cholecystitis v. Tumefactive sludge b. Malignant i. Gallbladder carcinoma ii. Malignant polyps 3. Role of CEUS in interventions a. Image guided biopsy b. Evaluation of cholecystostomy tube for cystic duct patency and leaks 4. Pitfalls

### **GIEE-9 Retrorectal Cystic Lesions: Utility of Magnetic Resonance Imaging for a Forbidden Space**

Participants

Lautaro Florentin, MD, Buenos Aires, Argentina (*Presenter*) Nothing to Disclose

#### **TEACHING POINTS**

- The retrorectal cystic lesions include a wide spectrum of etiologies.- The magnetic resonance imaging (MRI) allows approximate the diagnosis and to determine complications.- Diffusion weighted imaging (DWI) sequence is a cornerstone to suggest the presence of a solid component within the cyst.- Surgical management is mainly influenced by the MRI findings. The third sacral vertebra (S3) level is the key point for surgical approach selection.

#### **TABLE OF CONTENTS/OUTLINE**

1) Introduction and anatomy2) Differential diagnosis. Definition and imaging characteristics a) Developmental cysts - Dermoid cysts - Epidermoid cysts - Retrorectal cystic hamartomas (tailgut cysts) b) Malignancy - Rectal carcinomas with atypical presentations - Metastases c) Abscess d) Others - Vascular malformations - Granulomas3) MRI advantagesa) Intracystic content characterization - What to look for? (Size, lobulations, septum, walls, dense, fat and/or solid component) - Malignancy signs - Complications: infection and fistula. b) Malignant transformation - Why does it matter? Prognosis and management implications. - How to diagnose? DWI/ADC utility. Avoiding pitfalls: teratomas and dense-content lesions. c) Surgical planning. What radiologist apport to the surgeon? - Surgical approach selection. The S3 level. - Non-surgical treatment. The MRI role

### **GIEE-90 When the Bile Goes Sour: A Case-based Review of Unusual Complications of Biliary Procedures**

Participants

Cynthia Borborema, MD, Sao Paulo, Brazil (*Presenter*) Nothing to Disclose

#### **TEACHING POINTS**

To review the expected imaging appearance after hepatobiliary surgeries. To list radiologic features of early and late usual biliary postsurgical complications to provide a practical resource for radiologists to standardize examination. To illustrate cases of unusual complications after biliary procedures to improve the clarity and clinical impact of radiology reports.

#### **TABLE OF CONTENTS/OUTLINE**

Anatomy of the normal biliary tract. Most common variants of the biliary tree and their surgical relevance. Role of imaging in surgical planning and relevant report information. List of most common biliary surgeries and procedures. Epidemiological background of biliary procedures and associated complications. Usual complications after biliary procedures (biliary and nonbiliary, early and late ones), including key patient history, risk factors, imaging findings, and pitfalls. Unusual postsurgical biliary complications, including right hepatic artery pseudoaneurysm, post-cholecystectomy Mirizzi syndrome, late cholangitis after Kasai procedure, lung abscess due to retained gallstones, subcapsular liver hematoma after cholecystectomy, foreign-body granuloma caused by dropped gallstones simulating abdominal wall tumor, and others. Diagnostic tools, including magnetic resonance cholangiopancreatography (MRCP). Optimal imaging protocols.

### **GIEE-91 Misses and Misinterpretations of Pancreatic Adenocarcinoma: Recognizing Its Atypical Manifestations**

Participants

Pavan Shah, MD, Sayreville, NJ (*Presenter*) Nothing to Disclose

#### **TEACHING POINTS**

Pancreatic adenocarcinomas are highly lethal and timely detection is key to improving patient prognosis. While most cases present with typical features of pancreatic ductal dilatation, hypo enhancing mass and mass with restricted diffusion, some cases can present a diagnostic dilemma and are frequently misdiagnosed. Recognizing the atypical features helps in early diagnosis. We present atypical cross-sectional imaging findings of pancreatic adenocarcinoma.To review the epidemiology, pathology, and prognosis of pancreatic ductal adenocarcinomaTo describe typical imaging characteristics of PDAC along with atypical features to improve diagnostic accuracyTo discuss optimization of imaging techniques with the goal of preventing diagnostic delays and improving prognosis

#### **TABLE OF CONTENTS/OUTLINE**

Introduction, epidemiology, clinical manifestations, histopathology, typical CT/MRI findings, atypical CT/ MRI findings including

lesions without pancreatic ductal dilatation, lesions without restricted diffusion, lesions masquerading as cystic lesions, lesions presenting as acute pancreatitis, groove pancreatitis. Discussion on optimization of CT technique including use of dual energy, optimization of MRI techniques including use of MRCP, and T1 weighted sequences. Conclusion.

## **GIEE-92 Inflammatory Bowel Disease: Fluoroscopic Assessment and Postoperative Complications**

### **Awards**

#### **Certificate of Merit**

#### **Participants**

Linda Kelahan, MD, Chicago, IL (*Presenter*) Nothing to Disclose

#### **TEACHING POINTS**

1. Revisiting fluoroscopic findings in inflammatory bowel disease (IBD) with cross sectional correlation. 2. Outline possible surgical interventions for IBD. 3. Steps to successful fluoroscopic evaluation prior to ileostomy reversal 4. Fluoroscopic assessment of postoperative surgical complications.

#### **TABLE OF CONTENTS/OUTLINE**

1. Introduction a. Definition of IBD b. Epidemiology 2. Multimodality imaging of IBD a. Small bowel follow-through and barium enema examination. i. Technique ii. Imaging findings b. Cross sectional imaging findings 3. Fluoroscopic evaluation prior to ileostomy reversal a. Evaluate records to determine anatomy and surgical anastomoses b. Scout images in multiple obliquities c. Water-soluble fluoroscopic LGI steps to success d. Troubleshooting common complications during LGI: how to navigate enterocutaneous fistulas, severe anastomotic strictures, no contrast progression into the ostomy bag, multiple anastomoses. 4. Common surgical procedures (Fluoroscopic assessment of the altered anatomy) a. Small bowel resection b. Small bowel strictureplasty c. Total abdominal colectomy with ileorectal anastomosis d. Total abdominal colectomy with end ileostomy e. Colectomy (segmental/total) f. Proctectomy g. Restorative proctocolectomy with ileal pouch anal anastomosis h. Balloon dilatation 5. Postoperative complications: Fluoroscopic assessment with cross sectional correlation a. Strictures b. Pelvic infections c. Anastomotic site leakage d. Pouch failure e. Pouch cancer f. Fecal incontinence 6. Conclusion and take-home messages

## **GIEE-93 Early Postoperative GI Tract Evaluation: From Expected Findings to Complications**

### **Awards**

#### **Identified for RadioGraphics**

#### **Participants**

Louise Cavalcanti, MD, Sao Paulo, Brazil (*Presenter*) Nothing to Disclose

#### **TEACHING POINTS**

1. Distinguishing frequent and expected postoperative image findings after gastrointestinal tract surgical procedures from complications is essential in the early postoperative period, as well as detecting signs of possible complications that require further investigation. 2. Intraoperative free air and fluid, fat stranding and bowel dilatation are extremely common findings in the early postoperative image and, although are expected, they can sometimes represent signs of complications. The imaging characteristics and evolution are key for this differentiation. 3. Contrast-enhanced CT is the imaging method of choice for the evaluation of patients in the early postoperative period, with good characterization of gas and free fluid and the possibility of using positive oral contrast in patients with suspected anastomotic leakage or bowel perforation.

#### **TABLE OF CONTENTS/OUTLINE**

a. Introduction. b. CT protocol for early postoperative evaluation. c. Evaluation of intraperitoneal air: residual postoperative pneumoperitoneum or complication? d. Evaluation of intraabdominal fluids: sterile postoperative content or infected collections - imaging features and score systems. e. Fat stranding patterns of the mesentery that may suggest postoperative complications. f. Identification of dilated bowel and differentiation between metabolic, obstructive or ischemic conditions. g. Other expected postoperative findings and major early complications. h. Take home messages.

## **GIEE-94 Magnetic Resonance Imaging Evaluation of Perianal Fistulas: Making It Easier For Surgeons and Radiologists!**

#### **Participants**

Joao Manoel Santos, MD, Sao Paulo, Brazil (*Presenter*) Nothing to Disclose

#### **TEACHING POINTS**

The purpose of this exhibit is:- To review usual and unusual cases of perianal fistulas.- To correlate important findings with the anatomy and pathophysiology.- To discuss image findings according to Parks and St James's University Hospital classifications, in order to enhance surgeons and radiologists' skills.- To review MRI protocols in the evaluation of patients with perianal fistulas.- To highlight their characteristics in order to familiarize surgeons and radiologists with these conditions, preventing unfavorable patient outcome.

#### **TABLE OF CONTENTS/OUTLINE**

Applied anatomy of the anal sphincter complex. MRI protocols in the evaluation of patients with perianal fistula. Parks classification with sample cases of:- Intersphincteric Suprasphincteric- Transsphincteric- Extrasphincteric. St James's University Hospital classification with sample cases of:- Grade 1: simple linear intersphincteric fistula- Grade 2: intersphincteric fistula with an abscess or secondary track- Grade 3: transsphincteric fistula- Grade 4: transsphincteric fistula with an abscess or secondary track in the ischioanal or ischioanal fossa- Grade 5: supralelevator and translevator disease. Correlation between Parks and St James's University Hospital classifications. Submucosal fistula. How do I report?- Location- Track o Relationship to sphincters o Simple or complex? Sample cases of pearls, pitfalls, diagnostic difficulties, and mimics. Summary and take-home messages.

## **GIEE-95 Most Common Gastrointestinal Post-surgical Anatomy on CT: A Pictorial Review. Radiologists- Don't Be Afraid**

#### **Participants**

Louise Cavalcanti, MD, Sao Paulo, Brazil (*Presenter*) Nothing to Disclose

#### TEACHING POINTS

1. Radiological evaluation of the post-operative abdomen can be challenging and knowledge of normal post-operative anatomy is important to identify possible complications. 2. The intention of this pictorial review is to describe the most important gastrointestinal surgical techniques, their clinical indications and show their normal post-operative appearance on computed tomography (CT). 3. Besides that, this essay provides some signs to identifying the procedure, which can be helpful particularly when surgical history is missing, with recognition of the organ(s) involved, determination of what was resected and familiarity with the type of anastomoses used.

#### TABLE OF CONTENTS/OUTLINE

a. Introduction b. Imaging methods and protocols for postoperative evaluation. c. Identification of mechanical stapling patterns and radio-opaque markers from the anastomosis. d. Evaluation of gastric surgical techniques, including bariatric procedures and expected results. e. Evaluation of small bowel surgical techniques. f. Evaluation of the most common colorectal surgical techniques, including Hartmann procedure and restoration of intestinal continuity. g. Take-home messages.

#### GIEE-96 A "Spectral-acular" Ileus

Participants

Reza Al-Saudi, MD, Belfast, United Kingdom (*Presenter*) Nothing to Disclose

#### TEACHING POINTS

1. Gallstone ileus represents a rare cause of small bowel obstruction. 2. Sensitivity of CT in the diagnosis of gallstone ileus is > 90%. 3. CT diagnosis of gallstone ileus is dependent on establishing the features of Rigler's triad - small bowel obstruction, pneumobilia, and an ectopic calcified gallstone. 4. 15% - 20% of gallstones are radio-opaque. This fact limits the Radiologist's ability to definitively establish the presence of an ectopic gallstone, although this presence is usually inferred based on associated features. 5. Spectral CT offers numerous advantages over standard CT. Spectral CT utilises the principle that elements and by extension mixed-composition materials cause differing attenuation of photons (via photo-electric absorption) at energy levels near the k-edge of the element in question, as compared to the remainder of the energy spectrum. The differing behaviour of elements across the energy spectrum allows material differentiation and the determination of material composition. 6. Effective atomic number (Z effective), mono-energetic (mono keV), and iodine density spectral reformats all aide in material differentiation. Z effective reformats provide the most reliable and reproducible results in relation to the detection of radio-lucent gallstones.

#### TABLE OF CONTENTS/OUTLINE

1. Introduction. 2. Role of conventional CT. 3. Conventional CT vs Spectral CT. 4. Spectral CT - options for diagnosis.

#### GIEE-97 Pancreas Allograft biopsies: What do you need to know?

Participants

Dayhane De Souza, MD, Sao Paulo, Brazil (*Presenter*) Nothing to Disclose

#### TEACHING POINTS

1 - Describe the anatomy of the main pancreatic transplantation technique.??2 - Discuss the Pancreas graft biopsy and Percutaneous needle biopsy technique guided by Ultrasound (US) and Computed Tomography (CT).3 - Discuss the sample of the pancreas considered adequate for evaluation.

#### TABLE OF CONTENTS/OUTLINE

1 - Review indications for pancreas transplantation and causes of graft injury.2 - Illustrate anatomy and surgical techniques supported by the use of graphics and cross-sectional imaging cases. 3 - Discuss the indication for pancreas graft biopsy and biopsy access routes.4 - Discuss what constitutes a satisfactory graft sample and what are the histopathological findings.5 - Summary and take home messages.

#### GIEE-98 Hepatocellular Lesions In Patients with Vascular Liver Diseases : Radiologic-Pathologic Correlation

Participants

Mayu Uka, (*Presenter*) Nothing to Disclose

#### TEACHING POINTS

The purpose of this exhibit is: 1)To review imaging features on contrast enhanced CT, MRI of hepatocellular nodules found in vascular liver diseases with histopathological correlations. 2) To discuss the point of differential diagnosis.

#### TABLE OF CONTENTS/OUTLINE

Hepatocellular nodules have been recognized in vascular liver diseases (Budd-Chiari syndrome, congenital portosystemic shunt, hereditary hemorrhagic telangiectasia, extrahepatic portal vein obstruction and congenital heart disease etc.). They may be related to portal venous deprivation, venous outflow obstruction, or arterial diseases, imbalances in arterial, portal, and venous blood flow have been reported to cause nodule formation. These nodules include nodular regenerative hyperplasia, large regenerative nodule, partial nodular transformation, focal nodular hyperplasia, and others, as well as hepatocellular adenoma and hepatocellular carcinoma, which are true neoplastic lesions. Some confusions in their identification and overlap in their definitions exist. This exhibit will describe the imaging appearances of each type of hepatocellular nodules found in the vascular liver diseases, by correlating with histology, and provide some clues for their differential diagnosis.

#### GIEE-99 Deep Learning Reconstruction of MR Imaging: Technical Features and Clinical Impact on Abdominal MR Imaging

Participants

Hiroimitsu Onishi, MD, Suita, Japan (*Presenter*) Research Grant, General Electric Company;Speakers Bureau, General Electric Company

## **TEACHING POINTS**

Deep learning reconstruction (DLR) has been introduced by several vendors to improve MR image quality. DLR has various benefits such as effective noise reduction in the diagnosis with MR imaging. The purpose of this presentation is: 1. To illustrate technical features of DLR compared with conventional reconstruction, 2. To discuss image quality of MR imaging using DLR, and 3. To discuss clinical impact on MR study in the diagnosis of abdominal diseases.

## **TABLE OF CONTENTS/OUTLINE**

1. Overview 2. Principle of DLR 3. Difference from the conventional reconstruction technique 4. Sequences applicable to DLR: fast spin echo T2WI, single-shot fast spin echo T2WI, DWI, small field-of-view DWI, fast imaging employing steady-state acquisition (FIESTA), etc. 5. Effective reduction of image noise with DLR 6. Improved spatial resolution with DLR 7. Reduction of truncation artifacts with DLR 8. What purpose can DLR be used for in clinical practice? To improve image quality, to increase the spatial resolution of the images, to save acquisition time, or combination of them 9. Clinical impact on the diagnosis of liver diseases 10. Clinical impact on the diagnosis of pancreatic diseases 11. Summary

Printed on: 02/07/23



## Abstract Archives of the RSNA, 2022

GIEE-1

### Split Scar Sign (SSS): How to Interpret It In The Context of Response to Neoadjuvant Treatment in Rectal Cancer

Sunday, Nov. 27 8:00AM - 9:00AM Room: Learning Center - GI

#### Participants

Ana Uski, MD, Sao Paulo, Brazil (*Presenter*) Nothing to Disclose

#### TEACHING POINTS

Describe the typical MRI imaging findings in cases of SSS+ and SSS-. Demonstrate the applicability of MRI in the context of neoadjuvant radiotherapy in rectal cancer and its potential limitations. Propose a structured report for local re-staging purposes.

#### TABLE OF CONTENTS/OUTLINE

Radical mesorectal excision surgery contributes substantially to patient morbidity in the context of rectal cancer. A number of clinical trials support the use of neoadjuvant radiation as a form of initial approach in an attempt at more conservative treatment, and responders to this modality have a favorable prognosis and similar outcomes to those who underwent radical surgery. In this context, MRI is the imaging modality of choice in response assessment to predict fibrosis or suspicious areas of viable neoplastic tissue. The split scar sign (SSS) is assessed on high-resolution T2-WI, positive or present when a thin regular 1-2 mm layer of hypointense "fibrosis" is well defined on the endoluminal aspect of the tumor site (corresponding to fibrous submucosa). Whenever the tumor site is not "organized" and this T2WI hypointensity layer is broken focally, the signal should be considered absent or negative. The positive or present SSS (+) has a very high specificity (97%) and positive predictive value (93/94%) for sustained complete response in case of neoadjuvant radiotherapy in rectal cancer. A good quality examination with the appropriate technique is necessary as well as the recognition of the imaging findings related to the presence or absence of this sign (SSS) and potential limitations of MRI.

Printed on: 02/07/23



## Abstract Archives of the RSNA, 2022

GIEE-10

### Management of Incidentally Detected Gallbladder Polyps: Review of Clinical Scenarios Using the 2021 SRU Gallbladder Polyp Consensus Guideline

Sunday, Nov. 27 8:00AM - 9:00AM Room: Learning Center - GI

#### Participants

Christopher Fung, MD, Edmonton, AB (*Presenter*) Stockholder, Mikata Health

#### TEACHING POINTS

Incidental gallbladder (GB) polyps are common, seen in 3-6% of the general population, often benign cholesterol polyps. Few GB polyps (6%) are neoplastic (intracholecystic papillary neoplasm, ICPN). While ICPNs have malignant potential, malignant transformation is believed rare. GB cancers also typically arise from flat dysplastic epithelium, not polyps. Yet the concern a small polyp may harbor a future or early neoplasm has led past guidelines to suggest relatively aggressive management; recent studies show significant overtreatment of predominantly benign GB lesions. In 2021 the Society of Radiologists in Ultrasound (SRU) convened a multidisciplinary committee to review current literature and construct updated guidelines for the management of incidentally detected GB polyps. The SRU Guidelines, to be published in 2022 (Radiology), stratify risk into three categories: Extremely Low, Low, and Indeterminate Risk. Clinical examples and common questions will be addressed.

#### TABLE OF CONTENTS/OUTLINE

1. Background and review of prior guidelines
  - a. Overview of gallbladder polyps and underlying pathology
  - b. Discussion of current literature and recommendations
2. 2021 SRU Gallbladder Polyp Consensus Recommendations
  - a. Applicable and excluded patient populations
  - b. Risk Categories: Extremely Low Risk, Low Risk, Indeterminate Risk
3. Common and uncommon clinical scenarios
  - a. Polyp measurement
  - b. Sessile versus pedunculated
  - c. Determination of growth
  - d. Doppler assessment
  - e. Multiple versus single gallbladder polyps
  - f. The role of alternative modalities such as contrast-enhanced ultrasound and MRI
  - g. Other risk factors: primary sclerosing cholangitis, age, ethnicity, geographic location

Printed on: 02/07/23

## Abstract Archives of the RSNA, 2022

GIEE-100

### **Gastrointestinal Neuroendocrine Neoplasms on Multimodality Imaging With Emphasis on Dynamic CT: Case Review with Radiology Pathology Correlation**

Sunday, Nov. 27 8:00AM - 9:00AM Room: Learning Center - GI

#### **Awards**

**Certificate of Merit**

#### **Participants**

Nobuyuki Takeyama, MD, (*Presenter*) Nothing to Disclose

#### **TEACHING POINTS**

To describe the comprehensive categorization system between well-differentiated neuroendocrine tumors (NETs), poorly differentiated neuroendocrine carcinomas (NECs), and mixed neuroendocrine-non-neuroendocrine neoplasms (MiNENs) on the basis of the WHO 2019 classification for gastrointestinal neuroendocrine neoplasms (GI-NENs). To review multimodality imaging of endoscopy, enteroscopy, endoscopic ultrasound, and cross-sectional images (CT, MRI, SPECT, and PET) in this case-based review presentation correlated with pathology.

#### **TABLE OF CONTENTS/OUTLINE**

1.Introduction including definition, epidemiology, genetic evidence, clinical features, and TNM staging in GI-NENs.2.Pathology of the WHO 2019 classification for grading and differentiation of GI-NENs to discuss differentiation, mitosis index, Ki-67 index and immunostaining. 3.Case-based review presentations with multimodality imaging for esophageal NEC, gastric NET, NEC and MiNEN, ampullary NET, duodenal NET, duodenal gastrinomas with MEN 1, small bowel NET, metastases of

Printed on: 02/07/23



## Abstract Archives of the RSNA, 2022

GIEE-101

### Anal Cancer Imaging: What We Know and What is On The Horizon

Sunday, Nov. 27 8:00AM - 9:00AM Room: Learning Center - GI

#### Awards

Certificate of Merit

#### Participants

Jessica Gomes, MD, Sao Paulo, Brazil (*Presenter*) Nothing to Disclose

#### TEACHING POINTS

Know the epidemiology, increasing number of cases, and risk factors of anal squamous cell carcinoma (SCC) Recognize the imaging differences between rectal adenocarcinoma and anal SCC Be familiar with future directions in anal SCC staging

#### TABLE OF CONTENTS/OUTLINE

INTRODUCTION Epidemiology Risk factors RECTAL ADENOCARCINOMA X ANAL SQUAMOUS CELL CARCINOMA ANAL SCC  
TREATMENT Chemoradiation therapy (CRT) and how to prevent sequelae Surgery Tumor recurrence/persistence Anal margin tumor approach  
ROLE OF IMAGING Staging scenario Restaging scenario THE MOST RECENT CONSENSUS How to staging How to restaging post CRT  
WHAT'S ON THE HORIZON INTERACTIVE CHALLENGING SCENARIOS

Printed on: 02/07/23



## Abstract Archives of the RSNA, 2022

GIEE-102

### Hepatobiliary and Pancreatic Tumor Board Primer for Radiologists: Review of AJCC Staging and NCCN Guidelines

Sunday, Nov. 27 8:00AM - 9:00AM Room: Learning Center - GI

#### Participants

Madiha Aslam, MD, Darby, PA (*Presenter*) Nothing to Disclose

#### TEACHING POINTS

Review of AJCC for radiological staging of hepatobiliary and pancreatic tumors. Review of NCCN guidelines for stage-based treatment planning of hepatobiliary and pancreatic tumors. Review of NCCN guidelines for follow up of post treatment hepato-bilio pancreatic tumors. Radiological implication of AJCC and NCCN guidelines in tumor boards for determining the further diagnostic steps and making decisions about the appropriate treatment. Pitfalls in imaging.

#### TABLE OF CONTENTS/OUTLINE

Tumor staging and stage-based treatment planning is a crucial step in appropriate cancer treatment and being a part of multidisciplinary team in tumor boards, radiologists play a critical role in diagnosing, characterizing, initial staging, determining resectability, and surveillance of cancer patients. This helps the rest of the team to choose the appropriate treatment therapies and determine the follow up interval for post treatment cases. We will provide a comprehensive review of the AJCC staging and NCCN guidelines for hepato bilio pancreatic tumors using multiple imaging modalities, which will help the radiologists in day-to-day tumor boards to solve the staging and decision dilemmas.

Printed on: 02/07/23



## Abstract Archives of the RSNA, 2022

GIEE-103

### Imaging Assessment of Small Gastrointestinal Lesions. How Can we Improve the Detection or Suspect of Early Tumors?

Sunday, Nov. 27 8:00AM - 9:00AM Room: Learning Center - GI

#### Participants

Tomas Lacerda, MD, Sao Paulo, Brazil (*Presenter*) Nothing to Disclose

#### TEACHING POINTS

TEACHING POINTS: Initial malignant lesions may be an incidental finding. We must pay special attention to small findings in patients with a background that favors malignancy, such as neoplastic syndromes and a known primary tumor. Understand how we can and should improve our imaging protocol according to each patient's background. Review when we should consider complementation with different methods and how to choose the best protocol. Understand which characteristics of small lesions may favor malignancy. Protocol pearls for certain tumor types.

#### TABLE OF CONTENTS/OUTLINE

Epidemiological considerations that may change our interpretation and pretest probability of a disease when characterizing a small lesion. Imaging examples of small lesions that were confirmed as malignant on follow up, biopsy or surgery: Neuroendocrine tumors; Initial metastasis; Small cholangiocarcinoma; Early CHC imaging protocol and imaging methods discussion regarding small lesions: When to include additional phases in our protocol; When to consider MRI evaluation; Hepatocyte-specific contrast indications; PET scan evaluation considerations.

Printed on: 02/07/23



## Abstract Archives of the RSNA, 2022

GIEE-104

### Do Not Forget the Pipes: Inferior Vena Cava: Abnormal Finding and Their Imaging Appearance

Sunday, Nov. 27 8:00AM - 9:00AM Room: Learning Center - GI

#### Participants

Teresa Garcia, MD, Buenos Aires, Argentina (*Presenter*) Nothing to Disclose

#### TEACHING POINTS

To review the usual anatomy and the most common congenital variants of the inferior vena cava (IVC). To describe the most used IVC imaging techniques, its relevance and usefulness. To highlight the pathologies that may affect the IVC and the associated radiological findings. To describe the most frequent IVC pitfalls.

#### TABLE OF CONTENTS/OUTLINE

Brief review of the anatomy and embryology of the inferior vena cava Imaging techniques and its relevance. Most common IVC congenital variants. Pathologies that can involve IVC ( primary and secondary involvement) Pitfalls at IVC imaging and miscellaneous imaging.

Printed on: 02/07/23



## Abstract Archives of the RSNA, 2022

GIEE-105

### Acute Mesenteric Ischemia: A Primer

Sunday, Nov. 27 8:00AM - 9:00AM Room: Learning Center - GI

#### Participants

Ken Nakanote, MD, Salt Lake City, UT (*Presenter*) Nothing to Disclose

#### TEACHING POINTS

Understand the different etiologies of acute mesenteric ischemia  
Recall the CT protocol used in the evaluation of acute mesenteric ischemia  
Evaluate for the radiological features associated with each etiology of acute mesenteric ischemia

#### TABLE OF CONTENTS/OUTLINE

A. Background  
B. Etiology and pathophysiology  
C. Clinical presentation  
D. Evaluation  
Imaging- ACR appropriateness guidelines- CT protocol- Imaging findings for different etiologies  
E. Treatment and management  
F. Summary

Printed on: 02/07/23



## Abstract Archives of the RSNA, 2022

GIEE-106

### Demistifying the Mesentery: A Differential-Based Approach to Mesenteric Pathology

Sunday, Nov. 27 8:00AM - 9:00AM Room: Learning Center - GI

#### Participants

Daniel Schneider, MD, Ann Arbor, MI (*Presenter*) Nothing to Disclose

#### TEACHING POINTS

- Review anatomy of the mesentery with illustrations - Review common and rare, focal and diffuse mesenteric pathologies with imaging examples - Present an imaging-based approach to various mesenteric pathology

#### TABLE OF CONTENTS/OUTLINE

1. Mesenteric anatomy 2. Differential diagnoses for mesenteric infiltration a. Edema i. Hepatic failure, hypoproteinemia ii. Venous thrombosis iii. Angioedema (angiotensin converting enzyme inhibitor-associated angioedema) b. Hemorrhage i. Trauma c. Inflammation i. Pancreatitis ii. Crohn's disease iii. Post-operative iv. Sclerosing encapsulating peritonitis v. COVID-19 d. Neoplasm i. Peritoneal carcinomatosis ii. Lymphoma iii. Carcinoid iv. Mesothelioma v. Primary peritoneal serous neoplasm vi. Pseudomyxoma peritonei vii. Desmoid viii. Lymphangioma e. Sclerosing mesenteritis i. Mesenteric panniculitis ii. Retractable mesenteritis f. Idiopathic 3. Conclusion a. Mesenteric infiltration is often nonspecific and can pose diagnostic challenges to the radiologist. Knowledge of key imaging features associated with various mesenteric pathologies can help narrow the differential diagnosis in appropriate clinical setting.

Printed on: 02/07/23

## Abstract Archives of the RSNA, 2022

GIEE-107

### Seeing Through the Mist: An Interactive Tour of Mesenteric Pathology

Sunday, Nov. 27 8:00AM - 9:00AM Room: Learning Center - GI

#### Awards

Certificate of Merit

Identified for RadioGraphics

#### Participants

Amelia Kernizan, MD, (*Presenter*) Nothing to Disclose

#### TEACHING POINTS

Mesenteric lesions are frequently encountered incidentally on abdominal imaging. As many of the underlying etiologies appear similar on CT and/or MRI, they often pose a diagnostic dilemma. The broad differential diagnosis for these lesions ranges from benign etiologies including infection, inflammation, and benign neoplasia to malignant etiologies such as carcinoid, lymphoma and metastatic disease. Via a multiple-choice case-based approach, this presentation will provide a framework for approaching solid mesenteric lesions, while providing pathologic correlation to highlight their similarities and differences, as well as how the histology influences their imaging appearance.

#### TABLE OF CONTENTS/OUTLINE

I. Review of normal peritoneal anatomy and histology. II. Quiz-style case-based review of solid mesenteric masses. IIa. Discussion of sclerosing mesenteritis with cases of mesenteric panniculitis and retractile mesenteritis showing radiologic-pathologic correlation. IIb. Case of multiple mesenteric masses highlighting the differential and pertinent imaging findings. IIc. Case of mesenteric mass with associated small bowel masses. IId. Case of a <sup>68</sup>Ga-DOTATATE-avid mass with potential pitfalls to avoid with this imaging modality. III. Summary with our method for approaching and differentiating between commonly encountered incidental mesenteric lesions.

Printed on: 02/07/23



## Abstract Archives of the RSNA, 2022

GIEE-108

### All Around the Liver: The Perihepatic Space and Why It Matters

Sunday, Nov. 27 8:00AM - 9:00AM Room: Learning Center - GI

#### Participants

Helena de Souza, MD, Sao Paulo, Brazil (*Presenter*) Nothing to Disclose

#### TEACHING POINTS

- The perihepatic space is often involved in a spectrum of diseases, including intrahepatic lesions that extend into the capsule and conditions arising from adjacent or pelvic organs. It is covered by the peritoneum, and it includes the right subphrenic space, the subhepatic space, the lesser sac, and the left perihepatic space.- The distribution and dynamics of the peritoneal fluid influence the spread of inflammatory and tumor processes to the perihepatic space. The correct evaluation of this space is part of abdominal radiology workup and the knowledge of the main abnormalities is crucial for the best report.- The objectives of this exhibit are to highlight different etiologies of perihepatic involvement, from inflammatory/infectious diseases (stone-related abscesses, Fitz-Hugh-Curtis Syndrome, peritoneal tuberculosis, echinococcosis), endometriotic and metastatic lesions, to rare primary peritoneal tumors (peritoneal malignant mesothelioma, desmoplastic small round cell tumor, peritoneal serous papillary carcinoma, periportal plexiform neurofibroma, and hepatic hilum lymphoma), with illustrative cases (CT and MRI).

#### TABLE OF CONTENTS/OUTLINE

Background of the perihepatic space. Evaluation of the anatomy and physiology of the perihepatic space and its peritoneal fluid dynamic. Case-based review of a range of cases including the main and rarer abnormalities of the perihepatic space with respective MRI and CT findings. Radiological correlation with the peritoneal fluid flow distribution.

Printed on: 02/07/23



## Abstract Archives of the RSNA, 2022

GIEE-109

### **GIST: What The Radiologist Should Know**

Sunday, Nov. 27 8:00AM - 9:00AM Room: Learning Center - GI

#### **Participants**

Cristina Cano Pardo, MD, Pontevedra, Spain (*Presenter*) Nothing to Disclose

#### **TEACHING POINTS**

To identify typical and atypical radiological findings of gastrointestinal stromal tumors (GIST). To know the radiological criteria used in GIST for the evaluation of tumor response. To review what factors have been proposed as relevant when predicting prognosis and response to treatment.

#### **TABLE OF CONTENTS/OUTLINE**

Relevant information towards the diagnosis of GIST will be clearly exposed using examples of different cases seen in our center. We will review the main radiological characteristics of GIST in order to suggest a correct differential diagnosis and adequately suggest this pathology. GIST complications and their different responses to treatment are not rare, especially in the emergency room. That is why we will display some key points to identify those situations and ensure a rapid diagnosis and treatment. Likewise, it is interesting to know the different response criteria to treatment so as not to confuse a favorable evolution with a progression of the disease.

Printed on: 02/07/23



## Abstract Archives of the RSNA, 2022

GIEE-11

### Vascular Ultrasound in the Setting of Post-kidney, Liver, and Pancreas Transplantation: The Ins and Outs of Post-surgical Anatomy and Need-to-know Pathology

Sunday, Nov. 27 8:00AM - 9:00AM Room: Learning Center - GI

#### Participants

Harrison Lee, MD, MBA, (*Presenter*) Nothing to Disclose

#### TEACHING POINTS

1. Ultrasound is typically the first-line option for post-surgical evaluation in the setting of kidney, liver, and pancreas transplantation. A focused review of vascular complications across these organ transplantations can enable a comparative and more conceptual-based approach toward this topic. 2. Kidney, liver, and pancreas transplantation can be performed using different surgical techniques leading to variable post-surgical vascular configurations. 3. Post-transplant vascular complications differ across etiology, timing, and clinical presentations, largely falling into categories of thrombosis, stenosis, and post-biopsy complications, with early and accurate detection being essential to preventing graft failure.

#### TABLE OF CONTENTS/OUTLINE

I. Kidney transplantation A. Post-transplant vascular anatomy and variations B. Common indications for ultrasound C. Vascular complications 1. Renal artery thrombosis, stenosis 2. Renal vein thrombosis, stenosis 3. Post-biopsy vascular complications (arteriovenous fistula, pseudoaneurysm) II. Liver transplantation A. Post-transplant vascular anatomy and variations B. Common indications for ultrasound C. Vascular complications 1. Hepatic artery thrombosis, stenosis 2. Portal vein thrombosis, stenosis 3. Hepatic vein stenosis 4. IVC thrombosis, stenosis III. Pancreas transplantation A. Post-transplant vascular anatomy and variations B. Common indications for ultrasound C. Vascular complications 1. Thrombosis, stenosis 2. Post-biopsy vascular complications

Printed on: 02/07/23



## Abstract Archives of the RSNA, 2022

GIEE-110

### Up Your Game: A Masterclass on CT Contrast in Abdominal Imaging

Sunday, Nov. 27 8:00AM - 9:00AM Room: Learning Center - GI

#### Participants

Alex Chan, DO, Rochester, MN (*Presenter*) Nothing to Disclose

#### TEACHING POINTS

-Review how contrast agent distribution reflects physiology and provides a foundation for diagnosis, problem-solving, and avoiding imaging pitfalls.-Discuss diagnostic advantages and pitfalls related to iodinated contrast distribution, altered hemodynamics, x-ray interaction, and contrast timing.-Collaborative use of gained knowledge to focus on problem solving complex post-surgical cases

#### TABLE OF CONTENTS/OUTLINE

The goal of this education exhibit is to review how contrast agent distribution reflects physiology in normal and diseased states which provides the foundation for understanding how CT contrast agent enhancement patterns can be used for diagnosis, problem-solving, and avoiding imaging pitfalls. We will first discuss the physiologic redistribution effect of typical iodinated contrast agent from the intravascular to interstitial space. Next, we will discuss the effects of altered vascular hemodynamics, for example, in the setting of VA-ECMO and inhomogeneous venous return. Following, the physics of x-ray interaction with iodinated contrast will be discussed accompanied with its diagnostic challenges and exploitation with dual energy CT. Additionally, we will discuss the diagnostic sensitivity of various pathologies related to CT technique/contrast timing and explore the utility of bowel contrast agents. Throughout the presentation, we will use these main ideas to problem solve complex postsurgical patients. In conclusion, the audience will gain a higher level of understanding of CT contrast agents and apply these concepts to improve diagnostic confidence at daily practice.

Printed on: 02/07/23

## Abstract Archives of the RSNA, 2022

GIEE-111

### Imaging in The Spectrum of Periportal Soft Tissue Pathologies

Sunday, Nov. 27 8:00AM - 9:00AM Room: Learning Center - GI

#### Participants

Sinduja Sivaramalingam, DMRD, MBBS, (*Presenter*) Nothing to Disclose

#### TEACHING POINTS

1.Learning the anatomical structures involving the porta hepatis and their importance.2.To classify various periportal pathologies based upon the structure of origin.3.To study the radiological features of the individual pathologies, the unique patterns and differentiating points from other pathologies.

#### TABLE OF CONTENTS/OUTLINE

BACKGROUND:ANATOMY OF THE PORTA HEPATIS: ROLE OF IMAGING MODALITIES:CLASSIFICATION OF PERIportal PATHOLOGIES BASED ON THE STRUCTURE OF ORIGIN1) DUCTAL AND PERI-DUCTAL PATHOLOGIES: • Cholangiocarcinoma (large duct carcinoma)-periductal and infiltrating, hilar types, advanced locally aggressive spread • Intraductal papillary neoplasm of the bile duct (IPNB)/ biliary papillomatosis • Primary neuroendocrine tumors of the bile ducts Cholangitis • IgG4 related sclerosing cholangitis • Langerhans cell histiocytosis - proliferative and fibrotic phase 2) LYMPH NODAL PATHOLOGIES: • Benign reactive hyperplasia of periportal nodes. • Infective nodes • Peritoneal carcinomatosis / Loco-regional spread of tumor 3) NERVES AND CONNECTIVE TISSUE:• Schwannoma, Neurofibroma • Sarcomas 4) POST SURGICAL OR POST TRANSPLANT CASES: • Periportal inflammatory soft tissue • Tumor recurrence • Post Transplant lymphoproliferative disorder.IMPORTANCE OF PREVIOUS IMAGES/ FOLLOW UP.ROLE OF TUMOUR MARKERS.CONCLUSION: Primary step in the diagnostic approach would be identification of the structure or epicenter of origin and then considering the relevant differentials.

Printed on: 02/07/23



## Abstract Archives of the RSNA, 2022

GIEE-112

### Test Your Knowledge: Reviewing Classic Hepatobiliary Radiologic Signs

Sunday, Nov. 27 8:00AM - 9:00AM Room: Learning Center - GI

#### Participants

Larissa Lima, Sao Paulo, Brazil (*Presenter*) Nothing to Disclose

#### TEACHING POINTS

The purposes of this quiz are:1. Recognize some classic radiologic signs (a way that makes easier to achieve diferent diagnosis).2. To discuss the pathophysiologic characteristics associated with these radiologic findings.3. Improve the memorize process making associations, since many signs use metaphorical language, such as comparision with objects.4. At the end of the quiz, the reader must be able to recognize these signs and associated pathologies, consolidating the acquired knowledge.

#### TABLE OF CONTENTS/OUTLINE

1. The presentation describes classic signs associated with hepatobiliary diseases through Computed Tomography (CT) and Magnetic Resonance (MR) images, in a cased-based quiz format.2. Illustrative key points: improve understanding of the correlation between the sign and pathophysiologic process involved.3. Pictorial review of most frequent hepatobiliary signs and associated disease, for example: adenomyomatosis (pearl neklace/rosary sign; hourglass gallbladder), inflamatory hepatic adenoma (atoll sign), hepatic hydatid disease (water-lily sign ) and more.4. Key images that the radiologist must actively look to recognize the sign.

Printed on: 02/07/23



## Abstract Archives of the RSNA, 2022

GIEE-113

### Imaging of Small Bowel Tumors: What Radiologists Should Know

Sunday, Nov. 27 8:00AM - 9:00AM Room: Learning Center - GI

#### Participants

Kiyoka Maeba, MD, Kurashiki-City, Japan (*Presenter*) Nothing to Disclose

#### TEACHING POINTS

The purpose of this presentation is:1) To demonstrate epidemiology of small bowel tumors and the characteristic imaging findings of ultrasound, endoscopy, computed tomography and magnetic resonance imaging including the radiologic-pathologic correlation.2) To learn about the differentiation between benign and malignant small bowel tumors by imaging of various modalities.

#### TABLE OF CONTENTS/OUTLINE

CONTENTS ORGANIZATION  
DECISION TREE FOR SMALL BOWEL TUMORS  
BENIGN BOWEL TUMORS - Polyp/Polyposis syndromes-  
Lipoma - Ectopic endometriosis- Hemangioma  
MALIGNANT SMALL BOWEL TUMORS- Adenocarcinoma- Neuroendocrine tumor: NET-  
Gastrointestinal stromal tumor: GIST- Malignant lymphoma - Metastatic disease- Sarcoma

Printed on: 02/07/23



## Abstract Archives of the RSNA, 2022

GIEE-114

### Simplified Approach to Lateral Pelvic Nodes in Rectal Cancer Addressing Controversies, Categorization and Involvement

Sunday, Nov. 27 8:00AM - 9:00AM Room: Learning Center - GI

#### Awards

Certificate of Merit

#### Participants

Harmeet Kaur, MD, Houston, TX (*Presenter*) Stock options, Health Catalyst; Stock options, Nuance Communications, Inc

#### TEACHING POINTS

•What constitute LPLN compartments in the pelvis  
•What are the boundaries of LPLN compartments on CT/MR  
•What are the pathways of lymphatic rectum and why are these important  
•What the most commonly involved LPLN compartments in rectal cancer  
•What are the currently proposed size criteria for LPLN involvement?  
•What are the circumstances in which these criteria should be applied?

#### TABLE OF CONTENTS/OUTLINE

Definition of LPLN compartments based on existing surgical literature  
Definition of boundaries of LPLN compartments on CT/MR  
Simplified imaging criteria to define LPLN on cross sectional imaging  
Clarification of pathways of lymphatic spread in the pelvis and how this impacts nodal involvement  
Survey of the current criteria of LPLN involvement in the literature  
Implication for radiologists  
Size criteria for LPLN what do these really mean?

Printed on: 02/07/23



## Abstract Archives of the RSNA, 2022

GIEE-115

### Clinical And Radiological Features Of Hepatocellular Carcinoma: An Update In The Era Of Systemic Therapy

Sunday, Nov. 27 8:00AM - 9:00AM Room: Learning Center - GI

#### Awards

Cum Laude

#### Participants

Mariko Irizato, Kashihara, Japan (*Presenter*) Nothing to Disclose

#### TEACHING POINTS

The purpose of the exhibit is to update knowledge of hyperintense HCC on the hepatobiliary phase (HBP) of EOB-MRI, not only for diagnosis but also for early prediction of treatment effect, leading to personalized therapy in the future, and to recognize various cases of HCC with atypical imaging features on multimodality imaging.

#### TABLE OF CONTENTS/OUTLINE

With recent advances in systemic therapy for HCC, treatment strategies for HCC are changing. Now radiologists are required not only to diagnose but also to predict early treatment effects and contribute to appropriate treatment selection. As an imaging finding linked to predicting treatment effects, the signal intensity of HCC on HBP of EOB-MRI has recently attracted attention. Hyperintense HCC on HBP of EOB-MRI showed a correlation with the therapeutic effects of various treatments, such as immunotherapy, TACE, and hepatic arterial infusion chemotherapy (HAIC). HCC is also a genetically and molecularly diverse group. Actually, approximately 40% of HCCs do not show typical imaging features, such as Li-RADS major imaging feature of HCC, including hyperenhancement (APHE), portal venous phase, delayed phase washout, and capsule appearance. The atypical imaging features of HCC are generally associated with pathological type and molecular phenotype. Understanding HCC with atypical imaging features can improve diagnostic accuracy and help clinicians plan strategies for better treatment. 1) Hyperintense HCC on HBP of EOB-MRIa) Etiology and Imaging findingsb) Treatment prediction: TACE, HAIC, and systemic therapy c) Differential diagnosis: the hepatic tumor with hyperintensity on HBP 2) Multimodality imaging of HCC with atypical imaging features

Printed on: 02/07/23



## Abstract Archives of the RSNA, 2022

GIEE-116

### MR of Anorectal Fistulas: Current and Evolving Concepts Simplified

Sunday, Nov. 27 8:00AM - 9:00AM Room: Learning Center - GI

#### Participants

Nabih Nakrou, MD, Boston, MA (*Presenter*) Nothing to Disclose

#### TEACHING POINTS

The purpose of this exhibit is to: Review anatomy of the anorectal region and MR imaging landmarks relative to anorectal fistula classification. Demonstrate the role of MR in presurgical planning for anorectal fistulas, including anatomic mapping, fistula track relation to the sphincters and pelvic organs, detecting internal and external fistula openings, assessing the degree of fistula complexity, and associate fluid collections. Discuss current and evolving concepts of anorectal fistula management and imaging features predicting prognosis. Validate with sample cases MR contribution to diagnosis and decision-making.

#### TABLE OF CONTENTS/OUTLINE

The present role of MR in diagnosis and management of anorectal fistula: -Anatomy of the anorectal regions and anal sphincters. MR protocols and optimizing imaging techniques in detecting anorectal fistulas. -Anorectal fistula classifications. Imaging manifestation and diagnostic pearls for each fistula subtype. Surgical approach and treatment options. Radiologic appearance of postsurgical devices. Example cases and illustrations of the above contents.

Printed on: 02/07/23



## Abstract Archives of the RSNA, 2022

GIEE-117

### Evaluating the Performance of Segmentation Models for Liver, Spleen, and Fat by Radiologists

Sunday, Nov. 27 8:00AM - 9:00AM Room: Learning Center - GI

#### Participants

Ari Borthakur, PhD, MBA, Philadelphia, PA (*Presenter*) Nothing to Disclose

#### TEACHING POINTS

Opportunistic screening (1) with abdominal CT examinations, capturing anatomic structures beyond the main clinical indication for performing the exam, may provide the opportunity for more comprehensive analyses of the entire abdomen and pelvis (2). It provides additional value to both patients, by uncovering incidental findings without additional scans, and providers, by improving both quality and service offerings, potentially mitigating risk and improving revenue without additional scan costs (3). The challenge, however, is that opportunistic screening has the potential to increase the burden of unnecessary work for providers. Artificial Intelligence (AI) based machine learning (ML) approaches can help reduce some of this burden particularly in the automation of tedious tasks like image segmentation (4). We present a comprehensive approach to evaluating the performance of an AI algorithm for fully automated CT-based body composition measurements (5) with automated reporting to PACS prior to deployment in routine clinical workflow. References Cited 1. P. J. Pickhardt, *Radiology*, 211561 (2022). 2. L. L. Berland et al., *J Am Coll Radiol* 7, 754-773 (2010). 3. P. J. Pickhardt et al., *Radiology* 249, 151-159 (2008). 4. J. Mongan, A. Vagal, C. C. Wu, *Radiol Artif Intell* 4, e220039 (2022). 5. M. T. MacLean et al., *J Am Med Inform Assoc* 28, 1178-1187 (2021).

#### TABLE OF CONTENTS/OUTLINE

A. Clinical need for an AI solution a. Current approaches to body organ segmentation b. Our solution i. Automated phenotyping ii. Structured reporting c. Impact on patient care d. Cost implications B. Evaluating the value of the output for radiologists a. Reader studies b. Analyses of Concordance

Printed on: 02/07/23



## Abstract Archives of the RSNA, 2022

GIEE-118

### **Biliopancreatic Anatomic Variants: Radiologic Findings And Clinical Relevance**

Sunday, Nov. 27 8:00AM - 9:00AM Room: Learning Center - GI

#### **Participants**

Kamila Albuquerque, Vila Velha, Brazil (*Presenter*) Nothing to Disclose

#### **TEACHING POINTS**

Biliopancreatic anatomic variants are common and they are more frequently diagnosed nowadays due to the increasing number of patients submitted to radiology exams. Recognizing these variants is essential to avoid misdiagnosis of pathologies and in the preoperative of biliopancreatic surgeries. The purpose of this exhibit is to make a brief review of pancreatic and biliary tract embryology and review the main biliopancreatic anatomic variants and their clinical relevance.

#### **TABLE OF CONTENTS/OUTLINE**

Introduction with a schematic review of the embryology of the pancreas and biliary tract. Present with images from CT, MR, ERCP, and USG illustrative cases of biliopancreatic anatomic variants and anomalies including annular pancreas, pancreas divisum, ectopic pancreas, ansa pancreatica, pancreatic hypoplasia, circumportal pancreas, dorsal pancreatic agenesis, anomalous biliopancreatic junction, low cystic duct insertion, gallbladder duplication, Caroli disease, intrahepatic bile ducts variations, among others. Correlate each one of these cases with its clinical/surgical relevance. Summary and take-home notes.

Printed on: 02/07/23



## Abstract Archives of the RSNA, 2022

GIEE-119HC

### Radiologic Review of Small Bowel Malignancies with Their Mimicking Lesions

Sunday, Nov. 27 8:00AM - 9:00AM Room: Learning Center - GI

#### Participants

Jongsoo Lee, MD, Incheon, Korea, Republic Of (*Presenter*) Nothing to Disclose

#### TEACHING POINTS

When radiologists inspect computed tomography (CT) images, small bowel malignancies are often easy to miss because of the small size, which can lead to mistake for normal small bowel due to their similar enhancement to small bowel or non-specific enhancement. In addition, small bowel malignancies are sometimes mistaken for masses from other origins, such as the uterus, rectum, or omentum. In this article, we illustrate various small bowel malignancies and their mimicking lesions with typical and atypical features on CT imaging as well as their clinical manifestations.

#### TABLE OF CONTENTS/OUTLINE

1. Introduction 2. Small bowel gastrointestinal stromal tumor (GIST) 3. Small bowel adenocarcinoma 4. Small bowel lymphoma 5. Small bowel sarcoma 6. Small bowel plasmacytoma (Extramedullary plasmacytoma) 7. Small bowel neuroendocrine tumor (NET) 8. Mass-like small bowel lesions mimicking small bowel malignancies 9. Clinical history of small bowel malignancy: anemia, weight loss, vomiting, nonspecific abdominal pain Small bowel malignancies can be easily missed or misdiagnosed by radiologists because of their rarity, nonspecific symptoms, and overlapping imaging features, especially when manifesting with small sizes. However, if radiologists know some characteristic imaging features of small bowel malignancies and their mimicking lesions, and perform a careful inspection of the entire small bowel loops, especially when patients present with gastrointestinal bleeding symptoms, optimal detection and diagnosis of small bowel malignancies can be achieved. Please visit the Learning Center to also view this presentation in hardcopy format.

Printed on: 02/07/23



## Abstract Archives of the RSNA, 2022

GIEE-12

### High Frequency Imaging in Hepatobiliary Ultrasound: Zooming In

Sunday, Nov. 27 8:00AM - 9:00AM Room: Learning Center - GI

#### Awards

Identified for RadioGraphics

#### Participants

Michael Enea, DO, Philadelphia, PA (*Presenter*) Nothing to Disclose

#### TEACHING POINTS

1. Understand the benefits and limitations of using a high frequency linear transducer (= 12 MHz) for adult hepatobiliary imaging and how it can improve confidence in ultrasound interpretations.2. Compare routine and high frequency imaging of liver parenchyma and surface contour in patients on a spectrum including normal, steatosis, fibrosis, and cirrhosis.3. Demonstrate the usefulness of high frequency liver imaging for focal hepatic lesions.4. Understand the advantage of high frequency imaging for biliary pathology including dilatation, sludge, and calculi.5. Compare low and high frequency imaging for the evaluation of gallbladder wall thickening, integrity, focal lesions, and calculi.

#### TABLE OF CONTENTS/OUTLINE

1. General- how technique affects high frequency imaginga. Variable transducer frequenciesb. Different machine settingsc. Patient habitus2. Livera. Diffuse parenchymal liver diseasei. Steatosis1. Homogeneous increased echogenicity2. Focal fatii. Fibrosis1. Coarse echotexture2. Correlate with shear wave elastographyiii. Cirrhosis1. Nodular surface2. Regenerative nodules3. Parenchymal atrophyb. Focal liver lesionsi. Hepatocellular carcinomaii. Metastasesiii. Cystsc. Otheri. Fulminant liver failureii. Periportal edemaiii. Portal thrombosis- benign and malignantiv. Varices3. Biliary Ductsa. Choledocholithiasisb. Biliary duct dilationc. Biliary castsd. Von Meyenburg Complexes4. Gallbladdera. Wall thickeningb. Integrity of wallc. Adenomyomatosisb. Focal lesions: polyps, masses

Printed on: 02/07/23



## Abstract Archives of the RSNA, 2022

GIEE-120

### Imaging of External Hernias of The Abdomen: Revisited

Sunday, Nov. 27 8:00AM - 9:00AM Room: Learning Center - GI

#### Participants

Manabu Minami, MD, PhD, (*Presenter*) Nothing to Disclose

#### TEACHING POINTS

External hernias of the abdomen are clinically common problems and frequently require imaging evaluation preoperatively. Various kinds of external hernias can occur in the abdominal wall. In the era of three-dimensional imaging using CT and MRI, a more precise evaluation of the structure of each hernia (hernia orifice, hernia sac, its content, and its covering) and complications such as inflammation, bowel obstruction/incarceration, and strangulation can be analyzed than before. In this presentation, we review various kinds of external hernias of the abdomen and show radiological anatomy using three-dimensional images with representative cases as well as their rare types. Understanding the membranous structures of the abdominal wall related to external hernias will be essential for GI radiologists to provide more critical information to surgeons in patient management and surgical planning.

#### TABLE OF CONTENTS/OUTLINE

1. General consideration of external hernias of the abdomen  
2. Classification of external abdominal hernias and their imaging findings:  
case presentations  
a. groin (inguinal): indirect (external), direct (internal), femoral  
b. umbilical/periumbilical: cf. omphalocele  
c. ventral (anterior): epigastric/hypogastric (linea alba), suprapubic, Spigelian (linea semilunaris)  
d. lumbar (lateral): superior lumbar (Grynfeltt-Lesshaft), inferior lumbar (Petit)  
e. pelvic floor (inferior): obturator foramen, sciatic foramen, perineal  
f. cicatricial: traumatic, incisional, parastomal, trocar site  
3. Conclusions

Printed on: 02/07/23



## Abstract Archives of the RSNA, 2022

GIEE-121

### MR Enterography in Chron Disease: Detection of Complications

Sunday, Nov. 27 8:00AM - 9:00AM Room: Learning Center - GI

#### Participants

Maria Luisa Rosa, MD, (*Presenter*) Nothing to Disclose

#### TEACHING POINTS

MR Enterography is the gold-standard method for studying the small-bowel in patients with Chron's Disease, not only to depict active inflammatory disease, but to exclude complications, as the presence of fibrostenosing and/or penetrating disease alters medical treatment and may imply surgical intervention. The aim of this work is to depict the imaging findings of complicated Crohn's disease on MR Enterography and discuss the correct terminology and potential differential diagnoses of such findings.

#### TABLE OF CONTENTS/OUTLINE

Through pictorial review we illustrate the different aspects of penetrating disease such as such as sinuses, simple and complex fistulas, inflammatory masses and abscesses, concentrating on what defines and differentiates them from pseudo-sacculations or deep ulcers and from adhesions, that can be misinterpreted on imaging studies as sinuses and fistulas, respectively. In regards to stenosing disease, we explain the criteria for defining a stricture and provide examples of strictures with and without active inflammation as the distinction is important for determining the treatment plan. We will also clarify the circumstances in which you can consider a probable stricture even when there is no upstream dilation. We will discuss how to potentially differentiate occlusion due to peritoneal adhesions from fibrotic strictures; and from functional abnormalities sometimes seen in these patients who demonstrate dilated small bowel loops without mechanical obstruction.

Printed on: 02/07/23



## Abstract Archives of the RSNA, 2022

GIEE-122

### Do You Remember The Meckel Diverticulum?

Sunday, Nov. 27 8:00AM - 9:00AM Room: Learning Center - GI

#### Participants

Cristina Berastegi Santamaria, MD, Bilbao, Spain (*Presenter*) Nothing to Disclose

#### TEACHING POINTS

The purpose of this exhibit is: 1. To describe Meckel diverticulum's characteristics 2. To review imaging findings of Meckel's diverticulum on computer tomography 3. To describe the radiologic features of complications of Meckel diverticulum 4. To correlate the histological findings with the radiological perspective

#### TABLE OF CONTENTS/OUTLINE

1. Embriology of Meckel diverticulum 2. Pathology of Meckel diverticulum 3. Review of imaging findings on CT and pathological correlation (sample cases) - Non complicated Meckel diverticulum - Complicated Mecel diverticulum Hemorrhage Bezoar Intestinal obstruction Diverticulitis Neoplasms Volvulation Intususpection 4. Conclussions and taking-home messages

Printed on: 02/07/23

## Abstract Archives of the RSNA, 2022

GIEE-123

### Anisakiasis: What Radiologists Need to Know

Sunday, Nov. 27 8:00AM - 9:00AM Room: Learning Center - GI

#### Participants

Ines Alonso Sanchez, MD, Bilbao, Spain (*Presenter*) Nothing to Disclose

#### TEACHING POINTS

- Become familiar with the radiological findings of anisakiasis, because it is an underdiagnosed parasitosis with an increasing incidence worldwide.- Initial clinical suspicion is sometimes difficult as the symptoms are non-specific, and a multidisciplinary approach is important to make an accurate diagnosis.

#### TABLE OF CONTENTS/OUTLINE

Objectives: Review and describe the main clinical, radiological and epidemiological features of the different forms of Anisakiasis. Background: Anisakiasis is a zoonosis caused by accidental infection by *Anisakis simplex* due to the ingestion of raw or undercooked fish that affects mainly the gastrointestinal tract. Although the highest prevalence of anisakiasis is found in Asia and it is rare in the United States and Europe, the incidence is expected to increase worldwide as cultural globalization of food habits increases opportunities to eat raw or undercooked seafood. Imaging findings: Severe submucosal edema, ascites, fluid collection and mesenteric fat infiltration. Diagnosis: Clinical suspicion is helpful but difficult in some cases, especially in intestinal anisakiasis, and CT findings may suggest the possibility of anisakiasis when characteristic imaging features are present. Laboratory tests or endoscopic direct visualization give a definite diagnosis. Treatment: Generally symptomatic and in some cases endoscopic larvae removal. Conclusions: Anisakiasis is a rare and underdiagnosed parasitosis that affects the gastrointestinal tract. As its incidence is increasing worldwide, it is important that we are familiar with the characteristic clinical and radiological manifestations.

Printed on: 02/07/23



## Abstract Archives of the RSNA, 2022

GIEE-124

### The Many Faces Of Colitis: An Imaging Review

Sunday, Nov. 27 8:00AM - 9:00AM Room: Learning Center - GI

#### Participants

Gustavo Alonzo Correa I, MD, Mexico City, Mexico (*Presenter*) Nothing to Disclose

#### TEACHING POINTS

To describe the normal appearance of the colon in the different imaging modalities. To explain the appearances, pathogenesis and differential diagnosis of CT colonic enhancement patterns. To discuss the differential diagnosis of colitis based on imaging findings, epidemiology and clinical history.

#### TABLE OF CONTENTS/OUTLINE

Introduction  
Normal anatomy of the colon in the different imaging modalities  
Classification of CT colonic enhancement patterns  
Infectious colitis  
Pseudomembranous colitis  
Neutropenic colitis (Typhlitis)  
Radiation colitis  
Inflammatory bowel disease  
Ischemic colitis  
Take home points

Printed on: 02/07/23



## Abstract Archives of the RSNA, 2022

GIEE-126

### Post-operative Abdominal Complications Following Colorectal Surgery on CT: Pearls and Pitfalls

Sunday, Nov. 27 8:00AM - 9:00AM Room: Learning Center - GI

#### Awards

Certificate of Merit

#### Participants

Deevia Kotecha, MBChB, BSc, Wilmslow, United Kingdom (*Presenter*) Nothing to Disclose

#### TEACHING POINTS

1) To illustrate the spectrum of early post-operative complications, emphasizing the importance of the timing of surgery. 2) To distinguish expected post-operative CT appearances versus a complication, highlighting useful tips and potential pitfalls. 3) To relate the type of surgery to key review areas on post operative imaging (including recent advances in endoluminal and robotic surgery). 4) To discuss the utility of positive luminal contrast in problem solving.

#### TABLE OF CONTENTS/OUTLINE

The post-operative abdomen is challenging. Knowledge of the potential complications is important to every radiologist so that life-threatening conditions can be quickly diagnosed and treated. Post-operative GI complications covered will be broadly categorised into the following headings. A range of examples with key learning points will be illustrated and where relevant correlate with any pre-operative imaging.

- Abnormal gas patterns
- o Location and volume of free gas.
- o Retained surgical swabs
- o Haemostatic agents.
- Fluid collections
- o Anastomotic leaks
- o Urinoma
- Vascular complications
- o Bowel ischemia
- o Arterio-venous fistula
- o Pseudo-aneurysm

Printed on: 02/07/23



## Abstract Archives of the RSNA, 2022

GIEE-127

### Improving CT Colonography Standards

Sunday, Nov. 27 8:00AM - 9:00AM Room: Learning Center - GI

#### Participants

Aishwariya Vegunta, MD, Stratford, CT (*Presenter*) Nothing to Disclose

#### TEACHING POINTS

Discuss various standards to maximize the quality of CT colonography.

#### TABLE OF CONTENTS/OUTLINE

Background: There is an increasing incidence of colorectal cancer which is a largely preventable disease if identified at precursor polyp stage and removed. CTC Performance standards: a. Patient Information and experience. b. Bowel Preparation: 1. Diet. 2. Catharsis: Dry versus wet agents and 3. Tagging of residual stool and fluid. Bowel preparation for same-day CTC after incomplete colonoscopy. c. Imaging: A. CT technique/ Scanning parameters and radiation risk. B. Colonic distension with carbon dioxide, using an automated insufflator. C. Scout to assess for adequate bowel distension. D. Dual-position scanning in Supine and prone positions versus decubitus position. d. Interpretation: A. Colonic and extracolonic findings are reported in a standard examination as per CT Colonography Reporting and Data System (C-RADS). B. Colonic interpretation involving primary 2-D and primary 3-D reviews. Flat lesions measuring 3 mm or less in height are better depicted with contrast tagging at 2D while 3D reviews are better at smaller polyp detection and greater conspicuity of polyps at or near the folds. C. CTC descriptors including polyp morphology, location and measurements. D. Pitfalls in CTC interpretation. e. Management decisions and interval surveillance: Follow-up recommendations on polyp management and role of surveillance CTC. f. CTC outcome measures: Audits and ACR's CTC registry.

Printed on: 02/07/23

## Abstract Archives of the RSNA, 2022

GIEE-128

### **Roux-en-Y Gastric Bypass: Post-surgical Anatomy and Most Common Complications**

Sunday, Nov. 27 8:00AM - 9:00AM Room: Learning Center - GI

#### **Participants**

Ines Alonso Sanchez, MD, Bilbao, Spain (*Presenter*) Nothing to Disclose

#### **TEACHING POINTS**

- Review the Roux-en-Y gastric bypass surgical technique and understand the normal post-surgical anatomy and radiological findings. - Describe and explain the most frequent complications and their imaging manifestations using a series of cases from our institution as examples.

#### **TABLE OF CONTENTS/OUTLINE**

Background Obesity is a disease of epidemic proportions. Non-surgical treatment fails in 95% of the patients, and therefore bariatric surgery is the most effective, yet invasive, treatment. There are two surgical approaches for achieving weight loss: bypass procedures and restrictive procedures. Roux-en-Y gastric bypass is the most popular technique and obtains greater sustained weight loss and higher sustained long-term success than other techniques. Findings: As radiologists, we should be familiar with the anatomic changes caused by this surgery, in order to be able to recognize them and identify possible complications. Complications In this presentation, we describe the most common complications of gastric bypass surgery (mainly post-operative leaks, small bowel obstruction, gastro-gastric fistula and ulceration) and their imaging features based on cases of our centre. We revise the imaging techniques recommended to examine each type of complication and key findings to identify them. Conclusions Bariatric surgery is increasing dramatically, especially Roux-en-Y gastric bypass and radiologists should be able to recognize the anatomic changes that this surgery involves and the most frequent complications it may have.

Printed on: 02/07/23



## Abstract Archives of the RSNA, 2022

GIEE-129

### Barium Swallow Radiological Technique to Evaluate Hiatal Hernias and Other Commonly Associated Findings

Sunday, Nov. 27 8:00AM - 9:00AM Room: Learning Center - GI

#### Participants

Tatiana J. Ludena Camacho I, MD, Mexico City, Mexico (*Presenter*) Nothing to Disclose

#### TEACHING POINTS

- Explain the anatomy thorough diagrams as well as the typical imaging findings.- Review the different types of hernia and much more frequently observed in radiological practice.- Simplify the correct technique for the execution of the esophagogram.- Present through real clinical cases usual findings during an esophagogram.

#### TABLE OF CONTENTS/OUTLINE

1. Introduction.2. Anatomy3. Technique4. Hiatal hernias- Definitions.- Pearls and pitfalls.- Key terms of the radiographic lexicon terms.- Categories.5. Other common findings in Barium Esophagogram.6. Conclusions.

Printed on: 02/07/23



## Abstract Archives of the RSNA, 2022

GIEE-13

### Anatomic Basis of Rectal Cancer Staging: Clarifying Controversies and Confusion

Sunday, Nov. 27 8:00AM - 9:00AM Room: Learning Center - GI

#### Awards

Identified for RadioGraphics

Cum Laude

#### Participants

Muhammad Awiwi, MD, Houston, TX (*Presenter*) Nothing to Disclose

#### TEACHING POINTS

Despite the adoption of rectal MRI as a mandatory staging tool for rectal cancer, inconsistencies still exist in defining anatomic landmarks even among experts (Lambregts DMJ et al. 2022).

#### TABLE OF CONTENTS/OUTLINE

This exhibit aims to review controversies in anatomic issues, propose the best opinion based on the evolving literature, and discuss impact on management. Anatomic landmarks to be discussed include: Re-definition of the rectum and its upper/lower boundaries. - The anatomy of the anal sphincter and staging of tumors involving this structure. - The definition of circumferential resection margin (CRM) will vary depending on surgical procedure and does not equate to mesorectal fascia (MRF). - Clarify the difference between peritoneal involvement and mesorectal fascia involvement in the upper rectum. - Clarify the anatomic boundaries of lateral pelvic nodes and their clinical significance.

Printed on: 02/07/23



## Abstract Archives of the RSNA, 2022

GIEE-130

### Complications of Percutaneous Liver Procedures: Bleeding and Beyond

Sunday, Nov. 27 8:00AM - 9:00AM Room: Learning Center - GI

#### Participants

James Palmer, MD, Tucson, AZ (*Presenter*) Nothing to Disclose

#### TEACHING POINTS

1.) Percutaneous diagnostic and therapeutic liver procedures are commonly performed and range from biopsy to more invasive treatments such as ablation and biliary interventions. 2.) While these procedures are generally safe, major complications do occur usually at a rate of 0.1-5%. Bleeding is one of the most common complications and various manifestations of bleeding are important to recognize as they may require different treatment approaches. 3.) Non-hemorrhagic complications are diagnosed primarily by imaging and the radiologist should be aware of the range of complications so that timely treatment can be instituted.

#### TABLE OF CONTENTS/OUTLINE

1.) Brief overview of literature regarding complications of percutaneous liver procedures a.) Definition of minor vs. major complications 2.) Multimodality case-based review of complications with teaching points and discussion of treatment implications. a.) Hemorrhagic and Vascular i.) Subcapsular hematoma, hemoperitoneum ii.) Pseudoaneurysm, active bleeding, AVF iii.) Arterial vs. Venous bleeding iv.) Thrombosis b.) Biliary i.) Bile leak/biloma ii.) Stricture iii.) Hemobilia c.) Infectious i.) Liver abscess ii.) Biliary sepsis d.) Local i.) Organ injury (diaphragm, GB, stomach, colon) ii.) Residual/recurrent tumor iii.) Liver infarction iv.) Tumor seeding e.) Thoracic i.) Pneumothorax, hemothorax Hemopericardium

Printed on: 02/07/23



## Abstract Archives of the RSNA, 2022

GIEE-131

### Multimodality Imaging of Tumor Thrombus in Hepatocellular Carcinoma

Sunday, Nov. 27 8:00AM - 9:00AM Room: Learning Center - GI

#### Participants

Ulysses Torres, MD, PhD, Sao Paulo, Brazil (*Presenter*) Nothing to Disclose

#### TEACHING POINTS

- To review and illustrate the vascular involvement in hepatocellular carcinoma (HCC) on ultrasound, computerized tomography (CT), and magnetic resonance imaging (MRI).
- To prepare abdominal radiologists to identify the most common hepatic venous thrombosis sites on imaging in HCC, with emphasis on portal vein.
- To present imaging features of tumor thrombosis according to LI-RADS v2018.
- To present clinical cases from our institution with a multidisciplinary approach, some correlated with pathology results and individualized treatment.
- To recognize potential pitfalls in image interpretation and differential diagnosis of tumor thrombus.

#### TABLE OF CONTENTS/OUTLINE

- Background: the importance of a multimodality assessment of vascular involvement in HCC, which can be subtle.
- The impact of tumor thrombus on management in patient care.
- Categorization according to LI-RADS v2018.
- Illustrative cases of our institution with the main hepatic tumor thrombus sites with imaging features and interpretation on:
  - o Ultrasound.
  - o CT.
  - o MRI.
- Challenging cases of tumor thrombosis in HCC (as infiltrative carcinoma).
- Differential diagnosis with hematic thrombosis.
- Tips and tricks.

Printed on: 02/07/23



## Abstract Archives of the RSNA, 2022

GIEE-132

### Advanced CT Techniques In the Evaluation of Hepatocellular Carcinoma: Roles of Ultra-high-resolution CT, Dual-energy CT, Contrast Enhancement Boost Technique, and Radiomics

Sunday, Nov. 27 8:00AM - 9:00AM Room: Learning Center - GI

#### Participants

Masatoshi Hori, MD, Kobe, Japan (*Presenter*) Research Grant, Canon Medical Systems Corporation

#### TEACHING POINTS

1. Understanding the characteristics of advanced techniques such as 1024-matrix ultra-high resolution (UHR) CT, dual-energy CT, contrast enhancement boost (CE boost) technique, and radiomics. 2. Understanding how radiologists can use advanced techniques to detect and characterize hepatocellular carcinoma (HCC). 3. Understanding the prospects for advanced techniques to improve the management of patients with HCC.

#### TABLE OF CONTENTS/OUTLINE

A. Introduction B. Ultra-high-resolution (UHR) CT with a 1024 matrix B-1. Spatial resolution, image noise, and deep learning reconstruction B-2. Tumor margin can be better delineated, potentially resulting in improved assessment of microvascular invasion C. Dual-energy CT (DECT) C-1. Material decomposition C-2. Virtual monochromatic imaging (VMI) can enhance tumor-to-liver contrast C-3. Beyond the dual-energy CT: Hope for photon counting CT D. Contrast enhancement boost (CE boost) technique: a postprocessing technique for increasing the degree of contrast enhancement D-1. Principles: Roles of image subtraction, non-rigid registration, and denoising D-2. CE boost combined with multiphase CT can improve the detection of small HCC D-3. CE boost can be combined with low-keV VMI in DECT to further increase the conspicuity of HCC E. Radiomics F. Clinical roles of the advanced techniques in evaluating HCC G. Conclusion

Printed on: 02/07/23

## Abstract Archives of the RSNA, 2022

GIEE-133

### Hepatic Hydatid Disease: Typical and Atypical Imaging Features with Clinical Correlation and Impact on Management

Sunday, Nov. 27 8:00AM - 9:00AM Room: Learning Center - GI

#### Awards

Certificate of Merit

#### Participants

Mohamed Ibrahim, MBCh, Rochester, MN (*Presenter*) Nothing to Disclose

#### TEACHING POINTS

1. Understand the etiopathogenesis of hydatid disease 2. Highlight hepatic and extrahepatic hydatidosis imaging features (cardiac, brain, spine, muscular, subcutaneous, and adrenal) 3. Highlight different IR management for hepatic hydatid cysts

#### TABLE OF CONTENTS/OUTLINE

1. Etiopathogenesis of hydatid disease: • Historical overview • Echinococci types, lifecycle, infection sources, and clinical relevance • Hydatid cyst composition and imaging features 2. Imaging features of different stages: • WHO IWG 2001 management classification and radiological classification (Active vs transient vs inactive) • Extrahepatic lesions (brain, spleen, pulmonary, spine, pyriformis muscle, subcutaneous and adrenal) • CT vs MRI, which is better? 3. Management; indications, contraindications, procedural steps, and imaging follow-up • Surgical: conservative (partial cystectomy, and deroofing) vs radical (pericystectomy vs hepatic resection) • IR options. Discussing PAIR cases and highlighting why it is better i. PAIR "Percutaneous puncture under sonographic guidance, Aspiration of a substantial amount, Injection of scolicidal agent, Re-aspiration) ii. D-PAI: Double puncture-aspiration-injection iii. PEVAC: Percutaneous evacuate on of cyst content

Printed on: 02/07/23

## Abstract Archives of the RSNA, 2022

GIEE-134

### Uncommon Primary Liver Tumors in Adults: An Image Review

Sunday, Nov. 27 8:00AM - 9:00AM Room: Learning Center - GI

#### Participants

Guillem Dolz Alvarez De La Ballina, MD, Valldoreix, Spain (*Presenter*) Nothing to Disclose

#### TEACHING POINTS

To show the wide spectrum of unusual primary liver tumors that can arise from the different progenitor cells in the liver, and review the imaging findings of these uncommon lesions. To assess features that may help in the diagnosis of rare hepatic tumors.

#### TABLE OF CONTENTS/OUTLINE

Introduction to unusual hepatic tumors  
Description of hepatocellular tumors:- Fibrolamellar hepatocarcinoma- Hepatocoangiocarcinoma- Hepatoblastoma  
Review of epithelial/cholangiocellular tumors:- Intraductal papillary tumor of the bile ducts- Cystic mucinous tumor  
Mesenchymal tumors:- Angiomyolipoma- Angiosarcoma- Hepatic epithelioid hemangioendothelioma- Inflammatory myofibroblastic tumor- Solitary fibrous tumor  
Primary hepatic neuroendocrine carcinoma. Primary hepatic lymphoma.  
Others:- Necrotic nodule of the liver- Brucellar liver abscess ( brucelloma).  
Conclusions

Printed on: 02/07/23



## Abstract Archives of the RSNA, 2022

GIEE-135

### In Between Peritoneal and Retroperitoneal Layers: The Spread of Disease in The Abdominal Cavity

Sunday, Nov. 27 8:00AM - 9:00AM Room: Learning Center - GI

#### Participants

Marcela Santos Conde, MD, Sao Paulo, Brazil (*Presenter*) Nothing to Disclose

#### TEACHING POINTS

1. Recognizing the types of disease spread in the abdominal cavity (interfascial, intraperitoneal, subperitoneal and transperitoneal).
2. Understanding the anatomy of the peritoneum and retroperitoneum and its correlation with disease spread.
3. Expected findings on disease spread in the abdominal cavity, from tumoral dissemination to inflammatory disease and trauma.

#### TABLE OF CONTENTS/OUTLINE

Introduction: general aspects of the disease spread in the peritoneum and retroperitoneum. Anatomy of the retroperitoneum as it relates to interfascial spread of diseases. Peritoneal cavity and the circulation of ascitic fluid as it relates to intraperitoneal disease spread. Anatomy of peritoneal ligaments and omental sacs as it relates to subperitoneal spread of diseases. Understanding the relation of retroperitoneal and peritoneal organs with the peritoneal membrane as it relates to transperitoneal spread of disease. Take home messages.

Printed on: 02/07/23



## Abstract Archives of the RSNA, 2022

GIEE-136

### Peritoneal MRI: Dedicated Protocol, Tips and Tricks

Sunday, Nov. 27 8:00AM - 9:00AM Room: Learning Center - GI

#### Awards

Certificate of Merit

#### Participants

Anais Delagnes, Angers, France (*Presenter*) Nothing to Disclose

#### TEACHING POINTS

-To know the MRI sequences to be performed and the order of execution-To understand usefulness of each sequence for the detection of peritoneal malignancies-To know how to adapt patient preparation and sequence parameters in case of MRI artifacts

#### TABLE OF CONTENTS/OUTLINE

Magnetic Resonance Imaging (MRI) has an emerging role in the exploration of peritoneal malignancy. The knowledge and the management of peritoneal pathologies have considerably evolved over the last decade, especially with the possibility of curative treatment of peritoneal metastatic disease. Peritoneal MRI is routinely performed in referral centers and play essential role at different stages of the management: for the selection of patients for curative surgery, in the preoperative phase to optimize mapping of lesions, and in surveillance for early detection of recurrence. A dedicated and detailed protocol is proposed to perform a peritoneal MRI. Each step are explained including the preparation of the patient, oral and intravenous contrast agent and drugs used. Then each sequences (recommended and optional) with their parameters and the optimized order of realization are detailed, as well as their usefulness to detect peritoneal lesions and their limits. Finally, tips and tricks to limit artifacts are given, in particular to reduce artifacts related to the MR technique like susceptibility artifact and related to the patient condition (for exemple the black hole artifact caused by the presence of ascites).

Printed on: 02/07/23



## Abstract Archives of the RSNA, 2022

GIEE-137

### Illustrative Cases of Acute Pancreatitis and Commonly Encountered Complications

Sunday, Nov. 27 8:00AM - 9:00AM Room: Learning Center - GI

#### Participants

Klaudio Gjeluci, MD, MS, (*Presenter*) Nothing to Disclose

#### TEACHING POINTS

1. Demonstrate the wide array of acute pancreatitis encountered on imaging. 2. Discuss the utility of imaging. 3. Evolution of interstitial edematous pancreatitis and necrotizing pancreatitis. 4. Summarize the nomenclature of the 2012 Revised Atlanta Classification for acute pancreatitis. 5. Review of common complications of acute pancreatitis through illustrative cases.

#### TABLE OF CONTENTS/OUTLINE

Utility of imaging in acute pancreatitis and complications: Limited in the early phase of the disease process  
Clinical diagnosis: epigastric pain and elevated pancreatic enzymes three times the normal level  
Diagnostic in cases where elevated pancreatic enzymes do not meet the threshold criteria. Typically, in late presentation of acute pancreatitis  
Determining unclear etiology  
Gallstone pancreatitis  
Obstructive neoplastic process  
Predictor of mortality in the late phase of disease process  
Extent of necrosis  
Infection  
Local complications: pseudoaneurysm/bleeding, venous thrombosis, CBD stricture, pancreatic duct stricture  
Discuss Case Examples with Imaging Findings: Acute interstitial edematous pancreatitis  
Acute necrotizing pancreatitis  
Acute pancreatic fluid collection  
Acute necrotic collection  
Pseudocyst  
Walled-off necrosis  
Infected walled-off necrosis  
Bleeding splenic artery pseudoaneurysm  
Large gastroduodenal artery pseudoaneurysm  
Interesting case of splenic vein thrombosis

Printed on: 02/07/23



## Abstract Archives of the RSNA, 2022

GIEE-138

### What Radiologists Should Know for The Early Detection of Small Pancreatic Ductal Adenocarcinoma

Sunday, Nov. 27 8:00AM - 9:00AM Room: Learning Center - GI

#### Participants

Yoshihiko Fukukura, MD, PhD, Kagoshima, Japan (*Presenter*) Nothing to Disclose

#### TEACHING POINTS

Pancreatic ductal adenocarcinoma (PDAC) still has a dismal prognosis because of the difficulty in early diagnosis, although small PDAC has a good prognosis with a 5-year survival rate of 68.7% for stage IA disease. CT and MR are the most frequent imaging modalities used for evaluating patients with clinically suspected PDAC. However, these modalities often fail to demonstrate small PDAC. The possibility of diagnosing precursor lesions of the pancreas (pancreatic intraepithelial neoplasia [PanIN-3]) and small PDAC may greatly improve the prognosis of PDAC. The purpose of this exhibit is 1. To illustrate CT and MR imaging findings of PanIN and small PDAC 2. To discuss how to improve the detection of PDAC.

#### TABLE OF CONTENTS/OUTLINE

1. Summarize the definition, etiology, and clinical and histological features of PanIN and small PDAC (<20 mm)
2. Describe the characteristic CT and MR imaging findings of PanIN and small PDAC (<20 mm) with histopathological correlation
3. Highlight how to improve the detection of PDAC (tumor delineation and important secondary signs)
4. Discuss the diagnostic approach to potentially achieve earlier detection of PDAC
5. Summary: Knowledge of characteristic CT and MRI features and how to improve tumor delineation is important to improve the prognosis of patients with PDAC.

Printed on: 02/07/23



## Abstract Archives of the RSNA, 2022

GIEE-139

### **Bubbles and Marbles in the Pancreas: Demystifying Cystic and Solid Pancreatic Lesions with Emphasis on Management**

Sunday, Nov. 27 8:00AM - 9:00AM Room: Learning Center - GI

#### **Participants**

Katherine Chung, MD, Stony Brook, NY (*Presenter*) Nothing to Disclose

#### **TEACHING POINTS**

Imaging characteristics of cystic and solid lesions of the pancreas are well studied. However, with ongoing research in management and prognosis of these pancreatic lesions, it can be confusing for practicing radiologists and trainees to form recommendations for patients and clinicians. In this education exhibit, we will describe classic imaging findings of pancreatic lesions, review their clinical features, and discuss the latest recommendations on treatment options and management of these lesions. We present a pictorial review of cystic and solid lesions of the pancreas to guide radiologists on the management of these lesions.

#### **TABLE OF CONTENTS/OUTLINE**

Solid pancreatic lesions: Ductal adenocarcinoma, Neuroendocrine tumors, Metastasis, Lymphoma. Cystic pancreatic lesions: Intrapancreatic Mucinous Neoplasms (IPMN), Serous Cystadenoma, Mucinous cystadenoma, Solid Pseudopapillary Neoplasm. Mimickers: Pseudocyst, Duodenal diverticulum.

Printed on: 02/07/23



## Abstract Archives of the RSNA, 2022

GIEE-14

### CT and MR Enterography in Celiac Disease: What Should Residents Know?

Sunday, Nov. 27 8:00AM - 9:00AM Room: Learning Center - GI

#### Awards

Identified for RadioGraphics

#### Participants

Andrea Penizzotto, DMRD, (*Presenter*) Nothing to Disclose

#### TEACHING POINTS

The role of small bowel imaging is most important in patients with nonresponsive celiac disease and to exclude celiac disease related complications. The most specific imaging finding of celiac disease is the jejunoileal fold reversal pattern, but other findings are those of a nonspecific malabsorptive pattern. Ulcerative jejunitis, small bowel wall thickening, and small bowel dilation are more commonly seen in patients with refractory celiac disease. Ascites, pleural effusion and/or subcutaneous edema are related to severe malnutrition secondary to refractory celiac disease.

#### TABLE OF CONTENTS/OUTLINE

1) Introduction 2) Imaging protocols CT enterography MR enterography 3) Imaging analysis: Systemic approach 4) Intestinal findings Ileal jejunitis Jejunum fold flattening Fold pattern reversal Intestine wall thickening Bowel dilatation Stricture Intussusception 5) Extra-intestinal findings Mesenteric adenopathy Mesenteric vascular engorgement Hyposplenism Ascites 6) Complications Ulcerative jejunoileitis Malignancy Cavitory mesenteric lymph node syndrome 7) Take home messages

Printed on: 02/07/23

## Abstract Archives of the RSNA, 2022

GIEE-140

### Mimickers of Pancreatic Adenocarcinoma: What to Watch for at Tumor Board and the Workstation

Sunday, Nov. 27 8:00AM - 9:00AM Room: Learning Center - GI

#### Participants

Andrea Esquivel Mora, MD, San Jose, Costa Rica (*Presenter*) Nothing to Disclose

#### TEACHING POINTS

Neoplastic and non-neoplastic pancreatic conditions can mimic pancreatic ductal adenocarcinoma (PDAC) on cross-sectional imaging. Our purpose is to: • Highlight distinguishing clinical and radiologic features that provide a clue to the correct (non-PDAC) diagnosis • Understand treatment and outcome implications for these mimics

#### TABLE OF CONTENTS/OUTLINE

Around 90% of pancreatic cancers are pancreatic adenocarcinoma while other pancreatic tumors are infrequently seen. This exhibit will highlight distinguishing radiologic and clinical features of PDAC mimics. 1. Uncommon exocrine pancreatic neoplasms. \*Acinar cell carcinoma \*Pancreatoblastoma \*Squamous and Adenosquamous Ca \*Colloid Carcinoma \*Invasive IPMN \*Mucinous cystadenocarcinoma 2. Non-exocrine pancreatic neoplasms that can mimic pancreatic cancer. \*Pancreatic neuroendocrine neoplasms \*Metastasis 3. Benign mimics of pancreatic cancer: "groove pancreatitis", focal autoimmune pancreatitis, mass forming chronic pancreatitis, obstructive chronic pancreatitis, and focal steatosis 4. Key imaging features that can distinguish these entities from PDAC: multifocality, multiple ductal strictures, hemorrhage, duct-penetrating sign, low duct-to-parenchyma ratio, collateral duct dilatation, "sandwich sign", hyperenhancement, calcifications, and capsule like rim or loss of lobulations. 5. Clinical features that can support the differential diagnosis are the history of a primary tumor, sex, age, predisposing genetic syndromes, and serum markers (IgG4, tryptase).

Printed on: 02/07/23



## Abstract Archives of the RSNA, 2022

GIEE-141

### The Perceptual Problem in Pancreatic Imaging

Sunday, Nov. 27 8:00AM - 9:00AM Room: Learning Center - GI

#### Participants

Abraham Fourie Bezuidenhout, MD, Boston, MA (*Presenter*) Nothing to Disclose

#### TEACHING POINTS

Diagnostic errors are common and can affect overall patient care, none more so than in the setting of pancreatic ductal adenocarcinoma (PDAC). In the absence of a PDAC screening program for the general population, the onus of early diagnosis is primarily placed on radiologists which largely determine patient outcomes and is an understandable source of anxiety to radiologists. Diagnostic errors can occur at any time in the process, from initial perception to final image interpretation. Cognitive errors include perceptual challenges and a myriad of cognitive biases which are particularly common and impactful in pancreatic imaging. Becoming aware of perceptual challenges specifically related to PDAC as well as understanding the various biases, related to internal and external pressures, can allow radiologists to minimize diagnostic errors and thereby help improve patient outcomes. In this exhibit we will provide explanations, insight and a framework for understanding the basis of these diagnostic errors and potential avenues to minimize them.

#### TABLE OF CONTENTS/OUTLINE

What contributes to diagnostic errors in the setting of PDAC? What's the unique perceptual challenges of PDAC? Direct vs indirect signs of PDAC. Which cognitive biases are in play in pancreatic imaging? Internal and external factors contributing to bias. Common vs newly described biases as it pertains to pancreatic imaging. How to overcome biases with guidelines to create an environment of peer learning which enables systematic improvement, rather than viewing it as individual failures.

Printed on: 02/07/23



## Abstract Archives of the RSNA, 2022

GIEE-142

### Ultrasound: Lumps and Bumps in the Anterior Abdominal Wall

Sunday, Nov. 27 8:00AM - 9:00AM Room: Learning Center - GI

#### Participants

Marie Vogel, MD, (*Presenter*) Nothing to Disclose

#### TEACHING POINTS

1. Ultrasound is a low cost, low risk, widely accessible imaging tool that can serve as a first line imaging modality in characterizing superficial lesions. 2. A thorough understanding of abdominal wall anatomy and scanning techniques will allow the radiologist to confidently identify common abdominal wall pathologies. 3. By combining scanning technique, anatomic knowledge and patient history, the radiologist can troubleshoot challenging cases and confidently arrive at the correct diagnosis.

#### TABLE OF CONTENTS/OUTLINE

1. A brief overview of the advantages and disadvantages of ultrasound in the assessment of superficial lumps and bumps in the abdominal wall. 2. Review the anatomy of the abdominal wall and its ultrasonographic appearance. 3. Review use and limitations of ultrasound and key ultrasound scanning techniques. 4. Case based presentation of common lumps and bumps, describing key ultrasound findings, scanning tips and tricks, common mimics and/or complications, clinical presentation and management of these pathologies including but not limited to: Subcutaneous lesions: lipoma and epidermal inclusion cyst; Hernias: direct versus indirect inguinal hernia, femoral hernia, incisional hernia; Sequelae of trauma and infection: hematoma, abscess, Morax-Lavallee lesion; Neoplasms: desmoid tumor, liposarcoma, melanoma; Miscellaneous lesions: adenopathy, endometriosis.

Printed on: 02/07/23



## Abstract Archives of the RSNA, 2022

GIEE-143

### Ultrasound of the Portal Vein: ImPORTant Things to Know

Sunday, Nov. 27 8:00AM - 9:00AM Room: Learning Center - GI

#### Awards

Identified for RadioGraphics

#### Participants

Matthew Simon, MD, Philadelphia, PA (*Presenter*) Nothing to Disclose

#### TEACHING POINTS

1. Understand normal ultrasound appearance of portal veins in grayscale, color and spectral Doppler 2. Recognize abnormalities of the portal vein including thrombus (bland and tumor), cavernous transformation and portal venous gas 3. Identify abnormal waveforms and abnormal direction of flow in the portal veins and formulate a differential diagnosis 4. Understand the normal ultrasound appearance of a TIPS and recognize complications

#### TABLE OF CONTENTS/OUTLINE

1. Normal ultrasound of portal vein a. Anatomy i. 3D rendering of portal venous system b. Grayscale c. Doppler i. Color ii. Waveforms iii. Velocities 2. Abnormalities of flow a. Slow flow b. Helical flow c. Abnormal flow due to portal hypertension i. Alterations of velocity and direction 1. Hepatofugal flow: partial and complete 2. Perihepatic varices: paraumbilical, coronary, gallbladder 3. Portal Vein Thrombosis a. Bland thrombus 1. Causes 2. Acute versus chronic 3. Differentiating occlusive from non-occlusive b. Tumor thrombus 1. Hepatocellular carcinoma and other tumors 2. Grayscale, cine clips 3. Doppler: arterial flow within thrombus c. Chronic occlusion/Cavernous Transformation 4. Portal venous gas a. Causes b. Differentiate from pneumobilia c. Gray scale and Doppler appearance 5. Other a. Effect of cardiac disease on portal system b. Portal fistula i. Portal-hepatic venous ii. Portal-hepatic arterial 6. TIPS a. Normal appearance on Grayscale and Doppler i. when to image a TIPS after insertion ii. protocol for imaging a TIPS iii. effect on other vessels b. Complications i. Thrombus ii. Stenosis

Printed on: 02/07/23



## Abstract Archives of the RSNA, 2022

GIEE-144

### Big Kids with Tummy Pains: Classically Pediatric Acute Abdominal Presentations in Adults

Sunday, Nov. 27 8:00AM - 9:00AM Room: Learning Center - GI

#### Participants

Neel Jain, MA, MBBS, (*Presenter*) Nothing to Disclose

#### TEACHING POINTS

1. Review of the adult presentation of pediatric acute abdominal pathology with discussion of imaging findings. 2. Illustrated conditions include Meckel's diverticulum, intussusception, anatomical variants, intestinal malrotation, mesenteric adenitis. 3. Highlight important review areas and implications. 4. Insight into their clinical management.

#### TABLE OF CONTENTS/OUTLINE

Pediatric pathology is often not a primary focus for adult GI radiologists and clinicians. Whilst uncommon, pediatric abdominal pathologies can also present later in life. It is therefore crucial that the radiologist on call considers pediatric illnesses and underlying congenital structural abnormalities within their differential diagnosis. We present a case-based educational exhibit to familiarize radiologists with the key imaging findings.

Printed on: 02/07/23



## Abstract Archives of the RSNA, 2022

GIEE-145

### Hidden Gem: Ultrasonography Detection Differentiation of Sclerosing Cholangitis

Sunday, Nov. 27 8:00AM - 9:00AM Room: Learning Center - GI

#### Participants

Moran Drucker Iarovich, MD, (*Presenter*) Nothing to Disclose

#### TEACHING POINTS

Teaching Points • Review different etiologies of sclerosing cholangitis • Discuss specific SC manifestations, including: background, clinical presentation, mechanism, treatment • Emphasize sonographic features of each, to allow an educated query of appropriate diagnosis

#### TABLE OF CONTENTS/OUTLINE

Sclerosing cholangitis is a progressive cholestatic disease, characterized by inflammation, fibrosis strictures. It is divided into primary sclerosing cholangitis (PSC) secondary sclerosing cholangitis (SSC). PSC is idiopathic, often seen in young males with concomitant ulcerative colitis, while SSC denotes a spectrum of progressive cholestatic diseases which have an identifiable, even treatable cause. SSC etiologies are divided into five mechanistic categories: immune-mediated, drug-induced, infectious, obstructive, or ischemic. Differentiation between the various causes of sclerosing cholangitis is imperative for appropriate patient management. Ultrasound (U/S) is the primary imaging of choice for evaluation of the biliary tree, being accurate, available, cost-effective, impervious to motion, safe. U/S is underrecognized as a diagnostic and problem-solving tool in assessment of PSC SSC. U/S's high spatial resolution allows detection of fine ductal features not often seen by MRCP. Subcapular ducts are often only visible on U/S. As well, it has the highest sensitivity for detection of intrahepatic stones bile duct casts. However, lack of familiarity means that many diagnostic features of biliary diseases are often missed. In this review we will describe the typical U/S features of PSC SSC.

Printed on: 02/07/23

## Abstract Archives of the RSNA, 2022

GIEE-146

### **Spectrum of Clinically Important Isolated and Concomitant Anatomical Variations of Biliary Ducts, Pancreatic Duct and Gall Bladder on MR Cholangiopancreatography (MRCP): What Not to Miss and What Radiologist Should Know to Help the Clinician in This Era of Advanced Hepato-Biliary Surgery!"**

Sunday, Nov. 27 8:00AM - 9:00AM Room: Learning Center - GI

#### **Participants**

Aruna Pallewatte, MD, FRCR, (*Presenter*) Nothing to Disclose

#### **TEACHING POINTS**

1) Learn embryological basis of anomalies of hepatic, biliary and pancreatic ducts 2) Optimal MRCP protocol/Physics 3) Know classification of anatomical variants in configuration of intra/extrahepatic biliary ducts (BD) with clinical relevance 4) Appreciate classification of cystic duct pancreatic duct (PD) variations based on course insertion 5) Classification MRI features of Gall bladder (GB) variations such as duplication, intrahepatic GB. 6) Learn incidence of variations with literature comparison 7) Learn clinical significance (eg longterm effects, Surgeon's needs) of identified hepato-biliary-pancreatic duct variations and how to document them accurately on pre-op MRCP report to answer clinical needs 8) Learn to avoid diagnostic pitfalls and mimics causing misinterpretation on MRI/MRCP

#### **TABLE OF CONTENTS/OUTLINE**

1) Introduction to spectrum of BD, PD, Cystic duct GB anatomical variants, aberrant anatomy embryological basis with illustrations 2) Optimised MRCP protocol 3) Huang classification of Right Left intra hepatic BD illustrated with our MRCP images - Demography incidence 4) Classification of extrahepatic BD, PD and cystic duct variants with our sample cases 5) MRCP of Intrahepatic GB, double GB and classification 6) Pictorial depiction of concomitant BD, PD, GB variants and choledochal cysts with sample MRI cases 7) Diagnostic Mimics pitfalls, clues to avoid them 8) Potential longterm complications of variants such as pancreatitis 9) Challenges to Hepatobiliary surgery and value of pre operative documenting of anatomical variants 10) Guidance for systematic MRI/MRCP reporting focused specially for hepatic transplantation, hepatic resection, ERCP, laparoscopic surgery etc.

Printed on: 02/07/23



## Abstract Archives of the RSNA, 2022

GIEE-147

### Gallbladder Malignancy and its Many Mimics

Sunday, Nov. 27 8:00AM - 9:00AM Room: Learning Center - GI

#### Participants

Matthew Carr, MD, (*Presenter*) Nothing to Disclose

#### TEACHING POINTS

Gallbladder Malignancy and its Many Mimics Teaching Points: 1. Gallbladder malignancy tends to predominantly present in several different ways on imaging as an: intraluminal mass lesion, asymmetric wall thickening, or polyp. 2: Many potential mimics of gallbladder malignancy exist. Use the clinical history, all available views, and all modalities to create a more informed differential. 3: How the lesion evolves (or doesn't evolve) over time can help narrow or change the differential. 4: Sometimes you don't know if it is malignancy or a benign process. When in doubt take it out! (Or biopsy).

#### TABLE OF CONTENTS/OUTLINE

Table of Contents: - 1. Different gall bladder malignancies and their presentations (some with rad-path correlation). - 2. Metastatic diseases to the gallbladder (including lung and melanoma).- 3. The different potential mimics of gall bladder cancer (cholecystitis, adenomyomatosis, etc) - 4. Multiple case-based examples where specifics of the patient presentation help aid the differential diagnosis. - 5. Multiple case-based examples where the temporal course of the lesion changes the differential. - 6. Xanthogranulomatous cholecystitis cases (the great mimicker) with rad path correlation.

Printed on: 02/07/23



## Abstract Archives of the RSNA, 2022

GIEE-148

### What Went Wrong? Hepatobiliopancreatic Postoperative Complications: A Primer for Radiologists

Sunday, Nov. 27 8:00AM - 9:00AM Room: Learning Center - GI

#### Awards

Certificate of Merit

#### Participants

Lucas Roberto Lelis Oliveira, MD, Sao Paulo, Brazil (*Presenter*) Nothing to Disclose

#### TEACHING POINTS

- Recognize hepatobiliopancreatic (HBP) anatomy and anatomical variations.
- Understand most common types of HBP surgeries.
- Know radiologists role in the pre- and postoperative settings.
- Recognize HBP postoperative complications through multimodality imagings.

#### TABLE OF CONTENTS/OUTLINE

INTRODUCTION: o Overview of frequency, relevance, and cost of HBP surgeries. o HBP anatomy including key anatomical variations as they relate to surgical complications. o Summary of most common types of HBP surgeries. 2. IMAGING ON THE PREOPERATIVE SETTING: o Presurgical roadmap to optimize the surgery and avoid complications. o Pros and cons of each imaging modality. 3. IMAGING ON THE POSTOPERATIVE SETTING: o Step by step didactic approach in assessing patients after HBP surgery: § Surgical notes; § What to ask to the multidisciplinary team; § Clinical notes and laboratory tests; § How to decide which imaging modality; § Best protocol; § Ultrasound approach; § CT approach; § MRI approach; § How to report and communicate; o Surgical complications: § Acute versus chronic; § Main groups: vascular, biliary, GI tract, infectious, other. 4. WHAT IS THE ROLE OF INTERVENTIONAL RADIOLOGY. 5. WHAT'S ON THE HORIZON. 6. INTERACTIVE CHALLENGING SCENARIOS.

Printed on: 02/07/23



## Abstract Archives of the RSNA, 2022

GIEE-149

### Back to the Basics: US Findings in Acute Cholecystitis-Tips for New Residents

Sunday, Nov. 27 8:00AM - 9:00AM Room: Learning Center - GI

#### Participants

Mariana De Los Santos Carmona, MD, Ciudad de Mexico, Mexico (*Presenter*) Nothing to Disclose

#### TEACHING POINTS

To show normal anatomy, pathology and its variants.-To identify in a simpler way the ultrasonographic characteristics of acute cholecystitis, in special for new residents.-To recognize different clinical characteristics that help to recognize acute cholecystitis.- To give advice for new residents when performing an ultrasound, to help base the most accurate diagnosis and thus decide on interdisciplinary management.-To be familiar with the sonographic technique, tips, pitfalls, limitations and troubleshooting for the right upper quadrant pain.-This discussion will help residents to reinforce the radiological and clinical features of acute cholecystitis, keeping in mind that interdisciplinary consensus remains the gold standard for diagnosis

#### TABLE OF CONTENTS/OUTLINE

1.Objectives.2.Review the anatomy of the gallbladder and its variants. 3.Discuss the global panorama about the importance of acute cholecystitis. 4.Explain the clinical characteristics based on Tokyo's criteria for acute cholecystitis as a multidisciplinary approach. 5.Discuss the algorithm of the ultrasound technique used to evaluate the right upper quadrant pain. 6.Recognize and illustrate the main ultrasonographic findings in this pathology. 7.Present a series of cases to exemplify the most important ultrasonographic findings of acute cholecystitis, as well tips for the correct approach. 8.Recognize differential diagnoses of right upper quadrant pain. 9.Conclusions. 10.References

Printed on: 02/07/23



## Abstract Archives of the RSNA, 2022

GIEE-15

### Clinical Photon Counting Abdominopelvic CT: A Crash Course!

Sunday, Nov. 27 8:00AM - 9:00AM Room: Learning Center - GI

#### Awards

Certificate of Merit

#### Participants

Bari Dane, MD, New York, NY (*Presenter*) Nothing to Disclose

#### TEACHING POINTS

Conventional CT uses energy integrating detectors (EID), in which x-rays create visible light that is converted to electrical pulses to create images. Photon counting CT (PCCT) detectors directly convert photons into electrical pulses, allowing electronic noise elimination and leading to significant dose reduction. Unlike EID, PCCT counts the energy of each photon, including low energy photons. This improves image contrast, makes every CT multienergy, and permits electronic baseline noise removal. Downsides include K-escape and charge sharing in PCCT can reduce spectral separation.

#### TABLE OF CONTENTS/OUTLINE

1. PCCT versus EID physics  
2. Clinical benefits  
a. Improved spatial and contrast resolution, without dose penalty - Small vessel visualization - Small lesion visibility and characterization in low contrast areas (pancreas, liver, peritoneum) - Better iodine contrast to noise ratio, lower intravenous contrast dose  
b. Multienergy every scan - Simultaneous high pitch and multienergy - Incidental finding characterization  
c. Remove electronic noise - Better image quality in obese patients - Lower dose CT - Better virtual noncontrast (VNC) image quality  
3. Current Version Pitfalls  
a. Cross-scatter artifact with dual-source mode  
b. Urographic phase derived VNC artifact  
c. Slower reconstruction time

Printed on: 02/07/23



## Abstract Archives of the RSNA, 2022

GIEE-150

### MRI Anal Fistula: Anatomy of Anal Canal

Sunday, Nov. 27 8:00AM - 9:00AM Room: Learning Center - GI

#### Participants

Christian Torres Ramirez, MD, (*Presenter*) Nothing to Disclose

#### TEACHING POINTS

Learning objective Identify the anatomy of the anal canal by MRI to achieve an adequate classification of anal fistula. Introduction The anal fistula corresponds to an anomalous path that connects the anal canal with the skin. MRI is the imaging modality of choice due to its high resolution, allowing an adequate characterization of the anatomy and also greater precision in the classification of the anal fistula. Teaching points The anal canal is limited between the dentate line and the anal verge. The layers of this wall are mucosa, submucosa and muscularis. The muscularis layer is composed from the innermost to the outermost layer, by the internal anal sphincter (IAS), the intersphincteric liner and the external anal sphincter (EAS). The IAS is a continuation of the muscular layer of the rectum, and the EAS is composed of skeletal muscle. The MRI is the imaging modality recommended in ESGAR consensus. The protocol used in our institution is performed in 1.5 T and 3 T, the MRI sequences and the planes are axial, coronal and sagittal T2-weighted, and post-contrast T1-weighted sequences are performed. The axial acquisition performed align with respect to anal canal axis. By magnetic resonance imaging in axial T2-weighted sequences, the anal canal is a circumference of 5 layers: the innermost layer mucosa (hyperintense), submucosa (hypointense), IAS (hyperintense), intersphincteric liner (hyperintense) and the outermost layer EAS (hypointense). The Parks classification is used for anal fistula: intersphincteric, transsphincteric, suprasphincteric and extrasphincteric.

#### TABLE OF CONTENTS/OUTLINE

1. Learning objective  
2. Introduction  
3. Teaching points

Printed on: 02/07/23



## Abstract Archives of the RSNA, 2022

GIEE-152

### The Anterior and Sub-peritoneal Compartments of The Extraperitoneal Space: Comprehensive Imaging Review of Anatomy and Pathologies

Sunday, Nov. 27 8:00AM - 9:00AM Room: Learning Center - GI

#### Participants

Arvin Saremi, MS, (*Presenter*) Nothing to Disclose

#### TEACHING POINTS

Review the relevant anatomy of the structures participating in formation of the anterior extraperitoneal space Review characteristic imaging findings of common and uncommon pathologies involving this region

#### TABLE OF CONTENTS/OUTLINE

Normal embryology and anatomy of the anterior extraperitoneal space Development Transversalis fascia Umbilical prevesical fascia Umbilicovesical fascia Fascia around the round ligament Imaging characteristics with cadaveric correlation Abdominal above the umbilicus Retropubic or prevesical space of Retzius Prevesical, perivesical, and paravesical spaces The retroinguinal space of Bogros Connections to Subperitoneal pelvic space, presacral space and retroperitoneum Relationship to the vessels, median and medial umbilical ligaments Anatomical variations Abnormalities of the anterior extraperitoneal space Infection and abscess Post trauma changes Malignancies Relevance for extraperitoneal laparoscopic surgery Relevant considerations for percutaneous interventions

Printed on: 02/07/23



## Abstract Archives of the RSNA, 2022

GIEE-153

### All of the Guts, None of the Glory: An Overview of the Abdominal Radiograph

Sunday, Nov. 27 8:00AM - 9:00AM Room: Learning Center - GI

#### Participants

Elainea Smith, MD, Birmingham, AL (*Presenter*) Nothing to Disclose

#### TEACHING POINTS

1. Review the most common bowel pathology and gas appearances on abdominal radiographs and understand clinical relevance. 2. Discuss common and uncommon calcifications that can be seen on the abdominal radiograph. 3. Highlight most common "corner" pitfalls to increase sensitivity for these commonly missed pathologies.

#### TABLE OF CONTENTS/OUTLINE

Introduction  
Bowel- Small bowel obstruction- Large bowel obstruction- Ileus- Enteritis/colitis- Pneumatosis  
Air- Free intraperitoneal air- Portal venous gas- Retroperitoneal gas- Emphysematous cholecystitis- Emphysematous cystitis  
Calcifications- Renal stones- Gallstones- Calcified mass(es)- Vascular  
Corners- Lung bases- Cardiac- Proximal thighs  
Conclusion

Printed on: 02/07/23



## Abstract Archives of the RSNA, 2022

GIEE-154

### The Spectrum of Interpretive and Perceptual Biases in Abdominal Radiology

Sunday, Nov. 27 8:00AM - 9:00AM Room: Learning Center - GI

#### Awards

Identified for RadioGraphics

#### Participants

Jonathan Kruskal, MBChB, Boston, MA (*Presenter*) Nothing to Disclose

#### TEACHING POINTS

For abdominal radiologists, cognitive biases impact our interpretive and perceptual skills predisposing to diagnostic errors. Published data suggests that such biases are particularly common and impactful in abdominal radiology. A broad spectrum of recognized (common and less common) as well as newly emerging biases occur in abdominal radiology. Being aware of one's personal diagnostic biases, as well as strategies for mitigating their occurrence, is likely to improve our diagnostic performance. Familiarity with the spectrum of biases enables cases to be categorized in the peer learning and improvement meeting.

#### TABLE OF CONTENTS/OUTLINE

What are cognitive biases? How do biases impact abdominal radiologists? How to construct your Personal Bias Profile? Brief explanations, clinical examples and strategies for mitigating the following biases: Common biases: anchoring, confirmation, availability, automation, bandwagon, satisfaction of search and of report, premature closure, zebra retreat, representative, outcomes, framing, attribution, context, authority, premature closure, provider, hindsight, alliterative, blind spot, regret, scout neglect and inattention biases. Newly recognized biases: hanging protocol, risk averse, clinical trial, demographic, productivity, follow up, trainee assumption, provisional report, structured report and remote reader biases.

Printed on: 02/07/23

## Abstract Archives of the RSNA, 2022

GIEE-155

### Drug-associated Hepatobiliary and Pancreatic Disorders: Pictorial Essay

Sunday, Nov. 27 8:00AM - 9:00AM Room: Learning Center - GI

#### Participants

Shintaro Ichikawa, MD, PhD, Hamamatsu, Japan (*Presenter*) Nothing to Disclose

#### TEACHING POINTS

Various disorders of the hepatobiliary system and pancreas are caused by several drugs, and imaging diagnosis is often challenging. Familiarity with these conditions may improve diagnostic accuracy and patient management. The purpose of this presentation is to describe the imaging findings of drug-associated hepatobiliary and pancreatic disorders and to identify tips for correct diagnosis.

#### TABLE OF CONTENTS/OUTLINE

The following drug-associated hepatobiliary and pancreatic disorders are discussed along with their key imaging findings: 1. Drug-induced acute liver failure Imaging findings are non-specific and include hepatomegaly with heterogeneous parenchymal enhancement, periportal edema, gallbladder wall thickening, and ascites. 2. Sinusoidal obstruction syndrome (SOS) A diffuse hypointense reticular pattern in the hepatobiliary phase is a highly specific sign for the diagnosis. 3. Pseudocirrhosis Imaging manifestations may be identical to those of liver cirrhosis. 4. Immune-related adverse events (irAEs) Cholangitis and pancreatitis may develop after immune checkpoint inhibitors therapy. 5. Methotrexate-associated lymphoproliferative disorders It is visible as a periportal infiltrating hypodense mass on computed tomography and is weakly enhanced. 6. Amiodarone deposition in the liver 7. Ceftriaxone-associated gallbladder pseudolithiasis 8. Secondary iron overload

Printed on: 02/07/23



## Abstract Archives of the RSNA, 2022

GIEE-156

### "Don't Forget Me!" Said the Spleen: Multimodality Imaging of The Spleen and Its Pathology

Sunday, Nov. 27 8:00AM - 9:00AM Room: Learning Center - GI

#### Participants

Adrian Xu, MD, Salt Lake City, UT (*Presenter*) Nothing to Disclose

#### TEACHING POINTS

Know the normal anatomy of the spleen  
Identify congenital anomalies of the spleen and their associated systemic pathologies  
Understand the multiple imaging modalities used in the assessment of splenic pathologies and the pitfalls  
Know and accurately diagnose focal and diffuse pathologies in the spleen on imaging

#### TABLE OF CONTENTS/OUTLINE

A. Anatomy  
B. Multimodality imaging of the spleen and associated pitfalls  
C. Splenic pathologies  
1. Congenital including asplenia and polysplenia and their associated imaging findings in other systems  
2. Focal masses  
i. Benign  
ii. Indeterminant  
iii. Malignant  
3. Diffuse processes (Splenomegaly/granulomas)  
4. Other  
i. Rupture  
ii. Infarct  
iii. Splenosis  
iv. Peliosis  
D. Summary

Printed on: 02/07/23



## Abstract Archives of the RSNA, 2022

GIEE-158

### Spectrum of Findings After Radiation-based Therapy In the Liver

Sunday, Nov. 27 8:00AM - 9:00AM Room: Learning Center - GI

#### Participants

Emre Altinmakas, MD, New York, NY (*Presenter*) Nothing to Disclose

#### TEACHING POINTS

Stereotactic body radiotherapy (SBRT) and transarterial radioembolization (TARE) with Yttrium-90 are the two commonly used treatment options for primary liver cancer and liver metastasis in patients unsuitable for surgery. Patients receiving such treatments require to undergo imaging surveillance with CT or MRI as there is possibility of incomplete tumor response. Careful assessment of these follow-up studies is essential to proper patient management. It is also crucial for radiologist to be aware of expected treatment-specific changes within the treatment zone as well as non-treated liver parenchyma following each type of treatment. The purposes of this exhibit are: 1. To discuss the concept of tumor response assessment after radiation-based therapies 2. Demonstrate expected posttreatment changes within the targeted as well as surrounding non-targeted liver parenchyma following SBRT and TARE 3. To review potential complications of radiation-based therapies

#### TABLE OF CONTENTS/OUTLINE

Table of contents/outline: 1. What are the optimal imaging follow-up strategies after radiation-based therapies for liver cancer? 2. How should we assess response after SBRT? • Imaging features of non-viable tumor • Imaging features of viable tumor 3. How should we assess response after TARE? • Imaging features of non-viable tumor • Imaging features of viable tumor 4. What are the expected posttreatment findings within targeted region as well as surrounding off-target liver following TARE and SBRT? 5. Potential complications of radiation-based therapies 6. Summary

Printed on: 02/07/23

## Abstract Archives of the RSNA, 2022

GIEE-159

### Atypical Focal Nodular Hyperplasia: Don't Let It Fool You

Sunday, Nov. 27 8:00AM - 9:00AM Room: Learning Center - GI

#### Awards

**Cum Laude**

#### Participants

Brendan O'Connor, MD, (*Presenter*) Nothing to Disclose

#### TEACHING POINTS

-Focal nodular hyperplasia (FNH) is a benign hepatic lesion with a typical imaging presentation at CT and MR imaging.-Rarely, FNH may show histological components that lead to an atypical imaging presentation mimicking other benign and malignant lesions. Atypical features include intralesional fat, iron, calcifications, sinusoidal dilatation, and significant growth. FNH occurring in an abnormal liver, defined as FNH-like lesions, may present a diagnostic challenge.-Illustrated overview of typical and atypical presentations of FNH and FNH-like lesions with representative rad-path correlation cases, along with key diagnostic clues for an accurate diagnosis of FNH and FNH-like lesions based on a constellation of multiple imaging features to include iso-to-hyperintensity on hepatobiliary phase imaging.

#### TABLE OF CONTENTS/OUTLINE

-Epidemiology, pathology of FNH-Typical features of FNH on CT and MR imaging (with extra-cellular and hepatobiliary Gd-based contrast agents).-Atypical imaging presentation of FNH to include steatotic and steatohepatic FNHs, calcification, intralesional sinusoidal dilatation, abnormal growth and intralesional iron-Definition and pathology of FNH-like lesions.-Imaging presentation of FNH-like lesions.-Key clues for accurate diagnosis of FNH and FNH-like lesions and differential diagnosis with other hepatic lesions (e.g hepatocellular adenoma).

Printed on: 02/07/23



## Abstract Archives of the RSNA, 2022

GIEE-16

### Hepatocellular Carcinoma: A Primer for Residents

Sunday, Nov. 27 8:00AM - 9:00AM Room: Learning Center - GI

#### Awards

Certificate of Merit

#### Participants

Marika Pitot, MD, Rochester, MN (*Presenter*) Nothing to Disclose

#### TEACHING POINTS

1) Review the typical imaging appearance of HCC on CT and MRI 2) Learn about the various patterns of HCC presentation 3) Review the recognized histologic subtypes of HCC with an emphasis on characteristic differentiating imaging features 4) Understand HCC imaging features that correlate with favorable versus poor outcome 5) Review LIRADS categorization with some examples

#### TABLE OF CONTENTS/OUTLINE

1. HCC overview a. Typical HCC appearance on imaging b. Patterns of presentation on imaging i. Nodular (expansive) - single, dominant nodule, with or without satellite nodules ii. Multifocal nodules iii. Infiltrative (massive) iv. Cirrhotomimetic v. Pedunculated c. Histologic growth patterns of HCC 2. Histologic subtypes of HCC a. Frequency b. Characteristic and "buzzword" imaging features 3. Favorable and poor prognostic features of HCCs a. Favorable imaging signs include single, small nodule with smooth margins, no necrosis, and homogenous enhancement. Other favorable features include low tumor stiffness on elastography, uptake of hepatobiliary contrast suggestive of beta-catenin activation, and occurrence in a normal or non-cirrhotic liver b. Poor prognostic imaging signs include large size at presentation, multifocality, evidence of necrosis, heterogeneous enhancement, ill-defined margins, and macroscopic vascular invasion. 4. LIRADS characterization overview a. Explanation of LIRADS categorization with examples

Printed on: 02/07/23



## Abstract Archives of the RSNA, 2022

GIEE-160

### **This Is Not a Soap Bubble-What's Going on In The Liver?: A Surviving Guide for Radiological Workup of Cystic Liver Lesions**

Sunday, Nov. 27 8:00AM - 9:00AM Room: Learning Center - GI

#### **Participants**

Gabriella Cagliari, Sao Paulo, Brazil (*Presenter*) Nothing to Disclose

#### **TEACHING POINTS**

Cystic hepatic lesions are very common in daily practice. The differential diagnosis ranges from benign lesions with no clinical significance to malignant neoplasms and potentially lethal conditions. Some cystic hepatic lesions have classical findings, allowing a correct diagnosis based on imaging findings only. On the other hand, some presentations may be challenging. In most cases, familiarity with the most relevant radiologic key features in combination with critical clinical and laboratory information is enough for adequate lesion characterization. The purpose of this presentation is to review the main cystic liver lesions, recalling imaging features from typical to challenging cases; a series of diagnostic tips will be presented, as well as a practical guide on how to develop objective reasoning in face of such cases.

#### **TABLE OF CONTENTS/OUTLINE**

1) Review the most common liver cystic lesions and their imaging features with didactical cases.2) Provide a didactic approach to differential diagnoses.3) Tips that can be helpful in face of challenging cases.4) Surviving guide that can be useful for a quick consultation.

Printed on: 02/07/23



## Abstract Archives of the RSNA, 2022

GIEE-161

### A to Z of Focal Nodular Hyperplasia (FNH)

Sunday, Nov. 27 8:00AM - 9:00AM Room: Learning Center - GI

#### Participants

Sophie Cheshire, MBChB, FRCR, (*Presenter*) Nothing to Disclose

#### TEACHING POINTS

1. Imaging features of FNH including typical findings and rarer features  
2. Multiple imaging modalities presented  
3. A unique method of presenting the findings using letters of the alphabet as an aide memoir

#### TABLE OF CONTENTS/OUTLINE

FNH is a common benign lesion, encountered on multiple imaging modalities. It is therefore important to recognise the key features of both typical and atypical lesions for accurate diagnosis in order to prevent unnecessary intervention. This display will include ultrasound examples, using both colour doppler and contrast enhanced techniques. All MRI sequences will be demonstrated with key learning points illustrated. The importance of liver specific contrast agents is highlighted, along with the pathology and aetiology of the lesion. The unique selling point for this presentation is the format which should be easy to remember and help in consolidating knowledge. The points to be covered using an A to Z format are as follows: Arterialisation, Biopsy, Contrast enhanced ultrasound, Doppler, Exophytic lesion, Fat, Glutamine synthetase, Hepatobiliary phase, Isointensity, Juicy orange, Kupffer cells, Lobulated, MRI, Nodules, OATP receptors, Pathology, Question, Ring on hepatobiliary phase, Scar, Telangiectatic, Ultrasound, Vascular malformation, Washout, Xtra fun fact, Young, Zero malignant.

Printed on: 02/07/23



## Abstract Archives of the RSNA, 2022

GIEE-162

### Pumping Iron: Iron Overload Imaging

Sunday, Nov. 27 8:00AM - 9:00AM Room: Learning Center - GI

#### Participants

Timothy McMahon, MD, MS, New York, NY (*Presenter*) Nothing to Disclose

#### TEACHING POINTS

Iron is an essential mineral critical to oxygen transport but it can have a toxic effect at high concentration. Absorption is regulated, but primary hemochromatosis and hemosiderosis lead to toxicity. The liver stores and regulates iron. Primary hemochromatosis and hemosiderosis cause toxic buildup of iron in the liver which has characteristic imaging appearances. Primary hemochromatosis typically affects the liver and pancreas on MRI. Hemosiderosis, which is usually due to frequent blood transfusions secondary to various anemias, typically affects the liver, spleen, and bone marrow. Intravascular hemolysis can affect the kidneys. MRI can qualitatively and quantitatively assess iron overload and assists in diagnosing and managing hemochromatosis and hemosiderosis.

#### TABLE OF CONTENTS/OUTLINE

Intro Iron absorption, transport, and regulation Iron overload causes and clinical impact Diagnosis, treatment, and management of iron overload Imaging Noncontrast CT Typical appearance Confounding factors and differential with cases Dual energy CT Methodology and typical appearance Iron content quantification MRI Basic physics Qualitative assessment In/out of phase imaging analysis Imaging patterns with case examples Quantitative assessment Methodology - Benefits and drawbacks Signal Intensity ratios T2/R2 relaxometry (FerriScan) T2\* and R2\* relaxometry Quantitative Susceptibility Mapping Example cases with effects of treatment SQUID Biomagnetometry - Advantages, disadvantages, and relevance Conclusion

Printed on: 02/07/23



## Abstract Archives of the RSNA, 2022

GIEE-163

### A Multimodality Approach to Inflammatory Bowel Disease and Complications

Sunday, Nov. 27 8:00AM - 9:00AM Room: Learning Center - GI

#### Awards

Certificate of Merit

#### Participants

Weibo Fu, BS, Augusta, GA (*Presenter*) Nothing to Disclose

#### TEACHING POINTS

1) To review the pathophysiology of common imaging findings seen in inflammatory bowel disease. 2) To demonstrate barium enema, CT, and MRI findings of acute and chronic inflammatory bowel disease, associated findings, and diverse complications. 3) To discuss the advantages and disadvantages of currently available imaging modalities for inflammatory bowel disease.

#### TABLE OF CONTENTS/OUTLINE

Inflammatory bowel disease (IBD) most commonly occurs in North America and Europe, with an estimated combined patient population of 4-5 million in both regions. Incidence of IBD has been gradually rising since the mid-20th century, likely due to widespread changes in dietary patterns along with environmental factors. Cross-sectional imaging modalities such as computed tomography (CT) and magnetic resonance (MR) enterography are now more commonly utilized because of their ability to detect subtle changes in inflammation, high clinical sensitivity, and ability to detect complications such as a) fistulae, b) bowel obstruction, c) intussusception, and d) abscesses outside the bowel lumen. Though resolution for both CT and MR are comparable, MR has the added benefit of zero radiation exposure.

Printed on: 02/07/23



## Abstract Archives of the RSNA, 2022

GIEE-164

### Prediction of Cirrhosis-related Complications at Dual-energy CT and MRI

Sunday, Nov. 27 8:00AM - 9:00AM Room: Learning Center - GI

#### Participants

Ra On Kang, MD, Jinju, Korea, Republic Of (*Presenter*) Nothing to Disclose

#### TEACHING POINTS

\* Describe the clinical states of cirrhosis according to the development of disease complications (varices and decompensation events) with the progression of pathophysiological mechanisms and hemodynamic. \* Discuss the clinical importance of noninvasive prediction of these complications in cirrhosis. \* Discuss how and whether routine dual-energy CT (DECT) and MRI can predict future complications in cirrhosis based on the recent quantitative studies.

#### TABLE OF CONTENTS/OUTLINE

Epidemiology  
Clinical states in cirrhosis  
Management implications of clinical states of cirrhosis  
DECT and MRI-based techniques for prediction of cirrhosis-related complications- DECT- T1 mapping- T2 mapping  
Future directions  
Summary

Printed on: 02/07/23



## Abstract Archives of the RSNA, 2022

GIEE-165

### Multiparametric MRI of The Liver: Practical Tips For Starters

Sunday, Nov. 27 8:00AM - 9:00AM Room: Learning Center - GI

#### Participants

Marina Raze, MD, Sao Paulo, Brazil (*Presenter*) Nothing to Disclose

#### TEACHING POINTS

-MAFLD, aprendendo mais sobre a nova 'epidemia'- Learn and review basic protocol sequences for a complete liver assessment- Execution and preparation tips- Limitations for measures of steatosis and iron overload- Illustrate the findings and correlate them with clinic application- Learn how to make illustrative radiology reports- Attention to the most common pitfalls

#### TABLE OF CONTENTS/OUTLINE

- Imaging protocols- Imaging aspects that may be mistaken- Pitfalls- Practical examples- Impact the liver evaluation and clinical application in everyday life- Illustrated and structured report

Printed on: 02/07/23

## Abstract Archives of the RSNA, 2022

GIEE-166

### Evaluation of Hepatic Steatosis, Inflammation and Fibrosis in NAFLD by Imaging: An Overview

Sunday, Nov. 27 8:00AM - 9:00AM Room: Learning Center - GI

#### Participants

Jong Yeong Kim, MD, Seoul, Korea, Republic Of (*Presenter*) Nothing to Disclose

#### TEACHING POINTS

Since significant differences are found in the prognosis of NAFLD depending on histological findings including fibrosis and steatosis, exact diagnosis of these conditions is clinically crucial. Many studies for non-invasive methods to estimate the histological severity of NAFLD instead of liver biopsy have been undertaken, mainly in the field of radiological and biochemical examinations. The purposes of this review are 1) to explain the principal, clinical application, pros/cons and limitations of imaging techniques for hepatic steatosis, fibrosis and hepatitis 2) to review the recently developed machine-learning based evaluations (computer aided diagnosis and radiomics) of conventional US, CT and MR images for the measurement of intrahepatic fat and fibrosis, 3) to discuss the future of these techniques, the possibility for wider clinical applications and roles in clinical trials for the treatment of diffuse liver disease

#### TABLE OF CONTENTS/OUTLINE

- Background
- Hepatic steatosis1. US based techniques 1) Gray scale imaging 2) Controlled attenuation parameter 3) Attenuation imaging2. Unenhanced CT 3. MRI based techniques 1) Two point DIXON 2) MR spectroscopy 3) MRI-PDFF
- Differentiation of NASH from simple steatosis
- Hepatic fibrosis1. US based techniques 1) Transient elastography 2) Shear wave-based elastography: Point SWE, ARFI, Supersonic shearwave2. MRI based techniques 1) Diffusion weighted imaging 2) Hepatocyte-specific contrast agent enhanced imaging 3) MR elastography
- Machine learning based evaluation of hepatic steatosis and fibrosis with US, CT, MR images
- Can we replace liver biopsy by imaging studies for hepatic steatosis or fibrosis?
- Conclusion

Printed on: 02/07/23



## Abstract Archives of the RSNA, 2022

GIEE-167

### Don't Be So thick! A Practical Approach to Common and Uncommon Causes of Gastric Wall Thickening

Sunday, Nov. 27 8:00AM - 9:00AM Room: Learning Center - GI

#### Participants

Edward Lawrence, MD, PhD, (*Presenter*) Nothing to Disclose

#### TEACHING POINTS

Gastric wall thickening can present a diagnostic challenge due the overlapping features of normal rugal folds, inflammation, and neoplasm. Features that suggest true gastric wall thickening include altered wall enhancement, asymmetric thickening, adjacent stranding, or local adenopathy Lower attenuation (edema) or mural stratification favors a benign process related to infection or inflammation. Intermediate/soft tissue attenuation favors neoplastic processes such as lymphoma or adenocarcinoma. Additional diagnostic work-up will frequently include further evaluation with endoscopy and endoscopic biopsy

#### TABLE OF CONTENTS/OUTLINE

1. Basics of gastric wall evaluation 2. Tips and tricks a. Differentiating true versus pseudo-thickening b. Differentiating malignant versus benign thickening 3. Malignant causes (e.g., linitis plastica, lymphoma, gastric adenocarcinoma) 4. Benign causes - common (e.g., gastritis) and uncommon (e.g., Ménétrier's disease) a. Inflammatory/infiltrative b. Infectious

Printed on: 02/07/23



## Abstract Archives of the RSNA, 2022

GIEE-168

### Spaces and Places: A Radiologist's Roadmap to the Peritoneum and Retroperitoneum

Sunday, Nov. 27 8:00AM - 9:00AM Room: Learning Center - GI

#### Participants

Christopher Sears, MD, (*Presenter*) Nothing to Disclose

#### TEACHING POINTS

Teaching PointsThe peritoneum and retroperitoneum, with their myriad spaces, pouches, and ligaments, are difficult to comprehend, let alone identify on imaging. However, understanding how the peritoneal reflections limit, circulate, and react to disease can facilitate the correct diagnosis and proper care. After reviewing this education exhibit, the learner will be able to: Understand and identify structures and spaces of the peritoneum and retroperitoneum. Appreciate the significance of the peritoneum and retroperitoneum, with respect to the spread of and response to infection, the staging of cancers, and the severity and localization of traumatic injuries. Recognize how medical and surgical management changes when peritoneal borders are violated.

#### TABLE OF CONTENTS/OUTLINE

Outline1.) Overview of the anatomy, spaces, and pouches of the peritoneum and retroperitoneum.2.) Differences regarding the peritoneum of males and females.3.) Case-based demonstration of the significance of the peritoneum, with regards to management and outcomes in cancer, trauma, and infection.

Printed on: 02/07/23



## Abstract Archives of the RSNA, 2022

GIEE-169

### Unraveling the Superficial, Internal and Complex Hernias: Case-based Guide for Accurate Diagnosis

Sunday, Nov. 27 8:00AM - 9:00AM Room: Learning Center - GI

#### Participants

Hunter Sellers, BS, MD, Houston, TX (*Presenter*) Nothing to Disclose

#### TEACHING POINTS

1. Hernias are a very common pathology found on imaging with a large variety of presentation types. We provide multiple examples of hernias, both superficial and internal. 2. Superficial hernias can occur anywhere along the anterior, lateral, or posterior abdominal wall and can be simple containing only fat, or complex containing organs. We have cases of these simple and complex hernias, and hernias which contain pathology in the hernia sac. 3. Internal hernias can be intimidating to radiologists who are unfamiliar with the specific imaging patterns, our goal is to provide examples of these hernias along with the etiologies to help improve diagnostic acumen and accuracy. 4. The important goal of reporting pertinent information of type of hernias to clinicians to ensure that patients receive the best treatment possible.

#### TABLE OF CONTENTS/OUTLINE

Discussion of superficial hernias, which include inguinal, umbilical, Spigelian, amyand, Richter, incisional and others. Elucidate internal hernias, which include paraduodenal, Foramen of Winslow, Petersen and others. Highlight features of complex hernias. Imaging tips on recognizing specific hernia types. Report pertinent information that the clinicians want to know. Conclusion.

Printed on: 02/07/23



## Abstract Archives of the RSNA, 2022

GIEE-17

### Imaging Diagnosis of Hepatocellular Carcinoma in the Era of Molecular Targeted Therapy and Immunotherapy

Sunday, Nov. 27 8:00AM - 9:00AM Room: Learning Center - GI

#### Awards

Certificate of Merit

#### Participants

Azusa Kitao, MD, PhD, Kanazawa, Japan (*Presenter*) Nothing to Disclose

#### TEACHING POINTS

1. To understand the mechanisms and application of molecular targeted therapy and immuno-therapy for HCC2. To know the role of imaging in evaluation and prediction of treatment response of HCC3. To learn the adverse events of these systemic therapies for HCC that can be assessed by imaging

#### TABLE OF CONTENTS/OUTLINE

1. History and treatment mechanisms-Molecular targeted therapy-Immunotherapy2. Application-Clinical and imaging criteria-Roles in multidisciplinary therapy3. Evaluation of treatment response-Guidelines, especially in modified response evaluation criteria in solid tumors (RECIST)-Imaging modalities and techniques: dynamic CT, dynamic MRI, contrast enhanced US and radiomics-Pitfalls4. Prediction of treatment response based on molecular subclassification of HCC-Molecular targeted therapy: dynamic CT, intravoxel incoherent motion (IVIM) and 18F-FDG PET/CT-Immunotherapy: gadoxetate-enhanced MRI5. Adverse reactions of molecular targeted therapy and immunotherapy-Tumor related reactions-Systemic reactionsSummaryThe radiologists should know the imaging features related to molecular targeted therapy and immunotherapy for HCC in the era of personalized medicine.

Printed on: 02/07/23



## Abstract Archives of the RSNA, 2022

GIEE-170

### Imaging Postoperative Abdomen: What A Radiologist Should Know?

Sunday, Nov. 27 8:00AM - 9:00AM Room: Learning Center - GI

#### Participants

Smily Sharma, MD, MBBS, Jodhpur, India (*Presenter*) Nothing to Disclose

#### TEACHING POINTS

1) To understand the anatomical basis of common and uncommon surgical procedures2) To elaborate on the salient features of various pathologies encountered in cross-sectional imaging of the post-operative abdomen3) To illustrate the distinguishing imaging features of complications of laparotomy4) To propose an algorithmic approach to the differential diagnosis of various pathologies5) To highlight red flag imaging biomarkers with implications on management strategies

#### TABLE OF CONTENTS/OUTLINE

1) Introduction2) Radiological anatomy of common and uncommon abdominal surgeries3) Imaging of complications of Hepatobiliary surgeries including Whipple, Extended hepatectomy, Roux en Y jejunostomy, resection and anastomosis, rectal surgeries and Cholecystectomy4) Imaging of complications of Genitourinary surgeries including nephrectomy, hysterectomy and caesarean section5) Understanding the chronology and pathophysiology of early and late complications6) Tailored regimens of cross sectional imaging to optimise image acquisition7) Diagnostic challenges posed by sequelae of laparotomy including structures, adhesions and scar8) Endovascular management of Vascular complications of Abdominal surgery9) Conclusion

Printed on: 02/07/23



## Abstract Archives of the RSNA, 2022

GIEE-171

### Basics of RUQ Ultrasound for Trainees: Anatomy, How to Scan and Diagnoses to Know for Call

Sunday, Nov. 27 8:00AM - 9:00AM Room: Learning Center - GI

#### Awards

Identified for RadioGraphics  
Magna Cum Laude

#### Participants

Gail Stanton, MD, Milwaukie, OR (*Presenter*) Nothing to Disclose

#### TEACHING POINTS

1.) Understand basic principles of ultrasound and how to acquire ultrasound images of the right upper quadrant. 2.) Review anatomy of the RUQ on cine ultrasound images including hepatobiliary, pancreatic and regional anatomy. 3.) Identify common pathology seen in the right upper quadrant, with a focus on high yield on-call ultrasound findings and diagnoses for trainees.

#### TABLE OF CONTENTS/OUTLINE

1.) Basic principles of ultrasound imaging. a.) Ultrasound probe selection and sonographic windows to assess the liver, gallbladder, and pancreas illustrated with images/movies. b.) Knobology basics: Image optimization for best image quality. 2.) Imaging review of labelled cine images of right upper quadrant anatomy. a.) Hepatobiliary - hepatic segments, vasculature, biliary system. b.) Pancreas and upper abdominal vasculature. c.) Regional anatomy - Bowel, right kidney, thorax. 3.) Review imaging of RUQ pathology. a.) Hepatic - diffuse liver disease, mass, abscess, TIPS, portal vein thrombus, portal vein gas. b.) Biliary - Cholecystitis, cholelithiasis, obstruction, choledocholithiasis, adenomyomatosis, gallbladder cancer, pneumobilia. c.) Pancreatic - pancreatic mass, pancreatitis. d.) Peritoneum.

Printed on: 02/07/23



## Abstract Archives of the RSNA, 2022

GIEE-172

### Fantastic 'Four': Imaging of Hepatic Segment 4 - Management and Surgical Implications

Sunday, Nov. 27 8:00AM - 9:00AM Room: Learning Center - GI

#### Awards

Certificate of Merit

#### Participants

Bryce Carson, MD, San Antonio, TX (*Presenter*) Nothing to Disclose

#### TEACHING POINTS

Discuss anatomy, embryology, arterial, portal venous supply hepatic venous drainage biliary drainage of segment 4 (S4) Review select pseudotumors, developmental, inflammatory, and neoplastic pathologies specific to S4 Discuss the clinical significance of S4 vasculature, bile ducts in living donor liver transplant viability complications

#### TABLE OF CONTENTS/OUTLINE

Introduction Anatomy: Couinaud, International Hepato-Pancreatico-Biliary Association New World Terminology Classifications Embryology Hepatic arteries Portal veins Hepatic veins Bile ducts Imaging Modalities: US, CT MRI Implications of living donor transplant hepatic resection surgeries: Hepatic artery thrombosis, venous congestion post-operative bile leak Pseudotumors: Focal fat deposition, sparing perfusion abnormalities due to aberrant vessels Hot quadrant lobe sign in superior vena cava syndrome Target-like lesions in S4 Ciliary Hepatic Foregut cyst Ingested gastric foreign bodies perforating S4: Toothpicks, fish bones wires bristles from grill cleaning brush Mucinous cystic neoplasm of the liver (MCN) Direct tumor extension from stomach gastrohepatic ligament Conclusion Clinical Implications Knowledge of arterial, portal venous, hepatic venous, bile duct anatomy of S4 vascular variations is crucial in successful liver donor liver transplant other left lobe resections. Focal fat sparing, deposition are more common in S4 due to peculiar venous drainage. Given embryologic origin in close proximity to esophagus stomach, MCN ciliated foregut cyst develop exclusively in S4.

Printed on: 02/07/23

## Abstract Archives of the RSNA, 2022

GIEE-173

### Utility and Limitations of 18F-FDG PET/CT For the Evaluation of Hepatic Lesions

Sunday, Nov. 27 8:00AM - 9:00AM Room: Learning Center - GI

#### Participants

Shota Kondo, Hiroshima, Japan (*Presenter*) Nothing to Disclose

#### TEACHING POINTS

a. In well-to-moderately differentiated hepatocellular carcinoma (HCC), the 18F-fluorodeoxy-glucose (FDG) uptake tends to be poor. A high FDG uptake is associated with histologically poor differentiation, microvascular invasion, and a poor prognosis. Therefore, 18F-FDG-PET is useful for estimating the malignancy grade of HCC. b. Although most intrahepatic cholangiocellular carcinomas (ICC) show elevated FDG uptake, in some the uptake may be poor. c. A marked FDG uptake may identify rare malignant hepatic tumors such as malignant lymphoma and leiomyosarcoma. d. As it is difficult to differentiate malignant hepatic tumors from inflammation with only the degree of FDG uptake, findings of other imaging modalities should be considered.

#### TABLE OF CONTENTS/OUTLINE

1. Molecular background of 18F-FDG 2. Technical and physiological pitfalls of 18F-FDG PET/CT 3. Imaging findings of various hepatic lesions on 18F-FDG-PET/CT scans 4. The advantages and limitations of 18F-FDG-PET/CT vis-à-vis other imaging modalities for the diagnosis of hepatic lesions 5. The future prospects of nuclear imaging for the diagnosis of hepatic lesions

Printed on: 02/07/23



## Abstract Archives of the RSNA, 2022

GIEE-174

### Multimodality Comprehensive Imaging Review of Benign and Malignant Hepatic Vascular Abnormalities: Pearls and Pitfalls

Sunday, Nov. 27 8:00AM - 9:00AM Room: Learning Center - GI

#### Participants

Mohd Zahid, MD, Birmingham, AL (*Presenter*) Nothing to Disclose

#### TEACHING POINTS

Hepatic vascular lesions have a wide spectrum of clinical presentations and varying degrees of malignancies. They range from benign tumors such as hepatic hemangiomas, benign/low-grade malignancies such as hepatic small vessel neoplasia, tumors with high malignant potential such as hepatic perivascular epithelioid cell tumors, and hepatic hemangiopericytomas, other tumors with intermediate degrees of malignancy such as hepatic epithelioid hemangioendothelioma, up to malignancies developed more often in the context of immunodeficiency syndrome-Kaposi sarcomas, and high-grade malignancies with a poor outcome such as hepatic angiosarcomas. On Imaging, differentiation of primary malignant vascular tumors of the liver from benign neoplasms or vascular abnormalities is often difficult. After reviewing this exhibit, the learner will be able to: 1. Understand the epidemiology, pathology, and imaging appearance of common and uncommon benign and malignant hepatic vascular lesions or neoplasms 2. Imaging tips to differentiate vascular lesions from other non-vascular abnormalities.

#### TABLE OF CONTENTS/OUTLINE

A. WHO Classification of hepatic vascular neoplasms B. Epidemiology and pathophysiology. C. Multimodality imaging of benign and vascular lesions with imaging tips and pitfalls

Printed on: 02/07/23



## Abstract Archives of the RSNA, 2022

GIEE-175

### Pearls in Imaging of Biliary and Vascular Complications of Orthotopic Liver Transplant

Sunday, Nov. 27 8:00AM - 9:00AM Room: Learning Center - GI

#### Participants

Ana Gonzalez, Chicago, IL (*Presenter*) Nothing to Disclose

#### TEACHING POINTS

1) Orthotopic liver transplantation (OLT) is the definitive treatment for patients with end-stage liver disease accounting for 22.8% of all organ transplantations in the United States (OPTN).2) Although the advances in OLT have led to reduced morbidity and mortality, the procedure continues to be associated with a high rate of complications occurring in 25-30% of cases (NG 2015).3) We will highlight the surgical technique and anatomy of OLT with a brief overview of different anastomosis techniques.4) We will review the imaging techniques for peri- and post-operative evaluation of transplanted grafts including normal imaging appearance post-transplantation.5) We will summarize the most common post-operative complications following OLT with their associated radiologic findings and discuss possible interventional solutions.

#### TABLE OF CONTENTS/OUTLINE

Summary of OLT surgical approach Surgical anatomy with location of anastomoses for the hepatic artery, portal vein, inferior vena cava, and biliary duct system accompanied with illustrations.Imaging of transplanted grafts Grayscale and Doppler ultrasound for routine surveillance post-transplantation. Describe common waveform characteristics seen with specific complications.The use of CT and MRI to further explore suspected abnormalities followed by angiography.Common OLT complications with associated radiologic findings i. Biliary complications including biliary strictures and bilomas. ii. Vascular complications including arterial and venous stenosis, thrombosis, and pseudoaneurysm formation.Brief imaging review of OLT complications pre- and post- treatment with interventional radiology procedures.

Printed on: 02/07/23



## Abstract Archives of the RSNA, 2022

GIEE-176

### Imaging Findings of Post-chemotherapy Non-Metastatic Hepatic Parenchymal Changes

Sunday, Nov. 27 8:00AM - 9:00AM Room: Learning Center - GI

#### Participants

San Yu Leung, MBBS, (*Presenter*) Nothing to Disclose

#### TEACHING POINTS

Use of chemotherapy has revolutionized management of cancer in past decades. Liver toxicity is commonly observed among different types of chemotherapy drugs. The aim of this exhibit is to illustrate radiological features of various chemotherapy-associated hepatic parenchymal changes, with examples in different imaging modalities, and to demonstrate potential complications of these liver injury patterns with representative cases. Early recognition of these liver conditions allow prompt clinical action to be taken, thus optimizing management and avoiding severe complications.

#### TABLE OF CONTENTS/OUTLINE

1. Introduction 2. To illustrate cases and radiological features of: a. Pseudocirrhosis in breast cancer and non breast cancer patients with liver metastasis, as well as its potential complications b. Chemotherapy-related hepatic steatosis c. Chemotherapy-related hepatitis d. Chemotherapy-related cholangiopathy 3. Summary of key teaching points

Printed on: 02/07/23



## Abstract Archives of the RSNA, 2022

GIEE-177

### Ultrasound Based Hepatic Fat Quantification

Sunday, Nov. 27 8:00AM - 9:00AM Room: Learning Center - GI

#### Participants

Nuran Seneviratne, MA, MBBS, London, United Kingdom (*Presenter*) Nothing to Disclose

#### TEACHING POINTS

Non-alcoholic fatty liver disease (NAFLD) is a growing cause of cirrhosis, hepatocellular carcinoma and liver transplant. Currently, steatosis is graded by subjective assessment of liver echogenicity and attenuation, with significant interobserver variability and sub-optimal detection of mild or greater steatosis (S>0). Controlled Attenuation Parameter is widely used (found in the Fibroscan® system, Echosens). Different disease states and probes impact measurement and for S>0 steatosis, it has a high false negative rate and low sensitivity. Quantitative metrics are now offered by various vendors, relying on changes in backscatter, attenuation and the speed of sound found in steatotic livers. Attenuation Imaging (Canon) and Ultrasound Guided Attenuation Parameter (General Electric) show excellent S>0 performance in NAFLD and other aetiologies of hepatic steatosis compared to both MRI and histology. Fatty Liver Attenuation Index (Samsung) shows moderate performance at the S>0 task in 351 patients with mixed aetiologies of chronic liver disease at histology. Ultrasound Derived Fat Fraction (Siemens Healthineers) obtains 15 point shear wave and a steatosis percentage from a single large region of interest, also showing excellent S>0 performance. These technologies are in their early stages. Larger clinical trials are needed to determine optimal steatosis grade cut-off values and compare results across vendors.

#### TABLE OF CONTENTS/OUTLINE

Introduction Qualitative Assessment Quantitative Assessment Conclusion

Printed on: 02/07/23



## Abstract Archives of the RSNA, 2022

GIEE-178

### Diffuse Liver Disease and Its Quantification in MRI for Rookies

Sunday, Nov. 27 8:00AM - 9:00AM Room: Learning Center - GI

#### Participants

Camilo Soler Becerra, PhD, Bogota, Colombia (*Presenter*) Nothing to Disclose

#### TEACHING POINTS

- NAFLD is the most common chronic liver disease worldwide. It has increasing prevalence among adults and children.
- Iron overload may lead to liver cirrhosis, hepatocellular carcinoma, and cardiac and endocrine complications.
- Fibrosis is the final stage of diffuse liver disease, with its complications and which we want to anticipate.
- Measurement of fat, iron overload and liver stiffness by MRI is a noninvasive and accurate approach.
- Knowledge of the protocol and the post-process will lead more hospitals worldwide to diagnose and quantify these pathologies, being of great help to the patient and other specialties. For example, we observe two similar liver parenchyma in images A and B. Still, we identify greater hardness in image B when quantifying liver stiffness, which alerts us about an inflammatory process.

#### TABLE OF CONTENTS/OUTLINE

1. Introduction.2. FatFrac.3. Iron quantification.4. Elastography.5. Conclusions.

Printed on: 02/07/23



## Abstract Archives of the RSNA, 2022

GIEE-179

### The Falciform Ligament and Ligamentum Teres Hepatis Revisited

Sunday, Nov. 27 8:00AM - 9:00AM Room: Learning Center - GI

#### Participants

Tomoya Nishiyama, MD, (*Presenter*) Nothing to Disclose

#### TEACHING POINTS

The falciform ligament and the ligamentum teres hepatis have been considered as insignificant embryological remnants that include umbilical artery and vein. The purpose of this educational exhibit is to spotlight the clinical importance of the falciform ligament and the ligamentum teres hepatis in the radiological perspective.

#### TABLE OF CONTENTS/OUTLINE

This education exhibit includes 4 categories;(i) clinical embryology;(ii) clinical anatomy;(iii) clinical use for packing material; (iv) pathological conditions and disease process. Schematic illustrations of the embryology and anatomy and case based-presentations using CT images, macroscopic specimens and operative findings will be presented.

Printed on: 02/07/23



## Abstract Archives of the RSNA, 2022

GIEE-18

### **It Looks Like Liver Cancer, But What Is It Really?: Pearls and Pitfalls for Diagnosis of Pathological Entities Mimicking Liver Malignancies**

Sunday, Nov. 27 8:00AM - 9:00AM Room: Learning Center - GI

#### **Awards**

**Certificate of Merit**

#### **Participants**

Hanna Ferreira Dalla Pria, MD, MD Anderson, Houston, TX (*Presenter*) Nothing to Disclose

#### **TEACHING POINTS**

- Recognize the most common mimickers of liver malignancies.
- Illustrate key clinical and imaging findings that may help distinguishing benign from malignant liver lesions.
- Discuss relevant tips including clinical information, and diagnostic workup which could help in making precise diagnosis
- Discuss appropriate management options including, tissue sampling or follow-up.

#### **TABLE OF CONTENTS/OUTLINE**

1. Overview of liver findings on imaging modalities -Prevalence, relevance, costs -Cancer facts and statistics 2022 -ACR white paper recommendations for management of incidental liver lesions 2. Clinical and Pathological Background -Symptoms -Key pathological and laboratorial findings 3. Imaging-based approach to assess mimickers of liver malignancies on imaging -Background liver -Pattern of the liver findings -Combined clinical and imaging algorithm 4. Illustrate a spectrum of imaging findings, differentiation with pathological correlation -Benign nodules: e.g. atypical hemangiomas, inflammatory pseudotumor, FNH-like lesions. -Inflammatory: IgG4-related disease, eosinophilic hepatitis, confluent fibrosis. -Infectious: ex. parasitic infections, pseudotumoral granulomatosis, abscess. -Precancerous: ex. dysplastic nodules, bile duct adenoma. -Miscellaneous: ex. vascular shunts, infarction. 5. Multidisciplinary liver tumor board -What do non-radiologist liver physicians and surgeons need to know -What do radiologists need to ask. 6. Interactive case examples -Sample cases to illustrate challenging scenarios and provide tips to reach a specific diagnoses

Printed on: 02/07/23



## Abstract Archives of the RSNA, 2022

GIEE-180

### Ultrasound and Computed Tomography in The Evaluation of Mesenteric Lesions

Sunday, Nov. 27 8:00AM - 9:00AM Room: Learning Center - GI

#### Participants

Snehal Kose, MBBS, MD, (*Presenter*) Nothing to Disclose

#### TEACHING POINTS

Explain the anatomy and contents of the mesentery Describe ultrasound (USG) and computed tomographic (CT) features of primary and secondary solid mesenteric lesions, mesenteric cystic lesions, secondary mesenteric involvement in inflammatory/ infectious conditions like tuberculosis and inflammatory bowel disease and vascular lesions affecting mesentery. Highlight the importance of cross sectional imaging in diagnosis, detection of complications and management of mesenteric lesions Discuss a stepwise algorithm to approach mesenteric lesions for providing thoughtful differentials

#### TABLE OF CONTENTS/OUTLINE

Anatomy and contents of the small bowel mesentery USG and computed tomographic (CT) features of - Primary mesenteric solid neoplasms Mesenteric cystic lesions Unilocular cysts Multilocular cysts Secondary mesenteric solid lesions and their routes of spread Deposits Lymphadenopathy Stellate mesentery Mesenteric involvement in tuberculosis and inflammatory bowel disease Vascular anomalies of mesentery SMA thrombosis with acute mesenteric ischemia SMA-SMV arteriovenous fistula Complications due to mesenteric lesions Bowel Urological Vascular Management of mesenteric lesions Image guided biopsy Planning surgical strategy Stepwise algorithm for imaging evaluation of mesenteric lesions

Printed on: 02/07/23



## Abstract Archives of the RSNA, 2022

GIEE-181

### Diagnostic Approach to Peritoneal Lesions

Sunday, Nov. 27 8:00AM - 9:00AM Room: Learning Center - GI

#### Participants

Mihran Khdir, MBChB, (*Presenter*) Nothing to Disclose

#### TEACHING POINTS

A wide spectrum of abnormalities affect the peritoneum; including neoplastic, infectious, and inflammatory etiologies as well as spread of ectopic tissues. Anatomy of the peritoneal cavity and its ligaments determine the patterns of disease spread. In this educational exhibit, we provide a comprehensive radiologic diagnostic approach to peritoneal lesions based of the predominant composition (solid, cystic, hemorrhagic, calcific, lipomatous, and gas containing). Each entity will be discussed briefly along with illustrated images of various cases.

#### TABLE OF CONTENTS/OUTLINE

Peritoneal Anatomy; Outline of Diagnostic Approach to Peritoneal Lesions; Solid Lesions; Cystic Lesions; Hemorrhagic Lesions; Calcific Lesions; Lipomatous Lesions; Gas Containing Lesions

Printed on: 02/07/23

## Abstract Archives of the RSNA, 2022

GIEE-182

### Peritoneal Carcinomatosis on CT and MR: How Not to Miss A Single Case

Sunday, Nov. 27 8:00AM - 9:00AM Room: Learning Center - GI

#### Participants

Ana Veron, MD, (*Presenter*) Nothing to Disclose

#### TEACHING POINTS

To depict the most frequent and the not so common sites and imaging features of peritoneal carcinomatosis on CT and MR. To propose how to systematically look for peritoneal implants on CT and MR, acknowledging the technical limitations. To describe the differential diagnosis and pitfalls

#### TABLE OF CONTENTS/OUTLINE

IntroductionThe peritoneum is the second most common metastatic localization for abdominal tumors, only surpassed by the liver. Peritoneal metastases in tumors of an extraabdominal origin occur less frequently. Early diagnosis of peritoneal carcinomatosis based on imaging findings is not always easy but it is essential in staging and managing primary tumors. CT is usually the first diagnostic tool but its performance is poor when it comes to detecting subcentimetric implants and those in anatomically difficult sites. MR has proved to have a better performance due to its better contrast resolution. Material and methodsThe revision of 300 peritoneal carcinomatosis cases from our database (comprising tumors of digestive origin, breast, gynecologic, testicular, renal, neuroendocrine, melanoma, lung, head and neck and soft tissue) has allowed us to establish a systematic diagnostic approach. Examples of the how and where to look for peritoneal implants, bearing in mind the anatomical sites and the major pathways of spread will be described, enhancing the added value of multiplanar reconstructions. Typical and less common presentations will be described using a case-based approach. Despite the non-specificity of the imaging findings, in some cases there are helpful hints to suggest the origin of the primary tumor. Examples of pitfalls and differential diagnosis will also be discussed.

Printed on: 02/07/23



## Abstract Archives of the RSNA, 2022

GIEE-183HC

### MR Defecography For the Evaluation of Pelvic Floor Dysfunction

Sunday, Nov. 27 8:00AM - 9:00AM Room: Learning Center - GI

#### Participants

EUNBYUL CHO, (*Presenter*) Nothing to Disclose

#### TEACHING POINTS

Among the worldwide women, pelvic floor disorder is common health problem which is hard to say other people. and it is significant problem lowering their quality of life and causing to morbidity. Pelvic floor disorder means overall pelvic floor functional disorders caused by impairment of the ligament, fasiae, muscles supporting the pelvic organs. Conventional defecography is performed with fluoroscopy after injection of barium contrast to rectum. But it can evaluate pelvic floor disorder concentrating posterior compartment of pelvic floor and has risk of exposure to ionizing radiation to patient and doctor. MR defecography is dynamic study to evaluate pelvic floor disorder during defecation using US gel in real time and has been proven accurate and reliable for checking multiple compartments of pelvic floor. It is used to diagnosis of rectocele, intussusception, and anismus. we review normal female pelvic floor anatomy and MR defecography which can accurate diagnosis of pelvic floor disorder involving all three compartments of pelvic floor and improve the postoperative results. Our teaching points are as follows. To review normal anatomy of the pelvic floor, To compare MR defecography to fluor defecography, To introduce the concepts of the integral theory ; anatomically-based diagnostic methods locate damaged structure.

#### TABLE OF CONTENTS/OUTLINE

1) Subdivisions of female pelvic anatomy (three compartment) : anterior compartment -middle compartment -posterior compartment  
2) Defecation function evaluation 3) Comparison of fluoro defecography and MR defecography. 4) Introduce the concepts of the integral theory  
Please visit the Learning Center to also view this presentation in hardcopy format.

Printed on: 02/07/23



## Abstract Archives of the RSNA, 2022

GIEE-184

### MRCP Image Optimization

Sunday, Nov. 27 8:00AM - 9:00AM Room: Learning Center - GI

#### Participants

Khyati Bidani, MBBS, New Delhi, India (*Presenter*) Nothing to Disclose

#### TEACHING POINTS

1. Using ultrafast technique (RARE< HASTE< SSFSE) reduces artifacts and improves acquisition time.2. Use breathing independent sequences

#### TABLE OF CONTENTS/OUTLINE

1. Applications of MRCP (Congenital anomalies, choledocholithiasis, biliary strictures, cystic pancreatic tumors, biliary injuries).2. Common indications (Failed MRCP, contraindication to MRCP and post biliary-enteric anastomosis case).3. Advantages and disadvantages of MRCP over ERCP4. Techniques (2D Vs. 3D).5. Factors affecting image quality.6. Artifacts (Susceptibility, motion and other artifacts).7. Image optimization techniques.

Printed on: 02/07/23



## Abstract Archives of the RSNA, 2022

GIEE-185

### Gastric Cancer: Pearls, Pitfalls and Lessons Learned from The Multidisciplinary Tumor Board

Sunday, Nov. 27 8:00AM - 9:00AM Room: Learning Center - GI

#### Participants

Stephen Kwak, MD, Rochester, NY (*Presenter*) Nothing to Disclose

#### TEACHING POINTS

Gastric carcinoma is one of the most common malignancies worldwide and is currently the fourth leading cause of cancer-related deaths. While early gastric cancers are limited to the mucosa and submucosa and usually manifest as focal wall thickening with possible ulceration, advanced cancers involve the muscularis propria or even deeper, manifesting as diffuse, infiltrative thickening with ulceration and possible linitis plastica. Upper gastrointestinal endoscopy is currently accepted as the gold standard for detection of gastric cancer, while Multidetector Computed Tomography (MDCT) is preferred for staging of the tumor. MDCT allows for assessment of tumor depth, lymph node involvement, and disease spread which may be through subperitoneal dissemination, direct invasion, transperitoneal dissemination, or hematogenous spread. Careful preoperative staging is essential for proper surgical treatment, as complete resection of the tumor and surrounding lymph nodes is the only cure. In this exhibit we will discuss the MDCT technique and imaging features of gastric cancer with treatment approaches and various pearls and pitfalls learned during our experience at gastric cancer tumor board.

#### TABLE OF CONTENTS/OUTLINE

Introduction; Staging of gastric cancer; Imaging modalities; Treatment algorithm; Medical management; Surgical management; Imaging; Pearls and Pitfalls

Printed on: 02/07/23



## Abstract Archives of the RSNA, 2022

GIEE-186

### Postoperative Upper Gastrointestinal Fluoroscopy: What the Radiologist Needs to Know

Sunday, Nov. 27 8:00AM - 9:00AM Room: Learning Center - GI

#### Participants

Matheus Fritzen, MD, Sao Paulo, Brazil (*Presenter*) Nothing to Disclose

#### TEACHING POINTS

- Describe the surgical anatomy and normal imaging findings of the main upper gastrointestinal surgeries in fluoroscopy. - Evaluate the main imaging findings of the routine use of postoperative contrast swallow. - Illustrate the major complications of upper gastrointestinal surgeries.

#### TABLE OF CONTENTS/OUTLINE

- Describe major headings (e.g., anatomy, physiology, imaging techniques, etc.) - Describe the following surgeries and identify the major complications of these: Bariatric Surgery (Sleeve and Y-Roux), gastrectomy, Nissen fundoplication, hiatus hernia repair, Peroral endoscopic myotomy (POEM)- Imaging in postoperative barium or iodine contrast to diagnose the main postoperative complications.

Printed on: 02/07/23



## Abstract Archives of the RSNA, 2022

GIEE-187HC

### Preoperative MRCP for Laparoscopic Cholecystectomy: What Radiologists Need to Know

Sunday, Nov. 27 8:00AM - 9:00AM Room: Learning Center - GI

#### Participants

Young-Hwan Lee, MD, Iksan, Korea, Republic Of (*Presenter*) Nothing to Disclose

#### TEACHING POINTS

1. To clarify the role of MRCP in preoperative evaluation of acute or chronic cholecystitis. 2. To understand the normal variations of bile duct anatomy to avoid surgical injury in laparoscopic cholecystectomy. 3. To describe the useful MRCP findings for differential diagnosis of various wall thickening gallbladder lesions.

#### TABLE OF CONTENTS/OUTLINE

1. Review of various MRCP techniques 2. Classification of bile duct anatomy using MRCP of a total of 879 patients were examined before laparoscopic cholecystectomy. Cases of bile duct injury during cholecystectomy were added. 3. Representative cases of gallbladder diseases, such as acute cholecystitis, chronic cholecystitis, gallstones, adenomyomatosis, xanthogranulomatous cholecystitis, Mirizzi syndrome, cholangitis with common bile duct stones, and wall thickening type gallbladder carcinoma, were included, and their imaging findings with literature review were illustrated. Conclusion: MRCP is a useful method for preoperative evaluation of biliary anatomy to prevent surgical complications. In various cases such as inflammatory and malignant diseases, accurate diagnosis is possible through preoperative MRCP. Please visit the Learning Center to also view this presentation in hardcopy format.

Printed on: 02/07/23



## Abstract Archives of the RSNA, 2022

GIEE-188

### The Typical and Atypical Appearances of Pancreatic Neuroendocrine Tumors: The Role of CT Angiography and Cinematic Rendering

Sunday, Nov. 27 8:00AM - 9:00AM Room: Learning Center - GI

#### Participants

Elliot Fishman, MD, Owings Mills, MD (*Presenter*) Co-founder, HipGraphics, Inc; Stockholder, HipGraphics, Inc; Institutional Grant support, Siemens AG; Institutional Grant support, General Electric Company; Consultant, Exact Sciences Corporation; Consultant, Imaging Endpoints

#### TEACHING POINTS

1. Understand how to use multiphase CT with CT angiography and 3D mapping with Cinematic Rendering to optimize detection of pancreatic neuroendocrine tumors
2. understand the range of appearance of pancreatic neuroendocrine tumors and how to distinguish them from other pancreatic tumors
3. learn how to optimize staging of pancreatic neuroendocrine tumors by creating vascular 3D maps for staging of vascular involvement and for pre-op surgical planning
4. understand the challenges and pitfalls in the diagnosis of pancreatic neuroendocrine tumors
5. understand how cinematic rendering can be valuable in small tumor detection and staging of larger tumors

#### TABLE OF CONTENTS/OUTLINE

1. CT scan protocols and role of dual phase imaging and CTA
2. role of Cinematic Rendering and how to optimize cinematic rendering for lesion detection and staging
3. learn how to generate and interpret the images created by Cinematic rendering
4. case studies and examples showing typical and atypical appearances
5. potential pitfalls and challenges
6. role of CT and AI in the near time to help build on cinematic rendering over time.

Printed on: 02/07/23



## Abstract Archives of the RSNA, 2022

GIEE-189

### Covid-19- Associated Secondary Sclerosing Cholangitis: Imaging Features on Magnetic Resonance Imaging and Magnetic Resonance Cholangiopancreatography

Sunday, Nov. 27 8:00AM - 9:00AM Room: Learning Center - GI

#### Participants

Manon Germann, Zurich, Switzerland (*Presenter*) Nothing to Disclose

#### TEACHING POINTS

- Prolonged cholestasis in critically ill patients after severe COVID-19 infection may indicate the presence of secondary sclerosing cholangitis (SSC).
- Affected patients are at high risk of progression to biliary cirrhosis requiring liver transplantation.
- Since differential diagnosis to other causes of cholestatic liver injury can be difficult based on clinical and laboratory findings alone, imaging with MRI and MRCP can be crucial to help confirm the diagnosis.
- COVID 19-associated SSC mostly affects intrahepatic bile ducts showing strictures with or without upstream dilatation, bile duct beading, vanishing ducts and periductal edema.
- The extrahepatic bile ducts are typically spared.
- Changes of the liver parenchyma are commonly observed including patchy arterial enhancement, reduced uptake of hepatobiliary contrast agent and signal changes on T2- and diffusion weighted-images.
- Hepatic macrovascular changes and periportal lymphadenopathy are not typically seen.

#### TABLE OF CONTENTS/OUTLINE

1) Background a. Epidemiology b. Pathogenesis c. Clinical presentation d. Diagnosis 2) Imaging findings a. Biliary tree b. Liver parenchyma c. Hepatic vessels d. Other findings 3) Clinical implication and prognosis 4) Conclusion

Printed on: 02/07/23



## Abstract Archives of the RSNA, 2022

GIEE-19

### Response Evaluation Criteria in GI Cancers: What to Use and How to Measure: An Emerging Challenge in the Era of Novel Cancer Treatments

Sunday, Nov. 27 8:00AM - 9:00AM Room: Learning Center - GI

#### Awards

Identified for RadioGraphics

#### Participants

Francesca Castagnoli, MD, (*Presenter*) Nothing to Disclose

#### TEACHING POINTS

- Therapeutic response is assessed by tumour diameter measurements (WHO, RECIST 1.1, and iRECIST), tumour enhancement (mRECIST, EASL, RECICL) or CT density (CHOI). Metabolic response is measured on PET by the standardized uptake value (SUV) normalized to the lean body weight (PERCIST).
- Novel therapeutics and therapy-induced non-tumoral changes can lead to interpretation pitfalls.
- In rectal cancer, MRI-derived tumour regression grade (TRG) infers pathological response to guide treatment and disease prognosis.
- Functional imaging, radiomics, artificial intelligence and machine learning provide new and early biomarkers of response but require further qualification.

#### TABLE OF CONTENTS/OUTLINE

- GI Cancer therapies: 1) FDA-approved chemotherapies, targeted therapies and immunotherapies 2) external/internal radiotherapy
- Imaging response criteria: when, where and how?
- Patterns of response, stable disease and progression.
- Atypical response patterns: pseudo-progression, hyper-progression, dissociated response, abscopal effect.
- Potential pitfalls from non-tumoral effects of treatment: Hepatic steatosis, Sinusoidal obstruction syndrome, Others.
- MRI-TRG [after Mandard/Rode] applied to rectal cancer after neoadjuvant treatment.
- LI-RADS, a structured reporting system, for treatment response of hepatocellular carcinoma.
- Imaging response evaluation after neoadjuvant treatments of pancreatic cancer.
- Functional imaging: DCE-MRI, DWI and others; myth or reality?
- Radiomics: summary of current evidence.
- AI and machine learning: potential applications

Printed on: 02/07/23

## Abstract Archives of the RSNA, 2022

GIEE-190

### Hyperthermic Intraperitoneal Chemotherapy (HIPEC): A Radiological Primer

Sunday, Nov. 27 8:00AM - 9:00AM Room: Learning Center - GI

#### Participants

Mary Renton, MBBCh, (*Presenter*) Nothing to Disclose

#### TEACHING POINTS

- The treatment of peritoneal carcinomatosis has been revolutionised by cytoreductive surgery with hyperthermic intraperitoneal chemotherapy (HIPEC).- HIPEC is used in a combined approach immediately following surgery and involves heated chemotherapy agents being temporarily instilled into the abdominopelvic cavity.- The associated high morbidity means an optimised patient selection process is vital.- We review key patterns of peritoneal disease and their prognostic implications.- We summarise common and important HIPEC complications.

#### TABLE OF CONTENTS/OUTLINE

- Background into the clinical indications and outcomes for HIPEC.- Review of common sites of peritoneal disease and types (nodular, mass or plaque-like).- Review of prognostic imaging features, including, gastrointestinal involvement, mesenteric and retroperitoneal lymphadenopathy, ureteric obstruction, psoas or pelvic sidewall involvement and gastrohepatic ligament disease.- Review of radiological contraindications to HIPEC, including extra-abdominal metastases and massive retroperitoneal lymphadenopathy.- Review of post-HIPEC complications, including ascites, splenic/ovarian venous thrombosis, pseudoaneurysm, haemoperitoneum, lymphocyte, perihepatic hematoma, pancreatic fistula and ureteric injury.- Importance of radiological assessment in the selection and management of HIPEC patients.

Printed on: 02/07/23



## Abstract Archives of the RSNA, 2022

GIEE-191

### Spleen Doppler and Elastography: What the Radiologist Needs to Know

Sunday, Nov. 27 8:00AM - 9:00AM Room: Learning Center - GI

#### Participants

Mariana Del Rio Gonzalez, MD, Monterrey, Mexico (*Presenter*) Nothing to Disclose

#### TEACHING POINTS

1- To review splenic and vascular anatomy. 2- To discuss the differences in Strain and Shear Wave Elastography. 3- To identify the different techniques of Shear Wave Elastography. 4- To learn the indications and adequate protocol of splenic Doppler and Elastography. 5- To teach how to interpret and report findings.

#### TABLE OF CONTENTS/OUTLINE

1. Introduction  
2. Splenic anatomy: A) Parenchyma B) Circulation  
3. Elastography: A) Strain vs Shear Wave  
4. Shear Wave Techniques: A) 1D Transient Elastography B) Point Shear Wave Elastography C) 2D Shear Wave Elastography  
5. Indications  
6. Protocol: A) Technique B) Errors C) Artifacts  
7. Report: A) Interpretation B) Suggested Reporting

Printed on: 02/07/23

## Abstract Archives of the RSNA, 2022

GIEE-2

### **In Search of Harmony: Where Do We Still Disagree in the Radiological TNM Staging of Rectal Cancer?: A Pictorial Review Based on the Published Findings of a Recent International Survey and Multidisciplinary Expert Consensus**

Sunday, Nov. 27 8:00AM - 9:00AM Room: Learning Center - GI

#### **Participants**

Ulysses Torres, MD, PhD, Sao Paulo, Brazil (*Presenter*) Nothing to Disclose

#### **TEACHING POINTS**

- Recently, a global online survey was carried out among 321 experts from 32 countries to identify points of controversy in the applicability of the TNM system (8th ed.) for the radiological staging of rectal cancer. A total of 16 problem areas were identified, grouped in topics related to clinical tumor staging in low-rectal cancers, definitions for cT4b and cM1a disease, definitions for mesorectal fascia involvement, evaluation of lymph nodes versus tumor deposits, and staging of lateral lymph nodes.- These critical areas remain considerable points of dissensus even among experts in rectal cancer imaging, and their awareness by residents, general radiologists, and even abdominal radiologists is paramount for better and more consistent use of the TNM system in the everyday radiological practice.- An illustrated case-based review with schematic drawings may be a didactical and straightforward way of exhibiting such a range of controversies, facilitating their comprehension by a general audience. Secondly, it may also help make more understandable the points of consensus proposed and published by the international multidisciplinary panel of specialists.

#### **TABLE OF CONTENTS/OUTLINE**

1) Presentation of the 16 problem areas identified, illustrating them with schematical drawings. 2) Imaging-based review with didactical clinical cases exhibiting such critical points of controversies. 3) Tips on how to report the radiological findings in such cases in the light of the consensus proposed by the panel of experts.

Printed on: 02/07/23

## Abstract Archives of the RSNA, 2022

GIEE-20

### Early Detection of Pancreas Adenocarcinoma: Time to Give Up or Time to Double Survival?

Sunday, Nov. 27 8:00AM - 9:00AM Room: Learning Center - GI

#### Participants

Hala Khasawneh, MBBS, Rochester, MN (*Presenter*) Nothing to Disclose

#### TEACHING POINTS

Highlight the emerging concepts and recent advances in the domain of early detection of pancreas ductal adenocarcinoma (PDA):  
1. Dire prognosis of PDA: Early detection is the only intervention with the highest potential to improve outcomes  
2. Rationale for early detection: Substantial differences in the 5-year survival between stage I (26-months) versus stage IV disease (4.8-months)  
3. Challenges of early detection including inability of imaging to identify early PDA  
4. Emerging evidence supporting the role of Artificial Intelligence (AI) to augment imaging-based screening efforts for early detection of PDA in high-risk cohorts

#### TABLE OF CONTENTS/OUTLINE

1. PDA as an almost uniformly fatal disease  
2. Rationale for early PDA detection: What is "early" PDA and why is it critical to detect PDA at a stage when surgical cure is a possibility?  
3. Challenges and opportunities for population-based screening for PDA  
a) The Define (D)-Enrich (E)-Find (F) protocol as an emerging paradigm  
4. High-risk cohorts:  
a) Familial PDA and subjects with germline mutations  
b) New-onset diabetes (NOD) with high Enriching New-Onset Diabetes for Pancreas Cancer model (END-PAC) score  
c) Potential precursor lesions such as intraductal papillary mucinous neoplasms  
5. Limitations of imaging to detect early or incidental PDA:  
a) Imaging findings of early PDA  
b) Factors contributing to missed PDA on imaging  
6. AI tools being developed to augment screening efforts for PDA:  
a) Pancreas segmentation tools  
b) Imaging signature of pancreatic carcinogenesis at the prediagnostic stage  
c) AI-augmented detection of PDA on CTs  
7. Potential utility of molecular imaging for early detection of PDA

Printed on: 02/07/23

## Abstract Archives of the RSNA, 2022

GIEE-21

### Imaging of Young-onset Colorectal Cancer

Sunday, Nov. 27 8:00AM - 9:00AM Room: Learning Center - GI

#### Participants

James Fish, MBBS, London, United Kingdom (*Presenter*) Nothing to Disclose

#### TEACHING POINTS

Young onset colorectal cancer is defined as a colorectal tumour diagnosed at < 50 years. The incidence of young-onset colorectal cancer is on the rise, currently constituting approximately 10% of all cases. As such, reporting radiologists should have a good understanding of the imaging features and considerations associated with such patients including: • The risk factors and pre-disposing conditions associated with young-onset colorectal cancer. • The imaging manifestations frequently encountered on CT and MRI with correlation to histopathology and genetic markers. • Imaging appearances during the disease course including complex surgical management.

#### TABLE OF CONTENTS/OUTLINE

A case based educational exhibit including multiple examples of young-onset colorectal cancer with referenced teaching points. To include: • Demographics and epidemiology • Risk factors associated with young-onset colorectal cancer and associated imaging features. Including Hereditary syndromes (e.g. Lynch syndrome), genetic mutations and inflammatory bowel disease • Imaging presentations on MRI and CT with histopathological and genetic correlation, including synchronous or metachronous cancers. • Staging imaging and imaging during the disease course. • Post-treatment appearances, including complex surgical management e.g. exenteration, pelvic side wall clearance and peritoneal therapies. • Risk stratification and follow-up imaging surveillance.

Printed on: 02/07/23



## Abstract Archives of the RSNA, 2022

GIEE-22

### Posttreatment Challenges in Rectal Cancer MRI: A Systematic Approach

Sunday, Nov. 27 8:00AM - 9:00AM Room: Learning Center - GI

#### Awards

Cum Laude

#### Participants

Lucas Roberto Leis Oliveira, MD, Sao Paulo, Brazil (*Presenter*) Nothing to Disclose

#### TEACHING POINTS

- Understanding the critical role that MRI plays in rectal cancer staging and restaging.
- Comprehend that several histopathologic changes may occur within rectal tumors after chemoradiation treatment, such as fibrosis or increased mucin production.
- Radiologists play a crucial role in "watch-and-wait" programs for select patients with rectal cancer and should understand how to differentiate the several types of response, as well as how these posttreatment changes may be evaluated with high-spatial-resolution MRI.

#### TABLE OF CONTENTS/OUTLINE

- INTRODUCTION: o Rectal cancer treatment guidelines overview: § Selecting whether primary surgery or neoadjuvant treatment is an optimal approach; § Neoadjuvant treatment options: chemoradiotherapy versus total neoadjuvant therapy (TNT). o Primary tumor and nodal assessment with MRI.
- ASSESSMENT OF TREATMENT RESPONSE: A SYSTEMATIC APPROACH. o Posttreatment changes in the primary tumor o Tumor Restaging: Histopathologic and MRI regression grades: § Identifying incomplete/poor responders, as well as "near-complete" and complete responders. o Patterns of tumor response: shrinking versus fragmentation; fibrosis and increased mucin production.
- "WATCH-AND-WAIT": PATIENT SELECTION AND CURRENT CONTROVERSIES.
- FUTURE DIRECTIONS IN RECTAL CANCER TREATMENT AND IMAGING.
- TAKE HOME MESSAGES.

Printed on: 02/07/23



## Abstract Archives of the RSNA, 2022

GIEE-23

### #PRO TuMor# Becoming a PRO in Rectal TuMor: A Simple Way and Quiz Not to Miss the Tumoral Regression Grade After Neoadjuvant Therapy

Sunday, Nov. 27 8:00AM - 9:00AM Room: Learning Center - GI

#### Participants

Aaron Alarcon Novillo, Rio De Janeiro, Brazil (*Presenter*) Nothing to Disclose

#### TEACHING POINTS

> To demonstrate the importance of the radiologist in the context of rectal cancer, with a special interest in post-neoadjuvant evaluation.> To familiarize radiologists with the tumor regression grade (TRG) and its importance.> To demonstrate a simple way to minimize possible errors in the tumor regression grade (TRG).> To train the correct characterization of the tumor regression grade (TRG) based on recent cases using a simple way.

#### TABLE OF CONTENTS/OUTLINE

IntroductionRectal neoplasm is the third most common type of tumor in men and the second in women. Surgical treatment with total mesorectal excision is the gold standard, however, in cases of locally advanced tumors at diagnosis, neoadjuvant chemotherapy and radiotherapy are required. Magnetic resonance imaging is one of the mainstays in the management of patients with rectal tumors, providing primary staging and re-staging after neoadjuvant therapy. In the latter context, the response to treatment is evaluated by MRI, which provides the tumor regression grade (TRG) and re-staging, fundamental factors directly related to patient survival, which is again managed according to the imaging findings.We evaluated several MRI scans of post-neoadjuvant rectal tumors, with emphasis on the adequate qualification of the TRG, and we also developed a simple sequence of questions with a mnemonic (PRO TuMor) to assist in the proper characterization of the TRG, reducing possible errors.At the end of the presentation, we selected some MRI images in a quiz format for training purposes, using PRO TuMor.

Printed on: 02/07/23

## Abstract Archives of the RSNA, 2022

GIEE-24

### Post Pancreatic Surgery Complications: Diagnostic Imaging Approach

Sunday, Nov. 27 8:00AM - 9:00AM Room: Learning Center - GI

#### Awards

Identified for RadioGraphics  
Certificate of Merit

#### Participants

Ayman H. Gaballah, MD, FRCR, Columbia, MO (*Presenter*) Nothing to Disclose

#### TEACHING POINTS

- Review indications of pancreatic surgeries
- Illustrate types of pancreatic surgeries
- Discuss complications of pancreatic surgeries and their imaging features, including pancreas transplant
- Highlight management options of these complications

#### TABLE OF CONTENTS/OUTLINE

1. Introduction a. Normal anatomy b. Indications for pancreatic surgery 2. Approaches to pancreatic surgeries: a. Endoscopic b. Minimally invasive- laparoscopic and robotic c. Open pancreatectomy 3. Types of pancreatic surgeries: a. Necrosectomy and abscess drainage b. Lateral pancreaticojejunostomy (Puestow) c. Beger procedure d. Frey procedure e. Pancreaticoduodenectomy (Whipple's procedure) f. Distal/central pancreatectomy g. Total pancreatectomy h. Pancreatic transplant surgery 4. Normal postoperative imaging findings 5. Multimodality Imaging features of post-surgical complications: a. Pancreatico-biliary complications i. Transient fluid collection ii. Biliary leaks/bilomas iii. Pseudocysts iv. Pancreatitis v. Pancreatic fistulas 1. Pancreatic-enteric fistulas 2. Pancreatic-cutaneous fistulas vi. Anastomotic stenosis vii. Infections (abscess and peritonitis) viii. Local disease recurrence b. Vascular complications i. Arterial injuries ii. Hematomas iii. Arteriovenous fistulas iv. Vascular thrombosis c. Bowel complications i. Delayed gastric emptying ii. Bowel ischemia iii. Bowel injury iv. Anastomotic leak v. Anastomotic stenosis vi. Afferent loop syndrome d. Solid-organ complications: (e.g., liver infarction, splenic injury, etc.) e. Abdominal compartment syndrome f. Pancreatic transplantation i. Rejection ii. Vascular complications Inflammation, infection, necrosis

Printed on: 02/07/23



## Abstract Archives of the RSNA, 2022

GIEE-25

### The Postoperative Pancreas

Sunday, Nov. 27 8:00AM - 9:00AM Room: Learning Center - GI

#### Participants

Ryan Clayton, MD, (*Presenter*) Nothing to Disclose

#### TEACHING POINTS

\* Review indications for various pancreatic surgeries and circumstances under which they are done.\* Understand the postoperative anatomy after common and uncommon pancreatic surgeries, as seen on radiologic studies including CT, MRI, Ultrasound, fluoroscopy and nuclear medicine.\* Be aware of the complications of the postoperative pancreas, and their imaging appearance. \* After reviewing this material, the radiologist will more easily and accurately identify normal postoperative anatomy after pancreatic surgeries (both common and uncommon), leading to improved diagnosis of potential complications and avoiding pitfalls such as misinterpreting postoperative anatomy as pathology.

#### TABLE OF CONTENTS/OUTLINE

\* Indications, anatomy and radiologic appearance of common pancreatic procedures: Whipple procedure (Classic, Pylorus-sparing), Distal pancreatectomy, Total pancreatectomy, Puestow procedure. Devices (CIVA sheet, Cystgastrostomy device).\* Complications of common pancreatic procedures and their radiologic appearance: Leaks (Anastomotic leak, Pancreatic fistula, Bile leak), Other collections (Abscess, Hematoma), Strictures (Gastrojejunal anastomotic stricture, Bile duct stricture, Pancreatic duct stricture), Delayed gastric emptying, Vascular complications (Portomesenteric venous thrombosis, Portomesenteric venous stenosis, Aneurysms and pseudoaneurysms), Tumor recurrence.

Printed on: 02/07/23



## Abstract Archives of the RSNA, 2022

GIEE-26

### Out of Place: Ectopic and Accessory Tissues

Sunday, Nov. 27 8:00AM - 9:00AM Room: Learning Center - GI

#### Awards

Certificate of Merit

#### Participants

Patricia Dantas I, MD, Sao Paulo, Brazil (*Presenter*) Nothing to Disclose

#### TEACHING POINTS

The purposes of this exhibit are:1) Review the most relevant imaging findings of ectopic and accessory tissue types, using a didactic approach by illustrations and cased-based imaging.2) Review the pathophysiology and embryology that are related to ectopic tissues, helping to understand the imaging findings in Computed Tomography (CT) and Magnetic Resonance (MR) imaging.3) Discuss the relevance of different ectopic tissue imaging presentations correlating with possible clinical complications.4) Improve knowledge about the main differential diagnoses and the main patterns of image appearance that are the key points to clarify diagnostic challenges.

#### TABLE OF CONTENTS/OUTLINE

1) Pictorial review of most frequent image findings of different ectopic and accessory tissue types.2) Cased-based review of ectopic tissue clinical presentation, frequent location, imaging findings, possible complications and differential diagnosis: pancreas, spleen, liver, gallbladder, leiomyomatosis, genitourinary system and endometriosis.3) Illustrative key points: improve understanding of the correlation between embryology and ectopic tissue imaging findings.4) Highlight the relevant imaging findings that aid surgical decisions.5) Conclusions and "take home messages": consolidate the acquired knowledge.

Printed on: 02/07/23



## Abstract Archives of the RSNA, 2022

GIEE-27

### Postoperative Complications of Hepatobiliopancreatic Surgeries: Where To Look?

Sunday, Nov. 27 8:00AM - 9:00AM Room: Learning Center - GI

#### Participants

Cristiane Costa, Sao Paulo, Brazil (*Presenter*) Nothing to Disclose

#### TEACHING POINTS

Revisit the surgical techniques involving the pancreas, liver, and bile ducts for the various pathologies that involve these organs. To review the most relevant complications of hepatobiliopancreatic surgeries and correlate with the imaging findings of computed tomography (CT), magnetic resonance imaging (MRI), and cholangiopancreatography (MRCP). Illustrate the cases of complications and demonstrate the therapeutical options.

#### TABLE OF CONTENTS/OUTLINE

Surgical techniques of hepatobiliopancreatic surgeries. Imaging protocols. Advantages and disadvantages of CT, MRI, and MRCP. Expected findings on postoperative imaging evaluation. Key sites where the radiologist should actively look for complications. Illustrate with cases the imaging findings of complications that must be described in the report. Demonstrate surgical and non-surgical treatment options.

Printed on: 02/07/23



## Abstract Archives of the RSNA, 2022

GIEE-28

### Fixing The Edges: A Critical Analysis of Rectal Carcinoma After Neoadjuvant Therapy

Sunday, Nov. 27 8:00AM - 9:00AM Room: Learning Center - GI

#### Participants

Paulo Antunes, MD, Niteroi, Brazil (*Presenter*) Nothing to Disclose

#### TEACHING POINTS

1. To recognize the MRI pitfalls in restaging rectal cancer after neoadjuvant treatment with chemotherapy and/or radiotherapy. 2. Test the limits of MRI rectal cancer re-staging emphasizing the difference between the misdiagnosis that is a limitation of the MRI and those that can be avoided thru a careful analysis by the radiologist

#### TABLE OF CONTENTS/OUTLINE

Introduction: Basic concepts of image analysis in rectal carcinoma after neoadjuvant treatment. Discussion- Correlation between MRI TRG scoring and histopathological TRG in selected cases. - Is that fibrosis or tumor cells? Follow-up results for patients eligible for watch and wait; - Mesorectal e pelvic nodes: the assessment of response comparing MRI and histopathologic or MRI follow-up; - Detecting complete clinical response after neoadjuvant therapy. Conclusion Summary with pearls and best tips of the analysis of MR rectal carcinoma after neoadjuvant treatment.

Printed on: 02/07/23



## Abstract Archives of the RSNA, 2022

GIEE-29

### Cruisin' the Lumen: Fluoroscopic Evaluation of Normal and Abnormal Gastrointestinal Tract Luminal Anatomy in the Postoperative Setting

Sunday, Nov. 27 8:00AM - 9:00AM Room: Learning Center - GI

#### Awards

Cum Laude

#### Participants

Sonia Gaur, MD, (Presenter) Nothing to Disclose

#### TEACHING POINTS

1. Fluoroscopy is a cost-effective method of postoperatively distending the esophagus, stomach, and bowel to assess for postoperative anastomotic leak and other complications. Learning fluoroscopy requires exposure to high volume of cases including those performed in the postoperative setting. 2. Identify common postoperative settings in which fluoroscopy is performed for anatomic evaluation. 3. Review normal postoperative luminal anatomy and the fluoroscopic appearance of postoperative complications. 4. Review fluoroscopic techniques that are helpful in diagnosing postoperative complications.

#### TABLE OF CONTENTS/OUTLINE

1. Introduction - commonly encountered postprocedural scenarios in the fluoroscopy suite 2. Postoperative scenarios including explanation of surgery, expected postoperative appearance, possible complications, and corresponding normal and abnormal fluoroscopic cases. Technique and important views will be emphasized for each case. Case selection includes -- a) Zenker's diverticulotomy/diverticulectomy; b) evaluation for iatrogenic esophageal perforation; c) transhiatal esophagectomy; d) hiatal hernia repair; e) bariatric surgery (gastric sleeve surgery roux-en-y gastric bypass); f) percutaneous gastrostomy evaluation and g) colorectal surgeries (low anterior resection, ileoanal J-pouch creation, ileocolonic anastomosis).

Printed on: 02/07/23



## Abstract Archives of the RSNA, 2022

GIEE-3

### Surgery or Follow-up? That is the Question: The Diagnostic Dilemma of Intraductal Papillary Mucinous Neoplasms

Sunday, Nov. 27 8:00AM - 9:00AM Room: Learning Center - GI

#### Awards

Certificate of Merit

#### Participants

Akio Tamura, MD, (*Presenter*) Nothing to Disclose

#### TEACHING POINTS

The diagnosis of intraductal papillary mucinous neoplasms (IPMNs) is complex because adherence to the clinical guidelines depends on numerous imaging features and clinician opinions. The rate of accuracy of diagnostic guidelines for the presence of advanced dysplasia or cancer is 50-80%. Therefore, a small percentage of patients will be overtreated and some patients with IPMNs with high-grade dysplasia or cancer will be overlooked. This educational exhibit explains the key diagnostic imaging aspects of IPMNs and suggests methods to solve this dilemma in real-world clinical practice.

#### TABLE OF CONTENTS/OUTLINE

1. Why do IPMNs matter? 2. Algorithm for the management of suspected IPMNs 3. Solving the imaging dilemma of IPMN 4. Pancreatic cystic disease vs. IPMN

Printed on: 02/07/23



## Abstract Archives of the RSNA, 2022

GIEE-30

### Diffuse Infiltrative Small Bowel Disease and Its Mimics

Sunday, Nov. 27 8:00AM - 9:00AM Room: Learning Center - GI

#### Awards

Identified for RadioGraphics

#### Participants

Preet Dhillon, MD, Rochester, MN (*Presenter*) Nothing to Disclose

#### TEACHING POINTS

1. Review the differential for a diffuse infiltrative small bowel disease process. 2. Present the clinical presentation and imaging findings of several diffusely infiltrative diseases within the small bowel, in order to delineate the unique features of each entity. 3. Review entities that may mimic infiltrative bowel disease on imaging.

#### TABLE OF CONTENTS/OUTLINE

The presentation will present the following disease categories and examples of infiltrative bowel disease within them. A non-exhaustive list of example cases by category is provided. 1. Infectious: Mycobacterium avium intracellulare (MAI), Whipple disease, Histoplasmosis, Coccidiomycosis 2. Inflammatory: IgA vasculitis, graft-vs-host disease, radiation enteritis 3. Neoplastic: Metastatic lobular breast carcinoma, acute myelogenous leukemia, diffuse large B-cell lymphoma, post-transplant lymphoproliferative disorder 4. Other: Amyloidosis, endometriosis, hemorrhage, lymphangiectasia Summary: An infiltrative small bowel disease will manifest as a segmental or diffuse degree of small bowel wall thickening. Although these disease processes may share many characteristics, there are key clinical and imaging attributes of each that can be examined. This education exhibit aims to present several cases demonstrating disease processes in which the small bowel is diffusely infiltrated. The unique features of each disease entity will be examined in order to best differentiate them, with additional cases presented as potential mimics.

Printed on: 02/07/23



## Abstract Archives of the RSNA, 2022

GIEE-31

### Postoperative Colon Tract: What's That Hookup and What Could Go Wrong?

Sunday, Nov. 27 8:00AM - 9:00AM Room: Learning Center - GI

#### Participants

Aman Khurana, MD, Lexington, KY (*Presenter*) Nothing to Disclose

#### TEACHING POINTS

Review indications and techniques of the common colonic surgical procedures with diagrammatic depiction. Multimodality imaging review of the normal post-surgical anatomy and associated complications with diagrammatic correlation. Summarize the appropriate imaging workup of patients suspected of postoperative gastrointestinal complications.

#### TABLE OF CONTENTS/OUTLINE

1. Review indications for colon surgeries and relevant variants that would alter surgical approach (robotic vs. other).
2. Review post-surgical anatomy of ileal-anal anastomosis, Hartmann pouch and its reversal, APR, colostomy complications and reversal, rectopexy, etc.
3. Imaging of post-operative complications such as anastomotic leaks, afferent loop syndrome, and parastomal hernias, lower abdominal resection, etc.
4. Review multimodality imaging evaluation including the role of barium studies, CT, MRI, and relevant endoscopic correlation.
5. Algorithmic approach in the setting of unknown surgical anatomy.

Printed on: 02/07/23



## Abstract Archives of the RSNA, 2022

GIEE-32

### Advanced CT Imaging Techniques for Characterization of Suspected Hepatocellular Carcinoma: Spectral CT, Low kVp Technique, Deep Learning, and Beyond

Sunday, Nov. 27 8:00AM - 9:00AM Room: Learning Center - GI

#### Participants

Amir Borhani, MD, Chicago, IL (*Presenter*) Institutional research agreement, Siemens AG

#### TEACHING POINTS

1. Advanced CT techniques and novel CT-based software are increasingly used in daily clinical practice. These new approaches can improve accuracy of CT in detection and characterization of focal liver lesions while ensuring optimized radiation dose and image quality. 2. The appropriate use of these new techniques can improve characterization of focal hepatic lesions in at-risk population.

#### TABLE OF CONTENTS/OUTLINE

Current Status of CT in Liver Imaging • Overview of techniques and protocols • Dosage and timing of iodinated contrast • Effect on detection and conspicuity of hepatic lesions • ACR LI-RADS CT technical recommendations Spectral CT: Dual-energy and Multi-energy CT • Overview of basic principles of spectral CT • Review of current acquisition techniques • Advantages of spectral CT for LI-RADS classification • Suggested protocols and workflow Low kVp CT • Overview of physical principles of mass attenuation coefficient • Advantages and disadvantages of low kVp CT imaging • Added value of low kVp CT technique for LI-RADS classification Deep Learning (DL) Techniques • Background • Novel DL-based noise reduction and image reconstruction techniques • Role in detection and characterization of focal hepatic lesions • Computer-assisted detection (CAD) Novel Post-Processing Techniques • Background • Image subtraction • Value in assessment of focal hepatic lesions and classification

Printed on: 02/07/23



## Abstract Archives of the RSNA, 2022

GIEE-33

### **Congestive Hepatopathy: Pathophysiology, Workup, and Typical and Atypical Imaging Findings with Pathological Correlation**

Sunday, Nov. 27 8:00AM - 9:00AM Room: Learning Center - GI

#### **Participants**

Marta Flory, MD, Redwood City, CA (*Presenter*) Nothing to Disclose

#### **TEACHING POINTS**

Understand the pathophysiology of congestive hepatopathy and its effects on the liver parenchyma Recognize the imaging findings of congestive hepatopathy Know the benign and malignant lesions that develop in congested livers and how to use imaging features and techniques to distinguish them

#### **TABLE OF CONTENTS/OUTLINE**

1. Liver vascular anatomy and sinusoidal architecture2. Pathophysiology of congestive hepatopathy3. Etiologies of congestive hepatopathy4. Imaging findings of congestive hepatopathy a. Diffuse liver abnormalities b. Focal lesions associated with congestive hepatopathy5. Challenges and pitfalls in imaging of congestive hepatopathy a. Assessment of hepatic fibrosis b. Differentiation of benign hypervascular lesions from hepatocellular carcinoma c. Proposed algorithm for workup of focal hepatic lesions in setting of congestive hepatopathy?

Printed on: 02/07/23



## Abstract Archives of the RSNA, 2022

GIEE-34

### Upset Stomach: CT and Fluoroscopic Imaging of the Stomach after Surgery, Endoscopic Interventions, and Unusual Devices

Sunday, Nov. 27 8:00AM - 9:00AM Room: Learning Center - GI

#### Awards

Identified for RadioGraphics

#### Participants

Preethi Raghu, MD, San Francisco, CA (*Presenter*) Nothing to Disclose

#### TEACHING POINTS

1) Review normal postsurgical CT and fluoroscopic imaging appearance after gastric surgical interventions for weight loss, reflux management, and gastroparesis treatment. 2) Discuss normal postprocedural CT and fluoroscopic imaging appearance after endoscopic sleeve gastropasty, transoral incisionless fundoplication (TIF), gastric peroral endoscopic myotomy (G-POEM), and other specialized endoscopic procedures. 3) Recognize the normal CT and fluoroscopic appearance of various gastric devices, including those used for weight loss, reflux management, and pancreatitis. 4) Understand the CT and fluoroscopic imaging appearance of the complications associated with these gastric surgeries, procedures, and devices.

#### TABLE OF CONTENTS/OUTLINE

1) Postsurgical Stomach: a) Roux-en-Y gastric bypass b) Laparoscopic sleeve gastrectomy c) Laparoscopic banding d) Nissen/complete fundoplication e) Toupet/partial fundoplication f) Gastric pacemaker placement. 2) Postprocedural Stomach: a) Endoscopic sleeve gastropasty b) Transoral incisionless fundoplication (TIF) c) Transgastric Rendezvous technique d) Endoscopic Ultrasound Directed Transgastric ERCP (EDGE) e) Gastric Peroral Endoscopic Myotomy (G-POEM). 3) Unusual Devices: a) LINX Reflux Management System b) Intra-gastric balloon c) AspireAssist Device d) Axios stent and drainage e) Metallic gastric stent for cancer

Printed on: 02/07/23



## Abstract Archives of the RSNA, 2022

GIEE-35

### Choices, Choices, Choices: What Your Multidisciplinary HCC Treatment Team Wants to Know?

Sunday, Nov. 27 8:00AM - 9:00AM Room: Learning Center - GI

#### Participants

Omar Kamal, MD, MSc, Portland, OR (*Presenter*) Nothing to Disclose

#### TEACHING POINTS

1. Different treatment options exist for hepatocellular carcinoma (HCC) including surgical, locoregional and systemic therapies. Appropriate choice of therapy is crucial to improve clinical outcomes. 2. HCC treatment guidelines incorporate different clinical and imaging variables to guide treatment options. 3. Radiologists need to be familiar with how imaging findings can change treatment planning for HCC and what is the crucial information that the multidisciplinary liver team (MDLT) wants to know.

#### TABLE OF CONTENTS/OUTLINE

1. Brief overview of HCC management: a. Surveillance. b. Overview of HCC staging and treatment options. i. Describe various treatment options. ii. Status of stereotactic body radiation therapy (SBRT). iii. Goals of noncurative treatments. c. HCC imaging features and role of biopsy in diagnosis and management. 2. Tumor burden and treatment considerations: a. Single vs. Multipleb. Size. c. Location in relation to other structures. 3. Liver status and treatment considerations: a. Background liver disease. b. Liver volume. c. Signs and symptoms of Portal hypertension. d. Portal vein thrombosis. e. Arterial anatomy. f. Metastasis. g. Liver transplant candidacy. h. Performance status. 4. Treatment response: a. Size vs. viability. b. LI-RADS treatment response criteria. c. Specific challenges for TARE and SBRT. 5. Common questions for radiologists during MDLTs.

Printed on: 02/07/23



## Abstract Archives of the RSNA, 2022

GIEE-36

### Peritumoral Area of Focal Liver Lesions: Imaging-pathological Correlation and Clinical Significance

Sunday, Nov. 27 8:00AM - 9:00AM Room: Learning Center - GI

#### Awards

Certificate of Merit

#### Participants

Kumi Ozaki, MD, PhD, Fukui, Japan (*Presenter*) Nothing to Disclose

#### TEACHING POINTS

Peritumoral area of focal liver lesions is the liver parenchyma adjacent to focal hepatic lesions, which is often altered due to compression of the tumors, drainage of blood flow of the lesion, vascular or bile duct invasion as well as due to malignant infiltration in some cases. These histological findings are plainly reflected in the imaging findings. In some tumors, the imaging findings of peritumoral area could be helpful for an accurate diagnosis and could be biomarkers of malignant grades or prognosis. The radiologist should pay attention to not only the tumor itself but also peritumoral area.

#### TABLE OF CONTENTS/OUTLINE

1. Introduction. 2. The definition of "peritumoral area," and several imaging findings of peritumoral area. 3. Imaging-pathological correlation of peritumoral area of each lesion as follows; peritumoral arterial enhancement (corona enhancement) of hepatocellular carcinoma, peritumoral hyper- or hypointensity on hepatobiliary phase of hepatocellular carcinoma, peritumoral arterial enhancement and peritumoral hypointensity on hepatobiliary phase of colorectal liver metastases, peritumoral hyperintensity on hepatobiliary phase of liver metastases from neuroendocrine tumor, and peritumoral arterial enhancement (arteriportal shunt) of cavernous hemangioma. 4. Non-existence of peritumoral changes of simple cysts or focal nodular hyperplasia 5. Clinical significance of peritumoral area of each lesions such as microvascular invasion, prognosis, the effect of chemotherapy, and the influence on the results of radiomics analyses. 6. Summary of the clinical significance of peritumoral area of focal liver lesions. 7. Conclusion.

Printed on: 02/07/23

## Abstract Archives of the RSNA, 2022

GIEE-37

### Why Do Mucin-producing Cystic Neoplasms of the Liver Confuse Us?: Top Tips To Get the Right Diagnosis

Sunday, Nov. 27 8:00AM - 9:00AM Room: Learning Center - GI

#### Awards

Certificate of Merit

#### Participants

Sofia Santos, MD, Lisbon, Portugal (*Presenter*) Nothing to Disclose

#### TEACHING POINTS

This exhibit intends to: (1) To clarify and to compare the old and the new nomenclature of mucin-producing cystic neoplasms of the liver. (2) To summarize the characteristic features of hepatic mucinous cystic neoplasms (MCN) and intraductal papillary neoplasms of the bile duct (IPNB). (3) To highlight the key differences between MCN and IPNB and to present the main differential diagnoses. (4) To understand the impact of an adequate differential diagnosis. The main teaching points are: Mucinous cystic neoplasms of the liver are rare neoplasms that include hepatic mucinous cystic neoplasms (MCN), previously known as cystadenoma and cystadenocarcinoma, and intraductal papillary neoplasms of the bile duct (IPNB). The keys for distinguishing MCN and IPNB are based on the presence of bile ductal communication (only in the case of IPNB) and the presence of sub-epithelial ovarian stroma (only in the case of MCN). The differential diagnosis encompasses non-neoplastic cystic lesions and cystic metastases. The five top tips to the radiologist are: (1) to look for ductal communication, (2) to assess for bile duct dilation, (3) to look for thickened enhancing septa, mural solid nodules and calcifications, (4) to take into account location and number of lesion(s), and (5) to review the clinical data (namely primary extra-hepatic malignancy).

#### TABLE OF CONTENTS/OUTLINE

- Mucin-producing cystic neoplasms of the liver: the old and the new nomenclature- Hepatic mucinous cystic neoplasms (MCN) and intraductal papillary neoplasms of the bile duct (IPNB): epidemiologic, clinical, histological, and imaging features- MCN versus IPNB: top tips to the radiologist- Therapeutic insights- Diagnostic flowchart

Printed on: 02/07/23

## Abstract Archives of the RSNA, 2022

GIEE-38

### **Imaging Assessment after Partial Hepatectomies: Surgical Technique and Type of Parenchymal Transection Performed: Normal Findings and Complications**

Sunday, Nov. 27 8:00AM - 9:00AM Room: Learning Center - GI

#### **Participants**

Juan C. Spina JR, MD, (*Presenter*) Nothing to Disclose

#### **TEACHING POINTS**

1- In the last two decades there has been an increase in the number of hepatic surgeries performed, together with an improvement in surgical techniques and new dissection devices. 2- Radiologists play a key role in the process of surgical planning and post surgical evaluation. Knowledge of types of resection is important to interpret postsurgical liver appearance. 3- In the acute post surgical period, imaging helps to identify complications and contributes to define treatment.

#### **TABLE OF CONTENTS/OUTLINE**

1) Introduction. 2) Type of hepatectomies and technique- left hepatectomy, right hepatectomy, trisegmentectomy, segmentectomy, atypical segmentectomy, alpps, mini alpps.- liver hanging maneuver- Pringle Maneuver- liver transection methods: clamp crushing, electric scalpel, CUSA, water jet, tissue link. When and why?. 3)- Imaging findings after hepatectomies.- Normal findings: fluid collection, hypodense line, hepatic perfusion abnormalities, air bubbles, omentum adipose tissue, extraluminal gas.- Pathologic findings: biloma, hematoma, abscess, pulmonary complications. Tips for the correct diagnosis and differentiation. Example cases and evaluation test. Conclusion

Printed on: 02/07/23



## Abstract Archives of the RSNA, 2022

GIEE-39

### Liver MR Elastography: A Case-based Approach on Quality Control and Main Technical Failures

Sunday, Nov. 27 8:00AM - 9:00AM Room: Learning Center - GI

#### Participants

Marcelo Mota, (*Presenter*) Nothing to Disclose

#### TEACHING POINTS

- Review the basic principles of elastography, focusing on the liver
- Summarize the liver magnetic resonance elastography technique
- Describe the steps in the evaluation and quality control of elastography images
- Recognize the main causes of low-quality and nondiagnostic elastograms
- Illustrate with didactic cases some technical failures of liver MR elastography and how to potentially correct them

#### TABLE OF CONTENTS/OUTLINE

? INTRODUCTION - Important concepts - Basic principles of elastography ? LIVER MR ELASTOGRAPHY TECHNIQUE - Typical liver MR elastography configuration - Raw data and post-processed images ? IMAGES QUALITY CONTROL - How to evaluate elastography images and ensure their quality ? LOW-QUALITY AND NONDIAGNOSTIC ELASTOGRAMS - Main causes of technical failures during the liver MR elastography ? INTERACTIVE CASE-BASED DIDACTICS - Sample cases to illustrate and solidify the concepts - How to potentially correct low-quality and nondiagnostic elastograms ? TAKE HOME MESSAGES

Printed on: 02/07/23



## Abstract Archives of the RSNA, 2022

GIEE-4

### Postoperative Complications of Hepatobiliary Surgery: An Imaging Review

Sunday, Nov. 27 8:00AM - 9:00AM Room: Learning Center - GI

#### Awards

Certificate of Merit

#### Participants

John Kirby, MD, Rochester, MN (*Presenter*) Nothing to Disclose

#### TEACHING POINTS

- Review normal liver segmentation, vascular, biliary anatomy, and variants
- Recognize the normal appearance of the postoperative liver
- Recognize early complications such as abscess, parenchymal necrosis, and bile leak
- Describe pertinent vascular findings such as active bleeding, pseudoaneurysm, stenoses, and thrombosis
- Understand the post ablation appearance of the liver and potential complications
- Many of our cases will contain a QR code that will allow the reader to open a fully functional PACS interface on their mobile device

#### TABLE OF CONTENTS/OUTLINE

- Background: Liver surgery is a common procedure and complication rates can be as high as 50%. With the high-risk nature, radiologists can play an important role in the early detection and management of potential complications.
- Review normal hepatic anatomy including the conventional segmental divisions, vasculature, and biliary system.
- Terminology including wedge resections, segmentectomy, and hepatectomy to assist the radiologist in reviewing operative reports and accurately describing imaging findings.
- Normal/expected post operative appearances
- Case based examples illustrated utilizing multiple modalities to demonstrate common complications that radiologists may encounter:
  - o CT and MR examples of early complications requiring hospital admission
  - o Vascular and biliary complications and interventions
  - o Utility of nuclear medicine studies
  - o Evaluation of long-term complications.
  - o Post ablation appearance and potential complications.

Printed on: 02/07/23

## Abstract Archives of the RSNA, 2022

GIEE-40

### Colitis in Cancer: Going Beyond Immune Checkpoint Inhibitors: Diagnosis, Monitoring and Management

Sunday, Nov. 27 8:00AM - 9:00AM Room: Learning Center - GI

#### Participants

Kaustav Bera, MD, Cleveland, OH (*Presenter*) Nothing to Disclose

#### TEACHING POINTS

1. To review cancer drugs that are primarily responsible for causing colitis 2. Review the different etiologies of colitis and imaging findings that help differentiate them from cancer-therapy associated colitis 3. To discuss the CT imaging patterns of colitis of different etiologies 4. To discuss the crucial role of the radiologist in monitoring/management of treatment-related colitis. 5. Review established grading and management guidelines for treatment related colitis

#### TABLE OF CONTENTS/OUTLINE

1. Discuss common anti-neoplastic agents that cause colitis 2. Enumerate etiologies of colitis, along with their typical imaging findingsi) Immune checkpoint inhibitor associated colitisii) Drug-induced colitisiii) Infectious colitis -a. Neutropenic colitisb. Pseudomembranous colitisiv) Radiation induced colitis v) Inflammatory - Ulcerative colitis/Crohn disease vi) Ischemic colitis 3. Discuss clinical findings, history and risk factors for developing colitis 4. Discuss mimics of colitis a. Diverticulitis b. Appendicitis c. Epiploic appendagitis 5. Discuss presenting clinical symptoms and grading system for drug-induced colitis6. Management guidelines for drug-induced colitis with special focus on checkpoint inhibitors (ICI), targeted therapy, Car-T cell therapy 7. How a Radiologist plays an important role in monitoring and management 8. Prognosis and clinical outcome of patients developing drug-induced colitis 9. Real-world cases showing management and clinical course of drug-induced colitis in cancer therapies from to combination ICI and CAR-T cells as well as additional causes of colitis in cancer patients

Printed on: 02/07/23



## Abstract Archives of the RSNA, 2022

GIEE-41

### Fundamentals of Response Evaluation for Abdominal Tumors

Sunday, Nov. 27 8:00AM - 9:00AM Room: Learning Center - GI

#### Participants

Marcelo Cortes, MD, Petropolis, Brazil (*Presenter*) Nothing to Disclose

#### TEACHING POINTS

? Overview of the application of tumor response criteria and quantitative imaging and its benefits for clinical trials and novel oncology therapeutics. ? The role of radiologists in the standardization of tumor evaluation for clinical trials. ? Basics on response assessment and quantitative analysis of the most prevalent abdominopelvic tumors. ? Updates in imaging management and surveillance strategies for abdominal tumors. ? The role of imaging and genetic/molecular evaluation

#### TABLE OF CONTENTS/OUTLINE

Based on extensive imaging experience from a leading cancer center: ? A brief review of abdominopelvic tumors, highlighting the clinical and laboratory features that can be helpful in diagnosis and management. ? Review of the main criteria for clinical trials and clinical decision support employed to evaluate abdominopelvic tumors, for instance, RECIST 1.1, irRECIST, iRECIST, irRC, Lugano, Cheson, EASL, imRECIST, itRECIST, PERCIST, RECIL, and Choi. ? Tumor metrics criteria evaluation for abdominal tumors response compared to radiomics and imaging genomics role. ? Evaluation of immunotherapy: main concepts and practical application of tumor response evaluation. ? Interactive imaging-based approach with teaching points for response evaluation, work-up and recurrence of abdominopelvic tumors, challenges of immunotherapy evaluation, and equivocal cases on anatomic (CT/MRI) and functional (PET/CT and PET MRI) cross-sectional imaging. ? Current guidelines. ? Limitations of current imaging methods and new directions. ? Take-home messages.

Printed on: 02/07/23



## Abstract Archives of the RSNA, 2022

GIEE-42

### Typical and Atypical Findings in Cirrhotic Liver: Pearls and Pitfalls for Diagnosis of Benign and Malignant Lesions

Sunday, Nov. 27 8:00AM - 9:00AM Room: Learning Center - GI

#### Participants

Xiaoyang Liu, MD, PhD, (Presenter) Nothing to Disclose

#### TEACHING POINTS

1. Case-based review on imaging pitfalls and pearls of focal liver lesions in cirrhosis. 2. The distortion of normal liver parenchyma by fibrous and regenerative tissue can change the typical appearance of many benign lesions, causing misdiagnosis as malignancy. 3. As the most common primary malignancy arising from cirrhotic liver, hepatocellular carcinomas (HCC) can have atypical imaging appearance. 4. Contrast enhanced ultrasound (CEUS) can provide characterization of focal liver lesions in addition to CT and MRI to achieve accurate diagnosis.

#### TABLE OF CONTENTS/OUTLINE

Technical pitfalls in cirrhotic liver imaging: 1) HCC may be nearly isointense to background liver on heavily T2 weighted MR images. 2) CT and MRI can miss early enhancement pattern of HCC due to mistiming. 3) Replacement of liver parenchyma by fibrous and regenerative tissue in cirrhosis can lead to decreased penetration by ultrasound. Benign lesions mimicking malignancy: 1) Regenerative nodules. 2) Siderotic nodules. 3) Confluent fibrosis. 4) Hemangioma with pseudo washout. Atypical appearance of HCC 1) Hypovascular. 2) Cystic. 3) Fat containing HCC. 4) Nodule in nodule HCC. Other malignancies mimicking HCC 1) Intrahepatic cholangiocarcinoma. 2) Metastases. CEUS providing added value to CT and MRI, for differentiation of benign versus malignant lesions 1) HCC washout not shown on CT or MRI, but demonstrated by CEUS, due to the purely intravascular nature. 2) More sensitive detection of arterial hyperenhancement, due to its real-time nature.

Printed on: 02/07/23



## Abstract Archives of the RSNA, 2022

GIEE-43

### 2022 Update of the Barcelona Clinic Liver Cancer Recommendations: What the Radiologist Needs to Know

Sunday, Nov. 27 8:00AM - 9:00AM Room: Learning Center - GI

#### Awards

Certificate of Merit

#### Participants

Vikrant Khare, MD, (*Presenter*) Nothing to Disclose

#### TEACHING POINTS

Teaching Points Although many hepatocellular carcinoma staging systems exist, the Barcelona Clinic Liver Cancer (BCLC) staging system is the most widely validated system which provides guidelines for therapy based on tumor stage and underlying liver function. Following the BCLC treatment guidelines has survival benefits for HCC patients, and the 2022 expanded upon its previous iteration for a more personalized and individualized approach, taking into consideration local technical and expertise availability in conjunction with the tumor profile. Knowledge of the imaging findings for each BCLC stage and understanding the updated treatment recommendations for each stage are required to ensure appropriate clinical decisions and management for each patient. This exhibit aims to highlight the imaging appearance of HCC for various BCLC stages while highlighting the key differences in the 2022 version.

#### TABLE OF CONTENTS/OUTLINE

Outline  
Brief background on HCC and the BCLC staging system  
Highlight key updates of the BCLC 2022 staging system  
Case based review illustrating the key imaging features of each stage  
BCLC-0, very early stage  
BCLC-A, early stage  
BCLC-B, intermediate stage  
BCLC-C, advanced stage  
BCLC-D, terminal stage  
Case-based review highlighting the various treatment options recommended by the updated BCLC system for each stage, with an emphasis on locoregional interventional treatments

Printed on: 02/07/23



## Abstract Archives of the RSNA, 2022

GIEE-44

### Imaging Findings of Early Gastrointestinal and Hepatobiliary Cancers: Pitfalls and Pearls

Sunday, Nov. 27 8:00AM - 9:00AM Room: Learning Center - GI

#### Awards

Certificate of Merit

#### Participants

Alecio Lombardi, MD, San Diego, CA (*Presenter*) Nothing to Disclose

#### TEACHING POINTS

Describe the imaging modalities of choice for the detection of early gastrointestinal and hepatobiliary cancers; Understand MRI technique and protocols, common challenges, and how to overcome them; Highlight imaging pearls and pitfalls for the characterization of early lesions on each modality; Underscore imaging characteristics that help in the differential diagnosis; Recognize key anatomical landmarks for surgical planning; Know what to include in the radiology report; Discuss future directions in the image analysis of early gastrointestinal and hepatobiliary cancers.

#### TABLE OF CONTENTS/OUTLINE

INTRODUCTION: General overview and definitions; Common gastrointestinal and hepatobiliary cancers. IMAGING TECHNIQUE: Modalities of choice; Sensitivity, specificity, and accuracy across methods; Protocols; Difficulties and how to overcome them to obtain high-quality images. IMAGING INTERPRETATION: Structured imaging analysis; Pitfalls and pearls; Anatomic Landmarks: What the Surgeon wants to know?; What should be included in the radiology report. STRATEGIES TO OVERCOME THE CHALLENGING CASES: Imaging characteristics that help in the differential diagnosis; WHAT'S ON THE HORIZON TO ASSESS EARLY GASTROINTESTINAL AND HEPATOBILIARY CANCER: Dual-energy CT; Digital Subtraction Angiography; DWI; Radiomics; Artificial Intelligence applied to image acquisition, reconstruction; Quantitative Imaging Analysis; PET/MRI; New nuclear medicine radionuclides; Nanoparticles.

Printed on: 02/07/23



## Abstract Archives of the RSNA, 2022

GIEE-45

### Renal Transplant Complications From A-Z: A Multimodality Case Based Review

Sunday, Nov. 27 8:00AM - 9:00AM Room: Learning Center - GI

#### Participants

Meghan Stanton, MD, Syracuse, NY (*Presenter*) Nothing to Disclose

#### TEACHING POINTS

- The kidney is the most commonly transplanted solid organ and therefore it is imperative that the radiologist be familiar with the surgical procedure, as well as the post operative complications.
- Understanding the general timeline of specific complications in order to narrow the differential of imaging findings.
- Recognize the imaging findings of the most common and the rare postoperative complications related to renal transplantation.

#### TABLE OF CONTENTS/OUTLINE

- Review of the renal transplant surgical procedure and normal post-operative anatomy
- Imaging modalities used to assess the allograft
- Complication timeline
- Perinephric fluid collections
- Vascular complications
- Collecting system complications
- Parenchymal abnormalities
- Abdominopelvic complications
- Conclusion

Printed on: 02/07/23



## Abstract Archives of the RSNA, 2022

GIEE-46

### Mimickers of Pancreatic Cancer: Lessons Learned

Sunday, Nov. 27 8:00AM - 9:00AM Room: Learning Center - GI

#### Awards

Identified for RadioGraphics  
Magna Cum Laude

#### Participants

Camila Vendrami, MD, Chicago, IL (*Presenter*) Nothing to Disclose

#### TEACHING POINTS

· Review of characteristic and atypical pancreatic ductal adenocarcinoma imaging and clinical findings · Review of imaging and clinical features that allow differentiation between pancreatic ductal adenocarcinoma and its mimickers

#### TABLE OF CONTENTS/OUTLINE

Pancreatic ductal adenocarcinoma is the most common primary tumor of the pancreas. Several pancreatic conditions can mimic the appearance of pancreatic ductal adenocarcinoma, including inflammatory conditions, uncommon primary pancreatic tumors, and metastases to the pancreas. Imaging differentiation between these lesions and pancreatic ductal adenocarcinoma can be difficult because of overlapping features; however, knowledge of their typical imaging characteristics and clinical presentation may assist in their differentiation. 1. Introduction 2. What key imaging and clinical features of pancreatic ductal adenocarcinoma suggest this diagnosis and what are the atypical findings? 3. What clinical and imaging features differentiate mimickers (acute and chronic pancreatitis, groove pancreatitis, autoimmune pancreatitis, high-grade neuroendocrine tumors, metastases, other less common benign and malignant tumors) from pancreatic ductal adenocarcinoma? 4. Take home points

Printed on: 02/07/23



## Abstract Archives of the RSNA, 2022

GIEE-47

### Liver MR Elastography: Practical Guidance for Interpretation and Reporting

Sunday, Nov. 27 8:00AM - 9:00AM Room: Learning Center - GI

#### Awards

**Magna Cum Laude**

#### Participants

Guilherme M. Cunha, MD, Seattle, WA (*Presenter*) Nothing to Disclose

#### TEACHING POINTS

1) Review principles of MR elastography (MRE) for noninvasive assessment of liver fibrosis. 2) Summarize the literature on diagnostic accuracy of MRE in different liver disease etiologies. 3) Review pitfalls and confounders. 4) Provide guidance on liver MRE reporting and interpretation. 5) Discuss future directions.

#### TABLE OF CONTENTS/OUTLINE

1) Introduction: Stiffness as a biomarker of liver fibrosis and clinical significance. 2) Basic principles of MRE. 3) Clinical application detection and staging of liver fibrosis, liver stiffness and histology fibrosis stages, contexts of use and populations. 4) Diagnostic performance: overview of meta-analyses, MRE sequence, disease-specific MRE-determined liver stiffness thresholds. 5) Pitfalls and confounders a. Technical: improper hardware setup, left lobe vs right lobe, wave frequency dependencies, region of interest (ROI) placement. b. Biological: steatosis, iron overload, inflammation, cholestasis and venous congestion, expiration vs inspiration, fasting vs postprandial state. 6) Image interpretation Image analysis and interpretation (wave and elastograms), ROI approaches, stiffness thresholds and disease-specific interpretation. 7) Reporting: what to report, how to report it, QIBA recommendations. 8) Future directions: new contexts of use and applications, technical innovations.

Printed on: 02/07/23

## Abstract Archives of the RSNA, 2022

GIEE-48

### A Beginners Guide to Liver Iron Quantification: What a Radiology Resident Ought to Know

Sunday, Nov. 27 8:00AM - 9:00AM Room: Learning Center - GI

#### Participants

Archit Dikshit, MBBS, (Presenter) Nothing to Disclose

#### TEACHING POINTS

(1) Iron overload could be due to primary hemochromatosis (hereditary) or secondary hemochromatosis (acquired by blood transfusions) and can cause serious complications including liver cirrhosis and heart failure. (2) MRI based iron quantification is increasingly being preferred to biopsy which is invasive, and not representative in inhomogenous distribution and serum ferritin which can be inaccurate in inflammatory states. (3) MRI based liver iron quantification is the recommended technique for estimating liver iron concentration in patients with increased serum Ferritin levels and assessing its trend in patients with repeated blood transfusions. (4) Superparamagnetic property of iron is the basis of quantification by MRI as it creates magnetic field inhomogeneity (estimated by QSM), which leads to signal drop of liver (measured by SIR method) and shortening of T2 and T2\* times (measured by relaxometry). (5) The choice of method of iron quantification is made according to the availability of resources, and level of iron overload. (6) In cases with very high iron overload, R2\* based relaxometry mapping gives error and use of signal intensity ratio method is preferred.

#### TABLE OF CONTENTS/OUTLINE

(1) Iron metabolism (2) Iron Overload and its clinical implications (3) Monitoring of Iron Overload (4) Clinical Indication for liver iron quantification (5) Principle of MRI based Iron Quantification (a) Principles (b) Relaxometry: T2 and T2\* (c) Signal Intensity Ratio (SIR) Method (d) Quantum Susceptibility Mapping (QSM) Method (6) Merits and Demerits of MRI based Iron Quantification methods in practical usage (a) T2 Relaxometry (b) T2\* Relaxometry (c) SIR (d) QSM (7) How to practically use different tools and methods

Printed on: 02/07/23

## Abstract Archives of the RSNA, 2022

GIEE-49

### Ultrasound of the Abdominal Wall: Pearls and Pitfalls

Sunday, Nov. 27 8:00AM - 9:00AM Room: Learning Center - GI

#### Participants

Christian Burgos-Sanchez, MD, (*Presenter*) Nothing to Disclose

#### TEACHING POINTS

-Recognize normal anatomy of the abdominal wall-Know and identify the types of hernias that occur in the abdominal wall-Identify normal and pathologic conditions that may clinically mimic hernias

#### TABLE OF CONTENTS/OUTLINE

1. Introductiona. Hernia general terms and definitionsb. Hernia ultrasound protocolc. Normal abdominal wall anatomy2. Abdominal wall hernia casesa. Umbilical herniab. Indirect inguinal herniac. Direct inguinal herniad. Spigelian herniae. Lumbar herniaf. Incisional hernia3. Abdominal wall pathology mimicking herniaa. Lipomab. Cellulitisc. Post op fat necrosisd. Rectus sheath hematomae. Endometrioma in C-section scarf. Lung cancer metastasis4. Inguinal pathology mimicking herniaa. Metastatic lymph nodeb. Hydrocelec. Rhabdomyosarcomad. Spermatic cord lipomae. Encysted hydrocelef. Undescended testicle5. Vascular pathology mimicking herniaa. Varicose veinsb. Pseudoaneurysmc. Thrombosed veins6. Conclusion and summary

Printed on: 02/07/23



## Abstract Archives of the RSNA, 2022

GIEE-5

### The Portal Vein: A Comprehensive Review

Sunday, Nov. 27 8:00AM - 9:00AM Room: Learning Center - GI

#### Awards

Identified for RadioGraphics

#### Participants

Ben Layton, BMBS, FRCR, Blackburn, United Kingdom (*Presenter*) Nothing to Disclose

#### TEACHING POINTS

Combining radiological case examples with succinct explanation and illustrations this exhibit will provide a comprehensive summary of the portal vein (PV). This will:

- Guide the radiologist in successful description of PV anatomy and branching patterns leading to optimal surgical approach.
- Teach recognition and correct interpretation of rare topographic portal vein variations such as circumportal pancreas and preduodenal PV.
- Provide an understanding of the appearances, associations and complications of PV shunts including congenital (E.g., Abernethy malformations, hereditary hemorrhagic telangiectasia) and acquired shunts (E.g., cirrhosis, traumatic).
- Examine all pathology of the PV, including tips to differentiate between bland and tumour thrombus and explain sequelae with case examples (E.g., cavernous transformation, THAD/hepatic artery buffer response and portal biliopathy)
- Deliver an overview of the newly described disease entity "porto-sinusoidal vascular disorder" clarifying the nomenclature associated with it and distinguishing it from cirrhosis and non-cirrhotic portal hypertension

#### TABLE OF CONTENTS/OUTLINE

Portal vein anatomy: branching pattern variations and extrahepatic topography  
Malformations of the portal vein: associations and sequelae  
Disease processes affecting the portal vein  
Portal vein intervention  
Summary and recommendations

Printed on: 02/07/23



## Abstract Archives of the RSNA, 2022

GIEE-50

### Beyond the Images: A Simplified Approach for Rectal Cancer Mimics and Variants

Sunday, Nov. 27 8:00AM - 9:00AM Room: Learning Center - GI

#### Participants

Katherine Wei, MD, Orange, CA (*Presenter*) Nothing to Disclose

#### TEACHING POINTS

This exhibit aims to provide an overview of the different benign and neoplastic mimickers of rectal cancer that can be encountered and provide an evidence-based framework for how to approach the differential diagnoses for rectal masses.

#### TABLE OF CONTENTS/OUTLINE

Different categories of rectal masses/rectal cancer mimickers to be discussed include: -Large rectal masses: In addition to advanced stage or poorly differentiated adenocarcinoma, high grade neoplasms such as poorly differentiated squamous cell carcinoma, high-grade neuroendocrine tumor, adenosquamous carcinoma, or lymphoma may be considered. If the tumor is eccentrically located, non-epithelial/mesenchymal tumors such as gastrointestinal stromal tumor or tumor of adjacent organ origin should be in the differential. -Anorectal junction masses of unknown histology: These lesions present a dilemma, as staging and treatment of anal cancer differ from rectal adenocarcinoma. -Precancerous/early-stage rectal cancer: These lesions have differing morphological and enhancement patterns compared to more locally advanced disease. -Benign rectal masses: Differentials include vascular malformations/hemangiomas, solitary rectal ulcer syndrome, and endometriosis implants. -Metastasis, including direct invasion of adjacent organs and commonly confused non-rectal cancer origin metastasis.

Printed on: 02/07/23

## Abstract Archives of the RSNA, 2022

GIEE-51

### **Beyond Infectious, Inflammatory, or Ischemic" Morphologic Approach to Bowel Wall Thickening**

Sunday, Nov. 27 8:00AM - 9:00AM Room: Learning Center - GI

#### **Participants**

Nabih Nakrour, MD, Boston, MA (*Presenter*) Nothing to Disclose

#### **TEACHING POINTS**

The purpose of this exhibit is to: Identify imaging patterns of wall thickening in the stomach, small bowel, and colon. Discuss the differential diagnosis of bowel wall thickening based on imaging characteristics, morphology, distribution, secondary signs, and clinical presentation. Present correlative endoscopic gross images when available.

#### **TABLE OF CONTENTS/OUTLINE**

The presentation will include Anatomic layers of the bowel wall. Pathophysiology of bowel wall thickening including wall layers involvement with edema, hemorrhage, inflammatory and neoplastic cells, fatty deposits, and fibrotic replacement. Differential diagnosis, example cases, and concurrent endoscopic images of gastric wall thickening are classified into diffuse, segmental, focal, and multifocal wall thickening. Differential diagnosis, example cases, and concurrent capsule endoscopic images of bowel wall thickening are classified into diffuse, segmental, and nodular fold thickening. Differential diagnosis, example cases, and concurrent colonoscopy images of bowel wall thickening are classified into diffuse, segmental, and nodular fold thickening. Address secondary signs favoring one diagnosis over others.

Printed on: 02/07/23



## Abstract Archives of the RSNA, 2022

GIEE-52

### Periampullary Disorders: Running Away From the Obvious - A Pictorial Essay of Periampullary Lesions

Sunday, Nov. 27 8:00AM - 9:00AM Room: Learning Center - GI

#### Awards

Certificate of Merit

#### Participants

Ulysses Torres, MD, PhD, Sao Paulo, Brazil (*Presenter*) Nothing to Disclose

#### TEACHING POINTS

- To review the general anatomy of the ampullary region and its variants with schematic drawings correlated with CT and MRI.
- Expose the possible periampullary disorders categorized into four large groups (anatomical variations, tumoral, inflammatory, and miscellaneous). To unravel the main differential diagnoses of periampullary involvement with didactic cases, literature review, and main imaging aspects.

#### TABLE OF CONTENTS/OUTLINE

Diagram and educational schematic drawings for diagnostic of the ampullary and periampullary lesions, dividing them as:- Anatomical variations: including cases of pancreas divisum, annular pancreas, and independent drainage of the common bile duct and pancreatic duct. - Tumoral disorders: including cases of a duodenum GIST, a papilla tumor, and a Frantz Tumor - Inflammatory disorders: such as paraduodenal pancreatitis, bulging duodenal papilla, and HIV papillitis. - Miscellaneous disorders: presenting other kinds of periampullary involvement, including a case of collateral circulation mimicking a neoplastic pathology, ischemic cholangiopathy, and intradiverticular papilla.

Printed on: 02/07/23



## Abstract Archives of the RSNA, 2022

GIEE-53

### Body MRI Pulse Sequences: An Atlas and User Guide

Sunday, Nov. 27 8:00AM - 9:00AM Room: Learning Center - GI

#### Awards

Identified for RadioGraphics  
Certificate of Merit

#### Participants

Anup Shetty, MD, Saint Louis, MO (*Presenter*) Nothing to Disclose

#### TEACHING POINTS

Body MRI protocols can be daunting for the new trainee or novice reader, with a multitude of pulse sequences and a wide variety of acronyms. Understanding of basic MRI physics provides a framework for how to optimally use these sequences in clinical practice. Knowledge of the sequences as building blocks also informs efficient protocol design. This exhibit will: 1) Highlight basic MRI physics principles that underpin core body MRI sequences 2) Provide a framework of the families of sequences used in body MRI protocols, including individual vendors sequence names and key parameters 3) Illustrate technical considerations and clinical utility of each sequence through case examples 4) Describe how to build efficient protocols for indications such as liver masses, pancreaticobiliary imaging, renal/adrenal imaging, pelvic imaging, and imaging the moving patient

#### TABLE OF CONTENTS/OUTLINE

- relevant body MRI physics: single-shot, free-breathing, respiratory navigation, chemical shift, hepatobiliary contrast- sequence families: single-shot fast-spin echo, balanced steady-state free-precession, diffusion-weighted, spoiled gradient echo (chemical shift, quantitative multi-echo imaging, dynamic imaging), high resolution/small field of view imaging- for each sequence: vendor names/acronyms, key sequence parameters (TR, TE, flip angle, acquisition time, breath-holding strategy), technical considerations (SNR, artifacts, sensitivity to motion and susceptibility, need for fat suppression), and clinical applications- body MRI protocols: what sequences to include and why, using examples such as liver mass, pancreaticobiliary, renal/adrenal, and pelvic imaging, and how to image the moving patient

Printed on: 02/07/23



## Abstract Archives of the RSNA, 2022

GIEE-54

### Success is Best When Shared: A Multidisciplinary Interpretation of Rectal Adenocarcinoma Regression

Sunday, Nov. 27 8:00AM - 9:00AM Room: Learning Center - GI

#### Participants

Olivia Errecondo, MD, (*Presenter*) Nothing to Disclose

#### TEACHING POINTS

? To review the role of MRI in restaging rectal cancer, emphasizing the use of T2 weighted images and diffusion weighted images. ? To describe the basis of neoadjuvant treatment in rectal cancer, making a brief analysis of the Prodigy, Opra and Rapido Trial. ? To accomplish a description of the tumor regression grade system (TRG) using cases from our database as examples. ? To highlight the importance of multidisciplinary approach between imaging findings, endoscopy and histopathologic results.

#### TABLE OF CONTENTS/OUTLINE

? Introduction. ? Rectal MRI basis. ? Neoadjuvant chemoradiotherapy in rectal cancer. ? TRG review. ? Conclusion.

Printed on: 02/07/23



## Abstract Archives of the RSNA, 2022

GIEE-55

### Hepatic Nodular Regenerative Hyperplasia: Radiologic-Pathologic Correlation

Sunday, Nov. 27 8:00AM - 9:00AM Room: Learning Center - GI

#### Participants

Arpan Patel, MD, (*Presenter*) Nothing to Disclose

#### TEACHING POINTS

This educational exhibit will aim to: Describe and define Nodular Regenerative Hyperplasia (NRH) from a clinical, radiological and histopathological perspective with the use of CT and MRI imaging. Compare and contrast NRH from other liver pathology. Distinguish NRH from other adaptive liver reactions that precede non-cirrhotic portal hypertension. Describe the causes and associations of NRH.

#### TABLE OF CONTENTS/OUTLINE

- NRH Background
- o NRH and other liver adaptive reactions causing non-cirrhotic intrahepatic portal hypertension
- o Epidemiology
- o Aetiology and pathogenesis
- Histopathological-Radiological correlation with CT and MRI Imaging
- o Molecular background
- o Imaging features
- Imaging pearls and pitfalls
- o Mimics of NRH
- o Appearance with hepatobiliary phase Gadoteric Acid- enhanced MR imaging
- Summary

Printed on: 02/07/23



## Abstract Archives of the RSNA, 2022

GIEE-56

### Imaging Techniques for Quantification of Liver Fat and Iron

Sunday, Nov. 27 8:00AM - 9:00AM Room: Learning Center - GI

#### Participants

Sarah Bastawrous, DO, Seattle, WA (*Presenter*) Nothing to Disclose

#### TEACHING POINTS

1. Review the importance of identifying liver fat and iron in the general population and in patients with liver disease. 2. Discuss ultrasound and MR imaging techniques for detection and quantification of liver fat and iron. 3. Illustrate these imaging techniques with clinical vignettes, including pearls and pitfalls.

#### TABLE OF CONTENTS/OUTLINE

1. Background and clinical importance of identifying abnormal accumulation of liver fat and iron. 2. Risks, clinical implications, impact on health care costs and mortality in patients with abnormal liver fat or iron. 3. Benefits of early detection and intervention in patients with abnormal fat and/or iron in the liver. 4. Ultrasound and MR imaging techniques for detection and quantification of liver fat and iron, including physical concepts, technique, interpretation, limitations, and future trends. 5. Multimodality case-based examples and appropriate clinical indications. 6. How to calculate and report fat and iron content.

Printed on: 02/07/23



## Abstract Archives of the RSNA, 2022

GIEE-57

### Back to our Origins: Abdominal Radiography and Its Uses

Sunday, Nov. 27 8:00AM - 9:00AM Room: Learning Center - GI

#### Participants

Elisa Antolinos Macho, MD, Madrid, Spain (*Presenter*) Nothing to Disclose

#### TEACHING POINTS

- Going over current abdominal X-ray purposes and indications. - Optimal technique review and basic projections. - Learning basic radiological anatomy. - Knowing most common abnormalities and underlying disease.

#### TABLE OF CONTENTS/OUTLINE

Indications Technique Basic projections 1) AP supine view 2) AP erect view 3) Lateral decubitus view 4) PA erect view Regional anatomy - Air (luminogram) - Organ silhouettes - Fat stripes - Bone Abdominal X-Ray semiology - Hepatobiliary Hepatomegaly, Splenomegaly, Cholelithiasis, Calcified cysts - Genitourinary Urolithiasis and other calcified structures - Gastrointestinal Bowel obstruction (Small bowel obstruction, large bowel obstruction and volvulus), and pneumoperitoneum - Foreign bodies - Medical devices

Printed on: 02/07/23



## Abstract Archives of the RSNA, 2022

GIEE-58

### MRI Findings of the Rectum and Anus: Beyond Tumor Staging

Sunday, Nov. 27 8:00AM - 9:00AM Room: Learning Center - GI

#### Awards

Certificate of Merit

#### Participants

Sergio Jimenez Serrano, Barcelona, Spain (*Presenter*) Nothing to Disclose

#### TEACHING POINTS

The purpose of this educational exhibit is:- To analyze the different pathological processes that can be found in the imaging modalities intended for the characterization and staging of rectoanal or perirectal pathology, beyond the adenocarcinoma and squamous neoplasia.- To illustrate the characteristic image features of these processes, especially on MRI, emphasizing those aspects that can be clues to orientate the diagnosis.

#### TABLE OF CONTENTS/OUTLINE

We have realized a retrospective review of patients in whom an imaging study, mostly MRI, has been requested to evaluate rectoanal or perirectal diseases in the last 12 years and whose definitive diagnosis has been other than primary neoplasia (adenocarcinoma or squamous neoplasia) or perianal fistula extension study. The final diagnosis was histologically confirmed. In this way, we present 44 patients and we have classified them into six groups:- Inflammatory/infectious pathology. - Endometriosis.- Neoplastic pathology Benign: schwannoma, leiomyoma, myelolipoma, hemangioma, diffuse rectal hemangiomatosis. Malign: neuroendocrine tumor, melanoma, plasmablastic lymphoma, undifferentiated pleomorphic sarcoma.- Secondary neoplastic involvement ? highlights a rare and specific form of involvement such as rectal linitis.- Congenital and developmental lesions.- Other benign processes.

Printed on: 02/07/23



## Abstract Archives of the RSNA, 2022

GIEE-59

### Pancreas-kidney Transplant: Imaging Before, During and After Transplant

Sunday, Nov. 27 8:00AM - 9:00AM Room: Learning Center - GI

#### Participants

Carlos Felipe Reyna, MD, Sao Paulo, Brazil (*Presenter*) Nothing to Disclose

#### TEACHING POINTS

To better understand pancreas-kidney transplant, its technique and complications using a didactic approach using images and illustrations. To show the different imaging methods for evaluating transplant complications, such as Computed Tomography (CT) and Ultrasound (US). To highlight the surgical complications using cases from our database and the importance of their detection. To highlight the importance of a structured report.

#### TABLE OF CONTENTS/OUTLINE

1. Review of the pancreas-kidney transplant and its technique through illustrations and images.
2. Explore pancreas-kidney complications supported by cross-sectional imaging cases, such as CT and US.
3. Preoperative and postoperative knowledge of pancreas-kidney transplant is mandatory for surgical planning and thus helping to identify postoperative complications. This information must be a part of the structured report.
4. Summary and take home messages.

Printed on: 02/07/23

## Abstract Archives of the RSNA, 2022

GIEE-6

### Tough to Swallow: Adventures in Postoperative GI Fluoroscopy

Sunday, Nov. 27 8:00AM - 9:00AM Room: Learning Center - GI

#### Participants

Elainea Smith, MD, Birmingham, AL (*Presenter*) Nothing to Disclose

#### TEACHING POINTS

1. Review the most common gastrointestinal surgical procedures performed and common indications - from pharynx to anus.2. Discuss case examples of the expected postoperative appearance of these procedures.3. Highlight the most common post operative complications and their fluoroscopic appearance.

#### TABLE OF CONTENTS/OUTLINE

IntroductionPharynx- LaryngectomyEsophagus- Zenker's diverticulectomy and diverticulectomy- Reflux management devices (such as Linx device)- POEM- Esophagectomy- Hiatal hernia repair- Heller myotomyStomach- Fundoplication- Sleeve gastrectomy- Roux-en-Y gastric bypass- Total gastrectomySmall bowel - Gastrostomy or gastrojejunostomy catheters- Whipple procedure- Pylorus sparing whippleLarge bowel- Partial colectomy- LAR versus APRSummary

Printed on: 02/07/23

## Abstract Archives of the RSNA, 2022

GIEE-60

### Strictures in Crohn's Disease: What a Radiologist Needs to Know

Sunday, Nov. 27 8:00AM - 9:00AM Room: Learning Center - GI

#### Participants

Antonio Bevere, Rome, Italy (*Presenter*) Nothing to Disclose

#### TEACHING POINTS

- Illustrate how to recognize bowel stenosis in Patients with Crohn's disease (CD), show the differences between inflammatory and fibrotic strictures, and explain their implication on the treatment choice. - How to describe intestinal stenosis in CD patients and which information should be included in the report to guide the management. - Exclude other potential differential diagnosis, including adhesive disease and bowel cancer.

#### TABLE OF CONTENTS/OUTLINE

Stricture is a frequent complication in CD. The precise definition of stricture has not been defined yet, and varies across studies, comprising either luminal stenosis with intestinal wall thickening with or without pre-stenotic dilatation, and lesion-causing stenosis lower than 1 cm. The site of strictures usually follows the distribution of inflammation, frequently involving the ileum. Even though CT- and MR-enterography offer great visualization of the intestinal tract, defining strictures remains challenging. Assessing strictures, the transition point should be carefully evaluated to establish the cause of bowel obstruction and exclude other potential differential diagnosis, including adhesive disease and bowel cancer. In addition, in CD inflammation and fibrosis are strictly connected mechanisms, which usually coexist in the same Patient and even in the same intestinal tract in varying degrees, making the diagnosis even more complex. MR exams can accurately differentiate between inflammatory and fibrotic strictures, guiding the correct treatment choice. Inflammatory strictures are treated with anti-inflammatory drugs; on the other hand, fibrotic strictures are treated mechanically with intestinal resection or endoscopic dilatation.

Printed on: 02/07/23



## Abstract Archives of the RSNA, 2022

GIEE-61

### Clinical and Radiological Scores for Assessing Inflammation in Crohn's Disease

Sunday, Nov. 27 8:00AM - 9:00AM Room: Learning Center - GI

#### Participants

Jordi Rimola, MD, PhD, (*Presenter*) Consultant, Alimentiv Health Trust; Speaker, Takeda Pharmaceutical Company Limited; Consultant, Johnson & Johnson; Consultant, Boehringer Ingelheim GmbH; Research Grant, AbbVie Inc

#### TEACHING POINTS

1-To familiarize radiologists with activity indices of Crohn's disease (CD) used by gastroenterologists including clinical and endoscopic scores  
2-To describe the main validated activity scores and other imaging biomarkers for assessing inflammation in patients with CD  
3-To provide a practical guide on the correct use and interpretation of imaging biomarkers in CD  
4-To discuss the potential contribution of imaging biomarkers in assessing therapeutic efficacy and to applied as endpoints in clinical research

#### TABLE OF CONTENTS/OUTLINE

1- Limitation of endoscopy as reference standard to assess inflammation and therapeutic response in patients with CD  
Cross-sectional imaging may overcome these limitations and offers additional advantages  
2- Description of Magnetic Resonance Enterography (MRE) and intestinal ultrasound (IUS) activity scores have been developed and validated  
Detailed list of MRE and IUS activity scores and other imaging biomarkers (e.g. motility) in CD  
Evidence supporting their satisfactory inter- and intra-reader reproducibility, and validity against a range of reference standards  
Optimal use and interpretation. Not forget ulcerative colitis  
3- Rational and limitations to consider activity scores as endpoints in clinical research in CD.

Printed on: 02/07/23



## Abstract Archives of the RSNA, 2022

GIEE-62

### Rectal MR: A Refresher on Low Rectal Cancers at Initial Staging

Sunday, Nov. 27 8:00AM - 9:00AM Room: Learning Center - GI

#### Awards

Identified for RadioGraphics  
Certificate of Merit

#### Participants

David Kim, MD, Madison, WI (*Presenter*) Shareholder, Elucent Medical

#### TEACHING POINTS

1. The 'anorectal junction to tumor' distance can estimate potential distal surgical margin and thus helps to determine the surgical approach. 2. MRF involvement at the pelvic floor can be inferred by the T category status for low cancers. 3. Cancer involvement of the anal sphincter in the context of T staging is remains undefined by AJCC. The recommendation is to be descriptive. It is important to have a strong grasp of anal sphincter anatomy to accurately describe tumor involvement with particular emphasis regarding the tumor relationship to the intersphincteric space. 4. External iliac and inguinal lymph nodes are regional (N+) not M disease when there is cancer involvement of the anal sphincter. 5. The histology of the tumor must be confirmed as adenocarcinoma. If squamous in histology, a low cancer is staged and treated as an anal cancer.

#### TABLE OF CONTENTS/OUTLINE

Background • Rectal MR and clinical staging • Classification (high/mid/low) Low rectal cancers (special considerations) • Anatomy of the anal sphincter • Treatment approaches • Staging issues and areas of controversy • Histology Summary

Printed on: 02/07/23



## Abstract Archives of the RSNA, 2022

GIEE-63

### MR and CT Enterography: Expanding the Knowledge and Digesting the Information

Sunday, Nov. 27 8:00AM - 9:00AM Room: Learning Center - GI

#### Participants

Martin Horwarth, Sao Paulo, Brazil (*Presenter*) Nothing to Disclose

#### TEACHING POINTS

1 - Review the imaging findings for inflammatory bowel disease when using enterography protocols in CT and MR.2 - Illustrate these findings and correlate them with the correct terms to use on radiology reports.3 - Showcase the most common pitfalls that can be mistaken for active inflammatory disease and what to look for besides the bowel.

#### TABLE OF CONTENTS/OUTLINE

1 - Advantages and disadvantages of CT and MR.2 - Exam protocols.3 - Imaging findings in Crohn's disease and their descriptors.4 - Imaging findings in non-specific intestinal inflammatory conditions.5 - Pitfalls that may be mistaken for active inflammation.6 - Other sites of interest for when analyzing a patient with Crohn's disease.

Printed on: 02/07/23



## Abstract Archives of the RSNA, 2022

GIEE-64

### When it is NOT Appendicitis: What to Look for in Appendiceal Disease Besides Inflammation

Sunday, Nov. 27 8:00AM - 9:00AM Room: Learning Center - GI

#### Participants

Joao Stern, MD, Rio de Janeiro, Brazil (*Presenter*) Nothing to Disclose

#### TEACHING POINTS

- Review literature in appendiceal malignancies and benign disease.- Demonstrate images patterns of the different diseases of the appendix- Postulate a flowchart to investigate appendiceal disease

#### TABLE OF CONTENTS/OUTLINE

Appendicitis is one of the most common acute abdominal inflammatory disease and demands surgical treatment. Other appendix afflictions are rare in comparison and frequently overlooked. Radiologists must know the different diagnosis, to recognize when it's not appendicitis and impact the surgical or clinical management.

Printed on: 02/07/23



## Abstract Archives of the RSNA, 2022

GIEE-65

### Icing on the Cake: Added Value of Dual Energy CT (DECT) in Challenging Biliary Pathologies

Sunday, Nov. 27 8:00AM - 9:00AM Room: Learning Center - GI

#### Participants

Victoria Kim, MD, (*Presenter*) Nothing to Disclose

#### TEACHING POINTS

1. Understand basic technique of dual energy CT (DECT) imaging.2. Describe the role of DECT in complex biliary pathologies.3. Show how DECT aids appropriate management of challenging biliary cases.

#### TABLE OF CONTENTS/OUTLINE

1. Background: DECT has a variety of emerging clinical applications. By acquiring images at both high and low x-ray energies, computer software analysis can estimate chemical composition of materials. Images are reconstructed to enhance or suppress appearance of different materials. CT is often first choice of cross-sectional imaging in outpatient and acute care settings due its relative ease of acquisition and lower cost compared to MRI. DECT is a particularly useful tool in imaging biliary pathologies to add greater information and value from a single imaging encounter.2. Gallstone disease: Noncalcified cholesterol stones are less apparent on single-energy contrast enhanced CT, but attenuate differently at various energies and are better visualized on monoenergetic images.3. Postoperative cases: Iodine map and virtual non-contrast (VNC) images distinguish true postoperative abscesses.4. Biliary malignancy: Iodine map and VNC images distinguish enhancing tissue versus biliary hematoma.5. Other pathology: In unusual cases such as gallbladder volvulus, iodine map and VNC images identify gallbladder ischemia and expedite management.VI. Conclusions: DECT has an exciting range of applications for biliary pathology, aiding in appropriate management and minimizing additional studies and delayed care.

Printed on: 02/07/23



## Abstract Archives of the RSNA, 2022

GIEE-66

### Save Your Tears for Another Day: Unmasking Pancreatic Adenocarcinoma

Sunday, Nov. 27 8:00AM - 9:00AM Room: Learning Center - GI

#### Participants

Ahmed Elsakka, MD, Rutherford, NJ (*Presenter*) Nothing to Disclose

#### TEACHING POINTS

- Recognize early focal pancreatic abnormalities on CT associated with subsequent diagnosis of early-stage pancreatic ductal adenocarcinoma (PDAC).
- Understand the role and limitations of radiology on primary staging and restaging.
- Comprehend common imaging pitfalls and benign mimickers of PDAC.
- Recognize post-surgical complications.
- Recognize different patterns of recurrence on imaging.
- Understand imaging response to CRT and current limitations.
- Be familiar with future directions on PDAC.

#### TABLE OF CONTENTS/OUTLINE

1.INTRODUCTION oWorld prevalence and cancer Facts and statistics 2022. oRelevance, costs. 2.TREATMENT SUMMARY 3.ROLE OF IMAGING oEarly detection oInitial staging oCommon pitfalls •Vascular involvement from surgical perspective •Peritoneal carcinomatosis versus inflammatory changes or congestion. •Regional and extra-regional nodal metastasis. •Perineural invasion: myth or fact? oMimickers •Pancreatitis. •Duodenal diverticulitis. •Prominent pancreatic lobulations. •Uneven fat deposition oRestaging •Imaging criteria and limitations. oTumor recurrence •Common locations. •Imaging patterns. •Role of follow up comparison 4.RADIOSURGICAL CORRELATION oWhen we were wrong 5.POST-OPERATIVE COMPLICATIONS oPre-surgical red flags. oConcerning imaging findings. 6.MULTIDISCIPLINARY TUMOR BOARD oWhat they need to know and what we need to ask 7.WHAT'S ON THE HORIZON

Printed on: 02/07/23



## Abstract Archives of the RSNA, 2022

GIEE-67

### NCCN Guideline Driven Gastrointestinal Tract Tumor Board: A Primer for Radiologists

Sunday, Nov. 27 8:00AM - 9:00AM Room: Learning Center - GI

#### Participants

Basem Jaber, MD, Darby, PA (*Presenter*) Nothing to Disclose

#### TEACHING POINTS

\* Demonstrating a radiologist's role in the clinical management of GI tumors.\* Reviewing NCCN guidelines for GI tumors.\* Highlighting the use of different imaging modalities in management decisions.\* Identifying possible pitfalls in multidisciplinary tumor board discussions from a radiology standpoint.

#### TABLE OF CONTENTS/OUTLINE

GI tract cancers are one of the most common malignancies discussed during multidisciplinary tumor board meetings. The National Cancer Committee Network (NCCN) publishes guidelines that are considered the gold standard for management of malignancies. This exhibit is a pictorial review of cancers of the stomach, small bowel, colon and rectum with emphasis on the NCCN guidelines. Key points: \* Description of the role of imaging in cancer staging.\* Multimodality imaging for initial workup.\* Outline of impact of radiology on the surgical management and medical treatment of GI cancers.\* Highlight of potential conflicts and pitfalls in tumor boards discussions.\* Imaging principles for active surveillance.

Printed on: 02/07/23



## Abstract Archives of the RSNA, 2022

GIEE-68

### Multimodality Approach to Complications of Pancreatitis

Sunday, Nov. 27 8:00AM - 9:00AM Room: Learning Center - GI

#### Participants

Kaustubh Shiralkar, MD, Houston, TX (*Presenter*) Nothing to Disclose

#### TEACHING POINTS

Acute and chronic pancreatitis may lead to a wide array of complications which can be visualized on imaging. Our exhibit will focus on understanding the use and unique advantages of ultrasound, CT, and MRI including secretin enhanced MRI to better characterize complications of acute and chronic pancreatitis to aid in management decisions. Acute pancreatitis may lead to numerous local complications including acute peripancreatic fluid collections, necrosis with or without superimposed infection, fistula formation, and vascular complications such as hemorrhage from erosion of nearby vessels, pseudoaneurysm formation, and adjacent venous thrombosis. Chronic pancreatitis may lead to pseudocyst formation with possible dissection into the mediastinum or adjacent peritoneal compartments, parenchymal atrophy or enlargement with or without calcifications, and decreased exocrine reserve which may be evaluated on secretin enhanced MRI. This exhibit will also focus on effective reporting for management and clinical decision making.

#### TABLE OF CONTENTS/OUTLINE

Peripancreatic fluid collections, pancreatic and peripancreatic necrosis, emphysematous pancreatitis, fistula formation, vascular complications, chronic pancreatitis pseudocyst formation, ductal stenosis

Printed on: 02/07/23

## Abstract Archives of the RSNA, 2022

GIEE-69

### **Congenital Cystic Lesions of the Biliary Tract: A Pictorial Review**

Sunday, Nov. 27 8:00AM - 9:00AM Room: Learning Center - GI

#### **Participants**

Abel Gonzalez Huete, MD, Madrid, Spain (*Presenter*) Nothing to Disclose

#### **TEACHING POINTS**

1. To explain congenital cystic lesions of the biliary tree: congenital hepatic fibrosis, biliary hamartomas (von Meyenburg complexes), autosomal dominant polycystic disease, Caroli disease and choledochal cysts. 2. To review the embryology, physiology and pathogenesis. 3. To illustrate the imaging findings. 4. To discuss their differential diagnosis illustrated by sample cases.

#### **TABLE OF CONTENTS/OUTLINE**

1. Introduction. 2. Embryopathogenesis. 3. Anomalies of the intrahepatic bile ducts. - Congenital hepatic fibrosis: Etiopathogenesis, Imaging findings. - Biliary hamartomas (von Meyenburg complexes): Etiopathogenesis, Imaging findings (Ultrasound, CT, MR), Differential diagnosis. - Caroli disease: Etiopathogenesis, Types (Caroli disease proper, Caroli Syndrome), Imaging findings (Ultrasound, CT, MR), Complications, Differential diagnosis. - Autosomal dominant polycystic disease: Etiopathogenesis, Imaging findings (Ultrasound, CT, MR), Complications, Extrahepatic associations. 4. Anomalies of the extrahepatic bile ducts. - Choledochal cysts: Etiopathogenesis, Imaging findings, Classification, Complications. 5. Summary.

Printed on: 02/07/23



## Abstract Archives of the RSNA, 2022

GIEE-7

### Multimodality Imaging Evaluation of Gastroenteropancreatic Neuroendocrine Neoplasms: A Diagnostic Challenge

Sunday, Nov. 27 8:00AM - 9:00AM Room: Learning Center - GI

#### Participants

Monica Munoz-Lopez, MD, Mexico City, Mexico (*Presenter*) Nothing to Disclose

#### TEACHING POINTS

- To review the origin, pathophysiology and classification of gastroenteropancreatic neuroendocrine neoplasms.- To recognize the utility of anatomical and somatostatine receptor functional imaging in the diagnosis, staging, prognosis and selection of treatment.- To identify, in a case- based review, the main challenges and pitfalls of functional imaging in the diagnosis and follow- up of GEP NETs.- To understand the radiologists role in the selection of treatment with theranostic agents.

#### TABLE OF CONTENTS/OUTLINE

- Introduction to gastroenteropancreatic neuroendocrine neoplasms (GEP NENs): origin, pathophysiology and clinical syndromes- The WHO 2019 classification of GEP NENs: well- differentiated neuroendocrine tumor versus poorly differentiated neuroendocrine carcinoma- Multimodality anatomical and somatostatine receptor imaging criteria in diagnosis and staging- Pitfalls in interpretation of somatostatine receptor imaging- Prognostic value of dual positron emission tomography imaging with 18F-FDG and 18F-OC for NENs- Overview of theranostic agents for treatment of NENs

Printed on: 02/07/23



## Abstract Archives of the RSNA, 2022

GIEE-70

### Multimodality Imaging of Biliary Tract Conditions: What Radiologists Should Know

Sunday, Nov. 27 8:00AM - 9:00AM Room: Learning Center - GI

#### Awards

Identified for RadioGraphics

#### Participants

Camila Vendrami, MD, Chicago, IL (*Presenter*) Nothing to Disclose

#### TEACHING POINTS

· Review of biliary tract imaging technique · Identify the multimodality imaging features of benign and malignant conditions of the biliary tract · Discuss pitfalls in the interpretation of MR imaging and CT findings in the biliary tract

#### TABLE OF CONTENTS/OUTLINE

The biliary tract may be affected by a wide variety of pathologic conditions, some with similar clinical presentations. Biliary tract imaging plays a key role in determining the etiology, location, and severity of the condition and any complications. Imaging also guides management of biliary tract diseases including the most appropriate intervention when required. 1. Introduction 2. Imaging technique: what are the uses and how are standard MR cholangiopancreatography, 3D isotropic MR cholangiopancreatography and contrast-enhanced MR cholangiography and DECT performed? 3. What features characterize, on multimodality imaging including but not malignant to benign biliary (choledochal cysts including Caroli disease, cholangitis, recurrent pyogenic cholangitis, primary sclerosing cholangitis, ischemic cholangiopathy) and pre-malignant and malignant conditions (intraductal papillary neoplasm of the bile duct-IPNB-, cholangiocarcinoma and metastases)? 4. Review imaging pitfalls in the biliary tract imaging: blooming artifact, physiologic variants of the biliary system and pulsation/compression artifact 5. Take home points

Printed on: 02/07/23



## Abstract Archives of the RSNA, 2022

GIEE-71

### Extramural Venous Invasion in Rectal Cancer Before and After Neoadjuvant Therapy Beyond Classic Findings: Recognition of Detailed Characteristics and Tumor Deposit

Sunday, Nov. 27 8:00AM - 9:00AM Room: Learning Center - GI

#### Participants

Akitoshi Inoue, MD, PhD, Rochester, MN (*Presenter*) Nothing to Disclose

#### TEACHING POINTS

Extramural venous invasion (EMVI) is a well-investigated prognostic factor predicting poor survival in rectal cancer despite no statement in American Joint Committee on Cancer TNM staging system. EMVI was described as an expanded, irregular vessel with intermediate tumor-signal intensity; however, detailed characteristics such as the number, diameter, and location of the involved vessel, and treatment response are gathering attention, aiming to predict precise patient outcomes and stratify risk. Tumor deposits (TDs), defined as cancer nodules located in the mesorectum without evidence of underlying lymph node architecture on histopathology, are recently reported as irregular nodules in the mesorectum directly interrupting the course of the vein with tapering into the vein on MRI. MR-detected TDs are reported to be a prognostic factor as well as pathological TDs. The purposes of this exhibit are: 1. To review imaging findings of EMVI and TDs in rectal cancer 2. To discuss the clinical significance of EMVI and TDs in contemporary therapeutic strategy in rectal cancer.

#### TABLE OF CONTENTS/OUTLINE

1. Detection of EMVI and imaging pitfalls 2. What are TDs? Imaging findings and cutting-edge knowledge. 3. Detailed characteristics of EMVI and difference between EMVI and TDs 4. Assessing response of EMVI and TDs after neoadjuvant therapy 5. Summary

Printed on: 02/07/23



## Abstract Archives of the RSNA, 2022

GIEE-72

### Closing the Loop on Challenging and Complex Small Bowel Obstructions

Sunday, Nov. 27 8:00AM - 9:00AM Room: Learning Center - GI

#### Participants

Michael Hartung, MD, Madison, WI (*Presenter*) Consultant, Innovenn, Inc; Consultant, Otsuka Holdings Co, Ltd

#### TEACHING POINTS

1. Complex small bowel obstructions often bring both diagnostic and management dilemmas to the radiology and surgical teams. 2. The radiologist plays a major role in providing a confident interpretation of the baseline CT exam that influences management and follow-up. 3. Complex small bowel obstructions can be divided up into mechanical, neoplastic, and closed-loop categories. The key findings that raise the concern of closed-loop physiology include the beak sign, asymmetric edema, clustered loops with radial vessels, dilated C or U-shaped loops, and swirling narrowed vasculature. 4. Important mimics and pitfalls to consider when evaluating a complex bowel case include ischemia, angioedema, inflammatory enteritides, and graft versus host disease.

#### TABLE OF CONTENTS/OUTLINE

A. Defining simple versus complex small bowel obstruction- Mechanical- Abdominal and pelvic external hernias- Gallstone ileus - Afferent loop syndrome- Endometriosis B. Neoplastic- Benign- Primary tumors- Secondary tumors C. Closed-loop- Key signs of CLO- Adhesive disease- Internal hernia- Gastric bypass related- Volvulus D. Mimics and pitfalls- Non-obstructive ischemia- Angioedema- Inflammatory enteritides (vasculitis, eosinophilic, IBD)- Radiation and GVHDE. A practical approach to reporting challenging cases

Printed on: 02/07/23



## Abstract Archives of the RSNA, 2022

GIEE-73

### Bariatric Surgery: Imaging of Normal Post Operative Appearance and Complications

Sunday, Nov. 27 8:00AM - 9:00AM Room: Learning Center - GI

#### Participants

Adina Laufer, MD, New York, NY (*Presenter*) Nothing to Disclose

#### TEACHING POINTS

The goal of this exhibit is to familiarize the participants with the surgical anatomy of the most common forms of bariatric surgery. Participants can then use that knowledge as a basis to identify complications of bariatric surgery and corresponding CT and fluoroscopic imaging features. Upon completion of this educational exhibit, participants will be familiar with the normal CT and fluoroscopic imaging appearance as well as the CT and fluoroscopic appearance of postoperative complications for the most commonly performed bariatric procedures. Familiarity with this subject will allow for prompt diagnosis and management for bariatric patients.

#### TABLE OF CONTENTS/OUTLINE

CT and GI fluoroscopic appearance of: -Gastric bypass-Gastric band-Sleeve gastrectomy This exhibit will highlight the CT and fluoroscopic appearance for the gamut of postoperative complications including but not limited to: -leaks-strictures-marginal ulcers-hernias-small bowel obstruction-intussusception-gastroesophageal reflux

Printed on: 02/07/23



## Abstract Archives of the RSNA, 2022

GIEE-74

### The Art of Letting It Flow: Small Bowel Follow-Through in the Age of Cross-Sectional Imaging

Sunday, Nov. 27 8:00AM - 9:00AM Room: Learning Center - GI

#### Awards

Identified for RadioGraphics

#### Participants

Shamus Moran, MD, Seattle, WA (*Presenter*) Nothing to Disclose

#### TEACHING POINTS

1) Review the indications, contraindications, and technique for the small bowel follow-through 2) Review the normal fluoroscopic appearance of small bowel anatomy 3) Provide a practical algorithmic approach to small bowel pathologies on fluoroscopy with an emphasis on clinical significance 4) Discuss the role of the small bowel follow-through in small bowel motility assessment 5) Fluoroscopic - cross-sectional imaging correlation

#### TABLE OF CONTENTS/OUTLINE

Introduction. Indications, contraindications, and technique. Discussion of the following entities with case examples and an approach for diagnosis and further management  
Motility Assessment: • Normal small bowel transit times • Bedside SBFT for assessment of small bowel obstruction.  
Congenital: • Duplication cyst communicating with ileum • Cystic fibrosis • Meckel's diverticulum • Malrotation.  
Infectious: • Ascariasis • Giardiasis • Mononucleosis • Strongyloides • Tuberculous enteritis • Typhoid ileitis • Whipple's disease.  
Inflammatory: • Crohn disease (stenosis, diffuse mucosal thickening, colonic fistulae, enteroenteric fistula, sacculations, polyps, cobblestone) • Eosinophilic enterocolitis • Radiation enteritis • Scleroderma • Celiac Sprue • Amyloidosis • Henoch-Schoenlein Purpura • GVHD • Sclerosing mesenteritis.  
Neoplastic: • Adenocarcinoma • Carcinoid • Gastrointestinal stromal tumors • Lymphoma • Zollinger-Ellison syndrome • Metastasis.  
Miscellaneous: • Ischemia • Intestinal neuropathy • Small bowel - small bowel intussusception • Diverticulosis • Hypoalbuminemia

Printed on: 02/07/23

## Abstract Archives of the RSNA, 2022

GIEE-75

### Ulcerative Colitis on MR Enterography: Beyond the Scope of Endoscope!

Sunday, Nov. 27 8:00AM - 9:00AM Room: Learning Center - GI

#### Awards

Identified for RadioGraphics

#### Participants

Mehrnam Amouei, MD, (*Presenter*) Nothing to Disclose

#### TEACHING POINTS

Ulcerative colitis (UC) is a chronic inflammatory disease that can present at various stages of disease activity. Ileocolonoscopy and biopsy are the tests of choice to diagnose ulcerative colitis and assess disease severity. The value of MR enterography (MRE) is its usefulness in transmural/extramural assessment and identification of disease complications and extraintestinal manifestations. On the other hand, a complete colonoscopy might be unachievable in some patients, even in the expert hands, due to anatomical limitations or disease severity. However, this role is less emphasized compared to Crohn's disease due to the gradual course of UC, which is confined to the mucosa/submucosal layers of the colon. Beyond describing UC extension and severity, after completing this educational material, the readers will be able to recognize the value of MRE in: 1. Assessment of GI tract abnormalities beyond the colon in UC. 2. Identifying acute complications related to UC. 3. Describing benign and malignant disorders superimposed on UC. 4. Diagnosis of post-surgical complications in UC.

#### TABLE OF CONTENTS/OUTLINE

Ø Background Ø Technical considerations Ø Imaging features of UC variants in MRE Ø Acute complications Ø Extra-colonic manifestations Ø Benign disorders superimposed on UC Ø Malignant disorders superimposed on UC Ø Post-surgical imaging findings and complications Ø Mimickers Ø A practical algorithm for interpretation of MRE in UC Ø Conclusion Ø References

Printed on: 02/07/23



## Abstract Archives of the RSNA, 2022

GIEE-76

### Liver Transplant Primer For Radiologists: A Question-Based and Case-Based Review

Sunday, Nov. 27 8:00AM - 9:00AM Room: Learning Center - GI

#### Awards

Certificate of Merit

#### Participants

Roberta Catania, MD, Chicago, IL (*Presenter*) Institutional Research Grant, Siemens AG

#### TEACHING POINTS

1. Familiarity with surgical techniques for deceased-donor and living-donor liver transplantation and postoperative anatomy 2. Familiarity with pertinent variant anatomies affecting the future transplant and role of imaging for their pre-operative assessment 3. Familiarity with role of imaging in early post-operative assessment of liver allograft 4. Familiarity with the common post-transplant complications and their imaging findings

#### TABLE OF CONTENTS/OUTLINE

[All information will be presented and highlighted in an interactive questions-based and case-based format.]Indications• Current and expanding indications for liver transplantation• The issues with organ availability and organ allocationSurgical Techniques• Surgical techniques for deceased liver transplant• Surgical techniques for living donor liver transplant• Postsurgical anatomyPretransplant evaluation• Imaging assessment of recipient for surgical candidacy• Imaging assessment of living donor candidate o Overview of different imaging techniques and protocols o Pertinent variant biliary and vascular anatomy that may affect surgical planning o Segmentation and calculation of liver volumesPostoperative complications• Early post-operative complications• Delayed post-operative complications o Post-Transplant Lymphoproliferative Disorder (PTLD) and other malignancies

Printed on: 02/07/23



## Abstract Archives of the RSNA, 2022

GIEE-77

### Diffuse Bile Ducts Abnormalities: A Case Base Review with Histopathologic Correlation

Sunday, Nov. 27 8:00AM - 9:00AM Room: Learning Center - GI

#### Participants

Francisco Manuel Moreno SR, (*Presenter*) Nothing to Disclose

#### TEACHING POINTS

o To provide a comprehensive review of bile pathway anatomy and a basic approach to Its histology o To be able to identify abnormal appearance of the biliary tree on radiologic images, image patterns and the most common causes of diffuse biliary tree diseases o To include anatomopathological correlation for the pathologies reviewed so the radiologic signs associated to each entity can be better understood. o Key signs to be considered to differentiate malignance from other diseases

#### TABLE OF CONTENTS/OUTLINE

1. Overview 2. Possible etiologies3. Case based - review with histopathologic correlation4. Pearls5. Conclusions

Printed on: 02/07/23



## Abstract Archives of the RSNA, 2022

GIEE-78

### Vascular Complications of Hepatopancreatobiliary Surgeries and Liver Transplant

Sunday, Nov. 27 8:00AM - 9:00AM Room: Learning Center - GI

#### Participants

Dayhane De Souza, MD, Sao Paulo, Brazil (*Presenter*) Nothing to Disclose

#### TEACHING POINTS

1 - To demonstrate the vascular reconstructions techniques in hepatopancreatobiliary surgeries, including the liver transplant scenario. 2 - To recognize the vascular surgical complications and how to elaborate a structured report that may help the clinical management. 3 - To Illustrate the different imaging methods for evaluating vascular complications, such as Computed Tomography (CT) and ultrasonography (US).

#### TABLE OF CONTENTS/OUTLINE

1 - Illustration of typical imaging features of vascular complications supported by the use of graphics and cross-sectional imaging cases, such as arterial and venous stenosis and thrombosis. 2 - Knowledge of hepatic vascular reconstruction is mandatory for early recognition of postoperative complications. 3 - Summary and take home messages.

Printed on: 02/07/23



## Abstract Archives of the RSNA, 2022

GIEE-79

### A Step-by-Step Approach to the Understanding of Dysphagia: What Not to Miss in a Swallow Mechanism!

Sunday, Nov. 27 8:00AM - 9:00AM Room: Learning Center - GI

#### Participants

Yumi Kimura Sandoval, MD, Mexico City, Mexico (*Presenter*) Nothing to Disclose

#### TEACHING POINTS

- Recognize the importance of swallow mechanism in the diagnostic algorithm of dysphagia- Learn the indications and technique used in the performance of a swallow mechanism- Review the normal anatomy of the oral cavity, oropharynx, hypopharynx, and esophagus- Understand the physiology and different phases involved in deglutition- Case-based review of the main radiologic signs and features observed in deglutition alterations leading to dysphagia

#### TABLE OF CONTENTS/OUTLINE

1. Normal anatomy - Oral cavity - Oropharynx - Hypopharynx - Esophagus - Anatomic variants  
2. Indications and technique of swallow mechanism - Useful projections - Oral contrast consistencies  
3. Deglutition physiology - Oral phase - Pharyngeal phase - Esophageal phase  
4. Deglutition pathology  
a) Oral phase: - Lip incompetence - Leakage to the oropharynx - Nasopharyngeal reflux  
b) Pharyngeal phase: - Functional alterations: penetration, aspiration, asymmetry, stasis, cricopharyngeal dysfunction- Structural alterations: esophageal web, Killian Jamieson`s diverticulum, Zenker`s diverticulum  
c) Esophageal phase: - Functional: achalasia, diffuse esophageal spasm - Structural: epiphrenic diverticulum

Printed on: 02/07/23



## Abstract Archives of the RSNA, 2022

GIEE-8

### From A to Z(ebras): Vascular Findings and Complications After Liver Transplant

Sunday, Nov. 27 8:00AM - 9:00AM Room: Learning Center - GI

#### Participants

Heba Albasha, MD, Cincinnati, OH (*Presenter*) Nothing to Disclose

#### TEACHING POINTS

- Review surgical techniques of liver transplant with a focus on vascular anatomy.
- Discuss imaging findings of common vascular complications after liver transplant.
- Understand and recognize unique imaging findings of uncommon vascular findings and complications of liver transplant.

#### TABLE OF CONTENTS/OUTLINE

1. Liver transplant surgical techniques
  - a. Review of liver transplant anatomy, including that of conventional, piggyback, deceased donor, and split liver techniques
2. Imaging work-up of liver transplant complications
3. Hepatic artery complications
  - a. Hepatic artery thrombosis
  - b. Hepatic artery stenosis
  - c. Hepatic artery kinking
  - d. Reversal of hepatic arterial flow
  - e. Hepatic arterial-portal venous fistula
  - f. Hepatic artery pseudoaneurysm
4. Portal vein complications
  - a. Portal vein thrombosis
  - b. Portal vein stenosis
  - c. Portal vein compression
  - d. Portal vein size discrepancy
  - e. Portal steal
  - f. Primary nonfunction
5. Hepatic vein/IVC complications
  - a. IVC thrombosis
  - b. IVC stenosis
  - c. Venocaval anastomotic stricture

Printed on: 02/07/23



## Abstract Archives of the RSNA, 2022

GIEE-80

### LR-M in LI-RADS v2018: Non-HCC Malignancies and Atypical HCC

Sunday, Nov. 27 8:00AM - 9:00AM Room: Learning Center - GI

#### Awards

Cum Laude

#### Participants

Tatsuyuki Tonan, MD, Kurume, Japan (*Presenter*) Nothing to Disclose

#### TEACHING POINTS

Illustrate the malignant tumor (non-HCC malignancies and atypical HCC), which are classified as LR-M in the LI-RADS v2018 as follows: 1. The definition of LR-M criteria including "targetoid" and "nontargetoid" imaging appearance on EOB-enhanced MRI. 2. The relationship between the targetoid/nontargetoid imaging appearances and pathological findings (i.e., fibrosis, peliotic change, mucin, cell density/ ischemia, necrosis). 3. The relationship between delayed (or persistent) extracellular contrast enhancement effects and targetoid imaging appearances. 4. Exhibit of non-HCC malignancies with targetoid or nontargetoid imaging appearance (i.e., intrahepatic cholangiocarcinoma, cholangiolocellular carcinoma, sarcomatous HCC, neuroendocrine tumors, mucinous carcinoma, intraductal papillary neoplasm of the bile duct and primary hepatic lymphoma). 5. New knowledge about the atypical HCCs with targetoid or nontargetoid imaging appearance favoring non-HCC malignancies.

#### TABLE OF CONTENTS/OUTLINE

LI-RADS v2017 introduced an important update to the LI-RADS-M (LR-M; probably or definitely malignant but not HCC specific) category to clarify appropriate use. Specifically, LR-M was modified as follows: "targetoid mass" including peripheral hypercellularity and central stromal fibrosis or "nontargetoid mass" including an infiltrative appearance, marked diffusion restriction, necrosis or severe ischemia, in addition to features that suggest a non-HCC malignancy in radiologist's judgment. While these imaging findings are not specific finding, to understand these imaging findings are helpful in the diagnosis of hepatic tumors, and is important in assignment of the LI-RADS.

Printed on: 02/07/23



## Abstract Archives of the RSNA, 2022

GIEE-81

### Post-Operative CT Findings After Whipple Procedure: Normal Findings and Complications

Sunday, Nov. 27 8:00AM - 9:00AM Room: Learning Center - GI

#### Participants

Vamshi Mugu, MD, Rochester, MN (*Presenter*) Nothing to Disclose

#### TEACHING POINTS

1) Identify components of post-operative anatomy for a) Standard Whipple b) Pylorus-sparing Whipple 2) Identify normal post-operative findings and distinguish them from complications

#### TABLE OF CONTENTS/OUTLINE

1) Conventional Whipple consists of a) Partial pancreatectomy and pancreaticojejunostomy b) Duodenectomy c) Distal gastrectomy and gastrojejunostomy d) Cholecystectomy and hepaticojejunostomy 2) Pylorus-sparing Whipple consists of a) Partial pancreatectomy and pancreaticojejunostomy b) Partial duodenectomy and duodenojejunostomy c) Cholecystectomy and hepaticojejunostomy 3) Common normal post-operative findings a) Post-operative anatomy: 1) Hepaticojejunostomy 2) Pancreaticojejunostomy 3) Gastrojejunostomy b) Vascular reconstructions c) Jejunal limb edema 4) CT appearance of post-operative complications a) Delayed gastric emptying (a clinical diagnosis) b) Pancreatic fistula c) Biliary leak d) Hemorrhage e) Acute pancreatitis f) Vascular thrombus

Printed on: 02/07/23



## Abstract Archives of the RSNA, 2022

GIEE-82

### Fat's All Folks: A Case-Based Tour of Benign and Malignant Abdominopelvic Lesions

Sunday, Nov. 27 8:00AM - 9:00AM Room: Learning Center - GI

#### Participants

Alana Fruauff, MD, BS, New York, NY (*Presenter*) Nothing to Disclose

#### TEACHING POINTS

Intralesional fat within the abdominopelvic viscera narrows differential diagnosis for benign and malignant disease processes. Abdominal and pelvic fat distribution can help diagnose co-existent and unrecognized disease. The presence of fat within a lesion does not automatically suggest a benign diagnosis. It is critical for radiologists to identify when a fat-containing lesion is most likely malignant.

#### TABLE OF CONTENTS/OUTLINE

1. Introduction of fat-containing lesions and typical appearance on ultrasound, CT, and MRI. Case-based review of benign and malignant fatty lesions in the following locations: a. Right upper abdomen. b. GI tract. c. Renal and adrenal glands. d. Reproductive system. e. Retroperitoneum. f. Mesentery/peritoneum

Printed on: 02/07/23



## Abstract Archives of the RSNA, 2022

GIEE-83

### **GISTS and the Limits of RECIST: State of the Art Imaging and Treatment of Gastrointestinal Stromal Tumors**

Sunday, Nov. 27 8:00AM - 9:00AM Room: Learning Center - GI

#### **Participants**

Xin Zhan, MD, (*Presenter*) Nothing to Disclose

#### **TEACHING POINTS**

GIST is the most common single type of sarcoma and the most common mesenchymal tumor in the GI tract. Teaching points include 1) Approximately 25% of GIST are discovered incidentally. GISTs have 3 morphologic patterns: spindle, epithelioid, and Wild-Type which can be associated with genetic syndromes and worse prognosis. 2) The diagnostic workup of GIST consists of the initial imaging with contrast-enhanced CT (CECT), detection of metastasis with CECT or PET/MRI, and definitive diagnosis by histopathology. Given its propensity for the stomach, CT protocols for GIST can be optimized with changes in patient position, use of oral water, CO<sub>2</sub> crystals or positive enteric contrast. Multiphase CECT is useful in differentiating enhancement patterns of GIST vs other tumors. 3) Surgery remains the standard of care for localized tumors, but systemic therapy may be indicated based off unfavorable tumor locations, metastases, and genetic mutations. New biologic treatments (Imatinib, Sunitinib) have changed the clinical management of GIST and radiomic response evaluation continues to evolve to better assess disease progression. RECIST focuses on unidimensional, anatomic measurements, CHOI evaluates both anatomic and functional measurements, while PERCIST measures the metabolic response of tumors. We will discuss the strengths and weaknesses of these different criteria and how they impact patient management.

#### **TABLE OF CONTENTS/OUTLINE**

GIST Outline:- Pathophysiology- Clinical manifestations- Diagnostic imaging modalities/imaging features- Optimizing imaging protocols - Differential diagnoses on imaging- Treatment options, new biologic drugs- Radiomics (RECIST, PERCIST, CHOI) strengths and weaknesses

Printed on: 02/07/23



## Abstract Archives of the RSNA, 2022

GIEE-84

### What Do You Look at Plain Radiograph Abdomen?

Sunday, Nov. 27 8:00AM - 9:00AM Room: Learning Center - GI

#### Participants

Axel Torres Monarrez, MD, Tlalpan, Mexico (*Presenter*) Nothing to Disclose

#### TEACHING POINTS

\* To review the indications, limitations, and benefits of plain abdominal radiographs.\* To discuss the basic projections in the abdominal radiograph.\* To show normal anatomy and its variants.\* To analyze the systematic approach for interpretation of abdominal radiographs and provide a guide for residents.\* To recognize normal bowel from the abnormal small and large bowel. \* To be familiarize with descriptive terms for common bone and soft tissue abnormalities seen on abdominal radiographs.\* To review abnormal calcification on an abdominal radiograph. \* To review the lines, tubes, and other devices commonly seen on AXR including their purposes and proper positions.

#### TABLE OF CONTENTS/OUTLINE

1. Review of indications, advantages, and disadvantages of plain abdominal radiographs. 2. Discuss the basic projections in the abdominal radiograph. 3. Explain the normal anatomy and its variants. 4. Discuss the algorithm for the evaluation of abdominal x-ray. 5. Present a series of cases to exemplify the most important diseases presented in AXR: - Abnormal calcifications: solid organs, hollow organs, and others. - Classification of bowel gas patterns: intraluminal and extraluminal. - Fluid/Soft Tissue Density: intraluminal and extraluminal. - Displacement of Structures: splenomegaly and hepatomegaly. - Bone and soft tissue abnormalities: osteophytes, neoplasms, post traumatic, and metabolic. 6. Recognize and illustrate devices commonly seen on AXR, the lines, tubes, and drains with demonstrative cases. 7. Conclusions and a complete section of key points of what residents need to know of abdominal X-rays. 8. References.

Printed on: 02/07/23



## Abstract Archives of the RSNA, 2022

GIEE-85

### Cosmetic Surgery in the Abdomen and Pelvis: Post-Operative Appearances and Complications

Sunday, Nov. 27 8:00AM - 9:00AM Room: Learning Center - GI

#### Participants

Madeleine Sertic, MBBCh, Boston, MA (*Presenter*) Nothing to Disclose

#### TEACHING POINTS

Since the turn of the 21st century, there has been a significant increase in the number of Cosmetic Surgeries performed. In 2020 alone, there were more than 2 million cosmetic procedures in the United States, including over 200,000 liposuction procedures, over 90,000 abdominoplasties, and more than 20,000 gluteal augmentation surgeries. While most of these cases do not undergo routine pre- or post-operative imaging, the increased incidence of these surgeries has led to an increased number of post-op patients who are imaged for other reasons. It is important to understand the expected post-operative appearances of these procedures so as to not misdiagnose pathology, and to correctly identify complications, if present. The expected post-surgical appearances and possible complications vary depending on the specific surgery. Gluteal injections and implants can be complicated by silicone granuloma formation or implant rupture. Abdominoplasty with gluteal fat transfer (i.e. "Brazilian Butt Lift") can be complicated by fat embolism; the risk varies with the surgical technique used. Complications for most procedures include infection, hematoma, and dehiscence.

#### TABLE OF CONTENTS/OUTLINE

Background on Cosmetic Surgery  
Abdominal Wall Augmentation  
Liposuction  
Abdominoplasty  
Abdominoplasty with Gluteal Fat Transfer  
Gluteal Augmentation  
Implants  
Injections  
Pelvic Augmentation  
Cosmetic Phalloplasty  
Cosmetic Labiaplasty  
Complications  
Hematoma  
Infection  
Dehiscence  
Fat Embolism  
Granuloma Formation  
Implant Rupture

Printed on: 02/07/23



## Abstract Archives of the RSNA, 2022

GIEE-86

### Utilization of Perfusion CT to Improve the Diagnostic Accuracy of Pancreatic Cancer

Sunday, Nov. 27 8:00AM - 9:00AM Room: Learning Center - GI

#### Participants

Konno Yoshihiro, PhD, (*Presenter*) Nothing to Disclose

#### TEACHING POINTS

The accuracy improvement of diagnostic imaging of pancreatic cancer including the early lesion is necessary. Functional information obtained by perfusion CT (PCT) would be able to address unmet clinical needs in conventional diagnostic imaging based on morphological images. We have developed a novel protocol that incorporates volumetric PCT into multiphase contrast-enhanced CT, enabling broad clinical use. Besides reducing radiation exposure, this method provides high-resolution perfusion information through parametric map fused with morphological images. In general, pancreatic cancer is depicted as a decreased area of blood flow and blood volume and a prolonged area of mean transit time compared with the background pancreatic parenchyma. Imaging assessment using PCT increased the diagnostic accuracy of small pancreatic cancers and helped detect minute lesion that was not visible as a mass. Perfusion information is associated with histopathological features, and its detailed examination may be useful in the management of pancreatic cancer.

#### TABLE OF CONTENTS/OUTLINE

1. Clinical issues in imaging diagnosis of pancreatic cancer. 2. Development of PCT imaging protocol. 3. High-resolution perfusion imaging: Parametric map analysis. 4. Reduction of exposure dose. 5. Imaging evaluation of pancreatic cancer using PCT. 6. Clinical usefulness and research applications.

Printed on: 02/07/23



## Abstract Archives of the RSNA, 2022

GIEE-88

### The Forgotten Organ: Role of Contrast Ultrasound in the Evaluation of Splenic Lesion

Sunday, Nov. 27 8:00AM - 9:00AM Room: Learning Center - GI

#### Participants

Paula Garcia, MEd, PhD, (*Presenter*) Nothing to Disclose

#### TEACHING POINTS

- To assess the role of contrast enhanced ultrasound (CEUS) in the characterization of non-traumatic splenic focal lesions.
- To review the technique used and the main fundamentals of CEUS as well as the main indications.
- To analyze the different focal splenic lesions through representative cases with special emphasis on the semiology of the lesions and their behavior after the injection of ultrasound contrast material.

#### TABLE OF CONTENTS/OUTLINE

Focal splenic lesions (FSL) are rare compared to those of other organs such as the liver and are often discovered incidentally. Conventional ultrasound and Doppler ultrasound have a limited role in the characterization of FSL, many of them being non-specific due to the wide spectrum of radiological manifestations they may present. CEUS is an accessible, inexpensive and safe technique that can help in the characterization of FSL. We analyzed the main imaging findings supporting us in the anatomopathological diagnosis, through representative cases performed in our center of both benign (simple cyst, abscesses, cystic lymphangioma, hemangioma, hamartoma) and malignant (lymphoma, metastasis) lesions. CEUS has an added role in the characterization of FSL allowing to see the enhancement of lesions in real time. Therefore, the spleen presents a special appetite for contrast due to the unique histological characteristics of this organ. CEUS may become a good alternative when other diagnostic techniques such as computed tomography (CT) and magnetic resonance imaging (MRI) are not available.

Printed on: 02/07/23

## Abstract Archives of the RSNA, 2022

GIEE-89

### Role of Ultrasound Contrast in the Evaluation of Gallbladder Pathology

Sunday, Nov. 27 8:00AM - 9:00AM Room: Learning Center - GI

#### Participants

Kanupriya Vijay, MBBS, MD, Jacksonville, FL (*Presenter*) Nothing to Disclose

#### TEACHING POINTS

1. Conventional grayscale ultrasound (US) is useful in evaluating various gallbladder diseases; however, assessment of microvascularity is often needed for detailed wall assessment and to distinguish many benign from malignant processes. 2. Contrast-enhanced ultrasound (CEUS) is an easy and effective modality to differentiate conditions such as tumefactive sludge from gallbladder cancer. 3. CEUS may be useful in differentiating benign wall thickening from adenomyomatosis and chronic cholecystitis and gallbladder cancer. 4. CEUS can accurately demonstrate the microvascularity used to differentiate adherent biliary precipitate from polyps, and can help identify features of malignancy. 5. Cholecystectomy tube injection of ultrasound contrast can be used to determine cystic duct patency and identify leak.

#### TABLE OF CONTENTS/OUTLINE

1. Introduction: a. Briefly review microbubble formulation and pharmacokinetics b. Discuss imaging techniques with CEUS to optimize image quality 2. Case guided review of various gallbladder pathologies a. Benign i. Stones ii. Adenomyomatosis iii. Polyps iv. Chronic cholecystitis v. Tumefactive sludge b. Malignant i. Gallbladder carcinoma ii. Malignant polyps 3. Role of CEUS in interventions a. Image guided biopsy b. Evaluation of cholecystostomy tube for cystic duct patency and leaks 4. Pitfalls

Printed on: 02/07/23

## Abstract Archives of the RSNA, 2022

GIEE-9

### Retrorectal Cystic Lesions: Utility of Magnetic Resonance Imaging for a Forbidden Space

Sunday, Nov. 27 8:00AM - 9:00AM Room: Learning Center - GI

#### Participants

Lautaro Florentin, MD, Buenos Aires, Argentina (*Presenter*) Nothing to Disclose

#### TEACHING POINTS

- The retrorectal cystic lesions include a wide spectrum of etiologies.- The magnetic resonance imaging (MRI) allows approximate the diagnosis and to determine complications.- Diffusion weighted imaging (DWI) sequence is a cornerstone to suggest the presence of a solid component within the cyst.- Surgical management is mainly influenced by the MRI findings. The third sacral vertebra (S3) level is the key point for surgical approach selection.

#### TABLE OF CONTENTS/OUTLINE

1) Introduction and anatomy 2) Differential diagnosis. Definition and imaging characteristics a) Developmental cysts - Dermoid cysts - Epidermoid cysts - Retrorectal cystic hamartomas (tailgut cysts) b) Malignancy - Rectal carcinomas with atypical presentations - Metastases c) Abscess d) Others - Vascular malformations - Granulomas 3) MRI advantages a) Intracystic content characterization - What to look for? (Size, lobulations, septum, walls, dense, fat and/or solid component) - Malignancy signs - Complications: infection and fistula. b) Malignant transformation - Why does it matter? Prognosis and management implications. - How to diagnose? DWI/ADC utility. Avoiding pitfalls: teratomas and dense-content lesions. c) Surgical planning. What radiologist apports to the surgeon? - Surgical approach selection. The S3 level. - Non-surgical treatment. The MRI role

Printed on: 02/07/23



## Abstract Archives of the RSNA, 2022

GIEE-90

### When the Bile Goes Sour: A Case-based Review of Unusual Complications of Biliary Procedures

Sunday, Nov. 27 8:00AM - 9:00AM Room: Learning Center - GI

#### Participants

Cynthia Borborema, MD, Sao Paulo, Brazil (*Presenter*) Nothing to Disclose

#### TEACHING POINTS

To review the expected imaging appearance after hepatobiliary surgeries. To list radiologic features of early and late usual biliary postsurgical complications to provide a practical resource for radiologists to standardize examination. To illustrate cases of unusual complications after biliary procedures to improve the clarity and clinical impact of radiology reports.

#### TABLE OF CONTENTS/OUTLINE

Anatomy of the normal biliary tract. Most common variants of the biliary tree and their surgical relevance. Role of imaging in surgical planning and relevant report information. List of most common biliary surgeries and procedures. Epidemiological background of biliary procedures and associated complications. Usual complications after biliary procedures (biliary and nonbiliary, early and late ones), including key patient history, risk factors, imaging findings, and pitfalls. Unusual postsurgical biliary complications, including right hepatic artery pseudoaneurysm, post-cholecystectomy Mirizzi syndrome, late cholangitis after Kasai procedure, lung abscess due to retained gallstones, subcapsular liver hematoma after cholecystectomy, foreign-body granuloma caused by dropped gallstones simulating abdominal wall tumor, and others. Diagnostic tools, including magnetic resonance cholangiopancreatography (MRCP). Optimal imaging protocols.

Printed on: 02/07/23



## Abstract Archives of the RSNA, 2022

GIEE-91

### Misses and Misinterpretations of Pancreatic Adenocarcinoma: Recognizing Its Atypical Manifestations

Sunday, Nov. 27 8:00AM - 9:00AM Room: Learning Center - GI

#### Participants

Pavan Shah, MD, Sayreville, NJ (*Presenter*) Nothing to Disclose

#### TEACHING POINTS

Pancreatic adenocarcinomas are highly lethal and timely detection is key to improving patient prognosis. While most cases present with typical features of pancreatic ductal dilatation, hypo enhancing mass and mass with restricted diffusion, some cases can present a diagnostic dilemma and are frequently misdiagnosed. Recognizing the atypical features helps in early diagnosis. We present atypical cross-sectional imaging findings of pancreatic adenocarcinoma. To review the epidemiology, pathology, and prognosis of pancreatic ductal adenocarcinoma. To describe typical imaging characteristics of PDAC along with atypical features to improve diagnostic accuracy. To discuss optimization of imaging techniques with the goal of preventing diagnostic delays and improving prognosis.

#### TABLE OF CONTENTS/OUTLINE

Introduction, epidemiology, clinical manifestations, histopathology, typical CT/MRI findings, atypical CT/ MRI findings including lesions without pancreatic ductal dilatation, lesions without restricted diffusion, lesions masquerading as cystic lesions, lesions presenting as acute pancreatitis, groove pancreatitis. Discussion on optimization of CT technique including use of dual energy, optimization of MRI techniques including use of MRCP, and T1 weighted sequences. Conclusion.

Printed on: 02/07/23



## Abstract Archives of the RSNA, 2022

GIEE-92

### Inflammatory Bowel Disease: Fluoroscopic Assessment and Postoperative Complications

Sunday, Nov. 27 8:00AM - 9:00AM Room: Learning Center - GI

#### Awards

Certificate of Merit

#### Participants

Linda Kelahan, MD, Chicago, IL (*Presenter*) Nothing to Disclose

#### TEACHING POINTS

1. Revisiting fluoroscopic findings in inflammatory bowel disease (IBD) with cross sectional correlation. 2. Outline possible surgical interventions for IBD. 3. Steps to successful fluoroscopic evaluation prior to ileostomy reversal 4. Fluoroscopic assessment of postoperative surgical complications.

#### TABLE OF CONTENTS/OUTLINE

1. Introduction a. Definition of IBD b. Epidemiology 2. Multimodality imaging of IBD a. Small bowel follow-through and barium enema examination. i. Technique ii. Imaging findings b. Cross sectional imaging findings 3. Fluoroscopic evaluation prior to ileostomy reversal a. Evaluate records to determine anatomy and surgical anastomoses b. Scout images in multiple obliquities c. Water-soluble fluoroscopic LGI steps to success d. Troubleshooting common complications during LGI: how to navigate enterocutaneous fistulas, severe anastomotic strictures, no contrast progression into the ostomy bag, multiple anastomoses. 4. Common surgical procedures (Fluoroscopic assessment of the altered anatomy) a. Small bowel resection b. Small bowel strictureplasty c. Total abdominal colectomy with ileorectal anastomosis d. Total abdominal colectomy with end ileostomy e. Colectomy (segmental/total) f. Proctectomy g. Restorative proctocolectomy with ileal pouch anal anastomosis h. Balloon dilatation 5. Postoperative complications: Fluoroscopic assessment with cross sectional correlation a. Strictures b. Pelvic infections c. Anastomotic site leakage d. Pouch failure e. Pouch cancer f. Fecal incontinence 6. Conclusion and take-home messages

Printed on: 02/07/23



## Abstract Archives of the RSNA, 2022

GIEE-93

### Early Postoperative GI Tract Evaluation: From Expected Findings to Complications

Sunday, Nov. 27 8:00AM - 9:00AM Room: Learning Center - GI

#### Awards

Identified for RadioGraphics

#### Participants

Louise Cavalcanti, MD, Sao Paulo, Brazil (*Presenter*) Nothing to Disclose

#### TEACHING POINTS

1. Distinguishing frequent and expected postoperative image findings after gastrointestinal tract surgical procedures from complications is essential in the early postoperative period, as well as detecting signs of possible complications that require further investigation. 2. Intraperitoneal free air and fluid, fat stranding and bowel dilatation are extremely common findings in the early postoperative image and, although are expected, they can sometimes represent signs of complications. The imaging characteristics and evolution are key for this differentiation. 3. Contrast-enhanced CT is the imaging method of choice for the evaluation of patients in the early postoperative period, with good characterization of gas and free fluid and the possibility of using positive oral contrast in patients with suspected anastomotic leakage or bowel perforation.

#### TABLE OF CONTENTS/OUTLINE

a. Introduction. b. CT protocol for early postoperative evaluation. c. Evaluation of intraperitoneal air: residual postoperative pneumoperitoneum or complication? d. Evaluation of intraabdominal fluids: sterile postoperative content or infected collections - imaging features and score systems. e. Fat stranding patterns of the mesentery that may suggest postoperative complications. f. Identification of dilated bowel and differentiation between metabolic, obstructive or ischemic conditions. g. Other expected postoperative findings and major early complications. h. Take home messages.

Printed on: 02/07/23



## Abstract Archives of the RSNA, 2022

GIEE-94

### Magnetic Resonance Imaging Evaluation of Perianal Fistulas: Making It Easier For Surgeons and Radiologists!

Sunday, Nov. 27 8:00AM - 9:00AM Room: Learning Center - GI

#### Participants

Joao Manoel Santos, MD, Sao Paulo, Brazil (*Presenter*) Nothing to Disclose

#### TEACHING POINTS

The purpose of this exhibit is:- To review usual and unusual cases of perianal fistulas.- To correlate important findings with the anatomy and pathophysiology.- To discuss image findings according to Parks and St James's University Hospital classifications, in order to enhance surgeons and radiologists' skills.- To review MRI protocols in the evaluation of patients with perianal fistulas.- To highlight their characteristics in order to familiarize surgeons and radiologists with these conditions, preventing unfavorable patient outcome.

#### TABLE OF CONTENTS/OUTLINE

Applied anatomy of the anal sphincter complex.MRI protocols in the evaluation of patients with perianal fistula.Parks classification with sample cases of:- Intersphincteric Suprasphincteric- Transsphincteric- Extrasphincteric.St James's University Hospital classification with sample cases of:- Grade 1: simple linear intersphincteric fistula- Grade 2: intersphincteric fistula with an abscess or secondary track- Grade 3: transsphincteric fistula- Grade 4: transsphincteric fistula with an abscess or secondary track in the ischioanal or ischioanal fossa- Grade 5: supralelevator and translevator disease.Correlation between Parks and St James's University Hospital classifications.Submucosal fistula.How do I report?- Location- Track o Relationship to sphincters o Simple or complex? Sample cases of pearls, pitfalls, diagnostic difficulties, and mimics.Summary and take-home messages.

Printed on: 02/07/23



## Abstract Archives of the RSNA, 2022

GIEE-95

### Most Common Gastrointestinal Post-surgical Anatomy on CT: A Pictorial Review. Radiologists- Don't Be Afraid

Sunday, Nov. 27 8:00AM - 9:00AM Room: Learning Center - GI

#### Participants

Louise Cavalcanti, MD, Sao Paulo, Brazil (*Presenter*) Nothing to Disclose

#### TEACHING POINTS

1. Radiological evaluation of the post-operative abdomen can be challenging and knowledge of normal post-operative anatomy is important to identify possible complications. 2. The intention of this pictorial review is to describe the most important gastrointestinal surgical techniques, their clinical indications and show their normal post-operative appearance on computed tomography (CT). 3. Besides that, this essay provides some signs to identifying the procedure, which can be helpful particularly when surgical history is missing, with recognition of the organ(s) involved, determination of what was resected and familiarity with the type of anastomoses used.

#### TABLE OF CONTENTS/OUTLINE

a. Introduction b. Imaging methods and protocols for postoperative evaluation. c. Identification of mechanical stapling patterns and radio-opaque markers from the anastomosis. d. Evaluation of gastric surgical techniques, including bariatric procedures and expected results. e. Evaluation of small bowel surgical techniques. f. Evaluation of the most common colorectal surgical techniques, including Hartmann procedure and restoration of intestinal continuity. g. Take-home messages.

Printed on: 02/07/23



## Abstract Archives of the RSNA, 2022

GIEE-96

### A "Spectral-acular" Ileus

Sunday, Nov. 27 8:00AM - 9:00AM Room: Learning Center - GI

#### Participants

Reza Al-Saudi, MD, Belfast, United Kingdom (*Presenter*) Nothing to Disclose

#### TEACHING POINTS

1. Gallstone ileus represents a rare cause of small bowel obstruction. 2. Sensitivity of CT in the diagnosis of gallstone ileus is > 90%. 3. CT diagnosis of gallstone ileus is dependent on establishing the features of Rigler's triad - small bowel obstruction, pneumobilia, and an ectopic calcified gallstone. 4. 15% - 20% of gallstones are radio-opaque. This fact limits the Radiologist's ability to definitively establish the presence of an ectopic gallstone, although this presence is usually inferred based on associated features. 5. Spectral CT offers numerous advantages over standard CT. Spectral CT utilises the principle that elements and by extension mixed-composition materials cause differing attenuation of photons (via photo-electric absorption) at energy levels near the k-edge of the element in question, as compared to the remainder of the energy spectrum. The differing behaviour of elements across the energy spectrum allows material differentiation and the determination of material composition. 6. Effective atomic number (Z effective), mono-energetic (mono keV), and iodine density spectral reformats all aide in material differentiation. Z effective reformats provide the most reliable and reproducible results in relation to the detection of radio-lucent gallstones.

#### TABLE OF CONTENTS/OUTLINE

1. Introduction. 2. Role of conventional CT. 3. Conventional CT vs Spectral CT. 4. Spectral CT - options for diagnosis.

Printed on: 02/07/23



## Abstract Archives of the RSNA, 2022

GIEE-97

### Pancreas Allograft biopsies: What do you need to know?

Sunday, Nov. 27 8:00AM - 9:00AM Room: Learning Center - GI

#### Participants

Dayhane De Souza, MD, Sao Paulo, Brazil (*Presenter*) Nothing to Disclose

#### TEACHING POINTS

1 - Describe the anatomy of the main pancreatic transplantation technique.??2 - Discuss the Pancreas graft biopsy and Percutaneous needle biopsy technique guided by Ultrasound (US) and Computed Tomography (CT).3 - Discuss the sample of the pancreas considered adequate for evaluation.

#### TABLE OF CONTENTS/OUTLINE

1 - Review indications for pancreas transplantation and causes of graft injury.2 - Illustrate anatomy and surgical techniques supported by the use of graphics and cross-sectional imaging cases. 3 - Discuss the indication for pancreas graft biopsy and biopsy access routes.4 - Discuss what constitutes a satisfactory graft sample and what are the histopathological findings.5 - Summary and take home messages.

Printed on: 02/07/23



## Abstract Archives of the RSNA, 2022

GIEE-98

### Hepatocellular Lesions In Patients with Vascular Liver Diseases : Radiologic-Pathologic Correlation

Sunday, Nov. 27 8:00AM - 9:00AM Room: Learning Center - GI

#### Participants

Mayu Uka, (*Presenter*) Nothing to Disclose

#### TEACHING POINTS

The purpose of this exhibit is: 1) To review imaging features on contrast enhanced CT, MRI of hepatocellular nodules found in vascular liver diseases with histopathological correlations. 2) To discuss the point of differential diagnosis.

#### TABLE OF CONTENTS/OUTLINE

Hepatocellular nodules have been recognized in vascular liver diseases (Budd-Chiari syndrome, congenital portosystemic shunt, hereditary hemorrhagic telangiectasia, extrahepatic portal vein obstruction and congenital heart disease etc.). They may be related to portal venous deprivation, venous outflow obstruction, or arterial diseases, imbalances in arterial, portal, and venous blood flow have been reported to cause nodule formation. These nodules include nodular regenerative hyperplasia, large regenerative nodule, partial nodular transformation, focal nodular hyperplasia, and others, as well as hepatocellular adenoma and hepatocellular carcinoma, which are true neoplastic lesions. Some confusions in their identification and overlap in their definitions exist. This exhibit will describe the imaging appearances of each type of hepatocellular nodules found in the vascular liver diseases, by correlating with histology, and provide some clues for their differential diagnosis.

Printed on: 02/07/23



## Abstract Archives of the RSNA, 2022

GIEE-99

### Deep Learning Reconstruction of MR Imaging: Technical Features and Clinical Impact on Abdominal MR Imaging

Sunday, Nov. 27 8:00AM - 9:00AM Room: Learning Center - GI

#### Participants

Hironitsu Onishi, MD, Suita, Japan (*Presenter*) Research Grant, General Electric Company; Speakers Bureau, General Electric Company

#### TEACHING POINTS

Deep learning reconstruction (DLR) has been introduced by several vendors to improve MR image quality. DLR has various benefits such as effective noise reduction in the diagnosis with MR imaging. The purpose of this presentation is: 1. To illustrate technical features of DLR compared with conventional reconstruction, 2. To discuss image quality of MR imaging using DLR, and 3. To discuss clinical impact on MR study in the diagnosis of abdominal diseases.

#### TABLE OF CONTENTS/OUTLINE

1. Overview 2. Principle of DLR 3. Difference from the conventional reconstruction technique 4. Sequences applicable to DLR: fast spin echo T2WI, single-shot fast spin echo T2WI, DWI, small field-of-view DWI, fast imaging employing steady-state acquisition (FIESTA), etc. 5. Effective reduction of image noise with DLR 6. Improved spatial resolution with DLR 7. Reduction of truncation artifacts with DLR 8. What purpose can DLR be used for in clinical practice? To improve image quality, to increase the spatial resolution of the images, to save acquisition time, or combination of them 9. Clinical impact on the diagnosis of liver diseases 10. Clinical impact on the diagnosis of pancreatic diseases 11. Summary

Printed on: 02/07/23



## Abstract Archives of the RSNA, 2022

GUEE

### Genitourinary Education Exhibits

Sunday, Nov. 27 8:00AM - 9:00AM Room: Learning Center - GU

#### Sub-Events

#### **GUEE-1 Imaging of Perirenal Retroperitoneal Lymphatic Systems: Anatomy, Function and Conditions**

##### Awards

Identified for RadioGraphics

Cum Laude

##### Participants

Hiroaki Takahashi, MD, PhD, Rochester, MN (*Presenter*) Nothing to Disclose

##### TEACHING POINTS

Normal perirenal lymphatic drain is difficult to identify on conventional imaging. It is partially visualized by CT- and MRI- lymphangiogram. It is also occasionally depicted as pyelolymphatic backflow on retrograde pyelogram, intravenous urogram and CT urogram secondary to acute rise of pressure in the collecting system. However, the knowledge of perirenal lymphatic flow is of clinical importance to understand the conditions involving the perirenal retroperitoneal lymphatics and behavior of lymph node metastases from renal or upper tract urothelial malignancy. This exhibit will review the fundamental concept about perirenal lymphatic systems, and imaging assessment for non-neoplastic and neoplastic conditions involving the perirenal lymphatics. Further, differential diagnosis and treatment strategy of these conditions are discussed. The purposes of this exhibit are: 1. To review the fundamental anatomy, physiology and imaging of normal perirenal lymphatic systems. 2. To review the imaging findings, differential diagnoses and treatment options for various conditions associated with perirenal lymphatic systems.

##### TABLE OF CONTENTS/OUTLINE

1. Overview of the lymphatic system. 2. Fundamental anatomy and physiology of perirenal lymphatic systems. 3. Imaging of perirenal lymphatics and their communication with other lymphatic chains. 4. Imaging findings of various conditions of perirenal lymphatic systems with discussion of their differential diagnoses and treatment strategies. 5. Summary

#### **GUEE-10 Malignant Neoplasms of the Penis with Radiologic Pathologic Correlation**

##### Participants

Jamie Marko, MD, (*Presenter*) Nothing to Disclose

##### TEACHING POINTS

1. Most malignant tumors of the penis are squamous cell carcinomas (SCC) arising from the mucosal lining of the glans, coronal sulcus and foreskin. Non-epithelial tumors do not demonstrate the same anatomical predilection. 2. HPV infection is associated with subtypes of penile SCC. Additional risk factors are lack of circumcision, phimosis, chronic inflammation, lichen sclerosis, smoking, and radiotherapy. 3. Penile cancer commonly presents as a discrete mass, ulcer or erythematous lesion on the glans or foreskin in a male in their 5th or 6th decade of life. 4. Imaging may be used to evaluate the local extent of a penile neoplasm and to detect metastases. Penile SCC has a predictable pattern of spread from the inguinal lymph nodes (LN) to the pelvic LN and lastly to the periaortic LN. Systemic metastases, including to the liver, lungs, mediastinal LN, are a late event.

##### TABLE OF CONTENTS/OUTLINE

1. Review penile anatomy with an emphasis on frequent sites of tumor origin and local spread. We will emphasize the anatomic structures that affect local staging and impact management. 2. Illustrate the pathologic spectrum of malignant penile neoplasms. The pathologic descriptions will serve as the basis for understanding the imaging appearances. 3. Describe the multimodality imaging evaluation of penile cancer. 4. Illustrate the spectrum of penile cancer at imaging providing radiologic-pathologic correlation.

#### **GUEE-11 Benign Lesions of the Urinary Tract Mimicking Malignancy - Test Your Skills with this Case-based Review**

##### Participants

Javier Azpeitia Arman, MD, Madrid, Spain (*Presenter*) Nothing to Disclose

##### TEACHING POINTS

To illustrate equivocal imaging findings of upper and lower urinary tract lesions including normal variants, inflammatory/infectious diseases and benign tumors mimicking genitourinary malignancy. To analyze the correlation between cystourethrogram, IVU, US, CT and MR imaging features with pathology in urinary tract lesions. To emphasize pitfalls, diagnostic difficulties and differential diagnosis.

##### TABLE OF CONTENTS/OUTLINE

Although a mass or a thickening in the upper and lower urinary tract may be caused by urothelial carcinoma, several benign and

malignant entities should also be included in differential diagnosis. We review images of the urinary tract (pelvic/ureteral system, ureters, bladder and urethra) in different entities mimicking cancers in a quiz format, with clues to interpretation and providing images of malignant lesions for comparison. Imaging findings (cystourethrogram, IVU, US, CT and MR) and pathologic correlation will be presented. How pathologic correlation informs imaging interpretation will be highlighted. The list of cases presented includes: inflammatory diseases (pyelitis and cystitis cystica, eosinophilic ureteritis and cystitis, Keratinizing desquamative squamous metaplasia (cholesteatoma) of the ureter, polypoid, papillary, granulomatous BCG), secondary to chemotherapy or irradiation, benign tumors (papilloma, leiomyoma), extrinsic lesions (prostate hyperplasia and carcinoma, uterine and ovarian tumors, colonic cancer, diverticulitis, Crohn's disease, varicose ureteral veins), filling defects (lithiasis, ureterocele, blood clot), addition images (diverticula).

## **GUEE-12 Keeping it Retro: Reflecting on the Spaces, Planes, Pathologies of the Retroperitoneum**

### **Awards**

#### **Certificate of Merit**

Participants

Jessica Lovett, MD, (*Presenter*) Nothing to Disclose

### **TEACHING POINTS**

The purpose of this exhibit is to: 1. Review abdominopelvic anatomy, including the borders of the peritoneum and retroperitoneum. 2. Identify imaging findings to localize abdominal pathology to the peritoneum versus the retroperitoneum. 3. Examine the imaging signs used to localize pathology to a particular organ or space, focusing on retroperitoneal pathology. 4. Distinguish the pathways of spread of disease amongst the retroperitoneal compartments and surrounding compartments. 5. Apply these concepts with illustrative, interactive cases.

### **TABLE OF CONTENTS/OUTLINE**

1. Anatomic borders of the peritoneal and retroperitoneal compartments within the abdomen and pelvis, and communicating foramina. 2. Localizing signs to assist radiologists in localizing pathology to peritoneum, retroperitoneum, or a specific organ. 3. Key imaging findings and differential diagnosis, with focus on retroperitoneal pathology. 4. Relevance of anatomical boundaries and disease spread for surgical planning. 5. Challenging cases to demonstrate teaching points.

## **GUEE-13 Follow the Yellow Brick Road: An Educational Review of Current Imaging in Urethral Stricture Disease with a Focus on MRI**

Participants

Daniel Harris, (*Presenter*) Nothing to Disclose

### **TEACHING POINTS**

1. Provide important definitions and principles in urethral stricture disease including a brief overview of clinical assessment, treatment, and current diagnostic imaging guidelines as suggested by the AUA and EAU. 2. In-depth discussion of retrograde urethrography, sonourethrography, and magnetic resonance urethrography including their advantages, disadvantages, and best uses with examples from our practice including our own protocol for each imaging modality. 3. Suggest supported uses for magnetic resonance urethrography by compiling case series data from over the last decade. Then, discuss an example case where multiple imaging modalities were used, providing direct comparison of magnetic resonance urethrography to the other modalities.

### **TABLE OF CONTENTS/OUTLINE**

1. Introduction: definitions, clinical assessment, and treatment modalities for urethral strictures 2. Imaging modality sections: Current uses, advantages, disadvantages, potential future applications for each respective modality 2a. Retrograde urethrography, Sonourethrography, Magnetic resonance urethrography 2b. Table summarizing MRU case findings from prominent case series 3. Example case: comparison of modalities

## **GUEE-14 Adrenal Lesions Inside Out" - A Pictorial Review of the Correlation Between Radiologic and Anatomopathological Patterns of Benign and Malign Adrenal Lesions**

Participants

Camila Franco, BMedSc, (*Presenter*) Nothing to Disclose

### **TEACHING POINTS**

1. Review adrenal gland anatomy and discuss how it is important in the evaluation of adrenal lesions 2. Discuss the role of imaging and pathological evaluation in the assessment of adrenal gland lesions 3. Review the most common and uncommon imaging and anatomopathological patterns of benign and malignant adrenal lesions. 4. Understand the correlation between radiologic and anatomopathological findings

### **TABLE OF CONTENTS/OUTLINE**

Adrenal gland lesions have a prevalence of 4-7% in imaging tests among adults. The prevalence of these lesions increases with the greater availability of imaging tests and as the population gets older. Once the adrenal gland is made of different types of tissues that produce various types of hormones, adrenal lesions may present different features. This pictorial review will discuss: 1. Adrenal gland anatomy and histology review 2. The role of different imaging and anatomopathological techniques in evaluation of adrenal lesions (a) Ultrasound (b) Computed tomography (c) Magnetic resonance (d) PET/CT (e) Gross specimen evaluation (f) Histology - Morphological criteria - Immunohistochemical studies (g). Molecular pathology 3. Different (usual and unusual) imaging and anatomopathological patterns of benign and malignant adrenal lesions and how they correlate (a) Adenoma (lipid-rich and lipid-poor) (b) Aldosteronoma (c) Myelolipoma (d) Hematoma (e) Macronodular adrenal bilateral hyperplasia (f) Neural crest tumors (g) Cysts (h) Pheochromocytoma (i) Adrenocortical carcinoma (j) Metastatic neoplasms (k) Miscellaneous

## **GUEE-15 What Do We See When We Don't See the Bladder? Review of the Main Urinary Diversion Techniques and Their Complications**

### **Awards**

#### **Certificate of Merit**

Participants

Alba Salgado Parente, MD, Madrid, Spain (*Presenter*) Nothing to Disclose

#### TEACHING POINTS

1. Review the different types of urinary diversion techniques.2. To understand the common findings to be expected in a postoperative study using the different imaging techniques (MDCT, MRI, fluoroscopy).3. To recognize the main postoperative complications, both early and late, grouped according to pathological groups.

#### TABLE OF CONTENTS/OUTLINE

1. Introduction2. Radiological protocol for post-operative evaluation (MDCT, MRI, fluoroscopy, US).3. Main surgical techniques and expected post-operative findings.3.1 Cutaneous incontinent diversions: Cutaneous diversion (Uretero-ureterocutaneostomy), Ileal conduit.3.2 Continent diversions: Indiana pouch, Orthotopic Bladder Replacement.4. Post-operative complications: Pictorial review4.1 Collecting system: Hydronephrosis, Urolithiasis, Urinary leakage, Ureteral stricture.4.2 Intestinal loops: Alteration of the intestinal rhythm, Intestinal leakage, Stomal stricture, Parastomal herniation, Fistulas, ileal conduit necrosis.4.3 Infection: pyelonephritis, abscesses, and other collections (hematoma, lymphocele).4.4 Tumoral: Local recurrence, Distant recurrence.5. Systematic approach to urinary diversions5.1 What type of urinary diversion surgery has been performed?5.2 Points of particular interest when assessing the presence of each type of complication6. Take home messages7. Bibliography

#### GUEE-16 Radiological Lexicon for Renal Mass Characterization: Pictorial Review

Participants

Rebeca Gil Vallano, Madrid, Spain (*Presenter*) Nothing to Disclose

#### TEACHING POINTS

- Revise a list of standardized terms employed to describe renal masses: basic imaging, CT, MR and miscellaneous terms.
- Correlate each term with several cases from our institution with pathologic correlation.

#### TABLE OF CONTENTS/OUTLINE

Radiology reports need to employ a standardized language to improve their understanding for the rest of radiologists, clinicians and patients. In February 2021 the Society of Abdominal Radiology disease-focused panel on renal cell carcinoma published a consensus statement of recommended terms to be employed when reporting renal masses at CT and MR. We have revised the 31 terms described in this consensus: 14 basic terms such as definition of solid or cystic mass, 8 CT terms for example macroscopic fat or CT enhancement, 6 MR terms as MR enhancement and 3 miscellaneous terms like growth rate. Each term will be reviewed, explained and illustrated with different cases of our institution. In addition, we will offer an interesting anatomopathological approach to the cases presented. Knowledge of this lexicon will improve radiological reports, decrease interobserver variability, and facilitate communication with physicians.

#### GUEE-17 To Infinity and Beyond: Present and Future of Contrast Enhanced Ultrasound (CEUS) in Renal Transplant

##### Awards

Certificate of Merit

Identified for RadioGraphics

Participants

Tomas Fernandez, MD, Barcelona, Spain (*Presenter*) Nothing to Disclose

#### TEACHING POINTS

Assessment of renal transplant complications with CEUS. Review of unusual and latest complications associated with up-to-date surgical techniques and immunosuppressant therapies. Future of CEUS on renal transplant patients, focusing on radiomics.

#### TABLE OF CONTENTS/OUTLINE

Immediate complications Intracavitary ultrasound in robot renal transplant. CEUS in hyperacute rejection. CEUS in acute tubular necrosis. CEUS in cortical necrosis. CEUS in arterial and venous thrombosis. CEUS in compartmental syndrome. CEUS in segmentary infarcts. Living renal donor transplant pseudostenosis. Urological complications: CEUS guide for nephrostomy. CEUS anatomy of the intracavitary upper urinary tract (UUT). CEUS in UUT leak. CEUS in the differentiation of benign and malignant diseases of UUT. CEUS in ureteral kinking and stenosis. Collections CEUS in posttransplant collections. Late subcapsular lymphocele and sinus lymphatic ingurgitation due to mTOR. Subcapsular hematoma due to hemorrhagic cyst. Presurgical ureteral map for marsupialization of lymphoceles. CEUS in renal infection. Malignancies associated with renal transplant: Malignancies associated with immunosuppression and more prevalence of tumors due to extended age inclusion on donor lists. Malignancies associated with acquired cystic disease in long hemodialysis. Known malignancies, partial nephrectomy ex vivo. CEUS in active surveillance of complicated cysts and biopsied benign tumors. Biopsy CEUS as a guide for biopsy. CEUS in arteriovenous fistula and pseudoaneurysm. CEUS in the diagnosis of active bleeding. CEUS in US-guided thrombin treatment of pseudoaneurysm/bleeding. Future: CEUS perfusion. Elastography. Radiomics.

#### GUEE-18 What's New in Classification, Pathology, Imaging Findings, and Management of Renal Cell Carcinomas? 2022 Update for Radiologists

Participants

Varshaa Koneru, Telangana, India (*Presenter*) Nothing to Disclose

#### TEACHING POINTS

Review updated, current classification of renal cell carcinomas (RCCs) that are based on histomorphology/molecular diagnostic criteria with special emphasis on novel tumor entities Discuss select pathologic/molecular features and genetic alterations that influence natural history, prognosis, metastatic disease targeted therapies Describe imaging findings of existing 'new' RCCs with an update on radiogenomics of select tumors Review novel treatment strategies for metastatic RCCs role of imaging in assessing efficacy of novel drugs

#### TABLE OF CONTENTS/OUTLINE

Introduction RCC Classification: Existing tumors, New tumors Emerging entities Pathology Updates: Molecular signatures, histopathology patterns TNM staging Imaging Findings Clear cell RCC Papillary RCC Chromophobe RCC Oncocytoma other oncocytic-hybrid tumors Clear cell papillary RCC Tubulocystic RCC MiTF Family RCC: Xp11 translocation TFEB-fused Acquired cystic disease-associated RCC SMARCB1-deficient RCC: Medullary carcinoma unclassified RCC with medullary phenotype Mucinous tubular spindle cell carcinoma Metanephric adenoma related tumors Hereditary RCC syndromes: Fumarate-deficient RCC, Succinate Dehydrogenase-deficient RCC Birt-Hogg-Dube syndrome RCC in Post-Radiation/Chemotherapy Multilocular Cystic Neoplasm of Low Malignant Potential RCC in Neuroblastoma Survivors Thyroid-like Follicular RCCs RCCs associated with ALK-Gene Rearrangements Molecular Imaging biomarkers Novel targeted therapies Role of Imaging Summary RCCs are genetically heterogeneous and demonstrate characteristic molecular features imaging findings that dictate prognosis survival

## **GUEE-19 Biochemical Recurrence of Prostate Cancer: Where Cancer Recurs, Where MRI Fails, and Where PSMA PET Fails?**

### **Awards**

**Identified for RadioGraphics**

Participants

Muhammad Awiwi, MD, Houston, TX (*Presenter*) Nothing to Disclose

### **TEACHING POINTS**

Prostate cancer can recur in up to 40% of patients who receive treatment (radical prostatectomy, androgen deprivation therapy, or radiotherapy) and the definition of biochemical recurrence varies according to the treatment type. There are typical sites of prostate cancer recurrence, but the disease can also recur in unusual sites in the pelvis. These sites should be interrogated when interpreting pelvic MRI. Both MRI and PSMA-PET have limitations/pitfalls and they complement each other.

### **TABLE OF CONTENTS/OUTLINE**

To review the definition of biochemical recurrence To review expected imaging findings after prostate cancer treatment Describe common sites of prostate cancer recurrence Describe uncommon sites of prostate cancer recurrence in the pelvis Describe potential pitfalls of MRI and PSMA-PET in detection of recurrent prostate cancer.

## **GUEE-2 Renal Mass Imaging with the Clear Cell Likelihood Score v2: A User Guide**

### **Awards**

**Identified for RadioGraphics**

Participants

Anup Shetty, MD, Saint Louis, MO (*Presenter*) Nothing to Disclose

### **TEACHING POINTS**

Solid small renal masses (SSRM), defined as < 4 cm in diameter, are increasingly detected but can be complex to manage. A framework for approaching the SSRM is critical in providing optimal management, as clear cell RCC is the most common and aggressive subtype, and a high likelihood of this diagnosis can influence management. The recently updated MRI clear cell likelihood score (ccLS) provides the radiologist with tools to optimize their assessment of the SSRM. This exhibit will: 1) Familiarize the reader with the ccLS and why it was developed 2) Discuss key considerations in MRI protocol, eligibility criteria, and imaging features for using the ccLS algorithm 3) Illustrate how to use the ccLS algorithm to assess the SSRM through a series of cases 4) Highlight pitfalls of the ccLS algorithm and other considerations in MRI of SSRM not included in ccLS

### **TABLE OF CONTENTS/OUTLINE**

- ccLS: rationale (moving beyond "is it enhancing, does it contain fat") and diagnostic performance- MRI protocol- Eligibility criteria and imaging features- How to use the algorithm- Case examples of working through the algorithm and pitfalls, including off-ramps when the ccLS is inappropriate to utilize (fat-rich angiomyolipoma, cystic renal mass, hemorrhagic renal cysts)- Reporting using ccLS: template and nomenclature- Potential management strategies based on ccLS

## **GUEE-20 Multicenter Lessons from Adrenal Multidisciplinary Tumor Boards: Expert Evidence-Based Views of the Society of Abdominal Radiology Adrenal Neoplasm Disease Focused Panel**

### **Awards**

**Certificate of Merit**

Participants

Ryan Chung, MD, Boston, MA (*Presenter*) Consultant, ScanMed, LLC; Stockholder, ScanMed, LLC

### **TEACHING POINTS**

While some adrenal pathology is easily diagnosed radiologically, there are many common errors in adrenal imaging that may arise due to a lack of familiarity with technical, anatomic, physiologic, hemodynamic, and biologic factors. This is compounded by a deficiency of modern clinical and radiologic knowledge of adrenal pathology. These challenges arise when the radiologist encounters atypical presentations of common benign and malignant adrenal masses, mimics of benign and malignant adrenal masses, and rare adrenal pathology. This may lead to misdiagnosis, suboptimal management, and potentially adverse outcomes. In this exhibit, we present cases commonly encountered in clinical practice and presented to adrenal multidisciplinary tumor boards of major tertiary centers. Evidence-based expert views will be discussed to provide clues to the correct diagnosis and further guide appropriate management. 1. Describe common errors encountered in clinical practice and presented to adrenal multidisciplinary tumor boards of major tertiary centers 2. Illustrate relevant technical, anatomic, pathophysiologic, hemodynamic, and biologic factors leading to these errors 3. Review evidence-based literature and discuss expert opinions to provide useful tips in diagnosis 4. Correlate cross-sectional imaging findings with clinical and pathologic findings

### **TABLE OF CONTENTS/OUTLINE**

1. Technical errors 2. Atypical presentations of common benign masses 3. Atypical presentations of common malignant masses 4. Benign mimics of malignant masses 5. Malignant mimics of benign masses 6. Rare adrenal pathology

## **GUEE-21 Participants**

## Postoperative Changes and Complications of the Urinary Tract at Imaging

Weibo Fu, BS, Augusta, GA (*Presenter*) Nothing to Disclose

### TEACHING POINTS

1) To review changes to the anatomy of the genitourinary tract after urological procedures 2) To provide imaging examples of postoperative appearance and complications of the urinary tract 3) To distinguish between expected and unexpected postoperative imaging findings following urological surgery and image-guided procedures

### TABLE OF CONTENTS/OUTLINE

The incidence of urological pathologies such as renal cell carcinoma and renal stones has risen over time, in part due to improved detection with increased use of imaging in clinical practice. In turn, rates of urologic interventions performed have also increased, some of which include a) partial nephrectomy, b) ureteroneocystostomy, c) cryoablation, d) diversions, and e) neobladder placement. Potential complications can arise from these procedures such as a) hematomas, b) conduits, c) strictures, and d) lymphoceles. Such complications are important to distinguish from common postoperative changes in clinical practice. Computed tomography scan is the most common imaging modality used when potential complications are suspected, though MRI may be considered for complex cases. For radiologists to provide appropriate recommendations for care following surgical urology procedures, a clear understanding of normal and abnormal post-operative anatomy is necessary.

### GUEE-22 Imaging Peyronie disease Before and After Treatment: A Guide for Radiologists Urologists

Participants

Lauren F. Alexander, MD, Jacksonville Beach, FL (*Presenter*) Spouse, Stockholder, Abbott Laboratories; Spouse, Stockholder, AbbVie Inc; Spouse, Stockholder, General Electric Company; Spouse, Stockholder, Myriad Genetics, Inc

### TEACHING POINTS

Ultrasound (US) is primary imaging modality for assessment of plaque and erectile dysfunction in patients with Peyronie disease to guide medical vs. surgical treatment planning; however, magnetic resonance imaging (MRI) and computed tomography (CT) can be used in the pretreatment and post treatment setting as well. After reviewing this exhibit the learner will: (1) Understand the pathophysiology of acute and chronic fibrosing Peyronie disease. (2) Recognize US findings of Peyronie plaques and US Doppler features of erectile dysfunction. (3) Describe role of noncontrast CT for calcified Peyronie plaques. (4) Determine when to use imaging after penile surgery. (5) Recognize normal and abnormal imaging findings of penile implants.

### TABLE OF CONTENTS/OUTLINE

A. Background (1) Pathophysiology of Peyronie's disease (2) Clinical exam findings: acute and chronic phases (3) AUA management algorithm B. Pre-treatment imaging with case examples (1) Penile US grayscale: plaque Doppler: erectile function (2) CT and MR when to use, typical protocols, findings (C) Surgical treatment options (1) tunical plication vs. plaque incision/excision +/- grafting (2) role of penile prosthesis (D) Post operative imaging (1) typical findings complications

### GUEE-23 Post-treatment MRI in Cervical Cancer - What To Look For

Participants

Mayra V. Soares, MD, Brasilia, Brazil (*Presenter*) Nothing to Disclose

### TEACHING POINTS

Basic technical key points of pelvic MRI for a targeted assessment. Quick review of the latest FIGO MRI staging system, with the anatomical landmarks. Correlation between staging and therapeutic options. MRI findings of post-treatment and post-intervention procedures. Challenges in differentiating post-treatment and tumor recurrence. Identify the main complications of cervical cancer treatments.

### TABLE OF CONTENTS/OUTLINE

Introduction: recurrency up to 30% of treated patients, which 66% occur in the next 2 year post initial treatment and 90% until 5 year, and survival rate can reach 15-20%. Technical points: MRI high-resolution oblique T2WI planes (small thickness and FOV) are critical to evaluate lesions. Anatomical landmarks: pelvic intricate anatomy requires the understanding of its compartments, cervix zones, vessels, sidewalls, ligaments, and lymph nodes. Staging and therapeutic correlation: Stage IIB (parametrial invasion) as a landmark for prognosis and therapeutic decision. Lower stages allow surgery with or without RT/QT. Stages IIB requires neoadjuvant treatment before reassessment. Main treatments MRI findings: trachelectomy and fertility-preserving treatment; hysterectomy/lymphadenectomy; RT/QT. Acute (vaginal edema/erythema, cystitis) and chronic (stenosis, fistulations, enteritis, insufficiency fractures, and urological) complications.

### GUEE-24 Prostate MRI Quality - A Pictorial Review Using the PI-QUAL Score

Participants

Francesco Giganti, MD, London, United Kingdom (*Presenter*) Nothing to Disclose

### TEACHING POINTS

The PI-RADS guidelines set out the minimal technical requirements for the acquisition of multiparametric MRI of the prostate. The rapid diffusion of prostate MRI has led to variability in vendor and scan quality across the world. The Prostate Imaging Quality (PI-QUAL) score was created to standardize the reporting of prostate MRI quality. Our education exhibit has 3 teaching points: 1) PI-RADS technical requirements for good quality prostate MRI; 2) Application of the PI-QUAL score; 3) Pictorial review of images from different vendors and magnets and quiz.

### TABLE OF CONTENTS/OUTLINE

All those involved in the acquisition and interpretation of prostate MRI (radiologists, MR physicists and radiographers) should be aware of the PI-RADS technical recommendations and could benefit from a learning module on the PI-QUAL score. We will: 1) discuss the technical requirements (e.g., FOV, in-plane resolution, b values, etc) for a good quality prostate MR scan for each sequence, as outlined in the PI-RADS document; 2) discuss the PI-QUAL score and its ambition to standardize image quality both at a center level (i.e., up-to-date MR scanners and dedicated radiologists/radiographers highly experienced in prostate MRI) and at a

patient level (i.e., patient-related artefacts such as rectal air/stools or movement should be minimized with prior preparation); 3) present a set of images of adequate and suboptimal image quality (ranging from PI-QUAL 1 to PI-QUAL 5) to stress the importance of reducing practice variability in prostate MRI; 4) discuss the current limitations of PI-QUAL and what should be addressed in the next version.

## **GUEE-25 Beyond Prostatic Adenocarcinoma - Confusing MRI Findings and How to Recognize Them**

Participants

Camila Reifegerste, MD, Curitiba, Brazil (*Presenter*) Nothing to Disclose

### **TEACHING POINTS**

Review normal prostate anatomy and possible neoplasm mimickers. Review benign conditions of the prostate that may mimic neoplasia. Review some rare histological subtypes of prostate neoplasia. To propose a systematic approach of the prostate MRI that allows differentiating findings suggestive of clinically significant neoplasia from the more common pitfalls.

### **TABLE OF CONTENTS/OUTLINE**

Prostate cancer is the most common neoplasm in American men and the second leading cause of cancer death in this population. Its diagnosis is based on rectal examination, elevated prostate specific antigen (PSA), ultrasound-guided prostate biopsy and magnetic resonance imaging (MRI), which has become an important tool in detection of possible neoplasms, risk stratification and follow-up, thanks to the standardization of examination protocols and their interpretation with the development of the Prostate Imaging-Reporting and Data System (PI-RADS). Since prostate MRI is becoming more relevant in clinical decision making, it is important that the radiologist be familiar with pitfalls in its interpretation, whether they are normal anatomical structures, benign prostate changes, or even rare malignant neoplasms, different from traditional adenocarcinoma. That's why we propose a review of challenging cases, in order to discuss some of these pitfalls.

## **GUEE-26 V Steps to Assess VI-RADS**

Participants

Vivianne Reis Guimaraes, MD, (*Presenter*) Nothing to Disclose

### **TEACHING POINTS**

1. Practice guide for radiologists, identify five steps in the process to create a systematic approach to report bladder MRI findings as well as define the risk of muscle invasion. 2. Provide radiologists an overview of Vesical Imaging-Reporting and Data System (VI-RADS) that indicates the possibility of detrusor muscle invasion by bladder cancer through the five-point scoring system. 3. Discuss resources for radiologists to improve diagnostic performance through VI-RADS.

### **TABLE OF CONTENTS/OUTLINE**

Step 1: Bladder wall anatomy and appearance of the muscularis propria on MRI. Step 2: Staging and how to subdivide bladder cancer into with and without muscle invasion. Step 3: Technical considerations about MR equipment and protocol. Step 4: Scoring tumors using appearances in T2W images, DWI and DCE to create an overall risk of muscle invasion score. Step 5: Final VI-RADS score and likelihood of muscle invasion.

## **GUEE-27 Gender Affirming Genitourinary Surgeries - What Surgeons Do and What We Need to Know**

Participants

Susana Fernandez, MD, Madrid, Spain (*Presenter*) Nothing to Disclose

### **TEACHING POINTS**

Define the concept of gender incongruence and transgender. Learn different types of genitourinary procedures employed for gender affirming surgery. Review imaging modalities used to evaluate surgical changes and complications. Show different cases presented at our institution.

### **TABLE OF CONTENTS/OUTLINE**

Gender incongruence is defined as a discrepancy between gender identity and the assigned sex. Those individuals in whom gender incongruence exists are referred to as transgender. The gender affirming therapy involves multidisciplinary care that can improve quality of life of transgender people. Genital reconstruction surgery includes vaginoplasty, phalloplasty and metoidioplasty. Radiology department plays an important role in this process. We have reviewed affirming surgeries performed at our institution in the last 10 years. 78 patients have undergone this process, 67 transwomen and 11 transmen. Surgical procedures performed were: 67 vaginoplasty, 6 phalloplasties (using most often anterolateral flaps) and 5 metoidioplasties. These surgeries and normal surgical changes will be explained and reviewed. Frequent complications such as fistulas (5), leaks (1) and stenosis (4) which are recurrent in some patients, will be exposed. Retrograde urethrocytography and cystourethrography are the methods of choice for postoperative assessment, allowing the diagnosis of most common complications. TC, RM or enema are other imaging techniques that may be necessary. They will be illustrated with different imaging techniques and images of different surgeries.

## **GUEE-28 Expect the Unexpected - Postoperative and Postintervention Imaging of the GU Tract**

Participants

Janelle West, MD, Pelham, AL (*Presenter*) Nothing to Disclose

### **TEACHING POINTS**

- To understand expected appearance of genitourinary structures after common and uncommon surgeries and interventions- To illustrate acute and chronic complications of genitourinary organs following intervention and/or surgery- To briefly discuss potential treatment of complications secondary to genitourinary interventions

### **TABLE OF CONTENTS/OUTLINE**

? Introduction? Renal: Expected appearance post ablation, Expected appearance post partial nephrectomy, Postablation renal infarct, Postablation residual/recurrent tumor, Postablation bleeding, Postablation organ injury/fistula, Post partial nephrectomy pseudoaneurysm? Ureter: Postsurgical stricture, Postsurgical leak/urinoma? Bladder: Expected appearance of augmented urinary

bladder/neobladder/ileal conduit/Indiana pouch, Augmented bladder rupture, Ileal conduit leak/rupture, Recurrent tumor in ileal conduit, Bladder neck leak status post prostatectomy? Urethra: Expected appearance post urethroplasty, Expected appearance status post transurethral resection of the prostate, Urethral leak status post urethroplasty, Urethral leak status post diverticulectomy, Recurrent urethral stricture status post TURP and brachytherapy, Urethrocutaneous fistula? Male GU: Expected appearance of penile prosthesis and artificial urinary sphincter, Postintervention arteriovenous fistula, Malfunctioning artificial urinary sphincter, Malpositioned penile prosthesis, Recurrent penile cancer status post penectomy, Puboprostic fistula status post brachytherapy/pelvic radiation? Female GU: Post DC uterine AVF (and subsequent embolization), Recurrent GYN malignancy, Retained products of conception

### **GUEE-29 Imaging Findings Following Renal Tumor Treatment**

Participants

Leonardo Kenji Mitsutake, MD, Sao Paulo, Brazil (*Presenter*) Nothing to Disclose

#### **TEACHING POINTS**

The purpose of this exhibit is to:- Brief review renal cancer epidemiology and the main societies management guidelines.- Describe CT and MRI renal mass protocols.- Describe and illustrate the main initial and late imaging findings after renal tumor treatment.- Discuss the most frequent complications following renal tumor treatment.

#### **TABLE OF CONTENTS/OUTLINE**

1. Introduction:- Renal cancer epidemiology.- Society guidelines (AUA and EUA) for renal cancer management.- Overview the approach for renal cancer treatment (systemic treatment, radical and partial nephrectomy, ablation treatment). 2. Diagnostic Imaging evaluation:- CT and MRI renal mass protocols. 3. Imaging findings after renal tumor treatment:- Procedure complications.- Initial and late expected post-treatment imaging features.- Features of tumor recurrence. 4. Take home messages.

### **GUEE-3 "Mesh Mash"- Multimodality Imaging of Pelvic Floor Repair**

#### **Awards**

**Cum Laude**

**Identified for RadioGraphics**

Participants

Kanupriya Vijay, MBBS, MD, Jacksonville, FL (*Presenter*) Nothing to Disclose

#### **TEACHING POINTS**

1. Review the expected postsurgical appearances after surgical and non-surgical repair of pelvic floor/urethral dysfunction. 2. Ultrasound is superior to MRI for assessing synthetic slings in suburethral space and evaluate for complications such as urethral erosion and vaginal exposure. 3. Ultrasound can accurately demonstrate the distribution of injected bulking agent, and determine the need and location for reinjection; as well as migrated bulking agent. 4. Radiologists play an important role in the detection of normal and abnormal appearances of postsurgical pelvic floor repair, and guide for future intervention.

#### **TABLE OF CONTENTS/OUTLINE**

1. Introduction: a. Briefly review pelvic floor dysfunction and various surgical and nonsurgical treatment options 2. Discuss imaging techniques and protocol: a. Ultrasound b. MRI 3. Case based review of various treatment options: a. Normal imaging appearances b. Complications: i. Misplacement ii. Urethral erosion iii. Vaginal exposure iv. Infection

### **GUEE-30 Ups and Downs in the Andes: Soft Tissue Sarcomas of the Genitourinary Tract with Radiologic-pathologic Correlation**

#### **Awards**

**Certificate of Merit**

**Identified for RadioGraphics**

Participants

Jorge Huayanay, MD, (*Presenter*) Nothing to Disclose

#### **TEACHING POINTS**

1. Soft tissue sarcomas of the genitourinary tract are uncommon, constituting less than 2% of all soft tissue sarcomas. This presentation will illustrate imaging features of these rare soft tissue sarcomas of the genitourinary tract. 2. The exhibit will review the spectrum of histopathologic correlations. 3. This review will emphasize diagnostic difficulties, potential imaging pitfalls and differential diagnoses of these entities.

#### **TABLE OF CONTENTS/OUTLINE**

The goals of this exhibit are to: Provide a pictorial review of the diverse imaging appearances of the soft tissue sarcomas of the genitourinary tract. Discuss specific imaging and pathological characteristics of the soft tissue sarcomas of the genitourinary tract. Familiarize the audience with the imaging features of the soft tissue sarcomas of the genitourinary tract, thereby helping in formulation of a complete differential diagnosis. These major featured entities include: • Renal leiomyosarcoma • Perirenal and pararenal liposarcoma • Vesical rhabdomyosarcoma • Prostate sarcomas • Paratesticular liposarcoma • Penile sarcoma • Uterine rhabdomyosarcoma • Uterine endometrial stromal sarcoma • Uterine adenocarcinoma

### **GUEE-31 MR Imaging of the Penis - What a Radiologist Needs to Know**

#### **Awards**

**Certificate of Merit**

Participants

Pankaj Nepal, MD, Bridgeport, CT (*Presenter*) Nothing to Disclose

#### **TEACHING POINTS**

To emphasize role of MRI in the evaluation of penile pathologies To illustrate normal MR anatomy of the penis and its importance on

To emphasize role of MRI in the evaluation of penile pathologies To illustrate normal MR anatomy of the penis, and its importance on local staging of penile cancer with reference to surgical outcomes To evaluate the role of MRI in evaluation of penile prosthesis To demonstrate role of MRI in diagnosis of unexplained cases of priapism or erectile dysfunction

#### TABLE OF CONTENTS/OUTLINE

Normal MR anatomy of penis, MR imaging protocol, different protocols (e.g. artificial erection) Etiologies Tumors - primary and metastasis, some rare tumors Trauma - penile fractures, hematoma, urethral injury Infarction- sickle cell disease, intracavernosal injection Infection Penoscrotal fistulas Peyronie's disease - diagnosis, follow up, plication, plication failure Penile prosthesis - types, parts, and complications Future directions

#### GUEE-32 How Fluent Are You in PI-RADS Terminology?

Participants

Ana Cristina Delgado, MD, Porto Alegre, Brazil (*Presenter*) Nothing to Disclose

#### TEACHING POINTS

The use of standard terminology, correct report organization, clear knowledge of the PI-RADS guides, understanding prostate anatomy, allows radiologist to certainly communicate the image findings of the prostate gland and organize the final report. For radiology residents/radiologists, a good understanding of terminology used on PI-RADS is one prerequisite for starting the image interpretation as well as knowing the anatomy. The idea of this exhibit is to expose residents/radiologist to a series of cases to reinforce concepts in an interactive activity.

#### TABLE OF CONTENTS/OUTLINE

Prostate anatomy / sector map case / review PI-RADS classification , what to evaluate on each sequence cases / review Benign findings, how to describe them, cases / review Extra prostatic invasion cases / review Final remarks

#### GUEE-33 Blast From the Past: Post-ablation Imaging of Renal Tumors Post-ablation Imaging of Small Renal Tumors

Participants

Lucas Daniel Pereira Lopes, (*Presenter*) Nothing to Disclose

#### TEACHING POINTS

Title: Blast from the past: Post-ablation imaging of small renal tumors Teaching Points 1. Review features of renal masses appropriate for ablation 2. Outline timeline for post-ablation surveillance 3. Distinguish between expected post-ablation appearance and pathological findings 4. Identify red flags and potential complications to look out for in the post-ablation period Table of Contents • Background o Types and mechanisms of thermal ablative techniques o Features of renal tumors for pre-ablation planning • Post-ablation expectations o Overview of timeline for post-ablation surveillance o Technical requirements of imaging o Expected appearance in imaging • Pathological changes in post-ablation o Red flags in appearance o Complications to look out for

#### TABLE OF CONTENTS/OUTLINE

Title: Blast from the past: Post-ablation imaging of small renal tumors Teaching Points 1. Review features of renal masses appropriate for ablation 2. Outline timeline for post-ablation surveillance 3. Distinguish between expected post-ablation appearance and pathological findings 4. Identify red flags and potential complications to look out for in the post-ablation period Table of Contents • Background o Types and mechanisms of thermal ablative techniques o Features of renal tumors for pre-ablation planning • Post-ablation expectations o Overview of timeline for post-ablation surveillance o Technical requirements of imaging o Expected appearance in imaging • Pathological changes in post-ablation o Red flags in appearance o Complications to look out for

#### GUEE-34 Pheochromocytoma and Paraganglioma: Key Findings, Clinical Features, and Their Association with Anatomic and Functional Imaging - Tutorial for Residents

##### Awards

##### Certificate of Merit

Participants

Leonela Ramirez Almanza, (*Presenter*) Nothing to Disclose

#### TEACHING POINTS

Pheochromocytoma and paraganglioma are chromaffin cell tumors that require early diagnosis due to their potentially serious and sometimes fatal cardiovascular sequelae. CT density of pheochromocytoma greater than 20 HU in the proper clinical context should be suggestive of this pathology. Hypercellularity in pheochromocytoma results in restricted diffusion and should not be confused with malignancy. Pheochromocytoma and larger paragangliomas may have areas of necrosis and intratumoral vessels with a "salt and pepper" appearance on MRI. Functional imaging is key to the diagnosis of pheochromocytoma and paraganglioma when no tumor is identified on anatomic imaging.

#### TABLE OF CONTENTS/OUTLINE

1. Introduction 2. Imaging protocols a. CT b. MRI c. PET/CT 3. Systematic analysis of images in relation to the clinic. a. Incidental finding b. Clinical Context and findings suggestive of pheochromocytoma and paraganglioma 4. Paraganglioma clinical and imaging features 5. Pheochromocytoma clinical and imaging features 6. Differential diagnoses 7. Take home messages

#### GUEE-35 Variant Bladder Cancer: MR Imaging, VIRADS Score, Clinical Feature and Management

Participants

Arisa Kameda, (*Presenter*) Nothing to Disclose

#### TEACHING POINTS

Variant bladder cancer is relatively rare and associated with increased risks of disease recurrence. Since these subtypes are often more advanced in stage than pure urothelial bladder cancer and is likely to underestimate the myometrial invasion, immediate total bladder resection is recommended in these patients. However, there has been few reports about MR imaging of Variant bladder

cancer. The purpose of this exhibit is To clarify the feature of the MR findings of variant bladder cancer To depict the VIRADS score of variant bladder cancer To discuss the clinical feature and management comparing pure urothelial bladder cancer.

#### **TABLE OF CONTENTS/OUTLINE**

1, Over view of histological classification of bladder cancer based on WHO 2016 2, Demonstrate the MR imaging of variant bladder cancer (Glandular differentiation, Squamous differentiation, Micropapillary type, Nested type, Sarcomatoid type) 3, VIRADS scoring of variant bladder cancer with histological correlation 4, Discussion of clinical feature and management of variant bladder cancer 5, Summary

#### **GUEE-36 DCE MRI: A Superhero Or Villain In Prostate MRI?**

Participants  
Samantha Jayasinghe, MD, Cleveland, OH (*Presenter*) Nothing to Disclose

#### **TEACHING POINTS**

1. Review different rationales and imaging protocols in prostate MRI. 2. Discuss the strengths and limitations of using or not using DCE in prostate MRI for diagnosis of clinically significant cancer (csPCa). 3. Review the available evidence on the diagnostic performance of prostate MRI without versus with contrast. 4. Provide a risk-based workflow to optimize the choice between contrast and non-contrast MRI utilization.

#### **TABLE OF CONTENTS/OUTLINE**

1. Imaging Protocols in Prostate MRIa. from standard and optional mpMRIb. MRI without contrastc. "fast MRI". 2. Dynamic Contrast enhancement imaging in prostate MRIa. Acquisition technique, Interpretation, and Post-processing methodsb. Strengthsi. Increased detection and confidence of csPCa. ii. Helpful to inexperienced readers. iii. Excellent PI-RADS staging tool. iv. Accurate estimation of index PCa volume. Limitationsi. Cost. ii. Time. iii. Nephrotoxicity. iv. Limited role in Transitional Zone. 3. Non-contrast MRI imaging (i.e., bpMRI) Strengths: a. Non-inferior in sensitivity and specificity. b. Increased safety and cost effectiveness. Limitations: a. Requires higher reader expertise. b. Follow-up safety net. Increased patient in indeterminate category. 4. When to choose between contrast or non-contrast prostate MRI: Is it always one or the other? 5. Risk-based approach to Workflow

#### **GUEE-37 Iatrogenic Injuries of the Urinary System: Radiologic Features and Imaging-guided Intervention**

Participants  
Emanuele Barabino, MD, (*Presenter*) Nothing to Disclose

#### **TEACHING POINTS**

- Iatrogenic Injuries of the urinary system could occur during percutaneous/endoscopic procedure involving the urinary system or during surgery; in recent years, due to the diffusion of laparoscopic and robotic surgery, the incidence of these lesions is increasing.
- The spectrum of radiologic findings is wide and heterogeneous and depends on the type of injury, the procedure that cause it and time-to-diagnosis.
- Imaging-guided intervention maintains a fundamental role in the management of iatrogenic injuries to the urinary system.

#### **TABLE OF CONTENTS/OUTLINE**

1. Introduction 2. Anatomical Considerations 3. Mechanisms of Injury 3.1 Transection and Avulsion 3.2 Ligation 3.3 Mixed lesions 4. Imaging Techniques 5. Radiologic Features 5.1 Percutaneous Treatments 5.1.1 Thermal Ablation 5.1.2 Nephrostomy/Anterograde ureteral stenting 5.1.3 Lithotripsy 5.2 Endoscopic Treatments 5.3 Urologic Surgery 5.4 Gastrointestinal Surgery 5.5 Gynecologic Surgery 5.6 Vascular Surgery and Endovascular Procedures 6. Imaging-guided intervention 6.1 Kidney derivation 6.2 Recanalization and Stenting 7. Conclusion

#### **GUEE-38 Pitfalls in Prostate MRI: How to Avoid These Common Errors of Under and Over Diagnosis**

**Awards**  
**Certificate of Merit**

Participants  
Omar Kamal, MD, MSc, Portland, OR (*Presenter*) Nothing to Disclose

#### **TEACHING POINTS**

- Prostate MRI has a steep learning curve and experts suggest attending a course and a minimum of 100 supervised cases prior to independent practice.
- There is a tendency for inexperienced readers to overcall normal anatomy and benign lesions as cancer as they do not want to "miss" cancer.
- At the same time underdiagnosis is a problem due to poor technique and/or failure to recognize small or subtle cancers.

#### **TABLE OF CONTENTS/OUTLINE**

1. Brief overview of typical and atypical appearance of prostate cancer on multiparametric MRI: a. Discussion of learning curve, expert opinion, lack of standardization in training/certification/performance. 2. MRI technique: a. Optimal technique to avoid under- or overdiagnosis. b. Examples of poor technique side by side with proper technique. 3. Pitfalls: a. Overview of the literature in prostate interpretation errors. b. Mimics of peripheral zone cancer. i. Normal central zone ii. Exophytic BPH nodules iii. Midline pseudolesion iv. Periprostatic vein v. Prostatitis/scar/atrophy (PIRADS 2) lesions overcalled as PIRADS 4/5 vi. DWI and coil artifact vii. Post biopsy hemorrhage viii. Calcification c. Mimics of transition zone cancer. i. Failure to recognize encapsulated or heterogeneous nodules ii. Atypical and asymmetric BPH nodules iii. Thick anterior fibromuscular stroma iv. Thickening of the pseudocapsule. d. Underdiagnosis. i. Failure to recognize small/subtle lesions ii. Failure to recognize very large lesions replacing most of the normal gland. e. Other Lesions Mimicking Cancer. i. Seminal vesicle collapse ii. Granulomatous and IgG4 prostatitis iii. Cowper's gland hyperplasia. 4. Practical ideas for self-improvement.

#### **GUEE-4 MR Imaging of Postoperative Endometriosis**

**Awards**  
**Identified for RadioGraphics**  
**Magna Cum Laude**

Participants

Patricia Dantas I, MD, Sao Paulo, Brazil (*Presenter*) Nothing to Disclose

#### **TEACHING POINTS**

The purposes of this exhibit are:1) Discuss the roles of surgical treatment of different types of endometriosis using a didactic approach by illustrations and MR images.2) Clarify significant MRI image postoperative findings and meaningful information to radiology reports.3) Illustrate imaging patterns and pitfalls of postoperative complications, residual endometriosis and recurrence after surgery.

#### **TABLE OF CONTENTS/OUTLINE**

1) Review preoperative imaging findings that aid in surgical decisions.2) Describe surgical treatment of different types of endometriosis: endometrioma, posterior compartment, bowel endometriosis, uterus/vagina, bladder and ureters.3) Recognition of patterns normal MR postoperative findings.4) Cased-based imaging of postoperative complications.5) Illustrative key points: residual disease and recurrence after surgery.6) Pitfalls.7) Conclusions and "take home messages": consolidate the acquired knowledge.

#### **GUEE-40 Non-Wilms Kidney Tumors in Childhood - What the Radiologist Should Know**

Participants

Elena Paz Calzada, MD, Madrid, Spain (*Presenter*) Nothing to Disclose

#### **TEACHING POINTS**

Wilms tumor is the fifth most common malignant neoplasm in childhood and the most common renal tumor in children. It is estimated that the annual incidence is 1 case per 10,000 children under 15 years of age. However, there are other childhood kidney tumors with which the radiologist should be familiar. The aim is to present epidemiological, clinical and radiological findings that better guide us to a differential diagnosis of renal mass in pediatric patients.

#### **TABLE OF CONTENTS/OUTLINE**

We have carried out a review of the cases of non-Wilms kidney tumors in childhood in our institution, spanning from 2008 to 2021. Regarding the case review, a literature research of the main kidney tumors: Wilms and non-Wilms, as well as their characteristics, was performed. We found several cases of:- Clear cell renal carcinoma- Renal clear cell sarcoma- Renal angiomyolipoma- Inferior vena cava thrombosis mimicking a renal tumor- Renal Ewing sarcoma- Chromophobic carcinoma Both the ultrasound, CT and MRI images of each case are exposed, as well as a brief summary of the epidemiology, symptoms, radiological characteristics and prognosis of each one.

#### **GUEE-41 Propensity for Density: Hyperdense and Calcified Disease throughout the Genitourinary System on CT**

##### **Awards**

**Certificate of Merit**

Participants

Virginia Planz, MD, Nashville, TN (*Presenter*) Nothing to Disclose

#### **TEACHING POINTS**

- A wide spectrum of benign and malignant conditions in the GU system can be readily detected on CT as calcified or hyperdense findings.
- Recognizing distinguishing features and characteristic imaging appearances will determine the diagnosis or narrow the differential.
- Dual energy CT offers opportunity for further characterization of hyperdense and calcified pathology.

#### **TABLE OF CONTENTS/OUTLINE**

- Review the spectrum of diseases associated with GU calcification and intrinsic hyperdensity such as: hemorrhagic cysts, RCC, calculi, nephrocalcinosis, papillary necrosis, ADPKD, multicystic dysplastic kidney, renal transplant rejection, tuberculosis, schistosomiasis, alkaline encrusted pyelitis/cystitis, acute/chronic subcapsular hematoma, renal and gonadal vein thrombosis, renal artery aneurysm, urothelial carcinoma, radiation cystitis, bladder mucinous adenocarcinoma, urachal adenocarcinoma, amyloidosis, malakoplakia, serous ovarian carcinoma, colonic mucous adenocarcinoma ovarian metastasis, dermoid cyst, degenerated fibroids, prostate and vas deferens calcification
- Describe and classify hyperdense and calcified findings based on involved organ, distribution, appearance, and other accompanying findings, with an emphasis on pattern recognition in a case-based review.
- Apply teaching points to unknown cases.

#### **GUEE-42 Penile MRI - Normal and Abnormal**

Participants

Madhura Ghate, MD, MD, (*Presenter*) Nothing to Disclose

#### **TEACHING POINTS**

After viewing this exhibit, the readers will gain insight into penile anatomy on MRI. They will be able to independently carry out MR imaging of the penis. MR imaging protocol and utility of diffusion weighted imaging and I.V contrast will be discussed. Imaging appearances of various pathologies such as structural abnormalities, inflammatory/infective pathologies, neoplasms will be presented.

#### **TABLE OF CONTENTS/OUTLINE**

1)Imaging anatomy of the penis. 2)MRI protocols. 3)MR imaging of various penile and urethral abnormalities including congenital/structural anomalies, infective/inflammatory pathologies, vascular pathologies, neoplasms and post operative assessment.

#### **GUEE-43 Sonography of the Penis: Beyond Erectile Dysfunction - A Primer for Radiology Residents and Fellows**

##### **Awards**

**Identified for RadioGraphics**

Participants

Nanda Venkatanarasimha, MRCP, FRCR, Singapore, Singapore (*Presenter*) Nothing to Disclose

#### TEACHING POINTS

div>

#### TABLE OF CONTENTS/OUTLINE

1. Case based review of the various pathologies affecting the penis including Doppler studies. Pathologies presented: Non-vascular (Peyronie's disease, Trauma, infection, benign malignant lesions, Idiopathic calcinosis cutis) Vascular (arterial insufficiency, venous insufficiency, mixed disease, iatrogenic malignant priapism, Acute venous thrombosis Mondor's disease)2. Review Ultrasound anatomy3. Illustrate, discuss normal abnormal Doppler wave forms4. Demonstrate Ultrasound technique including pearls pitfalls5. Correlative imaging where appropriate will be discussed and illustrated6. Clinical presentation and management will be highlighted

#### GUEE-44 Novel Implantable Devices in the Abdomen and Pelvis: A Primer for Radiologists

Participants

Nabih Nakrou, MD, Boston, MA (*Presenter*) Nothing to Disclose

#### TEACHING POINTS

The purpose of this exhibit is to: Provide a multimodality review of novel implantable devices in the abdomen and pelvis with a focus on indications, proper anatomical positioning, and expected radiologic features. Recognize radiologic findings of devices malposition, malfunction, and resulting complications. Discuss imaging pearls and pitfalls of novel devices. Discuss imaging techniques and protocol modifications to optimize device assessment.

#### TABLE OF CONTENTS/OUTLINE

We will address the following novel devices: An artificial male sphincter. Sacrocolpoplexy mesh for pelvic floor descent. Bladder neck suspension. Urethral bulking agent. Midurethral and retropubic sling. Omentopexy and omental packing.Sacral nerve stimulator. Antibiotics beads for intraabdominal or intrapelvic infections. Bariatric intragastric balloon and Sleeve balloon device. Gastric electrical stimulators. Anti-reflux devices.

#### GUEE-45 Updates on Adrenal Imaging: from A(denomas) to Z(ebras)

Participants

Wendy Tu, MD, Edmonton, AB (*Presenter*) Nothing to Disclose

#### TEACHING POINTS

Incidental adrenal nodules are common, seen in 4-8% of patients. Although most are benign adenomas, the differential is broad, requiring an algorithmic approach to incidental adrenal nodules. This approach should incorporate relevant recent literature given the evolving use of CT, MRI, and PET-CT and their advantages/disadvantages. Beyond image interpretation, radiology plays a crucial role in guiding biochemical testing, referral, and management. Current literature on adrenal pathology and management outcomes are discussed.

#### TABLE OF CONTENTS/OUTLINE

1) Case-based comprehensive review of benign and malignant adrenal pathology highlighting clinical and imaging findings.a. Can imaging alone differentiate benign and malignant adrenal masses?b. What are the diagnostic criteria for adenoma?c. What is the radiologic workup?d. What are the strengths/limitations of CT washout and MR chemical shift imaging studies?e. When is PET/CT indicated?f. What are key imaging pitfalls?2) Learn an algorithmic pathway to the incidental adrenal nodule, incorporating current major guidelines.a. What are the first steps after finding an incidental adrenal nodule?b. Which guidelines are available?c. What imaging findings support each step?d. What reporting templates are available?3) Discuss management of adrenal nodules, highlighting the role of the radiologist in directing appropriate specialist referral, biochemical testing, and biopsy.4) Review the treatment options and prognosis of conditions including hormonally active tumors.

#### GUEE-46 Müllerian Duct Anomalies: New Classification Systems, Clinical Implications, and Treatment Frontiers

Participants

Moataz Ahmed Sayed Mohammed Soliman, MD, MSc, CHICAGO, IL (*Presenter*) Nothing to Disclose

#### TEACHING POINTS

- Understanding the evolution of Mullerian duct anomalies classification systems.
- Formulating a stepwise approach to report Mullerian duct anomalies considering the new American Society of Reproductive Medicine (ASRM) classification.
- Learning the impact of new classification systems on management.
- Familiarize with new surgical approaches for management.

#### TABLE OF CONTENTS/OUTLINE

- Introduction o Embryological background. o Normal anatomy.
- Normal Multimodality imaging of the female genital system: (US, 3D US, MRI, and hysterosalpingography (HSG).
- Classification of Mullerian duct anomalies: (American fertility society, ESHRE/ESGE, American society of fertility medicine).
- o Mullerian duct anomalies: (uterus, cervix, and vagina).
- o Comparison between old and new classification systems.
- Multimodality imaging approach diagnosing Mullerian duct anomalies: (US, 3D US, MRI, hysterosalpingography (HSG), and CT in selected cases)
- Clinical implications for fertility and patient outcomes.
- Management approach in light of the newly proposed classification systems.
- Multimodality imaging post corrective interventions.
- New treatment frontiers for the treatment of female infertility. o Hysteroscopic management. o Uterus transplantation.

#### GUEE-47 Pubic Symphyseal Urinary Fistulae with Osteomyelitis in the Setting of Treated Prostate Carcinoma

Participants

Paul Wojack, MD, Manhasset, NY (*Presenter*) Nothing to Disclose

#### TEACHING POINTS

Prostate cancer is the leading cause of cancer in men and a variety treatment options are available. Increasing population size and advancements in prostate cancer treatment has led to an increased number of patients who are living longer with prostate cancer.

Complications of prostate cancer treatment include erectile dysfunction, impotence, incontinence, gastrointestinal issues (such as radiation proctitis), and rarely posterior urethral strictures (secondary to radiation damage). Manipulation of these strictures with urethroplasty, stenting, and other urethral instrumentation can cause breakdown of the friable post-radiation tissues. Patients can develop urinary fistulae to the pubic symphysis which are often complicated by pubic osteomyelitis and often require aggressive surgical interventions. A paucity of literature regarding urosymphyseal fistulae, making this a rare complication of which radiologists should be aware, especially musculoskeletal and body imagers.

#### TABLE OF CONTENTS/OUTLINE

1. Introduction 2. Background 3. Prostate Cancer a. Epidemiology b. Treatments c. Complications 4. Urosymphyseal fistulae a. Normal and post-treatment anatomy b. Pathophysiology in the setting of treated prostate cancer c. Pubic osteomyelitis vs osteitis pubis. d. Imaging review of several cases of urosymphyseal fistulae 5. Summary 6. References

#### GUEE-48 Reporting a Renal Mass: Can We Do It Better?

Participants

Pablo Valdes Solis, PhD, (*Presenter*) Nothing to Disclose

#### TEACHING POINTS

Review the points that are considered most important when making a radiological report of a renal mass. Analyze why they are important and how to describe them. See examples of each of the points, with practical cases explaining what is reported, how and why.

#### TABLE OF CONTENTS/OUTLINE

Introduction: Importance of the correct description of the renal mass. Variability in how radiologists and urologists consider the most important points. Current situation: vision of the radiologist and the urologist. Points to be included in the report. In each point, the what, how and why will be described, accompanied by examples, as well as the importance that radiologists and urologists have given to each point. Examination type and description; CT or MRI, with or without contrast. Mass type: cystic or solid. Mass size, including methods. Size comparison: studies and measurements included for comparison. Enhancement, including methods. Importance of measurement comparing enhanced and unenhanced scans. Macroscopic fat: importance of detecting and describing the presence of fat in the mass. Mass margins: is there infiltration? Necrosis. Bosniak classification: a review of the classification of cystic masses. Nephrometry score: something that some urologist use. Estimated probability of malignancy: if included and method. Features predictive of indolent growth in solid masses. Lymph node size: how to measure and describe lymph nodes. Tumor thrombus: description, location and extension. Location inside the kidney: axial location, capsular location, distance to sinus fat, position relative to polar lines. Management options mentioned. Tumor-Node-Metastasis (TNM) staging reported: a review. Conclusions

#### GUEE-49 Not Kidneying Around: Multimodality Imaging of Renal Infectious and Inflammatory Conditions in Adults- Key Imaging Findings

Participants

Camila Vendrami, MD, Chicago, IL (*Presenter*) Nothing to Disclose

#### TEACHING POINTS

- Discuss the role of imaging in the evaluation of a wide spectrum of renal infections and inflammatory conditions
- Review their main pathophysiologic features
- Emphasize specific imaging features of certain renal infections and inflammatory conditions that aid in making the correct diagnosis

#### TABLE OF CONTENTS/OUTLINE

A wide spectrum of renal infectious and inflammatory conditions exists. Imaging plays a key role in many instances, including in immunocompromised patients, treatment non-responders, transplant patients, and cases with an equivocal clinical diagnosis. 1. Introduction 2. What is the role of multimodality imaging (US, CT, MR) in the evaluation of renal infections and inflammatory conditions? 3. What are the key imaging features of acute renal conditions (acute pyelonephritis, renal and perirenal abscesses, pyonephrosis, emphysematous pyelonephritis/cystitis)? 4. What are the key imaging features of fungal infections and their complications (such as aspergillus, candida and mucor) as well as of tuberculosis and parasitic infections (renal hydatid disease)? 5. What are the key imaging features of chronic renal conditions (chronic pyelonephritis, xanthogranulomatous pyelonephritis, eosinophilic cystitis, renal replacement lipomatosis, struvite stones)? 6. Take Home Points

#### GUEE-5 MR Imaging of the Penis: A Practical Guide for Radiologists

Participants

Renata Nascimento, MD, (*Presenter*) Nothing to Disclose

#### TEACHING POINTS

- Review the penile anatomy
- Describe our institutional protocol for penile magnetic resonance imaging (MRI)
- Create a practical guide to evaluate the penis at MRI
- Describe common and uncommon penile imaging findings
- Revisit the new TNM staging system used for squamous cell carcinoma of the penis

#### TABLE OF CONTENTS/OUTLINE

- Introduction
- Anatomy of the penis
- MR Imaging Technique
- Preparation
- MRI protocol and how to optimize it
- Magnetic resonance imaging findings of the penis
- Traumatic (eg: fracture)
- Infectious
- Inflammatory (eg: Peyronie's disease)
- Vascular (eg: fistula, segmental thrombosis of the corpus cavernosum, priapism, Mondor disease)
- Penile prosthesis
- Penile cancer

#### GUEE-50 The Postoperative Kidney: Multimodality Imaging Manifestations of Common and Uncommon Complications

Participants

Cole Thompson, MD, (*Presenter*) Nothing to Disclose

#### TEACHING POINTS

-Postoperative renal complications may be grouped into several broad categories: Fluid collections; vascular, lymphatic, and collecting system injuries; tumor seeding; trauma to adjacent organs; and general complications.-Postoperative fluid collections include hematoma, seroma, urinoma, abscess, and lymphocele, each at varied time intervals following surgery. Discernment of differences in key imaging features allows for appropriate management.-Vascular complications related to renal arterial injury or thrombosis include active hemorrhage, pseudoaneurysm, and renal infarction. Prompt recognition of imaging findings enables early intervention.-Postsurgical complications are not limited to the kidney or collecting system. The adjacent organs may also be injured, including the spleen, adrenal glands, liver, pancreas, bowel, and pleura.

#### TABLE OF CONTENTS/OUTLINE

-Expected imaging features of the post-operative kidney following partial nephrectomy, radical nephrectomy, and lithotripsy (ESWL) or nephrolithotomy.-Case-based review illustrating the role of imaging (CT, US, MRI, angiography) in complications following renal surgery: Fluid collections; vascular and lymphatic injuries; complications related to the collecting system; tumor seeding and recurrence; and injury to adjacent organs.-Recognition of key imaging features that warrant urgent therapeutic intervention.-Challenging clinical scenarios and strategies for optimal image interpretation to guide subsequent management and follow-up.

#### **GUEE-51 Preoperative Planning In Cancer Of The Urinary Tract: What Surgeon Wants to Know What Radiologists Need to Know**

Participants

Patricia E. Ortega Aragon, MD, MD, Mexico City, Mexico (*Presenter*) Nothing to Disclose

#### TEACHING POINTS

Bladder cancer (BC) is the most common cancer of the urinary tract in the United States. In bladder cancer, images play an important role in locoregional staging and remote evaluation of the disease. The RENAL nephrometry scoring system, VI-RADS, and PI-RADS provide preoperative information that is important in predicting long-term outcomes. It is important for radiologists to understand what information to provide in diagnostic reports to support the surgical plan and provide important data for making treatment decisions.

#### TABLE OF CONTENTS/OUTLINE

- Introduction- Systemic approach: kidney, prostate and bladder- The Rads and Scores.- Clinical radiological Review: pictorial cases.

#### **GUEE-52 Focal MRI-Guided Transurethral Ultrasound Ablation (TULSA) in Men with Prostate Cancer: Lessons Learned in 60+ Patients**

Participants

Daniel N. Costa, MD, Dallas, TX (*Presenter*) Research support, Bayer AG

#### TEACHING POINTS

1. Review the rationale for focal therapy in prostate cancer and the unique aspects of MRI-guided transurethral ablation (TULSA) of the prostate2. Discuss the multidisciplinary patient selection, treatment and follow-up strategies3. Review and discuss strategies to overcome challenging scenarios

#### TABLE OF CONTENTS/OUTLINE

1. Basic facts about prostate cancer (Disease prevalence and heterogeneity, Over- and under-diagnosis, Morbidity of standard of care treatment options)2. Different focal therapy modalities (Cryoablation, laser, irreversible electroporation, microwave ablation, transrectal high-intensity focused ultrasound; Transurethral ultrasound ablation (TULSA))3. TULSA - Multidisciplinary effort- Patient selection (Inclusion and exclusion criteria, Distances of interest, Critical anatomical relationships, Calcifications, Pre-treatment imaging and biopsy)- Treatment planning and patient-specific customization (Sextant, hemi-, near whole-gland, and whole-gland ablation Neurovascular bundle and ejaculatory duct sparing, Concurrent benign prostatic hypertrophy treatment)- Procedure duration- Strategies for workflow improvements- Post-treatment follow-up (Imaging - normal and abnormal appearance, PSA trends, Functional (sexual and urinary) recovery, Biopsy, Complications)- Challenging scenarios (Hip prosthesis, Radiation therapy fiducials and seeds, Motion, Calcifications)

#### **GUEE-53 T2-Hyperintense Prostatic and Periprostatic Lesions and Their MRI Characteristics**

Participants

Alfonso Iglesias, MD, PhD, (*Presenter*) Nothing to Disclose

#### TEACHING POINTS

Knowledge of the anatomy and embryological development of the inferior male genitourinary tract should allow the radiologist to classify the T2-hyperintense prostatic and periprostatic lesions according to localizationClinical presentation, MRI characteristics with pathological correlation can help us to accurately characterize T2-hyperintense prostatic and periprostatic lesions resulting in appropriate patient management.

#### TABLE OF CONTENTS/OUTLINE

Define, classify and review the clinical manifestations of T2-Hyperintense prostatic and periprostatic lesions Review imaging findings that can help us shorten the differential diagnosis and perform a correlation of imaging findings with clinical and therapeutic management Describe an imaging algorithm for T2-Hyperintense prostatic and periprostatic lesions that is based on MRI characteristics

#### **GUEE-54 Gonadal Vein - The Omitted by Lane**

Participants

Aruna R. Patil, MD, FRCR, (*Presenter*) Research Consultant, Koninklijke Philips NV

#### TEACHING POINTS

The gonadal veins are paired vessels that drain the testes and ovaries. This exhibit aims to:1. Review the imaging anatomy of

gonadal veins<sup>2</sup>. Its use as a landmark, collateral<sup>3</sup>. Its role in conditions such as pelvic congestion, varicocele<sup>4</sup>. Its role in spread of tumor and infection.

#### **TABLE OF CONTENTS/OUTLINE**

1. Anatomy of gonadal veins- male and female<sup>2</sup>. Variant anatomy and implications<sup>3</sup>. Use as landmark - ovaries, testes (normal and pathologies - torsion, germ cell tumor in undescended testes, upper ureter physiological narrowing<sup>4</sup>. Collateral pathways - varices, varicocele, pelvic congestion syndrome, mesentericogonadal shunts in CLD, Abernathy malformations<sup>5</sup>. Spread: gonadal vein thrombosis- septic in infections (PID) , bland or tumor thrombosis - leiomyomatosis, leiomyosarcoma, other carcinomas with gonadal vein spread.

#### **GUEE-55 Peritoneal and Retroperitoneal Anatomy as it Relates to Disease Spread**

##### **Awards**

##### **Identified for RadioGraphics**

##### **Participants**

Ayman H. Gaballah, MD, FRCR, Columbia, MO (*Presenter*) Nothing to Disclose

##### **TEACHING POINTS**

1- Review anatomy and anatomic landmarks of peritoneal and retroperitoneal (RP) spaces 2- Illustrate the intercommunications among different spaces and their effect on spread of related diseases 3- Differentiate peritoneal from RP diseases 4- Discuss imaging workup and imaging features of different pathologic entities and pathways of disease spread 5- Provide algorithmic approach to differential considerations 6- Review management options

#### **TABLE OF CONTENTS/OUTLINE**

1- Introduction 2- Anatomy of peritoneal and retroperitoneal (RP) spaces with diagrammatic illustrations 3- Differentiation of intraperitoneal from retroperitoneal pathology 4- Imaging features of different pathologic entities including, extraluminal gas, fluid collections, and masses 5- Case presentation 6- Algorithmic approach to differential considerations 7- Peritoneal carcinomatosis index 8- Management options including HIPEC for peritoneal carcinomatosis 9- Summary and conclusion

#### **GUEE-56 Don't Be Outsourced - A Practical Guide to VI-RADS, Including Differentials**

##### **Awards**

##### **Identified for RadioGraphics**

##### **Participants**

Jonatas Favero Prietto Dos Santos, MD, Porto Alegre, Brazil (*Presenter*) Nothing to Disclose

##### **TEACHING POINTS**

1) VI-RADS provides a five-point score to determine the risk of detrusor muscle invasion based on tumor appearances in T2WI, DWI and DCE; 2)Despite the high reproducibility verified so far, scoring is a trick process and requires supervised practicing. Along with a series of typical cases, some pitfalls and common errors are discussed; 3)As the VI-RADS only applies for urothelial lesions, it's important to be aware of MRI appearances of other malignant neoplasms and benign conditions that may mimic urothelial cancers.

#### **TABLE OF CONTENTS/OUTLINE**

Bladder neoplasms are classified as epithelial and nonepithelial, and they can emerge from any of the bladder layers. Urothelial carcinoma account for the majority of urinary bladder cancer and differentiating muscle-invasive (MI) from non-muscle-invasive (NMI) tumors is vital to choose the appropriate treatment. It is noteworthy that transurethral resection of bladder tumor may not sample the muscularis propria, leading to understaging in 25% to 40% of MI cancers. In this setting, VI-RADS is a reproducible and feasible guide for Radiologists to use a standardized approach to imaging and reporting multiparametric MRI. This system provides a five-point score which effectively indicates the likelihood of detrusor muscle invasion. MRI scoring is based on T2WI, DWI and DCE. It is also important to evaluate the presence of synchronous urothelial lesions, lymph node enlargement and distant metastasis. Aside from an accurate scoring of urothelial lesions, Radiologists should be able to recognize imaging findings of other malignant neoplasms and non-malignant conditions, which may simulate urothelial cancers.

#### **GUEE-57 Altered Nephrogram: What the Radiologist Needs to Know**

##### **Participants**

Elisa Antolinis Macho, MD, Madrid, Spain (*Presenter*) Nothing to Disclose

##### **TEACHING POINTS**

1 - Understanding what "nephrogram" means and normal kidney behavior in monophasic and multiphasic CT. 2 - Learning the most common abnormalities: absent (global or segmental), delayed, striated, spotted and persistent nephrogram. 3 - Correlating each altered nephrogram with its typical underlying pathophysiology.

#### **TABLE OF CONTENTS/OUTLINE**

1. Normal kidney vascularization 2. Normal kidney behavior in multiphasic CT: Normal nephrogram 3. Absent nephrogram - Global absence: Traumatic / Non-traumatic - Segmental absence: Vascular / Others 4. Delayed nephrogram - Vascular - Obstructive - Others 5. Striated nephrogram - Unilateral - Bilateral - Spotted nephrogram 6. Persistent nephrogram 7. Altered nephrogram: tips and tricks - Laterality - How to define it - Most common cause - The "rim sign" - Final diagram with every altered nephrogram

#### **GUEE-58 Urine Luck: Using the Nephrogram to Aid in Diagnosis**

##### **Participants**

Layne Kelley, MD, Dallas, TX (*Presenter*) Nothing to Disclose

##### **TEACHING POINTS**

1. An understanding of normal patterns of renal enhancement and contrast excretion can be utilized to optimize image acquisition for detection of abnormalities. 2. Recognizing abnormal enhancement patterns improves detection of subtle pathology.

## TABLE OF CONTENTS/OUTLINE

1. Introduction:A. Review of normal progression of contrast through the kidneys and urinary tract over time on CTB. Provide an overview of abnormal enhancement patterns with a "back to basics" approach referencing the normal and abnormal nephron function.2. Case-based review of abnormal enhancement patterns, including:A. Delayed nephrogram i. Arterial inflow1. Renal artery occlusion2. Renal artery dissectionii. Venous outflow1. Renal vein thrombosis2. Nutcracker syndromeiii. Urine outflow1. Obstructive urolithiasis2. Inflammatory stricture3. Malignancya. Invasive prostate carcinomab. Cervical cancerc. Subtle ureteral tumor implantB. Absent nephrogrami. Renal infarctC. Striated nephrogrami. PyelonephritisD. Persistent nephrogrami. Retained contrast in the setting of acute kidney injury3. Review how an understanding the nephrogram allows optimal evaluation for specific pathologies, with case examples:A. Unenhanced CT for nephrolithiasisB. Nephrographic phase for optimal detection of renal massesC. Excretory phase for detection of urothelial masses and suspected urine leak

### **GUEE-59 Updated 2019 Bosniak Classification: Examples, Challenges and Future Directions**

Participants

Srinivas Saripalli, MD, Jackson, MS (*Presenter*) Nothing to Disclose

#### **TEACHING POINTS**

Renal cystic lesions are commonly encountered incidentally as part of trauma workups and workup for other diseases, and also as part of workup for symptomatic presentation such as hematuria and flank pain. The management and treatment of these renal cystic lesions has been the focus of multiple efforts from the radiological and urological communities. The challenge posed by cystic renal lesions is to stratify those which are more likely to be malignant and require more invasive treatment and ventricles which can be managed conservatively with serial imaging and thereby avoid the morbidity of invasive treatment. The goal of the updated Bosniak classification in 2019 was to better encompasses the small renal masses that are commonly encountered in practice and to more systematically stratify these lesions such that variability in classification was decreased, with both CT and MRI classification schemes. The updated classification has many simplifications for practice which we will review. We will also show some continued challenges in the classification and how they can be addressed using multiparametric MRI and multimodality correlation.

## TABLE OF CONTENTS/OUTLINE

1. Review the 2019 Bosniak classification for cystic renal lesions. 2. Show multiple examples of cystic renal lesions and their classifications in the old and new Bosniak classifications. Particular focus on lesions which have different management in the old versus new classifications. 3. Review the varied appearances of lesions in each category in ultrasound, CT and MRI. 4. Discuss advantages, challenges, pitfalls and clinical implications of the updated system compared to the old.

### **GUEE-6 Imaging of the Enlarged Scrotum: A Vas(t) Deferens-tial Diagnosis**

Participants

Christopher Yu, MD, PhD, Los Angeles, CA (*Presenter*) Nothing to Disclose

#### **TEACHING POINTS**

Scrotal masses or masslike scrotal enlargement may cause substantial discomfort and anxiety to patients. While the clinical setting is often suggestive of the correct diagnosis, imaging is nearly always requested to confirm the suspected diagnosis, exclude other concerning differential possibilities, evaluate the disease extent, and/or assess for comorbidities and complications. The goal of the current educational exhibit is to review the differential diagnosis of scrotal masses/masslike scrotal enlargement, as outlined below. In addition to the rich imaging illustration of common etiologies, multiple less common but important causes will be provided with corresponding clinical and surgico-pathologic correlation. The exhibit will also include a review of inguino-scrotal fascial anatomy that is often very confusing for both trainees and practicing radiologists. Interactive (board-exam question/answer-type) pointers will also be provided to emphasize key principles.

## TABLE OF CONTENTS/OUTLINE

1. Developmental and gross anatomy of the inguino-scrotal region (fascial layers, scrotal contents, inguinal canal);2. Clinical and imaging diagnostic flowcharts;3. Role of imaging (US, CT, and MR);4. Casesa. Intratesticular (mass/cyst; torsion, infection);b. Extratesticular;i. Epididymal (mass/cyst, infection),ii. Spermatic cord (varicocele, masses),iii. Inguino-scrotal hernias (direct versus indirect);c. Scrotal wall:i. Diffuse swelling:1. Infection (cellulitis, Fournier gangrene),2. Lymphedema from systemic process (heart/liver/kidney failure),3. Hidradenitis suppurativa;ii. Focal masses/collections (hydrocele, abscess, hematoma).

### **GUEE-60 Renal Cell Carcinomas: Uncommon Clinical and Imaging Presentations and Uncommon Histological Subtypes**

Participants

Satomi Kawamoto, MD, Baltimore, MD (*Presenter*) Nothing to Disclose

#### **TEACHING POINTS**

1. To review uncommon clinical and imaging presentations of renal cell carcinomas (RCCs).2. To become familiar with uncommon histological subtypes of RCCs and their clinical features

## TABLE OF CONTENTS/OUTLINE

1. Uncommon clinical presentation of RCC. (1) Most RCCs in the developed world are incidentally discovered at imaging studies. (2) However, RCC may be discovered with uncommon presentations. Examples include spontaneous hemorrhage and paraneoplastic syndrome. Review uncommon clinical presentations with imaging findings. 2. Uncommon imaging features. (1) Unenhancing or equivocally enhancing RCCs. (2) RCC mimicking other entity such as renal abscess, lymphoma, pyelonephritis. (3) Other uncommon imaging features. 3. Uncommon histological subtypes of RCCs. (1) RCC subtypes emerged to 2016 WHO classification, and review their imaging and clinical features. (2) Review imaging and clinical features of other uncommon RCC subtypes.

### **GUEE-62 Direct MRI-Guided In-Bore Targeted Biopsies of the Prostate: Lessons Learned in 800+ Patients**

**Awards**

**Identified for RadioGraphics**

Participants  
Daniel N. Costa, MD, Dallas, TX (*Presenter*) Research support, Bayer AG

#### TEACHING POINTS

1. Review the unique aspects of direct MRI-guided in-bore biopsies compared to ultrasound-based targeted approaches. 2. Demonstrate strategies to leverage the direct lesion and needle visualization provided by the in-bore approach to overcome challenges encountered during targeted biopsies

#### TABLE OF CONTENTS/OUTLINE

1. Direct MRI-guided in-bore biopsy vs US-based (cognitive and MRI-TRUS fusion) biopsies • Advantages o Precise lesion-needle location verification • Disadvantages o Cost and duration o Lack of systematic sampling  
2. Steps of a direct MRI-guided in-bore biopsy • Review of diagnostic, pre-biopsy multiparametric MRI • Patient positioning, moderate sedation and needle guide placement • Pre-biopsy imaging • Target identification and biopsy planning • Needle guide location adjustment(s) • Tissue sampling and needle-lesion location verification • Specimen handling  
3. Challenging scenarios • Small lesion in large prostate • Tricky lesion location • Tumor heterogeneity • Plaque-like subcapsular lesions • Motion (whole body, rectal, pelvic floor) • Needle deflection • Anatomical changes secondary to hematomas • Suspected post-prostatectomy local recurrence • Prostates with unusual morphology (eg, post focal therapy) • Patients without rectal access • Unusual anorectal anatomy • "MRI-invisible" lesions • Patient selection (e.g., hip prosthesis) • Efficient imaging and tissue sampling

#### GUEE-63 Prostate Diffusion-weighted Imaging: Insatiable Challenge to Improve Tumor Detection and Characterization in Prostate Cancer

Participants  
Tsutomu Tamada, MD, Kurashiki, Japan (*Presenter*) Nothing to Disclose

#### TEACHING POINTS

The purpose of this presentation is: 1. To learn the role of diffusion-weighted imaging (DWI) in diagnosis of prostate cancer (PC) 2. To understand the problems for the detection and characterization of PC using standard DWI with single-shot echo-planar imaging (ssEPI) in patients with elevated PSA levels 3. To demonstrate the countermeasures for problems on ssEPI DWI

#### TABLE OF CONTENTS/OUTLINE

Role of DWI in diagnosis of prostate cancer (PC)- Primary PC detection: DWI scoring system in Prostate Imaging Reporting and Data System v2.1- Local recurrent PC detection: DWI scoring system in Prostate Magnetic Resonance Imaging for Local Recurrence Reporting (PI-RR)- Local staging: extracapsular extension and seminal vesicle invasion- Assessment of tumor aggressiveness in PC using quantitative DWI metrics- MRI-ultrasound Fusion-guided Prostate targeted Biopsy  
Problems and countermeasures for detection and characterization of PC using ssEPI DWI - Susceptibility artifact and geometric anatomic distortion: Reduced field-of-view DWI Turbo spin-echo DWI Multi-shot EPI DWI- Blurring: Multi-shot EPI DWI- Low SNR and CNR in high b-value and high spatial resolution acquisitions: Compressed SENSE- Insufficient image contrast between benign and PC tissues: Ultra-high b value DWI Synthetic DWI Synthetic DWI which enable to synthesize DW images with any TR and TE- Insufficient diagnostic performance of tumor aggressiveness in PC using mean apparent diffusion coefficient (ADC) ADC histogram analysis Non-Gaussian fitting models- DWI invisible clinically significant PC Microstructural MRI which is a quantitative technique that focuses on structural change in three typical microstructures of prostatic tissue

#### GUEE-64 Prostate Magnetic Resonance Imaging for Local Recurrence Reporting PI-RR in Clinical Practice - A Primer for Novice and Expert Radiologists

Participants  
Jorge Abreu Gomez, MD, Pickering, ON (*Presenter*) Nothing to Disclose

#### TEACHING POINTS

\* Local recurrence after radical treatment represent a diagnostic challenge for novice and experienced radiologists. Throughout review of oncologic history, MRI and histologic findings of the primary lesion are crucial for adequate assessment/interpretation.\* PI-RR system aims to standardize the performance, interpretation and reporting of MRI after radical treatment in order to reduce variability.\* Combination of DCE and DWI features of a given observation will determine the likelihood for local recurrence

#### TABLE OF CONTENTS/OUTLINE

\* PI-RR categories and applicability.\* PI-RR scoring after radiotherapy. Understanding the sequence with highest score!!\* PI-RR scoring after radical prostatectomy. DCE as dominant sequence!!\* Beyond PI-RR. MRI assessment of recurrent disease after focal therapy

#### GUEE-65 Post-treatment Prostatic Cancer: How To Perform an Adequate Imaging Evaluation

Participants  
Vivien Bonadio, MD, (*Presenter*) Nothing to Disclose

#### TEACHING POINTS

? Understand the current concepts of biochemical recurrence and its clinical impact ? Address the different treatment modalities used, as well as their indications ? Review the role of functional imaging in follow-up and detection of recurrent disease ? Discuss the highlight findings on post treatment images of patients with prostatic cancer

#### TABLE OF CONTENTS/OUTLINE

INTRODUCTION ? Brief discussion of epidemiology ? Review of the concept and current criteria of biochemical recurrence in prostate cancer TREATMENT MODALITIES AND THEIR INDICATIONS ? Androgen deprivation therapy ? Brachytherapy ? External radiation therapy ? High Intensity Focused Ultrasound - HIFU ? Prostatectomy INDICATIONS OF IMAGING IN THE ASSESSMENT OF LOCOREGIONAL AND DISTANT RECURRENCE ? MR ? PSMA PET/CT ? PSMA PET/MR IMAGING EVALUATION ? Systematic approach to the interpretation of MR images of patients in post-treatment of prostatic cancer ? Case based-review of PI-RR (Prostate Magnetic Resonance Imaging for Local Recurrence Reporting) ? Pitfalls, challenges, and how to overcome these

## **GUEE-66 Biparametric and Multiparametric Prostate MRI: How To and When To Use Them Properly**

Participants

Mitsuru Takeuchi, MD, PhD, Nagoya, Japan (*Presenter*) Nothing to Disclose

### **TEACHING POINTS**

Multiparametric MRI (mpMRI) is currently the standard imaging method for prostate MRI. All Prostate Imaging Reporting and Data System (PI-RADS) versions emphasized that prostate MRI protocols should include not only T2-weighted imaging (T2WI) but also diffusion-weighted imaging (DWI) and dynamic contrast-enhanced MRI (DCE-MRI). However, in the latest PI-RADS after version 2, DCE-MRI plays a minor role. Biparametric MRI (bpMRI) study excluding DCE-MRI can be performed in a shorter time and is free from the cost and potential risks of gadolinium-based contrast agents compared to mpMRI. Recently, several studies have reported bpMRI is not inferior to mpMRI in the prostate cancer (PCa) detection. In this educational exhibit, we review these articles and explain when to and how to use bpMRI and mpMRI while presenting clinical cases.

### **TABLE OF CONTENTS/OUTLINE**

1) Diagnostic accuracy of bpMRI and mpMRI for the PCa tumor detection in treatment naïve patients (primary PCa). 2) Clinical application of bpMRI bpMRI could be apply to the patients who is suspected primary PCa. mpMRI should be used to T-staging, locally recurrent PCa after radiotherapy and prostatectomy and active surveillance. 3) Imaging protocol of bpMRI High image quality of T2WI and DWI is mandatory for securing the diagnostic accuracy of bpMRI. T2WI should be acquired with multiplanes and high spatial resolution. DWI should be obtained with less artefacts and high contrast between lesion and normal tissue. 4) Clinical cases

## **GUEE-67 Spectrum of Male and Female Urethral Pathologies at MRI**

Participants

Nikolas Brozovich, MD, Augusta, GA (*Presenter*) Nothing to Disclose

### **TEACHING POINTS**

1. Recognize variety of pathological conditions of the urethra at MRI 2. Discuss advantages and disadvantages of the MR Imaging of the urethra 3. Describe Imaging techniques for evaluation of urethra

### **TABLE OF CONTENTS/OUTLINE**

Evaluation of the male and female urethra on conventional imaging studies including retrograde urethrography (RUG), voiding cystourethrography (VCUG), and ultrasonography (US) may be helpful in demonstrating urethral abnormalities however limited in providing information regarding the periurethral tissues. MRI due to multiplanar capability and excellent tissue contrast can provide anatomic details about both the urethra and periurethral tissues and also orientation of the lesion in three dimensions. In this presentation conditions affecting the urethra or periurethral tissues will be discussed. Specific topics of discussion will be anatomical detail, MR imaging techniques, diverticulum, inflammation, tumors, strictures and miscellaneous conditions of the male and female urethra. Summary: MRI is a noninvasive technique that does not require ionizing radiation and can provide anatomic and pathological details about both the urethra and periurethral tissues and the orientation of the lesion in three dimensions due its multiplanar capabilities and superior soft tissue contrast.

## **GUEE-8 Diverse Spectrum of Tumefactive, Non-neoplastic, Proliferative Pseudotumors of the GU Tract: Cross-sectional Imaging Findings**

**Awards**

**Identified for RadioGraphics**

Participants

Rashmi Balasubramanya, MD, Philadelphia,, PA (*Presenter*) Nothing to Disclose

### **TEACHING POINTS**

There is a wide spectrum of non-neoplastic conditions of the GU tract that show tumefactive growth pattern reminiscent of neoplasms. A diverse spectrum of inflammatory, infective, proliferative and idiopathic disorders with distinct histopathology occur in the kidneys and upper/lower urinary tracts. We present multi-modality cross-sectional imaging findings of a broad spectrum of these pseudo-tumors. To review taxonomy, epidemiology, clinical features, histopathology biology of a wide spectrum of tumefactive, non-neoplastic, proliferative conditions of the genitourinary tract. To describe multimodality cross-sectional imaging findings of these lesions and differentiate from neoplasms. To discuss management and prognosis.

### **TABLE OF CONTENTS/OUTLINE**

Organization Introduction, classification, epidemiology, clinical manifestations, histopathology, CT/MRI findings, management, prognosis, conclusion. Entities discussed Xanthogranulomatous pyelonephritis, Actinomycosis, Tuberculosis, Malakoplakia, IgG4 related disease, Amyloidosis, Perinephric myxoid pseudotumor of fat, Erdheim-Chester disease, Pseudosarcomatous myofibroblastic proliferation, Cystitis cystica, endometriosis of the ureters/urinary bladder, Nephrogenic adenoma, Adrenal rest, Echinococcal cyst.

## **GUEE-9 Unexpected Imaging Findings following Uterine Interventions**

**Awards**

**Identified for RadioGraphics**

Participants

Allan Brazier, MD, Sterling Heights, MI (*Presenter*) Nothing to Disclose

### **TEACHING POINTS**

1) Uterine and endometrial interventions include a spectrum of routine surgical, hysteroscopic, and interventional procedures. 2) Familiarity with the spectrum of interventions and recognition of their potential complications on imaging are essential to guide management and optimize patient outcomes. 3) An understanding of how these procedures are performed will lead to a better grasp of all potential complications that may ensue.

### **TABLE OF CONTENTS/OUTLINE**

1) A review of uterine and endometrial procedures and their techniques. 2) A case-based presentation of complications that result from these procedures as well as relevant management recommendations. Cases: -Retained fibroid after hysterectomy -Ureteral transection and ureterovaginal fistula after hysterectomy -Active extravasation after hysterectomy-Vesicovaginal fistula after do-it-yourself pessary placement -Regenerating uterine tissue after morcellation -Uterine perforation after dilatation and curettage (D C) -AVM after D C-Synechiae after D C -Hematometra after endometrial ablation -Uterine actinomycosis due to retained intrauterine device (IUD) -Uterine perforation by IUD -Avulsion of pedunculated fibroid after uterine artery embolization (UAE) -Utero-enteric fistula after UAE -Small bowel obstruction after UAE -Fascial dehiscence after cesarean section -Bladder flap hematoma after cesarean section -Vaginal cuff dehiscence and bowel herniation -Endometritis after embryo transfer -Peritoneal inclusion cysts following pelvic surgery -Scar endometriosis

Printed on: 02/07/23



## Abstract Archives of the RSNA, 2022

GUEE-1

### Imaging of Perirenal Retroperitoneal Lymphatic Systems: Anatomy, Function and Conditions

Sunday, Nov. 27 8:00AM - 9:00AM Room: Learning Center - GU

#### Awards

Identified for RadioGraphics  
Cum Laude

#### Participants

Hiroaki Takahashi, MD, PhD, Rochester, MN (*Presenter*) Nothing to Disclose

#### TEACHING POINTS

Normal perirenal lymphatic drain is difficult to identify on conventional imaging. It is partially visualized by CT- and MRI- lymphangiogram. It is also occasionally depicted as pyelolymphatic backflow on retrograde pyelogram, intravenous urogram and CT urogram secondary to acute rise of pressure in the collecting system. However, the knowledge of perirenal lymphatic flow is of clinical importance to understand the conditions involving the perirenal retroperitoneal lymphatics and behavior of lymph node metastases from renal or upper tract urothelial malignancy. This exhibit will review the fundamental concept about perirenal lymphatic systems, and imaging assessment for non-neoplastic and neoplastic conditions involving the perirenal lymphatics. Further, differential diagnosis and treatment strategy of these conditions are discussed. The purposes of this exhibit are: 1. To review the fundamental anatomy, physiology and imaging of normal perirenal lymphatic systems. 2. To review the imaging findings, differential diagnoses and treatment options for various conditions associated with perirenal lymphatic systems.

#### TABLE OF CONTENTS/OUTLINE

1. Overview of the lymphatic system. 2. Fundamental anatomy and physiology of perirenal lymphatic systems. 3. Imaging of perirenal lymphatics and their communication with other lymphatic chains. 4. Imaging findings of various conditions of perirenal lymphatic systems with discussion of their differential diagnoses and treatment strategies. 5. Summary

Printed on: 02/07/23



## Abstract Archives of the RSNA, 2022

GUEE-10

### Malignant Neoplasms of the Penis with Radiologic Pathologic Correlation

Sunday, Nov. 27 8:00AM - 9:00AM Room: Learning Center - GU

#### Participants

Jamie Marko, MD, (*Presenter*) Nothing to Disclose

#### TEACHING POINTS

1. Most malignant tumors of the penis are squamous cell carcinomas (SCC) arising from the mucosal lining of the glans, coronal sulcus and foreskin. Non-epithelial tumors do not demonstrate the same anatomical predilection. 2. HPV infection is associated with subtypes of penile SCC. Additional risk factors are lack of circumcision, phimosis, chronic inflammation, lichen sclerosis, smoking, and radiotherapy. 3. Penile cancer commonly presents as a discrete mass, ulcer or erythematous lesion on the glans or foreskin in a male in their 5th or 6th decade of life. 4. Imaging may be used to evaluate the local extent of a penile neoplasm and to detect metastases. Penile SCC has a predictable pattern of spread from the inguinal lymph nodes (LN) to the pelvic LN and lastly to the periaortic LN. Systemic metastases, including to the liver, lungs, mediastinal LN, are a late event.

#### TABLE OF CONTENTS/OUTLINE

1. Review penile anatomy with an emphasis on frequent sites of tumor origin and local spread. We will emphasize the anatomic structures that affect local staging and impact management. 2. Illustrate the pathologic spectrum of malignant penile neoplasms. The pathologic descriptions will serve as the basis for understanding the imaging appearances. 3. Describe the multimodality imaging evaluation of penile cancer. 4. Illustrate the spectrum of penile cancer at imaging providing radiologic-pathologic correlation.

Printed on: 02/07/23



## Abstract Archives of the RSNA, 2022

GUEE-11

### Benign Lesions of the Urinary Tract Mimicking Malignancy - Test Your Skills with this Case-based Review

Sunday, Nov. 27 8:00AM - 9:00AM Room: Learning Center - GU

#### Participants

Javier Azpeitia Arman, MD, Madrid, Spain (*Presenter*) Nothing to Disclose

#### TEACHING POINTS

To illustrate equivocal imaging findings of upper and lower urinary tract lesions including normal variants, inflammatory/infectious diseases and benign tumors mimicking genitourinary malignancy. To analyze the correlation between cystourethrogram, IVU, US, CT and MR imaging features with pathology in urinary tract lesions. To emphasize pitfalls, diagnostic difficulties and differential diagnosis.

#### TABLE OF CONTENTS/OUTLINE

Although a mass or a thickening in the upper and lower urinary tract may be caused by urothelial carcinoma, several benign and malignant entities should also be included in differential diagnosis. We review images of the urinary tract (pelvic/ureteral system, ureters, bladder and urethra) in different entities mimicking cancers in a quiz format, with clues to interpretation and providing images of malignant lesions for comparison. Imaging findings (cystourethrogram, IVU, US, CT and MR) and pathologic correlation will be presented. How pathologic correlation informs imaging interpretation will be highlighted. The list of cases presented includes: inflammatory diseases (pielitis and cystitis cystica, eosinophilic ureteritis and cystitis, Keratinizing desquamative squamous metaplasia (cholesteatoma) of the ureter, polypoid, papillary, granulomatous BCG), secondary to chemotherapy or irradiation, benign tumors (papilloma, leiomyoma), extrinsic lesions (prostate hyperplasia and carcinoma, uterine and ovarian tumors, colonic cancer, diverticulitis, Crohn's disease, varicose ureteral veins), filling defects (lithiasis, ureterocele, blood clot), addition images (diverticula).

Printed on: 02/07/23



## Abstract Archives of the RSNA, 2022

GUEE-12

### Keeping it Retro: Reflecting on the Spaces, Planes, Pathologies of the Retroperitoneum

Sunday, Nov. 27 8:00AM - 9:00AM Room: Learning Center - GU

#### Awards

Certificate of Merit

#### Participants

Jessica Lovett, MD, (*Presenter*) Nothing to Disclose

#### TEACHING POINTS

The purpose of this exhibit is to: 1. Review abdominopelvic anatomy, including the borders of the peritoneum and retroperitoneum. 2. Identify imaging findings to localize abdominal pathology to the peritoneum versus the retroperitoneum. 3. Examine the imaging signs used to localize pathology to a particular organ or space, focusing on retroperitoneal pathology. 4. Distinguish the pathways of spread of disease amongst the retroperitoneal compartments and surrounding compartments. 5. Apply these concepts with illustrative, interactive cases.

#### TABLE OF CONTENTS/OUTLINE

1. Anatomic borders of the peritoneal and retroperitoneal compartments within the abdomen and pelvis, and communicating foramina. 2. Localizing signs to assist radiologists in localizing pathology to peritoneum, retroperitoneum, or a specific organ. 3. Key imaging findings and differential diagnosis, with focus on retroperitoneal pathology. 4. Relevance of anatomical boundaries and disease spread for surgical planning. 5. Challenging cases to demonstrate teaching points.

Printed on: 02/07/23



## Abstract Archives of the RSNA, 2022

GUEE-13

### Follow the Yellow Brick Road: An Educational Review of Current Imaging in Urethral Stricture Disease with a Focus on MRI

Sunday, Nov. 27 8:00AM - 9:00AM Room: Learning Center - GU

#### Participants

Daniel Harris, (*Presenter*) Nothing to Disclose

#### TEACHING POINTS

1. Provide important definitions and principles in urethral stricture disease including a brief overview of clinical assessment, treatment, and current diagnostic imaging guidelines as suggested by the AUA and EAU. \2. In-depth discussion of retrograde urethrography, sonourethrography, and magnetic resonance urethrography including their advantages, disadvantages, and best uses with examples from our practice including our own protocol for each imaging modality. \3. Suggest supported uses for magnetic resonance urethrography by compiling case series data from over the last decade. Then, discuss an example case where multiple imaging modalities were used, providing direct comparison of magnetic resonance urethrography to the other modalities. \

#### TABLE OF CONTENTS/OUTLINE

1. Introduction: definitions, clinical assessment, and treatment modalities for urethral strictures2. Imaging modality sections: Current uses, advantages, disadvantages, potential future applications for each respective modality \2a. Retrograde urethrography, Sonourethrography, Magnetic resonance urethrography \2b. Table summarizing MRU case findings from prominent case series \3. Example case: comparison of modalities

Printed on: 02/07/23



## Abstract Archives of the RSNA, 2022

GUEE-14

### Adrenal Lesions Inside Out" - A Pictorial Review of the Correlation Between Radiologic and Anatomopathological Patterns of Benign and Malign Adrenal Lesions

Sunday, Nov. 27 8:00AM - 9:00AM Room: Learning Center - GU

#### Participants

Camila Franco, BMedSc, (*Presenter*) Nothing to Disclose

#### TEACHING POINTS

1. Review adrenal gland anatomy and discuss how it is important in the evaluation of adrenal lesions 2. Discuss the role of imaging and pathological evaluation in the assessment of adrenal gland lesions 3. Review the most common and uncommon imaging and anatomopathological patterns of benign and malign adrenal lesions. 4. Understand the correlation between radiologic and anatomopathological findings

#### TABLE OF CONTENTS/OUTLINE

Adrenal gland lesions have a prevalence of 4-7% in imaging tests among adults. The prevalence of these lesions increases with the greater availability of imaging tests and as the population gets older. Once the adrenal gland is made of different types of tissues that produce various types of hormones, adrenal lesions may present different features. This pictorial review will discuss: 1. Adrenal gland anatomy and histology review 2. The role of different imaging and anatomopathological techniques in evaluation of adrenal lesions (a) Ultrasound (b) Computed tomography (c) Magnetic resonance (d) PET/CT (e) Gross specimen evaluation (f) Histology - Morphological criteria - Immunohistochemical studies (g). Molecular pathology 3. Different (usual and unusual) imaging and anatomopathological patterns of benign and malign adrenal lesions and how they correlate (a) Adenoma (lipid-rich and lipid-poor) (b) Aldosteronoma (c) Myelolipoma (d) Hematoma (e) Macronodular adrenal bilateral hyperplasia (f) Neural crest tumors (g) Cysts (h) Pheochromocytoma (i) Adrenocortical carcinoma (j) Metastatic neoplasms (k) Miscellaneous

Printed on: 02/07/23



## Abstract Archives of the RSNA, 2022

GUEE-15

### What Do We See When We Don't See the Bladder? Review of the Main Urinary Diversion Techniques and Their Complications

Sunday, Nov. 27 8:00AM - 9:00AM Room: Learning Center - GU

#### Awards

Certificate of Merit

#### Participants

Alba Salgado Parente, MD, Madrid, Spain (*Presenter*) Nothing to Disclose

#### TEACHING POINTS

1. Review the different types of urinary diversion techniques.2. To understand the common findings to be expected in a postoperative study using the different imaging techniques (MDCT, MRI, fluoroscopy).3. To recognize the main postoperative complications, both early and late, grouped according to pathological groups.

#### TABLE OF CONTENTS/OUTLINE

1. Introduction2. Radiological protocol for post-operative evaluation (MDTC, MRI, fluoroscopy, US).3. Main surgical techniques and expected post-operative findings.3.1 Cutaneous incontinent diversions: Cutaneous diversion (Uretero-ureterocutaneostomy), Ileal conduit.3.2 Continent diversions: Indiana pouch, Orthotopic Bladder Replacement.4. Post-operative complications: Pictorial review4.1 Collecting system: Hydronephrosis, Urolithiasis, Urinary leakage, Ureteral stricture.4.2 Intestinal loops: Alteration of the intestinal rhythm, Intestinal leakage, Stomal stricture, Parastomal herniation, Fistulas, ileal conduit necrosis.4.3 Infection: pyelonephritis, abscesses, and other collections (hematoma, lymphocele).4.4 Tumoral: Local recurrence, Distant recurrence.5. Systematic approach to urinary diversions5.1 What type of urinary diversion surgery has been performed?5.2 Points of particular interest when assessing the presence of each type of complication6. Take home messages7. Bibliography

Printed on: 02/07/23



## Abstract Archives of the RSNA, 2022

GUEE-16

### Radiological Lexicon for Renal Mass Characterization: Pictorial Review

Sunday, Nov. 27 8:00AM - 9:00AM Room: Learning Center - GU

#### Participants

Rebeca Gil Vallano, Madrid, Spain (*Presenter*) Nothing to Disclose

#### TEACHING POINTS

- Revise a list of standardized terms employed to describe renal masses: basic imaging, CT, MR and miscellaneous terms. • Correlate each term with several cases from our institution with pathologic correlation.

#### TABLE OF CONTENTS/OUTLINE

Radiology reports need to employ a standardized language to improve their understanding for the rest of radiologists, clinicians and patients. In February 2021 the Society of Abdominal Radiology disease-focused panel on renal cell carcinoma published a consensus statement of recommended terms to be employed when reporting renal masses at CT and MR. We have revised the 31 terms described in this consensus: 14 basic terms such as definition of solid or cystic mass, 8 CT terms for example macroscopic fat or CT enhancement, 6 MR terms as MR enhancement and 3 miscellaneous terms like growth rate. Each term will be reviewed, explained and illustrated with different cases of our institution. In addition, we will offer an interesting anatomopathological approach to the cases presented. Knowledge of this lexicon will improve radiological reports, decrease interobserver variability, and facilitate communication with physicians.

Printed on: 02/07/23



## Abstract Archives of the RSNA, 2022

GUEE-17

### To Infinity and Beyond: Present and Future of Contrast Enhanced Ultrasound (CEUS) in Renal Transplant

Sunday, Nov. 27 8:00AM - 9:00AM Room: Learning Center - GU

#### Awards

Certificate of Merit

Identified for RadioGraphics

#### Participants

Tomas Fernandez, MD, Barcelona, Spain (*Presenter*) Nothing to Disclose

#### TEACHING POINTS

Assessment of renal transplant complications with CEUS. Review of unusual and latest complications associated with up-to-date surgical techniques and immunosuppressant therapies. Future of CEUS on renal transplant patients, focusing on radiomics.

#### TABLE OF CONTENTS/OUTLINE

Immediate complications Intrasurgical ultrasound in robot renal transplant. CEUS in hyperacute rejection. CEUS in acute tubular necrosis. CEUS in cortical necrosis. CEUS in arterial and venous thrombosis. CEUS in compartmental syndrome. CEUS in segmentary infarcts. Living renal donor transplant pseudostenosis. Urological complications: CEUS guide for nephrostomy. CEUS anatomy of the intracavitary upper urinary tract (UUT). CEUS in UUT leak. CEUS in the differentiation of benign and malignant diseases of UUT. CEUS in ureteral kinking and stenosis. Collections CEUS in posttransplant collections. Late subcapsular lymphocele and sinus lymphatic ingurgitation due to mTOR. Subcapsular hematoma due to hemorrhagic cyst. Presurgical ureteral map for marsupialization of lymphoceles. CEUS in renal infection. Malignancies associated with renal transplant: Malignancies associated with immunosuppression and more prevalence of tumors due to extended age inclusion on donor lists. Malignancies associated with acquired cystic disease in long hemodialysis. Known malignancies, partial nephrectomy ex vivo. CEUS in active surveillance of complicated cysts and biopsied benign tumors. Biopsy CEUS as a guide for biopsy. CEUS in arteriovenous fistula and pseudoaneurysm. CEUS in the diagnosis of active bleeding. CEUS in US-guided thrombin treatment of pseudoaneurysm/bleeding. Future: CEUS perfusion. Elastography. Radiomics.

Printed on: 02/07/23



## Abstract Archives of the RSNA, 2022

GUEE-18

### What's New in Classification, Pathology, Imaging Findings, and Management of Renal Cell Carcinomas? 2022 Update for Radiologists

Sunday, Nov. 27 8:00AM - 9:00AM Room: Learning Center - GU

#### Participants

Varshaa Koneru, Telangana, India (*Presenter*) Nothing to Disclose

#### TEACHING POINTS

Review updated, current classification of renal cell carcinomas (RCCs) that are based on histomorphology/molecular diagnostic criteria with special emphasis on novel tumor entities Discuss select pathologic/molecular features and genetic alterations that influence natural history, prognosis, metastatic disease targeted therapies Describe imaging findings of existing 'new' RCCs with an update on radiogenomics of select tumors Review novel treatment strategies for metastatic RCCs role of imaging in assessing efficacy of novel drugs

#### TABLE OF CONTENTS/OUTLINE

Introduction RCC Classification: Existing tumors, New tumors Emerging entities Pathology Updates: Molecular signatures, histopathology patterns TNM staging Imaging Findings Clear cell RCC Papillary RCC Chromophobe RCC Oncocytoma other oncocytic-hybrid tumors Clear cell papillary RCC Tubulocystic RCC MiTF Family RCC: Xp11 translocation TFEB-fused Acquired cystic disease-associated RCC SMARCB1-deficient RCC: Medullary carcinoma unclassified RCC with medullary phenotype Mucinous tubular spindle cell carcinoma Metanephric adenoma related tumors Hereditary RCC syndromes: Fumarate-deficient RCC, Succinate Dehydrogenase-deficient RCC Birt-Hogg-Dube syndrome RCC in Post-Radiation/Chemotherapy Multilocular Cystic Neoplasm of Low Malignant Potential RCC in Neuroblastoma Survivors Thyroid-like Follicular RCCs RCCs associated with ALK-Gene Rearrangements Molecular Imaging biomarkers Novel targeted therapies Role of Imaging Summary RCCs are genetically heterogeneous and demonstrate characteristic molecular features imaging findings that dictate prognosis survival

Printed on: 02/07/23



## Abstract Archives of the RSNA, 2022

GUEE-19

### Biochemical Recurrence of Prostate Cancer: Where Cancer Recurs, Where MRI Fails, and Where PSMA PET Fails?

Sunday, Nov. 27 8:00AM - 9:00AM Room: Learning Center - GU

#### Awards

Identified for RadioGraphics

#### Participants

Muhammad Awiwi, MD, Houston, TX (*Presenter*) Nothing to Disclose

#### TEACHING POINTS

Prostate cancer can recur in up to 40% of patients who receive treatment (radical prostatectomy, androgen deprivation therapy, or radiotherapy) and the definition of biochemical recurrence varies according to the treatment type. There are typical sites of prostate cancer recurrence, but the disease can also recur in unusual sites in the pelvis. These sites should be interrogated when interpreting pelvic MRI. Both MRI and PSMA-PET have limitations/pitfalls and they complement each other.

#### TABLE OF CONTENTS/OUTLINE

To review the definition of biochemical recurrence  
To review expected imaging findings after prostate cancer treatment  
Describe common sites of prostate cancer recurrence  
Describe uncommon sites of prostate cancer recurrence in the pelvis  
Describe potential pitfalls of MRI and PSMA-PET in detection of recurrent prostate cancer.

Printed on: 02/07/23



## Abstract Archives of the RSNA, 2022

GUEE-2

### Renal Mass Imaging with the Clear Cell Likelihood Score v2: A User Guide

Sunday, Nov. 27 8:00AM - 9:00AM Room: Learning Center - GU

#### Awards

Identified for RadioGraphics

#### Participants

Anup Shetty, MD, Saint Louis, MO (*Presenter*) Nothing to Disclose

#### TEACHING POINTS

Solid small renal masses (SSRM), defined as < 4 cm in diameter, are increasingly detected but can be complex to manage. A framework for approaching the SSRM is critical in providing optimal management, as clear cell RCC is the most common and aggressive subtype, and a high likelihood of this diagnosis can influence management. The recently updated MRI clear cell likelihood score (ccLS) provides the radiologist with tools to optimize their assessment of the SSRM. This exhibit will: 1) Familiarize the reader with the ccLS and why it was developed 2) Discuss key considerations in MRI protocol, eligibility criteria, and imaging features for using the ccLS algorithm 3) Illustrate how to use the ccLS algorithm to assess the SSRM through a series of cases 4) Highlight pitfalls of the ccLS algorithm and other considerations in MRI of SSRM not included in ccLS

#### TABLE OF CONTENTS/OUTLINE

- ccLS: rationale (moving beyond "is it enhancing, does it contain fat") and diagnostic performance- MRI protocol- Eligibility criteria and imaging features- How to use the algorithm- Case examples of working through the algorithm and pitfalls, including off-ramps when the ccLS is inappropriate to utilize (fat-rich angiomyolipoma, cystic renal mass, hemorrhagic renal cysts)- Reporting using ccLS: template and nomenclature- Potential management strategies based on ccLS

Printed on: 02/07/23



## Abstract Archives of the RSNA, 2022

GUEE-20

### Multicenter Lessons from Adrenal Multidisciplinary Tumor Boards: Expert Evidence-Based Views of the Society of Abdominal Radiology Adrenal Neoplasm Disease Focused Panel

Sunday, Nov. 27 8:00AM - 9:00AM Room: Learning Center - GU

#### Awards

Certificate of Merit

#### Participants

Ryan Chung, MD, Boston, MA (*Presenter*) Consultant, ScanMed, LLC; Stockholder, ScanMed, LLC

#### TEACHING POINTS

While some adrenal pathology is easily diagnosed radiologically, there are many common errors in adrenal imaging that may arise due to a lack of familiarity with technical, anatomic, physiologic, hemodynamic, and biologic factors. This is compounded by a deficiency of modern clinical and radiologic knowledge of adrenal pathology. These challenges arise when the radiologist encounters atypical presentations of common benign and malignant adrenal masses, mimics of benign and malignant adrenal masses, and rare adrenal pathology. This may lead to misdiagnosis, suboptimal management, and potentially adverse outcomes. In this exhibit, we present cases commonly encountered in clinical practice and presented to adrenal multidisciplinary tumor boards of major tertiary centers. Evidence-based expert views will be discussed to provide clues to the correct diagnosis and further guide appropriate management.

1. Describe common errors encountered in clinical practice and presented to adrenal multidisciplinary tumor boards of major tertiary centers
2. Illustrate relevant technical, anatomic, pathophysiologic, hemodynamic, and biologic factors leading to these errors
3. Review evidence-based literature and discuss expert opinions to provide useful tips in diagnosis
4. Correlate cross-sectional imaging findings with clinical and pathologic findings

#### TABLE OF CONTENTS/OUTLINE

1. Technical errors
2. Atypical presentations of common benign masses
3. Atypical presentations of common malignant masses
4. Benign mimics of malignant masses
5. Malignant mimics of benign masses
6. Rare adrenal pathology

Printed on: 02/07/23



## Abstract Archives of the RSNA, 2022

GUEE-21

### Postoperative Changes and Complications of the Urinary Tract at Imaging

Sunday, Nov. 27 8:00AM - 9:00AM Room: Learning Center - GU

#### Participants

Weibo Fu, BS, Augusta, GA (*Presenter*) Nothing to Disclose

#### TEACHING POINTS

1) To review changes to the anatomy of the genitourinary tract after urological procedures 2) To provide imaging examples of postoperative appearance and complications of the urinary tract 3) To distinguish between expected and unexpected postoperative imaging findings following urological surgery and image-guided procedures

#### TABLE OF CONTENTS/OUTLINE

The incidence of urological pathologies such as renal cell carcinoma and renal stones has risen over time, in part due to improved detection with increased use of imaging in clinical practice. In turn, rates of urologic interventions performed have also increased, some of which include a) partial nephrectomy, b) ureteroneocystostomy, c) cryoablation, d) diversions, and e) neobladder placement. Potential complications can arise from these procedures such as a) hematomas, b) conduits, c) strictures, and d) lymphoceles. Such complications are important to distinguish from common postoperative changes in clinical practice. Computed tomography scan is the most common imaging modality used when potential complications are suspected, though MRI may be considered for complex cases. For radiologists to provide appropriate recommendations for care following surgical urology procedures, a clear understanding of normal and abnormal post-operative anatomy is necessary.

Printed on: 02/07/23



## Abstract Archives of the RSNA, 2022

GUEE-22

### Imaging Peyronie disease Before and After Treatment: A Guide for Radiologists Urologists

Sunday, Nov. 27 8:00AM - 9:00AM Room: Learning Center - GU

#### Participants

Lauren F. Alexander, MD, Jacksonville Beach, FL (*Presenter*) Spouse, Stockholder, Abbott Laboratories; Spouse, Stockholder, AbbVie Inc; Spouse, Stockholder, General Electric Company; Spouse, Stockholder, Myriad Genetics, Inc

#### TEACHING POINTS

Ultrasound (US) is primary imaging modality for assessment of plaque and erectile dysfunction in patients with Peyronie disease to guide medical vs. surgical treatment planning; however, magnetic resonance imaging (MRI) and computed tomography (CT) can be used in the pretreatment and post treatment setting as well. After reviewing this exhibit the learner will: (1) Understand the pathophysiology of acute and chronic fibrosing Peyronie disease. (2) Recognize US findings of Peyronie plaques and US Doppler features of erectile dysfunction. (3) Describe role of noncontrast CT for calcified Peyronie plaques. (4) Determine when to use imaging after penile surgery. (5) Recognize normal and abnormal imaging findings of penile implants.

#### TABLE OF CONTENTS/OUTLINE

A. Background (1) Pathophysiology of Peyronie's disease (2) Clinical exam findings: acute and chronic phases (3) AUA management algorithm B. Pre-treatment imaging with case examples (1) Penile US grayscale: plaque Doppler: erectile function (2) CT and MR when to use, typical protocols, findings (C) Surgical treatment options (1) tunical plication vs. plaque incision/excision +/- grafting (2) role of penile prosthesis (D) Post operative imaging (1) typical findings complications

Printed on: 02/07/23



## Abstract Archives of the RSNA, 2022

GUEE-23

### Post-treatment MRI in Cervical Cancer - What To Look For

Sunday, Nov. 27 8:00AM - 9:00AM Room: Learning Center - GU

#### Participants

Mayra V. Soares, MD, Brasilia, Brazil (*Presenter*) Nothing to Disclose

#### TEACHING POINTS

Basic technical key points of pelvic MRI for a targeted assessment. Quick review of the latest FIGO MRI staging system, with the anatomical landmarks. Correlation between staging and therapeutic options. MRI findings of post-treatment and post-intervention procedures. Challenges in differentiating post-treatment and tumor recurrence. Identify the main complications of cervical cancer treatments.

#### TABLE OF CONTENTS/OUTLINE

Introduction: recurrency up to 30% of treated patients, which 66% occur in the next 2 year post initial treatment and 90% until 5 year, and survival rate can reach 15-20%. Technical points: MRI high-resolution oblique T2WI planes (small thickness and FOV) are critical to evaluate lesions. Anatomical landmarks: pelvic intricate anatomy requires the understanding of its compartments, cervix zones, vessels, sidewalls, ligaments, and lymph nodes. Staging and therapeutic correlation: Stage IIB (parametrial invasion) as a landmark for prognosis and therapeutics decision. Lower stages allow surgery with or without RT/QT. Stages IIB requires neoadjuvant treatment before reassessment. Main treatments MRI findings: trachelectomy and fertility-preserving treatment; hysterectomy/lymphadenectomy; RT/QT. Acute (vaginal edema/erythema, cystitis) and chronic (stenosis, fistulations, enteritis, insufficiency fractures, and urological) complications.

Printed on: 02/07/23



## Abstract Archives of the RSNA, 2022

GUEE-24

### Prostate MRI Quality - A Pictorial Review Using the PI-QUAL Score

Sunday, Nov. 27 8:00AM - 9:00AM Room: Learning Center - GU

#### Participants

Francesco Giganti, MD, London, United Kingdom (*Presenter*) Nothing to Disclose

#### TEACHING POINTS

The PI-RADS guidelines set out the minimal technical requirements for the acquisition of multiparametric MRI of the prostate. The rapid diffusion of prostate MRI has led to variability in vendor and scan quality across the world. The Prostate Imaging Quality (PI-QUAL) score was created to standardize the reporting of prostate MRI quality. Our education exhibit has 3 teaching points: 1) PI-RADS technical requirements for good quality prostate MRI; 2) Application of the PI-QUAL score; 3) Pictorial review of images from different vendors and magnets and quiz.

#### TABLE OF CONTENTS/OUTLINE

All those involved in the acquisition and interpretation of prostate MRI (radiologists, MR physicists and radiographers) should be aware of the PI-RADS technical recommendations and could benefit from a learning module on the PI-QUAL score. We will: 1) discuss the technical requirements (e.g., FOV, in-plane resolution, b values, etc) for a good quality prostate MR scan for each sequence, as outlined in the PI-RADS document; 2) discuss the PI-QUAL score and its ambition to standardize image quality both at a center level (i.e., up-to-date MR scanners and dedicated radiologists/radiographers highly experienced in prostate MRI) and at a patient level (i.e., patient-related artefacts such as rectal air/stools or movement should be minimized with prior preparation); 3) present a set of images of adequate and suboptimal image quality (ranging from PI-QUAL 1 to PI-QUAL 5) to stress the importance of reducing practice variability in prostate MRI; 4) discuss the current limitations of PI-QUAL and what should be addressed in the next version.

Printed on: 02/07/23



## Abstract Archives of the RSNA, 2022

GUEE-25

### Beyond Prostatic Adenocarcinoma - Confusing MRI Findings and How to Recognize Them

Sunday, Nov. 27 8:00AM - 9:00AM Room: Learning Center - GU

#### Participants

Camila Reifegerste, MD, Curitiba, Brazil (*Presenter*) Nothing to Disclose

#### TEACHING POINTS

Review normal prostate anatomy and possible neoplasm mimickers. Review benign conditions of the prostate that may mimic neoplasia. Review some rare histological subtypes of prostate neoplasia. To propose a systematic approach of the prostate MRI that allows differentiating findings suggestive of clinically significant neoplasia from the more common pitfalls.

#### TABLE OF CONTENTS/OUTLINE

Prostate cancer is the most common neoplasm in American men and the second leading cause of cancer death in this population. Its diagnosis is based on rectal examination, elevated prostate specific antigen (PSA), ultrasound-guided prostate biopsy and magnetic resonance imaging (MRI), which has become an important tool in detection of possible neoplasms, risk stratification and follow-up, thanks to the standardization of examination protocols and their interpretation with the development of the Prostate Imaging-Reporting and Data System (PI-RADS). Since prostate MRI is becoming more relevant in clinical decision making, it is important that the radiologist be familiar with pitfalls in its interpretation, whether they are normal anatomical structures, benign prostate changes, or even rare malignant neoplasms, different from traditional adenocarcinoma. That's why we propose a review of challenging cases, in order to discuss some of these pitfalls.

Printed on: 02/07/23



## Abstract Archives of the RSNA, 2022

GUEE-26

### V Steps to Assess VI-RADS

Sunday, Nov. 27 8:00AM - 9:00AM Room: Learning Center - GU

#### Participants

Vivianne Reis Guimaraes, MD, (*Presenter*) Nothing to Disclose

#### TEACHING POINTS

1. Practice guide for radiologists, identify five steps in the process to create a systematic approach to report bladder MRI findings as well as define the risk of muscle invasion. 2. Provide radiologists an overview of Vesical Imaging-Reporting and Data System (VI-RADS) that indicates the possibility of detrusor muscle invasion by bladder cancer through the five-point scoring system. 3. Discuss resources for radiologists to improve diagnostic performance through VI-RADS.

#### TABLE OF CONTENTS/OUTLINE

Step 1: Bladder wall anatomy and appearance of the muscularis propria on MRI. Step 2: Staging and how to subdivide bladder cancer into with and without muscle invasion. Step 3: Technical considerations about MR equipment and protocol. Step 4: Scoring tumors using appearances in T2W images, DWI and DCE to create an overall risk of muscle invasion score. Step 5: Final VI-RADS score and likelihood of muscle invasion.

Printed on: 02/07/23



## Abstract Archives of the RSNA, 2022

GUEE-27

### Gender Affirming Genitourinary Surgeries - What Surgeons Do and What We Need to Know

Sunday, Nov. 27 8:00AM - 9:00AM Room: Learning Center - GU

#### Participants

Susana Fernandez, MD, Madrid, Spain (*Presenter*) Nothing to Disclose

#### TEACHING POINTS

Define the concept of gender incongruence and transgender. Learn different types of genitourinary procedures employed for gender affirming surgery. Review imaging modalities used to evaluate surgical changes and complications. Show different cases presented at our institution.

#### TABLE OF CONTENTS/OUTLINE

Gender incongruence is defined as a discrepancy between gender identity and the assigned sex. Those individuals in whom gender incongruence exists are referred to as transgender. The gender affirming therapy involves multidisciplinary care that can improve quality of life of transgender people. Genital reconstruction surgery includes vaginoplasty, phalloplasty and metoidioplasty. Radiology department plays an important role in this process. We have reviewed affirming surgeries performed at our institution in the last 10 years. 78 patients have undergone this process, 67 transwomen and 11 transmen. Surgical procedures performed were: 67 vaginoplasty, 6 phalloplasties (using most often anterolateral flaps) and 5 metoidioplasties. These surgeries and normal surgical changes will be explained and reviewed. Frequent complications such as fistulas (5), leaks (1) and stenosis (4) which are recurrent in some patients, will be exposed. Retrograde urethrocytography and cystourethrography are the methods of choice for postoperative assessment, allowing the diagnosis of most common complications. TC, RM or enema are other imaging techniques that may be necessary. They will be illustrated with different imaging techniques and images of different surgeries.

Printed on: 02/07/23



## Abstract Archives of the RSNA, 2022

GUEE-28

### Expect the Unexpected - Postoperative and Postintervention Imaging of the GU Tract

Sunday, Nov. 27 8:00AM - 9:00AM Room: Learning Center - GU

#### Participants

Janelle West, MD, Pelham, AL (*Presenter*) Nothing to Disclose

#### TEACHING POINTS

- To understand expected appearance of genitourinary structures after common and uncommon surgeries and interventions- To illustrate acute and chronic complications of genitourinary organs following intervention and/or surgery-To briefly discuss potential treatment of complications secondary to genitourinary interventions

#### TABLE OF CONTENTS/OUTLINE

? Introduction? Renal: Expected appearance post ablation, Expected appearance post partial nephrectomy, Postablation renal infarct, Postablation residual/recurrent tumor, Postablation bleeding, Postablation organ injury/fistula, Post partial nephrectomy pseudoaneurysm? Ureter: Postsurgical stricture, Postsurgical leak/urinoma? Bladder: Expected appearance of augmented urinary bladder/neobladder/ileal conduit/Indiana pouch, Augmented bladder rupture, Ileal conduit leak/rupture, Recurrent tumor in ileal conduit, Bladder neck leak status post prostatectomy? Urethra: Expected appearance post urethroplasty, Expected appearance status post transurethral resection of the prostate, Urethral leak status post urethroplasty, Urethral leak status post diverticulectomy, Recurrent urethral stricture status post TURP and brachytherapy, Urethrocutaneous fistula? Male GU: Expected appearance of penile prosthesis and artificial urinary sphincter, Postintervention arteriovenous fistula, Malfunctioning artificial urinary sphincter, Malpositioned penile prosthesis, Recurrent penile cancer status post penectomy, Puboprostatic fistula status post brachytherapy/pelvic radiation? Female GU: Post DC uterine AVF (and subsequent embolization), Recurrent GYN malignancy, Retained products of conception

Printed on: 02/07/23



## Abstract Archives of the RSNA, 2022

GUEE-29

### Imaging Findings Following Renal Tumor Treatment

Sunday, Nov. 27 8:00AM - 9:00AM Room: Learning Center - GU

#### Participants

Leonardo Kenji Mitsutake, MD, Sao Paulo, Brazil (*Presenter*) Nothing to Disclose

#### TEACHING POINTS

The purpose of this exhibit is to:- Brief review renal cancer epidemiology and the main societies management guidelines.- Describe CT and MRI renal mass protocols.- Describe and illustrate the main initial and late imaging findings after renal tumor treatment.- Discuss the most frequent complications following renal tumor treatment.

#### TABLE OF CONTENTS/OUTLINE

1. Introduction:- Renal cancer epidemiology.- Society guidelines (AUA and EUA) for renal cancer management.- Overview the approach for renal cancer treatment (systemic treatment, radical and partial nephrectomy, ablation treatment). 2. Diagnostic Imaging evaluation:- CT and MRI renal mass protocols. 3. Imaging findings after renal tumor treatment:- Procedure complications.- Initial and late expected post-treatment imaging features.- Features of tumor recurrence. 4. Take home messages.

Printed on: 02/07/23



## Abstract Archives of the RSNA, 2022

GUEE-3

### "Mesh Mash"- Multimodality Imaging of Pelvic Floor Repair

Sunday, Nov. 27 8:00AM - 9:00AM Room: Learning Center - GU

#### Awards

**Cum Laude**

**Identified for RadioGraphics**

#### Participants

Kanupriya Vijay, MBBS, MD, Jacksonville, FL (*Presenter*) Nothing to Disclose

#### TEACHING POINTS

1. Review the expected postsurgical appearances after surgical and non-surgical repair of pelvic floor/urethral dysfunction. 2. Ultrasound is superior to MRI for assessing synthetic slings in suburethral space and evaluate for complications such as urethral erosion and vaginal exposure. 3. Ultrasound can accurately demonstrate the distribution of injected bulking agent, and determine the need and location for reinjection; as well as migrated bulking agent. 4. Radiologists play an important role in the detection of normal and abnormal appearances of postsurgical pelvic floor repair, and guide for future intervention.

#### TABLE OF CONTENTS/OUTLINE

1. Introduction: a. Briefly review pelvic floor dysfunction and various surgical and nonsurgical treatment options 2. Discuss imaging techniques and protocol: a. Ultrasound b. MRI 3. Case based review of various treatment options: a. Normal imaging appearances b. Complications: i. Misplacement ii. Urethral erosion iii. Vaginal exposure iv. Infection

Printed on: 02/07/23



## Abstract Archives of the RSNA, 2022

GUEE-30

### Ups and Downs in the Andes: Soft Tissue Sarcomas of the Genitourinary Tract with Radiologic-pathologic Correlation

Sunday, Nov. 27 8:00AM - 9:00AM Room: Learning Center - GU

#### Awards

**Certificate of Merit**

**Identified for RadioGraphics**

#### Participants

Jorge Huayanay, MD, (*Presenter*) Nothing to Disclose

#### TEACHING POINTS

1. Soft tissue sarcomas of the genitourinary tract are uncommon, constituting less than 2% of all soft tissue sarcomas. This presentation will illustrate imaging features of these rare soft tissue sarcomas of the genitourinary tract. 2. The exhibit will review the spectrum of histopathologic correlations. 3. This review will emphasize diagnostic difficulties, potential imaging pitfalls and differential diagnoses of these entities.

#### TABLE OF CONTENTS/OUTLINE

The goals of this exhibit are to: Provide a pictorial review of the diverse imaging appearances of the soft tissue sarcomas of the genitourinary tract. Discuss specific imaging and pathological characteristics of the soft tissue sarcomas of the genitourinary tract. Familiarize the audience with the imaging features of the soft tissue sarcomas of the genitourinary tract, thereby helping in formulation of a complete differential diagnosis. These major featured entities include: • Renal leiomyosarcoma • Perirenal and pararenal liposarcoma • Vesical rhabdomyosarcoma • Prostate sarcomas • Paratesticular liposarcoma • Penile sarcoma • Uterine rhabdomyosarcoma • Uterine endometrial stromal sarcoma • Uterine adenocarcinoma

Printed on: 02/07/23



## Abstract Archives of the RSNA, 2022

GUEE-31

### MR Imaging of the Penis - What a Radiologist Needs to Know

Sunday, Nov. 27 8:00AM - 9:00AM Room: Learning Center - GU

#### Awards

Certificate of Merit

#### Participants

Pankaj Nepal, MD, Bridgeport, CT (*Presenter*) Nothing to Disclose

#### TEACHING POINTS

To emphasize role of MRI in the evaluation of penile pathologies To illustrate normal MR anatomy of the penis, and its importance on local staging of penile cancer with reference to surgical outcomes To evaluate the role of MRI in evaluation of penile prosthesis To demonstrate role of MRI in diagnosis of unexplained cases of priapism or erectile dysfunction

#### TABLE OF CONTENTS/OUTLINE

Normal MR anatomy of penis, MR imaging protocol, different protocols (e.g. artificial erection) Etiologies Tumors - primary and metastasis, some rare tumors Trauma - penile fractures, hematoma, urethral injury Infarction- sickle cell disease, intracavernosal injection Infection Penoscrotal fistulas Peyronie's disease - diagnosis, follow up, plication, plication failure Penile prosthesis - types, parts, and complications Future directions

Printed on: 02/07/23



## Abstract Archives of the RSNA, 2022

GUEE-32

### How Fluent Are You in PI-RADS Terminology?

Sunday, Nov. 27 8:00AM - 9:00AM Room: Learning Center - GU

#### Participants

Ana Cristina Delgado, MD, Porto Alegre, Brazil (*Presenter*) Nothing to Disclose

#### TEACHING POINTS

The use of standard terminology, correct report organization, clear knowledge of the PI-RADS guides, understanding prostate anatomy, allows radiologist to certainly communicate the image findings of the prostate gland and organize the final report. For radiology residents/radiologists, a good understanding of terminology used on PI-RADS is one prerequisite for starting the image interpretation as well as knowing the anatomy. The idea of this exhibit is to expose residents/radiologist to a series of cases to reinforce concepts in an interactive activity.

#### TABLE OF CONTENTS/OUTLINE

Prostate anatomy / sector map case / review PI-RADS classification , what to evaluate on each sequence cases / review Benign findings, how to describe them, cases / review Extra prostatic invasion cases / review Final remarks

Printed on: 02/07/23



## Abstract Archives of the RSNA, 2022

GUEE-33

### Blast From the Past: Post-ablation Imaging of Renal Tumors Post-ablation Imaging of Small Renal Tumors

Sunday, Nov. 27 8:00AM - 9:00AM Room: Learning Center - GU

#### Participants

Lucas Daniel Pereira Lopes, (*Presenter*) Nothing to Disclose

#### TEACHING POINTS

Title: Blast from the past: Post-ablation imaging of small renal tumors Teaching Points 1. Review features of renal masses appropriate for ablation 2. Outline timeline for post-ablation surveillance 3. Distinguish between expected post-ablation appearance and pathological findings 4. Identify red flags and potential complications to look out for in the post-ablation period Table of Contents • Background o Types and mechanisms of thermal ablative techniques o Features of renal tumors for pre-ablation planning • Post-ablation expectations o Overview of timeline for post-ablation surveillance o Technical requirements of imaging o Expected appearance in imaging • Pathological changes in post-ablation o Red flags in appearance o Complications to look out for

#### TABLE OF CONTENTS/OUTLINE

Title: Blast from the past: Post-ablation imaging of small renal tumors Teaching Points 1. Review features of renal masses appropriate for ablation 2. Outline timeline for post-ablation surveillance 3. Distinguish between expected post-ablation appearance and pathological findings 4. Identify red flags and potential complications to look out for in the post-ablation period Table of Contents • Background o Types and mechanisms of thermal ablative techniques o Features of renal tumors for pre-ablation planning • Post-ablation expectations o Overview of timeline for post-ablation surveillance o Technical requirements of imaging o Expected appearance in imaging • Pathological changes in post-ablation o Red flags in appearance o Complications to look out for

Printed on: 02/07/23



## Abstract Archives of the RSNA, 2022

GUEE-34

### **Pheochromocytoma and Paraganglioma: Key Findings, Clinical Features, and Their Association with Anatomic and Functional Imaging - Tutorial for Residents**

Sunday, Nov. 27 8:00AM - 9:00AM Room: Learning Center - GU

#### **Awards**

**Certificate of Merit**

#### **Participants**

Leonela Ramirez Almanza, (*Presenter*) Nothing to Disclose

#### **TEACHING POINTS**

Pheochromocytoma and paraganglioma are chromaffin cell tumors that require early diagnosis due to their potentially serious and sometimes fatal cardiovascular sequelae. CT density of pheochromocytoma greater than 20 HU in the proper clinical context should be suggestive of this pathology. Hypercellularity in pheochromocytoma results in restricted diffusion and should not be confused with malignancy. Pheochromocytoma and larger paragangliomas may have areas of necrosis and intratumoral vessels with a "salt and pepper" appearance on MRI. Functional imaging is key to the diagnosis of pheochromocytoma and paraganglioma when no tumor is identified on anatomic imaging.

#### **TABLE OF CONTENTS/OUTLINE**

1. Introduction 2. Imaging protocols a. CT b. MRI c. PET/CT 3. Systematic analysis of images in relation to the clinic. a. Incidental finding b. Clinical Context and findings suggestive of pheochromocytoma and paraganglioma 4. Paraganglioma clinical and imaging features 5. Pheochromocytoma clinical and imaging features 6. Differential diagnoses 7. Take home messages

Printed on: 02/07/23



## Abstract Archives of the RSNA, 2022

GUEE-35

### Variant Bladder Cancer: MR Imaging, VIRADS Score, Clinical Feature and Management

Sunday, Nov. 27 8:00AM - 9:00AM Room: Learning Center - GU

#### Participants

Arisa Kameda, (*Presenter*) Nothing to Disclose

#### TEACHING POINTS

Variant bladder cancer is relatively rare and associated with increased risks of disease recurrence. Since these subtypes are often more advanced in stage than pure urothelial bladder cancer and is likely to underestimate the myometrial invasion, immediate total bladder resection is recommended in these patients. However, there has been few reports about MR imaging of Variant bladder cancer. The purpose of this exhibit is To clarify the feature of the MR findings of variant bladder cancer To depict the VIRADS score of variant bladder cancer To discuss the clinical feature and management comparing pure urothelial bladder cancer.

#### TABLE OF CONTENTS/OUTLINE

1, Over view of histological classification of bladder cancer based on WHO 2016 2, Demonstrate the MR imaging of variant bladder cancer (Glandular differentiation, Squamous differentiation, Micropapillary type, Nested type, Sarcomatoid type) 3, VIRADS scoring of variant bladder cancer with histological correlation 4, Discussion of clinical feature and management of variant bladder cancer 5, Summary

Printed on: 02/07/23



## Abstract Archives of the RSNA, 2022

GUEE-36

### DCE MRI: A Superhero Or Villain In Prostate MRI?

Sunday, Nov. 27 8:00AM - 9:00AM Room: Learning Center - GU

#### Participants

Samantha Jayasinghe, MD, Cleveland, OH (*Presenter*) Nothing to Disclose

#### TEACHING POINTS

1. Review different rationales and imaging protocols in prostate MRI. 2. Discuss the strengths and limitations of using or not using DCE in prostate MRI for diagnosis of clinically significant cancer (csPCa). 3. Review the available evidence on the diagnostic performance of prostate MRI without versus with contrast. 4. Provide a risk-based workflow to optimize the choice between contrast and non-contrast MRI utilization.

#### TABLE OF CONTENTS/OUTLINE

1. Imaging Protocols in Prostate MRIa. from standard and optional mpMRIb. MRI without contrastc. "fast MRI". 2. Dynamic Contrast enhancement imaging in prostate MRIa. Acquisition technique, Interpretation, and Post-processing methodsb. Strengthsi. Increased detection and confidence of csPCaii. Helpful to inexperienced readersiii. Excellent PI-RADS staging tooliv. Accurate estimation of index PCa volumeLimitationsi. Costii. Timeiii. Nephrotoxicityiv. Limited role in Transitional Zone3. Non-contrast MRI imaging (i.e., bpMRI)Strengths: a. Non-inferior in sensitivity and specificityb. Increased safety and cost effectivenessLimitations: a. Requires higher reader expertiseb. Follow-up safety netIncreased patient in indeterminate category4. When to choose between contrast or non-contrast prostate MRI: Is it always one or the other?5. Risk-based approach to Workflow

Printed on: 02/07/23

## Abstract Archives of the RSNA, 2022

GUEE-37

### Iatrogenic Injuries of the Urinary System: Radiologic Features and Imaging-guided Intervention

Sunday, Nov. 27 8:00AM - 9:00AM Room: Learning Center - GU

#### Participants

Emanuele Barabino, MD, (*Presenter*) Nothing to Disclose

#### TEACHING POINTS

• Iatrogenic Injuries of the urinary system could occur during percutaneous/endoscopic procedure involving the urinary system or during surgery; in recent years, due to the diffusion of laparoscopic and robotic surgery, the incidence of these lesions is increasing. • The spectrum of radiologic findings is wide and heterogeneous and depends on the type of injury, the procedure that cause it and time-to-diagnosis. • Imaging-guided intervention maintains a fundamental role in the management of iatrogenic injuries to the urinary system.

#### TABLE OF CONTENTS/OUTLINE

1. Introduction  
2. Anatomical Considerations  
3. Mechanisms of Injury  
3.1 Transection and Avulsion  
3.2 Ligation  
3.3 Mixed lesions  
4. Imaging Techniques  
5. Radiologic Features  
5.1 Percutaneous Treatments  
5.1.1 Thermal Ablation  
5.1.2 Nephrostomy/Anterograde ureteral stenting  
5.1.3 Lithotripsy  
5.2 Endoscopic Treatments  
5.3 Urologic Surgery  
5.4 Gastrointestinal Surgery  
5.5 Gynecologic Surgery  
5.6 Vascular Surgery and Endovascular Procedures  
6. Imaging-guided intervention  
6.1 Kidney derivation  
6.2 Recanalization and Stenting  
7. Conclusion

Printed on: 02/07/23



## Abstract Archives of the RSNA, 2022

GUEE-38

### Pitfalls in Prostate MRI: How to Avoid These Common Errors of Under and Over Diagnosis

Sunday, Nov. 27 8:00AM - 9:00AM Room: Learning Center - GU

#### Awards

Certificate of Merit

#### Participants

Omar Kamal, MD, MSc, Portland, OR (*Presenter*) Nothing to Disclose

#### TEACHING POINTS

- Prostate MRI has a steep learning curve and experts suggest attending a course and a minimum of 100 supervised cases prior to independent practice.
- There is a tendency for inexperienced readers to overcall normal anatomy and benign lesions as cancer as they do not want to "miss" cancer.
- At the same time underdiagnosis is a problem due to poor technique and/or failure to recognize small or subtle cancers.

#### TABLE OF CONTENTS/OUTLINE

1. Brief overview of typical and atypical appearance of prostate cancer on multiparametric MRI: a. Discussion of learning curve, expert opinion, lack of standardization in training/certification/performance.
2. MRI technique: a. Optimal technique to avoid under- or overdiagnosis. b. Examples of poor technique side by side with proper technique.
3. Pitfalls: a. Overview of the literature in prostate interpretation errors. b. Mimics of peripheral zone cancer. i. Normal central zone ii. Exophytic BPH nodules iii. Midline pseudolesion iv. Periprostatic vein v. Prostatitis/scar/atrophy (PIRADS 2) lesions overcalled as PIRADS 4/5 vi. DWI and coil artifact vii. Post biopsy hemorrhage viii. Calcification c. Mimics of transition zone cancer. i. Failure to recognize encapsulated or heterogeneous nodules ii. Atypical and asymmetric BPH nodules iii. Thick anterior fibromuscular stroma iv. Thickening of the pseudocapsule. d. Underdiagnosis. i. Failure to recognize small/subtle lesions ii. Failure to recognize very large lesions replacing most of the normal gland. e. Other Lesions Mimicking Cancer. i. Seminal vesicle collapse ii. Granulomatous and IgG4 prostatitis iii. Cowper's gland hyperplasia.
4. Practical ideas for self-improvement.

Printed on: 02/07/23



## Abstract Archives of the RSNA, 2022

GUEE-4

### MR Imaging of Postoperative Endometriosis

Sunday, Nov. 27 8:00AM - 9:00AM Room: Learning Center - GU

#### Awards

Identified for RadioGraphics

Magna Cum Laude

#### Participants

Patricia Dantas I, MD, Sao Paulo, Brazil (*Presenter*) Nothing to Disclose

#### TEACHING POINTS

The purposes of this exhibit are:1) Discuss the roles of surgical treatment of different types of endometriosis using a didactic approach by illustrations and MR images.2) Clarify significant MRI image postoperative findings and meaningful information to radiology reports.3) Illustrate imaging patterns and pitfalls of postoperative complications, residual endometriosis and recurrence after surgery.

#### TABLE OF CONTENTS/OUTLINE

1) Review preoperative imaging findings that aid in surgical decisions.2) Describe surgical treatment of different types of endometriosis: endometrioma, posterior compartment, bowel endometriosis, uterus/vagina, bladder and ureters.3) Recognition of patterns normal MR postoperative findings.4) Cased-based imaging of postoperative complications.5) Illustrative key points: residual disease and recurrence after surgery.6) Pitfalls.7) Conclusions and "take home messages": consolidate the acquired knowledge.

Printed on: 02/07/23



## Abstract Archives of the RSNA, 2022

GUEE-40

### Non-Wilms Kidney Tumors in Childhood - What the Radiologist Should Know

Sunday, Nov. 27 8:00AM - 9:00AM Room: Learning Center - GU

#### Participants

Elena Paz Calzada, MD, Madrid, Spain (*Presenter*) Nothing to Disclose

#### TEACHING POINTS

Wilms tumor is the fifth most common malignant neoplasm in childhood and the most common renal tumor in children. It is estimated that the annual incidence is 1 case per 10,000 children under 15 years of age. However, there are other childhood kidney tumors with which the radiologist should be familiar. The aim is to present epidemiological, clinical and radiological findings that better guide us to a differential diagnosis of renal mass in pediatric patients.

#### TABLE OF CONTENTS/OUTLINE

We have carried out a review of the cases of non-Wilms kidney tumors in childhood in our institution, spanning from 2008 to 2021. Regarding the case review, a literature research of the main kidney tumors: Wilms and non-Wilms, as well as their characteristics, was performed. We found several cases of: - Clear cell renal carcinoma- Renal clear cell sarcoma- Renal angiomyolipoma- Inferior vena cava thrombosis mimicking a renal tumor- Renal Ewing sarcoma- Chromophobic carcinoma Both the ultrasound, CT and MRI images of each case are exposed, as well as a brief summary of the epidemiology, symptoms, radiological characteristics and prognosis of each one.

Printed on: 02/07/23



## Abstract Archives of the RSNA, 2022

GUEE-41

### Propensity for Density: Hyperdense and Calcified Disease throughout the Genitourinary System on CT

Sunday, Nov. 27 8:00AM - 9:00AM Room: Learning Center - GU

#### Awards

Certificate of Merit

#### Participants

Virginia Planz, MD, Nashville, TN (*Presenter*) Nothing to Disclose

#### TEACHING POINTS

- A wide spectrum of benign and malignant conditions in the GU system can be readily detected on CT as calcified or hyperdense findings.
- Recognizing distinguishing features and characteristic imaging appearances will determine the diagnosis or narrow the differential.
- Dual energy CT offers opportunity for further characterization of hyperdense and calcified pathology.

#### TABLE OF CONTENTS/OUTLINE

- Review the spectrum of diseases associated with GU calcification and intrinsic hyperdensity such as: hemorrhagic cysts, RCC, calculi, nephrocalcinosis, papillary necrosis, ADPKD, multicystic dysplastic kidney, renal transplant rejection, tuberculosis, schistosomiasis, alkaline encrusted pyelitis/cystitis, acute/chronic subcapsular hematoma, renal and gonadal vein thrombosis, renal artery aneurysm, urothelial carcinoma, radiation cystitis, bladder mucinous adenocarcinoma, urachal adenocarcinoma, amyloidosis, malakoplakia, serous ovarian carcinoma, colonic mucous adenocarcinoma ovarian metastasis, dermoid cyst, degenerated fibroids, prostate and vas deferens calcification
- Describe and classify hyperdense and calcified findings based on involved organ, distribution, appearance, and other accompanying findings, with an emphasis on pattern recognition in a case-based review.
- Apply teaching points to unknown cases.

Printed on: 02/07/23



## Abstract Archives of the RSNA, 2022

GUEE-42

### Penile MRI - Normal and Abnormal

Sunday, Nov. 27 8:00AM - 9:00AM Room: Learning Center - GU

#### Participants

Madhura Ghatge, MD,MD, (*Presenter*) Nothing to Disclose

#### TEACHING POINTS

After viewing this exhibit, the readers will gain insight into penile anatomy on MRI. They will be able to independently carry out MR imaging of the penis. MR imaging protocol and utility of diffusion weighted imaging and I.V contrast will be discussed. Imaging appearances of various pathologies such as structural abnormalities, inflammatory/infective pathologies, neoplasms will be presented.

#### TABLE OF CONTENTS/OUTLINE

1) Imaging anatomy of the penis. 2) MRI protocols. 3) MR imaging of various penile and urethral abnormalities including congenital/structural anomalies, infective/inflammatory pathologies, vascular pathologies, neoplasms and post operative assessment.

Printed on: 02/07/23



## Abstract Archives of the RSNA, 2022

GUEE-43

### Sonography of the Penis: Beyond Erectile Dysfunction - A Primer for Radiology Residents and Fellows

Sunday, Nov. 27 8:00AM - 9:00AM Room: Learning Center - GU

#### Awards

Identified for RadioGraphics

#### Participants

Nanda Venkatanarasimha, MRCP, FRCR, Singapore, Singapore (*Presenter*) Nothing to Disclose

#### TEACHING POINTS

div>

#### TABLE OF CONTENTS/OUTLINE

1. Case based review of the various pathologies affecting the penis including Doppler studies. Pathologies presented: Non-vascular (Peyronie's disease, Trauma, infection, benign malignant lesions, Idiopathic calcinosis cutis) Vascular (arterial insufficiency, venous insufficiency, mixed disease, iatrogenic malignant priapism, Acute venous thrombosis Mondor's disease)2. Review Ultrasound anatomy3. Illustrate, discuss normal abnormal Doppler wave forms4. Demonstrate Ultrasound technique including pearls pitfalls5. Correlative imaging where appropriate will be discussed and illustrated6. Clinical presentation and management will be highlighted

Printed on: 02/07/23



## Abstract Archives of the RSNA, 2022

GUEE-44

### Novel Implantable Devices in the Abdomen and Pelvis: A Primer for Radiologists

Sunday, Nov. 27 8:00AM - 9:00AM Room: Learning Center - GU

#### Participants

Nabih Nakrour, MD, Boston, MA (*Presenter*) Nothing to Disclose

#### TEACHING POINTS

The purpose of this exhibit is to: Provide a multimodality review of novel implantable devices in the abdomen and pelvis with a focus on indications, proper anatomical positioning, and expected radiologic features. Recognize radiologic findings of devices malposition, malfunction, and resulting complications. Discuss imaging pearls and pitfalls of novel devices. Discuss imaging techniques and protocol modifications to optimize device assessment.

#### TABLE OF CONTENTS/OUTLINE

We will address the following novel devices: An artificial male sphincter. Sacrocolpoplexy mesh for pelvic floor descent. Bladder neck suspension. Urethral bulking agent. Midurethral and retropubic sling. Omentopexy and omental packing. Sacral nerve stimulator. Antibiotics beads for intraabdominal or intrapelvic infections. Bariatric intragastric balloon and Sleeve balloon device. Gastric electrical stimulators. Anti-reflux devices.

Printed on: 02/07/23



## Abstract Archives of the RSNA, 2022

GUEE-45

### Updates on Adrenal Imaging: from A(denomas) to Z(ebras)

Sunday, Nov. 27 8:00AM - 9:00AM Room: Learning Center - GU

#### Participants

Wendy Tu, MD, Edmonton, AB (*Presenter*) Nothing to Disclose

#### TEACHING POINTS

Incidental adrenal nodules are common, seen in 4-8% of patients. Although most are benign adenomas, the differential is broad, requiring an algorithmic approach to incidental adrenal nodules. This approach should incorporate relevant recent literature given the evolving use of CT, MRI, and PET-CT and their advantages/disadvantages. Beyond image interpretation, radiology plays a crucial role in guiding biochemical testing, referral, and management. Current literature on adrenal pathology and management outcomes are discussed.

#### TABLE OF CONTENTS/OUTLINE

1) Case-based comprehensive review of benign and malignant adrenal pathology highlighting clinical and imaging findings.a. Can imaging alone differentiate benign and malignant adrenal masses?b. What are the diagnostic criteria for adenoma?c. What is the radiologic workup?d. What are the strengths/limitations of CT washout and MR chemical shift imaging studies?e. When is PET/CT indicated?f. What are key imaging pitfalls?2) Learn an algorithmic pathway to the incidental adrenal nodule, incorporating current major guidelines.a. What are the first steps after finding an incidental adrenal nodule?b. Which guidelines are available?c. What imaging findings support each step?d. What reporting templates are available?3) Discuss management of adrenal nodules, highlighting the role of the radiologist in directing appropriate specialist referral, biochemical testing, and biopsy.4) Review the treatment options and prognosis of conditions including hormonally active tumors.

Printed on: 02/07/23



## Abstract Archives of the RSNA, 2022

GUEE-46

### Müllerian Duct Anomalies: New Classification Systems, Clinical Implications, and Treatment Frontiers

Sunday, Nov. 27 8:00AM - 9:00AM Room: Learning Center - GU

#### Participants

Moataz Ahmed Sayed Mohammed Soliman, MD, MSc, CHICAGO, IL (*Presenter*) Nothing to Disclose

#### TEACHING POINTS

- Understanding the evolution of Mullerian duct anomalies classification systems.
- Formulating a stepwise approach to report Mullerian duct anomalies considering the new American Society of Reproductive Medicine (ASRM) classification.
- Learning the impact of new classification systems on management.
- Familiarize with new surgical approaches for management.

#### TABLE OF CONTENTS/OUTLINE

- Introduction o Embryological background. o Normal anatomy.
- Normal Multimodality imaging of the female genital system: (US, 3D US, MRI, and hysterosalpingography (HSG).
- Classification of Mullerian duct anomalies: (American fertility society, ESHRE/ESGE, American society of fertility medicine).
- o Mullerian duct anomalies: (uterus, cervix, and vagina).
- o Comparison between old and new classification systems.
- Multimodality imaging approach diagnosing Mullerian duct anomalies: (US, 3D US, MRI, hysterosalpingography (HSG), and CT in selected cases)
- Clinical implications for fertility and patient outcomes.
- Management approach in light of the newly proposed classification systems.
- Multimodality imaging post corrective interventions.
- New treatment frontiers for the treatment of female infertility. o Hysteroscopic management. o Uterus transplantation.

Printed on: 02/07/23



## Abstract Archives of the RSNA, 2022

GUEE-47

### Pubic Symphyseal Urinary Fistulae with Osteomyelitis in the Setting of Treated Prostate Carcinoma

Sunday, Nov. 27 8:00AM - 9:00AM Room: Learning Center - GU

#### Participants

Paul Wojack, MD, Manhasset, NY (*Presenter*) Nothing to Disclose

#### TEACHING POINTS

Prostate cancer is the leading cause of cancer in men and a variety treatment options are available. Increasing population size and advancements in prostate cancer treatment has led to an increased number of patients who are living longer with prostate cancer. Complications of prostate cancer treatment include erectile dysfunction, impotence, incontinence, gastrointestinal issues (such as radiation proctitis), and rarely posterior urethral strictures (secondary to radiation damage). Manipulation of these strictures with urethroplasty, stenting, and other urethral instrumentation can cause breakdown of the friable post-radiation tissues. Patients can develop urinary fistulae to the pubic symphysis which are often complicated by pubic osteomyelitis and often require aggressive surgical interventions. A paucity of literature regarding urosymphyseal fistulae, making this a rare complication of which radiologists should be aware, especially musculoskeletal and body imagers.

#### TABLE OF CONTENTS/OUTLINE

1. Introduction 2. Background 3. Prostate Cancer a. Epidemiology b. Treatments c. Complications 4. Urosymphyseal fistulae a. Normal and post-treatment anatomy b. Pathophysiology in the setting of treated prostate cancer c. Pubic osteomyelitis vs osteitis pubis. d. Imaging review of several cases of urosymphyseal fistulae 5. Summary 6. References

Printed on: 02/07/23



## Abstract Archives of the RSNA, 2022

GUEE-48

### Reporting a Renal Mass: Can We Do It Better?

Sunday, Nov. 27 8:00AM - 9:00AM Room: Learning Center - GU

#### Participants

Pablo Valdes Solis, PhD, (*Presenter*) Nothing to Disclose

#### TEACHING POINTS

Review the points that are considered most important when making a radiological report of a renal mass. Analyze why they are important and how to describe them. See examples of each of the points, with practical cases explaining what is reported, how and why.

#### TABLE OF CONTENTS/OUTLINE

Introduction: Importance of the correct description of the renal mass. Variability in how radiologists and urologists consider the most important points. Current situation: vision of the radiologist and the urologist. Points to be included in the report. In each point, the what, how and why will be described, accompanied by examples, as well as the importance that radiologists and urologists have given to each point. Examination type and description; CT or MRI, with or without contrast. Mass type: cystic or solid. Mass size, including methods. Size comparison: studies and measurements included for comparison. Enhancement, including methods. Importance of measurement comparing enhanced and unenhanced scans. Macroscopic fat: importance of detecting and describing the presence of fat in the mass. Mass margins: is there infiltration? Necrosis. Bosniak classification: a review of the classification of cystic masses. Nephrometry score: something that some urologist use. Estimated probability of malignancy: if included and method. Features predictive of indolent growth in solid masses. Lymph node size: how to measure and describe lymph nodes. Tumor thrombus: description, location and extension. Location inside the kidney: axial location, capsular location, distance to sinus fat, position relative to polar lines. Management options mentioned. Tumor-Node-Metastasis (TNM) staging reported: a review. Conclusions

Printed on: 02/07/23



## Abstract Archives of the RSNA, 2022

GUEE-49

### Not Kidneying Around: Multimodality Imaging of Renal Infectious and Inflammatory Conditions in Adults- Key Imaging Findings

Sunday, Nov. 27 8:00AM - 9:00AM Room: Learning Center - GU

#### Participants

Camila Vendrami, MD, Chicago, IL (*Presenter*) Nothing to Disclose

#### TEACHING POINTS

· Discuss the role of imaging in the evaluation of a wide spectrum of renal infections and inflammatory conditions· Review their main pathophysiologic features · Emphasize specific imaging features of certain renal infections and inflammatory conditions that aid in making the correct diagnosis

#### TABLE OF CONTENTS/OUTLINE

A wide spectrum of renal infectious and inflammatory conditions exists. Imaging plays a key role in many instances, including in immunocompromised patients, treatment non-responders, transplant patients, and cases with an equivocal clinical diagnosis.1. Introduction 2. What is the role of multimodality imaging (US, CT, MR) in the evaluation of renal infections and inflammatory conditions? 3. What are the key imaging features of acute renal conditions (acute pyelonephritis, renal and perirenal abscesses, pyonephrosis, emphysematous pyelonephritis/cystitis)?4. What are the key imaging features of fungal infections and their complications (such as aspergillus, candida and mucor) as well as of tuberculosis and parasitic infections (renal hydatid disease)?5. What are the key imaging features of chronic renal conditions (chronic pyelonephritis, xanthogranulomatous pyelonephritis, eosinophilic cystitis, renal replacement lipomatosis, struvite stones)?6. Take Home Points

Printed on: 02/07/23



## Abstract Archives of the RSNA, 2022

GUEE-5

### MR Imaging of the Penis: A Practical Guide for Radiologists

Sunday, Nov. 27 8:00AM - 9:00AM Room: Learning Center - GU

#### Participants

Renata Nascimento, MD, (*Presenter*) Nothing to Disclose

#### TEACHING POINTS

- Review the penile anatomy - Describe our institutional protocol for penile magnetic resonance imaging (MRI) - Create a practical guide to evaluate the penis at MRI - Describe common and uncommon penile imaging findings - Revisit the new TNM staging system used for squamous cell carcinoma of the penis

#### TABLE OF CONTENTS/OUTLINE

- Introduction Anatomy of the penis - MR Imaging Technique Preparation MRI protocol and how to optimize it - Magnetic resonance imaging findings of the penis Traumatic (eg: fracture) Infectious Inflammatory (eg: Peyronie's disease) Vascular (eg: fistula, segmental thrombosis of the corpus cavernosum, priapism, mondor disease) Penile prosthesis Penile cancer

Printed on: 02/07/23



## Abstract Archives of the RSNA, 2022

GUEE-50

### The Postoperative Kidney: Multimodality Imaging Manifestations of Common and Uncommon Complications

Sunday, Nov. 27 8:00AM - 9:00AM Room: Learning Center - GU

#### Participants

Cole Thompson, MD, (*Presenter*) Nothing to Disclose

#### TEACHING POINTS

-Postoperative renal complications may be grouped into several broad categories: Fluid collections; vascular, lymphatic, and collecting system injuries; tumor seeding; trauma to adjacent organs; and general complications.-Postoperative fluid collections include hematoma, seroma, urinoma, abscess, and lymphocele, each at varied time intervals following surgery. Discernment of differences in key imaging features allows for appropriate management.-Vascular complications related to renal arterial injury or thrombosis include active hemorrhage, pseudoaneurysm, and renal infarction. Prompt recognition of imaging findings enables early intervention.-Postsurgical complications are not limited to the kidney or collecting system. The adjacent organs may also be injured, including the spleen, adrenal glands, liver, pancreas, bowel, and pleura.

#### TABLE OF CONTENTS/OUTLINE

-Expected imaging features of the post-operative kidney following partial nephrectomy, radical nephrectomy, and lithotripsy (ESWL) or nephrolithotomy.-Case-based review illustrating the role of imaging (CT, US, MRI, angiography) in complications following renal surgery: Fluid collections; vascular and lymphatic injuries; complications related to the collecting system; tumor seeding and recurrence; and injury to adjacent organs.-Recognition of key imaging features that warrant urgent therapeutic intervention.-Challenging clinical scenarios and strategies for optimal image interpretation to guide subsequent management and follow-up.

Printed on: 02/07/23



## Abstract Archives of the RSNA, 2022

GUEE-51

### Preoperative Planning In Cancer Of The Urinary Tract: What Surgeon Wants to Know What Radiologists Need to Know

Sunday, Nov. 27 8:00AM - 9:00AM Room: Learning Center - GU

#### Participants

Patricia E. Ortega Aragon, MD, MD, Mexico City, Mexico (*Presenter*) Nothing to Disclose

#### TEACHING POINTS

Bladder cancer (BC) is the most common cancer of the urinary tract in the United States. In bladder cancer, images play an important role in locoregional staging and remote evaluation of the disease. The RENAL nephrometry scoring system, VI-RADS, and PI-RADS provide preoperative information that is important in predicting long-term outcomes. It is important for radiologists to understand what information to provide in diagnostic reports to support the surgical plan and provide important data for making treatment decisions.

#### TABLE OF CONTENTS/OUTLINE

- Introduction- Systemic approach: kidney, prostate and bladder- The Rads and Scores.- Clinical radiological Review: pictorial cases.

Printed on: 02/07/23

## Abstract Archives of the RSNA, 2022

GUEE-52

### **Focal MRI-Guided Transurethral Ultrasound Ablation (TULSA) in Men with Prostate Cancer: Lessons Learned in 60+ Patients**

Sunday, Nov. 27 8:00AM - 9:00AM Room: Learning Center - GU

#### **Participants**

Daniel N. Costa, MD, Dallas, TX (*Presenter*) Research support, Bayer AG

#### **TEACHING POINTS**

1. Review the rationale for focal therapy in prostate cancer and the unique aspects of MRI-guided transurethral ablation (TULSA) of the prostate  
2. Discuss the multidisciplinary patient selection, treatment and follow-up strategies  
3. Review and discuss strategies to overcome challenging scenarios

#### **TABLE OF CONTENTS/OUTLINE**

1. Basic facts about prostate cancer (Disease prevalence and heterogeneity, Over- and under-diagnosis, Morbidity of standard of care treatment options)  
2. Different focal therapy modalities (Cryoablation, laser, irreversible electroporation, microwave ablation, transrectal high-intensity focused ultrasound; Transurethral ultrasound ablation (TULSA))  
3. TULSA - Multidisciplinary effort - Patient selection (Inclusion and exclusion criteria, Distances of interest, Critical anatomical relationships, Calcifications, Pre-treatment imaging and biopsy)- Treatment planning and patient-specific customization (Sextant, hemi-, near whole-gland, and whole-gland ablation)  
Neurovascular bundle and ejaculatory duct sparing, Concurrent benign prostatic hypertrophy treatment)- Procedure duration- Strategies for workflow improvements- Post-treatment follow-up (Imaging - normal and abnormal appearance, PSA trends, Functional (sexual and urinary) recovery, Biopsy, Complications)- Challenging scenarios (Hip prosthesis, Radiation therapy fiducials and seeds, Motion, Calcifications)

Printed on: 02/07/23



## Abstract Archives of the RSNA, 2022

GUEE-53

### T2-Hyperintense Prostatic and Periprostatic Lesions and Their MRI Characteristics

Sunday, Nov. 27 8:00AM - 9:00AM Room: Learning Center - GU

#### Participants

Alfonso Iglesias, MD, PhD, (*Presenter*) Nothing to Disclose

#### TEACHING POINTS

Knowledge of the anatomy and embryological development of the inferior male genitourinary tract should allow the radiologist to classify the T2-hyperintense prostatic and periprostatic lesions according to localization. Clinical presentation, MRI characteristics with pathological correlation can help us to accurately characterize T2-hyperintense prostatic and periprostatic lesions resulting in appropriate patient management.

#### TABLE OF CONTENTS/OUTLINE

Define, classify and review the clinical manifestations of T2-Hyperintense prostatic and periprostatic lesions. Review imaging findings that can help us shorten the differential diagnosis and perform a correlation of imaging findings with clinical and therapeutic management. Describe an imaging algorithm for T2-Hyperintense prostatic and periprostatic lesions that is based on MRI characteristics.

Printed on: 02/07/23

## Abstract Archives of the RSNA, 2022

GUEE-54

### Gonadal Vein - The Omitted by Lane

Sunday, Nov. 27 8:00AM - 9:00AM Room: Learning Center - GU

#### Participants

Aruna R. Patil, MD, FRCR, (*Presenter*) Research Consultant, Koninklijke Philips NV

#### TEACHING POINTS

The gonadal veins are paired vessels that drain the testes and ovaries. This exhibit aims to: 1. Review the imaging anatomy of gonadal veins 2. Its use as a landmark, collateral 3. Its role in conditions such as pelvic congestion, varicocele 4. Its role in spread of tumor and infection.

#### TABLE OF CONTENTS/OUTLINE

1. Anatomy of gonadal veins- male and female 2. Variant anatomy and implications 3. Use as landmark - ovaries, testes (normal and pathologies - torsion, germ cell tumor in undescended testes, upper ureter physiological narrowing) 4. Collateral pathways - varices, varicocele, pelvic congestion syndrome, mesentericogonadal shunts in CLD, Abernathy malformations 5. Spread: gonadal vein thrombosis- septic in infections (PID), bland or tumor thrombosis - leiomyomatosis, leiomyosarcoma, other carcinomas with gonadal vein spread.

Printed on: 02/07/23



## Abstract Archives of the RSNA, 2022

GUEE-55

### Peritoneal and Retroperitoneal Anatomy as it Relates to Disease Spread

Sunday, Nov. 27 8:00AM - 9:00AM Room: Learning Center - GU

#### Awards

Identified for RadioGraphics

#### Participants

Ayman H. Gaballah, MD, FRCR, Columbia, MO (*Presenter*) Nothing to Disclose

#### TEACHING POINTS

1- Review anatomy and anatomic landmarks of peritoneal and retroperitoneal (RP) spaces 2- Illustrate the intercommunications among different spaces and their effect on spread of related diseases 3- Differentiate peritoneal from RP diseases 4- Discuss imaging workup and imaging features of different pathologic entities and pathways of disease spread 5- Provide algorithmic approach to differential considerations 6- Review management options

#### TABLE OF CONTENTS/OUTLINE

1- Introduction 2- Anatomy of peritoneal and retroperitoneal (RP) spaces with diagrammatic illustrations 3- Differentiation of intraperitoneal from retroperitoneal pathology 4- Imaging features of different pathologic entities including, extraluminal gas, fluid collections, and masses 5- Case presentation 6- Algorithmic approach to differential considerations 7- Peritoneal carcinomatosis index 8- Management options including HIPEC for peritoneal carcinomatosis 9- Summary and conclusion

Printed on: 02/07/23



## Abstract Archives of the RSNA, 2022

GUEE-56

### Don't Be Outscored - A Practical Guide to VI-RADS, Including Differentials

Sunday, Nov. 27 8:00AM - 9:00AM Room: Learning Center - GU

#### Awards

Identified for RadioGraphics

#### Participants

Jonatas Favero Prietto Dos Santos, MD, Porto Alegre, Brazil (*Presenter*) Nothing to Disclose

#### TEACHING POINTS

1) VI-RADS provides a five-point score to determine the risk of detrusor muscle invasion based on tumor appearances in T2WI, DWI and DCE; 2) Despite the high reproducibility verified so far, scoring is a trick process and requires supervised practicing. Along with a series of typical cases, some pitfalls and common errors are discussed; 3) As the VI-RADS only applies for urothelial lesions, it's important to be aware of MRI appearances of other malignant neoplasms and benign conditions that may mimic urothelial cancers.

#### TABLE OF CONTENTS/OUTLINE

Bladder neoplasms are classified as epithelial and nonepithelial, and they can emerge from any of the bladder layers. Urothelial carcinoma account for the majority of urinary bladder cancer and differentiating muscle-invasive (MI) from non-muscle-invasive (NMI) tumors is vital to choose the appropriate treatment. It is noteworthy that transurethral resection of bladder tumor may not sample the muscularis propria, leading to understaging in 25% to 40% of MI cancers. In this setting, VI-RADS is a reproducible and feasible guide for Radiologists to use a standardized approach to imaging and reporting multiparametric MRI. This system provides a five-point score which effectively indicates the likelihood of detrusor muscle invasion. MRI scoring is based on T2WI, DWI and DCE. It is also important to evaluate the presence of synchronous urothelial lesions, lymph node enlargement and distant metastasis. Aside from an accurate scoring of urothelial lesions, Radiologists should be able to recognize imaging findings of other malignant neoplasms and non-malignant conditions, which may simulate urothelial cancers.

Printed on: 02/07/23



## Abstract Archives of the RSNA, 2022

GUEE-57

### Altered Nephrogram: What the Radiologist Needs to Know

Sunday, Nov. 27 8:00AM - 9:00AM Room: Learning Center - GU

#### Participants

Elisa Antolinos Macho, MD, Madrid, Spain (*Presenter*) Nothing to Disclose

#### TEACHING POINTS

1 - Understanding what "nephrogram" means and normal kidney behavior in monophasic and multiphasic CT. 2 - Learning the most common abnormalities: absent (global or segmental), delayed, striated, spotted and persistent nephrogram. 3 - Correlating each altered nephrogram with its typical underlying pathophysiology.

#### TABLE OF CONTENTS/OUTLINE

1. Normal kidney vascularization 2. Normal kidney behavior in multiphasic CT: Normal nephrogram 3. Absent nephrogram - Global absence: Traumatic / Non-traumatic - Segmental absence: Vascular / Others 4. Delayed nephrogram - Vascular - Obstructive - Others 5. Striated nephrogram - Unilateral - Bilateral - Spotted nephrogram 6. Persistent nephrogram 7. Altered nephrogram: tips and tricks - Laterality - How to define it - Most common cause - The "rim sign" - Final diagram with every altered nephrogram

Printed on: 02/07/23



## Abstract Archives of the RSNA, 2022

GUEE-58

### Urine Luck: Using the Nephrogram to Aid in Diagnosis

Sunday, Nov. 27 8:00AM - 9:00AM Room: Learning Center - GU

#### Participants

Layne Kelley, MD, Dallas, TX (*Presenter*) Nothing to Disclose

#### TEACHING POINTS

1. An understanding of normal patterns of renal enhancement and contrast excretion can be utilized to optimize image acquisition for detection of abnormalities. 2. Recognizing abnormal enhancement patterns improves detection of subtle pathology.

#### TABLE OF CONTENTS/OUTLINE

1. Introduction: A. Review of normal progression of contrast through the kidneys and urinary tract over time on CT. B. Provide an overview of abnormal enhancement patterns with a "back to basics" approach referencing the normal and abnormal nephron function. 2. Case-based review of abnormal enhancement patterns, including: A. Delayed nephrogram i. Arterial inflow 1. Renal artery occlusion 2. Renal artery dissection ii. Venous outflow 1. Renal vein thrombosis 2. Nutcracker syndrome iii. Urine outflow 1. Obstructive urolithiasis 2. Inflammatory stricture 3. Malignancy a. Invasive prostate carcinoma b. Cervical cancer c. Subtle ureteral tumor implant B. Absent nephrogram i. Renal infarct C. Striated nephrogram i. Pyelonephritis D. Persistent nephrogram i. Retained contrast in the setting of acute kidney injury 3. Review how an understanding of the nephrogram allows optimal evaluation for specific pathologies, with case examples: A. Unenhanced CT for nephrolithiasis B. Nephrographic phase for optimal detection of renal masses C. Excretory phase for detection of urothelial masses and suspected urine leak

Printed on: 02/07/23



## Abstract Archives of the RSNA, 2022

GUEE-59

### Updated 2019 Bosniak Classification: Examples, Challenges and Future Directions

Sunday, Nov. 27 8:00AM - 9:00AM Room: Learning Center - GU

#### Participants

Srinivas Saripalli, MD, Jackson, MS (*Presenter*) Nothing to Disclose

#### TEACHING POINTS

Renal cystic lesions are commonly encountered incidentally as part of trauma workups and workup for other diseases, and also as part of workup for symptomatic presentation such as hematuria and flank pain. The management and treatment of these renal cystic lesions has been the focus of multiple efforts from the radiological and urological communities. The challenge posed by cystic renal lesions is to stratify those which are more likely to be malignant and require more invasive treatment and ventricles which can be managed conservatively with serial imaging and thereby avoid the morbidity of invasive treatment. The goal of the updated Bosniak classification in 2019 was to better encompass the small renal masses that are commonly encountered in practice and to more systematically stratify these lesions such that variability in classification was decreased, with both CT and MRI classification schemes. The updated classification has many simplifications for practice which we will review. We will also show some continued challenges in the classification and how they can be addressed using multiparametric MRI and multimodality correlation.

#### TABLE OF CONTENTS/OUTLINE

1. Review the 2019 Bosniak classification for cystic renal lesions.
2. Show multiple examples of cystic renal lesions and their classifications in the old and new Bosniak classifications. Particular focus on lesions which have different management in the old versus new classifications.
3. Review the varied appearances of lesions in each category in ultrasound, CT and MRI.
4. Discuss advantages, challenges, pitfalls and clinical implications of the updated system compared to the old.

Printed on: 02/07/23

## Abstract Archives of the RSNA, 2022

GUEE-6

### Imaging of the Enlarged Scrotum: A Vas(t) Deferens-tial Diagnosis

Sunday, Nov. 27 8:00AM - 9:00AM Room: Learning Center - GU

#### Participants

Christopher Yu, MD, PhD, Los Angeles, CA (*Presenter*) Nothing to Disclose

#### TEACHING POINTS

Scrotal masses or masslike scrotal enlargement may cause substantial discomfort and anxiety to patients. While the clinical setting is often suggestive of the correct diagnosis, imaging is nearly always requested to confirm the suspected diagnosis, exclude other concerning differential possibilities, evaluate the disease extent, and/or assess for comorbidities and complications. The goal of the current educational exhibit is to review the differential diagnosis of scrotal masses/masslike scrotal enlargement, as outlined below. In addition to the rich imaging illustration of common etiologies, multiple less common but important causes will be provided with corresponding clinical and surgico-pathologic correlation. The exhibit will also include a review of inguino-scrotal fascial anatomy that is often very confusing for both trainees and practicing radiologists. Interactive (board-exam question/answer-type) pointers will also be provided to emphasize key principles.

#### TABLE OF CONTENTS/OUTLINE

1. Developmental and gross anatomy of the inguino-scrotal region (fascial layers, scrotal contents, inguinal canal); 2. Clinical and imaging diagnostic flowcharts; 3. Role of imaging (US, CT, and MR); 4. Cases. Intratesticular (mass/cyst; torsion, infection); b. Extratesticular; i. Epididymal (mass/cyst, infection), ii. Spermatic cord (varicocele, masses), iii. Inguino-scrotal hernias (direct versus indirect); c. Scrotal wall: i. Diffuse swelling: 1. Infection (cellulitis, Fournier gangrene), 2. Lymphedema from systemic process (heart/liver/kidney failure), 3. Hidradenitis suppurativa; ii. Focal masses/collections (hydrocele, abscess, hematoma).

Printed on: 02/07/23



## Abstract Archives of the RSNA, 2022

GUEE-60

### Renal Cell Carcinomas: Uncommon Clinical and Imaging Presentations and Uncommon Histological Subtypes

Sunday, Nov. 27 8:00AM - 9:00AM Room: Learning Center - GU

#### Participants

Satomi Kawamoto, MD, Baltimore, MD (*Presenter*) Nothing to Disclose

#### TEACHING POINTS

1. To review uncommon clinical and imaging presentations of renal cell carcinomas (RCCs). 2. To become familiar with uncommon histological subtypes of RCCs and their clinical features

#### TABLE OF CONTENTS/OUTLINE

1. Uncommon clinical presentation of RCC. (1) Most RCCs in the developed world are incidentally discovered at imaging studies. (2) However, RCC may be discovered with uncommon presentations. Examples include spontaneous hemorrhage and paraneoplastic syndrome. Review uncommon clinical presentations with imaging findings. 2. Uncommon imaging features. (1) Unenhancing or equivocally enhancing RCCs. (2) RCC mimicking other entity such as renal abscess, lymphoma, pyelonephritis. (3) Other uncommon imaging features. 3. Uncommon histological subtypes of RCCs. (1) RCC subtypes emerged to 2016 WHO classification, and review their imaging and clinical features. (2) Review imaging and clinical features of other uncommon RCC subtypes.

Printed on: 02/07/23



## Abstract Archives of the RSNA, 2022

GUEE-62

### Direct MRI-Guided In-Bore Targeted Biopsies of the Prostate: Lessons Learned in 800+ Patients

Sunday, Nov. 27 8:00AM - 9:00AM Room: Learning Center - GU

#### Awards

Identified for RadioGraphics

#### Participants

Daniel N. Costa, MD, Dallas, TX (*Presenter*) Research support, Bayer AG

#### TEACHING POINTS

1. Review the unique aspects of direct MRI-guided in-bore biopsies compared to ultrasound-based targeted approaches. 2. Demonstrate strategies to leverage the direct lesion and needle visualization provided by the in-bore approach to overcome challenges encountered during targeted biopsies

#### TABLE OF CONTENTS/OUTLINE

1. Direct MRI-guided in-bore biopsy vs US-based (cognitive and MRI-TRUS fusion) biopsies • Advantages o Precise lesion-needle location verification • Disadvantages o Cost and duration o Lack of systematic sampling 2. Steps of a direct MRI-guided in-bore biopsy • Review of diagnostic, pre-biopsy multiparametric MRI • Patient positioning, moderate sedation and needle guide placement • Pre-biopsy imaging • Target identification and biopsy planning • Needle guide location adjustment(s) • Tissue sampling and needle-lesion location verification • Specimen handling 3. Challenging scenarios • Small lesion in large prostate • Tricky lesion location • Tumor heterogeneity • Plaque-like subcapsular lesions • Motion (whole body, rectal, pelvic floor) • Needle deflection • Anatomical changes secondary to hematomas • Suspected post-prostatectomy local recurrence • Prostates with unusual morphology (eg, post focal therapy) • Patients without rectal access • Unusual anorectal anatomy • "MRI-invisible" lesions • Patient selection (e.g., hip prosthesis) • Efficient imaging and tissue sampling

Printed on: 02/07/23



## Abstract Archives of the RSNA, 2022

GUEE-63

### Prostate Diffusion-weighted Imaging: Insatiable Challenge to Improve Tumor Detection and Characterization in Prostate Cancer

Sunday, Nov. 27 8:00AM - 9:00AM Room: Learning Center - GU

#### Participants

Tsutomu Tamada, MD, Kurashiki, Japan (*Presenter*) Nothing to Disclose

#### TEACHING POINTS

The purpose of this presentation is:1. To learn the role of diffusion-weighted imaging (DWI) in diagnosis of prostate cancer (PC)2. To understand the problems for the detection and characterization of PC using standard DWI with single-shot echo-planar imaging (ssEPI) in patients with elevated PSA levels3. To demonstrate the countermeasures for problems on ssEPI DWI

#### TABLE OF CONTENTS/OUTLINE

Role of DWI in diagnosis of prostate cancer (PC)- Primary PC detection: DWI scoring system in Prostate Imaging Reporting and Data System v2.1- Local recurrent PC detection: DWI scoring system in Prostate Magnetic Resonance Imaging for Local Recurrence Reporting (PI-RR)- Local staging: extracapsular extension and seminal vesicle invasion- Assessment of tumor aggressiveness in PC using quantitative DWI metrics- MRI-ultrasound Fusion-guided Prostate targeted BiopsyProblems and countermeasures for detection and characterization of PC using ssEPI DWI - Susceptibility artifact and geometric anatomic distortion:Reduced field-of-view DWITurbo spin-echo DWIMulti-shot EPI DWI- Blurring:Multi-shot EPI DWI- Low SNR and CNR in high b-value and high spatial resolution acquisitions:Compressed SENSE- Insufficient image contrast between benign and PC tissues:Ultra-high b value DWI Synthetic DWISynthetic DWI which enable to synthesize DW images with any TR and TE- Insufficient diagnostic performance of tumor aggressiveness in PC using mean apparent diffusion coefficient (ADC)ADC histogram analysisNon-Gaussian fitting models- DWI invisible clinically significant PCMicrostructural MRI which is a quantitative technique that focuses on structural change in three typical microstructures of prostatic tissue

Printed on: 02/07/23



## Abstract Archives of the RSNA, 2022

GUEE-64

### Prostate Magnetic Resonance Imaging for Local Recurrence Reporting PI-RR in Clinical Practice - A Primer for Novice and Expert Radiologists

Sunday, Nov. 27 8:00AM - 9:00AM Room: Learning Center - GU

#### Participants

Jorge Abreu Gomez, MD, Pickering, ON (*Presenter*) Nothing to Disclose

#### TEACHING POINTS

\* Local recurrence after radical treatment represent a diagnostic challenge for novice and experienced radiologists. Throughout review of oncologic history, MRI and histologic findings of the primary lesion are crucial for adequate assessment/interpretation.\* PI-RR system aims to standardize the performance, interpretation and reporting of MRI after radical treatment in order to reduce variability.\* Combination of DCE and DWI features of a given observation will determine the likelihood for local recurrence

#### TABLE OF CONTENTS/OUTLINE

\* PI-RR categories and applicability.\* PI-RR scoring after radiotherapy. Understanding the sequence with highest score!!\* PI-RR scoring after radical prostatectomy. DCE as dominant sequence!!\* Beyond PI-RR. MRI assessment of recurrent disease after focal therapy

Printed on: 02/07/23



## Abstract Archives of the RSNA, 2022

GUEE-65

### Post-treatment Prostatic Cancer: How To Perform an Adequate Imaging Evaluation

Sunday, Nov. 27 8:00AM - 9:00AM Room: Learning Center - GU

#### Participants

Vivien Bonadio, MD, (*Presenter*) Nothing to Disclose

#### TEACHING POINTS

? Understand the current concepts of biochemical recurrence and its clinical impact ? Address the different treatment modalities used, as well as their indications ? Review the role of functional imaging in follow-up and detection of recurrent disease ? Discuss the highlight findings on post treatment images of patients with prostatic cancer

#### TABLE OF CONTENTS/OUTLINE

INTRODUCTION ? Brief discussion of epidemiology ? Review of the concept and current criteria of biochemical recurrence in prostate cancer TREATMENT MODALITIES AND THEIR INDICATIONS ? Androgen deprivation therapy ? Brachytherapy ? External radiation therapy ? High Intensity Focused Ultrasound - HIFU ? Prostatectomy INDICATIONS OF IMAGING IN THE ASSESSMENT OF LOCOREGIONAL AND DISTANT RECURRENCE ? MR ? PSMA PET/CT ? PSMA PET/MR IMAGING EVALUATION ? Systematic approach to the interpretation of MR images of patients in post-treatment of prostatic cancer ? Case based-review of PI-RR (Prostate Magnetic Resonance Imaging for Local Recurrence Reporting) ? Pitfalls, challenges, and how to overcome these

Printed on: 02/07/23



## Abstract Archives of the RSNA, 2022

GUEE-66

### Biparametric and Multiparametric Prostate MRI: How To and When To Use Them Properly

Sunday, Nov. 27 8:00AM - 9:00AM Room: Learning Center - GU

#### Participants

Mitsuru Takeuchi, MD, PhD, Nagoya, Japan (*Presenter*) Nothing to Disclose

#### TEACHING POINTS

Multiparametric MRI (mpMRI) is currently the standard imaging method for prostate MRI. All Prostate Imaging Reporting and Data System (PI-RADS) versions emphasized that prostate MRI protocols should include not only T2-weighted imaging (T2WI) but also diffusion-weighted imaging (DWI) and dynamic contrast-enhanced MRI (DCE-MRI). However, in the latest PI-RADS after version 2, DCE-MRI plays a minor role. Biparametric MRI (bpMRI) study excluding DCE-MRI can be performed in a shorter time and is free from the cost and potential risks of gadolinium-based contrast agents compared to mpMRI. Recently, several studies have reported bpMRI is not inferior to mpMRI in the prostate cancer (PCa) detection. In this educational exhibit, we review these articles and explain when to and how to use bpMRI and mpMRI while presenting clinical cases.

#### TABLE OF CONTENTS/OUTLINE

1) Diagnostic accuracy of bpMRI and mpMRI for the PCa tumor detection in treatment naïve patients (primary PCa). 2) Clinical application of bpMRI bpMRI could be apply to the patients who is suspected primary PCa. mpMRI should be used to T-staging, locally recurrent PCa after radiotherapy and prostatectomy and active surveillance. 3) Imaging protocol of bpMRI High image quality of T2WI and DWI is mandatory for securing the diagnostic accuracy of bpMRI. T2WI should be acquired with multiplanes and high spatial resolution. DWI should be obtained with less artefacts and high contrast between lesion and normal tissue. 4) Clinical cases

Printed on: 02/07/23



## Abstract Archives of the RSNA, 2022

GUEE-67

### Spectrum of Male and Female Urethral Pathologies at MRI

Sunday, Nov. 27 8:00AM - 9:00AM Room: Learning Center - GU

#### Participants

Nikolas Brozovich, MD, Augusta, GA (*Presenter*) Nothing to Disclose

#### TEACHING POINTS

1. Recognize variety of pathological conditions of the urethra at MRI 2. Discuss advantages and disadvantages of the MR Imaging of the urethra 3. Describe Imaging techniques for evaluation of urethra

#### TABLE OF CONTENTS/OUTLINE

Evaluation of the male and female urethra on conventional imaging studies including retrograde urethrography (RUG), voiding cystourethrography (VCUG), and ultrasonography (US) may be helpful in demonstrating urethral abnormalities however limited in providing information regarding the periurethral tissues. MRI due to multiplanar capability and excellent tissue contrast can provide anatomic details about both the urethra and periurethral tissues and also orientation of the lesion in three dimensions. In this presentation conditions affecting the urethra or periurethral tissues will be discussed. Specific topics of discussion will be anatomical detail, MR imaging techniques, diverticulum, inflammation, tumors, strictures and miscellaneous conditions of the male and female urethra. Summary: MRI is a noninvasive technique that does not require ionizing radiation and can provide anatomic and pathological details about both the urethra and periurethral tissues and the orientation of the lesion in three dimensions due its multiplanar capabilities and superior soft tissue contrast.

Printed on: 02/07/23



## Abstract Archives of the RSNA, 2022

GUEE-8

### Diverse Spectrum of Tumefactive, Non-neoplastic, Proliferative Pseudotumors of the GU Tract: Cross-sectional Imaging Findings

Sunday, Nov. 27 8:00AM - 9:00AM Room: Learning Center - GU

#### Awards

Identified for RadioGraphics

#### Participants

Rashmi Balasubramanya, MD, Philadelphia,, PA (*Presenter*) Nothing to Disclose

#### TEACHING POINTS

There is a wide spectrum of non-neoplastic conditions of the GU tract that show tumefactive growth pattern reminiscent of neoplasms. A diverse spectrum of inflammatory, infective, proliferative and idiopathic disorders with distinct histopathology occur in the kidneys and upper/lower urinary tracts. We present multi-modality cross-sectional imaging findings of a broad spectrum of these pseudo-tumors. To review taxonomy, epidemiology, clinical features, histopathology biology of a wide spectrum of tumefactive, non-neoplastic, proliferative conditions of the genitourinary tract. To describe multimodality cross-sectional imaging findings of these lesions and differentiate from neoplasms. To discuss management and prognosis.

#### TABLE OF CONTENTS/OUTLINE

Organization Introduction, classification, epidemiology, clinical manifestations, histopathology, CT/MRI findings, management, prognosis, conclusion. Entities discussed Xanthogranulomatous pyelonephritis, Actinomycosis, Tuberculosis, Malakoplakia, IgG4 related disease, Amyloidosis, Perinephric myxoid pseudotumor of fat, Erdheim-Chester disease, Pseudosarcomatous myofibroblastic proliferation, Cystitis cystica, endometriosis of the ureters/urinary bladder, Nephrogenic adenoma, Adrenal rest, Echinococcal cyst.

Printed on: 02/07/23



## Abstract Archives of the RSNA, 2022

GUEE-9

### Unexpected Imaging Findings following Uterine Interventions

Sunday, Nov. 27 8:00AM - 9:00AM Room: Learning Center - GU

#### Awards

Identified for RadioGraphics

#### Participants

Allan Brazier, MD, Sterling Heights, MI (*Presenter*) Nothing to Disclose

#### TEACHING POINTS

1) Uterine and endometrial interventions include a spectrum of routine surgical, hysteroscopic, and interventional procedures. 2) Familiarity with the spectrum of interventions and recognition of their potential complications on imaging are essential to guide management and optimize patient outcomes. 3) An understanding of how these procedures are performed will lead to a better grasp of all potential complications that may ensue.

#### TABLE OF CONTENTS/OUTLINE

1) A review of uterine and endometrial procedures and their techniques. 2) A case-based presentation of complications that result from these procedures as well as relevant management recommendations. Cases: -Retained fibroid after hysterectomy -Ureteral transection and ureterovaginal fistula after hysterectomy -Active extravasation after hysterectomy -Vesicovaginal fistula after do-it-yourself pessary placement -Regenerating uterine tissue after morcellation -Uterine perforation after dilatation and curettage (D C) -AVM after D C -Synechiae after D C -Hematometra after endometrial ablation -Uterine actinomyces due to retained intrauterine device (IUD) -Uterine perforation by IUD -Avulsion of pedunculated fibroid after uterine artery embolization (UAE) -Utero-enteric fistula after UAE -Small bowel obstruction after UAE -Fascial dehiscence after cesarean section -Bladder flap hematoma after cesarean section -Vaginal cuff dehiscence and bowel herniation -Endometritis after embryo transfer -Peritoneal inclusion cysts following pelvic surgery -Scar endometriosis

Printed on: 02/07/23

## Abstract Archives of the RSNA, 2022

HNEE

### Head and Neck Education Exhibits

Sunday, Nov. 27 8:00AM - 9:00AM Room: Learning Center - HN

#### Sub-Events

#### HNEE-1 A Blurry Confusion-Optic Neuropathy Etiologies And Imaging

##### Awards

##### Certificate of Merit

##### Participants

Luis Souza, MD, (*Presenter*) Nothing to Disclose

##### TEACHING POINTS

Optic neuropathy is a broad definition that encompasses a myriad of different diagnoses. Objectives: Understand what is expected from the radiologist when faced with this difficult group of diseases, which the imaging findings can be subtle and often missed. To illustrate the most common imaging findings of optic neuropathy. To show the useful imaging hallmarks that help differentiate active disease from sequelar changes and differential diagnosis.

##### TABLE OF CONTENTS/OUTLINE

Imaging investigation protocol: optic neuropathy standard imaging protocol and useful additional MRI sequences that can help in the diagnosis. General and common imaging findings in optic neuropathy. Differentiating active disease and sequelae? Main imaging characteristics and differential diagnosis of the different etiologies.- Inflammatory / Infectious (Viral, Bacterial, Other).- Inflammatory / Autoimmune. (Demyelinating - NMOSD, MS, Anti-MOG+, Paraneoplastic - and Non-Demyelinating).- Ischemic (anterior and posterior ischemic neuropathy).- Toxic-metabolic.- Compressive.- Infiltrative.- Traumatic. Take-home messages and tips and tricks to differential diagnosis.

#### HNEE-10 Perimarginal Nodes - An Underestimated Site for Metastatic Squamous Cell Oral Cancer: A CT Pictorial Review

##### Awards

##### Certificate of Merit

##### Participants

Erik Radin, MD, Trieste, Italy (*Presenter*) Nothing to Disclose

##### TEACHING POINTS

(1) Definition of perimarginal nodes (PMN). (2) To explain the clinical relevance of the PMN. (3) To illustrate the spatial identification of PMN on CT imaging.

##### TABLE OF CONTENTS/OUTLINE

Head and neck squamous cell cancer is notoriously affected by an elevated risk for metastatic nodal disease, one of the most important prognostic factors. Nodal status represents one of the fundamental parameters of the TNM staging system; it is also essential for the therapeutical approach, with elective neck dissection as the leading treatment. Perimarginal nodes (PMN) are often considered as facial rather than cervical lymph nodes, even though they could be regarded as a submandibular nodal subgroup (level IB). They lie close to the marginal mandibular nerve (MMN), within a clinically defined distance cut-off of 1 to 2 cm from the mandibular border. CECT imaging has high accuracy for PMN identification and allows to divide them into four different sites, depending on their relationship with the anterior facial vein (AFV) and the submandibular gland: pre glandular, prevascular, retrovascular, and retro glandular nodes. Perimarginal nodes could represent a miscalculated site for occult metastases in head and neck cancers, especially those located in oral cavity. Unintentionally, small perimarginal nodes could be left in the surgical site in order to protect the MMN during neck dissection through the Hayes Martin maneuver; this would affect the patient's prognosis, precluding a complete therapeutic response, with an increased risk of disease relapse.

#### HNEE-11 Facial Ultrasound Anatomy of the Aging Skin and the Growing Role of the Radiologist in the Aesthetic Medicine Field

##### Participants

Slavina Mancheva, MD, MD, (*Presenter*) Nothing to Disclose

##### TEACHING POINTS

To evaluate the normal facial anatomy. Causes of normal aging visible and quantified by imaging studies. To evaluate pre, during and post-treatment status of beauty treatments using autologous and FDA authorized dermal fillers. The use of ultrasound to guide dermal filler injections. To identify facial danger zones.

##### TABLE OF CONTENTS/OUTLINE

1. Facial anatomy depiction. Nowadays there is continuous growth of the aesthetic facial treatments using fillers and neurotoxins. In order to prevent complications it is very important to analyze the area of interest using ultrasound- being a safe and handy technique. 2. Aging of upper, mid and lower face. In this exhibit a couple of patients in their mid 20s, mid 30s and late 60s are analyzed using ultrasound. Some patients are followed pre and post treatment sessions in order to identify the causes of their individual aging and also offer them follow up of their treatment. 3. The difficult case and the role of the radiologist in a multidisciplinary aesthetic medicine team. Many patients has been using different type filler treatments and some appear with different and unknown secondary effects. The radiologist must identify the relevant variation anatomy, possible iatrogenic effects and help during invasive treatments. 4. The facial danger zones. Identify the major danger zones where the practitioner must be very careful and decide what options of treatments must be offered in a safe manner.

## **HNEE-12 A Joint Affair: Radiologic Findings of TMJ Anatomy and Pathology**

### **Awards**

#### **Certificate of Merit**

#### **Participants**

Samantha Platt, MD, New York, NY (*Presenter*) Nothing to Disclose

#### **TEACHING POINTS**

1. Review TMJ anatomy and variation with function through radiologic and medical illustration. 2. Review Wilke's criteria and relevant findings for internal derangement including disc displacement with or without reduction, disc morphology, joint effusion and bony changes such as sclerosis and subcortical cysts. 3. Demonstrate imaging findings associated with the diverse spectrum of TMJ disorders through varied modalities. 4. Describe features of TMJ disorders that are helpful to include in report for general radiologists and neuroradiologists.

#### **TABLE OF CONTENTS/OUTLINE**

Temporomandibular joint (TMJ) disorders exhibit variable radiographic presentation. Many causes of extra-articular pain (i.e. muscle fatigue, fibromyalgia) do not have imaging findings. The best modalities to evaluate the TMJ include MRI and CT and should be chosen based on clinical symptoms and the anticipated pathology. We have curated images from various modalities for TMJ pathologies: osteoarthritis, mandibular hypoplasia, bifid mandibular condyle, hemicranimegaly, infectious synovitis, osteomyelitis, malignant otitis externa, osteonecrosis, rheumatoid arthritis, ankylosing spondylitis, chondromatosis, giant cell granuloma, squamous cell carcinoma, metastatic disease, nasopharyngeal carcinoma, mandibular fractures, pseudoarthrosis, myositis ossificans, ankylosis, osteoradionecrosis, and surgical implants. Additionally, we have curated MR views that exemplify the pathology seen in each of Wilke's classification for internal derangement along with pictorial representation. Imaging is crucial to noninvasive assessment of the TMJ and subsequent management plans.

## **HNEE-13 Don't Wait Till Neck Time: Learn the "Spatial" Way to Master Neck Anatomy on Ultrasound Now**

#### **Participants**

Paran Davari, MD, (*Presenter*) Nothing to Disclose

#### **TEACHING POINTS**

1. Describe the concept of spaces of the neck and highlight spaces that can be evaluated on ultrasound. 2. Provide a sonographic atlas for the spaces using multimodality comparison to better understand spatial relationships. 3. Learn contents of each space to help guide a space specific differential diagnosis. 4. Overall increase familiarity with anatomic structures that might often be ignored while interpreting a neck ultrasound obtained for frequent indications such as thyroid gland, cervical lymph node or carotid evaluation, as well as increased knowledge of relevant anatomy for less frequent indications such as parotid or submandibular gland evaluation. 5. Provide examples of clinical applications of this anatomic knowledge on ultrasound for diagnostic and potentially procedural purposes.

#### **TABLE OF CONTENTS/OUTLINE**

1. Learning objectives 2. Introduction to neck anatomy on ultrasound: current practices 3. Introduction to spaces of the neck 4. Describe sonographically visualized spaces of neck, content and clinical considerations A. Superficial space of neck B. Deep neck spaces limited to suprahyoid neck: i. Parotid space ii. Submandibular space iii. Floor of mouth or sublingual space iv. Masticator space C. Deep neck spaces limited to infrahyoid neck: i. Visceral space ii. Anterior cervical space iii. Posterior cervical space D. Deep neck spaces spanning entire neck: i. Carotid space ii. Perivertebral space

## **HNEE-14 Practical Applications of the Permeability Study in Head and Neck Imaging**

#### **Participants**

Beatriz Prado, MD, Sao Paulo, Brazil (*Presenter*) Nothing to Disclose

#### **TEACHING POINTS**

Permeability imaging or quantitative DCE-MRI is a functional MRI modality that involves repeated acquisition of images of the same lesion and analyses of the Time-signal intensity curves (TICs) of the tumor and feeding artery to yield various parameters related to perfusion and permeability within the tumor. It has been reported to be useful in the differentiation of head and neck tumors, most commonly of the parotid gland, as well as tumors in other organs. This panel aims to: Define what is the permeability study Review of the technique Cite the main clinical indications for permeability study in head and neck imaging Illustrate through clinical cases the applications of perfusion permeability imaging in head and neck

#### **TABLE OF CONTENTS/OUTLINE**

Salivary gland tumors (i.e.: pleomorphic adenoma, Warthin's tumor and carcinoma) Distinction of benign versus malignant tumor (i.e.: lymphoma, spinocellular carcinoma, paraganglioma and schwannoma) Histologic differentiation among lesions, in combination with DWI and conventional T1 and T2 imaging (i.e.: pleomorphic adenoma, Warthin's tumor, lymphoma, paraganglioma) Differentiation of recurrent tumor versus post-therapeutic changes Prediction of response to radiotherapy and chemotherapy Biopsy guidance Metastatic cervical lymph nodes

## **HNEE-15 One Nerve is Just Right, Two is Too Many, Three is Not Enough - Unraveling the Trigeminal Nerve and Its Alterations**

Participants

Fernanda Guedes, MD, (*Presenter*) Nothing to Disclose

#### TEACHING POINTS

-Review the anatomy of the trigeminal nerve from its sensory and motor nucleus, the branches and peripheral segments.-Review the most common trigeminal nerve diseases in each segment and their radiological findings.-Learn more about some important differential diagnoses for each nerve segment.

#### TABLE OF CONTENTS/OUTLINE

1. Simplify trigeminal nerve anatomy, the largest of the twelve pairs of cranial nerves, and its segments (intraaxial, cisternal, Meckel's cave/cavernous sinus and peripheral). 2. Describe the relationship between trigeminal nerve segments and adjacent anatomical structures like skull base foramina, cavernous sinus, infraorbital canal and pterygopalatine fossa. 3. Summarize the different diseases that affect each trigeminal nerve segment, from the most common injuries, such as neurovascular conflicts, to the rarer pure motor neuropathy, highlighting some pathologies like: - Hypoplasia; - Herpes Zoster; - Trigeminal nerve schwannoma; - Meningioma; - Demyelinating disorders; - IgG4 related disease; - Lymphoproliferative disease; - Dermoid cyst; - Perineural facial tumor spread; - Post surgical trigeminal alterations; - Leptomeningeal carcinomatosis; - Neurosyphilis.

#### HNEE-16 Post-treatment Head and Neck Cancer Imaging: Anatomical Considerations Based on Cancer Subsites

##### Awards

Identified for RadioGraphics

Magna Cum Laude

Participants

Takashi Hiyama, MD, PhD, Kashiwa, Japan (*Presenter*) Nothing to Disclose

#### TEACHING POINTS

Recurrence of head and neck cancer occurs in approximately 10-20% of patients with early stage cancer, and 50-60% of those with advanced cancer. Detecting recurrent tumors at a treatable stage contributes to improved prognosis. The interpretation of follow-up images should be considered separately for each subsite as head and neck cancers can arise at various anatomical subsites. For each subsite, knowledge of normal imaging changes after surgery or chemoradiotherapy and patterns that are prone to recurrence are essential for detecting recurrence. When a lesion is detected, a differential diagnosis of recurrence, posttreatment changes, or other pathologies may be required. NIRADS is a useful tool for these evaluations. In addition, radiologists should assess the extent of recurrent tumors to select optimal salvage treatment. The purposes of this exhibit are: 1) To discuss normal post-treatment imaging at each subsite 2) To discuss the imaging findings of early local recurrence at each subsite, and neck recurrence 3) To discuss how to assess recurrence to allow subsequent optimal treatment

#### TABLE OF CONTENTS/OUTLINE

1. Introduction 2. Overview Epidemiology of head and neck cancer recurrence Roles of CT/MRI and PET/CT in follow-up NIRADS 3. Case illustrations Imaging findings of post-treatment change and recurrence: Oral cavity, Nasopharynx, Oropharynx, Hypopharynx, Sinonasal cavity, Larynx, Neck Imaging evaluation of recurrent tumor extension for salvage treatment 4. Summary 5. Conclusion

#### HNEE-17 Shedding Light On Lymphoproliferative Disorders: Extranodal and Nodal Lesions of the Head and Neck

Participants

Thayssa Leite, Sao Paulo, Brazil (*Presenter*) Nothing to Disclose

#### TEACHING POINTS

Teaching points:The purpose of this exhibit is:To identify the most common anatomic locations of lymphoproliferative disorders of the head and neck.To review the main imaging modalities, such as ultrasound (US), computed tomography (CT), magnetic resonance imaging (MRI), including functional methods (DCE imaging).To describe the radiological patterns and propose differential diagnosis of lesions including congenital anomalies, neoplasms, vascular, inflammatory or infectious diseases.To suggest practical tips and discuss common pitfalls of lymphoproliferative disorders of the head and neck, emphasizing the utility of a systematic approach for accurate evaluation.

#### TABLE OF CONTENTS/OUTLINE

Table of contents:Introduction.Anatomy.Imaging modalities.Differential diagnoses and clues to diagnosis.Practical tips and Pitfalls.Conclusion/Take home message.

#### HNEE-18 Multimodality Imaging of The Lacrimal Drainage System

##### Awards

Certificate of Merit

Participants

Viviana Loureiro, MD, (*Presenter*) Nothing to Disclose

#### TEACHING POINTS

To recognize the anatomy of the lacrimal drainage system.To understand the indications and technique of multiple imaging modalities forevaluation of the lacrimal drainage apparatus, as well as the advantages anddrawbacks of each modality.To review the spectrum of imaging findings of various diseases that affect the lacrimal drainage system on multiple modalities.

#### TABLE OF CONTENTS/OUTLINE

- Introduction- Anatomy- Multimodality Imaging Technique- Congenital and Developmental Lesions- Inflammatory and Infectious Diseases- Traumatic Lesions- Neoplasms- Nasolacrimal Drainage System Surgery- Pearls and Pitfalls- Conclusion

#### HNEE-19 Awards

## Facial Pain: Classification, Clinical Features, and Imaging Findings

### Certificate of Merit

Participants

Rodrigo De Azevedo, MD, Santo Andre, Brazil (*Presenter*) Nothing to Disclose

### TEACHING POINTS

To understand the classification, pathophysiology, and clinical features of facial pain. To review the role of imaging in the assessment of facial pain, including imaging techniques and protocols. To review the spectrum of imaging findings in multiple causes of facial pain.

### TABLE OF CONTENTS/OUTLINE

- Introduction - Relevant Anatomy - Classification and etiology of facial pain: nociceptive, neuropathic (neuralgia and painful neuropathy), trigeminal autonomic cephalalgias, and other causes. - Imaging Technique and Protocol (CT, conventional MRI, MRI angiography, and MRI neurography) - Imaging of Trigeminal Neuralgia - Imaging of Glossopharyngeal Neuralgia - Imaging of Painful Cranial Neuropathies - Other Causes of Facial Pain - Imaging after Ablative and Surgical Treatment of Cranial Neuralgia - Conclusions - References

### HNEE-2 Neuroendocrine Neoplasms of Head and Neck: Spectrum

Participants

Shreya Shukla, MBBS, Mumbai, India (*Presenter*) Nothing to Disclose

### TEACHING POINTS

The spectrum of neuroendocrine neoplasms (NENs) of the head and neck varies from benign neoplasms which may require just observation to poorly differentiated malignant neoplasms that may require multimodality treatment or palliative care. According to the fifth edition Classification of by the World Health Organization (WHO) International Agency for Research on Cancer (IARC) consensus meeting held in Lyon on 2-3 November 2017, NENs can be of epithelial or non-epithelial origin. Epithelial variety can range from well-differentiated NENs known to occur in small intestine, ovary etc to poorly-differentiated neuroendocrine carcinoma NECs (lung, colon). These tumors may be functional or non-functional. Nuclear imaging has an important role.

### TABLE OF CONTENTS/OUTLINE

This educational exhibit contains: • Review of classification of neuroendocrine neoplasms (NENs) • Enlists the common site of occurrence of NENs in the head and neck. • Review of the imaging appearance of these neoplasms at various sub-sites. • Briefly reviews the management of these neoplasms.

### HNEE-20 Novel Imaging Techniques in the Management of Thyroid Nodules and Diffuse Thyroid Disease

Participants

Thiago Jose Pinheiro Lopes, MD, Sao Paulo, Brazil (*Presenter*) Nothing to Disclose

### TEACHING POINTS

1) The gold standard of thyroid nodules diagnostics is conventional ultrasonography followed by fine-needle aspiration biopsy of qualified lesions, an invasive procedure related to inconclusive cytological results in up to 10-25% patients. 2) There is a need to search for novel imaging procedures or markers, that would allow a non-invasive estimation of malignancy risk with satisfying sensitivity and specificity. 3) Our purpose is to review imaging innovative applications in the management of thyroid nodules and diffuse thyroid disease, with focus in shear wave elastography (SWE) and contrast-enhanced ultrasonography (CEUS).

### TABLE OF CONTENTS/OUTLINE

1) Introduction 2) Conventional Techniques: B-mode and Doppler 3) Novel imaging techniques 3.1) Elastography (SWE) 3.2) CEUS 3.3) Next-generation molecular imaging 4) Radiological-pathological correlations 4.1) Thyroid nodules 4.2) Autoimmune thyroid disease 5) Challenges, pearls and pitfalls 5.1) Detecting extra-thyroid extension 5.2) Assessing lymph node metastases 5.3) Thyroid nodules in pediatric population 6) Future directions 6.1) Novel biochemical and genetic markers 6.2) Artificial intelligence (radiomics) 7) Take home messages

### HNEE-21 Imaging of Head and Neck Vascular Anomalies (Tumors and Malformations)

Participants

Augusto B. Antunes, MD, MSc, Nova Lima, Brazil (*Presenter*) Nothing to Disclose

### TEACHING POINTS

Vascular tumors and vascular malformations are commonly found in the head and neck region and have distinctive features. Radiologists should be aware of their presentation features and clinical history to establish the correct diagnosis and provide appropriate care. Imaging allows for high spatial and temporal resolutions and is essential for the correct diagnosis of these pathologies, but also for assessing the extension and anatomical relationships, as well as for studying blood flow patterns. We will highlight proliferating vascular tumors and vascular malformations, often misdiagnosed due to confusing definitions and classifications. After completing this reading, participants will be able to comprehend and to recognize specific features for various such anomalies, including infantile hemangioma, congenital hemangioma, lymphatic, venous, arteriovenous and capillary malformations, and combined anomalies.

### TABLE OF CONTENTS/OUTLINE

Classification, clinical presentation, and evolutionary history of the most common vascular anomalies of the head and neck. Case-based review illustrating the findings of vascular tumors and vascular malformations on different imaging modalities Take-home messages References

### HNEE-22 Differential Diagnosis Between Chondrosarcoma and Synovial Chondromatosis of the Temporomandibular Joint Using CT and MRI

Participants  
Kyung-Hoe Huh, PhD, DDS, (Presenter) Nothing to Disclose

#### TEACHING POINTS

Chondrosarcoma and synovial chondromatosis are a representative tumor or tumor-like arthropathy of the temporomandibular joint, producing cartilaginous calcification within the mass and causing bone changes of the mandibular condyle and/or articular eminence/glenoid fossa. Imaging differentiation between chondrosarcoma and synovial chondromatosis of the TMJ is very important, because they share clinical and histopathological features. CT and MR imaging features such as lesion epicenter of the mandibular condyle, infiltration into the tendon of the lateral pterygoid muscle, destruction of the mandibular condyle, no destruction/sclerosis of the articular eminence/glenoid fossa, calcification pattern (absence or stippled), periosteal reaction, and internal enhancement can be an effective tool to differentiate between chondrosarcoma and synovial chondromatosis. The single imaging feature with the highest performance for differential diagnosis is infiltration into the tendon of the lateral pterygoid muscle. With combination of the several imaging features, the diagnostic performance can be improved.

#### TABLE OF CONTENTS/OUTLINE

1. Introduction 2. Anatomy of the temporomandibular joint a. comparison of lesion epicenter b. infiltration of the tendon of the lateral pterygoid muscle 3. Imaging parameters of the TMJ on CT and MR image 4. Imaging features of chondrosarcoma 5. Imaging features of synovial chondromatosis 6. Differentiation between chondrosarcoma and synovial chondromatosis 7. Conclusion

#### HNEE-23 SMARCB1-Deficient Sinonasal Cancer- Imaging Features of An Emerging Entity

Participants  
Renuka Ashtekar, MBBS, MD, Mumbai, India (Presenter) Nothing to Disclose

#### TEACHING POINTS

1. Enumerate the various subtypes of sinonasal malignancies. 2. Describe CT and MR imaging features of SMARCB1-deficient sinonasal cancer (SdSNC). 3. Distinguishing SdSNC from other close imaging differentials.

#### TABLE OF CONTENTS/OUTLINE

1. Introduction to sinonasal malignancies and their various subtypes. 2. What is SMARCB-1 and how are these tumors diagnosed? 3. Imaging characteristics of SdSNC on CT and MRI. 4. Common differential diagnoses and their imaging features. 5. Case-based review of uncommon presentations of SdSNC.

#### HNEE-24 The Hidden Windows Between the Neck Spaces

Participants  
Daniel Sebastian Chaves Burbano, MD, (Presenter) Nothing to Disclose

#### TEACHING POINTS

- To identify the limits, content and communication between the neck spaces, it is useful the understanding that some of them are virtual spaces. - The cervical fasciae are non-continuous connective tissue structures that surround the muscles, nerves, and vessels of the neck and establish the spaces in the neck. Its functions are to be a barrier and reduce friction between structures. These are two: superficial cervical fasciae and deep cervical fasciae. - Some of the neck spaces have no boundaries between them, so they are connected to each other. Identifying the communication between them is an important step approaching the images. - The communication between the spaces of the neck is not only between them, but also with the base of the skull, thorax and the back, and they are not usually easy to find. They can be a route of dissemination of pathologies.

#### TABLE OF CONTENTS/OUTLINE

- Gross anatomy - Superficial cervical fascia - Deep cervical fascia - Suprahyoid deep neck spaces - Infrahyoid deep neck spaces - Supra and infrahyoid deep neck spaces - The windows between the neck spaces - Conclusions

#### HNEE-25HC Virtual Reality Module Reinforcing Cranial Nerve Deficits with Physical Examination

Participants  
Christopher Lack, MD, PhD, (Presenter) Consultant, PhenoMx, Inc

#### TEACHING POINTS

The relationship between cranial nerve anatomy, function, pathology and physical examination findings requires a deep understanding of multiple domains. Virtual reality has the potential to be a powerful tool in teaching, reinforcing concepts that are not well represented by textbooks. Using our interactive 3D model, the learner can easily examine the important anatomic structures and be exposed to many pathologic states without the need for multiple unique patient encounters. This module could easily be used around the world if the end-user has an appropriate VR headset.

#### TABLE OF CONTENTS/OUTLINE

Using MRI and CT data, we developed an interactive high-fidelity 3D model, in a virtual environment, that highlights the anatomy of the orbits and cranial nerves II, III, IV, VI. The user can view and interact with the anatomic structures using a VR headset and perform an exam of the extraocular muscles. Using the "Quiz-mode" users will be tested on an unknown cranial nerve deficit and will have to identify the deficit based on an actual physical exam in the virtual environment. The module can be seen both in 3D by wearing the VR goggles but also in 2D on the attached laptop screen. Since the power of 3D and physical exam is best demonstrated using the VR headset, please come to the exhibit to experience the headset demo. Please visit the Learning Center to also view this presentation in hardcopy format.

#### HNEE-26 Advanced Imaging Biomarkers in Head and Neck Cancer: Precision Diagnosis, Gene Mutation Detection, and Treatment Response Assessment and Prediction

Participants  
Yoshiaki Ota, MD, Ann Arbor, MI (Presenter) Nothing to Disclose

## TEACHING POINTS

Teaching point1. To review physics of DWI, CT perfusion, MR spectroscopy, dynamic susceptibility contrast perfusion MRI (DSC-MRI), and dynamic contrast-enhanced MRI (DCE-MRI)2. To demonstrate head and neck tumors and application of advanced imaging for tumor differentiation, gene mutation detection, and assessment of treatment effect3. To demonstrate pitfalls of advanced imaging

## TABLE OF CONTENTS/OUTLINE

Outline1. Physics and clinical application- DWI: Assessment of cellularity, cytotoxic/vasogenic edema- CT perfusion: Assessment of vascular space of the lesions- MR spectroscopy: Detection and quantification of abnormal metabolites related to gene mutation- DSC-MRI: Assessment of vascularity, permeability, and hemodynamic pattern (First pass)- DCE-MRI: Assessment of vascularity, permeability, and hemodynamic pattern 2. Head and neck tumors- Infratentorial extra-axial tumorsa. Common tumors/meningiomas, schwannomas, paragangliomasb. Atypical/metastasis, chordoma, chondrosarcoma, endolymphatic sac tumor- Tumors in the head and neck mucosal surface- Tumors in the head and neck deep tissues 3. Clinical and academic application of DWI, CT perfusion, DSC-MRI, and DCE-MRI- Tumor differentiation- Detection of tumor mutation- Assessment of treatment effect- Post-operative risk assessment 4. Pitfalls of applications of DWI, DSC-MRI and DCE-MRI- DWI: Geographic artifact - CT perfusion: Motion artifacts, severe beam-hardening- DSC-MRI: Susceptibility artifacts at tissue interfaces or skull base area- DCE-MRI: Different magnetic field (1.5T or 3T) and parameters (such as TE, TR, or temporal resolution) in DCE-MRI can affect quantitative parameters (Vp, Ve, Ktrans, and Kep).

## HNEE-27 Don't Let Your Mouth Water - Everything You Need to Know About the Parotid Glands

### Awards

#### Certificate of Merit

Participants

Marcio Ricardo Garcia, MD, Sao Paulo, Brazil (*Presenter*) Nothing to Disclose

## TEACHING POINTS

1. To review the anatomy of the parotid gland and adjacent anatomical structures. 2. To review the most common parotid gland diseases and their radiological findings. 3. To learn more about some important differential diagnoses.

## TABLE OF CONTENTS/OUTLINE

1. Simplifying the anatomy of the parotid gland and adjacent anatomical structures (temporomandibular joint, external auditory canal and masticator space). 2. Summarize the main key points of some different diseases that affect the parotid gland with a focus on computed tomography and magnetic resonance findings, highlighting some pathologies like: developmental variations, first branquial cleft cyst, lymphatic venous malformation, lipoma, dermoid cyst, acute parotitis, abscess, chronic parotitis, necrotizing otitis externa with parotid extension, Sjögren syndrome, IgG4-related disease, intraparotid facial neuropathy and perineural spread, lithiasis, iatrogenic injury of the Stensen duct after bichectomy, Warthin tumor, pleomorphic adenoma, oncocytoma, mucoepidermoid carcinoma, lymphoma and metastasis. 3. Elaboration of a flowchart to help in the analysis of focal lesions of the parotid gland, including analysis of diffusion and permeability. 4. Conclusion.

## HNEE-28 A Head Turner: Diffusion Restricting Head and Neck Lesions

Participants

Yasasvi Tadavarthi, MD, (*Presenter*) Nothing to Disclose

## TEACHING POINTS

Diffusion-weighted imaging has been shown promising in tissue characterization of primary tumors (benign and malignant), nodal metastases, differentiation of recurrent tumor from post therapeutic changes, monitoring treatment response, and many other clinical scenarios in head and neck. In this presentation we will discuss different aspects of using diffusion weighted imaging in head and neck and their added value over anatomic imaging.

## TABLE OF CONTENTS/OUTLINE

1. Brief review of diffusion weighted imaging technique and its use in head and neck imaging.2. Review imaging features of different pathologic conditions seen in the head and neck demonstrating diffusion restriction including:a. Benign neoplasms - Warthin tumor. b. Malignant neoplasms - Lymphoma, Carcinomas (Squamous cell carcinoma and Adenocarcinoma), Rhabdomyosarcoma. c. Infectious and inflammatory lesions - Abscess, Pseudotumor. d. Miscellaneous lesions- Hematoma, Cholesteatoma, Epidermoid cyst, Lymphadenopathy3. Challenges and limitations of diffusion weighted imaging in the head and neck.4. Mimics and special circumstances - Artifacts, Monitoring treatment response

## HNEE-29 The Sound of Silence: Clinical and Imaging Aspects of Sudden Hearing Loss

Participants

Stephanie Nagano, MD, Sao Paulo, Brazil (*Presenter*) Nothing to Disclose

## TEACHING POINTS

Sudden hearing loss occurs within a 72-hour period. It is essential to define whether the hearing loss is conductive, sensorineural or mixed to guide the investigation.Sudden sensorineural hearing loss is a clinical emergency and must be evaluated quickly to decrease the chances of becoming permanent.The diagnosis is predominantly clinical and imaging tests can provide additional information regarding the etiology. In cases of conductive deafness, the best method is computed tomography and in sensorineural deafness, resonance. Both methods can be used in cases of mixed deafness and surgical planning.Systematic analysis by topography can be useful to identify causes of sudden neurosensory deafness. Is recommended to start the evaluation with retrocochlear causes such as brain lesions, cerebellopontine angle and internal auditory canal, moving on to vestibular and cochlear causes.

## TABLE OF CONTENTS/OUTLINE

Definition and clinical aspects of sudden hearing loss: how to define neurosensory, conductive or mixed?Imaging methods and pertinent ear anatomy in sudden deafness.Sudden conductive hearing loss examples.Neurosensory hearing loss

examples. Systematic clinical and imaging evaluation in sudden hearing loss: summing up.

### **HNEE-3 Show some nerve! - Neurography in Head and Neck**

#### **Awards**

##### **Certificate of Merit**

Participants

Samya Alves, MD, Sao Paulo, Brazil (*Presenter*) Nothing to Disclose

#### **TEACHING POINTS**

- Review anatomy and imaging aspects of cranial nerves and their branches.- Discuss specific sequences for nerve evaluation (PSIF, DESS, 3D SPACE).- List the main indications for performing neurography studies.- Illustrate concepts by a case-based review and original drawings.

#### **TABLE OF CONTENTS/OUTLINE**

ANATOMY: REVIEW- Review the anatomy, formation and imaging features of the nerves. NEUROGRAPHY IN HEAD AND NECK- Indications- Magnetic Resonance (MR) sequences- Advanced sequences ALTERATED NEUROGRAPHIES- Sample cases to illustrate and solidify the conceptsWHAT'S ON THE HORIZON- What's new on cranial nerves and its branches evaluation.- What do we need to improve?

### **HNEE-30 Hypopharynx - Beyond Squamous Cell Carcinoma**

Participants

Guilherme Chaves, MD, Sao Paulo, Brazil (*Presenter*) Nothing to Disclose

#### **TEACHING POINTS**

- Hypopharynx comprehends the most inferior part of the pharynx, as the continuation of the oropharynx, extending from the hyoid bone level (between C3-C4 vertebral bodies) to the inferior margin of the cricoid cartilage. It's bounded anteriorly by the laryngeal vestibule (separated by the aryepiglottic folds) and posteriorly by the retropharyngeal space.
- Can be divided into piriform sinuses, anterior wall (post cricoid area) and posterior wall. Anterior and posterior walls are usually close to each other, unless there is liquid or gaseous content between them.
- The most common pathology of the hypopharynx is squamous cell carcinoma. However, some other pathologies may cause similar symptoms and be quite confusing: congenital, inflammatory, foreign bodies and post treatment complications.
- It's extremely important for every radiologist to understand hypopharynx anatomy and pathologies cause some of them can present high morbidity.

#### **TABLE OF CONTENTS/OUTLINE**

1. Review hypopharynx anatomy and boundaries. 2. Briefly discuss hypopharynx embryology 3. List non-neoplastic pathologies of the hypopharynx: congenital, inflammatory, foreign bodies and post treatment complications. 4. Identify imaging patterns that facilitate distinction between the entities listed above and neoplastic lesions.

### **HNEE-31 Tympanoplasty: A Review of Indications, Surgical Techniques and Complications for the Radiologist**

Participants

Beatriz Prado, MD, Sao Paulo, Brazil (*Presenter*) Nothing to Disclose

#### **TEACHING POINTS**

Tympanoplasty is the surgical repair of the tympanic membrane with or without grafting and usually performed with reconstruction of the ossicular chain. Encompasses a range of procedures that vary according to the extent of the underlying pathology and required surgical exposure. This panel aims to: Define tympanoplasty Quote the main clinical indications Depict surgical aspects: Types of tympanoplasty Grafting of the tympanic membrane Illustrate complications Discuss and outline through clinical cases the expected postoperative findings and complications after tympanoplasty.

#### **TABLE OF CONTENTS/OUTLINE**

Definition of tympanoplasty Main clinical indications of tympanoplasty Types of tympanoplasty: Types 1 to 5 Complications: Thickening, Retraction, and Reperforation of the Tympanic Membrane Recurrent Cholesteatoma Granulation Tissue Extrusion, Intrusion, or Dislocation of Ossicular Prostheses Infection

### **HNEE-32 Clinical Impact of MR Bone Imaging on Head and Neck Diseases**

#### **Awards**

##### **Cum Laude**

Participants

Miho Gomyo, Miraka, Japan (*Presenter*) Nothing to Disclose

#### **TEACHING POINTS**

1. To learn the basic principles of MR bone imaging that can visualize bony and calcified structures like CT. 2. To know clinical applications to head and neck lesions of MR bone imaging. 3. To review pitfalls of MR bone imaging.

#### **TABLE OF CONTENTS/OUTLINE**

1. Basic principles and various scanning methods 2. Clinical applications to depict the following structures/lesions: physiological calcifications (basal ganglia, pineal body, choroid plexus, dura mater), skull tumors (primary and malignant tumors including metastasis), reactive bone sclerosis/erosion, bone deformity by tumors and tumor calcification 3. Applications to vessel wall imaging: segment diagnosis with the vertebral body in the carotid artery stenosis, calcified plaque and arterial wall calcification of the intracranial aneurysm 4. Pitfalls

### **HNEE-33 Rhinoseptoplasty for Radiologists: Recognizing the Main Early and Late Complications**

Participants

Beatriz Prado, MD, Sao Paulo, Brazil (*Presenter*) Nothing to Disclose

#### **TEACHING POINTS**

The purposes of this exhibit are: To show and exemplify rhinoseptoplasty early and late complications; To discuss and illustrate through clinical cases the imaging features of different complications which can be seen in the post operative state; To give some tips of when to raise suspicion of rhinoseptoplasty complications as the main responsible cause of patients symptoms.

#### **TABLE OF CONTENTS/OUTLINE**

Introduction. Early and late complications list. Clinical cases and imaging findings of different early and late rhinoseptoplasty complications. Early: Infection, Nasal septum perforation, Nasal septum hematoma. Late: Empty nose syndrome, Depression of the nasal dorsum, Depression of nasal alae, Post septoplasty cystic formation, Pinch tip deformity, Synechia, Nasal cartilage necrosis. Take home messages and final remarks.

### **HNEE-34 Ultrasound of the Post-thyroidectomy Neck in Well Differentiated Thyroid Cancer - Pearls and Pitfalls**

Participants

Sepideh Sefidbakht, MD, Powel, OH (*Presenter*) Nothing to Disclose

#### **TEACHING POINTS**

- To review the imaging appearance of thyroid bed recurrence post-thyroidectomy in well-differentiated thyroid cancers
- To review the pitfalls of ultrasound diagnosis of thyroid bed recurrence in well-differentiated thyroid cancers
- To review the ultrasound appearance of lymph node recurrence in well-differentiated thyroid cancer
- To review the pitfalls of ultrasound diagnosis of lymph node recurrence in well-differentiated thyroid cancers
- To integrate I<sup>123</sup> images, basic clinical data, including knowledge of surgical technique, cumulative dose of I<sup>131</sup> already received, laterality of the cancer in the thyroid gland, and basic lab data including Tg, TgAb to refine decision-making in ultrasound

#### **TABLE OF CONTENTS/OUTLINE**

1-Introduction: • Thyroid cancer, the prevalence, types, and recurrence pattern; implications for ultrasound diagnosis • Thyroid cancer surgery; thyroidectomy, suture, and suture-less techniques; implications for ultrasound diagnosis • Neck lymphadenectomy, central versus peripheral, indications and implications for ultrasound diagnosis • Thyroid cancer; post-op management, surveillance modalities, and their limitations  
2-The thyroid bed recurrence, appearance • Echogenicity, size, vascularity, calcification • The thyroid bed recurrence, pitfalls • Granulation tissue and edema • Suture granuloma • The upward extension of thymus • The parathyroid gland • EBRT implants  
3-Lymph node recurrence, • Appearance, Echogenicity, size, shape, central hilum; and location • Lymphadenectomy; central versus peripheral • Pre-operative lymph node mapping; what the surgeon needs and doesn't need to know

### **HNEE-35 Imaging Aspects of the New Classification for Carotid Body Tumors: Understanding Mehanna Classification Using Computed Tomography Images**

Participants

Alessandra d. Borges, MD, (*Presenter*) Nothing to Disclose

#### **TEACHING POINTS**

Discuss the new classification for carotid body tumors. Review anatomical neck landmarks of Mehanna classification in computed tomography images.

#### **TABLE OF CONTENTS/OUTLINE**

Paragangliomas are commonly located in the carotid body, usually in carotid bifurcation. Although histopathologically benign, its involvement in neurovascular structures and intracranial invasion are associated with high morbidity. The surgery of paraganglioma in the carotid body can be very challenging and for that reason, an accurate classification to predict the risk of potential complications is vital for treatment decision-making. Mehanna et al developed a new classification and risk stratification system for carotid body tumors which demonstrated better prognostic power for the risk of developing neurovascular complications after surgery, including the widely used modified Shamblin classification system. It classifies in type 1 to 4 based on the fact that the main cause of complications was the level of cranial extension. The risk of complications increases significantly with increasing Mehanna type. Type 1 extends up to but not above the superior-most aspect of the body of hyoid bone. Type 2 extends up to but not above the lower border of the angle of mandible. Type 3 extends up to but not above the superior-most aspect of the body of C2 vertebra. Type 4 extends above superior-most aspect of the body of C2 vertebra. An additional subclassification can be added for surgical planning: E: encircling bifurcation, internal or common carotid artery. F: functional, secreting catecholamines. S: skull base reached.

### **HNEE-36 Osteoradionecrosis Of Mandible- Addressing The Raging Bull In Head And Neck Surgical Oncology**

Participants

Ankush Jajodia, MD, MBBS, New Delhi, India (*Presenter*) Nothing to Disclose

#### **TEACHING POINTS**

1. Treatment of oral cavity malignancies includes primary surgical resection which may include marginal or segmental mandibulectomy followed by adjuvant radiation. Radiation comes at its own cost in producing adverse effects on neighboring tissues, like osteoradionecrosis (ORN). 2. ORN is a condition in which irradiated bone becomes exposed to an ulcer in the overlying skin or mucosa and persists without healing for a period of 3 to 6 months. Clinically the condition may manifest with pain, swelling, orocutaneous fistula or trismus. The overall incidence of ORN of the mandible is 2.6% -15%. 3. Mandible is a compact bone and has a higher mineral content that may lead to a higher absorbed dose. The ramus and condylar processes are comparatively resistant to the development of ORN, whereas the mandibular body, symphysis, and parasymphysis regions supplied mainly by the inferior alveolar artery are at higher risk to develop ORN. 4. The pathophysiology of ORN described by Marx in 1983 (3-H principle), radiation therapy causes hypoxia, hypovascularity, and hypocellularity of tissue, thus inhibiting substitution of cells to complete the turnover

for the maintenance of homeostasis and wound cicatrization, leading to a chronic nonhealing wound. The affected cells are the ones of vascular endothelium, fibroblasts which make stroma and parenchyma cells. 5. MR imaging during follow-up help strained radiologists to detect ORN.

#### TABLE OF CONTENTS/OUTLINE

Clinical cases with pictorial depiction of Osteoradionecrosis of mandible on conventional MR Imaging

#### **HNEE-37 Multi-modality Imaging Including MR Diffusion, T2 Signal Intensity and 18 FDG PET-CT for Neck Imaging Reporting and Data System Categorization**

Participants

Ankush Jajodia, MD, MBBS, New Delhi, India (*Presenter*) Nothing to Disclose

#### TEACHING POINTS

- Previous studies documented an overall PPV of 54-56% for NI-RADS 3 posttreatment PET/CT, which was advocated as low. • NI-RADS favors NPV over PPV to potentially capture treatable lesions, even if it comes at the cost of performing additional biopsies. • Functional imaging like DWI and ADC parameters derived from DWI have shown promise for identifying true disease recurrence with higher specificity than conventional PET-CT, with a reported pooled sensitivity and specificity of 85 % and 93 %, for PET/CT. • NIRADS can serve as an assessment tool, wherein individual radiologists or groups of radiologists can utilize the PPV and NPV, to evaluate their own performance.

#### TABLE OF CONTENTS/OUTLINE

National Comprehensive Cancer Network suggests posttreatment baseline imaging after six months of therapy for advanced HNSCC but does not formally advocate imaging for asymptomatic patients. Ideal timing and frequency for using PET- CT in the posttreatment context have not yet been established. ACR "Neck Imaging Reporting and Data System" (NI-RADS) lexicon defines NIRADS 2b lesions as deep soft tissue lesions with ill-defined or mildly enhancing soft tissue or soft tissue with only mild FDG uptake. These are indeterminate lesions and should have a short-term interval follow-up. NIRADS 3 lesions should have a short-term interval follow-up or biopsy, depending on the degree of FDG uptake. Recurrence rates in NIRADS 2b and NIRADS 3 lesions were 5.6 % and 60-80%, respectively. The template was initially designed for CECT with concentration on PET-CT for detecting recurrence; MR imaging has been done in few centres. Although diffusion imaging has become a routine sequence in head and neck imaging, it is not yet a criterion in NI-RADS.

#### **HNEE-38 Ultrasound of Neck Masses - Pearls and Pitfalls**

Participants

Pooya Iranpour, MD, Shiraz, Iran, Islamic Republic Of (*Presenter*) Nothing to Disclose

#### TEACHING POINTS

To review the zonal anatomy of the neck • To understand the sonographic anatomy and the surface land marks of neck triangles • To be able to propose a primary differential diagnosis for adult neck masses list based on the location of the lesion • To review the gray scale, color Doppler and elastographic features of most common neck lesions seen in the adult • To review the key sonographic features in adult patients with cervical LAP • To review the similarities and differences of metastatic lymphnodes, versus reactive lymph nodes versus lymphoma • Using the anatomic location, and ultrasound features to determine the most likely diagnosis

#### TABLE OF CONTENTS/OUTLINE

- Neck triangles; Back to the Basics • Ultrasound of normal neck anatomy; Sonographic landmarks • Differential diagnosis of the most common neck lesions; location, location, location • Ultrasound of a neck lump; the good, the bad, and the ugly • Solid neck lesions, an overview • Lymphoma, reactive or metastasis? that is the question! • Cysts; where do they sit?

#### **HNEE-39 Addressing Pertinent Surgical Questions in Skull Base Onco-imaging Reports: Case Based Approach**

Participants

Shreya Shukla, MBBS, Mumbai, India (*Presenter*) Nothing to Disclose

#### TEACHING POINTS

Radiological reporting of cross-sectional oncological imaging including Computed Tomography (CT) and Magnetic Resonance Imaging (MRI) can be inadequate and futile for clinicians if it is unsculpted and descriptive. A checklist of vital imaging findings should be strictly used in radiological reporting to give maximum useful information to the treating clinicians. We have created such a checklist and proposed its use as a standardized synoptic reporting format to address all essential questions that need to be answered to help reach a diagnosis and optimize the management plan in skull base neoplasms. Our checklist has been designed after a thorough discussion of a multitude of skull base neoplasms cases between radiologists and clinicians at weekly multi-disciplinary joint clinics (JCs) in our tertiary cancer centre.

#### TABLE OF CONTENTS/OUTLINE

This educational exhibit contains:- Checklist of relevant and essential findings in baseline radiological reporting of skull base neoplasms.- Proposed synoptic reporting format for skull base neoplasms.- Case-based approach to understanding how including essential details in the radiology reports can affect the management plan.

#### **HNEE-4 Preoperative Orthognathic Surgery: What Radiologists Should Know**

Participants

Andre Formiga, MD, (*Presenter*) Nothing to Disclose

#### TEACHING POINTS

The purposes of this exhibit are:- To review the anatomical landmarks of the face and the angles they make on computed tomography images.- To discuss the main facial patterns made from these angles and usual changes in dental occlusion that accompany them.- To review the main osteotomy techniques employed on orthognathic surgeries.- To highlight a few craniofacial cases with either tumoral, malformation or vascular etiologies that could be subjected to orthognathic surgeries.

## TABLE OF CONTENTS/OUTLINE

Orthognathic surgery uses repositioning of the mandible and maxilla to correct imbalances in facial proportions that can affect everything from physiological dental occlusion and sleep apnea to aesthetic problems related to asymmetries and facial disharmonies that affect patient self-esteem. The objectives of this presentation are to describe the pre operative imaging findings and cephalometric parameters, mainly on CT scans, of some of the main conditions where orthognathic surgery can act, their reflections on dental occlusion, and how to report them.

### **HNEE-40 Imaging Considerations in Head and Neck Reconstruction with 3D Printed Surgical Guides and Implants**

Participants  
Mark Tan, MBBS, FRCR, (*Presenter*) Nothing to Disclose

#### TEACHING POINTS

1. Common indications for Head and Neck reconstruction:(a) Tumour (i) SCC (ii) ACC(b) Deformity correction (i) post Radiotherapy Osteonecrosis (ii) post Traumatic - midface(iii) Post surgical temporal hollowing2. Options for Head and Neck Reconstruction:(a) Maxillectomy (b) Mandibulectomy (c) Fibula flap (d) PEEK and Titanium3. Radiological interpretation considerations (a) Objectives (i) Differential diagnosis (ii) lesion extent (iii) resectability (iv) fibula vasculature (branching, septocutaneous perforator and periosteal branches)4. Workflow for 3D Printed surgical guide and implant production5. Application of Workflow: Fibula flap reconstruction with 3D printing: Virtual surgical planning: Resection with 3D printed guides, dental implant placement, 3D printed titanium plate6. Imaging acquisition considerations (i) Protocols (ii) Artefacts (iii) Patient positioning(iv) Artefact reduction: MAR (v) Reconstruction algorithms(vi) Reconstruction slice thickness(vii) CT-MRI fusion(viii) Scalar and Vector DICOM Data

## TABLE OF CONTENTS/OUTLINE

To appreciate for Head and Neck surgical reconstruction:1. Common indications 2. Surgical options 3. Radiological interpretation considerations 4. Workflow for 3D Printed surgical guide and implant production - Process Overview 5. Application of Workflow: 3D Printed Fibula Resection Guide and Titanium Plate 6. Radiographic imaging acquisition considerations for 3D Printed surgical guides and implants7. Radiographic imaging post-processing considerations for 3D Printed surgical guides and implants

### **HNEE-41 Laryngeal Protrusion, Prolapse and Eversion - Diagnoses Forgotten by Radiology**

Participants  
Ricardo Fujiki, MD, (*Presenter*) Nothing to Disclose

#### TEACHING POINTS

Protrusion, prolapse and eversion are definitions often used as synonyms, but they have totally different clinicopathological entities and have not been updated or revisited in the radiological scientific environment for a long time. Imaging findings in the head and neck were recognized and evaluated and may serve as supporting markers to differentiate protrusion, prolapse and eversion, and thus help to define the clinicopathological causes and the need or not to continue the investigation.

## TABLE OF CONTENTS/OUTLINE

- Objectives: 1 - Review definitions and clinicopathological differences between protrusion, prolapse and eversion. 2 - Illustrate through clinical cases the different entities by radiological methods. - Methods: Head and neck imaging findings were highlighted in this pictorial review. We also discussed the imaging findings in order to demonstrate the differences between the laryngeal findings. - Discussion (based on cases): Characteristic radiological findings for the differentiation between protrusion, prolapse and eversion were reported in conjunction with the development of didactic schemes to facilitate learning and recognition and differentiation in clinical practice. - Conclusion: Early and accurate recognition of the causes of laryngeal prolapse through imaging methods can help assisting physicians in defining the need for biopsy.

### **HNEE-42 What the Eye Can't See but the Radiologists Do: Clinical-radiological Correlation in the Assessment of Visual Disturbances**

**Awards**  
**Identified for RadioGraphics**

Participants  
Ewa Joanna Maciag, (*Presenter*) Nothing to Disclose

#### TEACHING POINTS

Patients with visual disturbances may present a wide variety of symptoms that can be divided into three main categories: (1) Visual dysfunction, such as blurred vision, vision loss, and visual field defects. (2) Extrinsic ocular motility disorders, which usually cause binocular diplopia. (3) Pupillary motility impairment. This review aims to analyze the correlation between the different radiological presentation patterns and the clinical manifestations, with an emphasis on the anatomical localization of the causative lesion and an approach to an appropriate selection and interpretation of the different imaging techniques.

## TABLE OF CONTENTS/OUTLINE

1. Introduction. 2. Main symptoms and anatomical background. 3. Imaging techniques: appropriate selection and application. 4. Intrinsic ocular motility disorders: miosis and mydriasis. 5. Alterations of the extrinsic ocular motility: neurogenic and myogenic causes and an evidence-based diagnostic algorithm of diplopia. 6. Disorders of visual function: a case-based overview of the causative pathology. 7. Diagnostic pathway to determine the cause of the visual disturbances. 8. Conclusions.

### **HNEE-43 Head and Neck Manifestations of Autoimmune Disease - A Didactical Review**

Participants  
Mayne Brandao, MD, (*Presenter*) Nothing to Disclose

#### TEACHING POINTS

Little is said about the manifestations of autoimmune diseases and their imaging aspects in Head and Neck. This panel is intended

to show challenging cases that are part of this group of diseases, which affect the various areas of this region. The diversity of findings shows us the importance of disclosing these imaging aspects and makes it a useful tool for consultation. Unusual places such as ossicular involvement, the Eustachian tube, the sternocleidomastoid muscle and other structures illustrate this diversity of places. There are other diseases that will also be addressed in this exhibit as for example lupus; seronegative spondyloarthropathies; systemic sclerosis. Correlation of the imaging findings with the clinical features and laboratory findings is also important for the diagnosis and the recognition of the disease activity, and the identification of possible complications or even the occurrence of associated neoplasms.

#### **TABLE OF CONTENTS/OUTLINE**

Introduction of the main acquired immunologically mediated inflammatory disorders. These disorders may be associated with paraneoplastic syndrome, especially hematologic tumors, or may increase the risk for the development of malignancies, predominantly lymphoproliferative disorders. Also, these patients may be associated with infection and granulomatous lesions of the head and neck. We will provide with didactical cases a review presenting the imaging findings in the head and neck in patients with these diseases. Conclusions. References.

#### **HNEE-44 Temporal Bone Osteodystrophies**

Participants  
Afonso Santos, MD, Sao Paulo, Brazil (*Presenter*) Nothing to Disclose

#### **TEACHING POINTS**

The purposes of this exhibit are: To exemplify all forms of otospongiosis presentation (typical and atypical) and discuss possible pitfalls (eg, foci at the internal acoustic meatus versus diverticula). To demonstrate other osteodystrophies of the temporal bone, including osteogenesis imperfecta, osteopetrosis, Paget's disease and fibrous dysplasia.

#### **TABLE OF CONTENTS/OUTLINE**

Introduction. CT and MRI temporal bone studies. Imaging of typical and atypical cases of otospongiosis. Practical tips and pitfalls on otospongiosis analysis. Other osteodystrophies of the temporal bone: osteogenesis imperfecta, osteopetrosis, Paget's disease and fibrous dysplasia. Take-home messages.

#### **HNEE-45 Surgical Pitfalls in the Otospongiosis Evaluation: What the Otorhinolaryngologist Needs to Know**

Participants  
Marcio Ricardo Garcia, MD, Sao Paulo, Brazil (*Presenter*) Nothing to Disclose

#### **TEACHING POINTS**

To describe imaging findings in CT scan evaluation of otosclerosis with preoperative relevance. To warn the radiologists about the detection of relevant features that could lead to surgical failure or complications in the stapedotomy and improve patient outcomes

#### **TABLE OF CONTENTS/OUTLINE**

1. Introduction - A brief discussion about physiopathology and classical imaging findings of fenestral and retrofenestral otosclerosis - The role of CT and MR in the diagnosis of otosclerosis - A little explanation about the surgical treatment of otosclerosis with emphasis on stapedotomy and possible postoperative complications (untreatable vertigo, anacusis, facial palsy, and meningitis). 2. Imaging findings on preoperative evaluation before stapedotomy - Oval or round window involvement (atresia, narrowing, thickened stapes footplate) and their relation with close structures - Facial nerve anomalies as congenital abnormalities, deviation of facial nerve, or dehiscence - Vestibular aqueduct anomalies as enlargement or dehiscence - Persistent stapedial artery - Semicircular canal dehiscence- Cochlear-facial nerve dehiscence- Lateral semicircular canal dysplasia- Ossicular chain fixation 3. Conclusion 4. Take-home messages

#### **HNEE-46 Advanced Imaging of Head and Neck Infection**

**Awards**  
**Cum Laude**

Participants  
Akira Baba, Ann Arbor, MI (*Presenter*) Nothing to Disclose

#### **TEACHING POINTS**

Advanced cross-sectional imaging plays a critical role in providing differential diagnoses, treatment decisions, and prognostic implications in head and neck infections. Contrast-enhanced CT is the imaging modality of choice for head and neck infections; however, other imaging modalities may be complementary and diagnostic. MRI is excellent for evaluation of intracranial spread of inflammation/abscess formation and osteomyelitis, etc. DWI and ADC values are useful in providing differential diagnoses and evaluating treatment response of head and neck infections. 18F-FDG-PET/CT is helpful in the follow-up of skull base osteomyelitis. Dual energy CT allows for various techniques such as metal artifact reduction and material decomposition imaging that can help reduce dental metal artifacts, increase salivary stone detection. Metal artifact reduction algorithm can help reduce dental metal artifacts. Subtraction CT techniques are used to reduce dental metal artifacts and detect destructive osseous changes. This presentation will provide an overview of must-know head and neck infections with updated advanced imaging techniques and their imaging findings.

#### **TABLE OF CONTENTS/OUTLINE**

1. Imaging techniques 2. Temporal bone/skull base 3. Pharynx 4. Deep neck 5. Oral cavity 6. Salivary Glands

#### **HNEE-47 Skull Base Osteomyelitis in COVID-19 related Acute Invasive Fungal Rhino Sinusitis: Spectrum of Findings**

Participants  
Gayatri Senapathy, FRCR, (*Presenter*) Nothing to Disclose

#### **TEACHING POINTS**

- SBO is a dreaded condition with high morbidity and mortality and fungal rhinosinusitis is one among the many causes of SBO
- Incidence of AIFRS showed a significant increase during the second wave of COVID-19 pandemic and Diabetes Mellitus and Steroid use were found to be the major associated factors.
- AIFRS was seen in patients with active or recent COVID-19 infection. SBO was seen as a complication at presentation in some cases of AIFRS, and beyond the 3rd week of onset in treated patients who had progressive disease.
- AIFRS has a predilection for both vascular and perineural spread across intact bony boundaries. Patients with early involvement of the pterygopalatine fossa, orbital apex and the cavernous sinus are at high risk of developing SBO due to perineural and vascular spread.
- Contrast enhanced MRI (CE MRI) is superior to CT in the early detection of SBO as the marrow signal changes and the adjacent soft tissue changes are detected before bone erosion becomes evident on CT.
- Intracranial complications such as meningitis, vascular complications, cerebritis and abscesses are also depicted earlier on MRI.

#### TABLE OF CONTENTS/OUTLINE

- Revisit skull base anatomy
- Elucidate the pathways of spread of sinonasal fungal infection to involve the skull base
- Illustrate the various findings of skull base osteomyelitis (SBO) in cases of COVID-19 related Acute Invasive Fungal Rhino Sinusitis (AIFRS) in our institute between March and September 2021
- Demonstrate the associated intracranial and extracranial complications.

#### HNEE-48 Extraocular Muscle Pathology: That's How Eye Roll

Participants

Juliana Sitta, MD, Jackson, MS (*Presenter*) Nothing to Disclose

#### TEACHING POINTS

To review the normal orbital imaging anatomy highlighting the advantages of each imaging modality. To discuss the differential diagnosis of extraocular muscle (EOM) pathology including inflammatory, infectious, neoplastic, congenital, and traumatic etiologies. To recognize the importance of systematic EOM assessment in the diagnosis of systemic diseases and potential complications

#### TABLE OF CONTENTS/OUTLINE

The differential diagnosis of EOM pathology is broad and often challenging including inflammatory, infectious, neoplastic, and traumatic causes. Although eye movement disorders may be unclear on initial imaging, modalities including CT, MRI, and PET-CT along with clinical findings play a key role in identifying or ruling out important differential diagnosis. In this presentation we will review the imaging features of normal orbital anatomy and the spectrum of EOM pathology. We will illustrate a wide range of etiologies including key imaging findings to narrow down the differential diagnosis in various categories of disease such as congenital orbital fibrosis of the EOM, anophthalmia-micropthalmia, spontaneous hematoma, thyroid orbitopathy, orbital metastases, PET-CT findings in nerve palsy, idiopathic orbital inflammation, and IgG4 sclerosing disease of the orbit.

#### HNEE-49 Branchial Apparatus Lesions and Thyroglossal Duct Lesions: Embryology, Typical Imaging Findings of Those Lesions and Mimics

Participants

Yoshiko Y. Kurihara, MD, (*Presenter*) Nothing to Disclose

#### TEACHING POINTS

Many structures in the head and neck region arise from branchial apparatus. To learn congenital lesions secondary to abnormal embryogenesis in this region, the knowledge of these structures including embryology can make those diseases easier to understand. The thyroglossal duct also causes abnormal embryogenesis. On this presentation, the embryological changes of branchial clefts, pouches and thyroglossal duct are demonstrated. This presentation shows many developmental abnormalities as 1) fistulae, sinuses and cysts originated from branchial clefts and thyroglossal duct with typical location according to the embryology 2) complicated status of these lesions ; infection, neoplastic change including malignancy 3) ectopic thymus, ectopic parathyroid gland and ectopic thyroid tissue according to their migrating tract 4) neoplastic changes of these ectopic lesions, with CT, MRI, RI images and interpretations. In addition, 5) mimics should be differentiate from these lesions as well.

#### TABLE OF CONTENTS/OUTLINE

1) Figure of branchial apparatus developing structures anomalies. 2) Embryology of branchial apparatus. 3) Developmental abnormalities related to branchial cleft, complicated lesions and mimics. 4) Developmental abnormalities related to branchial pouch, complicated lesions and mimics. 5) Figure and embryology of thyroglossal duct. 6) Developmental abnormalities related thyroglossal duct, complicated lesions and mimics.

#### HNEE-5 High Resolution CT Angiography of the Orbits, Skull Base and Pterygopalatine Fossa

Awards

Certificate of Merit

Participants

Norbert Campeau, MD, Rochester, MN (*Presenter*) Nothing to Disclose

#### TEACHING POINTS

1. To detail the arterial anatomy of the orbit, anterior skull base and pterygopalatine fossa through high resolution CT angiography images and corresponding anatomic legends. 2. Discuss several of the more commonly occurring congenital arterial variants. 3. Review relevant skull base foramina and fissures.

#### TABLE OF CONTENTS/OUTLINE

High resolution computed tomography angiography (CTA) of the brain and skull base has continued to improve substantially over the past two decades, now routinely obtained with sub-millimeter voxel resolution. In this educational exhibit, we present a detailed review of the arterial anatomy of the orbit and pterygopalatine fossa using high resolution CTA images obtained from a state of the art 510k cleared photon counting CT scanner. Arterial supply to the optic nerve, ocular globe, lacrimal gland will be detailed. Anatomy of internal maxillary artery branches will also be described, including course of the arteries of the pterygopalatine canal, foramen rotundum, sphenopalatine, greater and lesser palatine arteries. Anastomotic connections between meningeal, external carotid, and internal carotid artery branches via the inferolateral trunk will also be discussed.

## **HNEE-50 Open Your Eyes and Look Out for All the Windows - Evaluation of the Oval, the Round and Other Windows of the Inner Ear**

Participants

Bruna Gherardi, MD, Rio de Janeiro, Brazil (*Presenter*) Nothing to Disclose

### **TEACHING POINTS**

To illustrate the pathophysiology of third window syndrome. To demonstrate the most common imaging aspects of oval, round, and other pathologic window changes and the clinical implications.

### **TABLE OF CONTENTS/OUTLINE**

Physiology of air and bone auditory conduction. Imaging protocol. Mastoid trauma involving oval and round windows. Labyrinthine fistula. Fenestral and retrofenestral otospongiosis. Cochleofacial dehiscence. Carotid-cochlear dehiscence. Dehiscence of semicircular canals. Enlarged vestibular aqueduct syndrome. Round window stenosis.

## **HNEE-51 Facing the Challenge: Imaging of Facial Nerve Paralysis**

Participants

Hugo Tames, MD, Sao Paulo, Brazil (*Presenter*) Nothing to Disclose

### **TEACHING POINTS**

To review the anatomy of the normal facial nerve and its expected normal imaging appearances on CT and MR. To review causes of facial nerve paralysis, ranging from the commonest and less common diseases. To present the imaging appearances on CT and MR of facial nerve when affected by these pathologies. To present different cases of facial paralysis from the teaching files of a tertiary center, including typical appearance and atypical variants.

### **TABLE OF CONTENTS/OUTLINE**

1. Introduction  
2. Review of facial nerve anatomy and its expected normal imaging appearance on CT and MR  
The central nervous system segment  
The cisternal segment  
The meatal segment  
The labyrinthine segment  
The tympanic segment  
The mastoid segment  
The extra-temporal segment  
3. Review of different causes of facial paralysis  
Bell's palsy / idiopathic paralysis  
Facial nerve arteriovenous malformation  
Facial nerve schwannoma  
Facial nerve meningioma  
Ramsay-Hunt syndrome  
Moebius syndrome  
Melkersson-Rosenthal syndrome  
Metaphyseal chondrodysplasia  
Facial nerve paralysis secondary to perineural spread of adenoid cystic carcinoma  
Central facial paralysis secondary to ischaemic event  
4. To present the imaging appearances on CT and MR of facial nerve when affected by these pathologies

## **HNEE-52 Skull Base Osteomyelitis: Imaging checklist**

Participants

Sri Lakshmi J P Rao G, MBBS, MD, (*Presenter*) Nothing to Disclose

### **TEACHING POINTS**

1. Should be suspected in all cases of infiltrative skull base lesions, particularly in diabetics and immunocompromised people, when repeated biopsies turn negative for malignancy.  
2. Imaging checklist to be followed while reporting a case of Skull base osteomyelitis.  
3. Mimics of Skull base osteomyelitis.

### **TABLE OF CONTENTS/OUTLINE**

1. Introduction and types of SBO  
2. Imaging protocol  
3. Checklist for SBO reporting  
4. Role of imaging in follow-up  
5. Imaging mimics of SBO

## **HNEE-53 Head and Neck Sarcoma: A Magnetic Resonance Imaging Review Based on the 2020 World Health Organization Classification**

Participants

Simone Caprioli, MD, Genova, Italy (*Presenter*) Nothing to Disclose

### **TEACHING POINTS**

1. Magnetic resonance imaging (MRI) characteristics of head and neck sarcomas are often nonspecific and may be difficult to identify the precise diagnosis. 2. The recognition of the epicenter of the mass allows to differentiate a soft tissue from a bone or cartilage tumor. 3. MRI may narrow the differential diagnosis by analyzing the signal of the matrix of the tumor. 4. MRI is useful for identifying orbital and intracranial invasion.

### **TABLE OF CONTENTS/OUTLINE**

In 2020 a novel classification system for soft tissue and bone tumors was published by the World Health Organization (WHO). Even though it is usually applied for trunk and extremities sarcoma, it may be a guide for characterizing non-epithelial lesions of head and neck. Magnetic resonance imaging (MRI) plays a pivotal role in the diagnosis of head and neck sarcoma, supporting the hypothesis of the non-epithelial origin of a mass and suggesting clues about histology. This work aims to review the MRI characteristics of non-epithelial neoplasms of head and neck as they are grouped in the 2020 WHO classification. Moreover, it offers a guide for precise local staging and for narrowing the differential diagnosis, thanks to a combination of criteria: location, epicenter, and MRI signal characteristics. The present work was based on a ten-years long multicentric record of 248 cases of head and neck sarcomas.

## **HNEE-54 Unboxing the Voice Box: Imaging in Laryngeal Malignancy**

**Awards**

**Identified for RadioGraphics**

**Certificate of Merit**

Participants

Anu Kamalasanan, FRCR, MBBS, East Renfrewshire, United Kingdom (*Presenter*) Nothing to Disclose

#### TEACHING POINTS

1) T1 lesions may be radiologically occult . 2) Nodal disease occurs late in glottic malignancy due to the relative paucity of lymphatic drainage of vocal cords 3) Anterior commissure involvement precludes hemilaryngectomy and may be associated with early cartilage invasion from extension along Broyle ligament 4) Paraglottic/ pre-epiglottic fat infiltration upstages disease to T3. Assessment can be done with CT/ MRI and USS 5) Thyroid cartilage has a variable appearance - ossified thyroid cartilage can make it difficult to differentiate from infiltration. USS and MRI can be used to differentiate between the two.

#### TABLE OF CONTENTS/OUTLINE

1) Illustrate with images, normal laryngeal anatomy including TNM subsites 2) Describe Imaging modalities for assessment and staging of laryngeal malignancy. 3) Update on Ultrasound and MRI as imaging adjuncts 4) TNM staging with examples 5) Illustrate various patterns of spread 6) Discuss management pathway.

#### HNEE-55 Anatomic Approach to Pharyngeal SCC Staging and Patterns of Spread

Participants

Daniel Warren, MD, (*Presenter*) Nothing to Disclose

#### TEACHING POINTS

1. Brief discussion of the revised 8th edition of the American Joint Committee staging of pharyngeal squamous cell carcinomas (SCCs). 2. Overview of anatomic landmarks vital for staging of pharyngeal SCCs and discussion of imaging evaluation of invasion and extranodal extension. 3. Image-based review of common routes of spread based on the location of origin.

#### TABLE OF CONTENTS/OUTLINE

1. Background 2. HPV status and outcomes 3. Nasopharyngeal SCC 3a. Staging 3b. Imaging Features 3c. Common and Easily Missed Locations 3d. Routes of Spread 4. HPV/P16(+) Oropharyngeal SCC 4a. Staging 4b. Imaging Features 4c. Common and Easily Missed Locations 4d. Routes of Spread 5. HPV/P16(-) Oropharyngeal SCC and Hypopharyngeal SCC 5a. Staging 5b. Imaging Features 5c. Common and Easily Missed Locations 5d. Routes of Spread 6. Conclusion

#### HNEE-56 Fire in the Hole!: Jugular Foramen Pathology and Pitfalls

Participants

Fernando Ferraro IV, MD, Buenos Aires, Argentina (*Presenter*) Nothing to Disclose

#### TEACHING POINTS

Explain the anatomical content and content of the jugular foramen. Based on clinical findings, interpret the location of lesions involving the jugular foramen. Review of various lesions, variants and pitfalls involving the jugular foramen. Describe radiological findings secondary to cranial nerve deficit.

#### TABLE OF CONTENTS/OUTLINE

Technical specifications and protocol to study the jugular foramen. Schematic summary of the anatomy of the jugular foramen, including anatomical variations, and its importance for interpreting clinical examination. Illustrate the principal imaging findings with clinical examples (such as Vernet's syndrome, schwannomas, desmoid tumor, etc).

#### HNEE-57 Lymphoproliferative Lesions of the Orbit

Awards

Certificate of Merit

Participants

Taisa Santos, MD, Salvador, Brazil (*Presenter*) Nothing to Disclose

#### TEACHING POINTS

Lymphoproliferative lesions represent the most common primary orbital disease, manifesting mainly in the elderly, and may also be a manifestation of systemic lymphoproliferative disease. Imaging evaluation is essential to guide the diagnosis, follow-up and treatment response, since the clinical presentation is nonspecific signs and symptoms and can mimic other orbital pathologies. CT image pattern is not very specific, usually presenting as a mass that molds to the orbital walls, isoattenuating/hyperattenuating, with homogeneous contrast enhancement. It rarely presents with bone erosion, when present, it is usually associated with diffuse large B-cell lymphoma. MRI is the imaging method of choice and some sequences are essential for distinguishing pathologies that may mimic lymphoproliferative lesions, especially idiopathic orbital inflammatory disease, which may have similar signs and symptoms, being clinically different by association with painful proptosis and findings of image, as high ADC values ?? on MRI. The main differential diagnoses include idiopathic orbital inflammatory syndrome, orbital cellulitis, thyroidopathy, sarcoidosis, IgG4, granulomatosis with polyangiitis, and metastases.

#### TABLE OF CONTENTS/OUTLINE

Introduction  
Histological classification  
Clinical findings  
Image protocol  
Image patterns  
Diferenciais diagnósticos  
Prognosis and follow up

#### HNEE-58 Breathe In Breathe Out: Obtaining Clarity in Imaging of Sino Nasal Malignancy

Participants

Janani Baradwaj, MBBS, MD, (*Presenter*) Nothing to Disclose

#### TEACHING POINTS

±Sino-nasal malignancies are mostly squamous cell types ±Historically Ohngren's line was used in prognostication and management. It is an imaginary line drawn from the angle of the mandible to the medial canthus of the eye, dividing the antrum. Disease involvement above the line is associated with a poor prognosis. ±CT demonstrates the extent of osseous involvement better. Soft tissue and nodal disease are assessed with post-contrast CT. ±MRI helps differentiate between mass and inflammatory change in

the sinuses.°Tumour - Low T1, Low T2 signal, Heterogeneous enhancement °Mucosa - Low T1, High T2 signal, Intense homogeneous enhancement °Secretions - Low T1, Very high T2 signal, No enhancement ±MRI also helps to assess orbital, intracranial and perineural spread ±MRI is more sensitive for assessment of perineural spread - Enlarged affected nerves have high T2 signal with perineural enhancement, loss of normal T1 fat signal and normal CSF signal in the foramina. ±Perineural spread on CT - Enlargement and erosion of foramina, loss of normal low attenuating fat, Soft tissue attenuation of foramen.±Sino-nasal malignancies have a moderate incidence of loco-regional recurrence with late nodal disease. The presence of positive neck nodes is associated with higher incidence of disease recurrence. Retropharyngeal nodal involvement should be actively looked for on CT and MRI

#### **TABLE OF CONTENTS/OUTLINE**

±Describe normal paranasal sinus anatomy with images ±TNM staging of sino-nasal malignancy ±Illustrate with images routes of spread of malignancy ±Describe histopathological types of malignancies involving the sino-nasal cavity with images ±Radiological prognosticating factors ±Discuss management pathway

#### **HNEE-59 What You Need to Know Before Reporting a Nasopharyngeal Tumor**

Participants  
Maria Rocha, MD, (*Presenter*) Nothing to Disclose

#### **TEACHING POINTS**

Simplifying and help less experienced radiologists know how to actively look for the critical areas that changes the treatment and staging of the patient. Review basic anatomy highlighting the main anatomical milestones in tumor staging. Illustrate common path of nasopharyngeal tumor.

#### **TABLE OF CONTENTS/OUTLINE**

Introduction to nasopharyngeal tumors A comprehensible guide of key anatomy and correlating to TNM / prognostic information Flowchart that resumes the critical points of the staging Didactical cases following the proposed flowchart

#### **HNEE-6 Temporomandibular Joint Imaging from Basic to Advanced**

Participants  
Eduardo Valadares, MD, Sao Paulo, Brazil (*Presenter*) Nothing to Disclose

#### **TEACHING POINTS**

Describe the anatomy and biomechanics of temporomandibular joint Exhibit the normal appearance of temporomandibular joint in advanced imaging (CT and MRI) Summarize the main temporomandibular joint dysfunctions and disorders with a group-based approach

#### **TABLE OF CONTENTS/OUTLINE**

Introduction Anatomy and biomechanics of temporomandibular joint Normal CT and MRI appearance Abnormal development of the temporomandibular joint (aplasia/hypoplasia/hyperplasia) Temporomandibular joint dysfunction (direct and indirect signs) Traumatic lesions Inflammatory arthritis • Osteoarthritis • Rheumatoid arthritis • Juvenile inflammatory arthritis • 7. Tumor and tumorlike lesions • Metastasis • Fibrous dysplasia • Synovial chondromatosis • Pigmented villonodular synovitis Take-home messages/Conclusions

#### **HNEE-60 Multimodality Imaging of Carotid Paragangliomas**

Participants  
Ingrid Alonso Ramon, MD, Mexico City, Mexico (*Presenter*) Nothing to Disclose

#### **TEACHING POINTS**

Teaching points 1. To review general characteristics of paragangliomas for a better understanding of carotid glomus 2. To discuss general concepts of a carotid glomus, including the different types and their incidence 3. To describe different multimodality imaging characteristics (ultrasound, CT, MRI, PET/CT and angiography) including the recommended protocols and pros and cons of each one. 4. To recognize importance of diagnosis, treatment and follow up

#### **TABLE OF CONTENTS/OUTLINE**

Table of contents 1. Description of general characteristics of paragangliomas including common sites of occurrence, incidence, pathophysiology and embryology. 2. Description of general features of carotid paraganglioma a. Epidemiology b. Anatomy c. Detailed pathologic characteristics d. Clinical presentation including functional paraganglioma e. Differential diagnosis 3. Review of multimodality imaging findings including recommended protocol and expected findings for each one 4. Discussion of management and outcome including Shambling classification and prognosis based on pathology or imaging findings

#### **HNEE-61 Postoperative Imaging of Sinonasal Surgery and its Complications: What To Look for?**

Participants  
Raphael Correia, MD, Sao Paulo, Brazil (*Presenter*) Nothing to Disclose

#### **TEACHING POINTS**

To recognize the main sinonasal surgeries and their anatomic landmarks. To understand the expected postoperative findings of sinonasal surgery. To review the clinical presentations and imaging findings of sinonasal surgery complications.

#### **TABLE OF CONTENTS/OUTLINE**

Introduction. Sinonasal Anatomy. Main Surgical Procedures and Their Anatomic Landmarks. Imaging Technique and Protocols. Expected Postoperative Appearance, Including Grafts and Prosthesis. Clinical Presentations and Imaging Features of Postoperative Complications With Teaching Cases. Conclusions. References.

## **HNEE-62 The radiologist's guide to the Pterygopalatine Fossa**

### **Awards**

#### **Identified for RadioGraphics**

#### **Participants**

Alba Salgado Parente, MD, Madrid, Spain (*Presenter*) Nothing to Disclose

#### **TEACHING POINTS**

1. Review in detail the anatomy and communications of the pterygopalatine fossa (PPF).2. To expose the main keys to recognize and evaluate the perineural extension of tumors.3. To review the main pathologies that can affect this anatomical area.4. To develop a systematic approach to facilitate the evaluation of this space and avoid diagnostic errors.

#### **TABLE OF CONTENTS/OUTLINE**

1. Introduction2. Imaging anatomy, content and communications of the PPF2.1 Where is and what are the boundaries of the PPF?2.2 What does the PPF contain?2.3 Anatomical relationships and communications of the PPF.3. Pathology of the PPF3.1 Perineural extension: Concept, radiological signs and pathology (cavum carcinoma, palatal carcinoma and paranasal sinus carcinoma).3.2 Other pathologies: Direct tumor dissemination, masticatory space sarcomas, nasopharyngeal angiofibroma, invasive fungal disease, schwannomas and inflammatory pseudotumor.4. Pitfalls and how to avoid them: post-surgical changes and mimics5. Systematic approach to PPF: The nerve pathways that must be carefully evaluated depending on the pathology we are facing6. Take Home Points7. Bibliography

## **HNEE-63HC Lessons From Dental School: What the General Radiologist Needs to Know About Teeth**

#### **Participants**

Cameron Spence, MBChB, (*Presenter*) Nothing to Disclose

#### **TEACHING POINTS**

Radiologists who have not attended dental school are at a disadvantage when interpreting OPGs and other oral images such as CT. Whilst radiology curricula include frequently examined pathologies, such as periapical infections and cystic mandibular lesions, limited understanding of the basics of dentistry hamper our interpretation in clinical practice. This pictorial review will highlight the most important background concepts for radiologists that the authors learned during their dental degrees. Understanding these concepts will aid interpretation and help your delegates to provide more useful reports for the extended clinical team and patients.

#### **TABLE OF CONTENTS/OUTLINE**

Relevant radiographic dental anatomy. Restorative dentistry - how to recognize different restorations, including composite/amalgam/temporary fillings, root canal fillings, crowns, bridges, dentures, implants, and orthodontic appliances. Dental caries - where this begins, how it spreads through the dentine to the pulp, and how it leads to periapical pathology. Periodontal disease - generalized and localized types, assessing alveolar bone loss and recognizing commonly overlooked acute periodontal infections. Pericoronitis and impacted wisdom teeth. OPG limitations compared with intraoral dental radiographs. Please visit the Learning Center to also view this presentation in hardcopy format.

## **HNEE-64 Imaging Evaluation of Pulsatile Tinnitus: Case Based Review**

#### **Participants**

Sang Soo Shin, MD, Gwangju, Korea, Republic Of (*Presenter*) Nothing to Disclose

#### **TEACHING POINTS**

1. To review the etiologic causes of pulsatile tinnitus2. To review the imaging role and technique in evaluation of pulsatile tinnitus3. To review the imaging findings and differential diagnosis4. To discuss the endovascular treatment of pulsatile tinnitus

#### **TABLE OF CONTENTS/OUTLINE**

1. Introduction2. Imaging role and technique in evaluation of pulsatile tinnitus3. Imaging findings and differential diagnosis: case based review1) Neoplastic: glomus tympanicum paraganglioma, glomus jugulare paraganglioma, meningioma2) Osseous: otosclerosis, intraosseous hemangioma, Paget's disease3) Arterial: aberrant ICA, persistent stapedia artery, ICA dissection/stenosis4) Venous: high riding jugular bulb, jugular bulb diverticulum, jugular bulb/sigmoid plate dehiscence, transverse sinus stenosis, dilated emissary vein5) Arteriovenous: dural AV fistula, AVM4. Endovascular treatment5. Summary

## **HNEE-65 A review of Uncommon Benign Pathologies of Larynx**

#### **Participants**

Pooja Muddana, MBBS, (*Presenter*) Nothing to Disclose

#### **TEACHING POINTS**

The larynx can be affected by a multitude of pathologies of which squamous cell carcinomas are commonly encountered. Benign pathologies demonstrate typical imaging features, which aid in narrowing the list of differential diagnoses and differentiating them from malignant conditions. In this presentation we will: 1) Review the typical clinical presentation and pathology of the uncommon benign conditions. 2) Review imaging appearance of benign conditions that involve the larynx. 3) Review differential diagnoses for these conditions.

#### **TABLE OF CONTENTS/OUTLINE**

1) Introduction 2) Congenital - Laryngeal clefts, congenital high airway obstruction, laryngomalacia3) Laryngocoele and laryngopyocoele4) Infective conditions- Tuberculosis, Actinomycosis, Fungal infections, Scleroma, Leprosy5) Immunological conditions - Granulomatous with polyangiitis, Relapsing polychondritis, Sarcoidosis, Rheumatoid arthritis, Ankylosing spondylitis 6) Amyloidosis 7) Thyroglossal duct cyst 8) Vascular malformations- Lymphatic malformation, Arteriovenous malformations 9) Conclusion

## **HNEE-66 New Pathways: Postoperative Changes in Aerodigestive Tract After Neck Surgery**

Participants

Naomi Murakami SR, MBBS, Niteroi, Brazil (*Presenter*) Nothing to Disclose

#### **TEACHING POINTS**

Review normal neck anatomy in order to identify surgical manipulations. Recognize the anatomic changes that are associated with aerodigestive tract surgery. Discuss important complications of these procedures.

#### **TABLE OF CONTENTS/OUTLINE**

Different types of devices are used in surgery for neck injuries and diseases. They can be either parts of organs, such as neoesophagus with colon, or medical devices, such as metallic prosthesis. It's important to identify correctly these neck changes and complications that may be associated. This pictorial review will discuss. 1. Neck anatomy review. 2. The role of different imaging techniques in evaluation of medical devices, anatomic changes and complications: a. Computed tomography b. Magnetic resonance imaging c. Esophagogram 3. Surgical techniques and anatomic changes: Esophagectomy: gastric tube and colon interposition Prosthesis in upper airway Esophageal prosthesis Tracheoesophageal phonation prosthesis 4. Complications: Collection/ abscess Fistulas: tracheoesophageal, esophagocutaneous, pharyngocutaneous Necrosis

### **HNEE-67 The Face of Beauty: Image Features and Complications of Facial Cosmetics Procedures**

#### **Awards**

#### **Identified for RadioGraphics**

Participants

Beatriz Prado, MD, Sao Paulo, Brazil (*Presenter*) Nothing to Disclose

#### **TEACHING POINTS**

Review the anatomy of facial fat compartments To discuss and illustrate, through clinical cases, the imaging aspects expected after a facial aesthetic procedure, as well some relevant complications and common diagnostic pitfalls.

#### **TABLE OF CONTENTS/OUTLINE**

Anatomy of fat compartments Contribution of different non-invasive imaging methods to detect facial cosmetic material Types of cosmetic procedures Facial Implants Fillers: Fat filler, hyaluronic acid, polymethylmethacrylate, calcium hydroxyapatite, paraffin, silicone Thread-Lifting Blepharoplasty Bichectomy Complications of facial filler injections and role of imaging Hematoma and seroma formation Infections Migration of injected substances Asymmetries Formation of foreign body granuloma Vascular occlusion leading to skin necrosis or blindness Inadvertent injury to adjacent structures Pitfalls in image interpretations

### **HNEE-7 Vocal Cord Paralysis: A Practical Approach**

Participants

Thiago Martins Fernandes Vilela, Mogi das Cruzes, Brazil (*Presenter*) Nothing to Disclose

#### **TEACHING POINTS**

-- To review the normal anatomy of vagal and recurrent laryngeal nerves and the larynx.-- To illustrate the specific and secondary imaging features found in vocal cord paralysis and its mimics and pitfalls.-- To develop an analysis roadmap that should be performed when faced with a vocal cord paralysis.-- Illustrated review of a series of cases of vocal cord paralysis and lesions that may possibly be related to vocal cord paralysis.-- To demonstrate the treatments that can be performed in these cases, their imaging aspects and possible complications.

#### **TABLE OF CONTENTS/OUTLINE**

-- Introduction-- Epidemiology-- Clinical scenarios-- Anatomy- Vagus nerves and their nuclei- Recurrent laryngeal nerves- Larynx-- Typical and secondary imaging features-- Pitfalls and mimics-- Analysis roadmap-- Series of cases of vocal cord paralysis-- Treatments and their image appearance-- Conclusion

### **HNEE-8 Fungal Infections of the Head and Neck: Imaging Spectrum**

Participants

Niels Vinicius Padua Carvalho, MD, Sao Paulo, Brazil (*Presenter*) Nothing to Disclose

#### **TEACHING POINTS**

1. The aim of this exhibition is to: 2. Review the spectrum of fungal infections of the head and neck. 3. Discuss the main findings across all imaging techniques, overall CT and MRI. 4. Unify all these conditions in a single article/presentation. 5. Highlight the importance of imaging in the diagnosis and treatment process.

#### **TABLE OF CONTENTS/OUTLINE**

1. INTRODUCTION a. Considerations on fungal infections and its prevalence and relevance affecting head and neck structures. 2. IMAGING INTERPRETATION a. Imaging techniques and findings. b. When to do imaging screening, control and surveillance for these diseases. 3. INTERACTIVE CASE-BASED DIDACTICS a. Sample cases to illustrate and solidify the concepts about the main findings of these diseases, separated through head and neck spaces: i. Temporal bones ii. Pharynx iii. Larynx iv. Orbit v. Sinuses 4. FURTHER DIRECTIONS AND TAKE HOME MESSAGES

Printed on: 02/07/23



## Abstract Archives of the RSNA, 2022

HNEE-1

### A Blurry Confusion-Optic Neuropathy Etiologies And Imaging

Sunday, Nov. 27 8:00AM - 9:00AM Room: Learning Center - HN

#### Awards

Certificate of Merit

#### Participants

Luis Souza, MD, (*Presenter*) Nothing to Disclose

#### TEACHING POINTS

Optic neuropathy is a broad definition that encompasses a myriad of different diagnoses. Objectives: Understand what is expected from the radiologist when faced with this difficult group of diseases, which the imaging findings can be subtle and often missed. To illustrate the most common imaging findings of optic neuropathy. To show the useful imaging hallmarks that help differentiate active disease from sequela changes and differential diagnosis.

#### TABLE OF CONTENTS/OUTLINE

Imaging investigation protocol: optic neuropathy standard imaging protocol and useful additional MRI sequences that can help in the diagnosis. General and common imaging findings in optic neuropathy. Differentiating active disease and sequelae? Main imaging characteristics and differential diagnosis of the different etiologies.- Inflammatory / Infectious (Viral, Bacterial, Other).- Inflammatory / Autoimmune. (Demyelinating - NMOSD, MS, Anti-MOG+, Paraneoplastic - and Non-Demyelinating).- Ischemic (anterior and posterior ischemic neuropathy).- Toxic-metabolic.- Compressive.- Infiltrative.- Traumatic. Take-home messages and tips and tricks to differential diagnosis.

Printed on: 02/07/23



## Abstract Archives of the RSNA, 2022

HNEE-10

### Perimarginal Nodes - An Underestimated Site for Metastatic Squamous Cell Oral Cancer: A CT Pictorial Review

Sunday, Nov. 27 8:00AM - 9:00AM Room: Learning Center - HN

#### Awards

Certificate of Merit

#### Participants

Erik Radin, MD, Trieste, Italy (*Presenter*) Nothing to Disclose

#### TEACHING POINTS

(1) Definition of perimarginal nodes (PMN). (2) To explain the clinical relevance of the PMN. (3) To illustrate the spatial identification of PMN on CT imaging.

#### TABLE OF CONTENTS/OUTLINE

Head and neck squamous cell cancer is notoriously affected by an elevated risk for metastatic nodal disease, one of the most important prognostic factors. Nodal status represents one of the fundamental parameters of the TNM staging system; it is also essential for the therapeutical approach, with elective neck dissection as the leading treatment. Perimarginal nodes (PMN) are often considered as facial rather than cervical lymph nodes, even though they could be regarded as a submandibular nodal subgroup (level IB). They lie close to the marginal mandibular nerve (MMN), within a clinically defined distance cut-off of 1 to 2 cm from the mandibular border. CECT imaging has high accuracy for PMN identification and allows to divide them into four different sites, depending on their relationship with the anterior facial vein (AFV) and the submandibular gland: preglandular, prevascular, retrovascular, and retroglandular nodes. Perimarginal nodes could represent a miscalculated site for occult metastases in head and neck cancers, especially those located in oral cavity. Unintentionally, small perimarginal nodes could be left in the surgical site in order to protect the MMN during neck dissection through the Hayes Martin maneuver; this would affect the patient's prognosis, precluding a complete therapeutic response, with an increased risk of disease relapse.

Printed on: 02/07/23



## Abstract Archives of the RSNA, 2022

HNEE-11

### Facial Ultrasound Anatomy of the Aging Skin and the Growing Role of the Radiologist in the Aesthetic Medicine Field

Sunday, Nov. 27 8:00AM - 9:00AM Room: Learning Center - HN

#### Participants

Slavina Mancheva, MD, MD, (*Presenter*) Nothing to Disclose

#### TEACHING POINTS

To evaluate the normal facial anatomy. Causes of normal aging visible and quantified by imaging studies. To evaluate pre, during and post-treatment status of beauty treatments using autologous and FDA authorized dermal fillers. The use of ultrasound to guide dermal filler injections. To identify facial danger zones.

#### TABLE OF CONTENTS/OUTLINE

1. Facial anatomy depiction. Nowadays there is continuous growth of the aesthetic facial treatments using fillers and neurotoxins. In order to prevent complications it is very important to analyze the area of interest using ultrasound- being a safe and handy technique. 2. Aging of upper, mid and lower face. In this exhibit a couple of patients in their mid 20s, mid 30s and late 60s are analyzed using ultrasound. Some patients are followed pre and post treatment sessions in order to identify the causes of their individual aging and also offer them follow up of their treatment. 3. The difficult case and the role of the radiologist in a multidisciplinary aesthetic medicine team. Many patients have been using different type filler treatments and some appear with different and unknown secondary effects. The radiologist must identify the relevant variation anatomy, possible iatrogenic effects and help during invasive treatments. 4. The facial danger zones. Identify the major danger zones where the practitioner must be very careful and decide what options of treatments must be offered in a safe manner.

Printed on: 02/07/23



## Abstract Archives of the RSNA, 2022

HNEE-12

### A Joint Affair: Radiologic Findings of TMJ Anatomy and Pathology

Sunday, Nov. 27 8:00AM - 9:00AM Room: Learning Center - HN

#### Awards

Certificate of Merit

#### Participants

Samantha Platt, MD, New York, NY (*Presenter*) Nothing to Disclose

#### TEACHING POINTS

1. Review TMJ anatomy and variation with function through radiologic and medical illustration. 2. Review Wilke's criteria and relevant findings for internal derangement including disc displacement with or without reduction, disc morphology, joint effusion and bony changes such as sclerosis and subcortical cysts. 3. Demonstrate imaging findings associated with the diverse spectrum of TMJ disorders through varied modalities. 4. Describe features of TMJ disorders that are helpful to include in report for general radiologists and neuroradiologists.

#### TABLE OF CONTENTS/OUTLINE

Temporomandibular joint (TMJ) disorders exhibit variable radiographic presentation. Many causes of extra-articular pain (i.e. muscle fatigue, fibromyalgia) do not have imaging findings. The best modalities to evaluate the TMJ include MRI and CT and should be chosen based on clinical symptoms and the anticipated pathology. We have curated images from various modalities for TMJ pathologies: osteoarthritis, mandibular hypoplasia, bifid mandibular condyle, hemicranimegaly, infectious synovitis, osteomyelitis, malignant otitis externa, osteonecrosis, rheumatoid arthritis, ankylosing spondylitis, chondromatosis, giant cell granuloma, squamous cell carcinoma, metastatic disease, nasopharyngeal carcinoma, mandibular fractures, pseudoarthrosis, myositis ossificans, ankylosis, osteoradionecrosis, and surgical implants. Additionally, we have curated MR views that exemplify the pathology seen in each of Wilke's classification for internal derangement along with pictorial representation. Imaging is crucial to noninvasive assessment of the TMJ and subsequent management plans.

Printed on: 02/07/23



## Abstract Archives of the RSNA, 2022

HNEE-13

### Don't Wait Till Neck Time: Learn the "Spatial" Way to Master Neck Anatomy on Ultrasound Now

Sunday, Nov. 27 8:00AM - 9:00AM Room: Learning Center - HN

#### Participants

Paran Davari, MD, (*Presenter*) Nothing to Disclose

#### TEACHING POINTS

1. Describe the concept of spaces of the neck and highlight spaces that can be evaluated on ultrasound. 2. Provide a sonographic atlas for the spaces using multimodality comparison to better understand spatial relationships. 3. Learn contents of each space to help guide a space specific differential diagnosis. 4. Overall increase familiarity with anatomic structures that might often be ignored while interpreting a neck ultrasound obtained for frequent indications such as thyroid gland, cervical lymph node or carotid evaluation, as well as increased knowledge of relevant anatomy for less frequent indications such as parotid or submandibular gland evaluation. 5. Provide examples of clinical applications of this anatomic knowledge on ultrasound for diagnostic and potentially procedural purposes.

#### TABLE OF CONTENTS/OUTLINE

1. Learning objectives 2. Introduction to neck anatomy on ultrasound: current practices 3. Introduction to spaces of the neck 4. Describe sonographically visualized spaces of neck, content and clinical considerations A. Superficial space of neck B. Deep neck spaces limited to suprahyoid neck: i. Parotid space ii. Submandibular space iii. Floor of mouth or sublingual space iv. Masticator space C. Deep neck spaces limited to infrahyoid neck: i. Visceral space ii. Anterior cervical space iii. Posterior cervical space D. Deep neck spaces spanning entire neck: i. Carotid space ii. Perivertebral space

Printed on: 02/07/23



## Abstract Archives of the RSNA, 2022

HNEE-14

### Practical Applications of the Permeability Study in Head and Neck Imaging

Sunday, Nov. 27 8:00AM - 9:00AM Room: Learning Center - HN

#### Participants

Beatriz Prado, MD, Sao Paulo, Brazil (*Presenter*) Nothing to Disclose

#### TEACHING POINTS

Permeability imaging or quantitative DCE-MRI is a functional MRI modality that involves repeated acquisition of images of the same lesion and analyses of the Time-signal intensity curves (TICs) of the tumor and feeding artery to yield various parameters related to perfusion and permeability within the tumor. It has been reported to be useful in the differentiation of head and neck tumors, most commonly of the parotid gland, as well as tumors in other organs. This panel aims to: Define what is the permeability study  
Review of the technique Cite the main clinical indications for permeability study in head and neck imaging  
Illustrate through clinical cases the applications of perfusion permeability imaging in head and neck

#### TABLE OF CONTENTS/OUTLINE

Salivary gland tumors (i.e.: pleomorphic adenoma, Warthin's tumor and carcinoma) Distinction of benign versus malignant tumor (i.e.: lymphoma, spinocellular carcinoma, paraganglioma and schwannoma) Histologic differentiation among lesions, in combination with DWI and conventional T1 and T2 imaging (i.e.: pleomorphic adenoma, Warthin's tumor, lymphoma, paraganglioma)  
Differentiation of recurrent tumor versus post-therapeutic changes  
Prediction of response to radiotherapy and chemotherapy  
Biopsy guidance  
Metastatic cervical lymph nodes

Printed on: 02/07/23



## Abstract Archives of the RSNA, 2022

HNEE-15

### One Nerve is Just Right, Two is Too Many, Three is Not Enough - Unraveling the Trigeminal Nerve and It's Alterations

Sunday, Nov. 27 8:00AM - 9:00AM Room: Learning Center - HN

#### Participants

Fernanda Guedes, MD, (*Presenter*) Nothing to Disclose

#### TEACHING POINTS

-Review the anatomy of the trigeminal nerve from its sensory and motor nucleus, the branches and peripheral segments.-Review the most common trigeminal nerve diseases in each segment and their radiological findings.-Learn more about some important differential diagnoses for each nerve segment.

#### TABLE OF CONTENTS/OUTLINE

1. Simplify trigeminal nerve anatomy, the largest of the twelve pairs of cranial nerves, and its segments (intraaxial, cisternal, Meckel's cave/cavernous sinus and peripheral). 2. Describe the relationship between trigeminal nerve segments and adjacent anatomical structures like skull base foramina, cavernous sinus, infraorbital canal and pterygopalatine fossa. 3. Summarize the different diseases that affect each trigeminal nerve segment, from the most common injuries, such as neurovascular conflicts, to the rarer pure motor neuropathy, highlighting some pathologies like: - Hypoplasia; - Herpes Zoster; - Trigeminal nerve schwannoma; - Meningioma; - Demyelinating disorders; - IgG4 related disease; - Lymphoproliferative disease; - Dermoid cyst; - Perineural facial tumor spread; - Post surgical trigeminal alterations; - Leptomeningeal carcinomatosis; - Neurosyphilis.

Printed on: 02/07/23



## Abstract Archives of the RSNA, 2022

HNEE-16

### Post-treatment Head and Neck Cancer Imaging: Anatomical Considerations Based on Cancer Subsites

Sunday, Nov. 27 8:00AM - 9:00AM Room: Learning Center - HN

#### Awards

Identified for RadioGraphics

Magna Cum Laude

#### Participants

Takashi Hiyama, MD, PhD, Kashiwa, Japan (*Presenter*) Nothing to Disclose

#### TEACHING POINTS

Recurrence of head and neck cancer occurs in approximately 10-20% of patients with early stage cancer, and 50-60% of those with advanced cancer. Detecting recurrent tumors at a treatable stage contributes to improved prognosis. The interpretation of follow-up images should be considered separately for each subsite as head and neck cancers can arise at various anatomical subsites. For each subsite, knowledge of normal imaging changes after surgery or chemoradiotherapy and patterns that are prone to recurrence are essential for detecting recurrence. When a lesion is detected, a differential diagnosis of recurrence, posttreatment changes, or other pathologies may be required. NIRADS is a useful tool for these evaluations. In addition, radiologists should assess the extent of recurrent tumors to select optimal salvage treatment. The purposes of this exhibit are: 1) To discuss normal post-treatment imaging at each subsite 2) To discuss the imaging findings of early local recurrence at each subsite, and neck recurrence 3) To discuss how to assess recurrence to allow subsequent optimal treatment

#### TABLE OF CONTENTS/OUTLINE

1. Introduction 2. Overview Epidemiology of head and neck cancer recurrence Roles of CT/MRI and PET/CT in follow-up NIRADS 3. Case illustrations Imaging findings of post-treatment change and recurrence: Oral cavity, Nasopharynx, Oropharynx, Hypopharynx, Sinonasal cavity, Larynx, Neck Imaging evaluation of recurrent tumor extension for salvage treatment 4. Summary 5. Conclusion

Printed on: 02/07/23



## Abstract Archives of the RSNA, 2022

HNEE-17

### Shedding Light On Lymphoproliferative Disorders: Extranodal and Nodal Lesions of the Head and Neck

Sunday, Nov. 27 8:00AM - 9:00AM Room: Learning Center - HN

#### Participants

Thayssa Leite, Sao Paulo, Brazil (*Presenter*) Nothing to Disclose

#### TEACHING POINTS

Teaching points: The purpose of this exhibit is: To identify the most common anatomic locations of lymphoproliferative disorders of the head and neck. To review the main imaging modalities, such as ultrasound (US), computed tomography (CT), magnetic resonance imaging (MRI), including functional methods (DCE imaging). To describe the radiological patterns and propose differential diagnosis of lesions including congenital anomalies, neoplasms, vascular, inflammatory or infectious diseases. To suggest practical tips and discuss common pitfalls of lymphoproliferative disorders of the head and neck, emphasizing the utility of a systematic approach for accurate evaluation.

#### TABLE OF CONTENTS/OUTLINE

Table of contents: Introduction. Anatomy. Imaging modalities. Differential diagnoses and clues to diagnosis. Practical tips and Pitfalls. Conclusion/ Take home message.

Printed on: 02/07/23



## Abstract Archives of the RSNA, 2022

HNEE-18

### Multimodality Imaging of The Lacrimal Drainage System

Sunday, Nov. 27 8:00AM - 9:00AM Room: Learning Center - HN

#### Awards

Certificate of Merit

#### Participants

Viviana Loureiro, MD, (*Presenter*) Nothing to Disclose

#### TEACHING POINTS

To recognize the anatomy of the lacrimal drainage system. To understand the indications and technique of multiple imaging modalities for evaluation of the lacrimal drainage apparatus, as well as the advantages and drawbacks of each modality. To review the spectrum of imaging findings of various diseases that affect the lacrimal drainage system on multiple modalities.

#### TABLE OF CONTENTS/OUTLINE

- Introduction- Anatomy- Multimodality Imaging Technique- Congenital and Developmental Lesions- Inflammatory and Infectious Diseases- Traumatic Lesions- Neoplasms- Nasolacrimal Drainage System Surgery- Pearls and Pitfalls- Conclusion

Printed on: 02/07/23



## Abstract Archives of the RSNA, 2022

HNEE-19

### Facial Pain: Classification, Clinical Features, and Imaging Findings

Sunday, Nov. 27 8:00AM - 9:00AM Room: Learning Center - HN

#### Awards

Certificate of Merit

#### Participants

Rodrigo De Azevedo, MD, Santo Andre, Brazil (*Presenter*) Nothing to Disclose

#### TEACHING POINTS

To understand the classification, pathophysiology, and clinical features of facial pain. To review the role of imaging in the assessment of facial pain, including imaging techniques and protocols. To review the spectrum of imaging findings in multiple causes of facial pain.

#### TABLE OF CONTENTS/OUTLINE

- Introduction - Relevant Anatomy - Classification and etiology of facial pain: nociceptive, neuropathic (neuralgia and painful neuropathy), trigeminal autonomic cephalalgias, and other causes. - Imaging Technique and Protocol (CT, conventional MRI, MRI angiography, and MRI neurography) - Imaging of Trigeminal Neuralgia - Imaging of Glossopharyngeal Neuralgia - Imaging of Painful Cranial Neuropathies - Other Causes of Facial Pain - Imaging after Ablative and Surgical Treatment of Cranial Neuralgia - Conclusions - References

Printed on: 02/07/23



## Abstract Archives of the RSNA, 2022

HNEE-2

### Neuroendocrine Neoplasms of Head and Neck: Spectrum

Sunday, Nov. 27 8:00AM - 9:00AM Room: Learning Center - HN

#### Participants

Shreya Shukla, MBBS, Mumbai, India (*Presenter*) Nothing to Disclose

#### TEACHING POINTS

The spectrum of neuroendocrine neoplasms (NENs) of the head and neck varies from benign neoplasms which may require just observation to poorly differentiated malignant neoplasms that may require multimodality treatment or palliative care. According to the fifth edition Classification of by the World Health Organization (WHO) International Agency for Research on Cancer (IARC) consensus meeting held in Lyon on 2-3 November 2017, NENs can be of epithelial or non-epithelial origin. Epithelial variety can range from well-differentiated NENs known to occur in small intestine, ovary etc to poorly-differentiated neuroendocrine carcinoma NECs (lung, colon). These tumors may be functional or non-functional. Nuclear imaging has an important role.

#### TABLE OF CONTENTS/OUTLINE

This educational exhibit contains: • Review of classification of neuroendocrine neoplasms (NENs) • Enlists the common site of occurrence of NENs in the head and neck. • Review of the imaging appearance of these neoplasms at various sub-sites. • Briefly reviews the management of these neoplasms.

Printed on: 02/07/23



## Abstract Archives of the RSNA, 2022

HNEE-20

### Novel Imaging Techniques in the Management of Thyroid Nodules and Diffuse Thyroid Disease

Sunday, Nov. 27 8:00AM - 9:00AM Room: Learning Center - HN

#### Participants

Thiago Jose Pinheiro Lopes, MD, Sao Paulo, Brazil (*Presenter*) Nothing to Disclose

#### TEACHING POINTS

1) The gold standard of thyroid nodules diagnostics is conventional ultrasonography followed by fine-needle aspiration biopsy of qualified lesions, an invasive procedure related to inconclusive cytological results in up to 10-25% patients. 2) There is a need to search for novel imaging procedures or markers, that would allow a non-invasive estimation of malignancy risk with satisfying sensitivity and specificity. 3) Our purpose is to review imaging innovative applications in the management of thyroid nodules and diffuse thyroid disease, with focus in shear wave elastography (SWE) and contrast-enhanced ultrasonography (CEUS).

#### TABLE OF CONTENTS/OUTLINE

1) Introduction 2) Conventional Techniques: B-mode and Doppler 3) Novel imaging techniques 3.1) Elastography (SWE) 3.2) CEUS 3.3) Next-generation molecular imaging 4) Radiological-pathological correlations 4.1) Thyroid nodules 4.2) Autoimmune thyroid disease 5) Challenges, pearls and pitfalls 5.1) Detecting extra-thyroid extension 5.2) Assessing lymph node metastases 5.3) Thyroid nodules in pediatric population 6) Future directions 6.1) Novel biochemical and genetic markers 6.2) Artificial intelligence (radiomics) 7) Take home messages

Printed on: 02/07/23



## Abstract Archives of the RSNA, 2022

HNEE-21

### Imaging of Head and Neck Vascular Anomalies (Tumors and Malformations)

Sunday, Nov. 27 8:00AM - 9:00AM Room: Learning Center - HN

#### Participants

Augusto B. Antunes, MD, MSc, Nova Lima, Brazil (*Presenter*) Nothing to Disclose

#### TEACHING POINTS

Vascular tumors and vascular malformations are commonly found in the head and neck region and have distinctive features. Radiologists should be aware of their presentation features and clinical history to establish the correct diagnosis and provide appropriate care. Imaging allows for high spatial and temporal resolutions and is essential for the correct diagnosis of these pathologies, but also for assessing the extension and anatomical relationships, as well as for studying blood flow patterns. We will highlight proliferating vascular tumors and vascular malformations, often misdiagnosed due to confusing definitions and classifications. After completing this reading, participants will be able to comprehend and to recognize specific features for various such anomalies, including infantile hemangioma, congenital hemangioma, lymphatic, venous, arteriovenous and capillary malformations, and combined anomalies.

#### TABLE OF CONTENTS/OUTLINE

Classification, clinical presentation, and evolutionary history of the most common vascular anomalies of the head and neck. Case-based review illustrating the findings of vascular tumors and vascular malformations on different imaging modalities  
Take-home messages  
References

Printed on: 02/07/23



## Abstract Archives of the RSNA, 2022

HNEE-22

### Differential Diagnosis Between Chondrosarcoma and Synovial Chondromatosis of the Temporomandibular Joint Using CT and MRI

Sunday, Nov. 27 8:00AM - 9:00AM Room: Learning Center - HN

#### Participants

Kyung-Hoe Huh, PhD, DDS, (Presenter) Nothing to Disclose

#### TEACHING POINTS

Chondrosarcoma and synovial chondromatosis are a representative tumor or tumor-like arthropathy of the temporomandibular joint, producing cartilaginous calcification within the mass and causing bone changes of the mandibular condyle and/or articular eminence/glenoid fossa. Imaging differentiation between chondrosarcoma and synovial chondromatosis of the TMJ is very important, because they share clinical and histopathological features. CT and MR imaging features such as lesion epicenter of the mandibular condyle, infiltration into the tendon of the lateral pterygoid muscle, destruction of the mandibular condyle, no destruction/sclerosis of the articular eminence/glenoid fossa, calcification pattern (absence or stippled), periosteal reaction, and internal enhancement can be an effective tool to differentiate between chondrosarcoma and synovial chondromatosis. The single imaging feature with the highest performance for differential diagnosis is infiltration into the tendon of the lateral pterygoid muscle. With combination of the several imaging features, the diagnostic performance can be improved.

#### TABLE OF CONTENTS/OUTLINE

1. Introduction 2. Anatomy of the temporomandibular joint a. comparison of lesion epicenter b. infiltration of the tendon of the lateral pterygoid muscle 3. Imaging parameters of the TMJ on CT and MR image 4. Imaging features of chondrosarcoma 5. Imaging features of synovial chondromatosis 6. Differentiation between chondrosarcoma and synovial chondromatosis 7. Conclusion

Printed on: 02/07/23



## Abstract Archives of the RSNA, 2022

HNEE-23

### SMARCB1-Deficient Sinonasal Cancer- Imaging Features of An Emerging Entity

Sunday, Nov. 27 8:00AM - 9:00AM Room: Learning Center - HN

#### Participants

Renuka Ashtekar, MBBS, MD, Mumbai, India (*Presenter*) Nothing to Disclose

#### TEACHING POINTS

1. Enumerate the various subtypes of sinonasal malignancies.2. Describe CT and MR imaging features of SMARCB1-deficient sinonasal cancer (SdSNC).3. Distinguishing SdSNC from other close imaging differentials.

#### TABLE OF CONTENTS/OUTLINE

1. Introduction to sinonasal malignancies and their various subtypes.2. What is SMARCB-1 and how are these tumors diagnosed?3. Imaging characteristics of SdSNC on CT and MRI.4. Common differential diagnoses and their imaging features.5. Case-based review of uncommon presentations of SdSNC.

Printed on: 02/07/23



## Abstract Archives of the RSNA, 2022

HNEE-24

### The Hidden Windows Between the Neck Spaces

Sunday, Nov. 27 8:00AM - 9:00AM Room: Learning Center - HN

#### Participants

Daniel Sebastian Chaves Burbano, MD, (*Presenter*) Nothing to Disclose

#### TEACHING POINTS

- To identify the limits, content and communication between the neck spaces, it is useful the understanding that some of them are virtual spaces.- The cervical fasciae are non-continuous connective tissue structures that surround the muscles, nerves, and vessels of the neck and establish the spaces in the neck. Its functions are to be a barrier and reduce friction between structures. These are two: superficial cervical fasciae and deep cervical fasciae.- Some of the neck spaces have no boundaries between them, so they are connected to each other. Identifying the communication between them is an important step approaching the images.- The communication between the spaces of the neck is not only between them, but also with the base of the skull, thorax and the back, and they are not usually easy to find. They can be a route of dissemination of pathologies.

#### TABLE OF CONTENTS/OUTLINE

- Gross anatomy- Superficial cervical fascia- Deep cervical fascia- Suprahyoid deep neck spaces- Infrahyoid deep neck spaces- Supra and infrahyoid deep neck spaces- The windows between the neck spaces- Conclusions

Printed on: 02/07/23



## Abstract Archives of the RSNA, 2022

HNEE-25HC

### Virtual Reality Module Reinforcing Cranial Nerve Deficits with Physical Examination

Sunday, Nov. 27 8:00AM - 9:00AM Room: Learning Center - HN

#### Participants

Christopher Lack, MD, PhD, (*Presenter*) Consultant, PhenoMx, Inc

#### TEACHING POINTS

The relationship between cranial nerve anatomy, function, pathology and physical examination findings requires a deep understanding of multiple domains. Virtual reality has the potential to be a powerful tool in teaching, reinforcing concepts that are not well represented by textbooks. Using our interactive 3D model, the learner can easily examine the important anatomic structures and be exposed to many pathologic states without the need for multiple unique patient encounters. This module could easily be used around the world if the end-user has an appropriate VR headset.

#### TABLE OF CONTENTS/OUTLINE

Using MRI and CT data, we developed an interactive high-fidelity 3D model, in a virtual environment, that highlights the anatomy of the orbits and cranial nerves II, III, IV, VI. The user can view and interact with the anatomic structures using a VR headset and perform an exam of the extraocular muscles. Using the "Quiz-mode" users will be tested on an unknown cranial nerve deficit and will have to identify the deficit based on an actual physical exam in the virtual environment. The module can be seen both in 3D by wearing the VR goggles but also in 2D on the attached laptop screen. Since the power of 3D and physical exam is best demonstrated using the VR headset, please come to the exhibit to experience the headset demo. Please visit the Learning Center to also view this presentation in hardcopy format.

Printed on: 02/07/23

## Abstract Archives of the RSNA, 2022

HNEE-26

### Advanced Imaging Biomarkers in Head and Neck Cancer: Precision Diagnosis, Gene Mutation Detection, and Treatment Response Assessment and Prediction

Sunday, Nov. 27 8:00AM - 9:00AM Room: Learning Center - HN

#### Participants

Yoshiaki Ota, MD, Ann Arbor, MI (*Presenter*) Nothing to Disclose

#### TEACHING POINTS

Teaching point1. To review physics of DWI, CT perfusion, MR spectroscopy, dynamic susceptibility contrast perfusion MRI (DSC-MRI), and dynamic contrast-enhanced MRI (DCE-MRI)2. To demonstrate head and neck tumors and application of advanced imaging for tumor differentiation, gene mutation detection, and assessment of treatment effect3. To demonstrate pitfalls of advanced imaging

#### TABLE OF CONTENTS/OUTLINE

Outline1. Physics and clinical application- DWI: Assessment of cellularity, cytotoxic/vasogenic edema- CT perfusion: Assessment of vascular space of the lesions- MR spectroscopy: Detection and quantification of abnormal metabolites related to gene mutation- DSC-MRI: Assessment of vascularity, permeability, and hemodynamic pattern (First pass)- DCE-MRI: Assessment of vascularity, permeability, and hemodynamic pattern 2. Head and neck tumors- Infratentorial extra-axial tumorsa. Common tumors/meningiomas, schwannomas, paragangliomasb. Atypical/metastasis, chordoma, chondrosarcoma, endolymphatic sac tumor- Tumors in the head and neck mucosal surface- Tumors in the head and neck deep tissues 3. Clinical and academic application of DWI, CT perfusion, DSC-MRI, and DCE-MRI- Tumor differentiation- Detection of tumor mutation- Assessment of treatment effect- Post-operative risk assessment 4. Pitfalls of applications of DWI, DSC-MRI and DCE-MRI- DWI: Geographic artifact - CT perfusion: Motion artifacts, severe beam-hardening- DSC-MRI: Susceptibility artifacts at tissue interfaces or skull base area- DCE-MRI: Different magnetic field (1.5T or 3T) and parameters (such as TE, TR, or temporal resolution) in DCE-MRI can affect quantitative parameters (Vp, Ve, Ktrans, and Kep).

Printed on: 02/07/23



## Abstract Archives of the RSNA, 2022

HNEE-27

### Don't Let Your Mouth Water - Everything You Need to Know About the Parotid Glands

Sunday, Nov. 27 8:00AM - 9:00AM Room: Learning Center - HN

#### Awards

Certificate of Merit

#### Participants

Marcio Ricardo Garcia, MD, Sao Paulo, Brazil (*Presenter*) Nothing to Disclose

#### TEACHING POINTS

1. To review the anatomy of the parotid gland and adjacent anatomical structures. 2. To review the most common parotid gland diseases and their radiological findings. 3. To learn more about some important differential diagnoses.

#### TABLE OF CONTENTS/OUTLINE

1. Simplifying the anatomy of the parotid gland and adjacent anatomical structures (temporomandibular joint, external auditory canal and masticator space). 2. Summarize the main key points of some different diseases that affect the parotid gland with a focus on computed tomography and magnetic resonance findings, highlighting some pathologies like: developmental variations, first branquial cleft cyst, lymphatic venous malformation, lipoma, dermoid cyst, acute parotitis, abscess, chronic parotitis, necrotizing otitis externa with parotid extension, Sjögren syndrome, IgG4-related disease, intraparotid facial neuropathy and perineural spread, lithiasis, iatrogenic injury of the Stensen duct after bichectomy, Warthin tumor, pleomorphic adenoma, oncocytoma, mucoepidermoid carcinoma, lymphoma and metastasis. 3. Elaboration of a flowchart to help in the analysis of focal lesions of the parotid gland, including analysis of diffusion and permeability. 4. Conclusion.

Printed on: 02/07/23



## Abstract Archives of the RSNA, 2022

HNEE-28

### A Head Turner: Diffusion Restricting Head and Neck Lesions

Sunday, Nov. 27 8:00AM - 9:00AM Room: Learning Center - HN

#### Participants

Yasasvi Tadavarthi, MD, (*Presenter*) Nothing to Disclose

#### TEACHING POINTS

Diffusion-weighted imaging has been shown promising in tissue characterization of primary tumors (benign and malignant), nodal metastases, differentiation of recurrent tumor from post therapeutic changes, monitoring treatment response, and many other clinical scenarios in head and neck. In this presentation we will discuss different aspects of using diffusion weighted imaging in head and neck and their added value over anatomic imaging.

#### TABLE OF CONTENTS/OUTLINE

1. Brief review of diffusion weighted imaging technique and its use in head and neck imaging.2. Review imaging features of different pathologic conditions seen in the head and neck demonstrating diffusion restriction including:a. Benign neoplasms - Warthin tumor. b. Malignant neoplasms - Lymphoma, Carcinomas (Squamous cell carcinoma and Adenocarcinoma), Rhabdomyosarcoma. c. Infectious and inflammatory lesions - Abscess, Pseudotumor. d. Miscellaneous lesions- Hematoma, Cholesteatoma, Epidermoid cyst, Lymphadenopathy3. Challenges and limitations of diffusion weighted imaging in the head and neck.4. Mimics and special circumstances - Artifacts, Monitoring treatment response

Printed on: 02/07/23



## Abstract Archives of the RSNA, 2022

HNEE-29

### The Sound of Silence: Clinical and Imaging Aspects of Sudden Hearing Loss

Sunday, Nov. 27 8:00AM - 9:00AM Room: Learning Center - HN

#### Participants

Stephanie Nagano, MD, Sao Paulo, Brazil (*Presenter*) Nothing to Disclose

#### TEACHING POINTS

Sudden hearing loss occurs within a 72-hour period. It is essential to define whether the hearing loss is conductive, sensorineural or mixed to guide the investigation. Sudden sensorineural hearing loss is a clinical emergency and must be evaluated quickly to decrease the chances of becoming permanent. The diagnosis is predominantly clinical and imaging tests can provide additional information regarding the etiology. In cases of conductive deafness, the best method is computed tomography and in sensorineural deafness, resonance. Both methods can be used in cases of mixed deafness and surgical planning. Systematic analysis by topography can be useful to identify causes of sudden neurosensory deafness. It is recommended to start the evaluation with retrocochlear causes such as brain lesions, cerebellopontine angle and internal auditory canal, moving on to vestibular and cochlear causes.

#### TABLE OF CONTENTS/OUTLINE

Definition and clinical aspects of sudden hearing loss: how to define neurosensorial, conductive or mixed? Imaging methods and pertinent ear anatomy in sudden deafness. Sudden conductive hearing loss examples. Neurosensorial hearing loss examples. Systematic clinical and imaging evaluation in sudden hearing loss: summing up.

Printed on: 02/07/23



## Abstract Archives of the RSNA, 2022

HNEE-3

### Show some nerve! - Neurography in Head and Neck

Sunday, Nov. 27 8:00AM - 9:00AM Room: Learning Center - HN

#### Awards

Certificate of Merit

#### Participants

Samya Alves, MD, Sao Paulo, Brazil (*Presenter*) Nothing to Disclose

#### TEACHING POINTS

- Review anatomy and imaging aspects of cranial nerves and their branches.- Discuss specific sequences for nerve evaluation (PSIF, DESS, 3D SPACE).- List the main indications for performing neurography studies.- Illustrate concepts by a case-based review and original drawings.

#### TABLE OF CONTENTS/OUTLINE

ANATOMY: REVIEW- Review the anatomy, formation and imaging features of the nerves. NEUROGRAPHY IN HEAD AND NECK- Indications- Magnetic Resonance (MR) sequences- Advanced sequences ALTERATED NEUROGRAPHIES- Sample cases to illustrate and solidify the conceptsWHAT'S ON THE HORIZON- What's new on cranial nerves and its branches evaluation.- What do we need to improve?

Printed on: 02/07/23

## Abstract Archives of the RSNA, 2022

HNEE-30

### Hypopharynx - Beyond Squamous Cell Carcinoma

Sunday, Nov. 27 8:00AM - 9:00AM Room: Learning Center - HN

#### Participants

Guilherme Chaves, MD, Sao Paulo, Brazil (*Presenter*) Nothing to Disclose

#### TEACHING POINTS

- Hypopharynx comprehends the most inferior part of the pharynx, as the continuation of the oropharynx, extending from the hyoid bone level (between C3-C4 vertebral bodies) to the inferior margin of the cricoid cartilage. It's bounded anteriorly by the laryngeal vestibule (separated by the aryepiglottic folds) and posteriorly by the retropharyngeal space.
- Can be divided into piriform sinuses, anterior wall (post cricoid area) and posterior wall. Anterior and posterior walls are usually close to each other, unless there is liquid or gaseous content between them.
- The most common pathology of the hypopharynx is squamous cell carcinoma. However, some other pathologies may cause similar symptoms and be quite confusing: congenital, inflammatory, foreign bodies and post treatment complications.
- It's extremely important for every radiologist to understand hypopharynx anatomy and pathologies cause some of them can present high morbidity.

#### TABLE OF CONTENTS/OUTLINE

1. Review hypopharynx anatomy and boundaries.
2. Briefly discuss hypopharynx embryology
3. List non-neoplastic pathologies of the hypopharynx: congenital, inflammatory, foreign bodies and post treatment complications.
4. Identify imaging patterns that facilitate distinction between the entities listed above and neoplastic lesions.

Printed on: 02/07/23



## Abstract Archives of the RSNA, 2022

HNEE-31

### **Tympanoplasty: A Review of Indications, Surgical Techniques and Complications for the Radiologist**

Sunday, Nov. 27 8:00AM - 9:00AM Room: Learning Center - HN

#### **Participants**

Beatriz Prado, MD, Sao Paulo, Brazil (*Presenter*) Nothing to Disclose

#### **TEACHING POINTS**

Tympanoplasty is the surgical repair of the tympanic membrane with or without grafting and usually performed with reconstruction of the ossicular chain. Encompasses a range of procedures that vary according to the extent of the underlying pathology and required surgical exposure. This panel aims to: Define tympanoplasty Quote the main clinical indications Depict surgical aspects: Types of tympanoplasty Grafting of the tympanic membrane Illustrate complications Discuss and outline through clinical cases the expected postoperative findings and complications after tympanoplasty.

#### **TABLE OF CONTENTS/OUTLINE**

Definition of tympanoplasty Main clinical indications of tympanoplasty Types of tympanoplasty: Types 1 to 5 Complications: Thickening, Retraction, and Reperforation of the Tympanic Membrane Recurrent Cholesteatoma Granulation Tissue Extrusion, Intrusion, or Dislocation of Ossicular Prostheses Infection

Printed on: 02/07/23

## Abstract Archives of the RSNA, 2022

HNEE-32

### Clinical Impact of MR Bone Imaging on Head and Neck Diseases

Sunday, Nov. 27 8:00AM - 9:00AM Room: Learning Center - HN

#### Awards

Cum Laude

#### Participants

Miho Gomyo, Miraka, Japan (*Presenter*) Nothing to Disclose

#### TEACHING POINTS

1. To learn the basic principles of MR bone imaging that can visualize bony and calcified structures like CT. 2. To know clinical applications to head and neck lesions of MR bone imaging. 3. To review pitfalls of MR bone imaging.

#### TABLE OF CONTENTS/OUTLINE

1. Basic principles and various scanning methods 2. Clinical applications to depict the following structures/lesions: physiological calcifications (basal ganglia, pineal body, choroid plexus, dura mater), skull tumors (primary and malignant tumors including metastasis), reactive bone sclerosis/erosion, bone deformity by tumors and tumor calcification 3. Applications to vessel wall imaging: segment diagnosis with the vertebral body in the carotid artery stenosis, calcified plaque and arterial wall calcification of the intracranial aneurysm 4. Pitfalls

Printed on: 02/07/23



## Abstract Archives of the RSNA, 2022

HNEE-33

### Rhinoseptoplasty for Radiologists: Recognizing the Main Early and Late Complications

Sunday, Nov. 27 8:00AM - 9:00AM Room: Learning Center - HN

#### Participants

Beatriz Prado, MD, Sao Paulo, Brazil (*Presenter*) Nothing to Disclose

#### TEACHING POINTS

The purposes of this exhibit are: To show and exemplify rhinoseptoplasty early and late complications; To discuss and illustrate through clinical cases the imaging features of different complications which can be seen in the post operative state; To give some tips of when to raise suspicion of rhinoseptoplasty complications as the main responsible cause of patients symptoms.

#### TABLE OF CONTENTS/OUTLINE

Introduction. Early and late complications list. Clinical cases and imaging findings of different early and late rhinoseptoplasty complications. Early: Infection, Nasal septum perforation, Nasal septum hematoma. Late: Empty nose syndrome, Depression of the nasal dorsum, Depression of nasal alae, Post septoplasty cystic formation, Pinch tip deformity, Synechiae, Nasal cartilage necrosis. Take home messages and final remarks.

Printed on: 02/07/23

## Abstract Archives of the RSNA, 2022

HNEE-34

### Ultrasound of the Post-thyroidectomy Neck in Well Differentiated Thyroid Cancer - Pearls and Pitfalls

Sunday, Nov. 27 8:00AM - 9:00AM Room: Learning Center - HN

#### Participants

Sepideh Sefidbakht, MD, Powel, OH (*Presenter*) Nothing to Disclose

#### TEACHING POINTS

- To review the imaging appearance of thyroid bed recurrence post-thyroidectomy in well-differentiated thyroid cancers
- To review the pitfalls of ultrasound diagnosis of thyroid bed recurrence in well-differentiated thyroid cancers
- To review the ultrasound appearance of lymph node recurrence in well-differentiated Thyroid cancer
- To review the pitfalls of ultrasound diagnosis of lymph node recurrence in well-differentiated thyroid cancers
- To integrate I<sup>123</sup> images, basic clinical data, including knowledge of surgical technique, cumulative dose of I<sup>131</sup> already received, laterality of the cancer in the thyroid gland, and basic lab data including Tg TgAb to refine decision-making in ultrasound

#### TABLE OF CONTENTS/OUTLINE

1-Introduction: • Thyroid cancer, the prevalence, types, and recurrence pattern; implications for ultrasound diagnosis • Thyroid cancer surgery; thyroidectomy, suture, and suture-less techniques; implications for ultrasound diagnosis • Neck lymphadenectomy, central versus peripheral, indications and implications for ultrasound diagnosis • Thyroid cancer; post-op management, surveillance modalities, and their limitations  
2-The thyroid bed recurrence, appearance • Echogenicity, size, vascularity, calcification • The thyroid bed recurrence, pitfalls • Granulation tissue and edema • Suture granuloma • The upward extension of thymus • The parathyroid gland • EBRT implants  
3-Lymph node recurrence, • Appearance, Echogenicity, size, shape, central hilum; and location • Lymphadenectomy; central versus peripheral • Pre-operative lymph node mapping; what the surgeon needs and doesn't need to know

Printed on: 02/07/23



## Abstract Archives of the RSNA, 2022

HNEE-35

### Imaging Aspects of the New Classification for Carotid Body Tumors: Understanding Mehanna Classification Using Computed Tomography Images

Sunday, Nov. 27 8:00AM - 9:00AM Room: Learning Center - HN

#### Participants

Alessandra d. Borges, MD, (*Presenter*) Nothing to Disclose

#### TEACHING POINTS

Discuss the new classification for carotid body tumors Review anatomical neck landmarks of Mehanna classification in computed tomography images

#### TABLE OF CONTENTS/OUTLINE

Paragangliomas is commonly located in the carotid body, usually in carotid bifurcation. Although histopathologically benign, its involvement in neurovascular structures and intracranial invasion are associated with high morbidity. The surgery of paraganglioma in the carotid body can be very challenging and for that reason, an accurate classification to predict the risk of potential complications is vital for treatment decision-making. Mehanna et al developed a new classification and risk stratification system for carotid body tumors which demonstrated better prognostic power for the risk of developing neurovascular complications after surgery, including the widely used modified Shamblyn classification system. It classifies in type 1 to 4 based on the fact that the main cause of complications was the level of cranial extension. The risk of complications increases significantly with increasing Mehanna type. Type 1 extends up to but not above the superior-most aspect of the body of hyoid bone Type 2 extends up to but not above the lower border of the angle of mandible Type 3 extends up to but not above the superior-most aspect of the body of C2 vertebra Type 4 extends above superior-most aspect of the body of C2 vertebra An additional subclassification can be added for surgical planning: E: encircling bifurcation, internal or common carotid artery F: functional, secreting catecholamines S: skull base reached.

Printed on: 02/07/23

## Abstract Archives of the RSNA, 2022

HNEE-36

### Osteoradionecrosis Of Mandible- Addressing The Raging Bull In Head And Neck Surgical Oncology

Sunday, Nov. 27 8:00AM - 9:00AM Room: Learning Center - HN

#### Participants

Ankush Jajodia, MD, MBBS, New Delhi, India (*Presenter*) Nothing to Disclose

#### TEACHING POINTS

1. Treatment of oral cavity malignancies includes primary surgical resection which may include marginal or segmental mandibulectomy followed by adjuvant radiation. Radiation comes at its own cost in producing adverse effects on neighboring tissues, like osteoradionecrosis (ORN) 2. ORN is a condition in which irradiated bone becomes exposed to an ulcer in the overlying skin or mucosa and persists without healing for a period of 3 to 6 months. Clinically the condition may manifest with pain, swelling, oro-cutaneous fistula or trismus. The overall incidence of ORN of the mandible is 2.6% -15%. 3. Mandible is a compact bone and has a higher mineral content that may lead to a higher absorbed dose. The ramus and condylar processes are comparatively resistant to the development of ORN, whereas the mandibular body, symphysis, and parasymphysis regions supplied mainly by the inferior alveolar artery are at higher risk to develop ORN. 4. The pathophysiology of ORN described by Marx in 1983 (3-H principle), radiation therapy causes hypoxia, hypovascularity, and hypocellularity of tissue, thus inhibiting substitution of cells to complete the turnover for the maintenance of homeostasis and wound cicatrization, leading to a chronic nonhealing wound. The affected cells are the ones of vascular endothelium, fibroblasts which make stroma and parenchyma cells. 5. MR imaging during follow-up helps radiologists to detect ORN.

#### TABLE OF CONTENTS/OUTLINE

Clinical cases with pictorial depiction of Osteoradionecrosis of mandible on conventional MR Imaging

Printed on: 02/07/23



## Abstract Archives of the RSNA, 2022

HNEE-37

### Multi-modality Imaging Including MR Diffusion, T2 Signal Intensity and 18 FDG PET-CT for Neck Imaging Reporting and Data System Categorization

Sunday, Nov. 27 8:00AM - 9:00AM Room: Learning Center - HN

#### Participants

Ankush Jajodia, MD, MBBS, New Delhi, India (*Presenter*) Nothing to Disclose

#### TEACHING POINTS

- Previous studies documented an overall PPV of 54-56% for NI-RADS 3 posttreatment PET/CT, which was advocated as low.
- NI-RADS favors NPV over PPV to potentially capture treatable lesions, even if it comes at the cost of performing additional biopsies.
- Functional imaging like DWI and ADC parameters derived from DWI have shown promise for identifying true disease recurrence with higher specificity than conventional PET-CT, with a reported pooled sensitivity and specificity of 85 % and 93 %, for PET/CT.
- NIRADS can serve as an assessment tool, wherein individual radiologists or groups of radiologists can utilize the PPV and NPV, to evaluate their own performance.

#### TABLE OF CONTENTS/OUTLINE

National Comprehensive Cancer Network suggests posttreatment baseline imaging after six months of therapy for advanced HNSCC but does not formally advocate imaging for asymptomatic patients. Ideal timing and frequency for using PET- CT in the posttreatment context have not yet been established. ACR "Neck Imaging Reporting and Data System" (NI-RADS) lexicon defines NIRADS 2b lesions as deep soft tissue lesions with ill-defined or mildly enhancing soft tissue or soft tissue with only mild FDG uptake. These are indeterminate lesions and should have a short-term interval follow-up. NIRADS 3 lesions should have a short-term interval follow-up or biopsy, depending on the degree of FDG uptake. Recurrence rates in NIRADS 2b and NIRADS 3 lesions were 5.6 % and 60-80%, respectively. The template was initially designed for CECT with concentration on PET-CT for detecting recurrence; MR imaging has been done in few centres. Although diffusion imaging has become a routine sequence in head and neck imaging, it is not yet a criterion in NI-RADS.

Printed on: 02/07/23



## Abstract Archives of the RSNA, 2022

HNEE-38

### Ultrasound of Neck Masses - Pearls and Pitfalls

Sunday, Nov. 27 8:00AM - 9:00AM Room: Learning Center - HN

#### Participants

Pooya Iranpour, MD, Shiraz, Iran, Islamic Republic Of (*Presenter*) Nothing to Disclose

#### TEACHING POINTS

To review the zonal anatomy of the neck• To understand the sonographic anatomy and the surface land marks of neck triangles• To be able to propose a primary differential diagnosis for adult neck masses list based on the location of the lesion• To review the gray scale, color Doppler and elastographic features of most common neck lesions seen in the adult• To review the key sonographic features in adult patients with cervical LAP• To review the similarities and differences of metastatic lymphnodes, versus reactive lymph nodes versus lymphoma• Using the anatomic location, and ultrasound features to determine the mostlikely diagnosis

#### TABLE OF CONTENTS/OUTLINE

- Neck triangles; Back to the Basics• Ultrasound of normal neck anatomy; Sonographic landmarks• Differential diagnosis of the most common neck lesions; location, location, location• Ultrasound of a neck lump; the good, the bad, and the ugly• Solid neck lesions, an overview• Lymphoma, reactive or metastasis? that is the question!• Cysts; where do they sit?

Printed on: 02/07/23



## Abstract Archives of the RSNA, 2022

HNEE-39

### Addressing Pertinent Surgical Questions in Skull Base Onco-imaging Reports: Case Based Approach

Sunday, Nov. 27 8:00AM - 9:00AM Room: Learning Center - HN

#### Participants

Shreya Shukla, MBBS, Mumbai, India (*Presenter*) Nothing to Disclose

#### TEACHING POINTS

Radiological reporting of cross-sectional oncological imaging including Computed Tomography (CT) and Magnetic Resonance Imaging (MRI) can be inadequate and futile for clinicians if it is unsculpted and descriptive. A checklist of vital imaging findings should be strictly used in radiological reporting to give maximum useful information to the treating clinicians. We have created such a checklist and proposed its use as a standardized synoptic reporting format to address all essential questions that need to be answered to help reach a diagnosis and optimize the management plan in skull base neoplasms. Our checklist has been designed after a thorough discussion of a multitude of skull base neoplasms cases between radiologists and clinicians at weekly multi-disciplinary joint clinics (JCs) in our tertiary cancer centre.

#### TABLE OF CONTENTS/OUTLINE

This educational exhibit contains:- Checklist of relevant and essential findings in baseline radiological reporting of skull base neoplasms.- Proposed synoptic reporting format for skull base neoplasms.- Case-based approach to understanding how including essential details in the radiology reports can affect the management plan.

Printed on: 02/07/23



## Abstract Archives of the RSNA, 2022

HNEE-4

### Preoperative Orthognathic Surgery: What Radiologists Should Know

Sunday, Nov. 27 8:00AM - 9:00AM Room: Learning Center - HN

#### Participants

Andre Formiga, MD, (*Presenter*) Nothing to Disclose

#### TEACHING POINTS

The purposes of this exhibit are:- To review the anatomical landmarks of the face and the angles they make on computed tomography images.- To discuss the main facial patterns made from these angles and usual changes in dental occlusion that accompany them.- To review the main osteotomy techniques employed on orthognathic surgeries.- To highlight a few craniofacial cases with either tumoral, malformation or vascular etiologies that could be subjected to orthognathic surgeries.

#### TABLE OF CONTENTS/OUTLINE

Orthognathic surgery uses repositioning of the mandible and maxilla to correct imbalances in facial proportions that can affect everything from physiological dental occlusion and sleep apnea to aesthetic problems related to asymmetries and facial disharmonies that affect patient self-esteem. The objectives of this presentation are to describe the pre operator imaging findings and cephalometric parameters, mainly on CT scans, of some of the main conditions where orthognathic surgery can act, their reflections on dental occlusion, and how to report them.

Printed on: 02/07/23



## Abstract Archives of the RSNA, 2022

HNEE-40

### Imaging Considerations in Head and Neck Reconstruction with 3D Printed Surgical Guides and Implants

Sunday, Nov. 27 8:00AM - 9:00AM Room: Learning Center - HN

#### Participants

Mark Tan, MBBS, FRCR, (*Presenter*) Nothing to Disclose

#### TEACHING POINTS

1. Common indications for Head and Neck reconstruction:(a) Tumour (i) SCC (ii) ACC(b) Deformity correction (i) post Radiotherapy Osteonecrosis (ii) post Traumatic - midface(iii) Post surgical temporal hollowing2. Options for Head and Neck Reconstruction:(a) Maxillectomy (b) Mandibulectomy (c) Fibula flap (d) PEEK and Titanium3. Radiological interpretation considerations (a) Objectives (i) Differential diagnosis (ii) lesion extent (iii) resectability (iv) fibula vasculature (branching, septocutaneous perforator and periosteal branches)4. Workflow for 3D Printed surgical guide and implant production5. Application of Workflow: Fibula flap reconstruction with 3D printing: Virtual surgical planning: Resection with 3D printed guides, dental implant placement, 3D printed titanium plate6. Imaging acquisition considerations (i) Protocols (ii) Artefacts (iii) Patient positioning(iv) Artefact reduction: MAR (v) Reconstruction algorithms(vi) Reconstruction slice thickness(vii) CT-MRI fusion(viii) Scalar and Vector DICOM Data

#### TABLE OF CONTENTS/OUTLINE

To appreciate for Head and Neck surgical reconstruction:1. Common indications 2. Surgical options 3. Radiological interpretation considerations 4. Workflow for 3D Printed surgical guide and implant production - Process Overview 5. Application of Workflow: 3D Printed Fibula Resection Guide and Titanium Plate 6. Radiographic imaging acquisition considerations for 3D Printed surgical guides and implants7. Radiographic imaging post-processing considerations for 3D Printed surgical guides and implants

Printed on: 02/07/23



## Abstract Archives of the RSNA, 2022

HNEE-41

### Laryngeal Protrusion, Prolapse and Eversion - Diagnoses Forgotten by Radiology

Sunday, Nov. 27 8:00AM - 9:00AM Room: Learning Center - HN

#### Participants

Ricardo Fujiki, MD, (*Presenter*) Nothing to Disclose

#### TEACHING POINTS

Protrusion, prolapse and eversion are definitions often used as synonyms, but they have totally different clinicopathological entities and have not been updated or revisited in the radiological scientific environment for a long time. Imaging findings in the head and neck were recognized and evaluated and may serve as supporting markers to differentiate protrusion, prolapse and eversion, and thus help to define the clinicopathological causes and the need or not to continue the investigation.

#### TABLE OF CONTENTS/OUTLINE

- Objectives: 1 - Review definitions and clinicopathological differences between protrusion, prolapse and eversion. 2 - Illustrate through clinical cases the different entities by radiological methods. - Methods: Head and neck imaging findings were highlighted in this pictorial review. We also discussed the imaging findings in order to demonstrate the differences between the laryngeal findings. - Discussion (based on cases): Characteristic radiological findings for the differentiation between protrusion, prolapse and eversion were reported in conjunction with the development of didactic schemes to facilitate learning and recognition and differentiation in clinical practice. - Conclusion: Early and accurate recognition of the causes of laryngeal prolapse through imaging methods can help assisting physicians in defining the need for biopsy.

Printed on: 02/07/23



## Abstract Archives of the RSNA, 2022

HNEE-42

### What the Eye Can't See but the Radiologists Do: Clinical-radiological Correlation in the Assessment of Visual Disturbances

Sunday, Nov. 27 8:00AM - 9:00AM Room: Learning Center - HN

#### Awards

Identified for RadioGraphics

#### Participants

Ewa Joanna Maciag, (*Presenter*) Nothing to Disclose

#### TEACHING POINTS

Patients with visual disturbances may present a wide variety of symptoms that can be divided into three main categories: (1) Visual dysfunction, such as blurred vision, vision loss, and visual field defects. (2) Extrinsic ocular motility disorders, which usually cause binocular diplopia. (3) Pupillary motility impairment. This review aims to analyze the correlation between the different radiological presentation patterns and the clinical manifestations, with an emphasis on the anatomical localization of the causative lesion and an approach to an appropriate selection and interpretation of the different imaging techniques.

#### TABLE OF CONTENTS/OUTLINE

1. Introduction. 2. Main symptoms and anatomical background. 3. Imaging techniques: appropriate selection and application. 4. Intrinsic ocular motility disorders: miosis and mydriasis. 5. Alterations of the extrinsic ocular motility: neurogenic and myogenic causes and an evidence-based diagnostic algorithm of diplopia. 6. Disorders of visual function: a case-based overview of the causative pathology. 7. Diagnostic pathway to determine the cause of the visual disturbances. 8. Conclusions.

Printed on: 02/07/23



## Abstract Archives of the RSNA, 2022

HNEE-43

### Head and Neck Manifestations of Autoimmune Disease - A Didactical Review

Sunday, Nov. 27 8:00AM - 9:00AM Room: Learning Center - HN

#### Participants

Mayne Brandao, MD, (*Presenter*) Nothing to Disclose

#### TEACHING POINTS

Little is said about the manifestations of autoimmune diseases and their imaging aspects in Head and Neck. This panel is intended to show challenging cases that are part of this group of diseases, which affect the various areas of this region. The diversity of findings shows us the importance of disclosing these imaging aspects and makes it a useful tool for consultation. Unusual places such as ossicular involvement, the Eustachian tube, the sternocleidomastoid muscle and other structures illustrate this diversity of places. There are other diseases that will also be addressed in this exhibit as for example lupus; seronegative spondyloarthropathies; systemic sclerosis. Correlation of the imaging findings with the clinical features and laboratory findings is also important for the diagnosis and the recognition of the disease activity, and the identification of possible complications or even the occurrence of associated neoplasms.

#### TABLE OF CONTENTS/OUTLINE

Introduction of the main acquired immunologically mediated inflammatory disorders. These disorders may be associated with paraneoplastic syndrome, especially hematologic tumors, or may increase the risk for the development of malignancies, predominantly lymphoproliferative disorders. Also, these patients may be associated with infection and granulomatous lesions of the head and neck. We will provide with didactical cases a review presenting the imaging findings in the head and neck in patients with these diseases. Conclusions. References.

Printed on: 02/07/23



## Abstract Archives of the RSNA, 2022

HNEE-44

### Temporal Bone Osteodystrophies

Sunday, Nov. 27 8:00AM - 9:00AM Room: Learning Center - HN

#### Participants

Afonso Santos, MD, Sao Paulo, Brazil (*Presenter*) Nothing to Disclose

#### TEACHING POINTS

The purposes of this exhibit are: To exemplify all forms of otospongiosis presentation (typical and atypical) and discuss possible pitfalls (eg, foci at the internal acoustic meatus versus diverticula). To demonstrate other osteodystrophies of the temporal bone, including osteogenesis imperfecta, osteopetrosis, Paget's disease and fibrous dysplasia.

#### TABLE OF CONTENTS/OUTLINE

Introduction. CT and MRI temporal bone studies. Imaging of typical and atypical cases of otospongiosis. Practical tips and pitfalls on otospongiosis analysis. Other osteodystrophies of the temporal bone: osteogenesis imperfecta, osteopetrosis, Paget's disease and fibrous dysplasia. Take-home messages.

Printed on: 02/07/23



## Abstract Archives of the RSNA, 2022

HNEE-45

### Surgical Pitfalls in the Otospongiosis Evaluation: What the Otorhinolaryngologist Needs to Know

Sunday, Nov. 27 8:00AM - 9:00AM Room: Learning Center - HN

#### Participants

Marcio Ricardo Garcia, MD, Sao Paulo, Brazil (*Presenter*) Nothing to Disclose

#### TEACHING POINTS

To describe imaging findings in CT scan evaluation of otosclerosis with preoperative relevance. To warn the radiologists about the detection of relevant features that could lead to surgical failure or complications in the stapedotomy and improve patient outcomes

#### TABLE OF CONTENTS/OUTLINE

1. Introduction - A brief discussion about physiopathology and classical imaging findings of fenestral and retrofenestral otosclerosis - The role of CT and MR in the diagnosis of otosclerosis - A little explanation about the surgical treatment of otosclerosis with emphasis on stapedotomy and possible postoperative complications (untreatable vertigo, anacusis, facial palsy, and meningitis). 2. Imaging findings on preoperative evaluation before stapedotomy - Oval or round window involvement (atresia, narrowing, thickened stapes footplate) and their relation with close structures - Facial nerve anomalies as congenital abnormalities, deviation of facial nerve, or dehiscence - Vestibular aqueduct anomalies as enlargement or dehiscence - Persistent stapedial artery - Semicircular canal dehiscence- Cochlear-facial nerve dehiscence- Lateral semicircular canal dysplasia- Ossicular chain fixation 3. Conclusion 4. Take-home messages

Printed on: 02/07/23



## Abstract Archives of the RSNA, 2022

HNEE-46

### Advanced Imaging of Head and Neck Infection

Sunday, Nov. 27 8:00AM - 9:00AM Room: Learning Center - HN

#### Awards

Cum Laude

#### Participants

Akira Baba, Ann Arbor, MI (*Presenter*) Nothing to Disclose

#### TEACHING POINTS

Advanced cross-sectional imaging plays a critical role in providing differential diagnoses, treatment decisions, and prognostic implications in head and neck infections. Contrast-enhanced CT is the imaging modality of choice for head and neck infections; however, other imaging modalities may be complementary and diagnostic. MRI is excellent for evaluation of intracranial spread of inflammation/abscess formation and osteomyelitis, etc. DWI and ADC values are useful in providing differential diagnoses and evaluating treatment response of head and neck infections. 18F-FDG-PET/CT is helpful in the follow-up of skull base osteomyelitis. Dual energy CT allows for various techniques such as metal artifact reduction and material decomposition imaging that can help reduce dental metal artifacts, increase salivary stone detection. Metal artifact reduction algorithm can help reduce dental metal artifacts. Subtraction CT techniques are used to reduce dental metal artifacts and detect destructive osseous changes. This presentation will provide an overview of must-know head and neck infections with updated advanced imaging techniques and their imaging findings.

#### TABLE OF CONTENTS/OUTLINE

1. Imaging techniques 2. Temporal bone/skull base 3. Pharynx 4. Deep neck 5. Oral cavity 6. Salivary Glands

Printed on: 02/07/23

## Abstract Archives of the RSNA, 2022

HNEE-47

### Skull Base Osteomyelitis in COVID-19 related Acute Invasive Fungal Rhino Sinusitis: Spectrum of Findings

Sunday, Nov. 27 8:00AM - 9:00AM Room: Learning Center - HN

#### Participants

Gayatri Senapathy, FRCR, (*Presenter*) Nothing to Disclose

#### TEACHING POINTS

- SBO is a dreaded condition with high morbidity and mortality and fungal rhinosinusitis is one among the many causes of SBO
- Incidence of AIFRS showed a significant increase during the second wave of COVID-19 pandemic and Diabetes Mellitus and Steroid use were found to be the major associated factors.
- AIFRS was seen in patients with active or recent COVID-19 infection. SBO was seen as a complication at presentation in some cases of AIFRS, and beyond the 3rd week of onset in treated patients who had progressive disease.
- AIFRS has a predilection for both vascular and perineural spread across intact bony boundaries. Patients with early involvement of the pterygopalatine fossa, orbital apex and the cavernous sinus are at high risk of developing SBO due to perineural and vascular spread.
- Contrast enhanced MRI (CE MRI) is superior to CT in the early detection of SBO as the marrow signal changes and the adjacent soft tissue changes are detected before bone erosion becomes evident on CT.
- Intracranial complications such as meningitis, vascular complications, cerebritis and abscesses are also depicted earlier on MRI.

#### TABLE OF CONTENTS/OUTLINE

- Revisit skull base anatomy
- Elucidate the pathways of spread of sinonasal fungal infection to involve the skull base
- Illustrate the various findings of skull base osteomyelitis (SBO) in cases of COVID-19 related Acute Invasive Fungal Rhino Sinusitis (AIFRS) in our institute between March and September 2021
- Demonstrate the associated intracranial and extracranial complications.

Printed on: 02/07/23



## Abstract Archives of the RSNA, 2022

HNEE-48

### Extraocular Muscle Pathology: That's How Eye Roll

Sunday, Nov. 27 8:00AM - 9:00AM Room: Learning Center - HN

#### Participants

Juliana Sitta, MD, Jackson, MS (*Presenter*) Nothing to Disclose

#### TEACHING POINTS

To review the normal orbital imaging anatomy highlighting the advantages of each imaging modality. To discuss the differential diagnosis of extraocular muscle (EOM) pathology including inflammatory, infectious, neoplastic, congenital, and traumatic etiologies. To recognize the importance of systematic EOM assessment in the diagnosis of systemic diseases and potential complications

#### TABLE OF CONTENTS/OUTLINE

The differential diagnosis of EOM pathology is broad and often challenging including inflammatory, infectious, neoplastic, and traumatic causes. Although eye movement disorders may be unclear on initial imaging, modalities including CT, MRI, and PET-CT along with clinical findings play a key role in identifying or ruling out important differential diagnosis. In this presentation we will review the imaging features of normal orbital anatomy and the spectrum of EOM pathology. We will illustrate a wide range of etiologies including key imaging findings to narrow down the differential diagnosis in various categories of disease such as congenital orbital fibrosis of the EOM, anophthalmia-microphthalmia, spontaneous hematoma, thyroid orbitopathy, orbital metastases, PET-CT findings in nerve palsy, idiopathic orbital inflammation, and IgG4 sclerosing disease of the orbit.

Printed on: 02/07/23

## Abstract Archives of the RSNA, 2022

HNEE-49

### **Branchial Apparatus Lesions and Thyroglossal Duct Lesions: Embryology, Typical Imaging Findings of Those Lesions and Mimics**

Sunday, Nov. 27 8:00AM - 9:00AM Room: Learning Center - HN

#### **Participants**

Yoshiko Y. Kurihara, MD, (*Presenter*) Nothing to Disclose

#### **TEACHING POINTS**

Many structures in the head and neck region arise from branchial apparatus. To learn congenital lesions secondary to abnormal embryogenesis in this region, the knowledge of these structures including embryology can make those diseases easier to understand. The thyroglossal duct also causes abnormal embryogenesis. On this presentation, the embryological changes of branchial clefts, pouches and thyroglossal duct are demonstrated. This presentation shows many developmental abnormalities as 1) fistulae, sinuses and cysts originated from branchial clefts and thyroglossal duct with typical location according to the embryology 2) complicated status of these lesions ; infection, neoplastic change including malignancy 3) ectopic thymus, ectopic parathyroid gland and ectopic thyroid tissue according to their migrating tract 4) neoplastic changes of these ectopic lesions, with CT, MRI, RI images and interpretations. In addition, 5) mimics should be differentiate from these lesions as well.

#### **TABLE OF CONTENTS/OUTLINE**

1) Figure of branchial apparatus developing structures anomalies. 2) Embryology of branchial apparatus. 3) Developmental abnormalities related to branchial cleft, complicated lesions and mimics. 4) Developmental abnormalities related to branchial pouch, complicated lesions and mimics. 5) Figure and embryology of thyroglossal duct. 6) Developmental abnormalities related thyroglossal duct, complicated lesions and mimics.

Printed on: 02/07/23



## Abstract Archives of the RSNA, 2022

HNEE-5

### High Resolution CT Angiography of the Orbits, Skull Base and Pterygopalatine Fossa

Sunday, Nov. 27 8:00AM - 9:00AM Room: Learning Center - HN

#### Awards

Certificate of Merit

#### Participants

Norbert Campeau, MD, Rochester, MN (*Presenter*) Nothing to Disclose

#### TEACHING POINTS

1. To detail the arterial anatomy of the orbit, anterior skull base and pterygopalatine fossa through high resolution CT angiography images and corresponding anatomic legends.2. Discuss several of the more commonly occurring congenital arterial variants.3. Review relevant skull base foramina and fissures.

#### TABLE OF CONTENTS/OUTLINE

High resolution computed tomography angiography (CTA) of the brain and skull base has continued to improve substantially over the past two decades, now routinely obtained with sub-millimeter voxel resolution. In this educational exhibit, we present a detailed review of the arterial anatomy of the orbit and pterygopalatine fossa using high resolution CTA images obtained from a state of the art 510k cleared photon counting CT scanner. Arterial supply to the optic nerve, ocular globe, lacrimal gland will be detailed. Anatomy of internal maxillary artery branches will also be described, including course of the arteries of the pterygopalatine canal, foramen rotundum, sphenopalatine, greater and lesser palatine arteries. Anastomotic connections between meningeal, external carotid, and internal carotid artery branches via the inferolateral trunk will also be discussed.

Printed on: 02/07/23



## Abstract Archives of the RSNA, 2022

HNEE-50

### Open Your Eyes and Look Out for All the Windows - Evaluation of the Oval, the Round and Other Windows of the Inner Ear

Sunday, Nov. 27 8:00AM - 9:00AM Room: Learning Center - HN

#### Participants

Bruna Gherardi, MD, Rio de Janeiro, Brazil (*Presenter*) Nothing to Disclose

#### TEACHING POINTS

To illustrate the pathophysiology of third window syndrome. To demonstrate the most common imaging aspects of oval, round, and other pathologic window changes and the clinical implications.

#### TABLE OF CONTENTS/OUTLINE

Physiology of air and bone auditory conduction. Imaging protocol. Mastoid trauma involving oval and round windows. Labyrinthine fistula. Fenestral and retrofenestral otospongiosis. Cochleofacial dehiscence. Carotid-cochlear dehiscence. Dehiscence of semicircular canals. Enlarged vestibular aqueduct syndrome. Round window stenosis.

Printed on: 02/07/23

## Abstract Archives of the RSNA, 2022

HNEE-51

### Facing the Challenge: Imaging of Facial Nerve Paralysis

Sunday, Nov. 27 8:00AM - 9:00AM Room: Learning Center - HN

#### Participants

Hugo Tames, MD, Sao Paulo, Brazil (*Presenter*) Nothing to Disclose

#### TEACHING POINTS

To review the anatomy of the normal facial nerve and its expected normal imaging appearances on CT and MR. To review causes of facial nerve paralysis, ranging from the commonest and less common diseases. To present the imaging appearances on CT and MR of facial nerve when affected by these pathologies. To present different cases of facial paralysis from the teaching files of a tertiary center, including typical appearance and atypical variants.

#### TABLE OF CONTENTS/OUTLINE

1. Introduction  
2. Review of facial nerve anatomy and its expected normal imaging appearance on CT and MR  
The central nervous system segment  
The cisternal segment  
The meatal segment  
The labyrinthine segment  
The tympanic segment  
The mastoid segment  
The extra-temporal segment  
3. Review of different causes of facial paralysis  
Bell's palsy / idiopathic paralysis  
Facial nerve arteriovenous malformation  
Facial nerve schwannoma  
Facial nerve meningioma  
Ramsay-Hunt syndrome  
Moebius syndrome  
Melkersson-Rosenthal syndrome  
Metaphyseal chondrodysplasia  
Facial nerve paralysis secondary to perineural spread of adenoid cystic carcinoma  
Central facial paralysis secondary to ischaemic event  
4. To present the imaging appearances on CT and MR of facial nerve when affected by these pathologies

Printed on: 02/07/23



## Abstract Archives of the RSNA, 2022

HNEE-52

### Skull Base Osteomyelitis: Imaging checklist

Sunday, Nov. 27 8:00AM - 9:00AM Room: Learning Center - HN

#### Participants

Sri Lakshmi J P Rao G, MBBS, MD, (*Presenter*) Nothing to Disclose

#### TEACHING POINTS

1. Should be suspected in all cases of infiltrative skull base lesions, particularly in diabetics and immunocompromised people, when repeated biopsies turn negative for malignancy.2. Imaging checklist to be followed while reporting a case of Skull base osteomyelitis.3. Mimics of Skull base osteomyelitis.

#### TABLE OF CONTENTS/OUTLINE

1. Introduction and types of SBO2. Imaging protocol3. Checklist for SBO reporting4. Role of imaging in follow-up5. Imaging mimics of SBO

Printed on: 02/07/23



## Abstract Archives of the RSNA, 2022

HNEE-53

### Head and Neck Sarcoma: A Magnetic Resonance Imaging Review Based on the 2020 World Health Organization Classification

Sunday, Nov. 27 8:00AM - 9:00AM Room: Learning Center - HN

#### Participants

Simone Caprioli, MD, Genova, Italy (*Presenter*) Nothing to Disclose

#### TEACHING POINTS

1. Magnetic resonance imaging (MRI) characteristics of head and neck sarcomas are often nonspecific and may be difficult to identify the precise diagnosis. 2. The recognition of the epicenter of the mass allows to differentiate a soft tissue from a bone or cartilage tumor. 3. MRI may narrow the differential diagnosis by analyzing the signal of the matrix of the tumor. 4. MRI is useful for identifying orbital and intracranial invasion.

#### TABLE OF CONTENTS/OUTLINE

In 2020 a novel classification system for soft tissue and bone tumors was published by the World Health Organization (WHO). Even though it is usually applied for trunk and extremities sarcoma, it may be a guide for characterizing non-epithelial lesions of head and neck. Magnetic resonance imaging (MRI) plays a pivotal role in the diagnosis of head and neck sarcoma, supporting the hypothesis of the non-epithelial origin of a mass and suggesting clues about histology. This work aims to review the MRI characteristics of non-epithelial neoplasms of head and neck as they are grouped in the 2020 WHO classification. Moreover, it offers a guide for precise local staging and for narrowing the differential diagnosis, thanks to a combination of criteria: location, epicenter, and MRI signal characteristics. The present work was based on a ten-years long multicentric record of 248 cases of head and neck sarcomas.

Printed on: 02/07/23

## Abstract Archives of the RSNA, 2022

HNEE-54

### Unboxing the Voice Box: Imaging in Laryngeal Malignancy

Sunday, Nov. 27 8:00AM - 9:00AM Room: Learning Center - HN

#### Awards

Identified for RadioGraphics  
Certificate of Merit

#### Participants

Anu Kamalasanan, FRCR, MBBS, East Renfrewshire, United Kingdom (*Presenter*) Nothing to Disclose

#### TEACHING POINTS

1) T1 lesions may be radiologically occult . 2) Nodal disease occurs late in glottic malignancy due to the relative paucity of lymphatic drainage of vocal cords 3) Anterior commissure involvement precludes hemilaryngectomy and may be associated with early cartilage invasion from extension along Broyle ligament 4) Paraglottic/ pre-epiglottic fat infiltration upstages disease to T3. Assessment can be done with CT/ MRI and USS 5) Thyroid cartilage has a variable appearance - unossified thyroid cartilage can make it difficult to differentiate from infiltration. USS and MRI can be used to differentiate between the two.

#### TABLE OF CONTENTS/OUTLINE

1) Illustrate with images, normal laryngeal anatomy including TNM subsites 2) Describe Imaging modalities for assessment and staging of laryngeal malignancy. 3) Update on Ultrasound and MRI as imaging adjuncts 4) TNM staging with examples 5) Illustrate various patterns of spread 6) Discuss management pathway.

Printed on: 02/07/23



## Abstract Archives of the RSNA, 2022

HNEE-55

### Anatomic Approach to Pharyngeal SCC Staging and Patterns of Spread

Sunday, Nov. 27 8:00AM - 9:00AM Room: Learning Center - HN

#### Participants

Daniel Warren, MD, (*Presenter*) Nothing to Disclose

#### TEACHING POINTS

1. Brief discussion of the revised 8th edition of the American Joint Committee staging of pharyngeal squamous cell carcinomas (SCCs).2. Overview of anatomic landmarks vital for staging of pharyngeal SCCs and discussion of imaging evaluation of invasion and extranodal extension.3. Image-based review of common routes of spread based on the location of origin.

#### TABLE OF CONTENTS/OUTLINE

1. Background2. HPV status and outcomes3. Nasopharyngeal SCC 3a. Staging 3b. Imaging Features 3c. Common and Easily Missed Locations 3d. Routes of Spread4. HPV/P16(+) Oropharyngeal SCC 4a. Staging 4b. Imaging Features 4c. Common and Easily Missed Locations 4d. Routes of Spread5. HPV/P16(-) Oropharyngeal SCC and Hypopharyngeal SCC 5a. Staging 5b. Imaging Features 5c. Common and Easily Missed Locations 5d. Routes of Spread6. Conclusion

Printed on: 02/07/23



## Abstract Archives of the RSNA, 2022

HNEE-56

### Fire in the Hole!: Jugular Foramen Pathology and Pitfalls

Sunday, Nov. 27 8:00AM - 9:00AM Room: Learning Center - HN

#### Participants

Fernando Ferraro IV, MD, Buenos Aires, Argentina (*Presenter*) Nothing to Disclose

#### TEACHING POINTS

Explain the anatomical content and content of the jugular foramen. Based on clinical findings, interpret the location of lesions involving the jugular foramen. Review of various lesions, variants and pitfalls involving the jugular foramen. Describe radiological findings secondary to cranial nerve deficit.

#### TABLE OF CONTENTS/OUTLINE

Technical specifications and protocol to study the jugular foramen. Schematic summary of the anatomy of the jugular foramen, including anatomical variations, and its importance for interpreting clinical examination. Illustrate the principal imaging findings with clinical examples (such as Vernet's syndrome, schwannomas, desmoid tumor, etc).

Printed on: 02/07/23



## Abstract Archives of the RSNA, 2022

HNEE-57

### Lymphoproliferative Lesions of the Orbit

Sunday, Nov. 27 8:00AM - 9:00AM Room: Learning Center - HN

#### Awards

Certificate of Merit

#### Participants

Taisa Santos, MD, Salvador, Brazil (*Presenter*) Nothing to Disclose

#### TEACHING POINTS

Lymphoproliferative lesions represent the most common primary orbital disease, manifesting mainly in the elderly, and may also be a manifestation of systemic lymphoproliferative disease. Imaging evaluation is essential to guide the diagnosis, follow-up and treatment response, since the clinic presentation is nonspecific signs and symptoms and can mimic other orbital pathologies. CT image pattern is not very specific, usually presenting as a mass that molds to the orbital walls, isoattenuating/hyperattenuating, with homogeneous contrast enhancement. It rarely presents with bone erosion, when present, it is usually associated with diffuse large B-cell lymphoma. MRI is the imaging method of choice and some sequences are essential for distinguishing pathologies that may mimic lymphoproliferative lesions, especially idiopathic orbital inflammatory disease, which may have similar signs and symptoms, being clinically different by association with painful proptosis and findings of image, as high ADC values on MRI. The main differential diagnoses include idiopathic orbital inflammatory syndrome, orbital cellulitis, thyroidopathy, sarcoidosis, IgG4, granulomatosis with polyangiitis, and metastases.

#### TABLE OF CONTENTS/OUTLINE

Introduction Histological classification Clinical findings Image protocol Image patterns Diagnósticos diferenciais Prognosis and follow up

Printed on: 02/07/23

## Abstract Archives of the RSNA, 2022

HNEE-58

### Breathe In Breathe Out: Obtaining Clarity in Imaging of Sino Nasal Malignancy

Sunday, Nov. 27 8:00AM - 9:00AM Room: Learning Center - HN

#### Participants

Janani Baradwaj, MBBS, MD, (*Presenter*) Nothing to Disclose

#### TEACHING POINTS

±Sino-nasal malignancies are mostly squamous cell types ±Historically Ohngren's line was used in prognostication and management. It is an imaginary line drawn from the angle of the mandible to the medial canthus of the eye, dividing the antrum. Disease involvement above the line is associated with a poor prognosis. ±CT demonstrates the extent of osseous involvement better. Soft tissue and nodal disease are assessed with post-contrast CT. ±MRI helps differentiate between mass and inflammatory change in the sinuses. °Tumour - Low T1, Low T2 signal, Heterogeneous enhancement °Mucosa - Low T1, High T2 signal, Intense homogeneous enhancement °Secretions - Low T1, Very high T2 signal, No enhancement ±MRI also helps to assess orbital, intracranial and perineural spread ±MRI is more sensitive for assessment of perineural spread - Enlarged affected nerves have high T2 signal with perineural enhancement, loss of normal T1 fat signal and normal CSF signal in the foramina. ±Perineural spread on CT - Enlargement and erosion of foramina, loss of normal low attenuating fat, Soft tissue attenuation of foramen.±Sino-nasal malignancies have a moderate incidence of loco-regional recurrence with late nodal disease. The presence of positive neck nodes is associated with higher incidence of disease recurrence. Retropharyngeal nodal involvement should be actively looked for on CT and MRI

#### TABLE OF CONTENTS/OUTLINE

±Describe normal paranasal sinus anatomy with images ±TNM staging of sino-nasal malignancy ±Illustrate with images routes of spread of malignancy ±Describe histopathological types of malignancies involving the sino-nasal cavity with images ±Radiological prognosticating factors ±Discuss management pathway

Printed on: 02/07/23



## Abstract Archives of the RSNA, 2022

HNEE-59

### What You Need to Know Before Reporting a Nasopharyngeal Tumor

Sunday, Nov. 27 8:00AM - 9:00AM Room: Learning Center - HN

#### Participants

Maria Rocha, MD, (*Presenter*) Nothing to Disclose

#### TEACHING POINTS

Simplifying and help less experienced radiologists know how to actively look for the critical areas that changes the treatment and staging of the patient. Review basic anatomy highlighting the main anatomical milestones in tumor staging. Illustrate common path of nasopharyngeal tumor.

#### TABLE OF CONTENTS/OUTLINE

Introduction to nasopharyngeal tumors A comprehensible guide of key anatomy and correlating to TNM / prognostic information  
Flowchart that resumes the critical points of the staging Didactical cases following the proposed flowchart

Printed on: 02/07/23



## Abstract Archives of the RSNA, 2022

HNEE-6

### Temporomandibular Joint Imaging from Basic to Advanced

Sunday, Nov. 27 8:00AM - 9:00AM Room: Learning Center - HN

#### Participants

Eduardo Valadares, MD, Sao Paulo, Brazil (*Presenter*) Nothing to Disclose

#### TEACHING POINTS

Describe the anatomy and biomechanics of temporomandibular joint  
Exhibit the normal appearance of temporomandibular joint in advanced imaging (CT and MRI)  
Summarize the main temporomandibular joint dysfunctions and disorders with a group-based approach

#### TABLE OF CONTENTS/OUTLINE

Introduction  
Anatomy and biomechanics of temporomandibular joint  
Normal CT and MRI appearance  
Abnormal development of the temporomandibular joint (aplasia/hypoplasia/hyperplasia)  
Temporomandibular joint dysfunction (direct and indirect signs)  
Traumatic lesions  
Inflammatory arthritis • Osteoarthritis • Rheumatoid arthritis • Juvenile inflammatory arthritis • 7. Tumor and tumorlike lesions • Metastasis • Fibrous dysplasia • Synovial chondromatosis • Pigmented villonodular synovitis  
Take-home messages/Conclusions

Printed on: 02/07/23



## Abstract Archives of the RSNA, 2022

HNEE-60

### Multimodality Imaging of Carotid Paragangliomas

Sunday, Nov. 27 8:00AM - 9:00AM Room: Learning Center - HN

#### Participants

Ingrid Alonso Ramon, MD, Mexico City, Mexico (*Presenter*) Nothing to Disclose

#### TEACHING POINTS

Teaching points1. To review general characteristics of paragangliomas for a better understanding of carotid glomus2. To discuss general concepts of a carotid glomus, including the different types and their incidence3. To describe different multimodality imaging characteristics (ultrasound, CT, MRI, PET/CT and angiography) including the recommended protocols and pros and cons of each one. 4. To recognize importance of diagnosis, treatment and follow up

#### TABLE OF CONTENTS/OUTLINE

Table of contents1. Description of general characteristics of paragangliomas including common sites of occurrence, incidence, pathophysiology and embryology.2. Description of general features of carotid paragangliomasa. Epidemiologyb. Anatomyc. Detailed pathologic characteristicsd. Clinical presentation including functional paragangliomase. Differential diagnosis3. Review of multimodality imaging findings including recommended protocol and expected findings for each one4. Discussion of management and outcome including Shambling classification and prognosis based on pathology or imaging findings

Printed on: 02/07/23



## Abstract Archives of the RSNA, 2022

HNEE-61

### Postoperative Imaging of Sinonasal Surgery and its Complications: What To Look for?

Sunday, Nov. 27 8:00AM - 9:00AM Room: Learning Center - HN

#### Participants

Raphael Correia, MD, Sao Paulo, Brazil (*Presenter*) Nothing to Disclose

#### TEACHING POINTS

To recognize the main sinonasal surgeries and their anatomic landmarks. To understand the expected postoperative findings of sinonasal surgery. To review the clinical presentations and imaging findings of sinonasal surgery complications.

#### TABLE OF CONTENTS/OUTLINE

Introduction. Sinonasal Anatomy. Main Surgical Procedures and Their Anatomic Landmarks. Imaging Technique and Protocols. Expected Postoperative Appearance, Including Grafts and Prosthesis. Clinical Presentations and Imaging Features of Postoperative Complications With Teaching Cases. Conclusions. References.

Printed on: 02/07/23



## Abstract Archives of the RSNA, 2022

HNEE-62

### The radiologist's guide to the Pterygopalatine Fossa

Sunday, Nov. 27 8:00AM - 9:00AM Room: Learning Center - HN

#### Awards

Identified for RadioGraphics

#### Participants

Alba Salgado Parente, MD, Madrid, Spain (*Presenter*) Nothing to Disclose

#### TEACHING POINTS

1. Review in detail the anatomy and communications of the pterygopalatine fossa (PPF).2. To expose the main keys to recognize and evaluate the perineural extension of tumors.3. To review the main pathologies that can affect this anatomical area.4. To develop a systematic approach to facilitate the evaluation of this space and avoid diagnostic errors.

#### TABLE OF CONTENTS/OUTLINE

1. Introduction2. Imaging anatomy, content and communications of the PPF2.1 Where is and what are the boundaries of the PPF?2.2 What does the PPF contain?2.3 Anatomical relationships and communications of the PPF.3. Pathology of the PPF3.1 Perineural extension: Concept, radiological signs and pathology (cavum carcinoma, palatal carcinoma and paranasal sinus carcinoma).3.2 Other pathologies: Direct tumor dissemination, masticatory space sarcomas, nasopharyngeal angiofibroma, invasive fungal disease, schwannomas and inflammatory pseudotumor.4. Pitfalls and how to avoid them: post-surgical changes and mimics5. Systematic approach to PPF: The nerve pathways that must be carefully evaluated depending on the pathology we are facing6. Take Home Points7. Bibliography

Printed on: 02/07/23



## Abstract Archives of the RSNA, 2022

HNEE-63HC

### Lessons From Dental School: What the General Radiologist Needs to Know About Teeth

Sunday, Nov. 27 8:00AM - 9:00AM Room: Learning Center - HN

#### Participants

Cameron Spence, MBChB, (*Presenter*) Nothing to Disclose

#### TEACHING POINTS

Radiologists who have not attended dental school are at a disadvantage when interpreting OPGs and other oral images such as CT. Whilst radiology curricula include frequently examined pathologies, such as periapical infections and cystic mandibular lesions, limited understanding of the basics of dentistry hamper our interpretation in clinical practice. This pictorial review will highlight the most important background concepts for radiologists that the authors learned during their dental degrees. Understanding these concepts will aid interpretation and help your delegates to provide more useful reports for the extended clinical team and patients.

#### TABLE OF CONTENTS/OUTLINE

Relevant radiographic dental anatomy. Restorative dentistry - how to recognize different restorations, including composite/amalgam/temporary fillings, root canal fillings, crowns, bridges, dentures, implants, and orthodontic appliances. Dental caries - where this begins, how it spreads through the dentine to the pulp, and how it leads to periapical pathology. Periodontal disease - generalized and localized types, assessing alveolar bone loss and recognizing commonly overlooked acute periodontal infections. Pericoronitis and impacted wisdom teeth. OPG limitations compared with intraoral dental radiographs. Please visit the Learning Center to also view this presentation in hardcopy format.

Printed on: 02/07/23



## Abstract Archives of the RSNA, 2022

HNEE-64

### Imaging Evaluation of Pulsatile Tinnitus: Case Based Review

Sunday, Nov. 27 8:00AM - 9:00AM Room: Learning Center - HN

#### Participants

Sang Soo Shin, MD, Gwangju, Korea, Republic Of (*Presenter*) Nothing to Disclose

#### TEACHING POINTS

1. To review the etiologic causes of pulsatile tinnitus2. To review the imaging role and technique in evaluation of pulsatile tinnitus3. To review the imaging findings and differential diagnosis4. To discuss the endovascular treatment of pulsatile tinnitus

#### TABLE OF CONTENTS/OUTLINE

1. Introduction2. Imaging role and technique in evaluation of pulsatile tinnitus3. Imaging findings and differential diagnosis: case based review1) Neoplastic: glomus tympanicum paraganglioma, glomus jugulare paraganglioma, meningioma2) Osseous: otosclerosis, intraosseous hemangioma, Paget's disease3) Arterial: aberrant ICA, persistent stapedial artery, ICA dissection/stenosis4) Venous: high riding jugular bulb, jugular bulb diverticulum, jugular bulb/sigmoid plate dehiscence, transverse sinus stenosis, dilated emissary vein5) Arteriovenous: dural AV fistula, AVM4. Endovascular treatment5. Summary

Printed on: 02/07/23



## Abstract Archives of the RSNA, 2022

HNEE-65

### A review of Uncommon Benign Pathologies of Larynx

Sunday, Nov. 27 8:00AM - 9:00AM Room: Learning Center - HN

#### Participants

Pooja Muddana, MBBS, (*Presenter*) Nothing to Disclose

#### TEACHING POINTS

The larynx can be affected by a multitude of pathologies of which squamous cell carcinomas are commonly encountered. Benign pathologies demonstrate typical imaging features, which aid in narrowing the list of differential diagnoses and differentiating them from malignant conditions. In this presentation we will: 1) Review the typical clinical presentation and pathology of the uncommon benign conditions. 2) Review imaging appearance of benign conditions that involve the larynx. 3) Review differential diagnoses for these conditions.

#### TABLE OF CONTENTS/OUTLINE

1) Introduction 2) Congenital - Laryngeal clefts, congenital high airway obstruction, laryngomalacia 3) Laryngocoele and laryngopyocoele 4) Infective conditions- Tuberculosis, Actinomycosis, Fungal infections, Scleroma, Leprosy 5) Immunological conditions - Granulomatous with polyangiitis, Relapsing polychondritis, Sarcoidosis, Rheumatoid arthritis, Ankylosing spondylitis 6) Amyloidosis 7) Thyroglossal duct cyst 8) Vascular malformations- Lymphatic malformation, Arteriovenous malformations 9) Conclusion

Printed on: 02/07/23



## Abstract Archives of the RSNA, 2022

HNEE-66

### New Pathways: Postoperative Changes in Aerodigestive Tract After Neck Surgery

Sunday, Nov. 27 8:00AM - 9:00AM Room: Learning Center - HN

#### Participants

Naomi Murakami SR, MBBS, Niteroi, Brazil (*Presenter*) Nothing to Disclose

#### TEACHING POINTS

Review normal neck anatomy in order to identify surgical manipulations. Recognize the anatomic changes that are associated with aerodigestive tract surgery. Discuss important complications of these procedures.

#### TABLE OF CONTENTS/OUTLINE

Different types of devices are used in surgery for neck injuries and diseases. They can be either parts of organs, such as neoesophagus with colon, or medical devices, such as metallic prosthesis. It's important to identify correctly these neck changes and complications that may be associated. This pictorial review will discuss. 1. Neck anatomy review. 2. The role of different imaging techniques in evaluation of medical devices, anatomic changes and complications: a. Computed tomography b. Magnetic resonance imaging c. Esophagogram 3. Surgical techniques and anatomic changes: Esophagectomy: gastric tube and colon interposition Prosthesis in upper airway Esophageal prosthesis Tracheoesophageal phonation prosthesis 4. Complications: Collection/ abscess Fistulas: tracheoesophageal, esophagocutaneous, pharyngocutaneous Necrosis

Printed on: 02/07/23

## Abstract Archives of the RSNA, 2022

HNEE-67

### The Face of Beauty: Image Features and Complications of Facial Cosmetics Procedures

Sunday, Nov. 27 8:00AM - 9:00AM Room: Learning Center - HN

#### Awards

Identified for RadioGraphics

#### Participants

Beatriz Prado, MD, Sao Paulo, Brazil (*Presenter*) Nothing to Disclose

#### TEACHING POINTS

Review the anatomy of facial fat compartments To discuss and illustrate, through clinical cases, the imaging aspects expected after a facial aesthetic procedure, as well some relevant complications and common diagnostic pitfalls.

#### TABLE OF CONTENTS/OUTLINE

Anatomy of fat compartments Contribution of different non-invasive imaging methods to detect facial cosmetic material Types of cosmetic procedures Facial Implants Fillers: Fat filler, hyaluronic acid, polymethylmethacrylate, calcium hydroxyapatite, paraffin, silicone Thread-Lifting Blepharoplasty Bichectomy Complications of facial filler injections and role of imaging Hematoma and seroma formation Infections Migration of injected substances Asymmetries Formation of foreign body granuloma Vascular occlusion leading to skin necrosis or blindness Inadvertent injury to adjacent structures Pitfalls in image interpretations

Printed on: 02/07/23



## Abstract Archives of the RSNA, 2022

HNEE-7

### Vocal Cord Paralysis: A Practical Approach

Sunday, Nov. 27 8:00AM - 9:00AM Room: Learning Center - HN

#### Participants

Thiago Martins Fernandes Vilela, Mogi das Cruzes, Brazil (*Presenter*) Nothing to Disclose

#### TEACHING POINTS

-- To review the normal anatomy of vagal and recurrent laryngeal nerves and the larynx.-- To illustrate the specific and secondary imaging features found in vocal cord paralysis and its mimics and pitfalls.-- To develop an analysis roadmap that should be performed when faced with a vocal cord paralysis.-- Illustrated review of a series of cases of vocal cord paralysis and lesions that may possible be related to vocal cord paralysis.-- To demonstrate the treatments that can be performed in these cases, their imaging aspects and possible complications.

#### TABLE OF CONTENTS/OUTLINE

-- Introduction-- Epidemiology-- Clinical scenarios-- Anatomy- Vagus nerves and their nuclei- Recurrent laryngeal nerves- Larynx-- Typical and secondary imaging features-- Pitfalls and mimics-- Analysis roadmap-- Series of cases of vocal cord paralysis-- Treatments and their image appearance-- Conclusion

Printed on: 02/07/23



## Abstract Archives of the RSNA, 2022

HNEE-8

### Fungal Infections of the Head and Neck: Imaging Spectrum

Sunday, Nov. 27 8:00AM - 9:00AM Room: Learning Center - HN

#### Participants

Niels Vinicius Padua Carvalho, MD, Sao Paulo, Brazil (*Presenter*) Nothing to Disclose

#### TEACHING POINTS

1. The aim of this exhibition is to:2. Review the spectrum of fungal infections of the head and neck.3. Discuss the main findings across all imaging techniques, overall CT and MRI4. Unify all this conditions in a single article/presentation.5. Highlight the importance of imaging in the diagnosis and treatment process.

#### TABLE OF CONTENTS/OUTLINE

1. INTRODUCTIONa. Considerations on fungal infections and its prevalence and relevance affecting head and neck structures.2. IMAGING INTERPRETATIONa. Imaging techniques and findings.b. When to do imaging screening, control and surveillance for these diseases.3. INTERACTIVE CASE-BASED DIDACTICSa. Sample cases to illustrate and solidify the concepts about the main findings of these diseases, separated through head and neck spaces: i. Temporal bones ii. Pharynx iii. Larynx iv. Orbit v. Sinuses4. FURTHER DIRECTIONS AND TAKE HOME MESSAGES

Printed on: 02/07/23



## Abstract Archives of the RSNA, 2022

INEE

### Informatics Education Exhibits

Sunday, Nov. 27 8:00AM - 9:00AM Room: Learning Center - IN

#### Sub-Events

#### INEE-10 Developing a Prostate Cancer Radiologic-Pathologic Correlated Quality Reporting Dashboard

Participants

Ryan Ward, MD, (*Presenter*) Nothing to Disclose

#### TEACHING POINTS

Prostate cancer is an important cause of morbidity and mortality in men. The Prostate Imaging Reporting and Data System (PI-RADS) provides a framework for systematically scoring lesions on prostate MRI based on clinical suspicion for prostate cancer. Using this data, combined with actual pathologic outcomes, we developed a robust system for tracking patients being evaluated for prostate cancer. The system allows the user to evaluate diagnostic performance at physician, department, and enterprise level and easily identify patients where discordance may exist between MRI findings and pathologic result.

#### TABLE OF CONTENTS/OUTLINE

1) Provide a brief overview of prostate cancer and the PI-RADS scoring system. 2) Describe the importance of tracking and analyzing prostate MRI data. 3) Describe the underlying technology/architecture for extracting, transforming, and loading the data into the data warehouse. 4) Provide examples of the dashboard and the different visualizations available.

#### INEE-12 Standardized Operational Log of Events (SOLE) for Artificial Intelligence (AI) Monitoring

Awards

Certificate of Merit

Identified for RadioGraphics

Participants

Ali Tejani, MD, Frisco, TX (*Presenter*) Nothing to Disclose

#### TEACHING POINTS

1. Provide an overview of IHE standardized operational log of events (SOLE)2. Review the interoperability advantages of using SOLE application programming interfaces (APIs) and codes in practice3. Describe specific metrics defined by SOLE to monitor deployed AI solutions4. Demonstrate how processes monitored by SOLE codes can be visualized through business analytics/dashboards5. Describe challenges with adopting SOLE APIs and codes in practice

#### TABLE OF CONTENTS/OUTLINE

1. Introductiona. Describe the problem: lack of interoperability and an efficient means of monitoring AI solutions workflowsb. SOLE for business analytics/process miningi. Review SOLE APIsii. Review select SOLE codesc. Introduce the concept of SOLE for AI monitoring2. Review how SOLE can be applied for AI monitoringa. Describe specific use cases to demonstrate how SOLE codes can be used to monitor AIi. Frequency of AI tool useii. Disagreement rate with AI resultsiii. Effect of AI tool use on time from study ordered to study readiv. Clinical monitoring for the impact of AI on patient care1. Time to treatment based on urgent AI alert2. Time to ED admissionv. Aggregating history of events over an extended time (i.e., if needing to justify ROI for annual budget)b. Demonstrate visualization of processes captured by SOLE codes with business analytics/dashboards3. Challenges associated with adopting SOLE APIs and codesa. Presence of multiple profiles (SYSLOG, ATNA, FHIR)b. Distilling the list of codesc. Encouraging vendor adoptiond. Flexibility to capture all potential AI-radiologist interactions

#### INEE-13CS Try Before You Buy: A One-Stop-Shop Approach for Testing and Procuring Commercial AI Applications

Participants

Vidur Mahajan, MBBS, New Delhi, India (*Presenter*) Employee, CARPL.ai

#### TEACHING POINTS

1. There are more than 150 FDA approved AI applications and the new approvals are growing at 50% per annum. There are 100s of other commercial AI applications available around the world.2. This makes it nearly impossible for radiologists to effectively discover and test these AI solutions on their own data.3. We present a software system with pre-integrated commercial AI applications, i.e. an AI marketplace, which allows radiologists to upload their own data and rigorously test the performance of the application.4. The software includes in built data management, anonymisation, cohort creation, annotation and statistical analysis tools.5. The option to ensemble AI outputs to improve performance also exists.

#### TABLE OF CONTENTS/OUTLINE

Our exhibit will be a computer system with 3 monitors, replicating the radiologists workstation. Radiologists at RSNA would be able to

bring their own data and upload it into this system and choose to run commercial AI applications and compare their performance. This would allow them to make informed purchase decisions, and optimize for productivity / quality gains. We believe that ours is a unique offering which can exponentially drive the adoption of clinical AI.

#### **INEE-14      Ultrasound-guided Peripheral Insertion System using Deep Learning**

Participants

Yuina Ezawa, Maebashi, Japan (*Presenter*) Nothing to Disclose

##### **TEACHING POINTS**

Puncture of peripheral blood vessels in the elderly and children is a difficult activity. Ultrasound-guided venipuncture is a widely used method to facilitate peripheral venipuncture. In this method, the positional relationship between the target blood vessel and the needle is confirmed, and the target blood vessel is punctured while operating the probe and needle at the same time. However, it is very difficult to confirm the positional relationship between the target blood vessel and the needle. To solve this problem, we propose a method that uses a convolutional neural network (DCNN) to automatically extract blood vessels and needles on the image. It is possible to display the optimum needle approach angle by computer-assisted detection. This method can show the positional relationship between the peripheral vein and the needle and provide useful information to assist in the puncture. The major teaching points of this exhibit are to: 1. automatically extract blood vessels and needles from ultrasound images. 2. understand how to extract blood vessels and needles using DCNN. 3. be useful for ultrasonic-guided venipuncture.

##### **TABLE OF CONTENTS/OUTLINE**

To discuss the clinical usefulness for accurate examination in ultrasound-guided venipuncture using DCNN extraction.

#### **INEE-15      The New 3D Slicer Version 5.0 Open Source Platform for Medical Image Analysis, 3D Visualization and Image-guided Intervention**

Participants

Sonia M. Pujol, PhD, MSc, (*Presenter*) Nothing to Disclose

##### **TEACHING POINTS**

3D Slicer is an open-source and extensible software platform used in clinical research worldwide. The new Slicer 5.0 release version provides hundreds essential core modules and extensions, and builds on the success of the version 4 downloaded over 1 million times since RSNA 2011. The goal of the exhibit is: 1. To review a brief history of 3D Slicer development in the past 20 years; 2. To discover the DICOMweb browser for cloud-based DICOM workflows; 3. To visualize GPU-based volume-rendering of DICOM images; 4. To discover the new Markups features; 5. To perform interactive segmentation of 2D/3D/4D images; 6. To discover the new MONAI Label extension for AI-assisted image annotation; 7. To learn new Slicer features for COVID-19 data analysis; 8. To create 3D solid objects for 3D printing; 9. To perform real-time data fusion for image-guided therapy; 10. To connect Slicer with robots, scanners, and trackers; 11. To interact with 3D scenes using virtual and augmented reality headsets; 12. To perform cloud-based computing in a Web browser using AWS AppStream 2.0, in a Docker container or a Jupyter notebook kernel; 13. To understand how to use 3D Slicer in clinical research applications.

##### **TABLE OF CONTENTS/OUTLINE**

Overview of the new 3D Slicer version 5.0; DICOM Standard Interoperability: import/export and structured reporting; DICOMweb features; GPU-based 3D and 4D Volume Rendering; Markups and Automated Measurements; Interactive 2D/3D/4D Image Segmentation; 3D Printing; Artificial Intelligence; Virtual and Augmented Reality; Cloud-based Computing; Clinical Applications in COVID-19, Surgical Navigation, and Image-Guided Intervention; Slicer Community Resources: Forum, Training Compendium, and Documentation.

#### **INEE-16HC      Understanding Patient Needs and Gaps in Radiology Reports Through Online Discussion Forum Analysis**

Participants

Mohammad Alarifi, PhD, (*Presenter*) Nothing to Disclose

##### **TEACHING POINTS**

Our objective is to investigate patient needs and understand information gaps in radiology reports using patient questions that were posted on online discussion forums. We leveraged online question and answer platforms to collect questions posted by patients to understand current gaps and patient needs. We retrieved six hundred fifty-nine (659) questions using the following sites: Yahoo Answers, Reddit.com, Quora, and Wiki Answers. The questions retrieved were classified into eight major themes. The themes were related to the following topics: radiology report, safety, price, preparation, procedure, meaning, medical staff, and patient portal. Among the 659 questions, 35.50% were concerned with the radiology report. The most common question topics in the radiology report focused on patient understanding of the radiology report (62 of 234 [26.49%]), image visualization (53 of 234 [22.64%]), and report representation (46 of 234 [19.65%]). We also found that most patients were concerned about understanding the MRI report (32%; n = 143) compared with the other imaging modalities (n = 434). Using online discussion forums, we discussed major unmet patient needs and information gaps in radiology reports. These issues could be improved to enhance radiology design in the future.

##### **TABLE OF CONTENTS/OUTLINE**

Introduction  
Methods  
Data sources and collection  
Thematic analysis  
Patient-centered approach  
Results  
( Summary of the four data sources, Analysis of patient question themes, Radiology report results; Safety, Procedure processing, Meaning, Preparation Patient portal, Preparation, The medical staff and Price  
Conclusion  
Please visit the Learning Center to also view this presentation in hardcopy format.

#### **INEE-17      Adding Value in Radiology: 3D Imaging Lab**

Participants

Larson Hsu, MD, (*Presenter*) Nothing to Disclose

##### **TEACHING POINTS**

In contrast to conventional volume rendering static images, segmentations of the patient's anatomy can be exported as a 3D model and further utilized in different applications for better spatial understanding of the disease. For example, the 3D model can be reviewed with an interactive viewer on the computer or other flat-screen devices, or visualized in virtual or augmented realities. It can also be 3D printed as an anatomical model for presurgical planning, or used as the basis to design patient-specific medical devices such as cutting guides or wearable prostheses. In this exhibit we will share the experience of our 3D imaging lab in a cancer center, and demonstrate how it can add value to the Radiology Department and potentially improve patient care.

#### TABLE OF CONTENTS/OUTLINE

1) Introduction/background: radiology 3D imaging lab 2) Volume rendering vs. 3D segmentation model 3) Advanced visualization using virtual and augmented realities 4) 3D printing of anatomical models and patient-specific medical devices at the point-of-care 5) Showcase and examples of 3D model applications in different disciplines 6) Future directions

#### INEE-18 Demystifying Coloring and Surface Labeled 3D Printed Anatomical Models

Participants

Muhammad Rehman, BA, Virginia, VA (*Presenter*) Nothing to Disclose

#### TEACHING POINTS

? Discussion on the relevance and importance of multi-color 3D printing with emphasis on models with special surface characteristics such as text, image and texture ? Highlighting various applications of color 3D models such as educational models, in clinical cases or for research purposes ? Pros and cons of de novo creation of multi-part STL files vs working on pre-existing STL files ? Advantages and disadvantages of graphically designing STL files vs using cross-sectional imaging to 3D reconstruct STL files in the educational setting ? Introducing UV surface mapping ? Detailing multiple software programs that can be used to color, label and imprint images onto the surface of a preexisting STL file and providing brief methodology for each ? Discussion of different 3D printing techniques that allow for color 3D printing, especially highlighting novel Multi Jet Fusion technology that allows for development of highly durable and versatile models with fully customizable surface appearance, not previously as robustly available ? A chart detailing subjective learning curve, user friendliness and cost of the software programs and 3D printers/printing services

#### TABLE OF CONTENTS/OUTLINE

? Background ? Discussion ? Software programs ? Meshmixer ? Microsoft Paint 3D ? Blender ? Autodesk 3d Studio Max ? Color 3D printing techniques ? PolyJet ? Stereolithography ? Paper Based ? Binder Jetting ? Multi Jet Fusion ? Summary chart

#### INEE-19 Quantitative Evaluation of a Large-scale Multi-year Artificial Intelligence (AI) Deployment at a Large Academic Radiology Department - Key Metrics, Trends, and Milestones

Participants

Axel Wismueller, MD, PhD, Pittsford, NY (*Presenter*) Nothing to Disclose

#### TEACHING POINTS

A) We present key analytics, trends, and milestones that are extracted from a multi-year large-scale AI clinical deployment of a radiology triage and prioritization solution in a large academic hospital setting. B) The analytics, trends and milestones are extracted from the hospital system's experience of taking a single-pathology AI module and scaling it out to cover nine different pathologies. Our analysis provides a set of recommended metrics to measure growth, performance, and user engagement. C) We present trends for various milestones and how the metrics change as an AI solution scales up to cover a greater number of imaging examinations. D) Our case study may provide insights and value to other radiology practices and hospital systems as a basis for defining best practice guidelines, and for contributing to the calculation of business metrics, such as Return-on-Investment (ROI) or Total Cost of Ownership (TCO) in the clinical adoption of AI solutions.

#### TABLE OF CONTENTS/OUTLINE

A) Introduction: 1. Description of project goals and timeline 2. Overview of the AI integration into the radiologist workflow B) Metrics: 1. Description and visualization of metrics for measuring: a) Growth of the AI adoption b) Performance of the AI c) User engagement 2. Highlights of the key trends milestones C) Summary of key metrics: 1. Overview of the value of each metric 2. Identified minimum thresholds for success criteria 3. Summary of teaching points

#### INEE-1CS Using the Open Health Imaging Foundation (OHIF) Framework To Build Web-based Imaging Applications

Participants

Erik Ziegler, MSc, PhD, (*Presenter*) Consultant, Radical Imaging LLC; Consultant, Novometrics LLC; Stockholder, Yunu Inc

#### TEACHING POINTS

The purpose of this exhibit is to: 1. Explain how radiologists can build their own imaging tools and applications using the open source Open Health Imaging Foundation (OHIF) framework to address their custom use cases. 2. Discuss the components of a full fledged zero-footprint web-based imaging application and how they interact using various APIs (e.g. DICOMweb). 3. Explain how advanced functionality, such as 3D visualization, image fusion, and segmentation, can be incorporated in these applications. 4. Demonstrate how to organize specific function sets into custom workflow modes for optimizing efficiency. 5. Demonstrate how this type of system can be deployed both securely and cost effectively.

#### TABLE OF CONTENTS/OUTLINE

- Open source resources for radiology and AI applications- Relationships between components in web imaging applications- Building custom measurement tools- Incorporating advanced visualization and segmentation tools- Building custom workflow modes for the OHIF Viewer (e.g. configuring the application to provide functionality for use cases like ProstateCancer.ai, NCI Imaging Data Commons, XNAT)- Deploying scalable secure web imaging applications locally or using cloud resources- Future directions

#### INEE-2 Development of A Training Simulator of Plain Radiography Using Augmented Reality Technology

Awards

Certificate of Merit

Participants  
Kaito Oikawa, (*Presenter*) Nothing to Disclose

#### TEACHING POINTS

Radiographers need to acquire proficient skills through a great deal of experience to perform plain radiography accurately. Lack of such skills may lead to misdiagnosis and unnecessary radiation exposure. Conventional training methods for plain radiography were phantom radiography and radiography role-playing. They were insufficient to develop proficient skills because of the unlike clinical settings. Recently, a radiography training simulator using virtual reality was proposed. This simulator allowed the trainee to perform plain radiography on a virtual subject in a virtual space. However, the trainee cannot touch the virtual subject in this training simulator. This is the same as the conventional training methods in that it is different from the clinical settings. Therefore, we developed a training simulator of plain radiography using augmented reality technology. Our simulator can output virtual x-ray images similar to clinical settings, adapting positions and angles obtained by tracking human subjects in real time. The training using our simulator allows trainees to acquire proficient skills in preclinical training.

#### TABLE OF CONTENTS/OUTLINE

Lack of skills in plain radiography may lead to misdiagnosis and unnecessary radiation exposure in clinical settings. Our simulator can output the virtual x-ray images that reflect the positions and angles of the subject. Radiographers can acquire proficient skills by training the plain radiography repeatedly using our simulator.

#### INEE-20HC Taking the Medical Devices Through the Regulatory Gatekeepers: How To Do It Right!

Participants  
Bhanushree Bahl, New Delhi, India (*Presenter*) Employee, CARPL.ai

#### TEACHING POINTS

The clinical trial of AI-based Investigational Devices (AID) will look at the device performance through the lens of business capabilities, while evaluating technologies. Our exhibit will showcase the clinical trial workflow of AI algorithms with multiple scenarios for different regulatory approvals. Regulatory approvals are necessary for an AI model to be used clinically, and to add value to the business. AI companies can run clinical trials, which will help them get comprehensive results through data analysis for improved decision making. Conducting clinical trials on extensive data allows AI companies to detect patterns for enhanced business performance. We will highlight the steps needed to conduct a successful clinical trial for various scenarios. In addition to this, the exhibit will also feature protocols required to follow for different regulatory approvals.

#### TABLE OF CONTENTS/OUTLINE

Protocol Synopsis: Study name, objective and type of the study, with the design procedure along with the calculated sample size and investigator selection (Screener / Reader / Gter). Study procedure: Ethical committee approval, Data collection and de-identifying studies, Screening, Ground Truthing, Standalone performance evaluation, Reader test Data Management Plan / Flow: Annotation Platform (Ex: CARPL), System verification and UAT, Security and maintenance of account External Data Management Process: Data collection and archiving and cleaning, Master data Set creation Study Endpoints and Statistical Analysis: Threshold of study endpoints and statistical analysis, Endpoints in standalone performance test Preparation of Violation List Please visit the Learning Center to also view this presentation in hardcopy format.

#### INEE-21 The Day After Tomorrow: How to Monitor A Deployed AI Model and Automate the Radiologist Feedback Loop

Participants  
Victor Menezes, MD, Sao Paulo, Brazil (*Presenter*) Nothing to Disclose

#### TEACHING POINTS

To describe how an Artificial Intelligence (AI) model can lose performance due to data drift / concept drift; To describe other biases that can affect an AI model; To explain the importance of monitoring an AI model over time; To explain how to sustain and monitor the performance of an AI model after the deployment. To illustrate with an example of how we built an automated feedback loop. To explore a few options on how to maintain performance in the long run and retrain the model if necessary.

#### TABLE OF CONTENTS/OUTLINE

1. Model degradation: Data drift, Concept drift and Upstream data changes; 2. How to automatically gather and analyze AI model inferences; 3. Types of AI model scenarios and the possible types of analysis; 4. Main metrics to evaluate the performance of an AI model; 5. When and how to retrain an AI model and other options to maintain performance in the long run.

#### INEE-22HC A Practical Guideline for Safely Deploying Continuous Machine Learning Systems

Participants  
Camila Gonzalez, MS, Darmstadt, Germany (*Presenter*) Nothing to Disclose

#### TEACHING POINTS

A central advantage of successful learning systems is their ability to adapt to new conditions in the dynamic real world. In clinical practice, common changes range from developments in image acquisition protocols to shifts in the patient population. When designing AI-powered systems, building mechanisms that allow such adjustments is necessary for preventing dangerous performance declines. Yet no continuous learning system is in use as of now. In this abstract, we summarize the central obstacles preventing the deployment of such solutions, and present practical advice on how to overcome them. We explore FDA and European Commission regulations (both in-effect and works-on-progress), consider the daily work of clinicians, and review under which conditions continuous learning systems can be a better return on investment than statically trained models. Our guide is useful for all relevant stakeholders, from data scientists to hospital administration.

#### TABLE OF CONTENTS/OUTLINE

(1) Continuous learning systems: definitions, technical challenges and benefits (2) Regulatory frameworks for the approval of continuous learning solutions in the USA and EU (3) Considerations for medical professionals when deploying continuously trained models in clinical practice (4) Cost-benefit analysis from an economic perspective: why continuous Machine Learning is

advantageous despite the regulatory overhead Please visit the Learning Center to also view this presentation in hardcopy format.

### **INEE-23 Selection and Maintenance of Consumer Grade Displays for Home Reading Workstations**

Participants

Douglas Nachand, MD, Shaker Heights, OH (*Presenter*) Nothing to Disclose

#### **TEACHING POINTS**

- Describe the display specifications of a consumer grade display that meets the suggested guidelines for non-mammographic diagnostic imaging- Design a workflow to properly calibrate the monitor for diagnostic purposes at baseline and at set intervals

#### **TABLE OF CONTENTS/OUTLINE**

Choosing a diagnostic display- What are the guidelines and who sets them -- Guidelines for non-mammography displays-- Mammography displays are regulated (specifications and quality control) and will not be covered- Pros and cons of displays marketed as consumer and medical grade- Ensuring your monitor meets the standards and additional features to consider Acceptance Testing and Initial Setup- Necessary equipment and software- Describe baseline and periodic calibration workflows-- How to perform-- Estimated time to complete Maintenance and Quality Control- Expected points of failure- QC tests, frequency, expected radiologist time Conclusions

### **INEE-24 Educational Applications of Metaverse and XR Extended Reality (VR, AR, MR) for Radiology and Telemedicine**

**Awards**

**Identified for RadioGraphics**

Participants

Maki Sugimoto, MD, PhD, (*Presenter*) Officer, Holoeyes Inc

#### **TEACHING POINTS**

To define the metaverse in radiology and to explain the potential and limitations of its educational applications. 1) To learn the utilization of metaverse and XR (virtual-augmented-mixed reality) in medical imaging. 2) To learn how to segment and export polygons of targeting organs from DICOM data from CT or MRI. 3) To learn how to utilize metaverse systems and XR devices. 4) To show clinical examples, such as in medical education, surgical planning, simulation, and navigation. 5) To learn how to integrate metaverse and XR to improve visual-spatial ability to mentally manipulate medical anatomy in three dimensions.

#### **TABLE OF CONTENTS/OUTLINE**

1. Terminology: The representative forms such as XR (VR/AR/MR) are referring to all real-and-virtual combined environments and human-machine interactions generated by computer technology and wearables. 2. Beneficial applications of the XR devices and metaverse. 3. How to integrate the spatial imaging system and metaverse using avatars by interactive superimposing 3D holograms. 4. Effectiveness: Enhancing scene visualization is a feasible strategy for augmenting spatial awareness in complex anatomy education.

### **INEE-25 Estimating Vascular Age in Carotid Ultrasound using Deep Learning**

Participants

Rena Nishimaki, Maebashi, Japan (*Presenter*) Nothing to Disclose

#### **TEACHING POINTS**

Heart and cerebrovascular diseases are caused by atherosclerosis, which is associated with the aging of blood vessels. Understanding vascular age plays a major role in the prevention of vascular diseases. The progression of arteriosclerosis is measured by ultrasonography (US), pulse wave velocity, and cardio-ankle vascular index. Carotid US is an excellent examination for early detection and evaluation of patients and indicates the degree of atherosclerosis as a whole body. However, carotid US alone cannot evaluate vascular age as an indicator of atherosclerosis. In this study, we propose estimating vascular age in the carotid US using a deep convolutional neural network (DCNN). It can provide useful information on the appropriate diagnosis of atherosclerosis. The major teaching points of this exhibit are to: 1. classify and regress the carotid US using DCNN. 2. understand how to estimate vascular age with a computer-aided diagnosis (CAD) system. 3. be useful for diagnosing atherosclerosis.

#### **TABLE OF CONTENTS/OUTLINE**

To provide CAD using DCNN regarding estimation of vascular age and discuss clinical usefulness toward accurate diagnosis of the arteriosclerosis in ultrasonography.

### **INEE-26 Unsupervised Learning Classification of Rectum Region for Prostate Cancer During Image-guided Radiation Therapy in CBCT**

Participants

Haruyuki Watanabe, PhD, (*Presenter*) Nothing to Disclose

#### **TEACHING POINTS**

Intensity-modulated radiotherapy (IMRT) is a more effective curative treatment option for prostate cancer patients than surgery. IMRT uses for tumor and normal organ detection to generate treatment plans that confine the prescribed dose to cancer while maximally excluding the adjacent normal organs. Image-guided radiation therapy using cone-beam CT (CBCT) associated with IMRT provides a safe and reliable radiotherapy treatment. Because the rectal size and shape cause prostate motion, it is necessary to confirm in CBCT images. If necessary, after checking the CBCT images, defecation and exhaust gas treatment are required. However, there is no clear standard as to whether to take the treatment. Thus, we propose an unsupervised learning classification to support the decision of treatment such as defecation and exhaust gas. The major teaching points of this exhibit are to: 1. automatically classify the rectum region. 2. understand how to use unsupervised learning schemes. 3. be useful for prostate cancer during image-guided radiation therapy in CBCT.

#### **TABLE OF CONTENTS/OUTLINE**

To provide unsupervised learning classification regarding validation of image-guided radiation therapy in CBCT.

## **INEE-27 Natural Language Processing in Radiology: State of the Art and Future Directions**

### **Awards**

**Magna Cum Laude**

Participants

Pratheek Bobba, BS, New Haven, CT (*Presenter*) Nothing to Disclose

### **TEACHING POINTS**

1. The need for Natural Language Processing (NLP) in Radiology. 2. History of NLP and milestones. 3. Current clinical applications of NLP in radiology. 4. Applications and future directions of NLP in radiology.

### **TABLE OF CONTENTS/OUTLINE**

1. The need for NLP in radiology: Cures act for radiology benefits and challenges including health literacy, increased anxiety from patients reading reports without guidance, increased calls to clinicians which may disrupt workflow. 2. History and milestones: brief review of the history of NLP and the current NLP models, focusing on Bidirectional Encoder Representations from Transformers (BERT). 3. Current state of the art: there has been an exponential increase in rate of NLP in radiology publications, with a 3-fold increase in publications about NLP in radiology from 2015 to 2019, focusing on extracting disease information from reports/labelling disease phenotypes rather than clinical applications. 4. A review of the need for the following applications of NLP in radiology: text simplification, text summarization, extracting information, cohort creation/entity recognition, reporting accuracy/quality assurance, revenue loss, billing code generation, appropriate communication of disease acuity, and a special focus on structured reporting and NLP.

## **INEE-28HC Introduction to Clinical Workflow to Engineer 3D Printed Patient Specific Models with Specified Tissue Mechanical Properties**

Participants

Kelsey Sommer, PhD, Buffalo, NY (*Presenter*) Stockholder, QAS.AI

### **TEACHING POINTS**

Learn how to design and 3D print patient-specific phantoms on a multi-material anatomical printer which allows selection of specific mechanical properties for various tissues. Exemplification of multi-material 3D printed phantoms with specified mechanical properties: coronary arteries, neurovasculature and spine. Exemplification of using multi-material 3D printed phantoms for testing, residency training and treatment planning. 3D printing of patient specific phantoms is a benchtop tool that has high precision in geometric modelling and material properties. The latest advances in 3D printing allows mixing of polymers to simulate mechanical properties for various tissues and diseased state. Such advances allow performance of precise biomechanical, imaging or flow experimentation with controlled parameters such as pressure, flow rates, compliance, and range of motion.

### **TABLE OF CONTENTS/OUTLINE**

- Exemplification of multi-material use for coronary arteries, neurovasculature and spine
- Segmentation workflow, with focus on separation of various tissues
- 3D printing process, including optimal selection of materials for a Stratasys J750 Anatomical Printer
- Post-processing of 3D printed models
- Applications of 3D printed patient-specific anatomical modelling
- Discussion of the advantages and limitation of the new materials

Please visit the Learning Center to also view this presentation in hardcopy format.

## **INEE-29 Systematic Review of Evidence-Based Medical AI**

Participants

Terumasa Kondo, Toyoake, Japan (*Presenter*) Nothing to Disclose

### **TEACHING POINTS**

Deep learning is beginning to be used as an essential tool in radiology. However, the use of deep learning can lead to black-boxing of the technology due to the complexity of the process. To solve these problems, Deep learning visualization methods have attracted attention in recent years. When AI technology surpasses human classification performance, the basis for decision-making by deep learning is expected to bring new knowledge to the human race. This exhibition aims to introduce how deep learning can be visualized, and will also show examples of research using CAM (Class activation map) and the development of a prognosis prediction method for CCU patients using electrocardiogram images. Main teaching point 1. Black box problem of deep learning 2. What is Explainable AI technology? 3. Examples of Explainable AI Technology using GradCAM

### **TABLE OF CONTENTS/OUTLINE**

TABLE OF CONTENTS 1. Black box problem of deep learning 2. What is Explainable AI technology? 3. Various types of Explainable 4. Example of Explainable AI technology 5. Our study

## **INEE-3 Prognostic AI-imaging Biomarkers: How to Predict the Survival of Patients With Idiopathic Pulmonary Fibrosis (IPF)**

### **Awards**

**Certificate of Merit**

Participants

Chinatsu Watari, MD, Boston, MA (*Presenter*) Nothing to Disclose

### **TEACHING POINTS**

Idiopathic pulmonary fibrosis (IPF) is a major chronic progressive interstitial lung disease, with a median survival of 2-5 years from the time of diagnosis without anti-fibrotic medication. The teaching points of this exhibit are to (1) review currently established clinical prognostic biomarkers for IPF, (2) review the most promising emerging radiomic and AI-based biomarkers for imaging-based prediction of the survival in IPF, and (3) review the comparative performance between clinically established and AI-based prognostic biomarkers in the image-based prediction of the survival in IPF.

## TABLE OF CONTENTS/OUTLINE

1. Why IPF is a problem. 2. Clinically established prognostic biomarkers for IPF (visual high-resolution CT (HRCT) pattern; gender, age, and physiology (GAP) index and staging system). 3. Radiomic biomarkers (traditional radiomics; hyper-curvature features; deep-learning radiomics) for survival analysis. 4. Why machine learning for survival analysis (AI-radiomics) outperforms clinical and radiomic biomarkers. 5. Comparative performance in terms of survival prediction and Kaplan-Meier survival curves. 6. Clinical case studies.

### INEE-30 **Mastering Basic Machine Learning Principles Without Coding Experience: A Tutorial on Google's Teaching Machine**

#### Awards

Certificate of Merit

Participants

Adam Flanders, MD, Philadelphia, PA (*Presenter*) Nothing to Disclose

#### TEACHING POINTS

1) Understanding machine learning requires developing a conceptual framework. 2) Recognize that fundamental machine learning principles can be learned without coding experience. 3) Understand the overall process to train a deep learning model. 4) Learn basic concepts on how to assess model generalizability and performance. 5) Appreciate that several free and easy to use non-coding solutions exist where you can experience training, validating and testing an image-based machine learning model. 6) Understand that adjustment of training hyperparameters and dataset balance/bias significantly affects the performance of your model.

## TABLE OF CONTENTS/OUTLINE

I) Introduction: Building a conceptual framework: introduction to hyperparameters (e.g. learning rate, batch size, epochs). II) Introduction to performance metrics: loss function, confusion matrix, accuracy. III) Datasets: tips to build an effective dataset. IV) Introduction to Google's Teachable Machine. V) Creating your classes / loading your data. VI) Train and view the performance live. VII) Adjust hyperparameters and observe the effect on training with loss curve and confusion matrix. VIII) Readjust the distribution of your positive and negative classes in your training dataset. IX) Observe the effects of data redistribution. X) Observe the effect of pre-processing to accuracy of the model. XI) Summary.

### INEE-31 **Robust AI in Brain MRI's Large-Factor Super-Resolution - And Its Application In Improving Brain CAD System's Precision**

#### Awards

Certificate of Merit

Participants

Tong Zheng, Nagoya, Japan (*Presenter*) Nothing to Disclose

#### TEACHING POINTS

1. To learn the concept of super-resolution (SR) and its applications in brain MRI. 2. To understand difficulties in brain MRI's SR and how does our proposed AI overcome these difficulties. 3. To learn how to train a registration-error robust AI for SR on low- and high-resolution images dataset. 4. To learn our SR AI's application in brain CAD system and how does our AI improve precision of the CAD system

## TABLE OF CONTENTS/OUTLINE

1. AI-based super-resolution (SR): fundamental concepts and application in medical imaging- SR technique enhances the resolution of a given image- AI can perform SR of medical images such as brain MRI. 2. Problems in training an AI for medical image SR- Training the AI needs precisely-registered low- and high-resolution image pairs- Existing AI for SR are not registration-error robust. 3. Techniques of our registration-error robust AI in medical image SR: newly-designed structure- Pre-train a StyleGAN as latent memory bank- Encoder-decoder structure to decompose images into high- and low-dimensional features. 4. Techniques of our registration-error robust AI in medical image SR: loss terms and pre-processing- Novel loss term to stabilize training procedure- Multi-channel input to obtain more spatial information. 5. SR results and its application in improving brain CAD system's precision- Our AI successfully performed SR of brain MRI images, made it easier for radiologists to observe brain structures only from low-resolution (LR) images taken with shorter scanning time- With our AI for SR, CAD systems can proceed more accurate diagnosis from LR MRI

### INEE-33 **Ready or Not, The Metaverse Will Have a Presence in Radiology**

Participants

Aditya Khurana, MD, Scottsdale, AZ (*Presenter*) Nothing to Disclose

#### TEACHING POINTS

(1) To present an initial discussion on the metaverse, its current state, and existing but limited literature within healthcare; (2) Present a thought experiment with key thought leaders as to what can the metaverse mean for Radiology in the future; (3) Outline future concepts with specific examples in which the metaverse can enhance the education, application, and visibility of radiology

## TABLE OF CONTENTS/OUTLINE

The "metaverse" is a relatively new concept emerging within technology in which humans can interact within a digital environment - it is the intersection of the virtual and real worlds and the emergence of a second digital life. The metaverse will have a presence in healthcare. As of May 1, 2022, Pubmed search for 'Metaverse' identified 33 articles thus far. Because the literature on this topic and its applications in radiology is still in its infancy, we present this exhibit as a thought experiment with key opinion leaders on how the metaverse will enhance radiology. We will discuss the integration of the metaverse with concepts such as: (1) Real time image analysis and insight, (2) Trainee education and experience, (3) Patient education, (4) Teleradiology, (5) Research, (6) Industry relations, (7) Knowledge sharing, and (8) Quality improvement patient safety.

## **INEE-35 Leveraging Virtual Containers for High-Powered-Collaborative AI Research in Radiology**

Participants

Lucas Aronson, BS, Madison, WI (*Presenter*) Nothing to Disclose

### **TEACHING POINTS**

(1) Multi-institutional collaboration of AI research poses challenges due to variations in hardware and software specifications. (2) No two users are likely to have the exact same requirements to execute their code, so even sharing between members of the same lab can present challenges. (3) Virtual containers alleviate many obstacles related to compatibility and portability and also offer a wide variety of tools to aid developers. (4) Virtual containers: (4a) Streamline remote access to high-powered computers and GPU servers. (4b) Can serve as a foundation for new projects with various base containers tailored to certain project types. This can save developers time as opposed to starting from scratch. (4c) Allow users to create portable, fully functional, self-contained coding environments for seamless operation irrespective of the computer/server employed. (4d) Facilitate multi-institutional collaboration and potential large-scale AI projects.

### **TABLE OF CONTENTS/OUTLINE**

(1) Why do we need virtual containers? (1a) Address hurdles researchers face when collaborating and sharing AI algorithms. (1b) Highlight some features of containers that mitigate these obstacles, including the specification of software versions and dependencies. (2) A guide to getting started with virtual containers. (2a) Demonstrate an example virtual container termed Docker, including: (2a1) The Dockerfile and requirements file (2a2) How to build a Docker Image (2a3) How to run a Docker Container (2a4) Useful commands in Docker (3) An example of how Docker was used to facilitate a large-scale AI project.

## **INEE-37 International Outreach in Medical Imaging Research: 3D Slicer Internationalization and Localization to French**

Participants

Sonia M. Pujol, PhD, MSc, (*Presenter*) Nothing to Disclose

### **TEACHING POINTS**

3D Slicer is an open-source software platform used in medical imaging research around the world. However, the application is currently available in the English language only. While English is the language of science, radiologists and medical imaging researchers in non-English speaking countries work and communicate with their scientific colleagues in their own languages. Through current Essential Open Source Software for Science funding of the Chan Zuckerberg Initiative, we have created a 3D Slicer internationalization team in the US, Canada, and Senegal to facilitate access to the platform for the global medical imaging research community. We have begun internationalizing 3D Slicer and localizing the user interface, tutorials, and documentation to French. The goal of the exhibit is 1. to provide an overview of the current 3D Slicer internationalization effort; 2. to introduce the new internationalization infrastructure for translating 3D Slicer user interface; 3. to present the 3D Slicer glossary for medical imaging research; 4. to teach how to contribute translations in multiple languages on the 3D Slicer translation repository; 5. to showcase 3D Slicer global outreach activities for medical imaging research in Senegal.

### **TABLE OF CONTENTS/OUTLINE**

Overview of 3D Slicer Internationalization effort; Language Packs extension; 3D Slicer Glossary; 3D Slicer Weblate Repository; 3D Slicer Community Resources in French; 3D Slicer Outreach in Senegal.

## **INEE-38 Statistical Plots in Oncologic Imaging: A Primer for Radiologists**

Participants

Sina Bagheri, MD, Philadelphia, PA (*Presenter*) Nothing to Disclose

### **TEACHING POINTS**

Visual illustrations of quantitative information, including graphs and figures, are often practical and powerful methods of presenting scientific research results. Appropriate implementation of graphs improves the accuracy of readers' interpretation and understanding of the data, particularly for complex information. Recently, an increasing number of novel diagrams and plots have been used to visually display the outcome in radio-oncologic and radiogenomic studies. Thus, it is crucial for radiologists to be familiar with these kinds of data representations. In this educational exhibit, we describe the potential application of these various statistical plots and guide radiologists to interpret them in such reports. We also highlight the specific features of each graph type and review its advantages and drawbacks/pitfalls.

### **TABLE OF CONTENTS/OUTLINE**

1. Brief introduction describing different ways for graphical representation of data 2. Graphical illustrations of tumor response 3. Graphical illustrations of survival 4. Graphical illustrations of cancer genotypes 5. Drawbacks and pitfalls 6. Conclusions

## **INEE-39CS NCI Imaging Data Commons: Towards Transparency and Reproducibility in Imaging AI**

### **Awards**

#### **Identified for RadioGraphics**

Participants

Andriy Fedorov, PhD, Arlington, MA (*Presenter*) Nothing to Disclose

### **TEACHING POINTS**

NCI Imaging Data Commons (IDC) is a cloud-based repository of publicly available cancer imaging data co-located with the analysis and exploration tools and resources. IDC is part of the NCI Cancer Research Data Commons (CRDC) infrastructure that provides secure access to a large, comprehensive, and expanding collection of cancer research data. IDC uses a combination of the commercially available Google Cloud Platform and open source components. The DICOM standard is used for representation and communication of the data. Google Healthcare API enables the use of SQL for DICOM metadata exploration. The IDC portal (<https://imaging.datacommons.cancer.gov>) enables exploration and visualization of data and cohort building. As of Spring 2022, IDC hosts over 30 TB of public radiology and digital pathology images and image-derived data. IDC is intended for cloud-based data

processing, but data can be freely downloaded for on-premise analysis. Cloud-based workflows co-locating persistent data with software tools and compute resources enable reproducible analysis workflows. Attendees will learn about the scope and status of IDC (e.g., new features of the image viewers and IDC portal), accompanying learning resources (e.g., interactive notebooks with reproducible AI workflows applied to the data within IDC), and plans for future development. Live interactive demonstrations will be presented.

#### TABLE OF CONTENTS/OUTLINE

Overview of CRDC and IDC; Data curation and the role of The Cancer Imaging Archive; Portal; Viewer; Organization of data; Data versioning; Integration of tools; Use case development; Documentation and user support resources; IDC cloud credit program; Status update and plans for future development.

#### INEE-40 COVID-19 Surveillance System Based On a Nationwide Medical Image Database and Machine Learning

##### Participants

Kensaku Mori, PhD, Nagoya, Japan (*Presenter*) Research Grant, Cybernet Systems Co, Ltd;Intellectual Property, Cybernet Systems Co, Ltd;Research Grant, J Morita Corporation;Intellectual Property, J Morita Corporation;Developer, J Morita Corporation

##### TEACHING POINTS

- To understand what is nationwide CT image database- To understand how cloud-computing environments are constructed for CT image analysis- To understand how a nationwide CT image database is utilized for COVID-19 surveillance- To understand how machine learning techniques can be used for COVID-19 surveillance

#### TABLE OF CONTENTS/OUTLINE

Introduction- COVID-19 related disease shows several findings on CT images, including GGO.- Machine learning-based methods enable us to analyze CT images of COVID-19 cases.Nationwide medical image database-A nationwide medical image database is constructed in collaboration with medical societies and National Institutes of Informatics.- Medical images taken at hospitals are transferred daily to the cloud data center through the Japanese academic network SINET in L2VPN connection.- The data center has GPU servers for machine learningCOVID-19 CT image analysis- Machine learning-based COVID-19 CT image analysis algorithm has been developed- The algorithm consist of lung area segmentation and CT image appearance classification (typical COVID-19 cases or atypical COVID-19 cases)- In-house neural network architecture has been developed.COVID-19 CT daily surveillance- All of CT images having "lung" words in diagnosis reports are targets for analysis- Only CT images, including lung areas, are selected for further analysis.- Number of lung CT cases, typical COVID-19 cases and atypical COVID-19 cases are measured.Discussion- Nationwide CT image database has potential to become one of the information sources to know COVID-19 disease spread in a nation- Surveillance based on automated CT image analysis on a nationwide database can be used for monitoring many disease spreads.

#### INEE-41 An Overview of Artificial Intelligence for Multiple Sclerosis Analysis in MRI

##### Participants

Leiner Barba, PhD, (*Presenter*) Nothing to Disclose

##### TEACHING POINTS

Purposes: 1) Provide an overview of artificial intelligence (AI) methods, experts team and technological needs, and their potential use in Radiology; 2) Review of Multiple Sclerosis (MS) affectations and biomarkers from MRI; 3) Discuss about how AI methods have been used for MS analysis; 4) Know the basis for application of AI to MS lesion detection and segmentation.

#### TABLE OF CONTENTS/OUTLINE

A. Overview of AI methods and MS affectations; B. Segmentation of MS lesions using AI techniques; C. Analysis of MS activity; D. How to use AI for analysis of affected regions in patient with MS; E. Challenges of applying AI for analysis of MS in clinical practice; F. Future trends of AI applied to MS analysis.

#### INEE-42 Generating Rapid Multiparametric Prostate MRI Protocols Using Deep Learning Reconstruction

##### Participants

David Wang, MD, (*Presenter*) Nothing to Disclose

##### TEACHING POINTS

Multiparametric Prostate MRI (mpMRI) protocol consists of high resolution multiplanar T2, diffusion weighted imaging (DWI), and dynamic contrast enhanced acquisitions. An ideal mpMRI protocol meeting or exceeding PIRADS recommendations can take ~25 minutes, even after optimizing protocols using commercially available acceleration techniques. The biggest time sinks within these protocols are the T2 weighted and high b-value DWI acquisitions. Recently, a Deep Learning (DL) reconstruction technology (AIR™ Recon DL, GE Healthcare) was leveraged to reduce the multiplanar T2 acquisition time by 3-fold, without loss in signal-to-noise ratio (SNR). In this exhibit, we will review the application of this DL reconstruction technology to both T2-weighted and DWI acquisitions, focusing on comparisons of the DL reconstruction to conventional reconstructions, as well as benefits in SNR and scan time reduction. Potential pitfalls and remaining artifacts from the accelerated acquisitions will be discussed as well as the requirements and trade-offs needed to achieve a fast and robust PI-RADS 2.1-compliant protocol in less than 10 minutes.

#### TABLE OF CONTENTS/OUTLINE

1. Key components of mpMRI for prostate cancer 2. Standard acquisitions and associated scan times. 3. Synopsis of DL technique and application to accelerated multiplanar T2-weighted imaging. 4. Application of DL reconstruction for DWI and synthetic b-value calculation. 5. Potential pitfalls and artifacts post DL reconstruction. 6. Overview of PI-RADS 2.1 compliant rapid protocols utilizing DL reconstruction. 7. Summary.

#### INEE-43 Federated Learning Environment in The ACRs AI Lab: Are Those Rubbers (AI models) Meant For Our Roads (Imaging Data)?

##### Participants

Lina Karout, MD, Boston, MA (*Presenter*) Nothing to Disclose

## TEACHING POINTS

(1) Understanding generalizability, reproducibility, and biases in AI models. (2) Foundation and application of federated learning environment for AI models. (3) Construction and deployment of data for federated learning. (4) Validation of AI models in ACR's AI Lab environment: Steps and Stats

## TABLE OF CONTENTS/OUTLINE

(1) Foundational aspects of federated learning in AI model validation: What is it and why do we need it? How does it help? What does it entail? (2) Case-based demonstration of how you can use ACR's AI Lab to test and optimize AI models in a federated learning environment: (a) Understanding steps in data format, gathering, and uploading to the AI Lab. (b) Running AI models in the AI-Lab. (c) Analyzing AI outputs and performance statistics. (d) Improving AI model performance from local to global level. (3) Strengths and limitations of federated learning and its environment

## INEE-44CS The Federated Tumor Segmentation Initiative: The Largest To-date Real-World Federation Focusing on NeuroOncology

Participants

Alexander Getka, Philadelphia, PA (*Presenter*) Nothing to Disclose

## TEACHING POINTS

There is a growing body of literature offering evidence of the potential impact that artificial intelligence (AI) methods can have towards healthcare. To ensure robustness and generalizability of AI methods, ample and diverse multi-site patient datasets are desired. However, there are various factors that hinder access to such data in the current paradigm of multi-site collaborations, which include the tedious bureaucratic processes, data ownership concerns, and legal considerations reflected in patient privacy regulations. To tackle these issues, we introduce the Federated Tumor Segmentation (FeTS) Initiative, which includes an open-source software toolkit for data-private collaborative learning of AI methods across multiple international institutions using federated learning (FL). The goals of the exhibit are to: (i) broaden the understanding of the general community regarding FL, (ii) showcase how a user can leverage FL to train a model across various sites, (iii) present results of the first real-world federation across 71 collaborating sites across 6 continents with 25,256 MRI scans from 6,314 patients focusing on the rare disease of glioblastoma, (iv) discuss privacy and data protection concerns and how FeTS hopes to solve it.

## TABLE OF CONTENTS/OUTLINE

This exhibit will present a toolkit to define a FL-based model training problem and deploy it across multiple partnering sites, ensuring a data-private AI training paradigm. Specific principles to protect data privacy will be described, along with common pitfalls to avoid when performing an FL-based study.

## INEE-45 A Practical Approach Into Artificial Intelligence: Ultrasonography and Artificial Intelligence Pipeline for Developmental Hip Dysplasia Screening

Participants

Sebastian Gallo-Bernal, MD, Boston, MA (*Presenter*) Nothing to Disclose

## TEACHING POINTS

- Artificial intelligence (AI) algorithms have demonstrated remarkable progress in image-recognition tasks.
- We aim to exemplify AI integration into clinical workflows, by assessing the feasibility of an ultrasound (US) AI (xAI) pipeline to increase the availability of sonographic screening for developmental hip dysplasia (DDH).
- US screening for DDH is based on the Graf method. The main drawback of this method is the high inter-operator variability. Primary sources of image acquisition variability arise from the manual selection of anatomical points and the difficulties to acquire images in the adequate anatomical plane.
- An AI-based computer-aided diagnosis (CAD) system can standardize image acquisition and reduce diagnosis time, improving the accuracy and objectivity of DDH diagnosis.
- Problem-solving in practical approaches towards AI: Class Imbalance.
- US x AI pipeline product: preprocessing techniques, image adequacy assessment and diagnosis models, atlas creation and nearest neighbor retrieval modules, and modules for post-hoc quantification of prediction uncertainty

## TABLE OF CONTENTS/OUTLINE

INTRODUCTION AND BACKGROUND: • Artificial intelligence and radiology: AI for image quality assessment and image selection and standardization  
PROBLEM STATEMENT: • Ultrasonography for DDH screening and follow-up. Graf technique: image quality consideration; drawbacks and limitations on radiology workflows  
US x AI PIPELINE: PRACTICAL APPROACH TOWARDS IMPLEMENTATION • Ultrasonography x AI pipeline architecture and outputs • Comparison of undersampling and class weights for addressing class imbalance • Performance metrics for binary classification of image adequacy  
LIMITATIONS/FUTURE

## INEE-46 A Hands-on Guide to Designing Cloud-based Web Platforms with Radiological Applications

Participants

Adrian Serapio, Berkeley, CA (*Presenter*) Nothing to Disclose

## TEACHING POINTS

Learning what goes into the design of cloud-based radiological web platforms will empower radiologists to truly leverage the power of the cloud and enhance their everyday workflow. We will walk through designing one such application, RadSim, an interactive reader performance study application that streamlines the process of conducting image based surveys. We demonstrate: - Why and how to apply cloud-based applications to a radiologist's everyday workflow- How to design a basic web application from ideation to testing- How to use the REST framework to develop the web application (using Node.js, MySQL, AWS)- How to visualize data generated by the web platform (using Python's Matplotlib library)

## TABLE OF CONTENTS/OUTLINE

Problem Statement - Paucity of easy-to-learn, open-source, platform-agnostic, cloud-based web applications matching the needs of radiologists- Introduce and walkthrough a product design framework to build simple cloud-based applications in radiology  
Prerequisite/Background- Basic understanding of any programming language  
Walkthrough1. Product design framework2. Cloud-based web development3. Data visualization4. Integration to radiological workflow  
Conclusion

## INEE-47 Understanding and Mitigating Bias in Artificial Intelligence

### Awards

Identified for RadioGraphics

Cum Laude

Participants

Ali Tejani, MD, Frisco, TX (*Presenter*) Nothing to Disclose

### TEACHING POINTS

1. Define and review categories of bias in AI. 2. Raise awareness of the sources of bias to promote mindfulness when using AI solutions in practice. 3. Understand how models can perpetuate prejudices and bias inherent in datasets. 4. Propose solutions to combat bias in AI.

### TABLE OF CONTENTS/OUTLINE

1. Introduction  
a. Define bias in AI  
i. Broad categories (i.e., implicit versus explicit, cognitive biases)  
ii. Model development (i.e., dataset, algorithm, and prediction bias)  
2. Scope of bias in AI  
a. Bias in AI along the radiology value chain  
b. Workflow diagram of the effect of bias in AI beyond the reading room (i.e., referring clinician and enterprise-level effects)  
i. Exacerbation of healthcare inequities  
3. Sources of bias in AI  
a. Model development  
i. Dataset curation  
1. Training/validation set demographics  
2. Confounding clinical comorbidities  
ii. Technical dataset variables  
1. Dataset shift  
2. Data leakage  
3. Varying post-processing techniques  
iii. Annotations  
1. Varying expertise  
2. Lack of standard guidelines  
3. Heterogeneous imaging scanners and protocols  
iv. Bias-variance tradeoff  
b. Model utilization and clinical impact  
i. Automation bias  
ii. Inequality considerations  
1. Exacerbation of inherent algorithm bias (i.e., underdiagnosis)  
2. Amplification of resource inequality and implications of inadequate access to AI tools  
3. Heterogeneous monitoring and adjustment of deployed AI tools  
4. Proposed solutions to mitigate bias in AI  
a. "Checkpoints" throughout AI workflow  
b. Involving statisticians in the model development process  
c. Require diverse datasets  
d. Monitoring AI performance across diverse populations and varying modalities/hardware

## INEE-48 Building A Multi-institution and Multi-expert Annotators Dataset for Machine Learning: Experience From

Participants

Felipe C. Kitamura, MD, PhD, Sao Paulo, SP (*Presenter*) Consultant, MD.ai, Inc; Speaker, General Electric Company

### TEACHING POINTS

Creating Machine Learning (ML) datasets is a laborious and tricky team effort. Errors in the planning phase can undermine the final result. Baking a refined ML dataset can be viewed as a multi-step process, including use-case definition, IRB approval, multi-institutional agreement, imaging protocol definition, data de-identification, data collection, labeling scheme definition, collaborating with annotators, annotation and data quality control, and license definition. A recipe approach is suggested with a list of ingredients and preparation instructions.

### TABLE OF CONTENTS/OUTLINE

Why is it important to create ML datasets? ML dataset recipe  
Key ingredients of a useful dataset  
Dataset preparation instructions  
Most common pitfalls and mistakes  
Logistics and quality control when generating expert annotations  
Examples of RSNA datasets  
How the dataset structure affects model development.

## INEE-49 Impact-sensitive Management of Prediction Uncertainty in Artificial Intelligence for Healthcare

Participants

Michelle Chua, Brookline, MA (*Presenter*) Nothing to Disclose

### TEACHING POINTS

Unsafe prediction failure occurs when a machine learning model is unable to convey lack of confidence, or deceitfully conveys high confidence, in an erroneous prediction  
Standard performance metrics measure overall model performance on limited test data and provide no indication of model confidence in the correctness of individual predictions  
Post-hoc prediction uncertainty metrics, such as calibrated classifier confidence, measures of visual similarity, and information entropy, may be used to quantify prediction uncertainty  
Classifier confidence and information entropy do not capture out-of-distribution uncertainty  
Prevention of unsafe prediction failure requires task-specific and impact-sensitive selection of prediction uncertainty metrics and prediction uncertainty thresholds  
Prediction uncertainty metrics may be calibrated to precision if the desired safety threshold is zero tolerance for false positives or to negative predictive value if the desired safety threshold is zero tolerance for false negatives

### TABLE OF CONTENTS/OUTLINE

Understanding prediction uncertainty and prediction uncertainty metrics  
Comparative evaluation of prediction uncertainty metrics  
Selection of prediction uncertainty metrics for zero tolerance and error tolerant clinical applications

## INEE-4HC Building the Administrative and Operational Infrastructure for an AI Enabled Radiology Department

### Awards

Certificate of Merit

Participants

Holly Meyer, RT, Rochester, MN (*Presenter*) Nothing to Disclose

### TEACHING POINTS

The goal of this exhibit is to provide an administrator's perspective on building an artificial intelligence (AI) team in the Department of Radiology, as well as the framework for successful discovery, translation, application, and commercialization of AI software technology. To establish a thriving AI program, careful consideration must be given to the organizational structure, key job roles and responsibilities, and an effective program structure must be established within which to operate.

### TABLE OF CONTENTS/OUTLINE

1. Radiology AI Ecosystem 2. Program Stakeholder Network 3. Pathways to Navigate a. Technical b. Administrative c. Regulatory 4. Clinical AI Pillars 5. Program Structure a. Leadership b. Organization c. Team d. Roles Responsibilities e. Information Management f. Communication g. Training and Education h. Quality Management System i. Architecture Infrastructure 6. Process a. Idea Submission b. Feasibility Analysis c. Intake d. Discovery e. Translation f. Limited Rollout g. Full Rollout h. Post-Production Please visit the Learning Center to also view this presentation in hardcopy format.

#### **INEE-5 Lessons Learned from a Cyberattack on the Healthcare System: A Radiology Perspective**

Participants

Hilary Strong, MD, (Presenter) Nothing to Disclose

##### **TEACHING POINTS**

We wish to share our insight and lessons learned from navigating a response to the cyberattack on province-wide healthcare authorities which rendered medical information technology systems inaccessible. Prompt, accurate, and consistent communication with all medical imaging staff, referring physicians, and healthcare authorities, is a crucial first step. Effective communication involves various modalities, such as secure applications, texts, emails, calls, and frequent face-to-face discussions/meetings. Following effective communication, having an existing cyberattack response system in place to immediately modify workflow and adapt to technology limitations is a priority. Finding an effective modified workflow system is not a linear process. However, judicious trial and error of solutions is more effective than remaining idle during a cyberattack. Modified workflow included entirely paper-based medical imaging requisitions and patient safety identification systems, as well as workflow limited to urgent and emergent studies only. With patient-centered care at the forefront of the radiology department's response to the cyberattack, safe and effective medical imaging services were provided to the patients of our province.

##### **TABLE OF CONTENTS/OUTLINE**

1. Introduction 2. Four Lessons Learned from a Cyberattack on Our Provinces' Healthcare System a. Prompt and consistent communication is paramount. b. (Not completely) out with the old (paper-based system). c. Correct patient identification prioritizes safety. d. Judicious trial and error is the way forward. 3. Conclusion

#### **INEE-6 All-in-One workplace for Radiologists: How to Build Your Personal Radiology Knowledge**

Participants

Ken Oba, MD, Chuoku, Japan (Presenter) Nothing to Disclose

##### **TEACHING POINTS**

At the end of this presentation, you will be able to: -Learn about Notion and Cloud PACS basics and start practicing with simple lessons and review concepts. -Make the all-in-one workspace and notes for research, education, and conference. -Build a system for collecting, maintaining, and serving knowledge to the right person at the right time.

##### **TABLE OF CONTENTS/OUTLINE**

-Introduction. -What is Notion, and what is Cloud PACS. -How to start Notion and Cloud PACS. -How to make a database for scientific research. -How to make a database for education. -How to make flashcards for exams. -How to make a database for conferences. -Advanced techniques will be introduced through Twitter using templates and short movies. -Conclusion

#### **INEE-7 Medical imaging AI In the Real World: Decoding Bias in Under-represented Populations**

Participants

Eduardo Freire, MD, Sao Paulo, Brazil (Presenter) Nothing to Disclose

##### **TEACHING POINTS**

Patterns of health inequality permeate artificial intelligence (AI) systems when bias and discrimination become entrenched in the conception, design, and use of these systems. Underserved patients, who have historically faced greater challenges accessing care, including imaging, may be underrepresented in the development of AI systems, leading to bias and compromising model performance. We aim to present a literature review on how to identify and mitigate existing and potential bias related to healthy inequality in medical imaging AI.

##### **TABLE OF CONTENTS/OUTLINE**

1) Introduction 1.1) Basic concepts and definitions: diversity, equity and inclusion in the AI era 1.2) Fairness and ethics of artificial intelligence in radiology: where are we? 2) Categories of AI bias 3) Sources of bias in AI development lifecycle 3.1) Human factors 3.2) Dataset challenges 4) Identifying bias in medical imaging AI: Case studies 4.1) How gender and race imbalance in a medical imaging dataset influences AI performance 4.2) Transgender population and health care disparities 5) Strategies to managing and mitigating bias in medical imaging AI 5.1) Transparency and data sharing 5.2) Policy and Regulations

#### **INEE-8 3D Printing and Digital Surgical Rehearsal in Complex Spine Surgery**

**Awards**

**Identified for RadioGraphics**

Participants

Lumarie Santiago, MD, Houston, TX (Presenter) Nothing to Disclose

##### **TEACHING POINTS**

The approach to complex spine surgery requires a multidisciplinary team and multimodality imaging to delineate the extent of disease as well as the structures at risk during surgery. Integration of the information provided by the various imaging exams may be difficult, particularly as each surgical discipline may have different take away points. This case-based exhibit provides information on the process of 3D printing including segmentation using multimodality imaging exams, validation (QA) and post processing. The use of digital and 3D printed models in surgical rehearsal with a focus on their impact on prescribing digital surgical planes will be discussed. The integration of .STL files into intraoperative navigation systems and validation of the digital surgical plan using the 3D printed model will also be reviewed.

## TABLE OF CONTENTS/OUTLINE

1. The 3D printing workflow used to integrate multimodality imaging exams. 2. 3D printing material selection to enhance surgical rehearsal. 3. Quality assurance steps in 3D printing. 4. Prescribing digital surgical planes. 5. Validation of digital surgical planes using the 3D printed model. 6. Intraoperative use of digital surgical planes.

## INEE-9 3D Printing from Medical Imaging Data: What the Resident Needs to Know

Participants

Nicole Wake, PhD, Aurora, OH (*Presenter*) Employee, General Electric Company

## TEACHING POINTS

A. Patient-specific 3D printed anatomic models and guides can aid in surgical planning, can provide intra-operative guidance, can be utilized for simulations, and can be used for trainee and patient education. B. Volumetric medical imaging data with high spatial resolution, good signal-to-noise ratio (SNR), and good contrast-to-noise ratio (CNR) is recommended if 3D printing will be performed. C. The workflow to create 3D printed anatomic models from volumetric imaging data includes image acquisition, image segmentation, conversion to 3D mesh geometries, and printing. D. Reimbursement for 3D printed anatomic models and anatomic guides can be pursued using Category III CPT Codes. E. The medical 3D printing process should be formally documented and recorded in the electronic medical record system and this is required for reimbursement. F. Hospital-based 3D printing labs should establish quality management systems to ensure the accuracy of 3D printed models.

## TABLE OF CONTENTS/OUTLINE

1. Review of the common applications of 3D printed medical models. 2. Description of major imaging recommendations for the creation of 3D printed anatomic models and guides derived from medical imaging data. 3. Overview of the workflow required to create 3D printed patient-specific anatomic models from volumetric medical imaging data. 4. Review of CPT codes including the Category III CPT Codes for 3D Printed anatomic models and anatomic guides, and introduction to the RSNA-ACR 3D printed model registry. 5. Synopsis of a formal documentation system for 3D printed anatomic models and guides. 6. Summary of the quality assurance steps required to ensure the accuracy of 3D printed medical models.

Printed on: 02/07/23



## Abstract Archives of the RSNA, 2022

INEE-10

### Developing a Prostate Cancer Radiologic-Pathologic Correlated Quality Reporting Dashboard

Sunday, Nov. 27 8:00AM - 9:00AM Room: Learning Center - IN

#### Participants

Ryan Ward, MD, (*Presenter*) Nothing to Disclose

#### TEACHING POINTS

Prostate cancer is an important cause of morbidity and mortality in men. The Prostate Imaging Reporting and Data System (PI-RADS) provides a framework for systematically scoring lesions on prostate MRI based on clinical suspicion for prostate cancer. Using this data, combined with actual pathologic outcomes, we developed a robust system for tracking patients being evaluated for prostate cancer. The system allows the user to evaluate diagnostic performance at physician, department, and enterprise level and easily identify patients where discordance may exist between MRI findings and pathologic result.

#### TABLE OF CONTENTS/OUTLINE

1) Provide a brief overview of prostate cancer and the PI-RADS scoring system. 2) Describe the importance of tracking and analyzing prostate MRI data. 3) Describe the underlying technology/architecture for extracting, transforming, and loading the data into the data warehouse. 4) Provide examples of the dashboard and the different visualizations available.

Printed on: 02/07/23



## Abstract Archives of the RSNA, 2022

INEE-12

### Standardized Operational Log of Events (SOLE) for Artificial Intelligence (AI) Monitoring

Sunday, Nov. 27 8:00AM - 9:00AM Room: Learning Center - IN

#### Awards

Certificate of Merit

Identified for RadioGraphics

#### Participants

Ali Tejani, MD, Frisco, TX (*Presenter*) Nothing to Disclose

#### TEACHING POINTS

1. Provide an overview of IHE standardized operational log of events (SOLE)  
2. Review the interoperability advantages of using SOLE application programming interfaces (APIs) and codes in practice  
3. Describe specific metrics defined by SOLE to monitor deployed AI solutions  
4. Demonstrate how processes monitored by SOLE codes can be visualized through business analytics/dashboards  
5. Describe challenges with adopting SOLE APIs and codes in practice

#### TABLE OF CONTENTS/OUTLINE

1. Introduction  
a. Describe the problem: lack of interoperability and an efficient means of monitoring AI solutions workflows  
b. SOLE for business analytics/process mining  
i. Review SOLE APIs  
ii. Review select SOLE codes  
c. Introduce the concept of SOLE for AI monitoring  
2. Review how SOLE can be applied for AI monitoring  
a. Describe specific use cases to demonstrate how SOLE codes can be used to monitor AI  
i. Frequency of AI tool use  
ii. Disagreement rate with AI results  
iii. Effect of AI tool use on time from study ordered to study read  
iv. Clinical monitoring for the impact of AI on patient care  
1. Time to treatment based on urgent AI alert  
2. Time to ED admission  
v. Aggregating history of events over an extended time (i.e., if needing to justify ROI for annual budget)  
b. Demonstrate visualization of processes captured by SOLE codes with business analytics/dashboards  
3. Challenges associated with adopting SOLE APIs and codes  
a. Presence of multiple profiles (SYSLOG, ATNA, FHIR)  
b. Distilling the list of codes  
c. Encouraging vendor adoption  
d. Flexibility to capture all potential AI-radiologist interactions

Printed on: 02/07/23



## Abstract Archives of the RSNA, 2022

INEE-13CS

### Try Before You Buy: A One-Stop-Shop Approach for Testing and Procuring Commercial AI Applications

Sunday, Nov. 27 8:00AM - 9:00AM Room: Learning Center - IN

#### Participants

Vidur Mahajan, MBBS, New Delhi, India (*Presenter*) Employee, CARPL.ai

#### TEACHING POINTS

1. There are more than 150 FDA approved AI applications and the new approvals are growing at 50% per annum. There are 100s of other commercial AI applications available around the world.2. This makes it nearly impossible for radiologists to effectively discover and test these AI solutions on their own data.3. We present a software system with pre-integrated commercial AI applications, i.e. an AI marketplace, which allows radiologists to upload their own data and rigorously test the performance of the application.4. The software includes in built data management, anonymisation, cohort creation, annotation and statistical analysis tools.5. The option to ensemble AI outputs to improve performance also exists.

#### TABLE OF CONTENTS/OUTLINE

Our exhibit will be a computer system with 3 monitors, replicating the radiologists workstation. Radiologists at RSNA would be able to bring their own data and upload it into this system and choose to run commercial AI applications and compare their performance. This would allow them to make informed purchase decisions, and optimize for productivity / quality gains. We believe that ours is a unique offering which can exponentially drive the adoption of clinical AI.

Printed on: 02/07/23



## Abstract Archives of the RSNA, 2022

INEE-14

### Ultrasound-guided Peripheral Insertion System using Deep Learning

Sunday, Nov. 27 8:00AM - 9:00AM Room: Learning Center - IN

#### Participants

Yuina Ezawa, Maebashi, Japan (*Presenter*) Nothing to Disclose

#### TEACHING POINTS

Puncture of peripheral blood vessels in the elderly and children is a difficult activity. Ultrasound-guided venipuncture is a widely used method to facilitate peripheral venipuncture. In this method, the positional relationship between the target blood vessel and the needle is confirmed, and the target blood vessel is punctured while operating the probe and needle at the same time. However, it is very difficult to confirm the positional relationship between the target blood vessel and the needle. To solve this problem, we propose a method that uses a convolutional neural network (DCNN) to automatically extract blood vessels and needles on the image. It is possible to display the optimum needle approach angle by computer-assisted detection. This method can show the positional relationship between the peripheral vein and the needle and provide useful information to assist in the puncture. The major teaching points of this exhibit are to: 1. automatically extract blood vessels and needles from ultrasound images. 2. understand how to extract blood vessels and needles using DCNN. 3. be useful for ultrasonic-guided venipuncture.

#### TABLE OF CONTENTS/OUTLINE

To discuss the clinical usefulness for accurate examination in ultrasound-guided venipuncture using DCNN extraction.

Printed on: 02/07/23



## Abstract Archives of the RSNA, 2022

INEE-15

### The New 3D Slicer Version 5.0 Open Source Platform for Medical Image Analysis, 3D Visualization and Image-guided Intervention

Sunday, Nov. 27 8:00AM - 9:00AM Room: Learning Center - IN

#### Participants

Sonia M. Pujol, PhD, MSc, (*Presenter*) Nothing to Disclose

#### TEACHING POINTS

3D Slicer is an open-source and extensible software platform used in clinical research worldwide. The new Slicer 5.0 release version provides hundreds essential core modules and extensions, and builds on the success of the version 4 downloaded over 1 million times since RSNA 2011. The goal of the exhibit is: 1. To review a brief history of 3D Slicer development in the past 20 years; 2. To discover the DICOMweb browser for cloud-based DICOM workflows; 3. To visualize GPU-based volume-rendering of DICOM images; 4. To discover the new Markups features; 5. To perform interactive segmentation of 2D/3D/4D images; 6. To discover the new MONAI Label extension for AI-assisted image annotation; 7. To learn new Slicer features for COVID-19 data analysis; 8. To create 3D solid objects for 3D printing; 9. To perform real-time data fusion for image-guided therapy; 10. To connect Slicer with robots, scanners, and trackers; 11. To interact with 3D scenes using virtual and augmented reality headsets; 12. To perform cloud-based computing in a Web browser using AWS AppStream 2.0, in a Docker container or a Jupyter notebook kernel; 13. To understand how to use 3D Slicer in clinical research applications.

#### TABLE OF CONTENTS/OUTLINE

Overview of the new 3D Slicer version 5.0; DICOM Standard Interoperability: import/export and structured reporting; DICOMweb features; GPU-based 3D and 4D Volume Rendering; Markups and Automated Measurements; Interactive 2D/3D/4D Image Segmentation; 3D Printing; Artificial Intelligence; Virtual and Augmented Reality; Cloud-based Computing; Clinical Applications in COVID-19, Surgical Navigation, and Image-Guided Intervention; Slicer Community Resources: Forum, Training Compendium, and Documentation.

Printed on: 02/07/23



## Abstract Archives of the RSNA, 2022

INEE-16HC

### Understanding Patient Needs and Gaps in Radiology Reports Through Online Discussion Forum Analysis

Sunday, Nov. 27 8:00AM - 9:00AM Room: Learning Center - IN

#### Participants

Mohammad Alarifi, PhD, (*Presenter*) Nothing to Disclose

#### TEACHING POINTS

Our objective is to investigate patient needs and understand information gaps in radiology reports using patient questions that were posted on online discussion forums. We leveraged online question and answer platforms to collect questions posted by patients to understand current gaps and patient needs. We retrieved six hundred fifty-nine (659) questions using the following sites: Yahoo Answers, Reddit.com, Quora, and Wiki Answers. The questions retrieved were classified into eight major themes. The themes were related to the following topics: radiology report, safety, price, preparation, procedure, meaning, medical staff, and patient portal. Among the 659 questions, 35.50% were concerned with the radiology report. The most common question topics in the radiology report focused on patient understanding of the radiology report (62 of 234 [26.49%]), image visualization (53 of 234 [22.64%]), and report representation (46 of 234 [19.65%]). We also found that most patients were concerned about understanding the MRI report (32%; n = 143) compared with the other imaging modalities (n = 434). Using online discussion forums, we discussed major unmet patient needs and information gaps in radiology reports. These issues could be improved to enhance radiology design in the future.

#### TABLE OF CONTENTS/OUTLINE

Introduction  
Methods  
Data sources and collection  
Thematic analysis  
Patient-centered approach  
Results ( Summary of the four data sources, Analysis of patient question themes, Radiology report results; Safety, Procedure processing, Meaning, Preparation Patient portal, Preparation, The medical staff and Price  
Conclusion  
Please visit the Learning Center to also view this presentation in hardcopy format.

Printed on: 02/07/23



## Abstract Archives of the RSNA, 2022

INEE-17

### Adding Value in Radiology: 3D Imaging Lab

Sunday, Nov. 27 8:00AM - 9:00AM Room: Learning Center - IN

#### Participants

Larson Hsu, MD, (*Presenter*) Nothing to Disclose

#### TEACHING POINTS

In contrast to conventional volume rendering static images, segmentations of the patient's anatomy can be exported as a 3D model and further utilized in different applications for better spatial understanding of the disease. For example, the 3D model can be reviewed with an interactive viewer on the computer or other flat-screen devices, or visualized in virtual or augmented realities. It can also be 3D printed as an anatomical model for presurgical planning, or used as the basis to design patient-specific medical devices such as cutting guides or wearable prostheses. In this exhibit we will share the experience of our 3D imaging lab in a cancer center, and demonstrate how it can add value to the Radiology Department and potentially improve patient care.

#### TABLE OF CONTENTS/OUTLINE

1) Introduction/background: radiology 3D imaging lab 2) Volume rendering vs. 3D segmentation model 3) Advanced visualization using virtual and augmented realities 4) 3D printing of anatomical models and patient-specific medical devices at the point-of-care 5) Showcase and examples of 3D model applications in different disciplines 6) Future directions

Printed on: 02/07/23



## Abstract Archives of the RSNA, 2022

INEE-18

### Demystifying Coloring and Surface Labeled 3D Printed Anatomical Models

Sunday, Nov. 27 8:00AM - 9:00AM Room: Learning Center - IN

#### Participants

Muhammad Rehman, BA, Virginia, VA (*Presenter*) Nothing to Disclose

#### TEACHING POINTS

? Discussion on the relevance and importance of multi-color 3D printing with emphasis on models with special surface characteristics such as text, image and texture ? Highlighting various applications of color 3D models such as educational models, in clinical cases or for research purposes ? Pros and cons of de novo creation of multi-part STL files vs working on pre-existing STL files ? Advantages and disadvantages of graphically designing STL files vs using cross-sectional imaging to 3D reconstruct STL files in the educational setting ? Introducing UV surface mapping ? Detailing multiple software programs that can be used to color, label and imprint images onto the surface of a preexisting STL file and providing brief methodology for each ? Discussion of different 3D printing techniques that allow for color 3D printing, especially highlighting novel Multi Jet Fusion technology that allows for development of highly durable and versatile models with fully customizable surface appearance, not previously as robustly available ? A chart detailing subjective learning curve, user friendliness and cost of the software programs and 3D printers/printing services

#### TABLE OF CONTENTS/OUTLINE

? Background ? Discussion ? Software programs ? Meshmixer ? Microsoft Paint 3D ? Blender ? Autodesk 3d Studio Max ? Color 3D printing techniques ? PolyJet ? Stereolithography ? Paper Based ? Binder Jetting ? Multi Jet Fusion ? Summary chart

Printed on: 02/07/23



## Abstract Archives of the RSNA, 2022

INEE-19

### Quantitative Evaluation of a Large-scale Multi-year Artificial Intelligence (AI) Deployment at a Large Academic Radiology Department - Key Metrics, Trends, and Milestones

Sunday, Nov. 27 8:00AM - 9:00AM Room: Learning Center - IN

#### Participants

Axel Wismueller, MD, PhD, Pittsford, NY (*Presenter*) Nothing to Disclose

#### TEACHING POINTS

A) We present key analytics, trends, and milestones that are extracted from a multi-year large-scale AI clinical deployment of a radiology triage and prioritization solution in a large academic hospital setting. B) The analytics, trends and milestones are extracted from the hospital system's experience of taking a single-pathology AI module and scaling it out to cover nine different pathologies. Our analysis provides a set of recommended metrics to measure growth, performance, and user engagement. C) We present trends for various milestones and how the metrics change as an AI solution scales up to cover a greater number of imaging examinations. D) Our case study may provide insights and value to other radiology practices and hospital systems as a basis for defining best practice guidelines, and for contributing to the calculation of business metrics, such as Return-on-Investment (ROI) or Total Cost of Ownership (TCO) in the clinical adoption of AI solutions.

#### TABLE OF CONTENTS/OUTLINE

A) Introduction: 1. Description of project goals and timeline 2. Overview of the AI integration into the radiologist workflow B) Metrics: 1. Description and visualization of metrics for measuring: a) Growth of the AI adoption b) Performance of the AI c) User engagement 2. Highlights of the key trends milestones C) Summary of key metrics: 1. Overview of the value of each metric 2. Identified minimum thresholds for success criteria 3. Summary of teaching points

Printed on: 02/07/23



## Abstract Archives of the RSNA, 2022

INEE-1CS

### Using the Open Health Imaging Foundation (OHIF) Framework To Build Web-based Imaging Applications

Sunday, Nov. 27 8:00AM - 9:00AM Room: Learning Center - IN

#### Participants

Erik Ziegler, MSc, PhD, (*Presenter*) Consultant, Radical Imaging LLC; Consultant, Novometrics LLC; Stockholder, Yunu Inc

#### TEACHING POINTS

The purpose of this exhibit is to: 1. Explain how radiologists can build their own imaging tools and applications using the open source Open Health Imaging Foundation (OHIF) framework to address their custom use cases. 2. Discuss the components of a full fledged zero-footprint web-based imaging application and how they interact using various APIs (e.g. DICOMweb). 3. Explain how advanced functionality, such as 3D visualization, image fusion, and segmentation, can be incorporated in these applications. 4. Demonstrate how to organize specific function sets into custom workflow modes for optimizing efficiency. 5. Demonstrate how this type of system can be deployed both securely and cost effectively.

#### TABLE OF CONTENTS/OUTLINE

- Open source resources for radiology and AI applications
- Relationships between components in web imaging applications
- Building custom measurement tools
- Incorporating advanced visualization and segmentation tools
- Building custom workflow modes for the OHIF Viewer (e.g. configuring the application to provide functionality for use cases like ProstateCancer.ai, NCI Imaging Data Commons, XNAT)
- Deploying scalable secure web imaging applications locally or using cloud resources
- Future directions

Printed on: 02/07/23



## Abstract Archives of the RSNA, 2022

INEE-2

### Development of A Training Simulator of Plain Radiography Using Augmented Reality Technology

Sunday, Nov. 27 8:00AM - 9:00AM Room: Learning Center - IN

#### Awards

Certificate of Merit

#### Participants

Kaito Oikawa, (*Presenter*) Nothing to Disclose

#### TEACHING POINTS

Radiographers need to acquire proficient skills through a great deal of experience to perform plain radiography accurately. Lack of such skills may lead to misdiagnosis and unnecessary radiation exposure. Conventional training methods for plain radiography were phantom radiography and radiography role-playing. They were insufficient to develop proficient skills because of the unlike clinical settings. Recently, a radiography training simulator using virtual reality was proposed. This simulator allowed the trainee to perform plain radiography on a virtual subject in a virtual space. However, the trainee cannot touch the virtual subject in this training simulator. This is the same as the conventional training methods in that it is different from the clinical settings. Therefore, we developed a training simulator of plain radiography using augmented reality technology. Our simulator can output virtual x-ray images similar to clinical settings, adapting positions and angles obtained by tracking human subjects in real time. The training using our simulator allows trainees to acquire proficient skills in preclinical training.

#### TABLE OF CONTENTS/OUTLINE

Lack of skills in plain radiography may lead to misdiagnosis and unnecessary radiation exposure in clinical settings. Our simulator can output the virtual x-ray images that reflect the positions and angles of the subject. Radiographers can acquire proficient skills by training the plain radiography repeatedly using our simulator.

Printed on: 02/07/23



## Abstract Archives of the RSNA, 2022

INEE-20HC

### Taking the Medical Devices Through the Regulatory Gatekeepers: How To Do It Right!

Sunday, Nov. 27 8:00AM - 9:00AM Room: Learning Center - IN

#### Participants

Bhanushree Bahl, New Delhi, India (*Presenter*) Employee, CARPL.ai

#### TEACHING POINTS

The clinical trial of AI-based Investigational Devices (AID) will look at the device performance through the lens of business capabilities, while evaluating technologies. Our exhibit will showcase the clinical trial workflow of AI algorithms with multiple scenarios for different regulatory approvals. Regulatory approvals are necessary for an AI model to be used clinically, and to add value to the business. AI companies can run clinical trials, which will help them get comprehensive results through data analysis for improved decision making. Conducting clinical trials on extensive data allows AI companies to detect patterns for enhanced business performance. We will highlight the steps needed to conduct a successful clinical trial for various scenarios. In addition to this, the exhibit will also feature protocols required to follow for different regulatory approvals.

#### TABLE OF CONTENTS/OUTLINE

Protocol Synopsis: Study name, objective and type of the study, with the design procedure along with the calculated sample size and investigator selection (Screener / Reader / Gter). Study procedure: Ethical committee approval, Data collection and de-identifying studies, Screening, Ground Truthing, Standalone performance evaluation, Reader test Data Management Plan / Flow: Annotation Platform (Ex: CARPL), System verification and UAT, Security and maintenance of account External Data Management Process: Data collection and archiving and cleaning, Master data Set creation Study Endpoints and Statistical Analysis: Threshold of study endpoints and statistical analysis, Endpoints in standalone performance test Preparation of Violation List Please visit the Learning Center to also view this presentation in hardcopy format.

Printed on: 02/07/23



## Abstract Archives of the RSNA, 2022

INEE-21

### The Day After Tomorrow: How to Monitor A Deployed AI Model and Automate the Radiologist Feedback Loop

Sunday, Nov. 27 8:00AM - 9:00AM Room: Learning Center - IN

#### Participants

Victor Menezes, MD, Sao Paulo, Brazil (*Presenter*) Nothing to Disclose

#### TEACHING POINTS

To describe how an Artificial Intelligence (AI) model can lose performance due to data drift / concept drift; To describe other biases that can affect an AI model; To explain the importance of monitoring an AI model over time; To explain how to sustain and monitor the performance of an AI model after the deployment. To illustrate with an example of how we built an automated feedback loop. To explore a few options on how to maintain performance in the long run and retrain the model if necessary.

#### TABLE OF CONTENTS/OUTLINE

1. Model degradation: Data drift, Concept drift and Upstream data changes; 2. How to automatically gather and analyze AI model inferences; 3. Types of AI model scenarios and the possible types of analysis; 4. Main metrics to evaluate the performance of an AI model; 5. When and how to retrain an AI model and other options to maintain performance in the long run.

Printed on: 02/07/23



## Abstract Archives of the RSNA, 2022

INEE-22HC

### A Practical Guideline for Safely Deploying Continuous Machine Learning Systems

Sunday, Nov. 27 8:00AM - 9:00AM Room: Learning Center - IN

#### Participants

Camila Gonzalez, MS, Darmstadt, Germany (*Presenter*) Nothing to Disclose

#### TEACHING POINTS

A central advantage of successful learning systems is their ability to adapt to new conditions in the dynamic real world. In clinical practice, common changes range from developments in image acquisition protocols to shifts in the patient population. When designing AI-powered systems, building mechanisms that allow such adjustments is necessary for preventing dangerous performance declines. Yet no continuous learning system is in use as of now. In this abstract, we summarize the central obstacles preventing the deployment of such solutions, and present practical advice on how to overcome them. We explore FDA and European Commission regulations (both in-effect and works-on-progress), consider the daily work of clinicians, and review under which conditions continuous learning systems can be a better return on investment than statically trained models. Our guide is useful for all relevant stakeholders, from data scientists to hospital administration.

#### TABLE OF CONTENTS/OUTLINE

(1) Continuous learning systems: definitions, technical challenges and benefits(2) Regulatory frameworks for the approval of continuous learning solutions in the USA and EU(3) Considerations for medical professionals when deploying continuously trained models in clinical practice(4) Cost-benefit analysis from an economic perspective: why continuous Machine Learning is advantageous despite the regulatory overheadPlease visit the Learning Center to also view this presentation in hardcopy format.

Printed on: 02/07/23



## Abstract Archives of the RSNA, 2022

INEE-23

### Selection and Maintenance of Consumer Grade Displays for Home Reading Workstations

Sunday, Nov. 27 8:00AM - 9:00AM Room: Learning Center - IN

#### Participants

Douglas Nachand, MD, Shaker Heights, OH (*Presenter*) Nothing to Disclose

#### TEACHING POINTS

- Describe the display specifications of a consumer grade display that meets the suggested guidelines for non-mammographic diagnostic imaging- Design a workflow to properly calibrate the monitor for diagnostic purposes at baseline and at set intervals

#### TABLE OF CONTENTS/OUTLINE

Choosing a diagnostic display- What are the guidelines and who sets them -- Guidelines for non-mammography displays-- Mammography displays are regulated (specifications and quality control) and will not be covered- Pros and cons of displays marketed as consumer and medical grade- Ensuring your monitor meets the standards and additional features to consider Acceptance Testing and Initial Setup- Necessary equipment and software- Describe baseline and periodic calibration workflows-- How to perform-- Estimated time to complete Maintenance and Quality Control- Expected points of failure- QC tests, frequency, expected radiologist time Conclusions

Printed on: 02/07/23



## Abstract Archives of the RSNA, 2022

INEE-24

### Educational Applications of Metaverse and XR Extended Reality (VR, AR, MR) for Radiology and Telemedicine

Sunday, Nov. 27 8:00AM - 9:00AM Room: Learning Center - IN

#### Awards

Identified for RadioGraphics

#### Participants

Maki Sugimoto, MD, PhD, (*Presenter*) Officer, Holoeyes Inc

#### TEACHING POINTS

To define the metaverse in radiology and to explain the potential and limitations of its educational applications. 1) To learn the utilization of metaverse and XR (virtual-augmented-mixed reality) in medical imaging. 2) To learn how to segment and export polygons of targeting organs from DICOM data from CT or MRI. 3) To learn how to utilize metaverse systems and XR devices. 4) To show clinical examples, such as in medical education, surgical planning, simulation, and navigation. 5) To learn how to integrate metaverse and XR to improve visual-spatial ability to mentally manipulate medical anatomy in three dimensions.

#### TABLE OF CONTENTS/OUTLINE

1. Terminology: The representative forms such as XR (VR/AR/MR) are referring to all real-and-virtual combined environments and human-machine interactions generated by computer technology and wearables. 2. Beneficial applications of the XR devices and metaverse. 3. How to integrate the spatial imaging system and metaverse using avatars by interactive superimposing 3D holograms. 4. Effectiveness: Enhancing scene visualization is a feasible strategy for augmenting spatial awareness in complex anatomy education.

Printed on: 02/07/23



## Abstract Archives of the RSNA, 2022

INEE-25

### Estimating Vascular Age in Carotid Ultrasound using Deep Learning

Sunday, Nov. 27 8:00AM - 9:00AM Room: Learning Center - IN

#### Participants

Rena Nishimaki, Maebashi, Japan (*Presenter*) Nothing to Disclose

#### TEACHING POINTS

Heart and cerebrovascular diseases are caused by atherosclerosis, which is associated with the aging of blood vessels. Understanding vascular age plays a major role in the prevention of vascular diseases. The progression of arteriosclerosis is measured by ultrasonography (US), pulse wave velocity, and cardio-ankle vascular index. Carotid US is an excellent examination for early detection and evaluation of patients and indicates the degree of atherosclerosis as a whole body. However, carotid US alone cannot evaluate vascular age as an indicator of atherosclerosis. In this study, we propose estimating vascular age in the carotid US using a deep convolutional neural network (DCNN). It can provide useful information on the appropriate diagnosis of atherosclerosis. The major teaching points of this exhibit are to: 1. classify and regress the carotid US using DCNN. 2. understand how to estimate vascular age with a computer-aided diagnosis (CAD) system. 3. be useful for diagnosing atherosclerosis.

#### TABLE OF CONTENTS/OUTLINE

To provide CAD using DCNN regarding estimation of vascular age and discuss clinical usefulness toward accurate diagnosis of the arteriosclerosis in ultrasonography.

Printed on: 02/07/23



## Abstract Archives of the RSNA, 2022

INEE-26

### Unsupervised Learning Classification of Rectum Region for Prostate Cancer During Image-guided Radiation Therapy in CBCT

Sunday, Nov. 27 8:00AM - 9:00AM Room: Learning Center - IN

#### Participants

Haruyuki Watanabe, PhD, (*Presenter*) Nothing to Disclose

#### TEACHING POINTS

Intensity-modulated radiotherapy (IMRT) is a more effective curative treatment option for prostate cancer patients than surgery. IMRT uses for tumor and normal organ detection to generate treatment plans that confine the prescribed dose to cancer while maximally excluding the adjacent normal organs. Image-guided radiation therapy using cone-beam CT (CBCT) associated with IMRT provides a safe and reliable radiotherapy treatment. Because the rectal size and shape cause prostate motion, it is necessary to confirm in CBCT images. If necessary, after checking the CBCT images, defecation and exhaust gas treatment are required. However, there is no clear standard as to whether to take the treatment. Thus, we propose an unsupervised learning classification to support the decision of treatment such as defecation and exhaust gas. The major teaching points of this exhibit are to: 1. automatically classify the rectum region. 2. understand how to use unsupervised learning schemes. 3. be useful for prostate cancer during image-guided radiation therapy in CBCT.

#### TABLE OF CONTENTS/OUTLINE

To provide unsupervised learning classification regarding validation of image-guided radiation therapy in CBCT.

Printed on: 02/07/23



## Abstract Archives of the RSNA, 2022

INEE-27

### Natural Language Processing in Radiology: State of the Art and Future Directions

Sunday, Nov. 27 8:00AM - 9:00AM Room: Learning Center - IN

#### Awards

**Magna Cum Laude**

#### Participants

Pratheek Bobba, BS, New Haven, CT (*Presenter*) Nothing to Disclose

#### TEACHING POINTS

1. The need for Natural Language Processing (NLP) in Radiology.2. History of NLP and milestones.3. Current clinical applications of NLP in radiology. 4. Applications and future directions of NLP in radiology.

#### TABLE OF CONTENTS/OUTLINE

1. The need for NLP in radiology: Cures act for radiology benefits and challenges including health literacy, increased anxiety from patients reading reports without guidance, increased calls to clinicians which may disrupt workflow.2. History and milestones: brief review of the history of NLP and the current NLP models, focusing on Bidirectional Encoder Representations from Transformers (BERT).3. Current state of the art: there has been an exponential increase in rate of NLP in radiology publications, with a 3-fold increase in publications about NLP in radiology from 2015 to 2019, focusing on extracting disease information from reports/labelling disease phenotypes rather than clinical applications.4. A review of the need for the following applications of NLP in radiology: text simplification, text summarization, extracting information, cohort creation/entity recognition, reporting accuracy/quality assurance, revenue loss, billing code generation, appropriate communication of disease acuity, and a special focus on structured reporting and NLP.

Printed on: 02/07/23



## Abstract Archives of the RSNA, 2022

INEE-28HC

### Introduction to Clinical Workflow to Engineer 3D Printed Patient Specific Models with Specified Tissue Mechanical Properties

Sunday, Nov. 27 8:00AM - 9:00AM Room: Learning Center - IN

#### Participants

Kelsey Sommer, PhD, Buffalo, NY (*Presenter*) Stockholder, QAS.AI

#### TEACHING POINTS

Learn how to design and 3D print patient-specific phantoms on a multi-material anatomical printer which allows selection of specific mechanical properties for various tissues. Exemplification of multi-material 3D printed phantoms with specified mechanical properties: coronary arteries, neurovasculature and spine. Exemplification of using multi-material 3D printed phantoms for testing, residency training and treatment planning. 3D printing of patient specific phantoms is a benchtop tool that has high precision in geometric modelling and material properties. The latest advances in 3D printing allows mixing of polymers to simulate mechanical properties for various tissues and diseased state. Such advances allow performance of precise biomechanical, imaging or flow experimentation with controlled parameters such as pressure, flow rates, compliance, and range of motion.

#### TABLE OF CONTENTS/OUTLINE

- Exemplification of multi-material use for coronary arteries, neurovasculature and spine
  - Segmentation workflow, with focus on separation of various tissues
  - 3D printing process, including optimal selection of materials for a Stratasys J750 Anatomical Printer
  - Post-processing of 3D printed models
  - Applications of 3D printed patient-specific anatomical modelling
  - Discussion of the advantages and limitation of the new materials
- Please visit the Learning Center to also view this presentation in hardcopy format.

Printed on: 02/07/23



## Abstract Archives of the RSNA, 2022

INEE-29

### Systematic Review of Evidence-Based Medical AI

Sunday, Nov. 27 8:00AM - 9:00AM Room: Learning Center - IN

#### Participants

Terumasa Kondo, Toyoake, Japan (*Presenter*) Nothing to Disclose

#### TEACHING POINTS

Deep learning is beginning to be used as an essential tool in radiology. However, the use of deep learning can lead to black-boxing of the technology due to the complexity of the process. To solve these problems, Deep learning visualization methods have attracted attention in recent years. When AI technology surpasses human classification performance, the basis for decision-making by deep learning is expected to bring new knowledge to the human race. This exhibition aims to introduce how deep learning can be visualized, and will also show examples of research using CAM (Class activation map) and the development of a prognosis prediction method for CCU patients using electrocardiogram images. Main teaching point 1. Black box problem of deep learning 2. What is Explainable AI technology? 3. Examples of Explainable AI Technology using GradCAM

#### TABLE OF CONTENTS/OUTLINE

TABLE OF CONTENTS 1. Black box problem of deep learning 2. What is Explainable AI technology? 3. Various types of Explainable 4. Example of Explainable AI technology 5. Our study

Printed on: 02/07/23



## Abstract Archives of the RSNA, 2022

INEE-3

### Prognostic AI-imaging Biomarkers: How to Predict the Survival of Patients With Idiopathic Pulmonary Fibrosis (IPF)

Sunday, Nov. 27 8:00AM - 9:00AM Room: Learning Center - IN

#### Awards

**Certificate of Merit**

#### Participants

Chinatsu Watari, MD, Boston, MA (*Presenter*) Nothing to Disclose

#### TEACHING POINTS

Idiopathic pulmonary fibrosis (IPF) is a major chronic progressive interstitial lung disease, with a median survival of 2-5 years from the time of diagnosis without anti-fibrotic medication. The teaching points of this exhibit are to (1) review currently established clinical prognostic biomarkers for IPF, (2) review the most promising emerging radiomic and AI-based biomarkers for imaging-based prediction of the survival in IPF, and (3) review the comparative performance between clinically established and AI-based prognostic biomarkers in the image-based prediction of the survival in IPF.

#### TABLE OF CONTENTS/OUTLINE

1. Why IPF is a problem. 2. Clinically established prognostic biomarkers for IPF (visual high-resolution CT (HRCT) pattern; gender, age, and physiology (GAP) index and staging system). 3. Radiomic biomarkers (traditional radiomics; hyper-curvature features; deep-learning radiomics) for survival analysis. 4. Why machine learning for survival analysis (AI-radiomics) outperforms clinical and radiomic biomarkers. 5. Comparative performance in terms of survival prediction and Kaplan-Meier survival curves. 6. Clinical case studies.

Printed on: 02/07/23



## Abstract Archives of the RSNA, 2022

INEE-30

### Mastering Basic Machine Learning Principles Without Coding Experience: A Tutorial on Googles Teaching Machine

Sunday, Nov. 27 8:00AM - 9:00AM Room: Learning Center - IN

#### Awards

Certificate of Merit

#### Participants

Adam Flanders, MD, Philadelphia, PA (*Presenter*) Nothing to Disclose

#### TEACHING POINTS

1) Understanding machine learning requires developing a conceptual framework.2) Recognize that fundamental machine learning principles can be learned without coding experience.3) Understand the overall process to train a deep learning model.4) Learn basic concepts on how to assess model generalizability and performance.5) Appreciate that several free and easy to use non-coding solutions exist where you can experience training, validating and testing an image-based machine learning model.6) Understand that adjustment of training hyperparameters and dataset balance/bias significantly affects the performance of your model.

#### TABLE OF CONTENTS/OUTLINE

I) Introduction: Building a conceptual framework: introduction to hyperparameters (e.g. learning rate, batch size, epochs).II) Introduction to performance metrics: loss function, confusion matrix, accuracy.III) Datasets: tips to build an effective dataset.IV) Introduction to Google's Teachable Machine.V) Creating your classes / loading your data.VI) Train and view the performance live.VII) Adjust hyperparameters and observe the effect on training with loss curve and confusion matrix.VIII) Readjust the distribution of your positive and negative classes in your training dataset.IX) Observe the effects of data redistribution.X) Observe the effect of pre-processing to accuracy of the model.XI) Summary.

Printed on: 02/07/23



## Abstract Archives of the RSNA, 2022

INEE-31

### Robust AI in Brain MRI's Large-Factor Super-Resolution - And Its Application In Improving Brain CAD System's Precision

Sunday, Nov. 27 8:00AM - 9:00AM Room: Learning Center - IN

#### Awards

Certificate of Merit

#### Participants

Tong Zheng, Nagoya, Japan (*Presenter*) Nothing to Disclose

#### TEACHING POINTS

1. To learn the concept of super-resolution (SR) and its applications in brain MRI<sup>2</sup>. To understand difficulties in brain MRI's SR and how does our proposed AI overcome these difficulties<sup>3</sup>. To learn how to train a registration-error robust AI for SR on low- and high-resolution images dataset<sup>4</sup>. To learn our SR AI's application in brain CAD system and how does our AI improve precision of the CAD system

#### TABLE OF CONTENTS/OUTLINE

1. AI-based super-resolution (SR): fundamental concepts and application in medical imaging- SR technique enhances the resolution of a given image- AI can perform SR of medical images such as brain MRI<sup>2</sup>. Problems in training an AI for medical image SR- Training the AI needs precisely-registered low- and high-resolution image pairs- Existing AI for SR are not registration-error robust<sup>3</sup>. Techniques of our registration-error robust AI in medical image SR: newly-designed structure- Pre-train a StyleGAN as latent memory bank- Encoder-decoder structure to decompose images into high- and low-dimensional features<sup>4</sup>. Techniques of our registration-error robust AI in medical image SR: loss terms and pre-processing- Novel loss term to stabilize training procedure- Multi-channel input to obtain more spatial information<sup>5</sup>. SR results and its application in improving brain CAD system's precision- Our AI successfully performed SR of brain MRI images, made it easier for radiologists to observe brain structures only from low-resolution (LR) images taken with shorter scanning time- With our AI for SR, CAD systems can proceed more accurate diagnosis from LR MRI

Printed on: 02/07/23



## Abstract Archives of the RSNA, 2022

INEE-33

### Ready or Not, The Metaverse Will Have a Presence in Radiology

Sunday, Nov. 27 8:00AM - 9:00AM Room: Learning Center - IN

#### Participants

Aditya Khurana, MD, Scottsdale, AZ (*Presenter*) Nothing to Disclose

#### TEACHING POINTS

(1) To present an initial discussion on the metaverse, its current state, and existing but limited literature within healthcare; (2) Present a thought experiment with key thought leaders as to what can the metaverse mean for Radiology in the future; (3) Outline future concepts with specific examples in which the metaverse can enhance the education, application, and visibility of radiology

#### TABLE OF CONTENTS/OUTLINE

The "metaverse" is a relatively new concept emerging within technology in which humans can interact within a digital environment - it is the intersection of the virtual and real worlds and the emergence of a second digital life. The metaverse will have a presence in healthcare. As of May 1, 2022, Pubmed search for 'Metaverse' identified 33 articles thus far. Because the literature on this topic and its applications in radiology is still in its infancy, we present this exhibit as a thought experiment with key opinion leaders on how the metaverse will enhance radiology. We will discuss the integration of the metaverse with concepts such as: (1) Real time image analysis and insight, (2) Trainee education and experience, (3) Patient education, (4) Teleradiology, (5) Research, (6) Industry relations, (7) Knowledge sharing, and (8) Quality improvement patient safety.

Printed on: 02/07/23



## Abstract Archives of the RSNA, 2022

INEE-35

### Leveraging Virtual Containers for High-Powered-Collaborative AI Research in Radiology

Sunday, Nov. 27 8:00AM - 9:00AM Room: Learning Center - IN

#### Participants

Lucas Aronson, BS, Madison, WI (*Presenter*) Nothing to Disclose

#### TEACHING POINTS

(1) Multi-institutional collaboration of AI research poses challenges due to variations in hardware and software specifications. (2) No two users are likely to have the exact same requirements to execute their code, so even sharing between members of the same lab can present challenges. (3) Virtual containers alleviate many obstacles related to compatibility and portability and also offer a wide variety of tools to aid developers. (4) Virtual containers: (4a) Streamline remote access to high-powered computers and GPU servers. (4b) Can serve as a foundation for new projects with various base containers tailored to certain project types. This can save developers time as opposed to starting from scratch. (4c) Allow users to create portable, fully functional, self-contained coding environments for seamless operation irrespective of the computer/server employed. (4d) Facilitate multi-institutional collaboration and potential large-scale AI projects.

#### TABLE OF CONTENTS/OUTLINE

(1) Why do we need virtual containers? (1a) Address hurdles researchers face when collaborating and sharing AI algorithms. (1b) Highlight some features of containers that mitigate these obstacles, including the specification of software versions and dependencies. (2) A guide to getting started with virtual containers. (2a) Demonstrate an example virtual container termed Docker, including: (2a1) The Dockerfile and requirements file (2a2) How to build a Docker Image (2a3) How to run a Docker Container (2a4) Useful commands in Docker (3) An example of how Docker was used to facilitate a large-scale AI project.

Printed on: 02/07/23



## Abstract Archives of the RSNA, 2022

INEE-37

### International Outreach in Medical Imaging Research: 3D Slicer Internationalization and Localization to French

Sunday, Nov. 27 8:00AM - 9:00AM Room: Learning Center - IN

#### Participants

Sonia M. Pujol, PhD, MSc, (*Presenter*) Nothing to Disclose

#### TEACHING POINTS

3D Slicer is an open-source software platform used in medical imaging research around the world. However, the application is currently available in the English language only. While English is the language of science, radiologists and medical imaging researchers in non-English speaking countries work and communicate with their scientific colleagues in their own languages. Through current Essential Open Source Software for Science funding of the Chan Zuckerberg Initiative, we have created a 3D Slicer internationalization team in the US, Canada, and Senegal to facilitate access to the platform for the global medical imaging research community. We have begun internationalizing 3D Slicer and localizing the user interface, tutorials, and documentation to French. The goal of the exhibit is 1. to provide an overview of the current 3D Slicer internationalization effort; 2. to introduce the new internationalization infrastructure for translating 3D Slicer user interface; 3. to present the 3D Slicer glossary for medical imaging research; 4. to teach how to contribute translations in multiple languages on the 3D Slicer translation repository; 5. to showcase 3D Slicer global outreach activities for medical imaging research in Senegal.

#### TABLE OF CONTENTS/OUTLINE

Overview of 3D Slicer Internationalization effort; Language Packs extension; 3D Slicer Glossary; 3D Slicer Weblate Repository; 3D Slicer Community Resources in French; 3D Slicer Outreach in Senegal.

Printed on: 02/07/23



## Abstract Archives of the RSNA, 2022

INEE-38

### Statistical Plots in Oncologic Imaging: A Primer for Radiologists

Sunday, Nov. 27 8:00AM - 9:00AM Room: Learning Center - IN

#### Participants

Sina Bagheri, MD, Philadelphia, PA (*Presenter*) Nothing to Disclose

#### TEACHING POINTS

Visual illustrations of quantitative information, including graphs and figures, are often practical and powerful methods of presenting scientific research results. Appropriate implementation of graphs improves the accuracy of readers' interpretation and understanding of the data, particularly for complex information. Recently, an increasing number of novel diagrams and plots have been used to visually display the outcome in radio-oncologic and radiogenomic studies. Thus, it is crucial for radiologists to be familiar with these kinds of data representations. In this educational exhibit, we describe the potential application of these various statistical plots and guide radiologists to interpret them in such reports. We also highlight the specific features of each graph type and review its advantages and drawbacks/pitfalls.

#### TABLE OF CONTENTS/OUTLINE

1. Brief introduction describing different ways for graphical representation of data 2. Graphical illustrations of tumor response 3. Graphical illustrations of survival 4. Graphical illustrations of cancer genotypes 5. Drawbacks and pitfalls 6. Conclusions

Printed on: 02/07/23



## Abstract Archives of the RSNA, 2022

INEE-39CS

### NCI Imaging Data Commons: Towards Transparency and Reproducibility in Imaging AI

Sunday, Nov. 27 8:00AM - 9:00AM Room: Learning Center - IN

#### Awards

Identified for RadioGraphics

#### Participants

Andriy Fedorov, PhD, Arlington, MA (*Presenter*) Nothing to Disclose

#### TEACHING POINTS

NCI Imaging Data Commons (IDC) is a cloud-based repository of publicly available cancer imaging data co-located with the analysis and exploration tools and resources. IDC is part of the NCI Cancer Research Data Commons (CRDC) infrastructure that provides secure access to a large, comprehensive, and expanding collection of cancer research data. IDC uses a combination of the commercially available Google Cloud Platform and open source components. The DICOM standard is used for representation and communication of the data. Google Healthcare API enables the use of SQL for DICOM metadata exploration. The IDC portal (<https://imaging.datacommons.cancer.gov>) enables exploration and visualization of data and cohort building. As of Spring 2022, IDC hosts over 30 TB of public radiology and digital pathology images and image-derived data. IDC is intended for cloud-based data processing, but data can be freely downloaded for on-premise analysis. Cloud-based workflows co-locating persistent data with software tools and compute resources enable reproducible analysis workflows. Attendees will learn about the scope and status of IDC (e.g., new features of the image viewers and IDC portal), accompanying learning resources (e.g., interactive notebooks with reproducible AI workflows applied to the data within IDC), and plans for future development. Live interactive demonstrations will be presented.

#### TABLE OF CONTENTS/OUTLINE

Overview of CRDC and IDC; Data curation and the role of The Cancer Imaging Archive; Portal; Viewer; Organization of data; Data versioning; Integration of tools; Use case development; Documentation and user support resources; IDC cloud credit program; Status update and plans for future development.

Printed on: 02/07/23



## Abstract Archives of the RSNA, 2022

INEE-40

### COVID-19 Surveillance System Based On a Nationwide Medical Image Database and Machine Learning

Sunday, Nov. 27 8:00AM - 9:00AM Room: Learning Center - IN

#### Participants

Kensaku Mori, PhD, Nagoya, Japan (*Presenter*) Research Grant, Cybernet Systems Co, Ltd;Intellectual Property, Cybernet Systems Co, Ltd;Research Grant, J Morita Corporation;Intellectual Property, J Morita Corporation;Developer, J Morita Corporation

#### TEACHING POINTS

- To understand what is nationwide CT image database- To understand how cloud-computing environments are constructed for CT image analysis- To understand how a nationwide CT image database is utilized for COVID-19 surveillance- To understand how machine learning techniques can be used for COVID-19 surveillance

#### TABLE OF CONTENTS/OUTLINE

Introduction- COVID-19 related disease shows several findings on CT images, including GGO.- Machine learning-based methods enable us to analyze CT images of COVID-19 cases.Nationwide medical image database-A nationwide medical image database is constructed in collaboration with medical societies and National Institutes of Informatics.- Medical images taken at hospitals are transferred daily to the cloud data center through the Japanese academic network SINET in L2VPN connection.- The data center has GPU servers for machine learningCOVID-19 CT image analysis- Machine learning-based COVID-19 CT image analysis algorithm has been developed- The algorithm consist of lung area segmentation and CT image appearance classification (typical COVID-19 cases or atypical COVID-19 cases)- In-house neural network architecture has been developed.COVID-19 CT daily surveillance- All of CT images having "lung" words in diagnosis reports are targets for analysis- Only CT images, including lung areas, are selected for further analysis.- Number of lung CT cases, typical COVID-19 cases and atypical COVID-19 cases are measured.Discussion- Nationwide CT image database has potential to become one of the information sources to know COVID-19 disease spread in a nation- Surveillance based on automated CT image analysis on a nationwide database can be used for monitoring many disease spreads.

Printed on: 02/07/23



## Abstract Archives of the RSNA, 2022

INEE-41

### An Overview of Artificial Intelligence for Multiple Sclerosis Analysis in MRI

Sunday, Nov. 27 8:00AM - 9:00AM Room: Learning Center - IN

#### Participants

Leiner Barba, PhD, (*Presenter*) Nothing to Disclose

#### TEACHING POINTS

Purposes: 1) Provide an overview of artificial intelligence (AI) methods, experts team and technological needs, and their potential use in Radiology; 2) Review of Multiple Sclerosis (MS) affectations and biomarkers from MRI; 3) Discuss about how AI methods have been used for MS analysis; 4) Know the basis for application of AI to MS lesion detection and segmentation.

#### TABLE OF CONTENTS/OUTLINE

A. Overview of AI methods and MS affectations; B. Segmentation of MS lesions using AI techniques; C. Analysis of MS activity; D. How to use AI for analysis of affected regions in patient with MS; E. Challenges of applying AI for analysis of MS in clinical practice; F. Future trends of AI applied to MS analysis.

Printed on: 02/07/23



## Abstract Archives of the RSNA, 2022

INEE-42

### Generating Rapid Multiparametric Prostate MRI Protocols Using Deep Learning Reconstruction

Sunday, Nov. 27 8:00AM - 9:00AM Room: Learning Center - IN

#### Participants

David Wang, MD, (*Presenter*) Nothing to Disclose

#### TEACHING POINTS

Multiparametric Prostate MRI (mpMRI) protocol consists of high resolution multiplanar T2, diffusion weighted imaging (DWI), and dynamic contrast enhanced acquisitions. An ideal mpMRI protocol meeting or exceeding PIRADS recommendations can take ~25 minutes, even after optimizing protocols using commercially available acceleration techniques. The biggest time sinks within these protocols are the T2 weighted and high b-value DWI acquisitions. Recently, a Deep Learning (DL) reconstruction technology (AIR™ Recon DL, GE Healthcare) was leveraged to reduce the multiplanar T2 acquisition time by 3-fold, without loss in signal-to-noise ratio (SNR). In this exhibit, we will review the application of this DL reconstruction technology to both T2-weighted and DWI acquisitions, focusing on comparisons of the DL reconstruction to conventional reconstructions, as well as benefits in SNR and scan time reduction. Potential pitfalls and remaining artifacts from the accelerated acquisitions will be discussed as well as the requirements and trade-offs needed to achieve a fast and robust PI-RADS 2.1-compliant protocol in less than 10 minutes.

#### TABLE OF CONTENTS/OUTLINE

1. Key components of mpMRI for prostate cancer 2. Standard acquisitions and associated scan times. 3. Synopsis of DL technique and application to accelerated multiplanar T2-weighted imaging. 4. Application of DL reconstruction for DWI and synthetic b-value calculation. 5. Potential pitfalls and artifacts post DL reconstruction. 6. Overview of PI-RADS 2.1 compliant rapid protocols utilizing DL reconstruction. 7. Summary.

Printed on: 02/07/23



## Abstract Archives of the RSNA, 2022

INEE-43

### Federated Learning Environment in The ACRs AI Lab: Are Those Rubbers (AI models) Meant For Our Roads (Imaging Data)?

Sunday, Nov. 27 8:00AM - 9:00AM Room: Learning Center - IN

#### Participants

Lina Karout, MD, Boston, MA (*Presenter*) Nothing to Disclose

#### TEACHING POINTS

(1) Understanding generalizability, reproducibility, and biases in AI models. (2) Foundation and application of federated learning environment for AI models. (3) Construction and deployment of data for federated learning. (4) Validation of AI models in ACR's AI Lab environment: Steps and Stats

#### TABLE OF CONTENTS/OUTLINE

(1) Foundational aspects of federated learning in AI model validation: What is it and why do we need it? How does it help? What does it entail? (2) Case-based demonstration of how you can use ACR's AI Lab to test and optimize AI models in a federated learning environment: (a) Understanding steps in data format, gathering, and uploading to the AI Lab. (b) Running AI models in the AI-Lab. (c) Analyzing AI outputs and performance statistics. (d) Improving AI model performance from local to global level. (3) Strengths and limitations of federated learning and its environment

Printed on: 02/07/23



## Abstract Archives of the RSNA, 2022

INEE-44CS

### The Federated Tumor Segmentation Initiative: The Largest To-date Real-World Federation Focusing on NeuroOncology

Sunday, Nov. 27 8:00AM - 9:00AM Room: Learning Center - IN

#### Participants

Alexander Getka, Philadelphia, PA (*Presenter*) Nothing to Disclose

#### TEACHING POINTS

There is a growing body of literature offering evidence of the potential impact that artificial intelligence (AI) methods can have towards healthcare. To ensure robustness and generalizability of AI methods, ample and diverse multi-site patient datasets are desired. However, there are various factors that hinder access to such data in the current paradigm of multi-site collaborations, which include the tedious bureaucratic processes, data ownership concerns, and legal considerations reflected in patient privacy regulations. To tackle these issues, we introduce the Federated Tumor Segmentation (FeTS) Initiative, which includes an open-source software toolkit for data-private collaborative learning of AI methods across multiple international institutions using federated learning (FL). The goals of the exhibit are to: (i) broaden the understanding of the general community regarding FL, (ii) showcase how a user can leverage FL to train a model across various sites, (iii) present results of the first real-world federation across 71 collaborating sites across 6 continents with 25,256 MRI scans from 6,314 patients focusing on the rare disease of glioblastoma, (iv) discuss privacy and data protection concerns and how FeTS hopes to solve it.

#### TABLE OF CONTENTS/OUTLINE

This exhibit will present a toolkit to define a FL-based model training problem and deploy it across multiple partnering sites, ensuring a data-private AI training paradigm. Specific principles to protect data privacy will be described, along with common pitfalls to avoid when performing an FL-based study.

Printed on: 02/07/23



## Abstract Archives of the RSNA, 2022

INEE-45

### A Practical Approach Into Artificial Intelligence: Ultrasonography and Artificial Intelligence Pipeline for Developmental Hip Dysplasia Screening

Sunday, Nov. 27 8:00AM - 9:00AM Room: Learning Center - IN

#### Participants

Sebastian Gallo-Bernal, MD, Boston, MA (*Presenter*) Nothing to Disclose

#### TEACHING POINTS

- Artificial intelligence (AI) algorithms have demonstrated remarkable progress in image-recognition tasks.
- We aim to exemplify AI integration into clinical workflows, by assessing the feasibility of an ultrasound (US) AI (xAI) pipeline to increase the availability of sonographic screening for developmental hip dysplasia (DDH).
- US screening for DDH is based on the Graf method. The main drawback of this method is the high inter-operator variability. Primary sources of image acquisition variability arise from the manual selection of anatomical points and the difficulties to acquire images in the adequate anatomical plane.
- An AI-based computer-aided diagnosis (CAD) system can standardize image acquisition and reduce diagnosis time, improving the accuracy and objectivity of DDH diagnosis.
- Problem-solving in practical approaches towards AI: Class Imbalance.
- US x AI pipeline product: preprocessing techniques, image adequacy assessment and diagnosis models, atlas creation and nearest neighbor retrieval modules, and modules for post-hoc quantification of prediction uncertainty

#### TABLE OF CONTENTS/OUTLINE

INTRODUCTION AND BACKGROUND: • Artificial intelligence and radiology: AI for image quality assessment and image selection and standardization  
PROBLEM STATEMENT: • Ultrasonography for DDH screening and follow-up. Graf technique: image quality consideration; drawbacks and limitations on radiology workflows  
US x AI PIPELINE: PRACTICAL APPROACH TOWARDS IMPLEMENTATION • Ultrasonography x AI pipeline architecture and outputs • Comparison of undersampling and class weights for addressing class imbalance • Performance metrics for binary classification of image adequacy  
LIMITATIONS/FUTURE

Printed on: 02/07/23



## Abstract Archives of the RSNA, 2022

INEE-46

### A Hands-on Guide to Designing Cloud-based Web Platforms with Radiological Applications

Sunday, Nov. 27 8:00AM - 9:00AM Room: Learning Center - IN

#### Participants

Adrian Serapio, Berkeley, CA (*Presenter*) Nothing to Disclose

#### TEACHING POINTS

Learning what goes into the design of cloud-based radiological web platforms will empower radiologists to truly leverage the power of the cloud and enhance their everyday workflow. We will walk through designing one such application, RadSim, an interactive reader performance study application that streamlines the process of conducting image based surveys. We demonstrate: - Why and how to apply cloud-based applications to a radiologist's everyday workflow- How to design a basic web application from ideation to testing- How to use the REST framework to develop the web application (using Node.js, MySQL, AWS)- How to visualize data generated by the web platform (using Python's Matplotlib library)

#### TABLE OF CONTENTS/OUTLINE

Problem Statement - Paucity of easy-to-learn, open-source, platform-agnostic, cloud-based web applications matching the needs of radiologists- Introduce and walkthrough a product design framework to build simple cloud-based applications in radiologyPrerequisite/Background- Basic understanding of any programming languageWalkthrough1. Product design framework2. Cloud-based web development 3. Data visualization4. Integration to radiological workflowConclusion

Printed on: 02/07/23



## Abstract Archives of the RSNA, 2022

INEE-47

### Understanding and Mitigating Bias in Artificial Intelligence

Sunday, Nov. 27 8:00AM - 9:00AM Room: Learning Center - IN

#### Awards

Identified for RadioGraphics  
Cum Laude

#### Participants

Ali Tejani, MD, Frisco, TX (*Presenter*) Nothing to Disclose

#### TEACHING POINTS

1. Define and review categories of bias in AI. 2. Raise awareness of the sources of bias to promote mindfulness when using AI solutions in practice. 3. Understand how models can perpetuate prejudices and bias inherent in datasets. 4. Propose solutions to combat bias in AI.

#### TABLE OF CONTENTS/OUTLINE

1. Introduction  
a. Define bias in AI  
i. Broad categories (i.e., implicit versus explicit, cognitive biases)  
ii. Model development (i.e., dataset, algorithm, and prediction bias)  
2. Scope of bias in AI  
a. Bias in AI along the radiology value chain  
b. Workflow diagram of the effect of bias in AI beyond the reading room (i.e., referring clinician and enterprise-level effects)  
i. Exacerbation of healthcare inequities  
3. Sources of bias in AI  
a. Model development  
i. Dataset curation  
1. Training/validation set demographics  
2. Confounding clinical comorbidities  
ii. Technical dataset variables  
1. Dataset shift  
2. Data leakage  
3. Varying post-processing techniques  
iii. Annotations  
1. Varying expertise  
2. Lack of standard guidelines  
3. Heterogeneous imaging scanners and protocols  
iv. Bias-variance tradeoff  
b. Model utilization and clinical impact  
i. Automation bias  
ii. Inequality considerations  
1. Exacerbation of inherent algorithm bias (i.e., underdiagnosis)  
2. Amplification of resource inequality and implications of inadequate access to AI tools  
3. Heterogeneous monitoring and adjustment of deployed AI tools  
4. Proposed solutions to mitigate bias in AI  
a. "Checkpoints" throughout AI workflow  
b. Involving statisticians in the model development process  
c. Require diverse datasets  
d. Monitoring AI performance across diverse populations and varying modalities/hardware

Printed on: 02/07/23



## Abstract Archives of the RSNA, 2022

INEE-48

### Building A Multi-institution and Multi-expert Annotators Dataset for Machine Learning: Experience From

Sunday, Nov. 27 8:00AM - 9:00AM Room: Learning Center - IN

#### Participants

Felipe C. Kitamura, MD, PhD, Sao Paulo, SP (*Presenter*) Consultant, MD.ai, Inc; Speaker, General Electric Company

#### TEACHING POINTS

Creating Machine Learning (ML) datasets is a laborious and tricky team effort. Errors in the planning phase can undermine the final result. Baking a refined ML dataset can be viewed as a multi-step process, including use-case definition, IRB approval, multi-institutional agreement, imaging protocol definition, data de-identification, data collection, labeling scheme definition, collaborating with annotators, annotation and data quality control, and license definition. A recipe approach is suggested with a list of ingredients and preparation instructions.

#### TABLE OF CONTENTS/OUTLINE

Why is it important to create ML datasets? ML dataset recipe Key ingredients of a useful dataset Dataset preparation instructions Most common pitfalls and mistakes Logistics and quality control when generating expert annotations Examples of RSNA datasets How the dataset structure affects model development.

Printed on: 02/07/23



## Abstract Archives of the RSNA, 2022

INEE-49

### Impact-sensitive Management of Prediction Uncertainty in Artificial Intelligence for Healthcare

Sunday, Nov. 27 8:00AM - 9:00AM Room: Learning Center - IN

#### Participants

Michelle Chua, Brookline, MA (*Presenter*) Nothing to Disclose

#### TEACHING POINTS

Unsafe prediction failure occurs when a machine learning model is unable to convey lack of confidence, or deceitfully conveys high confidence, in an erroneous prediction. Standard performance metrics measure overall model performance on limited test data and provide no indication of model confidence in the correctness of individual predictions. Post-hoc prediction uncertainty metrics, such as calibrated classifier confidence, measures of visual similarity, and information entropy, may be used to quantify prediction uncertainty. Classifier confidence and information entropy do not capture out-of-distribution uncertainty. Prevention of unsafe prediction failure requires task-specific and impact-sensitive selection of prediction uncertainty metrics and prediction uncertainty thresholds. Prediction uncertainty metrics may be calibrated to precision if the desired safety threshold is zero tolerance for false positives or to negative predictive value if the desired safety threshold is zero tolerance for false negatives.

#### TABLE OF CONTENTS/OUTLINE

Understanding prediction uncertainty and prediction uncertainty metrics  
Comparative evaluation of prediction uncertainty metrics  
Selection of prediction uncertainty metrics for zero tolerance and error tolerant clinical applications

Printed on: 02/07/23



## Abstract Archives of the RSNA, 2022

INEE-4HC

### Building the Administrative and Operational Infrastructure for an AI Enabled Radiology Department

Sunday, Nov. 27 8:00AM - 9:00AM Room: Learning Center - IN

#### Awards

Certificate of Merit

#### Participants

Holly Meyer, RT, Rochester, MN (*Presenter*) Nothing to Disclose

#### TEACHING POINTS

The goal of this exhibit is to provide an administrator's perspective on building an artificial intelligence (AI) team in the Department of Radiology, as well as the framework for successful discovery, translation, application, and commercialization of AI software technology. To establish a thriving AI program, careful consideration must be given to the organizational structure, key job roles and responsibilities, and an effective program structure must be established within which to operate.

#### TABLE OF CONTENTS/OUTLINE

1. Radiology AI Ecosystem 2. Program Stakeholder Network 3. Pathways to Navigate a. Technical b. Administrative c. Regulatory 4. Clinical AI Pillars 5. Program Structure a. Leadership b. Organization c. Team d. Roles Responsibilities e. Information Management f. Communication g. Training and Education h. Quality Management System i. Architecture Infrastructure 6. Process a. Idea Submission b. Feasibility Analysis c. Intake d. Discovery e. Translation f. Limited Rollout g. Full Rollout h. Post-Production Please visit the Learning Center to also view this presentation in hardcopy format.

Printed on: 02/07/23



## Abstract Archives of the RSNA, 2022

INEE-5

### Lessons Learned from a Cyberattack on the Healthcare System: A Radiology Perspective

Sunday, Nov. 27 8:00AM - 9:00AM Room: Learning Center - IN

#### Participants

Hilary Strong, MD, (*Presenter*) Nothing to Disclose

#### TEACHING POINTS

We wish to share our insight and lessons learned from navigating a response to the cyberattack on province-wide healthcare authorities which rendered medical information technology systems inaccessible. Prompt, accurate, and consistent communication with all medical imaging staff, referring physicians, and healthcare authorities, is a crucial first step. Effective communication involves various modalities, such as secure applications, texts, emails, calls, and frequent face-to-face discussions/meetings. Following effective communication, having an existing cyberattack response system in place to immediately modify workflow and adapt to technology limitations is a priority. Finding an effective modified workflow system is not a linear process. However, judicious trial and error of solutions is more effective than remaining idle during a cyberattack. Modified workflow included entirely paper-based medical imaging requisitions and patient safety identification systems, as well as workflow limited to urgent and emergent studies only. With patient-centered care at the forefront of the radiology department's response to the cyberattack, safe and effective medical imaging services were provided to the patients of our province.

#### TABLE OF CONTENTS/OUTLINE

1. Introduction  
2. Four Lessons Learned from a Cyberattack on Our Provinces' Healthcare System  
a. Prompt and consistent communication is paramount.  
b. (Not completely) out with the old (paper-based system).  
c. Correct patient identification prioritizes safety.  
d. Judicious trial and error is the way forward.  
3. Conclusion

Printed on: 02/07/23



## Abstract Archives of the RSNA, 2022

INEE-6

### All-in-One workplace for Radiologists: How to Build Your Personal Radiology Knowledge

Sunday, Nov. 27 8:00AM - 9:00AM Room: Learning Center - IN

#### Participants

Ken Oba, MD, Chuoku, Japan (*Presenter*) Nothing to Disclose

#### TEACHING POINTS

At the end of this presentation, you will be able to:-Learn about Notion and Cloud PACS basics and start practicing with simple lessons and review concepts.-Make the all-in-one workspace and notes for research, education, and conference.-Build a system for collecting, maintaining, and serving knowledge to the right person at the right time.

#### TABLE OF CONTENTS/OUTLINE

-Introduction.-What is Notion, and what is Cloud PACS.-How to start Notion and Cloud PACS.-How to make a database for scientific research.-How to make a database for education.-How to make flashcards for exams.-How to make a database for conferences.-Advanced techniques will be introduced through Twitter using templates and short movies.-Conclusion

Printed on: 02/07/23



## Abstract Archives of the RSNA, 2022

INEE-7

### Medical imaging AI In the Real World: Decoding Bias in Under-represented Populations

Sunday, Nov. 27 8:00AM - 9:00AM Room: Learning Center - IN

#### Participants

Eduardo Freire, MD, Sao Paulo, Brazil (*Presenter*) Nothing to Disclose

#### TEACHING POINTS

Patterns of health inequality permeate artificial intelligence (AI) systems when bias and discrimination become entrenched in the conception, design, and use of these systems. Underserved patients, who have historically faced greater challenges accessing care, including imaging, may be underrepresented in the development of AI systems, leading to bias and compromising model performance. We aim to present a literature review on how to identify and mitigate existing and potential bias related to healthy inequality in medical imaging AI.

#### TABLE OF CONTENTS/OUTLINE

1) Introduction 1.1) Basic concepts and definitions: diversity, equity and inclusion in the AI era 1.2) Fairness and ethics of artificial intelligence in radiology: where are we? 2) Categories of AI bias 3) Sources of bias in AI development lifecycle 3.1) Human factors 3.2) Dataset challenges 4) Identifying bias in medical imaging AI: Case studies 4.1) How gender and race imbalance in a medical imaging dataset influences AI performance 4.2) Transgender population and health care disparities 5) Strategies to managing and mitigating bias in medical imaging AI 5.1) Transparency and data sharing 5.2) Policy and Regulations

Printed on: 02/07/23



## Abstract Archives of the RSNA, 2022

INEE-8

### 3D Printing and Digital Surgical Rehearsal in Complex Spine Surgery

Sunday, Nov. 27 8:00AM - 9:00AM Room: Learning Center - IN

#### Awards

Identified for RadioGraphics

#### Participants

Lumarie Santiago, MD, Houston, TX (*Presenter*) Nothing to Disclose

#### TEACHING POINTS

The approach to complex spine surgery requires a multidisciplinary team and multimodality imaging to delineate the extent of disease as well as the structures at risk during surgery. Integration of the information provided by the various imaging exams may be difficult, particularly as each surgical discipline may have different take away points. This case-based exhibit provides information on the process of 3D printing including segmentation using multimodality imaging exams, validation (QA) and post processing. The use of digital and 3D printed models in surgical rehearsal with a focus on their impact on prescribing digital surgical planes will be discussed. The integration of .STL files into intraoperative navigation systems and validation of the digital surgical plan using the 3D printed model will also be reviewed.

#### TABLE OF CONTENTS/OUTLINE

1. The 3D printing workflow used to integrate multimodality imaging exams. 2. 3D printing material selection to enhance surgical rehearsal. 3. Quality assurance steps in 3D printing. 4. Prescribing digital surgical planes. 5. Validation of digital surgical planes using the 3D printed model. 6. Intraoperative use of digital surgical planes.

Printed on: 02/07/23



## Abstract Archives of the RSNA, 2022

INEE-9

### 3D Printing from Medical Imaging Data: What the Resident Needs to Know

Sunday, Nov. 27 8:00AM - 9:00AM Room: Learning Center - IN

#### Participants

Nicole Wake, PhD, Aurora, OH (*Presenter*) Employee, General Electric Company

#### TEACHING POINTS

A. Patient-specific 3D printed anatomic models and guides can aid in surgical planning, can provide intra-operative guidance, can be utilized for simulations, and can be used for trainee and patient education. B. Volumetric medical imaging data with high spatial resolution, good signal-to-noise ratio (SNR), and good contrast-to-noise ratio (CNR) is recommended if 3D printing will be performed. C. The workflow to create 3D printed anatomic models from volumetric imaging data includes image acquisition, image segmentation, conversion to 3D mesh geometries, and printing. D. Reimbursement for 3D printed anatomic models and anatomic guides can be pursued using Category III CPT Codes. E. The medical 3D printing process should be formally documented and recorded in the electronic medical record system and this is required for reimbursement. F. Hospital-based 3D printing labs should establish quality management systems to ensure the accuracy of 3D printed models.

#### TABLE OF CONTENTS/OUTLINE

1. Review of the common applications of 3D printed medical models.
2. Description of major imaging recommendations for the creation of 3D printed anatomic models and guides derived from medical imaging data.
3. Overview of the workflow required to create 3D printed patient-specific anatomic models from volumetric medical imaging data.
4. Review of CPT codes including the Category III CPT Codes for 3D Printed anatomic models and anatomic guides, and introduction to the RSNA-ACR 3D printed model registry.
5. Synopsis of a formal documentation system for 3D printed anatomic models and guides.
6. Summary of the quality assurance steps required to ensure the accuracy of 3D printed medical models.

Printed on: 02/07/23

## Abstract Archives of the RSNA, 2022

IREE

### Interventional Education Exhibits

Sunday, Nov. 27 8:00AM - 9:00AM Room: Learning Center - IR

#### Sub-Events

#### **IREE-1 Arterial Embolization for Gynecological and Obstetric Hemorrhage - Indications, Preparation, Technique, Results, and Complications**

##### Awards

##### Certificate of Merit

##### Participants

Mario Matute Gonzalez, MD, Barcelona, Spain (*Presenter*) Nothing to Disclose

##### TEACHING POINTS

1. To describe the diagnostic and therapeutic management of patients with gynecological and obstetric hemorrhage (GOH) suitable to transcatheter embolization.2. To review main gynecologic and obstetric indications for arterial embolization, providing key imaging findings before and after embolization.3. To explain the technique and intraprocedural considerations, results and complications of GOH embolization.

##### TABLE OF CONTENTS/OUTLINE

1. Introduction.1.1. Vascular anatomy of the female pelvis.2. Management of patients with GOH.2.1. Therapeutic algorithm.2.2. Pre-treatment imaging assessment.3. Indications for arterial embolization: imaging findings.3.1. Obstetric hemorrhage.- Abnormal placentation.- Postpartum hemorrhage.3.2. Gynecological hemorrhage.- Malignancies.- Post-surgical bleeding.- Vascular anomalies: Uterine AVMs and AV fistulas.3.3. Beyond hemostasis.- Uterine fibroids.- Pelvic Congestion Syndrome.4. Procedural features.4.1. Patient preparation.4.2. Materials.4.3. Technical considerations.4.4. Results.4.5. Complications.5. Summarize.6. Conclusion.

#### **IREE-10 Minimally Invasive Prostate Cancer Treatments- An Update**

##### Participants

Riddhi Borse, MD, New Haven, MA (*Presenter*) Nothing to Disclose

##### TEACHING POINTS

The purpose of this exhibit is:1.To provide rationale for minimally invasive prostate cancer (PCa) treatment.The "index" lesion is responsible for driving risk associated with localized PCa. However, imaging underestimates lesion volume it is important to have adequate treatment zone margins.2.To review modalities and devices available for minimally invasive PCa treatment. Understanding the nuances of available devices along with their FDA approval/ reimbursement status and current evidence about their efficacy is crucial towards building a successful PCa treatment program.

##### TABLE OF CONTENTS/OUTLINE

1. Need for minimally invasive prostate cancer therapy. 2. Defining the index lesion. 3. Treatment margins - How much prostate should you ablate? 4. Treatment modality specific review including device capabilities/limitations, cost, side effect profile and efficacy evidence;Laser Ablation CryoablationIrreversible Electroporation Therapeutic Ultrasound Photodynamic Therapy Aquablation Bipolar radiofrequency ablation5. Post treatment prostate MRI 6. FDA Approval Status and Insurance Reimbursements for minimally invasive PCa treatment.

#### **IREE-12 How to Make It Right When Vessels Go Wrong: Demystifying Abdominal Vascular Anomalies**

##### Participants

Ece Meram, MD, Madison, WI (*Presenter*) Research Grant, Koninklijke Philips NV

##### TEACHING POINTS

The classification of vascular anomalies has been evolving and remains challenging with limited worldwide adoption and lingering of historically used terminology. Vascular anomalies are divided into two main categories (i.e. mass or malformation) based on their increased mitotic activity and cell turnover. Vascular masses, benign or malignant, are vasoproliferative lesions with increased endothelial cell turnover. Vascular malformations, on the other hand, are congenital, non-neoplastic entities of incorrectly formed vessels. This exhibit aims to 1) describe different types of abdominal vascular anomalies according to International Society for the Study of Vascular Anomalies (ISSVA) classification, 2) demonstrate examples of abdominal vascular tumors and malformations, including those associated with hereditary conditions and 3) highlight the interventional approaches utilized in the management (i.e. correction) of these anomalies.

##### TABLE OF CONTENTS/OUTLINE

A. When Vessels Go Wrong: Vascular Anomalies a. Definition/Types: Mass vs Malformation b. ISSVA Classification. B. Abdominal Vascular Tumors a. Benign (eg. Hepatic Hemangioma) b. Borderline c. Malignant (eg. Angiosarcoma). C. Abdominal Vascular

Malformations a. Simple i. Low-flow (Capillary, Lymphatic, Venous) ii. High-flow (Arteriovenous malformation or fistula) iii. Portosystemic Fistula (eg. Congenital Portosystemic Shunts) b. Combined c. Anomalies of Major Named Vessels d. Associated with Other Anomalies (Hereditary and/or Syndromic). D. How to Make it Right? a. Surgical Management b. Types of Interventional Procedures c. Case Examples. E. Quiz Cases

### **IREE-13 Adrenal Venous Sampling: Tips and Tricks for Non-Experts**

#### **Awards**

**Identified for RadioGraphics**

Participants

Katsuhiro Kobayashi, MD, , (Presenter) Nothing to Disclose

#### **TEACHING POINTS**

1) Review adrenal vein anatomy and anatomical landmarks for right adrenal vein cannulation. 2) Describe adjunctive techniques used for adrenal vein sampling (AVS). 3) Discuss adrenal vein sample interpretation and indication for repeat AVS

#### **TABLE OF CONTENTS/OUTLINE**

1) Overview of primary aldosteronism 2) Anatomy of adrenal veins relevant to AVS and anatomical landmarks for right adrenal vein cannulation (inferior emissary vein, communicating veins, inferior accessory hepatic vein) 3) Pre-procedural work-up including MDCT technique used for adrenal vein assessment 4) Protocol for AVS including antihypertensive medication modification, or cosyntropin infusion etc.) 5) Techniques used for AVS and adjunctive techniques used for right adrenal vein cannulation (Cone-Beam CT, coaxial guide wire- catheter technique, intraprocedural cortisol measurement) 6) Sample interpretation and indication for repeat AVS (double down Aldosterone/Cortisol) 7) Complications associated with AVS 8) Advances in AVS (subselective AVS) 9) Summary of Tips and Tricks

### **IREE-14 Portal Hypertension: A Comprehensive Clinico-Radiological Review.**

Participants

Antonio Hernandez Villegas, MD, Mexico City, Mexico (Presenter) Nothing to Disclose

#### **TEACHING POINTS**

- To review the physiopathology, classification and etiologies of different types of portal hypertension- To illustrate in a case based approach the different types and causes of portal hypertension (acute and chronic) with multimodality imaging findings- To mention key imaging findings that need to be assessed and provided to the clinician (GI, endoscopy and/or surgeon) in order to determine treatment options- To present interventional radiology treatment options for this pathology according to clinical scenario.

#### **TABLE OF CONTENTS/OUTLINE**

- Introduction: Epidemiology and risk factors.- Physiopathology: the basics for radiologists in order to understand imaging findings.- Classification: anatomy and timing.- Imaging: role of different imaging modalities and the main findings in the approach, diagnosis and follow-up of patients with portal hypertension.- Case-based approach: imaging findings, diagnosis and interventional treatments.- Take-home points.

### **IREE-15 Various Interventional Procedures Through Percutaneous Cholecystostomy Tract**

Participants

Jong Hyouk Yun, MD, PhD, Busan, Korea, Republic Of (Presenter) Nothing to Disclose

#### **TEACHING POINTS**

The purpose of this review is to illustrate the various transcholecystic interventions and to discuss the clinical significance, technical aspects and complications of this alternative access to the biliary tree.

#### **TABLE OF CONTENTS/OUTLINE**

Percutaneous cholecystostomy is a well-established procedure for management of acute cholecystitis. It has been used to provide GB decompression, biliary drainage and cholangiography. In patients who underwent previous surgery or who have intolerance or anxiety for endoscopy, in cases of having difficulties to perform PTBD, or in patients who have previously undergone percutaneous cholecystostomy, percutaneous transcholecystic interventions can be performed as an alternative route. Cystic duct (CD) cannulation is necessary to perform various transcholecystic interventions. For the successful cystic duct cannulation perform a GB puncture in the long axis direction of the GB, keep catheter drainage for 3 days or more to reduce inflammation of the biliary tree, insert a 8F sheath into the GB for the back support, and use guide wires with various sizes and tips. Through cystic duct cannulation, various interventional procedures such as CBD stone removal, biopsy, biliary dilation, biliary stent placement, and GI intervention can be performed. Percutaneous transcholecystic interventions seems to be safe, technically feasible and clinically effective procedures. Percutaneous transcholecystic approach can be used as an alternative route for the patient who could not use peroral or transhepatic route.

### **IREE-16 Cholangioscopy Guidance During Percutaneous Transhepatic Biliary Interventions**

Participants

Ayca Kutlu, MD, Madison, WI (Presenter) Nothing to Disclose

#### **TEACHING POINTS**

• Introduce readers to transhepatic cholangioscopy. • Provide an overview of transhepatic cholangioscopy technique, indications, and utility. • Improve readers' ability to interpret cholangioscopy imaging through representative cases. • Demonstrate through case examples how transhepatic cholangioscopy guidance can improve procedural success.

#### **TABLE OF CONTENTS/OUTLINE**

1. Title page 2. Teaching points 3. Background on current transhepatic biliary imaging techniques a. Fluoroscopic cholangiogram b. Intrahepatic cone-beam CT cholangiography 4. Introduction to percutaneous transhepatic cholangioscopy 5. Indications for

percutaneous transhepatic cholangioscopy a. Patients with indwelling biliary catheters with new concern for pathology b. Patients with history of previous failed ERCP or altered anatomy prohibiting ERCP 6. Percutaneous transhepatic cholangioscopy interventions a. Targeted tissue sampling b. Biliary stone/debris management c. Biliary Stent/drain placement 7. Case Examples a. Tissue sampling: Targeted biopsy via direct visualization b. Intraductal stone/debris manipulation: Identification of intrahepatic stone/debris with lithotripsy treatment, extraction, or sweeping c. Complex post-surgical anatomic delineation: Navigation across post-surgical benign biliary strictures 8. Conclusions a. Transhepatic cholangioscopy can improve diagnostic and therapeutic precision in the management of biliary pathology. b. Interventional radiologists becoming comfortable with transhepatic cholangioscopy image interpretation and procedural skill can increase procedural success for complex biliary pathology. 9. Quiz Case

## **IRRE-17      Interventional Management of Ectopic Varices**

### **Awards**

#### **Identified for RadioGraphics**

#### **Participants**

Jin Woo Choi, MD, Seoul, Korea, Republic Of (*Presenter*) Nothing to Disclose

#### **TEACHING POINTS**

Ectopic varices may occur around the duodenum, rectum, stoma, hepaticojejunostomy, etc. Although ectopic varices are not common, those can be a source of considerable bleeding. They usually occur in the setting of portal hypertension such as liver cirrhosis or portal vein occlusion/thrombosis. Whereas endoscopic management is commonly ineffective for ectopic varices, various interventional procedures including percutaneous varix embolization or modified retrograde transvenous obliteration can be performed depending on vascular anatomy. The purposes of this exhibit are: (1) To illustrate vascular anatomy related to ectopic varices, (2) To list various interventional procedures and their indications, (3) To review the technical tips and pitfalls of percutaneous varix embolization and modified retrograde transvenous obliteration.

#### **TABLE OF CONTENTS/OUTLINE**

1. Vascular anatomy related to ectopic varices. 2. Treatment modalities and indications for ectopic varices: retrograde transvenous obliteration, percutaneous embolization, and their modifications. 3. Technical tips and pitfalls of retrograde transvenous obliteration, percutaneous embolization, and their modifications.

## **IRRE-18      Overview of the Complications of Prostate Artery Embolization and its Management**

#### **Participants**

Richard Liang, (*Presenter*) Nothing to Disclose

#### **TEACHING POINTS**

Prostate Artery Embolization (PAE) is a safe, minimally invasive treatment for lower urinary tract symptoms (LUTS) secondary to benign prostatic hyperplasia (BPH). The purpose of this exhibit is to discuss the complications associated with PAE along with the management of those complications. Complications of PAE can be divided into access site complications, post-embolic complications, non-target embolization and radiation dermatitis. Though the majority of complications are considered self-limiting and can be managed conservatively, more severe complications such as bladder wall ischemia may require cystoscopic surgical resection. While reviewing non-target embolization complications, we will also discuss prostate artery anatomy and its relevance to these complications. Additionally, we will also compare the safety of PAE to some of the other common surgical treatments available for BPH.

#### **TABLE OF CONTENTS/OUTLINE**

1. What is PAE? 2. How to Perform PAE 3. Overview of the Complications in PAE 4. Access Site Complications and its Management 5. Post-Embolic Complications and its Management 6. Arterial Anatomy and Anatomical Variants of the Prostate 7. Non-Target Embolization Complications and its Management 8. Safety of PAE compared to Surgical Treatments

## **IRRE-19      A Comprehensive Approach to Image-guided Ablation in Primary Aldosteronism**

#### **Participants**

Mohamed Ibrahim, MBCh, Rochester, MN (*Presenter*) Nothing to Disclose

#### **TEACHING POINTS**

- Learn appropriate patient selection for image-guided ablation of PA
- Learn appropriate clinical evaluation and consultation of PA patients
- Understand key pre-procedural patient preparations
- Highlight pertinent intra-procedural techniques and considerations
- Highlight appropriate post-procedural follow-up and management

#### **TABLE OF CONTENTS/OUTLINE**

• Appropriate patient selection for image-guided ablation  
o Key laboratory analysis for diagnosis of PA  
o Confirming collateralization of imaging and AVS findings  
• The PA clinic consult  
o Pertinent HPI; positives and negatives  
o Consenting the PA patient, risks and expectations  
• Pre-procedural patient preparation  
o Anesthesia clearance  
o Adrenergic hypertensive crisis, strategies for prevention  
o Considerations for the day of the procedure  
• Pertinent intra-procedural techniques and considerations  
o Patient positioning  
o Ablation modalities and respective protocols  
o Accessing adrenal nodules in challenging anatomy  
• Post-procedural follow-up and management  
o Next day visit for serum potassium check, blood pressure measurement, and medication adjustments  
o Three months follow-up  
o Management of non-responders or relapsing patients

## **IRRE-2      Training of Interventional Radiology Procedures for Medical Students Using Virtual Reality**

#### **Participants**

Yukiko Honda, MD, Kure, Japan (*Presenter*) Nothing to Disclose

#### **TEACHING POINTS**

The COVID-19 pandemic made it difficult to train medical students on procedures that involve direct patient contact, such as interventional radiology (IR). For this reason, we developed training materials for medical students on endovascular procedures of the abdominal pelvis in IR using virtual reality (VR). Advantages of VR-based IR education include the ability to conduct training at

any time, repeated training exercises, no invasiveness to the patients, and no risk of infection to both the patient and the student. The disadvantages are that a large number of funds are needed to purchase or develop VR simulators and that there are few studies that have proven the effectiveness of education using VR. This educational exhibit will provide a brief overview of simulators available for purchase, and our VR-based training software, and discuss its advantages, current issues, and future prospects.

#### TABLE OF CONTENTS/OUTLINE

1 Features of the currently commercially available VR simulators of endovascular procedures A virtual and augmented reality: VIST(Mentice), ANGIO mentor (Simbionix), ORCAMP (Orzone). 2 Assessment of the educational validity of VR simulators. Face validity, content validity, Construct validity, Concurrent validity, Predictive validity. 3 Assessment tools of VR simulators. I Global rating scales: Likert scales etc, II Surveys: A subjective assessment tool, III Pre- and Post-tests: tests before and after the training, IV Time-action analysis, V Error analysis, VI Simulator metrics: metrics preprogrammed into the simulator to measure performance. 4 Review of reports on the educational validity of VR simulators. 5 Future challenges and our approach.

#### **IREE-20 Superselective Radioembolization for Hepatocellular Carcinoma: Radiation Segmentectomy and Beyond**

Participants

Hyo-Cheol Kim, MD, Seoul, Korea, Republic Of (*Presenter*) Nothing to Disclose

#### TEACHING POINTS

Radioembolization is an established treatment for unresectable hepatocellular carcinoma. Radioactive microspheres are preferentially deposited into the hypervascular tumor by siphoning effect so that injection of microspheres are commonly performed at the lobar artery level. However, superselective radioembolization is the best way to improve tumor response and to prevent potential complications. The purpose of this exhibit is : (1) To review the rationale of radiation segmentectomy. (2) To learn when superselective radioembolization is needed, (3) technical tips for superselective radioembolization.

#### TABLE OF CONTENTS/OUTLINE

1) Radiation segmentectomy : rationale and evidence 2) Dosimetry : Practical guide for dosimetry of superselective radioembolization 3) When superselective radioembolization is needed A. small single tumor : radiation segmentectomy B. Large single tumor saddling on both lobes C. Small remnant liver D. Hepatic artery branching at acute angle E. Extrahepatic collateral artery supplying the tumor 4) Technical consideration of superselective radioembolization A. Protection of distal normal liver by using balloon microcatheter and detachable coil B. Combination treatment of lobar and segmental artery C. Combination treatment of 1st and 2nd week dosing of glass microsphere 5) Follow-up imaging after superselective radioembolization A. Early loss of arterial enhancement of the tumor B. Focal radiation necrosis mimicking new hypovascular tumor

#### **IREE-21 Mesenteric Arteriovenous Malformations: A Rare Cause of Colonic Ischemia**

Participants

Lindsey Miley, MD, (*Presenter*) Nothing to Disclose

#### TEACHING POINTS

Learn the diagnostic and interventional imaging characteristics of mesenteric arteriovenous malformations. Review the current literature of mesenteric arteriovenous malformations associated with colonic ischemia. Review a case series of mesenteric arteriovenous malformations from our institution including etiology, diagnostic imaging, interventions, and outcomes. Understand the role of the Interventional Radiologist in diagnosis and treatment of these anomalies.

#### TABLE OF CONTENTS/OUTLINE

1. Define mesenteric arteriovenous malformation • Etiologies and incidence • Clinical versus imaging classification 2. Mesenteric arteriovenous malformations with associated colonic ischemia • Diagnostic imaging work-up • Literature review of treatment and outcomes • Review of case series from our institution 3. Role of the Interventional Radiologist in diagnosis and treatment of mesenteric arteriovenous malformations • Diagnostic angiography • Embolization • Challenges in work-up and treatment • Future directions

#### **IREE-23 Minimally Invasive Image-Guided Treatment of Primary, Recurrent and Metastatic Prostate Cancer**

Participants

Daniel Adamo, MD, Rochester, MN (*Presenter*) Nothing to Disclose

#### TEACHING POINTS

1.) Learn the diagnostic and treatment approach to prostate cancer within the National Comprehensive Cancer Network (NCCN) guidelines 2.) Learn the imaging appearance of native, in-gland recurrent and metastatic prostate cancer at multimodal imaging 3.) Understand the minimally invasive image-guided therapies for treating focal native, locally recurrent, and metastatic prostate cancer.

#### TABLE OF CONTENTS/OUTLINE

1. Diagnostic, staging and treatment approach to prostate cancer within the National Comprehensive Cancer Network (NCCN) guidelines • Prostate cancer epidemiology • Diagnostic and staging evaluation (history, physical exam, laboratory evaluation, imaging, biopsy) • NCCN treatment algorithm 2. Imaging appearance of native, locally recurrent, and metastatic prostate cancer at multimodal imaging with a focus on MRI and PET. • Ultrasound • CT • Bone Scintigraphy • PET (11C-Choline, 68Ga-PSMA, 18F-PSMA, 18F-Fluciclovine) • Dynamic Contrast Enhanced Multiparametric MRI 3. Minimally invasive image-guided therapies for treating focal native, locally recurrent, and metastatic prostate cancer • Focal native and locally recurrent prostate cancer o MRI-guided therapies (Cryoablation, Laser ablation, Focused Ultrasound (FUS)) o US-guided therapies (Cryoablation, Irreversible Electroporation (IRE), High-intensity focused ultrasound (HIFU)) • Focal metastatic prostate cancer o Bone metastases (Cryoablation, External beam radiation therapy (EBRT)) o Lymph node metastases (Cryoablation, External beam radiation therapy (EBRT)) o Hepatic metastases (Ablation, Transarterial Embolization). • Emerging targeted therapies o Theranostics o Radioembolization (90Y-TARE)

#### **IREE-24HC Endoscopic Biliary Interventions Performed by Interventional Radiology and Gastroenterology: A**

## Case Based Review

### Participants

Tushar Garg, MD, Baltimore, MD (*Presenter*) Conference Travel, Siemens Healthineers

### TEACHING POINTS

1) To learn about the different endoscopes and ancillary devices available for interventional radiology (IR) and gastroenterology (GI) biliary procedures 2) To learn about the basic and advanced endoscopy techniques 3) To review the endoscopic management of benign and malignant lesions of the biliary tree with the help of cases

### TABLE OF CONTENTS/OUTLINE

1) Types of devices available a. Endoscopes used in IR: BF-XP160F EVIS Exera video bronchoscope, LithoVue single-use digital flexible ureteroscope, SpyGlass digital catheter, AXIS Single-Use Digital Ureteroscopes b. Endoscopes used in GI: surgical cholangioscope (FCN-15X), Fiberoptic percutaneous cholangioscope (CHF-CB30L/S), SpyGlass direct visualization system c. Accessories used in IR and GI: biopsy forceps, electrohydraulic lithotripsy, laser lithotripsy, retrieval basket, retrieval snare, balloons 2) Basic techniques: a. IR techniques: percutaneous cholangioscopy with manual or pump irrigation b. GI techniques: dual operator mother-daughter per-oral cholangioscopy, single-operator per-oral cholangioscopy, direct per-oral cholangioscopy 3) Clinical applications of IR and GI biliary endoscopy and their outcomes: A case for each application will be shown a. Malignancy: indeterminate biliary stricture, staging of cholangiocarcinoma b. Bile stones treatment c. Primary sclerosing cholangitis diagnosis and treatment d. Selective cannulation of structures like cystic duct, gallbladder, intrahepatic ducts, anastomotic strictures e. Investigational uses Please visit the Learning Center to also view this presentation in hardcopy format.

### IREE-25HC Cryoablation for Vascular Malformations

### Participants

Shin Mei Chan, BS, New Haven, CT (*Presenter*) Nothing to Disclose

### TEACHING POINTS

Venous malformations (VM), the most common vascular anomaly that may cause significant pain, can be treated with percutaneous sclerotherapy. However, many do not achieve pain-free remission; in select patients, percutaneous cryoablation is an option. However, this is not routinely offered and there is a paucity in the literature describing techniques. Herein we review procedural aspects of cryoablation for VM.

### TABLE OF CONTENTS/OUTLINE

1. Pre-procedure a. Ultrasound is performed in clinic, in addition to MRI (T2-weighted fat-suppressed and T1-weighted images) 2. Procedure a. Under non-contrast CT ± US, a needle access route is selected and skin is marked b. A guiding needle is advanced and position confirmed under CT c. Hydrodissection, whereby a 21-gauge needle is used to instill saline to separate the skin and malformation, can be used for peripheral lesions with < 1 cm of overlying subcutaneous tissue to prevent injury to peripheral structures d. Warm packs applied to surrounding skin may also be used to avoid injury e. Freeze cycles and the number of cryoprobes varies, depending on lesion size and location i. In literature, a common regimen is two ten-minute freeze cycles per cryoprobe ii. When multiple probes are required, they are often placed ~2 cm apart f. Adequate ablation can be considered achieved when the iceball adequately covers the malformation corresponding to symptoms 3. Post-procedure a. Most can be done as an outpatient, with discharge within ~4 hours b. Clinic follow-up at 1 week for wound check, then 6 weeks for US and pain scale Please visit the Learning Center to also view this presentation in hardcopy format.

### IREE-26 Pulmonary Arteriovenous Malformation - General Issues and New Topics

### Participants

Ryo Takeshita, MD, (*Presenter*) Nothing to Disclose

### TEACHING POINTS

1. If possible, all PAVM lesions should be treated regardless of feeding artery diameter. 2. Embolized distal to last normal pulmonary artery branch results in low recanalization rate. 3. With a cutoff of 55% of preoperative, drainage vein diameter most accurately assess patency after embolization. 4. Diagnosis of Patency by Time-resolved MR Angiography more accurate than CT evaluation. 5. Systemic collateral development after PAVM embolization rarely causes hemoptysis.

### TABLE OF CONTENTS/OUTLINE

1. Definition and Epidemiology. A: Relationship with Hereditary Hemorrhagic Telangiectasia. B: Mimickers. 2. Life threatening complications of Pulmonary Arteriovenous Malformation. A: Hemoptysis. B: Paradoxical embolism. 3. Diagnosis. A: Classification of Pulmonary Arteriovenous Malformation. B: Treatment indications. 3. Embolization Procedure. A: Venous Access. B: Embolic Agents. 4: Catheter Equipments. 5: Embolization position. 4. Evaluation of patency after Embolization A: CT findings of Drainage Vein Diameter. B: Time-resolved Magnetic Resonance Angiography. 5. Systemic collateral development

### IREE-27 Review of the Experience of a Reference Hospital in Brazil on the Efficacy and Safety of Radiofrequency Ablation (RFA) of Autonomously Functioning Thyroid Nodules (AFTN)

### Participants

Leonardo Machado, MD, Sao Paulo, Brazil (*Presenter*) Nothing to Disclose

### TEACHING POINTS

- To demonstrate our service's experience using the RFA in AFTN treatment.
- To discuss imaging characteristics and distinguishing features of AFTN and post-RAF nodule imaging appearance.
- To demonstrate treatment efficacy and its related factors, as well as to compare characteristics of RFA treatment and complications.

### TABLE OF CONTENTS/OUTLINE

- Introduction.
- Criteria of patient's election.
- RFA technique and its limitations.
- Post-RFA nodule characteristics and treatment complications.
- Patient's follow-up using CEUS.
- Treatment efficacy and safety.

## **IREE-28 The Iceberg Technique: Bringing Diving Thyroid Nodules to the Surface**

Participants

Gabriela Merigue, MBBS, MD, (*Presenter*) Nothing to Disclose

### **TEACHING POINTS**

The purposes of this exhibit are: Present some cases of a new therapeutic approach to diving thyroid nodules in a minimally invasive way by interventional radiology; To overcome the difficulty of applying the "moving-shot" technique in the mediastinal component; Illustrate this new technique results.

### **TABLE OF CONTENTS/OUTLINE**

Thyroid nodules and its symptoms; Indications of radiofrequency thermal ablation; "Iceberg technique" two steps; Challenging nodules to approach; Outcomes after first RTA after second RTA

## **IREE-29 Middle Meningeal Artery Embolization for the Management of Chronic Subdural Hematoma**

### **Awards**

**Identified for RadioGraphics**

**Certificate of Merit**

Participants

Ángela Huete Schmolling, Madrid, Spain (*Presenter*) Nothing to Disclose

### **TEACHING POINTS**

- To describe the chronic subdural hematoma physiopathology. - To analyze the medial meningeal artery embolization as a novel and effective treatment modality for the management of chronic subdural hematoma.

### **TABLE OF CONTENTS/OUTLINE**

1. Introduction: Incidence, risk factors and physiopathology. 2. Treatment: Surgery vs. medial meningeal artery embolization. 3. Protocol (Clinico San Carlos Hospital). 4. Procedure.

## **IREE-3 Stepwise Percutaneous Approach to Treat Severe Benign Hepaticojejunostomy Strictures**

Participants

Charles Shelton, DO, Cincinnati, OH (*Presenter*) Nothing to Disclose

### **TEACHING POINTS**

1. Hepaticojejunostomy anastomosis (HJA) can be complicated by severe strictures or complete obstructions. Interventional radiologists should be aware of etiologies, complications, clinical evaluation, and treatment approaches. 2. Stepwise algorithm for percutaneous treatments of HJA strictures is provided. 3. Percutaneous techniques to treat severe HJA strictures include: a. Conventional antegrade fluoroscopic-guided recanalization b. Direct antegrade visualization with percutaneous cholangioscope and sharp recanalization c. Spyglass cholangioscopy with laser incision of HJA Stricture d. Combined percutaneous trans-jejunal retrograde approach with antegrade approach e. Combined percutaneous and endoscopic rendezvous technique f. Bio-degradable stents for benign strictures 4. Post-procedural complications and clinical outcomes

### **TABLE OF CONTENTS/OUTLINE**

1. Epidemiology and etiology of HJA strictures and complete occlusions. 2. Clinical presentation and evaluation 3. Stepwise management algorithm for HJA stricture recanalization: multi-disciplinary approach 4. Review of percutaneous techniques of biliary recanalization along with pictorial examples of percutaneous antegrade approach, combined approach, and recently developed techniques using cholangioscope and laser incision 5. Short- and long- term clinical outcomes of percutaneous treatments, and management of post-procedural complications

## **IREE-30 Radioembolization of Hepatocellular Carcinoma with Extrahepatic Collateral Blood Supply: Anatomic and Technical Considerations**

Participants

Jin Woo Choi, MD, Seoul, Korea, Republic Of (*Presenter*) Nothing to Disclose

### **TEACHING POINTS**

Radioembolization for hepatocellular carcinoma (HCC) has exploded in recent years. HCC typically received its blood supply from the hepatic artery, however, it can recruit a parasitic blood supply from extrahepatic collateral arteries (EHC). Whereas chemoembolization has been performed through EHC without serious complications, little experiences about radioembolization though EHC have been reported. The purpose of this exhibit is: (1) To review the key anatomy of EHC by using cone-beam CT. (2) To review when we suspect the presence of EHC supplying HCC. (3) To learn how to do safe radioembolization through EHC.

### **TABLE OF CONTENTS/OUTLINE**

1) List of treated EHC 2) Vascular anatomy of EHC by using cone-beam CT and safe point of each EHC 3) Suggestive findings of EHC on CT/MR and cone-beam CT 4) Special considerations for radioembolization through EHC: dosimetry, embolization of pulmonary shunt, protection of normal vessel, and redistribution by proximal embolization.

## **IREE-31 Updates on Combination TACE and Ablation Therapy for HCC: A Case-Based Review of Technique, Results and Complications**

Participants

Surbhi Trivedi, MD, (*Presenter*) Nothing to Disclose

### **TEACHING POINTS**

1) Review the current literature and treatment pathophysiology regarding combination transarterial chemoembolization (TACE) and

radiofrequency ablation (RFA) therapy in unresectable intermediate sized hepatocellular carcinoma. 2) Outline treatment timeline, procedural workflow and TACE-RFA technique. 3) Summarize post-treatment follow-up, patient outcomes and overall survival in our experience. 4) Review alternative forms of combination therapy including TACE and ethanol ablation. 4) Illustrate complications specific to combination therapy and subsequent management. 5) Discuss future directions for combination locoregional therapy in HCC management and emerging role for combination embolization-ablation therapies.

#### TABLE OF CONTENTS/OUTLINE

1) Hepatocellular carcinoma epidemiology and treatment algorithms 2) Combination therapy patient selection and contraindications 3) Literature review of combination therapy, overall survival and patient outcomes 4) Technique, workflow and timeline for combination therapy 5) Case-based illustration of successful combination therapy and post-procedure tumor response 6) Alternative forms of combination therapy including TACE and ethanol ablation 7) Case-based illustration of procedural complications and management 8) Future directions

#### **IREE-32 Building an Interventional Radiology Consult Service: Considerations for Improving Referring Physician Communication and Patient Care**

Participants  
Jacob Conroy, (*Presenter*) Nothing to Disclose

#### TEACHING POINTS

1. Understand the impact of referring physician communication on inpatient care related to IR services. 2. Recognize barriers that may limit effective communication with referring physicians. 3. Understand the methods to implement an IR consult service and how this improves communication and patient care.

#### TABLE OF CONTENTS/OUTLINE

LEARNING OBJECTIVES: To discuss methods for improving inpatient communication with referring physicians and patients concerning IR services. BACKGROUND: Limited awareness, understanding, and access to IR procedures continue to be limiting factors in patient care and the growth development for IR practices. Effective communication with referring physicians is essential for combatting these limiting factors. Several barriers exist that prevent effective communication with referring physicians and thus, negatively impact patient care and the continued growth of IR services. Recent strategies to overcome these barriers have focused on the development of IR consult services that are prominent and visible on hospital floors, in clinics, and in electronic medical records. CLINICAL FINDINGS/PROCEDURE DETAILS: This exhibit will: 1. Summarize the findings of previous studies on referring physician awareness and utilization of IR services. 2. Discuss the barriers to effective communication with referring physicians. 3. Describe the impact these communication barriers have on patient care and IR practices. 4. Explore methods to develop and execute a successful IR consult service, describing experiences from our institution as well as those from the literature. CONCLUSION/TEACHING POINTS:

#### **IREE-33 Making Sense of Stents: An Evidence-Based Review of Classes of Arterial Stents**

Participants  
Stephanie Jankovic, MD, (*Presenter*) Nothing to Disclose

#### TEACHING POINTS

-There are several permutations of stents today, including: covered/uncovered; balloon-expandable/self-expanding; drug-eluting/bare metal; and metal/absorbable. These different classes of stents have particular characteristics which make them optimal for various indications in the arteries throughout the body. -Primary, primary-assisted, and secondary patency rates vary amongst the classes of stents in different vascular beds throughout the body. -Appropriate stent choice influences vessel patency, reintervention rate, and resolution of underlying clinical symptoms. An understanding of these factors will allow the interventional radiologist to best treat each patient.

#### TABLE OF CONTENTS/OUTLINE

1. Brief review of history of stents 2. Classes of stents 3. Evidence for stent selection is reviewed for the following arteries, highlighting key papers, clinical trials, and device indications for use (IFUs) that guide stent selection, with critique of the quality of evidence: -Subclavian/upper extremity -Celiac axis -Splenic -Hepatic - native and transplant -Superior mesenteric -Renal -Iliac -Superficial femoral -Popliteal (P1, P2, and P3 segments) -Tibial 4. Characteristics underlying patency rates, including indication (e.g., atherosclerosis versus aneurysms), size, trackability, radial force, and fracturing are also discussed.

#### **IREE-34 Adrenal Vein Sampling: A Failure Mode Analysis**

Participants  
Praneeth Kalva, Dallas, TX (*Presenter*) Nothing to Disclose

#### TEACHING POINTS

Adrenal vein sampling (AVS) differentiates unilateral from bilateral adrenal disease and plays a pivotal role in deciding surgical vs medical management in patients with a diagnosis of primary hyperaldosteronism (PA). Cannulating the right adrenal vein can be technically challenging with high variability in procedural success rates. Factors contributing to failure of cannulating the right adrenal vein include failure to locate the adrenal vein, misidentification of another vessel as the adrenal vein, and dilution of the sample from accessory vein blood flow. This educational exhibit will cover each of these failure modes. A brief description of the technique with imaging correlates, review of literature and how to identify and overcome the scenarios contributing to the failure with examples will be discussed.

#### TABLE OF CONTENTS/OUTLINE

A. Introduction to AVS B. Typical success rates and non-procedural determinants of success C. Utility of unilateral adrenal vein sampling using a mathematical model for prediction D. Alternate imaging techniques for localization after failed AVS E. Pre-operative planning a. Medications that affect success of AVS: Physiology and Plasma Renin levels b. Pre procedural imaging: What to look for to maximize the success during AVS c. Logistics of specimen processing and analysis d. Required catheters/equipment F. Procedural steps: a. Adrenal vein identification: Anatomical patterns, Role of cone beam CT b. Sampling: End hole vs Side hole catheters, utility of microcatheters c. Complications: Adrenal hematoma contributing to failure of sampling G. Illustrative cases of failed AVS and how

these cases are managed in the author's institution. Conclusion

### **IREE-36 Percutaneous Transjejunal Biliary Intervention: A Primer for the Diagnostic and Interventional Radiologist**

#### **Awards**

##### **Certificate of Merit**

#### **Participants**

Ryan Gabos, San Antonio, TX (*Presenter*) Nothing to Disclose

#### **TEACHING POINTS**

-Review imaging and biliary anatomy of patients selected for percutaneous transjejunal biliary intervention (PTJBI).-Discuss common indications and interventions performed via PTJBI.-Review current techniques, maintenance, advantages, and complications of PTJBI.-Review cases of successful and challenging interventions with periprocedural imaging.

#### **TABLE OF CONTENTS/OUTLINE**

IntroductionHistory of PTJBI, modern practice, and role of IR in biliary management.Postsurgical changes and imaging (CT, MRI) following hepaticojejunostomy or roux-en-y reconstruction.Common and uncommon biliary anatomy.Common indications for PTJBI access with periprocedural imaging.Steps, maintenance, and advantages of PTJBI access.Complications of initial PTJBI procedure.Case PresentationsCholangiocarcinomaLiver transplantCholedochal cyst, s/p hepaticojejunostomyCholecystectomy complications, s/p hepaticojejunostomyConclusionClinical ImplicationsPTJBI is a proven method to manage biliary disease in patients with surgically altered small bowel anatomy. In patients requiring repeat intervention or those with diffuse biliary disease, retrograde biliary access via PTJBI represents an attractive and underutilized resource.

### **IREE-37HC Spinal Dural and Extradural Arteriovenous Fistulas: Imaging Features and Endovascular Treatments**

#### **Participants**

Hiro Kiyosue, MD, (*Presenter*) Research Grant, Koninklijke Philips NV

#### **TEACHING POINTS**

Despite of recent developments in technology of imaging and endovascular treatments, some cases are often incorrectly diagnosed or inadequately treated even now. In this presentation, we demonstrate imaging features and endovascular treatments of spinal dural AVFs and various types of extradural AVFs with illustrative case presentation. 1. Spinal dural AVFs are usually located in the dorsal spinal dura matter at lower thoracic spine, which are fed by small dural feeders from the radiculomeningeal artery or the prelaminar artery and drain into a bridging vein. Typical case shows horizontal T sign on frontal view of spinal angiography. 2. Spinal epidural AVFs are the most common type in extradural AVFs, which are frequently located in the ventral epidural space at lumbar spine. They are fed by multiple epidural feeders from the somatic branches and drains into an epidural venous pouch to a radiculomedullary vein and/or paravertebral veins. 3. Mixed AVFs is the second common type of extradural AVFs, which involve multiple spaces of osseous, epidural, and paravertebral spaces and often associated with spinal arteriovenous metamerism syndrome.

#### **TABLE OF CONTENTS/OUTLINE**

1. Spinal dural AVFs: Clinical features, Imaging features, Transarterial embolization 2. Spinal extradural AVFs: Classification 2-1 Epidural AVFs: Clinical features, Imaging features, Transarterial and transvenous embolization 2-2 Osseous AVFs: Clinical features, Imaging features, Transarterial and transvenous embolization, and direct puncture embolization 2-3 Paravertebral AVFs: Clinical features, Imaging features, Endovascular techniques 2-4 Mixed AVFs: Clinical features, Imaging features, Endovascular techniquesPlease visit the Learning Center to also view this presentation in hardcopy format.

### **IREE-38 Irreversible Electroporation in Locally Advanced Pancreatic Cancer**

#### **Awards**

##### **Certificate of Merit**

#### **Participants**

Kenneth Huynh, BS, Orange, CA (*Presenter*) Nothing to Disclose

#### **TEACHING POINTS**

1. To provide an overview of the role and literature of percutaneous irreversible electroporation (IRE) in locally advanced pancreatic cancer (LAPC) including a review of ongoing trials. 2. To present, through case-based review, the techniques utilized in percutaneous IRE to safely target pancreatic lesions. 3. To illustrate the multi-modality imaging fusion and navigation for IRE of LAPC, with emphasis on intra-procedural cone-beam computed tomography (CBCT).

#### **TABLE OF CONTENTS/OUTLINE**

Locally advanced pancreatic cancer (LAPC) is considered unresectable due to tumoral encasement of the superior mesenteric or celiac arteries or non-reconstructable venous involvement. Percutaneous irreversible electroporation (IRE) in LAPC has shown promising outcomes with respect to median overall survival, especially when combined with chemotherapy. IRE provides non-thermal ablation of LAPC while mitigating risk of thermal injury to nearby structures compared to thermal techniques. Given the location of the pancreas and proximity to nearby structures, safe percutaneous targeting may be difficult with high risk of complication. This educational exhibit will: (1) provide an overview of the role and literature of percutaneous IRE in LAPC including ongoing trials, (2) present different procedural techniques used to safely target pancreatic lesions and minimize complications. Techniques including electrode steering, gantry tilting, bolus chasing, and CT arteriography will be discussed, and (3) illustrate the multi-modality imaging fusion and navigation for IRE of LAPC with emphasis on intra-procedural CBCT.

### **IREE-39 Priapism: Types and Interventional Treatment**

#### **Participants**

Benjamin Reichardt, Hattingen, Germany (*Presenter*) Nothing to Disclose

#### **TEACHING POINTS**

Priapism is defined as a sustained tumescence or erection lasting more than 6 hours. The erection is limited to the penile tissue

Priapism is defined as a sustained tumescence or erection lasting more than 6 hours. The erection is limited to the erectile tissue without affecting the corpus spongiosum. There are two different types of priapism: 1. Low flow (ischemic / venous occlusive) 2. High flow (non-ischemic or arterial): Does not require emergency treatment. Genitoperitoneal trauma is the most common etiology. The trauma results in a rupture in the cavernous artery with subsequent development of a high flow fistula or a pseudoaneurysm. Interventional Therapeutic options: 1. Autologous blood clot 2. Gel foam 3. Polyvinyl alcohol (PVA) 4. Spherical Particles 5. Micro-spirals 6. Alcohol - lipiodol mixture 7. N-butyl cyanoacrylate (NBCA)

#### TABLE OF CONTENTS/OUTLINE

The success rates are up to 89%. Sexual function may be impaired after embolization, although potency is fully restored in about 80% of cases. With decongestion and potency rates of 100% and 86-91%; superior to surgery. Relapse: rates vary between 7% and 27%, regardless of the type of embolotherapy. Erectile dysfunction: occurs in around 39% of the time with the use of permanent embolic agents and in only 5% with the use of temporary embolic agents. Conclusion: Superselective embolization is the gold standard in the treatment of HFP because of its safety and efficacy profile. The type of embolic agent does not appear to be a major factor influencing treatment outcomes in terms of recurrence of priapism or deterioration in erectile quality. The embolic product should be tailored to each patient and the procedures should be performed by well trained and experienced operators, who should know his embolic materials.

#### IREE-4 Finding the Adenoma in Cushing's Disease: Bilateral Inferior Petrosal Sinus Sampling and Pituitary MRI

Participants  
Celia Alonso, MD, Madrid, Spain (*Presenter*) Nothing to Disclose

#### TEACHING POINTS

The objective of this educational exhibit is to emphasize the role of bilateral inferior petrosal sinus sampling (BIPSS) in the diagnosis of Cushing's disease. After reading it, you will:- Learn the pathophysiology underlying Cushing's syndrome. Differentiation between ACTH-dependent and ACTH-independent hypercortisolism.- Comprehend the relevance of radiological techniques identifying the etiology of hypercortisolism, focusing on the diagnosis of ACTH-secreting pituitary microadenomas.- Deepen the knowledge about BIPSS indications, technique, safety and possible complications.

#### TABLE OF CONTENTS/OUTLINE

- Introduction.- Cushing's syndrome diagnostic algorithm: clinical, biochemical and radiological analyses. BIPSS as the gold standard test in Cushing's disease and comparison with pituitary MRI. Experience in our institution, a tertiary care center, in the last sixteen years.- BIPSS technique and rationale. Indications, relevant venous anatomy and variants, technical considerations and possible complications.- Conclusion.

#### IREE-40 Magnetic Resonance Lymphangiography (MRL): Past, Present, and Future Directions

**Awards**  
Identified for RadioGraphics

Participants  
Ahmed Negm, MBBCh, (*Presenter*) Nothing to Disclose

#### TEACHING POINTS

Learn the lymphatic system anatomy and the historical development of MRL. Review the MRI sequences and techniques currently used for transpedal and intranodal MRL. Understand current indications and applications of MRL including diagnosis and treatment of lymphatic disorders.

#### TABLE OF CONTENTS/OUTLINE

1. Lymphatic system anatomy and Historical development of MRL • Embryological development of peripheral and central lymphatic system • Location and territorial drainage of central, hepatic, and mesenteric lymphatics • Other methods of lymphatic imaging (Lymphoscintigraphy, Fluoroscopic lymphangiography, Fluorescence lymphography) • Historical development of MRL 2. MRI sequences and techniques currently used in MRL • Intranodal Dynamic contrast-enhanced MRL (DCE-MRL) • Interstitial transpedal MRL (tMRL) • Intra-hepatic DCE-MRL (IH-DCE-MRL) • Retrograde thoracic duct dynamic contrast-enhanced MRL • Utility of T2W MR Sequences • Procedural aspects (Saline, Contrast, Needles, Catheters, Scanner, Anesthesia, ±Ultrasound) 3. Indications and applications of MRL • DCE-MRL o Evaluation of lymphatic flow (Pulmonary lymphatic perfusion syndrome, Plastic bronchitis, Protein-losing enteropathy, Chylothorax, Chylous ascites, Leaks, Edema) o Lymphatic malformations o Identification of aberrant lymphatic vessels for embolization o Localization (Sentinel lymph nodes, Leaks, Pre-operative planning) • tMRL o Alternative to DCE-MRL (Simple, Fast, No ultrasound) o Diagnosis pre-treatment plan o Localization (Peripheral or Central lymphatic leakage) • IH-DCE-MRL o Diagnosis (Protein-losing enteropathy, Chylous ascites, Contrast leakage to peritoneum/duodenum) • Limitations of DCE-MRL tMRL

#### IREE-41 Hydro, Pneumo, and Balloon-assisted Separation of Critical Structures in Ablation Procedures

Participants  
Mohamed Ibrahim, MBBCh, Rochester, MN (*Presenter*) Nothing to Disclose

#### TEACHING POINTS

- Learn the role and limitation of hydro-dissection in the separation of critical structure during image-guided ablation procedures
- Learn the role and limitation of pneumo-dissection in the separation of critical structure during image-guided ablation procedures
- Learn the role and limitation of balloon-assisted separation of the critical structure during image-guided ablation procedures

#### TABLE OF CONTENTS/OUTLINE

- Role and limitation of hydro-dissection of critical structures o Appropriate clinical scenarios for hydro-dissection o Limitations of hydro-dissection and how to manage them; avoiding streak artifact and fluid redistribution
- Role and limitation of pneumo-dissection of critical structures o Appropriate clinical scenarios for pneumo-dissection o Limitations of pneumo-dissection and how to manage them; gas absorption and redistribution
- Role and limitation of balloon-assisted separation of critical structures o Appropriate clinical scenarios for balloon-assisted separation o Limitations of balloon-assisted separation and how to manage them; placement of multiple balloons

## **IREE-42 Principles of Tissue Sampling, Handling, and Processing: A Primer for Procedural Radiologists**

Participants

Majid Chalian, MD, Seattle, WA (*Presenter*) Grant, The Boeing Company

### **TEACHING POINTS**

1) Provide a broad overview of pathology to demystify subdivisions and associated protocols and procedures 2) Discuss best practices for tissue sampling and handling, based on organ system (including thyroid, breast, lung, liver, kidney, bone, and musculoskeletal soft tissue) 3) Familiarize with different sample media, their functions, and indications 4) Learn about common histopathology artifacts and mitigation strategies 5) Learn how to implement clinical and imaging findings to sample adequately and handle tissue appropriately

### **TABLE OF CONTENTS/OUTLINE**

Introduction? Significance of collaboration between radiology and pathology departments and impact on patient care? Pathology subdivisions? Anatomic pathology? Clinical pathology (AKA "laboratory medicine") Anatomic pathology workflow ? Pre-analytical steps ? Gross examination and description? Tissue processing ? Tissue staining? Final diagnosis and pathology report Best practices for specimen sampling ? Small lesions? Metastases? Location dependent ? Thyroid? Breast? Lung? Liver? Kidney? Bone? Musculoskeletal soft tissue? Uncertain cases that may benefit from pathology's consultation/presence before and/or during the procedure Best practices for specimen handling/processing? Formalin? Saline/RPMI? EM fixative (glutaraldehyde)? Decalcifying agents? RDO (dilute hydrochloric acid) ? EDTA? Fresh tissue ? How the differential impacts handling/processing Common Artifacts and Mitigation Techniques ? Fixation ? Crush ? Cautery? Air Dry Core Needle Biopsy vs FNA ? Specimen processing basics ? Advantages of each? Disadvantages of each Tips to use clinical and imaging findings for proper tissue sampling and handling

## **IREE-43 Interventional Pain Management in Extraplural Osseous Metastases**

### **Awards**

#### **Certificate of Merit**

Participants

Kenneth Huynh, BS, Orange, CA (*Presenter*) Nothing to Disclose

### **TEACHING POINTS**

1. To review the indications and procedural considerations for percutaneous management of extrapural osseous metastases. 2. To review cases of interventional pain management of extrapural osseous metastases including embolization, thermal ablation, and bone stabilization.

### **TABLE OF CONTENTS/OUTLINE**

Extrapural bone metastases can cause significant morbidity to many patients due to localized pain, referred pain, impaired mobility, and pathological fractures. This commonly leads to long-term narcotic use, prolonged bedrest, and poor quality of life. Percutaneous interventions have been shown to provide sustained palliative relief of pain associated with metastatic osseous disease, in addition to improving mobility and quality of life. A multi-disciplinary approach to oncologic pain associated with bony lesions including interventional radiology can improve patient's pain and quality of life. This educational exhibit will: (1) review the indications and procedural considerations for percutaneous management of extrapural osseous metastases with palliative intent, and (2) present different procedural techniques used in pain palliation and bone stabilization. Techniques include embolization for hypervascular metastatic lesions, radiofrequency ablation, microwave ablation, cryoablation, and cementoplasty. An overview on these techniques and possible procedural complications with measures for prevention and management will also be discussed.

## **IREE-44 Interventional Approach to the Cancer Pain Patient: A Case-Based Review**

### **Awards**

#### **Cum Laude**

Participants

Omair Ali, BS, (*Presenter*) Nothing to Disclose

### **TEACHING POINTS**

Chronic pain is a common concern among patients with cancer, resulting in frequent utilization of emergency room visits and hospitalizations. Pharmacotherapy is a widely used approach for cancer pain relief, although long-term opioid use is often inadequate in treating cancer pain and has a significant side effect profile. Interventions for cancer pain offer unique solutions to improve quality of life and provide more effective long-term pain relief. The purpose of this exhibit is to provide a case-based approach to interventional radiology's role in the management of cancer pain.

### **TABLE OF CONTENTS/OUTLINE**

1) Introduction to cancer pain a) Nociceptive pain b) Neuropathic pain 2) Decision-making algorithm for cancer pain interventions a) Correlation of pain to imaging b) Source and location of cancer pain i) Nerve-related pain ii) Bone pain (spinal pain, non-spinal pain, and presence of fracture in the setting of bone pain) c) Available non-IR treatment options d) Available IR treatment options 3) Cancer pain intervention cases: clinical history, imaging, decision-making, intervention a) Celiac plexus neurolysis b) Intercostal cryoneurolysis c) Vertebral augmentation for pathologic compression fractures d) Thermal ablation for painful bone metastasis e) Percutaneous screw fixation for pelvic metastasis f) Palliative embolization of bone metastasis

## **IREE-45 Insulinoma: Role of the Interventional Radiologist**

Participants

Ali Abbas Saifuddin, MD, (*Presenter*) Nothing to Disclose

### **TEACHING POINTS**

Radiologically occult insulinomas should be assessed with selective arterial calcium stimulation test (SACST) with hepatic venous sampling prior to surgical treatment.

## TABLE OF CONTENTS/OUTLINE

Insulinomas typically present with Whipple's triad which is composed of hypoglycemia, low fasting plasma glucose, and alleviation of symptoms by glucose administration. Factitious hypoglycemia (i.e., exogenous insulin administration) must be excluded to make a diagnosis of insulinoma, and this is accomplished by a supervised 72-hour (or 48-hour) fast. Localization of tumor can be accomplished using transabdominal ultrasound (TUS), triple phase CT, gadolinium enhanced MR abdomen, gallium-68 dotatate PET/CT, Octreoscan, or a combination of these tests. If non-invasive modalities cannot localize the tumor, then invasive tests, such as SACST with hepatic venous sampling or endoscopic ultrasound (EUS), can be utilized. SACST involves injecting calcium solution at a dose of 0.0125 mmol Ca<sup>2+</sup>/kg (0.005 mmol Ca<sup>2+</sup>/kg for obese patients) into the superior mesenteric, proximal splenic, mid-splenic, gastroduodenal, and proper hepatic arteries. 5 mL right hepatic venous samples at 0, 20, 40, and 60 seconds are obtained after calcium solution injection in each artery. Diagnostic criterion for a positive response is an insulin response 2x of baseline. Positive response when injecting the gastroduodenal artery or the superior mesenteric artery localizes to the pancreatic head or neck. Positive response when injecting the splenic artery localizes to the pancreatic body or tail. Positive response when injecting the proper hepatic artery suggests liver metastases. Localization is critical prior to surgical treatment.

### IREE-46 Introducing Pre-Clinical Medical Students to IR - Medical Student IR Symposia 2.0

Participants

Robert Weinstein, Baltimore, MD (*Presenter*) Nothing to Disclose

#### TEACHING POINTS

To review the importance of introducing IR to pre-clinical medical students. To learn about the different methods by which pre-clinical medical students are introduced to IR. To recognize that the traditional medical student IR symposium relying solely on didactic lectures is being replaced by a new IR symposium consisting of interactive and hands-on exercises and simulation sessions. To review the available literature regarding the use of new IR symposia consisting of interactive and hands-on simulation sessions.

## TABLE OF CONTENTS/OUTLINE

Why is introducing IR into pre-clinical medical training important? The new integrated IR residency. IR Residency Match competitiveness. The evolution of medical student symposia. Traditional didactic lecture-based symposia. Interactive and hands-on symposia. Target audience. Factors effecting participation in medical student symposia. Choosing the right format. In-person vs. virtual formats. Didactic vs. interactive/hands-on vs. mix. Choosing the appropriate faculty. Involving trainees/medical students. Data Collection. The importance of pre- and post-symposia surveys. Polling questions during the event Performance during simulations. Feedback allows for improvements Future directions. Simulation and clinical IR bootcamps. The role of national meetings

### IREE-47 Fistula Fix: Maturation, Maintenance, and De-Clots

Awards

Identified for RadioGraphics

Cum Laude

Participants

Anne Sailer, MD, New Haven, CT (*Presenter*) Nothing to Disclose

#### TEACHING POINTS

1. Discuss epidemiology, cases, and clinical presentations of hemodialysis (HD) access failure requiring intervention and literature based treatment interventions. 2. Review role of imaging in the diagnosis of hemodialysis access malfunction/failure. 3. Briefly review characteristic area of stenosis/failure based on HD access anatomy. 4. Review main interventional therapies for management of HD access with emphasis on angioplasty, stent placement and DeClot interventions.

## TABLE OF CONTENTS/OUTLINE

1. Ultrasound and conventional angiogram evaluation and function and HD access maturity (rules of sixes), including common artifacts and pitfalls and advanced ultrasound techniques. 2. Overview of the anatomy and physiology of characteristic HD areas of stenosis. 3. Overview of the current literature of HD access failure treatment: drug-coated vs non-drug-coated balloons, covered vs bare-metal stents, etc. 4. Case-based review of various endovascular techniques in management of fistula malfunction including: failure to mature, outflow stenosis treatment (characteristic HD access areas of stenosis such as the swing-point in BVT fistulas, cephalic arch stenosis, etc.), DeClot (traditional vs IJ access), coil embolization of accessory veins to aid in maturation, anastomotic narrowing, and intraprocedural complications.

### IREE-48 Various Approaches to the Portal Venous System

Awards

Certificate of Merit

Participants

Yoshitaka Tamura, Kumamoto, Japan (*Presenter*) Nothing to Disclose

#### TEACHING POINTS

Portal venous (PV) interventions including transjugular intrahepatic portosystemic shunt (TIPS), antegrade transportal obliteration (ATO), PV stenting, PV embolization (PVE), and islet transplantation have developed for a few decades. Approach to the PV system is an essential step in PV intervention. Various approaches are described. Transjugular approach is usually as a part of TIPS procedure. Puncture from the proximal portion of the right hepatic vein to the right PV is often done under fluoroscopy. Intravascular ultrasonographic guidance can facilitate the safety. Transhepatic approach is a classical approach for various interventions. It has potential risks of bleeding and transpleural puncture. Transsplenic approach is useful for cases with PV/splenic vein occlusion. Tract embolization is important because of higher risk of bleeding from puncture site. Transumbilical venous and portosystemic collateral approaches are the safest approaches. Catheterization through the tortuous way is required. Surgical approaches (transiliocolic venous approach and round ligament approach) are reliable for catheterization. They provide good controllability of devices, and effective for selected cases.

## TABLE OF CONTENTS/OUTLINE

1 Basics of PV interventions (TIPS, ATO, stenting, PVE and islet transplantation) 2 Transjugular approach 3 Transhepatic approach

4 Transsplenic approach 5 Transumbilical venous and portosystemic collateral approach 6 Surgical approach (Transiliocolic venous approach and round ligament approach)

#### **IREE-49 Percutaneous Management of Post-Liver Transplant Complications**

Participants

Ahsun Riaz, MD, Chicago, IL (*Presenter*) Consultant, Boston Scientific Corporation

##### **TEACHING POINTS**

1. Describe the complications of liver transplant (LT)2. Diagnosis of post-LT complications using various imaging modalities3. Highlight the techniques employed by interventional radiologists to manage post-transplant complications

##### **TABLE OF CONTENTS/OUTLINE**

Introduction1. Types of liver transplants and various anastomoses2. Normal imaging after transplant3. Pathophysiology of complicationsClinical Presentation, Risk Factors and Diagnostic ImagingComplications and Their Management by IR1. Vascular complicationsa) Transplant hepatic artery stenosis/thrombosis- Angioplasty/stenting/catheter-directed thrombolysisb) Arterial dissection/aneurysm/pseudoaneurysm and arterioportal fistulas- Coiling/stent grafting/stentingc) Splenic steal syndrome/"small-for-size" syndrome- Splenic artery embolization via coils/vascular plugsd) Transplant portal vein stenosis/thrombosis- Venoplasty/stentinge) Transplant hepatic vein stenosis- Venoplasty/stentingf) Inferior vena cava complications- Venoplasty/stenting2. Biliary Complicationsa) Biliary stricture- Percutaneous transhepatic/transjejunal cholangioplasty/stenting- Role of endoscopyb) Biliary leak/biloma- Percutaneous drainage- Embolization of leaking ductc) Stones/casts/debris

#### **IREE-50 Intraoperative Nerve Monitoring to Prevent Nerve Damage on Image-Guided Percutaneous Tumor Ablation**

Participants

Robert Weinstein, Baltimore, MD (*Presenter*) Nothing to Disclose

##### **TEACHING POINTS**

To describe the use of intraoperative nerve monitoring as a tool to prevent iatrogenic peripheral nerve injury during percutaneous thermal and cryo-ablation of tumors. Percutaneous ablation is a potentially curative minimally invasive treatment option for patients. Intraoperative Nerve Monitoring (IONM) is a group of electrophysiological modalities that can provide intraoperative assessment of neural structures to prevent iatrogenic nerve injury. IONM been shown to be valuable in reducing nerve injury during percutaneous thermal and cryo-ablation of tumors.

##### **TABLE OF CONTENTS/OUTLINE**

Percutaneous tumor ablation has become a popular tool for tumor treatment due to its minimally invasive approach and low risk profile. However, it has the potential to damage both sensory and motor nerves. Neurophysiologists can use several modalities to stimulate and measure responsiveness of at-risk neural pathways. IONM includes somatosensory evoked potentials (SSEPs) and motor nerve conduction studies (MNCSs). SSEPs monitor sensory pathways and MNCSs monitor peripheral motor nerve integrity. The interventional radiologist can be guided to avoid further ablation in each region as signal changes occur, which can limit long-term nerve damage. Regional anatomy of relevant nerves in the operational area is also key. Radiofrequency can produce interference which inhibits monitoring of neurotonic activity, and as such must be paused to record IONM signals. Cryoablation does not produce artifacts and as such real time monitoring is possible. Studies have shown the risk of major motor injury is significantly increased with persistent motor evoked potential change compared to transient or no motor evoked potential change.

#### **IREE-51HC Arterio-Biliary Fistula as a Rare Cause of Upper Gastrointestinal Bleed: Diagnostic and Procedural Considerations**

Participants

Mark Edelstein, MD, Bala Cynwyd, PA (*Presenter*) Nothing to Disclose

##### **TEACHING POINTS**

1. Arterio-biliary fistula is a rare cause of upper gastrointestinal bleeding.2. The most common clinical presentation of an arterio-biliary fistula is hemobilia, which refers to bleeding into the biliary tree.3. In the majority of cases, arterio-biliary fistulas are iatrogenic in etiology, such as occurring after transhepatic biliary interventions or transarterial chemoembolization.4. There is a scarcity of existing literature describing spontaneous arterio-biliary fistula in the absence of prior relevant intervention. In the absence of such procedural history, the possibility of a communication between the arterial and biliary systems may not be on a clinician's diagnostic radar when responding to a patient with active gastrointestinal bleeding.

##### **TABLE OF CONTENTS/OUTLINE**

1. Introduction to arterio-biliary fistula as a cause of upper gastrointestinal bleeding.2. Multimodality image-rich review of multiple cases of arterio-biliary fistula of both iatrogenic and spontaneous etiology.3. Angiographic demonstration of arterio-biliary fistula and unique considerations for the managing interventional radiologist.4. Conclusion.Please visit the Learning Center to also view this presentation in hardcopy format.

#### **IREE-52 A Practical Guide to RF Ablation for Treating Locoregional Recurrence of Well-Differentiated Thyroid Cancer**

Participants

Eun Ju Ha, MD, Suwon, Korea, Republic Of (*Presenter*) Nothing to Disclose

##### **TEACHING POINTS**

While the mortality rate for well-differentiated thyroid cancer tends to be favorable, the risk of recurrent papillary thyroid cancer can range from 20 - 59% depending on patient and tumor risk factors. Various thermal ablative techniques (RFA, LA or MA) and chemical ablative approaches (ethanol ablation) can be used as an alternative method in patients deemed to be at high surgical risk, those in whom the surgeon deems non-operable or for those refusing to undergo repeat surgery. In this educational exhibit, we would like to 1) provide updated evidences of RFA for recurrent thyroid cancers and to 2) describe practical tips regarding

indication, pre-procedural evaluation, techniques, post-procedural evaluation and complications.

#### TABLE OF CONTENTS/OUTLINE

1. A systematic review of the current evidences 2. Practical tips for RFA to treat recurrent thyroid cancers 2-1) How to select patients - curative vs. palliative management strategies 2-2) Pre-procedural checklist before RFA - US, CT, and laboratory tests 2-3) Standard techniques - approach route based on the tumor location, hydro-dissection technique, moving-shot/fixed-electrode technique 2-4) Post-procedural checklist after RFA- US, CT, and laboratory tests 2-5) How to prevent complications- US-based nerve anatomy, cold 5% dextrose injection, medication

#### **IREE-53HC Applicability of Irreversible Electroporation for Therapeutic Management of Pancreatic Adenocarcinoma**

Participants

Raquel Moreno, MD, New York, NY (*Presenter*) Nothing to Disclose

#### TEACHING POINTS

Review fundamental concepts about pancreatic ductal adenocarcinoma (PDAC), including relevant vascular anatomy in axial image; disease staging and therapeutic management according to each stage. Introduce the participant to the fundamentals of Irreversible Electroporation (IRE) ablation therapy, including its eligibility criteria and contraindications. Present a pictorial essay to illustrate IRE indications based on imaging criteria of key anatomic structures involvement - arteries, veins and miscellaneous - highlighting teaching points in each case. Summarize the role of the IRE in the Therapeutic Management of the PDAC through a Flowchart.

#### TABLE OF CONTENTS/OUTLINE

- Introduction: PDAC- Relevant Anatomy- Irreversible Electroporation (IRE): Fundamentals- Irreversible Electroporation (IRE): Applications- Imaging Criteria: Arterial Involvement- Imaging Criteria: Venous Involvement- Imaging Criteria: Non-vascular Involvement- Final Considerations Please visit the Learning Center to also view this presentation in hardcopy format.

#### **IREE-54HC Development of a New Drug-eluting Stent for Peripheral Arterial Diseases by General Radiologists: What You Need to Know Before You Start**

Participants

Shunsuke Kamei, MD, Hachioji, Japan (*Presenter*) Nothing to Disclose

#### TEACHING POINTS

What do you need to know to develop a new stent? The first author, a general radiologist with no specific background, has played a central role in developing a stent platform for below-the-knee (BTK) atherosclerotic diseases. Based on this experience, we will explain the tangible and intangible methods how to develop a new stent system in general practice.

#### TABLE OF CONTENTS/OUTLINE

1. Arteriosclerosis in BTK lesions is a severe disease, and the treatment is still underdeveloped. Therefore, we are developing a new drug-eluting stent for BTK. 2. The first step in stent fabrication is to draw stent design using 3-dimensional Computer-Aided Design (CAD) software. 3. Self-expanding stents are manufactured through laser cutting, diameter expansion, annealing, and electropolishing. The prototype is intended to improve the design through mechanical evaluation. However, since prototyping takes a long time, effective simulation (Finite element analysis using Abaqus® ) can shorten the development period. 4. The stent is completed by applying our original technology, hybrid nano-coating (anti-thrombogenic base-coating with drug-eluting polymer), on the newly developed stent platform. We have evaluated the ability of the device to withstand a 10-year equivalent fatigue life due to the cyclic pulsation from blood flow. 5. In animal studies on the requirements of FDA's Good Laboratory Practices (GLP) regulations, we should confirm stent coverage by the vascular endothelium, drug-release profiles, and good stent patency rate at six months after implantation. After approval by FDA, a pivotal clinical trial can be started in humans using a newly developed stent system. Please visit the Learning Center to also view this presentation in hardcopy format.

#### **IREE-55 Interventional Radiology and Childbirth: From Conception through Delivery and Beyond**

**Awards**

**Identified for RadioGraphics**

Participants

Joseph Moirano, BS, Massapequa, NY (*Presenter*) Nothing to Disclose

#### TEACHING POINTS

1. To review radiation exposure risk at different points in pregnancy and assess how to decrease exposure risk during IR procedures 2. To discuss the role of IR in promoting male and female fertility 3. To highlight the various procedures that interventionalists perform during the antepartum and postpartum period.

#### TABLE OF CONTENTS/OUTLINE

1. Pregnancy and Radiation Exposure a. Radiation Effects on Fetal Development b. Ways to Minimize Fetal Exposure Risk 2. Procedures to Promote Fertility a. Male Infertility Treatments (Varicocele Embolization) b. Female Infertility Treatments (Fallopian Tube Recanalization, Uterine Artery Embolization (for fibroids), and Management of Complications of Ovarian Hyperstimulation Syndrome) 3. Procedures in the Pregnant Patient a. Venous Access (Midline and Peripherally Inserted Central Catheter, Dialysis Access, Medi-port) b. Genitourinary Interventions (Percutaneous Nephrostomy Tube/Nephroureterostomy Tube, Ureteral Stent Placement) c. Biliary Interventions (Cholecystostomy Tube, Percutaneous Biliary Drainage Catheter Placement) d. Venous Thromboembolism Interventions (IVC Filter Placement, Venous/Pulmonary Artery Thrombectomy) e. Ectopic Pregnancy Management f. Ovarian Cyst Aspiration g. Trauma Interventions (Arterial Embolization) 4. Procedures in the Peri/Postpartum Period a. Invasive Placenta Spectrum Management (Pre-operative Balloon Occlusion) b. Postpartum Hemorrhage after Vaginal Delivery (Prophylactic Uterine/Internal Iliac Artery Embolization, Retained POC, Uterine AVM) c. Post-Cesarean Section Procedures (Abscess Drainage, Embolization of Surgically Injured Vessel, Urinary Diversion after Ureteral Injury)

#### **IREE-56 Magnetic Resonance Guided Focused Ultrasound (MRgFUS) for Treatment of Uterine Fibroids: Patient Selection, Contraindications and Operative Execution**

Participants

Monica Mattone, MD, Roma, Italy (*Presenter*) Nothing to Disclose

#### TEACHING POINTS

Different treatments have been proposed for uterine fibroids. Magnetic Resonance Focused Ultrasound (MRgFUS) has been proposed in the last years as a new non invasive method to treat symptomatic fibroids without any complication. It associates the spatial resolution of a MR scanner with a focused high intensity ultrasound beam. The purpose of this educational exhibit is to illustrate indications to MRgFUS treatment for uterine fibroids, contraindications and possible risks related to the procedure. We are going to describe how this system works, to show expected results after the procedure and to discuss results from the literature.

#### TABLE OF CONTENTS/OUTLINE

1. Current treatment for uterine fibroids: their indications, contraindications and complications. 2. Patient selection and contraindications to MRgFUS. 3. MRgFUS system and how does it work. 4. Imaging technique to evaluate size, number, accessibility, viability and texture of fibroids. 5. Results from the literature.

#### **IREE-58 Radioembolization for Hepatocellular Carcinomas: Consideration of Non-hepatic Artery Originating from the Hepatic Artery**

##### Awards

##### Certificate of Merit

Participants

Hyo-Cheol Kim, MD, Seoul, Korea, Republic Of (*Presenter*) Nothing to Disclose

#### TEACHING POINTS

Radioembolization is increasingly used for the treatment of patients with hepatocellular carcinoma. The knowledge of the hepatic artery anatomy is pivotal for effective and safe treatment. Several non-hepatic arteries, which should not be treated or should be protected, can originate from the hepatic artery. However, non-hepatic arteries may be frequently overlooked or be inadvertently treated, resulting in variable consequences from mild postembolization syndrome to catastrophic gastrointestinal radiation ulcer. The purpose of this exhibit is : (1) To list non-hepatic arteries originating from the hepatic artery. (2) To review the vascular anatomy of non-hepatic arteries on digital subtraction angiography (DSA) and cone-beam CT. (3) To learn how to deal with non-hepatic arteries prior to/during radioembolization. (4) To review the possible complications when they are inadvertently treated.

#### TABLE OF CONTENTS/OUTLINE

1) Cystic artery, right gastric artery, accessory left gastric artery, hepatic falciform artery, left inferior phrenic artery, and supraduodenal artery 2) Vascular anatomy of non-hepatic artery on CT/MR, DSA and cone-beam CT 3) Tips of non-hepatic artery detection on cone-beam CT as well as planning angiography and SPECT/CT 4) Technical considerations : permanent embolization, temporary embolization, and by-pass 5) Complications related with non-hepatic artery and their management : ischemic cholecystitis, radiation cholecystitis, radiation gastroduodenal ulcer, radiation dermatitis, epigastric pain.

#### **IREE-59 Interventional Radiologic Procedures in Pelvic Bone Tumors**

Participants

Yet Yen Yan, MBBS, (*Presenter*) Nothing to Disclose

#### TEACHING POINTS

Pelvic bone tumours are frequently encountered in the daily practice of the musculoskeletal radiologists. In addition, the pelvis is the 2nd most common site for bone metastases. As the array of pelvic bone interventional procedures have gradually widened from diagnostic to therapeutic, the musculoskeletal radiologist plays an important role in the care of such patients in terms of relieving pain, disease control and improving quality of life. This educational exhibit aims to equip the radiologist with the necessary information on the various interventions that be performed.

#### TABLE OF CONTENTS/OUTLINE

Bone biopsy, embolisation, osteoplasty and osteosynthesis will be covered.

#### **IREE-6 Balloon Pulmonary Angioplasty for Chronic Thromboembolic Pulmonary Hypertension: Indications, Preparation, Technique, Results and Complications.**

##### Awards

##### Certificate of Merit

Participants

Mario Matute Gonzalez, MD, Barcelona, Spain (*Presenter*) Nothing to Disclose

#### TEACHING POINTS

To describe the clinical manifestations, imaging findings, and diagnostic and therapeutic algorithms available in patients with chronic thromboembolic pulmonary hypertension (CTEPH) amenable to balloon pulmonary angioplasty (BPA). To discuss the importance of a proper selection, evaluation, and preparation of patients undergoing BPA, including protocols, applications, and a systematic clinical and imaging management proposal. To explain the technique, intraprocedural clinical evaluation, expected clinical and imaging findings, results and complications of BPA.

#### TABLE OF CONTENTS/OUTLINE

1. Introduction. 2. Management of patients with CTEPH. 2.1. Clinical manifestations. 2.2. Imaging modalities and typical findings. 2.3. Diagnostic algorithm. 2.4. Therapeutic algorithm. 3. Assessment before BPA. 3.1. Patient selection. 3.2. Preprocedural evaluation and preparation. 3.3. Proposal of a systematic protocol used in our institution. 4. BPA procedure. 4.1. 10-step technique. 4.2. Intraprocedural clinical evaluation. 4.3. Immediate clinical and imaging findings. 4.4. Complications. 5. BPA Follow-up. 5.1. Clinical and imaging evaluation. 5.2. Results. 6. Summarize. 7. Conclusion.

## **IREE-60 Bariatric Arterial Embolization: How To Build a Clinical Program**

Participants

Adham Khalil, MD, Baltimore, MD (*Presenter*) Research Grant, Siemens AG

### **TEACHING POINTS**

Obesity is a major public health issue that contributes to significant disability, cardiovascular risk, mortality, and healthcare costs. Over the last 50 years, there has been a dramatic increase in the prevalence of obesity in the United States. Obesity is associated with an increased risk of all-cause mortality and a significant reduction in life expectancy. For these reasons, obesity has been labeled a major healthcare epidemic in the United States. Thus, there is an urgent need to develop new therapies for obesity. BAE is an emerging, minimally-invasive therapy for patients with obesity. This image-guided transcatheter procedure involves occlusion of the arteries supplying the gastric fundus, which contains the majority of ghrelin-producing cells. BAE has an excellent safety profile with more than 100 patients with obesity having undergone the procedure worldwide, without any significant adverse sequelae. These early findings suggest that BAE may represent an additional tool in the treatment of patients with obesity that could be used alone or in conjunction with a dedicated lifestyle management program. The goal of the exhibit is to educate the reader on our experience with building a clinical, insurance-supported BAE program and how to integrate BAE as a part of the care path for treating obesity.

### **TABLE OF CONTENTS/OUTLINE**

1. Structure of the bariatric program  
2. Patient acquisition and workflow  
3. Patient referral and assessment  
4. Multidisciplinary discussion  
5. Peri-procedural patient care  
6. Procedure technique  
7. Insurance and billing  
8. Pearls / Lessons learnt

## **IREE-61 Transjugular Venous Access in Upper Extremity Hemodialysis Arteriovenous Fistula / Graft Interventions**

Participants

Louis Fanucci, DO, Orange, CA (*Presenter*) Nothing to Disclose

### **TEACHING POINTS**

1. To review the indications for use of transjugular venous access in upper extremity hemodialysis arteriovenous fistula / graft (AVF / AVG) interventions  
2. To describe the procedural technique involved with transjugular venous access  
3. To discuss the specific clinical applications for transjugular venous access

### **TABLE OF CONTENTS/OUTLINE**

Transjugular venous approaches were originally described in the context of upper extremity AVF / AVG interventions in 1998, for patients with thrombosed dialysis grafts. A clotted fistula / graft presents a situation where a direct puncture into that AVF / AVG is undesirable. A transjugular approach facilitates intervention using a single puncture site that does not involve the AVF / AVG outflow vein. Pre-procedure access assessment includes ultrasound evaluation of anastomotic sites, inflow artery and outflow vein, and patency of the internal jugular veins. IV access is obtained with a micropuncture system under ultrasound guidance, followed by insertion of 7-French vascular sheath. A guidewire and reverse-curve catheter are most commonly used to perform retrograde catheterization of the outflow vein of interest. After successful retrograde access is established and the procedure completed, hemostasis is achieved by simply applying pressure at the puncture site of the internal jugular vein. Clinical applications of the transjugular access approach include interventions to assist an AVF's maturation and de-clotting of an AVF. This approach is a safe and effective alternative approach to AVF / AVG interventions for patients whose target arteriovenous systems are not amenable to direct puncture.

## **IREE-62 History of Histotripsy: Bench to Clinical Translation**

Participants

Nathan Loudon, MD, Ann Arbor, MI (*Presenter*) Nothing to Disclose

### **TEACHING POINTS**

Histotripsy is a new non-invasive, non-thermal, non-radiation ablative modality that uses mechanical cavitation to destroy tissues. Histotripsy began as a basic science bioengineering research project, where the investigation of ultrasound generated cavitation eventually progressed to small and large animal trials, ultimately leading to clinical translation with a Phase I FDA approved clinical trial in the US and Europe. This exhibit will review the basic physics of the technology, review the history of development from small animal to large animal to clinical translation, and finally review the clinical applications and early clinical data.

### **TABLE OF CONTENTS/OUTLINE**

Overview of the technology  
Review of basic science and animal trials  
Small animal feasibility studies  
Large animal feasibility studies  
pre-clinical translation  
Small animal abscopal trials  
Early clinical trials  
Review of early human clinical trials  
Phase I efficacy trial: TERESA trial in Spain  
Phase I safety and efficacy trial: #HOPE4LIVER trial in the U.S. and Europe

## **IREE-63HC Common Vascular and Bleeding Complications of Percutaneous Biliary Interventions**

Participants

Aziz Tejani, (*Presenter*) Nothing to Disclose

### **TEACHING POINTS**

With the increase in percutaneous biliary tract interventions (PBTI) being performed over the past few years, it is important for radiologists to be aware of the many associated post-procedural complications. While there are several complications that are commonly seen, bleeding can be one of the more serious ones that should readily be assessed for. Bleeding is typically seen in 2-3% of all PBTI cases (3). Injuries to the portal vein, hepatic artery, hepatic vein, and pseudoaneurysms are common vascular injuries that are encountered. Signs and symptoms of such vascular injury can be subtle and non-specific. Although morbidity and mortality is rare, a delay in detection may lead to significant adverse outcomes in some patients. After reviewing this educational exhibit, the individual will be able to: 1. Detect the various vascular and bleeding complications of PBTI on imaging modalities 2. Understand the best practices for diagnostic evaluation 3. Understand the therapeutic percutaneous interventions for treatment

## TABLE OF CONTENTS/OUTLINE

This Exhibit Will Provide:1. An overview of the various types of iatrogenic vascular injury seen with percutaneous biliary interventions2. Demonstrate the clinical signs and symptoms of vascular injury for the clinician to be aware of3. Review appropriate imaging modalities and how to detect such vascular complications on the particular studies4. An overview of therapeutic procedures from an interventional radiology standpoint to manage these bleeding complications5. An assessment of future direction and summary of teaching pointsPlease visit the Learning Center to also view this presentation in hardcopy format.

### **IREE-65 Tips for TIPS: An Update on Transjugular Intrahepatic Portosystemic Shunt Complications for Radiologists**

Participants

Andrew Ni, San Antonio, TX (*Presenter*) Nothing to Disclose

#### TEACHING POINTS

Learning Objectives:Present common TIPS complications and their etiologyPresent an update for the diagnostic radiologist in early detection and management of TIPS complicationsReview management of common TIPS complications

## TABLE OF CONTENTS/OUTLINE

Content/Outline IntroductionProcedural complications, imaging findings, and management:Venous access complications: pneumothorax, carotid artery puncture, cardiac perforationPortal access needle punctures: puncture (hepatic artery, biliary ducts, gallbladder), hemoperitoneum, and liver capsule perforationStent related: stent length, occlusion, and deployment issuesPost-procedural complications, imaging findings, and management:Shunt thrombosis: stent occlusion, portal vein thrombosis, Budd Chiari syndromeDevice-related: stent migration, hemolysisHepatic pathology: liver failure, encephalopathy, hepatic abscess, hepatic infarctOther: sepsis, radiation injury, right sided cardiac failure, hernia incarceration Routine and clinically indicated follow-up imaging Ultrasound to ensure patency and for long-term observation Imaging for detection and treatment of stent stenosis and obstruction Contrast enhanced CT to determine etiology of acute hepatic failure (vessel occlusion, thrombosis)

### **IREE-66 Thoracic Central Venous Occlusion: Pathogenesis, Imaging Findings, and Recanalization Techniques**

Participants

Carlos Ortiz, MD, San Antonio, TX (*Presenter*) Consultant, Argon Medical Devices, Inc

#### TEACHING POINTS

- Discuss the pathophysiology, imaging findings, and common presentations of thoracic central venous occlusions (TCVOs)- Review collateral pathways formed in response to TCVO and associated findings on imaging- Discuss current endovascular techniques for central venous recanalization- Review the role of imaging in assessing stent patency and complications after venous recanalization

## TABLE OF CONTENTS/OUTLINE

Introduction - Pathogenesis of TCVOs in the context of hemodialysis, indwelling catheters, extrinsic compression, and associated pathophysiology- Imaging of TCVOs on CT and diagnostic venogram, including review of collateral venous pathway formation- Current recanalization techniques employed in the treatment of TCVOs and indications for specific techniques (standard wire crossing, sharp recanalization, radiofrequency wire, and endovascular stenting)- Immediate complications (hemothorax, pneumothorax, hemopericardium) and subsequent complications (stent thrombosis, occlusion, dialysis issues) after endovascular recanalization- Medical management after TCVO endovascular stentingConclusionIdentification of a TCVO is important for patients as symptoms can be life altering and compromise hemodialysis. Successful recanalization requires technical skill, appropriate planning, and postprocedural management. Complications from TCVO revascularization can be severe and familiarity with this procedure is important for radiologists.

### **IREE-67 "Burning Questions": What Every Radiologist Should Know about the Diagnosis and Management of Bleeding Duodenal Ulcers**

Participants

Roberto Chavez Appendini, MD, (*Presenter*) Nothing to Disclose

#### TEACHING POINTS

1. Vascular supply of the duodenum arises from the anterior and posterior division of the superior pancreaticoduodenal arteries which are branches of the gastroduodenal artery, these arteries anastomose with the inferior pancreaticoduodenal artery which is a branch of the superior mesenteric artery.2. Diagnosis and treatment of bleeding duodenal ulcers are traditionally endoscopic, when bleeding is refractory to treatment, Three-phase GI bleed CT protocol (non-contrast, arterial and venous phases) is an important diagnostic tool, nuclear medicine studies are helpful when CT contraindicated.3. CT findings of duodenal ulcers are subtle and include, mural enhancement of the duodenum, fat stranding, submucosal edema, regional lymphadenopathy, and active extravasation of contrast into the duodenal lumen.4. Endovascular treatment must be considered for bleeding ulcer refractory to endoscopic treatment. Selective embolization of the GDA is done when active bleeding is identified either on CT or angiographically. Empiric embolization of the GDA is an effective alternative, especially for clinically unstable patients.5. Selective and empiric embolization of the GDA for bleeding duodenal ulcers refractory to endoscopic treatment has a low complication rate, for which rebleeding is the most common, in these cases angiogram with potential re-embolization can be considered as well as surgical treatment.

## TABLE OF CONTENTS/OUTLINE

1. Introduction and epidemiology2.Diagnostic approach for suspected bleeding duodenal ulcer3.Treatment modalities4.Case series5.Conclusion

### **IREE-68 Complications After Radioembolization of Hepatic Tumors: Spectrum of Imaging Findings**

**Awards**

**Certificate of Merit**

Participants

Hyo-Cheol Kim, MD, Seoul, Korea, Republic Of (*Presenter*) Nothing to Disclose

#### TEACHING POINTS

Radioembolization is a potent intra-arterial therapy used to treat primary liver tumors and liver metastases. However, this treatment may result in various hepatic and extrahepatic complications which could be alleviated or prevented. The common complications include biliary necrosis, benign biliary stricture, liver abscess, radioembolization-induced liver disease, radiation cholecystitis, gastrointestinal radiation ulcer, radiation pneumonitis, and radiation dermatitis. The purpose of this exhibit is : (1) To review the hepatic and extrahepatic complications related with radioembolization. (2) To learn how to manage these complications. (3) To learn how to prevent or alleviate these complications.

#### TABLE OF CONTENTS/OUTLINE

1) Hepatic complications associated with radioembolization A. biliary complication (biliary necrosis, biliary stricture, biloma, liver abscess) B. radiation hepatitis and focal radiation necrosis C. radiation-induced liver disease 2) Extrahepatic complications associated with radioembolization A. Radiation cholecystitis B. Radiation ulcer C. Radiation pneumonitis D. Radiation dermatitis 3) Management of each complication 4) Prevention method of each complication

#### IREE-69 Percutaneous Sclerotherapy for Orbital Low Flow Lympho-venous Malformations (LFVM)

Participants

Shyamal Patel, MBBS, FRCR, London, United Kingdom (*Presenter*) Nothing to Disclose

#### TEACHING POINTS

1. Orbital sclerotherapy is effective with low complication rates, and is therefore an important minimally invasive option in the management of orbital low flow lympho-venous malformations. 2. Bleomycin is the sclerosant of choice as it is associated with less local inflammatory response - important for lesions in/around the orbit where significant swelling can result in visual loss. 3. Treatment is performed under a general anaesthetic and prior to bleomycin use, adequate pre-assessment is required including appropriate imaging and ophthalmology review. 4. The entire team should be aware of specific precautions related to bleomycin use including potential for lung fibrosis, skin marking and the need for cytotoxic precautions. 5. Important complications to be aware of are retro-orbital haemorrhage, requiring emergency lateral canthotomy and the oculocardiac reflex which is rare but may result in bradycardia, arrhythmias and potentially asystole.

#### TABLE OF CONTENTS/OUTLINE

1. What are orbital LFVMs (Primary vs Secondary; Venous, lymphatic and mixed). 2. Imaging appearances (US, CT, MRI). 3. Bleomycin use: pre-assessment, bleomycin precautions. 4. Sclerotherapy procedure - dosage, technique and assessment for deep venous drainage. 5. Complications (retro-orbital haemorrhage, oculocardiac reflex).

#### IREE-7 Recent Development of Augmented Reality and Mixed Reality for Needle Guidance

Awards

Certificate of Merit

Participants

Satoru Morita, MD, PhD, Tokyo, Japan (*Presenter*) Nothing to Disclose

#### TEACHING POINTS

Augmented reality (AR) and mixed reality (MR) can expand the possibilities of image guidance procedures. Some needle guidance applications using AR/MR on smartphones and smartglasses have been developed recently. Various resources are available for developing applications using AR/MR. The purpose of this exhibit is to 1). Review the current situations of AR/MR for image guidance procedures. 2). Introduce the recent needle guidance applications using AR/MR and discuss each advantage and disadvantage. 3). Introduce how to develop needle guidance applications using AR/MR.

#### TABLE OF CONTENTS/OUTLINE

1). Introduction 2). Definitions of AR/MR 3). Devices for AR/MR 4). Platforms to develop AR/MR applications 5). Registration methods for AR/MR 6). Current needle guidance applications using AR/MR 7). Limitations 8). Future perspectives 9). Conclusions and take home messages

#### IREE-70 Interventional Pain Frontiers: Role of IR in Median Arcuate Ligament Syndrome (MALS) Management

Awards

Certificate of Merit

Participants

Mohamed Ibrahim, MBCh, Rochester, MN (*Presenter*) Nothing to Disclose

#### TEACHING POINTS

• Understand the current hypothesis of MALS etiology and highlight pertinent anatomy • Learn the role of IR in the diagnosis and determination of surgical candidacy for MALS patients • Learn the role of IR in the treatment of MALS patients

#### TABLE OF CONTENTS/OUTLINE

• MALS etiology and pertinent anatomy o A neurogenic disorder rather than a compression syndrome o Celiac plexus and splanchnic plexus anatomy • Role of IR in the diagnosis and determination of surgical candidacy MALS patients o Role of celiac plexus block in the diagnosis of MALS o Common approaches and protocols for celiac plexus block in the diagnosis of MALS • Role of IR in treatment of MALS patients o Celiac plexus neurolysis; technical considerations, and expected outcomes o Splanchnic plexus neurolysis; technical considerations, and expected outcomes

#### IREE-71 Interventional Management of Portal Vein Thrombosis: A Problem-solving Approach

Participants

Daniel Cardoso, MD, Fortaleza, Brazil (*Presenter*) Nothing to Disclose

## TEACHING POINTS

Recognize the anatomy of the portal venous system (PVS) and its most common variants. Understand the causes of Portal Vein thrombosis (PVT) and related clinical features. Comprehend imaging patterns of PVT through a wide variety of imaging modalities. Recognize the complications associated to PVT and its imaging patterns. Understand PVT treatment methods and criteria.

## TABLE OF CONTENTS/OUTLINE

1. INTRODUCTION: PVS anatomy and most common anatomical variations. Definition of PVT (acute x recent x chronic). Epidemiology of the most common causes of PVT. Signs and symptoms associated to the obstruction site (Portal Vein (PV), Superior Mesenteric Vein (SMV) and Splenic Vein (SV)). 2. DIAGNOSIS AND IMAGING FINDINGS: PV: Benign PV / Cirrhotic and non-cirrhotic PVT / Infectious/septic PVT - thrombophlebitis / Transplant-associated PVT. Malignant PVT: Tumor Invasion/PV Tumor Thrombosis (Hepatocellular carcinoma) / External Constriction of the PV within a Tumor (Pancreatic Cancer or Cholangiocarcinoma) / Complications associated to PVT. SMV: SMV thrombosis / Complications associated to SMV thrombosis. SV: SV thrombosis / Complications associated to SV thrombosis. 3. MANAGEMENT OF PVT: Fundamentals of Anticoagulation Therapy / Interventional Approach / Techniques / Follow-up and Early Identification of Possible Complications.

## IREE-73 Venous Access Ports: What Every Radiology Resident Should Know

Participants

Nicholas Champagne-Aves, BS, (*Presenter*) Nothing to Disclose

## TEACHING POINTS

List indications and contraindications of venous access ports Describe port placement and confirmatory imaging Describe associated complications, imaging findings, and management

## TABLE OF CONTENTS/OUTLINE

Indications Long term intravascular access with minimal disruption to patient's life (medications, transfusions, blood draws) Contraindications Absolute: bacteremia/sepsis, infection at access site Relative: coagulopathy, chest wall deformity, pneumothorax, distorted anatomy (trauma/thrombosis) Procedural Steps Visualize desired vein under ultrasound (US) guidance Sterilize field Obtain planned venous access with micropuncture kit under US guidance Measure desired length of catheter using micropuncture guidewire Exchange for 0.035" wire and place in the SV Create port reservoir site and tunnel catheter to venotomy Trim catheter to length and ensure adequate port connection Advance peel away sheath over wire, remove inner dilator Insert catheter completely through sheath and peel away sheath Confirm proper placement with fluoroscopy Test and flush port with heparin, close incision Complications, imaging findings, management Early: malposition, hemorrhage, hemothorax, pneumothorax, air embolism Late: infection, catheter occlusion/thrombosis, catheter pinch off/migration Port Removal: catheter calcification, fracture, pseudo-fracture A systematic approach to venous access port placement minimizes complications and improves outcomes. Radiologists must be familiar with indications, procedural steps, and complications for accurate management.

## IREE-74HC Acute Calculous Cholecystitis: The Role of the Radiologist in Diagnosis and Treatment

Participants

Darius Jonasch, BEng, (*Presenter*) Nothing to Disclose

## TEACHING POINTS

1. Review diagnostic approach for Acute Calculous Cholecystitis 2. Define the grading of Acute Calculous Cholecystitis 3. Discuss treatment options based on the patient's presentation and history

## TABLE OF CONTENTS/OUTLINE

1. Introduction a. Anatomy of the Hepatobiliary System b. Pathophysiology of Acute Calculous Cholecystitis c. Epidemiology and Clinical Presentation of Acute Calculous Cholecystitis 2. Imaging Appearance a. Ultrasound b. Cholescintigraphy c. Magnetic Resonance Cholangiopancreatography d. Computed Tomography e. Endoscopic Retrograde Cholangiopancreatography f. Percutaneous Biliary Endoscopy 3. Clinical Severity a. Introduction to Tokyo Guidelines i. Grade I ii. Grade II iii. Grade III 4. Risk Stratification and Treatment a. Low Risk Patients i. Surgical Therapy 1. Surgical Cholecystectomy b. High Risk Patients i. Medical Therapy 1. Antibiotics ii. Endoscopic Therapy 1. Endoscopic Drainage iii. Interventional Radiology Therapy 1. Percutaneous Drainage 2. Percutaneous Transhepatic Stone Retrieval iv. Surgical Therapy 1. Surgical Candidacy 2. Surgical Timing 5. Potential Complications a. Complications of Acute Cholecystitis - Sepsis, Choledocholithiasis, Gangrenous Cholecystitis, Gallbladder Perforation, Emphysematous Cholecystitis, Cholecystoenteric Fistula, Gallstone Ileus b. Complications of Treatment of Acute Calculous Cholecystitis - Hemorrhage, Bile Leak, Biloma, Common Bile Duct Injury, Bowel Injury, Tube Complications Please visit the Learning Center to also view this presentation in hardcopy format.

## IREE-75 Biliary Leaks: There Are Many Ways to Fix

Awards

Identified for RadioGraphics

Participants

Christopher Mao, Sugar Land, TX (*Presenter*) Nothing to Disclose

## TEACHING POINTS

Biliary leaks are most seen in patients as iatrogenic complications after surgeries such as cholecystectomy. Postoperative leaks occur in 1% of laparoscopic cholecystectomies and 0.5% of open cholecystectomies but can occur in other procedures such as RFA (Radiofrequency Ablation) of primary and secondary liver tumors. As the number of hepatobiliary surgeries performed continue to increase, biliary leaks will become even more prevalent. Since clinical signs and symptoms of bile leaks are nonspecific and delay in the recognition of bile leaks is associated with high morbidity and mortality rates, imaging is crucial for establishing an early diagnosis and guiding the treatment algorithm. After reviewing this exhibit, learners should be able to: 1. Recognize emergent biliary leaks from key image findings. 2. Use best practices for diagnosing biliary leaks. 3. Understand the options for percutaneous management.

## TABLE OF CONTENTS/OUTLINE

1. Provide an overview of the different types of biliary leaks. 2. Illustrate the clinical and imaging features of biliary leaks with a focus on iatrogenic etiologies. 3. Review the framework for selecting the best imaging practice of the biliary duct system. 4. Address relevant management as applicable to the interventional radiologist to aid in expedient and appropriate management. 5. Discuss future directions. 6. Conclude with a summary of key teaching points.

#### **IREE-76 MRI Guided Transurethral Ultrasound Ablation (TULSA) of Prostate: Initial Experience at Wellspan Hospital**

Participants

Edward Steiner, MD, (*Presenter*) Key Opinion Leader, Koninklijke Philips NV ;Speaker, Koninklijke Philips NV;Speaker, Quantib BV;Research support, Profound Medical Inc ;Speaker, Profound Medical Inc

##### **TEACHING POINTS**

Teaching points - To present the capabilities of TULSA-TULSA-PRO is a minimally invasive procedure that combines real-time MRI with robotically-driven directional thermal ultrasound to treat prostate cancer, with the goal of achieving comparable disease control to radiation therapy or prostatectomy and significantly improved functional preservation. TULSA can also treat BPH concurrent with cancer in a single procedure. Examples of TULSA whole-gland and hemi-ablation procedures performed at our institution are provided. - To report lessons learned with the TULSA procedure Critical lessons and technical points are presented including patient preparation, considerations on treating radio-recurrent disease, sparing of sphincter and bladder tissue, maintaining ejaculatory function, and workup of patients with intermediate to high grade lesions with PSMA scans. - To report early functional, oncological, and safety outcomes Discussion of post procedure care and follow-up, monitoring, repeat MRI and PSA trends, continence and erectile function data analysis as well as preliminary tumor recurrence data.

##### **TABLE OF CONTENTS/OUTLINE**

Table of contents - Basics of TULSA procedure and workflow - Lessons learned, and treatment planning strategies - Early functional, oncological, and safety outcomes - Applications of TULSA for sparing functionally important structures and treating radio-recurrent disease

#### **IREE-77 Intra-arterial Treatment for Hepatocellular Carcinomas: How to Manage Shunting From the Artery**

**Awards**

**Magna Cum Laude**

Participants

Hyo-Cheol Kim, MD, Seoul, Korea, Republic Of (*Presenter*) Nothing to Disclose

##### **TEACHING POINTS**

Intra-arterial therapy including chemoembolization and radioembolization is a workhorse for the treatment of patients with hepatocellular carcinomas. Occasionally, the operators encounter shunts from the artery (arterioportal, arteriovenous, and arteriopulmonary shunts) that prevent effective treatment. The causes of these shunts include tumor invasion to the vessels, previous percutaneous procedures, chronic inflammation, and congenital acquisition. Unless the shunt is properly occluded, embolic material can pass through the shunt and cause non-target embolization or serious complications. The purpose of this exhibit is : (1) To review radiologic appearance of arterioportal, arteriovenous, and arteriopulmonary shunts. (2) To learn how to manage these shunts with proper embolic materials. (3) To list the possible complications and their management.

##### **TABLE OF CONTENTS/OUTLINE**

1) List of shunts Arteriportal shunt (hepatic artery - portal vein), Arteriovenous shunt (hepatic artery - hepatic vein), Arteriopulmonary shunt (hepatic artery - pulmonary artery/vein), 2) Imaging findings on CT/MR and angiography according to the cause (tumorous vs non-tumorous condition) 3) Embolization strategy and materials for shunts 4) Complications related with non-target embolization and their management

#### **IREE-78 To Glue or Not to Glue, That Was the Question - Misadventures with Glue Embolization in Peripheral Applications**

Participants

Jorge Lopera, MD, San Antonio, TX (*Presenter*) Shareholder, Tecnostent SA;Consultant, Merit Medical Systems, Inc;Research Grant, AngioDynamics, Inc

##### **TEACHING POINTS**

Embolization using N butyl acrylate (NBCA) or glue is showing very promising results with better and faster occlusion results than particles or coils in areas that are susceptible to recanalization after embolization such as bronchial arteries, portal vein embolization and endoleaks after EVAR, among others. Emerging uses of glue include trauma, uterine artery embolization in placental insertion abnormalities, cyst sclerosis and gastrointestinal bleeding. As with other liquid embolization agents, using glue has a steep learning curve and serious complications can occur. The purpose of this exhibit is to illustrate in a case by case presentation, different complications with the use of glue with emphasis in ways to prevent them.

##### **TABLE OF CONTENTS/OUTLINE**

1. When to use and not to use glue 2. How to prepare glue; basic steps 3. Complications a. Lung glue embolization after portal vein embolization. b. Portal vein embolization after treatment of arterio-portal fistula in HCC c. SMA glue migration after percutaneous aneurysm embolization d. Iliac artery glue embolization after trans lumbar endoleak embolization e. Glue cast adhered to catheter in the aorta- ways to fix this. f. Stroke after peripheral glue embolization, beware of PFO. Conclusions : Glue is a very versatile embolization agent, showing very promising results with lesser recanalization rates than particles or coils in many areas. As a liquid embolization agent, serious complications can occur that require a clear understanding of the different mechanisms of glue migration and ways to mitigate them.

#### **IREE-79 Benign Prostatic Hyperplasia Treatments: A Review of the Fundamentals to Assist in Optimal Prostate Artery Embolization Patient Selection**

Participants

Miltiadis Tembelis, Mineola, NY (*Presenter*) Nothing to Disclose

#### TEACHING POINTS

1. A thorough understanding of benign prostatic hyperplasia (BPH) pathophysiology and management options is essential before embarking on developing a prostate artery embolization (PAE) program. 2. While the risks of PAE are low when done with proper technique, major complications can occur and have negative impact on a patient and/or a PAE program. 3. An understanding of PAE indications as well as alternative BPH treatment is essential to ensure appropriate patient selection and PAE procedural advocacy.

#### TABLE OF CONTENTS/OUTLINE

-Review BPH pathophysiology-Discuss lower urinary tract symptoms (LUTS), their diagnosis, and that a variety of causes exist (not just bladder outlet obstruction from BPH)-Provide the learner with a thorough review of BPH management options, including medications, minimally invasive surgical therapies, PAE, and more invasive surgical interventions (TURP, HoLEP, and prostatectomy)-Review relevant literature on indications and outcomes of these procedures, with the goal of providing radiologists and trainees with key fundamental knowledge to allow for optimal PAE patient selection and also for guiding patients towards other management options when more appropriate

#### IREE-8 **The Pelvic Venous Disease Continuum: Nutcracker Phenomenon, Non-thrombotic Iliac Vein Lesion (NIVL), Ovarian and Pelvic Vein Reflux**

Participants

Navpreet Khurana, MBBS, (*Presenter*) Nothing to Disclose

#### TEACHING POINTS

1. Discuss the complex pathophysiological interactions between Nutcracker syndrome, Nonthrombotic Iliac Vein Lesion (NIVL), and ovarian pelvic venous reflux leading to the constellation of findings known as Pelvic Venous Disease (PeVD). PeVD is often misdiagnosed and inappropriately treated. 2. Describe the key imaging findings in the diagnosis of PeVD. 3. Review the algorithm and pearls/pitfalls of IR management.

#### TABLE OF CONTENTS/OUTLINE

1. Key anatomical and pathophysiological concepts a) Nutcracker Phenomenon - Compression between aorta and superior mesenteric artery results in stenosis and increased pressure in the left renal vein, often with blow-out retrograde flow down the ovarian vein resulting in pelvic varicosities to act as collateral. b) NIVL - Stenosis of left common iliac vein between right common iliac artery and aorta, either by mechanical compression or with superimposed chronic microtrauma secondary to proximity and pulsatility causing venous wall thickening and/or webs. c) Ovarian Pelvic Vein Reflux - Incompetence and reflux of ovarian and/or pelvic veins resulting in pooling of blood into "reservoirs", classically in the pelvis. Blood may also leak out of the pelvis from "escape points" due to gravity and venous hypertension. 2. Diagnostic imaging algorithm and findings with a case-based discussion. 3. Role of Interventional Radiology: a) Initial consultation with focused history/physical exam. b) Diagnostic evaluation for PeVD - US, CT Venography, MR Venography. c) Nutcracker Phenomenon its dynamic role in PeVD. d) In NIVL, understanding the interplay of iliac stenosis with ovarian reflux, role of its treatment in PeVD. 4. Complications/misdiagnosis case examples of PeVD.

#### IREE-80 **Prostate Artery Embolization Practice Building - With a Focus on Understanding the Current Literature**

Participants

Nathan Mickinac, MD, Mineola, NY (*Presenter*) Nothing to Disclose

#### TEACHING POINTS

1. A thorough understanding of benign prostatic hyperplasia (BPH) pathophysiology and management options is essential before embarking on developing a PAE program. 2. While the risks of PAE are low when done with proper technique, major complications can occur and have negative impact on a patient and/or a PAE program. 3. Thoughtful implementation, careful patient selection, meticulous procedural technique, collaboration with other specialties, and appropriate marketing are keys to building a successful PAE program.

#### TABLE OF CONTENTS/OUTLINE

-Review BPH pathophysiology and epidemiology-Brief review of BPH treatment options, with a focus on PAE-Review relevant literature on PAE, including large prostates (>80g), acute urinary retention, and/or hematuria-Provide basic review of sexual health relating to BPH, including erectile dysfunction (ED) and ejaculatory dysfunction (EjD), and review relevant evaluation tools/scales-Highlight data regarding ED and EjD across multiple BPH procedures, including PAE-Review current AUA BPH guidelines and discuss why PAE is not supported in those guidelines currently-Detail current data regarding repeat PAE-Share practice building advice, with a focus on utilizing PAE data to engage other specialties as a part of building a successful program

#### IREE-9 **Cryoablation of Aneurysmal Bone Cyst: Current Status and Management**

Participants

Elisabet Vila, (*Presenter*) Nothing to Disclose

#### TEACHING POINTS

This exhibit will: 1) Describe imaging features of primary ABC using different imaging modalities. 2) Discuss this novel interventional technique and how it works (low dose CT protocol, needle placement method and ice ball formation). 3) Illustrate normal post treatment imaging findings of aneurysmal bone cyst using cryoablation on MRI. 4) Characterize the radiological appearance of relapse.

#### TABLE OF CONTENTS/OUTLINE

Aneurysmal bone cysts are benign and expansile bone lesions with locally aggressive behavior. Diagnosis is achieved using different imaging modalities. Cryoablation is a percutaneous ablation technique that uses extreme low temperatures for tumor destruction and is becoming increasingly accepted for treatment of aneurysmal bone cysts. It uses liquefied gas (nitrogen or argon), through cryoprobes that expand into a gaseous state at the end of the probe to create temperatures as low as -190 °C. Intra-procedure computed tomography (CT) is used to identify the ablated zone in real time appearing as a low-density area which corresponds to

the generated ice ball. In this exhibit we will review how cryoablation works, procedure planning and imaging appearance of post procedural interventions, showing different examples of normal findings and relapse.

Printed on: 02/07/23



## Abstract Archives of the RSNA, 2022

IREE-1

### Arterial Embolization for Gynecological and Obstetric Hemorrhage - Indications, Preparation, Technique, Results, and Complications

Sunday, Nov. 27 8:00AM - 9:00AM Room: Learning Center - IR

#### Awards

Certificate of Merit

#### Participants

Mario Matute Gonzalez, MD, Barcelona, Spain (*Presenter*) Nothing to Disclose

#### TEACHING POINTS

1. To describe the diagnostic and therapeutic management of patients with gynecological and obstetric hemorrhage (GOH) suitable to transcatheter embolization.2. To review main gynecologic and obstetric indications for arterial embolization, providing key imaging findings before and after embolization.3. To explain the technique and intraprocedural considerations, results and complications of GOH embolization.

#### TABLE OF CONTENTS/OUTLINE

1. Introduction.1.1. Vascular anatomy of the female pelvis.2. Management of patients with GOH.2.1. Therapeutic algorithm.2.2. Pre-treatment imaging assessment.3. Indications for arterial embolization: imaging findings.3.1. Obstetric hemorrhage.- Abnormal placentation.- Postpartum hemorrhage.3.2. Gynecological hemorrhage.- Malignancies.- Post-surgical bleeding.- Vascular anomalies: Uterine AVMs and AV fistulas.3.3. Beyond hemostasis.- Uterine fibroids.- Pelvic Congestion Syndrome.4. Procedural features.4.1. Patient preparation.4.2. Materials.4.3. Technical considerations.4.4. Results.4.5. Complications.5. Summarize.6. Conclusion.

Printed on: 02/07/23



## Abstract Archives of the RSNA, 2022

IREE-10

### Minimally Invasive Prostate Cancer Treatments- An Update

Sunday, Nov. 27 8:00AM - 9:00AM Room: Learning Center - IR

#### Participants

Riddhi Borse, MD, New Haven, MA (*Presenter*) Nothing to Disclose

#### TEACHING POINTS

The purpose of this exhibit is: 1. To provide rationale for minimally invasive prostate cancer (PCa) treatment. The "index" lesion is responsible for driving risk associated with localized PCa. However, imaging underestimates lesion volume it is important to have adequate treatment zone margins. 2. To review modalities and devices available for minimally invasive PCa treatment. Understanding the nuances of available devices along with their FDA approval/ reimbursement status and current evidence about their efficacy is crucial towards building a successful PCa treatment program.

#### TABLE OF CONTENTS/OUTLINE

1. Need for minimally invasive prostate cancer therapy. 2. Defining the index lesion. 3. Treatment margins - How much prostate should you ablate? 4. Treatment modality specific review including device capabilities/limitations, cost, side effect profile and efficacy evidence; Laser Ablation Cryoablation Irreversible Electroporation Therapeutic Ultrasound Photodynamic Therapy Aquablation Bipolar radiofrequency ablation. 5. Post treatment prostate MRI. 6. FDA Approval Status and Insurance Reimbursements for minimally invasive PCa treatment.

Printed on: 02/07/23



## Abstract Archives of the RSNA, 2022

IREE-12

### How to Make It Right When Vessels Go Wrong: Demystifying Abdominal Vascular Anomalies

Sunday, Nov. 27 8:00AM - 9:00AM Room: Learning Center - IR

#### Participants

Ece Meram, MD, Madison, WI (*Presenter*) Research Grant, Koninklijke Philips NV

#### TEACHING POINTS

The classification of vascular anomalies has been evolving and remains challenging with limited worldwide adoption and lingering of historically used terminology. Vascular anomalies are divided into two main categories (i.e. mass or malformation) based on their increased mitotic activity and cell turnover. Vascular masses, benign or malignant, are vasoproliferative lesions with increased endothelial cell turnover. Vascular malformations, on the other hand, are congenital, non-neoplastic entities of incorrectly formed vessels. This exhibit aims to 1) describe different types of abdominal vascular anomalies according to International Society for the Study of Vascular Anomalies (ISSVA) classification, 2) demonstrate examples of abdominal vascular tumors and malformations, including those associated with hereditary conditions and 3) highlight the interventional approaches utilized in the management (i.e. correction) of these anomalies.

#### TABLE OF CONTENTS/OUTLINE

A. When Vessels Go Wrong: Vascular Anomalies a. Definition/Types: Mass vs Malformation b. ISSVA Classification. B. Abdominal Vascular Tumors a. Benign (eg. Hepatic Hemangioma) b. Borderline c. Malignant (eg. Angiosarcoma). C. Abdominal Vascular Malformations a. Simple i. Low-flow (Capillary, Lymphatic, Venous) ii. High-flow (Arteriovenous malformation or fistula) iii. Portosystemic Fistula (eg. Congenital Portosystemic Shunts) b. Combined c. Anomalies of Major Named Vessels d. Associated with Other Anomalies (Hereditary and/or Syndromic). D. How to Make it Right? a. Surgical Management b. Types of Interventional Procedures c. Case Examples. E. Quiz Cases

Printed on: 02/07/23



## Abstract Archives of the RSNA, 2022

IREE-13

### Adrenal Venous Sampling: Tips and Tricks for Non-Experts

Sunday, Nov. 27 8:00AM - 9:00AM Room: Learning Center - IR

#### Awards

Identified for RadioGraphics

#### Participants

Katsuhiro Kobayashi, MD, , (Presenter) Nothing to Disclose

#### TEACHING POINTS

1) Review adrenal vein anatomy and anatomical landmarks for right adrenal vein cannulation. 2) Describe adjunctive techniques used for adrenal vein sampling (AVS). 3) Discuss adrenal vein sample interpretation and indication for repeat AVS

#### TABLE OF CONTENTS/OUTLINE

1) Overview of primary aldosteronism 2) Anatomy of adrenal veins relevant to AVS and anatomical landmarks for right adrenal vein cannulation (inferior emissary vein, communicating veins, inferior accessory hepatic vein) 3) Pre-procedural work-up including MDCT technique used for adrenal vein assessment 4) Protocol for AVS including antihypertensive medication modification, or cosyntropin infusion etc.) 5) Techniques used for AVS and adjunctive techniques used for right adrenal vein cannulation (Cone-Bean CT, coaxial guide wire- catheter technique, intraprocedural cortisol measurement) 6) Sample interpretation and indication for repeat AVS (double down Aldosterone/Cortisol) 7) Complications associated with AVS 8) Advances in AVS (subselective AVS) 9) Summary of Tips and Tricks

Printed on: 02/07/23



## Abstract Archives of the RSNA, 2022

IREE-14

### Portal Hypertension: A Comprehensive Clinico-Radiological Review.

Sunday, Nov. 27 8:00AM - 9:00AM Room: Learning Center - IR

#### Participants

Antonio Hernandez Villegas, MD, Mexico City, Mexico (*Presenter*) Nothing to Disclose

#### TEACHING POINTS

- To review the physiopathology, classification and etiologies of different types of portal hypertension- To illustrate in a case based approach the different types and causes of portal hypertension (acute and chronic) with multimodality imaging findings- To mention key imaging findings that need to be assessed and provided to the clinician (GI, endoscopy and/or surgeon) in order to determine treatment options- To present interventional radiology treatment options for this pathology according to clinical scenario.

#### TABLE OF CONTENTS/OUTLINE

- Introduction: Epidemiology and risk factors.- Physiopathology: the basics for radiologists in order to understand imaging findings.- Classification: anatomy and timing.- Imaging: role of different imaging modalities and the main findings in the approach, diagnosis and follow-up of patients with portal hypertension.- Case-based approach: imaging findings, diagnosis and interventional treatments.- Take-home points.

Printed on: 02/07/23

## Abstract Archives of the RSNA, 2022

IREE-15

### Various Interventional Procedures Through Percutaneous Cholecystostomy Tract

Sunday, Nov. 27 8:00AM - 9:00AM Room: Learning Center - IR

#### Participants

Jong Hyouk Yun, MD, PhD, Busan, Korea, Republic Of (*Presenter*) Nothing to Disclose

#### TEACHING POINTS

The purpose of this review is to illustrate the various transcholecystic interventions and to discuss the clinical significance, technical aspects and complications of this alternative access to the biliary tree.

#### TABLE OF CONTENTS/OUTLINE

Percutaneous cholecystostomy is a well-established procedure for management of acute cholecystitis. It has been used to provide GB decompression, biliary drainage and cholangiography. In patients who underwent previous surgery or who have intolerance or anxiety for endoscopy, in cases of having difficulties to perform PTBD, or in patients who have previously undergone percutaneous cholecystostomy, percutaneous transcholecystic interventions can be performed as an alternative route. Cystic duct (CD) cannulation is necessary to perform various transcholecystic interventions. For the successful cystic duct cannulation perform a GB puncture in the long axis direction of the GB, keep catheter drainage for 3 days or more to reduce inflammation of the biliary tree, insert a 8F sheath into the GB for the back support, and use guide wires with various sizes and tips. Through cystic duct cannulation, various interventional procedures such as CBD stone removal, biopsy, biliary dilation, biliary stent placement, and GI intervention can be performed. Percutaneous transcholecystic interventions seems to be safe, technically feasible and clinically effective procedures. Percutaneous transcholecystic approach can be used as an alternative route for the patient who could not use peroral or transhepatic route.

Printed on: 02/07/23



## Abstract Archives of the RSNA, 2022

IREE-16

### Cholangioscopy Guidance During Percutaneous Transhepatic Biliary Interventions

Sunday, Nov. 27 8:00AM - 9:00AM Room: Learning Center - IR

#### Participants

Ayca Kutlu, MD, Madison, WI (*Presenter*) Nothing to Disclose

#### TEACHING POINTS

- Introduce readers to transhepatic cholangioscopy.
- Provide an overview of transhepatic cholangioscopy technique, indications, and utility.
- Improve readers' ability to interpret cholangioscopy imaging through representative cases.
- Demonstrate through case examples how transhepatic cholangioscopy guidance can improve procedural success.

#### TABLE OF CONTENTS/OUTLINE

1. Title page 2. Teaching points 3. Background on current transhepatic biliary imaging techniques a. Fluoroscopic cholangiogram b. Intrahepatic cone-beam CT cholangiography 4. Introduction to percutaneous transhepatic cholangioscopy 5. Indications for percutaneous transhepatic cholangioscopy a. Patients with indwelling biliary catheters with new concern for pathology b. Patients with history of previous failed ERCP or altered anatomy prohibiting ERCP 6. Percutaneous transhepatic cholangioscopy interventions a. Targeted tissue sampling b. Biliary stone/debris management c. Biliary Stent/drain placement 7. Case Examples a. Tissue sampling: Targeted biopsy via direct visualization b. Intraductal stone/debris manipulation: Identification of intrahepatic stone/debris with lithotripsy treatment, extraction, or sweeping c. Complex post-surgical anatomic delineation: Navigation across post-surgical benign biliary strictures 8. Conclusions a. Transhepatic cholangioscopy can improve diagnostic and therapeutic precision in the management of biliary pathology. b. Interventional radiologists becoming comfortable with transhepatic cholangioscopy image interpretation and procedural skill can increase procedural success for complex biliary pathology. 9. Quiz Case

Printed on: 02/07/23



## Abstract Archives of the RSNA, 2022

IREE-17

### Interventional Management of Ectopic Varices

Sunday, Nov. 27 8:00AM - 9:00AM Room: Learning Center - IR

#### Awards

Identified for RadioGraphics

#### Participants

Jin Woo Choi, MD, Seoul, Korea, Republic Of (*Presenter*) Nothing to Disclose

#### TEACHING POINTS

Ectopic varices may occur around the duodenum, rectum, stoma, hepaticojejunostomy, etc. Although ectopic varices are not common, those can be a source of considerable bleeding. They usually occur in the setting of portal hypertension such as liver cirrhosis or portal vein occlusion/thrombosis. Whereas endoscopic management is commonly ineffective for ectopic varices, various interventional procedures including percutaneous varix embolization or modified retrograde transvenous obliteration can be performed depending on vascular anatomy. The purposes of this exhibit are: (1) To illustrate vascular anatomy related to ectopic varices, (2) To list various interventional procedures and their indications, (3) To review the technical tips and pitfalls of percutaneous varix embolization and modified retrograde transvenous obliteration.

#### TABLE OF CONTENTS/OUTLINE

1. Vascular anatomy related to ectopic varices. 2. Treatment modalities and indications for ectopic varices: retrograde transvenous obliteration, percutaneous embolization, and their modifications. 3. Technical tips and pitfalls of retrograde transvenous obliteration, percutaneous embolization, and their modifications.

Printed on: 02/07/23



## Abstract Archives of the RSNA, 2022

IREE-18

### Overview of the Complications of Prostate Artery Embolization and its Management

Sunday, Nov. 27 8:00AM - 9:00AM Room: Learning Center - IR

#### Participants

Richard Liang, (*Presenter*) Nothing to Disclose

#### TEACHING POINTS

Prostate Artery Embolization (PAE) is a safe, minimally invasive treatment for lower urinary tract symptoms (LUTS) secondary to benign prostatic hyperplasia (BPH). The purpose of this exhibit is to discuss the complications associated with PAE along with the management of those complications. Complications of PAE can be divided into access site complications, post-embolic complications, non-target embolization and radiation dermatitis. Though the majority of complications are considered self-limiting and can be managed conservatively, more severe complications such as bladder wall ischemia may require cystoscopic surgical resection. While reviewing non-target embolization complications, we will also discuss prostate artery anatomy and its relevance to these complications. Additionally, we will also compare the safety of PAE to some of the other common surgical treatments available for BPH.

#### TABLE OF CONTENTS/OUTLINE

1. What is PAE?
2. How to Perform PAE
3. Overview of the Complications in PAE
4. Access Site Complications and its Management
5. Post-Embolic Complications and its Management
6. Arterial Anatomy and Anatomical Variants of the Prostate
7. Non-Target Embolization Complications and its Management
8. Safety of PAE compared to Surgical Treatments

Printed on: 02/07/23



## Abstract Archives of the RSNA, 2022

IREE-19

### A Comprehensive Approach to Image-guided Ablation in Primary Aldosteronism

Sunday, Nov. 27 8:00AM - 9:00AM Room: Learning Center - IR

#### Participants

Mohamed Ibrahim, MBBCh, Rochester, MN (*Presenter*) Nothing to Disclose

#### TEACHING POINTS

- Learn appropriate patient selection for image-guided ablation of PA
- Learn appropriate clinical evaluation and consultation of PA patients
- Understand key pre-procedural patient preparations
- Highlight pertinent intra-procedural techniques and considerations
- Highlight appropriate post-procedural follow-up and management

#### TABLE OF CONTENTS/OUTLINE

- Appropriate patient selection for image-guided ablation
  - o Key laboratory analysis for diagnosis of PA
  - o Confirming collateralization of imaging and AVS findings
- The PA clinic consult
  - o Pertinent HPI; positives and negatives
  - o Consenting the PA patient, risks and expectations
- Pre-procedural patient preparation
  - o Anesthesia clearance
  - o Adrenergic hypertensive crisis, strategies for prevention
  - o Considerations for the day of the procedure
- Pertinent intra-procedural techniques and considerations
  - o Patient positioning
  - o Ablation modalities and respective protocols
  - o Accessing adrenal nodules in challenging anatomy
- Post-procedural follow-up and management
  - o Next day visit for serum potassium check, blood pressure measurement, and medication adjustments
  - o Three months follow-up
  - o Management of non-responders or relapsing patients

Printed on: 02/07/23



## Abstract Archives of the RSNA, 2022

IREE-2

### Training of Interventional Radiology Procedures for Medical Students Using Virtual Reality

Sunday, Nov. 27 8:00AM - 9:00AM Room: Learning Center - IR

#### Participants

Yukiko Honda, MD, Kure, Japan (*Presenter*) Nothing to Disclose

#### TEACHING POINTS

The COVID-19 pandemic made it difficult to train medical students on procedures that involve direct patient contact, such as interventional radiology (IR). For this reason, we developed training materials for medical students on endovascular procedures of the abdominal pelvis in IR using virtual reality (VR). Advantages of VR-based IR education include the ability to conduct training at any time, repeated training exercises, no invasiveness to the patients, and no risk of infection to both the patient and the student. The disadvantages are that a large number of funds are needed to purchase or develop VR simulators and that there are few studies that have proven the effectiveness of education using VR. This educational exhibit will provide a brief overview of simulators available for purchase, and our VR-based training software, and discuss its advantages, current issues, and future prospects.

#### TABLE OF CONTENTS/OUTLINE

1 Features of the currently commercially available VR simulators of endovascular procedures A virtual and augmented reality: VIST(Mentice), ANGIO mentor (Simbionix), ORCAMP (Orzone). 2 Assessment of the educational validity of VR simulators. Face validity, content validity, Construct validity, Concurrent validity, Predictive validity. 3 Assessment tools of VR simulators. I Global rating scales: Likert scales etc, II Surveys: A subjective assessment tool, III Pre- and Post-tests: tests before and after the training, IV Time-action analysis, V Error analysis, VI Simulator metrics: metrics preprogrammed into the simulator to measure performance. 4 Review of reports on the educational validity of VR simulators. 5 Future challenges and our approach.

Printed on: 02/07/23



## Abstract Archives of the RSNA, 2022

IREE-20

### Superselective Radioembolization for Hepatocellular Carcinoma: Radiation Segmentectomy and Beyond

Sunday, Nov. 27 8:00AM - 9:00AM Room: Learning Center - IR

#### Participants

Hyo-Cheol Kim, MD, Seoul, Korea, Republic Of (*Presenter*) Nothing to Disclose

#### TEACHING POINTS

Radioembolization is an established treatment for unresectable hepatocellular carcinoma. Radioactive microspheres are preferentially deposited into the hypervascular tumor by siphoning effect so that injection of microspheres are commonly performed at the lobar artery level. However, superselective radioembolization is the best way to improve tumor response and to prevent potential complications. The purpose of this exhibit is : (1) To review the rationale of radiation segmentectomy. (2) To learn when superselective radioembolization is needed, (3) technical tips for superselective radioembolization.

#### TABLE OF CONTENTS/OUTLINE

1) Radiation segmentectomy : rationale and evidence 2) Dosimetry : Practical guide for dosimetry of superselective radioembolization 3) When superselective radioembolization is needed A. small single tumor : radiation segmentectomy B. Large single tumor saddling on both lobes C. Small remnant liver D. Hepatic artery branching at acute angle E. Extrahepatic collateral artery supplying the tumor 4) Technical consideration of superselective radioembolization A. Protection of distal normal liver by using balloon microcatheter and detachable coil B. Combination treatment of lobar and segmental artery C. Combination treatment of 1st and 2nd week dosing of glass microsphere 5) Follow-up imaging after superselective radioembolization A. Early loss of arterial enhancement of the tumor B. Focal radiation necrosis mimicking new hypovascular tumor

Printed on: 02/07/23



## Abstract Archives of the RSNA, 2022

IREE-21

### Mesenteric Arteriovenous Malformations: A Rare Cause of Colonic Ischemia

Sunday, Nov. 27 8:00AM - 9:00AM Room: Learning Center - IR

#### Participants

Lindsey Miley, MD, (*Presenter*) Nothing to Disclose

#### TEACHING POINTS

Learn the diagnostic and interventional imaging characteristics of mesenteric arteriovenous malformations. Review the current literature of mesenteric arteriovenous malformations associated with colonic ischemia. Review a case series of mesenteric arteriovenous malformations from our institution including etiology, diagnostic imaging, interventions, and outcomes. Understand the role of the Interventional Radiologist in diagnosis and treatment of these anomalies.

#### TABLE OF CONTENTS/OUTLINE

1. Define mesenteric arteriovenous malformation • Etiologies and incidence • Clinical versus imaging classification 2. Mesenteric arteriovenous malformations with associated colonic ischemia • Diagnostic imaging work-up • Literature review of treatment and outcomes • Review of case series from our institution 3. Role of the Interventional Radiologist in diagnosis and treatment of mesenteric arteriovenous malformations • Diagnostic angiography • Embolization • Challenges in work-up and treatment • Future directions

Printed on: 02/07/23

## Abstract Archives of the RSNA, 2022

IREE-23

### Minimally Invasive Image-Guided Treatment of Primary, Recurrent and Metastatic Prostate Cancer

Sunday, Nov. 27 8:00AM - 9:00AM Room: Learning Center - IR

#### Participants

Daniel Adamo, MD, Rochester, MN (*Presenter*) Nothing to Disclose

#### TEACHING POINTS

1.) Learn the diagnostic and treatment approach to prostate cancer within the National Comprehensive Cancer Network (NCCN) guidelines 2.) Learn the imaging appearance of native, in-gland recurrent and metastatic prostate cancer at multimodal imaging 3.) Understand the minimally invasive image-guided therapies for treating focal native, locally recurrent, and metastatic prostate cancer.

#### TABLE OF CONTENTS/OUTLINE

1. Diagnostic, staging and treatment approach to prostate cancer within the National Comprehensive Cancer Network (NCCN) guidelines • Prostate cancer epidemiology • Diagnostic and staging evaluation (history, physical exam, laboratory evaluation, imaging, biopsy) • NCCN treatment algorithm 2. Imaging appearance of native, locally recurrent, and metastatic prostate cancer at multimodal imaging with a focus on MRI and PET. • Ultrasound • CT • Bone Scintigraphy • PET (11C-Choline, 68Ga-PSMA, 18F-PSMA, 18F-Fluciclovine) • Dynamic Contrast Enhanced Multiparametric MRI 3. Minimally invasive image-guided therapies for treating focal native, locally recurrent, and metastatic prostate cancer • Focal native and locally recurrent prostate cancer o MRI-guided therapies (Cryoablation, Laser ablation, Focused Ultrasound (FUS)) o US-guided therapies (Cryoablation, Irreversible Electroporation (IRE), High-intensity focused ultrasound (HIFU)) • Focal metastatic prostate cancer o Bone metastases (Cryoablation, External beam radiation therapy (EBRT)) o Lymph node metastases (Cryoablation, External beam radiation therapy (EBRT)) o Hepatic metastases (Ablation, Transarterial Embolization). • Emerging targeted therapies o Theranostics o Radioembolization (90Y-TARE)

Printed on: 02/07/23



## Abstract Archives of the RSNA, 2022

IREE-24HC

### Endoscopic Biliary Interventions Performed by Interventional Radiology and Gastroenterology: A Case Based Review

Sunday, Nov. 27 8:00AM - 9:00AM Room: Learning Center - IR

#### Participants

Tushar Garg, MD, Baltimore, MD (*Presenter*) Conference Travel, Siemens Healthineers

#### TEACHING POINTS

1) To learn about the different endoscopes and ancillary devices available for interventional radiology (IR) and gastroenterology (GI) biliary procedures 2) To learn about the basic and advanced endoscopy techniques 3) To review the endoscopic management of benign and malignant lesions of the biliary tree with the help of cases

#### TABLE OF CONTENTS/OUTLINE

1) Types of devices available a. Endoscopes used in IR: BF-XP160F EVIS Exera video bronchoscope, LithoVue single-use digital flexible ureteroscope, SpyGlass digital catheter, AXIS Single-Use Digital Ureteroscopes b. Endoscopes used in GI: surgical cholangioscope (FCN-15X), Fiberoptic percutaneous cholangioscope (CHF-CB30L/S), SpyGlass direct visualization system c. Accessories used in IR and GI: biopsy forceps, electrohydraulic lithotripsy, laser lithotripsy, retrieval basket, retrieval snare, balloons 2) Basic techniques: a. IR techniques: percutaneous cholangioscopy with manual or pump irrigation b. GI techniques: dual operator mother-daughter per-oral cholangioscopy, single-operator per-oral cholangioscopy, direct per-oral cholangioscopy 3) Clinical applications of IR and GI biliary endoscopy and their outcomes: A case for each application will be shown a. Malignancy: indeterminate biliary stricture, staging of cholangiocarcinoma b. Bile stones treatment c. Primary sclerosing cholangitis diagnosis and treatment d. Selective cannulation of structures like cystic duct, gallbladder, intrahepatic ducts, anastomotic strictures e. Investigational uses Please visit the Learning Center to also view this presentation in hardcopy format.

Printed on: 02/07/23



## Abstract Archives of the RSNA, 2022

IREE-25HC

### Cryoablation for Vascular Malformations

Sunday, Nov. 27 8:00AM - 9:00AM Room: Learning Center - IR

#### Participants

Shin Mei Chan, BS, New Haven, CT (*Presenter*) Nothing to Disclose

#### TEACHING POINTS

Venous malformations (VM), the most common vascular anomaly that may cause significant pain, can be treated with percutaneous sclerotherapy. However, many do not achieve pain-free remission; in select patients, percutaneous cryoablation is an option. However, this is not routinely offered and there is a paucity in the literature describing techniques. Herein we review procedural aspects of cryoablation for VM.

#### TABLE OF CONTENTS/OUTLINE

1. Pre-procedure a. Ultrasound is performed in clinic, in addition to MRI (T2-weighted fat-suppressed and T1-weighted images)2. Procedurea. Under non-contrast CT ± US, a needle access route is selected and skin is marked b. A guiding needle is advanced and position confirmed under CT c. Hydrodissection, whereby a 21-gauge needle is used to instill saline to separate the skin and malformation, can be used for peripheral lesions with < 1 cm of overlying subcutaneous tissue to prevent injury to peripheral structures d. Warm packs applied to surrounding skin may also be used to avoid injury e. Freeze cycles and the number of cryoprobes varies, depending on lesion size and location i. In literature, a common regimen is two ten-minute freeze cycles per cryoprobe ii. When multiple probes are required, they are often placed ~2 cm apart f. Adequate ablation can be considered achieved when the iceball adequately covers the malformation corresponding to symptoms 3. Post-procedure a. Most can be done as an outpatient, with discharge within ~4 hours b. Clinic follow-up at 1 week for wound check, then 6 weeks for US and pain scalePlease visit the Learning Center to also view this presentation in hardcopy format.

Printed on: 02/07/23



## Abstract Archives of the RSNA, 2022

IREE-26

### Pulmonary Arteriovenous Malformation - General Issues and New Topics

Sunday, Nov. 27 8:00AM - 9:00AM Room: Learning Center - IR

#### Participants

Ryo Takeshita, MD, (*Presenter*) Nothing to Disclose

#### TEACHING POINTS

1. If possible, all PAVM lesions should be treated regardless of feeding artery diameter. 2. Embolized distal to last normal pulmonary artery branch results in low recanalization rate. 3. With a cutoff of 55% of preoperative, drainage vein diameter most accurately assess patency after embolization. 4. Diagnosis of Patency by Time-resolved MR Angiography more accurate than CT evaluation. 5. Systemic collateral development after PAVM embolization rarely causes hemoptysis.

#### TABLE OF CONTENTS/OUTLINE

1. Definition and Epidemiology. A: Relationship with Hereditary Hemorrhagic Telangiectasia. B: Mimickers. 2. Life threatening complications of Pulmonary Arteriovenous Malformation. A: Hemoptysis. B: Paradoxical embolism. 3. Diagnosis. A: Classification of Pulmonary Arteriovenous Malformation. B: Treatment indications. 3. Embolization Procedure. A: Venous Access. B: Embolic Agents. 4. Catheter Equipments. 5. Embolization position. 4. Evaluation of patency after Embolization A: CT findings of Drainage Vein Diameter. B: Time-resolved Magnetic Resonance Angiography. 5. Systemic collateral development

Printed on: 02/07/23



## Abstract Archives of the RSNA, 2022

IREE-27

### Review of the Experience of a Reference Hospital in Brazil on the Efficacy and Safety of Radiofrequency Ablation (RFA) of Autonomously Functioning Thyroid Nodules (AFTN)

Sunday, Nov. 27 8:00AM - 9:00AM Room: Learning Center - IR

#### Participants

Leonardo Machado, MD, Sao Paulo, Brazil (*Presenter*) Nothing to Disclose

#### TEACHING POINTS

- To demonstrate our service's experience using the RFA in AFTN treatment.
- To discuss imaging characteristics and distinguishing features of AFTN and post-RAF nodule imaging appearance.
- To demonstrate treatment efficacy and its related factors, as well as to compare characteristics of RFA treatment and complications.

#### TABLE OF CONTENTS/OUTLINE

- Introduction.
- Criteria of patient's election.
- RFA technique and its limitations.
- Post-RFA nodule characteristics and treatment complications.
- Patient's follow-up using CEUS.
- Treatment efficacy and safety.

Printed on: 02/07/23



## Abstract Archives of the RSNA, 2022

IREE-28

### The Iceberg Technique: Bringing Diving Thyroid Nodules to the Surface

Sunday, Nov. 27 8:00AM - 9:00AM Room: Learning Center - IR

#### Participants

Gabriela Merigue, MBBS, MD, (*Presenter*) Nothing to Disclose

#### TEACHING POINTS

The purposes of this exhibit are: Present some cases of a new therapeutic approach to diving thyroid nodules in a minimally invasive way by interventional radiology; To overcome the difficulty of applying the "moving-shot" technique in the mediastinal component; Illustrate this new technique results.

#### TABLE OF CONTENTS/OUTLINE

Thyroid nodules and its symptoms; Indications of radiofrequency thermal ablation; "Iceberg technique" two steps; Challenging nodules to approach; Outcomes after first RTA after second RTA

Printed on: 02/07/23



## Abstract Archives of the RSNA, 2022

IREE-29

### Middle Meningeal Artery Embolization for the Management of Chronic Subdural Hematoma

Sunday, Nov. 27 8:00AM - 9:00AM Room: Learning Center - IR

#### Awards

Identified for RadioGraphics  
Certificate of Merit

#### Participants

Ángela Huete Schmolling, Madrid, Spain (*Presenter*) Nothing to Disclose

#### TEACHING POINTS

- To describe the chronic subdural hematoma physiopathology. - To analyze the medial meningeal artery embolization as a novel and effective treatment modality for the management of chronic subdural hematoma.

#### TABLE OF CONTENTS/OUTLINE

1. Introduction: Incidence, risk factors and physiopathology. 2. Treatment: Surgery vs. medial meningeal artery embolization.3. Protocol (Clinico San Carlos Hospital). 4. Procedure.

Printed on: 02/07/23



## Abstract Archives of the RSNA, 2022

IREE-3

### Stepwise Percutaneous Approach to Treat Severe Benign Hepaticojejunostomy Strictures

Sunday, Nov. 27 8:00AM - 9:00AM Room: Learning Center - IR

#### Participants

Charles Shelton, DO, Cincinnati, OH (*Presenter*) Nothing to Disclose

#### TEACHING POINTS

1. Hepaticojejunostomy anastomosis (HJA) can be complicated by severe strictures or complete obstructions. Interventional radiologists should be aware of etiologies, complications, clinical evaluation, and treatment approaches. 2. Stepwise algorithm for percutaneous treatments of HJA strictures is provided. 3. Percutaneous techniques to treat severe HJA strictures include: a. Conventional antegrade fluoroscopic-guided recanalization b. Direct antegrade visualization with percutaneous cholangioscope and sharp recanalization c. Spyglass cholangioscopy with laser incision of HJA Stricture d. Combined percutaneous trans-jejunal retrograde approach with antegrade approach e. Combined percutaneous and endoscopic rendezvous technique f. Bio-degradable stents for benign strictures 4. Post-procedural complications and clinical outcomes

#### TABLE OF CONTENTS/OUTLINE

1. Epidemiology and etiology of HJA strictures and complete occlusions. 2. Clinical presentation and evaluation 3. Stepwise management algorithm for HJA stricture recanalization: multi-disciplinary approach 4. Review of percutaneous techniques of biliary recanalization along with pictorial examples of percutaneous antegrade approach, combined approach, and recently developed techniques using cholangioscope and laser incision 5. Short- and long- term clinical outcomes of percutaneous treatments, and management of post-procedural complications

Printed on: 02/07/23



## Abstract Archives of the RSNA, 2022

IREE-30

### Radioembolization of Hepatocellular Carcinoma with Extrahepatic Collateral Blood Supply: Anatomic and Technical Considerations

Sunday, Nov. 27 8:00AM - 9:00AM Room: Learning Center - IR

#### Participants

Jin Woo Choi, MD, Seoul, Korea, Republic Of (*Presenter*) Nothing to Disclose

#### TEACHING POINTS

Radioembolization for hepatocellular carcinoma (HCC) has exploded in recent years. HCC typically received its blood supply from the hepatic artery, however, it can recruit a parasitic blood supply from extrahepatic collateral arteries (EHC). Whereas chemoembolization has been performed through EHC without serious complications, little experiences about radioembolization though EHC have been reported. The purpose of this exhibit is: (1) To review the key anatomy of EHC by using cone-beam CT. (2) To review when we suspect the presence of EHC supplying HCC. (3) To learn how to do safe radioembolization through EHC.

#### TABLE OF CONTENTS/OUTLINE

1) List of treated EHC 2) Vascular anatomy of EHC by using cone-beam CT and safe point of each EHC 3) Suggestive findings of EHC on CT/MR and cone-beam CT 4) Special considerations for radioembolization through EHC: dosimetry, embolization of pulmonary shunt, protection of normal vessel, and redistribution by proximal embolization.

Printed on: 02/07/23



## Abstract Archives of the RSNA, 2022

IREE-31

### Updates on Combination TACE and Ablation Therapy for HCC: A Case-Based Review of Technique, Results and Complications

Sunday, Nov. 27 8:00AM - 9:00AM Room: Learning Center - IR

#### Participants

Surbhi Trivedi, MD, (*Presenter*) Nothing to Disclose

#### TEACHING POINTS

1) Review the current literature and treatment pathophysiology regarding combination transarterial chemoembolization (TACE) and radiofrequency ablation (RFA) therapy in unresectable intermediate sized hepatocellular carcinoma. 2) Outline treatment timeline, procedural workflow and TACE-RFA technique. 3) Summarize post-treatment follow-up, patient outcomes and overall survival in our experience. 4) Review alternative forms of combination therapy including TACE and ethanol ablation. 4) Illustrate complications specific to combination therapy and subsequent management. 5) Discuss future directions for combination locoregional therapy in HCC management and emerging role for combination embolization-ablation therapies.

#### TABLE OF CONTENTS/OUTLINE

1) Hepatocellular carcinoma epidemiology and treatment algorithms 2) Combination therapy patient selection and contraindications 3) Literature review of combination therapy, overall survival and patient outcomes 4) Technique, workflow and timeline for combination therapy 5) Case-based illustration of successful combination therapy and post-procedure tumor response 6) Alternative forms of combination therapy including TACE and ethanol ablation 7) Case-based illustration of procedural complications and management 8) Future directions

Printed on: 02/07/23



## Abstract Archives of the RSNA, 2022

IREE-32

### **Building an Interventional Radiology Consult Service: Considerations for Improving Referring Physician Communication and Patient Care**

Sunday, Nov. 27 8:00AM - 9:00AM Room: Learning Center - IR

#### **Participants**

Jacob Conroy, (*Presenter*) Nothing to Disclose

#### **TEACHING POINTS**

1. Understand the impact of referring physician communication on inpatient care related to IR services. 2. Recognize barriers that may limit effective communication with referring physicians. 3. Understand the methods to implement an IR consult service and how this improves communication and patient care.

#### **TABLE OF CONTENTS/OUTLINE**

**LEARNING OBJECTIVES:** To discuss methods for improving inpatient communication with referring physicians and patients concerning IR services. **BACKGROUND:** Limited awareness, understanding, and access to IR procedures continue to be limiting factors in patient care and the growth development for IR practices. Effective communication with referring physicians is essential for combatting these limiting factors. Several barriers exist that prevent effective communication with referring physicians and thus, negatively impact patient care and the continued growth of IR services. Recent strategies to overcome these barriers have focused on the development of IR consult services that are prominent and visible on hospital floors, in clinics, and in electronic medical records. **CLINICAL FINDINGS/PROCEDURE DETAILS:** This exhibit will: 1. Summarize the findings of previous studies on referring physician awareness and utilization of IR services. 2. Discuss the barriers to effective communication with referring physicians. 3. Describe the impact these communication barriers have on patient care and IR practices. 4. Explore methods to develop and execute a successful IR consult service, describing experiences from our institution as well as those from the literature. **CONCLUSION/TEACHING POINTS:**

Printed on: 02/07/23



## Abstract Archives of the RSNA, 2022

IREE-33

### Making Sense of Stents: An Evidence-Based Review of Classes of Arterial Stents

Sunday, Nov. 27 8:00AM - 9:00AM Room: Learning Center - IR

#### Participants

Stephanie Jankovic, MD, (*Presenter*) Nothing to Disclose

#### TEACHING POINTS

-There are several permutations of stents today, including: covered/uncovered; balloon-expandable/self-expanding; drug-eluting/bare metal; and metal/absorbable. These different classes of stents have particular characteristics which make them optimal for various indications in the arteries throughout the body.-Primary, primary-assisted, and secondary patency rates vary amongst the classes of stents in different vascular beds throughout the body.-Appropriate stent choice influences vessel patency, reintervention rate, and resolution of underlying clinical symptoms. An understanding of these factors will allow the interventional radiologist to best treat each patient.

#### TABLE OF CONTENTS/OUTLINE

1. Brief review of history of stents  
2. Classes of stents  
3. Evidence for stent selection is reviewed for the following arteries, highlighting key papers, clinical trials, and device indications for use (IFUs) that guide stent selection, with critique of the quality of evidence:  
--Subclavian/upper extremity  
--Celiac axis  
--Splenic  
--Hepatic - native and transplant  
--Superior mesenteric  
--Renal  
--Iliac  
--Superficial femoral  
--Popliteal (P1, P2, and P3 segments)  
--Tibial  
4. Characteristics underlying patency rates, including indication (e.g., atherosclerosis versus aneurysms), size, trackability, radial force, and fracturing are also discussed.

Printed on: 02/07/23



## Abstract Archives of the RSNA, 2022

IREE-34

### Adrenal Vein Sampling: A Failure Mode Analysis

Sunday, Nov. 27 8:00AM - 9:00AM Room: Learning Center - IR

#### Participants

Praneeth Kalva, Dallas, TX (*Presenter*) Nothing to Disclose

#### TEACHING POINTS

Adrenal vein sampling (AVS) differentiates unilateral from bilateral adrenal disease and plays a pivotal role in deciding surgical vs medical management in patients with a diagnosis of primary hyperaldosteronism (PA). Cannulating the right adrenal vein can be technically challenging with high variability in procedural success rates. Factors contributing to failure of cannulating the right adrenal vein include failure to locate the adrenal vein, misidentification of another vessel as the adrenal vein, and dilution of the sample from accessory vein blood flow. This educational exhibit will cover each of these failure modes. A brief description of the technique with imaging correlates, review of literature and how to identify and overcome the scenarios contributing to the failure with examples will be discussed.

#### TABLE OF CONTENTS/OUTLINE

A. Introduction to AVS B. Typical success rates and non-procedural determinants of success C. Utility of unilateral adrenal vein sampling using a mathematical model for prediction D. Alternate imaging techniques for localization after failed AVS E. Pre-operative planning a. Medications that affect success of AVS: Physiology and Plasma Renin levels b. Pre procedural imaging: What to look for to maximize the success during AVS c. Logistics of specimen processing and analysis d. Required catheters/equipment F. Procedural steps: a. Adrenal vein identification: Anatomical patterns, Role of cone beam CT b. Sampling: End hole vs Side hole catheters, utility of microcatheters c. Complications: Adrenal hematoma contributing to failure of sampling G. Illustrative cases of failed AVS and how these cases are managed in the author's institution H. Conclusion

Printed on: 02/07/23



## Abstract Archives of the RSNA, 2022

IREE-36

### Percutaneous Transjejun Biliary Intervention: A Primer for the Diagnostic and Interventional Radiologist

Sunday, Nov. 27 8:00AM - 9:00AM Room: Learning Center - IR

#### Awards

Certificate of Merit

#### Participants

Ryan Gabos, San Antonio, TX (*Presenter*) Nothing to Disclose

#### TEACHING POINTS

-Review imaging and biliary anatomy of patients selected for percutaneous transjejun biliary intervention (PTJBI).-Discuss common indications and interventions performed via PTJBI.-Review current techniques, maintenance, advantages, and complications of PTJBI.-Review cases of successful and challenging interventions with periprocedural imaging.

#### TABLE OF CONTENTS/OUTLINE

IntroductionHistory of PTJBI, modern practice, and role of IR in biliary management.Postsurgical changes and imaging (CT, MRI) following hepaticojejunostomy or roux-en-y reconstruction.Common and uncommon biliary anatomy.Common indications for PTJBI access with periprocedural imaging.Steps, maintenance, and advantages of PTJBI access.Complications of initial PTJBI procedure.Case PresentationsCholangiocarcinomaLiver transplantCholedochal cyst, s/p hepaticojejunostomyCholecystectomy complications, s/p hepaticojejunostomyConclusionClinical ImplicationsPTJBI is a proven method to manage biliary disease in patients with surgically altered small bowel anatomy. In patients requiring repeat intervention or those with diffuse biliary disease, retrograde biliary access via PTJBI represents an attractive and underutilized resource.

Printed on: 02/07/23



## Abstract Archives of the RSNA, 2022

IREE-37HC

### Spinal Dural and Extradural Arteriovenous Fistulas: Imaging Features and Endovascular Treatments

Sunday, Nov. 27 8:00AM - 9:00AM Room: Learning Center - IR

#### Participants

Hiro Kiyosue, MD, (*Presenter*) Research Grant, Koninklijke Philips NV

#### TEACHING POINTS

Despite of recent developments in technology of imaging and endovascular treatments, some cases are often incorrectly diagnosed or inadequately treated even now. In this presentation, we demonstrate imaging features and endovascular treatments of spinal dural AVFs and various types of extradural AVFs with illustrative case presentation. 1. Spinal dural AVFs are usually located in the dorsal spinal dura matter at lower thoracic spine, which are fed by small dural feeders from the radiculomeningeal artery or the prelaminar artery and drain into a bridging vein. Typical case shows horizontal T sign on frontal view of spinal angiography. 2. Spinal epidural AVFs are the most common type in extradural AVFs, which are frequently located in the ventral epidural space at lumbar spine. They are fed by multiple epidural feeders from the somatic branches and drains into an epidural venous pouch to a radiculomedullary vein and/or paravertebral veins. 3. Mixed AVFs is the second common type of extradural AVFs, which involve multiple spaces of osseous, epidural, and paravertebral spaces and often associated with spinal arteriovenous metamerism syndrome.

#### TABLE OF CONTENTS/OUTLINE

1. Spinal dural AVFs: Clinical features, Imaging features, Transarterial embolization 2. Spinal extradural AVFs: Classification 2-1 Epidural AVFs: Clinical features, Imaging features, Transarterial and transvenous embolization 2-2 Osseous AVFs: Clinical features, Imaging features, Transarterial and transvenous embolization, and direct puncture embolization 2-3 Paravertebral AVFs: Clinical features, Imaging features, Endovascular techniques 2-4 Mixed AVFs: Clinical features, Imaging features, Endovascular techniques Please visit the Learning Center to also view this presentation in hardcopy format.

Printed on: 02/07/23



## Abstract Archives of the RSNA, 2022

IREE-38

### Irreversible Electroporation in Locally Advanced Pancreatic Cancer

Sunday, Nov. 27 8:00AM - 9:00AM Room: Learning Center - IR

#### Awards

Certificate of Merit

#### Participants

Kenneth Huynh, BS, Orange, CA (*Presenter*) Nothing to Disclose

#### TEACHING POINTS

1. To provide an overview of the role and literature of percutaneous irreversible electroporation (IRE) in locally advanced pancreatic cancer (LAPC) including a review of ongoing trials. 2. To present, through case-based review, the techniques utilized in percutaneous IRE to safely target pancreatic lesions. 3. To illustrate the multi-modality imaging fusion and navigation for IRE of LAPC, with emphasis on intra-procedural cone-beam computed tomography (CBCT).

#### TABLE OF CONTENTS/OUTLINE

Locally advanced pancreatic cancer (LAPC) is considered unresectable due to tumoral encasement of the superior mesenteric or celiac arteries or non-reconstructable venous involvement. Percutaneous irreversible electroporation (IRE) in LAPC has shown promising outcomes with respect to median overall survival, especially when combined with chemotherapy. IRE provides non-thermal ablation of LAPC while mitigating risk of thermal injury to nearby structures compared to thermal techniques. Given the location of the pancreas and proximity to nearby structures, safe percutaneous targeting may be difficult with high risk of complication. This educational exhibit will: (1) provide an overview of the role and literature of percutaneous IRE in LAPC including ongoing trials, (2) present different procedural techniques used to safely target pancreatic lesions and minimize complications. Techniques including electrode steering, gantry tilting, bolus chasing, and CT arteriography will be discussed, and (3) illustrate the multi-modality imaging fusion and navigation for IRE of LAPC with emphasis on intra-procedural CBCT.

Printed on: 02/07/23



## Abstract Archives of the RSNA, 2022

IREE-39

### Priapism: Types and Interventional Treatment

Sunday, Nov. 27 8:00AM - 9:00AM Room: Learning Center - IR

#### Participants

Benjamin Reichardt, Hattingen, Germany (*Presenter*) Nothing to Disclose

#### TEACHING POINTS

Priapism is defined as a sustained tumescence or erection lasting more than 6 hours. The erection is limited to the erectile tissue without affecting the corpus spongiosum. There are two different types of priapism: 1. Low flow (ischemic / venous occlusive) 2. High flow (non-ischemic or arterial): Does not require emergency treatment. Genitoperitoneal trauma is the most common etiology. The trauma results in a rupture in the cavernous artery with subsequent development of a high flow fistula or a pseudoaneurysm. Interventional Therapeutic options: 1. Autologous blood clot 2. Gel foam 3. Polyvinyl alcohol (PVA) 4. Spherical Particles 5. Micro-spirals 6. Alcohol - lipiodol mixture 7. N-butyl cyanoacrylate (NBCA)

#### TABLE OF CONTENTS/OUTLINE

The success rates are up to 89%. Sexual function may be impaired after embolization, although potency is fully restored in about 80% of cases. With decongestion and potency rates of 100% and 86-91%; superior to surgery. Relapse: rates vary between 7% and 27%, regardless of the type of embolotherapy. Erectile dysfunction: occurs in around 39% of the time with the use of permanent embolic agents and in only 5% with the use of temporary embolic agents. Conclusion: Superselective embolization is the gold standard in the treatment of HFP because of its safety and efficacy profile. The type of embolic agent does not appear to be a major factor influencing treatment outcomes in terms of recurrence of priapism or deterioration in erectile quality. The embolic product should be tailored to each patient and the procedures should be performed by well trained and experienced operators, who should know his embolic materials.

Printed on: 02/07/23



## Abstract Archives of the RSNA, 2022

IREE-4

### Finding the Adenoma in Cushing's Disease: Bilateral Inferior Petrosal Sinus Sampling and Pituitary MRI

Sunday, Nov. 27 8:00AM - 9:00AM Room: Learning Center - IR

#### Participants

Celia Alonso, MD, Madrid, Spain (*Presenter*) Nothing to Disclose

#### TEACHING POINTS

The objective of this educational exhibit is to emphasize the role of bilateral inferior petrosal sinus sampling (BIPSS) in the diagnosis of Cushing's disease. After reading it, you will:- Learn the pathophysiology underlying Cushing's syndrome. Differentiation between ACTH-dependent and ACTH-independent hypercortisolism.- Comprehend the relevance of radiological techniques identifying the etiology of hypercortisolism, focusing on the diagnosis of ACTH-secreting pituitary microadenomas.- Deepen the knowledge about BIPSS indications, technique, safety and possible complications.

#### TABLE OF CONTENTS/OUTLINE

- Introduction.- Cushing's syndrome diagnostic algorithm: clinical, biochemical and radiological analyses. BIPSS as the gold standard test in Cushing's disease and comparison with pituitary MRI. Experience in our institution, a tertiary care center, in the last sixteen years.- BIPSS technique and rationale. Indications, relevant venous anatomy and variants, technical considerations and possible complications.- Conclusion.

Printed on: 02/07/23

## Abstract Archives of the RSNA, 2022

IREE-40

### Magnetic Resonance Lymphangiography (MRL): Past, Present, and Future Directions

Sunday, Nov. 27 8:00AM - 9:00AM Room: Learning Center - IR

#### Awards

Identified for RadioGraphics

#### Participants

Ahmed Negm, MBBCh, (*Presenter*) Nothing to Disclose

#### TEACHING POINTS

Learn the lymphatic system anatomy and the historical development of MRL. Review the MRI sequences and techniques currently used for transpedal and intranodal MRL. Understand current indications and applications of MRL including diagnosis and treatment of lymphatic disorders.

#### TABLE OF CONTENTS/OUTLINE

1. Lymphatic system anatomy and Historical development of MRL • Embryological development of peripheral and central lymphatic system • Location and territorial drainage of central, hepatic, and mesenteric lymphatics • Other methods of lymphatic imaging (Lymphoscintigraphy, Fluoroscopic lymphangiography, Fluorescence lymphography) • Historical development of MRL 2. MRI sequences and techniques currently used in MRL • Intranodal Dynamic contrast-enhanced MRL (DCE-MRL) • Interstitial transpedal MRL (tMRL) • Intra-hepatic DCE-MRL (IH-DCE-MRL) • Retrograde thoracic duct dynamic contrast-enhanced MRL • Utility of T2W MR Sequences • Procedural aspects (Saline, Contrast, Needles, Catheters, Scanner, Anesthesia, ±Ultrasound) 3. Indications and applications of MRL • DCE-MRL o Evaluation of lymphatic flow (Pulmonary lymphatic perfusion syndrome, Plastic bronchitis, Protein-losing enteropathy, Chylothorax, Chylous ascites, Leaks, Edema) o Lymphatic malformations o Identification of aberrant lymphatic vessels for embolization o Localization (Sentinel lymph nodes, Leaks, Pre-operative planning) • tMRL o Alternative to DCE-MRL (Simple, Fast, No ultrasound) o Diagnosis pre-treatment plan o Localization (Peripheral or Central lymphatic leakage) • IH-DCE-MRL o Diagnosis (Protein-losing enteropathy, Chylous ascites, Contrast leakage to peritoneum/duodenum) • Limitations of DCE-MRL tMRL

Printed on: 02/07/23



## Abstract Archives of the RSNA, 2022

IREE-41

### Hydro, Pneumo, and Balloon-assisted Separation of Critical Structures in Ablation Procedures

Sunday, Nov. 27 8:00AM - 9:00AM Room: Learning Center - IR

#### Participants

Mohamed Ibrahim, MBCh, Rochester, MN (*Presenter*) Nothing to Disclose

#### TEACHING POINTS

- Learn the role and limitation of hydro-dissection in the separation of critical structure during image-guided ablation procedures
- Learn the role and limitation of pneumo-dissection in the separation of critical structure during image-guided ablation procedures
- Learn the role and limitation of balloon-assisted separation of the critical structure during image-guided ablation procedures

#### TABLE OF CONTENTS/OUTLINE

- Role and limitation of hydro-dissection of critical structures
  - o Appropriate clinical scenarios for hydro-dissection
  - o Limitations of hydro-dissection and how to manage them; avoiding streak artifact and fluid redistribution
- Role and limitation of pneumo-dissection of critical structures
  - o Appropriate clinical scenarios for pneumo-dissection
  - o Limitations of pneumo-dissection and how to manage them; gas absorption and redistribution
- Role and limitation of balloon-assisted separation of critical structures
  - o Appropriate clinical scenarios for balloon-assisted separation
  - o Limitations of balloon-assisted separation and how to manage them; placement of multiple balloons

Printed on: 02/07/23



## Abstract Archives of the RSNA, 2022

IREE-42

### Principles of Tissue Sampling, Handling, and Processing: A Primer for Procedural Radiologists

Sunday, Nov. 27 8:00AM - 9:00AM Room: Learning Center - IR

#### Participants

Majid Chalian, MD, Seattle, WA (*Presenter*) Grant, The Boeing Company

#### TEACHING POINTS

1) Provide a broad overview of pathology to demystify subdivisions and associated protocols and procedures 2) Discuss best practices for tissue sampling and handling, based on organ system (including thyroid, breast, lung, liver, kidney, bone, and musculoskeletal soft tissue) 3) Familiarize with different sample media, their functions, and indications 4) Learn about common histopathology artifacts and mitigation strategies 5) Learn how to implement clinical and imaging findings to sample adequately and handle tissue appropriately

#### TABLE OF CONTENTS/OUTLINE

Introduction? Significance of collaboration between radiology and pathology departments and impact on patient care? Pathology subdivisions? Anatomic pathology? Clinical pathology (AKA "laboratory medicine") Anatomic pathology workflow ? Pre-analytical steps ? Gross examination and description? Tissue processing ? Tissue staining? Final diagnosis and pathology report Best practices for specimen sampling ? Small lesions? Metastases? Location dependent ? Thyroid? Breast? Lung? Liver? Kidney? Bone? Musculoskeletal soft tissue? Uncertain cases that may benefit from pathology's consultation/presence before and/or during the procedure Best practices for specimen handling/processing? Formalin? Saline/RPMI? EM fixative (glutaraldehyde)? Decalcifying agents? RDO (dilute hydrochloric acid) ? EDTA? Fresh tissue ? How the differential impacts handling/processing Common Artifacts and Mitigation Techniques ? Fixation ? Crush ? Cautery? Air Dry Core Needle Biopsy vs FNA ? Specimen processing basics ? Advantages of each? Disadvantages of each Tips to use clinical and imaging findings for proper tissue sampling and handling

Printed on: 02/07/23



## Abstract Archives of the RSNA, 2022

IREE-43

### Interventional Pain Management in Extraplinal Osseous Metastases

Sunday, Nov. 27 8:00AM - 9:00AM Room: Learning Center - IR

#### Awards

Certificate of Merit

#### Participants

Kenneth Huynh, BS, Orange, CA (*Presenter*) Nothing to Disclose

#### TEACHING POINTS

1. To review the indications and procedural considerations for percutaneous management of extrapinal osseous metastases. 2. To review cases of interventional pain management of extrapinal osseous metastases including embolization, thermal ablation, and bone stabilization.

#### TABLE OF CONTENTS/OUTLINE

Extraplinal bone metastases can cause significant morbidity to many patients due to localized pain, referred pain, impaired mobility, and pathological fractures. This commonly leads to long-term narcotic use, prolonged bedrest, and poor quality of life.

Percutaneous interventions have been shown to provide sustained palliative relief of pain associated with metastatic osseous disease, in addition to improving mobility and quality of life. A multi-disciplinary approach to oncologic pain associated with bony lesions including interventional radiology can improve patient's pain and quality of life. This educational exhibit will: (1) review the indications and procedural considerations for percutaneous management of extrapinal osseous metastases with palliative intent, and (2) present different procedural techniques used in pain palliation and bone stabilization. Techniques include embolization for hypervascular metastatic lesions, radiofrequency ablation, microwave ablation, cryoablation, and cementoplasty. An overview on these techniques and possible procedural complications with measures for prevention and management will also be discussed.

Printed on: 02/07/23



## Abstract Archives of the RSNA, 2022

IREE-44

### Interventional Approach to the Cancer Pain Patient: A Case-Based Review

Sunday, Nov. 27 8:00AM - 9:00AM Room: Learning Center - IR

#### Awards

Cum Laude

#### Participants

Omar Ali, BS, (*Presenter*) Nothing to Disclose

#### TEACHING POINTS

Chronic pain is a common concern among patients with cancer, resulting in frequent utilization of emergency room visits and hospitalizations. Pharmacotherapy is a widely used approach for cancer pain relief, although long-term opioid use is often inadequate in treating cancer pain and has a significant side effect profile. Interventions for cancer pain offer unique solutions to improve quality of life and provide more effective long-term pain relief. The purpose of this exhibit is to provide a case-based approach to interventional radiology's role in the management of cancer pain.

#### TABLE OF CONTENTS/OUTLINE

1) Introduction to cancer pain a) Nociceptive pain b) Neuropathic pain 2) Decision-making algorithm for cancer pain interventions a) Correlation of pain to imaging b) Source and location of cancer pain i) Nerve-related pain ii) Bone pain (spinal pain, non-spinal pain, and presence of fracture in the setting of bone pain) c) Available non-IR treatment options d) Available IR treatment options 3) Cancer pain intervention cases: clinical history, imaging, decision-making, intervention a) Celiac plexus neurolysis b) Intercostal cryoneurolysis c) Vertebral augmentation for pathologic compression fractures d) Thermal ablation for painful bone metastasis e) Percutaneous screw fixation for pelvic metastasis f) Palliative embolization of bone metastasis

Printed on: 02/07/23



## Abstract Archives of the RSNA, 2022

IREE-45

### Insulinoma: Role of the Interventional Radiologist

Sunday, Nov. 27 8:00AM - 9:00AM Room: Learning Center - IR

#### Participants

Ali Abbas Saifuddin, MD, (*Presenter*) Nothing to Disclose

#### TEACHING POINTS

Radiologically occult insulinomas should be assessed with selective arterial calcium stimulation test (SACST) with hepatic venous sampling prior to surgical treatment.

#### TABLE OF CONTENTS/OUTLINE

Insulinomas typically present with Whipple's triad which is composed of hypoglycemia, low fasting plasma glucose, and alleviation of symptoms by glucose administration. Factitious hypoglycemia (i.e., exogenous insulin administration) must be excluded to make a diagnosis of insulinoma, and this is accomplished by a supervised 72-hour (or 48-hour) fast. Localization of tumor can be accomplished using transabdominal ultrasound (TUS), triple phase CT, gadolinium enhanced MR abdomen, gallium-68 dotatate PET/CT, Octreoscan, or a combination of these tests. If non-invasive modalities cannot localize the tumor, then invasive tests, such as SACST with hepatic venous sampling or endoscopic ultrasound (EUS), can be utilized. SACST involves injecting calcium solution at a dose of 0.0125 mmol Ca<sup>2+</sup>/kg (0.005 mmol Ca<sup>2+</sup>/kg for obese patients) into the superior mesenteric, proximal splenic, mid-splenic, gastroduodenal, and proper hepatic arteries. 5 mL right hepatic venous samples at 0, 20, 40, and 60 seconds are obtained after calcium solution injection in each artery. Diagnostic criterion for a positive response is an insulin response 2x of baseline. Positive response when injecting the gastroduodenal artery or the superior mesenteric artery localizes to the pancreatic head or neck. Positive response when injecting the splenic artery localizes to the pancreatic body or tail. Positive response when injecting the proper hepatic artery suggests liver metastases. Localization is critical prior to surgical treatment.

Printed on: 02/07/23



## Abstract Archives of the RSNA, 2022

IREE-46

### Introducing Pre-Clinical Medical Students to IR - Medical Student IR Symposia 2.0

Sunday, Nov. 27 8:00AM - 9:00AM Room: Learning Center - IR

#### Participants

Robert Weinstein, Baltimore, MD (*Presenter*) Nothing to Disclose

#### TEACHING POINTS

To review the importance of introducing IR to pre-clinical medical students. To learn about the different methods by which pre-clinical medical students are introduced to IR. To recognize that the traditional medical student IR symposium relying solely on didactic lectures is being replaced by a new IR symposium consisting of interactive and hands-on exercises and simulation sessions. To review the available literature regarding the use of new IR symposia consisting of interactive and hands-on simulation sessions.

#### TABLE OF CONTENTS/OUTLINE

Why is introducing IR into pre-clinical medical training important? The new integrated IR residency. IR Residency Match competitiveness. The evolution of medical student symposia. Traditional didactic lecture-based symposia. Interactive and hands-on symposia. Target audience. Factors effecting participation in medical student symposia. Choosing the right format. In-person vs. virtual formats. Didactic vs. interactive/hands-on vs. mix. Choosing the appropriate faculty. Involving trainees/medical students. Data Collection. The importance of pre- and post-symposia surveys. Polling questions during the event Performance during simulations. Feedback allows for improvements Future directions. Simulation and clinical IR bootcamps. The role of national meetings

Printed on: 02/07/23



## Abstract Archives of the RSNA, 2022

IREE-47

### Fistula Fix: Maturation, Maintenance, and De-Clots

Sunday, Nov. 27 8:00AM - 9:00AM Room: Learning Center - IR

#### Awards

Identified for RadioGraphics  
Cum Laude

#### Participants

Anne Sailer, MD, New Haven, CT (*Presenter*) Nothing to Disclose

#### TEACHING POINTS

1. Discuss epidemiology, cases, and clinical presentations of hemodialysis (HD) access failure requiring intervention and literature based treatment interventions. 2. Review role of imaging in the diagnosis of hemodialysis access malfunction/failure. 3. Briefly review characteristic area of stenosis/failure based on HD access anatomy. 4. Review main interventional therapies for management of HD access with emphasis on angioplasty, stent placement and DeClot interventions.

#### TABLE OF CONTENTS/OUTLINE

1. Ultrasound and conventional angiogram evaluation and function and HD access maturity (rules of sixes), including common artifacts and pitfalls and advanced ultrasound techniques. 2. Overview of the anatomy and physiology of characteristic HD areas of stenosis. 3. Overview of the current literature of HD access failure treatment: drug-coated vs non-drug-coated balloons, covered vs bare-metal stents, etc. 4. Case-based review of various endovascular techniques in management of fistula malfunction including: failure to mature, outflow stenosis treatment (characteristic HD access areas of stenosis such as the swing-point in BVT fistulas, cephalic arch stenosis, etc.), DeClot (traditional vs IJ access), coil embolization of accessory veins to aid in maturation, anastomotic narrowing, and intraprocedural complications.

Printed on: 02/07/23



## Abstract Archives of the RSNA, 2022

IREE-48

### Various Approaches to the Portal Venous System

Sunday, Nov. 27 8:00AM - 9:00AM Room: Learning Center - IR

#### Awards

Certificate of Merit

#### Participants

Yoshitaka Tamura, Kumamoto, Japan (*Presenter*) Nothing to Disclose

#### TEACHING POINTS

Portal venous (PV) interventions including transjugular intrahepatic portosystemic shunt (TIPS), antegrade transportal obliteration (ATO), PV stenting, PV embolization (PVE), and islet transplantation have developed for a few decades. Approach to the PV system is an essential step in PV intervention. Various approaches are described. Transjugular approach is usually as a part of TIPS procedure. Puncture from the proximal portion of the right hepatic vein to the right PV is often done under fluoroscopy. Intravascular ultrasonographic guidance can facilitate the safety. Transhepatic approach is a classical approach for various interventions. It has potential risks of bleeding and transpleural puncture. Transsplenic approach is useful for cases with PV/splenic vein occlusion. Tract embolization is important because of higher risk of bleeding from puncture site. Transumbilical venous and portosystemic collateral approaches are the safest approaches. Catheterization through the tortuous way is required. Surgical approaches (transiliocolic venous approach and round ligament approach) are reliable for catheterization. They provide good controllability of devices, and effective for selected cases.

#### TABLE OF CONTENTS/OUTLINE

1 Basics of PV interventions (TIPS, ATO, stenting, PVE and islet transplantation) 2 Transjugular approach 3 Transhepatic approach 4 Transsplenic approach 5 Transumbilical venous and portosystemic collateral approach 6 Surgical approach (Transiliocolic venous approach and round ligament approach)

Printed on: 02/07/23



## Abstract Archives of the RSNA, 2022

IREE-49

### Percutaneous Management of Post-Liver Transplant Complications

Sunday, Nov. 27 8:00AM - 9:00AM Room: Learning Center - IR

#### Participants

Ahsun Riaz, MD, Chicago, IL (*Presenter*) Consultant, Boston Scientific Corporation

#### TEACHING POINTS

1. Describe the complications of liver transplant (LT)  
2. Diagnosis of post-LT complications using various imaging modalities  
3. Highlight the techniques employed by interventional radiologists to manage post-transplant complications

#### TABLE OF CONTENTS/OUTLINE

Introduction  
1. Types of liver transplants and various anastomoses  
2. Normal imaging after transplant  
3. Pathophysiology of complications  
Clinical Presentation, Risk Factors and Diagnostic Imaging  
Complications and Their Management by IR  
1. Vascular complications  
a) Transplant hepatic artery stenosis/thrombosis- Angioplasty/stenting/catheter-directed thrombolysis  
b) Arterial dissection/aneurysm/pseudoaneurysm and arterioportal fistulas- Coiling/stent grafting/stenting  
c) Splenic steal syndrome/"small-for-size" syndrome- Splenic artery embolization via coils/vascular plugs  
d) Transplant portal vein stenosis/thrombosis- Venoplasty/stenting  
e) Transplant hepatic vein stenosis- Venoplasty/stenting  
f) Inferior vena cava complications- Venoplasty/stenting  
2. Biliary Complications  
a) Biliary stricture- Percutaneous transhepatic/transjejunal cholangioplasty/stenting- Role of endoscopy  
b) Biliary leak/biloma- Percutaneous drainage- Embolization of leaking duct  
c) Stones/casts/debris

Printed on: 02/07/23



## Abstract Archives of the RSNA, 2022

IREE-50

### Intraoperative Nerve Monitoring to Prevent Nerve Damage on Image-Guided Percutaneous Tumor Ablation

Sunday, Nov. 27 8:00AM - 9:00AM Room: Learning Center - IR

#### Participants

Robert Weinstein, Baltimore, MD (*Presenter*) Nothing to Disclose

#### TEACHING POINTS

To describe the use of intraoperative nerve monitoring as a tool to prevent iatrogenic peripheral nerve injury during percutaneous thermal and cryo-ablation of tumors. Percutaneous ablation is a potentially curative minimally invasive treatment option for patients. Intraoperative Nerve Monitoring (IONM) is a group of electrophysiological modalities that can provide intraoperative assessment of neural structures to prevent iatrogenic nerve injury. IONM been shown to be valuable in reducing nerve injury during percutaneous thermal and cryo-ablation of tumors.

#### TABLE OF CONTENTS/OUTLINE

Percutaneous tumor ablation has become a popular tool for tumor treatment due to its minimally invasive approach and low risk profile. However, it has the potential to damage both sensory and motor nerves. Neurophysiologists can use several modalities to stimulate and measure responsiveness of at-risk neural pathways. IONM includes somatosensory evoked potentials (SSEPs) and motor nerve conduction studies (MNCSs). SSEPs monitor sensory pathways and MNCSs monitor peripheral motor nerve integrity. The interventional radiologist can be guided to avoid further ablation in each region as signal changes occur, which can limit long-term nerve damage. Regional anatomy of relevant nerves in the operational area is also key. Radiofrequency can produce interference which inhibits monitoring of neurotronic activity, and as such must be paused to record IONM signals. Cryoablation does not produce artifacts and as such real time monitoring is possible. Studies have shown the risk of major motor injury is significantly increased with persistent motor evoked potential change compared to transient or no motor evoked potential change.

Printed on: 02/07/23



## Abstract Archives of the RSNA, 2022

IREE-51HC

### Arterio-Biliary Fistula as a Rare Cause of Upper Gastrointestinal Bleed: Diagnostic and Procedural Considerations

Sunday, Nov. 27 8:00AM - 9:00AM Room: Learning Center - IR

#### Participants

Mark Edelstein, MD, Bala Cynwyd, PA (*Presenter*) Nothing to Disclose

#### TEACHING POINTS

1. Arterio-biliary fistula is a rare cause of upper gastrointestinal bleeding.2. The most common clinical presentation of an arterio-biliary fistula is hemobilia, which refers to bleeding into the biliary tree.3. In the majority of cases, arterio-biliary fistulas are iatrogenic in etiology, such as occurring after transhepatic biliary interventions or transarterial chemoembolization.4. There is a scarcity of existing literature describing spontaneous arterio-biliary fistula in the absence of prior relevant intervention. In the absence of such procedural history, the possibility of a communication between the arterial and biliary systems may not be on a clinician's diagnostic radar when responding to a patient with active gastrointestinal bleeding.

#### TABLE OF CONTENTS/OUTLINE

1. Introduction to arterio-biliary fistula as a cause of upper gastrointestinal bleeding.2. Multimodality image-rich review of multiple cases of arterio-biliary fistula of both iatrogenic and spontaneous etiology.3. Angiographic demonstration of arterio-biliary fistula and unique considerations for the managing interventional radiologist.4. Conclusion.Please visit the Learning Center to also view this presentation in hardcopy format.

Printed on: 02/07/23



## Abstract Archives of the RSNA, 2022

IREE-52

### A Practical Guide to RF Ablation for Treating Locoregional Recurrence of Well-Differentiated Thyroid Cancer

Sunday, Nov. 27 8:00AM - 9:00AM Room: Learning Center - IR

#### Participants

Eun Ju Ha, MD, Suwon, Korea, Republic Of (*Presenter*) Nothing to Disclose

#### TEACHING POINTS

While the mortality rate for well-differentiated thyroid cancer tends to be favorable, the risk of recurrent papillary thyroid cancer can range from 20 - 59% depending on patient and tumor risk factors. Various thermal ablative techniques (RFA, LA or MA) and chemical ablative approaches (ethanol ablation) can be used as an alternative method in patients deemed to be at high surgical risk, those in whom the surgeon deems non-operable or for those refusing to undergo repeat surgery. In this educational exhibit, we would like to 1) provide updated evidences of RFA for recurrent thyroid cancers and to 2) describe practical tips regarding indication, pre-procedural evaluation, techniques, post-procedural evaluation and complications.

#### TABLE OF CONTENTS/OUTLINE

1. A systematic review of the current evidences 2. Practical tips for RFA to treat recurrent thyroid cancers 2-1) How to select patients - curative vs. palliative management strategies 2-2) Pre-procedural checklist before RFA - US, CT, and laboratory tests 2-3) Standard techniques - approach route based on the tumor location, hydro-dissection technique, moving-shot/fixed-electrode technique 2-4) Post-procedural checklist after RFA- US, CT, and laboratory tests 2-5) How to prevent complications- US-based nerve anatomy, cold 5% dextrose injection, medication

Printed on: 02/07/23



## Abstract Archives of the RSNA, 2022

IREE-53HC

### Applicability of Irreversible Electroporation for Therapeutic Management of Pancreatic Adenocarcinoma

Sunday, Nov. 27 8:00AM - 9:00AM Room: Learning Center - IR

#### Participants

Raquel Moreno, MD, New York, NY (*Presenter*) Nothing to Disclose

#### TEACHING POINTS

Review fundamental concepts about pancreatic ductal adenocarcinoma (PDAC), including relevant vascular anatomy in axial image; disease staging and therapeutic management according to each stage. Introduce the participant to the fundamentals of Irreversible Electroporation (IRE) ablation therapy, including its eligibility criteria and contraindications. Present a pictorial essay to illustrate IRE indications based on imaging criteria of key anatomic structures involvement - arteries, veins and miscellaneous - highlighting teaching points in each case. Summarize the role of the IRE in the Therapeutic Management of the PDAC through a Flowchart.

#### TABLE OF CONTENTS/OUTLINE

- Introduction: PDAC- Relevant Anatomy- Irreversible Electroporation (IRE): Fundamentals- Irreversible Electroporation (IRE): Applications- Imaging Criteria: Arterial Involvement- Imaging Criteria: Venous Involvement- Imaging Criteria: Non-vascular Involvement- Final Considerations Please visit the Learning Center to also view this presentation in hardcopy format.

Printed on: 02/07/23



## Abstract Archives of the RSNA, 2022

IREE-54HC

### Development of a New Drug-eluting Stent for Peripheral Arterial Diseases by General Radiologists: What You Need to Know Before You Start

Sunday, Nov. 27 8:00AM - 9:00AM Room: Learning Center - IR

#### Participants

Shunsuke Kamei, MD, Hachioji, Japan (*Presenter*) Nothing to Disclose

#### TEACHING POINTS

What do you need to know to develop a new stent? The first author, a general radiologist with no specific background, has played a central role in developing a stent platform for below-the-knee (BTK) atherosclerotic diseases. Based on this experience, we will explain the tangible and intangible methods how to develop a new stent system in general practice.

#### TABLE OF CONTENTS/OUTLINE

1. Arteriosclerosis in BTK lesions is a severe disease, and the treatment is still underdeveloped. Therefore, we are developing a new drug-eluting stent for BTK. 2. The first step in stent fabrication is to draw stent design using 3-dimensional Computer-Aided Design (CAD) software. 3. Self-expanding stents are manufactured through laser cutting, diameter expansion, annealing, and electropolishing. The prototype is intended to improve the design through mechanical evaluation. However, since prototyping takes a long time, effective simulation (Finite element analysis using Abaqus® ) can shorten the development period. 4. The stent is completed by applying our original technology, hybrid nano-coating (anti-thrombogenic base-coating with drug-eluting polymer), on the newly developed stent platform. We have evaluated the ability of the device to withstand a 10-year equivalent fatigue life due to the cyclic pulsation from blood flow. 5. In animal studies on the requirements of FDA's Good Laboratory Practices (GLP) regulations, we should confirm stent coverage by the vascular endothelium, drug-release profiles, and good stent patency rate at six months after implantation. After approval by FDA, a pivotal clinical trial can be started in humans using a newly developed stent system. Please visit the Learning Center to also view this presentation in hardcopy format.

Printed on: 02/07/23



## Abstract Archives of the RSNA, 2022

IREE-55

### Interventional Radiology and Childbirth: From Conception through Delivery and Beyond

Sunday, Nov. 27 8:00AM - 9:00AM Room: Learning Center - IR

#### Awards

Identified for RadioGraphics

#### Participants

Joseph Moirano, BS, Massapequa, NY (*Presenter*) Nothing to Disclose

#### TEACHING POINTS

1. To review radiation exposure risk at different points in pregnancy and assess how to decrease exposure risk during IR procedures  
2. To discuss the role of IR in promoting male and female fertility  
3. To highlight the various procedures that interventionalists perform during the antepartum and postpartum period.

#### TABLE OF CONTENTS/OUTLINE

1. Pregnancy and Radiation Exposure  
a. Radiation Effects on Fetal Development  
b. Ways to Minimize Fetal Exposure Risk  
2. Procedures to Promote Fertility  
a. Male Infertility Treatments (Varicocele Embolization)  
b. Female Infertility Treatments (Fallopian Tube Recanalization, Uterine Artery Embolization (for fibroids), and Management of Complications of Ovarian Hyperstimulation Syndrome)  
3. Procedures in the Pregnant Patient  
a. Venous Access (Midline and Peripherally Inserted Central Catheter, Dialysis Access, Medi-port)  
b. Genitourinary Interventions (Percutaneous Nephrostomy Tube/Nephroureterostomy Tube, Ureteral Stent Placement)  
c. Biliary Interventions (Cholecystostomy Tube, Percutaneous Biliary Drainage Catheter Placement)  
d. Venous Thromboembolism Interventions (IVC Filter Placement, Venous/Pulmonary Artery Thrombectomy)  
e. Ectopic Pregnancy Management  
f. Ovarian Cyst Aspiration  
g. Trauma Interventions (Arterial Embolization)  
4. Procedures in the Peri/Postpartum Period  
a. Invasive Placenta Spectrum Management (Pre-operative Balloon Occlusion)  
b. Postpartum Hemorrhage after Vaginal Delivery (Prophylactic Uterine/Internal Iliac Artery Embolization, Retained POC, Uterine AVM)  
c. Post-Cesarean Section Procedures (Abscess Drainage, Embolization of Surgically Injured Vessel, Urinary Diversion after Ureteral Injury)

Printed on: 02/07/23



## Abstract Archives of the RSNA, 2022

IREE-56

### Magnetic Resonance Guided Focused Ultrasound (MRgFUS) for Treatment of Uterine Fibroids: Patient Selection, Contraindications and Operative Execution

Sunday, Nov. 27 8:00AM - 9:00AM Room: Learning Center - IR

#### Participants

Monica Mattone, MD, Roma, Italy (*Presenter*) Nothing to Disclose

#### TEACHING POINTS

Different treatments have been proposed for uterine fibroids. Magnetic Resonance Focused Ultrasound (MRgFUS) has been proposed in the last years as a new non invasive method to treat symptomatic fibroids without any complication. It associates the spatial resolution of a MR scanner with a focused high intensity ultrasound beam. The purpose of this educational exhibit is to illustrate indications to MRgFUS treatment for uterine fibroids, contraindications and possible risks related to the procedure. We are going to describe how this system works, to show expected results after the procedure and to discuss results from the literature.

#### TABLE OF CONTENTS/OUTLINE

1. Current treatment for uterine fibroids: their indications, contraindications and complications. 2. Patient selection and contraindications to MRgFUS. 3. MRgFUS system and how does it work. 4. Imaging technique to evaluate size, number, accessibility, viability and texture of fibroids. 5. Results from the literature.

Printed on: 02/07/23

## Abstract Archives of the RSNA, 2022

IREE-58

### Radioembolization for Hepatocellular Carcinomas: Consideration of Non-hepatic Artery Originating from the Hepatic Artery

Sunday, Nov. 27 8:00AM - 9:00AM Room: Learning Center - IR

#### Awards

**Certificate of Merit**

#### Participants

Hyo-Cheol Kim, MD, Seoul, Korea, Republic Of (*Presenter*) Nothing to Disclose

#### TEACHING POINTS

Radioembolization is increasingly used for the treatment of patients with hepatocellular carcinoma. The knowledge of the hepatic artery anatomy is pivotal for effective and safe treatment. Several non-hepatic arteries, which should not be treated or should be protected, can originate from the hepatic artery. However, non-hepatic arteries may be frequently overlooked or be inadvertently treated, resulting in variable consequences from mild postembolization syndrome to catastrophic gastrointestinal radiation ulcer. The purpose of this exhibit is : (1) To list non-hepatic arteries originating from the hepatic artery. (2) To review the vascular anatomy of non-hepatic arteries on digital subtraction angiography (DSA) and cone-beam CT. (3) To learn how to deal with non-hepatic arteries prior to/during radioembolization. (4) To review the possible complications when they are inadvertently treated.

#### TABLE OF CONTENTS/OUTLINE

1) Cystic artery, right gastric artery, accessory left gastric artery, hepatic falciform artery, left inferior phrenic artery, and supraduodenal artery 2) Vascular anatomy of non-hepatic artery on CT/MR, DSA and cone-beam CT 3) Tips of non-hepatic artery detection on cone-beam CT as well as planning angiography and SPECT/CT 4) Technical considerations : permanent embolization, temporary embolization, and by-pass 5) Complications related with non-hepatic artery and their management : ischemic cholecystitis, radiation cholecystitis, radiation gastroduodenal ulcer, radiation dermatitis, epigastric pain.

Printed on: 02/07/23



## Abstract Archives of the RSNA, 2022

IREE-59

### Interventional Radiologic Procedures in Pelvic Bone Tumors

Sunday, Nov. 27 8:00AM - 9:00AM Room: Learning Center - IR

#### Participants

Yet Yen Yan, MBBS, (*Presenter*) Nothing to Disclose

#### TEACHING POINTS

Pelvic bone tumours are frequently encountered in the daily practice of the musculoskeletal radiologists. In addition, the pelvis is the 2nd most common site for bone metastases. As the array of pelvic bone interventional procedures have gradually widened from diagnostic to therapeutic, the musculoskeletal radiologist plays an important role in the care of such patients in terms of relieving pain, disease control and improving quality of life. This educational exhibit aims to equip the radiologist with the necessary information on the various interventions that be performed.

#### TABLE OF CONTENTS/OUTLINE

Bone biopsy, embolisation, osteoplasty and osteosynthesis will be covered.

Printed on: 02/07/23



## Abstract Archives of the RSNA, 2022

IREE-6

### **Balloon Pulmonary Angioplasty for Chronic Thromboembolic Pulmonary Hypertension: Indications, Preparation, Technique, Results and Complications.**

Sunday, Nov. 27 8:00AM - 9:00AM Room: Learning Center - IR

#### **Awards**

**Certificate of Merit**

#### **Participants**

Mario Matute Gonzalez, MD, Barcelona, Spain (*Presenter*) Nothing to Disclose

#### **TEACHING POINTS**

To describe the clinical manifestations, imaging findings, and diagnostic and therapeutic algorithms available in patients with chronic thromboembolic pulmonary hypertension (CTEPH) amenable to balloon pulmonary angioplasty (BPA). To discuss the importance of a proper selection, evaluation, and preparation of patients undergoing BPA, including protocols, applications, and a systematic clinical and imaging management proposal. To explain the technique, intraprocedural clinical evaluation, expected clinical and imaging findings, results and complications of BPA.

#### **TABLE OF CONTENTS/OUTLINE**

1. Introduction. 2. Management of patients with CTEPH. 2.1. Clinical manifestations. 2.2. Imaging modalities and typical findings. 2.3. Diagnostic algorithm. 2.4. Therapeutic algorithm. 3. Assessment before BPA. 3.1. Patient selection. 3.2. Preprocedural evaluation and preparation. 3.3. Proposal of a systematic protocol used in our institution. 4. BPA procedure. 4.1. 10-step technique. 4.2. Intraprocedural clinical evaluation. 4.3. Immediate clinical and imaging findings. 4.4. Complications. 5. BPA Follow-up. 5.1. Clinical and imaging evaluation. 5.2. Results. 6. Summarize. 7. Conclusion.

Printed on: 02/07/23



## Abstract Archives of the RSNA, 2022

IREE-60

### **Bariatric Arterial Embolization: How To Build a Clinical Program**

Sunday, Nov. 27 8:00AM - 9:00AM Room: Learning Center - IR

#### **Participants**

Adham Khalil, MD, Baltimore, MD (*Presenter*) Research Grant, Siemens AG

#### **TEACHING POINTS**

Obesity is a major public health issue that contributes to significant disability, cardiovascular risk, mortality, and healthcare costs. Over the last 50 years, there has been a dramatic increase in the prevalence of obesity in the United States. Obesity is associated with an increased risk of all-cause mortality and a significant reduction in life expectancy. For these reasons, obesity has been labeled a major healthcare epidemic in the United States. Thus, there is an urgent need to develop new therapies for obesity. BAE is an emerging, minimally-invasive therapy for patients with obesity. This image-guided transcatheter procedure involves occlusion of the arteries supplying the gastric fundus, which contains the majority of ghrelin-producing cells. BAE has an excellent safety profile with more than 100 patients with obesity having undergone the procedure worldwide, without any significant adverse sequelae. These early findings suggest that BAE may represent an additional tool in the treatment of patients with obesity that could be used alone or in conjunction with a dedicated lifestyle management program. The goal of the exhibit is to educate the reader on our experience with building a clinical, insurance-supported BAE program and how to integrate BAE as a part of the care path for treating obesity.

#### **TABLE OF CONTENTS/OUTLINE**

1. Structure of the bariatric program  
2. Patient acquisition and workflow  
3. Patient referral and assessment  
4. Multidisciplinary discussion  
5. Peri-procedural patient care  
6. Procedure technique  
7. Insurance and billing  
8. Pearls / Lessons learnt

Printed on: 02/07/23



## Abstract Archives of the RSNA, 2022

IREE-61

### Transjugular Venous Access in Upper Extremity Hemodialysis Arteriovenous Fistula / Graft Interventions

Sunday, Nov. 27 8:00AM - 9:00AM Room: Learning Center - IR

#### Participants

Louis Fanucci, DO, Orange, CA (*Presenter*) Nothing to Disclose

#### TEACHING POINTS

1. To review the indications for use of transjugular venous access in upper extremity hemodialysis arteriovenous fistula / graft (AVF / AVG) interventions
2. To describe the procedural technique involved with transjugular venous access
3. To discuss the specific clinical applications for transjugular venous access

#### TABLE OF CONTENTS/OUTLINE

Transjugular venous approaches were originally described in the context of upper extremity AVF / AVG interventions in 1998, for patients with thrombosed dialysis grafts. A clotted fistula / graft presents a situation where a direct puncture into that AVF / AVG is undesirable. A transjugular approach facilitates intervention using a single puncture site that does not involve the AVF / AVG outflow vein. Pre-procedure access assessment includes ultrasound evaluation of anastomotic sites, inflow artery and outflow vein, and patency of the internal jugular veins. IV access is obtained with a micropuncture system under ultrasound guidance, followed by insertion of 7-French vascular sheath. A guidewire and reverse-curve catheter are most commonly used to perform retrograde catheterization of the outflow vein of interest. After successful retrograde access is established and the procedure completed, hemostasis is achieved by simply applying pressure at the puncture site of the internal jugular vein. Clinical applications of the transjugular access approach include interventions to assist an AVF's maturation and de-clotting of an AVF. This approach is a safe and effective alternative approach to AVF / AVG interventions for patients whose target arteriovenous systems are not amenable to direct puncture.

Printed on: 02/07/23



## Abstract Archives of the RSNA, 2022

IREE-62

### History of Histotripsy: Bench to Clinical Translation

Sunday, Nov. 27 8:00AM - 9:00AM Room: Learning Center - IR

#### Participants

Nathan Loudon, MD, Ann Arbor, MI (*Presenter*) Nothing to Disclose

#### TEACHING POINTS

Histotripsy is a new non-invasive, non-thermal, non-radiation ablative modality that uses mechanical cavitation to destroy tissues. Histotripsy began as a basic science bioengineering research project, where the investigation of ultrasound generated cavitation eventually progressed to small and large animal trials, ultimately leading to clinical translation with a Phase I FDA approved clinical trial in the US and Europe. This exhibit will review the basic physics of the technology, review the history of development from small animal to large animal to clinical translation, and finally review the clinical applications and early clinical data.

#### TABLE OF CONTENTS/OUTLINE

Overview of the technology  
Review of basic science and animal trials  
Small animal feasibility studies  
Large animal feasibility studies  
pre-clinical translation  
Small animal abscopal trials  
Early clinical trials  
Review of early human clinical trials  
Phase I efficacy trial: TERESA trial in Spain  
Phase I safety and efficacy trial: #HOPE4LIVER trial in the U.S. and Europe

Printed on: 02/07/23



## Abstract Archives of the RSNA, 2022

IREE-63HC

### Common Vascular and Bleeding Complications of Percutaneous Biliary Interventions

Sunday, Nov. 27 8:00AM - 9:00AM Room: Learning Center - IR

#### Participants

Aziz Tejani, (*Presenter*) Nothing to Disclose

#### TEACHING POINTS

With the increase in percutaneous biliary tract interventions (PBTI) being performed over the past few years, it is important for radiologists to be aware of the many associated post-procedural complications. While there are a several complications that are commonly seen, bleeding can be one of the more serious ones that should readily be assessed for. Bleeding is typically seen in 2-3% of all PBTI cases (3). Injuries to the portal vein, hepatic artery, hepatic vein, and pseudoaneurysms are common vascular injuries that are encountered. Signs and symptoms of such vascular injury can be subtle and non-specific. Although morbidity and mortality is rare, a delay in detection may lead to significant adverse outcomes in some patients. After reviewing this educational exhibit, the individual will be able to: 1. Detect the various vascular and bleeding complications of PBTI on imaging modalities2. Understand the best practices for diagnostic evaluation3. Understand the therapeutic percutaneous interventions for treatment

#### TABLE OF CONTENTS/OUTLINE

This Exhibit Will Provide:1. An overview of the various types of iatrogenic vascular injury seen with percutaneous biliary interventions2. Demonstrate the clinical signs and symptoms of vascular injury for the clinician to be aware of3. Review appropriate imaging modalities and how to detect such vascular complications on the particular studies4. An overview of therapeutic procedures from an interventional radiology standpoint to manage these bleeding complications5. An assessment of future direction and summary of teaching pointsPlease visit the Learning Center to also view this presentation in hardcopy format.

Printed on: 02/07/23



## Abstract Archives of the RSNA, 2022

IREE-65

### Tips for TIPS: An Update on Transjugular Intrahepatic Portosystemic Shunt Complications for Radiologists

Sunday, Nov. 27 8:00AM - 9:00AM Room: Learning Center - IR

#### Participants

Andrew Ni, San Antonio, TX (*Presenter*) Nothing to Disclose

#### TEACHING POINTS

Learning Objectives: Present common TIPS complications and their etiology Present an update for the diagnostic radiologist in early detection and management of TIPS complications Review management of common TIPS complications

#### TABLE OF CONTENTS/OUTLINE

Content/Outline Introduction Procedural complications, imaging findings, and management: Venous access complications: pneumothorax, carotid artery puncture, cardiac perforation Portal access needle punctures: puncture (hepatic artery, biliary ducts, gallbladder), hemoperitoneum, and liver capsule perforation Stent related: stent length, occlusion, and deployment issues Post-procedural complications, imaging findings, and management: Shunt thrombosis: stent occlusion, portal vein thrombosis, Budd Chiari syndrome Device-related: stent migration, hemolysis Hepatic pathology: liver failure, encephalopathy, hepatic abscess, hepatic infarct Other: sepsis, radiation injury, right sided cardiac failure, hernia incarceration Routine and clinically indicated follow-up imaging Ultrasound to ensure patency and for long-term observation Imaging for detection and treatment of stent stenosis and obstruction Contrast enhanced CT to determine etiology of acute hepatic failure (vessel occlusion, thrombosis)

Printed on: 02/07/23



## Abstract Archives of the RSNA, 2022

IREE-66

### Thoracic Central Venous Occlusion: Pathogenesis, Imaging Findings, and Recanalization Techniques

Sunday, Nov. 27 8:00AM - 9:00AM Room: Learning Center - IR

#### Participants

Carlos Ortiz, MD, San Antonio, TX (*Presenter*) Consultant, Argon Medical Devices, Inc

#### TEACHING POINTS

- Discuss the pathophysiology, imaging findings, and common presentations of thoracic central venous occlusions (TCVOs)- Review collateral pathways formed in response to TCVO and associated findings on imaging- Discuss current endovascular techniques for central venous recanalization- Review the role of imaging in assessing stent patency and complications after venous recanalization

#### TABLE OF CONTENTS/OUTLINE

Introduction - Pathogenesis of TCVOs in the context of hemodialysis, indwelling catheters, extrinsic compression, and associated pathophysiology- Imaging of TCVOs on CT and diagnostic venogram, including review of collateral venous pathway formation- Current recanalization techniques employed in the treatment of TCVOs and indications for specific techniques (standard wire crossing, sharp recanalization, radiofrequency wire, and endovascular stenting)- Immediate complications (hemothorax, pneumothorax, hemopericardium) and subsequent complications (stent thrombosis, occlusion, dialysis issues) after endovascular recanalization- Medical management after TCVO endovascular stentingConclusionIdentification of a TCVO is important for patients as symptoms can be life altering and compromise hemodialysis. Successful recanalization requires technical skill, appropriate planning, and postprocedural management. Complications from TCVO revascularization can be severe and familiarity with this procedure is important for radiologists.

Printed on: 02/07/23



## Abstract Archives of the RSNA, 2022

IREE-67

### "Burning Questions": What Every Radiologist Should Know about the Diagnosis and Management of Bleeding Duodenal Ulcers

Sunday, Nov. 27 8:00AM - 9:00AM Room: Learning Center - IR

#### Participants

Roberto Chavez Appendini, MD, (*Presenter*) Nothing to Disclose

#### TEACHING POINTS

1. Vascular supply of the duodenum arises from the anterior and posterior division of the superior pancreaticoduodenal arteries which are branches of the gastroduodenal artery, these arteries anastomose with the inferior pancreaticoduodenal artery which is a branch of the superior mesenteric artery. 2. Diagnosis and treatment of bleeding duodenal ulcers are traditionally endoscopic, when bleeding is refractory to treatment, Three-phase GI bleed CT protocol (non-contrast, arterial and venous phases) is an important diagnostic tool, nuclear medicine studies are helpful when CT contraindicated. 3. CT findings of duodenal ulcers are subtle and include, mural enhancement of the duodenum, fat stranding, submucosal edema, regional lymphadenopathy, and active extravasation of contrast into the duodenal lumen. 4. Endovascular treatment must be considered for bleeding ulcer refractory to endoscopic treatment. Selective embolization of the GDA is done when active bleeding is identified either on CT or angiographically. Empiric embolization of the GDA is an effective alternative, especially for clinically unstable patients. 5. Selective and empiric embolization of the GDA for bleeding duodenal ulcers refractory to endoscopic treatment has a low complication rate, for which rebleeding is the most common, in these cases angiogram with potential re-embolization can be considered as well as surgical treatment.

#### TABLE OF CONTENTS/OUTLINE

1. Introduction and epidemiology 2. Diagnostic approach for suspected bleeding duodenal ulcer 3. Treatment modalities 4. Case series 5. Conclusion

Printed on: 02/07/23



## Abstract Archives of the RSNA, 2022

IREE-68

### Complications After Radioembolization of Hepatic Tumors: Spectrum of Imaging Findings

Sunday, Nov. 27 8:00AM - 9:00AM Room: Learning Center - IR

#### Awards

Certificate of Merit

#### Participants

Hyo-Cheol Kim, MD, Seoul, Korea, Republic Of (*Presenter*) Nothing to Disclose

#### TEACHING POINTS

Radioembolization is a potent intra-arterial therapy used to treat primary liver tumors and liver metastases. However, this treatment may result in various hepatic and extrahepatic complications which could be alleviated or prevented. The common complications include biliary necrosis, benign biliary stricture, liver abscess, radioembolization-induced liver disease, radiation cholecystitis, gastrointestinal radiation ulcer, radiation pneumonitis, and radiation dermatitis. The purpose of this exhibit is : (1) To review the hepatic and extrahepatic complications related with radioembolization. (2) To learn how to manage these complications. (3) To learn how to prevent or alleviate these complications.

#### TABLE OF CONTENTS/OUTLINE

1) Hepatic complications associated with radioembolization A. biliary complication (biliary necrosis, biliary stricture, biloma, liver abscess) B. radiation hepatitis and focal radiation necrosis C. radiation-induced liver disease 2) Extrahepatic complications associated with radioembolization A. Radiation cholecystitis B. Radiation ulcer C. Radiation pneumonitis D. Radiation dermatitis 3) Management of each complication 4) Prevention method of each complication

Printed on: 02/07/23

## Abstract Archives of the RSNA, 2022

IREE-69

### Percutaneous Sclerotherapy for Orbital Low Flow Lympho-venous Malformations (LFVM)

Sunday, Nov. 27 8:00AM - 9:00AM Room: Learning Center - IR

#### Participants

Shyamal Patel, MBBS, FRCR, London, United Kingdom (*Presenter*) Nothing to Disclose

#### TEACHING POINTS

1. Orbital sclerotherapy is effective with low complication rates, and is therefore an important minimally invasive option in the management of orbital low flow lympho-venous malformations. 2. Bleomycin is the sclerosant of choice as it is associated with less local inflammatory response - important for lesions in/around the orbit where significant swelling can result in visual loss. 3. Treatment is performed under a general anaesthetic and prior to bleomycin use, adequate pre-assessment is required including appropriate imaging and ophthalmology review. 4. The entire team should be aware of specific precautions related to bleomycin use including potential for lung fibrosis, skin marking and the need for cytotoxic precautions. 5. Important complications to be aware of are retro-orbital haemorrhage, requiring emergency lateral canthotomy and the oculocardiac reflex which is rare but may result in bradycardia, arrhythmias and potentially asystole.

#### TABLE OF CONTENTS/OUTLINE

1. What are orbital LFVMs (Primary vs Secondary; Venous, lymphatic and mixed). 2. Imaging appearances (US, CT, MRI). 3. Bleomycin use: pre-assessment, bleomycin precautions. 4. Sclerotherapy procedure - dosage, technique and assessment for deep venous drainage. 5. Complications (retro-orbital haemorrhage, oculocardiac reflex).

Printed on: 02/07/23



## Abstract Archives of the RSNA, 2022

IREE-7

### Recent Development of Augmented Reality and Mixed Reality for Needle Guidance

Sunday, Nov. 27 8:00AM - 9:00AM Room: Learning Center - IR

#### Awards

Certificate of Merit

#### Participants

Satoru Morita, MD, PhD, Tokyo, Japan (*Presenter*) Nothing to Disclose

#### TEACHING POINTS

Augmented reality (AR) and mixed reality (MR) can expand the possibilities of image guidance procedures. Some needle guidance applications using AR/MR on smartphones and smartglasses have been developed recently. Various resources are available for developing applications using AR/MR. The purpose of this exhibit is to 1). Review the current situations of AR/MR for image guidance procedures. 2). Introduce the recent needle guidance applications using AR/MR and discuss each advantage and disadvantage. 3). Introduce how to develop needle guidance applications using AR/MR.

#### TABLE OF CONTENTS/OUTLINE

1). Introduction 2). Definitions of AR/MR 3). Devices for AR/MR 4). Platforms to develop AR/MR applications 5). Registration methods for AR/MR 6). Current needle guidance applications using AR/MR 7). Limitations 8). Future perspectives 9). Conclusions and take home messages

Printed on: 02/07/23



## Abstract Archives of the RSNA, 2022

IREE-70

### Interventional Pain Frontiers: Role of IR in Median Arcuate Ligament Syndrome (MALS) Management

Sunday, Nov. 27 8:00AM - 9:00AM Room: Learning Center - IR

#### Awards

Certificate of Merit

#### Participants

Mohamed Ibrahim, MBBCh, Rochester, MN (*Presenter*) Nothing to Disclose

#### TEACHING POINTS

- Understand the current hypothesis of MALS etiology and highlight pertinent anatomy
- Learn the role of IR in the diagnosis and determination of surgical candidacy for MALS patients
- Learn the role of IR in the treatment of MALS patients

#### TABLE OF CONTENTS/OUTLINE

- MALS etiology and pertinent anatomy
  - o A neurogenic disorder rather than a compression syndrome
  - o Celiac plexus and splanchnic plexus anatomy
- Role of IR in the diagnosis and determination of surgical candidacy MALS patients
  - o Role of celiac plexus block in the diagnosis of MALS
  - o Common approaches and protocols for celiac plexus block in the diagnosis of MALS
- Role of IR in treatment of MALS patients
  - o Celiac plexus neurolysis; technical considerations, and expected outcomes
  - o Splanchnic plexus neurolysis; technical considerations, and expected outcomes

Printed on: 02/07/23



## Abstract Archives of the RSNA, 2022

IREE-71

### Interventional Management of Portal Vein Thrombosis: A Problem-solving Approach

Sunday, Nov. 27 8:00AM - 9:00AM Room: Learning Center - IR

#### Participants

Daniel Cardoso, MD, Fortaleza, Brazil (*Presenter*) Nothing to Disclose

#### TEACHING POINTS

Recognize the anatomy of the portal venous system (PVS) and its most common variants. Understand the causes of Portal Vein thrombosis (PVT) and related clinical features. Comprehend imaging patterns of PVT through a wide variety of imaging modalities. Recognize the complications associated to PVT and its imaging patterns. Understand PVT treatment methods and criteria.

#### TABLE OF CONTENTS/OUTLINE

1. INTRODUCTION: PVS anatomy and most common anatomical variations. Definition of PVT (acute x recent x chronic). Epidemiology of the most common causes of PVT. Signs and symptoms associated to the obstruction site (Portal Vein (PV), Superior Mesenteric Vein (SMV) and Splenic Vein (SV)). 2. DIAGNOSIS AND IMAGING FINDINGS: PV: Benign PV / Cirrhotic and non-cirrhotic PVT / Infectious/septic PVT - thrombophlebitis / Transplant-associated PVT. Malignant PVT: Tumor Invasion/PV Tumor Thrombosis (Hepatocellular carcinoma) / External Constriction of the PV within a Tumor (Pancreatic Cancer or Cholangiocarcinoma) / Complications associated to PVT. SMV: SMV thrombosis / Complications associated to SMV thrombosis. SV: SV thrombosis / Complications associated to SV thrombosis. 3. MANAGEMENT OF PVT: Fundamentals of Anticoagulation Therapy / Interventional Approach / Techniques / Follow-up and Early Identification of Possible Complications.

Printed on: 02/07/23



## Abstract Archives of the RSNA, 2022

IREE-73

### Venous Access Ports: What Every Radiology Resident Should Know

Sunday, Nov. 27 8:00AM - 9:00AM Room: Learning Center - IR

#### Participants

Nicholas Champagne-Aves, BS, (*Presenter*) Nothing to Disclose

#### TEACHING POINTS

List indications and contraindications of venous access ports Describe port placement and confirmatory imaging Describe associated complications, imaging findings, and management

#### TABLE OF CONTENTS/OUTLINE

Indications Long term intravascular access with minimal disruption to patient's life (medications, transfusions, blood draws) Contraindications Absolute: bacteremia/sepsis, infection at access site Relative: coagulopathy, chest wall deformity, pneumothorax, distorted anatomy (trauma/thrombosis) Procedural Steps Visualize desired vein under ultrasound (US) guidance Sterilize field Obtain planned venous access with micropuncture kit under US guidance Measure desired length of catheter using micropuncture guidewire Exchange for 0.035" wire and place in the SVC Create port reservoir site and tunnel catheter to venotomy Trim catheter to length and ensure adequate port connection Advance peel away sheath over wire, remove inner dilator Insert catheter completely through sheath and peel away sheath Confirm proper placement with fluoroscopy Test and flush port with heparin, close incision Complications, imaging findings, management Early: malposition, hemorrhage, hemothorax, pneumothorax, air embolism Late: infection, catheter occlusion/thrombosis, catheter pinch off/migration Port Removal: catheter calcification, fracture, pseudo-fracture A systematic approach to venous access port placement minimizes complications and improves outcomes. Radiologists must be familiar with indications, procedural steps, and complications for accurate management.

Printed on: 02/07/23



## Abstract Archives of the RSNA, 2022

IREE-74HC

### Acute Calculous Cholecystitis: The Role of the Radiologist in Diagnosis and Treatment

Sunday, Nov. 27 8:00AM - 9:00AM Room: Learning Center - IR

#### Participants

Darius Jonasch, BEng, (Presenter) Nothing to Disclose

#### TEACHING POINTS

1. Review diagnostic approach for Acute Calculous Cholecystitis2. Define the grading of Acute Calculous Cholecystitis3. Discuss treatment options based on the patient's presentation and history

#### TABLE OF CONTENTS/OUTLINE

1. Introductiona. Anatomy of the Hepatobiliary Systemb. Pathophysiology of Acute Calculous Cholecystitisc. Epidemiology and Clinical Presentation of Acute Calculous Cholecystitis2. Imaging Appearancea. Ultrasoundb. Cholescintigraphyc. Magnetic Resonance Cholangiopancreatographyd. Computed Tomographye. Endoscopic Retrograde Cholangiopancreatographyf. Percutaneous Biliary Endoscopy3. Clinical Severitya. Introduction to Tokyo Guidelinesi. Grade Iii. Grade IIiii. Grade III4. Risk Stratification and Treatmenta. Low Risk Patientsi. Surgical Therapy1. Surgical Cholecystectomyb. High Risk Patientsi. Medical Therapy1. Antibioticsii. Endoscopic Therapy1. Endoscopic Drainageiii. Interventional Radiology Therapy1. Percutaneous Drainage2. Percutaneous Transhepatic Stone Retrievaliv. Surgical Therapy1. Surgical Candidacy2. Surgical Timing5. Potential Complicationsa. Complications of Acute Cholecystitis - Sepsis, Choledocholithiasis, Gangrenous Cholecystitis, Gallbladder Perforation, Emphysematous Cholecystitis, Cholecystoenteric Fistula, Gallstone Ileusb. Complications of Treatment of Acute Calculous Cholecystitis - Hemorrhage, Bile Leak, Biloma, Common Bile Duct Injury, Bowel Injury, Tube ComplicationsPlease visit the Learning Center to also view this presentation in hardcopy format.

Printed on: 02/07/23



## Abstract Archives of the RSNA, 2022

IREE-75

### Biliary Leaks: There Are Many Ways to Fix

Sunday, Nov. 27 8:00AM - 9:00AM Room: Learning Center - IR

#### Awards

Identified for RadioGraphics

#### Participants

Christopher Mao, Sugar Land, TX (*Presenter*) Nothing to Disclose

#### TEACHING POINTS

Biliary leaks are most seen in patients as iatrogenic complications after surgeries such as cholecystectomy. Postoperative leaks occur in 1% of laparoscopic cholecystectomies and 0.5% of open cholecystectomies but can occur in other procedures such as RFA (Radiofrequency Ablation) of primary and secondary liver tumors. As the number of hepatobiliary surgeries performed continue to increase, biliary leaks will become even more prevalent. Since clinical signs and symptoms of bile leaks are nonspecific and delay in the recognition of bile leaks is associated with high morbidity and mortality rates, imaging is crucial for establishing an early diagnosis and guiding the treatment algorithm. After reviewing this exhibit, learners should be able to: 1. Recognize emergent biliary leaks from key image findings. 2. Use best practices for diagnosing biliary leaks. 3. Understand the options for percutaneous management.

#### TABLE OF CONTENTS/OUTLINE

1. Provide an overview of the different types of biliary leaks. 2. Illustrate the clinical and imaging features of biliary leaks with a focus on iatrogenic etiologies. 3. Review the framework for selecting the best imaging practice of the biliary duct system. 4. Address relevant management as applicable to the interventional radiologist to aid in expedient and appropriate management. 5. Discuss future directions. 6. Conclude with a summary of key teaching points.

Printed on: 02/07/23



## Abstract Archives of the RSNA, 2022

IREE-76

### MRI Guided Transurethral Ultrasound Ablation (TULSA) of Prostate: Initial Experience at Wellspan Hospital

Sunday, Nov. 27 8:00AM - 9:00AM Room: Learning Center - IR

#### Participants

Edward Steiner, MD, (*Presenter*) Key Opinion Leader, Koninklijke Philips NV ;Speaker, Koninklijke Philips NV;Speaker, Quantib BV;Research support, Profound Medical Inc ;Speaker, Profound Medical Inc

#### TEACHING POINTS

Teaching points - To present the capabilities of TULSA TULSA-PRO is a minimally invasive procedure that combines real-time MRI with robotically-driven directional thermal ultrasound to treat prostate cancer, with the goal of achieving comparable disease control to radiation therapy or prostatectomy and significantly improved functional preservation. TULSA can also treat BPH concurrent with cancer in a single procedure. Examples of TULSA whole-gland and hemi-ablation procedures performed at our institution are provided. - To report lessons learned with the TULSA procedure Critical lessons and technical points are presented including patient preparation, considerations on treating radio-recurrent disease, sparing of sphincter and bladder tissue, maintaining ejaculatory function, and workup of patients with intermediate to high grade lesions with PSMA scans. - To report early functional, oncological, and safety outcomes Discussion of post procedure care and follow-up, monitoring, repeat MRI and PSA trends, continence and erectile function data analysis as well as preliminary tumor recurrence data.

#### TABLE OF CONTENTS/OUTLINE

Table of contents - Basics of TULSA procedure and workflow - Lessons learned, and treatment planning strategies - Early functional, oncological, and safety outcomes - Applications of TULSA for sparing functionally important structures and treating radio-recurrent disease

Printed on: 02/07/23



## Abstract Archives of the RSNA, 2022

IREE-77

### Intra-arterial Treatment for Hepatocellular Carcinomas: How to Manage Shunting From the Artery

Sunday, Nov. 27 8:00AM - 9:00AM Room: Learning Center - IR

#### Awards

**Magna Cum Laude**

#### Participants

Hyo-Cheol Kim, MD, Seoul, Korea, Republic Of (*Presenter*) Nothing to Disclose

#### TEACHING POINTS

Intra-arterial therapy including chemoembolization and radioembolization is a workhorse for the treatment of patients with hepatocellular carcinomas. Occasionally, the operators encounter shunts from the artery (arteriportal, arteriovenous, and arteriopulmonary shunts) that prevent effective treatment. The causes of these shunts include tumor invasion to the vessels, previous percutaneous procedures, chronic inflammation, and congenital acquisition. Unless the shunt is properly occluded, embolic material can pass through the shunt and cause non-target embolization or serious complications. The purpose of this exhibit is : (1) To review radiologic appearance of arteriportal, arteriovenous, and arteriopulmonary shunts. (2) To learn how to manage these shunts with proper embolic materials. (3) To list the possible complications and their management.

#### TABLE OF CONTENTS/OUTLINE

1) List of shunts Arteriportal shunt (hepatic artery - portal vein), Arteriovenous shunt (hepatic artery - hepatic vein), Arteriopulmonary shunt (hepatic artery - pulmonary artery/vein), 2) Imaging findings on CT/MR and angiography according to the cause (tumorous vs non-tumorous condition) 3) Embolization strategy and materials for shunts 4) Complications related with non-target embolization and their management

Printed on: 02/07/23



## Abstract Archives of the RSNA, 2022

IREE-78

### To Glue or Not to Glue, That Was the Question - Misadventures with Glue Embolization in Peripheral Applications

Sunday, Nov. 27 8:00AM - 9:00AM Room: Learning Center - IR

#### Participants

Jorge Lopera, MD, San Antonio, TX (*Presenter*) Shareholder, Tecnostent SA; Consultant, Merit Medical Systems, Inc; Research Grant, AngioDynamics, Inc

#### TEACHING POINTS

Embolization using N butyl acrylate (NBCA) or glue is showing very promising results with better and faster occlusion results than particles or coils in areas that are susceptible to recanalization after embolization such as bronchial arteries, portal vein embolization and endoleaks after EVAR, among others. Emerging uses of glue include trauma, uterine artery embolization in placental insertion abnormalities, cyst sclerosis and gastrointestinal bleeding. As with other liquid embolization agents, using glue has a steep learning curve and serious complications can occur. The purpose of this exhibit is to illustrate in a case by case presentation, different complications with the use of glue with emphasis in ways to prevent them.

#### TABLE OF CONTENTS/OUTLINE

1. When to use and not to use glue 2. How to prepare glue; basic steps 3. Complications a. Lung glue embolization after portal vein embolization . b. Portal vein embolization after treatment of arterio-portal fistula in HCC c. SMA glue migration after percutaneous aneurysm embolization d. Iliac artery glue embolization after trans lumbar endoleak embolization e. Glue cast adhered to catheter in the aorta- ways to fix this . f. Stroke after peripheral glue embolization, beware of PFO .Conclusions : Glue is a very versatile embolization agent, showing very promising results with lesser recanalization rates than particles or coils in many areas. As a liquid embolization agent, serious complications can occur that require a clear understanding of the different mechanisms of glue migration and ways to mitigate them.

Printed on: 02/07/23



## Abstract Archives of the RSNA, 2022

IREE-79

### **Benign Prostatic Hyperplasia Treatments: A Review of the Fundamentals to Assist in Optimal Prostate Artery Embolization Patient Selection**

Sunday, Nov. 27 8:00AM - 9:00AM Room: Learning Center - IR

#### **Participants**

Miltiadis Tembelis, Mineola, NY (*Presenter*) Nothing to Disclose

#### **TEACHING POINTS**

1. A thorough understanding of benign prostatic hyperplasia (BPH) pathophysiology and management options is essential before embarking on developing a prostate artery embolization (PAE) program. 2. While the risks of PAE are low when done with proper technique, major complications can occur and have negative impact on a patient and/or a PAE program. 3. An understanding of PAE indications as well as alternative BPH treatment is essential to ensure appropriate patient selection and PAE procedural advocacy.

#### **TABLE OF CONTENTS/OUTLINE**

-Review BPH pathophysiology-Discuss lower urinary tract symptoms (LUTS), their diagnosis, and that a variety of causes exist (not just bladder outlet obstruction from BPH)-Provide the learner with a thorough review of BPH management options, including medications, minimally invasive surgical therapies, PAE, and more invasive surgical interventions (TURP, HoLEP, and prostatectomy)-Review relevant literature on indications and outcomes of these procedures, with the goal of providing radiologists and trainees with key fundamental knowledge to allow for optimal PAE patient selection and also for guiding patients towards other management options when more appropriate

Printed on: 02/07/23



## Abstract Archives of the RSNA, 2022

IREE-8

### The Pelvic Venous Disease Continuum: Nutcracker Phenomenon, Non-thrombotic Iliac Vein Lesion (NIVL), Ovarian and Pelvic Vein Reflux

Sunday, Nov. 27 8:00AM - 9:00AM Room: Learning Center - IR

#### Participants

Navpreet Khurana, MBBS, (Presenter) Nothing to Disclose

#### TEACHING POINTS

1. Discuss the complex pathophysiological interactions between Nutcracker syndrome, Nonthrombotic Iliac Vein Lesion (NIVL), and ovarian pelvic venous reflux leading to the constellation of findings known as Pelvic Venous Disease (PeVD). PeVD is often misdiagnosed and inappropriately treated. 2. Describe the key imaging findings in the diagnosis of PeVD. 3. Review the algorithm and pearls/pitfalls of IR management.

#### TABLE OF CONTENTS/OUTLINE

1. Key anatomical and pathophysiological concepts a) Nutcracker Phenomenon - Compression between aorta and superior mesenteric artery results in stenosis and increased pressure in the left renal vein, often with blow-out retrograde flow down the ovarian vein resulting in pelvic varicosities to act as collateral. b) NIVL - Stenosis of left common iliac vein between right common iliac artery and aorta, either by mechanical compression or with superimposed chronic microtrauma secondary to proximity and pulsatility causing venous wall thickening and/or webs. c) Ovarian Pelvic Vein Reflux - Incompetence and reflux of ovarian and/or pelvic veins resulting in pooling of blood into "reservoirs", classically in the pelvis. Blood may also leak out of the pelvis from "escape points" due to gravity and venous hypertension. 2. Diagnostic imaging algorithm and findings with a case-based discussion. 3. Role of Interventional Radiology: a) Initial consultation with focused history physical exam. b) Diagnostic evaluation for PeVD - US, CT Venography, MR Venography. c) Nutcracker Phenomenon its dynamic role in PeVD. d) In NIVL, understanding the interplay of iliac stenosis with ovarian reflux, role of its treatment in PeVD. 4. Complications/misdiagnosis case examples of PeVD.

Printed on: 02/07/23



## Abstract Archives of the RSNA, 2022

IREE-80

### Prostate Artery Embolization Practice Building - With a Focus on Understanding the Current Literature

Sunday, Nov. 27 8:00AM - 9:00AM Room: Learning Center - IR

#### Participants

Nathan Mickinac, MD, Mineola, NY (*Presenter*) Nothing to Disclose

#### TEACHING POINTS

1. A thorough understanding of benign prostatic hyperplasia (BPH) pathophysiology and management options is essential before embarking on developing a PAE program. 2. While the risks of PAE are low when done with proper technique, major complications can occur and have negative impact on a patient and/or a PAE program. 3. Thoughtful implementation, careful patient selection, meticulous procedural technique, collaboration with other specialties, and appropriate marketing are keys to building a successful PAE program.

#### TABLE OF CONTENTS/OUTLINE

-Review BPH pathophysiology and epidemiology-Brief review of BPH treatment options, with a focus on PAE-Review relevant literature on PAE, including large prostates (>80g), acute urinary retention, and/or hematuria-Provide basic review of sexual health relating to BPH, including erectile dysfunction (ED) and ejaculatory dysfunction (EjD), and review relevant evaluation tools/scales-Highlight data regarding ED and EjD across multiple BPH procedures, including PAE-Review current AUA BPH guidelines and discuss why PAE is not supported in those guidelines currently-Detail current data regarding repeat PAE-Share practice building advice, with a focus on utilizing PAE data to engage other specialties as a part of building a successful program

Printed on: 02/07/23



## Abstract Archives of the RSNA, 2022

IREE-9

### Cryoablation of Aneurysmal Bone Cyst: Current Status and Management

Sunday, Nov. 27 8:00AM - 9:00AM Room: Learning Center - IR

#### Participants

Elisabet Vila, (*Presenter*) Nothing to Disclose

#### TEACHING POINTS

This exhibit will: 1) Describe imaging features of primary ABC using different imaging modalities. 2) Discuss this novel interventional technique and how it works (low dose CT protocol, needle placement method and ice ball formation). 3) Illustrate normal post treatment imaging findings of aneurysmal bone cyst using cryoablation on MRI. 4) Characterize the radiological appearance of relapse.

#### TABLE OF CONTENTS/OUTLINE

Aneurysmal bone cysts are benign and expansile bone lesions with locally aggressive behavior. Diagnosis is achieved using different imaging modalities. Cryoablation is a percutaneous ablation technique that uses extreme low temperatures for tumor destruction and is becoming increasingly accepted for treatment of aneurysmal bone cysts. It uses liquefied gas (nitrogen or argon), through cryoprobes that expands into a gaseous state at the end of the probe to create temperatures as low as -190 °C. Intra-procedure computed tomography (CT) is used to identify the ablated zone in real time appearing as a low-density area which corresponds to the generated ice ball. In this exhibit we will review how cryoablation works, procedure planning and imaging appearance of post procedural interventions, showing different examples of normal findings and relapse.

Printed on: 02/07/23

## Abstract Archives of the RSNA, 2022

MKEE

### Musculoskeletal Education Exhibits

Sunday, Nov. 27 8:00AM - 9:00AM Room: Learning Center - MK

#### Sub-Events

#### MKEE-1 Achilles-calcaneus-plantar fascia system: Anatomy, Biomechanics and Patterns of Injury

##### Awards

Certificate of Merit

Identified for RadioGraphics

##### Participants

Dyan V. Flores, MD, Ottawa, ON (*Presenter*) Nothing to Disclose

##### TEACHING POINTS

The Achilles tendon, calcaneus and plantar fascia comprise an interconnected complex or system of structures that play a vital role in the load distribution of the foot, including absorbing mechanical shock, stabilizing and preventing the collapse of the longitudinal arch during propulsion. Failure, overload or repetitive stress to any or a combination of these structures leads to a multitude of disorders and imaging findings. The objectives of this educational exhibit are: • Review normal anatomy and biomechanics of the Achilles tendon, calcaneus and plantar fascia • Discuss patterns of failure and injury involving the Achilles tendon, calcaneus and plantar fascia • Identify imaging findings that may aid in differentiating these disorders when clinical findings are equivocal

##### TABLE OF CONTENTS/OUTLINE

Pertinent anatomy and biomechanics • Calcaneal crescent • Windlass mechanism Imaging techniques Disorders Achilles Complete and partial tear Insertional tendinopathy and tendinitis Peritendinitis Peri-Achilles bursal fluid Calcaneus Stress fracture Haglund syndrome Posterior ankle impingement Plantar fascia Fasciitis Rupture Fibromatosis Plantar fat pad abnormalities

#### MKEE-10 Current Trends in Total Ankle Arthroplasty

##### Awards

Identified for RadioGraphics

##### Participants

Jason Ha, (*Presenter*) Nothing to Disclose

##### TEACHING POINTS

Describe indications for total ankle arthroplasty (TAA) vs. arthrodesis. Recognize different types of TAA, including semi-constrained and minimally constrained designs. Understand normal tibiotalar and distal anterior tibia angles. Define normal and abnormal imaging appearance of TAA.

##### TABLE OF CONTENTS/OUTLINE

1. Indications for TAA vs. arthrodesis. 2. Types of TAA: Differences between 1st generation, 2nd generation, 3rd generation. Comparison of Agility, Salto-Talaris, Inbone, STAR, Hintegra, Mobility, and Zimmer Trabecular Metal. 3. Normal imaging appearance: Radiolucency, Tibiotalar Angle, Distal Anterior Tibia Angle. 4. Complications: Radiolucency, Hardware Subsidence, Perihardware fracture, Syndesmotic screw loosening, Heterotopic ossification, Increased varus or valgus angulation of the ankle, Ankle gutter narrowing, Infection, Syndesmotic or fibula osteotomy nonunion, Aseptic loosening, Expansile osteolysis (also known as ballooning osteolysis, periprosthetic cysts)

#### MKEE-100 Pain in the Rear-Exploration of MRI Findings Useful in Distinguishing Septic Arthritis from Inflammatory Spondyloarthritis of the Sacroiliac (SI) joints

##### Participants

Matin Goldooz, MD, Jackson, MS (*Presenter*) Nothing to Disclose

##### TEACHING POINTS

Review the sacroiliac joint anatomy. Illustrate MRI findings specific for inflammatory sacroiliitis and review updated Assessment of SpondyloArthritis international Society (ASAS) criteria. Illustrate common MR findings in infectious sacroiliitis. Review manifestations of degenerative sacroiliitis. Discuss common procedures for SI joint aspiration and therapeutic injection.

##### TABLE OF CONTENTS/OUTLINE

Infectious sacroiliitis is a destructive, monoarticular arthropathy typically caused by hematogenous seeding of bacterial pathogen. Clinical symptoms of SI joint disease are often nonspecific and may be attributed to pathology in hips or spine. Early recognition and prompt treatment of the condition is important to prevent permanent joint damage or abscess formation. Spondyloarthritides such as ankylosing spondylitis commonly involve the SI joints. The most recently updated classification criteria of axial

spondyloarthropathies are based on specific MRI findings, which facilitates prompt diagnosis. Differentiation between infectious and spondyloarthropathy associated sacroiliitis is incredibly important given the different prognosis and treatment regimens. MRI is the most relevant modality in evaluation of sacroiliitis, that can assist in differentiation of infectious and inflammatory etiology. Radiologists should be familiar with the MRI features that are more indicative of infectious sacroiliitis given the urgency required in making this diagnosis. In this educational exhibit we illustrate MRI findings of infectious and inflammatory sacroiliitis with emphasis on findings useful in differentiation of the two and in distinguishing both from degenerative sacroiliitis.

### **MKEE-101 Cervical Spine Infections and their Mimics**

#### **Awards**

##### **Certificate of Merit**

#### **Participants**

Samantha Salmon, MD, Columbia, MO (*Presenter*) Nothing to Disclose

#### **TEACHING POINTS**

1. Discuss shared key clinical and imaging characteristics of inflammatory and infectious diseases of the cervical spine. 2. To detail, in a case-based format, typical imaging features of infection of the cervical spine, organized by the site of origin. 3. To detail, in a case-based format, disease states that mimic infection and highlight key imaging and clinical factors that assist in the differentiation.

#### **TABLE OF CONTENTS/OUTLINE**

This presentation will be a case-based discussion reviewing cervical infections, differentiated by their site of origin. Cases will be presented alongside cases that mimic infection. Overview of shared presentation of infection and inflammatory diseases. Features of perivertebral infections. Prevertebral infection compared to longus coli tendinitis. Spondylodiscitis compared to renal osteodystrophy. Epidural infection, highlighting progression from phlegmon to abscess, compared to epidural tumor and hematoma. Intramedullary abscess compared to demyelination and infarction. Facet septic arthritis compared to CPPD arthropathy and neoplasm. Posterior soft tissue infections compared to post-operative seroma.

### **MKEE-102 3T Magnetic Resonance Neurography - From Head to Toe!**

#### **Awards**

##### **Cum Laude**

#### **Participants**

Flavia M. Costa, MD, PhD, Rio de Janeiro, Brazil (*Presenter*) Nothing to Disclose

#### **TEACHING POINTS**

1) 3T MR neurography is a technique involving regional MRI that allows evaluation of the peripheral nerves and is more effective than electrodiagnostic studies in the evaluation of deep structures. 2) Create a didactic script of what should be evaluated in neurography exams and how to recognize a normal or altered nerve. 3) Make a pictorial essay of the main peripheral nerves and their differential diagnoses.

#### **TABLE OF CONTENTS/OUTLINE**

1) Overview of what is magnetic resonance neurography and the examination technique. 2) 3T magnetic resonance of a traumatic lesion. 3) Tumoral lesion. 4) Inflammatory neuronal lesion. 5) Step by step for the evaluation of lesions and table with a summary of findings expected.

### **MKEE-104 Pediatric Spine and Spinal Cord Tumors: Imaging Answers to Clinical and Surgical Needs**

#### **Awards**

##### **Certificate of Merit**

#### **Participants**

VINICIUS BRAMBILLA, MD, Sao Paulo, Brazil (*Presenter*) Nothing to Disclose

#### **TEACHING POINTS**

Review the most frequent spinal, spinal cord and paravertebral tumors in childhood; Briefly discuss imaging modalities and protocols; Discuss differential diagnosis; Illustrate pseudotumoral findings and pitfalls.

#### **TABLE OF CONTENTS/OUTLINE**

**INTRODUCTION** Overview of spinal and paravertebral tumors in childhood seeking to illustrate and review the lesions split by compartments (paravertebral, vertebral, extradural and intradural) based on clinical cases from our institutional database. **PARAVERTEBRAL NEOPLASMS** Including neurofibromatosis benign findings and malign degeneration, neuroblastic tumors, paravertebral primary PNET. **VERTEBRAL NEOPLASMS** Including Langerhans cell histiocytosis, metastasis, osteoblastoma, chondrosarcoma; **EXTRADURAL NEOPLASMS** Including chloroma, primary extradural lymphoma; epidural metastasis. **INTRADURAL NEOPLASMS** Including astrocytoma, ependymoma, hemangioblastoma, intradural lipomatous lesions, primary diffuse leptomeningeal glioneuronal tumor, meningioma; **PSEUDOTUMORS** Including infectious diseases, extramedullary hematopoiesis, chronic recurrent multifocal osteomyelitis, arachnoid cysts; vascular lesions, spinal dysraphisms.

### **MKEE-105 A Nocturnal Nuisance: Diagnosis and Treatment of Osteoid Osteoma**

#### **Participants**

Meghan Jardon, MD, (*Presenter*) Nothing to Disclose

#### **TEACHING POINTS**

1. Osteoid osteoma is a benign tumor of bone that presents with nocturnal pain in children and young adults, classically relieved by non-steroidal anti-inflammatory drugs (NSAIDs). Common locations include the femur, tibia, and posterior elements of the spine. 2. The classic imaging appearance of a calcified nidus with surrounding sclerosis that is described on CT can be difficult to appreciate

on MRI. Thus, the radiologist must maintain a high level of suspicion when interpreting MRI, as misinterpretation may delay appropriate patient management. 3. Radiofrequency ablation provides a safe and effective means of treating osteoid osteomas, but additional consideration should be given in difficult locations (i.e. adjacent to neural elements, articular cartilage, etc.)

#### TABLE OF CONTENTS/OUTLINE

1. Background/Introduction 2. Clinical and Imaging Manifestations of Osteoid Osteomas 3. Case Examples from a variety of different anatomic locations A. Long bones: femur, tibia B. Spine: T12 posterior elements C. Others: talus, calcaneus D. Intra-articular examples: hip, elbow 4. Differential Diagnostic considerations for osteoid osteoma 5. Management of Osteoid Osteoma A. Medical management B. Radiofrequency ablation: Equipment, technique, special considerations in difficult locations C. Surgical resection

#### MKEE-106 Many Faces of Bone Metastasis: How to Detect and Not be Surprised

Participants

Eduarda Bernal, MD, Sao Paulo, Brazil (*Presenter*) Nothing to Disclose

#### TEACHING POINTS

Teaching points? Be prepared to do early detection of skeletal metastases.? Understand the biological mechanisms by which tumors metastasize to bone.? Recognize the appearance of skeletal metastases.? Review typical and atypical forms of secondary musculoskeletal involvement in different imaging methods

#### TABLE OF CONTENTS/OUTLINE

Introduction and objectives Metastases are the most common malignant tumors of the skeleton, and bone is the third most frequent site of metastasis, behind only the lung and liver. Early detection of skeletal metastases is essential for accurate staging and optimal treatment, in addition to improving the patient's quality of life. Bone metastases are a major cause of morbidity in cancer patients, characterized by severe pain, impaired mobility, pathological fractures and spinal cord compression. Understanding of the biological mechanisms by which tumors metastasize to bone and the diverse image appearance of skeletal metastases are important to detect disseminated disease. Methods We will review typical and atypical forms of secondary musculoskeletal involvement in different imaging methods through several cases and discuss the ideal method for diagnosis and monitoring of response to treatment of skeletal metastases. Conclusions Bone metastases have an important impact on the quality of life of cancer patients, and therefore, new strategies are needed to detect skeletal disease and attenuate established skeletal events. Radiologists are essential for this diagnosis since most bone metastases are asymptomatic at the beginning and knowing typical and atypical forms of skeletal metastatic involvement helps in early diagnosis and monitoring of response to treatment.

#### MKEE-107 Recognizing Pediatric Bone Tumors: Growing Your Knowledge

Participants

Vitor Cardoso Linhares, MD, Sao Paulo, Brazil (*Presenter*) Nothing to Disclose

#### TEACHING POINTS

There is a vast variety of bone tumors proposed by WHO 2020 classification, divided, among other aspects, into its tissue matrix type and biological behavior (benign, intermediate and malign). Considering the bone tumors of the pediatric population, the most common malign tumors are osteosarcoma and ewing sarcoma, and the most common benign tumours includes simple bone cyst and aneurysmal bone cyst. To identify the main characteristic of this tumours, especially in the pediatric age, can help patients to receive the adequate treatment and avoid unnecessary procedures. The purpose of this exhibit is to: • Briefly review the most recent World Health Organization (WHO) bone tumours classification. • Demonstrate cases of the most prevalent pediatric bone tumours. • Review the image findings of radiographic, CT and MRI studies of the most prevalent bone neoplasms in children.

#### TABLE OF CONTENTS/OUTLINE

(1) Briefly review the World Health Organization (WHO) bone tumours classification, and correlacionate with the most prevalent tumours in the pediatric population. (2) Approach the characteristics and image findings to help distinguish non aggressive and aggressive bone neoplasms. (3) Classify the most prevalent groups of benign, intermediate and malignant bone tumours in the pediatric population. (4) Describe radiographic, CT and MRI findings of each of the most prevalent groups of bone neoplasm in children. (5) Systematic approach to help the radiologist in the correct diagnosis of the bone tumours in the pediatric population.

#### MKEE-108 Fractures of the Appendicular Skeleton and Criteria for Their Surgical Management: What the Orthopedic Surgeon Wants to Know

Participants

Lucas Miyahara, MD, Sao Paulo, Brazil (*Presenter*) Nothing to Disclose

#### TEACHING POINTS

The purpose of this exhibit is to: 1. Review and illustrate some of the main appendicular skeleton fractures with surgical management, with emphasis on radiography and computed tomography, methods most commonly used in the emergency. 2. Didactically summarize the imaging findings that indicate the surgical treatment of appendicular skeleton fractures.

#### TABLE OF CONTENTS/OUTLINE

Introduction: general illustration of the fractures to be addressed. Demonstrate didactic and illustrative cases contemplating the following fractures: proximal humerus fracture, terrible triad of the elbow, Monteggia fracture-dislocation, Galeazzi fracture-dislocation, Barton fracture, scaphoid fracture, pelvic ring fracture, intertrochanteric fracture, femoral neck fracture, tibial plateau fracture, ankle fracture and Lisfranc fracture-dislocation. Provide schematic illustrations reviewing fracture classifications and discussing important concepts to understand the imaging findings. Present two tables that summarizes the trauma mechanisms and imaging findings that indicate the surgical treatment of appendicular skeleton fractures in each affected segment. Bibliographical references.

#### MKEE-109 Uncommon Manifestations of Bone Trauma: Focus on Medullary Fat

Participants

Pablo Rengifo, MD, (*Presenter*) Nothing to Disclose

## TEACHING POINTS

1. Following a high energy bone injury, a macroscopic fracture or a bone contusion (trabecular microfractures) is produced. In either case, medullary fat is compromised and typically shows high signal on fluid-sensitive MRI sequences. However, medullary fat might have other manifestations secondary to bone injuries.2. Uncommon manifestations of medullary fat related to bone trauma can be classified in intramedullary and extramedullary (extraosseus) fat accumulation. The last one could be categorized in intra-articular, intra-tendon sheath, intra-bursal, subperiosteal and systemic (fat embolism).3. Familiarity with imaging characteristics of intramedullary and extramedullary fat accumulation related to a high energy bone injury is essential in order to prompt further studies to demonstrate a possible occult fracture.

## TABLE OF CONTENTS/OUTLINE

1. Introduction.2. Anatomy of the Medullary Cavity.3. Types of uncommon manifestations of medullary fat after bone trauma: Overview.4. Intramedullary fat accumulation after bone trauma.5. Extramedullary (extraosseus) fat accumulation after bone trauma.5.1. Intra-articular.5.2. Intra-tendon sheath. 5.3. Intra-bursal. 5.4. Subperiosteal. 5.5. Systemic (fat embolism).5. Summary.6. References.

## MKEE-11 Gluteal Tendon Injuries: Anatomy, Pathological Conditions and Postoperative Imaging

Participants

Carlos H. Longo, MD, Sao Paulo, Brazil (*Presenter*) Nothing to Disclose

## TEACHING POINTS

The purpose of this exhibit is to: • Review and illustrate the anatomy of the gluteal tendons and their relationship to adjacent structures; • Illustrate and discuss the patterns of injuries involving these structures with didactic cases and their clinical relevance; • Illustrate and discuss types of surgical treatment and postoperative imaging findings of gluteal tendon injuries, and discuss its relation to hip arthroplasty.

## TABLE OF CONTENTS/OUTLINE

The gluteus medius and minimus muscles are hip abductors, with a crucial role in maintaining pelvic stability and normal gait. Although gluteal lesions are common, there is a relative paucity of detailed descriptions of features and patterns of tendon pathology in the literature compared to upper limb rotator cuff tendinopathy. Anatomy: • Imaging of gluteal bundles, subgluteus bursa and insertional anatomy exemplified by cases and didactic illustrations. Pathological conditions: • Function considerations and clinical relevance: Tendinopathy of the gluteus tendons are a cause of lateral hip pain and gait instability, particularly in older adults. Asymptomatic gluteal tendinopathies have been shown to have a negative effect on the outcomes of total hip arthroplasty. Surgical treatment and postoperative imaging: • Surgical indications and types of surgeries, modalities and complications.

## MKEE-110 World Cup is Coming - Recall the Typical Soccer Lesions

Participants

Gillis Lago, MD, (*Presenter*) Nothing to Disclose

## TEACHING POINTS

The purpose of this exhibition is:1. Review the main orthopedic injuries that occur in soccer.2. Correlate the trauma mechanism with the type of injury found3. Discuss the most common injuries, including muscle strains and injuries that occur in the knee, ankle and foot, as well as less common injuries that can occur in the upper limbs, through imaging methods in a multimodality approach.

## TABLE OF CONTENTS/OUTLINE

1 - Most common orthopedic injuries that occur after playing soccer, correlated with the main imaging findings in a multimodality approach (CR, US, CT and MRI).2 - Correlate the trauma mechanism with the main injuries found.3 - Most common orthopedic injuries and imaging findings in a multimodal approach, including:- Muscle injuries: - Acute; - Chronic;- Hip and pelvis: - Symphysis pubic dysfunction.- Knee injuries: - Ligament injuries, especially rupture of the anterior cruciate, medial collateral and posterior cruciate ligaments (less common). - Meniscal injuries; - Posterolateral corner injuries;- Ankle/foot injuries: - Ligament injuries, especially the lateral complex, which is the most affected; - Less common injuries, such as foot plate and ligament injuries;- Upper limb injuries: - Acute injuries to the shoulder, wrist and finger.- Miscellaneous and pediatric skeletal injuries, as osteochondrosis.

## MKEE-111 The Great Pretender: Benign Soft Tissue Tumors Mimicking Malignancy

Participants

Tina Shiang, MD, Worcester, MA (*Presenter*) Nothing to Disclose

## TEACHING POINTS

The aim of this educational exhibit is to present a case-based multimodality review of benign soft tissue tumors mimicking malignancy and provide a systematic approach to challenging cases of "lumps and bumps."1. Review the systematic approach to evaluating "lumps and bumps" and general principles for distinguishing benign vs malignant soft tissue masses.2. Present a series of challenging soft tissue tumor/pseudotumor cases that provided a diagnostic dilemma for the radiologist using a multimodality approach.3. Highlight the importance of a multidisciplinary approach in improving patient experience, including clinical, radiologic, and histopathologic correlation.

## TABLE OF CONTENTS/OUTLINE

1. Systematic approach to evaluating "lumps and bumps" in MSK practice.2. Presentation of benign soft tissue masses with imaging features suggestive of malignancy (XR, US, CT and MRI). a. Trauma: Myositis ossificans b. Neurologic: granular cell tumor, schwannoma c. Vascular: glomus tumor, vascular malformation d. Inflammatory: rheumatoid nodule e. Other: desmoplastic fibroelastoma, nodular fasciitis, pigmented villonodular synovitis3. Discussion of challenging aspects of clinical decision-making, management, and patient outcome.

## MKEE-112 Soft Tissue Tumors: What to Include in the Report - A Primer for General Radiologists

Awards

Cum Laude

## Identified for RadioGraphics

### Participants

Geoffrey M. Riley, MD, Portola Valley, CA (*Presenter*) Nothing to Disclose

### TEACHING POINTS

1. Provide general facts about soft tissue tumors  
2. List the 10 most important items that should be described in an MRI report on soft tissue tumors  
3. Show examples of how to report each item

### TABLE OF CONTENTS/OUTLINE

1. Introduction-General facts on imaging of soft tissue tumors  
2. Top 10 important components of the report-Compartment-Anatomic structure-Size and shape-Location relative to bony landmark-Description of borders-Relationship to adjacent structures-Signal characteristics and contrast enhancement-Peritumoral signal and tail-Feeding and draining vessels-Lymph nodes  
3. Conclusion  
4. References

## MKEE-113 I Feel Something in My Hand - What Could it Be?

### Participants

Cecilia Ruiz de Castaneda, Toledo, Spain (*Presenter*) Nothing to Disclose

### TEACHING POINTS

The purpose of this exhibit is: 1. To review the spectrum of soft tissue tumors of the hand and illustrate the typical and atypical imaging features. 2. To describe the main tumor-like lesions of the hand and wrist. 3. To analyze the differential diagnosis and provide diagnostic keys to identify pitfalls.

### TABLE OF CONTENTS/OUTLINE

Soft tissue masses of the hand and wrist are very prevalent in clinical practice. For this reason, the radiologist should be familiar with the most common benign and malignant tumors to develop and narrow the differential diagnosis. Multimodality imaging approach is mandatory for therapeutic planning. Although magnetic resonance imaging is an important imaging modality to diagnose soft tissue tumors, other initially ordered imaging modalities such as radiographs and ultrasound can also add valuable information about the lesions. We provide a comprehensive approach to tumors and tumor-like lesions of the hand, including demographics, clinical presentation, and imaging findings required to make an appropriate differential diagnosis

## MKEE-114 Vascular Changes that Every Musculoskeletal Radiologist Should be Aware of

### Awards

#### Certificate of Merit

### Participants

Eduarda Bernal, MD, Sao Paulo, Brazil (*Presenter*) Nothing to Disclose

### TEACHING POINTS

Teaching points- MRI of joints is often performed for presumed musculoskeletal conditions. There is a wide variety of variant vascular anatomy and vascular pathology that can occur around the joint, including an aberrant artery, vascular trauma that occurs with joint dislocation, artery aneurysm, vein thrombosis, cystic adventitial disease, and vascular anomalies like arteriovenous malformation.- Peripheral artery disease (PAD) is currently the leading cause of morbidity and mortality in the western world. The identification of PAD incidentally in a musculoskeletal examination can make the diagnosis and improve the survival of this patient.- Venous thrombosis is an important and frequent diagnosis with clinical signs and symptoms that can mimic musculoskeletal pathologies.- Cystic adventitial disease is an uncommon vascular pathology that have a predilection in the popliteal region, manifesting rapidly progressive calf claudication and lower extremity pain.

### TABLE OF CONTENTS/OUTLINE

IntroductionVascular abnormalities are an important and frequent diagnosis with clinical signs and symptoms that can mimic musculoskeletal pathologies. Due to this clinical similarity, MR examinations are frequently requested for patients with vascular abnormalities, under an equivocate suspicion of a musculotendineous or articular injury.ObjectivesThe purpose of this study is review unexpected and expected vascular findings, that can mimic musculoskeletal pathologies with the same clinical signs and symptoms.ConclusionsReviewing cases with vascular abnormalities on musculoskeletal examinations can help the radiologist to detect some patterns and extend the differential diagnosis.

## MKEE-115 More Than Just a Pinch: A Comprehensive Review of Ankle Impingement Syndromes

### Participants

Hira Qureshi, BA, Mason, OH (*Presenter*) Nothing to Disclose

### TEACHING POINTS

1. Review anatomy of the ankle and spaces at risk for impingement  
2. Describe clinical presentation and spectrum  
3. Discuss causes of impingement  
4. Imaging overview  
5. Discuss treatment

### TABLE OF CONTENTS/OUTLINE

-Introduction-Background-Review of anatomy-Role of imaging-Impingement syndromes: presentation, pathophysiology, imaging - Anterolateral-Soft tissue pathology-MRI: High signal intensity and thickening of ATFL andAITFL, synovial hypertrophy and distortion of anterolateral gutter-Tx: Conservative, arthroscopy-Anterior -Osseous outgrowth causing synovial reactivity-Radiographs: anterior tibiotalar osseous prominence-MRI: osteophytes, synovial thickening, scarring-Tx: Conservative, arthroscopy-Anteromedial-Soft tissue and osseous pathology-Radiographs: Medial malleolar osteophytes-MRI: Anterior deltoid thickening, synovitis, osteophyte formation-Tx: Conservative, arthroscopy-Posteromedial-Soft tissue pathology-MRI: intermediate signal of posterior tibiotalar ligament with thickening and loss of normal fibrillation-Tx: Conservative, arthroscopy-Posterior-Soft tissue pathology with anatomic predisposition, os trigonum -MRI: Bone marrow edema, edema at synchondrosis, thickening of posterior ligaments-Tx: Conservative, arthroscopy-Extra-articular-Biomechanical-MRI: cystic changes and bone marrow edema of lateral

talus-Tx: osseous correction or arthrodesis-Summary

### **MKEE-116 Do Not Let It Go:Frozen Shoulder and Capsulitis At Other Sinovial Joints**

Participants

Deodato Cartaxo, MD, Sao Paulo, Brazil (*Presenter*) Nothing to Disclose

#### **TEACHING POINTS**

Review the normal anatomy of shoulder, hip and other joints. Describe the pathophysiological mechanism and clinical evolution of adhesive capsulitis. Review the main image findings present on MRI, ultrasound and arthrography through didactically illustrative cases of adhesive capsulitis and its differential diagnosis. Exemplify the importance of a precise diagnosis in terms of treatment planning.

#### **TABLE OF CONTENTS/OUTLINE**

Review anatomy, pathophysiological mechanism and discuss about the different radiological findings of adhesive capsulitis of the shoulder and other joints, based on cases obtained from the digital file of our magnetic resonance institution and other methods. We also provide literature review, teaching points, take home message and references.

### **MKEE-117 Ultrasound-guided Intervention of Small Joints**

**Awards**

**Certificate of Merit**

Participants

Dyan V. Flores, MD, Ottawa, ON (*Presenter*) Nothing to Disclose

#### **TEACHING POINTS**

Ultrasound-guided intervention of small joints can be technically challenging because of irregular bony contour, size of joints disproportionately small compared to utilized tools and superficial location of intended targets. The objectives of this educational exhibit are: • 1. To identify clinical manifestations and indications of US-guided small joint interventions • 2. To describe the various indications for, contraindications to and expected outcomes associated with US-guided small joint interventions • 3. To demonstrate techniques, tips and tricks in performing these procedures by correlating with cross sectional images and graphic illustrations

#### **TABLE OF CONTENTS/OUTLINE**

Axial skeleton • Temporomandibular joint • Sternoclavicular • Symphysis Upper extremity • Tenotomies at the elbow • Ulnar nerve at cubital tunnel • De Quervain's tenosynovitis • Trigger finger • Median nerve at carpal tunnel • DRUJ Lower extremity • PeriAchilles region • Plantar fascia • Morton's neuroma

### **MKEE-118 Extensor Pollicis Longus: Imaging Review of Anatomy, Function and Pathology**

Participants

Cedric Bohyn, MD, Antwerp, Belgium (*Presenter*) Nothing to Disclose

#### **TEACHING POINTS**

1. Learn normal anatomy and variants 2. Learn the EPL's function 3. How to image and normal findings 4. Learn specific pathology:- Tenosynovitis- Distal intersection syndrome- Tendon tear- Delayed tendon rupture- Tendon subluxation and dislocation- Tendon entrapment

#### **TABLE OF CONTENTS/OUTLINE**

1. Anatomy, variants and associated structures:- Extensor Pollicis Longus- Lister's tubercle- Extensor retinaculum- Sagittal band of the first metacarpal joint 2. Function 3. Imaging Considerations 3. Dysfunction/Pathology- Tenosynovitis- Distal intersection syndrome- Tendon tear- Delayed tendon rupture- Tendon subluxation and dislocation- Tendon entrapment

### **MKEE-119 Anything is Possible if You've Got Enough Nerve! Ultrasound (US) Approach to the Upper Limb Nerves**

Participants

Michaela Cellina, (*Presenter*) Nothing to Disclose

#### **TEACHING POINTS**

To show the US approach to the nerves of the upper limb, involving the technique, patient's positioning, and anatomical landmarks. To describe dimensional and echo-structural characteristics of non-pathological nerves.

#### **TABLE OF CONTENTS/OUTLINE**

Thanks to its spatial resolution, wide availability, and possibility of real-time and dynamic evaluation, US is the first level exam for the peripheral nerves study, but its use is still limited by a lack of knowledge and expertise. One of the most common indications is suspected nerve entrapment (e.g. carpal and cubital tunnel syndromes). Peripheral nerves should be studied with high-frequency linear array probes. Nerves are usually identified on the axial planes in defined anatomical landmarks. Normal nerves show a fascicular, honeycomb appearance in the short axis and are surrounded by hyperechoic connective tissue. In the long axis, the nerve aspect is coarse and hypoechoic. Important landmarks for median nerve identification are the brachial artery in the upper arm and elbow, the flexor digitorum profundus and flexor digitorum superficialis in the forearm and the carpal tunnel in the wrist. Cross-sectional area (CSA) at three sites of the median nerve ranges from 5.38 to 8.43 mm<sup>2</sup>. The ulnar nerve is evaluated posteriorly to the brachial artery in the upper arm, at the level of the medial epicondyle of the elbow and the pisiform bone of the wrist. CSA at various points for the ulnar nerve ranges from 2.76 to 5.21 mm<sup>2</sup>. The radial nerve is assessed at the level of the arm-spiral sulcus on the posterior aspect of the humerus and has a normal CSA of 4.72 mm<sup>2</sup>. The thickening of the nerve sheath is a very common finding in the main demyelinating neuropathies, both hereditary and acquired.

## **MKEE-12    Participants    Your Weakest Link: The Kinetic Chain and Pitching Injuries of the Elbow**

Akwasi Opoku, MD, Nashville, TN (*Presenter*) Nothing to Disclose

### **TEACHING POINTS**

The "kinetic chain" is the coordinated translation of force and motion from the lower extremity/core into the upper extremity during pitching. Any deviation-abnormal anatomy, physiology, or mechanics- places increased forces across joints, predisposing to injury, especially of the elbow. This multimodality imaging review of repetitive valgus stress injury of the elbow in pitchers emphasizes important imaging findings for surgical intervention. Intra-operative correlation is provided. After viewing this exhibit, the learner should be able to: 1) Understand the biomechanics of pitching, including the concept of the kinetic chain, and recognize potential chain disruptors. 2) Recognize patterns of valgus injury of the elbow in pitchers. 3) Discuss important preoperative imaging findings for ulnar collateral ligament and osteochondral injuries.

### **TABLE OF CONTENTS/OUTLINE**

Introduction: (1) Biomechanics of pitching: kinetic chain (2) Deviations in the kinetic chain (anatomy, physiology, mechanics) Elbow injury of the elite pitcher: Repetitive valgus overload (1) Medial Tensile force overload: UCL and common flexor tendon origin) (a) anatomy (b) pathology (tear grade and location, ligament edema, associated osseous changes) (c) Role of MR arthrography (2) Lateral compressive force overload: radiocapitellar joint (a) anatomy (capitellar bare area mimic) (b) pathology (osteochondral injury, Panner's disease) (3) Valgus extension overload (a) pathology (asymmetric osteoarthritis, ulnohumeral impaction) (4) Management of elbow injury: important imaging findings (a) surgical vs non-surgical (b) surgical technique

## **MKEE-120    Pointing to the Problem: A Comprehensive Approach to Finger Disorders**

Participants

Augusto Altoe, Rio de Janeiro, Brazil (*Presenter*) Nothing to Disclose

### **TEACHING POINTS**

1. To understand the anatomical basis involved in finger injuries; 2. To describe the imaging patterns of the finger pathologies; 3. To recognize common and uncommon finger disorders.

### **TABLE OF CONTENTS/OUTLINE**

1- Background. 2- MRI acquisition considerations. 3- Finger ligaments; a. Review of the finger ligaments; b. Collateral ligament injuries of the finger; c. Locked metacarpophalangeal joint; d. Ulnar collateral ligament tears of the thumb; e. Volar plate injuries. 4- Flexor tendons and pulley system; a. Review of the flexor tendons anatomy and pulley system; b. Flexor tendon injuries and lacerations; c. Pulley injuries; d. Trigger finger. 5 - Extensor mechanism; a. Review of the extensor mechanism anatomy; b. Terminal extensor tendon injury (Mallet Finger); c. Central slip injury; d. Sagittal band injury. 6- Miscellaneous; a. Macrodystrophia lipomatosa; b. Acro-osteolysis; c. Palmar fibromatosis (Dupuytren's contracture); d. Tenosynovial giant cell tumor; e. Fibroma of the tendon sheath. 7 - Take home messages.

## **MKEE-121    Talk to the Hand - Ultrasound evaluation of Tendon, Ligament, and Support Structure Injury in the Hand with MRI Correlation**

**Awards**

**Cum Laude**

Participants

Peter Hoeksema, MD, Detroit, MI (*Presenter*) Nothing to Disclose

### **TEACHING POINTS**

1. Normal appearance of the flexor and extensor tendons of the hand on ultrasound. Review of scanning technique to optimize imaging of desired structures. Discussion of normal anatomy and insertion of tendons. Review of the pulleys on the flexor surfaces of the hand. Discussion of the extensor hood and sagittal bands. Review of the UCL at the first MCP joint. 2. Ultrasound examples of injury involving the FDP, and FDS. Ultrasound example of pulley abnormalities with trigger finger. Concurrent MRI examples of pathology demonstrated on US. 3. Ultrasound examples of injury extensor tendons. Example of sagittal band injury with dynamic subluxation of the tendon. Concurrent MRI examples. 4. Ultrasound examples of UCL injuries (partial and full thickness tear). Example of a Stener type lesion.

### **TABLE OF CONTENTS/OUTLINE**

- Anatomy and Imaging Review of optimal imaging technique for the flexor and extensor tendons. Review of associated normal anatomy. Review of the normal location of the flexor pulleys and imaging appearance. Review of optimal position and technique to visualize the UCL of the thumb. Volar Pathology with radiographic and MRI correlates as available. Ultrasound examples of FDP/FDS tendon tears with static and dynamic images. Ultrasound of injury to the flexor pulley apparatus. Dynamic US imaging of trigger finger. Dorsal Pathology with radiographic and MRI correlates as available. Ultrasound example of extensor tendon tear. Ultrasound examples of sagittal band injury with dynamic examples of tendon subluxation. UCL. Example of injury to the thumb UCL on ultrasound with MRI example. Example of Stener lesion on ultrasound

## **MKEE-122    Hypermobility Syndrome - Findings on an Underestimated Diagnosis of Carpal Instability Non-dissociative by the Radiologist**

Participants

André Henrique Toledo, Campinas, Brazil (*Presenter*) Nothing to Disclose

### **TEACHING POINTS**

Carpal instability is a complex and heterogeneous clinical condition. Management requires accurate identification of the structural lesion involved. Midcarpal instability is a form of non-dissociative carpal instability and can be caused by various combinations of extrinsic ligament injuries with abnormal kinematics between the carpal rows. Such instability is related to biomechanical alterations of multiple causes that, if not identified and treated in a timely manner, will lead to gradual joint collapse. It is important to note that unstable wrist initially does not show relevant signs on standard radiographs and studies such as Magnetic resonance imaging

(MRI) and MRI arthrography can detect initial findings of instability. In more advanced stages, carpal instability can progress to static wrist misalignment and osteoarthritis, both of which are associated with significant morbidity and disability. To prevent complications and joint sequelae, the radiologist must be aware of this challenge for the early and accurate diagnosis of carpal instability as an important entity, but often undervalued and remembered.

#### TABLE OF CONTENTS/OUTLINE

Role of the Radiologist - What differential diagnosis would you think? - Step by step in imaging and classic instability signs - Classification and what to look for Differential diagnosis review - is there room for hypermobility syndrome? - Carpal instability x joint hypermobility syndrome - What to expect? - Take home message.

#### MKEE-124 Spectral CT Imaging of the Bone Marrow: How To Do It"

Participants

Bernhard Petritsch, MD, Wuerzburg, Germany (*Presenter*) Research Consultant, Siemens AG

#### TEACHING POINTS

To review the indications, contraindications and limitations of spectral CT imaging in terms of photon counting detector computed tomography (PCD-CT) and conventional energy integrating detector (EID) dual-energy computed tomography (DECT) for bone marrow imaging. To learn about the basic physical principles of PCD-CT and conventional DECT imaging with emphasis on bone marrow applications. To interpret spectral bone marrow CT scans of healthy subjects, patients with acute fractures or malignant bone marrow infiltration. To highlight the potential benefits of spectral CT investigation as a comprehensive examination of osseous morphology and additional bone marrow information.

#### TABLE OF CONTENTS/OUTLINE

A. Basic principles of photon counting detector (PCD) and energy integrating detector dual-energy computed tomography (DECT).B. Technical differences in data acquisition: PCD CT vs. Single-Source EID vs. Dual-Source EID CT-scanners (differences between 1st-3rd generation dual-source scanners).C. Post-processing: Material-decomposition algorithm, creation of VNCA ("virtual non-calcium") images.D. Data acquisition: Parameter settings for PCD and dual-energy CT of the extremities, spine and pelvis.E. Current applications of spectral CT for the detection of acute fractures and malignant bone marrow infiltrations (e.g. in multiple myeloma): examples in the spine, pelvis and extremities.F. Pitfalls and limitations of spectral bone marrow Imaging; alternative imaging modalities.

#### MKEE-125 Don't Let the Foot Drop: Review of the Anatomy, Imaging, and Pathologies of the Sciatic Nerve and its Branches

Participants

Andrew Liu, MD, (*Presenter*) Nothing to Disclose

#### TEACHING POINTS

Foot drop is a common reason for consultation and deserves a quick clinical and radiological assessment. Knowledge of the anatomy, the course and the division of the sciatic nerve and its branches is required so that the radiologist can image the adequate anatomical area whether by ultrasound or by MR imaging. The advantages of ultrasound lie in the possibility to survey the entire nerve and its branches in a short period of time. However, this modality remains operator-dependent. Through this Education Presentation, a review of the anatomy of the sciatic nerve and its branches, the different modern modalities available, and pathologies that might affect the sciatic nerve and its branches nerve is propose.

#### TABLE OF CONTENTS/OUTLINE

Revise the anatomy of the sciatic nerve, the common peroneal nerve, the superficial and deep peroneal nerves Understand, revise and optimize cross-section imaging (MRI neurography and ultrasound). Navigate through traumatic (traumatic neuroma, post-amputation neuroma), tumoral (BNPST, MPNST, neurofibromatosis, etc.), and miscellaneous pathologies (intra-neuronal and extra-neuronal ganglion cyst) of the lower extremity nerves.

#### MKEE-126 Musculoskeletal Ultrasound: No Pain, No Gain - A Compilation of Techniques and Lesions

Participants

Cleiton Freitas, MD, Sao Paulo, Brazil (*Presenter*) Nothing to Disclose

#### TEACHING POINTS

A) Musculoskeletal ultrasound should be based on systematized image acquisition techniques and on the recognition of multiple pathologies. B) Importance of documenting and visualizing the appropriate musculoskeletal anatomical structures, focusing on teaching the Radiology Resident physicians the most recommended techniques. C) For each analyzed body segment, pathologies of significant clinical importance, including common and uncommon pathologies will be analyzed. D) More than 40 pathologies and their differential diagnoses will be analyzed, because no pain no gain.

#### TABLE OF CONTENTS/OUTLINE

- Introduction- Anatomy review- Ultrasound imaging capture sequence- Lesions and their differential diagnosis- Take-home messages

#### MKEE-127 Imaging of Postoperative Pectoralis Major Tendon: What Radiologists Need to Know

Participants

Luana Maciel, (*Presenter*) Nothing to Disclose

#### TEACHING POINTS

- To evaluate the appearance of pectoralis major tendon after surgical correction.
- To assess the MRI aspects of the pectoralis major muscle tendon after surgical repair, using different approaches, such as anchors, cortical buttons, bone holes or surgical reconstruction using autologous graft (semitendinosus, gracilis) or allograft.

## TABLE OF CONTENTS/OUTLINE

• Anabolic steroids usage by weightlifting athletes gym work out men has led to a significant increase in the incidence of pectoralis major injuries. • Ecchymosis and local hematomas followed to those lesions limits clinical evaluation and make imaging crucial for injury graduation and repair planning. Magnetic resonance imaging and ultrasonography are established as methods of choice. • Surgical treatment is the best approach for pectoralis major injuries. • Humeral tendon reinsertion using either surgical wires or metallic anchors are chosen for acute lesions and orthopedic screws for chronic ones. Old injuries with tendon retraction may require reconstruction with autologous graft, commonly from the hamstrings or allograft. • Surgical treatment reported a lower degree of strength loss compared to conservative conduct. In addition, it was superior regarding aesthetic and functional gain, with a high rate of sports activity return. • Imaging plays an important role not only for diagnose and surgical planning but also to postoperative follow-up, depicting early changes not seen in clinical evaluation.

### MKEE-128 Normal and Abnormal MRI Finding of Rotator Interval Correlated with Arthroscopy

Participants

Ji Yoon Lee, (*Presenter*) Nothing to Disclose

#### TEACHING POINTS

1. To describe normal MRI anatomy of rotator interval, with associated arthroscopy finding. 2. To present MRI finding of rotator interval pathology, correlation with arthroscopy. 3. To present associated findings at long head of biceps tendon and subscapularis tendon, correlation with arthroscopy. 4. To enhance rotator interval image interpretation and let better coordination between radiologists and orthopedic surgeons in terms of surgical planning or retrospective image review.

## TABLE OF CONTENTS/OUTLINE

1. Normal MRI and arthroscopy finding of rotator interval. 2. Abnormal MRI findings of rotator interval, including biceps tendon tear and subluxation, subscapularis tendon lesion, synovitis, adhesive capsulitis are presented, with corresponding arthroscopy image.

### MKEE-129 The Repaired Rotator Cuff: Normal and Abnormal Appearance with Focus on US and MRI

**Awards**

**Cum Laude**

Participants

Paola Kuenzer Goes, MD, Sao Paulo, Brazil (*Presenter*) Nothing to Disclose

#### TEACHING POINTS

The repaired rotator cuff frequently appears abnormal on ultrasound (US) and magnetic resonance imaging (MRI). While the appearance of tendons and surrounding tissues typically normalize, they can demonstrate clinically insignificant abnormal imaging appearances for longer than 6 months. US and MRI are useful in the postoperative assessment of the rotator cuff, not only for evaluation of the integrity of the rotator cuff, but also for detecting hardware complications and ruling out other sources of shoulder pain. The objectives of this educational exhibit are: 1. Briefly review the US and MRI findings of the normal postoperative rotator cuff 2. Discuss US and MRI findings of various types of repair and fixation 3. Illustrate US and MRI findings of post rotator cuff repair complications according to three potential sources (tendon, hardware and soft tissues)

## TABLE OF CONTENTS/OUTLINE

Normal postoperative rotator cuff • Types of repair Which tendon(s) was repaired, method of repair (tendon suture, reinsertion, transfer of tendons or grafts), and types of fixation (transosseous, double-row, double-row bridged) • US findings • Early MRI findings • Late MRI findings • Complications • Tendon Partial re-tear Complete re-tear • Hardware complications Fracture Migration • Soft tissues Infection Bursitis Adhesive capsulitis

### MKEE-13 Imaging Review of the Healing Process in Sport Muscle Injuries

**Awards**

**Identified for RadioGraphics**

Participants

Jaime Isem, PhD, (*Presenter*) Nothing to Disclose

#### TEACHING POINTS

1. To review the mechanisms of muscle injury, repair and regeneration. 2. To present the imaging technique of choice for the healing process study. 3. To describe the MRI findings of reparative changes of a muscle tear. 4. To show the muscle adaptive changes by MRI during the healing process. 5. To show the imaging findings that suggest aberrant progression of the healing process.

## TABLE OF CONTENTS/OUTLINE

Physiological mechanism of the healing process after muscle sport injury. MRI protocol to assess the reparative process of sports muscle injury. Review of imaging findings of the healing process and adaptive changes. Discuss the influence of MRI findings on the therapeutic decision.

### MKEE-130 Postoperative Rotator Cuff (Surgical Indications, Normal and Pathological Postoperative Findings) - A Practical Guide for Radiologists

Participants

Camila Munaro I, MD, (*Presenter*) Nothing to Disclose

#### TEACHING POINTS

1. To review the anatomy of the rotator cuff and discuss common tendon tears 2. To review surgical procedures and indications for treatment of rotator cuff tears 3. To review the challenging clinical and radiologic scenario of postoperative shoulder 4. To describe normal expected postoperative appearances of the rotator cuff tendons 5. To discuss the most common pathological postoperative

findings, including recurrent tears, infection, anchor migration, nerve injury and muscle degeneration.

#### TABLE OF CONTENTS/OUTLINE

1 - Anatomy of rotator cuff  
2 - MR Imaging of rotator cuff tears  
3 - Treatment of rotator cuff tears  
4 - Surgical indications  
5 - MR evaluation of the expected postoperative rotator cuff  
6 - Recurrent tears  
7 - Infection  
8 - Anchor migration  
9 - Nerve injury  
10 - Muscle atrophy and fatty degeneration

#### MKEE-131 Multimodality Review of Sclerotic Lesions in the Spine

Participants

William Holden, MD, BS, (*Presenter*) Nothing to Disclose

#### TEACHING POINTS

Sclerotic lesions of the spine can be challenging to characterize due to their broad differential and overlapping imaging features. A methodical approach is necessary when formulating a differential diagnosis for these lesions. This educational exhibit will review patterns of focal, multifocal, and diffuse vertebral body sclerosis on multiple modalities, including plain radiographs, CT, MRI, MDP bone scan, and FDG-PET. This review will provide a framework for evaluating different categories of osseous sclerosis, including infectious/inflammatory, neoplastic, metabolic, and developmental causes. Familiarity with specific imaging patterns and assessment of pertinent clinical information will allow the radiologist to more accurately interpret sclerotic lesions of the spine, and recommend appropriate follow-up and additional imaging evaluation.

#### TABLE OF CONTENTS/OUTLINE

1. Provide an overview of modalities used for the evaluation of sclerotic bone lesions, including plain radiographs, CT, MRI, MDP bone scan, and FDG-PET. 2. Review common and uncommon cases of focal, multifocal, and diffuse sclerotic vertebral lesions. a. Cases will include 3-4 examples from each category: i. Infectious/inflammatory ii. Neoplastic iii. Metabolic iv. Developmental b. For each lesion, the discussion will include: i. Multimodality imaging findings ii. Pertinent clinical history iii. Diagnostic pearls 3. Provide a diagnostic algorithm for the evaluation of sclerotic vertebral lesions.

#### MKEE-132 Sacral Lesion - Recognizing the Most Common Lesions

Participants

Andre Y. Aihara, MD, PhD, Sao Paulo, Brazil (*Presenter*) Nothing to Disclose

#### TEACHING POINTS

The purpose of this study is:- Review the normal anatomy and imaging appearance of the sacrum, using CT and MR images.- Didactically discuss sacrum lesion, dividing into 4 categories: Tumors, trauma, infections, and non-infectious inflammatory arthropathies.- Elucidate the typical findings of sacral tumors, frequent locations, age and sex distribution, and characteristic imaging findings.

#### TABLE OF CONTENTS/OUTLINE

The sacrum is a structure located in the pelvis with an important role in spinal biomechanics. It is composed of multiple tissues: cartilage, bone marrow, nerves, meninges and notochord remnants. This diversity of components can originate different primary tumors, most of them with predicted location and imaging findings. Since the sacrum is rich in hematopoietic bone marrow, metastasis is frequent. Sacral fractures can result from high-energy trauma or be related to low-energy impact, as in insufficiency stress fractures. The typical H-shaped pattern can be seen in bilateral sacral insufficiency fractures. Most sacrum infection is by continuity spread, common with the infection of the pelvic adjacent organs. Finally, it is important to remember inflammatory arthropathy and those resulting from local mechanical overload.

#### MKEE-133 Atlantoaxial Injuries: Don't Lose Your Head!

**Awards**

**Identified for RadioGraphics**

Participants

Leticia Morimoto, MD, Sao Paulo, Brazil (*Presenter*) Nothing to Disclose

#### TEACHING POINTS

The purpose of this study is:• Revisit the anatomy of the atlantoaxial joint, highlighting the ligamentous structures• Review with didactic cases the main atlantoaxial fractures and its associated injury mechanisms• Present several cases of non-traumatic lesions of the atlantoaxial joint, including inflammatory, infectious and tumoral conditions

#### TABLE OF CONTENTS/OUTLINE

• Introduction and overview of the atlantoaxial joint, including normal anatomy with didactic illustration. • Demonstrate the ligamentous anatomy and how to recognize it on MRI. • Demonstrate didactically the radiographic, CT and MRI findings of several traumatic atlantoaxial traumatic injuries. • Overview the classifications for atlantoaxial trauma injuries. • Review the management treatment options for each injury, and their post-operative exams, highlighting what the radiologist should look for. • Challenging cases of non-traumatic diseases, including rheumatoid arthritis, villonodular synovitis, infections, neurofibromatosis, Langerhans cell histiocytosis, and others. • Summary.

#### MKEE-134 Bone-RADS Classification - What the Radiologist Needs to Know

Participants

Verena Pires, MD, (*Presenter*) Nothing to Disclose

#### TEACHING POINTS

To review the Bone-RADS (bone reporting and data system) classification with a simple guide using examples. To provide radiologists with a general overview enabling them to understand and interpret Bone-RADS in different lesions.

#### TABLE OF CONTENTS/OUTLINE

Incidental solitary bone lesions are frequently encountered on computed tomography (CT) and magnetic resonance imaging (MRI) in routine clinical practice. Despite the prevalence of these unexpected lesions, clear and consistent guidelines for their management have not been defined in the literature. The purpose is to present algorithms for the diagnostic management of solitary bone lesions incidentally encountered on CT and MRI in adults. For risk stratification, the Bone-RADS recommends four categories, incorporating the range of benign to suspicious for malignancy or need for treatment (Bone-RADS1, leave alone; Bone-RADS2, perform different imaging modality; Bone-RADS3, perform follow-up imaging; Bone-RADS4, biopsy and/or oncologic referral). Two algorithms for CT based on lesion density (lucent or sclerotic/mixed) and two for MRI allow the user to arrive at a specific Bone-RADS management recommendation. Representative cases are provided to illustrate the usability of the algorithms. The ultimate goal is to optimize bone lesion outcomes while minimizing unnecessary surgical procedures in patients at low risk of malignancy and to provide a management recommendation for each risk category. Then, this classification can standardize lesions and decrease ambiguity reporting to enhance communication among the multidisciplinary team.

### **MKEE-135 The Role of Conventional Radiography in the Diagnosis of Bone Tumors**

#### **Awards**

#### **Identified for RadioGraphics**

#### **Participants**

Abel Gonzalez Huete, MD, Madrid, Spain (*Presenter*) Nothing to Disclose

#### **TEACHING POINTS**

1. To provide an educational review of bone tumors and their appearance in conventional radiography. 2. To review differential diagnosis and discuss a systematic approach to the diagnosis of bone tumors and tumor-like lesions based on conventional radiography features and clinical presentation.

#### **TABLE OF CONTENTS/OUTLINE**

1. Introduction. 2. Age of presentation. 3. Review of imaging findings. - Opacity (lytic, sclerotic, mixed). - Margin and destruction patterns. - Periosteal Reaction. - Cortical Involvement. - Mineralization (chondroid matrix, osteoid matrix). - Location: skeleton, longitudinal (epiphyseal, metaphyseal, diaphyseal), transverse (centric, eccentric, cortical, juxtacortical). - Number (solitary, multiple, polyostotic). - Soft Tissue Component. 4. Sample cases and mimics. 5. Summary.

### **MKEE-136 Whole-body Imaging on Multiple Myeloma: Imaging Modalities and Applications**

#### **Participants**

Henrique Lino, MD, Sao Paulo, Brazil (*Presenter*) Nothing to Disclose

#### **TEACHING POINTS**

Multiple myeloma is the most common primary tumour of bone with an incidence of 10 per 100,000. Multiple myeloma whole-body imaging techniques (MM-WB) can help detect subclinical lesions and determine early treatment, increasing prognostic and avoiding fractures and other complications.

#### **TABLE OF CONTENTS/OUTLINE**

Introduction: The MM-WB modalities are x-ray skeletal survey, computed tomography (CT), magnetic resonance (MRI), computed tomography 18F-fluorodeoxyglucose positron emission tomography (PET-CT). Objectives: (1) to review the use of MM-WB. (2) to exemplify cases and compare the imaging modalities. Methods: We queried cases to illustrate the imaging methods. Discussion: Although skeletal survey is the reference method, it has a high false negative rate (30-70%). Axial methods have a higher sensitivity (68-100 %) for the condition. The general diagnostic criteria for axial methods, by the International Myeloma Working Group, is one or more focal lesions with 5 mm or more, with osteolytic behaviour. Among these methods, MRI has the advantage of no radiation, and it has the best diagnostic performance for the evaluation of soft tissue lesions and bone marrow compromise as well it has a high specificity from 83 to 100%, and also treatment response (as well as PET-CT). Conclusion: multiple modalities of MM-WB can detect focal and diffuse disease, quantify burden, and predict treatment response as well it is able to detect mechanical complications.

### **MKEE-137 Sacral Insufficiency Fractures in Cancer: Is There a Met Hiding in Plain Sight?**

#### **Participants**

Kaustav Bera, MD, Cleveland, OH (*Presenter*) Nothing to Disclose

#### **TEACHING POINTS**

1. Review the different causes of sacral insufficiency fractures (SIFs) 2. Review the various imaging modalities used to diagnose SIFs 3. Discuss the role of imaging findings along with clinical and laboratory findings to determine the cause of the SIFs 4. Review ways to differentiate SIFs from metastatic lesions of the sacrum 5. Discuss management and outcomes of SIFs

#### **TABLE OF CONTENTS/OUTLINE**

1. Introduction and history of sacral insufficiency fractures (SIF) as an entity 2. Epidemiology and demographics of SIF 3. Risk factors for SIF 4. Clinical History and symptoms in SIF 5. Association of SIF with disease conditions (Renal osteodystrophy, Rheumatoid Arthritis, Paget disease) 6. Different imaging modalities that help in diagnosing SIF 7. Different etiologies that cause SIF a) Age induced/Osteoporotic b) Inflammatory arthropathy c) Radiation induced d) Hormone induced e) Other Drug induced (Steroids/Bisphosphonate) 8. Cancers that often metastasize to the sacrum and can mimic SIF 9. Imaging findings coupled with clinical and laboratory parameters that help you distinguish between different etiologies of SIF as well as contrast it from Metastatic disease 10. Management of SIF 11. Prognosis and clinical outcome of SIF

### **MKEE-138 The Role of Cinematic Rendering in the Evaluation of Complex Vascular Injury of the Lower Extremities: How We Do It**

#### **Participants**

Elliot Fishman, MD, Owings Mills, MD (*Presenter*) Co-founder, HipGraphics, Inc; Stockholder, HipGraphics, Inc; Institutional Grant support, Siemens AG; Institutional Grant support, General Electric Company; Consultant, Exact Sciences Corporation; Consultant, Imaging Endpoints

## TEACHING POINTS

1. CT with CTA is the state of the art for the evaluation of the patient with lower extremity trauma regardless of whether the trauma is an MVA,, gunshot wound or stabbing or simply a fall2. diagnosis of injury is but step one in patient management and the role of 3D has classically been to help with management decisions by improving understanding of the true extent of the injury.3. Cinematic rendering is an advanced form of volume rendering which is ideal in the trauma setting by visualization of muscle and soft tissue, the vascular map and underlying bony structures. When optimized it provides a clear understanding of the "personality" of the specific injury4. the use of Cinematic Rendering provides an opportunity to provide extra value in the interpretation and management of complex trauma to the lower extremities. A paradigm for use of cinematic rendering is addressed.

## TABLE OF CONTENTS/OUTLINE

1. Imaging protocols for lower extremity trauma including the role of dual energy CT2. imaging protocols for using cinematic rendering for the range of lower extremity trauma3. analysis of case studies showing the added value of cinematic rendering in trauma of soft tissue/muscle, the bony anatomy and the vascular map. Specific presets for optimizing workflow and analysis are presented4. case studies showing the impact of cinematic rendering on patient management are presented, and discussed5. role of Cinematic Rendering for patient management dcisions is addressed and illustrated as well. potential pitfalls and limitations of Cinematic Rendering are also discussed and illustrated

### MKEE-139 Staying Afloat With the Competitive Swimmer - Common and Uncommon Injuries

Participants

Sonja Oppen, DO, Pittsburgh, PA (*Presenter*) Nothing to Disclose

## TEACHING POINTS

1. Athletic injuries have been well documented in the literature, particularly in mainstream sports such as football, soccer and baseball. A sport that is poorly represented in the literature is swimming. 2. Swimmers are susceptible to chronic types of stress on their bodies as a result of varying repetitive physical movements, as well as unique environmental and chemical exposures. The majority of swimming related injuries are a result of repetitive microtrauma in the shoulders, elbows, and knees. 3. Acute injuries often relate to the flip turn, starts/finishes and the dive where there are rapid accelerations and decelerations as well as the potential for barotrauma while submerged. 4. In this presentation we will review common and uncommon injuries in avid swimmers and review the mechanism of injury in these athletes with special attention to the physiology of different strokes.

## TABLE OF CONTENTS/OUTLINE

1. Review the 4 basic strokes (freestyle, backstroke, breaststroke, and butterfly) and flip turns with videos illustrating the mechanics, areas of stress, and potential for injuries. 2. Review imaging of the common injuries related to competitive swimmers. a. Shoulder injuries b. Knee injuries c. Foot injuries d. Hip injuries 3. Discuss the environmental and chemical exposures that predispose swimmers to unique injuries. 4. Interactive cases

### MKEE-14 Let's be "Franc" about the Lisfranc: A Review of Anatomy, Pathology, and Disease Mimics

Participants

Sirui Jiang, MD, PhD, Cleveland, OH (*Presenter*) Nothing to Disclose

## TEACHING POINTS

1. Review the anatomy of the Lisfranc joint complex2. Review the clinical presentation and causes of injuries to the Lisfranc joint complex3. Multimodality imaging overview of Lisfranc joint complex injuries including common measurements and hallmark findings4. Discuss common radiographic mimics of Lisfranc injuries5. Overview of orthopedic management of Lisfranc injuries

## TABLE OF CONTENTS/OUTLINE

Background-Image-based anatomy review of the Lisfranc joint complex-Incidence of Lisfranc injuries and diagnostic missesEtiology of Disease -Biomechanical/Traumatic Causes-Soft tissue injuries without dislocation-Bony injury with mild displacement -Bony injury with marked displacement-Clinical Presentation-Physical Examination Imaging Studies-Radiographs-AP, lateral, and oblique views during weight-bearing-How to identify dislocation of the Lisfranc joint complex-Spectrum of findings in alternative views - Spontaneous reduction during radiographic evaluation-Other Imaging Modalities-CT-MRI-Ultrasound Common Mimics -Vascular calcifications -Os intermetatarsale Complications-Post-traumatic arthrosis-Instability-Chronic painManagement-Non-operative management-Surgical fixation-Repeat imaging-Post-operative physical therapy

### MKEE-140 Traumatic Instabilities of the Cervical Spine: What the Radiologists Need to Know

Participants

Alan Strapasson, MD, (*Presenter*) Nothing to Disclose

## TEACHING POINTS

The purpose of this exhibit is: 1. Review the anatomy in the different imaging methods and their main variations relevant to trauma assessment.2. Review measurement techniques.3. Correlate the trauma mechanism with the main injuries related to each one of them.4. Address the most common ligament injuries with a focus on MRI.5. Discuss atlantoaxial dissociation and odontoid fracture. 6. Classification of lesion instability (Vaccaro, NEXUS).

## TABLE OF CONTENTS/OUTLINE

1. Anatomy and assessment of CR, CT and MRI in adults and children and their main anatomical variations relevant to the assessment of trauma. 2. Measurement techniques: Wackenheim, Chamberlain, Mcgregor, Power Ratio, basion-axial interval, atlantodental interval. 3. Flexion injuries: wedge compression fracture, flexion teardrop fracture, anterior subluxation, bilateral facet dislocation, Clay Shoveler, anterior atlantoaxial dislocation. 4. Hyperflexion and rotation: unilateral facet displacement (locked facet). 5. Extension: hangman's fracture, teardrop fracture by extension.6. Axial compression: Jefferson fracture, burst fracture.7. Odontoid fracture.8. Atlantoaxial Dissociation.9. Ligament injuries: alar and transverse ligament.10. Vaccaro Classification (2007), Harris.11. Unstable fractures in order.12. NEXUS Criteria.

## **MKEE-141 Myxofibrosarcoma Imaging with Pathological and Clinical Correlation**

Participants

Robert W. Morris, MD, (*Presenter*) Nothing to Disclose

### **TEACHING POINTS**

Myxofibrosarcoma is one of the most common sarcomas in older patients, but has only relatively recently been defined as a distinct pathological entity. There is also limited information about myxofibrosarcoma in the radiology literature. After viewing this exhibit, the viewer should be able to: 1. Describe the pathological features of myxofibrosarcoma. 2. Describe the typical imaging appearance of both low-grade and high-grade myxofibrosarcoma. 3. Discuss ancillary imaging and post-treatment imaging. 4. Recognize important features for staging, treatment and prognosis.

### **TABLE OF CONTENTS/OUTLINE**

Table of Contents: 1. Myxofibrosarcoma overview 2. Pathology 3. Imaging characteristics 4. Low-grade myxofibrosarcoma 5. High-grade myxofibrosarcoma 6. Ancillary imaging and staging 7. Treatment 8. Post-treatment imaging 9. Prognosis 10. Conclusion

## **MKEE-142 Checkmate to Chest Wall Tumors: A Strategic Approach to Diagnosis**

Participants

Rebeca Francelino, MD, (*Presenter*) Nothing to Disclose

### **TEACHING POINTS**

The purpose of this exhibit is: 1. To review the most common tumors and their characteristic imaging findings. 2. To discuss the diagnosis and management of benign and malignant tumors. 3. To correlate the imaging findings and clinical clues on a systematic approach to help narrowing the differential diagnosis.

### **TABLE OF CONTENTS/OUTLINE**

1- Institutional Protocol to evaluate the chest wall; 2- Epidemiological assessment of the main lesions and best imaging modality; 3- Bening bone and cartilaginous tumors: Osteochondroma; Fibrous dysplasia; Aneurysmal bone cyst (ABC); Giant cell tumor (GCT); Ossifying fibromyxoid tumor; Chondromyxoid fibroma 4- Malignant bone and cartilaginous tumors: Chondrosarcoma; Multiple Myeloma; Metastasis; Osteosarcoma 5- Benign soft tissue lesions: Hemangioma; Elastofibroma dorsi; Fibrous Hamartoma of Infancy; Lipoma; Schwannoma; Desmoid Tumor; Neurofibroma; Ganglioneuroma; Paraganglioma; Hemangiopericytoma 6- Malignant soft tissue lesions: Ewing sarcoma; Rhabdomyosarcoma; Synovial sarcoma; Pleomorphic sarcoma; Ganglioneuroblastoma; Neuroblastoma; Angiosarcoma; Leiomyosarcoma; Malignant fibrous histiocytoma (MFH); Malignant peripheral nerve sheath tumor; Dermatofibrosarcoma protuberans 7- Miscellaneous Brown Tumor

## **MKEE-143 3D-MERGE MRI Sequence in the Assessment of Foot and Ankle Bone Abnormalities**

Participants

Tatiane Rodrigues, MD, Sao Paulo, Brazil (*Presenter*) Nothing to Disclose

### **TEACHING POINTS**

1) Discuss the use of MERGE MRI sequence in the assessment of bone abnormalities in the foot and ankle. 2) Discuss clinical applications of synthetic-CT based images on MERGE sequence in the foot and ankle through a case-based approach.

### **TABLE OF CONTENTS/OUTLINE**

Different techniques have been used to generate MRI-based synthetic-CT and have demonstrated equivalence to conventional CT. While MRI has superior soft tissue contrast when compared to CT, abnormalities that usually manifest as areas of low-signal intensity on conventional MRI scans, such as fracture lines, are better depicted on CT. Both modalities may complement each other in the characterization of several musculoskeletal disorders. Performing CT in association with MRI not only increases costs but also exposes the patient to ionizing radiation. MERGE (Multiple Echo Recombined Gradient Echo, GE Healthcare) is a spoiled T2\*-weighted 3D sequence for spinal and musculoskeletal imaging, which has the acquisition and combination of multiple echoes with a high receiver bandwidth instead of using a single low bandwidth echo, that provides high resolution and isotropic images of the extremities with optimized contrast between the ligaments and soft tissue. The purpose of this work is to show the 3D-MERGE MRI sequence in the assessment of bone abnormalities of the foot and ankle in a case-based discussion. Radiologists need to be familiarized with MRI-based synthetic-CT techniques, such as MERGE, and their imaging findings to obtain an optimal evaluation of musculoskeletal conditions with the combination of conventional and innovative sequences.

## **MKEE-144 Shipwrecked: Spontaneous Osteonecrosis of the Navicular Bone**

Participants

Juliana Sitta, MD, Jackson, MS (*Presenter*) Nothing to Disclose

### **TEACHING POINTS**

To review the anatomy, joints, ligaments, function, and vascularization of the navicular bone. Discuss the clinical features and mechanism of pediatric and adult avascular necrosis of the navicular bone. Illustrate the imaging characteristics of navicular osteonecrosis and complications in multimodality imaging at different stages of the disease

### **TABLE OF CONTENTS/OUTLINE**

Navicular bone osteonecrosis, also known as Kohler disease, is a relatively uncommon, self-limited abnormality with typically good prognosis. It differs in imaging presentation and prognosis from its adult counterpart, known as Mueller Weiss disease, which often results in progressive navicular bone deformity and midfoot biomechanical impairment. This educational exhibit aims to explore the anatomic predispositions of the navicular to osteonecrosis as well as the imaging features of these two pathologically similar entities that affect patients at opposite ends of the age spectrum. This educational exhibit provide an overview of the navicular bone anatomy, including common anatomic variants and mimickers, relationship with neighboring bones, function, and vascularization. We discuss imaging features, imaging anatomy, and potential complications in the pediatric and adult types of avascular osteonecrosis of the navicular bone. Multimodality imaging and didactic illustrations will explore the injury mechanism and presentation spectrum. The authors raise attention to the role of imaging in assessing potential secondary biomechanical

complications and pitfalls.

#### **MKEE-145 Working "Smarter" : A Review of Artificial Intelligence in Musculoskeletal Radiology**

Participants

Vidya Sankar Viswanathan, MBBS, Shaker Heights, OH (*Presenter*) Nothing to Disclose

##### **TEACHING POINTS**

1. Define Artificial Intelligence (AI) and other commonly associated terminology  
2. Review current applications of FDA approved AI tools in Musculoskeletal (MSK) Radiology (diagnostics, image processing)  
3. Describe ways that integration of AI can improve clinical workflow  
4. Discuss future technologies in AI, including Radiomics and Autonomous AI  
5. Review limitations of AI, including challenges that need to be addressed for clinical translation of these tools.

##### **TABLE OF CONTENTS/OUTLINE**

1. Introduction -Define Artificial Intelligence (AI), Machine learning, Deep learning, Convolutional Neural Networks(CNN), Generative Adversarial Networks (GAN)  
2. Current applications of FDA approved AI tools in Musculoskeletal Radiology  
A. Image Processing/Quantification -Improved visualization -Surgical planning  
B. Computer-aided diagnosis  
3. Improved Clinical Workflow with AI  
A. Image Acquisition Time  
B. Study Triaging  
C. Image Interpretation Time  
D. Scheduling  
4. Future of AI  
A. Interpretive tools - Device placement assessment -Augment Radiology Assistants  
B. Non-interpretive tools -Reduce noise and artifacts -Enhance contrast -Improved visualization of pathology -Worklist Prioritization -Improving Radiology Resident Education  
C. Radiomics  
D. Autonomous AI  
5. Challenges  
A. Clinical - Reluctance toward implementation -Information/knowledge gap -Reimbursement strategies  
B. Medico-legal -Liability: Physician vs. software developer vs healthcare institution -Advocacy for guidelines and legislation

#### **MKEE-146 The Role of MRI in Evaluation of Soft Tissue Lesions of the Hand and Fingers: An Imaging Review of the Common Differential Diagnoses, Artifacts and Normal Findings Which Can Simulate Disease**

Participants

Cormac O'Brien, MRCPI, MRCP, Dublin 4, Ireland (*Presenter*) Nothing to Disclose

##### **TEACHING POINTS**

Soft tissue lesions of the hand and fingers are frequently encountered in everyday clinical practice. They can be detected incidentally or present as painfully or painless lumps. Lesions may be idiopathic or arise secondary to trauma, foreign body, infection or systemic illness. These lesions provide a unique diagnostic challenge due to the small size of the lesions, the wide differential and the intricate anatomy. Our teaching aim is to present a practical illustration of hand and finger soft tissue lesions along with relevant clinical findings, illustrate the normal MRI appearance's which can simulate disease and help the radiologist to provide a more accurate diagnosis, allowing improved recommendations to the referring clinicians and minimize unnecessary investigations or biopsy.

##### **TABLE OF CONTENTS/OUTLINE**

First we describe the MRI protocols used to work up soft tissue lesions of hand and fingers. Secondly we evaluate the most common artifacts in hand and finger MRI such as pulsation, aliasing and phase-encoded motion artifacts and the review practical tips to optimize image quality. Third we provide an outline of the normal findings which simulate disease including Pacinian corpuscles and submatrical hyperintense area. Finally we illustrate the key MRI imaging features of common soft tissue lesions of the hand and fingers including cystic lesions (glomus tumors, inclusion cyst), tumor like lesions (fibroma, keratoacanthoma, peripheral nerve sheath tumor), vascular lesions such as haemangioma and malignant lesions which include squamous cell carcinoma, malignant melanoma and metastasis, with plain film, CT and Ultrasound correlation.

#### **MKEE-147 MRI of The Midhand: The Lesser Known Anatomy**

Participants

Michel De Maeseneer, PhD, (*Presenter*) Nothing to Disclose

##### **TEACHING POINTS**

-The anatomy of the midhand is complex and not well known. We illustrate this anatomy by MR-anatomical correlation. -It includes the distal tendon insertions, the muscles of thenar and hypothenar, the midpalmar compartment, the palmar bursa and synovial sheaths, the sesamoid apparatus of the thumb base, the palmar aponeurosis. -For each structure we illustrate and refer to the most important pathological conditions -A good knowledge of anatomy is essential to adequately assess normal and abnormal MR imaging of this region.

##### **TABLE OF CONTENTS/OUTLINE**

Outline  
1. Distal tendon insertions: AP, EPB, ECRB and ECRL, EPL, ED, EDM, ECU  
2. Muscles of the hypothenar: opponens, abductor, interosseous  
3. Muscles of the thenar: opponens, abductor, flexor brevis, flexor pollicis longus, adductor, interosseous  
4. Midpalmar compartment: interosseous, lumbricals, neurovascular bundle, transverse metacarpal ligament  
5. Bursae and synovial sheaths: palmar bursa, synovial sheath of finger 1 and 5, synovial sheath of finger 2-4  
6. Thumb base; sesamoid bones, intersesamoid ligament, accessory collateral ligament, collateral ligament, dorsal aponeurotic expansion (hood) from abductor and adductor tendons  
7. Palmar aponeurosis: palmaris longus, apex of aponeurosis, pretendinous bands, transverse ligament of Skoog, natatory ligament

#### **MKEE-149 Meniscus Repair: What Radiologists Need to Know**

Participants

Camila De Paula Silva, MD, Botucatu, Brazil (*Presenter*) Nothing to Disclose

##### **TEACHING POINTS**

The purpose of this exhibit is 1. To review and illustrate the surgical techniques of meniscal repair. 2. To show MRI images appearance of the repaired meniscus. 3. To show the postoperative normal and abnormal findings.

##### **TABLE OF CONTENTS/OUTLINE**

1. Imaging appearance of meniscus injuries before and after repair 2. Types of surgical techniques of meniscal repair, including:

1- Imaging appearance of meniscus injuries before and after repair. 2- Types of surgical techniques of meniscal repair, including: Inside-out suture repairs, outside-in suture repairs and all-inside repairs. 3- Normal post surgery findings and how to differentiate it from abnormalities. 4- Main postoperative complications of meniscal repairs in MRI images, including: avulsion of the repair, progressive meniscal extrusion and progressive articular cartilage damage.

#### **MKEE-15 Soft Tissue Calcifications on Ultrasound - Differentials and Radiographic Correlate**

Participants

Alex Ward, MD, (*Presenter*) Nothing to Disclose

#### **TEACHING POINTS**

1) Ultrasound is not the modality of choice for evaluation of calcifications, however practitioners frequently encounter calcifications during diagnostic and procedural musculoskeletal ultrasound. These calcifications may be challenging to diagnose, especially if discovered incidentally. 2) Knowledge of the sonographic appearance of calcifications and their respective radiographic correlate can help clinicians comfortably diagnose soft tissue calcifications. 3) Review of commonly encountered calcifications focusing on their typical location, distribution, imaging appearance and mechanism of formation. 4) Focus on companion cases, potential pitfalls, and unique sonographic/radiographic features to distinguish and accurately identify calcifications (ex. HADD vs enthesopathy, ultrasound appearance of Gout vs CPPD, benign vs malignant causes of calcifications)

#### **TABLE OF CONTENTS/OUTLINE**

1) Terminology and categorization of calcification vs ossification. 2) Review of commonly encountered calcifications, including typical location/distribution, mechanism of formation, sonographic appearance with radiographic correlate, potential pitfalls of the following: A. Calcium hydroxyapatite deposition disease (HADD) B. Calcium pyrophosphate deposition C. Gout D. Enthesophytes E. Normal variant ossicles F. Myositis ossificans and other forms of heterotopic ossification G. Scleroderma H. Tumoral calcinosis in End Stage Renal Disease I. Phleboliths seen in vascular malformation J. Malignancy, including chondrosarcoma and calcification in synovial sarcoma

#### **MKEE-150 MSK Word Salad: Making Sense of the Most Frequently Encountered Metabolic Bone Disorders**

Participants

Andrew Liu, MD, (*Presenter*) Nothing to Disclose

#### **TEACHING POINTS**

Metabolic bone disorders encompass those diseases which affect bone structure and/or mass and are caused by metabolic derangements. They are important to recognize as they are common and affect patients of all age groups. Metabolic bone disorders lead to considerable morbidity and mortality, as they weaken bones, regardless of the underlying morphologic changes, increasing the risk of fractures in elderly patients and stunting skeletal growth in children. Due to the lack of acute symptoms of many of these disorders, the radiologist is likely to make the initial diagnosis and facilitate subsequent workup.

#### **TABLE OF CONTENTS/OUTLINE**

This presentation covers the more commonly encountered metabolic bone disorders. For each disease, a brief summary of the pathophysiology precedes a discussion of characteristic imaging features to provide a basis for understanding WHY those findings occur. Each slide is centered on radiographic features, with cross-sectional imaging findings shown as correlates. This is because metabolic bone diseases are most often initially detected on radiographs. Disorders discussed will be categorized as osteopenic, osteosclerotic, or mixed pattern lesions.

#### **MKEE-151 Skeletal Dysplasias: The Role of Radiologist's Report**

Participants

Mateus Andreoni, MD, Sao Paulo, Brazil (*Presenter*) Nothing to Disclose

#### **TEACHING POINTS**

TEACHING POINTS: The purpose of this pictorial essay is to review the main characteristics of the most prevalent bone dysplasias and highlight the key points of the radiological report: Most prevalent types of skeletal dysplasias and the latest classification Review of bone dysplasias radiological appearance The role of radiologist's report for early diagnosis and family counseling

#### **TABLE OF CONTENTS/OUTLINE**

TABLE OF CONTENTS/OUTLINE: Most prevalent types of skeletal dysplasias Skeletal dysplasias are a group of more than 450 heritable disorders with specific type of inheritance. The latest discoveries have added embryological and genetic data which provided a detailed classification in 42 groups. Review of bone dysplasias radiological appearance: Despite being a large group of pathologies, radiological appearance may be diagnostic or narrow to a small amount of differentials in most cases. The role of radiologist's report: It is important to determine a precise diagnosis to aid in management, familial recurrence and to report those disorders highly associated with mortality. Even tenuous radiologic findings should be correctly interpreted and reported because, added to clinical context, can be decisive in the correct diagnosis.

#### **MKEE-152 Ultrasound (US) Imaging of The Peripheral Nerves: Normality and Abnormalities**

Participants

Michaela Cellina, (*Presenter*) Nothing to Disclose

#### **TEACHING POINTS**

To describe the technique of the lower limb US nerve study and the appearance of the nerves to help the radiologist become confident with this US application. To show the anatomical landmarks to identify the nerves.

#### **TABLE OF CONTENTS/OUTLINE**

Thanks to its wide availability, low costs, fast execution, high soft-tissue resolution, real-time dynamic evaluation, and direct correlation with signs and symptoms, high-frequency US is considered the first-line imaging tool for the study of the peripheral nerve. Moreover, US does not suffer the limitations of MRI, such as metal implants, claustrophobia, and pacemakers. The exam is

performed with high-frequency linear array probes. The nerves are identifiable on the axial plane at defined anatomical landmarks, then the nerve is followed with the probe in the axial plane proximally and distally. If abnormalities are recognizable, the nerve should be also studied on the long axis. Common indications for US nerves study include tarsal tunnel syndrome, entrapments, traumas, suspected neuromas, and polyneuropathies. Non-pathological nerves have a characteristic honeycomb appearance in the short axis, as they are formed by hypoechoic nerve fascicles surrounded by hyperechoic connective tissue and collagen. They can be detected in the adipose tissue or in fascial planes among or superficial to the muscles and each nerve is surrounded by a portion of fat. Pathological nerves show increased diameter with a hypoechoic appearance proximal to the site of the entrapment. Post-traumatic damages can be visible as nervous focal discontinuation with swollen retracted portions.

### **MKEE-153 Radiographic Signs of Musculotendinous and Ligament Injuries**

Participants

Diego dos Santos, MD, Sao Paulo, Brazil (*Presenter*) Nothing to Disclose

#### **TEACHING POINTS**

- Review some general information about radiographic signs of musculotendinous and ligament injuries- Describe the radiographic findings of musculotendinous and ligament injuries in the different joints of the body and in both adult and pediatric population through cases illustrated in our service- Highlight some anatomical considerations, the mechanism and some quick tips and pitfalls involving the musculotendinous and ligament injuries- Correlate the radiographic findings of musculotendinous and ligament injuries with other imaging methods

#### **TABLE OF CONTENTS/OUTLINE**

Introduction- General information about radiographic signs of musculotendinous and ligament injuries  
Radiographic findings of musculotendinous and ligament injuries in the different joints- Quadriceps tendon tear with patella baja- Patellar tendon tear with patella alta- Fibularis longus tear with posterior deviation of the accessory peroneal ossicle- Elbow dislocation associated with fracture of the radial head and coronoid process and ligament injuries- Turf toe with posterior deviation of the hallux sesamoids- Rotator cuff tear with coracohumeral interval shortening / superior subluxation of the humeral head- Bone avulsions in different body sites associated to ligaments and tendon tears- Periarticular soft tissue densification associated to ligaments and tendon tears- Other cases  
Anatomical considerations  
Injury mechanism  
Quick tips and pitfalls  
Correlation with other imaging methods-  
Ultrasound- Magnetic Resonance Imaging

### **MKEE-154 Preoperative Planification and Postoperative CT-Scan Imaging Assessment of Latarjet Procedure for Anterior Shoulder Instability: What's On The Menu?**

Participants

Ulrike Novo, MD, (*Presenter*) Nothing to Disclose

#### **TEACHING POINTS**

- To review the most important findings in preoperative CT scan planning before Latarjet.- To describe the key points to be considered in the postoperative CT scan evaluation. - To illustrate a wide spectrum of normal and pathological findings in postsurgical CT scans in a case-based scenario.

#### **TABLE OF CONTENTS/OUTLINE**

The Latarjet procedure is an operation for recurrent anterior shoulder instability consists of transferring the coracoid process to the anterior glenoid rim.  
Appetizer  
PREOPERATIVE CT SCAN PLANNING  
Preoperative planning of the arthroscopic Latarjet procedure based on the CT scan is necessary to achieve satisfactory clinical and radiographic results:  
• Coracoid dimensions • Measurement of bone defects, Hill-Sachs lesion, bony Bankart and glenoid track  
Main course  
HOW TO PERFORM ARTHROSCOPIC LATARJET SURGERY AND POSTOPERATIVE CT SCAN EVALUATION  
Adequate coracoid graft positioning:  
Coronal view: Coracoid graft should be flush with the articular surface along its lateral aspect.  
Axial view is the most useful view to judge the mediolateral position and the "angulation" of the graft. Coracoid graft should be flush with the articular surface. The angulation of the graft (open, closed or neutral) is evaluated with the circle method.  
Axial plane to analyze the angle of the screw (alpha angle) with the articular surface.  
Sagittal view allows assessment of craneocaudal position respect to glenoid equator  
Dessert  
COMPLICATIONS  
• Short term: Graf fracture/ avulsion and graft non-union  
• Long term: Osteoarthritis  
In conclusion, the radiologist plays a key role in Latarjet, to know what pre-surgical CT findings are important to help with preoperative planning and to diagnose potential complications that may occur.

### **MKEE-155 Main Sacral Lesions and Their Radiological Findings**

Participants

Bárbara Moreira Machado, Sao Paulo, Brazil (*Presenter*) Nothing to Disclose

#### **TEACHING POINTS**

1- Review and understand the most common sacral tumors. 2- Debate over imaging patterns and their prevalence

#### **TABLE OF CONTENTS/OUTLINE**

1- Introduction and anatomy of the sacrum. 2- Epidemiology of sacral tumors. 3- Limitations of diagnostic imaging methods. 4- Differential diagnosis of sacral lesions and main imaging features  
a) primary bone tumors: Sacral chordoma; chondrosarcoma; osteosarcoma; multiple myeloma/plasmacytoma; giant cell tumor; aneurysmal bone cyst; osteoid osteoma; osteoblastoma.  
b) secondary bone tumors: metastases. c) neural tumors: Ependymoma; schwannoma; neurofibroma; Ganglioneuroma / neuroblastoma / ganglioneuroblastoma. d) germ cell tumors: teratoma; yolk sac tumor

### **MKEE-156 Whole body MRI in The Analysis of Multiple Myeloma: A Overview of Evolution, Imaging Methods and Future Perspectives**

Participants

Eduardo Zukovski, MD, Umuarama, Brazil (*Presenter*) Nothing to Disclose

#### **TEACHING POINTS**

- Recognize the updated diagnostic criteria for MM, indications and limitations of each imaging option, and recommendations for

follow-up. - Know MR imaging protocol for MM evaluation, indications and general technical parameters. - Comprehend MM imaging features in the different whole body MRI sequences. - Recognize the imaging response criteria in MM treatment. - Understand future perspectives of monoclonal gammopathies imaging analysis and flowcharts.

#### TABLE OF CONTENTS/OUTLINE

Introduction: • - Epidemiology of MM and indications of each imaging option • - Definition of MM updated diagnosis criteria • - Different indications of whole body MRI for bone diseases • - Whole body MRI sequences, technical parameters and MM imaging findings  
Diagnosis and imaging findings: • - Flowcharts of monoclonal gammopathies imaging methods • - Whole body MRI useful in MM treatment response assessment • - MRI patterns of bone marrow infiltration in MM • - Definition of unequivocal focal active lesion of MM in whole body MRI • - MRI findings correlated with poor patient survival • - Imaging follow-up for MM and identification of possible complications

#### MKEE-157 A Whole-body MRI Experience in The ProstateCancer

Participants

Augusto Altoe, Rio de Janeiro, Brazil (*Presenter*) Nothing to Disclose

#### TEACHING POINTS

1. To describe whole-body MRI protocol and its general considerations; 2. To understand the anatomical and functional techniques and their applications; 3. To illustrate the image findings of whole-body MRI in prostate cancer; 4. To identify potential imaging pitfalls, differential diagnoses, and post-therapeutic assessment.

#### TABLE OF CONTENTS/OUTLINE

1- Introduction. 2- MRI acquisition a. Anatomical techniques; b. Functional techniques; c. Recommended protocol. 3- Clinical indications of whole-body MRI in prostate cancer; a. Newly diagnosed prostate cancer; b. Biochemical recurrence; c. Advanced disease and response assessment. 4 - Image findings of whole-body MRI in prostate cancer; a. Locoregional disease; b. Metastatic lymph node disease; c. Metastatic bone disease; d. Post-therapeutic findings. 5 - Imaging pitfalls and differential diagnoses. 6 - Take home messages and teaching points.

#### MKEE-158 Pitch Perfect: Biomechanics and Patterns of Injury In the Throwing Arm

Awards

Identified for RadioGraphics  
Certificate of Merit

Participants

Dyan V. Flores, MD, Ottawa, ON (*Presenter*) Nothing to Disclose

#### TEACHING POINTS

The exceptional velocity required by sporting activities relying on overhead throwing predisposes the shoulder to extreme forces, leading to both adaptive changes and pathologic cascade of findings that can be detected on imaging. The objectives of this educational exhibit are: • 1. To review the phases of pitching and associated biomechanics that predispose the overhead-throwing shoulder and elbow to injury • 2. To highlight unique sites of injury in the overhead-throwing athlete • 3. To discuss imaging findings of common shoulder and elbow injuries in the overhead-throwing athlete

#### TABLE OF CONTENTS/OUTLINE

Throwing biomechanics and arc of motion  
Shoulder • Glenohumeral internal rotation deficit (GIRD) • Internal impingement • Superior labral anteroposterior (SLAP) tear • Partial thickness rotator cuff tear • Anterior capsule injury • Subscapularis tendon injury • Bennett lesion • Posterior muscle injury  
Elbow • Flexor tendinitis • UCL injury • Valgus extension overload • Olecranon stress fracture • Ulnar neuritis  
Pediatric • Little leaguer's shoulder and elbow

#### MKEE-159 Spectrum of Musculoskeletal Involvement in COVID-19 Infection Diseases: Pictorial Essay

Participants

Pedro Martins, MD, Rio de Janeiro, Brazil (*Presenter*) Nothing to Disclose

#### TEACHING POINTS

Covid-19 has a broad spectrum of musculoskeletal involvement that can mimic other diseases and trigger the development of rheumatic disease. After almost two years of the coronavirus pandemic, some countries are starting to treat COVID-19 infection as an endemic disease and we will probably continue to live with the virus. Although musculoskeletal involvement is uncommon, it's important to recognize its most common neuromuscular and rheumatologist complications associated with the infection, and also the musculoskeletal changes related to the long term hospitalization and the vaccine side effects.

#### TABLE OF CONTENTS/OUTLINE

- To explain how COVID-19 infection can involve the musculoskeletal system. - To illustrate with ultrasound, computed tomography, and magnetic resonance images the most common musculoskeletal changes of covid infection, including myositis, neuropathy, synovitis, arthritis and soft tissue abnormalities. - To demonstrate the differential diagnosis of others musculoskeletal infections and inflammatory conditions  
The global COVID-19 pandemic is not over yet, and may become an endemic disease within the next few years. Musculoskeletal changes can be related to the infection itself, and also be found in patients with prolonged hospitalizations and due vaccine side effects. It is important to recognize the most common musculoskeletal changes to avoid unnecessary procedures and to prevent misdiagnosis of other inflammatory and infectious conditions.

#### MKEE-16 The Navicular: Keystone of the Foot

Participants

Scott Wuertzer, MD, Winston Salem, NC (*Presenter*) Nothing to Disclose

#### TEACHING POINTS

1. Review the anatomy of the tarsal navicular with an emphasis on the three arches of the foot. 2. Review the biomechanics of the

1. Review the anatomy of the tarsal navicular with an emphasis on the three arches of the foot. 2. Review the biomechanics of the navicular, including the osseous keystone and the peri-navicular soft tissue stabilizers. 3. Describe various pathologies of the navicular with an emphasis on the associated pathomechanics. 4. Through case examples, highlight the expected imaging characteristics of navicular pathology.

#### TABLE OF CONTENTS/OUTLINE

1. Anatomy and Biomechanics. A. Osseous and vascular anatomy of the navicular. B. The arches of the foot - medial, lateral, and transverse. C. Peri-navicular soft tissue stabilizers - dorsal and plantar cuneonavicular ligaments, bifurcate ligament, spring ligament, dorsal talonavicular ligaments, cuboideonavicular ligaments, and the posterior tibial tendon. D. Joints - naviculocuneiform, cuboideonavicular, and talocalcaneonavicular. 2. Pathology, Pathomechanics, and Imaging Characteristics. A. Accessory ossicles - os navicularis, os supranaviculare. B. Tarsal coalitions - calcaneonavicular, talonavicular. C. Acute fractures - avulsion, body, and tuberosity. D. Stress fractures and osteochondral lesions. D. Köhler's disease. E. Osteonecrosis - Mueller-Weiss, secondary osteonecrosis. F. Arthropathies - osteoarthritis, rheumatoid arthritis, and neuropathic arthropathy. G. Adult acquired flatfoot deformity.

#### MKEE-160 A Stepwise Approach to Finally Understanding Arthritis

Participants

Bryan Wessel, BS, MD, Cincinnati, OH (*Presenter*) Nothing to Disclose

#### TEACHING POINTS

1. Understand the differences between inflammatory and degenerative arthritis. 2. Understand the progression of various forms of arthritis. 3. Identify the different radiographic findings that help distinguish between the different causes of arthritis.

#### TABLE OF CONTENTS/OUTLINE

- Characteristics of inflammatory and degenerative arthritis. o Symmetric vs Asymmetric joint space narrowing o Erosions vs subchondral cysto What are osteophytes?
- Stepwise algorithm for determining the specific type of arthritis.
- Explanation of subtypes of inflammatory arthritis with examples. o Septic Arthritis o Rheumatoid Arthritis o Seronegative Arthropathies
- Explanation of subtypes of degenerative arthritis with examples. o Typical Osteoarthritis o Atypical Osteoarthritis
- Application of knowledge to unknown cases.

#### MKEE-161 Not All Erosions are Created Equal - Approach to Hand and Wrist Arthropathy: What a Radiologist Needs to Know?

Awards

Certificate of Merit

Participants

Neha Antil, MD, Mountain View, CA (*Presenter*) Nothing to Disclose

#### TEACHING POINTS

The purpose of this exhibit is to: 1. Outline the various arthritides that have a predilection for the hand and wrist. 2. Classify arthritides based on the clinical presentation, site of involvement in the hand and wrist and further differentiate them based on characteristic imaging appearances. 3. Discuss advanced imaging techniques that can be used as a problem-solving tool in rheumatology. 4. Summarize and develop a practical imaging approach to making an accurate diagnosis.

#### TABLE OF CONTENTS/OUTLINE

- Review the causes of arthritis in hand and wrist joints. o Classify arthritides based on clinical presentation and site of involvement in the hand and wrist. o Describe imaging appearances for each arthropathy. o Differentiate the arthritides based on characteristic imaging findings.
- Illustrate advanced imaging techniques that can help differentiate arthropathies affecting the wrist and hand.

#### MKEE-162 Ultrasound for Ultra-Insight into Diagnosing and Treating the Painful Joint Arthroplasty

Participants

Brendan Franz, MD, (*Presenter*) Nothing to Disclose

#### TEACHING POINTS

Overview of utilizing ultrasound for the evaluation of periprosthetic joint infections, as well as for US-guided aspiration of infectious material in a periprosthetic joint infection. Review of the expected sonographic appearance of reactions to metallic debris at the joint arthroplasty site, including conditions such as metallosis, trunnionosis, and metal-on-metal pseudotumors. Using ultrasound for the evaluation of tendon pathology with arthroplasties, including dynamic maneuvers to evaluate for tendon impingement or snapping. Indications for joint arthroplasty injections and precautions to be taken.

#### TABLE OF CONTENTS/OUTLINE

Introduction Brief review of current trends in arthroplasty placement Ultrasound evaluation in periprosthetic joint infections Expected appearance of a periprosthetic joint infection on ultrasound imaging. US-guided aspiration and important biomarkers. Saline Lavage. Major pathogen causing periprosthetic joint infections at the shoulder; Cutibacterium acnes. Adverse Reactions to Metallic Debris Metallosis Trunnionosis Metal-on-metal pseudotumors Tendon pathology in joint arthroplasty Subscapularis tendon tears Gluteal tendon tears Quadriceps and patellar tendon tears Iliopsoas tendinopathy, bursitis, and impingement/snapping Joint arthroplasty injections Indications Risks Precautions Summary

#### MKEE-163HC3D Printed Kyphoplasty Simulator Build Guide

Participants

Caleb Heiberger, MD, Sioux Falls, SD (*Presenter*) Nothing to Disclose

#### TEACHING POINTS

We demonstrate the creation of a functional kyphoplasty simulator using computed tomography (CT) images, a "desktop grade printer" and open-source software. To do so, we obtained three CT Digital Imaging and Communications in Medicine (DICOM) files

including spinal compression fractures with 1) Standard Anatomy, 2) Scoliosis and 3) Severe Arthrosis. Segmentation was performed using 3D Slicer with post-processing in Mesh-Mixer and Fusion 360 to repair segmentation defects. Printing was performed on a Prusa i3 MK3S fused deposition modeling printer using Polylactic acid (PLA) for the vertebrae and Thermoplastic Polyurethane (TPU) for the intervertebral disks. Soft tissue was simulated using a 1:1 mixture of Knox Gelatin and water, activated by a freeze/boil cycle. The mixture was poured into a custom printed container with the printed spine and allowed to solidify. Simulations were performed under fluoroscopic guidance. Early usage reviews indicated high satisfaction with device fidelity compared to other models, including cadavers. The production of this kyphoplasty model demonstrates the effective use of 3D printing in image guided interventional training.

#### TABLE OF CONTENTS/OUTLINE

Segmenting a DICOM in 3D Slicer  
Editing segmented DICOM in Mesh Mixer and Fusion 360  
Preparing a print in 3D CAD  
Software  
Selecting filaments for specific anatomy  
Printing the model  
Creating soft-tissue mold and embedding spine  
Demonstration  
fluoroscopic fidelity of the model  
Usage reviews and future directions  
Please visit the Learning Center to also view this presentation in hardcopy format.

#### MKEE-164 A Pictorial Review of the Different Radiological Presentations and Differential Diagnosis of Gout in Atypical Sites

Participants

Lin Liu, MD, Guangzhou, China (*Presenter*) Nothing to Disclose

#### TEACHING POINTS

1. Monosodium urate crystals commonly deposit at the joints or tendons of the foot or ankle, especially at the first metatarsophalangeal joint, but rarely deposit at the joints of upper limbs and other extra-articular sites.
2. Intraspinal gout is difficult to diagnose before surgery and its clinical presentations and imaging findings mimic tumors and degenerative spinal diseases. Early diagnosis of intraspinal gout is extremely significant because timely urate-lowering therapy may avoid surgical intervention.
3. The confirmation of MSU crystals in synovial fluid or tophaceous material is considered the gold standard for gout diagnosis. Gout in the atypical sites may misdiagnose because of the nonspecific clinical and imaging findings. Therefore, DECT as an auxiliary tool should be performed as soon as possible for suspected gout lesions, which may avoid unnecessary invasive operations.

#### TABLE OF CONTENTS/OUTLINE

1. A case-based review of sixteen different radiological presentations of gout in the atypical sites including upper limbs, spine, ligaments, and other rare joints.
2. Recognize different findings of gout in atypical sites in radiography, CT, MRI, and dual-energy CT.
3. Identify the differential diagnosis of gout in atypical sites.

#### MKEE-165 Tips and Tricks for Ablating an Osteoid osteoma: Plan It Right!

Participants

Roshni Anand, MBBS, New Delhi, India (*Presenter*) Nothing to Disclose

#### TEACHING POINTS

Approach the lesion perpendicular to the cortical surface and avoid the sclerotic part of bone. This may require a prone, oblique, or lateral decubitus position. The shortest path to the lesion enables minimum injury to surrounding tissues. Avoiding neurovascular bundle (NVB): Lesions may be targeted through the longer route and farther cortex to avoid injury to the NVB. Dextrose may be injected to keep at least 1 cm distance. Tandem needle technique or use of protractor in case of the angulated route. Drill bit is a superior option compared to hammering, especially in the case of a longer osseous path and sclerosis. Two or more electrodes may be required for lesions measuring >1.5cm. A single electrode is sufficient for smaller lesions. Dextrose may be injected to prevent soft tissue injury in superficial bones like in digits. Intra-articular lesions: Trans-articular approach is avoided. Iatrogenic joint effusion by instilling dextrose may protect from articular cartilage injury. Spinal lesions: Entering the facet joint or neural foramen should be strictly avoided. A bipolar RF probe can avoid damage to the surrounding structures. Reducing Post-procedure pain and swelling: Injecting lignocaine-bupivacaine mixture along the tract up to the periosteum and local site compression for 5 minutes after ablation

#### TABLE OF CONTENTS/OUTLINE

Learning objectives: To demonstrate the practical tips and tricks for abating an osteoid osteoma by correct planning  
Cases demonstrating the teaching points  
Conclusion

#### MKEE-166HC Quantitative Analysis of Water Material Density Values by Dual Energy CT for Osteoblastic Vertebral Metastases

Participants

Hirotaaka Nakashima, MSc, RT, (*Presenter*) Nothing to Disclose

#### TEACHING POINTS

1. Virtual non-calcium (VNCa) images were created by two-material decomposition processing.
2. Clinically diagnosed 81 osteoblastic metastatic vertebrae and 301 normal vertebrae were compared by water material density values quantitatively.
3. The area under the curve value obtained from receiver operating characteristic (ROC) analysis was 0.93, and the water material density value was a highly discriminative index for osteoblastic metastases.
4. The cutoff value between lesion and normal was 1047.8 mg/cm<sup>3</sup> based on ROC analysis with a sensitivity of 85.7% and a specificity of 98.1%.
5. New image display method was developed that reflects the cut-off value calculated from water material density values.

#### TABLE OF CONTENTS/OUTLINE

Vertebral metastases are the most common bone metastases. CT can detect bone calcification with high sensitivity and is therefore excellent for the diagnosis of osteolytic bone metastases with bone cortex destruction. However, osteoblastic bone metastases without destruction are difficult to diagnose and are easily overlooked. VNCa image is one of the material discrimination images produced by dual-energy CT and is a material density image obtained by highlighting the water component and removing the calcium component. By measuring the VNCa image, water material density values can be obtained. Quantitative evaluation using water material density values was a gap of knowledge. In this exhibition, water material density values of osteoblastic vertebral

metastases and normal vertebrae were compared. And cutoff values were calculated by ROC analysis. The results showed that water material density values have a high discriminatory ability against osteoblastic metastases. Please visit the Learning Center to also view this presentation in hardcopy format.

#### **MKEE-167 Don't Stress About Stress Injuries: A Review of Stress Related Injuries of Bone**

Participants

Samantha Jayasinghe, MD, Cleveland, OH (*Presenter*) Nothing to Disclose

##### **TEACHING POINTS**

1. Discuss clinical presentation and pathophysiology of stress related fractures including fatigue, atypical, and insufficiency fractures. 2. Role of imaging for stress related injuries of bone. 3. Discuss common stress fracture patterns and locations. 4. Discuss uncommon stress fracture patterns and locations related to competitive athletes or surgical changes. 5. Review treatment algorithms.

##### **TABLE OF CONTENTS/OUTLINE**

Background 1. Clinical presentation of Stress injuries 2. Anatomy, Biomechanical tensile/compressive forces 3. Pathophysiology 4. Optimal imaging modalities for evaluation Stress Fracture Subtypes Fatigue Common 1. Metatarsal 2. Compression side femoral neck 3. Calcaneal 4. Tibial Fredericson classification Uncommon 1. Patellar 2. Tensile side femoral neck 3. Pubic ramus fractures status post periacetabular osteotomy 4. Rib stress in competitive swimmers Atypical Bisphosphonate or monoclonal antibody associated lateral femoral fractures 1. Imaging/treatment recommendations Insufficiency 1. Femoral Condylar 2. Femoral Head 3. Sacral Unilateral, H-shaped 4. Acetabular Pediatric 1. Little Leaguer Shoulder 2. Acromial Apophysiolyis 3. Elbow-Olecranon 4. Elbow-Pannars 5. Gymnast wrist 6. Distal Femoral Stress Injury 7. Sinding-Larsen-Johannson 8. Osgood-Schlatter Treatment of Stress Fractures 1. Stratifying fracture risk 2. Low Risk Conservative Management Continued Weight Bearing 3. High Risk Rehabilitation Protected Weight Bearing Surgical Intervention

#### **MKEE-168 Imaging Findings That Should Never Be Forgotten In Non-accidental Trauma in Children**

Participants

Giovana Mesquita, MD, Sao Paulo, Brazil (*Presenter*) Nothing to Disclose

##### **TEACHING POINTS**

Revise the most important muscle-skeletal image findings related to non-accidental trauma in children, by using original schematic drawings and images from suspect cases of child physical abuse. Most of the cases presented were confirmed by assistant physicians. Therefore, this paper has also the aim of highlighting the fundamental role of the muscle-skeletal radiologist in identifying and documenting the skeletal injuries so as to protect the children involved and help bring victims away from their offenders as fast as possible, to stop further abuse.

##### **TABLE OF CONTENTS/OUTLINE**

1. Classical metaphyseal fracture 1.1 Traumatic mechanism 1.2 Image findings 2. Non-accidental trauma in long bones 2.1 Traumatic mechanism 2.2 Image findings 3. Non-accidental trauma in ribs 3.1 Traumatic mechanism 3.2 Image findings 4. Non-accidental trauma in pelvis 4.1 Traumatic mechanism 4.2 Image findings

#### **MKEE-169 Whole-Body Diffusion-Weighted Magnetic Resonance Imaging in Non-tumoral Bone Marrow Diseases and Their Mimics**

Participants

Carolina Almeida, MD, Rio de Janeiro, Brazil (*Presenter*) Nothing to Disclose

##### **TEACHING POINTS**

TEACHING POINTS 1) Identify correct MR protocol that should be used to analyse bone marrow in whole-body MR imaging (WBMRI) owing to detect tumoral involvement and their differential diagnosis. 2) Know basic principals of DWI WBMRI and typical lesion appearances and awareness of potential pitfalls. 3) Make a pictorial essay of lesions that mimic bone marrow tumoral lesions including conventional MRI sequences, DIXON and DWI and understand the characteristic features which allow discrimination between them and true neoplasms in order to avoid unnecessary additional workup. 4) The usefulness of DWI whole-body MR in diagnostic algorithms of non oncological disorders including differentiate diagnosis as inflammatory, infectious and pseudotumoral conditions.

##### **TABLE OF CONTENTS/OUTLINE**

TABLE OF CONTENTS AND OUTLINE 1) Case discussion regarding imaging that mimic bone marrow tumoral lesions as: 2) SAPHO syndrome 3) CRMO 4) Tuberculosis 5) Syphilis 6) Sarcoidosis 7) Bone Marrow hiperplasia 8) Differential diagnosis 9) Report structuring step by step

#### **MKEE-17 Congenital Talipes Equinovarus Made Easy: What Radiologists Need to Know and How to Evaluate the Idiopathic Congenital Clubfoot**

**Awards**

**Identified for RadioGraphics**

Participants

Julia Peixoto, Sao Paulo, Brazil (*Presenter*) Nothing to Disclose

##### **TEACHING POINTS**

Teaching Points: Emphasize a minimum of two major teaching points of this exhibit. What should the viewer accomplish by viewing this exhibit? The purpose of this exhibit is: 1. Review the main aspects related to idiopathic congenital clubfoot (congenital talipes equinovarus), including anatomy, etiology, pathophysiology, epidemiology, clinical classification and treatment. 2. To illustrate the main imaging findings and how to assess this condition in a multimodality approach, focusing on US and MRI studies.

##### **TABLE OF CONTENTS/OUTLINE**

Describe major headings (e.g., anatomy, physiology, imaging techniques, tumor disease states, etc.) 1. Review the main aspects related to idiopathic congenital clubfoot (congenital talipes equinovarus), including anatomy, etiology, pathophysiology, epidemiology, clinical classification and treatment. 2. Clinical and imaging findings in a multimodality approach. 3. US assessment protocol. 4. MRI assessment protocol. 5. Clubfoot major differential diagnoses, including: (simple metatarsus adductus, skewfoot, and oblique and vertical talus).

### **MKEE-18 Ultrasonography of Thumb Metacarpophalangeal Joint: Normal Anatomy and Mechanism-based Injury Approach**

Participants

Kyu-Chong Lee, (*Presenter*) Nothing to Disclose

#### **TEACHING POINTS**

1. The difference between metacarpal joint of thumb and other fingers 2. Anatomy and ultrasonographic normal images of thumb MCP joint 3. Mechanism based thumb MCP injury

#### **TABLE OF CONTENTS/OUTLINE**

1. Introduction 1) What is the difference between MCP joint of thumb and other fingers? 2) Biomechanism: Condylod joint: freedom of flexion/extension, valgus/varus + opposition 3) Imaging technique for MCP joint evaluation 2. Normal anatomy (1) Osseous anatomy: 1st proximal phalanx metacarpal bone + two sesamoid bones (2) Soft tissue 1) Palmar side: a. Muscle tendon: Adductor pollicis (ADP), Abductor pollicis brevis (APB), Flexor pollicis brevis (FPB), Flexor pollicis longus (FPL) b. Volar plate c. Pulley system (A1, Av, Ao + A2) 2) Dorsal side: a. Tendon: Extensor pollicis brevis (EPB) + Extensor pollicis longus (EPL) b. Dorsal plate c. Extensor hood or apparatus (sagittal band + triangular extension) 3) Collateral system (capsule-ligamentous system) a. Ulnar collateral ligament (UCL = proper/principle + accessory) + adductor aponeurosis b. Radial collateral ligament (RCL = proper/principle + accessory) + APB, FPB aponeurosis 3. Mechanism based injury approach 1) Valgus or abduction injury (most common) a. Skier thumb (UCL injury) b. Stener lesion 2) Varus or adduction injury a. RCL injury b. Stener like lesion c. Varus deformity 3) Hyperextension injury a. Volar plate injury b. Tendon pulley injury c. Muscle injury 4) Hyperflexion injury a. Dorsal plate injury b. Extensor tendon tear 5) Combination damage 4. Summary

### **MKEE-2 Imaging Dancers' Injuries**

Participants

María Carvajo, MD, (*Presenter*) Nothing to Disclose

#### **TEACHING POINTS**

1. To present the most common dancers' injuries and their underlying mechanisms. 2. To show the different imaging techniques. 3. To describe the semiology in imaging.

#### **TABLE OF CONTENTS/OUTLINE**

1. Most frequent types, mechanisms and structures injured in ballet dancers. 2. Injuries classification according to their mechanism. 2.1. Extreme ankle inversion and plantar flexion. 2.1.1. Lateral ankle sprains. 2.1.2. Acute fifth metatarsal fractures. 2.2. Ankle dorsiflexion, knee flexion and plantar stress. 2.2.1. Patellar tendinopathy. 2.2.2. Tibial stress injuries. 2.2.3. Acute Achilles tendon injury. 2.2.4. Tarsal stress injuries and fractures. 2.2.5. Plantar fasciitis. 2.3. Extreme ankle plantar flexion. 2.3.1. Posterior ankle impingement. 2.3.2. Peroneal tendinopathy. 2.3.3. Achilles tendinopathy. 2.3.4. Tarsal, metatarsal and phalanx stress injuries and fractures. 2.4. Knee flexo-extension. 2.4.1. Patellar tendinopathy. 2.4.2. Medial plica syndrome. 2.4.3. Patellofemoral maltracking. 2.5. Hip external rotation. 2.6. Hip external rotation, abduction and flexion. 2.6.1. Snapping hip syndrome. 2.7. Extreme hip adduction. Hip flexion/knee extension. 2.7.1. Adductor muscles injuries. 2.7.2. Stress pelvis injuries. 2.8. Lumbar spine hyperextension. 2.8.1. Spondylolysis/spondylolisthesis.

### **MKEE-20 Ultrasound-guided Injection of Botulinum Toxin in Neurogenic Thoracic Outlet Syndrome: Technical Aspects and Experience Over 15 Years**

Participants

Ronald Mercer, MD, (*Presenter*) Nothing to Disclose

#### **TEACHING POINTS**

-Thoracic outlet syndrome (TOS) includes a group of upper extremity disorders believed to occur due to isolated or combined neurovascular compression. -Neurogenic TOS (NTOS) constitutes 95% of all TOS patients, but presents diagnostic difficulty due to nonspecific findings during electro-diagnostic and imaging evaluation. -Botulinum toxin A (BTX) injections are useful to evaluate the diagnosis of NTOS, with symptom relief correlating with good response to subsequent treatments. -Our group pioneered ultrasound guided BTX injections since 2007, having performed over 5,000 procedures in patients being investigated for NTOS. -Injection of BTX into the anterior (ASM) and middle (MSM) scalene muscles as well as the pectoralis minor muscle (PMM) has been effective in reducing the symptoms of NTOS and may contribute to patient selection criteria for surgical management. -Ultrasound guided injection has been demonstrated to be safe and well tolerated.

#### **TABLE OF CONTENTS/OUTLINE**

-Discuss NTOS and the use of imaging-guided BTX injection in diagnosis and management. -Present relevant anatomy and safe approach to ultrasound-guided BTX injection into the ASM, MSM, and PMM. -Described complications and documented rate of symptom relief of these injections.

### **MKEE-21 Use of Soft Modeling Compound to Teach Musculoskeletal Anatomy and Pathology**

Participants

Osvaldo Velez-Martinez, MMedSc, (*Presenter*) Nothing to Disclose

#### **TEACHING POINTS**

1. Medical imaging is a 2D representation of 3D structures. It can be challenging for trainees to conceptualize 3D structures from 2D slices. 2. Soft modeling compound is an interactive and cost effective medium to teach musculoskeletal pathology. 3. 3D models

allow trainees to view anatomical structures in space and therefore conceptualize normal anatomy and pathology.4. Soft modeling can be integrated into any teaching program and its impact can be quantified.

#### TABLE OF CONTENTS/OUTLINE

Introduction to soft modeling compound as a teaching medium -Types-Pros-ConsSet-up-3D Model generation-Modeling tools-Documenting examplesTeaching Algorithm-Attending mediated "Show and Tell"-Trainee modeling and gradingResident Survey-Design-ResultsShoulder -Anatomy-Pathology-Labral Tears-Cartilage Injury-Rotator Cuff Tears-Long Head Biceps-CapsuloligamentousElbow AnatomyPathologyTendon TearsLigament Cartilage InjuryWrist -Anatomy-Pathology-Triangular Fibrocartilage-Scapholunate and Lunotriquetral Ligaments Hip -Anatomy-Pathology-Labral Tears-Cartilage Injury-Femoroacetabular ImpingementKnee -Anatomy-Pathology-Meniscus Tears-Cartilage Injury-Ligament Tendon Foot-Anatomy-Pathology-Ligament -Cartilage InjuryFuture Developments-Resident Grading-Quantitation of Competency Improvement-Other Applications

#### MKEE-22 Low-dose CT Approach to Tendon Delineation Using Deep Learning Technology

Participants

Takato Yanagisawa, Ueda, Japan (*Presenter*) Nothing to Disclose

#### TEACHING POINTS

The three-dimensional tendons image has a highly usefulness as surgical support. However, the difference in CT values between tendons and muscles is small. Therefore, it is necessary to reduce image noise in order to distinguish them. As a result, increased patient dose becomes a problem. We have tried to use Deep Learning Reconstruction (DLR) to solve this problem. This report introduces scanning techniques and patient dose reduction for creating 3D images of tendons. The 3D tendons imaging requires increased contrast and reduced patient dose reconstruction. The DLR for the brain LCD met this goal. This is because the diagnosis of the brain and the diagnosis of tendons are performed with the same low contrast. Compared to the conventional reconstruction method, DLR produced low-noise images at 75% lower dose and improved contrast, significantly enhancing the ability to visualize the finger flexor tendons.

#### TABLE OF CONTENTS/OUTLINE

1. Problems with imaging techniques in tendon morphology diagnosis 2. Improvement of image contrast using DLR 3. Reducing patient dose using DLR 4. Ingenuity when scanning tendons 5. Ingenuity for creating 3D tendons images 6. Verification of Clinical Effectiveness

#### MKEE-23 Brachial Plexus: Don't Be Afraid Anymore - A Guide for Brachial Plexus Anatomy and Injuries

Participants

LEON PERIN, Araras, Brazil (*Presenter*) Nothing to Disclose

#### TEACHING POINTS

The purpose of this study is to:1. Review with didactic illustrations the brachial plex anatomy, including how to recognize it on MRI.2. Demonstrate how several brachial plex injuries manifest clinically and on imaging exams.3. Present didactic cases of brachial plex injuries highlighting the main findings the radiologist should expect, untangling brachial plexus exams.

#### TABLE OF CONTENTS/OUTLINE

Introduction and review of the brachial plexus anatomy, with didactic illustration.Review the normal anatomy no MRI, highlighting the anatomic landmarks on coronal and sagittal exams.Overview the main injuries of the brachial plexus, including pre and post-ganglionar injuries, their clinical manifestations and epidemiology, and their imaging findings.Demonstrate with challenging clinical cases non-traumatic pathologies involving inflammatory and compressive causes, including Parsonage-Turner, thoracic outlet syndrome, post-Covid plexopathy.Present a serie of cases of brachial plex injuries, and what you should actively look for depending on clinical history.Propose a diagnostic checklist when evaluating brachial plexus injuries, simplifying the reading of these challenging exams.Summary.

#### MKEE-24 Axial Spondyloarthritis: What the Radiologist Needs to Know

**Awards**

**Certificate of Merit**

Participants

Taiki Nozaki, MD, Tokyo, Japan (*Presenter*) Nothing to Disclose

#### TEACHING POINTS

The purposes of this exhibit are 1) To demonstrate the classification of spondyloarthritis and anatomy of sacroiliac joint. 2) To know basic imaging findings of axial spondyloarthritis. 3) To review the imaging findings of mimickers of axial spondyloarthritis that radiologists should be familiar with.

#### TABLE OF CONTENTS/OUTLINE

1) Introduction 2) Classification of spondyloarthritis 3) Anatomy of sacroiliac joint for the proper evaluation on MRI 4) MR findings of axial spondyloarthritis i) Signs of activity -bone marrow edema, capsulitis, joint space fluid- ii) Signs of structural change -erosion, fat metaplasia, backfill, sclerosis, ankylosis- 5) Mimickers of axial spondyloarthritis -early post-partum, osteitis condensans ilii, pyogenic sacroiliitis, Paget disease, fibrous dysplasia, tuberculosis, spondyloepiphyseal dysplasia, bone metastases, SAPHO syndrome, DISH-

#### MKEE-25 The Sword in the Bone: A Review of the Sternum and Parasternal Region

**Awards**

**Certificate of Merit**

Participants

Sean Rodich, MD, MS, (*Presenter*) Nothing to Disclose

## TEACHING POINTS

1. Review anatomy of sternal bone landmarks, sternal and parasternal joints, and surrounding muscle attachments for a comprehensive understanding of the anterior chest wall. 2. Identify developmental variants and anomalies of the sternum to avoid confusion with other sternal pathologies. 3. Illustrate various pathologies of the sternum and parasternal region, which are often overlooked in the broad differential diagnosis for chest pain.

## TABLE OF CONTENTS/OUTLINE

1. Anatomy of the sternum- Bone landmarks- Sternal and parasternal joints (manubriosternal, xiphisternal, sternoclavicular, sternocostal, costochondral, and interchondral joints)- Muscle attachments 2. Developmental variants and anomalies of the sternum- Sclerotic bars and clefts- Sternal foramen- Episternal ossicles- Xiphoid process variants- Pectus excavatum/carinatum- Ectopia cordis- Miscellaneous syndromes (PHACES, Pentology of Cantrell) 3. Pathology of the sternum and parasternal region- Trauma (sternal and costal cartilage fractures, sternoclavicular joint dislocation)- Arthropathy (osteoarthritis, calcium pyrophosphate deposition disease, rheumatoid arthritis, seronegative spondyloarthropathy)- SAPHO (Synovitis, Acne, Palmoplantar pustulosis, Hyperostosis, Osteitis)- Condensing osteitis of the clavicle- Costochondritis versus Tietze syndrome- Sternotomy complications (sternal dehiscence, infection)- Neoplasm

## MKEE-26 Calcaneal Fracture Guide: Don't Miss a Thing - Beware of the Ugly Stuff

### Awards

#### Certificate of Merit

Participants

Marina Akuri, MD, Marilia, Brazil (*Presenter*) Nothing to Disclose

## TEACHING POINTS

The purpose of this exhibit is to: 1. Review calcaneal anatomy, fracture classifications, possible complications and the management for each kind of fracture. 2. Highlight the main information that radiologists should include in the report when analyzing a calcaneal fracture and their post-operative imaging, including normal and abnormal findings. 3. Illustrate several cases of calcaneal fractures, including postoperative evaluation with normal findings and complications, as well as differential diagnosis cases.

## TABLE OF CONTENTS/OUTLINE

Introduction: general review of calcaneal fractures, including classifications and what the report should include. Provide didactic and challenging cases of calcaneal fractures, including several complications, highlighting what is important for the report and for the orthopedic surgeon. Overview operative indications and modalities of surgical treatment. Present didactic cases of the different surgical modalities, discussing the normal and abnormal postoperative findings. Bibliographical references.

## MKEE-27 Stain the Eyes-Utility of high Resolution CT Dacryocystography in Imaging Lacrimal Duct Pathology Following Facial Trauma

Participants

Sudha Pyla, MBBS, Vijayawada, India (*Presenter*) Nothing to Disclose

## TEACHING POINTS

To demonstrate the common complications encountered in lacrimal drainage as a complication of facial injuries.

## TABLE OF CONTENTS/OUTLINE

Nasolacrimal duct injury may be due to blunt or penetrating trauma involving naso-orbitoethmoidal complex, maxillofacial fractures especially Le fort type-II, Le fort type-III, also secondary to postoperative cases due to inadequate surgical repair. In early post-injury period, nasolacrimal duct obstruction can occur as a result of post-traumatic compression by bone fragments or due to soft tissue edema. Inflammatory reaction followed by cicatrization resulting in delayed lacrimal duct blockade can present as late complication. Patients usually present with epiphora with or without purulent discharge. Long-term complication includes dacryocystocele formation. CT dacryocystography gives detailed information about the cause of obstruction, level of blockade, associated fractures and bony displacements. 1.5ml of diluted nonionic contrast (Ultravist 300mg iodine/ml) is administered into the inferior canaliculi and high resolution CT is performed. Depending on the level of blockage dacryocystorhinostomy is performed. In complete cut-off of duct or chronic dacryocystitis dacryocystectomy is done. This exhibit will demonstrate various spectrum of post-traumatic nasolacrimal drainage abnormality on CT dacryocystography.

## MKEE-28 Lumpy-Bumpy Ride Made Easy ! - A Sonographic Guide Through Soft Tissue Lesions

Participants

Saakshi Aggarwal, MBBS, (*Presenter*) Nothing to Disclose

## TEACHING POINTS

1. To review imaging features of various soft tissue lesions to be able to differentiate pseudo masses and pseudo tumors like dermoid, sebaceous cyst, abscess, hematoma from true tumors 2. To make a schematic approach towards suspected soft tissue lesions in order to assess nature of them based on internal characteristics of the lesion 3. To prime young budding radiologists towards diagnosis of benign "leave alone" lesions such as lipomas so as to reduce patient anxiety and limit further investigations unless indicated 4. To pick up suspicious morphology on ultrasonography and suggest the next appropriate step for further assessment

## TABLE OF CONTENTS/OUTLINE

1. Introduction 2. Importance of ultrasonography in assessing soft tissue lesions 3. Ultrasonographic Technique to assess soft tissue lesions 4. Imaging features to differentiate pseudo masses and pseudo tumors from true tumors 5. Simplified schematic approach towards suspected true tumors 6. Review of imaging features of various soft tissue tumors with histopathological diagnosis 7. Practical pearls for successful and complete diagnosis

## MKEE-29HC Baseline, Posttreatment and Surveillance Advanced Magnetic Resonance Imaging of Soft-Tissue Sarcomas

Participants

Mathew Canjirathinkal, MD, Houston, TX (*Presenter*) Nothing to Disclose

#### TEACHING POINTS

1. Soft-Tissue Sarcoma is a rare malignant tumor of mesenchymal and primitive neuroectodermal origin, more common than primary malignant bone tumors. 2. Traditional response criteria such as RECIST inadequate rely on physical measurements, as tumor diameter does not reflect all response types. 3. Diffusion-weighted imaging analysis could rely upon Whole tumor ADC histograms, focusing on mean ADC, Kurtosis, and Skewness. 4. Whole tumor Perfusion Weighted Imaging (PWI) with Dynamic Contrast-enhanced imaging (DCE) could rely on morphologic patterns (nodular vs. linear) and time-intensity curves (TIC) analysis, where the presence of early arterial enhancement (TIC III, IV, and V) correlates with untreated or unsuccessfully treated sarcomas, while TIC II with successfully treated sarcomas. 5. DCE MR imaging reliably distinguishes recurrent sarcoma from postsurgical scarring. TICs III, IV, and V highly raise suspicion of local tumor recurrence, while TIC type II usually represents granulation.

#### TABLE OF CONTENTS/OUTLINE

1. Introduction 2. Learning objectives 3. Soft tissue sarcoma 4. The Armamentarium: MR sequences: DWI/ADC, PWI/DCE and SWI 5. ABASTI (Advanced bone and soft tissue tumor imaging) 6. Worth knowing: Hemorrhage and ADC, Fat and ADC. 7. Responding tumor ABASTI patterns 8. Non-responding tumor ABASTI patterns 9. Tumor recurrence and DCE 10. References Please visit the Learning Center to also view this presentation in hardcopy format.

#### MKEE-3 Radial Tunnel Anatomy in Supination and Pronation: Guidance for Imaging Interpretation and Interventional Procedures

##### Awards

##### Magna Cum Laude

Participants

Aurea Mohana-Borges, MD, MSc, San Diego, CA (*Presenter*) Nothing to Disclose

#### TEACHING POINTS

To provide a guide for radial tunnel anatomy that emphasizes the relationship of soft tissue (nerve, vessel, muscle) and osseous structures in supination and pronation with High Resolution Ultrasound (HRUS) and magnetic resonance imaging (MRI). This guide will highlight anatomic landmarks implicated in entrapment syndromes of the radial nerve. It will emphasize the dynamic nature of radial tunnel and its spatial relationships through range of motion. It will compare and contrast normal anatomy with examples of commonly encountered pathology about the radial tunnel.

#### TABLE OF CONTENTS/OUTLINE

Explanation of the concept, constituents, and anatomic boundaries of the radial tunnel. Demonstration of normal anatomy of the radial tunnel with HRUS and MRI with emphasis on the relationship of deep branch of radial nerve (DBRN), leash of Henry, and superior arcade of supinator muscle (arcade of Frohse). Examples of dynamic ultrasound of the DBRN, DBRN hydrodissection, and commonly encountered pathology about the radial tunnel.

#### MKEE-30HC Susceptibility-Weighted Imaging (SWI) Emerging Role in Musculoskeletal (MSK) Oncology

##### Awards

##### Certificate of Merit

Participants

Mathew Canjirathinkal, MD, Houston, TX (*Presenter*) Nothing to Disclose

#### TEACHING POINTS

1. Susceptibility-weighted imaging (SWI) is a 3D high-spatial-resolution, velocity-corrected gradient-echo MRI sequence that uses magnitude and filtered-phase information to create images. 2. Distinguishing between calcification and blood products is possible through the filtered phase images, helping to recognize osteoblastic and osteolytic bone metastases or demonstrating calcifications and osteoid production in liposarcoma and osteosarcoma. 3. Contrast-enhanced SWI (CE-SWI) can simultaneously detect the T2\* susceptibility effect and spontaneous T1 shortening. 4. Various Bone and soft tissue masses SWI features are described. 5. CE SWI demonstrates the viable, enhancing portions of a soft tissue sarcoma separately from hemorrhagic/necrotic components, suggesting its utility as a biomarker of tumor grade and treatment response. CE-SWI shows superior differentiation between mature fibrotic T2\* dark components and active enhancing T1 shortening components in Desmoid Fibromatosis. 6. Ring-like hemosiderin SWI pattern is observed in successfully treated sarcomas. 7. CE-SWI also separates healthy T2\* blooming iron-loaded bone marrow from T1-shortening enhancing bone marrow replacing tumor.

#### TABLE OF CONTENTS/OUTLINE

1. Introduction to SWI and SWI with contrast CE-SWI 2. CE-SWI in Benign and malignant soft tissue masses 3. CE-SWI of primary bone tumors and metastasis 4. CE-SWI features of soft tissue sarcoma tumor response 5. References Please visit the Learning Center to also view this presentation in hardcopy format.

#### MKEE-31 Stand and Deliver: Weight-Bearing Extremity CT in Clinical Practice

##### Awards

##### Identified for RadioGraphics

Participants

Matthew Doan, BS, Phoenix, AZ (*Presenter*) Nothing to Disclose

#### TEACHING POINTS

The structures of the foot and ankle are ideally assessed during weight-bearing. Cross-sectional imaging of the foot and ankle using CT and MRI can overcome the limitations of radiographs but is typically performed with patients in the supine position. Recently standing cone-beam CT (CBCT) scanners have been introduced to combine the value of cross-sectional CT imaging with the

anatomic assessment of structures during weight-bearing.

#### TABLE OF CONTENTS/OUTLINE

Purpose/Aim: This educational exhibit will spotlight the implementation and utilization of a standing CBCT scanner in a tertiary care medical center. The exhibit will cover the scanner and room setup, basic scanner physics, patient preparation and positioning, and image acquisition. Illustrative example cases will be included. Content Organization: Describe the room requirements for installing a standing CBCT scanner. Review the CT physics involved in obtaining a standing CBCT image. Provide a workflow model for standing CBCT scanner use in musculoskeletal radiology practice. Showcase patient positioning during standing CBCT acquisition. Highlight additional uses of a standing CBCT scanner for hand and wrist imaging. Provide illustrative clinical cases spotlighting the value of standing CBCT imaging. Summary: Radiographs of the foot and ankle obtained with weight-bearing are fundamental in initial imaging assessment. In cases requiring cross-sectional imaging, standing CBCT provides weight-bearing advanced imaging at lower dosing than traditional CT. This educational exhibit highlights the role a standing CBCT scanner can play in clinical practice.

#### MKEE-32 Sonography of the Wrist and Hand in Clinical Practice: Diagnosis and Intervention

##### Awards

##### Identified for RadioGraphics

##### Participants

Dyan V. Flores, MD, Ottawa, ON (*Presenter*) Nothing to Disclose

##### TEACHING POINTS

Diagnostic and interventional sonography of the wrist and hand may be daunting in clinical practice due to the plethora of structures and abnormalities that need to be evaluated. In this education exhibit, we describe a compartment approach in detecting common wrist and hand disorders and performing the corresponding interventional procedures. The objectives of this educational exhibit are: • To review normal sonographic anatomy of the wrist and hand • To illustrate and highlight a compartment approach in diagnostic and interventional sonography of the hand and wrist • To discuss common abnormalities encountered in clinical practice and the corresponding interventions in each compartment

#### TABLE OF CONTENTS/OUTLINE

Extensor compartment • Extensor compartments 2 and 3 (EPL rupture, distal intersection syndrome) • Intrinsic ligaments of the wrist • Extensor hood/Ulnar compartment • DRUJ • TFCC • Extensor compartment 6/Volar compartment • Median nerve at carpal tunnel • Ulnar nerve in Guyon's canal • Flexor tendons and retinaculum • Finger pulleys/Radial compartment • 1st CMC and STT • Extensor compartment 1 (De Quervain's tenosynovitis, proximal intersection syndrome) • UCL of thumb

#### MKEE-33 MRI of the Metabolic Knee

##### Participants

Bruno C. Vande Berg, MD, PhD, (*Presenter*) Nothing to Disclose

##### TEACHING POINTS

\* Metabolic disorders of the MSK system are frequent disorders that are usually clinically silent for a long period of time. All components of the musculo-skeletal system can be involved including bones, marrow, cartilage, tendons, ligaments, capsule, synovium and muscles. \* Despite the fact that knee MRI is one of the most frequently performed examination, radiologists rarely suggest the presence of an underlying metabolic disorder at knee MRI. The vast majority of the metabolic disorders of the MSK system remains occult at knee MRI until complications occur. \* Knee MRI can depict a spectrum of complications associated with metabolic disorders including typical and atypical fractures, bone necrosis, acute and chronic arthritis, peri-arthritis, tendinopathies and tendon rupture, synovial and capsule deposits, red marrow reconversion and serous transformation. \* The radiologists should recognize these complications at knee MRI and suggest a possible link with an underlying metabolic disorder. \* The current exhibit aims at presenting a series of clinical cases in which knee MRI was performed and led to the diagnosis of a systemic metabolic disorder.

#### TABLE OF CONTENTS/OUTLINE

\* Insufficiency and avulsion fractures in osteoporosis/osteomalacia/renal osteodystrophy. \* Crystal-associated acute arthritis and peri-arthritis. \* Chronic tophaceous arthritis. \* Drug-associated tendinopathies and tendon rupture. \* Unusual osteoarthritis associated with calcium pyrophosphate crystals. \* Marrow reconversion and marrow necrosis associated with anemias. \* fat and serous atrophy of the bone marrow associated with cachexia. \* Synovial and cartilage deposits of iron and copper. \* Synovial and capsule amyloidosis.

#### MKEE-34 The Many Faces of Ramp Lesions of the Medial Meniscus

##### Participants

Alfonso Iglesias, MD, PhD, (*Presenter*) Nothing to Disclose

##### TEACHING POINTS

Meniscal ramp injury is a meniscus-capsular vertical longitudinal tear of the posterior horn of the internal meniscus, often associated, with an anterior cruciate ligament injury. In MRI, an injury of the internal meniscal ramp must be suspected when a rupture of the ACL and/or bone edema in the posteromedial slope of the tibial plateau is observed. It is important to detect meniscal ramp injuries in MRI and alert the traumatologist, since they are hidden meniscal lesions with the usual arthroscopic portals, and require accessory portals for a diagnostic confirmation. The decision of either a conservative or a surgical treatment will depend primary on the stability and the extent of the injury.

#### TABLE OF CONTENTS/OUTLINE

Recognize and identify a ramp lesion of the medial meniscus on MR images Describe and classify ramp lesion of the medial meniscus on MR images with arthroscopic correlation Review of surgical technique for the detection and repair of these types of lesions

## **MKEE-35    Shoulder Microinstability: Demystifying the Interplay of Static and Dynamic Stabilizers of the Glenohumeral Joint**

Participants

Juliana Sitta, MD, Jackson, MS (*Presenter*) Nothing to Disclose

### **TEACHING POINTS**

Microinstability is a relatively new concept defined by rotational or directional pathologic movement of the glenohumeral joint without true (macro) instability on physical examination. The pathophysiology may include abnormalities involving static and dynamic stabilizers of the glenohumeral joint, the anterosuperior labrum, rotator interval, or middle glenohumeral ligament. Causes of microinstability may include acute or chronic recurrent traumatic etiology (including overuse), iatrogenic, and congenital osseous and soft tissue abnormalities. Clinical and imaging findings including those of internal impingement syndromes are often subtle and radiologists play an important role in identifying these patients to guide appropriate treatment and avoid delay in diagnosis which can lead to osteoarthritis.

### **TABLE OF CONTENTS/OUTLINE**

Glenohumeral anatomy and congenital variants. Pathophysiology of shoulder microinstability, glenoid dysplasia, anterior and posterior internal impingement syndromes. Multimodality imaging findings and differential diagnosis. Clinical and surgical management. Complications and post treatment imaging findings.

## **MKEE-36    Imaging Features of Glenohumeral Osteoarthritis: The Power of Simplicity**

Participants

Paulo de Tarso Perez, MD, (*Presenter*) Nothing to Disclose

### **TEACHING POINTS**

The purpose of this exhibit is to: To briefly review the concepts of glenohumeral osteoarthritis. To review the most used classifications, image findings and measures of glenoid. Highlight the Walch classification, glenoid morphology changes and what we should report that can change the management and treatment. To make the differential diagnosis with entities that may cause osteoarthritis.

### **TABLE OF CONTENTS/OUTLINE**

Introduction: to review the concepts of glenohumeral osteoarthritis. Show didactic and illustrative cases reviewing the classifications and the main imaging findings according to the different etiologies, highlighting what we should report in order to assist in the correct and early diagnosis and treatment. Present a schematic table and imaging of the most used classifications and showing measures of glenoid and its morphology changes. Conclusions. Bibliographical references.

## **MKEE-37    Is This DISH?": Radiological Findings with Special Attention to Extraspinal Involvement**

Participants

Dario Herran de la Gala, MD, Santander, Spain (*Presenter*) Nothing to Disclose

### **TEACHING POINTS**

This exhibit will: 1) Describe the most frequent radiological findings of DISH in the spine. 2) Establish the diagnostic criteria and their usefulness in DISH differential diagnosis. 3) Show the most frequent extraspinal findings. 4) Illustrate the most frequent DISH complications.

### **TABLE OF CONTENTS/OUTLINE**

Diffuse idiopathic skeletal hyperostosis (DISH) is an underdiagnosed disease whose prevalence increases with age. This disease consist in an ossification of both spinal and extraspinal tendons, ligaments, periosteum and joint capsules. It can cause pain, stiffness, compressive syndromes or spinal fractures after minor traumas. Radiological findings in the spine and DISH diagnostic criteria are widely known. On the other hand, extraspinal involvement, especially in isolation, may go unnoticed. Moreover, extraspinal involvement precedes spinal radiological findings and can be found in younger patients.

## **MKEE-38    Haemophilic Artropathy: An Imaging Overview**

Participants

Marina Akuri, MD, Marilia, Brazil (*Presenter*) Nothing to Disclose

### **TEACHING POINTS**

The purpose of this exhibit is to: 1. Review and illustrate classifications and spectrum of imaging findings of haemophilic arthropathies in a multimodality approach including radiographs, ultrasound, computed tomography and magnetic resonance in different joints. 2. Highlight and discuss other musculoskeletal complications of haemophilia that the radiologist must be aware in these patients, such as hematomas, pseudotumors, heterotopic calcification, and others. 3. Provide a guidebook for all the typical and atypical musculoskeletal findings in hemophilic arthropathy.

### **TABLE OF CONTENTS/OUTLINE**

Introduction: general presentation, epidemiology, pathology and clinical manifestation of haemophilic arthropathies. Present a schematic illustration with the distribution of the most common joints affected by haemophilic arthropathy while discussing the main findings on didactic cases. Overview some of main haemophilic arthropathy classification including a schematic illustration of Arnold-Hilgartner classification. Provide didactic cases of the all image modality of different joints with typical and atypical findings. Provide other musculoskeletal manifestations and complication with challenging cases of hematomas, pseudotumors and heterotopic calcification. Present differential diagnosis cases with some similar intra-articular findings that should not be mistaken with hemophilic disease, including inflammatory arthropathies, amyloidosis, gout, among others. Bibliographical references.

## **MKEE-39 A Radiological Overview of Ankle Arthroplasty - Practical Keys in the Assessment of Ankle Replacement**

Participants

Javier Azpeitia Arman, MD, Madrid, Spain (*Presenter*) Nothing to Disclose

### **TEACHING POINTS**

-To know the different types of total ankle replacement. -To review imaging techniques for preoperative imaging and in the evaluation of prostheses (plain radiograph, CT, MR, US, scintigraphy). -To understand the usefulness and limitations of plain radiographs in the evaluation of ankle replacements, emphasizing useful parameters and illustrating image analysis and interpretation. -To become familiar with normal and abnormal postoperative imaging findings and signs of complications.

### **TABLE OF CONTENTS/OUTLINE**

We review imaging of total ankle replacement, highlighting key concepts perceived as important variables by the surgeon and correlating images with clinical considerations and functional outcomes. We present: 1. A review of types of ankle replacement 2. Surgery. Aims. 3. Imaging. Role of CT, MR, US, and scintigraphy. 4. Plain radiographs: -Technique and views. Standard image acquisition: beam and anatomical landmarks -Parameters that should be evaluated: alignment of tibial and talar components, position, rotation, radiolucent lines and subtle abnormalities such as subsidence, early osteolysis, and angular deformities that may indicate aseptic loosening or possible infection -Imaging of complications: aseptic loosening, expansile osteolysis, subsidence and component migration, infection, periprosthetic fracture, heterotopic ossification, and PE spacer displacement or fracture

## **MKEE-4 Apophyseal Athletic Injuries Around the Hip: Why You Shouldn't Be Afraid**

**Awards**

**Certificate of Merit**

Participants

Vitor Sato, MD, Sao Paulo, Brazil (*Presenter*) Nothing to Disclose

### **TEACHING POINTS**

The purpose of this exhibit is to: Illustrate and discuss hip anatomy in individuals with immature bone skeleton, focusing on the apophysis; Describe and illustrate the maturation process of apophysis; Discuss and illustrate with classical and challenging cases the imaging findings of different apophysitis and apophyseal lesion around the hip; Show common and uncommon pitfalls that mimic apophyseal lesion in the hip; Show imaging findings of sequelae of apophysitis in the hip.

### **TABLE OF CONTENTS/OUTLINE**

Introduction: general presentation of anatomy with MRI of hip apophysis in the immature bone skeleton, including the complex anatomy of tendinous and aponeurosis insertion in the pubic apophysis; Present schematic cases and illustration to show maturation process of apophysis, with emphasis in the pubic apophysis; Describe schematically the algorithm and imaging protocol for assessing apophyseal injury in skeletal immature athletes; Show imaging findings of classical and challenging cases of apophyseal injury around the hip in athletes and also pitfalls that could mimic this pathologic condition; Show imaging findings of sequelae of apophysitis in the hip; Bibliographical references with recent articles highlighting what's new in the topic.

## **MKEE-40 Chip on the Shoulder: Multimodality Review of Reverse Shoulder Arthroplasties**

Participants

Akwasi Opoku, MD, Nashville, TN (*Presenter*) Nothing to Disclose

### **TEACHING POINTS**

The reverse shoulder arthroplasty (RSA) is a significant advance in shoulder reconstruction, reversing the normal ball and socket anatomy, stabilizing the glenohumeral center of rotation, and allowing the deltoid to function as the main muscular force. RSA has been shown to provide pain relief and functional improvement. Radiologists must be aware of the importance of certain preoperative imaging findings in patients under consideration for RSA, such as deltoid integrity, as well as potential postoperative complications unique to RSA, such as acromial and scapular fractures, and scapular notching. After viewing this exhibit, the learner should understand: 1. Shoulder anatomy and biomechanics 2. Indications for RSA 3. Role of preoperative imaging and measurements 4. Advantages, disadvantages, and specific complications of RSA 5. Normal imaging findings and imaging findings of complications

### **TABLE OF CONTENTS/OUTLINE**

Introduction Shoulder anatomy and biomechanics 1. Bones, joints, muscles, other soft tissues (cartilage, labrum, capsule) 2. Unconstrained ball and socket, static and dynamic stabilizers Design, function, and success of RSA Indications 1. Arthropathy, trauma, cuff disease, osteonecrosis, prior infection, failed arthroplasty Role of preoperative imaging (multimodality) 1. Evaluation of cuff, bone stock, cartilage 2. Glenoid morphology and version Complications 1. Acromial and scapular fractures 2. Scapular notching 3. Hardware fracture and disengagement 4. Periprosthetic fracture 5. Loosening 6. Infection 7. Instability 8. Nerve injury Imaging appearances 1. Normal and complications

## **MKEE-41 Hip Dysplasia: Evaluation Beyond Diagnosis - What the Radiologist Should Know About Its Management Treatment**

Participants

Mariana Batista Rosa Pinto, MD, (*Presenter*) Nothing to Disclose

### **TEACHING POINTS**

The purpose of this study is to: Briefly approach the pathophysiology and epidemiology of hip dysplasia. Discuss the imaging modalities used to evaluate hip dysplasia and list the imaging findings and measurable parameters that most accurately reflect the disorder. Review and didactically illustrate the most frequent treatments, complications and differential diagnoses of the disease. Provide a guide with several examples of post-treatment imaging, highlighting what the radiologist should know about the management of hip dysplasia.

### **TABLE OF CONTENTS/OUTLINE**

Introduction: general presentation of the epidemiology, pathophysiology and clinical findings of hip dysplasia. Present schematic illustrations of findings and measurable parameters that most accurately help the diagnosis of the disorder. Provide didactic cases of the manifestation related to each type of imaging method. Discuss treatments and what radiologists should know when evaluating the postoperative exams, while providing pre and postoperative imaging examples. Point complications and show differential diagnoses. Provide an imaging guide of the several hip dysplasia treatment options. Conclusions. Bibliographical references with recent articles on what is new in the topic.

#### **MKEE-42 Musculoskeletal Complications of Cosmetic Procedures: When Things Get Ugly**

Participants

Ligia Couceiro, MD, Sao Paulo, Brazil (*Presenter*) Nothing to Disclose

##### **TEACHING POINTS**

According to the American Society of Plastic Surgery (ASPS), aesthetic procedures have increased exponentially in recent years. A wide variety of cosmetic techniques are performed in healthy patients to improve body image or for reconstructive reasons. Those procedures can be either incidental findings or the cause of symptoms on imaging exams. It is indispensable for radiologists to learn identification of the common aesthetic procedures on different imaging techniques and be capable of evaluating their normal appearance and complications. The purpose of this study is: • To recognize the most common aesthetic procedures and their normal appearance, focusing on musculoskeletal system imaging. • To discuss the cosmetic procedures complications and their imaging findings. • Illustrate imaging findings through sample cases • Propose a systematic approach to image interpretation.

##### **TABLE OF CONTENTS/OUTLINE**

• INTRODUCTION • Review aesthetic procedures and their complications. • COSMETIC PROCEDURES INVOLVING THE MUSCULOSKELETAL SYSTEM AND THEIR COMPLICATIONS: • Gluteal augmentation (gluteal implants, autologous fat grafting, filler injections): implants displacement/ rupture, capsular contraction; infection; compressive syndromes, etc • Abdominoplasty: wound dehiscence, infection, etc • Body contouring with silicone implants (arms, legs): infection, implants rupture, etc • Pectoral augmentation (implants, filler injections): infection, implants displacement or rupture, etc • IMAGING INTERPRETATION • Cosmetic procedures normal and pathological findings • Systematic approach to evaluate image exams • INTERACTIVE CASE-BASED DIDACTICS • Sample cases to illustrate and solidify the concepts

#### **MKEE-43 Fungal Musculoskeletal Infections: Who, When, Where and How? A Comprehensive Approach to Proper Diagnosis**

**Awards**

**Certificate of Merit**

**Identified for RadioGraphics**

Participants

Julia Peixoto, Sao Paulo, Brazil (*Presenter*) Nothing to Disclose

##### **TEACHING POINTS**

Teaching points: The purpose of this exhibit is to: 1. Provide a comprehensive overview, yet a didactic practical guide to assess fungal musculoskeletal infections imaging; 2. Integrate imaging, clinical and epidemiological aspects, reviewing and illustrating the most frequent and some rare presentations of fungal musculoskeletal infections;

##### **TABLE OF CONTENTS/OUTLINE**

Outlines: Introduction: epidemiology, etiology, pathophysiology and clinical findings. Section-structured overview emphasizing the main imaging findings and relevant clinical and epidemiological features of each group of fungus. Illustrative cases, exemplifying classic imaging signs, and challenging cases addressing differential diagnoses with practical tips. Bibliography: broad-researched references highlighting what's useful to the radiologist.

#### **MKEE-44 A Guide to Tibiofibular Syndesmosis: Anatomy, Imaging and Surgical Techniques**

Participants

Cristyano Leite, MD, Sao Paulo, Brazil (*Presenter*) Nothing to Disclose

##### **TEACHING POINTS**

Comprehend clinic indications for imaging evaluation. Recognize the most useful image methods. Learn the anatomic features and relationships of the tibiofibular syndesmosis. Understand role and limitations of each method.

##### **TABLE OF CONTENTS/OUTLINE**

INTRODUCTION. Epidemiology of the tibiofibular syndesmosis injury. Different Imaging methods to evaluate the syndesmosis. ANATOMICAL CONCEPTS. Anatomic description of the syndesmosis ligaments. Normal syndesmosis in the different methods. CASE-BASED DIDACTICS. Ligaments and syndesmotic injuries in the different methods. SURGICAL TECHNIQUES. Most used surgical techniques: indication and examples.

#### **MKEE-45 Ultrasound of Medial Elbow Pain: Beyond the Epicondylitis**

Participants

Jee Won Chai, MD, Seoul, Korea, Republic Of (*Presenter*) Nothing to Disclose

##### **TEACHING POINTS**

Although it is less common than lateral elbow pain, medial elbow pain is a musculoskeletal problem more commonly encountered in the population participating repetitive activities. Ultrasonography has advantages in focused and dynamic evaluation of medial elbow structures, and subsequently enables to establish the differential diagnosis. The various anatomic structures more than common flexor tendon, such as ulnar collateral ligament, ulnar nerve, medial antebrachial cutaneous nerve and elbow joint can cause medial elbow pain, and some characteristic clinical features and physical examinations would be helpful for more focused evaluation on the clinically suspicious structures. Even with positive finding on one structure, other structures also should be evaluated for screening of coexisting pathology or other possible diagnosis; for instance, medial epicondylitis can accompany ulnar

neuropathy or ulnar collateral ligament injury as well, and proper treatment would be differed in such cases.

#### TABLE OF CONTENTS/OUTLINE

1. Differential diagnosis of medial elbow pain 2. Scanning technique and normal medial elbow on ultrasonography 3. Medial elbow pathology  
A. Medial epicondylitis  
B. Ulnar collateral ligament injury  
C. Ulnar neuropathy i. Cubital tunnel syndrome ii. Ulnar nerve instability  
D. Snapping triceps syndrome  
E. Medial antecubital cutaneous neuropathy  
F. Arthritis i. Ulnohumeral osteoarthritis ii. Gouty arthritis  
G. Others i. Cervical radiculopathy ii. Basilic vein thrombophlebitis

#### MKEE-46 Comparing US and MRI for Hand and Wrist Diseases: Which Weapon to Choose?

Participants

Young Ju Song, MD, Jeonju, Korea, Republic Of (*Presenter*) Nothing to Disclose

#### TEACHING POINTS

Ultrasound imaging uses sound waves to produce pictures of muscles, tendons, ligaments, nerves and joints throughout the body. It is used to help diagnose sprains, strains, tears, trapped nerves, arthritis and other conditions. However, there are some diseases that US cannot fully detect, whereas MRI can easily and quickly find. Magnetic resonance imaging (MRI) uses a powerful magnetic field, radio waves and a computer to produce detailed pictures of joints, soft tissues and especially intraosseous lesions. It is usually the best choice for evaluating the body for injuries, tumors, and degenerative disorders. But in some cases, US is superior to MRI for detecting certain pathologies. The ability of a radiologist to understand the fundamental physics of US and MRI, recognize US and MRI competencies, and provide recommendations for using the most suitable imaging modality is essential for proper image interpretation, troubleshooting, and utilization of the full potential of each modality.

#### TABLE OF CONTENTS/OUTLINE

1. Basic Physics of Ultrasound 2. Basic Physics of MRI 3. Hand and Wrist Lesions : Comparison of Ultrasound vs. MRI  
1) Cases that show how Ultrasound is superior to MRI: Gout, Calcific Tendinosis, Extensor Carpi Ulnaris Dislocation (in dynamic study), Digital Nerve Adhesion, Pulley Thickening (Trigger finger)  
2) Cases that show how MRI is superior to Ultrasound: Triangular Fibrocartilage Complex Tear, Osteomyelitis, Bone Tumor, Complex Regional Pain Syndrome, Infectious Arthritis  
3) Cases that show how both Ultrasound and MRI are equally useful: Tenosynovitis, Sagittal Band Rupture, Volar Plate Injury, Collateral Ligament Injury, Rheumatoid Arthritis, Ganglion Cyst, Tenosynovial Giant Cell Tumor

#### MKEE-47 "Go With the Flow" - Vascular Pathology Encountered on Knee MRI

Participants

Kathryn Stevens, MBBS, FRCR, Stanford, CA (*Presenter*) Nothing to Disclose

#### TEACHING POINTS

The purpose of this exhibit is to: 1. Review common and uncommon pathology of the popliteal artery and veins that can be encountered on knee MRI 2. Describe the signal characteristics of vascular masses occurring within and around the knee, as well as some of the potential pitfalls The major teaching points of this exhibit are: 1. Vascular pathology can often be seen on knee MRI, and is important to recognize 2. Knowledge of normal variants in vascular and muscle anatomy occurring around the knee has important implications for surgical planning 3. Detecting a DVT on routine MRI may significantly affect subsequent patient management 4. Intra- and extra-articular vascular malformations are not infrequently encountered around the knee, and it is important to identify characteristic imaging findings together with some of the potential pitfalls in diagnosis

#### TABLE OF CONTENTS/OUTLINE

1. Discuss classification and imaging findings of popliteal entrapment syndrome 2. Illustrate pathologies affecting the popliteal artery, including popliteal artery dissection, transection, aneurysm/pseudoaneurysm, cystic adventitial disease of the popliteal artery, and arterial calcification due to deficiency of CD73 (ACDC) 3. Review the aberrant anterior tibial artery, a commonly encountered normal variant, and emphasize the importance of including a description of this common variant in an MR report, particularly if the patient is to undergo subsequent knee surgery 4. Highlight the importance of evaluating for deep venous thrombosis on routine MRI 5. Outline imaging characteristics of vascular malformations occurring around the knee 6. Illustrate potential pitfalls mimicking vascular pathology around the knee

#### MKEE-48 Don't Be Afraid About T2 Mapping of the Knee Articular Cartilage: A Simple Way to Decrease Reports Ambiguity and Improve the Communication with Arthroscopists

Awards

Certificate of Merit

Participants

Estefania Gallego Diaz, MD, MD, Mexico City, Mexico (*Presenter*) Nothing to Disclose

#### TEACHING POINTS

- T2 mapping sequence improves the sensibility of detecting cartilage lesions within the knee joint, especially in the early stages. - To explain the importance of adding a T2 mapping sequence to a routine MRI protocol. - To instruct the radiologist on who applies the T2 mapping and how to do it. - To Review the main classifications of chondral (cartilage) lesions. - To implement the use of validated evaluation scales. - To present an algorithm approach and protocol that facilitates a uniform lexicon between radiologists and arthroscopists. - To simplify the technique and reports used in these patients to improve communication with the arthroscopy specialists.

#### TABLE OF CONTENTS/OUTLINE

1. Introduction 2. Definitions 3. Understanding the chondral(cartilage) lesion 4. Classifications of chondral lesions and correlation with arthroscopy 5. Validated evaluation scales 6. T2 mapping sequence · Indications · Physics · Technique and protocol recommendations 7. How to report it: · Pictorial review · Algorithm approach and templates tips. · Case-based learning 8. Conclusions

## **MKEE-49 The Patellofemoral Joint: From Joint Stability to Articular Pathologies**

Participants

Andre Rosenfeld, MD, Sao Paulo, Brazil (*Presenter*) Nothing to Disclose

### **TEACHING POINTS**

The purpose of this educational exhibit is:- Review the normal anatomy and imaging evaluation of the stabilizers of the patellofemoral joint and their pathologies, exemplifying the pathologies with didactic cases- Illustrate and discuss knee extensor mechanism injuries, patellar fat pad and bursae pathologies- Review patellofemoral joint pathologies, including degenerative osteoarthritis, inflammatory and crystal arthropathy

### **TABLE OF CONTENTS/OUTLINE**

Patellofemoral congruency depends on dynamic stabilizers (extensor muscles and medial patellofemoral retinaculum/ligament) and static (bone) stabilizers. Imaging evaluation includes patellar and trochlear measurements, patellar translation distance (TT-TG) and torsional measurements. The knee extensor mechanism is composed of the quadriceps muscle and tendon, medial and lateral patellar retinaculum, patella, patellar tendon and tibial tuberosity. Its pathologies can be divided by location and chronology (acute vs chronic). Associated extensor mechanism pathologies include patellar fat pad and bursa abnormalities. The patellofemoral joint is a synovial joint that can be affected by degenerative, inflammatory and crystal arthropathies and synovial processes, with typical imaging findings. The radiologist needs to be familiar with the complete imaging evaluation of the patellofemoral joint, from joint stability to articular pathologies.

## **MKEE-5 Musculoskeletal Manifestations of Dermatomyositis: An Imaging Overview**

Participants

Marina Akuri, MD, Marilia, Brazil (*Presenter*) Nothing to Disclose

### **TEACHING POINTS**

The purpose of this exhibit is to:1. Review and illustrate musculoskeletal manifestation of dermatomyositis with imaging findings on radiographs, ultrasound, computed tomography scan and magnetic resonance imaging.2. Review and discuss diagnoses related to dermatomyositis as paraneoplastic manifestation. 3. Review and discuss differential diagnoses.

### **TABLE OF CONTENTS/OUTLINE**

Introduction: overview of clinical manifestation of the disease, including epidemiology, physiopathology, also presenting musculoskeletal clinical features of dermatomyositis. Present an illustrated scheme with the most common manifestations of dermatomyositis. Exemplify the manifestations of dermatomyositis such as skin involvement, subcutaneous tissue involvement, musculoskeletal involvement, and correlate with different imaging modalities. Present clinical case with differential diagnosis. References.

## **MKEE-50 Posterior Meniscal Roots Injury: What Radiologists Need to Know**

Participants

Camila De Paula Silva, MD, Botucatu, Brazil (*Presenter*) Nothing to Disclose

### **TEACHING POINTS**

To review and illustrate the anatomy of the posterior meniscal roots in schematic figures and MRI. To review and illustrate the lesions and classification of posterior root meniscal tears in schematic figures and MRI. To review and illustrate the surgical techniques to repair meniscal posterior root tears in schematic figures, intra-operative imaging, and post-operative imaging in a multimodality approach.

### **TABLE OF CONTENTS/OUTLINE**

1- Anatomy of the posterior meniscus root. 2- MRI of posterior meniscus root tears and their classifications: - type 1 (partial radial root tears without any tear in the adjacent posterior horn or body); - type 2 (complete radial root tears); - type 3 (longitudinal bucket-handle tears with a complete tear of the root attachment); - type 4 (complex oblique tears with a complete tear of the root attachment); - type 5 (avulsion fractures of the tibial plateau). 3- Types of surgical techniques to repair meniscal root tears, include - Surgical indications.- Intra-operative imaging.- Partial meniscectomy.- Meniscal repair (transtibial pullout repair, suture anchor repair, and side-to-side repair).

## **MKEE-51 Update on Orthopedic Procedures in the Knee**

Participants

Eduarda Bernal, MD, Sao Paulo, Brazil (*Presenter*) Nothing to Disclose

### **TEACHING POINTS**

Review new methods to repair cartilage of the knee like allograft and autologous transplantation associated with collagen membrane. Demonstrate that extra-articular anterolateral procedures improve clinical outcome when performed as an augmentation of the anterior cruciate ligament reconstruction in specific groups of patients. Review normal and abnormal postoperative MRI findings of arthroscopic transtibial pullout repair (ATPR) for medial meniscus posterior root tear (MMPRT). Talk about future prospects of minimally invasive knee surgery.

### **TABLE OF CONTENTS/OUTLINE**

Cartilage defects of the knee are often debilitating and predispose to osteoarthritis. Seeking methods that combined can effectively repair cartilage and prevent progression to osteoarthritis is the goal of orthopedists. For larger lesions with a substantial amount of cartilage loss, autologous chondrocyte implantation using a bilayer collagen membrane has been demonstrated excellent results. Currently, the most commonly used technique for root repair is ATPR. The role of postoperative MRI is confirm the reduction of the posterior meniscus root to the original footprint of the tibial surface, identify the integrity of this structure, note the decrease in intra-meniscal signal intensity. The anterolateral ligament and capsule of the knee are anatomical structures involved in rotational stability and pivot-shift control. As such, it has been demonstrated that the extra-articular anterolateral procedures improve clinical outcome when performed as an augmentation of the anterior cruciate ligament reconstruction in specific groups of

patients.

## **MKEE-52 Osteosarcopenia: A New Geriatric Syndrome with Great Impact on Our Life**

Participants

Jimi Huh, MD, (*Presenter*) Nothing to Disclose

### **TEACHING POINTS**

The purpose of this exhibit is 1. To explain the concept and updated knowledge about osteosarcopenia 2. To systematically review the current researches about clinical importance of osteosarcopenia 3. To understand the concept and future directions of body composition imaging for evaluation of osteosarcopenia Major teaching points are: 1. Osteosarcopenia, a combination of osteoporosis and sarcopenia is a distinct disease entity with unique pathophysiology. 2. Osteosarcopenia is highly associated with frailty and mortality in elderly people and cancer patients. 3. Advances in imaging have enabled detailed analysis of osteosarcopenia.

### **TABLE OF CONTENTS/OUTLINE**

1. Concept and updated knowledge about osteosarcopenia - Changing concepts: From sarcopenia to osteosarcopenia and myosteatosis - Osteosarcopenia: combination of sarcopenia and osteoporosis - Distinct pathophysiology focusing on interaction between muscle and bone 2. Systematic review for clinical importance of osteosarcopenia - Prognostic markers for overall survival in cancer patients - Independent risk factors for osteoporotic fractures and frailty - Increase in mortality/morbidity after major surgery 3. Body composition imaging for evaluation of osteosarcopenia - Current leading diagnostic modalities of osteosarcopenia : CT, MRI and DXA - Imaging methods to measure the skeletal muscle area (SMA) and bone mineral density (BMD) - Evolution of AI techniques: AI segmentation and pattern analysis for BMD 4. Future directions of body composition imaging - Standardization of diagnostic modality, measuring level, and diagnostic cut-off and criteria - Accurate methods to assess muscle and bone tissue composition in opportunistic CT

## **MKEE-53 Sonography of Anatomical Variations in the Hand Innervation**

Participants

Afarine Madani, PhD, Bruxelles, Belgium (*Presenter*) Nothing to Disclose

### **TEACHING POINTS**

- Less than 10% of individuals show the classical hand innervation pattern as described in anatomical books
- More than 90% of individuals display at least one or up to five anastomoses between ulnar nerve and median nerve
- 50% of the anastomoses are localized within the forearm
- Knowledge of anatomical variations in the hand innervation is essential because they induce variations in symptomatology, clinical findings, imaging results, and "routine" electrodiagnostic tests, but also because they may lead to wrong diagnosis, inadequate treatment and/or iatrogenic lesions
- In case of anastomosis between motor branches, diagnosis is based on the distribution of atrophic pattern and fatty degeneration of intrinsic muscles of the hand
- In case of anastomosis between sensitive branches, diagnosis is mainly focused on patient's complaints

### **TABLE OF CONTENTS/OUTLINE**

- The 4 most frequent anastomoses in the upper extremity are between motor branches, -Martin-Gruber, Marinacci, Riché-Cannieu, and between sensitive branches, -Berrettini-
- Description of US technique that helps their identification
- Discussion of the clinical implications

## **MKEE-54 Using Dynamic Maneuvers in the Computer Tomography/Magnetic Resonance Assessment of Musculoskeletal Pathologies**

Participants

Thais de Souza, MD, Sao Paulo, Brazil (*Presenter*) Nothing to Disclose

### **TEACHING POINTS**

Radiologic assessment of certain musculoskeletal lesions may still pose difficulties. Certain maneuvers have been described to overcome these difficulties. Although dynamic ultrasound is a well established diagnostic technique, TC and MR dynamic imaging have particular indications and are also valuable tools in certain musculoskeletal pathologies. This study aims to review the use of dynamic maneuvers in MR and CT for evaluation of some specific musculoskeletal pathologies including: Hirayama disease, ankle syndesmosis injury, radioulnar instability, chronic compartmental syndrome and others. We intend to illustrate and highlight the utility and benefits of dynamic maneuvers for the diagnosis of different musculoskeletal pathologies.

### **TABLE OF CONTENTS/OUTLINE**

INTRODUCTION: Dynamic Acquisitions. Diseases caused by dynamic abnormalities and dynamic instability SAMPLE CASES Hirayama disease: flexion maneuvers allow to demonstrate anterior displacement of the dura mater. Ankle syndesmosis injury: flexion knee maneuvers. Radioulnar instability: supine maneuvers allow sensibilization for ulnar subluxation. Chronic compartmental syndrome: effort maneuvers. Thoracic outlet syndrome (TOC): arm abduction maneuvers allow sensibilization for TOC. Extrinsic median nerve compression: flexion/extension of fingers allow better visualization of dynamic compression. CONCLUSION Dynamic musculoskeletal imaging in CT and MR are important tools that allow detection of different musculoskeletal pathologies. Being able to recognize its indications, to guide targeted protocols and to know how to interpret the imaging findings both in neutral and dynamic positions is imperative for radiologists.

## **MKEE-55 Don't Forget the Atlantoaxial Joint: From Anatomy to Pathological Findings**

Participants

Alan Strapasson, MD, (*Presenter*) Nothing to Disclose

### **TEACHING POINTS**

The purpose of this exhibit is: 1. Review developmental embryology, anatomy, biomechanics, measurement of the atlantodental interval in the adult and pediatric population and its main anatomical variations that can simulate solutions. 2. Review imaging protocols for their evaluation according to clinical suspicion (X-ray, CT and MRI). 3. Discuss the main traumatic and non-traumatic injuries that can affect the joint, correlating their findings with imaging methods.

## TABLE OF CONTENTS/OUTLINE

1. Developmental embryology (ossification nuclei). 2. Atlanto-axial joint anatomy: CT, X-ray, ligaments (MRI), craniometry (basion-dens interval, power ratio, basion-axial interval, atlantodental interval, spinolamine distance C1-C2) 3. Normal variants that mimic lesions: fusion anomalies, posterior/anterior rachischisis, persistence of the terminal ossicle (Bergman), "os odontoideum", calcification of the alar ligament. 4. Biomechanics: extension, flexion, lateral flexion, axial rotation. 5. Imaging assessment: RX, CT and MRI protocols (ligaments and spinal cord injury). 6. Differentiation of normal/positional findings from pathological alignment changes. 7. Atlas fracture (Jefferson). 8. Odontoid fracture (Anderson and D'Alonzo classification). 9. Traumatic spondylolisthesis of C2 (hangman's fracture). 10. Atlanto-axial subluxation (anteroposterior, rotational, vertical and lateral). 11. Alar ligament deformity-rupture. 12. Rupture of the transverse ligaments. 13. Rheumatoid arthritis. 14. CPPD

## MKEE-56 Update on Cartilaginous Tumors

### Awards

#### Certificate of Merit

#### Participants

Sara Gomez Pena, Madrid, Spain (*Presenter*) Nothing to Disclose

### TEACHING POINTS

- To review the new concepts of the 2020 WHO classification of tumors of bone
- To describe the radiological spectrum of cartilaginous tumors
- To recognize the radiologic manifestations that may allow differentiation of the various types of chondrosarcoma
- To discuss the role of different imaging modalities in the diagnosis and follow-up of chondrosarcomas
- To deepen the role of imaging biomarkers and artificial intelligence in the diagnosis and follow-up of cartilaginous tumors

## TABLE OF CONTENTS/OUTLINE

1.Introduction: generalities and the 2020 WHO classification of tumors of bone 2.Enchondroma vs. chondrosarcoma 3.Imaging features in the diagnosis, follow-up and local recurrence in chondrosarcomas 4.Imaging biomarkers and IA in chondrosarcomas 5.Conclusions

## MKEE-57 Bone Tumors in the Spine: A Simplified Approach

#### Participants

Tatiane Moriwaki, MD, Sao Paulo, Brazil (*Presenter*) Nothing to Disclose

### TEACHING POINTS

The purpose of this exhibit is to: Review and illustrate features of spinal bone tumors with imaging findings on radiography, computed tomography and magnetic resonance; Illustrate and discuss differential diagnosis with didactic and challenging cases; Provide a basic guide to characterizing bone tumors of the spine.

## TABLE OF CONTENTS/OUTLINE

Introduction: general presentation of the epidemiology of bone tumors in the spine. Distribution of bone tumors: schematic flowchart showing the rationale for bone lesions based on age, distribution, and location of the main spinal tumors to help narrow differential diagnoses and identify "don't touch" lesions. • In patients younger than 30 years, spinal tumors are uncommon and usually benign, except for Ewing's sarcoma and osteosarcoma, while in patients older than 30 years, metastases should be included in the differential diagnoses. Infections should also be considered when there are signs of aggression. Evaluation of spinal tumors: •Characteristics of the main bone tumors in terms of epidemiology, matrix type, typical, and atypical imaging findings; • Summary of management and prognosis; •Didactic and challenging cases: benign and malignant spinal tumors. Bibliographical references with recent articles highlighting what is new in the topic.

## MKEE-58 Spondylarthritis (SpA): A Practical Imaging Diagnostic Approach and Current Definitions

### Awards

#### Cum Laude

#### Participants

Damaris Goncalves, MD, Sao Paulo, Brazil (*Presenter*) Nothing to Disclose

### TEACHING POINTS

SpA is a heterogeneous group of diseases that share common genetic, clinical, and imaging features. The diagnosis is complex and multifactorial, there is no gold standard exam or diagnostic criterion, and the classification criterion is often misused in clinical practice, which can lead to diagnostic errors, mostly false positives. In its last update of the definition of sacroiliitis in 2021, the ASAS highlighted the high rates of false positives when using previous definitions of sacroiliitis, expressed concern about the misuse of the classification criteria in clinical practice and reformulated the definition, now more specific, including both inflammatory and structural lesions, although still for research purposes. Imaging diagnosis of SpA in clinical practice can be made with any combination of inflammatory and/or structural lesions in the sacroiliac joints, spine, peripheral joints and/or entheses, as long as these findings are "highly suggestive of SpA", although this definition is subjective and there is considerable interobserver variability, even among experienced readers. The distribution of the lesions must also be considered either in the sacroiliac joint, spine or peripheral joints. The differential diagnoses must be excluded, especially mechanical pathologies, which are much more prevalent and a common cause of false positive results. In addition, knowledge of habitual skeletal maturation in children is essential, as it can mimic sacroiliitis or enthesitis.

## TABLE OF CONTENTS/OUTLINE

1. Introduction 2. Sacroiliac joint 3. Spine 4. Peripheral Findings 5. WBMRI 6. Conclusion

## MKEE-59 2022: A Spacer Odyssey: Imaging of Antibiotic Spacers for Periprosthetic Joint Infection-

#### Participants

Jason Matakas, MD, MS, (*Presenter*) Nothing to Disclose

## TEACHING POINTS

• Educate the reader regarding two-stage revision surgery with antibiotic spacers and why it has become the gold standard for periprosthetic joint infection (PJI) management. • Highlight advances in antibiotic spacer design. • Depict radiographic appearance of various types of spacers and how they can be differentiated. • Discuss common complications of antibiotic spacers the radiologist should be aware of.

## TABLE OF CONTENTS/OUTLINE

• Background/Indication for two-staged revision with antibiotic spacer. • Benefits: Maintains tissue tension, provides high local concentration of antibiotics, preserves cavity for subsequent revision; articulating spacers additionally allow preserved range of motion, prevent immobilization, and allow weightbearing. • Spacer types and radiographic appearance: o Knee: static, intraoperative mold, prefabricated cement, metal/polyethylene. o Hip: non-articulating, intraoperative mold, prefabricated cement, metal/polyethylene. o Shoulder: non-articulating, intraoperative mold, prefabricated cement, cement-coated hemiarthroplasty. • Case-based discussion of complications: prosthetic and periprosthetic fracture, bone loss, dislocation/subluxation, persistent infection. • Outcomes: High efficacy of infection eradication; some patients decline further revision.

## MKEE-6 Pain in the Calf! - Musculoskeletal Ultrasound in the Diagnosis of Calf Pain

### Awards

#### Certificate of Merit

Participants

Kristin Shute, DO, (*Presenter*) Nothing to Disclose

## TEACHING POINTS

Review the normal anatomy of the calf. Demonstrate the optimal patient positioning and ultrasound technique for the evaluation of various causes of calf pain. Illustrate the ultrasound appearance of various pathologic conditions about the calf. Highlight pitfalls of calf ultrasound to avoid misinterpretation of pathology.

## TABLE OF CONTENTS/OUTLINE

Anatomy overview with correlate of normal ultrasound appearance. Clinical imaging and findings of disease Muscle Injuries/Pathologies Tennis leg Muscle strain, tear, hematoma Muscle hernia Accessory soleus Bursae Baker's cyst (simple and complex) Ruptured Baker's cyst PseudoBaker's cyst/mimics Pes Anserine bursa Achilles rupture Nerves Neuroma PNST Nerve entrapments Fracture Conclusion and discussion References

## MKEE-60 Don't Be Very Nervous": Neurovascular Structures to Avoid During Ultrasound-guided Interventions in the Extremities

Participants

Jenifer Pitman, MD, New York, NY (*Presenter*) Nothing to Disclose

## TEACHING POINTS

1. Ultrasound is extremely useful for guiding injections and other procedures in the extremities, but a firm grasp of the regional anatomy is important for the procedures to be performed safely. 2. Neurovascular structures need to be avoided, and awareness of their characteristic locations relative to the structure of interest will allow safe needle advancement. 3. This education exhibit will review the typical needle orientation for many ultrasound-guided procedures in the extremities, focusing on important neurovascular structures to avoid for each.

## TABLE OF CONTENTS/OUTLINE

1. Introduction 2. Shoulder: a. Paralabral cyst aspiration (Avoiding the suprascapular nerve (N)) 3. Elbow: a. Elbow joint injection (Avoiding the deep branch of the radial N) b. Medial epicondylitis injection (Avoiding the ulnar N) c. Biceps tendon injection (Avoiding the lateral antebrachial cutaneous N) 4. Wrist/Hand: a. Dorsal and volar ganglion cyst aspirations of the wrist (Avoiding the posterior interosseous N and radial artery (A), respectively) b. 1st carpometacarpal and triscaphe joint injections (Avoiding the radial A) c. 1st dorsal extensor compartment injections (Avoiding the sensory branch of the radial N) d. Finger flexor tendon retinacular cyst aspiration/tendon sheath injection (Avoiding the proper digital N) 5. Hip: a. Iliopsoas bursal injection (Avoiding the femoral neurovascular bundle) b. Hamstring injection/aspiration (Avoiding the sciatic N) 6. Knee: a. Baker's cyst aspiration (Avoiding the saphenous N) 7. Ankle: a. Tibiotalar joint injection (Avoiding the dorsalis pedis and deep peroneal N) b. Flexor hallucis longus sheath / os trigonum injection (Avoiding the tibial N and medial and lateral plantar N)

## MKEE-61 Opportunistic Evaluation of Sarcopenia and Osteoporosis - Focus on Musculoskeletal Imaging

Participants

Jennifer Padwal, MD, MS, Palo Alto, CA (*Presenter*) Nothing to Disclose

## TEACHING POINTS

1) Sarcopenia and osteoporosis are independent risk factors for poor clinical outcomes 2) Abdominal CTs have been most thoroughly studied for the evaluation of sarcopenia and osteoporosis, although other anatomic regions on CT, MRI, and ultrasound may offer valuable information on muscle and bone quality 3) Reporting of sarcopenia and osteoporosis on imaging may influence patient management

## TABLE OF CONTENTS/OUTLINE

I. Epidemiology and clinical significance of sarcopenia and osteoporosis II. Definitions of sarcopenia and osteoporosis: From DXA to opportunistic CT, MRI, and ultrasound III. CT and MRI screening of sarcopenia and osteoporosis on musculoskeletal imaging examinations (spine and extremities), including CT attenuation (e.g., Hounsfield unit thresholds) and MRI-derived biomarkers (e.g., T2 relaxation time, functional anisotropy) IV. Translating clinical research into clinical practice: Terminology and templates for reporting sarcopenia and osteoporosis on CT, MRI, and ultrasound

## **MKEE-62 Congenital Femoral Deficiency and Its Imaging and Surgical Evolution Over Time**

Participants

Denny Marcela Achicanoy I, MEd, Ciudad De Mexico, Mexico (*Presenter*) Nothing to Disclose

### **TEACHING POINTS**

Congenital femoral deficiency is hypoplasia of the proximal portion of the femur without a known specific etiology. Its prevalence is 0.1 to 0.2 cases per 10,000 newborns it is mainly associated with fibular hemimelia, patellar absence, acetabular dysplasia. Paley's imaging classification depends on the degree of development of the integrity of the femur without depending on age or degree of ossification.

### **TABLE OF CONTENTS/OUTLINE**

1. Definition. 2. Embryological origin. 3. Etiology associated factors. 4. Imaging findings. 5. Treatment. Congenital femoral deficiency is the specific partial absence (hypoplasia) of the proximal portion of the femur with shortening of the entire lower limb without an etiology. Its prevalence is 0.1 to 0.2 cases per 10,000 newborns it is mainly associated with fibular hemimelia, patellar absence and acetabular dysplasia mainly due to the association with its postaxial embryonic origin. Initially it was classified by Gillespie Torode into two groups: I or congenital hypoplastic femur, where the hip knee are functional after surgical treatment symmetry of the limbs can be achieved; II or proximal focal femoral deficiency where the hip is abnormal the knee is considered non-functional, in these cases prosthetic management is suggested. However, Paley created an imaging classification with the intention of offering a guide for surgical treatment depending on the degree of development of the integrity of the femur. The Paley Classification is aimed at facilitating decisions treatment protocols to follow. In this poster we will present cases of femoral hypoplasia with different classification according to Paley.

## **MKEE-63 Uncomplicating Spinal Cord Disorders - A Practical Guide for the Musculoskeletal Radiologist**

Participants

Alexandre Goncalves, MD, Sao Paulo, Brazil (*Presenter*) Nothing to Disclose

### **TEACHING POINTS**

The purpose of this exhibit is: 1. To review anatomy of the spinal cord. 2. Narrow the differential of spinal cord diseases according to location. 3. Differentiate between inflammatory, infection, demyelinating, metabolic, neoplastic lesions and vascular disorders.

### **TABLE OF CONTENTS/OUTLINE**

1 - Topographic and cross section detailed anatomy of the spinal cord. 2 - Correlate spinal cord diseases that manifest with high signal within the spinal cord on T2WI with their locations to narrow the differential diagnosis. 3 - Illustrate the most common causes and imaging findings in MRI, including - Inflammatory; - Vasculitis; - Infection; - HIV; - Bacteria; - Fungus; - Cysticercosis; - Demyelinating disorders; - Multiple sclerosis; - Transverse myelitis; - Neuromyelitis optica; - Acute disseminated encephalomyelitis; - Metabolic; - B12 hypovitaminosis; - Neoplastic; - Ependymoma; - Astrocytoma - Hemangioblastoma; - Lymphoma; - Metastases; - Vascular disorders; - Ischemia due to spinal arteriovenous malformation. 4 - Summary and practical guide to narrow the differential diagnosis of MRI findings according to location and how to relate the findings to the patients' relevant clinical and laboratory data.

## **MKEE-64 Spectrum of Imaging Findings of Iatrogenic Vascular Injuries After Orthopedic Surgery**

Participants

Emanuele Barabino, MD, (*Presenter*) Nothing to Disclose

### **TEACHING POINTS**

- Despite the establishment of safety zones to place screws and metallic devices, the rate of vascular injuries during orthopedic surgery has been keeping increasing in the last decades due to the increasing employment and revision of prosthetic devices.
- Severe injuries (i.e., tearing of major vessels) cause severe bleeding and hypotension and are usually promptly recognized intraoperatively; despite not life-threatening, minor injuries are typically more insidious, and they could determine significant functional losses and postpone the healing process.
- The spectrum of imaging findings of the iatrogenic vascular injuries after orthopedic surgery is wide and heterogeneous and the radiologic evaluation of surgical field is often impaired by artifacts generated by metallic devices.

### **TABLE OF CONTENTS/OUTLINE**

1. Introduction  
2. Anatomical Considerations  
3. Mechanisms of Injury  
3.1 Vascular injuries after elective surgery  
3.2 Vascular injuries after trauma surgery  
4. Risk Factors  
4.1 Anticoagulation and Antiplatelet therapy  
4.2 Atherosclerosis  
4.3 Infection  
5. Imaging Techniques and Technical Consideration  
5.1 CT Protocol  
5.2 Metal Artifact reduction Protocol  
6. Radiologic Features  
6.1 Hematoma  
6.2 Pseudoaneurysm  
6.3 Vessel Transection  
6.4 Occlusion  
7. Conclusion

## **MKEE-65 I Want to Ride My Bicycle! A Pictorial Essay on Cycling-related Musculoskeletal Injuries**

Participants

Damaris Goncalves, MD, Sao Paulo, Brazil (*Presenter*) Nothing to Disclose

### **TEACHING POINTS**

? Overview on epidemiology of cycling-related musculoskeletal injuries; ? To demonstrate the most common mechanisms that lead to the development of musculoskeletal lesions during cycling (lesions of contact, overuse and traumatic); ? To summarize the main musculoskeletal lesions related to cycling according to the affected musculoskeletal structures; ? To demonstrate the typical findings related to such lesions in a variety of imaging methods.

### **TABLE OF CONTENTS/OUTLINE**

? Introduction: concept of bicycling-related injuries, epidemiology; ? Mechanisms of musculoskeletal injuries that occur during cycling; ? Overview of the main musculoskeletal injuries among cyclists in different parts of the musculoskeletal system; ? Pictorial essay on the typical imaging findings related to those lesions, including brief discussion on clinical presentation.

## **MKEE-66 First Metatarsophalangeal Trauma: The Complete Spectrum of Osseous and Soft Tissue Injuries**

Participants

Collin Edwards, MD, New York, NY (*Presenter*) Nothing to Disclose

#### **TEACHING POINTS**

Injuries to the first metatarsophalangeal (MTP) joint, including but not limited to "turf toe", have long been associated with athletic trauma and overuse. Imaging plays an important role in the determination of severity and extent of damaged structures within this complex. Multiple classification systems frequently combine both the imaging characteristics and clinical presentation in an effort to guide management and predict return to play. This session reviews injuries to the first MTP joint to increase participants' understanding of the following: 1. Mechanisms of injury and epidemiological risk factors 2. MRI findings of 1st MTP injury and classification systems 3. Management pathways. We use multiple case examples to demonstrate the relationship between MRI findings and management decisions/outcomes. Increased understanding of these clinical, radiologic and surgical factors will further inform the radiologist's interpretation of MRI for first MTP trauma.

#### **TABLE OF CONTENTS/OUTLINE**

Review of normal 1st MTP osseous and ligamentous anatomy; Mechanisms and epidemiology of 1st MTP injury; Classifications of 1st MTP injuries; Case examples of osseous and ligamentous pathology, including: - Hallux sesamoid fracture and stress injuries - Osteochondral lesions - Capsuloligamentous injuries (Sesamoidophalangeal, intersesamoid, metatarsos sesamoid, collateral ligament injuries) - Musculotendinous injuries; Non-surgical and surgical management

#### **MKEE-68 MRI evaluation of Post-operative Peripheral Nerve Injury**

##### **Awards**

##### **Certificate of Merit**

Participants

Hye Yang, MD, New York, NY (*Presenter*) Nothing to Disclose

#### **TEACHING POINTS**

1. To review common types of procedures that are prone to causing peripheral nerve injury. 2. To recognize the MRI appearance of peripheral nerve injury including the changes to the related muscles. 3. To review the patterns of peripheral nerve injury. 4. To review the common appearances and presentations of peripheral nerve injury on MRI

#### **TABLE OF CONTENTS/OUTLINE**

1. Normal Anatomy: a. Normal appearance of peripheral nerve. b. Normal appearance of muscle. 2. Procedures that predispose to peripheral nerve injury: a. Types of procedures. b. Areas that are prone to injury. 3. Classification of peripheral nerve injury: a. Seddon Classification. b. Sunderland Classification. 4. MRI appearance of injury: a. Grades/Types of nerve injury. b. Neuroma. c. Peripheral muscle changes. 5. Treatment

#### **MKEE-69 Complications of Reverse Total Shoulder Arthroplasty: What a Radiologist Should Know**

##### **Awards**

##### **Certificate of Merit**

Participants

Timothy T. Klostermeier, MD, Lebanon, OH (*Presenter*) Nothing to Disclose

#### **TEACHING POINTS**

1. Reverse Total Shoulder Arthroplasty (RTSA) restores glenohumeral mobility and function to patients with rotator cuff arthropathy and other severe glenohumeral conditions. Radiologists should understand the biomechanical advantages, expected appearance, and anatomy of this arthroplasty (and its design variations). 2. Basic examples of types of RTSA will be presented. 3. Complications related to RTSA need to be promptly recognized and communicated. Radiologists should be familiar with the appearance of these complications. 4. Mechanical failures will be highlighted with pictorial examples. 5. Recognition of signs of infection and role in component failure.

#### **TABLE OF CONTENTS/OUTLINE**

1. Epidemiology of RTSA Incidence, prevalence, and rising complications 2. Role of radiologist: - Normal biomechanics - Identifying types of RTSA, medialized and lateralized and expected appearance - Recognizing and addressing complications 3. Components of RTSA 4. Complications (a) Scapular notching (b) Acromial stress fractures (c) Periprosthetic fractures (d) Infections and treatment (e) Implant failures • Implant loosening • glenoid/ humeral stem • Intra implant unscrewing: humerus • Disengaged glenosphere • Broken screws • Canal filling of stem and stress shielding of greater tuberosity 5. Dislocation - Assessment of implant orientation

#### **MKEE-7 A Pain in the Neck: Magnetic Resonance Neurography of Neurogenic and Disputed Subtypes of Thoracic Outlet Syndrome**

Participants

Emily Davidson, MD, (*Presenter*) Nothing to Disclose

#### **TEACHING POINTS**

1. Thoracic outlet syndrome (TOS) is thought to result from compression of the upper limb neurovascular structures traversing the thoracic outlet. TOS remains poorly understood, despite extensive available literature describing clinical features, imaging findings and approaches to the syndrome. 2. TOS due to compression on the brachial plexus causes upper limb neurological symptoms, varying from mild sensory disturbance to motor function loss. 3. Subtypes of neurological TOS have been divided into Neurogenic TOS (nTOS) and Disputed TOS (dTOS), based on clinical features and electrodiagnostic results. nTOS have positive motor nerve involvement, whilst dTOS have preserved motor nerve function with a predominant sensory disturbance. 4. Magnetic resonance neurography (MRN) is increasingly being used to investigate nTOS and dTOS and identify focal areas of compression on the brachial plexus. MRN has become an important test within the diagnostic algorithm for TOS investigation and management (non-operative vs operative).

## TABLE OF CONTENTS/OUTLINE

1. Update on brachial plexus MRN imaging techniques including coil selection, imaging acquisition protocols, and imaging reconstruction protocols that employ deep learning algorithms. 2. Overview of TOS brachial plexus anatomy. 3. Review clinical features/electrodiagnostics of nTOS and dTOS. 4. Review MRN case examples of nTOS and dTOS subtypes, including: overhead throwing athlete, postoperative complications resulting in perineural scar and muscle denervation, and osseous abnormalities (cervical and first rib).

### **MKEE-71 Exploiting the Technical Possibilities and Advancements of Photon-Counting CT for Musculoskeletal Imaging: The Way Forward**

Participants

Jeffrey De Groen, BSc, (*Presenter*) Nothing to Disclose

#### TEACHING POINTS

To demonstrate the possibilities regarding acquisition and reconstruction techniques of PCCT for musculoskeletal imaging To provide insights and knowledge needed for optimal utilization of PCCT in musculoskeletal imaging To give an outlook on the future prospects of PCCT in MSK imaging

## TABLE OF CONTENTS/OUTLINE

With the recent introduction of a clinical photon-counting computed tomography (PCCT) scanner, it has become possible to combine ultra-high image resolution with spectral information. Image data obtained with PCCT may provide clinicians and radiologists with improved diagnostic confidence. For example, a better visualization of metastatic bone might offer valuable information about how to best stabilize the bone with metal plate placement. However, there is still limited knowledge about what the best choices are for PCCT acquisitions (e.g. x-ray spectra) and reconstructions (e.g. kernels, mono-energetic and metal artifact reduction techniques) for the various areas of interest. This exhibit will provide you with examples of clinical PCCT scans obtained in two different institutions, compared to previously acquired energy-integrating detector (EID) CT scans and other modalities in e.g., the diagnosis and follow-up of fractures, the evaluation of osteolysis, osseointegration of orthopedic joint replacement implants, and the assessment of bone tumor and metastasis. Finally, an outlook on the future utilization of PCCT to extract quantitative bone biomarkers and the assessment of bone quality and structure is provided.

### **MKEE-72 Osteotomies - Indications, Imaging Appearance, and Surgical Techniques**

Participants

Majid Chalian, MD, Seattle, WA (*Presenter*) Grant, The Boeing Company

#### TEACHING POINTS

1. Review of the common osteotomy procedures and techniques 2. Review of different techniques for each osteotomy procedure Review of the common osteotomies' clinical indications and complications Review of the common osteotomies normal postoperative imaging findings.

## TABLE OF CONTENTS/OUTLINE

• Craniotomy • Lateral nasal osteotomy • Bilateral sagittal split osteotomy • Reduction malarplasty • Thoracolumbar vertebral osteotomy • Rib osteotomy • External rotation humeral osteotomy • Ulnar shortening Osteotomy • Distal radius corrective osteotomy • Scaphoid corrective osteotomy • Periacetabular osteotomy • High tibial osteotomy • Talar neck osteotomy • Calcaneal osteotomy • Hallux valgus osteotomy

### **MKEE-73 Normal and Abnormal MRI of the CapsuloLabral Complex of the Hip**

Awards

**Magna Cum Laude**

**Identified for RadioGraphics**

Participants

Dyan V. Flores, MD, Ottawa, ON (*Presenter*) Nothing to Disclose

#### TEACHING POINTS

Contrary to its counterpart in the glenohumeral joint, the anatomy, biomechanics and patterns of injury involving the femoroacetabular capsulo-labral complex may be less familiar to radiologists. The labrum and articular capsule of the femoroacetabular (hip) joint work in conjunction to stabilize the articulation. At lesser degrees of distraction, the labrum is the most important hip stabilizer, whereas in greater distraction states, the contribution of the capsule to hip stability increases. The objectives of this educational exhibit are as follows: • Review normal anatomy and biomechanics of the femoroacetabular or hip labrum and capsular ligaments • Discuss patterns of failure and injury involving the capsulo-labral complex of the hip • Define MR imaging pearls and pitfalls in diagnosing these capsulo-labral injuries

## TABLE OF CONTENTS/OUTLINE

NORMAL MRI • Hip labrum and anatomic variants • Capsular ligaments of the hip • Ligamentum teres IMAGING CONSIDERATIONS • Radial sequences • MR arthrography ABNORMAL MRI • Labral tears • Posterior hip dislocation • Isolated injuries of the capsular ligaments

### **MKEE-74 Imaging Review of Beach Tennis Injuries: A New Sport Trend and Related Musculoskeletal Lesions**

Participants

Andre Mannato, MD, Sao Paulo, Brazil (*Presenter*) Nothing to Disclose

#### TEACHING POINTS

The exponential growth of Beach Tennis (BT) has been observed in Brazil, mainly in coastal cities. The origin of this sport dates back to Italy in the 80s. Only in 1996 the official rules of the sport were determined. Worldwide it is estimated that more than 1 million people are practicing which is played using Beach Tennis paddles and a low compression tennis ball. BT is mainly played

overhead, including serving, defensive moves and attacking, this may have contributed to rotator cuff tendinopathy. Explosive sprinting in the serve with sudden plantarflexion of the foot with knee extended, contributed to more injuries in the leg and ankle muscles and tendon. Moving on sand requires more energy due to the mechanical work related to the sand's compliance and the lower efficacy of positive muscular work. For this reason, is important for the radiologist to correlate the clinical scenarios for the correct radiologic diagnosis.

#### TABLE OF CONTENTS/OUTLINE

1. Overview on epidemiology of beach tennis related musculoskeletal injuries 2. To demonstrate the most common mechanisms that lead to the development of musculoskeletal lesions during the match (serving, attacking, defense) 3. To summarize the main musculoskeletal lesion related to beach tennis according to the affected musculoskeletal structures To demonstrate the typical findings related to such lesions in a variety of imaging methods

#### MKEE-75 Midfoot Strains Illustrated with Global Illumination Rendering

Participants

Fatma Boubaker, Nancy, France (*Presenter*) Nothing to Disclose

#### TEACHING POINTS

Midfoot strains are clinically and radiologically underdiagnosed. They require a more aggressive treatment than classical lateral ankle sprains, with which they are often associated, because of higher sequelae risk. The Chopart joint is sustained by the spring ligament complex, the talonavicular, bifurcate, and calcaneocuboid (lateral and plantar) ligaments. Inversion lesions are the most frequent and lead to talonavicular impaction and calcaneocuboid distraction injuries. The Lisfranc joint is composed of 3 columns, inter-connected by dorsal, plantar, and intermetatarsal ligaments, and especially by an inter-osseous (Lisfranc) ligament, linking the medial and intermediate columns, which attempt leads to joint instability. Radiographs allow sub-optimal evaluation in a post-traumatic context. CT must be performed if a fracture is suspected and permits a good depiction of small bony avulsions, as MRI, considered the gold standard for ligamentous study, is usually not available in the acute phase. Moreover, Global Illumination rendering provides information beyond the reach of 2D images. Even though midfoot anatomy is considered complex, a clear knowledge of its anatomy improves the early detection of traumatic lesions requiring more aggressive treatment to avoid degenerative changes, especially using CT in the very early setting.

#### TABLE OF CONTENTS/OUTLINE

1. Chopart injuries. 1.1 - Introduction, 1.2 - Anatomy, 1.3 - Imaging findings 2. Lisfranc Injuries. 2.1 - Introduction, 2.2 - Anatomy, 2.3 - Imaging findings

#### MKEE-76 Non-traumatic Mid and Forefoot Pain: Must-know Findings to Radiologists in Training

Participants

Marcos Assuncao, MD, Sao Paulo, Brazil (*Presenter*) Nothing to Disclose

#### TEACHING POINTS

The mid and forefoot pain is a common complaint among patients in a non-traumatic scenario, especially the forefoot. Many pathologies with different etiopathogenesis and difficult differentiation based only on clinical aspects can cause pain in these regions, from biomechanical disarrangements to infections or neoplasms. An important aspect in the initial evaluation is differentiation between mechanical and non-mechanical causes. The first is related to structural changes that lead to overload of the joints, primary the metatarsophalangeals, and may present with varied findings. The non-mechanical causes comprises the degenerative and inflammatory arthropathies, infections, tendinosis, metabolic or vascular disorders, tumors and alterations associated with foreign bodies. Imaging of the mid and forefoot allows the complete evaluation of these primary causes and their relationship with anatomy and biomechanics, granting correct and fast therapeutic alignment with better outcomes. Radiologists should be familiar with the method of choice in each clinical presumption and promptly recognize the typical findings of each pathology.

#### TABLE OF CONTENTS/OUTLINE

Introduction to primary causes of non-traumatic pain of the mid and forefoot. Pictorial essay with the typical imaging findings. Discussion about the methods of choice and what to evaluate in each disorder.

#### MKEE-77 No Strings Attached - Tendon and Tendon Sheath Pathologies of the Hand

Participants

Jan Grunz, MD, Wuerzburg, Germany (*Presenter*) Research Consultant, Siemens AG

#### TEACHING POINTS

The tendons of the hand run in close proximity to each other and within reticular tunnels adjacent to articular joints, while forming intersections in characteristic locations. This particular anatomy can lead to stenosis in the fibrous outer layers of the extensor retinaculum and A1 annular pulleys, resulting in tendinosis and functional disability. In contrast, proliferative tenosynovitis is a disease of the synovial inner layer of the tendon sheath with tendon infiltration and ensuing tendinitis, most frequently seen in rheumatoid arthritis. Phlegmonous or purulent tenosynovitis is more common in the flexor compartments, potentially resulting in tenosynovial necrosis and tendon dislocation. Diseases of the tendons and tendon sheaths may have mechanical, degenerative, metabolic or inflammatory etiology. Fibrous tunnels and bony prominences in close proximity to crossing tendons predispose to mechanical tendon irritation at typical sites of the hand. Requiring high-resolution techniques due to the small size of the compartments involved, the tendons and tendon sheaths of the hand can be precisely assessed in ultrasound and MRI.

#### TABLE OF CONTENTS/OUTLINE

1. Anatomy of the tendon and tenosynovium 1.1. The extensor mechanism 1.2. The flexor mechanism 2. Imaging principles 2.1 Ultrasound 2.2 MRI 3. Common pathologies 3.1. Tendinosis 3.2. Tendinitis 3.3. Paratendinitis 3.4. Reactive tenosynovialosis 3.5. Stenosing tenovaginitis 3.6. Proliferative tenosynovitis 3.7. Traumatic ruptures 3.8. Tumors of the tendon sheath 4. Discussion

#### MKEE-78 Stay Flexible! Diagnosis and Treatment of Flexor Tendon Injuries

**Awards**

## Certificate of Merit

### Participants

Steven Daniels, MD, New York, NY (*Presenter*) Nothing to Disclose

### TEACHING POINTS

1. To review anatomy of the flexor tendon and flexor tendon sheath 2. To review imaging findings in flexor tendon tears highlighting those important to the treating surgeon 3. To discuss the different treatment options in flexor tendon tears and demonstrate how imaging helps guide patient management 4. To discuss complications of primary flexor tendon repair and flexor tendon reconstruction

### TABLE OF CONTENTS/OUTLINE

1. Anatomy of the flexor tendon and flexor tendon sheath a. Flexor tendon anatomy b. Flexor tendon sheath and pulley system c. Flexor zones of injury 2. Zone 1 injuries - Leddy and Packer classification 3. Zone 2 injuries - Injury types 4. Zone 3,4,5 injuries - Injuries by location 5. Treatment options a. Primary tendon repair b. One-stage reconstruction c. Two-stage reconstruction 6. Imaging of potential tendon grafts 7. Post-operative clinical care 8. Post-operative imaging and complications a. Normal findings b. Adhesions c. Re-tear

## MKEE-79 **Finger It to Know It: A Detailed Walk Through from Anatomy, Imaging and Pathology to Post-treatment Follow-up of Finger**

### Participants

Amit Sahu, MBBS, MD, New Delhi, India (*Presenter*) Nothing to Disclose

### TEACHING POINTS

1. Review the normal anatomy of finger and the appearance on ultrasound, radiograph, CT and MRI. 2. Discuss common bony injuries affecting the finger. 3. Discuss soft tissue injuries affecting the finger. 4. Review common bone tumours of finger and their imaging appearance. 5. Review common soft tissue tumours of finger and their imaging appearance.

### TABLE OF CONTENTS/OUTLINE

1. Normal anatomy of finger on radiograph, ultrasound, CT and MRI including the bony and soft tissue structures (tendons, ligaments, volar plates and pulleys). 2. Advantages and pitfalls of ultrasound and MRI in imaging of finger. 3. Various types of fracture of metacarpal and phalanges, their imaging approach and what the orthopedic surgeon wants to know. 4. Types of soft tissue injuries like avulsion injuries of flexor and extensor tendons, volar plate injuries, collateral ligament injuries, their imaging appearance, what a radiologist should describe and post surgical follow-up. 5. Various common and uncommon bony and soft tissue tumours of finger, their imaging appearance and common differentials. Need of time for radiologist is not just lesion detection but also guiding the treating doctor for further management.

## MKEE-8 **Glenoid Track Assessment on Imaging in Anterior Shoulder Instability: Its Rationale and A Step-By-Step Guide**

### Awards

#### Certificate of Merit

#### Identified for RadioGraphics

### Participants

Ustun Aydingoz, MD, (*Presenter*) Nothing to Disclose

### TEACHING POINTS

1. To explain the concept of glenoid track and how it relates to the management of glenohumeral instability associated with bipolar (humeral and glenoid) fractures. 2. To describe how to make the glenoid track assessment on CT or with the help of CT-like images generated with zero echo-time (ZTE) MR imaging in bipolar (humeral and glenoid) fractures associated with anterior shoulder instability. 3. To explain how on-track/off-track status influences strategizing treatment and selecting the type of surgery.

### TABLE OF CONTENTS/OUTLINE

1. Pathophysiologic background of glenoid track assessment and why this evaluation is important. 2. Step-by-step guide to assessment of the glenoid track on CT or MRI with the CT-like ZTE sequence: (a) establishing the bipolarity of the shoulder fracture dislocation; (b) estimating the glenoid bone stock; (c) calculating the glenoid track; (d) determining the Hill-Sachs interval; (e) ascertaining the on-track/off-track status of the Hill-Sachs lesion. 3. Case examples with pearls, pitfalls, and sample radiology reports (e.g., how to decide on erosive/compressive versus fragmented osseous Bankart lesions; how correlation of the Hill-Sachs interval on ZTE and conventional MRI sequences overcomes a shortcoming of CT in ascertaining this interval; what to put into the imaging report). 4. How the on-track/off-track status influences the treatment strategy or type of surgery.

## MKEE-80 **Doctor, I Can't Bend My Finger": Diagnostic Strategies for the Radiologists**

### Participants

Jiwoon Seo, MD, Seoul, Korea, Republic Of (*Presenter*) Nothing to Disclose

### TEACHING POINTS

Patients with impaired finger flexion are often encountered in our daily clinical practice. There are many etiologies, such as tendon injuries or neuropathy, that cause difficulty in finger flexion. Radiologist must understand the basic anatomy of the finger flexor system and corresponding structural failure to make diagnostic decision. The major teaching points of this exhibit are: 1. To review the basic anatomy of the finger flexor system and mechanism. 2. To review the etiologies of impaired finger flexion and correlate with imaging (US, MRI) findings.

### TABLE OF CONTENTS/OUTLINE

1. Anatomy and Mechanism of the Finger Flexor System. a. Tendons and extrinsic muscles. b. Flexor pulley system. c. Intrinsic muscles. d. Nerve innervation. 2. Etiologies of the Impaired Finger Flexion. a. Flexor tendon injuries. b. Trigger finger. c. Flexor

tenosynovitis.d. Neuropathy.e. Intrinsic muscle injuries.f. Miscellaneous.3. Summary and Take-home Messages.

### **MKEE-81 Scratching the Surface: MSK Pathology Involving the Skin Subcutaneous Tissues**

Participants

Mark Manganaro, DO, Rochester, NY (*Presenter*) Nothing to Disclose

#### **TEACHING POINTS**

1. Familiarize radiologists with musculoskeletal diseases that have associated manifestations of the skin and subcutaneous tissues including causes from: infectious, inflammatory, tumor, congenital and connective tissue disorders.2. Be able to identify and diagnosis these various entities using radiography, CT, and MRI.3. Clinically correlate the radiographic findings with the dermatologic appearances.4. An emphasis will be placed on uncommon musculoskeletal disorders which have known dermatological manifestations.

#### **TABLE OF CONTENTS/OUTLINE**

The following diseases/syndromes will be shown using radiographs, CT, and MRI as well as having dermatologic correlate images when applicable. Cases that will be in the exhibit include:1. Infectious: Disseminated Mycobacterium chelonae.2. Inflammatory/Connective tissue disorders: Psoriasis/Acrodermatitis of Hallopeau, CREST syndrome/Scleroderma, SAPHO syndrome, dermatomyositis, granuloma annulare, eosinophilic fasciitis.3. Tumor: Rothmund-Thomson Syndrome, Maffucci Syndrome, Neurofibromatosis 1, etc, basal cell and squamous cell carcinoma (Marjolin's ulcer), Dermatofibrosarcoma protuberans.4. Congenital: McCune-Albright Syndrome, Nail-Patella Syndrome, Osteopoikilosis / Osteopathia Striata, Tuberous Sclerosis.

### **MKEE-82 Peripheral Nerve Assessment of Typical and Atypical Lesions - An Ultrasound Review**

Participants

Ligia Couceiro, MD, Sao Paulo, Brazil (*Presenter*) Nothing to Disclose

#### **TEACHING POINTS**

Peripheral nerve injuries are important causes of loss of functionality what makes early diagnosis and treatment indispensable. High resolution ultrasound stands out as a cost-effective, accessible method with high diagnostic potential. The purpose of this study is:• To review peripheral nerve anatomy and correlation with the ultrasound imaging. • To discuss the method's advantages and disadvantages. • To identify normal nerve appearance and also pathological findings. • To recognize the multiple causes of neuropathies, including the most prevalent ones and some atypical or rare presentations. • Illustrate imaging findings through sample cases - atypical and typical cases.

#### **TABLE OF CONTENTS/OUTLINE**

• INTRODUCTION- Review peripheral nerve anatomy and correlate to the ultrasound imaging.- To compare high frequency ultrasound advantages and disadvantages to evaluate peripheral neuropathies compared to other methods.- Evaluation of peripheral nerve's normal appearance and pathological findings. • PERIPHERAL NEUROPATHIES - DIFFERENTIAL DIAGNOSIS- Trauma - Compressive syndromes- Inflammatory processes- Infection- Neoplastic • IMAGING INTERPRETATION• Systematic approach to evaluate image exams• Template reporting system • INTERACTIVE CASE-BASED DIDACTICS• Sample typical and atypical cases to illustrate and solidify the concepts.

### **MKEE-83 Sports Injuries in the Rectus Femoris - What, How, Why and Where**

**Awards**

**Certificate of Merit**

Participants

Leandro Mazza, MD, La Plata, Argentina (*Presenter*) Nothing to Disclose

#### **TEACHING POINTS**

Know the anatomy and biodynamic characteristics of the rectus femoris. Recognize the spectrum of muscle injuries that compromise the rectus femoris in various sports, analyzing its production mechanism. Analyze the different diagnostic methods of the different injuries in order to establish the precise location and particular characteristics of each injury. Establish an estimated prognostic criterion for recovery and sports return.

#### **TABLE OF CONTENTS/OUTLINE**

The anterior rectus has a complex anatomy that allows it to fulfill very characteristic functions, being essential in many current sports practices. Its "muscle within a muscle" morphology and its insertions, added to the type of contractile fibers it presents, mean that its lesions can be grouped and classified, with characteristic compromise sites that are repeated in the different sports practices, presenting a mechanism of similar injury. Indirect type injuries (muscle tears) can be divided into central or peripheral according to the myoconnective junction, being in the case of central injuries of capital importance to assess the status of the adjacent tendon. According to its extension and location, we can roughly predict the potential evolution of the lesions and the approximate return to play time. In turn, there are also direct type injuries (muscle contusions) that will have another treatment and evolution. Finally, we must include epiphysitis in children - adolescents, and tendon disinsertions, which are more frequent in adults.

### **MKEE-84 Give It Another Shot": A Radiologist's Guide to Shoulder Injury Related to Vaccine Administration (SIRVA) Imaging Features**

Participants

Hadas Benhabib, MD, MSc, (*Presenter*) Nothing to Disclose

#### **TEACHING POINTS**

1) Review procedural considerations for the administration of intramuscular injections, including anatomical landmarking and injection technique; 2) Discuss the variety of anatomical structures that can be injured, depending on the different locations of a non-target deltoid intramuscular injection; 3) Describe the imaging features of patients with recent vaccinations and the spectrum of imaging findings in patients with SIRVA, including subacromial/subdeltoid bursitis, glenohumeral synovitis, adhesive capsulitis, septic

arthritis, osteitis/periostitis, and rotator cuff tears.

#### **TABLE OF CONTENTS/OUTLINE**

Shoulder injury related to vaccine administration (SIRVA) is a preventable outcome that can occur when an intramuscular deltoid injection is inadvertently administered into the shoulder capsule or surrounding musculoskeletal structures. Imaging studies are frequently requested in the diagnostic evaluation of SIRVA, with the reported utilization of MRI in SIRVA patients being as high as 81%. This exhibit provides a case-based review of the variety of SIRVA-related events, including rotator cuff injuries, bursitis, adhesive capsulitis, and osteomyelitis. Given the importance and growing prevalence of recent COVID-19 inoculations, with 660 million vaccinations having been administered in Canada and the United States to date, prompt recognition of symptomatic non-target vaccinations is essential in providing quality care for our patients and preventing long-term impairments.

#### **MKEE-85 Scoliosis: A Review of Surgical Treatment Options**

Participants

Lucas Miyahara, MD, Sao Paulo, Brazil (*Presenter*) Nothing to Disclose

#### **TEACHING POINTS**

The purpose of this exhibit is to: 1. Review the modalities of scoliosis surgical treatment and their indications, including the main findings in scoliosis exams that needs to be highlighted when choosing surgical management. 2. Illustrate several cases of scoliosis with emphasis on postoperative findings, what to expect and their complications. 3. Discuss and provide a guide for what the radiologist must actively look for and report in these cases, supporting surgeons in decision making.

#### **TABLE OF CONTENTS/OUTLINE**

Introduction: review general presentation of scoliosis, including their complete evaluation and what the report should include. Provide several challenging scoliosis cases due to defects of formation, segmentation and mixed ones, in the context of various syndromic conditions. Overview and discuss the several operative indications and modalities of surgical treatment. Present didactic illustrations and cases of the different surgical modalities, with their pre and post-operative imaging exams. Propose a guidebook for post-operative scoliosis imaging, including several complications that the radiologist needs to be aware and how they should report. Relevant bibliographical references.

#### **MKEE-86 Soft Tissue Imaging Findings of Critically Ill Patients**

Participants

Ana Carolina Augusto, MD, MSc, Sao Paulo, Brazil (*Presenter*) Nothing to Disclose

#### **TEACHING POINTS**

The purpose of this pictorial essay is to: • Review the imaging appearance of soft tissue findings commonly seen critically ill patients, mainly in MRI. • Differentiate infectious from non-infectious soft tissue diseases in the intensive care unit patient setting.

#### **TABLE OF CONTENTS/OUTLINE**

Patients in intensive care units commonly spend long periods of time restrict to the hospital bed, vulnerable to infections and going through multiple venipunctures. Not rarely, imaging is required to further examine possible complications related to the primal disease or long-term hospitalization. Early diagnosis of possible soft tissues changes can prevent further complications and poor outcomes, specially in elder population. In addition, it is possible to help the surgeon clarify the extent of the damage and prepare the best approach. Muscle edema is a common MRI finding in critically ill patients and the differential diagnosis includes critical illness myopathy (a common acquired condition in an ICU setting), rhabdomyolysis, infections, among others. Correct distinction of infectious from noninfectious soft tissue diseases can be an important factor in determining patient survival.

#### **MKEE-87 Declawed: A Review of Claw Toe Pathology and Treatment**

##### **Awards**

##### **Certificate of Merit**

Participants

Tristan Cooper-Roth, (*Presenter*) Nothing to Disclose

#### **TEACHING POINTS**

The purpose of this educational exhibit is to provide the learner with the following information: 1. Define anatomically what a claw toe deformity is, what this looks like on a radiograph, and what the most common causes are 2. What are the key distinguishing features of other lesser toe deformities and their corresponding radiographic appearances 3. Identify claw toe abnormalities seen on MRI 4. Summarize the types of therapeutic non-surgical and surgical approaches of a claw toe deformity 5. Characterize the post-surgical changes of a Weil lesser metatarsal osteotomy on diagnostic imaging

#### **TABLE OF CONTENTS/OUTLINE**

1. Define anatomically what a claw toe deformity is, providing a radiographic example, and what are the most common causes 2. Examples of other lesser toe deformities and their appearance on radiographs 3. Characteristics of claw toe abnormalities on MRI 4. Assess atrophy of intrinsic foot musculature on diagnostic imaging 5. Types of therapeutic non-surgical and surgical approaches to a claw toe deformity 6. Post-surgical changes on diagnostic imaging

#### **MKEE-88HC Qualitative and Quantitative Anatomic Investigation of the Lateral Ankle Ligaments for Surgical Reconstruction Procedures Using 3D High-Resolution MRI in Chronic Ankle Instability**

Participants

Meng Dai, (*Presenter*) Nothing to Disclose

#### **TEACHING POINTS**

To quantitatively investigate the anatomy of the ATFL and CFL for surgical reconstruction procedures in chronic ankle instability.

## TABLE OF CONTENTS/OUTLINE

Purpose: To quantitatively investigate the anatomy of the anterior talofibular ligament (ATFL) and calcaneofibular ligament (CFL) for surgical reconstruction procedures in chronic ankle instability. Materials and Methods: 3D MRI were performed on five fresh-frozen cadaveric ankles with six different spatial resolutions. Resolution of 0.45x0.45x0.45mm<sup>3</sup> was performed on 24 healthy adult volunteers on bilateral ankles. A four-point subjective score system was used to evaluate the imaging quality. Morphologic parameters including the classification of ATFL, the length of ATFL and CFL, and the four distances of surgically relevant bony landmarks were measured and analyzed. Results: In subjective evaluation, the interobserver ICC was 0.95 [95% confidence interval (CI): 0.94-0.97] between two readers. The spatial resolution of 0.3x0.3x0.3mm<sup>3</sup> and 0.45x0.45x0.45mm<sup>3</sup> received highest subjective score on average and demonstrated highest consistency with autopsy measurements in objective evaluation. Regarding the measurements on the 48 volunteer ankles, distance 1 in type I and II were 12.65±2.08mm, 13.43±2.06mm (superior-banded in Type II) and 7.69±2.56mm (inferior-banded in Type II) (means ± SD), respectively. Distance 2 in type I and II were 10.90±2.24mm, 11.07±2.66mm (superior-banded in Type II), and 18.44±3.28mm (inferior-banded in Type II), respectively. Distance 3 and 4 were 4.71±1.04mm and 14.35±2.22mm, respectively. Conclusion: The feasibility to quantify the distances of surgically relevant bony landmarks. Please visit the Learning Center to also view this presentation in hardcopy format.

### MKEE-89 Multimodality Review of Important Musculoskeletal Measurements in the Upper Extremity

Participants

Jennifer S. Weaver, MD, Albuquerque, NM (*Presenter*) Nothing to Disclose

#### TEACHING POINTS

Many image-based measurements are used by orthopedic surgeons to plan treatment. This educational exhibit will discuss the indications and measurement techniques for several commonly used upper extremity measurements, and will detail the technical requirements of imaging needed to obtain precise and accurate measurements. After viewing this exhibit, the learner should be able to: (1) Understand important technical considerations and limitations in measurement techniques of various modalities, including radiographs, CT, MRI, and ultrasound (2) Discuss commonly encountered measurements in the upper extremity, including clinical indication, specific technique, and potential pitfalls

## TABLE OF CONTENTS/OUTLINE

Introduction General Measurement Techniques Shoulder 1. Acromioclavicular Interval 2. Acromiohumeral Distance 3. Coracoclavicular Interval 4. Acromial Angle, Tilt, and Slope 5. Humeral Neck Shaft Angle 6. Lateral Glenohumeral Offset Angle 7. Glenoid Version Angle 8. On track/off track Hill Sachs Elbow 1. Humero-condylar Angle 2. Ulnar Collateral Ligament Thickness 3. Ulnar Collateral Ligament Medial Joint Gap with Valgus Stress 4. Nerve Cross Sectional Area Wrist-hand 1. Capitulunate, Lunotriquetral, and Scapholunate Angles 2. Scapholunate Interval 3. Radial Inclination 4. Dorsal Radial Tilt 5. Radial Height 6. Radioulnar Angle 7. Radioscaphoid Angle 8. Ulnar Variance and Inclination 9. Carpal Tunnel Bowing and Area 10. Median Nerve Cross Sectional Area 11. Carpal Height, Height Ratio, and Height Index Shear wave elastography Conclusion

### MKEE-9 Musculoskeletal Manifestations of Systemic Lupus Erythematosus: An Imaging Overview

Participants

Marina Akuri, MD, Marilia, Brazil (*Presenter*) Nothing to Disclose

#### TEACHING POINTS

The purpose of this exhibit is to: 1. Review the most frequent and also atypical presentations of musculoskeletal involvement of systemic lupus erythematosus (SLE). 2. Illustrate with didactic cases while discussing the imaging findings and main complications of these disease

## TABLE OF CONTENTS/OUTLINE

Introduction: general presentation of the epidemiology and clinical findings of musculoskeletal involvement of systemic lupus erythematosus. Review the multi-modality imaging findings of musculoskeletal SLE with didactic illustrations. Present challenging cases with musculoskeletal manifestations related to systemic lupus erythematosus as insufficiency fracture, tenosynovitis, arthropathy, avascular necrosis, bone infarction, vasculitis and infection. Differential diagnosis including other inflammatory conditions and arthropathy helping the radiologist how to differentiate them. Relevant bibliographical references.

### MKEE-90 Shouldering the Burden: A Pictorial Review of Shoulder Arthroplasties

Participants

Akwasi Opoku, MD, Nashville, TN (*Presenter*) Nothing to Disclose

#### TEACHING POINTS

Advancements in shoulder arthroplasty has increased its use, particularly over the past two decades. The shoulder is the third most common replaced joint after hip and knee, with its overall incidence increasing at a greater rate than those of total knee and hip replacements. After viewing this exhibit, the learner should understand: 1. Shoulder anatomy and biomechanics 2. Indications for shoulder arthroplasty 3. Role of preoperative imaging and measurements 4. Advantages, disadvantages, and specific complications of various shoulder arthroplasties 5. Normal imaging findings and imaging findings of complications

## TABLE OF CONTENTS/OUTLINE

Introduction - history and evolution Shoulder anatomy and biomechanics 1. Bones, joints, muscles, other soft tissues (cartilage, labrum, capsule) 2. Unconstrained ball and socket, static and dynamic stabilizers Indications 1. Arthropathy, trauma, cuff pathology, osteonecrosis, prior infection Role of preoperative imaging (multimodality) 1. Evaluation of cuff, bone stock, cartilage 2. Glenoid morphology and version Types of shoulder arthroplasties, indications, advantages, disadvantages 1. Humeral head resurfacing arthroplasty 2. Hemiarthroplasty 3. Anatomic total shoulder arthroplasty 4. Reverse total shoulder arthroplasty Imaging appearances 1. Normal and complications

### MKEE-91 What's Your Carbon Footprint? Carbon-Fiber Implants in Orthopedic Oncology

Awards

Certificate of Merit

Participants

Erik Verhey, Reno, NV (*Presenter*) Nothing to Disclose

#### TEACHING POINTS

\*Carbon fiber reinforced polyetheretherketone (CFR-PEEK) is a composite material which can be used to create orthopedic implants for use in the appendicular skeleton and spine\*CFR-PEEK implants are nearly radiolucent and produce relatively little artifact when imaged with CT and MRI\*Owing to their favorable imaging profile, CFR-PEEK implants facilitate post-operative imaging follow up of tumor patients\*Post-operative radiation therapy in oncologic patients with CFR-PEEK implants is also improved due to lower artifact on planning CT scans and enabling the use of photon therapy

#### TABLE OF CONTENTS/OUTLINE

\*Background of CFR-PEEK as a composite material and its use in implants\*Surgical perspective: CFR-PEEK implant use in the spine\*Surgical perspective: CFR-PEEK implant use in the appendicular skeleton\*Radiographic and fluoroscopic appearance of CFR-PEEK implants with example cases\*CT appearance of CFR-PEEK implants with example cases\*MRI appearance of CFR-PEEK implants with example cases\*Value of CFR-PEEK implants in radiation oncology \*Conclusions

#### MKEE-92 Exchange Arthroplasty for Periprosthetic Joint Infection: What the Radiologist Needs to Know

Participants

Nicholas G. Rhodes, MD, Rochester, MN (*Presenter*) Nothing to Disclose

#### TEACHING POINTS

1. Management of periprosthetic joint infection (PJI) is a complex task.2. The radiologist should be familiar with the varied constructs employed following resection arthroplasty for infection.3. The presence of polymethylmethacrylate bone cement is often the radiologist's initial clue to the presence of joint infection undergoing treatment.4. Serial radiographs play an important role in the management of periprosthetic joint infection.

#### TABLE OF CONTENTS/OUTLINE

1. Review imaging of PJI a. Role of radiographs b. Role of advanced imaging c. Role of joint aspiration 2. Review clinical features of PJI 3. Review treatment options for PJI 4. Discuss imaging related to various treatment options a. Review of imaging appearance during and after treatment of PJI at various joints i. Resected arthroplasty ii. Spacers iii. Articulating spacers iv. Destination spacers b. Review how the radiologist puts it all together i. Discuss clinical findings and thought behind and directing this process ii. Define the role of the radiologist iii. Define appropriate terminology concerning joint resection/prosthesis explantation and employed spacers iv. Highlight role of serial radiographs v. Highlight expected and unexpected imaging findings during this process

#### MKEE-93 Intercondylar Notch Beyond the Cruciate Ligaments: Light at the End of the Tunnel

Participants

Sergio Atala, MD, Las Condes, Chile (*Presenter*) Nothing to Disclose

#### TEACHING POINTS

1. The intercondylar notch is a commonly neglected area in the knee anatomy and in the assessment of radiologic studies. 2. Knowledge of the consistent normal anatomy of this notch is easily and swiftly assessed with several imaging modalities, particularly with MR Imaging. 3. Some anatomic variations should be well recognized, not be confused with pathologic conditions. 4. Meniscal root pathology is critical and dedicated examination in the MR Imaging studies is recommended. In the case of meniscal root tears LaPrade classification can be utilized preoperatively, with prognostic relevance. Surgical techniques for meniscal root tears are presented to be assessed in the postoperative MR Imaging studies. 5. Solid and cystic masses can be primarily originated in the intercondylar notch, and a brief pictorial review is presented. 6. The medial synovial fold of the posterior cruciate ligament is a well-recognized structure, and pathologic conditions are presented, with therapeutic implications.

#### TABLE OF CONTENTS/OUTLINE

1. Introduction. 2. Anatomy. 3. Intercondylar morphology and insertion (tibial / femoral) of intercondylar structures. 4. Tibial spine tubercles. 5. Changes in the anatomy of the intercondylar notch during lifetime. 6. Meniscal roots variants, tears and postoperative changes. 7. Ganglion cyst in meniscal roots. 8. Oblique meniscal ligaments. Meniscomfemoral ligaments. 9. Ligamentum mucosum. 10. Synovial fringe. 11. Intercondylar meniscal fragments. 12. Ganglion cysts. 13. Solid Masses. 14. Medial synovial fold PCL. 15. Conclusion.

#### MKEE-94 Adipose Tissue Around the Knee - A Review of Normal Anatomy and MRI Findings of Common Pathologies

Participants

Majid Chalian, MD, Seattle, WA (*Presenter*) Grant, The Boeing Company

#### TEACHING POINTS

1. Anatomy of intraarticular fat pads and subcutaneous adipose tissue2. Review the role of intraarticular fat pads and subcutaneous adipose tissue3. Review the clinical presentation of intraarticular fat pads and subcutaneous adipose tissue pathologies and provide case examples 4. Review the MRI presentation of the pathologies involving intraarticular fat pads and Subcutaneous adipose tissue

#### TABLE OF CONTENTS/OUTLINE

Review of anatomy:• Infrapatellar fat pad and related structures• Suprapatellar fat pad• Prefemoral fat pad• Pericruciate fat pad• Subcutaneous fat Review of the role:• Non-mechanical roleo Inflammatory roleo Endocrine roleo Proprioceptive role• Mechanical roleo The dynamic role of anterior intraarticular fat pads during knee flexion and extensiono Shock absorbing roleo The route for surgical probingReview of the clinical presentation in pathological changes:• Infrapatellar fat pad and related structures• Suprapatellar fat pad• Prefemoral fat pad• Pericruciate fat pad• Subcutaneous fat Review of the MRI presentation:• Pathologies involving the synovial lining• Pathologies presenting with edema like changes • Space occupying pathologies

#### MKEE-95 The Multiple Applications of Dixon Sequences in Musculoskeletal MRI

## Awards

### Certificate of Merit

Participants

Massimo Donalisio, MD, (*Presenter*) Nothing to Disclose

### TEACHING POINTS

The Dixon method has gained much interest in musculoskeletal MRI, and many applications have been validated by the literature. The four sets of images generated by the Dixon technique can each provide specific qualitative or quantitative information, and they may serve to optimise acquisition protocols in various applications including bone marrow, whole body, oncological and rheumatological imaging. Water only images provide robust fat suppression that can be useful in large field of view applications or MRI of the extremities. Fat only images are particularly useful for the assessment of bone marrow lesions and may replace the information provided by T1-weighted sequences in certain indications. There are some pitfalls and disadvantages that radiologists must be familiar with.

### TABLE OF CONTENTS/OUTLINE

1. Brief review of the physics of Dixon sequences: from one sequence to four sets of images; 2. Illustrated review of common applications of Dixon sequences in musculoskeletal practice: a) Fat suppression technique in extremities, large field of view applications (comparison to CHESS and STIR techniques), b) Spine and bone marrow imaging: advantages of the use of fat only images in replacement of T1 weighted sequences, c) Whole body MRI: the use of Dixon technique to optimise whole-body protocols with a focus on neuromuscular disorders, d) MRI in rheumatology: the use of Dixon sequences to scan more regions with less sequences, e) MRI of sarcomas: the benefits of including Dixon sequences in the acquisition protocol, f) The Dixon technique as a quantitative MRI tool to assess the fat fraction; 3. Pitfalls and disadvantages of Dixon sequences.

### MKEE-96 Mismatch Findings of WB DWI MRI and PET-CT in Oncology

Participants

Carolina Almeida, MD, Rio de Janeiro, Brazil (*Presenter*) Nothing to Disclose

### TEACHING POINTS

TEACHING POINTS To evaluate the performance of WB-DWI MRI in the diagnosis and follow-up of cancer patients in situations of false positive or negative results in the PET-CT study (18F-FDG and PSMA). PET/CT is used in the evaluation of oncology patients to identify malignancy, but could be non-specific. Identify what sequences should be used to analyse bone marrow and soft tissue in whole-body MR imaging protocols to detect neoplastic lesions and pseudotumoral in oncological patients. To be aware of the conditions and the mechanisms by which false positive and negative results occur on 18F-FDG-PET-CT scans and to compare with WB MRI-DWI study. Make a pictorial essay of the main false false negative PET-CT PSMA cases comparing with WB MRI study. An understanding of the limitations of this nuclear medicine technology is necessary to avoid making inaccurate diagnosis and potentially limiting the right treatment for our patients.

### TABLE OF CONTENTS/OUTLINE

TABLE OF CONTENTS AND OUTLINE 1) The value of WB-DWI MRI IN the diagnosis and follow-up of cancer patients. 2) Case discussion to demonstrate 18F-FDG PET/CT false positive and false negative examples: Small lesions (less than 1,0 cm) Osteoblastic sclerotic metastases Patient anxiety can result in increased uptake Bone marrow infiltration Low grade lymphoma 3) To demonstrate PET/CT-PSMA false positive and false negative examples: small tumors neuroendocrine prostate tumor Small tumors near bladder 4) Common pitfalls 5) Differential diagnosis 6) Structured reporting step by step

### MKEE-97 Review of the Effects of Diabetes Mellitus on the Musculoskeletal System

Participants

Jimmy Saade, MD, (*Presenter*) Nothing to Disclose

### TEACHING POINTS

- Epidemiology and financial burden of diabetes mellitus (DM).
- DM affects nearly every organ system.
- Beyond the well-known manifestations of diabetes, such as neuropathy and nephropathy, DM can also have damaging effects on the musculoskeletal (MSK) system.
- As the prevalence of DM continues to increase, the lesser-known musculoskeletal complications are to increase as well.
- We demonstrate some of these MSK manifestations. Early recognition and diagnosis of the many DM-related complications will lead to earlier intervention, and ultimately, less morbidity for patients and financial burden on the healthcare system.
- DM-related disease entities discussed include osteoporosis, diffuse idiopathic skeletal hyperostosis (DISH), Dupuytren's contractures, trigger finger, rotator cuff tendinopathy, adhesive capsulitis, and calcaneal insufficiency fractures.
- We demonstrate a multimodality approach to the diagnosis of these pathologies including MSK ultrasound.

### TABLE OF CONTENTS/OUTLINE

- Diabetes Mellitus: Epidemiology and pathology.
- DM-related osteoporosis and diagnosis with DEXA, radiographs, and CT.
- DISH with imaging findings across multiple imaging modalities.
- Dupuytren's contractures utilizing ultrasound for diagnosis.
- Trigger finger with confirmatory findings on MRI.
- Adhesive capsulitis and rotator cuff tendinopathy findings on MRI.
- Calcaneal insufficiency fracture and confirmatory findings on CT and x-ray.
- Conclusion.

### MKEE-98 Imaging of Calf Pain

## Awards

### Certificate of Merit

### Identified for RadioGraphics

Participants

Allison Khoo, MD, (*Presenter*) Nothing to Disclose

### TEACHING POINTS

1. Understand the muscular anatomy of the calf including the gastrocnemius, soleus, plantaris, and Achilles tendon. 2. Recognize

subtle radiographic findings of calf and posterior ankle pathology such as obliteration of Kager's fat pad. 3. Develop a differential for calf pain spanning traumatic, metabolic, infectious/inflammatory, neoplastic, congenital, and vascular etiologies.

#### **TABLE OF CONTENTS/OUTLINE**

1. Introduction. 2. Relevant anatomy: a. Kager's fat pad on ankle radiograph: obliterated by pathology from adjacent structures including Achilles tendon, calcaneus, and tibiotalar joint. b. Review of gastrocnemius, soleus, and plantaris anatomy. 3. Case-based review of calf and posterior ankle pathology organized by etiology. a) trauma/overuse- Achilles tendinopathy and tear, Haglund deformity, Tennis leg/plantar rupture. b) metabolic-xanthoma. c) infectious/inflammatory: myositis, rhabdomyolysis. d) neoplastic: sarcoma, lymphoma. e) congenital: accessory soleus, cortical desmoid. f) vascular: popliteal artery (aneurysm, entrapment, stenosis), deep venous thrombosis

#### **MKEE-99 Triceps Surae Muscle Injuries: What the Radiologist Should Know?**

Participants

Jaime Isem, PhD, (*Presenter*) Nothing to Disclose

#### **TEACHING POINTS**

1. To review the pathophysiological mechanism of Triceps surae muscle injuries. 2. To Assess the imaging technique of choice for the study of acute and chronic injuries. 3. To show the US and MRI findings in Triceps surae muscle injuries. 4. To describe the reparative process in the favorable or unfavorable evolution of these injuries and the residual findings.

#### **TABLE OF CONTENTS/OUTLINE**

Pathophysiological mechanism of Triceps surae muscle injuries. US and MRI protocols for an adequate diagnosis of Triceps surae muscle injuries. Current severity classification systems. Review of imaging findings of the acute injury according to the type of damage. Range of imaging healing process in lesions and residual changes.

Printed on: 02/07/23



## Abstract Archives of the RSNA, 2022

MKEE-1

### Achilles-calcaneus-plantar fascia system: Anatomy, Biomechanics and Patterns of Injury

Sunday, Nov. 27 8:00AM - 9:00AM Room: Learning Center - MK

#### Awards

Certificate of Merit

Identified for RadioGraphics

#### Participants

Dyan V. Flores, MD, Ottawa, ON (*Presenter*) Nothing to Disclose

#### TEACHING POINTS

The Achilles tendon, calcaneus and plantar fascia comprise an interconnected complex or system of structures that play a vital role in the load distribution of the foot, including absorbing mechanical shock, stabilizing and preventing the collapse of the longitudinal arch during propulsion. Failure, overload or repetitive stress to any or a combination of these structures leads to a multitude of disorders and imaging findings. The objectives of this educational exhibit are: • Review normal anatomy and biomechanics of the Achilles tendon, calcaneus and plantar fascia • Discuss patterns of failure and injury involving the Achilles tendon, calcaneus and plantar fascia • Identify imaging findings that may aid in differentiating these disorders when clinical findings are equivocal

#### TABLE OF CONTENTS/OUTLINE

Pertinent anatomy and biomechanics • Calcaneal crescent • Windlass mechanism Imaging techniques Disorders Achilles Complete and partial tear Insertional tendinopathy and tendinitis Peritendinitis Peri-Achilles bursal fluid Calcaneus Stress fracture Haglund syndrome Posterior ankle impingement Plantar fascia Fasciitis Rupture Fibromatosis Plantar fat pad abnormalities

Printed on: 02/07/23



## Abstract Archives of the RSNA, 2022

MKEE-10

### Current Trends in Total Ankle Arthroplasty

Sunday, Nov. 27 8:00AM - 9:00AM Room: Learning Center - MK

#### Awards

Identified for RadioGraphics

#### Participants

Jason Ha, (*Presenter*) Nothing to Disclose

#### TEACHING POINTS

Describe indications for total ankle arthroplasty (TAA) vs. arthrodesis. Recognize different types of TAA, including semi-constrained and minimally constrained designs. Understand normal tibiotalar and distal anterior tibia angles. Define normal and abnormal imaging appearance of TAA.

#### TABLE OF CONTENTS/OUTLINE

1. Indications for TAA vs. arthrodesis. 2. Types of TAA: Differences between 1st generation, 2nd generation, 3rd generation. Comparison of Agility, Salto-Talaris, Inbone, STAR, Hinteagra, Mobility, and Zimmer Trabecular Metal. 3. Normal imaging appearance: Radiolucency, Tibiotalar Angle, Distal Anterior Tibia Angle. 4. Complications: Radiolucency, Hardware Subsidence, Perihardware fracture, Syndesmotic screw loosening, Heterotopic ossification, Increased varus or valgus angulation of the ankle, Ankle gutter narrowing, Infection, Syndesmotic or fibula osteotomy nonunion, Aseptic loosening, Expansile osteolysis (also known as ballooning osteolysis, periprosthetic cysts)

Printed on: 02/07/23



## Abstract Archives of the RSNA, 2022

MKEE-100

### **Pain in the Rear-Exploration of MRI Findings Useful in Distinguishing Septic Arthritis from Inflammatory Spondyloarthritis of the Sacroiliac (SI) joints**

Sunday, Nov. 27 8:00AM - 9:00AM Room: Learning Center - MK

#### **Participants**

Matin Goldooz, MD, Jackson, MS (*Presenter*) Nothing to Disclose

#### **TEACHING POINTS**

Review the sacroiliac joint anatomy. Illustrate MRI findings specific for inflammatory sacroiliitis and review updated Assessment of SpondyloArthritis international Society (ASAS) criteria. Illustrate common MR findings in infectious sacroiliitis. Review manifestations of degenerative sacroiliitis. Discuss common procedures for SI joint aspiration and therapeutic injection.

#### **TABLE OF CONTENTS/OUTLINE**

Infectious sacroiliitis is a destructive, monoarticular arthropathy typically caused by hematogenous seeding of bacterial pathogen. Clinical symptoms of SI joint disease are often nonspecific and may be attributed to pathology in hips or spine. Early recognition and prompt treatment of the condition is important to prevent permanent joint damage or abscess formation. Spondyloarthritides such as ankylosing spondylitis commonly involve the SI joints. The most recently updated classification criteria of axial spondyloarthropathies are based on specific MRI findings, which facilitates prompt diagnosis. Differentiation between infectious and spondyloarthropathy associated sacroiliitis is incredibly important given the different prognosis and treatment regimens. MRI is the most relevant modality in evaluation of sacroiliitis, that can assist in differentiation of infectious and inflammatory etiology. Radiologists should be familiar with the MRI features that are more indicative of infectious sacroiliitis given the urgency required in making this diagnosis. In this educational exhibit we illustrate MRI findings of infectious and inflammatory sacroiliitis with emphasis on findings useful in differentiation of the two and in distinguishing both from degenerative sacroiliitis.

Printed on: 02/07/23



## Abstract Archives of the RSNA, 2022

MKEE-101

### Cervical Spine Infections and their Mimics

Sunday, Nov. 27 8:00AM - 9:00AM Room: Learning Center - MK

#### Awards

Certificate of Merit

#### Participants

Samantha Salmon, MD, Columbia, MO (*Presenter*) Nothing to Disclose

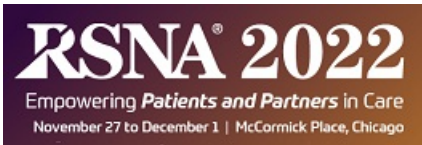
#### TEACHING POINTS

1. Discuss shared key clinical and imaging characteristics of inflammatory and infectious diseases of the cervical spine<sup>2</sup>. To detail, in a case-based format, typical imaging features of infection of the cervical spine, organized by the site of origin<sup>3</sup>. To detail, in a case-based format, disease states that mimic infection and highlight key imaging and clinical factors that assist in the differentiation

#### TABLE OF CONTENTS/OUTLINE

This presentation will be a case-based discussion reviewing cervical infections, differentiated by their site of origin. Cases will be presented alongside cases that mimic infection.· Overview of shared presentation of infection and inflammatory diseases· Features of perivertebral infections· Prevertebral infection compared to longus coli tendinitis· Spondylodiscitis compared to renal osteodystrophy· Epidural infection, highlighting progression from phlegmon to abscess, compared to epidural tumor and hematoma· Intramedullary abscess compared to demyelination and infarction· Facet septic arthritis compared to CPPD arthropathy and neoplasm· Posterior soft tissue infections compared to post-operative seroma

Printed on: 02/07/23



## Abstract Archives of the RSNA, 2022

MKEE-102

### 3T Magnetic Resonance Neurography - From Head to Toe!

Sunday, Nov. 27 8:00AM - 9:00AM Room: Learning Center - MK

#### Awards

Cum Laude

#### Participants

Flavia M. Costa, MD, PhD, Rio de Janeiro, Brazil (*Presenter*) Nothing to Disclose

#### TEACHING POINTS

1) 3T MR neurography is a technique involving regional MRI that allows evaluation of the peripheral nerves and is more effective than electrodiagnostic studies in the evaluation of deep structures. 2) Create a didactic script of what should be evaluated in neurography exams and how to recognize a normal or altered nerve. 3) Make a pictorial essay of the main peripheral nerves and their differential diagnoses.

#### TABLE OF CONTENTS/OUTLINE

1) Overview of what is magnetic resonance neurography and the examination technique. 2) 3T magnetic resonance of a traumatic lesion. 3) Tumoral lesion. 4) Inflammatory neuronal lesion. 5) Step by step for the evaluation of lesions and table with a summary of findings expected.

Printed on: 02/07/23



## Abstract Archives of the RSNA, 2022

MKEE-104

### Pediatric Spine and Spinal Cord Tumors: Imaging Answers to Clinical and Surgical Needs

Sunday, Nov. 27 8:00AM - 9:00AM Room: Learning Center - MK

#### Awards

Certificate of Merit

#### Participants

VINICIUS BRAMBILLA, MD, Sao Paulo, Brazil (*Presenter*) Nothing to Disclose

#### TEACHING POINTS

Review the most frequent spinal, spinal cord and paravertebral tumors in childhood; Briefly discuss imaging modalities and protocols; Discuss differential diagnosis; Illustrate pseudotumoral findings and pitfalls.

#### TABLE OF CONTENTS/OUTLINE

INTRODUCTION Overview of spinal and paravertebral tumors in childhood seeking to illustrate and review the lesions split by compartments (paravertebral, vertebral, extradural and intradural) based on clinical cases from our institutional database. PARAVERTEBRAL NEOPLASMS Including neurofibromatosis benign findings and malign degeneration, neuroblastic tumors, paravertebral primary PNET. VERTEBRAL NEOPLASMS Including Langerhans cell histiocytosis, metastasis, osteblastoma, chondrosarcoma; EXTRADURAL NEOPLASMS Including chloroma, primary extradural lymphoma; epidural metastasis. INTRADURAL NEOPLASMS Including astrocytoma, ependimoma, hemangioblastoma, intradural lipomatous lesions, primary diffuse leptomeningeal glioneuronal tumor, meningioma; PSEUDOTUMORS Including infectious diseases, extramedullary hematopoiesis, chronic recurrent multifocal osteomyelitis, arachnoid cysts; vascular lesions, spinal dysraphisms.

Printed on: 02/07/23

## Abstract Archives of the RSNA, 2022

MKEE-105

### A Nocturnal Nuisance: Diagnosis and Treatment of Osteoid Osteoma

Sunday, Nov. 27 8:00AM - 9:00AM Room: Learning Center - MK

#### Participants

Meghan Jardon, MD, (*Presenter*) Nothing to Disclose

#### TEACHING POINTS

1. Osteoid osteoma is a benign tumor of bone that presents with nocturnal pain in children and young adults, classically relieved by non-steroidal anti-inflammatory drugs (NSAIDs). Common locations include the femur, tibia, and posterior elements of the spine. 2. The classic imaging appearance of a calcified nidus with surrounding sclerosis that is described on CT can be difficult to appreciate on MRI. Thus, the radiologist must maintain a high level of suspicion when interpreting MRI, as misinterpretation may delay appropriate patient management. 3. Radiofrequency ablation provides a safe and effective means of treating osteoid osteomas, but additional consideration should be given in difficult locations (i.e. adjacent to neural elements, articular cartilage, etc.)

#### TABLE OF CONTENTS/OUTLINE

1. Background/Introduction  
2. Clinical and Imaging Manifestations of Osteoid Osteomas  
3. Case Examples from a variety of different anatomic locations  
A. Long bones: femur, tibia  
B. Spine: T12 posterior elements  
C. Others: talus, calcaneus  
D. Intra-articular examples: hip, elbow  
4. Differential Diagnostic considerations for osteoid osteoma  
5. Management of Osteoid Osteoma  
A. Medical management  
B. Radiofrequency ablation: Equipment, technique, special considerations in difficult locations  
C. Surgical resection

Printed on: 02/07/23



## Abstract Archives of the RSNA, 2022

MKEE-106

### Many Faces of Bone Metastasis: How to Detect and Not be Surprised

Sunday, Nov. 27 8:00AM - 9:00AM Room: Learning Center - MK

#### Participants

Eduarda Bernal, MD, Sao Paulo, Brazil (*Presenter*) Nothing to Disclose

#### TEACHING POINTS

Teaching points? Be prepared to do early detection of skeletal metastases.? Understand the biological mechanisms by which tumors metastasize to bone.? Recognize the appearance of skeletal metastases.? Review typical and atypical forms of secondary musculoskeletal involvement in different imaging methods

#### TABLE OF CONTENTS/OUTLINE

Introduction and objectives Metastases are the most common malignant tumors of the skeleton, and bone is the third most frequent site of metastasis, behind only the lung and liver. Early detection of skeletal metastases is essential for accurate staging and optimal treatment, in addition to improving the patient's quality of life. Bone metastases are a major cause of morbidity in cancer patients, characterized by severe pain, impaired mobility, pathological fractures and spinal cord compression. Understanding of the biological mechanisms by which tumors metastasize to bone and the diverse image appearance of skeletal metastases are important to detect disseminated disease. Methods We will review typical and atypical forms of secondary musculoskeletal involvement in different imaging methods through several cases and discuss the ideal method for diagnosis and monitoring of response to treatment of skeletal metastases. Conclusions Bone metastases have an important impact on the quality of life of cancer patients, and therefore, new strategies are needed to detect skeletal disease and attenuate established skeletal events. Radiologists are essential for this diagnosis since most bone metastases are asymptomatic at the beginning and knowing typical and atypical forms of skeletal metastatic involvement helps in early diagnosis and monitoring of response to treatment.

Printed on: 02/07/23



## Abstract Archives of the RSNA, 2022

MKEE-107

### Recognizing Pediatric Bone Tumors: Growing Your Knowledge

Sunday, Nov. 27 8:00AM - 9:00AM Room: Learning Center - MK

#### Participants

Vitor Cardoso Linhares, MD, Sao Paulo, Brazil (*Presenter*) Nothing to Disclose

#### TEACHING POINTS

There is a vast variety of bone tumors proposed by WHO 2020 classification, divided, among other aspects, into its tissue matrix type and biological behavior (benign, intermediate and malign). Considering the bone tumors of the pediatric population, the most common malign tumours are osteosarcoma and ewing sarcoma, and the most common benign tumours includes simple bone cyst and aneurysmal bone cyst. To identify the main characteristic of this tumours, especially in the pediatric age, can help patients to receive the adequate treatment and avoid unnecessary procedures. The purpose of this exhibit is to:

- Briefly review the most recent World Health Organization (WHO) bone tumours classification.
- Demonstrate cases of the most prevalent pediatric bone tumours.
- Review the image findings of radiographic, CT and MRI studies of the most prevalent bone neoplasms in children.

#### TABLE OF CONTENTS/OUTLINE

(1) Briefly review the World Health Organization (WHO) bone tumours classification, and correlacionate with the most prevalent tumours in the pediatric population. (2) Approach the characteristics and image findings to help distinguish non aggressive and aggressive bone neoplasms. (3) Classify the most prevalent groups of benign, intermediate and malignant bone tumours in the pediatric population. (4) Describe radiographic, CT and MRI findings of each of the most prevalent groups of bone neoplasm in children. (5) Systematic approach to help the radiologist in the correct diagnosis of the bone tumours in the pediatric population.

Printed on: 02/07/23



## Abstract Archives of the RSNA, 2022

MKEE-108

### Fractures of the Appendicular Skeleton and Criteria for Their Surgical Management: What the Orthopedic Surgeon Wants to Know

Sunday, Nov. 27 8:00AM - 9:00AM Room: Learning Center - MK

#### Participants

Lucas Miyahara, MD, Sao Paulo, Brazil (*Presenter*) Nothing to Disclose

#### TEACHING POINTS

The purpose of this exhibit is to: 1. Review and illustrate some of the main appendicular skeleton fractures with surgical management, with emphasis on radiography and computed tomography, methods most commonly used in the emergency. 2. Didactically summarize the imaging findings that indicate the surgical treatment of appendicular skeleton fractures.

#### TABLE OF CONTENTS/OUTLINE

Introduction: general illustration of the fractures to be addressed. Demonstrate didactic and illustrative cases contemplating the following fractures: proximal humerus fracture, terrible triad of the elbow, Monteggia fracture-dislocation, Galeazzi fracture-dislocation, Barton fracture, scaphoid fracture, pelvic ring fracture, intertrochanteric fracture, femoral neck fracture, tibial plateau fracture, ankle fracture and Lisfranc fracture-dislocation. Provide schematic illustrations reviewing fracture classifications and discussing important concepts to understand the imaging findings. Present two tables that summarize the trauma mechanisms and imaging findings that indicate the surgical treatment of appendicular skeleton fractures in each affected segment. Bibliographical references.

Printed on: 02/07/23

## Abstract Archives of the RSNA, 2022

MKEE-109

### Uncommon Manifestations of Bone Trauma: Focus on Medullary Fat

Sunday, Nov. 27 8:00AM - 9:00AM Room: Learning Center - MK

#### Participants

Pablo Rengifo, MD, (*Presenter*) Nothing to Disclose

#### TEACHING POINTS

1. Following a high energy bone injury, a macroscopic fracture or a bone contusion (trabecular microfractures) is produced. In either case, medullary fat is compromised and typically shows high signal on fluid-sensitive MRI sequences. However, medullary fat might have other manifestations secondary to bone injuries. 2. Uncommon manifestations of medullary fat related to bone trauma can be classified in intramedullary and extramedullary (extraosseus) fat accumulation. The last one could be categorized in intra-articular, intra-tendon sheath, intra-bursal, subperiosteal and systemic (fat embolism). 3. Familiarity with imaging characteristics of intramedullary and extramedullary fat accumulation related to a high energy bone injury is essential in order to prompt further studies to demonstrate a possible occult fracture.

#### TABLE OF CONTENTS/OUTLINE

1. Introduction. 2. Anatomy of the Medullary Cavity. 3. Types of uncommon manifestations of medullary fat after bone trauma: Overview. 4. Intramedullary fat accumulation after bone trauma. 5. Extramedullary (extraosseus) fat accumulation after bone trauma. 5.1. Intra-articular. 5.2. Intra-tendon sheath. 5.3. Intra-bursal. 5.4. Subperiosteal. 5.5. Systemic (fat embolism). 5. Summary. 6. References.

Printed on: 02/07/23



## Abstract Archives of the RSNA, 2022

MKEE-11

### Gluteal Tendon Injuries: Anatomy, Pathological Conditions and Postoperative Imaging

Sunday, Nov. 27 8:00AM - 9:00AM Room: Learning Center - MK

#### Participants

Carlos H. Longo, MD, Sao Paulo, Brazil (*Presenter*) Nothing to Disclose

#### TEACHING POINTS

The purpose of this exhibit is to: • Review and illustrate the anatomy of the gluteal tendons and their relationship to adjacent structures; • Illustrate and discuss the patterns of injuries involving these structures with didactic cases and their clinical relevance; • Illustrate and discuss types of surgical treatment and postoperative imaging findings of gluteal tendon injuries, and discuss its relation to hip arthroplasty.

#### TABLE OF CONTENTS/OUTLINE

The gluteus medius and minimus muscles are hip abductors, with a crucial role in maintaining pelvic stability and normal gait. Although gluteal lesions are common, there is a relative paucity of detailed descriptions of features and patterns of tendon pathology in the literature compared to upper limb rotator cuff tendinopathy. Anatomy: • Imaging of gluteal bundles, subgluteus bursa and insertional anatomy exemplified by cases and didactic illustrations. Pathological conditions: • Function considerations and clinical relevance: Tendinopathy of the gluteus tendons are a cause of lateral hip pain and gait instability, particularly in older adults. Asymptomatic gluteal tendinopathies have been shown to have a negative effect on the outcomes of total hip arthroplasty. Surgical treatment and postoperative imaging: • Surgical indications and types of surgeries, modalities and complications.

Printed on: 02/07/23



## Abstract Archives of the RSNA, 2022

MKEE-110

### World Cup is Coming - Recall the Typical Soccer Lesions

Sunday, Nov. 27 8:00AM - 9:00AM Room: Learning Center - MK

#### Participants

Gillis Lago, MD, (*Presenter*) Nothing to Disclose

#### TEACHING POINTS

The purpose of this exhibition is: 1. Review the main orthopedic injuries that occur in soccer. 2. Correlate the trauma mechanism with the type of injury found. 3. Discuss the most common injuries, including muscle strains and injuries that occur in the knee, ankle and foot, as well as less common injuries that can occur in the upper limbs, through imaging methods in a multimodality approach.

#### TABLE OF CONTENTS/OUTLINE

1 - Most common orthopedic injuries that occur after playing soccer, correlated with the main imaging findings in a multimodality approach (CR, US, CT and MRI). 2 - Correlate the trauma mechanism with the main injuries found. 3 - Most common orthopedic injuries and imaging findings in a multimodal approach, including: - Muscle injuries: - Acute; - Chronic; - Hip and pelvis: - Symphysis pubic dysfunction. - Knee injuries: - Ligament injuries, especially rupture of the anterior cruciate, medial collateral and posterior cruciate ligaments (less common). - Meniscal injuries; - Posterolateral corner injuries; - Ankle/foot injuries: - Ligament injuries, especially the lateral complex, which is the most affected; - Less common injuries, such as foot plate and ligament injuries; - Upper limb injuries: - Acute injuries to the shoulder, wrist and finger. - Miscellaneous and pediatric skeletal injuries, as osteochondrosis.

Printed on: 02/07/23



## Abstract Archives of the RSNA, 2022

MKEE-111

### The Great Pretender: Benign Soft Tissue Tumors Mimicking Malignancy

Sunday, Nov. 27 8:00AM - 9:00AM Room: Learning Center - MK

#### Participants

Tina Shiang, MD, Worcester, MA (*Presenter*) Nothing to Disclose

#### TEACHING POINTS

The aim of this educational exhibit is to present a case-based multimodality review of benign soft tissue tumors mimicking malignancy and provide a systematic approach to challenging cases of "lumps and bumps."1. Review the systematic approach to evaluating "lumps and bumps" and general principles for distinguishing benign vs malignant soft tissue masses.2. Present a series of challenging soft tissue tumor/pseudotumor cases that provided a diagnostic dilemma for the radiologist using a multimodality approach.3. Highlight the importance of a multidisciplinary approach in improving patient experience, including clinical, radiologic, and histopathologic correlation.

#### TABLE OF CONTENTS/OUTLINE

1. Systematic approach to evaluating "lumps and bumps" in MSK practice.2. Presentation of benign soft tissue masses with imaging features suggestive of malignancy (XR, US, CT and MRI). a. Trauma: Myositis ossificans b. Neurologic: granular cell tumor, schwannoma c. Vascular: glomus tumor, vascular malformation d. Inflammatory: rheumatoid nodule e. Other: desmoplastic fibroelastoma, nodular fasciitis, pigmented villonodular synovitis3. Discussion of challenging aspects of clinical decision-making, management, and patient outcome.

Printed on: 02/07/23



## Abstract Archives of the RSNA, 2022

MKEE-112

### Soft Tissue Tumors: What to Include in the Report - A Primer for General Radiologists

Sunday, Nov. 27 8:00AM - 9:00AM Room: Learning Center - MK

#### Awards

**Cum Laude**

**Identified for RadioGraphics**

#### Participants

Geoffrey M. Riley, MD, Portola Valley, CA (*Presenter*) Nothing to Disclose

#### TEACHING POINTS

1. Provide general facts about soft tissue tumors  
2. List the 10 most important items that should be described in an MRI report on soft tissue tumors  
3. Show examples of how to report each item

#### TABLE OF CONTENTS/OUTLINE

1. Introduction- General facts on imaging of soft tissue tumors  
2. Top 10 important components of the report- Compartment- Anatomic structure- Size and shape- Location relative to bony landmark- Description of borders- Relationship to adjacent structures- Signal characteristics and contrast enhancement- Peritumoral signal and tail- Feeding and draining vessels- Lymph nodes  
3. Conclusion  
4. References

Printed on: 02/07/23



## Abstract Archives of the RSNA, 2022

MKEE-113

### I Feel Something in My Hand - What Could it Be?

Sunday, Nov. 27 8:00AM - 9:00AM Room: Learning Center - MK

#### Participants

Cecilia Ruiz de Castaneda, Toledo, Spain (*Presenter*) Nothing to Disclose

#### TEACHING POINTS

The purpose of this exhibit is: 1. To review the spectrum of soft tissue tumors of the hand and illustrate the typical and atypical imaging features. 2. To describe the main tumor-like lesions of the hand and wrist. 3. To analyze the differential diagnosis and provide diagnostic keys to identify pitfalls.

#### TABLE OF CONTENTS/OUTLINE

Soft tissue masses of the hand and wrist are very prevalent in clinical practice. For this reason, the radiologist should be familiar with the most common benign and malignant tumors to develop and narrow the differential diagnosis. Multimodality imaging approach is mandatory for therapeutic planning. Although magnetic resonance imaging is an important imaging modality to diagnose soft tissue tumors, other initially ordered imaging modalities such as radiographs and ultrasound can also add valuable information about the lesions. We provide a comprehensive approach to tumors and tumor-like lesions of the hand, including demographics, clinical presentation, and imaging findings required to make an appropriate differential diagnosis

Printed on: 02/07/23



## Abstract Archives of the RSNA, 2022

MKEE-114

### Vascular Changes that Every Musculoskeletal Radiologist Should be Aware of

Sunday, Nov. 27 8:00AM - 9:00AM Room: Learning Center - MK

#### Awards

Certificate of Merit

#### Participants

Eduarda Bernal, MD, Sao Paulo, Brazil (*Presenter*) Nothing to Disclose

#### TEACHING POINTS

Teaching points- MRI of joints is often performed for presumed musculoskeletal conditions. There is a wide variety of variant vascular anatomy and vascular pathology that can occur around the joint, including an aberrant artery, vascular trauma that occurs with joint dislocation, artery aneurysm, vein thrombosis, cystic adventitial disease, and vascular anomalies like arteriovenous malformation.- Peripheral artery disease (PAD) is currently the leading cause of morbidity and mortality in the western world. The identification of PAD incidentally in a musculoskeletal examination can make the diagnosis and improve the survival of this patient.- Venous thrombosis is an important and frequent diagnosis with clinical signs and symptoms that can mimic musculoskeletal pathologies.- Cystic adventitial disease is an uncommon vascular pathology that have a predilection in the popliteal region, manifesting rapidly progressive calf claudication and lower extremity pain.

#### TABLE OF CONTENTS/OUTLINE

IntroductionVascular abnormalities are an important and frequent diagnosis with clinical signs and symptoms that can mimic musculoskeletal pathologies. Due to this clinical similarity, MR examinations are frequently requested for patients with vascular abnormalities, under an equivocate suspicion of a musculotendineous or articular injury.ObjectivesThe purpose of this study is review unexpected and expected vascular findings, that can mimic musculoskeletal pathologies with the same clinical signs and symptoms.ConclusionsReviewing cases with vascular abnormalities on musculoskeletal examinations can help the radiologist to detect some patterns and extend the differential diagnosis.

Printed on: 02/07/23

## Abstract Archives of the RSNA, 2022

MKEE-115

### More Than Just a Pinch: A Comprehensive Review of Ankle Impingement Syndromes

Sunday, Nov. 27 8:00AM - 9:00AM Room: Learning Center - MK

#### Participants

Hira Qureshi, BA, Mason, OH (*Presenter*) Nothing to Disclose

#### TEACHING POINTS

1. Review anatomy of the ankle and spaces at risk for impingement  
2. Describe clinical presentation and spectrum  
3. Discuss causes of impingement  
4. Imaging overview  
5. Discuss treatment

#### TABLE OF CONTENTS/OUTLINE

-Introduction-Background-Review of anatomy-Role of imaging-Impingement syndromes: presentation, pathophysiology, imaging -  
Anterolateral-Soft tissue pathology-MRI: High signal intensity and thickening of ATFL andAITFL, synovial hypertrophy and distortion of anterolateral gutter-Tx: Conservative, arthroscopy-Anterior -Osseous outgrowth causing synovial reactivity-Radiographs: anterior tibiotalar osseous prominence-MRI: osteophytes, synovial thickening, scarring-Tx: Conservative, arthroscopy-  
Anteromedial-Soft tissue and osseous pathology-Radiographs: Medial malleolar osteophytes-MRI: Anterior deltoid thickening, synovitis, osteophyte formation-Tx: Conservative, arthroscopy-Posteromedial-Soft tissue pathology-MRI: intermediate signal of posterior tibiotalar ligament with thickening and loss of normal fibrillation-Tx: Conservative, arthroscopy-Posterior-Soft tissue pathology with anatomic predisposition, os trigonum -MRI: Bone marrow edema, edema at synchondrosis, thickening of posterior ligaments-Tx: Conservative, arthroscopy-Extra-articular-Biomechanical-MRI: cystic changes and bone marrow edema of lateral talus-Tx: osseous correction or arthrodesis-Summary

Printed on: 02/07/23



## Abstract Archives of the RSNA, 2022

MKEE-116

### Do Not Let It Go:Frozen Shoulder and Capsulitis At Other Sinovial Joints

Sunday, Nov. 27 8:00AM - 9:00AM Room: Learning Center - MK

#### Participants

Deodato Cartaxo, MD, Sao Paulo, Brazil (*Presenter*) Nothing to Disclose

#### TEACHING POINTS

Review the normal anatomy of shoulder, hip and other joints. Describe the pathophysiological mechanism and clinical evolution of adhesive capsulitis. Review the main image findings present on MRI, ultrasound and arthrography through didactically illustrative cases of adhesive capsulitis and its differential diagnosis. Exemplify the importance of a precise diagnosis in terms of treatment planning.

#### TABLE OF CONTENTS/OUTLINE

Review anatomy, pathophysiological mechanism and discuss about the different radiological findings of adhesive capsulitis of the shoulder and other joints, based on cases obtained from the digital file of our magnetic resonance institution and other methods. We also provide literature review, teaching points, take home message and references.

Printed on: 02/07/23



## Abstract Archives of the RSNA, 2022

MKEE-117

### Ultrasound-guided Intervention of Small Joints

Sunday, Nov. 27 8:00AM - 9:00AM Room: Learning Center - MK

#### Awards

Certificate of Merit

#### Participants

Dyan V. Flores, MD, Ottawa, ON (*Presenter*) Nothing to Disclose

#### TEACHING POINTS

Ultrasound-guided intervention of small joints can be technically challenging because of irregular bony contour, size of joints disproportionately small compared to utilized tools and superficial location of intended targets. The objectives of this educational exhibit are: • 1. To identify clinical manifestations and indications of US-guided small joint interventions • 2. To describe the various indications for, contraindications to and expected outcomes associated with US-guided small joint interventions • 3. To demonstrate techniques, tips and tricks in performing these procedures by correlating with cross sectional images and graphic illustrations

#### TABLE OF CONTENTS/OUTLINE

Axial skeleton • Temporomandibular joint • Sternoclavicular • Symphysis Upper extremity • Tenotomies at the elbow • Ulnar nerve at cubital tunnel • De Quervain's tenosynovitis • Trigger finger • Median nerve at carpal tunnel • DRUJ Lower extremity • PeriAchilles region • Plantar fascia • Morton's neuroma

Printed on: 02/07/23



## Abstract Archives of the RSNA, 2022

MKEE-118

### Extensor Pollicis Longus: Imaging Review of Anatomy, Function and Pathology

Sunday, Nov. 27 8:00AM - 9:00AM Room: Learning Center - MK

#### Participants

Cedric Bohyn, MD, Antwerp, Belgium (*Presenter*) Nothing to Disclose

#### TEACHING POINTS

1. Learn normal anatomy and variants  
2. Learn the EPL's function  
3. How to image and normal findings  
4. Learn specific pathology:-  
Tenosynovitis- Distal intersection syndrome- Tendon tear- Delayed tendon rupture- Tendon subluxation and dislocation- Tendon entrapment

#### TABLE OF CONTENTS/OUTLINE

1. Anatomy, variants and associated structures:- Extensor Pollicis Longus- Lister's tubercle- Extensor retinaculum- Sagittal band of the first metacarpal joint  
2. Function  
3. Imaging Considerations  
3. Dysfunction/Pathology- Tenosynovitis- Distal intersection syndrome- Tendon tear- Delayed tendon rupture- Tendon subluxation and dislocation- Tendon entrapment

Printed on: 02/07/23

## Abstract Archives of the RSNA, 2022

MKEE-119

### Anything is Possible if You've Got Enough Nerve! Ultrasound (US) Approach to the Upper Limb Nerves

Sunday, Nov. 27 8:00AM - 9:00AM Room: Learning Center - MK

#### Participants

Michaela Cellina, (*Presenter*) Nothing to Disclose

#### TEACHING POINTS

To show the US approach to the nerves of the upper limb, involving the technique, patient's positioning, and anatomical landmarks. To describe dimensional and echo-structural characteristics of non-pathological nerves.

#### TABLE OF CONTENTS/OUTLINE

Thanks to its spatial resolution, wide availability, and possibility of real-time and dynamic evaluation, US is the first level exam for the peripheric nerves study, but its use is still limited by a lack of knowledge and expertise. One of the most common indications is suspected nerve entrapment (e.g. carpal and cubital tunnel syndromes). Peripheral nerves should be studied with high-frequency linear array probes. Nerves are usually identified on the axial planes in defined anatomical landmarks. Normal nerves show a fascicular, honeycomb appearance in the short axis and are surrounded by hyperechoic connective tissue. In the long axis, the nerve aspect is coarse and hypoechoic. Important landmarks for median nerve identification are the brachial artery in the upper arm and elbow, the flexor digitorum profundus and flexor digitorum superficialis in the forearm and the carpal tunnel in the wrist. Cross-sectional area (CSA) at three sites of the median nerve ranges from 5.38 to 8.43 mm<sup>2</sup>. The ulnar nerve is evaluated posteriorly to the brachial artery in the upper arm, at the level of the medial epicondyle of the elbow and the pisiform bone of the wrist. CSA at various points for the ulnar nerve ranges from 2.76 to 5.21 mm<sup>2</sup>. The radial nerve is assessed at the level of the arm-spiral sulcus on the posterior aspect of the humerus and has a normal CSA of 4.72 mm<sup>2</sup>. The thickening of the nerve sheath is a very common finding in the main demyelinating neuropathies, both hereditary and acquired.

Printed on: 02/07/23



## Abstract Archives of the RSNA, 2022

MKEE-12

### Strong as Your Weakest Link: The Kinetic Chain and Pitching Injuries of the Elbow

Sunday, Nov. 27 8:00AM - 9:00AM Room: Learning Center - MK

#### Participants

Akwasi Opoku, MD, Nashville, TN (*Presenter*) Nothing to Disclose

#### TEACHING POINTS

The "kinetic chain" is the coordinated translation of force and motion from the lower extremity/core into the upper extremity during pitching. Any deviation-abnormal anatomy, physiology, or mechanics- places increased forces across joints, predisposing to injury, especially of the elbow. This multimodality imaging review of repetitive valgus stress injury of the elbow in pitchers emphasizes important imaging findings for surgical intervention. Intra-operative correlation is provided. After viewing this exhibit, the learner should be able to: 1) Understand the biomechanics of pitching, including the concept of the kinetic chain, and recognize potential chain disruptors. 2) Recognize patterns of valgus injury of the elbow in pitchers. 3) Discuss important preoperative imaging findings for ulnar collateral ligament and osteochondral injuries.

#### TABLE OF CONTENTS/OUTLINE

Introduction: (1) Biomechanics of pitching: kinetic chain (2) Deviations in the kinetic chain (anatomy, physiology, mechanics) Elbow injury of the elite pitcher: Repetitive valgus overload (1) Medial Tensile force overload: UCL and common flexor tendon origin) (a) anatomy (b) pathology (tear grade and location, ligament edema, associated osseous changes) (c) Role of MR arthrography (2) Lateral compressive force overload: radiocapitellar joint (a) anatomy (capitellar bare area mimic) (b) pathology (osteochondral injury, Panner's disease) (3) Valgus extension overload (a) pathology (asymmetric osteoarthritis, ulnohumeral impaction) (4) Management of elbow injury: important imaging findings (a) surgical vs non-surgical (b) surgical technique

Printed on: 02/07/23

## Abstract Archives of the RSNA, 2022

MKEE-120

### Pointing to the Problem: A Comprehensive Approach to Finger Disorders

Sunday, Nov. 27 8:00AM - 9:00AM Room: Learning Center - MK

#### Participants

Augusto Altoe, Rio de Janeiro, Brazil (*Presenter*) Nothing to Disclose

#### TEACHING POINTS

1. To understand the anatomical basis involved in finger injuries; 2. To describe the imaging patterns of the finger pathologies; 3. To recognize common and uncommon finger disorders.

#### TABLE OF CONTENTS/OUTLINE

1- Background. 2- MRI acquisition considerations. 3- Finger ligaments; a. Review of the finger ligaments; b. Collateral ligament injuries of the finger; c. Locked metacarpophalangeal joint; d. Ulnar collateral ligament tears of the thumb; e. Volar plate injuries. 4- Flexor tendons and pulley system; a. Review of the flexor tendons anatomy and pulley system; b. Flexor tendon injuries and lacerations; c. Pulley injuries; d. Trigger finger. 5 - Extensor mechanism; a. Review of the extensor mechanism anatomy; b. Terminal extensor tendon injury (Mallet Finger); c. Central slip injury; d. Sagittal band injury. 6- Miscellaneous; a. Macrodystrophia lipomatosa; b. Acro-osteolysis; c. Palmar fibromatosis (Dupuytren's contracture); d. Tenosynovial giant cell tumor; e. Fibroma of the tendon sheath. 7 - Take home messages.

Printed on: 02/07/23

## Abstract Archives of the RSNA, 2022

MKEE-121

### Talk to the Hand - Ultrasound evaluation of Tendon, Ligament, and Support Structure Injury in the Hand with MRI Correlation

Sunday, Nov. 27 8:00AM - 9:00AM Room: Learning Center - MK

#### Awards

**Cum Laude**

#### Participants

Peter Hoeksema, MD, Detroit, MI (*Presenter*) Nothing to Disclose

#### TEACHING POINTS

1. Normal appearance of the flexor and extensor tendons of the hand on ultrasound. Review of scanning technique to optimize imaging of desired structures. Discussion of normal anatomy and insertion of tendons. Review of the pulleys on the flexor surfaces of the hand. Discussion of the extensor hood and sagittal bands. Review of the UCL at the first MCP joint. 2. Ultrasound examples of injury involving the FDP, and FDS. Ultrasound example of pulley abnormalities with trigger finger. Concurrent MRI examples of pathology demonstrated on US. 3. Ultrasound examples of injury extensor tendons. Example of sagittal band injury with dynamic subluxation of the tendon. Concurrent MRI examples. 4. Ultrasound examples of UCL injuries (partial and full thickness tear). Example of a Stener type lesion.

#### TABLE OF CONTENTS/OUTLINE

- Anatomy and Imaging Review  
o Review of optimal imaging technique for the flexor and extensor tendons. Review of associated normal anatomy  
o Review of the normal location of the flexor pulleys and imaging appearance  
o Review of optimal position and technique to visualize the UCL of the thumb  
- Volar Pathology with radiographic and MRI correlates as available  
o Ultrasound examples of FDP/FDS tendon tears with static and dynamic images  
o Ultrasound of injury to the flexor pulley apparatus. Dynamic US imaging of trigger finger  
- Dorsal Pathology with radiographic and MRI correlates as available  
o Ultrasound example of extensor tendon tear  
o Ultrasound examples of sagittal band injury with dynamic examples of tendon subluxation  
- UCL  
o Example of injury to the thumb UCL on ultrasound with MRI examples  
o Example of Stener lesion on ultrasound

Printed on: 02/07/23

## Abstract Archives of the RSNA, 2022

MKEE-122

### Hypermobility Syndrome - Findings on an Underestimated Diagnosis of Carpal Instability Non-dissociative by the Radiologist

Sunday, Nov. 27 8:00AM - 9:00AM Room: Learning Center - MK

#### Participants

André Henrique Toledo, Campinas, Brazil (*Presenter*) Nothing to Disclose

#### TEACHING POINTS

Carpal instability is a complex and heterogeneous clinical condition. Management requires accurate identification of the structural lesion involved. Midcarpal instability is a form of non-dissociative carpal instability and can be caused by various combinations of extrinsic ligament injuries with abnormal kinematics between the carpal rows. Such instability is related to biomechanical alterations of multiple causes that, if not identified and treated in a timely manner, will lead to gradual joint collapse. It is important to note that unstable wrist initially does not show relevant signs on standard radiographs and studies such as Magnetic resonance imaging (MRI) and MRI arthrography can detect initial findings of instability. In more advanced stages, carpal instability can progress to static wrist misalignment and osteoarthritis, both of which are associated with significant morbidity and disability. To prevent complications and joint sequelae, the radiologist must be aware of this challenge for the early and accurate diagnosis of carpal instability as an important entity, but often undervalued and remembered.

#### TABLE OF CONTENTS/OUTLINE

Role of the Radiologist - What differential diagnosis would you think? - Step by step in imaging and classic instability signs - Classification and what to look for Differential diagnosis review - is there room for hypermobility syndrome? - Carpal instability x joint hypermobility syndrome - What to expect? - Take home message.

Printed on: 02/07/23



## Abstract Archives of the RSNA, 2022

MKEE-124

### Spectral CT Imaging of the Bone Marrow: How To Do It'

Sunday, Nov. 27 8:00AM - 9:00AM Room: Learning Center - MK

#### Participants

Bernhard Petritsch, MD, Wuerzburg, Germany (*Presenter*) Research Consultant, Siemens AG

#### TEACHING POINTS

To review the indications, contraindications and limitations of spectral CT imaging in terms of photon counting detector computed tomography (PCD-CT) and conventional energy integrating detector (EID) dual-energy computed tomography (DECT) for bone marrow imaging. To learn about the basic physical principles of PCD-CT and conventional DECT imaging with emphasis on bone marrow applications. To interpret spectral bone marrow CT scans of healthy subjects, patients with acute fractures or malignant bone marrow infiltration. To highlight the potential benefits of spectral CT investigation as a comprehensive examination of osseous morphology and additional bone marrow information.

#### TABLE OF CONTENTS/OUTLINE

A. Basic principles of photon counting detector (PCD) and energy integrating detector dual-energy computed tomography (DECT).B. Technical differences in data acquisition: PCD CT vs. Single-Source EID vs. Dual-Source EID CT-scanners (differences between 1st-3rd generation dual-source scanners).C. Post-processing: Material-decomposition algorithm, creation of VNCa ("virtual non-calcium") images.D. Data acquisition: Parameter settings for PCD and dual-energy CT of the extremities, spine and pelvis.E. Current applications of spectral CT for the detection of acute fractures and malignant bone marrow infiltrations (e.g. in multiple myeloma): examples in the spine, pelvis and extremities.F. Pitfalls and limitations of spectral bone marrow Imaging; alternative imaging modalities.

Printed on: 02/07/23



## Abstract Archives of the RSNA, 2022

MKEE-125

### Don't Let the Foot Drop: Review of the Anatomy, Imaging, and Pathologies of the Sciatic Nerve and its Branches

Sunday, Nov. 27 8:00AM - 9:00AM Room: Learning Center - MK

#### Participants

Andrew Liu, MD, (*Presenter*) Nothing to Disclose

#### TEACHING POINTS

Foot drop is a common reason for consultation and deserves a quick clinical and radiological assessment. Knowledge of the anatomy, the course and the division of the sciatic nerve and its branches is required so that the radiologist can image the adequate anatomical area whether by ultrasound or by MR imaging. The advantages of ultrasound lie in the possibility to survey the entire nerve and its branches in a short period of time. However, this modality remains operator-dependent. Through this Education Presentation, a review of the anatomy of the sciatic nerve and its branches, the different modern modalities available, and pathologies that might affect the sciatic nerve and its branches nerve is propose.

#### TABLE OF CONTENTS/OUTLINE

Revise the anatomy of the sciatic nerve, the common peroneal nerve, the superficial and deep peroneal nerves Understand, revise and optimize cross-section imaging (MRI neurography and ultrasound). Navigate through traumatic (traumatic neuroma, post-amputation neuroma), tumoral (BNPST, MPNST, neurofibromatosis, etc.), and miscellaneous pathologies (intra-neuronal and extra-neuronal ganglion cyst) of the lower extremity nerves.

Printed on: 02/07/23



## Abstract Archives of the RSNA, 2022

MKEE-126

### Musculoskeletal Ultrasound: No Pain, No Gain - A Compilation of Techniques and Lesions

Sunday, Nov. 27 8:00AM - 9:00AM Room: Learning Center - MK

#### Participants

Cleiton Freitas, MD, Sao Paulo, Brazil (*Presenter*) Nothing to Disclose

#### TEACHING POINTS

A) Musculoskeletal ultrasound should be based on systematized image acquisition techniques and on the recognition of multiple pathologies. B) Importance of documenting and visualizing the appropriate musculoskeletal anatomical structures, focusing on teaching the Radiology Resident physicians the most recommended techniques. C) For each analyzed body segment, pathologies of significant clinical importance, including common and uncommon pathologies will be analyzed. D) More than 40 pathologies and their differential diagnoses will be analyzed, because no pain no gain.

#### TABLE OF CONTENTS/OUTLINE

- Introduction- Anatomy review- Ultrasound imaging capture sequence- Lesions and their differential diagnosis- Take-home messages

Printed on: 02/07/23

## Abstract Archives of the RSNA, 2022

MKEE-127

### Imaging of Postoperative Pectoralis Major Tendon: What Radiologists Need to Know

Sunday, Nov. 27 8:00AM - 9:00AM Room: Learning Center - MK

#### Participants

Luana Maciel, (*Presenter*) Nothing to Disclose

#### TEACHING POINTS

- To evaluate the appearance of pectoralis major tendon after surgical correction.
- To assess the MRI aspects of the pectoralis major muscle tendon after surgical repair, using different approaches, such as anchors, cortical buttons, bone holes or surgical reconstruction using autologous graft (semitendinosus, gracilis) or allograft.

#### TABLE OF CONTENTS/OUTLINE

- Anabolic steroids usage by weightlifting athletes gym work out men has led to a significant increase in the incidence of pectoralis major injuries.
- Ecchymosis and local hematomas followed to those lesions limits clinical evaluation and make imaging crucial for injury graduation and repair planning. Magnetic resonance imaging and ultrasonography are established as methods of choice.
- Surgical treatment is the best approach for pectoralis major injuries.
- Humeral tendon reinsertion using either surgical wires or metallic anchors are chosen for acute lesions and orthopedic screws for chronic ones. Old injuries with tendon retraction may require reconstruction with autologous graft, commonly from the hamstrings or allograft.
- Surgical treatment reported a lower degree of strength loss compared to conservative conduct. In addition, it was superior regarding aesthetic and functional gain, with a high rate of sports activity return.
- Imaging plays an important role not only for diagnose and surgical planning but also to postoperative follow-up, depicting early changes not seen in clinical evaluation.

Printed on: 02/07/23

## Abstract Archives of the RSNA, 2022

MKEE-128

### Normal and Abnormal MRI Finding of Rotator Interval Correlated with Arthroscopy

Sunday, Nov. 27 8:00AM - 9:00AM Room: Learning Center - MK

#### Participants

Ji Yoon Lee, (*Presenter*) Nothing to Disclose

#### TEACHING POINTS

1. To describe normal MRI anatomy of rotator interval, with associated arthroscopy finding. 2. To present MRI finding of rotator interval pathology, correlation with arthroscopy. 3. To present associated findings at long head of biceps tendon and subscapularis tendon, correlation with arthroscopy. 4. To enhance rotator interval image interpretation and let better coordination between radiologists and orthopedic surgeons in terms of surgical planning or retrospective image review.

#### TABLE OF CONTENTS/OUTLINE

1. Normal MRI and arthroscopy finding of rotator interval. 2. Abnormal MRI findings of rotator interval, including biceps tendon tear and subluxation, subscapularis tendon lesion, synovitis, adhesive capsulitis are presented, with corresponding arthroscopy image.

Printed on: 02/07/23



## Abstract Archives of the RSNA, 2022

MKEE-129

### The Repaired Rotator Cuff: Normal and Abnormal Appearance with Focus on US and MRI

Sunday, Nov. 27 8:00AM - 9:00AM Room: Learning Center - MK

#### Awards

Cum Laude

#### Participants

Paola Kuenzer Goes, MD, Sao Paulo, Brazil (*Presenter*) Nothing to Disclose

#### TEACHING POINTS

The repaired rotator cuff frequently appears abnormal on ultrasound (US) and magnetic resonance imaging (MRI). While the appearance of tendons and surrounding tissues typically normalize, they can demonstrate clinically insignificant abnormal imaging appearances for longer than 6 months. US and MRI are useful in the postoperative assessment of the rotator cuff, not only for evaluation of the integrity of the rotator cuff, but also for detecting hardware complications and ruling out other sources of shoulder pain. The objectives of this educational exhibit are: 1. Briefly review the US and MRI findings of the normal postoperative rotator cuff 2. Discuss US and MRI findings of various types of repair and fixation 3. Illustrate US and MRI findings of post rotator cuff repair complications according to three potential sources (tendon, hardware and soft tissues)

#### TABLE OF CONTENTS/OUTLINE

Normal postoperative rotator cuff • Types of repair Which tendon(s) was repaired, method of repair (tendon suture, reinsertion, transfer of tendons or grafts), and types of fixation (transosseous, double-row, double-row bridged) • US findings • Early MRI findings • Late MRI findings Complications • Tendon Partial re-tear Complete re-tear • Hardware complications Fracture Migration • Soft tissues Infection Bursitis Adhesive capsulitis

Printed on: 02/07/23



## Abstract Archives of the RSNA, 2022

MKEE-13

### Imaging Review of the Healing Process in Sport Muscle Injuries

Sunday, Nov. 27 8:00AM - 9:00AM Room: Learning Center - MK

#### Awards

Identified for RadioGraphics

#### Participants

Jaime Isern, PhD, (*Presenter*) Nothing to Disclose

#### TEACHING POINTS

1. To review the mechanisms of muscle injury, repair and regeneration. 2. To present the imaging technique of choice for the healing process study. 3. To describe the MRI findings of reparative changes of a muscle tear. 4. To show the muscle adaptive changes by MRI during the healing process. 5. To show the imaging findings that suggest aberrant progression of the healing process.

#### TABLE OF CONTENTS/OUTLINE

Physiological mechanism of the healing process after muscle sport injury. MRI protocol to assess the reparative process of sports muscle injury. Review of imaging findings of the healing process and adaptive changes. Discuss the influence of MRI findings on the therapeutic decision.

Printed on: 02/07/23



## Abstract Archives of the RSNA, 2022

MKEE-130

### Postoperative Rotator Cuff (Surgical Indications, Normal and Pathological Postoperative Findings) - A Practical Guide for Radiologists

Sunday, Nov. 27 8:00AM - 9:00AM Room: Learning Center - MK

#### Participants

Camila Munaro I, MD, (*Presenter*) Nothing to Disclose

#### TEACHING POINTS

1.To review the anatomy of the rotator cuff and discuss common tendon tears2.To review surgical procedures and indications for treatment of rotator cuff tears3. To review the challenging clinical and radiologic scenario of postoperative shoulder4.To describe normal expected postoperative appearances of the rotator cuff tendons5. To discuss the most common pathological postoperative findings, including recurrent tears, infection, anchor migration, nerve injury and muscle degeneration.

#### TABLE OF CONTENTS/OUTLINE

1 - Anatomy of rotator cuff2 - MR Imaging of rotator cuff tears3 - Treatment of rotator cuff tears4 - Surgical indications5 - MR evaluation of the expected postoperative rotator cuff6 - Recurrent tears7 - Infection8 - Anchor migration9 - Nerve injury10 - Muscle atrophy and fatty degeneration

Printed on: 02/07/23



## Abstract Archives of the RSNA, 2022

MKEE-131

### Multimodality Review of Sclerotic Lesions in the Spine

Sunday, Nov. 27 8:00AM - 9:00AM Room: Learning Center - MK

#### Participants

William Holden, MD, BS, (*Presenter*) Nothing to Disclose

#### TEACHING POINTS

Sclerotic lesions of the spine can be challenging to characterize due to their broad differential and overlapping imaging features. A methodical approach is necessary when formulating a differential diagnosis for these lesions. This educational exhibit will review patterns of focal, multifocal, and diffuse vertebral body sclerosis on multiple modalities, including plain radiographs, CT, MRI, MDP bone scan, and FDG-PET. This review will provide a framework for evaluating different categories of osseous sclerosis, including infectious/inflammatory, neoplastic, metabolic, and developmental causes. Familiarity with specific imaging patterns and assessment of pertinent clinical information will allow the radiologist to more accurately interpret sclerotic lesions of the spine, and recommend appropriate follow-up and additional imaging evaluation.

#### TABLE OF CONTENTS/OUTLINE

1. Provide an overview of modalities used for the evaluation of sclerotic bone lesions, including plain radiographs, CT, MRI, MDP bone scan, and FDG-PET. 2. Review common and uncommon cases of focal, multifocal, and diffuse sclerotic vertebral lesions. a. Cases will include 3-4 examples from each category: i. Infectious/inflammatory ii. Neoplastic iii. Metabolic iv. Developmental b. For each lesion, the discussion will include: i. Multimodality imaging findings ii. Pertinent clinical history iii. Diagnostic pearls 3. Provide a diagnostic algorithm for the evaluation of sclerotic vertebral lesions.

Printed on: 02/07/23

## Abstract Archives of the RSNA, 2022

MKEE-132

### Sacral Lesion - Recognizing the Most Common Lesions

Sunday, Nov. 27 8:00AM - 9:00AM Room: Learning Center - MK

#### Participants

Andre Y. Aihara, MD, PhD, Sao Paulo, Brazil (*Presenter*) Nothing to Disclose

#### TEACHING POINTS

The purpose of this study is:- Review the normal anatomy and imaging appearance of the sacrum, using CT and MR images.- Didactically discuss sacrum lesion, dividing into 4 categories: Tumors, trauma, infections, and non-infectious inflammatory arthropathies.- Elucidate the typical findings of sacral tumors, frequent locations, age and sex distribution, and characteristic imaging findings.

#### TABLE OF CONTENTS/OUTLINE

The sacrum is a structure located in the pelvis with an important role in spinal biomechanics. It is composed of multiple tissues: cartilage, bone marrow, nerves, meninges and notochord remnants. This diversity of components can originate different primary tumors, most of them with predicted location and imaging findings. Since the sacrum is rich in hematopoietic bone marrow, metastasis is frequent. Sacral fractures can result from high-energy trauma or be related to low-energy impact, as in insufficiency stress fractures. The typical H-shaped pattern can be seen in bilateral sacral insufficiency fractures. Most sacrum infection is by continuity spread, common with the infection of the pelvic adjacent organs. Finally, it is important to remember inflammatory arthropathy and those resulting from local mechanical overload.

Printed on: 02/07/23

## Abstract Archives of the RSNA, 2022

MKEE-133

### Atlantoaxial Injuries: Don't Lose Your Head!

Sunday, Nov. 27 8:00AM - 9:00AM Room: Learning Center - MK

#### Awards

Identified for RadioGraphics

#### Participants

Leticia Morimoto, MD, Sao Paulo, Brazil (*Presenter*) Nothing to Disclose

#### TEACHING POINTS

The purpose of this study is:• Revisit the anatomy of the atlantoaxial joint, highlighting the ligamentous structures• Review with didactic cases the main atlantoaxial fractures and its associated injury mechanisms• Present several cases of non-traumatic lesions of the atlantoaxial joint, including inflammatory, infectious and tumoral conditions

#### TABLE OF CONTENTS/OUTLINE

- Introduction and overview of the atlantoaxial joint, including normal anatomy with didactic illustration.
- Demonstrate the ligamentous anatomy and how to recognize it on MRI.
- Demonstrate didactically the radiographic, CT and MRI findings of several traumatic atlantoaxial traumatic injuries.
- Overview the classifications for atlantoaxial trauma injuries.
- Review the management treatment options for each injury, and their post-operative exams, highlighting what the radiologist should look for.
- Challenging cases of non-traumatic diseases, including rheumatoid arthritis, villonodular synovitis, infections, neurofibromatosis, Langerhans cell histiocytosis, and others.
- Summary.

Printed on: 02/07/23



## Abstract Archives of the RSNA, 2022

MKEE-134

### Bone-RADS Classification - What the Radiologist Needs to Know

Sunday, Nov. 27 8:00AM - 9:00AM Room: Learning Center - MK

#### Participants

Verena Pires, MD, (Presenter) Nothing to Disclose

#### TEACHING POINTS

To review the Bone-RADS (bone reporting and data system) classification with a simple guide using examples. To provide radiologists with a general overview enabling them to understand and interpret Bone-RADS in different lesions.

#### TABLE OF CONTENTS/OUTLINE

Incidental solitary bone lesions are frequently encountered on computed tomography (CT) and magnetic resonance imaging (MRI) in routine clinical practice. Despite the prevalence of these unexpected lesions, clear and consistent guidelines for their management have not been defined in the literature. The purpose is to present algorithms for the diagnostic management of solitary bone lesions incidentally encountered on CT and MRI in adults. For risk stratification, the Bone-RADS recommends four categories, incorporating the range of benign to suspicious for malignancy or need for treatment (Bone-RADS1, leave alone; Bone-RADS2, perform different imaging modality; Bone-RADS3, perform follow-up imaging; Bone-RADS4, biopsy and/or oncologic referral). Two algorithms for CT based on lesion density (lucent or sclerotic/mixed) and two for MRI allow the user to arrive at a specific Bone-RADS management recommendation. Representative cases are provided to illustrate the usability of the algorithms. The ultimate goal is to optimize bone lesion outcomes while minimizing unnecessary surgical procedures in patients at low risk of malignancy and to provide a management recommendation for each risk category. Then, this classification can standardize lesions and decrease ambiguity reporting to enhance communication among the multidisciplinary team.

Printed on: 02/07/23



## Abstract Archives of the RSNA, 2022

MKEE-135

### The Role of Conventional Radiography in the Diagnosis of Bone Tumors

Sunday, Nov. 27 8:00AM - 9:00AM Room: Learning Center - MK

#### Awards

Identified for RadioGraphics

#### Participants

Abel Gonzalez Huete, MD, Madrid, Spain (*Presenter*) Nothing to Disclose

#### TEACHING POINTS

1. To provide an educational review of bone tumors and their appearance in conventional radiography. 2. To review differential diagnosis and discuss a systematic approach to the diagnosis of bone tumors and tumor-like lesions based on conventional radiography features and clinical presentation.

#### TABLE OF CONTENTS/OUTLINE

1. Introduction. 2. Age of presentation. 3. Review of imaging findings. - Opacity (lytic, sclerotic, mixed). - Margin and destruction patterns. - Periosteal Reaction. - Cortical Involvement. - Mineralization (chondroid matrix, osteoid matrix). - Location: skeleton, longitudinal (epiphyseal, metaphyseal, diaphyseal), transverse (centric, eccentric, cortical, juxtacortical). - Number (solitary, multiple, polyostotic). - Soft Tissue Component. 4. Sample cases and mimics. 5. Summary.

Printed on: 02/07/23



## Abstract Archives of the RSNA, 2022

MKEE-136

### Whole-body Imaging on Multiple Myeloma: Imaging Modalities and Applications

Sunday, Nov. 27 8:00AM - 9:00AM Room: Learning Center - MK

#### Participants

Henrique Lino, MD, Sao Paulo, Brazil (*Presenter*) Nothing to Disclose

#### TEACHING POINTS

Multiple myeloma is the most common primary tumour of bone with an incidence of 10 per 100,000. Multiple myeloma whole-body imaging techniques (MM-WB) can help detect subclinical lesions and determine early treatment, increasing prognostic and avoiding fractures and other complications.

#### TABLE OF CONTENTS/OUTLINE

Introduction: The MM-WB modalities are x-ray skeletal survey, computed tomography (CT), magnetic resonance (MRI), computed tomography 18F-fluorodeoxyglucose positron emission tomography (PET-CT). Objectives: (1) to review the use of MM-WB. (2) to exemplify cases and compare the imaging modalities. Methods: We queried cases to illustrate the imaging methods. Discussion: Although skeletal survey is the reference method, it has a high false negative rate (30-70%). Axial methods have a higher sensitivity (68-100 %) for the condition. The general diagnostic criteria for axial methods, by the International Myeloma Working Group, is one or more focal lesions with 5 mm or more, with osteolytic behaviour. Among these methods, MRI has the advantage of no radiation, and it has the best diagnostic performance for the evaluation of soft tissue lesions and bone marrow compromise as well it has a high specificity from 83 to 100%, and also treatment response (as well as PET-CT). Conclusion: multiple modalities of MM-WB can detect focal and diffuse disease, quantify burden, and predict treatment response as well it is able to detect mechanical complications.

Printed on: 02/07/23



## Abstract Archives of the RSNA, 2022

MKEE-137

### Sacral Insufficiency Fractures in Cancer: Is There a Met Hiding in Plain Sight?

Sunday, Nov. 27 8:00AM - 9:00AM Room: Learning Center - MK

#### Participants

Kaustav Bera, MD, Cleveland, OH (*Presenter*) Nothing to Disclose

#### TEACHING POINTS

1. Review the different causes of sacral insufficiency fractures (SIFs)2. Review the various imaging modalities used to diagnose SIFs3. Discuss the role of imaging findings along with clinical and laboratory findings to determine the cause of the SIFs4. Review ways to differentiate SIFs from metastatic lesions of th sacrum5. Discuss management and outcomes of SIFs

#### TABLE OF CONTENTS/OUTLINE

1. Introduction and history of sacral insufficiency fractures (SIF) as an entity2. Epidemiology and demographics of SIF3. Risk factors for SIF4. Clinical History and symptoms in SIF5. Association of SIF with disease conditions (Renal osteodystrophy, Rheumatoid Arthritis, Paget disease)6. Different imaging modalities that help in diagnosing SIF 7. Different etiologies that cause SIFa) Age induced/Osteoporoticb) Inflammatory arthropathyc) Radiation inducedd) Hormone inducede) Other Drug induced (Steroids/Bisphosphonate)8. Cancers that often metastasize to the sacrum and can mimic SIF9. Imaging findings coupled with clinical and laboratory parameters that help you distinguish between different etiologies of SIF as well as contrast it from Metastatic disease10. Management of SIF11. Prognosis and clinical outcome of SIF

Printed on: 02/07/23



## Abstract Archives of the RSNA, 2022

MKEE-138

### The Role of Cinematic Rendering in the Evaluation of Complex Vascular Injury of the Lower Extremities: How We Do It

Sunday, Nov. 27 8:00AM - 9:00AM Room: Learning Center - MK

#### Participants

Elliot Fishman, MD, Owings Mills, MD (*Presenter*) Co-founder, HipGraphics, Inc; Stockholder, HipGraphics, Inc; Institutional Grant support, Siemens AG; Institutional Grant support, General Electric Company; Consultant, Exact Sciences Corporation; Consultant, Imaging Endpoints

#### TEACHING POINTS

1. CT with CTA is the state of the art for the evaluation of the patient with lower extremity trauma regardless of whether the trauma is an MVA, gunshot wound or stabbing or simply a fall. 2. diagnosis of injury is but step one in patient management and the role of 3D has classically been to help with management decisions by improving understanding of the true extent of the injury. 3. Cinematic rendering is an advanced form of volume rendering which is ideal in the trauma setting by visualization of muscle and soft tissue, the vascular map and underlying bony structures. When optimized it provides a clear understanding of the "personality" of the specific injury. 4. the use of Cinematic Rendering provides an opportunity to provide extra value in the interpretation and management of complex trauma to the lower extremities. A paradigm for use of cinematic rendering is addressed.

#### TABLE OF CONTENTS/OUTLINE

1. Imaging protocols for lower extremity trauma including the role of dual energy CT. 2. imaging protocols for using cinematic rendering for the range of lower extremity trauma. 3. analysis of case studies showing the added value of cinematic rendering in trauma of soft tissue/muscle, the bony anatomy and the vascular map. Specific presets for optimizing workflow and analysis are presented. 4. case studies showing the impact of cinematic rendering on patient management are presented, and discussed. 5. role of Cinematic Rendering for patient management decisions is addressed and illustrated as well. potential pitfalls and limitations of Cinematic Rendering are also discussed and illustrated.

Printed on: 02/07/23



## Abstract Archives of the RSNA, 2022

MKEE-139

### Staying Afloat With the Competitive Swimmer - Common and Uncommon Injuries

Sunday, Nov. 27 8:00AM - 9:00AM Room: Learning Center - MK

#### Participants

Sonja Opper, DO, Pittsburgh, PA (*Presenter*) Nothing to Disclose

#### TEACHING POINTS

1. Athletic injuries have been well documented in the literature, particularly in mainstream sports such as football, soccer and baseball. A sport that is poorly represented in the literature is swimming. 2. Swimmers are susceptible to chronic types of stress on their bodies as a result of varying repetitive physical movements, as well as unique environmental and chemical exposures. The majority of swimming related injuries are a result of repetitive microtrauma in the shoulders, elbows, and knees. 3. Acute injuries often relate to the flip turn, starts/finishes and the dive where there are rapid accelerations and decelerations as well as the potential for barotrauma while submerged. 4. In this presentation we will review common and uncommon injuries in avid swimmers and review the mechanism of injury in these athletes with special attention to the physiology of different strokes.

#### TABLE OF CONTENTS/OUTLINE

1. Review the 4 basic strokes (freestyle, backstroke, breaststroke, and butterfly) and flip turns with videos illustrating the mechanics, areas of stress, and potential for injuries. 2. Review imaging of the common injuries related to competitive swimmers. a. Shoulder injuries b. Knee injuries c. Foot injuries d. Hip injuries 3. Discuss the environmental and chemical exposures that predispose swimmers to unique injuries. 4. Interactive cases

Printed on: 02/07/23



## Abstract Archives of the RSNA, 2022

MKEE-14

### Let's be "Franc" about the Lisfranc: A Review of Anatomy, Pathology, and Disease Mimics

Sunday, Nov. 27 8:00AM - 9:00AM Room: Learning Center - MK

#### Participants

Sirui Jiang, MD, PhD, Cleveland, OH (*Presenter*) Nothing to Disclose

#### TEACHING POINTS

1. Review the anatomy of the Lisfranc joint complex  
2. Review the clinical presentation and causes of injuries to the Lisfranc joint complex  
3. Multimodality imaging overview of Lisfranc joint complex injuries including common measurements and hallmark findings  
4. Discuss common radiographic mimics of Lisfranc injuries  
5. Overview of orthopedic management of Lisfranc injuries

#### TABLE OF CONTENTS/OUTLINE

Background-Image-based anatomy review of the Lisfranc joint complex-Incidence of Lisfranc injuries and diagnostic misses  
Etiology of Disease -Biomechanical/Traumatic Causes-Soft tissue injuries without dislocation-Bony injury with mild displacement -Bony injury with marked displacement-Clinical Presentation-Physical Examination  
Imaging Studies-Radiographs-AP, lateral, and oblique views during weight-bearing-How to identify dislocation of the Lisfranc joint complex-Spectrum of findings in alternative views - Spontaneous reduction during radiographic evaluation-Other Imaging Modalities-CT-MRI-Ultrasound  
Common Mimics -Vascular calcifications -Os intermetatarsum Complications-Post-traumatic arthrosis-Instability-Chronic pain  
Management-Non-operative management-Surgical fixation-Repeat imaging-Post-operative physical therapy

Printed on: 02/07/23



## Abstract Archives of the RSNA, 2022

MKEE-140

### Traumatic Instabilities of the Cervical Spine: What the Radiologists Need to Know

Sunday, Nov. 27 8:00AM - 9:00AM Room: Learning Center - MK

#### Participants

Alan Strapasson, MD, (*Presenter*) Nothing to Disclose

#### TEACHING POINTS

The purpose of this exhibit is: 1. Review the anatomy in the different imaging methods and their main variations relevant to trauma assessment. 2. Review measurement techniques. 3. Correlate the trauma mechanism with the main injuries related to each one of them. 4. Address the most common ligament injuries with a focus on MRI. 5. Discuss atlantoaxial dissociation and odontoid fracture. 6. Classification of lesion instability (Vaccaro, NEXUS).

#### TABLE OF CONTENTS/OUTLINE

1. Anatomy and assessment of CR, CT and MRI in adults and children and their main anatomical variations relevant to the assessment of trauma. 2. Measurement techniques: Wackenheim, Chamberlain, McGregor, Power Ratio, basion-axial interval, atlantodental interval. 3. Flexion injuries: wedge compression fracture, flexion teardrop fracture, anterior subluxation, bilateral facet dislocation, Clay Shoveler, anterior atlantoaxial dislocation. 4. Hyperflexion and rotation: unilateral facet displacement (locked facet). 5. Extension: hangman's fracture, teardrop fracture by extension. 6. Axial compression: Jefferson fracture, burst fracture. 7. Odontoid fracture. 8. Atlantoaxial Dissociation. 9. Ligament injuries: alar and transverse ligament. 10. Vaccaro Classification (2007), Harris. 11. Unstable fractures in order. 12. NEXUS Criteria.

Printed on: 02/07/23



## Abstract Archives of the RSNA, 2022

MKEE-141

### Myxofibrosarcoma Imaging with Pathological and Clinical Correlation

Sunday, Nov. 27 8:00AM - 9:00AM Room: Learning Center - MK

#### Participants

Robert W. Morris, MD, (*Presenter*) Nothing to Disclose

#### TEACHING POINTS

Myxofibrosarcoma is one of the most common sarcomas in older patients, but has only relatively recently been defined as a distinct pathological entity. There is also limited information about myxofibrosarcoma in the radiology literature. After viewing this exhibit, the viewer should be able to: 1. Describe the pathological features of myxofibrosarcoma. 2. Describe the typical imaging appearance of both low-grade and high-grade myxofibrosarcoma. 3. Discuss ancillary imaging and post-treatment imaging. 4. Recognize important features for staging, treatment and prognosis.

#### TABLE OF CONTENTS/OUTLINE

Table of Contents: 1. Myxofibrosarcoma overview 2. Pathology 3. Imaging characteristics 4. Low-grade myxofibrosarcoma 5. High-grade myxofibrosarcoma 6. Ancillary imaging and staging 7. Treatment 8. Post-treatment imaging 9. Prognosis 10. Conclusion

Printed on: 02/07/23

## Abstract Archives of the RSNA, 2022

MKEE-142

### Checkmate to Chest Wall Tumors: A Strategical Approach to Diagnosis

Sunday, Nov. 27 8:00AM - 9:00AM Room: Learning Center - MK

#### Participants

Rebeca Francelino, MD, (*Presenter*) Nothing to Disclose

#### TEACHING POINTS

The purpose of this exhibit is: 1. To review the most common tumors and their characteristic imaging findings. 2. To discuss the diagnosis and management of benign and malignant tumors. 3. To correlate the imaging findings and clinical clues on a systematic approach to help narrowing the differential diagnosis.

#### TABLE OF CONTENTS/OUTLINE

1- Institutional Protocol to evaluate the chest wall; 2- Epidemiological assessment of the main lesions and best imaging modality; 3- Benign bone and cartilaginous tumors: Osteochondroma; Fibrous dysplasia; Aneurysmal bone cyst (ABC); Giant cell tumor (GCT); Ossifying fibromyxoid tumor; Chondromyxoid fibroma 4- Malignant bone and cartilaginous tumors: Chondrosarcoma; Multiple Myeloma; Metastasis; Osteosarcoma 5- Benign soft tissue lesions: Hemangioma; Elastofibroma dorsi; Fibrous Hamartoma of Infancy; Lipoma; Schwannoma; Desmoid Tumor; Neurofibroma; Ganglioneuroma; Paraganglioma; Hemangiopericytoma 6- Malignant soft tissue lesions: Ewing sarcoma; Rhabdomyosarcoma; Synovial sarcoma; Pleomorphic sarcoma; Ganglioneuroblastoma; Neuroblastoma; Angiosarcoma; Leiomyosarcoma; Malignant fibrous histiocytoma (MFH); Malignant peripheral nerve sheath tumor; Dermatofibrosarcoma protuberans 7- Miscellaneous Brown Tumor

Printed on: 02/07/23

## Abstract Archives of the RSNA, 2022

MKEE-143

### 3D-MERGE MRI Sequence in the Assessment of Foot and Ankle Bone Abnormalities

Sunday, Nov. 27 8:00AM - 9:00AM Room: Learning Center - MK

#### Participants

Tatiane Rodrigues, MD, Sao Paulo, Brazil (*Presenter*) Nothing to Disclose

#### TEACHING POINTS

1) Discuss the use of MERGE MRI sequence in the assessment of bone abnormalities in the foot and ankle. 2) Discuss clinical applications of synthetic-CT based images on MERGE sequence in the foot and ankle through a case-based approach.

#### TABLE OF CONTENTS/OUTLINE

Different techniques have been used to generate MRI-based synthetic-CT and have demonstrated equivalence to conventional CT. While MRI has superior soft tissue contrast when compared to CT, abnormalities that usually manifest as areas of low-signal intensity on conventional MRI scans, such as fracture lines, are better depicted on CT. Both modalities may complement each other in the characterization of several musculoskeletal disorders. Performing CT in association with MRI not only increases costs but also exposes the patient to ionizing radiation. MERGE (Multiple Echo Recombined Gradient Echo, GE Healthcare) is a spoiled T2\*-weighted 3D sequence for spinal and musculoskeletal imaging, which has the acquisition and combination of multiple echoes with a high receiver bandwidth instead of using a single low bandwidth echo, that provides high resolution and isotropic images of the extremities with optimized contrast between the ligaments and soft tissue. The purpose of this work is to show the 3D-MERGE MRI sequence in the assessment of bone abnormalities of the foot and ankle in a case-based discussion. Radiologists need to be familiarized with MRI-based synthetic-CT techniques, such as MERGE, and their imaging findings to obtain an optimal evaluation of musculoskeletal conditions with the combination of conventional and innovative sequences.

Printed on: 02/07/23



## Abstract Archives of the RSNA, 2022

MKEE-144

### Shipwrecked: Spontaneous Osteonecrosis of the Navicular Bone

Sunday, Nov. 27 8:00AM - 9:00AM Room: Learning Center - MK

#### Participants

Juliana Sitta, MD, Jackson, MS (*Presenter*) Nothing to Disclose

#### TEACHING POINTS

To review the anatomy, joints, ligaments, function, and vascularization of the navicular bone. Discuss the clinical features and mechanism of pediatric and adult avascular necrosis of the navicular bone. Illustrate the imaging characteristics of navicular osteonecrosis and complications in multimodality imaging at different stages of the disease

#### TABLE OF CONTENTS/OUTLINE

Navicular bone osteonecrosis, also known as Kohler disease, is a relatively uncommon, self-limited abnormality with typically good prognosis. It differs in imaging presentation and prognosis from its adult counterpart, known as Mueller Weiss disease, which often results in progressive navicular bone deformity and midfoot biomechanical impairment. This educational exhibit aims to explore the anatomic predispositions of the navicular to osteonecrosis as well as the imaging features of these two pathologically similar entities that affect patients at opposite ends of the age spectrum. This educational exhibit provide an overview of the navicular bone anatomy, including common anatomic variants and mimickers, relationship with neighboring bones, function, and vascularization. We discuss imaging features, imaging anatomy, and potential complications in the pediatric and adult types of avascular osteonecrosis of the navicular bone. Multimodality imaging and didactic illustrations will explore the injury mechanism and presentation spectrum. The authors raise attention to the role of imaging in assessing potential secondary biomechanical complications and pitfalls.

Printed on: 02/07/23



## Abstract Archives of the RSNA, 2022

MKEE-145

### Working "Smarter" : A Review of Artificial Intelligence in Musculoskeletal Radiology

Sunday, Nov. 27 8:00AM - 9:00AM Room: Learning Center - MK

#### Participants

Vidya Sankar Viswanathan, MBBS, Shaker Heights, OH (*Presenter*) Nothing to Disclose

#### TEACHING POINTS

1. Define Artificial Intelligence (AI) and other commonly associated terminology  
2. Review current applications of FDA approved AI tools in Musculoskeletal (MSK) Radiology (diagnostics, image processing)  
3. Describe ways that integration of AI can improve clinical workflow  
4. Discuss future technologies in AI, including Radiomics and Autonomous AI  
5. Review limitations of AI, including challenges that need to be addressed for clinical translation of these tools.

#### TABLE OF CONTENTS/OUTLINE

1. Introduction - Define Artificial Intelligence (AI), Machine learning, Deep learning, Convolutional Neural Networks (CNN), Generative Adversarial Networks (GAN)  
2. Current applications of FDA approved AI tools in Musculoskeletal Radiology  
A. Image Processing/Quantification - Improved visualization - Surgical planning  
B. Computer-aided diagnosis  
3. Improved Clinical Workflow with AI  
A. Image Acquisition Time  
B. Study Triaging  
C. Image Interpretation Time  
D. Scheduling  
4. Future of AI  
A. Interpretive tools - Device placement assessment - Augment Radiology Assistants  
B. Non-interpretive tools - Reduce noise and artifacts - Enhance contrast - Improved visualization of pathology - Worklist Prioritization - Improving Radiology Resident Education  
C. Radiomics  
D. Autonomous AI  
5. Challenges  
A. Clinical - Reluctance toward implementation - Information/knowledge gap - Reimbursement strategies  
B. Medico-legal - Liability: Physician vs. software developer vs healthcare institution - Advocacy for guidelines and legislation

Printed on: 02/07/23



## Abstract Archives of the RSNA, 2022

MKEE-146

### The Role of MRI in Evaluation of Soft Tissue Lesions of the Hand and Fingers: An Imaging Review of the Common Differential Diagnoses, Artifacts and Normal Findings Which Can Simulate Disease

Sunday, Nov. 27 8:00AM - 9:00AM Room: Learning Center - MK

#### Participants

Cormac O'Brien, MRCPI, MRCP, Dublin 4, Ireland (*Presenter*) Nothing to Disclose

#### TEACHING POINTS

Soft tissue lesions of the hand and fingers are frequently encountered in everyday clinical practice. They can be detected incidentally or present as painfully or painless lumps. Lesions may be idiopathic or arise secondary to trauma, foreign body, infection or systemic illness. These lesions provide a unique diagnostic challenge due to the small size of the lesions, the wide differential and the intricate anatomy. Our teaching aim is to present a practical illustration of hand and finger soft tissue lesions along with relevant clinical findings, illustrate the normal MRI appearances which can simulate disease and help the radiologist to provide a more accurate diagnosis, allowing improved recommendations to the referring clinicians and minimize unnecessary investigations or biopsy.

#### TABLE OF CONTENTS/OUTLINE

First we describe the MRI protocols used to work up soft tissue lesions of hand and fingers. Secondly we evaluate the most common artifacts in hand and finger MRI such as pulsation, aliasing and phase-encoded motion artifacts and the review practical tips to optimize image quality. Third we provide an outline of the normal findings which simulate disease including Pacinian corpuscles and submatrical hyperintense area. Finally we illustrate the key MRI imaging features of common soft tissue lesions of the hand and fingers including cystic lesions (glomus tumors, inclusion cyst), tumor like lesions (fibroma, keratoacanthoma, peripheral nerve sheath tumor), vascular lesions such as haemangioma and malignant lesions which include squamous cell carcinoma, malignant melanoma and metastasis, with plain film, CT and Ultrasound correlation.

Printed on: 02/07/23

## Abstract Archives of the RSNA, 2022

MKEE-147

### **MRI of The Midhand: The Lesser Known Anatomy**

Sunday, Nov. 27 8:00AM - 9:00AM Room: Learning Center - MK

#### **Participants**

Michel De Maeseneer, PhD, (*Presenter*) Nothing to Disclose

#### **TEACHING POINTS**

-The anatomy of the midhand is complex and not well known. We illustrate this anatomy by MR-anatomical correlation. -It includes the distal tendon insertions, the muscles of thenar and hypothenar, the midpalmar compartment, the palmar bursa and synovial sheaths, the sesamoid apparatus of the thumb base, the palmar aponeurosis. -For each structure we illustrate and refer to the most important pathological conditions -A good knowledge of anatomy is essential to adequately assess normal and abnormal MR imaging of this region.

#### **TABLE OF CONTENTS/OUTLINE**

Outline1. Distal tendon insertions: AP, EPB, ECRB and ECRL, EPL, ED, EDM, ECU2. Muscles of the hypothenar: opponens, abductor, interosseous3. Muscles of the thenar: opponens, abductor, flexor brevis, flexor pollicis longus, adductor, interosseous.4. Midpalmar compartment: interosseous, lumbricals, neurovascular bundle, transverse metacarpal ligament5. Bursae and synovial sheaths: palmar bursa, synovial sheath of finger 1 and 5, synovial sheath of finger 2-4. 6. Thumb base; sesamoid bones, intersesamoid ligament, accessory collateral ligament, collateral ligament, dorsal aponeurotic expansion (hood) from abductor and adductor tendons7. Palmar aponeurosis: palmaris longus, apex of aponeurosis, pretendinous bands, transverse ligament of Skoog, natatory ligament

Printed on: 02/07/23



## Abstract Archives of the RSNA, 2022

MKEE-149

### Meniscus Repair: What Radiologists Need to Know

Sunday, Nov. 27 8:00AM - 9:00AM Room: Learning Center - MK

#### Participants

Camila De Paula Silva, MD, Botucatu, Brazil (*Presenter*) Nothing to Disclose

#### TEACHING POINTS

The purpose of this exhibit is 1. To review and illustrate the surgical techniques of meniscal repair. 2. To show MRI images appearance of the repaired meniscus. 3. To show the postoperative normal and abnormal findings.

#### TABLE OF CONTENTS/OUTLINE

1- Imaging appearance of meniscus injuries before and after repair. 2- Types of surgical techniques of meniscal repair, including: Inside-out suture repairs, outside-in suture repairs and all-inside repairs. 3- Normal post surgery findings and how to differentiate it from abnormalities. 4- Main postoperative complications of meniscal repairs in MRI images, including: avulsion of the repair, progressive meniscal extrusion and progressive articular cartilage damage.

Printed on: 02/07/23



## Abstract Archives of the RSNA, 2022

MKEE-15

### Soft Tissue Calcifications on Ultrasound - Differentials and Radiographic Correlate

Sunday, Nov. 27 8:00AM - 9:00AM Room: Learning Center - MK

#### Participants

Alex Ward, MD, (Presenter) Nothing to Disclose

#### TEACHING POINTS

1) Ultrasound is not the modality of choice for evaluation of calcifications, however practitioners frequently encounter calcifications during diagnostic and procedural musculoskeletal ultrasound. These calcifications may be challenging to diagnose, especially if discovered incidentally. 2) Knowledge of the sonographic appearance of calcifications and their respective radiographic correlate can help clinicians comfortably diagnose soft tissue calcifications. 3) Review of commonly encountered calcifications focusing on their typical location, distribution, imaging appearance and mechanism of formation. 4) Focus on companion cases, potential pitfalls, and unique sonographic/radiographic features to distinguish and accurately identify calcifications (ex. HADD vs enthesopathy, ultrasound appearance of Gout vs CPPD, benign vs malignant causes of calcifications)

#### TABLE OF CONTENTS/OUTLINE

1) Terminology and categorization of calcification vs ossification. 2) Review of commonly encountered calcifications, including typical location/distribution, mechanism of formation, sonographic appearance with radiographic correlate, potential pitfalls of the following: A. Calcium hydroxyapatite deposition disease (HADD) B. Calcium pyrophosphate deposition C. Gout D. Enthesophytes E. Normal variant ossicles F. Myositis ossificans and other forms of heterotopic ossification G. Scleroderma H. Tumoral calcinosis in End Stage Renal Disease I. Phleboliths seen in vascular malformation J. Malignancy, including chondrosarcoma and calcification in synovial sarcoma

Printed on: 02/07/23



## Abstract Archives of the RSNA, 2022

MKEE-150

### MSK Word Salad: Making Sense of the Most Frequently Encountered Metabolic Bone Disorders

Sunday, Nov. 27 8:00AM - 9:00AM Room: Learning Center - MK

#### Participants

Andrew Liu, MD, (*Presenter*) Nothing to Disclose

#### TEACHING POINTS

Metabolic bone disorders encompass those diseases which affect bone structure and/or mass and are caused by metabolic derangements. They are important to recognize as they are common and affect patients of all age groups. Metabolic bone disorders lead to considerable morbidity and mortality, as they weaken bones, regardless of the underlying morphologic changes, increasing the risk of fractures in elderly patients and stunting skeletal growth in children. Due to the lack of acute symptoms of many of these disorders, the radiologist is likely to make the initial diagnosis and facilitate subsequent workup.

#### TABLE OF CONTENTS/OUTLINE

This presentation covers the more commonly encountered metabolic bone disorders. For each disease, a brief summary of the pathophysiology precedes a discussion of characteristic imaging features to provide a basis for understanding WHY those findings occur. Each slide is centered on radiographic features, with cross-sectional imaging findings shown as correlates. This is because metabolic bone diseases are most often initially detected on radiographs. Disorders discussed will be categorized as osteopenic, osteosclerotic, or mixed pattern lesions.

Printed on: 02/07/23



## Abstract Archives of the RSNA, 2022

MKEE-151

### Skeletal Dysplasias: The Role of Radiologist's Report

Sunday, Nov. 27 8:00AM - 9:00AM Room: Learning Center - MK

#### Participants

Mateus Andreoni, MD, Sao Paulo, Brazil (*Presenter*) Nothing to Disclose

#### TEACHING POINTS

TEACHING POINTS: The purpose of this pictorial essay is to review the main characteristics of the most prevalent bone dysplasias and highlight the key points of the radiological report: Most prevalent types of skeletal dysplasias and the latest classification  
Review of bone dysplasias radiological appearance  
The role of radiologist's report for early diagnosis and family counseling

#### TABLE OF CONTENTS/OUTLINE

TABLE OF CONTENTS/OUTLINE: Most prevalent types of skeletal dysplasias  
Skeletal dysplasias are a group of more than 450 heritable disorders with specific type of inheritance. The latest discoveries have added embryological and genetic data which provided a detailed classification in 42 groups.  
Review of bone dysplasias radiological appearance: Despite being a large group of pathologies, radiological appearance may be diagnostic or narrow to a small amount of differentials in most cases. The role of radiologist's report: It is important to determine a precise diagnosis to aid in management, familial recurrence and to report those disorders highly associated with mortality. Even tenuous radiologic findings should be correctly interpreted and reported because, added to clinical context, can be decisive in the correct diagnosis.

Printed on: 02/07/23

## Abstract Archives of the RSNA, 2022

MKEE-152

### Ultrasound (US) Imaging of The Peripheral Nerves: Normality and Abnormalities

Sunday, Nov. 27 8:00AM - 9:00AM Room: Learning Center - MK

#### Participants

Michaela Cellina, (*Presenter*) Nothing to Disclose

#### TEACHING POINTS

To describe the technique of the lower limb US nerve study and the appearance of the nerves to help the radiologist become confident with this US application. To show the anatomical landmarks to identify the nerves.

#### TABLE OF CONTENTS/OUTLINE

Thanks to its wide availability, low costs, fast execution, high soft-tissue resolution, real-time dynamic evaluation, and direct correlation with signs and symptoms, high-frequency US is considered the first-line imaging tool for the study of the peripheral nerve. Moreover, US does not suffer the limitations of MRI, such as metal implants, claustrophobia, and pacemakers. The exam is performed with high-frequency linear array probes. The nerves are identifiable on the axial plane at defined anatomical landmarks, then the nerve is followed with the probe in the axial plane proximally and distally. If abnormalities are recognizable, the nerve should be also studied on the long axis. Common indications for US nerves study include tarsal tunnel syndrome, entrapments, traumas, suspected neuromas, and polyneuropathies. Non-pathological nerves have a characteristic honeycomb appearance in the short axis, as they are formed by hypoechoic nerve fascicles surrounded by hyperechoic connective tissue and collagen. They can be detected in the adipose tissue or in fascial planes among or superficial to the muscles and each nerve is surrounded by a portion of fat. Pathological nerves show increased diameter with a hypoechoic appearance proximal to the site of the entrapment. Post-traumatic damages can be visible as nervous focal discontinuation with swollen retracted portions.

Printed on: 02/07/23

## Abstract Archives of the RSNA, 2022

MKEE-153

### Radiographic Signs of Musculotendinous and Ligament Injuries

Sunday, Nov. 27 8:00AM - 9:00AM Room: Learning Center - MK

#### Participants

Diego dos Santos, MD, Sao Paulo, Brazil (*Presenter*) Nothing to Disclose

#### TEACHING POINTS

- Review some general information about radiographic signs of musculotendinous and ligament injuries- Describe the radiographic findings of musculotendinous and ligament injuries in the different joints of the body and in both adult and pediatric population through cases illustrated in our service- Highlight some anatomical considerations, the mechanism and some quick tips and pitfalls involving the musculotendinous and ligament injuries- Correlate the radiographic findings of musculotendinous and ligament injuries with other imaging methods

#### TABLE OF CONTENTS/OUTLINE

Introduction- General information about radiographic signs of musculotendinous and ligament injuriesRadiographic findings of musculotendinous and ligament injuries in the different joints- Quadriceps tendon tear with patella baja- Patellar tendon tear with patella alta- Fibularis longus tear with posterior deviation of the accessory peroneal ossicle- Elbow dislocation associated with fracture of the radial head and coronoid process and ligament injuries- Turf toe with posterior deviation of the hallux sesamoids- Rotator cuff tear with coracohumeral interval shortening / superior subluxation of the humeral head- Bone avulsions in different body sites associated to ligaments and tendon tears- Periarticular soft tissue densification associated to ligaments and tendon tears- Other casesAnatomical considerationsInjury mechanismQuick tips and pitfallsCorrelation with other imaging methods- Ultrasound- Magnetic Resonance Imaging

Printed on: 02/07/23



## Abstract Archives of the RSNA, 2022

MKEE-154

### Preoperative Planification and Postoperative CT-Scan Imaging Assessment of Latarjet Procedure for Anterior Shoulder Instability: What's On The Menu?

Sunday, Nov. 27 8:00AM - 9:00AM Room: Learning Center - MK

#### Participants

Ulrike Novo, MD, (*Presenter*) Nothing to Disclose

#### TEACHING POINTS

- To review the most important findings in preoperative CT scan planning before Latarjet.- To describe the key points to be considered in the postoperative CT scan evaluation. - To illustrate a wide spectrum of normal and pathological findings in postsurgical CT scans in a case-based scenario.

#### TABLE OF CONTENTS/OUTLINE

The Latarjet procedure is an operation for recurrent anterior shoulder instability consists of transferring the coracoid process to the anterior glenoid rim. Appetizer PREOPERATIVE CT SCAN PLANNING Preoperative planning of the arthroscopic Latarjet procedure based on the CT scan is necessary to achieve satisfactory clinical and radiographic results: • Coracoid dimensions • Measurement of bone defects, Hill-Sachs lesion, bony Bankart and glenoid track Main course HOW TO PERFORM ARTHROSCOPIC LATARJET SURGERY AND POSTOPERATIVE CT SCAN EVALUATION Adequate coracoid graft positioning: Coronal view: Coracoid graft should be flush with the articular surface along its lateral aspect. Axial view is the most useful view to judge the mediolateral position and the "angulation" of the graft. Coracoid graft should be flush with the articular surface. The angulation of the graft (open, closed or neutral) is evaluated with the circle method. Axial plane to analyze the angle of the screw (alpha angle) with the articular surface. Sagittal view allows assessment of cranio-caudal position respect to glenoid equator Dessert COMPLICATIONS • Short term: Graf fracture/ avulsion and graft non-union • Long term: Osteoarthritis In conclusion, the radiologist plays a key role in Latarjet, to know what pre-surgical CT findings are important to help with preoperative planning and to diagnose potential complications that may occur.

Printed on: 02/07/23

## Abstract Archives of the RSNA, 2022

MKEE-155

### Main Sacral Lesions and Their Radiological Findings

Sunday, Nov. 27 8:00AM - 9:00AM Room: Learning Center - MK

#### Participants

Bárbara Moreira Machado, Sao Paulo, Brazil (*Presenter*) Nothing to Disclose

#### TEACHING POINTS

1- Review and understand the most common sacral tumors. 2- Debate over imaging patterns and their prevalence

#### TABLE OF CONTENTS/OUTLINE

1- Introduction and anatomy of the sacrum. 2- Epidemiology of sacral tumors. 3- Limitations of diagnostic imaging methods. 4- Differential diagnosis of sacral lesions and main imaging features a) primary bone tumors: Sacral chordoma; chondrosarcoma; osteosarcoma; multiple myeloma/plasmacytoma; giant cell tumor; aneurysmal bone cyst; osteoid osteoma; osteoblastoma. b) secondary bone tumors: metastases. c) neural tumors: Ependymoma; schwannoma; neurofibroma; Ganglioneuroma / neuroblastoma / ganglioneuroblastoma. d) germ cell tumors: teratoma; yolk sac tumor

Printed on: 02/07/23



## Abstract Archives of the RSNA, 2022

MKEE-156

### Whole body MRI in The Analysis of Multiple Myeloma: A Overview of Evolution, Imaging Methods and Future Perspectives

Sunday, Nov. 27 8:00AM - 9:00AM Room: Learning Center - MK

#### Participants

Eduardo Zukovski, MD, Umuarama, Brazil (*Presenter*) Nothing to Disclose

#### TEACHING POINTS

- Recognize the updated diagnostic criteria for MM, indications and limitations of each imaging option, and recommendations for follow-up. - Know MR imaging protocol for MM evaluation, indications and general technical parameters. - Comprehend MM imaging features in the different whole body MRI sequences. - Recognize the imaging response criteria in MM treatment. - Understand future perspectives of monoclonal gammopathies imaging analysis and flowcharts.

#### TABLE OF CONTENTS/OUTLINE

Introduction: • - Epidemiology of MM and indications of each imaging option • - Definition of MM updated diagnosis criteria • - Different indications of whole body MRI for bone diseases • - Whole body MRI sequences, technical parameters and MM imaging findings  
Diagnosis and imaging findings: • - Flowcharts of monoclonal gammopathies imaging methods • - Whole body MRI useful in MM treatment response assessment • - MRI patterns of bone marrow infiltration in MM • - Definition of unequivocal focal active lesion of MM in whole body MRI • - MRI findings correlated with poor patient survival • - Imaging follow-up for MM and identification of possible complications

Printed on: 02/07/23



## Abstract Archives of the RSNA, 2022

MKEE-157

### A Whole-body MRI Experience in The ProstateCancer

Sunday, Nov. 27 8:00AM - 9:00AM Room: Learning Center - MK

#### Participants

Augusto Altoe, Rio de Janeiro, Brazil (*Presenter*) Nothing to Disclose

#### TEACHING POINTS

1. To describe whole-body MRI protocol and its general considerations; 2. To understand the anatomical and functional techniques and their applications; 3. To illustrate the image findings of whole-body MRI in prostate cancer; 4. To identify potential imaging pitfalls, differential diagnoses, and post-therapeutic assessment.

#### TABLE OF CONTENTS/OUTLINE

1- Introduction. 2- MRI acquisition a. Anatomical techniques; b. Functional techniques; c. Recommended protocol. 3- Clinical indications of whole-body MRI in prostate cancer; a. Newly diagnosed prostate cancer; b. Biochemical recurrence; c. Advanced disease and response assessment. 4 - Image findings of whole-body MRI in prostate cancer; a. Locoregional disease; b. Metastatic lymph node disease; c. Metastatic bone disease; d. Post-therapeutic findings. 5 - Imaging pitfalls and differential diagnoses. 6 - Take home messages and teaching points.

Printed on: 02/07/23



## Abstract Archives of the RSNA, 2022

MKEE-158

### Pitch Perfect: Biomechanics and Patterns of Injury In the Throwing Arm

Sunday, Nov. 27 8:00AM - 9:00AM Room: Learning Center - MK

#### Awards

Identified for RadioGraphics  
Certificate of Merit

#### Participants

Dyan V. Flores, MD, Ottawa, ON (*Presenter*) Nothing to Disclose

#### TEACHING POINTS

The exceptional velocity required by sporting activities relying on overhead throwing predisposes the shoulder to extreme forces, leading to both adaptive changes and pathologic cascade of findings that can be detected on imaging. The objectives of this educational exhibit are: • 1. To review the phases of pitching and associated biomechanics that predispose the overhead-throwing shoulder and elbow to injury • 2. To highlight unique sites of injury in the overhead-throwing athlete • 3. To discuss imaging findings of common shoulder and elbow injuries in the overhead-throwing athlete

#### TABLE OF CONTENTS/OUTLINE

Throwing biomechanics and arc of motion Shoulder • Glenohumeral internal rotation deficit (GIRD) • Internal impingement • Superior labral anteroposterior (SLAP) tear • Partial thickness rotator cuff tear • Anterior capsule injury • Subscapularis tendon injury • Bennett lesion • Posterior muscle injury Elbow • Flexor tendinitis • UCL injury • Valgus extension overload • Olecranon stress fracture • Ulnar neuritis Pediatric • Little leaguer's shoulder and elbow

Printed on: 02/07/23



## Abstract Archives of the RSNA, 2022

MKEE-159

### Spectrum of Musculoskeletal Involvement in COVID-19 Infection Diseases: Pictorial Essay

Sunday, Nov. 27 8:00AM - 9:00AM Room: Learning Center - MK

#### Participants

Pedro Martins, MD, Rio de Janeiro, Brazil (*Presenter*) Nothing to Disclose

#### TEACHING POINTS

Covid-19 has a broad spectrum of musculoskeletal involvement that can mimic other diseases and trigger the development of rheumatic disease. After almost two years of the coronavirus pandemic, some countries are starting to treat COVID-19 infection as an endemic disease and we will probably continue to live with the virus. Although musculoskeletal involvement is uncommon, it's important to recognize its most common neuromuscular and rheumatologist complications associated with the infection, and also the musculoskeletal changes related to the long term hospitalization and the vaccine side effects.

#### TABLE OF CONTENTS/OUTLINE

- To explain how COVID-19 infection can involve the musculoskeletal system. - To illustrate with ultrasound, computed tomography, and magnetic resonance images the most common musculoskeletal changes of covid infection, including myositis, neuropathy, synovitis, arthritis and soft tissue abnormalities. - To demonstrate the differential diagnosis of others musculoskeletal infections and inflammatory conditions. The global COVID-19 pandemic is not over yet, and may become an endemic disease within the next few years. Musculoskeletal changes can be related to the infection itself, and also be found in patients with prolonged hospitalizations and due vaccine side effects. It is important to recognize the most common musculoskeletal changes to avoid unnecessary procedures and to prevent misdiagnosis of other inflammatory and infectious conditions.

Printed on: 02/07/23



## Abstract Archives of the RSNA, 2022

MKEE-16

### The Navicular: Keystone of the Foot

Sunday, Nov. 27 8:00AM - 9:00AM Room: Learning Center - MK

#### Participants

Scott Wuertzer, MD, Winston Salem, NC (*Presenter*) Nothing to Disclose

#### TEACHING POINTS

1. Review the anatomy of the tarsal navicular with an emphasis on the three arches of the foot. 2. Review the biomechanics of the navicular, including the osseous keystone and the peri-navicular soft tissue stabilizers. 3. Describe various pathologies of the navicular with an emphasis on the associated pathomechanics. 4. Through case examples, highlight the expected imaging characteristics of navicular pathology.

#### TABLE OF CONTENTS/OUTLINE

1. Anatomy and Biomechanics. A. Osseous and vascular anatomy of the navicular. B. The arches of the foot - medial, lateral, and transverse. C. Peri-navicular soft tissue stabilizers - dorsal and plantar cuneonavicular ligaments, bifurcate ligament, spring ligament, dorsal talonavicular ligaments, cuboideonavicular ligaments, and the posterior tibial tendon. D. Joints - naviculocuneiform, cuboideonavicular, and talocalcaneonavicular. 2. Pathology, Pathomechanics, and Imaging Characteristics. A. Accessory ossicles - os navicularis, os supranaviculare. B. Tarsal coalitions - calcaneonavicular, talonavicular. C. Acute fractures - avulsion, body, and tuberosity. D. Stress fractures and osteochondral lesions. D. Kohler's disease. E. Osteonecrosis - Mueller-Weiss, secondary osteonecrosis. F. Arthropathies - osteoarthritis, rheumatoid arthritis, and neuropathic arthropathy. G. Adult acquired flatfoot deformity.

Printed on: 02/07/23



## Abstract Archives of the RSNA, 2022

MKEE-160

### A Stepwise Approach to Finally Understanding Arthritis

Sunday, Nov. 27 8:00AM - 9:00AM Room: Learning Center - MK

#### Participants

Bryan Wessel, BS, MD, Cincinnati, OH (*Presenter*) Nothing to Disclose

#### TEACHING POINTS

1. Understand the differences between inflammatory and degenerative arthritis. 2. Understand the progression of various forms of arthritis. 3. Identify the different radiographic findings that help distinguish between the different causes of arthritis.

#### TABLE OF CONTENTS/OUTLINE

- Characteristics of inflammatory and degenerative arthritis.
  - o Symmetric vs Asymmetric joint space narrowing
  - o Erosions vs subchondral cysto What are osteophytes?
- Stepwise algorithm for determining the specific type of arthritis.
- Explanation of subtypes of inflammatory arthritis with examples.
  - o Septic Arthritis
  - o Rheumatoid Arthritis
  - o Seronegative Arthropathies
- Explanation of subtypes of degenerative arthritis with examples.
  - o Typical Osteoarthritis
  - o Atypical Osteoarthritis
- Application of knowledge to unknown cases.

Printed on: 02/07/23



## Abstract Archives of the RSNA, 2022

MKEE-161

### Not All Erosions are Created Equal - Approach to Hand and Wrist Arthropathy: What a Radiologist Needs to Know?

Sunday, Nov. 27 8:00AM - 9:00AM Room: Learning Center - MK

#### Awards

Certificate of Merit

#### Participants

Neha Antil, MD, Mountain View, CA (*Presenter*) Nothing to Disclose

#### TEACHING POINTS

The purpose of this exhibit is to: 1. Outline the various arthritides that have a predilection for the hand and wrist. 2. Classify arthritides based on the clinical presentation, site of involvement in the hand and wrist and further differentiate them based on characteristic imaging appearances. 3. Discuss advanced imaging techniques that can be used as a problem-solving tool in rheumatology. 4. Summarize and develop a practical imaging approach to making an accurate diagnosis.

#### TABLE OF CONTENTS/OUTLINE

- Review the causes of arthritis in hand and wrist joints.
- o Classify arthritides based on clinical presentation and site of involvement in the hand and wrist.
- o Describe imaging appearances for each arthropathy.
- o Differentiate the arthritides based on characteristic imaging findings.
- Illustrate advanced imaging techniques that can help differentiate arthropathies affecting the wrist and hand.

Printed on: 02/07/23



## Abstract Archives of the RSNA, 2022

MKEE-162

### Ultrasound for Ultra-Insight into Diagnosing and Treating the Painful Joint Arthroplasty

Sunday, Nov. 27 8:00AM - 9:00AM Room: Learning Center - MK

#### Participants

Brendan Franz, MD, (*Presenter*) Nothing to Disclose

#### TEACHING POINTS

Overview of utilizing ultrasound for the evaluation of periprosthetic joint infections, as well as for US-guided aspiration of infectious material in a periprosthetic joint infection. Review of the expected sonographic appearance of reactions to metallic debris at the joint arthroplasty site, including conditions such as metallosis, trunnionosis, and metal-on-metal pseudotumors. Using ultrasound for the evaluation of tendon pathology with arthroplasties, including dynamic maneuvers to evaluate for tendon impingement or snapping. Indications for joint arthroplasty injections and precautions to be taken.

#### TABLE OF CONTENTS/OUTLINE

Introduction Brief review of current trends in arthroplasty placement Ultrasound evaluation in periprosthetic joint infections Expected appearance of a periprosthetic joint infection on ultrasound imaging. US-guided aspiration and important biomarkers. Saline Lavage. Major pathogen causing periprosthetic joint infections at the shoulder; Cutibacterium acnes. Adverse Reactions to Metallic Debris Metallosis Trunnionosis Metal-on-metal pseudotumors Tendon pathology in joint arthroplasty Subscapularis tendon tears Gluteal tendon tears Quadriceps and patellar tendon tears Iliopsoas tendinopathy, bursitis, and impingement/snapping Joint arthroplasty injections Indications Risks Precautions Summary

Printed on: 02/07/23



## Abstract Archives of the RSNA, 2022

MKEE-163HC

### 3D Printed Kyphoplasty Simulator Build Guide

Sunday, Nov. 27 8:00AM - 9:00AM Room: Learning Center - MK

#### Participants

Caleb Heiberger, MD, Sioux Falls, SD (*Presenter*) Nothing to Disclose

#### TEACHING POINTS

We demonstrate the creation of a functional kyphoplasty simulator using computed tomography (CT) images, a "desktop grade printer" and open-source software. To do so, we obtained three CT Digital Imaging and Communications in Medicine (DICOM) files including spinal compression fractures with 1) Standard Anatomy, 2) Scoliosis and 3) Severe Arthrosis. Segmentation was performed using 3D Slicer with post-processing in Mesh-Mixer and Fusion 360 to repair segmentation defects. Printing was performed on a Prussa i3 MK3S fused deposition modeling printer using Polylactic acid (PLA) for the vertebrae and Thermoplastic Polyurethane (TPU) for the intervertebral disks. Soft tissue was simulated using a 1:1 mixture of Knox Gelatin and water, activated by a freeze/boil cycle. The mixture was poured into a custom printed container with the printed spine and allowed to solidify. Simulations were performed under fluoroscopic guidance. Early usage reviews indicated high satisfaction with device fidelity compared to other models, including cadavers. The production of this kyphoplasty model demonstrates the effective use of 3D printing in image guided interventional training.

#### TABLE OF CONTENTS/OUTLINE

Segmenting a DICOM in 3D Slicer  
Editing segmented DICOM in Mesh Mixer and Fusion 360  
Preparing a print in 3D CAD Software  
Selecting filaments for specific anatomy  
Printing the model  
Creating soft-tissue mold and embedding spine  
Demonstration of fluoroscopic fidelity of the model  
Usage reviews and future directions  
Please visit the Learning Center to also view this presentation in hardcopy format.

Printed on: 02/07/23



## Abstract Archives of the RSNA, 2022

MKEE-164

### A Pictorial Review of the Different Radiological Presentations and Differential Diagnosis of Gout in Atypical Sites

Sunday, Nov. 27 8:00AM - 9:00AM Room: Learning Center - MK

#### Participants

Lin Liu, MD, Guangzhou, China (*Presenter*) Nothing to Disclose

#### TEACHING POINTS

1. Monosodium urate crystals commonly deposit at the joints or tendons of the foot or ankle, especially at the first metatarsophalangeal joint, but rarely deposit at the joints of upper limbs and other extra-articular sites. 2. Intraspinous gout is difficult to diagnose before surgery and its clinical presentations and imaging findings mimic tumors and degenerative spinal diseases. Early diagnosis of intraspinal gout is extremely significant because timely urate-lowering therapy may avoid surgical intervention. 3. The confirmation of MSU crystals in synovial fluid or tophaceous material is considered the gold standard for gout diagnosis. Gout in the atypical sites may misdiagnose because of the nonspecific clinical and imaging findings. Therefore, DECT as an auxiliary tool should be performed as soon as possible for suspected gout lesions, which may avoid unnecessary invasive operations.

#### TABLE OF CONTENTS/OUTLINE

1. A case-based review of sixteen different radiological presentations of gout in the atypical sites including upper limbs, spine, ligaments, and other rare joints. 2. Recognize different findings of gout in atypical sites in radiography, CT, MRI, and dual-energy CT. 3. Identify the differential diagnosis of gout in atypical sites.

Printed on: 02/07/23



## Abstract Archives of the RSNA, 2022

MKEE-165

### Tips and Tricks for Ablating an Osteoid osteoma: Plan It Right!

Sunday, Nov. 27 8:00AM - 9:00AM Room: Learning Center - MK

#### Participants

Roshni Anand, MBBS, New Delhi, India (*Presenter*) Nothing to Disclose

#### TEACHING POINTS

Approach the lesion perpendicular to the cortical surface and avoid the sclerotic part of bone. This may require a prone, oblique, or lateral decubitus position. The shortest path to the lesion enables minimum injury to surrounding tissues. Avoiding neurovascular bundle (NVB): Lesions may be targeted through the longer route and farther cortex to avoid injury to the NVB. Dextrose may be injected to keep at least 1 cm distance. Tandem needle technique or use of protractor in case of the angulated route. Drill bit is a superior option compared to hammering, especially in the case of a longer osseous path and sclerosis. Two or more electrodes may be required for lesions measuring >1.5cm. A single electrode is sufficient for smaller lesions. Dextrose may be injected to prevent soft tissue injury in superficial bones like in digits. Intra-articular lesions: Trans-articular approach is avoided. Iatrogenic joint effusion by instilling dextrose may protect from articular cartilage injury. Spinal lesions: Entering the facet joint or neural foramen should be strictly avoided. A bipolar RF probe can avoid damage to the surrounding structures. Reducing Post-procedure pain and swelling: Injecting lignocaine-bupivacaine mixture along the tract up to the periosteum and local site compression for 5 minutes after ablation

#### TABLE OF CONTENTS/OUTLINE

Learning objectives: To demonstrate the practical tips and tricks for abating an osteoid osteoma by correct planning  
Cases demonstrating the teaching points  
Conclusion

Printed on: 02/07/23



## Abstract Archives of the RSNA, 2022

MKEE-166HC

### Quantitative Analysis of Water Material Density Values by Dual Energy CT for Osteoblastic Vertebral Metastases

Sunday, Nov. 27 8:00AM - 9:00AM Room: Learning Center - MK

#### Participants

Hiroataka Nakashima, MSc, RT, (*Presenter*) Nothing to Disclose

#### TEACHING POINTS

1. Virtual non-calcium (VNCa) images were created by two-material decomposition processing. 2. Clinically diagnosed 81 osteoblastic metastatic vertebrae and 301 normal vertebrae were compared by water material density values quantitatively. 3. The area under the curve value obtained from receiver operating characteristic (ROC) analysis was 0.93, and the water material density value was a highly discriminative index for osteoblastic metastases. 4. The cutoff value between lesion and normal was 1047.8 mg/cm<sup>3</sup> based on ROC analysis with a sensitivity of 85.7% and a specificity of 98.1%. 5. New image display method was developed that reflects the cut-off value calculated from water material density values.

#### TABLE OF CONTENTS/OUTLINE

Vertebral metastases are the most common bone metastases. CT can detect bone calcification with high sensitivity and is therefore excellent for the diagnosis of osteolytic bone metastases with bone cortex destruction. However, osteoblastic bone metastases without destruction are difficult to diagnose and are easily overlooked. VNCa image is one of the material discrimination images produced by dual-energy CT and is a material density image obtained by highlighting the water component and removing the calcium component. By measuring the VNCa image, water material density values can be obtained. Quantitative evaluation using water material density values was a gap of knowledge. In this exhibition, water material density values of osteoblastic vertebral metastases and normal vertebrae were compared. And cutoff values were calculated by ROC analysis. The results showed that water material density values have a high discriminatory ability against osteoblastic metastases. Please visit the Learning Center to also view this presentation in hardcopy format.

Printed on: 02/07/23



## Abstract Archives of the RSNA, 2022

MKEE-167

### Don't Stress About Stress Injuries: A Review of Stress Related Injuries of Bone

Sunday, Nov. 27 8:00AM - 9:00AM Room: Learning Center - MK

#### Participants

Samantha Jayasinghe, MD, Cleveland, OH (*Presenter*) Nothing to Disclose

#### TEACHING POINTS

1. Discuss clinical presentation and pathophysiology of stress related fractures including fatigue, atypical, and insufficiency fractures. 2. Role of imaging for stress related injuries of bone. 3. Discuss common stress fracture patterns and locations. 4. Discuss uncommon stress fracture patterns and locations related to competitive athletes or surgical changes. 5. Review treatment algorithms.

#### TABLE OF CONTENTS/OUTLINE

Background 1. Clinical presentation of Stress injuries 2. Anatomy, Biomechanical tensile/compressive forces 3. Pathophysiology 4. Optimal imaging modalities for evaluation  
Stress Fracture Subtypes  
Fatigue  
Common 1. Metatarsal 2. Compression side femoral neck 3. Calcaneal 4. Tibial Fredericson classification  
Uncommon 1. Patellar 2. Tensile side femoral neck 3. Pubic ramus fractures status post periacetabular osteotomy 4. Rib stress in competitive swimmers  
Atypical  
Bisphosphonate or monoclonal antibody associated lateral femoral fractures  
1. Imaging/treatment recommendations  
Insufficiency 1. Femoral Condylar 2. Femoral Head 3. Sacral Unilateral, H-shaped 4. Acetabular  
Pediatric 1. Little Leaguer Shoulder 2. Acromial Apophysiolysis 3. Elbow-Olecranon 4. Elbow-Panners 5. Gymnast wrist 6. Distal Femoral Stress Injury 7. Sinding-Larsen-Johannson 8. Osgood-Schlatter  
Treatment of Stress Fractures 1. Stratifying fracture risk 2. Low Risk  
Conservative Management  
Continued Weight Bearing 3. High Risk  
Rehabilitation  
Protected Weight Bearing  
Surgical Intervention

Printed on: 02/07/23



## Abstract Archives of the RSNA, 2022

MKEE-168

### Imaging Findings That Should Never Be Forgotten In Non-accidental Trauma in Children

Sunday, Nov. 27 8:00AM - 9:00AM Room: Learning Center - MK

#### Participants

Giovana Mesquita, MD, Sao Paulo, Brazil (*Presenter*) Nothing to Disclose

#### TEACHING POINTS

Revise the most important muscle-skeletal image findings related to non-accidental trauma in children, by using original schematic drawings and images from suspect cases of child physical abuse. Most of the cases presented were confirmed by assistant physicians. Therefore, this paper has also the aim of highlighting the fundamental role of the muscle-skeletal radiologist in identifying and documenting the skeletal injuries so as to protect the children involved and help bring victims away from their offenders as fast as possible, to stop further abuse.

#### TABLE OF CONTENTS/OUTLINE

1. Classical metaphyseal fracture 1.1 Traumatic mechanism 1.2 Image findings 2. Non-accidental trauma in long bones 2.1 Traumatic mechanism 2.2 Image findings 3. Non-accidental trauma in ribs 3.1 Traumatic mechanism 3.2 Image findings 4. Non-accidental trauma in pelvis 4.1 Traumatic mechanism 4.2 Image findings

Printed on: 02/07/23



## Abstract Archives of the RSNA, 2022

MKEE-169

### Whole-Body Diffusion-Weighted Magnetic Resonance Imaging in Non-tumoral Bone Marrow Diseases and Their Mimics

Sunday, Nov. 27 8:00AM - 9:00AM Room: Learning Center - MK

#### Participants

Carolina Almeida, MD, Rio de Janeiro, Brazil (*Presenter*) Nothing to Disclose

#### TEACHING POINTS

TEACHING POINTS 1) Identify correct MR protocol that should be used to analyse bone marrow in whole-body MR imaging (WBMRI) owing to detect tumoral involvement and their differential diagnosis. 2) Know basic principals of DWI WBMRI and typical lesion appearances and awareness of potential pitfalls. 3) Make a pictorial essay of lesions that mimic bone marrow tumoral lesions including conventional MRI sequences, DIXON and DWI and understand the characteristic features which allow discrimination between them and true neoplasms in order to avoid unnecessary additional workup. 4) The usefulness of DWI whole-body MR in diagnostic algorithms of non oncological disorders including differentiate diagnosis as inflammatory, infectious and pseudotumoral conditions.

#### TABLE OF CONTENTS/OUTLINE

TABLE OF CONTENTS AND OUTLINE 1) Case discussion regarding imaging that mimick bone marrow tumoral lesions as: 2) SAPHO syndrome 3) CRMO 4) Tuberculosis 5) Syphilis 6) Sarcoidosis 7) Bone Marrow hiperplasia 8) Differential diagnosis 9) Report structuring step by step

Printed on: 02/07/23



## Abstract Archives of the RSNA, 2022

MKEE-17

### **Congenital Talipes Equinovarus Made Easy: What Radiologists Need to Know and How to Evaluate the Idiopathic Congenital Clubfoot**

Sunday, Nov. 27 8:00AM - 9:00AM Room: Learning Center - MK

#### **Awards**

**Identified for RadioGraphics**

#### **Participants**

Julia Peixoto, Sao Paulo, Brazil (*Presenter*) Nothing to Disclose

#### **TEACHING POINTS**

Teaching Points: Emphasize a minimum of two major teaching points of this exhibit. What should the viewer accomplish by viewing this exhibit? The purpose of this exhibit is: 1. Review the main aspects related to idiopathic congenital clubfoot (congenital talipes equinovarus), including anatomy, etiology, pathophysiology, epidemiology, clinical classification and treatment. 2. To illustrate the main imaging findings and how to assess this condition in a multimodality approach, focusing on US and MRI studies.

#### **TABLE OF CONTENTS/OUTLINE**

Describe major headings (e.g., anatomy, physiology, imaging techniques, tumor disease states, etc.) 1. Review the main aspects related to idiopathic congenital clubfoot (congenital talipes equinovarus), including anatomy, etiology, pathophysiology, epidemiology, clinical classification and treatment. 2. Clinical and imaging findings in a multimodality approach. 3. US assessment protocol. 4. MRI assessment protocol. 5. Clubfoot major differential diagnoses, including: (simple metatarsus adductus, skewfoot, and oblique and vertical talus).

Printed on: 02/07/23

## Abstract Archives of the RSNA, 2022

MKEE-18

### Ultrasonography of Thumb Metacarpophalangeal Joint: Normal Anatomy and Mechanism-based Injury Approach

Sunday, Nov. 27 8:00AM - 9:00AM Room: Learning Center - MK

#### Participants

Kyu-Chong Lee, (*Presenter*) Nothing to Disclose

#### TEACHING POINTS

1. The difference between metacarpal joint of thumb and other fingers 2. Anatomy and ultrasonographic normal images of thumb MCP joint 3. Mechanism based thumb MCP injury

#### TABLE OF CONTENTS/OUTLINE

1. Introduction 1) What is the difference between MCP joint of thumb and other fingers? 2) Biomechanism: Condylod joint: freedom of flexion/extension, valgus/varus + opposition 3) Imaging technique for MCP joint evaluation 2. Normal anatomy (1) Osseous anatomy: 1st proximal phalanx metacarpal bone + two sesamoid bones (2) Soft tissue 1) Palmar side: a. Muscle tendon: Adductor pollicis (ADP), Abductor pollicis brevis (APB), Flexor pollicis brevis (FPB), Flexor pollicis longus (FPL) b. Volar plate c. Pulley system (A1, Av, Ao + A2) 2) Dorsal side: a. Tendon: Extensor pollicis brevis (EPB) + Extensor pollicis longus (EPL) b. Dorsal plate c. Extensor hood or apparatus (sagittal band + triangular extension) 3) Collateral system (capsule-ligamentous system) a. Ulnar collateral ligament (UCL = proper/principle + accessory) + adductor aponeurosis b. Radial collateral ligament (RCL = proper/principle + accessory) + APB, FPB aponeurosis 3. Mechanism based injury approach 1) Valgus or abduction injury (most common) a. Skier thumb (UCL injury) b. Stener lesion 2) Varus or adduction injury a. RCL injury b. Stener like lesion c. Varus deformity 3) Hyperextension injury a. Volar plate injury b. Tendon pulley injury c. Muscle injury 4) Hyperflexion injury a. Dorsal plate injury b. Extensor tendon tear 5) Combination damage 4. Summary

Printed on: 02/07/23

## Abstract Archives of the RSNA, 2022

MKEE-2

### Imaging Dancers' Injuries

Sunday, Nov. 27 8:00AM - 9:00AM Room: Learning Center - MK

#### Participants

María Carvajo, MD, (*Presenter*) Nothing to Disclose

#### TEACHING POINTS

1. To present the most common dancers' injuries and their underlying mechanisms. 2. To show the different imaging techniques. 3. To describe the semiology in imaging.

#### TABLE OF CONTENTS/OUTLINE

1. Most frequent types, mechanisms and structures injured in ballet dancers. 2. Injuries classification according to their mechanism. 2.1. Extreme ankle inversion and plantar flexion. 2.1.1. Lateral ankle sprains. 2.1.2. Acute fifth metatarsal fractures. 2.2. Ankle dorsiflexion, knee flexion and plantar stress. 2.2.1. Patellar tendinopathy. 2.2.2. Tibial stress injuries. 2.2.3. Acute Achilles tendon injury. 2.2.4. Tarsal stress injuries and fractures. 2.2.5. Plantar fasciitis. 2.3. Extreme ankle plantar flexion. 2.3.1. Posterior ankle impingement. 2.3.2. Peroneal tendinopathy. 2.3.3. Achilles tendinopathy. 2.3.4. Tarsal, metatarsal and phalanx stress injuries and fractures. 2.4. Knee flexo-extension. 2.4.1. Patellar tendinopathy. 2.4.2. Medial plica syndrome. 2.4.3. Patellofemoral maltracking. 2.5. Hip external rotation. 2.6. Hip external rotation, abduction and flexion. 2.6.1. Snapping hip syndrome. 2.7. Extreme hip adduction. Hip flexion/knee extension. 2.7.1. Adductor muscles injuries. 2.7.2. Stress pelvis injuries. 2.8. Lumbar spine hyperextension. 2.8.1. Spondylolysis/spondylolisthesis.

Printed on: 02/07/23



## Abstract Archives of the RSNA, 2022

MKEE-20

### Ultrasound-guided Injection of Botulinum Toxin in Neurogenic Thoracic Outlet Syndrome: Technical Aspects and Experience Over 15 Years

Sunday, Nov. 27 8:00AM - 9:00AM Room: Learning Center - MK

#### Participants

Ronald Mercer, MD, (*Presenter*) Nothing to Disclose

#### TEACHING POINTS

-Thoracic outlet syndrome (TOS) includes a group of upper extremity disorders believed to occur due to isolated or combined neurovascular compression. -Neurogenic TOS (NTOS) constitutes 95% of all TOS patients, but presents diagnostic difficulty due to nonspecific findings during electro-diagnostic and imaging evaluation. -Botulinum toxin A (BTX) injections are useful to evaluate the diagnosis of NTOS, with symptom relief correlating with good response to subsequent treatments. -Our group pioneered ultrasound guided BTX injections since 2007, having performed over 5,000 procedures in patients being investigated for NTOS. -Injection of BTX into the anterior (ASM) and middle (MSM) scalene muscles as well as the pectoralis minor muscle (PMM) has been effective in reducing the symptoms of NTOS and may contribute to patient selection criteria for surgical management. -Ultrasound guided injection has been demonstrated to be safe and well tolerated.

#### TABLE OF CONTENTS/OUTLINE

-Discuss NTOS and the use of imaging-guided BTX injection in diagnosis and management. -Present relevant anatomy and safe approach to ultrasound-guided BTX injection into the ASM, MSM, and PMM. -Described complications and documented rate of symptom relief of these injections.

Printed on: 02/07/23



## Abstract Archives of the RSNA, 2022

MKEE-21

### Use of Soft Modeling Compound to Teach Musculoskeletal Anatomy and Pathology

Sunday, Nov. 27 8:00AM - 9:00AM Room: Learning Center - MK

#### Participants

Oswaldo Velez-Martinez, MMedSc, (*Presenter*) Nothing to Disclose

#### TEACHING POINTS

1. Medical imaging is a 2D representation of 3D structures. It can be challenging for trainees to conceptualize 3D structures from 2D slices. 2. Soft modeling compound is an interactive and cost effective medium to teach musculoskeletal pathology. 3. 3D models allow trainees to view anatomical structures in space and therefore conceptualize normal anatomy and pathology. 4. Soft modeling can be integrated into any teaching program and its impact can be quantified.

#### TABLE OF CONTENTS/OUTLINE

Introduction to soft modeling compound as a teaching medium -Types-Pros-ConsSet-up-3D Model generation-Modeling tools-Documenting examplesTeaching Algorithm-Attending mediated "Show and Tell"-Trainee modeling and gradingResident Survey-Design-ResultsShoulder -Anatomy-Pathology-Labral Tears-Cartilage Injury-Rotator Cuff Tears-Long Head Biceps-CapsuloligamentousElbow AnatomyPathologyTendon TearsLigament Cartilage InjuryWrist -Anatomy-Pathology-Triangular Fibrocartilage-Scapholunate and Lunotriquetral Ligaments Hip -Anatomy-Pathology-Labral Tears-Cartilage Injury-Femoroacetabular ImpingementKnee -Anatomy-Pathology-Meniscus Tears-Cartilage Injury-Ligament Tendon Foot-Anatomy-Pathology-Ligament -Cartilage InjuryFuture Developments-Resident Grading-Quantitation of Competency Improvement-Other Applications

Printed on: 02/07/23



## Abstract Archives of the RSNA, 2022

MKEE-22

### Low-dose CT Approach to Tendon Delineation Using Deep Learning Technology

Sunday, Nov. 27 8:00AM - 9:00AM Room: Learning Center - MK

#### Participants

Takato Yanagisawa, Ueda, Japan (*Presenter*) Nothing to Disclose

#### TEACHING POINTS

The three-dimensional tendons image has a highly usefulness as surgical support. However, the difference in CT values between tendons and muscles is small. Therefore, it is necessary to reduce image noise in order to distinguish them. As a result, increased patient dose becomes a problem. We have tried to use Deep Learning Reconstruction (DLR) to solve this problem. This report introduces scanning techniques and patient dose reduction for creating 3D images of tendons. The 3D tendons imaging requires increased contrast and reduced patient dose reconstruction. The DLR for the brain LCD met this goal. This is because the diagnosis of the brain and the diagnosis of tendons are performed with the same low contrast. Compared to the conventional reconstruction method, DLR produced low-noise images at 75% lower dose and improved contrast, significantly enhancing the ability to visualize the finger flexor tendons.

#### TABLE OF CONTENTS/OUTLINE

1. Problems with imaging techniques in tendon morphology diagnosis 2. Improvement of image contrast using DLR 3. Reducing patient dose using DLR 4. Ingenuity when scanning tendons 5. Ingenuity for creating 3D tendons images 6. Verification of Clinical Effectiveness

Printed on: 02/07/23



## Abstract Archives of the RSNA, 2022

MKEE-23

### Brachial Plexus: Don't Be Afraid Anymore - A Guide for Brachial Plexus Anatomy and Injuries

Sunday, Nov. 27 8:00AM - 9:00AM Room: Learning Center - MK

#### Participants

LEON PERIN, Araras, Brazil (*Presenter*) Nothing to Disclose

#### TEACHING POINTS

The purpose of this study is to: 1. Review with didactic illustrations the brachial plex anatomy, including how to recognize it on MRI. 2. Demonstrate how several brachial plex injuries manifest clinically and on imaging exams. 3. Present didactic cases of brachial plex injuries highlighting the main findings the radiologist should expect, untangling brachial plex exams.

#### TABLE OF CONTENTS/OUTLINE

Introduction and review of the brachial plexus anatomy, with didactic illustration. Review the normal anatomy on MRI, highlighting the anatomic landmarks on coronal and sagittal exams. Overview the main injuries of the brachial plexus, including pre and post-ganglionic injuries, their clinical manifestations and epidemiology, and their imaging findings. Demonstrate with challenging clinical cases non-traumatic pathologies involving inflammatory and compressive causes, including Parsonage-Turner, thoracic outlet syndrome, post-Covid plexopathy. Present a series of cases of brachial plex injuries, and what you should actively look for depending on clinical history. Propose a diagnostic checklist when evaluating brachial plexus injuries, simplifying the reading of these challenging exams. Summary.

Printed on: 02/07/23



## Abstract Archives of the RSNA, 2022

MKEE-24

### Axial Spondyloarthritis: What the Radiologist Needs to Know

Sunday, Nov. 27 8:00AM - 9:00AM Room: Learning Center - MK

#### Awards

Certificate of Merit

#### Participants

Taiki Nozaki, MD, Tokyo, Japan (*Presenter*) Nothing to Disclose

#### TEACHING POINTS

The purposes of this exhibit are 1) To demonstrate the classification of spondyloarthritis and anatomy of sacroiliac joint. 2) To know basic imaging findings of axial spondyloarthritis. 3) To review the imaging findings of mimickers of axial spondyloarthritis that radiologists should be familiar with.

#### TABLE OF CONTENTS/OUTLINE

1) Introduction 2) Classification of spondyloarthritis 3) Anatomy of sacroiliac joint for the proper evaluation on MRI 4) MR findings of axial spondyloarthritis i) Signs of activity -bone marrow edema, capsulitis, joint space fluid- ii) Signs of structural change -erosion, fat metaplasia, backfill, sclerosis, ankylosis- 5) Mimickers of axial spondyloarthritis -early post-partum, osteitis condensans ilii, pyogenic sacroiliitis, Paget disease, fibrous dysplasia, tuberculosis, spondyloepiphyseal dysplasia, bone metastases, SAPHO syndrome, DISH-

Printed on: 02/07/23



## Abstract Archives of the RSNA, 2022

MKEE-25

### The Sword in the Bone: A Review of the Sternum and Parasternal Region

Sunday, Nov. 27 8:00AM - 9:00AM Room: Learning Center - MK

#### Awards

Certificate of Merit

#### Participants

Sean Rodich, MD, MS, (*Presenter*) Nothing to Disclose

#### TEACHING POINTS

1. Review anatomy of sternal bone landmarks, sternal and parasternal joints, and surrounding muscle attachments for a comprehensive understanding of the anterior chest wall. 2. Identify developmental variants and anomalies of the sternum to avoid confusion with other sternal pathologies. 3. Illustrate various pathologies of the sternum and parasternal region, which are often overlooked in the broad differential diagnosis for chest pain.

#### TABLE OF CONTENTS/OUTLINE

1. Anatomy of the sternum- Bone landmarks- Sternal and parasternal joints (manubriosternal, xiphisternal, sternoclavicular, sternocostal, costochondral, and interchondral joints)- Muscle attachments 2. Developmental variants and anomalies of the sternum- Sclerotic bars and clefts- Sternal foramen- Episternal ossicles- Xiphoid process variants- Pectus excavatum/carinatum- Ectopia cordis- Miscellaneous syndromes (PHACES, Pentalogy of Cantrell) 3. Pathology of the sternum and parasternal region- Trauma (sternal and costal cartilage fractures, sternoclavicular joint dislocation)- Arthropathy (osteoarthritis, calcium pyrophosphate deposition disease, rheumatoid arthritis, seronegative spondyloarthropathy)- SAPHO (Synovitis, Acne, Palmoplantar pustulosis, Hyperostosis, Osteitis)- Condensing osteitis of the clavicle- Costochondritis versus Tietze syndrome- Sternotomy complications (sternal dehiscence, infection)- Neoplasm

Printed on: 02/07/23



## Abstract Archives of the RSNA, 2022

MKEE-26

### Calcaneal Fracture Guide: Don't Miss a Thing - Beware of the Ugly Stuff

Sunday, Nov. 27 8:00AM - 9:00AM Room: Learning Center - MK

#### Awards

Certificate of Merit

#### Participants

Marina Akuri, MD, Marilia, Brazil (*Presenter*) Nothing to Disclose

#### TEACHING POINTS

The purpose of this exhibit is to:1. Review calcaneal anatomy, fracture classifications, possible complications and the management for each kind of fracture.2. Highlight the main information that radiologists should include in the report when analyzing a calcaneal fracture and their post-operative imaging, including normal and abnormal findings.3. Illustrate several cases of calcaneal fractures, including postoperative evaluation with normal findings and complications, as well as differential diagnosis cases.

#### TABLE OF CONTENTS/OUTLINE

Introduction: general review of calcaneal fractures, including classifications and what the report should include. Provide didactic and challenging cases of calcaneal fractures, including several complications, highlighting what is important for the report and for the orthopedic surgeon. Overview operative indications and modalities of surgical treatment. Present didactic cases of the different surgical modalities, discussing the normal and abnormal postoperative findings. Bibliographical references.

Printed on: 02/07/23

## Abstract Archives of the RSNA, 2022

MKEE-27

### Stain the Eyes-Utility of high Resolution CT Dacryocystography in Imaging Lacrimal Duct Pathology Following Facial Trauma

Sunday, Nov. 27 8:00AM - 9:00AM Room: Learning Center - MK

#### Participants

Sudha Pyla, MBBS, Vijayawada, India (*Presenter*) Nothing to Disclose

#### TEACHING POINTS

To demonstrate the common complications encountered in lacrimal drainage as a complication of facial injuries.

#### TABLE OF CONTENTS/OUTLINE

Nasolacrimal duct injury may be due to blunt or penetrating trauma involving naso orbitoethmoidal complex, maxillofacial fractures especially Le fort type-II, Le fort type-III, also secondary to postoperative cases due to inadequate surgical repair. In early post injury period, nasolacrimal duct obstruction can occur as a result of post traumatic compression by bone fragments or due to soft tissue edema. Inflammatory reaction followed by cicatrization resulting in delayed lacrimal duct blockade can present as late complication. Patients usually present with epiphora with or without purulent discharge. Long term complication include dacryocystocele formation. CT dacryocystography gives detailed information about the cause of obstruction, level of blockade, associated fractures and bony displacements. 1.5ml of diluted nonionic contrast (Ultravist 300mg iodine/ml) is administered into the inferior canaliculi and high resolution CT is performed. Depending on the level of blockage dacryocystorhinostomy is performed. In complete cut off of duct or chronic dacryocystitis dacryocystectomy is done. This exhibit will demonstrate various spectrum of post traumatic nasolacrimal drainage abnormality on CT dacryocystography.

Printed on: 02/07/23



## Abstract Archives of the RSNA, 2022

MKEE-28

### Lumpy-Bumpy Ride Made Easy ! - A Sonographic Guide Through Soft Tissue Lesions

Sunday, Nov. 27 8:00AM - 9:00AM Room: Learning Center - MK

#### Participants

Saakshi Aggarwal, MBBS, (*Presenter*) Nothing to Disclose

#### TEACHING POINTS

1. To review imaging features of various soft tissue lesions to be able to differentiate pseudo masses and pseudo tumors like dermoid, sebaceous cyst, abscess, hematoma from true tumors 2. To make a schematic approach towards suspected soft tissue lesions in order to assess nature of them based on internal characteristics of the lesion 3. To prime young budding radiologists towards diagnosis of benign "leave alone" lesions such as lipomas so as to reduce patient anxiety and limit further investigations unless indicated 4.To pick up suspicious morphology on ultrasonography and suggest the next appropriate step for further assessment

#### TABLE OF CONTENTS/OUTLINE

1. Introduction 2. Importance of ultrasonography in assessing soft tissue lesions 3. Ultrasonographic Technique to assess soft tissue lesions 4. Imaging features to differentiate pseudo masses and pseudo tumors from true tumors 5. Simplified schematic approach towards suspected true tumors 6. Review of imaging features of various soft tissue tumors with histopathological diagnosis 7. Practical pearls for successful and complete diagnosis

Printed on: 02/07/23



## Abstract Archives of the RSNA, 2022

MKEE-29HC

### Baseline, Posttreatment and Surveillance Advanced Magnetic Resonance Imaging of Soft-Tissue Sarcomas

Sunday, Nov. 27 8:00AM - 9:00AM Room: Learning Center - MK

#### Participants

Mathew Canjirathinkal, MD, Houston, TX (*Presenter*) Nothing to Disclose

#### TEACHING POINTS

1. Soft-Tissue Sarcoma is a rare malignant tumor of mesenchymal and primitive neuroectodermal origin, more common than primary malignant bone tumors. 2. Traditional response criteria such as RECIST inadequate rely on physical measurements, as tumor diameter does not reflect all response types. 3. Diffusion-weighted imaging analysis could rely upon Whole tumor ADC histograms, focusing on mean ADC, Kurtosis, and Skewness. 4. Whole tumor Perfusion Weighted Imaging (PWI) with Dynamic Contrast-enhanced imaging (DCE) could rely on morphologic patterns (nodular vs. linear) and time-intensity curves (TIC) analysis, where the presence of early arterial enhancement (TIC III, IV, and V) correlates with untreated or unsuccessfully treated sarcomas, while TIC II with successfully treated sarcomas. 5. DCE MR imaging reliably distinguishes recurrent sarcoma from postsurgical scarring. TICs III, IV, and V highly raise suspicion of local tumor recurrence, while TIC type II usually represents granulation.

#### TABLE OF CONTENTS/OUTLINE

1. Introduction 2. Learning objectives 3. Soft tissue sarcoma 4. The Armamentarium: MR sequences: DWI/ADC, PWI/DCE and SWI 5. ABASTI (Advanced bone and soft tissue tumor imaging) 6. Worth knowing: Hemorrhage and ADC, Fat and ADC. 7. Responding tumor ABASTI patterns 8. Non-responding tumor ABASTI patterns 9. Tumor recurrence and DCE 10. References Please visit the Learning Center to also view this presentation in hardcopy format.

Printed on: 02/07/23



## Abstract Archives of the RSNA, 2022

MKEE-3

### Radial Tunnel Anatomy in Supination and Pronation: Guidance for Imaging Interpretation and Interventional Procedures

Sunday, Nov. 27 8:00AM - 9:00AM Room: Learning Center - MK

#### Awards

**Magna Cum Laude**

#### Participants

Aurea Mohana-Borges, MD, MSc, San Diego, CA (*Presenter*) Nothing to Disclose

#### TEACHING POINTS

To provide a guide for radial tunnel anatomy that emphasizes the relationship of soft tissue (nerve, vessel, muscle) and osseous structures in supination and pronation with High Resolution Ultrasound (HRUS) and magnetic resonance imaging (MRI). This guide will highlight anatomic landmarks implicated in entrapment syndromes of the radial nerve. It will emphasize the dynamic nature of radial tunnel and its spatial relationships through range of motion. It will compare and contrast normal anatomy with examples of commonly encountered pathology about the radial tunnel.

#### TABLE OF CONTENTS/OUTLINE

Explanation of the concept, constituents, and anatomic boundaries of the radial tunnel. Demonstration of normal anatomy of the radial tunnel with HRUS and MRI with emphasis on the relationship of deep branch of radial nerve (DBRN), leash of Henry, and superior arcade of supinator muscle (arcade of Frohse). Examples of dynamic ultrasound of the DBRN, DBRN hydrodissection, and commonly encountered pathology about the radial tunnel.

Printed on: 02/07/23



## Abstract Archives of the RSNA, 2022

MKEE-30HC

### Susceptibility-Weighted Imaging (SWI) Emerging Role in Musculoskeletal (MSK) Oncology

Sunday, Nov. 27 8:00AM - 9:00AM Room: Learning Center - MK

#### Awards

Certificate of Merit

#### Participants

Mathew Canjirathinkal, MD, Houston, TX (*Presenter*) Nothing to Disclose

#### TEACHING POINTS

1. Susceptibility-weighted imaging (SWI) is a 3D high-spatial-resolution, velocity-corrected gradient-echo MRI sequence that uses magnitude and filtered-phase information to create images. 2. Distinguishing between calcification and blood products is possible through the filtered phase images, helping to recognize osteoblastic and osteolytic bone metastases or demonstrating calcifications and osteoid production in liposarcoma and osteosarcoma. 3. Contrast-enhanced SWI (CE-SWI) can simultaneously detect the T2\* susceptibility effect and spontaneous T1 shortening. 4. Various Bone and soft tissue masses SWI features are described. 5. CE SWI demonstrates the viable, enhancing portions of a soft tissue sarcoma separately from hemorrhagic/necrotic components, suggesting its utility as a biomarker of tumor grade and treatment response. CE-SWI shows superior differentiation between mature fibrotic T2\* dark components and active enhancing T1 shortening components in Desmoid Fibromatosis. 6. Ring-like hemosiderin SWI pattern is observed in successfully treated sarcomas. 7. CE-SWI also separates healthy T2\* blooming iron-loaded bone marrow from T1-shortening enhancing bone marrow replacing tumor.

#### TABLE OF CONTENTS/OUTLINE

1. Introduction to SWI and SWI with contrast CE-SWI. 2. CE-SWI in Benign and malignant soft tissue masses. 3. CE-SWI of primary bone tumors and metastasis. 4. CE-SWI features of soft tissue sarcoma tumor response. 5. References. Please visit the Learning Center to also view this presentation in hardcopy format.

Printed on: 02/07/23



## Abstract Archives of the RSNA, 2022

MKEE-31

### Stand and Deliver: Weight-Bearing Extremity CT in Clinical Practice

Sunday, Nov. 27 8:00AM - 9:00AM Room: Learning Center - MK

#### Awards

Identified for RadioGraphics

#### Participants

Matthew Doan, BS, Phoenix, AZ (*Presenter*) Nothing to Disclose

#### TEACHING POINTS

The structures of the foot and ankle are ideally assessed during weight-bearing. Cross-sectional imaging of the foot and ankle using CT and MRI can overcome the limitations of radiographs but is typically performed with patients in the supine position. Recently standing cone-beam CT (CBCT) scanners have been introduced to combine the value of cross-sectional CT imaging with the anatomic assessment of structures during weight-bearing.

#### TABLE OF CONTENTS/OUTLINE

Purpose/Aim: This educational exhibit will spotlight the implementation and utilization of a standing CBCT scanner in a tertiary care medical center. The exhibit will cover the scanner and room setup, basic scanner physics, patient preparation and positioning, and image acquisition. Illustrative example cases will be included. Content Organization: Describe the room requirements for installing a standing CBCT scanner. Review the CT physics involved in obtaining a standing CBCT image. Provide a workflow model for standing CBCT scanner use in musculoskeletal radiology practice. Showcase patient positioning during standing CBCT acquisition. Highlight additional uses of a standing CBCT scanner for hand and wrist imaging. Provide illustrative clinical cases spotlighting the value of standing CBCT imaging. Summary: Radiographs of the foot and ankle obtained with weight-bearing are fundamental in initial imaging assessment. In cases requiring cross-sectional imaging, standing CBCT provides weight-bearing advanced imaging at lower dosing than traditional CT. This educational exhibit highlights the role a standing CBCT scanner can play in clinical practice.

Printed on: 02/07/23



## Abstract Archives of the RSNA, 2022

MKEE-32

### Sonography of the Wrist and Hand in Clinical Practice: Diagnosis and Intervention

Sunday, Nov. 27 8:00AM - 9:00AM Room: Learning Center - MK

#### Awards

Identified for RadioGraphics

#### Participants

Dyan V. Flores, MD, Ottawa, ON (*Presenter*) Nothing to Disclose

#### TEACHING POINTS

Diagnostic and interventional sonography of the wrist and hand may be daunting in clinical practice due to the plethora of structures and abnormalities that need to be evaluated. In this education exhibit, we describe a compartment approach in detecting common wrist and hand disorders and performing the corresponding interventional procedures. The objectives of this educational exhibit are: • To review normal sonographic anatomy of the wrist and hand • To illustrate and highlight a compartment approach in diagnostic and interventional sonography of the hand and wrist • To discuss common abnormalities encountered in clinical practice and the corresponding interventions in each compartment

#### TABLE OF CONTENTS/OUTLINE

Extensor compartment • Extensor compartments 2 and 3 (EPL rupture, distal intersection syndrome) • Intrinsic ligaments of the wrist • Extensor hood/Ulnar compartment • DRUJ • TFCC • Extensor compartment 6/Volar compartment • Median nerve at carpal tunnel • Ulnar nerve in Guyon's canal • Flexor tendons and retinaculum • Finger pulleys/Radial compartment • 1st CMC and STT • Extensor compartment 1 (De Quervain's tenosynovitis, proximal intersection syndrome) • UCL of thumb

Printed on: 02/07/23

## Abstract Archives of the RSNA, 2022

MKEE-33

### MRI of the Metabolic Knee

Sunday, Nov. 27 8:00AM - 9:00AM Room: Learning Center - MK

#### Participants

Bruno C. Vande Berg, MD, PhD, (*Presenter*) Nothing to Disclose

#### TEACHING POINTS

\* Metabolic disorders of the MSK system are frequent disorders that are usually clinically silent for a long period of time. All components of the musculo-skeletal system can be involved including bones, marrow, cartilage, tendons, ligaments, capsule, synovium and muscles. \* Despite the fact that knee MRI is one of the most frequently performed examination, radiologists rarely suggest the presence of an underlying metabolic disorder at knee MRI. The vast majority of the metabolic disorders of the MSK system remains occult at knee MRI until complications occur. \* Knee MRI can depict a spectrum of complications associated with metabolic disorders including typical and atypical fractures, bone necrosis, acute and chronic arthritis, peri-arthritis, tendinopathies and tendon rupture, synovial and capsule deposits, red marrow reconversion and serous transformation. \* The radiologists should recognize these complications at knee MRI and suggest a possible link with an underlying metabolic disorder. \* The current exhibit aims at presenting a series of clinical cases in which knee MRI was performed and led to the diagnosis of a systemic metabolic disorder.

#### TABLE OF CONTENTS/OUTLINE

\* Insufficiency and avulsion fractures in osteoporosis/osteomalacia/renal osteodystrophy.\* Crystal-associated acute arthritis and peri-arthritis. \* Chronic tophaceous arthritis. \* Drug-associated tendinopathies and tendon rupture. \* Unusual osteoarthritis associated with calcium pyrophosphate crystals.\* Marrow reconversion and marrow necrosis associated with anemias.\* fat and serous atrophy of the bone marrow associated with cachexia.\* Synovial and cartilage deposits of iron and copper. \* Synovial and capsule amyloidosis.

Printed on: 02/07/23



## Abstract Archives of the RSNA, 2022

MKEE-34

### The Many Faces of Ramp Lesions of the Medial Meniscus

Sunday, Nov. 27 8:00AM - 9:00AM Room: Learning Center - MK

#### Participants

Alfonso Iglesias, MD, PhD, (*Presenter*) Nothing to Disclose

#### TEACHING POINTS

Meniscal ramp injury is a meniscus-capsular vertical longitudinal tear of the posterior horn of the internal meniscus, often associated, with an anterior cruciate ligament injury. In MRI, an injury of the internal meniscal ramp must be suspected when a rupture of the ACL and/or bone edema in the posteromedial slope of the tibial plateau is observed. It is important to detect meniscal ramp injuries in MRI and alert the traumatologist, since they are hidden meniscal lesions with the usual arthroscopic portals, and require accessory portals for a diagnostic confirmation. The decision of either a conservative or a surgical treatment will depend primary on the stability and the extent of the injury.

#### TABLE OF CONTENTS/OUTLINE

Recognize and identify a ramp lesion of the medial meniscus on MR images Describe and classify ramp lesion of the medial meniscus on MR images with arthroscopic correlation Review of surgical technique for the detection and repair of these types of lesions

Printed on: 02/07/23



## Abstract Archives of the RSNA, 2022

MKEE-35

### Shoulder Microinstability: Demystifying the Interplay of Static and Dynamic Stabilizers of the Glenohumeral Joint

Sunday, Nov. 27 8:00AM - 9:00AM Room: Learning Center - MK

#### Participants

Juliana Sitta, MD, Jackson, MS (*Presenter*) Nothing to Disclose

#### TEACHING POINTS

Microinstability is a relatively new concept defined by rotational or directional pathologic movement of the glenohumeral joint without true (macro) instability on physical examination. The pathophysiology may include abnormalities involving static and dynamic stabilizers of the glenohumeral joint, the anterosuperior labrum, rotator interval, or middle glenohumeral ligament. Causes of microinstability may include acute or chronic recurrent traumatic etiology (including overuse), iatrogenic, and congenital osseous and soft tissue abnormalities. Clinical and imaging findings including those of internal impingement syndromes are often subtle and radiologists play an important role in identifying these patients to guide appropriate treatment and avoid delay in diagnosis which can lead to osteoarthritis.

#### TABLE OF CONTENTS/OUTLINE

Glenohumeral anatomy and congenital variants. Pathophysiology of shoulder microinstability, glenoid dysplasia, anterior and posterior internal impingement syndromes. Multimodality imaging findings and differential diagnosis. Clinical and surgical management. Complications and post treatment imaging findings.

Printed on: 02/07/23



## Abstract Archives of the RSNA, 2022

MKEE-36

### Imaging Features of Glenohumeral Osteoarthritis: The Power of Simplicity

Sunday, Nov. 27 8:00AM - 9:00AM Room: Learning Center - MK

#### Participants

Paulo de Tarso Perez, MD, (*Presenter*) Nothing to Disclose

#### TEACHING POINTS

The purpose of this exhibit is to: To briefly review the concepts of glenohumeral osteoarthritis. To review the most used classifications, image findings and measures of glenoid. Highlight the Walch classification, glenoid morphology changes and what we should report that can change the management and treatment. To make the differential diagnosis with entities that may cause osteoarthritis.

#### TABLE OF CONTENTS/OUTLINE

Introduction: to review the concepts of glenohumeral osteoarthritis. Show didactic and illustrative cases reviewing the classifications and the main imaging findings according to the different etiologies, highlighting what we should report in order to assist in the correct and early diagnosis and treatment. Present a schematic table and imaging of the most used classifications and showing measures of glenoid and its morphology changes. Conclusions. Bibliographical references.

Printed on: 02/07/23



## Abstract Archives of the RSNA, 2022

MKEE-37

### Is This DISH?": Radiological Findings with Special Attention to Extraplinal Involvement

Sunday, Nov. 27 8:00AM - 9:00AM Room: Learning Center - MK

#### Participants

Dario Herran de la Gala, MD, Santander, Spain (*Presenter*) Nothing to Disclose

#### TEACHING POINTS

This exhibit will: 1) Describe the most frequent radiological findings of DISH in the spine. 2) Establish the diagnostic criteria and their usefulness in DISH differential diagnosis. 3) Show the most frequent extraplnal findings. 4) Illustrate the most frequent DISH complications.

#### TABLE OF CONTENTS/OUTLINE

Diffuse idiopathic skeletal hyperostosis (DISH) is an underdiagnosed disease whose prevalence increases with age. This disease consist in an ossification of both spinal and extraplnal tendons, ligaments, periosteum and joint capsules. It can cause pain, stiffness, compressive syndromes or spinal fractures after minor traumas. Radiological findings in the spine and DISH diagnostic criteria are widely known. On the other hand, extraplnal involvement, especially in isolation, may go unnoticed. Moreover, extraplnal involvement precedes spinal radiological findings and can be found in younger patients.

Printed on: 02/07/23

## Abstract Archives of the RSNA, 2022

MKEE-38

### Haemophilic Arthropathy: An Imaging Overview

Sunday, Nov. 27 8:00AM - 9:00AM Room: Learning Center - MK

#### Participants

Marina Akuri, MD, Marilia, Brazil (*Presenter*) Nothing to Disclose

#### TEACHING POINTS

The purpose of this exhibit is to: 1. Review and illustrate classifications and spectrum of imaging findings of haemophilic arthropathies in a multimodality approach including radiographs, ultrasound, computed tomography and magnetic resonance in different joints. 2. Highlight and discuss other musculoskeletal complications of haemophilia that the radiologist must be aware in these patients, such as hematomas, pseudotumors, heterotopic calcification, and others. 3. Provide a guidebook for all the typical and atypical musculoskeletal findings in hemophilic arthropathy.

#### TABLE OF CONTENTS/OUTLINE

Introduction: general presentation, epidemiology, pathology and clinical manifestation of haemophilic arthropathies. Present a schematic illustration with the distribution of the most common joints affected by haemophilic arthropathy while discussing the main findings on didactic cases. Overview some of main haemophilic arthropathy classification including a schematic illustration of Arnold-Hilgartner classification. Provide didactic cases of the all image modality of different joints with typical and atypical findings. Provide other musculoskeletal manifestations and complication with challenging cases of hematomas, pseudotumors and heterotopic calcification. Present differential diagnosis cases with some similar intra-articular findings that should not be mistaken with hemophilic disease, including inflammatory arthropathies, amyloidosis, gout, among others. Bibliographical references.

Printed on: 02/07/23



## Abstract Archives of the RSNA, 2022

MKEE-39

### A Radiological Overview of Ankle Arthroplasty - Practical Keys in the Assessment of Ankle Replacement

Sunday, Nov. 27 8:00AM - 9:00AM Room: Learning Center - MK

#### Participants

Javier Azpeitia Arman, MD, Madrid, Spain (*Presenter*) Nothing to Disclose

#### TEACHING POINTS

-To know the different types of total ankle replacement. -To review imaging techniques for preoperative imaging and in the evaluation of prostheses (plain radiograph, CT, MR, US, scintigraphy). -To understand the usefulness and limitations of plain radiographs in the evaluation of ankle replacements, emphasizing useful parameters and illustrating image analysis and interpretation. -To become familiar with normal and abnormal postoperative imaging findings and signs of complications.

#### TABLE OF CONTENTS/OUTLINE

We review imaging of total ankle replacement, highlighting key concepts perceived as important variables by the surgeon and correlating images with clinical considerations and functional outcomes. We present: 1. A review of types of ankle replacement 2. Surgery. Aims. 3. Imaging. Role of CT, MR, US, and scintigraphy. 4. Plain radiographs: -Technique and views. Standard image acquisition: beam and anatomical landmarks -Parameters that should be evaluated: alignment of tibial and talar components, position, rotation, radiolucent lines and subtle abnormalities such as subsidence, early osteolysis, and angular deformities that may indicate aseptic loosening or possible infection -Imaging of complications: aseptic loosening, expansile osteolysis, subsidence and component migration, infection, periprosthetic fracture, heterotopic ossification, and PE spacer displacement or fracture

Printed on: 02/07/23



## Abstract Archives of the RSNA, 2022

MKEE-4

### Apophyseal Athletic Injuries Around the Hip: Why You Shouldn't Be Afraid

Sunday, Nov. 27 8:00AM - 9:00AM Room: Learning Center - MK

#### Awards

Certificate of Merit

#### Participants

Vitor Sato, MD, Sao Paulo, Brazil (*Presenter*) Nothing to Disclose

#### TEACHING POINTS

The purpose of this exhibit is to: Illustrate and discuss hip anatomy in individuals with immature bone skeleton, focusing on the apophysis; Describe and illustrate the maturation process of apophysis; Discuss and illustrate with classical and challenging cases the imaging findings of different apophysitis and apophyseal lesion around the hip; Show common and uncommon pitfalls that mimic apophyseal lesion in the hip; Show imaging findings of sequelae of apophysitis in the hip.

#### TABLE OF CONTENTS/OUTLINE

Introduction: general presentation of anatomy with MRI of hip apophysis in the immature bone skeleton, including the complex anatomy of tendinous and aponeurosis insertion in the pubic apophysis; Present schematic cases and illustration to show maturation process of apophysis, with emphasis in the pubic apophysis; Describe schematically the algorithm and imaging protocol for assessing apophyseal injury in skeletal immature athletes; Show imaging findings of classical and challenging cases of apophyseal injury around the hip in athletes and also pitfalls that could mimic this pathologic condition; Show imaging findings of sequelae of apophysitis in the hip; Bibliographical references with recent articles highlighting what's new in the topic.

Printed on: 02/07/23



## Abstract Archives of the RSNA, 2022

MKEE-40

### Chip on the Shoulder: Multimodality Review of Reverse Shoulder Arthroplasties

Sunday, Nov. 27 8:00AM - 9:00AM Room: Learning Center - MK

#### Participants

Akwasi Opoku, MD, Nashville, TN (*Presenter*) Nothing to Disclose

#### TEACHING POINTS

The reverse shoulder arthroplasty (RSA) is a significant advance in shoulder reconstruction, reversing the normal ball and socket anatomy, stabilizing the glenohumeral center of rotation, and allowing the deltoid to function as the main muscular force. RSA has been shown to provide pain relief and functional improvement. Radiologists must be aware of the importance of certain preoperative imaging findings in patients under consideration for RSA, such as deltoid integrity, as well as potential postoperative complications unique to RSA, such as acromial and scapular fractures, and scapular notching. After viewing this exhibit, the learner should understand: 1. Shoulder anatomy and biomechanics 2. Indications for RSA 3. Role of preoperative imaging and measurements 4. Advantages, disadvantages, and specific complications of RSA 5. Normal imaging findings and imaging findings of complications

#### TABLE OF CONTENTS/OUTLINE

Introduction Shoulder anatomy and biomechanics 1. Bones, joints, muscles, other soft tissues (cartilage, labrum, capsule) 2. Unconstrained ball and socket, static and dynamic stabilizers Design, function, and success of RSA Indications 1. Arthropathy, trauma, cuff disease, osteonecrosis, prior infection, failed arthroplasty Role of preoperative imaging (multimodality) 1. Evaluation of cuff, bone stock, cartilage 2. Glenoid morphology and version Complications 1. Acromial and scapular fractures 2. Scapular notching 3. Hardware fracture and disengagement 4. Periprosthetic fracture 5. Loosening 6. Infection 7. Instability 8. Nerve injury Imaging appearances 1. Normal and complications

Printed on: 02/07/23



## Abstract Archives of the RSNA, 2022

MKEE-41

### **Hip Dysplasia: Evaluation Beyond Diagnosis - What the Radiologist Should Know About Its Management Treatment**

Sunday, Nov. 27 8:00AM - 9:00AM Room: Learning Center - MK

#### **Participants**

Mariana Batista Rosa Pinto, MD, (*Presenter*) Nothing to Disclose

#### **TEACHING POINTS**

The purpose of this study is to: Briefly approach the pathophysiology and epidemiology of hip dysplasia. Discuss the imaging modalities used to evaluate hip dysplasia and list the imaging findings and measurable parameters that most accurately reflect the disorder. Review and didactically illustrate the most frequent treatments, complications and differential diagnoses of the disease. Provide a guide with several examples of post-treatment imaging, highlighting what the radiologist should know about the management of hip dysplasia.

#### **TABLE OF CONTENTS/OUTLINE**

Introduction: general presentation of the epidemiology, pathophysiology and clinical findings of hip dysplasia. Present schematic illustrations of findings and measurable parameters that most accurately help the diagnosis of the disorder. Provide didactic cases of the manifestation related to each type of imaging method. Discuss treatments and what radiologists should know when evaluating the postoperative exams, while providing pre and postoperative imaging examples. Point complications and show differential diagnoses. Provide an imaging guide of the several hip dysplasia treatment options. Conclusions. Bibliographical references with recent articles on what is new in the topic.

Printed on: 02/07/23



## Abstract Archives of the RSNA, 2022

MKEE-42

### Musculoskeletal Complications of Cosmetic Procedures: When Things Get Ugly

Sunday, Nov. 27 8:00AM - 9:00AM Room: Learning Center - MK

#### Participants

Ligia Couceiro, MD, Sao Paulo, Brazil (*Presenter*) Nothing to Disclose

#### TEACHING POINTS

According to the American Society of Plastic Surgery (ASPS), aesthetic procedures have increased exponentially in recent years. A wide variety of cosmetic techniques are performed in healthy patients to improve body image or for reconstructive reasons. Those procedures can be either incidental findings or the cause of symptoms on imaging exams. It is indispensable for radiologists to learn identification of the common aesthetic procedures on different imaging techniques and be capable of evaluating their normal appearance and complications. The purpose of this study is: • To recognize the most common aesthetic procedures and their normal appearance, focusing on musculoskeletal system imaging. • To discuss the cosmetic procedures complications and their imaging findings. • Illustrate imaging findings through sample cases • Propose a systematic approach to image interpretation.

#### TABLE OF CONTENTS/OUTLINE

• INTRODUCTION • Review aesthetic procedures and their complications. • COSMETIC PROCEDURES INVOLVING THE MUSCULOSKELETAL SYSTEM AND THEIR COMPLICATIONS: • Gluteal augmentation (gluteal implants, autologous fat grafting, filler injections): implants displacement/ rupture, capsular contraction; infection; compressive syndromes, etc • Abdominoplasty: wound dehiscence, infection, etc • Body contouring with silicone implants (arms, legs): infection, implants rupture, etc • Pectoral augmentation (implants, filler injections): infection, implants displacement or rupture, etc • IMAGING INTERPRETATION • Cosmetic procedures normal and pathological findings • Systematic approach to evaluate image exams • INTERACTIVE CASE-BASED DIDACTICS • Sample cases to illustrate and solidify the concepts

Printed on: 02/07/23



## Abstract Archives of the RSNA, 2022

MKEE-43

### Fungal Musculoskeletal Infections: Who, When, Where and How? A Comprehensive Approach to Proper Diagnosis

Sunday, Nov. 27 8:00AM - 9:00AM Room: Learning Center - MK

#### Awards

**Certificate of Merit**

**Identified for RadioGraphics**

#### Participants

Julia Peixoto, Sao Paulo, Brazil (*Presenter*) Nothing to Disclose

#### TEACHING POINTS

Teaching points: The purpose of this exhibit is to: 1. Provide a comprehensive overview, yet a didactic practical guide to assess fungal musculoskeletal infections imaging; 2. Integrate imaging, clinical and epidemiological aspects, reviewing and illustrating the most frequent and some rare presentations of fungal musculoskeletal infections;

#### TABLE OF CONTENTS/OUTLINE

Outlines: Introduction: epidemiology, etiology, pathophysiology and clinical findings. Section-structured overview emphasizing the main imaging findings and relevant clinical and epidemiological features of each group of fungus. Illustrative cases, exemplifying classic imaging signs, and challenging cases addressing differential diagnoses with practical tips. Bibliography: broad-researched references highlighting what's useful to the radiologist.

Printed on: 02/07/23



## Abstract Archives of the RSNA, 2022

MKEE-44

### A Guide to Tibiofibular Syndesmosis: Anatomy, Imaging and Surgical Techniques

Sunday, Nov. 27 8:00AM - 9:00AM Room: Learning Center - MK

#### Participants

Cristyano Leite, MD, Sao Paulo, Brazil (*Presenter*) Nothing to Disclose

#### TEACHING POINTS

Comprehend clinic indications for imaging evaluation. Recognize the most useful image methods. Learn the anatomic features and relationships of the tibiofibular syndesmosis. Understand role and limitations of each method.

#### TABLE OF CONTENTS/OUTLINE

INTRODUCTION. Epidemiology of the tibiofibular syndesmosis injury. Different Imaging methods to evaluate the syndesmosis. ANATOMICAL CONCEPTS. Anatomic description of the syndesmosis ligaments. Normal syndesmosis in the different methods. CASE-BASED DIDACTICS. Ligaments and syndesmotic injuries in the different methods. SURGICAL TECHNIQUES. Most used surgical techniques: indication and examples.

Printed on: 02/07/23



## Abstract Archives of the RSNA, 2022

MKEE-45

### Ultrasound of Medial Elbow Pain: Beyond the Epicondylitis

Sunday, Nov. 27 8:00AM - 9:00AM Room: Learning Center - MK

#### Participants

Jee Won Chai, MD, Seoul, Korea, Republic Of (*Presenter*) Nothing to Disclose

#### TEACHING POINTS

Although it is less common than lateral elbow pain, medial elbow pain is a musculoskeletal problem more commonly encountered in the population participating repetitive activities. Ultrasonography has advantages in focused and dynamic evaluation of medial elbow structures, and subsequently enables to establish the differential diagnosis. The various anatomic structures more than common flexor tendon, such as ulnar collateral ligament, ulnar nerve, medial antebrachial cutaneous nerve and elbow joint can cause medial elbow pain, and some characteristic clinical features and physical examinations would be helpful for more focused evaluation on the clinically suspicious structures. Even with positive finding on one structure, other structures also should be evaluated for screening of coexisting pathology or other possible diagnosis; for instance, medial epicondylitis can accompany ulnar neuropathy or ulnar collateral ligament injury as well, and proper treatment would be differed in such cases.

#### TABLE OF CONTENTS/OUTLINE

1. Differential diagnosis of medial elbow pain 2. Scanning technique and normal medial elbow on ultrasonography 3. Medial elbow pathology  
A. Medial epicondylitis  
B. Ulnar collateral ligament injury  
C. Ulnar neuropathy  
i. Cubital tunnel syndrome  
ii. Ulnar nerve instability  
D. Snapping triceps syndrome  
E. Medial antecubital cutaneous neuropathy  
F. Arthritis  
i. Ulnohumeral osteoarthritis  
ii. Gouty arthritis  
G. Others  
i. Cervical radiculopathy  
ii. Basilic vein thrombophlebitis

Printed on: 02/07/23



## Abstract Archives of the RSNA, 2022

MKEE-46

### Comparing US and MRI for Hand and Wrist Diseases: Which Weapon to Choose?

Sunday, Nov. 27 8:00AM - 9:00AM Room: Learning Center - MK

#### Participants

Young Ju Song, MD, Jeonju, Korea, Republic Of (*Presenter*) Nothing to Disclose

#### TEACHING POINTS

Ultrasound imaging uses sound waves to produce pictures of muscles, tendons, ligaments, nerves and joints throughout the body. It is used to help diagnose sprains, strains, tears, trapped nerves, arthritis and other conditions. However, there are some diseases that US cannot fully detect, whereas MRI can easily and quickly find. Magnetic resonance imaging (MRI) uses a powerful magnetic field, radio waves and a computer to produce detailed pictures of joints, soft tissues and especially intraosseous lesions. It is usually the best choice for evaluating the body for injuries, tumors, and degenerative disorders. But in some cases, US is superior to MRI for detecting certain pathologies. The ability of a radiologist to understand the fundamental physics of US and MRI, recognize US and MRI competencies, and provide recommendations for using the most suitable imaging modality is essential for proper image interpretation, troubleshooting, and utilization of the full potential of each modality.

#### TABLE OF CONTENTS/OUTLINE

1. Basic Physics of Ultrasound 2. Basic Physics of MRI 3. Hand and Wrist Lesions : Comparison of Ultrasound vs. MRI 1) Cases that show how Ultrasound is superior to MRI: Gout, Calcific Tendinosis, Extensor Carpi Ulnaris Dislocation (in dynamic study), Digital Nerve Adhesion, Pulley Thickening (Trigger finger) 2) Cases that show how MRI is superior to Ultrasound: Triangular Fibrocartilage Complex Tear, Osteomyelitis, Bone Tumor, Complex Regional Pain Syndrome, Infectious Arthritis 3) Cases that show how both Ultrasound and MRI are equally useful: Tenosynovitis, Sagittal Band Rupture, Volar Plate Injury, Collateral Ligament Injury, Rheumatoid Arthritis, Ganglion Cyst, Tenosynovial Giant Cell Tumor

Printed on: 02/07/23



## Abstract Archives of the RSNA, 2022

MKEE-47

### "Go With the Flow" - Vascular Pathology Encountered on Knee MRI

Sunday, Nov. 27 8:00AM - 9:00AM Room: Learning Center - MK

#### Participants

Kathryn Stevens, MBBS, FRCR, Stanford, CA (*Presenter*) Nothing to Disclose

#### TEACHING POINTS

The purpose of this exhibit is to: 1. Review common and uncommon pathology of the popliteal artery and veins that can be encountered on knee MRI 2. Describe the signal characteristics of vascular masses occurring within and around the knee, as well as some of the potential pitfalls The major teaching points of this exhibit are: 1. Vascular pathology can often be seen on knee MRI, and is important to recognize 2. Knowledge of normal variants in vascular and muscle anatomy occurring around the knee has important implications for surgical planning 3. Detecting a DVT on routine MRI may significantly affect subsequent patient management 4. Intra- and extra-articular vascular malformations are not infrequently encountered around the knee, and it is important to identify characteristic imaging findings together with some of the potential pitfalls in diagnosis

#### TABLE OF CONTENTS/OUTLINE

1. Discuss classification and imaging findings of popliteal entrapment syndrome 2. Illustrate pathologies affecting the popliteal artery, including popliteal artery dissection, transection, aneurysm/pseudoaneurysm, cystic adventitial disease of the popliteal artery, and arterial calcification due to deficiency of CD73 (ACDC) 3. Review the aberrant anterior tibial artery, a commonly encountered normal variant, and emphasize the importance of including a description of this common variant in an MR report, particularly if the patient is to undergo subsequent knee surgery 4. Highlight the importance of evaluating for deep venous thrombosis on routine MRI 5. Outline imaging characteristics of vascular malformations occurring around the knee 6. Illustrate potential pitfalls mimicking vascular pathology around the knee

Printed on: 02/07/23



## Abstract Archives of the RSNA, 2022

MKEE-48

### Don't Be Afraid About T2 Mapping of the Knee Articular Cartilage: A Simple Way to Decrease Reports Ambiguity and Improve the Communication with Arthroscopists

Sunday, Nov. 27 8:00AM - 9:00AM Room: Learning Center - MK

#### Awards

Certificate of Merit

#### Participants

Estefania Gallego Diaz, MD, MD, Mexico City, Mexico (*Presenter*) Nothing to Disclose

#### TEACHING POINTS

- T2 mapping sequence improves the sensibility of detecting cartilage lesions within the knee joint, especially in the early stages.- To explain the importance of adding a T2 mapping sequence to a routine MRI protocol. - To instruct the radiologist on who applies the T2 mapping and how to do it. - To Review the main classifications of chondral (cartilage) lesions. - To implement the use of validated evaluation scales. - To present an algorithm approach and protocol that facilitates a uniform lexicon between radiologists and arthroscopists.- To simplify the technique and reports used in these patients to improve communication with the arthroscopy specialists.

#### TABLE OF CONTENTS/OUTLINE

1. Introduction 2. Definitions 3. Understanding the chondral(cartilage) lesion 4. Classifications of chondral lesions and correlation with arthroscopy 5. Validated evaluation scales 6. T2 mapping sequence · Indications · Physics · Technique and protocol recommendations 7. How to report it: · Pictorial review · Algorithm approach and templates tips. · Case-based learning 8. Conclusions

Printed on: 02/07/23



## Abstract Archives of the RSNA, 2022

MKEE-49

### The Patellofemoral Joint: From Joint Stability to Articular Pathologies

Sunday, Nov. 27 8:00AM - 9:00AM Room: Learning Center - MK

#### Participants

Andre Rosenfeld, MD, Sao Paulo, Brazil (*Presenter*) Nothing to Disclose

#### TEACHING POINTS

The purpose of this educational exhibit is:- Review the normal anatomy and imaging evaluation of the stabilizers of the patellofemoral joint and their pathologies, exemplifying the pathologies with didactic cases- Illustrate and discuss knee extensor mechanism injuries, patellar fat pad and bursae pathologies- Review patellofemoral joint pathologies, including degenerative osteoarthritis, inflammatory and crystal arthropathy

#### TABLE OF CONTENTS/OUTLINE

Patellofemoral congruency depends on dynamic stabilizers (extensor muscles and medial patellofemoral retinaculum/ligament) and static (bone) stabilizers. Imaging evaluation includes patellar and trochlear measurements, patellar translation distance (TT-TG) and torsional measurements. The knee extensor mechanism is composed of the quadriceps muscle and tendon, medial and lateral patellar retinaculum, patella, patellar tendon and tibial tuberosity. Its pathologies can be divided by location and chronology (acute vs chronic). Associated extensor mechanism pathologies include patellar fat pad and bursa abnormalities. The patellofemoral joint is a synovial joint that can be affected by degenerative, inflammatory and crystal arthropathies and synovial processes, with typical imaging findings. The radiologist needs to be familiar with the complete imaging evaluation of the patellofemoral joint, from joint stability to articular pathologies.

Printed on: 02/07/23



## Abstract Archives of the RSNA, 2022

MKEE-5

### Musculoskeletal Manifestations of Dermatomyositis: An Imaging Overview

Sunday, Nov. 27 8:00AM - 9:00AM Room: Learning Center - MK

#### Participants

Marina Akuri, MD, Marilia, Brazil (*Presenter*) Nothing to Disclose

#### TEACHING POINTS

The purpose of this exhibit is to: 1. Review and illustrate musculoskeletal manifestation of dermatomyositis with imaging findings on radiographs, ultrasound, computed tomography scan and magnetic resonance imaging. 2. Review and discuss diagnoses related to dermatomyositis as paraneoplastic manifestation. 3. Review and discuss differential diagnoses.

#### TABLE OF CONTENTS/OUTLINE

Introduction: overview of clinical manifestation of the disease, including epidemiology, physiopathology, also presenting musculoskeletal clinical features of dermatomyositis. Present an illustrated scheme with the most common manifestations of dermatomyositis. Exemplify the manifestations of dermatomyositis such as skin involvement, subcutaneous tissue involvement, musculoskeletal involvement, and correlate with different imaging modalities. Present clinical case with differential diagnosis. References.

Printed on: 02/07/23

## Abstract Archives of the RSNA, 2022

MKEE-50

### Posterior Meniscal Roots Injury: What Radiologists Need to Know

Sunday, Nov. 27 8:00AM - 9:00AM Room: Learning Center - MK

#### Participants

Camila De Paula Silva, MD, Botucatu, Brazil (*Presenter*) Nothing to Disclose

#### TEACHING POINTS

To review and illustrate the anatomy of the posterior meniscal roots in schematic figures and MRI. To review and illustrate the lesions and classification of posterior root meniscal tears in schematic figures and MRI. To review and illustrate the surgical techniques to repair meniscal posterior root tears in schematic figures, intra-operative imaging, and post-operative imaging in a multimodality approach.

#### TABLE OF CONTENTS/OUTLINE

1- Anatomy of the posterior meniscus root. 2- MRI of posterior meniscus root tears and their classifications: - type 1 (partial radial root tears without any tear in the adjacent posterior horn or body); - type 2 (complete radial root tears); - type 3 (longitudinal bucket-handle tears with a complete tear of the root attachment); - type 4 (complex oblique tears with a complete tear of the root attachment); - type 5 (avulsion fractures of the tibial plateau). 3- Types of surgical techniques to repair meniscal root tears, include - Surgical indications.- Intra-operative imaging.- Partial meniscectomy.- Meniscal repair (transtibial pullout repair, suture anchor repair, and side-to-side repair).

Printed on: 02/07/23



## Abstract Archives of the RSNA, 2022

MKEE-51

### Update on Orthopedic Procedures in the Knee

Sunday, Nov. 27 8:00AM - 9:00AM Room: Learning Center - MK

#### Participants

Eduarda Bernal, MD, Sao Paulo, Brazil (*Presenter*) Nothing to Disclose

#### TEACHING POINTS

Review new methods to repair cartilage of the knee like allograft and autologous transplantation associated with collagen membrane. Demonstrate that extra-articular anterolateral procedures improve clinical outcome when performed as an augmentation of the anterior cruciate ligament reconstruction in specific groups of patients. Review normal and abnormal postoperative MRI findings of arthroscopic transtibial pullout repair (ATPR) for medial meniscus posterior root tear (MMPRT). Talk about future prospects of minimally invasive knee surgery.

#### TABLE OF CONTENTS/OUTLINE

Cartilage defects of the knee are often debilitating and predispose to osteoarthritis. seeking methods that combined can effectively repair cartilage and prevent progression to osteoarthritis is the goal of orthopedists. For larger lesions with a substantial amount of cartilage loss, autologous chondrocyte implantation using a bilayer collagen membrane has been demonstrated excellent results. Currently, the most commonly used technique for root repair is ATPR. The role of postoperative MRI is confirm the reduction of the posterior meniscus root to the original footprint of the tibial surface, identify the integrity of this structure, note the decrease in intra-meniscal signal intensity. The anterolateral ligament and capsule of the knee are anatomical structures involved in rotational stability and pivot-shift control. As such, it has been demonstrated that the extra-articular anterolateral procedures improve clinical outcome when performed as an augmentation of the anterior cruciate ligament reconstruction in specific groups of patients.

Printed on: 02/07/23



## Abstract Archives of the RSNA, 2022

MKEE-52

### Osteosarcopenia: A New Geriatric Syndrome with Great Impact on Our Life

Sunday, Nov. 27 8:00AM - 9:00AM Room: Learning Center - MK

#### Participants

Jimi Huh, MD, (*Presenter*) Nothing to Disclose

#### TEACHING POINTS

The purpose of this exhibit is 1. To explain the concept and updated knowledge about osteosarcopenia 2. To systematically review the current researches about clinical importance of osteosarcopenia 3. To understand the concept and future directions of body composition imaging for evaluation of osteosarcopenia Major teaching points are: 1. Osteosarcopenia, a combination of osteoporosis and sarcopenia is a distinct disease entity with unique pathophysiology. 2. Osteosarcopenia is highly associated with frailty and mortality in elderly people and cancer patients. 3. Advances in imaging have enabled detailed analysis of osteosarcopenia.

#### TABLE OF CONTENTS/OUTLINE

1. Concept and updated knowledge about osteosarcopenia - Changing concepts: From sarcopenia to osteosarcopenia and myosteatosis - Osteosarcopenia: combination of sarcopenia and osteoporosis - Distinct pathophysiology focusing on interaction between muscle and bone 2. Systematic review for clinical importance of osteosarcopenia - Prognostic markers for overall survival in cancer patients - Independent risk factors for osteoporotic fractures and frailty - Increase in mortality/morbidity after major surgery 3. Body composition imaging for evaluation of osteosarcopenia - Current leading diagnostic modalities of osteosarcopenia : CT, MRI and DXA - Imaging methods to measure the skeletal muscle area (SMA) and bone mineral density (BMD) - Evolution of AI techniques: AI segmentation and pattern analysis for BMD 4. Future directions of body composition imaging - Standardization of diagnostic modality, measuring level, and diagnostic cut-off and criteria - Accurate methods to assess muscle and bone tissue composition in opportunistic CT

Printed on: 02/07/23



## Abstract Archives of the RSNA, 2022

MKEE-53

### Sonography of Anatomical Variations in the Hand Innervation

Sunday, Nov. 27 8:00AM - 9:00AM Room: Learning Center - MK

#### Participants

Afarine Madani, PhD, Bruxelles, Belgium (*Presenter*) Nothing to Disclose

#### TEACHING POINTS

- Less than 10% of individuals show the classical hand innervation pattern as described in anatomical books
- More than 90% of individuals display at least one or up to five anastomoses between ulnar nerve and median nerve
- 50% of the anastomoses are localized within the forearm
- Knowledge of anatomical variations in the hand innervation is essential because they induce variations in symptomatology, clinical findings, imaging results, and "routine" electrodiagnostic tests, but also because they may lead to wrong diagnosis, inadequate treatment and/or iatrogenic lesions
- In case of anastomosis between motor branches, diagnosis is based on the distribution of atrophic pattern and fatty degeneration of intrinsic muscles of the hand
- In case of anastomosis between sensitive branches, diagnosis is mainly focused on patient's complaints

#### TABLE OF CONTENTS/OUTLINE

- The 4 most frequent anastomoses in the upper extremity are between motor branches, -Martin-Gruber, Marinacci, Riché-Cannieu, and between sensitive branches, -Berrettini-
- Description of US technique that helps their identification
- Discussion of the clinical implications

Printed on: 02/07/23



## Abstract Archives of the RSNA, 2022

MKEE-54

### Using Dynamic Maneuvers in the Computer Tomography/Magnetic Resonance Assessment of Musculoskeletal Pathologies

Sunday, Nov. 27 8:00AM - 9:00AM Room: Learning Center - MK

#### Participants

Thais de Souza, MD, Sao Paulo, Brazil (*Presenter*) Nothing to Disclose

#### TEACHING POINTS

Radiologic assessment of certain musculoskeletal lesions may still pose difficulties. Certain maneuvers have been described to overcome these difficulties. Although dynamic ultrasound is a well established diagnostic technique, TC and MR dynamic imaging have particular indications and are also valuable tools in certain musculoskeletal pathologies. This study aims to review the use of dynamic maneuvers in MR and CT for evaluation of some specific musculoskeletal pathologies including: Hirayama disease, ankle syndesmosis injury, radioulnar instability, chronic compartmental syndrome and others. We intend to illustrate and highlight the utility and benefits of dynamic maneuvers for the diagnosis of different musculoskeletal pathologies.

#### TABLE OF CONTENTS/OUTLINE

INTRODUCTION: Dynamic Acquisitions. Diseases caused by dynamic abnormalities and dynamic instability SAMPLE CASES Hirayama disease: flexion maneuvers allow to demonstrate anterior displacement of the dura mater. Ankle syndesmosis injury: flexion knee maneuvers. Radioulnar instability: supine maneuvers allow sensibilization for ulnar subluxation. Chronic compartmental syndrome: effort maneuvers. Thoracic outlet syndrome (TOC): arm abduction maneuvers allow sensibilization for TOC. Extrinsic median nerve compression: flexion/extension of fingers allow better visualization of dynamic compression. CONCLUSION Dynamic musculoskeletal imaging in CT and MR are important tools that allow detection of different musculoskeletal pathologies. Being able to recognize its indications, to guide targeted protocols and to know how to interpret the imaging findings both in neutral and dynamic positions is imperative for radiologists.

Printed on: 02/07/23



## Abstract Archives of the RSNA, 2022

MKEE-55

### Don't Forget the Atlantoaxial Joint: From Anatomy to Pathological Findings

Sunday, Nov. 27 8:00AM - 9:00AM Room: Learning Center - MK

#### Participants

Alan Strapasson, MD, (*Presenter*) Nothing to Disclose

#### TEACHING POINTS

The purpose of this exhibit is: 1. Review developmental embryology, anatomy, biomechanics, measurement of the atlantodental interval in the adult and pediatric population and its main anatomical variations that can simulate solutions. 2. Review imaging protocols for their evaluation according to clinical suspicion (X-ray, CT and MRI). 3. Discuss the main traumatic and non-traumatic injuries that can affect the joint, correlating their findings with imaging methods.

#### TABLE OF CONTENTS/OUTLINE

1. Developmental embryology (ossification nuclei). 2. Atlanto-axial joint anatomy: CT, X-ray, ligaments (MRI), craniometry (basion-dens interval, power ratio, basion-axial interval, atlantodental interval, spinolamine distance C1-C2) 3. Normal variants that mimic lesions: fusion anomalies, posterior/anterior rachischisis, persistence of the terminal ossicle (Bergman), "os odontoideum", calcification of the alar ligament. 4. Biomechanics: extension, flexion, lateral flexion, axial rotation. 5. Imaging assessment: RX, CT and MRI protocols (ligaments and spinal cord injury). 6. Differentiation of normal/positional findings from pathological alignment changes. 7. Atlas fracture (Jefferson). 8. Odontoid fracture (Anderson and D'Alonzo classification). 9. Traumatic spondylolisthesis of C2 (hangman's fracture). 10. Atlanto-axial subluxation (anteroposterior, rotational, vertical and lateral). 11. Alar ligament deformity-rupture. 12. Rupture of the transverse ligaments. 13. Rheumatoid arthritis. 14. CPPD

Printed on: 02/07/23

## Abstract Archives of the RSNA, 2022

MKEE-56

### Update on Cartilaginous Tumors

Sunday, Nov. 27 8:00AM - 9:00AM Room: Learning Center - MK

#### Awards

Certificate of Merit

#### Participants

Sara Gomez Pena, Madrid, Spain (*Presenter*) Nothing to Disclose

#### TEACHING POINTS

•To review the new concepts of the 2020 WHO classification of tumors of bone •To describe the radiological spectrum of cartilaginous tumors •To recognize the radiologic manifestations that may allow differentiation of the various types of chondrosarcoma •To discuss the role of different imaging modalities in the diagnosis and follow-up of chondrosarcomas •To deepen the role of imaging biomarkers and artificial intelligence in the diagnosis and follow-up of cartilaginous tumors

#### TABLE OF CONTENTS/OUTLINE

1.Introduction: generalities and the 2020 WHO classification of tumors of bone 2.Enchondroma vs. chondrosarcoma 3.Imaging features in the diagnosis, follow-up and local recurrence in chondrosarcomas 4.Imaging biomarkers and IA in chondrosarcomas 5.Conclusions

Printed on: 02/07/23



## Abstract Archives of the RSNA, 2022

MKEE-57

### **Bone Tumors in the Spine: A Simplified Approach**

Sunday, Nov. 27 8:00AM - 9:00AM Room: Learning Center - MK

#### **Participants**

Tatiane Moriwaki, MD, Sao Paulo, Brazil (*Presenter*) Nothing to Disclose

#### **TEACHING POINTS**

The purpose of this exhibit is to: Review and illustrate features of spinal bone tumors with imaging findings on radiography, computed tomography and magnetic resonance; Illustrate and discuss differential diagnosis with didactic and challenging cases; Provide a basic guide to characterizing bone tumors of the spine.

#### **TABLE OF CONTENTS/OUTLINE**

Introduction: general presentation of the epidemiology of bone tumors in the spine. Distribution of bone tumors: schematic flowchart showing the rationale for bone lesions based on age, distribution, and location of the main spinal tumors to help narrow differential diagnoses and identify "don't touch" lesions. • In patients younger than 30 years, spinal tumors are uncommon and usually benign, except for Ewing's sarcoma and osteosarcoma, while in patients older than 30 years, metastases should be included in the differential diagnoses. Infections should also be considered when there are signs of aggression. Evaluation of spinal tumors: •Characteristics of the main bone tumors in terms of epidemiology, matrix type, typical, and atypical imaging findings; • Summary of management and prognosis; •Didactic and challenging cases: benign and malignant spinal tumors. Bibliographical references with recent articles highlighting what is new in the topic.

Printed on: 02/07/23



## Abstract Archives of the RSNA, 2022

MKEE-58

### Spondylarthritis (SpA): A Practical Imaging Diagnostic Approach and Current Definitions

Sunday, Nov. 27 8:00AM - 9:00AM Room: Learning Center - MK

#### Awards

Cum Laude

#### Participants

Damaris Goncalves, MD, Sao Paulo, Brazil (*Presenter*) Nothing to Disclose

#### TEACHING POINTS

SpA is a heterogeneous group of diseases that share common genetic, clinical, and imaging features. The diagnosis is complex and multifactorial, there is no gold standard exam or diagnostic criterion, and the classification criterion is often misused in clinical practice, which can lead to diagnostic errors, mostly false positives. In its last update of the definition of sacroiliitis in 2021, the ASAS highlighted the high rates of false positives when using previous definitions of sacroiliitis, expressed concern about the misuse of the classification criteria in clinical practice and reformulated the definition, now more specific, including both inflammatory and structural lesions, although still for research purposes. Imaging diagnosis of SpA in clinical practice can be made with any combination of inflammatory and/or structural lesions in the sacroiliac joints, spine, peripheral joints and/or entheses, as long as these findings are "highly suggestive of SpA", although this definition is subjective and there is considerable interobserver variability, even among experienced readers. The distribution of the lesions must also be considered either in the sacroiliac joint, spine or peripheral joints. The differential diagnoses must be excluded, especially mechanical pathologies, which are much more prevalent and a common cause of false positive results. In addition, knowledge of habitual skeletal maturation in children is essential, as it can mimic sacroiliitis or enthesitis.

#### TABLE OF CONTENTS/OUTLINE

1. Introduction 2. Sacroiliac joint 3. Spine 4. Peripheral Findings 5. WBMRI 6. Conclusion

Printed on: 02/07/23



## Abstract Archives of the RSNA, 2022

MKEE-59

### 2022: A Spacer Odyssey: Imaging of Antibiotic Spacers for Periprosthetic Joint Infection-

Sunday, Nov. 27 8:00AM - 9:00AM Room: Learning Center - MK

#### Participants

Jason Matakas, MD, MS, (*Presenter*) Nothing to Disclose

#### TEACHING POINTS

- Educate the reader regarding two-stage revision surgery with antibiotic spacers and why it has become the gold standard for periprosthetic joint infection (PJI) management.
- Highlight advances in antibiotic spacer design.
- Depict radiographic appearance of various types of spacers and how they can be differentiated.
- Discuss common complications of antibiotic spacers the radiologist should be aware of.

#### TABLE OF CONTENTS/OUTLINE

- Background/Indication for two-staged revision with antibiotic spacer.
- Benefits: Maintains tissue tension, provides high local concentration of antibiotics, preserves cavity for subsequent revision; articulating spacers additionally allow preserved range of motion, prevent immobilization, and allow weightbearing.
- Spacer types and radiographic appearance:
  - o Knee: static, intraoperative mold, prefabricated cement, metal/polyethylene.
  - o Hip: non-articulating, intraoperative mold, prefabricated cement, metal/polyethylene.
  - o Shoulder: non-articulating, intraoperative mold, prefabricated cement, cement-coated hemiarthroplasty.
- Case-based discussion of complications: prosthetic and periprosthetic fracture, bone loss, dislocation/subluxation, persistent infection.
- Outcomes: High efficacy of infection eradication; some patients decline further revision.

Printed on: 02/07/23



## Abstract Archives of the RSNA, 2022

MKEE-6

### Pain in the Calf! - Musculoskeletal Ultrasound in the Diagnosis of Calf Pain

Sunday, Nov. 27 8:00AM - 9:00AM Room: Learning Center - MK

#### Awards

Certificate of Merit

#### Participants

Kristin Shute, DO, (*Presenter*) Nothing to Disclose

#### TEACHING POINTS

Review the normal anatomy of the calf. Demonstrate the optimal patient positioning and ultrasound technique for the evaluation of various causes of calf pain. Illustrate the ultrasound appearance of various pathologic conditions about the calf. Highlight pitfalls of calf ultrasound to avoid misinterpretation of pathology.

#### TABLE OF CONTENTS/OUTLINE

Anatomy overview with correlate of normal ultrasound appearance. Clinical imaging and findings of disease Muscle Injuries/Pathologies Tennis leg Muscle strain, tear, hematoma Muscle hernia Accessory soleus Bursae Baker's cyst (simple and complex) Ruptured Baker's cyst PseudoBaker's cyst/mimics Pes Anserine bursa Achilles rupture Nerves Neuroma PNST Nerve entrapments Fracture Conclusion and discussion References

Printed on: 02/07/23



## Abstract Archives of the RSNA, 2022

MKEE-60

### Don't Be Very Nervous": Neurovascular Structures to Avoid During Ultrasound-guided Interventions in the Extremities

Sunday, Nov. 27 8:00AM - 9:00AM Room: Learning Center - MK

#### Participants

Jenifer Pitman, MD, New York, NY (*Presenter*) Nothing to Disclose

#### TEACHING POINTS

1. Ultrasound is extremely useful for guiding injections and other procedures in the extremities, but a firm grasp of the regional anatomy is important for the procedures to be performed safely. 2. Neurovascular structures need to be avoided, and awareness of their characteristic locations relative to the structure of interest will allow safe needle advancement. 3. This education exhibit will review the typical needle orientation for many ultrasound-guided procedures in the extremities, focusing on important neurovascular structures to avoid for each.

#### TABLE OF CONTENTS/OUTLINE

1. Introduction  
2. Shoulder:  
a. Paralabral cyst aspiration (Avoiding the suprascapular nerve (N))  
b. Medial epicondylitis injection (Avoiding the ulnar N)  
c. Biceps tendon injection (Avoiding the lateral antebrachial cutaneous N)  
3. Wrist/Hand:  
a. Dorsal and volar ganglion cyst aspirations of the wrist (Avoiding the posterior interosseous N and radial artery (A), respectively)  
b. 1st carpometacarpal and triscaphe joint injections (Avoiding the radial A)  
c. 1st dorsal extensor compartment injections (Avoiding the sensory branch of the radial N)  
d. Finger flexor tendon retinacular cyst aspiration/tendon sheath injection (Avoiding the proper digital N)  
4. Hip:  
a. Iliopsoas bursal injection (Avoiding the femoral neurovascular bundle)  
b. Hamstring injection/aspiration (Avoiding the sciatic N)  
5. Knee:  
a. Baker's cyst aspiration (Avoiding the saphenous N)  
6. Ankle:  
a. Tibiotalar joint injection (Avoiding the dorsalis pedis and deep peroneal N)  
b. Flexor hallucis longus sheath / os trigonum injection (Avoiding the tibial N and medial and lateral plantar N)

Printed on: 02/07/23



## Abstract Archives of the RSNA, 2022

MKEE-61

### Opportunistic Evaluation of Sarcopenia and Osteoporosis - Focus on Musculoskeletal Imaging

Sunday, Nov. 27 8:00AM - 9:00AM Room: Learning Center - MK

#### Participants

Jennifer Padwal, MD, MS, Palo Alto, CA (*Presenter*) Nothing to Disclose

#### TEACHING POINTS

1) Sarcopenia and osteoporosis are independent risk factors for poor clinical outcomes 2) Abdominal CTs have been most thoroughly studied for the evaluation of sarcopenia and osteoporosis, although other anatomic regions on CT, MRI, and ultrasound may offer valuable information on muscle and bone quality 3) Reporting of sarcopenia and osteoporosis on imaging may influence patient management

#### TABLE OF CONTENTS/OUTLINE

I. Epidemiology and clinical significance of sarcopenia and osteoporosis II. Definitions of sarcopenia and osteoporosis: From DXA to opportunistic CT, MRI, and ultrasound III. CT and MRI screening of sarcopenia and osteoporosis on musculoskeletal imaging examinations (spine and extremities), including CT attenuation (e.g., Hounsfield unit thresholds) and MRI-derived biomarkers (e.g., T2 relaxation time, functional anisotropy) IV. Translating clinical research into clinical practice: Terminology and templates for reporting sarcopenia and osteoporosis on CT, MRI, and ultrasound

Printed on: 02/07/23



## Abstract Archives of the RSNA, 2022

MKEE-62

### **Congenital Femoral Deficiency and Its Imaging and Surgical Evolution Over Time**

Sunday, Nov. 27 8:00AM - 9:00AM Room: Learning Center - MK

#### **Participants**

Denny Marcela Achicanoy I, MEd, Ciudad De Mexico, Mexico (*Presenter*) Nothing to Disclose

#### **TEACHING POINTS**

Congenital femoral deficiency is hypoplasia of the proximal portion of the femur without a known specific etiology. Its prevalence is 0.1 to 0.2 cases per 10,000 newborns it is mainly associated with fibular hemimelia, patellar absence, acetabular dysplasia. Paley's imaging classification depends on the degree of development of the integrity of the femur without depending on age or degree of ossification.

#### **TABLE OF CONTENTS/OUTLINE**

1. Definition. 2. Embryological origin. 3. Etiology associated factors. 4. Imaging findings. 5. Treatment. Congenital femoral deficiency is the specific partial absence (hypoplasia) of the proximal portion of the femur with shortening of the entire lower limb without an etiology. Its prevalence is 0.1 to 0.2 cases per 10,000 newborns it is mainly associated with fibular hemimelia, patellar absence and acetabular dysplasia mainly due to the association with its postaxial embryonic origin. Initially it was classified by Guillespie Torode into two groups: I or congenital hypoplastic femur, where the hip knee are functional after surgical treatment symmetry of the limbs can be achieved; II or proximal focal femoral deficiency where the hip is abnormal the knee is considered non-functional, in these cases prosthetic management is suggested. However, Paley created an imaging classification with the intention of offering a guide for surgical treatment depending on the degree of development of the integrity of the femur. The Paley Classification is aimed at facilitating decisions treatment protocols to follow. In this poster we will present cases of femoral hypoplasia with different classification according to Paley.

Printed on: 02/07/23



## Abstract Archives of the RSNA, 2022

MKEE-63

### Uncomplicating Spinal Cord Disorders - A Practical Guide for the Musculoskeletal Radiologist

Sunday, Nov. 27 8:00AM - 9:00AM Room: Learning Center - MK

#### Participants

Alexandre Goncalves, MD, Sao Paulo, Brazil (*Presenter*) Nothing to Disclose

#### TEACHING POINTS

The purpose of this exhibit is: 1. To review anatomy of the spinal cord. 2. Narrow the differential of spinal cord diseases according to location. 3. Differentiate between inflammatory, infection, demyelinating, metabolic, neoplastic lesions and vascular disorders.

#### TABLE OF CONTENTS/OUTLINE

1 - Topographic and cross section detailed anatomy of the spinal cord. 2 - Correlate spinal cord diseases that manifest with high signal within the spinal cord on T2WI with their locations to narrow the differential diagnosis. 3 - Illustrate the most common causes and imaging findings in MRI, including - Inflammatory; - Vasculitis; - Infection; - HIV; - Bacteria; - Fungus; - Cysticercosis; - Demyelinating disorders; - Multiple sclerosis; - Transverse myelitis; - Neuromyelitis optica; - Acute disseminated encephalomyelitis; - Metabolic; - B12 hypovitaminosis; - Neoplastic; - Ependymoma; - Astrocytoma - Hemangioblastoma; - Lymphoma; - Metastases; - Vascular disorders; - Ischemia due to spinal arteriovenous malformation. 4 - Summary and practical guide to narrow the differential diagnosis of MRI findings according to location and how to relate the findings to the patients' relevant clinical and laboratory data.

Printed on: 02/07/23



## Abstract Archives of the RSNA, 2022

MKEE-64

### Spectrum of Imaging Findings of Iatrogenic Vascular Injuries After Orthopedic Surgery

Sunday, Nov. 27 8:00AM - 9:00AM Room: Learning Center - MK

#### Participants

Emanuele Barabino, MD, (*Presenter*) Nothing to Disclose

#### TEACHING POINTS

- Despite the establishment of safety zones to place screws and metallic devices, the rate of vascular injuries during orthopedic surgery has been increasing in the last decades due to the increasing employment and revision of prosthetic devices.
- Severe injuries (i.e., tearing of major vessels) cause severe bleeding and hypotension and are usually promptly recognized intraoperatively; despite not life-threatening, minor injuries are typically more insidious, and they could determine significant functional losses and postpone the healing process.
- The spectrum of imaging findings of the iatrogenic vascular injuries after orthopedic surgery is wide and heterogeneous and the radiologic evaluation of surgical field is often impaired by artifacts generated by metallic devices.

#### TABLE OF CONTENTS/OUTLINE

1. Introduction
2. Anatomical Considerations
3. Mechanisms of Injury
  - 3.1 Vascular injuries after elective surgery
  - 3.2 Vascular injuries after trauma surgery
4. Risk Factors
  - 4.1 Anticoagulation and Antiplatelet therapy
  - 4.2 Atherosclerosis
  - 4.3 Infection
5. Imaging Techniques and Technical Consideration
  - 5.1 CT Protocol
  - 5.2 Metal Artifact reduction Protocol
6. Radiologic Features
  - 6.1 Hematoma
  - 6.2 Pseudoaneurysm
  - 6.3 Vessel Transection
  - 6.4 Occlusion
7. Conclusion

Printed on: 02/07/23



## Abstract Archives of the RSNA, 2022

MKEE-65

### I Want to Ride My Bicycle! A Pictorial Essay on Cycling-related Musculoskeletal Injuries

Sunday, Nov. 27 8:00AM - 9:00AM Room: Learning Center - MK

#### Participants

Damaris Goncalves, MD, Sao Paulo, Brazil (*Presenter*) Nothing to Disclose

#### TEACHING POINTS

? Overview on epidemiology of cycling-related musculoskeletal injuries; ? To demonstrate the most common mechanisms that lead to the development of musculoskeletal lesions during cycling (lesions of contact, overuse and traumatic); ? To summarize the main musculoskeletal lesions related to cycling according to the affected musculoskeletal structures; ? To demonstrate the typical findings related to such lesions in a variety of imaging methods.

#### TABLE OF CONTENTS/OUTLINE

? Introduction: concept of bicycling-related injuries, epidemiology; ? Mechanisms of musculoskeletal injuries that occur during cycling; ? Overview of the main musculoskeletal injuries among cyclists in different parts of the musculoskeletal system; ? Pictorial essay on the typical imaging findings related to those lesions, including brief discussion on clinical presentation.

Printed on: 02/07/23



## Abstract Archives of the RSNA, 2022

MKEE-66

### First Metatarsophalangeal Trauma: The Complete Spectrum of Osseous and Soft Tissue Injuries

Sunday, Nov. 27 8:00AM - 9:00AM Room: Learning Center - MK

#### Participants

Collin Edwards, MD, New York, NY (*Presenter*) Nothing to Disclose

#### TEACHING POINTS

Injuries to the first metatarsophalangeal (MTP) joint, including but not limited to "turf toe", have long been associated with athletic trauma and overuse. Imaging plays an important role in the determination of severity and extent of damaged structures within this complex. Multiple classification systems frequently combine both the imaging characteristics and clinical presentation in an effort to guide management and predict return to play. This session reviews injuries to the first MTP joint to increase participants' understanding of the following: 1. Mechanisms of injury and epidemiological risk factors 2. MRI findings of 1st MTP injury and classification systems 3. Management pathways. We use multiple case examples to demonstrate the relationship between MRI findings and management decisions/outcomes. Increased understanding of these clinical, radiologic and surgical factors will further inform the radiologist's interpretation of MRI for first MTP trauma.

#### TABLE OF CONTENTS/OUTLINE

Review of normal 1st MTP osseous and ligamentous anatomy; Mechanisms and epidemiology of 1st MTP injury; Classifications of 1st MTP injuries; Case examples of osseous and ligamentous pathology, including: - Hallux sesamoid fracture and stress injuries - Osteochondral lesions - Capsuloligamentous injuries (Sesamoidophalangeal, intersesamoid, metatarsos sesamoid, collateral ligament injuries) - Musculotendinous injuries; Non-surgical and surgical management

Printed on: 02/07/23



## Abstract Archives of the RSNA, 2022

MKEE-68

### MRI evaluation of Post-operative Peripheral Nerve Injury

Sunday, Nov. 27 8:00AM - 9:00AM Room: Learning Center - MK

#### Awards

Certificate of Merit

#### Participants

Hye Yang, MD, New York, NY (*Presenter*) Nothing to Disclose

#### TEACHING POINTS

1. To review common types of procedures that are prone to causing peripheral nerve injury. 2. To recognize the MRI appearance of peripheral nerve injury including the changes to the related muscles. 3. To review the patterns of peripheral nerve injury. 4. To review the common appearances and presentations of peripheral nerve injury on MRI

#### TABLE OF CONTENTS/OUTLINE

1. Normal Anatomy: a. Normal appearance of peripheral nerve. b. Normal appearance of muscle. 2. Procedures that predispose to peripheral nerve injury: a. Types of procedures. b. Areas that are prone to injury. 3. Classification of peripheral nerve injury: a. Seddon Classification. b. Sunderland Classification. 4. MRI appearance of injury: a. Grades/Types of nerve injury. b. Neuroma. c. Peripheral muscle changes. 5. Treatment

Printed on: 02/07/23



## Abstract Archives of the RSNA, 2022

MKEE-69

### Complications of Reverse Total Shoulder Arthroplasty: What a Radiologist Should Know

Sunday, Nov. 27 8:00AM - 9:00AM Room: Learning Center - MK

#### Awards

Certificate of Merit

#### Participants

Timothy T. Klostermeier, MD, Lebanon, OH (*Presenter*) Nothing to Disclose

#### TEACHING POINTS

1. Reverse Total Shoulder Arthroplasty (RTSA) restores glenohumeral mobility and function to patients with rotator cuff arthropathy and other severe glenohumeral conditions. Radiologists should understand the biomechanical advantages, expected appearance, and anatomy of this arthroplasty (and its design variations).2. Basic examples of types of RTSA will be presented.3. Complications related to RTSA need to be promptly recognized and communicated. Radiologists should be familiar with the appearance of these complications.4. Mechanical failures will be highlighted with pictorial examples.5. Recognition of signs of infection and role in component failure.

#### TABLE OF CONTENTS/OUTLINE

1. Epidemiology of RTSAINcidence, prevalence, and rising complications 2. Role of radiologist:-Normal biomechanics-Identifying types of RTSA, medialized and lateralized and expected appearance-Recognizing and addressing complications 3. Components of RTSA4. Complications(a) Scapular notching (b) Acromial stress fractures(c) Periprosthetic fractures (d) Infections and treatment(e) Implant failures• Implant loosening• glenoid/ humeral stem• Intra implant unscrewing: humerus• Disengaged glenosphere• Broken screws• Canal filling of stem and stress shielding of greater tuberosity5. Dislocation-Assessment of implant orientation

Printed on: 02/07/23



## Abstract Archives of the RSNA, 2022

MKEE-7

### A Pain in the Neck: Magnetic Resonance Neurography of Neurogenic and Disputed Subtypes of Thoracic Outlet Syndrome

Sunday, Nov. 27 8:00AM - 9:00AM Room: Learning Center - MK

#### Participants

Emily Davidson, MD, (*Presenter*) Nothing to Disclose

#### TEACHING POINTS

1. Thoracic outlet syndrome (TOS) is thought to result from compression of the upper limb neurovascular structures traversing the thoracic outlet. TOS remains poorly understood, despite extensive available literature describing clinical features, imaging findings and approaches to the syndrome. 2. TOS due to compression on the brachial plexus causes upper limb neurological symptoms, varying from mild sensory disturbance to motor function loss. 3. Subtypes of neurological TOS have been divided into Neurogenic TOS (nTOS) and Disputed TOS (dTOS), based on clinical features and electrodiagnostic results. nTOS have positive motor nerve involvement, whilst dTOS have preserved motor nerve function with a predominant sensory disturbance. 4. Magnetic resonance neurography (MRN) is increasingly being used to investigate nTOS and dTOS and identify focal areas of compression on the brachial plexus. MRN has become an important test within the diagnostic algorithm for TOS investigation and management (non-operative vs operative).

#### TABLE OF CONTENTS/OUTLINE

1. Update on brachial plexus MRN imaging techniques including coil selection, imaging acquisition protocols, and imaging reconstruction protocols that employ deep learning algorithms. 2. Overview of TOS brachial plexus anatomy. 3. Review clinical features/electrodiagnostics of nTOS and dTOS. 4. Review MRN case examples of nTOS and dTOS subtypes, including: overhead throwing athlete, postoperative complications resulting in perineural scar and muscle denervation, and osseous abnormalities (cervical and first rib).

Printed on: 02/07/23



## Abstract Archives of the RSNA, 2022

MKEE-71

### Exploiting the Technical Possibilities and Advancements of Photon-Counting CT for Musculoskeletal Imaging: The Way Forward

Sunday, Nov. 27 8:00AM - 9:00AM Room: Learning Center - MK

#### Participants

Jeffrey De Groen, BSc, (*Presenter*) Nothing to Disclose

#### TEACHING POINTS

To demonstrate the possibilities regarding acquisition and reconstruction techniques of PCCT for musculoskeletal imaging To provide insights and knowledge needed for optimal utilization of PCCT in musculoskeletal imaging To give an outlook on the future prospects of PCCT in MSK imaging

#### TABLE OF CONTENTS/OUTLINE

With the recent introduction of a clinical photon-counting computed tomography (PCCT) scanner, it has become possible to combine ultra-high image resolution with spectral information. Image data obtained with PCCT may provide clinicians and radiologists with improved diagnostic confidence. For example, a better visualization of metastatic bone might offer valuable information about how to best stabilize the bone with metal plate placement. However, there is still limited knowledge about what the best choices are for PCCT acquisitions (e.g. x-ray spectra) and reconstructions (e.g. kernels, mono-energetic and metal artifact reduction techniques) for the various areas of interest. This exhibit will provide you with examples of clinical PCCT scans obtained in two different institutions, compared to previously acquired energy-integrating detector (EID) CT scans and other modalities in e.g., the diagnosis and follow-up of fractures, the evaluation of osteolysis, osseointegration of orthopedic joint replacement implants, and the assessment of bone tumor and metastasis. Finally, an outlook on the future utilization of PCCT to extract quantitative bone biomarkers and the assessment of bone quality and structure is provided.

Printed on: 02/07/23



## Abstract Archives of the RSNA, 2022

MKEE-72

### Osteotomies - Indications, Imaging Appearance, and Surgical Techniques

Sunday, Nov. 27 8:00AM - 9:00AM Room: Learning Center - MK

#### Participants

Majid Chalian, MD, Seattle, WA (*Presenter*) Grant, The Boeing Company

#### TEACHING POINTS

1. Review of the common osteotomy procedures and techniques  
2. Review of different techniques for each osteotomy procedure  
Review of the common osteotomies' clinical indications and complications  
Review of the common osteotomies normal postoperative imaging findings.

#### TABLE OF CONTENTS/OUTLINE

- Craniotomy
- Lateral nasal osteotomy
- Bilateral sagittal split osteotomy
- Reduction malarplasty
- Thoracolumbar vertebral osteotomy
- Rib osteotomy
- External rotation humeral osteotomy
- Ulnar shortening Osteotomy
- Distal radius corrective osteotomy
- Scaphoid corrective osteotomy
- Periacetabular osteotomy
- High tibial osteotomy
- Talar neck osteotomy
- Calcaneal osteotomy
- Hallux valgus osteotomy

Printed on: 02/07/23



## Abstract Archives of the RSNA, 2022

MKEE-73

### Normal and Abnormal MRI of the CapsuloLabral Complex of the Hip

Sunday, Nov. 27 8:00AM - 9:00AM Room: Learning Center - MK

#### Awards

**Magna Cum Laude**

**Identified for RadioGraphics**

#### Participants

Dyan V. Flores, MD, Ottawa, ON (*Presenter*) Nothing to Disclose

#### TEACHING POINTS

Contrary to its counterpart in the glenohumeral joint, the anatomy, biomechanics and patterns of injury involving the femoroacetabular capsulo-labral complex may be less familiar to radiologists. The labrum and articular capsule of the femoroacetabular (hip) joint work in conjunction to stabilize the articulation. At lesser degrees of distraction, the labrum is the most important hip stabilizer, whereas in greater distraction states, the contribution of the capsule to hip stability increases. The objectives of this educational exhibit are as follows: • Review normal anatomy and biomechanics of the femoroacetabular or hip labrum and capsular ligaments • Discuss patterns of failure and injury involving the capsulo-labral complex of the hip • Define MR imaging pearls and pitfalls in diagnosing these capsulo-labral injuries

#### TABLE OF CONTENTS/OUTLINE

NORMAL MRI • Hip labrum and anatomic variants • Capsular ligaments of the hip • Ligamentum teres  
IMAGING CONSIDERATIONS • Radial sequences • MR arthrography  
ABNORMAL MRI • Labral tears • Posterior hip dislocation • Isolated injuries of the capsular ligaments

Printed on: 02/07/23



## Abstract Archives of the RSNA, 2022

MKEE-74

### Imaging Review of Beach Tennis Injuries: A New Sport Trend and Related Musculoskeletal Lesions

Sunday, Nov. 27 8:00AM - 9:00AM Room: Learning Center - MK

#### Participants

Andre Mannato, MD, Sao Paulo, Brazil (*Presenter*) Nothing to Disclose

#### TEACHING POINTS

The exponential growth of Beach Tennis (BT) has been observed in Brazil, mainly in coastal cities. The origin of this sport dates back to Italy in the 80s. Only in 1996 the official rules of the sport were determined. Worldwide it is estimated that more than 1 million people are practicing which is played using Beach Tennis paddles and a low compression tennis ball. BT is mainly played overhead, including serving, defensive moves and attacking, this may have contributed to rotator cuff tendinopathy. Explosive sprinting in the serve with sudden plantarflexion of the foot with knee extended, contributed to more injuries in the leg and ankle muscles and tendon. Moving on sand requires more energy due to the mechanical work related to the sand's compliance and the lower efficacy of positive muscular work. For this reason, is important for the radiologist to correlate the clinical scenarios for the correct radiologic diagnosis.

#### TABLE OF CONTENTS/OUTLINE

1. Overview on epidemiology of beach tennis related musculoskeletal injuries 2. To demonstrate the most common mechanisms that lead to the development of musculoskeletal lesions during the match (serving, attacking, defense) 3. To summarize the main musculoskeletal lesion related to beach tennis according to the affected musculoskeletal structures To demonstrate the typical findings related to such lesions in a variety of imaging methods

Printed on: 02/07/23

## Abstract Archives of the RSNA, 2022

MKEE-75

### Midfoot Strains Illustrated with Global Illumination Rendering

Sunday, Nov. 27 8:00AM - 9:00AM Room: Learning Center - MK

#### Participants

Fatma Boubaker, Nancy, France (*Presenter*) Nothing to Disclose

#### TEACHING POINTS

Midfoot strains are clinically and radiologically underdiagnosed. They require a more aggressive treatment than classical lateral ankle sprains, with which they are often associated, because of higher sequelae risk. The Chopart joint is sustained by the spring ligament complex, the talonavicular, bifurcate, and calcaneocuboid (lateral and plantar) ligaments. Inversion lesions are the most frequent and lead to talonavicular impaction and calcaneocuboid distraction injuries. The Lisfranc joint is composed of 3 columns, inter-connected by dorsal, plantar, and intermetatarsal ligaments, and especially by an inter-osseous (Lisfranc) ligament, linking the medial and intermediate columns, which attempt leads to joint instability. Radiographs allow sub-optimal evaluation in a post-traumatic context. CT must be performed if a fracture is suspected and permits a good depiction of small bony avulsions, as MRI, considered the gold standard for ligamentous study, is usually not available in the acute phase. Moreover, Global Illumination rendering provides information beyond the reach of 2D images. Even though midfoot anatomy is considered complex, a clear knowledge of its anatomy improves the early detection of traumatic lesions requiring more aggressive treatment to avoid degenerative changes, especially using CT in the very early setting.

#### TABLE OF CONTENTS/OUTLINE

1. Chopart injuries. 1.1 - Introduction, 1.2 - Anatomy, 1.3 - Imaging findings  
2. Lisfranc Injuries. 2.1 - Introduction, 2.2 - Anatomy, 2.3 - Imaging findings

Printed on: 02/07/23





## Abstract Archives of the RSNA, 2022

MKEE-77

### No Strings Attached - Tendon and Tendon Sheath Pathologies of the Hand

Sunday, Nov. 27 8:00AM - 9:00AM Room: Learning Center - MK

#### Participants

Jan Grunz, MD, Wuerzburg, Germany (*Presenter*) Research Consultant, Siemens AG

#### TEACHING POINTS

The tendons of the hand run in close proximity to each other and within reticular tunnels adjacent to articular joints, while forming intersections in characteristic locations. This particular anatomy can lead to stenosis in the fibrous outer layers of the extensor retinaculum and A1 annular pulleys, resulting in tendinosis and functional disability. In contrast, proliferative tenosynovitis is a disease of the synovial inner layer of the tendon sheath with tendon infiltration and ensuing tendinitis, most frequently seen in rheumatoid arthritis. Phlegmonous or purulent tenosynovitis is more common in the flexor compartments, potentially resulting in tenosynovial necrosis and tendon dislocation. Diseases of the tendons and tendon sheaths may have mechanical, degenerative, metabolic or inflammatory etiology. Fibrous tunnels and bony prominences in close proximity to crossing tendons predispose to mechanical tendon irritation at typical sites of the hand. Requiring high-resolution techniques due to the small size of the compartments involved, the tendons and tendon sheaths of the hand can be precisely assessed in ultrasound and MRI.

#### TABLE OF CONTENTS/OUTLINE

1. Anatomy of the tendon and tenosynovium 1.1. The extensor mechanism 1.2. The flexor mechanism 2. Imaging principles 2.1 Ultrasound 2.2 MRI 3. Common pathologies 3.1. Tendinosis 3.2. Tendinitis 3.3. Paratendinitis 3.4. Reactive tenosynovialosis 3.5. Stenosing tenovaginitis 3.6. Proliferative tenosynovitis 3.7. Traumatic ruptures 3.8. Tumors of the tendon sheath 4. Discussion

Printed on: 02/07/23



## Abstract Archives of the RSNA, 2022

MKEE-78

### Stay Flexible! Diagnosis and Treatment of Flexor Tendon Injuries

Sunday, Nov. 27 8:00AM - 9:00AM Room: Learning Center - MK

#### Awards

Certificate of Merit

#### Participants

Steven Daniels, MD, New York, NY (*Presenter*) Nothing to Disclose

#### TEACHING POINTS

1. To review anatomy of the flexor tendon and flexor tendon sheath 2. To review imaging findings in flexor tendon tears highlighting those important to the treating surgeon 3. To discuss the different treatment options in flexor tendon tears and demonstrate how imaging helps guide patient management 4. To discuss complications of primary flexor tendon repair and flexor tendon reconstruction

#### TABLE OF CONTENTS/OUTLINE

1. Anatomy of the flexor tendon and flexor tendon sheath a. Flexor tendon anatomy b. Flexor tendon sheath and pulley system c. Flexor zones of injury 2. Zone 1 injuries - Leddy and Packer classification 3. Zone 2 injuries - Injury types 4. Zone 3,4,5 injuries - Injuries by location 5. Treatment options a. Primary tendon repair b. One-stage reconstruction c. Two-stage reconstruction 6. Imaging of potential tendon grafts 7. Post-operative clinical care 8. Post-operative imaging and complications a. Normal findings b. Adhesions c. Re-tear

Printed on: 02/07/23

## Abstract Archives of the RSNA, 2022

MKEE-79

### **Finger It to Know It: A Detailed Walk Through from Anatomy, Imaging and Pathology to Post-treatment Follow-up of Finger**

Sunday, Nov. 27 8:00AM - 9:00AM Room: Learning Center - MK

#### **Participants**

Amit Sahu, MBBS, MD, New Delhi, India (*Presenter*) Nothing to Disclose

#### **TEACHING POINTS**

1. Review the normal anatomy of finger and the appearance on ultrasound, radiograph, CT and MRI. 2. Discuss common bony injuries affecting the finger. 3. Discuss soft tissue injuries affecting the finger. 4. Review common bone tumours of finger and their imaging appearance. 5. Review common soft tissue tumours of finger and their imaging appearance.

#### **TABLE OF CONTENTS/OUTLINE**

1. Normal anatomy of finger on radiograph, ultrasound, CT and MRI including the bony and soft tissue structures (tendons, ligaments, volar plates and pulleys). 2. Advantages and pitfalls of ultrasound and MRI in imaging of finger. 3. Various types of fracture of metacarpal and phalanges, their imaging approach and what the orthopedic surgeon wants to know. 4. Types of soft tissue injuries like avulsion injuries of flexor and extensor tendons, volar plate injuries, collateral ligament injuries, their imaging appearance, what a radiologist should describe and post surgical follow-up. 5. Various common and uncommon bony and soft tissue tumors of finger, their imaging appearance and common differentials. Need of time for radiologist is not just lesion detection but also guiding the treating doctor for further management.

Printed on: 02/07/23



## Abstract Archives of the RSNA, 2022

MKEE-8

### Glenoid Track Assessment on Imaging in Anterior Shoulder Instability: Its Rationale and A Step-By-Step Guide

Sunday, Nov. 27 8:00AM - 9:00AM Room: Learning Center - MK

#### Awards

**Certificate of Merit**

**Identified for RadioGraphics**

#### Participants

Ustun Aydingoz, MD, (*Presenter*) Nothing to Disclose

#### TEACHING POINTS

1. To explain the concept of glenoid track and how it relates to the management of glenohumeral instability associated with bipolar (humeral and glenoid) fractures. 2. To describe how to make the glenoid track assessment on CT or with the help of CT-like images generated with zero echo-time (ZTE) MR imaging in bipolar (humeral and glenoid) fractures associated with anterior shoulder instability. 3. To explain how on-track/off-track status influences strategizing treatment and selecting the type of surgery.

#### TABLE OF CONTENTS/OUTLINE

1. Pathophysiologic background of glenoid track assessment and why this evaluation is important. 2. Step-by-step guide to assessment of the glenoid track on CT or MRI with the CT-like ZTE sequence: (a) establishing the bipolarity of the shoulder fracture dislocation; (b) estimating the glenoid bone stock; (c) calculating the glenoid track; (d) determining the Hill-Sachs interval; (e) ascertaining the on-track/off-track status of the Hill-Sachs lesion. 3. Case examples with pearls, pitfalls, and sample radiology reports (e.g., how to decide on erosive/compressive versus fragmented osseous Bankart lesions; how correlation of the Hill-Sachs interval on ZTE and conventional MRI sequences overcomes a shortcoming of CT in ascertaining this interval; what to put into the imaging report). 4. How the on-track/off-track status influences the treatment strategy or type of surgery.

Printed on: 02/07/23



## Abstract Archives of the RSNA, 2022

MKEE-80

### Doctor, I Can't Bend My Finger": Diagnostic Strategies for the Radiologists

Sunday, Nov. 27 8:00AM - 9:00AM Room: Learning Center - MK

#### Participants

Jiwoon Seo, MD, Seoul, Korea, Republic Of (*Presenter*) Nothing to Disclose

#### TEACHING POINTS

Patients with impaired finger flexion are often encountered in our daily clinical practice. There are many etiologies, such as tendon injuries or neuropathy, that cause difficulty in finger flexion. Radiologist must understand the basic anatomy of the finger flexor system and corresponding structural failure to made diagnostic decision. The major teaching points of this exhibit are: 1. To review the basic anatomy of the finger flexor system and mechanism. 2. To review the etiologies of impaired finger flexion and correlate with imaging (US, MRI) findings.

#### TABLE OF CONTENTS/OUTLINE

1. Anatomy and Mechanism of the Finger Flexor System. a. Tendons and extrinsic muscles. b. Flexor pulley system. c. Intrinsic muscles. d. Nerve innervation. 2. Etiologies of the Impaired Finger Flexion. a. Flexor tendon injuries. b. Trigger finger. c. Flexor tenosynovitis. d. Neuropathy. e. Intrinsic muscle injuries. f. Miscellaneous. 3. Summary and Take-home Messages.

Printed on: 02/07/23



## Abstract Archives of the RSNA, 2022

MKEE-81

### Scratching the Surface: MSK Pathology Involving the Skin Subcutaneous Tissues

Sunday, Nov. 27 8:00AM - 9:00AM Room: Learning Center - MK

#### Participants

Mark Manganaro, DO, Rochester, NY (*Presenter*) Nothing to Disclose

#### TEACHING POINTS

1. Familiarize radiologists with musculoskeletal diseases that have associated manifestations of the skin and subcutaneous tissues including causes from: infectious, inflammatory, tumor, congenital and connective tissue disorders.2. Be able to identify and diagnosis these various entities using radiography, CT, and MRI.3. Clinically correlate the radiographic findings with the dermatologic appearances.4. An emphasis will be placed on uncommon musculoskeletal disorders which have known dermatological manifestations.

#### TABLE OF CONTENTS/OUTLINE

The following diseases/syndromes will be shown using radiographs, CT, and MRI as well as having dermatologic correlate images when applicable. Cases that will be in the exhibit include:1. Infectious: Disseminated Mycobacterium chelonae.2. Inflammatory/Connective tissue disorders: Psoriasis/Acrodermatitis of Hallopeau, CREST syndrome/Scleroderma, SAPHO syndrome, dermatomyositis, granuloma annulare, eosinophilic fasciitis.3. Tumor: Rothmund-Thomson Syndrome, Maffucci Syndrome, Neurofibromatosis 1, etc, basal cell and squamous cell carcinoma (Marjolin's ulcer), Dermatofibrosarcoma protuberans.4. Congenital: McCune-Albright Syndrome, Nail-Patella Syndrome, Osteopoikilosis / Osteopathia Striata, Tuberous Sclerosis.

Printed on: 02/07/23



## Abstract Archives of the RSNA, 2022

MKEE-82

### Peripheral Nerve Assessment of Typical and Atypical Lesions - An Ultrasound Review

Sunday, Nov. 27 8:00AM - 9:00AM Room: Learning Center - MK

#### Participants

Ligia Couceiro, MD, Sao Paulo, Brazil (*Presenter*) Nothing to Disclose

#### TEACHING POINTS

Peripheral nerve injuries are important causes of loss of functionality what makes early diagnosis and treatment indispensable. High resolution ultrasound stands out as a cost-effective, accessible method with high diagnostic potential. The purpose of this study is: • To review peripheral nerve anatomy and correlation with the ultrasound imaging. • To discuss the method's advantages and disadvantages. • To identify normal nerve appearance and also pathological findings. • To recognize the multiple causes of neuropathies, including the most prevalent ones and some atypical or rare presentations. • Illustrate imaging findings through sample cases - atypical and typical cases.

#### TABLE OF CONTENTS/OUTLINE

- INTRODUCTION- Review peripheral nerve anatomy and correlate to the ultrasound imaging.- To compare high frequency ultrasound advantages and disadvantages to evaluate peripheral neuropathies compared to other methods.- Evaluation of peripheral nerve's normal appearance and pathological findings.
- PERIPHERAL NEUROPATHIES - DIFFERENTIAL DIAGNOSIS- Trauma - Compressive syndromes- Inflammatory processes- Infection- Neoplastic
- IMAGING INTERPRETATION• Systematic approach to evaluate image exams• Template reporting system
- INTERACTIVE CASE-BASED DIDACTICS• Sample typical and atypical cases to illustrate and solidify the concepts.

Printed on: 02/07/23



## Abstract Archives of the RSNA, 2022

MKEE-83

### Sports Injuries in the Rectus Femoris - What, How, Why and Where

Sunday, Nov. 27 8:00AM - 9:00AM Room: Learning Center - MK

#### Awards

Certificate of Merit

#### Participants

Leandro Mazza, MD, La Plata, Argentina (*Presenter*) Nothing to Disclose

#### TEACHING POINTS

Know the anatomy and biodynamic characteristics of the rectus femoris. Recognize the spectrum of muscle injuries that compromise the rectus femoris in various sports, analyzing its production mechanism. Analyze the different diagnostic methods of the different injuries in order to establish the precise location and particular characteristics of each injury. Establish an estimated prognostic criterion for recovery and sports return.

#### TABLE OF CONTENTS/OUTLINE

The anterior rectus has a complex anatomy that allows it to fulfill very characteristic functions, being essential in many current sports practices. Its "muscle within a muscle" morphology and its insertions, added to the type of contractile fibers it presents, mean that its lesions can be grouped and classified, with characteristic compromise sites that are repeated in the different sports practices, presenting a mechanism of similar injury. Indirect type injuries (muscle tears) can be divided into central or peripheral according to the myoconnective junction, being in the case of central injuries of capital importance to assess the status of the adjacent tendon. According to its extension and location, we can roughly predict the potential evolution of the lesions and the approximate return to play time. In turn, there are also direct type injuries (muscle contusions) that will have another treatment and evolution. Finally, we must include epiphysitis in children - adolescents, and tendon disinsertions, which are more frequent in adults.

Printed on: 02/07/23



## Abstract Archives of the RSNA, 2022

MKEE-84

### Give It Another Shot™: A Radiologist's Guide to Shoulder Injury Related to Vaccine Administration (SIRVA) Imaging Features

Sunday, Nov. 27 8:00AM - 9:00AM Room: Learning Center - MK

#### Participants

Hadas Benhabib, MD, MSc, (Presenter) Nothing to Disclose

#### TEACHING POINTS

1) Review procedural considerations for the administration of intramuscular injections, including anatomical landmarking and injection technique; 2) Discuss the variety of anatomical structures that can be injured, depending on the different locations of a non-target deltoid intramuscular injection; 3) Describe the imaging features of patients with recent vaccinations and the spectrum of imaging findings in patients with SIRVA, including subacromial/subdeltoid bursitis, glenohumeral synovitis, adhesive capsulitis, septic arthritis, osteitis/periostitis, and rotator cuff tears.

#### TABLE OF CONTENTS/OUTLINE

Shoulder injury related to vaccine administration (SIRVA) is a preventable outcome that can occur when an intramuscular deltoid injection is inadvertently administered into the shoulder capsule or surrounding musculoskeletal structures. Imaging studies are frequently requested in the diagnostic evaluation of SIRVA, with the reported utilization of MRI in SIRVA patients being as high as 81%. This exhibit provides a case-based review of the variety of SIRVA-related events, including rotator cuff injuries, bursitis, adhesive capsulitis, and osteomyelitis. Given the importance and growing prevalence of recent COVID-19 inoculations, with 660 million vaccinations having been administered in Canada and the United States to date, prompt recognition of symptomatic non-target vaccinations is essential in providing quality care for our patients and preventing long-term impairments.

Printed on: 02/07/23



## Abstract Archives of the RSNA, 2022

MKEE-85

### Scoliosis: A Review of Surgical Treatment Options

Sunday, Nov. 27 8:00AM - 9:00AM Room: Learning Center - MK

#### Participants

Lucas Miyahara, MD, Sao Paulo, Brazil (*Presenter*) Nothing to Disclose

#### TEACHING POINTS

The purpose of this exhibit is to: 1. Review the modalities of scoliosis surgical treatment and their indications, including the main findings in scoliosis exams that need to be highlighted when choosing surgical management. 2. Illustrate several cases of scoliosis with emphasis on postoperative findings, what to expect and their complications. 3. Discuss and provide a guide for what the radiologist must actively look for and report in these cases, supporting surgeons in decision making.

#### TABLE OF CONTENTS/OUTLINE

Introduction: review general presentation of scoliosis, including their complete evaluation and what the report should include. Provide several challenging scoliosis cases due to defects of formation, segmentation and mixed ones, in the context of various syndromic conditions. Overview and discuss the several operative indications and modalities of surgical treatment. Present didactic illustrations and cases of the different surgical modalities, with their pre and post-operative imaging exams. Propose a guidebook for post-operative scoliosis imaging, including several complications that the radiologist needs to be aware of and how they should report. Relevant bibliographical references.

Printed on: 02/07/23



## Abstract Archives of the RSNA, 2022

MKEE-86

### Soft Tissue Imaging Findings of Critically Ill Patients

Sunday, Nov. 27 8:00AM - 9:00AM Room: Learning Center - MK

#### Participants

Ana Carolina Augusto, MD, MSc, Sao Paulo, Brazil (*Presenter*) Nothing to Disclose

#### TEACHING POINTS

The purpose of this pictorial essay is to: • Review the imaging appearance of soft tissue findings commonly seen critically ill patients, mainly in MRI. • Differentiate infectious from non-infectious soft tissue diseases in the intensive care unit patient setting.

#### TABLE OF CONTENTS/OUTLINE

Patients in intensive care units commonly spend long periods of time restrict to the hospital bed, vulnerable to infections and going through multiple venipunctures. Not rarely, imaging is required to further examine possible complications related to the primal disease or long-term hospitalization. Early diagnosis of possible soft tissues changes can prevent further complications and poor outcomes, specially in elder population. In addition, it is possible to help the surgeon clarify the extent of the damage and prepare the best approach. Muscle edema is a common MRI finding in critically ill patients and the differential diagnosis includes critical illness myopathy (a common acquired condition in an ICU setting), rhabdomyolysis, infections, among others. Correct distinction of infectious from noninfectious soft tissue diseases can be an important factor in determining patient survival.

Printed on: 02/07/23



## Abstract Archives of the RSNA, 2022

MKEE-87

### Declawed: A Review of Claw Toe Pathology and Treatment

Sunday, Nov. 27 8:00AM - 9:00AM Room: Learning Center - MK

#### Awards

Certificate of Merit

#### Participants

Tristan Cooper-Roth, (*Presenter*) Nothing to Disclose

#### TEACHING POINTS

The purpose of this educational exhibit is to provide the learner with the following information: 1. Define anatomically what a claw toe deformity is, what this looks like on a radiograph, and what the most common causes are 2. What are the key distinguishing features of other lesser toe deformities and their corresponding radiographic appearances 3. Identify claw toe abnormalities seen on MRI 4. Summarize the types of therapeutic non-surgical and surgical approaches of a claw toe deformity 5. Characterize the post-surgical changes of a Weil lesser metatarsal osteotomy on diagnostic imaging

#### TABLE OF CONTENTS/OUTLINE

1. Define anatomically what a claw toe deformity is, providing a radiographic example, and what are the most common causes 2. Examples of other lesser toe deformities and their appearance on radiographs 3. Characteristics of claw toe abnormalities on MRI 4. Assess atrophy of intrinsic foot musculature on diagnostic imaging 5. Types of therapeutic non-surgical and surgical approaches to a claw toe deformity 6. Post-surgical changes on diagnostic imaging

Printed on: 02/07/23

## Abstract Archives of the RSNA, 2022

MKEE-88HC

### Qualitative and Quantitative Anatomic Investigation of the Lateral Ankle Ligaments for Surgical Reconstruction Procedures Using 3D High-Resolution MRI in Chronic Ankle Instability

Sunday, Nov. 27 8:00AM - 9:00AM Room: Learning Center - MK

#### Participants

Meng Dai, (*Presenter*) Nothing to Disclose

#### TEACHING POINTS

To quantitatively investigate the anatomy of the ATFL and CFL for surgical reconstruction procedures in chronic ankle instability.

#### TABLE OF CONTENTS/OUTLINE

Purpose: To quantitatively investigate the anatomy of the anterior talofibular ligament (ATFL) and calcaneofibular ligament (CFL) for surgical reconstruction procedures in chronic ankle instability. Materials and Methods: 3D MRI were performed on five fresh-frozen cadaveric ankles with six different spatial resolutions. Resolution of  $0.45 \times 0.45 \times 0.45 \text{mm}^3$  was performed on 24 healthy adult volunteers on bilateral ankles. A four-point subjective score system was used to evaluate the imaging quality. Morphologic parameters including the classification of ATFL, the length of ATFL and CFL, and the four distances of surgically relevant bony landmarks were measured and analyzed. Results: In subjective evaluation, the interobserver ICC was 0.95 [95% confidence interval (CI): 0.94-0.97] between two readers. The spatial resolution of  $0.3 \times 0.3 \times 0.3 \text{mm}^3$  and  $0.45 \times 0.45 \times 0.45 \text{mm}^3$  received highest subjective score on average and demonstrated highest consistency with autopsy measurements in objective evaluation. Regarding the measurements on the 48 volunteer ankles, distance 1 in type I and II were  $12.65 \pm 2.08 \text{mm}$ ,  $13.43 \pm 2.06 \text{mm}$  (superior-banded in Type II) and  $7.69 \pm 2.56 \text{mm}$  (inferior-banded in Type II) (means  $\pm$  SD), respectively. Distance 2 in type I and II were  $10.90 \pm 2.24 \text{mm}$ ,  $11.07 \pm 2.66 \text{mm}$  (superior-banded in Type II), and  $18.44 \pm 3.28 \text{mm}$  (inferior-banded in Type II), respectively. Distance 3 and 4 were  $4.71 \pm 1.04 \text{mm}$  and  $14.35 \pm 2.22 \text{mm}$ , respectively. Conclusion: The feasibility to quantify the distances of surgically relevant bony landmarks. Please visit the Learning Center to also view this presentation in hardcopy format.

Printed on: 02/07/23



## Abstract Archives of the RSNA, 2022

MKEE-89

### Multimodality Review of Important Musculoskeletal Measurements in the Upper Extremity

Sunday, Nov. 27 8:00AM - 9:00AM Room: Learning Center - MK

#### Participants

Jennifer S. Weaver, MD, Albuquerque, NM (*Presenter*) Nothing to Disclose

#### TEACHING POINTS

Many image-based measurements are used by orthopedic surgeons to plan treatment. This educational exhibit will discuss the indications and measurement techniques for several commonly used upper extremity measurements, and will detail the technical requirements of imaging needed to obtain precise and accurate measurements. After viewing this exhibit, the learner should be able to: (1) Understand important technical considerations and limitations in measurement techniques of various modalities, including radiographs, CT, MRI, and ultrasound (2) Discuss commonly encountered measurements in the upper extremity, including clinical indication, specific technique, and potential pitfalls

#### TABLE OF CONTENTS/OUTLINE

Introduction  
General Measurement Techniques  
Shoulder  
1. Acromioclavicular Interval  
2. Acromiohumeral Distance  
3. Coracoclavicular Interval  
4. Acromial Angle, Tilt, and Slope  
5. Humeral Neck Shaft Angle  
6. Lateral Glenohumeral Offset Angle  
7. Glenoid Version Angle  
8. On track/off track Hill Sachs  
Elbow  
1. Humero-condylar Angle  
2. Ulnar Collateral Ligament Thickness  
3. Ulnar Collateral Ligament Medial Joint Gap with Valgus Stress  
4. Nerve Cross Sectional Area  
Wrist-hand  
1. Capitolunate, Lunotriquetral, and Scapholunate Angles  
2. Scapholunate Interval  
3. Radial Inclination  
4. Dorsal Radial Tilt  
5. Radial Height  
6. Radioulnar Angle  
7. Radioscaphoid Angle  
8. Ulnar Variance and Inclination  
9. Carpal Tunnel Bowing and Area  
10. Median Nerve Cross Sectional Area  
11. Carpal Height, Height Ratio, and Height Index  
Shear wave elastography  
Conclusion

Printed on: 02/07/23



## Abstract Archives of the RSNA, 2022

MKEE-9

### Musculoskeletal Manifestations of Systemic Lupus Erythematosus: An Imaging Overview

Sunday, Nov. 27 8:00AM - 9:00AM Room: Learning Center - MK

#### Participants

Marina Akuri, MD, Marilia, Brazil (*Presenter*) Nothing to Disclose

#### TEACHING POINTS

The purpose of this exhibit is to: 1. Review the most frequent and also atypical presentations of musculoskeletal involvement of systemic lupus erythematosus (SLE). 2. Illustrate with didactic cases while discussing the imaging findings and main complications of these disease

#### TABLE OF CONTENTS/OUTLINE

Introduction: general presentation of the epidemiology and clinical findings of musculoskeletal involvement of systemic lupus erythematosus. Review the multi-modality imaging findings of musculoskeletal SLE with didactic illustrations. Present challenging cases with musculoskeletal manifestations related to systemic lupus erythematosus as insufficiency fracture, tenosynovitis, arthropathy, avascular necrosis, bone infarction, vasculitis and infection. Differential diagnosis including other inflammatory conditions and arthropathy helping the radiologist how to differentiate them. Relevant bibliographical references.

Printed on: 02/07/23



## Abstract Archives of the RSNA, 2022

MKEE-90

### Shouldering the Burden: A Pictorial Review of Shoulder Arthroplasties

Sunday, Nov. 27 8:00AM - 9:00AM Room: Learning Center - MK

#### Participants

Akwasi Opoku, MD, Nashville, TN (*Presenter*) Nothing to Disclose

#### TEACHING POINTS

Advancements in shoulder arthroplasty has increased its use, particularly over the past two decades. The shoulder is the third most common replaced joint after hip and knee, with its overall incidence increasing at a greater rate than those of total knee and hip replacements. After viewing this exhibit, the learner should understand:1. Shoulder anatomy and biomechanics2. Indications for shoulder arthroplasty3. Role of preoperative imaging and measurements4. Advantages, disadvantages, and specific complications of various shoulder arthroplasties5. Normal imaging findings and imaging findings of complications

#### TABLE OF CONTENTS/OUTLINE

Introduction - history and evolution Shoulder anatomy and biomechanics1. Bones, joints, muscles, other soft tissues (cartilage, labrum, capsule)2. Unconstrained ball and socket, static and dynamic stabilizers Indications 1. Arthropathy, trauma, cuff pathology, osteonecrosis, prior infectionRole of preoperative imaging (multimodality)1. Evaluation of cuff, bone stock, cartilage2. Glenoid morphology and versionTypes of shoulder arthroplasties, indications, advantages, disadvantages 1. Humeral head resurfacing arthroplasty2. Hemiarthroplasty3. Anatomic total shoulder arthroplasty4. Reverse total should arthroplastyImaging appearances1. Normal and complications

Printed on: 02/07/23

## Abstract Archives of the RSNA, 2022

MKEE-91

### What's Your Carbon Footprint? Carbon-Fiber Implants in Orthopedic Oncology

Sunday, Nov. 27 8:00AM - 9:00AM Room: Learning Center - MK

#### Awards

Certificate of Merit

#### Participants

Erik Verhey, Reno, NV (*Presenter*) Nothing to Disclose

#### TEACHING POINTS

\*Carbon fiber reinforced polyetheretherketone (CFR-PEEK) is a composite material which can be used to create orthopedic implants for use in the appendicular skeleton and spine\*CFR-PEEK implants are nearly radiolucent and produce relatively little artifact when imaged with CT and MRI\*Owing to their favorable imaging profile, CFR-PEEK implants facilitate post-operative imaging follow up of tumor patients\*Post-operative radiation therapy in oncologic patients with CFR-PEEK implants is also improved due to lower artifact on planning CT scans and enabling the use of photon therapy

#### TABLE OF CONTENTS/OUTLINE

\*Background of CFR-PEEK as a composite material and its use in implants\*Surgical perspective: CFR-PEEK implant use in the spine\*Surgical perspective: CFR-PEEK implant use in the appendicular skeleton\*Radiographic and fluoroscopic appearance of CFR-PEEK implants with example cases\*CT appearance of CFR-PEEK implants with example cases\*MRI appearance of CFR-PEEK implants with example cases\*Value of CFR-PEEK implants in radiation oncology \*Conclusions

Printed on: 02/07/23



## Abstract Archives of the RSNA, 2022

MKEE-92

### Exchange Arthroplasty for Periprosthetic Joint Infection: What the Radiologist Needs to Know

Sunday, Nov. 27 8:00AM - 9:00AM Room: Learning Center - MK

#### Participants

Nicholas G. Rhodes, MD, Rochester, MN (*Presenter*) Nothing to Disclose

#### TEACHING POINTS

1. Management of periprosthetic joint infection (PJI) is a complex task. 2. The radiologist should be familiar with the varied constructs employed following resection arthroplasty for infection. 3. The presence of polymethylmethacrylate bone cement is often the radiologist's initial clue to the presence of joint infection undergoing treatment. 4. Serial radiographs play an important role in the management of periprosthetic joint infection.

#### TABLE OF CONTENTS/OUTLINE

1. Review imaging of PJI a. Role of radiographs b. Role of advanced imaging c. Role of joint aspiration 2. Review clinical features of PJI 3. Review treatment options for PJI 4. Discuss imaging related to various treatment options a. Review of imaging appearance during and after treatment of PJI at various joints i. Resected arthroplasty ii. Spacers iii. Articulating spacers iv. Destination spacers b. Review how the radiologist puts it all together i. Discuss clinical findings and thought behind and directing this process ii. Define the role of the radiologist iii. Define appropriate terminology concerning joint resection/prosthesis explantation and employed spacers iv. Highlight role of serial radiographs v. Highlight expected and unexpected imaging findings during this process

Printed on: 02/07/23

## Abstract Archives of the RSNA, 2022

MKEE-93

### Intercondylar Notch Beyond the Cruciate Ligaments: Light at the End of the Tunnel

Sunday, Nov. 27 8:00AM - 9:00AM Room: Learning Center - MK

#### Participants

Sergio Atala, MD, Las Condes, Chile (*Presenter*) Nothing to Disclose

#### TEACHING POINTS

1. The intercondylar notch is a commonly neglected area in the knee anatomy and in the assessment of radiologic studies. 2. Knowledge of the consistent normal anatomy of this notch is easily and swiftly assessed with several imaging modalities, particularly with MR Imaging. 3. Some anatomic variations should be well recognized, not be confused with pathologic conditions. 4. Meniscal root pathology is critical and dedicated examination in the MR Imaging studies is recommended. In the case of meniscal root tears LaPrade classification can be utilized preoperatively, with prognostic relevance. Surgical techniques for meniscal root tears are presented to be assessed in the postoperative MR Imaging studies. 5. Solid and cystic masses can be primarily originated in the intercondylar notch, and a brief pictorial review is presented. 6. The medial synovial fold of the posterior cruciate ligament is a well-recognized structure, and pathologic conditions are presented, with therapeutic implications.

#### TABLE OF CONTENTS/OUTLINE

1. Introduction. 2. Anatomy. 3. Intercondylar morphology and insertion (tibial / femoral) of intercondylar structures. 4. Tibial spine tubercles. 5. Changes in the anatomy of the intercondylar notch during lifetime. 6. Meniscal roots variants, tears and postoperative changes. 7. Ganglion cyst in meniscal roots. 8. Oblique meniscal ligaments. Meniscomfemoral ligaments. 9. Ligamentum mucosum. 10. Synovial fringe. 11. Intercondylar meniscal fragments. 12. Ganglion cysts. 13. Solid Masses. 14. Medial synovial fold PCL. 15. Conclusion.

Printed on: 02/07/23

## Abstract Archives of the RSNA, 2022

MKEE-94

### Adipose Tissue Around the Knee - A Review of Normal Anatomy and MRI Findings of Common Pathologies

Sunday, Nov. 27 8:00AM - 9:00AM Room: Learning Center - MK

#### Participants

Majid Chalian, MD, Seattle, WA (*Presenter*) Grant, The Boeing Company

#### TEACHING POINTS

1. Anatomy of intraarticular fat pads and subcutaneous adipose tissue  
2. Review the role of intraarticular fat pads and subcutaneous adipose tissue  
3. Review the clinical presentation of intraarticular fat pads and subcutaneous adipose tissue pathologies and provide case examples  
4. Review the MRI presentation of the pathologies involving intraarticular fat pads and Subcutaneous adipose tissue

#### TABLE OF CONTENTS/OUTLINE

Review of anatomy:  
• Infrapatellar fat pad and related structures  
• Suprapatellar fat pad  
• Prefemoral fat pad  
• Pericruciate fat pad  
• Subcutaneous fat  
Review of the role:  
• Non-mechanical role  
• Inflammatory role  
• Endocrine role  
• Proprioceptive role  
• Mechanical role  
The dynamic role of anterior intraarticular fat pads during knee flexion and extension  
• Shock absorbing role  
The route for surgical probing  
Review of the clinical presentation in pathological changes:  
• Infrapatellar fat pad and related structures  
• Suprapatellar fat pad  
• Prefemoral fat pad  
• Pericruciate fat pad  
• Subcutaneous fat  
Review of the MRI presentation:  
• Pathologies involving the synovial lining  
• Pathologies presenting with edema like changes  
• Space occupying pathologies

Printed on: 02/07/23



## Abstract Archives of the RSNA, 2022

MKEE-95

### The Multiple Applications of Dixon Sequences in Musculoskeletal MRI

Sunday, Nov. 27 8:00AM - 9:00AM Room: Learning Center - MK

#### Awards

Certificate of Merit

#### Participants

Massimo Donalisio, MD, (*Presenter*) Nothing to Disclose

#### TEACHING POINTS

The Dixon method has gained much interest in musculoskeletal MRI, and many applications have been validated by the literature. The four sets of images generated by the Dixon technique can each provide specific qualitative or quantitative information, and they may serve to optimise acquisition protocols in various applications including bone marrow, whole body, oncological and rheumatological imaging. Water only images provide robust fat suppression that can be useful in large field of view applications or MRI of the extremities. Fat only images are particularly useful for the assessment of bone marrow lesions and may replace the information provided by T1-weighted sequences in certain indications. There are some pitfalls and disadvantages that radiologists must be familiar with.

#### TABLE OF CONTENTS/OUTLINE

1. Brief review of the physics of Dixon sequences: from one sequence to four sets of images; 2. Illustrated review of common applications of Dixon sequences in musculoskeletal practice: a) Fat suppression technique in extremities, large field of view applications (comparison to CHESS and STIR techniques), b) Spine and bone marrow imaging: advantages of the use of fat only images in replacement of T1 weighted sequences, c) Whole body MRI: the use of Dixon technique to optimise whole-body protocols with a focus on neuromuscular disorders, d) MRI in rheumatology: the use of Dixon sequences to scan more regions with less sequences, e) MRI of sarcomas: the benefits of including Dixon sequences in the acquisition protocol, f) The Dixon technique as a quantitative MRI tool to assess the fat fraction; 3. Pitfalls and disadvantages of Dixon sequences.

Printed on: 02/07/23

## Abstract Archives of the RSNA, 2022

MKEE-96

### Mismatch Findings of WB DWI MRI and PET-CT in Oncology

Sunday, Nov. 27 8:00AM - 9:00AM Room: Learning Center - MK

#### Participants

Carolina Almeida, MD, Rio de Janeiro, Brazil (*Presenter*) Nothing to Disclose

#### TEACHING POINTS

TEACHING POINTS To evaluate the performance of WB-DWI MRI in the diagnosis and follow-up of cancer patients in situations of false positive or negative results in the PET-CT study (18F-FDG and PSMA). PET/CT is used in the evaluation of oncology patients to identify malignancy, but could be non-specific. Identify what sequences should be used to analyse bone marrow and soft tissue in whole-body MR imaging protocols to detect neoplastic lesions and pseudotumoral in oncological patients. To be aware of the conditions and the mechanisms by which false positive and negative results occur on 18F-FDG-PET-CT scans and to compare with WB MRI-DWI study. Make a pictorial essay of the main false false negative PET-CT PSMA cases comparing with WB MRI study. An understanding of the limitations of this nuclear medicine technology is necessary to avoid making inaccurate diagnosis and potentially limiting the right treatment for our patients.

#### TABLE OF CONTENTS/OUTLINE

TABLE OF CONTENTS AND OUTLINE 1) The value of WB-DWI MRI IN in the diagnosis and follow-up of cancer patients. 2) Case discussion to demonstrate 18F-FDG PET/CT false positive and false negative examples: Small lesions (less than 1,0 cm) Osteoblastic sclerotic metastases Patient anxiety can result in increased uptake Bone marrow infiltration Low grade lymphoma 3) To demonstrate PET/CT-PSMA false positive and false negative examples: small tumors neuroendocrine prostate tumor Small tumors near bladder 4) Common pitfalls 5) Differential diagnosis 6) Structured reporting step by step

Printed on: 02/07/23



## Abstract Archives of the RSNA, 2022

MKEE-97

### Review of the Effects of Diabetes Mellitus on the Musculoskeletal System

Sunday, Nov. 27 8:00AM - 9:00AM Room: Learning Center - MK

#### Participants

Jimmy Saade, MD, (*Presenter*) Nothing to Disclose

#### TEACHING POINTS

- Epidemiology and financial burden of diabetes mellitus (DM).
- DM affects nearly every organ system.
- Beyond the well-known manifestations of diabetes, such as neuropathy and nephropathy, DM can also have damaging effects on the musculoskeletal (MSK) system.
- As the prevalence of DM continues to increase, the lesser-known musculoskeletal complications are to increase as well.
- We demonstrate some of these MSK manifestations. Early recognition and diagnosis of the many DM-related complications will lead to earlier intervention, and ultimately, less morbidity for patients and financial burden on the healthcare system.
- DM-related disease entities discussed include osteoporosis, diffuse idiopathic skeletal hyperostosis (DISH), Dupuytren's contractures, trigger finger, rotator cuff tendinopathy, adhesive capsulitis, and calcaneal insufficiency fractures.
- We demonstrate a multimodality approach to the diagnosis of these pathologies including MSK ultrasound.

#### TABLE OF CONTENTS/OUTLINE

- Diabetes Mellitus: Epidemiology and pathology.
- DM-related osteoporosis and diagnosis with DEXA, radiographs, and CT.
- DISH with imaging findings across multiple imaging modalities.
- Dupuytren's contractures utilizing ultrasound for diagnosis.
- Trigger finger with confirmatory findings on MRI.
- Adhesive capsulitis and rotator cuff tendinopathy findings on MRI.
- Calcaneal insufficiency fracture and confirmatory findings on CT and x-ray.
- Conclusion.

Printed on: 02/07/23



## Abstract Archives of the RSNA, 2022

MKEE-98

### Imaging of Calf Pain

Sunday, Nov. 27 8:00AM - 9:00AM Room: Learning Center - MK

#### Awards

Certificate of Merit

Identified for RadioGraphics

#### Participants

Allison Khoo, MD, (*Presenter*) Nothing to Disclose

#### TEACHING POINTS

1. Understand the muscular anatomy of the calf including the gastrocnemius, soleus, plantaris, and Achilles tendon. 2. Recognize subtle radiographic findings of calf and posterior ankle pathology such as obliteration of Kager's fat pad. 3. Develop a differential for calf pain spanning traumatic, metabolic, infectious/inflammatory, neoplastic, congenital, and vascular etiologies.

#### TABLE OF CONTENTS/OUTLINE

1. Introduction. 2. Relevant anatomy: a. Kager's fat pad on ankle radiograph: obliterated by pathology from adjacent structures including Achilles tendon, calcaneus, and tibiotalar joint. b. Review of gastrocnemius, soleus, and plantaris anatomy. 3. Case-based review of calf and posterior ankle pathology organized by etiology. a) trauma/overuse- Achilles tendinopathy and tear, Haglund deformity, Tennis leg/plantar rupture. b) metabolic-xanthoma. c) infectious/inflammatory: myositis, rhabdomyolysis. d) neoplastic: sarcoma, lymphoma. e) congenital: accessory soleus, cortical desmoid. f) vascular: popliteal artery (aneurysm, entrapment, stenosis), deep venous thrombosis

Printed on: 02/07/23



## Abstract Archives of the RSNA, 2022

MKEE-99

### Triceps Surae Muscle Injuries: What the Radiologist Should Know?

Sunday, Nov. 27 8:00AM - 9:00AM Room: Learning Center - MK

#### Participants

Jaime Isem, PhD, (*Presenter*) Nothing to Disclose

#### TEACHING POINTS

1. To review the pathophysiological mechanism of Triceps surae muscle injuries. 2. To Assess the imaging technique of choice for the study of acute and chronic injuries. 3. To show the US and MRI findings in Triceps surae muscle injuries. 4. To describe the reparative process in the favorable or unfavorable evolution of these injuries and the residual findings.

#### TABLE OF CONTENTS/OUTLINE

Pathophysiological mechanism of Triceps surae muscle injuries. US and MRI protocols for an adequate diagnosis of Triceps surae muscle injuries. Current severity classification systems. Review of imaging findings of the acute injury according to the type of damage. Range of imaging healing process in lesions and residual changes.

Printed on: 02/07/23



## Abstract Archives of the RSNA, 2022

MSEE

### Multisystem Education Exhibits

Sunday, Nov. 27 8:00AM - 9:00AM Room: Learning Center - MS

#### Sub-Events

#### **MSEE-1 Pre-and Post Procedure CT for Cardiac Implantable Electronic Devices Extraction: A Primer for Radiologists**

Participants

Samuel Cesconetto, MD, SAO PAULO, Brazil (*Presenter*) Nothing to Disclose

#### TEACHING POINTS

Learning objectives: - To review the principles of extraction technique and the role of computed tomography for planning the extraction of cardiac implantable electronic devices - To illustrate a spectrum of different complications related to cardiac electronic devices and their extraction - To discuss how to assess by imaging the risk of major complications during the procedure - To propose a systematic approach and a structured reporting.

#### TABLE OF CONTENTS/OUTLINE

Table of contents: - Introduction: - Cardiac implantable electronic devices: Overview, types, components, follow up and complications. - Extraction technique. - Patient selection. - CT: Acquisition protocol, image interpretation and clinical application. - Case-based review. - Pre-and postprocedure multidisciplinary assessment and complication score. - Proposal for a structured reporting. - Future directions and take home messages.

#### **MSEE-11 MRI Safety: Bullets, Ballistics, Shrapnel**

Participants

Kyle Stumetz, DO, (*Presenter*) Nothing to Disclose

#### TEACHING POINTS

In the United States, more than 100,000 patients per year present to the emergency room for gun-related trauma or other ballistic related injuries. Many of these patients may require an MRI (during the initial visit or years later), and thus the presence of retained bullet fragments and/or metallic shrapnel impose important safety concerns. With this information in mind, the goal of this presentation is to: 1) Review an algorithmic approach to imaging patients with suspected retained bullets and/or shrapnel. 2) Identify the most common types of bullets and projectiles, including their metallic compositions. 3) Explain commonly encountered MRI metallic artifacts and common techniques employed to diminish them. 4) Identify scenarios in which MRI imaging is and is not appropriate for retained bullet fragments via a case-based review.

#### TABLE OF CONTENTS/OUTLINE

1. Can my patient with a bullet in their \_\_\_\_ get an MRI? 2. Most common questions 3. Algorithmic Approach 4. Types of Projectiles 5. Bullet/Projectile Composition 6. MR Metal Artifacts 7. MR Metal Artifact Reduction Sequences (MARS) 8. Case-based review

#### **MSEE-12 Genetics and Its Advances: What a Pediatric Radiologist Needs to Know?**

Participants

Sara Rodriguez, MD, (*Presenter*) Nothing to Disclose

#### TEACHING POINTS

1. New advances and understanding in genetics is driving the diagnostic workup, management and clinical practice. 2. Learning the basic concepts of genetics can help radiologists to have a better understanding of diseases and their imaging characteristics, and help decide imaging workup and screening protocols. 3. In this primer, we aim to provide basic concepts and terminology in genetics, to familiarize radiologists with different types of genetic testing and to understand the impact of genetics in different groups of pediatric diseases including cancers and cancer predisposition syndromes, skeletal dysplasia, vascular anomalies, autoimmune diseases and others.

#### TABLE OF CONTENTS/OUTLINE

Introduction Basic concepts and terminology in genetics: Gene expression and regulation: from DNA to mRNA to amino acids to protein Gene inheritance, transmission and genetic imprinting Genetic dominance: genotype-phenotype relationships, phenotype variability Genetic mutations Genes and diseases: monogenetic, chromosomal, multifactorial. Genetic testing: Molecular test (target single variant, single gene, gene panel, whole genome sequence) Chromosomal microarray Gene expression test Biochemical tests. Genetics in cancer predisposition syndromes: Tumor suppressor genes Proto oncogenes Radiological screening in cancer predisposition syndromes. Genetics in skeletal dysplasia: Skeletal dysplasia panel Implications on imaging. Genetics in vascular malformations: RAS/ MEK/ERK and PI3 kinase/mTOR signaling pathway. Genetics in autoimmune diseases. Genetics in other pediatric diseases. Summary

## **MSEE-13 Abdominal Abbreviated MRI Protocols: From Description to Implementation**

Participants

Maria Tello, MD, (*Presenter*) Nothing to Disclose

### **TEACHING POINTS**

1. Understand the need of having abbreviated MRI protocols and describe their role. 2. Explain the clinical scenarios where they can be applied. 3. Describe how to perform some of these abdominal abbreviated MRI protocols. 4. Illustrate the workflow of how to implement the described above protocols

### **TABLE OF CONTENTS/OUTLINE**

1. MRI nowadays, why to perform abbreviated protocols, advantages and disadvantages. 2. Description of the MRI situation at our institution, selecting the abbreviated protocols that we can benefit the most. 3. Description of the abbreviated MRI protocols we are going to implement: Pancreatic cystic lesions, Liver metastases, including the role in colorectal cancer, Adrenal incidentalomas, Active surveillance for small renal masses. 4. Implementation at our institution, how we are going to do it? A brief guide step by step.

## **MSEE-14 DECT In The Emergency Room: Play Your Best Game and Leave It All Out On The Field!**

### **Awards**

#### **Certificate of Merit**

Participants

Kirbi Sullivan, MD, (*Presenter*) Nothing to Disclose

### **TEACHING POINTS**

1. Dual Energy CT (DECT) may aid in diagnosis for Emergency Department (ED) patients but is only impactful if radiologists maximize utilization of the extra information. 2. Workflow changes are needed to optimally incorporate DECT into a busy ED.

### **TABLE OF CONTENTS/OUTLINE**

1. Introduction: a. Discuss patient selection strategies for DECT from both the radiologist and technologist perspective. b. Review high-yield DECT reconstructions to detect pathology and problem-solve. 2. DECT wins: a. Avoiding downstream testing. i. Differentiating between gastrointestinal bleeding and ingested contents, avoiding endoscopy. ii. Differentiating hematoma from tumor in a hypotensive patient with peritoneal carcinomatosis. b. Expediting care. i. Detection of postoperative hemorrhage on a portal venous phase CT, bypassing CT angiography for rapid embolization. ii. Detection of early bowel ischemia on iodine maps, leading to rapid surgery and avoiding bowel resection. iii. Subtle fracture detection with bone marrow edema maps. iv. Active extravasation detection in intracranial hemorrhage on iodine maps. 3. DECT losses: underutilized information negatively impacted downstream testing and care. a. Unnecessary testing. i. Mischaracterization of suture material as active extravasation in a postoperative patient, leading to unnecessary angiography. ii. Unnecessary workup of incidentalomas not fully characterized with DECT at the time of detection. b. Delayed care. i. Missed subtle pyelonephritis, leading to a second ED visit 1 month later.

## **MSEE-15 Recent Advances in Cardiothoracic Imaging**

Participants

Joshua Hunter, Cleveland, OH (*Presenter*) Nothing to Disclose

### **TEACHING POINTS**

1. Review novel techniques in cardiothoracic imaging and how they improve upon existing methodologies. 2. Discuss technical parameters and protocol considerations of the new techniques. 3. Illustrate use cases of novel cardiothoracic imaging techniques.

### **TABLE OF CONTENTS/OUTLINE**

1. Discuss existing cardiothoracic imaging modalities and briefly cover the pathologies that they diagnose. 2. Discuss limitations of existing techniques. 3. Enumerate the new techniques in cardiothoracic imaging and how they alleviate some of the existing limitations. 4. Discuss technical and protocol implications of the new techniques. 5. Compare the advantages and disadvantages afforded by the new techniques, when compared to existing imaging methodologies. 6. Brief overview of several novel imaging techniques. 7. Novel Cardiothoracic Imaging: a. Radiography: i. Dual energy subtraction radiography (DESR). 1. Bone-selective radiograph improves detection of bony lesions. 2. Soft tissue-selective radiograph eliminates potential for obstruction by bones. ii. AI-enabled detection. 1. Thoracic Pathologies (Pneumothorax, Pneumonia). 2. Lines and tube malpositioning (ET tube, Enteric tube). iii. AI-enabled prognostication. 1. COVID-19 patients needing urgent mechanical ventilation. CT: i. Dual Energy CT. ii. Photon counting CT. iii. CT-FFR. iv. AI-enabled tools. 1. Automated coronary artery calcium scoring. 2. Automated PE detection and nodule analysis on CT. c. MRI: i. Parametric mapping and ECV. ii. MR Strain imaging. iii. 4D Flow MRI. iv. PET/MRI. d. Ultrasound: i. IVUS. ii. 3D Echocardiography. 8. Disadvantages of new imaging techniques. 9. Other emerging techniques currently in the research sphere; and not in clinical use. 10. Future goals and directions.

## **MSEE-16 Low Field Body MRI: Challenges and Opportunities at 0.55T**

### **Awards**

#### **Identified for RadioGraphics**

Participants

Anup Shetty, MD, Saint Louis, MO (*Presenter*) Nothing to Disclose

### **TEACHING POINTS**

Low-field MRI (0.55T) for body imaging presents challenges and opportunities for patients, radiologists, and enterprises compared to high-field (1.5T or 3T) MRI. This exhibit will: 1. Discuss imaging advantages and challenges of low-field body MRI compared to high-field body MRI. 2. Discuss logistical and workflow challenges of low-field body MRI compared to high-field body MRI. 3. Illustrate use cases, strategies, and nuances in low-field body MRI through a series of case examples.

### **TABLE OF CONTENTS/OUTLINE**

- Low-field MRI advantages: lower cost; easier installation (including lighter weight, less shielding, less helium), larger bore size, MR physics benefits (longer T2\* [i.e., reduced susceptibility], lower SAR, shorter T1 [i.e., faster acquisition], easier shimming for B0 homogeneity), less acoustic noise- Low-field MRI challenges: lower SNR, fewer receiver coil options, weaker gradients, longer acquisition times, longer TE for chemical-shift imaging- Comparison of sequences across field strengths, highlighting key limitations and observations of each sequence at 0.55T- comparison of lesion conspicuity with example cases acquired at both low and high field strengths- discussion of sequence modifications and strategies at 0.55T to overcome imaging limitations and maintain comparable image quality- exploration of uses cases (lung imaging, pancreatic cyst follow-up, hepatic imaging after locoregional therapy, emergency imaging, adrenal/renal imaging, pelvic imaging, etc.)

### **MSEE-17HC Whole Body MRI In Children: A Primer for Beginners**

Participants

Daniela Carrascal-Penaranda, MD, MSc, Bogota D.C, Colombia (*Presenter*) Nothing to Disclose

#### **TEACHING POINTS**

To explain the usefulness of Whole body MRI in the pediatric population, its utility and indications. To review basic concepts on used sequences and different protocols, which one is the most appropriate to make a successful evaluation of the body. To discuss and exemplify through cases the possible scenarios of imaging findings in patients with cancer and the broad spectrum of cancer predisposition syndromes. To discuss the principal indications of whole body MRI in infectious - inflammatory disease as well as in general population.

#### **TABLE OF CONTENTS/OUTLINE**

Introduction - Definitions. Applications and indications Standard protocol - Technical requirements Cancer predisposition syndromes Indications in non-oncological pathology: Miscellaneous Incidental findings and further implications to the patient Structured report in pediatrics Summary Conclusions Please visit the Learning Center to also view this presentation in hardcopy format.

### **MSEE-18 Imaging of Oncologic Pain: A Multi System Approach**

Participants

Thais Kuwazuru, MD, Sao Paulo, Brazil (*Presenter*) Nothing to Disclose

#### **TEACHING POINTS**

The aim of this exhibition is to: 1. Review the current concepts about oncologic pain syndromes; 2. Describe the role of imaging in oncologic pain, focusing on diagnosis; 3. Correlate imaging findings with clinical syndromes and therapeutic strategies; 4. Illustrate the causes of oncologic pain with illustrative cases.

#### **TABLE OF CONTENTS/OUTLINE**

1. INTRODUCTION: a. Definitions and classification of oncologic pain; b. Impact of pain syndromes in patient quality of life and prognosis. 2. ACUTE PAIN SYNDROMES: a. Associated with tumor: Tumor bleeding, pathologic fractures, obstruction and perforation of viscera, superior vena cava syndrome, acute thrombosis; b. Associated with treatment: Chemotherapy-induced neuropathy, radiation therapy-induced bone pain and plexopathy, oral mucositis, enteritis and proctitis. 3. CHRONIC PAIN SYNDROMES: a. Somatic pain: Bone and soft tissue pain; b. Visceral pain: Abdominal pain syndromes; c. Neuropathic pain: Leptomeningeal metastasis, cranial and peripheral neuropathies; d. Headaches; e. Related to treatment: Post-chemotherapy, post-surgical and post-radiation pain syndromes; 4. CONCLUSION: a. Pain assessment in cancer patients very often include imaging investigation; b. When interpreting imaging exams, it is essential to understand the imaging patterns of each syndrome and the important findings for therapeutic planning.

### **MSEE-19HC Strategies to Identify, Treat, and Eliminate MRI Radiofrequency Burns**

Participants

Anshuman Panda, PhD, Scottsdale, AZ (*Presenter*) Nothing to Disclose

#### **TEACHING POINTS**

1. Thermal burns are a potential cause of injury during MRI scans. Recognition, diagnosis, and management of these burns can be challenging and may often go unrecognized. 2. We implemented a multidisciplinary team, led by a radiology physician assistant, to help in the timely identification, assessment, and management of patients with suspected MRI burns. 3. As a result of this initiative, we have collected numerous cases of MRI burns. In this exhibit, we will use these cases to demonstrate causes of MRI burns, physical findings of these burns, and discuss management strategies.

#### **TABLE OF CONTENTS/OUTLINE**

A. Background of MRI burns with an emphasis on physics aspect of burns and excessive power deposition. B. Pathophysiology of radiofrequency burns. C. Clinical presentation and treatment. D. Discussion of our local burn initiative including physical assessment of patients and the review by MR technologists and physicists to address root cause of burn cases. E. Case based review and management of burn cases identified in our practice Please visit the Learning Center to also view this presentation in hardcopy format.

### **MSEE-2 Solitary Fibrous Tumor in the Brain, Head and Neck, and Spine: Basic and Advanced Neuroimaging**

**Awards**

**Certificate of Merit**

Participants

Ryo Kurokawa, MD, PhD, Ann Arbor, MI (*Presenter*) Nothing to Disclose

#### **TEACHING POINTS**

The aim of this exhibit is to 1. Review the etiology, histology, and epidemiology of solitary fibrous tumor (SFT) in the brain, head and neck, and spine 2. Demonstrate the imaging characteristics on the conventional modalities/sequences 3. Show how advanced modalities/sequences can help diagnose SFT

## TABLE OF CONTENTS/OUTLINE

Content organization 1. Introduction-Etiology, histology, and epidemiology of SFT in the brain, head and neck, and spine 2. Typical imaging findings 3. Advanced imaging-MRS-Diffusion-weighted imaging-Contrast-enhanced perfusion-weighted imaging-FDG-PET 4. Atypical imaging findings-Atypical localization: Cavernous sinus, Orbit-Atypical manifestation: Metastasis, Doege-Potter syndrome, Intracranial hemorrhage 5. Differential diagnosis-Various neoplasms 6. Summary

### MSEE-20 The Forgotten System: Lymphatics of Abdomen and Pelvis

Participants

Rodrigo Loto, MD, Rosario, Argentina (*Presenter*) Nothing to Disclose

#### TEACHING POINTS

-Presentation of the organization and function of the lymphatic vascular system.-Overview of lymphatic vascular development (lymphangiogenesis).-Importantly, lymphangiogenesis occurs in adult tissues during inflammation, wound healing, and tumor metastasis.-Radiology is playing an important and growing role in the diagnosis and treatment of many lymphatic conditions.

## TABLE OF CONTENTS/OUTLINE

Studies of the last decades have revealed the importance of angiogenesis for normal growth and for the pathogenesis of numerous diseases. Much less studied is lymphangiogenesis, the growth of lymphatic vessels, which drain extravasated fluid, proteins, and cells and transport them back to the venous circulation. Nonetheless, insufficient lymphangiogenesis causes incapacitating lymphedema, while lymphatic growth around tumors may facilitate metastatic spread of malignant cells that ultimately kill the patient. During inflammation, lymph flow increases to limit edema and prevents tissue antigen-presenting cell transport. Lymphatics also adjust their contractile activity to increase fluid transfer during acute inflammation. Conversely, chronic inflammation can provoke lymphostasis, which might limit pathogen spread within the circulation; however, decreased lymph flow leads to the persistence of immune cells and mediators in tissues to intensifying injury. Knowledge of lymphatic anatomy, physiology, and expected imaging appearances is crucial in understanding the pattern of cancer spread. Lymphatics have been proposed as transperineal dissemination pathway for multiple phenomena, including neoplasms, septic processes, urinothorax, and porous diaphragm syndromes.

### MSEE-21 Not Too Young to Know: Multimodality Imaging Review of Commonly Encountered Pathologies in Institution-Living Elderly

Participants

Andy Guo, MD, (*Presenter*) Nothing to Disclose

#### TEACHING POINTS

1- Define the institutional elderly patient population and explain how they are a vulnerable population 2- Learn about common pathologic conditions specifically affecting the institutional elderly 3- There are special considerations in clinical and imaging approach for evaluating these patients that are different from the general population including compassionate care, imaging techniques and accounting for limitations in the institutional elderly

## TABLE OF CONTENTS/OUTLINE

1- Review examples of common pathologies in the institutional elderly, including but not limited to: Musculoskeletal- falls and trauma Infectious disease- aspiration pneumonia Gastrointestinal- chronic constipation Genitourinary- incontinence Drug Toxicity- confusion and over-sedation Neurological- dementia and stroke Underlying Medical Condition- heart failure, hypertension and type 2 diabetes 2- Describe specific imaging findings in evaluation of example pathologies, with teaching points about underlying pathophysiology 3- Review special considerations that radiologists and technologists must make in evaluating this vulnerable patient population to align with compassionate care

### MSEE-23 Lymphatics: Imaging and Interventions- A Comprehensive Review

Participants

Smily Sharma, MD, MBBS, Jodhpur, India (*Presenter*) Nothing to Disclose

#### TEACHING POINTS

1. To study the anatomy of the lymphatic system and its pathophysiological basis 2. To study in detail the methodology and protocols of MR and Conventional Lymphangiography 3. To discuss imaging features of various disorders of the lymphatic system including macrocystic, microcystic, mixed lymphatic malformations, renal lymphangiectasia and syndromes associated with lymphatic disorders 4. To discuss imaging features of congenital abnormalities of lymphatics like vanishing bone disease, primary lymphedema 5. To discuss imaging features of acquired lymphatic disorders like chyle leak, pulmonary lymphatic perfusion syndrome, and the role of MR and conventional lymphangiogram in these disorders using state of the art cases 6. To discuss the role of Interventional Radiology in the management of lymphatic disorders including sclerosing agents and thoracic duct embolization

## TABLE OF CONTENTS/OUTLINE

1. Anatomy of Lymphatic System and Pathophysiological Basis of Lymphatic Disorders 2. Conventional Lymphangiography: Method 3. MR Lymphangiography: Method and Protocols 4. Lymphatic Malformations 5. Renal Lymphangiectasia 6. Syndromes associated with Lymphatic disorders 7. Congenital Lymphatic Disorders: Generalized Lymphatic Anomaly, Gorham Stout Disease, Primary Lymphedema 8. Acquired Lymphatic disorders: chyle leak, pulmonary lymphatic perfusion syndrome, secondary lymphedema 9. Interventional Radiology in treatment of lymphatics: Sclerosing Agents, Thoracic Duct Embolization 10. Summary

### MSEE-24 Free-Breathing T1-Weighted Motion Correction in Abdominal MRI: Technical Principles, Applications, and Current Limitations

Awards

Identified for RadioGraphics

Participants

Ebru Yaman Akcicek, Seattle, WA (*Presenter*) Nothing to Disclose

## TEACHING POINTS

1. Understand the technical principles of free breathing T1 weighted pulse sequences 2. Learn the difference between non-dynamic and dynamic contrast enhanced acquisitions using radial k space trajectories 3. Examine the currently established indications for motion corrected contrast techniques 4. Discuss limitations of current free breathing techniques and accelerated cartesian acquisitions 5. Learn how to identify the best patient-adapted protocol strategy 6. Review newly emerging techniques for motion reduction

## TABLE OF CONTENTS/OUTLINE

1. Principals of radial imaging: description of radial k-space trajectories (stack of stars) 2. Dynamic contrast acquisitions with view sharing 3. Abdominal applications of free breathing motion correction indications in liver, pancreas and kidneys 4. Strategies for patient-adapted abdominal examination protocols using free breathing techniques 5. Limitations of motion correction techniques, and mitigation strategies 6. Novel developments of free breathing pulse sequences

## MSEE-25 **Focusing the Retrospectroscope: Challenging and Easily Overlooked Patterns of Recurrence and Metastases in Abdominopelvic Oncologic Imaging**

Participants

Molly Roseland, MD, Northville, MI (*Presenter*) Nothing to Disclose

## TEACHING POINTS

1. Accurate recognition of recurrent and metastatic cancers by CT, MRI, and PET/CT may be challenging. 2. Post-surgical scarring and distortion is a common mimic of recurrence. Enlarging enhancing tissue should be considered suspicious. 3. Common features of missed recurrent malignancy include small size, slow or infiltrative growth pattern, obscuration by irregular surgical margins, or location in an imaging "blind-spot." Comparisons over time, surgical history, and thorough search pattern are essential. PET may improve detection.

## TABLE OF CONTENTS/OUTLINE

1. General principles: use history, many comparisons 2. Individual Cancer Recurrence Patterns A. Pancreatic adenocarcinoma - Recurrence: perivascular cuffing, pancreatic mass; Mimic: Post-Whipple fibrosis -Metastases: peritoneum, liver; mimic: fat necrosis, micro-abscesses B. Cholangiocarcinoma -Recurrence: mass at surgical margin, biliary stricture; mimic: postsurgical change, cholangitis C. Colorectal cancer -Recurrence: perianastomotic, lymph nodes; mimic: scarring (presacral) D. Renal cell carcinoma - Recurrence: surgical bed, IVC; Pitfall: post-treatment change (noncontrast) -Metastases: Adrenal, pancreas (unique), bone; Pitfall: Small; no arterial-phase; adrenal washout E. Bladder cancer -Recurrence: ureteral stricture, mass; Mimic: Reflux post-cystectomy F. Prostate cancer -Local Recurrence; PSMA PET Pitfall: obscuration by urinary excretion -Metastases: bone, lymph nodes; Pitfall: epidural extension, fracture; Pitfall: rare sites (sacral nerves, penis) 3. Summary and recommendations

## MSEE-26 **Lymph Nodes in Abdominal and Pelvis Neoplasms: Evaluation From Stagn to Post - Treatment: Messengers of the Force or Dark Side Sentinel?**

### Awards

#### Certificate of Merit

Participants

Thamiris De Sousa Garcia, MD, MD, Sao Paulo, Brazil (*Presenter*) Nothing to Disclose

## TEACHING POINTS

- Use of different imaging methods to assess lymph nodes for tumor dissemination, what each method can add and how to proceed for further investigation. - Evaluation of heterogeneity of staging criteria and treatment response of lymph nodes involved in abdominal and pelvic neoplasms. - Better understanding of regional lymph nodes involved in different neoplasms, with revision of the anatomy of lymph node chains and dissemination routes.

## TABLE OF CONTENTS/OUTLINE

- Introduction - Lymph nodes of abdomen and pelvis: anatomy. - Evaluation of lymph nodes using different imaging methods: findings of normality and criteria for tumor involvement. - Staging of the main neoplasms of the abdomen and pelvis with characterization of regional involvement and dissemination pathways, as well as its particularities. - Comparison between different types of methods and criteria for evaluating lymph node response to surgical and non-surgical treatment. - Teaching points.

## MSEE-27 **Flap Anatomy After Pelvic Reconstructive Surgery: A Brief Survival Guide**

Participants

Paula Otermin Barrera, MD, Madrid, Spain (*Presenter*) Nothing to Disclose

## TEACHING POINTS

To describe in a practical way the resulting anatomy after various flap-based reconstructive surgery techniques, as well as potential complications, providing specific iconography selected from our tertiary referral center, with special emphasis on myocutaneous flaps and their application in pelvic reconstruction after oncological resections

## TABLE OF CONTENTS/OUTLINE

1. Introduction. Definition of flap and benefits provided by flap coverage.2. Types of flap according to their vascular anatomy and tissue composition.3. Myocutaneous flaps. Imaging characteristics and applications in pelvic reconstruction of rectus abdominis muscle flaps (TRAM, VRAM and variants) and gracilis muscle flaps. 4. Omental flap.5. Deep Inferior Epigastric Perforator flap (DIEP). Preoperative CT study for selection and marking of optimal perforators. Imaging characteristics and applications in pelvic reconstruction.6. Complications (flap and donor area): post-surgical fluid collections and surgical wound infection, fat necrosis, flap ischemia, dehiscence, tumor recurrence.

## MSEE-28 **Ciliopathy Syndromes: Pathogenesis and Multisystem Multimodality Imaging Review**

Participants

Yarik Bezkor, BS, MD, Lexington, KY (*Presenter*) Nothing to Disclose

#### TEACHING POINTS

Teaching Points: 1. Ciliopathies are a diverse group of disorders occurring secondary to abnormal development and/or structural or functional defects of the cilia. 2. Cilia are highly evolved, complex organelles, found ubiquitously on the surface of almost all the cell types, and have diverse mechanosensory and chemosensory signal transduction roles and there have been significant recent advances in the understanding of these key organelles. 3. Ciliopathy syndromes affecting non-motile cilia are associated with multisystem developmental disorders predominantly affecting renal, skeletal, and nervous systems. 4. Renal ciliopathies are the most common which include autosomal polycystic kidney disease, and nephronophthisis, Ciliopathy syndromes associated with neurodevelopmental features include Meckel-Gruber syndrome, Joubert syndrome, orofacial digital syndrome as well as Bardet-Biedl syndrome. Motile ciliopathies, grouped as "primary ciliary dyskinesia" most commonly present as Kartagener's syndrome. 5. Multimodality imaging with Ultrasound, CT, and MRI is crucial for the diagnosis and management of these syndromes.

#### TABLE OF CONTENTS/OUTLINE

1. A. Embryology and pathogenesis of ciliopathy syndromes 2. B. Multimodality imaging of Motile and non-motile ciliopathy syndromes.

#### MSEE-29 **New CT Technology: A Practical Approach to Convert CT Acquisition Protocols from Energy Integrating Detector (EID) CT to Photon Counting Detector (PCD) CT**

Participants

Nikkole Weber, ARRT, RT, Rochester, MN (*Presenter*) Nothing to Disclose

#### TEACHING POINTS

1. Explain the differences between energy integrating detector (EID) and photon counting detector (PCD) technologies 2. Understand critical differences in PCD technology that need to be taken into account when designing PCD scanning acquisition protocols.

#### TABLE OF CONTENTS/OUTLINE

1. Explain differences between PCD and EID technologies used on commercial CT scanners a. PCD: Directly convert X-ray into electronic signals, count individual photon and record its energy b. EID: Indirect, 2 stage conversion of X-ray of light to electronic signal. No information on individual photon energy 2. Create a core team of experts a. Medical Physicists b. CT technologists c. Subspecialized radiologists 3. Explore new CT scanner technology and its benefits 4. As a practice, decide protocol conversion approach: a. Apples-to-apples: i. Acquisitions with similar appearance and diagnostic quality as current EID CT b. Apples-to-oranges: i. Acquisitions leveraging technical advantages of PCD technology (high matrix, sharper kernels, higher IR) 5. Define parameters that do not allow an apples-to-apples protocol conversion a. Scan modes (high res, multi-energy, combined-lower kV) b. Conventional tube potential selection (conventional) vs. Virtual monoenergetic selection (PCD) c. System-specific reconstruction kernels and reconstruction nomenclature 6. Protocol evaluation through image review sessions a. Define two lists of protocols i. Commonly used protocols in your practice ii. Protocols or indications that would benefit from new technology b. Change acquisition and reconstruction parameters, iteratively reevaluating images with core experts

#### MSEE-3 **Don't Burst That Bubble!: A Guide to Skin Cysts**

Participants

Carolina Almeida, MD, Rio de Janeiro, Brazil (*Presenter*) Nothing to Disclose

#### TEACHING POINTS

TEACHING POINTS 1) Palpable skin lesions are a common complaint in dermatology offices and ultrasounds are often requested to clarify the origin. 2) High-frequency ultrasound is the imaging modality chosen for skin examination due to its cost and availability. 3) Cutaneous cystic lesions are very common and have specific characteristics that help in the diagnosis. 4) Make a pictorial essay of the main cutaneous cysts and their differential diagnoses, such as trichilemmal cyst, dermoid cyst, epidermic cyst, and hidradenoma.

#### TABLE OF CONTENTS/OUTLINE

TABLE OF CONTENTS/OUTLINE 1) Overview of cystic structures and their definition; 2) High-frequency ultrasound of cystic skin lesions - epidermal cyst and hidradenoma; 3) Trichilemmal cyst and dermoid cyst; 4) Report structuring step by step; 5) Differential diagnosis.

#### MSEE-30 **Thinking IN and OUT of the Box: Using Chemical Shift Imaging as a Problem-Solving Tool**

Participants

Anthony Larder, DO, Milford, OH (*Presenter*) Nothing to Disclose

#### TEACHING POINTS

-Review basic physics concepts of chemical shift and magnetic susceptibility in MRI-Discuss tissue characteristics that can be used for diagnosis with chemical shift imaging including: macroscopic fat, microscopic fat, calcifications, gas, and iron-Review imaging findings and associated pathophysiology of multiple scenarios in which chemical shift artifact aids in diagnosis

#### TABLE OF CONTENTS/OUTLINE

Review of physics concepts related to chemical shift imaging including original illustrations and relevant case examples-Precession of fat and water-Signal characteristics and physical properties of Type 1 and Type 2 chemical shift artifact-Liver fat quantification-Magnetic susceptibility-T2\* decay based on TE-Properties of diamagnetic, paramagnetic, and ferromagnetic substances-Liver iron quantification-Review of chemical shift as a diagnostic tool, including differential diagnoses, discussion of relevant pathophysiology, and clinical issues. Case examples including-Macroscopic fat:-Renal angiomyolipoma-Mature teratoma-Liposarcoma-Fat-containing hepatocellular carcinoma-Microscopic fat:-Hepatic steatosis-Nodular-Companion case of hepatic melanoma metastases -Hepatic adenoma-Adrenal adenoma-Metastatic marrow replacement -Fat-containing hepatocellular carcinoma-Magnetic Susceptibility:-Iron deposition-Primary hemochromatosis-Hemosiderosis-Gamma-Gandy bodies-Hepatic siderotic nodules-Including case of Wilson's disease with siderotic nodules-Metallic Susceptibility-Surgical clip localization-Calcifications-Cholelithiasis-Nephrolithiasis-Blood

products-Gas-Within infected pancreatic necrosis-Pneumoperitoneum-Pneumobilia

### **MSEE-31 Introduction to Oncology Imaging: A Primer For Residents and Fellows**

Participants

Jordan LeGout, MD, Ponte Vedra Beach, FL (*Presenter*) Nothing to Disclose

#### **TEACHING POINTS**

Learning to interpret oncology imaging can be a complex and daunting topic for residents and fellows. In this exhibit we will:- Provide a framework for approaching oncology cases for the trainee-Review the various tumor response criterion and their main takeaways for clinical use-Discuss differences in imaging assessment for chemotherapy and immunotherapy-Examine imaging response for local-regional therapies-Highlight the benefit of high-yield disease specific search patterns

#### **TABLE OF CONTENTS/OUTLINE**

1. Introduction a. Role of radiologist and importance of imaging in patient care b. Words matter! "Loaded words" and definitions i. Stable, response, progression2. Clinical history (the "what, when, and how") a. Key history elements to know for each case i. Original presentation 1. Always review the first scan = Each case a teaching file! 2. Establishes disease appearance and sites pre-therapy ii. Therapy type 1. Start date 2. How treatment type influences image interpretation iv. Time crunch: what are the highest yield priors v. Tumor markers and trend3. Tumor response criteria (the takeaways) a. RECIST 1.1 b. mRECIST c. iRECIST d. Choi e. Cheson/Lugano4. Immunotherapy a. Pseudoprogression b. Unique adverse effects5. Local-regional therapies a. Ablations and embolizations b. Radioembolization6. Disease specific high-yield search patterns a. Examples of common malignancies

### **MSEE-32 The Role of the Radiologist in LGBTQ+ Patient Care: A Comprehensive Curriculum**

Participants

Janis Yee, MD, (*Presenter*) Nothing to Disclose

#### **TEACHING POINTS**

? Understand the radiologist's role in delivering inclusive and culturally sensitive care to LGBTQ+ patients. ? Understand the current cancer screening guidelines for transgender patients. ? Recognize the normal postoperative appearance and postoperative complications related to gender affirmation surgeries. ? List complications related to hormone therapy, including increased risk of venous thromboembolism, ischemic heart disease, cerebrovascular events, and hormone-sensitive organ atrophy or cancers. ? Recognize complications related to HIV and highly active antiretroviral therapy (HAART).

#### **TABLE OF CONTENTS/OUTLINE**

? Background and definitions of LGBTQ+ ? Challenges to caring for the LGBTQ+ community ? Discuss imaging relevant to trans patients ? Preoperative imaging in planning for feminization surgery ? Preoperative imaging in planning for masculinization surgery ? Postoperative complications in gender-affirming surgery ? Normal appearance of feminization and masculinization after medical transition ? Complications of gender-affirming hormone therapy ? Provide an overview of imaging findings in lesbian, gay, bisexual, and queer patients related to stigmatized health concerns such as STDS, substance abuse, and certain types of cancer ? Review complications from common preventative medications prescribed to patients, for example, pre-exposure prophylaxis (PrEP) ? Qualitatively assess the availability of multidisciplinary care to LGBTQ+ patients at three different academic institutions across the country ? Discuss how radiology departments can improve their role in the care of this patient population ? Conclusion

### **MSEE-33 Skin Ultrasound in Lipolytic Aesthetic Procedures**

Participants

Luciana Zattar, MD, Sao Paulo, Brazil (*Presenter*) Nothing to Disclose

#### **TEACHING POINTS**

Lipolysis and lipolytic aesthetic procedures are increasingly being performed, and minimal invasive types are preferable. Nonsurgical body contouring techniques, aimed at reducing the subcutaneous adipose tissue, includes cryolipolysis, injectable lipolytic (meso-therapy), low and high-intensity focused ultrasound and others therapies. In this context, the radiologist has been requested to recognize their usual aspects as well as to assess possible complications. To achieve accurate and timely detection and appropriate approach of each case, High frequency ultrasound (HFUS/24-33MHz) is the most effective method since it provides optimal anatomical information of the skin and allows evaluation before, during and after these procedures. This study aims to discuss and illustrate the radiologist's role in the evaluation of lipolytic aesthetic procedures with HFUS. The purpose of this exhibit is:- To describe the preprocedure evaluation.- To illustrate the anatomy of the skin layers.- To show the main image patterns and effects of the lipolytic aesthetic procedures.- To list and describe the most common procedures complications.- To highlight the importance of HFUS before, during and after nonsurgical body contouring techniques.

#### **TABLE OF CONTENTS/OUTLINE**

1. INTRODUCTION.2. NORMAL ANATOMY.3. PREPROCEDURAL EVALUATION.4. PROCEDURES CHARACTERISTICS AND IMAGING FINDINGS5. COMPLICATIONS.6. PROCEDURE GUIDANCE.7. CONCLUSION.

### **MSEE-34 Polyps From Head to Toe: What's Your Impression?**

Participants

Carlos Padula, MD, (*Presenter*) Nothing to Disclose

#### **TEACHING POINTS**

To understand the pathophysiology of polyps. To review most common presenting locations. To review imaging features of polyps across multiple modalities including ultrasound, fluoroscopy, CT, and MRI. To review differential diagnoses of polypoid lesions. To review current guidelines and literature regarding management of polyps.

#### **TABLE OF CONTENTS/OUTLINE**

1. Pathophysiology of polyps. 2. Anatomical locations 3. Imaging features of polyps 4. Case examples: Aural, sinonasal, oropharyngeal, vocal cord, esophageal, gastric, gallbladder, small bowel, colorectal, endometrial, and cervical.

## **MSEE-35 Metabolic Syndrome: Imaging Features and Clinical Outcomes**

Participants

Mohamed Badawy, MD, Houston, TX (*Presenter*) Nothing to Disclose

### **TEACHING POINTS**

- Discuss obesity prevalence and different types of fat distribution - Review imaging techniques used to evaluate the obesity effects on different body organs - Describe clinical outcomes and imaging artifacts related to obesity Table of content

### **TABLE OF CONTENTS/OUTLINE**

- Introduction- Differences between white and brown fat and between central and peripheral adipose tissue- Methods of obesity evaluation and the superiority of anthropometric measurement over body mass index (BMI) - Imaging quantitative assessment of visceral fat volume - MetS effects on the o Liver § Imaging used to diagnose non-alcoholic fatty liver disease including ultrasonography (ULS), elastography, magnetic resonance (MR) spectroscopy, MR proton density fat fraction § Liver fat quantification o Pancreas § Imaging features of pancreatic infiltration and its mimics o Heart § Imaging and clinical effects of increased epicardial fat o Gastrointestinal tract § CT and MR appearances of fat deposition (e.g submucosal fat deposition, diffuse fat lipomatosis and fat halo sign) o Urinary tract § Imaging and mimics of fat deposition in the urinary bladder wall o Lumbosacral edema § Imaging features of lumbosacral edema correlated with MetS o Tumors development in different body organs § Malignancies associated with obesity and their imaging features - Obesity Imaging artifacts - Obesity surgery pre and post-operative imaging

## **MSEE-36 A Confusion of Wild Catheters: A Review of Abdominal Medical Devices**

Participants

Victoria Kim, MD, (*Presenter*) Nothing to Disclose

### **TEACHING POINTS**

1. Recognize the normal appearance of various abdominal devices on multi-modality imaging.2. Identify potential complications related to abdominal devices which may have acute clinical implications.

### **TABLE OF CONTENTS/OUTLINE**

I. Background: In the continuously changing landscape of medicine, abdominal imaging often captures a wide variety of medical devices. These can be bewildering when seen for the first time, especially for residents early in training. Recognizing potential complications related to unfamiliar devices is an even greater challenge but can have acute clinical implications for patient safety and outcomes.II. Gastrointestinal tract devices: Traditional enteric catheters; Gastrostomy/gastrojejunostomy tubes; Gastrointestinal and biliary stents.III. Genitourinary devices: Ureteral stents; Nephrostomy tubes; Contraceptive devices; Prosthetics.IV. Vascular devices: IVC filters; Vascular stents and grafts; ECMO cannulas and other vascular catheters; Ventricular assist device drivelines.V. Miscellaneous devices: Spinal catheters; Electronic stimulator devices; Peritoneal dialysis catheters; Surgical clips, sutures, and drains.

## **MSEE-37 Multimodality Imaging in Metabolic Syndrome: A State-of-the-Art Review**

**Awards**

**Cum Laude**

**Identified for RadioGraphics**

Participants

Prabhakar Rajiah, MD, FRCR, Rochester, MN (*Presenter*) Nothing to Disclose

### **TEACHING POINTS**

1. To review the etiology and complications of metabolic syndrome 2. To understand the role of multimodality imaging in metabolic syndrome 3. To illustrate the utility of imaging in diagnosis of metabolic syndrome and assessment of target organ injury

### **TABLE OF CONTENTS/OUTLINE**

• METABOLIC SYNDROME- Definition and criteria • CAUSES AND RISK FACTORS • ROLE OF IMAGING - Diagnosis, target organ injury assessment, biomarkers for novel therapy • MODALITIES- CT, MRI (including MR spectroscopy, Elastography, PET/MRI), nuclear medicine, Ultrasound, DXA • FAT ASSESSMENT - Subcutaneous abdominal fat - Visceral abdominal fat- US (thickness, fat index), CT (inc single slice CT ) MRI (FSE, chemical shift, fat selective), DXA - Parenchymal fat- MRS - Fat around organs- Eg. Pericardiac fat (echo, CT/MRI) - Fat around vessels- CT, MRI, 1H-MRS • INSULIN RESISTANCE - Intramyocellular lipid in skeletal muscle biopsy, 1H- MRS - Glucose metabolism using 18F-FDG PET, dynamic triple-tracer PET with 15O-H<sub>2</sub>O, 11C-3-O-methylglucose, and 18F-FDG • TARGET ORGAN INJURY - Vessels- Atherosclerosis, elevated arterial stiffness- Doppler, CT, MRI - Cardiac- Dilation/hypertrophy, diastolic dysfunction, impaired strain, coronary atherosclerosis, ischemic heart disease- Echo, CT, MRI, Nuclear perfusion - Liver- Nonalcoholic fatty liver, cirrhosis- Ultrasound, CT, 1H- MRS, Dixon MRI, 31P- MRS, MRI, MR Elastography, US elastography - Pancreas- Fatty disease- US, CT, MR, 1HMRS - Kidney- Chronic renal disease, renal stone- Ultrasound, CT, MRI, 99mTc-DTPA, dynamic CE- MRI, ASL-MRI, DWI, BOLD-MRI - Brain- Cognitive impairment, dementia, stroke- MRI, DTI, MTI, 18F-FDG PET • ALGORITHMIC APPROACH for diagnosis and target organ injury assessment

## **MSEE-38 Imaging Spectrum of Amyloidosis: What A Radiologist Should Know ?**

Participants

Smily Sharma, MD, MBBS, Jodhpur, India (*Presenter*) Nothing to Disclose

### **TEACHING POINTS**

Using a case-based approach: 1. To study the types of Amyloidosis and their pathophysiological basis 2. To study the imaging manifestations of Amyloidosis from head to toe. including CNS, Cardiothoracic, gastrointestinal and visceral manifestations 3. To study in details features of Airway and Pulmonary Amyloidosis 4. Using state of the art cases, discussing the role of Cardiac MRI in Amyloidosis including recent advances like T1 mapping

### **TABLE OF CONTENTS/OUTLINE**

1. Amyloidosis: Classifications and Pathophysiological basis 2. CNS Manifestations of Amyloidosis 3. Airway Amyloidosis 4. Pulmonary

1. Amyloidosis: Classifications and Pathophysiological basis 2. CNS manifestations of Amyloidosis 3. Airway Amyloidosis 4. Pulmonary Amyloidosis 5. Cardiac Amyloidosis: Role of Cardiac MRI, Spectrum of cases, Differentials 6. GIT manifestations of Amyloidosis: Imaging features of Tongue, Esophagus, Stomach, Bowel involvement 7. Visceral Manifestations: Hepatosplenomegaly, Renal Involvement 8. Complications and Prognosis 9. Summary 10. References

### **MSEE-39 Imaging Features of Erdheim-Chester Disease**

#### **Awards**

#### **Certificate of Merit**

#### **Participants**

Irene Dixe de Oliveira Santo, MD, New Haven, CT (*Presenter*) Nothing to Disclose

#### **TEACHING POINTS**

1. Review the pathogenesis and epidemiology of Erdheim-Chester disease; 2. Discuss possible clinical presentations and main organ systems affected; 3. Describe main imaging findings and modalities used in suspected diagnosis and follow-up; 4. Provide an overview of the main currently available therapies and their side effects

#### **TABLE OF CONTENTS/OUTLINE**

1. Pathogenesis, epidemiology, and clinical manifestations; 2. Role of imaging in diagnosis and follow-up, including main radiological findings: (a) Radiographs (eg, bilateral, symmetric, preponderance for lower extremities); (b) Bone scan (eg, lower extremity metaphysis diaphysis); (c) Whole body PET-CT (eg, avid 18F-FDG activity in the affected regions); (d) MRI brain orbits (eg, absence of pituitary bright spot on T1-weighted images, posterior fossa T2-hyperintense white matter lesions); (e) Cardiac MRI/CT (eg, right atrial pseudotumor, thickened interatrial septum); (f) CT chest, abdomen pelvis (eg, periaortic perinephric infiltration, ie, "coated aorta" "hairy kidney"); 3. Definitive diagnosis including markers and specific mutations (eg, BRAF V600E); 4. Management of symptomatic versus asymptomatic patients; 5. Targeted (eg, BRAF and MEK inhibitors) and non-targeted (eg, steroids, interferon- $\alpha$ , pegylated-interferon alfa-2a, IL-1 inhibitors, cladribine, etc) therapies

### **MSEE-4 Diverse Spectrum of Visceral and Somatic PEComas: Current Update on Pathology and Cross-sectional Imaging Findings**

#### **Participants**

Akhilesh Pillai, (*Presenter*) Nothing to Disclose

#### **TEACHING POINTS**

1. Discuss the taxonomy, epidemiology, clinical features, histopathology and biology of the diverse spectrum of PEComas. 2. Describe the salient multimodality cross-sectional imaging features of these tumors. 3. Review the genetics, management and prognosis of these tumors.

#### **TABLE OF CONTENTS/OUTLINE**

1. Introduction, epidemiology and clinical features. 2. Histopathology, immunocytochemistry and molecular pathology. 3. CT, MR and PET/CT imaging features and tumor biology of wide spectrum of PEComas. 4. Prognosis and management. 5. Diverse group of PEComas of varying biological potential. 6. Heterogeneous imaging characteristics of tumors; advanced pathology techniques permit definitive diagnosis. 7. Accurate diagnosis is essential for optimal treatment and management. 8. Conclusion

### **MSEE-40 The Invasion of Fat-Silent and Dangerous: A Radiologic-Pathologic Correlation of Lipo-sarcoma in Usual and Unusual Locations**

#### **Participants**

Nancy Margarita Gutierrez Castaneda, MD, Mexico City, Mexico (*Presenter*) Nothing to Disclose

#### **TEACHING POINTS**

-To describe the general characteristics and subtypes of the liposarcoma.-To review liposarcoma subtypes and imaging characteristics for each subtypes.-To know clinical features and pathogenesis of liposarcoma.-To identify the imaging characteristics for each liposarcoma subtypes and all the radiological modalities (X-ray, CT- scan, PET-CT, SPECT-CT and others).-To associate the clinical presentation, the radiological studies and the histopathological result.-To discuss the appropriate management and follow up of the liposarcoma based on recent literature guideline and expert opinions.

#### **TABLE OF CONTENTS/OUTLINE**

-Introduction-General features of liposarcoma How to identify it?-Liposarcoma background and molecular pathogenesis-Usual and unusual locations of liposarcoma-Clinical presentation-Imaging findings and pathology of different subtypes of liposarcoma(Well-differentiated, dedifferentiated, myxoid, pleomorphic)-Illustrative pathological cases-Appropriate management and follow up of the liposarcoma-Conclusion

### **MSEE-41 Li Fraumeni Syndrome (LFS): Multimodality Imaging Features from Head to Toe and Imaging Guidelines**

#### **Awards**

#### **Identified for RadioGraphics**

#### **Participants**

Babina Gosangi, MD, MPH, New Haven, MA (*Presenter*) Nothing to Disclose

#### **TEACHING POINTS**

• LFS occurs due to TP53 mutation, is transmitted in an autosomal dominant mode and is associated with early onset of cancers and more than one cancer in a lifetime. • The most common tumors associated with LFS are Sarcomas, Leukemia, Adrenocortical carcinoma and Breast tumors (SLAB syndrome). • Individuals with LFS are screened from childhood for early detection of cancer with imaging including annual MRI brain, annual whole-body MRI, ultrasound of the abdomen every 3-4 months in children and once in 6 months in adults, annual breast MRI in women older than 20 years.

## TABLE OF CONTENTS/OUTLINE

Imaging guidelines for LFS Head to toe description of tumors based on location• Brain tumors- medulloblastoma, glioblastoma, meningioma, choroid plexus carcinoma• Breast tumors- phyllodes tumor• Chest tumors- lung cancer, thymoma, thyroid cancer• Abdomen tumors- adrenocortical carcinoma, renal cell cancer, colon cancer, pancreatic cancer• Pelvic tumors- Ovarian cancer, testicular cancer, prostate cancer• Musculoskeletal- rhabdomyosarcomas, osteosarcomas• Skin cancer- melanoma• Others - Leukemia

### MSEE-42 Don't Forget About Abdomen Radiographs Just Yet: Take Advantage of Natural "Contrast Agents"

#### Awards

#### Identified for RadioGraphics

#### Participants

David Disantis, MD, Jacksonville, FL (*Presenter*) Nothing to Disclose

#### TEACHING POINTS

As of 2019, in the U.S. alone, 10.1 million abdomen radiographs were performed. Being able to interpret them is still relevant. Abdominal radiographs have 3 innate "contrast agents" as clues to diagnoses: Gas: Normal (bowel gas) and abnormal (extra-luminal, mural pneumatosis, portal venous, biliary, abscess). Calcium: Benign (calculi, vascular, inflammatory, neoplasms) and malignant. Fat: Around things (organomegaly, masses) and in things (benign and malignant neoplasms)• Case-based examples will illustrate each

## TABLE OF CONTENTS/OUTLINE

1. Recognizing the normal abdomen film 2. Clues from gas as "contrast": bowel obstruction/ileus, pneumoperitoneum/retroperitoneum; bowel/gallbladder/kidney/bladder pneumatosis, abscess. 3. Clues from calcium as "contrast": urinary tract and biliary calculi, milk of calcium, nephrocalcinosis, porcelain gallbladder, calcified neoplasms. 4. Clues from fat as "contrast": outlining organomegaly and masses; within masses.

### MSEE-43 Abdominopelvic Applications for Intra-operative Ultrasound

#### Participants

Omar Shwaiqi, MD, Canton, OH (*Presenter*) Nothing to Disclose

#### TEACHING POINTS

Intraoperative ultrasound (IOUS) is a useful technique that a radiologist can leverage to add value to his/her practice. The use of high frequency probes, often directly upon the organ of interest, allows one to obtain crisp images at resolutions not possible with other modalities. The use cases for IOUS are numerous but generally include localization and marking of lesions, lesion characterization, and survey for metastases. IOUS may also be used to facilitate intraoperative biopsy and/or device placement.

## TABLE OF CONTENTS/OUTLINE

1) Provide overview of IOUS equipment and describe appropriate sterilization procedures for both the equipment and the radiologist. 2) Illustrate intraoperative ultrasound techniques and describe the advantages and disadvantages of each. Where appropriate, describe the relevant ultrasound anatomy. 3) Provide case examples of intraoperative ultrasound utility of various organ systems including the liver, pancreas, kidneys, and female pelvis. 4) Describe limitations and pitfalls of intraoperative IOUS.

### MSEE-44 Bone Marrow Lesions on MRI: A Proliferative Discussion

#### Participants

Blake Marmie, MD, (*Presenter*) Nothing to Disclose

#### TEACHING POINTS

1. Highlight the World Health Organization (WHO) classification scheme of myeloid and lymphoid neoplasms. 2. Review magnetic resonance imaging (MRI) techniques and approaches for evaluating bone marrow disorders. 3. Discuss imaging features of common marrow disorders and provide an imaging-based stratification approach via illustrations and case examples. 4. Provide a suggested imaging lexicon of common marrow lesions that allows for conforming radiology to the histopathology classification of marrow lesions.

## TABLE OF CONTENTS/OUTLINE

1. Marrow tumor classification 1.1. WHO classification of hematopoietic and lymphoid tissue tumors 1.1.1. Myeloid neoplasms 1.1.2. Lymphoid neoplasms 1.2. Imaging-based stratifications of marrow neoplasms 1.2.1. Diffuse or multifocal marrow infiltration 1.2.2. Diffuse or multifocal marrow replacement 2. Imaging technique and concepts 2.1. Radiographs and computed tomography (CT) 2.2. MRI 2.2.1. Conventional sequences (T1-weighted and fluid-sensitive) 2.2.2. Contrast enhanced images 2.2.3. Chemical Shift (in-phase and out-of-phase) 2.2.4. Diffusion-weighted images 3. MRI pattern-based stratification of marrow lesions 3.1. Focal pattern 3.1.1. Unifocal 3.1.2. Multifocal 3.2. Variegated pattern 3.3. Diffuse 4. Proposed MR imaging lexicon for marrow lesions

### MSEE-45 Skin Ultrasound (US): Not Everything Is Cellulitis Nor Lipoma

#### Participants

Fatima Lezcano Sticchi SR, MD, (*Presenter*) Nothing to Disclose

#### TEACHING POINTS

To review the different imaging presentations of common daily practice skin lesions. To identify the key findings in order to approach the correct diagnosis and to learn how to report them. To identify suspicious features that should prompt further evaluation. To enhance the radiologist role into the differentiation of common soft tissue masses and its impact on the dermatologist practice.

## TABLE OF CONTENTS/OUTLINE

Introduction Sonographic Anatomy Technique Benign skins lesions and cases Malignant skin lesions and cases Inflammatory/Infectious diseases and cases Conclusion

## **MSEE-46 Fibroblastic and Myofibroblastic Soft Tissue Tumors (WHO Classification 2020):Imaging Spectrum and Pathology Correlation - Benign Lesions (Part 1)**

### **Awards**

**Certificate of Merit**

**Identified for RadioGraphics**

Participants

Majid Chalian, MD, Seattle, WA (*Presenter*) Grant, The Boeing Company

### **TEACHING POINTS**

1. Review of benign fibroblastic and myofibroblastic soft tissue tumors based on the most recent WHO classification. Review of radiologic features of fibroblastic and myofibroblastic tumors. Radiology-Pathology correlation for each tumor.

### **TABLE OF CONTENTS/OUTLINE**

1. Nodular fasciitis 2. Proliferative fasciitis and proliferative myositis 3. Myositis ossificans and fibro-osseous pseudotumor of digits 4. Ischaemic fasciitis 5. Elastofibroma 6. Fibrous hamartoma of infancy 7. Fibromatosis colli 8. Juvenile hyaline fibromatosis 9. Inclusion body fibromatosis 10. Fibroma of tendon sheath 11. Desmoplastic fibroblastoma 12. Myofibroblastoma 13. Mammary-type myofibroblastoma 14. Calcifying aponeurotic fibroma 15. EWSR1-SMAD3-positive fibroblastic tumour (emerging) 16. Angiomyofibroblastoma 17. Cellular angiofibroma 18. Angiofibroma NOS 19. Nuchal fibroma 20. Acral fibromyxoma 21. Gardner fibroma

## **MSEE-47 I Can Be Anywhere On Your Body: Manifestations and Complications of Hydatid Disease**

Participants

Cecilia Ruiz de Castaneda, Toledo, Spain (*Presenter*) Nothing to Disclose

### **TEACHING POINTS**

The purpose of this exhibit is: 1. To describe hydatid cyst structure and the life cycle of Echinococcus tapeworm 2. To review and illustrate the imaging features in US, CT, and MRI of hydatid disease throughout the body. 3. To review and illustrate the main potential complications of hydatid cysts.

### **TABLE OF CONTENTS/OUTLINE**

Hydatid disease is a worldwide zoonosis produced by the larval stage of the Echinococcus tapeworm. Hydatid cyst demonstrates a variety of imaging features, varying according to growth stage, affected tissue, and complications. For this reason, a hydatid cyst should be kept in mind when a cystic lesion is encountered anywhere in the body, especially in endemic areas. Clinical symptoms may be related to the mass effect of the cyst, its infection, or anaphylactic reactions secondary to its rupture. The classical findings in hydatid disease are well known. However, we review unusual anatomic locations and complications providing images of cases from our experience.

## **MSEE-48 Imaging Review of Diabetes Mellitus**

### **Awards**

**Certificate of Merit**

Participants

Thurl Hugh Cledera, MD, Taguig, Philippines (*Presenter*) Nothing to Disclose

### **TEACHING POINTS**

Diabetes Mellitus (DM) is a metabolic disorder characterized by a chronic hyperglycemic state and impairment of protein, fat, and carbohydrate metabolism due to alterations in insulin action. Complications in DM include microvascular (diabetic retinopathy, neuropathy, and nephropathy) and macrovascular (coronary artery, peripheral artery, and cerebrovascular disease). Non-ketotic hyperglycemia hemichorea may present with asymmetric hyperdensity or T1-weighted hyperintensity in the basal ganglia contralateral to the patient's neurologic deficit. Cardiac MRI can demonstrate the presence of scar or fibrosis and even underlying ischemia. Diabetic mastopathy is a rare complication that is usually seen in late-stage diabetes. Imaging is not primarily indicated in assessing acute urinary tract infection but may be necessary for the presence in the clinical setting of known diabetes.

### **TABLE OF CONTENTS/OUTLINE**

1. Introduction 2. Pathogenesis 3. Head and Neck a. Non-Ketotic Hyperglycemia Hemichorea b. Stroke 4. Cardiac a. Diabetic Cardiomyopathy b. Peripheral Artery Disease c. Coronary Artery Disease 5. Breast a. Diabetic Mastopathy 6. Gastrointestinal a. Subcapsular Fatty Infiltration of the Liver b. Emphysematous Cholecystitis 7. Genitourinary a. Renal Abscess b. Emphysematous Pyelonephritis c. Emphysematous Cystitis d. Ductus Deferens Calcification 8. Musculoskeletal a. Fasciitis b. Fournier Gangrene c. Diabetic Neuroarthropathy d. Diabetic Myopathy e. Medial Calcific Sclerosis f. Subcutaneous Amyloid Deposits

## **MSEE-49 Lose The Battle and Win the War: Multimodality Imaging of Diseases Unique to Immuno-Suppressed**

### **Awards**

**Certificate of Merit**

Participants

Pegah Khoshpouri, MD, Seattle, WA (*Presenter*) Nothing to Disclose

### **TEACHING POINTS**

- Suppression of immune system can be primary-congenital immunodeficiency, secondary to chemo- or immuno-therapy medications, or acquired immunodeficiency syndrome (AIDS).
- Immunosuppression predisposes patients to various opportunistic infections, inflammatory responses such as drug toxicity, or malignancies.
- There are unique and overlapping imaging manifestations. Learning about unique radiologic findings can lead to earlier and more precise diagnosis.

### **TABLE OF CONTENTS/OUTLINE**

To provide a comprehensive review of multimodality and multisystem unique imaging appearances of various scenarios in

immunocompromised patients in a case-based format. These scenarios are including but not limited to: • Infections such as pneumocystis jiroveci pneumonia, tuberculosis in patients with leukemia or HIV, aspergillosis in neutropenic patients or those on immunosuppressants after transplantation. • Malignancies such as Kaposi' sarcoma in HIV and post-transplant lymphoproliferative disorder after transplant. • Lymphoproliferative disorders in patients with congenital hypogammaglobulinemia. • Medication-induced pneumonitis or sarcoid-like reaction. • Table summarizing various predisposing diseases and commonly seen associated infections.

#### **MSEE-5 Castleman Disease: A Multifaceted Diagnostic Dilemma**

##### **Awards**

##### **Identified for RadioGraphics**

Participants

Marika Pitot, MD, Rochester, MN (*Presenter*) Nothing to Disclose

##### **TEACHING POINTS**

1. Review Castleman Disease, clinical subtypes, and implications for disease presentation and identification. 2. Describe the imaging features of Castleman Disease on different imaging modalities. 3. Raise awareness of Castleman Disease as a mimicker of other disease processes. 4. Discuss the potential known associations with and complications of Castleman Disease.

##### **TABLE OF CONTENTS/OUTLINE**

1. General overview of Castleman disease (CD) a. Unicentric (UCD) or multicentric (MCD) lymphoproliferative processes b. Several distinct clinical subtypes c. Histopathologic subtypes: hyaline vascular, plasma cell, mixed d. Spectrum of presentation and association with subtype: UCD - Localized, asymptomatic, indolent, incidentally discovered - localized mass; MCD - Systemic disease presenting acutely with constitutional symptoms, widespread lymphadenopathy, and hepatosplenomegaly 2. Imaging appearances on ultrasound, CT, MRI and PET a. Lymphadenopathy - single, regional, or widespread b. Soft tissue masses - thoracic, abdominal, retroperitoneal etc c. Specific organ involvement and appropriate imaging modalities for evaluation - hepatomegaly, splenomegaly, adrenal gland, salivary glands 3. Potential mimickers 4. Known associations and complications - POEMS syndrome

#### **MSEE-50 A Call for Vigilance: Multimodality Imaging Evaluation of Malignancy in Solid Organ Transplant Recipients**

Participants

Anthony Micetich, MD, (*Presenter*) Nothing to Disclose

##### **TEACHING POINTS**

Solid organ transplant recipients are at risk of numerous postoperative complications. A particularly dreaded immediate and long-term complication is malignancy. Development of these cancers is multifactorial and related to elements inherent to solid organ transplantation, with classification dependent on pathogenesis. Radiologists are often the first providers to identify these malignancies. We will review multimodality imaging presentation of various transplant related malignancies and their mimickers and emphasize the role of the radiologist in the care team.

##### **TABLE OF CONTENTS/OUTLINE**

1. Review various solid organ transplants with diagrammatic depiction 2. Review risk factors for malignancy in transplant recipients a. Increased risk compared to the general population b. Can develop in the transplanted organ(s) or elsewhere in the body 3. Review pathogenesis of malignancy in solid organ transplants: a. Pre-existing risk factors in the recipient, donor, and transplanted organ b. Long-term immunosuppression: type, intensity, duration of use c. Oncogenic and non-oncogenic viral infections 4. Three major classifications of solid organ malignancy in transplant recipients: a. De novo b. Recurrent malignancy c. Donor transmission i. Donor transmitted ii. Donor derived 5. Multimodality imaging of mimics of malignancy in solid organ transplants (including opportunistic infections and graft versus host disease) 6. Role of the radiologist (screening, biopsy, follow up, surveillance) 7. Summary table listing solid organs, related malignancies, and mimickers

#### **MSEE-51 Comprehensive Imaging Review of Peritoneum and Implications of Disease Spread**

Participants

Shruti Kumar, MBBS, Little Rock, AR (*Presenter*) Nothing to Disclose

##### **TEACHING POINTS**

Review embryogenesis and complex imaging anatomy of peritoneal spaces, folds and ligaments. Formulate a differential diagnosis based on disease localization in different peritoneal compartments. Discuss the interconnections between peritoneal and extra-peritoneal spaces, with focus on interfascial disease spread.

##### **TABLE OF CONTENTS/OUTLINE**

Review embryogenesis of ventral and dorsal mesentery and their subsequent specialization into different peritoneal ligaments. Imaging examples of peritoneal ligaments and folds of the liver and stomach, small bowel mesentery, large bowel mesocolon, pelvic ligaments. Demonstrate peritoneal spaces on cross-sectional imaging including lesser sac, greater sac, perihepatic, supramesocolic, inframesocolic compartments, paracolic, and pelvic peritoneal spaces. CT/MRI examples of pathologies that frequently involve peritoneal ligaments and spaces, e.g acute pancreatitis, internal hernias, primary/metastatic peritoneal malignancies, intra-abdominal hematomas, sclerosing encapsulating peritonitis. Discuss clinical impact of peritoneal compartmentalization on disease pathogenesis and management decisions e.g. dissemination of gastric adenocarcinoma along perigastric ligaments, borderline resectability of pancreatic adenocarcinoma with mesocolon invasion. Peritoneal Cancer Index (PCI)

#### **MSEE-52 A Comprehensive Review of Oncologic Emergencies: Update for Radiologists**

Participants

Koichiro Mori, (*Presenter*) Nothing to Disclose

##### **TEACHING POINTS**

• Describe some of the oncologic emergencies for which diagnostic imaging has a significant impact on patient management •

Describe treatment-related oncologic emergencies in which imaging findings are useful for diagnosis • In particular, we also address complications associated with immune checkpoint inhibitors and CAR-T therapy, in which diagnostic imaging is now playing a significant role, including whether or not treatment should be continued.

#### TABLE OF CONTENTS/OUTLINE

I. Introduction and Imaging Findings &1;Classification of Oncologic Emergencies &1;Direct effects of a tumor -Neurological complication- II. Direct effects of a tumor -Thoracic, Abdominal complication- &1;Superior Vena Cava Syndrome &1;Pulmonary thromboembolism III. Treatment-related complications: Radiation therapy &1;Radiation-Induced Myelitis IV. Treatment-related complications: Immune checkpoint inhibitors &1;Myositis &1;Colitis V. Treatment-related complications: CAR-T therapy &1;Cytokine Release Syndrome

#### MSEE-53 Precision Cancer Treatment Toxicity: What the Radiologist Should Know

Participants

Rozan Bokhari, MD, (*Presenter*) Nothing to Disclose

#### TEACHING POINTS

1. Review precision cancer treatments, 2. Review the general mechanisms of anticancer treatment toxicity, 3. Present the spectrum of toxicities, 4. Illustrate the common and uncommon toxicities

#### TABLE OF CONTENTS/OUTLINE

1. Overview of anticancer treatment in the era of precision medicine: Molecular targeted therapies and immune checkpoint inhibitors, Illustrations on the mechanism of drugs and their toxicities (on-target and off-target), 2. Spectrum of toxicities: Acute, Chronic, Delayed, Recurrent, Marker for response and survival, 3. Representative examples with an organ based approach

#### MSEE-54 A Beginners Guide to Cinematic Rendering in Clinical Practice: What You Need to Know

Participants

Elliot Fishman, MD, Owings Mills, MD (*Presenter*) Co-founder, HipGraphics, Inc;Stockholder, HipGraphics, Inc;Institutional Grant support, Siemens AG;Institutional Grant support, General Electric Company;Consultant, Exact Sciences Corporation;Consultant, Imaging Endpoints

#### TEACHING POINTS

1. What is Cinematic Rendering and what are its advantages over classic 3D medical imaging?2. What are the clinical applications where Cinematic Rendering is helpful in either diagnosis or staging of disease or in guiding patient management.3. What CT techniques are needed for Cinematic Rendering and what is the Radiologists role in using Cinematic Rendering in clinical practice4. what is the role of Cinematic Rendering in pre-operative planning for surgery using Cinematic Rendering5. what are the future directions of Cinematic Rendering including Augmented Reality display with HoloLens and multimodality imaging like PET/CT

#### TABLE OF CONTENTS/OUTLINE

1. what is Cinematic Rendering and why is it different from other 3D rendering techniques like MIP and VRT2. what are the specific advantages of Cinematic Rendering from a technical perspective as a computer graphics technique3. what clinical applications is Cinematic Rendering ideal for and why4. what is the role of Cinematic Rendering in applications like Oncologic Staging and Surgical planning5. what is the role of Cinematic Rendering in applications like trauma and vascular imaging6. what are future direction of Cinematic Rendering including improved Augmented Reality displays as well as multimodality imaging like PET/CT7. what role can Cinematic Rendering play in medical education and in patient education

#### MSEE-55 Novel Uses of Contrast-Enhanced Ultrasound

Participants

Clayton Douglas, MD, (*Presenter*) Nothing to Disclose

#### TEACHING POINTS

Contrast-enhanced ultrasound is a well-established modality to characterize liver and renal masses in the setting of contraindication to both MRI and CT. Given this is generally a rare occurrence, many small- and medium-sized hospitals have yet to find adequate utility in adopting this imaging modality. Since the implementation of contrast-enhanced ultrasound at our institution, we have discovered many unique uses of US contrast in common and uncommon clinical scenarios. We aim to share these unique uses in order to increase contrast-enhanced ultrasound usage in medical practice.

#### TABLE OF CONTENTS/OUTLINE

1. Introduction to contrast-enhanced ultrasound and well-established uses in the literature. 2. Present unique uses of contrast-enhanced ultrasound to answer common and uncommon clinical questions. Case examples include evaluating central line location/functionality, solid organ transplant perfusion, solid organ mass versus abscess, and identification of subtle liver lesions for biopsy localization. 3. Discuss potential future applications.

#### MSEE-56 Imaging Spectrum of Radiation Induced"

Participants

Kota Yokoyama, MD, (*Presenter*) Nothing to Disclose

#### TEACHING POINTS

- Imaging findings after radiotherapy are diverse, ranging from transient changes to irreversible tissue damage, fibrosis, angiogenesis, and radiation-induced tumors. - Transient imaging changes are seen in a variety of organs and are more often seen as reversible hyperaccumulation on FDG PET with subtle change in morphologic imaging. - Irreversible tissue damage and fibrosis can be seen on CT and MRI as leukoencephalopathy, lung damage, skin scarring, and vascular stenosis. Fragility fractures of the ribs and sacrum are also commonly encountered. - Angiogenesis can result in trabecular vascular malformation, especially hemorrhage and calcification. - Radiation-induced tumors often occur long after treatment. Meningiomas and gliomas tend to occur after whole-brain irradiation. Squamous cell carcinoma, adenocarcinoma, and hematologic tumors can also occur. Osteosarcoma

after tangential irradiation of breast cancer is also important to recognize.

#### TABLE OF CONTENTS/OUTLINE

Transient imaging changes after radiation therapy Irreversible tissue damage, fibrosis, and angiogenesis after radiation therapy  
Radiation-induced tumors

#### MSEE-57HC **Not All Lumps Are The Same! The Role of High-frequency Ultrasound In the Differential Diagnosis of Benign Skin Lesions**

Participants

Victor Alguz, MD, Santos, Brazil (*Presenter*) Nothing to Disclose

#### TEACHING POINTS

Cystic and solid benign skin lesions are commonly observed in clinical practice and high-frequency ultrasound (HFU) has been increasingly used to characterize them. HFU (>15 MHz) clearly define the skin layers and adnexal structures, allowing better characterization of the lesion's location, morphology, thickness and vascularity. Radiologists must know the ultrasound features of the most common benign skin lesions to avoid misdiagnosis. Epidermoid or epidermal inclusion cysts can appear anywhere in the body and typically present as a well-defined, oval, hypoechoic or heterogeneous, subcutaneous mass with an orifice in the epidermis (punctum). Other cysts may show typical locations, such as synovial or ganglion cysts, located near a joint or tendon, and trichilemmal cysts, originated from the outer hair root sheath, most commonly on the scalp. Common solid benign skin lesions include lipoma, dermatofibroma, pilomatricoma, glomus tumor, plantar fibromatosis, nevus sebaceous of Jadassohn, among others. Each lesion has characteristic findings on high-frequency ultrasound and proper correlation with dermoscopic evaluation can help in the differential diagnosis.

#### TABLE OF CONTENTS/OUTLINE

General aspects of benign skin lesions. High-frequency ultrasound assessment of the most common lesions with dermoscopic correlation (eg. epidermoid cysts, synovial cysts, trichilemmal cysts, lipoma, dermatofibroma, pilomatricoma, glomus tumor, plantar fibromatosis and nevus sebaceous of Jadassohn). Summary and Differential Diagnosis. Please visit the Learning Center to also view this presentation in hardcopy format.

#### MSEE-58 **Neoplastic and Non-neoplastic Conditions of the Skin and Superficial Tissue at Imaging**

Participants

Nikolas Brozovich, MD, Augusta, GA (*Presenter*) Nothing to Disclose

#### TEACHING POINTS

1. Describe classification of superficial tissue lesions on the basis of cellular origin 2. Discuss symptomatic and incidental cutaneous and subcutaneous lesions identified by imaging 3. Discuss systematic approach to achieve definitive diagnosis and limit the differential diagnosis

#### TABLE OF CONTENTS/OUTLINE

Superficial soft-tissue masses are common in clinical practice, and the expanding availability of radiologic imaging has increased radiologists' familiarity with these entities. Superficial soft-tissue masses may be classified in one of the following general diagnostic categories: neoplastic and non-neoplastic conditions. Neoplastic lesions: Neurofibroma, Lipoma, Lipofibroma, Desmoid tumors. Extra mammary Paget's disease of the skin, Liposarcoma, Squamous cell carcinoma, Melanoma. Metastases. Non neoplastic conditions Lymph node, Pilonidal cyst, Epidermoid inclusion cyst, Vascular malformation, Infection and inflammation Cellulitis and panniculitis, Dermatomyositis, Scleroderma, Injection granuloma, Hidradenitis suppurativa, Keloid, Abscess, Endometriosis, Inflammatory bowel disease (IBD), Post traumatic and iatrogenic Hematoma/seroma, Silicone injection

#### MSEE-59 **Imaging Pearls for Post-Operative Complications in Simultaneous Liver-Kidney Transplant-**

##### Awards

##### Certificate of Merit

Participants

Eric Cooper, Chicago, IL (*Presenter*) Nothing to Disclose

#### TEACHING POINTS

Simultaneous liver-kidney transplantations (SLKTs) are increasing in incidence in patients with end-stage liver disease (ESLD) and end-stage renal disease (ESRD). Understanding of the imaging findings for these transplants is crucial for timely detection and management of post-transplant complications. 1. We will review the operative technique and anatomy of traditional and en-bloc SLKTs. 2. We will discuss a systematic imaging approach for evaluation of transplanted grafts. 3. We will review the imaging pearls and techniques to work up common complications following SLKT.

#### TABLE OF CONTENTS/OUTLINE

I. Brief overview of the surgical anatomy of traditional and en-bloc approaches to SLKT II. Imaging approach and normal findings of transplanted grafts. Ultrasound evaluation including major vessel evaluation with doppler waveform characteristics and analysis. CT, MRI and angiography for confirmation of sonographic abnormalities and treatment planning III. Imaging patterns and workup for the most common SLKT complications including - Arterial: hepatic artery stenosis and thrombosis, renal artery stenosis; - Venous: hepatic vein and IVC stenosis and thrombosis; - Portal: portal vein stenosis and thrombosis; - Biliary: biliary leaks, biliary strictures, biliary duct dilation; - Ureteral: urinary tract obstruction, urinary leaks, and vesicoureteral reflux; - Fluid collections (e.g., seromas, hematomas, urinomas).

#### MSEE-6 **Beyond Staging: A Genitourinary Tumor Board Navigation Guide for Radiologists with Emphasis on NCCN Guidelines**

Participants

Daniela Garcia, MBBS, Philadelphia, PA (*Presenter*) Nothing to Disclose

## TEACHING POINTS

- Oncological management requires multidisciplinary approach driven by the NCCN guidelines
- Radiologists fulfill a fundamental role in the decision making for best treatment available
- Radiologist should be familiar with the association between different staging levels and their impact in surgical, systemic, adjuvant and neoadjuvant therapies

## TABLE OF CONTENTS/OUTLINE

Modern day diagnosis and treatment of cancer has transformed what was once a somber sentence into a treatable condition with favorable outcomes. Oncological management is no longer limited to oncologists and surgeons, but requires a multidisciplinary discussion including radiologists, radiation oncologists, and pathologists, among others. In this setting, the radiologist fulfills the important role of custodian in every step of patient management. Radiologists are in a privileged position where we can understand the "big picture" and recommend the best next step in treatment algorithm. In this educational exhibit, we will review updated NCCN management guidelines for genitourinary tumors including kidney, ovarian, cervical, prostate, and penile cancer; highlighting pivotal points where imaging can determine change in management. The accessible format of this presentation is particularly targeted to help create an efficient work frame to successfully navigate tumor board discussion in clinical practice.

## MSEE-60 Evolutionary Fails: A Radiological Exploration of Human Vestigiality and Associated Pathology

Participants

Akito Nicol, (*Presenter*) Nothing to Disclose

## TEACHING POINTS

Vestigiality refers to evolutionarily conserved structures that have lost their original function These holdovers are useful in understanding patterns of organismal change Vestigial structures are usually harmless but may cause disease Knowledge of human evolution can further the radiologist's understanding and imaging analysis of diseases of vestigial structures

## TABLE OF CONTENTS/OUTLINE

1. Vestigial structures in animals 2. Examples in humans organized by system and pathology (as follows)1) Gastrointestinal and Genitourinary Radiology a. Appendix (Appendicitis) b. Meckel's diverticulum (Hemorrhage, intussusception, perforation) c. Urachus (Patent urachus, urachal sinus/cyst)2) Neuroradiology a. Head and Neck i. Recurrent laryngeal nerve (Mediastinal trauma, neoplasms) ii. Wisdom teeth (Impaction, infection, cysts) iii. Platysma (Inflammation, infection, trauma) iv. Tonsils (Infection, neoplasm)b. Spine i. Lumbar degenerative disease related to bipedalism (Disc herniation and spondylolysis) ii. Coccyx (Trauma, infections)3) Musculoskeletal Imaging a. Levator claviculae (Confused for mass/lymphadenopathy; thoracic outlet syndrome) b. Fabella (Fabella pain syndrome, arthritis) c. Plantaris (Tendon graft source, rupture)4) Breast Imaging a. Male breast tissue (Gynecomastia, cancer) b. Supranumerary nipples (Cancer)5) Cardiac Imaging a. Left atrial appendage (Thrombus)

## MSEE-61 Cystic Fibrosis in Children: A Multi-organ Approach From a Radiological Perspective

Participants

Alfonso Escobar Villalba, MD, Madrid, Spain (*Presenter*) Nothing to Disclose

## TEACHING POINTS

1. The lungs are often severely affected, being the presence of thick-walled bronchiectasis the most characteristic finding.2. The pancreas is the most frequently involved abdominal organ, being fatty replacement the most common imaging finding. 3. Liver disease is frequent. SWE elastography and ATI are useful for diagnosis and management. 4. Meconium ileus is the earliest clinical manifestation of cystic fibrosis. 5. The appendix is often distended so its diameter alone is not an adequate parameter for diagnosing appendicitis.

## TABLE OF CONTENTS/OUTLINE

- Etiology, epidemiology - Diagnosis, role of advanced techniques (elastography, ATI, SMI, lung MRI) - Imaging findings- Chest: bronchiectasis, hyperinflation, mucous plugging, consolidation, tree-in-bud, mosaic attenuation/air trapping, pneumothorax, pulmonary and bronchial arterial enlargement.- Abdomen: pancreatic disease (fatty replacement, cystosis, pancreatitis calcifications), liver disease (steatosis, focal biliary fibrosis, cirrhosis, portal hypertension), biliary system (cholelithiasis, microgallbladder, intrahepatic ductal strictures, sclerosing cholangitis), gastrointestinal tract (distal intestinal obstruction syndrome, meconium ileus, rectal prolapse, gastroesophageal reflux, distension of appendix, fibrosing colonopathy, ileocolic intussusception) - Genito-urinary: nephrolithiasis, vas deferens absence, testicular microlithiasis - Head and neck: chronic sinusitis, nasal polyposis - Musculoskeletal: low bone mineral density, kyphosis- Treatment, prognosis

## MSEE-62 Imaging Features in Paroxysmal Nocturnal Hemoglobinuria (PNH)

Participants

Carlos Rubio Sanchez, MD, Madrid, Spain (*Presenter*) Nothing to Disclose

## TEACHING POINTS

- Paroxysmal nocturnal hemoglobinuria (PNH) is a rare, acquired, clonal hematopoietic stem cell disorder.
- Physiopathology: PIG-A gene mutation - glycosylphosphatidylinositol (GPI) molecule deficit - abnormal complement regulatory proteins CD55, CD59 - complement-mediated intravascular hemolysis - hemoglobinuria
- Triad of clinical features: intravascular hemolysis, thromboembolic events, and cytopenia.
- Thromboembolic events represent the leading cause of morbidity and mortality. They can occur in atypical locations in the body (venous sinus thrombosis, Budd-Chiari syndrome?), sometimes silent.
- Imaging plays an important role in the diagnosis of thromboembolic events, infarcts, and abnormal iron deposits.
- The follow-up protocol for PNH patients includes: CT, MRI, or Doppler-ultrasound techniques. MRI is the most sensitive test for detecting silent thrombosis and quantifying iron deposits.
- The treatment with eculizumab has changed the paradigm of this disease, prolonging the life expectancy and quality of life of these patients.

## TABLE OF CONTENTS/OUTLINE

- Introduction: pathogenesis, clinical manifestations, diagnosis criteria.
- Imaging features: -Brain: thrombosis, infarcts, leukoencephalopathy, iron deposit. -Thoracic: cardiac infarcts, pulmonary thromboembolism, pulmonary hypertension signs. -Abdominal: Thrombosis (Sd. Budd Chiari, portal venous, cava?) infarcts, iron deposits. - Osteomuscular: deep vein thrombosis, osteonecrosis
- Conclusions.

## MSEE-63 You Are Not Alone: Solitary Fibrous Tumors Beyond the Chest

Participants

Flavia M. Starling, MD, Belo Horizonte, Brazil (*Presenter*) Nothing to Disclose

### TEACHING POINTS

For a long time, solitary fibrous tumors (SFTs) were thought to be exclusive to the pleura. In fact, this is still the most common place to diagnose this rare pathology. With the advances in histologic, molecular, and genetic techniques and the discovery of the SFT fusion gene, other names of tumors with the same histologic spectrum were abandoned and after classified as SFT, such as hemangiopericytomas. This fact has changed the perception about its restricted location. Although visceral pleura is the most common site of this pathology, it can affect several body structures, such as the head and neck, thoracic and abdominal cavities. The radiological features are generally nonspecific, except for the low signal intensity foci on MRI T1 and T2-weighted sequences corresponding to collagen content, producing a chocolate chip cookie appearance, which may aid in the diagnosis. The behavior of TFS on 18 FDG PET-CT can also raise suspicion for this tumor. This work intends to demonstrate that solitary fibrous tumors are not solitary anymore, being found in many locations in the body, by demonstrating and reviewing their imaging features in the many possible topographies.

### TABLE OF CONTENTS/OUTLINE

- Case-based review in different imaging methods illustrating the solitary fibrous tumor in its different locations.
- Obtaining and understanding characteristic imaging findings of solitary fibrous tumor enables a proper diagnosis for early treatment.
- Discuss different radiological findings of solitary fibrous tumor.

## MSEE-64 Imaging Manifestations of Trisomy 21, from Pediatrics to Adults

Awards

Certificate of Merit

Participants

Christian Gomez, MD, (*Presenter*) Nothing to Disclose

### TEACHING POINTS

Trisomy 21 is the most common chromosomal anomaly in humans, affecting approximately 1 in every 700 babies and more than 350,000 people living in the United States. As medical management evolves, the average life expectancy for people living with Trisomy 21 has increased exponentially, with individuals now commonly living beyond their fifth decade of life. Medical imaging not only plays a critical role in prenatal diagnosis, but also aids in diagnosis and management of associated multiorgan anomalies throughout a patient's life.

### TABLE OF CONTENTS/OUTLINE

Brief introduction to Trisomy 21  
Fetal US/MRI/EchoSoft Markers  
Cardiovascular  
Congenital heart anomalies  
Pulmonary  
Pulmonary congenital anomalies  
Pulmonary hypoplasia and hypertension  
Upper airway obstruction  
Lower airway obstruction  
GI  
Foregut pathology  
Midgut pathology  
Hindgut pathology  
Diaphragmatic herniation  
Musculoskeletal  
Atlantoaxial instability, hypoplastic C1 arch  
Joint laxity/dislocation  
Hands/feet - Kimer deformity  
Eleven ribs  
Hypersegmented sternum  
Developmental hip dysplasia, mickey mouse pelvis  
GU  
Cryptorchidism  
Neuro  
Hearing loss secondary to temporal bone pathology  
Moyamoya  
Early age neurodegeneration  
Cerebellar and vermian hypoplasia  
Oncology  
Leukemia - ALL, AML  
Testicular Cancer

## MSEE-65 Imaging Atlas for Childhood Whole-body MRI

Participants

Mary-Louise Greer, MBBS, (*Presenter*) Research Grant, AbbVie Inc

### TEACHING POINTS

1. To describe whole-body MRI imaging protocols and strategies to optimize these to the patient's developmental and chronological age, co-morbidities and the clinical indication; 2. To illustrate the spectrum of normal anatomy from the neonatal period to adolescence seen on different whole-body MRI imaging sequences, 3. To demonstrate and compare normal, normal variant and abnormal imaging findings on pediatric whole-body MRI to improve diagnostic accuracy for a range of oncologic and non-oncologic diseases

### TABLE OF CONTENTS/OUTLINE

\*Outline  
Whole-body MRI is now standardly performed in pediatric patients for a range of oncologic and non-oncologic indications, used for diagnostic and/or screening purposes. Diagnostic accuracy depends upon the recognition of disease patterns and familiarity with normal maturation that can be mimickers for disease. The purpose of this atlas is to provide an anatomy-based overview of specific imaging features to improve lesion detection and aid distinction from normal and normal variant observations, that can lead to a high rate of false positive findings, as well as offer a differential for imaging findings where the disease entity is as yet unknown.  
Whole-body MRI Protocols - generic: standard optional sequences coverage - indication-specific sequences coverage  
Anatomy-based Spectrum of Normal and Abnormal Whole-body MRI - normal for age - focal, multifocal and diffuse pathology - bones joints, muscle soft tissue, head neck, chest, abdomen pelvis

## MSEE-66 Imaging Spectrum of Tuberculosis from Head to Toe with Updates

Participants

Onur Simsek, MD, (*Presenter*) Nothing to Disclose

### TEACHING POINTS

The purpose of the exhibit is to: Explain pathogenesis and classical imaging findings of tuberculosis · Describe typical and atypical imaging spectrum of tuberculosis from head to toe with updates · Review the recent literature and discuss what changed through the years in imaging of tuberculosis · Highlight pearls and pitfalls in imaging tuberculosis

### TABLE OF CONTENTS/OUTLINE

Background  
Tuberculosis is an infectious disease caused by the mycobacterium tuberculosis complex, and it is one of the leading

Background Tuberculosis is an infectious disease caused by the Mycobacterium tuberculosis complex, and it is one of the leading causes of death due to infectious diseases worldwide. Although tuberculosis is primarily seen as pulmonary infection, it can cause disease in almost any part of the body. Method and Outline: In line with the exhibit's purpose, cases that will set an example for different organ involvements of tuberculosis from the PACS system of our hospital were selected retrospectively. Selected cases include the following examples of tuberculosis: Meningitis, Gastrointestinal tuberculosis, Genitourinary tuberculosis, Spondylodiscitis, Arthritis, Splenic tuberculosis, Pulmonary patterns, Lymphadenitis. Imaging findings were discussed and evaluated with current literature. Conclusion Tuberculosis is still a public health issue in most countries and an essential differential diagnosis all over the world. Even tuberculosis is mainly known for its pulmonary infiltration; it can be detected in almost any part of the body. Hereby, we provide different organ involvements with case examples. This educational exhibit will assist the radiologist in understanding the unexpected presentations of tuberculosis.

#### **MSEE-67 Vasculitides from Head to Toe: Multimodality Imaging Diagnosis, Treatment, and Management**

Participants

Anne Sailer, MD, New Haven, CT (*Presenter*) Nothing to Disclose

##### **TEACHING POINTS**

Vasculitides and arterial wall diseases are rare conditions of the arterial system that may result in significant complications including luminal stenosis, arterial thrombosis, and infarction of the corresponding organs and structures. Development of pseudoaneurysms and dissections and arterial rupture are additional serious complications in this patient population. Doppler US is a first line imaging modality utilized for the assessment of the peripheral arterial system, abdominal aorta and its branches. a) types of arterial wall pathologies b) normal arterial wall anatomy and physiology of waveforms on Doppler US c) sonographic findings associated with vasculitides and arterial wall disease with multi-imaging correlation

##### **TABLE OF CONTENTS/OUTLINE**

Review pathophysiology of various types of vasculitides and pathologies affecting the arterial wall (collagen vascular disease, giant cell arteritis, temporal arteritis, Systemic Lupus Erythematosus (SLE), Takayasu arteritis, Polyarteritis nodosa, Wegener's granulomatosis, and Kawasaki disease, radiation-induced, disease. Discuss general concepts of the assessment of the peripheral arterial system and abdominal aorta using Doppler US and CEUS: technique protocol, image optimization). Demonstrate key sonographic features of the discussed arterial pathologies with correlation other imaging modalities correlation. Review role of ultrasound in the diagnosis and surveillance of complications in this group of patients. Discuss management options with interventional radiology procedures.

#### **MSEE-68 Pediatric Applications of Photon Counting Detector Computed Tomography (PCD CT)**

Participants

Kelly Horst, MD, Rochester, MN (*Presenter*) Nothing to Disclose

##### **TEACHING POINTS**

1) Photon counting detector computed tomography (PCD-CT) technology has qualities that stand to optimize pediatric imaging. 2) The spatial and contrast resolution are optimized by this technique. 3) Dose reduction is accomplished by the combined use of a decreased detector size, without septae, the addition of a tin filter, and the high resolution mode.

##### **TABLE OF CONTENTS/OUTLINE**

Multimodality imaging of pediatric cases illustrating the benefits of PCD CT, including: 1) Increased spatial resolution. 2) Decreased electronic noise. 3) Increased contrast to noise ratio. 4) Decreased beam-hardening artifact. 5) Multi-energy data acquisition 6) The ability to distinguish multiple contrast agents simultaneously.

#### **MSEE-69 3D Printed Models for Pre-surgical Planning: What the Surgeon Wants to Know and Touch**

**Awards**

**Certificate of Merit**

Participants

Sarah Bastawrous, DO, Seattle, WA (*Presenter*) Nothing to Disclose

##### **TEACHING POINTS**

1. Discuss the role, applications and benefits of 3D printed models in presurgical planning 2. Provide case-based examples of presurgical 3D printed models with applicable surgeon feedback 3. Explore success strategies for radiologists and radiology departments to create impactful 3D printing models 4. Define intended use of 3D printed models

##### **TABLE OF CONTENTS/OUTLINE**

1. Clinical impact and potential of presurgical 3D printed models in medicine and role of the radiologist. 2. Brief literature reports of applications and benefits of 3D presurgical printed models. 3. Multimodality, illustrative examples of 3D printed pre-surgical models. 4. Elements important to the surgeon and why. 5. End user and surgeon feedback. 6. "In-surgery" and "out-of-surgery" intended uses, to include patient education/informed consent, trainee simulation, procedure rehearsal, device/guide sizing. 7. Success strategies to include quality management and considerations for radiology departments. 8. Standardization and guidelines to include professional societies, ACR data registry, and appropriateness criteria to guide 3D printing of presurgical models.

#### **MSEE-7 Diversity of Spinal Manifestations in Systemic Disease**

Participants

Ryo Kurokawa, MD, PhD, Ann Arbor, MI (*Presenter*) Nothing to Disclose

##### **TEACHING POINTS**

The aim of this review is to summarize the spectrum of clinical and radiological findings of spinal abnormalities associated with systemic diseases.

##### **TABLE OF CONTENTS/OUTLINE**

I. Vertebral abnormalities- Infection: Tuberculous and Non-tuberculous infections.- Inflammation/autoimmune: Scleroderma, SAPHO syndrome, rheumatoid arthritis- Neoplasm: Systemic mastocytosis, metastasis, lymphoma, leukemia- Neoplasm-like: POEMS syndrome, IgG4-related disease, Langerhans cell histiocytosis- Phacomatosis- Miscellaneous: Alkaptonuria, acromegaly, dialysis-associated, spinal neuroarthropathy (Charcot spine) II. Spinal cord abnormalities- Infection: Varicella-zoster virus, Acute flaccid myelitis- Inflammation, autoimmune: Inflammatory bowel disease, Vasculitis, Systemic lupus erythematosus, Sjogren syndrome, Behcet's disease, HTLV-1-associated myelopathy, Sarcoidosis, GFAP astrocytopathy, Hereditary hemorrhagic telangiectasia- Demyelination: Adrenoleukodystrophy,- Neoplasm: Metastasis, Lymphoma, Leukemia, Paraneoplastic syndrome- Metabolic: Copper deficiency, Hepatic myelopathy, Subacute combined degeneration of the cord- Drug-induced: Heroin, TNF-alpha inhibitor-related demyelination, Immune-checkpoint-inhibitor-related polyradiculoneuropathy- Phacomatosis- Miscellaneous: amyloidosis, superficial siderosis with meningocele or Marfan syndrome Summary1. Imaging findings of the vertebrae, spinal cord and cauda equina, and associated clinical features in various systemic diseases are important for the correct diagnosis.2. Knowledge of X-ray, CT, MRI, bone scintigraphy, and PET imaging findings is essential for identifying these abnormalities.

## **MSEE-70 Neurologic Manifestations of Thoracic Conditions**

Participants

Julian Sison, MD, (*Presenter*) Nothing to Disclose

### **TEACHING POINTS**

Radiologists frequently encounter multisystem diseases that produce findings across multiple subspecialties. This is true of several thoracic diseases with neurologic manifestations. When viewed in isolation many of these findings are nonspecific. However, correlation with imaging across both organ systems can provide clarity to the underlying diagnosis, or at least to the underlying etiology, which can then guide ordering clinicians to the next appropriate step in management so that these conditions can be recognized.

### **TABLE OF CONTENTS/OUTLINE**

We will stratify diseases by etiology: 1) infectious - tuberculosis, nocardiosis, aspergillosis, mucormycosis, COVID-19, 2) inflammatory - sarcoidosis, polymyositis, 3) autoimmune - IgG4 sclerosing disease, 4) genetic - neurofibromatosis-1, tuberous sclerosis, Ehlers-Danlos syndrome, 5) vascular - hereditary hemorrhagic telangiectasia, and 6) neoplastic - lung cancer, lymphoma, paragangliomas. Within these subcategories we will conduct a case-based review of several diseases that demonstrate both thoracic and neurologic manifestations.

## **MSEE-71 Tumors Associated with Tobacco Use: Pathophysiology, Clinical Features Role of Imaging**

Participants

Sanjana Dhakshinamoorthy, Houston, TX (*Presenter*) Nothing to Disclose

### **TEACHING POINTS**

1. Tobacco is the most important risk factor for lung cancers, with nearly 9 out of 10 cancers being related to smoking cigarettes or from exposure to second hand smoke. However, there is a wide spectrum of tobacco-induced cancers that can involve multiple organ systems, including in the oropharynx, larynx, esophagus, liver, pancreas, stomach, colon rectum, urinary bladder, kidney and uterine cervix. 2. Given that many tumors from various different organ systems can occur in patients with tobacco use, radiologists play a vital role in being able to detect these synchronous or metachronous tumors, even before they become symptomatic. 3. Lung-RADS (Lung Imaging Reporting and Data System), is a classification proposed to aid with findings in low-dose CT screening exams for lung cancer. The goal of the classification system is to standardize follow-up and management decisions.

### **TABLE OF CONTENTS/OUTLINE**

1. Review the epidemiology, pathophysiology and clinical features of all the neoplasms associated with tobacco use 2. Discuss the multimodality imaging features of tobacco-induced neoplasms 3. Review the role of imaging in screening, diagnosis and surveillance of malignancies associated with tobacco use

## **MSEE-73 Emerging Complications in the Era of COVID-19 Vaccination: Role of Radiologist and Imaging**

Participants

Janardhana Ponnatapura, MD, Winston Salem, NC (*Presenter*) Nothing to Disclose

### **TEACHING POINTS**

In November 2019, a new RNA Coronavirus (SARS-CoV-2) responsible for a severe acute respiratory syndrome was identified in China. In early 2022, there were nearly 5.8 million deaths and a total of 10 billion doses of vaccination administered. Benefit of vaccine protecting against severe COVID-19 infection far outweighs the very small risk of development of some rare adverse events. Gaining familiarity with various adverse events following COVID-19 vaccination and their clinical presentation is important for radiologist as they come across different imaging modalities. Optimal utilization of imaging and promptly recognize these adverse events helps in better management of patients.

### **TABLE OF CONTENTS/OUTLINE**

• Types and mechanisms of COVID-19 vaccines• Common reactions and adverse events• Emerging rare complications of COVID-19 vaccines-Radiation recall pneumonitis-Radiation recall dermatitis-Breast nodules-Axillary lymphadenopathy-Myocarditis• Role of Imaging• Differentiation from neoplastic disease• What radiologist need to know• Recommendations to oncology providers• Management of these complications• Multidisciplinary team approach

## **MSEE-74 Don't Overlook the Skin! Multimodality Imaging Review of Skin Subcutaneous Malignancies with Radiology-Pathology Correlation**

**Awards**

**Cum Laude**

**Identified for RadioGraphics**

Participants

Priya Pathak, MBBS,MD, (*Presenter*) Nothing to Disclose

## TEACHING POINTS

1) Overview of the spectrum of primary and secondary skin and subcutaneous malignancies with a focus on the role of various imaging modalities for diagnosis, evaluation of anatomical extension, management, and surveillance. 2) Highlight the clinical features, prognosis and modes of spread of cutaneous malignancies. 3) Review relevant radiologic-pathologic correlation, differential diagnoses, imaging artifacts and pitfalls with a systematic approach to narrow the final diagnosis.

## TABLE OF CONTENTS/OUTLINE

- Introduction: Multimodality imaging approach to skin and subcutaneous malignancies for an accurate evaluation of the lesion location, size, extension, margins, metabolic activity and spread patterns. Outline
- Primary malignancies: Squamous cell carcinoma, Basal cell carcinoma, Merkel cell carcinoma and Melanoma
- Secondary malignancies: -Mesenchymal: Dermatofibrosarcoma, Leiomyosarcoma, Angiosarcoma, liposarcoma, Desmoid tumor. -Lymphoma: Mycosis Fungoides, NK T cell lymphoma, Primary cutaneous B cell lymphoma, Follicular lymphoma. - Metastasis: Breast cancer, Lung cancer, Head and neck cancer, GI cancers, RCC, Ovarian cancer, endometrial cancer, Prostate cancer.
- Benign entities/tumor-like lesions: -Systemic disorder: Sarcoidosis, Gout, vasculitis. -Autoimmune, inflammatory and infectious disorders. -Subcutaneous disorders: Fat necrosis, Lipodystrophy, Panniculitis, Epidermoid cyst, pilonidal cysts. -Iatrogenic: Keloids, scars, Injection granulomas, Foreign bodies.

## MSEE-75 Multimodality Imaging in End-Stage Renal Disease

### Awards

Identified for RadioGraphics  
Certificate of Merit

### Participants

Prabhakar Rajiah, MD, FRCR, Rochester, MN (*Presenter*) Nothing to Disclose

## TEACHING POINTS

1. To define and review the pathophysiology of end-stage renal disease (ESRD). 2. To discuss the renal and extrarenal manifestations of ESRD. 3. To describe the role of imaging in the evaluation of ESRD. 4. To illustrate the imaging appearances of various manifestations of ESRD

## TABLE OF CONTENTS/OUTLINE

1. ESRD- DEFINITION, PATHOPHYSIOLOGY 2. ROLE OF IMAGING-Radiograph, ultrasound, CT, MRI, nuclear medicine, echocardiogram, 3. DISCUSSION AND ILLUSTRATION OF THE FOLLOWING MANIFESTATIONS OF ESRD A. Renal - Decreased size; Increased echogenicity; Decreased vascularity; Cystic disease; Renal neoplasms B. Musculoskeletal -Secondary hyperparathyroidism; Osteosclerosis, osteoporosis; Subchondral erosions; Osteomalacia/rickets; Brown tumors; Amyloidosis-arthritis; Destructive spondyloarthropathy; Crystal deposition; Soft tissue calcification; Aluminium toxicity ; AVN, Osteomyelitis C. Cardiac - Coronary atherosclerosis; Concentric LV thickening, cardiomegaly; Diastolic/systolic dysfunction; Cardiac failure; Myocardial calcification; Myocardial ischemia/infarction; Pericardial effusion D. Vascular - Calcifications; Decreased compliance; Peripheral vascular disease; PE; Thrombus in catheters E. Thoracic - Alveolar edema; Metastatic calcification; Calcifications; Infections F. Neurological - Cerebral atrophy, white matter lesions; Encephalopathy; Cerebral infarction/hemorrhage ; Posterior reversible encephalopathy; Osmotic demyelination ; Infection; Sinus thrombosis; Dialysis disequilibrium syndrome G. Abdominal - Encapsulating peritoneal sclerosis H. Dialysis access complications - Vascular stenosis; Thrombus/infection; Aneurysm/pseudoaneurysm

## MSEE-76 What's New in Pathogenesis, Imaging Findings, Prevention, and Management of Human Papillomavirus (HPV)-Related Malignancies? 2022 Update

### Awards

Identified for RadioGraphics  
Magna Cum Laude

### Participants

Sammar Ghannam, MD, MPH, San Antonio, TX (*Presenter*) Nothing to Disclose

## TEACHING POINTS

Review epidemiology pathogenesis of human papillomavirus (HPV)-associated neoplasms Discuss imaging findings of benign and malignant HPV-related neoplasms Describe role of imaging in screening, staging surveillance of HPV-associated cancers Review 2022 updates in treatment vaccination strategies

## TABLE OF CONTENTS/OUTLINE

Introduction Epidemiology Pathogenesis: Molecular pathways Benign tumors: Respiratory Papillomas condyloma acuminata (genital warts) Malignancies: Squamous cell cancer of the oropharyngeal region (oral cavity, palatine/lingual tonsils, tongue base, oropharynx larynx), bronchopulmonary anogenital region (penis, vagina, vulva, cervix anal canal) Updates in WHO Classification Imaging Techniques: CT, MRI 18FDG PET/CT Imaging Findings HPV positive vs. HPV negative cancers: How to differentiate on Imaging? HPV Vaccination: Type of vaccines Current guidelines Role of imaging in screening surveillance Novel treatment strategies: Immunotherapy Imaging Biomarkers: treatment response prognosis Conclusion Summary and Clinical Implications Novel immunotherapies are being investigated and updated screening vaccination guidelines are used to improve outcomes in HPV-related cancers. HPV-positive oropharyngeal SCCs show well-defined borders cystic nodal metastases; have good treatment response, prognosis with better survival. Imaging plays an important role in the diagnosis, staging, and surveillance of HPV-associated lesions in both men women.

## MSEE-8 Twists and Turns: The Torsion Tour

### Participants

Mary J. Clingan, MD, Ponte Vedra Beach, FL (*Presenter*) Nothing to Disclose

## TEACHING POINTS

Teaching points Torsion can affect a number of organs and has a variety of imaging appearances. Abnormal ligamentous attachments and/or increased laxity can lead to increased mobility and predispose to torsion. Increased organ size or a focal mass

can also predispose to torsion. Alternatively, an organ may herniate and twist into a defect left by organ removal or surgical change. Clues to diagnosis vary by location, but include organ displacement, organ enlargement, and a twisted vascular pedicle. Torsion can be intermittent, incomplete, acute, or chronic. In late cases, decreased vascular flow can lead to infarction. There are clues with color and spectral doppler that may be seen in cases of incomplete or intermittent torsion.

#### **TABLE OF CONTENTS/OUTLINE**

OutlineChest: Lung; RUQ: Gallbladder, Wandering liver, Omental Infarct; LUQ: Splenic, epiploic appendage; Pelvis: Adnexal, fibroid, renal transplant; Scrotum: epididymal appendix, testicular/spermatic cord; Bowel: gastric, small bowel, colon

Printed on: 02/07/23



## Abstract Archives of the RSNA, 2022

MSEE-1

### Pre-and Post Procedure CT for Cardiac Implantable Electronic Devices Extraction: A Primer for Radiologists

Sunday, Nov. 27 8:00AM - 9:00AM Room: Learning Center - MS

#### Participants

Samuel Cesconetto, MD, SAO PAULO, Brazil (*Presenter*) Nothing to Disclose

#### TEACHING POINTS

Learning objectives: - To review the principles of extraction technique and the role of computed tomography for planning the extraction of cardiac implantable electronic devices - To illustrate a spectrum of different complications related to cardiac electronic devices and their extraction - To discuss how to assess by imaging the risk of major complications during the procedure - To propose a systematic approach and a structured reporting.

#### TABLE OF CONTENTS/OUTLINE

Table of contents: - Introduction: - Cardiac implantable electronic devices: Overview, types, components, follow up and complications. - Extraction technique. - Patient selection. - CT: Acquisition protocol, image interpretation and clinical application. - Case-based review. - Pre-and postprocedure multidisciplinary assessment and complication score. - Proposal for a structured reporting. - Future directions and take home messages.

Printed on: 02/07/23



## Abstract Archives of the RSNA, 2022

MSEE-11

### MRI Safety: Bullets, Ballistics, Shrapnel

Sunday, Nov. 27 8:00AM - 9:00AM Room: Learning Center - MS

#### Participants

Kyle Stumetz, DO, (Presenter) Nothing to Disclose

#### TEACHING POINTS

In the United States, more than 100,000 patients per year present to the emergency room for gun-related trauma or other ballistic related injuries. Many of these patients may require an MRI (during the initial visit or years later), and thus the presence of retained bullet fragments and/or metallic shrapnel impose important safety concerns. With this information in mind, the goal of this presentation is to: 1) Review an algorithmic approach to imaging patients with suspected retained bullets and/or shrapnel. 2) Identify the most common types of bullets and projectiles, including their metallic compositions. 3) Explain commonly encountered MRI metallic artifacts and common techniques employed to diminish them. 4) Identify scenarios in which MRI imaging is and is not appropriate for retained bullet fragments via a case-based review.

#### TABLE OF CONTENTS/OUTLINE

1. Can my patient with a bullet in their \_\_\_\_ get an MRI? 2. Most common questions 3. Algorithmic Approach 4. Types of Projectiles 5. Bullet/Projectile Composition 6. MR Metal Artifacts 7. MR Metal Artifact Reduction Sequences (MARS) 8. Case-based review

Printed on: 02/07/23



## Abstract Archives of the RSNA, 2022

MSEE-12

### Genetics and Its Advances: What a Pediatric Radiologist Needs to Know?

Sunday, Nov. 27 8:00AM - 9:00AM Room: Learning Center - MS

#### Participants

Sara Rodriguez, MD, (*Presenter*) Nothing to Disclose

#### TEACHING POINTS

1. New advances and understanding in genetics is driving the diagnostic workup, management and clinical practice. 2. Learning the basic concepts of genetics can help radiologists to have a better understanding of diseases and their imaging characteristics, and help decide imaging workup and screening protocols. 3. In this primer, we aim to provide basic concepts and terminology in genetics, to familiarize radiologists with different types of genetic testing and to understand the impact of genetics in different groups of pediatric diseases including cancers and cancer predisposition syndromes, skeletal dysplasia, vascular anomalies, autoimmune diseases and others.

#### TABLE OF CONTENTS/OUTLINE

Introduction  
Basic concepts and terminology in genetics: Gene expression and regulation: from DNA to mRNA to amino acids to protein  
Gene inheritance, transmission and genetic imprinting  
Genetic dominance: genotype-phenotype relationships, phenotype variability  
Genetic mutations  
Genes and diseases: monogenetic, chromosomal, multifactorial.  
Genetic testing: Molecular test (target single variant, single gene, gene panel, whole genome sequence)  
Chromosomal microarray  
Gene expression test  
Biochemical tests.  
Genetics in cancer predisposition syndromes: Tumor suppressor genes  
Proto oncogenes  
Radiological screening in cancer predisposition syndromes.  
Genetics in skeletal dysplasia: Skeletal dysplasia panel  
Implications on imaging.  
Genetics in vascular malformations: RAS/ MEK/ERK and PI3 kinase/mTOR signaling pathway.  
Genetics in autoimmune diseases.  
Genetics in other pediatric diseases.  
Summary

Printed on: 02/07/23



## Abstract Archives of the RSNA, 2022

MSEE-13

### Abdominal Abbreviated MRI Protocols: From Description to Implementation

Sunday, Nov. 27 8:00AM - 9:00AM Room: Learning Center - MS

#### Participants

Maria Tello, MD, (*Presenter*) Nothing to Disclose

#### TEACHING POINTS

1. Understand the need of having abbreviated MRI protocols and describe their role. 2. Explain the clinical scenarios where they can be applied. 3. Describe how to perform some of these abdominal abbreviated MRI protocols. 4. Illustrate the workflow of how to implement the described above protocols

#### TABLE OF CONTENTS/OUTLINE

1. MRI nowadays, why to perform abbreviated protocols, advantages and disadvantages. 2. Description of the MRI situation at our institution, selecting the abbreviated protocols that we can benefit the most. 3. Description of the abbreviated MRI protocols we are going to implement: Pancreatic cystic lesions, Liver metastases, including the role in colorectal cancer, Adrenal incidentalomas, Active surveillance for small renal masses. 4. Implementation at our institution, how we are going to do it? A brief guide step by step.

Printed on: 02/07/23



## Abstract Archives of the RSNA, 2022

MSEE-14

### DECT In The Emergency Room: Play Your Best Game and Leave It All Out On The Field!

Sunday, Nov. 27 8:00AM - 9:00AM Room: Learning Center - MS

#### Awards

Certificate of Merit

#### Participants

Kirbi Sullivan, MD, (*Presenter*) Nothing to Disclose

#### TEACHING POINTS

1. Dual Energy CT (DECT) may aid in diagnosis for Emergency Department (ED) patients but is only impactful if radiologists maximize utilization of the extra information. 2. Workflow changes are needed to optimally incorporate DECT into a busy ED.

#### TABLE OF CONTENTS/OUTLINE

1. Introductiona. Discuss patient selection strategies for DECT from both the radiologist and technologist perspectiveb. Review high-yield DECT reconstructions to detect pathology and problem-solve2. DECT winsa. Avoiding downstream testingi. Differentiating between gastrointestinal bleeding and ingested contents, avoiding endoscopyii. Differentiating hematoma from tumor in a hypotensive patient with peritoneal carcinomatosisb. Expediting carei. Detection of postoperative hemorrhage on a portal venous phase CT, bypassing CT angiography for rapid embolizationii. Detection of early bowel ischemia on iodine maps, leading to rapid surgery and avoiding bowel resectioniii. Subtle fracture detection with bone marrow edema mapsiv. Active extravasation detection in intracranial hemorrhage on iodine maps3. DECT losses: underutilized information negatively impacted downstream testing and carea. Unnecessary testingi. Mischaracterization of suture material as active extravasation in a postoperative patient, leading to unnecessary angiographyii. Unnecessary workup of incidentalomas not fully characterized with DECT at the time of detectionb. Delayed carei. Missed subtle pyelonephritis, leading to a second ED visit 1 month later

Printed on: 02/07/23



## Abstract Archives of the RSNA, 2022

MSEE-15

### Recent Advances in Cardiothoracic Imaging

Sunday, Nov. 27 8:00AM - 9:00AM Room: Learning Center - MS

#### Participants

Joshua Hunter, Cleveland, OH (*Presenter*) Nothing to Disclose

#### TEACHING POINTS

1. Review novel techniques in cardiothoracic imaging and how they improve upon existing methodologies. 2. Discuss technical parameters and protocol considerations of the new techniques. 3. Illustrate use cases of novel cardiothoracic imaging techniques.

#### TABLE OF CONTENTS/OUTLINE

1. Discuss existing cardiothoracic imaging modalities and briefly cover the pathologies that they diagnose  
2. Discuss limitations of existing techniques  
3. Enumerate the new techniques in cardiothoracic imaging and how they alleviate some of the existing limitations  
4. Discuss technical and protocol implications of the new techniques  
5. Compare the advantages and disadvantages afforded by the new techniques, when compared to existing imaging methodologies  
6. Brief overview of several novel imaging techniques  
7. Novel Cardiothoracic Imaginga. Radiography i. Dual energy subtraction radiography (DESR)  
1. Bone-selective radiograph improves detection of bony lesions  
2. Soft tissue-selective radiograph eliminates potential for obstruction by bones  
ii. AI-enabled detection  
1. Thoracic Pathologies (Pneumothorax, Pneumonia)  
2. Lines and tube malpositioning (ET tube, Enteric tube)  
iii. AI-enabled prognostication  
1. COVID-19 patients needing urgent mechanical ventilation. CT  
i. Dual Energy CT  
ii. Photon counting CT  
iii. CT-FFR  
iv. AI-enabled tools  
1. Automated coronary artery calcium scoring  
2. Automated PE detection and nodule analysis on CT  
c. MRI  
i. Parametric mapping and ECV  
ii. MR Strain imaging  
iii. 4D Flow MRI  
iv. PET/MRI  
d. Ultrasound  
i. IVUS  
ii. 3D Echocardiography  
8. Disadvantages of new imaging techniques  
9. Other emerging techniques currently in the research sphere; and not in clinical use  
10. Future goals and directions

Printed on: 02/07/23



## Abstract Archives of the RSNA, 2022

MSEE-16

### Low Field Body MRI: Challenges and Opportunities at 0.55T

Sunday, Nov. 27 8:00AM - 9:00AM Room: Learning Center - MS

#### Awards

Identified for RadioGraphics

#### Participants

Anup Shetty, MD, Saint Louis, MO (*Presenter*) Nothing to Disclose

#### TEACHING POINTS

Low-field MRI (0.55T) for body imaging presents challenges and opportunities for patients, radiologists, and enterprises compared to high-field (1.5T or 3T) MRI. This exhibit will: 1. Discuss imaging advantages and challenges of low-field body MRI compared to high-field body MRI. 2. Discuss logistical and workflow challenges of low-field body MRI compared to high-field body MRI. 3. Illustrate use cases, strategies, and nuances in low-field body MRI through a series of case examples

#### TABLE OF CONTENTS/OUTLINE

- Low-field MRI advantages: lower cost; easier installation (including lighter weight, less shielding, less helium), larger bore size, MR physics benefits (longer T2\* [i.e., reduced susceptibility], lower SAR, shorter T1 [i.e., faster acquisition], easier shimming for B0 homogeneity), less acoustic noise- Low-field MRI challenges: lower SNR, fewer receiver coil options, weaker gradients, longer acquisition times, longer TE for chemical-shift imaging- Comparison of sequences across field strengths, highlighting key limitations and observations of each sequence at 0.55T- comparison of lesion conspicuity with example cases acquired at both low and high field strengths- discussion of sequence modifications and strategies at 0.55T to overcome imaging limitations and maintain comparable image quality- exploration of use cases (lung imaging, pancreatic cyst follow-up, hepatic imaging after locoregional therapy, emergency imaging, adrenal/renal imaging, pelvic imaging, etc.)

Printed on: 02/07/23



## Abstract Archives of the RSNA, 2022

MSEE-17HC

### Whole Body MRI In Children: A Primer for Beginners

Sunday, Nov. 27 8:00AM - 9:00AM Room: Learning Center - MS

#### Participants

Daniela Carrascal-Penaranda, MD, MSc, Bogota D.C, Colombia (*Presenter*) Nothing to Disclose

#### TEACHING POINTS

To explain the usefulness of Whole body MRI in the pediatric population, its utility and indications. To review basic concepts on used sequences and different protocols, which one is the most appropriate to make a successful evaluation of the body. To discuss and exemplify through cases the possible scenarios of imaging findings in patients with cancer and the broad spectrum of cancer predisposition syndromes. To discuss the principal indications of whole body MRI in infectious - inflammatory disease as well as in general population.

#### TABLE OF CONTENTS/OUTLINE

Introduction - Definitions. Applications and indications Standard protocol - Technical requirements Cancer predisposition syndromes Indications in non-oncological pathology: Miscellaneous Incidental findings and further implications to the patient Structured report in pediatrics Summary Conclusions Please visit the Learning Center to also view this presentation in hardcopy format.

Printed on: 02/07/23



## Abstract Archives of the RSNA, 2022

MSEE-18

### Imaging of Oncologic Pain: A Multi System Approach

Sunday, Nov. 27 8:00AM - 9:00AM Room: Learning Center - MS

#### Participants

Thais Kuwazuru, MD, Sao Paulo, Brazil (*Presenter*) Nothing to Disclose

#### TEACHING POINTS

The aim of this exhibition is to:1. Review the current concepts about oncologic pain syndromes;2. Describe the role of imaging in oncologic pain, focusing on diagnosis;3. Correlate imaging findings with clinical syndromes and therapeutic strategies;4. Illustrate the causes of oncologic pain with illustrative cases.

#### TABLE OF CONTENTS/OUTLINE

1. INTRODUCTION:a. Definitions and classification of oncologic pain;b. Impact of pain syndromes in patient quality of life and prognosis.2. ACUTE PAIN SYNDROMES:a. Associated with tumor: Tumor bleeding, pathologic fractures, obstruction and perforation of viscera, superior vena cava syndrome, acute thrombosis;b. Associated with treatment: Chemotherapy-induced neuropathy, radiation therapy-induced bone pain and plexopathy, oral mucositis, enteritis and proctitis.3. CHRONIC PAIN SYNDROMES:a. Somatic pain: Bone and soft tissue pain;b. Visceral pain: Abdominal pain syndromes;c. Neuropathic pain: Leptomeningeal metastasis, cranial and peripheral neuropathies;d. Headaches;e. Related to treatment: Post-chemotherapy, post-surgical and post-radiation pain syndromes;4. CONCLUSION:a. Pain assessment in cancer patients very often include imaging investigation;b. When interpreting imaging exams, it is essential to understand the imaging patterns of each syndrome and the important findings for therapeutic planning.

Printed on: 02/07/23



## Abstract Archives of the RSNA, 2022

MSEE-19HC

### Strategies to Identify, Treat, and Eliminate MRI Radiofrequency Burns

Sunday, Nov. 27 8:00AM - 9:00AM Room: Learning Center - MS

#### Participants

Anshuman Panda, PhD, Scottsdale, AZ (*Presenter*) Nothing to Disclose

#### TEACHING POINTS

1. Thermal burns are a potential cause of injury during MRI scans. Recognition, diagnosis, and management of these burns can be challenging and may often go unrecognized.2. We implemented a multidisciplinary team, led by a radiology physician assistant, to help in the timely identification, assessment, and management of patients with suspected MRI burns.3. As a result of this initiative, we have collected numerous cases of MRI burns. In this exhibit, we will use these cases to demonstrate causes of MRI burns, physical findings of these burns, and discuss management strategies.

#### TABLE OF CONTENTS/OUTLINE

A. Background of MRI burns with an emphasis on physics aspect of burns and excessive power deposition.B. Pathophysiology of radiofrequency burns.C. Clinical presentation and treatment.D. Discussion of our local burn initiative including physical assessment of patients and the review by MR technologists and physicists to address root cause of burn cases.E. Case based review and management of burn cases identified in our practicePlease visit the Learning Center to also view this presentation in hardcopy format.

Printed on: 02/07/23



## Abstract Archives of the RSNA, 2022

MSEE-2

### Solitary Fibrous Tumor in the Brain, Head and Neck, and Spine: Basic and Advanced Neuroimaging

Sunday, Nov. 27 8:00AM - 9:00AM Room: Learning Center - MS

#### Awards

Certificate of Merit

#### Participants

Ryo Kurokawa, MD, PhD, Ann Arbor, MI (*Presenter*) Nothing to Disclose

#### TEACHING POINTS

The aim of this exhibit is to 1. Review the etiology, histology, and epidemiology of solitary fibrous tumor (SFT) in the brain, head and neck, and spine 2. Demonstrate the imaging characteristics on the conventional modalities/sequences 3. Show how advanced modalities/sequences can help diagnose SFT

#### TABLE OF CONTENTS/OUTLINE

Content organization 1. Introduction-Etiology, histology, and epidemiology of SFT in the brain, head and neck, and spine 2. Typical imaging findings 3. Advanced imaging-MRS-Diffusion-weighted imaging-Contrast-enhanced perfusion-weighted imaging-FDG-PET 4. Atypical imaging findings-Atypical localization: Cavernous sinus, Orbit-Atypical manifestation: Metastasis, Doege-Potter syndrome, Intracranial hemorrhage 5. Differential diagnosis-Variou neoplasms 6. Summary

Printed on: 02/07/23

## Abstract Archives of the RSNA, 2022

MSEE-20

### The Forgotten System: Lymphatics of Abdomen and Pelvis

Sunday, Nov. 27 8:00AM - 9:00AM Room: Learning Center - MS

#### Participants

Rodrigo Loto, MD, Rosario, Argentina (*Presenter*) Nothing to Disclose

#### TEACHING POINTS

-Presentation of the organization and function of the lymphatic vascular system.-Overview of lymphatic vascular development (lymphangiogenesis).-Importantly, lymphangiogenesis occurs in adult tissues during inflammation, wound healing, and tumor metastasis.-Radiology is playing an important and growing role in the diagnosis and treatment of many lymphatic conditions.

#### TABLE OF CONTENTS/OUTLINE

Studies of the last decades have revealed the importance of angiogenesis for normal growth and for the pathogenesis of numerous diseases. Much less studied is lymphangiogenesis, the growth of lymphatic vessels, which drain extravasated fluid, proteins, and cells and transport them back to the venous circulation. Nonetheless, insufficient lymphangiogenesis causes incapacitating lymphedema, while lymphatic growth around tumors may facilitate metastatic spread of malignant cells that ultimately kill the patient. During inflammation, lymph flow increases to limit edema and prevents tissue antigen-presenting cell transport. Lymphatics also adjust their contractile activity to increase fluid transfer during acute inflammation. Conversely, chronic inflammation can provoke lymphostasis, which might limit pathogen spread within the circulation; however, decreased lymph flow leads to the persistence of immune cells and mediators in tissues to intensifying injury. Knowledge of lymphatic anatomy, physiology, and expected imaging appearances is crucial in understanding the pattern of cancer spread. Lymphatics have been proposed as transphrenic dissemination pathway for multiple phenomena, including neoplasms, septic processes, urinothorax, and porous diaphragm syndromes.

Printed on: 02/07/23



## Abstract Archives of the RSNA, 2022

MSEE-21

### Not Too Young to Know: Multimodality Imaging Review of Commonly Encountered Pathologies in Institution-Living Elderly

Sunday, Nov. 27 8:00AM - 9:00AM Room: Learning Center - MS

#### Participants

Andy Guo, MD, (*Presenter*) Nothing to Disclose

#### TEACHING POINTS

1- Define the institutional elderly patient population and explain how they are a vulnerable population  
2- Learn about common pathologic conditions specifically affecting the institutional elderly  
3- There are special considerations in clinical and imaging approach for evaluating these patients that are different from the general population including compassionate care, imaging techniques and accounting for limitations in the institutional elderly

#### TABLE OF CONTENTS/OUTLINE

1- Review examples of common pathologies in the institutional elderly, including but not limited to:  
Musculoskeletal- falls and trauma  
Infectious disease- aspiration pneumonia  
Gastrointestinal- chronic constipation  
Genitourinary- incontinence  
Drug Toxicity- confusion and over-sedation  
Neurological- dementia and stroke  
Underlying Medical Condition- heart failure, hypertension and type 2 diabetes  
2- Describe specific imaging findings in evaluation of example pathologies, with teaching points about underlying pathophysiology  
3- Review special considerations that radiologists and technologists must make in evaluating this vulnerable patient population to align with compassionate care

Printed on: 02/07/23

## Abstract Archives of the RSNA, 2022

MSEE-23

### Lymphatics: Imaging and Interventions- A Comprehensive Review

Sunday, Nov. 27 8:00AM - 9:00AM Room: Learning Center - MS

#### Participants

Smily Sharma, MD, MBBS, Jodhpur, India (*Presenter*) Nothing to Disclose

#### TEACHING POINTS

1. To study the anatomy of the lymphatic system and its pathophysiological basis 2. To study in detail the methodology and protocols of MR and Conventional Lymphangiography 3. To discuss imaging features of various disorders of the lymphatic system including macrocystic, microcystic, mixed lymphatic malformations, renal lymphangiectasia and syndromes associated with lymphatic disorders 4. To discuss imaging features of congenital abnormalities of lymphatics like vanishing bone disease, primary lymphedema 5. To discuss imaging features of acquired lymphatic disorders like chyle leak, pulmonary lymphatic perfusion syndrome, and the role of MR and conventional lymphangiogram in these disorders using state of the art cases 6. To discuss the role of Interventional Radiology in the management of lymphatic disorders including sclerosing agents and thoracic duct embolization

#### TABLE OF CONTENTS/OUTLINE

1. Anatomy of Lymphatic System and Pathophysiological Basis of Lymphatic Disorders 2. Conventional Lymphangiography: Method 3. MR Lymphangiography: Method and Protocols 4. Lymphatic Malformations 5. Renal Lymphangiectasia 6. Syndromes associated with Lymphatic disorders 7. Congenital Lymphatic Disorders: Generalized Lymphatic Anomaly, Gorham Stout Disease, Primary Lymphedema 8. Acquired Lymphatic disorders: chyle leak, pulmonary lymphatic perfusion syndrome, secondary lymphedema 9. Interventional Radiology in treatment of lymphatics: Sclerosing Agents, Thoracic Duct Embolization 10. Summary

Printed on: 02/07/23



## Abstract Archives of the RSNA, 2022

MSEE-24

### Free-Breathing T1-Weighted Motion Correction in Abdominal MRI: Technical Principles, Applications, and Current Limitations

Sunday, Nov. 27 8:00AM - 9:00AM Room: Learning Center - MS

#### Awards

Identified for RadioGraphics

#### Participants

Ebru Yaman Akcicek, Seattle, WA (*Presenter*) Nothing to Disclose

#### TEACHING POINTS

1. Understand the technical principles of free breathing T1 weighted pulse sequences 2. Learn the difference between non-dynamic and dynamic contrast enhanced acquisitions using radial k space trajectories 3. Examine the currently established indications for motion corrected contrast techniques 4. Discuss limitations of current free breathing techniques and accelerated cartesian acquisitions 5. Learn how to identify the best patient-adapted protocol strategy 6. Review newly emerging techniques for motion reduction

#### TABLE OF CONTENTS/OUTLINE

1. Principals of radial imaging: description of radial k-space trajectories (stack of stars) 2. Dynamic contrast acquisitions with view sharing 3. Abdominal applications of free breathing motion correction indications in liver, pancreas and kidneys 4. Strategies for patient-adapted abdominal examination protocols using free breathing techniques 5. Limitations of motion correction techniques, and mitigation strategies 6. Novel developments of free breathing pulse sequences

Printed on: 02/07/23



## Abstract Archives of the RSNA, 2022

MSEE-25

### Focusing the Retrospectroscope: Challenging and Easily Overlooked Patterns of Recurrence and Metastases in Abdominopelvic Oncologic Imaging

Sunday, Nov. 27 8:00AM - 9:00AM Room: Learning Center - MS

#### Participants

Molly Roseland, MD, Northville, MI (*Presenter*) Nothing to Disclose

#### TEACHING POINTS

1. Accurate recognition of recurrent and metastatic cancers by CT, MRI, and PET/CT may be challenging. 2. Post-surgical scarring and distortion is a common mimic of recurrence. Enlarging enhancing tissue should be considered suspicious. 3. Common features of missed recurrent malignancy include small size, slow or infiltrative growth pattern, obscuration by irregular surgical margins, or location in an imaging "blind-spot." Comparisons over time, surgical history, and thorough search pattern are essential. PET may improve detection.

#### TABLE OF CONTENTS/OUTLINE

1. General principles: use history, many comparisons 2. Individual Cancer Recurrence Patterns A. Pancreatic adenocarcinoma - Recurrence: perivascular cuffing, pancreatic mass; Mimic: Post-Whipple fibrosis -Metastases: peritoneum, liver; mimic: fat necrosis, micro-abscesses B. Cholangiocarcinoma -Recurrence: mass at surgical margin, biliary stricture; mimic: postsurgical change, cholangitis C. Colorectal cancer -Recurrence: perianastomotic, lymph nodes; mimic: scarring (presacral) D. Renal cell carcinoma - Recurrence: surgical bed, IVC; Pitfall: post-treatment change (noncontrast) -Metastases: Adrenal, pancreas (unique), bone; Pitfall: Small; no arterial-phase; adrenal washout E. Bladder cancer -Recurrence: ureteral stricture, mass; Mimic: Reflux post-cystectomy F. Prostate cancer -Local Recurrence; PSMA PET Pitfall: obscuration by urinary excretion -Metastases: bone, lymph nodes; Pitfall: epidural extension, fracture; Pitfall: rare sites (sacral nerves, penis) 3. Summary and recommendations

Printed on: 02/07/23



## Abstract Archives of the RSNA, 2022

MSEE-26

### Lymph Nodes in Abdominal and Pelvis Neoplasms: Evaluation From Staging to Post - Treatment: Messengers of the Force or Dark Side Sentinel?

Sunday, Nov. 27 8:00AM - 9:00AM Room: Learning Center - MS

#### Awards

Certificate of Merit

#### Participants

Thamiris De Sousa Garcia, MD, MD, Sao Paulo, Brazil (*Presenter*) Nothing to Disclose

#### TEACHING POINTS

- Use of different imaging methods to assess lymph nodes for tumor dissemination, what each method can add and how to proceed for further investigation. - Evaluation of heterogeneity of staging criteria and treatment response of lymph nodes involved in abdominal and pelvic neoplasms. - Better understanding of regional lymph nodes involved in different neoplasms, with revision of the anatomy of lymph node chains and dissemination routes.

#### TABLE OF CONTENTS/OUTLINE

- Introduction - Lymph nodes of abdomen and pelvis: anatomy. - Evaluation of lymph nodes using different imaging methods: findings of normality and criteria for tumor involvement. - Staging of the main neoplasms of the abdomen and pelvis with characterization of regional involvement and dissemination pathways, as well as its particularities. - Comparison between different types of methods and criteria for evaluating lymph node response to surgical and non-surgical treatment. - Teaching points.

Printed on: 02/07/23



## Abstract Archives of the RSNA, 2022

MSEE-27

### Flap Anatomy After Pelvic Reconstructive Surgery: A Brief Survival Guide

Sunday, Nov. 27 8:00AM - 9:00AM Room: Learning Center - MS

#### Participants

Paula Otermin Barrera, MD, Madrid, Spain (*Presenter*) Nothing to Disclose

#### TEACHING POINTS

To describe in a practical way the resulting anatomy after various flap-based reconstructive surgery techniques, as well as potential complications, providing specific iconography selected from our tertiary referral center, with special emphasis on myocutaneous flaps and their application in pelvic reconstruction after oncological resections

#### TABLE OF CONTENTS/OUTLINE

1. Introduction. Definition of flap and benefits provided by flap coverage. 2. Types of flap according to their vascular anatomy and tissue composition. 3. Myocutaneous flaps. Imaging characteristics and applications in pelvic reconstruction of rectus abdominis muscle flaps (TRAM, VRAM and variants) and gracilis muscle flaps. 4. Omental flap. 5. Deep Inferior Epigastric Perforator flap (DIEP). Preoperative CT study for selection and marking of optimal perforators. Imaging characteristics and applications in pelvic reconstruction. 6. Complications (flap and donor area): post-surgical fluid collections and surgical wound infection, fat necrosis, flap ischemia, dehiscence, tumor recurrence.

Printed on: 02/07/23



## Abstract Archives of the RSNA, 2022

MSEE-28

### Ciliopathy Syndromes: Pathogenesis and Multisystem Multimodality Imaging Review

Sunday, Nov. 27 8:00AM - 9:00AM Room: Learning Center - MS

#### Participants

Yarik Bezkor, BS, MD, Lexington, KY (*Presenter*) Nothing to Disclose

#### TEACHING POINTS

Teaching Points: 1. Ciliopathies are a diverse group of disorders occurring secondary to abnormal development and/or structural or functional defects of the cilia. 2. Cilia are highly evolved, complex organelles, found ubiquitously on the surface of almost all the cell types, and have diverse mechanosensory and chemosensory signal transduction roles and there have been significant recent advances in the understanding of these key organelles. 3. Ciliopathy syndromes affecting non-motile cilia are associated with multisystem developmental disorders predominantly affecting renal, skeletal, and nervous systems. 4. Renal ciliopathies are the most common which include autosomal polycystic kidney disease, and nephronophthisis, Ciliopathy syndromes associated with neurodevelopmental features include Meckel-Gruber syndrome, Joubert syndrome, orofacial digital syndrome as well as Bardet-Biedl syndrome. Motile ciliopathies, grouped as "primary ciliary dyskinesia" most commonly present as Kartagener's syndrome. 5. Multimodality imaging with Ultrasound, CT, and MRI is crucial for the diagnosis and management of these syndromes.

#### TABLE OF CONTENTS/OUTLINE

1. A. Embryology and pathogenesis of ciliopathy syndromes 2. B. Multimodality imaging of Motile and non-motile ciliopathy syndromes.

Printed on: 02/07/23



## Abstract Archives of the RSNA, 2022

MSEE-29

### **New CT Technology: A Practical Approach to Convert CT Acquisition Protocols from Energy Integrating Detector (EID) CT to Photon Counting Detector (PCD) CT**

Sunday, Nov. 27 8:00AM - 9:00AM Room: Learning Center - MS

#### **Participants**

Nikkole Weber, ARRT, RT, Rochester, MN (*Presenter*) Nothing to Disclose

#### **TEACHING POINTS**

1. Explain the differences between energy integrating detector (EID) and photon counting detector (PCD) technologies 2. Understand critical differences in PCD technology that need to be taken into account when designing PCD scanning acquisition protocols.

#### **TABLE OF CONTENTS/OUTLINE**

1. Explain differences between PCD and EID technologies used on commercial CT scanners a. PCD: Directly convert X-ray into electronic signals, count individual photon and record its energy b. EID: Indirect, 2 stage conversion of X-ray of light to electronic signal. No information on individual photon energy 2. Create a core team of experts a. Medical Physicists b. CT technologists c. Subspecialized radiologists 3. Explore new CT scanner technology and its benefits 4. As a practice, decide protocol conversion approach: a. Apples-to-apples: i. Acquisitions with similar appearance and diagnostic quality as current EID CT b. Apples-to-oranges: i. Acquisitions leveraging technical advantages of PCD technology (high matrix, sharper kernels, higher IR) 5. Define parameters that do not allow an apples-to-apples protocol conversion a. Scan modes (high res, multi-energy, combined-lower kV) b. Conventional tube potential selection (conventional) vs. Virtual monoenergetic selection (PCD) c. System-specific reconstruction kernels and reconstruction nomenclature 6. Protocol evaluation through image review sessions a. Define two lists of protocols i. Commonly used protocols in your practice ii. Protocols or indications that would benefit from new technology b. Change acquisition and reconstruction parameters, iteratively reevaluating images with core experts

Printed on: 02/07/23



## Abstract Archives of the RSNA, 2022

MSEE-3

### Don't Burst That Bubble!: A Guide to Skin Cysts

Sunday, Nov. 27 8:00AM - 9:00AM Room: Learning Center - MS

#### Participants

Carolina Almeida, MD, Rio de Janeiro, Brazil (*Presenter*) Nothing to Disclose

#### TEACHING POINTS

TEACHING POINTS1) Palpable skin lesions are a common complaint in dermatology offices and ultrasounds are often requested to clarify the origin.2) High-frequency ultrasound is the imaging modality chosen for skin examination due to its cost and availability.3) Cutaneous cystic lesions are very common and have specific characteristics that help in the diagnosis.4) Make a pictorial essay of the main cutaneous cysts and their differential diagnoses, such as trichilemmal cyst, dermoid cyst, epidermic cyst, and hidradenoma.

#### TABLE OF CONTENTS/OUTLINE

TABLE OF CONTENTS/OUTLINE1) Overview of cystic structures and their definition;2) High-frequency ultrasound of cystic skin lesions - epidermal cyst and hidradenoma;3) Trichilemmal cyst and dermoid cyst;4) Report structuring step by step;5) Differential diagnosis.

Printed on: 02/07/23

## Abstract Archives of the RSNA, 2022

MSEE-30

### Thinking IN and OUT of the Box: Using Chemical Shift Imaging as a Problem-Solving Tool

Sunday, Nov. 27 8:00AM - 9:00AM Room: Learning Center - MS

#### Participants

Anthony Larder, DO, Milford, OH (*Presenter*) Nothing to Disclose

#### TEACHING POINTS

-Review basic physics concepts of chemical shift and magnetic susceptibility in MRI-Discuss tissue characteristics that can be used for diagnosis with chemical shift imaging including: macroscopic fat, microscopic fat, calcifications, gas, and iron-Review imaging findings and associated pathophysiology of multiple scenarios in which chemical shift artifact aids in diagnosis

#### TABLE OF CONTENTS/OUTLINE

Review of physics concepts related to chemical shift imaging including original illustrations and relevant case examples-Precession of fat and water-Signal characteristics and physical properties of Type 1 and Type 2 chemical shift artifact-Liver fat quantification-Magnetic susceptibility-T2\* decay based on TE-Properties of diamagnetic, paramagnetic, and ferromagnetic substances-Liver iron quantification-Review of chemical shift as a diagnostic tool, including differential diagnoses, discussion of relevant pathophysiology, and clinical issues. Case examples including-Macroscopic fat:-Renal angiomyolipoma-Mature teratoma-Liposarcoma-Fat-containing hepatocellular carcinoma-Microscopic fat:-Hepatic steatosis-Nodular-Companion case of hepatic melanoma metastases -Hepatic adenoma-Adrenal adenoma-Metastatic marrow replacement -Fat-containing hepatocellular carcinoma-Magnetic Susceptibility:-Iron deposition-Primary hemochromatosis-Hemosiderosis-Gamma-Gandy bodies-Hepatic siderotic nodules-Including case of Wilson's disease with siderotic nodules-Metallic Susceptibility-Surgical clip localization-Calcifications-Cholelithiasis-Nephrolithiasis-Blood products-Gas-Within infected pancreatic necrosis-Pneumoperitoneum-Pneumobilia

Printed on: 02/07/23



## Abstract Archives of the RSNA, 2022

MSEE-31

### Introduction to Oncology Imaging: A Primer For Residents and Fellows

Sunday, Nov. 27 8:00AM - 9:00AM Room: Learning Center - MS

#### Participants

Jordan LeGout, MD, Ponte Vedra Beach, FL (*Presenter*) Nothing to Disclose

#### TEACHING POINTS

Learning to interpret oncology imaging can be a complex and daunting topic for residents and fellows. In this exhibit we will:- Provide a framework for approaching oncology cases for the trainee-Review the various tumor response criterion and their main takeaways for clinical use-Discuss differences in imaging assessment for chemotherapy and immunotherapy-Examine imaging response for local-regional therapies-Highlight the benefit of high-yield disease specific search patterns

#### TABLE OF CONTENTS/OUTLINE

1. Introduction a. Role of radiologist and importance of imaging in patient care b. Words matter! "Loaded words" and definitions i. Stable, response, progression2. Clinical history (the "what, when, and how") a. Key history elements to know for each case i. Original presentation 1. Always review the first scan = Each case a teaching file! 2. Establishes disease appearance and sites pre-therapy ii. Therapy type 1. Start date 2. How treatment type influences image interpretation iv. Time crunch: what are the highest yield priors v. Tumor markers and trend3. Tumor response criteria (the takeaways) a. RECIST 1.1 b. mRECIST c. iRECIST d. Choi e. Cheson/Lugano4. Immunotherapy a. Pseudoprogression b. Unique adverse effects5. Local-regional therapies a. Ablations and embolizations b. Radioembolization6. Disease specific high-yield search patterns a. Examples of common malignancies

Printed on: 02/07/23



## Abstract Archives of the RSNA, 2022

MSEE-32

### The Role of the Radiologist in LGBTQ+ Patient Care: A Comprehensive Curriculum

Sunday, Nov. 27 8:00AM - 9:00AM Room: Learning Center - MS

#### Participants

Janis Yee, MD, (*Presenter*) Nothing to Disclose

#### TEACHING POINTS

? Understand the radiologist's role in delivering inclusive and culturally sensitive care to LGBTQ+ patients. ? Understand the current cancer screening guidelines for transgender patients. ? Recognize the normal postoperative appearance and postoperative complications related to gender affirmation surgeries. ? List complications related to hormone therapy, including increased risk of venous thromboembolism, ischemic heart disease, cerebrovascular events, and hormone-sensitive organ atrophy or cancers. ? Recognize complications related to HIV and highly active antiretroviral therapy (HAART).

#### TABLE OF CONTENTS/OUTLINE

? Background and definitions of LGBTQ+ ? Challenges to caring for the LGBTQ+ community ? Discuss imaging relevant to trans patients ? Preoperative imaging in planning for feminization surgery ? Preoperative imaging in planning for masculinization surgery ? Postoperative complications in gender-affirming surgery ? Normal appearance of feminization and masculinization after medical transition ? Complications of gender-affirming hormone therapy ? Provide an overview of imaging findings in lesbian, gay, bisexual, and queer patients related to stigmatized health concerns such as STDS, substance abuse, and certain types of cancer ? Review complications from common preventative medications prescribed to patients, for example, pre-exposure prophylaxis (PrEP) ? Qualitatively assess the availability of multidisciplinary care to LGBTQ+ patients at three different academic institutions across the country ? Discuss how radiology departments can improve their role in the care of this patient population ? Conclusion

Printed on: 02/07/23



## Abstract Archives of the RSNA, 2022

MSEE-33

### Skin Ultrasound in Lipolytic Aesthetic Procedures

Sunday, Nov. 27 8:00AM - 9:00AM Room: Learning Center - MS

#### Participants

Luciana Zattar, MD, Sao Paulo, Brazil (*Presenter*) Nothing to Disclose

#### TEACHING POINTS

Lipolysis and lipolytic aesthetic procedures are increasingly being performed, and minimal invasive types are preferable. Nonsurgical body contouring techniques, aimed at reducing the subcutaneous adipose tissue, includes cryolipolysis, injectable lipolytic (meso-therapy), low and high-intensity focused ultrasound and others therapies. In this context, the radiologist has been requested to recognize their usual aspects as well as to assess possible complications. To achieve accurate and timely detection and appropriate approach of each case, High frequency ultrasound (HFUS/24-33MHz) is the most effective method since it provides optimal anatomical information of the skin and allows evaluation before, during and after these procedures. This study aims to discuss and illustrate the radiologist's role in the evaluation of lipolytic aesthetic procedures with HFUS. The purpose of this exhibit is:- To describe the preprocedure evaluation.- To illustrate the anatomy of the skin layers.- To show the main image patterns and effects of the lipolytic aesthetic procedures.- To list and describe the most common procedures complications.- To highlight the importance of HFUS before, during and after nonsurgical body contouring techniques.

#### TABLE OF CONTENTS/OUTLINE

1. INTRODUCTION.2. NORMAL ANATOMY.3. PREPROCEDURAL EVALUATION.4. PROCEDURES CHARACTERISTICS AND IMAGING FINDINGS5. COMPLICATIONS.6. PROCEDURE GUIDANCE.7. CONCLUSION.

Printed on: 02/07/23



## Abstract Archives of the RSNA, 2022

MSEE-34

### Polyps From Head to Toe: What's Your Impression?

Sunday, Nov. 27 8:00AM - 9:00AM Room: Learning Center - MS

#### Participants

Carlos Padula, MD, (*Presenter*) Nothing to Disclose

#### TEACHING POINTS

To understand the pathophysiology of polyps. To review most common presenting locations. To review imaging features of polyps across multiple modalities including ultrasound, fluoroscopy, CT, and MRI. To review differential diagnoses of polypoid lesions. To review current guidelines and literature regarding management of polyps.

#### TABLE OF CONTENTS/OUTLINE

1. Pathophysiology of polyps. 2. Anatomical locations 3. Imaging features of polyps 4. Case examples: Aural, sinonasal, oropharyngeal, vocal cord, esophageal, gastric, gallbladder, small bowel, colorectal, endometrial, and cervical.

Printed on: 02/07/23



## Abstract Archives of the RSNA, 2022

MSEE-35

### Metabolic Syndrome: Imaging Features and Clinical Outcomes

Sunday, Nov. 27 8:00AM - 9:00AM Room: Learning Center - MS

#### Participants

Mohamed Badawy, MD, Houston, TX (*Presenter*) Nothing to Disclose

#### TEACHING POINTS

- Discuss obesity prevalence and different types of fat distribution - Review imaging techniques used to evaluate the obesity effects on different body organs - Describe clinical outcomes and imaging artifacts related to obesity Table of content

#### TABLE OF CONTENTS/OUTLINE

- Introduction- Differences between white and brown fat and between central and peripheral adipose tissue- Methods of obesity evaluation and the superiority of anthropometric measurement over body mass index (BMI) - Imaging quantitative assessment of visceral fat volume - MetS effects on the o Liver § Imaging used to diagnose non-alcoholic fatty liver disease including ultrasonography (ULS), elastography, magnetic resonance (MR) spectroscopy, MR proton density fat fraction § Liver fat quantification o Pancreas § Imaging features of pancreatic infiltration and its mimics o Heart § Imaging and clinical effects of increased epicardial fat o Gastrointestinal tract § CT and MR appearances of fat deposition (e.g submucosal fat deposition, diffuse fat lipomatosis and fat halo sign) o Urinary tract § Imaging and mimics of fat deposition in the urinary bladder wall o Lumbosacral edema § Imaging features of lumbosacral edema correlated with MetS o Tumors development in different body organs § Malignancies associated with obesity and their imaging features - Obesity Imaging artifacts - Obesity surgery pre and post-operative imaging

Printed on: 02/07/23



## Abstract Archives of the RSNA, 2022

MSEE-36

### A Confusion of Wild Catheters: A Review of Abdominal Medical Devices

Sunday, Nov. 27 8:00AM - 9:00AM Room: Learning Center - MS

#### Participants

Victoria Kim, MD, (*Presenter*) Nothing to Disclose

#### TEACHING POINTS

1. Recognize the normal appearance of various abdominal devices on multi-modality imaging.2. Identify potential complications related to abdominal devices which may have acute clinical implications.

#### TABLE OF CONTENTS/OUTLINE

I. Background: In the continuously changing landscape of medicine, abdominal imaging often captures a wide variety of medical devices. These can be bewildering when seen for the first time, especially for residents early in training. Recognizing potential complications related to unfamiliar devices is an even greater challenge but can have acute clinical implications for patient safety and outcomes.II. Gastrointestinal tract devices: Traditional enteric catheters; Gastrostomy/gastrojejunostomy tubes; Gastrointestinal and biliary stents.III. Genitourinary devices: Ureteral stents; Nephrostomy tubes; Contraceptive devices; Prosthetics.IV. Vascular devices: IVC filters; Vascular stents and grafts; ECMO cannulas and other vascular catheters; Ventricular assist device drivelines.V. Miscellaneous devices: Spinal catheters; Electronic stimulator devices; Peritoneal dialysis catheters; Surgical clips, sutures, and drains.

Printed on: 02/07/23

## Abstract Archives of the RSNA, 2022

MSEE-37

### Multimodality Imaging in Metabolic Syndrome: A State-of-the-Art Review

Sunday, Nov. 27 8:00AM - 9:00AM Room: Learning Center - MS

#### Awards

**Cum Laude**

**Identified for RadioGraphics**

#### Participants

Prabhakar Rajiah, MD, FRCR, Rochester, MN (*Presenter*) Nothing to Disclose

#### TEACHING POINTS

1. To review the etiology and complications of metabolic syndrome 2. To understand the role of multimodality imaging in metabolic syndrome 3. To illustrate the utility of imaging in diagnosis of metabolic syndrome and assessment of target organ injury

#### TABLE OF CONTENTS/OUTLINE

• METABOLIC SYNDROME- Definition and criteria • CAUSES AND RISK FACTORS • ROLE OF IMAGING - Diagnosis, target organ injury assessment, biomarkers for novel therapy • MODALITIES- CT, MRI (including MR spectroscopy, Elastography, PET/MRI), nuclear medicine, Ultrasound, DXA • FAT ASSESSMENT - Subcutaneous abdominal fat - Visceral abdominal fat- US (thickness, fat index), CT (inc single slice CT ) MRI (FSE, chemical shift, fat selective), DXA - Parenchymal fat- MRS - Fat around organs- Eg. Pericardiac fat (echo, CT/MRI) - Fat around vessels- CT, MRI, 1H-MRS • INSULIN RESISTANCE - Intramyocellular lipid in skeletal muscle biopsy, 1H- MRS - Glucose metabolism using 18F-FDG PET, dynamic triple-tracer PET with 15O-H<sub>2</sub>O, 11C-3-0-methylglucose, and 18F-FDG • TARGET ORGAN INJURY - Vessels- Atherosclerosis, elevated arterial stiffness- Doppler, CT, MRI - Cardiac- Dilation/hypertrophy, diastolic dysfunction, impaired strain, coronary atherosclerosis, ischemic heart disease- Echo, CT, MRI, Nuclear perfusion - Liver- Nonalcoholic fatty liver, cirrhosis- Ultrasound, CT, 1H- MRS, Dixon MRI, 31P- MRS, MRI, MR Elastography, US elastography - Pancreas- Fatty disease- US, CT, MR, 1HMRS - Kidney- Chronic renal disease, renal stone- Ultrasound, CT, MRI, 99mTc-DTPA, dynamic CE- MRI, ASL-MRI, DWI, BOLD-MRI - Brain- Cognitive impairment, dementia, stroke- MRI, DTI, MTI, 18F-FDG PET • ALGORITHMIC APPROACH for diagnosis and target organ injury assessment

Printed on: 02/07/23



## Abstract Archives of the RSNA, 2022

MSEE-38

### Imaging Spectrum of Amyloidosis: What A Radiologist Should Know ?

Sunday, Nov. 27 8:00AM - 9:00AM Room: Learning Center - MS

#### Participants

Smily Sharma, MD, MBBS, Jodhpur, India (*Presenter*) Nothing to Disclose

#### TEACHING POINTS

Using a case-based approach: 1. To study the types of Amyloidosis and their pathophysiological basis 2. To study the imaging manifestations of Amyloidosis from head to toe. including CNS, Cardiothoracic, gastrointestinal and visceral manifestations 3. To study in details features of Airway and Pulmonary Amyloidosis 4. Using state of the art cases, discussing the role of Cardiac MRI in Amyloidosis including recent advances like T1 mapping

#### TABLE OF CONTENTS/OUTLINE

1. Amyloidosis: Classifications and Pathophysiological basis 2. CNS Manifestations of Amyloidosis 3. Airway Amyloidosis 4. Pulmonary Amyloidosis 5. Cardiac Amyloidosis: Role of Cardiac MRI, Spectrum of cases, Differentials 6. GIT manifestations of Amyloidosis: Imaging features of Tongue, Esophagus, Stomach, Bowel involvement 7. Visceral Manifestations: Hepatosplenomegaly, Renal Involvement 8. Complications and Prognosis 9. Summary 10. References

Printed on: 02/07/23

## Abstract Archives of the RSNA, 2022

MSEE-39

### Imaging Features of Erdheim-Chester Disease

Sunday, Nov. 27 8:00AM - 9:00AM Room: Learning Center - MS

#### Awards

Certificate of Merit

#### Participants

Irene Dixe de Oliveira Santo, MD, New Haven, CT (*Presenter*) Nothing to Disclose

#### TEACHING POINTS

1. Review the pathogenesis and epidemiology of Erdheim-Chester disease; 2. Discuss possible clinical presentations and main organ systems affected; 3. Describe main imaging findings and modalities used in suspected diagnosis and follow-up; 4. Provide an overview of the main currently available therapies and their side effects

#### TABLE OF CONTENTS/OUTLINE

1. Pathogenesis, epidemiology, and clinical manifestations; 2. Role of imaging in diagnosis and follow-up, including main radiological findings: (a) Radiographs (eg, bilateral, symmetric, preponderance for lower extremities); (b) Bone scan (eg, lower extremity metaphysis diaphysis); (c) Whole body PET-CT (eg, avid 18F-FDG activity in the affected regions); (d) MRI brain orbits (eg, absence of pituitary bright spot on T1-weighted images, posterior fossa T2-hyperintense white matter lesions); (e) Cardiac MRI/CT (eg, right atrial pseudotumor, thickened interatrial septum); (f) CT chest, abdomen pelvis (eg, periaortic perinephric infiltration, ie, "coated aorta" "hairy kidney"); 3. Definitive diagnosis including markers and specific mutations (eg, BRAF V600E); 4. Management of symptomatic versus asymptomatic patients; 5. Targeted (eg, BRAF and MEK inhibitors) and non-targeted (eg, steroids, interferon- $\alpha$ , pegylated-interferon alfa-2a, IL-1 inhibitors, cladribine, etc) therapies

Printed on: 02/07/23



## Abstract Archives of the RSNA, 2022

MSEE-4

### Diverse Spectrum of Visceral and Somatic PEComas: Current Update on Pathology and Cross-sectional Imaging Findings

Sunday, Nov. 27 8:00AM - 9:00AM Room: Learning Center - MS

#### Participants

Akhilesh Pillai, (*Presenter*) Nothing to Disclose

#### TEACHING POINTS

1. Discuss the taxonomy, epidemiology, clinical features, histopathology and biology of the diverse spectrum of PEComas.2. Describe the salient multimodality cross-sectional imaging features of these tumors.3. Review the genetics, management and prognosis of these tumors.

#### TABLE OF CONTENTS/OUTLINE

1. Introduction, epidemiology and clinical features.2. Histopathology, immunocytochemistry and molecular pathology.3. CT, MR and PET/CT imaging features and tumor biology of wide spectrum of PEComas.4. Prognosis and management.5. Diverse group of PEComas of varying biological potential.6. Heterogeneous imaging characteristics of tumors; advanced pathology techniques permit definitive diagnosis.7. Accurate diagnosis is essential for optimal treatment and management.8. Conclusion

Printed on: 02/07/23



## Abstract Archives of the RSNA, 2022

MSEE-40

### The Invasion of Fat-Silent and Dangerous: A Radiologic-Pathologic Correlation of Lipo-sarcoma in Usual and Unusual Locations

Sunday, Nov. 27 8:00AM - 9:00AM Room: Learning Center - MS

#### Participants

Nancy Margarita Gutierrez Castaneda, MD, Mexico City, Mexico (*Presenter*) Nothing to Disclose

#### TEACHING POINTS

-To describe the general characteristics and subtypes of the liposarcoma.-To review liposarcoma subtypes and imaging characteristics for each subtypes.-To know clinical features and pathogenesis of liposarcoma.-To identify the imaging characteristics for each liposarcoma subtypes and all the radiological modalities (X-ray, CT- scan, PET-CT, SPECT-CT and others).- To associate the clinical presentation, the radiological studies and the histopathological result.-To discuss the appropriate management and follow u of the liposarcoma based on recent literature guideline and expert opinions.

#### TABLE OF CONTENTS/OUTLINE

-Introduction-General features of liposarcoma How to identify it?-Liposarcoma background and molecular pathogenesis-Usual and unusual locations of liposarcoma-Clinical presentation-Imaging findings and pathology of different subtypes of liposarcoma(Well-differentiated, dedifferentiated, myxoid, pleomorphic)-Ilustrative pathological cases-Appropriate management and follow up of the liposarcoma-Conclusion

Printed on: 02/07/23



## Abstract Archives of the RSNA, 2022

MSEE-41

### Li Fraumeni Syndrome (LFS): Multimodality Imaging Features from Head to Toe and Imaging Guidelines

Sunday, Nov. 27 8:00AM - 9:00AM Room: Learning Center - MS

#### Awards

Identified for RadioGraphics

#### Participants

Babina Gosangi, MD, MPH, New Haven, MA (*Presenter*) Nothing to Disclose

#### TEACHING POINTS

- LFS occurs due to TP53 mutation, is transmitted in an autosomal dominant mode and is associated with early onset of cancers and more than one cancer in a lifetime.
- The most common tumors associated with LFS are Sarcomas, Leukemia, Adrenocortical carcinoma and Breast tumors (SLAB syndrome).
- Individuals with LFS are screened from childhood for early detection of cancer with imaging including annual MRI brain, annual whole-body MRI, ultrasound of the abdomen every 3-4 months in children and once in 6 months in adults, annual breast MRI in women older than 20 years.

#### TABLE OF CONTENTS/OUTLINE

Imaging guidelines for LFS Head to toe description of tumors based on location

- Brain tumors- medulloblastoma, glioblastoma, meningioma, choroid plexus carcinoma
- Breast tumors- phyllodes tumor
- Chest tumors- lung cancer, thymoma, thyroid cancer
- Abdomen tumors- adrenocortical carcinoma, renal cell cancer, colon cancer, pancreatic cancer
- Pelvic tumors- Ovarian cancer, testicular cancer, prostate cancer
- Musculoskeletal- rhabdomyosarcomas, osteosarcomas
- Skin cancer- melanoma
- Others - Leukemia

Printed on: 02/07/23



## Abstract Archives of the RSNA, 2022

MSEE-42

### Don't Forget About Abdomen Radiographs Just Yet: Take Advantage of Natural "Contrast Agents"

Sunday, Nov. 27 8:00AM - 9:00AM Room: Learning Center - MS

#### Awards

Identified for RadioGraphics

#### Participants

David Disantis, MD, Jacksonville, FL (*Presenter*) Nothing to Disclose

#### TEACHING POINTS

As of 2019, in the U.S. alone, 10.1 million abdomen radiographs were performed. Being able to interpret them is still relevant. Abdominal radiographs have 3 innate "contrast agents" as clues to diagnoses: Gas: Normal (bowel gas) and abnormal (extra-luminal, mural pneumatosis, portal venous, biliary, abscess). Calcium: Benign (calculi, vascular, inflammatory, neoplasms) and malignant. Fat: Around things (organomegaly, masses) and in things (benign and malignant neoplasms)• Case-based examples will illustrate each

#### TABLE OF CONTENTS/OUTLINE

1. Recognizing the normal abdomen film 2. Clues from gas as "contrast": bowel obstruction/ileus, pneumoperitoneum/retroperitoneum; bowel/gallbladder/kidney/bladder pneumatosis, abscess.3. Clues from calcium as "contrast": urinary tract and biliary calculi, milk of calcium, nephrocalcinosis, porcelain gallbladder, calcified neoplasms.4. Clues from fat as "contrast": outlining organomegaly and masses; within masses.

Printed on: 02/07/23



## Abstract Archives of the RSNA, 2022

MSEE-43

### Abdominopelvic Applications for Intra-operative Ultrasound

Sunday, Nov. 27 8:00AM - 9:00AM Room: Learning Center - MS

#### Participants

Omar Shwaiki, MD, Canton, OH (*Presenter*) Nothing to Disclose

#### TEACHING POINTS

Intraoperative ultrasound (IOUS) is a useful technique that a radiologist can leverage to add value to his/her practice. The use of high frequency probes, often directly upon the organ of interest, allows one to obtain crisp images at resolutions not possible with other modalities. The use cases for IOUS are numerous but generally include localization and marking of lesions, lesion characterization, and survey for metastases. IOUS may also be used to facilitate intraoperative biopsy and/or device placement.

#### TABLE OF CONTENTS/OUTLINE

- 1) Provide overview of IOUS equipment and describe appropriate sterilization procedures for both the equipment and the radiologist.
- 2) Illustrate intraoperative ultrasound techniques and describe the advantages and disadvantages of each. Where appropriate, describe the relevant ultrasound anatomy.
- 3) Provide case examples of intraoperative ultrasound utility of various organ systems including the liver, pancreas, kidneys, and female pelvis.
- 4) Describe limitations and pitfalls of intraoperative IOUS.

Printed on: 02/07/23



## Abstract Archives of the RSNA, 2022

MSEE-44

### Bone Marrow Lesions on MRI: A Proliferative Discussion

Sunday, Nov. 27 8:00AM - 9:00AM Room: Learning Center - MS

#### Participants

Blake Marmie, MD, (*Presenter*) Nothing to Disclose

#### TEACHING POINTS

1. Highlight the World Health Organization (WHO) classification scheme of myeloid and lymphoid neoplasms. 2. Review magnetic resonance imaging (MRI) techniques and approaches for evaluating bone marrow disorders. 3. Discuss imaging features of common marrow disorders and provide an imaging-based stratification approach via illustrations and case examples. 4. Provide a suggested imaging lexicon of common marrow lesions that allows for conforming radiology to the histopathology classification of marrow lesions.

#### TABLE OF CONTENTS/OUTLINE

1. Marrow tumor classification 1.1. WHO classification of hematopoietic and lymphoid tissue tumors 1.1.1. Myeloid neoplasms 1.1.2. Lymphoid neoplasms 1.2. Imaging-based stratifications of marrow neoplasms 1.2.1. Diffuse or multifocal marrow infiltration 1.2.2. Diffuse or multifocal marrow replacement 2. Imaging technique and concepts 2.1. Radiographs and computed tomography (CT) 2.2. MRI 2.2.1. Conventional sequences (T1-weighted and fluid-sensitive) 2.2.2. Contrast enhanced images 2.2.3. Chemical Shift (in-phase and out-of-phase) 2.2.4. Diffusion-weighted images 3. MRI pattern-based stratification of marrow lesions 3.1. Focal pattern 3.1.1. Unifocal 3.1.2. Multifocal 3.2. Variegated pattern 3.3. Diffuse 4. Proposed MR imaging lexicon for marrow lesions

Printed on: 02/07/23



## Abstract Archives of the RSNA, 2022

MSEE-45

### **Skin Ultrasound (US): Not Everything Is Cellulitis Nor Lipoma**

Sunday, Nov. 27 8:00AM - 9:00AM Room: Learning Center - MS

#### **Participants**

Fatima Lezcano Sticchi SR, MD, (*Presenter*) Nothing to Disclose

#### **TEACHING POINTS**

To review the different imaging presentations of common daily practice skin lesions. To identify the key findings in order to approach the correct diagnosis and to learn how to report them. To identify suspicious features that should prompt further evaluation. To enhance the radiologist role into the differentiation of common soft tissue masses and its impact on the dermatologist practice.

#### **TABLE OF CONTENTS/OUTLINE**

Introduction Sonographic Anatomy Technique Benign skins lesions and cases Malignant skin lesions and cases  
Inflammatory/Infectious diseases and cases Conclusion

Printed on: 02/07/23



## Abstract Archives of the RSNA, 2022

MSEE-46

### Fibroblastic and Myofibroblastic Soft Tissue Tumors (WHO Classification 2020): Imaging Spectrum and Pathology Correlation - Benign Lesions (Part 1)

Sunday, Nov. 27 8:00AM - 9:00AM Room: Learning Center - MS

#### Awards

**Certificate of Merit**

**Identified for RadioGraphics**

#### Participants

Majid Chalian, MD, Seattle, WA (*Presenter*) Grant, The Boeing Company

#### TEACHING POINTS

1. Review of benign fibroblastic and myofibroblastic soft tissue tumors based on the most recent WHO classification. Review of radiologic features of fibroblastic and myofibroblastic tumors. Radiology-Pathology correlation for each tumor.

#### TABLE OF CONTENTS/OUTLINE

1. Nodular fasciitis 2. Proliferative fasciitis and proliferative myositis 3. Myositis ossificans and fibro-osseous pseudotumor of digits 4. Ischaemic fasciitis 5. Elastofibroma 6. Fibrous hamartoma of infancy 7. Fibromatosis colli 8. Juvenile hyaline fibromatosis 9. Inclusion body fibromatosis 10. Fibroma of tendon sheath 11. Desmoplastic fibroblastoma 12. Myofibroblastoma 13. Mammary-type myofibroblastoma 14. Calcifying aponeurotic fibroma 15. EWSR1-SMAD3-positive fibroblastic tumour (emerging) 16. Angiomyofibroblastoma 17. Cellular angiofibroma 18. Angiofibroma NOS 19. Nuchal fibroma 20. Acral fibromyxoma 21. Gardner fibroma

Printed on: 02/07/23



## Abstract Archives of the RSNA, 2022

MSEE-47

### I Can Be Anywhere On Your Body: Manifestations and Complications of Hydatid Disease

Sunday, Nov. 27 8:00AM - 9:00AM Room: Learning Center - MS

#### Participants

Cecilia Ruiz de Castaneda, Toledo, Spain (*Presenter*) Nothing to Disclose

#### TEACHING POINTS

The purpose of this exhibit is: 1. To describe hydatid cyst structure and the life cycle of Echinococcus tapeworm 2. To review and illustrate the imaging features in US, CT, and MRI of hydatid disease throughout the body. 3. To review and illustrate the main potential complications of hydatid cysts.

#### TABLE OF CONTENTS/OUTLINE

Hydatid disease is a worldwide zoonosis produced by the larval stage of the Echinococcus tapeworm. Hydatid cyst demonstrates a variety of imaging features, varying according to growth stage, affected tissue, and complications. For this reason, a hydatid cyst should be kept in mind when a cystic lesion is encountered anywhere in the body, especially in endemic areas. Clinical symptoms may be related to the mass effect of the cyst, its infection, or anaphylactic reactions secondary to its rupture. The classical findings in hydatid disease are well known. However, we review unusual anatomic locations and complications providing images of cases from our experience.

Printed on: 02/07/23



## Abstract Archives of the RSNA, 2022

MSEE-48

### Imaging Review of Diabetes Mellitus

Sunday, Nov. 27 8:00AM - 9:00AM Room: Learning Center - MS

#### Awards

Certificate of Merit

#### Participants

Thurl Hugh Cledera, MD, Taguig, Philippines (*Presenter*) Nothing to Disclose

#### TEACHING POINTS

Diabetes Mellitus (DM) is a metabolic disorder characterized by a chronic hyperglycemic state and impairment of protein, fat, and carbohydrate metabolism due to alterations in insulin action. Complications in DM include microvascular (diabetic retinopathy, neuropathy, and nephropathy) and macrovascular (coronary artery, peripheral artery, and cerebrovascular disease). Non-ketotic hyperglycemia hemichorea may present with asymmetric hyperdensity or T1-weighted hyperintensity in the basal ganglia contralateral to the patient's neurologic deficit. Cardiac MRI can demonstrate the presence of scar or fibrosis and even underlying ischemia. Diabetic mastopathy is a rare complication that is usually seen in late-stage diabetes. Imaging is not primarily indicated in assessing acute urinary tract infection but may be necessary for the presence in the clinical setting of known diabetes.

#### TABLE OF CONTENTS/OUTLINE

1. Introduction 2. Pathogenesis 3. Head and Neck a. Non-Ketotic Hyperglycemia Hemichorea b. Stroke 4. Cardiac a. Diabetic Cardiomyopathy b. Peripheral Artery Disease c. Coronary Artery Disease 5. Breast a. Diabetic Mastopathy 6. Gastrointestinal a. Subcapsular Fatty Infiltration of the Liver b. Emphysematous Cholecystitis 7. Genitourinary a. Renal Abscess b. Emphysematous Pyelonephritis c. Emphysematous Cystitis d. Ductus Deferens Calcification 8. Musculoskeletal a. Fasciitis b. Fournier Gangrene c. Diabetic Neuroarthropathy d. Diabetic Myopathy e. Medial Calcific Sclerosis f. Subcutaneous Amyloid Deposits

Printed on: 02/07/23



## Abstract Archives of the RSNA, 2022

MSEE-49

### Lose The Battle and Win the War: Multimodality Imaging of Diseases Unique to Immuno-Suppressed

Sunday, Nov. 27 8:00AM - 9:00AM Room: Learning Center - MS

#### Awards

Certificate of Merit

#### Participants

Pegah Khoshpouri, MD, Seattle, WA (*Presenter*) Nothing to Disclose

#### TEACHING POINTS

- Suppression of immune system can be primary-congenital immunodeficiency, secondary to chemo- or immuno-therapy medications, or acquired immunodeficiency syndrome (AIDS).
- Immunosuppression predisposes patients to various opportunistic infections, inflammatory responses such as drug toxicity, or malignancies.
- There are unique and overlapping imaging manifestations. Learning about unique radiologic findings can lead to earlier and more precise diagnosis.

#### TABLE OF CONTENTS/OUTLINE

To provide a comprehensive review of multimodality and multisystem unique imaging appearances of various scenarios in immunocompromised patients in a case-based format. These scenarios are including but not limited to:

- Infections such as pneumocystis jiroveci pneumonia, tuberculosis in patients with leukemia or HIV, aspergillosis in neutropenic patients or those on immunosuppressants after transplantation.
- Malignancies such as Kaposi' sarcoma in HIV and post-transplant lymphoproliferative disorder after transplant.
- Lymphoproliferative disorders in patients with congenital hypogammaglobulinemia.
- Medication-induced pneumonitis or sarcoid-like reaction.
- Table summarizing various predisposing diseases and commonly seen associated infections.

Printed on: 02/07/23

## Abstract Archives of the RSNA, 2022

MSEE-5

### Castleman Disease: A Multifaceted Diagnostic Dilemma

Sunday, Nov. 27 8:00AM - 9:00AM Room: Learning Center - MS

#### Awards

Identified for RadioGraphics

#### Participants

Marika Pitot, MD, Rochester, MN (*Presenter*) Nothing to Disclose

#### TEACHING POINTS

1. Review Castleman Disease, clinical subtypes, and implications for disease presentation and identification. 2. Describe the imaging features of Castleman Disease on different imaging modalities. 3. Raise awareness of Castleman Disease as a mimicker of other disease processes. 4. Discuss the potential known associations with and complications of Castleman Disease.

#### TABLE OF CONTENTS/OUTLINE

1. General overview of Castleman disease (CD) a. Unicentric (UCD) or multicentric (MCD) lymphoproliferative processes b. Several distinct clinical subtypes c. Histopathologic subtypes: hyaline vascular, plasma cell, mixed d. Spectrum of presentation and association with subtype: UCD - Localized, asymptomatic, indolent, incidentally discovered - localized mass; MCD - Systemic disease presenting acutely with constitutional symptoms, widespread lymphadenopathy, and hepatosplenomegaly 2. Imaging appearances on ultrasound, CT, MRI and PET a. Lymphadenopathy - single, regional, or widespread b. Soft tissue masses - thoracic, abdominal, retroperitoneal etc c. Specific organ involvement and appropriate imaging modalities for evaluation - hepatomegaly, splenomegaly, adrenal gland, salivary glands 3. Potential mimickers 4. Known associations and complications - POEMS syndrome

Printed on: 02/07/23



## Abstract Archives of the RSNA, 2022

MSEE-50

### A Call for Vigilance: Multimodality Imaging Evaluation of Malignancy in Solid Organ Transplant Recipients

Sunday, Nov. 27 8:00AM - 9:00AM Room: Learning Center - MS

#### Participants

Anthony Micetich, MD, (*Presenter*) Nothing to Disclose

#### TEACHING POINTS

Solid organ transplant recipients are at risk of numerous postoperative complications. A particularly dreaded immediate and long-term complication is malignancy. Development of these cancers is multifactorial and related to elements inherent to solid organ transplantation, with classification dependent on pathogenesis. Radiologists are often the first providers to identify these malignancies. We will review multimodality imaging presentation of various transplant related malignancies and their mimickers and emphasize the role of the radiologist in the care team.

#### TABLE OF CONTENTS/OUTLINE

1. Review various solid organ transplants with diagrammatic depiction
2. Review risk factors for malignancy in transplant recipients
  - a. Increased risk compared to the general population
  - b. Can develop in the transplanted organ(s) or elsewhere in the body
3. Review pathogenesis of malignancy in solid organ transplants:
  - a. Pre-existing risk factors in the recipient, donor, and transplanted organ
  - b. Long-term immunosuppression: type, intensity, duration of use
  - c. Oncogenic and non-oncogenic viral infections
4. Three major classifications of solid organ malignancy in transplant recipients:
  - a. De novo
  - b. Recurrent malignancy
  - c. Donor transmission
    - i. Donor transmitted
    - ii. Donor derived
5. Multimodality imaging of mimics of malignancy in solid organ transplants (including opportunistic infections and graft versus host disease)
6. Role of the radiologist (screening, biopsy, follow up, surveillance)
7. Summary table listing solid organs, related malignancies, and mimickers

Printed on: 02/07/23

## Abstract Archives of the RSNA, 2022

MSEE-51

### Comprehensive Imaging Review of Peritoneum and Implications of Disease Spread

Sunday, Nov. 27 8:00AM - 9:00AM Room: Learning Center - MS

#### Participants

Shruti Kumar, MBBS, Little Rock, AR (*Presenter*) Nothing to Disclose

#### TEACHING POINTS

Review embryogenesis and complex imaging anatomy of peritoneal spaces, folds and ligaments. Formulate a differential diagnosis based on disease localization in different peritoneal compartments. Discuss the interconnections between peritoneal and extra-peritoneal spaces, with focus on interfascial disease spread.

#### TABLE OF CONTENTS/OUTLINE

Review embryogenesis of ventral and dorsal mesentery and their subsequent specialization into different peritoneal ligaments. Imaging examples of peritoneal ligaments and folds of the liver and stomach, small bowel mesentery, large bowel mesocolon, pelvic ligaments. Demonstrate peritoneal spaces on cross-sectional imaging including lesser sac, greater sac, perihepatic, supramesocolic, inframesocolic compartments, paracolic, and pelvic peritoneal spaces. CT/MRI examples of pathologies that frequently involve peritoneal ligaments and spaces, e.g. acute pancreatitis, internal hernias, primary/metastatic peritoneal malignancies, intra-abdominal hematomas, sclerosing encapsulating peritonitis. Discuss clinical impact of peritoneal compartmentalization on disease pathogenesis and management decisions e.g. dissemination of gastric adenocarcinoma along perigastric ligaments, borderline resectability of pancreatic adenocarcinoma with mesocolon invasion. Peritoneal Cancer Index (PCI)

Printed on: 02/07/23



## Abstract Archives of the RSNA, 2022

MSEE-52

### A Comprehensive Review of Oncologic Emergencies: Update for Radiologists

Sunday, Nov. 27 8:00AM - 9:00AM Room: Learning Center - MS

#### Participants

Koichiro Mori, (*Presenter*) Nothing to Disclose

#### TEACHING POINTS

- Describe some of the oncologic emergencies for which diagnostic imaging has a significant impact on patient management
- Describe treatment-related oncologic emergencies in which imaging findings are useful for diagnosis
- In particular, we also address complications associated with immune checkpoint inhibitors and CAR-T therapy, in which diagnostic imaging is now playing a significant role, including whether or not treatment should be continued.

#### TABLE OF CONTENTS/OUTLINE

I. Introduction and Imaging Findings &1;Classification of Oncologic Emergencies &1;Direct effects of a tumor -Neurological complication- II. Direct effects of a tumor -Thoracic, Abdominal complication- &1;Superior Vena Cava Syndrome &1;Pulmonary thromboembolism III. Treatment-related complications: Radiation therapy &1;Radiation-Induced Myelitis IV. Treatment-related complications: Immune checkpoint inhibitors &1;Myositis &1;Colitis V. Treatment-related complications: CAR-T therapy &1;Cytokine Release Syndrome

Printed on: 02/07/23



## Abstract Archives of the RSNA, 2022

MSEE-53

### Precision Cancer Treatment Toxicity: What the Radiologist Should Know

Sunday, Nov. 27 8:00AM - 9:00AM Room: Learning Center - MS

#### Participants

Rozan Bokhari, MD, (*Presenter*) Nothing to Disclose

#### TEACHING POINTS

1. Review precision cancer treatments, 2. Review the general mechanisms of anticancer treatment toxicity, 3. Present the spectrum of toxicities, 4. Illustrate the common and uncommon toxicities

#### TABLE OF CONTENTS/OUTLINE

1. Overview of anticancer treatment in the era of precision medicine: Molecular targeted therapies and immune checkpoint inhibitors, Illustrations on the mechanism of drugs and their toxicities (on-target and off-target), 2. Spectrum of toxicities: Acute, Chronic, Delayed, Recurrent, Marker for response and survival, 3. Representative examples with an organ based approach

Printed on: 02/07/23



## Abstract Archives of the RSNA, 2022

MSEE-54

### A Beginners Guide to Cinematic Rendering in Clinical Practice: What You Need to Know

Sunday, Nov. 27 8:00AM - 9:00AM Room: Learning Center - MS

#### Participants

Elliot Fishman, MD, Owings Mills, MD (*Presenter*) Co-founder, HipGraphics, Inc; Stockholder, HipGraphics, Inc; Institutional Grant support, Siemens AG; Institutional Grant support, General Electric Company; Consultant, Exact Sciences Corporation; Consultant, Imaging Endpoints

#### TEACHING POINTS

1. What is Cinematic Rendering and what are its advantages over classic 3D medical imaging? 2. What are the clinical applications where Cinematic Rendering is helpful in either diagnosis or staging of disease or in guiding patient management? 3. What CT techniques are needed for Cinematic Rendering and what is the Radiologists role in using Cinematic Rendering in clinical practice? 4. what is the role of Cinematic Rendering in pre-operative planning for surgery using Cinematic Rendering? 5. what are the future directions of Cinematic Rendering including Augmented Reality display with HoloLens and multimodality imaging like PET/CT

#### TABLE OF CONTENTS/OUTLINE

1. what is Cinematic Rendering and why is it different from other 3D rendering techniques like MIP and VRT? 2. what are the specific advantages of Cinematic Rendering from a technical perspective as a computer graphics technique? 3. what clinical applications is Cinematic Rendering ideal for and why? 4. what is the role of Cinematic Rendering in applications like Oncologic Staging and Surgical planning? 5. what is the role of Cinematic Rendering in applications like trauma and vascular imaging? 6. what are future direction of Cinematic Rendering including improved Augmented Reality displays as well as multimodality imaging like PET/CT? 7. what role can Cinematic Rendering play in medical education and in patient education

Printed on: 02/07/23



## Abstract Archives of the RSNA, 2022

MSEE-55

### Novel Uses of Contrast-Enhanced Ultrasound

Sunday, Nov. 27 8:00AM - 9:00AM Room: Learning Center - MS

#### Participants

Clayton Douglas, MD, (*Presenter*) Nothing to Disclose

#### TEACHING POINTS

Contrast-enhanced ultrasound is a well-established modality to characterize liver and renal masses in the setting of contraindication to both MRI and CT. Given this is generally a rare occurrence, many small- and medium-sized hospitals have yet to find adequate utility in adopting this imaging modality. Since the implementation of contrast-enhanced ultrasound at our institution, we have discovered many unique uses of US contrast in common and uncommon clinical scenarios. We aim to share these unique uses in order to increase contrast-enhanced ultrasound usage in medical practice.

#### TABLE OF CONTENTS/OUTLINE

1. Introduction to contrast-enhanced ultrasound and well-established uses in the literature. 2. Present unique uses of contrast-enhanced ultrasound to answer common and uncommon clinical questions. Case examples include evaluating central line location/functionality, solid organ transplant perfusion, solid organ mass versus abscess, and identification of subtle liver lesions for biopsy localization. 3. Discuss potential future applications.

Printed on: 02/07/23



## Abstract Archives of the RSNA, 2022

MSEE-56

### “Imaging Spectrum of Radiation Induced”

Sunday, Nov. 27 8:00AM - 9:00AM Room: Learning Center - MS

#### Participants

Kota Yokoyama, MD, (*Presenter*) Nothing to Disclose

#### TEACHING POINTS

- Imaging findings after radiotherapy are diverse, ranging from transient changes to irreversible tissue damage, fibrosis, angiogenesis, and radiation-induced tumors. - Transient imaging changes are seen in a variety of organs and are more often seen as reversible hyperaccumulation on FDG PET with subtle change in morphologic imaging. - Irreversible tissue damage and fibrosis can be seen on CT and MRI as leukoencephalopathy, lung damage, skin scarring, and vascular stenosis. Fragility fractures of the ribs and sacrum are also commonly encountered. - Angiogenesis can result in trabecular vascular malformation, especially hemorrhage and calcification. - Radiation-induced tumors often occur long after treatment. Meningiomas and gliomas tend to occur after whole-brain irradiation. Squamous cell carcinoma, adenocarcinoma, and hematologic tumors can also occur. Osteosarcoma after tangential irradiation of breast cancer is also important to recognize.

#### TABLE OF CONTENTS/OUTLINE

Transient imaging changes after radiation therapy  
Irreversible tissue damage, fibrosis, and angiogenesis after radiation therapy  
Radiation-induced tumors

Printed on: 02/07/23



## Abstract Archives of the RSNA, 2022

MSEE-57HC

### Not All Lumps Are The Same! The Role of High-frequency Ultrasound In the Differential Diagnosis of Benign Skin Lesions

Sunday, Nov. 27 8:00AM - 9:00AM Room: Learning Center - MS

#### Participants

Victor Alguz, MD, Santos, Brazil (*Presenter*) Nothing to Disclose

#### TEACHING POINTS

Cystic and solid benign skin lesions are commonly observed in clinical practice and high-frequency ultrasound (HFU) has been increasingly used to characterize them. HFU (>15 MHz) clearly define the skin layers and adnexal structures, allowing better characterization of the lesion's location, morphology, thickness and vascularity. Radiologists must know the ultrasound features of the most common benign skin lesions to avoid misdiagnosis. Epidermoid or epidermal inclusion cysts can appear anywhere in the body and typically present as a well-defined, oval, hypoechoic or heterogeneous, subcutaneous mass with an orifice in the epidermis (punctum). Other cysts may show typical locations, such as synovial or ganglion cysts, located near a joint or tendon, and trichilemmal cysts, originated from the outer hair root sheath, most commonly on the scalp. Common solid benign skin lesions include lipoma, dermatofibroma, pilomatricoma, glomus tumor, plantar fibromatosis, nevus sebaceous of Jadassohn, among others. Each lesion has characteristic findings on high-frequency ultrasound and proper correlation with dermoscopic evaluation can help in the differential diagnosis.

#### TABLE OF CONTENTS/OUTLINE

General aspects of benign skin lesions. High-frequency ultrasound assessment of the most common lesions with dermoscopic correlation (eg. epidermoid cysts, synovial cysts, trichilemmal cysts, lipoma, dermatofibroma, pilomatricoma, glomus tumor, plantar fibromatosis and nevus sebaceous of Jadassohn). Summary and Differential Diagnosis. Please visit the Learning Center to also view this presentation in hardcopy format.

Printed on: 02/07/23



## Abstract Archives of the RSNA, 2022

MSEE-58

### Neoplastic and Non-neoplastic Conditions of the Skin and Superficial Tissue at Imaging

Sunday, Nov. 27 8:00AM - 9:00AM Room: Learning Center - MS

#### Participants

Nikolas Brozovich, MD, Augusta, GA (*Presenter*) Nothing to Disclose

#### TEACHING POINTS

1. Describe classification of superficial tissue lesions on the basis of cellular origin 2. Discuss symptomatic and incidental cutaneous and subcutaneous lesions identified by imaging 3. Discuss systematic approach to achieve definitive diagnosis and limit the differential diagnosis

#### TABLE OF CONTENTS/OUTLINE

Superficial soft-tissue masses are common in clinical practice, and the expanding availability of radiologic imaging has increased radiologists' familiarity with these entities. Superficial soft-tissue masses may be classified in one of the following general diagnostic categories: neoplastic and non-neoplastic conditions. Neoplastic lesions: Neurofibroma, Lipoma, Lipofibroma, Desmoid tumors. Extra mammary Paget's disease of the skin, Liposarcoma, Squamous cell carcinoma, Melanoma. Metastases. Non neoplastic conditions Lymph node, Pilonidal cyst, Epidermoid inclusion cyst, Vascular malformation, Infection and inflammation Cellulitis and panniculitis, Dermatomyositis, Scleroderma, Injection granuloma, Hidradenitis suppurativa, Keloid, Abscess, Endometriosis, Inflammatory bowel disease (IBD), Post traumatic and iatrogenic Hematoma/seroma, Silicone injection

Printed on: 02/07/23



## Abstract Archives of the RSNA, 2022

MSEE-59

### Imaging Pearls for Post-Operative Complications in Simultaneous Liver-Kidney Transplant-

Sunday, Nov. 27 8:00AM - 9:00AM Room: Learning Center - MS

#### Awards

Certificate of Merit

#### Participants

Eric Cooper, Chicago, IL (*Presenter*) Nothing to Disclose

#### TEACHING POINTS

Simultaneous liver-kidney transplantations (SLKTs) are increasing in incidence in patients with end-stage liver disease (ESLD) and end-stage renal disease (ESRD). Understanding of the imaging findings for these transplants is crucial for timely detection and management of post-transplant complications. 1. We will review the operative technique and anatomy of traditional and en-bloc SLKTs. 2. We will discuss a systematic imaging approach for evaluation of transplanted grafts. 3. We will review the imaging pearls and techniques to work up common complications following SLKT.

#### TABLE OF CONTENTS/OUTLINE

I. Brief overview of the surgical anatomy of traditional and en-bloc approaches to SLKT II. Imaging approach and normal findings of transplanted grafts. Ultrasound evaluation including major vessel evaluation with doppler waveform characteristics and analysis. CT, MRI and angiography for confirmation of sonographic abnormalities and treatment planning III. Imaging patterns and workup for the most common SLKT complications including - Arterial: hepatic artery stenosis and thrombosis, renal artery stenosis; - Venous: hepatic vein and IVC stenosis and thrombosis; - Portal: portal vein stenosis and thrombosis; - Biliary: biliary leaks, biliary strictures, biliary duct dilation; - Ureteral: urinary tract obstruction, urinary leaks, and vesicoureteral reflux; - Fluid collections (e.g., seromas, hematomas, urinomas).

Printed on: 02/07/23



## Abstract Archives of the RSNA, 2022

MSEE-6

### **Beyond Staging: A Genitourinary Tumor Board Navigation Guide for Radiologists with Emphasis on NCCN Guidelines**

Sunday, Nov. 27 8:00AM - 9:00AM Room: Learning Center - MS

#### **Participants**

Daniela Garcia, MBBS, Philadelphia, PA (*Presenter*) Nothing to Disclose

#### **TEACHING POINTS**

- Oncological management requires multidisciplinary approach driven by the NCCN guidelines
- Radiologists fulfill a fundamental role in the decision making for best treatment available
- Radiologist should be familiar with the association between different staging levels and their impact in surgical, systemic, adjuvant and neoadjuvant therapies

#### **TABLE OF CONTENTS/OUTLINE**

Modern day diagnosis and treatment of cancer has transformed what was once a somber sentence into a treatable condition with favorable outcomes. Oncological management is no longer limited to oncologists and surgeons, but requires a multidisciplinary discussion including radiologists, radiation oncologists, and pathologists, among others. In this setting, the radiologist fulfills the important role of custodian in every step of patient management. Radiologists are in a privileged position where we can understand the "big picture" and recommend the best next step in treatment algorithm. In this educational exhibit, we will review updated NCCN management guidelines for genitourinary tumors including kidney, ovarian, cervical, prostate, and penile cancer; highlighting pivotal points where imaging can determine change in management. The accessible format of this presentation is particularly targeted to help create an efficient work frame to successfully navigate tumor board discussion in clinical practice.

Printed on: 02/07/23

## Abstract Archives of the RSNA, 2022

MSEE-60

### Evolutionary Fails: A Radiological Exploration of Human Vestigiality and Associated Pathology

Sunday, Nov. 27 8:00AM - 9:00AM Room: Learning Center - MS

#### Participants

Akito Nicol, (*Presenter*) Nothing to Disclose

#### TEACHING POINTS

Vestigiality refers to evolutionarily conserved structures that have lost their original function. These holdovers are useful in understanding patterns of organismal change. Vestigial structures are usually harmless but may cause disease. Knowledge of human evolution can further the radiologist's understanding and imaging analysis of diseases of vestigial structures.

#### TABLE OF CONTENTS/OUTLINE

1. Vestigial structures in animals  
2. Examples in humans organized by system and pathology (as follows)  
1) Gastrointestinal and Genitourinary Radiology  
a. Appendix (Appendicitis)  
b. Meckel's diverticulum (Hemorrhage, intussusception, perforation)  
c. Urachus (Patent urachus, urachal sinus/cyst)  
2) Neuroradiology  
a. Head and Neck  
i. Recurrent laryngeal nerve (Mediastinal trauma, neoplasms)  
ii. Wisdom teeth (Impaction, infection, cysts)  
iii. Platysma (Inflammation, infection, trauma)  
iv. Tonsils (Infection, neoplasm)  
b. Spine  
i. Lumbar degenerative disease related to bipedalism (Disc herniation and spondylolysis)  
ii. Coccyx (Trauma, infections)  
3) Musculoskeletal Imaging  
a. Levator claviculae (Confused for mass/lymphadenopathy; thoracic outlet syndrome)  
b. Fabella (Fabella pain syndrome, arthritis)  
c. Plantaris (Tendon graft source, rupture)  
4) Breast Imaging  
a. Male breast tissue (Gynecomastia, cancer)  
b. Supranumerary nipples (Cancer)  
5) Cardiac Imaging  
a. Left atrial appendage (Thrombus)

Printed on: 02/07/23

## Abstract Archives of the RSNA, 2022

MSEE-61

### Cystic Fibrosis in Children: A Multi-organ Approach From a Radiological Perspective

Sunday, Nov. 27 8:00AM - 9:00AM Room: Learning Center - MS

#### Participants

Alfonso Escobar Villalba, MD, Madrid, Spain (*Presenter*) Nothing to Disclose

#### TEACHING POINTS

1. The lungs are often severely affected, being the presence of thick-walled bronchiectasis the most characteristic finding. 2. The pancreas is the most frequently involved abdominal organ, being fatty replacement the most common imaging finding. 3. Liver disease is frequent. SWE elastography and ATI are useful for diagnosis and management. 4. Meconium ileus is the earliest clinical manifestation of cystic fibrosis. 5. The appendix is often distended so its diameter alone is not an adequate parameter for diagnosing appendicitis.

#### TABLE OF CONTENTS/OUTLINE

- Etiology, epidemiology - Diagnosis, role of advanced techniques (elastography, ATI, SMI, lung MRI) - Imaging findings- Chest: bronchiectasis, hyperinflation, mucous plugging, consolidation, tree-in-bud, mosaic attenuation/air trapping, pneumothorax, pulmonary and bronchial arterial enlargement.- Abdomen: pancreatic disease (fatty replacement, cystosis, pancreatitis calcifications), liver disease (steatosis, focal biliary fibrosis, cirrhosis, portal hypertension), biliary system (cholelithiasis, microgallbladder, intrahepatic ductal strictures, sclerosing cholangitis), gastrointestinal tract (distal intestinal obstruction syndrome, meconium ileus, rectal prolapse, gastroesophageal reflux, distension of appendix, fibrosing colonopathy, ileocolic intussusception) - Genito-urinary: nephrolithiasis, vas deferens absence, testicular microlithiasis - Head and neck: chronic sinusitis, nasal polyposis - Musculoskeletal: low bone mineral density, kyphosis- Treatment, prognosis

Printed on: 02/07/23



## Abstract Archives of the RSNA, 2022

MSEE-62

### Imaging Features in Paroxysmal Nocturnal Hemoglobinuria (PNH)

Sunday, Nov. 27 8:00AM - 9:00AM Room: Learning Center - MS

#### Participants

Carlos Rubio Sanchez, MD, Madrid, Spain (*Presenter*) Nothing to Disclose

#### TEACHING POINTS

- Paroxysmal nocturnal hemoglobinuria (PNH) is a rare, acquired, clonal hematopoietic stem cell disorder.
- Physiopathology: PIG-A gene mutation - glycosylphosphatidylinositol (GPI) molecule deficit - abnormal complement regulatory proteins CD55, CD59 - complement-mediated intravascular hemolysis - hemoglobinuria
- Triad of clinical features: intravascular hemolysis, thromboembolic events, and cytopenia.
- Thromboembolic events represent the leading cause of morbidity and mortality. They can occur in atypical locations in the body (venous sinus thrombosis, Budd-Chiari syndrome?), sometimes silent.
- Imaging plays an important role in the diagnosis of thromboembolic events, infarcts, and abnormal iron deposits.
- The follow-up protocol for PNH patients includes: CT, MRI, or Doppler-ultrasound techniques. MRI is the most sensitive test for detecting silent thrombosis and quantifying iron deposits.
- The treatment with eculizumab has changed the paradigm of this disease, prolonging the life expectancy and quality of life of these patients.

#### TABLE OF CONTENTS/OUTLINE

- Introduction: pathogenesis, clinical manifestations, diagnosis criteria.
- Imaging features: -Brain: thrombosis, infarcts, leukoencephalopathy, iron deposit. -Thoracic: cardiac infarcts, pulmonary thromboembolism, pulmonary hypertension signs. -Abdominal: Thrombosis (Sd. Budd Chiari, portal venous, cava?) infarcts, iron deposits. - Osteomuscular: deep vein thrombosis, osteonecrosis
- Conclusions.

Printed on: 02/07/23

## Abstract Archives of the RSNA, 2022

MSEE-63

### You Are Not Alone: Solitary Fibrous Tumors Beyond the Chest

Sunday, Nov. 27 8:00AM - 9:00AM Room: Learning Center - MS

#### Participants

Flavia M. Starling, MD, Belo Horizonte, Brazil (*Presenter*) Nothing to Disclose

#### TEACHING POINTS

For a long time, solitary fibrous tumors (SFTs) were thought to be exclusive to the pleura. In fact, this is still the most common place to diagnose this rare pathology. With the advances in histologic, molecular, and genetic techniques and the discovery of the SFT fusion gene, other names of tumors with the same histologic spectrum were abandoned and after classified as SFT, such as hemangiopericytomas. This fact has changed the perception about its restricted location. Although visceral pleura is the most common site of this pathology, it can affect several body structures, such as the head and neck, thoracic and abdominal cavities. The radiological features are generally nonspecific, except for the low signal intensity foci on MRI T1 and T2-weighted sequences corresponding to collagen content, producing a chocolate chip cookie appearance, which may aid in the diagnosis. The behavior of TFS on 18 FDG PET-CT can also raise suspicion for this tumor. This work intends to demonstrate that solitary fibrous tumors are not solitary anymore, being found in many locations in the body, by demonstrating and reviewing their imaging features in the many possible topographies.

#### TABLE OF CONTENTS/OUTLINE

- Case-based review in different imaging methods illustrating the solitary fibrous tumor in its different locations.
- Obtaining and understanding characteristic imaging findings of solitary fibrous tumor enables a proper diagnosis for early treatment.
- Discuss different radiological findings of solitary fibrous tumor.

Printed on: 02/07/23



## Abstract Archives of the RSNA, 2022

MSEE-64

### Imaging Manifestations of Trisomy 21, from Pediatrics to Adults

Sunday, Nov. 27 8:00AM - 9:00AM Room: Learning Center - MS

#### Awards

Certificate of Merit

#### Participants

Christian Gomez, MD, (*Presenter*) Nothing to Disclose

#### TEACHING POINTS

Trisomy 21 is the most common chromosomal anomaly in humans, affecting approximately 1 in every 700 babies and more than 350,000 people living in the United States. As medical management evolves, the average life expectancy for people living with Trisomy 21 has increased exponentially, with individuals now commonly living beyond their fifth decade of life. Medical imaging not only plays a critical role in prenatal diagnosis, but also aids in diagnosis and management of associated multiorgan anomalies throughout a patient's life.

#### TABLE OF CONTENTS/OUTLINE

Brief introduction to Trisomy 21  
Fetal US/MRI/EchoSoft Markers  
Cardiovascular  
Congenital heart anomalies  
Pulmonary  
Pulmonary congenital anomalies  
Pulmonary hypoplasia and hypertension  
Upper airway obstruction  
Lower airway obstruction  
GI  
Foregut pathology  
Midgut pathology  
Hindgut pathology  
Diaphragmatic herniation  
Musculoskeletal  
Atlantoaxial instability, hypoplastic C1 arch  
Joint laxity/dislocation  
Hands/feet - Kimer deformity  
Eleven ribs  
Hypersegmented sternum  
Developmental hip dysplasia, mickey mouse pelvis  
GU  
Cryptorchidism  
Neuro  
Hearing loss secondary to temporal bone pathology  
Moyamoya  
Early age neurodegeneration  
Cerebellar and vermian hypoplasia  
Oncology  
Leukemia - ALL, AML  
Testicular Cancer

Printed on: 02/07/23



## Abstract Archives of the RSNA, 2022

MSEE-65

### Imaging Atlas for Childhood Whole-body MRI

Sunday, Nov. 27 8:00AM - 9:00AM Room: Learning Center - MS

#### Participants

Mary-Louise Greer, MBBS, (*Presenter*) Research Grant, AbbVie Inc

#### TEACHING POINTS

1. To describe whole-body MRI imaging protocols and strategies to optimize these to the patient's developmental and chronological age, co-morbidities and the clinical indication; 2. To illustrate the spectrum of normal anatomy from the neonatal period to adolescence seen on different whole-body MRI imaging sequences, 3. To demonstrate and compare normal, normal variant and abnormal imaging findings on pediatric whole-body MRI to improve diagnostic accuracy for a range of oncologic and non-oncologic diseases

#### TABLE OF CONTENTS/OUTLINE

\*Outline Whole-body MRI is now standardly performed in pediatric patients for a range of oncologic and non-oncologic indications, used for diagnostic and/or screening purposes. Diagnostic accuracy depends upon the recognition of disease patterns and familiarity with normal maturation that can be mimickers for disease. The purpose of this atlas is to provide an anatomy-based overview of specific imaging features to improve lesion detection and aid distinction from normal and normal variant observations, that can lead to a high rate of false positive findings, as well as offer a differential for imaging findings where the disease entity is as yet unknown. Whole-body MRI Protocols - generic: standard optional sequences coverage - indication-specific sequences coverage Anatomy-based Spectrum of Normal and Abnormal Whole-body MRI - normal for age - focal, multifocal and diffuse pathology - bones joints, muscle soft tissue, head neck, chest, abdomen pelvis

Printed on: 02/07/23



## Abstract Archives of the RSNA, 2022

MSEE-66

### Imaging Spectrum of Tuberculosis from Head to Toe with Updates

Sunday, Nov. 27 8:00AM - 9:00AM Room: Learning Center - MS

#### Participants

Onur Simsek, MD, (*Presenter*) Nothing to Disclose

#### TEACHING POINTS

The purpose of the exhibit is to· Explain pathogenesis and classical imaging findings of tuberculosis· Describe typical and atypical imaging spectrum of tuberculosis from head to toe with updates· Review the recent literature and discuss what changed through the years in imaging of tuberculosis · Highlight pearls and pitfalls in imaging tuberculosis

#### TABLE OF CONTENTS/OUTLINE

BackgroundTuberculosis is an infectious disease caused by the mycobacterium tuberculosis complex, and it is one of the leading causes of death due to infectious diseases worldwide. Although tuberculosis is primarily seen as pulmonary infection, it can cause disease in almost any part of the body.Method and Outline: In line with the exhibit's purpose, cases that will set an example for different organ involvements of tuberculosis from the PACS system of our hospital were selected retrospectively.Selected cases include the following examples of tuberculosis:MeningitidisGastrointestinal tuberculosisGenitourinary tuberculosisSpondylodiscitisArthritisSplenic tuberculosisPulmonary patternsLymphadenitisImaging findings were discussed and evaluated with current literature. ConclusionTuberculosis is still a public health issue in most countries and an essential differential diagnosis all over the world. Even tuberculosis is mainly known for its pulmonary infiltration; it can be detected in almost any part of the body. Hereby, we provide different organ involvements with case examples. This educational exhibit will assist the radiologist in understanding the unexpected presentations of tuberculosis.

Printed on: 02/07/23



## Abstract Archives of the RSNA, 2022

MSEE-67

### Vasculitides from Head to Toe: Multimodality Imaging Diagnosis, Treatment, and Management

Sunday, Nov. 27 8:00AM - 9:00AM Room: Learning Center - MS

#### Participants

Anne Sailer, MD, New Haven, CT (*Presenter*) Nothing to Disclose

#### TEACHING POINTS

Vasculitides and arterial wall diseases are rare conditions of the arterial system that may result in significant complications including luminal stenosis, arterial thrombosis, and infarction of the corresponding organs and structures. Development of pseudoaneurysms and dissections and arterial rupture are additional serious complications in this patient population. Doppler US is a first line imaging modality utilized for the assessment of the peripheral arterial system, abdominal aorta and its branches.a) types of arterial wall pathologiesb) normal arterial wall anatomy and physiology of waveforms on Doppler USc) sonographic findings associated with vasculitides and arterial wall disease with multi-imaging correlation

#### TABLE OF CONTENTS/OUTLINE

Review pathophysiology of various types of vasculitides and pathologies affecting the arterial wall (collagen vascular disease, giant cell arteritis, temporal arteritis, Systemic Lupus Erythematosus (SLE), Takayasu arteritis, Polyarteritis nodosa, Wegener's granulomatosis, and Kawasaki disease, radiation-induced, disease. Discuss general concepts of the assessment of the peripheral arterial system and abdominal aorta using Doppler US and CEUS: technique protocol, image optimization).Demonstrate key sonographic features of the discussed arterial pathologies with correlation other imaging modalities correlation. Review role of ultrasound is the diagnosis and surveillance of complications in this group of patients. Discuss management options with interventional radiology procedures.

Printed on: 02/07/23



## Abstract Archives of the RSNA, 2022

MSEE-68

### Pediatric Applications of Photon Counting Detector Computed Tomography (PCD CT)

Sunday, Nov. 27 8:00AM - 9:00AM Room: Learning Center - MS

#### Participants

Kelly Horst, MD, Rochester, MN (*Presenter*) Nothing to Disclose

#### TEACHING POINTS

1) Photon counting detector computed tomography (PCD-CT) technology has qualities that stand to optimize pediatric imaging. 2) The spatial and contrast resolution are optimized by this technique. 3) Dose reduction is accomplished by the combined use of a decreased detector size, without septae, the addition of a tin filter, and the high resolution mode.

#### TABLE OF CONTENTS/OUTLINE

Multimodality imaging of pediatric cases illustrating the benefits of PCD CT, including: 1) Increased spatial resolution. 2) Decreased electronic noise. 3) Increased contrast to noise ratio. 4) Decreased beam-hardening artifact. 5) Multi-energy data acquisition 6) The ability to distinguish multiple contrast agents simultaneously.

Printed on: 02/07/23



## Abstract Archives of the RSNA, 2022

MSEE-69

### 3D Printed Models for Pre-surgical Planning: What the Surgeon Wants to Know and Touch

Sunday, Nov. 27 8:00AM - 9:00AM Room: Learning Center - MS

#### Awards

Certificate of Merit

#### Participants

Sarah Bastawrous, DO, Seattle, WA (*Presenter*) Nothing to Disclose

#### TEACHING POINTS

1. Discuss the role, applications and benefits of 3D printed models in presurgical planning 2. Provide case-based examples of presurgical 3D printed models with applicable surgeon feedback 3. Explore success strategies for radiologists and radiology departments to create impactful 3D printing models 4. Define intended use of 3D printed models

#### TABLE OF CONTENTS/OUTLINE

1. Clinical impact and potential of presurgical 3D printed models in medicine and role of the radiologist. 2. Brief literature reports of applications and benefits of 3D presurgical printed models. 3. Multimodality, illustrative examples of 3D printed pre-surgical models. 4. Elements important to the surgeon and why. 5. End user and surgeon feedback. 6. "In-surgery" and "out-of-surgery" intended uses, to include patient education/informed consent, trainee simulation, procedure rehearsal, device/guide sizing. 7. Success strategies to include quality management and considerations for radiology departments. 8. Standardization and guidelines to include professional societies, ACR data registry, and appropriateness criteria to guide 3D printing of presurgical models.

Printed on: 02/07/23

## Abstract Archives of the RSNA, 2022

MSEE-7

### Diversity of Spinal Manifestations in Systemic Disease

Sunday, Nov. 27 8:00AM - 9:00AM Room: Learning Center - MS

#### Participants

Ryo Kurokawa, MD, PhD, Ann Arbor, MI (*Presenter*) Nothing to Disclose

#### TEACHING POINTS

The aim of this review is to summarize the spectrum of clinical and radiological findings of spinal abnormalities associated with systemic diseases.

#### TABLE OF CONTENTS/OUTLINE

I. Vertebral abnormalities- Infection: Tuberculous and Non-tuberculous infections.- Inflammation/autoimmune: Scleroderma, SAPHO syndrome, rheumatoid arthritis- Neoplasm: Systemic mastocytosis, metastasis, lymphoma, leukemia- Neoplasm-like: POEMS syndrome, IgG4-related disease, Langerhans cell histiocytosis- Phacomatosis- Miscellaneous: Alkaptonuria, acromegaly, dialysis-associated, spinal neuroarthropathy (Charcot spine) II. Spinal cord abnormalities- Infection: Varicella-zoster virus, Acute flaccid myelitis- Inflammation, autoimmune: Inflammatory bowel disease, Vasculitis, Systemic lupus erythematosus, Sjogren syndrome, Behcet's disease, HTLV-1-associated myelopathy, Sarcoidosis, GFAP astrocytopathy, Hereditary hemorrhagic telangiectasia- Demyelination: Adrenoleukodystrophy,- Neoplasm: Metastasis, Lymphoma, Leukemia, Paraneoplastic syndrome- Metabolic: Copper deficiency, Hepatic myelopathy, Subacute combined degeneration of the cord- Drug-induced: Heroin, TNF-alpha inhibitor-related demyelination, Immune-checkpoint-inhibitor-related polyradiculoneuropathy- Phacomatosis- Miscellaneous: amyloidosis, superficial siderosis with meningocele or Marfan syndrome Summary1. Imaging findings of the vertebrae, spinal cord and cauda equina, and associated clinical features in various systemic diseases are important for the correct diagnosis.2. Knowledge of X-ray, CT, MRI, bone scintigraphy, and PET imaging findings is essential for identifying these abnormalities.

Printed on: 02/07/23



## Abstract Archives of the RSNA, 2022

MSEE-70

### Neurologic Manifestations of Thoracic Conditions

Sunday, Nov. 27 8:00AM - 9:00AM Room: Learning Center - MS

#### Participants

Julian Sison, MD, (*Presenter*) Nothing to Disclose

#### TEACHING POINTS

Radiologists frequently encounter multisystem diseases that produce findings across multiple subspecialties. This is true of several thoracic diseases with neurologic manifestations. When viewed in isolation many of these findings are nonspecific. However, correlation with imaging across both organ systems can provide clarity to the underlying diagnosis, or at least to the underlying etiology, which can then guide ordering clinicians to the next appropriate step in management so that these conditions can be recognized.

#### TABLE OF CONTENTS/OUTLINE

We will stratify diseases by etiology: 1) infectious - tuberculosis, nocardiosis, aspergillosis, mucormycosis, COVID-19, 2) inflammatory - sarcoidosis, polymyositis, 3) autoimmune - IgG4 sclerosing disease, 4) genetic - neurofibromatosis-1, tuberous sclerosis, Ehlers-Danlos syndrome, 5) vascular - hereditary hemorrhagic telangiectasia, and 6) neoplastic - lung cancer, lymphoma, paragangliomas. Within these subcategories we will conduct a case-based review of several diseases that demonstrate both thoracic and neurologic manifestations.

Printed on: 02/07/23



## Abstract Archives of the RSNA, 2022

MSEE-71

### Tumors Associated with Tobacco Use: Pathophysiology, Clinical Features Role of Imaging

Sunday, Nov. 27 8:00AM - 9:00AM Room: Learning Center - MS

#### Participants

Sanjana Dhakshinamoorthy, Houston, TX (*Presenter*) Nothing to Disclose

#### TEACHING POINTS

1. Tobacco is the most important risk factor for lung cancers, with nearly 9 out of 10 cancers being related to smoking cigarettes or from exposure to second hand smoke. However, there is a wide spectrum of tobacco-induced cancers that can involve multiple organ systems, including in the oropharynx, larynx, esophagus, liver, pancreas, stomach, colon rectum, urinary bladder, kidney and uterine cervix. 2. Given that many tumors from various different organ systems can occur in patients with tobacco use, radiologists play a vital role in being able to detect these synchronous or metachronous tumors, even before they become symptomatic. 3. Lung-RADS (Lung Imaging Reporting and Data System), is a classification proposed to aid with findings in low-dose CT screening exams for lung cancer. The goal of the classification system is to standardize follow-up and management decisions.

#### TABLE OF CONTENTS/OUTLINE

1. Review the epidemiology, pathophysiology and clinical features of all the neoplasms associated with tobacco use 2. Discuss the multimodality imaging features of tobacco-induced neoplasms 3. Review the role of imaging in screening, diagnosis and surveillance of malignancies associated with tobacco use

Printed on: 02/07/23



## Abstract Archives of the RSNA, 2022

MSEE-73

### Emerging Complications in the Era of COVID-19 Vaccination: Role of Radiologist and Imaging

Sunday, Nov. 27 8:00AM - 9:00AM Room: Learning Center - MS

#### Participants

Janardhana Ponnatapura, MD, Winston Salem, NC (*Presenter*) Nothing to Disclose

#### TEACHING POINTS

In November 2019, a new RNA Coronavirus (SARS-CoV-2) responsible for a severe acute respiratory syndrome was identified in China. In early 2022, there were nearly 5.8 million deaths and a total of 10 billion doses of vaccination administered. Benefit of vaccine protecting against severe COVID-19 infection far outweighs the very small risk of development of some rare adverse events. Gaining familiarity with various adverse events following COVID-19 vaccination and their clinical presentation is important for radiologist as they come across different imaging modalities. Optimal utilization of imaging and promptly recognize these adverse events helps in better management of patients.

#### TABLE OF CONTENTS/OUTLINE

- Types and mechanisms of COVID-19 vaccines
- Common reactions and adverse events
- Emerging rare complications of COVID-19 vaccines-Radiation recall pneumonitis-Radiation recall dermatitis-Breast nodules-Axillary lymphadenopathy-Myocarditis
- Role of Imaging
- Differentiation from neoplastic disease
- What radiologist need to know
- Recommendations to oncology providers
- Management of these complications
- Multidisciplinary team approach

Printed on: 02/07/23



## Abstract Archives of the RSNA, 2022

MSEE-74

### Don't Overlook the Skin! Multimodality Imaging Review of Skin Subcutaneous Malignancies with Radiology-Pathology Correlation

Sunday, Nov. 27 8:00AM - 9:00AM Room: Learning Center - MS

#### Awards

**Cum Laude**

**Identified for RadioGraphics**

#### Participants

Priya Pathak, MBBS,MD, (Presenter) Nothing to Disclose

#### TEACHING POINTS

1) Overview of the spectrum of primary and secondary skin and subcutaneous malignancies with a focus on the role of various imaging modalities for diagnosis, evaluation of anatomical extension, management, and surveillance.2) Highlight the clinical features, prognosis and modes of spread of cutaneous malignancies.3) Review relevant radiologic-pathologic correlation, differential diagnoses, imaging artifacts and pitfalls with a systematic approach to narrow the final diagnosis.

#### TABLE OF CONTENTS/OUTLINE

- Introduction: Multimodality imaging approach to skin and subcutaneous malignancies for an accurate evaluation of the lesion location, size, extension, margins, metabolic activity and spread patterns. Outline
- Primary malignancies: Squamous cell carcinoma, Basal cell carcinoma, Merkel cell carcinoma and Melanoma
- Secondary malignancies: -Mesenchymal: Dermatofibrosarcoma, Leiomyosarcoma, Angiosarcoma, liposarcoma, Desmoid tumor. -Lymphoma: Mycosis Fungoides, NK T cell lymphoma, Primary cutaneous B cell lymphoma, Follicular lymphoma. - Metastasis: Breast cancer, Lung cancer, Head and neck cancer, GI cancers, RCC, Ovarian cancer, endometrial cancer, Prostate cancer.
- Benign entities/tumor-like lesions: -Systemic disorder: Sarcoidosis, Gout, vasculitis. -Autoimmune, inflammatory and infectious disorders. -Subcutaneous disorders: Fat necrosis, Lipodystrophy, Panniculitis, Epidermoid cyst, pilonidal cysts. -Iatrogenic: Keloids, scars, Injection granulomas, Foreign bodies.

Printed on: 02/07/23



## Abstract Archives of the RSNA, 2022

MSEE-75

### Multimodality Imaging in End-Stage Renal Disease

Sunday, Nov. 27 8:00AM - 9:00AM Room: Learning Center - MS

#### Awards

Identified for RadioGraphics  
Certificate of Merit

#### Participants

Prabhakar Rajiah, MD, FRCR, Rochester, MN (*Presenter*) Nothing to Disclose

#### TEACHING POINTS

1. To define and review the pathophysiology of end-stage renal disease (ESRD). 2. To discuss the renal and extrarenal manifestations of ESRD. 3. To describe the role of imaging in the evaluation of ESRD. 4. To illustrate the imaging appearances of various manifestations of ESRD

#### TABLE OF CONTENTS/OUTLINE

1. ESRD- DEFINITION, PATHOPHYSIOLOGY 2. ROLE OF IMAGING-Radiograph, ultrasound, CT, MRI, nuclear medicine, echocardiogram, 3. DISCUSSION AND ILLUSTRATION OF THE FOLLOWING MANIFESTATIONS OF ESRD A. Renal - Decreased size; Increased echogenicity; Decreased vascularity; Cystic disease; Renal neoplasms B. Musculoskeletal -Secondary hyperparathyroidism; Osteosclerosis, osteoporosis; Subchondral erosions; Osteomalacia/rickets; Brown tumors; Amyloidosis-arthritis; Destructive spondyloarthropathy; Crystal deposition; Soft tissue calcification; Aluminium toxicity ; AVN, Osteomyelitis C. Cardiac - Coronary atherosclerosis; Concentric LV thickening, cardiomegaly; Diastolic/systolic dysfunction; Cardiac failure; Myocardial calcification; Myocardial ischemia/infarction; Pericardial effusion D. Vascular - Calcifications; Decreased compliance; Peripheral vascular disease; PE; Thrombus in catheters E. Thoracic - Alveolar edema; Metastatic calcification; Calcifications; Infections F. Neurological - Cerebral atrophy, white matter lesions; Encephalopathy; Cerebral infarction/hemorrhage ; Posterior reversible encephalopathy; Osmotic demyelination ; Infection; Sinus thrombosis; Dialysis disequilibrium syndrome G. Abdominal - Encapsulating peritoneal sclerosis H. Dialysis access complications - Vascular stenosis; Thrombus/infection; Aneurysm/pseudoaneurysm

Printed on: 02/07/23



## Abstract Archives of the RSNA, 2022

MSEE-76

### What's New in Pathogenesis, Imaging Findings, Prevention, and Management of Human Papillomavirus (HPV)-Related Malignancies? 2022 Update

Sunday, Nov. 27 8:00AM - 9:00AM Room: Learning Center - MS

#### Awards

Identified for RadioGraphics

Magna Cum Laude

#### Participants

Sammar Ghannam, MD, MPH, San Antonio, TX (*Presenter*) Nothing to Disclose

#### TEACHING POINTS

Review epidemiology pathogenesis of human papillomavirus (HPV)-associated neoplasms Discuss imaging findings of benign and malignant HPV-related neoplasms Describe role of imaging in screening, staging surveillance of HPV-associated cancers Review 2022 updates in treatment vaccination strategies

#### TABLE OF CONTENTS/OUTLINE

Introduction Epidemiology Pathogenesis: Molecular pathways Benign tumors: Respiratory Papillomas condyloma acuminata (genital warts) Malignancies: Squamous cell cancer of the oropharyngeal region (oral cavity, palatine/lingual tonsils, tongue base, oropharynx larynx), bronchopulmonary anogenital region (penis, vagina, vulva, cervix anal canal) Updates in WHO Classification Imaging Techniques: CT, MRI 18FDG PET/CT Imaging Findings HPV positive vs. HPV negative cancers: How to differentiate on Imaging? HPV Vaccination: Type of vaccines Current guidelines Role of imaging in screening surveillance Novel treatment strategies: Immunotherapy Imaging Biomarkers: treatment response prognosis Conclusion Summary and Clinical Implications Novel immunotherapies are being investigated and updated screening vaccination guidelines are used to improve outcomes in HPV-related cancers. HPV-positive oropharyngeal SCCs show well-defined borders cystic nodal metastases; have good treatment response, prognosis with better survival. Imaging plays an important role in the diagnosis, staging, and surveillance of HPV-associated lesions in both men women.

Printed on: 02/07/23



## Abstract Archives of the RSNA, 2022

MSEE-8

### Twists and Turns: The Torsion Tour

Sunday, Nov. 27 8:00AM - 9:00AM Room: Learning Center - MS

#### Participants

Mary J. Clingan, MD, Ponte Vedra Beach, FL (*Presenter*) Nothing to Disclose

#### TEACHING POINTS

Teaching points Torsion can affect a number of organs and has a variety of imaging appearances. Abnormal ligamentous attachments and/or increased laxity can lead to increased mobility and predispose to torsion. Increased organ size or a focal mass can also predispose to torsion. Alternatively, an organ may herniate and twist into a defect left by organ removal or surgical change. Clues to diagnosis vary by location, but include organ displacement, organ enlargement, and a twisted vascular pedicle. Torsion can be intermittent, incomplete, acute, or chronic. In late cases, decreased vascular flow can lead to infarction. There are clues with color and spectral doppler that may be seen in cases of incomplete or intermittent torsion.

#### TABLE OF CONTENTS/OUTLINE

OutlineChest: Lung; RUQ: Gallbladder, Wandering liver, Omental Infarct; LUQ: Splenic, epiploic appendage; Pelvis: Adnexal, fibroid, renal transplant; Scrotum: epididymal appendix, testicular/spermatic cord; Bowel: gastric, small bowel, colon

Printed on: 02/07/23



## Abstract Archives of the RSNA, 2022

NMMIEE

### Nuclear Medicine & Molecular Imaging Education Exhibits

Sunday, Nov. 27 8:00AM - 9:00AM Room: Learning Center - NMMI

#### Sub-Events

#### **NMMIEE-1 Integrating Molecular Imaging to Meningiomas: Is PET with Somatostatin Receptors Our New Buddy?**

Participants

Rodrigo Hernandez Ramirez, MD, Leon, Mexico (*Presenter*) Nothing to Disclose

#### TEACHING POINTS

To identify the importance of somatostatin receptors in meningioma. To show the applications of PET in the evaluation of meningiomas specifically in detection and delimitation of the tumor, diagnosis of recurrence and radiotherapy planning.

#### TABLE OF CONTENTS/OUTLINE

Meningiomas are the most common primary brain tumors and represent about 30% of intracranial tumors. Neuro-Oncology guidelines recommend contrast-enhanced MRI as the primary radiologic modality of choice because it has a sensitivity of 90%. Meningiomas can express somatostatin receptors type 2. Molecular imaging techniques allow the incorporation of functional information for diagnostic purposes. PET tracers for SSTR evaluation provide high sensitivity with excellent target-to-background contrast due to low uptake in bone and healthy brain tissue. SSTR PET has demonstrated benefits for noninvasive differential diagnosis, delineation tumor and treatment planning. Although PET plays only a minor role in the initial diagnosis of meningiomas, it may add value for meningioma detection, with a sensitivity of 100%. Clinically, this is relevant because meningiomas located at the skull base or nearby the falx cerebri, with transosseous extension, or equivocal imaging findings related to artifacts or calcifications were difficult to detect by MRI. For the differentiation of scar tissue from active tumor, SSTR PET has a high sensitivity of 90%, outperforming standard MRI with 79%. PET can obtain an optimized target volume delineation for fractionated radiation therapy in patients with meningiomas grade I-III.

#### **NMMIEE-10 Punctiliously Perfect PSMA PET: Pearls and Pitfalls**

Participants

Daniel Wale, DO, (*Presenter*) Nothing to Disclose

#### TEACHING POINTS

1. Several PET radiopharmaceuticals targeting prostate specific membrane antigen (PSMA) are now FDA-approved for assessment of metastatic prostate cancer. 2. PSMA PET agents have a normal biodistribution that includes salivary and lacrimal glands, kidneys, and small bowel, as well as urinary excretion. Familiarity with normal uptake decreases potential for misdiagnosis. 3. PSMA expression is not prostate-specific, and uptake can be identified in a variety of other benign and malignant processes. Awareness of commonly encountered non-prostatic lesions, combined with knowledge of common metastatic patterns of prostate cancer, allows the radiologist to avoid potential pitfalls.

#### TABLE OF CONTENTS/OUTLINE

I. Introduction  
II. Prostate cancer  
A. PSMA expression  
B. Utility of PSMA expression for diagnosis  
C. Utility of PSMA expression for treatment  
III. Nuclear imaging  
A. Indium 111 capromab pendetide (historical)  
B. PET agents targeting PSMA  
1. Gallium 68 PSMA-112  
2. Fluorine 18 piflufolastat  
C. Clinical indications  
D. Imaging protocols  
IV. Pearls and pitfalls  
A. Normal biodistribution  
B. Pitfalls regarding normal biodistribution  
1. Accessory salivary gland tissue  
2. Urine activity  
C. Parasympathetic ganglia  
D. Osseous  
1. Degenerative disease and inflammation  
2. Fibro-osseous lesions  
E. Non-prostatic neoplasms  
1. Meningioma  
2. Thyroid nodule  
3. Hemangioma  
4. PSMA avid non-prostate malignancies  
V. Treatment utilizing PSMA  
A. Lutetium 177 PSMA  
B. Localize anatomically occult disease for external radiation  
VI. Conclusion

#### **NMMIEE-11 Hybrid PSMA Imaging of The Prostate: A Guide For the Beginner- A Reference For the Expert**

Participants

Felipe Furtado, MD, Boston, MA (*Presenter*) Nothing to Disclose

#### TEACHING POINTS

Prostate-specific membrane antigen (PSMA) PET is revolutionizing the management of prostate cancer in all clinical settings, from treatment-naïve cancer to biochemical recurrence. Different PSMA ligands share a high affinity toward PSMA but differ in sensitivity, specificity, half-life, biodistribution, pitfalls, and excretion profile. Workflows, acquisition protocols, hybrid imaging modality (PET/CT vs. PET/MRI), and interpretation must be tailored to the appropriate clinical scenario and specific PSMA radiopharmaceutical. Adequately performed and interpreted PSMA hybrid imaging will revolutionize personalized medicine in prostate cancer patients.

#### TABLE OF CONTENTS/OUTLINE

1) PSMA ligands; 2) PET/CT and PET/MRI strengths, weaknesses, acquisition protocols, and workflows; 3) How to perform the best PSMA hybrid study for each clinical scenario; 4) PSMA PET/CT and PET/MRI interpretation, for the beginner and the expert

### **NMMIEE-12 Post PRRT Imaging: What To Look For On Routine and Emergent Imaging?**

Participants

Malak Itani, MD, Saint Louis, MO (*Presenter*) Nothing to Disclose

#### **TEACHING POINTS**

The purpose of this exhibit is for radiologists, nuclear medicine physicians, radiation oncologists and medical oncologists and trainees to:- Know what to look for on post-PRRT SPECT-CT imaging- Be familiar with most common complications of PRRT and their imaging manifestations in the acute, subacute, and chronic setting- Understand the appropriate timeline for routine follow-up after PRRT- Evaluate response to treatment after PRRT using anatomic and functional imaging modalities

#### **TABLE OF CONTENTS/OUTLINE**

I. Brief overview of PRRT complications with no imaging correlate  
A. Myelosuppression  
B. Renal toxicity  
C. Hepatotoxicity  
D. Neuroendocrine hormonal crisis  
E. Secondary leukemia and myelodysplastic syndrome  
F. Reproductive side effects  
II. Post-PRRT Imaging by Timeline:  
A. Post-PRRT SPECT/CT:  
i. SPECT: Localize sites of uptake, compare intensity relative to pre-treatment SSTR-PET  
ii. CT: Correlate gross tumor burden with pre-PRRT imaging, evaluate for immediate post-treatment complications, general CT read  
B. Acute presentations after PRRT:  
i. CT/MRI: tumor necrosis, hepatitis, cholangitis, hepatic abscess, radiation peritonitis, ascites, perforation, vascular thrombosis  
C. Routine follow-up post-treatment:  
i. CT/MRI: timing, changes in lesion size, criteria for progression vs pseudo-progression, potential side effects  
ii. PET: Indications, timing, comparison, quantitative measures and scores, potential complications

### **NMMIEE-13 18F-DCFPyL PSMA PET/CT for Prostate Cancer Imaging: A Primer on Technique, Interpretation Structured reporting**

Participants

Harit Kapoor, MD, Dallas, TX (*Presenter*) Nothing to Disclose

#### **TEACHING POINTS**

1) 18F-DCFPyL (PyL) is the first commercially available PSMA PET agent for Prostate Cancer (PCa) evaluation, FDA approved for both staging and biochemical recurrence. 2) PyL has an unprecedented diagnostic performance, especially in the setting of small volume recurrence, detecting nodal metastasis in the 2-5 mm range. 3) Aside from superior logistics inherent to being a F-18 based agent, PyL also shows higher spatial resolution and tumor to background ratio compared to Ga-68 PSMA-11 PET. 4) PyL imaging has been hailed as a paradigm shift, altering patient management in >50% of published cohorts. 5) Radiologist's awareness of the interpretative limitations and pitfalls as well as the use of standardized evaluation criteria, is vital in order to prepare for anticipated rapid utilization. 6) Initiation of androgen deprivation therapy can create flare-like imaging appearance due to PSMA upregulation.

#### **TABLE OF CONTENTS/OUTLINE**

1) Role and evolution of PET tracers in the clinical continuum of recurrent prostate cancer  
2) Imaging protocol and normal biodistribution for PyL PSMA PET/CT  
3) Standardized evaluation criteria for staging, recurrence and treatment response.  
4) Case examples of pearls and pitfalls (e.g. ganglionic uptake, follicular hyperplasia and tumor-neovascularity etc.)  
5) Into the future: Metastasis directed therapy 177Lu-PSMA theranostics

### **NMMIEE-14 An Illustrative Review of Nuclear Medicine Thyroid Studies**

#### **Awards**

**Identified for RadioGraphics  
Certificate of Merit**

Participants

Andrew Schneider, MD, MPH, Boston, MA (*Presenter*) Nothing to Disclose

#### **TEACHING POINTS**

Nuclear medicine thyroid studies are a common type of imaging that require a broad understanding of the microbiology, physiology, and clinical manifestations of the underlying disease in order to interpret successfully. For trainees who are learning to interpret these studies, the intricate integration of multiple lines of clinical, laboratory, imaging, and pathological evidence can be intimidating and confusing. Here we provide an educational resource for trainees designed to build understanding by walking through the basic biology, radiopharmaceuticals, principles, indications, protocols, and interpretation of nuclear medicine thyroid studies. A key component of this resource is a representative collection of illustrative cases with a combination of clinical information, laboratory data, nuclear medicine and other imaging studies, and pathology findings.

#### **TABLE OF CONTENTS/OUTLINE**

Thyroid Anatomy / Physiology; Radiopharmaceuticals; Study Indications; Imaging Protocols; Decision-Making; Illustrative Cases

### **NMMIEE-15 PSMA-Targeted PET Imaging Interpretation Frameworks Comparison of PROMISE Classification and PSMA RADS Version 1.0**

#### **Awards**

**Certificate of Merit**

Participants

Vanessa Murad, MD, Bogota, Colombia (*Presenter*) Nothing to Disclose

#### **TEACHING POINTS**

1) PSMA-targeted PET imaging interpretation schemes have been devised to ensure consistency in reporting and avoid potential pitfalls. 2) PROMISE classification is based on the molecular imaging PSMA (miPSMA) expression score, assigned to each lesion with

respect to uptake in reference tissues (Figure 1). mPSMA score together with the presence or absence of morphological findings provide diagnostic certainty (positive, negative or equivocal). 3) When applying PROMISE classification for PSMA-targeted imaging with predominantly hepatobiliary excretion (e.g. 18F-PSMA-1007), the spleen is recommended as the intermediate reference. 4) On PSMA-RADS, findings are categorized on a 5-point scale according to PSMA-uptake and morphological characteristics, where the higher the number, the greater the likelihood of a cancer related lesion (Table 3)

#### **TABLE OF CONTENTS/OUTLINE**

1) Introduction/Aim. 2) PROMISE Classification 2.1) Description and interpretation: Tables 1,2. 2.2) Illustrative examples: Figure 2. 2.3) Advantages and disadvantages. 3) PSMA-RADS Version 1.0. 3.1) Description and interpretation. 3.2) Illustrative examples: Figure 3. 3.3) Advantages and disadvantages

#### **NMMIEE-16 Practical Interpretation of 18F PSMA PET/CT: Spectrum of Findings**

Participants

Kenneth Huynh, BS, Orange, CA (*Presenter*) Nothing to Disclose

#### **TEACHING POINTS**

1.To familiarize the viewers with 18F PSMA normal biodistribution 2.To present all potential incidental findings detected by 18F PSMA PET/CT. 3.To review the staging and monitoring of prostate cancer and its locoregional and distant metastasis depicted by PET/CT.

#### **TABLE OF CONTENTS/OUTLINE**

The exhibit has three components: (1) the presentation of normal 18F PSMA features with characteristic physiologic uptake at lacrimal glands, glottis and sympathetic ganglion chains, differentiating this tracer from 18F FACBC and 11C Choline, (2) the review of incidental findings such as accessory parotid gland, lung inflammatory and infectious processes, osseous fractures, splenosis, and hibernoma, and (3) the description of common and atypical/rare features of prostate cancer and metastasis such as lesions of bones, nodes, liver, peritoneum, penis, adrenal glands and thyroid cartilage. The 177 Lu PSMA therapy of prostate cancer with related imaging is also addressed in the exhibit.

#### **NMMIEE-18 The History and Evolution of the Molecular Evaluation of Neuroendocrine Tumors**

Participants

Jorge Espinosa, MD,MS, (*Presenter*) Nothing to Disclose

#### **TEACHING POINTS**

To understand the pathophysiology of the neuroendocrine tumors.To briefly know the history of radiotracers.To show the current radiotracers and its different applications in nuclear and imaging medicine.

#### **TABLE OF CONTENTS/OUTLINE**

Table of contents1. Introduction on neuroendocrine tumors2. Brief history of radiotracers and its evolutions3. Line time of evolutions of radiotracers and its applications4. Comparative table.5. The newest radiotracers and new applications6. CT-PET protocols7. Comparative images8. Examples of CT-PETOutline Since the discovery of In-111 OctreoScan in 1983, the role of molecular imaging in the diagnosis, follow-up and even treatment of neuroendocrine tumors has revolutionized the management of these lesions.Twenty years ago, the introduction of somatostatin analogues labeled with Ga68 in PET studies, improved the diagnostic sensitivity mainly as a result of improvements in spatial resolution.Knowledge of the evolution of molecular imaging during the diagnostic approach on neuroendocrine tumors aids in better selection of the method in patients with suspected neuroendocrine tumors.

#### **NMMIEE-19 Incidental Uptake on FAPI PET/CT Imaging: Physiologies, Pathologies, and Pitfalls**

Participants

Masatoshi Hotta, (*Presenter*) Nothing to Disclose

#### **TEACHING POINTS**

FAPI PET/CT can identify tumor lesions with a higher tumor-to-background ratio in various tumor entities, and has sparked considerable interest in the oncologic community. As studies on FAPI PET grow in number and size, incidental findings related to non-oncologic conditions have been increasingly reported.The purpose of this exhibit is to:1) Review the physiological FAPI uptake of each organ system2) Describe the main pathologies of non-oncological uptake3) Demonstrate FAPI PET/CT of non-oncologic diseases.

#### **TABLE OF CONTENTS/OUTLINE**

1. Introduction2. Physiological and non-oncological uptake of each organ system:a) Brainb) Head and Neck (Thyroid, Salivary glands, Dental)c) Thorax (Lung, Cardiac, Breast, Esophagus)d) Abdomen (Gastrointestinal, Liver, Pancreas, Bile duct, Spleen, Kidney, Uterus)e) Musculoskeletal (Bone, Joint, Muscle, Skin)f) Other systems (Vascular, Lymph node)

#### **NMMIEE-2 Multimodality Imaging of Adenoid Cystic Carcinoma With Emphasis On PET/CT**

**Awards**

**Certificate of Merit**

Participants

Ba D. Nguyen, MD, (*Presenter*) Nothing to Disclose

#### **TEACHING POINTS**

1. To review the clinical, pathological and imaging features of Adenoid Cystic Carcinoma (ACC). 2. To present the PET/CT impact of ACC evaluation for metastases, recurrence, and treatment monitoring.

#### **TABLE OF CONTENTS/OUTLINE**

ACC is a rare cancer that typically arises in the head and neck region as a salivary gland tumor, composing 1% of head and neck tumors and 10% of salivary gland tumors. Other presenting locations within the head and neck include the hard palate, auditory canal, nasopharynx, epiglottis, lacrimal gland, and tongue. Outside of the head and neck, ACC may target the skin, trachea, breast, and reproductive tract. Most ACC are indolent, presenting as a slow growing, painless mass. However, perineural invasion is common and there are potential distant metastases via lymphatic or hematogenous spread. Primary management is via complete resection, often with adjuvant radiation and chemotherapy. MRI and CT are most useful for head and neck assessment of ACC. Diagnosis relies on histology. PET/CT is used for staging, evaluating for metastasis, and monitoring for recurrence. This exhibit reviews PET/CT features of ACC at common and atypical sites of the body with emphasis on the PET/CT impact on staging and post-therapeutic surveillance of ACC.

## **NMMIEE-20 Myocardial Perfusion Imaging: Past, Present, and Future**

Participants

Saif Azam, MD, Los Angeles, CA (*Presenter*) Nothing to Disclose

### **TEACHING POINTS**

1. Explore the physiology underlying the distribution of radiopharmaceuticals used in myocardial perfusion imaging  
2. Review classic patterns of uptake and how they may guide clinical management  
3. Understand the pros and cons of different modalities available for the assessment of myocardial perfusion  
4. Increase awareness of factors that can cause false positive and false negative results

### **TABLE OF CONTENTS/OUTLINE**

- Introduction and review of anatomy and physiology pertaining to myocardial perfusion imaging
- Exercise versus pharmaceutical stress testing
- Cadmium-zinc-telluride camera utility
- Logistics of radiotracers used in cardiac single photon emission computed tomography (SPECT): Thallium-201 (201-Tl), Technetium-99m sestamibi, Technetium-99m tetrofosmin
- Case-based review of positron emission tomography (PET) radiotracers: Rubidium-82 (82-Rb), Nitrogen-13 ammonia (13N-NH<sub>3</sub>), Oxygen-15 water (15O-H<sub>2</sub>O), Fluorine-18 flurpiridaz
- Spectrum of imaging findings in the evaluation of ischemic heart disease
- Causes and troubleshooting of false positives, false negatives, and other artifacts
- Questions

## **NMMIEE-21 Essentials of Theranostics: A Guide for Physicians and Medical Physicists**

**Awards**

**Identified for RadioGraphics**

Participants

Celeste Winters, PHD, Portland, OR (*Presenter*) Nothing to Disclose

### **TEACHING POINTS**

1) Understand the basic physics principles and radiation biology involved in Theranostics. 2) Describe the factors involved in the choice and application of radionuclide therapies, including eligibility for treatment based on patient and tumor factors. 3) Apply the concepts above to currently available radionuclide therapies.

### **TABLE OF CONTENTS/OUTLINE**

1) Physics overview of radionuclides used in theranostics: a. Decay pathways of radionuclides used for imaging ( $\beta^-$ ,  $\beta^+$  emissions) and therapy ( $\beta^-$  and  $\alpha$  emissions) b. Desirable characteristics of theranostics agents c. Clinical examples of imaging/therapeutic pairs, with the characteristics of radionuclides used (half-life, energies, range, and imaging modality): i. 123I-MIBG/ 131I-MIBG (Azedra®) ii. 68Ga/64Cu-DOTATATE/ 177Lu-DOTATATE (Luthatera®) iii. 68Ga-PSMA-11/ 177Lu-PSMA-617 (Pluvicto®) iv. 99mTc-MDP/223Ra (Xofigo®) 2) Concepts of radiation biology and dosimetry: a. Biological descriptors of uptake pathways and pharmacokinetics b. Types of dosimetry calculation: Tumor, blood and solid organ at risk (OAR) i. MIRD Schema and Voxel Based ii. Generating time activity curves c. Implications on side effects from the therapy 3) Additional factors involved in the choice and application of radionuclide therapies: a. Patient factors: such as clearance rates and baseline function of OAR b. Tumor factors: level of uptake of the therapeutic agent by the tumor, and tumor heterogeneity

## **NMMIEE-22 Towards Structured PET Reporting with PSMA Tracers in Prostate Cancer**

Participants

Patricia Romero Fernandez, MBBS, Madrid, Spain (*Presenter*) Nothing to Disclose

### **TEACHING POINTS**

To highlight the importance of having a solo criteria for performance and interpretation of PET-CT images using prostate-specific membrane antigen based tracers  
To discuss the role of different imaging modalities in the biochemical recurrence of prostate cancer  
To distinguish between physiological findings and those that could be consider as positive for prostate cancer recurrence  
To describe 18F-DCFPyL PET-CT findings in our department according to PROMISE system

### **TABLE OF CONTENTS/OUTLINE**

-Introduction: generalities, biochemical recurrence definitions, other imaging modalities -Imaging findings characteristics with 18F-DCFPyL-Standardization of PSMA-PET interpretation: Prostate cancer recurrence sites classification PROMISE (Prostate Cancer Molecular Imaging Standardized Evaluation)1/E-PSMA: the EANM standardized reporting guidelines v1.0 for PSMA-PET2: our experience-Conclusions(1) Eiber M, Herrmann K, Calais J, Hadaschik B, Giesel FL, Hartenbach M, Hope T, Reiter R, Maurer T, Weber WA, Fendler WP. Prostate Cancer Molecular Imaging Standardized Evaluation (PROMISE): Proposed mITNM Classification for the Interpretation of PSMA-Ligand PET/CT. J Nucl Med. 2018 Mar;59(3):469-478. doi: 10.2967/jnumed.117.198119. Epub 2017 Nov 9. Erratum in: J Nucl Med. 2018 Jun;59(6):992. PMID: 29123012.(2) Ceci F, Oprea-Lager DE, Emmett L, Adam JA, Bomanji J, Czernin J, Eiber M, Haberkorn U, Hofman M, Hope TA, Kumar R, Rowe SP, Schwarzenboeck SM, Fanti S, Herrmann K. E-PSMA: the EANM standardized reporting guidelines v1.0 for PSMA-PET. Eur J Nucl Med Mol Imaging 2021;48:1626-38. <https://doi.org/10.1007/s00259-021-05245-y>

## **NMMIEE-23 Added Value of FDG-PET/MRI in Gynecologic Oncology: A Pictorial Review**

**Awards**

**Identified for RadioGraphics**

**Cum Laude**

Participants  
Malak Itani, MD, Saint Louis, MO (*Presenter*) Nothing to Disclose

#### TEACHING POINTS

PET/MRI is becoming increasingly available and provides physiologic information from the PET with accurate localization to high soft-tissue contrast images from MRI. PET/MRI plays an important role in staging and assessing treatment response in patients with uterine, cervical, vulvar and vaginal cancers. PET/MRI has a more limited role in ovarian malignancies but can be used as a problem solving tool in patients with negative CT scan and persistent concern for disease recurrence

#### TABLE OF CONTENTS/OUTLINE

- Review of instrumentation and techniques- Role of FDG PET/MRI in specific malignancies: o Endometrial cancer o Cervical cancer o Ovarian cancer o Vaginal cancer o Vulvar cancer- Future directions

#### NMMIEE-24 First Pass PET Imaging of Various Cardiovascular Disease

Participants  
Takashi Norikane, MD, PhD, Kita-gun, Japan (*Presenter*) Nothing to Disclose

#### TEACHING POINTS

Positron emission tomography (PET) is usually used for evaluating metabolic activity of the cells of body tissues. However, adding first pass PET imaging to standard imaging can provide information about vessel morphology and perfusion. The major teaching points of this exhibit are: 1: Knowledge of technique of first pass PET is important for an alternative imaging to conventional angiography for evaluation of vessels. 2: Knowledge of combination first pass and standard PET imaging provides further findings for radiologists to understand the disease condition accurately.

#### TABLE OF CONTENTS/OUTLINE

Technique List mode dynamic scan in selected region ECG-gated early phase scan Whole body PET angiography using continuous bed motion mode Disease Takayasu arteritis Giant cell arteritis Infectious aortitis Behcet's disease IgG4-related disease Pulmonary arterial venous malformation Pelvic arterial venous malformation Tubulointerstitial nephritis and uveitis Leriche syndrome Carotid artery stenosis Cardiac amyloidosis Constrictive pericarditis

#### NMMIEE-25 Imaging Features of Atypical Thoracic Metastases From Biochemically Recurrent Prostate Adenocarcinoma

Participants  
Hala Khasawneh, MBBS, Rochester, MN (*Presenter*) Nothing to Disclose

#### TEACHING POINTS

Using a case-based approach we will reinforce the following: 1. Treatment advancements and improved patient survival have led to an increase in the frequency of encountering atypical sites of biochemically recurrent (BCR) prostate cancer (PCa) metastasis 2. Novel PET radiotracers including 11C-choline and 68Ga-PSMA have the potential to detect atypical sites of metastases early in the disease course and often at very low PSA levels 3. Multimodality imaging evaluation of atypical sites of tracer uptake is essential for metastasis detection and characterization 4. Information on the site and burden of disease is required for personalized management of BCR PCa 5. Awareness of atypical sites of metastasis is critical given the essential role of radiologists in guiding patient care

#### TABLE OF CONTENTS/OUTLINE

1. Brief overview of BCR in PCa 2. Available imaging modalities used in patients with suspected BCR; Conventional versus PET imaging. 3. PET radiotracers used in early detection of BCR PCa: a) Comparison of available PET radiotracers for imaging of BCR PCa. b) Imaging protocol and patient preparation. c) Normal biodistribution of commonly used PET radiotracers. 4. Metastatic pattern in BCR PCa a) Typical versus atypical metastases sites b) Oligo-metastasis versus widespread disease 5. Case-based review of imaging features for a variety of atypical sites of BCR metastasis in the thorax with multimodality correlation: a) The respiratory system; lungs, pleura, and airways b) Supradiaphragmatic lymph nodes c) Breast metastasis d) Atypical bone metastasis and mimickers 6. Discuss relevant differential diagnosis and potential imaging pitfalls 7. Impact of early BCR localization on clinical management

#### NMMIEE-26 Always Wear Sunscreen: Conventional and Hybrid Imaging of Melanoma

Participants  
Craig Ferguson, BMBS, (*Presenter*) Nothing to Disclose

#### TEACHING POINTS

- To describe the variety of imaging investigations to detect disease extent and evaluate their relative merits and limitations (including ultrasound, CT, MRI and 18F-FDG PET/CT)- To define the rationale of sentinel lymph node biopsy and highlight the benefit of SPECT over conventional planar lymphoscintigraphy for sentinel node localization- To discuss the role of imaging in surveillance and response assessment, and associated challenges relating to novel therapies including immunotherapy- To identify disease mimics that the radiologist must recognize to ensure patients are not inappropriately denied treatment- To highlight the role of MRI in assessing CNS disease, including characteristic imaging appearances and common pitfalls

#### TABLE OF CONTENTS/OUTLINE

Background- Melanoma subtypes (cutaneous and non-cutaneous) including histopathology- Epidemiology, pathogenesis and management- Review of current guidelines relating to imaging workup in melanoma- Lymphoscintigraphy to identify the sentinel node; indications and technique- Role of cross-sectional imaging for initial staging, surveillance and response assessment; focusing on the benefits and limitations of 18F-FDG PET/CT- Top-to-toe review of multimodality imaging throughout a range of organ systems using selected case studies, including atypical presentations, important mimics, and imaging pitfalls

#### NMMIEE-27 Assessment of Response to Androgen Deprivation Therapy in Patients With Metastatic Castration-Resistant or Hormone-Sensitive Prostate Cancer by Radiolabeled Choline PET/CT: A Pictorial Essay

Participants  
Elisabet Vila, (*Presenter*) Nothing to Disclose

#### TEACHING POINTS

This exhibit will:- Review the concept of castration resistant prostate carcinoma (CRPC) and the use of choline PET/CT for response assessment.- Discuss the role of androgen receptor blockers in CRPC, and their mechanism of action.- Present radiological choline PET/CT CRPC cases and their different responses to treatment.- Assess the overall response to therapy and management in patients with CRPC as well as the utility of choline PET/CT in this scenario.

#### TABLE OF CONTENTS/OUTLINE

1. Introduction to prostate cancer  
1.1 Background and epidemiology  
1.2 Clinical Course  
1.3 Imaging findings of prostate cancer recurrence  
1.4 Metastatic Castration Resistant Prostate Carcinoma (mCRPC)  
1.4.1 Definition  
1.4.2 Metastatic spread  
2. Treatment options  
2.1 Androgen receptor blockers (enzalutamide, abiraterone)  
2.2 Chemotherapies (docetaxel)  
2.3 Actual management  
3. Role of Choline PET/CT in the evaluation of tumor response  
3.1 Target and normal distribution of choline  
3.2 Strengths and weaknesses  
3.3 Use of choline PET/CT in mCRPC  
3.4 Pitfalls and artifacts  
4. Presentation of mCRPC cases at our center and evaluation of the response to treatment

#### NMMIEE-28 Nuking Dementia: Adding Some Colour to The Dementia Diagnostic Pathway

Participants  
Peter Jarvis, FRCR, MBBS, Bournemouth, United Kingdom (*Presenter*) Nothing to Disclose

#### TEACHING POINTS

1. Provide an overview of the different molecular imaging techniques, with sample protocols, used in the diagnostic work up of dementia. 2. Appreciate normal images (including typical ageing) and give a strategy to identify the most common dementia subtypes using FDG-PET examples. 3. Overview of the specific role of DaTscan imaging in the diagnosis of Parkinson's disease and Lewy body dementia. 4. Determine which patients would benefit from functional imaging and lay out a suggested diagnostic pathway to be used in conjunction with conventional structural imaging. 5. Explore some of the newer molecular imaging techniques currently in practice and under development.

#### TABLE OF CONTENTS/OUTLINE

\*Aims? \*Background and purpose of nuclear imaging? \*Molecules overexpressed in dementia subtypes? \*Overview of HMPAO SPECT/CT? \*Overview of FDG PET/CT? \*Comparison of HMPAO and FDG PET? \*Statistical parametric mapping? \*Important regions for interpretation? \*Normal images (FDG PET and HMPAO)? \*Normal ageing (FDG PET)? \*FDG PET imaging of dementia subtypes? \*Alzheimer's disease?(typical) \*Mild cognitive impairment? \*Logophenic aphasia \*Posterior cortical atrophy \*Fronto-temporal dementia?(typical) \*Behavioral variant FTD \*Semantic dementia? \*Progressive non-fluent aphasia \*Lewy body dementia? \*Cautions and pitfalls? \*DaTscan?- overview and clinical uses? \*Newer PET imaging agents? \*Amyloid PET? \*Tau PET? \*TSPO PET (neuroinflammation)? \*When functional imaging should be used / pathway? \*Summary? \*References?

#### NMMIEE-29 Practical Overview of I-123 Ioflupane (DaTscan) Imaging for Parkinsonian Syndromes: Clinical Applications Findings and Pitfalls of Interpretation

#### Awards Identified for RadioGraphics

Participants  
Megan Mercer, MD, Charleston, SC (*Presenter*) Nothing to Disclose

#### TEACHING POINTS

I-123 Ioflupane (DaTscan) imaging is routinely performed in nuclear medicine departments nationwide. The clinical symptoms of Parkinsonian syndromes are not always specific, and radiologists are frequently called upon to help provide a diagnosis. The goal of this exhibit is to provide a focused guide for radiologists on important aspects of patient preparation, protocoling, troubleshooting, interpretation, and reporting of DaTscan imaging, through both a didactic and case-based approach. Multimodality correlation of DaTscan findings with other molecular (FDG PET-CT) and cross-sectional imaging (CT, MRI) is also incorporated.

#### TABLE OF CONTENTS/OUTLINE

1. Introduction 2. Pathophysiology 3. Indications 4. Protocol 5. Patient Preparation 6. Troubleshooting 7. Pitfalls 8. Interpretation 9. Reporting 10. Case examples with multimodality correlation 11. Conclusion.

#### NMMIEE-3 Musculoskeletal Involvement in Oncological Diseases: Strengths and Weaknesses of 18F-FDG-PET/CT

Participants  
Patricia Garcia, MD, PhD, Madrid, Spain (*Presenter*) Nothing to Disclose

#### TEACHING POINTS

-To illustrate the spectrum of hematological diseases and oncological pathologies with musculoskeletal involvement in FDG-PET/CT with histological correlation -To discuss strengths and limitations of FDG-PET/CT in the diagnostic and follow up of these diseases

#### TABLE OF CONTENTS/OUTLINE

FDG-PET/CT is proved to be the best technique for diagnosis and follow up of myeloma and lymphoma. One limitation in these diseases is the diffuse affection of the bone marrow, where there can be false negatives and positives findings. FDG-PET/CT plays also an important role for detection of metastases. FDG uptake alone is not adequate for characterizing primary bone tumors and morphologic evaluation is an important factor in the interpretation of FDG-PET/CT scans. In many cases other imaging studies or biopsy is required for definitive diagnosis. We reviewed the hematological and oncological FDG-PET/CT studies from the last 10 years in two institutions. Regarding the musculoskeletal involvement we divided them in: - Bone lesions: I.e. scapular telangiectatic sarcoma, different patterns of presentation of myeloma, lymphoma, metastases - Soft tissue lesions: I.e. cell T skin lymphoma, cell

B lymphoma - Complications: spinal cord compressions and pathological fractures We discuss the actual importance of FDG-PET/CT in each pathology and its limitations.

### **NMMIEE-31 Neoplastic Neurocristopathies in Nuclear Medicine: Embryology, Pathophysiology, and Theranostics**

Participants

Edgar Zamora, MD, (*Presenter*) Nothing to Disclose

#### **TEACHING POINTS**

Familiarize the reader with neural crest cell (NCC) embryology, pathophysiology of neoplastic neurocristopathies (NCP) and biochemical phenotypes, and the role of nuclear imaging and therapy. The exhibit includes illustrations and cases categorized based on primary NCC lineages involved (i.e., cranial, truncal, vagal, sacral).

#### **TABLE OF CONTENTS/OUTLINE**

NCCs arise from unfused neural folds, migrate extensively, and differentiate into specialized tissues in multiple systems. Mutations in crucial genes can lead to various neoplasms and dysgenetic conditions, originally presumed unrelated. Neuroblastomas (sympathoadrenal progenitor cells) result from epigenetic alterations (MYCN overexpression) or mutations in key genes (ALK, PHOX2B), while pheochromocytomas/paragangliomas (chromaffin/ chief cells) are more often familial (SDHx, VHL, RET). Targeted imaging can be performed with 123I-MIBG, and 111In- or 68Ga-SSTR binding agents, the latter also available for differentiated NETs. Theranostic  $\beta$ - and  $\alpha$  emitting radiopharmaceuticals are useful in select conditions. Familial syndromes such as NF1 and MEN are associated with various NCPs, such as MTC, pancreatic islet cell tumors, and parathyroid adenomas. Radiolabeled SSTR binding agents can be used for pancreatic islet cell tumors, 18F-FDG for MTC, and 99mTc-Sestamibi for parathyroid adenomas. Other conditions resulting from dysgenesis or abnormal migration/differentiation of NCCs include meningioma, melanoma, and neurocutaneous syndromes. Biochemical phenotypes have an important role in radiopharmaceutical selection. Therefore, understanding the pathophysiology of NCPs is essential for diagnosis and management strategy.

### **NMMIEE-32 PSMA PET/CT: A Pictorial Review of Common Pitfalls in Interpretation**

Participants

Venkata Kal Byrapogu, (*Presenter*) Nothing to Disclose

#### **TEACHING POINTS**

Our studies indicate that uptake of PSMA by PCa bone metastatic lesions tends to be homogeneous and more intense. In contrast, uptake by other pathologies presented here tend to be heterogenous and less intense.

#### **TABLE OF CONTENTS/OUTLINE**

Introduction: Prostate cancer (PCa) is the one of the most common cancers affecting men in the United States and worldwide[1]. Advanced PCa presents with bone metastases - most commonly osteoblastic while rarely osteolytic metastases. Accurate and reliable detection of these bone metastases is critical for patient survival as well as for improving patient's quality of life[2]. Technique: Prostate-specific membrane antigen (PSMA) is a cell surface glycoprotein that is predominantly expressed in prostate epithelium, proximal tubules of the kidney, jejunal brush border of the small intestine and ganglia of nervous system[3]. Hence, PSMA can be expressed in benign processes of these tissues, PCa, and other cancers. PCa expresses significantly higher (100x - 1000x) PSMA than normal tissues making PSMA an excellent target for nuclear imaging[4]. PSMA PET/CT technique has emerged as a novel receptor-based imaging technique for whole-body detection of PCa bone metastases[5]. Pathologic Correlation: It is important for radiologists to be aware of false-positives when evaluating PSMA PET/CT studies. In this study, we present examples of false positive uptake in patients with PCa. For comparison, we also present a typical sclerotic bone lesion of PCa. References: 1. Fitzmaurice, C., et al., 2017. 2. Lin, S.C., et al 2018. 3. Chang, S.S., et al., 2004. 4. Evans, J.D., et al., 2018. 5. Rowe, S., et al., 2019. 6. Savir-Baruch, B., et al., 2021.

### **NMMIEE-33 Assessing Tumor Response to Therapy With Hybrid Imaging: Practical Aspects**

Participants

Laith Abandeh, MD, Seattle, WA (*Presenter*) Nothing to Disclose

#### **TEACHING POINTS**

- Illustrate the primary role of conventional and hybrid imaging in the evaluation of tumor response to treatment.
- Review the general concepts and existing imaging-based criteria for evaluating tumor response to therapy.
- Outline the challenges encountered during tumor response assessment using anatomic imaging/size-based criteria.
- Learn the emerging approaches and challenges in evaluating imaging-based tumor response to immunotherapeutic agents and targeted treatment.
- Outline the synergy between PET and CT to overcome diagnostic challenges and achieve a comprehensive tumor response assessment.

#### **TABLE OF CONTENTS/OUTLINE**

§ Introduction and U.S Cancer Facts § Treatment Outcome Prediction via Response Monitoring § Cancers Evade Therapy: Mechanisms § Role of Anatomic Imaging - WHO Response Criteria - Limitations - Responses RECIST does not capture § Treatment Monitoring: Role of Hybrid Imaging (Integration of Data) § Practical Use of SUV § Artifacts and Pitfalls § Cases/Examples § Conclusion

### **NMMIEE-34 Expect the Unexpected! Pictorial Review of Acute and Emergent Findings on Oncologic F18-FDG PET/CT**

Participants

Priya Pathak, MBBS, MD, (*Presenter*) Nothing to Disclose

#### **TEACHING POINTS**

1. Overview of FDG uptake patterns in commonly encountered oncologic emergencies and non-cancer related acute findings in oncologic patients on F18-FDG PET/CT.
2. Encourage identification of key imaging findings based on the attenuation corrected PET images with approach to differential diagnosis.
3. Highlight the clinical features, prognosis and treatment options for these entities.
4. Provide correlation between PET and anatomic imaging (US/CT/MRI).

## TABLE OF CONTENTS/OUTLINE

Introduction: Discussion of the following entities with case examples and approach to imaging features. ONCOLOGIC EMERGENCIES AND ACUTE DISORDERS Vascular: SVC syndrome, DVT, Pulmonary embolism CNS: Brain metastasis, Spinal cord compression Chest: Airway obstruction, Pneumonia, Esophagorespiratory fistula, Pericardial effusion tamponade Abdomen Pelvis: Bowel obstruction, Typhilitis, Biliary obstruction, Cholangitis, Pancreatitis, Urinary tract obstruction Treatment related: Intracranial bleed, Pneumothorax, Invasive fungal pneumonia, Drug radiation related pneumonitis, Pericarditis, Pancreatitis, Enterocolitis MSK: Pathological fractures, Radiation osteonecrosis NON-CANCER RELATED ACUTE DISORDERS Vascular: Aortic dissection, Aneurysm, Vasculitis Chest: COVID, Aspiration pneumonitis, Lung abscess, Atrial fibrillation Abdomen: Infective and inflammatory enteritis, Diverticulitis, Appendicitis, Obstructed hernia, Cholecystitis, Hepatic abscess MSK: Discitis, Osteomyelitis, Septic arthritis, AVN, Myositis

### **NMMIEE-35 Gastrointestinal Motility on Nuclear Scintigraphy: Protocols, and Pathologies with Multimodality Correlates**

#### **Awards**

**Certificate of Merit**

**Identified for RadioGraphics**

Participants

Jonathan Revels, DO, Albuquerque, NM (*Presenter*) Nothing to Disclose

#### **TEACHING POINTS**

Teaching Points 1- Learn the clinical approach and role of radiology in the assessment and management of patients with GI motility disorders. 2- Recognize imaging patterns of normal and abnormal gastric, small bowel, and large bowel motility on nuclear scintigraphy. 3- Learn potential limitations of nuclear medicine examinations for GI motility assessment. 4- Learn the complimentary role nuclear scintigraphy and other radiologic examinations have in evaluation of GI motility disorders.

## TABLE OF CONTENTS/OUTLINE

1- Introduction a. Review gastrointestinal motility disorder epidemiology and pathophysiology. b. Review the clinical approach to diagnosis of gastric, small bowel, and large bowel dysmotility, and the role of nuclear scintigraphy in evaluation of these patients. 2- Review protocols for gastrointestinal motility patient preparation and evaluation with nuclear scintigraphy. a. Various approaches to gastric emptying studies, and small bowel and large bowel transit studies. b. Briefly review gastric motility assessment in pre and post-operative setting (gastric bypass, colectomy) and following medical therapy (initiation of prokinetic medication). 3- Review how to evaluate GI motility scintigraphy examinations visually and quantitatively. a. Intragastric meal distribution for gastric emptying i. Fundal -vs- antral dysfunction, rapid gastric emptying. b. Quality control of regions of interest and quantitative assessment. 4- Provide case examples of: a. GI dysmotility on nuclear scintigraphy with fluoroscopic, radiographic, and cross-sectional correlates. b. Incidental findings on nuclear scintigraphy with clinical implications (gastroesophageal reflux, hiatal hernia).

### **NMMIEE-4 Triaging Frostbite Injuries with Tc99 MDP Multiphase Imaging**

Participants

Austin Promersberger, Fargo, ND (*Presenter*) Nothing to Disclose

#### **TEACHING POINTS**

- Extreme cold exposure/frostbite leads to distal arterial vasoconstriction and ischemia. • Management of frostbite varies widely based on the severity of injury. Treatments range from noninvasive care to catheter directed thrombolytic therapy and amputation.
- Patient selection for invasive frostbite management requires timely decision making. • NM multiphase Tc99 MDP scintigraphy provides a noninvasive evaluation demarcating viable perfused tissue from ischemic/infarcted tissue. • MDP imaging can be used to select patients for catheter directed thrombolytic therapy as well as guide amputation planning.

## TABLE OF CONTENTS/OUTLINE

1. Review the pathophysiology of frostbite and staging classifications. 2. Illustrate utility of early Tc99 MDP multiphase imaging in guiding thrombolytic therapy. 3. Emphasize the use of delayed Tc99 MDP planar imaging and SPECT/CT for assessing depth and extent of infarcted tissue for surgical debridement and amputation. 4. Pictorially review lessons and caveats learned at a level 1 trauma center during algorithmic implementation of MDP frostbite imaging including sequelae of bandaging, early rewarming, and distal digital marker use to improve diagnostic abilities and patient outcome. 5. Provide a detailed protocol for institutional frostbite imaging implementation.

### **NMMIEE-5 Spectrum of Vocal Cord FDG Avidity on 18F-FDG PET/CT: Presentations Causes and Sites of Nerve Injury**

Participants

Reema Goel, MD, (*Presenter*) Nothing to Disclose

#### **TEACHING POINTS**

Objectives 1. Describe the course of the vagus and recurrent laryngeal nerves. 2. Identify accurate PET/CT signs of unilateral vocal cord paralysis and avoid mimics and pitfalls. 3. Recognize the role of FDG PET/CT in assessing common and uncommon head and neck as well as mediastinal benign and malignant conditions that may lead to vocal cord paralysis as well as its role in evaluating primary vocal cord tumors

## TABLE OF CONTENTS/OUTLINE

Examples of FDG PET/CT imaging highlighting the following benign and malignant causes of vocal cord paralysis : 1. 1. Masses, tumors compressing vagal nerve/its branches at various levels-at base of the skull, neck, thyroid region, and thoracic cavity especially as the recurrent laryngeal nerve (RLN) loops around the aorta at aorticopulmonary window 2. 2. Surgical interventions (especially thyroid surgery)-It would be highlighted that in the lower neck, the course of the right RLN is more lateral and oblique than the left, making it prone to injury particularly secondary to trauma and surgery, most commonly thyroid dissection. However, the length of the left RLN is at times more than double that of the right RLN causing the left RLN to a higher rate of injury from nontraumatic causes, such as neoplastic infiltration. 3. 3. Being secondary to intubation 4. 4. Viral neuritis and

idiopathic/paraneoplastic conditions 5. Additionally examples of role of FDG PET in assessing vocal cord tumors at initial diagnosis and post treatment stage/follow up would also be included.

## **NMMIEE-6 What Do We Know About Emerging Methods for Imaging The Glymphatic System?**

Participants

Yuichi Morita, Bunkyo, Japan (*Presenter*) Nothing to Disclose

### **TEACHING POINTS**

The glymphatic system describes the brain perivascular network promoting cerebrospinal and interstitial fluids exchange that facilitates the clearance of solutes and waste from the brain. Dysfunction of the glymphatic system is related to numerous neurological disorders. MRI tracer-based methods have been used to evaluate glymphatic function in humans; however, tracer administration is relatively invasive and limited in its clinical application. Recent studies have showed the potential of structural and diffusion MRI to investigate the glymphatic system non-invasively. The teaching points are: 1. To review the current knowledge of the glymphatic system. 2. To overview invasive and non-invasive methods for imaging the glymphatic system. 3. To introduce clinical applications of glymphatic imaging using MRI.

### **TABLE OF CONTENTS/OUTLINE**

1. The description of the glymphatic system hypothesis. 2. Glymphatic imaging methods using tracers (i.e., Gadolinium-based contrast agents and <sup>17O</sup> isotope). 3. Non-invasive glymphatic imaging methods (i.e., perivascular space volumetry, diffusion tensor image analysis along the perivascular space, free water imaging, etc.). 4. Clinical applications of glymphatic imaging methods, including Alzheimer's disease, Parkinson's disease, idiopathic normal pressure hydrocephalus, etc., and the future prospective application.

## **NMMIEE-8 Keep Calm and Image On: Safely Employing PET/CT In Pediatric Malignancies**

Participants

Jaron Hansen, MD, San Antonio, TX (*Presenter*) Nothing to Disclose

### **TEACHING POINTS**

1. Learn the oncologic indications for performing PET/CT in pediatric patients. 2. Recognize the normal biodistribution of <sup>18F</sup>-FDG in pediatric patients. 3. Present case examples which highlight the utility of pediatric PET/CT in oncologic conditions. 4. Discuss mechanisms for reducing pediatric radiation doses while still obtaining a diagnostic imaging exam.

### **TABLE OF CONTENTS/OUTLINE**

1. Pediatric oncologic PET/CT a. Indications for PET/CT in the work up of pediatric cancer patients b. PET radiopharmaceuticals i. <sup>18F</sup>-FDG in cancer staging and treatment response assessment ii. <sup>68Ga</sup>-DOTATATE in neuroblastoma and neuroendocrine tumor imaging 2. Oncologic case examples a. Lymphoma i. <sup>18F</sup>-FDG PET/CT imaging in staging and treatment response assessment b. Sarcomas i. <sup>18F</sup>-FDG PET/CT for staging, treatment response assessment, and PET-guided biopsies c. Neural origin tumors i. <sup>18F</sup>-FDG PET/CT to characterize peripheral nerve sheath tumors ii. <sup>68Ga</sup>-DOTATATE in neuroblastoma staging d. Malignancies associated with congenital syndromes i. Using <sup>18F</sup>-FDG PET/CT to identify and stage malignancy in cancer predisposition syndromes, including Li Fraumeni and Lynch Syndrome 3. Pediatric PET/CT scanning considerations a. Understanding the balance between dose reduction and high-quality imaging, including the pros and cons of anesthesia and radiation in pediatric patients b. Technologies that help reduce dose or scan time for PET/CT scans c. Targeting the right PET/CT protocol for the clinical management decision

## **NMMIEE-9 Spectrum of PET Emergent Findings Among Various Radiotracers**

### **Awards**

#### **Certificate of Merit**

Participants

Hiroaki Takahashi, MD, PhD, Rochester, MN (*Presenter*) Nothing to Disclose

### **TEACHING POINTS**

Unexpected emergent findings are occasionally detected on PET. Since PET scans routinely cover almost the entire body, there is a higher probability of incidental emergent findings than focused imaging. However, anatomical assessment is limited on the portion of these exams that are performed primarily for attenuation correction and colocalization of PET findings. While the appearance of emergent findings on FDG PET has been well-documented, reports on these findings as seen with other newly emerging PET radiotracers are scarce. In this exhibit we will present methods to detect the most common emergent diagnostic challenges radiologists will face on PET, focusing on their different appearance on various radiotracers including FDG, Choline, DOTATATE, Ammonia and PSMA. The purposes of this exhibit are: 1. To review varying appearances of incidental emergent conditions detected with different PET radiotracers. 2. To review appropriate management.

### **TABLE OF CONTENTS/OUTLINE**

1. Overview of emergent findings on PET. 2. Basic mechanism and imaging of various PET radiotracers. 3. Findings of the emergent abdomen, including diverticulitis, cholecystitis/cholangitis, appendicitis, bowel obstruction, pyelonephritis, and pancreatitis. 4. Findings of the emergent chest, including pulmonary embolism, pneumothorax, and infection including COVID-19. 5. Findings of vascular emergencies, including deep venous thrombus, intramural hematoma, and pseudoaneurysm. 6. Findings of neurological emergencies, including intracranial hemorrhage, and large volume brain metastasis/tumor. 7. Findings of spine and musculoskeletal emergencies, including spinal stenosis, osteomyelitis and unstable fracture.

Printed on: 02/07/23



## Abstract Archives of the RSNA, 2022

NMMIEE-1

### Integrating Molecular Imaging to Meningiomas: Is PET with Somatostatin Receptors Our New Buddy?

Sunday, Nov. 27 8:00AM - 9:00AM Room: Learning Center - NMMI

#### Participants

Rodrigo Hernandez Ramirez, MD, Leon, Mexico (*Presenter*) Nothing to Disclose

#### TEACHING POINTS

To identify the importance of somatostatin receptors in meningioma. To show the applications of PET in the evaluation of meningiomas specifically in detection and delimitation of the tumor, diagnosis of recurrence and radiotherapy planning.

#### TABLE OF CONTENTS/OUTLINE

Meningiomas are the most common primary brain tumors and represent about 30% of intracranial tumors. Neuro-Oncology guidelines recommend contrast-enhanced MRI as the primary radiologic modality of choice because it has a sensitivity of 90%. Meningiomas can express somatostatin receptors type 2. Molecular imaging techniques allow the incorporation of functional information for diagnostic purposes. PET tracers for SSTR evaluation provide high sensitivity with excellent target-to-background contrast due to low uptake in bone and healthy brain tissue. SSTR PET has demonstrated benefits for noninvasive differential diagnosis, delineation tumor and treatment planning. Although PET plays only a minor role in the initial diagnosis of meningiomas, it may add value for meningioma detection, with a sensitivity of 100%. Clinically, this is relevant because meningiomas located at the skull base or nearby the falx cerebri, with transosseous extension, or equivocal imaging findings related to artifacts or calcifications were difficult to detect by MRI. For the differentiation of scar tissue from active tumor, SSTR PET has a high sensitivity of 90%, outperforming standard MRI with 79%. PET can obtain an optimized target volume delineation for fractionated radiation therapy in patients with meningiomas grade I-III.

Printed on: 02/07/23



## Abstract Archives of the RSNA, 2022

NMMIEE-10

### Punctiliously Perfect PSMA PET: Pearls and Pitfalls

Sunday, Nov. 27 8:00AM - 9:00AM Room: Learning Center - NMMI

#### Participants

Daniel Wale, DO, (*Presenter*) Nothing to Disclose

#### TEACHING POINTS

1. Several PET radiopharmaceuticals targeting prostate specific membrane antigen (PSMA) are now FDA-approved for assessment of metastatic prostate cancer. 2. PSMA PET agents have a normal biodistribution that includes salivary and lacrimal glands, kidneys, and small bowel, as well as urinary excretion. Familiarity with normal uptake decreases potential for misdiagnosis. 3. PSMA expression is not prostate-specific, and uptake can be identified in a variety of other benign and malignant processes. Awareness of commonly encountered non-prostatic lesions, combined with knowledge of common metastatic patterns of prostate cancer, allows the radiologist to avoid potential pitfalls.

#### TABLE OF CONTENTS/OUTLINE

I. Introduction  
II. Prostate cancer  
A. PSMA expression  
B. Utility of PSMA expression for diagnosis  
C. Utility of PSMA expression for treatment  
III. Nuclear imaging  
A. Indium 111 capromab pendetide (historical)  
B. PET agents targeting PSMA  
1. Gallium 68 PSMA-112.  
2. Fluorine 18 piflufolastat  
C. Clinical indications  
D. Imaging protocols  
IV. Pearls and pitfalls  
A. Normal biodistribution  
B. Pitfalls regarding normal biodistribution  
1. Accessory salivary gland tissue  
2. Urine activity  
3. Parasympathetic ganglia  
4. Osseous  
a. Degenerative disease and inflammation  
b. Fibro-osseous lesions  
E. Non-prostatic neoplasms  
1. Meningioma  
2. Thyroid nodules  
3. Hemangioma  
4. PSMA avid non-prostate malignancies  
V. Treatment utilizing PSMA  
A. Lutetium 177 PSMA  
B. Localize anatomically occult disease for external radiation  
VI. Conclusion

Printed on: 02/07/23



## Abstract Archives of the RSNA, 2022

NMMIEE-11

### Hybrid PSMA Imaging of The Prostate: A Guide For the Beginner- A Reference For the Expert

Sunday, Nov. 27 8:00AM - 9:00AM Room: Learning Center - NMMI

#### Participants

Felipe Furtado, MD, Boston, MA (*Presenter*) Nothing to Disclose

#### TEACHING POINTS

Prostate-specific membrane antigen (PSMA) PET is revolutionizing the management of prostate cancer in all clinical settings, from treatment-naive cancer to biochemical recurrence. Different PSMA ligands share a high affinity toward PSMA but differ in sensitivity, specificity, half-life, biodistribution, pitfalls, and excretion profile. Workflows, acquisition protocols, hybrid imaging modality (PET/CT vs. PET/MRI), and interpretation must be tailored to the appropriate clinical scenario and specific PSMA radiopharmaceutical. Adequately performed and interpreted PSMA hybrid imaging will revolutionize personalized medicine in prostate cancer patients.

#### TABLE OF CONTENTS/OUTLINE

1) PSMA ligands; 2)PET/CT and PET/MRI strengths, weaknesses, acquisition protocols, and workflows; 3) How to perform the best PSMA hybrid study for each clinical scenario; 4) PSMA PET/CT and PET/MRI interpretation, for the beginner and the expert

Printed on: 02/07/23



## Abstract Archives of the RSNA, 2022

NMMIEE-12

### Post PRRT Imaging: What To Look For On Routine and Emergent Imaging?

Sunday, Nov. 27 8:00AM - 9:00AM Room: Learning Center - NMMI

#### Participants

Malak Itani, MD, Saint Louis, MO (*Presenter*) Nothing to Disclose

#### TEACHING POINTS

The purpose of this exhibit is for radiologists, nuclear medicine physicians, radiation oncologists and medical oncologists and trainees to:- Know what to look for on post-PRRT SPECT-CT imaging- Be familiar with most common complications of PRRT and their imaging manifestations in the acute, subacute, and chronic setting- Understand the appropriate timeline for routine follow-up after PRRT- Evaluate response to treatment after PRRT using anatomic and functional imaging modalities

#### TABLE OF CONTENTS/OUTLINE

I. Brief overview of PRRT complications with no imaging correlate  
A. Myelosuppression  
B. Renal toxicity  
C. Hepatotoxicity  
D. Neuroendocrine hormonal crisis  
E. Secondary leukemia and myelodysplastic syndrome  
F. Reproductive side effects  
II. Post-PRRT Imaging by Timeline:  
A. Post-PRRT SPECT/CT:  
i. SPECT: Localize sites of uptake, compare intensity relative to pre-treatment SSTR-PET  
ii. CT: Correlate gross tumor burden with pre-PRRT imaging, evaluate for immediate post-treatment complications, general CT read  
B. Acute presentations after PRRT:  
i. CT/MRI: tumor necrosis, hepatitis, cholangitis, hepatic abscess, radiation peritonitis, ascites, perforation, vascular thrombosis  
C. Routine follow-up post-treatment:  
i. CT/MRI: timing, changes in lesion size, criteria for progression vs pseudo-progression, potential side effects  
ii. PET: Indications, timing, comparison, quantitative measures and scores, potential complications

Printed on: 02/07/23



## Abstract Archives of the RSNA, 2022

NMMIEE-13

### **18F-DCFPyL PSMA PET/CT for Prostate Cancer Imaging: A Primer on Technique, Interpretation Structured reporting**

Sunday, Nov. 27 8:00AM - 9:00AM Room: Learning Center - NMMI

#### **Participants**

Harit Kapoor, MD, Dallas, TX (*Presenter*) Nothing to Disclose

#### **TEACHING POINTS**

1) 18F-DCFPyL (PyL) is the first commercially available PSMA PET agent for Prostate Cancer (PCa) evaluation, FDA approved for both staging and biochemical recurrence.2) PyL has an unprecedented diagnostic performance, especially in the setting of small volume recurrence, detecting nodal metastasis in the 2-5 mm range.3) Aside from superior logistics inherent to being a F-18 based agent, PyL also shows higher spatial resolution and tumor to background ratio compared to Ga-68 PSMA-11 PET.4) PyL imaging has been hailed as a paradigm shift, altering patient management in >50% of published cohorts.5) Radiologist's awareness of the interpretative limitations and pitfalls as well as the use of standardized evaluation criteria, is vital in order to prepare for anticipated rapid utilization.6) Initiation of androgen deprivation therapy can create flare-like imaging appearance due to PSMA upregulation.

#### **TABLE OF CONTENTS/OUTLINE**

1) Role and evolution of PET tracers in the clinical continuum of recurrent prostate cancer2) Imaging protocol and normal biodistribution for PyL PSMA PET/CT3) Standardized evaluation criteria for staging, recurrence and treatment response.4) Case examples of pearls and pitfalls (e.g. ganglionic uptake, follicular hyperplasia and tumor-neovascularity etc.)5) Into the future: Metastasis directed therapy 177Lu-PSMA theranostics

Printed on: 02/07/23



## Abstract Archives of the RSNA, 2022

NMMIEE-14

### An Illustrative Review of Nuclear Medicine Thyroid Studies

Sunday, Nov. 27 8:00AM - 9:00AM Room: Learning Center - NMMI

#### Awards

Identified for RadioGraphics  
Certificate of Merit

#### Participants

Andrew Schneider, MD, MPH, Boston, MA (*Presenter*) Nothing to Disclose

#### TEACHING POINTS

Nuclear medicine thyroid studies are a common type of imaging that require a broad understanding of the microbiology, physiology, and clinical manifestations of the underlying disease in order to interpret successfully. For trainees who are learning to interpret these studies, the intricate integration of multiple lines of clinical, laboratory, imaging, and pathological evidence can be intimidating and confusing. Here we provide an educational resource for trainees designed to build understanding by walking through the basic biology, radiopharmaceuticals, principles, indications, protocols, and interpretation of nuclear medicine thyroid studies. A key component of this resource is a representative collection of illustrative cases with a combination of clinical information, laboratory data, nuclear medicine and other imaging studies, and pathology findings.

#### TABLE OF CONTENTS/OUTLINE

Thyroid Anatomy / Physiology; Radiopharmaceuticals; Study Indications; Imaging Protocols; Decision-Making; Illustrative Cases

Printed on: 02/07/23



## Abstract Archives of the RSNA, 2022

NMMIEE-15

### PSMA-Targeted PET Imaging Interpretation Frameworks Comparison of PROMISE Classification and PSMA RADS Version 1.0

Sunday, Nov. 27 8:00AM - 9:00AM Room: Learning Center - NMMI

#### Awards

**Certificate of Merit**

#### Participants

Vanessa Murad, MD, Bogota, Colombia (*Presenter*) Nothing to Disclose

#### TEACHING POINTS

1) PSMA-targeted PET imaging interpretation schemes have been devised to ensure consistency in reporting and avoid potential pitfalls. 2) PROMISE classification is based on the molecular imaging PSMA (miPSMA) expression score, assigned to each lesion with respect to uptake in reference tissues (Figure 1). miPSMA score together with the presence or absence of morphological findings provide diagnostic certainty (positive, negative or equivocal). 3) When applying PROMISE classification for PSMA-targeted imaging with predominantly hepatobiliary excretion (e.g. 18F-PSMA-1007), the spleen is recommended as the intermediate reference. 4) On PSMA-RADS, findings are categorized on a 5-point scale according to PSMA-uptake and morphological characteristics, where the higher the number, the greater the likelihood of a cancer related lesion (Table 3)

#### TABLE OF CONTENTS/OUTLINE

1) Introduction/Aim. 2) PROMISE Classification 2.1) Description and interpretation: Tables 1,2. 2.2) Illustrative examples: Figure 2. 2.3) Advantages and disadvantages. 3) PSMA-RADS Version 1.0. 3.1) Description and interpretation. 3.2) Illustrative examples: Figure 3. 3.3) Advantages and disadvantages

Printed on: 02/07/23



## Abstract Archives of the RSNA, 2022

NMMIEE-16

### Practical Interpretation of 18F PSMA PET/CT: Spectrum of Findings

Sunday, Nov. 27 8:00AM - 9:00AM Room: Learning Center - NMMI

#### Participants

Kenneth Huynh, BS, Orange, CA (*Presenter*) Nothing to Disclose

#### TEACHING POINTS

1.To familiarize the viewers with 18F PSMA normal biodistribution 2.To present all potential incidental findings detected by 18F PSMA PET/CT. 3.To review the staging and monitoring of prostate cancer and its locoregional and distant metastasis depicted by PET/CT.

#### TABLE OF CONTENTS/OUTLINE

The exhibit has three components: (1) the presentation of normal 18F PSMA features with characteristic physiologic uptake at lacrimal glands, glottis and sympathetic ganglion chains, differentiating this tracer from 18F FACBC and 11C Choline, (2) the review of incidental findings such as accessory parotid gland, lung inflammatory and infectious processes, osseous fractures, splenosis, and hibernoma, and (3) the description of common and atypical/rare features of prostate cancer and metastasis such as lesions of bones, nodes, liver, peritoneum, penis, adrenal glands and thyroid cartilage. The 177 Lu PSMA therapy of prostate cancer with related imaging is also addressed in the exhibit.

Printed on: 02/07/23



## Abstract Archives of the RSNA, 2022

NMMIEE-18

### The History and Evolution of the Molecular Evaluation of Neuroendocrine Tumors

Sunday, Nov. 27 8:00AM - 9:00AM Room: Learning Center - NMMI

#### Participants

Jorge Espinosa, MD,MS, (*Presenter*) Nothing to Disclose

#### TEACHING POINTS

To understand the pathophysiology of the neuroendocrine tumors. To briefly know the history of radiotracers. To show the current radiotracers and its different applications in nuclear and imaging medicine.

#### TABLE OF CONTENTS/OUTLINE

Table of contents  
1. Introduction on neuroendocrine tumors  
2. Brief history of radiotracers and its evolutions  
3. Line time of evolutions of radiotracers and its applications  
4. Comparative table  
5. The newest radiotracers and new applications  
6. CT-PET protocols  
7. Comparative images  
8. Examples of CT-PET  
Outline  
Since the discovery of In-111 OctreoScan in 1983, the role of molecular imaging in the diagnosis, follow-up and even treatment of neuroendocrine tumors has revolutionized the management of these lesions. Twenty years ago, the introduction of somatostatin analogues labeled with Ga68 in PET studies, improved the diagnostic sensitivity mainly as a result of improvements in spatial resolution. Knowledge of the evolution of molecular imaging during the diagnostic approach on neuroendocrine tumors aids in better selection of the method in patients with suspected neuroendocrine tumors.

Printed on: 02/07/23



## Abstract Archives of the RSNA, 2022

NMMIEE-19

### Incidental Uptake on FAPI PET/CT Imaging: Physiologies, Pathologies, and Pitfalls

Sunday, Nov. 27 8:00AM - 9:00AM Room: Learning Center - NMMI

#### Participants

Masatoshi Hotta, (*Presenter*) Nothing to Disclose

#### TEACHING POINTS

FAPI PET/CT can identify tumor lesions with a higher tumor-to-background ratio in various tumor entities, and has sparked considerable interest in the oncologic community. As studies on FAPI PET grow in number and size, incidental findings related to non-oncologic conditions have been increasingly reported. The purpose of this exhibit is to: 1) Review the physiological FAPI uptake of each organ system 2) Describe the main pathologies of non-oncological uptake 3) Demonstrate FAPI PET/CT of non-oncologic diseases.

#### TABLE OF CONTENTS/OUTLINE

1. Introduction  
2. Physiological and non-oncological uptake of each organ system:  
a) Brain  
b) Head and Neck (Thyroid, Salivary glands, Dental)  
c) Thorax (Lung, Cardiac, Breast, Esophagus)  
d) Abdomen (Gastrointestinal, Liver, Pancreas, Bile duct, Spleen, Kidney, Uterus)  
e) Musculoskeletal (Bone, Joint, Muscle, Skin)  
f) Other systems (Vascular, Lymph node)

Printed on: 02/07/23



## Abstract Archives of the RSNA, 2022

NMMIEE-2

### Multimodality Imaging of Adenoid Cystic Carcinoma With Emphasis On PET/CT

Sunday, Nov. 27 8:00AM - 9:00AM Room: Learning Center - NMMI

#### Awards

Certificate of Merit

#### Participants

Ba D. Nguyen, MD, (*Presenter*) Nothing to Disclose

#### TEACHING POINTS

1. To review the clinical, pathological and imaging features of Adenoid Cystic Carcinoma (ACC). 2. To present the PET/CT impact of ACC evaluation for metastases, recurrence, and treatment monitoring.

#### TABLE OF CONTENTS/OUTLINE

ACC is a rare cancer that typically arises in the head and neck region as a salivary gland tumor, composing 1% of head and neck tumors and 10% of salivary gland tumors. Other presenting locations within the head and neck include the hard palate, auditory canal, nasopharynx, epiglottis, lacrimal gland, and tongue. Outside of the head and neck, ACC may target the skin, trachea, breast, and reproductive tract. Most ACC are indolent, presenting as a slow growing, painless mass. However, perineurial invasion is common and there are potential distant metastases via lymphatic or hematogenous spread. Primary management is via complete resection, often with adjuvant radiation and chemotherapy. MRI and CT are most useful for head and neck assessment of ACC. Diagnosis relies on histology. PET/CT is used for staging, evaluating for metastasis, and monitoring for recurrence. This exhibit reviews PET/CT features of ACC at common and atypical sites of the body with emphasis on the PET/CT impact on staging and post-therapeutic surveillance of ACC.

Printed on: 02/07/23



## Abstract Archives of the RSNA, 2022

NMMIEE-20

### Myocardial Perfusion Imaging: Past, Present, and Future

Sunday, Nov. 27 8:00AM - 9:00AM Room: Learning Center - NMMI

#### Participants

Saif Azam, MD, Los Angeles, CA (*Presenter*) Nothing to Disclose

#### TEACHING POINTS

1. Explore the physiology underlying the distribution of radiopharmaceuticals used in myocardial perfusion imaging  
2. Review classic patterns of uptake and how they may guide clinical management  
3. Understand the pros and cons of different modalities available for the assessment of myocardial perfusion  
4. Increase awareness of factors that can cause false positive and false negative results

#### TABLE OF CONTENTS/OUTLINE

- Introduction and review of anatomy and physiology pertaining to myocardial perfusion imaging
- Exercise versus pharmaceutical stress testing
- Cadmium-zinc-telluride camera utility
- Logistics of radiotracers used in cardiac single photon emission computed tomography (SPECT): Thallium-201 (201-Tl), Technetium-99m sestamibi, Technetium-99m tetrofosmin
- Case-based review of positron emission tomography (PET) radiotracers: Rubidium-82 (82-Rb), Nitrogen-13 ammonia (13N-NH<sub>3</sub>), Oxygen-15 water (15O-H<sub>2</sub>O), Fluorine-18 flurpiridaz
- Spectrum of imaging findings in the evaluation of ischemic heart disease
- Causes and troubleshooting of false positives, false negatives, and other artifacts
- Questions

Printed on: 02/07/23



## Abstract Archives of the RSNA, 2022

NMMIEE-21

### Essentials of Theranostics: A Guide for Physicians and Medical Physicists

Sunday, Nov. 27 8:00AM - 9:00AM Room: Learning Center - NMMI

#### Awards

Identified for RadioGraphics

#### Participants

Celeste Winters, PHD, Portland, OR (*Presenter*) Nothing to Disclose

#### TEACHING POINTS

1) Understand the basic physics principles and radiation biology involved in Theranostics. 2) Describe the factors involved in the choice and application of radionuclide therapies, including eligibility for treatment based on patient and tumor factors. 3) Apply the concepts above to currently available radionuclide therapies.

#### TABLE OF CONTENTS/OUTLINE

1) Physics overview of radionuclides used in theranostics: a. Decay pathways of radionuclides used for imaging ( $\gamma$ ,  $\beta^+$  emissions) and therapy ( $\beta^-$  and  $\alpha$  emissions) b. Desirable characteristics of theranostics agents c. Clinical examples of imaging/therapeutic pairs, with the characteristics of radionuclides used (half-life, energies, range, and imaging modality): i.  $^{123}\text{I}$ -MIBG/  $^{131}\text{I}$ -MIBG (Azedra®) ii.  $^{68}\text{Ga}/^{64}\text{Cu}$ -DOTATATE/  $^{177}\text{Lu}$ -DOTATATE (Luthatera®) iii.  $^{68}\text{Ga}$ -PSMA-11/  $^{177}\text{Lu}$ -PSMA-617 (Pluvicto®) iv.  $^{99\text{m}}\text{Tc}$ -MDP/ $^{223}\text{Ra}$  (Xofigo®) 2) Concepts of radiation biology and dosimetry: a. Biological descriptors of uptake pathways and pharmacokinetics b. Types of dosimetry calculation: Tumor, blood and solid organ at risk (OAR) i. MIRD Schema and Voxel Based ii. Generating time activity curves c. Implications on side effects from the therapy 3) Additional factors involved in the choice and application of radionuclide therapies: a. Patient factors: such as clearance rates and baseline function of OAR b. Tumor factors: level of uptake of the therapeutic agent by the tumor, and tumor heterogeneity

Printed on: 02/07/23



## Abstract Archives of the RSNA, 2022

NMMIEE-22

### Towards Structured PET Reporting with PSMA Tracers in Prostate Cancer

Sunday, Nov. 27 8:00AM - 9:00AM Room: Learning Center - NMMI

#### Participants

Patricia Romero Fernandez, MBBS, Madrid, Spain (*Presenter*) Nothing to Disclose

#### TEACHING POINTS

To highlight the importance of having a solo criteria for performance and interpretation of PET-CT images using prostate-specific membrane antigen based tracers  
To discuss the role of different imaging modalities in the biochemical recurrence of prostate cancer  
To distinguish between physiological findings and those that could be consider as positive for prostate cancer recurrence  
To describe 18F-DCFPyL PET-CT findings in our department according to PROMISE system

#### TABLE OF CONTENTS/OUTLINE

-Introduction: generalities, biochemical recurrence definitions, other imaging modalities -Imaging findings characteristics with 18F-DCFPyL-Standardization of PSMA-PET interpretation: Prostate cancer recurrence sites classification PROMISE (Prostate Cancer Molecular Imaging Standardized Evaluation)1/E-PSMA: the EANM standardized reporting guidelines v1.0 for PSMA-PET2: our experience-Conclusions(1) Eiber M, Herrmann K, Calais J, Hadaschik B, Giesel FL, Hartenbach M, Hope T, Reiter R, Maurer T, Weber WA, Fendler WP. Prostate Cancer Molecular Imaging Standardized Evaluation (PROMISE): Proposed mTNM Classification for the Interpretation of PSMA-Ligand PET/CT. J Nucl Med. 2018 Mar;59(3):469-478. doi: 10.2967/jnumed.117.198119. Epub 2017 Nov 9. Erratum in: J Nucl Med. 2018 Jun;59(6):992. PMID: 29123012.(2) Ceci F, Oprea-Lager DE, Emmett L, Adam JA, Bomanji J, Czernin J, Eiber M, Haberkorn U, Hofman M, Hope TA, Kumar R, Rowe SP, Schwarzenboeck SM, Fanti S, Herrmann K. E-PSMA: the EANM standardized reporting guidelines v1.0 for PSMA-PET. Eur J Nucl Med Mol Imaging 2021;48:1626-38. <https://doi.org/10.1007/s00259-021-05245-y>

Printed on: 02/07/23



## Abstract Archives of the RSNA, 2022

NMMIEE-23

### Added Value of FDG-PET/MRI in Gynecologic Oncology: A Pictorial Review

Sunday, Nov. 27 8:00AM - 9:00AM Room: Learning Center - NMMI

#### Awards

Identified for RadioGraphics

Cum Laude

#### Participants

Malak Itani, MD, Saint Louis, MO (*Presenter*) Nothing to Disclose

#### TEACHING POINTS

PET/MRI is becoming increasingly available and provides physiologic information from the PET with accurate localization to high soft-tissue contrast images from MRI. PET/MRI plays an important role in staging and assessing treatment response in patients with uterine, cervical, vulvar and vaginal cancers. PET/MRI has a more limited role in ovarian malignancies but can be used as a problem solving tool in patients with negative CT scan and persistent concern for disease recurrence

#### TABLE OF CONTENTS/OUTLINE

- Review of instrumentation and techniques- Role of FDG PET/MRI in specific malignancies: o Endometrial cancer o Cervical cancer o Ovarian cancer o Vaginal cancer o Vulvar cancer- Future directions

Printed on: 02/07/23



## Abstract Archives of the RSNA, 2022

NMMIEE-24

### First Pass PET Imaging of Various Cardiovascular Disease

Sunday, Nov. 27 8:00AM - 9:00AM Room: Learning Center - NMMI

#### Participants

Takashi Norikane, MD, PhD, Kita-gun, Japan (*Presenter*) Nothing to Disclose

#### TEACHING POINTS

Positron emission tomography (PET) is usually used for evaluating metabolic activity of the cells of body tissues. However, adding first pass PET imaging to standard imaging can provide information about vessel morphology and perfusion. The major teaching points of this exhibit are: 1: Knowledge of technique of first pass PET is important for an alternative imaging to conventional angiography for evaluation of vessels. 2: Knowledge of combination first pass and standard PET imaging provides further findings for radiologists to understand the disease condition accurately.

#### TABLE OF CONTENTS/OUTLINE

Technique List mode dynamic scan in selected region ECG-gated early phase scan Whole body PET angiography using continuous bed motion mode Disease Takayasu arteritis Giant cell arteritis Infectious aortitis Behcet's disease IgG4-related disease Pulmonary arterial venous malformation Pelvic arterial venous malformation Tubulointerstitial nephritis and uveitis Leriche syndrome Carotid artery stenosis Cardiac amyloidosis Constrictive pericarditis

Printed on: 02/07/23



## Abstract Archives of the RSNA, 2022

NMMIEE-25

### Imaging Features of Atypical Thoracic Metastases From Biochemically Recurrent Prostate Adenocarcinoma

Sunday, Nov. 27 8:00AM - 9:00AM Room: Learning Center - NMMI

#### Participants

Hala Khasawneh, MBBS, Rochester, MN (*Presenter*) Nothing to Disclose

#### TEACHING POINTS

Using a case-based approach we will reinforce the following: 1. Treatment advancements and improved patient survival have led to an increase in the frequency of encountering atypical sites of biochemically recurrent (BCR) prostate cancer (PCa) metastasis 2. Novel PET radiotracers including 11C-choline and 68Ga-PSMA have the potential to detect atypical sites of metastases early in the disease course and often at very low PSA levels 3. Multimodality imaging evaluation of atypical sites of tracer uptake is essential for metastasis detection and characterization 4. Information on the site and burden of disease is required for personalized management of BCR PCa 5. Awareness of atypical sites of metastasis is critical given the essential role of radiologists in guiding patient care

#### TABLE OF CONTENTS/OUTLINE

1. Brief overview of BCR in PCa 2. Available imaging modalities used in patients with suspected BCR; Conventional versus PET imaging. 3. PET radiotracers used in early detection of BCR PCa: a) Comparison of available PET radiotracers for imaging of BCR PCa. b) Imaging protocol and patient preparation. c) Normal biodistribution of commonly used PET radiotracers. 4. Metastatic pattern in BCR PCa a) Typical versus atypical metastases sites b) Oligo-metastasis versus widespread disease 5. Case-based review of imaging features for a variety of atypical sites of BCR metastasis in the thorax with multimodality correlation: a) The respiratory system; lungs, pleura, and airways b) Supradiaphragmatic lymph nodes c) Breast metastasis d) Atypical bone metastasis and mimickers 6. Discuss relevant differential diagnosis and potential imaging pitfalls 7. Impact of early BCR localization on clinical management

Printed on: 02/07/23



## Abstract Archives of the RSNA, 2022

NMMIEE-26

### Always Wear Sunscreen: Conventional and Hybrid Imaging of Melanoma

Sunday, Nov. 27 8:00AM - 9:00AM Room: Learning Center - NMMI

#### Participants

Craig Ferguson, BMBS, (*Presenter*) Nothing to Disclose

#### TEACHING POINTS

- To describe the variety of imaging investigations to detect disease extent and evaluate their relative merits and limitations (including ultrasound, CT, MRI and 18F-FDG PET/CT)- To define the rationale of sentinel lymph node biopsy and highlight the benefit of SPECT over conventional planar lymphoscintigraphy for sentinel node localization- To discuss the role of imaging in surveillance and response assessment, and associated challenges relating to novel therapies including immunotherapy- To identify disease mimics that the radiologist must recognize to ensure patients are not inappropriately denied treatment- To highlight the role of MRI in assessing CNS disease, including characteristic imaging appearances and common pitfalls

#### TABLE OF CONTENTS/OUTLINE

Background- Melanoma subtypes (cutaneous and non-cutaneous) including histopathology- Epidemiology, pathogenesis and management- Review of current guidelines relating to imaging workup in melanoma- Lymphoscintigraphy to identify the sentinel node; indications and technique- Role of cross-sectional imaging for initial staging, surveillance and response assessment; focusing on the benefits and limitations of 18F-FDG PET/CT- Top-to-toe review of multimodality imaging throughout a range of organ systems using selected case studies, including atypical presentations, important mimics, and imaging pitfalls

Printed on: 02/07/23



## Abstract Archives of the RSNA, 2022

NMMIEE-27

### Assessment of Response to Androgen Deprivation Therapy in Patients With Metastatic Castration-Resistant or Hormone-Sensitive Prostate Cancer by Radiolabeled Choline PET/CT: A Pictorial Essay

Sunday, Nov. 27 8:00AM - 9:00AM Room: Learning Center - NMMI

#### Participants

Elisabet Vila, (*Presenter*) Nothing to Disclose

#### TEACHING POINTS

This exhibit will:- Review the concept of castration resistant prostate carcinoma (CRPC) and the use of choline PET/CT for response assessment.- Discuss the role of androgen receptor blockers in CRPC, and their mechanism of action.- Present radiological choline PET/CT CRPC cases and their different responses to treatment.- Assess the overall response to therapy and management in patients with CRPC as well as the utility of choline PET/CT in this scenario.

#### TABLE OF CONTENTS/OUTLINE

1. Introduction to prostate cancer  
1.1 Background and epidemiology  
1.2 Clinical Course  
1.3 Imaging findings of prostate cancer recurrence  
1.4 Metastatic Castration Resistant Prostate Carcinoma (mCRPC)  
1.4.1 Definition  
1.4.2 Metastatic spread  
2. Treatment options  
2.1 Androgen receptor blockers (enzalutamide, abiraterone)  
2.2 Chemotherapies (docetaxel)  
2.3 Actual management  
3. Role of Choline PET/CT in the evaluation of tumor response  
3.1 Target and normal distribution of choline  
3.2 Strengths and weaknesses  
3.3 Use of choline PET/CT in mCRPC  
3.4 Pitfalls and artifacts  
4. Presentation of mCRPC cases at our center and evaluation of the response to treatment

Printed on: 02/07/23

## Abstract Archives of the RSNA, 2022

NMMIEE-28

### Nuking Dementia: Adding Some Colour to The Dementia Diagnostic Pathway

Sunday, Nov. 27 8:00AM - 9:00AM Room: Learning Center - NMMI

#### Participants

Peter Jarvis, FRCR, MBBS, Bournemouth, United Kingdom (*Presenter*) Nothing to Disclose

#### TEACHING POINTS

1. Provide an overview of the different molecular imaging techniques, with sample protocols, used in the diagnostic work up of dementia. 2. Appreciate normal images (including typical ageing) and give a strategy to identify the most common dementia subtypes using FDG-PET examples. 3. Overview of the specific role of DaTscan imaging in the diagnosis of Parkinson's disease and Lewy body dementia. 4. Determine which patients would benefit from functional imaging and lay out a suggested diagnostic pathway to be used in conjunction with conventional structural imaging. 5. Explore some of the newer molecular imaging techniques currently in practice and under development.

#### TABLE OF CONTENTS/OUTLINE

\*Aims? \*Background and purpose of nuclear imaging? \*Molecules overexpressed in dementia subtypes? \*Overview of HMPAO SPECT/CT? \*Overview of FDG PET/CT? \*Comparison of HMPAO and FDG PET? \*Statistical parametric mapping? \*Important regions for interpretation? \*Normal images (FDG PET and HMPAO)? \*Normal ageing (FDG PET)? \*FDG PET imaging of dementia subtypes? \*Alzheimer's disease?(typical) \*Mild cognitive impairment? \*Logophenic aphasia \*Posterior cortical atrophy \*Fronto-temporal dementia?(typical) \*Behavioral variant FTD \*Semantic dementia? \*Progressive non-fluent aphasia \*Lewy body dementia? \*Cautions and pitfalls? \*DaTscan?- overview and clinical uses? \*Newer PET imaging agents? \*Amyloid PET? \*Tau PET? \*TSPO PET (neuroinflammation)? \*When functional imaging should be used / pathway? \*Summary? \*References?

Printed on: 02/07/23



## Abstract Archives of the RSNA, 2022

NMMIEE-29

### Practical Overview of I-123 Ioflupane (DaTscan) Imaging for Parkinsonian Syndromes: Clinical Applications Findings and Pitfalls of Interpretation

Sunday, Nov. 27 8:00AM - 9:00AM Room: Learning Center - NMMI

#### Awards

Identified for RadioGraphics

#### Participants

Megan Mercer, MD, Charleston, SC (*Presenter*) Nothing to Disclose

#### TEACHING POINTS

I-123 Ioflupane (DaTscan) imaging is routinely performed in nuclear medicine departments nationwide. The clinical symptoms of Parkinsonian syndromes are not always specific, and radiologists are frequently called upon to help provide a diagnosis. The goal of this exhibit is to provide a focused guide for radiologists on important aspects of patient preparation, protocoling, troubleshooting, interpretation, and reporting of DaTscan imaging, through both a didactic and case-based approach. Multimodality correlation of DaTscan findings with other molecular (FDG PET-CT) and cross-sectional imaging (CT, MRI) is also incorporated.

#### TABLE OF CONTENTS/OUTLINE

1. Introduction 2. Pathophysiology 3. Indications 4. Protocol 5. Patient Preparation 6. Troubleshooting 7. Pitfalls 8. Interpretation 9. Reporting 10. Case examples with multimodality correlation 11. Conclusion.

Printed on: 02/07/23



## Abstract Archives of the RSNA, 2022

NMMIEE-3

### Musculoskeletal Involvement in Oncological Diseases: Strengths and Weaknesses of 18F-FDG- PET/CT

Sunday, Nov. 27 8:00AM - 9:00AM Room: Learning Center - NMMI

#### Participants

Patricia Garcia, MD, PhD, Madrid, Spain (*Presenter*) Nothing to Disclose

#### TEACHING POINTS

-To illustrate the spectrum of hematological diseases and oncological pathologies with musculoskeletal involvement in FDG-PET/CT with histological correlation -To discuss strengths and limitations of FDG-PET/CT in the diagnostic and follow up of these diseases

#### TABLE OF CONTENTS/OUTLINE

FDG-PET/CT is proved to be the best technique for diagnosis and follow up of myeloma and lymphoma. One limitation in these diseases is the diffuse affection of the bone marrow, where there can be false negatives and positives findings. FDG-PET/CT plays also an important role for detection of metastases. FDG uptake alone is not adequate for characterizing primary bone tumors and morphologic evaluation is an important factor in the interpretation of FDG-PET/CT scans. In many cases other imaging studies or biopsy is required for definitive diagnosis. We reviewed the hematological and oncological FDG-PET/CT studies from the last 10 years in two institutions. Regarding the musculoskeletal involvement we divided them in: - Bone lesions: I.e. scapular telangiectatic sarcoma, different patterns of presentation of myeloma, lymphoma, metastases - Soft tissue lesions: I.e. cell T skin lymphoma, cell B lymphoma - Complications: spinal cord compressions and pathological fractures We discuss the actual importance of FDG-PET/CT in each pathology and its limitations.

Printed on: 02/07/23



## Abstract Archives of the RSNA, 2022

NMMIEE-31

### Neoplastic Neurocristopathies in Nuclear Medicine: Embryology, Pathophysiology, and Theranostics

Sunday, Nov. 27 8:00AM - 9:00AM Room: Learning Center - NMMI

#### Participants

Edgar Zamora, MD, (*Presenter*) Nothing to Disclose

#### TEACHING POINTS

Familiarize the reader with neural crest cell (NCC) embryology, pathophysiology of neoplastic neurocristopathies (NCP) and biochemical phenotypes, and the role of nuclear imaging and therapy. The exhibit includes illustrations and cases categorized based on primary NCC lineages involved (i.e., cranial, truncal, vagal, sacral).

#### TABLE OF CONTENTS/OUTLINE

NCCs arise from unfused neural folds, migrate extensively, and differentiate into specialized tissues in multiple systems. Mutations in crucial genes can lead to various neoplasms and dysgenetic conditions, originally presumed unrelated. Neuroblastomas (sympathoadrenal progenitor cells) result from epigenetic alterations (MYCN overexpression) or mutations in key genes (ALK, PHOX2B), while pheochromocytomas/paragangliomas (chromaffin/ chief cells) are more often familial (SDHx, VHL, RET). Targeted imaging can be performed with <sup>123</sup>I-MIBG, and <sup>111</sup>In- or <sup>68</sup>Ga-SSTR binding agents, the latter also available for differentiated NETs. Theranostic  $\beta$ - and  $\gamma$  emitting radiopharmaceuticals are useful in select conditions. Familial syndromes such as NF1 and MEN are associated with various NCPs, such as MTC, pancreatic islet cell tumors, and parathyroid adenomas. Radiolabeled SSTR binding agents can be used for pancreatic islet cell tumors, <sup>18</sup>F-FDG for MTC, and <sup>99m</sup>Tc-Sestamibi for parathyroid adenomas. Other conditions resulting from dysgenesis or abnormal migration/differentiation of NCCs include meningioma, melanoma, and neurocutaneous syndromes. Biochemical phenotypes have an important role in radiopharmaceutical selection. Therefore, understanding the pathophysiology of NCPs is essential for diagnosis and management strategy.

Printed on: 02/07/23

## Abstract Archives of the RSNA, 2022

NMMIEE-32

### PSMA PET/CT: A Pictorial Review of Common Pitfalls in Interpretation

Sunday, Nov. 27 8:00AM - 9:00AM Room: Learning Center - NMMI

#### Participants

Venkata Kal Byrapogu, (*Presenter*) Nothing to Disclose

#### TEACHING POINTS

Our studies indicate that uptake of PSMA by PCa bone metastatic lesions tends to be homogeneous and more intense. In contrast, uptake by other pathologies presented here tend to be heterogenous and less intense.

#### TABLE OF CONTENTS/OUTLINE

Introduction: Prostate cancer (PCa) is the one of the most common cancers affecting men in the United States and worldwide[1]. Advanced PCa presents with bone metastases - most commonly osteoblastic while rarely osteolytic metastases. Accurate and reliable detection of these bone metastases is critical for patient survival as well as for improving patient's quality of life[2]. Technique: Prostate-specific membrane antigen (PSMA) is a cell surface glycoprotein that is predominantly expressed in prostate epithelium, proximal tubules of the kidney, jejunal brush border of the small intestine and ganglia of nervous system[3]. Hence, PSMA can be expressed in benign processes of these tissues, PCa, and other cancers. PCa expresses significantly higher (100x - 1000x) PSMA than normal tissues making PSMA an excellent target for nuclear imaging[4]. PSMA PET/CT technique has emerged as a novel receptor-based imaging technique for whole-body detection of PCa bone metastases[5]. Pathologic Correlation: It is important for radiologists to be aware of false-positives when evaluating PSMA PET/CT studies. In this study, we present examples of false positive uptake in patients with PCa. For comparison, we also present a typical sclerotic bone lesion of PCa. References: 1. Fitzmaurice, C., et al., 2017. 2. Lin, S.C., et al 2018. 3. Chang, S.S., et al., 2004. 4. Evans, J.D., et al., 2018. 5. Rowe, S., et al., 2019. 6. Savir-Baruch, B., et al., 2021.

Printed on: 02/07/23



## Abstract Archives of the RSNA, 2022

NMMIEE-33

### Assessing Tumor Response to Therapy With Hybrid Imaging: Practical Aspects

Sunday, Nov. 27 8:00AM - 9:00AM Room: Learning Center - NMMI

#### Participants

Laith Abandeh, MD, Seattle, WA (*Presenter*) Nothing to Disclose

#### TEACHING POINTS

- Illustrate the primary role of conventional and hybrid imaging in the evaluation of tumor response to treatment.
- Review the general concepts and existing imaging-based criteria for evaluating tumor response to therapy.
- Outline the challenges encountered during tumor response assessment using anatomic imaging/size-based criteria.
- Learn the emerging approaches and challenges in evaluating imaging-based tumor response to immunotherapeutic agents and targeted treatment.
- Outline the synergy between PET and CT to overcome diagnostic challenges and achieve a comprehensive tumor response assessment.

#### TABLE OF CONTENTS/OUTLINE

§ Introduction and U.S Cancer Facts § Treatment Outcome Prediction via Response Monitoring § Cancers Evade Therapy: Mechanisms § Role of Anatomic Imaging - WHO Response Criteria -Limitations -Responses RECIST does not capture § Treatment Monitoring: Role of Hybrid Imaging (Integration of Data) § Practical Use of SUV § Artifacts and Pitfalls § Cases/Examples § Conclusion

Printed on: 02/07/23



## Abstract Archives of the RSNA, 2022

NMMIEE-34

### Expect the Unexpected! Pictorial Review of Acute and Emergent Findings on Oncologic F18-FDG PET/CT

Sunday, Nov. 27 8:00AM - 9:00AM Room: Learning Center - NMMI

#### Participants

Priya Pathak, MBBS,MD, (Presenter) Nothing to Disclose

#### TEACHING POINTS

1. Overview of FDG uptake patterns in commonly encountered oncologic emergencies and non-cancer related acute findings in oncologic patients on F18-FDG PET/CT.2. Encourage identification of key imaging findings based on the attenuation corrected PET images with approach to differential diagnosis.3. Highlight the clinical features, prognosis and treatment options for these entities.4. Provide correlation between PET and anatomic imaging (US/CT/MRI).

#### TABLE OF CONTENTS/OUTLINE

Introduction: Discussion of the following entities with case examples and approach to imaging features. ONCOLOGIC EMERGENCIES AND ACUTE DISORDERS Vascular: SVC syndrome, DVT, Pulmonary embolism CNS: Brain metastasis, Spinal cord compression Chest: Airway obstruction, Pneumonia, Esophagorespiratory fistula, Pericardial effusion tamponade Abdomen Pelvis: Bowel obstruction, Typhilitis, Biliary obstruction, Cholangitis, Pancreatitis, Urinary tract obstruction Treatment related: Intracranial bleed, Pneumothorax, Invasive fungal pneumonia, Drug radiation related pneumonitis, Pericarditis, Pancreatitis, Enterocolitis MSK: Pathological fractures, Radiation osteonecrosis NON-CANCER RELATED ACUTE DISORDERS Vascular: Aortic dissection, Aneurysm, Vasculitis Chest: COVID, Aspiration pneumonitis, Lung abscess, Atrial fibrillation Abdomen: Infective and inflammatory enteritis, Diverticulitis, Appendicitis, Obstructed hernia, Cholecystitis, Hepatic abscess MSK: Discitis, Osteomyelitis, Septic arthritis, AVN, Myositis

Printed on: 02/07/23



## Abstract Archives of the RSNA, 2022

NMMIEE-35

### Gastrointestinal Motility on Nuclear Scintigraphy: Protocols, and Pathologies with Multimodality Correlates

Sunday, Nov. 27 8:00AM - 9:00AM Room: Learning Center - NMMI

#### Awards

Certificate of Merit

Identified for RadioGraphics

#### Participants

Jonathan Revels, DO, Albuquerque, NM (*Presenter*) Nothing to Disclose

#### TEACHING POINTS

Teaching Points 1- Learn the clinical approach and role of radiology in the assessment and management of patients with GI motility disorders. 2- Recognize imaging patterns of normal and abnormal gastric, small bowel, and large bowel motility on nuclear scintigraphy. 3- Learn potential limitations of nuclear medicine examinations for GI motility assessment. 4- Learn the complimentary role nuclear scintigraphy and other radiologic examinations have in evaluation of GI motility disorders.

#### TABLE OF CONTENTS/OUTLINE

1- Introduction a. Review gastrointestinal motility disorder epidemiology and pathophysiology. b. Review the clinical approach to diagnosis of gastric, small bowel, and large bowel dysmotility, and the role of nuclear scintigraphy in evaluation of these patients. 2- Review protocols for gastrointestinal motility patient preparation and evaluation with nuclear scintigraphy. a. Various approaches to gastric emptying studies, and small bowel and large bowel transit studies. b. Briefly review gastric motility assessment in pre and post-operative setting (gastric bypass, colectomy) and following medical therapy (initiation of prokinetic medication). 3- Review how to evaluate GI motility scintigraphy examinations visually and quantitatively. a. Intragastric meal distribution for gastric emptying i. Fundal -vs- antral dysfunction, rapid gastric emptying. b. Quality control of regions of interest and quantitative assessment. 4- Provide case examples of: a. GI dysmotility on nuclear scintigraphy with fluoroscopic, radiographic, and cross-sectional correlates. b. Incidental findings on nuclear scintigraphy with clinical implications (gastroesophageal reflux, hiatal hernia).

Printed on: 02/07/23



## Abstract Archives of the RSNA, 2022

NMMIEE-4

### Triaging Frostbite Injuries with Tc99 MDP Multiphase Imaging

Sunday, Nov. 27 8:00AM - 9:00AM Room: Learning Center - NMMI

#### Participants

Austin Promersberger, Fargo, ND (*Presenter*) Nothing to Disclose

#### TEACHING POINTS

- Extreme cold exposure/frostbite leads to distal arterial vasoconstriction and ischemia.
- Management of frostbite varies widely based on the severity of injury. Treatments range from noninvasive care to catheter directed thrombolytic therapy and amputation.
- Patient selection for invasive frostbite management requires timely decision making.
- NM multiphase Tc99 MDP scintigraphy provides a noninvasive evaluation demarcating viable perfused tissue from ischemic/infarcted tissue.
- MDP imaging can be used to select patients for catheter directed thrombolytic therapy as well as guide amputation planning.

#### TABLE OF CONTENTS/OUTLINE

1. Review the pathophysiology of frostbite and staging classifications. 2. Illustrate utility of early Tc99 MDP multiphase imaging in guiding thrombolytic therapy. 3. Emphasize the use of delayed Tc99 MDP planar imaging and SPECT/CT for assessing depth and extent of infarcted tissue for surgical debridement and amputation. 4. Pictorially review lessons and caveats learned at a level 1 trauma center during algorithmic implementation of MDP frostbite imaging including sequelae of bandaging, early rewarming, and distal digital marker use to improve diagnostic abilities and patient outcome. 5. Provide a detailed protocol for institutional frostbite imaging implementation.

Printed on: 02/07/23



## Abstract Archives of the RSNA, 2022

NMMIEE-5

### Spectrum of Vocal Cord FDG Avidity on 18F-FDG PET/CT: Presentations Causes and Sites of Nerve Injury

Sunday, Nov. 27 8:00AM - 9:00AM Room: Learning Center - NMMI

#### Participants

Reema Goel, MD, (*Presenter*) Nothing to Disclose

#### TEACHING POINTS

Objectives 1. Describe the course of the vagus and recurrent laryngeal nerves. 2. Identify accurate PET/CT signs of unilateral vocal cord paralysis and avoid mimics and pitfalls. 3. Recognize the role of FDG PET/CT in assessing common and uncommon head and neck as well as mediastinal benign and malignant conditions that may lead to vocal cord paralysis as well as its role in evaluating primary vocal cord tumors

#### TABLE OF CONTENTS/OUTLINE

Examples of FDG PET/CT imaging highlighting the following benign and malignant causes of vocal cord paralysis : 1. 1. Masses, tumors compressing vagal nerve/its branches at various levels-at base of the skull, neck, thyroid region, and thoracic cavity especially as the recurrent laryngeal nerve (RLN) loops around the aorta at aorticopulmonary window 2. 2. Surgical interventions (especially thyroid surgery)-It would be highlighted that in the lower neck, the course of the right RLN is more lateral and oblique than the left, making it prone to injury particularly secondary to trauma and surgery, most commonly thyroid dissection. However, the length of the left RLN is at times more than double that of the right RLN causing the left RLN to a higher rate of injury from nontraumatic causes, such as neoplastic infiltration. 3. 3. Being secondary to intubation 4. 4. Viral neuritis and idiopathic/paraneoplastic conditions 5. Additionally examples of role of FDG PET in assessing vocal cord tumors at initial diagnosis and post treatment stage/follow up would also be included.

Printed on: 02/07/23



## Abstract Archives of the RSNA, 2022

NMMIEE-6

### What Do We Know About Emerging Methods for Imaging The Glymphatic System?

Sunday, Nov. 27 8:00AM - 9:00AM Room: Learning Center - NMMI

#### Participants

Yuichi Morita, Bunkyo, Japan (*Presenter*) Nothing to Disclose

#### TEACHING POINTS

The glymphatic system describes the brain perivascular network promoting cerebrospinal and interstitial fluids exchange that facilitates the clearance of solutes and waste from the brain. Dysfunction of the glymphatic system is related to numerous neurological disorders. MRI tracer-based methods have been used to evaluate glymphatic function in humans; however, tracer administration is relatively invasive and limited in its clinical application. Recent studies have showed the potential of structural and diffusion MRI to investigate the glymphatic system non-invasively. The teaching points are: 1. To review the current knowledge of the glymphatic system. 2. To overview invasive and non-invasive methods for imaging the glymphatic system. 3. To introduce clinical applications of glymphatic imaging using MRI.

#### TABLE OF CONTENTS/OUTLINE

1. The description of the glymphatic system hypothesis. 2. Glymphatic imaging methods using tracers (i.e., Gadolinium-based contrast agents and <sup>17</sup>O isotope). 3. Non-invasive glymphatic imaging methods (i.e., perivascular space volumetry, diffusion tensor image analysis along the perivascular space, free water imaging, etc.). 4. Clinical applications of glymphatic imaging methods, including Alzheimer's disease, Parkinson's disease, idiopathic normal pressure hydrocephalus, etc., and the future prospective application.

Printed on: 02/07/23

## Abstract Archives of the RSNA, 2022

NMMIEE-8

### Keep Calm and Image On: Safely Employing PET/CT In Pediatric Malignancies

Sunday, Nov. 27 8:00AM - 9:00AM Room: Learning Center - NMMI

#### Participants

Jaron Hansen, MD, San Antonio, TX (*Presenter*) Nothing to Disclose

#### TEACHING POINTS

1. Learn the oncologic indications for performing PET/CT in pediatric patients  
2. Recognize the normal biodistribution of 18F-FDG in pediatric patients  
3. Present case examples which highlight the utility of pediatric PET/CT in oncologic conditions  
4. Discuss mechanisms for reducing pediatric radiation doses while still obtaining a diagnostic imaging exam

#### TABLE OF CONTENTS/OUTLINE

1. Pediatric oncologic PET/CT  
a. Indications for PET/CT in the work up of pediatric cancer patients  
b. PET radiopharmaceuticals  
i. 18F-FDG in cancer staging and treatment response assessment  
ii. 68Ga-DOTATATE in neuroblastoma and neuroendocrine tumor imaging  
2. Oncologic case examples  
a. Lymphoma  
i. 18F-FDG PET/CT imaging in staging and treatment response assessment  
b. Sarcomas  
i. 18F-FDG PET/CT for staging, treatment response assessment, and PET-guided biopsies  
c. Neural origin tumors  
i. 18F-FDG PET/CT to characterize peripheral nerve sheath tumors  
ii. 68Ga-DOTATATE in neuroblastoma staging  
d. Malignancies associated with congenital syndromes  
i. Using 18F-FDG PET/CT to identify and stage malignancy in cancer predisposition syndromes, including Li Fraumeni and Lynch Syndrome  
3. Pediatric PET/CT scanning considerations  
a. Understanding the balance between dose reduction and high-quality imaging, including the pros and cons of anesthesia and radiation in pediatric patients  
b. Technologies that help reduce dose or scan time for PET/CT scans  
c. Targeting the right PET/CT protocol for the clinical management decision

Printed on: 02/07/23



## Abstract Archives of the RSNA, 2022

NMMIEE-9

### Spectrum of PET Emergent Findings Among Various Radiotracers

Sunday, Nov. 27 8:00AM - 9:00AM Room: Learning Center - NMMI

#### Awards

Certificate of Merit

#### Participants

Hiroaki Takahashi, MD, PhD, Rochester, MN (*Presenter*) Nothing to Disclose

#### TEACHING POINTS

Unexpected emergent findings are occasionally detected on PET. Since PET scans routinely cover almost the entire body, there is a higher probability of incidental emergent findings than focused imaging. However, anatomical assessment is limited on the portion of these exams that are performed primarily for attenuation correction and colocalization of PET findings. While the appearance of emergent findings on FDG PET has been well-documented, reports on these findings as seen with other newly emerging PET radiotracers are scarce. In this exhibit we will present methods to detect the most common emergent diagnostic challenges radiologists will face on PET, focusing on their different appearance on various radiotracers including FDG, Choline, DOTATATE, Ammonia and PSMA. The purposes of this exhibit are: 1. To review varying appearances of incidental emergent conditions detected with different PET radiotracers. 2. To review appropriate management.

#### TABLE OF CONTENTS/OUTLINE

1. Overview of emergent findings on PET. 2. Basic mechanism and imaging of various PET radiotracers. 3. Findings of the emergent abdomen, including diverticulitis, cholecystitis/cholangitis, appendicitis, bowel obstruction, pyelonephritis, and pancreatitis. 4. Findings of the emergent chest, including pulmonary embolism, pneumothorax, and infection including COVID-19. 5. Findings of vascular emergencies, including deep venous thrombus, intramural hematoma, and pseudoaneurysm. 6. Findings of neurological emergencies, including intracranial hemorrhage, and large volume brain metastasis/tumor. 7. Findings of spine and musculoskeletal emergencies, including spinal stenosis, osteomyelitis and unstable fracture.

Printed on: 02/07/23



## Abstract Archives of the RSNA, 2022

NPMEE

### Noninterpretive Education Exhibits

Sunday, Nov. 27 8:00AM - 9:00AM Room: Learning Center - NPM

#### Sub-Events

#### **NPMEE-1 Up the Game for Radiology Education in Medical School: A New Approach Using Virtual Case-based Learning With Resident Mentorship**

Participants

Sagar Wagle, MD, Rochester, MN (*Presenter*) Nothing to Disclose

#### TEACHING POINTS

- Free online curricula combined with guided mentorship by radiology residents can provide a structured educational experience for a week-long medical student radiology rotation, hosted virtually.- Two examples of online curricula, including LearnAbdominal.com and LearningNeuroradiology.com, offer interactive resources such as search-pattern videos and scrollable DICOM cases. - The radiology rotation consisted of initial resident-student meetings, either in person or online, to discuss search patterns and review introductory cases. This was followed by students completing a self-paced curriculum. The resident remained available if students had questions. - The educational experience has several benefits: the students learn basic radiology skills, establish relationships with radiology residents, and are exposed to radiology as a potential career. The residents reinforce teaching skills, and explore interest in academic radiology. - Online curricula with mentorship is a scalable model that can increase access to radiology education, especially in underserved training programs nationally or internationally.

#### TABLE OF CONTENTS/OUTLINE

Rotation outline and structure. Curriculum content examples. Role of the radiology resident mentor. Challenges of implementing an online rotation. Outcomes of the rotation. Medical student and resident feedback. Application of this model for underserved training environments.

#### **NPMEE-10 Beyond the Reading Room: Creating an Engaging Radiology Screening Elective Emphasizing Public Health Principles and Healthcare Disparities**

Awards

**Certificate of Merit**

Participants

Alison Gegios, MD, Whitefish Bay, WI (*Presenter*) Nothing to Disclose

#### TEACHING POINTS

1. Engaging medical students in a radiology screening elective highlighting basic principles of screening and contemporary screening guidelines provides exposure to radiology and the role of radiology in public health. 2. Students embrace novel methods of delivering educational content, such as "enduring learning objects" (i.e. online learning modules) and interactive case sets, in addition to more traditional lectures and reading room observation. 3. Students are motivated to synthesize learned material and create educational content through innovative assignments with an emphasis on public health education and analysis of healthcare disparities.

#### TABLE OF CONTENTS/OUTLINE

(1) How to develop a new course, including designing objectives and key course components: a. Review basics of screening and select most impactful exams to emphasize in the course (e.g., breast, lung, colorectal cancer screening) b. Implement progressive ways of delivering educational content through a flipped classroom model c. Construct novel assessment methods (e.g., infographic presentations) (2) Engagement in and beyond the reading room, including how to create interactive experiences, such as: a. Role-play sessions b. Curated case sets c. Patient experiences in radiology (i.e., image acquisition with technologists, delivering information to patients about next steps) (3) Future goals, including creating an interactive website (4) Analysis of course feedback

#### **NPMEE-11 Challenges and Opportunities in Creating an Interactive Student Focused Radiology Curriculum for Medical Students**

Participants

Danielle Cadoret, BS, (*Presenter*) Nothing to Disclose

#### TEACHING POINTS

Medical school curricula for radiology are not standardized, although some guidelines do exist. As radiology has become more central to the day-to-day practice of clinical medicine, it is critical that this is reflected in how we teach our medical students. If we can produce medical school graduates who are competent and confident in their radiology knowledge base, it will be beneficial both in maintaining the quality of graduates choosing a career in radiology and facilitating communication between radiologists and non-radiologist clinicians going forward. It is the responsibility of the Radiologist to teach these students what we want them to know,

but time is the most precious, limited resource and medical student teaching tends to be the lowest priority for many. However, methods of delivery of education have changed drastically, emphasizing independent active learning, online and in-person. This exhibit will highlight best practices when designing a new medical school radiology curriculum, including high yield core content, teaching modalities used, and interactive delivery strategies tailored to current educational standards. It will also highlight the challenges encountered in this process, and the solutions used to overcome them based on our experience creating a new curriculum at our institution. This exhibit aims to enable fellow radiologists to grow their educational roles expeditiously and in accordance with current best practices in medical education.

#### TABLE OF CONTENTS/OUTLINE

Current standards of medical school radiology curricula. Evolving learning styles. Key considerations in building a new curriculum. Delivery: Interactive, Student focused Online Models. Challenges solutions

### **NPMEE-12 Constructing Clinically Relevant, Indication Driven Reports: An Institutional Web-Based Platform for Musculoskeletal Radiography Reference Materials**

#### **Awards**

##### **Certificate of Merit**

Participants

Blake Bartholomew, MD, (*Presenter*) Nothing to Disclose

#### **TEACHING POINTS**

- An institutional web-based platform provides quick access to musculoskeletal radiography search patterns and reference materials to optimize report dictation.
- Indication and location specific pathology guides with example reports may assist radiology trainees with technical vocabulary development.

#### TABLE OF CONTENTS/OUTLINE

1. Background: a. Novice residents report difficulty with identifying and describing relevant normal and pathologic findings for a given indication. b. A web-based platform has been created at our institution to serve as a comprehensive, easily accessible tool to help users develop indication specific search patterns and the technical vocabulary to create tailored, clinically relevant musculoskeletal radiograph reports. 2. Utility: a. Trainees develop indication specific search patterns. b. Quick access to high-yield example cases, diagrams, and measurement guides to assist with report dictation. 3. Structure: a. Homepage i. Hyperlinks to pages organized by anatomic location and specific pathology. b. Section content i. Review of indication specific search patterns (i.e. trauma, atraumatic pain, post-operative assessment) • Anatomic diagrams • Measurement guides ii. Overview of common pathologic findings and relevant descriptors iii. Case-based review with example reports iv. External links to high-yield resources 4. User data and feedback 5. Conclusion

### **NPMEE-13 Optimising Human Factors to Promote the Learning in Radiology**

Participants

Rachel Magennis, Manchester, United Kingdom (*Presenter*) Nothing to Disclose

#### **TEACHING POINTS**

- The handling of error or discrepancy within radiology departments can have a very negative impact on individuals and the wider team depending on relationships, environment and culture.
- Individuals can feel targeted and unsupported in a process that should be 'safe' and blame free and for the benefit of all reporters.
- We have a unique opportunity in radiology to review scan findings from a given time and consider alternate diagnoses, learn from missed opportunities or celebrate the 'good spots'.
- This allows radiologists to engage in a learning process, outlined by the Royal College of Radiologists, called 'Radiology Events and Learning' or REAL in the UK.

#### TABLE OF CONTENTS/OUTLINE

A better understanding of human factors in the wider healthcare setting has started to impact positively on the culture in many trusts. Human factors and their impact on the well being of staff and on the safety of our patients has also influenced radiology error management in recent years. With the movement away from 'Mistakes meeting' and advent of 'Radiology Events and Learning', the terminology has softened and judgement gone. The focus now is all about the learning and this culture shift has enhanced engagement and participation. 'Good spots' as well as errors and discrepancies are shared anonymously, in a 'safe' environment. With human factors in mind, we have strived to create an environment of psychological safety with anonymous submission of cases and sharing without judgement, for the benefit of all reporters. We highlight how human factors interplay with the process of learning in radiology with reference to the college standards and our own practice.

### **NPMEE-14 A New (Digital) Era in Medical Journalism: Leveraging Social Media and Other Online Tools to Increase Reach and Engagement**

#### **Awards**

##### **Identified for RadioGraphics**

Participants

Katie S. Traylor, DO, Pittsburgh, PA (*Presenter*) Nothing to Disclose

#### **TEACHING POINTS**

1. Social media and other digital tools offer many advantages and opportunities to medical journals with the vision and expertise to leverage them.
2. The purpose of this exhibit is to highlight these advantages from the standpoints of journal editors, authors, and readers, particularly emphasizing ways all stakeholders can benefit

#### TABLE OF CONTENTS/OUTLINE

A. Background/Introduction. 1. Available tools. a. Pros and cons of each. B. Editor Advantages. 1. Expand audience through global reach. a. Increase diversity. b. Bolster pipelines. c. Identify talented and interested individuals for future journal involvement. \*RG Team. d. Tracking metrics. 2. Receive and incorporate reader feedback. 3. Define brand. 4. Altmetrics and article citations. C. Author Advantages. 1. Increased visibility of work. 2. Engage with readers in active discussions. 3. Receive reader feedback to

inform future work. D. Reader Advantages. 1. Ease of access to content for 'on-the-go' consumption. 2. Engage editors and authors in active discussions. 3. Discover opportunities to get involved/volunteer. 4. Low cost (often free). E. How RadioGraphics Does It. 1. Social Media and Digital Innovation Team. a. Article summary tweets. b. Tweetorials. c. Tweet chats. d. Live audio journal discussions. e. #RGphx. 2. Visual abstracts. a. Digital Table of Contents. 3. Podcasts. 4. RadDiscord collaboration.

### **NPMEE-15 Climate Change and Radiology: What Radiologists Need to Know**

Participants

Cameron Nosrat, San Francisco, CA (*Presenter*) Nothing to Disclose

#### **TEACHING POINTS**

1. The health care contribution to overall greenhouse gas emissions in the U.S. was estimated at 10% in 2013, with radiology responsible for a substantial share of carbon footprint. 2. Historically marginalized groups are most vulnerable to impacts of climate change. 3. A strong interrelationship exists between radiology and climate change. Current radiology practices produce excessive waste and energy consumption while the changing climate makes it increasingly more difficult for underserved communities to receive the health care and imaging they need. 4. Solutions addressing climate change and health equity should focus on promoting sustainable radiology practices through education and research.

#### **TABLE OF CONTENTS/OUTLINE**

1. Introduction a. Current climate outlook b. Urgency c. Health care contribution to climate change 2. Impact of radiology on climate change a. Current research on environmental costs of radiology b. Energy cost of imaging modalities c. ACR appropriateness and sustainable alternatives including clinical cases d. Education, policy, and advocacy 3. Impact of climate change on radiology a. Natural disasters b. Supply chain c. Endemic disease patterns d. Disproportionate burden on underserved communities 4. Future directions for institutional initiatives

### **NPMEE-16 A Color Doppler Picture is Worth a Thousand Words**

**Awards**

**Cum Laude**

Participants

Sinan Bana, MD, (*Presenter*) Nothing to Disclose

#### **TEACHING POINTS**

As radiologists' workload increases and the amount of time they have to interpret each study decreases, it can become easy to rely on sonographers' worksheets for most of the findings. Over time, sonographers are reviewing their studies to radiologists less and less, and with the increase in teleradiology across the world, many radiologists don't know the sonographers producing the studies or have a convenient way to contact them with questions about their images or findings. When radiologists choose where to spend their limited time interpreting a Doppler study, they often overlook the color Doppler image that accompanies the spectral Doppler waveform. If the radiologist knows the sonographer well and has proven to be strong, they can more easily overlook this portion of the image. However, if a radiologist doesn't know or trust the sonographers performing the studies they are interpreting, this crucial part of study interpretation cannot be ignored. This exhibit will show many examples of how the color Doppler portion of an image accompanied by a spectral Doppler waveform will tell a very different story than the spectral waveform and bring enhanced awareness of how critically important it is not to overlook these color images and rely solely on the spectral waveform or the sonographers' worksheets.

#### **TABLE OF CONTENTS/OUTLINE**

1. Review proper technical settings for the gray-scale, color Doppler and spectral Doppler waveform images. 2. Show examples of how the color Doppler images tell a different story than the spectral waveform or the sonographers' worksheet. 3. Provide advice on how to handle issues of inconsistency for high quality patient care.

### **NPMEE-17 Pre-med Shadowing: Establishing a Week Long Introductory Experience for College Students Interested in Radiology**

Participants

Matthew Miller, MD, Sewickley, PA (*Presenter*) Editor, Aquifer Inc

#### **TEACHING POINTS**

1. Student interest in a career in radiology will be piqued if opportunities to observe are readily available 2. Establish an organized week long radiology shadowing experience for premedical college students. 3. Create a comprehensive self-learning curriculum for the shadowers. 4. Facilitate a mentorship pipeline through which premedical students and radiologists can collaborate.

#### **TABLE OF CONTENTS/OUTLINE**

1. Pre-medical student timeline a. MCAT and application timing 2. Purposes for establishing a week long organized shadowing experience a. Child labor limitations b. Lack of radiology exposure c. Post-COVID 3. Goals for the week a. Observe the breadth of radiology subspecialties and partake in reading room learning similar to medical student rotators i. Breast ii. Abdominal iii. Musculoskeletal iv. Chest v. Neuro b. Observe specialty "field trips" outside of the reading room i. X-Ray, Mammogram, CT, MRI, Fluoro c. Partake in organized self-learning curriculum i. Recorded lectures ii. Selected readings d. Establish a mentorship pipeline with a few radiologists

### **NPMEE-18 Making Radiology Reports Great Again**

Participants

Uffan Zafar, MBBS, Karachi, Pakistan (*Presenter*) Nothing to Disclose

#### **TEACHING POINTS**

To review the perspectives on reporting styles and fundamentals of concise radiology reporting. Components of the findings and impression sections of radiology reports and underlying concepts. Navigating the use and abuse of perception-related terminology in radiology report. Impact of radiology reports on delivering high quality clinical care. Adapting radiology report to evolving practices

and communication styles in medicine. Exploring the role of artificial intelligence in formulating radiology reports.

#### TABLE OF CONTENTS/OUTLINE

Background Speaking like a radiologist Improving radiology report Differences findings and impression sections Key principles for the findings section Key principles for the impression section Key structural Components of an Impression Radiology report audience and their needs Role of artificial intelligence Summary References Acknowledgements Author information Ethics declaration Rights and permissions Further Reading

#### **NPMEE-19 The Price Is Right...Sometimes: CMS Price Transparency Requirements, Intra-Institutional Inconsistencies in Published Charges, and Imaging Charge Variability**

Participants  
Matthew Petterson, MD, (*Presenter*) Nothing to Disclose

#### TEACHING POINTS

1. Introduce the Centers for Medicare and Medicaid Services hospital price transparency requirements, including the charges which must be made publicly available via chargemasters and consumer-friendly displays. 2. Discuss widespread intra-institutional inconsistency between charges for the same examinations published in chargemasters versus consumer-friendly displays. 3. Highlight the marked heterogeneity in total charges for common imaging examinations across prominent U.S. academic medical centers.

#### TABLE OF CONTENTS/OUTLINE

1. Centers for Medicare and Medicaid Services Price Transparency Rule a. Goals b. Affected institutions c. Required data publication formats i. Chargemasters 1. Required data ii. Consumer-friendly display of shoppable services 1. Required data 2. Mandatory imaging examinations 3. Common consumer-friendly displays d. Penalties 2. Intra-institutional inconsistencies between total charges published in chargemasters and consumer-friendly displays a. Rates and magnitudes b. Other commonly incomplete charge data c. Sources d. Implications for institutions e. Implications for patients 3. Variability in total charges for C.M.S. mandated imaging examinations a. CT i. CPT 70450, 72193, 74177 b. MRI i. CPT 70553, 72148, 73721 c. US i. CPT 76700, 76805, 76830 d. Radiography i. CPT 72110 e. Mammography i. CPT 77065, 77066, 77067

#### **NPMEE-2 How To Develop The Best Radiology Clerkship?: A Guide for Educators**

Participants  
Francisco Garrido Cisterna, MD, Santiago, Chile (*Presenter*) Nothing to Disclose

#### TEACHING POINTS

1. Increasing workload and continued specialization of radiology practice are challenge for medical educators planning in-person activities in the reading room of medical students during their elective radiology clerkships. 2. Radiology clerkships require a structure that will enable the proposed educational goals to be met: known learning objectives, available and user friendly consult materials, feedback sessions and assessment. 3. In the reading room, various educational strategies can be applied such as: patient history review from the EMR, involvement in clinical-radiological discussions, creation of a portfolio of interesting cases, selection of topics based on cases encountered for further presentation in the journal club, among others. 4. Radiology residents may spend more time with medical students that with supervisions fellows or staff radiologists, playing a central role in the overall quality of medical student experience in the reading room. Therefore, they must learn and apply a few teaching techniques specifically for this environment.

#### TABLE OF CONTENTS/OUTLINE

1. Introduction 2. What is the current status in the world? 3. The educational challenge in the reading room 4. What elements do you need to build a clerkship? 5. Teaching and learning methods in the reading room and at home 6. The impact of the residents in the radiology clerkship (resident as teachers) 7. Assessment 8. Conclusions

#### **NPMEE-20 MRI Safety of Commonly Used Implants and Devices: What the Radiologist Needs to Know**

##### **Awards** **Certificate of Merit**

Participants  
Vivek Pai, MBBS, MD, Toronto, Singapore (*Presenter*) Nothing to Disclose

#### TEACHING POINTS

Requests for MRIs in patients with medical and/or surgical devices are frequently encountered in practice. The aims of this exhibit are: 1. To review the concepts of static magnetic fields, gradient fields, and RF pulse with regard to MRI safety 2. To review the concept of Specific Absorption Rate (SAR) and B1+rms 3. To review standard MRI safety terminology 4. To review general guidelines with respect to MRI safety in patients with implants and devices 5. To review the specific MRI safety concerns of the most commonly used devices and implants.

#### TABLE OF CONTENTS/OUTLINE

1. Basic concepts and definitions in MRI safety 2. Review of MRI safety for: a. Deep Brain Stimulators b. Epidural and Peripheral Nerve Catheters c. Spinal Cord Stimulators d. Peripheral Nerve Stimulators e. Cochlear Implants f. Scleral Buckles g. Pacemakers and Defibrillators h. Vascular Stents i. Endoscopic Hemostatic Clips and Video Capsule Endoscopic Recording Devices j. Intrauterine and Fallopian Tube Closure Devices k. Bullets, Shrapnel, and Foreign Metallic Objects.

#### **NPMEE-21HC Fostering Organizational Excellence Through Inclusive Leadership: A Practical Guide for Radiology Leaders**

##### **Awards** **Identified for RadioGraphics**

Participants

Anand Narayan, MD, PhD, Verona, WI (*Presenter*) Nothing to Disclose

#### TEACHING POINTS

- Increasing the diversity of Radiology departments can drive performance by leveraging the collective experiences of different backgrounds, age groups, and genders.
- The potential of diverse teams can only be actualized when team members feel valued, respected, included, confident, and inspired.
- Inclusive work cultures promote innovation, productivity, higher quality decision making, and profitability.
- Inclusive leadership training can provide radiology leaders with tools to foster healthy, diverse and inclusive environments and teams.

#### TABLE OF CONTENTS/OUTLINE

1. Rationale for Inclusive Leadershipa. Backgroundb. Impact of Inclusion on Team Performance2. Inclusive Leadershipa. Inclusive versus Exclusive Leadership Stylesi. Transformative Leadershipii. Transactional Leadershipiii. Authoritarian Leadershipiv. Laissez Faire Leadershipv. Democratic Leadershipvi. Servant Leadershipb. Characteristics of Highly Inclusive Leadersi. Cognizanceii. Curiosityiii. Courageiv. Cultural Intelligencev. Commitmentvi. Collaborationc. Unconscious biasesi. Definitionii. Impact on Decision-Making in the Workplaceiii. Strategies for Reducing Unconscious Biases3. Strategies for Radiology Leadersa. Increase Diversityb. Nurture Authentic, Brave Dialoguec. Inclusive Meetingsd. Transparent Processes for Assignments and Promotione. Foster Community BuildingPlease visit the Learning Center to also view this presentation in hardcopy format.

#### NPMEE-22 Mapping Our Journey Towards Gender-Affirming Imaging Care

Participants

Kristen L. Dean, Boston, MA (*Presenter*) Nothing to Disclose

#### TEACHING POINTS

It is critical for radiology practices to know how to provide a welcoming care environment for gender diverse patients such as transgender patients. We employed a structured patient experience mapping process to identify potential barriers associated with each aspect of the imaging exam. The purpose of this exhibit is: 1. To learn how to provide a safe, affirming, and inclusive environment for transgender patients and their families by understanding the patient journey from their perspective. 2. To describe our 'Gender Diverse Patient Experience' initiative to improve the care journey and support staff in gaining cultural competency.

#### TABLE OF CONTENTS/OUTLINE

1. Mapping the Journey • Potential Scenarios o Transgender male having a transvaginal US o Transgender female having a RUG/VCUG o Transgender male having a mammogram • Step-by-Step • Actions, Motivations, Questions, Barriers • Staff concerns 2. Framework to Map • Patient Journey template • Documentation 3. Key Findings • Causes of Patient Distress • Information Gap • Semblance of Control 4. Informing Improvements • Patient Workflow Across Journey o Patient preparation information o Welcoming greeting: Chosen name, pronouns o History, intake and control forms (sexual orientation, gender identity, sex assigned at birth) o Patient preferences during exam (changing, conversation, students) o Radiology reports use of pronouns • Physical Environment o Affirming inclusive silent indicators (Healthcare Equality Index, Non- Discrimination policy) o Changing rooms, waiting rooms restrooms o Reflect across online environment touchpoints • Awareness, Education Training o Experiential, safe to make mistakes, multi-pronged o Culturally competent workforce

#### NPMEE-23 International Medical Graduates: A Primer for Program Directors

Participants

Jose Armando Rodriguez Hernandez, MD, Tegucigalpa, Honduras (*Presenter*) Nothing to Disclose

#### TEACHING POINTS

1. Define International Medical Graduates (IMG)2. Understand composition and historic trends of IMGs in the U.S. medical and radiology workforce3. Discuss the steps IMGs need to take to be eligible to apply to residency positions in the U.S.4. Recognize common misconceptions IMGs face in the interview trail5. Recognize attributes IMGs bring to the U.S. healthcare system

#### TABLE OF CONTENTS/OUTLINE

1. Define International Medical Graduateso US-citizens IMGo Non-US citizens IMG2. IMG composition and trends in the U.S. medical and radiology workforce3. Steps IMG need to take to apply to a residency position in the U.S.o Medical school requirements (established by the Educational Commission for Foreign Medical Graduates, or ECFMG)o Application for ECFMG certificationo Examination requirements Medical education credential requirements4. Common misconceptions IMG face in the interview trailo Medical schools unknown to selection committeeso "Gap" years from graduation for non-US IMGs, commonly spent on:Mandatory service at their home countryClinical and research rotations in the U.S.Preparing for USMLE examsApplying for ECFMG certificationo English language proficiencyo Understanding of the U.S. medical systemo Difficulty acquiring visas5. Attributes IMG bring to the U.S. healthcare systemo Diverse medical and cultural backgroundso Contribute to peers' cultural competencyo Fluency in multiple languageso Experience working unsupervised as primary care providers

#### NPMEE-24 Avenues Of Advocacy For Healthcare Disparities In Breast Imaging

Participants

Connie Ge, (*Presenter*) Nothing to Disclose

#### TEACHING POINTS

- Understand how healthcare disparities (HCD) affect morbidity and mortality in breast cancer- Identify 3 domains of HCD advocacy in breast imaging (Patient centeredness, Imaging processes, Healthcare systems)- Examine the literature on efforts to address each of these domains- Apply this knowledge to problem solving in real-life patient vignettes.

#### TABLE OF CONTENTS/OUTLINE

- Background and objectives- Overview of literature examining HCD in context of breast imaging- Overview of 3 domains of HCD advocacy in breast imaging1. Patient centeredness--Patient education--Patient-centered reporting and guidelines--Cultural competency training and diversification of workforce--Language accessibility2. Imaging processes--R-Scan--ACR Select--Tools to examine data through lens of health equity3. Healthcare systems--Structural barriers to accessing care--Targeted outreach efforts for specific vulnerable populations--Collaboration with local organizations- Patient vignettes with guided brainstorming- Conclusions

## **NPMEE-25 What Radiologists Need to Know About Workplace Ergonomics**

Participants

Tyler Yan, MD, (*Presenter*) Nothing to Disclose

### **TEACHING POINTS**

- Substantial workstation-related MSK discomfort is experienced by Canadian radiologists
- Adjustable furniture is not often available or used
- Provision of adjustable equipment is an important component in the creation of accessible and inclusive radiology departments
- There is great opportunity to improve the wellbeing and productivity of radiologists and trainees by addressing workstation ergonomics

### **TABLE OF CONTENTS/OUTLINE**

- Why workstation ergonomics are important in radiology
- We use workstations all day (and night)
- Many workstations are shared
- Workstations are often not fully adjustable
- Musculoskeletal (MSK) discomfort can affect productivity
- Increased knowledge of ergonomics is associated with decreased likelihood of MSK discomfort
- Optimal workstation ergonomics
- Shoulders and arms are relaxed
- Monitor is at arm's length with top of screen at eye level
- Wrists are relatively flat
- Elbows at 90degrees
- Feet flat on floor/footstool
- Chair with lumbar support
- Substantial workstation-related MSK discomfort in radiologists
- Impact on productivity
- Requires symptom management
- Radiologists have limited ergonomic knowledge
- Recommendations to Radiology Departments
- Provide ergonomics training and ergonomics evaluation
- Provide adjustable equipment
- Recommendations to Radiologists and Trainees
- Advocate for inclusive workplace
- Make adjustments before using shared workstation (when possible)

## **NPMEE-26 A Guide to Using YouTube Live for Radiology Education**

Participants

Lilly Kauffman, BA, (*Presenter*) Nothing to Disclose

### **TEACHING POINTS**

- YouTube Live is the most popular streaming platform on social media-
- Livestreaming is a way to reach and interact with a large audience for radiology education-
- There are several advantages, including interactivity and analytics, that come with YouTube Live-
- However there are also disadvantages, such as limited streaming abilities within the YouTube platform

### **TABLE OF CONTENTS/OUTLINE**

1. Understanding YouTube Live
- 1a. YouTube Live Statistics
- 2a. How to create a YouTube Live segment
2. Our experience
3. The pros of using YouTube Live
4. The drawbacks of using YouTube Live

## **NPMEE-27 Next Level Cases: Strategies for Creating Dynamic and Interactive Radiology Presentations**

Participants

Lucas Aronson, BS, Madison, WI (*Presenter*) Nothing to Disclose

### **TEACHING POINTS**

- (1) Traditional radiology presentations rely on a few images of cross-sectional studies rather than scrollable images. While this is more efficient for content delivery, this can decrease learner engagement and emphasizes the "classic" appearance of diseases.
- (2) There are several techniques and tools to boost interaction and integrate scrollable cross-sectional imaging in radiology presentations. These help facilitate a diagnostic simulation environment and provide a stronger bridge to making independent diagnoses.
- (3) Interactive and scrollable cases permit the teacher to more confidently teach complex pathologies that do not display well in a few-image presentation.
- (4) Interactive presentations create more flexibility in teaching methods, including flipped-model, group work, and learner-directed exploration of topics.
- (5) Interactive presentations can reach a broader variety of learners, as individuals can approach the material from their current skill set and are not confined by a few-image presentation of pathology.

### **TABLE OF CONTENTS/OUTLINE**

- (1) Limitations of traditional presentations
- (1a) Use of single images from cross-sectional studies
- (1b) Reduced interactivity
- (1c) Selection biased toward "Aunt Minnie" images
- (1d) Barriers for teaching complex topics
- (2) How to make presentations more engaging and dynamic
- (2a) Include scrollable cross-sectional imaging
- (2b) Utilize links for multiple choice questions
- (2c) Implement polling software for group engagement
- (2d) Toggle annotations with links
- (2e) Zoom into regions of interest with hover-links

## **NPMEE-3 Immersive Imaging: Structure and Outcomes from a Novel One-year Medical Student Fellowship in Radiology**

Participants

Sohum D. Patel, BA, White River Junction, VT (*Presenter*) Nothing to Disclose

### **TEACHING POINTS**

1. Identify challenges to medical student recruitment/engagement with radiology given the conventional clerkship framework.
2. Describe our institution's novel medical student fellowship in radiology.
3. Analyze outcome metrics from past fellows, including specialty choice influence, perceived educational utility, and contribution to professional development.
4. Summarize resident and faculty perceptions of adding a medical student fellow and its effect on clinical workflow.
5. Explore potential future directions of immersive radiology experiences.

### **TABLE OF CONTENTS/OUTLINE**

Introduction- Limitations of current student engagement strategies in radiology- Current state of affairs for radiology recruitment

The Robert Jeffery Medical Student Fellowship in Radiology

1. Fellowship overview - History, philosophy, and structure - Responsibilities and opportunities
2. Outcomes: Perspectives from Prior Fellows - Preparedness for rotations, internship, and residency - Perceived importance for residency application - Mentorship, advising, and professional development
3. Outcomes: Perspectives from Radiology Residents Faculty - Perceived contribution to workflow and department
4. Challenges
5. The Road Ahead - Plans for future fellowships - Considerations for implementation at other institutions

Conclusion: Student fellowships in radiology provide an incredible opportunity to both students and the department to recruit and train future radiologists.

## **NPMEE-4 Global Learning Centers: Sustainable and Impactful Radiology Outreach**

### Participants

Sucari Vlok, MBChB, MMed, Tygerberg, South Africa (*Presenter*) Nothing to Disclose

### TEACHING POINTS

- Evolution in radiology education and outreach
- Power of conceptual thinking
- Beauty of collaboration and ability to listen

### TABLE OF CONTENTS/OUTLINE

• Introduction o Previously the RSNA relied on the International Visiting Program (IVP) for international outreach. o In 2018, the RSNA board re-envisioned the IVP, and the Global Learning Centers (GLC) were birthed. • Planning phase o Stellenbosch University/Tygerberg Hospital was chosen as the inaugural GLC program. A curriculum was derived from perceived greatest areas of need. • Implementation phase o The COVID pandemic struck as the first RSNA team was preparing an on-site visit. It forced the program to pivot to an online curriculum, utilizing the RSNA's considerable back catalog of lecture material from annual meetings. • Online continuing education phase o RSNA Department of Education staff curated online content into course modules. An online classroom and ultrasound facilities for distance-based teaching were installed. • Exit phase o The GLC will be implemented over a three-year period, but relationships and collaboration will hopefully endure long after and ascertain sustainability of the program. • Conclusion o The COVID pandemic forced us all to conceptualize new ways of thinking, planning and learning. o The board of RSNA Radiologists' rich history of visionary thinking transformed and led Radiology from its inception to where we are today.

## **NPMEE-5 Nothing Humerus About it: Recognizing, Preventing and Treating Radiologist Elbow**

### Participants

Kathleen MacMillan, PharmD, (*Presenter*) Nothing to Disclose

### TEACHING POINTS

1. Lateral epicondylitis is an overuse injury related to wrist extension and is commonly known as tennis elbow. 2. Due to wrist positioning during computer-mouse related work, radiologists are at risk of occupational lateral epicondylitis, "radiologist elbow". 3. Lateral epicondylitis can usually be diagnosed clinically, but ultrasound or MRI may be helpful to confirm the diagnosis and to determine the severity of tendinopathy or tearing. 4. Prevention of lateral epicondylitis centers on reduction of wrist extension. For radiologists this includes supports for the forearm, use of a vertical mouse, and use of voice recognition software where possible. 5. Treatment of lateral epicondylitis can include rest, ice, therapeutic ultrasound interventions, physiotherapy, NSAIDs, corticosteroid injections, or surgery.

### TABLE OF CONTENTS/OUTLINE

1. Detailed explanation of the anatomy and pathophysiology of lateral epicondylitis in computer-users focusing on specific occupational risks of radiologists. 2. Review the symptoms of lateral epicondylitis, clinical diagnostic criteria, and typical diagnostic imaging findings. 3. Using a structured literature review, summarize evidence-based recommendations to prevent radiologist elbow. Explain the ergonomic basis of the interventions. 4. Provide recommendations to reduce and treat associated symptoms in radiologists.

## **NPMEE-6 Magnetic Resonance Nail Evaluation With The Use Of Conductive Gel: Technical and Clinical Aspects**

### Participants

Paula Lucio, MSc, (*Presenter*) Nothing to Disclose

### TEACHING POINTS

- To review clinical aspects of MRI nail evaluation. - To summarize main challenges related to MRI nail evaluation, including patient positioning, image quality and technical factors that undermine the individualization of structures and possible alterations. - To discuss the importance of conductive gel using illustrative and comparative cases. - To discuss other technical factors that impact in imaging quality using illustrative and comparative cases, including the use of the coilLoop Small-Siemens®.

### TABLE OF CONTENTS/OUTLINE

1. Clinical indications of nail evaluation of fingers and pododactyls by Magnetic Resonance a. Suspected retronychia b. Suspected ligament injury c. Suspected tumor d. Trauma e. Infectious/inflammatory processes 2. Use on the finger and glove to apply the conductive gel. 3. Positioning for fingers and pododactyls. 4. How the structures and conductive gel appear on T2 images with FAT and T1. 5. Use of the coil Loop Small-Siemens® and image quality. 6. Take home messages.

## **NPMEE-7 What Radiologists Need to Know About Gender-Inclusive Naming**

### Participants

Tyler Yan, MD, (*Presenter*) Nothing to Disclose

### TEACHING POINTS

• Transgender individuals experience significant inequalities in radiology • Using gender-inclusive terminology is one of many ways to combat structural stigma • Barriers to gender-inclusive naming include the lack of provider education, departmental equity, diversity, and inclusion (EDI) committees, and public online presence of EDI efforts • Individual and systems level strategies exist to promote transgender inclusivity in radiology.

### TABLE OF CONTENTS/OUTLINE

• Why transgender inclusivity is important in radiology Transgender individuals face numerous inequalities in medicine Inequalities faced in radiology departments specifically Downstream detrimental effects, like suicide risk • Example of inclusive practice: fellowship naming Importance of gender-inclusive naming Current landscape of naming in Canada and the United States Gender-inclusive naming among continuing medical education (CME) courses • Barriers to gender-inclusive naming Current landscape of departmental EDI committees, EDI CME courses • Recommendations to individuals Importance of patient names and pronouns; provider normalizing practice too Provider self-education Recognizing unconscious biases • Recommendations to radiology departments Advocate for gender-inclusive naming of fellowships and CME courses Establish departmental committees, EDI training Increasing public visibility of EDI efforts

## **NPMEE-8    Microaggressions With a Macro-Impact: What the Radiologist Needs to Know About Microaggressions**

Participants

Sheikh Ahmed, BSc, MD, (*Presenter*) Nothing to Disclose

### **TEACHING POINTS**

By reviewing the definitions of microaggressions and their impact in radiology, the learner will be able to: 1. Define and identify microaggressions and their subtypes 2. Recognize the impact of microaggressions in medicine and radiology 3. Recognize the link between microaggressions and challenges of developing diversity in radiology 4. Employ strategies to combat and address microaggressions

### **TABLE OF CONTENTS/OUTLINE**

1. Introduction - Definitions of Microaggressions 2. Micro-insults - Definitions and Examples 3. Micro-invalidation- Definitions and Examples 4. Micro-assault- Definitions and Examples 5. Microaggressions as a negative determinant of diversity in medicine and radiology - literature examples 6. Gender-based microaggressions as a negative predictor of diversity in radiology and contributor to the "leaky pipe" concept 7. How to combat microaggressions - strategies and applications to training programs and departments

## **NPMEE-9    A Program Director's Guide to Recruiting for Excellence and Diversity**

Participants

Mai A. Elezaby, MD, Madison, WI (*Presenter*) Investigator, Exact Sciences Corporation; Research Grant, Exact Sciences Corporation

### **TEACHING POINTS**

The average percentage of female radiology residents remains at 26-27% despite improvement and equity in medical school applicants. Several reported factors accounting for fewer female applicants to Radiology include perceived lack of patient contact, lack of female role models, paucity of females in leadership positions and hostile work environment. A diverse healthcare team with parity in gender representation provides more opportunities for success and improved patient care. This presentation describes best practices for residency recruitment to achieve excellence and diversity using examples from a Midwestern Academic Radiology Residency program's experience with standardized virtual recruitment strategies.

### **TABLE OF CONTENTS/OUTLINE**

I. Current Radiology Residency Recruitment Data in the U.S. II. Outline of a Standardized Recruitment Process to increase Diversity  
a. Building a diverse search committee b. Recruiting a pool of highly qualified, diverse candidates c. Strategies to mitigate unconscious bias d. Tenants of holistic review process e. Standardized behavioral questions III. How to leverage virtual interviews to increase Diversity IV. Future proposals for residency interviews and potential pitfalls

Printed on: 02/07/23



## Abstract Archives of the RSNA, 2022

NPMEE-1

### Up the Game for Radiology Education in Medical School: A New Approach Using Virtual Case-based Learning With Resident Mentorship

Sunday, Nov. 27 8:00AM - 9:00AM Room: Learning Center - NPM

#### Participants

Sagar Wagle, MD, Rochester, MN (*Presenter*) Nothing to Disclose

#### TEACHING POINTS

- Free online curricula combined with guided mentorship by radiology residents can provide a structured educational experience for a week-long medical student radiology rotation, hosted virtually.- Two examples of online curricula, including LearnAbdominal.com and LearningNeuroradiology.com, offer interactive resources such as search-pattern videos and scrollable DICOM cases. - The radiology rotation consisted of initial resident-student meetings, either in person or online, to discuss search patterns and review introductory cases. This was followed by students completing a self-paced curriculum. The resident remained available if students had questions. - The educational experience has several benefits: the students learn basic radiology skills, establish relationships with radiology residents, and are exposed to radiology as a potential career. The residents reinforce teaching skills, and explore interest in academic radiology. - Online curricula with mentorship is a scalable model that can increase access to radiology education, especially in underserved training programs nationally or internationally.

#### TABLE OF CONTENTS/OUTLINE

Rotation outline and structure. Curriculum content examples. Role of the radiology resident mentor. Challenges of implementing an online rotation. Outcomes of the rotation. Medical student and resident feedback. Application of this model for underserved training environments.

Printed on: 02/07/23



## Abstract Archives of the RSNA, 2022

NPMEE-10

### Beyond the Reading Room: Creating an Engaging Radiology Screening Elective Emphasizing Public Health Principles and Healthcare Disparities

Sunday, Nov. 27 8:00AM - 9:00AM Room: Learning Center - NPM

#### Awards

Certificate of Merit

#### Participants

Alison Gegios, MD, Whitefish Bay, WI (*Presenter*) Nothing to Disclose

#### TEACHING POINTS

1. Engaging medical students in a radiology screening elective highlighting basic principles of screening and contemporary screening guidelines provides exposure to radiology and the role of radiology in public health. 2. Students embrace novel methods of delivering educational content, such as "enduring learning objects" (i.e. online learning modules) and interactive case sets, in addition to more traditional lectures and reading room observation. 3. Students are motivated to synthesize learned material and create educational content through innovative assignments with an emphasis on public health education and analysis of healthcare disparities.

#### TABLE OF CONTENTS/OUTLINE

(1) How to develop a new course, including designing objectives and key course components: a. Review basics of screening and select most impactful exams to emphasize in the course (e.g., breast, lung, colorectal cancer screening) b. Implement progressive ways of delivering educational content through a flipped classroom model c. Construct novel assessment methods (e.g., infographic presentations) (2) Engagement in and beyond the reading room, including how to create interactive experiences, such as: a. Role-play sessions b. Curated case sets c. Patient experiences in radiology (i.e., image acquisition with technologists, delivering information to patients about next steps) (3) Future goals, including creating an interactive website (4) Analysis of course feedback

Printed on: 02/07/23



## Abstract Archives of the RSNA, 2022

NPMEE-11

### Challenges and Opportunities in Creating an Interactive Student Focused Radiology Curriculum for Medical Students

Sunday, Nov. 27 8:00AM - 9:00AM Room: Learning Center - NPM

#### Participants

Danielle Cadoret, BS, (*Presenter*) Nothing to Disclose

#### TEACHING POINTS

Medical school curricula for radiology are not standardized, although some guidelines do exist. As radiology has become more central to the day-to-day practice of clinical medicine, it is critical that this is reflected in how we teach our medical students. If we can produce medical school graduates who are competent and confident in their radiology knowledge base, it will be beneficial both in maintaining the quality of graduates choosing a career in radiology and facilitating communication between radiologists and non-radiologist clinicians going forward. It is the responsibility of the Radiologist to teach these students what we want them to know, but time is the most precious, limited resource and medical student teaching tends to be the lowest priority for many. However, methods of delivery of education have changed drastically, emphasizing independent active learning, online and in-person. This exhibit will highlight best practices when designing a new medical school radiology curriculum, including high yield core content, teaching modalities used, and interactive delivery strategies tailored to current educational standards. It will also highlight the challenges encountered in this process, and the solutions used to overcome them based on our experience creating a new curriculum at our institution. This exhibit aims to enable fellow radiologists to grow their educational roles expeditiously and in accordance with current best practices in medical education.

#### TABLE OF CONTENTS/OUTLINE

Current standards of medical school radiology curricula. Evolving learning styles. Key considerations in building a new curriculum. Delivery: Interactive, Student focused Online Models. Challenges solutions

Printed on: 02/07/23



## Abstract Archives of the RSNA, 2022

NPMEE-12

### Constructing Clinically Relevant, Indication Driven Reports: An Institutional Web-Based Platform for Musculoskeletal Radiography Reference Materials

Sunday, Nov. 27 8:00AM - 9:00AM Room: Learning Center - NPM

#### Awards

**Certificate of Merit**

#### Participants

Blake Bartholomew, MD, (*Presenter*) Nothing to Disclose

#### TEACHING POINTS

- An institutional web-based platform provides quick access to musculoskeletal radiography search patterns and reference materials to optimize report dictation.
- Indication and location specific pathology guides with example reports may assist radiology trainees with technical vocabulary development.

#### TABLE OF CONTENTS/OUTLINE

1. Background: a. Novice residents report difficulty with identifying and describing relevant normal and pathologic findings for a given indication. b. A web-based platform has been created at our institution to serve as a comprehensive, easily accessible tool to help users develop indication specific search patterns and the technical vocabulary to create tailored, clinically relevant musculoskeletal radiograph reports. 2. Utility: a. Trainees develop indication specific search patterns. b. Quick access to high-yield example cases, diagrams, and measurement guides to assist with report dictation. 3. Structure: a. Homepage i. Hyperlinks to pages organized by anatomic location and specific pathology. b. Section content i. Review of indication specific search patterns (i.e. trauma, atraumatic pain, post-operative assessment) • Anatomic diagrams • Measurement guides ii. Overview of common pathologic findings and relevant descriptors iii. Case-based review with example reports iv. External links to high-yield resources 4. User data and feedback 5. Conclusion

Printed on: 02/07/23



## Abstract Archives of the RSNA, 2022

NPMEE-13

### Optimising Human Factors to Promote the Learning in Radiology

Sunday, Nov. 27 8:00AM - 9:00AM Room: Learning Center - NPM

#### Participants

Rachel Magennis, Manchester, United Kingdom (*Presenter*) Nothing to Disclose

#### TEACHING POINTS

- The handling of error or discrepancy within radiology departments can have a very negative impact on individuals and the wider team depending on relationships, environment and culture.
- Individuals can feel targeted and unsupported in a process that should be 'safe' and blame free and for the benefit of all reporters.
- We have a unique opportunity in radiology to review scan findings from a given time and consider alternate diagnoses, learn from missed opportunities or celebrate the 'good spots'.
- This allows radiologists to engage in a learning process, outlined by the Royal College of Radiologists, called 'Radiology Events and Learning' or REAL in the UK.

#### TABLE OF CONTENTS/OUTLINE

A better understanding of human factors in the wider healthcare setting has started to impact positively on the culture in many trusts. Human factors and their impact on the well being of staff and on the safety of our patients has also influenced radiology error management in recent years. With the movement away from 'Mistakes meeting' and advent of 'Radiology Events and Learning', the terminology has softened and judgement gone. The focus now is all about the learning and this culture shift has enhanced engagement and participation. 'Good spots' as well as errors and discrepancies are shared anonymously, in a 'safe' environment. With human factors in mind, we have strived to create an environment of psychological safety with anonymous submission of cases and sharing without judgement, for the benefit of all reporters. We highlight how human factors interplay with the process of learning in radiology with reference to the college standards and our own practice.

Printed on: 02/07/23



## Abstract Archives of the RSNA, 2022

NPMEE-14

### A New (Digital) Era in Medical Journalism: Leveraging Social Media and Other Online Tools to Increase Reach and Engagement

Sunday, Nov. 27 8:00AM - 9:00AM Room: Learning Center - NPM

#### Awards

Identified for RadioGraphics

#### Participants

Katie S. Traylor, DO, Pittsburgh, PA (*Presenter*) Nothing to Disclose

#### TEACHING POINTS

1. Social media and other digital tools offer many advantages and opportunities to medical journals with the vision and expertise to leverage them. 2. The purpose of this exhibit is to highlight these advantages from the standpoints of journal editors, authors, and readers, particularly emphasizing ways all stakeholders can benefit

#### TABLE OF CONTENTS/OUTLINE

A. Background/Introduction. 1. Available tools. a. Pros and cons of each. B. Editor Advantages. 1. Expand audience through global reach. a. Increase diversity. b. Bolster pipelines. c. Identify talented and interested individuals for future journal involvement. \*RG Team. d. Tracking metrics. 2. Receive and incorporate reader feedback. 3. Define brand. 4. Altmetrics and article citations. C. Author Advantages. 1. Increased visibility of work. 2. Engage with readers in active discussions. 3. Receive reader feedback to inform future work. D. Reader Advantages. 1. Ease of access to content for 'on-the-go' consumption. 2. Engage editors and authors in active discussions. 3. Discover opportunities to get involved/volunteer. 4. Low cost (often free). E. How RadioGraphics Does It. 1. Social Media and Digital Innovation Team. a. Article summary tweets. b. Tweetorials. c. Tweet chats. d. Live audio journal discussions. e. #RGphx. 2. Visual abstracts. a. Digital Table of Contents. 3. Podcasts. 4. RadDiscord collaboration.

Printed on: 02/07/23



## Abstract Archives of the RSNA, 2022

NPMEE-15

### Climate Change and Radiology: What Radiologists Need to Know

Sunday, Nov. 27 8:00AM - 9:00AM Room: Learning Center - NPM

#### Participants

Cameron Nosrat, San Francisco, CA (*Presenter*) Nothing to Disclose

#### TEACHING POINTS

1. The health care contribution to overall greenhouse gas emissions in the U.S. was estimated at 10% in 2013, with radiology responsible for a substantial share of carbon footprint.2. Historically marginalized groups are most vulnerable to impacts of climate change.3. A strong interrelationship exists between radiology and climate change. Current radiology practices produce excessive waste and energy consumption while the changing climate makes it increasingly more difficult for underserved communities to receive the health care and imaging they need.4. Solutions addressing climate change and health equity should focus on promoting sustainable radiology practices through education and research.

#### TABLE OF CONTENTS/OUTLINE

1. Introduction a. Current climate outlook b. Urgency c. Health care contribution to climate change2. Impact of radiology on climate change a. Current research on environmental costs of radiology b. Energy cost of imaging modalities c. ACR appropriateness and sustainable alternatives including clinical cases d. Education, policy, and advocacy3. Impact of climate change on radiology a. Natural disasters b. Supply chain c. Endemic disease patterns d. Disproportionate burden on underserved communities4. Future directions for institutional initiatives

Printed on: 02/07/23



## Abstract Archives of the RSNA, 2022

NPMEE-16

### A Color Doppler Picture is Worth a Thousand Words

Sunday, Nov. 27 8:00AM - 9:00AM Room: Learning Center - NPM

#### Awards

Cum Laude

#### Participants

Sinan Bana, MD, (*Presenter*) Nothing to Disclose

#### TEACHING POINTS

As radiologists' workload increases and the amount of time they have to interpret each study decreases, it can become easy to rely on sonographers' worksheets for most of the findings. Over time, sonographers are reviewing their studies to radiologists less and less, and with the increase in teleradiology across the world, many radiologists don't know the sonographers producing the studies or have a convenient way to contact them with questions about their images or findings. When radiologists choose where to spend their limited time interpreting a Doppler study, they often overlook the color Doppler image that accompanies the spectral Doppler waveform. If the radiologist knows the sonographer well and has proven to be strong, they can more easily overlook this portion of the image. However, if a radiologist doesn't know or trust the sonographers performing the studies they are interpreting, this crucial part of study interpretation cannot be ignored. This exhibit will show many examples of how the color Doppler portion of an image accompanied by a spectral Doppler waveform will tell a very different story than the spectral waveform and bring enhanced awareness of how critically important it is not to overlook these color images and rely solely on the spectral waveform or the sonographers' worksheets.

#### TABLE OF CONTENTS/OUTLINE

1. Review proper technical settings for the gray-scale, color Doppler and spectral Doppler waveform images. 2. Show examples of how the color Doppler images tell a different story than the spectral waveform or the sonographers' worksheet. 3. Provide advice on how to handle issues of inconsistency for high quality patient care.

Printed on: 02/07/23



## Abstract Archives of the RSNA, 2022

NPMEE-17

### Pre-med Shadowing: Establishing a Week Long Introductory Experience for College Students Interested in Radiology

Sunday, Nov. 27 8:00AM - 9:00AM Room: Learning Center - NPM

#### Participants

Matthew Miller, MD, Sewickley, PA (*Presenter*) Editor, Aquifer Inc

#### TEACHING POINTS

1. Student interest in a career in radiology will be piqued if opportunities to observe are readily available  
2. Establish an organized week long radiology shadowing experience for premedical college students.  
3. Create a comprehensive self-learning curriculum for the shadowers.  
4. Facilitate a mentorship pipeline through which premedical students and radiologists can collaborate.

#### TABLE OF CONTENTS/OUTLINE

1. Pre-medical student timelinea. MCAT and application timing  
2. Purposes for establishing a week long organized shadowing experiencea. Child labor limitationsb. Lack of radiology exposurec. Post-COVID  
3. Goals for the weeka. Observe the breadth of radiology subspecialties and partake in reading room learning similar to medical student rotatorsi. Breastii. Abdominaliii. Musculoskeletaliv. Chestv. Neurob. Observe specialty "field trips" outside of the reading roomi. X-Ray, Mammogram, CT, MRI, Fluoroc. Partake in organized self-learning curriculumi. Recorded lecturesii. Selected readingsd. Establish a mentorship pipeline with a few radiologists

Printed on: 02/07/23



## Abstract Archives of the RSNA, 2022

NPMEE-18

### Making Radiology Reports Great Again

Sunday, Nov. 27 8:00AM - 9:00AM Room: Learning Center - NPM

#### Participants

Uffan Zafar, MBBS, Karachi, Pakistan (*Presenter*) Nothing to Disclose

#### TEACHING POINTS

To review the perspectives on reporting styles and fundamentals of concise radiology reporting. Components of the findings and impression sections of radiology reports and underlying concepts. Navigating the use and abuse of perception-related terminology in radiology report. Impact of radiology reports on delivering high quality clinical care. Adapting radiology report to evolving practices and communication styles in medicine. Exploring the role of artificial intelligence in formulating radiology reports.

#### TABLE OF CONTENTS/OUTLINE

Background Speaking like a radiologist Improving radiology report Differences findings and impression sections Key principles for the findings section Key principles for the impression section Key structural Components of an Impression Radiology report audience and their needs Role of artificial intelligence Summary References Acknowledgements Author information Ethics declaration Rights and permissions Further Reading

Printed on: 02/07/23



## Abstract Archives of the RSNA, 2022

NPMEE-19

### **The Price Is Right...Sometimes: CMS Price Transparency Requirements, Intra-Institutional Inconsistencies in Published Charges, and Imaging Charge Variability**

Sunday, Nov. 27 8:00AM - 9:00AM Room: Learning Center - NPM

#### **Participants**

Matthew Petterson, MD, (*Presenter*) Nothing to Disclose

#### **TEACHING POINTS**

1. Introduce the Centers for Medicare and Medicaid Services hospital price transparency requirements, including the charges which must be made publicly available via chargemasters and consumer-friendly displays. 2. Discuss widespread intra-institutional inconsistency between charges for the same examinations published in chargemasters versus consumer-friendly displays. 3. Highlight the marked heterogeneity in total charges for common imaging examinations across prominent U.S. academic medical centers.

#### **TABLE OF CONTENTS/OUTLINE**

1. Centers for Medicare and Medicaid Services Price Transparency Rule a. Goals b. Affected institutions c. Required data publication formats i. Chargemasters 1. Required data ii. Consumer-friendly display of shoppable services 1. Required data 2. Mandatory imaging examinations 3. Common consumer-friendly displays d. Penalties 2. Intra-institutional inconsistencies between total charges published in chargemasters and consumer-friendly displays a. Rates and magnitudes b. Other commonly incomplete charge data c. Sources d. Implications for institutions e. Implications for patients 3. Variability in total charges for C.M.S. mandated imaging examinations a. CT i. CPT 70450, 72193, 74177 b. MRI i. CPT 70553, 72148, 73721 c. US i. CPT 76700, 76805, 76830 d. Radiography i. CPT 72110 e. Mammography i. CPT 77065, 77066, 77067

Printed on: 02/07/23



## Abstract Archives of the RSNA, 2022

NPMEE-2

### How To Develop The Best Radiology Clerkship?: A Guide for Educators

Sunday, Nov. 27 8:00AM - 9:00AM Room: Learning Center - NPM

#### Participants

Francisco Garrido Cisterna, MD, Santiago, Chile (*Presenter*) Nothing to Disclose

#### TEACHING POINTS

1. Increasing workload and continued specialization of radiology practice are challenge for medical educators planning in-person activities in the reading room of medical students during their elective radiology clerkships. 2. Radiology clerkships require a structure that will enable the proposed educational goals to be met: known learning objectives, available and user friendly consult materials, feedback sessions and assessment. 3. In the reading room, various educational strategies can be applied such as: patient history review from the EMR, involvement in clinical-radiological discussions, creation of a portfolio of interesting cases, selection of topics based on cases encountered for further presentation in the journal club, among others. 4. Radiology residents may spend more time with medical students that with supervisions fellows or staff radiologists, playing a central role in the overall quality of medical student experience in the reading room. Therefore, they must learn and apply a few teaching techniques specifically for this environment.

#### TABLE OF CONTENTS/OUTLINE

1. Introduction 2. What is the current status in the world? 3. The educational challenge in the reading room 4. What elements do you need to build a clerkship? 5. Teaching and learning methods in the reading room and at home 6. The impact of the residents in the radiology clerkship (resident as teachers) 7. Assessment 8. Conclusions

Printed on: 02/07/23



## Abstract Archives of the RSNA, 2022

NPMEE-20

### MRI Safety of Commonly Used Implants and Devices: What the Radiologist Needs to Know

Sunday, Nov. 27 8:00AM - 9:00AM Room: Learning Center - NPM

#### Awards

Certificate of Merit

#### Participants

Vivek Pai, MBBS,MD, Toronto, Singapore (*Presenter*) Nothing to Disclose

#### TEACHING POINTS

Requests for MRIs in patients with medical and/or surgical devices are frequently encountered in practice. The aims of this exhibit are: 1. To review the concepts of static magnetic fields, gradient fields, and RF pulse with regard to MRI safety 2. To review the concept of Specific Absorption Rate (SAR) and B1+rms 3. To review standard MRI safety terminology 4. To review general guidelines with respect to MRI safety in patients with implants and devices 5. To review the specific MRI safety concerns of the most commonly used devices and implants.

#### TABLE OF CONTENTS/OUTLINE

1. Basic concepts and definitions in MRI safety 2. Review of MRI safety for: a. Deep Brain Stimulators b. Epidural and Peripheral Nerve Catheters c. Spinal Cord Stimulators d. Peripheral Nerve Stimulators e. Cochlear Implants f. Scleral Buckles g. Pacemakers and Defibrillators h. Vascular Stents i. Endoscopic Hemostatic Clips and Video Capsule Endoscopic Recording Devices j. Intrauterine and Fallopian Tube Closure Devices k. Bullets, Shrapnel, and Foreign Metallic Objects.

Printed on: 02/07/23



## Abstract Archives of the RSNA, 2022

NPMEE-21HC

### Fostering Organizational Excellence Through Inclusive Leadership: A Practical Guide for Radiology Leaders

Sunday, Nov. 27 8:00AM - 9:00AM Room: Learning Center - NPM

#### Awards

Identified for RadioGraphics

#### Participants

Anand Narayan, MD, PhD, Verona, WI (*Presenter*) Nothing to Disclose

#### TEACHING POINTS

- Increasing the diversity of Radiology departments can drive performance by leveraging the collective experiences of different backgrounds, age groups, and genders.
- The potential of diverse teams can only be actualized when team members feel valued, respected, included, confident, and inspired.
- Inclusive work cultures promote innovation, productivity, higher quality decision making, and profitability.
- Inclusive leadership training can provide radiology leaders with tools to foster healthy, diverse and inclusive environments and teams.

#### TABLE OF CONTENTS/OUTLINE

1. Rationale for Inclusive Leadershipa. Backgroundb. Impact of Inclusion on Team Performance2. Inclusive Leadershipa. Inclusive versus Exclusive Leadership Stylesi. Transformative Leadershipii. Transactional Leadershipiii. Authoritarian Leadershipiv. Laissez Faire Leadershipv. Democratic Leadershipvi. Servant Leadershipb. Characteristics of Highly Inclusive Leadersi. Cognizanceii. Curiosityiii. Courageiv. Cultural Intelligencev. Commitmentvi. Collaborationc. Unconscious biasesi. Definitionii. Impact on Decision-Making in the Workplaceiii. Strategies for Reducing Unconscious Biases3. Strategies for Radiology Leadersa. Increase Diversityb. Nurture Authentic, Brave Dialoguec. Inclusive Meetingsd. Transparent Processes for Assignments and Promotione. Foster Community BuildingPlease visit the Learning Center to also view this presentation in hardcopy format.

Printed on: 02/07/23



## Abstract Archives of the RSNA, 2022

NPMEE-22

### Mapping Our Journey Towards Gender-Affirming Imaging Care

Sunday, Nov. 27 8:00AM - 9:00AM Room: Learning Center - NPM

#### Participants

Kristen L. Dean, Boston, MA (*Presenter*) Nothing to Disclose

#### TEACHING POINTS

It is critical for radiology practices to know how to provide a welcoming care environment for gender diverse patients such as transgender patients. We employed a structured patient experience mapping process to identify potential barriers associated with each aspect of the imaging exam. The purpose of this exhibit is: 1. To learn how to provide a safe, affirming, and inclusive environment for transgender patients and their families by understanding the patient journey from their perspective. 2. To describe our 'Gender Diverse Patient Experience' initiative to improve the care journey and support staff in gaining cultural competency.

#### TABLE OF CONTENTS/OUTLINE

1. Mapping the Journey • Potential Scenarios o Transgender male having a transvaginal US o Transgender female having a RUG/VCUG o Transgender male having a mammogram • Step-by-Step • Actions, Motivations, Questions, Barriers • Staff concerns 2. Framework to Map • Patient Journey template • Documentation 3. Key Findings • Causes of Patient Distress • Information Gap • Semblance of Control 4. Informing Improvements • Patient Workflow Across Journey o Patient preparation information o Welcoming greeting: Chosen name, pronouns o History, intake and control forms (sexual orientation, gender identity, sex assigned at birth) o Patient preferences during exam (changing, conversation, students) o Radiology reports use of pronouns • Physical Environment o Affirming inclusive silent indicators (Healthcare Equality Index, Non- Discrimination policy) o Changing rooms, waiting rooms restrooms o Reflect across online environment touchpoints • Awareness, Education Training o Experiential, safe to make mistakes, multi-pronged o Culturally competent workforce

Printed on: 02/07/23



## Abstract Archives of the RSNA, 2022

NPMEE-23

### International Medical Graduates: A Primer for Program Directors

Sunday, Nov. 27 8:00AM - 9:00AM Room: Learning Center - NPM

#### Participants

Jose Armando Rodriguez Hernandez, MD, Tegucigalpa, Honduras (*Presenter*) Nothing to Disclose

#### TEACHING POINTS

1. Define International Medical Graduates (IMG)  
2. Understand composition and historic trends of IMGs in the U.S. medical and radiology workforce  
3. Discuss the steps IMGs need to take to be eligible to apply to residency positions in the U.S.  
4. Recognize common misconceptions IMGs face in the interview trail  
5. Recognize attributes IMGs bring to the U.S. healthcare system

#### TABLE OF CONTENTS/OUTLINE

1. Define International Medical Graduates  
o US-citizens IMG  
o Non-US citizens IMG  
2. IMG composition and trends in the U.S. medical and radiology workforce  
3. Steps IMG need to take to apply to a residency position in the U.S.  
o Medical school requirements (established by the Educational Commission for Foreign Medical Graduates, or ECFMG)  
o Application for ECFMG certification  
o Examination requirements  
o Medical education credential requirements  
4. Common misconceptions IMG face in the interview trail  
o Medical schools unknown to selection committees  
o "Gap" years from graduation for non-US IMGs, commonly spent on:  
Mandatory service at their home country  
Clinical and research rotations in the U.S.  
Preparing for USMLE exams  
Applying for ECGME certification  
English language proficiency  
o Understanding of the U.S. medical system  
o Difficulty acquiring visas  
5. Attributes IMG bring to the U.S. healthcare system  
o Diverse medical and cultural backgrounds  
o Contribute to peers' cultural competency  
o Fluency in multiple languages  
o Experience working unsupervised as primary care providers

Printed on: 02/07/23



## Abstract Archives of the RSNA, 2022

NPMEE-24

### Avenues Of Advocacy For Healthcare Disparities In Breast Imaging

Sunday, Nov. 27 8:00AM - 9:00AM Room: Learning Center - NPM

#### Participants

Connie Ge, (*Presenter*) Nothing to Disclose

#### TEACHING POINTS

- Understand how healthcare disparities (HCD) affect morbidity and mortality in breast cancer- Identify 3 domains of HCD advocacy in breast imaging (Patient centeredness, Imaging processes, Healthcare systems)- Examine the literature on efforts to address each of these domains- Apply this knowledge to problem solving in real-life patient vignettes.

#### TABLE OF CONTENTS/OUTLINE

- Background and objectives- Overview of literature examining HCD in context of breast imaging- Overview of 3 domains of HCD advocacy in breast imaging1. Patient centeredness--Patient education--Patient-centered reporting and guidelines--Cultural competency training and diversification of workforce--Language accessibility2. Imaging processes--R-Scan--ACR Select--Tools to examine data through lens of health equity3. Healthcare systems--Structural barriers to accessing care--Targeted outreach efforts for specific vulnerable populations--Collaboration with local organizations- Patient vignettes with guided brainstorming- Conclusions

Printed on: 02/07/23



## Abstract Archives of the RSNA, 2022

NPMEE-25

### What Radiologists Need to Know About Workplace Ergonomics

Sunday, Nov. 27 8:00AM - 9:00AM Room: Learning Center - NPM

#### Participants

Tyler Yan, MD, (*Presenter*) Nothing to Disclose

#### TEACHING POINTS

- Substantial workstation-related MSK discomfort is experienced by Canadian radiologists
- Adjustable furniture is not often available or used
- Provision of adjustable equipment is an important component in the creation of accessible and inclusive radiology departments
- There is great opportunity to improve the wellbeing and productivity of radiologists and trainees by addressing workstation ergonomics

#### TABLE OF CONTENTS/OUTLINE

- Why workstation ergonomics are important in radiology
- We use workstations all day (and night)
- Many workstations are shared
- Workstations are often not fully adjustable
- Musculoskeletal (MSK) discomfort can affect productivity
- Increased knowledge of ergonomics is associated with decreased likelihood of MSK discomfort
- Optimal workstation ergonomics
- Shoulders and arms are relaxed
- Monitor is at arm's length with top of screen at eye level
- Wrists are relatively flat
- Elbows at 90degrees
- Feet flat on floor/footstool
- Chair with lumbar support
- Substantial workstation-related MSK discomfort in radiologists
- Impact on productivity
- Requires symptom management
- Radiologists have limited ergonomic knowledge
- Recommendations to Radiology Departments
- Provide ergonomics training and ergonomics evaluation
- Provide adjustable equipment
- Recommendations to Radiologists and Trainees
- Advocate for inclusive workplace
- Make adjustments before using shared workstation (when possible)

Printed on: 02/07/23



## Abstract Archives of the RSNA, 2022

NPMEE-26

### A Guide to Using YouTube Live for Radiology Education

Sunday, Nov. 27 8:00AM - 9:00AM Room: Learning Center - NPM

#### Participants

Lilly Kauffman, BA, (*Presenter*) Nothing to Disclose

#### TEACHING POINTS

- YouTube Live is the most popular streaming platform on social media- Livestreaming is a way to reach and interact with a large audience for radiology education- There are several advantages, including interactivity and analytics, that come with YouTube Live- However there are also disadvantages, such as limited streaming abilities within the YouTube platform

#### TABLE OF CONTENTS/OUTLINE

1. Understanding YouTube Live  
1a. YouTube Live Statistics  
2a. How to create a YouTube Live segment  
2. Our experience  
3. The pros of using YouTube Live  
4. The drawbacks of using YouTube Live

Printed on: 02/07/23



## Abstract Archives of the RSNA, 2022

NPMEE-27

### Next Level Cases: Strategies for Creating Dynamic and Interactive Radiology Presentations

Sunday, Nov. 27 8:00AM - 9:00AM Room: Learning Center - NPM

#### Participants

Lucas Aronson, BS, Madison, WI (*Presenter*) Nothing to Disclose

#### TEACHING POINTS

(1) Traditional radiology presentations rely on a few images of cross-sectional studies rather than scrollable images. While this is more efficient for content delivery, this can decrease learner engagement and emphasizes the "classic" appearance of diseases. (2) There are several techniques and tools to boost interaction and integrate scrollable cross-sectional imaging in radiology presentations. These help facilitate a diagnostic simulation environment and provide a stronger bridge to making independent diagnoses. (3) Interactive and scrollable cases permit the teacher to more confidently teach complex pathologies that do not display well in a few-image presentation. (4) Interactive presentations create more flexibility in teaching methods, including flipped-model, group work, and learner-directed exploration of topics. (5) Interactive presentations can reach a broader variety of learners, as individuals can approach the material from their current skill set and are not confined by a few-image presentation of pathology.

#### TABLE OF CONTENTS/OUTLINE

(1) Limitations of traditional presentations (1a) Use of single images from cross-sectional studies (1b) Reduced interactivity (1c) Selection biased toward "Aunt Minnie" images (1d) Barriers for teaching complex topics (2) How to make presentations more engaging and dynamic (2a) Include scrollable cross-sectional imaging (2b) Utilize links for multiple choice questions (2c) Implement polling software for group engagement (2d) Toggle annotations with links (2e) Zoom into regions of interest with hover-links

Printed on: 02/07/23



## Abstract Archives of the RSNA, 2022

NPMEE-3

### Immersive Imaging: Structure and Outcomes from a Novel One-year Medical Student Fellowship in Radiology

Sunday, Nov. 27 8:00AM - 9:00AM Room: Learning Center - NPM

#### Participants

Sohum D. Patel, BA, White River Junction, VT (*Presenter*) Nothing to Disclose

#### TEACHING POINTS

1. Identify challenges to medical student recruitment/engagement with radiology given the conventional clerkship framework.2. Describe our institution's novel medical student fellowship in radiology.3. Analyze outcome metrics from past fellows, including specialty choice influence, perceived educational utility, and contribution to professional development.4. Summarize resident and faculty perceptions of adding a medical student fellow and its effect on clinical workflow.5. Explore potential future directions of immersive radiology experiences.

#### TABLE OF CONTENTS/OUTLINE

Introduction- Limitations of current student engagement strategies in radiology- Current state of affairs for radiology recruitmentThe Robert Jeffery Medical Student Fellowship in Radiology1. Fellowship overview - History, philosophy, and structure - Responsibilities and opportunities2. Outcomes: Perspectives from Prior Fellows - Preparedness for rotations, internship, and residency - Perceived importance for residency application - Mentorship, advising, and professional development3. Outcomes: Perspectives from Radiology Residents Faculty - Perceived contribution to workflow and department4. Challenges5. The Road Ahead - Plans for future fellowships - Considerations for implementation at other institutionsConclusion: Student fellowships in radiology provide an incredible opportunity to both students and the department to recruit and train future radiologists.

Printed on: 02/07/23



## Abstract Archives of the RSNA, 2022

NPMEE-4

### Global Learning Centers: Sustainable and Impactful Radiology Outreach

Sunday, Nov. 27 8:00AM - 9:00AM Room: Learning Center - NPM

#### Participants

Sucari Vlok, MBChB, MMed, Tygerberg, South Africa (*Presenter*) Nothing to Disclose

#### TEACHING POINTS

- Evolution in radiology education and outreach
- Power of conceptual thinking
- Beauty of collaboration and ability to listen

#### TABLE OF CONTENTS/OUTLINE

- Introduction
  - o Previously the RSNA relied on the International Visiting Program (IVP) for international outreach.
  - o In 2018, the RSNA board re-envisioned the IVP, and the Global Learning Centers (GLC) were birthed.
- Planning phase
  - o Stellenbosch University/Tygerberg Hospital was chosen as the inaugural GLC program. A curriculum was derived from perceived greatest areas of need.
- Implementation phase
  - o The COVID pandemic struck as the first RSNA team was preparing an on-site visit. It forced the program to pivot to an online curriculum, utilizing the RSNA's considerable back catalog of lecture material from annual meetings.
- Online continuing education phase
  - o RSNA Department of Education staff curated online content into course modules. An online classroom and ultrasound facilities for distance-based teaching were installed.
- Exit phase
  - o The GLC will be implemented over a three-year period, but relationships and collaboration will hopefully endure long after and ascertain sustainability of the program.
- Conclusion
  - o The COVID pandemic forced us all to conceptualize new ways of thinking, planning and learning.
  - o The board of RSNA Radiologists' rich history of visionary thinking transformed and led Radiology from its inception to where we are today.

Printed on: 02/07/23



## Abstract Archives of the RSNA, 2022

NPMEE-5

### Nothing Humerus About it: Recognizing, Preventing and Treating Radiologist Elbow

Sunday, Nov. 27 8:00AM - 9:00AM Room: Learning Center - NPM

#### Participants

Kathleen MacMillan, PharmD, (*Presenter*) Nothing to Disclose

#### TEACHING POINTS

1. Lateral epicondylitis is an overuse injury related to wrist extension and is commonly known as tennis elbow.2. Due to wrist positioning during computer-mouse related work, radiologists are at risk of occupational lateral epicondylitis, "radiologist elbow".3. Lateral epicondylitis can usually be diagnosed clinically, but ultrasound or MRI may be helpful to confirm the diagnosis and to determine the severity of tendinopathy or tearing.4. Prevention of lateral epicondylitis centers on reduction of wrist extension. For radiologists this includes supports for the forearm, use of a vertical mouse, and use of voice recognition software where possible.5. Treatment of lateral epicondylitis can include rest, ice, therapeutic ultrasound interventions, physiotherapy, NSAIDs, corticosteroid injections, or surgery.

#### TABLE OF CONTENTS/OUTLINE

1. Detailed explanation of the anatomy and pathophysiology of lateral epicondylitis in computer-users focusing on specific occupational risks of radiologists.2. Review the symptoms of lateral epicondylitis, clinical diagnostic criteria, and typical diagnostic imaging findings.3. Using a structured literature review, summarize evidence-based recommendations to prevent radiologist elbow. Explain the ergonomic basis of the interventions.4. Provide recommendations to reduce and treat associated symptoms in radiologists.

Printed on: 02/07/23



## Abstract Archives of the RSNA, 2022

NPMEE-6

### Magnetic Resonance Nail Evaluation With The Use Of Conductive Gel: Technical and Clinical Aspects

Sunday, Nov. 27 8:00AM - 9:00AM Room: Learning Center - NPM

#### Participants

Paula Lucio, MSc, (Presenter) Nothing to Disclose

#### TEACHING POINTS

- To review clinical aspects of MRI nail evaluation. - To summarize main challenges related to MRI nail evaluation, including patient positioning, image quality and technical factors that undermine the individualization of structures and possible alterations. - To discuss the importance of conductive gel using illustrative and comparative cases. - To discuss other technical factors that impact in imaging quality using illustrative and comparative cases, including the use of the coilLoop Small-Siemens®.

#### TABLE OF CONTENTS/OUTLINE

1. Clinical indications of nail evaluation of fingers and pododactyls by Magnetic Resonance a. Suspected retronychia b. Suspected ligament injury c. Suspected tumor d. Trauma e. Infectious/inflammatory processes 2. Use on the finger and glove to apply the conductive gel. 3. Positioning for fingers and pododactyls. 4. How the structures and conductive gel appear on T2 images with FAT and T1. 5. Use of the coil Loop Small-Siemens® and image quality. 6. Take home messages.

Printed on: 02/07/23



## Abstract Archives of the RSNA, 2022

NPMEE-7

### What Radiologists Need to Know About Gender-Inclusive Naming

Sunday, Nov. 27 8:00AM - 9:00AM Room: Learning Center - NPM

#### Participants

Tyler Yan, MD, (*Presenter*) Nothing to Disclose

#### TEACHING POINTS

- Transgender individuals experience significant inequalities in radiology
- Using gender-inclusive terminology is one of many ways to combat structural stigma
- Barriers to gender-inclusive naming include the lack of provider education, departmental equity, diversity, and inclusion (EDI) committees, and public online presence of EDI efforts
- Individual and systems level strategies exist to promote transgender inclusivity in radiology.

#### TABLE OF CONTENTS/OUTLINE

- Why transgender inclusivity is important in radiology
- Transgender individuals face numerous inequalities in medicine
- Inequalities faced in radiology departments specifically
- Downstream detrimental effects, like suicide risk
- Example of inclusive practice: fellowship naming
- Importance of gender-inclusive naming
- Current landscape of naming in Canada and the United States
- Gender-inclusive naming among continuing medical education (CME) courses
- Barriers to gender-inclusive naming
- Current landscape of departmental EDI committees, EDI CME courses
- Recommendations to individuals
- Importance of patient names and pronouns; provider normalizing practice too
- Provider self-education
- Recognizing unconscious biases
- Recommendations to radiology departments
- Advocate for gender-inclusive naming of fellowships and CME courses
- Establish departmental committees, EDI training
- Increasing public visibility of EDI efforts

Printed on: 02/07/23



## Abstract Archives of the RSNA, 2022

NPMEE-8

### Microaggressions With a Macro-Impact: What the Radiologist Needs to Know About Microaggressions

Sunday, Nov. 27 8:00AM - 9:00AM Room: Learning Center - NPM

#### Participants

Sheikh Ahmed, BSc, MD, (*Presenter*) Nothing to Disclose

#### TEACHING POINTS

By reviewing the definitions of microaggressions and their impact in radiology, the learner will be able to: 1. Define and identify microaggressions and their subtypes 2. Recognize the impact of microaggressions in medicine and radiology 3. Recognize the link between microaggressions and challenges of developing diversity in radiology 4. Employ strategies to combat and address microaggressions

#### TABLE OF CONTENTS/OUTLINE

1. Introduction - Definitions of Microaggressions 2. Micro-insults - Definitions and Examples 3. Micro-invalidation- Definitions and Examples 4. Micro-assault- Definitions and Examples 5. Microaggressions as a negative determinant of diversity in medicine and radiology - literature examples 6. Gender-based microaggressions as a negative predictor of diversity in radiology and contributor to the "leaky pipe" concept 7. How to combat microaggressions - strategies and applications to training programs and departments

Printed on: 02/07/23



## Abstract Archives of the RSNA, 2022

NPMEE-9

### A Program Director's Guide to Recruiting for Excellence and Diversity

Sunday, Nov. 27 8:00AM - 9:00AM Room: Learning Center - NPM

#### Participants

Mai A. Elezaby, MD, Madison, WI (*Presenter*) Investigator, Exact Sciences Corporation; Research Grant, Exact Sciences Corporation

#### TEACHING POINTS

The average percentage of female radiology residents remains at 26-27% despite improvement and equity in medical school applicants. Several reported factors accounting for fewer female applicants to Radiology include perceived lack of patient contact, lack of female role models, paucity of females in leadership positions and hostile work environment. A diverse healthcare team with parity in gender representation provides more opportunities for success and improved patient care. This presentation describes best practices for residency recruitment to achieve excellence and diversity using examples from a Midwestern Academic Radiology Residency program's experience with standardized virtual recruitment strategies.

#### TABLE OF CONTENTS/OUTLINE

I. Current Radiology Residency Recruitment Data in the U.S. II. Outline of a Standardized Recruitment Process to increase Diversity  
a. Building a diverse search committee b. Recruiting a pool of highly qualified, diverse candidates c. Strategies to mitigate unconscious bias d. Tenants of holistic review process e. Standardized behavioral questions III. How to leverage virtual interviews to increase Diversity IV. Future proposals for residency interviews and potential pitfalls

Printed on: 02/07/23

## Abstract Archives of the RSNA, 2022

NREE

### Neuroradiology Education Exhibits

Sunday, Nov. 27 8:00AM - 9:00AM Room: Learning Center - NR

#### Sub-Events

##### NREE-1 **Cranial Nerves Cavernoma: A Rare Presentation of an Usual Lesion**

#### Awards

##### Cum Laude

Participants

Danielly Santos SR, Sao Paulo, Brazil (*Presenter*) Nothing to Disclose

#### TEACHING POINTS

Through this pictorial essay a review will be made based on cases and original drawings about atypical location of Cavernous Malformations (CM's). The purposes of this exhibit are:- To review the normal anatomy of cranial nerves using schematic illustrations and imaging MRI.- To discuss imaging features of cavernous malformations (CM's) and their classification.- To display a compendium of cases of CM's involving the origin and path of cranial nerves.- To show the examination protocols and the best MRI sequence for assessing these cases.

#### TABLE OF CONTENTS/OUTLINE

Cavernous angiomas or malformations are angiographically occult vascular malformations found in approximately 0.4%-0.9% of the population, and they account for 10-20% of all cerebrovascular malformations. Their location is variable, with 70-80% having a supratentorial origin, followed by infratentorial location (15%) within the spinal cord (5%). Isolated cranial nerves CMs are extremely rare, and there are very few reports. Although rare, it poses a significant threat to nerve functions. Due to the limited number of cases and scarce evidence, no definite recommendation is available on the indications of surgery and treatment. However, it seems essential to treat patients with progressive neurological deficits. MRI imaging is crucial for the evaluation of CMs. It can be safely stated that the CISS/FIESTA sequence should be considered as a tool for evaluating the CM origin and nerve continuity and planning a surgical approach.

##### NREE-10 **Ocular Trauma: There is More Than Meets the Eye**

Participants

Atefeh Zeinoddini, MD, St. Clair Shores, TX (*Presenter*) Nothing to Disclose

#### TEACHING POINTS

Describe the relevant ocular anatomy. Identify the common post traumatic ocular injuries. Discuss potential pitfalls and complications of traumatic ocular injuries. List imaging findings that require immediate (surgical) intervention.

#### TABLE OF CONTENTS/OUTLINE

Relevant ocular anatomy. Ocular Trauma Score Points. Types of Detachments. Types of globe rupture, ocular foreign body (FB) and their potential pitfalls. Complications of ocular trauma.

##### NREE-100 **Bilateral Thalamic Lesions Report: Imaging Statistics and Facts**

Participants

Pedro Castro, MD, Rio de Janeiro, Brazil (*Presenter*) Nothing to Disclose

#### TEACHING POINTS

To illustrate the spectrum of bilateral thalamic lesions on MRI. To demonstrate that the MRI assessment of bilateral thalamic lesions can be simplified through a practical approach, listing the most valuable key imaging points. To identify potential imaging pitfalls, make possible the implementation of precise therapeutic measures, and avoid potentially harmful biopsies.

#### TABLE OF CONTENTS/OUTLINE

1. Anatomy of the thalamic region. 2. Main neoplasms presenting with bilateral involvement of the thalamus, including astrocytomas and lymphomas. 3. Inflammatory, infectious, and demyelinating lesions that can manifest with bilateral thalamic involvement, including West Nile and Mycoplasma encephalitis. 4. Vascular causes: deep venous thrombosis, arterial infarction, and hypoxic-ischemic encephalopathy. 5. Toxic and metabolic causes, including Wernicke's encephalopathy, Fahr disease, and Leigh disease. 6. Clues for a practical imaging assessment and the avoidance of pitfalls.

##### NREE-101 **Case Based Review of Meningeal Disorders**

Participants

Etsushi Iida, MD, Ube, Japan (*Presenter*) Nothing to Disclose

#### TEACHING POINTS

To review normal anatomy of the meninges and imaging techniques for evaluation of meningeal pathologies To be familiar with imaging diagnosis of meningeal diseases with case based review

#### TABLE OF CONTENTS/OUTLINE

1. Anatomy of meninges and extra-axial spaces 2. Imaging techniques for detection of meningeal abnormality 3. Representative abnormal imaging findings on various sequences including FLAIR, DWI, SWI, ASL-PWI, and contrast enhanced FLAIR and T1WI 4. List of Case based review | Case1 tubercular meningitis | Case2 sarcoidosis | Case3 intracranial hypotension | Case4 dural AVF | Case5 Sturge Weber syndrome | Case6 MOG related disease

##### NREE-102 **Shedding light on the Substantia Nigra: Anatomy, Function, Imaging Technique and Pathophysiology.**

Participants

Guillaume Curaudeau, MD, (*Presenter*) Nothing to Disclose

## TEACHING POINTS

Anatomic features of the substantia nigra beget predictable imaging presentations of common and uncommon pathologies. Multi-modality and multi-sequence approach, including conventional T1 and T2-weighted images, DWI, SWI, and perfusion imaging are necessary to segregate different etiologies that affect the substantia nigra. The spectrum in imaging is reinforced via case based learning. Whereas DAT-SPECT scans have traditionally been used to evaluate Parkinsonian pathologies, improved high-resolution volumetric and susceptibility-weighted imaging are being leveraged for both Parkinsonian and non-Parkinsonian evaluation of etiologies affecting the substantia nigra. Understanding the difference between Wallerian and transneuronal degeneration Cellular idiosyncrasies of the nigrostriatal pathways including dense aquaporin-4 and elevated GABA receptor concentrations, as well as increased axonal arborization, contribute to higher metabolic burden and therefore lower threshold for development of oxidative stress. Genetic predispositions, some of which are newly characterized, foster accelerated pathways for nigrostriatal injury, and increased bionergetic burden.

## TABLE OF CONTENTS/OUTLINE

Anatomy and Cellular underpinnings Function Imaging techniques Cases Summary and implications for clinical practice

### NREE-103 Immunodeficiency-associated Primary CNS Lymphoma in Non-AIDS Patients - Clinico-Radiological Update

Participants

Francis Astrid Garay Buitron, MD, Barcelona, Spain (*Presenter*) Nothing to Disclose

## TEACHING POINTS

-Presurgical suspicion of CNS lymphoma is crucial for initial patient management: corticoids avoidance prior to biopsy.-Imaging features of CNS lymphoma are T2 hypointensity, homogeneous enhancement, and restricted diffusion, without hemorrhage. These features refer to diffuse large B-cell lymphoma of the CNS (Epstein-Barr virus-negative, immunocompetent hosts).-Immunodeficiency-associated CNS lymphoma (diffuse large B-cell, Epstein-Barr virus-positive) does not fulfill these imaging criteria and it appears ring-enhancing with necrosis and hemorrhage; mimicking glioblastoma or metastasis.-It has been mainly associated with AIDS, which incidence is decreasing; while other causes of immunocompromise are increasing.-MRI interpretations usually misdiagnose this entity as glioblastoma or metastasis, and it is not uncommon that patients undergo avoidable surgical resection.-We noted a TSE-T2 hypointensity of the central non-enhancing component in these tumors, which may provide an easily-recognizable clue. Also, DSC-PWI (low CBV and high percentage of signal recovery) could be very useful.-In this presentation, clinical and radiological features of patients with non-AIDS DLBC EBV-positive CNS lymphoma are described with emphasis on 'imaging pearls'.-Radiologists must be aware of any cause of immunocompromise when facing a ring-enhancing tumor and know the imaging pearls for immunodeficiency-associated CNS lymphoma.

## TABLE OF CONTENTS/OUTLINE

-CNS lymphomas WHO classification-Epidemiology-Clinico-radiological features of immunodeficiency-associated CNS lymphoma: clinical experience literature review-Differential diagnosis-Key-imaging features-Conclusions

### NREE-104 Do Not Touch Lesions in Neuroradiology

Awards

Certificate of Merit

Participants

Joshua Litchman, MD, (*Presenter*) Nothing to Disclose

## TEACHING POINTS

Define the concept of a Do Not Touch lesion in radiology Identify and describe representative Do Not Touch lesions in the brain, head and neck, and spine Compare and contrast these Do Not Touch lesions with their radiologic mimics on the basis of their respective clinical and imaging features

## TABLE OF CONTENTS/OUTLINE

Do Not Touch Lesions in Radiology Definition Examples Do Not Touch Lesions of the Brain Dilated perivascular space Dural sinus and aberrant arachnoid granulations Benign enlarged subarachnoid spaces Capillary telangiectasia Porencephalic cyst Colloid cyst Do Not Touch Lesions of the Head and Neck Petrous apex asymmetric marrow Skull base fibrous dysplasia Jugular bulb pseudolesion Intratemporal facial nerve enhancement Facial nerve hemangioma Ranula Do Not Touch Lesions of the Spine Split atlas Odontoid process variants Limbus vertebra Ventriculus terminalis Perineural root sleeve cyst Extramedullary hematopoiesis

### NREE-105 Imaging Features of CNS Neuroblastoma with FOXR2 Activation

Participants

Lohith Kini, MD, PhD, (*Presenter*) Consultant, Blackfynn Inc

## TEACHING POINTS

Primitive neuroectodermal tumors of the central nervous system (CNS-PNETs) are a heterogeneous group of highly aggressive, poorly differentiated embryonal tumors occurring predominantly in young children. With the discovery and advances in molecular and genetic diagnostics led to a reclassification of CNS embryonal tumors in the most recent 2021 WHO Classification of CNS Tumors. The varied molecular and genetic alterations, as well as distinct histopathological and imaging features, described in this new taxonomy could inform future targeted clinical decision-making and reduce diagnostic challenge due to a lack of defining molecular markers. Using gene methylation profiling, CNS neuroblastoma with FOXR2 activation (CNS NB-FOXR2) has been identified as a distinct subtype. This educational exhibit will discuss the key radiographic and molecular features of CNS NB-FOXR2, as well as similar entities on the radiologic differential diagnoses.

## TABLE OF CONTENTS/OUTLINE

I. Overview of CNS neuroblastoma with FOXR2 activation (CNS NB-FOXR2). II. Characteristic imaging features and molecular classification of CNS NB-FOXR2. III. Radiologic differences between CNS NB-FOXR2 and other embryonic tumors. Medulloblastoma b. CNS tumor with BCOR internal tandem duplication IV. Summary and Quiza. Summary of key radiologic findings of CNS NB-FOXR2. b. Quiz: apply this new knowledge to a few example cases to improve diagnostic precision.

### NREE-106 Circumscribed Astrocytic Gliomas: Key Findings You Need to Know

Participants

Seulkee Kim, MD, PhD, Gwangju, Korea, Republic Of (*Presenter*) Nothing to Disclose

## TEACHING POINTS

1. To review the major changes of the fifth edition of the WHO Classification of Tumors of the CNS (WHO CNS5) 2. To review the key radiologic and clinical findings of circumscribed astrocytic gliomas.

## TABLE OF CONTENTS/OUTLINE

1. Introduction 2. The major changes in the WHO CNS5 of circumscribed astrocytic gliomas 3. Diagnostic key radiologic and clinical findings: case-based review 1) Pilocytic astrocytoma 2) Pleomorphic xanthoastrocytoma 3) Subependymal giant cell astrocytoma 4) Chordoid glioma 5) Astroblastoma 4. Differential diagnosis 1) Ganglioglioma 2) Dysembryoplastic neuroepithelial tumor 5. Summary

### NREE-107 The Lymphoma Game Show: Imaging Review of Primary CNS Lymphoma and Its Differential Diagnoses

Participants

Karla Jonguitud, MD, (*Presenter*) Nothing to Disclose

#### TEACHING POINTS

The purpose of this exhibit is Review the most common imaging manifestations of primary CNS lymphoma. To know the purpose of radiological imaging of primary CNS lymphoma. Explain the most common manifestations encountered with neuroimaging (CT, MRI, MR spectroscopy and MR perfusion) and assess their role in the initial diagnosis and monitoring of primary CNS lymphoma. Discuss imaging findings of differential diagnosis of primary CNS lymphoma with a "choose your answer" game.

#### TABLE OF CONTENTS/OUTLINE

General features of primary CNS lymphoma. Clinical presentation in primary CNS lymphoma. Diagnostic procedures in primary CNS lymphoma. Purpose of radiological imaging in primary CNS lymphoma. Imaging diagnostic clues in primary CNS lymphoma. Imaging CT findings in primary CNS lymphoma. Imaging MR findings in primary CNS lymphoma. Game: Differential diagnosis of primary CNS lymphoma. Toxoplasmosis. Glioblastoma. Abscess. Progressive multifocal leukoencephalopathy. Demyelination. Metastases. Neurosarcooidosis. Diagnostic considerations and pearls in primary CNS lymphoma. Conclusions.

#### NREE-108 Imaging Features of Primary Intracranial Sarcoma with DICER1 Mutation

Participants

Lohith Kini, MD, PhD, (*Presenter*) Consultant, Blackfynn Inc

#### TEACHING POINTS

A broad spectrum of primary intracranial sarcoma subtypes is now recognized, presumably arising from mesenchymal progenitor cells within the meningeal covering of the brain and along perivascular spaces. Building on the key advancements in radiographic and genetic and molecular diagnostics including DNA methylation profiling, primary intracranial sarcoma with DICER1 mutation (PISD) can now be characterized as a distinct tumor entity, newly defined by the 2021 WHO Classification of CNS Tumors. The significant histological variability of PISD makes diagnosis challenging, but DNA methylation profiling and gene panel sequencing have elucidated it as a homogenous entity. This educational exhibit will highlight the important and distinct radiographic and molecular features of PISD in contrast to other intracranial mesenchymal, non-meningothelial tumors such as rhabdomyosarcoma, CIC-rearranged sarcoma and solitary fibrous tumors.

#### TABLE OF CONTENTS/OUTLINE

I. Overview of primary intracranial sarcoma with DICER1 mutation (PISD). II. Characteristic imaging features and molecular classification of PISD. III. Radiologic differences between PISD and other intracranial mesenchymal, non-meningothelial tumors a. Rhabdomyosarcoma b. CIC-rearranged sarcoma c. Solitary fibrous tumors IV. Summary and Quiz a. Summary of key radiologic findings of PISD. b. Quiz: apply this new knowledge to a few example cases to improve diagnostic precision.

#### NREE-109 Hypothalamic-pituitary Region and the Neighborhood

Participants

Eduardo Valadares, MD, Sao Paulo, Brazil (*Presenter*) Nothing to Disclose

#### TEACHING POINTS

Describe the embryology, anatomy and physiology of hypothalamic-pituitary axis and anatomy of structures around the sella turcica. Exhibit the normal appearance of pituitary gland and hypothalamus in CT and MRI imaging. Summarize the main anatomy variants, congenital anomalies, neoplasms, inflammatory diseases, tumor-like lesions and other disorders of hypothalamic-pituitary axis and neighborhood

#### TABLE OF CONTENTS/OUTLINE

Introduction Embryology, anatomy and physiology of hypothalamic-pituitary axis Normal CT and MRI appearance Main anatomy variants Pituitary hyperplasia Empty sella Congenital anomalies • Pituitary anomalies • Hypothalamic hamartoma • Rathke Cleft cyst Neoplasms • Pituitary adenomas • Craniopharyngioma • Lymphoma • Germinoma • Meningioma • Histiocytosis • Astrocytoma • Teratoma • Lipoma • Metastasis Inflammatory diseases • Hypophysitis • Infectious processes Tumor-like lesions and other disorders • Pituitary apoplexy • Hypothalamic hamartoma • Aneurysm • Wernicke disease • Wyburn-Mason syndrome • Neuromyelitis optica (NMO) Take-home messages/Conclusions

#### NREE-11 Brain Arteriovenous Malformations (AVMs): A Practical Approach

Participants

Danielly Santos SR, Sao Paulo, Brazil (*Presenter*) Nothing to Disclose

#### TEACHING POINTS

To make the correct diagnosis, distinguishing brain AVMs from other intracranial vascular malformations and identify any complications at the time of presentation that may require immediate management; To stratify the risk of future complications, especially hemorrhage, perilesional hypoxemia or venous congestion, and thereby, establishing the appropriateness of conservative management or treatment; If AVM treatment is indicated, to choose the most effective modality for treatment with the lowest risk of adverse events; To follow the AVM over time, monitoring responses to treatment or ensuring stability with conservative management.

#### TABLE OF CONTENTS/OUTLINE

A AVM is a nidus of abnormal blood vessels connecting arteries and veins in the brain parenchyma through a shunt, primarily composed of enlarged feeding arteries through which arteriovenous shunting occurs with draining veins. Brain AVMs are rare lesions and most occur sporadically, although there are known associations with syndromes, such as hereditary hemorrhagic telangiectasia and cerebrofacial arteriovenous metamerism. When imaging AVMs, it is important to first identify features suggesting elevated risk of hemorrhage or other morbidity, such as perinidal hypoxemia, and secondly, to inform the choice of treatment or observation that provides the best balance of risk and benefit to the individual patient. Longitudinal imaging surveillance, either with conservative management or after treatment, enables monitoring for resolution of the AVM or the development of adverse findings that may necessitate a change in management.

#### NREE-110 Post-treatment Imaging Findings of Brain Metastases

Participants

Neudy Junior, MD, Sao Paulo, Brazil (*Presenter*) Nothing to Disclose

#### TEACHING POINTS

The purpose of this exhibit is: Illustrate typical and atypical post-treatment findings of brain metastases, including stereotactic radiotherapy, surgery resection, whole-brain irradiation, and immunotherapy. Describe characteristic imaging findings with sample cases from our institution's database. Highlight key imaging points and differential diagnosis.

#### TABLE OF CONTENTS/OUTLINE

Introduction. Epidemiology. Brain metastasis's location. Treatment options and complications. Series of cases of post-treatment imaging findings, complications, differential diagnosis and pitfalls. Conclusion.

#### NREE-111 Signs or Sins of Stroke in the Young Population: The Unforgivable Vascular Imaging Mystery

#### Participants

Pedro Castro, MD, Rio de Janeiro, Brazil (*Presenter*) Nothing to Disclose

#### TEACHING POINTS

To demonstrate that other vasculopathies besides atherosclerosis can cause ischemic stroke in young patients. To review the inflammatory, metabolic, coagulopathic, and genetic vasculopathies. To illustrate the imaging pearls of reversible cerebral vasoconstriction syndrome, carotid and vertebral dissection, carotid web, moyamoya, vasculitis, CADASIL, and drug abuse. To review these fewer common causes of stroke, sometimes misdiagnosed, and encourage the radiologist to go deeper into investigating these diseases.

#### TABLE OF CONTENTS/OUTLINE

1. Background of non-atherosclerotic vasculopathy causing ischemic stroke in young people. 2. Terminology, etiology, and pathology. 3. How CT and MRI angiography can help in differential diagnoses. 4. Vessel Wall MRI. 5. Carotid and vertebral dissection. 6. Carotid web. 7. Moya-Moya syndrome. 8. RCVS. 9. CADASIL. 10. Vasculitis. 11. Flowchart of imaging assessment. 12. Summary and Take-home messages.

#### **NREE-112 Recanalization Therapy is a Matter of Mismatch**

#### Participants

Pedro Castro, MD, Rio de Janeiro, Brazil (*Presenter*) Nothing to Disclose

#### TEACHING POINTS

To review the most beneficial practices in the ischemic stroke imaging assessment, emphasizing perfusion-diffusion evaluation of ischemic penumbra and FLAIR-diffusion mismatch. To show the importance of perfusion-diffusion mismatch evaluation in ischemic strokes with more than 6 hours of evolution. To explain the importance of FLAIR-diffusion mismatch evaluation in ischemic strokes with unknown onset time. To re-examine the current AHA/ASA Guidelines for the Early Management of Patients with Acute Ischemic Stroke Update.

#### TABLE OF CONTENTS/OUTLINE

1. Brief pathophysiological considerations of ischemic penumbra. 2. Flowchart of the objectives traced by the radiologist: critical objectives for stroke management. 3. Potentially salvageable brain: definition of ischemic penumbra through CT perfusion. 4. Potentially salvageable brain: definition of ischemic penumbra through MR perfusion-diffusion mismatch. 5. Strokes with unknown onset time: the importance of FLAIR-diffusion mismatch for clinical management. 7. Take-home messages.

#### **NREE-113 Dose Size Matter? Going Beyond Large Vessels in Stroke Imaging**

#### Participants

Humza Haque, MD, Newark, NJ (*Presenter*) Nothing to Disclose

#### TEACHING POINTS

1. To appreciate the importance of more distal vasculature when a patient presents with clinical appreciable stroke symptoms- High clinical suspicion, such as with a high NIH Stroke Scale, without occlusion of a large vessel (ICA, M1, basilar), should prompt careful inspection of more distal vasculature. Latest research trends have shown success with intervention upon smaller vessels, making the radiologist's role for detection vital.<sup>1,2</sup> To understand the utility of CT perfusion to guide identification of smaller vessel occlusion.- CT perfusion increases sensitivity and specificity of the detection of an occluded vessel.<sup>3</sup> To gain insight on pearls and pitfalls regarding vascular anatomy, CT technique, and to avoid common errors when faced with stroke imaging. Saver et al. (2020) Stroke 51:2872. Amukotuwa et al. (2021) Stroke 52:3308.

#### TABLE OF CONTENTS/OUTLINE

Define commonly used terms and abbreviations in the world of stroke and its imaging, including medium vessel occlusions (M2/3 middle cerebral artery, A2/3 anterior cerebral artery, and P2/3 posterior cerebral artery segments)<sup>3</sup> Review literature regarding large and more distal vessel occlusion. Cases and teaching points of medium vessel occlusions involving the ACA, MCA, and PCA with pertinent clinical information, non-contrast CT head, CT angiogram, CT perfusion, and MRI. Conclusion. Ospel et al. (2020) Stroke 51:2817

#### **NREE-114 2022: a Stroke Flowchart Odyssey in the Emergency Room**

#### Participants

Heber Colares Costa, MD, Rio de Janeiro, Brazil (*Presenter*) Nothing to Disclose

#### TEACHING POINTS

To illustrate the current flowchart protocol for assessing acute ischemic stroke in the emergency room. To clarify the better protocol selection indications, including CT, CT angiography, and MRI. To explain the advantages of employing MRI for acute stroke evaluation. To demonstrate the optimal therapeutic implementation, including intravenous thrombolysis and mechanical thrombectomy.

#### TABLE OF CONTENTS/OUTLINE

1. Background. 2. Current flowchart protocol. 3. Clinical perspective and relevance of determining the correct stroke diagnosis, considering stroke mimics, and excluding hemorrhage. 4. Imaging perspective: CT, CT angiography, and MRI - advantages and disadvantages. 5. Critical Objectives Outlined by the Radiologist for Initial Conduct. 6. Tissue Viability: Definition of Ischemic Penumbra through CT and MRI Perfusion. 7. Update in the therapeutic assessment of stroke. 8. Take-Home messages.

#### **NREE-115 Arachnoid Cysts: Not Always Benign**

#### Participants

Glauber Siqueira I, MD, ARRT, (*Presenter*) Nothing to Disclose

#### TEACHING POINTS

The purpose of this exhibit is: The objective of this iconographic essay is to highlight the main imaging aspects of computed tomography (CT) and magnetic resonance imaging (MRI) of complications related to arachnoid cysts through illustrative cases. Among the main findings, that stand out, are rupture with the formation of extra-axial collections such as subdural hygroma or hematoma, intracystic hemorrhage, herniations, and hydrocephalus. It is crucial that radiologists become familiar with the main diagnostic aspects in cross-sectional imaging of this frequent cause that is not always devoid of clinical significance.

#### TABLE OF CONTENTS/OUTLINE

Anatomical considerations: location, anatomical variants and its implications. Cystic characteristics on CT and MRI. Adjacent structures: brain, bone, vessel and nerves. Atypical imaging appearance: red flags on differential diagnosis Arachnoid cysts post-operative imaging.

#### **NREE-116 Clues to Suspect Dural Arteriovenous Fistulas at Cross-sectional Imaging: Case-based Quiz and Review with Anatomic Correlation**

#### Participants

Carlota Garcia de Andoin Sojo, MD, Bilbao, Spain (*Presenter*) Nothing to Disclose

#### TEACHING POINTS

Even if arteriography is the gold standard radiological technique to confirm the presence of dural arteriovenous fistulas, some CT and MRI direct and indirect findings can suggest the diagnosis if seen.

#### TABLE OF CONTENTS/OUTLINE

**Objectives**To describe different radiological signs that suggest the presence of dural arteriovenous fistulas in cross-sectional image modalities (CT and MRI).To show the correlation between the signs described before and the angiographic findings.**Methods**A CT and MRI illustrated quiz with cases from our institution has been made to introduce the revision of each sign that suggests the presence of dural arteriovenous fistulas in non-invasive radiological tests.**Direct signs:** high signal of venous structures seen on time of flight (TOF) angiography MRI sequence; early enhancement of venous structures on contrast-enhanced angio-CT or MRI. **Indirect signs:** congestive parenchymatous or spinal oedema with variable hemorrhagic foci on MRI; intracranial intraparenchymal, subarachnoid or subdural haemorrhages; cerebral venous sinus thrombosis; prominent vascular structures in absence of nidus; area of increased blood flow in neuroperfusion studies; proptosis and orbital oedema; abnormally enlarged dural vascular channels in the skull. **Conclusion:**The knowledge of these findings in cross-sectional image modalities is useful for approaching the diagnosis and before performing an invasive test.

#### **NREE-117 Reversible Cerebral Vasoconstriction Syndrome Learning Methods - How to Tighten the Mind**

##### **Awards**

**Certificate of Merit**

Participants

Elissandra Lima, MD, Rio de Janeiro, Brazil (*Presenter*) Nothing to Disclose

#### TEACHING POINTS

To illustrate the imaging assessment of reversible cerebral vasoconstriction syndrome (RCVS). To describe the terminology, etiology, and physiopathology of RCVS. To explain the complications, disease associations, and treatment options involved in the RCVS.

#### TABLE OF CONTENTS/OUTLINE

1. Background. 2. MRI and CT angiography imaging protocol. 3. Physiopathology and related disorders. 4. Imaging assessment of RCVS and associations, like Posterior reversible encephalopathy syndrome and cortical subarachnoid hemorrhage. 5. Differential diagnoses. 6. Digital subtraction angiography assessment with emphasis on therapeutics. 7. Flowchart for assessment of RCVS. 8. Take-Home messages.

#### **NREE-118 Arterial Wall Irregularities in Cerebral Vessels: Radiological Findings of Cerebral Vasculopathy**

Participants

Mariano Lozano Gomez, MD, Almeria, Spain (*Presenter*) Nothing to Disclose

#### TEACHING POINTS

- To recognize imaging appearances of various forms of cerebral vasculopathy at CT, MRI and Digital Subtraction Angiography (DSA)- To describe key aspects to distinguish some types of cerebral nervous system (CNS) vasculopathy.- To discuss the correlation of clinical presentation and laboratory test results with imaging findings to aid the diagnosis of cerebral vasculopathy.

#### TABLE OF CONTENTS/OUTLINE

- Introduction.- Cerebral vascular anatomy: - Circle of Willis. - Vertebrobasilar circulation.- Analysis of CNS vasculopathies: - Description. - Clinical presentation. - Radiological features (CT, MRI, DSA).- Conclusion. - Take-home points.

#### **NREE-119 CT Myelography: From Technical Aspects to Imaging Evaluation**

##### **Awards**

**Identified for RadioGraphics**

**Certificate of Merit**

Participants

Irlene Cordeiro de Macedo Pontes, MD, Sao Paulo, Brazil (*Presenter*) Nothing to Disclose

#### TEACHING POINTS

Although MRI has increased in importance, CT myelography still has a key role in delineating the spinal anatomy, especially to demonstrate dural sac and its contents pathologies. Therefore the radiologists must be aware of the main indications and the principles of the exam technique. The aim of this exhibit is to:1. Detail the technique from lumbar and C1-C2 punctures.2. Demonstrate the differences between the acquisition techniques from CT myelography.3. Describe the differences between the contrast agents and the most suitable choice for the procedure.4. Display and illustrate the needles available for lumbar puncture and the best selection for each case. 5. Exhibit forms of prevention of post-dural puncture headache. 6. Demonstrate imaging findings from erroneous contrast administration.7. Illustrate the main indications from CT myelography with imaging findings.

#### TABLE OF CONTENTS/OUTLINE

1. INTRODUCTION2. THE TECHNICAL ASPECTS FROM CT MYELOGRAPHY a. Lumbar and cervical punctures b. Acquisition techniques c. Contrast selection. Ionicii. Nonionic d. Needles selectioni. Conventional typeii. Pencil-point type e. Erroneous contrast administration: imaging findings.f. Post-dural puncture headache3. MAIN INDICATIONS AND IMAGING FINDINGS a. Main indications b. Imaging findings from pathologiesi. Radiation planning treatmentii. Spontaneous intracranial hypotensioniii. MRI contraindicationsiv. Older uses/ indications

#### **NREE-12 Pearls and Pitfalls of Diagnosing Spinal Cord Abnormalities: Emphasis on Patterns in T2-, Postcontrast T1- and Diffusion-Weighted Images**

##### **Awards**

**Certificate of Merit**

Participants

Mariko Kurokawa, MD, Ann Arbor, MI (*Presenter*) Nothing to Disclose

#### TEACHING POINTS

The aim of this review is to summarize the clinical and imaging features of spinal cord disorders with focus on the distribution and enhancement patterns and diffusion-weighted images (DWI).**Abstract****Teaching Points:**• Understand the anatomy of the spinal cord and surrounding structures in correlation with symptomatology and pathophysiologic mechanisms• Describe the pattern and distribution on axial and sagittal T2, postcontrast T1, and DWI in the spinal cord and surrounding structures, and discuss the appropriate imaging techniques and pitfalls.• Summarize typical and atypical imaging features of various common and uncommon diseases

#### TABLE OF CONTENTS/OUTLINE

1. Spinal imaging techniques:MR protocols including single or multi-shot EPI and non-EPI DWI; pitfalls and artifacts2. Anatomy of the spine and spinal cordAscending tracts, descending tracts, and arterial territory3. Axial imagesWhite matter or gray matter (anterior, lateral, and posterior segments)4. Sagittal imagesLong cord lesion or short cord lesion5. Enhancement patternRim or ring enhancement, single nodular enhancement, multiple nodular enhancement, and patchy enhancement, pial or dural enhancement6. Diffusion pattern7. CasesSpinal cord infarction/ischemia, dural AVF, neurosarcoidosis, transverse myelitis, viral myelitis, demyelinating diseases, compressive myelopathy, subacute combined degeneration, traumatic cord

injury, spinal cord injury without radiographic abnormality (SCIWORA), and benign and malignant spinal tumors<sup>8</sup>. Systemic diseases with spinal cord abnormalities<sup>9</sup>. Summary

### **NREE-120 Correlation of Magnetic Resonance Imaging with Neuroinflammatory and Neuroimmune Responses in Acute, Subacute and Chronic Phases of Traumatic Spinal Cord Injury**

Participants

Mabel Torres - Llacsa, MD, (*Presenter*) Nothing to Disclose

#### **TEACHING POINTS**

1- Describe the normal appearance of spinal cord in adult and after traumatic SCI. 2- Distribution of oligodendrocyte cell subpopulations in the adult CNS 3- Recognize the radiological appearance of the spinal cord in the acute, subacute and chronic phases after a traumatic spinal cord injury

#### **TABLE OF CONTENTS/OUTLINE**

1- Describe the inflammatory process that occurs in the spinal cord after a traumatic injury to the spinal cord. 2- Relationship of the radiological uptakes by magnetic resonance with the inflammatory phases that occur after a traumatic SCI. 3- Discuss the possible use of oligodendrocyte cells as cell therapy in traumatic spinal cord injury due to its ability to facilitate axonal re-growth re-myelination. 3.1- Cure by stimulation of resident oligodendrocyte cells near lesion area in SCI. 3.2- Injection of autologous oligodendrocyte cells grown ex vivo.

### **NREE-121 Sick Spine - A Review Of Differential Diagnosis Of Intramedullary Lesions On MRI**

Participants

Pedro Gama Carpentieri Primo, MD, Rio De Janeiro, Brazil (*Presenter*) Nothing to Disclose

#### **TEACHING POINTS**

Summarize the main strategy of the differential diagnosis for intramedullary signal alterations Explore the differential diagnosis of intramedullary pathology with focus on unusual and rare cases Characterize the imaging aspects of the main lesions

#### **TABLE OF CONTENTS/OUTLINE**

Differential of intramedullary lesions based on MRI signal findings T1 hyperintense/hypointense T2 hyperintense/hypointense Anatomical distribution findings Ventral cord Dorsal cord Central cord Important differential diagnosis and its imaging features Angiomyolipoma Cavematomatous malformation Embryonal tumor with multilayered rosettes Hemangioblastoma Syringocephalus Medullary congestion Medullary tuberculosis Neuromyelitis optica spectrum Transverse myelitis post-COVID vaccination Leukemic infiltration Syphilis myelitis Intramedullary metastasis Medullary cone ependymoma Acute disseminated encephalomyelitis Systemic lupus erythematosus related myelitis Multiple sclerosis Medullary schistosomiasis

### **NREE-122 Spinal Epidural Lesions: A Case-Based Review**

Participants

Izaely Prates, MD, Sao Paulo, Brazil (*Presenter*) Nothing to Disclose

#### **TEACHING POINTS**

1 - TEACHING POINTS- Review the normal anatomy of the epidural space and its relationship to adjacent structures- to illustrate a variety of rare cases in order to avoid misinterpretations and pitfalls;- propose an interpretation algorithm to try to reduce the number of differential diagnoses to help the referring physician.

#### **TABLE OF CONTENTS/OUTLINE**

2 - TABLE OF CONTENTS/OUTLINE INTRODUCTION. RELEVANT IMAGING ANATOMY. SPINAL EPIDURAL LESIONS: Clinical cases illustrating the spectrum of common and uncommon spinal epidural space findings in CT and MRI). Primary neoplasms of epidural space; Neoplasms that invade the epidural space; Hematomas; Infection and collections; Other lesions. A STEP-BY-STEP ALGORITHM TO APPROACH SPINAL EPIDURAL LESIONS. TAKE-HOME MESSAGES REFERENCES

### **NREE-123 Diffusion for Clearing Confusion: Role of the Diffusion-weighted Imaging in the Spine and Spinal Cord**

Participants

Melih Akyuz, MD, Chicago, IL (*Presenter*) Nothing to Disclose

#### **TEACHING POINTS**

TEACHING POINTS: 1. Diffusion-weighted imaging (DWI) in the spine is relatively new, yet has been a reliable imaging method for the characterization of a variety of disease entities 2. DWI provides information on the tissue microstructure depending on the alterations of the water-proton mobility. The efficacy of this technique has been proven in the evaluation of the abnormalities of not only the brain but also the spinal cord and spine 3. Previous studies have shown that DWI might be useful in the evaluation of vertebral fractures, degenerative changes of the spine, infection, infarction of the spinal cord, neoplasms, and various inflammatory conditions involving the spine and spinal cord

#### **TABLE OF CONTENTS/OUTLINE**

TABLE OF CONTENTS OUTLINE: 1. Describing different techniques of diffusion-weighted imaging in the spine 2. Discuss various abnormalities involving the spine spinal cord their clinical manifestations 3. Briefly discuss the sources and mechanisms of actions of different disease entities involving the spine 4. Case-based imaging review of the abnormalities of the spine spinal cord with distinctive imaging findings emphasis on the use of the DWI in each entity

### **NREE-124 Magnetic Resonance Imaging Findings in Infectious and Granulomatous Spinal Cord Lesions**

Participants

Alice Abreu Mota, MD, Sao Paulo, Brazil (*Presenter*) Nothing to Disclose

#### **TEACHING POINTS**

• Magnetic Resonance findings, associated with clinical and laboratorial exams, may help differentiate the specific etiology for infectious and granulomatous medulla and spinal cord pathologies. • Linear and nodular enhancement pattern with an "arborized" appearance is typical in neuroschistosomiasis. • The tuberculosis infection may lead to many complications like meningitis, radiculomyelitis, tuberculoma, myelitis, syringomyelia and spinal abscess. • Sarcoidosis lesions are frequently multiple and centrally located. • Toxoplasmosis is often indistinguishable from tuberculoma. • Abnormalities are mainly found in the dorsal columns in HTLV-1 and usually involve the posterior and lateral region of the cord in HIV. • In Varicella Zoster the T2 hyperintensity is in the lateral portion. • Myeloradiculopathy, myeloradiculitis, myelitis, myeloneuropathy, Guillain-Barre syndrome, have been reported in arboviruses.

#### **TABLE OF CONTENTS/OUTLINE**

Viral Myelitis • Varicella Zoster • Arboviruses ( Chikungunya ) • Citomegalovirus • HIV • HTLV-1 Others Infectious diseases • Tuberculosis • Neuroschistosomiasis • Neurotoxoplasmosis Non-infectious granulomatous disease • Sarcoidosis

### **NREE-125 Non-traumatic Spine Emergencies -A Primer for the On-Call Radiology Resident**

Participants

Emily Convery, MD, (*Presenter*) Nothing to Disclose

#### TEACHING POINTS

Although trauma remains a common indication for emergency room clinician to order spine imaging study, there are several atraumatic causes that warrant emergent spine imaging. This differential includes acute disc herniations with compressive myelopathy, pyogenic osteomyelitis with epidural abscess, and acute inflammatory process such as Guillain Barre syndrome or demyelinating disease, as well as direct or leptomeningeal spread of metastatic disease and vascular pathologies. Having familiarity with typical clinical manifestations and emergent management of such disease process can aid the radiologist with obtaining the proper spinal level of imaging with appropriate imaging modality and if need be recommend further imaging outside the neural axis.

#### TABLE OF CONTENTS/OUTLINE

1) Overview of spinal anatomy imaging search pattern 2) Signs and symptoms of myelopathy 3) Degenerative disease 4) Infectious and inflammatory diseases 5) Malignant compressive pathology 6) Vascular pathology 7) Treatment/management options

#### **NREE-126 Diffusion Kurtosis Imaging (DKI) in Neuroradiology: Technique and Clinical Applications**

Participants

Silvia Lanzarote Vargas, MD, Madrid, Spain (*Presenter*) Nothing to Disclose

#### TEACHING POINTS

DKI is a diffusion technique based on the use of very high values  $b=2000$  s/mm<sup>2</sup> and on the complex tissue structural technique with interesting applications in neuroradiology, mainly in the diagnosis and follow-up of gliomas.

#### TABLE OF CONTENTS/OUTLINE

Kurtosis is a statistical measure that determines the degree of concentration that the values of a variable present around the central zone of the frequency distribution. Diffusion imaging (DWI) with low b values assumes that the movement of water molecules after the application of the gradients of the diffusion sequence is the same in any direction in space and follows a Gaussian distribution. In biological tissues the movement of water molecules varies from the Gaussian distribution. This degree of deviation is related to tissue structural complexity and barriers to the free diffusion of water and it can be calculated using DKI. This presentation will explain in a simple way what are the technical requirements necessary to obtain the DKI as well as the parameters that can be calculated, such as the kurtosis coefficient (K). It is intended to provide information that may be useful in routine clinical practice, illustrating representative cases. Examples of the different applications of DKI in the diagnosis and monitoring of different pathologies will be given. In brain tumors, it can be useful to differentiate high-grade and low-grade gliomas, as well as to distinguish between recurrence of high-grade gliomas and pseudoprogression or radionecrosis and gliomas from other tumors such as primary CNS lymphomas. We will also show the usefulness of DKI in the diagnosis of head and neck tumors as well as in neurodegenerative diseases.

#### **NREE-127 Cavernous Sinus Hyperintense on Magnetic Resonance Angiography - Can You Differentiate Dural Arteriovenous Fistula from Cerebral Venous Reflux?**

Participants

Keizo Tanitame, MD, Hiroshima, Japan (*Presenter*) Nothing to Disclose

#### TEACHING POINTS

Diagnostic radiologists often encounter cavernous sinus hyperintense on three-dimensional time-of-flight magnetic resonance angiography (MRA). Even if detailed evaluation of the source images of MRA is performed, differentiation between dural arteriovenous fistula (DAVF) and cerebral venous reflux (CVR) is occasionally difficult. Cerebral digital subtraction angiography (DSA) is useful for differentiating them, but it is invasive and has a small risk of cerebral embolisms. CVR is observed mostly on the left side, and considered to be retrograde venous flow due to compression of the left brachiocephalic vein between the sternum and aortic arch or branches. We demonstrate several cases with diagnostic difficulty and focus the cause of retrograde venous flow in left cavernous sinus and some techniques suppressing the CVR on MRA.

#### TABLE OF CONTENTS/OUTLINE

1. Representative MRA and DSA images of cavernous sinus DAVF - Small arteriovenous shunts near the cavernous sinus 2. Representative MRA and DSA images of upward venous reflux in the cavernous sinus - Retrograde venous flow of the cavernous sinus and other venous sinuses 3. The cause of retrograde venous flow in the left cavernous sinus - Images and schematic illustration of left brachiocephalic vein compression 4. Suppression techniques against intracranial retrograde venous flow - The usefulness of MRA scanning in the supine position with shoulder pillows and small breathing

#### **NREE-128 Probing Metabolism: The Role of Proton MR Spectroscopy in Neurometabolic Diseases**

Participants

Milena Kriek Farche, MD, Campinas, Brazil (*Presenter*) Nothing to Disclose

#### TEACHING POINTS

1- Describe the basic principles of magnetic resonance spectroscopy (MRS), with an emphasis on protocol acquisition and optimal technique in a variety of neurometabolic conditions. 2- Illustrate the normal spectra and main abnormal patterns of brain metabolites, integrating the spectroscopy information with the analysis of conventional MRI sequences. 3- To review the main neurometabolic diseases in which spectroscopy can aid in establishing the correct diagnosis, presenting radiological tips for each clinical context.

#### TABLE OF CONTENTS/OUTLINE

1 - Introduction 2 - Principles of Proton MR spectroscopy A) Choosing the localization technique B) Choosing the echo-time (TE) C) Deciding between single-voxel vs multi-voxel D) Choosing the voxel location 3 - Normal spectra and main abnormal patterns of brain metabolites, including potential pitfalls and normal variants. 4 - Role of spectroscopy in the diagnosis of specific neurometabolic diseases with a series of illustrative cases 5 - A spectroscopy-based approach to narrow the differential diagnosis in certain clinico-radiological scenarios (leukodystrophies, mitochondrial diseases, etc.) 6 - Conclusion

#### **NREE-129 Abnormalities Associated with Cerebral Cortical (AACs) on MRI**

Participants

Zhiqiang Zhang, MD, PhD, (*Presenter*) Nothing to Disclose

#### TEACHING POINTS

Abnormalities associated with cerebral cortical (AACs) present specific anatomic, pathological, clinical and radiological features, but have less been addressed. We proposed a diagnostic framework by categorizing AACs into focal, regional and diffuse types according to the shape on MRI. In summary, AACs cover a variety of pathologies, show radiological gyrus-thickness sign in focal AACs, outline-sketch sign in regional AACs and flower-mimic sign in diffuse AACs, and are well demonstrated with IR-based T1WI, SWI and DWI on MRI.

#### TABLE OF CONTENTS/OUTLINE

Regional AACs, mainly include diseases of MCD of FCD-I and tumors of long-term epilepsy. Diseases mainly present symptoms of seizures, and are well demonstrated as focal gyrus thickness on IR based T1WI. Regional AACs, lesions are within a lobe at a hemisphere, pathologically diversified into (1) MCDs of polymicrogyria, (2) VDs of cortical laminar necrosis, Isolated cortical venous thrombosis and meningoangiomatosis. (3) tumors of gliomas and MVNT. (4) Brain injury of status epilepticus and (5) CNS infections/inflammation. The diseases feature with consciousness disorders and are well

demonstrated on SWI or DWI with outline-sketches of gyrus. Diffuse AACS, are mostly bilaterally distributed and cover widely cortical areas, include more pathological types of (1) VD of HIE and SSCNS. (2) Tumor of DLGNT. (3) Metabolic of MELAS, hypoglycemic and hyperammonia encephalopathy; (4) CJD (5) NIID and (7) Toxicosis of mercury and benzene. Diseases feature with cognitive impairments, are pathologically associated with energy metabolic abnormality in cortex, and presented with regular geometric/vivid flower-mimic shapes on DWI and FLAIR.

### **NREE-13 Spinal Vascular Lesions: What to Know, and How it Should be Reported**

Participants

Thiago Martins Fernandes Vilela, Mogi das Cruzes, Brazil (*Presenter*) Nothing to Disclose

#### **TEACHING POINTS**

- To review the normal anatomy of the spinal cord, the modified classification of spinal vascular lesions (by Spletz), a more practical classification based on the vascular anatomy of the spinal cord and the inborn or acquired nature of the lesion (Bicentre group). - To review the pathophysiological mechanisms and their clinical correlations. - To present and review some of the metamer and myelomeric syndromes. - To point out what information is expected beyond the diagnosis in each of the cases presented. - To propose a structured report. - To review post-operative image findings and complications of the most used procedures and techniques.

#### **TABLE OF CONTENTS/OUTLINE**

-- Introduction - Anatomy - Classifications - Pathophysiological mechanisms and their clinical correlations - MRI and digital angiography techniques -- Description of the image features, pointing out the most important information that is to be provided. -- Review of the post-operative image findings and complications of the most used procedures and techniques. -- Proposal of a structured report. -- Conclusion

### **NREE-130 Neurosyphilis: Findings From a Reemerging Disease**

Participants

Pedro Henrique Andrade, MD, Sao Paulo, Brazil (*Presenter*) Nothing to Disclose

#### **TEACHING POINTS**

1. To review the syphilis natural history. 2. To review the CNS syphilis involvement. 3. To illustrate imaging findings related to neurosyphilis.

#### **TABLE OF CONTENTS/OUTLINE**

1. Introduction 2. Pathogenesis and natural course of untreated syphilis a. Primary syphilis b. Secondary syphilis c. Tertiary syphilis 3. CNS involvement in syphilis a. meningitis b. meningovascular syphilis c. parenchymal neurosyphilis d. syphilitic dementia (general paresis) e. otologic syphilis f. ocular syphilis g. tabes dorsalis h. congenital neurosyphilis 4. Imaging in syphilis neurological manifestations and differential diagnosis 5. Conclusion 6. Take-home messages 7. References

### **NREE-131 Inborn Errors of Metabolism: A Step by Step Clinico-radiological Approach**

Participants

Gabriela Bandeira, MD, Sao Paulo, Brazil (*Presenter*) Nothing to Disclose

#### **TEACHING POINTS**

1- To review the classification of inborn errors of metabolism. 2- To review the pathophysiology basic principles of the inborn errors of metabolism. 3- To illustrate imaging findings related to genetically determined metabolic disorders.

#### **TABLE OF CONTENTS/OUTLINE**

1 - Introduction 2 - Classification of inborn errors of metabolism Disorders of intermediary metabolism: aminoacidopathies, organic acidurias, lactic acidemias, hyperammonemia and disorders of the urea cycle, disorders of fatty acid oxidation. Disorders of the biosynthesis and breakdown of complex molecules: purine and pyrimidine metabolism, lipoprotein metabolism, lysosomal storage disorders, peroxisomal disorders, porphyrias. Mitochondrial disorders: mitochondrial encephalomyopathy, lactic acidosis and stroke-like episodes (MELAS), Kearns-Sayre syndrome, MERRF (myoclonus epilepsy with ragged red fibers). Neurotransmitter defects and related disorders: disorders of glycine and serine metabolism. Disorders of mineral metabolism: Menkes disease, Wilson disease, others. 3- General and specific clinical features of inborn errors of metabolism 4 - Clinico-radiological approach to inborn errors of metabolism with illustrative cases 5 - Take home message 6 - Conclusion 7 - References

### **NREE-132 Molecular and Genetic Features of Adult Diffuse Gliomas: Essential Updates from WHO 2021 CNS Tumor Classification**

Participants

Ilan Benador, MD, PhD, (*Presenter*) Nothing to Disclose

#### **TEACHING POINTS**

Diffuse adult gliomas have been previously organized into 15 separate entities primarily based on histological features. WHO CNS tumor classification 2021 has reorganized diffuse gliomas into only three subtypes based on molecular and genetic characteristics that better correlate with prognosis and treatment response: 1) astrocytoma, IDH-mutant, 2) oligodendroglioma, IDH-mutant, and 1p19q-codeleted, 3) glioblastoma, IDH-wildtype. Additionally, the following entities have been retired from the tumor nomenclature in the classification scheme: glioblastoma, IDH-mutant, astrocytoma, IDH-wildtype, and oligoastroglioma. This educational exhibit will highlight the key advancements in radiographic and molecular diagnosis of diffuse gliomas.

#### **TABLE OF CONTENTS/OUTLINE**

I. Overview of WHO 2021 CNS Tumor Classification of adult-type diffuse gliomas. II. Characteristic imaging features and molecular classification of adult-type gliomas. A) Astrocytoma, IDH mutant: ATRX mutation, CDKN2A/B deletion. B) Oligodendroglioma, IDH-mutant: 1p19q co-deleted, TERT promoter mutation. C) GBM, IDH-wildtype: TERT promoter mutation, EGFR amplification, Trisomy 7 Monosomy 10. III. Summary of key molecular signatures of each subtype. IV. Quiz: apply this new knowledge to a few example cases to improve diagnostic precision.

### **NREE-133 Distinguishing Mimics from the Great Mimicker: CNS Lymphoma in Immunocompromised Hosts**

Participants

Nima Omid-Fard, MD, BSc, (*Presenter*) Nothing to Disclose

#### **TEACHING POINTS**

• In the immunocompromised setting, there are distinct radiologic findings of CNS lymphoma, including necrotic ring-enhancing lesions, increased propensity for intrasial hemorrhage, and multiplicity. • In this clinical context, advanced imaging with MR perfusion, spectroscopy and diffusion-weighted imaging can be used to increase accuracy in the diagnosis of lymphoma over mimics such as GBM, metastases or infection. • This knowledge is particularly relevant to radiologists as the incidence of immunodeficiency-related CNS lymphoma may be increasing.

#### **TABLE OF CONTENTS/OUTLINE**

• Briefly review typical imaging findings of primary and secondary CNS lymphoma • Discuss the potential for rare and atypical presentations of CNS lymphoma • A greater emphasis will then be placed on the unique imaging findings in immunodeficiency-associated CNS lymphoma, reviewing advanced imaging techniques including MR spectroscopy, diffusion, and MR perfusion. • Side-by-side multisequence comparison of immunocompromised vs immunocompetent CNS lymphoma • Side-by-side multisequence comparison of immunocompromised CNS lymphoma vs glioblastoma • Side-by-side multisequence comparison of immunocompromised CNS lymphoma vs metastasis • Side-by-side multisequence comparison of immunocompromised CNS

lymphoma vs infection (toxoplasmosis)

### **NREE-134 The B - T Guide of Lymphomas**

Participants

Pedro Castro, MD, Rio de Janeiro, Brazil (*Presenter*) Nothing to Disclose

#### **TEACHING POINTS**

To demonstrate the typical MRI patterns and the classification of central nervous system (CNS) lymphomas. To explain the difference between intra-axial and extra-axial primary CNS lymphoma. To illustrate the importance of MRI in the trivial and atypical features of CNS lymphomas. To depict the importance of MRI in the differential diagnosis.

#### **TABLE OF CONTENTS/OUTLINE**

1. Background. 2. Diffuse large B-cell lymphoma and high-grade Burkitt-like B-cell lymphoma. 3. Low-grade T-cell lymphoma. 4. Lymphomas in the immunocompromised patient: AIDS-related diffuse large B-cell lymphoma. 5 EBV-positive diffuse large B-cell lymphoma, NOS. 6. Lymphomatoid granulomatosis. 7. Primary CNS posttransplant lymphoproliferative disorder. 8. Intravascular lymphoma. 9. MALT lymphoma of the dura. 10. Typical features, including hypercellularity and moderate to low perfusion. 11. Imaging assessment of the atypical imaging patterns of CNS lymphomas, including spontaneous remission and relapsing presentation, and corticospinal tract infiltration. 12. Differential diagnoses: meningioma, sarcoidosis, non-Langerhans cell histiocytosis, and IgG4-related disease. 13. Flowchart of evaluation. 14. Take-Home messages.

### **NREE-135 Unraveling Lesions of Chiasmatic-Hypothalamic Region: A Case Based Approach**

**Awards**

**Certificate of Merit**

Participants

Virginia Simonini, MD, Sao Paulo, Brazil (*Presenter*) Nothing to Disclose

#### **TEACHING POINTS**

- The hypothalamus is a midline structure located below the thalamus, and together with the epithalamus and subthalamus, they constitute the diencephalon and its main function is homeostasis. - The optic chiasm is also a midline structure located anteriorly to the hypothalamus and is the point where both optic nerves meet and continue posteriorly as the optic tracts. - The hypothalamic-chiasmatic region can be affected by many diseases from multiple etiologies, such as neoplastic, developmental abnormalities and inflammatory/granulomatous, and the aim of this study is to didactically illustrate such cases. - Many important structures surround the hypothalamic-chiasmatic region, such as mamillary bodies (MB), pituitary stalk (PS), neuro and adenohypophysis, and can also be affected by those diseases. - Computed tomography (CT) is a limited method for the hypothalamic-chiasmatic region evaluation, since it has low contrast between structures. Hence, the imaging modality of choice for examination of this area is magnetic resonance imaging (MRI), specially midline sagittal slices.

#### **TABLE OF CONTENTS/OUTLINE**

- Illustrate normal hypothalamic-chiasmatic region anatomy. - Expose didactic cases of hypothalamic-chiasmatic region lesions, from many etiologies and how to evaluate through imaging, illustrating described findings to consolidate the acquired knowledge. - Bibliographical references.

### **NREE-136 Retinoblastoma: A Giant for the Little Ones**

Participants

Karolina Cancela, MD, Sao Paulo, Brazil (*Presenter*) Nothing to Disclose

#### **TEACHING POINTS**

The purposes of this exhibition are: review the anatomy of the eyeball, including its main anatomical limits and the structures that compose it. Review vascularization characteristics and normal MR imaging findings. Correlated clinical syndromes. Discuss and illustrate the main imaging patterns of retinoblastoma. Detail the lesions according to their topography, whether unilateral, bilateral or even trilateral, configuring pineoblastoma. Describe diagnostic scenarios through illustrative cases, focusing on typical imaging patterns, unexpected tumor findings, dissemination patterns and imaging aspects of complications and post-treatment.

#### **TABLE OF CONTENTS/OUTLINE**

Retinoblastoma with its imaging patterns on MRI sequences; unilateral, bilateral or trilateral; structures involved: intra-orbital and/or extra-orbital; unexpected findings: other tumors as main differential diagnoses; post-treatment evaluation and complications; final considerations.

### **NREE-137 Imaging of Common and Uncommon Post-treatment Related Complications in the Brain and Spinal Cord**

Participants

David Michaels, MD, (*Presenter*) Nothing to Disclose

#### **TEACHING POINTS**

• Present cases which highlight both common and uncommon complications related to neurological treatment • Identify specific imaging findings to look for when presented with post-treatment cases • Give a brief summary of the natural time course of the above mentioned complications and how they will evolve over time on follow up imaging studies

#### **TABLE OF CONTENTS/OUTLINE**

Complications from treatment, whether related to medical, surgical, or radiation treatments, are important for the neuroradiologist to recognize and diagnose. Often, recognition of such complications is crucial, as it can change future care of the patient. This education exhibit will present cases which illustrate both common and uncommon complications related to neurological treatment. We will provide a succinct overview of patient history, followed by a comprehensive interpretation of pertinent imaging studies. Our institution functions as a large tertiary care referral center for the region, which translates into both rare complications of common treatments, and common complications of rare treatments. Finally, we will end each case with a brief comment on the prognosis of each complication, and what to look for on future imaging studies. Cases include acute toxic leukoencephalopathy from both immunosuppressive and chemotherapeutic agents, radiation-induced leukoencephalopathy and meningioma formation, and postsurgical complications to include Teflon granuloma and remote cerebellar hemorrhage, among others.

### **NREE-138CS Development and Clinical Translation of a Neuro-analysis Pipeline for Automatic Quantitative Analysis Using the Kaapana Platform**

Participants

Vikas Bommineni, Orlando, FL (*Presenter*) Nothing to Disclose

#### **TEACHING POINTS**

Quantitative measures, such as brain atrophy patterns related to neurodegenerative diseases, may provide complementary information to radiologists. However, translation of quantitative biomarkers to clinical practice has been limited. Recent advances in image analysis allow automated and rapid processing of medical image data, while new statistical methods enable collection of large harmonized reference datasets to perform comparative analyses of individual measures. We present a workflow on Kaapana, an open-source framework for medical data analysis, for translating laboratory-validated, quantitative measures into next-generation, precise biomarkers towards personalized diagnostics. The pipeline includes pretrained deep

learning(DL) models for segmentation of brain anatomy, data harmonization to a cognitively normal reference population, and calculation of machine-learning based individualized summary scores that quantify neurodegeneration and brain aging. The pipeline inputs DICOM scans directly from scanners or Picture Archival and Communications Systems (PACS) and generates segmentation maps and a patient-specific summary report to visualize measures in comparison to expected distributions based on reference populations. Outputs are converted to DICOM for archival on PACS.

#### TABLE OF CONTENTS/OUTLINE

1) Introduction2) Neurodegeneration biomarkers3) Neuro-analysis pipeline:a) Pre-processing: Nifti conversion, skull stripping tissue segmentationb) Analysis: Data harmonization extraction of quantitative biomarkersc) Generation of summary reportd) DICOM output4) Workflow: Push data to Kaapana, trigger pipeline, QC results and push to PACS5) Future enhancements

#### **NREE-139 Improving Automated Substantia Nigra Segmentation Accuracy Using a Novel Test-time Normalization Method**

Participants

Tao Hu, MSc, Nagoya, Japan (*Presenter*) Nothing to Disclose

#### TEACHING POINTS

1. To understand the feasibility and benefits of substantia nigra (SN) segmentation using T2-weighted magnetic resonance imaging (MRI).2. To understand how the proposed test-time normalization (TTN) can be used for improving segmentation accuracy.3. To understand the the potential applications of the segmentation results and estimated uncertainty maps in clinical scenarios.

#### TABLE OF CONTENTS/OUTLINE

1. Review of automated SN segmentation using MRI- Relationship between SN and progression of Parkinson Disease (PD)- Difficulties of automated SN segmentation from MRI- Conventional methods for automated SN segmentation2. Automated SN segmentation with the proposed TTN- Review of test-time augmentations in segmentation tasks- Detailed explanations of the proposed TTN- Algorithm of the proposed TTN and its application in segmentation- Review of losses for tiny structure segmentation- Combination of the proposed TTN and investigated losses in segmentation- Segmentation results with and without TTN- Benefits of the proposed TTN3. Potential applications of automated SN segmentation- SN volume and asymmetric metric estimation using segmentation results- Indicating vague boundaries of SN using uncertainty maps- longitudinal SN inspection using automated segmentation results

#### **NREE-14 Lumbar Spine MR Examination (2 Minutes, 30 seconds) Faster than Instant Noodles Using GRAPPA and Deep Learning Reconstruction with High Acceleration Factor**

Participants

Takeshi Hasuda, RT, Ueda-Shi, Japan (*Presenter*) Nothing to Disclose

#### TEACHING POINTS

This exhibition was approved by our Medical Ethics Committee. One of the disadvantages of MRI examinations is the relatively long time required to acquire MR images. In MRI examinations of the spine, there are cases in which the examination needs to be performed quickly due to trauma, or patients with hernias or other pain that make it impossible to perform the examination in the same position for long periods of time due to rounded backs. In recent years, reconstruction technology using Deep Learning has been attracting attention, and high-speed and high-resolution MRI have been attracting attention. This education focused on Deep Resolve (DR), a Deep Learning Reconstruction (DLR) method, to understand the characteristics of DR and to optimize the imaging protocol. The teaching points of this exhibition are to (1) understand the outline of DR by validation using phantoms and to examine the optimal conditions in combination with parallel imaging (GRRAPPA), (2) practice the validation results in clinical practice and to analyze problems, and (3) optimize the parameters of Spine's imaging conditions based on the results and demonstrate scan times faster than instant noodles.

#### TABLE OF CONTENTS/OUTLINE

1. overview 2. understanding the characteristics of DR (Deep Resolve) 3. phantom verification 4. trial and error in actual clinical practice 5. MR images (comparison of original and optimized images) Faster than instant noodles

#### **NREE-140 Synthetic MRI Evaluation of Sella Pathologies**

Participants

Ranliang Hu, MD, (*Presenter*) Stockholder, Moderna, Inc;Stockholder, Pfizer Inc

#### TEACHING POINTS

Synthetic MRI is an emerging technique for clinical imaging, able to generate multiple contrast weighted images and parametric maps based on a single acquisition using multiple delay and and echo times. While Synthetic MRI has become available from multiple vendors and recent studies have shown it to produce comparable image quality to that of conventional brain MRI, it is still underutilized in part due to lack of experience among radiologists with the technique and post-processing. The sella region is complex for neuroradiologic evaluation due its small anatomy, subtle pathologies, complex tissue/enhancement characteristics. Technical developments in 3D synthetic MRI with higher spatial resolution has made sella imaging feasible, with ability to perform qualitative and quantitative tissue characterization. This education exhibit will review recent developments in Synthetic MRI for neuroimaging and through case examples demonstrate its role in the evaluation of pathologies in the sella region.

#### TABLE OF CONTENTS/OUTLINE

1. Background: a. Brief review of current literature2. Technical Overview: a. Acquisition b. Post-processing3. Case Review: a. Pituitary hyperplasia b. Rathke's cleft cyst c. Epidermoid cyst d. Pituitary adenoma e. Post-treatment adenoma f. Meningioma g. Craniopharyngioma4. Summary: a. Key points for qualitative interpretation b. Quantitative differences between pathologies c. Challenges and limitations

#### **NREE-141 Trigeminal, Facial, Hypoglossal and Greater Occipital Nerves: Had You Seen Them Like This Before?**

Participants

Marta Barrios Lopez, MD, Santander, Spain (*Presenter*) Nothing to Disclose

#### TEACHING POINTS

-To summarize the most important anatomical relationships of the extracranial segments of the main cranial nerves (including the trigeminal, facial and hypoglossal nerves). We will also include those of the greater occipital nerve, the thickest cutaneous nerve in the human body. -To demonstrate the ability of 3D CRANI, an innovative MRI sequence, to help visualize these branches.

#### TABLE OF CONTENTS/OUTLINE

-INTRODUCTION- THE 3D CRANI SEQUENCE: a relatively new MRI technique that combines a STIR TSE black-blood sequence, a motion-sensitized driven equilibrium (MSDE) pulse and a pseudo steady-state (PSS) sweep.- TRIGEMINAL NERVE: introduction and origin. Extracranial segment.- Ophthalmic nerve. Maxillary nerve. Mandibular nerve: main anatomical relationships and branches. Useful details and their correlation with the clinic. - FACIAL NERVE: introduction and origin. Extracranial segment. Main extracranial branches and their relationship to the parotid gland. - HYPOGLOSSAL NERVE: introduction and origin. Main anatomical relationships in the neck.- GREATER OCCIPITAL NERVE: introduction, importance, anatomical landmarks. -CONCLUSIONS: 3D CRANI is useful to visualize the extraforaminal segments of the major cranial nerves.

#### **NREE-142 Perfusion Imaging: The Cerebral Path to the Final Diagnose**

Participants

Pedro Castro, MD, Rio de Janeiro, Brazil (*Presenter*) Nothing to Disclose

#### TEACHING POINTS

To depict the perfusion imaging applications to assess neoplastic, ischemic, post-ictal, and infectious diseases. To clarify the physics and how to interpret the brain perfusion maps. To elucidate the advantages and disadvantages of utilizing perfusion compared to the permeability.

#### TABLE OF CONTENTS/OUTLINE

1. Background. 2. Imaging protocol and physics. 3. Advantages and disadvantages of perfusion versus permeability. 4. Applications in CNS tumors. 5. Perfusion and the therapeutic and molecular diagnosis implications in neoplastic disease. 6. Applications in stroke. 7. The therapeutic implications of the perfusion in ischemia. 8. Differential diagnosis, including infectious diseases and post-ictal changes. 9. Flowchart for assessment of brain diseases with perfusion. 10. Take-Home messages.

#### **NREE-143 Mismatch of Arterial Spin Labeling (ASL) Compared to MR Dynamic Susceptibility Contrast Perfusion Weighted Imaging (DSC-PWI) in the Central Nervous System Diseases**

Participants

Xiang Liu, MD, PhD, (*Presenter*) Nothing to Disclose

#### TEACHING POINTS

MR dynamic susceptibility contrast perfusion weighted imaging (DSC-PWI) is the most commonly used perfusion imaging technique in the central nervous system (CNS) diseases, including brain tumors. MR arterial spin labeling (ASL) is a novel noninvasive MR sequence to quantify tissue blood flow. Most published studies showed that the relative cerebral blood volume (rCBV) derived from DSC-PWI and cerebral blood flow (CBF) of ASL. Based on our experience of more than 950 patients who had concurrent ASL and DSCPWI examinations, the purpose of this Education Exhibit is to present following teaching points of mismatch between ASL and DSCPWI in the evaluation of hemodynamic changes in the CNS diseases. 1. Learning the principle of DSC-PWI; 2. Learning the principle of ASL; 3. Learning advantages and limitations of DSC-PWI and ASL in the CNS diseases;

#### TABLE OF CONTENTS/OUTLINE

1. Introduction of the principle of DSC-PWI; 2. Introduction of the principle of ASL; 3. Sample cases comparing between DSC-PWI and ASL in glioma, brain metastasis, meningioma, vascular malformation, and MELAS, etc ; 4. Summary of advantages and limitations of DSC-PWI and ASL in the CNS diseases;

#### **NREE-15 How Diffusion Tensor Imaging Enables Direct Targeting for Focused Ultrasound Surgery**

Participants

Hiroki Hori, (*Presenter*) Nothing to Disclose

#### TEACHING POINTS

The purpose of this exhibit is to summarize how to implement diffusion tensor imaging (DTI) as a direct targeting method in transcranial MR-guided focused ultrasound surgery (TcMRgFUS). Although the atlas-based targeting method of indirect measuring the ventral intermediate nucleus (VIM) of the thalamus from the posterior commissure (PC) was widely used, it may not be precise, as the locations of the VIM, ventral caudal nucleus (Vc) and pyramidal tract (PT) etc., may vary in each subject based on our pilot study. Especially in the case of atrophic brain, it is difficult to measure the precise location of the VIM using the conventional indirect targeting method, hence a direct targeting strategy is more desired. DTI enables visualization and characterization of fibrous structures in the brain, and tractography-based direct targeting may become the method of choice for surgical targeting as it is capable of providing patient-specific coordinates. DSI studio is an open source, high spec image processing software tool that facilitates DTI data analysis. DSI studio assisted tractography-based direct targeting offers a practical and flexible approach to improve treatment efficacy and safety profiles after TcMRgFUS treatments.

#### TABLE OF CONTENTS/OUTLINE

1. What is TcMRgFUS a. Overview b. Traditional method of assessment c. Ablating location 2. How to visualize each fiber a. Visualize VIM b. Visualize Vc c. Visualize PT 3. Location of the nucleus and ablation outcome a. Mild adverse event b. Severe adverse event c. Recurrence and mild adverse event d. Perfect treatment 4. Future outlook

#### **NREE-16 The Role of APTw with fMRI, and DTI in Preoperative Planning**

Participants

Sevcan Turk, MD, Ann Arbor, MI (*Presenter*) Nothing to Disclose

#### TEACHING POINTS

- Highlight the role of amide proton transfer weighted (APTw) imaging for preoperative planning of the brain tumors; grading, genetic mutations, peritumoral invasion, and white matter tumor infiltration• Discuss the potential of using APTw imaging in assessing treatment response and discrimination of true tumor progression from pseudoprogression• APTw high signals: hypercellular components of the tumor, extracellular tumor matrix, hematoma, necrosis. • Discuss the pros and cons, artifacts in interpreting APTw, fMRI, DTI, PWI

#### TABLE OF CONTENTS/OUTLINE

- Overview of imaging characteristics of brain tumors with emphasis on APTw in conjunction with fMRI, DTI, and PWI for preoperative planning. • Demonstrate cases of tumor progression versus treatment effects, peritumoral invasion, and genetic mutation and grade correlation APT, PWI, DWI parameters with the role of fMRI and DTI. • Differences of pediatric tumors on advanced imaging, the added value of APTw imaging • Necrosis, hemorrhage, calcification, and extracellular matrix effects on the signal intensity in APT, fMRI, DTI, and perfusion-weighted imaging. Pitfalls and accuracy of each advanced imaging method.

#### **NREE-17 Neuronal and Mixed Glioneuronal Tumors: Image Correlation X Molecular Profile**

Participants

Milena Ouchar Sabino, MD, Sao Paulo, Brazil (*Presenter*) Nothing to Disclose

#### TEACHING POINTS

- To review the main imaging findings of neuronal and mixed glioneuronal tumors with cases from three hospitals imaging departments. - To correlate some of the neuronal and mixed glioneuronal tumors to specific altered molecular profiles.

#### TABLE OF CONTENTS/OUTLINE

- A brief discussion of the new WHO 2021 CNS tumors classification, focusing on neuronal and mixed glioneuronal tumors.- The most frequently altered molecular pathways.- Correlation of neuronal and mixed glioneuronal tumors according to their most frequent location and clinical presentation.- A review of the main imaging features - cases of neuronal and mixed glioneuronal tumors and their associated altered molecular profiles: gangliogliomas, desmoplastic infantile ganglioglioma/astrocytoma, papillary glioneuronal tumor, DNET, rosette-forming glioneuronal tumor, multinodular and vacuolating neuronal tumor, diffuse leptomeningeal glioneuronal tumor, central neurocytoma, extraventricular neurocytoma, dysplastic cerebellar gangliocytoma (Lhermitte-Duclos), myxoid glioneuronal tumor.- An approach to neuronal and mixed glioneuronal tumors according to their imaging appearance (solid or cystic-solid and pseudocystic).

#### **NREE-18 Diffuse Gliomas Genomics: What Radiology Residents Need to Know**

## Participants

Yu Bin Lee, MD, Gwang Ju, Korea, Republic Of (*Presenter*) Nothing to Disclose

### TEACHING POINTS

1. Two review the major changes of the fifth edition of the WHO Classification of Tumors of the CNS (WHO CNS5).2. Two review the clinical implications and related imaging findings of the representative genetic mutations associated with diffuse gliomas.

### TABLE OF CONTENTS/OUTLINE

1. Introduction2. The major changes of the WHO CNS53. Clinical implications and imaging evaluation of tumor genomics1) Adult-type diffuse gliomas- Isocitrate dehydrogenase (IDH) mutation- 1p/19q codeletion- O-6-Methylguanine-DNA-Methyltransferase (MGMT)- ATRX loss- TP53 mutation- TERT promoter mutation- EGFR amplification2) Pediatric-type diffuse low-grade gliomas- BRAF mutation in MAPK pathway3) Pediatric-type diffuse high-grade gliomas- H3 K27-altered- H3 G34-mutant4. AI approaches in radiogenomics5. Summary

## **NREE-19 Update on Radiophenotypes of Central Nervous System Tumors After 5th Edition WHO Classification 2021**

## Participants

Taina Estruzani, MD, Sao Paulo, Brazil (*Presenter*) Nothing to Disclose

### TEACHING POINTS

Recognize high specificity imaging phenotypes of CNS Tumors. Discuss modifications of taxonomy. Characterize pediatric and adult CNS tumors. Differentiate between high-grade and low-grade gliomas. Correlate imaging and molecular features.

### TABLE OF CONTENTS/OUTLINE

Imaging phenotypes of CNS Tumors. Gliomas imaging classification. Pediatric-type diffuse low-grade gliomas. Pediatric-type diffuse high-grade gliomas. Adult-type diffuse gliomas. Some new types of tumors according to molecular biomarkers. Modifications of new CNS tumors taxonomy. Differential diagnosis of CNS tumors.

## **NREE-2 Photon-Counting CT Applications in Neuroradiology**

## Awards

### Certificate of Merit

## Participants

Fides Schwartz, MD, Durham, NC (*Presenter*) Nothing to Disclose

### TEACHING POINTS

Photon-counting computed tomography (PCCT) is a new CT technology. PCCT uses energy-resolving detectors, instead of integrating the entire x-ray signal (energy integrating detectors: EID), enabling spectral acquisitions without the need of specialized acquisition strategies (e.g., dual-source). PCCT records photons in different energy bins, starting at a minimum energy threshold, so electronic noise can be avoided altogether. PCCT detectors use a two-step conversion (x-rays to electrical signal), rather than the 3-step conversion EID (x-rays to light to electrical signal), and inherently have higher spatial resolution as no septa (to separate voxels) are needed. This project is geared toward introducing the emerging technology of PCCT to the RSNA neuroradiology imaging community. The details of this technology will be explained using diagrams of the physics principles, and examples of standard EID vs PCCT patient scans to demonstrate the performance of the new scanner system.

### TABLE OF CONTENTS/OUTLINE

1. PCCT - Detectors a. Comparison of energy-integrating vs photon-counting detectors b. How is higher spatial resolution of PCCT achieved? 2. PCCT - Photon Binning a. How does photon binning work? b. How are energy thresholds defined? c. How do thresholds help with electronic noise? 3. PCCT - Spectral Data a. How is it always available? b. What can it be used for? 4. Clinical examples a. Temporal Bone - superior spatial resolution b. Brain without contrast - higher image contrast c. CTA - improved contrast conspicuity d. Myelograms - material decomposition capabilities

## **NREE-20 Retinoblastoma Management: Emphasis on RB-RECIST Criteria with MRI Correlation after Intra-arterial Treatment**

## Participants

Sevcan Turk, MD, Ann Arbor, MI (*Presenter*) Nothing to Disclose

### TEACHING POINTS

• Highlight the role of MRI and diffusion-weighted imaging in the evaluation of retinoblastoma treatment response. • Discuss the ultrasound and MRI correlation of the different treatment response types of retinoblastoma. • Discuss the pearls and pitfalls in interpreting ultrasound and MRI.

### TABLE OF CONTENTS/OUTLINE

• Clinical presentation, genetics, and epidemiology from the ophthalmologist field of view: evaluation of retinoblastoma with orbital US, CT, and MRI. • Retinoblastoma classification: what radiologists need to know. • When Intra-arterial treatment is indicated and how we do it. • Overview of imaging characteristics of retinoblastoma after intraarterial treatment with emphasis on ultrasound- MRI correlation of the RB-RECIST criteria assessment. • Discuss type 0-IV tumor regression patterns with MRI correlate. • Discuss the role of diffusion-weighted imaging in the discrimination of treatment effect and tumor progression. • DCE and DSC perfusion, SWI value in treatment response assessment. • The role of MRI in the evaluation of extraocular extension, optic nerve invasion, post-treatment complications, and intracranial abnormalities. • Surveillance: radiation field, secondary tumors, and beyond the optic nerve.

## **NREE-21 CSF Circulation and Glymphatic System of the Spinal Cord**

## Participants

Shotaro Naganawa, MD, Ann Arbor, MI (*Presenter*) Nothing to Disclose

### TEACHING POINTS

1. To review CSF circulation in the spinal cord2. To review glymphatic system of the spinal cord3. To explore spinal cord diseases related to CSF circulation and glymphatic system in the spinal cord

### TABLE OF CONTENTS/OUTLINE

CSF circulation in the spineGlymphatic-lymphatic fluid transport system of the spinal cordSpinal cord diseases related to CSF production, absorption, and loss (leakage)-CSF leakage and CSF venous fistulas -Hypersecretion of CSF after subarachnoid hemorrhageSpinal cord diseases related to CSF flow abnormality-Chiari malformation-Spinal canal stenosis-Amyotrophic lateral sclerosis (ALS)-Spinal web, spinal cord herniation Spinal cord diseases related to glymphatic system-Iatrogenic intrathecal Gd administration -Spinal neurosarcoidosis-Neuromyelitis optica-Preyrix stateDrug delivery and glymphatic system-Spinal muscular atrophy -ALS and other neurodegenerative diseases

## **NREE-22 Deep Brain Stimulation (DBS) - Pre and Post Operative Imaging, From Adequate Nucleus and Fiber Tract Localization to Electrode Misplacement**

## Awards

### Cum Laude

#### Participants

Leandro Souza, MD, Sao Paulo, Brazil (*Presenter*) Nothing to Disclose

#### TEACHING POINTS

This panel aims to guide a good quality exam acquisition for Deep Brain Stimulator (DBS) study, in both pre and post operative evaluations. It will be shown how to accurately localize the targets for DBS implantation in different scenarios, such as Parkinson Disease (PD), tremors, dystonias and obsessive-compulsive disorder (OCD), with images acquired on CT and MRI, these from 1,5T, 3T and 7T, correlating the electrode targets in each case with the anatomy and histology. To showcase the MRI and CT imaging protocols, with advanced sequences that are useful for evaluation, such as diffusion tensor imaging (DTI) and functional brain MRI, for each scenario (pre e post operative), its uses and limitations. Post operative protocol and images to assert possible structural reasons for clinical failure of the DBS procedure and electrode misplacement.

#### TABLE OF CONTENTS/OUTLINE

1 - pre operative study: 1.1 - indications, physiology of action, and scientifically proven improvement 1.1.1 - PD, tremor and dystonias 1.1.2 - OCD 1.2 - anatomy of the targets: 1.2.1 - histology 1.2.2 - MRI 1,5T, 3T and 7T 1.3. - acquisition protocol: 1.3.1 - CT 1.3.2 - structural MRI: IR, T2, FGATIR, DP 1.3.3 - functional MRI: DTI, fMRI 2 - post operative study 2.1 - acquisition protocol: 2.1.1 - CT 2.1.2 - MRI 2.2 - imaging evaluation 2.2.1 - electrode positioning 2.2.2 - other possible structural causes of failure

#### **NREE-23 Beyond Five Millimeters Below the Foramen Magnum: Exploring the Depths of the Chiari 1 Deformity**

#### Participants

James Loftus, MD, Rochester, NY (*Presenter*) Nothing to Disclose

#### TEACHING POINTS

1. Define the proper nomenclature and terminology of the Chiari 1 and related deformities including 0/0.5 and 1.5 and how they differ in pathogenesis and embryology from the other subtypes (Don't call it a malformation!). 2. Detail the imaging evaluation of the Chiari 1 and related deformities including conventional and phase contrast magnetic resonance imaging. 3. Review surgical techniques and post-surgical imaging of the Chiari 1 and related deformities including expected findings and complications.

#### TABLE OF CONTENTS/OUTLINE

I. Review of the pathogenesis, embryology, nomenclature, and proper terminology surrounding the Chiari 1 and related deformities. a. Subtypes of the Chiari deformities (0-1.5) and malformations (2-5) and their pathologic and embryologic basis. b. Further description of the anatomic changes in Chiari 0/0.5, 1, and 1.5 compared to normal patients. II. Imaging evaluation of the Chiari 0/0.5, 1, and 1.5 deformities. a. Conventional brain and cervical spine MRI. i. Proper measurement of tonsillar herniation and controversies. ii. Clues to abnormal CSF flow dynamics on conventional MRI sequences (No phase contrast, no problem!). b. Phase contrast MRI (PC-MRI). i. Evaluating the re-phased image, magnitude image, and phase image. ii. Brief note on quantitative PC-MRI. III. Surgical techniques and post-surgical imaging and complications. a. Surgical techniques and expected post-surgical imaging findings including evaluation of the adequacy of decompression on PC-MRI. b. Post-surgical complications the radiologist must recognize.

#### **NREE-24 Transfontanellar Ultrasound Beyond Hemorrhages In Infants**

#### Participants

Pedro Da Silva, MD, Sao Paulo, Brazil (*Presenter*) Nothing to Disclose

#### TEACHING POINTS

Transfontanellar ultrasound (TFUS) has been increasingly used as a diagnostic and screening tool in pediatrics, even as a first-line imaging technique, due to its advantages over other imaging methods, especially for critical ill newborns, often unable to perform the other ones. In addition, ultrasound (US) is possible to be repeated whenever necessary, without harm to the patient. In this context, grey-scale, color and spectral Doppler assessment with TFUS plays an important role in the evaluation and screening of findings beyond hemorrhages in infants, including ventriculomegaly, cerebral ischemia and its progression, as well as cerebral blood flow patterns and complications related to the use of Extracorporeal Membrane Oxygenation (ECMO) in seriously ill children. Assessment of ventricular measurements in infants allows for rapid diagnoses, monitoring of ventricular dilatations in children who need several exams, and suggests early interventions, avoiding unnecessary and expensive additional imaging methods. Several US measurements of ventricular dimensions have been proposed and increasingly used in control and clinical or surgical decisions. Furthermore, due to the great impact on morbidity and mortality of hypoxic-ischemic encephalopathy in the neonatal population, the TFUS also plays an important role in the characterization and progression of ischemic lesions and their variations, such as ischemic lesion with hemorrhagic transformation.

#### TABLE OF CONTENTS/OUTLINE

· Review and discuss the advantages of transfontanellar ultrasound as an imaging method in infants · Discuss and understand ultrasound imaging and its sensitivity and specificity of intracranial findings beyond hemorrhages

#### **NREE-25 Craniosynostosis and Craniofacial Malformations: A Radiological and Surgical Perspective**

#### Participants

Jameson Da Silva, MD, Teresina, Brazil (*Presenter*) Nothing to Disclose

#### TEACHING POINTS

Discuss important anatomical features of craniosynostosis which have surgical implications and should be included in imaging reports. Consider the role of CT, especially with 3D reconstruction, in preoperative planning. Briefly describe main strategies of surgical approaches for craniosynostosis, with technique considerations relevant for the imaging specialist.

#### TABLE OF CONTENTS/OUTLINE

Summary- Introduction.- Relevant Anatomy.- Craniosynostosis classification and types.- Craniofacial malformations associated.- Imaging technique and protocol (Radiography, CT, conventional MRI and MRI angiography).- Imaging of normal and pathologic sutures.- Craniosynostosis clinical syndromes associated.- Postoperative follow-up imaging.- The different surgical options available for the treatment of different types of craniosynostosis.- Conclusions.- References.

#### **NREE-26 One Side at a Time - Unilateral or Asymmetric Centrencephalic Lesions**

#### Awards

#### Certificate of Merit

#### Participants

Samya Alves, MD, Sao Paulo, Brazil (*Presenter*) Nothing to Disclose

#### TEACHING POINTS

Centrencephalic abnormalities can be detected on neuroimaging in a wide variety of pathological conditions. Bilateral and symmetrical alterations are well established in the literature, however, when we look at unilateral conditions, there is a gap in the systematization of the approach. Unilateral or asymmetric centrencephalic lesions will be addressed by an algorithm developed according to typical imaging patterns, such as diffusion restriction, SWI, expansive lesions and T1 contrast enhancement. The purpose of this exhibition is to:- Review anatomy and imaging aspects of the basal ganglia and thalamus;- List normal variations, common benign findings and main diseases that present by unilateral or asymmetric centrencephalic involvement;- Review of the main pathologies on a case-based approach;- Organize the radiologic reasoning with an algorithm.

## TABLE OF CONTENTS/OUTLINE

1. ANATOMY AND IMAGING- Basal ganglia and thalamus- Imaging techniques 2. DIFFERENTIAL DIAGNOSIS OF UNILATERAL/ASYMMETRIC CENTRECEPHALIC LESIONS- Normal variants- Restricted diffusion- SWI- Volumetric alterations: enlargement and atrophy- T1 alteration: hypersignal, contrast enhancement and morphologic change.

### NREE-27 Pediatric Neurodegenerative Diseases: Pathophysiology and Neuroimaging Features

#### Awards Certificate of Merit

Participants  
Ryo Kurokawa, MD, PhD, Ann Arbor, MI (*Presenter*) Nothing to Disclose

#### TEACHING POINTS

The aim of this review is to 1. Understand the concept of pediatric neurodegenerative disorders (pedND) 2. Demonstrate the brain imaging findings of pedND 3. Show how clinical features can contribute to the diagnosis of pedND

## TABLE OF CONTENTS/OUTLINE

1. Overview and definition of pedND 2. Triplet Repeat Disease: Huntington disease (HD), Myotonic dystrophy type 1 (DM1), Spinocerebellar ataxia (SCA) type 1, SCA2, SCA3/Machado-Joseph disease (MJD), SCA7, SCA17, Fragile X syndrome (FXS), Friedreich's ataxia (FRDA) 3. Autosomal Dominant: HD, DM1, SCA1, SCA2, SCA3/MJD, SCA7, SCA17. Autosomal Recessive: FRDA, Ataxia with Oculomotor Apraxia type 1 (AOA1), AOA2, Autosomal recessive spastic ataxia of Charlevoix-Saguenay (ARSACS), Ataxia telangiectasia (AT), Marinesco-Sjogren syndrome (MSS), Ataxia with vitamin E syndrome (AVED), Progressive myoclonus epilepsy type 1 (EPM1), Chorea-acanthocytosis (CHAC) 5. X-linked: FXS, X-linked Charcot-Marie-Tooth disease (CMTX1) 6. Cerebellar ataxia in pedND 7. Diseases associated with secondary neurodegeneration: Amino acid metabolism disorders, Urea cycle disorders, Carbohydrate metabolism disorders, Mitochondrial disorders, Lysosomal storage disease, Peroxisomal disorders, Metal metabolism disorders Summary 1. PedND have diverse pathomechanisms. 2. Some pedNDs have pathognomonic radiological features that can help in differentiation. 3. Clinical features can help diagnose pedNDs, especially when radiological findings are similar to others.

### NREE-28 Neuroimaging of Hypophysitis: Anatomy, Etiology, Pathology, and Imaging Mimics

Participants  
Ryo Kurokawa, MD, PhD, Ann Arbor, MI (*Presenter*) Nothing to Disclose

#### TEACHING POINTS

The purpose of this exhibit is: 1. To review the embryology and anatomy of the pituitary gland 2. To summarize the various etiologies and pathologies of hypophysitis and the mimics 3. To demonstrate how neuroimaging contributes to the diagnosis of hypophysitis

## TABLE OF CONTENTS/OUTLINE

Outline 1. The embryology and anatomy of the pituitary gland 2. Etiology, epidemiology, pathology and clinical features of hypophysitis 3. Neuroimaging findings in hypophysitis- Lymphocytic hypophysitis- Granulomatous hypophysitis (primary or secondary: Crohn D, sarcoidosis, GPA, tuberculosis, fungal infection)- Plasmacytic/immunoglobulin G4-related hypophysitis- Xanthomatous hypophysitis- Necrotizing hypophysitis- Immune checkpoint inhibitor-related pituitary adverse effects: isolated adrenocorticotropic hormone deficiency, hypophysitis- Anti-pituitary-specific transcriptional factor (PIT)-1 antibody-related hypophysitis- Differential diagnosis: pituitary adenoma, pituitary tumor, pituitary blastoma, craniopharyngioma, metastasis, lymphoma, histiocytosis, germ cell tumor, abscess

### NREE-29 Diversity of Hyperammonemia-associated CNS Abnormalities: Pathophysiology and Neuroimaging Features

Participants  
Ryo Kurokawa, MD, PhD, Ann Arbor, MI (*Presenter*) Nothing to Disclose

#### TEACHING POINTS

The aim of this exhibit is to 1. Review the various causes and mechanisms of hyperammonemia 2. Demonstrate the imaging characteristics associated with the causes of hyperammonemia 3. Show how clinical features can contribute to a diagnosis

## TABLE OF CONTENTS/OUTLINE

Content organization 1. Introduction-Mechanisms of hyperammonemia-Mechanisms of hyperammonemic encephalopathy 2. High ammonia production-Infection: Urease-producing bacteria (Proteus, E-coli, Klebsiella)-Increased protein load: Gastrointestinal bleeding, Total parenteral nutrition-Elevated catabolism: Exercise, Seizure/ Eclampsia, Trauma/Burn 3. Portosystemic shunt-Cirrhosis-Neoplasm-Congenital: Congenital portosystemic shunt syndrome, Noonan syndrome-Transjugular intrahepatic portosystemic shunt (TIPS) 4. Metabolic disorders-Congenital: Urea cycle disorders, Organic acidemias, Fatty acid oxidation disorders, Mitochondrial diseases-Drugs: Valproic acid, Acetaminophen, Carbamazepine, 5-Fluorouracil (5-FU), etc. 5. Decreased urine excretion-Renal failure-Urinary retention 6. Miscellaneous Multiple myeloma 7. Summary 1. Various etiologies cause hyperammonemia and its associated CNS manifestations 2. Knowledge of neuroimaging features and clinical findings helps in diagnosis and appropriate management

### NREE-3 Clinical Applications of MR Spectroscopy in the Era of Molecular and Genetic Diagnosis and Treatment

#### Awards Magna Cum Laude

Participants  
Mariko Kurokawa, MD, Ann Arbor, MI (*Presenter*) Nothing to Disclose

#### TEACHING POINTS

- Understand the basic principle of MRS: the methodology to acquire the spectrum of chemical shifts
- Describe main pathologies related to common metabolites found in MRS as well as novel genetic markers such as SDHB mutation and IDH mutation
- Identify the common and uncommon MRS findings, especially focusing on metabolic diseases and their differential diagnoses.

## TABLE OF CONTENTS/OUTLINE

1. Introduction Physics and methodology 2. Pathologies related to common and uncommon metabolites N-acetyl aspartyl glutamate (NAA), Creatine, Choline, Myo-inositol, Gamma-aminobutyric acid (GABA), Glutamine/glutamate, Lipid, Lactate, Taurine, Glycine, Alanine, Succinate, and 2-HG 3. Metabolic diseases Mitochondrial diseases, arginase deficiency, Salla disease, Sandhoff disease, nonketotic hyperglycinemia, Phenylketonuria, Canavan disease, Creatine transporter deficiency, and maple syrup urine disease 4. Hypoxic ischemic encephalopathy 5. Demyelination diseases (multiple sclerosis, acute disseminated encephalomyelopathy) 6. Tumors (low-grade gliomas, high-grade gliomas, medulloblastomas, and other malignant tumors) 7. Genetic diseases Vanishing white matter disease, Alexander disease, Adrenoleukodystrophy 8. Summary

### NREE-30 An Unusual Relation: A Walk to Remember, Neurological Manifestations of Inflammatory Bowel Disease, An Underdiagnosed Pathology

Participants  
Angela Sosa, MD, (*Presenter*) Nothing to Disclose

## TEACHING POINTS

After reviewing this exhibit, you will be able to: Describe the neurological disorders associated with inflammatory bowel diseases such as ulcerative colitis and Crohn's disease. Understand the mechanisms involved in the pathophysiology of these manifestations. Recognize the most common imaging findings in central and peripheral nervous system manifestations of patients with inflammatory bowel diseases.

## TABLE OF CONTENTS/OUTLINE

1. Neurological complications of inflammatory bowel diseases 1.1 Epidemiology 1.2 Pathophysiology 2. Imaging findings of central and peripheral nervous system manifestations of inflammatory bowel diseases. 2.1 Cerebrovascular: Stroke, vasculitis, and Cerebral venous thrombosis.2.2. Demyelinating2.3. Asymptomatic white matter lesions2.4. Peripheral neuropathy2.5. Toxic treatment-related3. Other central nervous systemsComplications.3.1. Dementia3.2. Headaches3.3 Encephalopathy

## NREE-31 Imaging of Cranial Nerve Disorders in Pediatric and Adult Patients

Participants

Minako Azuma, MD, PhD, (*Presenter*) Nothing to Disclose

## TEACHING POINTS

1. In pediatric and adult patients, a wide variety of diseases are related to cranial nerves, including tumors, inflammations, vascular, and so on. 2. It is necessary for radiologists to know typical and atypical radiological findings of cranial nerve disorders. 3. Radiologists have to select the best imaging modality and protocol for the detection of lesions.

## TABLE OF CONTENTS/OUTLINE

1. Anatomy of cranial nerves (1) Locations, structure, and function (2) Foramina related to cranial nerves 2. Techniques for the imaging of cranial nerve disorders (1) CT (2) MRI 3. Cranial nerve disorders (1) Tumor Schwannoma Optic nerve sheath meningioma Optic nerve glioma Olfactory neuroblastoma AT/RT (atypical teratoid/rhabdoid tumor) Malignant lymphoma Leukemia Metastasis / Dissemination (2) Inflammation Optic neuritis Neuromyelitis optica spectrum disorder (NMOSD) Myelin oligodendrocyte glycoprotein (MOG) antibody-associated disease Multiple sclerosis IgG4 related disease Tolosa-Hunt syndrome Bell's palsy Sarcoidosis HTLV-1 Cerebrotendinous Xanthomatosis (3) Hemorrhage Superficial siderosis (4) Secondary compressive disorders a) Orbital and sellar-suprasellar mass b) Neurovascular compression and aneurysm c) Thyroid orbitopathy (5) Toxic neuropathy (6) Congenital (7) Vascular Carotid-cavernous fistula Dural arteriovenous fistula Dural sinus thrombosis Acute cerebral infarction 4. Take home points 5. References

## NREE-33 Top 7 Must Know Movement Disorders: Imaging with Clinical Videography Correlation

Participants

Leslie Starkey, MD, Portland, OR (*Presenter*) Nothing to Disclose

## TEACHING POINTS

Diagnosis of movement disorders is challenging due to the varied clinical manifestations and heterogeneity, so the integration of imaging and clinical features plays an extremely important role. We have selected seven important movement disorders and provide multidisciplinary learning by introducing their imaging and clinical manifestations through a series of unknown cases followed by a clinical discussion including videos. In addition to important imaging manifestations, in collaboration with a neurologist, we present the typical diagnostic criteria and clinical examination findings that would be useful for radiologists to understand, such as the ataxia findings in spinocerebellar ataxia.

## TABLE OF CONTENTS/OUTLINE

1. Amyotrophic lateral sclerosis imaging findings, followed by clinical pearls with video demonstration. 2. Multiple system atrophy imaging findings, followed by clinical pearls with video demonstration. 3. Spinocerebellar ataxia imaging findings, followed by clinical pearls with video demonstration. 4. Huntington disease imaging findings, followed by clinical pearls with video demonstration. 5. Fahr disease imaging findings, followed by clinical pearls with video demonstration. 6. Creutzfeldt-Jakob disease imaging findings, followed by clinical pearls with video demonstration. 7. Wilson disease imaging findings, followed by clinical pearls with video demonstration.

## NREE-34 Visual Summary of the 2021 WHO Central Nervous System Tumor Classification

Awards

Certificate of Merit

Participants

Neiladri Khan, DO, Pittsburgh, PA (*Presenter*) Nothing to Disclose

## TEACHING POINTS

The 2021 WHO Classification of Tumors of the Central Nervous System (CNS) is the fifth edition of the classification system, and it succeeds the fourth edition released in 2016. The 2021 classification incorporates changes in diagnostic principles, with a particular emphasis on the molecular profiling of tumors. A description of the new diagnostic principles, along with visual examples and graphics demonstrating their significance. We include two peculiar cases of IDH wild-type gliomas from our home institution which benefit from the new classification system. In addition to changes in diagnostic principles, several tumor-specific changes were also made. There are now also several entirely new tumor entities. The new concept of layered pathological reporting, and the impact of this new system on radiologists.

## TABLE OF CONTENTS/OUTLINE

Title page - Disclosures - Introduction to the WHO classification system - Objectives - Brief overview of what is new in the 2021 update - Radiological and pathological visual examples of changes made to the diagnostic principles - IDH wild-type glioma, home institution interesting case 1 - IDH wild-type glioma, home institution interesting case 2 - Graphic rendition of changes made to specific tumor types - Introducing and explaining the concept of integrated diagnoses and layered reports, and what these changes mean for the radiologist - Conclusion - Biography

## NREE-35 Genetics and Epigenetics of Brain Tumors for Radiologists

Awards

Certificate of Merit

Participants

Gabriela Bandeira, MD, Sao Paulo, Brazil (*Presenter*) Nothing to Disclose

## TEACHING POINTS

1- To review the oncogenesis of primary brain tumors. 2- To understand the main molecular pathways involved in primary brain tumors. 3- To integrate the oncogenesis knowledge with the new molecular parameters from the 5th edition of the WHO Classification of Tumors of the Central Nervous System (WHO CNS5). 4- To review the phenotypic and the genotypic key features of some primary brain tumors (radiogenomics).

## TABLE OF CONTENTS/OUTLINE

1- Introduction 2- Oncogenesis in CNS Fundamental Concepts Cell Cycle Ligands and Receptors Cyclin-Dependent Kinases (CDKs) Cellular Signaling Pathways involved in brain tumors Epigenetics : Histone modifications, DNA Methylation 4- New molecular parameters from the 5th edition of the WHO Classification of Tumors of the Central Nervous System (WHO CNS5). 5- Illustrative cases of primary brain tumors with confirmed genetic and epigenetic profiles. 6- Take-home messages 7- Conclusion 8- References

## **NREE-36 Intracranial Cystic-appearing Images More than a Simple Find**

### **Participants**

Eugenio César Rocha Santos Filho, SAO PAULO, Brazil (*Presenter*) Nothing to Disclose

### **TEACHING POINTS**

The purpose of this exhibit is: To show different types of diseases that have cystic presentation. To demonstrate sites that are typically affected by each disease To help expand the differential diagnoses through the distinct imaging patterns of cystic lesions by a pictorial essay.

### **TABLE OF CONTENTS/OUTLINE**

Overview of all pathologies and their division by etiology  
Congenital: Arachnoid cyst: different locations and sizes  
Ectodermal Inclusion Cysts  
Dermoid cyst  
Epidermoid cyst  
White epidermoid cyst  
Neuroglial cyst  
Blake pouch cyst  
Rathke's cleft cyst  
Corpus callosum agenesis and interhemispheric cyst  
Choroid plexus cyst  
Choroidal fissure cyst  
Colloid cysts of the third ventricle  
Pineal cysts  
Perivascular spaces and its association  
Infectious: Viral: Cytomegalovirus  
Bacterial: Neurosyphilis  
Neurotuberculosis  
Abscess  
Protozoa  
Neurotoxoplasmosis  
Parasitic  
Neurocysticercosis  
Chagas disease  
Fungi  
Aspergillosis  
Neurocryptococcosis  
Neoplastic: Intra-axial: Multinodular and vacuolating neuronal tumor  
Dysembryoplastic neuroepithelial tumors (DNET)  
Primitive neuroectodermal tumors (PNET)  
Multinodular and vacuolating neuronal tumor  
Central neurocytoma  
Ependymoma  
Hemangioblastoma  
Gliomas  
Ganglioglioma  
Medulloblastoma  
Metastasis  
Extra-axial: Meningioma  
Schwannoma  
Macroadenoma  
Craniopharyngioma  
Hemangioma  
Germinomas  
Pineal tumors  
Demyelinating: Demyelinating pseudotumor  
Balo disease  
Others  
Cobblestone malformation  
Hypomelanosis of Ito  
Megalecephalic leukoencephalopathy with subcortical cysts  
Porencephalic cyst

## **NREE-37 Posterior Circulation Stroke: How Much Do You Know About It?**

### **Participants**

Celia Alonso, MD, Madrid, Spain (*Presenter*) Nothing to Disclose

### **TEACHING POINTS**

The objective of this educational exhibit is to shine a light on the acute management of vertebrobasilar stroke. Therefore, after reading it, the reader will: -Comprehend the epidemiology of vertebrobasilar strokes, their clinical presentation and etiology depending on the affected anatomical territory. - Learn the indications and limitations of imaging techniques in posterior circulation strokes, as well as their most frequent imaging features. -Know how to apply the two most important imaging prognostic scores in large vessel occlusions: pc-ASPECTS and BATMAN.

### **TABLE OF CONTENTS/OUTLINE**

-Introduction. -Clinical considerations: its symptoms are frequently non-focal, overlap with those of anterior circulation strokes and simulate other neurological conditions ('stroke chameleons'), which usually leads to delayed diagnosis. -Etiology of posterior circulation strokes: ASCOD and topographic classification. -Vertebrobasilar anatomy, relevant variants shown with images. -Imaging techniques: indications, limitations and semiology. Imaging prognostic scores in large vessel occlusions: pc-ASPECTS and BATMAN. Its application will be shown using real cases. -All possible clinical scenarios (small, medium-sized and large vessel disease) will be shown with real cases studied with multimodal CT and/or brain MRI from our institution. -Treatment considerations. -Conclusion.

## **NREE-38 Imaging Cerebrospinal Fluid Hypotension: Cerebrospinal Fluid Fistula Hyper-knowledge**

### **Participants**

Pedro Castro, MD, Rio de Janeiro, Brazil (*Presenter*) Nothing to Disclose

### **TEACHING POINTS**

To illustrate the most common symptoms related to cerebrospinal fluid (CSF) hypotension. To demonstrate the imaging aspects of spontaneous intracranial hypotension, a well-recognized entity. To explain that depicting the CSF leak location is the radiologist's goal, allowing effective treatment. To show that CSF leak imaging can be challenging and often misdiagnosed, leading to severe CSF hypotension.

### **TABLE OF CONTENTS/OUTLINE**

1. Revision of epidemiology and clinical presentation, including headache, rhinorrhea, and severe CSF hypotension. 2. Etiologies of intracranial hypotension and CSF leaks, including surgery and trauma. 3. Imaging strategies and findings of CSF leaks, including MRI and CT myelography assessment. 4. MRI vs. CT cisternography in the assessment of CSF fistulas. 5. CT cisternography in the assessment of spinal CSF fistulas. 4. Differential diagnosis of CSF hypotension. 5. Treatment options: epidural blood patches and surgery. 6. Take-home messages.

## **NREE-39 Ultrahigh-resolution CTA of the Brain as a Tool for Pre- and Postoperative Imaging**

### **Participants**

Miho Gomyo, Miraka, Japan (*Presenter*) Nothing to Disclose

### **TEACHING POINTS**

1. To learn the basic principles and characteristics of ultrahigh-resolution CT. 2. To learn the kinds of image denoising reconstruction processing and understand their characteristics. 3. To learn the clinical importance of small arteries such as cortical arteries and perforators depicted by ultrahigh-resolution brain CTA.

### **TABLE OF CONTENTS/OUTLINE**

1. Basic principles and characteristics 2. Image denoising reconstruction processing: FBP (filtered back-projection), hybrid IR (iterative reconstruction), full IR and deep learning reconstruction 3. Imaging anatomy and clinical importance the following arteries: cortical arteries, branches of main arteries and perforating arteries 4. Clinical application to preoperative and postoperative images: aneurysm, infectious aneurysm, dissecting aneurysm, arteriovenous malformation, moyamoya disease, arterial stenosis, temporal arteritis, superficial temporal artery-middle cerebral artery bypass and brain tumor

## **NREE-4 Dural and Leptomeningeal Diseases: Anatomy, Etiology, and Neuroimaging**

### **Awards**

Identified for RadioGraphics

### **Participants**

Ryo Kurokawa, MD, PhD, Ann Arbor, MI (*Presenter*) Nothing to Disclose

### **TEACHING POINTS**

This review summarizes the clinical and radiological findings of dural and leptomeningeal diseases caused by various etiologies.

### **TABLE OF CONTENTS/OUTLINE**

Outline  
I. Overview of dural and leptomeningeal diseases  
Anatomy  
Etiology  
Recommended workups  
II. Content  
-Idiopathic-  
Infection: tuberculosis, syphilis, fungi, Lyme disease, HTLV-1, Q fever  
Autoimmune: ANCA-related vasculitis, PCNSV, sarcoidosis, systemic lupus erythematosus, rheumatoid arthritis, Behçet's disease, Sjogren's disease, Vogt-Koyanagi-Harada disease, inflammatory bowel disease, SAPHO syndrome  
Lymphoproliferative: POEMS syndrome and lymphoma  
Neoplasm: metastasis (breast cancer, lung cancer, melanoma, gliomatosis), leukemia, medulloblastoma, multiple myeloma, meningioma  
Histiocytosis: Erdheim-Chester disease, Rosai-Dorfman disease, Langerhans cell histiocytosis, juvenile xanthogranuloma  
Intracranial

hypotension: lumbar puncture, CSF leak, CSF shunting, craniotomy  
Miscellaneous: Multiple sclerosis, amyloidosis, and neurocutaneous melanosis III.  
Summary  
1. Various entities cause the development of dural and leptomeningeal diseases.  
2. Clinical and radiological findings can help in the diagnosis of the etiology.  
3. Appropriate workup can lead to timely diagnosis and management.

#### **NREE-41 Don't Tense About It: MRI Findings of Idiopathic Intracranial Hypertension and Intracranial Hypotension**

Participants

Ana Paula Fonseca, MD, Sao Paulo, Brazil (*Presenter*) Nothing to Disclose

##### **TEACHING POINTS**

This review focuses on the imaging of idiopathic intracranial hypertension and spontaneous intracranial hypotension. Both have salient imaging findings that are important to recognize to help prevent their misdiagnosis from other neurological disorders. This panel aims to: Review the pathophysiology of these two important intracranial pressure disorders. Discuss and illustrate their imaging patterns. Describe through illustrative cases the scenarios for diagnosis, typical imaging patterns, unexpected findings and red flags that aid the diagnosis.

##### **TABLE OF CONTENTS/OUTLINE**

Pathophysiology of these two ICP disorders: Idiopathic intracranial hypertension and spontaneous intracranial hypotension  
Definition  
The Monroe-Kellie doctrine  
Main causes  
Clinical syndrome  
Imaging findings  
Spontaneous intracranial hypotension  
Brain swelling  
Distension of the venous sinuses  
Bilateral subdural collections  
Dural thickening and enhancement  
Enlarged pituitary  
Flattened pons  
Inferior displacement of the third ventricle  
Sagging brain  
Idiopathic intracranial hypertension  
Partially empty sella turcica  
Distension of the optic nerve sheath  
CSF space  
Increased vertical tortuosity of the optic nerve  
Flattening of the posterior sclera/  
intraocular protrusion of the optic nerve head  
Cerebellar tonsilla ectopia  
Meningoceles  
Hypoplastic and/or stenosis of the venous sinus  
Prominence of the occipital emissary vein  
Associated Conditions  
Superficial Siderosis  
Ventral Epidural Collection  
Venous Sinus Thrombosis  
Pituitary Apoplexy  
Mimickers  
Chiari Type I Malformation  
Subdural Fluid Collections or Hematomas  
Other Conditions with Dural Thickening  
Red flags and diagnostic tips  
Diagnostic Approach  
Final remarks

#### **NREE-42 Quantitative Susceptibility Mapping: Overview and Applications**

Participants

Alexey Dimov, (*Presenter*) Nothing to Disclose

##### **TEACHING POINTS**

Quantitative susceptibility mapping (QSM) is an automated technique that post-processes three-dimensional (3D) gradient echo phase images to depict local tissue magnetic properties, which are blurred in conventional MRI sequences, such as T2w, T2\*w and phase images. QSM makes use of the already acquired phase data, does not add scan time, and can be easily integrated into the clinical workflow. QSM provides superb contrast-to-noise ratio (CNR) for depicting deep gray nuclei that are rich with iron, which is useful for precise guidance of deep brain stimulation. QSM provides high fidelity and quantitative measurements of iron in proinflammatory activated microglia in neuroinflammatory disorders, such as in multiple sclerosis, Parkinson's disease, Alzheimer's disease. QSM allows unambiguous differentiation of diamagnetic calcification from paramagnetic iron such as in microbleeds.

##### **TABLE OF CONTENTS/OUTLINE**

1. Revision of the basic physics of tissue magnetism, gradient echo data, and phase post-processing for QSM  
2. Description of how QSM can be used to measure iron overloading in neurodegenerative diseases, such as Parkinson's disease.  
3. Overview of how QSM can be used to define deep brain stimulation targets.  
4. Synopsis of how QSM can be used to eliminate gadolinium injection in MRI monitoring of multiple sclerosis (MS) patients and to adjust therapy to measure chronic lesion activity for improved patient care.  
5. Summary of how QSM processing of phase plus quantitative blood oxygenation level dependent (qBOLD) modeling of magnitude can enable oxygen extraction fraction (OEF) mapping from the widely available multiecho gradient echo data without vascular challenge.

#### **NREE-43 Applications of MR Bone Imaging to Vertebral Lesions**

Participants

Kazuhiro Tsuchiya, PhD, Tokyo, Japan (*Presenter*) Nothing to Disclose

##### **TEACHING POINTS**

1. To learn basic concepts and technical aspects of bone imaging like CT by MRI.  
2. To know how MR bone images depict the normal vertebra and adjacent structures compared with CT.  
3. To know the differences, especially the advantages, of MR bone images from CT and conventional MR images in miscellaneous vertebral lesions.

##### **TABLE OF CONTENTS/OUTLINE**

1. Basic issues of MR bone imaging including currently employed scanning sequences and postprocessing methods.  
2. Characteristics of MR bone images of the normal vertebra, placing emphasis on the difference from conventional MR images as well as CT.  
3. Presentation of clinical cases with discussion of implications. Cases will cover spine degeneration (Modic changes), neoplastic lesions including primary and metastatic vertebral tumors, inflammatory changes such as spondylitis, vertebral fractures, and so on.  
4. Additional discussion including current limitations as well as future directions of this technique.

#### **NREE-44 Synthetic MRI, STAGE, and MR Acceleration through Deep-Learning: A Comparison of Time-Efficient MR Techniques in Neuroimaging**

**Awards**

**Certificate of Merit**

Participants

Marc Von Reppert, New Haven, CT (*Presenter*) Nothing to Disclose

##### **TEACHING POINTS**

1. To provide a structured overview of main approaches to shortening neuroimaging protocols.  
2. To review recent developments in the field: STAGE, synthetic MRI and Deep Learning-based image enhancement.  
3. To provide an understanding of current applications and perspectives for clinical use.  
4. To highlight current shortcomings of these techniques and potential remedies.

##### **TABLE OF CONTENTS/OUTLINE**

Background: Highlighting the need for Time-Efficient MRI // Overview of Rapid Imaging Techniques // Synthetic MRI: Acquisition // Comparison of IRTrueFISP, MPME and QRAPMASTER // Application in MS and CNS Tumors // Summary // STAGE: Acquisition // AI-based Automated Microbleed Detection // STAGE for different clinical applications // Summary // DL-based Reconstruction: Introduction and Workflow // Example Case // Introduction of Uncertainty Estimation in Image Enhancement // Outlook // Take Home Points

#### **NREE-45 Implementing Perfusion Protocols for Tumor Differentiation and Analysis of Post-Treatment Changes into Busy Clinical Practice**

Participants

Christopher Atkins, MD, New Haven, CT (*Presenter*) Nothing to Disclose

##### **TEACHING POINTS**

1. To review the fundamentals of MR perfusion and applications in Neuro-Oncology  
2. To review protocol considerations for clinical applications concerning image acquisition, processing, and analysis.  
3. To review the current developments in standardization efforts for perfusion imaging.

#### TABLE OF CONTENTS/OUTLINE

I. Review the fundamentals of perfusion imaging including explaining techniques of dynamic susceptibility contrast MRI, dynamic contrast enhanced MRI, and arterial spin labelling as well as highlighting their strengths and pitfalls.  
II. Review various clinical applications of MR perfusion including differentiation of tumor recurrence from radiation necrosis, distinction of different tumors, and differentiation of cerebral tumor entities using clinical examples.  
III. Review protocol considerations for each technique including technical requirements and choice of labeling approach.  
IV. Review the current standardization efforts for MR perfusion protocols.

#### NREE-46 Reversible Restricted Diffusion Lesions in Excitotoxic Brain Injury and Acute Ischemic Stroke

Participants

Yun Young Lee, Gwangju, Korea, Republic Of (*Presenter*) Nothing to Disclose

#### TEACHING POINTS

1. To review the etiologies of excitotoxic brain injury and its pathomechanisms.  
2. To review the reversible diffusion weighted imaging lesions in acute ischemic stroke and its clinical implications.

#### TABLE OF CONTENTS/OUTLINE

1. Introduction- The importance of diffusion weighted imaging (DWI) in the neuroimaging area and the basic mechanisms of diffusion restriction.- Representative etiologies of diffusion restriction  
2. Reversible restricted diffusion lesions in excitotoxic brain injury- Review the pathomechanisms of excitotoxic brain injury- Possible explanations for reversible diffusion restriction in excitotoxic brain injury- Case based review: toxic, metabolic, trauma, seizure, infection  
3. Reversible restricted diffusion lesions in acute ischemic stroke- A systematic review the literature for reversible restricted diffusion lesions in acute ischemic stroke- Clinical implications of reversible diffusion restriction in acute ischemic stroke and plausible mechanisms- Permanent reversible diffusion restriction- Transient reversible diffusion restriction  
4. Summary

#### NREE-47 Multi-modality Imaging of Skull Base Tumors and Tumor-like Lesions

Participants

Justin Caskey, MD, (*Presenter*) Nothing to Disclose

#### TEACHING POINTS

1. Basic skull base anatomy and anatomic landmarks relevant to the evaluation of skull base tumors and tumor-like lesions.  
2. Common skull base tumors and tumor-like lesions.  
3. Practical benefit of multi-modality imaging evaluation of skull base tumors and tumor-like lesions. Skull base pathology represents an often-challenging topic in neuroradiology. Anatomically, the skull base is a complex space formed by the ethmoid, sphenoid, occipital and paired frontal and temporal bones. Contained within and traversing through the skull base are critical neurovascular structures which must be carefully considered at radiologic evaluation. In many cases, multi-modality imaging, including perfusion weighted imaging, diffusion weighted imaging, and positron emission tomography, can provide a useful adjunct to standard neuroimaging techniques (CT, MRI) in evaluation of skull base pathology.

#### TABLE OF CONTENTS/OUTLINE

I. Introduction  
II. Review of basic skull base anatomy  
III. Brief overview of diffusion and perfusion imaging and positron emission tomography  
IV. Case based examples of multi-modality imaging of skull base pathology  
a. Bone metastases from various primary sites, lymphoma, rhabdomyosarcoma  
b. Primary bone tumor, chordoma, chondrosarcoma, giant cell tumor  
c. Skull base invasion from carcinoma, pituitary adenoma, meningioma  
d. Inflammatory pseudotumor  
e. Bacterial and fungal osteomyelitis  
f. Benign tumor-like lesions, cholesterol granuloma, cholesteroloma, notochord origin lesion

#### NREE-48HC Imaging features of Diffuse Pediatric-type High-grade Glioma, H3- /IDH-wildtype, and Diffuse Hemispheric Glioma, H3 G34-Mutant

Participants

Andrew Chang, MD, San Francisco, CA (*Presenter*) Nothing to Disclose

#### TEACHING POINTS

Diffuse pediatric high-grade gliomas (pHGG) are a heterogeneous group of brain tumors comprising 3-15% of all pediatric CNS tumors. In the 2021 WHO Classification of tumors of the CNS, two new subtypes of pHGG have been added to reflect the unique molecular features underlying each tumor: (1) diffuse pediatric-type high-grade glioma, H3-wildtype and IDH-wildtype (DPHGG H3/IDH-wt), and (2) diffuse hemispheric glioma, H3 G34-mutant (DHG H3G34M). This educational exhibit highlights the key MR imaging features of the two new tumor subtypes with emphasis on unique feature of each subtype that may aid in differential diagnosis. DPHGG H3/IDH-wt and DHG H3G34M demonstrate similar MRI features to other pHGGs, with low T2, high T2, and high FLAIR signal intensities, restricted diffusion, and variable enhancement pattern. Distinct features of DPHGG H3/IDH-wt include its propensity for frank intratumoral hemorrhage resulting in extensive edema, mass-effect, and hydrocephalus. In contrast, DHG H3G34M rarely develops hemorrhage and instead demonstrates cyst-and-nodule morphology with minimal surrounding edema or mass-effect.

#### TABLE OF CONTENTS/OUTLINE

[I] Overview of 2021 WHO Classification of diffuse pediatric-type high-grade gliomas. [II] Summary of key molecular genetic classification schemes. [III] Characteristic MRI features of diffuse pediatric-type high-grade gliomas (a) DPHGG H3/IDH-wt (b) DHG H3G34M  
Please visit the Learning Center to also view this presentation in hardcopy format.

#### NREE-5 Multimodality Imaging of Typical and Atypical Pilocytic Astrocytomas with Pathological Correlations

Participants

Toshio Moritani, MD, PhD, Ann Arbor, MI (*Presenter*) Nothing to Disclose

#### TEACHING POINTS

-To demonstrate imaging findings of typical and atypical pilocytic astrocytomas using multimodal imaging including CT, MRI, diffusion, perfusion (DSC and DCE), APTw, MR spectroscopy and PET.  
-To learn genetic and oncogenic pathways of tumor development of pilocytic astrocytoma with or without NF1  
-To discuss the pathological correlation

#### TABLE OF CONTENTS/OUTLINE

-Genetic and oncogenic pathways: tumor development of pilocytic astrocytomas with or without NF1  
-Pathology: microcystic change, myxoid degeneration, Rosenthal fiber, pilocytic variants such as diffuse variant or pilomyxoid astrocytoma  
-Multimodal Imaging and imaging techniques: CT, MRI, diffusion, perfusion (DSC and DCE), APTw, MR spectroscopy and PET  
Classically high ADC values, while high grade gliomas and embryonal tumors show lower ADC. Relatively wide range of ADC values in PAs. Classically low rCBV and rCBF and high K2 on DSC, and low VP, high VE, and partially high Ktrans on DCE  
Increased choline and lactate peak on MRS which can be a pitfall of the diagnosis. APT maps often show high values for PA even this is low grade tumor.  
-Case presentations: Typical findings: Well-defined infratentorial cystic lesion with enhancing mural nodule and supratentorial enhancing mass, with facilitated diffusion, high ADC value, typical perfusion pattern, increased APTw  
Atypical findings: unusual locations, non-enhancing, exophytic, hemorrhagic, multicentric/dissemination, relatively low ADC value, atypical perfusion pattern.  
Pediatric versus adult cases NF1 versus non NF1  
Differential diagnosis

## **NREE-50 Pictorial Depiction of a Lexicon Based Approach to BT-RADS**

Participants

Ankush Jajodia, MD, MBBS, New Delhi, India (*Presenter*) Nothing to Disclose

### **TEACHING POINTS**

Background: Imaging evaluation of brain tumor patients is challenging since imaging findings of tumor development and treatment-related alterations overlap significantly. The accurate interpretation of these tumors causes significant inter-observer variability going to tumor heterogeneity, especially in complex circumstances. Imaging evaluation of brain tumors with MRI plays a crucial role in managing these patients, who face poor survival [median 15 months]. A structured reporting system (BT-RADS) aims to increase uniformity among radiologists. The need for a structured glioma surveillance reporting system with a standardized management-based suggestion, which has the potential to improve clinical interpretation and facilitate more effective patient communication, has already been voiced. There has been a dearth of lexicon depiction and illustration in the literature review. Clinical relevance: A standardized reporting system with the BT-RADS is encouraged using the various sequence-based lexicon. The published lexicon and report template will improve the completeness and accuracy of generated reports.

### **TABLE OF CONTENTS/OUTLINE**

Characterize lexicon on MRI using BT-RADS Review case examples using the BT-RADS descriptive parameters.

## **NREE-51 Stepwise Application of RANO Criteria on Follow-up Imaging and Treatment of Gliomas: A Guide for Residents**

**Awards**

**Certificate of Merit**

Participants

Thurl Hugh Cledera, MD, Taguig, Philippines (*Presenter*) Nothing to Disclose

### **TEACHING POINTS**

Gliomas are the most common intra-axial tumor of the central nervous system, among which the most common type is glioblastoma, which incidentally is a highly aggressive tumor. Imaging plays a pivotal role in the management of glioblastomas; hence guidelines have been developed to facilitate the interpretation of studies from pre-treatment studies down to post-surgical and post-radiation changes, one of which is known as the Response Assessment in Neuro-Oncology (RANO) Criteria. The criteria are broken down to complete response, partial response, stable disease, and progressive disease must be applied to all post-treatment glioma cases to guide therapy. Pseudoprogression and pseudoresponse are necessary to distinguish from the standard response criteria as they will have an effect on the treatment and follow-up of patients.

### **TABLE OF CONTENTS/OUTLINE**

1. Introduction and Background 2. Step 1: Confirm Patient History and Treatment 3. Step 2: Know the Natural Course and Management of Glioblastoma 4. Step 3: Identifying Lesions 5. Step 4: Identifying Response Criteria a. Complete Response b. Partial Response c. Stable Disease d. Progressive Disease 6. Step 5: Check for Imaging Pitfalls a. Pseudoprogression (Post-surgical, Post-radiation, Post-chemotherapy) b. Pseudoresponse (VEGF Therapy)

## **NREE-52 Uncertainty Estimation in Auto-Segmentation and Image Reconstruction Tasks**

**Awards**

**Certificate of Merit**

Participants

Marc Von Reppert, New Haven, CT (*Presenter*) Nothing to Disclose

### **TEACHING POINTS**

1. To provide a structured overview of the concept of uncertainty estimation (UE) in the context of Machine Learning and Deep Learning. 2. To summarize and review different approaches to measuring uncertainty. 3. To provide a perspective on current applications of UE in the literature of neuroimaging in tasks like segmentation and image enhancement. 4. To highlight sources of uncertainty in neuroimaging and provide an outlook on potential developments in the field.

### **TABLE OF CONTENTS/OUTLINE**

1. Principles of Uncertainty Estimation: // Background: Understanding Uncertainty // Background: Machine Learning and Deep Learning // Types of Uncertainty // Methods of Measuring Uncertainty 2. Application of Uncertainty Estimation in Neuroimaging: // Summary of Current Neuroimaging Applications // Brain Anatomical Segmentation // Brain Tumor Segmentation // Image Super-Resolution and Denoising // Collection of Publications 3. Take Home Points

## **NREE-53 Diffusion Weighted Imaging in the Spine: A Magic Key**

**Awards**

**Certificate of Merit**

Participants

Mahmoud Shalaby, MD, Lansdowne, PA (*Presenter*) Nothing to Disclose

### **TEACHING POINTS**

1- Illustrate the role of diffusion weighted imaging (DWI) in spine infectious, neoplastic, and inflammatory disease 2- Demonstrate the role of DWI in spine trauma and degenerative disease 3- Emphasize the role of DWI in spinal cord ischemia 4- Highlight the challenges of spine DWI acquisition 5- Discuss technical tips and considerations for protocol optimization for 1.5T and 3T MRI

### **TABLE OF CONTENTS/OUTLINE**

- Clinical applications of DWI in common spinal pathologies: o Infectious and inflammatory disease o Primary and metastatic spine tumor o Degenerative disease o Trauma o Spinal cord ischemia o Compression fractures o Demyelinating disease - Challenges of spine DWI acquisition - Protocol optimization with practical tips to improve spine DWI for 1.5T and 3T MRI

## **NREE-54 Amide Proton Transfer Weighted Imaging (APTwi) in Brain Tumors: A Pictorial Review**

**Awards**

**Magna Cum Laude**

Participants

Guillaume Hamon, MD, Rennes, France (*Presenter*) Nothing to Disclose

### **TEACHING POINTS**

The aims of this exhibit are: 1. To describe the basic theory and advantages of the APTwi technique 2. To illustrate brain tumors and differential's features in APTwi 3. To highlight and discuss potential pitfalls in APTwi 4. To review the current clinical applications of APTwi in neuro-oncology

### **TABLE OF CONTENTS/OUTLINE**

I. Understanding the APTwi technique1. Introduction to the Chemical Exchange Saturation Transfer (CEST) technique2. Basic physical principles of the amide-CEST contrast, so-called APTwi3. Technical consideration and limitations4. Image analysisII. Brain tumors, tumor mimics pitfalls in APTwi: an image-based approach1. Why to image amide protons in brain tumors?2. Primary and secondary brain tumors3. Tumor mimics4. Potential pitfalls in technique and image interpretationIII. Clinical applications of APTwi in neuro-oncology1. Main current published clinical applications of APTwi to image brain tumors2. Ongoing research and potential perspectives

#### **NREE-55      Imaging Abnormalities Associated With Pediatric Pituitary Disorders**

Participants

Yun Song Choo, MBBS, FRCR, (Presenter) Nothing to Disclose

##### **TEACHING POINTS**

The pituitary gland occupies a small footprint in terms of volume within the cranium, but pathologies arising from or involving it can have profound and long-lasting effects on the growth and development of the pediatric patient. It is hence important to appreciate the range of abnormalities in the pituitary gland and sellar region arising from both congenital and acquired pathologies that may be seen on neuroimaging studies. In this education exhibit, we revisit the development of the pituitary gland and share approaches to pediatric pituitary abnormalities on imaging with illustrative cases. Some of the major teaching points are: • MRI is the modality of choice to investigate suspected pituitary abnormalities in the pediatric patient. • The anterior and posterior pituitary gland have different embryological origins. • On top of masses that involve the sella and suprasellar region, the radiologist should be aware of mass-like lesions and mimics that have previously resulted in unnecessary surgical intervention.

##### **TABLE OF CONTENTS/OUTLINE**

• Pituitary Gland Development and Anatomy • Imaging the Pediatric Pituitary Gland • Abnormalities of Size and Number • Abnormalities of the Posterior Pituitary • Pituitary Stalk Thickening • Masses and Mass-like Lesions

#### **NREE-56      Checklist Based Approach to Interpret Pediatric Brain MRI Studies**

Awards

Certificate of Merit

Participants

Anvita Pauranik, MD, FRCPC, VANCOUVER, BC (Presenter) Nothing to Disclose

##### **TEACHING POINTS**

1. To develop a checklist-based methodical approach while interpreting pediatric brain MRI studies by knowing what to look for on different MR imaging planes and sequences, driven by the clinical question. 2. To understand the spectrum of age-related changes in a developing brain.3. To differentiate subtle pathology from normal variants using various case examples.

##### **TABLE OF CONTENTS/OUTLINE**

1. Midline sagittal brain. A. Commissures- size, shape, dysmorphisms. B. Sellar and Suprasellar region- Anterior/posterior pituitary gland, Infundibulum, Optic Chiasm, Floor of Third ventricle. Pineal gland C. Posterior fossa- Brainstem, Vermis and Cerebellar tonsils D. CSF Spaces- Cisterns, Aqueduct, Retrocerebellar space. E. Skull base including craniocervical junction, Scalp 2. Brain parenchyma-assessment on T1/T2/DWI/SWI. Age related changes, terminal zones of myelination versus white matter injury, subtle findings in altered sensorium- basal ganglia/ brainstem lesions.3 Ventricles- focal dilatation in PVHI, puckering in PVL, extra axial CSF spaces- prominence, collections, asymmetry, BESSI, cisterns- utility of Sagittal CISS 4. Flow Voids. 5. Extracranial - orbits, mastoids, paranasal sinuses.2. Checklist for focal seizure evaluation A. Midline- Hypothalamic Hamartoma versus inter-hypothalamic adhesion B.Cortical ribbon-blind spots C. Focal cortical Dysplasias-search patterns- Asymmetry in Grey-White matter signal, Sulcation. D. Mesial temporal lobe- early hippocampal sclerosis, dual lesions, temporo-polar changes, skull base defects3. Checklist for Neonatal brain MRI PLIC, Deep gray nuclei, Peri-Rolandic cortex, T1 bright punctate white matter lesions. Normal anisotropy on DWI.

#### **NREE-57      Mind-Bending Cerebellar Anatomy Techniques**

Participants

Elissandra Lima, MD, Rio de Janeiro, Brazil (Presenter) Nothing to Disclose

##### **TEACHING POINTS**

To demonstrate the anatomy of the cerebellum by illustrations and imaging, with phylogenetic and functional considerations. To correlate the most frequent diseases with anatomic regions. To depict the importance of precise localization of the disease according to the anatomical point of the cerebellum.

##### **TABLE OF CONTENTS/OUTLINE**

1. Background. 2. Imaging protocol. 3. Embryonic development. 4. Cerebellum anatomy. 5. Cerebellar functional anatomy. 6. Phylogenetic considerations of the cerebellar segments. 7. Cerebellar connections and function. 8. Cerebellum vascular anatomy. 9. Clinical perspective: symptoms and diseases - including neoplastic, inflammatory, infections, congenital and degenerative. 10. Flowchart for imaging assessment of cerebellar anatomic regions. 11. Take-Home messages.

#### **NREE-58      Anatomy and Functionality: Solidifying the Sulci, Gyri, and Brain Segmentation**

Participants

Elissandra Lima, MD, Rio de Janeiro, Brazil (Presenter) Nothing to Disclose

##### **TEACHING POINTS**

To illustrate the anatomy of the sulci, gyri, and brain segmentation with MRI imaging and illustrations. To correlate the anatomic segments with their functionality. To demonstrate the significance of accurate localization of the disease according to the anatomical locations, considering the clinical perspective.

##### **TABLE OF CONTENTS/OUTLINE**

1. Background. 2. Imaging protocol. 3. Sulci, gyri, and brain segmentation anatomy based on MRI imaging and illustrations. 4. Anatomic region and functionality. 5. Clinical perspective: brain diseases and their correlation with anatomy and neurological deficits. 6. Take-Home messages.

#### **NREE-59      Need-to-know Neuroimaging with Clinical Correlation: Parkinson's Disease and Related Movement Disorders**

Participants

Leslie Starkey, MD, Portland, OR (Presenter) Nothing to Disclose

##### **TEACHING POINTS**

Although Parkinson's disease is a relatively common movement disorder (MD), the onset is insidious and diagnosis challenging due to the varied clinical manifestations and heterogeneity, so the integration of imaging and clinical features plays an extremely important role. Other MD can simulate Parkinson's disease, including progressive supranuclear palsy, essential tremor, corticobasal degeneration, and carbon monoxide poisoning, among others. One area neurologists may have interest but little opportunity for learning is the clinical side, e.g. classic neurological findings in MD. In this presentation, we teach imaging and clinical manifestations. Imaging is presented as cases followed by the neurologist's perspective, including diagnostic criteria and videos of findings useful for radiologists to know, such as the eye findings in supranuclear palsy.

## TABLE OF CONTENTS/OUTLINE

General topics: 1) Parkinson's disease 2) PSP 3) Corticobasal degeneration 4) CO poisoning. Radiology cases and videos of neurologic findings include: •DAT scan, Nigrosome-1 and the absent swallow tail sign, classic and spectrum. •Clinical videos: motor features: fascial masking, bradykinesia, rest tremors, and gate. •Scans without Evidence of Dopamine Deficit (SWEDDS). •Differential: dopa responsive dystonia, paroxysmal kinesigenic dyskinesia, juvenile Huntington disease. •Deep brain stimulators, locations: VIM, GPi, STN. •Clinical videos: off meds, on meds, on meds and on DBS. •PSP: hummingbird sign. •Clinical videos: blink rate, eye movements, freezing speech, gait. •Corticobasal degeneration: asymmetric atrophy. •CO poisoning: globus pallidus lesions. •Clinical videos: gait freezing.

### **NREE-6      **Neuroradiological Aspects of Congenital Infections and Mimics****

#### **Awards**

#### **Certificate of Merit**

Participants

Luiz Uchoa, MD, Sao Paulo, Brazil (*Presenter*) Nothing to Disclose

#### **TEACHING POINTS**

To review imaging findings of congenital infection according to clinical suspicion. Identify the neurologic imaging findings of congenital infection and mimics with CT and MR images. A practical approach to interpreting these conditions systematizing the evaluation based on main neurologic imaging findings and clinical features.

## TABLE OF CONTENTS/OUTLINE

Introduction. Congenital Disease: Genetical x Disruptive. Visual Systematization of congenital infection and mimics. Congenital Infections and neurologic imaging findings. Main mimics of congenital infections. Take home messages.

### **NREE-60      **Moving to Diagnosis: Neuroimaging Systematic Approach to Neurometabolic Diseases Manifested as Movement Disorders****

Participants

Andres Abad, MD, (*Presenter*) Nothing to Disclose

#### **TEACHING POINTS**

To propose a neuroimaging systematic approach for the patients with movements disorders and suspicion of inborn error of metabolism etiology. To review the different neuroimaging presentation of the main inborn error of metabolism associated with movement disorders. To enrich the radiologist role into the diagnosis process of inborn error of metabolism To familiarize the radiologist with the neuroimaging findings present in uncommon congenital diseases that can produce movements disorders.

## TABLE OF CONTENTS/OUTLINE

Introduction. Movements disorders classification. Inborn errors of metabolism associated with each movement disorder. Cases and images of neurometabolic diseases associated with chorea. Cases and images of neurometabolic diseases associated with dystonia. Cases and images of neurometabolic diseases associated with myoclonus. Cases and images of neurometabolic diseases associated with parkinsonism. Conclusion.

### **NREE-61      **"Live and in Color": Imaging of Neurovascular Devices****

Participants

Camila Barbosa, MD, Sao Paulo, Brazil (*Presenter*) Nothing to Disclose

#### **TEACHING POINTS**

Illustrate the most common intracranial and cervical neurointerventional and neurosurgical devices, such as clips, coils, stents and intrasaccular flow disruptors, used for treatment of neurovascular conditions as intracranial aneurysms, arterial stenosis and vascular malformations. Understand the clinical indication of each dispositive. Present cases treated with neurovascular devices, recognizing the importance of the radiologist familiarity with the dispositives in order to proper evaluate post-operative images. Understand the best imaging method on the post-operative evaluation for each dispositive. Review the possible limitations of imaging methods for the follow-up and diagnosis of complications.

## TABLE OF CONTENTS/OUTLINE

Illustrated neurovascular devices. Algorithms for the post-treatment follow up. Case-based didactics: sample cases to demonstrate the devices, its appearance on different imaging methods and clinical use. Case-based post treatment discussion of complications.

### **NREE-62      **Far Beyond Atheromatosis: Unusual Findings of Carotid Duplex Scan****

#### **Awards**

#### **Certificate of Merit**

Participants

Iza Vieira, MD, Sao Paulo, Brazil (*Presenter*) Nothing to Disclose

#### **TEACHING POINTS**

The purposes of this exhibit are: 1. Comprehend the normal anatomy of the common carotid artery (CCA), internal carotid artery (ICA) and external carotid artery (ECA) on B-mode ultrasound; 2. Recognize anatomy variations and uncommon findings on B-mode ultrasound and duplex scan, with the correlation of CT-angiography (CTA) when necessary; 3. Correlate imaging findings with clinical presentation; 4. Recognize complications and possible outcomes; 5. Brief review of management options.

## TABLE OF CONTENTS/OUTLINE

- Normal anatomy of the extracranial carotid system on ultrasound; - Anatomy variations of the extracranial carotid system; - Carotid kinking; - Carotid aneurysms; - Endoleak following endovascular aneurysm repair; - Carotid artery pseudoaneurysm; - Carotid dissection; - Carotid web; - Carotid-jugular arteriovenous fistula; - Occlusion of the CCA and internalization of the ECA; - Takayasu arteritis; - Carotidynia; - Complications and outcomes.

### **NREE-63      **A Checklist Approach to Interpreting Cerebral Digital Subtraction Angiography****

#### **Awards**

#### **Certificate of Merit**

Participants

Charlotte Chung, MD, PhD, (*Presenter*) Nothing to Disclose

#### **TEACHING POINTS**

As diagnostic and interventional neuroradiology become increasingly siloed, most diagnostic neuroradiologists no longer perform catheter-based neuroangiography. However, basic understanding of cerebral digital subtraction angiography (DSA), the gold standard for diagnosis of cerebrovascular pathologies, remains crucial for accurate interpretation of noninvasive brain CT and MR angiogram. This exhibit introduces the art of interpreting 2-

dimensional (2D) cerebral DSA to the contemporary diagnostic neuroradiologist. Educational objectives of this exhibit include:- Outline imaging techniques and protocol for a typical diagnostic cerebral angiogram- Provide an annotated atlas for normal cerebral arterial and venous anatomy on 2D DSA- Introduce a checklist approach for interpretation of 2D cerebral DSA- Illustrate angiographic appearance of variant anatomy and various pathologies

#### TABLE OF CONTENTS/OUTLINE

I. 2D DSA imaging techniques II. Diagnostic cerebral angiogram imaging protocol III. Annotated atlas of normal anterior and posterior circulation on 2D DSA IV. Step-by-step checklist for interpretation of 2D cerebral DSA V. Systemic checklist-based illustration of variant and abnormal angiographic findings VI. Application of the checklist approach using case-based examples

#### **NREE-65 Neurovascular Imaging at 7T: Small Vessel Anatomy**

Participants

Neethu Gopal, MBBS, Jacksonville, FL (*Presenter*) Nothing to Disclose

#### TEACHING POINTS

Ultra-high resolution MR angiography (MRA) of the brain with a voxel size=0.3 x 0.3 x 0.3 mm is now achievable thanks to more readily available 7 Tesla clinical MR scanners and modern acceleration techniques. This advancement in our imaging capability allows for visualization of small normal vascular structures that were previously imperceptible on routine non-invasive vascular imaging. Teaching Points: 1. Revisit normal arterial anatomy of the smaller branches of the circle of Willis including normal anatomic variants. A combination of 2D and cinematic rendered images as well as illustrations will be utilized. 2. Demonstrate the normal cross sectional imaging appearance of these small vessels. In many cases, MRA images will be fused with 3D T1-weighted or T2-weighted sequences to better orient the viewer and demonstrate the spatial relationship of these vessels with gray-matter and white matter structures within the brain parenchyma. 3. Review pathological conditions associated with the smaller circle of Willis branches.

#### TABLE OF CONTENTS/OUTLINE

1. Introduction 2. Serial review of normal anatomy followed by cross-sectional images. Arteries will be reviewed systematically from anterior circulation to posterior circulation. Arteries that will be covered include but are not limited to: Anterior Choroidal Artery and its Branches, Superior Hypophyseal Artery, Anatomic Variations of the Posterior Communicating Artery, Medial Lenticulostriate Arteries, Recurrent Artery of Heubner, Lateral Lenticulostriate Arteries, Posterior Cerebral Artery Branches, Artery of Percheron, Basilar Perforator Vessels. 3. Review of cases with pathology 4. Conclusion

#### **NREE-66 Challenging Procedures at the C1-2 Spinal Level - Using CT Guidance to Improve Patient Care and Safety**

Participants

Ross Frederick, MD, Phoenix, AZ (*Presenter*) Nothing to Disclose

#### TEACHING POINTS

- There are several important procedures at the C1-2 level that can significantly improve patient quality of life. CT guidance makes these otherwise dangerous procedures safer and easier to perform.
- There are key anatomical structures that must be avoided when performing these procedures, most notably the vertebral artery, posterior inferior cerebellar artery, C2 nerve, and spinal cord. A thorough understanding of anatomy in this region is crucial to perform these procedures confidently and safely.
- Cervicogenic headache is an underrecognized and therefore undertreated condition that radiologists can treat with C1-2 facet joint injection, C2 nerve root block, or C2 ablation.
- For patients with a contraindication to lumbar puncture, cervical puncture at the C1-2 level provides an alternative approach for CSF collection, injection of contrast for myelography, or injection of chemotherapy.

#### TABLE OF CONTENTS/OUTLINE

1. Introduction: types of procedures and the patients who can benefit from them 2. Critical regional anatomy a. Vertebral artery b. PICAC. C2 nerved. Spinal cord 3. Cervicogenic headache and atlantoaxial osteoarthritis a. C1-2 facet injection i. Indications ii. Technical considerations b. C2 nerve root block i. Indications ii. Technical considerations c. C2 nerve ablation i. Indications ii. Technical considerations 4. Cervical puncture a. Indication - contraindication to lumbar puncture i. CSF collection ii. Injection of contrast for myelography iii. Injection of chemotherapy b. Technical considerations

#### **NREE-67 Spinal Vascular Pathologies: An Approach for Diagnosis and Management**

Participants

Moataz Ahmed Sayed Mohammed Soliman, MD, MSc, CHICAGO, IL (*Presenter*) Nothing to Disclose

#### TEACHING POINTS

- Describe normal vascular supply and drainage of the spine.
- Outline various types of spinal arteriovenous shunting and hyper-vascular spinal lesions: Common imaging findings and pitfalls.
- Discuss imaging features of common differential diagnosis
- Illustrate therapeutic options for spinal arteriovenous shunts and outcomes.

#### TABLE OF CONTENTS/OUTLINE

1. Introduction a. Normal arterial supply of the spinal cord b. Normal venous drainage of the spinal cord 2. Classification and cross-sectional imaging findings of spinal vascular lesions with angiographic correlation a. Spinal Arteriovenous shunts i. Type I: Spinal Dural Arteriovenous Fistula. ii. Type II: Spinal Glomus AVM iii. Type III: juvenile Spinal AVM iv. Type IV: Intradural Peri-medullary AVF b. Intramedullary hypervascular neoplastic lesions i. Cavernous malformation ii. Hemangioblastoma iii. Paraganglioma c. Spinal cord aneurysms i. Imaging features ii. Therapeutic interventions d. Cord infarct i. Etiology ii. Imaging manifestations 3. Role of interventional radiology in management of spinal vascular lesions a. Therapeutic embolization b. Preoperative devascularization 4. Conclusion and take-home messages

#### **NREE-68 Intramedullary Spinal Cord Injuries: A Potpourri"**

Participants

Juliana Benez, Sao Paulo, Brazil (*Presenter*) Nothing to Disclose

#### TEACHING POINTS

The purpose of this exhibit is: • To illustrate the imaging features found in different intramedullary pathologies, including their location, affected vertebral segment, contrast media uptake, and specific features. • To demonstrate intramedullary pathologies didactically divided into five groups: demyelinating, neoplastic, vascular, metabolic, and other lesions. • Illustrated review of a case series of intramedullary pathologies.

#### TABLE OF CONTENTS/OUTLINE

- Introduction - Epidemiology - Clinical scenarios - Typical imaging findings, with differences between the various intramedullary pathologies
- Case series of Intramedullary spinal cord injuries
- References
- Conclusion

#### **NREE-69 What Can it be in the Conus Medullaris? A Pictorial Review**

Participants

Felipe Pacheco, MD, PhD, Sao Paulo, Brazil (*Presenter*) Nothing to Disclose

#### TEACHING POINTS

The conus medullaris is affected by many conditions, including congenital, vascular, tumoral, inflammatory and infectious diseases, which many times

are hardly differentiated because of the similarity of their clinical history and physical examination among different etiologies. Magnetic resonance imaging presents high sensitivity in the detection of these lesions and plays a relevant role in the diagnosis and in the evolutive control. This panel aims to: Review the anatomy of the conus medullaris, including its anatomical limits, normal MR imaging findings and related clinical syndromes. Discuss and illustrate the imaging patterns of the main lesions in the conus medullaris, including congenital, vascular, tumoral, inflammatory, infectious, among others. - Describe through illustrative cases the scenarios for diagnosis, focusing on typical imaging patterns, unexpected findings and red flags that aid the diagnosis.

#### TABLE OF CONTENTS/OUTLINE

- Anatomy of the conus medullaris - Normal appearance on CT and MRI - Main pathologies involving the conus medullaris, involving: - Congenital lesions: Caudal regression syndrome types 1 and 2, Ventriculus terminalis, Myelomeningocele - Neoplastic lesions: myxopapillary ependymoma, tanyocytic ependymoma, leptomeningeal carcinomatosis, metastatic lesion, glioblastoma, dermoid cyst - Vascular lesions: arteriovenous dural fistula, cavernoma, ischemia - Systemic inflammatory diseases: IGG-4 related disease, Sarcoidosis, Dermatomyositis - Infectious diseases: Schistosomiasis, Tuberculosis, Herpes Virus, Polio-like - Auto-immune diseases: MOG antibody disease, Multiple Sclerosis, NMSOD - Red flags and diagnostic tips - Diagnostic Approach - Final remarks

#### NREE-7 What Can Go Wrong? Advanced Imaging of Malformation of Cortical Development

**Awards**  
Identified for RadioGraphics  
Cum Laude

Participants  
Julia Brunelli, MD, Sao Paulo, Brazil (*Presenter*) Nothing to Disclose

#### TEACHING POINTS

This pictorial essay will review the main etiologies of malformations of cortical development (MCDs) based on illustrative cases and original drawings. MCD will be addressed according to the last consensus update, considering pathological, genetic and neuroimaging features. The entities are divided into three major groups, according to the pathophysiological path that leads to that malformation. The purpose of this exhibition is to: - Review the cortical development, and its three main stages: cellular proliferation and differentiation, neuronal migration, and cortical organization; - Describe the new consensus of MCDs; - Recognize the main etiologies of MCDs, according to their imaging findings, and understand how different etiologies, when damaging the same pathway, can cause the same radiologic pattern.

#### TABLE OF CONTENTS/OUTLINE

NORMAL CORTICAL DEVELOPMENT - Didactic original drawings of the stages of cortex formation. MALFORMATIONS OF CORTICAL DEVELOPMENT - The new consensus taking account pathological, genetic and neuroimaging features. CASE-BASED DIDACTICS - Sample cases to illustrate and solidify the concepts; - Review of the main pathologies, addressing the pathophysiological and genetic aspects that leads to each image pattern.

#### NREE-70 Spinal Dysraphisms: Step-by-Step

Participants  
María José Risco Fernandez, Toledo, Spain (*Presenter*) Nothing to Disclose

#### TEACHING POINTS

• Knowledge of the normal embryologic development of the spinal cord is crucial for understanding spinal dysraphisms (SD). • They have been divided into open (OSD) and closed spinal dysraphisms (CSD), depending on the absence or presence of skin covering the defect. • Magnetic resonance imaging (MRI) is the modality of choice for the evaluation of these.

#### TABLE OF CONTENTS/OUTLINE

Spinal dysraphisms (SD) make reference to a wide spectrum of congenital abnormalities of the spine and spinal cord. Spinal development occurs throughout the 2nd and 6th week along embryologic stages of gastrulation, and primary and secondary neurulation. Anomalies in any of these stages can result in a defective or incomplete closure of the neural tube and structures of the dorsal midline. The clinical manifestations of these entities are heterogeneous: from being unnoticed to becoming incompatible with life outside the uterus. SD has been classically divided into two main groups depending on whether there is skin covering the defect: OSD and CSD. Magnetic resonance imaging (MRI) is the modality of choice for the detailed evaluation of these conditions. A step-by-step evaluation of the normal and abnormal imaging findings is critical to providing accurate surgical information. The aim of this pictorial review is to offer a systematic evaluation of SD on MRI, including normal and abnormal findings, classifying the type and the site of SD, and additional or associated findings both in pre and postnatal patients of our clinical practice.

#### NREE-71 Traumatic Spine Injury Classification: A Review of the AO Spine Injury Classification Systems Through Case Examples

Participants  
Chad Farris, MD, PhD, (*Presenter*) Nothing to Disclose

#### TEACHING POINTS

- Review the AO Spine Injury Classification Systems for traumatic injuries to the thoracolumbar spine (Thoracolumbar Injury Classification System), subaxial cervical spine (Subaxial Injury Classification System), and the upper cervical spine (Upper Cervical Injury Classification System). - Review case examples of traumatic spine injuries fitting into all of the morphological classifications based on the AO Spine Injury Classification Systems.

#### TABLE OF CONTENTS/OUTLINE

A. What are the AO Spine Classification Systems? B. Three basic parameters that all AO Spine Classification Systems are based on: 1. Morphological Classification of the Fracture, 2. Neurological Status, 3. Clinical Modifiers C. Case examples fitting into all of the morphological classifications within the AO Spine Classification Systems in the thoracolumbar spine, subaxial cervical spine, and upper cervical spine. 1. Thoracolumbar Spine Examples: a. Type A0 Injury, b. Type A1 Injury, c. Type A2 Injury, d. Type A3 Injury, e. Type A4 Injury, f. Type B1 Injury, g. Type B2 Injury, h. Type B3 Injury, i. Type C Injury 2. Subaxial Cervical Spine Examples: a. Type A0 Injury, b. Type A1 Injury, c. Type A2 Injury, d. Type A3 Injury, e. Type A4 Injury, f. Type B1 Injury, g. Type B2 Injury, h. Type B3 Injury, i. Type C Injury, j. Type F1 Injury, k. Type F2 Injury, l. Type F3 Injury, m. Type F4 Injury 3. Upper Cervical Spine: a. Occipital Condyle and Occipital Cervical Joint Complex: i. Type A Injury, ii. Type B Injury, iii. Type C Injury, b. C1 Ring and C1-2 Joint Complex Injuries: i. Type A Injury, ii. Type B Injury, iii. Type C Injury

#### NREE-72 Resting-state FMRI Seed-based Connectivity Map as a Diagnostic Visualization Biomarkers in Different Brain Disorders

Participants  
Mohamed Eid, MD, PhD, (*Presenter*) Nothing to Disclose

#### TEACHING POINTS

We plotted seed based connectivity (SBC) for about 40 main dynamic functional connectivity networks for each cases, then we reviewed the homogeneity of cerebral and cerebellar brain activity in both sides and we determined for epileptic case visualization the sign of Bull's eye of abnormal disrupted brain activity as a reference for seizure's onset zone (SOZ). And as regards to the alcohol toxicity induced bilateral total blindness we determine the visualization of normal bilateral dynamic functional connectivity and activity in the occipital networks and compared it to the normal control cases. 30 Normal controls cases, 25 clinical confirmed uncontrolled epileptic patients and one case of alcohol toxicity induced total bilateral

eyes blindness although normal signal intensities of both optic nerves and chiasm in conventional MRI sequences and MRI post gad contrast. Methods We obtained raw data from MRI Toshiba and Siemens 1.5 Tesla for all cases after written Informed consent as follow ; Bold EPI sequences (as a functional raw data ) about 3:40 minute duration ,High resolution axial T1 WI ( as an anatomical raw data ) , about 3:20 minute.All data preprocessed ,post processed and analysed used MATLAB based softwares , CONN toolbox .

#### TABLE OF CONTENTS/OUTLINE

Abstract Patient Methods Cases and figures / pdf

#### **NREE-74 Neurogenetics: What Should the Radiologist Know?**

Participants

Mario Abizaid, Sao Paulo, Brazil (*Presenter*) Nothing to Disclose

#### TEACHING POINTS

- The autosomal recessive inheritance pattern, although rare, when considered as a group becomes prevalent. Those diseases have an increased prevalence in consanguineous marriage and restricted geographic areas, known as "founder effect".- The autosomal dominant inheritance pattern is seen in heterozygosis and it is inherited from a parent who had the disease (family history). Less frequently, can emerge from a new mutation (mutation of de novo).- The trinucleotide repeat, as in Huntington's disease, is amplified with each generation, due to a misreading in the DNA.- There are mitochondrial proteins produced in the organelle itself (maternal inheritance pattern), as well as produced in the cell nucleus (autosomal or X-linked inheritance pattern).

#### TABLE OF CONTENTS/OUTLINE

Autosomal recessive inheritance patternMetachromatic leukodystrophyHorizontal gaze palsy with progressive scoliosisCARASILMaple syrup urine diseasePKANWilson's diseasePhenylketonuriaAutosomal dominant inheritance pattern CADASILNeurofibromatosis type 1Von Hippel LindauMarfan SyndromeTuberous sclerosis .X linked disorders patternX linked adrenoleukodystrophyPelizaeus-Merzbacher diseaseRett syndromeIncontinentia pigmentiTrinucleotide repeat expansion Huntington's diseaseFragile x associated tremor ataxia syndromeFriedreich ataxiaMitochondrial diseaseMELASLeigh SyndromeLHONKern-Sayres SyndromeOncogeneticproto-oncogene and tumor suppressor geneIDH-wildtype and IDH-mutant H3 K27M-mutant RELA fusion-positive ependymomamedulloblastoma: WNT-activated and SHH-activatedC19MC-altered

#### **NREE-75 Genetic Complexity and Imaging Assessment of the Mitochondrial Disorders**

Participants

Heber Colares Costa, MD, Rio de Janeiro, Brazil (*Presenter*) Nothing to Disclose

#### TEACHING POINTS

To review the terminology, epidemiology, pathology, clinical and genetic issues of the mitochondrial disorders. To illustrate the imaging highlights of the primary mitochondrial disorders. To demonstrate the most common differential diagnosis based on imaging and epidemiology.

#### TABLE OF CONTENTS/OUTLINE

1. Background with pathological, physiopathological, epidemiological, clinical, and genetic revision of the mitochondrial disorders. 2. Imaging pearls of mitochondrial disorders with an emphasis on MRI patterns and specific diagnoses. 3. Flowchart of assessment of the mitochondrial disorders. 4. Take-home messages.

#### **NREE-76HC Imaging Approach to Intraventricular Masses: Common and Uncommon MR Imaging Findings**

Participants

Hee Soo Won, (*Presenter*) Nothing to Disclose

#### TEACHING POINTS

To identify normal anatomy of ventricular system. To help narrow the differential diagnosis in intraventricular masses according to their location, patient's age, gender and underlying conditions. To describe the imaging features of intraventricular masses. To review common and uncommon location of intraventricular masses with MR imaging.

#### TABLE OF CONTENTS/OUTLINE

Imaging anatomy of ventricular system Imaging approach to intraventricular mass Review of common and uncommon MR imaging features of the following intraventricular neoplastic and nonneoplastic masses 1. Central neurocytoma 2. Subependymoma 3. glioblastoma 4. Subependymal giant cell astrocytoma 5. Lymphoma 6. Metastasis 7. Choroid plexus tumor 8. Choroid plexus cyst 9. Meningioma 10. Colloid cyst 11. Craniopharyngioma 12. Ependymoma 13. Epidermoid cyst 14. Pleomorphic xanthoastrocytoma 15. Multiple myeloma Summary and conclusionPlease visit the Learning Center to also view this presentation in hardcopy format.

#### **NREE-77 Consensus Recommendations on Clinical APT-weighted Imaging Approaches at 3T for Brain Tumors**

Participants

Jinyuan Zhou, PhD, Baltimore, MD (*Presenter*) Inventor, Koninklijke Philips NV;Institutional license agreement, Koninklijke Philips NV;Speaker, Koninklijke Philips NV

#### TEACHING POINTS

Currently used amide proton transfer-weighted (APT<sub>w</sub>) MRI protocols vary substantially among different institutes. Thus, the results acquired from different patient studies are difficult to compare, which hampers uniform clinical application and interpretation. The purpose of this education exhibit is: 1) To review challenging issues for clinical APT<sub>w</sub> imaging at 3T. 2) To provide a rationale for optimized and standardized APT<sub>w</sub> brain tumor imaging. 3) To review specific recommendations for pulse sequences, acquisition protocols, and data processing methods for APT<sub>w</sub> imaging of brain tumors. 4) To provide tips for using APT<sub>w</sub> imaging in the clinical setting.

#### TABLE OF CONTENTS/OUTLINE

1) Introduction. 2) APT<sub>w</sub> MRI background and theory. 3) History of the mechanism and the evolution of its understanding. 4) APT<sub>w</sub> imaging pulse sequences, including RF saturation approaches and parameters, lipid suppression, and readout. 5) Acquisition protocols. 6) Data processing and display. 7) Brain tumor APT<sub>w</sub> imaging data interpretation and pitfalls. 8) Conclusions and remarks.

#### **NREE-78 Paragangliomas of the Head, Neck, and Spine: Radiologic-Pathologic Correlation**

Participants

Robert Y. Shih, MD, (*Presenter*) Nothing to Disclose

#### TEACHING POINTS

1. The paraganglia are non-neuronal neuroendocrine cells that are part of the autonomic nervous system and derived from the neural crest. They are named for the location beside the paravertebral sympathetic ganglia.2. Pheochromocytomas (chromaffin cells) are named for a characteristic brown color change of the paraganglia tissues when fixed in chromium salts, which reflects oxidation of stored catecholamines. These chromaffin cells are found in the adrenal medulla or beside sympathetic ganglia in the abdomen.3. There is another type of paraganglia, which has chemoreceptor rather than neuroendocrine functions, responsible for increasing respiration in response to acidosis, hypoxia, or hypercarbia. These parasympathetic paraganglia are

composed of glomus cells and give rise to paragangliomas of the head and neck.4. Aside from paragangliomas of the head and neck, paragangliomas of the spine (specifically the cauda equina) are also encountered in neuroradiology. With the 2022 WHO Classification of Endocrine and Neuroendocrine Tumors, these are being reclassified as cauda equina neuroendocrine tumor (NET).5. Approximately 40% of paragangliomas are related to germline mutations, therefore genetic testing is indicated for all patients. While there are many familial endocrine tumor syndromes, hereditary paraganglioma syndromes involve mutations in succinate dehydrogenase (SDH).

#### TABLE OF CONTENTS/OUTLINE

1. What are the paraganglia?2. What is the relationship of paragangliomas and pheochromocytomas?3. What are the classic locations for paragangliomas of the head and neck?4. What is the classic location for paraganglioma of the spine?5. What is the significance of germline mutations for paragangliomas?

#### NREE-79 T2-FLAIR Mismatch Sign: My Favorite Evil

Participants

Larissa Martins, MD, Sao Paulo, Brazil (*Presenter*) Nothing to Disclose

#### TEACHING POINTS

The purposes of this exhibit are:• To elucidate the characterization and criteria for the application of the T2-FLAIR mismatch signal, described as one of the main radiophenotypes in neuroradiology, with a specificity close to 100% in the identification of IDH-mutant, 1p/19q-intact lower-grade glioma• Propose a checklist for the proper identification of the T2-FLAIR mismatch radiophenotype• Demonstrate practical tips and possible pitfalls to achieve the highest possible positive predictive value when faced with a probable T2-FLAIR mismatch• Discuss the differential diagnoses of lesions that present a sign of partial T2-FLAIR mismatch\*?αβ?e ?? ??te?ts/?t???e • Introduction:ο Mismatch T2-FLAIR: What is it?ο Differential Diagnosis• Checklist for the proper identification of the T2-FLAIR mismatch• Practical examples of lesions with true T2-FLAIR mismatch and lesions that mimic this radiophenotype• Differential diagnoses of lesions that present a sign of partial T2-FLAIR mismatch

#### NREE-8 Expand The Differential - An Interesting Case Series of Bithalamic Pathology

Participants

David Wessling, MD, Council Bluffs, IA (*Presenter*) Nothing to Disclose

#### TEACHING POINTS

This education exhibit presents a series of unique pathologies that lead to bilateral thalamic region imaging abnormalities. Our intention is to demonstrate numerous pathologies, expand the differential considerations of bithalamic lesions and raise the awareness of less commonly encountered disease processes. Many of the cases chosen were either were initially misinterpreted or puzzled the neuroradiologists at our academic institution. Many of the cases required multiple imaging modalities including advanced imaging techniques such as perfusion, diffusion tensor imaging and spectroscopy to either make a diagnosis, narrow the differential, or guide further management. Our aim with creating this exhibit is to describe the clinical presentation, demonstrate imaging appearances and defining characteristics, and provide interpretation of studies across multiple imaging modalities. Additionally, an explanation for how each study aids the radiologist's impression is provided. Our exhibit will advance the audience's comfort when faced with interpreting bithalamic imaging abnormalities. This will help to minimize patient harm from unnecessary intervention or delayed diagnosis.

#### TABLE OF CONTENTS/OUTLINE

This exhibit is intended to serve as a collection of interesting disease processes with bithalamic involvement. Specific interests will be given to cases utilizing multiple different imaging modalities and those which required advanced imaging techniques. These cases will be organized categorically; vascular, metabolic/toxic, neoplastic, inflammatory, infectious and seizures. Tables and diagrams will be created to highlight similarities and differences when applicable.

#### NREE-80HC Machine Learning in Alzheimer's Disease: Diagnostic Classification Using MR Neuroimaging Data

Participants

Stephanos Leandrou, PhD, MSc, (*Presenter*) Nothing to Disclose

#### TEACHING POINTS

Alzheimer's Disease (AD) is a neurodegenerative disease and its diagnosis relies mainly on cognitive tests. An important limitation of cognitive tests is the diagnosis of AD after structural changes have occurred within the brain. Therefore, these patients have a long prodromal phase when effective treatment strategies may be applied to delay or alter the onset of the symptoms. Research on quantitative MRI-derived biomarkers is an active research area which detects brain neurodegeneration before AD symptoms appear. In this study multi-modal features from both entorhinal cortex (ERC) and hippocampus were extracted from 194 normal controls (NC), 284 mild cognitive impairment (MCI) and 130 AD subjects. Texture analysis was mainly used which evaluates statistical properties of the tissue image quantitatively; therefore, it could detect smaller-scale changes of neurodegeneration. The use of ERC texture features is very limited in the literature, however, it is the first structure affected. We hypothesized that through the earlier involvement of ERC and the use of texture features, it is likely to detect microscopic alterations of the disease before atrophy spreads. This study used Machine Learning (ML) methods to address high dimensional data and discover new biomarkers in the assessment of AD. These directions will help to manage the disease progression and develop novel treatment strategies. This study innovates by using multi-modal data (incl. ERC) in the assessment of AD through a ML-based classification. An area under curve of 0.940, 0.806, and 0.786 was seen between NC vs AD, NC vs MCI and MCI vs AD subjects, respectively.

#### TABLE OF CONTENTS/OUTLINE

PurposeReviewMethodsResultsConclusionsReferencesPlease visit the Learning Center to also view this presentation in hardcopy format.

#### NREE-82 Learning from Machines: A Resident's Guide to AI Mistakes in Neuroradiology and What Residents Can Learn From Them

Awards

Certificate of Merit

Participants

Austin Young, (*Presenter*) Nothing to Disclose

#### TEACHING POINTS

With the steady advancement of computer vision technology, artificial intelligence (AI) algorithms have been shown to outperform radiologists in certain imaging interpretation tasks [1]. These technologies have been increasingly applied in clinical practice to aid in detection/diagnosis, disease prediction, and image segmentation [2]. Our institution has recently acquired an AI software package that allows for detection of acute hemorrhage, large vessel occlusion, and quantitative evaluation of perfusion deficits. This software package is expected to help provide a more prompt and accurate diagnosis by delivering qualitative and quantitative analysis of critical findings [3]. In this exhibit we highlight common pathologies where AI interpretation was discordant with the underlying pathology as determined by final attending interpretation, highlighting potential pitfalls in overreliance on this new technology in imaging interpretation. As we analyze these cases, an emphasis will be placed on the human component of imaging, how information must be integrated and synthesized to arrive at a proper diagnosis with the goal of providing direction for future deep learning algorithms and improved resident education.

#### TABLE OF CONTENTS/OUTLINE

Case 1: Pseudo-subarachnoid hemorrhage incorrectly interpreted as true hemorrhage Case 2: Erroneous interpretation of decreased blood vessel

density secondary to subdural hematoma Case 3: Presence of endovascular coils causing false interpretation of large vessel occlusion Case 4: Erroneous interpretation of decreased blood vessel density due to intraparenchymal hemorrhage Case 5: Cortical laminar necrosis wrongly interpreted as subarachnoid hemorrhage

#### **NREE-83 Decoding White Matter Tracts in Brain : Role of Diffusion Tensor Imaging (DTI) and Tractography in Brain Tumors**

Participants

Dinesh Meher, MBBS, MD, Delhi, India (*Presenter*) Nothing to Disclose

##### **TEACHING POINTS**

The purpose of this exhibit is to : 1.Discuss the construction of various white matter tractograms using appropriate regions of interest (ROIs). 2.Illustrate white matter tract pathological spectrum in various intra and extra axial brain tumors. 3.Review the importance of information provided by Diffusion tensor imaging (DTI) in addition to conventional MR imaging. 4.Discuss the importance of DTI in pre operative evaluation of brain tumors.

##### **TABLE OF CONTENTS/OUTLINE**

1.Introduction 2.DTI Physics 3.Normal white matter tracts in DTI 4.DTI patterns in brain tumors 5.Cases 6.Take home message

#### **NREE-84 OpenAI, SciSpacy, Supervised Machine Learning, and Deep Learning for Automated Data Extraction from Radiology Reports**

Participants

Ethan Wang, Dallas, TX (*Presenter*) Nothing to Disclose

##### **TEACHING POINTS**

1. Review how various natural language processing (NLP) techniques can be applied to optimize radiological text analysis involving binary classification and disease entity recognition. 2. Review the intricacies of Bag of Words text representation, supervised machine learning, pre-trained SciSpacy models, and fine-tuned OpenAI engine implementation for radiological text analysis. 3. Review the advantages, limitations, and optimal scenarios of different NLP approaches for radiological text analysis.

##### **TABLE OF CONTENTS/OUTLINE**

1. Introduction to NLP 2. Traditional NLP Applications for Binary Classification (BoW text representation, Deep Neural Networks, Supervised Machine Learning Algorithms) 3. Pre-Trained SciSpacy Models for Binary Classification and Disease Entity Extraction 4. Fine-Tuning OpenAI Engines for Binary Classification and Disease Entity Extraction 5. Advantages and Limitations of NLP (Time Expenditure, Flexibility, Integration with Traditional Statistics, Association with Task Complexity)

#### **NREE-86 Arterial Spin Labeling Perfusion Technique in Neurovascular Diseases: Technical Aspects, Artifacts and Clinical Applications**

Participants

Carlos Basoa Ramos, MD, Bilbao, Spain (*Presenter*) Nothing to Disclose

##### **TEACHING POINTS**

- To review the technical principles of the Arterial Spin Labelling (ASL) technique.
- To list the main artifacts that radiologists should be aware of.
- To review the main applications of the ASL technique, with special attention to neurovascular pathology (acute and chronic ischemia, arteriovenous shunt and moya-moya disease, among others).

##### **TABLE OF CONTENTS/OUTLINE**

ASL is an underused magnetic resonance imaging (MRI) technique that uses water molecules within arterial blood as endogenous contrast to obtain quantitative information of cerebral blood flow (CBF). Thus, ASL does not use exogenous contrast agents, being an alternative to other more established MRI perfusion techniques. Radiofrequency pulses are applied proximal to the brain, at neck vessels, to obtain an inversion of longitudinal magnetization of arterial blood water molecules. This process is called labelling. After a short period of time called post labelling delay (PLD) imaging is performed. Two imaging acquisitions are made, one unlabelled and one labelled. Subtraction of the unlabelled images will provide cerebral perfusion data. There are multiple labelling techniques but nowadays guidelines recommend implementation of 3D pseudocontinuous ASL (PCASL) in clinical practice. ASL has been studied and compared as well with other perfusion MRI techniques in neurodegenerative diseases, neuro-oncology, and neurovascular diseases. ASL technique is a useful technique in neurovascular pathology, especially in the control of patients with treated arteriovenous malformations.

#### **NREE-87 What Brain Perfusion is Telling You and You Might Not Have Noticed**

Participants

David Castanedo SR, MD, Santander, Spain (*Presenter*) Nothing to Disclose

##### **TEACHING POINTS**

- To analyze the most frequent perfusion alterations on perfusion CT (TCP) associated with "stroke mimics" .
- To differentiate between real and false ischemic penumbras.
- To identify the main pitfalls when analyzing these studies.

##### **TABLE OF CONTENTS/OUTLINE**

1. Introduction. 2. Analysis parameters. 3. Introduction to perfusion anomalies. 4. Imaging protocol. 5. Clinical cases. 5.1. Hyperperfusion. 5.1.1. Epileptic seizure (ictal phase). 5.1.2. High-grade gliomas. 5.1.3. Reversible Posterior Encephalopathy Syndrome (PRES). 5.1.4. Reperfusion/Hyperperfusion Syndrome. 5.1.5. Viral encephalitis. 5.2. Hypoperfusion. 5.2.1. Transient ischemic accident (TIA). 5.2.2. Vasospasm. 5.2.3. Bilateral carotid stenosis. 5.2.4. Cerebral venous thrombosis. 5.2.5. Migraine with aura. 5.2.6. Hypoglycemia. 5.2.6. Arterio-Venous Fistula Dural. 5.3. Gray or conflictive areas. 5.3.1. Chronic infarctions and "luxury perfusion". 5.3.2. Lacunary infarctions. 5.3.3. Crossed cerebellar diaschisis. 5.3.4. Motion artifacts. 5.3.5. Arterial and venous time-attenuation curves. 5.3.6. Threshold values in color maps. 5.3.7. Post-processing software. 6. Take Home Messages.

#### **NREE-88 The Multiple Faces of Typical Atypical Primary Central Nervous System Lymphomas**

Participants

Irene Dixe de Oliveira Santo, MD, New Haven, CT (*Presenter*) Nothing to Disclose

##### **TEACHING POINTS**

1. Review the demographics, differential diagnosis, and current standard for definitive diagnosis of primary central nervous system lymphoma 2. Describe the imaging features of typical and atypical PCNSL, including location, enhancement pattern, signal intensity in multiple sequences, presence or absence of hemorrhage, necrosis and calcification 3. Educate the radiologist regarding the differences in management of PCNSL and its main differential diagnoses, and discuss why prompt diagnosis is crucial for improved outcomes 4. Provide a brief outline of currently under investigation alternative methods for earlier and less invasive PCNSL diagnosis and classification, including the role of systematic classification tools and machine learning algorithms

##### **TABLE OF CONTENTS/OUTLINE**

- Demographics of PCNSL
- Presentation, important clinical features and imaging findings of multiple typical and atypical histologically-proven PCNSL

patients from our institution (71 patients available) • Differential diagnoses of PCNSL • Definitive diagnosis of PCNSL • Management of PCNSL vs management of its main differential diagnosis • Alternative methods for earlier and less invasive PCNSL diagnosis and classification

### **NREE-89 Finding the Specific in Non-Specific: Imaging in Acute Decompensation in Inherited Metabolic Disorders**

Participants

Garima Sharma, MBBS, MD, (*Presenter*) Nothing to Disclose

#### **TEACHING POINTS**

Most inherited metabolic disorders present as a severe progressive illness, however, some of them are often complicated by acute decompensation. These events are precipitated by the accumulation of toxic metabolites leading to encephalopathy and severe neurological injury. The factors triggering such episodes are generally states of an increased catabolic state, i.e., infection, trauma, or even increased consumption of any specific food component. While imaging is often ordered along with other investigations for a complete evaluation, most of the time the findings are labeled as non-specific. Hence, it is important for the radiologist to know: a) The metabolic disorders which can present as metabolic compensation b) Clinical clues and biochemistry c) Specific imaging features for various entities d) Mimics and major differential diagnosis. The most important mimics for these entities are hypoxic-ischemic injuries, sepsis, and vascular events (e.g. stroke). Magnetic Resonance Imaging (MRI) is the most important imaging modality for adequate evaluation of these patients.

#### **TABLE OF CONTENTS/OUTLINE**

1. Introduction 2. Causes of acute decompensation in inherited metabolic disorders 3. Clinical presentations 4. Understanding the biochemistry 5. Role of imaging 6. Specific imaging features a. Organic acidemias b. Urea cycle disorders c. Maple syrup urine disease d. Fatty acid oxidation defects e. Glycogen storage disease (type I) f. Leighs Disease

### **NREE-9 Cytokines and the Central Nervous System: What the Radiologists Should Know**

Awards

Identified for RadioGraphics

Participants

Mariko Kurokawa, MD, Ann Arbor, MI (*Presenter*) Nothing to Disclose

#### **TEACHING POINTS**

• Understand the role and mechanism of cytokines that affect the central nervous system (CNS), which often cause encephalitis/encephalopathy and cerebrovascular diseases. • Identify the causes, clinical features, and imaging features of cytokine storm. • Summarize cytokine engaging therapy including interferon-beta and chimeric antigen receptor (CAR) T-cell therapy with focus on the neuroradiological changes before and after treatment.

#### **TABLE OF CONTENTS/OUTLINE**

1. Cytokines and signaling pathways 2. Cytokine storm and CNS: Mechanisms, Acute necrotizing encephalopathy (ANE), Cytotoxic lesion of the corpus callosum (CLOCC), Virus-associated necrotizing disseminated acute leukoencephalopathy (VANDEL), Acute disseminated encephalomyelitis (ADEM), Thromboembolism, Hemorrhage 3. Cytokines and neurological diseases (multiple sclerosis, MS), Acute and chronic infarction, Tumors (Chordoma and angiomatoid fibrous histiocytoma), Castleman's diseases, and Mastocytosis 4. Cytokine engaging therapy and neuroimaging Interferon (IFN) beta for MS treatment, IFN alpha for lymphoma and malignant melanoma, Cytokine releasing syndrome in CAR-T therapy 5. Summary

### **NREE-90 Retinoblastoma: Beyond What the Eyes Can See**

Awards

Cum Laude

Participants

Taisa Guarilha, MD, Sao Paulo, Brazil (*Presenter*) Nothing to Disclose

#### **TEACHING POINTS**

Retinoblastomas are the most prevalent form of eye cancer in children, mostly occurring in first infancy. Most of them are diagnosed by the detection of leukocoria at ophthalmologist clinics. Nonetheless, image analysis performed by a radiologist can provide an assessment of key features that highly impact prognosis and treatment definition. We can see beyond the eye by detecting optic nerve involvement, extraocular tumor, and intracranial extension. The goal of this paper are: Review the anatomy of the orbit region Discuss epidemiology and clinical findings Demonstrate how retinoblastomas can present itself Exemplify the six groups according to the Grouping Classification of Retinoblastoma Features Demonstrate common and uncommon metastasis Show differential diagnosis

#### **TABLE OF CONTENTS/OUTLINE**

> Anatomy of the orbit region > Epidemiology and clinical findings > Imaging features > Present and explain cases from groups A to F from the Grouping Classification of Retinoblastoma Features > Metastasis: -optic nerve involvement- trilateral retinoblastoma- intracranial metastasis- spinal metastasis- leptomeningeal metastasis - abdominal metastasis- bone metastasis > Differential diagnosis: - Coats Disease- Medulloepithelioma- Retinal Hamartoma - Persistent hyperplastic primary vitreous- Optic pathway glioma- Meningioma > Postoperative control findings

### **NREE-91 The New Horizons of Neuroimaging in Recognition of Patterns of Genetic-Phenotypic Lissencephaly Spectrum**

Participants

Heber Colares Costa, MD, Rio de Janeiro, Brazil (*Presenter*) Nothing to Disclose

#### **TEACHING POINTS**

To illustrate the imaging spectrum of lissencephaly spectrum along with their genetic relationship. To exemplify the classification systems based on the most likely causative genes. To demonstrate the challenges of the new imaging and severity classification tools to guide and prioritize genetic testing for patients' clinical management and genetic counseling. To depict the differential diagnoses and a flowchart for assessing the lissencephaly spectrum.

#### **TABLE OF CONTENTS/OUTLINE**

1. Background. 2. Imaging protocol. 3. Clinical perspective and importance of analysis of lissencephaly spectrum. 4. The genetic cascade of events implicated in cortical development. 5. Imaging assessment and their correlation with the genetic abnormalities. 6. Imaging pearls correlated with the lissencephaly spectrum. 7. Differential diagnoses. 8. Flowchart for imaging assessment. 9. Take-Home messages.

### **NREE-92 Neurocutaneous Diseases, Clues for Neuroradiology Findings**

Participants

Karla Fuentes Badillo, MD, (*Presenter*) Nothing to Disclose

#### **TEACHING POINTS**

Neurofibromatosis Type I Characterized by the involvement of the nerve sheath. Imaging findings include white matter lesions, bone lesion associated with plexiform neurofibromas, focal areas of signal intensity hyperintense in T2, plexiform and paraspinal neurofibromas. Neurofibromatosis Type II NF2 is a hereditary syndrome characterized by multiple cranial nerve schwannomas, specifically with bilateral vestibular schwannomas, meningiomas and spinal

tumors. They can be evaluated on CT but are better characterized by MRI. Tuberous Sclerosis Complex Characterized by the presence of hamartomas. Cortical tubers appear in 95% of patients, subependymal giant cell astrocytomas tend to have intense enhancement, white matter abnormalities with variable appearance and subependymal nodules. Sturge Weber Syndrome Characterized by detects subcortical calcification at an earlier age than plain film and can also demonstrate associated parenchymal volume loss, tram-track sign of cortical and subcortical calcification. Von Hippel Lindau The most common lesions are retinal angiomas, hemangioblastomas of the cerebellum and spinal cord, visceral cyst and tumors. HGBL is seen as a well-defined cerebellar cyst with nodule on NECT, on MR imaging on T1 is observed as an iso/hypointense nodule with Flow voids (large feeding vessels within the periphery), while on T2/FLAIR is evidenced as a hyperintense nodule, which blooms in case of hemorrhage and enhances strongly without changes on cyst wall.

#### TABLE OF CONTENTS/OUTLINE

Neurofibromatosis Type I, Neurofibromatosis Type II, Tuberous Sclerosis, Sturge Weber, Von Hippel Lindau

#### NREE-93 Reinvent the Dragonfly: Pontocerebellar Hypoplasia Imaging and Genetics

Participants

Heber Colares Costa, MD, Rio de Janeiro, Brazil (*Presenter*) Nothing to Disclose

#### TEACHING POINTS

To demonstrate the spectrum of pontocerebellar hypoplasia through MRI, emphasizing the dragonfly signal sometimes present. To explain the physiopathology and genetic cascade involved. To demonstrate the imaging pearls with emphasis on the differential diagnosis.

#### TABLE OF CONTENTS/OUTLINE

1. Background. 2. Imaging protocol. 3. Clinical perspective and importance of analysis of pontocerebellar hypoplasia through MRI. 4. The genetic cascade of events implicated in the pontocerebellar hypoplasia. 5. Imaging pearls, including the dragonfly signal. 6. Differential diagnosis. 7. Flowchart for imaging assessment. 8. Take-Home messages.

#### NREE-94 Microtubulin Dysfunction - Key Imaging Features

Participants

Joel Samuel, MBBS, MD, (*Presenter*) Nothing to Disclose

#### TEACHING POINTS

Neurological abnormalities found on MRI brain in tubulinopathies predominantly consists of dysmorphic basal ganglia(90%),cerebral cortical malformations(60%), microcephaly(30%),callosal abnormalities(80%), ventriculomegaly(90%), asymmetric brain stem(60%), andsmall cerebellar vermis or hemispheres(50%).

#### TABLE OF CONTENTS/OUTLINE

LEARNING OBJECTIVE:The aim of this study is to describe the spectrum of key imaging findings associated with Tubulinopathies. BACKGROUND:Tubulinopathies are a heterogenous group of rare disorders that lead to complex brain malformation ,caused by mutation in tubulin genes.Study design:The study included MRI brain of 10 patients with symptoms of developmental delay, microcephaly, seizures and imaging features suggestive of tubulinopathies were studied over a period of three years.Microcephaly, cerebral cortical malformations, callosal abnormalities,ventriculomegaly, dysmorphic basal ganglia,hypoplasia of internal capsule, asymmetric brain stem, and small cerebellar vermis or hemispheres were the predominant finding seen in MRI.CONCLUSION:Knowledge of the main imaging findings of tubulinopathies is critical. Given the rarity of these conditions and lack of discriminating clinical features, imaging may be the only clue to an underlying tubulinopathy. Also helps in further genetic workup for these patients and identifying the gene mutated and helps in treatment .

#### NREE-95 Imaging Abnormalities in Patients with Alzheimers Disease Treated with Anti-Amyloid Beta Therapy

Awards

Identified for RadioGraphics

Participants

Amit K. Agarwal, MD, MBBS, Jacksonville, FL (*Presenter*) Stockholder, Gilead Sciences, Inc

#### TEACHING POINTS

-To discuss the novel therapeutic strategies for Alzheimer's disease, with focus on the recently approved anti-amyloid beta therapy- To illustrate the imaging abnormalities in patients with Alzheimer's Disease treated with Anti-Amyloid Beta Therapy- To discuss the protocol for monitoring and assessment for imaging abnormalities in patients on Anti-Amyloid Beta Therapy- To discuss the imaging differentials of ARIA ( with focus on cerebral amyloid angiopathy)

#### TABLE OF CONTENTS/OUTLINE

-Neuropathology of Alzheimer's disease (AD)-Role of cerebral amyloid-B (Ab) in Alzheimer's disease-Brief discussion on current imaging modalities for diagnosis and monitoring of AD (MRI, Amyloid PET,Tau PET)-Therapeutic strategies against amyloid- $\beta$  peptides in Alzheimer's disease- Imaging Abnormalities in Patients with Alzheimer's Disease Treated with Anti-Amyloid Beta Therapy - Amyloid-related imaging abnormalities: edema (ARIA-E) and hemorrhage(ARIA-H)- International Collaboration for Real-World Evidence in Alzheimer's Disease (ICARE AD) -MRI Acquisition Protocol Proposed to ICARE AD Sites ARIA Monitoring- Imaging differentials of ARIA (cerebral amyloid angiopathy, PRES)

#### NREE-96 How Much Do You Know About MRI Patterns of Brainstem Inflammatory Lesions?

Participants

Carlota Garcia de Andoin Sojo, MD, Bilbao, Spain (*Presenter*) Nothing to Disclose

#### TEACHING POINTS

When facing inflammatory lesions of the brainstem there are a number of differential diagnoses and accurate diagnosis can be difficult. Knowing clinical features and MRI findings, especially on the extent of dissemination, number, morphology and appearance of the lesions in different MRI sequences radiologists will be able to reach the correct diagnosis.

#### TABLE OF CONTENTS/OUTLINE

Objective: To describe MRI findings of major inflammatory and immune-mediated diseases that affect the brainstem.Methods A revision of the most characteristic inflammatory lesions of the brainstem has been made in MRI-illustrated challenging quiz format.Findings 1. Immune-mediated inflammatory disorders: illustrated quiz-mode cases will lead to the revision of disorders that involve the brainstem, including Multiple Sclerosis, Neuromyelitis Optica Spectrum Disorder, Myelin Oligodendrocyte Glycoprotein antibody-induced demyelination, Neuro-Behçet, Neurosarcoidosis, Histiocytic disorders, Bickerstaff Brainstem Encephalitis, Acute Haemorrhagic Encephalomyelitis, Hurst disease, Systemic Lupus Erythematosus2. Differential diagnosis should be done having in mind MRI and clinical features of other diseases that also cause brainstem inflammation, such as paraneoplastic encephalitis, Alexander leukodystrophy, Wilson disease, Wernicke-Korsakoff syndrome and CNS infections (listeria, tuberculosis and enterovirus).Conclusion Knowing the typical MRI presentation of each of the disorders that cause brainstem inflammations radiologists can give important information to achieve an accurate diagnosis and establish appropriate treatments.

## **NREE-97      The Radiologist's Guide to Non-Traumatic Orbital Pathology**

### Participants

Emily Haas, MD, (*Presenter*) Nothing to Disclose

### **TEACHING POINTS**

Orbital pathology identification and diagnosis is of critical importance as delayed diagnosis and management may ultimately result in vision loss for many patients. Development of an appropriate differential diagnosis of orbital lesions is vital as to guide our clinician colleagues in appropriate next steps and future follow-up. This educational exhibit aims to review orbital anatomy and explore non-traumatic orbital pathology by underlying etiology. While there may be overlap in imaging features, we will discuss characteristic imaging findings for each diagnosis that help to distinguish them amongst each other and alleviate diagnostic dilemma.

### **TABLE OF CONTENTS/OUTLINE**

1. Vascular: Venous Malformation, Capillary Hemangioma, Orbital Varix, Carotid-Cavernous Fistula, Lymphatic Malformation, Granulomatosis with Polyangiitis (GPA). 2. Infectious/ Inflammatory: Pre-septal Cellulitis, Post-septal Cellulitis, Orbital Abscess, Dacryocystitis, Invasive Fungal Infection, Optic Neuritis, Idiopathic Orbital Inflammation, Thyroid-Associated Orbitopathy, Papilledema. 3. Neoplastic: Optic Nerve Sheath Meningioma, Optic Glioma, Rhabdomyosarcoma, Dermoid, Lymphoproliferative Disorders, Metastases.

## **NREE-98      Imaging of Headache in Relation to CSF Pressure/Volume Problem: What Radiologists Need to Know**

### Participants

Hyeonwoo Kim, MD, Seoul, Korea, Republic Of (*Presenter*) Nothing to Disclose

### **TEACHING POINTS**

Brain and spine imaging are key components in diagnosis and treatment strategy of SIH and IIH. After reviewing this educational exhibition, radiology residents should be able to understand clinical manifestations in headaches with CSF pressure/volume problem and how to approach imaging diagnosis with better imaging protocols.

### **TABLE OF CONTENTS/OUTLINE**

New onset or progressive headache is often the most common symptom of intracranial hypotension or hypertension syndrome. In spite of imaging advances, spontaneous intracranial hypotension (SIH) and idiopathic intracranial hypertension (IIH) are often misdiagnosed and if untreated, lead to severe neurologic impairment such as cognitive decline for SIH or visual impairment for IIH. The purpose of this educational exhibition is to review the related imaging findings of intracranial hypotension or hypertension and the suggested imaging protocols in patients with headache associated with CSF problem. We retrospectively evaluated MR images and clinical reports of headache patients collected at our hospital from 2011 to 2021. Contents Organization 1. Introduction 2. SIH 1) clinical manifestation 2) brain imaging for SIH 3) spine imaging for CSF leak 4) suggested imaging protocol 3. IIH 1) clinical manifestation 2) brain imaging for IIH 3) suggested imaging protocol 4. New concept of CSF physiology and glymphatic in relation to SIH and IIH 5. Summary

## **NREE-99      Carotid Cavernous Fistula: Classification, Arterial and Venous Anatomy, Clinical Presentation and Diagnosis and Endovascular Approach**

### Participants

Shadab Alam, MBBS, BANGALORE, India (*Presenter*) Nothing to Disclose

### **TEACHING POINTS**

1) Carotid cavernous fistula (CCF) are classified hemodynamically as high flow and low flow, etiologically as spontaneous, traumatic and Iatrogenic and anatomically as direct and indirect. 2) Clinical presentation is influenced by venous drainage patterns and shunt flow rate. 3) Endovascular approach depends on the type of CCF and angiographic findings which could be transarterial or transvenous. 4) Alternative approach for indirect CCF include transorbital superior ophthalmic vein approach and transfemoral Superior Petrosal Sinus Approach

### **TABLE OF CONTENTS/OUTLINE**

The exhibit will include: Classification of CCF. Arterial and venous anatomy with emphasis on the ECA and ICA anastomosis. Various clinical presentation. Imaging appearance of CCF. Angiographic anatomy and angiographic check list to plan treatment. Illustration interventional hardware for treatment planning. Case illustration of various treatment options like Transarterial coiling, parent artery occlusion, coil plus EVOH Embolisation, transvenous approach, various alternative approaches with case illustrations. Tips and tricks planning and execution of cases.

Printed on: 02/07/23



## Abstract Archives of the RSNA, 2022

NREE-1

### Cranial Nerves Cavernoma: A Rare Presentation of an Usual Lesion

Sunday, Nov. 27 8:00AM - 9:00AM Room: Learning Center - NR

#### Awards

Cum Laude

#### Participants

Danielly Santos SR, Sao Paulo, Brazil (*Presenter*) Nothing to Disclose

#### TEACHING POINTS

Through this pictorial essay a review will be made based on cases and original drawings about atypical location of Cavernous Malformations (MC's). The purposes of this exhibit are:- To review the normal anatomy of cranial nerves using schematic illustrations and imaging MRI.- To discuss imaging features of cavernous malformations (CM's) and their classification.- To display a compendium of cases of CM's involving the origin and path of cranial nerves.- To show the examination protocols and the best MRI sequence for assessing these cases.

#### TABLE OF CONTENTS/OUTLINE

Cavernous angiomas or malformations are angiographically occult vascular malformations found in approximately 0.4%-0.9% of the population, and they account for 10-20% of all cerebrovascular malformations. Their location is variable, with 70-80% having a supratentorial origin, followed by infratentorial location (15%) within the spinal cord (5%). Isolated cranial nerves CMs are extremely rare, and there are very few reports. Although rare, it poses a significant threat to nerve functions. Due to the limited number of cases and scarce evidence, no definite recommendation is available on the indications of surgery and treatment. However, it seems essential to treat patients with progressive neurological deficits. MRI imaging is crucial for the evaluation of CMs. It can be safely stated that the CISS/FIESTA sequence should be considered as a tool for evaluating the CM origin and nerve continuity and planning a surgical approach.

Printed on: 02/07/23



## Abstract Archives of the RSNA, 2022

NREE-10

### Ocular Trauma: There is More Than Meets the Eye

Sunday, Nov. 27 8:00AM - 9:00AM Room: Learning Center - NR

#### Participants

Atefeh Zeinoddini, MD, St. Clair Shores, TX (*Presenter*) Nothing to Disclose

#### TEACHING POINTS

Describe the relevant ocular anatomy. Identify the common post traumatic ocular injuries. Discuss potential pitfalls and complications of traumatic ocular injuries. List imaging findings that require immediate (surgical) intervention.

#### TABLE OF CONTENTS/OUTLINE

Relevant ocular anatomy. Ocular Trauma Score Points. Types of Detachments. Types of globe rupture, ocular foreign body (FB) and their potential pitfalls. Complications of ocular trauma.

Printed on: 02/07/23



## Abstract Archives of the RSNA, 2022

NREE-100

### Bilateral Thalamic Lesions Report: Imaging Statistics and Facts

Sunday, Nov. 27 8:00AM - 9:00AM Room: Learning Center - NR

#### Participants

Pedro Castro, MD, Rio de Janeiro, Brazil (*Presenter*) Nothing to Disclose

#### TEACHING POINTS

To illustrate the spectrum of bilateral thalamic lesions on MRI. To demonstrate that the MRI assessment of bilateral thalamic lesions can be simplified through a practical approach, listing the most valuable key imaging points. To identify potential imaging pitfalls, make possible the implementation of precise therapeutic measures, and avoid potentially harmful biopsies.

#### TABLE OF CONTENTS/OUTLINE

1. Anatomy of the thalamic region. 2. Main neoplasms presenting with bilateral involvement of the thalamus, including astrocytomas and lymphomas. 3. Inflammatory, infectious, and demyelinating lesions that can manifest with bilateral thalamic involvement, including West Nile and Mycoplasma encephalitis. 4. Vascular causes: deep venous thrombosis, arterial infarction, and hypoxic-ischemic encephalopathy. 5. Toxic and metabolic causes, including Wernicke's encephalopathy, Fahr disease, and Leigh disease. 6. Clues for a practical imaging assessment and the avoidance of pitfalls.

Printed on: 02/07/23



## Abstract Archives of the RSNA, 2022

NREE-101

### Case Based Review of Meningeal Disorders

Sunday, Nov. 27 8:00AM - 9:00AM Room: Learning Center - NR

#### Participants

Etsushi Iida, MD, Ube, Japan (*Presenter*) Nothing to Disclose

#### TEACHING POINTS

To review normal anatomy of the meninges and imaging techniques for evaluation of meningeal pathologies To be familiar with imaging diagnosis of meningeal diseases with case based review

#### TABLE OF CONTENTS/OUTLINE

1. Anatomy of meninges and extra-axial spaces 2. Imaging techniques for detection of meningeal abnormality 3. Representative abnormal imaging findings on various sequences including FLAIR, DWI, SWI, ASL-PWI, and contrast enhanced FLAIR and T1WI 4. List of Case based review | Case1 tubercular meningitis | Case2 sarcoidosis | Case3 intracranial hypotension | Case4 dural AVF | Case5 Sturge Weber syndrome | Case6 MOG related disease

Printed on: 02/07/23



## Abstract Archives of the RSNA, 2022

NREE-102

### Shedding light on the Substantia Nigra: Anatomy, Function, Imaging Technique and Pathophysiology.

Sunday, Nov. 27 8:00AM - 9:00AM Room: Learning Center - NR

#### Participants

Guillaume Curaudeau, MD, (*Presenter*) Nothing to Disclose

#### TEACHING POINTS

Anatomic features of the substantia nigra beget predictable imaging presentations of common and uncommon pathologies. Multi-modality and multi-sequence approach, including conventional T1 and T2-weighted images, DWI, SWI, and perfusion imaging are necessary to segregate different etiologies that affect the substantia nigra. The spectrum in imaging is reinforced via case based learning. Whereas DAT-SPECT scans have traditionally been used to evaluate Parkinsonian pathologies, improved high-resolution volumetric and susceptibility-weighted imaging are being leveraged for both Parkinsonian and non-Parkinsonian evaluation of etiologies affecting the substantia nigra. Understanding the difference between Wallerian and transneuronal degeneration Cellular idiosyncrasies of the nigrostriatal pathways including dense aquaporin-4 and elevated GABA receptor concentrations, as well as increased axonal aborization, contribute to higher metabolic burden and therefore lower threshold for development of oxidative stress. Genetic predispositions, some of which are newly characterized, foster accelerated pathways for nigrostriatal injury, and increased bionergetic burden.

#### TABLE OF CONTENTS/OUTLINE

Anatomy and Cellular underpinnings Function Imaging techniques Cases Summary and implications for clinical practice

Printed on: 02/07/23

## Abstract Archives of the RSNA, 2022

NREE-103

### Immunodeficiency-associated Primary CNS Lymphoma in Non-AIDS Patients - Clinico-Radiological Update

Sunday, Nov. 27 8:00AM - 9:00AM Room: Learning Center - NR

#### Participants

Francis Astrid Garay Buitron, MD, Barcelona, Spain (*Presenter*) Nothing to Disclose

#### TEACHING POINTS

-Presurgical suspicion of CNS lymphoma is crucial for initial patient management: corticoids avoidance prior to biopsy.-Imaging features of CNS lymphoma are T2 hypointensity, homogeneous enhancement, and restricted diffusion, without hemorrhage. These features refer to diffuse large B-cell lymphoma of the CNS (Epstein-Barr virus-negative, immunocompetent hosts).- Immunodeficiency-associated CNS lymphoma (diffuse large B-cell, Epstein-Barr virus-positive) does not fulfill these imaging criteria and it appears ring-enhancing with necrosis and hemorrhage; mimicking glioblastoma or metastasis.-It has been mainly associated with AIDS, which incidence is decreasing; while other causes of immunocompromise are increasing.-MRI interpretations usually misdiagnose this entity as glioblastoma or metastasis, and it is not uncommon that patients undergo avoidable surgical resection.- We noted a TSE-T2 hypointensity of the central non-enhancing component in these tumors, which may provide an easily-recognizable clue. Also, DSC-PWI (low CBV and high percentage of signal recovery) could be very useful.-In this presentation, clinical and radiological features of patients with non-AIDS DLBC EBV-positive CNS lymphoma are described with emphasis on 'imaging pearls'.-Radiologists must be aware of any cause of immunocompromise when facing a ring-enhancing tumor and know the imaging pearls for immunodeficiency-associated CNS lymphoma.

#### TABLE OF CONTENTS/OUTLINE

-CNS lymphomas WHO classification-Epidemiology-Clinico-radiological features of immunodeficiency-associated CNS lymphoma: clinical experience literature review-Differential diagnosis-Key-imaging features-Conclusions

Printed on: 02/07/23



## Abstract Archives of the RSNA, 2022

NREE-104

### Do Not Touch Lesions in Neuroradiology

Sunday, Nov. 27 8:00AM - 9:00AM Room: Learning Center - NR

#### Awards

Certificate of Merit

#### Participants

Joshua Litchman, MD, (*Presenter*) Nothing to Disclose

#### TEACHING POINTS

Define the concept of a Do Not Touch lesion in radiology  
Identify and describe representative Do Not Touch lesions in the brain, head and neck, and spine  
Compare and contrast these Do Not Touch lesions with their radiologic mimics on the basis of their respective clinical and imaging features

#### TABLE OF CONTENTS/OUTLINE

Do Not Touch Lesions in Radiology  
Definition  
Examples  
Do Not Touch Lesions of the Brain  
Dilated perivascular space  
Dural sinus and aberrant arachnoid granulations  
Benign enlarged subarachnoid spaces  
Capillary telangiectasia  
Porencephalic cyst  
Colloid cyst  
Do Not Touch Lesions of the Head and Neck  
Petrous apex asymmetric marrow  
Skull base fibrous dysplasia  
Jugular bulb pseudolesion  
Intratemporal facial nerve enhancement  
Facial nerve hemangioma  
Ranula  
Do Not Touch Lesions of the Spine  
Split atlas  
Odontoid process variants  
Limbus vertebra  
Ventriculus terminalis  
Perineural root sleeve cyst  
Extramedullary hematopoiesis

Printed on: 02/07/23



## Abstract Archives of the RSNA, 2022

NREE-105

### Imaging Features of CNS Neuroblastoma with FOXR2 Activation

Sunday, Nov. 27 8:00AM - 9:00AM Room: Learning Center - NR

#### Participants

Lohith Kini, MD, PhD, (*Presenter*) Consultant, Blackfynn Inc

#### TEACHING POINTS

Primitive neuroectodermal tumors of the central nervous system (CNS-PNETs) are a heterogeneous group of highly aggressive, poorly differentiated embryonal tumors occurring predominantly in young children. With the discovery and advances in molecular and genetic diagnostics led to a reclassification of CNS embryonal tumors in the most recent 2021 WHO Classification of CNS Tumors. The varied molecular and genetic alterations, as well as distinct histopathological and imaging features, described in this new taxonomy could inform future targeted clinical decision-making and reduce diagnostic challenge due to a lack of defining molecular markers. Using gene methylation profiling, CNS neuroblastoma with FOXR2 activation (CNS NB-FOXR2) has been identified as a distinct subtype. This educational exhibit will discuss the key radiographic and molecular features of CNS NB-FOXR2, as well as similar entities on the radiologic differential diagnoses.

#### TABLE OF CONTENTS/OUTLINE

I. Overview of CNS neuroblastoma with FOXR2 activation (CNS NB-FOXR2). II. Characteristic imaging features and molecular classification of CNS NB-FOXR2. III. Radiologic differences between CNS NB-FOXR2 and other embryonic tumors. Medulloblastoma. CNS tumor with BCOR internal tandem duplication IV. Summary and Quiza. Summary of key radiologic findings of CNS NB-FOXR2.b. Quiz: apply this new knowledge to a few example cases to improve diagnostic precision.

Printed on: 02/07/23



## Abstract Archives of the RSNA, 2022

NREE-106

### Circumscribed Astrocytic Gliomas: Key Findings You Need to Know

Sunday, Nov. 27 8:00AM - 9:00AM Room: Learning Center - NR

#### Participants

Seulkee Kim, MD, PhD, Gwangju, Korea, Republic Of (*Presenter*) Nothing to Disclose

#### TEACHING POINTS

1. To review the major changes of the fifth edition of the WHO Classification of Tumors of the CNS (WHO CNS5)2. To review the key radiologic and clinical findings of circumscribed astrocytic gliomas.

#### TABLE OF CONTENTS/OUTLINE

1. Introduction2. The major changes in the WHO CNS5 of circumscribed astrocytic gliomas3. Diagnostic key radiologic and clinical findings: case-based review1) Pilocytic astrocytoma2) Pleomorphic xanthoastrocytoma3) Subependymal giant cell astrocytoma4) Chordoid glioma5) Astroblastoma4. Differential diagnosis1) Ganglioglioma2) Dysembryoplastic neuroepithelial tumor5. Summary

Printed on: 02/07/23



## Abstract Archives of the RSNA, 2022

NREE-107

### The Lymphoma Game Show: Imaging Review of Primary CNS Lymphoma and Its Differential Diagnoses

Sunday, Nov. 27 8:00AM - 9:00AM Room: Learning Center - NR

#### Participants

Karla Jongitud, MD, (*Presenter*) Nothing to Disclose

#### TEACHING POINTS

The purpose of this exhibit is to review the most common imaging manifestations of primary CNS lymphoma. To know the purpose of radiological imaging of primary CNS lymphoma. Explain the most common manifestations encountered with neuroimaging (CT, MRI, MR spectroscopy and MR perfusion) and assess their role in the initial diagnosis and monitoring of primary CNS lymphoma. Discuss imaging findings of differential diagnosis of primary CNS lymphoma with a "choose your answer" game.

#### TABLE OF CONTENTS/OUTLINE

General features of primary CNS lymphoma. Clinical presentation in primary CNS lymphoma. Diagnostic procedures in primary CNS lymphoma. Purpose of radiological imaging in primary CNS lymphoma. Imaging diagnostic clues in primary CNS lymphoma. Imaging CT findings in primary CNS lymphoma. Imaging MR findings in primary CNS lymphoma. Game: Differential diagnosis of primary CNS lymphoma. Toxoplasmosis. Glioblastoma. Abscess. Progressive multifocal leukoencephalopathy. Demyelination. Metastases. Neurosarcoidosis. Diagnostic considerations and pearls in primary CNS lymphoma. Conclusions.

Printed on: 02/07/23

## Abstract Archives of the RSNA, 2022

NREE-108

### Imaging Features of Primary Intracranial Sarcoma with DICER1 Mutation

Sunday, Nov. 27 8:00AM - 9:00AM Room: Learning Center - NR

#### Participants

Lohith Kini, MD, PhD, (*Presenter*) Consultant, Blackfynn Inc

#### TEACHING POINTS

A broad spectrum of primary intracranial sarcoma subtypes is now recognized, presumably arising from mesenchymal progenitor cells within the meningeal covering of the brain and along perivascular spaces. Building on the key advancements in radiographic and genetic and molecular diagnostics including DNA methylation profiling, primary intracranial sarcoma with DICER1 mutation (PISD) can now be characterized as a distinct tumor entity, newly defined by the 2021 WHO Classification of CNS Tumors. The significant histological variability of PISD makes diagnosis challenging, but DNA methylation profiling and gene panel sequencing have elucidated it as a homogenous entity. This educational exhibit will highlight the important and distinct radiographic and molecular features of PISD in contrast to other intracranial mesenchymal, non-meningothelial tumors such as rhabdomyosarcoma, CIC-rearranged sarcoma and solitary fibrous tumors.

#### TABLE OF CONTENTS/OUTLINE

I. Overview of primary intracranial sarcoma with DICER1 mutation (PISD). II. Characteristic imaging features and molecular classification of PISD. III. Radiologic differences between PISD and other intracranial mesenchymal, non-meningothelial tumors a. Rhabdomyosarcoma b. CIC-rearranged sarcoma c. Solitary fibrous tumors IV. Summary and Quiz a. Summary of key radiologic findings of PISD. b. Quiz: apply this new knowledge to a few example cases to improve diagnostic precision.

Printed on: 02/07/23



## Abstract Archives of the RSNA, 2022

NREE-109

### Hypothalamic-pituitary Region and the Neighborhood

Sunday, Nov. 27 8:00AM - 9:00AM Room: Learning Center - NR

#### Participants

Eduardo Valadares, MD, Sao Paulo, Brazil (*Presenter*) Nothing to Disclose

#### TEACHING POINTS

Describe the embryology, anatomy and physiology of hypothalamic-pituitary axis and anatomy of structures around the sella turcica. Exhibit the normal appearance of pituitary gland and hypothalamus in CT and MRI imaging. Summarize the main anatomy variants, congenital anomalies, neoplasms, inflammatory diseases, tumor-like lesions and other disorders of hypothalamic-pituitary axis and neighborhood.

#### TABLE OF CONTENTS/OUTLINE

Introduction Embryology, anatomy and physiology of hypothalamic-pituitary axis Normal CT and MRI appearance Main anatomy variants Pituitary hyperplasia Empty sella Congenital anomalies • Pituitary anomalies • Hypothalamic hamartoma • Rathke Cleft cyst Neoplasms • Pituitary adenomas • Craniopharyngioma • Lymphoma • Germinoma • Meningioma • Histiocytosis • Astrocytoma • Teratoma • Lipoma • Metastasis Inflammatory diseases • Hypophysitis • Infectious processes Tumor-like lesions and other disorders • Pituitary apoplexy • Hypothalamic hamartoma • Aneurysm • Wernicke disease • Wyburn-Mason syndrome • Neuromyelitis optica (NMO) Take-home messages/Conclusions

Printed on: 02/07/23



## Abstract Archives of the RSNA, 2022

NREE-11

### Brain Arteriovenous Malformations (AVMs): A Practical Approach

Sunday, Nov. 27 8:00AM - 9:00AM Room: Learning Center - NR

#### Participants

Danielly Santos SR, Sao Paulo, Brazil (*Presenter*) Nothing to Disclose

#### TEACHING POINTS

To make the correct diagnosis, distinguishing brain AVMs from other intracranial vascular malformations and identify any complications at the time of presentation that may require immediate management; To stratify the risk of future complications, especially hemorrhage, perilesional hypoxemia or venous congestion, and thereby, establishing the appropriateness of conservative management or treatment; If AVM treatment is indicated, to choose the most effective modality for treatment with the lowest risk of adverse events; To follow the AVM over time, monitoring responses to treatment or ensuring stability with conservative management.

#### TABLE OF CONTENTS/OUTLINE

A AVM is a nidus of abnormal blood vessels connecting arteries and veins in the brain parenchyma through a shunt, primarily composed of enlarged feeding arteries through which arteriovenous shunting occurs with draining veins. Brain AVMs are rare lesions and most occur sporadically, although there are known associations with syndromes, such as hereditary hemorrhagic telangiectasia and cerebrofacial arteriovenous metamerism syndrome. When imaging AVMs, it is important to first identify features suggesting elevated risk of hemorrhage or other morbidity, such as perinidal hypoxemia, and secondly, to inform the choice of treatment or observation that provides the best balance of risk and benefit to the individual patient. Longitudinal imaging surveillance, either with conservative management or after treatment, enables monitoring for resolution of the AVM or the development of adverse findings that may necessitate a change in management.

Printed on: 02/07/23



## Abstract Archives of the RSNA, 2022

NREE-110

### Post-treatment Imaging Findings of Brain Metastases

Sunday, Nov. 27 8:00AM - 9:00AM Room: Learning Center - NR

#### Participants

Neudy Junior, MD, Sao Paulo, Brazil (*Presenter*) Nothing to Disclose

#### TEACHING POINTS

The purpose of this exhibit is: Illustrate typical and atypical post-treatment findings of brain metastases, including stereotactic radiotherapy, surgery resection, whole-brain irradiation, and immunotherapy. Describe characteristic imaging findings with sample cases from our institution's database. Highlight key imaging points and differential diagnosis.

#### TABLE OF CONTENTS/OUTLINE

Introduction. Epidemiology. Brain metastasis's location. Treatment options and complications. Series of cases of post-treatment imaging findings, complications, differential diagnosis and pitfalls. Conclusion.

Printed on: 02/07/23



## Abstract Archives of the RSNA, 2022

NREE-111

### Signs or Sins of Stroke in the Young Population: The Unforgivable Vascular Imaging Mystery

Sunday, Nov. 27 8:00AM - 9:00AM Room: Learning Center - NR

#### Participants

Pedro Castro, MD, Rio de Janeiro, Brazil (*Presenter*) Nothing to Disclose

#### TEACHING POINTS

To demonstrate that other vasculopathies besides atherosclerosis can cause ischemic stroke in young patients. To review the inflammatory, metabolic, coagulopathic, and genetic vasculopathies. To illustrate the imaging pearls of reversible cerebral vasoconstriction syndrome, carotid and vertebral dissection, carotid web, moyamoya, vasculitis, CADASIL, and drug abuse. To review these fewer common causes of stroke, sometimes misdiagnosed, and encourage the radiologist to go deeper into investigating these diseases.

#### TABLE OF CONTENTS/OUTLINE

1. Background of non-atherosclerotic vasculopathy causing ischemic stroke in young people. 2. Terminology, etiology, and pathology. 3. How CT and MRI angiography can help in differential diagnoses. 4. Vessel Wall MRI. 5. Carotid and vertebral dissection. 6. Carotid web. 7. Moya-Moya syndrome. 8. RCVS. 9. CADASIL. 10. Vasculitis. 11. Flowchart of imaging assessment. 12. Summary and Take-home messages.

Printed on: 02/07/23



## Abstract Archives of the RSNA, 2022

NREE-112

### Recanalization Therapy is a Matter of Mismatch

Sunday, Nov. 27 8:00AM - 9:00AM Room: Learning Center - NR

#### Participants

Pedro Castro, MD, Rio de Janeiro, Brazil (*Presenter*) Nothing to Disclose

#### TEACHING POINTS

To review the most beneficial practices in the ischemic stroke imaging assessment, emphasizing perfusion-diffusion evaluation of ischemic penumbra and FLAIR-diffusion mismatch. To show the importance of perfusion-diffusion mismatch evaluation in ischemic strokes with more than 6 hours of evolution. To explain the importance of FLAIR-diffusion mismatch evaluation in ischemic strokes with unknown onset time. To re-examine the current AHA/ASA Guidelines for the Early Management of Patients with Acute Ischemic Stroke Update.

#### TABLE OF CONTENTS/OUTLINE

1. Brief pathophysiological considerations of ischemic penumbra. 2. Flowchart of the objectives traced by the radiologist: critical objectives for stroke management. 3. Potentially salvageable brain: definition of ischemic penumbra through CT perfusion. 4. Potentially salvageable brain: definition of ischemic penumbra through MR perfusion-diffusion mismatch. 5. Strokes with unknown onset time: the importance of FLAIR-diffusion mismatch for clinical management. 7. Take-home messages.

Printed on: 02/07/23



## Abstract Archives of the RSNA, 2022

NREE-113

### Dose Size Matter? Going Beyond Large Vessels in Stroke Imaging

Sunday, Nov. 27 8:00AM - 9:00AM Room: Learning Center - NR

#### Participants

Humza Haque, MD, Newark, NJ (*Presenter*) Nothing to Disclose

#### TEACHING POINTS

1. To appreciate the importance of more distal vasculature when a patient presents with clinical appreciable stroke symptoms- High clinical suspicion, such as with a high NIH Stroke Scale, without occlusion of a large vessel (ICA, M1, basilar), should prompt careful inspection of more distal vasculature Latest research trends have shown success with intervention upon smaller vessels, making the radiologist's role for detection vital <sup>1</sup>2. To understand the utility of CT perfusion to guide identification of smaller vessel occlusion.- CT perfusion increases sensitivity and specificity of the detection of an occluded vessel <sup>2</sup>3. To gain insight on pearls and pitfalls regarding vascular anatomy, CT technique, and to avoid common errors when faced with stroke imaging Saver et al. (2020) Stroke 51:2872. Amukotuwa et al. (2021) Stroke 52:3308.

#### TABLE OF CONTENTS/OUTLINE

Define commonly used terms and abbreviations in the world of stroke and its imaging, including medium vessel occlusions (M2/3 middle cerebral artery, A2/3 anterior cerebral artery, and P2/3 posterior cerebral artery segments) <sup>3</sup>Review literature regarding large and more distal vessel occlusion Cases and teaching points of medium vessel occlusions involving the ACA, MCA, and PCA with pertinent clinical information, non-contrast CT head, CT angiogram, CT perfusion, and MRI. Conclusion <sup>3</sup>. Ospel et al. (2020) Stroke 51:2817

Printed on: 02/07/23



## Abstract Archives of the RSNA, 2022

NREE-114

### 2022: a Stroke Flowchart Odyssey in the Emergency Room

Sunday, Nov. 27 8:00AM - 9:00AM Room: Learning Center - NR

#### Participants

Heber Colares Costa, MD, Rio de Janeiro, Brazil (*Presenter*) Nothing to Disclose

#### TEACHING POINTS

To illustrate the current flowchart protocol for assessing acute ischemic stroke in the emergency room. To clarify the better protocol selection indications, including CT, CT angiography, and MRI. To explain the advantages of employing MRI for acute stroke evaluation. To demonstrate the optimal therapeutic implementation, including intravenous thrombolysis and mechanic thrombectomy.

#### TABLE OF CONTENTS/OUTLINE

1. Background. 2. Current flowchart protocol. 3. Clinical perspective and relevance of determining the correct stroke diagnosis, considering stroke mimics, and excluding hemorrhage. 4. Imaging perspective: CT, CT angiography, and MRI - advantages and disadvantages. 5. Critical Objectives Outlined by the Radiologist for Initial Conduct. 6. Tissue Viability: Definition of Ischemic Penumbra through CT and MRI Perfusion. 7. Update in the therapeutic assessment of stroke. 8. Take-Home messages.

Printed on: 02/07/23



## Abstract Archives of the RSNA, 2022

NREE-115

### Arachnoid Cysts: Not Always Benign

Sunday, Nov. 27 8:00AM - 9:00AM Room: Learning Center - NR

#### Participants

Glauber Siqueira I, MD,ARRT, (*Presenter*) Nothing to Disclose

#### TEACHING POINTS

The purpose of this exhibit is: The objective of this iconographic essay is to highlight the main imaging aspects of computed tomography (CT) and magnetic resonance imaging (MRI) of complications related to arachnoid cysts through illustrative cases. Among the main findings, that stand out, are rupture with the formation of extra-axial collections such as subdural hygroma or hematoma, intracystic hemorrhage, herniations, and hydrocephalus. It is crucial that radiologists become familiar with the main diagnostic aspects in cross-sectional imaging of this frequent cause that is not always devoid of clinical significance.

#### TABLE OF CONTENTS/OUTLINE

Anatomical considerations: location, anatomical variants and its implications. Cystic characteristics on CT and MRI. Adjacent structures: brain, bone, vessel and nerves. Atypical imaging appearance: red flags on differential diagnosis Arachnoid cysts post-operative imaging.

Printed on: 02/07/23

## Abstract Archives of the RSNA, 2022

NREE-116

### Clues to Suspect Dural Arteriovenous Fistulas at Cross-sectional Imaging: Case-based Quiz and Review with Angiographic Correlation

Sunday, Nov. 27 8:00AM - 9:00AM Room: Learning Center - NR

#### Participants

Carlota Garcia de Andoin Sojo, MD, Bilbao, Spain (*Presenter*) Nothing to Disclose

#### TEACHING POINTS

Even if arteriography is the gold standard radiological technique to confirm the presence of dural arteriovenous fistulas, some CT and MRI direct and indirect findings can suggest the diagnosis if seen.

#### TABLE OF CONTENTS/OUTLINE

**Objectives**To describe different radiological signs that suggest the presence of dural arteriovenous fistulas in cross-sectional image modalities (CT and MRI).To show the correlation between the signs described before and the angiographic findings.**Methods**A CT and MRI illustrated quiz with cases from our institution has been made to introduce the revision of each sign that suggests the presence of dural arteriovenous fistulas in non-invasive radiological tests.**Direct signs:** high signal of venous structures seen on time of flight (TOF) angiography MRI sequence; early enhancement of venous structures on contrast-enhanced angio-CT or MRI.**Indirect signs:** congestive parenchymatous or spinal oedema with variable hemorrhagic foci on MRI; intracranial intraparenchymal, subarachnoid or subdural haemorrhages; cerebral venous sinus thrombosis; prominent vascular structures in absence of nidus; area of increased blood flow in neuroperfusion studies; proptosis and orbital oedema; abnormally enlarged dural vascular channels in the skull. **Conclusion:**The knowledge of these findings in cross-sectional image modalities is useful for approaching the diagnosis and before performing an invasive test.

Printed on: 02/07/23



## Abstract Archives of the RSNA, 2022

NREE-117

### Reversible Cerebral Vasoconstriction Syndrome Learning Methods - How to Tighten the Mind

Sunday, Nov. 27 8:00AM - 9:00AM Room: Learning Center - NR

#### Awards

Certificate of Merit

#### Participants

Elissandra Lima, MD, Rio de Janeiro, Brazil (*Presenter*) Nothing to Disclose

#### TEACHING POINTS

To illustrate the imaging assessment of reversible cerebral vasoconstriction syndrome (RCVS). To describe the terminology, etiology, and physiopathology of RCVS. To explain the complications, disease associations, and treatment options involved in the RCVS.

#### TABLE OF CONTENTS/OUTLINE

1. Background. 2. MRI and CT angiography imaging protocol. 3. Physiopathology and related disorders. 4. Imaging assessment of RCVS and associations, like Posterior reversible encephalopathy syndrome and cortical subarachnoid hemorrhage. 5. Differential diagnoses. 6. Digital subtraction angiography assessment with emphasis on therapeutics. 7. Flowchart for assessment of RCVS. 8. Take-Home messages.

Printed on: 02/07/23



## Abstract Archives of the RSNA, 2022

NREE-118

### Arterial Wall Irregularities in Cerebral Vessels: Radiological Findings of Cerebral Vasculopathy

Sunday, Nov. 27 8:00AM - 9:00AM Room: Learning Center - NR

#### Participants

Mariano Lozano Gomez, MD, Almeria, Spain (*Presenter*) Nothing to Disclose

#### TEACHING POINTS

- To recognize imaging appearances of various forms of cerebral vasculopathy at CT, MRI and Digital Subtraction Angiography (DSA)- To describe key aspects to distinguish some types of cerebral nervous system (CNS) vasculopathy.- To discuss the correlation of clinical presentation and laboratory test results with imaging findings to aid the diagnosis of cerebral vasculopathy.

#### TABLE OF CONTENTS/OUTLINE

- Introduction.- Cerebral vascular anatomy: - Circle of Willis. - Vertebrobasilar circulation.- Analysis of CNS vasculopathies: - Description. - Clinical presentation. - Radiological features (CT, MRI, DSA).- Conclusion. - Take-home points.

Printed on: 02/07/23



## Abstract Archives of the RSNA, 2022

NREE-119

### CT Myelography: From Technical Aspects to Imaging Evaluation

Sunday, Nov. 27 8:00AM - 9:00AM Room: Learning Center - NR

#### Awards

Identified for RadioGraphics  
Certificate of Merit

#### Participants

Irlene Cordeiro de Macedo Pontes, MD, Sao Paulo, Brazil (*Presenter*) Nothing to Disclose

#### TEACHING POINTS

Although MRI has increased in importance, CT myelography still has a key role in delineating the spinal anatomy, especially to demonstrate dural sac and its contents pathologies. Therefore the radiologists must be aware of the main indications and the principles of the exam technique. The aim of this exhibit is to: 1. Detail the technique from lumbar and C1-C2 punctures. 2. Demonstrate the differences between the acquisition techniques from CT myelography. 3. Describe the differences between the contrast agents and the most suitable choice for the procedure. 4. Display and illustrate the needles available for lumbar puncture and the best selection for each case. 5. Exhibit forms of prevention of post-dural puncture headache. 6. Demonstrate imaging findings from erroneous contrast administration. 7. Illustrate the main indications from CT myelography with imaging findings.

#### TABLE OF CONTENTS/OUTLINE

1. INTRODUCTION  
2. THE TECHNICAL ASPECTS FROM CT MYELOGRAPHY  
a. Lumbar and cervical punctures  
b. Acquisition techniques  
c. Contrast selection  
i. Ionic  
ii. Nonionic  
d. Needles selection  
i. Conventional type  
ii. Pencil-point type  
e. Erroneous contrast administration: imaging findings  
f. Post-dural puncture headache  
3. MAIN INDICATIONS AND IMAGING FINDINGS  
a. Main indications  
b. Imaging findings from pathologies  
i. Radiation planning treatment  
ii. Spontaneous intracranial hypotension  
iii. MRI contraindications  
iv. Older uses/ indications

Printed on: 02/07/23



## Abstract Archives of the RSNA, 2022

NREE-12

### Pearls and Pitfalls of Diagnosing Spinal Cord Abnormalities: Emphasis on Patterns in T2-, Postcontrast T1- and Diffusion-Weighted Images

Sunday, Nov. 27 8:00AM - 9:00AM Room: Learning Center - NR

#### Awards

Certificate of Merit

#### Participants

Mariko Kurokawa, MD, Ann Arbor, MI (*Presenter*) Nothing to Disclose

#### TEACHING POINTS

The aim of this review is to summarize the clinical and imaging features of spinal cord disorders with focus on the distribution and enhancement patterns and diffusion-weighted images (DWI). Abstract Teaching Points: • Understand the anatomy of the spinal cord and surrounding structures in correlation with symptomatology and pathophysiologic mechanisms • Describe the pattern and distribution on axial and sagittal T2, postcontrast T1, and DWI in the spinal cord and surrounding structures, and discuss the appropriate imaging techniques and pitfalls. • Summarize typical and atypical imaging features of various common and uncommon diseases

#### TABLE OF CONTENTS/OUTLINE

1. Spinal imaging techniques: MR protocols including single or multi-shot EPI and non-EPI DWI; pitfalls and artifacts
2. Anatomy of the spine and spinal cord: Ascending tracts, descending tracts, and arterial territory
3. Axial images: White matter or gray matter (anterior, lateral, and posterior segments)
4. Sagittal images: Long cord lesion or short cord lesion
5. Enhancement pattern: Rim or ring enhancement, single nodular enhancement, multiple nodular enhancement, and patchy enhancement, pial or dural enhancement
6. Diffusion pattern
7. Cases: Spinal cord infarction/ischemia, dural AVF, neurosarcoidosis, transverse myelitis, viral myelitis, demyelinating diseases, compressive myelopathy, subacute combined degeneration, traumatic cord injury, spinal cord injury without radiographic abnormality (SCIWORA), and benign and malignant spinal tumors
8. Systemic diseases with spinal cord abnormalities
9. Summary

Printed on: 02/07/23



## Abstract Archives of the RSNA, 2022

NREE-120

### Correlation of Magnetic Resonance Imaging with Neuroinflammatory and Neuroimmune Responses in Acute, Subacute and Chronic Phases of Traumatic Spinal Cord Injury

Sunday, Nov. 27 8:00AM - 9:00AM Room: Learning Center - NR

#### Participants

Mabel Torres - Llacsá, MD, (*Presenter*) Nothing to Disclose

#### TEACHING POINTS

1- Describe the normal appearance of spinal cord in adult and after traumatic SCI. 2- Distribution of aldynoglia cell subpopulations in the adult CNS 3- Recognize the radiological appearance of the spinal cord in the acute, subacute and chronic phases after a traumatic spinal cord injury

#### TABLE OF CONTENTS/OUTLINE

1- Describe the inflammatory process that occurs in the spinal cord after a traumatic injury to the spinal cord. 2- Relationship of the radiological uptakes by magnetic resonance with the inflammatory phases that occur after a traumatic SCI. 3- Discuss the possible use of aldynoglia cells as cell therapy in traumatic spinal cord injury due to its ability to facilitate axonal re-growth re-myelination. 3.1- Cure by stimulation of resident aldynoglia cells near lesion area in SCI. 3.2- Injection of autologous aldynoglia cells grown ex vivo.

Printed on: 02/07/23



## Abstract Archives of the RSNA, 2022

NREE-121

### Sick Spine - A Review Of Differential Diagnosis Of Intramedullary Lesions On MRI

Sunday, Nov. 27 8:00AM - 9:00AM Room: Learning Center - NR

#### Participants

Pedro Gama Carpentieri Primo, MD, Rio De Janeiro, Brazil (*Presenter*) Nothing to Disclose

#### TEACHING POINTS

Summarize the main strategy of the differential diagnosis for intramedullary signal alterations Explore the differential diagnosis of intramedullary pathology with focus on unusual and rare cases Characterize the imaging aspects of the main lesions

#### TABLE OF CONTENTS/OUTLINE

Differential of intramedullary lesions based on MRI signal findings T1 hyperintense/hypointense T2 hyperintense/hypointense Anatomical distribution findings Ventral cord Dorsal cord Central cord Important differential diagnosis and its imaging features Angiomyolipoma Cavemomatous malformation Embryonal tumor with multilayered rosettes Hemangioblastoma Syringocephalus Medullary congestion Medullary tuberculosis Neuromyelitis optica spectrum Transverse myelitis post-COVID vaccination Leukemic infiltration Syphilis myelitis Intramedullary metastasis Medullary cone ependymoma Acute disseminated encephalomyelitis Systemic lupus erythematosus related myelitis Multiple sclerosis Medullary schistosomiasis

Printed on: 02/07/23



## Abstract Archives of the RSNA, 2022

NREE-122

### Spinal Epidural Lesions: A Case-Based Review

Sunday, Nov. 27 8:00AM - 9:00AM Room: Learning Center - NR

#### Participants

Izaely Prates, MD, Sao Paulo, Brazil (*Presenter*) Nothing to Disclose

#### TEACHING POINTS

1 - TEACHING POINTS- Review the normal anatomy of the epidural space and its relationship to adjacent structures- to illustrate a variety of rare cases in order to avoid misinterpretations and pitfalls;- propose an interpretation algorithm to try to reduce the number of differential diagnoses to help the referring physician.

#### TABLE OF CONTENTS/OUTLINE

2 - TABLE OF CONTENTS/OUTLINEINTRODUCTION.RELEVANT IMAGING ANATOMY.SPINAL EPIDURAL LESIONS: Clinical cases illustrating the spectrum of common and uncommon spinal epidural space findings in CT and MRI).Primary neoplasms of epidural space;Neoplasms that invade the epidural space;Hematomas;Infection and collections;Other lesions.A STEP-BY-STEP ALGORITHM TO APPROACH SPINAL EPIDURAL LESIONS.TAKE-HOME MESSAGESREFERENCES

Printed on: 02/07/23



## Abstract Archives of the RSNA, 2022

NREE-123

### Diffusion for Clearing Confusion: Role of the Diffusion-weighted Imaging in the Spine and Spinal Cord

Sunday, Nov. 27 8:00AM - 9:00AM Room: Learning Center - NR

#### Participants

Melih Akyuz, MD, Chicago, IL (*Presenter*) Nothing to Disclose

#### TEACHING POINTS

TEACHING POINTS: 1. Diffusion-weighted imaging (DWI) in the spine is relatively new, yet has been a reliable imaging method for the characterization of a variety of disease entities 2. DWI provides information on the tissue microstructure depending on the alterations of the water-proton mobility. The efficacy of this technique has been proven in the evaluation of the abnormalities of not only the brain but also the spinal cord and spine 3. Previous studies have shown that DWI might be useful in the evaluation of vertebral fractures, degenerative changes of the spine, infection, infarction of the spinal cord, neoplasms, and various inflammatory conditions involving the spine and spinal cord

#### TABLE OF CONTENTS/OUTLINE

TABLE OF CONTENTS OUTLINE: 1. Describing different techniques of diffusion-weighted imaging in the spine 2. Discuss various abnormalities involving the spine spinal cord their clinical manifestations 3. Briefly discuss the sources and mechanisms of actions of different disease entities involving the spine 4. Case-based imaging review of the abnormalities of the spine spinal cord with distinctive imaging findings emphasis on the use of the DWI in each entity

Printed on: 02/07/23



## Abstract Archives of the RSNA, 2022

NREE-124

### Magnetic Resonance Imaging Findings in Infectious and Granulomatous Spinal Cord Lesions

Sunday, Nov. 27 8:00AM - 9:00AM Room: Learning Center - NR

#### Participants

Alice Abreu Mota, MD, Sao Paulo, Brazil (*Presenter*) Nothing to Disclose

#### TEACHING POINTS

• Magnetic Resonance findings, associated with clinical and laboratorial exams, may help differentiate the specific etiology for infectious and granulomatous medulla and spinal cord pathologies. • Linear and nodular enhancement pattern with an “arborized” appearance is typical in neuroschistosomiasis. • The tuberculosis infection may lead to many complications like meningitis, radiculomyelitis, tuberculoma, myelitis, syringomyelia and spinal abscess. • Sarcoidosis lesions are frequently multiple and centrally located. • Toxoplasmosis is often indistinguishable from tuberculoma. • Abnormalities are mainly found in the dorsal columns in HTLV-1 and usually involve the posterior and lateral region of the cord in HIV. • In Varicella Zoster the T2 hyperintensity is in the lateral portion. • Myeloradiculopathy, myeloradiculitis, myelitis, myeloneuropathy, Guillain-Barre syndrome, have been reported in arboviruses.

#### TABLE OF CONTENTS/OUTLINE

Viral Myelitis • Varicella Zoster • Arboviruses ( Chikungunya) • Citomegalovirus • HIV • HTLV-1 Others Infectious diseases • Tuberculosis • Neuroschistosomiasis • Neurotoxoplasmosis Non-infectious granulomatous disease • Sarcoidosis

Printed on: 02/07/23



## Abstract Archives of the RSNA, 2022

NREE-125

### Non-traumatic Spine Emergencies -A Primer for the On-Call Radiology Resident

Sunday, Nov. 27 8:00AM - 9:00AM Room: Learning Center - NR

#### Participants

Emily Convery, MD, (*Presenter*) Nothing to Disclose

#### TEACHING POINTS

Although trauma remains a common indication for emergency room clinician to order spine imaging study, there are several atraumatic causes that warrant emergent spine imaging. This differential includes acute disc herniations with compressive myelopathy, pyogenic osteomyelitis with epidural abscess, and acute inflammatory process such as Guillain Barre syndrome or demyelinating disease, as well as direct or leptomeningeal spread of metastatic disease and vascular pathologies. Having familiarity with typical clinical manifestations and emergent management of such disease process can aid the radiologist with obtaining the proper spinal level of imaging with appropriate imaging modality and if need be recommend further imaging outside the neural axis.

#### TABLE OF CONTENTS/OUTLINE

1) Overview of spinal anatomy imaging search pattern 2) Signs and symptoms of myelopathy 3) Degenerative disease 4) Infectious and inflammatory diseases 5) Malignant compressive pathology 6) Vascular pathology 7) Treatment/management options

Printed on: 02/07/23



## Abstract Archives of the RSNA, 2022

NREE-126

### Diffusion Kurtosis Imaging (DKI) in Neuroradiology: Technique and Clinical Applications

Sunday, Nov. 27 8:00AM - 9:00AM Room: Learning Center - NR

#### Participants

Silvia Lanzarote Vargas, MD, Madrid, Spain (*Presenter*) Nothing to Disclose

#### TEACHING POINTS

DKI is a diffusion technique based on the use of very high values  $b=2000$  s/mm<sup>2</sup> and on the complex tissue structural technique with interesting applications in neuroradiology, mainly in the diagnosis and follow-up of gliomas.

#### TABLE OF CONTENTS/OUTLINE

Kurtosis is a statistical measure that determines the degree of concentration that the values of a variable present around the central zone of the frequency distribution. Diffusion imaging (DWI) with low  $b$  values assumes that the movement of water molecules after the application of the gradients of the diffusion sequence is the same in any direction in space and follows a Gaussian distribution. In biological tissues the movement of water molecules varies from the Gaussian distribution. This degree of deviation is related to tissue structural complexity and barriers to the free diffusion of water and it can be calculated using DKI. This presentation will explain in a simple way what are the technical requirements necessary to obtain the DKI as well as the parameters that can be calculated, such as the kurtosis coefficient ( $K$ ). It is intended to provide information that may be useful in routine clinical practice, illustrating representative cases. Examples of the different applications of DKI in the diagnosis and monitoring of different pathologies will be given. In brain tumors, it can be useful to differentiate high-grade and low-grade gliomas, as well as to distinguish between recurrence of high-grade gliomas and pseudoprogression or radionecrosis and gliomas from other tumors such as primary CNS lymphomas. We will also show the usefulness of DKI in the diagnosis of head and neck tumors as well as in neurodegenerative diseases.

Printed on: 02/07/23



## Abstract Archives of the RSNA, 2022

NREE-127

### Cavernous Sinus Hyperintense on Magnetic Resonance Angiography - Can You Differentiate Dural Arteriovenous Fistula from Cerebral Venous Reflux?

Sunday, Nov. 27 8:00AM - 9:00AM Room: Learning Center - NR

#### Participants

Keizo Tanitame, MD, Hiroshima, Japan (*Presenter*) Nothing to Disclose

#### TEACHING POINTS

Diagnostic radiologists often encounter cavernous sinus hyperintense on three-dimensional time-of-flight magnetic resonance angiography (MRA). Even if detailed evaluation of the source images of MRA is performed, differentiation between dural arteriovenous fistula (DAVF) and cerebral venous reflux (CVR) is occasionally difficult. Cerebral digital subtraction angiography (DSA) is useful for differentiating them, but it is invasive and has a small risk of cerebral embolisms. CVR is observed mostly on the left side, and considered to be retrograde venous flow due to compression of the left brachiocephalic vein between the sternum and aortic arch or branches. We demonstrate several cases with diagnostic difficulty and focus the cause of retrograde venous flow in left cavernous sinus and some techniques suppressing the CVR on MRA.

#### TABLE OF CONTENTS/OUTLINE

1. Representative MRA and DSA images of cavernous sinus DAVF - Small arteriovenous shunts near the cavernous sinus
2. Representative MRA and DSA images of upward venous reflux in the cavernous sinus - Retrograde venous flow of the cavernous sinus and other venous sinuses
3. The cause of retrograde venous flow in the left cavernous sinus - Images and schematic illustration of left brachiocephalic vein compression
4. Suppression techniques against intracranial retrograde venous flow - The usefulness of MRA scanning in the supine position with shoulder pillows and small breathing

Printed on: 02/07/23

## Abstract Archives of the RSNA, 2022

NREE-128

### Probing Metabolism: The Role of Proton MR Spectroscopy in Neurometabolic Diseases

Sunday, Nov. 27 8:00AM - 9:00AM Room: Learning Center - NR

#### Participants

Milena Kriek Farche, MD, Campinas, Brazil (*Presenter*) Nothing to Disclose

#### TEACHING POINTS

1- Describe the basic principles of magnetic resonance spectroscopy (MRS), with an emphasis on protocol acquisition and optimal technique in a variety of neurometabolic conditions. 2- Illustrate the normal spectra and main abnormal patterns of brain metabolites, integrating the spectroscopy information with the analysis of conventional MRI sequences. 3- To review the main neurometabolic diseases in which spectroscopy can aid in establishing the correct diagnosis, presenting radiological tips for each clinical context.

#### TABLE OF CONTENTS/OUTLINE

1 - Introduction  
2 - Principles of Proton MR spectroscopy  
A) Choosing the localization technique  
B) Choosing the echo-time (TE)  
C) Deciding between single-voxel vs multi-voxel  
D) Choosing the voxel location  
3 - Normal spectra and main abnormal patterns of brain metabolites, including potential pitfalls and normal variants.  
4 - Role of spectroscopy in the diagnosis of specific neurometabolic diseases with a series of illustrative cases  
5 - A spectroscopy-based approach to narrow the differential diagnosis in certain clinico-radiological scenarios (leukodystrophies, mitochondrial diseases, etc.)  
6 - Conclusion

Printed on: 02/07/23

## Abstract Archives of the RSNA, 2022

NREE-129

### Abnormalities Associated with Cerebral Cortical (AACs) on MRI

Sunday, Nov. 27 8:00AM - 9:00AM Room: Learning Center - NR

#### Participants

Zhiqiang Zhang, MD, PhD, (*Presenter*) Nothing to Disclose

#### TEACHING POINTS

Abnormalities associated with cerebral cortical (AACs) present specific anatomic, pathological, clinical and radiological features, but have less been addressed. We proposed a diagnostic framework by categorizing AACs into focal, regional and diffuse types according to the shape on MRI. In summary, AACs cover a variety of pathologies, show radiological gyrus-thickness sign in focal AACs, outline-sketch sign in regional AACs and flower-mimic sign in diffuse AACs, and are well demonstrated with IR-based T1WI, SWI and DWI on MRI.

#### TABLE OF CONTENTS/OUTLINE

Regional AACs, mainly include diseases of MCD of FCD-I and tumors of long-term epilepsy. Diseases mainly present symptoms of seizures, and are well demonstrated as focal gyrus thickness on IR based T1WI. Regional AACs, lesions are within a lobe at a hemisphere, pathologically diversified into (1) MCDs of polymicrogyria, (2) VDs of cortical laminar necrosis, Isolated cortical venous thrombosis and meningioangiomas. (3) tumors of gliomas and MVNT. (4) Brain injury of status epilepticus and (5) CNS infections/inflammation. The diseases feature with consciousness disorders and are well demonstrated on SWI or DWI with outline-sketch sign of gyrus. Diffuse AACs, are mostly bilaterally distributed and cover widely cortical areas, include more pathological types of (1) VD of HIE and SSCNS. (2) Tumor of DLGNT. (3) Metabolic of MELAS, hypoglycemic and hyperammonia encephalopathy; (4) CJD (5) NIID and (7) Toxicosis of mercury and benzene. Diseases feature with cognitive impairments, are pathologically associated with energy metabolic abnormality in cortex, and presented with regular geometric/vivid flower-mimic shapes on DWI and FLAIR.

Printed on: 02/07/23

## Abstract Archives of the RSNA, 2022

NREE-13

### Spinal Vascular Lesions: What to Know, and How it Should be Reported

Sunday, Nov. 27 8:00AM - 9:00AM Room: Learning Center - NR

#### Participants

Thiago Martins Fernandes Vilela, Mogi das Cruzes, Brazil (*Presenter*) Nothing to Disclose

#### TEACHING POINTS

- To review the normal anatomy of the spinal cord, the modified classification of spinal vascular lesions (by Spletz), a more practical classification based on the vascular anatomy of the spinal cord and the inborn or acquired nature of the lesion (Bicentre group).- To review the pathophysiological mechanisms and their clinical correlations.- To present and review some of the metameric and myelomeric syndromes.- To point out what information is expected beyond the diagnosis in each of the cases presented.- To propose a structured report.- To review post-operative image findings and complications of the most used procedures and techniques.

#### TABLE OF CONTENTS/OUTLINE

-- Introduction - Anatomy - Classifications - Pathophysiological mechanisms and their clinical correlations - MRI and digital angiography techniques -- Description of the image features, pointing out the most important information that is to be provided. - Review of the post-operative image findings and complications of the most used procedures and techniques. -- Proposal of a structured report. -- Conclusion

Printed on: 02/07/23



## Abstract Archives of the RSNA, 2022

NREE-130

### Neurosyphilis: Findings From a Reemerging Disease

Sunday, Nov. 27 8:00AM - 9:00AM Room: Learning Center - NR

#### Participants

Pedro Henrique Andrade, MD, Sao Paulo, Brazil (*Presenter*) Nothing to Disclose

#### TEACHING POINTS

1. To review the syphilis natural history. 2. To review the CNS syphilis involvement. 3. To illustrate imaging findings related to neurosyphilis.

#### TABLE OF CONTENTS/OUTLINE

1. Introduction 2. Pathogenesis and natural course of untreated syphilis a.Primary syphilis b.Secondary syphilis c.Tertiary syphilis3. CNS involvement in syphilis a.meningitis b.meningovascular syphilis c.parenchymal neurosyphilis d.syphilitic dementia (general paresis) e.otologic syphilis f.ocular syphilis g.tabes dorsalis h.congenital neurosyphilis4. Imaging in syphilis neurological manifestations and differential diagnosis 5. Conclusion 6. Take-home messages 7. References

Printed on: 02/07/23

## Abstract Archives of the RSNA, 2022

NREE-131

### **Inborn Errors of Metabolism: A Step by Step Clinico-radiological Approach**

Sunday, Nov. 27 8:00AM - 9:00AM Room: Learning Center - NR

#### **Participants**

Gabriela Bandeira, MD, Sao Paulo, Brazil (*Presenter*) Nothing to Disclose

#### **TEACHING POINTS**

1-To review the classification of inborn errors of metabolism.2- To review the pathophysiology basic principles of the inborn errors of metabolism.3-To illustrate imaging findings related to genetically determined metabolic disorders.

#### **TABLE OF CONTENTS/OUTLINE**

1 - Introduction  
2 - Classification of inborn errors of metabolism  
Disorders of intermediary metabolism : aminoacidopathies, organic acidurias, lactic acidemias, hyperammonemia and disorders of the urea cycle, disorders of fatty acid oxidation. Disorders of the biosynthesis and breakdown of complex molecules: purine and pyrimidine metabolism, lipoprotein metabolism, lysosomal storage disorders, peroxisomal disorders, porphyrias. Mitochondrial disorders: mitochondrial encephalomyopathy, lactic acidosis and stroke-like episodes (MELAS), Kearns-Sayre syndrome, MERRF (myoclonus epilepsy with ragged red fibers). Neurotransmitter defects and related disorders: disorders of glycine and serine metabolism. Disorders of mineral metabolism: Menkes disease, Wilson disease, others.  
3- General and specific clinical features of inborn errors of metabolism  
4 - Clinico-radiological approach to inborn errors of metabolism with illustrative cases  
5- Take home message  
6 - Conclusion  
7 - References

Printed on: 02/07/23



## Abstract Archives of the RSNA, 2022

NREE-132

### Molecular and Genetic Features of Adult Diffuse Gliomas: Essential Updates from WHO 2021 CNS Tumor Classification

Sunday, Nov. 27 8:00AM - 9:00AM Room: Learning Center - NR

#### Participants

Ilan Benador, MD, PhD, (Presenter) Nothing to Disclose

#### TEACHING POINTS

Diffuse adult gliomas have been previously organized into 15 separate entities primarily based on histological features. WHO CNS tumor classification 2021 has reorganized diffuse gliomas into only three subtypes based on molecular and genetic characteristics that better correlate with prognosis and treatment response: 1) astrocytoma, IDH-mutant, 2) oligodendroglioma, IDH-mutant, and 1p19q-codeleted, 3) glioblastoma, IDH-wildtype. Additionally, the following entities have been retired from the tumor nomenclature in the classification scheme: glioblastoma, IDH-mutant, astrocytoma, IDH-wildtype, and oligoastroglioma. This educational exhibit will highlight the key advancements in radiographic and molecular diagnosis of diffuse gliomas.

#### TABLE OF CONTENTS/OUTLINE

I. Overview of WHO 2021 CNS Tumor Classification of adult-type diffuse gliomas. II. Characteristic imaging features and molecular classification of adult-type gliomas. A) Astrocytoma, IDH mutant: ATRX mutation, CDKN2A/B deletion. B) Oligodendroglioma, IDH-mutant: 1p19q co-deleted, TERT promoter mutation. C) GBM, IDH-wildtype: TERT promoter mutation, EGFR amplification, Trisomy 7 Monosomy 10. III. Summary of key molecular signatures of each subtype. IV. Quiz: apply this new knowledge to a few example cases to improve diagnostic precision.

Printed on: 02/07/23



## Abstract Archives of the RSNA, 2022

NREE-133

### Distinguishing Mimics from the Great Mimicker: CNS Lymphoma in Immunocompromised Hosts

Sunday, Nov. 27 8:00AM - 9:00AM Room: Learning Center - NR

#### Participants

Nima Omid-Fard, MD, BSc, (*Presenter*) Nothing to Disclose

#### TEACHING POINTS

• In the immunocompromised setting, there are distinct radiologic findings of CNS lymphoma, including necrotic ring-enhancing lesions, increased propensity for intralesional hemorrhage, and multiplicity. • In this clinical context, advanced imaging with MR perfusion, spectroscopy and diffusion-weighted imaging can be used to increase accuracy in the diagnosis of lymphoma over mimics such as GBM, metastases or infection. • This knowledge is particularly relevant to radiologists as the incidence of immunodeficiency-related CNS lymphoma may be increasing.

#### TABLE OF CONTENTS/OUTLINE

• Briefly review typical imaging findings of primary and secondary CNS lymphoma • Discuss the potential for rare and atypical presentations of CNS lymphoma • A greater emphasis will then be placed on the unique imaging findings in immunodeficiency-associated CNS lymphoma, reviewing advanced imaging techniques including MR spectroscopy, diffusion, and MR perfusion. • Side-by-side multisequence comparison of immunocompromised vs immunocompetent CNS lymphoma • Side-by-side multisequence comparison of immunocompromised CNS lymphoma vs glioblastoma • Side-by-side multisequence comparison of immunocompromised CNS lymphoma vs metastasis • Side-by-side multisequence comparison of immunocompromised CNS lymphoma vs infection (toxoplasmosis)

Printed on: 02/07/23



## Abstract Archives of the RSNA, 2022

NREE-134

### The B - T Guide of Lymphomas

Sunday, Nov. 27 8:00AM - 9:00AM Room: Learning Center - NR

#### Participants

Pedro Castro, MD, Rio de Janeiro, Brazil (*Presenter*) Nothing to Disclose

#### TEACHING POINTS

To demonstrate the typical MRI patterns and the classification of central nervous system (CNS) lymphomas. To explain the difference between intra-axial and extra-axial primary CNS lymphoma. To illustrate the importance of MRI in the trivial and atypical features of CNS lymphomas. To depict the importance of MRI in the differential diagnosis.

#### TABLE OF CONTENTS/OUTLINE

1. Background. 2. Diffuse large B-cell lymphoma and high-grade Burkitt-like B-cell lymphoma. 3. Low-grade T-cell lymphoma. 4. Lymphomas in the immunocompromised patient: AIDS-related diffuse large B-cell lymphoma. 5 EBV-positive diffuse large B-cell lymphoma, NOS. 6. Lymphomatoid granulomatosis. 7. Primary CNS posttransplant lymphoproliferative disorder. 8. Intravascular lymphoma. 9. MALT lymphoma of the dura. 10. Typical features, including hypercellularity and moderate to low perfusion. 11. Imaging assessment of the atypical imaging patterns of CNS lymphomas, including spontaneous remission and relapsing presentation, and corticospinal tract infiltration. 12. Differential diagnoses: meningioma, sarcoidosis, non-Langerhans cell histiocytosis, and IgG4-related disease. 13. Flowchart of evaluation. 14. Take-Home messages.

Printed on: 02/07/23

## Abstract Archives of the RSNA, 2022

NREE-135

### Unraveling Lesions of Chiasmatic-Hypothalamic Region: A Case Based Approach

Sunday, Nov. 27 8:00AM - 9:00AM Room: Learning Center - NR

#### Awards

Certificate of Merit

#### Participants

Virginia Simonini, MD, Sao Paulo, Brazil (*Presenter*) Nothing to Disclose

#### TEACHING POINTS

- The hypothalamus is a midline structure located below the thalamus, and together with the epithalamus and subthalamus, they constitute the diencephalon and its main function is homeostasis. - The optic chiasm is also a midline structure located anteriorly to the hypothalamus and is the point where both optic nerves meet and continue posteriorly as the optic tracts. - The hypothalamic-chiasmatic region can be affected by many diseases from multiple etiologies, such as neoplastic, developmental abnormalities and inflammatory/granulomatous, and the aim of this study is to didactically illustrate such cases. - Many important structures surround the hypothalamic-chiasmatic region, such as mamillary bodies (MB), pituitary stalk (PS), neuro and adenohipophysis, and can also be affected by those diseases. - Computed tomography (CT) is a limited method for the hypothalamic-chiasmatic region evaluation, since it has low contrast between structures. Hence, the imaging modality of choice for examination of this area is magnetic resonance imaging (MRI), specially midline sagittal slices.

#### TABLE OF CONTENTS/OUTLINE

- Illustrate normal hypothalamic-chiasmatic region anatomy. - Expose didactic cases of hypothalamic-chiasmatic region lesions, from many etiologies and how to evaluate through imaging, illustrating described findings to consolidate the acquired knowledge. - Bibliographical references.

Printed on: 02/07/23



## Abstract Archives of the RSNA, 2022

NREE-136

### Retinoblastoma: A Giant for the Little Ones

Sunday, Nov. 27 8:00AM - 9:00AM Room: Learning Center - NR

#### Participants

Karolina Cancela, MD, Sao Paulo, Brazil (*Presenter*) Nothing to Disclose

#### TEACHING POINTS

The purposes of this exhibition are: review the anatomy of the eyeball, including its main anatomical limits and the structures that compose it. Review vascularization characteristics and normal MR imaging findings. Correlated clinical syndromes. Discuss and illustrate the main imaging patterns of retinoblastoma. Detail the lesions according to their topography, whether unilateral, bilateral or even trilateral, configuring pineoblastoma. Describe diagnostic scenarios through illustrative cases, focusing on typical imaging patterns, unexpected tumor findings, dissemination patterns and imaging aspects of complications and post-treatment.

#### TABLE OF CONTENTS/OUTLINE

Retinoblastoma with its imaging patterns on MRI sequences; unilateral, bilateral or trilateral; structures involved: intra-orbital and/or extra-orbital; unexpected findings: other tumors as main differential diagnoses; post-treatment evaluation and complications; final considerations.

Printed on: 02/07/23



## Abstract Archives of the RSNA, 2022

NREE-137

### Imaging of Common and Uncommon Post-treatment Related Complications in the Brain and Spinal Cord

Sunday, Nov. 27 8:00AM - 9:00AM Room: Learning Center - NR

#### Participants

David Michaels, MD, (*Presenter*) Nothing to Disclose

#### TEACHING POINTS

- Present cases which highlight both common and uncommon complications related to neurological treatment
- Identify specific imaging findings to look for when presented with post-treatment cases
- Give a brief summary of the natural time course of the above mentioned complications and how they will evolve over time on follow up imaging studies

#### TABLE OF CONTENTS/OUTLINE

Complications from treatment, whether related to medical, surgical, or radiation treatments, are important for the neuroradiologist to recognize and diagnose. Often, recognition of such complications is crucial, as it can change future care of the patient. This education exhibit will present cases which illustrate both common and uncommon complications related to neurological treatment. We will provide a succinct overview of patient history, followed by a comprehensive interpretation of pertinent imaging studies. Our institution functions as a large tertiary care referral center for the region, which translates into both rare complications of common treatments, and common complications of rare treatments. Finally, we will end each case with a brief comment on the prognosis of each complication, and what to look for on future imaging studies. Cases include acute toxic leukoencephalopathy from both immunosuppressive and chemotherapeutic agents, radiation-induced leukoencephalopathy and meningioma formation, and postsurgical complications to include Teflon granuloma and remote cerebellar hemorrhage, among others.

Printed on: 02/07/23



## Abstract Archives of the RSNA, 2022

NREE-138CS

### Development and Clinical Translation of a Neuro-analysis Pipeline for Automatic Quantitative Analysis Using the Kaapana Platform

Sunday, Nov. 27 8:00AM - 9:00AM Room: Learning Center - NR

#### Participants

Vikas Bommineni, Orlando, FL (*Presenter*) Nothing to Disclose

#### TEACHING POINTS

Quantitative measures, such as brain atrophy patterns related to neurodegenerative diseases, may provide complementary information to radiologists. However, translation of quantitative biomarkers to clinical practice has been limited. Recent advances in image analysis allow automated and rapid processing of medical image data, while new statistical methods enable collection of large harmonized reference datasets to perform comparative analyses of individual measures. We present a workflow on Kaapana, an open-source framework for medical data analysis, for translating laboratory-validated, quantitative measures into next-generation, precise biomarkers towards personalized diagnostics. The pipeline includes pretrained deep learning(DL) models for segmentation of brain anatomy, data harmonization to a cognitively normal reference population, and calculation of machine-learning based individualized summary scores that quantify neurodegeneration and brain aging. The pipeline inputs DICOM scans directly from scanners or Picture Archival and Communications Systems (PACS) and generates segmentation maps and a patient-specific summary report to visualize measures in comparison to expected distributions based on reference populations. Outputs are converted to DICOM for archival on PACS.

#### TABLE OF CONTENTS/OUTLINE

1) Introduction  
2) Neurodegeneration biomarkers  
3) Neuro-analysis pipeline:  
a) Pre-processing: Nifti conversion, skull stripping tissue segmentation  
b) Analysis: Data harmonization extraction of quantitative biomarkers  
c) Generation of summary report  
d) DICOM output  
4) Workflow: Push data to Kaapana, trigger pipeline, QC results and push to PACS  
5) Future enhancements

Printed on: 02/07/23



## Abstract Archives of the RSNA, 2022

NREE-139

### Improving Automated Substantia Nigra Segmentation Accuracy Using a Novel Test-time Normalization Method

Sunday, Nov. 27 8:00AM - 9:00AM Room: Learning Center - NR

#### Participants

Tao Hu, MSc, Nagoya, Japan (*Presenter*) Nothing to Disclose

#### TEACHING POINTS

1. To understand the feasibility and benefits of substantia nigra (SN) segmentation using T2-weighted magnetic resonance imaging (MRI). 2. To understand how the proposed test-time normalization (TTN) can be used for improving segmentation accuracy. 3. To understand the potential applications of the segmentation results and estimated uncertainty maps in clinical scenarios.

#### TABLE OF CONTENTS/OUTLINE

1. Review of automated SN segmentation using MRI- Relationship between SN and progression of Parkinson Disease (PD)- Difficulties of automated SN segmentation from MRI- Conventional methods for automated SN segmentation 2. Automated SN segmentation with the proposed TTN- Review of test-time augmentations in segmentation tasks- Detailed explanations of the proposed TTN- Algorithm of the proposed TTN and its application in segmentation- Review of losses for tiny structure segmentation- Combination of the proposed TTN and investigated losses in segmentation- Segmentation results with and without TTN- Benefits of the proposed TTN 3. Potential applications of automated SN segmentation- SN volume and asymmetric metric estimation using segmentation results- Indicating vague boundaries of SN using uncertainty maps- longitudinal SN inspection using automated segmentation results

Printed on: 02/07/23



## Abstract Archives of the RSNA, 2022

NREE-14

### Lumbar Spine MR Examination (2 Minutes, 30 seconds) Faster than Instant Noodles Using GRAPPA and Deep Learning Reconstruction with High Acceleration Factor

Sunday, Nov. 27 8:00AM - 9:00AM Room: Learning Center - NR

#### Participants

Takeshi Hasuda, RT, Ueda-Shi, Japan (*Presenter*) Nothing to Disclose

#### TEACHING POINTS

This exhibition was approved by our Medical Ethics Committee. One of the disadvantages of MRI examinations is the relatively long time required to acquire MR images. In MRI examinations of the spine, there are cases in which the examination needs to be performed quickly due to trauma, or patients with hernias or other pain that make it impossible to perform the examination in the same position for long periods of time due to rounded backs. In recent years, reconstruction technology using Deep Learning has been attracting attention, and high-speed and high-resolution MRI have been attracting attention. This education focused on Deep Resolve (DR), a Deep Learning Reconstruction (DLR) method, to understand the characteristics of DR and to optimize the imaging protocol. The teaching points of this exhibition are to (1) understand the outline of DR by validation using phantoms and to examine the optimal conditions in combination with parallel imaging (GRRAPPA), (2) practice the validation results in clinical practice and to analyze problems, and (3) optimize the parameters of Spine's imaging conditions based on the results and demonstrate scan times faster than instant noodles.

#### TABLE OF CONTENTS/OUTLINE

1. overview 2. understanding the characteristics of DR (Deep Resolve) 3. phantom verification 4. trial and error in actual clinical practice 5. MR images (comparison of original and optimized images) Faster than instant noodles

Printed on: 02/07/23



## Abstract Archives of the RSNA, 2022

NREE-140

### Synthetic MRI Evaluation of Sella Pathologies

Sunday, Nov. 27 8:00AM - 9:00AM Room: Learning Center - NR

#### Participants

Ranliang Hu, MD, (*Presenter*) Stockholder, Moderna, Inc; Stockholder, Pfizer Inc

#### TEACHING POINTS

Synthetic MRI is an emerging technique for clinical imaging, able to generate multiple contrast weighted images and parametric maps based on a single acquisition using multiple delay and and echo times. While Synthetic MRI has become available from multiple vendors and recent studies have shown it to produce comparable image quality to that of conventional brain MRI, it is still underutilized in part due to lack of experience among radiologists with the technique and post-processing. The sella region is complex for neuroradiologic evaluation due its small anatomy, subtle pathologies, complex tissue/enhancement characteristics. Technical developments in 3D synthetic MRI with higher spatial resolution has made sella imaging feasible, with ability to perform qualitative and quantitative tissue characterization. This education exhibit will review recent developments in Synthetic MRI for neuroimaging and through case examples demonstrate its role in the evaluation of pathologies in the sella region.

#### TABLE OF CONTENTS/OUTLINE

1. Background: a. Brief review of current literature2. Technical Overview: a. Acquisition b. Post-processing3. Case Review: a. Pituitary hyperplasia b. Rathke's cleft cyst c. Epidermoid cyst d. Pituitary adenoma e. Post-treatment adenoma f. Meningioma g. Craniopharyngioma4. Summary: a. Key points for qualitative interpretation b. Quantitative differences between pathologies c. Challenges and limitations

Printed on: 02/07/23

## Abstract Archives of the RSNA, 2022

NREE-141

### Trigeminal, Facial, Hypoglossal and Greater Occipital Nerves: Had You Seen Them Like This Before?

Sunday, Nov. 27 8:00AM - 9:00AM Room: Learning Center - NR

#### Participants

Marta Barrios Lopez, MD, Santander, Spain (*Presenter*) Nothing to Disclose

#### TEACHING POINTS

-To summarize the most important anatomical relationships of the extracranial segments of the main cranial nerves (including the trigeminal, facial and hypoglossal nerves). We will also include those of the greater occipital nerve, the thickest cutaneous nerve in the human body. -To demonstrate the ability of 3D CRANI, an innovative MRI sequence, to help visualize these branches.

#### TABLE OF CONTENTS/OUTLINE

-INTRODUCTION- THE 3D CRANI SEQUENCE: a relatively new MRI technique that combines a STIR TSE black-blood sequence, a motion-sensitized driven equilibrium (MSDE) pulse and a pseudo steady-state (PSS) sweep.- TRIGEMINAL NERVE: introduction and origin. Extracranial segment.-Ophthalmic nerve. Maxillary nerve. Mandibular nerve: main anatomical relationships and branches. Useful details and their correlation with the clinic. - FACIAL NERVE: introduction and origin. Extracranial segment. Main extracranial branches and their relationship to the parotid gland. - HYPOGLOSSAL NERVE: introduction and origin. Main anatomical relationships in the neck.- GREATER OCCIPITAL NERVE: introduction, importance, anatomical landmarks. -CONCLUSIONS: 3D CRANI is useful to visualize the extraforaminal segments of the major cranial nerves.

Printed on: 02/07/23



## Abstract Archives of the RSNA, 2022

NREE-142

### Perfusion Imaging: The Cerebral Path to the Final Diagnose

Sunday, Nov. 27 8:00AM - 9:00AM Room: Learning Center - NR

#### Participants

Pedro Castro, MD, Rio de Janeiro, Brazil (*Presenter*) Nothing to Disclose

#### TEACHING POINTS

To depict the perfusion imaging applications to assess neoplastic, ischemic, post-ictal, and infectious diseases. To clarify the physics and how to interpret the brain perfusion maps. To elucidate the advantages and disadvantages of utilizing perfusion compared to the permeability.

#### TABLE OF CONTENTS/OUTLINE

1. Background. 2. Imaging protocol and physics. 3. Advantages and disadvantages of perfusion versus permeability. 4. Applications in CNS tumors. 5. Perfusion and the therapeutic and molecular diagnosis implications in neoplastic disease. 6. Applications in stroke. 7. The therapeutic implications of the perfusion in ischemia. 8. Differential diagnosis, including infectious diseases and post-ictal changes. 9. Flowchart for assessment of brain diseases with perfusion. 10. Take-Home messages.

Printed on: 02/07/23



## Abstract Archives of the RSNA, 2022

NREE-143

### Mismatch of Arterial Spin Labeling (ASL) Compared to MR Dynamic Susceptibility Contrast Perfusion Weighted Imaging (DSC-PWI) in the Central Nervous System Diseases

Sunday, Nov. 27 8:00AM - 9:00AM Room: Learning Center - NR

#### Participants

Xiang Liu, MD, PhD, (*Presenter*) Nothing to Disclose

#### TEACHING POINTS

MR dynamic susceptibility contrast perfusion weighted imaging (DSC-PWI) is the most commonly used perfusion imaging technique in the central nervous system (CNS) diseases, including brain tumors. MR arterial spin labeling (ASL) is a novel noninvasive MR sequence to quantify tissue blood flow. Most published studies showed that the relative cerebral blood volume (rCBV) derived from DSC-PWI and cerebral blood flow (CBF) of ASL. Based on our experience of more than 950 patients who had concurrent ASL and DSCPWI examinations, the purpose of this Education Exhibit is to present following teaching points of mismatch between ASL and DSCPWI in the evaluation of hemodynamic changes in the CNS diseases. 1. Learning the principle of DSC-PWI; 2. Learning the principle of ASL; 3. Learning advantages and limitations of DSC-PWI and ASL in the CNS diseases;

#### TABLE OF CONTENTS/OUTLINE

1. Introduction of the principle of DSC-PWI; 2. Introduction of the principle of ASL; 3. Sample cases comparing between DSC-PWI and ASL in glioma, brain metastasis, meningioma, vascular malformation, and MELAS, etc ; 4. Summary of advantages and limitations of DSC-PWI and ASL in the CNS diseases;

Printed on: 02/07/23



## Abstract Archives of the RSNA, 2022

NREE-15

### How Diffusion Tensor Imaging Enables Direct Targeting for Focused Ultrasound Surgery

Sunday, Nov. 27 8:00AM - 9:00AM Room: Learning Center - NR

#### Participants

Hiroki Hori, (*Presenter*) Nothing to Disclose

#### TEACHING POINTS

The purpose of this exhibit is to summarize how to implement diffusion tensor imaging (DTI) as a direct targeting method in transcranial MR-guided focused ultrasound surgery (TcMRgFUS). Although the atlas-based targeting method of indirect measuring the ventral intermediate nucleus (VIM) of the thalamus from the posterior commissure (PC) was widely used, it may not be precise, as the locations of the VIM, ventral caudal nucleus (Vc) and pyramidal tract (PT) etc., may vary in each subject based on our pilot study. Especially in the case of atrophic brain, it is difficult to measure the precise location of the VIM using the conventional indirect targeting method, hence a direct targeting strategy is more desired. DTI enables visualization and characterization of fibrous structures in the brain, and tractography-based direct targeting may become the method of choice for surgical targeting as it is capable of providing patient-specific coordinates. DSI studio is an open source, high spec image processing software tool that facilitates DTI data analysis. DSI studio assisted tractography-based direct targeting offers a practical and flexible approach to improve treatment efficacy and safety profiles after TcMRgFUS treatments.

#### TABLE OF CONTENTS/OUTLINE

1. What is TcMRgFUS a. Overview b. Traditional method of assessment c. Ablating location  
2. How to visualize each fiber a. Visualize VIM b. Visualize Vc c. Visualize PT  
3. Location of the nucleus and ablation outcome a. Mild adverse event b. Severe adverse event c. Recurrence and mild adverse event d. Perfect treatment  
4. Future outlook

Printed on: 02/07/23



## Abstract Archives of the RSNA, 2022

NREE-16

### The Role of APTw with fMRI, and DTI in Preoperative Planning

Sunday, Nov. 27 8:00AM - 9:00AM Room: Learning Center - NR

#### Participants

Sevcan Turk, MD, Ann Arbor, MI (*Presenter*) Nothing to Disclose

#### TEACHING POINTS

- Highlight the role of amide proton transfer weighted (APT<sub>w</sub>) imaging for preoperative planning of the brain tumors; grading, genetic mutations, peritumoral invasion, and white matter tumor infiltration
- Discuss the potential of using APT<sub>w</sub> imaging in assessing treatment response and discrimination of true tumor progression from pseudoprogression
- APT<sub>w</sub> high signals: hypercellular components of the tumor, extracellular tumor matrix, hematoma, necrosis
- Discuss the pros and cons, artifacts in interpreting APT<sub>w</sub>, fMRI, DTI, PWI

#### TABLE OF CONTENTS/OUTLINE

- Overview of imaging characteristics of brain tumors with emphasis on APT<sub>w</sub> in conjunction with fMRI, DTI, and PWI for preoperative planning
- Demonstrate cases of tumor progression versus treatment effects, peritumoral invasion, and genetic mutation and grade correlation APT, PWI, DWI parameters with the role of fMRI and DTI
- Differences of pediatric tumors on advanced imaging, the added value of APT<sub>w</sub> imaging
- Necrosis, hemorrhage, calcification, and extracellular matrix effects on the signal intensity in APT, fMRI, DTI, and perfusion-weighted imaging. Pitfalls and accuracy of each advanced imaging method.

Printed on: 02/07/23

## Abstract Archives of the RSNA, 2022

NREE-17

### Neuronal and Mixed Glioneuronal Tumors: Image Correlation X Molecular Profile

Sunday, Nov. 27 8:00AM - 9:00AM Room: Learning Center - NR

#### Participants

Milena Ouchar Sabino, MD, Sao Paulo, Brazil (*Presenter*) Nothing to Disclose

#### TEACHING POINTS

- To review the main imaging findings of neuronal and mixed glioneuronal tumors with cases from three hospitals imaging departments. - To correlate some of the neuronal and mixed glioneuronal tumors to specific altered molecular profiles.

#### TABLE OF CONTENTS/OUTLINE

- A brief discussion of the new WHO 2021 CNS tumors classification, focusing on neuronal and mixed glioneuronal tumors.- The most frequently altered molecular pathways.- Correlation of neuronal and mixed glioneuronal tumors according to their most frequent location and clinical presentation.- A review of the main imaging features - cases of neuronal and mixed glioneuronal tumors and their associated altered molecular profiles: gangliogliomas, desmoplastic infantile ganglioglioma/astrocytoma, papillary glioneuronal tumor, DNET, rosette-forming glioneuronal tumor, multinodular and vacuolating neuronal tumor, diffuse leptomeningeal glioneuronal tumor, central neurocytoma, extraventricular neurocytoma, dysplastic cerebellar gangliocytoma (Lhermitte-Duclos), myxoid glioneuronal tumor.- An approach to neuronal and mixed glioneuronal tumors according to their imaging appearance (solid or cystic-solid and pseudocystic).

Printed on: 02/07/23



## Abstract Archives of the RSNA, 2022

NREE-18

### Diffuse Gliomas Genomics: What Radiology Residents Need to Know

Sunday, Nov. 27 8:00AM - 9:00AM Room: Learning Center - NR

#### Participants

Yu Bin Lee, MD, Gwang Ju, Korea, Republic Of (*Presenter*) Nothing to Disclose

#### TEACHING POINTS

1. Two review the major changes of the fifth edition of the WHO Classification of Tumors of the CNS (WHO CNS5).2. Two review the clinical implications and related imaging findings of the representative genetic mutations associated with diffuse gliomas.

#### TABLE OF CONTENTS/OUTLINE

1. Introduction2. The major changes of the WHO CNS53. Clinical implications and imaging evaluation of tumor genomics1) Adult-type diffuse gliomas- Isocitrate dehydrogenase (IDH) mutation- 1p/19q codeletion- O-6-Methylguanine-DNA-Methyltransferase (MGMT)- ATRX loss- TP53 mutation- TERT promotor mutation- EGFR amplification2) Pediatric-type diffuse low-grade gliomas- BRAF mutation in MAPK pathway3) Pediatric-type diffuse high-grade gliomas- H3 K27-altered- H3 G34-mutant4. AI approaches in radiogenomics5. Summary

Printed on: 02/07/23



## Abstract Archives of the RSNA, 2022

NREE-19

### Update on Radiophenotypes of Central Nervous System Tumors After 5th Edition WHO Classification 2021

Sunday, Nov. 27 8:00AM - 9:00AM Room: Learning Center - NR

#### Participants

Taina Estruzani, MD, Sao Paulo, Brazil (*Presenter*) Nothing to Disclose

#### TEACHING POINTS

Recognize high specificity imaging phenotypes of CNS Tumors. Discuss modifications of taxonomy. Characterize pediatric and adult CNS tumors. Differentiate between high-grade and low-grade gliomas. Correlate imaging and molecular features.

#### TABLE OF CONTENTS/OUTLINE

Imaging phenotypes of CNS Tumors. Gliomas imaging classification. Pediatric-type diffuse low-grade gliomas. Pediatric-type diffuse high-grade gliomas. Adult-type diffuse gliomas. Some new types of tumors according to molecular biomarkers. Modifications of new CNS tumors taxonomy. Differential diagnosis of CNS tumors.

Printed on: 02/07/23



## Abstract Archives of the RSNA, 2022

NREE-2

### Photon-Counting CT Applications in Neuroradiology

Sunday, Nov. 27 8:00AM - 9:00AM Room: Learning Center - NR

#### Awards

Certificate of Merit

#### Participants

Fides Schwartz, MD, Durham, NC (*Presenter*) Nothing to Disclose

#### TEACHING POINTS

Photon-counting computed tomography (PCCT) is a new CT technology. PCCT uses energy-resolving detectors, instead of integrating the entire x-ray signal (energy integrating detectors: EID), enabling spectral acquisitions without the need of specialized acquisition strategies (e.g., dual-source). PCCT records photons in different energy bins, starting at a minimum energy threshold, so electronic noise can be avoided altogether. PCCT detectors use a two-step conversion (x-rays to electrical signal), rather than the 3-step conversion EID (x-rays to light to electrical signal), and inherently have higher spatial resolution as no septa (to separate voxels) are needed. This project is geared toward introducing the emerging technology of PCCT to the RSNA neuroradiology imaging community. The details of this technology will be explained using diagrams of the physics principles, and examples of standard EID vs PCCT patient scans to demonstrate the performance of the new scanner system.

#### TABLE OF CONTENTS/OUTLINE

1. PCCT - Detectors a. Comparison of energy-integrating vs photon-counting detectors b. How is higher spatial resolution of PCCT achieved?
2. PCCT - Photon Binning a. How does photon binning work? b. How are energy thresholds defined? c. How do thresholds help with electronic noise?
3. PCCT - Spectral Data a. How is it always available? b. What can it be used for?
4. Clinical examples a. Temporal Bone - superior spatial resolution b. Brain without contrast - higher image contrast c. CTA - improved contrast conspicuity d. Myelograms - material decomposition capabilities

Printed on: 02/07/23



## Abstract Archives of the RSNA, 2022

NREE-20

### Retinoblastoma Management: Emphasis on RB-RECIST Criteria with MRI Correlation after Intra-arterial Treatment

Sunday, Nov. 27 8:00AM - 9:00AM Room: Learning Center - NR

#### Participants

Sevcan Turk, MD, Ann Arbor, MI (*Presenter*) Nothing to Disclose

#### TEACHING POINTS

- Highlight the role of MRI and diffusion-weighted imaging in the evaluation of retinoblastoma treatment response.
- Discuss the ultrasound and MRI correlation of the different treatment response types of retinoblastoma.
- Discuss the pearls and pitfalls in interpreting ultrasound and MRI.

#### TABLE OF CONTENTS/OUTLINE

- Clinical presentation, genetics, and epidemiology from the ophthalmologist field of view: evaluation of retinoblastoma with orbital US, CT, and MRI.
- Retinoblastoma classification: what radiologists need to know.
- When Intra-arterial treatment is indicated and how we do it.
- Overview of imaging characteristics of retinoblastoma after intraarterial treatment with emphasis on ultrasound- MRI correlation of the RB-RECIST criteria assessment.
- Discuss type 0-IV tumor regression patterns with MRI correlate.
- Discuss the role of diffusion-weighted imaging in the discrimination of treatment effect and tumor progression.
- DCE and DSC perfusion, SWI value in treatment response assessment.
- The role of MRI in the evaluation of extraocular extension, optic nerve invasion, post-treatment complications, and intracranial abnormalities.
- Surveillance: radiation field, secondary tumors, and beyond the optic nerve.

Printed on: 02/07/23



## Abstract Archives of the RSNA, 2022

NREE-21

### CSF Circulation and Glymphatic System of the Spinal Cord

Sunday, Nov. 27 8:00AM - 9:00AM Room: Learning Center - NR

#### Participants

Shotaro Naganawa, MD, Ann Arbor, MI (*Presenter*) Nothing to Disclose

#### TEACHING POINTS

1. To review CSF circulation in the spinal cord  
2. To review glymphatic system of the spinal cord  
3. To explore spinal cord diseases related to CSF circulation and glymphatic system in the spinal cord

#### TABLE OF CONTENTS/OUTLINE

CSF circulation in the spine  
Glymphatic-lymphatic fluid transport system of the spinal cord  
Spinal cord diseases related to CSF production, absorption, and loss (leakage)-CSF leakage and CSF venous fistulas -Hypersecretion of CSF after subarachnoid hemorrhage  
Spinal cord diseases related to CSF flow abnormality-Chiari malformation-Spinal canal stenosis-Amyotrophic lateral sclerosis (ALS)-Spinal web, spinal cord herniation  
Spinal cord diseases related to glymphatic system-Iatrogenic intrathecal Gd administration -Spinal neurosarcoidosis-Neuromyelitis optica-Presyrinx state  
Drug delivery and glymphatic system-Spinal muscular atrophy -ALS and other neurodegenerative diseases

Printed on: 02/07/23



## Abstract Archives of the RSNA, 2022

NREE-22

### Deep Brain Stimulation (DBS) - Pre and Post Operative Imaging, From Adequate Nucleus and Fiber Tract Localization to Electrode Misplacement

Sunday, Nov. 27 8:00AM - 9:00AM Room: Learning Center - NR

#### Awards

Cum Laude

#### Participants

Leandro Souza, MD, Sao Paulo, Brazil (*Presenter*) Nothing to Disclose

#### TEACHING POINTS

This panel aims to guide a good quality exam acquisition for Deep Brain Stimulator (DBS) study, in both pre and post operative evaluations. It will be shown how to accurately localize the targets for DBS implantation in different scenarios, such as Parkinson Disease (PD), tremors, dystonias and obsessive-compulsive disorder (OCD), with images acquired on CT and MRI, these from 1,5T, 3T and 7T, correlating the electrode targets in each case with the anatomy and histology. To showcase the MRI and CT imaging protocols, with advanced sequences that are useful for evaluation, such as diffusion tensor imaging (DTI) and functional brain MRI, for each scenario (pre e post operative), its uses and limitations. Post operative protocol and images to assert possible structural reasons for clinical failure of the DBS procedure and electrode misplacement.

#### TABLE OF CONTENTS/OUTLINE

1 - pre operative study: 1.1 - indications, physiology of action, and scientifically proven improvement  
1.1.1 - PD, tremor and dystonias  
1.1.2 - OCD  
1.2 - anatomy of the targets: 1.2.1 - histology  
1.2.2 - MRI 1,5T, 3T and 7T  
1.3. - acquisition protocol: 1.3.1 - CT  
1.3.2 - structural MRI: IR, T2, FGATIR, DP  
1.3.3 - functional MRI: DTI, fMRI  
2 - post operative study  
2.1 - acquisition protocol: 2.1.1 - CT  
2.1.2 - MRI  
2.2 - imaging evaluation  
2.2.1 - electrode positioning  
2.2.2 - other possible structural causes of failure

Printed on: 02/07/23

## Abstract Archives of the RSNA, 2022

NREE-23

### Beyond Five Millimeters Below the Foramen Magnum: Exploring the Depths of the Chiari 1 Deformity

Sunday, Nov. 27 8:00AM - 9:00AM Room: Learning Center - NR

#### Participants

James Loftus, MD, Rochester, NY (*Presenter*) Nothing to Disclose

#### TEACHING POINTS

1. Define the proper nomenclature and terminology of the Chiari 1 and related deformities including 0/0.5 and 1.5 and how they differ in pathogenesis and embryology from the other subtypes (Don't call it a malformation!). 2. Detail the imaging evaluation of the Chiari 1 and related deformities including conventional and phase contrast magnetic resonance imaging. 3. Review surgical techniques and post-surgical imaging of the Chiari 1 and related deformities including expected findings and complications.

#### TABLE OF CONTENTS/OUTLINE

I. Review of the pathogenesis, embryology, nomenclature, and proper terminology surrounding the Chiari 1 and related deformities.  
a. Subtypes of the Chiari deformities (0-1.5) and malformations (2-5) and their pathologic and embryologic basis. b. Further description of the anatomic changes in Chiari 0/0.5, 1, and 1.5 compared to normal patients. II. Imaging evaluation of the Chiari 0/0.5, 1, and 1.5 deformities. a. Conventional brain and cervical spine MRI. i. Proper measurement of tonsillar herniation and controversies. ii. Clues to abnormal CSF flow dynamics on conventional MRI sequences (No phase contrast, no problem!). b. Phase contrast MRI (PC-MRI). i. Evaluating the re-phased image, magnitude image, and phase image. ii. Brief note on quantitative PC-MRI. III. Surgical techniques and post-surgical imaging and complications. a. Surgical techniques and expected post-surgical imaging findings including evaluation of the adequacy of decompression on PC-MRI. b. Post-surgical complications the radiologist must recognize.

Printed on: 02/07/23



## Abstract Archives of the RSNA, 2022

NREE-24

### Transfontanellar Ultrasound Beyond Hemorrhages In Infants

Sunday, Nov. 27 8:00AM - 9:00AM Room: Learning Center - NR

#### Participants

Pedro Da Silva, MD, Sao Paulo, Brazil (*Presenter*) Nothing to Disclose

#### TEACHING POINTS

Transfontanellar ultrasound (TFUS) has been increasingly used as a diagnostic and screening tool in pediatrics, even as a first-line imaging technique, due to its advantages over other imaging methods, especially for critical ill newborns, often unable to perform the other ones. In addition, ultrasound (US) is possible to be repeated whenever necessary, without harm to the patient. In this context, grey-scale, color and spectral Doppler assessment with TFUS plays an important role in the evaluation and screening of findings beyond hemorrhages in infants, including ventriculomegaly, cerebral ischemia and its progression, as well as cerebral blood flow patterns and complications related to the use of Extracorporeal Membrane Oxygenation (ECMO) in seriously ill children. Assessment of ventricular measurements in infants allows for rapid diagnoses, monitoring of ventricular dilatations in children who need several exams, and suggests early interventions, avoiding unnecessary and expensive additional imaging methods. Several US measurements of ventricular dimensions have been proposed and increasingly used in control and clinical or surgical decisions. Furthermore, due to the great impact on morbidity and mortality of hypoxic-ischemic encephalopathy in the neonatal population, the TFUS also plays an important role in the characterization and progression of ischemic lesions and their variations, such as ischemic lesion with hemorrhagic transformation.

#### TABLE OF CONTENTS/OUTLINE

- Review and discuss the advantages of transfontanellar ultrasound as an imaging method in infants· Discuss and understand ultrasound imaging and its sensitivity and specificity of intracranial findings beyond hemorrhages

Printed on: 02/07/23



## Abstract Archives of the RSNA, 2022

NREE-25

### **Craniosynostosis and Craniofacial Malformations: A Radiological and Surgical Perspective**

Sunday, Nov. 27 8:00AM - 9:00AM Room: Learning Center - NR

#### **Participants**

Jameson Da Silva, MD, Teresina, Brazil (*Presenter*) Nothing to Disclose

#### **TEACHING POINTS**

Discuss important anatomical features of craniosynostosis which have surgical implications and should be included in imaging reports. Consider the role of CT, especially with 3D reconstruction, in preoperative planning. Briefly describe main strategies of surgical approaches for craniosynostosis, with technique considerations relevant for the imaging specialist.

#### **TABLE OF CONTENTS/OUTLINE**

Summary- Introduction.- Relevant Anatomy.- Craniosynostosis classification and types.- Craniofacial malformations associated.- Imaging technique and protocol (Radiography, CT, conventional MRI and MRI angiography).- Imaging of normal and pathologic sutures.- Craniosynostosis clinical syndromes associated.- Postoperative follow-up imaging.- The different surgical options available for the treatment of different types of craniosynostosis.- Conclusions.- References.

Printed on: 02/07/23



## Abstract Archives of the RSNA, 2022

NREE-26

### One Side at a Time - Unilateral or Asymmetric Centrencephalic Lesions

Sunday, Nov. 27 8:00AM - 9:00AM Room: Learning Center - NR

#### Awards

Certificate of Merit

#### Participants

Samya Alves, MD, Sao Paulo, Brazil (*Presenter*) Nothing to Disclose

#### TEACHING POINTS

Centrencephalic abnormalities can be detected on neuroimaging in a wide variety of pathological conditions. Bilateral and symmetrical alterations are well established in the literature, however, when we look at unilateral conditions, there is a gap in the systematization of the approach. Unilateral or asymmetric centrencephalic lesions will be addressed by an algorithm developed according to typical imaging patterns, such as diffusion restriction, SWI, expansive lesions and T1 contrast enhancement. The purpose of this exhibition is to:- Review anatomy and imaging aspects of the basal ganglia and thalamus;- List normal variations, common benign findings and main diseases that present by unilateral or asymmetric centrencephalic involvement;- Review of the main pathologies on a case-based approach;- Organize the radiologic reasoning with an algorithm.

#### TABLE OF CONTENTS/OUTLINE

1. ANATOMY AND IMAGING- Basal ganglia and thalamus- Imaging techniques 2. DIFFERENTIAL DIAGNOSIS OF UNILATERAL/ASYMMETRIC CENTRENCEPHALIC LESIONS- Normal variants- Restricted diffusion- SWI- Volumetric alterations: enlargement and atrophy- T1 alteration: hypersignal, contrast enhancement and morphologic change.

Printed on: 02/07/23



## Abstract Archives of the RSNA, 2022

NREE-27

### Pediatric Neurodegenerative Diseases: Pathophysiology and Neuroimaging Features

Sunday, Nov. 27 8:00AM - 9:00AM Room: Learning Center - NR

#### Awards

Certificate of Merit

#### Participants

Ryo Kurokawa, MD, PhD, Ann Arbor, MI (*Presenter*) Nothing to Disclose

#### TEACHING POINTS

The aim of this review is to 1. Understand the concept of pediatric neurodegenerative disorders (pedND) 2. Demonstrate the brain imaging findings of pedND 3. Show how clinical features can contribute to the diagnosis of pedND

#### TABLE OF CONTENTS/OUTLINE

1. Overview and definition of pedND 2. Triplet Repeat Disease: Huntington disease (HD), Myotonic dystrophy type 1 (DM1), Spinocerebellar ataxia (SCA) type 1, SCA2, SCA3/Machado-Joseph disease (MJD), SCA7, SCA17, Fragile X syndrome (FXS), Friedreich's ataxia (FRDA) 3. Autosomal Dominant: HD, DM1, SCA1, SCA2, SCA3/MJD, SCA7, SCA17 4. Autosomal Recessive: FRDA, Ataxia with Oculomotor Apraxia type 1 (AOA1), AOA2, Autosomal recessive spastic ataxia of Charlevoix-Saguenay (ARSACS), Ataxia telangiectasia (AT), Marinesco-Sjogren syndrome (MSS), Ataxia with vitamin E syndrome (AVED), Progressive myoclonus epilepsy type 1 (EPM1), Chorea-acanthocytosis (CHAC) 5. X-linked: FXS, X-linked Charcot-Marie-Tooth disease (CMTX1) 6. Cerebellar ataxia in pedND 7. Diseases associated with secondary neurodegeneration: Amino acid metabolism disorders, Urea cycle disorders, Carbohydrate metabolism disorders, Mitochondrial disorders, Lysosomal storage disease, Peroxisomal disorders, Metal metabolism disorders Summary 1. PedND have diverse pathomechanisms. 2. Some pedNDs have pathognomonic radiological features that can help in differentiation. 3. Clinical features can help diagnose pedNDs, especially when radiological findings are similar to others.

Printed on: 02/07/23



## Abstract Archives of the RSNA, 2022

NREE-28

### Neuroimaging of Hypophysitis: Anatomy, Etiology, Pathology, and Imaging Mimics

Sunday, Nov. 27 8:00AM - 9:00AM Room: Learning Center - NR

#### Participants

Ryo Kurokawa, MD, PhD, Ann Arbor, MI (*Presenter*) Nothing to Disclose

#### TEACHING POINTS

The purpose of this exhibit is:1. To review the embryology and anatomy of the pituitary gland2. To summarize the various etiologies and pathologies of hypophysitis and the mimics3. To demonstrate how neuroimaging contributes to the diagnosis of hypophysitis

#### TABLE OF CONTENTS/OUTLINE

Outline1. The embryology and anatomy of the pituitary gland 2. Etiology, epidemiology, pathology and clinical features of hypophysitis 3. Neuroimaging findings in hypophysitis- Lymphocytic hypophysitis- Granulomatous hypophysitis (primary or secondary: Crohn D, sarcoidosis, , GPA, tuberculosis, fungal infection)- Plasmacytic/immunoglobulin G4-related hypophysitis- Xanthomatous hypophysitis- Necrotizing hypophysitis- Immune checkpoint inhibitor-related pituitary adverse effects: isolated adrenocorticotrophic hormone deficiency, hypophysitis- Anti-pituitary-specific transcriptional factor (PIT)-1 antibody-related hypophysitis- Differential diagnosis: pituitary adenoma, pituicytoma, pituitary blastoma craniopharyngioma, metastasis, lymphoma, histiocytosis, germ cell tumor, abscess

Printed on: 02/07/23



## Abstract Archives of the RSNA, 2022

NREE-29

### Diversity of Hyperammonemia-associated CNS Abnormalities: Pathophysiology and Neuroimaging Features

Sunday, Nov. 27 8:00AM - 9:00AM Room: Learning Center - NR

#### Participants

Ryo Kurokawa, MD, PhD, Ann Arbor, MI (*Presenter*) Nothing to Disclose

#### TEACHING POINTS

The aim of this exhibit is to 1. Review the various causes and mechanisms of hyperammonemia 2. Demonstrate the imaging characteristics associated with the causes of hyperammonemia 3. Show how clinical features can contribute to a diagnosis

#### TABLE OF CONTENTS/OUTLINE

Content organization 1. Introduction-Mechanisms of hyperammonemia-Mechanisms of hyperammonemic encephalopathy 2. High ammonia production-Infection: Urease-producing bacteria (Proteus, E-coli, Klebsiella)-Increased protein load: Gastrointestinal bleeding, Total parenteral nutrition-Elevated catabolism: Exercise, Seizure/ Eclampsia, Trauma/Burn 3. Portosystemic shunt-Cirrhosis-Neoplasm-Congenital: Congenital portosystemic shunt syndrome, Noonan syndrome-Transjugular intrahepatic portosystemic shunt (TIPS) 4. Metabolic disorders-Congenital: Urea cycle disorders, Organic acidemias, Fatty acid oxidation disorders, Mitochondrial diseases-Drugs: Valproic acid, Acetaminophen, Carbamazepine, 5-Fluorouracil (5-FU), etc. 5. Decreased urine excretion-Renal failure-Urinary retention 6. Miscellaneous Multiple myeloma 7. Summary 1. Various etiologies cause hyperammonemia and its associated CNS manifestations 2. Knowledge of neuroimaging features and clinical findings helps in diagnosis and appropriate management

Printed on: 02/07/23



## Abstract Archives of the RSNA, 2022

NREE-3

### Clinical Applications of MR Spectroscopy in the Era of Molecular and Genetic Diagnosis and Treatment

Sunday, Nov. 27 8:00AM - 9:00AM Room: Learning Center - NR

#### Awards

**Magna Cum Laude**

#### Participants

Mariko Kurokawa, MD, Ann Arbor, MI (*Presenter*) Nothing to Disclose

#### TEACHING POINTS

- Understand the basic principle of MRS: the methodology to acquire the spectrum of chemical shifts
- Describe main pathologies related to common metabolites found in MRS as well as novel genetic markers such as SDHB mutation and IDH mutation
- Identify the common and uncommon MRS findings, especially focusing on metabolic diseases and their differential diagnoses.

#### TABLE OF CONTENTS/OUTLINE

1. Introduction  
Physics and methodology  
2. Pathologies related to common and uncommon metabolites  
N-acetyl aspartyl glutamate (NAA), Creatine, Choline, Myo-inositol, Gamma-aminobutyric acid (GABA), Glutamine/glutamate, Lipid, Lactate, Taurine, Glycine, Alanine, Succinate, and 2-HG  
3. Metabolic diseases  
Mitochondrial diseases, arginase deficiency, Salla disease, Sandhoff disease, nonketotic hyperglycinemia, Phenylketonuria, Canavan disease, Creatine transporter deficiency, and maple syrup urine disease  
4. Hypoxic ischemic encephalopathy  
5. Demyelination diseases (multiple sclerosis, acute disseminated encephalomyelopathy)  
6. Tumors (low-grade gliomas, high-grade gliomas, medulloblastomas, and other malignant tumors)  
7. Genetic diseases  
Vanishing white matter disease, Alexander disease, Adrenoleukodystrophy  
8. Summary

Printed on: 02/07/23



## Abstract Archives of the RSNA, 2022

NREE-30

### **An Unusual Relation: A Walk to Remember, Neurological Manifestations of Inflammatory Bowel Disease, An Underdiagnosed Pathology**

Sunday, Nov. 27 8:00AM - 9:00AM Room: Learning Center - NR

#### **Participants**

Angela Sosa, MD, (*Presenter*) Nothing to Disclose

#### **TEACHING POINTS**

After reviewing this exhibit, you will be able to: Describe the neurological disorders associated with inflammatory bowel diseases such as ulcerative colitis and Crohn's disease. Understand the mechanisms involved in the pathophysiology of these manifestations. Recognize the most common imaging findings in central and peripheral nervous system manifestations of patients with inflammatory bowel diseases.

#### **TABLE OF CONTENTS/OUTLINE**

1. Neurological complications of inflammatory bowel diseases 1.1 Epidemiology 1.2 Pathophysiology 2. Imaging findings of central and peripheral nervous system manifestations of inflammatory bowel diseases. 2.1 Cerebrovascular: Stroke, vasculitis, and Cerebral venous thrombosis.2.2. Demyelinating2.3. Asymptomatic white matter lesions2.4. Peripheral neuropathy2.5. Toxic treatment-related3. Other central nervous systemsComplications.3.1. Dementia3.2. Headaches3.3 Encephalopathy

Printed on: 02/07/23

## Abstract Archives of the RSNA, 2022

NREE-31

### Imaging of Cranial Nerve Disorders in Pediatric and Adult Patients

Sunday, Nov. 27 8:00AM - 9:00AM Room: Learning Center - NR

#### Participants

Minako Azuma, MD, PhD, (*Presenter*) Nothing to Disclose

#### TEACHING POINTS

1. In pediatric and adult patients, a wide variety of diseases are related to cranial nerves, including tumors, inflammations, vascular, and so on. 2. It is necessary for radiologists to know typical and atypical radiological findings of cranial nerve disorders. 3. Radiologists have to select the best imaging modality and protocol for the detection of lesions.

#### TABLE OF CONTENTS/OUTLINE

1. Anatomy of cranial nerves (1) Locations, structure, and function (2) Foramina related to cranial nerves 2. Techniques for the imaging of cranial nerve disorders (1) CT (2) MRI 3. Cranial nerve disorders (1) Tumor Schwannoma Optic nerve sheath meningioma Optic nerve glioma Olfactory neuroblastoma AT/RT (atypical teratoid/rhabdoid tumor) Malignant lymphoma Leukemia Metastasis / Dissemination (2) Inflammation Optic neuritis Neuromyelitis optica spectrum disorder (NMOSD) Myelin oligodendrocyte glycoprotein (MOG) antibody-associated disease Multiple sclerosis IgG4 related disease Tolosa-Hunt syndrome Bell's palsy Sarcoidosis HTLV-1 Cerebrotendinous Xanthomatosis (3) Hemorrhage Superficial siderosis (4) Secondary compressive disorders a) Orbital and sellar-suprasellar mass b) Neurovascular compression and aneurysm c) Thyroid orbitopathy (5) Toxic neuropathy (6) Congenital (7) Vascular Carotid-cavernous fistula Dural arteriovenous fistula Dural sinus thrombosis Acute cerebral infarction 4. Take home points 5. References

Printed on: 02/07/23



## Abstract Archives of the RSNA, 2022

NREE-33

### Top 7 Must Know Movement Disorders: Imaging with Clinical Videography Correlation

Sunday, Nov. 27 8:00AM - 9:00AM Room: Learning Center - NR

#### Participants

Leslie Starkey, MD, Portland, OR (*Presenter*) Nothing to Disclose

#### TEACHING POINTS

Diagnosis of movement disorders is challenging due to the varied clinical manifestations and heterogeneity, so the integration of imaging and clinical features plays an extremely important role. We have selected seven important movement disorders and provide multidisciplinary learning by introducing their imaging and clinical manifestations through a series of unknown cases followed by a clinical discussion including videos. In addition to important imaging manifestations, in collaboration with a neurologist, we present the typical diagnostic criteria and clinical examination findings that would be useful for radiologists to understand, such as the ataxia findings in spinocerebellar ataxia.

#### TABLE OF CONTENTS/OUTLINE

1. Amyotrophic lateral sclerosis imaging findings, followed by clinical pearls with video demonstration. 2. Multiple system atrophy imaging findings, followed by clinical pearls with video demonstration. 3. Spinocerebellar ataxia imaging findings, followed by clinical pearls with video demonstration. 4. Huntington disease imaging findings, followed by clinical pearls with video demonstration. 5. Fahr disease imaging findings, followed by clinical pearls with video demonstration. 6. Creutzfeldt-Jakob disease imaging findings, followed by clinical pearls with video demonstration. 7. Wilson disease imaging findings, followed by clinical pearls with video demonstration.

Printed on: 02/07/23



## Abstract Archives of the RSNA, 2022

NREE-34

### Visual Summary of the 2021 WHO Central Nervous System Tumor Classification

Sunday, Nov. 27 8:00AM - 9:00AM Room: Learning Center - NR

#### Awards

Certificate of Merit

#### Participants

Neiladri Khan, DO, Pittsburgh, PA (*Presenter*) Nothing to Disclose

#### TEACHING POINTS

The 2021 WHO Classification of Tumors of the Central Nervous System (CNS) is the fifth edition of the classification system, and it succeeds the fourth edition released in 2016. The 2021 classification incorporates changes in diagnostic principles, with a particular emphasis on the molecular profiling of tumors. A description of the new diagnostic principles, along with visual examples and graphics demonstrating their significance. We include two peculiar cases of IDH wild-type gliomas from our home institution which benefit from the new classification system. In addition to changes in diagnostic principles, several tumor-specific changes were also made. There are now also several entirely new tumor entities. The new concept of layered pathological reporting, and the impact of this new system on radiologists.

#### TABLE OF CONTENTS/OUTLINE

Title page - Disclosures - Introduction to the WHO classification system - Objectives - Brief overview of what is new in the 2021 update - Radiological and pathological visual examples of changes made to the diagnostic principles - IDH wild-type glioma, home institution interesting case 1 - IDH wild-type glioma, home institution interesting case 2 - Graphic rendition of changes made to specific tumor types - Introducing and explaining the concept of integrated diagnoses and layered reports, and what these changes mean for the radiologist - Conclusion - Biography

Printed on: 02/07/23



## Abstract Archives of the RSNA, 2022

NREE-35

### Genetics and Epigenetics of Brain Tumors for Radiologists

Sunday, Nov. 27 8:00AM - 9:00AM Room: Learning Center - NR

#### Awards

Certificate of Merit

#### Participants

Gabriela Bandeira, MD, Sao Paulo, Brazil (*Presenter*) Nothing to Disclose

#### TEACHING POINTS

1- To review the oncogenesis of primary brain tumors.2- To understand the main molecular pathways involved in primary brain tumors.3- To integrate the oncogenesis knowledge with the new molecular parameters from the 5th edition of the WHO Classification of Tumors of the Central Nervous System (WHO CNS5).4- To review the phenotypic and the genotypic key features of some primary brain tumors (radiogenomics).

#### TABLE OF CONTENTS/OUTLINE

1- Introduction2- Oncogenesis in CNSFundamental ConceptsCell CycleLigands and ReceptorsCyclin-Dependent Kinases (CDKs)Cellular Signaling Pathways involved in brain tumorsEpigenetics : Histone modifications, DNA Methylation4- New molecular parameters from the 5th edition of the WHO Classification of Tumors of the Central Nervous System (WHO CNS5).5- Illustrative cases of primary brain tumors with confirmed genetic and epigenetic profiles.6- Take-home messages7- Conclusion8- References

Printed on: 02/07/23

## Abstract Archives of the RSNA, 2022

NREE-36

### Intracranial Cystic-appearing Images More than a Simple Find

Sunday, Nov. 27 8:00AM - 9:00AM Room: Learning Center - NR

#### Participants

Eugenio César Rocha Santos Filho, SAO PAULO, Brazil (*Presenter*) Nothing to Disclose

#### TEACHING POINTS

The purpose of this exhibit is: To show different types of diseases that have cystic presentation. To demonstrate sites that are typically affected by each disease To help expand the differential diagnoses through the distinct imaging patterns of cystic lesions by a pictorial essay.

#### TABLE OF CONTENTS/OUTLINE

Overview of all pathologies and their division by etiology  
Congenital: Arachnoid cyst: different locations and sizes  
Ectodermal Inclusion Cysts  
Dermoid cyst  
Epidermoid cyst  
White epidermoid cyst  
Neuroglial cyst  
Blake pouch cyst  
Rathke's cleft cyst  
Corpus callosum agenesis and interhemispheric cyst  
Choroid plexus cyst  
Choroidal fissure cyst  
Colloid cysts of the third ventricle  
Pineal cysts  
Perivascular spaces and its association  
Infectious: Viral: Cytomegalovirus  
Bacterial: Neurosyphilis  
Neurotuberculosis  
Abscess  
Protozoa  
Neurotoxoplasmosis  
Parasitic  
Neurocysticercosis  
Chagas disease  
Fungi  
Aspergillosis  
Neurocryptococcosis  
Neoplastic: Intra-axial: Multinodular and vacuolating neuronal tumor  
Dysembryoplastic neuroepithelial tumors (DNET)  
Primitive neuroectodermal tumors (PNET)  
Multinodular and vacuolating neuronal tumor  
Central neurocytoma  
Ependymoma  
Hemangioblastoma  
Gliomas  
Ganglioglioma  
Medulloblastoma  
Metastasis  
Extra-axial: Meningioma  
Schwannoma  
Macroadenoma  
Craniopharyngioma  
Hemangioma  
Germinomas  
Pineal tumors  
Demyelinating: Demyelinating pseudotumor  
Balo disease  
Others  
Cobblestone malformation  
Hypomelanosis of Ito  
Megalecephalic leukoencephalopathy with subcortical cysts  
Porencephalic cyst

Printed on: 02/07/23

## Abstract Archives of the RSNA, 2022

NREE-37

### Posterior Circulation Stroke: How Much Do You Know About It?

Sunday, Nov. 27 8:00AM - 9:00AM Room: Learning Center - NR

#### Participants

Celia Alonso, MD, Madrid, Spain (*Presenter*) Nothing to Disclose

#### TEACHING POINTS

The objective of this educational exhibit is to shine a light on the acute management of vertebrobasilar stroke. Therefore, after reading it, the reader will: -Comprehend the epidemiology of vertebrobasilar strokes, their clinical presentation and etiology depending on the affected anatomical territory. -Learn the indications and limitations of imaging techniques in posterior circulation strokes, as well as their most frequent imaging features. -Know how to apply the two most important imaging prognostic scores in large vessel occlusions: pc-ASPECTS and BATMAN.

#### TABLE OF CONTENTS/OUTLINE

-Introduction. -Clinical considerations: its symptoms are frequently non-focal, overlap with those of anterior circulation strokes and simulate other neurological conditions ('stroke chameleons'), which usually leads to delayed diagnosis. -Etiology of posterior circulation strokes: ASCOD and topographic classification. -Vertebrobasilar anatomy, relevant variants shown with images. -Imaging techniques: indications, limitations and semiology. Imaging prognostic scores in large vessel occlusions: pc-ASPECTS and BATMAN. Its application will be shown using real cases. -All possible clinical scenarios (small, medium-sized and large vessel disease) will be shown with real cases studied with multimodal CT and/or brain MRI from our institution. -Treatment considerations. -Conclusion.

Printed on: 02/07/23



## Abstract Archives of the RSNA, 2022

NREE-38

### Imaging Cerebrospinal Fluid Hypotension: Cerebrospinal Fluid Fistula Hyper-knowledge

Sunday, Nov. 27 8:00AM - 9:00AM Room: Learning Center - NR

#### Participants

Pedro Castro, MD, Rio de Janeiro, Brazil (*Presenter*) Nothing to Disclose

#### TEACHING POINTS

To illustrate the most common symptoms related to cerebrospinal fluid (CSF) hypotension. To demonstrate the imaging aspects of spontaneous intracranial hypotension, a well-recognized entity. To explain that depicting the CSF leak location is the radiologist's goal, allowing effective treatment. To show that CSF leak imaging can be challenging and often misdiagnosed, leading to severe CSF hypotension.

#### TABLE OF CONTENTS/OUTLINE

1. Revision of epidemiology and clinical presentation, including headache, rhinorrhea, and severe CSF hypotension. 2. Etiologies of intracranial hypotension and CSF leaks, including surgery and trauma. 3. Imaging strategies and findings of CSF leaks, including MRI and CT myelography assessment. 4. MRI vs. CT cisternography in the assessment of CSF fistulas. 5. CT myelography in the assessment of spinal CSF fistulas. 4. Differential diagnosis of CSF hypotension. 5. Treatment options: epidural blood patches and surgery. 6. Take-home messages.

Printed on: 02/07/23



## Abstract Archives of the RSNA, 2022

NREE-39

### Ultrahigh-resolution CTA of the Brain as a Tool for Pre- and Postoperative Imaging

Sunday, Nov. 27 8:00AM - 9:00AM Room: Learning Center - NR

#### Participants

Miho Gomyo, Miraka, Japan (*Presenter*) Nothing to Disclose

#### TEACHING POINTS

1. To learn the basic principles and characteristics of ultrahigh-resolution CT. 2. To learn the kinds of image denoising reconstruction processing and understand their characteristics. 3. To learn the clinical importance of small arteries such as cortical arteries and perforators depicted by ultrahigh-resolution brain CTA.

#### TABLE OF CONTENTS/OUTLINE

1. Basic principles and characteristics 2. Image denoising reconstruction processing: FBP (filtered back-projection), hybrid IR (iterative reconstruction), full IR and deep learning reconstruction 3. Imaging anatomy and clinical importance the following arteries: cortical arteries, branches of main arteries and perforating arteries 4. Clinical application to preoperative and postoperative images: aneurysm, infectious aneurysm, dissecting aneurysm, arteriovenous malformation, moyamoya disease, arterial stenosis, temporal arteritis, superficial temporal artery-middle cerebral artery bypass and brain tumor

Printed on: 02/07/23

## Abstract Archives of the RSNA, 2022

NREE-4

### Dural and Leptomeningeal Diseases: Anatomy, Etiology, and Neuroimaging

Sunday, Nov. 27 8:00AM - 9:00AM Room: Learning Center - NR

#### Awards

Identified for RadioGraphics

#### Participants

Ryo Kurokawa, MD, PhD, Ann Arbor, MI (*Presenter*) Nothing to Disclose

#### TEACHING POINTS

This review summarizes the clinical and radiological findings of dural and leptomeningeal diseases caused by various etiologies.

#### TABLE OF CONTENTS/OUTLINE

Outline. I. Overview of dural and leptomeningeal diseases. Anatomy. Etiology. Recommended workups. II. Content. -Idiopathic-Infection: tuberculosis, syphilis, fungi, Lyme disease, HTLV-1, Q fever. -Autoimmune: ANCA-related vasculitis, PCNSV, sarcoidosis, systemic lupus erythematosus, rheumatoid arthritis, Behçet's disease, Sjogren's disease, Vogt-Koyanagi-Harada disease, inflammatory bowel disease, SAPHO syndrome. -Lymphoproliferative: POEMS syndrome and lymphoma. -Neoplasm: metastasis (breast cancer, lung cancer, melanoma, gliomatosis), leukemia, medulloblastoma, multiple myeloma, meningioma. -Histiocytosis: Erdheim-Chester disease, Rosai-Dorfman disease, Langerhans cell histiocytosis, juvenile xanthogranuloma. -Intracranial hypotension: lumbar puncture, CSF leak, CSF shunting, craniotomy. -Miscellaneous: Multiple sclerosis, amyloidosis, and neurocutaneous melanosis III. Summary. 1. Various entities cause the development of dural and leptomeningeal diseases. 2. Clinical and radiological findings can help in the diagnosis of the etiology. 3. Appropriate workup can lead to timely diagnosis and management.

Printed on: 02/07/23



## Abstract Archives of the RSNA, 2022

NREE-41

### Don't Tense About It: MRI Findings of Idiopathic Intracranial Hypertension and Intracranial Hypotension

Sunday, Nov. 27 8:00AM - 9:00AM Room: Learning Center - NR

#### Participants

Ana Paula Fonseca, MD, Sao Paulo, Brazil (*Presenter*) Nothing to Disclose

#### TEACHING POINTS

This review focuses on the imaging of idiopathic intracranial hypertension and spontaneous intracranial hypotension. Both have salient imaging findings that are important to recognize to help prevent their misdiagnosis from other neurological disorders. This panel aims to: Review the pathophysiology of these two important intracranial pressure disorders. Discuss and illustrate their imaging patterns. Describe through illustrative cases the scenarios for diagnosis, typical imaging patterns, unexpected findings and red flags that aid the diagnosis.

#### TABLE OF CONTENTS/OUTLINE

Pathophysiology of these two ICP disorders: Idiopathic intracranial hypertension and spontaneous intracranial hypotension  
Definition  
The Monro-Kellie doctrine  
Main causes  
Clinical syndrome  
Imaging findings  
Spontaneous intracranial hypotension  
Brain swelling  
Distension of the venous sinuses  
Bilateral subdural collections  
Dural thickening and enhancement  
Enlarged pituitary  
Flattened pons  
Inferior displacement of the third ventricle  
Sagging brain  
Idiopathic intracranial hypertension  
Partially empty sella turcica  
Distension of the optic nerve sheath  
CSF space  
Increased vertical tortuosity of the optic nerve  
Flattening of the posterior sclera/  
intraocular protrusion of the optic nerve head  
Cerebellar tonsilla ectopia  
Meningoceles  
Hypoplastic and/or stenosis of the venous sinus  
Prominence of the occipital emissary vein  
Associated Conditions  
Superficial Siderosis  
Ventral Epidural Collection  
Venous Sinus Thrombosis  
Pituitary Apoplexy  
Mimickers  
Chiari Type I Malformation  
Subdural Fluid Collections or Hematomas  
Other Conditions with Dural Thickening  
Red flags and diagnostic tips  
Diagnostic Approach  
Final remarks

Printed on: 02/07/23



## Abstract Archives of the RSNA, 2022

NREE-42

### Quantitative Susceptibility Mapping: Overview and Applications

Sunday, Nov. 27 8:00AM - 9:00AM Room: Learning Center - NR

#### Participants

Alexey Dimov, (*Presenter*) Nothing to Disclose

#### TEACHING POINTS

Quantitative susceptibility mapping (QSM) is an automated technique that post-processes three-dimensional (3D) gradient echo phase images to depict local tissue magnetic properties, which are blurred in conventional MRI sequences, such as T2w, T2\*w and phase images. QSM makes use of the already acquired phase data, does not add scan time, and can be easily integrated into the clinical workflow. QSM provides superb contrast-to-noise ratio (CNR) for depicting deep gray nuclei that are rich with iron, which is useful for precise guidance of deep brain stimulation. QSM provides high fidelity and quantitative measurements of iron in proinflammatory activated microglia in neuroinflammatory disorders, such as in multiple sclerosis, Parkinson's disease, Alzheimer's disease. QSM allows unambiguous differentiation of diamagnetic calcification from paramagnetic iron such as in microbleeds.

#### TABLE OF CONTENTS/OUTLINE

1. Revision of the basic physics of tissue magnetism, gradient echo data, and phase post-processing for QSM
2. Description of how QSM can be used to measure iron overloading in neurodegenerative diseases, such as Parkinson's disease.
3. Overview of how QSM can be used to define deep brain stimulation targets.
4. Synopsis of how QSM can be used to eliminate gadolinium injection in MRI monitoring of multiple sclerosis (MS) patients and to adjust therapy to measure chronic lesion activity for improved patient care.
5. Summary of how QSM processing of phase plus quantitative blood oxygenation level dependent (qBOLD) modeling of magnitude can enable oxygen extraction fraction (OEF) mapping from the widely available multiecho gradient echo data without vascular challenge.

Printed on: 02/07/23



## Abstract Archives of the RSNA, 2022

NREE-43

### Applications of MR Bone Imaging to Vertebral Lesions

Sunday, Nov. 27 8:00AM - 9:00AM Room: Learning Center - NR

#### Participants

Kazuhiro Tsuchiya, PhD, Tokyo, Japan (*Presenter*) Nothing to Disclose

#### TEACHING POINTS

1. To learn basic concepts and technical aspects of bone imaging like CT by MRI.2. To know how MR bone images depict the normal vertebra and adjacent structures compared with CT.3. To know the differences, especially the advantages, of MR bone images from CT and conventional MR images in miscellaneous vertebral lesions.

#### TABLE OF CONTENTS/OUTLINE

1. Basic issues of MR bone imaging including currently employed scanning sequences and postprocessing methods.2. Characteristics of MR bone images of the normal vertebra, placing emphasis on the difference from conventional MR images as well as CT.3. Presentation of clinical cases with discussion of implications. Cases will cover spine degeneration (Modic changes), neoplastic lesions including primary and metastatic vertebral tumors, inflammatory changes such as spondylitis, vertebral fractures, and so on.4. Additional discussion including current limitations as well as future directions of this technique.

Printed on: 02/07/23



## Abstract Archives of the RSNA, 2022

NREE-44

### Synthetic MRI, STAGE, and MR Acceleration through Deep-Learning: A Comparison of Time-Efficient MR Techniques in Neuroimaging

Sunday, Nov. 27 8:00AM - 9:00AM Room: Learning Center - NR

#### Awards

Certificate of Merit

#### Participants

Marc Von Reppert, New Haven, CT (*Presenter*) Nothing to Disclose

#### TEACHING POINTS

1. To provide a structured overview of main approaches to shortening neuroimaging protocols.2. To review recent developments in the field: STAGE, synthetic MRI and Deep Learning-based image enhancement.3. To provide an understanding of current applications and perspectives for clinical use.4. To highlight current shortcomings of these techniques and potential remedies.

#### TABLE OF CONTENTS/OUTLINE

Background: Highlighting the need for Time-Efficient MRI // Overview of Rapid Imaging Techniques // Synthetic MRI: Acquisition // Comparison of IRTTrueFISP, MPME and QRAPMASTER // Application in MS and CNS Tumors // Summary // STAGE: Acquisition // AI-based Automated Microbleed Detection // STAGE for different clinical applications // Summary // DL-based Reconstruction: Introduction and Workflow // Example Case // Introduction of Uncertainty Estimation in Image Enhancement // Outlook // Take Home Points

Printed on: 02/07/23



## Abstract Archives of the RSNA, 2022

NREE-45

### Implementing Perfusion Protocols for Tumor Differentiation and Analysis of Post-Treatment Changes into Busy Clinical Practice

Sunday, Nov. 27 8:00AM - 9:00AM Room: Learning Center - NR

#### Participants

Christopher Atkins, MD, New Haven, CT (*Presenter*) Nothing to Disclose

#### TEACHING POINTS

1. To review the fundamentals of MR perfusion and applications in Neuro-Oncology  
2. To review protocol considerations for clinical applications concerning image acquisition, processing, and analysis.  
3. To review the current developments in standardization efforts for perfusion imaging.

#### TABLE OF CONTENTS/OUTLINE

I. Review the fundamentals of perfusion imaging including explaining techniques of dynamic susceptibility contrast MRI, dynamic contrast enhanced MRI, and arterial spin labelling as well as highlighting their strengths and pitfalls.  
II. Review various clinical applications of MR perfusion including differentiation of tumor recurrence from radiation necrosis, distinction of different tumors, and differentiation of cerebral tumor entities using clinical examples.  
III. Review protocol considerations for each technique including technical requirements and choice of labeling approach.  
IV. Review the current standardization efforts for MR perfusion protocols.

Printed on: 02/07/23



## Abstract Archives of the RSNA, 2022

NREE-46

### Reversible Restricted Diffusion Lesions in Excitotoxic Brain Injury and Acute Ischemic Stroke

Sunday, Nov. 27 8:00AM - 9:00AM Room: Learning Center - NR

#### Participants

Yun Young Lee, Gwangju, Korea, Republic Of (*Presenter*) Nothing to Disclose

#### TEACHING POINTS

1. To review the etiologies of excitotoxic brain injury and its pathomechanisms. 2. To review the reversible diffusion weighted imaging lesions in acute ischemic stroke and its clinical implications.

#### TABLE OF CONTENTS/OUTLINE

1. Introduction- The importance of diffusion weighted imaging (DWI) in the neuroimaging area and the basic mechanisms of diffusion restriction.- Representative etiologies of diffusion restriction 2. Reversible restricted diffusion lesions in excitotoxic brain injury- Review the pathomechanisms of excitotoxic brain injury- Possible explanations for reversible diffusion restriction in excitotoxic brain injury- Case based review: toxic, metabolic, trauma, seizure, infection 3. Reversible restricted diffusion lesions in acute ischemic stroke- A systematic review the literature for reversible restricted diffusion lesions in acute ischemic stroke- Clinical implications of reversible diffusion restriction in acute ischemic stroke and plausible mechanisms- Permanent reversible diffusion restriction- Transient reversible diffusion restriction 4. Summary

Printed on: 02/07/23



## Abstract Archives of the RSNA, 2022

NREE-47

### Multi-modality Imaging of Skull Base Tumors and Tumor-like Lesions

Sunday, Nov. 27 8:00AM - 9:00AM Room: Learning Center - NR

#### Participants

Justin Caskey, MD, (*Presenter*) Nothing to Disclose

#### TEACHING POINTS

1. Basic skull base anatomy and anatomic landmarks relevant to the evaluation of skull base tumors and tumor-like lesions.2. Common skull base tumors and tumor-like lesions.3. Practical benefit of multi-modality imaging evaluation of skull base tumors and tumor-like lesions. Skull base pathology represents an often-challenging topic in neuroradiology. Anatomically, the skull base is a complex space formed by the ethmoid, sphenoid, occipital and paired frontal and temporal bones. Contained within and traversing through the skull base are critical neurovascular structures which must be carefully considered at radiologic evaluation. In many cases, multi-modality imaging, including perfusion weighted imaging, diffusion weighted imaging, and positron emission tomography, can provide a useful adjunct to standard neuroimaging techniques (CT, MRI) in evaluation of skull base pathology.

#### TABLE OF CONTENTS/OUTLINE

I. IntroductionII. Review of basic skull base anatomyIII. Brief overview of diffusion and perfusion imaging and positron emission tomographyIV. Case based examples of multi-modality imaging of skull base pathologya. Bone metastases from various primary sites, lymphoma, rhabdomyosarcoma b. Primary bone tumor, chordoma, chondrosarcoma, giant cell tumor c. Skull base invasion from carcinoma, pituitary adenoma, meningioma d. Inflammatory pseudotumor e. Bacterial and fungal osteomyelitis f. Benign tumor-like lesions, cholesterol granuloma, cholesteatoma, notochord origin lesion

Printed on: 02/07/23



## Abstract Archives of the RSNA, 2022

NREE-48HC

### Imaging features of Diffuse Pediatric-type High-grade Glioma, H3- /IDH-wildtype, and Diffuse Hemispheric Glioma, H3 G34-Mutant

Sunday, Nov. 27 8:00AM - 9:00AM Room: Learning Center - NR

#### Participants

Andrew Chang, MD, San Francisco, CA (*Presenter*) Nothing to Disclose

#### TEACHING POINTS

Diffuse pediatric high-grade gliomas (pHGG) are a heterogeneous group of brain tumors comprising 3-15% of all pediatric CNS tumors. In the 2021 WHO Classification of tumors of the CNS, two new subtypes of pHGG have been added to reflect the unique molecular features underlying each tumor: (1) diffuse pediatric-type high-grade glioma, H3-wildtype and IDH-wildtype (DPHGG H3/IDH-wt), and (2) diffuse hemispheric glioma, H3 G34-mutant (DHG H3G34M). This educational exhibit highlights the key MR imaging features of the two new tumor subtypes with emphasis on unique feature of each subtype that may aid in differential diagnosis. DPHGG H3/IDH-wt and DHG H3G34M demonstrate similar MRI features to other pHGGs, with low T2, high T2, and high FLAIR signal intensities, restricted diffusion, and variable enhancement pattern. Distinct features of DPHGG H3/IDH-wt include its propensity for frank intratumoral hemorrhage resulting in extensive edema, mass-effect, and hydrocephalus. In contrast, DHG H3G34M rarely develops hemorrhage and instead demonstrates cyst-and-nodule morphology with minimal surrounding edema or mass-effect.

#### TABLE OF CONTENTS/OUTLINE

[I] Overview of 2021 WHO Classification of diffuse pediatric-type high-grade gliomas. [II] Summary of key molecular genetic classification schemes. [III] Characteristic MRI features of diffuse pediatric-type high-grade gliomas (a) DPHGG H3/IDH-wt (b) DHG H3G34M Please visit the Learning Center to also view this presentation in hardcopy format.

Printed on: 02/07/23

## Abstract Archives of the RSNA, 2022

NREE-5

### Multimodality Imaging of Typical and Atypical Pilocytic Astrocytomas with Pathological Correlations

Sunday, Nov. 27 8:00AM - 9:00AM Room: Learning Center - NR

#### Participants

Toshio Moritani, MD, PhD, Ann Arbor, MI (*Presenter*) Nothing to Disclose

#### TEACHING POINTS

-To demonstrate imaging findings of typical and atypical pilocytic astrocytomas using multimodal imaging including CT, MRI, diffusion, perfusion (DSC and DCE), APTw, MR spectroscopy and PET. -To learn genetic and oncogenic pathways of tumor development of pilocytic astrocytoma with or without NF1 -To discuss the pathological correlation

#### TABLE OF CONTENTS/OUTLINE

-Genetic and oncogenic pathways: tumor development of pilocytic astrocytomas with or without NF1-Pathology: microcystic change, myxoid degeneration, Rosenthal fiber, pilocytic variants such as diffuse variant or pilomyxoid astrocytoma -Multimodal Imaging and imaging techniques: CT, MRI, diffusion, perfusion (DSC and DCE), APTw, MR spectroscopy and PET Classically high ADC values, while high grade gliomas and embryonal tumors show lower ADC. Relatively wide range of ADC values in PAs. Classically low rCBV and rCBF and high K2 on DSC, and low VP, high VE, and partially high Ktrans on DCEIncreased choline and lactate peak on MRS which can be a pitfall of the diagnosis. APT maps often show high values for PA even this is low grade tumor. -Case presentations:Typical findings: Well-defined infratentorial cystic lesion with enhancing mural nodule and supratentorial enhancing mass, with facilitated diffusion, high ADC value, typical perfusion pattern, increased APTw Atypical findings: unusual locations, non-enhancing, exophytic, hemorrhagic, multicentric/dissemination, relatively low ADC value, atypical perfusion pattern. Pediatric versus adult cases NF1 versus non NF1 Differential diagnosis

Printed on: 02/07/23



## Abstract Archives of the RSNA, 2022

NREE-50

### Pictorial Depiction of a Lexicon Based Approach to BT-RADS

Sunday, Nov. 27 8:00AM - 9:00AM Room: Learning Center - NR

#### Participants

Ankush Jajodia, MD, MBBS, New Delhi, India (*Presenter*) Nothing to Disclose

#### TEACHING POINTS

Background: Imaging evaluation of brain tumor patients is challenging since imaging findings of tumor development and treatment-related alterations overlap significantly. The accurate interpretation of these tumors causes significant inter-observer variability going to tumor heterogeneity, especially in complex circumstances. Imaging evaluation of brain tumors with MRI plays a crucial role in managing these patients, who face poor survival [median 15 months]. A structured reporting system (BT-RADS) aims to increase uniformity among radiologists. The need for a structured glioma surveillance reporting system with a standardized management-based suggestion, which has the potential to improve clinical interpretation and facilitate more effective patient communication, has already been voiced. There has been a dearth of lexicon depiction and illustration in the literature review. Clinical relevance: A standardized reporting system with the BT-RADS is encouraged using the various sequence-based lexicon. The published lexicon and report template will improve the completeness and accuracy of generated reports.

#### TABLE OF CONTENTS/OUTLINE

Characterize lexicon on MRI using BT-RADS Review case examples using the BT-RADS descriptive parameters.

Printed on: 02/07/23



## Abstract Archives of the RSNA, 2022

NREE-51

### Stepwise Application of RANO Criteria on Follow-up Imaging and Treatment of Gliomas: A Guide for Residents

Sunday, Nov. 27 8:00AM - 9:00AM Room: Learning Center - NR

#### Awards

Certificate of Merit

#### Participants

Thurl Hugh Cledera, MD, Taguig, Philippines (*Presenter*) Nothing to Disclose

#### TEACHING POINTS

Gliomas are the most common intra-axial tumor of the central nervous system, among which the most common type is glioblastoma, which incidentally is a highly aggressive tumor. Imaging plays a pivotal role in the management of glioblastomas; hence guidelines have been developed to facilitate the interpretation of studies from pre-treatment studies down to post-surgical and post-radiation changes, one of which is known as the Response Assessment in Neuro-Oncology (RANO) Criteria. The criteria are broken down to complete response, partial response, stable disease, and progressive disease must be applied to all post-treatment glioma cases to guide therapy. Pseudoprogression and pseudoresponse are necessary to distinguish from the standard response criteria as they will have an effect on the treatment and follow-up of patients.

#### TABLE OF CONTENTS/OUTLINE

1. Introduction and Background 2. Step 1: Confirm Patient History and Treatment 3. Step 2: Know the Natural Course and Management of Glioblastoma 4. Step 3: Identifying Lesions 5. Step 4: Identifying Response Criteria a. Complete Response b. Partial Response c. Stable Disease d. Progressive Disease 6. Step 5: Check for Imaging Pitfalls a. Pseudoprogression (Post-surgical, Post-radiation, Post-chemotherapy) b. Pseudoresponse (VEGF Therapy)

Printed on: 02/07/23



## Abstract Archives of the RSNA, 2022

NREE-52

### Uncertainty Estimation in Auto-Segmentation and Image Reconstruction Tasks

Sunday, Nov. 27 8:00AM - 9:00AM Room: Learning Center - NR

#### Awards

Certificate of Merit

#### Participants

Marc Von Reppert, New Haven, CT (*Presenter*) Nothing to Disclose

#### TEACHING POINTS

1. To provide a structured overview of the concept of uncertainty estimation (UE) in the context of Machine Learning and Deep Learning.2. To summarize and review different approaches to measuring uncertainty.3. To provide a perspective on current applications of UE in the literature of neuroimaging in tasks like segmentation and image enhancement.4. To highlight sources of uncertainty in neuroimaging and provide an outlook on potential developments in the field.

#### TABLE OF CONTENTS/OUTLINE

1. Principles of Uncertainty Estimation: // Background: Understanding Uncertainty // Background: Machine Learning and Deep Learning // Types of Uncertainty // Methods of Measuring Uncertainty2. Application of Uncertainty Estimation in Neuroimaging: // Summary of Current Neuroimaging Applications // Brain Anatomical Segmentation // Brain Tumor Segmentation // Image Super-Resolution and Denoising // Collection of Publications3. Take Home Points

Printed on: 02/07/23



## Abstract Archives of the RSNA, 2022

NREE-53

### Diffusion Weighted Imaging in the Spine: A Magic Key

Sunday, Nov. 27 8:00AM - 9:00AM Room: Learning Center - NR

#### Awards

Certificate of Merit

#### Participants

Mahmoud Shalaby, MD, Lansdowne, PA (*Presenter*) Nothing to Disclose

#### TEACHING POINTS

1- Illustrate the role of diffusion weighted imaging (DWI) in spine infectious, neoplastic, and inflammatory disease  
2- Demonstrate the role of DWI in spine trauma and degenerative disease  
3- Emphasize the role of DWI in spinal cord ischemia  
4- Highlight the challenges of spine DWI acquisition  
5- Discuss technical tips and considerations for protocol optimization for 1.5T and 3T MRI

#### TABLE OF CONTENTS/OUTLINE

- Clinical applications of DWI in common spinal pathologies:  
o Infectious and inflammatory disease  
o Primary and metastatic spine tumor  
o Degenerative disease  
o Trauma  
o Spinal cord ischemia  
o Compression fractures  
o Demyelinating disease  
- Challenges of spine DWI acquisition  
- Protocol optimization with practical tips to improve spine DWI for 1.5T and 3T MRI

Printed on: 02/07/23



## Abstract Archives of the RSNA, 2022

NREE-54

### Amide Proton Transfer Weighted Imaging (APTwi) in Brain Tumors: A Pictorial Review

Sunday, Nov. 27 8:00AM - 9:00AM Room: Learning Center - NR

#### Awards

**Magna Cum Laude**

#### Participants

Guillaume Hamon, MD, Rennes, France (*Presenter*) Nothing to Disclose

#### TEACHING POINTS

The aims of this exhibit are:1. To describe the basic theory and advantages of the APTwi technique2. To illustrate brain tumors and differential's features in APTwi3. To highlight and discuss potential pitfalls in APTwi4. To review the current clinical applications of APTwi in neuro-oncology

#### TABLE OF CONTENTS/OUTLINE

I. Understanding the APTwi technique1. Introduction to the Chemical Exchange Saturation Transfer (CEST) technique2. Basic physical principles of the amide-CEST contrast, so-called APTwi3. Technical consideration and limitations4. Image analysisII. Brain tumors, tumor mimics pitfalls in APTwi: an image-based approach1. Why to image amide protons in brain tumors?2. Primary and secondary brain tumors3. Tumor mimics4. Potential pitfalls in technique and image interpretationIII. Clinical applications of APTwi in neuro-oncology1. Main current published clinical applications of APTwi to image brain tumors2. Ongoing research and potential perspectives

Printed on: 02/07/23



## Abstract Archives of the RSNA, 2022

NREE-55

### Imaging Abnormalities Associated With Pediatric Pituitary Disorders

Sunday, Nov. 27 8:00AM - 9:00AM Room: Learning Center - NR

#### Participants

Yun Song Choo, MBBS, FRCR, (*Presenter*) Nothing to Disclose

#### TEACHING POINTS

The pituitary gland occupies a small footprint in terms of volume within the cranium, but pathologies arising from or involving it can have profound and long-lasting effects on the growth and development of the pediatric patient. It is hence important to appreciate the range of abnormalities in the pituitary gland and sellar region arising from both congenital and acquired pathologies that may be seen on neuroimaging studies. In this education exhibit, we revisit the development of the pituitary gland and share approaches to pediatric pituitary abnormalities on imaging with illustrative cases. Some of the major teaching points are: • MRI is the modality of choice to investigate suspected pituitary abnormalities in the pediatric patient. • The anterior and posterior pituitary gland have different embryological origins. • On top of masses that involve the sella and suprasellar region, the radiologist should be aware of mass-like lesions and mimics that have previously resulted in unnecessary surgical intervention.

#### TABLE OF CONTENTS/OUTLINE

• Pituitary Gland Development and Anatomy • Imaging the Pediatric Pituitary Gland • Abnormalities of Size and Number • Abnormalities of the Posterior Pituitary • Pituitary Stalk Thickening • Masses and Mass-like Lesions

Printed on: 02/07/23



## Abstract Archives of the RSNA, 2022

NREE-56

### Checklist Based Approach to Interpret Pediatric Brain MRI Studies

Sunday, Nov. 27 8:00AM - 9:00AM Room: Learning Center - NR

#### Awards

Certificate of Merit

#### Participants

Anvita Pauranik, MD, FRCPC, VANCOUVER, BC (*Presenter*) Nothing to Disclose

#### TEACHING POINTS

1. To develop a checklist-based methodical approach while interpreting pediatric brain MRI studies by knowing what to look for on different MR imaging planes and sequences, driven by the clinical question. 2. To understand the spectrum of age-related changes in a developing brain. 3. To differentiate subtle pathology from normal variants using various case examples.

#### TABLE OF CONTENTS/OUTLINE

1. Midline sagittal brain. A. Commissures- size, shape, dysmorphisms. B. Sellar and Suprasellar region- Anterior/posterior pituitary gland, Infundibulum, Optic Chiasm, Floor of Third ventricle. Pineal gland C. Posterior fossa- Brainstem, Vermis and Cerebellar tonsils D. CSF Spaces- Cisterns, Aqueduct, Retrocerebellar space. E. Skull base including craniocervical junction, Scalp 2. Brain parenchyma- assessment on T1/T2/DWI/SWI. Age related changes, terminal zones of myelination versus white matter injury, subtle findings in altered sensorium- basal ganglia/ brainstem lesions. 3. Ventricles- focal dilatation in PVHI, puckering in PVL, extra axial CSF spaces- prominence, collections, asymmetry, BESSI, cisterns- utility of Sagittal CISS 4. Flow Voids. 5. Extracranial - orbits, mastoids, paranasal sinuses. 2. Checklist for focal seizure evaluation A. Midline- Hypothalamic Hamartoma versus inter-hypothalamic adhesion B. Cortical ribbon-blind spots C. Focal cortical Dysplasias-search patterns- Asymmetry in Grey-White matter signal, Sulcation. D. Mesial temporal lobe- early hippocampal sclerosis, dual lesions, temporo-polar changes, skull base defects 3. Checklist for Neonatal brain MRI PLIC, Deep gray nuclei, Peri-Rolandic cortex, T1 bright punctate white matter lesions. Normal anisotropy on DWI.

Printed on: 02/07/23

## Abstract Archives of the RSNA, 2022

NREE-57

### Mind-Bending Cerebellar Anatomy Techniques

Sunday, Nov. 27 8:00AM - 9:00AM Room: Learning Center - NR

#### Participants

Elissandra Lima, MD, Rio de Janeiro, Brazil (*Presenter*) Nothing to Disclose

#### TEACHING POINTS

To demonstrate the anatomy of the cerebellum by illustrations and imaging, with phylogenetic and functional considerations. To correlate the most frequent diseases with anatomic regions. To depict the importance of precise localization of the disease according to the anatomical point of the cerebellum.

#### TABLE OF CONTENTS/OUTLINE

1. Background. 2. Imaging protocol. 3. Embryonic development. 4. Cerebellum anatomy. 5. Cerebellar functional anatomy. 6. Phylogenetic considerations of the cerebellar segments. 7. Cerebellar connections and function. 8. Cerebellum vascular anatomy. 9. Clinical perspective: symptoms and diseases - including neoplastic, inflammatory, infections, congenital and degenerative. 10. Flowchart for imaging assessment of cerebellar anatomic regions. 11. Take-Home messages.

Printed on: 02/07/23



## Abstract Archives of the RSNA, 2022

NREE-58

### **Anatomy and Functionality: Solidifying the Sulci, Gyri, and Brain Segmentation**

Sunday, Nov. 27 8:00AM - 9:00AM Room: Learning Center - NR

#### **Participants**

Elissandra Lima, MD, Rio de Janeiro, Brazil (*Presenter*) Nothing to Disclose

#### **TEACHING POINTS**

To illustrate the anatomy of the sulci, gyri, and brain segmentation with MRI imaging and illustrations. To correlate the anatomic segments with their functionality. To demonstrate the significance of accurate localization of the disease according to the anatomical locations, considering the clinical perspective.

#### **TABLE OF CONTENTS/OUTLINE**

1. Background. 2. Imaging protocol. 3. Sulci, gyri, and brain segmentation anatomy based on MRI imaging and illustrations. 4. Anatomic region and functionality. 5. Clinical perspective: brain diseases and their correlation with anatomy and neurological deficits. 6. Take-Home messages.

Printed on: 02/07/23



## Abstract Archives of the RSNA, 2022

NREE-59

### Need-to-know Neuroimaging with Clinical Correlation: Parkinson's Disease and Related Movement Disorders

Sunday, Nov. 27 8:00AM - 9:00AM Room: Learning Center - NR

#### Participants

Leslie Starkey, MD, Portland, OR (*Presenter*) Nothing to Disclose

#### TEACHING POINTS

Although Parkinson's disease is a relatively common movement disorder (MD), the onset is insidious and diagnosis challenging due to the varied clinical manifestations and heterogeneity, so the integration of imaging and clinical features plays an extremely important role. Other MD can simulate Parkinson's disease, including progressive supranuclear palsy, essential tremor, corticobasal degeneration, and carbon monoxide poisoning, among others. One area neuroradiologists may have interest but little opportunity for learning is the clinical side, e.g. classic neurological findings in MD. In this presentation, we teach imaging and clinical manifestations. Imaging is presented as cases followed by the neurologist's perspective, including diagnostic criteria and videos of findings useful for radiologists to know, such as the eye findings in supranuclear palsy.

#### TABLE OF CONTENTS/OUTLINE

General topics: 1) Parkinson's disease 2) PSP 3) Corticobasal degeneration 4) CO poisoning. Radiology cases and videos of neurologic findings include: •DAT scan, Nigrosome-1 and the absent swallow tail sign, classic and spectrum. •Clinical videos: motor features: fascial masking, bradykinesia, rest tremors, and gait. •Scans without Evidence of Dopamine Deficit (SWEDDS). •Differential: dopa responsive dystonia, paroxysmal kinesigenic dyskinesia, juvenile Huntington disease. •Deep brain stimulators, locations: VIM, GPi, STN. •Clinical videos: off meds, on meds, on meds and on DBS. •PSP: hummingbird sign. •Clinical videos: blink rate, eye movements, freezing speech, gait. •Corticobasal degeneration: asymmetric atrophy. •CO poisoning: globus pallidus lesions. •Clinical videos: gait freezing.

Printed on: 02/07/23



## Abstract Archives of the RSNA, 2022

NREE-6

### Neuroradiological Aspects of Congenital Infections and Mimics

Sunday, Nov. 27 8:00AM - 9:00AM Room: Learning Center - NR

#### Awards

Certificate of Merit

#### Participants

Luiz Uchoa, MD, Sao Paulo, Brazil (*Presenter*) Nothing to Disclose

#### TEACHING POINTS

To review imaging findings of congenital infection according to clinical suspicion. Identify the neurologic imaging findings of congenital infection and mimics with CT and MR images. A practical approach to interpreting these conditions systematizing the evaluation based on main neurologic imaging findings and clinical features.

#### TABLE OF CONTENTS/OUTLINE

Introduction. Congenital Disease: Genetical x Disruptive. Visual Systematization of congenital infection and mimics. Congenital Infections and neurologic imaging findings. Main mimics of congenital infections. Take home messages.

Printed on: 02/07/23



## Abstract Archives of the RSNA, 2022

NREE-60

### Moving to Diagnosis: Neuroimaging Systematic Approach to Neurometabolic Diseases Manifested as Movement Disorders

Sunday, Nov. 27 8:00AM - 9:00AM Room: Learning Center - NR

#### Participants

Andres Abad, MD, (*Presenter*) Nothing to Disclose

#### TEACHING POINTS

To propose a neuroimaging systematic approach for the patients with movements disorders and suspicion of inborn error of metabolism etiology. To review the different neuroimaging presentation of the main inborn error of metabolism associated with movement disorders. To enrich the radiologist role into the diagnosis process of inborn error of metabolism To familiarize the radiologist with the neuroimaging findings present in uncommon congenital diseases that can produce movements disorders.

#### TABLE OF CONTENTS/OUTLINE

Introduction. Movements disorders classification. Inborn errors of metabolism associated with each movement disorder. Cases and images of neurometabolic diseases associated with chorea. Cases and images of neurometabolic diseases associated with dystonia. Cases and images of neurometabolic diseases associated with myoclonus. Cases and images of neurometabolic diseases associated with tremor. Cases and images of neurometabolic diseases associated with parkinsonism. Conclusion.

Printed on: 02/07/23



## Abstract Archives of the RSNA, 2022

NREE-61

### "Live and in Color": Imaging of Neurovascular Devices

Sunday, Nov. 27 8:00AM - 9:00AM Room: Learning Center - NR

#### Participants

Camila Barbosa, MD, Sao Paulo, Brazil (*Presenter*) Nothing to Disclose

#### TEACHING POINTS

Illustrate the most common intracranial and cervical neurointerventional and neurosurgical devices, such as clips, coils, stents and intrasaccular flow disruptors, used for treatment of neurovascular conditions as intracranial aneurysms, arterial stenosis and vascular malformations. Understand the clinical indication of each dispositive. Present cases treated with neurovascular devices, recognizing the importance of the radiologist familiarity with the dispositives in order to proper evaluate post-operative images. Understand the best imaging method on the post-operative evaluation for each dispositive. Review the possible limitations of imaging methods for the follow-up and diagnosis of complications.

#### TABLE OF CONTENTS/OUTLINE

Illustrated neurovascular devices. Algorithms for the post-treatment follow up. Case-based didactics: sample cases to demonstrate the devices, its appearance on different imaging methods and clinical use. Case-based post treatment discussion of complications.

Printed on: 02/07/23



## Abstract Archives of the RSNA, 2022

NREE-62

### Far Beyond Atheromatosis: Unusual Findings of Carotid Duplex Scan

Sunday, Nov. 27 8:00AM - 9:00AM Room: Learning Center - NR

#### Awards

Certificate of Merit

#### Participants

Iza Vieira, MD, Sao Paulo, Brazil (*Presenter*) Nothing to Disclose

#### TEACHING POINTS

The purposes of this exhibit are: 1. Comprehend the normal anatomy of the common carotid artery (CCA), internal carotid artery (ICA) and external carotid artery (ECA) on B-mode ultrasound; 2. Recognize anatomy variations and uncommon findings on B-mode ultrasound and duplex scan, with the correlation of CT-angiography (CTA) when necessary; 3. Correlate imaging findings with clinical presentation; 4. Recognize complications and possible outcomes; 5. Brief review of management options.

#### TABLE OF CONTENTS/OUTLINE

- Normal anatomy of the extracranial carotid system on ultrasound; - Anatomy variations of the extracranial carotid system; - Carotid kinking; - Carotid aneurysms; - Endoleak following endovascular aneurysm repair; - Carotid artery pseudoaneurysm; - Carotid dissection; - Carotid web; - Carotid-jugular arteriovenous fistula; - Occlusion of the CCA and internalization of the ECA; - Takayasu arteritis; - Carotidynia; - Complications and outcomes.

Printed on: 02/07/23



## Abstract Archives of the RSNA, 2022

NREE-63

### A Checklist Approach to Interpreting Cerebral Digital Subtraction Angiography

Sunday, Nov. 27 8:00AM - 9:00AM Room: Learning Center - NR

#### Awards

Certificate of Merit

#### Participants

Charlotte Chung, MD, PhD, (*Presenter*) Nothing to Disclose

#### TEACHING POINTS

As diagnostic and interventional neuroradiology become increasingly siloed, most diagnostic neuroradiologists no longer perform catheter-based neuroangiography. However, basic understanding of cerebral digital subtraction angiography (DSA), the gold standard for diagnosis of cerebrovascular pathologies, remains crucial for accurate interpretation of noninvasive brain CT and MR angiogram. This exhibit introduces the art of interpreting 2-dimensional (2D) cerebral DSA to the contemporary diagnostic neuroradiologist. Educational objectives of this exhibit include:- Outline imaging techniques and protocol for a typical diagnostic cerebral angiogram- Provide an annotated atlas for normal cerebral arterial and venous anatomy on 2D DSA- Introduce a checklist approach for interpretation of 2D cerebral DSA- Illustrate angiographic appearance of variant anatomy and various pathologies

#### TABLE OF CONTENTS/OUTLINE

I. 2D DSA imaging techniques  
II. Diagnostic cerebral angiogram imaging protocol  
III. Annotated atlas of normal anterior and posterior circulation on 2D DSA  
IV. Step-by-step checklist for interpretation of 2D cerebral DSA  
V. Systemic checklist-based illustration of variant and abnormal angiographic findings  
VI. Application of the checklist approach using case-based examples

Printed on: 02/07/23



## Abstract Archives of the RSNA, 2022

NREE-65

### Neurovascular Imaging at 7T: Small Vessel Anatomy

Sunday, Nov. 27 8:00AM - 9:00AM Room: Learning Center - NR

#### Participants

Neethu Gopal, MBBS, Jacksonville, FL (*Presenter*) Nothing to Disclose

#### TEACHING POINTS

Ultra-high resolution MR angiography (MRA) of the brain with a voxel size=0.3 x 0.3 x 0.3 mm is now achievable thanks to more readily available 7 Tesla clinical MR scanners and modern acceleration techniques. This advancement in our imaging capability allows for visualization of small normal vascular structures that were previously imperceptible on routine non-invasive vascular imaging. Teaching Points: 1. Revisit normal arterial anatomy of the smaller branches of the circle of Willis including normal anatomic variants. A combination of 2D and cinematic rendered images as well as illustrations will be utilized. 2. Demonstrate the normal cross sectional imaging appearance of these small vessels. In many cases, MRA images will be fused with 3D T1-weighted or T2-weighted sequences to better orient the viewer and demonstrate the spatial relationship of these vessels with gray-matter and white matter structures within the brain parenchyma. 3. Review pathological conditions associated with the smaller circle of Willis branches.

#### TABLE OF CONTENTS/OUTLINE

1. Introduction 2. Serial review of normal anatomy followed by cross-sectional images. Arteries will be reviewed systematically from anterior circulation to posterior circulation. Arteries that will be covered include but are not limited to: Anterior Choroidal Artery and its Branches, Superior Hypophyseal Artery, Anatomic Variations of the Posterior Communicating Artery, Medial Lenticulostriate Arteries, Recurrent Artery of Heubner, Lateral Lenticulostriate Arteries, Posterior Cerebral Artery Branches, Artery of Percheron, Basilar Perforator Vessels. 3. Review of cases with pathology 4. Conclusion

Printed on: 02/07/23



## Abstract Archives of the RSNA, 2022

NREE-66

### Challenging Procedures at the C1-2 Spinal Level - Using CT Guidance to Improve Patient Care and Safety

Sunday, Nov. 27 8:00AM - 9:00AM Room: Learning Center - NR

#### Participants

Ross Frederick, MD, Phoenix, AZ (*Presenter*) Nothing to Disclose

#### TEACHING POINTS

- There are several important procedures at the C1-2 level that can significantly improve patient quality of life. CT guidance makes these otherwise dangerous procedures safer and easier to perform.
- There are key anatomical structures that must be avoided when performing these procedures, most notably the vertebral artery, posterior inferior cerebellar artery, C2 nerve, and spinal cord. A thorough understanding of anatomy in this region is crucial to perform these procedures confidently and safely.
- Cervicogenic headache is an underrecognized and therefore undertreated condition that radiologists can treat with C1-2 facet joint injection, C2 nerve root block, or C2 ablation.
- For patients with a contraindication to lumbar puncture, cervical puncture at the C1-2 level provides an alternative approach for CSF collection, injection of contrast for myelography, or injection of chemotherapy.

#### TABLE OF CONTENTS/OUTLINE

1. Introduction: types of procedures and the patients who can benefit from them
2. Critical regional anatomya. Vertebral arteryb. PICAc. C2 nerved. Spinal cord
3. Cervicogenic headache and atlantoaxial osteoarthritisa. C1-2 facet injection i. Indications ii. Technical considerationsb. C2 nerve root block i. Indications ii. Technical considerationsc. C2 nerve ablation i. Indications ii. Technical considerations
4. Cervical puncturea. Indication - contraindication to lumbar puncturei. CSF collection ii. Injection of contrast for myelography iii. Injection of chemotherapyb. Technical considerations

Printed on: 02/07/23



## Abstract Archives of the RSNA, 2022

NREE-67

### Spinal Vascular Pathologies: An Approach for Diagnosis and Management

Sunday, Nov. 27 8:00AM - 9:00AM Room: Learning Center - NR

#### Participants

Moataz Ahmed Sayed Mohammed Soliman, MD, MSc, CHICAGO, IL (*Presenter*) Nothing to Disclose

#### TEACHING POINTS

- Describe normal vascular supply and drainage of the spine.
- Outline various types of spinal arteriovenous shunting and hyper-vascular spinal lesions: Common imaging findings and pitfalls.
- Discuss imaging features of common differential diagnosis
- Illustrate therapeutic options for spinal arteriovenous shunting and outcomes.

#### TABLE OF CONTENTS/OUTLINE

1. Introduction
  - a. Normal arterial supply of the spinal cord
  - b. Normal venous drainage of the spinal cord
2. Classification and cross-sectional imaging findings of spinal vascular lesions with angiographic correlation
  - a. Spinal Arteriovenous shunts
    - i. Type I: Spinal Dural Arteriovenous Fistula.
    - ii. Type II: Spinal Glomus AVM
    - iii. Type III: juvenile Spinal AVM
    - iv. Type IV: Intradural Peri-medullary AVF
  - b. Intramedullary hypervascular neoplastic lesions
    - i. Cavernous malformation
    - ii. Hemangioblastoma
    - iii. Paraganglioma
  - c. Spinal cord aneurysms
    - i. Imaging features
    - ii. Therapeutic interventions
  - d. Cord infarct
    - i. Etiology
    - ii. Imaging manifestations
3. Role of interventional radiology in management of spinal vascular lesions
  - a. Therapeutic embolization
  - b. Preoperative devascularization
4. Conclusion and take-home messages

Printed on: 02/07/23



## Abstract Archives of the RSNA, 2022

NREE-68

### Intramedullary Spinal Cord Injuries: A Potpourri"

Sunday, Nov. 27 8:00AM - 9:00AM Room: Learning Center - NR

#### Participants

Juliana Benez, Sao Paulo, Brazil (*Presenter*) Nothing to Disclose

#### TEACHING POINTS

The purpose of this exhibit is: • To illustrate the imaging features found in different intramedullary pathologies, including their location, affected vertebral segment, contrast media uptake, and specific features. • To demonstrate intramedullary pathologies didactically divided into five groups: demyelinating, neoplastic, vascular, metabolic, and other lesions. • Illustrated review of a case series of intramedullary pathologies.

#### TABLE OF CONTENTS/OUTLINE

• Introduction - Epidemiology - Clinical scenarios - Typical imaging findings, with differences between the various intramedullary pathologies • Case series of Intramedullary spinal cord injuries • References • Conclusion

Printed on: 02/07/23

## Abstract Archives of the RSNA, 2022

NREE-69

### What Can it be in the Conus Medullaris? A Pictorial Review

Sunday, Nov. 27 8:00AM - 9:00AM Room: Learning Center - NR

#### Participants

Felipe Pacheco, MD, PhD, Sao Paulo, Brazil (*Presenter*) Nothing to Disclose

#### TEACHING POINTS

The conus medullaris is affected by many conditions, including congenital, vascular, tumoral, inflammatory and infectious diseases, which many times are hardly differentiated because of the similarity of their clinical history and physical examination among different etiologies. Magnetic resonance imaging presents high sensitivity in the detection of these lesions and plays a relevant role in the diagnosis and in the evolutive control. This panel aims to: Review the anatomy of the conus medullaris, including its anatomical limits, normal MR imaging findings and related clinical syndromes. Discuss and illustrate the imaging patterns of the main lesions in the conus medullaris, including congenital, vascular, tumoral, inflammatory, infectious, among others. - Describe through illustrative cases the scenarios for diagnosis, focusing on typical imaging patterns, unexpected findings and red flags that aid the diagnosis.

#### TABLE OF CONTENTS/OUTLINE

- Anatomy of the conus medullaris - Normal appearance on CT and MRI - Main pathologies involving the conus medullaris, involving: - Congenital lesions: Caudal regression syndrome types 1 and 2, Ventriculus terminalis, Myelomeningocele - Neoplastic lesions: myxopapilar ependymoma, tanicytic ependymoma, leptomeningeal carcinomatosis, metastatic lesion, glioblastoma, dermoid cyst - Vascular lesions: arteriovenous dural fistula, cavernoma, ischemia - Systemic inflammatory diseases: IGG-4 related disease, Sarcoidosis, Dermatomyositis - Infectious diseases: Schistosomiasis, Tuberculosis, Herpes Virus, Polio-like - Auto-immune diseases: MOG antibody disease, Multiple Sclerosis, NMSOD - Red flags and diagnostic tips - Diagnostic Approach - Final remarks

Printed on: 02/07/23



## Abstract Archives of the RSNA, 2022

NREE-7

### What Can Go Wrong? Advanced Imaging of Malformation of Cortical Development

Sunday, Nov. 27 8:00AM - 9:00AM Room: Learning Center - NR

#### Awards

Identified for RadioGraphics  
Cum Laude

#### Participants

Julia Brunelli, MD, Sao Paulo, Brazil (*Presenter*) Nothing to Disclose

#### TEACHING POINTS

This pictorial essay will review the main etiologies of malformations of cortical development (MCDs) based on illustrative cases and original drawings. MCD will be addressed according to the last consensus update, considering pathological, genetic and neuroimaging features. The entities are divided into three major groups, according to the pathophysiological path that leads to that malformation. The purpose of this exhibition is to:- Review the cortical development, and its three main stages: cellular proliferation and differentiation, neuronal migration, and cortical organization;- Describe the new consensus of MCDs;- Recognize the main etiologies of MCDs, according to their imaging findings, and understand how different etiologies, when damaging the same pathway, can cause the same radiologic pattern.

#### TABLE OF CONTENTS/OUTLINE

NORMAL CORTICAL DEVELOPMENT- Didactic original drawings of the stages of cortex formation. MALFORMATIONS OF CORTICAL DEVELOPMENT- The new consensus taking account pathological, genetic and neuroimaging features. CASE-BASED DIDACTICS- Sample cases to illustrate and solidify the concepts;- Review of the main pathologies, addressing the pathophysiological and genetic aspects that leads to each image pattern.

Printed on: 02/07/23



## Abstract Archives of the RSNA, 2022

NREE-70

### Spinal Dysraphisms: Step-by-Step

Sunday, Nov. 27 8:00AM - 9:00AM Room: Learning Center - NR

#### Participants

María José Risco Fernandez, Toledo, Spain (*Presenter*) Nothing to Disclose

#### TEACHING POINTS

- Knowledge of the normal embryologic development of the spinal cord is crucial for understanding spinal dysraphisms (SD).
- They have been divided into open (OSD) and closed spinal dysraphisms (CSD), depending on the absence or presence of skin covering the defect.
- Magnetic resonance imaging (MRI) is the modality of choice for the evaluation of these.

#### TABLE OF CONTENTS/OUTLINE

Spinal dysraphisms (DS) make reference to a wide spectrum of congenital abnormalities of the spine and spinal cord. Spinal development occurs throughout the 2nd and 6th week along embryologic stages of gastrulation, and primary and secondary neurulation. Anomalies in any of these stages can result in a defective or incomplete closure of the neural tube and structures of the dorsal midline. The clinical manifestations of these entities are heterogeneous: from being unnoticed to becoming incompatible with life outside the uterus. SD has been classically divided into two main groups depending on whether there is skin covering the defect: OSD and CSD. Magnetic resonance imaging (MRI) is the modality of choice for the detailed evaluation of these conditions. A step-by-step evaluation of the normal and abnormal imaging findings is critical to providing accurate surgical information. The aim of this pictorial review is to offer a systematic evaluation of SD on MRI, including normal and abnormal findings, classifying the type and the site of SD, and additional or associated findings both in pre and postnatal patients of our clinical practice.

Printed on: 02/07/23



## Abstract Archives of the RSNA, 2022

NREE-71

### Traumatic Spine Injury Classification: A Review of the AO Spine Injury Classification Systems Through Case Examples

Sunday, Nov. 27 8:00AM - 9:00AM Room: Learning Center - NR

#### Participants

Chad Farris, MD, PhD, (Presenter) Nothing to Disclose

#### TEACHING POINTS

-Review the AO Spine Injury Classification Systems for traumatic Injuries to the thoracolumbar spine (Thoracolumbar Injury Classification System), subaxial cervical spine (Subaxial Injury Classification System), and the upper cervical spine (Upper Cervical Injury Classification System).-Review case examples of traumatic spine injuries fitting into all of the morphological classifications based on the AO Spine Injury Classification Systems.

#### TABLE OF CONTENTS/OUTLINE

A. What are the AO Spine Classification Systems?B. Three basic parameters that all AO Spine Classification Systems are based on1. Morphological Classification of the Fracture, 2. Neurological Status, 3. Clinical ModifiersC. Case examples fitting into all of the morphological classifications within the AO Spine Classification Systems in the thoracolumbar spine, subaxial cervical spine, and upper cervical spine.1. Thoracolumbar Spine Examples: a. Type A0 Injury, b. Type A1 Injury, c. Type A2 Injury, d. Type A3 Injury, e. Type A4 Injury, f. Type B1 Injury, g. Type B2 Injury, h. Type B3 Injury, i. Type C Injury2. Subaxial Cervical Spine Examples: a. Type A0 Injury, b. Type A1 Injury, c. Type A2 Injury, d. Type A3 Injury, e. Type A4 Injury, f. Type B1 Injury, g. Type B2 Injury, h. Type B3 Injury, i. Type C Injury, j. Type F1 Injury, k. Type F2 Injury, l. Type F3 Injury, m. Type F4 Injury3. Upper Cervical Spine: a. Occipital Condyle and Occipital Cervical Joint Complex: i. Type A Injury, ii. Type B Injury, iii. Type C Injury, b. C1 Ring and C1-2 Joint Complex Injuries: i. Type A Injury, ii. Type B Injury, iii. Type C Injury, c. C2 and C2-3 Joint Complex Injuries: i. Type A Injury, ii. Type B Injury, iii. Type C Injury

Printed on: 02/07/23



## Abstract Archives of the RSNA, 2022

NREE-72

### Resting-state fMRI Seed-based Connectivity Map as a Diagnostic Visualization Biomarkers in Different Brain Disorders

Sunday, Nov. 27 8:00AM - 9:00AM Room: Learning Center - NR

#### Participants

Mohamed Eid, MD, PhD, (*Presenter*) Nothing to Disclose

#### TEACHING POINTS

We plotted seed based connectivity (SBC) for about 40 main dynamic functional connectivity networks for each cases , then we reviewed the homogeneity of cerebral and cerebellar brain activity in both sides and we determined for epileptic case visualization the sign of Bull's eye of as abnormal disrupted brain activity as a reference for seizer's onset zone (SOZ) .And as regards to the alcohol toxicity induced bilateral total blindness we determine the visualization of normal bilateral dynamic functional connectivity and activity in the occipital networks and compared it to the normal control cases.3o Normal controls cases , 25 clinical confirmed uncontrolled epileptic patients and one case of alcohol toxicity induced total bilateral eyes blindness although normal signal intensities of both optic nerves and chiasm in conventional MRI sequences and MRI post gad contrast.Methods We obtained raw data from MRI Toshiba and Siemens 1.5 Tesla for all cases after written Informed consent as follow ; Bold EPI sequences (as a functional raw data ) about 3:40 minute duration ,High resolution axial T1 WI ( as an anatomical raw data ) , about 3:20 minute.All data preprocessed ,post processed and analysed used MATLAB based softwares , CONN toolbox .

#### TABLE OF CONTENTS/OUTLINE

Abstract Patient Methods Cases and figures / pdf

Printed on: 02/07/23



## Abstract Archives of the RSNA, 2022

NREE-74

### Neurogenetics: What Should the Radiologist Know?

Sunday, Nov. 27 8:00AM - 9:00AM Room: Learning Center - NR

#### Participants

Mario Abizaid, Sao Paulo, Brazil (*Presenter*) Nothing to Disclose

#### TEACHING POINTS

- The autosomal recessive inheritance pattern, although rare, when considered as a group becomes prevalent. Those diseases have an increased prevalence in consanguineous marriage and restricted geographic areas, known as "founder effect".- The autosomal dominant inheritance pattern is seen in heterozygosis and it is inherited from a parent who had the disease (family history). Less frequently, can emerge from a new mutation (mutation of de novo).- The trinucleotide repeat, as in Huntington's disease, is amplified with each generation, due to a misreading in the DNA.- There are mitochondrial proteins produced in the organelle itself (maternal inheritance pattern), as well as produced in the cell nucleus (autosomal or X-linked inheritance pattern).

#### TABLE OF CONTENTS/OUTLINE

Autosomal recessive inheritance pattern  
Metachromatic leukodystrophy  
Horizontal gaze palsy with progressive scoliosis  
CARASIL  
Maple syrup urine disease  
PKAN  
Wilson's disease  
Phenylketonuria  
Autosomal dominant inheritance pattern  
CADASIL  
Neurofibromatosis type 1  
Von Hippel Lindau  
Marfan Syndrome  
Tuberous sclerosis  
.X linked disorders pattern  
X linked adrenoleukodystrophy  
Pelizaeus-Merzbacher disease  
Rett syndrome  
Incontinentia pigmenti  
Trinucleotide repeat expansion  
Huntington's disease  
Fragile x associated tremor ataxia syndrome  
Friedreich ataxia  
Mitochondrial disease  
MELAS  
Leight Syndrome  
LHON  
Kern-Sayres Syndrome  
Oncogenetic proto-oncogene and tumor suppressor gene  
IDH-wildtype and IDH-mutant H3 K27M-mutant  
RELA fusion-positive ependymoma  
medulloblastoma: WNT-activated and SHH-activated  
C19MC-altered

Printed on: 02/07/23



## Abstract Archives of the RSNA, 2022

NREE-75

### Genetic Complexity and Imaging Assessment of the Mitochondrial Disorders

Sunday, Nov. 27 8:00AM - 9:00AM Room: Learning Center - NR

#### Participants

Heber Colares Costa, MD, Rio de Janeiro, Brazil (*Presenter*) Nothing to Disclose

#### TEACHING POINTS

To review the terminology, epidemiology, pathology, clinical and genetic issues of the mitochondrial disorders. To illustrate the imaging highlights of the primary mitochondrial disorders. To demonstrate the most common differential diagnosis based on imaging and epidemiology.

#### TABLE OF CONTENTS/OUTLINE

1. Background with pathological, physiopathological, epidemiological, clinical, and genetic revision of the mitochondrial disorders. 2. Imaging pearls of mitochondrial disorders with an emphasis on MRI patterns and specific diagnoses. 3. Flowchart of assessment of the mitochondrial disorders. 4. Take-home messages.

Printed on: 02/07/23

## Abstract Archives of the RSNA, 2022

NREE-76HC

### Imaging Approach to Intraventricular Masses: Common and Uncommon MR Imaging Findings

Sunday, Nov. 27 8:00AM - 9:00AM Room: Learning Center - NR

#### Participants

Hee Soo Won, (*Presenter*) Nothing to Disclose

#### TEACHING POINTS

To identify normal anatomy of ventricular system. To help narrow the differential diagnosis in intraventricular masses according to their location, patient's age, gender and underlying conditions. To describe the imaging features of intraventricular masses. To review common and uncommon location of intraventricular masses with MR imaging.

#### TABLE OF CONTENTS/OUTLINE

Imaging anatomy of ventricular system Imaging approach to intraventricular mass Review of common and uncommon MR imaging features of the following intraventricular neoplastic and nonneoplastic masses 1. Central neurocytoma 2. Subependymoma 3. glioblastoma 4. Subependymal giant cell astrocytoma 5. Lymphoma 6. Metastasis 7. Choroid plexus tumor 8. Choroid plexus cyst 9. Meningioma 10. Colloid cyst 11. Craniopharyngioma 12. Ependymoma 13. Epidermoid cyst 14. Pleomorphic xanthoastrocytoma 15. Multiple myeloma Summary and conclusion Please visit the Learning Center to also view this presentation in hardcopy format.

Printed on: 02/07/23



## Abstract Archives of the RSNA, 2022

NREE-77

### Consensus Recommendations on Clinical APT-weighted Imaging Approaches at 3T for Brain Tumors

Sunday, Nov. 27 8:00AM - 9:00AM Room: Learning Center - NR

#### Participants

Jinyuan Zhou, PhD, Baltimore, MD (*Presenter*) Inventor, Koninklijke Philips NV; Institutional license agreement, Koninklijke Philips NV; *Speaker*, Koninklijke Philips NV

#### TEACHING POINTS

Currently used amide proton transfer-weighted (APT<sub>w</sub>) MRI protocols vary substantially among different institutes. Thus, the results acquired from different patient studies are difficult to compare, which hampers uniform clinical application and interpretation. The purpose of this education exhibit is: 1) To review challenging issues for clinical APT<sub>w</sub> imaging at 3T. 2) To provide a rationale for optimized and standardized APT<sub>w</sub> brain tumor imaging. 3) To review specific recommendations for pulse sequences, acquisition protocols, and data processing methods for APT<sub>w</sub> imaging of brain tumors. 4) To provide tips for using APT<sub>w</sub> imaging in the clinical setting.

#### TABLE OF CONTENTS/OUTLINE

1) Introduction. 2) APT<sub>w</sub> MRI background and theory. 3) History of the mechanism and the evolution of its understanding. 4) APT<sub>w</sub> imaging pulse sequences, including RF saturation approaches and parameters, lipid suppression, and readout. 5) Acquisition protocols. 6) Data processing and display. 7) Brain tumor APT<sub>w</sub> imaging data interpretation and pitfalls. 8) Conclusions and remarks.

Printed on: 02/07/23



## Abstract Archives of the RSNA, 2022

NREE-78

### Paragangliomas of the Head, Neck, and Spine: Radiologic-Pathologic Correlation

Sunday, Nov. 27 8:00AM - 9:00AM Room: Learning Center - NR

#### Participants

Robert Y. Shih, MD, (*Presenter*) Nothing to Disclose

#### TEACHING POINTS

1. The paraganglia are non-neuronal neuroendocrine cells that are part of the autonomic nervous system and derived from the neural crest. They are named for the location beside the paravertebral sympathetic ganglia. 2. Pheochromocytomas (chromaffin cells) are named for a characteristic brown color change of the paraganglia tissues when fixed in chromium salts, which reflects oxidation of stored catecholamines. These chromaffin cells are found in the adrenal medulla or beside sympathetic ganglia in the abdomen. 3. There is another type of paraganglia, which has chemoreceptor rather than neuroendocrine functions, responsible for increasing respiration in response to acidosis, hypoxia, or hypercarbia. These parasympathetic paraganglia are composed of glomus cells and give rise to paragangliomas of the head and neck. 4. Aside from paragangliomas of the head and neck, paragangliomas of the spine (specifically the cauda equina) are also encountered in neuroradiology. With the 2022 WHO Classification of Endocrine and Neuroendocrine Tumors, these are being reclassified as cauda equina neuroendocrine tumor (NET). 5. Approximately 40% of paragangliomas are related to germline mutations, therefore genetic testing is indicated for all patients. While there are many familial endocrine tumor syndromes, hereditary paraganglioma syndromes involve mutations in succinate dehydrogenase (SDH).

#### TABLE OF CONTENTS/OUTLINE

1. What are the paraganglia? 2. What is the relationship of paragangliomas and pheochromocytomas? 3. What are the classic locations for paragangliomas of the head and neck? 4. What is the classic location for paraganglioma of the spine? 5. What is the significance of germline mutations for paragangliomas?

Printed on: 02/07/23



## Abstract Archives of the RSNA, 2022

NREE-79

### T2-FLAIR Mismatch Sign: My Favorite Evil

Sunday, Nov. 27 8:00AM - 9:00AM Room: Learning Center - NR

#### Participants

Larissa Martins, MD, Sao Paulo, Brazil (*Presenter*) Nothing to Disclose

#### TEACHING POINTS

The purposes of this exhibit are:

- To elucidate the characterization and criteria for the application of the T2-FLAIR mismatch signal, described as one of the main radiophenotypes in neuroradiology, with a specificity close to 100% in the identification of IDH-mutant, 1p/19q-intact lower-grade glioma
- Propose a checklist for the proper identification of the T2-FLAIR mismatch radiophenotype
- Demonstrate practical tips and possible pitfalls to achieve the highest possible positive predictive value when faced with a probable T2-FLAIR mismatch
- Discuss the differential diagnoses of lesions that present a sign of partial T2-FLAIR mismatch\*

• Introduction:

- o Mismatch T2-FLAIR: What is it?
- o Differential Diagnosis
- Checklist for the proper identification of the T2-FLAIR mismatch
- Practical examples of lesions with true T2-FLAIR mismatch and lesions that mimic this radiophenotype
- Differential diagnoses of lesions that present a sign of partial T2-FLAIR mismatch

Printed on: 02/07/23



## Abstract Archives of the RSNA, 2022

NREE-8

### Expand The Differential - An Interesting Case Series of Bithalamic Pathology

Sunday, Nov. 27 8:00AM - 9:00AM Room: Learning Center - NR

#### Participants

David Wessling, MD, Council Bluffs, IA (*Presenter*) Nothing to Disclose

#### TEACHING POINTS

This education exhibit presents a series of unique pathologies that lead to bilateral thalamic region imaging abnormalities. Our intention is to demonstrate numerous pathologies, expand the differential considerations of bithalamic lesions and raise the awareness of less commonly encountered disease processes. Many of the cases chosen were either were initially misinterpreted or puzzled the neuroradiologists at our academic institution. Many of the cases required multiple imaging modalities including advanced imaging techniques such as perfusion, diffusion tensor imaging and spectroscopy to either make a diagnosis, narrow the differential, or guide further management. Our aim with creating this exhibit is to describe the clinical presentation, demonstrate imaging appearances and defining characteristics, and provide interpretation of studies across multiple imaging modalities. Additionally, an explanation for how each study aids the radiologist's impression is provided. Our exhibit will advance the audience's comfort when faced with interpreting bithalamic imaging abnormalities. This will help to minimize patient harm from unnecessary intervention or delayed diagnosis.

#### TABLE OF CONTENTS/OUTLINE

This exhibit is intended to serve as a collection of interesting disease processes with bithalamic involvement. Specific interests will be given to cases utilizing multiple different imaging modalities and those which required advanced imaging techniques. These cases will be organized categorically; vascular, metabolic/toxic, neoplastic, inflammatory, infectious and seizures. Tables and diagrams will be created to highlight similarities and differences when applicable.

Printed on: 02/07/23



## Abstract Archives of the RSNA, 2022

NREE-80HC

### Machine Learning in Alzheimer's Disease: Diagnostic Classification Using MR Neuroimaging Data

Sunday, Nov. 27 8:00AM - 9:00AM Room: Learning Center - NR

#### Participants

Stephanos Leandrou, PhD, MSc, (*Presenter*) Nothing to Disclose

#### TEACHING POINTS

Alzheimer's Disease (AD) is a neurodegenerative disease and its diagnosis relies mainly on cognitive tests. An important limitation of cognitive tests is the diagnosis of AD after structural changes have occurred within the brain. Therefore, these patients have a long prodromal phase when effective treatment strategies may be applied to delay or alter the onset of the symptoms. Research on quantitative MRI-derived biomarkers is an active research area which detects brain neurodegeneration before AD symptoms appear. In this study multi-modal features from both entorhinal cortex (ERC) and hippocampus were extracted from 194 normal controls (NC), 284 mild cognitive impairment (MCI) and 130 AD subjects. Texture analysis was mainly used which evaluates statistical properties of the tissue image quantitatively; therefore, it could detect smaller-scale changes of neurodegeneration. The use of ERC texture features is very limited in the literature, however, it is the first structure affected. We hypothesized that through the earlier involvement of ERC and the use of texture features, it is likely to detect microscopic alterations of the disease before atrophy spreads. This study used Machine Learning (ML) methods to address high dimensional data and discover new biomarkers in the assessment of AD. These directions will help to manage the disease progression and develop novel treatment strategies. This study innovates by using multi-modal data (incl. ERC) in the assessment of AD through a ML-based classification. An area under curve of 0.940, 0.806, and 0.786 was seen between NC vs AD, NC vs MCI and MCI vs AD subjects, respectively.

#### TABLE OF CONTENTS/OUTLINE

PurposeReviewMethodsResultsConclusionsReferencesPlease visit the Learning Center to also view this presentation in hardcopy format.

Printed on: 02/07/23



## Abstract Archives of the RSNA, 2022

NREE-82

### Learning from Machines: A Resident's Guide to AI Mistakes in Neuroradiology and What Residents Can Learn From Them

Sunday, Nov. 27 8:00AM - 9:00AM Room: Learning Center - NR

#### Awards

Certificate of Merit

#### Participants

Austin Young, (*Presenter*) Nothing to Disclose

#### TEACHING POINTS

With the steady advancement of computer vision technology, artificial intelligence (AI) algorithms have been shown to outperform radiologists in certain imaging interpretation tasks [1]. These technologies have been increasingly applied in clinical practice to aid in detection/diagnosis, disease prediction, and image segmentation [2]. Our institution has recently acquired an AI software package that allows for detection of acute hemorrhage, large vessel occlusion, and quantitative evaluation of perfusion deficits. This software package is expected to help provide a more prompt and accurate diagnosis by delivering qualitative and quantitative analysis of critical findings [3]. In this exhibit we highlight common pathologies where AI interpretation was discordant with the underlying pathology as determined by final attending interpretation, highlighting potential pitfalls in overreliance on this new technology in imaging interpretation. As we analyze these cases, an emphasis will be placed on the human component of imaging, how information must be integrated and synthesized to arrive at a proper diagnosis with the goal of providing direction for future deep learning algorithms and improved resident education.

#### TABLE OF CONTENTS/OUTLINE

Case 1: Pseudo-subarachnoid hemorrhage incorrectly interpreted as true hemorrhage Case 2: Erroneous interpretation of decreased blood vessel density secondary to subdural hematoma Case 3: Presence of endovascular coils causing false interpretation of large vessel occlusion Case 4: Erroneous interpretation of decreased blood vessel density due to intraparenchymal hemorrhage Case 5: Cortical laminar necrosis wrongly interpreted as subarachnoid hemorrhage

Printed on: 02/07/23



## Abstract Archives of the RSNA, 2022

NREE-83

### Decoding White Matter Tracts in Brain : Role of Diffusion Tensor Imaging (DTI) and Tractography in Brain Tumors

Sunday, Nov. 27 8:00AM - 9:00AM Room: Learning Center - NR

#### Participants

Dinesh Meher, MBBS, MD, Delhi, India (*Presenter*) Nothing to Disclose

#### TEACHING POINTS

The purpose of this exhibit is to : 1.Discuss the construction of various white matter tractograms using appropriate regions of interest (ROIs). 2.Illustrate white matter tract pathological spectrum in various intra and extra axial brain tumors. 3.Review the importance of information provided by Diffusion tensor imaging (DTI) in addition to conventional MR imaging. 4.Discuss the importance of DTI in pre operative evaluation of brain tumors.

#### TABLE OF CONTENTS/OUTLINE

1.Introduction 2.DTI Physics 3.Normal white matter tracts in DTI 4.DTI patterns in brain tumors 5.Cases 6.Take home message

Printed on: 02/07/23



## Abstract Archives of the RSNA, 2022

NREE-84

### OpenAI, SciSpacy, Supervised Machine Learning, and Deep Learning for Automated Data Extraction from Radiology Reports

Sunday, Nov. 27 8:00AM - 9:00AM Room: Learning Center - NR

#### Participants

Ethan Wang, Dallas, TX (*Presenter*) Nothing to Disclose

#### TEACHING POINTS

1. Review how various natural language processing (NLP) techniques can be applied to optimize radiological text analysis involving binary classification and disease entity recognition. 2. Review the intricacies of Bag of Words text representation, supervised machine learning, pre-trained SciSpacy models, and fine-tuned OpenAI engine implementation for radiological text analysis. 3. Review the advantages, limitations, and optimal scenarios of different NLP approaches for radiological text analysis.

#### TABLE OF CONTENTS/OUTLINE

1. Introduction to NLP 2. Traditional NLP Applications for Binary Classification (BoW text representation, Deep Neural Networks, Supervised Machine Learning Algorithms) 3. Pre-Trained SciSpacy Models for Binary Classification and Disease Entity Extraction 4. Fine-Tuning OpenAI Engines for Binary Classification and Disease Entity Extraction 5. Advantages and Limitations of NLP (Time Expenditure, Flexibility, Integration with Traditional Statistics, Association with Task Complexity)

Printed on: 02/07/23



## Abstract Archives of the RSNA, 2022

NREE-86

### Arterial Spin Labeling Perfusion Technique in Neurovascular Diseases: Technical Aspects, Artifacts and Clinical Applications

Sunday, Nov. 27 8:00AM - 9:00AM Room: Learning Center - NR

#### Participants

Carlos Basoa Ramos, MD, Bilbao, Spain (*Presenter*) Nothing to Disclose

#### TEACHING POINTS

- To review the technical principles of the Arterial Spin Labelling (ASL) technique.
- To list the main artifacts that radiologists should be aware of.
- To review the main applications of the ASL technique, with special attention to neurovascular pathology (acute and chronic ischemia, arteriovenous shunt and moya-moya disease, among others).

#### TABLE OF CONTENTS/OUTLINE

ASL is an underused magnetic resonance imaging (MRI) technique that uses water molecules within arterial blood as endogenous contrast to obtain quantitative information of cerebral blood flow (CBF). Thus, ASL does not use exogenous contrast agents, being an alternative to other more established MRI perfusion techniques. Radiofrequency pulses are applied proximal to the brain, at neck vessels, to obtain an inversion of longitudinal magnetization of arterial blood water molecules. This process is called labelling. After a short period of time called post labelling delay (PLD) imaging is performed. Two imaging acquisitions are made, one unlabelled and one labelled. Subtraction of the unlabelled images will provide cerebral perfusion data. There are multiple labelling techniques but nowadays guidelines recommend implementation of 3D pseudocontinuous ASL (PCASL) in clinical practice. ASL has been studied and compared as well with other perfusion MRI techniques in neurodegenerative diseases, neuro-oncology, and neurovascular diseases. ASL technique is a useful technique in neurovascular pathology, especially in the control of patients with treated arteriovenous malformations.

Printed on: 02/07/23



## Abstract Archives of the RSNA, 2022

NREE-87

### What Brain Perfusion is Telling You and You Might Not Have Noticed

Sunday, Nov. 27 8:00AM - 9:00AM Room: Learning Center - NR

#### Participants

David Castanedo SR, MD, Santander, Spain (*Presenter*) Nothing to Disclose

#### TEACHING POINTS

- To analyze the most frequent perfusion alterations on perfusion CT (TCP) associated with "stroke mimics" . - To differentiate between real and false ischemic penumbras. - To identify the main pitfalls when analyzing these studies.

#### TABLE OF CONTENTS/OUTLINE

1. Introduction.2. Analysis parameters.3. Introduction to perfusion anomalies.4. Imaging protocol.5. Clinical cases.5.1. Hyperperfusion.5.1.1. Epileptic seizure (ictal phase).5.1.2. High-grade gliomas.5.1.3. Reversible Posterior Encephalopathy Syndrome (PRES).5.1.4. Reperfusion/Hyperperfusion Syndrome.5.1.5. Viral encephalitis.5.2. Hypoperfusion.5.2.1. Transient ischemic accident (TIA).5.2.2. Vasospasm. 5.2.3.Bilateral carotid stenosis.5.2.4. Cerebral venous thrombosis.5.2.5. Migraine with aura.5.2.6. Hypoglycemia.5.2.6. Arterio-Venous Fistula Dural.5.3. Gray or conflictive areas.5.3.1. Chronic infarctions and "luxury perfusion"5.3.2. Lacunary infarctions.5.3.3. Crossed cerebellar diaschisis.5.3.4. Motion artifacts.5.3.5. Arterial and venous time-attenuation curves.5.3.6. Threshold values in color maps.5.3.7. Post-processing software.6. Take Home Messages.

Printed on: 02/07/23



## Abstract Archives of the RSNA, 2022

NREE-88

### The Multiple Faces of Typical Atypical Primary Central Nervous System Lymphomas

Sunday, Nov. 27 8:00AM - 9:00AM Room: Learning Center - NR

#### Participants

Irene Dixe de Oliveira Santo, MD, New Haven, CT (*Presenter*) Nothing to Disclose

#### TEACHING POINTS

1. Review the demographics, differential diagnosis, and current standard for definitive diagnosis of primary central nervous system lymphoma 2. Describe the imaging features of typical and atypical PCNSL, including location, enhancement pattern, signal intensity in multiple sequences, presence or absence of hemorrhage, necrosis and calcification 3. Educate the radiologist regarding the differences in management of PCNSL and its main differential diagnoses, and discuss why prompt diagnosis is crucial for improved outcomes 4. Provide a brief outline of currently under investigation alternative methods for earlier and less invasive PCNSL diagnosis and classification, including the role of systematic classification tools and machine learning algorithms

#### TABLE OF CONTENTS/OUTLINE

- Demographics of PCNSL
- Presentation, important clinical features and imaging findings of multiple typical and atypical histologically-proven PCNSL patients from our institution (71 patients available)
- Differential diagnoses of PCNSL
- Definitive diagnosis of PCNSL
- Management of PCNSL vs management of its main differential diagnosis
- Alternative methods for earlier and less invasive PCNSL diagnosis and classification

Printed on: 02/07/23



## Abstract Archives of the RSNA, 2022

NREE-89

### Finding the Specific in Non-Specific: Imaging in Acute Decompensation in Inherited Metabolic Disorders

Sunday, Nov. 27 8:00AM - 9:00AM Room: Learning Center - NR

#### Participants

Garima Sharma, MBBS, MD, (*Presenter*) Nothing to Disclose

#### TEACHING POINTS

Most inherited metabolic disorders present as a severe progressive illness, however, some of them are often complicated by acute decompensation. These events are precipitated by the accumulation of toxic metabolites leading to encephalopathy and severe neurological injury. The factors triggering such episodes are generally states of an increased catabolic state, i.e., infection, trauma, or even increased consumption of any specific food component. While imaging is often ordered along with other investigations for a complete evaluation, most of the time the findings are labeled as non-specific. Hence, it is important for the radiologist to know: a)The metabolic disorders which can present as metabolic compensation b)Clinical clues and biochemistry c)Specific imaging features for various entities d) Mimics and major differential diagnosis. The most important mimics for these entities are hypoxic-ischemic injuries, sepsis, and vascular events (e.g. stroke). Magnetic Resonance Imaging (MRI) is the most important imaging modality for adequate evaluation of these patients.

#### TABLE OF CONTENTS/OUTLINE

1. Introduction
2. Causes of acute decompensation in inherited metabolic disorders
3. Clinical presentations
4. Understanding the biochemistry
5. Role of imaging
6. Specific imaging features
  - a. Organic acidemias
  - b. Urea cycle disorders
  - c. Maple syrup urine disease
  - d. Fatty acid oxidation defects
  - e. Glycogen storage disease (type I)
  - f. Leighs Disease

Printed on: 02/07/23



## Abstract Archives of the RSNA, 2022

NREE-9

### Cytokines and the Central Nervous System: What the Radiologists Should Know

Sunday, Nov. 27 8:00AM - 9:00AM Room: Learning Center - NR

#### Awards

Identified for RadioGraphics

#### Participants

Mariko Kurokawa, MD, Ann Arbor, MI (*Presenter*) Nothing to Disclose

#### TEACHING POINTS

- Understand the role and mechanism of cytokines that affect the central nervous system (CNS), which often cause encephalitis/encephalopathy and cerebrovascular diseases.
- Identify the causes, clinical features, and imaging features of cytokine storm.
- Summarize cytokine engaging therapy including interferon-beta and chimeric antigen receptor (CAR) T-cell therapy with focus on the neuroradiological changes before and after treatment.

#### TABLE OF CONTENTS/OUTLINE

1. Cytokines and signaling pathways  
2. Cytokine storm and CNS: Mechanisms, Acute necrotizing encephalopathy (ANE), Cytotoxic lesion of the corpus callosum (CLOCC), Virus-associated necrotizing disseminated acute leukoencephalopathy (VANDEL), Acute disseminated encephalomyelitis (ADEM), Thromboembolism, Hemorrhage  
3. Cytokines and neurological diseases: Demyelinating diseases (multiple sclerosis, MS), Acute and chronic infarction, Tumors (Chordoma and angiomatoid fibrous histiocytoma), Castleman's diseases, and Mastocytosis  
4. Cytokine engaging therapy and neuroimaging: Interferon (IFN) beta for MS treatment, IFN alpha for lymphoma and malignant melanoma, Cytokine releasing syndrome in CAR-T therapy  
5. Summary

Printed on: 02/07/23



## Abstract Archives of the RSNA, 2022

NREE-90

### Retinoblastoma: Beyond What the Eyes Can See

Sunday, Nov. 27 8:00AM - 9:00AM Room: Learning Center - NR

#### Awards

Cum Laude

#### Participants

Taisa Guarilha, MD, Sao Paulo, Brazil (*Presenter*) Nothing to Disclose

#### TEACHING POINTS

Retinoblastomas are the most prevalent form of eye cancer in children, mostly occurring in first infancy. Most of them are diagnosed by the detection of leukocoria at ophthalmologist clinics. Nonetheless, image analysis performed by a radiologist can provide an assessment of key features that highly impact prognosis and treatment definition. We can see beyond the eye by detecting optic nerve involvement, extraocular tumor, and intracranial extension. The goal of this paper are: Review the anatomy of the orbit region Discuss epidemiology and clinical findings Demonstrate how retinoblastomas can present itself Exemplify the six groups according to the Grouping Classification of Retinoblastoma Features Demonstrate common and uncommon metastasis Show differential diagnosis

#### TABLE OF CONTENTS/OUTLINE

> Anatomy of the orbit region > Epidemiology and clinical findings > Imaging features > Present and explain cases from groups A to F from the Grouping Classification of Retinoblastoma Features > Metastasis: -optic nerve involvement-trilateral retinoblastoma-intracranial metastasis-spinal metastasis-leptomeningeal metastasis -abdominal metastasis-bone metastasis > Differential diagnosis: - Coats Disease- Medulloepithelioma- Retinal Hamartoma - Persistent hyperplastic primary vitreous- Optic pathway glioma-Meningioma > Postoperative control findings

Printed on: 02/07/23



## Abstract Archives of the RSNA, 2022

NREE-91

### The New Horizons of Neuroimaging in Recognition of Patterns of Genetic-Phenotypic Lissencephaly Spectrum

Sunday, Nov. 27 8:00AM - 9:00AM Room: Learning Center - NR

#### Participants

Heber Colares Costa, MD, Rio de Janeiro, Brazil (*Presenter*) Nothing to Disclose

#### TEACHING POINTS

To illustrate the imaging spectrum of lissencephaly spectrum along with their genetic relationship. To exemplify the classification systems based on the most likely causative genes. To demonstrate the challenges of the new imaging and severity classification tools to guide and prioritize genetic testing for patients' clinical management and genetic counseling. To depict the differential diagnoses and a flowchart for assessing the lissencephaly spectrum.

#### TABLE OF CONTENTS/OUTLINE

1. Background. 2. Imaging protocol. 3. Clinical perspective and importance of analysis of lissencephaly spectrum. 4. The genetic cascade of events implicated in cortical development. 5. Imaging assessment and their correlation with the genetic abnormalities. 6. Imaging pearls correlated with the lissencephaly spectrum. 7. Differential diagnoses. 8. Flowchart for imaging assessment. 9. Take-Home messages.

Printed on: 02/07/23



## Abstract Archives of the RSNA, 2022

NREE-92

### Neurocutaneous Diseases, Clues for Neuroradiology Findings

Sunday, Nov. 27 8:00AM - 9:00AM Room: Learning Center - NR

#### Participants

Karla Fuentes Badillo, MD, (*Presenter*) Nothing to Disclose

#### TEACHING POINTS

Neurofibromatosis Type I Characterized by the involvement of the nerve sheath. Imaging findings include white matter lesions, bone lesion associated with plexiform neurofibromas, focal areas of signal intensity hyperintense in T2, plexiform and paraspinal neurofibromas. Neurofibromatosis Type II NF2 is a hereditary syndrome characterized by multiple cranial nerve schwannomas, specifically with bilateral vestibular schwannomas, meningiomas and spinal tumors. They can be evaluated on CT but are better characterized by MRI. Tuberous Sclerosis Complex Characterized by the presence of hamartomas. Cortical tubers appear in 95% of patients, subependymal giant cell astrocytomas tend to have intense enhancement, white matter abnormalities with variable appearance and subependymal nodules. Sturge Weber Syndrome Characterized by detects subcortical calcification at an earlier age than plain film and can also demonstrate associated parenchymal volume loss, tram-track sign of cortical and subcortical calcification. Von Hippel Lindau The most common lesions are retinal angiomas, hemangioblastomas of the cerebellum and spinal cord, visceral cyst and tumors. HGBL is seen as a well-defined cerebellar cyst with nodule on NECT, on MR imaging on T1 is observed as an iso/hypointense nodule with Flow voids (large feeding vessels within the periphery), while on T2/FLAIR is evidenced as a hyperintense nodule, which blooms in case of hemorrhage and enhances strongly without changes on cyst wall.

#### TABLE OF CONTENTS/OUTLINE

Neurofibromatosis Type I, Neurofibromatosis Type II, Tuberous Sclerosis, Sturge Weber, Von Hippel Lindau

Printed on: 02/07/23



## Abstract Archives of the RSNA, 2022

NREE-93

### Reinvent the Dragonfly: Pontocerebellar Hypoplasia Imaging and Genetics

Sunday, Nov. 27 8:00AM - 9:00AM Room: Learning Center - NR

#### Participants

Heber Colares Costa, MD, Rio de Janeiro, Brazil (*Presenter*) Nothing to Disclose

#### TEACHING POINTS

To demonstrate the spectrum of pontocerebellar hypoplasia through MRI, emphasizing the dragonfly signal sometimes present. To explain the physiopathology and genetic cascade involved. To demonstrate the imaging pearls with emphasis on the differential diagnosis.

#### TABLE OF CONTENTS/OUTLINE

1. Background. 2. Imaging protocol. 3. Clinical perspective and importance of analysis of pontocerebellar hypoplasia through MRI. 4. The genetic cascade of events implicated in the pontocerebellar hypoplasia. 5. Imaging pearls, including the dragonfly signal. 6. Differential diagnosis. 7. Flowchart for imaging assessment. 8. Take-Home messages.

Printed on: 02/07/23

## Abstract Archives of the RSNA, 2022

NREE-94

### Microtubulin Dysfunction - Key Imaging Features

Sunday, Nov. 27 8:00AM - 9:00AM Room: Learning Center - NR

#### Participants

Joel Samuel, MBBS, MD, (*Presenter*) Nothing to Disclose

#### TEACHING POINTS

Neurological abnormalities found on MRI brain in tubulinopathies predominantly consists of dysmorphic basal ganglia(90%),cerebral cortical malformations(60%), microcephaly(30%),callosal abnormalities(80%), ventriculomegaly(90%), asymmetric brain stem(60%), andsmall cerebellar vermis or hemispheres(50%).

#### TABLE OF CONTENTS/OUTLINE

**LEARNING OBJECTIVE:**The aim of this study is to describe the spectrum of key imaging findings associated with Tubulinopathies.

**BACKGROUND:**Tubulinopathies are a heterogenous group of rare disorders that lead to complex brain malformation ,caused by mutation in tubulin genes.**Study design:**The study included MRI brain of 10 patients with symptoms of developemental delay, microcephaly, seizures and imaging features suggestive of tubulinopathies were studied over a period of three years.**Microcephaly, cerebral cortical malformations, callosal abnormalities,ventriculomegaly, dysmorphic basal ganglia,hypoplasia of internal capsule, asymmetric brain stem, and small cerebellar vermis or hemispheres were the predominant finding seen in**

**MRI.CONCLUSION:**Knowledge of the main imaging findings of tubulinopathies is critical. Given the rarity of these conditions and lack of discriminating clinical features, imaging may be the only clue to an underlying tubulinopathy. Also helps in further genetic workup for these patients and identifying the gene mutated and helps in treatment .

Printed on: 02/07/23



## Abstract Archives of the RSNA, 2022

NREE-95

### Imaging Abnormalities in Patients with Alzheimers Disease Treated with Anti-Amyloid Beta Therapy

Sunday, Nov. 27 8:00AM - 9:00AM Room: Learning Center - NR

#### Awards

Identified for RadioGraphics

#### Participants

Amit K. Agarwal, MD, MBBS, Jacksonville, FL (*Presenter*) Stockholder, Gilead Sciences, Inc

#### TEACHING POINTS

-To discuss the novel therapeutic strategies for Alzheimer's disease, with focus on the recently approved anti-amyloid beta therapy- To illustrate the imaging abnormalities in patients with Alzheimer's Disease treated with Anti-Amyloid Beta Therapy- To discuss the protocol for monitoring and assessment for imaging abnormalities in patients on Anti-Amyloid Beta Therapy- To discuss the imaging differentials of ARIA ( with focus on cerebral amyloid angiopathy)

#### TABLE OF CONTENTS/OUTLINE

-Neuropathology of Alzheimer's disease (AD)-Role of cerebral amyloid-B (Ab) in Alzheimer's disease-Brief discussion on current imaging modalities for diagnosis and monitoring of AD (MRI, Amyloid PET,Tau PET)-Therapeutic strategies against amyloid- $\beta$  peptides in Alzheimer's disease- Imaging Abnormalities in Patients with Alzheimer's Disease Treated with Anti-Amyloid Beta Therapy - Amyloid-related imaging abnormalities: edema (ARIA-E) and hemorrhage(ARIA-H)- International Collaboration for Real-World Evidence in Alzheimer's Disease (ICARE AD) -MRI Acquisition Protocol Proposed to ICARE AD Sites ARIA Monitoring- Imaging differentials of ARIA (cerebral amyloid angiopathy, PRES)

Printed on: 02/07/23

## Abstract Archives of the RSNA, 2022

NREE-96

### How Much Do You Know About MRI Patterns of Brainstem Inflammatory Lesions?

Sunday, Nov. 27 8:00AM - 9:00AM Room: Learning Center - NR

#### Participants

Carlota Garcia de Andoin Sojo, MD, Bilbao, Spain (*Presenter*) Nothing to Disclose

#### TEACHING POINTS

When facing inflammatory lesions of the brainstem there are a number of differential diagnoses and accurate diagnosis can be difficult. Knowing clinical features and MRI findings, especially on the extent of dissemination, number, morphology and appearance of the lesions in different MRI sequences radiologists will be able to reach the correct diagnosis.

#### TABLE OF CONTENTS/OUTLINE

Objective: To describe MRI findings of major inflammatory and immune-mediated diseases that affect the brainstem. Methods A revision of the most characteristic inflammatory lesions of the brainstem has been made in MRI-illustrated challenging quiz format. Findings 1. Immune-mediated inflammatory disorders: illustrated quiz-mode cases will lead to the revision of disorders that involve the brainstem, including Multiple Sclerosis, Neuromyelitis Optica Spectrum Disorder, Myelin Oligodendrocyte Glycoprotein antibody-induced demyelination, Neuro-Behçet, Neurosarcoidosis, Histiocytic disorders, Bickerstaff Brainstem Encephalitis, Acute Haemorrhagic Encephalomyelitis, Hurst disease, Systemic Lupus Erythematosus 2. Differential diagnosis should be done having in mind MRI and clinical features of other diseases that also cause brainstem inflammation, such as paraneoplastic encephalitis, Alexander leukodystrophy, Wilson disease, Wernicke-Korsakoff syndrome and CNS infections (listeria, tuberculosis and enterovirus). Conclusion Knowing the typical MRI presentation of each of the disorders that cause brainstem inflammations radiologists can give important information to achieve an accurate diagnosis and establish appropriate treatments.

Printed on: 02/07/23



## Abstract Archives of the RSNA, 2022

NREE-97

### The Radiologist's Guide to Non-Traumatic Orbital Pathology

Sunday, Nov. 27 8:00AM - 9:00AM Room: Learning Center - NR

#### Participants

Emily Haas, MD, (*Presenter*) Nothing to Disclose

#### TEACHING POINTS

Orbital pathology identification and diagnosis is of critical importance as delayed diagnosis and management may ultimately result in vision loss for many patients. Development of an appropriate differential diagnosis of orbital lesions is vital as to guide our clinician colleagues in appropriate next steps and future follow-up. This educational exhibit aims to review orbital anatomy and explore non-traumatic orbital pathology by underlying etiology. While there may be overlap in imaging features, we will discuss characteristic imaging findings for each diagnosis that help to distinguish them amongst each other and alleviate diagnostic dilemma.

#### TABLE OF CONTENTS/OUTLINE

1. Vascular: Venous Malformation, Capillary Hemangioma, Orbital Varix, Carotid-Cavernous Fistula, Lymphatic Malformation, Granulomatosis with Polyangiitis (GPA). 2. Infectious/ Inflammatory: Pre-septal Cellulitis, Post-septal Cellulitis, Orbital Abscess, Dacryocystitis, Invasive Fungal Infection, Optic Neuritis, Idiopathic Orbital Inflammation, Thyroid-Associated Orbitopathy, Papilledema. 3. Neoplastic: Optic Nerve Sheath Meningioma, Optic Glioma, Rhabdomyosarcoma, Dermoid, Lymphoproliferative Disorders, Metastases.

Printed on: 02/07/23



## Abstract Archives of the RSNA, 2022

NREE-98

### Imaging of Headache in Relation to CSF Pressure/Volume Problem: What Radiologists Need to Know

Sunday, Nov. 27 8:00AM - 9:00AM Room: Learning Center - NR

#### Participants

Hyeonwoo Kim, MD, Seoul, Korea, Republic Of (*Presenter*) Nothing to Disclose

#### TEACHING POINTS

Brain and spine imagings are key components in diagnosis and treatment strategy of SIH and IIH. After reviewing this educational exhibition, radiology residents should be able to understand clinical manifestations in headaches with CSF pressure/volume problem and how to approach imaging diagnosis with better imaging protocols.

#### TABLE OF CONTENTS/OUTLINE

New onset or progressive headache is often the most common symptom of intracranial hypotension or hypertension syndrome. In spite of imaging advances, spontaneous intracranial hypotension (SIH) and idiopathic intracranial hypertension (IIH) are often misdiagnosed and if untreated, lead to severe neurologic impairment such as cognitive decline for SIH or visual impairment for IIH. The purpose of this educational exhibition is to review the related imaging findings of intracranial hypotension or hypertension and the suggested imaging protocols in patients with headache associated with CSF problem. We retrospectively evaluated MR images and clinical reports of headache patients collected at our hospital from 2011 to 2021. Contents Organization 1. Introduction 2. SIH 1) clinical manifestation 2) brain imaging for SIH 3) spine imaging for CSF leak 4) suggested imaging protocol 3. IIH 1) clinical manifestation 2) brain imaging for IIH 3) suggested imaging protocol 4. New concept of CSF physiology and glymphatic in relation to SIH and IIH 5. Summary

Printed on: 02/07/23



## Abstract Archives of the RSNA, 2022

NREE-99

### Carotid Cavernous Fistula: Classification, Arterial and Venous Anatomy, Clinical Presentation and Diagnosis and Endovascular Approach

Sunday, Nov. 27 8:00AM - 9:00AM Room: Learning Center - NR

#### Participants

Shadab Alam, MBBS, BANGALORE, India (*Presenter*) Nothing to Disclose

#### TEACHING POINTS

1) Carotid cavernous fistula (CCF) are classified hemodynamically as high flow and low flow, etiologically as spontaneous, traumatic and Iatrogenic and anatomically as direct and indirect. 2) Clinical presentation is influenced by venous drainage patterns and shunt flow rate. 3) Endovascular approach depends on the type of CCF and angiographic findings which could be transarterial or transvenous. 4) Alternative approach for indirect CCF include transorbital superior ophthalmic vein approach and transfemoral Superior Petrosal Sinus Approach

#### TABLE OF CONTENTS/OUTLINE

The exhibit will include: Classification of CCF. Arterial and venous anatomy with emphasis on the ECA and ICA anastomosis. Various clinical presentation. Imaging appearance of CCF. Angiographic anatomy and angiographic check list to plan treatment. Illustration interventional hardware for treatment planning. Case illustration of various treatment options like Transarterial coiling, parent artery occlusion, coil plus EVOH Embolisation, transvenous approach, various alternative approaches with case illustrations. Tips and tricks planning and execution of cases.

Printed on: 02/07/23

## Abstract Archives of the RSNA, 2022

OBEE

### OB/Gynecology Education Exhibits

Sunday, Nov. 27 8:00AM - 9:00AM Room: Learning Center - OB

#### Sub-Events

#### **OBEE-1 How To Expand Your Diagnosis of Deep Endometriosis on Routine Pelvic Imaging**

Participants

Scott Young, MD, Phoenix, AZ (*Presenter*) Nothing to Disclose

#### TEACHING POINTS

Review uterine video clips on routine pelvic ultrasound and evaluate sliding sign maneuvers, differences in technique depending on uterine version. -Accurately locate important anatomical landmarks, including the torus uterinus and uterosacral ligaments on TVUS. -Understand how DE observations may appear different depending on uterine version and transducer position in the anterior and posterior vaginal fornices. -Recognize characteristics of DE bowel observations and assess bowel DE size and depth of invasion, critical factors which guide the level of surgical expertise required for resection. How to recognize DE on routine CT and MR examinations performed for clinical indications other than endometriosis. -Recognize characteristics of DE observations outside the pelvic compartments on routine CT, MSK pelvic, and non-dedicated abdominopelvic MR. -Utilize cues including location, signal, and enhancement characteristics to make an early diagnosis of DE.

#### TABLE OF CONTENTS/OUTLINE

1. Title 2. Disclosures 3. Learning objectives 4. Pelvic anatomy review-Uterosacral ligament (USL)/torus uterinus-Relationship of USL to transducer position and uterine version-Surgically relevant measurements/observations-Case examples of normal and abnormal TVUS video sweeps of anterior and posterior fornix view for each uterine flexion/version-5. US of bowel endometriosis-Schematic/operative images-Case examples with pertinent measurements 6. Extrapelvic and uncommon DE locations-Anatomic hypothesis of extraperitoneal spread-CT and MR enhancement/signal characteristics-Schematic/operative images 7. Conclusion 8. References

#### **OBEE-10 Post-treatment Complications of Gynecologic Malignancies**

Participants

Tsukasa Saida, MD, Tsukuba, Japan (*Presenter*) Nothing to Disclose

#### TEACHING POINTS

Radiologists need to be familiar with the imaging findings of the various complications that can occur in the treatment of gynecologic tumors and understand the urgency and symptoms of each. In this exhibition, we introduce various complications derived from gynecologic surgery and pelvis radiation therapy, and explain the diagnostic points of each complication. The teaching points of this exhibit are: 1. We classified postoperative complications immediately after surgery, subacute, and delayed complications. Complications immediately after surgery are caused by direct injury caused by surgical procedures. Subacute complications include infection, chylous ascites, deep venous thrombosis, and neuropathy. Delayed include, intestinal obstruction, hydronephrosis, lymphedema, and abdominal incisional hernia. 2. Radiation-induced complications can be divided into acute and chronic effects. Acute effects occur during or immediately after radiation therapy, are reversible, and in most cases, the conservative treatment leaves no disability. Chronic effects include cervical stenosis, small bowel stricture, fistula formation, and insufficiency fractures that occur a few months later.

#### TABLE OF CONTENTS/OUTLINE

A. Complications after surgery (Immediately after surgery, Subacute, Delayed) B. Radiation-induced effects (Early effects, Late effects)

#### **OBEE-11 Phenotypic Diversity of Uterine Mesenchymal Tumors (Excluding Smooth Muscle Tumors): Current Update on Genetics and Imaging**

Participants

Steven Chua, MD, PhD, Houston, TX (*Presenter*) Nothing to Disclose

#### TEACHING POINTS

1. Discuss the taxonomy, epidemiology, clinical features, histopathology and biology of the diverse spectrum of mesenchymal, non-smooth muscle tumors of the uterus. 2. Describe the salient multimodality cross-sectional imaging features of these tumors. 3. Review the genetics, management and prognosis of these tumors.

#### TABLE OF CONTENTS/OUTLINE

1. Introduction, epidemiology and clinical features of mesenchymal, non-smooth muscle tumors of the uterus. 2. Histopathological, immunohistochemistry and molecular pathology. 3. CT, MR and PET/CT imaging features and tumor biology of this wide spectrum of

tumors.4. Prognosis and management. \* Low grade Endometrial stromal sarcoma.\* High grade Endometrial stroma sarcoma.\* Adenosarcoma\* Carcinosarcoma\* Undifferentiated sarcoma.\* Uterine tumor resembling sex cord stromal tumor.\* PEComa.\* Inflammatory myofibroblastic tumor.\* Solitary fibrous tumor. Conclusion.

#### **OBEE-12 Management and Imaging Evaluation of Peripartum Hemorrhage: What Radiologists Need to Know**

Participants

Moataz Ahmed Sayed Mohammed Soliman, MD, MSc, CHICAGO, IL (*Presenter*) Nothing to Disclose

##### **TEACHING POINTS**

- Understand normal imaging findings of the utero-fetal complex.
- Recognize multimodality imaging findings of conditions predisposing to peripartum hemorrhage.
- Discuss Imaging pitfalls for peripartum hemorrhage.
- Impact of the preoperative radiological diagnosis on management and role of radiologists.

##### **TABLE OF CONTENTS/OUTLINE**

1. Introduction: a. Normal imaging anatomy of the uteroplacental complex 2. Ante-partum hemorrhage: a. Definitions b. Etiology: (Placental abruption, Placenta previa, Gestational trophoblastic disease, Vasa Previa, Uterine rupture) c. Management 3. Postpartum hemorrhage a. Definitions b. Normal imaging findings of the postpartum uterus. c. Classification and risk factors i. Primary postpartum hemorrhage: (Uterine atony, traumatic pelvic hematoma, bladder flap hematoma, retained products of conception, coagulopathies, and placenta accrete spectrum) ii. Secondary postpartum hemorrhage: (Retained products of conception, Infection, Uterine subinvolution, Coagulopathies, Delayed presentation of genital tract hematoma, Vascular bleeding from vascular malformation, and pseudoaneurysms)

#### **OBEE-13 The Postop Pelvis: A Review of Complications Following Surgery for Gynecological Malignancies**

Participants

Marie Vogel, MD, (*Presenter*) Nothing to Disclose

##### **TEACHING POINTS**

1. The radiologist plays a crucial role in detecting and characterizing acute and chronic complications following surgery for gynecologic malignancies.2. Knowledge of the multimodality imaging spectrum of common complications can lead to timely diagnoses and improved patient care.3. A thorough understanding of the common surgical techniques available and identification of pertinent findings on the preoperative imaging can help to identify a subset of patients who may be at higher risk for certain postsurgical complications.

##### **TABLE OF CONTENTS/OUTLINE**

This educational exhibit will: 1. Briefly overview the common management options and surgical techniques for uterine, cervical, endometrial and ovarian cancer.2. Review and illustrate common acute postoperative complications in a case-based format including: - Hemorrhage - Infection/Abscess - Vaginal Cuff Dehiscence - Bowel injury - Ureteral and bladder injury 3. Review and illustrate common subacute to chronic postoperative complications, including: - Lymphocele/Seroma - Peritoneal inclusion cyst - Adhesive disease and bowel obstruction - Pelvic floor dysfunction - Recurrence, including a detailed discussion of the most common pattern of recurrence for each gynecological malignancy

#### **OBEE-14 Elucidating the Spectrum of Extra-uterine Smooth Muscle Neoplasms in Women: Cross-sectional Imaging Findings.**

Participants

Steven Chua, MD, PhD, Houston, TX (*Presenter*) Nothing to Disclose

##### **TEACHING POINTS**

1. Describe taxonomy and histopathology of the diverse spectrum of extra-uterine smooth muscle tumors. 2. Discuss examples of different growth patterns, clinical features and locations of these extra-uterine tumors.3. Highlight the salient imaging features of these tumors by multimodality cross-sectional imaging.

##### **TABLE OF CONTENTS/OUTLINE**

1. Introduction, epidemiology and clinical features.2. Different growth patterns, including benign metastasizing leiomyoma, diffuse peritoneal leiomyomatosis, intravenous leiomyomatosis, parasitic and retroperitoneal.3. Histopathology and biological behavior.4. Multimodality imaging.5. Prognosis and Management.\* Leiomyoma.\* STUMP.\* Leiomyosarcoma.\* Angioleiomyoma.\* Extruterine leiomyomas of the urethra, vagina, broad ligament, round ligament and adnexum.\* Retroperitoneal leiomyoma with Mullerian Features. 6. Conclusion.

#### **OBEE-15 Pictorial guide to O-RADS MRI and online calculator**

Participants

Priyanka Jha, MBBS, San Francisco, CA (*Presenter*) Nothing to Disclose

##### **TEACHING POINTS**

1. Review and understand the O-RADS MRI lexicon terminology with imaging examples 2. Understand protocol requirements to adequately assess adnexal lesion with O-RADS MRI 3. Develop an algorithmic approach, guiding the readers through 4 key questions, to arrive at a final score

##### **TABLE OF CONTENTS/OUTLINE**

1. O-RADS MRI governing principles 2. Technical Requirements for O-RADS MRI assessment 3. Essential O-RADS MRI Calculator Definitionsa. Adnexal b. Lesion c. Cystic lesion d. Types of fluid e. Solid tissue f. Enhancement 4. Understanding types of enhancing solid tissue a. Mural nodule b. Papillary projection c. Irregular septation d. Irregular wall e. Large solid component 5. Lesion assessment on dynamic contrast enhancement a. Low risk curves b. Intermediate risk curves c. High risk curves 6. O-RADS MRI assessment of non-ovarian lesions: Fallopian tubes and para-ovarian cysts

## **OBEE-16 The path to mri expertise in endometriosis - correlation of mri cases with videolaparoscopy**

### **Awards**

#### **Certificate of Merit**

#### **Participants**

Alan Hummel, Sao Paulo, Brazil (*Presenter*) Nothing to Disclose

#### **TEACHING POINTS**

Radiologist training in endometriosis assessment by MRI should be ongoing. Videolaparoscopic correlation is consensually a key part of this development towards expertise. To assess the anatomy of the female pelvis on MRI and videolaparoscopy with the particularities, advantages, and disadvantages of each one. To review the imaging manifestations and the radiological approach in MRI endometriosis workup. To explain in a simplified and didactic way how to interpret the videolaparoscopy for endometriosis. To correlate the findings of pelvic resonance with videolaparoscopy filming in simple, complex, and challenging cases

#### **TABLE OF CONTENTS/OUTLINE**

Anatomy review for MRI and Videolaparoscopy based on key images, videos, and schematic illustrations. What surgeons see and we don't, and what we need to tell them, otherwise they won't see. Simplifying the approach to MRI endometriosis appraisal. Understanding videolaparoscopy surgeries for endometriosis research and treatment. Case-based review of: - Endometriosis in the ANTERIOR compartment - MRI and Videolaparoscopy correlated. - Endometriosis in the MIDDLE compartment - MRI and Videolaparoscopy correlated. - Endometriosis in the POSTERIOR compartment - MRI and Videolaparoscopy correlated. - Limitations of the methods - How far can the radiologist go? - Post-operative features on MRI and videolaparoscopy.

## **OBEE-17 DWI Fast MRI: Optimization of Pelvic MRI Pulse Sequences in Gynecologic Imaging**

### **Awards**

#### **Identified for RadioGraphics**

#### **Certificate of Merit**

#### **Participants**

Rebecca Rakow-Penner, MD, PhD, San Diego, CA (*Presenter*) Research Grant, General Electric Company; Consultant, Human Longevity Inc; Stockholder, CureMetrix, Inc; Stock options, CorTechs Labs, Inc

#### **TEACHING POINTS**

Understand the clinical utility of MR imaging of the female pelvis Describe the underlying principles of rapid and diffusion weighted imaging techniques used to optimize female pelvic MRI evaluation Illustrate the applications of these MRI techniques in the evaluation of different gynecological malignancies

#### **TABLE OF CONTENTS/OUTLINE**

Background a) Female pelvic anatomy and types of gynecologic malignancies b) Standard female pelvic MRI protocol MR Imaging Techniques Rapid Imaging Fast Spin Echo (FSE) / Turbo Spin Echo (TSE) Gradient Echo (GRE) Radial K-Space Radial Volume Interpolated Breath Hold Exam (VIBE) Golden Angle Radial Sparse Parallel (GRASP) Parallel Imaging Compressed Sense Diffusion weighted imaging Parallel Imaging (PI) Reduced FOV Distortion Correction How are these used to evaluate gynecologic malignancies? Review key cases Test yourself with MCQ assessment Conclusion

## **OBEE-18 Spectrum of Cystic and solid tumors of the Ovary at Imaging : Simplified Classification and Practical approach**

#### **Participants**

Nikolas Brozovich, MD, Augusta, GA (*Presenter*) Nothing to Disclose

#### **TEACHING POINTS**

1. Review cystic and solid tumors of the ovary on the basis of tumor origin including differential diagnosis. 2. Describe latest WHO classification of ovarian tumors. 3. Discuss a practical approach to determine key imaging features along with clinical information to narrow down the differential diagnosis.

#### **TABLE OF CONTENTS/OUTLINE**

Although ovarian tumors have similar clinical and radiologic features, predominant or specific imaging features may be present in some types of ovarian tumors. Familiarity with the clinical and imaging features of various ovarian tumors is important in narrowing the differential Classification of ovarian tumors on the basis of tumor of origin Epithelial tumors -serous -mucinous tumors, -Endometrioid -clear cell -Brenner tumor Germ cell tumors -Mature and immature teratoma, -Dysgerminoma, -Endodermal sinus tumor, Sex cord-stromal tumors -Fibrothecoma -Granulosa cell, -Sertoli-Leydig cell tumors

## **OBEE-19 Imaging the posttreatment pelvis with gynecologic cancer**

#### **Participants**

Stephanie Nougaret, MD, PhD, Montpellier, (*Presenter*) Nothing to Disclose

#### **TEACHING POINTS**

- To become familiar with the CT and MR imaging appearances of the treated female pelvis following chemotherapy, radiation therapy or surgery.
- To describe the most common complications of the treated female pelvis for gynecologic malignancies.
- To recognize the patterns of recurrence.
- To list the potential pitfalls in the interpretation of posttreatment imaging findings.

#### **TABLE OF CONTENTS/OUTLINE**

Gynecologic malignancies are usually treated with surgery, chemotherapy, or radiation therapy. Posttreatment imaging plays a crucial role in the assessment of treatment response, tumor recurrence and post treatment complication. Imaging of the treated pelvis following for example chemotherapy and radiation therapy is particularly challenging due to alteration of the normal anatomy and loss of tissue planes. Outline: Ovarian and endometrial cancer: Post-surgical normal aspect Post-surgical complications: Most

common complications Hematoma Infection and abscess formation Other complications Lymphocele Surgically-induced fistula and sinus tracts  
Recurrence: imaging presentation: what and where to look for: the essential role of baseline imaging. Cervical cancer: Post chemoradiotherapy normal aspect Post chemoradiotherapy complications: induced cystitis, induced gastrointestinal complications, fistulas, bone changes Assessment of response after CRT Recurrence: imaging presentation: what and where to look for, evaluation for exenteration

## **OBEE-2      How to Start an Endometriosis Imaging Program: the American Experience**

### **Awards**

#### **Certificate of Merit**

Participants

Lekui Xiao, MD, (*Presenter*) Nothing to Disclose

#### **TEACHING POINTS**

1. A dedicated MRI protocol is crucial for identifying endometriosis. 2. Templated reports for endometriosis are high yield for clinicians because they ensure that all anatomic areas of interest are reviewed. 3. Pre-operative review of MRI in multidisciplinary rounds can alter patient management. 4. Re-evaluation of post-operative MRI exams and associated intraoperative findings and pathology serve as a teaching guide for all parties involved. Specifically, for radiologists, review of concordance/discordance between imaging and intraoperative findings helps refine our imaging protocols and detection accuracy while recognizing the limitations of imaging. 5. Understanding the medical and surgical ramifications of endometriosis develops our relationship with gynecology colleagues to better manage complex cases. 6. Ultimately, earlier diagnosis of endometriosis reduces unnecessary distress and improves disease management.

#### **TABLE OF CONTENTS/OUTLINE**

1. Introduction: Significance of endometriosis and importance of accurate diagnosis 2. Role of imaging, with emphasis on MRI, in evaluating endometriosis 3. MRI protocol to optimize visualization 4. Details discussed in multidisciplinary cases 5. How multidisciplinary cases help radiologists, gynecology, and patients 6. Example cases demonstrating how reporting MRI findings can be refined through multidisciplinary rounds. a. Deep infiltrative endometriosis b. Bladder endometriosis c. Bowel endometriosis d. Ovarian endometriomas e. Malignant Transformation f. Clues for diagnosing subtle disease 7. Teaching Points 8. Conclusion

## **OBEE-20      Imaging of Post-treatment Complications in Gynecologic Malignancies**

Participants

Renuka Ashtekar, MBBS, MD, Mumbai, India (*Presenter*) Nothing to Disclose

#### **TEACHING POINTS**

1. Enumerate expected changes in the pelvis following radiation therapy and chemotherapy. 2. Describe common as well as uncommon complications following chemotherapy (CT), radiation therapy (RT) and surgery. 3. Complications associated with the advent of targeted therapy and immunotherapy.

#### **TABLE OF CONTENTS/OUTLINE**

1. Introduction- Imaging modalities in pre-treatment workup and post-treatment monitoring of gynecologic malignancies.- Overview of treatment options in different types of gynecologic cancers. 2. Expected changes in the pelvic structures post radiation therapy and chemotherapy. 3. Post-surgical imaging- expected post-operative findings. 4. Gastrointestinal complications following surgery/RT/CT and their imaging features. 5. Genitourinary complications following surgery/RT/CT and their imaging features. 6. Musculoskeletal complications following RT/CT and their imaging features. 7. Post treatment vascular complications and their imaging features. 8. Emerging treatments and associated complications and their imaging features.

## **OBEE-21      You should not pass: Simplifying MR Defecography**

### **Awards**

#### **Magna Cum Laude**

Participants

Brenda Hemandes dos Santos Teixeira, MD, Sao Paulo, Brazil (*Presenter*) Nothing to Disclose

#### **TEACHING POINTS**

1. Describe and highlight image acquisition protocols in Magnetic Resonance (MR) Defecography. 2. Improve the understanding of female pelvic floor anatomy using a didactic approach by illustrations and MR images. 3. Recognition of MR Defecography imaging patterns of pelvic floor dysfunctions and diagnostic value.

#### **TABLE OF CONTENTS/OUTLINE**

Review of the main imaging female pelvic floor anatomy. MR Defecography protocols. Case-based examples and illustrative key points of the main pelvic floor disorders: Anterior compartment: - Cystocele - Urethra Hypermobility. Middle compartment: - Uterine prolapse. Posterior compartment: - Enterocoele - Rectocele - Rectal prolapse - Rectal intussusception - Anismus 4. Discuss the perspectives for MR Defecography in clinical routine and imaging findings that aid surgical decisions. 5. Conclusions and "take home messages": consolidate the acquired knowledge.

## **OBEE-22      It's Not All About the Bump- Imaging of the Adnexa During Pregnancy**

### **Awards**

#### **Certificate of Merit**

Participants

Catherine Phillips, MD, Nashville, TN (*Presenter*) Nothing to Disclose

#### **TEACHING POINTS**

1. Complete OB assessment should include dedicated adnexal imaging. Early recognition of adnexal pathology permits timely

diagnosis and necessary treatment. 2. First trimester offers a unique opportunity to identify adnexal pathology before the enlarging uterus displaces the adnexa and possibly conceals lesions. 3. Adnexal pathology findings during pregnancy may be subtle. Diagnosis may be facilitated by transvaginal scanning, which provides superior resolution and is particularly helpful in obese patients. 4. US remains the diagnostic imaging test of choice to not only localize patient's symptoms and characterize incidental masses of pregnancy, but also guide therapeutic planning if needed. MRI can be helpful as a supplemental modality, particularly if lesions are large or of uncertain origin.

#### TABLE OF CONTENTS/OUTLINE

1. Diagrammatic depiction and imaging of normal anatomy of the adnexa (US, CT and MRI) 2. Review of imaging appearance of benign adnexal lesions with focus on how their appearance can differ during pregnancy including: Corpus luteum, Hemorrhagic cysts, Dermoid, Endometriomas including decidualized endometriomas, Hydrosalpinx, Fibroma, Torsion, Ovarian hyperstimulation (hormonal or treatment related), Subserosal fibroid projecting into the adnexa (and associated torsion), Complications related to prior surgeries. 3. Imaging appearance of neoplastic adnexal lesions including: Borderline tumors, Struma ovarii, Cystadenoma and adenocarcinoma, Immature ovarian teratoma. 4. Adnexal pregnancies including interstitial, ectopic pregnancies, and pregnancies in uterine Mullerian anomalies. 5. Mimics of adnexal pathology in pregnancy.

#### OBEE-23 A Game of Patterns: A Case based review on Ultrasonographic Imaging of Ovarian-Adnexal lesions

Participants

Madhumitha B, MBBS, (*Presenter*) Nothing to Disclose

#### TEACHING POINTS

This exhibit aims to 1. Review the ACR US- ORADS risk stratification method. 2. Precisely identify and characterize the common ovarian and adnexal lesions. 3. Apply ORADS to these lesions and categorize them based on their risk for malignancy.

#### TABLE OF CONTENTS/OUTLINE

1. Introduction 2. ORADS 3. A Detective's Perspective -Observation -Deduction -Knowledge 4. Case Series 5. Conclusion

#### OBEE-24 The right iliac fossa: from a new perspective

##### Awards

##### Certificate of Merit

Participants

Giovanna Andreani, MD, Sao Paulo, Brazil (*Presenter*) Nothing to Disclose

#### TEACHING POINTS

Endometriosis is defined as the presence of endometrial tissue outside the uterine cavity and frequently affects about 10% of women of reproductive age, generating symptoms such as dysmenorrhea, dyspareunia and pelvic pain, and infertility. Endometriotic involvement of structures of the right iliac fossa accounts for about 29% of women diagnosed with endometriosis and may affect the distal ileum, cecum, appendix, round ligament, among others. Although it is not such a frequent site of involvement, radiologists must be familiar with the imaging findings for the hypothesis of endometriosis in this topography to be raised. The objective of this study is to didactically illustrate cases of endometriosis affecting the right iliac fossa, how to systemize imaging exams to not miss possible lesions, and what information must be provided, in order to allow proper diagnosis and therapeutic planning.

#### TABLE OF CONTENTS/OUTLINE

Discussion of the different radiological findings of endometriosis and its involvement in structures of the right iliac fossa, based on cases obtained in our institution's digital archive in different imaging modalities, including ultrasound and magnetic resonance imaging. We also provide literature review, teaching points and references.

#### OBEE-25 Peripartum and Post-Partum Hemorrhage

##### Awards

##### Identified for RadioGraphics

##### Certificate of Merit

Participants

Nicole M. Hindman, MD, New York, NY (*Presenter*) Nothing to Disclose

#### TEACHING POINTS

1. Bleeding during pregnancy can be due to a wide variety of etiologies, for which the majority will be evaluated by ultrasound as the first and often the only modality required. 2. Post-partum bleeding /hemorrhage (PPH) can be due to a wide variety of etiologies. US remains the first line of imaging, however often additional modalities may be helpful to further discern etiology, extent and potential treatment options.

#### TABLE OF CONTENTS/OUTLINE

Section 1 will discuss relevant imaging modalities available. Section 2 will discuss the common etiologies of intrapartum bleeding, with a focus on late pregnancy. Some of the topics covered will include: Normal appearance of the placenta Bleeding related to the placenta including hematoma and abruption. Placenta previa Vasa previa Uterine rupture Diagnostic pitfalls. Section 3 will review the etiologies of bleeding in the post-partum period, typically termed post-partum hemorrhage (PPH) to include the following: Normal post-partum bleeding Retained products of conception, subinvolution of trophoblastic tissue and enhanced myometrial vascularity Review the distinction between AVM and enhanced myometrial vascularity Discuss rare etiologies of postpartum hemorrhage, such as uterine artery pseudoaneurysm. Various types of hematomas associated with caesarean section. Uterine dehiscence and/or rupture and their etiologies

#### OBEE-26 Vaginal Rejuvenation: Radiological Approach for Female Genital Anatomy and Procedures

Participants

Luciana Zattar, MD, Sao Paulo, Brazil (*Presenter*) Nothing to Disclose

## TEACHING POINTS

Female genital minimal-invasive procedures are increasingly being performed. In this context, the radiologist has been requested to evaluate this region in order to recognize the anatomical aspects as well as to identify procedures or materials, including fillers, thread lifts, injectable lipolytic, collagen biostimulators, and its complications. To achieve accurate and timely detection and appropriate approach of each case, High frequency ultrasound (HFUS/24-33MHz) is the most effective method since it provides optimal anatomical information of the region and allows identification of different materials and procedures effects. This study aims to discuss and illustrate the radiologist's role in the evaluation of the female genital region with HFUS. The purpose of this exhibit is:- To describe the correct examination technique and preprocedure evaluation- To illustrate the anatomy of the female genital region- To show the main image patterns of the genital minimal-invasive aesthetic procedures- To list, classify and describe the most common related complications in genital region- To discuss the differential diagnosis in genital female lesions- To highlight the importance of HFUS guidance in genital procedures with videos

## TABLE OF CONTENTS/OUTLINE

1. PREPROCEDURAL EVALUATION: Anatomical aspects and Female genital layers.2. PROCEDURES IMAGING FINDINGS AND GUIDANCE.3. COMPLICATIONS.4. DIFFERENTIAL DIAGNOSIS: most common genital lesions.5. CONCLUSION.

### OBEE-27 **Distal Mesonephric Anomalies:What Radiologists Need to Know about OHVIRA Syndrome**

Participants

Mariko Kumazawa, MD, Shimotsuga-gun, Japan (*Presenter*) Nothing to Disclose

## TEACHING POINTS

Werner-Herlyn-Wunderlich syndrome (WHWS) is known as obstructed hemivagina and ipsilateral renal anomaly (OHVIRA), and it has also been reported using various other names. Distal mesonephric anomalies result in the inhibition of appropriate development, fusion between the Müllerian ducts (the origin of the uterus and the vagina), resorption of the separating walls, and abnormal kidney development. There are many reports of various subtypes of WHWS by degree of development. The purposes of this educational exhibit are as follows:- To understand the embryology of this syndrome; what kind of malformation may occur?- To be able to predict what malformation causes a clinical presentation given clinical information, such as a patient's complaint and age.- To know the points of interpretation that contribute to treatment.

## TABLE OF CONTENTS/OUTLINE

1. Present embryology explaining OHVIRA and a classification of uterine malformations according to embryology published by Acién.2. Describe the relationship between various uterine and renal-urinary malformations and their clinical presentation.3. Discuss the key points of magnetic resonance imaging and interpretation that contribute to appropriate treatments with case presentations as follows: i) two cases of OHVIRA with ipsilateral ectopic ureter, ii) two cases of acute abdominal pain by hematometra or peritonitis, and iii) a case of Gardner's cyst.4. Summarize the history of the various terms.

### OBEE-28 **What's going on with the uterus: getting to know the new ASRM classification of Müllerian structures anomalies**

Participants

Paolo Franco, MD, Milano, Italy (*Presenter*) Nothing to Disclose

## TEACHING POINTS

Müllerian structures anomalies are developmental malformations of the female genital tract, with prevalence estimated from 0.5 to 6.7% in the general population. Many of these conditions may lead to significant health and reproductive consequences. Over the years, several systems have been proposed to classify müllerian anomalies. The most used ones are the American Fertility Society (AFS) Classification from 1988 and the European Society of Human Reproduction (ESHRE) and Embryology-European Society for Gynecological Endoscopy (ESGE) Classification, which includes not only uterine but also cervical and vaginal anomalies. The 2021 American Society for Reproductive Medicine (ASRM) Classification (MAC2021) was recently developed to update previous classification systems, include all malformations categories, and promote a more standardized terminology. The purposes of this exhibit are: (1) to review female genitourinary system embryology; (2) to get familiar with congenital female malformations; (3) to explore the new 2021 ASMR Müllerian anomalies classification; (4) to compare it with previous classifications, particularly those developed by AFS and ESHRE-ESGE; (5) to describe MRI findings of female genital anomalies by showing interesting cases.

## TABLE OF CONTENTS/OUTLINE

1. Female genitourinary system embryology and normal anatomy 2. Previous Mullerian anomalies classifications 3. The new 2021 ASMR Mullerian anomalies classification 4. MR female imaging protocols 5. MRI findings of the different female genital malformations

### OBEE-29 **MRI in uterine cancers with uncertain origin: endometrial or cervical. A radiological point of view**

Participants

Luca Russo, MD, Roma, Italy (*Presenter*) Grant, Elekta AB

## TEACHING POINTS

Therapeutic options and clinical management of cervical and endometrial cancers differs significantly. When clinical and histological analysis of a uterine mass are inconclusive, pelvic magnetic resonance imaging (MRI) may help establish the site of origin, allowing appropriate management and treatment planning. Radiologists should be aware of the morphologic (location, shape and different patterns of growth) and functional (enhancement pattern, tumor perfusion, diffusion-weighted imaging and spectroscopy) MRI features that can support the correct assessment of the site of origin.

## TABLE OF CONTENTS/OUTLINE

1. Introduction to the clinical problem and suggested MRI protocol 2. Typical MRI features of primary cervical and endometrial cancers 3. Morphologic MRI features that can help discriminate between endocervical and endometrial cancers, including location, shape and locoregional spread 4. Functional MRI features that can help discriminate between endocervical and endometrial cancers, including enhancement pattern and tumor perfusion, diffusion-weighted imaging and spectroscopy 5. Conclusion

### OBEE-3 **How to Improve Your Routine Transvaginal Ultrasound for Detection of Endometriosis - A Practical**

## Guide for General Radiologists

### Awards

#### Certificate of Merit

#### Participants

Luciana P. Chamie, MD, PhD, Sao Paulo, Brazil (*Presenter*) Nothing to Disclose

#### TEACHING POINTS

1. Endometriosis is a chronic inflammatory disease with significant diagnostic delays varying from four to 11 years 2. Although characteristically multifocal, the retrocervical space is the most common location of deep infiltrative endometriosis (DIE), present in most patients at the initial diagnosis as a hypoechogenic nodule or thickening affecting the uterosacral ligaments. 3. This repetitive and predictable characteristic of retrocervical endometriosis makes it suitable for early diagnosis. 4. Accurate diagnosis can have a tremendous impact on the evolution of the disease, quality of life, and fertility outcomes. 5. Transvaginal sonography (TVS) is the first-line imaging modality to investigate endometriosis and a cost-effective tool. 6. The standard TVS protocol misses the evaluation of the most common locations of endometriosis 7. The addition of a simple algorithm to the standard TVS protocol can reduce the late diagnosis and improve clinical care in patients suffering from long-standing undiagnosed endometriosis.

#### TABLE OF CONTENTS/OUTLINE

1. Title 2. Disclosures 3. Learning Objectives 4. Background information about endometriosis including last updates. Review the most common sites of endometriosis and anatomical landmarks . Discuss the typical presentation of DIE though TVS 5. Standard TVS limitations- discuss why basic ultrasound protocol miss endometriosis detection 6. Dedicated TVS protocol- comprehensive description on how to perform the maneuvers emphasizing advantages and limitations as well as potential pitfalls. 7. Imaging findings of endometriosis on TVS through case examples from mild to severe DIE 8. Conclusion 9. References

### OBEE-30 Problems are opportunities in disguise: Added value of contrast enhanced US (CEUS) in evaluation of the female pelvic disease

### Awards

#### Identified for RadioGraphics

#### Participants

Mariam Moshiri, MD, Brentwood, TN (*Presenter*) Nothing to Disclose

#### TEACHING POINTS

Ultrasound is the first imaging modality for evaluation of female pelvic disease followed by problem-solving or further evaluation with MRI and in rare cases other modalities such as CT, PET, angiography. Ultrasound Contrast agents (UCAs) have emerged as a valuable adjunct to ultrasound and allow visualization and evaluation of lesions that may not be possible on standard ultrasound imaging alone. We aim to describe and illustrate the utility of CEUS as a valuable adjunct in evaluation of disease in the female pelvis using a case-based approach. We will describe common pitfalls and offer some tips for optimizing the use of CEUS during such examinations. Lastly, we will suggest a workflow pattern that describes when CEUS use is appropriate

#### TABLE OF CONTENTS/OUTLINE

1. Stepwise review of technique for use of CEUS in the pelvis. 2. Review application through case-based approach with correlative imaging from other modalities and pathologic specimens( Cervical cancer; Fibroid; Ovarian lesions; Endometrial disease/lesions; Post-partum complications such as retained products of conception; AVM, etc; Hysterosalpingo contrast sonography (HyCoSy); Transperineal invasive procedures using CEUS such as biopsy, drainage, etc; 3.Tips and tricks-Lesion visualization: Compression, patient position, etc; Avoiding pitfalls of CEUS (avoiding accelerated bubble destruction, troubleshooting artifacts) 4.Table summarizing recommended utilization and techniques

### OBEE-31 Hysterosalpingography as a useful tool for the study of fallopian tubes and uterine cavity when MRI is not available

#### Participants

Victor Lara Ameca, MD, (*Presenter*) Nothing to Disclose

#### TEACHING POINTS

- Hysterosalpingography is a diagnostic procedure of great utility in the evaluation of the female reproductive tract. It provides useful information outlining the uterine cavity and the fallopian tubes. Radiologists should become familiar with the technique and the interpretation of HSG images.
- The knowledge of the anatomy and common findings is necessary for the accuracy in the diagnosis and adequate interpretation of image findings.
- There are several implications that should be taken into account performing these studies; patient preparation, good communication with the patient explaining the procedure and answering all the questions. An adequate technique is necessary to limit factors leading misinterpretation and to identify morphologic changes and corroborate them with complementary projections.
- Describe step by step procedure to successfully perform this studies and achieve diagnostic images.
- Present a systematic approach to adequate interpretation of hysterosalpingography.
- Describe and illustrate findings related to anatomical abnormalities of the uterine cavity such as polyps, fibroids, adhesions, adenomyosis and congenital abnormalities. Describe and illustrate findings related to abnormalities of the fallopian tubes as hydrosalpinx, salpingitis isthmica nodosa and surgical changes.

#### TABLE OF CONTENTS/OUTLINE

- Introduction.
- Indication.
- Normal anatomy and variations.
- Step by step procedure.
- Illustrative and imaging findings of polyps, fibroids, adhesions, adenomyosis and congenital abnormalities. Describe and illustrate findings related to abnormalities of the fallopian tubes as hydrosalpinx, salpingitis isthmica nodosa and surgical changes
- Conclusion.

### OBEE-32 Normal and abnormal appearance of the ovaries during assisted reproduction: a multimodality review

### Awards

#### Identified for RadioGraphics

Participants  
Katherine Smith, MD, (*Presenter*) Nothing to Disclose

#### TEACHING POINTS

- Assisted reproductive technology (ART) is increasing in utilization, thus increasing the likelihood that radiologists will encounter both the normal and abnormal imaging findings associated with these treatments.
- Sonographic monitoring is used for follicle tracking during ART cycles, but these images are usually acquired and interpreted by obstetricians. Thus, many radiologists are unfamiliar with the normal imaging appearance of the female pelvis during ART treatments.
- Radiologists should be familiar with the acute complications related to ART treatments.

#### TABLE OF CONTENTS/OUTLINE

A. Background• Overview of population data regarding the utilization of ART• Brief discussion of the clinical medicine involved with ARTB. Multimodality review of the normal appearance of the ovaries in patients undergoing ARTC. Abnormal ovarian appearance and complications in patients undergoing ART• Review of the Golan classification system for ovarian hyperstimulation syndrome• Discussion of the acute complications related to ART, including ovarian torsion and ectopic pregnancyD. Challenging and unusual cases• Case-based discussion of unique presentations in patients undergoing ART therapy• Problem-solving approach to challenging clinical or imaging scenarios

#### OBEE-33 Characterization of (minimally, partially, and predominantly) Solid Ovarian Masses

Participants  
Manasi Arora, MBBS, (*Presenter*) Nothing to Disclose

#### TEACHING POINTS

Imaging characteristics (size, shape, vascularity, contrast enhancement) of solid ovarian masses (SOM) can help differentiate between malignant and benign lesions. Early and accurate imaging diagnosis of SOM has significant therapeutic and prognostic implications. The presence of solid components (greater than 3 mm) arising from the cyst wall or septation and protruding into the cyst cavity (papillary projections) has been shown to be the single most important predictor of malignancy. Through this exhibit, we aim to 1) outline the role of imaging in the diagnosis of SOM, 2) characterization of SOM based on their imaging features (ultrasound, CT, and MRI), 3) review the common and uncommon solid ovarian lesions, and 4) highlight the key imaging findings that allow differentiation of malignant solid ovarian tumors from benign and pseudo-lesions.

#### TABLE OF CONTENTS/OUTLINE

A case-based discussion of the imaging features of minimally, partially, and predominantly SOM, with emphasis on the characteristics of their solid components. Our discussion will outline a comparison between mixed solid and cystic as well as predominantly solid ovarian neoplasms that will include but are not limited to clear cell carcinoma, serous and mucinous carcinomas, endometroid carcinoma, dysgerminoma, granulosa cell tumors, and similar appearing benign lesions (fibromas, mature teratoma, Brenner tumors) as well as pseudo-lesions that mimic a SOM on imaging.

#### OBEE-34 Anatomy and Functional Pathology of the Female Pelvic Girdle: From Bones to Bladder

Participants  
Julie An, MD, San Diego, CA (*Presenter*) Nothing to Disclose

#### TEACHING POINTS

- The female pelvic floor including bony structures, the pelvic organs, and supportive myofascial components- These normal structures not only maintains the anatomic position of the pelvic organs but also allow for normal function- Pelvic floor dysfunction encompasses a group of disorders affected by deficit in these various structures and can lead to bladder, bowel, and/or sexual dysfunction which may inhibit daily activities and negatively impact

#### TABLE OF CONTENTS/OUTLINE

- Review the anatomy of the female pelvis by layers (the most physiologic system for organizing female pelvis):-- Osseous structures, with an emphasis on variations of the female pelvic bones-- Visceral organs and attachments-- Endopelvic Fascia- Cardinal, uterosacral, urethral ligaments, vaginal viscera-- Levator Ani- puborectalis, pubococcygeus, iliococcygeus, and coccygeus-- Perineal Membrane- insertion of perineal muscles, external anal sphincter, and superficial perineal muscles- Present normal and pathologic MRI cases resulting from injury to normal structures-- Endometriosis with scarring of the uterosacral ligament and broad ligament resulting in chronic pelvic pain-- Rectal cancer status post radiation with thinning and fat containing hernia adjacent to the levator ani resulting in rectal prolapse-- Sacral fracture resulting in injury of bilateral coccygeus and iliococcygeus at the level of fracture-- Multiparity with multiple vaginal delivery and subsequent injury to the coccygeus resulting in multi-compartmental prolapse

#### OBEE-35 FIGO Staging Classification for Cervical Cancer - A Practical Guide for Radiologists

Participants  
Bruna Alexandre, MD, Sao Paulo, Brazil (*Presenter*) Nothing to Disclose

#### TEACHING POINTS

Review the female pelvis anatomy; Describe cervical cancer MRI protocol; Describe current management, treatment, and surgical techniques; Recognize the most important imaging features to report in tumor detection, primary staging and restaging, and post-treatment evaluation; Briefly review the 2018 FIGO Staging Classification; Discuss the key points that every radiologist needs to know about cervical cancer.

#### TABLE OF CONTENTS/OUTLINE

INTRODUCTION: Cervical cancer epidemiology; Cervical cancer prevention.FEMALE PELVIS ANATOMY: Review the female pelvis anatomy, highlighting the important landmarks for an adequate staging, correlating didactic illustrations with MRI.MANAGEMENT OF CERVICAL CANCER: Treatment guidelines and algorithmMRI IMAGING PROTOCOL: Exam preparation; MRI protocol.IMAGING EVALUATION: Step by step approach to evaluate cervical cancer; Didactic clinical cases approach to cervical cancer staging; Template reporting system; Limitations and pitfalls of cervical cancer MRI imaging; The most important information that

gynecologists/oncologists want to know from imaging; Post-treatment imaging evaluation.

### **OBEE-36 Imaging of Female Pelvic Masses of Unknown Origin: Tips and Tricks**

#### **Awards**

#### **Cum Laude**

Participants

Francesca Rosa, MD, Savona, Italy (*Presenter*) Nothing to Disclose

#### **TEACHING POINTS**

1. To illustrate a step-by-step approach to female pelvic lesions to define the epicentre of a pelvic mass and to reach the proper diagnosis. 2. To describe the radiological findings and specific imaging "signs" of a wide spectrum of pelvic disease.

#### **TABLE OF CONTENTS/OUTLINE**

1. Pelvic space anatomy description. 2. Anatomic pelvic space-based approach to pelvic mass. 3. Spectrum of imaging "signs" as imaging key to define the space of origin of a pelvic mass. 4. List differential diagnosis peculiar to each space.

### **OBEE-37 Post-surgical Complications of Gynecological Procedures: An Updated Review**

Participants

Ana Uski, MD, Sao Paulo, Brazil (*Presenter*) Nothing to Disclose

#### **TEACHING POINTS**

Know the "new normal anatomy" of the pelvis depending on the type of surgical procedure used. Discuss imaging modalities in the assessment of potential complications after gynecological surgery, focusing on CT and MRI. Recognize the radiological findings of these complications according to the type of procedure used.

#### **TABLE OF CONTENTS/OUTLINE**

Post-surgical gynecological complications are more frequent in extensive procedures, especially in the context of neoplasms, and may be seen less frequently in less invasive procedures such as myomectomies, placement of intrauterine devices, collection of endometrial sampling, endometriosis resection or repair pelvic floor. The most frequent complications include hematomas/hemorrhages, collections, infections, vascular injuries, intestinal and urinary injuries, suture dehiscence, fistulas and lymphoceles, and different imaging modalities play an important role in their diagnosis and follow-up. In stable patients, an initial approach with ultrasound should be considered, but in cases of clinical worsening, computed tomography (CT) is the most indicated exam, while magnetic resonance imaging (MRI) is relevant in the evaluation of mainly late complications. Recognizing normal postsurgical anatomy, expected postoperative findings, complications of each procedure, and pitfalls in image interpretation will facilitate diagnosis.

### **OBEE-38 Multi-Modality Imaging of Endometriosis with Correlative Operative Images: What the Surgeon Wants to Know**

Participants

Won-Kyung Sung, MBBS, Paddington, Australia (*Presenter*) Nothing to Disclose

#### **TEACHING POINTS**

- Endometriosis affect approximately 10% of women of reproductive age and approximately 35-50% of women who suffer from pelvic pain or infertility?
- Endometriotic lesions can exist in a variety of anatomic locations; this represents a diagnostic challenge that can lead to under- and delayed recognition of endometriosis due to lower degrees of suspicion
- In addition, the diversity of anatomic location of endometriotic lesions can change surgical plans
- While diagnostic laparoscopy with histological confirmation is a reliable method of diagnosis, imaging is a less invasive diagnostic alternative that can augment surgical interventions and aid in preoperative evaluation?
- Ultrasonographic imaging (particularly transvaginal sonography (TVS)) can determine the location and extent of endometriosis in patients with suggestive clinical examinations
- MR imaging is a high sensitivity and specificity second-line study, and it is especially useful in patients with previous equivocal TVS or involving structures poorly evaluated by US.

#### **TABLE OF CONTENTS/OUTLINE**

Purpose: The purpose of this study is to characterize and correlate laparoscopic and radiologic findings in the context of endometriosis and to highlight the role of radiologic interpretation in the surgical management of endometriosis patients. ?? Content Organization? ?? 1.???? Overview of endometriosis? 2.???? Laparoscopic operative approach to endometriosis? 3.???? Imaging techniques, advantages, and disadvantages? 4.???? Case examples?

### **OBEE-39 Don't Ovary-Act: O-RADS US/MRI updates and integration**

Participants

Daniela Garcia, MBBS, Philadelphia, PA (*Presenter*) Nothing to Disclose

#### **TEACHING POINTS**

1. O-RADS classifies adnexal masses into different risk categories only applicable to asymptomatic patients with average risk of malignancy. 2. Early familiarization with lexicon and standardized reporting decreases ambiguity in surveillance and management of adnexal masses. 3. Presence of solid component and high vascularity/enhancement are highly associated with malignancy. 4. Integration of O-RADS US and MRI can confidently rule out malignancy when imaging features are characteristic.

#### **TABLE OF CONTENTS/OUTLINE**

Radiologists are usually the first providers to encounter adnexal masses in daily practice and the ones guiding management and surveillance with serial imaging. In the setting of equivocal radiology reports, due to difficulty in obtaining tissue biopsy samples, adnexal lesions are often managed surgically. O-RADS is a standardized reporting system that identifies different risk groups according to specific imaging descriptors with the goal of improving communication between radiologist and referring providers, helping detect patients with potential malignancy and avoiding unnecessary surgery. Integration of O-RADS US and MRI has proven

to have good predictive value and is easily reproducible. This exhibit is a pictorial, multimodality imaging based review of the O-RADS lexicon and its application in the daily evaluation of patients with adnexal masses.

#### **OBEE-4 Postpartum Pelvis: Imaging Management of Early and Delayed Complications**

Participants

Marianna Konidari, MD, London, United Kingdom (*Presenter*) Nothing to Disclose

##### **TEACHING POINTS**

The postpartum period refers to the time interval from birth to 6-8 weeks later, when the uterus undergoes physiologic involution and returns to its nonpregnant state. Familiarization with normal postpartum imaging findings of the pelvis is essential to avoid misdiagnosis of disease. Normal appearances of the pelvis following vaginal delivery differ from those after caesarean section. During the first days after CS, it may be difficult to distinguish normal early postoperative changes from possible uterine complications. US, CT, and MRI can be used for imaging of the postpartum pelvis, each having different indications depending on the clinical setting. The role of imaging in the diagnosis of acute and delayed delivery complications is crucial since these are associated with greater morbidity and can even be fatal.

##### **TABLE OF CONTENTS/OUTLINE**

Normal anatomy and physiology of the postpartum pelvis and correlation with multimodality imaging: which are the most common normal imaging findings. Vaginal delivery vs caesarean section: what imaging findings to normally expect after each type of delivery. Rationale behind imaging during the postpartum period. Which is the best modality in different clinical scenarios and why. Acute complications: key imaging findings and the implications for morbidity and treatment. Case-based discussion on haemorrhage/hematomas; uterine rupture; endometritis; retained products of conception; pelvic vein thrombosis; intraoperative injuries. Delayed complications: when to suspect them and what signs to look for in imaging. Case-based discussion on endometriosis/ ectopic pregnancy on CS scar; placenta accreta spectrum disorder; gestational trophoblastic disease.

#### **OBEE-40 Rhombencephalosynapsis in fetal MRI: main findings and step-by-step evaluation**

Participants

Patricia Oliveira-Szejnfeld, MD, MD, Sao Paulo, Brazil (*Presenter*) Nothing to Disclose

##### **TEACHING POINTS**

1) Review the rhombencephalosynapsis disease spectrum concerning etiology, classification, epidemiological / clinical data and imaging features; 2) Demonstrate a structured evaluation of the fetal infratentorial structures through magnetic resonance imaging (MRI); 3) Depict the main findings of the rhombencephalosynapsis disease spectrum in fetal MRI as well as associated malformations and their implications in neonatal follow-up.

##### **TABLE OF CONTENTS/OUTLINE**

Teaching images will be employed to illustrate the following topics: 1) Embryology of infratentorial structures; 2) Rhombencephalosynapsis: underlying causes, disease spectrum, clinical findings and postnatal imaging; 3) Evaluation of infratentorial structures in fetal MRI (technical aspects and standardized imaging protocol; normal appearance; anatomical landmarks and how they change over time; pearls and pitfalls; potential limitations); 4) MR imaging findings in rhombencephalosynapsis disease spectrum (detailed and accurate analysis, with step-by-step morphological and biometric evaluation of the vermis and cerebellum); 5) Associated malformations in the antenatal period and their imaging findings, as well as a review of the additional evaluation required in the antenatal and postnatal period when the diagnosis is established.

#### **OBEE-41 MRI of the fetal midbrain: a step-by-step evaluation of normal and altered findings beyond aqueductal stenosis**

Participants

Patricia Oliveira-Szejnfeld, MD, MD, Sao Paulo, Brazil (*Presenter*) Nothing to Disclose

##### **TEACHING POINTS**

1) Conduct a brief review of antenatal ultrasound (US) findings that suggest midbrain anomalies; 2) Demonstrate a structured evaluation of the fetal midbrain through magnetic resonance imaging (MRI); 3) Highlight the main MRI findings of midbrain anomalies and associated malformations.

##### **TABLE OF CONTENTS/OUTLINE**

1) Brief review of midbrain embryology. 2) The antenatal sonographic evaluation concerning technical aspects and equipment features; time of best assessment; midbrain sonographic anatomy (size/growth normograms, shape, position, and texture; assessment of tectal length and anteroposterior diameter. Midbrain anomalies in fetal sonography (elongation, thinning, shortening, upward rotation) and potential limitations of antenatal US. 3) MRI evaluation of the fetal midbrain, concerning technical aspects and standardized imaging protocols; Main indications and when to perform; MRI anatomy and how to recognize the normal appearance and anatomical landmarks, as well as their changes over time. Detailed explanations will be provided on how to perform an accurate analysis, with step-by-step morphological and biometric evaluation. Finally, main midbrain malformations will be illustrated with teaching cases.

#### **OBEE-42 As easy as pie: MR imaging of the placenta made simple - a practical guide for beginners**

Participants

Ana De Ataíde Goes, MD, Sao Paulo, Brazil (*Presenter*) Nothing to Disclose

##### **TEACHING POINTS**

- To prepare radiologists to evaluate placental MRI based on a structured reporting model. - To review and illustrate the role of MRI in the diagnosis of the main abnormalities of the placenta. - To provide illustrations to clarify the anatomy and pathology of the placenta. - To present clinical cases in correlation with pathology results. - To review the literature and present tips to reduce interobserver variability.

##### **TABLE OF CONTENTS/OUTLINE**

1) Background: The importance of placental MR imaging in different diagnostic settings and in the management of placental conditions. 2) Correlation between anatomy and histology of normal placenta, including the normal appearance on MRI. 3) Brief description of MRI protocol for placental assessment. 4) Structured reporting model to guide MRI evaluation. 5) Illustrative cases of the main conditions of the placenta with their imaging features and interpretation: - Anatomical variations; - Placenta previa; - Umbilical cord insertion on placenta; - Placenta accreta spectrum; - Placenta disruption; - Placenta neoplasm (as chorioangioma). 6) Additional findings. 7) Potential pitfalls in placental MRI.

#### **OBEE-43 Non-Obstetrical Abdominal and Pelvic Imaging during Pregnancy: A Multimodality Review**

Participants

Kyle Jensen, MD, Portland, OR (*Presenter*) Nothing to Disclose

##### **TEACHING POINTS**

1. Pregnant patients present with non-obstetrical pathology, which must be included in the differential diagnosis. 2. Imaging pregnant patients requires specialized CT and MR protocols and considerations. 3. Pregnant patients require unique imaging, work-up, and treatment of benign and malignant pathologies.

##### **TABLE OF CONTENTS/OUTLINE**

1. Imaging protocols in the gravid patient for US, CT, and MR with discussion on intravenous contrast use. 2. Imaging of maternal infections including COVID-19. 3. Imaging of acute abdominal or pelvic pain during pregnancy by organ system. 4. Non-obstetrical, gynecologic pathology in the pregnant patient. 5. Trauma imaging in the pregnant patient. 6. Oncologic work-up during pregnancy. 7. Imaging work-up of benign/incidental findings.

#### **OBEE-44 Placental hemorrhage throughout gestation: from chorionic bump to Couvelaire uterus**

**Awards**

**Identified for RadioGraphics**

Participants

Roya Sohaey, MD, Portland, OR (*Presenter*) Nothing to Disclose

##### **TEACHING POINTS**

First trimester trophoblastic and early placental hemorrhage can present as chorionic bump or perigestational hemorrhage, and sonographic features can predict pregnancy outcome. Second and third trimester placental abruption can be marginal, retroplacental, preplacental, and intrauterine. Abruption is associated with maternal and fetal morbidity and mortality, therefore accurate imaging-guided classification is important.

##### **TABLE OF CONTENTS/OUTLINE**

1. Sonographic features of first trimester trophoblastic hemorrhage and which imaging findings predict outcome. We will focus on chorionic bump and perigestational hemorrhage. 2. Sonographic features of abruption and which imaging findings predict outcome: marginal abruption, retroplacental abruption, pre-placental abruption, Couvelaire uterus (intra-myometrial hemorrhage). 3. Pitfalls of hemorrhage: adenomyosis, accreta, acute blood mimics placenta, and other mimickers.

#### **OBEE-45 Endometriosis-related infertility: Hysterosalpingography, Ultrasound and MRI findings**

Participants

Luciana P. Chamie, MD, PhD, Sao Paulo, Brazil (*Presenter*) Nothing to Disclose

##### **TEACHING POINTS**

? Endometriosis is a common disease that affects women of reproductive age, being responsible for almost 60% of infertility cases. ? Laparoscopy is no longer the gold standard for the diagnosis of endometriosis, being replaced by imaging exams such as a transvaginal ultrasound (TVS) and pelvic MRI. ? Radiologists should identify typical imaging findings on hysterosalpingography, ultrasound (US) and MRI related to endometriosis that may impair fertility outcomes. ? Information provided by imaging methods is crucial for clinical counseling and surgical planning and to establish a fertility prognosis.

##### **TABLE OF CONTENTS/OUTLINE**

? Definition of infertility and endometriosis; ? Types of endometriosis and role of radiological exams; ? Illustrated teaching cases reviewing findings on hysterosalpingography, US and MR that should be considered in the management of infertility related to endometriosis; ? Didactic approach of relevant data, including: ? Clinical: ; Patient's age and anti-mullerian hormone dosage; ; Past obstetric history; ? Transvaginal ultrasound and MRI with bowel preparation: ; Antral follicle count; ; Endometriomas; ; Complex pelvic adhesions; ; Rectosigmoid endometriotic lesions; ; Subserous myometrial infiltration due to endometriosis; ; Hydrosalpinx; ; Post-operative findings (Isthmocele; thin uterine wall); ? Hysterosalpingography: ; Evaluation of tubal mobility and motility; ; Obliteration of fallopian tubes.

#### **OBEE-46 Hysterosalpingography and Caesarean section: A Niche subject**

Participants

Elizabeth J. Evans, MBChB, Glasgow, United Kingdom (*Presenter*) Nothing to Disclose

##### **TEACHING POINTS**

By reviewing this exhibit the viewer will appreciate: The hysterosalpingographic (HSG) appearances of caesarean section scars. The correlation between HSG appearances with other imaging modalities such as ultrasound and MRI. The importance of identifying adhesions, Asherman's syndrome, within the C-section scar and elsewhere in the cavity. The importance and relevance of other uterine and tubal abnormalities that may be contributing to secondary subfertility and which might influence future pregnancy outcomes.

##### **TABLE OF CONTENTS/OUTLINE**

Introduction. Background including data relating to increasing frequency of caesarean section and associated immediate and

chronic complications. The role of imaging in identifying uterine abnormality following caesarean section. Other uterine and tubal abnormalities which impact on the management of women with secondary subfertility and previous Caesarean section. Suggest a simple grading system to correlate with appearances, severity and prognosis of caesarean section defects.

#### **OBEE-47 Ovarian peritoneal carcinomatosis-Role of Radiologist in treatment**

Participants

Reefath Jabaraj, FRCR, (*Presenter*) Nothing to Disclose

##### **TEACHING POINTS**

To define the most common routes of ovarian peritoneal carcinomatosis dissemination in abdomen To recognise imaging characteristics of ovarian peritoneal carcinomatosis Role of radiologist in preoperative imaging in treatment of carcinomatosis

##### **TABLE OF CONTENTS/OUTLINE**

Introduction Routes of spread in abdomen Key radiological findings in surgical planning Resectable vs difficult to resect areas- a pictorial review Imaging in evaluating the effectiveness of chemotherapy Role of follow up imaging in surveillance Take home message

#### **OBEE-48 When Pregnancy Becomes a Problem"- Pictorial Essay of Common and Uncommon Gestational Complications in the Radiological Practice**

Participants

Ulysses Torres, MD, PhD, Sao Paulo, Brazil (*Presenter*) Nothing to Disclose

##### **TEACHING POINTS**

To recall the theoretical basis of the range of differential diagnoses of complications directly related to the gestational period - the obvious and non-obvious ones. To discuss the classical imaging features of these complications. To present examples of rare cases and typical images. To review which information matters for the differential diagnosis, especially when thinking of ectopic pregnancy. To present challenging diagnostic cases and demonstrate how radiologists can help in outcomes.

##### **TABLE OF CONTENTS/OUTLINE**

Diagram for diagnostic reasoning of gestational complication, dividing it as:- Related to location of pregnancy: including cases of ectopic pregnancy (cervical, cesarian scar, ampullar, interstitial, angular, intra-abdominal, cornual) and heterotopic pregnancy. - Related to gestational content: including cases of trophoblastic disease as complete and partial mola, invasive mola, and choriocarcinoma. - Related to placental issues such as placenta accreta, placenta previa, retroplacental hemorrhage, and placental mass (chorioangioma). - Related to systemic/extrauterine issues, such as hepatic subcapsular hematoma related to HELLP syndrome and the last but not the least decidualized endometriosis.

#### **OBEE-49 Imaging the post-treatment pelvis in gynecologic cancer**

Participants

Behnaz Moradi, MD, Tehran, Iran, Islamic Republic Of (*Presenter*) Nothing to Disclose

##### **TEACHING POINTS**

Complications of gynecologic cancer treatment can be categorized into early and late onset. They can be related to surgery or chemoradiotherapy. Different imaging modalities as ultrasound, CT scan and MRI based on the involved organ and their availability can be used for diagnosis.

##### **TABLE OF CONTENTS/OUTLINE**

In this exhibit, we will discuss about: 1) early complications as hematoma; genitourinary and gastrointestinal complications; infectious process; uterine rupture and wound dehiscence. 2) late complications as genitourinary and gastrointestinal complications; inclusion cyst and seroma formation; fistula; pelvic bone insufficiency fractures; neuritis; post radiotherapy vaginal and cervical stenosis and cystitis.

#### **OBEE-5 Pelvic Deep Endometriosis: What Radiologists Should Point Out in Preoperative Imaging**

Participants

Satoshi Asai, (*Presenter*) Nothing to Disclose

##### **TEACHING POINTS**

Endometriosis is one of the most common and burdening gynecological diseases, estimated to surpass 50% prevalence in women with infertility and chronic pelvic pain. Three types of endometriosis are recognized: ovarian, superficial, and deep. Of these, deep endometriosis (DE) is the most severe form, and surgery is the final solution for symptomatic cases. However, not only it is difficult to recognize all lesions in the surgical field, but it is also difficult to see the relationship to the surrounding organs, and even the lesion itself can be the invisible area. Therefore, preoperative MRI is the key to successful surgery. We advocate for diagnostic imaging that gives the surgeons the information they really need. First, we advocate separate reading and structured reporting for anterior, middle, and posterior compartment of pelvis, which can facilitate the diagnosis of DE and also help to estimate possible complications. Second, based on our experience with complications, we will also discuss the sites of lesions that are prone to be overlooked, and optimal views and imaging methods. Additionally, we show the correlation between MRI and laparoscopic appearance as an aid to understanding DE.

##### **TABLE OF CONTENTS/OUTLINE**

- Introduction to pelvic deep endometriosis with diagnostic and surgical problem - Complications of surgery - structured reporting - key images which are easy to find and often associated with DE - the surgical outcome after structured reporting

#### **OBEE-50 It's all about location, location, location: Distinguishing pregnancies in Mullerian anomalies from abnormally implanted pregnancies.**

Participants

Glynis Sacks-Sandler, MBBCh, Nashville, TN (*Presenter*) Nothing to Disclose

#### TEACHING POINTS

1. Congenital uterine anomalies are often asymptomatic, and the first trimester sonogram may be the first opportunity to diagnose Mullerian anomalies. 2. The recently updated ASRM classification (2021) relies on simple diagrams and descriptions to expand recognition of the multiple variations. More accurate diagnosis based on imaging will lead to improved clinical outcomes. 3. 3D transvaginal ultrasound imaging offers a high degree of diagnostic accuracy. 4. Mullerian anomalies have recognized obstetrical implications, with the most common septate uterus often requiring hysteroscopic septal resection. 5. Pregnancies in association with Mullerian anomalies need to be distinguished from abnormally implanted gestations including interstitial and cesarian scar pregnancies.

#### TABLE OF CONTENTS/OUTLINE

1. Illustrate Mullerian Duct anomalies (MDA) in the non-gravid uterus with correlating 3D ultrasound. 2. Optimal imaging of early intrauterine pregnancies in association with MDA's including Arcuate uterus, Bicornuate uterus, Septate uterus, and Uterus didelphys. 3. Clinical implications of pregnancies in septate uterus and in non-communicating horns. 4. Imaging of "Mimics" including Interstitial pregnancy, angular pregnancy as well as degenerating fibroids. 5. Review of unusual cases

#### OBEE-51 The Bulky Uterus: A Resident's Guide to Diffuse Uterine Pathology

Participants

Elizabeth Deans, MD, (*Presenter*) Nothing to Disclose

#### TEACHING POINTS

1. Diffuse uterine disease can be seen in several pathologies ranging from benign to malignant. 2. Knowledge of the normal appearance of the uterus and cervix by ultrasound, computed tomography (CT) and magnetic resonance imaging (MRI) is important for early detection of pathology. 3. The radiologist plays a vital role by using a combination of key imaging features to help distinguish between these benign and malignant pathologies.

#### TABLE OF CONTENTS/OUTLINE

This educational exhibit will:- Discuss the normal appearance of the uterus and cervix by ultrasound, computed tomography (CT), and magnetic resonance imaging (MRI)- For each of the following uterine pathologies, this exhibit will review pathophysiology and risk factors, describe and illustrate the spectrum of multimodality imaging appearances, and briefly discuss management options:- Diffuse uterine adenomyosis - Diffuse uterine leiomyomatosis - Post-radiation changes - Infection - Hormonal therapy changes - Postpartum changes - Uterine sarcoma/leiomyosarcoma - Invasive cervical/endometrial cancer - Metastatic uterine disease, including diffuse lymphomatous disease

#### OBEE-52 US and MRI of the Uterus: The Good, The Bad and The Ugly

Participants

Krupa Patel-Lippmann, MD, Nashville, TN (*Presenter*) Nothing to Disclose

#### TEACHING POINTS

1. US and MRI are complementary modalities in the evaluation of uterine lesions. US is the first line modality, with MRI utilized for equivocal or poorly visualized findings on US and delineation of suspected malignancy. 2. Benign lesions include endometrial polyps, adenomyosis and leiomyomas, which have a characteristic appearance on US and MR. When present, the radiologist can be confident of the diagnosis. 3. Malignant lesions include endometrial cancers and leiomyosarcomas. These lesions can be suggested based on their US appearance, with MRI used for confirmation and delineation of local tumor extent. 4. Features on multiparametric MRI can help distinguish leiomyomas and leiomyosarcoma.

#### TABLE OF CONTENTS/OUTLINE

- Introduction to imaging the uterus A. Normal anatomy B. Describe the complementary role of US and MRI
- Review imaging features of benign vs malignant endometrial and myometrial lesions A. Endometrial polyps and hyperplasia versus endometrial cancer B. Adenomyosis and leiomyomas versus leiomyosarcomas
- Differentiating leiomyomas versus leiomyosarcomas A. Features of leiomyomas o US: Well-defined and multiple areas of shadowing o MRI: Smooth border, dark T2 signal, no restricted diffusion; homogenous enhancement B. Features of leiomyosarcoma o US: Limited shadowing, irregular margin o MRI: Lobular/irregular margin, cloudy high signal on T1, intermediate T2 signal, restricts diffusion and enhancement C. Overlapping features can be seen in cases of atypical leiomyoma, STUMP, and low grade leiomyosarcoma

#### OBEE-53 From Leiomyoma to Leiomyosarcoma: A Review of the Imaging Spectrum of Uterine Smooth Muscle Tumors with Pathological Correlation

Participants

Keith A. Ferguson, MD, (*Presenter*) Stockholder, Hims & Hers Health, Inc

#### TEACHING POINTS

- - Describe the spectrum of uterine smooth muscle tumors, from benign to malignant - - Discuss pathology of LM variants and provide updated clarifications on different terms such as atypical, cellular, mitotic LMs, STUMP, etc. - - Identify radiological features of uterine leiomyosarcomata (LMS), ordinary leiomyomata (LM), and leiomyoma variants including smooth muscle tumors of uncertain malignant potential (STUMP) - - Demonstrate correlations between the radiological and histopathological features of uterine LMS, LM, and STUMP

#### TABLE OF CONTENTS/OUTLINE

- Title, names, institutions - Review of uterine smooth muscle tumors o Epidemiology Risk factors, Pathogenesis o Presentation - Diagnosis, Management and treatment options o Indications for imaging in assessing uterine tumors CT, MRI, US, PET/CT o Characteristic imaging features of benign and malignant uterine tumors - Our multi-institutional project - List patient cohorts, demographics - Show examples of ordinary LM including imaging and path characteristics o Non-degenerated o Degenerated Cystic Myxoid Hemorrhagic - Show examples of LM variants including imaging and path characteristics o Cellular o STUMP - Show examples of LMS including imaging and path characteristics o Routine and variants (myxoid, epithelioid) o Metastasis: patterns of recurrence

and spread - Summarize characteristic imaging and histopathological features of uterine smooth muscle tumors - Conclusions and future steps - Acknowledgements, references

#### **OBEE-54 Peritoneal Endometriosis and MRI: A New Look!**

Participants

Carolina Almeida, MD, Rio de Janeiro, Brazil (*Presenter*) Nothing to Disclose

##### **TEACHING POINTS**

TEACHING POINTS 1) Endometriosis is a disease that affects thousands of women and compromises their quality of life, causing chronic pain, infertility, and problems in sexual life. 2) Peritoneal endometriosis is often underdiagnosed and prevents adequate treatment. 3) Laparoscopy is the gold standard exam for the investigation of endometriosis, but it is an invasive method, and many women refuse or are afraid to undergo laparoscopy. 4) Clarify doubts about the appropriate exam protocol and what are the myths about MRI in endometriosis. 5) MRI allows the identification of signs that support the diagnosis of peritoneal endometriosis. These signs are subtle, and it is essential that the radiologist knows how to identify them. 6) Demonstrate MRI images and their correlation with exploratory laparoscopy in superficial endometriosis.

##### **TABLE OF CONTENTS/OUTLINE**

TABLE OF CONTENTS/OUTLINE 1) Overview of peritoneal endometriosis and a short quiz 2) Identification of focal, diffuse peritoneal thickening and peritoneal failure on MRI and laparoscopy 3) Identification of thickening and glandular tissue on the surface of organs 4) Identification of bloody fluid and septa on MRI and laparoscopy 5) Summary of changes found in each method.

#### **OBEE-55 Ultrasound in Endometriosis: Chocolate Cysts and Beyond**

Participants

Divya Singh, MD, MBBS, (*Presenter*) Nothing to Disclose

##### **TEACHING POINTS**

Ultrasonography is a widely available, inexpensive, real-time imaging modality which can be used to detect pelvic involvement by endometriosis beyond the classic ovarian endometriomas. Deep infiltrating endometriosis (DIE) implants are seen as well circumscribed, hypoechoic lesions with smooth or irregular margins using ultrasound. A systematic sonologic approach in evaluation of the pelvis is imperative for detection of DIE in the anterior and posterior compartments. Ultrasound offers the advantage of using soft markers like a negative sliding sign and probe tenderness to guide the search for DIE. Endometriomas undergo decidualisation during pregnancy which can mimic ovarian tumors on ultrasonography. Ultrasound can raise a red flag for occurrence of malignant transformation in long standing endometriomas.

##### **TABLE OF CONTENTS/OUTLINE**

Impact of endometriosis on women's health; Pathology; Clinical presentation: The great masquerader; Ultrasound evaluation technique; Sonographic features: Soft markers, overt findings; Changes in endometriosis in pregnancy; Malignant transformation of endometriomas; Conclusion

#### **OBEE-56HC Intrauterine Contraceptive Devices: History, Imaging and Complications**

Participants

Lisa Xuan, MD, BSc, Newmarket, ON (*Presenter*) Nothing to Disclose

##### **TEACHING POINTS**

1. For almost 100 years, iterations of intrauterine contraceptive devices (IUCD) have been in use. Older models are of historical interest and may be found incidentally on imaging. 2. Both copper and hormone-releasing IUCDs are as effective as tubal ligation in preventing pregnancy, but a 2 in 100 person per year pregnancy rate persists. 3. Malpositioning is the most common IUCD complication, and exists as a spectrum depending on severity. 4. All malpositioning should be communicated to the clinician as it may lead to decreased contraceptive efficacy or require intervention.

##### **TABLE OF CONTENTS/OUTLINE**

A brief history of IUCDs-1st generation-Non-copper metal devices-2nd generation-Plastic devices-3rd generation-Copper bearing devices-4th generation-Hormone bearing devices-5th generation-Frameless intrauterine implants Radiographic evaluation of IUCDs- Adequate positioning (on plain films, US and CT)-3D ultrasound as the gold standard in assessing malpositioning Complications of IUCDs- Malpositioning spectrum (expulsion, displacement, embedment, perforation)-Synchronous pregnancy- Ectopic pregnancy- Fragmentation of device- Clinical implications Cased Based Imaging Scenarios Summary Please visit the Learning Center to also view this presentation in hardcopy format.

#### **OBEE-6 Tips to Definitely Understand Pelvic Innervation in Endometriosis: The Guide You Asked For**

Participants

Helena de Souza, MD, Sao Paulo, Brazil (*Presenter*) Nothing to Disclose

##### **TEACHING POINTS**

- To prepare abdominal radiologists to evaluate magnetic resonance imaging (MRI) of pelvic innervation in the context of endometriosis.- To summarize the somatic and visceral neural anatomy in a practical way.- To illustrate the main findings of neural involvement by deep pelvic endometriosis with selected clinical cases.- To demonstrate the impact of such knowledge on patients' management and how radiologists may improve outcomes.

##### **TABLE OF CONTENTS/OUTLINE**

- Background: the importance of pelvic innervation MR imaging in diagnostic settings of deep pelvic endometriosis.- Description of the somatic and visceral neural anatomy and correlation with the normal appearance on MRI.- Interactive anatomical atlas and videos showing the pelvic innervation and its involvement in deep endometriosis based on anatomical diagrams and MRI imaging exams.- Tips and tricks.

## **OBEE-7 Plumbing Problems: Troubleshooting Tips for Complex Fetal Genitourinary Malformations**

### **Awards**

**Certificate of Merit**  
**Identified for RadioGraphics**

### **Participants**

April Griffith, MD, (*Presenter*) Nothing to Disclose

### **TEACHING POINTS**

1: Review all scans for development of urinoma, urinary ascites, obstructive dysplasia  
2: Assess bladder filling, changes in ureteric caliber, color Doppler for patent urethra  
3: Use MRI when low fluid, maternal habitus limit US assessment  
4: Confirm diagnoses with postnatal imaging, operative findings, genetic testing, autopsy

### **TABLE OF CONTENTS/OUTLINE**

Megacystis-1st trimester aneuploidy-Euploid fetus: Posterior urethral valves (PUV), prune belly (PB), megacystis microcolon intestinal hypoperistalsis (MMIH), urethral atresia-Evaluate genitalia (dilated urethra in PB, MMIH in female)-Pitfall dilated vagina for distended bladder  
Multicystic dysplastic kidney (MCDK) vs obstructive dysplasia (OD)-MCKD large kidney, large cysts, no pelvic dilation-OD small, echogenic kidney, small cysts-Look for ureterocele, ectopic more likely with duplication, can insert in vagina  
Urinary tract dilation (UTD)-Ureteropelvic junction obstruction: Pitfall MCDK-Duplicated system: Pitfall cystic adrenal mass vs obstructed upper moiety-Reflux: Variable ureter size-Report with 2014 UTD Classification System  
Genitourinary sinus malformation-Establish fetal sex (persistent cloaca, hydrocolpos, imperforate hymen in females)-Look for anal dimple-Fluid-fluid levels due to meconium/urine mixing in dilated vagina-  
Calcified meconium due to bowel-urinary tract fistula-MRI for evaluation of colon/rectum/anus--Meconium high T1, low T2, high GRE--Fluid low T1, high T2  
Anatomic variants-Crossed fused ectopia, pelvic kidney

## **OBEE-8 Pain Points: Making Sense of Pelvic Nerves Involved with Endometriosis and Chronic Pain**

### **Awards**

**Cum Laude**  
**Identified for RadioGraphics**

### **Participants**

Ceylan Colak, MD, MD, (*Presenter*) Nothing to Disclose

### **TEACHING POINTS**

1. Endometriosis is a common condition impacting approximately 1 out of every 10 women of childbearing age. 2. Deep infiltrating endometriosis most commonly occurs in the pelvis and is typically multifocal. 3. Although rarely reported, several lumbosacral nerves course through the pelvis and can be involved by deep infiltrating endometriosis including the sciatic, pudendal, obturator and hypogastric nerves. 4. Neural involvement by endometriosis may lead to pain or other neurological symptoms including muscle weakness, numbness, incontinence and paraplegia. 5. MRI is the most reliable noninvasive modality to diagnosis neural involvement by endometriosis. Protocol optimization can help increase conspicuity of nerves involved by endometriosis. 6. Imaging findings are variable and include identification of a deep infiltrative endometriotic lesion directly involving the nerve or nerve thickening with increased enhancement. In chronic cases, muscle atrophy may be present. 7. Identification of neural involvement is important for early diagnosis and treatment to avoid irreversible nerve injury and loss of function.

### **TABLE OF CONTENTS/OUTLINE**

1. Title 2. Disclosures 3. Learning Objectives 4. Background information about endometriosis with neural involvement 5. Normal anatomy of pelvic nerves with imaging examples 6. MRI protocol considerations 7. Imaging findings of nerves involved by endometriosis illustrated through case examples 8. Conclusion 9. References

## **OBEE-9 Postpartum and Post-abortion Complications - A Guide for Radiologists**

### **Participants**

Cynthia Borborema, MD, Sao Paulo, Brazil (*Presenter*) Nothing to Disclose

### **TEACHING POINTS**

To review the normal imaging appearance of postpartum and post-abortion period and to distinguish it from complications that require treatment. To list radiologic features of early and late postpartum and post-abortion complications to provide a practical guide to help radiologists. To emphasize an integrated radiologic and clinical approach in the assessment of challenging postpartum and post-abortion conditions to improve the clinical impact of radiology reports.

### **TABLE OF CONTENTS/OUTLINE**

Normal uterine changes in puerperium. Normal changes after cesarean delivery. Role of imaging in assessment of postpartum and post-abortion period and relevant report information. Diagnostic tools, with emphasis in computed tomography and magnetic resonance imaging. Usual and unusual postpartum and post-abortion complications (infectious, thromboembolic and hemorrhagic), including key patient history, risk factors, imaging findings, and pitfalls. Review of cesarean surgical technique (laparotomy, bladder flap creation and hysterotomy) and correlation with early related complications. Late cesarean delivery-related complications. Uterine complications after pregnancy-related curettage.



## Abstract Archives of the RSNA, 2022

OBEE-1

### How To Expand Your Diagnosis of Deep Endometriosis on Routine Pelvic Imaging

Sunday, Nov. 27 8:00AM - 9:00AM Room: Learning Center - OB

#### Participants

Scott Young, MD, Phoenix, AZ (*Presenter*) Nothing to Disclose

#### TEACHING POINTS

Review uterine video clips on routine pelvic ultrasound and evaluate sliding sign maneuvers, differences in technique depending on uterine version. -Accurately locate important anatomical landmarks, including the torus uterinus and uterosacral ligaments on TVUS. -Understand how DE observations may appear different depending on uterine version and transducer position in the anterior and posterior vaginal fornices. -Recognize characteristics of DE bowel observations and assess bowel DE size and depth of invasion, critical factors which guide the level of surgical expertise required for resection. How to recognize DE on routine CT and MR examinations performed for clinical indications other than endometriosis. -Recognize characteristics of DE observations outside the pelvic compartments on routine CT, MSK pelvic, and non-dedicated abdominopelvic MR. -Utilize cues including location, signal, and enhancement characteristics to make an early diagnosis of DE.

#### TABLE OF CONTENTS/OUTLINE

1. Title 2. Disclosures 3. Learning objectives 4. Pelvic anatomy review-Uterosacral ligament (USL)/torus uterinus-Relationship of USL to transducer position and uterine version-Surgically relevant measurements/observations-Case examples of normal and abnormal TVUS video sweeps of anterior and posterior fornix view for each uterine flexion/version-5. US of bowel endometriosis-Schematic/operative images-Case examples with pertinent measurements 6. Extrapelvic and uncommon DE locations-Anatomic hypothesis of extraperitoneal spread-CT and MR enhancement/signal characteristics-Schematic/operative images 7. Conclusion 8. References

Printed on: 02/07/23



## Abstract Archives of the RSNA, 2022

OBEE-10

### Post-treatment Complications of Gynecologic Malignancies

Sunday, Nov. 27 8:00AM - 9:00AM Room: Learning Center - OB

#### Participants

Tsukasa Saida, MD, Tsukuba, Japan (*Presenter*) Nothing to Disclose

#### TEACHING POINTS

Radiologists need to be familiar with the imaging findings of the various complications that can occur in the treatment of gynecologic tumors and understand the urgency and symptoms of each. In this exhibition, we introduce various complications derived from gynecologic surgery and pelvis radiation therapy, and explain the diagnostic points of each complication. The teaching points of this exhibit are: 1. We classified postoperative complications immediately after surgery, subacute, and delayed complications. Complications immediately after surgery are caused by direct injury caused by surgical procedures. Subacute complications include infection, chylous ascites, deep venous thrombosis, and neuropathy. Delayed include, intestinal obstruction, hydronephrosis, lymphedema, and abdominal incisional hernia. 2. Radiation-induced complications can be divided into acute and chronic effects. Acute effects occur during or immediately after radiation therapy, are reversible, and in most cases, the conservative treatment leaves no disability. Chronic effects include cervical stenosis, small bowel stricture, fistula formation, and insufficiency fractures that occur a few months later.

#### TABLE OF CONTENTS/OUTLINE

A. Complications after surgery (Immediately after surgery, Subacute, Delayed) B. Radiation-induced effects (Early effects, Late effects)

Printed on: 02/07/23



## Abstract Archives of the RSNA, 2022

OBEE-11

### Phenotypic Diversity of Uterine Mesenchymal Tumors (Excluding Smooth Muscle Tumors): Current Update on Genetics and Imaging

Sunday, Nov. 27 8:00AM - 9:00AM Room: Learning Center - OB

#### Participants

Steven Chua, MD, PhD, Houston, TX (*Presenter*) Nothing to Disclose

#### TEACHING POINTS

1. Discuss the taxonomy, epidemiology, clinical features, histopathology and biology of the diverse spectrum of mesenchymal, non-smooth muscle tumors of the uterus. 2. Describe the salient multimodality cross-sectional imaging features of these tumors. 3. Review the genetics, management and prognosis of these tumors.

#### TABLE OF CONTENTS/OUTLINE

1. Introduction, epidemiology and clinical features of mesenchymal, non-smooth muscle tumors of the uterus. 2. Histopathological, immunohistochemistry and molecular pathology. 3. CT, MR and PET/CT imaging features and tumor biology of this wide spectrum of tumors. 4. Prognosis and management. \* Low grade Endometrial stromal sarcoma. \* High grade Endometrial stroma sarcoma. \* Adenosarcoma. \* Carcinosarcoma. \* Undifferentiated sarcoma. \* Uterine tumor resembling sex cord stromal tumor. \* PEComa. \* Inflammatory myofibroblastic tumor. \* Solitary fibrous tumor. Conclusion.

Printed on: 02/07/23



## Abstract Archives of the RSNA, 2022

OBEE-12

### Management and Imaging Evaluation of Peripartum Hemorrhage: What Radiologists Need to Know

Sunday, Nov. 27 8:00AM - 9:00AM Room: Learning Center - OB

#### Participants

Moataz Ahmed Sayed Mohammed Soliman, MD, MSc, CHICAGO, IL (*Presenter*) Nothing to Disclose

#### TEACHING POINTS

- Understand normal imaging findings of the utero-fetal complex.
- Recognize multimodality imaging findings of conditions predisposing to peripartum hemorrhage.
- Discuss Imaging pitfalls for peripartum hemorrhage.
- Impact of the preoperative radiological diagnosis on management and role of radiologists.

#### TABLE OF CONTENTS/OUTLINE

1. Introduction: a. Normal imaging anatomy of the uteroplacental complex 2. Ante-partum hemorrhage: a. Definitions b. Etiology: (Placental abruption, Placenta previa, Gestational trophoblastic disease, Vasa Previa, Uterine rupture) c. Management 3. Postpartum hemorrhage a. Definitions b. Normal imaging findings of the postpartum uterus. c. Classification and risk factors i. Primary postpartum hemorrhage: (Uterine atony, traumatic pelvic hematoma, bladder flap hematoma, retained products of conception, coagulopathies, and placenta accrete spectrum) ii. Secondary postpartum hemorrhage: (Retained products of conception, Infection, Uterine subinvolution, Coagulopathies, Delayed presentation of genital tract hematoma, Vascular bleeding from vascular malformation, and pseudoaneurysms)

Printed on: 02/07/23



## Abstract Archives of the RSNA, 2022

OBEE-13

### The Postop Pelvis: A Review of Complications Following Surgery for Gynecological Malignancies

Sunday, Nov. 27 8:00AM - 9:00AM Room: Learning Center - OB

#### Participants

Marie Vogel, MD, (*Presenter*) Nothing to Disclose

#### TEACHING POINTS

1. The radiologist plays a crucial role in detecting and characterizing acute and chronic complications following surgery for gynecologic malignancies. 2. Knowledge of the multimodality imaging spectrum of common complications can lead to timely diagnoses and improved patient care. 3. A thorough understanding of the common surgical techniques available and identification of pertinent findings on the preoperative imaging can help to identify a subset of patients who may be at higher risk for certain postsurgical complications.

#### TABLE OF CONTENTS/OUTLINE

This educational exhibit will: 1. Briefly overview the common management options and surgical techniques for uterine, cervical, endometrial and ovarian cancer. 2. Review and illustrate common acute postoperative complications in a case-based format including: - Hemorrhage - Infection/Abscess - Vaginal Cuff Dehiscence - Bowel injury - Ureteral and bladder injury 3. Review and illustrate common subacute to chronic postoperative complications, including: - Lymphocele/Seroma - Peritoneal inclusion cyst - Adhesive disease and bowel obstruction - Pelvic floor dysfunction - Recurrence, including a detailed discussion of the most common pattern of recurrence for each gynecological malignancy

Printed on: 02/07/23



## Abstract Archives of the RSNA, 2022

OBEE-14

### Elucidating the Spectrum of Extra-uterine Smooth Muscle Neoplasms in Women: Cross-sectional Imaging Findings.

Sunday, Nov. 27 8:00AM - 9:00AM Room: Learning Center - OB

#### Participants

Steven Chua, MD, PhD, Houston, TX (*Presenter*) Nothing to Disclose

#### TEACHING POINTS

1. Describe taxonomy and histopathology of the diverse spectrum of extra-uterine smooth muscle tumors. 2. Discuss examples of different growth patterns, clinical features and locations of these extra-uterine tumors. 3. Highlight the salient imaging features of these tumors by multimodality cross-sectional imaging.

#### TABLE OF CONTENTS/OUTLINE

1. Introduction, epidemiology and clinical features. 2. Different growth patterns, including benign metastasizing leiomyoma, diffuse peritoneal leiomyomatosis, intravenous leiomyomatosis, parasitic and retroperitoneal. 3. Histopathology and biological behavior. 4. Multimodality imaging. 5. Prognosis and Management.\* Leiomyoma.\* STUMP.\* Leiomyosarcoma.\* Angioleiomyoma.\* Extruterine leiomyomas of the urethra, vagina, broad ligament, round ligament and adnexum.\* Retroperitoneal leiomyoma with Mullerian Features. 6. Conclusion.

Printed on: 02/07/23

## Abstract Archives of the RSNA, 2022

OBEE-15

### Pictorial guide to O-RADS MRI and online calculator

Sunday, Nov. 27 8:00AM - 9:00AM Room: Learning Center - OB

#### Participants

Priyanka Jha, MBBS, San Francisco, CA (*Presenter*) Nothing to Disclose

#### TEACHING POINTS

1. Review and understand the O-RADS MRI lexicon terminology with imaging examples 2. Understand protocol requirements to adequately assess adnexal lesion with O-RADS MRI 3. Develop an algorithmic approach, guiding the readers through 4 key questions, to arrive at a final score

#### TABLE OF CONTENTS/OUTLINE

1. O-RADS MRI governing principles 2. Technical Requirements for O-RADS MRI assessment 3. Essential O-RADS MRI Calculator Definitions a. Adnexal b. Lesion c. Cystic lesion d. Types of fluid e. Solid tissue f. Enhancement 4. Understanding types of enhancing solid tissue a. Mural nodule b. Papillary projection c. Irregular septation d. Irregular wall e. Large solid component 5. Lesion assessment on dynamic contrast enhancement a. Low risk curves b. Intermediate risk curves c. High risk curves 6. O-RADS MRI assessment of non-ovarian lesions: Fallopian tubes and para-ovarian cysts

Printed on: 02/07/23



## Abstract Archives of the RSNA, 2022

OBEE-16

### The path to mri expertise in endometriosis - correlation of mri cases with videolaparoscopy

Sunday, Nov. 27 8:00AM - 9:00AM Room: Learning Center - OB

#### Awards

Certificate of Merit

#### Participants

Alan Hummel, Sao Paulo, Brazil (*Presenter*) Nothing to Disclose

#### TEACHING POINTS

Radiologist training in endometriosis assessment by MRI should be ongoing. Videolaparoscopic correlation is consensually a key part of this development towards expertise. To assess the anatomy of the female pelvis on MRI and videolaparoscopy with the particularities, advantages, and disadvantages of each one. To review the imaging manifestations and the radiological approach in MRI endometriosis workup. To explain in a simplified and didactic way how to interpret the videolaparoscopy for endometriosis. To correlate the findings of pelvic resonance with videolaparoscopy filming in simple, complex, and challenging cases

#### TABLE OF CONTENTS/OUTLINE

Anatomy review for MRI and Videolaparoscopy based on key images, videos, and schematic illustrations. What surgeons see and we don't, and what we need to tell them, otherwise they won't see. Simplifying the approach to MRI endometriosis appraisal. Understanding videolaparoscopy surgeries for endometriosis research and treatment. Case-based review of: - Endometriosis in the ANTERIOR compartment - MRI and Videolaparoscopy correlated. - Endometriosis in the MIDDLE compartment - MRI and Videolaparoscopy correlated. - Endometriosis in the POSTERIOR compartment - MRI and Videolaparoscopy correlated. - Limitations of the methods - How far can the radiologist go? - Post operative features on MRI and videolaparoscopy.

Printed on: 02/07/23



## Abstract Archives of the RSNA, 2022

OBEE-17

### DWI Fast MRI: Optimization of Pelvic MRI Pulse Sequences in Gynecologic Imaging

Sunday, Nov. 27 8:00AM - 9:00AM Room: Learning Center - OB

#### Awards

Identified for RadioGraphics  
Certificate of Merit

#### Participants

Rebecca Rakow-Penner, MD, PhD, San Diego, CA (*Presenter*) Research Grant, General Electric Company; Consultant, Human Longevity Inc; Stockholder, CureMetrix, Inc; Stock options, CorTechs Labs, Inc

#### TEACHING POINTS

Understand the clinical utility of MR imaging of the female pelvis Describe the underlying principles of rapid and diffusion weighted imaging techniques used to optimize female pelvic MRI evaluation Illustrate the applications of these MRI techniques in the evaluation of different gynecological malignancies

#### TABLE OF CONTENTS/OUTLINE

Background a) Female pelvic anatomy and types of gynecologic malignancies b) Standard female pelvic MRI protocol MR Imaging Techniques Rapid Imaging Fast Spin Echo (FSE) / Turbo Spin Echo (TSE) Gradient Echo (GRE) Radial K-Space Radial Volume Interpolated Breath Hold Exam (VIBE) Golden Angle Radial Sparse Parallel (GRASP) Parallel Imaging Compressed Sense Diffusion weighted imaging Parallel Imaging (PI) Reduced FOV Distortion Correction How are these used to evaluate gynecologic malignancies? Review key cases Test yourself with MCQ assessment Conclusion

Printed on: 02/07/23

## Abstract Archives of the RSNA, 2022

OBEE-18

### Spectrum of Cystic and solid tumors of the Ovary at Imaging : Simplified Classification and Practical approach

Sunday, Nov. 27 8:00AM - 9:00AM Room: Learning Center - OB

#### Participants

Nikolas Brozovich, MD, Augusta, GA (*Presenter*) Nothing to Disclose

#### TEACHING POINTS

1. Review cystic and solid tumors of the ovary on the basis of tumor origin including differential diagnosis. 2. Describe latest WHO classification of ovarian tumors. 3. Discuss a practical approach to determine key imaging features along with clinical information to narrow down the differential diagnosis.

#### TABLE OF CONTENTS/OUTLINE

Although ovarian tumors have similar clinical and radiologic features, predominant or specific imaging features may be present in some types of ovarian tumors. Familiarity with the clinical and imaging features of various ovarian tumors is important in narrowing the differential Classification of ovarian tumors on the basis of tumor of origin Epithelial tumors -serous -mucinous tumors, - Endometrioid -clear cell -Brenner tumor Germ cell tumors -Mature and immature teratoma, -Dysgerminoma, -Endodermal sinus tumor, Sex cord-stromal tumors -Fibrothecoma -Granulosa cell, -Sertoli-Leydig cell tumors

Printed on: 02/07/23

## Abstract Archives of the RSNA, 2022

OBEE-19

### Imaging the posttreatment pelvis with gynecologic cancer

Sunday, Nov. 27 8:00AM - 9:00AM Room: Learning Center - OB

#### Participants

Stephanie Nougaret, MD, PhD, Montpellier, (*Presenter*) Nothing to Disclose

#### TEACHING POINTS

- To become familiar with the CT and MR imaging appearances of the treated female pelvis following chemotherapy, radiation therapy or surgery.
- To describe the most common complications of the treated female pelvis for gynecologic malignancies.
- To recognize the patterns of recurrence.
- To list the potential pitfalls in the interpretation of posttreatment imaging findings.

#### TABLE OF CONTENTS/OUTLINE

Gynecologic malignancies are usually treated with surgery, chemotherapy, or radiation therapy. Posttreatment imaging plays a crucial role in the assessment of treatment response, tumor recurrence and post treatment complication. Imaging of the treated pelvis following for example chemotherapy and radiation therapy is particularly challenging due to alteration of the normal anatomy and loss of tissue planes. Outline: Ovarian and endometrial cancer: Post-surgical normal aspect Post-surgical complications: Most common complications Hematoma Infection and abscess formation Other complications Lymphocele Surgically-induced fistula and sinus tracts Recurrence: imaging presentation: what and where to look for: the essential role of baseline imaging. Cervical cancer: Post chemoradiotherapy normal aspect Post chemoradiotherapy complications: induced cystitis, induced gastrointestinal complications, fistulas, bone changes Assessment of response after CRT Recurrence: imaging presentation: what and where to look for, evaluation for exenteration

Printed on: 02/07/23



## Abstract Archives of the RSNA, 2022

OBEE-2

### How to Start an Endometriosis Imaging Program: the American Experience

Sunday, Nov. 27 8:00AM - 9:00AM Room: Learning Center - OB

#### Awards

Certificate of Merit

#### Participants

Lekui Xiao, MD, (*Presenter*) Nothing to Disclose

#### TEACHING POINTS

1. A dedicated MRI protocol is crucial for identifying endometriosis. 2. Templated reports for endometriosis are high yield for clinicians because they ensure that all anatomic areas of interest are reviewed. 3. Pre-operative review of MRI in multidisciplinary rounds can alter patient management. 4. Re-evaluation of post-operative MRI exams and associated intraoperative findings and pathology serve as a teaching guide for all parties involved. Specifically, for radiologists, review of concordance/discordance between imaging and intraoperative findings helps refine our imaging protocols and detection accuracy while recognizing the limitations of imaging. 5. Understanding the medical and surgical ramifications of endometriosis develops our relationship with gynecology colleagues to better manage complex cases. 6. Ultimately, earlier diagnosis of endometriosis reduces unnecessary distress and improves disease management.

#### TABLE OF CONTENTS/OUTLINE

1. Introduction: Significance of endometriosis and importance of accurate diagnosis 2. Role of imaging, with emphasis on MRI, in evaluating endometriosis 3. MRI protocol to optimize visualization 4. Details discussed in multidisciplinary cases 5. How multidisciplinary cases help radiologists, gynecology, and patients 6. Example cases demonstrating how reporting MRI findings can be refined through multidisciplinary rounds. a. Deep infiltrative endometriosis b. Bladder endometriosis c. Bowel endometriosis d. Ovarian endometriomas e. Malignant Transformation f. Clues for diagnosing subtle disease 7. Teaching Points 8. Conclusion

Printed on: 02/07/23

## Abstract Archives of the RSNA, 2022

OBEE-20

### Imaging of Post-treatment Complications in Gynecologic Malignancies

Sunday, Nov. 27 8:00AM - 9:00AM Room: Learning Center - OB

#### Participants

Renuka Ashtekar, MBBS, MD, Mumbai, India (*Presenter*) Nothing to Disclose

#### TEACHING POINTS

1. Enumerate expected changes in the pelvis following radiation therapy and chemotherapy.2. Describe common as well as uncommon complications following chemotherapy (CT), radiation therapy (RT) and surgery.3. Complications associated with the advent of targeted therapy and immunotherapy.

#### TABLE OF CONTENTS/OUTLINE

1. Introduction- Imaging modalities in pre-treatment workup and post-treatment monitoring of gynecologic malignancies.- Overview of treatment options in different types of gynecologic cancers.2. Expected changes in the pelvic structures post radiation therapy and chemotherapy.3. Post-surgical imaging- expected post-operative findings.4. Gastrointestinal complications following surgery/RT/CT and their imaging features.5. Genitourinary complications following surgery/RT/CT and their imaging features.6. Musculoskeletal complications following RT/CT and their imaging features.7. Post treatment vascular complications and their imaging features.8. Emerging treatments and associated complications and their imaging features.

Printed on: 02/07/23



## Abstract Archives of the RSNA, 2022

OBEE-21

### You should not pass: Simplifying MR Defecography

Sunday, Nov. 27 8:00AM - 9:00AM Room: Learning Center - OB

#### Awards

**Magna Cum Laude**

#### Participants

Brenda Hernandes dos Santos Teixeira, MD, Sao Paulo, Brazil (*Presenter*) Nothing to Disclose

#### TEACHING POINTS

1. Describe and highlight image acquisition protocols in Magnetic Resonance (MR) Defecography. 2. Improve the understanding of female pelvic floor anatomy using a didactic approach by illustrations and MR images. 3. Recognition of MR Defecography imaging patterns of pelvic floor dysfunctions and diagnostic value.

#### TABLE OF CONTENTS/OUTLINE

Review of the main imaging female pelvic floor anatomy. MR Defecography protocols. Case-based examples and illustrative key points of the main pelvic floor disorders: Anterior compartment: - Cystocele - Urethra Hypermobility. Middle compartment: - Uterine prolapse. Posterior compartment: - Enterocele - Rectocele - Rectal prolapse - Rectal intussusception - Anismus<sup>4</sup>. Discuss the perspectives for MR Defecography in clinical routine and imaging findings that aid surgical decisions.5. Conclusions and "take home messages": consolidate the acquired knowledge.

Printed on: 02/07/23



## Abstract Archives of the RSNA, 2022

OBEE-22

### It's Not All About the Bump- Imaging of the Adnexa During Pregnancy

Sunday, Nov. 27 8:00AM - 9:00AM Room: Learning Center - OB

#### Awards

Certificate of Merit

#### Participants

Catherine Phillips, MD, Nashville, TN (*Presenter*) Nothing to Disclose

#### TEACHING POINTS

1. Complete OB assessment should include dedicated adnexal imaging. Early recognition of adnexal pathology permits timely diagnosis and necessary treatment. 2. First trimester offers a unique opportunity to identify adnexal pathology before the enlarging uterus displaces the adnexa and possibly conceals lesions. 3. Adnexal pathology findings during pregnancy may be subtle. Diagnosis may be facilitated by transvaginal scanning, which provides superior resolution and is particularly helpful in obese patients. 4. US remains the diagnostic imaging test of choice to not only localize patient's symptoms and characterize incidental masses of pregnancy, but also guide therapeutic planning if needed. MRI can be helpful as a supplemental modality, particularly if lesions are large or of uncertain origin.

#### TABLE OF CONTENTS/OUTLINE

1. Diagrammatic depiction and imaging of normal anatomy of the adnexa (US, CT and MRI) 2. Review of imaging appearance of benign adnexal lesions with focus on how their appearance can differ during pregnancy including: Corpus luteum, Hemorrhagic cysts, Dermoid, Endometriomas including decidualized endometriomas, Hydrosalpinx, Fibroma, Torsion, Ovarian hyperstimulation (hormonal or treatment related), Subserosal fibroid projecting into the adnexa (and associated torsion), Complications related to prior surgeries. 3. Imaging appearance of neoplastic adnexal lesions including: Borderline tumors, Struma ovarii, Cystadenoma and adenocarcinoma, Immature ovarian teratoma. 4. Adnexal pregnancies including interstitial, ectopic pregnancies, and pregnancies in uterine Mullerian anomalies. 5. Mimics of adnexal pathology in pregnancy.

Printed on: 02/07/23



## Abstract Archives of the RSNA, 2022

OBEE-23

### A Game of Patterns: A Case based review on Ultrasonographic Imaging of Ovarian-Adnexal lesions

Sunday, Nov. 27 8:00AM - 9:00AM Room: Learning Center - OB

#### Participants

Madhumitha B, MBBS, (*Presenter*) Nothing to Disclose

#### TEACHING POINTS

This exhibit aims to 1. Review the ACR US- ORADS risk stratification method. 2. Precisely identify and characterize the common ovarian and adnexal lesions. 3. Apply ORADS to these lesions and categorize them based on their risk for malignancy.

#### TABLE OF CONTENTS/OUTLINE

1. Introduction 2. ORADS 3. A Detective's Perspective -Observation -Deduction -Knowledge 4. Case Series 5. Conclusion

Printed on: 02/07/23



## Abstract Archives of the RSNA, 2022

OBEE-24

### The right iliac fossa: from a new perspective

Sunday, Nov. 27 8:00AM - 9:00AM Room: Learning Center - OB

#### Awards

Certificate of Merit

#### Participants

Giovanna Andreani, MD, Sao Paulo, Brazil (*Presenter*) Nothing to Disclose

#### TEACHING POINTS

Endometriosis is defined as the presence of endometrial tissue outside the uterine cavity and frequently affects about 10% of women of reproductive age, generating symptoms such as dysmenorrhea, dyspareunia and pelvic pain, and infertility. Endometriotic involvement of structures of the right iliac fossa accounts for about 29% of women diagnosed with endometriosis and may affect the distal ileum, cecum, appendix, round ligament, among others. Although it is not such a frequent site of involvement, radiologists must be familiar with the imaging findings for the hypothesis of endometriosis in this topography to be raised. The objective of this study is to didactically illustrate cases of endometriosis affecting the right iliac fossa, how to systemize imaging exams to not miss possible lesions, and what information must be provided, in order to allow proper diagnosis and therapeutic planning.

#### TABLE OF CONTENTS/OUTLINE

Discussion of the different radiological findings of endometriosis and its involvement in structures of the right iliac fossa, based on cases obtained in our institution's digital archive in different imaging modalities, including ultrasound and magnetic resonance imaging. We also provide literature review, teaching points and references.

Printed on: 02/07/23



## Abstract Archives of the RSNA, 2022

OBEE-25

### Peripartum and Post-Partum Hemorrhage

Sunday, Nov. 27 8:00AM - 9:00AM Room: Learning Center - OB

#### Awards

Identified for RadioGraphics  
Certificate of Merit

#### Participants

Nicole M. Hindman, MD, New York, NY (*Presenter*) Nothing to Disclose

#### TEACHING POINTS

1. Bleeding during pregnancy can be due to a wide variety of etiologies, for which the majority will be evaluated by ultrasound as the first and often the only modality required. 2. Post-partum bleeding /hemorrhage (PPH) can be due to a wide variety of etiologies. US remains the first line of imaging, however often additional modalities may be helpful to further discern etiology, extent and potential treatment options.

#### TABLE OF CONTENTS/OUTLINE

Section 1 will discuss relevant imaging modalities available. Section 2 will discuss the common etiologies of intrapartum bleeding, with a focus on late pregnancy. Some of the topics covered will include: Normal appearance of the placenta Bleeding related to the placenta including hematoma and abruption. Placenta previa Vasa previa Uterine rupture Diagnostic pitfalls. Section 3 will review the etiologies of bleeding in the post-partum period, typically termed post-partum hemorrhage (PPH) to include the following: Normal post-partum bleeding Retained products of conception, subinvolution of trophoblastic tissue and enhanced myometrial vascularity Review the distinction between AVM and enhanced myometrial vascularity Discuss rare etiologies of postpartum hemorrhage, such as uterine artery pseudoaneurysm. Various types of hematomas associated with caesarean section. Uterine dehiscence and/or rupture and their etiologies

Printed on: 02/07/23



## Abstract Archives of the RSNA, 2022

OBEE-26

### Vaginal Rejuvenation: Radiological Approach for Female Genital Anatomy and Procedures

Sunday, Nov. 27 8:00AM - 9:00AM Room: Learning Center - OB

#### Participants

Luciana Zattar, MD, Sao Paulo, Brazil (*Presenter*) Nothing to Disclose

#### TEACHING POINTS

Female genital minimal-invasive procedures are increasingly being performed. In this context, the radiologist has been requested to evaluate this region in order to recognize the anatomical aspects as well as to identify procedures or materials, including fillers, thread lifts, injectable lipolytic, collagen biostimulators, and its complications. To achieve accurate and timely detection and appropriate approach of each case, High frequency ultrasound (HFUS/24-33MHz) is the most effective method since it provides optimal anatomical information of the region and allows identification of different materials and procedures effects. This study aims to discuss and illustrate the radiologist's role in the evaluation of the female genital region with HFUS. The purpose of this exhibit is:- To describe the correct examination technique and preprocedure evaluation- To illustrate the anatomy of the female genital region- To show the main image patterns of the genital minimal-invasive aesthetic procedures- To list, classify and describe the most common related complications in genital region- To discuss the differential diagnosis in genital female lesions- To highlight the importance of HFUS guidance in genital procedures with videos

#### TABLE OF CONTENTS/OUTLINE

1. PREPROCEDURAL EVALUATION: Anatomical aspects and Female genital layers.2. PROCEDURES IMAGING FINDINGS AND GUIDANCE.3. COMPLICATIONS.4. DIFFERENTIAL DIAGNOSIS: most common genital lesions.5. CONCLUSION.

Printed on: 02/07/23

## Abstract Archives of the RSNA, 2022

OBEE-27

### Distal Mesonephric Anomalies: What Radiologists Need to Know about OHVIRA Syndrome

Sunday, Nov. 27 8:00AM - 9:00AM Room: Learning Center - OB

#### Participants

Mariko Kumazawa, MD, Shimotsuga-gun, Japan (*Presenter*) Nothing to Disclose

#### TEACHING POINTS

Werner-Herlyn-Wunderlich syndrome (WHWS) is known as obstructed hemivagina and ipsilateral renal anomaly (OHVIRA), and it has also been reported using various other names. Distal mesonephric anomalies result in the inhibition of appropriate development, fusion between the Müllerian ducts (the origin of the uterus and the vagina), resorption of the separating walls, and abnormal kidney development. There are many reports of various subtypes of WHWS by degree of development. The purposes of this educational exhibit are as follows:- To understand the embryology of this syndrome; what kind of malformation may occur?- To be able to predict what malformation causes a clinical presentation given clinical information, such as a patient's complaint and age.- To know the points of interpretation that contribute to treatment.

#### TABLE OF CONTENTS/OUTLINE

1. Present embryology explaining OHVIRA and a classification of uterine malformations according to embryology published by Ación.
2. Describe the relationship between various uterine and renal-urinary malformations and their clinical presentation.
3. Discuss the key points of magnetic resonance imaging and interpretation that contribute to appropriate treatments with case presentations as follows: i) two cases of OHVIRA with ipsilateral ectopic ureter, ii) two cases of acute abdominal pain by hematometra or peritonitis, and iii) a case of Gardner's cyst.
4. Summarize the history of the various terms.

Printed on: 02/07/23



## Abstract Archives of the RSNA, 2022

OBEE-28

### What's going on with the uterus: getting to know the new ASRM classification of Müllerian structures anomalies

Sunday, Nov. 27 8:00AM - 9:00AM Room: Learning Center - OB

#### Participants

Paolo Franco, MD, Milano, Italy (*Presenter*) Nothing to Disclose

#### TEACHING POINTS

Müllerian structures anomalies are developmental malformations of the female genital tract, with prevalence estimated from 0.5 to 6.7% in the general population. Many of these conditions may lead to significant health and reproductive consequences. Over the years, several systems have been proposed to classify müllerian anomalies. The most used ones are the American Fertility Society (AFS) Classification from 1988 and the European Society of Human Reproduction (ESHRE) and Embryology-European Society for Gynecological Endoscopy (ESGE) Classification, which includes not only uterine but also cervical and vaginal anomalies. The 2021 American Society for Reproductive Medicine (ASRM) Classification (MAC2021) was recently developed to update previous classification systems, include all malformations categories, and promote a more standardized terminology. The purposes of this exhibit are: (1) to review female genitourinary system embryology; (2) to get familiar with congenital female malformations; (3) to explore the new 2021 ASMR Müllerian anomalies classification; (4) to compare it with previous classifications, particularly those developed by AFS and ESHRE-ESGE; (5) to describe MRI findings of female genital anomalies by showing interesting cases.

#### TABLE OF CONTENTS/OUTLINE

1. Female genitourinary system embryology and normal anatomy 2. Previous Mullerian anomalies classifications 3. The new 2021 ASMR Mullerian anomalies classification 4. MR female imaging protocols 5. MRI findings of the different female genital malformations

Printed on: 02/07/23



## Abstract Archives of the RSNA, 2022

OBEE-29

### MRI in uterine cancers with uncertain origin: endometrial or cervical. A radiological point of view

Sunday, Nov. 27 8:00AM - 9:00AM Room: Learning Center - OB

#### Participants

Luca Russo, MD, Roma, Italy (*Presenter*) Grant, Elekta AB

#### TEACHING POINTS

Therapeutic options and clinical management of cervical and endometrial cancers differs significantly. When clinical and histological analysis of a uterine mass are inconclusive, pelvic magnetic resonance imaging (MRI) may help establish the site of origin, allowing appropriate management and treatment planning. Radiologists should be aware of the morphologic (location, shape and different patterns of growth) and functional (enhancement pattern, tumor perfusion, diffusion-weighted imaging and spectroscopy) MRI features that can support the correct assessment of the site of origin.

#### TABLE OF CONTENTS/OUTLINE

1. Introduction to the clinical problem and suggested MRI protocol 2. Typical MRI features of primary cervical and endometrial cancers 3. Morphologic MRI features that can help discriminate between endocervical and endometrial cancers, including location, shape and locoregional spread 4. Functional MRI features that can help discriminate between endocervical and endometrial cancers, including enhancement pattern and tumor perfusion, diffusion-weighted imaging and spectroscopy 5. Conclusion

Printed on: 02/07/23



## Abstract Archives of the RSNA, 2022

OBEE-3

### How to Improve Your Routine Transvaginal Ultrasound for Detection of Endometriosis - A Practical Guide for General Radiologists

Sunday, Nov. 27 8:00AM - 9:00AM Room: Learning Center - OB

#### Awards

Certificate of Merit

#### Participants

Luciana P. Chamie, MD, PhD, Sao Paulo, Brazil (*Presenter*) Nothing to Disclose

#### TEACHING POINTS

1. Endometriosis is a chronic inflammatory disease with significant diagnostic delays varying from four to 11 years 2. Although characteristically multifocal, the retrocervical space is the most common location of deep infiltrative endometriosis (DIE), present in most patients at the initial diagnosis as a hypoechogenic nodule or thickening affecting the uterosacral ligaments. 3. This repetitive and predictable characteristic of retrocervical endometriosis makes it suitable for early diagnosis. 4. Accurate diagnosis can have a tremendous impact on the evolution of the disease, quality of life, and fertility outcomes. 5. Transvaginal sonography (TVS) is the first-line imaging modality to investigate endometriosis and a cost-effective tool. 6. The standard TVS protocol misses the evaluation of the most common locations of endometriosis 7. The addition of a simple algorithm to the standard TVS protocol can reduce the late diagnosis and improve clinical care in patients suffering from long-standing undiagnosed endometriosis.

#### TABLE OF CONTENTS/OUTLINE

1. Title 2. Disclosures 3. Learning Objectives 4. Background information about endometriosis including last updates. Review the most common sites of endometriosis and anatomical landmarks . Discuss the typical presentation of DIE though TVS 5. Standard TVS limitations- discuss why basic ultrasound protocol miss endometriosis detection 6. Dedicated TVS protocol- comprehensive description on how to perform the maneuvers emphasizing advantages and limitations as well as potential pitfalls. 7. Imaging findings of endometriosis on TVS through case examples from mild to severe DIE 8. Conclusion 9. References

Printed on: 02/07/23



## Abstract Archives of the RSNA, 2022

OBEE-30

### Problems are opportunities in disguise: Added value of contrast enhanced US (CEUS) in evaluation of the female pelvic disease

Sunday, Nov. 27 8:00AM - 9:00AM Room: Learning Center - OB

#### Awards

Identified for RadioGraphics

#### Participants

Mariam Moshiri, MD, Brentwood, TN (*Presenter*) Nothing to Disclose

#### TEACHING POINTS

Ultrasound is the first imaging modality for evaluation of female pelvic disease followed by problem-solving or further evaluation with MRI and in rare cases other modalities such as CT, PET, angiography. Ultrasound Contrast agents (UCAs) have emerged as a valuable adjunct to ultrasound and allow visualization and evaluation of lesions that may not be possible on standard ultrasound imaging alone. We aim to describe and illustrate the utility of CEUS as a valuable adjunct in evaluation of disease in the female pelvis using a case-based approach. We will describe common pitfalls and offer some tips for optimizing the use of CEUS during such examinations. Lastly, we will suggest a workflow pattern that describes when CEUS use is appropriate

#### TABLE OF CONTENTS/OUTLINE

1. Stepwise review of technique for use of CEUS in the pelvis. 2. Review application through case-based approach with correlative imaging from other modalities and pathologic specimens( Cervical cancer; Fibroid; Ovarian lesions; Endometrial disease/lesions; Post-partum complications such as retained products of conception; AVM, etc; Hysterosalpingo contrast sonography (HyCoSy); Transperineal invasive procedures using CEUS such as biopsy, drainage, etc; 3.Tips and tricks-Lesion visualization: Compression, patient position, etc; Avoiding pitfalls of CEUS (avoiding accelerated bubble destruction, troubleshooting artifacts) 4.Table summarizing recommended utilization and techniques

Printed on: 02/07/23



## Abstract Archives of the RSNA, 2022

OBEE-31

### Hysterosalpingography as a useful tool for the study of fallopian tubes and uterine cavity when MRI is not available

Sunday, Nov. 27 8:00AM - 9:00AM Room: Learning Center - OB

#### Participants

Victor Lara Ameca, MD, (*Presenter*) Nothing to Disclose

#### TEACHING POINTS

- Hysterosalpingography is a diagnostic procedure of great utility in the evaluation of the female reproductive tract. It provides useful information outlining the uterine cavity and the fallopian tubes. Radiologists should become familiar with the technique and the interpretation of HSG images.
- The knowledge of the anatomy and common findings is necessary for the accuracy in the diagnosis and adequate interpretation of image findings.
- There are several implications that should be taken into account performing these studies; patient preparation, good communication with the patient explaining the procedure and answering all the questions. An adequate technique is necessary to limit factors leading to misinterpretation and to identify morphologic changes and corroborate them with complementary projections.
- Describe step by step procedure to successfully perform this studies and achieve diagnostic images.
- Present a systematic approach to adequate interpretation of hysterosalpingography.
- Describe and illustrate findings related to anatomical abnormalities of the uterine cavity such as polyps, fibroids, adhesions, adenomyosis and congenital abnormalities. Describe and illustrate findings related to abnormalities of the fallopian tubes as hydrosalpinx, salpingitis isthmica nodosa and surgical changes.

#### TABLE OF CONTENTS/OUTLINE

- Introduction.
- Indication.
- Normal anatomy and variations.
- Step by step procedure.
- Illustrative and imaging findings of polyps, fibroids, adhesions, adenomyosis and congenital abnormalities. Describe and illustrate findings related to abnormalities of the fallopian tubes as hydrosalpinx, salpingitis isthmica nodosa and surgical changes.
- Conclusion.

Printed on: 02/07/23



## Abstract Archives of the RSNA, 2022

OBEE-32

### Normal and abnormal appearance of the ovaries during assisted reproduction: a multimodality review

Sunday, Nov. 27 8:00AM - 9:00AM Room: Learning Center - OB

#### Awards

Identified for RadioGraphics

#### Participants

Katherine Smith, MD, (*Presenter*) Nothing to Disclose

#### TEACHING POINTS

- Assisted reproductive technology (ART) is increasing in utilization, thus increasing the likelihood that radiologists will encounter both the normal and abnormal imaging findings associated with these treatments.
- Sonographic monitoring is used for follicle tracking during ART cycles, but these images are usually acquired and interpreted by obstetricians. Thus, many radiologists are unfamiliar with the normal imaging appearance of the female pelvis during ART treatments.
- Radiologists should be familiar with the acute complications related to ART treatments.

#### TABLE OF CONTENTS/OUTLINE

A. Background• Overview of population data regarding the utilization of ART• Brief discussion of the clinical medicine involved with ARTB. Multimodality review of the normal appearance of the ovaries in patients undergoing ARTC. Abnormal ovarian appearance and complications in patients undergoing ART• Review of the Golan classification system for ovarian hyperstimulation syndrome• Discussion of the acute complications related to ART, including ovarian torsion and ectopic pregnancyD. Challenging and unusual cases• Case-based discussion of unique presentations in patients undergoing ART therapy• Problem-solving approach to challenging clinical or imaging scenarios

Printed on: 02/07/23



## Abstract Archives of the RSNA, 2022

OBEE-33

### Characterization of (minimally, partially, and predominantly) Solid Ovarian Masses

Sunday, Nov. 27 8:00AM - 9:00AM Room: Learning Center - OB

#### Participants

Manasi Arora, MBBS, (Presenter) Nothing to Disclose

#### TEACHING POINTS

Imaging characteristics (size, shape, vascularity, contrast enhancement) of solid ovarian masses (SOM) can help differentiate between malignant and benign lesions. Early and accurate imaging diagnosis of SOM has significant therapeutic and prognostic implications. The presence of solid components (greater than 3 mm) arising from the cyst wall or septation and protruding into the cyst cavity (papillary projections) has been shown to be the single most important predictor of malignancy. Through this exhibit, we aim to 1) outline the role of imaging in the diagnosis of SOM, 2) characterization of SOM based on their imaging features (ultrasound, CT, and MRI), 3) review the common and uncommon solid ovarian lesions, and 4) highlight the key imaging findings that allow differentiation of malignant solid ovarian tumors from benign and pseudo-lesions.

#### TABLE OF CONTENTS/OUTLINE

A case-based discussion of the imaging features of minimally, partially, and predominantly SOM, with emphasis on the characteristics of their solid components. Our discussion will outline a comparison between mixed solid and cystic as well as predominantly solid ovarian neoplasms that will include but are not limited to clear cell carcinoma, serous and mucinous carcinomas, endometrioid carcinoma, dysgerminoma, granulosa cell tumors, and similar appearing benign lesions (fibromas, mature teratoma, brenner tumors) as well as pseudo-lesions that mimic a SOM on imaging.

Printed on: 02/07/23

## Abstract Archives of the RSNA, 2022

OBEE-34

### Anatomy and Functional Pathology of the Female Pelvic Girdle: From Bones to Bladder

Sunday, Nov. 27 8:00AM - 9:00AM Room: Learning Center - OB

#### Participants

Julie An, MD, San Diego, CA (*Presenter*) Nothing to Disclose

#### TEACHING POINTS

- The female pelvic floor including bony structures, the pelvic organs, and supportive myofascial components- These normal structures not only maintains the anatomic position of the pelvic organs but also allow for normal function- Pelvic floor dysfunction encompasses a group of disorders affected by deficit in these various structures and can lead to bladder, bowel, and/or sexual dysfunction which may inhibit daily activities and negatively impact

#### TABLE OF CONTENTS/OUTLINE

- Review the anatomy of the female pelvis by layers (the most physiologic system for organizing female pelvis):-- Osseous structures, with an emphasis on variations of the female pelvic bones-- Visceral organs and attachments-- Endopelvic Fascia- Cardinal, uterosacral, urethral ligaments, vaginal viscera-- Levator Ani- puborectalis, pubococcygeus, iliococcygeus, and coccygeus-- Perineal Membrane- insertion of perineal muscles, external anal sphincter, and superficial perineal muscles- Present normal and pathologic MRI cases resulting from injury to normal structures-- Endometriosis with scarring of the uterosacral ligament and broad ligament resulting in chronic pelvic pain-- Rectal cancer status post radiation with thinning and fat containing hernia adjacent to the levator ani resulting in rectal prolapse-- Sacral fracture resulting in injury of bilateral coccygeus and iliococcygeus at the level of fracture-- Multiparity with multiple vaginal delivery and subsequent injury to the coccygeus resulting in multi-compartmental prolapse

Printed on: 02/07/23



## Abstract Archives of the RSNA, 2022

OBEE-35

### FIGO Staging Classification for Cervical Cancer - A Practical Guide for Radiologists

Sunday, Nov. 27 8:00AM - 9:00AM Room: Learning Center - OB

#### Participants

Bruna Alexandre, MD, Sao Paulo, Brazil (*Presenter*) Nothing to Disclose

#### TEACHING POINTS

Review the female pelvis anatomy; Describe cervical cancer MRI protocol; Describe current management, treatment, and surgical techniques; Recognize the most important imaging features to report in tumor detection, primary staging and restaging, and post-treatment evaluation; Briefly review the 2018 FIGO Staging Classification; Discuss the key points that every radiologist needs to know about cervical cancer.

#### TABLE OF CONTENTS/OUTLINE

INTRODUCTION: Cervical cancer epidemiology; Cervical cancer prevention.FEMALE PELVIS ANATOMY: Review the female pelvis anatomy, highlighting the important landmarks for an adequate staging, correlating didactic illustrations with MRI.MANAGEMENT OF CERVICAL CANCER: Treatment guidelines and algorithmMRI IMAGING PROTOCOL: Exam preparation; MRI protocol.IMAGING EVALUATION: Step by step approach to evaluate cervical cancer; Didactic clinical cases approach to cervical cancer staging; Template reporting system; Limitations and pitfalls of cervical cancer MRI imaging; The most important information that gynecologists/oncologists want to know from imaging; Post-treatment imaging evaluation.

Printed on: 02/07/23

## Abstract Archives of the RSNA, 2022

OBEE-36

### Imaging of Female Pelvic Masses of Unknown Origin: Tips and Tricks

Sunday, Nov. 27 8:00AM - 9:00AM Room: Learning Center - OB

#### Awards

Cum Laude

#### Participants

Francesca Rosa, MD, Savona, Italy (*Presenter*) Nothing to Disclose

#### TEACHING POINTS

1. To illustrate a step-by-step approach to female pelvic lesions to define the epicentre of a pelvic mass and to reach the proper diagnosis. 2. To describe the radiological findings and specific imaging "signs" of a wide spectrum of pelvic disease.

#### TABLE OF CONTENTS/OUTLINE

1. Pelvic space anatomy description. 2. Anatomic pelvic space-based approach to pelvic mass. 3. Spectrum of imaging "signs" as imaging key to define the space of origin of a pelvic mass. 4. List differential diagnosis peculiar to each space.

Printed on: 02/07/23

## Abstract Archives of the RSNA, 2022

OBEE-37

### Post-surgical Complications of Gynecological Procedures: An Updated Review

Sunday, Nov. 27 8:00AM - 9:00AM Room: Learning Center - OB

#### Participants

Ana Uski, MD, Sao Paulo, Brazil (*Presenter*) Nothing to Disclose

#### TEACHING POINTS

Know the “new normal anatomy” of the pelvis depending on the type of surgical procedure used. Discuss imaging modalities in the assessment of potential complications after gynecological surgery, focusing on CT and MRI. Recognize the radiological findings of these complications according to the type of procedure used.

#### TABLE OF CONTENTS/OUTLINE

Post-surgical gynecological complications are more frequent in extensive procedures, especially in the context of neoplasms, and may be seen less frequently in less invasive procedures such as myomectomies, placement of intrauterine devices, collection of endometrial sampling, endometriosis resection or repair pelvic floor. The most frequent complications include hematomas/hemorrhages, collections, infections, vascular injuries, intestinal and urinary injuries, suture dehiscence, fistulas and lymphoceles, and different imaging modalities play an important role in their diagnosis and follow-up. In stable patients, an initial approach with ultrasound should be considered, but in cases of clinical worsening, computed tomography (CT) is the most indicated exam, while magnetic resonance imaging (MRI) is relevant in the evaluation of mainly late complications. Recognizing normal postsurgical anatomy, expected postoperative findings, complications of each procedure, and pitfalls in image interpretation will facilitate diagnosis.

Printed on: 02/07/23



## Abstract Archives of the RSNA, 2022

OBEE-38

### Multi-Modality Imaging of Endometriosis with Correlative Operative Images: What the Surgeon Wants to Know

Sunday, Nov. 27 8:00AM - 9:00AM Room: Learning Center - OB

#### Participants

Won-Kyung Sung, MBBS, Paddington, Australia (*Presenter*) Nothing to Disclose

#### TEACHING POINTS

- Endometriosis affect approximately 10% of women of reproductive age and approximately 35-50% of women who suffer from pelvic pain or infertility?
- Endometriotic lesions can exist in a variety of anatomic locations; this represents a diagnostic challenge that can lead to under- and delayed recognition of endometriosis due to lower degrees of suspicion
- In addition, the diversity of anatomic location of endometriotic lesions can change surgical plans
- While diagnostic laparoscopy with histological confirmation is a reliable method of diagnosis, imaging is a less invasive diagnostic alternative that can augment surgical interventions and aid in preoperative evaluation?
- Ultrasonographic imaging (particularly transvaginal sonography (TVS)) can determine the location and extent of endometriosis in patients with suggestive clinical examinations
- MR imaging is a high sensitivity and specificity second-line study, and it is especially useful in patients with previous equivocal TVS or involving structures poorly evaluated by US.

#### TABLE OF CONTENTS/OUTLINE

Purpose: The purpose of this study is to characterize and correlate laparoscopic and radiologic findings in the context of endometriosis and to highlight the role of radiologic interpretation in the surgical management of endometriosis patients. ??  
Content Organization? ?? 1.???? Overview of endometriosis? 2.???? Laparoscopic operative approach to endometriosis? 3.???? Imaging techniques, advantages, and disadvantages? 4.???? Case examples?

Printed on: 02/07/23



## Abstract Archives of the RSNA, 2022

OBEE-39

### Don't Ovary-Act: O-RADS US/MRI updates and integration

Sunday, Nov. 27 8:00AM - 9:00AM Room: Learning Center - OB

#### Participants

Daniela Garcia, MBBS, Philadelphia, PA (*Presenter*) Nothing to Disclose

#### TEACHING POINTS

1. O-RADS classifies adnexal masses into different risk categories only applicable to asymptomatic patients with average risk of malignancy. 2. Early familiarization with lexicon and standardized reporting decreases ambiguity in surveillance and management of adnexal masses. 3. Presence of solid component and high vascularity/enhancement are highly associated with malignancy. 4. Integration of O-RADS US and MRI can confidently rule out malignancy when imaging features are characteristic.

#### TABLE OF CONTENTS/OUTLINE

Radiologists are usually the first providers to encounter adnexal masses in daily practice and the ones guiding management and surveillance with serial imaging. In the setting of equivocal radiology reports, due to difficulty in obtaining tissue biopsy samples, adnexal lesions are often managed surgically. O-RADS is a standardized reporting system that identifies different risk groups according to specific imaging descriptors with the goal of improving communication between radiologist and referring providers, helping detect patients with potential malignancy and avoiding unnecessary surgery. Integration of O-RADS US and MRI has proven to have good predictive value and is easily reproducible. This exhibit is a pictorial, multimodality imaging based review of the O-RADS lexicon and its application in the daily evaluation of patients with adnexal masses.

Printed on: 02/07/23



## Abstract Archives of the RSNA, 2022

OBEE-4

### Postpartum Pelvis: Imaging Management of Early and Delayed Complications

Sunday, Nov. 27 8:00AM - 9:00AM Room: Learning Center - OB

#### Participants

Marianna Konidari, MD, London, United Kingdom (*Presenter*) Nothing to Disclose

#### TEACHING POINTS

The postpartum period refers to the time interval from birth to 6-8 weeks later, when the uterus undergoes physiologic involution and returns to its nongravid state. Familiarization with normal postpartum imaging findings of the pelvis is essential to avoid misdiagnosis of disease. Normal appearances of the pelvis following vaginal delivery differ from those after caesarean section. During the first days after CS, it may be difficult to distinguish normal early postoperative changes from possible uterine complications. US, CT, and MRI can be used for imaging of the postpartum pelvis, each having different indications depending on the clinical setting. The role of imaging in the diagnosis of acute and delayed delivery complications is crucial since these are associated with greater morbidity and can even be fatal.

#### TABLE OF CONTENTS/OUTLINE

Normal anatomy and physiology of the postpartum pelvis and correlation with multimodality imaging: which are the most common normal imaging findings. Vaginal delivery vs caesarean section: what imaging findings to normally expect after each type of delivery. Rationale behind imaging during the postpartum period. Which is the best modality in different clinical scenarios and why. Acute complications: key imaging findings and the implications for morbidity and treatment. Case-based discussion on haemorrhage/hematomas; uterine rupture; endometritis; retained products of conception; pelvic vein thrombosis; intraoperative injuries. Delayed complications: when to suspect them and what signs to look for in imaging. Case-based discussion on endometriosis/ ectopic pregnancy on CS scar; placenta accreta spectrum disorder; gestational trophoblastic disease.

Printed on: 02/07/23



## Abstract Archives of the RSNA, 2022

OBEE-40

### Rhombencephalosynapsis in fetal MRI: main findings and step-by-step evaluation

Sunday, Nov. 27 8:00AM - 9:00AM Room: Learning Center - OB

#### Participants

Patricia Oliveira-Szejnfeld, MD, MD, Sao Paulo, Brazil (*Presenter*) Nothing to Disclose

#### TEACHING POINTS

1) Review the rhombencephalosynapsis disease spectrum concerning etiology, classification, epidemiological / clinical data and imaging features; 2) Demonstrate a structured evaluation of the fetal infratentorial structures through magnetic resonance imaging (MRI); 3) Depict the main findings of the rhombencephalosynapsis disease spectrum in fetal MRI as well as associated malformations and their implications in neonatal follow-up.

#### TABLE OF CONTENTS/OUTLINE

Teaching images will be employed to illustrate the following topics: 1) Embryology of infratentorial structures; 2) Rhombencephalosynapsis: underlying causes, disease spectrum, clinical findings and postnatal imaging; 3) Evaluation of infratentorial structures in fetal MRI (technical aspects and standardized imaging protocol; normal appearance; anatomical landmarks and how they change over time; pearls and pitfalls; potential limitations); 4) MR imaging findings in rhombencephalosynapsis disease spectrum (detailed and accurate analysis, with step-by-step morphological and biometric evaluation of the vermis and cerebellum); 5) Associated malformations in the antenatal period and their imaging findings, as well as a review of the additional evaluation required in the antenatal and postnatal period when the diagnosis is established.

Printed on: 02/07/23



## Abstract Archives of the RSNA, 2022

OBEE-41

### **MRI of the fetal midbrain: a step-by-step evaluation of normal and altered findings beyond aqueductal stenosis**

Sunday, Nov. 27 8:00AM - 9:00AM Room: Learning Center - OB

#### **Participants**

Patricia Oliveira-Szejnfeld, MD, MD, Sao Paulo, Brazil (*Presenter*) Nothing to Disclose

#### **TEACHING POINTS**

1) Conduct a brief review of antenatal ultrasound (US) findings that suggest midbrain anomalies; 2) Demonstrate a structured evaluation of the fetal midbrain through magnetic resonance imaging (MRI); 3) Highlight the main MRI findings of midbrain anomalies and associated malformations.

#### **TABLE OF CONTENTS/OUTLINE**

1) Brief review of midbrain embryology. 2) The antenatal sonographic evaluation concerning technical aspects and equipment features; time of best assessment; midbrain sonographic anatomy (size/growth nomograms, shape, position, and texture; assessment of tectal length and anteroposterior diameter. Midbrain anomalies in fetal sonography (elongation, thinning, shortening, upward rotation) and potential limitations of antenatal US. 3) MRI evaluation of the fetal midbrain, concerning technical aspects and standardized imaging protocols; Main indications and when to perform; MRI anatomy and how to recognize the normal appearance and anatomical landmarks, as well as their changes over time. Detailed explanations will be provided on how to perform an accurate analysis, with step-by-step morphological and biometric evaluation. Finally, main midbrain malformations will be illustrated with teaching cases.

Printed on: 02/07/23



## Abstract Archives of the RSNA, 2022

OBEE-42

### As easy as pie: MR imaging of the placenta made simple - a practical guide for beginners

Sunday, Nov. 27 8:00AM - 9:00AM Room: Learning Center - OB

#### Participants

Ana De Ataide Goes, MD, Sao Paulo, Brazil (*Presenter*) Nothing to Disclose

#### TEACHING POINTS

- To prepare radiologists to evaluate placental MRI based on a structured reporting model. - To review and illustrate the role of MRI in the diagnosis of the main abnormalities of the placenta. - To provide illustrations to clarify the anatomy and pathology of the placenta. - To present clinical cases in correlation with pathology results. - To review the literature and present tips to reduce interobserver variability.

#### TABLE OF CONTENTS/OUTLINE

1) Background: The importance of placental MR imaging in different diagnostic settings and in the management of placental conditions. 2) Correlation between anatomy and histology of normal placenta, including the normal appearance on MRI. 3) Brief description of MRI protocol for placental assessment. 4) Structured reporting model to guide MRI evaluation. 5) Illustrative cases of the main conditions of the placenta with their imaging features and interpretation:- Anatomical variations; - Placenta previa; - Umbilical cord insertion on placenta; - Placenta accreta spectrum; - Placenta disruption; - Placenta neoplasm (as chorioangioma). 6) Additional findings. 7) Potential pitfalls in placental MRI.

Printed on: 02/07/23



## Abstract Archives of the RSNA, 2022

OBEE-43

### Non-Obstetrical Abdominal and Pelvic Imaging during Pregnancy: A Multimodality Review

Sunday, Nov. 27 8:00AM - 9:00AM Room: Learning Center - OB

#### Participants

Kyle Jensen, MD, Portland, OR (*Presenter*) Nothing to Disclose

#### TEACHING POINTS

1. Pregnant patients present with non-obstetrical pathology, which must be included in the differential diagnosis. 2. Imaging pregnant patients requires specialized CT and MR protocols and considerations. 3. Pregnant patients require unique imaging, work-up, and treatment of benign and malignant pathologies.

#### TABLE OF CONTENTS/OUTLINE

1. Imaging protocols in the gravid patient for US, CT, and MR with discussion on intravenous contrast use. 2. Imaging of maternal infections including COVID-19. 3. Imaging of acute abdominal or pelvic pain during pregnancy by organ system. 4. Non-obstetrical, gynecologic pathology in the pregnant patient. 5. Trauma imaging in the pregnant patient. 6. Oncologic work-up during pregnancy. 7. Imaging work-up of benign/incidental findings.

Printed on: 02/07/23



## Abstract Archives of the RSNA, 2022

OBEE-44

### Placental hemorrhage throughout gestation: from chorionic bump to Couvelaire uterus

Sunday, Nov. 27 8:00AM - 9:00AM Room: Learning Center - OB

#### Awards

Identified for RadioGraphics

#### Participants

Roya Sohaey, MD, Portland, OR (*Presenter*) Nothing to Disclose

#### TEACHING POINTS

First trimester trophoblastic and early placental hemorrhage can present as chorionic bump or perigestational hemorrhage, and sonographic features can predict pregnancy outcome. Second and third trimester placental abruption can be marginal, retroplacental, preplacental, and intrauterine. Abruption is associated with maternal and fetal morbidity and mortality, therefore accurate imaging-guided classification is important.

#### TABLE OF CONTENTS/OUTLINE

1. Sonographic features of first trimester trophoblastic hemorrhage and which imaging findings predict outcome. We will focus on chorionic bump and perigestational hemorrhage 2. Sonographic features of abruption and which imaging findings predict outcome: marginal abruption, retroplacental abruption, pre-placental abruption, Couvelaire uterus (intra-myometrial hemorrhage) 3. Pitfalls of hemorrhage: adenomyosis, accreta, acute blood mimics placenta, and other mimickers

Printed on: 02/07/23



## Abstract Archives of the RSNA, 2022

OBEE-45

### Endometriosis-related infertility: Hysterosalpingography, Ultrasound and MRI findings

Sunday, Nov. 27 8:00AM - 9:00AM Room: Learning Center - OB

#### Participants

Luciana P. Chamie, MD, PhD, Sao Paulo, Brazil (*Presenter*) Nothing to Disclose

#### TEACHING POINTS

? Endometriosis is a common disease that affects women of reproductive age, being responsible for almost 60% of infertility cases ? Laparoscopy is no longer the gold standard for the diagnosis of endometriosis, being replaced by imaging exams such as a transvaginal ultrasound (TVS) and pelvic MRI ? Radiologists should identify typical imaging findings on hysterosalpingography, ultrasound (US) and MRI related to endometriosis that may impair fertility outcomes ? Information provided by imaging methods is crucial for clinical counseling and surgical planning and to establish a fertility prognosis

#### TABLE OF CONTENTS/OUTLINE

? Definition of infertility and endometriosis; ? Types of endometriosis and role of radiological exams; ? Illustrated teaching cases reviewing findings on hysterosalpingography, US and MR that should be considered in the management of infertility related to endometriosis; ? Didactic approach of relevant data, including: ? Clinical: ; Patient`s age and anti-mullerian hormone dosage; ; Past obstetric history; ? Transvaginal ultrasound and MRI with bowel preparation: ; Antral follicle count; ; Endometriomas; ; Complex pelvic adhesions; ; Rectosigmoid endometriotic lesions; ; Subserous myometrial infiltration due to endometriosis; ; Hydrosalpinx; ; Post-operative findings (Isthmocele; thin uterine wall); ? Hysterosalpingography: ; Evaluation of tubal mobility and motility; ; Obliteration of fallopian tubes

Printed on: 02/07/23



## Abstract Archives of the RSNA, 2022

OBEE-46

### Hysterosalpingography and Caesarean section: A Niche subject

Sunday, Nov. 27 8:00AM - 9:00AM Room: Learning Center - OB

#### Participants

Elizabeth J. Evans, MBChB, Glasgow, United Kingdom (*Presenter*) Nothing to Disclose

#### TEACHING POINTS

By reviewing this exhibit the viewer will appreciate: The hysterosalpingographic (HSG) appearances of caesarean section scars The correlation between HSG appearances with other imaging modalities such as ultrasound and MRI. The importance of identifying adhesions, Asherman's syndrome, within the C-section scar and elsewhere in the cavity. The importance and relevance of other uterine and tubal abnormalities that may be contributing to secondary subfertility and which might influence future pregnancy outcomes.

#### TABLE OF CONTENTS/OUTLINE

Introduction. Background including data relating to increasing frequency of caesarean section and associated immediate and chronic complications. The role of imaging in identifying uterine abnormality following caesarean section. Other uterine and tubal abnormalities which impact on the management of women with secondary subfertility and previous Caesarean section. Suggest a simple grading system to correlate with appearances, severity and prognosis of caesarean section defects.

Printed on: 02/07/23



## Abstract Archives of the RSNA, 2022

OBEE-47

### Ovarian peritoneal carcinomatosis-Role of Radiologist in treatment

Sunday, Nov. 27 8:00AM - 9:00AM Room: Learning Center - OB

#### Participants

Reefath Jabaraj, FRCR, (*Presenter*) Nothing to Disclose

#### TEACHING POINTS

To define the most common routes of ovarian peritoneal carcinomatosis dissemination in abdomen  
To recognise imaging characteristics of ovarian peritoneal carcinomatosis  
Role of radiologist in preoperative imaging in treatment of carcinomatosis

#### TABLE OF CONTENTS/OUTLINE

Introduction  
Routes of spread in abdomen  
Key radiological findings in surgical planning  
Resectable vs difficult to resect areas- a pictorial review  
Imaging in evaluating the effectiveness of chemotherapy  
Role of follow up imaging in surveillance  
Take home message

Printed on: 02/07/23



## Abstract Archives of the RSNA, 2022

OBEE-48

### When Pregnancy Becomes a Problem"- Pictorial Essay of Common and Uncommon Gestational Complications in the Radiological Practice

Sunday, Nov. 27 8:00AM - 9:00AM Room: Learning Center - OB

#### Participants

Ulysses Torres, MD, PhD, Sao Paulo, Brazil (*Presenter*) Nothing to Disclose

#### TEACHING POINTS

To recall the theoretical basis of the range of differential diagnoses of complications directly related to the gestational period - the obvious and non-obvious ones. To discuss the classical imaging features of these complications. To present examples of rare cases and typical images. To review which information matters for the differential diagnosis, especially when thinking of ectopic pregnancy. To present challenging diagnostic cases and demonstrate how radiologists can help in outcomes.

#### TABLE OF CONTENTS/OUTLINE

Diagram for diagnostic reasoning of gestational complication, dividing it as:- Related to location of pregnancy: including cases of ectopic pregnancy (cervical, cesarian scar, ampullar, interstitial, angular, intra-abdominal, cornual) and heterotopic pregnancy. - Related to gestational content: including cases of trophoblastic disease as complete and partial mola, invasive mola, and choriocarcinoma. - Related to placentary issues such as placenta accreta, placenta previa, retroplacental hemorrhage, and placental mass (chorioangioma). - Related to systemic/extrauterine issues, such as hepatic subcapsular hematoma related to HELLP syndrome and the last but not the least decidualized endometriosis.

Printed on: 02/07/23



## Abstract Archives of the RSNA, 2022

OBEE-49

### Imaging the post-treatment pelvis in gynecologic cancer

Sunday, Nov. 27 8:00AM - 9:00AM Room: Learning Center - OB

#### Participants

Behnaz Moradi, MD, Tehran, Iran, Islamic Republic Of (*Presenter*) Nothing to Disclose

#### TEACHING POINTS

Complications of gynecologic cancer treatment can be categorized into early and late onset. They can be related to surgery or chemoradiotherapy. Different imaging modalities as ultrasound, CT scan and MRI based on the involved organ and their availability can be used for diagnosis.

#### TABLE OF CONTENTS/OUTLINE

In this exhibit, we will discuss about: 1) early complications as hematoma; genitourinary and gastrointestinal complications; infectious process; uterine rupture and wound dehiscence. 2) late complications as genitourinary and gastrointestinal complications; inclusion cyst and seroma formation; fistula; pelvic bone insufficiency fractures; neuritis; post radiotherapy vaginal and cervical stenosis and cystitis.

Printed on: 02/07/23



## Abstract Archives of the RSNA, 2022

OBEE-5

### **Pelvic Deep Endometriosis: What Radiologists Should Point Out in Preoperative Imaging**

Sunday, Nov. 27 8:00AM - 9:00AM Room: Learning Center - OB

#### **Participants**

Satoshi Asai, (*Presenter*) Nothing to Disclose

#### **TEACHING POINTS**

Endometriosis is one of the most common and burdening gynecological diseases, estimated to surpass 50% prevalence in women with infertility and chronic pelvic pain. Three types of endometriosis are recognized: ovarian, superficial, and deep. Of these, deep endometriosis (DE) is the most severe form, and surgery is the final solution for symptomatic cases. However, not only it is difficult to recognize all lesions in the surgical field, but it is also difficult to see the relationship to the surrounding organs, and even the lesion itself can be the invisible area. Therefore, preoperative MRI is the key to successful surgery. We advocate for diagnostic imaging that gives the surgeons the information they really need. First, we advocate separate reading and structured reporting for anterior, middle, and posterior compartment of pelvis, which can facilitate the diagnosis of DE and also help to estimate possible complications. Second, based on our experience with complications, we will also discuss the sites of lesions that are prone to be overlooked, and optimal views and imaging methods. Additionally, we show the correlation between MRI and laparoscopic appearance as an aid to understanding DE.

#### **TABLE OF CONTENTS/OUTLINE**

- Introduction to pelvic deep endometriosis with diagnostic and surgical problem - Complications of surgery - structured reporting - key images which are easy to find and often associated with DE - the surgical outcome after structured reporting

Printed on: 02/07/23



## Abstract Archives of the RSNA, 2022

OBEE-50

**It's all about location, location, location: Distinguishing pregnancies in Mullerian anomalies from abnormally implanted pregnancies.**

Sunday, Nov. 27 8:00AM - 9:00AM Room: Learning Center - OB

### Participants

Glynis Sacks-Sandler, MBBCh, Nashville, TN (*Presenter*) Nothing to Disclose

### TEACHING POINTS

1. Congenital uterine anomalies are often asymptomatic, and the first trimester sonogram may be the first opportunity to diagnose Mullerian anomalies. 2. The recently updated ASRM classification (2021) relies on simple diagrams and descriptions to expand recognition of the multiple variations. More accurate diagnosis based on imaging will lead to improved clinical outcomes. 3. 3D transvaginal ultrasound imaging offers a high degree of diagnostic accuracy. 4. Mullerian anomalies have recognized obstetrical implications, with the most common septate uterus often requiring hysteroscopic septal resection. 5. Pregnancies in association with Mullerian anomalies need to be distinguished from abnormally implanted gestations including interstitial and cesarian scar pregnancies.

### TABLE OF CONTENTS/OUTLINE

1. Illustrate Mullerian Duct anomalies (MDA) in the non-gravid uterus with correlating 3D ultrasound. 2. Optimal imaging of early intrauterine pregnancies in association with MDA's including Arcuate uterus, Bicornuate uterus, Septate uterus, and Uterus didelphys. 3. Clinical implications of pregnancies in septate uterus and in non-communicating horns. 4. Imaging of "Mimics" including Interstitial pregnancy, angular pregnancy as well as degenerating fibroids. 5. Review of unusual cases

Printed on: 02/07/23



## Abstract Archives of the RSNA, 2022

OBEE-51

### The Bulky Uterus: A Resident's Guide to Diffuse Uterine Pathology

Sunday, Nov. 27 8:00AM - 9:00AM Room: Learning Center - OB

#### Participants

Elizabeth Deans, MD, (*Presenter*) Nothing to Disclose

#### TEACHING POINTS

1. Diffuse uterine disease can be seen in several pathologies ranging from benign to malignant. 2. Knowledge of the normal appearance of the uterus and cervix by ultrasound, computed tomography (CT) and magnetic resonance imaging (MRI) is important for early detection of pathology. 3. The radiologist plays a vital role by using a combination of key imaging features to help distinguish between these benign and malignant pathologies.

#### TABLE OF CONTENTS/OUTLINE

This educational exhibit will:- Discuss the normal appearance of the uterus and cervix by ultrasound, computed tomography (CT), and magnetic resonance imaging (MRI)- For each of the following uterine pathologies, this exhibit will review pathophysiology and risk factors, describe and illustrate the spectrum of multimodality imaging appearances, and briefly discuss management options:- Diffuse uterine adenomyosis - Diffuse uterine leiomyomatosis - Post-radiation changes - Infection - Hormonal therapy changes - Postpartum changes - Uterine sarcoma/leiomyosarcoma - Invasive cervical/endometrial cancer - Metastatic uterine disease, including diffuse lymphomatous disease

Printed on: 02/07/23



## Abstract Archives of the RSNA, 2022

OBEE-52

### US and MRI of the Uterus: The Good, The Bad and The Ugly

Sunday, Nov. 27 8:00AM - 9:00AM Room: Learning Center - OB

#### Participants

Krupa Patel-Lippmann, MD, Nashville, TN (*Presenter*) Nothing to Disclose

#### TEACHING POINTS

1. US and MRI are complementary modalities in the evaluation of uterine lesions. US is the first line modality, with MRI utilized for equivocal or poorly visualized findings on US and delineation of suspected malignancy. 2. Benign lesions include endometrial polyps, adenomyosis and leiomyomas, which have a characteristic appearance on US and MR. When present, the radiologist can be confident of the diagnosis. 3. Malignant lesions include endometrial cancers and leiomyosarcomas. These lesions can be suggested based on their US appearance, with MRI used for confirmation and delineation of local tumor extent. 4. Features on multiparametric MRI can help distinguish leiomyomas and leiomyosarcoma.

#### TABLE OF CONTENTS/OUTLINE

- Introduction to imaging the uterus A. Normal anatomy B. Describe the complementary role of US and MRI
- Review imaging features of benign vs malignant endometrial and myometrial lesions A. Endometrial polyps and hyperplasia versus endometrial cancer B. Adenomyosis and leiomyomas versus leiomyosarcomas
- Differentiating leiomyomas versus leiomyosarcomas A. Features of leiomyomas o US: Well-defined and multiple areas of shadowing o MRI: Smooth border, dark T2 signal, no restricted diffusion; homogenous enhancement B. Features of leiomyosarcoma o US: Limited shadowing, irregular margin o MRI: Lobular/irregular margin, cloudy high signal on T1, intermediate T2 signal, restricts diffusion and enhancement C. Overlapping features can be seen in cases of atypical leiomyoma, STUMP, and low grade leiomyosarcoma

Printed on: 02/07/23



## Abstract Archives of the RSNA, 2022

OBEE-53

### From Leiomyoma to Leiomyosarcoma: A Review of the Imaging Spectrum of Uterine Smooth Muscle Tumors with Pathological Correlation

Sunday, Nov. 27 8:00AM - 9:00AM Room: Learning Center - OB

#### Participants

Keith A. Ferguson, MD, (*Presenter*) Stockholder, Hims & Hers Health, Inc

#### TEACHING POINTS

- - Describe the spectrum of uterine smooth muscle tumors, from benign to malignant - - Discuss pathology of LM variants and provide updated clarifications on different terms such as atypical, cellular, mitotic LMs, STUMP, etc. - - Identify radiological features of uterine leiomyosarcomata (LMS), ordinary leiomyomata (LM), and leiomyoma variants including smooth muscle tumors of uncertain malignant potential (STUMP) - - Demonstrate correlations between the radiological and histopathological features of uterine LMS, LM, and STUMP

#### TABLE OF CONTENTS/OUTLINE

- Title, names, institutions - Review of uterine smooth muscle tumors o Epidemiology Risk factors, Pathogenesis o Presentation - Diagnosis, Management and treatment options o Indications for imaging in assessing uterine tumors CT, MRI, US, PET/CT o Characteristic imaging features of benign and malignant uterine tumors - Our multi-institutional project - List patient cohorts, demographics - Show examples of ordinary LM including imaging and path characteristics o Non-degenerated o Degenerated Cystic Myxoid Hemorrhagic - Show examples of LM variants including imaging and path characteristics o Cellular o STUMP - Show examples of LMS including imaging and path characteristics o Routine and variants (myxoid, epithelioid) o Metastasis: patterns of recurrence and spread - Summarize characteristic imaging and histopathological features of uterine smooth muscle tumors - Conclusions and future steps - Acknowledgements, references

Printed on: 02/07/23



## Abstract Archives of the RSNA, 2022

OBEE-54

### Peritoneal Endometriosis and MRI: A New Look!

Sunday, Nov. 27 8:00AM - 9:00AM Room: Learning Center - OB

#### Participants

Carolina Almeida, MD, Rio de Janeiro, Brazil (*Presenter*) Nothing to Disclose

#### TEACHING POINTS

TEACHING POINTS 1) Endometriosis is a disease that affects thousands of women and compromises their quality of life, causing chronic pain, infertility, and problems in sexual life. 2) Peritoneal endometriosis is often underdiagnosed and prevents adequate treatment. 3) Laparoscopy is the gold standard exam for the investigation of endometriosis, but it is an invasive method, and many women refuse or are afraid to undergo laparoscopy. 4) Clarify doubts about the appropriate exam protocol and what are the myths about MRI in endometriosis. 5) MRI allows the identification of signs that support the diagnosis of peritoneal endometriosis. These signs are subtle, and it is essential that the radiologist knows how to identify them. 6) Demonstrate MRI images and their correlation with exploratory laparoscopy in superficial endometriosis.

#### TABLE OF CONTENTS/OUTLINE

TABLE OF CONTENTS/OUTLINE 1) Overview of peritoneal endometriosis and a short quiz 2) Identification of focal, diffuse peritoneal thickening and peritoneal failure on MRI and laparoscopy 3) Identification of thickening and glandular tissue on the surface of organs 4) Identification of bloody fluid and septa on MRI and laparoscopy 5) Summary of changes found in each method.

Printed on: 02/07/23



## Abstract Archives of the RSNA, 2022

OBEE-55

### Ultrasound in Endometriosis: Chocolate Cysts and Beyond

Sunday, Nov. 27 8:00AM - 9:00AM Room: Learning Center - OB

#### Participants

Divya Singh, MD, MBBS, (*Presenter*) Nothing to Disclose

#### TEACHING POINTS

Ultrasonography is a widely available, inexpensive, real-time imaging modality which can be used to detect pelvic involvement by endometriosis beyond the classic ovarian endometriomas. Deep infiltrating endometriosis (DIE) implants are seen as well circumscribed, hypoechoic lesions with smooth or irregular margins using ultrasound. A systematic sonologic approach in evaluation of the pelvis is imperative for detection of DIE in the anterior and posterior compartments. Ultrasound offers the advantage of using soft markers like a negative sliding sign and probe tenderness to guide the search for DIE. Endometriomas undergo decidualisation during pregnancy which can mimic ovarian tumors on ultrasonography. Ultrasound can raise a red flag for occurrence of malignant transformation in long standing endometriomas.

#### TABLE OF CONTENTS/OUTLINE

Impact of endometriosis on women's health; Pathology; Clinical presentation: The great masquerader; Ultrasound evaluation technique; Sonographic features: Soft markers, overt findings; Changes in endometriosis in pregnancy; Malignant transformation of endometriomas; Conclusion

Printed on: 02/07/23



## Abstract Archives of the RSNA, 2022

OBEE-56HC

### Intrauterine Contraceptive Devices: History, Imaging and Complications

Sunday, Nov. 27 8:00AM - 9:00AM Room: Learning Center - OB

#### Participants

Lisa Xuan, MD, BSc, Newmarket, ON (*Presenter*) Nothing to Disclose

#### TEACHING POINTS

1. For almost 100 years, iterations of intrauterine contraceptive devices (IUCD) have been in use. Older models are of historical interest and may be found incidentally on imaging. 2. Both copper and hormone-releasing IUCDs are as effective as tubal ligation in preventing pregnancy, but a 2 in 100 person per year pregnancy rate persists. 3. Malpositioning is the most common IUCD complication, and exists as a spectrum depending on severity. 4. All malpositioning should be communicated to the clinician as it may lead to decreased contraceptive efficacy or require intervention.

#### TABLE OF CONTENTS/OUTLINE

A brief history of IUCDs-1st generation-Non-copper metal devices-2nd generation-Plastic devices-3rd generation-Copper bearing devices-4th generation-Hormone bearing devices-5th generation-Frameless intrauterine implants Radiographic evaluation of IUCDs- Adequate positioning (on plain films, US and CT)-3D ultrasound as the gold standard in assessing malpositioning Complications of IUCDs- Malpositioning spectrum (expulsion, displacement, embedment, perforation)-Synchronous pregnancy-Ectopic pregnancy- Fragmentation of device-Clinical implications Cased Based Imaging Scenarios Summary Please visit the Learning Center to also view this presentation in hardcopy format.

Printed on: 02/07/23



## Abstract Archives of the RSNA, 2022

OBEE-6

### Tips to Definitely Understand Pelvic Innervation in Endometriosis: The Guide You Asked For

Sunday, Nov. 27 8:00AM - 9:00AM Room: Learning Center - OB

#### Participants

Helena de Souza, MD, Sao Paulo, Brazil (*Presenter*) Nothing to Disclose

#### TEACHING POINTS

- To prepare abdominal radiologists to evaluate magnetic resonance imaging (MRI) of pelvic innervation in the context of endometriosis.- To summarize the somatic and visceral neural anatomy in a practical way.- To illustrate the main findings of neural involvement by deep pelvic endometriosis with selected clinical cases.- To demonstrate the impact of such knowledge on patients' management and how radiologists may improve outcomes.

#### TABLE OF CONTENTS/OUTLINE

- Background: the importance of pelvic innervation MR imaging in diagnostic settings of deep pelvic endometriosis.- Description of the somatic and visceral neural anatomy and correlation with the normal appearance on MRI.- Interactive anatomical atlas and videos showing the pelvic innervation and its involvement in deep endometriosis based on anatomical diagrams and MRI imaging exams.- Tips and tricks.

Printed on: 02/07/23

## Abstract Archives of the RSNA, 2022

OBEE-7

### Plumbing Problems: Troubleshooting Tips for Complex Fetal Genitourinary Malformations

Sunday, Nov. 27 8:00AM - 9:00AM Room: Learning Center - OB

#### Awards

Certificate of Merit

Identified for RadioGraphics

#### Participants

April Griffith, MD, (*Presenter*) Nothing to Disclose

#### TEACHING POINTS

1: Review all scans for development of urinoma, urinary ascites, obstructive dysplasia  
2: Assess bladder filling, changes in ureteric caliber, color Doppler for patent urethra  
3: Use MRI when low fluid, maternal habitus limit US assessment  
4: Confirm diagnoses with postnatal imaging, operative findings, genetic testing, autopsy

#### TABLE OF CONTENTS/OUTLINE

Megacystis-1st trimester aneuploidy-Euploid fetus: Posterior urethral valves (PUV), prune belly (PB), megacystis microcolon intestinal hypoperistalsis (MMIH), urethral atresia-Evaluate genitalia (dilated urethra in PB, MMIH in female)-Pitfall dilated vagina for distended bladder  
Multicystic dysplastic kidney (MCDK) vs obstructive dysplasia (OD)-MCKD large kidney, large cysts, no pelvic dilation-OD small, echogenic kidney, small cysts-Look for ureterocele, ectopic more likely with duplication, can insert in vagina  
Urinary tract dilation (UTD)-Ureteropelvic junction obstruction: Pitfall MCDK-Duplicated system: Pitfall cystic adrenal mass vs obstructed upper moiety-Reflux: Variable ureter size-Report with 2014 UTD Classification System  
Genitourinary sinus malformation-Establish fetal sex (persistent cloaca, hydrocolpos, imperforate hymen in females)-Look for anal dimple-Fluid-fluid levels due to meconium/urine mixing in dilated vagina-  
Calcified meconium due to bowel-urinary tract fistula-MRI for evaluation of colon/rectum/anus--Meconium high T1, low T2, high GRE--Fluid low T1, high T2  
Anatomic variants-Crossed fused ectopia, pelvic kidney

Printed on: 02/07/23



## Abstract Archives of the RSNA, 2022

OBEE-8

### Pain Points: Making Sense of Pelvic Nerves Involved with Endometriosis and Chronic Pain

Sunday, Nov. 27 8:00AM - 9:00AM Room: Learning Center - OB

#### Awards

Cum Laude

Identified for RadioGraphics

#### Participants

Ceylan Colak, MD, MD, (*Presenter*) Nothing to Disclose

#### TEACHING POINTS

1. Endometriosis is a common condition impacting approximately 1 out of every 10 women of childbearing age. 2. Deep infiltrating endometriosis most commonly occurs in the pelvis and is typically multifocal. 3. Although rarely reported, several lumbosacral nerves course through the pelvis and can be involved by deep infiltrating endometriosis including the sciatic, pudendal, obturator and hypogastric nerves. 4. Neural involvement by endometriosis may lead to pain or other neurological symptoms including muscle weakness, numbness, incontinence and paraplegia. 5. MRI is the most reliable noninvasive modality to diagnosis neural involvement by endometriosis. Protocol optimization can help increase conspicuity of nerves involved by endometriosis. 6. Imaging findings are variable and include identification of a deep infiltrative endometriotic lesion directly involving the nerve or nerve thickening with increased enhancement. In chronic cases, muscle atrophy may be present. 7. Identification of neural involvement is important for early diagnosis and treatment to avoid irreversible nerve injury and loss of function.

#### TABLE OF CONTENTS/OUTLINE

1. Title 2. Disclosures 3. Learning Objectives 4. Background information about endometriosis with neural involvement 5. Normal anatomy of pelvic nerves with imaging examples 6. MRI protocol considerations 7. Imaging findings of nerves involved by endometriosis illustrated through case examples 8. Conclusion 9. References

Printed on: 02/07/23



## Abstract Archives of the RSNA, 2022

OBEE-9

### Postpartum and Post-abortion Complications - A Guide for Radiologists

Sunday, Nov. 27 8:00AM - 9:00AM Room: Learning Center - OB

#### Participants

Cynthia Borborema, MD, Sao Paulo, Brazil (*Presenter*) Nothing to Disclose

#### TEACHING POINTS

To review the normal imaging appearance of postpartum and post-abortion period and to distinguish it from complications that require treatment. To list radiologic features of early and late postpartum and post-abortion complications to provide a practical guide to help radiologists. To emphasize an integrated radiologic and clinical approach in the assessment of challenging postpartum and post-abortion conditions to improve the clinical impact of radiology reports.

#### TABLE OF CONTENTS/OUTLINE

Normal uterine changes in puerperium. Normal changes after cesarean delivery. Role of imaging in assessment of postpartum and post-abortion period and relevant report information. Diagnostic tools, with emphasis in computed tomography and magnetic resonance imaging. Usual and unusual postpartum and post-abortion complications (infectious, thromboembolic and hemorrhagic), including key patient history, risk factors, imaging findings, and pitfalls. Review of cesarean surgical technique (laparotomy, bladder flap creation and hysterotomy) and correlation with early related complications. Late cesarean delivery-related complications. Uterine complications after pregnancy-related curettage.

Printed on: 02/07/23



## Abstract Archives of the RSNA, 2022

PDEE

### Pediatric Education Exhibits

Sunday, Nov. 27 8:00AM - 9:00AM Room: Learning Center - PD

#### Sub-Events

#### PDEE-1 Cardiac and Pericardial Neoplasm in Children: Radiologic-Pathologic Correlation

##### Awards

Identified for RadioGraphics

Cum Laude

##### Participants

Mariangeles Medina Perez, MD, Syracuse, NY (*Presenter*) Nothing to Disclose

##### TEACHING POINTS

· Illustrate the most common cardiac and pericardial masses in children and their relative prevalence. · Describe the characteristic imaging characteristics of primary pediatric benign and malignant cardiac and pericardial neoplasm based on pathologic features. · Identify imaging features that can help differentiate benign from malignant etiology.

##### TABLE OF CONTENTS/OUTLINE

· Role of imaging with delineation of technique and pediatric protocols. · Characterization of specific primary cardiac and pericardial tumors with description of clinical considerations, imaging features by different modalities, and pathologic features. · Appropriate differential diagnosis according to tumor location and imaging features.

#### PDEE-10 The Many Faces of Lymphomas in Pediatric Patients: Spectrum of Multimodality Imaging Findings in Thoracic and Abdominal Lymphomas

##### Participants

Luisa Faria, MD, Sao Paulo, Brazil (*Presenter*) Nothing to Disclose

##### TEACHING POINTS

Lymphomas account for 10%-15% of all cancers in the pediatric age group, being the third most common malignancy, following leukemia and malignant brain tumors. All organ systems may be involved, including the central nervous system, head and neck, thorax, abdomen, gonads, and bone, and several different histologic subtypes can be found. As a result, the spectrum of imaging findings is wide and the diagnosis can be challenging (particularly in extranodal disease), with considerable imaging overlap with other diseases. The purposes of this exhibit are: (1) to illustrate the spectrum of multimodality imaging findings in thoracic and abdominal lymphomas in the pediatric age group (2) to point out the most important differential diagnosis and lymphoma mimickers.

##### TABLE OF CONTENTS/OUTLINE

(1) Review of epidemiology and histologic subtypes. (2) Chest involvement (imaging findings, mimickers, and differential diagnosis): chest wall, pleura, lungs, mediastinal structures. (3) Abdominal involvement (imaging findings, mimickers, and differential diagnosis): liver, pancreas, biliary tree, spleen, small bowel, colon, kidney, ureters, peritoneum, and testes.

#### PDEE-11 Complications in Transjugular Liver Biopsy (TJLB) and Tips to Avoid Them

##### Participants

Juan Calle Toro, MD, MS, San Antonio, TX (*Presenter*) Nothing to Disclose

##### TEACHING POINTS

Different techniques can be used before, during, and after a TJLB to avoid potential complications

##### TABLE OF CONTENTS/OUTLINE

Liver biopsy remains the gold standard to diagnose cirrhosis, hepatitis, nonalcoholic fatty liver disease, primary biliary cirrhosis, autoimmune hepatitis and post-transplant for the diagnosis of rejection 1. Transjugular liver biopsy (TJLB) is preferred in patients with coagulopathies given the low risk of bleeding. Diagnostic sample rate in TJLB is 96.1% with low technical failure rate of 3.2%. Technical failure is usually due to failure to catheterize the hepatic vein 1. Complications of TJLB include subcapsular perforation in 1.4%, neck hematoma in 0.8%, intraperitoneal hemorrhage in 0.6%, arrhythmia in 0.05%, and pneumothorax in 0.05% 2. We recommend several tips to avoid complications. Ultrasound should be performed prior to the procedure to confirm the patency of the hepatic veins and jugular access. Secondly, we recommend using Tru-Cut (Quick-Core). Additionally; TJLB should be performed during breath hold. Finally, when in position to fire the biopsy needle, we advise wedging the cannula antero-lateral if the right hepatic vein is used, or lateral if the middle hepatic vein is used. The procedure should ideally be done in facilities equipped to handle bleeding complications 3. It is recommended to avoid TJLB in patients with thrombosis of the right IJ vein, thrombosis of hepatic veins, cholangitis, or lack of patient cooperation 4. In those cases, alternative routes can be considered such as transfemoral biopsy, endoscopic ultrasound-guided liver biopsy, or Laparoscopic liver biopsy 5.

## **PDEE-12      Ultrasound Evaluation of The Chest: Neonatal and Pediatric Cases**

Participants

Muhammad Khan, MD, Memphis, TN (*Presenter*) Nothing to Disclose

### **TEACHING POINTS**

1. To review proper chest ultrasound technique. 2. To discuss normal appearance of chest on US. 3. To discuss and illustrate ultrasound imaging appearance of neonatal and pediatric chest abnormalities by correlating the cases with cross sectional imaging. 4. Reinforcement of the ALARA principle along with the dictum of "Image gently"

### **TABLE OF CONTENTS/OUTLINE**

Ultrasound (US) is an excellent imaging modality for initial evaluation of chest due to its portable nature, lack of radiation and no need for contrast administration and sedation. Due to recent advances and improvement in technology the use of US in evaluation of chest has significantly increased. The main indications for chest US in children include, follow up and evaluation of antenatally detected lung abnormalities, assessment of an opaque hemithorax, differentiating cystic from solid lesions, evaluation of chest wall lesion, mediastinal masses, lung lesions, diaphragmatic hernia/eventration and clarify inconclusive plain film findings. Table of contents: Introduction - Chest Ultrasound Technique- normal anatomy and appearance - simple pleural effusion, empyema, ECMO and trauma related hemothorax, chest wall and mediastinal masses (teratoma, neuroblastoma, chest wall masses lipoblastoma, hemangioma), diaphragmatic hernia, eventration, hiatal hernia, pneumonia, necrotizing pneumonia, and atelectasis

## **PDEE-13      MR Insights into Fetal Brain Development: What is Normal and What is Not**

**Awards**

**Certificate of Merit**

Participants

Maria Camila Cortes Alborno, MD, (*Presenter*) Nothing to Disclose

### **TEACHING POINTS**

• 1. Fetal life is the most dynamic period of human brain development. • 2. MRI demonstrates all major developmental processes in vivo: hemispheric cleavage, sulcation, evolution of transient telencephalic zones, involution of germinal matrix, myelination, and growth of the corpus callosum and vermis. • 3. Awareness of normal fetal brain development enables the clinical fetal imager to identify abnormalities as they emerge.

### **TABLE OF CONTENTS/OUTLINE**

Illustration of normal processes of fetal brain development on structural images: Single-shot T2, Steady State Free Precession, T1-VIBE. Compare and contrast cases of normal development with pathologic cases. The collection includes: holoprosencephaly, polymicrogyria, cortical malformations, ventriculomegaly, callosal dysgenesis, vermian hypoplasia, rhombencephalosynapsis, among others. Review of emerging sequences on fetal MRI and their role in characterizing brain development: T2\*-weighted and DTI.

## **PDEE-14      Cancer Therapy-Related Hepatic Injury In Children: An Imaging Review From the Pediatric LI-RADS Workgroup**

**Awards**

**Cum Laude**

**Identified for RadioGraphics**

Participants

Cara Morin, PhD, Memphis, TN (*Presenter*) Nothing to Disclose

### **TEACHING POINTS**

The liver is the primary organ for the metabolism of many chemotherapeutic agents, and drug-induced liver injury is common in children undergoing cancer therapy. Acute toxic effects of cancer therapy in children include cholestasis, hepatitis, steatosis, steatohepatitis, hemosiderosis, and vascular complications such as sinusoidal obstruction syndrome. Longer-term effects of cancer therapy can include fibrosis, liver failure, and focal liver lesions that can be confused for metastatic disease.

### **TABLE OF CONTENTS/OUTLINE**

Introduction (including incidence and the effects of therapy on peri-operative morbidity) Imaging modalities Discussion of specific roles and pros/cons in children Description of quantitative sequences to assess for steatosis/iron deposition Specific etiologies of liver injury Hepatitis Cholestasis/biliary injury Vascular complications (e.g., SOS, PV thrombosis) Hepatic GVHD Steatosis steatohepatitis Iron deposition Radiation injury Expected appearance of treated metastatic disease (including post-ablation) Fibrosis cirrhosis Focal liver lesions FNH-like lesions, perfusion abnormalities, metastases, etc. Diagnostic challenges of underlying steatosis/siderosis Diagnostic challenges of differentiating benign lesions from recurrent/metastatic disease

## **PDEE-15      Ingested Foreign Bodies in Children-How Do We Image and What To Report**

Participants

Jeong Rye Kim, MD, PhD, Cheonan, Korea, Republic Of (*Presenter*) Nothing to Disclose

### **TEACHING POINTS**

1. Discuss the role of each imaging modality in the diagnosis of ingested foreign bodies in children 2. Review the general management considerations according to the location and the opacity of foreign bodies 3. Discuss imaging findings and management guidelines of specific types of ingested foreign bodies

### **TABLE OF CONTENTS/OUTLINE**

1. How to image children with ingested foreign bodies a. First imaging step: Radiography i. Guidelines for radiographic work-up ii. Things to report iii. What if there are negative findings on radiographs? b. Second line imaging modalities: CT versus US 2. General management considerations a. According to the location of FBs b. Radioopaque versus radiolucent FBs 3. Imaging findings and

management guidelines of specific types of ingested FBs. a. Magnets b. Battery c. Sharp FBs d. Blunt FBs (marbles, coins) e. Glass f. Water absorbent beads

## **PDEE-16 Visceral Torsions and Atypical Obstructions in the Pediatric Age Group**

Participants

Ankita Chauhan, MD,MBBS, (*Presenter*) Nothing to Disclose

### **TEACHING POINTS**

Background Information: Children often present to the pediatric emergency department with acute abdominal pain. It is particularly challenging to assess young children as they generally show nonspecific symptoms (fussiness, lethargy, inconsolable crying). An older child can often localize the pain and describe its character. The clinical signs of volvulus often are nonspecific, and radiologists often are consulted for diagnostic evaluations. Prompt diagnosis is crucial as a delay in diagnosis will result in increased morbidity and mortality. Teaching Points: 1. To learn the pathophysiology of visceral torsions and become familiar with their classic imaging appearances. 2. To become accustomed to identifying the twist in the hollow viscus and visceral torsions. 3. To become familiar with a few atypical but essential to know presentations of bowel obstruction in children. 4. To acquire a basic understanding of the radiographic obstructive bowel gas patterns.

### **TABLE OF CONTENTS/OUTLINE**

-Goals and objectives -Background information -Anatomy - Visceral torsions (midgut volvulus, gastric volvulus, small bowel internal hernia with volvulus, small bowel intussusception with volvulus, trichobezoar with volvulus, cecal volvulus, colonic volvulus, splenic torsion) -Atypical bowel obstruction (bezoars) -Summary

## **PDEE-17 Imaging Approach and Radiological Pitfalls of Pediatric Gastrostomy Tube Placement**

Participants

Lauren May, MD, (*Presenter*) Nothing to Disclose

### **TEACHING POINTS**

Teaching points: 1. Gastrostomy tubes are indicated for long term nutritional support, gastric decompression, or for future gastrojejunostomy conversion. 2. After placement or tube exchange, contrast can be administered through the gastrostomy to confirm intraluminal placement in the stomach. 3. Radiological technique may involve fluoroscopy by the radiologist or can be performed remotely with radiographs. 4. A checklist of findings to confirm placement includes contrast flowing dependently in the stomach away from the tube, contrast progressing to the small bowel, and visualization of the gastrostomy balloon. 5. Complications of gastrostomy tube placement include peritoneal leakage, enteric transgression, stomach perforation, buried bumper, gastric outlet obstruction, gastric or colonic cutaneous fistula formation, and gastrostomy site hernia. 6. Ultrasound and CT may be useful adjuncts for trouble-shooting challenging cases.

### **TABLE OF CONTENTS/OUTLINE**

Table of Contents/Outline: 1. Introduction 2. Clinical indications and gastrostomy tube placement technique 3. Fluoroscopy technique to confirm tube placement 4. Limited portable radiograph technique to confirm tube placement 5. Checklist to evaluate gastrostomy tube placement on radiographs and fluoroscopy 6. Ultrasound and CT: Useful problem-solving adjuncts 7. Illustrative case examples of complications highlighting pitfalls of imaging interpretation

## **PDEE-18 Typical and Not-so Typical Presentations of Childhood Intussusception**

Participants

Ankita Chauhan, MD,MBBS, (*Presenter*) Nothing to Disclose

### **TEACHING POINTS**

Background Information: Acute abdominal pain is a common complaint in pediatric emergency departments. Patients less than two years of age may present with inconsolable crying, fussiness, and/or lethargy, making the assessment particularly challenging compared to an older child able to localize the pain and describe its character. Intussusception's clinical symptoms are often nonspecific, and radiologists frequently perform diagnostic evaluations and therapeutic interventions. Teaching Points: 1. To acquire a basic understanding of the imaging features of intussusception with particular attention to the radiographic clues to the diagnosis. 2. To learn the pathophysiology of entero-enteric and entero-colic intussusceptions in the pediatric age group. 3. To become familiar with the atypical pathologic causes of intussusception. 4. To understand the radiologist's role in treating intussusception and recognizing complications of the disease or its treatment. 5. To recognize potential mimics of the disease.

### **TABLE OF CONTENTS/OUTLINE**

-Goals and objectives -Background information -Radiographic signs of intussusception - Types of intussusceptions -Management of entero-enteric intussusception -Management of ileocolic intussusception -Air enema (procedure, indications, contraindications, complications) -Mimics of Intussusception -Summary

## **PDEE-19 A Tour of Biliary Disorders, Anomalies, and Malignancies in Children**

**Awards**

**Identified for RadioGraphics**

Participants

Curtis Simmons, MD, (*Presenter*) Nothing to Disclose

### **TEACHING POINTS**

1. Distinct underlying genetic conditions can be made or suspected based on radiological/radiogenomic features. 2. Many congenital abnormalities can be understood from variations in embryological development. 3. While pediatric biliary malignancy is rare, rhabdomyosarcoma and cholangiocarcinoma are the two most likely entities. 4. Intra-operative cholangiograms can help visualize the biliary system not well evaluated with traditional imaging techniques. 5. The diagnosis of biliary atresia is evolving practice, with a delayed diagnosis causing a substantial increase in need for hepatic transplant.

## TABLE OF CONTENTS/OUTLINE

Introduction // Embryological Development of Ducts // Congenital Gallbladder Anomalies: Gallbladder agenesis, intrahepatic gallbladder, floating gallbladder, duplicated gallbladder, septate gallbladder // Anomalous pancreaticobiliary junctions: Aberrant cystic duct insertion, aberrant biliary ducts // Cholecystic processes: Neonatal hepatitis, biliary atresia, Alagille syndrome // Congenital cystic lesions: Choledochal cysts (types 1-4), Caroli's disease, Von Meyenburg complex, polycystic liver disease, complex and simple biliary cysts // Biliary filling anomalies: Cholelithiasis, choledocholithiasis, bile plug syndrome, sickle cell related cholelithiasis // Biliary changes in systemic genetic conditions: cystic fibrosis, autosomal dominant polycystic kidney disease, autosomal recessive polycystic kidney disease // Inflammatory biliary conditions: Sclerosis cholangitis // Pediatric biliary neoplasms: Rhabdomyosarcoma, cholangiocarcinoma // Conclusion

## PDEE-2 Pediatric Cardiac Masses: Multimodality Imaging with Rad-path Correlation

Participants  
Prabhakar Rajiah, MD, FRCR, Rochester, MN (*Presenter*) Nothing to Disclose

### TEACHING POINTS

Pediatric cardiac masses are rare, but it is important for radiologists to recognize these in time for initiating appropriate management. 1. To review the spectrum of cardiac masses in the pediatric population 2. To discuss the role of multimodality imaging in the evaluation of pediatric cardiac masses 3. To review optimal CT and MRI protocols of pediatric cardiac masses 4. To illustrate the imaging appearances of several pediatric masses with pathologic correlation

## TABLE OF CONTENTS/OUTLINE

- Introduction
- Spectrum of pediatric cardiac masses
- Multimodality imaging of pediatric cardiac masses- Ultrasound, CT, MRI, Nuclear medicine, cardiac cath
- Review and illustration of the following pediatric masses with case examples and path correlation where available - Benign tumors- Rhabdomyoma, fibroma, teratoma, myxoma, hemangioma, inflammatory myofibroblastic tumor - Malignant tumors- Metastases, sarcoma, lymphoma, leukemia - Non-neoplastic masses- Thrombus, Eosinophilic myocarditis, pericardial cyst, lipomatous hypertrophy of atrial septum, aneurysm, pseudoaneurysm, diverticulum, hamartomatous malformations - Anatomical variations- Prominent crista terminalis, Chiari network, taenia sagittalis, coumadin ridge

## PDEE-20CS Standardized Performance of Pediatric Appendix Ultrasound for Radiologists, Clinicians and Sonographers Introduction

Participants  
Lori L. Barr, MD, (*Presenter*) Nothing to Disclose

### TEACHING POINTS

Rationale of using a standardized exam protocol, sonographer worksheet and reporting template is explained. Identify and document the ultrasound characteristics of the normal and abnormal: appendix, right lower quadrant mesenteric fat, cecum, adjacent bowel loops, and right lower quadrant lymph nodes. Apply a standardized exam protocol to demonstrate presence or absence of primary and secondary appendicitis findings, a standardized sonographer worksheet and a standardized reporting template. Synthesize the imaging and sonographer worksheet information into a standardized report/impression that decreases the number of equivocal exams.

## TABLE OF CONTENTS/OUTLINE

Welcome and Pre-training Assessment has 4 activities, welcome, introduction to how the learning portal works, pre-training assessment and acknowledgments. Pediatric Ultrasound Appendix Exam Performance has 10 interactive activities: Minimum components of a complete exam, Required Images and Cines for a Complete Exam, Completing the Standardized Sonographer Worksheet, 10 Tips to Turn an Incomplete Exam into a Complete Exam, Normal Appendix, Appendix Not Identified No Appendicitis, Acute Appendicitis Not Perforated, 5 YO with right lower quadrant pain, Acute Appendicitis Perforated and Other Pathology That Presents with Right Lower Quadrant Pain. Pediatric Ultrasound Appendix Exam Interpretation has 7 activities: What is the Difference Between a Non-diagnostic Exam and an Equivocal Report?, Why use a standardized reporting template?, Download a Standardized Reporting Template, Definitive vs. Equivocal Interpretations, How to Minimize Equivocal Studies using a Template, 12 YO with RLQ Pain, Take This Post-training Assessment

## PDEE-22 Imaging Approach to Distal Neonatal Bowel Obstruction

### Awards Identified for RadioGraphics

Participants  
Samantha Gerrie, MBChB, FRANZCR, (*Presenter*) Nothing to Disclose

### TEACHING POINTS

1. Describe a structured approach to multimodality imaging workup of distal neonatal bowel obstruction including Hirschsprung disease, functional immaturity of the large bowel, meconium ileus, colonic atresia and segmental volvulus. 2. Highlight appropriate use of abdominal ultrasound (US) in specific problem solving scenarios.

## TABLE OF CONTENTS/OUTLINE

1. Introduction  
2. Hirschsprung disease  
a. Presentation, types, associations  
b. Radiographic finding  
c. Lower gastrointestinal (LGI) contrast study findings  
d. Pitfalls  
i. Total colonic Hirschsprung disease  
ii. Delayed or misdiagnosis in premature neonates  
iii. Delayed presentation in children with chronic constipation  
3. Functional immaturity of the large bowel  
a. Presentation  
b. Radiographic findings  
c. LGI contrast study findings  
d. Pitfalls  
i. Long-segment Hirschsprung disease mimicking functional immaturity  
ii. No clear caliber difference between right and left colon  
4. Meconium ileus  
a. Presentation, associations  
b. Radiographic findings  
c. LGI contrast study findings  
i. Simple meconium ileus  
ii. Meconium ileus complicated by segmental volvulus  
5. Ileal atresia  
a. Presentation  
b. Radiographic findings  
c. LGI contrast study findings  
6. Colonic atresia  
a. Presentation  
b. Radiographic findings  
c. LGI contrast study findings  
7. Segmental volvulus  
a. Presentation  
b. Radiographic findings  
c. US findings - "mini whirlpool" sign  
d. Upper and lower gastrointestinal contrast study findings  
8. Conclusion

## PDEE-23 Awards

## Imaging Approach to Proximal Neonatal Bowel Obstruction

### Identified for RadioGraphics

Participants  
Samantha Gerrie, MBChB, FRANZCR, (*Presenter*) Nothing to Disclose

### TEACHING POINTS

1. Describe a structured approach to multimodality imaging workup of proximal neonatal bowel obstruction including esophageal atresia, pyloric stenosis, duodenal atresia, duodenal web, malrotation with midgut volvulus and jejunal atresia. 2. Discuss the role of plain radiographs. 3. Discuss use of upper gastrointestinal (UGI) series and ultrasound (US) in establishing diagnosis or narrowing the differential diagnosis.

### TABLE OF CONTENTS/OUTLINE

1. Introduction 2. Esophageal atresia a. Types, presentation, associations b. Radiographic findings 3. Gastric/pyloric atresia a. Presentation b. Radiographic findings 4. Hypertrophic pyloric stenosis a. Presentation b. US findings i. Pylorus measurements ii. Pitfall - confusing gastroesophageal junction with pylorus 5. Duodenal atresia a. Presentation b. Radiographic findings i. Double bubble sign ii. Pitfall - Y-shaped hepatopancreatic duct anomaly 6. Duodenal web a. Presentation b. Radiographic, UGI series and US findings 7. Annular pancreas a. Presentation b. US findings 8. Malrotation with midgut volvulus a. Presentation b. Radiographic findings c. US findings i. SMA/SMV relationship ii. Position of third part of duodenum iii. Whirlpool sign d. UGI series findings i. Course of duodenum ii. Position of duodenojejunal junction (DJJ) iii. Corkscrew sign iv. Pitfalls - Abnormal position of DJJ due to extrinsic compression or displacement 9. Jejunal atresia a. Presentation b. Radiographic findings 10. Conclusion

### PDEE-24 Post-transplant Malignant Neoplasms in Pediatric Liver Transplantation

Participants  
Thaise Marquez, MD, (*Presenter*) Nothing to Disclose

### TEACHING POINTS

The objectives of this exhibit are: To review the frequency and the main types of malignancies in children post-liver transplantation, including: 1) "de novo" tumors and 2) recurrence of neoplasms in patients transplanted for oncological causes. To illustrate the aforementioned tumors with cases attended in our service. To highlight the importance of clinical follow-up in the post-transplant period, in order to diagnose neoplastic lesions at an early stage, reducing graft loss and increasing post-transplant survival.

### TABLE OF CONTENTS/OUTLINE

1. Recurrence of liver tumors in pediatric patients post-transplant. Review of the transplant criteria for children with liver tumors, as well as the most common tumors that require liver transplantation. Overview of the expected prognosis and usual management of those patients. Illustrated cases of our Pediatric Radiology group. 2. The occurrence of "de novo" tumors in children post-liver transplant. Post-Transplant Lymphoproliferative Disease (PTLD): definition, characteristics, risk factors, pathology, categories and radiographic features. Non-PTLD tumors: a brief mention of the main non-PTLD malignancies, focusing on Kaposi's sarcoma. Illustrated cases of our institute, including some rare "de novo" cancers.

### PDEE-25HC Postoperative Imaging Findings of Biliary Atresia in Children

Participants  
Jisun Hwang, MD, Hwaseong-si, Korea, Republic Of (*Presenter*) Nothing to Disclose

### TEACHING POINTS

- Describe the main surgical technique of Kasai portoenterostomy - Identify the imaging findings of complications after Kasai operation  
- Describe the indication and main surgical technique of liver transplantation - Identify the preoperative imaging evaluation and postoperative complications after liver transplantation

### TABLE OF CONTENTS/OUTLINE

- Kasai portoenterostomy procedure 1) Surgical technique 2) Imaging findings after Kasai portoenterostomy procedure \* Cholangitis and bile lakes \* Portal hypertension and variceal bleeding \* Hepatic tumor - Living-related liver transplantation for biliary atresia 1) Indication and surgical technique 2) Preoperative imaging evaluation (donor and recipient) 3) Imaging findings after liver transplantation \* Vascular complication (hepatic artery thrombosis, portal vein stenosis, hepatic vein stenosis) \* Nonvascular complication (biliary stricture, bile leak) Please visit the Learning Center to also view this presentation in hardcopy format.

### PDEE-26 Staging and Restaging Pediatric Abdominal Tumors: A Practical Guide

#### Awards

Identified for RadioGraphics  
Certificate of Merit

Participants  
Luisa Faria, MD, Sao Paulo, Brazil (*Presenter*) Nothing to Disclose

### TEACHING POINTS

The most common abdominal malignancies diagnosed in the pediatric population include neuroblastoma, nephroblastoma (Wilms' tumor), hepatoblastoma, lymphoma, germ cell tumors, and rhabdomyosarcomas. Each of these tumors has characteristic imaging findings and patterns of locoregional and distant spread. The staging systems are unique and the surgical and oncological management rely heavily on imaging evaluation. The purposes of this exhibit are: (1) to review imaging techniques and discuss the selection among imaging modalities, (2) to review the diagnostic approach of each tumor, (3) to organize the key points for determining tumor stage using a case-based approach, (4) to systematize the posttreatment response evaluation and surveillance and (5) to point out imaging findings of particular prognostic importance.

### TABLE OF CONTENTS/OUTLINE

(1) Epidemiology of pediatric abdominal tumors. (2) The role of each imaging modality in staging and restaging pediatric abdominal

(7) Epithelioid, or pleomorphic, embryonal sarcoma; (8) The role of positron-emitting tomography in staging and re-staging pleomorphic embryonal tumors. (3) Neuroblastoma: diagnostic approach, staging, and response assessment. (4) Nephroblastoma (Wilms' tumor): diagnostic approach, staging, and response assessment. (5) Hepatoblastoma: diagnostic approach, staging, and response assessment. (6) Lymphoma: diagnostic approach, staging, and response assessment. (7) Germ cell tumors: diagnostic approach, staging, and response assessment. (8) Rhabdomyosarcoma: diagnostic approach, staging, and response assessment.

### **PDEE-27 I Found a Mass in The Adrenal Region of A Neonate: Should I Be Concerned? Sonographic Findings In The Differential Diagnosis of Usual and Unusual Neonatal Suprarenal Masses**

Participants

Gabriela Pinho, MD, Sao Paulo, Brazil (*Presenter*) Nothing to Disclose

#### **TEACHING POINTS**

The purposes of this exhibit are: To review the normal sonographic aspect of the neonatal adrenal gland; To emphasize the importance of assessing the adrenal gland in our routine neonatal abdominal sonographic studies; To show based on cases from our Pediatric Radiology group, usual and unusual neonatal adrenal and suprarenal masses; To show the outcome of each case; To discuss risk factors and pathophysiology of the main neonatal adrenal and suprarenal masses.

#### **TABLE OF CONTENTS/OUTLINE**

Sonographic technique for the assessment of neonatal adrenal gland and suprarenal region. Usual sonographic aspects of the neonatal adrenal gland. Illustrated teaching cases from our Pediatric Radiology group showing the usual and unusual neonatal adrenal and suprarenal masses: Congenital adrenal hyperplasia associated with ambiguous genitalia and urogenital sinus demonstrated by transperineal ultrasound access; Fetal and neonatal congenital neuroblastoma; Adrenal hemorrhagic infarction: different sonographic aspects in the evolutionary stages of neonatal adrenal hemorrhage; Tips for the diagnosis of Infradiaphragmatic extralobar pulmonary sequestration associated with congenital cystic adenomatoid malformation / congenital pulmonary airway malformation by ultrasound.

### **PDEE-28 Biliary Atresia and the One Stick Wonder of Percutaneous Transhepatic Cholecystocholangiography**

Participants

Elliott Russell, MD, (*Presenter*) Nothing to Disclose

#### **TEACHING POINTS**

- The learner will review basic pathophysiology and types of biliary atresia and differential diagnosis for neonatal cholestatic jaundice
- The learner will gain familiarity with the diagnostic imaging pathways, including advantages and disadvantages of ultrasound, hepatobiliary iminodiacetic acid scan, and percutaneous transhepatic cholecystocholangiography (PTCC)
- The learner will discover the technique for PTCC, including patient selection, patient preparation, and materials and methods
- The learner will develop an understanding of PTCC image interpretation and implications for patient management through comprehensive case review

#### **TABLE OF CONTENTS/OUTLINE**

1. Clinical Scenario, Differential Diagnosis, and Importance of Timely Diagnosis 2. Biliary Atresia Pathophysiology/Types 3. Current Diagnostic Imaging Pathway, Including Advantages and Disadvantages 4. Percutaneous Transhepatic Cholecystocholangiography: Technique 5. Cases

### **PDEE-29 Pediatric Pancreaticobiliary Endoscopic Ultrasound Interventions as Primer for Radiologists-Case Based Review**

Participants

Emmanuel Owusu, MD, (*Presenter*) Nothing to Disclose

#### **TEACHING POINTS**

Diagnostic and therapeutic role of EUS in pediatric pancreaticobiliary conditions EUS. Preoperative and post-operative care of the pediatric patient. Evaluating safety, complications post EUS

#### **TABLE OF CONTENTS/OUTLINE**

What is EUS EUS equipment Indications for EUS in evaluation of Pediatric Pancreaticobiliary disease Pancreatic pathology Pancreatic collections, pseudocyst Pancreatic/gastric masses Biliary pathology CBD obstruction, cholestasis Congenital biliary anomalies EUS technique FNA, stenting, LAMS Pre-operative assessment of EUS Absolute contraindications Post procedure follow-up stent complications (splenic artery hemorrhage, stent migration, recurrent pseudocyst post stent removal) Imaging findings

### **PDEE-3 Pre and Post Operative CTS: Overview of Congenital Heart Defects**

Participants

Akinori Hata, MD, PhD, Suita, Japan (*Presenter*) Nothing to Disclose

#### **TEACHING POINTS**

Congenital heart defect (CHD) is the leading cause of death in infancy. CHDs often need interventions for complex structural cardiovascular abnormalities. Advances in the care for patients with CHD have improved survival. For radiologists, understanding pre- and post-operative status in patients with CHD is necessary for accurate interpretation of CT imaging. The purpose of this exhibit is 1) To overview structural abnormalities in typical types of CHDs on CT; 2) To know the procedure required in CHDs; and 3) To understand the hemodynamics in pre- and post-operative status of patients with CHD.

#### **TABLE OF CONTENTS/OUTLINE**

1. Overview of the types of typical CHDs 2. Introduction of the general concepts of surgeries for CHDs (palliative procedures and single-/two-ventricle repair) 3. Pre- and post-operative CTs for typical CHDs (Atrioventricular canal defect, Coarctation of the aorta, Double-outlet Right Ventricle, Ebstein anomaly, Heterotaxy syndrome, Hypoplastic left heart syndrome, Pulmonary atresia with intact ventricular septum, Tetralogy of Fallot, Transposition of the great arteries, Tricuspid atresia, Truncus Arteriosus, etc.)

**PDEE-30 RASopathies for Radiologists: Familiarizing Radiologists With the Common Genetic Thread Linking Diseases of the Ras/MAPK Signaling Pathway**

**Awards**

**Identified for RadioGraphics**  
**Certificate of Merit**

**Participants**

Atsuhiko Handa, MD, Boston, MA (*Presenter*) Nothing to Disclose

**TEACHING POINTS**

RASopathies are a clinically defined group of genetic syndromes caused by germline mutations in genes that encode components or regulators of Ras/MAPK signaling pathway. These disorders include neurofibromatosis type 1, Noonan syndrome, Noonan syndrome with multiple lentigines (formerly called LEOPARD syndrome), capillary malformation-arteriovenous malformation syndrome, Costello syndrome, cardio-facio-cutaneous syndrome, Legius syndrome, and other allied disorders (e.g. tuberous sclerosis). As a group, the RASopathies are among the most common genetic conditions, an incidence estimated to be about 1 per 1000 live births. Because of the common underlying Ras/MAPK pathway dysregulation, the RASopathies exhibit overlapping phenotypic features. The somatic mutations involving Ras/MAPK pathway have been well studied in cancer and appears to be a promising target for molecular inhibition to treat various malignancies. Similar treatment can potentially be used to ameliorate developmental defects in other RASopathies in the future. In fact, a pathway-based multidisciplinary clinic has already been established in many institutions to address unique challenges faced by individuals and families with RASopathies. The radiologist also needs to be aware of this emerging concept to participate in multidisciplinary care. Here we present the concept and imaging review of RASopathies with an emphasis on common features.

**TABLE OF CONTENTS/OUTLINE**

- Concept of RASopathies - NF1 - Noonan group - Other RASopathies - Allied disorders - Future directions

**PDEE-32 Pediatric Ribs: Roadmap to Become A Rib Expert**

**Awards**

**Identified for RadioGraphics**

**Participants**

Yuko Tsujioka, MD, Tokyo, Japan (*Presenter*) Nothing to Disclose

**TEACHING POINTS**

Pediatric rib lesions are diagnostic challenge for three reasons. First, they may be radiologically subtle. For example, a small costal mass that grows inward may be clinically silent. An early recognition of such a lesion that is at risk for serious complications, such as hemothorax or pneumothorax, is feasible only by well-trained eyes. Meticulous searching for trivial changes is essential. Second, they are diverse. There are a variety of rib changes that can lead to a diagnosis of hidden disorders. Examples include multiple posterior rib fractures in non-accidental injury, rib notch in coarctation of the aorta, thin ribs in severe neuromuscular diseases, twisted ribs in NF1, and canoe-paddle-like ribs in mucopolysaccharidosis. Radiologists need to know these rare, but diagnostic, radiological signs. Third, there are many normal variants. Radiologists should be familiar with the innocuous variants to avoid diagnostic errors and unnecessary imaging examinations. Here we provide a comprehensive imaging review of pediatric rib abnormalities and normal variants seen on routine chest radiographs to overcome these challenges. We also provide corresponding cross-sectional images, when available, to help understand the characteristic of each rib lesion.

**TABLE OF CONTENTS/OUTLINE**

Introduction - Normal rib variants - Tumors and tumor like-lesions - Inflammatory disorders - Rib abnormalities pointing to hidden disease (non-accidental injury, rib notch, twisted ribs, thin ribs, thin ribs with fractures, thin ribs with abnormal patterning, short ribs, broad ribs, dense ribs)

**PDEE-33 Perils by the Sea: Radiologic Manifestations of Coastal Related Injuries and Disorders in Pediatric Patients**

**Awards**

**Certificate of Merit**

**Participants**

Anna Fairfax, BS, MD, (*Presenter*) Nothing to Disclose

**TEACHING POINTS**

1. Review various injuries and disorders commonly seen in pediatric patients associated with coastal related activities. 2. Discuss the clinical presentations, management, and complications of various coastal, and broader water related, injuries and disorders. 3. Showcase imaging findings of coastal and water related injuries and disorders in pediatric patients via various imaging modalities.

**TABLE OF CONTENTS/OUTLINE**

1. Musculoskeletal a. Retained foreign bodies (e.g., oysters shells, impaled fishing hooks, stingray spines, shark teeth) b. Animal attacks/encounters (e.g., sharks, jellyfish, stingrays, sea urchins, crabs) c. Diving trauma d. Water sports trauma (e.g., boating and propeller injuries) 2. Lungs/airway a. Barotrauma/diving related disorders b. Aspiration of foreign bodies (e.g., shells and seafood) c. Drowning sequelae/pulmonary edema d. Laryngeal edema secondary to marine envenomation e. Hypersensitivity pneumonitis related to red tide 3. Neuro a. Anoxic brain injury secondary to drowning b. Trauma related to water sports and diving c. Barotrauma/diving related disorders 4. GI/abdomen a. Infection (I.e., Vibrio species) b. Water sports trauma

**PDEE-34 Infantile Hemangioma Pitfalls: Clinical and Radiological Evaluation**

**Awards**

**Certificate of Merit**  
**Identified for RadioGraphics**

Participants

Emilio Inarejos Clemente, MD, Barcelona, Spain (*Presenter*) Nothing to Disclose

#### TEACHING POINTS

After reviewing this exhibit, the learner should: 1. Be familiar with imaging modalities for vascular anomaly evaluation focused on hemangiomas 2. Discuss the role of photodocumentation with radiological correlation and importance in evaluation of pathologies with cutaneous involvement 3. Describe clinical features of infantile hemangiomas (IH) focusing on cutaneous lesions 4. Illustrate the most frequent pitfalls that may mimic IH and clinical appearance 5. Discuss most common imaging findings of these pitfalls and identify important differentiating imaging clues

#### TABLE OF CONTENTS/OUTLINE

1. Introduction of vascular anomalies and approach to ISSVA classification 2. Types of IH, demographics and clinical appearance 3. Imaging findings of different types of IH: Unifocal and multifocal diseases that can mimic IH Clinical photographs, pathology when available and imaging findings of frequent lesions that can mimic IH focusing on ultrasound and MRI: Vascular origin: Other vascular anomalies: venous or arterio-venous malformations Other hemangiomas: congenital hemangiomas Vascular neoplasms of intermediate behavior: Kaposiform hemangioendothelioma, tufted angioma Neoplasms: Benign: Lipomatous (lipoblastoma, angiolipoma), myofibroblastic tumors, fibrous hamartoma, neurofibromas Intermediate behavior: congenital fibrosarcoma Malignant: congenital sarcomas including rhabdomyosarcoma, lymphoma, metastatic neuroblastoma. Others: Fat necrosis, neural tube defects, ectopic thyroid 4. Summary

#### PDEE-35 Imaging Evaluation of The Post-surgical Foot and Ankle in Children

Participants

Emilio Inarejos Clemente, MD, Barcelona, Spain (*Presenter*) Nothing to Disclose

#### TEACHING POINTS

After reviewing this exhibit, the learner should be able to: 1. To discuss the most frequent pediatric disorders involving the foot and ankle that may require surgery 2. To illustrate the imaging findings of the post-surgical evaluation of the foot and ankle in different modalities 3. To describe the most frequent normal variants that may lead to misdiagnose

#### TABLE OF CONTENTS/OUTLINE

1. Technique: indications and protocols of the different imaging modalities in the post-surgical setting. 2. Illustrate the post-surgical imaging evaluation of the most frequent pediatric disorders involving the foot and ankle: 2.1. Congenital: congenital clubfoot, vertical talus, metatarsus adductus, tarsal coalition. Value of US and radiographs. 2.2 Traumatic: osteochondral lesions, fractures, ligamentoplasty 2.3. Infection secondary to surgery 2.4. Benign tumors: aneurysmal bone cyst, osteoid osteoma, chondroblastoma, osteochondroma, pigmented villonodular synovitis 2.5. Malignant tumors: Ewing sarcoma, osteosarcoma. soft tissue sarcomas. Use of multiparametric MRI evaluation and DWI. 3. Describe the most frequent normal variants involving the pediatric foot that may lead to misdiagnose: Hematopoietic marrow, bone marrow edema, Stieda process 4. Conclusion

#### PDEE-36 Role of Whole-body Magnetic Resonance Imaging In Pediatric Musculoskeletal System: Aside From Tumors

Participants

Joao Pedro Costa, MD, Sao Paulo, Brazil (*Presenter*) Nothing to Disclose

#### TEACHING POINTS

I) To review the main applications of whole-body magnetic resonance imaging (WB-MRI) focused on non-neoplastic musculoskeletal conditions in pediatric population. II) To discuss and present the technical aspects and WB-MRI protocol used in our pediatric radiology department including main limitations. III) To illustrate with clinical cases the use of WB-MRI to assess and follow musculoskeletal diseases in children. IV) To correlate imaging information given by WB-MRI with the clinical and laboratory data and compared with other imaging modalities.

#### TABLE OF CONTENTS/OUTLINE

1. Introduction: performance and applications of WB-MRI in the evaluation of pediatric musculoskeletal non-neoplastic diseases; discuss WB-MRI protocols, with not only the advantages but also with current limitations in comparison with different imaging methods. 2. Illustration of WB-MRI exams performed in our pediatric radiology department for diagnostic and follow-up evaluation of different musculoskeletal conditions: chronic recurrent multifocal osteomyelitis; pyogenic osteomyelitis; inflammatory myopathies; drug-induced myopathies; neuromuscular myopathies; fever of unknown origin; searching for rheumatologic inflammatory conditions.

#### PDEE-37 Intra-articular Osteoid Osteomas: Imaging Characteristics and Mimickers

##### Awards

**Magna Cum Laude**

Participants

Jade Iwasaka-Neder, MD, (*Presenter*) Nothing to Disclose

#### TEACHING POINTS

o Intra-articular osteoid osteomas (OOs) are rare and may pose a diagnostic challenge to radiologists, as they sometimes mimic other pathologies such as arthritis, stress fracture, avascular necrosis, osteomyelitis, and osteochondral lesions. o Although intra-articular OO may involve any joint, the majority of cases are localized to the hip. o Imaging findings of intra-articular OOs include focal edema, joint effusion and synovitis. However, these lesions often lack the usual reactive sclerosis and periosteal new bone formation, making their diagnoses more difficult. o CT scan is the best imaging modality to identify the nidus of the OO, and is particularly useful for treatment planning. o Na-F PET/CT can confirm the diagnosis of OO in equivocal cases.

#### TABLE OF CONTENTS/OUTLINE

o Typical imaging findings of extra-articular OO o Imaging findings of intra-articular OO § Imaging modality • Radiograph • MRI • CT • Bone scan • Na-F PET/CT § Anatomical locations • Elbow • Wrist • Acetabulum • Femoral head and neck • Knee • Ankle • Tarsal bones o

Differential diagnoses and mimickers§ Stress fracture§ Osteomyelitis with or without Brodie abscess§ Osteochondritis dissecans§ Osteomyelitis§ Arthritis§ Chondroblastoma§ Synovial cyst§ Normal variants (e.g. supra-acetabular fossa)

### **PDEE-38 Whole-body MRI in Pediatric Musculoskeletal Diseases: Clinical Applications and Technical Considerations**

Participants

Andre Mannato, MD, Sao Paulo, Brazil (*Presenter*) Nothing to Disclose

#### **TEACHING POINTS**

Discuss technical developments of WBMRI in musculoskeletal pediatric diseases, including acquisition and post-processing, as well as to propose an imaging protocol. Review the clinical applications of WBMRI in various disorders that involve the musculoskeletal system in children, especially in the oncology and rheumatology fields, exploring the typical and atypical imaging findings of each. Explore the role of WBMRI as a valuable imaging method for diagnosis, assessment of disease extent and follow-up, highlighting its advantages in comparison to standard imaging evaluation, specifically as they relate to the pediatric population.

#### **TABLE OF CONTENTS/OUTLINE**

In the last decades, WBMRI has emerged as a promising imaging method in musculoskeletal diseases, allowing a wide coverage assessment of bone and soft tissue in a single study. WBMRI is especially advantageous for the pediatric population since it avoids redundant examinations and exposure to ionizing radiation in patients who often undergo long-term surveillance. Also, due to patient's size, the examination can be performed with faster protocols and provide high quality images. For rheumatic and oncological diseases, WBMRI can have a large impact in diagnostic and follow-up workup of many pathologies such as chronic nonbacterial osteomyelitis, dermatomyositis, arthritis, tumor screening in cancer predisposition syndromes, evaluation of primary tumor, further investigation of distant lesions and other clinical applications. The development of new techniques and protocols makes WBMRI increasingly faster, safer and more accessible, and it is important for referring physicians and radiologists to recognize the role of this imaging method.

### **PDEE-39 Fast MRI: MSK Applications in Adults and Children**

Participants

Joey Gu, BS, (*Presenter*) Nothing to Disclose

#### **TEACHING POINTS**

1. Gain a foundational understanding of the physics behind accelerating MR image acquisition and the various techniques currently in use  
2. Discern the benefits and limitations that accelerated MRI offers for patients, providers, and healthcare systems  
3. Recognize the specific clinical applications, in both an adult and pediatric populations, for fast MR examinations of the shoulder, spine, hip, knee, and ankle

#### **TABLE OF CONTENTS/OUTLINE**

What is Fast MRI?- MR physics of accelerating image acquisition- Overview of various acceleration techniques--Fast spin-echo, turbo spin-echo--High gradient performance modes--Undersampling: matrix resolution/partial Fourier phase--Interpolation of matrix resolution--Fast radiofrequency pulses, high receiver bandwidth--Advanced techniques (PI, SMS, synthetic techniques, etc.)  
Why Use Fast MRI?- In adults--Efficiency of examinations (high volume of adult MSK MRI exams)--Reduce artifact from hardware/implants--Reduce motion artifact- In children--Decrease need for sedation--Reduce motion artifact  
MSK applications of Fast MRI (for each anatomical area of interest, disease processes evaluated, diagnostic accuracy, and imaging appearances will be covered)- In adults (shoulder, spine, hip, knee, ankle)- In children (knee, spine, infection)  
Limitations of Fast MRI - Medicolegal implications- Lack of studies demonstrating efficacy for various clinical applications

### **PDEE-4 Cardiac Evaluation in Pediatric Chest Radiographs: Back To the Future With CT/MRI Correlation**

Participants

Prabhakar Rajiah, MD, FRCR, Rochester, MN (*Presenter*) Nothing to Disclose

#### **TEACHING POINTS**

The last decade has seen tremendous growth of CT/MRI for evaluation of cardiac disorders. The humble chest radiograph still plays a key role, and it is important to interpret it accurately. The aim of this exhibit is 1. To discuss an approach to the interpretation of cardiac abnormalities in pediatric chest radiographs 2. To correlate radiographic cardiac abnormalities with CT/MRI appearances 3. To review common misses and pitfalls in radiographs

#### **TABLE OF CONTENTS/OUTLINE**

1. ROLE OF IMAGING IN CARDIAC DISEASES 2. ROLE OF CHEST RADIOGRAPH in pediatric cardiac disease 3. ENLARGED CARDIAC SILHOUETTE- Cardiomegaly- Criteria; Individual chamber enlargement; Pericardial effusion- double oreo cookie sign 4. PULMONARY VASCULATURE- Arterial, venous, edema 5. ALGORITHMIC APPROACH TO DIAGNOSIS OF CONGENITAL HEART DISEASES CYANOTIC HEART DISEASE A. Decreased blood flow - Normal size heart- TOF; Big heart- Ebstein, pulmonary atresia with intact septum B. increased blood flow - TGA- Egg-on-string; TAPVR- Snowman; Truncus- Right arch Single ventricle C. Pulmonary edema - Normal size heart- TAPVR infracardiac; Big heart- hypoplastic left heart ACYANOTIC HEART DISEASE A. Increased arterial flow- Normal LA- ASD; Large LA , normal aortic knob- VSD; Large LA and aortic knob- PDA B. Increased venous flow- Cardiac failure C. Normal flow- AS, Coarctation 6. OTHER FINDINGS -Box-shaped heart- Ebstein's; Boot-shaped- TOF; Wall-to-wall heart- Ebstein, pericardial effusion; Figure-of-3, rib notching- Coarctation; Scimitar sign- PAPVR; Asymmetric main, left PA enlargement- Pulmonic valve stenosis; 7. APPROACH TO VASCULAR RING/SLING- Tracheal and esophageal impressions. 8. PROSTHETIC VALVE EVALUATION 9. PITFALLS/MISSES

### **PDEE-40 Update On the Radiological Approach of Musculoskeletal Pediatric Infections: From Classical to Challenging Cases**

Participants

Stephanie Takara, MD, Sao Paulo, Brazil (*Presenter*) Nothing to Disclose

#### **TEACHING POINTS**

I) Review the main types of musculoskeletal infections and their particularities in children (epidemiology, etiology and pathophysiology), based on cases of our pediatric radiology department in correlation with clinical, laboratory and anatomopathological data. II) Discuss the use and indication of each imaging modality for the different types of musculoskeletal infections and purpose a diagnostic investigation flowchart. III) Present the main imaging findings, advantages and limitations of imaging modalities.

#### TABLE OF CONTENTS/OUTLINE

1. Introduction The importance of imaging exams for an early and correct diagnosis of pediatric musculoskeletal infection. The main uses of each imaging method. 2. Spondylodiscitis and intradural infections Epidemiology and pathophysiology The role of each imaging method and imaging findings 3. Osteomyelitis Pathophysiology The role of each imaging method and imaging aspects Chronic findings and sequelae 4. Septic arthritis Epidemiology and pathophysiology The role of each imaging method and imaging findings 5. Soft tissue infection Epidemiology and pathophysiology The role of each imaging method and imaging findings

#### PDEE-41 Clavicular Pathologies in the Pediatric Age Group: A Pictorial Review

Participants

Ankita Chauhan, MD, MBBS, (Presenter) Nothing to Disclose

#### TEACHING POINTS

Background Information: The clavicle connects the upper extremity to the axial skeleton. It is the first bone to ossify in the fetus. Epiphysis of the clavicle, however, is the last to ossify and fuse in adult life. The most common lesions of the clavicle are traumatic. Nontraumatic lesions of the clavicle are rare, more so in the pediatric age group. Radiologists need to know pathologies affecting the clavicle and their imaging appearance. Considering patient age, clinical symptoms, and other associated imaging findings can help make the correct diagnosis. Teaching Points 1. To discuss the development and normal anatomy of the clavicle. 2. To discuss various congenital (or developmental), traumatic, metabolic, infective, inflammatory, or benign and malignant neoplastic pathologic processes that can involve the clavicle. 3. To illustrate the imaging spectrum of clavicular pathologies in the pediatric age group. 4. To discuss various radiological features that can help make the correct diagnosis.

#### TABLE OF CONTENTS/OUTLINE

-Goals and objectives -Background information -Anatomy -Pathologic entities (fracture, pseudoarthrosis, infantile cortical hyperostosis (Caffey disease), hyperparathyroidism, cleidocranial dysostosis, chronic recurrent multifocal osteomyelitis, benign bone tumors such as unicameral bone cyst, aneurysmal bone cyst, malignant bone tumors, metastasis) -Summary

#### PDEE-42 Multimodality Imaging of Pediatric High Flow Vascular Malformations in the Brain and Spine

Participants

Amanda Baker, MD, (Presenter) Nothing to Disclose

#### TEACHING POINTS

Goal: To review multimodality imaging in the diagnosis and treatment of pediatric high flow vascular malformations in the brain and spine. Specifically, the exhibit will pinpoint features on US, CT, MRI, and catheter angiography that will allow the radiologist to accurately diagnosis the type of malformation and describe its characteristics.

#### TABLE OF CONTENTS/OUTLINE

Review diagnostic algorithms to aid in the classification of pediatric high flow vascular malformations in the brain and spine: Brain: 1. Nidal arteriovenous malformations 2. Dural arteriovenous fistulae. 3. Non-galenic pial arteriovenous fistulae. 4. Vein of Galen malformations. Spine: 1. Epidural spinal arteriovenous fistulae. 2. Dural spinal arteriovenous fistulae. 3. Perimedullary spinal arteriovenous fistulae. 4. Spinal arteriovenous malformations.

#### PDEE-43 Imaging Approach to Hypomyelinating Leukodystrophies (HLDs)

Participants

Prateek Malik, MD, Toronto, ON (Presenter) Nothing to Disclose

#### TEACHING POINTS

Hypomyelinating leukodystrophies (HLDs) are a rapidly expanding subgroup of inherited white matter disorders characterized by a permanent and substantial deficit in myelin. More than 50 genes are now linked with HLDs, the vast majority being discovered over the last 15 years. Since the first description of Pelizaeus-Merzbacher disease (PMD) in 1910, the understanding of white matter disorders and the key cellular players has improved tremendously. We discuss an updated review of the understanding of normal myelination, key terminologies in HLDs and provide a stepwise methodology in assessment of HLDs determined by key radiological findings.

#### TABLE OF CONTENTS/OUTLINE

1. Normal myelination - Neurobiology: Key players and myelin maintenance - Imaging normal myelination: key MRI changes, normal milestones and development of key structures - Pitfalls and caveats: Variable signal, permanent deficit Vs myelin stability, corrected gestational age 2. Hypomyelinating leukodystrophies (HLDs) - Updates in classification of white matter disorders including HLDs - Key terminologies - Stepwise approach to assessing HLDs: • Determining key pattern • Assessing for ABCDs • Assessing sub-patterns and clinical clues • Imaging differentials for specific patterns • Alternate imaging phenotypes

#### PDEE-44 Radiomics for Predicting Tumor Immune Profile of Pediatric Glioma

Participants

Nastaran Khalili, MD, MPH, (Presenter) Nothing to Disclose

#### TEACHING POINTS

Central nervous system (CNS) tumors are the leading cause of cancer-related death in children. Glioma accounts for more than half of pediatric CNS tumors. Complete resection is the mainstay of therapy but is not feasible for deeply seated or highly infiltrative

tumors. Hence, immunotherapeutic approaches are being increasingly applied in pediatric glioma. The immunological profile of the tumor microenvironment (TME) is regarded as a powerful tool for predicting tumor behavior and determining response to immunotherapy. Radiomics, which is the automated high-throughput extraction and processing of quantitative imaging based on intensity, shape, volume, and textural features provides insight into the underlying immunobiological processes within the TME. The purpose of this exhibit is to discuss how this non-invasive method facilitates the categorization and risk stratification of patients based on their tumor immune profile and to describe the role of radiomics in advancing personalized, patient-tailored therapy for pediatric glioma.

#### **TABLE OF CONTENTS/OUTLINE**

1. Brief review of the pathophysiology, prognosis, and current treatments for pediatric glioma. 2. Basic principles of radiomics and its role in understanding tumor immune biology. 3. Correlation between radiomics features, immune biomarkers and clinical outcomes in glioma according to existing literature. 4. Current challenges and future directions for the application of radiomics in the immune characterization of pediatric glioma.

#### **PDEE-45 Diffusion-weighted Imaging Patterns in Pediatric Neurometabolic Disorders**

Participants

Caleb Epps, MD, MS, (*Presenter*) Nothing to Disclose

#### **TEACHING POINTS**

The aim of this exhibit is to increase understanding of diffusion weighted-imaging patterns in pediatric neurometabolic disorders to improve diagnostic accuracy and characterization. By the end of this exhibit, the viewer should be able to recognize general DWI patterns and internalize a simplistic practical approach to pediatric neurometabolic disorders.

#### **TABLE OF CONTENTS/OUTLINE**

Pediatric neurometabolic disorders encompass an immense group of diseases that are diagnostically challenging for both clinicians and radiologists. Though they are rare individually, collectively they remain a source of significant pediatric morbidity. Though simple classification is problematic, one classification schema includes disorders of toxic accumulation, energy metabolism, complex molecules, and unique pathophysiology. Accurate and timely diagnosis is crucial as treatment depends on the underlying pathophysiology. Good clinical outcomes are associated with earlier intervention in some disorders. Cytotoxic, excitotoxic, and intramyelinic cerebral edema are pathologic processes common in many neurometabolic disorders and manifest on DWI. DWI signal abnormalities can be grossly categorized into white matter-dominant, peripheral gray matter, and deep gray matter. Of note, the practicality of this model compensates for its lack of specificity given that some disorders may demonstrate overlapping patterns. Though the work up of pediatric neurometabolic disorders largely remains a multi-disciplinary effort, an improved understanding of DWI patterns in pediatric neurometabolic disorders can facilitate timely diagnosis and help reduce long term morbidity.

#### **PDEE-46 An Imaging Review of Pediatric Monogenetic CNS Vasculopathy with Genetic Correlation**

**Awards**

**Identified for RadioGraphics**

Participants

Neetika Gupta, MBBS, MD, (*Presenter*) Nothing to Disclose

#### **TEACHING POINTS**

1. Review the current literature on rare genetic causes of CNS vasculopathy in children. 2. Describe the CNS and extra-CNS imaging findings in various genetic pediatric CNS vascular disorders. 3. Discuss the role of conventional imaging modalities and advanced imaging sequences in the diagnosis and prognosis of cerebral vascular disorders. 4. To emphasize the diagnostic and prognostic role of neuroimaging in the evaluation of pediatric monogenetic vascular disorders.

#### **TABLE OF CONTENTS/OUTLINE**

1. Comprehensive discussion of the various monogenetic disease resulting in CNS vascular disorders in children. 2. Identify and familiarize with the salient imaging features of rare genetic pediatric CNS vasculopathy that could help in the diagnosis and narrow the differentials. 3. Recommend a clinico-radiological approach pertinent genetic workup for the systematic evaluation of these rare genetic pediatric CNS vascular disorder. 4. Identify the genetic causes imperative to reach a final diagnosis and guide the appropriate treatment.

#### **PDEE-47 Advanced Imaging Evaluation of Pediatric Language Pathways: Where Do We Stand**

Participants

Monica Rebollo Polo, MD, (*Presenter*) Nothing to Disclose

#### **TEACHING POINTS**

- Review the major language pathways and their development in children from newborns to older children evaluated with advanced neuroimaging (DWI, fMRI) - Show the areas of activation related to language evaluated with resting state functional Magnetic Resonance (rsfMRI) - Task evaluation of language (presurgical language lateralization assessment) - Clinical indications of imaging language assessment - Show pathology that interferes with normal language pathways development

#### **TABLE OF CONTENTS/OUTLINE**

- Language pathways overview with deterministic and probabilistic tractography (arcuate fasciculus, uncinate fasciculus, inferior front-occipital fasciculus, inferior longitudinal fasciculus, frontal aslant tract) - Maturation and development of the language pathways - Dorsal and ventral language pathways representing auditory-motor integration and auditory-conceptual mapping - Rs fMRI language networks - Task evaluation of language (antonym generation, sentences completion, object naming, passive story listening) - Clinical examples (presurgical assessment in brain tumors, language lateralization in epilepsy, language pathways anomalies) Clinical entities that affect language pathways (prematurity, congenital infections, malformations of cortical development)

## **PDEE-48     Vertebral Artery Dissection in Children**

### **Awards**

**Identified for RadioGraphics  
Certificate of Merit**

### **Participants**

Stephen B. Little, MD, Atlanta, GA (*Presenter*) Nothing to Disclose

### **TEACHING POINTS**

1) Vertebral artery dissection (VAD) is the most common cause of isolated posterior circulation arterial ischemic stroke (PCAIS) in children. Posterior circulation infarcts due to VAD are often multifocal, occasionally of varying age, and may be associated with abrupt intracranial (downstream) arterial occlusions. 2) Extracranial VAD in children most often involves the proximal V3 segment. This portion of V3 is short, often transversely oriented, located in close proximity to bone and surrounded by fat and a periarterial venous plexus. Cervical vascular imaging protocols should take these challenging anatomic features into consideration. 3) VAD is often missed on clinically performed 2D TOF MRA and CE-MRA of the neck. In our experience, 3D TOF MRA or CTA of the neck are more reliable vascular imaging alternatives for VAD in children. 4) At presentation, extracranial VAD in children is most often characterized by segmental stenosis or occlusion at the C2 level, CASCADE 4a (3). Vertebral artery pseudoaneurysm (CASCADE 4a (1)) is less frequent and may be present at initial diagnosis or at follow-up. Intimal flap, double lumen and wall hematoma are infrequent findings on CTA or MRI/MRA. 5) Potentially pathogenic osseous anomalies are not uncommon and are best demonstrated on CT/CTA. 6) Digital subtraction angiography (DSA) with head turning may reveal dynamic vertebral artery compression but management is controversial.

### **TABLE OF CONTENTS/OUTLINE**

1. Stroke Patterns in VAD 2. Intracranial Vascular Findings in VAD 3. Extracranial Vascular Findings in VAD 4. Osseous Anomalies in VAD 5. Protocols - Optimizing MRA and CTA for Diagnosis of VAD in Children

## **PDEE-49     Imaging Diagnosis of Hydrocephalus and Ventricular Enlargement in Fetuses and Children**

### **Awards**

**Certificate of Merit**

### **Participants**

Hirozumi Mori, MD, (*Presenter*) Nothing to Disclose

### **TEACHING POINTS**

There are a wide variety of causative diseases that indicate hydrocephalus and ventricular enlargement during fetal and childhood, but first, a hint for differentiation can be obtained by classifying the mechanism. By picking up the findings in more detail in the classification and examining whether the causative disease is single or combined, more accurate diagnosis is possible. This time, we will explain how to pick up the findings and recent topics related to diseases.

### **TABLE OF CONTENTS/OUTLINE**

•The criteria for diagnosing hydrocephalus and ventricular enlargement during the fetal period are shown. •We will classify the causative diseases of hydrocephalus and ventricular enlargement in the fetal and childhood and outline them. 1. CSF circulation disorders-Posterior fossa malformation-Hereditary disease-Meningitis-Tumor-Cerebral hemorrhage 2. Encephaloclastic disorder-Cerebral Ischemia-Congenital infection 3. Encephalodysplasia-Neuronal migration disorders-Cerebral Hemisphere separation disorders •In particular, we will explain in detail about congenital malformations. 1. Posterior fossa malformation-Dandy-walker cyst-Blake's pouch cyst-Subarachnoid cyst-Arnold-chiari malformation 2. Neuronal migration disorders 3. Cerebral Hemisphere separation disorders-Holoprosencephaly-Callosal anomaly

## **PDEE-5     Examination of The Optimal Imaging Method for 3D-CT After Fontan Procedure**

### **Participants**

Norihiko Okamoto, (*Presenter*) Nothing to Disclose

### **TEACHING POINTS**

In 3D-CT after Fontan procedure, laminar flow of contrast agent caused by Fontan circulation occurs, which makes it difficult to accurately diagnose the presence or absence of thrombus. Also, the CT number required for 3D-imaging cannot be obtained. In addition, since it is necessary to diagnose Fontan-associated liver disease, multiphase CT scanning is unavoidable and the radiation dose increases. In order to solve this problem, we considered the optimal imaging method. We analyzed past clinical cases. Next, we prepared a tube simulating a blood vessel, injected a two-step diluted contrast agent (opposite ratio) into it, and performed CT scanning on it. The inside of the tube became uniform when the contrast agent and saline were injected at a ratio of 7 to 3/3 to 7. By monitoring the conduit immediately after systemic circulation, it became possible to easily determine the scan timing. At this scan timing, the occurrence of laminar flow was suppressed, and the CT number was sufficiently obtained. In addition to that, it is now possible to diagnose Fontan-associated liver disease. The double-concentration injection method (7 to 3/3 to 7 ratio) made it possible to simultaneously diagnose multiple findings after the Fontan procedure in one phase, and reduced the radiation dose.

### **TABLE OF CONTENTS/OUTLINE**

1. Clinical problems in 3D-CT after Fontan procedure. 2. Analyze past clinical cases. (Laminar flow) 3. Examination of contrast agent injection method. 4. Optimization of CT scanning. 5. Verification of clinical efficacy.

## **PDEE-50     Neuroimaging of Neonatal Stroke: Venous Focus**

### **Awards**

**Identified for RadioGraphics  
Certificate of Merit**

### **Participants**

Lilian Lai, MD, Iowa City, IA (*Presenter*) Nothing to Disclose

## TEACHING POINTS

Perinatal stroke is common and can result in lifelong morbidity. Perinatal stroke can be divided into arterial or venous ischemic stroke and hemorrhagic stroke (typically involving full-term neonates). Arterial ischemic infarcts can be recognized by their arterial distribution, but concurrent hypoxic ischemic injury can complicate interpretation. Less well recognized and under-diagnosed are venous infarcts. The majority of pediatric cerebral sinovenous thrombosis occurs in the neonatal period, and neonates may be more susceptible to venous thrombosis given their incomplete development of alternative indirect pathways of venous drainage. Hemorrhagic infarcts can be due to a myriad of causes and may require MR venogram or angiogram for further evaluation. This exhibit will review imaging patterns of perinatal stroke, with focus on neonatal venous thrombosis.

## TABLE OF CONTENTS/OUTLINE

1) Ischemic arterial perinatal stroke and potential mimics 2) Arterial versus venous drainage pathways and infarct patterns 3) Embryology and anatomy of cerebral venous system: emphasis on medullary and subpial veins 4) Cerebral venous thrombosis including dural venous sinus and cerebral vein thrombosis; medullary vein thrombosis (stand-alone or in association with intraventricular hemorrhage in premature and full-term neonates; subpial hemorrhage due to superficial subpial venous congestion 5) Hemorrhagic infarcts 6) Imaging techniques for perinatal stroke evaluation 7) Treatment and clinical implications of arterial/venous thrombosis

## PDEE-51 Pediatric Brain MRI: Normal For Age or Subtle Pathology?

Participants

Anvita Pauranik, MD, FRCPC, VANCOUVER, BC (*Presenter*) Nothing to Disclose

## TEACHING POINTS

1. To elucidate the difference between age-related changes and subtle pathology in pediatric brain MR studies 2. To understand the spectrum of normal variants in a developing brain.

## TABLE OF CONTENTS/OUTLINE

1. PARENCHYMA. Unmyelinated white matter versus edema in newborn. Normal T1 hyperintense basal ganglia versus hypoxic injury. Terminal zones of myelination versus white matter injury. Dorsal pontine tegmentum: normal hyperintensity versus encephalitis. Central tegmental tract hyperintensity- maturational signal versus metabolic etiology. Normal diffusion anisotropy of corticospinal tracts in newborn versus mild HIE. Peri-dentate hyperintensity-normal versus pathological. (Krabbe, LCH). Prematurity versus abnormal sulcation. Temporal pole-unmyelinated white matter versus Focal cortical dysplasia. SWI: deep gray abnormal mineralization. 2. VENTRICLES: developmental asymmetry versus dysmorphism. Perivascular spaces- normal distribution versus genetic etiology, overgrowth syndrome. Deep sulci: developmental asymmetry versus bottom of sulcus dysplasia. BESSI versus Glutaric aciduria, Abusive head injury. 3. MIDLINE: Cerebellar tonsils-normal variant tonsillar descent versus Chiari 1 deformity. Normal thinning at isthmus versus focal white matter loss. Commissural dysmorphism, abnormal thickening. InterHypothalamic adhesion versus hypothalamic hamartoma. Cysts: incidental versus pathological. PDH deficiency, Zellweger. Retrocerebellar CSF space- variant versus abnormal. Pineal gland- spectrum of cysts. Sella: Pars intermedia remnants versus craniopharyngioma. Marrow signal: clivus heterogeneity

## PDEE-52 What You Know About Rolling In the Deep: Pediatric Inflammatory and Infectious Conditions Involving the Thalami and Basal Ganglia in COVID Times

Participants

Kevin Oh, MD, Suwanee, GA (*Presenter*) Nothing to Disclose

## TEACHING POINTS

1. Introduce common and uncommon pediatric infectious and inflammatory disorders involving the bilateral thalami and/or basal ganglia using a case based approach to include etiologies relevant during the COVID pandemic. For example, acute disseminated encephalomyelitis including MOG antibody disease, acute necrotizing encephalopathy of childhood including that related to COVID-19, and viral encephalitis. 2. Discuss pathology, common imaging findings, and selected treatments for these patients. 3. Discuss briefly differential diagnoses to consider for bilateral thalamic/basal ganglia lesions, such as metabolic disorders and neoplasms.

## TABLE OF CONTENTS/OUTLINE

1. Introduction to pediatric infectious/inflammatory lesions in the basal ganglia and thalami. 2. Case based review of interesting cases within this category: Case presentation; Appropriate labs/pathology studies; Short description of the pathology/pathophysiology of the disease entity; Case images with explanation of common imaging features; Appropriate treatment if indicated; Prognosis. 3. Review of differential diagnoses that can mimic these appearances, such as metabolic (gangliosidosis), ischemic, and neoplastic processes (glioma) involving the bilateral thalami and/or basal ganglia.

## PDEE-53 What Now? Ultrasound or Computed Tomography? Decision Making Flowchart for Pediatric Head Trauma (PHT) and Birth Related Head Injuries (BRHI)

Participants

Gabriela Pinho, MD, Sao Paulo, Brazil (*Presenter*) Nothing to Disclose

## TEACHING POINTS

The purposes of this exhibit are: to review the anatomy of the layers of the scalp; To discuss the main sonographic findings of pediatric head trauma (PHT) and birth related head injuries (BRHI); To gain awareness of the frequency of computed tomography (CT) performed after PHT and BRHI in our service, and critically analyze its impact on patient's management; To propose a decision-making flowchart for the diagnostic management of initial assessment of PHT and BRHI focusing on the role of ultrasound (US) as an initial diagnostic tool.

## TABLE OF CONTENTS/OUTLINE

Anatomy of the scalp, skull and meninges; Risk factors for BRHI; Main indications of cranial ultrasound; Main types of injury observed after PHT and BRHI; Decision making flowchart for diagnostic management after PHT or BRHI: US or CT? Illustrative cases from our Pediatric Radiology group showing the proper conducts; Critically analyze the frequency of computed tomography

performed after PHT and BRHI, and evaluate its impact on patient's management in our service.

#### **PDEE-54 Pediatric Leukemia: How Can We Help?**

Participants

Maria Trujillo Ariza, MD, Villagarcia de Arosa, Spain (*Presenter*) Nothing to Disclose

##### **TEACHING POINTS**

Leukemia is the most common malignancy during childhood, is a multisystemic disease, as radiologist we don't play and important role at diagnosis but we must be aware of the possible imaging findings at the beginning of the disease, possible treatment complications and relapse:- To describe the typical imaging findings at diagnosis.- To summarize the imaging findings of possible complications during treatment.- To review the imaging findings that suggest relapse.

##### **TABLE OF CONTENTS/OUTLINE**

- Epidemiology and presentation of Pediatric Leukemia: Acute Lymphoblastic Leukemia (ALL) vs Acute Myeloblastic Leukemia (AML).-Utility of imaging techniques: x-ray, US, CT and MRI.- Imaging findings: at diagnosis, of treatment complications (short and long term) and in case of relapse.

#### **PDEE-55 Diagnosing VHL Disease By Understanding Morphology from Pathophysiology: What Radiologists Can Learn From The Nobel Prize**

Participants

Sho Koyasu, MD, PhD, (*Presenter*) Nothing to Disclose

##### **TEACHING POINTS**

The essence of the pathogenesis in VHL disease is the accumulation of the transcription factor HIF in cells with mutations in the VHL gene throughout the body, resulting in increased viability and tumorigenesis. This was highlighted by the Nobel Prize in Physiology or Medicine in 2019. VHL-associated tumors overexpress downstream genes of HIF, resulting in hypervascularization, clear cytoplasm, disrupted cell polarity, and cilia dysfunction. These characteristics can be observed from imaging of VHL-associated tumors throughout the body, with tumors showing strongly enhanced regions accompanied by cyst formations of various sizes. In clinical practice, the role of the radiologist becomes even more important after the diagnosis of VHL disease is made. In collaboration with other departments, it is necessary for radiologists to distinguish tumors that need to be treated from others. It is also important to be aware that there are some potential imaging pitfalls. The purpose of this exhibit is: 1. To introduce the history and molecular mechanisms of VHL disease. 2. To discuss the relationship between pathophysiology, morphology, and imaging findings. 3. To present images of common and uncommon VHL disease-related tumors. 4. To help the audience better understand problematic situations related to VHL disease in actual practice.

##### **TABLE OF CONTENTS/OUTLINE**

1. The history of VHL disease, including the discovery, the Nobel Prize, and the new drug approved by the FDA last year. 2. Discussion of imaging findings of VHL-related tumors from molecular mechanisms. 3. Explanation of common as well as rare VHL-related tumors from a morphological perspective. 4. Review of representative cases that are difficult to differentiate.

#### **PDEE-56HC Imaging Spectrum of Rhabdoid Predisposition Syndrome with underlying SMARCB1 and SMARCA4 Mutations**

Participants

Ayat Yousef, MBBS, (*Presenter*) Nothing to Disclose

##### **TEACHING POINTS**

1. List the manifestations of Rhabdoid tumor predisposition syndrome (RTPS) associated with SMARCB1 and SMARCA4 mutations in children. 2. Describe the imaging characteristics of rhabdoid tumors, specifically atypical rhabdoid teratoid tumors according to their molecular subtype. 3. Discuss the proposed imaging protocol for surveillance and post treatment assessment in RTPS.

##### **TABLE OF CONTENTS/OUTLINE**

Inactivation of the tumor suppressor gene SMARCB1 or rarely SMARCA4 is the hallmark of several types of tumors. Patients with SMARCB1 mutations have a high risk of developing synchronous and multifocal rhabdoid tumors (RTs) in early life as a part of rhabdoid tumor predisposition syndromes (RTPS). Other tumors with germline SMARCB1 mutations include cribriform neuroepithelial tumor (CRINET), schwannoma, meningioma, renal cell carcinoma, malignant peripheral nerve sheath tumor and ovarian cancer. RTs frequently arise in the central nervous system, known as atypical teratoid rhabdoid tumor (ATRT). Recently three molecular subtypes of ATRT have been described, each having location tendency and imaging characteristics. The second most common extra-cranial location is rhabdoid tumors of the kidneys (RTK) followed by other locations in the head and neck, liver and rest of the body grouped under extra-renal malignant rhabdoid tumors (ERMRT). Dedicated MRI is the main modality of choice for characterizing rhabdoid tumors and post treatment changes. Other studies like US abdomen, CT and whole-body MRI can be used for metastasis and surveillance in RTPS. Understanding the different imaging manifestations of SMARCB1 mutation can play a pivotal role in disease detection, surveillance and management approach. Please visit the Learning Center to also view this presentation in hardcopy format.

#### **PDEE-57 Imaging Guidelines for Common Pediatric Abdominal Tumors**

Participants

Zoe Winston, MBBS, Manchester, United Kingdom (*Presenter*) Nothing to Disclose

##### **TEACHING POINTS**

1. Review of international imaging guidelines for paediatric abdominal tumours including renal, adrenal gland and liver tumours. 2. Literature review of the advantages and disadvantages of MR compared to CT imaging in paediatric abdominal tumours. 3. Explore case examples of paediatric abdominal tumours, comparing multimodality imaging and also documenting findings from local experience

##### **TABLE OF CONTENTS/OUTLINE**

CT and MR imaging are both used for the diagnosis of common paediatric abdominal tumours. There are differing guidelines internationally for imaging paediatric abdominal tumours. The International Society of Paediatric Oncology (SIOP) and Children's Cancer and Leukaemia Group (CCLG) provide guidelines in Europe and the UK, and the Children's Oncology Group (COG) in North America. A literature review will provide an overview of the international guidelines for imaging of common paediatric abdominal tumours, exploring the advantages and disadvantages of MR and CT evaluation of paediatric abdominal tumours with review of relevant case-based imaging.

#### **PDEE-58 Retinoblastoma: Standardized Imaging Protocols and Reports with Relevance to Current Staging and Treatment**

##### **Awards**

**Identified for RadioGraphics  
Certificate of Merit**

##### **Participants**

Vivek Pai, MBBS, MD, Toronto, Singapore (*Presenter*) Nothing to Disclose

##### **TEACHING POINTS**

Retinoblastoma (RB) is the most common primary intraocular tumor of childhood. Diagnostic techniques and treatment have evolved rapidly over recent years. Accurate staging is key in initiating appropriate treatment for patients with RB, thereby maximizing survival and preserving vision potential. The aims of this educational exhibit are: 1. Review current standards of ocular and radiological imaging utilized in the staging of retinoblastoma. 2. Define the role of imaging in the clinical differentiation of the various stages of RB. 3. Discuss the importance of multimodal imaging in the assessment of the true clinical stage of the disease. 4. Suggest potential standard fields of reporting which are essential for the staging of children with RB.

##### **TABLE OF CONTENTS/OUTLINE**

1. Discussion on clinical and multimodal imaging evaluation in patients with RB 2. Discussion and development of imaging protocols and the importance of imaging in guiding treatment decisions. 3. Demonstrate multimodal images that describe: a) Anterior segment involvement, b) Vitreous and subretinal seeds, c) Intraocular hemorrhage, d) Choroidal invasion, e) Scleral and episcleral involvement, f) Optic nerve invasion, g) Trilateral lesions and intracranial involvement. h) Ophthalmic artery variants that impact chemo-embolization 4. Checklists and standardized reports

#### **PDEE-59 Complications After Pediatric Stem Cell Transplant: From Head to Toe**

##### **Participants**

Luisa Faria, MD, Sao Paulo, Brazil (*Presenter*) Nothing to Disclose

##### **TEACHING POINTS**

The number of disorders in the pediatric age group that benefit from hematopoietic stem cell transplantation (HSCT) is increasing. Nowadays, HSCT is being used for the treatment of leukemia, benign hematologic disorders, autoimmune diseases, certain genetic diagnoses, some forms of lymphoma, and even solid tumors. As a result of the expanding indications, there has been a year-to-year increase in the number of transplantations. Given this scenario, imaging plays a key role in the timely diagnosis of possible complications. The purposes of this multicentric educational exhibit are: (1) to understand the basic principles of HSCT and indications of this procedure in children, (2) to review the predictable timeline of immune suppression after HSCT (3) to systematize the main complications after HSCT in children, based in a multi-institutional experience in pediatric imaging.

##### **TABLE OF CONTENTS/OUTLINE**

(1) Review of the basic principles of HSCT, (2) Classical and novel indications of HSCT in children, (3) Timeline of immune suppression after HSCT and the expected infectious and non-infectious complications in each phase, (4) Case-based approach to the main complications following HSCT in each body segment, combining the clinical scenario with characteristic imaging findings: central nervous system, head and neck, chest, abdomen, and musculoskeletal.

#### **PDEE-6 Preventing Life-Threatening Respiratory Tract Bleeding in Kids!: A Systematic Imaging Approach to Shed Light on The Silent Killer**

##### **Participants**

Akari Makidono, MD, (*Presenter*) Nothing to Disclose

##### **TEACHING POINTS**

#1. Bleeding from the respiratory tract can stay undetected in children until major event occurs since small amount of hemoptysis is commonly veiled by swallowing bloody sputum. Even patients with potentially life-threatening conditions can present with non-specific symptoms, therefore, radiologists should be aware of minor signs and findings of these conditions to prevent major events to occur. #2. Among various diagnostic studies for major respiratory tract bleeding, multidetector CT plays a critical role in determining the cause, site of bleeding, and involved vessels and thus, guiding the caring team toward proper management. For this purpose, systematic imaging approach being demonstrated in this educational exhibit would be helpful for radiologists.

##### **TABLE OF CONTENTS/OUTLINE**

- Causes and pathophysiology - Diagnosis and management - Categories of causes - 1) Airway diseases: bronchiectasis, tracheostomy-related hemoptysis, foreign body aspiration, smoke inhalation - 2) Lung parenchymal diseases: infection, collagen vascular disease, idiopathic pulmonary hemosiderosis, coagulopathy, other causes of diffuse pulmonary hemorrhage - 3) Vascular diseases: congenital heart disease, pulmonary arterial hypertension, arteriovenous malformation/hereditary hemorrhagic telangiectasia, KCNT1 mutation-related hemoptysis - 4) Miscellaneous: trauma, tumor, catamenial hemoptysis, iatrogenic

#### **PDEE-60 Current Applications of PET/MR Imaging for Evaluation of Pediatric Musculoskeletal Disease**

##### **Participants**

Neetu Soni, MD, FRCR, Rochester, NY (*Presenter*) Nothing to Disclose

##### **TEACHING POINTS**

- PET-MR combines the excellent soft-tissue resolution and functional capabilities of MR with the quantitative information provided by positron emission tomography (PET)• “Hybrid” MR imaging implies concurrent acquisition of morphologic and functional MR data• Tumor metabolic response predates change in tumor cellularity/morphology; PET-MR is more sensitive than morphologic MR and DW-MRI for assessment of therapeutic response in oncology• PET-MR decreases total number of required imaging studies, simplifying clinical workflows, thus following the “lean” methodology of quality improvement

#### TABLE OF CONTENTS/OUTLINE

- Normal appearances of hybrid PET-MR in the growing skeleton on an illustrative case-based template• Interpretive pitfalls on PET-MR resulting from normal physiologic attributes of the growing skeleton and technique-related• Current applications and limitations of hybrid PET-MR for assessment of entities affecting the growing skeleton

#### PDEE-61 Hotchpotch in Germ Cell Tumors

Participants

Akanksha Joshi, MBBS, MD, Mumbai, India (*Presenter*) Nothing to Disclose

#### TEACHING POINTS

1. Imaging characteristics of the germ cell tumors on imaging modalities such as CT (Computed Tomography), MRI (Magnetic Resonance Imaging) and USG (Ultrasonography)
2. The imaging features in differentiating the tumors- teratoma, chorio-carcinoma, dysgerminoma, yolk sac, etc.
3. The management of these tumors depending on the location, and aggressiveness.

#### TABLE OF CONTENTS/OUTLINE

1. Classification of the germ cell tumors in the paediatric population based on the location, age, histology and tumor markers.
2. The spectrum of cases depending the location.
3. Imaging features on CT (Computed Tomography), MRI (Magnetic resonance Imaging) and USG (Ultrasonography) and management of these tumors.

#### PDEE-62 Cartilaginous Bone Lesions in Pediatric and Adolescent Age Group: A Case-based Review

Participants

Mahesh Kumar JR, MBBS, MD, Mumbai, India (*Presenter*) Nothing to Disclose

#### TEACHING POINTS

Classifying pediatric and adolescents cartilaginous bone lesions. Recognizing the radiological and pathological features of chondroid matrix. Learning the imaging features of benign, benign aggressive and malignant cartilaginous bone lesions. Special emphasize on chondrosarcoma in pediatric and adolescent age group. Management of cartilaginous bone lesions.

#### TABLE OF CONTENTS/OUTLINE

Disclosure. Introduction. Classification of pediatric and adolescents cartilaginous bone lesions. Chondrosarcoma in pediatric and adolescents age group. Cases

#### PDEE-63 Treatment-related Complications in Children with Hematolymphoid Malignancy: Emergent Conditions and Late Effects

#### Awards

Identified for RadioGraphics

Participants

Claudia Cheung, MBBS, Hong Kong, Hong Kong (*Presenter*) Nothing to Disclose

#### TEACHING POINTS

1. Treatment of childhood hematolymphoid malignancies depends on stages and risk of the specific disease, but generally comprises of intensive chemotherapy regimens, with addition of radiotherapy and/or allogenic hematopoietic stem cell transplantation (HSCT) and novel immunotherapy for certain conditions.
2. Severe myelosuppression and prolonged neutropenia are common, which are risk factors for invasive fungal infections from opportunistic organisms. Viral reactivation are common in HSCT recipients.
3. Acute treatment-related toxicity depends on the chemotherapeutic agents for specific disease. For example, methotrexate is associated with acute toxic leukoencephalopathy. Multiple chemotherapy agents are implicated in posterior reversible encephalopathy syndrome. L-asparaginase is associated with pancreatitis and venous thromboembolism. Anthracyclines can cause myocardial cell injury which leads to left ventricular dysfunction. Understanding the treatment regimen used is important in reaching the correct diagnosis.
4. Use of high dose corticosteroids can cause long term skeletal complications. Early recognition of avascular necrosis of femoral head is of particular importance as early orthopedic intervention is essential.
5. Use of intensive radiotherapy can lead to development of secondary cancer. For acute leukemia, secondary brain tumours are common in patients who received cranial radiotherapy.

#### TABLE OF CONTENTS/OUTLINE

- 1 Introduction
- 2 Brief overview of treatment regimens
- 3 Treatment-related complications (classified by body systems)
- 3(a) Infectious
- 3(b) Acute treatment toxicity
- 3(c) Late effects
- 4 Conclusion

#### PDEE-64 Radiologists Role In Establishing The Diagnosis, Evaluating Risk Factors, Detecting Recurrence, and Determining the Effectiveness of Treatment in Langerhans Cell Histiocytosis

Participants

Takahiro Hosokawa, (*Presenter*) Nothing to Disclose

#### TEACHING POINTS

Langerhans cell histiocytosis (LCH) predominantly affects children. Its clinical presentation varies significantly, from isolated and self-limiting to multisystem disorder with a life-threatening clinical course. Various organs are involved. Bone is affected most frequently, and the location of its involvement on imaging findings provides important clues for diagnosing LCH. After diagnosis, the

following risk factors should be evaluated: (1) risk of recurrence classified into three grades according to the degree of organ system involvement; I) multisystem (M-S) disease with involvement of high-risk organ (hematologic system, liver, and spleen), II) M-S disease without high-risk organ involvement, or III) single system involvement with one or multiple lesions; (2) risk of central nervous system involvement (manifesting as diabetes insipidus and neuro-degenerative complications); (3) risk of tracheal compression; anterior mediastinal or thyroid huge mass is a predictor of complications during general anesthesia. During follow-up, knowledge regarding the changes in imaging findings associated with pharmacotherapy and conservative treatment is required to evaluate the effectiveness of treatment and detect recurrence.

#### TABLE OF CONTENTS/OUTLINE

1. Introduction 2. Imaging findings of LCH; involvement of various organs 3. Key imaging findings for diagnosing LCH 4. Evaluation of risks of recurrence, central nervous system involvement, and tracheal compression 5. Imaging findings during follow-up of patients 6. Conclusion

#### PDEE-65 PET/CT in Pediatric Oncology

Participants

Flavio Garcia Pires, MD, (*Presenter*) Nothing to Disclose

#### TEACHING POINTS

After viewing this education exhibit, the learner should be able to: - Understand the principles of PET/CT as a hybrid imaging modality combining functional and anatomic information, which increases its diagnostic and prognostic accuracy; - Understand the importance of FDG PET/CT for the diagnosis, staging and posttreatment response assessment in pediatric oncology; - Identify specific malignancies when the use PET/CT is beneficial; - Instruct multidisciplinary team on the ideal patient preparation to minimize false positive and false negative sites of radiotracer uptake. - Identify expected/physiologic areas of radiotracer uptake and common pitfalls of imaging interpretation such as physiologic linear uptake in physes/apophyses and diffuse bone marrow uptake in generalized inflammatory states or gCSF administration.

#### TABLE OF CONTENTS/OUTLINE

1. RADIOTRACERS/MECHANISMS OF ACTION. 2. PATIENT PREPARATION. 3. PET INTERPRETATION. a. SUV. b. PHYSIOLOGIC FDG UPTAKE IN CHILDREN c. PITFALLS. 4. SPECIFIC DISEASES. a. LYMPHOMA/PTLD. b. SARCOMAS. i. OSTEOSARCOMA. ii. EWING'S SARCOMA. iii. RHABDOMYOSARCOMA. c. LESS INCIDENT TUMORS. i. GERM CELL TUMOR. ii. HEPATOBLASTOMA. iii. NEUROBLASTOMA. 1. FDG. 2. Ga-DOTATATE. iv. THYROID CANCER. 1. FDG. 2. Ga-DOTATE (FOR MEDULLARY SUBTYPE). v. MALIGNANT PERIPHERAL NERVE SHEATH TUMOR. vi. WILMS' TUMOR. vii. CNS TUMOR. 1. PITFALL: RADIATION NECROSIS. 5. FUTURE DIRECTIONS.

#### PDEE-66 Photon Counting Detector CT in Children: Advantages and Clinical Prospects

Participants

Juan Carlos Ramirez-Giraldo, PhD, Cary, NC (*Presenter*) Employee, Siemens AG

#### TEACHING POINTS

- Photon-counting detectors (PCD) technology directly converts individual x-ray photons into electrical pulses with small pixel size, that can be counted.
- Traditional energy-integrating detector (EID) CT uses an indirect conversion process where x-ray photons are converted to light, and the signal is integrated over a short period of time.
- PCD CT results in improved spatial resolution.
- PCD CT results in improved contrast of small structures in pediatric patients.
- PCD CT allows for substantial radiation dose reductions.
- PCD CT allows for spectral imaging all the time.

#### TABLE OF CONTENTS/OUTLINE

- Review basic principles of photon counting CT
- Discuss advantages of PCD CT
- Discuss applications PCD CT in pediatric imaging and advantages compared to traditional EID CT images.
- Ø High resolution temporal bone CT
- Ø High resolution chest CT
- Ø Contrast enhanced Chest CT
- Ø Cardiac CT
- Ø CT angiography
- Ø Abdominal CT
- Ø Head CT

#### PDEE-67 Baby Steps Toward a Proper Interpretation of Neonatal Chest and Abdominal Radiographs

Participants

Deborah Otto, Sao Paulo, Brazil (*Presenter*) Nothing to Disclose

#### TEACHING POINTS

The purposes of this exhibit are:- To review the normal radiological aspects of chest and abdominal radiographs in neonates.- To illustrate some of the main thoracic and abdominal disorders that can be diagnosed in neonates through plain radiographs.

#### TABLE OF CONTENTS/OUTLINE

Chest:- Normal anatomy- Lines and tubes (correct placement parameters, correct and incorrect placement examples and complications).- Diffuse lung disorders (Surfactant deficiency, retained fetal fluid, meconium aspiration, congenital surfactant dysfunction, alveolar growth disorders)- Focal lung disorders (Congenital Pulmonary Airway Malformations, Bronchopulmonary sequestration, congenital lobar hyperinflation)- Diffuse or Focal disorders(Pneumonia, Interstitial Emphysema)Abdomen:- Normal anatomy and expected bowel gas pattern- Lines and tubes (correct placement parameters, correct and incorrect placement examples and complications).- Congenital gastrointestinal disorders (tracheoesophageal fistula, duodenal atresia, ileal atresia, malrotation, Hirschsprung disease and congenital diaphragmatic hernia).- Acquired gastrointestinal disorders (necrotizing enterocolitis, pneumoperitoneum, meconium peritonitis, gastric volvulus and midgut volvulus)

#### PDEE-7 Imaging Features of Pediatric Sarcoidosis: From Head to Toe

Awards

Identified for RadioGraphics

Participants

Gozde Ozer IV, MD, (*Presenter*) Nothing to Disclose

#### TEACHING POINTS

Sarcoidosis occurs approximately ten times less frequently in children than in adults. Pediatric sarcoidosis predominantly involves the lungs and lymphatic system but can affect any organ in the body. Characteristic chest CT findings of pulmonary sarcoidosis are mediastinal, bilateral hilar lymphadenopathy, and nodules with the perilymphatic distribution along the interlobular septa, interlobar fissures, and subpleural regions. Abdominal sarcoidosis may manifest as numerous small nodules in the liver and spleen. In addition, abdominal lymphadenopathies can be seen in one-third of the patients. Neurosarcoidosis is most commonly manifested by leptomeningeal and pituitary gland involvement. Leptomeningeal sarcoidosis can be seen as nodular or plaque-like thickening and enhancement of the leptomeninges. Orbital involvement of sarcoidosis is the most common presentation in the head and neck region. Although any part of the orbit can be involved, uveitis is the most common condition and is often bilateral.

#### **TABLE OF CONTENTS/OUTLINE**

General information and diagnostic criteria of sarcoidosis. The role of radiology in the diagnosis. Imaging patterns of pulmonary, abdominal, central nervous system, head and neck, and musculoskeletal-cutaneous involvement of sarcoidosis.

#### **PDEE-8 Congenital Diaphragmatic Hernia: A Hole lot More than Morgagni**

Participants

Christian Pecoraro, DO, Rochester, NY (*Presenter*) Nothing to Disclose

#### **TEACHING POINTS**

Embryology of the diaphragm and cause of congenital diaphragmatic hernias. Role of pre-natal imaging including MR + US in the diagnosis and prognostication of CDH. Post-natal imaging findings of typical right and left CDH. Imaging findings of acute Late-Presenting CDH. Review of surgical strategies for CDH repair, as well as expected and un-expected post-operative findings. Associated anomalies, syndromic and non-syndromic including urogenital, musculoskeletal neurological.

#### **TABLE OF CONTENTS/OUTLINE**

Introduction, definition, and embryology. Classification of CDH. Prenatal imaging findings of CDH. Postnatal imaging findings of CDH. Review of fetoscopic endoluminal tracheal occlusion (FETO) for CDH. Expected post-operative appearance of the diaphragm following surgical prosthetic patch repair/graft. Acute and late post-operative related complications of CDH, including associated decreased ipsilateral lung perfusion. Associated anomalies, syndromic and non-syndromic including urogenital, musculoskeletal neurological. Describe the respiratory morbidities found in CDH survivors, including chronic cough, wheezing, chest wall deformities (pectus excavatum) and scoliosis.

#### **PDEE-9 Point of Care Ultrasound in Pulmonary Pathologies Applied to Intensive Care Unit Neonates**

Participants

Vitor Romano, MD, Sao Paulo, Brazil (*Presenter*) Nothing to Disclose

#### **TEACHING POINTS**

The purposes of this exhibit are: Make a didactic review of the point of care ultrasound in pulmonary pathologies in intensive care unit neonates; Point out the indications and limitations of the ultrasound on the evaluation of the pulmonary parenchyma; Review the techniques of the pulmonary ultrasound; Review the anatomy and the thoracic structures that can be evaluated by this method; Review the normal and abnormal findings on thoracic ultrasound; Review the main artifactuary lines on lung ultrasonography and it's pathological correlations; Review the main protocols of thoracic ultrasound.

#### **TABLE OF CONTENTS/OUTLINE**

We will discuss the following topics and focus on the echography features of the normal and abnormal thoracic ultrasound: Ultrasound technique Normal findings on pulmonary ultrasonography (A lines; B lines; I lines; Z lines; E lines) Pathologic findings on thoracic ultrasonography: Parenchyma (Consolidation; Atelectasia; Congestion) and Pleura (Pleural effusion; Pneumothorax) Protocols.

Printed on: 02/07/23



## Abstract Archives of the RSNA, 2022

PDEE-1

### Cardiac and Pericardial Neoplasm in Children: Radiologic-Pathologic Correlation

Sunday, Nov. 27 8:00AM - 9:00AM Room: Learning Center - PD

#### Awards

Identified for RadioGraphics  
Cum Laude

#### Participants

Mariangeles Medina Perez, MD, Syracuse, NY (*Presenter*) Nothing to Disclose

#### TEACHING POINTS

- Illustrate the most common cardiac and pericardial masses in children and their relative prevalence.
- Describe the characteristic imaging characteristics of primary pediatric benign and malignant cardiac and pericardial neoplasm based on pathologic features.
- Identify imaging features that can help differentiate benign from malignant etiology.

#### TABLE OF CONTENTS/OUTLINE

- Role of imaging with delineation of technique and pediatric protocols.
- Characterization of specific primary cardiac and pericardial tumors with description of clinical considerations, imaging features by different modalities, and pathologic features.
- Appropriate differential diagnosis according to tumor location and imaging features.

Printed on: 02/07/23



## Abstract Archives of the RSNA, 2022

PDEE-10

### The Many Faces of Lymphomas in Pediatric Patients: Spectrum of Multimodality Imaging Findings in Thoracic and Abdominal lymphomas

Sunday, Nov. 27 8:00AM - 9:00AM Room: Learning Center - PD

#### Participants

Luisa Faria, MD, Sao Paulo, Brazil (*Presenter*) Nothing to Disclose

#### TEACHING POINTS

Lymphomas account for 10%-15% of all cancers in the pediatric age group, being the third most common malignancy, following leukemia and malignant brain tumors. All organ systems may be involved, including the central nervous system, head and neck, thorax, abdomen, gonads, and bone, and several different histologic subtypes can be found. As a result, the spectrum of imaging findings is wide and the diagnosis can be challenging (particularly in extranodal disease), with considerable imaging overlap with other diseases. The purposes of this exhibit are: (1) to illustrate the spectrum of multimodality imaging findings in thoracic and abdominal lymphomas in the pediatric age group (2) to point out the most important differential diagnosis and lymphoma mimickers.

#### TABLE OF CONTENTS/OUTLINE

(1) Review of epidemiology and histologic subtypes. (2) Chest involvement (imaging findings, mimickers, and differential diagnosis): chest wall, pleura, lungs, mediastinal structures. (3) Abdominal involvement (imaging findings, mimickers, and differential diagnosis): liver, pancreas, biliary tree, spleen, small bowel, colon, kidney, ureters, peritoneum, and testes.

Printed on: 02/07/23



## Abstract Archives of the RSNA, 2022

PDEE-11

### Complications in Transjugular Liver Biopsy (TJLB) and Tips to Avoid Them

Sunday, Nov. 27 8:00AM - 9:00AM Room: Learning Center - PD

#### Participants

Juan Calle Toro, MD, MS, San Antonio, TX (*Presenter*) Nothing to Disclose

#### TEACHING POINTS

Different techniques can be used before, during, and after a TJLB to avoid potential complications

#### TABLE OF CONTENTS/OUTLINE

Liver biopsy remains the gold standard to diagnose cirrhosis, hepatitis, nonalcoholic fatty liver disease, primary biliary cirrhosis, autoimmune hepatitis and post-transplant for the diagnosis of rejection 1. Transjugular liver biopsy (TJLB) is preferred in patients with coagulopathies given the low risk of bleeding. Diagnostic sample rate in TJLB is 96.1% with low technical failure rate of 3.2%. Technical failure is usually due to failure to catheterize the hepatic vein 1. Complications of TJLB include subcapsular perforation in 1.4%, neck hematoma in 0.8%, intraperitoneal hemorrhage in 0.6%, arrhythmia in 0.05%, and pneumothorax in 0.05% 2. We recommend several tips to avoid complications. Ultrasound should be performed prior to the procedure to confirm the patency of the hepatic veins and jugular access. Secondly, we recommend using Tru-Cut (Quick-Core). Additionally; TJLB should be performed during breath hold. Finally, when in position to fire the biopsy needle, we advise wedging the cannula antero-lateral if the right hepatic vein is used, or lateral if the middle hepatic vein is used. The procedure should ideally be done in facilities equipped to handle bleeding complications 3. It is recommended to avoid TJLB in patients with thrombosis of the right IJ vein, thrombosis of hepatic veins, cholangitis, or lack of patient cooperation 4. In those cases, alternative routes can be considered such as transfemoral biopsy, endoscopic ultrasound-guided liver biopsy, or Laparoscopic liver biopsy 5.

Printed on: 02/07/23



## Abstract Archives of the RSNA, 2022

PDEE-12

### Ultrasound Evaluation of The Chest: Neonatal and Pediatric Cases

Sunday, Nov. 27 8:00AM - 9:00AM Room: Learning Center - PD

#### Participants

Muhammad Khan, MD, Memphis, TN (*Presenter*) Nothing to Disclose

#### TEACHING POINTS

1. To review proper chest ultrasound technique.2. To discuss normal appearance of chest on US.3. To discuss and illustrate ultrasound imaging appearance of neonatal and pediatric chest abnormalities by correlating the cases with cross sectional imaging.4. Reinforcement of the ALARA principle along with the dictum of "Image gently"

#### TABLE OF CONTENTS/OUTLINE

Ultrasound (US) is an excellent imaging modality for initial evaluation of chest due to its portable nature, lack of radiation and no need for contrast administration and sedation. Due to recent advances and improvement in technology the use of US in evaluation of chest has significantly increased. The main indications for chest US in children include, follow up and evaluation of antenatally detected lung abnormalities, assessment of an opaque hemithorax, differentiating cystic from solid lesions, evaluation of chest wall lesion, mediastinal masses, lung lesions, diaphragmatic hernia/eventration and clarify inconclusive plain film findings. Table of contents: Introduction - Chest Ultrasound Technique- normal anatomy and appearance - simple pleural effusion, empyema, ECMO and trauma related hemothorax, chest wall and mediastinal masses( teratoma, neuroblastoma, chest wall masses lipoblastoma, hemangioma), diaphragmatic hernia, eventration, hiatal hernia, pneumonia, necrotizing pneumonia, and atelectasis

Printed on: 02/07/23



## Abstract Archives of the RSNA, 2022

PDEE-13

### MR Insights into Fetal Brain Development: What is Normal and What is Not

Sunday, Nov. 27 8:00AM - 9:00AM Room: Learning Center - PD

#### Awards

Certificate of Merit

#### Participants

Maria Camila Cortes Albornoz, MD, (*Presenter*) Nothing to Disclose

#### TEACHING POINTS

- 1. Fetal life is the most dynamic period of human brain development.
- 2. MRI demonstrates all major developmental processes in vivo: hemispheric cleavage, sulcation, evolution of transient telencephalic zones, involution of germinal matrix, myelination, and growth of the corpus callosum and vermis.
- 3. Awareness of normal fetal brain development enables the clinical fetal imager to identify abnormalities as they emerge.

#### TABLE OF CONTENTS/OUTLINE

Illustration of normal processes of fetal brain development on structural images: Single-shot T2, Steady State Free Precession, T1-VIBE. Compare and contrast cases of normal development with pathologic cases. The collection includes: holoprosencephaly, polymicrogyria, cortical malformations, ventriculomegaly, callosal dysgenesis, vermian hypoplasia, rhombencephalosynapsis, among others. Review of emerging sequences on fetal MRI and their role in characterizing brain development: T2\*-weighted and DTI.

Printed on: 02/07/23



## Abstract Archives of the RSNA, 2022

PDEE-14

### Cancer Therapy-Related Hepatic Injury In Children: An Imaging Review From the Pediatric LI-RADS Workgroup

Sunday, Nov. 27 8:00AM - 9:00AM Room: Learning Center - PD

#### Awards

**Cum Laude**

Identified for RadioGraphics

#### Participants

Cara Morin, PhD, Memphis, TN (*Presenter*) Nothing to Disclose

#### TEACHING POINTS

The liver is the primary organ for the metabolism of many chemotherapeutic agents, and drug-induced liver injury is common in children undergoing cancer therapy. Acute toxic effects of cancer therapy in children include cholestasis, hepatitis, steatosis, steatohepatitis, hemosiderosis, and vascular complications such as sinusoidal obstruction syndrome. Longer-term effects of cancer therapy can include fibrosis, liver failure, and focal liver lesions that can be confused for metastatic disease.

#### TABLE OF CONTENTS/OUTLINE

Introduction (including incidence and the effects of therapy on peri-operative morbidity) Imaging modalities Discussion of specific roles and pros/cons in children Description of quantitative sequences to assess for steatosis/iron deposition Specific etiologies of liver injury Hepatitis Cholestasis/biliary injury Vascular complications (e.g., SOS, PV thrombosis) Hepatic GVHD Steatosis steatohepatitis Iron deposition Radiation injury Expected appearance of treated metastatic disease (including post-ablation) Fibrosis cirrhosis Focal liver lesions FNH-like lesions, perfusion abnormalities, metastases, etc. Diagnostic challenges of underlying steatosis/siderosis Diagnostic challenges of differentiating benign lesions from recurrent/metastatic disease

Printed on: 02/07/23



## Abstract Archives of the RSNA, 2022

PDEE-15

### Ingested Foreign Bodies in Children-How Do We Image and What To Report

Sunday, Nov. 27 8:00AM - 9:00AM Room: Learning Center - PD

#### Participants

Jeong Rye Kim, MD, PhD, Cheonan, Korea, Republic Of (*Presenter*) Nothing to Disclose

#### TEACHING POINTS

1. Discuss the role of each imaging modality in the diagnosis of ingested foreign bodies in children  
2. Review the general management considerations according to the location and the opacity of foreign bodies  
3. Discuss imaging findings and management guidelines of specific types of ingested foreign bodies

#### TABLE OF CONTENTS/OUTLINE

1. How to image children with ingested foreign bodies  
a. First imaging step: Radiography  
i. Guidelines for radiographic work-up  
ii. Things to report  
iii. What if there are negative findings on radiographs?  
b. Second line imaging modalities: CT versus US  
2. General management considerations  
a. According to the location of FBs  
b. Radioopaque versus radiolucent FBs  
3. Imaging findings and management guidelines of specific types of ingested FBs.  
a. Magnets  
b. Battery  
c. Sharp FBs  
d. Blunt FBs (marbles, coins)  
e. Glass  
f. Water absorbent beads

Printed on: 02/07/23



## Abstract Archives of the RSNA, 2022

PDEE-16

### Visceral Torsions and Atypical Obstructions in the Pediatric Age Group

Sunday, Nov. 27 8:00AM - 9:00AM Room: Learning Center - PD

#### Participants

Ankita Chauhan, MD,MBBS, (*Presenter*) Nothing to Disclose

#### TEACHING POINTS

Background Information: Children often present to the pediatric emergency department with acute abdominal pain. It is particularly challenging to assess young children as they generally show nonspecific symptoms (fussiness, lethargy, inconsolable crying). An older child can often localize the pain and describe its character. The clinical signs of volvulus often are nonspecific, and radiologists often are consulted for diagnostic evaluations. Prompt diagnosis is crucial as a delay in diagnosis will result in increased morbidity and mortality. Teaching Points: 1. To learn the pathophysiology of visceral torsions and become familiar with their classic imaging appearances. 2. To become accustomed to identifying the twist in the hollow viscus and visceral torsions. 3. To become familiar with a few atypical but essential to know presentations of bowel obstruction in children. 4. To acquire a basic understanding of the radiographic obstructive bowel gas patterns.

#### TABLE OF CONTENTS/OUTLINE

-Goals and objectives -Background information -Anatomy - Visceral torsions (midgut volvulus, gastric volvulus, small bowel internal hernia with volvulus, small bowel intussusception with volvulus, trichobezoar with volvulus, cecal volvulus, colonic volvulus, splenic torsion) -Atypical bowel obstruction (bezoars) -Summary

Printed on: 02/07/23



## Abstract Archives of the RSNA, 2022

PDEE-17

### Imaging Approach and Radiological Pitfalls of Pediatric Gastrostomy Tube Placement

Sunday, Nov. 27 8:00AM - 9:00AM Room: Learning Center - PD

#### Participants

Lauren May, MD, (*Presenter*) Nothing to Disclose

#### TEACHING POINTS

Teaching points: 1. Gastrostomy tubes are indicated for long term nutritional support, gastric decompression, or for future gastrojejunostomy conversion. 2. After placement or tube exchange, contrast can be administered through the gastrostomy to confirm intraluminal placement in the stomach. 3. Radiological technique may involve fluoroscopy by the radiologist or can be performed remotely with radiographs. 4. A checklist of findings to confirm placement includes contrast flowing dependently in the stomach away from the tube, contrast progressing to the small bowel, and visualization of the gastrostomy balloon. 5. Complications of gastrostomy tube placement include peritoneal leakage, enteric transgression, stomach perforation, buried bumper, gastric outlet obstruction, gastric or colonic cutaneous fistula formation, and gastrostomy site hernia. 6. Ultrasound and CT may be useful adjuncts for trouble-shooting challenging cases.

#### TABLE OF CONTENTS/OUTLINE

Table of Contents/Outline: 1. Introduction 2. Clinical indications and gastrostomy tube placement technique 3. Fluoroscopy technique to confirm tube placement 4. Limited portable radiograph technique to confirm tube placement 5. Checklist to evaluate gastrostomy tube placement on radiographs and fluoroscopy 6. Ultrasound and CT: Useful problem-solving adjuncts 7. Illustrative case examples of complications highlighting pitfalls of imaging interpretation

Printed on: 02/07/23



## Abstract Archives of the RSNA, 2022

PDEE-18

### Typical and Not-so Typical Presentations of Childhood Intussusception

Sunday, Nov. 27 8:00AM - 9:00AM Room: Learning Center - PD

#### Participants

Ankita Chauhan, MD,MBBS, (*Presenter*) Nothing to Disclose

#### TEACHING POINTS

Background Information: Acute abdominal pain is a common complaint in pediatric emergency departments. Patients less than two years of age may present with inconsolable crying, fussiness, and/or lethargy, making the assessment particularly challenging compared to an older child able to localize the pain and describe its character. Intussusception's clinical symptoms are often nonspecific, and radiologists frequently perform diagnostic evaluations and therapeutic interventions. Teaching Points: 1. To acquire a basic understanding of the imaging features of intussusception with particular attention to the radiographic clues to the diagnosis. 2. To learn the pathophysiology of entero-enteric and entero-colic intussusceptions in the pediatric age group. 3. To become familiar with the atypical pathologic causes of intussusception. 4. To understand the radiologist's role in treating intussusception and recognizing complications of the disease or its treatment. 5. To recognize potential mimics of the disease.

#### TABLE OF CONTENTS/OUTLINE

-Goals and objectives -Background information -Radiographic signs of intussusception - Types of intussusceptions -Management of entero-enteric intussusception -Management of ileocolic intussusception -Air enema (procedure, indications, contraindications, complications) -Mimics of Intussusception -Summary

Printed on: 02/07/23



## Abstract Archives of the RSNA, 2022

PDEE-19

### A Tour of Biliary Disorders, Anomalies, and Malignancies in Children

Sunday, Nov. 27 8:00AM - 9:00AM Room: Learning Center - PD

#### Awards

Identified for RadioGraphics

#### Participants

Curtis Simmons, MD, (*Presenter*) Nothing to Disclose

#### TEACHING POINTS

1. Distinct underlying genetic conditions can be made or suspected based on radiological/radiogenomic features. 2. Many congenital abnormalities can be understood from variations in embryological development. 3. While pediatric biliary malignancy is rare, rhabdomyosarcoma and cholangiocarcinoma are the two most likely entities. 4. Intra-operative cholangiograms can help visualize the biliary system not well evaluated with traditional imaging techniques. 5. The diagnosis of biliary atresia is evolving practice, with a delayed diagnosis causing a substantial increase in need for hepatic transplant.

#### TABLE OF CONTENTS/OUTLINE

Introduction // Embryological Development of Ducts // Congenital Gallbladder Anomalies: Gallbladder agenesis, intrahepatic gallbladder, floating gallbladder, duplicated gallbladder, septate gallbladder // Anomalous pancreaticobiliary junctions: Aberrant cystic duct insertion, aberrant biliary ducts // Cholecystic processes: Neonatal hepatitis, biliary atresia, Alagille syndrome // Congenital cystic lesions: Choledochal cysts (types 1-4), Caroli's disease, Von Meyenburg complex, polycystic liver disease, complex and simple biliary cysts // Biliary filling anomalies: Cholelithiasis, choledocholithiasis, bile plug syndrome, sickle cell related cholelithiasis // Biliary changes in systemic genetic conditions: cystic fibrosis, autosomal dominant polycystic kidney disease, autosomal recessive polycystic kidney disease // Inflammatory biliary conditions: Sclerosis cholangitis // Pediatric biliary neoplasms: Rhabdomyosarcoma, cholangiocarcinoma // Conclusion

Printed on: 02/07/23



## Abstract Archives of the RSNA, 2022

PDEE-2

### Pediatric Cardiac Masses: Multimodality Imaging with Rad-path Correlation

Sunday, Nov. 27 8:00AM - 9:00AM Room: Learning Center - PD

#### Participants

Prabhakar Rajiah, MD, FRCR, Rochester, MN (*Presenter*) Nothing to Disclose

#### TEACHING POINTS

Pediatric cardiac masses are rare, but it is important for radiologists to recognize these in time for initiating appropriate management. 1. To review the spectrum of cardiac masses in the pediatric population 2. To discuss the role of multimodality imaging in the evaluation of pediatric cardiac masses 3. To review optimal CT and MRI protocols of pediatric cardiac masses 4. To illustrate the imaging appearances of several pediatric masses with pathologic correlation

#### TABLE OF CONTENTS/OUTLINE

- Introduction
- Spectrum of pediatric cardiac masses
- Multimodality imaging of pediatric cardiac masses- Ultrasound, CT, MRI, Nuclear medicine, cardiac cath
- Review and illustration of the following pediatric masses with case examples and path correlation where available - Benign tumors- Rhabdomyoma, fibroma, teratoma, myxoma, hemangioma, inflammatory myofibroblastic tumor - Malignant tumors- Metastases, sarcoma, lymphoma, leukemia - Non-neoplastic masses- Thrombus, Eosinophilic myocarditis, pericardial cyst, lipomatous hypertrophy of atrial septum, aneurysm, pseudoaneurysm, diverticulum, hamartomatous malformations - Anatomical variations- Prominent crista terminalis, Chiari network, taenia sagittalis, coumadin ridge

Printed on: 02/07/23



## Abstract Archives of the RSNA, 2022

PDEE-20CS

### Standardized Performance of Pediatric Appendix Ultrasound for Radiologists, Clinicians and Sonographers Introduction

Sunday, Nov. 27 8:00AM - 9:00AM Room: Learning Center - PD

#### Participants

Lori L. Barr, MD, (*Presenter*) Nothing to Disclose

#### TEACHING POINTS

Rationale of using a standardized exam protocol, sonographer worksheet and reporting template is explained. Identify and document the ultrasound characteristics of the normal and abnormal: appendix, right lower quadrant mesenteric fat, cecum, adjacent bowel loops, and right lower quadrant lymph nodes. Apply a standardized exam protocol to demonstrate presence or absence of primary and secondary appendicitis findings, a standardized sonographer worksheet and a standardized reporting template. Synthesize the imaging and sonographer worksheet information into a standardized report/impression that decreases the number of equivocal exams.

#### TABLE OF CONTENTS/OUTLINE

Welcome and Pre-training Assessment has 4 activities, welcome, introduction to how the learning portal works, pre-training assessment and acknowledgments. Pediatric Ultrasound Appendix Exam Performance has 10 interactive activities: Minimum components of a complete exam, Required Images and Cines for a Complete Exam, Completing the Standardized Sonographer Worksheet, 10 Tips to Turn an Incomplete Exam into a Complete Exam, Normal Appendix, Appendix Not Identified No Appendicitis, Acute Appendicitis Not Perforated, 5 YO with right lower quadrant pain, Acute Appendicitis Perforated and Other Pathology That Presents with Right Lower Quadrant Pain. Pediatric Ultrasound Appendix Exam Interpretation has 7 activities: What is the Difference Between a Non-diagnostic Exam and an Equivocal Report?, Why use a standardized reporting template?, Download a Standardized Reporting Template, Definitive vs. Equivocal Interpretations, How to Minimize Equivocal Studies using a Template, 12 YO with RLQ Pain, Take This Post-training Assessment

Printed on: 02/07/23

## Abstract Archives of the RSNA, 2022

PDEE-22

### Imaging Approach to Distal Neonatal Bowel Obstruction

Sunday, Nov. 27 8:00AM - 9:00AM Room: Learning Center - PD

#### Awards

Identified for RadioGraphics

#### Participants

Samantha Gerrie, MBChB, FRANZCR, (*Presenter*) Nothing to Disclose

#### TEACHING POINTS

1. Describe a structured approach to multimodality imaging workup of distal neonatal bowel obstruction including Hirschsprung disease, functional immaturity of the large bowel, meconium ileus, colonic atresia and segmental volvulus. 2. Highlight appropriate use of abdominal ultrasound (US) in specific problem solving scenarios.

#### TABLE OF CONTENTS/OUTLINE

1. Introduction  
2. Hirschsprung disease  
a. Presentation, types, associations  
b. Radiographic finding  
c. Lower gastrointestinal (LGI) contrast study findings  
d. Pitfalls  
i. Total colonic Hirschsprung disease  
ii. Delayed or misdiagnosis in premature neonates  
iii. Delayed presentation in children with chronic constipation  
3. Functional immaturity of the large bowel  
a. Presentation  
b. Radiographic findings  
c. LGI contrast study findings  
d. Pitfalls  
i. Long-segment Hirschsprung disease mimicking functional immaturity  
ii. No clear caliber difference between right and left colon  
4. Meconium ileus  
a. Presentation, associations  
b. Radiographic findings  
c. LGI contrast study findings  
i. Simple meconium ileus  
ii. Meconium ileus complicated by segmental volvulus  
5. Ileal atresia  
a. Presentation  
b. Radiographic findings  
c. LGI contrast study findings  
6. Colonic atresia  
a. Presentation  
b. Radiographic findings  
c. LGI contrast study findings  
7. Segmental volvulus  
a. Presentation  
b. Radiographic findings  
c. US findings - "mini whirlpool" sign  
d. Upper and lower gastrointestinal contrast study findings  
8. Conclusion

Printed on: 02/07/23



## Abstract Archives of the RSNA, 2022

PDEE-23

### Imaging Approach to Proximal Neonatal Bowel Obstruction

Sunday, Nov. 27 8:00AM - 9:00AM Room: Learning Center - PD

#### Awards

Identified for RadioGraphics

#### Participants

Samantha Gerrie, MBChB, FRANZCR, (*Presenter*) Nothing to Disclose

#### TEACHING POINTS

1. Describe a structured approach to multimodality imaging workup of proximal neonatal bowel obstruction including esophageal atresia, pyloric stenosis, duodenal atresia, duodenal web, malrotation with midgut volvulus and jejunal atresia. 2. Discuss the role of plain radiographs. 3. Discuss use of upper gastrointestinal (UGI) series and ultrasound (US) in establishing diagnosis or narrowing the differential diagnosis.

#### TABLE OF CONTENTS/OUTLINE

1. Introduction 2. Esophageal atresia a. Types, presentation, associations b. Radiographic findings 3. Gastric/pyloric atresia a. Presentation b. Radiographic findings 4. Hypertrophic pyloric stenosis a. Presentation b. US findings i. Pylorus measurements ii. Pitfall - confusing gastroesophageal junction with pylorus 5. Duodenal atresia a. Presentation b. Radiographic findings i. Double bubble sign ii. Pitfall - Y-shaped hepatopancreatic duct anomaly 6. Duodenal web a. Presentation b. Radiographic, UGI series and US findings 7. Annular pancreas a. Presentation b. US findings 8. Malrotation with midgut volvulus a. Presentation b. Radiographic findings c. US findings i. SMA/SMV relationship ii. Position of third part of duodenum iii. Whirlpool sign d. UGI series findings i. Course of duodenum ii. Position of duodenojejunal junction (DJJ) iii. Corkscrew sign iv. Pitfalls - Abnormal position of DJJ due to extrinsic compression or displacement 9. Jejunal atresia a. Presentation b. Radiographic findings 10. Conclusion

Printed on: 02/07/23



## Abstract Archives of the RSNA, 2022

PDEE-24

### Post-transplant Malignant Neoplasms in Pediatric Liver Transplantation

Sunday, Nov. 27 8:00AM - 9:00AM Room: Learning Center - PD

#### Participants

Thaise Marquez, MD, (*Presenter*) Nothing to Disclose

#### TEACHING POINTS

The objectives of this exhibit are: To review the frequency and the main types of malignancies in children post-liver transplantation, including: 1) "de novo" tumors and 2) recurrence of neoplasms in patients transplanted for oncological causes. To illustrate the aforementioned tumors with cases attended in our service. To highlight the importance of clinical follow-up in the post-transplant period, in order to diagnose neoplastic lesions at an early stage, reducing graft loss and increasing post-transplant survival.

#### TABLE OF CONTENTS/OUTLINE

1. Recurrence of liver tumors in pediatric patients post-transplant. Review of the transplant criteria for children with liver tumors, as well as the most common tumors that require liver transplantation. Overview of the expected prognosis and usual management of those patients. Illustrated cases of our Pediatric Radiology group. 2. The occurrence of "de novo" tumors in children post-liver transplant. Post-Transplant Lymphoproliferative Disease (PTLD): definition, characteristics, risk factors, pathology, categories and radiographic features. Non-PTLD tumors: a brief mention of the main non-PTLD malignancies, focusing on Kaposi's sarcoma. Illustrated cases of our institute, including some rare "de novo" cancers.

Printed on: 02/07/23



## Abstract Archives of the RSNA, 2022

PDEE-25HC

### Postoperative Imaging Findings of Biliary Atresia in Children

Sunday, Nov. 27 8:00AM - 9:00AM Room: Learning Center - PD

#### Participants

Jisun Hwang, MD, Hwaseong-si, Korea, Republic Of (*Presenter*) Nothing to Disclose

#### TEACHING POINTS

-Describe the main surgical technique of Kasai portoenterostomy-Identify the imaging findings of complications after Kasai operation  
-Describe the indication and main surgical technique of liver transplantation -Identify the preoperative imaging evaluation and postoperative complications after liver transplantation

#### TABLE OF CONTENTS/OUTLINE

- Kasai portoenterostomy procedure 1) Surgical technique 2) Imaging findings after Kasai portoenterostomy procedure \* Cholangitis and bile lakes \* Portal hypertension and variceal bleeding \* Hepatic tumor - Living-related liver transplantation for biliary atresia 1) Indication and surgical technique 2) Preoperative imaging evaluation (donor and recipient) 3) Imaging findings after liver transplantation \* Vascular complication (hepatic artery thrombosis, portal vein stenosis, hepatic vein stenosis) \* Nonvascular complication (biliary stricture, bile leak)Please visit the Learning Center to also view this presentation in hardcopy format.

Printed on: 02/07/23



## Abstract Archives of the RSNA, 2022

PDEE-26

### Staging and Restaging Pediatric Abdominal Tumors: A Practical Guide

Sunday, Nov. 27 8:00AM - 9:00AM Room: Learning Center - PD

#### Awards

Identified for RadioGraphics  
Certificate of Merit

#### Participants

Luisa Faria, MD, Sao Paulo, Brazil (*Presenter*) Nothing to Disclose

#### TEACHING POINTS

The most common abdominal malignancies diagnosed in the pediatric population include neuroblastoma, nephroblastoma (Wilms' tumor), hepatoblastoma, lymphoma, germ cell tumors, and rhabdomyosarcomas. Each of these tumors has characteristic imaging findings and patterns of locoregional and distant spread. The staging systems are unique and the surgical and oncological management rely heavily on imaging evaluation. The purposes of this exhibit are: (1) to review imaging techniques and discuss the selection among imaging modalities, (2) to review the diagnostic approach of each tumor, (3) to organize the key points for determining tumor stage using a case-based approach, (4) to systematize the posttreatment response evaluation and surveillance and (5) to point out imaging findings of particular prognostic importance.

#### TABLE OF CONTENTS/OUTLINE

(1) Epidemiology of pediatric abdominal tumors. (2) The role of each imaging modality in staging and restaging pediatric abdominal tumors. (3) Neuroblastoma: diagnostic approach, staging, and response assessment. (4) Nephroblastoma (Wilms' tumor): diagnostic approach, staging, and response assessment. (5) Hepatoblastoma: diagnostic approach, staging, and response assessment. (6) Lymphoma: diagnostic approach, staging, and response assessment. (7) Germ cell tumors: diagnostic approach, staging, and response assessment. (8) Rhabdomyosarcoma: diagnostic approach, staging, and response assessment.

Printed on: 02/07/23



## Abstract Archives of the RSNA, 2022

PDEE-27

### **I Found a Mass in The Adrenal Region of A Neonate: Should I Be Concerned? Sonographic Findings In The Differential Diagnosis of Usual and Unusual Neonatal Suprarenal Masses**

Sunday, Nov. 27 8:00AM - 9:00AM Room: Learning Center - PD

#### **Participants**

Gabriela Pinho, MD, Sao Paulo, Brazil (*Presenter*) Nothing to Disclose

#### **TEACHING POINTS**

The purposes of this exhibit are: To review the normal sonographic aspect of the neonatal adrenal gland; To emphasize the importance of assessing the adrenal gland in our routine neonatal abdominal sonographic studies; To show based on cases from our Pediatric Radiology group, usual and unusual neonatal adrenal and suprarenal masses; To show the outcome of each case; To discuss risk factors and pathophysiology of the main neonatal adrenal and suprarenal masses.

#### **TABLE OF CONTENTS/OUTLINE**

Sonographic technique for the assessment of neonatal adrenal gland and suprarenal region. Usual sonographic aspects of the neonatal adrenal gland. Illustrated teaching cases from our Pediatric Radiology group showing the usual and unusual neonatal adrenal and suprarenal masses: Congenital adrenal hyperplasia associated with ambiguous genitalia and urogenital sinus demonstrated by transperineal ultrasound access; Fetal and neonatal congenital neuroblastoma; Adrenal hemorrhagic infarction: different sonographic aspects in the evolutionary stages of neonatal adrenal hemorrhage; Tips for the diagnosis of Infradiaphragmatic extralobar pulmonary sequestration associated with congenital cystic adenomatoid malformation / congenital pulmonary airway malformation by ultrasound.

Printed on: 02/07/23



## Abstract Archives of the RSNA, 2022

PDEE-28

### Biliary Atresia and the One Stick Wonder of Percutaneous Transhepatic Cholecystocholangiography

Sunday, Nov. 27 8:00AM - 9:00AM Room: Learning Center - PD

#### Participants

Elliott Russell, MD, (*Presenter*) Nothing to Disclose

#### TEACHING POINTS

- The learner will review basic pathophysiology and types of biliary atresia and differential diagnosis for neonatal cholestatic jaundice
- The learner will gain familiarity with the diagnostic imaging pathways, including advantages and disadvantages of ultrasound, hepatobiliary iminodiacetic acid scan, and percutaneous transhepatic cholecystocholangiography (PTCC)
- The learner will discover the technique for PTCC, including patient selection, patient preparation, and materials and methods
- The learner will develop an understanding of PTCC image interpretation and implications for patient management through comprehensive case review

#### TABLE OF CONTENTS/OUTLINE

1. Clinical Scenario, Differential Diagnosis, and Importance of Timely Diagnosis
2. Biliary Atresia Pathophysiology/Types
3. Current Diagnostic Imaging Pathway, Including Advantages and Disadvantages
4. Percutaneous Transhepatic Cholecystocholangiography: Technique
5. Cases

Printed on: 02/07/23



## Abstract Archives of the RSNA, 2022

PDEE-29

### **Pediatric Pancreaticobiliary Endoscopic Ultrasound Interventions as Primer for Radiologists-Case Based Review**

Sunday, Nov. 27 8:00AM - 9:00AM Room: Learning Center - PD

#### **Participants**

Emmanuel Owusu, MD, (*Presenter*) Nothing to Disclose

#### **TEACHING POINTS**

Diagnostic and therapeutic role of EUS in pediatric pancreaticobiliary conditions EUS.Preoperative and post-operative care of the pediatric patient.Evaluating safety, complications post EUS

#### **TABLE OF CONTENTS/OUTLINE**

What is EUS EUS equipment Indications for EUS in evaluation of Pediatric Pancreaticobiliary disease Pancreatic pathology Pancreatic collections, pseudocyst Pancreatic/gastric masses Biliary pathology CBD obstruction, cholestasis Congenital biliary anomalies EUS technique FNA, stenting, LAMS Pre-operative assessment of EUS Absolute contraindications Post procedure follow-up stent complications (splenic artery hemorrhage, stent migration, recurrent pseudocyst post stent removal) Imaging findings

Printed on: 02/07/23



## Abstract Archives of the RSNA, 2022

PDEE-3

### Pre and Post Operative CTS: Overview of Congenital Heart Defects

Sunday, Nov. 27 8:00AM - 9:00AM Room: Learning Center - PD

#### Participants

Akinori Hata, MD, PhD, Suita, Japan (*Presenter*) Nothing to Disclose

#### TEACHING POINTS

Congenital heart defect (CHD) is the leading cause of death in infancy. CHDs often need interventions for complex structural cardiovascular abnormalities. Advances in the care for patients with CHD have improved survival. For radiologists, understanding pre- and post-operative status in patients with CHD is necessary for accurate interpretation of CT imaging. The purpose of this exhibit is 1) To overview structural abnormalities in typical types of CHDs on CT; 2) To know the procedure required in CHDs; and 3) To understand the hemodynamics in pre- and post-operative status of patients with CHD.

#### TABLE OF CONTENTS/OUTLINE

1. Overview of the types of typical CHDs 2. Introduction of the general concepts of surgeries for CHDs (palliative procedures and single-/two-ventricle repair) 3. Pre- and post-operative CTs for typical CHDs (Atrioventricular canal defect, Coarctation of the aorta, Double-outlet Right Ventricle, Ebstein anomaly, Heterotaxy syndrome, Hypoplastic left heart syndrome, Pulmonary atresia with intact ventricular septum, Tetralogy of Fallot, Transposition of the great arteries, Tricuspid atresia, Truncus Arteriosus, etc.)

Printed on: 02/07/23

## Abstract Archives of the RSNA, 2022

PDEE-30

### **RASopathies for Radiologists: Familiarizing Radiologists With the Common Genetic Thread Linking Diseases of the Ras/MAPK Signaling Pathway**

Sunday, Nov. 27 8:00AM - 9:00AM Room: Learning Center - PD

#### **Awards**

**Identified for RadioGraphics  
Certificate of Merit**

#### **Participants**

Atsuhiko Handa, MD, Boston, MA (*Presenter*) Nothing to Disclose

#### **TEACHING POINTS**

RASopathies are a clinically defined group of genetic syndromes caused by germline mutations in genes that encode components or regulators of Ras/MAPK signaling pathway. These disorders include neurofibromatosis type 1, Noonan syndrome, Noonan syndrome with multiple lentigines (formerly called LEOPARD syndrome), capillary malformation-arteriovenous malformation syndrome, Costello syndrome, cardio-facio-cutaneous syndrome, Legius syndrome, and other allied disorders (e.g. tuberous sclerosis). As a group, the RASopathies are among the most common genetic conditions, an incidence estimated to be about 1 per 1000 live births. Because of the common underlying Ras/MAPK pathway dysregulation, the RASopathies exhibit overlapping phenotypic features. The somatic mutations involving Ras/MAPK pathway have been well studied in cancer and appears to be a promising target for molecular inhibition to treat various malignancies. Similar treatment can potentially be used to ameliorate developmental defects in other RASopathies in the future. In fact, a pathway-based multidisciplinary clinic has already been established in many institutions to address unique challenges faced by individuals and families with RASopathies. The radiologist also needs to be aware of this emerging concept to participate in multidisciplinary care. Here we present the concept and imaging review of RASopathies with an emphasis on common features.

#### **TABLE OF CONTENTS/OUTLINE**

- Concept of RASopathies - NF1 - Noonan group - Other RASopathies - Allied disorders - Future directions

Printed on: 02/07/23



## Abstract Archives of the RSNA, 2022

PDEE-32

### Pediatric Ribs: Roadmap to Become A Rib Expert

Sunday, Nov. 27 8:00AM - 9:00AM Room: Learning Center - PD

#### Awards

Identified for RadioGraphics

#### Participants

Yuko Tsujioka, MD, Tokyo, Japan (*Presenter*) Nothing to Disclose

#### TEACHING POINTS

Pediatric rib lesions are diagnostic challenge for three reasons. First, they may be radiologically subtle. For example, a small costal mass that grows inward may be clinically silent. An early recognition of such a lesion that is at risk for serious complications, such as hemothorax or pneumothorax, is feasible only by well-trained eyes. Meticulous searching for trivial changes is essential. Second, they are diverse. There are a variety of rib changes that can lead to a diagnosis of hidden disorders. Examples include multiple posterior rib fractures in non-accidental injury, rib notch in coarctation of the aorta, thin ribs in severe neuromuscular diseases, twisted ribs in NF1, and canoe-paddle-like ribs in mucopolysaccharidosis. Radiologists need to know these rare, but diagnostic, radiological signs. Third, there are many normal variants. Radiologists should be familiar with the innocuous variants to avoid diagnostic errors and unnecessary imaging examinations. Here we provide a comprehensive imaging review of pediatric rib abnormalities and normal variants seen on routine chest radiographs to overcome these challenges. We also provide corresponding cross-sectional images, when available, to help understand the characteristic of each rib lesion.

#### TABLE OF CONTENTS/OUTLINE

Introduction - Normal rib variants - Tumors and tumor like-lesions - Inflammatory disorders - Rib abnormalities pointing to hidden disease (non-accidental injury, rib notch, twisted ribs, thin ribs, thin ribs with fractures, thin ribs with abnormal patterning, short ribs, broad ribs, dense ribs)

Printed on: 02/07/23



## Abstract Archives of the RSNA, 2022

PDEE-33

### Perils by the Sea: Radiologic Manifestations of Coastal Related Injuries and Disorders in Pediatric Patients

Sunday, Nov. 27 8:00AM - 9:00AM Room: Learning Center - PD

#### Awards

Certificate of Merit

#### Participants

Anna Fairfax, BS, MD, (*Presenter*) Nothing to Disclose

#### TEACHING POINTS

1. Review various injuries and disorders commonly seen in pediatric patients associated with coastal related activities. 2. Discuss the clinical presentations, management, and complications of various coastal, and broader water related, injuries and disorders. 3. Showcase imaging findings of coastal and water related injuries and disorders in pediatric patients via various imaging modalities.

#### TABLE OF CONTENTS/OUTLINE

1. Musculoskeletal a. Retained foreign bodies (e.g., oysters shells, impaled fishing hooks, stingray spines, shark teeth) b. Animal attacks/encounters (e.g., sharks, jellyfish, stingrays, sea urchins, crabs) c. Diving trauma d. Water sports trauma (e.g., boating and propeller injuries) 2. Lungs/airway a. Barotrauma/diving related disorders b. Aspiration of foreign bodies (e.g., shells and seafood) c. Drowning sequelae/pulmonary edema d. Laryngeal edema secondary to marine envenomation e. Hypersensitivity pneumonitis related to red tide 3. Neuro a. Anoxic brain injury secondary to drowning b. Trauma related to water sports and diving c. Barotrauma/diving related disorders 4. GI/abdomen a. Infection (I.e., Vibrio species) b. Water sports trauma

Printed on: 02/07/23



## Abstract Archives of the RSNA, 2022

PDEE-34

### Infantile Hemangioma Pitfalls: Clinical and Radiological Evaluation

Sunday, Nov. 27 8:00AM - 9:00AM Room: Learning Center - PD

#### Awards

Certificate of Merit

Identified for RadioGraphics

#### Participants

Emilio Inarejos Clemente, MD, Barcelona, Spain (*Presenter*) Nothing to Disclose

#### TEACHING POINTS

After reviewing this exhibit, the learner should:1.Be familiar with imaging modalities for vascular anomaly evaluation focused on hemangiomas2.Discuss the role of photodocumentation with radiological correlation and importance in evaluation of pathologies with cutaneous involvement3.Describe clinical features of infantile hemangiomas (IH) focusing on cutaneous lesions4.Illustrate the most frequent pitfalls that may mimic IH and clinical appearance5.Discuss most common imaging findings of these pitfalls and identify important differentiating imaging clues

#### TABLE OF CONTENTS/OUTLINE

1.Introduction of vascular anomalies and approach to ISSVA classification2.Types of IH, demographics and clinical appearance3.Imaging findings of different types of IH:Unifocal and multifocal diseases that can mimic IHClinical photographs, pathology when available and imaging findings of frequent lesions that can mimic IH focusing on ultrasound and MRI:Vascular origin:Other vascular anomalies: venous or arterio-venous malformationsOther hemangiomas: congenital hemangiomasVascular neoplasms of intermediate behavior: Kaposiform hemangioendothelioma, tufted angiomaNeoplasms:Benign: Lipomatous (lipoblastoma, angiolipoma), myofibroblastic tumors, fibrous hamartoma, neurofibromasIntermediate behavior: congenital fibrosarcomaMalignant: congenital sarcomas including rhabdomyosarcoma, lymphoma, metastatic neuroblastoma.Others:Fat necrosis, neural tube defects, ectopic thyroid4.Summary

Printed on: 02/07/23

## Abstract Archives of the RSNA, 2022

PDEE-35

### Imaging Evaluation of The Post-surgical Foot and Ankle in Children

Sunday, Nov. 27 8:00AM - 9:00AM Room: Learning Center - PD

#### Participants

Emilio Inarejos Clemente, MD, Barcelona, Spain (*Presenter*) Nothing to Disclose

#### TEACHING POINTS

After reviewing this exhibit, the learner should be able to:1. To discuss the most frequent pediatric disorders involving the foot and ankle that may require surgery2. To illustrate the imaging findings of the post-surgical evaluation of the foot and ankle in different modalities3. To describe the most frequent normal variants that may lead to misdiagnose

#### TABLE OF CONTENTS/OUTLINE

1. Technique: indications and protocols of the different imaging modalities in the post-surgical setting.2. Illustrate the post-surgical imaging evaluation of the most frequent pediatric disorders involving the foot and ankle:2.1. Congenital: congenital clubfoot, vertical talus, metatarsus adductus, tarsal coalition. Value of US and radiographs.2.2 Traumatic: osteochondral lesions, fractures, ligamentoplasty2.3. Infection secondary to surgery2.4. Benign tumors: aneurysmal bone cyst, osteoid osteoma, condroblastoma, osteochondroma, pigmented villonodular synovitis2.5. Malignant tumors: Ewing sarcoma, osteosarcoma. soft tissue sarcomas. Use of multiparametric MRI evaluation and DWI.3. Describe the most frequent normal variants involving the pediatric foot that may lead to misdiagnose: Hematopoietic marrow, bone marrow edema, Stieda process4. Conclusion

Printed on: 02/07/23



## Abstract Archives of the RSNA, 2022

PDEE-36

### Role of Whole-body Magnetic Resonance Imaging In Pediatric Musculoskeletal System: Aside From Tumors

Sunday, Nov. 27 8:00AM - 9:00AM Room: Learning Center - PD

#### Participants

Joao Pedro Costa, MD, Sao Paulo, Brazil (*Presenter*) Nothing to Disclose

#### TEACHING POINTS

I) To review the main applications of whole-body magnetic resonance imaging (WB-MRI) focused on non-neoplastic musculoskeletal conditions in pediatric population.II) To discuss and present the technical aspects and WB-MRI protocol used in our pediatric radiology department including main limitations.III) To illustrate with clinical cases the use of WB-MRI to assess and follow musculoskeletal diseases in children.IV) To correlate imaging information given by WB-MRI with the clinical and laboratory data and compared with other imaging modalities.

#### TABLE OF CONTENTS/OUTLINE

1. Introduction: performance and applications of WB-MRI in the evaluation of pediatric musculoskeletal non-neoplastic diseases; discuss WB-MRI protocols, with not only the advantages but also with current limitations in comparison with different imaging methods.2. Illustration of WB-MRI exams performed in our pediatric radiology department for diagnostic and follow-up evaluation of different musculoskeletal conditions: chronic recurrent multifocal osteomyelitis; pyogenic osteomyelitis; inflammatory myopathies; drug-induced myopathies; neuromuscular myopathies; fever of unknown origin; searching for rheumatologic inflammatory conditions.

Printed on: 02/07/23



## Abstract Archives of the RSNA, 2022

PDEE-37

### Intra-articular Osteoid Osteomas: Imaging Characteristics and Mimickers

Sunday, Nov. 27 8:00AM - 9:00AM Room: Learning Center - PD

#### Awards

**Magna Cum Laude**

#### Participants

Jade Iwasaka-Neder, MD, (*Presenter*) Nothing to Disclose

#### TEACHING POINTS

o Intra-articular osteoid osteomas (OOs) are rare and may pose a diagnostic challenge to radiologists, as they sometimes mimic other pathologies such as arthritis, stress fracture, avascular necrosis, osteomyelitis, and osteochondral lesions. o Although intra-articular OO may involve any joint, the majority of cases are localized to the hip. o Imaging findings of intra-articular OOs include focal edema, joint effusion and synovitis. However, these lesions often lack the usual reactive sclerosis and periosteal new bone formation, making their diagnoses more difficult. o CT scan is the best imaging modality to identify the nidus of the OO, and is particularly useful for treatment planning. o Na-F PET/CT can confirm the diagnosis of OO in equivocal cases.

#### TABLE OF CONTENTS/OUTLINE

o Typical imaging findings of extra-articular OOo Imaging findings of intra-articular OO§ Imaging modality• Radiograph• MRI• CT• Bone scan• Na-F PET/CT§ Anatomical locations• Elbow• Wrist• Acetabulum• Femoral head and neck• Knee• Ankle• Tarsal boneso Differential diagnoses and mimickers§ Stress fracture§ Osteomyelitis with or without Brodie abscess§ Osteochondritis dissecans§ Osteomyelitis§ Arthritis§ Chondroblastoma§ Synovial cyst§ Normal variants (e.g. supra-acetabular fossa)

Printed on: 02/07/23



## Abstract Archives of the RSNA, 2022

PDEE-38

### Whole-body MRI in Pediatric Musculoskeletal Diseases: Clinical Applications and Technical Considerations

Sunday, Nov. 27 8:00AM - 9:00AM Room: Learning Center - PD

#### Participants

Andre Mannato, MD, Sao Paulo, Brazil (*Presenter*) Nothing to Disclose

#### TEACHING POINTS

Discuss technical developments of WBMRI in musculoskeletal pediatric diseases, including acquisition and post-processing, as well as to propose an imaging protocol. Review the clinical applications of WBMRI in various disorders that involve the musculoskeletal system in children, especially in the oncology and rheumatology fields, exploring the typical and atypical imaging findings of each. Explore the role of WBMRI as a valuable imaging method for diagnosis, assessment of disease extent and follow-up, highlighting its advantages in comparison to standard imaging evaluation, specifically as they relate to the pediatric population.

#### TABLE OF CONTENTS/OUTLINE

In the last decades, WBMRI has emerged as a promising imaging method in musculoskeletal diseases, allowing a wide coverage assessment of bone and soft tissue in a single study. WBMRI is especially advantageous for the pediatric population since it avoids redundant examinations and exposure to ionizing radiation in patients who often undergo long-term surveillance. Also, due to patient's size, the examination can be performed with faster protocols and provide high quality images. For rheumatic and oncological diseases, WBMRI can have a large impact in diagnostic and follow-up workup of many pathologies such as chronic nonbacterial osteomyelitis, dermatomyositis, arthritis, tumor screening in cancer predisposition syndromes, evaluation of primary tumor, further investigation of distant lesions and other clinical applications. The development of new techniques and protocols makes WBMRI increasingly faster, safer and more accessible, and it is important for referring physicians and radiologists to recognize the role of this imaging method.

Printed on: 02/07/23



## Abstract Archives of the RSNA, 2022

PDEE-39

### Fast MRI: MSK Applications in Adults and Children

Sunday, Nov. 27 8:00AM - 9:00AM Room: Learning Center - PD

#### Participants

Joey Gu, BS, (Presenter) Nothing to Disclose

#### TEACHING POINTS

1. Gain a foundational understanding of the physics behind accelerating MR image acquisition and the various techniques currently in use  
2. Discern the benefits and limitations that accelerated MRI offers for patients, providers, and healthcare systems  
3. Recognize the specific clinical applications, in both an adult and pediatric populations, for fast MR examinations of the shoulder, spine, hip, knee, and ankle

#### TABLE OF CONTENTS/OUTLINE

What is Fast MRI?- MR physics of accelerating image acquisition- Overview of various acceleration techniques--Fast spin-echo, turbo spin-echo--High gradient performance modes--Undersampling: matrix resolution/partial Fourier phase--Interpolation of matrix resolution--Fast radiofrequency pulses, high receiver bandwidth--Advanced techniques (PI, SMS, synthetic techniques, etc.)  
Why Use Fast MRI?- In adults--Efficiency of examinations (high volume of adult MSK MRI exams)--Reduce artifact from hardware/implants--Reduce motion artifact- In children--Decrease need for sedation--Reduce motion artifact  
MSK applications of Fast MRI (for each anatomical area of interest, disease processes evaluated, diagnostic accuracy, and imaging appearances will be covered)- In adults (shoulder, spine, hip, knee, ankle)- In children (knee, spine, infection)  
Limitations of Fast MRI - Medicolegal implications- Lack of studies demonstrating efficacy for various clinical applications

Printed on: 02/07/23



## Abstract Archives of the RSNA, 2022

PDEE-4

### Cardiac Evaluation in Pediatric Chest Radiographs: Back To the Future With CT/MRI Correlation

Sunday, Nov. 27 8:00AM - 9:00AM Room: Learning Center - PD

#### Participants

Prabhakar Rajiah, MD, FRCR, Rochester, MN (*Presenter*) Nothing to Disclose

#### TEACHING POINTS

The last decade has seen tremendous growth of CT/MRI for evaluation of cardiac disorders. The humble chest radiograph still plays a key role, and it is important to interpret it accurately. The aim of this exhibit is 1. To discuss an approach to the interpretation of cardiac abnormalities in pediatric chest radiographs 2. To correlate radiographic cardiac abnormalities with CT/MRI appearances 3. To review common misses and pitfalls in radiographs

#### TABLE OF CONTENTS/OUTLINE

1. ROLE OF IMAGING IN CARDIAC DISEASES 2. ROLE OF CHEST RADIOGRAPH in pediatric cardiac disease 3. ENLARGED CARDIAC SILHOUETTE- Cardiomegaly- Criteria; Individual chamber enlargement; Pericardial effusion- double oreo cookie sign 4. PULMONARY VASCULATURE- Arterial, venous, edema 5. ALGORITHMIC APPROACH TO DIAGNOSIS OF CONGENITAL HEART DISEASES CYANOTIC HEART DISEASE A. Decreased blood flow - Normal size heart- TOF; Big heart- Ebstein, pulmonary atresia with intact septum B. increased blood flow - TGA- Egg-on-string; TAPVR- Snowman; Truncus- Right arch Single ventricle C. Pulmonary edema - Normal size heart- TAPVR infracardiac; Big heart- hypoplastic left heart ACYANOTIC HEART DISEASE A. Increased arterial flow- Normal LA- ASD; Large LA , normal aortic knob- VSD; Large LA and aortic knob- PDA B. Increased venous flow- Cardiac failure C. Normal flow- AS, Coarctation 6. OTHER FINDINGS -Box-shaped heart- Ebstein's; Boot-shaped- TOF; Wall-to-wall heart- Ebstein, pericardial effusion; Figure-of-3, rib notching- Coarctation; Scimitar sign- PAPVR; Asymmetric main, left PA enlargement- Pulmonic valve stenosis; 7. APPROACH TO VASCULAR RING/SLING- Tracheal and esophageal impressions. 8. PROSTHETIC VALVE EVALUATION 9. PITFALLS/MISSES

Printed on: 02/07/23



## Abstract Archives of the RSNA, 2022

PDEE-40

### Update On the Radiological Approach of Musculoskeletal Pediatric Infections: From Classical to Challenging Cases

Sunday, Nov. 27 8:00AM - 9:00AM Room: Learning Center - PD

#### Participants

Stephanie Takara, MD, Sao Paulo, Brazil (*Presenter*) Nothing to Disclose

#### TEACHING POINTS

I) Review the main types of musculoskeletal infections and their particularities in children (epidemiology, etiology and pathophysiology), based on cases of our pediatric radiology department in correlation with clinical, laboratory and anatomopathological data. II) Discuss the use and indication of each imaging modality for the different types of musculoskeletal infections and purpose a diagnostic investigation flowchart. III) Present the main imaging findings, advantages and limitations of imaging modalities.

#### TABLE OF CONTENTS/OUTLINE

1. Introduction The importance of imaging exams for an early and correct diagnosis of pediatric musculoskeletal infection. The main uses of each imaging method.  
2. Spondylodiscitis and intradural infections Epidemiology and pathophysiology The role of each imaging method and imaging findings  
3. Osteomyelitis Pathophysiology The role of each imaging method and imaging aspects Chronic findings and sequelae  
4. Septic arthritis Epidemiology and pathophysiology The role of each imaging method and imaging findings  
5. Soft tissue infection Epidemiology and pathophysiology The role of each imaging method and imaging findings

Printed on: 02/07/23



## Abstract Archives of the RSNA, 2022

PDEE-41

### Clavicular Pathologies in the Pediatric Age Group: A Pictorial Review

Sunday, Nov. 27 8:00AM - 9:00AM Room: Learning Center - PD

#### Participants

Ankita Chauhan, MD,MBBS, (*Presenter*) Nothing to Disclose

#### TEACHING POINTS

Background Information: The clavicle connects the upper extremity to the axial skeleton. It is the first bone to ossify in the fetus. Epiphysis of the clavicle, however, is the last to ossify and fuse in adult life. The most common lesions of the clavicle are traumatic. Nontraumatic lesions of the clavicle are rare, more so in the pediatric age group. Radiologists need to know pathologies affecting the clavicle and their imaging appearance. Considering patient age, clinical symptoms, and other associated imaging findings can help make the correct diagnosis. Teaching Points 1. To discuss the development and normal anatomy of the clavicle. 2. To discuss various congenital (or developmental), traumatic, metabolic, infective, inflammatory, or benign and malignant neoplastic pathologic processes that can involve the clavicle. 3. To illustrate the imaging spectrum of clavicular pathologies in the pediatric age group. 4. To discuss various radiological features that can help make the correct diagnosis.

#### TABLE OF CONTENTS/OUTLINE

-Goals and objectives -Background information -Anatomy -Pathologic entities (fracture, pseudoarthrosis, infantile cortical hyperostosis (Caffey disease), hyperparathyroidism, cleidocranial dysostosis, chronic recurrent multifocal osteomyelitis, benign bone tumors such as unicameral bone cyst, aneurysmal bone cyst, malignant bone tumors, metastasis) -Summary

Printed on: 02/07/23



## Abstract Archives of the RSNA, 2022

PDEE-42

### Multimodality Imaging of Pediatric High Flow Vascular Malformations in the Brain and Spine

Sunday, Nov. 27 8:00AM - 9:00AM Room: Learning Center - PD

#### Participants

Amanda Baker, MD, (*Presenter*) Nothing to Disclose

#### TEACHING POINTS

Goal: To review multimodality imaging in the diagnosis and treatment of pediatric high flow vascular malformations in the brain and spine. Specifically, the exhibit will pinpoint features on US, CT, MRI, and catheter angiography that will allow the radiologist to accurately diagnosis the type of malformation and describe its characteristics.

#### TABLE OF CONTENTS/OUTLINE

Review diagnostic algorithms to aid in the classification of pediatric high flow vascular malformations in the brain and spine:Brain:1. Nidal arteriovenous malformations2. Dural arteriovenous fistulae.3. Non-galenic pial arteriovenous fistulae.4. Vein of Galen malformations.Spine:1. Epidural spinal arteriovenous fistulae.2. Dural spinal arteriovenous fistulae.3. Perimedullary spinal arteriovenous fistulae.4. Spinal arteriovenous malformations.

Printed on: 02/07/23

## Abstract Archives of the RSNA, 2022

PDEE-43

### Imaging Approach to Hypomyelinating Leukodystrophies (HLDs)

Sunday, Nov. 27 8:00AM - 9:00AM Room: Learning Center - PD

#### Participants

Prateek Malik, MD, Toronto, ON (*Presenter*) Nothing to Disclose

#### TEACHING POINTS

Hypomyelinating leukodystrophies (HLDs) are a rapidly expanding subgroup of inherited white matter disorders characterized by a permanent and substantial deficit in myelin. More than 50 genes are now linked with HLDs, the vast majority being discovered over the last 15 years. Since the first description of Pelizaeus-Merzbacher disease (PMD) in 1910, the understanding of white matter disorders and the key cellular players has improved tremendously. We discuss an updated review of the understanding of normal myelination, key terminologies in HLDs and provide a stepwise methodology in assessment of HLDs determined by key radiological findings.

#### TABLE OF CONTENTS/OUTLINE

1. Normal myelination - Neurobiology: Key players and myelin maintenance - Imaging normal myelination: key MRI changes, normal milestones and development of key structures - Pitfalls and caveats: Variable signal, permanent deficit Vs myelin stability, corrected gestational age  
2. Hypomyelinating leukodystrophies (HLDs) - Updates in classification of white matter disorders including HLDs - Key terminologies - Stepwise approach to assessing HLDs: • Determining key pattern • Assessing for ABCDs • Assessing sub-patterns and clinical clues • Imaging differentials for specific patterns • Alternate imaging phenotypes

Printed on: 02/07/23



## Abstract Archives of the RSNA, 2022

PDEE-44

### Radiomics for Predicting Tumor Immune Profile of Pediatric Glioma

Sunday, Nov. 27 8:00AM - 9:00AM Room: Learning Center - PD

#### Participants

Nastaran Khalili, MD, MPH, (*Presenter*) Nothing to Disclose

#### TEACHING POINTS

Central nervous system (CNS) tumors are the leading cause of cancer-related death in children. Glioma accounts for more than half of pediatric CNS tumors. Complete resection is the mainstay of therapy but is not feasible for deeply seated or highly infiltrative tumors. Hence, immunotherapeutic approaches are being increasingly applied in pediatric glioma. The immunological profile of the tumor microenvironment (TME) is regarded as a powerful tool for predicting tumor behavior and determining response to immunotherapy. Radiomics, which is the automated high-throughput extraction and processing of quantitative imaging based on intensity, shape, volume, and textural features provides insight into the underlying immunobiological processes within the TME. The purpose of this exhibit is to discuss how this non-invasive method facilitates the categorization and risk stratification of patients based on their tumor immune profile and to describe the role of radiomics in advancing personalized, patient-tailored therapy for pediatric glioma.

#### TABLE OF CONTENTS/OUTLINE

1. Brief review of the pathophysiology, prognosis, and current treatments for pediatric glioma. 2. Basic principles of radiomics and its role in understanding tumor immune biology. 3. Correlation between radiomics features, immune biomarkers and clinical outcomes in glioma according to existing literature. 4. Current challenges and future directions for the application of radiomics in the immune characterization of pediatric glioma.

Printed on: 02/07/23



## Abstract Archives of the RSNA, 2022

PDEE-45

### Diffusion-weighted Imaging Patterns in Pediatric Neurometabolic Disorders

Sunday, Nov. 27 8:00AM - 9:00AM Room: Learning Center - PD

#### Participants

Caleb Epps, MD, MS, (*Presenter*) Nothing to Disclose

#### TEACHING POINTS

The aim of this exhibit is to increase understanding of diffusion weighted-imaging patterns in pediatric neurometabolic disorders to improve diagnostic accuracy and characterization. By the end of this exhibit, the viewer should be able to recognize general DWI patterns and internalize a simplistic practical approach to pediatric neurometabolic disorders.

#### TABLE OF CONTENTS/OUTLINE

Pediatric neurometabolic disorders encompass an immense group of diseases that are diagnostically challenging for both clinicians and radiologists. Though they are rare individually, collectively they remain a source of significant pediatric morbidity. Though simple classification is problematic, one classification schema includes disorders of toxic accumulation, energy metabolism, complex molecules, and unique pathophysiology. Accurate and timely diagnosis is crucial as treatment depends on the underlying pathophysiology. Good clinical outcomes are associated with earlier intervention in some disorders. Cytotoxic, excitotoxic, and intramyelinic cerebral edema are pathologic processes common in many neurometabolic disorders and manifest on DWI. DWI signal abnormalities can be grossly categorized into white matter-dominant, peripheral gray matter, and deep gray matter. Of note, the practicality of this model compensates for its lack of specificity given that some disorders may demonstrate overlapping patterns. Though the work up of pediatric neurometabolic disorders largely remains a multi-disciplinary effort, an improved understanding of DWI patterns in pediatric neurometabolic disorders can facilitate timely diagnosis and help reduce long term morbidity.

Printed on: 02/07/23



## Abstract Archives of the RSNA, 2022

PDEE-46

### An Imaging Review of Pediatric Monogenetic CNS Vasculopathy with Genetic Correlation

Sunday, Nov. 27 8:00AM - 9:00AM Room: Learning Center - PD

#### Awards

Identified for RadioGraphics

#### Participants

Neetika Gupta, MBBS, MD, (*Presenter*) Nothing to Disclose

#### TEACHING POINTS

1. Review the current literature on rare genetic causes of CNS vasculopathy in children. 2. Describe the CNS and extra-CNS imaging findings in various genetic pediatric CNS vascular disorders. 3. Discuss the role of conventional imaging modalities and advanced imaging sequences in the diagnosis and prognosis of cerebral vascular disorders. 4. To emphasize the diagnostic and prognostic role of neuroimaging in the evaluation of pediatric monogenetic vascular disorders.

#### TABLE OF CONTENTS/OUTLINE

1. Comprehensive discussion of the various monogenetic disease resulting in CNS vascular disorders in children. 2. Identify and familiarize with the salient imaging features of rare genetic pediatric CNS vasculopathy that could help in the diagnosis and narrow the differentials. 3. Recommend a clinico-radiological approach pertinent genetic workup for the systematic evaluation of these rare genetic pediatric CNS vascular disorder. 4. Identify the genetic causes imperative to reach a final diagnosis and guide the appropriate treatment.

Printed on: 02/07/23



## Abstract Archives of the RSNA, 2022

PDEE-47

### Advanced Imaging Evaluation of Pediatric Language Pathways: Where Do We Stand

Sunday, Nov. 27 8:00AM - 9:00AM Room: Learning Center - PD

#### Participants

Monica Rebollo Polo, MD, (*Presenter*) Nothing to Disclose

#### TEACHING POINTS

- Review the major language pathways and their development in children from newborns to older children evaluated with advanced neuroimaging (DWI, fMRI) - - Show the areas of activation related to language evaluated with resting state functional Magnetic Resonance (rsfMRI) - Task evaluation of language (presurgical language lateralization assessment) - Clinical indications of imaging language assessment - Show pathology that interferes with normal language pathways development

#### TABLE OF CONTENTS/OUTLINE

- Language pathways overview with deterministic and probabilistic tractography (arcuate fasciculus, uncinate fasciculus, inferior front-occipital fasciculus, inferior longitudinal fasciculus, frontal aslant tract) - Maturation and development of the language pathways - Dorsal and ventral language pathways representing auditory-motor integration and auditory-conceptual mapping - Rs fMRI language networks - Task evaluation of language (antonym generation, sentences completion, object naming, passive story listening) - Clinical examples (presurgical assessment in brain tumors, language lateralization in epilepsy, language pathways anomalies) Clinical entities that affect language pathways (prematurity, congenital infections, malformations of cortical development)

Printed on: 02/07/23



## Abstract Archives of the RSNA, 2022

PDEE-48

### Vertebral Artery Dissection in Children

Sunday, Nov. 27 8:00AM - 9:00AM Room: Learning Center - PD

#### Awards

Identified for RadioGraphics  
Certificate of Merit

#### Participants

Stephen B. Little, MD, Atlanta, GA (*Presenter*) Nothing to Disclose

#### TEACHING POINTS

1) Vertebral artery dissection (VAD) is the most common cause of isolated posterior circulation arterial ischemic stroke (PCAIS) in children. Posterior circulation infarcts due to VAD are often multifocal, occasionally of varying age, and may be associated with abrupt intracranial (downstream) arterial occlusions. 2) Extracranial VAD in children most often involves the proximal V3 segment. This portion of V3 is short, often transversely oriented, located in close proximity to bone and surrounded by fat and a periarterial venous plexus. Cervical vascular imaging protocols should take these challenging anatomic features into consideration. 3) VAD is often missed on clinically performed 2D TOF MRA and CE-MRA of the neck. In our experience, 3D TOF MRA or CTA of the neck are more reliable vascular imaging alternatives for VAD in children. 4) At presentation, extracranial VAD in children is most often characterized by segmental stenosis or occlusion at the C2 level, CASCADE 4a (3). Vertebral artery pseudoaneurysm (CASCADE 4a (1)) is less frequent and may be present at initial diagnosis or at follow-up. Intimal flap, double lumen and wall hematoma are infrequent findings on CTA or MRI/MRA. 5) Potentially pathogenic osseous anomalies are not uncommon and are best demonstrated on CT/CTA. 6) Digital subtraction angiography (DSA) with head turning may reveal dynamic vertebral artery compression but management is controversial.

#### TABLE OF CONTENTS/OUTLINE

1. Stroke Patterns in VAD 2. Intracranial Vascular Findings in VAD 3. Extracranial Vascular Findings in VAD 4. Osseous Anomalies in VAD 5. Protocols - Optimizing MRA and CTA for Diagnosis of VAD in Children

Printed on: 02/07/23



## Abstract Archives of the RSNA, 2022

PDEE-49

### Imaging Diagnosis of Hydrocephalus and Ventricular Enlargement in Fetuses and Children

Sunday, Nov. 27 8:00AM - 9:00AM Room: Learning Center - PD

#### Awards

Certificate of Merit

#### Participants

Hirozumi Mori, MD, (*Presenter*) Nothing to Disclose

#### TEACHING POINTS

There are a wide variety of causative diseases that indicate hydrocephalus and ventricular enlargement during fetal and childhood, but first, a hint for differentiation can be obtained by classifying the mechanism. By picking up the findings in more detail in the classification and examining whether the causative disease is single or combined, more accurate diagnose is possible. This time, We will explain how to pick up the findings and recent topics related to diseases.

#### TABLE OF CONTENTS/OUTLINE

•The criteria for diagnosing hydrocephalus and ventricular enlargement during the fetal period are shown. •We will classify the causative diseases of hydrocephalus and ventricular enlargement in the fetal and childhood and outline them. 1. CSF circulation disorders-Posterior fossa malformation-Hereditary disease-Meningitis-Tumor-Cerebral hemorrhage 2. Encephaloclastic disorder-Cerebral Ischemia-Congenital infection 3. Encephalodysplasia-Neuronal migration disorders-Cerebral Hemisphere separation disorders •In particular, We will explain in detail about congenital malformations. 1. Posterior fossa malformation-Dandy-walker cyst-Blake's pouch cyst-Subarachnoid cyst-Arnold-chiari malformation 2. Neuronal migration disorders 3. Cerebral Hemisphere separation disorders-Holoprosencephaly-Callosal anomaly

Printed on: 02/07/23

## Abstract Archives of the RSNA, 2022

PDEE-5

### Examination of The Optimal Imaging Method for 3D-CT After Fontan Procedure

Sunday, Nov. 27 8:00AM - 9:00AM Room: Learning Center - PD

#### Participants

Norihiko Okamoto, (*Presenter*) Nothing to Disclose

#### TEACHING POINTS

In 3D-CT after Fontan procedure, laminar flow of contrast agent caused by Fontan circulation occurs, which makes it difficult to accurately diagnose the presence or absence of thrombus. Also, the CT number required for 3D-imaging cannot be obtained. In addition, since it is necessary to diagnose Fontan-associated liver disease, multiphase CT scanning is unavoidable and the radiation dose increases. In order to solve this problem, we considered the optimal imaging method. We analyzed past clinical cases. Next, we prepared a tube simulating a blood vessel, injected a two-step diluted contrast agent (opposite ratio) into it, and performed CT scanning on it. The inside of the tube became uniform when the contrast agent and saline were injected at a ratio of 7 to 3/3 to 7. By monitoring the conduit immediately after systemic circulation, it became possible to easily determine the scan timing. At this scan timing, the occurrence of laminar flow was suppressed, and the CT number was sufficiently obtained. In addition to that, it is now possible to diagnose Fontan-associated liver disease. The double-concentration injection method (7 to 3/3 to 7 ratio) made it possible to simultaneously diagnose multiple findings after the Fontan procedure in one phase, and reduced the radiation dose.

#### TABLE OF CONTENTS/OUTLINE

1. Clinical problems in 3D-CT after Fontan procedure. 2. Analyze past clinical cases. (Laminar flow) 3. Examination of contrast agent injection method. 4. Optimization of CT scanning. 5. Verification of clinical efficacy.

Printed on: 02/07/23



## Abstract Archives of the RSNA, 2022

PDEE-50

### Neuroimaging of Neonatal Stroke: Venous Focus

Sunday, Nov. 27 8:00AM - 9:00AM Room: Learning Center - PD

#### Awards

Identified for RadioGraphics  
Certificate of Merit

#### Participants

Lilian Lai, MD, Iowa City, IA (*Presenter*) Nothing to Disclose

#### TEACHING POINTS

Perinatal stroke is common and can result in lifelong morbidity. Perinatal stroke can be divided into arterial or venous ischemic stroke and hemorrhagic stroke (typically involving full-term neonates). Arterial ischemic infarcts can be recognized by their arterial distribution, but concurrent hypoxic ischemic injury can complicate interpretation. Less well recognized and under-diagnosed are venous infarcts. The majority of pediatric cerebral sinovenous thrombosis occurs in the neonatal period, and neonates may be more susceptible to venous thrombosis given their incomplete development of alternative indirect pathways of venous drainage. Hemorrhagic infarcts can be due to a myriad of causes and may require MR venogram or angiogram for further evaluation. This exhibit will review imaging patterns of perinatal stroke, with focus on neonatal venous thrombosis.

#### TABLE OF CONTENTS/OUTLINE

1) Ischemic arterial perinatal stroke and potential mimics 2) Arterial versus venous drainage pathways and infarct patterns 3) Embryology and anatomy of cerebral venous system: emphasis on medullary and subpial veins 4) Cerebral venous thrombosis including dural venous sinus and cerebral vein thrombosis; medullary vein thrombosis (stand-alone or in association with intraventricular hemorrhage in premature and full-term neonates; subpial hemorrhage due to superficial subpial venous congestion 5) Hemorrhagic infarcts 6) Imaging techniques for perinatal stroke evaluation 7) Treatment and clinical implications of arterial/venous thrombosis

Printed on: 02/07/23

## Abstract Archives of the RSNA, 2022

PDEE-51

### **Pediatric Brain MRI: Normal For Age or Subtle Pathology?**

Sunday, Nov. 27 8:00AM - 9:00AM Room: Learning Center - PD

#### **Participants**

Anvita Pauranik, MD, FRCPC, VANCOUVER, BC (*Presenter*) Nothing to Disclose

#### **TEACHING POINTS**

1. To elucidate the difference between age-related changes and subtle pathology in pediatric brain MR studies. 2. To understand the spectrum of normal variants in a developing brain.

#### **TABLE OF CONTENTS/OUTLINE**

1. PARENCHYMA. Unmyelinated white matter versus edema in newborn. Normal T1 hyperintense basal ganglia versus hypoxic injury. Terminal zones of myelination versus white matter injury. Dorsal pontine tegmentum: normal hyperintensity versus encephalitis. Central tegmental tract hyperintensity- maturational signal versus metabolic etiology. Normal diffusion anisotropy of corticospinal tracts in newborn versus mild HIE. Peri-dentate hyperintensity-normal versus pathological. (Krabbe, LCH). Prematurity versus abnormal sulcation. Temporal pole-unmyelinated white matter versus Focal cortical dysplasia. SWI: deep gray abnormal mineralization. 2. VENTRICLES: developmental asymmetry versus dysmorphism. Perivascular spaces- normal distribution versus genetic etiology, overgrowth syndrome. Deep sulci: developmental asymmetry versus bottom of sulcus dysplasia. BESSI versus Glutaric aciduria, Abusive head injury. 3. MIDLINE: Cerebellar tonsils-normal variant tonsillar descent versus Chiari 1 deformity. Normal thinning at isthmus versus focal white matter loss. Commissural dysmorphism, abnormal thickening. InterHypothalamic adhesion versus hypothalamic hamartoma. Cysts: incidental versus pathological. PDH deficiency, Zellweger. Retrocerebellar CSF space- variant versus abnormal. Pineal gland- spectrum of cysts. Sella: Pars intermedia remnants versus craniopharyngioma. Marrow signal: clivus heterogeneity

Printed on: 02/07/23



## Abstract Archives of the RSNA, 2022

PDEE-52

### What You Know About Rolling In the Deep: Pediatric Inflammatory and Infectious Conditions Involving the Thalami and Basal Ganglia in COVID Times

Sunday, Nov. 27 8:00AM - 9:00AM Room: Learning Center - PD

#### Participants

Kevin Oh, MD, Suwanee, GA (*Presenter*) Nothing to Disclose

#### TEACHING POINTS

1. Introduce common and uncommon pediatric infectious and inflammatory disorders involving the bilateral thalami and/or basal ganglia using a case based approach to include etiologies relevant during the COVID pandemic. For example, acute disseminated encephalomyelitis including MOG antibody disease, acute necrotizing encephalopathy of childhood including that related to COVID-19, and viral encephalitis. 2. Discuss pathology, common imaging findings, and selected treatments for these patients. 3. Discuss briefly differential diagnoses to consider for bilateral thalamic/basal ganglia lesions, such as metabolic disorders and neoplasms.

#### TABLE OF CONTENTS/OUTLINE

1. Introduction to pediatric infectious/inflammatory lesions in the basal ganglia and thalami. 2. Case based review of interesting cases within this category: Case presentation; Appropriate labs/pathology studies; Short description of the pathology/pathophysiology of the disease entity; Case images with explanation of common imaging features; Appropriate treatment if indicated; Prognosis. 3. Review of differential diagnoses that can mimic these appearances, such as metabolic (gangliosidosis), ischemic, and neoplastic processes (glioma) involving the bilateral thalami and/or basal ganglia.

Printed on: 02/07/23



## Abstract Archives of the RSNA, 2022

PDEE-53

### What Now? Ultrasound or Computed Tomography? Decision Making Flowchart for Pediatric Head Trauma (PHT) and Birth Related Head Injuries (BRHI)

Sunday, Nov. 27 8:00AM - 9:00AM Room: Learning Center - PD

#### Participants

Gabriela Pinho, MD, Sao Paulo, Brazil (*Presenter*) Nothing to Disclose

#### TEACHING POINTS

The purposes of this exhibit are: to review the anatomy of the layers of the scalp; To discuss the main sonographic findings of pediatric head trauma (PHT) and birth related head injuries (BRHI); To gain awareness of the frequency of computed tomography (CT) performed after PHT and BRHI in our service, and critically analyze its impact on patient's management; To propose a decision-making flowchart for the diagnostic management of initial assessment of PHT and BRHI focusing on the role of ultrasound (US) as an initial diagnostic tool.

#### TABLE OF CONTENTS/OUTLINE

Anatomy of the scalp, skull and meninges; Risk factors for BRHI; Main indications of cranial ultrasound; Main types of injury observed after PHT and BRHI; Decision making flowchart for diagnostic management after PHT or BRHI: US or CT? Illustrative cases from our Pediatric Radiology group showing the proper conducts; Critically analyze the frequency of computed tomography performed after PHT and BRHI, and evaluate its impact on patient's management in our service.

Printed on: 02/07/23



## Abstract Archives of the RSNA, 2022

PDEE-54

### **Pediatric Leukemia: How Can We Help?**

Sunday, Nov. 27 8:00AM - 9:00AM Room: Learning Center - PD

#### **Participants**

Maria Trujillo Ariza, MD, Villagarcia de Arosa, Spain (*Presenter*) Nothing to Disclose

#### **TEACHING POINTS**

Leukemia is the most common malignancy during childhood, is a multisystemic disease, as radiologist we don't play and important role at diagnosis but we must be aware of the possible imaging findings at the beginning of the disease, possible treatment complications and relapse:- To describe the typical imaging findings at diagnosis.- To summarize the imaging findings of possible complications during treatment.- To review the imaging findings that suggest relapse.

#### **TABLE OF CONTENTS/OUTLINE**

- Epidemiology and presentation of Pediatric Leukemia: Acute Lymphoblastic Leukemia (ALL) vs Acute Myeloblastic Leukemia (AML).-Utility of imaging techniques: x-ray, US, CT and MRI.- Imaging findings: at diagnosis, of treatment complications (short and long term) and in case of relapse.

Printed on: 02/07/23



## Abstract Archives of the RSNA, 2022

PDEE-55

### Diagnosing VHL Disease By Understanding Morphology from Pathophysiology: What Radiologists Can Learn From The Nobel Prize

Sunday, Nov. 27 8:00AM - 9:00AM Room: Learning Center - PD

#### Participants

Sho Koyasu, MD, PhD, (Presenter) Nothing to Disclose

#### TEACHING POINTS

The essence of the pathogenesis in VHL disease is the accumulation of the transcription factor HIF in cells with mutations in the VHL gene throughout the body, resulting in increased viability and tumorigenesis. This was highlighted by the Nobel Prize in Physiology or Medicine in 2019. VHL-associated tumors overexpress downstream genes of HIF, resulting in hypervascularization, clear cytoplasm, disrupted cell polarity, and cilia dysfunction. These characteristics can be observed from imaging of VHL-associated tumors throughout the body, with tumors showing strongly enhanced regions accompanied by cyst formations of various sizes. In clinical practice, the role of the radiologist becomes even more important after the diagnosis of VHL disease is made. In collaboration with other departments, it is necessary for radiologists to distinguish tumors that need to be treated from others. It is also important to be aware that there are some potential imaging pitfalls. The purpose of this exhibit is: 1. To introduce the history and molecular mechanisms of VHL disease. 2. To discuss the relationship between pathophysiology, morphology, and imaging findings. 3. To present images of common and uncommon VHL disease-related tumors. 4. To help the audience better understand problematic situations related to VHL disease in actual practice.

#### TABLE OF CONTENTS/OUTLINE

1. The history of VHL disease, including the discovery, the Nobel Prize, and the new drug approved by the FDA last year. 2. Discussion of imaging findings of VHL-related tumors from molecular mechanisms. 3. Explanation of common as well as rare VHL-related tumors from a morphological perspective. 4. Review of representative cases that are difficult to differentiate.

Printed on: 02/07/23

## Abstract Archives of the RSNA, 2022

PDEE-56HC

### Imaging Spectrum of Rhabdoid Predisposition Syndrome with underlying SMARCB1 and SMARCA4 Mutations

Sunday, Nov. 27 8:00AM - 9:00AM Room: Learning Center - PD

#### Participants

Ayat Yousef, MBBS, (*Presenter*) Nothing to Disclose

#### TEACHING POINTS

1. List the manifestations of Rhabdoid tumor predisposition syndrome (RTPS) associated with SMARCB1 and SMARCA4 mutations in children. 2. Describe the imaging characteristics of rhabdoid tumors, specifically atypical rhabdoid teratoid tumors according to their molecular subtype. 3. Discuss the proposed imaging protocol for surveillance and post treatment assessment in RTPS.

#### TABLE OF CONTENTS/OUTLINE

Inactivation of the tumor suppressor gene SMARCB1 or rarely SMARCA4 is the hallmark of several types of tumors. Patients with SMARCB1 mutations have a high risk of developing synchronous and multifocal rhabdoid tumors (RTs) in early life as a part of rhabdoid tumor predisposition syndromes (RTPS). Other tumors with germline SMARCB1 mutations include cribriform neuroepithelial tumor (CRINET), schwannoma, meningioma, renal cell carcinoma, malignant peripheral nerve sheath tumor and ovarian cancer. RTs frequently arise in the central nervous system, known as atypical teratoid rhabdoid tumor (ATRT). Recently three molecular subtypes of ATRT have been described, each having location tendency and imaging characteristics. The second most common extra-cranial location is rhabdoid tumors of the kidneys (RTK) followed by other locations in the head and neck, liver and rest of the body grouped under extra-renal malignant rhabdoid tumors (ERMRT). Dedicated MRI is the main modality of choice for characterizing rhabdoid tumors and post treatment changes. Other studies like US abdomen, CT and whole-body MRI can be used for metastasis and surveillance in RTPS. Understanding the different imaging manifestations of SMARCB1 mutation can play a pivotal role in disease detection, surveillance and management approach. Please visit the Learning Center to also view this presentation in hardcopy format.

Printed on: 02/07/23

## Abstract Archives of the RSNA, 2022

PDEE-57

### Imaging Guidelines for Common Pediatric Abdominal Tumors

Sunday, Nov. 27 8:00AM - 9:00AM Room: Learning Center - PD

#### Participants

Zoe Winston, MBBS, Manchester, United Kingdom (*Presenter*) Nothing to Disclose

#### TEACHING POINTS

1. Review of international imaging guidelines for paediatric abdominal tumours including renal, adrenal gland and liver tumours.2. Literature review of the advantages and disadvantages of MR compared to CT imaging in paediatric abdominal tumours3. Explore case examples of paediatric abdominal tumours, comparing multimodality imaging and also documenting findings from local experience

#### TABLE OF CONTENTS/OUTLINE

CT and MR imaging are both used for the diagnosis of common paediatric abdominal tumours. There are differing guidelines internationally for imaging paediatric abdominal tumours. The International Society of Paediatric Oncology (SIOP) and Children's Cancer and Leukaemia Group (CCLG) provide guidelines in Europe and the UK, and the Children's Oncology Group (COG) in North America. A literature review will provide an overview of the international guidelines for imaging of common paediatric abdominal tumours, exploring the advantages and disadvantages of MR and CT evaluation of paediatric abdominal tumours with review of relevant case-based imaging.

Printed on: 02/07/23



## Abstract Archives of the RSNA, 2022

PDEE-58

### Retinoblastoma: Standardized Imaging Protocols and Reports with Relevance to Current Staging and Treatment

Sunday, Nov. 27 8:00AM - 9:00AM Room: Learning Center - PD

#### Awards

Identified for RadioGraphics  
Certificate of Merit

#### Participants

Vivek Pai, MBBS,MD, Toronto, Singapore (*Presenter*) Nothing to Disclose

#### TEACHING POINTS

Retinoblastoma (RB) is the most common primary intraocular tumor of childhood. Diagnostic techniques and treatment have evolved rapidly over recent years. Accurate staging is key in initiating appropriate treatment for patients with RB, thereby maximizing survival and preserving vision potential. The aims of this educational exhibit are: 1. Review current standards of ocular and radiological imaging utilized in the staging of retinoblastoma. 2. Define the role of imaging in the clinical differentiation of the various stages of RB. 3. Discuss the importance of multimodal imaging in the assessment of the true clinical stage of the disease. 4. Suggest potential standard fields of reporting which are essential for the staging of children with RB.

#### TABLE OF CONTENTS/OUTLINE

1. Discussion on clinical and multimodal imaging evaluation in patients with RB 2. Discussion and development of imaging protocols and the importance of imaging in guiding treatment decisions. 3. Demonstrate multimodal images that describe: a) Anterior segment involvement, b) Vitreous and subretinal seeds, c) Intraocular hemorrhage, d) Choroidal invasion, e) Scleral and episcleral involvement, f) Optic nerve invasion, g) Trilateral lesions and intracranial involvement. h) Ophthalmic artery variants that impact chemo-embolization 4. Checklists and standardized reports

Printed on: 02/07/23



## Abstract Archives of the RSNA, 2022

PDEE-59

### Complications After Pediatric Stem Cell Transplant: From Head to Toe

Sunday, Nov. 27 8:00AM - 9:00AM Room: Learning Center - PD

#### Participants

Luisa Faria, MD, Sao Paulo, Brazil (*Presenter*) Nothing to Disclose

#### TEACHING POINTS

The number of disorders in the pediatric age group that benefit from hematopoietic stem cell transplantation (HSCT) is increasing. Nowadays, HSCT is being used for the treatment of leukemia, benign hematologic disorders, autoimmune diseases, certain genetic diagnoses, some forms of lymphoma, and even solid tumors. As a result of the expanding indications, there has been a year-to-year increase in the number of transplantations. Given this scenario, imaging plays a key role in the timely diagnosis of possible complications. The purposes of this multicentric educational exhibit are: (1) to understand the basic principles of HSCT and indications of this procedure in children, (2) to review the predictable timeline of immune suppression after HSCT (3) to systematize the main complications after HSCT in children, based in a multi-institutional experience in pediatric imaging.

#### TABLE OF CONTENTS/OUTLINE

(1) Review of the basic principles of HSCT, (2) Classical and novel indications of HSCT in children, (3) Timeline of immune suppression after HSCT and the expected infectious and non-infectious complications in each phase, (4) Case-based approach to the main complications following HSCT in each body segment, combining the clinical scenario with characteristic imaging findings: central nervous system, head and neck, chest, abdomen, and musculoskeletal.

Printed on: 02/07/23



## Abstract Archives of the RSNA, 2022

PDEE-6

### Preventing Life-Threatening Respiratory Tract Bleeding in Kids!: A Systematic Imaging Approach to Shed Light on The Silent Killer

Sunday, Nov. 27 8:00AM - 9:00AM Room: Learning Center - PD

#### Participants

Akari Makidono, MD, (*Presenter*) Nothing to Disclose

#### TEACHING POINTS

#1. Bleeding from the respiratory tract can stay undetected in children until major event occurs since small amount of hemoptysis is commonly veiled by swallowing bloody sputum. Even patients with potentially life-threatening conditions can present with non-specific symptoms, therefore, radiologists should be aware of minor signs and findings of these conditions to prevent major events to occur. #2. Among various diagnostic studies for major respiratory tract bleeding, multidetector CT plays a critical role in determining the cause, site of bleeding, and involved vessels and thus, guiding the caring team toward proper management. For this purpose, systematic imaging approach being demonstrated in this educational exhibit would be helpful for radiologists.

#### TABLE OF CONTENTS/OUTLINE

- Causes and pathophysiology - Diagnosis and management - Categories of causes - 1) Airway diseases: bronchiectasis, tracheostomy-related hemoptysis, foreign body aspiration, smoke inhalation - 2) Lung parenchymal diseases: infection, collagen vascular disease, idiopathic pulmonary hemosiderosis, coagulopathy, other causes of diffuse pulmonary hemorrhage - 3) Vascular diseases: congenital heart disease, pulmonary arterial hypertension, arteriovenous malformation/hereditary hemorrhagic telangiectasia, KCNT1 mutation-related hemoptysis - 4) Miscellaneous: trauma, tumor, catamenial hemoptysis, iatrogenic

Printed on: 02/07/23



## Abstract Archives of the RSNA, 2022

PDEE-60

### Current Applications of PET/MR Imaging for Evaluation of Pediatric Musculoskeletal Disease

Sunday, Nov. 27 8:00AM - 9:00AM Room: Learning Center - PD

#### Participants

Neetu Soni, MD, FRCR, Rochester, NY (*Presenter*) Nothing to Disclose

#### TEACHING POINTS

- PET-MR combines the excellent soft-tissue resolution and functional capabilities of MR with the quantitative information provided by positron emission tomography (PET)• "Hybrid" MR imaging implies concurrent acquisition of morphologic and functional MR data• Tumor metabolic response predates change in tumor cellularity/morphology; PET-MR is more sensitive than morphologic MR and DW-MRI for assessment of therapeutic response in oncology• PET-MR decreases total number of required imaging studies, simplifying clinical workflows, thus following the "lean" methodology of quality improvement

#### TABLE OF CONTENTS/OUTLINE

- Normal appearances of hybrid PET-MR in the growing skeleton on an illustrative case-based template• Interpretive pitfalls on PET-MR resulting from normal physiologic attributes of the growing skeleton and technique-related• Current applications and limitations of hybrid PET-MR for assessment of entities affecting the growing skeleton

Printed on: 02/07/23



## Abstract Archives of the RSNA, 2022

PDEE-61

### Hotchpotch in Germ Cell Tumors

Sunday, Nov. 27 8:00AM - 9:00AM Room: Learning Center - PD

#### Participants

Akanksha Joshi, MBBS, MD, Mumbai, India (*Presenter*) Nothing to Disclose

#### TEACHING POINTS

1. Imaging characteristics of the germ cell tumors on imaging modalities such as CT (Computed Tomography), MRI (Magnetic Resonance Imaging) and USG (Ultrasonography) 2. The imaging features in differentiating the tumors- teratoma, chorio-carcinoma, dysgerminoma, yolk sac, etc. 3. The management of these tumors depending on the location, and aggressiveness.

#### TABLE OF CONTENTS/OUTLINE

1. Classification of the germ cell tumors in the paediatric population based on the location, age, histology and tumor markers. 2. The spectrum of cases depending the location. 3. Imaging features on CT (Computed Tomography), MRI (Magnetic resonance Imaging) and USG (Ultrasonography) and management of these tumors.

Printed on: 02/07/23



## Abstract Archives of the RSNA, 2022

PDEE-62

### Cartilaginous Bone Lesions in Pediatric and Adolescent Age Group: A Case-based Review

Sunday, Nov. 27 8:00AM - 9:00AM Room: Learning Center - PD

#### Participants

Mahesh Kumar JR, MBBS, MD, Mumbai, India (*Presenter*) Nothing to Disclose

#### TEACHING POINTS

Classifying pediatric and adolescents cartilaginous bone lesions. Recognizing the radiological and pathological features of chondroid matrix. Learning the imaging features of benign, benign aggressive and malignant cartilaginous bone lesions. Special emphasize on chondrosarcoma in pediatric and adolescent age group. Management of cartilaginous bone lesions.

#### TABLE OF CONTENTS/OUTLINE

Disclosure. Introduction. Classification of pediatric and adolescents cartilaginous bone lesions. Chondrosarcoma in pediatric and adolescents age group. Cases

Printed on: 02/07/23

## Abstract Archives of the RSNA, 2022

PDEE-63

### Treatment-related Complications in Children with Hematolymphoid Malignancy: Emergent Conditions and Late Effects

Sunday, Nov. 27 8:00AM - 9:00AM Room: Learning Center - PD

#### Awards

Identified for RadioGraphics

#### Participants

Claudia Cheung, MBBS, Hong Kong, Hong Kong (*Presenter*) Nothing to Disclose

#### TEACHING POINTS

1. Treatment of childhood hematolymphoid malignancies depends on stages and risk of the specific disease, but generally comprises of intensive chemotherapy regimens, with addition of radiotherapy and/or allogenic hematopoietic stem cell transplantation (HSCT) and novel immunotherapy for certain conditions. 2. Severe myelosuppression and prolonged neutropenia are common, which are risk factors for invasive fungal infections from opportunistic organisms. Viral reactivation are common in HSCT recipients. 3. Acute treatment-related toxicity depends on the chemotherapeutic agents for specific disease. For example, methotrexate is associated with acute toxic leukoencephalopathy. Multiple chemotherapy agents are implicated in posterior reversible encephalopathy syndrome. L-asparaginase is associated with pancreatitis and venous thromboembolism. Anthracyclines can cause myocardial cell injury which leads to left ventricular dysfunction. Understanding the treatment regimen used is important in reaching the correct diagnosis. 4. Use of high dose corticosteroids can cause long term skeletal complications. Early recognition of avascular necrosis of femoral head is of particular importance as early orthopedic intervention is essential. 5. Use of intensive radiotherapy can lead to development of secondary cancer. For acute leukemia, secondary brain tumours are common in patients who received cranial radiotherapy.

#### TABLE OF CONTENTS/OUTLINE

1 Introduction  
2 Brief overview of treatment regimens  
3 Treatment-related complications (classified by body systems)  
3(a) Infectious  
3(b) Acute treatment toxicity  
3(c) Late effects  
4 Conclusion

Printed on: 02/07/23



## Abstract Archives of the RSNA, 2022

PDEE-64

### **Radiologists Role In Establishing The Diagnosis, Evaluating Risk Factors, Detecting Recurrence, and Determining the Effectiveness of Treatment in Langerhans Cell Histiocytosis**

Sunday, Nov. 27 8:00AM - 9:00AM Room: Learning Center - PD

#### **Participants**

Takahiro Hosokawa, (*Presenter*) Nothing to Disclose

#### **TEACHING POINTS**

Langerhans cell histiocytosis (LCH) predominantly affects children. Its clinical presentation varies significantly, from isolated and self-limiting to multisystem disorder with a life-threatening clinical course. Various organs are involved. Bone is affected most frequently, and the location of its involvement on imaging findings provides important clues for diagnosing LCH. After diagnosis, the following risk factors should be evaluated: (1) risk of recurrence classified into three grades according to the degree of organ system involvement; I) multisystem (M-S) disease with involvement of high-risk organ (hematologic system, liver, and spleen), II) M-S disease without high-risk organ involvement, or III) single system involvement with one or multiple lesions; (2) risk of central nervous system involvement (manifesting as diabetes insipidus and neuro-degenerative complications); (3) risk of tracheal compression; anterior mediastinal or thyroid huge mass is a predictor of complications during general anesthesia. During follow-up, knowledge regarding the changes in imaging findings associated with pharmacotherapy and conservative treatment is required to evaluate the effectiveness of treatment and detect recurrence.

#### **TABLE OF CONTENTS/OUTLINE**

1. Introduction 2. Imaging findings of LCH; involvement of various organs 3. Key imaging findings for diagnosing LCH 4. Evaluation of risks of recurrence, central nervous system involvement, and tracheal compression 5. Imaging findings during follow-up of patients 6. Conclusion

Printed on: 02/07/23



## Abstract Archives of the RSNA, 2022

PDEE-65

### PET/CT in Pediatric Oncology

Sunday, Nov. 27 8:00AM - 9:00AM Room: Learning Center - PD

#### Participants

Flavio Garcia Pires, MD, (*Presenter*) Nothing to Disclose

#### TEACHING POINTS

After viewing this education exhibit, the learner should be able to: - Understand the principles of PET/CT as a hybrid imaging modality combining functional and anatomic information, which increases its diagnostic and prognostic accuracy; - Understand the importance of FDG PET/CT for the diagnosis, staging and posttreatment response assessment in pediatric oncology; - Identify specific malignancies when the use PET/CT is beneficial; - Instruct multidisciplinary team on the ideal patient preparation to minimize false positive and false negative sites of radiotracer uptake. - Identify expected/physiologic areas of radiotracer uptake and common pitfalls of imaging interpretation such as physiologic linear uptake in physes/apophyses and diffuse bone marrow uptake in generalized inflammatory states or gCSF administration.

#### TABLE OF CONTENTS/OUTLINE

1. RADIOTRACERS/MECHANISMS OF ACTION. 2. PATIENT PREPARATION. 3. PET INTERPRETATION. a. SUV. b. PHYSIOLOGIC FDG UPTAKE IN CHILDREN c. PITFALLS. 4. SPECIFIC DISEASES. a. LYMPHOMA/PTLD. b. SARCOMAS. i. OSTEOSARCOMA. ii. EWING'S SARCOMA. iii. RHABDOMYOSARCOMA. c. LESS INCIDENT TUMORS. i. GERM CELL TUMOR. ii. HEPATOBLASTOMA. iii. NEUROBLASTOMA. 1. FDG. 2. Ga-DOTATATE. iv. THYROID CANCER. 1. FDG. 2. Ga-DOTATE (FOR MEDULLARY SUBTYPE). v. MALIGNANT PERIPHERAL NERVE SHEATH TUMOR. vi. WILMS' TUMOR. vii. CNS TUMOR. 1. PITFALL: RADIATION NECROSIS. 5. FUTURE DIRECTIONS.

Printed on: 02/07/23



## Abstract Archives of the RSNA, 2022

PDEE-66

### Photon Counting Detector CT in Children: Advantages and Clinical Prospects

Sunday, Nov. 27 8:00AM - 9:00AM Room: Learning Center - PD

#### Participants

Juan Carlos Ramirez-Giraldo, PhD, Cary, NC (*Presenter*) Employee, Siemens AG

#### TEACHING POINTS

- Photon-counting detectors (PCD) technology directly converts individual x-ray photons into electrical pulses with small pixel size, that can be counted.
- Traditional energy-integrating detector (EID) CT uses an indirect conversion process where x-ray photons are converted to light, and the signal is integrated over a short period of time.
- PCD CT results in improved spatial resolution.
- PCD CT results in improved contrast of small structures in pediatric patients.
- PCD CT allows for substantial radiation dose reductions.
- PCD CT allows for spectral imaging all the time.

#### TABLE OF CONTENTS/OUTLINE

- Review basic principles of photon counting CT
- Discuss advantages of PCD CT
- Discuss applications PCD CT in pediatric imaging and advantages compared to traditional EID CT images.
- High resolution temporal bone CT
- High resolution chest CT
- Contrast enhanced Chest CT
- Cardiac CT
- CT angiography
- Abdominal CT
- Head CT

Printed on: 02/07/23



## Abstract Archives of the RSNA, 2022

PDEE-67

### Baby Steps Toward a Proper Interpretation of Neonatal Chest and Abdominal Radiographs

Sunday, Nov. 27 8:00AM - 9:00AM Room: Learning Center - PD

#### Participants

Deborah Otto, Sao Paulo, Brazil (*Presenter*) Nothing to Disclose

#### TEACHING POINTS

The purposes of this exhibit are:- To review the normal radiological aspects of chest and abdominal radiographs in neonates.- To illustrate some of the main thoracic and abdominal disorders that can be diagnosed in neonates through plain radiographs.

#### TABLE OF CONTENTS/OUTLINE

Chest:- Normal anatomy- Lines and tubes (correct placement parameters, correct and incorrect placement examples and complications).- Diffuse lung disorders (Surfactant deficiency, retained fetal fluid, meconium aspiration, congenital surfactant dysfunction, alveolar growth disorders)- Focal lung disorders (Congenital Pulmonary Airway Malformations, Bronchopulmonary sequestration, congenital lobar hyperinflation)- Diffuse or Focal disorders(Pneumonia, Interstitial Emphysema)Abdomen:- Normal anatomy and expected bowel gas pattern- Lines and tubes (correct placement parameters, correct and incorrect placement examples and complications).- Congenital gastrointestinal disorders (tracheoesophageal fistula, duodenal atresia, ileal atresia, malrotation, Hirschsprung disease and congenital diaphragmatic hernia).- Acquired gastrointestinal disorders (necrotizing enterocolitis, pneumoperitoneum, meconium peritonitis, gastric volvulus and midgut volvulus)

Printed on: 02/07/23



## Abstract Archives of the RSNA, 2022

PDEE-7

### Imaging Features of Pediatric Sarcoidosis: From Head to Toe

Sunday, Nov. 27 8:00AM - 9:00AM Room: Learning Center - PD

#### Awards

Identified for RadioGraphics

#### Participants

Gozde Ozer IV, MD, (*Presenter*) Nothing to Disclose

#### TEACHING POINTS

Sarcoidosis occurs approximately ten times less frequently in children than in adults. Pediatric sarcoidosis predominantly involves the lungs and lymphatic system but can affect any organ in the body. Characteristic chest CT findings of pulmonary sarcoidosis are mediastinal, bilateral hilar lymphadenopathy, and nodules with the perilymphatic distribution along the interlobular septa, interlobar fissures, and subpleural regions. Abdominal sarcoidosis may manifest as numerous small nodules in the liver and spleen. In addition, abdominal lymphadenopathies can be seen in one-third of the patients. Neurosarcoidosis is most commonly manifested by leptomeningeal and pituitary gland involvement. Leptomeningeal sarcoidosis can be seen as nodular or plaque-like thickening and enhancement of the leptomeninges. Orbital involvement of sarcoidosis is the most common presentation in the head and neck region. Although any part of the orbit can be involved, uveitis is the most common condition and is often bilateral.

#### TABLE OF CONTENTS/OUTLINE

General information and diagnostic criteria of sarcoidosis. The role of radiology in the diagnosis. Imaging patterns of pulmonary, abdominal, central nervous system, head and neck, and musculoskeletal-cutaneous involvement of sarcoidosis.

Printed on: 02/07/23



## Abstract Archives of the RSNA, 2022

PDEE-8

### **Congenital Diaphragmatic Hernia: A Hole lot More than Morgagni**

Sunday, Nov. 27 8:00AM - 9:00AM Room: Learning Center - PD

#### **Participants**

Christian Pecoraro, DO, Rochester, NY (*Presenter*) Nothing to Disclose

#### **TEACHING POINTS**

Embryology of the diaphragm and cause of congenital diaphragmatic hernias. Role of pre-natal imaging including MR + US in the diagnosis and prognostication of CDH. Post-natal imaging findings of typical right and left CDH. Imaging findings of acute Late-Presenting CDH. Review of surgical strategies for CDH repair, as well as expected and un-expected post-operative findings. Associated anomalies, syndromic and non-syndromic including urogenital, musculoskeletal neurological.

#### **TABLE OF CONTENTS/OUTLINE**

Introduction, definition, and embryology. Classification of CDH. Prenatal imaging findings of CDH. Postnatal imaging findings of CDH. Review of fetoscopic endoluminal tracheal occlusion (FETO) for CDH. Expected post-operative appearance of the diaphragm following surgical prosthetic patch repair/graft. Acute and late post-operative related complications of CDH, including associated decreased ipsilateral lung perfusion. Associated anomalies, syndromic and non-syndromic including urogenital, musculoskeletal neurological. Describe the respiratory morbidities found in CDH survivors, including chronic cough, wheezing, chest wall deformities (pectus excavatum) and scoliosis.

Printed on: 02/07/23



## Abstract Archives of the RSNA, 2022

PDEE-9

### Point of Care Ultrasound in Pulmonary Pathologies Applied to Intensive Care Unit Neonates

Sunday, Nov. 27 8:00AM - 9:00AM Room: Learning Center - PD

#### Participants

Vitor Romano, MD, Sao Paulo, Brazil (*Presenter*) Nothing to Disclose

#### TEACHING POINTS

The purposes of this exhibit are: Make a didactic review of the point of care ultrasound in pulmonary pathologies in intensive care unit neonates; Point out the indications and limitations of the ultrasound on the evaluation of the pulmonary parenchyma; Review the techniques of the pulmonary ultrasound; Review the anatomy and the thoracic structures that can be evaluated by this method; Review the normal and abnormal findings on thoracic ultrasound; Review the main artifactuary lines on lung ultrasonography and it's pathological correlations; Review the main protocols of thoracic ultrasound.

#### TABLE OF CONTENTS/OUTLINE

We will discuss the following topics and focus on the echography features of the normal and abnormal thoracic ultrasound: Ultrasound technique Normal findings on pulmonary ultrasonography (A lines; B lines; I lines; Z lines; E lines) Pathologic findings on thoracic ultrasonography: Parenchyma (Consolidation; Atelectasia; Congestion) and Pleura (Pleural effusion; Pneumothorax) Protocols.

Printed on: 02/07/23

## Abstract Archives of the RSNA, 2022

PHEE

### Physics Education Exhibits

Sunday, Nov. 27 8:00AM - 9:00AM Room: Learning Center - PH

#### Sub-Events

#### **PHEE-10 Classification of Rectal Conditions in CBCT Images for Prostate Cancer Radiation Therapy Using Deep Learning**

Participants

Tomoki Kikuchi, Kiryu, Japan (*Presenter*) Nothing to Disclose

#### TEACHING POINTS

Radiation therapy for prostate cancer has the same outcome as surgery and is listed as a radical treatment option. Intensity-modulated radiotherapy is recommended as a treatment policy and is useful for reducing the risk of recurrence. It is necessary to give an appropriate dose distribution to the prostate to improve the therapeutic effect. Because of gas or stool dilation in the rectum, the position of the prostate becomes inaccurate. Positional inaccuracy causes excess or deficiency for dose distribution, so pretreatment such as exhaust gas and defecation is required before radiation therapy. The need for pretreatment is determined by the cone-beam computed tomography (CBCT) images. However, no clear criteria have been set, depending on the observer's subjectivity. Therefore, we propose a method of using deep learning to classify the rectal condition of CBCT images. Our method helps determine if pretreatment should be given before radiation therapy for prostate cancer patients. The main teaching points of this exhibition are to: 1. classify CBCT images according to the condition of the rectum. 2. understand how to use deep learning. 3. support observer decisions.

#### TABLE OF CONTENTS/OUTLINE

To support the decision on whether to perform pretreatment by classifying the rectal condition using deep learning in cone-beam CT.

#### **PHEE-11 Semiquantitative Evaluation of Image Quality of Clinical CT Images By Radiologists: From Physical Evaluation of Phantom to Semiquantitative Evaluation of Clinical Images**

Participants

Ikuo Kawashita, PhD, Hiroshima, Japan (*Presenter*) Nothing to Disclose

#### TEACHING POINTS

Physical characteristics such as the modulation transfer function (MTF), noise power spectrum (NPS), and detectability index are often measured on phantom CT images to obtain an objective evaluation of their quality. However, the image quality of phantom images is not always equivalent to that of clinical images and the physical evaluation of phantom images does not necessarily coincide with the subjective image quality on clinical images evaluated by radiologists. In this educational poster, we describe to diagnostic radiologists the semi-quantitative evaluation of the sharpness of structure contours (an MTF alternative), the image noise, and the detectability of objects on clinical CT images. We also discuss the limitations of semi-quantitative evaluation methods.

#### TABLE OF CONTENTS/OUTLINE

1. Introduction: a) Importance of semiquantitative evaluation of clinical images b) Limitations of general physical evaluations 2. Evaluation of the contour sharpness on clinical images a) MTF measurements using the blur of the edge profile curve on CT images b) Evaluation of the contour sharpness using the power spectrum 3. Evaluation of the noise characteristics of clinical CT images a) NPS measurement of flat areas without texture b) NPS measurement of non-flat textured areas 4. d'NPW: Detectability index measurements 5. Preconditions / limitations and estimation accuracy

#### **PHEE-12 Understanding the Dosimetric Effect of Contrast Agents on External Beam Radiation Therapy**

Participants

Zhou Wang, PhD, (*Presenter*) Nothing to Disclose

#### TEACHING POINTS

In radiation therapy (RT), contrast agents (CA) are used in CT simulation during treatment planning for better target/organ delineation. This educational exhibit demonstrates the different dominant photon interaction mechanisms between kV (CT) and MV (RT) photons and CA. Due to the K-edge enhanced photoelectric effect of CA in CT, CA's CT number (HU) can be misrepresented in MV beam dose computation by an exaggerated relative electron density. CA is not typically used during RT delivery, and the difference is accounted for by overriding the HU of CA in treatment plans to tissue equivalent (e.g. 0 HU). Image-guided radiation therapy (IGRT) using on-board cone-beam CT (CBCT) is common in RT and has potential for use in adaptive radiation therapy (ART). There is interest in using CA during CBCT for IGRT and/or ART, raising the question of the dosimetric effect of CA on RT delivery following CBCT with CA. Clinical cases recomputed with different levels of overridden HU are presented to understand the dosimetric effect caused by CA during RT.

## TABLE OF CONTENTS/OUTLINE

1) CA in CT simulation and HU value overridden in RT planning. 2) IGRT/ART and the use of CA in CBCT. 3) Difference in photon interactions - kV CBCT vs. MV RT beams. 4) Effect by HU of CA enhanced perirectal hydrogel spacer (e.g. SpaceOAR Vue) in prostate RT. 5) Recomputed IV/oral contrast clinical cases demonstrating the potential dosimetric effect when treating patient receiving CBCT CA imaging.

### **PHEE-13 Suggestion For The Dose Reduction of The Tomosynthesis Imaging By Using the Generated Interpolation Image Based On the Deep Learning**

Participants

Ryohei Fukui, PhD, (*Presenter*) Nothing to Disclose

#### TEACHING POINTS

Tomosynthesis is the 3-dimensional imaging technique used for the general X-ray and the mammography. The tomosynthesis imaging requires multiple projection images obtained from different angles. Although acquiring a large number of projection images improves an image quality of the reconstructed tomosynthesis image, however, a patient dose would be increased. If a precise interpolation image can be created and inserted into the dataset of reduced number of projection images instead of the real projection image, a significant reduction of the patient dose can be achieved. We are able to create a pseudo image easily by using the deep learning technique. The generative adversarial network (GAN) has improved its accuracy. We'll suggest the method for dose reduction by using a generated pseudo interpolation image based on the deep learning in the tomosynthesis. The aim of this exhibit is, 1. to learn the patient dose of the tomosynthesis, 2. to show the outline for generating the pseudo interpolation image by using the GAN, 3. to insert the generated pseudo image in the dataset of real projection images and reconstruct the tomosynthesis image, 4. to explain the problem of the proposed method. We hope that the patient dose would be reduced by our suggestion.

#### TABLE OF CONTENTS/OUTLINE

1. Patient dose of the tomosynthesis, 2. Image generation based on the deep learning. 3. Outline for generating the pseudo interpolation image, 4. Present the generated interpolation images and the reconstructed tomosynthesis image, 5. Dose reduction of the tomosynthesis.

### **PHEE-14 Routine Body Applications of Advanced Gemstone Spectral Imaging: What the Radiologist Need to Know**

Participants

Shingo Harashima, Tokyo, Japan (*Presenter*) Nothing to Disclose

#### TEACHING POINTS

1) To describe basic principles and various imaging/analyzing techniques of advanced Gemstone Spectral Imaging (GSI); 2) To introduce technological features and optimal imaging option in advanced GSI based on experimental and clinical data; 3) To illustrate routine body applications of advanced GSI by presenting various clinical images.

#### TABLE OF CONTENTS/OUTLINE

1) Basic principles imaging/analyzing techniques. Single-source dual-energy CT with fast kV switching; Virtual monochromatic/material decomposition imaging (VMI/MDI); Spectral HU curve/effective atomic number (Z) analysis. 2) Technological features optimal imaging option. Novel high output x-ray tube/kV mA synchronized switching/iterative deep-learning reconstruction for high-quality imaging/high-precision analysis/reasonable radiation contrast media (CM) dose reduction. 3) Routine body applications. Low-keV VMI (vs. low-kV CT): improved image contrast/reduced CM dose; High-keV VMI: reduced image noise/beam-hardening metallic artifact; Iodine-enhanced MDI: organ perfusion tumor viability assessment/cystic solid mass differentiation; Iodine-suppressed MDI: virtual non-contrast CT; Hydroxyapatite-suppressed MDI: bone marrow edema imaging/calcification-free CT angiography; Fat-enhanced MDI/Spectral HU curve/effective Z: lipid-rich lesion detection; Effective Z: nephrolithiasis composition analysis.

### **PHEE-15 How to Make Full Use of Ultra-High-Resolution CT: the Concepts of Imaging Condition and the Clinical Applications**

Participants

Yuta Miyamae, RT, Tokyo, Japan (*Presenter*) Nothing to Disclose

#### TEACHING POINTS

•Ultra-high-resolution CT (U-HRCT) can provide high-quality CT images depending on the optimum imaging conditions. Especially, it is important to know the characteristics of the three scan modes and the six focus sizes. •U-HRCT images tend to be increased image noise because of the extension of representable frequency band. Deep learning reconstruction (DLR) effectively reduces image noise while maintaining spatial resolution and low-contrast detectability. However, the image quality should be evaluated by proper methods in order to optimize the exposure dose because the excessive reducing exposure dose may cause unexpected deterioration of image quality. •This exhibition explains how to properly understand the physical characteristics of U-HRCT imaging and utilize high-quality images in clinical practice. In addition, we will review papers on clinical application of U-HRCT and discuss the usefulness of high-resolution images.

#### TABLE OF CONTENTS/OUTLINE

1. Explanation of the physical characteristics of U-HRCT images. The physical characteristics of U-HRCT images will be explained in terms of resolution characteristics for in-plane and z-axis direction, noise characteristics, low-contrast detectability and temporal resolution. 2. Investigation of exposure dose for clinical imaging. The exposure dose at clinical cases is shown about conventional MDCT and U-HRCT imaging. 3. Presentation of clinical U-HRCT images. We report clinical cases that U-HRCT imaging has been useful for the diagnostic imaging and surgical supports.

## **PHEE-16 ACR CT Accreditation Testing and Routine Quality Control for Clinical Photon-Counting Detector CT: Practical Tips and Tricks**

### **Awards**

#### **Certificate of Merit**

#### **Participants**

Michael R. Bruesewitz, RT, Rochester, MN (*Presenter*) Nothing to Disclose

#### **TEACHING POINTS**

- To explain the unique features of Photon-counting-detector (PCD) CT compared to conventional energy-integrating-detector (EID) CT
- To demonstrate the similarities and differences between PCD-CT and EID-CT for Quality Control (QC) and ACR accreditation
- To describe precautions needed to be taken in phantom and protocol selection for QC testing
- To discuss additional procedures to fully evaluate the performance of PCD-CT

#### **TABLE OF CONTENTS/OUTLINE**

1. What is PCD and how is it different from the energy integrating detectors (EID) used on commercial CT scanners? a. PCD: Directly convert X-ray into electronic signals, count individual photon and record its energy b. EID: Indirect, 2 stage conversion of X-ray to visible light then to electronic signal. Signal is proportional to total energy deposited, without information on individual photon 2. Similarities and Differences in PCD and EID for ACR and QC testing a. Higher spatial resolution in PCD vs EID b. CT number differences between PCD and EID due to different photon-weighting scheme c. CT number of virtual monoenergetic images (VMI) and its use in QC testing d. Slice thickness wire measurement differences, especially on the high resolution of PCD-CT 3. Protocol and Phantom selection a. Scanning with required Adult and Pediatric ACR protocols to meet specifications b. Obtaining correct CTDI measurements for QC and ACR accreditation 4. Future Directions a. Higher line pair/cm resolution scans b. MTF measurements c. Multi-Energy scans and testing d. Iodine quantification accuracy

## **PHEE-17 Demystifying the Radiation Dose Summary Page in Interventional Fluoroscopy**

### **Awards**

#### **Identified for RadioGraphics**

#### **Participants**

Anzi Zhao, MS, (*Presenter*) Nothing to Disclose

#### **TEACHING POINTS**

Interventional fluoroscopic procedures may lead to high radiation dose to the patient, it's paramount to understand the details of radiation exposure of a procedure. The radiation dose summary page generated by the interventional fluoroscope is a form that displays important information about a procedure. It is extremely helpful for clinicians to better understand the details of irradiation events and their imaging acquisition parameters, as well as the total radiation dose of the procedure. After reviewing this exhibit, learners will be able to: 1. Understand the two imaging modes of interventional fluoroscopy. 2. Understand important operating parameters of interventional fluoroscopy. 3. Understand radiation dose metrics in interventional fluoroscopy and how to interpret them on radiation dose summary page.

#### **TABLE OF CONTENTS/OUTLINE**

1. Review imaging modes of interventional fluoroscopy. 2. Review the operating parameters of interventional fluoroscopy - kV, mA, pulse width, pulse rate, filter, field of view, beam geometry. 3. Review radiation dose metrics in interventional fluoroscopy, including their usage and caveats about indicating of patient dose and associated risks - reference air kerma, DAP, peak skin dose. 4. How these above-mentioned contents are displayed in the radiation dose summary page from two major interventional fluoroscope manufacturers. 5. Review manufacturer specific content in radiation dose summary page.

## **PHEE-18 US and Doppler Artifacts: Real or Pitfall?**

#### **Participants**

Marina Akuri, MD, Marilia, Brazil (*Presenter*) Nothing to Disclose

#### **TEACHING POINTS**

1. To review and explain the most common ultrasound and Doppler artifacts;
2. To assess the clinical usefulness and downsides of US and Doppler artifacts;
3. To discuss how to emphasize, lessen, and avoid US artifacts and Doppler artifacts

#### **TABLE OF CONTENTS/OUTLINE**

1. Acoustic enhancement; 2. Acoustic shadowing; 3. Side lobe artifact; 4. Ring down artifact; 5. Reverberation artifact; 6. Anisotropy; 7. Aliasing artifact; 8. Twinkling artifact; 9. Blooming; 10. Color bruit artifact; 11. Comet tail artifact; 12. Mirror image artifact; 13. Beam width artifact; 14. Speed displacement artifact; 15. Hardware-related artifacts

## **PHEE-19 Protocol Management in MRI**

#### **Participants**

Joshua Yung, PhD, Houston, TX (*Presenter*) Nothing to Disclose

#### **TEACHING POINTS**

Outline MRI protocol management as a continuous quality improvement process with a focus on challenges and methods for protocol standardization across a fleet of scanners and technologists. Understand the need and discuss the steps required for checking technical compliance of an MR acquisition as a quality control metric. Understand the unique challenges in monitoring MR acquisitions for protocol standardization and tools for quantitative assessment.

#### **TABLE OF CONTENTS/OUTLINE**

1. MRI protocol management and quality assurance a. Consistent execution b. Protocol standardization vs. acquisition standardization c. Applications for MR protocol standardization d. Performance assessments and quality improvements to address

deficiencies 2. Measuring MR protocol acquisition compliance a. Relevant parameters and pitfalls b. Processing pipeline c. Example of results dashboard d. Other use cases benefiting from compliance checks 3. Monitoring of MR protocol acquisition performance a. Benchmarking performance for comparison and performance improvement b. Relevant parameters and pitfalls c. Workflow diagram d. Challenges with a large multi-vendor MR fleet e. Example of acquisition report 4. Additional protocol analytics tools a. Scanner and protocol utilization, performance profiles and lifecycle management b. Relating acquisition parameters and image quality for protocol development c. Image quality event reporting by radiologists, clinicians and technologists for feedback as part of the quality improvement process 5. Conclusion

### **PHEE-1HC    **Neuroradiology Applications with 7T Magnetom Terra Clinical MRI Scanner. A Single-Center Clinical Experience: Indications and Sequence Parameters****

Participants

Can Ozutemiz, MD, (*Presenter*) Nothing to Disclose

#### **TEACHING POINTS**

Point out the indications for the usage of 7T MRI in clinical neuroradiology practice. Provide the sequence parameters we developed for each indication

#### **TABLE OF CONTENTS/OUTLINE**

7-Tesla Ultra-Highfield Magnetom Terra Clinical MRI Scanner has been recently available for clinical use. Currently, the scanner is only approved for knee and brain imaging with dedicated coils. However, the presets and already built-in sequences within the machine are not optimized for patient care in neuroradiology. At our center, we have been testing healthy volunteers and selected patients to optimize our sequences for each indication. In this abstract, first, we will describe the indications where 7-Tesla MRI could be used. While a routine brain MRI can be performed with this machine, specific indications where high-field MRI can be beneficial will be discussed. These include brain tumor imaging with dynamic susceptibility contrast perfusion, epilepsy focus evaluation, high detail cranial MR angiogram/venogram, multiple sclerosis plaque assessment, pituitary MRI, movement disorder evaluation/deep brain stimulator planning, and vessel wall imaging. With each indication, we will provide a table where we describe the sequence parameters including the sequence name, slice thickness, matrix, field-of-view, slice plane, distance factor, voxel size, and time. Imaging examples for each indication will also be provided. Please visit the Learning Center to also view this presentation in hardcopy format.

### **PHEE-2        **Safely Imaging Patients Implanted with MRI Conditional, Non-conditional, and Other Active Devices****

#### **Awards**

**Identified for RadioGraphics  
Certificate of Merit**

Participants

Matthew Harwood, MD, Phoenix, AZ (*Presenter*) Nothing to Disclose

#### **TEACHING POINTS**

- Review device safety evaluation and patient scheduling processes.
- Demonstrate how to interpret vendor manuals.
- Demonstrate how and why decisions to refuse imaging are made.
- Demonstrate how MRI protocols can be modified for patients with implanted devices without compromising diagnostic ability.
- Discuss relevant background information for the above, such the MRI modes of operation, slew, SAR, and B1+rms

#### **TABLE OF CONTENTS/OUTLINE**

- Objectives
- Trend in Patients Presenting for MRI with Active Devices
- Overview of Devices, What Precisely Are We Talking About?
- Device Labeling
- MRI Safety Considerations: Torque, Induced Currents, RF Heating, Hearing Damage
- Specific Absorption Rate (SAR)
- B1+rms
- Examples of How to Modify Protocols to Reduce SAR/ B1+rms
- Gradient Slew Rate
- MRI Modes of Operation
- Suggested Device Assessment Strategy
- How to Read Vendor Manuals with Examples
- Scheduling and Evaluation Processes for Implanted Cardiac Devices
- Process Modifications for Non-Conditional Devices and Other Active Devices
- Case 1: MRI Was Requested but Not Performed
- Case 2: MRI Successfully Performed with Process Modifications
- Case 3: MRI Successfully Performed with Process Modifications
- Summary of Important Points

### **PHEE-20     **Basic Principles of Contrast Injection Protocols for Computed Tomography: Reintroduction for Clinicians by Simulation Software****

Participants

Takeshi Nakaura, MD, Kumamoto, Japan (*Presenter*) Nothing to Disclose

#### **TEACHING POINTS**

For contrast-enhanced computed tomography (CT) and CT angiography, it is necessary to stabilize the contrast enhancement using suitable contrast injection protocols. Furthermore, this protocol requires to be adjusted as CT evolves, and clinicians need to have a basic knowledge of it due to ongoing improvements such as photon-counting CT. The principles of the contrast injection protocols appear to be quite difficult; however, simulation software for contrast effects has been recently released, allowing doctors to use the program to test their understanding of the contrast injection protocol. The goal of this exhibition is to: 1. Demonstrate the fundamental principles of a contrast injection protocol. 2. Show contrast injection protocols and their contrast effects using simulation software under various conditions.

#### **TABLE OF CONTENTS/OUTLINE**

Table of Contents/Outline 1) The simulation of dilution and diffusion of contrast material in vivo Dilution by blood flow Passive diffusion using Fick's law 2) When and why does the peak enhancement occur? Simulation about the relationship between the contrast injection duration and enhancement curve 3) Patient factors that affect the contrast enhancement Patient body size Cardiac output Others 4) How to optimize the contrast injection protocol for various examinations

### **PHEE-3 Artifacts Caused by Left Ventricular Assist Devices in Digital Radiographic and Mammographic Environment**

Participants

Jill M. Lucas, RT, BA, (*Presenter*) Nothing to Disclose

#### **TEACHING POINTS**

- Identify electromagnetic interference artifacts in digital radiography and mammography
- Isolation and investigation of artifacts using phantom studies
- Potential reduction of artifacts due to LVAD devices

#### **TABLE OF CONTENTS/OUTLINE**

The use of left ventricular assist devices (LVAD) has been rapidly growing for patients with advanced heart failure, providing both a bridge-to-transplant and destination therapy. The presence of LVAD devices in clinical radiography and mammography exams have been accompanied by intermittent clinical complaints regarding line artifacts. Patient cases and artifact images were reviewed, from which electromagnetic interference (EMI) was determined to be the cause. Further investigation of two LVAD devices (HeartMate II and HeartMate 3, Abbott Inc.) in radiographic and mammographic environment was performed using phantoms. An appreciable difference was demonstrated in artifact appearance and magnitude depending on the LVAD model, flat panel detector type, and location of the LVAD pump relative to the detector. -Artifact identification; Examples clinical and phantom images will be shown - Variation in artifact appearance with differences in: LVAD model; Image receptor type and manufacturer; Imaging task, projection, and patient body habitus -Challenges; Breast imaging; Chest imaging, especially posteroanterior (PA) chest projection -Solutions: Positioning the patient so that LVAD is as far from image receptor as feasible; About 10 cm in PA chest imaging, or use anteroposterior projection if clinically acceptable; When possible, selecting a digital detector with improved EMI shielding, or utilizing a system with advanced processing for EMI artifact reduction

### **PHEE-4 Radiofrequency Safety in MR Imaging: What Are the Concerns?**

Participants

Zhongwei Zhang, MD, PhD, St. Louis, MO (*Presenter*) Nothing to Disclose

#### **TEACHING POINTS**

RF-induced thermal events including heating and burns in patients have become more common, concerns have accounted for more than half of the total adverse events according to FDA MRI-related adverse event reports. The purposes of this Education Exhibit are 1. Overview of RF-induced thermal events and thermal injury root causes analysis; 2. Explain the concept behind RF coils and B1 Field; 3. RF exposure and energy absorption: SAR definitions, types, methods for SAR calculation, factors affecting SAR, SAR reduction, B1+rms, Specific Energy Dose (SED), etc.; 4. Discuss RF heating mechanisms for tissues and implants; 5. Review current regulations and guidelines, RF energy monitoring approaches, and discuss strategies to prevent potential RF-induced thermal events; 6. Since SAR depends on system performance (B0, B1 field, RF transmission, etc), object properties (density, electrical conductivity, size, etc), geometry and patient positioning, and pulse sequences. A hands-on example will be presented to show SAR reduction in clinical protocols.

#### **TABLE OF CONTENTS/OUTLINE**

1. Introduction; 2. Overview of RF-induced thermal events and thermal injury root causes analysis; 3. RF coils and B1 field; 4. RF exposure and energy absorption; 5. RF heating mechanisms for tissues and implants; 6. RF safety and RF-induced thermal events prevention: emphasis on clinical protocols.

### **PHEE-5 A Picture Is Worth a Million Convolutions: A Simplified Explanation of Convolutional Neural Networks for Radiologists**

Participants

Tianyuan Fu, MD, Cleveland, OH (*Presenter*) Nothing to Disclose

#### **TEACHING POINTS**

1) To help radiologists gain a basic understanding of convolutional neural networks (ConvNets) for the purposes of interpreting literature on applications of artificial intelligence (AI), machine learning (ML), and deep learning (DL) in radiology. 2) Describe how ConvNets fit into the paradigm of AI, ML, and DL. 3) Touch on the similarities between ConvNets and biological human vision, and explain what makes ConvNets highly accurate and efficient at analyzing pictures. 4) Define important terminology associated with ConvNet architecture. 5) Explain the process through which ConvNets learn from imaging data with a simple illustration of how a raw image is translated into pixel data, passed as input and processed through the neural network, and translated into one or more outputs. 6) Give an overview of transfer learning and discuss examples of pre-trained ConvNet architectures.

#### **TABLE OF CONTENTS/OUTLINE**

1) Overview of artificial intelligence, machine learning, deep learning, and convolutional neural networks (ConvNets). 2) ConvNets and biological human vision. 3) What makes ConvNets accurate and efficient at image analysis? 4) Translating a raw image into training data for a ConvNet. 5) Describe how ConvNets process image data and in the process learn information stored as weights. 6) Illustrate what a complete ConvNet architecture looks like. 7) Discuss transfer learning and illustrate existing ConvNet architectures including VGG-16, Inception, ResNet, and others. 8) Summary of the essential basics of ConvNets for radiologists who are reading literature on AI and ML/DL applications in radiology.

### **PHEE-6 Emerging Applications of Cone-Beam Computed Tomography in Osseous Structure Assessment: A Pictorial Overview**

Participants

Hamza Ibad, MBBS, Baltimore, MD (*Presenter*) Nothing to Disclose

#### **TEACHING POINTS**

1. Flat-panel-detectors-based CBCT allows high-resolution osseous structural assessments. 2. CBCT enables investigation of joints at various motion states and weight-bearing (WB), providing physiological measurements of joints in diseased and non-diseased states. 3. Recently introduced motion compensation algorithms, such as regionally applied auto-focus, have the potential to greatly

improve the diagnostic yield of CBCT examinations.4. Fast and high-resolution CBCT protocols permit temporomandibular joint (TMJ) assessment in closed- and open-mouth states5. CBCT enables accurate volumetric cartilage and bone mineral density evaluation of the knee joint complex, TMJ, and various other joints.6. Long-term outcomes of intraoperative use of CBCT in the orthopedic, oral, and maxillofacial repair of skeletal defects are currently under investigation.

#### TABLE OF CONTENTS/OUTLINE

1. Introduction.2. Emerging developments in CBCT imaging - WB capabilities, motion artifact compensation algorithms, high-resolution dental protocols, and intraoperative CBCT systems (e.g. C-arms with three-dimensional capability).3. Use in MSK Imaging - Tibiofemoral joint space width quantification, ankle syndesmosis measurements, valgus hindfoot alignment measurements, and intraoperative fracture and joint reduction aid.4. Use in Dental Imaging - Volumetric TMJ analysis, fracture assessment and post-repair evaluation, endo- and periodontics.5. Limitations and prospects.

#### **PHEE-7 Photon-Counting CT: Physics of Alternative Detector Approaches, Impacts on Image Quality, and Potential Applications**

Participants

Paul E. Kinahan, PhD, Seattle, WA (*Presenter*) Co-founder, PET/X LLC

#### TEACHING POINTS

1. There are two established approaches for photon-counting CT detectors using silicon- and cadmium-based detectors, with different physical trade-offs.2. Photon-counting CT provides both lower noise and a much richer set of spectral (energy) information compared to CT scanners with standard energy-integrating detectors.3. Photon-counting CT also provides higher image resolution than CT scanners with standard energy-integrating detectors, albeit at a potentially higher cost and complexity.4. There are several clinical areas that can take advantage of the improved spatial and energy resolution of photon-counting CT systems.5. Developing appropriate workflows that take advantage of increased information per scan in an efficient manner is an important consideration.

#### TABLE OF CONTENTS/OUTLINE

Review the essential differences between photon-counting and energy-integrating CT systems, with an emphasis on the ability for lower noise and improved spectral (energy) information. Review the two established approaches for photon-counting CT detectors that use silicon- and cadmium-based detectors, with a discussion of the different physical trade-offs. Show how the silicon- and cadmium-based detector designs necessarily lead to improved spatial resolution. Describe the roughly 50-fold increase in raw (sinogram) data generated by a photon-counting CT system and how it may impact clinical workflows. Provide illustrations of where the improved spatial and energy resolution of photon-counting CT systems can lead to improvements in imaging for oncology, cardiovascular, thoracic, musculoskeletal, and head and neck imaging.

#### **PHEE-8 Seeing More with Super-Resolution Deep-Learning CT Reconstruction: Principles and Clinical Applications**

Participants

Yasunori Nagayama, MD, Kumamoto, Japan (*Presenter*) Nothing to Disclose

#### TEACHING POINTS

The acquisition of high-resolution and low-noise CT images is crucial for the detailed evaluation of fine anatomical and pathological structures. Recently, the super-resolution deep-learning-based reconstruction (SR-DLR) utilizing the convolutional neural networks (CNNs) to enhance the spatial resolution and reduce image noise has been clinically available. The purpose of this exhibit is: 1. To understand the basic concept and technical principles of the SR-DLR technique 2. To describe the image characteristics of SR-DLR and compare them with those of filtered back projection (FBP), hybrid iterative reconstruction (IR), model-based IR, and normal-resolution DLR (NR-DLR) 3. To review the impact of SR-DLR on the image quality and object detectability in the clinical examples

#### TABLE OF CONTENTS/OUTLINE

1. CNN-based super-resolution technique 2. Basic concept and technical details of SR-DLR 3. Image properties of SR-DLR: comparisons with FBP, hybrid IR, model-based IR, and NR-DLR algorithms A) Noise property B) Spatial resolution C) Low- and high-contrast object detectability 4. Clinical application of the SR-DLR technique A) Coronary CT for coronary plaque assessments B) Stent imaging C) Lung CT D) Cerebral CT angiogram E) Pediatric CT for the assessment of congenital heart diseases 5. Future directions A) Application to dual-energy CT B) Network training with photon counting CT

#### **PHEE-9 Current Status and Future of Personal Dose Management-Necessity for Real-Time Measurement of the Occupational Radiation Dose in Interventional Radiology**

Participants

Kenshin Hattori, (*Presenter*) Nothing to Disclose

#### TEACHING POINTS

To understand current personal dose management to interventional radiology (IVR) staff. To understand importance of lens dosimeter. To understand the need for real-time measurement of occupational radiation dose in IVR. To compare fundamental characteristics among several occupational real-time dosimeters. To understand the fundamental characteristics of a real-time occupational dosimetry and display system (i3 system). To show the usefulness of the i3 system in occupational dose management for IVR.

#### TABLE OF CONTENTS/OUTLINE

The 2011 ICRP Statement significantly lowered the cataract threshold dose for the eye lens from 8 Gy to 0.5 Gy. Accordingly, dose limits for medical personnel have been lowered in many countries, and in Japan the dose limit has been significantly reduced from 150 mSv per year to an average of 20 mSv per year over a five-year period. Therefore, personal dose management is becoming increasingly important. Currently, glass badges and pocket dosimeters are used for personal dose management for medical staff, but in the future, lens dosimeters and real-time dosimeters may become important. Until now, it has not been possible to determine the time of exposure, but with the use of this real-time dosimeter, it is possible to understand at a glance. The new real-time dosimeters evaluated in this study have sufficient performance for clinical use, especially good angular dependence. These

dosimeters will be important in the future.

Printed on: 02/07/23



## Abstract Archives of the RSNA, 2022

PHEE-10

### Classification of Rectal Conditions in CBCT Images for Prostate Cancer Radiation Therapy Using Deep Learning

Sunday, Nov. 27 8:00AM - 9:00AM Room: Learning Center - PH

#### Participants

Tomoki Kikuchi, Kiryu, Japan (*Presenter*) Nothing to Disclose

#### TEACHING POINTS

Radiation therapy for prostate cancer has the same outcome as surgery and is listed as a radical treatment option. Intensity-modulated radiotherapy is recommended as a treatment policy and is useful for reducing the risk of recurrence. It is necessary to give an appropriate dose distribution to the prostate to improve the therapeutic effect. Because of gas or stool dilation in the rectum, the position of the prostate becomes inaccurate. Positional inaccuracy causes excess or deficiency for dose distribution, so pretreatment such as exhaust gas and defecation is required before radiation therapy. The need for pretreatment is determined by the cone-beam computed tomography (CBCT) images. However, no clear criteria have been set, depending on the observer's subjectivity. Therefore, we propose a method of using deep learning to classify the rectal condition of CBCT images. Our method helps determine if pretreatment should be given before radiation therapy for prostate cancer patients. The main teaching points of this exhibition are to: 1. classify CBCT images according to the condition of the rectum. 2. understand how to use deep learning. 3. support observer decisions.

#### TABLE OF CONTENTS/OUTLINE

To support the decision on whether to perform pretreatment by classifying the rectal condition using deep learning in cone-beam CT.

Printed on: 02/07/23



## Abstract Archives of the RSNA, 2022

PHEE-11

### Semiquantitative Evaluation of Image Quality of Clinical CT Images By Radiologists: From Physical Evaluation of Phantom to Semiquantitative Evaluation of Clinical Images

Sunday, Nov. 27 8:00AM - 9:00AM Room: Learning Center - PH

#### Participants

Ikuo Kawashita, PhD, Hiroshima, Japan (*Presenter*) Nothing to Disclose

#### TEACHING POINTS

Physical characteristics such as the modulation transfer function (MTF), noise power spectrum (NPS), and detectability index are often measured on phantom CT images to obtain an objective evaluation of their quality. However, the image quality of phantom images is not always equivalent to that of clinical images and the physical evaluation of phantom images does not necessarily coincide with the subjective image quality on clinical images evaluated by radiologists. In this educational poster, we describe to diagnostic radiologists the semi-quantitative evaluation of the sharpness of structure contours (an MTF alternative), the image noise, and the detectability of objects on clinical CT images. We also discuss the limitations of semi-quantitative evaluation methods.

#### TABLE OF CONTENTS/OUTLINE

1. Introduction: a) Importance of semiquantitative evaluation of clinical images b) Limitations of general physical evaluations 2. Evaluation of the contour sharpness on clinical images a) MTF measurements using the blur of the edge profile curve on CT images b) Evaluation of the contour sharpness using the power spectrum 3. Evaluation of the noise characteristics of clinical CT images a) NPS measurement of flat areas without texture b) NPS measurement of non-flat textured areas 4. d'NPW: Detectability index measurements 5. Preconditions / limitations and estimation accuracy

Printed on: 02/07/23



## Abstract Archives of the RSNA, 2022

PHEE-12

### Understanding the Dosimetric Effect of Contrast Agents on External Beam Radiation Therapy

Sunday, Nov. 27 8:00AM - 9:00AM Room: Learning Center - PH

#### Participants

Zhou Wang, PhD, (*Presenter*) Nothing to Disclose

#### TEACHING POINTS

In radiation therapy (RT), contrast agents (CA) are used in CT simulation during treatment planning for better target/organ delineation. This educational exhibit demonstrates the different dominant photon interaction mechanisms between kV (CT) and MV (RT) photons and CA. Due to the K-edge enhanced photoelectric effect of CA in CT, CA's CT number (HU) can be misrepresented in MV beam dose computation by an exaggerated relative electron density. CA is not typically used during RT delivery, and the difference is accounted for by overriding the HU of CA in treatment plans to tissue equivalent (e.g. 0 HU). Image-guided radiation therapy (IGRT) using on-board cone-beam CT (CBCT) is common in RT and has potential for use in adaptive radiation therapy (ART). There is interest in using CA during CBCT for IGRT and/or ART, raising the question of the dosimetric effect of CA on RT delivery following CBCT with CA. Clinical cases recomputed with different levels of overridden HU are presented to understand the dosimetric effect caused by CA during RT.

#### TABLE OF CONTENTS/OUTLINE

1) CA in CT simulation and HU value overridden in RT planning. 2) IGRT/ART and the use of CA in CBCT. 3) Difference in photon interactions - kV CBCT vs. MV RT beams. 4) Effect by HU of CA enhanced perirectal hydrogel spacer (e.g. SpaceOAR Vue) in prostate RT. 5) Recomputed IV/oral contrast clinical cases demonstrating the potential dosimetric effect when treating patient receiving CBCT CA imaging.

Printed on: 02/07/23



## Abstract Archives of the RSNA, 2022

PHEE-13

### Suggestion For The Dose Reduction of The Tomosynthesis Imaging By Using the Generated Interpolation Image Based On the Deep Learning

Sunday, Nov. 27 8:00AM - 9:00AM Room: Learning Center - PH

#### Participants

Ryohei Fukui, PhD, (*Presenter*) Nothing to Disclose

#### TEACHING POINTS

Tomosynthesis is the 3-dimensional imaging technique used for the general X-ray and the mammography. The tomosynthesis imaging requires multiple projection images obtained from different angles. Although acquiring a large number of projection images improves an image quality of the reconstructed tomosynthesis image, however, a patient dose would be increased. If a precise interpolation image can be created and inserted into the dataset of reduced number of projection images instead of the real projection image, a significant reduction of the patient dose can be achieved. We are able to create a pseudo image easily by using the deep learning technique. The generative adversarial network (GAN) has improved its accuracy. We'll suggest the method for dose reduction by using a generated pseudo interpolation image based on the deep learning in the tomosynthesis. The aim of this exhibit is, 1. to learn the patient dose of the tomosynthesis, 2. to show the outline for generating the pseudo interpolation image by using the GAN, 3. to insert the generated pseudo image in the dataset of real projection images and reconstruct the tomosynthesis image, 4. to explain the problem of the proposed method. We hope that the patient dose would be reduced by our suggestion.

#### TABLE OF CONTENTS/OUTLINE

1. Patient dose of the tomosynthesis, 2. Image generation based on the deep learning. 3. Outline for generating the pseudo interpolation image, 4. Present the generated interpolation images and the reconstructed tomosynthesis image, 5. Dose reduction of the tomosynthesis.

Printed on: 02/07/23



## Abstract Archives of the RSNA, 2022

PHEE-14

### Routine Body Applications of Advanced Gemstone Spectral Imaging: What the Radiologist Need to Know

Sunday, Nov. 27 8:00AM - 9:00AM Room: Learning Center - PH

#### Participants

Shingo Harashima, Tokyo, Japan (*Presenter*) Nothing to Disclose

#### TEACHING POINTS

1) To describe basic principles and various imaging/analyzing techniques of advanced Gemstone Spectral Imaging (GSI); 2) To introduce technological features and optimal imaging option in advanced GSI based on experimental and clinical data; 3) To illustrate routine body applications of advanced GSI by presenting various clinical images.

#### TABLE OF CONTENTS/OUTLINE

1) Basic principles imaging/analyzing techniques. Single-source dual-energy CT with fast kV switching; Virtual monochromatic/material decomposition imaging (VMI/MDI); Spectral HU curve/effective atomic number (Z) analysis. 2) Technological features optimal imaging option. Novel high output x-ray tube/kV mA synchronized switching/iterative deep-learning reconstruction for high-quality imaging/high-precision analysis/reasonable radiation contrast media (CM) dose reduction. 3) Routine body applications. Low-keV VMI (vs. low-kV CT): improved image contrast/reduced CM dose; High-keV VMI: reduced image noise/beam-hardening metallic artifact; Iodine-enhanced MDI: organ perfusion tumor viability assessment/cystic solid mass differentiation; Iodine-suppressed MDI: virtual non-contrast CT; Hydroxyapatite-suppressed MDI: bone marrow edema imaging/calcification-free CT angiography; Fat-enhanced MDI/Spectral HU curve/effective Z: lipid-rich lesion detection; Effective Z: nephrolithiasis composition analysis.

Printed on: 02/07/23



## Abstract Archives of the RSNA, 2022

PHEE-15

### How to Make Full Use of Ultra-High-Resolution CT: the Concepts of Imaging Condition and the Clinical Applications

Sunday, Nov. 27 8:00AM - 9:00AM Room: Learning Center - PH

#### Participants

Yuta Miyamae, RT, Tokyo, Japan (*Presenter*) Nothing to Disclose

#### TEACHING POINTS

•Ultra-high-resolution CT (U-HRCT) can provide high-quality CT images depending on the optimum imaging conditions. Especially, it is important to know the characteristics of the three scan modes and the six focus sizes. •U-HRCT images tend to be increased image noise because of the extension of representable frequency band. Deep learning reconstruction (DLR) effectively reduces image noise while maintaining spatial resolution and low-contrast detectability. However, the image quality should be evaluated by proper methods in order to optimize the exposure dose because the excessive reducing exposure dose may cause unexpected deterioration of image quality. •This exhibition explains how to properly understand the physical characteristics of U-HRCT imaging and utilize high-quality images in clinical practice. In addition, we will review papers on clinical application of U-HRCT and discuss the usefulness of high-resolution images.

#### TABLE OF CONTENTS/OUTLINE

1. Explanation of the physical characteristics of U-HRCT images. The physical characteristics of U-HRCT images will be explained in terms of resolution characteristics for in-plane and z-axis direction, noise characteristics, low-contrast detectability and temporal resolution.
2. Investigation of exposure dose for clinical imaging. The exposure dose at clinical cases is shown about conventional MDCT and U-HRCT imaging.
3. Presentation of clinical U-HRCT images. We report clinical cases that U-HRCT imaging has been useful for the diagnostic imaging and surgical supports.

Printed on: 02/07/23



## Abstract Archives of the RSNA, 2022

PHEE-16

### ACR CT Accreditation Testing and Routine Quality Control for Clinical Photon-Counting Detector CT: Practical Tips and Tricks

Sunday, Nov. 27 8:00AM - 9:00AM Room: Learning Center - PH

#### Awards

##### Certificate of Merit

#### Participants

Michael R. Bruesewitz, RT, Rochester, MN (*Presenter*) Nothing to Disclose

#### TEACHING POINTS

- To explain the unique features of Photon-counting-detector (PCD) CT compared to conventional energy-integrating-detector (EID) CT
- To demonstrate the similarities and differences between PCD-CT and EID-CT for Quality Control (QC) and ACR accreditation
- To describe precautions needed to be taken in phantom and protocol selection for QC testing
- To discuss additional procedures to fully evaluate the performance of PCD-CT

#### TABLE OF CONTENTS/OUTLINE

1. What is PCD and how is it different from the energy integrating detectors (EID) used on commercial CT scanners?
  - a. PCD: Directly convert X-ray into electronic signals, count individual photon and record its energy
  - b. EID: Indirect, 2 stage conversion of X-ray to visible light then to electronic signal. Signal is proportional to total energy deposited, without information on individual photon
2. Similarities and Differences in PCD and EID for ACR and QC testing
  - a. Higher spatial resolution in PCD vs EID
  - b. CT number differences between PCD and EID due to different photon-weighting scheme
  - c. CT number of virtual monoenergetic images (VMI) and its use in QC testing
  - d. Slice thickness wire measurement differences, especially on the high resolution of PCD-CT
3. Protocol and Phantom selection
  - a. Scanning with required Adult and Pediatric ACR protocols to meet specifications
  - b. Obtaining correct CTDI measurements for QC and ACR accreditation
4. Future Directions
  - a. Higher line pair/cm resolution scans
  - b. MTF measurements
  - c. Multi-Energy scans and testing
  - d. Iodine quantification accuracy

Printed on: 02/07/23



## Abstract Archives of the RSNA, 2022

PHEE-17

### Demystifying the Radiation Dose Summary Page in Interventional Fluoroscopy

Sunday, Nov. 27 8:00AM - 9:00AM Room: Learning Center - PH

#### Awards

Identified for RadioGraphics

#### Participants

Anzi Zhao, MS, (*Presenter*) Nothing to Disclose

#### TEACHING POINTS

Interventional fluoroscopic procedures may lead to high radiation dose to the patient, it's paramount to understand the details of radiation exposure of a procedure. The radiation dose summary page generated by the interventional fluoroscope is a form that displays important information about a procedure. It is extremely helpful for clinicians to better understand the details of irradiation events and their imaging acquisition parameters, as well as the total radiation dose of the procedure. After reviewing this exhibit, learners will be able to: 1. Understand the two imaging modes of interventional fluoroscopy. 2. Understand important operating parameters of interventional fluoroscopy. 3. Understand radiation dose metrics in interventional fluoroscopy and how to interpret them on radiation dose summary page.

#### TABLE OF CONTENTS/OUTLINE

1. Review imaging modes of interventional fluoroscopy. 2. Review the operating parameters of interventional fluoroscopy - kV, mA, pulse width, pulse rate, filter, field of view, beam geometry. 3. Review radiation dose metrics in interventional fluoroscopy, including their usage and caveats about indicating of patient dose and associated risks - reference air kerma, DAP, peak skin dose. 4. How these above-mentioned contents are displayed in the radiation dose summary page from two major interventional fluoroscope manufacturers. 5. Review manufacturer specific content in radiation dose summary page.

Printed on: 02/07/23



## Abstract Archives of the RSNA, 2022

PHEE-18

### US and Doppler Artifacts: Real or Pitfall?

Sunday, Nov. 27 8:00AM - 9:00AM Room: Learning Center - PH

#### Participants

Marina Akuri, MD, Marilia, Brazil (*Presenter*) Nothing to Disclose

#### TEACHING POINTS

1. To review and explain the most common ultrasound and Doppler artifacts; 2. To assess the clinical usefulness and downsides of US and Doppler artifacts; 3. To discuss how to emphasize, lessen, and avoid US artifacts and Doppler artifacts

#### TABLE OF CONTENTS/OUTLINE

1. Acoustic enhancement; 2. Acoustic shadowing; 3. Side lobe artifact; 4. Ring down artifact; 5. Reverberation artifact; 6. Anisotropy; 7. Aliasing artifact; 8. Twinkling artifact; 9. Blooming; 10. Color bruit artifact; 11. Comet tail artifact; 12. Mirror image artifact; 13. Beam width artifact; 14. Speed displacement artifact; 15. Hardware-related artifacts

Printed on: 02/07/23



## Abstract Archives of the RSNA, 2022

PHEE-19

### Protocol Management in MRI

Sunday, Nov. 27 8:00AM - 9:00AM Room: Learning Center - PH

#### Participants

Joshua Yung, PhD, Houston, TX (*Presenter*) Nothing to Disclose

#### TEACHING POINTS

Outline MRI protocol management as a continuous quality improvement process with a focus on challenges and methods for protocol standardization across a fleet of scanners and technologists. Understand the need and discuss the steps required for checking technical compliance of an MR acquisition as a quality control metric. Understand the unique challenges in monitoring MR acquisitions for protocol standardization and tools for quantitative assessment.

#### TABLE OF CONTENTS/OUTLINE

1. MRI protocol management and quality assurance a. Consistent execution b. Protocol standardization vs. acquisition standardization c. Applications for MR protocol standardization d. Performance assessments and quality improvements to address deficiencies 2. Measuring MR protocol acquisition compliance a. Relevant parameters and pitfalls b. Processing pipeline c. Example of results dashboard d. Other use cases benefiting from compliance checks 3. Monitoring of MR protocol acquisition performance a. Benchmarking performance for comparison and performance improvement b. Relevant parameters and pitfalls c. Workflow diagram d. Challenges with a large multi-vendor MR fleet e. Example of acquisition report 4. Additional protocol analytics tools a. Scanner and protocol utilization, performance profiles and lifecycle management b. Relating acquisition parameters and image quality for protocol development c. Image quality event reporting by radiologists, clinicians and technologists for feedback as part of the quality improvement process 5. Conclusion

Printed on: 02/07/23



## Abstract Archives of the RSNA, 2022

PHEE-1HC

### Neuroradiology Applications with 7T Magnetom Terra Clinical MRI Scanner. A Single-Center Clinical Experience: Indications and Sequence Parameters

Sunday, Nov. 27 8:00AM - 9:00AM Room: Learning Center - PH

#### Participants

Can Ozutemiz, MD, (*Presenter*) Nothing to Disclose

#### TEACHING POINTS

Point out the indications for the usage of 7T MRI in clinical neuroradiology practice. Provide the sequence parameters we developed for each indication

#### TABLE OF CONTENTS/OUTLINE

7-Tesla Ultra-Highfield Magnetom Terra Clinical MRI Scanner has been recently available for clinical use. Currently, the scanner is only approved for knee and brain imaging with dedicated coils. However, the presets and already built-in sequences within the machine are not optimized for patient care in neuroradiology. At our center, we have been testing healthy volunteers and selected patients to optimize our sequences for each indication. In this abstract, first, we will describe the indications where 7-Tesla MRI could be used. While a routine brain MRI can be performed with this machine, specific indications where high-field MRI can be beneficial will be discussed. These include brain tumor imaging with dynamic susceptibility contrast perfusion, epilepsy focus evaluation, high detail cranial MR angiogram/venogram, multiple sclerosis plaque assessment, pituitary MRI, movement disorder evaluation/deep brain stimulator planning, and vessel wall imaging. With each indication, we will provide a table where we describe the sequence parameters including the sequence name, slice thickness, matrix, field-of-view, slice plane, distance factor, voxel size, and time. Imaging examples for each indication will also be provided. Please visit the Learning Center to also view this presentation in hardcopy format.

Printed on: 02/07/23



## Abstract Archives of the RSNA, 2022

PHEE-2

### Safely Imaging Patients Implanted with MRI Conditional, Non-conditional, and Other Active Devices

Sunday, Nov. 27 8:00AM - 9:00AM Room: Learning Center - PH

#### Awards

Identified for RadioGraphics  
Certificate of Merit

#### Participants

Matthew Harwood, MD, Phoenix, AZ (*Presenter*) Nothing to Disclose

#### TEACHING POINTS

- Review device safety evaluation and patient scheduling processes.
- Demonstrate how to interpret vendor manuals.
- Demonstrate how and why decisions to refuse imaging are made.
- Demonstrate how MRI protocols can be modified for patients with implanted devices without compromising diagnostic ability.
- Discuss relevant background information for the above, such the MRI modes of operation, slew, SAR, and B1+rms

#### TABLE OF CONTENTS/OUTLINE

- Objectives
- Trend in Patients Presenting for MRI with Active Devices
- Overview of Devices, What Precisely Are We Talking About?
- Device Labeling
- MRI Safety Considerations: Torque, Induced Currents, RF Heating, Hearing Damage
- Specific Absorption Rate (SAR)
- B1+rms
- Examples of How to Modify Protocols to Reduce SAR/ B1+rms
- Gradient Slew Rate
- MRI Modes of Operation
- Suggested Device Assessment Strategy
- How to Read Vendor Manuals with Examples
- Scheduling and Evaluation Processes for Implanted Cardiac Devices
- Process Modifications for Non-Conditional Devices and Other Active Devices
- Case 1: MRI Was Requested but Not Performed
- Case 2: MRI Successfully Performed with Process Modifications
- Case 3: MRI Successfully Performed with Process Modifications
- Summary of Important Points

Printed on: 02/07/23



## Abstract Archives of the RSNA, 2022

PHEE-20

### Basic Principles of Contrast Injection Protocols for Computed Tomography: Reintroduction for Clinicians by Simulation Software

Sunday, Nov. 27 8:00AM - 9:00AM Room: Learning Center - PH

#### Participants

Takeshi Nakaura, MD, Kumamoto, Japan (*Presenter*) Nothing to Disclose

#### TEACHING POINTS

For contrast-enhanced computed tomography (CT) and CT angiography, it is necessary to stabilize the contrast enhancement using suitable contrast injection protocols. Furthermore, this protocol requires to be adjusted as CT evolves, and clinicians need to have a basic knowledge of it due to ongoing improvements such as photon-counting CT. The principles of the contrast injection protocols appear to be quite difficult; however, simulation software for contrast effects has been recently released, allowing doctors to use the program to test their understanding of the contrast injection protocol. The goal of this exhibition is to:

1. Demonstrate the fundamental principles of a contrast injection protocol.
2. Show contrast injection protocols and their contrast effects using simulation software under various conditions.

#### TABLE OF CONTENTS/OUTLINE

Table of Contents/Outline

- 1) The simulation of dilution and diffusion of contrast material in vivo
  - Dilution by blood flow
  - Passive diffusion using Fick's law
- 2) When and why does the peak enhancement occur? Simulation about the relationship between the contrast injection duration and enhancement curve
- 3) Patient factors that affect the contrast enhancement
  - Patient body size
  - Cardiac output
  - Others
- 4) How to optimize the contrast injection protocol for various examinations

Printed on: 02/07/23



## Abstract Archives of the RSNA, 2022

PHEE-3

### Artifacts Caused by Left Ventricular Assist Devices in Digital Radiographic and Mammographic Environment

Sunday, Nov. 27 8:00AM - 9:00AM Room: Learning Center - PH

#### Participants

Jill M. Lucas, RT, BA, (*Presenter*) Nothing to Disclose

#### TEACHING POINTS

- Identify electromagnetic interference artifacts in digital radiography and mammography
- Isolation and investigation of artifacts using phantom studies
- Potential reduction of artifacts due to LVAD devices

#### TABLE OF CONTENTS/OUTLINE

The use of left ventricular assist devices (LVAD) has been rapidly growing for patients with advanced heart failure, providing both a bridge-to-transplant and destination therapy. The presence of LVAD devices in clinical radiography and mammography exams have been accompanied by intermittent clinical complaints regarding line artifacts. Patient cases and artifact images were reviewed, from which electromagnetic interference (EMI) was determined to be the cause. Further investigation of two LVAD devices (HeartMate II and HeartMate 3, Abbott Inc.) in radiographic and mammographic environment was performed using phantoms. An appreciable difference was demonstrated in artifact appearance and magnitude depending on the LVAD model, flat panel detector type, and location of the LVAD pump relative to the detector. -Artifact identification; Examples clinical and phantom images will be shown - Variation in artifact appearance with differences in: LVAD model; Image receptor type and manufacturer; Imaging task, projection, and patient body habitus -Challenges; Breast imaging; Chest imaging, especially posteroanterior (PA) chest projection -Solutions: Positioning the patient so that LVAD is as far from image receptor as feasible; About 10 cm in PA chest imaging, or use anteroposterior projection if clinically acceptable; When possible, selecting a digital detector with improved EMI shielding, or utilizing a system with advanced processing for EMI artifact reduction

Printed on: 02/07/23



## Abstract Archives of the RSNA, 2022

PHEE-4

### Radiofrequency Safety in MR Imaging: What Are the Concerns?

Sunday, Nov. 27 8:00AM - 9:00AM Room: Learning Center - PH

#### Participants

Zhongwei Zhang, MD, PhD, St. Louis, MO (*Presenter*) Nothing to Disclose

#### TEACHING POINTS

RF-induced thermal events including heating and burns in patients have become more common, concerns have accounted for more than half of the total adverse events according to FDA MRI-related adverse event reports. The purposes of this Education Exhibit are 1. Overview of RF-induced thermal events and thermal injury root causes analysis; 2. Explain the concept behind RF coils and B1 Field; 3. RF exposure and energy absorption: SAR definitions, types, methods for SAR calculation, factors affecting SAR, SAR reduction, B1+rms, Specific Energy Dose (SED), etc.; 4. Discuss RF heating mechanisms for tissues and implants; 5. Review current regulations and guidelines, RF energy monitoring approaches, and discuss strategies to prevent potential RF-induced thermal events; 6. Since SAR depends on system performance (B0, B1 field, RF transmission, etc), object properties (density, electrical conductivity, size, etc), geometry and patient positioning, and pulse sequences. A hands-on example will be presented to show SAR reduction in clinical protocols.

#### TABLE OF CONTENTS/OUTLINE

1. Introduction; 2. Overview of RF-induced thermal events and thermal injury root causes analysis; 3. RF coils and B1 field; 4. RF exposure and energy absorption; 5. RF heating mechanisms for tissues and implants; 6. RF safety and RF-induced thermal events prevention: emphasis on clinical protocols.

Printed on: 02/07/23



## Abstract Archives of the RSNA, 2022

PHEE-5

### **A Picture Is Worth a Million Convolutions: A Simplified Explanation of Convolutional Neural Networks for Radiologists**

Sunday, Nov. 27 8:00AM - 9:00AM Room: Learning Center - PH

#### **Participants**

Tianyuan Fu, MD, Cleveland, OH (*Presenter*) Nothing to Disclose

#### **TEACHING POINTS**

1) To help radiologists gain a basic understanding of convolutional neural networks (ConvNets) for the purposes of interpreting literature on applications of artificial intelligence (AI), machine learning (ML), and deep learning (DL) in radiology. 2) Describe how ConvNets fit into the paradigm of AI, ML, and DL. 3) Touch on the similarities between ConvNets and biological human vision, and explain what makes ConvNets highly accurate and efficient at analyzing pictures. 4) Define important terminology associated with ConvNet architecture. 5) Explain the process through which ConvNets learn from imaging data with a simple illustration of how a raw image is translated into pixel data, passed as input and processed through the neural network, and translated into one or more outputs. 6) Give an overview of transfer learning and discuss examples of pre-trained ConvNet architectures.

#### **TABLE OF CONTENTS/OUTLINE**

1) Overview of artificial intelligence, machine learning, deep learning, and convolutional neural networks (ConvNets). 2) ConvNets and biological human vision. 3) What makes ConvNets accurate and efficient at image analysis? 4) Translating a raw image into training data for a ConvNet. 5) Describe how ConvNets process image data and in the process learn information stored as weights. 6) Illustrate what a complete ConvNet architecture looks like. 7) Discuss transfer learning and illustrate existing ConvNet architectures including VGG-16, Inception, ResNet, and others. 8) Summary of the essential basics of ConvNets for radiologists who are reading literature on AI and ML/DL applications in radiology.

Printed on: 02/07/23



## Abstract Archives of the RSNA, 2022

PHEE-6

### Emerging Applications of Cone-Beam Computed Tomography in Osseous Structure Assessment: A Pictorial Overview

Sunday, Nov. 27 8:00AM - 9:00AM Room: Learning Center - PH

#### Participants

Hanza Ibad, MBBS, Baltimore, MD (*Presenter*) Nothing to Disclose

#### TEACHING POINTS

1. Flat-panel-detectors-based CBCT allows high-resolution osseous structural assessments. 2. CBCT enables investigation of joints at various motion states and weight-bearing (WB), providing physiological measurements of joints in diseased and non-diseased states. 3. Recently introduced motion compensation algorithms, such as regionally applied auto-focus, have the potential to greatly improve the diagnostic yield of CBCT examinations. 4. Fast and high-resolution CBCT protocols permit temporomandibular joint (TMJ) assessment in closed- and open-mouth states. 5. CBCT enables accurate volumetric cartilage and bone mineral density evaluation of the knee joint complex, TMJ, and various other joints. 6. Long-term outcomes of intraoperative use of CBCT in the orthopedic, oral, and maxillofacial repair of skeletal defects are currently under investigation.

#### TABLE OF CONTENTS/OUTLINE

1. Introduction. 2. Emerging developments in CBCT imaging - WB capabilities, motion artifact compensation algorithms, high-resolution dental protocols, and intraoperative CBCT systems (e.g. C-arms with three-dimensional capability). 3. Use in MSK Imaging - Tibiofemoral joint space width quantification, ankle syndesmosis measurements, valgus hindfoot alignment measurements, and intraoperative fracture and joint reduction aid. 4. Use in Dental Imaging - Volumetric TMJ analysis, fracture assessment and post-repair evaluation, endo- and periodontics. 5. Limitations and prospects.

Printed on: 02/07/23



## Abstract Archives of the RSNA, 2022

PHEE-7

### Photon-Counting CT: Physics of Alternative Detector Approaches, Impacts on Image Quality, and Potential Applications

Sunday, Nov. 27 8:00AM - 9:00AM Room: Learning Center - PH

#### Participants

Paul E. Kinahan, PhD, Seattle, WA (*Presenter*) Co-founder, PET/X LLC

#### TEACHING POINTS

1. There are two established approaches for photon-counting CT detectors using silicon- and cadmium-based detectors, with different physical trade-offs. 2. Photon-counting CT provides both lower noise and a much richer set of spectral (energy) information compared to CT scanners with standard energy-integrating detectors. 3. Photon-counting CT also provides higher image resolution than CT scanners with standard energy-integrating detectors, albeit at a potentially higher cost and complexity. 4. There are several clinical areas that can take advantage of the improved spatial and energy resolution of photon-counting CT systems. 5. Developing appropriate workflows that take advantage of increased information per scan in an efficient manner is an important consideration.

#### TABLE OF CONTENTS/OUTLINE

Review the essential differences between photon-counting and energy-integrating CT systems, with an emphasis on the ability for lower noise and improved spectral (energy) information. Review the two established approaches for photon-counting CT detectors that use silicon- and cadmium-based detectors, with a discussion of the different physical trade-offs. Show how the silicon- and cadmium-based detector designs necessarily lead to improved spatial resolution. Describe the roughly 50-fold increase in raw (sinogram) data generated by a photon-counting CT system and how it may impact clinical workflows. Provide illustrations of where the improved spatial and energy resolution of photon-counting CT systems can lead to improvements in imaging for oncology, cardiovascular, thoracic, musculoskeletal, and head and neck imaging.

Printed on: 02/07/23



## Abstract Archives of the RSNA, 2022

PHEE-8

### Seeing More with Super-Resolution Deep-Learning CT Reconstruction: Principles and Clinical Applications

Sunday, Nov. 27 8:00AM - 9:00AM Room: Learning Center - PH

#### Participants

Yasunori Nagayama, MD, Kumamoto, Japan (*Presenter*) Nothing to Disclose

#### TEACHING POINTS

The acquisition of high-resolution and low-noise CT images is crucial for the detailed evaluation of fine anatomical and pathological structures. Recently, the super-resolution deep-learning-based reconstruction (SR-DLR) utilizing the convolutional neural networks (CNNs) to enhance the spatial resolution and reduce image noise has been clinically available. The purpose of this exhibit is: 1. To understand the basic concept and technical principles of the SR-DLR technique 2. To describe the image characteristics of SR-DLR and compare them with those of filtered back projection (FBP), hybrid iterative reconstruction (IR), model-based IR, and normal-resolution DLR (NR-DLR) 3. To review the impact of SR-DLR on the image quality and object detectability in the clinical examples

#### TABLE OF CONTENTS/OUTLINE

1. CNN-based super-resolution technique 2. Basic concept and technical details of SR-DLR 3. Image properties of SR-DLR: comparisons with FBP, hybrid IR, model-based IR, and NR-DLR algorithms A) Noise property B) Spatial resolution C) Low- and high-contrast object detectability 4. Clinical application of the SR-DLR technique A) Coronary CT for coronary plaque assessments B) Stent imaging C) Lung CT D) Cerebral CT angiogram E) Pediatric CT for the assessment of congenital heart diseases 5. Future directions A) Application to dual-energy CT B) Network training with photon counting CT

Printed on: 02/07/23



## Abstract Archives of the RSNA, 2022

PHEE-9

### Current Status and Future of Personal Dose Management-Necessity for Real-Time Measurement of the Occupational Radiation Dose in Interventional Radiology

Sunday, Nov. 27 8:00AM - 9:00AM Room: Learning Center - PH

#### Participants

Kenshin Hattori, (*Presenter*) Nothing to Disclose

#### TEACHING POINTS

To understand current personal dose management to interventional radiology (IVR) staff. To understand importance of lens dosimeter. To understand the need for real-time measurement of occupational radiation dose in IVR. To compare fundamental characteristics among several occupational real-time dosimeters. To understand the fundamental characteristics of a real-time occupational dosimetry and display system (i3 system). To show the usefulness of the i3 system in occupational dose management for IVR.

#### TABLE OF CONTENTS/OUTLINE

The 2011 ICRP Statement significantly lowered the cataract threshold dose for the eye lens from 8 Gy to 0.5 Gy. Accordingly, dose limits for medical personnel have been lowered in many countries, and in Japan the dose limit has been significantly reduced from 150 mSv per year to an average of 20 mSv per year over a five-year period. Therefore, personal dose management is becoming increasingly important. Currently, glass badges and pocket dosimeters are used for personal dose management for medical staff, but in the future, lens dosimeters and real-time dosimeters may become important. Until now, it has not been possible to determine the time of exposure, but with the use of this real-time dosimeter, it is possible to understand at a glance. The new real-time dosimeters evaluated in this study have sufficient performance for clinical use, especially good angular dependence. These dosimeters will be important in the future.

Printed on: 02/07/23



## Abstract Archives of the RSNA, 2022

ROEE

### Radiation Oncology Education Exhibits

Sunday, Nov. 27 8:00AM - 9:00AM Room: Learning Center - RO

#### Sub-Events

#### ROEE-1 Chemoradiation Complications in the Head and Neck: What the Oncologist Wants to Know

##### Awards

##### Certificate of Merit

##### Participants

Cameron Overfield, MD, Jacksonville, FL (*Presenter*) Nothing to Disclose

##### TEACHING POINTS

1. Radiologists should be aware of current and novel oncologic treatment methods for head and neck cancer. After reviewing this presentation, the audience will understand the basics of the different oncologic treatment modalities for the head and neck. 2. Adverse effects with all treatment modalities may be early or delayed. It is imperative that these effects are recognized on imaging and not mistaken for residual, recurrent, or metastatic disease. The audience will be able to distinguish these entities in the head and neck as it relates to chemoradiation therapy and immunotherapy. 3. Treatment-induced malignancies are an unfortunate, but possible adverse delayed effect. An overview of the multimodality imaging characteristics of treatment-induced malignancies will be discussed.

##### TABLE OF CONTENTS/OUTLINE

1. Introduction 2. Teaching Points and Target Audience 3. Principal Radiation and Systemic Therapies a. Radiation therapy b. Chemotherapy c. Immunotherapy (check-point inhibitors) 4. Early Adverse Effects a. Skin and soft tissue abnormalities b. Mucositis c. Inflammatory responses (salivary gland edema, laryngeal edema, retropharyngeal fluid) 5. Delayed Adverse Effects a. Salivary gland changes b. Thyroid gland injury c. Osseous and Cartilage abnormalities (osteonecrosis of the mandible, laryngeal chondronecrosis, fatty marrow replacement) d. Vasculopathy (accelerated atherosclerotic disease, "carotid blowout") e. Tissue necrosis (brain, cord) f. Cranial neuropathies (optic neuropathy, ototoxicity, facial neuropathy) 6. Treatment-induced Malignancies a. Most common associated neoplasms b. Multimodality imaging characteristics and most common anatomical locations 7. Conclusion

#### ROEE-2 MRI-Guided Pelvic Radiotherapy: A Primer for Radiologists

##### Awards

##### Identified for RadioGraphics

##### Participants

Jim Zhong, MD, Leeds, United Kingdom (*Presenter*) Nothing to Disclose

##### TEACHING POINTS

- Discuss the rationale for Magnetic Resonance Imaging Guided Radiotherapy (MRIgRT), including external beam radiotherapy (EBRT), stereotactic ablative radiotherapy (SABR), brachytherapy, and highlight the current evidence base.
- Describe the current clinical experience of MRI-guided workflow for prostate, cervical and bladder cancer
- Describe translation of clinical workflow onto the Elekta Unity MR-Linac (MRL) and provide examples of treated cases
- Highlight the potential benefits and limitations of adaptive MRIgRT in prostate, cervical and bladder cancer
- Discuss opportunities for the development of biologically driven adapted radiotherapy (ART) using functional MRI sequences (e.g. DWI, DCE-MRI, T1 oxygen enhanced (OE) MRI)

##### TABLE OF CONTENTS/OUTLINE

Computed Tomography (CT) is the standard imaging modality for RT planning however due to poor tissue contrast, accurate delineation of pelvic tumors remains difficult with several limitations, including clear demarcation of tumors or normal structures, which influences dose delivered to surrounding organs. MRI is superior at visualising and staging pelvic malignancies. Using MRI in the therapeutic setting allows for comprehensive anatomic information to improve organ delineation and accurate RT delivery, particularly in the era of hypofractionated RT. The availability of hybrid systems incorporating MRI with a linear accelerator (MRL) offers the opportunity for real-time MRI at each radiotherapy fraction, with the ability of plan adaption while the patient is on the treatment table. This overview highlights the current evidence, workflow and future opportunities that this technology brings for treating pelvic tumors.

#### ROEE-3 Dual Energy Metal Artifact Reduction for Iodine-125 Seed Identification of Prostate Brachytherapy Planning

##### Participants

Chiaki Suzuki, (*Presenter*) Nothing to Disclose

##### TEACHING POINTS

In prostate brachytherapy, creating accurate post-planning dose distributions is important for defining the area to be treated. However, it was occasionally found on CT images that the exact number and location of sources could not be identified due to iodine-125 seed swelling and metal artifacts. In order to solve these problems, high-energy virtual monochromatic images (VMI) of dual-energy computed tomography (DECT) were used for treatment planning in combination with the metal artifact reduction processing technology (single energy metal artifact reduction: SEMER). To estimate iodine-125 seed swelling, the caliber of iodine-125 seed was calculated as the full width at half maximum. The metal artifacts were evaluated using the artifact index. The blooming artifacts were decreased at the higher keV levels. In addition, the SEMAR process markedly reduced the artifact index. As a result, the locations and number of iodine-125 seed were clearly identified in the dose distribution map of the treatment planning using high-energy (200keV) VMI with SEMAR. Reducing the overestimation of the high dose range helps us precisely reproduce the dose distribution near the urethra, which would be effective in reducing the risk of side effects.

#### **TABLE OF CONTENTS/OUTLINE**

1.Clinical problems with conventional CT. 2.Metal artifact reduction processing technology "SEMAR". 3.Blooming artifact reduction using high-energy VMI. 4.Adaptation of high-energy VMI with SEMAR to treatment planning 5.Effect on dose distribution

#### **ROEE-4 Imaging of Radiation Therapy for Lung Cancer**

Participants

Mylene T. Truong, MD, Houston, TX (*Presenter*) Nothing to Disclose

#### **TEACHING POINTS**

In the treatment of patients with lung cancer, radiation therapy is an integral component, using conventional fractionated external-beam or high-precision dose techniques including three-dimensional conformal radiotherapy, stereotactic body radiation therapy, intensity-modulated radiation therapy, and proton therapy. Knowledge of the radiation technique used, radiation treatment plan, expected evolution over time of radiation-induced lung injury and patient specific parameters, such as previous radiotherapy, concurrent chemoradiotherapy, and/or immunotherapy, is important in the interpretation of imaging studies to manage patients. This review discusses factors that affect the development and severity of radiation-induced lung injury and its radiological manifestations with emphasis on the differences between conventional radiation and high precision dose radiotherapy techniques. Complications of radiation therapy include radiation recall pneumonitis, in situ pulmonary artery thrombosis, tumor recurrence and secondary malignancies.

#### **TABLE OF CONTENTS/OUTLINE**

Introduction: 3D-conformal radiation therapy Intensity modulated RT Stereotactic body RT Proton therapy Radiation induced lung injury: Patient specific parameters include age, heavy smoking history, poor performance status, pulmonary fibrosis, previous RT, concurrent chemoradiotherapy and/or immunotherapy. Imaging findings: Timelines for conventional versus SBRT, Acute versus chronic. Complications: Radiation recall pneumonitis, Tumor recurrence, In situ pulmonary artery thrombosis.

#### **ROEE-5 Beware of the Radiation Changes! A Brief Pictorial Review of Post-Radiation Imaging Appearances in Pelvis Malignancies - Our Experience in MRI**

Participants

Mario Zelaya Villafranco, MD, (*Presenter*) Nothing to Disclose

#### **TEACHING POINTS**

Recognize the benefits and usefulness of radiotherapy in the treatment of numerous tumors of the abdominal-pelvic cavity as primary, adjuvant or palliative therapy. Emphasizing the sensitivity of tissues to radiation depends on the rate of cell turnover. The response of different organs to damage depends on the dominant tissue type. We will recognize the different post-radiotherapy appearances in the pelvic organs and tissues by magnetic resonance imaging, and they will be compared with the cases of patients in our institution.

#### **TABLE OF CONTENTS/OUTLINE**

A brief review of post-radiotherapy changes in different pelvic malignancies will be carried out, comparing the current theory on post-radiotherapy changes in different organs and tissues, with the cases obtained in our institution. The pictorial review will include key theory about the main post-radiotherapy changes in the different tissues in MRI, as well as their main complications. Post-radiotherapy changes and their complications in different tissues will be included, such as: uterus and ovaries, urinary bladder, intestines (post-radiation proctitis) and soft and bone tissues (bone marrow changes) and their different appearances exemplified with cases obtained in our institution.

#### **ROEE-6 Diagnosis and Management of Cholangiocarcinoma: Pearls and Pitfalls**

Participants

Zack Nigogosyan, MD, Saint Louis, MO (*Presenter*) Nothing to Disclose

#### **TEACHING POINTS**

1. Review epidemiology of cholangiocarcinoma 2. Review pathophysiology of cholangiocarcinoma 3. Review diagnostic criteria and staging of cholangiocarcinoma 4. Review imaging features to identify cholangiocarcinoma on CT, MRCP, and MRI 5. Evaluate cholangiocarcinoma on imaging post-treatment 6. Review clinical management of cholangiocarcinoma

#### **TABLE OF CONTENTS/OUTLINE**

1. Overview of cholangiocarcinoma based on evidence-based literature including incidence, pathophysiology, and risk factors 2. Discuss imaging methods such as CT, MRCP, and MRI in diagnosing cholangiocarcinoma 3. Review clinical management of cholangiocarcinoma including interventional radiology approaches, medical oncology approaches, and radiation oncology approaches 4. Discuss imaging findings of cholangiocarcinoma on CT and MRI post-treatment 5. Summary

#### **ROEE-7 How Advances in Imaging are Defining the Future of Precision Radiotherapy**

**Awards**

**Identified for RadioGraphics**

Participants

Sandra Baleato Gonzalez, MD, PhD, Santiago de Compostela, Spain (*Presenter*) Nothing to Disclose

#### **TEACHING POINTS**

Imaging has an essential role in radiotherapy (RT) planning. Recent advances in imaging have led to the development of new radiation therapy techniques and image-guided radiotherapy (IGRT). Furthermore, functional and molecular imaging techniques have allowed that tumor evaluation and treatment individualization are not only based on morphological criteria but also on biological tumor characteristics. The aim of this exhibit is: -To review the main biological effects of RT on tumor cells and tumor microenvironment. -To evaluate the importance of imaging in new radiotherapy techniques. -To discuss the contribution of advanced imaging techniques for tumor delineation, prognosis, prediction, and assessment of response/resistance to RT. -To review the future role of artificial intelligence, imaging biomarkers and radio(geno)mics in RT.

#### **TABLE OF CONTENTS/OUTLINE**

-Biological effects of RT on tumor cells and tumor microenvironment and how can imaging evaluate radiation effects. -The importance of imaging in new radiation therapy technologies (including IGRT, intensity-modulated RT, stereotactic body RT and proton beam therapy). -The complementary role of MRI and PET CT for tumor delineation and normal tissue identification. -Functional/molecular imaging techniques and multiparametric imaging in RT. -Precision RT and Imaging: the role of advanced imaging in tumor delineation and delivery, tumor heterogeneity (biologically targeted RT), prognosis, prediction, or assessment of response/resistance to RT. -Future directions in RT: artificial intelligence, imaging biomarkers and radio(geno)mics. -Conclusions

#### **ROEE-8 Solving The Neuroradiology Mystery: Progression, Pseudoprogession, or Radiation Necrosis in Post-treatment Imaging of Gliomas**

Participants

Maguy Farhat, MD, BS, Houston, TX (*Presenter*) Nothing to Disclose

#### **TEACHING POINTS**

Accurate timely diagnosis of treatment response in gliomas is crucial to avoid early inappropriate discontinuation of therapy or unnecessary toxic exposure to a treatment regimen. Pseudoprogession is a radiologic diagnosis defined by transient breakdown of the blood/brain barrier, with new contrast enhancement appearing within 3 months of completion of radiation therapy. Radiation necrosis can occur 3-12 months or even years after radiotherapy completion. Pseudoprogession is more likely to occur in patients with MGMT methylation promotion. Multiparametric imaging, including perfusion imaging and multivoxel MR Spectroscopy improves the ability to differentiate between tumor progression and treatment change. Delayed FDG PET optimizes conspicuity of progressive disease.

#### **TABLE OF CONTENTS/OUTLINE**

Overview of the standard of care approach for gliomas. Review conventional imaging findings of pseudoprogession. Review histologic and conventional imaging findings radiation necrosis and tumor progression. Discussion role of advanced MR sequences to improve confidence in differentiating between treatment changes and progressive tumor, including spectroscopy, perfusion and delayed time point FDG-PET.

Printed on: 02/07/23



## Abstract Archives of the RSNA, 2022

ROEE-1

### Chemoradiation Complications in the Head and Neck: What the Oncologist Wants to Know

Sunday, Nov. 27 8:00AM - 9:00AM Room: Learning Center - RO

#### Awards

Certificate of Merit

#### Participants

Cameron Overfield, MD, Jacksonville, FL (*Presenter*) Nothing to Disclose

#### TEACHING POINTS

1. Radiologists should be aware of current and novel oncologic treatment methods for head and neck cancer. After reviewing this presentation, the audience will understand the basics of the different oncologic treatment modalities for the head and neck. 2. Adverse effects with all treatment modalities may be early or delayed. It is imperative that these effects are recognized on imaging and not mistaken for residual, recurrent, or metastatic disease. The audience will be able to distinguish these entities in the head and neck as it relates to chemoradiation therapy and immunotherapy. 3. Treatment-induced malignancies are an unfortunate, but possible adverse delayed effect. An overview of the multimodality imaging characteristics of treatment-induced malignancies will be discussed.

#### TABLE OF CONTENTS/OUTLINE

1. Introduction 2. Teaching Points and Target Audience 3. Principal Radiation and Systemic Therapies a. Radiation therapy b. Chemotherapy c. Immunotherapy (check-point inhibitors) 4. Early Adverse Effects a. Skin and soft tissue abnormalities b. Mucositis c. Inflammatory responses (salivary gland edema, laryngeal edema, retropharyngeal fluid) 5. Delayed Adverse Effects a. Salivary gland changes b. Thyroid gland injury c. Osseous and Cartilage abnormalities (osteonecrosis of the mandible, laryngeal chondronecrosis, fatty marrow replacement) d. Vasculopathy (accelerated atherosclerotic disease, "carotid blowout") e. Tissue necrosis (brain, cord) f. Cranial neuropathies (optic neuropathy, ototoxicity, facial neuropathy) 6. Treatment-induced Malignancies a. Most common associated neoplasms b. Multimodality imaging characteristics and most common anatomical locations 7. Conclusion

Printed on: 02/07/23



## Abstract Archives of the RSNA, 2022

ROEE-2

### MRI-Guided Pelvic Radiotherapy: A Primer for Radiologists

Sunday, Nov. 27 8:00AM - 9:00AM Room: Learning Center - RO

#### Awards

Identified for RadioGraphics

#### Participants

Jim Zhong, MD, Leeds, United Kingdom (*Presenter*) Nothing to Disclose

#### TEACHING POINTS

- Discuss the rationale for Magnetic Resonance Imaging Guided Radiotherapy (MRIgRT), including external beam radiotherapy (EBRT), stereotactic ablative radiotherapy (SABR), brachytherapy, and highlight the current evidence base.
- Describe the current clinical experience of MRI-guided workflow for prostate, cervical and bladder cancer
- Describe translation of clinical workflow onto the Elekta Unity MR-Linac (MRL) and provide examples of treated cases
- Highlight the potential benefits and limitations of adaptive MRIgRT in prostate, cervical and bladder cancer
- Discuss opportunities for the development of biologically driven adapted radiotherapy (ART) using functional MRI sequences (e.g. DWI, DCE-MRI, T1 oxygen enhanced (OE) MRI)

#### TABLE OF CONTENTS/OUTLINE

Computed Tomography (CT) is the standard imaging modality for RT planning however due to poor tissue contrast, accurate delineation of pelvic tumors remains difficult with several limitations, including clear demarcation of tumors or normal structures, which influences dose delivered to surrounding organs. MRI is superior at visualising and staging pelvic malignancies. Using MRI in the therapeutic setting allows for comprehensive anatomic information to improve organ delineation and accurate RT delivery, particularly in the era of hypofractionated RT. The availability of hybrid systems incorporating MRI with a linear accelerator (MRL) offers the opportunity for real-time MRI at each radiotherapy fraction, with the ability of plan adaption while the patient is on the treatment table. This overview highlights the current evidence, workflow and future opportunities that this technology brings for treating pelvic tumors.

Printed on: 02/07/23

## Abstract Archives of the RSNA, 2022

ROEE-3

### Dual Energy Metal Artifact Reduction for Iodine-125 Seed Identification of Prostate Brachytherapy Planning

Sunday, Nov. 27 8:00AM - 9:00AM Room: Learning Center - RO

#### Participants

Chiaki Suzuki, (*Presenter*) Nothing to Disclose

#### TEACHING POINTS

In prostate brachytherapy, creating accurate post-planning dose distributions is important for defining the area to be treated. However, it was occasionally found on CT images that the exact number and location of sources could not be identified due to iodine-125 seed swelling and metal artifacts. In order to solve these problems, high-energy virtual monochromatic images (VMI) of dual-energy computed tomography (DECT) were used for treatment planning in combination with the metal artifact reduction processing technology (single energy metal artifact reduction: SEMAR). To estimate iodine-125 seed swelling, the caliber of iodine-125 seed was calculated as the full width at half maximum. The metal artifacts were evaluated using the artifact index. The blooming artifacts were decreased at the higher keV levels. In addition, the SEMAR process markedly reduced the artifact index. As a result, the locations and number of iodine-125 seed were clearly identified in the dose distribution map of the treatment planning using high-energy (200keV) VMI with SEMAR. Reducing the overestimation of the high dose range helps us precisely reproduce the dose distribution near the urethra, which would be effective in reducing the risk of side effects.

#### TABLE OF CONTENTS/OUTLINE

1.Clinical problems with conventional CT. 2.Metal artifact reduction processing technology "SEMAR". 3.Blooming artifact reduction using high-energy VMI. 4.Adaption of high-energy VMI with SEMAR to treatment planning 5.Effect on dose distribution

Printed on: 02/07/23



## Abstract Archives of the RSNA, 2022

ROEE-4

### Imaging of Radiation Therapy for Lung Cancer

Sunday, Nov. 27 8:00AM - 9:00AM Room: Learning Center - RO

#### Participants

Mylene T. Truong, MD, Houston, TX (*Presenter*) Nothing to Disclose

#### TEACHING POINTS

In the treatment of patients with lung cancer, radiation therapy is an integral component, using conventional fractionated external-beam or high-precision dose techniques including three-dimensional conformal radiotherapy, stereotactic body radiation therapy, intensity-modulated radiation therapy, and proton therapy. Knowledge of the radiation technique used, radiation treatment plan, expected evolution over time of radiation-induced lung injury and patient specific parameters, such as previous radiotherapy, concurrent chemoradiotherapy, and/or immunotherapy, is important in the interpretation of imaging studies to manage patients. This review discusses factors that affect the development and severity of radiation-induced lung injury and its radiological manifestations with emphasis on the differences between conventional radiation and high precision dose radiotherapy techniques. Complications of radiation therapy include radiation recall pneumonitis, in situ pulmonary artery thrombosis, tumor recurrence and secondary malignancies.

#### TABLE OF CONTENTS/OUTLINE

Introduction: 3D-conformal radiation therapy Intensity modulated RT Stereotactic body RT Proton therapy Radiation induced lung injury: Patient specific parameters include age, heavy smoking history, poor performance status, pulmonary fibrosis, previous RT, concurrent chemoradiotherapy and/or immunotherapy. Imaging findings: Timelines for conventional versus SBRT, Acute versus chronic. Complications: Radiation recall pneumonitis, Tumor recurrence, In situ pulmonary artery thrombosis.

Printed on: 02/07/23



## Abstract Archives of the RSNA, 2022

ROEE-5

### **Beware of the Raditation Changes! A Brief Pictorial Review of Post-Radiation Imaging Appearances in Pelvis Malignancies - Our Experience in MRI**

Sunday, Nov. 27 8:00AM - 9:00AM Room: Learning Center - RO

#### **Participants**

Mario Zelaya Villafranco, MD, (*Presenter*) Nothing to Disclose

#### **TEACHING POINTS**

Recognize the benefits and usefulness of radiotherapy in the treatment of numerous tumors of the abdominal-pelvic cavity as primary, adjuvant or palliative therapy. Emphasizing the sensitivity of tissues to radiation depends on the rate of cell turnover. The response of different organs to damage depends on the dominant tissue type. We will recognize the different post-radiotherapy appearances in the pelvic organs and tissues by magnetic resonance imaging, and they will be compared with the cases of patients in our institution.

#### **TABLE OF CONTENTS/OUTLINE**

A brief review of post-radiotherapy changes in different pelvic malignancies will be carried out, comparing the current theory on post-radiotherapy changes in different organs and tissues, with the cases obtained in our institution. The pictorial review will include key theory about the main post-radiotherapy changes in the different tissues in MRI, as well as their main complications. Post-radiotherapy changes and their complications in different tissues will be included, such as: uterus and ovaries, urinary bladder, intestines (post-radiation proctitis) and soft and bone tissues (bone marrow changes) and their different appearances exemplified with cases obtained in our institution.

Printed on: 02/07/23



## Abstract Archives of the RSNA, 2022

ROEE-6

### Diagnosis and Management of Cholangiocarcinoma: Pearls and Pitfalls

Sunday, Nov. 27 8:00AM - 9:00AM Room: Learning Center - RO

#### Participants

Zack Nigogosyan, MD, Saint Louis, MO (*Presenter*) Nothing to Disclose

#### TEACHING POINTS

1. Review epidemiology of cholangiocarcinoma  
2. Review pathophysiology of cholangiocarcinoma  
3. Review diagnostic criteria and staging of cholangiocarcinoma  
4. Review imaging features to identify cholangiocarcinoma on CT, MRCP, and MRI  
5. Evaluate cholangiocarcinoma on imaging post-treatment  
6. Review clinical management of cholangiocarcinoma

#### TABLE OF CONTENTS/OUTLINE

1. Overview of cholangiocarcinoma based on evidence-based literature including incidence, pathophysiology, and risk factors  
2. Discuss imaging methods such as CT, MRCP, and MRI in diagnosing cholangiocarcinoma  
3. Review clinical management of cholangiocarcinoma including interventional radiology approaches, medical oncology approaches, and radiation oncology approaches  
4. Discuss imaging findings of cholangiocarcinoma on CT and MRI post-treatment  
5. Summary

Printed on: 02/07/23



## Abstract Archives of the RSNA, 2022

ROEE-7

### How Advances in Imaging are Defining the Future of Precision Radiotherapy

Sunday, Nov. 27 8:00AM - 9:00AM Room: Learning Center - RO

#### Awards

Identified for RadioGraphics

#### Participants

Sandra Baleato Gonzalez, MD, PhD, Santiago de Compostela, Spain (*Presenter*) Nothing to Disclose

#### TEACHING POINTS

Imaging has an essential role in radiotherapy (RT) planning. Recent advances in imaging have led to the development of new radiation therapy techniques and image-guided radiotherapy (IGRT). Furthermore, functional and molecular imaging techniques have allowed that tumor evaluation and treatment individualization are not only based on morphological criteria but also on biological tumor characteristics. The aim of this exhibit is: -To review the main biological effects of RT on tumor cells and tumor microenvironment. -To evaluate the importance of imaging in new radiotherapy techniques. -To discuss the contribution of advanced imaging techniques for tumor delineation, prognosis, prediction, and assessment of response/resistance to RT. -To review the future role of artificial intelligence, imaging biomarkers and radio(geno)mics in RT.

#### TABLE OF CONTENTS/OUTLINE

-Biological effects of RT on tumor cells and tumor microenvironment and how can imaging evaluate radiation effects. -The importance of imaging in new radiation therapy technologies (including IGRT, intensity-modulated RT, stereotactic body RT and proton beam therapy). -The complementary role of MRI and PET CT for tumor delineation and normal tissue identification. -Functional/molecular imaging techniques and multiparametric imaging in RT. -Precision RT and Imaging: the role of advanced imaging in tumor delineation and delivery, tumor heterogeneity (biologically targeted RT), prognosis, prediction, or assessment of response/resistance to RT. -Future directions in RT: artificial intelligence, imaging biomarkers and radio(geno)mics. -Conclusions

Printed on: 02/07/23



## Abstract Archives of the RSNA, 2022

ROEE-8

### **Solving The Neuroradiology Mystery: Progression, Pseudoprogession, or Radiation Necrosis in Post-treatment Imaging of Gliomas**

Sunday, Nov. 27 8:00AM - 9:00AM Room: Learning Center - RO

#### **Participants**

Maguy Farhat, MD, BS, Houston, TX (*Presenter*) Nothing to Disclose

#### **TEACHING POINTS**

Accurate timely diagnosis of treatment response in gliomas is crucial to avoid early inappropriate discontinuation of therapy or unnecessary toxic exposure to a treatment regimen. Pseudoprogession is a radiologic diagnosis defined by transient breakdown of the blood/brain barrier, with new contrast enhancement appearing within 3 months of completion of radiation therapy. Radiation necrosis can occur 3-12 months or even years after radiotherapy completion. Pseudoprogession is more likely to occur in patients with MGMT methylation promotion. Multiparametric imaging, including perfusion imaging and multivoxel MR Spectroscopy improves the ability to differentiate between tumor progession and treatment change. Delayed FDG PET optimizes conspicuity of progressive disease.

#### **TABLE OF CONTENTS/OUTLINE**

Overview of the standard of care approach for gliomas. Review conventional imaging findings of pseudoprogession. Review histologic and conventional imaging findings radiation necrosis and tumor progession. Discussion role of advanced MR sequences to improve confidence in differentiating between treatment changes and progressive tumor, including spectroscopy, perfusion and delayed time point FDG-PET.

Printed on: 02/07/23



## Abstract Archives of the RSNA, 2022

VAEE

### Vascular Education Exhibits

Sunday, Nov. 27 8:00AM - 9:00AM Room: Learning Center - VA

#### Sub-Events

#### VAEE-1 Vascular Applications of Photon Counting Detector CT

##### Participants

Prabhakar Rajiah, MD, FRCR, Rochester, MN (*Presenter*) Nothing to Disclose

##### TEACHING POINTS

Photon-counting detector (PCD) CT is a recent technical innovation that uses novel detectors directly converting x-ray photons into electrical signals without the generation of light. In this exhibit, we aim 1. To discuss the physics and principles of PCD CT 2. To review the advantages of PCD CT over conventional energy integrating detector (EID) CT. 3. To illustrate the clinical applications of PCD CT in vascular imaging using multiple case examples

##### TABLE OF CONTENTS/OUTLINE

1. PCD CT TECHNOLOGIES- Single source, Dual-source 2. ADVANTAGES OF PCD-CT a. High spatial resolution b. Multi energy (ME) imaging c. Increased vascular signal d. Decreased electronic noise e. Decreased artifacts f. Lower radiation and contrast doses g. Potential K-edge imaging - Gadolinium + Iodine 3. APPLICATIONS OF PCD CT IN VASCULAR IMAGING WITH CASE EXAMPLES a. Ultra-high resolution- Improved visualization of small vessels (Artery of Adamkiewicz; Flaps including DIEP, fibular; arteries of hand, feet, head), calcified plaques, stents b. High iodine CNR (low-energy VMI's)- Low dose of iodinated contrast, salvage of suboptimal studies c. Decreased artifacts- Calcium blooming, beam hardening, metal d. ME calcium separation- Improved lumen visualization e. ME bone subtraction f. ME lesion characterization g. Vascular perfusion h. Potential for multi-contrast and novel contrast media- e.g. iodine and gadolinium i. Advanced material separation j. Radiation dose reduction- Virtual noncontrast images in multiphase studies, lower noise profile 4. LIMITATIONS, PITFALLS a. Increased data - storage and transfer issues b. Noise reduction in high resolution mode

#### VAEE-10 Applications of 4D Flow MRI from Head to Toe

##### Awards

**Cum Laude**

##### Participants

Prabhakar Rajiah, MD, FRCR, Rochester, MN (*Presenter*) Nothing to Disclose

##### TEACHING POINTS

1. To describe the principles and technique of 4D flow 2. To review the applications of 4D flow from head to toe 3. To illustrate the multi-systemic applications of 4D flow using case examples 4. To review common pitfalls and solutions in the use of 4D flow

##### TABLE OF CONTENTS/OUTLINE

1. 4D FLOW- Physics and principles 2. 4D FLOW PARAMETERS- Feraheme vs Gadolinium, spatial/ temporal resolution, plane, slice thickness, VENC, gating, flip angle 3. DISPLAY- Velocity MIPs, Streamlines, pathlines, vectors 4. ADVANCED PARAMETERS- Shear stress, pressure gradient, pulse wave velocity, turbulent kinetic energy 5. LIMITATIONS 6. ARTIFACTS 7. AI 8. REVIEW AND ILLUSTRATION OF THE FOLLOWING APPLICATIONS OF 4D FLOW FROM HEAD TO TOE A. Neurological - Vein of Galen malformations; Aneurysms- Pre and post procedure; AV malformations; Atherosclerotic stenosis B. Thoracic - Abnormal flow patterns- Novel biomarkers in aortopathies.e.g. bicuspid valve; Aortic dissection- Hemodynamics; Aortic coarctation- collateral blood flow; Vasculitis; Pulmonary hypertension C. Cardiac - Improved workflow in complex congenital heart diseases; Pre-surgical evaluation- E.g. Fontan shunt; Valvular heart disease; Detection of small shunts D. Abdominal - Dissection- False lumen Ejection fraction; Endoleak detection and characterization, type IIa vs IIb ; Mesenteric ischemia- Meal challenge; Portal hemodynamics in cirrhosis- shunting, AP fistula, vascular stenosis, Pre- and post TIPS; Splenic function; Pre transplant evaluation- Vascular anatomy, PV thrombus, portosystemic shunt; Uterine fibroid Pelvic venous congestion E. Peripheral - AV malformation; Lymphatic vessels

#### VAEE-11 US Of the Hemodialysis Patient: Mapping For Surgical And Percutaneous AVF, Grafts, And Postoperative US Evaluation, with Angiographic Correlation

##### Awards

**Certificate of Merit**

**Identified for RadioGraphics**

##### Participants

Kedar Sharbidre, MD, Birmingham, AL (*Presenter*) Nothing to Disclose

##### TEACHING POINTS

Patients with end stage renal disease (ESRD) requiring permanent hemodialysis (HD) access options of surgical creation of an

arteriovenous fistula (sAVF), percutaneous AVF (pAVF) creation, or surgical placement of synthetic arteriovenous graft. Superficial venous anatomy can be highly variable and hence accurate preoperative ultrasound (US) assessment is very important, particularly for pAVF planning. US can also help determine AVF maturity and evaluation for complications to guide management. After reviewing this exhibit, the learner will be able to: 1. Describe a typical US arterial and venous mapping protocol for upper extremity sAVF, pAVF, AVG, and thigh graft placement. 2. Understand postoperative US criteria for sAVF and pAVF maturation 3. Recognize abnormalities that may impede AVF maturation 4. Diagnose complications using the US including focal swelling or fluid collection at the fistula site, arterial steal, aneurysm, pseudoaneurysm, and graft degeneration

#### TABLE OF CONTENTS/OUTLINE

1. Venous and Arterial Anatomy of the Extremities for HD mapping a. Upper extremity arteries b. Upper extremity deep and superficial veins c. Groin arteries and veins for AVG 2. Preoperative vascular mapping a. Upper extremity protocol b. Specific mapping for pAVF c. Groin protocol 3. Postoperative assessment for fistula maturation a. sAVF b. pAVF 4. US assessment of complication with angiographic correlation showing treatment results as appropriate a. Abnormalities that prevent maturation i. stenosis (anastomotic, draining vein, central vein) ii. accessory draining veins b. Graft stenosis c. Thrombosis d. Fluid collections e. Arterial steal f. Pseudoaneurysm g. Graft degeneration.

#### VAEE-12 Thoracic Endovascular Aortic Repair: Past, Present, and Future

Participants

Jonathan Liu, MD, Palo Alto, CA (*Presenter*) Nothing to Disclose

#### TEACHING POINTS

-Knowledge of the nomenclature facilitates communication between radiologists and vascular/cardiothoracic surgeons.- Indications for TEVAR continues to evolve, with expanding indications. The proximal descending thoracic aorta, aortic arch, and even ascending aorta can be repaired endovascularly.- Awareness of the various types of repair will assist in the detection of repair complications.

#### TABLE OF CONTENTS/OUTLINE

I. Introduction/History and path to FDA approvalII. Indication for thoracic endovascular aortic repairIII. Anatomy for endovascular approach a. Aortic arch zones b. Aortic arch typesIV. Historical and contemporary devicesV. Novel techniques a. Petticoat technique b. Snorkel / Periscope technique c. In-situ laser fenestrationVI. Investigational devicesVII. Complications of TEVAR a. Birdbeaking b. Stent-graft induced new entry tear c. Endoleak / gutter leak d. Infection e. Fracture/migrationVIII. Conclusion

#### VAEE-13 Imaging Review and Management Update on Portal Vein Thrombosis

Participants

Maria Garcia, MD, (*Presenter*) Nothing to Disclose

#### TEACHING POINTS

1) Describe the anatomy of the portal vein (PV) and relevant anatomic relationships. 2) Describe the pathophysiology and common risk factors for portal vein thrombosis (PVT). 3) Identify the multimodality imaging features of acute, chronic and iatrogenic portal vein occlusion 4) Identify the role of imaging in diagnosis and management of PVT.

#### TABLE OF CONTENTS/OUTLINE

I. Background. II. Normal/Variant anatomy. III. Overview of PVT pathophysiology, broadly 3 etiologies: 1) Hereditary thrombophilia; 2) Acquired thrombophilia/hypercoagulable states, such as pregnancy and malignancy; 3) Intra-abdominal causes. IV. Definition and clinical manifestations of acute and chronic PVT. V. Imaging features of acute versus chronic PVT. VI. Illustration of PV occlusion: a) Bland thrombus: hematologic disorders, cirrhosis, pancreatitis, portal pyaemia, inflammatory bowel disease, pancreatic malignancy; b) Tumor thrombus: HCC and others such as sarcoma and NET; c) Intervention-related: Surgery/Liver transplant, TIPS stent thrombosis, Portal vein embolization; d) Chronic changes/complications: Cavemous transformation (adults/children), Portal hypertension, Portal biliopathy, Mesenteric ischemia; e) Mimics: Flow artifacts, Hepatic vein/IVC occlusion, Dilated bile duct. VII. Treatment: 1) Medical: Anticoagulation, highlight the reason for differential approach in the presence or absence of cirrhosis; 2) Endovascular: Two main interventions for portal vein recanalization (PVR) a) Thrombectomy +/- thrombolysis, b) PVR-TIPS stent placement. 3) Surgical: Bowel infarction or contraindication to thrombolytic therapy. VIII. Take home points.

#### VAEE-14 Ultrasound Evaluation of AV Fistulas for Hemodialysis: A Hands-on Approach

Participants

Mikel Elgezabal, MD, Barrika, Spain (*Presenter*) Nothing to Disclose

#### TEACHING POINTS

- To understand the importance of Chronic Kidney Disease in healthcare.- To make the reader confident to perform ultrasound on patients with AV fistulas as a vascular access for hemodialysis, using a simple step-by-step approach that can cover all the bases for a satisfactory evaluation.

#### TABLE OF CONTENTS/OUTLINE

Chronic Kidney Disease (CKD) Contemporary significance of CKD: definition, prevalence, burden. Ultrasound findings of CKD. Therapeutic options for CKD: Renal Replacement Therapy with a focus on hemodialysis. Arteriovenous Fistulas for Hemodialysis What is an AV fistula? A quick, basic review slide to get the reader up to speed. The upper extremity: vascular anatomy: We include labeled anatomy images of the upper limb arterial and venous system and discuss key anatomical landmarks along with their corresponding clinical significance. Planning an AV fistula: pre-surgical ultrasound. Types of AVF: Native vs. prosthetic, typical locations. Sonographic assessment of an AV fistula Before scanning: clinical assessment, patient position, ultrasound probe choice. Ultrasound exam. Components of an AV fistula and individual sonographic properties of each component. The afferent artery, the anastomosis, the efferent vein. Properties of the mature and healthy AV Fistula: ready to needle! Complications: We detail key diagnostic points of each one of the most common complications and support them with clinical cases and images from our institution.

#### VAEE-15 How Will 320-Row Multi Detector CT Change the Diagnosis of Pelvic Venous Congestion Syndrome?

Participants  
Kazuto Sakamoto, RT, (*Presenter*) Nothing to Disclose

#### **TEACHING POINTS**

The purpose of this exhibit is: 1. Pelvic venous congestion syndrome (PVC) is a cause of chronic pelvic pain in female patients. The cause of PVC is structural. It is the regurgitation of the gonadal vein with venous valve insufficiency due to compression have the left renal vein or the iliac vein. 2. PVC may not be accompanied by pelvic pain, and imaging by US or MRI may be useful. The most important reason for this is that US and MRI can determine the direction of blood flow in the refluxed gonadal vein. 3. The 320-row multi detector CT can acquire cine images up to 160 mm wide with 4D imaging. In addition, 4DCT angiography cine images can be used to evaluate gonadal vein reflux.

#### **TABLE OF CONTENTS/OUTLINE**

Major headings: 1. Describe PVC. 2. Usefulness of 4DCT angiography in PVC diagnosis.- 4DCT angiography cine imaging to evaluate gonadal vein reflux. - In all cases, the findings were comparable to catheter-based angiography. 3. Supporting imaging with 3DCT angiography in PVC revascularization. - Supporting imaging with 3DCT is expected to reduce the total radiation dose to the patient. - In other words, a reduction in fluoroscopic time due to shorter operative time. 4. Quantification of edema by CT imaging in determining treatment efficacy.- CT images are a useful tool for convenient volumetric measurements. - Volumetric evaluation is important to determine the efficacy of treatment of PVC with lower extremity edema.

#### **VAEE-16 Arteriovenous Fistula For Hemodialysis: A Thorough Analysis**

Participants  
Sofia Maksoud, MD, Sao Paulo, Brazil (*Presenter*) Nothing to Disclose

#### **TEACHING POINTS**

- The arteriovenous fistula is created from the anastomosis between native artery and vein, with the aim of providing chronic access for hemodialysis in patients with end-stage renal disease until they can receive a kidney transplant.- The most used are the anastomosis of the radial artery with the cephalic vein or brachial artery with the cephalic vein.- The structure created must be accessible and have the blood flow necessary to be cannulated repeatedly and thus allow adequate dialysis. For this, the minimum internal calibers must be 0.2 cm for the artery and 0.25 cm for the vein.- After the creation of the fistula, the blood vessels involved undergo a maturation process that can be evaluated by means of a color Doppler ultrasound study. The flow volume, calculated through the formula of the average velocity times the diameter of the opening, reaching 600 mL/minute is a parameter commonly associated with maturation.- Complications of arteriovenous fistula include failure of maturation, stenotic vascular lesions, thrombosis, aneurysms or pseudoaneurysms, and infection.

#### **TABLE OF CONTENTS/OUTLINE**

- Review expected ultrasound findings expected for a patent arteriovenous fistula for hemodialysis.- Evaluate the most common complications and their presentation on ultrasound.

#### **VAEE-17 Beware of The Dislodged Devices**

Participants  
Marcus Nascimento, MD, Sao Paulo, Brazil (*Presenter*) Fellow, Hospital Israelita Albert Einstein

#### **TEACHING POINTS**

The purpose of this exhibit is:- To briefly review and recognize some of the cardiovascular devices used in patient care.- To describe how to recognize and define the position of some devices in different imaging modalities.- Show examples of medical dislodged devices or with some kind of complication.

#### **TABLE OF CONTENTS/OUTLINE**

1) Basic anatomy of the chest and cardiovascular system. 2) Types and function of the devices 3) How the devices are represented in the different imaging modalities and their primary function in patient care. 4) Key Imaging Findings that define their malpositioning and/or deformation. 5) Take home messages.

#### **VAEE-18 Does Size Really Matter? Imaging in Visceral Artery Aneurysms**

Participants  
Tomas Lacerda, MD, Sao Paulo, Brazil (*Presenter*) Nothing to Disclose

#### **TEACHING POINTS**

The purpose of this exhibition is to review the most recent guideline on visceral aneurysms and its recommendations towards treatment indications and modalities. Also, discuss most common sites for visceral aneurysms, symptoms and complications and imaging findings in diagnostic and post treatment situations.

#### **TABLE OF CONTENTS/OUTLINE**

Understand the most common sites for visceral aneurysms and its potential complications; Reviewing the latest guideline on visceral aneurysms, its recommendations towards when and how to repair; Illustrate through a series of radiological cases the most common sites, findings on possible complications and imaging during and after endovascular repair.

#### **VAEE-19 Portal Vein Thrombosis: What a Radiologist Needs to Know In the Era of the Baveno VII Consensus Recommendations**

#### **Awards Identified for RadioGraphics**

Participants  
Alessandro Bozzato, MD, (*Presenter*) Nothing to Disclose

## TEACHING POINTS

-Illustrate the recommended standardized nomenclature for the description of portal vein thrombosis (PVT) and portal cavernoma, according to the Baveno VII consensus definitions. -Describe diagnosis and management of acute and chronic PVT in absence and presence of cirrhosis.

## TABLE OF CONTENTS/OUTLINE

Introduction PVT is characterized by the presence of a bland thrombus in the portal vein trunk and its branches. It occurs in non-cirrhotic patients, and, less frequently, in cirrhotic patients. Imaging methods should be used to diagnose PVT (ruling out malignant portal vein obstruction) and assess its extension. Recommended standardized nomenclature- Show typical imaging features illustrating the nomenclature: • Time course (acute and chronic thrombosis) • Percent occlusion of main portal vein (completely occlusive, partially occlusive, minimally occlusive thrombosis, and cavernous transformation) • Response to treatment or interval change (progressive, stable and regressive thrombosis) Portal vein thrombosis and portal cavernoma in the absence of cirrhosis- Illustrate acute and chronic PVT in the absence of cirrhosis: • Diagnosis and follow-up • Interventional management (image-guided interventions, thrombolysis, transjugular intrahepatic portosystemic shunt (TIPS), and other percutaneous recanalizations) Portal vein thrombosis and cirrhosis- Illustrate PVT in cirrhosis: • Diagnosis and follow-up • Interventional management ((TIPS), and other percutaneous recanalizations)

## VAEE-2 Multimodality Imaging of Portal Vein Thrombosis: Diagnosis and Influence on Clinical Management

Participants

Catherine Naidoo, MBBS, FRANZCR, Randwick, Australia (*Presenter*) Nothing to Disclose

## TEACHING POINTS

1- Learn how to diagnose portal vein thrombosis (PVT) on different imaging modalities 2- Determine the etiology (Benign vs. Malignant), onset (Acute vs. Chronic), and extent of PVT 3- Assess the acute and chronic complications of PVT

## TABLE OF CONTENTS/OUTLINE

Thrombosis of the portal venous system is a frequent and potentially life-threatening condition that can take place in a number of different clinical settings including liver cirrhosis, hepatocellular carcinoma, other solid tumors, abdominal septic foci, acute pancreatitis, hematological malignancies, and congenital or acquired prothrombotic disorders. Imaging plays a pivotal role in the clinical decision-making process in patients with thrombosis of the portal venous system. In this article, we will discuss the familiar and uncommon imaging findings of PVT at the ultrasound, contrast-enhanced ultrasound, CT, and MRI and the role of imaging in determining the underlying etiology (benign versus malignant) and onset (acute versus chronic). We will learn the available classification systems that provide a treatment-oriented assessment of PVT extension and degree of occlusion. We will recognize the acute and chronic morphologic changes of the liver parenchyma, such as nodular regenerative hyperplasia, secondary to PVT nodular regenerative hyperplasia. We will also review the complications of PVT such as portal biliopathy.

## VAEE-20 Ultrasound of Peripheral Arteries: An Update on Technique, Protocols, Interpretation and Applications

Participants

Prabhakar Rajiah, MD, FRCR, Rochester, MN (*Presenter*) Nothing to Disclose

## TEACHING POINTS

1. To review the indications of ultrasound (USG) in peripheral arterial diseases 2. To review the normal and abnormal flow patterns in peripheral arteries 3. To illustrate imaging appearances of common peripheral arterial abnormalities.

## TABLE OF CONTENTS/OUTLINE

1. INTRODUCTION 2. ANATOMY 3. ROLE, ADVANTAGES, LIMITATIONS OF USG- Comparison with other invasive and non-invasive modalities 4. TECHNICAL REQUIREMENTS- B-mode, doppler, color, power 5. OPTIMIZATION OF TECHNICAL PARAMETERS 6. TRANSDUCER AND PATIENT POSITION 6. NORMAL VESSEL- Normal caliber, laminar flow 7. WAVEFORMS - Normal - Triphasic or biphasic with sharp systolic upstroke; -Abnormal - Monophasic or biphasic without sharp systolic upstroke 8. VELOCITIES- Normal and abnormal at, proximal and distal to stenosis; grading of stenosis 9. ILLUSTRATION OF THE FOLLOWING ABNORMALITIES WITH SAMPLE CASES A. Atherosclerosis, native vessels- Indications; Diagnostic approach; Screening localization; Criteria for different grades of stenosis- Velocities, waveforms, pre and post stenotic vessels; Collaterals; Pitfalls, misses B. Bypass graft evaluation C. Stent evaluation D. Aneurysms E. Pseudoaneurysms- To-and-fro flow, guidance for management F. Popliteal artery entrapment G. Dissection H. Arteritis I. AV Fistula- High-velocity turbulent flow between vessels; low resistance proximal arterial waveforms; High, arterialized venous flow; vibration artifacts in perivascular tissues. J. Post-surgical/interventional follow-up- Grafts, thrombin injection

## VAEE-21HC Evaluation of Lower Extremity Peripheral Arterial Disease Using Ultrasonography: What Everyone Should Know

Participants

Omair Ali, BS, (*Presenter*) Nothing to Disclose

## TEACHING POINTS

1. To provide a clinical overview of peripheral arterial disease (PAD) of the lower extremities and its sequelae. 2. To examine the role of noninvasive imaging in the assessment of PAD 3. To provide a pictorial-based review of ultrasound (US) modalities and their utility in noninvasive evaluation of PAD 4. To discuss the role of US in unique clinical circumstances related to PAD

## TABLE OF CONTENTS/OUTLINE

1) Introduction to PAD a) Natural history 2) Overview of Noninvasive evaluation of PAD a) Indications for US evaluation of PAD 3) Arterial ultrasonography (US) of PAD a) Overview and limitations of US techniques for arterial imaging b) Arterial mapping by segment i) Aortoiliac ii) Femoropopliteal iii) Infrapopliteal c) B-mode Doppler i) Visualization of vascular anatomy ii) Abnormal findings (plaque, stenosis, calcification) Spectral Doppler i) Purpose: characterization of blood flow based on waveforms ii) Peak systolic velocity (PSV) and PSV ratio iii) Abnormal findings (spectral broadening, increase in PSV, monophasicity e) Color Doppler i)

Assessment of direction and speed of flow ii) Abnormal findings (aliasing, color bruit) f) Power Doppler i) Examining flow based on quantity of red blood cells ii) Abnormal findings (decreased flow, occlusion) g) Contrast-enhanced US i) Assessment of perfusion ii) Abnormal findings h) Pedal acceleration time i) Role in evaluating CLI and predicting limb salvage 4) Special considerations for US evaluation of PAD a) Chronic total occlusion b) Critical limb ischemia c) Calcified PAD d) Post-revascularization surveillance Please visit the Learning Center to also view this presentation in hardcopy format.

## **VAEE-22 Doppler US of Lower Limb Venous Insufficiency Made Simple**

Participants

Montserrat Torrent, (*Presenter*) Nothing to Disclose

### **TEACHING POINTS**

Chronic venous insufficiency of the lower limbs is very prevalent. Duplex ultrasound has the ability to demonstrate venous hemodynamic reflux, that why it become the method of choice to study this condition. We review the venous anatomy of the lower limbs, the pathophysiology of chronic venous insufficiency and explain the protocol for carrying out Duplex studies. These include venous mapping and a thorough evaluation of the superficial veins to identify all of the patterns of incompetence. We also evaluate patients with other treatment techniques such as thermal ablation, sclerotherapy. Therefore we can conclude the complications or the success of the applied procedure.

### **TABLE OF CONTENTS/OUTLINE**

Learning objectives: ? Review the venous anatomy of the lower limbs, the pathophysiology of chronic venous insufficiency and explain the protocol for carrying out Duplex studies? Perform venous mapping with the patterns of incompetence.? Evaluate patients after treatment to identify success, complications and recurrence.

## **VAEE-23 Abernethy Malformation: What You Need to Know**

Participants

Alexandra Panyukova, MD, (*Presenter*) Nothing to Disclose

### **TEACHING POINTS**

- To review the normal anatomy and embryology of the portal system. - To learn about Abernethy malformation - a rare congenital vascular pathology. - To illustrate the role of different imaging methods in diagnosis of Abernethy malformation. - To highlight the main points in radiology reports, which influence further patient evaluation and treatment.

### **TABLE OF CONTENTS/OUTLINE**

1. Introduction 2. Anatomy review 3. Embryology: portal venous system development 4. Abernethy malformation 4.1. Definition 4.2. Classification 4.3. Clinical manifestations, complications 4.4. Diagnostic methods 4.5. What else should you look for? 4.6. Follow-up and treatment 5. Take home points 6. Recommended bibliography

## **VAEE-24 Imaging in Hemodialysis: Role of Ultrasound in Assessment and Surveillance of Grafts and Fistulas**

### **Awards**

#### **Certificate of Merit**

Participants

Irene Dixe de Oliveira Santo, MD, New Haven, CT (*Presenter*) Nothing to Disclose

### **TEACHING POINTS**

Ultrasound (US) plays a major role in the assessment and surveillance of hemodialysis (HD) fistulas and grafts. Furthermore, it is essential in the evaluation of arterial and venous circulation before access creation. The complication rate of HD access is relatively high, and US is crucial for the accurate diagnosis of the different complications. (1) Discuss the role of US in preoperative planning; (2) Provide a step-by-step algorithm in the sonographic evaluation of the HD access; (3) Review the sonographic characteristic features of common and rare complications of HD access; (4) Briefly discuss the role of interventional radiology in the management of HD complications.

### **TABLE OF CONTENTS/OUTLINE**

Preoperative planning: discuss anatomy, major criteria for suitability of vascular system in creation of HD access Discuss various types of HD access based on access location, and operative techniques (graft versus fistula) Provide optimal protocol and diagnostic criteria for HD access assessment Review sonographic findings of uncomplicated HD access Discuss algorithmic approach to assess HD access complications using US Doppler (thrombosis, stenosis, ischemic steal syndrome, aneurysms and pseudoaneurysms formation, bleeding, hematoma and infection, and structural problems) Briefly discuss causes of nonmaturing fistula Review management options for HD complications and findings post-intervention

## **VAEE-25 Assessment of Tissue Vascularity: Non-contrast Micro-vascular Flow Imaging in Assessment of Vascularity, With Contrast and/or Pathological Correlation - Expanding the Horizons**

Participants

Muhammad Aziz, MBBS, Birmingham, AL (*Presenter*) Former Stockholder, Sorrento Therapeutics, Inc

### **TEACHING POINTS**

Ultrasound vascular imaging with color and power Doppler is an important tool in the assessment of various disease processes, with assessment of blood flow in organs, neoplasms and vessels; from infarction and ischemia to hyperemia, and is used in almost all ultrasound examinations. Recent development of small vessel, slow velocity flow without the utilization of contrast agents is more sensitive to microvasculature on comparison with color, Power and spectral Doppler - termed as "MicroVascular Flow Imaging (MVFI)". This results in a decreased need for follow-up contrast examinations (US, CT, MR) in many conditions. After reviewing this exhibit, the learner will be able to: 1 - Review the basics of physics of noncontrast MVFI. 2 - Understand the various applications of this novel technique in different adult and pediatric conditions - including benign and malignant conditions. 3 - Recognize different acute applications of MVFI; including in testes and gallbladder. 4 - Understand the potential future applications of MVFI. 5 - Review and diagnose many case examples of various conditions; including benign and malignant liver lesions, acute gallbladder and

testicular pathologies, benign and malignant renal lesions, role of MVFI in pre- and postsurgical cases.6- Describe the limitations of this technique

#### TABLE OF CONTENTS/OUTLINE

1 - Introduction to MVFI a. Background b. Physics of MVFI2 - Clinical Applications of US MVFI in Adults a. Liver b. Gallbladder c. Kidneys d. Superficial Organs - Testes, Lymph Nodes e. Vessel Disease3 - Clinical Applications of US MVFI in Pediatrics a. Liver b. Trauma4 - Future Potential and Direction5 - Limitations6 - Conclusion

#### VAEE-26 Imaging of Rare Intravascular Tumors and Tumorlike Lesions

Participants

Duygu Ekizalioglu, MD, (*Presenter*) Nothing to Disclose

#### TEACHING POINTS

- To overview rare miscellaneous intravascular tumors and tumorlike lesions that may pose difficulties for diagnosis. - To emphasize the imaging findings (US, CT, MRI, PET/CT) of rare neoplastic and nonneoplastic intravascular lesions. - To review the histopathological findings of neoplastic and nonneoplastic intravascular lesions.

#### TABLE OF CONTENTS/OUTLINE

Introduction. Overview of intravascular neoplastic lesions Primary Benign: Internal jugular vein hemangioma Primary Malign: Primary leiomyosarcoma of inferior vena cava (IVC) Secondary Benign: Renal angiomyolipoma extending into the renal vein Secondary Malign (Tumor Thrombus): Renal Ewing sarcoma with tumor thrombus in renal vein and IVC, Renal cell carcinoma with tumor thrombus in renal vein and IVC, Uterine sarcoma with tumor thrombus in ovarian vein and IVC, Hepatocellular carcinoma with tumor thrombus in IVC, Colon cancer liver metastasis and tumor thrombus in IVC. Overview of intravascular nonneoplastic lesions: Aortic hydatid cyst, Pyogenic granuloma of angular vein, Bland thrombus (associated with COVID-19). Review of imaging findings on US, CT, MRI, PET/CT of rare intravascular tumors and tumorlike lesions. Description of histopathological findings. Differential diagnostic algorithm for intravascular neoplastic and nonneoplastic lesions. Conclusion. References.

#### VAEE-3 A Practical Approach to the Interpretation of Arterial Waveforms on Duplex Doppler, Made Ridiculously Simple

Participants

Dana Galvan, MD, Albuquerque, NM (*Presenter*) Nothing to Disclose

#### TEACHING POINTS

Doppler US is the first line imaging modality for the evaluation of the vascular system. Various pathological processes affect vasculature and result in the characteristic appearance of the waveforms allowing to recognize the abnormality and correctly diagnose the disease process independent of its location. 1. Review normal appearance of the arterial and venous waveforms and underlying physiology 2. Discuss pathophysiology and waveform appearance of various pathological conditions affecting the vascular system 3. Discuss treatment management options and post treatment restoration of waveform pattern.

#### TABLE OF CONTENTS/OUTLINE

Outline: 1. Review normal arterial and venous waveform appearance on US and its physiology (dependence of waveform appearance on the cardiac cycle, principles of Doppler physics and Doppler technique of waveform acquisition) 2. Discuss correlation between the vascular process pathophysiology and waveform appearance (waveform pattern in the following conditions: stenosis (pre, at, and post stenosis, compensatory flow), thrombosis (proximal to occlusion, flow reversal), reconstitution (collateral waveform pattern), pseudoaneurysm, arteriovenous fistula, dissection, vascular torsion, neovascularity) 3. Discuss management options (stent, angioplasty, bypass graft) and post-treatment waveform appearance (flow restoration).

#### VAEE-4 Diagnosis and Treatment of Iliac Artery Aneurysms: From A to Z

Participants

Ruben Guerrero Vara, MD, (*Presenter*) Nothing to Disclose

#### TEACHING POINTS

1) To review the the main features of iliac artery aneurysms (IAA). 2) To highlight the importance of maintaining patency of the hypogastric artery during repair of IAA. 3) To describe the endovascular treatment options to preserve the hypogastric artery during endovascular repair.

#### TABLE OF CONTENTS/OUTLINE

1) IAA: definition and characteristics. 2) IAA: surgical indications 3) Description of the endovascular techniques developed to preserve internal iliac flow: Iliac branch device (IBD), bell bottom technique (BBT), sandwich technique (ST) and banana technique (BT). 4) Application of each procedure and anatomic limitations. 5) Potential complications of these methods. 6) Depiction of examples of every endovascular technique including preoperative CTA images, schematic illustrations, DSA images before and after stent implantation and control CTA pictures after the procedure. 7) Conclusions

#### VAEE-5 Vascular Ultrasound: A Primer on Arterial and Venous Doppler Waveforms, Interpretation, and Standardized Nomenclature

**Awards**

**Certificate of Merit**

Participants

Min Gyu Noh, MD, Seattle, WA (*Presenter*) Nothing to Disclose

#### TEACHING POINTS

1. Learn standard terminology for describing arterial and venous waveforms according to the consensus statement from the Society for Vascular Medicine (SVM) and the Society for Vascular Ultrasound (SVU)2. Recognize normal arterial and venous waveforms and

understand how physiologic and disease states can alter waveforms<sup>3</sup>. Review pearls and pitfalls of Doppler optimization<sup>4</sup>. Case-based review of normal physiologic and pathologic vascular ultrasound cases

#### TABLE OF CONTENTS/OUTLINE

1) Learn standardized terminology for describing arterial waveforms according to SVM and SVU:a. Flow directionb. Phasicityc. Resistance2) Review standardized terminology for describing venous waveforms according to SVM and SVU:a. Flow directionb. Flow patternc. Spontaneity3) Recognize normal and abnormal arterial waveforms and velocities based on anatomic function, with a focus on:a. Peripheral arteriesb. Mesenteric and renal arteriesd. Common carotid, internal carotid, and external carotid arteries4) Recognize normal and abnormal venous waveforms based on anatomic function:a. Deep and superficial peripheral venous structures (upper and lower extremities)b. Central veins (upper extremities)c. Abdominal veins (IVC, iliac, renal, hepatoportal)5) Pearls and pitfalls of Doppler optimization:a. PRFb. Wall filterc. Angle of insonation6) Utilize understanding of arterial and venous vascular physiology to review normal physiologic and pathologic vascular ultrasound cases, including:a. Mesenteric artery stenosisb. Deep vein thrombosisc. ICA/ECA stenosisd. Subclavian vein thrombosis and steal. Vertebral artery stenosisf. Peripheral artery stenosis

#### VAEE-6 Demystifying Ultrasound of the Standard Dialysis Fistula

Participants  
Sagar Desai, DO, Mountain Top, PA (*Presenter*) Nothing to Disclose

#### TEACHING POINTS

Describe the pathophysiology and anatomy of an arteriovenous dialysis fistula Discuss preoperative arterial and venous imaging required to support the high flow state Understand sonographic features indicative of a mature fistula Review the approach to a delayed or non-maturing fistula Describe the sonographic appearing of acute and chronic complications of dialysis fistulas with confirmatory angiography and treatment

#### TABLE OF CONTENTS/OUTLINE

Kidney Disease Outcomes Quality Initiative (KDOQI) Basic KDOQI guidelines pertaining to arteriovenous fistula (AVF) creation and management Pre-operative ultrasound planning Morphologic and functional data Arteries: course, relationship to vein, diameter, plaque, intimal medial thickness, waveforms and velocity Veins: anatomy, patency of superficial and deep veins including: depth, diameter, length, anomalies, fibrotic segments and waveforms Patency and perfusion of the palmar arch Examples of adequate and inadequate vessels US assessment of AVF maturity Physiologic requirements for adequate dialysis Evaluation of a delayed or non maturing fistula Ultrasound assessment Poor location (depth) Large or increased number of draining veins Stenosis Arterial inflow Venous outflow The interventional radiologist's approach Fundamental steps of a 'fistulogram' procedure Angiographic correlates and treatments to augment AVF maturation Complications: early and late Hematoma Thrombosis Stenosis (arterial and venous) Infection Aneurysm or pseudoaneurysm Steal Syndrome High output cardiac failure

#### VAEE-8 What to Do When the Aortic Aneurysm Keeps Growing After Endovascular Repair: An Illustrated Review of the CT Angiography Protocol and Most Important Complications of the Endoleaks

Participants  
Estefania Gallego Diaz, MD, MD, Mexico City, Mexico (*Presenter*) Nothing to Disclose

#### TEACHING POINTS

- The endoleak is defined as blood leak in an aneurysm sac excluded by stent-graft following endovascular aneurysm repair (EVAR), which means, flow outside the stent but into the aneurysm.
- To explain the importance of a timely diagnosis in this group of patients.
- To illustrate the detailed way to do an appropriate report.
- To review the consequences of an endoleak and its implication in morbidity and mortality for the patient.
- To simplify the imaging evaluation in patients with endoleaks.

#### TABLE OF CONTENTS/OUTLINE

1. Introduction. 2. What is an endoleak a. Indications. b. Classification. 3. CTA protocol and technical Recommendations. 4. Follow up. 5. How to report it / Algorithm for evaluation. 6. Which are the consequences of an endoleak a. Complications. b. Prognosis depending on the type of endoleak. 7. Clinical Cases and pictorial review. 8. Conclusions.

#### VAEE-9 Phenotypic Diversity of Intravascular Mesenchymal Tumors and Visceral Mesenchymal Tumors with Angioinvasion: Cross-sectional Imaging Spectrum

**Awards**  
**Certificate of Merit**

Participants  
Ajaykumar C. Morani, MD, Houston, TX (*Presenter*) Nothing to Disclose

#### TEACHING POINTS

There is a wide spectrum of primary intravascular mesenchymal neoplasms including smooth muscle tumors, intimal sarcomas and angiosarcomas. Diverse visceral mesenchymal tumors may demonstrate angio-invasion into contiguous veins. Cross-sectional imaging plays a critical role in accurate diagnosis and staging of these entities and guide management.

#### TABLE OF CONTENTS/OUTLINE

A. BackgroundB. Epidemiology, etio-pathogenesis, clinical findings and pathology of primary intravascular neoplasms as well as visceral mesenchymal tumors with angio-invasion.C. Classification with multimodality cross-sectional imaging illustrations:1. Primary vascular tumors a. Benign and intermediate biological aggressiveness - leiomyoma, intravenous leiomyomatosis, smooth muscle tumor of uncertain malignant potential b. Malignant - leiomyosarcoma, angiosarcoma2. Vascular invasion by mesenchymal tumors - Gynecological sarcomas, pelvic sarcomas, solitary fibrous tumorsD. Prognosis and management

Printed on: 02/07/23



## Abstract Archives of the RSNA, 2022

VAEE-1

### Vascular Applications of Photon Counting Detector CT

Sunday, Nov. 27 8:00AM - 9:00AM Room: Learning Center - VA

#### Participants

Prabhakar Rajiah, MD, FRCR, Rochester, MN (*Presenter*) Nothing to Disclose

#### TEACHING POINTS

Photon-counting detector (PCD) CT is a recent technical innovation that uses novel detectors directly converting x-ray photons into electrical signals without the generation of light. In this exhibit, we aim 1. To discuss the physics and principles of PCD CT 2. To review the advantages of PCD CT over conventional energy integrating detector (EID) CT. 3. To illustrate the clinical applications of PCD CT in vascular imaging using multiple case examples

#### TABLE OF CONTENTS/OUTLINE

1. PCD CT TECHNOLOGIES- Single source, Dual-source 2. ADVANTAGES OF PCD-CT a. High spatial resolution b. Multi energy (ME) imaging c. Increased vascular signal d. Decreased electronic noise e. Decreased artifacts f. Lower radiation and contrast doses g. Potential K-edge imaging - Gadolinium + Iodine 3. APPLICATIONS OF PCD CT IN VASCULAR IMAGING WITH CASE EXAMPLES a. Ultra-high resolution- Improved visualization of small vessels (Artery of Adamkiewicz; Flaps including DIEP, fibular; arteries of hand, feet, head), calcified plaques, stents b. High iodine CNR (low-energy VMI's)- Low dose of iodinated contrast, salvage of suboptimal studies c. Decreased artifacts- Calcium blooming, beam hardening, metal d. ME calcium separation- Improved lumen visualization e. ME bone subtraction f. ME lesion characterization g. Vascular perfusion h. Potential for multi-contrast and novel contrast media- e.g. iodine and gadolinium i. Advanced material separation j. Radiation dose reduction- Virtual noncontrast images in multiphase studies, lower noise profile 4. LIMITATIONS, PITFALLS a. Increased data - storage and transfer issues b. Noise reduction in high resolution mode

Printed on: 02/07/23



## Abstract Archives of the RSNA, 2022

VAEE-10

### Applications of 4D Flow MRI from Head to Toe

Sunday, Nov. 27 8:00AM - 9:00AM Room: Learning Center - VA

#### Awards

Cum Laude

#### Participants

Prabhakar Rajiah, MD, FRCR, Rochester, MN (*Presenter*) Nothing to Disclose

#### TEACHING POINTS

1. To describe the principles and technique of 4D flow 2. To review the applications of 4D flow from head to toe 3. To illustrate the multi-systemic applications of 4D flow using case examples 4. To review common pitfalls and solutions in the use of 4D flow

#### TABLE OF CONTENTS/OUTLINE

1. 4D FLOW- Physics and principles 2. 4D FLOW PARAMETERS- Feraheme vs Gadolinium, spatial/ temporal resolution, plane, slice thickness, VENC, gating, flip angle 3. DISPLAY- Velocity MIPs, Streamlines, pathlines, vectors 4. ADVANCED PARAMETERS- Shear stress, pressure gradient, pulse wave velocity, turbulent kinetic energy 5. LIMITATIONS 6. ARTIFACTS 7. AI 8. REVIEW AND ILLUSTRATION OF THE FOLLOWING APPLICATIONS OF 4D FLOW FROM HEAD TO TOE A. Neurological - Vein of Galen malformations; Aneurysms- Pre and post procedure; AV malformations; Atherosclerotic stenosis B. Thoracic - Abnormal flow patterns- Novel biomarkers in aortopathies.e.g. bicuspid valve; Aortic dissection- Hemodynamics; Aortic coarctation- collateral blood flow; Vasculitis; Pulmonary hypertension C. Cardiac - Improved workflow in complex congenital heart diseases; Pre-surgical evaluation- E.g. Fontan shunt; Valvular heart disease; Detection of small shunts D. Abdominal - Dissection- False lumen Ejection fraction; Endoleak detection and characterization, type IIa vs IIb ; Mesenteric ischemia- Meal challenge; Portal hemodynamics in cirrhosis- shunting, AP fistula, vascular stenosis, Pre- and post TIPS; Splenic function; Pre transplant evaluation- Vascular anatomy, PV thrombus, portosystemic shunt; Uterine fibroid Pelvic venous congestion E. Peripheral - AV malformation; Lymphatic vessels

Printed on: 02/07/23



## Abstract Archives of the RSNA, 2022

VAEE-11

### US Of the Hemodialysis Patient: Mapping For Surgical And Percutaneous AVF, Grafts, And Postoperative US Evaluation, with Angiographic Correlation

Sunday, Nov. 27 8:00AM - 9:00AM Room: Learning Center - VA

#### Awards

**Certificate of Merit**

**Identified for RadioGraphics**

#### Participants

Kedar Sharbidre, MD, Birmingham, AL (*Presenter*) Nothing to Disclose

#### TEACHING POINTS

Patients with end stage renal disease (ESRD) requiring permanent hemodialysis (HD) access options of surgical creation of an arteriovenous fistula (sAVF), percutaneous AVF (pAVF) creation, or surgical placement of synthetic arteriovenous graft. Superficial venous anatomy can be highly variable and hence accurate preoperative ultrasound (US) assessment is very important, particularly for pAVF planning. US can also help determine AVF maturity and evaluation for complications to guide management. After reviewing this exhibit, the learner will be able to: 1. Describe a typical US arterial and venous mapping protocol for upper extremity sAVF, pAVF, AVG, and thigh graft placement. 2. Understand postoperative US criteria for sAVF and pAVF maturation 3. Recognize abnormalities that may impede AVF maturation 4. Diagnose complications using the US including focal swelling or fluid collection at the fistula site, arterial steal, aneurysm, pseudoaneurysm, and graft degeneration

#### TABLE OF CONTENTS/OUTLINE

1. Venous and Arterial Anatomy of the Extremities for HD mapping a. Upper extremity arteries b. Upper extremity deep and superficial veins c. Groin arteries and veins for AVG 2. Preoperative vascular mapping a. Upper extremity protocol b. Specific mapping for pAVF c. Groin protocol 3. Postoperative assessment for fistula maturation a. sAVF b. pAVF 4. US assessment of complication with angiographic correlation showing treatment results as appropriate a. Abnormalities that prevent maturation i. stenosis (anastomotic, draining vein, central vein) ii. accessory draining veins b. Graft stenosis c. Thrombosis d. Fluid collections e. Arterial steal f. Pseudoaneurysm g. Graft degeneration.

Printed on: 02/07/23



## Abstract Archives of the RSNA, 2022

VAEE-12

### Thoracic Endovascular Aortic Repair: Past, Present, and Future

Sunday, Nov. 27 8:00AM - 9:00AM Room: Learning Center - VA

#### Participants

Jonathan Liu, MD, Palo Alto, CA (*Presenter*) Nothing to Disclose

#### TEACHING POINTS

-Knowledge of the nomenclature facilitates communication between radiologists and vascular/cardiothoracic surgeons.- Indications for TEVAR continues to evolve, with expanding indications. The proximal descending thoracic aorta, aortic arch, and even ascending aorta can be repaired endovascularly.- Awareness of the various types of repair will assist in the detection of repair complications.

#### TABLE OF CONTENTS/OUTLINE

I. Introduction/History and path to FDA approval  
II. Indication for thoracic endovascular aortic repair  
III. Anatomy for endovascular approach  
a. Aortic arch zones  
b. Aortic arch types  
IV. Historical and contemporary devices  
V. Novel techniques  
a. Petticoat technique  
b. Snorkel / Periscope technique  
c. In-situ laser fenestration  
VI. Investigational devices  
VII. Complications of TEVAR  
a. Birdbeaking  
b. Stent-graft induced new entry tear  
c. Endoleak / gutter leak  
d. Infection  
e. Fracture/migration  
VIII. Conclusion

Printed on: 02/07/23

## Abstract Archives of the RSNA, 2022

VAEE-13

### Imaging Review and Management Update on Portal Vein Thrombosis

Sunday, Nov. 27 8:00AM - 9:00AM Room: Learning Center - VA

#### Participants

Maria Garcia, MD, (*Presenter*) Nothing to Disclose

#### TEACHING POINTS

1) Describe the anatomy of the portal vein (PV) and relevant anatomic relationships. 2) Describe the pathophysiology and common risk factors for portal vein thrombosis (PVT). 3) Identify the multimodality imaging features of acute, chronic and iatrogenic portal vein occlusion 4) Identify the role of imaging in diagnosis and management of PVT.

#### TABLE OF CONTENTS/OUTLINE

I. Background. II. Normal/Variant anatomy. III. Overview of PVT pathophysiology, broadly 3 etiologies: 1) Hereditary thrombophilia; 2) Acquired thrombophilia/hypercoagulable states, such as pregnancy and malignancy; 3) Intra-abdominal causes. IV. Definition and clinical manifestations of acute and chronic PVT. V. Imaging features of acute versus chronic PVT. VI. Illustration of PV occlusion: a) Bland thrombus: hematologic disorders, cirrhosis, pancreatitis, portal pyaemia, inflammatory bowel disease, pancreatic malignancy; b) Tumor thrombus: HCC and others such as sarcoma and NET; c) Intervention-related: Surgery/Liver transplant, TIPS stent thrombosis, Portal vein embolization; d) Chronic changes/complications: Cavemous transformation (adults/children), Portal hypertension, Portal biliopathy, Mesenteric ischemia; e) Mimics: Flow artifacts, Hepatic vein/IVC occlusion, Dilated bile duct. VII. Treatment: 1) Medical: Anticoagulation, highlight the reason for differential approach in the presence or absence of cirrhosis; 2) Endovascular: Two main interventions for portal vein recanalization (PVR) a) Thrombectomy +/- thrombolysis, b) PVR-TIPS stent placement. 3) Surgical: Bowel infarction or contraindication to thrombolytic therapy. VIII. Take home points.

Printed on: 02/07/23



## Abstract Archives of the RSNA, 2022

VAEE-14

### Ultrasound Evaluation of AV Fistulas for Hemodialysis: A Hands-on Approach

Sunday, Nov. 27 8:00AM - 9:00AM Room: Learning Center - VA

#### Participants

Mikel Elgezabal, MD, Barrika, Spain (*Presenter*) Nothing to Disclose

#### TEACHING POINTS

- To understand the importance of Chronic Kidney Disease in healthcare.- To make the reader confident to perform ultrasound on patients with AV fistulas as a vascular access for hemodialysis, using a simple step-by-step approach that can cover all the bases for a satisfactory evaluation.

#### TABLE OF CONTENTS/OUTLINE

Chronic Kidney Disease (CKD) Contemporary significance of CKD: definition, prevalence, burden. Ultrasound findings of CKD. Therapeutic options for CKD: Renal Replacement Therapy with a focus on hemodialysis.Arteriovenous Fistulas for Hemodialysis What is an AV fistula? A quick, basic review slide to get the reader up to speed. The upper extremity: vascular anatomy: We include labeled anatomy images of the upper limb arterial and venous system and discuss key anatomical landmarks along with their corresponding clinical significance. Planning an AV fistula: pre-surgical ultrasound.Types of AVF: Native vs. prosthetic, typical locations.Sonographic assessment of an AV fistulaBefore scanning: clinical assessment, patient position, ultrasound probe choice. Ultrasound exam. Components of an AV fistula and individual sonographic properties of each component. The afferent artery, the anastomosis, the efferent vein. Properties of the mature and healthy AV Fistula: ready to needle! Complications: We detail key diagnostic points of each one of the most common complications and support them with clinical cases and images from our institution.

Printed on: 02/07/23



## Abstract Archives of the RSNA, 2022

VAEE-15

### How Will 320-Row Multi Detector CT Change the Diagnosis of Pelvic Venous Congestion Syndrome?

Sunday, Nov. 27 8:00AM - 9:00AM Room: Learning Center - VA

#### Participants

Kazuto Sakamoto, RT, (*Presenter*) Nothing to Disclose

#### TEACHING POINTS

The purpose of this exhibit is: 1. Pelvic venous congestion syndrome (PVCS) is a cause of chronic pelvic pain in female patients. The cause of PVCS may be structural. It is the regurgitation of the gonadal vein with venous valve insufficiency due to compression have the left renal vein or the iliac vein. 2. PVCS may not be accompanied by pelvic pain, and imaging by US or MRI may be useful. The most important reason for this is that US and MRI can determine the direction of blood flow in the refluxed gonadal vein. 3. The 320-row multi detector CT can acquire cine images up to 160 mm wide with 4D imaging. In addition, 4DCT angiography cine images can be used to evaluate gonadal vein reflux.

#### TABLE OF CONTENTS/OUTLINE

Major headings:1. Describe PVCS. 2. Usefulness of 4DCT angiography in PVCS diagnosis.- 4DCT angiography cine imaging to evaluate gonadal vein reflux. - In all cases, the findings were comparable to catheter-based angiography. 3. Supporting imaging with 3DCT angiography in PVCS revascularization. - Supporting imaging with 3DCT is expected to reduce the total radiation dose to the patient. - In other words, a reduction in fluoroscopic time due to shorter operative time. 4. Quantification of edema by CT imaging in determining treatment efficacy.- CT images are a useful tool for convenient volumetric measurements. - Volumetric evaluation is important to determine the efficacy of treatment of PVCS with lower extremity edema.

Printed on: 02/07/23



## Abstract Archives of the RSNA, 2022

VAEE-16

### Arteriovenous Fistula For Hemodialysis: A Thorough Analysis

Sunday, Nov. 27 8:00AM - 9:00AM Room: Learning Center - VA

#### Participants

Sofia Maksoud, MD, Sao Paulo, Brazil (*Presenter*) Nothing to Disclose

#### TEACHING POINTS

- The arteriovenous fistula is created from the anastomosis between native artery and vein, with the aim of providing chronic access for hemodialysis in patients with end-stage renal disease until they can receive a kidney transplant.- The most used are the anastomosis of the radial artery with the cephalic vein or brachial artery with the cephalic vein.- The structure created must be accessible and have the blood flow necessary to be cannulated repeatedly and thus allow adequate dialysis. For this, the minimum internal calibers must be 0.2 cm for the artery and 0.25 cm for the vein.- After the creation of the fistula, the blood vessels involved undergo a maturation process that can be evaluated by means of a color Doppler ultrasound study. The flow volume, calculated through the formula of the average velocity times the diameter of the opening, reaching 600 mL/minute is a parameter commonly associated with maturation.- Complications of arteriovenous fistula include failure of maturation, stenotic vascular lesions, thrombosis, aneurysms or pseudoaneurysms, and infection.

#### TABLE OF CONTENTS/OUTLINE

- Review expected ultrasound findings expected for a patent arteriovenous fistula for hemodialysis.- Evaluate the most common complications and their presentation on ultrasound.

Printed on: 02/07/23



## Abstract Archives of the RSNA, 2022

VAEE-17

### Beware of The Dislodged Devices

Sunday, Nov. 27 8:00AM - 9:00AM Room: Learning Center - VA

#### Participants

Marcus Nascimento, MD, Sao Paulo, Brazil (*Presenter*) Fellow, Hospital Israelita Albert Einstein

#### TEACHING POINTS

The purpose of this exhibit is:- To briefly review and recognize some of the cardiovascular devices used in patient care.- To describe how to recognize and define the position of some devices in different imaging modalities.- Show examples of medical dislodged devices or with some kind of complication.

#### TABLE OF CONTENTS/OUTLINE

1) Basic anatomy of the chest and cardiovascular system.2) Types and function of the devices3) How the devices are represented in the different images modalities and their primary function in patient care.4) Key Imaging Findings that define their malpositioning and/or deformation.5) Take home messages.

Printed on: 02/07/23



## Abstract Archives of the RSNA, 2022

VAEE-18

### Does Size Really Matter? Imaging in Visceral Artery Aneurysms

Sunday, Nov. 27 8:00AM - 9:00AM Room: Learning Center - VA

#### Participants

Tomas Lacerda, MD, Sao Paulo, Brazil (*Presenter*) Nothing to Disclose

#### TEACHING POINTS

The purpose of this exhibition is to review the most recent guideline on visceral aneurysms and its recommendations towards treatment indications and modalities. Also, discuss most common sites for visceral aneurysms, symptoms and complications and imaging findings in diagnostic and post treatment situations.

#### TABLE OF CONTENTS/OUTLINE

Understand the most common sites for visceral aneurysms and its potential potential complications; Reviewing the latest guideline on visceral aneurysms, its recommendations towards when and how to repair; Illustrate through a series of radiological cases the most common sites, findings on possible complications and imaging during and after endovascular repair.

Printed on: 02/07/23



## Abstract Archives of the RSNA, 2022

VAEE-19

### Portal Vein Thrombosis: What a Radiologist Needs to Know In the Era of the Baveno VII Consensus Recommendations

Sunday, Nov. 27 8:00AM - 9:00AM Room: Learning Center - VA

#### Awards

Identified for RadioGraphics

#### Participants

Alessandro Bozzato, MD, (Presenter) Nothing to Disclose

#### TEACHING POINTS

-Illustrate the recommended standardized nomenclature for the description of portal vein thrombosis (PVT) and portal cavernoma, according to the Baveno VII consensus definitions. -Describe diagnosis and management of acute and chronic PVT in absence and presence of cirrhosis.

#### TABLE OF CONTENTS/OUTLINE

Introduction PVT is characterized by the presence of a bland thrombus in the portal vein trunk and its branches. It occurs in non-cirrhotic patients, and, less frequently, in cirrhotic patients. Imaging methods should be used to diagnose PVT (ruling out malignant portal vein obstruction) and assess its extension. Recommended standardized nomenclature- Show typical imaging features illustrating the nomenclature: • Time course (acute and chronic thrombosis) • Percent occlusion of main portal vein (completely occlusive, partially occlusive, minimally occlusive thrombosis, and cavernous transformation) • Response to treatment or interval change (progressive, stable and regressive thrombosis) Portal vein thrombosis and portal cavernoma in the absence of cirrhosis- Illustrate acute and chronic PVT in the absence of cirrhosis: • Diagnosis and follow-up • Interventional management (image-guided interventions, thrombolysis, transjugular intrahepatic portosystemic shunt (TIPS), and other percutaneous recanalizations) Portal vein thrombosis and cirrhosis- Illustrate PVT in cirrhosis: • Diagnosis and follow-up • Interventional management ((TIPS), and other percutaneous recanalizations)

Printed on: 02/07/23



## Abstract Archives of the RSNA, 2022

VAEE-2

### Multimodality Imaging of Portal Vein Thrombosis: Diagnosis and Influence on Clinical Management

Sunday, Nov. 27 8:00AM - 9:00AM Room: Learning Center - VA

#### Participants

Catherine Naidoo, MBBS, FRANZCR, Randwick, Australia (*Presenter*) Nothing to Disclose

#### TEACHING POINTS

1- Learn how to diagnose portal vein thrombosis (PVT) on different imaging modalities 2- Determine the etiology (Benign vs. Malignant), onset (Acute vs. Chronic), and extent of PVT 3- Assess the acute and chronic complications of PVT

#### TABLE OF CONTENTS/OUTLINE

Thrombosis of the portal venous system is a frequent and potentially life-threatening condition that can take place in a number of different clinical settings including liver cirrhosis, hepatocellular carcinoma, other solid tumors, abdominal septic foci, acute pancreatitis, hematological malignancies, and congenital or acquired prothrombotic disorders. Imaging plays a pivotal role in the clinical decision-making process in patients with thrombosis of the portal venous system. In this article, we will discuss the familiar and uncommon imaging findings of PVT at the ultrasound, contrast-enhanced ultrasound, CT, and MRI and the role of imaging in determining the underlying etiology (benign versus malignant) and onset (acute versus chronic). We will learn the available classification systems that provide a treatment-oriented assessment of PVT extension and degree of occlusion. We will recognize the acute and chronic morphologic changes of the liver parenchyma, such as nodular regenerative hyperplasia, secondary to PVT nodular regenerative hyperplasia. We will also review the complications of PVT such as portal biliopathy.

Printed on: 02/07/23

## Abstract Archives of the RSNA, 2022

VAEE-20

### Ultrasound of Peripheral Arteries: An Update on Technique, Protocols, Interpretation and Applications

Sunday, Nov. 27 8:00AM - 9:00AM Room: Learning Center - VA

#### Participants

Prabhakar Rajiah, MD, FRCR, Rochester, MN (*Presenter*) Nothing to Disclose

#### TEACHING POINTS

1. To review the indications of ultrasound (USG) in peripheral arterial diseases 2. To review the normal and abnormal flow patterns in peripheral arteries 3. To illustrate imaging appearances of common peripheral arterial abnormalities.

#### TABLE OF CONTENTS/OUTLINE

1. INTRODUCTION 2. ANATOMY 3. ROLE, ADVANTAGES, LIMITATIONS OF USG- Comparison with other invasive and non-invasive modalities 4. TECHNICAL REQUIREMENTS- B-mode, doppler, color, power 5. OPTIMIZATION OF TECHNICAL PARAMETERS 6. TRANSDUCER AND PATIENT POSITION 7. NORMAL VESSEL- Normal caliber, laminar flow 8. WAVEFORMS - Normal - Triphasic or biphasic with sharp systolic upstroke; -Abnormal - Monophasic or biphasic without sharp systolic upstroke 9. VELOCITIES- Normal and abnormal at, proximal and distal to stenosis; grading of stenosis 10. ILLUSTRATION OF THE FOLLOWING ABNORMALITIES WITH SAMPLE CASES A. Atherosclerosis, native vessels- Indications; Diagnostic approach; Screening localization; Criteria for different grades of stenosis- Velocities, waveforms, pre and post stenotic vessels; Collaterals; Pitfalls, misses B. Bypass graft evaluation C. Stent evaluation D. Aneurysms E. Pseudoaneurysms- To-and-fro flow, guidance for management F. Popliteal artery entrapment G. Dissection H. Arteritis I. AV Fistula- High-velocity turbulent flow between vessels; low resistance proximal arterial waveforms; High, arterialized venous flow; vibration artifacts in perivascular tissues. J. Post-surgical/interventional follow-up- Grafts, thrombin injection

Printed on: 02/07/23



## Abstract Archives of the RSNA, 2022

VAEE-21HC

### Evaluation of Lower Extremity Peripheral Arterial Disease Using Ultrasonography: What Everyone Should Know

Sunday, Nov. 27 8:00AM - 9:00AM Room: Learning Center - VA

#### Participants

Omar Ali, BS, (Presenter) Nothing to Disclose

#### TEACHING POINTS

1. To provide a clinical overview of peripheral arterial disease (PAD) of the lower extremities and its sequelae. 2. To examine the role of noninvasive imaging in the assessment of PAD 3. To provide a pictorial-based review of ultrasound (US) modalities and their utility in noninvasive evaluation of PAD 4. To discuss the role of US in unique clinical circumstances related to PAD

#### TABLE OF CONTENTS/OUTLINE

1) Introduction to PAD a) Natural history 2) Overview of Noninvasive evaluation of PAD a) Indications for US evaluation of PAD 3) Arterial ultrasonography (US) of PAD a) Overview and limitations of US techniques for arterial imaging b) Arterial mapping by segment i) Aortoiliac ii) Femoropopliteal iii) Infrapopliteal c) B-mode Doppler i) Visualization of vascular anatomy ii) Abnormal findings (plaque, stenosis, calcification) Spectral Doppler i) Purpose: characterization of blood flow based on waveforms ii) Peak systolic velocity (PSV) and PSV ratio iii) Abnormal findings (spectral broadening, increase in PSV, monophasicity e) Color Doppler i) Assessment of direction and speed of flow ii) Abnormal findings (aliasing, color bruit) f) Power Doppler i) Examining flow based on quantity of red blood cells ii) Abnormal findings (decreased flow, occlusion) g) Contrast-enhanced US i) Assessment of perfusion ii) Abnormal findings h) Pedal acceleration time i) Role in evaluating CLI and predicting limb salvage 4) Special considerations for US evaluation of PAD a) Chronic total occlusion b) Critical limb ischemia c) Calcified PAD d) Post-revascularization surveillance Please visit the Learning Center to also view this presentation in hardcopy format.

Printed on: 02/07/23



## Abstract Archives of the RSNA, 2022

VAEE-22

### Doppler US of Lower Limb Venous Insufficiency Made Simple

Sunday, Nov. 27 8:00AM - 9:00AM Room: Learning Center - VA

#### Participants

Montserrat Torrent, (*Presenter*) Nothing to Disclose

#### TEACHING POINTS

Chronic venous insufficiency of the lower limbs is very prevalent. Duplex ultrasound has the ability to demonstrate venous hemodynamic reflux, that why it become the method of choice to study this condition. We review the venous anatomy of the lower limbs, the pathophysiology of chronic venous insufficiency and explain the protocol for carrying out Duplex studies. These include venous mapping and a thorough evaluation of the superficial veins to identify all of the patterns of incompetence. We also evaluate patients with other treatment techniques such as thermal ablation, sclerotherapy. Therefore we can conclude the complications or the success of the applied procedure.

#### TABLE OF CONTENTS/OUTLINE

Learning objectives: ? Review the venous anatomy of the lower limbs, the pathophysiology of chronic venous insufficiency and explain the protocol for carrying out Duplex studies? Perform venous mapping with the patterns of incompetence.? Evaluate patients after treatment to identify success, complications and recurrence.

Printed on: 02/07/23



## Abstract Archives of the RSNA, 2022

VAEE-23

### **Abernethy Malformation: What You Need to Know**

Sunday, Nov. 27 8:00AM - 9:00AM Room: Learning Center - VA

#### **Participants**

Alexandra Panyukova, MD, (*Presenter*) Nothing to Disclose

#### **TEACHING POINTS**

- To review the normal anatomy and embryology of the portal system. - To learn about Abernethy malformation - a rare congenital vascular pathology. - To illustrate the role of different imaging methods in diagnosis of Abernethy malformation. - To highlight the main points in radiology reports, which influence further patient evaluation and treatment.

#### **TABLE OF CONTENTS/OUTLINE**

1. Introduction 2. Anatomy review 3. Embryology: portal venous system development 4. Abernethy malformation 4.1. Definition 4.2. Classification 4.3. Clinical manifestations, complications 4.4. Diagnostic methods 4.5. What else should you look for? 4.6. Follow-up and treatment 5. Take home points 6. Recommended bibliography

Printed on: 02/07/23



## Abstract Archives of the RSNA, 2022

VAEE-24

### Imaging in Hemodialysis: Role of Ultrasound in Assessment and Surveillance of Grafts and Fistulas

Sunday, Nov. 27 8:00AM - 9:00AM Room: Learning Center - VA

#### Awards

Certificate of Merit

#### Participants

Irene Dixe de Oliveira Santo, MD, New Haven, CT (*Presenter*) Nothing to Disclose

#### TEACHING POINTS

Ultrasound (US) plays a major role in the assessment and surveillance of hemodialysis (HD) fistulas and grafts. Furthermore, it is essential in the evaluation of arterial and venous circulation before access creation. The complication rate of HD access is relatively high, and US is crucial for the accurate diagnosis of the different complications.(1) Discuss the role of US in preoperative planning; (2) Provide a step-by-step algorithm in the sonographic evaluation of the HD access;(3) Review the sonographic characteristic features of common and rare complications of HD access;(4) Briefly discuss the role of interventional radiology in the management of HD complications.

#### TABLE OF CONTENTS/OUTLINE

Preoperative planning: discuss anatomy, major criteria for suitability of vascular system in creation of HD access Discuss various types of HD access based on access location, and operative techniques (graft versus fistula) Provide optimal protocol and diagnostic criteria for HD access assessment Review sonographic findings of uncomplicated HD access Discuss algorithmic approach to assess HD access complications using US Doppler (thrombosis, stenosis, ischemic steal syndrome, aneurysms and pseudoaneurysms formation, bleeding, hematoma and infection, and structural problems) Briefly discuss causes of nonmaturing fistula Review management options for HD complications and findings post-intervention

Printed on: 02/07/23



## Abstract Archives of the RSNA, 2022

VAEE-25

### Assessment of Tissue Vascularity: Non-contrast Micro-vascular Flow Imaging in Assessment of Vascularity, With Contrast and/or Pathological Correlation - Expanding the Horizons

Sunday, Nov. 27 8:00AM - 9:00AM Room: Learning Center - VA

#### Participants

Muhammad Aziz, MBBS, Birmingham, AL (*Presenter*) Former Stockholder, Sorrento Therapeutics, Inc

#### TEACHING POINTS

Ultrasound vascular imaging with color and power Doppler is an important tool in the assessment of various disease processes, with assessment of blood flow in organs, neoplasms and vessels; from infarction and ischemia to hyperemia, and is used in almost all ultrasound examinations. Recent development of small vessel, slow velocity flow without the utilization of contrast agents is more sensitive to microvasculature on comparison with color, Power and spectral Doppler - termed as "MicroVascular Flow Imaging (MVFI)". This results in a decreased need for follow-up contrast examinations (US, CT, MR) in many conditions. After reviewing this exhibit, the learner will be able to: 1 - Review the basics of physics of noncontrast MVFI. 2 - Understand the various applications of this novel technique in different adult and pediatric conditions - including benign and malignant conditions. 3 - Recognize different acute applications of MVFI; including in testes and gallbladder. 4 - Understand the potential future applications of MVFI. 5 - Review and diagnose many case examples of various conditions; including benign and malignant liver lesions, acute gallbladder and testicular pathologies, benign and malignant renal lesions, role of MVFI in pre- and postsurgical cases. 6 - Describe the limitations of this technique

#### TABLE OF CONTENTS/OUTLINE

1 - Introduction to MVFI a. Background b. Physics of MVFI 2 - Clinical Applications of US MVFI in Adults a. Liver b. Gallbladder c. Kidneys d. Superficial Organs - Testes, Lymph Nodes e. Vessel Disease 3 - Clinical Applications of US MVFI in Pediatrics a. Liver b. Trauma 4 - Future Potential and Direction 5 - Limitations 6 - Conclusion

Printed on: 02/07/23



## Abstract Archives of the RSNA, 2022

VAEE-26

### Imaging of Rare Intravascular Tumors and Tumorlike Lesions

Sunday, Nov. 27 8:00AM - 9:00AM Room: Learning Center - VA

#### Participants

Duygu Ekizalioglu, MD, (*Presenter*) Nothing to Disclose

#### TEACHING POINTS

- To overview rare miscellaneous intravascular tumors and tumorlike lesions that may pose difficulties for diagnosis. - To emphasize the imaging findings (US, CT, MRI, PET/CT) of rare neoplastic and nonneoplastic intravascular lesions. - To review the histopathological findings of neoplastic and nonneoplastic intravascular lesions.

#### TABLE OF CONTENTS/OUTLINE

Introduction. Overview of intravascular neoplastic lesions Primary Benign: Internal jugular vein hemangioma Primary Malign: Primary leiomyosarcoma of inferior vena cava (IVC) Secondary Benign: Renal angiomyolipoma extending into the renal vein Secondary Malign (Tumor Thrombus): Renal Ewing sarcoma with tumor thrombus in renal vein and IVC, Renal cell carcinoma with tumor thrombus in renal vein and IVC, Uterine sarcoma with tumor thrombus in ovarian vein and IVC, Hepatocellular carcinoma with tumor thrombus in IVC, Colon cancer liver metastasis and tumor thrombus in IVC. Overview of intravascular nonneoplastic lesions: Aortic hydatid cyst, Pyogenic granuloma of angular vein, Bland thrombus (associated with COVID-19). Review of imaging findings on US, CT, MRI, PET/CT of rare intravascular tumors and tumorlike lesions. Description of histopathological findings. Differential diagnostic algorithm for intravascular neoplastic and nonneoplastic lesions. Conclusion. References.

Printed on: 02/07/23



## Abstract Archives of the RSNA, 2022

VAEE-3

### A Practical Approach to the Interpretation of Arterial Waveforms on Duplex Doppler, Made Ridiculously Simple

Sunday, Nov. 27 8:00AM - 9:00AM Room: Learning Center - VA

#### Participants

Dana Galvan, MD, Albuquerque, NM (*Presenter*) Nothing to Disclose

#### TEACHING POINTS

Doppler US is the first line imaging modality for the evaluation of the vascular system. Various pathological processes affect vasculature and result in the characteristic appearance of the waveforms allowing to recognize the abnormality and correctly diagnose the disease process independent of its location. 1. Review normal appearance of the arterial and venous waveforms and underlying physiology 2. Discuss pathophysiology and waveform appearance of various pathological conditions affecting the vascular system 3. Discuss treatment management options and post treatment restoration of waveform pattern.

#### TABLE OF CONTENTS/OUTLINE

Outline: 1. Review normal arterial and venous waveform appearance on US and its physiology (dependance of waveform appearance on the cardiac cycle, principles of Doppler physics and Doppler technique of waveform acquisition) 2. Discuss correlation between the vascular process pathophysiology and waveform appearance (waveform pattern in the following conditions: stenosis (pre, at, and post stenosis, compensatory flow), thrombosis (proximal to occlusion, flow reversal), reconstitution (collateral waveform pattern), pseudoaneurysm, arteriovenous fistula, dissection, vascular torsion, neovascularity 3. Discuss management options (stent, angioplasty, bypass graft) and post-treatment waveform appearance (flow restoration).

Printed on: 02/07/23



## Abstract Archives of the RSNA, 2022

VAEE-4

### Diagnosis and Treatment of Iliac Artery Aneurysms: From A to Z

Sunday, Nov. 27 8:00AM - 9:00AM Room: Learning Center - VA

#### Participants

Ruben Guerrero Vara, MD, (*Presenter*) Nothing to Disclose

#### TEACHING POINTS

1) To review the the main features of iliac artery aneurysms (IAA). 2) To highlight the importance of maintaining patency of the hypogastric artery during repair of IAA. 3) To describe the endovascular treatment options to preserve the hypogastric artery during endovascular repair.

#### TABLE OF CONTENTS/OUTLINE

1) IAA: definition and characteristics. 2) IAA: surgical indications 3) Description of the endovascular techniques developed to preserve internal iliac flow: Iliac branch device (IBD), bell bottom technique (BBT), sandwich technique (ST) and banana technique (BT). 4) Application of each procedure and anatomic limitations. 5) Potential complications of these methods. 6) Depiction of examples of every endovascular technique including preoperative CTA images, schematic illustrations, DSA images before and after stent implantation and control CTA pictures after the procedure. 7) Conclusions

Printed on: 02/07/23



## Abstract Archives of the RSNA, 2022

VAEE-5

### Vascular Ultrasound: A Primer on Arterial and Venous Doppler Waveforms, Interpretation, and Standardized Nomenclature

Sunday, Nov. 27 8:00AM - 9:00AM Room: Learning Center - VA

#### Awards

Certificate of Merit

#### Participants

Min Gyu Noh, MD, Seattle, WA (*Presenter*) Nothing to Disclose

#### TEACHING POINTS

1. Learn standard terminology for describing arterial and venous waveforms according to the consensus statement from the Society for Vascular Medicine (SVM) and the Society for Vascular Ultrasound (SVU)  
2. Recognize normal arterial and venous waveforms and understand how physiologic and disease states can alter waveforms  
3. Review pearls and pitfalls of Doppler optimization  
4. Case-based review of normal physiologic and pathologic vascular ultrasound cases

#### TABLE OF CONTENTS/OUTLINE

1) Learn standardized terminology for describing arterial waveforms according to SVM and SVU:  
a. Flow direction  
b. Phasicity  
c. Resistance  
2) Review standardized terminology for describing venous waveforms according to SVM and SVU:  
a. Flow direction  
b. Flow pattern  
c. Spontaneity  
3) Recognize normal and abnormal arterial waveforms and velocities based on anatomic function, with a focus on:  
a. Peripheral arteries  
b. Mesenteric and renal arteries  
c. Common carotid, internal carotid, and external carotid arteries  
4) Recognize normal and abnormal venous waveforms based on anatomic function:  
a. Deep and superficial peripheral venous structures (upper and lower extremities)  
b. Central veins (upper extremities)  
c. Abdominal veins (IVC, iliac, renal, hepatoportal)  
5) Pearls and pitfalls of Doppler optimization:  
a. PRF  
b. Wall filter  
c. Angle of insonation  
6) Utilize understanding of arterial and venous vascular physiology to review normal physiologic and pathologic vascular ultrasound cases, including:  
a. Mesenteric artery stenosis  
b. Deep vein thrombosis  
c. ICA/ECA stenosis  
d. Subclavian vein thrombosis and steal  
e. Vertebral artery stenosis  
f. Peripheral artery stenosis

Printed on: 02/07/23



## Abstract Archives of the RSNA, 2022

VAEE-6

### Demystifying Ultrasound of the Standard Dialysis Fistula

Sunday, Nov. 27 8:00AM - 9:00AM Room: Learning Center - VA

#### Participants

Sagar Desai, DO, Mountain Top, PA (*Presenter*) Nothing to Disclose

#### TEACHING POINTS

Describe the pathophysiology and anatomy of an arteriovenous dialysis fistula Discuss preoperative arterial and venous imaging required to support the high flow state Understand sonographic features indicative of a mature fistula Review the approach to a delayed or non-maturing fistula Describe the sonographic appearing of acute and chronic complications of dialysis fistulas with confirmatory angiography and treatment

#### TABLE OF CONTENTS/OUTLINE

Kidney Disease Outcomes Quality Initiative (KDOQI) Basic KDOQI guidelines pertaining to arteriovenous fistula (AVF) creation and management Pre-operative ultrasound planning Morphologic and functional data Arteries: course, relationship to vein, diameter, plaque, intimal medial thickness, waveforms and velocity Veins: anatomy, patency of superficial and deep veins including: depth, diameter, length, anomalies, fibrotic segments and waveforms Patency and perfusion of the palmar arch Examples of adequate and inadequate vessels US assessment of AVF maturity Physiologic requirements for adequate dialysis Evaluation of a delayed or non maturing fistula Ultrasound assessment Poor location (depth) Large or increased number of draining veins Stenosis Arterial inflow Venous outflow The interventional radiologist's approach Fundamental steps of a 'fistulogram' procedure Angiographic correlates and treatments to augment AVF maturation Complications: early and late Hematoma Thrombosis Stenosis (arterial and venous) Infection Aneurysm or pseudoaneurysm Steal Syndrome High output cardiac failure

Printed on: 02/07/23



## Abstract Archives of the RSNA, 2022

VAEE-8

### What to Do When the Aortic Aneurysm Keeps Growing After Endovascular Repair: An Illustrated Review of the CT Angiography Protocol and Most Important Complications of the Endoleaks

Sunday, Nov. 27 8:00AM - 9:00AM Room: Learning Center - VA

#### Participants

Estefania Gallego Diaz, MD, MD, Mexico City, Mexico (*Presenter*) Nothing to Disclose

#### TEACHING POINTS

- The endoleak is defined as blood leak in an aneurysm sac excluded by stent-graft following endovascular aneurysm repair (EVAR), which means, flow outside the stent but into the aneurysm.
- To explain the importance of a timely diagnosis in this group of patients.
- To illustrate the detailed way to do an appropriate report.
- To review the consequences of an endoleak and its implication in morbidity and mortality for the patient.
- To simplify the imaging evaluation in patients with endoleaks.

#### TABLE OF CONTENTS/OUTLINE

1. Introduction. 2. What is an endoleak a. Indications. b. Classification. 3. CTA protocol and technical Recommendations. 4. Follow up. 5. How to report it / Algorithm for evaluation. 6. Which are the consequences of an endoleak a. Complications. b. Prognosis depending on the type of endoleak. 7. Clinical Cases and pictorial review. 8. Conclusions.

Printed on: 02/07/23



## Abstract Archives of the RSNA, 2022

VAEE-9

### Phenotypic Diversity of Intravascular Mesenchymal Tumors and Visceral Mesenchymal Tumors with Angioinvasion: Cross-sectional Imaging Spectrum

Sunday, Nov. 27 8:00AM - 9:00AM Room: Learning Center - VA

#### Awards

Certificate of Merit

#### Participants

Ajaykumar C. Morani, MD, Houston, TX (*Presenter*) Nothing to Disclose

#### TEACHING POINTS

There is a wide spectrum of primary intravascular mesenchymal neoplasms including smooth muscle tumors, intimal sarcomas and angiosarcomas. Diverse visceral mesenchymal tumors may demonstrate angio-invasion into contiguous veins. Cross-sectional imaging plays a critical role in accurate diagnosis and staging of these entities and guide management.

#### TABLE OF CONTENTS/OUTLINE

A. Background  
B. Epidemiology, etio-pathogenesis, clinical findings and pathology of primary intravascular neoplasms as well as visceral mesenchymal tumors with angio-invasion.  
C. Classification with multimodality cross-sectional imaging illustrations:  
1. Primary vascular tumors  
a. Benign and intermediate biological aggressiveness - leiomyoma, intravenous leiomyomatosis, smooth muscle tumor of uncertain malignant potential  
b. Malignant - leiomyosarcoma, angiosarcoma  
2. Vascular invasion by mesenchymal tumors - Gynecological sarcomas, pelvic sarcomas, solitary fibrous tumors  
D. Prognosis and management

Printed on: 02/07/23



## Abstract Archives of the RSNA, 2022

DLL01

### Deep Learning Lab: DICOM Data Wrangling with Python

Sunday, Nov. 27 10:30AM - 11:30AM Room: NA

#### Participants

Katherine Andriole, PhD, Branford, CT (*Presenter*) Nothing to Disclose

#### COURSE DESCRIPTION

In Person Session Only. On-demand beginning on December 5. This introductory hands-on course will demonstrate the importance of fully understanding the data cohort used to train a machine learning model by stepping through a Jupyter Notebook in CoLab. Processes known as data wrangling will be used to investigate the data. Tools and libraries to perform textual and pixel/image data wrangling including pandas, NumPy, pydicom, and Seaborn libraries will be explored.

#### LEARNING OBJECTIVES

1) To understand the need for data wrangling of large data sets used in machine learning 2) To become familiar with the tools used for textual data wrangling 3) To become familiar with the tools used for image pixel data wrangling\*Course Description In Person Session Only. On-demand beginning on December 5. This introductory hands-on course will demonstrate the importance of fully understanding the data cohort used to train a machine learning model by stepping through a Jupyter Notebook in CoLab. Processes known as data wrangling will be used to investigate the data. Tools and libraries to perform textual and pixel/image data wrangling including pandas, NumPy, pydicom, and Seaborn libraries will be explored.

Printed on: 02/07/23



## Abstract Archives of the RSNA, 2022

DLL02

### Deep Learning Lab: Data Processing & Curation for Deep Learning

Sunday, Nov. 27 12:00PM - 1:00PM Room: NA

#### Participants

Kirti Magudia, MD, PhD, Durham, NC (*Presenter*) Nothing to Disclose  
Walter Wiggins, MD, PhD, Durham, NC (*Presenter*) Advisor, Qure.ai;

#### COURSE DESCRIPTION

In Person Session Only. On-demand beginning on December 5th. This course will provide attendees with the essential tools to perform data processing and curation necessary for deep learning projects. Attendees will start with free text radiology and pathology reports as well as anonymized DICOM data and process data into a unified data file ready for deep learning applications.

#### LEARNING OBJECTIVES

1) Extract relevant data from radiology and pathology reports 2) Understand how to manage and process image-based annotations 3) Perform image registration and normalization 4) Recognize features of data formats ideal for deep learning\*Course Description In Person Session Only. On-demand beginning on December 5th. This course will provide attendees with the essential tools to perform data processing and curation necessary for deep learning projects. Attendees will start with free text radiology and pathology reports as well as anonymized DICOM data and process data into a unified data file ready for deep learning applications.

Printed on: 02/07/23



## Abstract Archives of the RSNA, 2022

DLL03

### Deep Learning Lab: Basics of NLP in Radiology

Sunday, Nov. 27 2:00PM - 3:00PM Room: NA

#### Participants

Timothy Chen, San Jose, CA (*Presenter*) Nothing to Disclose  
Gunvant Chaudhari, BS, San Francisco, CA (*Presenter*) Nothing to Disclose  
Jae Ho Sohn, MD, San Francisco, CA (*Presenter*) Nothing to Disclose

#### COURSE DESCRIPTION

In Person Session Only. On-demand beginning on December 5th. This session will feature a brief lecture introducing the basics of natural language processing (NLP) and highlight potential uses for it in radiology. The goal is to survey standard text preprocessing techniques and traditional NLP approaches as well as modern neural network based approaches. We will follow up the didactic portion with a hands-on Google Colab demo implementing discussed concepts for a text classification task. For best experience, we highly recommend attendees bring a laptop with a keyboard as well as have a Gmail account to access Google Colab.

#### LEARNING OBJECTIVES

1) Understand common terminology and preprocessing techniques in NLP 2) Identify several classic and modern approaches used to capture semantic meaning in text 3) Learn how to implement a basic NLP pipeline from preprocessing to performance evaluation\*Course Description In Person Session Only. On-demand beginning on December 5th. This session will feature a brief lecture introducing the basics of natural language processing (NLP) and highlight potential uses for it in radiology. The goal is to survey standard text preprocessing techniques and traditional NLP approaches as well as modern neural network based approaches. We will follow up the didactic portion with a hands-on Google Colab demo implementing discussed concepts for a text classification task. For best experience, we highly recommend attendees bring a laptop with a keyboard as well as have a Gmail account to access Google Colab.

Printed on: 02/07/23



## Abstract Archives of the RSNA, 2022

DLL04

### Deep Learning Lab: NCI Imaging Data Commons-Curated Data and Reproducible AI Workflows

Monday, Nov. 28 9:00AM - 10:00AM Room: NA

#### Participants

Andriy Fedorov, PhD, Arlington, MA (*Presenter*) Nothing to Disclose

#### COURSE DESCRIPTION

In Person Session Only. On-demand beginning on December 5th. NCI Imaging Data Commons (IDC), <https://imaging.datacommons.cancer.gov>, is a cloud-based repository of publicly available cancer imaging data co-located with the analysis and exploration tools and resources. IDC contains over 35TB of publicly available images and image annotations spanning a variety of cancer types and modalities. Attendees of this course will learn how to search, visualize and download IDC data, and how to build reproducible and shareable analysis workflows using Google Colab. The educational format will combine a lecture followed by a hands-on component and interactive discussions to gain familiarity with this resource.

#### LEARNING OBJECTIVES

1) Learn about the functionality of NCI Imaging Data Commons related to selection and preparation of data cohorts for developing AI workflows 2) Introduce the basic capabilities of IDC in support of development of reproducible AI workflows 3) Experiment with the application of open source AI tools to public imaging datasets\*Course Description In Person Session Only. On-demand beginning on December 5th. NCI Imaging Data Commons (IDC), <https://imaging.datacommons.cancer.gov>, is a cloud-based repository of publicly available cancer imaging data co-located with the analysis and exploration tools and resources. IDC contains over 35TB of publicly available images and image annotations spanning a variety of cancer types and modalities. Attendees of this course will learn how to search, visualize and download IDC data, and how to build reproducible and shareable analysis workflows using Google Colab. The educational format will combine a lecture followed by a hands-on component and interactive discussions to gain familiarity with this resource.

Printed on: 02/07/23



## Abstract Archives of the RSNA, 2022

DLL05

### Deep Learning Lab: Accessing Freely Available Public Datasets from The Cancer Imaging Archive (TCIA)

Monday, Nov. 28 10:30AM - 11:30AM Room: NA

#### Participants

Justin Kirby, Rockville, MD (*Presenter*) Nothing to Disclose

#### COURSE DESCRIPTION

In Person Session Only. On-demand beginning on December 5th. Access to large, high quality data is essential for researchers to understand disease and precision medicine pathways, especially in cancer. However HIPAA constraints make sharing medical images outside an individual institution a complex process. The Cancer Imaging Archive (TCIA) (TCIA) is a free public service funded by the National Cancer Institute which addresses this challenge by providing hosting and de-identification services to take major burdens of data sharing off researchers. TCIA has published over 170 unique data collections containing more than 70 million images. Recognizing that images alone are not enough to conduct meaningful research, most collections are linked to rich supporting data including patient outcomes, treatment information, genomic / proteomic analyses, and expert image analyses (segmentations, annotations, and radiomic / radiogenomic features). This deep learning lab will teach the skills needed to fully access our existing data as well as learn how to submit new data for potential inclusion in TCIA so that it can be used for artificial intelligence research.

#### LEARNING OBJECTIVES

1) Learn how TCIA makes data sharing easier for researchers, and hear a summary of existing datasets that are freely available for download 2) Practice utilizing TCIA for data exploration, cohort definition, and downloading of data 3) Learn how to access public and restricted access datasets using TCIA's REST APIs and other command line tools via Google Colab\*Course Description In Person Session Only. On-demand beginning on December 5th. Access to large, high quality data is essential for researchers to understand disease and precision medicine pathways, especially in cancer. However HIPAA constraints make sharing medical images outside an individual institution a complex process. The Cancer Imaging Archive (TCIA) (TCIA) is a free public service funded by the National Cancer Institute which addresses this challenge by providing hosting and de-identification services to take major burdens of data sharing off researchers. TCIA has published over 170 unique data collections containing more than 70 million images. Recognizing that images alone are not enough to conduct meaningful research, most collections are linked to rich supporting data including patient outcomes, treatment information, genomic / proteomic analyses, and expert image analyses (segmentations, annotations, and radiomic / radiogenomic features). This deep learning lab will teach the skills needed to fully access our existing data as well as learn how to submit new data for potential inclusion in TCIA so that it can be used for artificial intelligence research.

Printed on: 02/07/23



## Abstract Archives of the RSNA, 2022

DLL06

### Deep Learning Lab: MedNIST Exam Classification with MONAI

Monday, Nov. 28 12:00PM - 1:00PM Room: NA

#### Participants

Bradley Erickson, MD, PhD, Rochester, MN (*Presenter*) Board of Directors, VoiceIt Technologies, LLC; Stockholder, VoiceIt Technologies, LLC; Board of Directors, FLOWSIGMA Inc; Officer, FLOWSIGMA Inc; Stockholder, FLOWSIGMA Inc; Officer, Yunu Inc; Stockholder, Yunu Inc

Kuan Zhang, PhD, , MN (*Presenter*) Nothing to Disclose

Jayashree Kalpathy-Cramer, MS, PhD, Charlestown, MA (*Presenter*) Institutional Research Grant, General Electric Company; Institutional Research Grant, F. Hoffmann-La Roche Ltd; Institutional Research Grant, Bayer AG

#### COURSE DESCRIPTION

In Person Session Only. On-demand beginning on December 5th. Medical image classification plays an essential role in aiding clinical diagnosis and treatment. With the rapid development of artificial intelligence (AI) and computer vision (CV), deep learning-based methods become more accurate and applicable to a variety of clinical tasks ---- potentially serving as a valuable ally for radiologists and pathologists. In this course, learners will get a hands-on practical introduction to deep learning for radiology and medical imaging. An end-to-end training and evaluation example based on the MedNIST dataset will be covered. We will introduce the "MONAI" deep learning platform, which is a Pytorch-based, open-source framework for deep learning in healthcare imaging.

#### LEARNING OBJECTIVES

1) Learn how to collect, format, and standardize medical image data 2) Use MONAI transforms to pre-process data 3) Learn to architect and train a convolutional neural network (CNN) in Pytorch for classification 4) Learn how to evaluate the trained model on test dataset\*Course Description In Person Session Only. On-demand beginning on December 5th. Medical image classification plays an essential role in aiding clinical diagnosis and treatment. With the rapid development of artificial intelligence (AI) and computer vision (CV), deep learning-based methods become more accurate and applicable to a variety of clinical tasks ---- potentially serving as a valuable ally for radiologists and pathologists. In this course, learners will get a hands-on practical introduction to deep learning for radiology and medical imaging. An end-to-end training and evaluation example based on the MedNIST dataset will be covered. We will introduce the "MONAI" deep learning platform, which is a Pytorch-based, open-source framework for deep learning in healthcare imaging.

Printed on: 02/07/23



## Abstract Archives of the RSNA, 2022

DLL07

### Deep Learning Lab: CT Body Part Classification

Monday, Nov. 28 1:30PM - 2:30PM Room: NA

#### Participants

Ish Talati, MSc, Lake Forest, CA (*Presenter*) Nothing to Disclose

Ross Filice, MD, Washington, DC (*Presenter*) Advisor, BunkerHill Health, Inc;Shareholder, BunkerHill Health, Inc;Speaker, General Electric Company;Speaker, Koios Medical;Researcher, Koios Medical

#### COURSE DESCRIPTION

In Person Session Only. On-demand beginning on December 5th.Learn what you can do with an artificial intelligence model after development is complete. We will review an existing tool that automatically determines body part in CT and inspect raw outputs, consider different ways to use these outputs depending on the target application, and display and visualize these outputs in rich intuitive means. Feel free to take the existing architecture and weights home to build a better one!

#### LEARNING OBJECTIVES

1) Evaluate an artificial intelligence model designed to determine body part in CT after development2) Learn how to interpret raw outputs from this model3) Build graphs and visualizations to help understand performance\*Course Description In Person Session Only. On-demand beginning on December 5th.Learn what you can do with an artificial intelligence model after development is complete. We will review an existing tool that automatically determines body part in CT and inspect raw outputs, consider different ways to use these outputs depending on the target application, and display and visualize these outputs in rich intuitive means. Feel free to take the existing architecture and weights home to build a better one!

Printed on: 02/07/23



## Abstract Archives of the RSNA, 2022

DLL08

### Deep Learning Lab: NLP - Text Classification with RNNs & Transformers

Monday, Nov. 28 3:00PM - 4:00PM Room: NA

#### Participants

Kirti Magudia, MD, PhD, Durham, NC (*Presenter*) Nothing to Disclose  
Walter Wiggins, MD, PhD, Durham, NC (*Presenter*) Advisor, Qure.ai;

#### COURSE DESCRIPTION

In Person Session Only. On-demand beginning on December 5th. This interactive course will provide participants with the opportunity to learn the basic principles of information extraction from radiology reports by working through a step-by-step example using radiology reports from a chest radiograph data set. Learners will train a model to classify radiology reports as positive or negative for opacity. This session will cover basics of text analysis and concepts in preprocessing and model training. No prior coding or machine learning experience is necessary.

#### LEARNING OBJECTIVES

1) Understand the basic steps required to prepare data for information extraction with natural language processing (NLP) tools. 2) Define the basic terminology of NLP for text analysis (e.g. preprocessing, tokenization). 3) Train an NLP model to classify chest radiograph reports as 'positive' or 'negative' for abnormal findings. \*Course Description In Person Session Only. On-demand beginning on December 5th. This interactive course will provide participants with the opportunity to learn the basic principles of information extraction from radiology reports by working through a step-by-step example using radiology reports from a chest radiograph data set. Learners will train a model to classify radiology reports as positive or negative for opacity. This session will cover basics of text analysis and concepts in preprocessing and model training. No prior coding or machine learning experience is necessary.

Printed on: 02/07/23



## Abstract Archives of the RSNA, 2022

DLL09

### Deep Learning Lab: YOLO-Bounding Box Segmentation & Classification (Part 1)

Tuesday, Nov. 29 10:00AM - 11:00AM Room: NA

#### Participants

Bradley Erickson, MD, PhD, Rochester, MN (*Presenter*) Board of Directors, VoiceIt Technologies, LLC; Stockholder, VoiceIt Technologies, LLC; Board of Directors, FLOWSIGMA Inc; Officer, FLOWSIGMA Inc; Stockholder, FLOWSIGMA Inc; Officer, Yunu Inc; Stockholder, Yunu Inc  
Pouria Rouzrokh, MD, MPH, Rochester, MN (*Presenter*) Nothing to Disclose

#### COURSE DESCRIPTION

In Person Session Only. On-demand beginning on December 5th. Deep learning is attracting more and more attention in all medical fields, especially medical imaging. Nowadays we have access to many valid and reliable deep learning models that can help radiologists in detecting pathologies, differentiating benign and malignant masses, segmenting organs, or even enhancing the quality of different imaging modalities. This course aims to further improve the toolbox diversity of those interested in applying deep learning to medical imaging by introducing an easy way to train and apply object detection deep learning models. These models are used to detect objects of interest in given images and put bounding boxes around them. We will start our course with a brief review of the field of object detection and then proceed to introduce You Look Only Once (YOLO) which is probably the most recognized and easy-to-use object detection model. This training workshop covers the theories of the object detection models and introduces the different components of a modern YOLO architecture. However, it is worth mentioning that immediately after the current workshop, we will hold another session that is hands-on, and will let you practice training and applying the YOLO model in Python and using Google Colab notebooks. So, we recommend you take part in both workshops together.

#### LEARNING OBJECTIVES

1) Define object detection deep learning models, their scope, and applications in medical imaging 2) Introduce the object detection model "You Look Only Once (YOLO)" and explain its general underlying principles, different versions, and recent advancements\*Course Description In Person Session Only. On-demand beginning on December 5th. Deep learning is attracting more and more attention in all medical fields, especially medical imaging. Nowadays we have access to many valid and reliable deep learning models that can help radiologists in detecting pathologies, differentiating benign and malignant masses, segmenting organs, or even enhancing the quality of different imaging modalities. This course aims to further improve the toolbox diversity of those interested in applying deep learning to medical imaging by introducing an easy way to train and apply object detection deep learning models. These models are used to detect objects of interest in given images and put bounding boxes around them. We will start our course with a brief review of the field of object detection and then proceed to introduce You Look Only Once (YOLO) which is probably the most recognized and easy-to-use object detection model. This training workshop covers the theories of the object detection models and introduces the different components of a modern YOLO architecture. However, it is worth mentioning that immediately after the current workshop, we will hold another session that is hands-on, and will let you practice training and applying the YOLO model in Python and using Google Colab notebooks. So, we recommend you take part in both workshops together.

Printed on: 02/07/23



## Abstract Archives of the RSNA, 2022

DLL10

### Deep Learning Lab: Generative Adversarial Networks

Tuesday, Nov. 29 11:30AM - 12:30PM Room: NA

#### Participants

Bradley Erickson, MD, PhD, Rochester, MN (*Presenter*) Board of Directors, VoiceIt Technologies, LLC; Stockholder, VoiceIt Technologies, LLC; Board of Directors, FLOWSIGMA Inc; Officer, FLOWSIGMA Inc; Stockholder, FLOWSIGMA Inc; Officer, Yunu Inc; Stockholder, Yunu Inc

Bardia Khosravi, MD, MPH, Rochester, MN (*Presenter*) Nothing to Disclose

#### COURSE DESCRIPTION

In Person Session Only. On-demand beginning on December 5th. Generative adversarial networks (GANs) have evolved over the past several years and are being widely used for faster image acquisition, image quality improvement, and data augmentation, among many other applications. This hands-on workshop will cover the theoretical bases of GAN training and its applications in Radiology and introduce some of the well-known algorithms in this field. Finally, we will train a GAN to create synthetic lesions for data augmentation.

#### LEARNING OBJECTIVES

1) Identify the applications of generative adversarial networks (GANs) in Radiology  
2) Explain the general intuition behind GAN training  
3) Train a GAN-based model to create synthetic lesions to augment the real data.\*Course Description In Person Session Only. On-demand beginning on December 5th. Generative adversarial networks (GANs) have evolved over the past several years and are being widely used for faster image acquisition, image quality improvement, and data augmentation, among many other applications. This hands-on workshop will cover the theoretical bases of GAN training and its applications in Radiology and introduce some of the well-known algorithms in this field. Finally, we will train a GAN to create synthetic lesions for data augmentation.

Printed on: 02/07/23



## Abstract Archives of the RSNA, 2022

DLL11

### Deep Learning Lab: Best Practices for Model Training: Architectures, Hyperparameters & Optimization

Tuesday, Nov. 29 1:00PM - 2:00PM Room: NA

#### Participants

Peter Chang, MD, Irvine, CA (*Presenter*) Co-founder, Avicenna.ai; Stockholder, Avicenna.ai; Research Grant, Canon Medical Systems Corporation; Speakers Bureau, Canon Medical Systems Corporation; Research Grant, General Electric Company

#### COURSE DESCRIPTION

In Person Session Only. On-demand beginning on December 7.

Printed on: 02/07/23



## Abstract Archives of the RSNA, 2022

DLL12

### Deep Learning Lab: YOLO-Bounding Box Segmentation & Classification (Part 2)

Wednesday, Nov. 30 10:00AM - 11:00AM Room: NA

#### Participants

Bradley Erickson, MD, PhD, Rochester, MN (*Presenter*) Board of Directors, VoiceIt Technologies, LLC; Stockholder, VoiceIt Technologies, LLC; Board of Directors, FLOWSIGMA Inc; Officer, FLOWSIGMA Inc; Stockholder, FLOWSIGMA Inc; Officer, Yunu Inc; Stockholder, Yunu Inc  
Pouria Rouzrokh, MD, MPH, Rochester, MN (*Presenter*) Nothing to Disclose

#### COURSE DESCRIPTION

In Person Session Only. On-demand beginning on December 5th. Deep learning is attracting more and more attention in all medical fields, especially medical imaging. Nowadays we have access to many valid and reliable deep learning models that can help radiologists in detecting pathologies, differentiating benign and malignant masses, segmenting organs, or even enhancing the quality of different imaging modalities. This course aims to further improve the toolbox diversity of those interested in applying deep learning to medical imaging by introducing an easy way to train and apply object detection deep learning models. These models are used to detect objects of interest in given images and put bounding boxes around them. We will start our course with a brief review of the field of object detection and then proceed to introduce You Look Only Once (YOLO), version 5, which is probably the most recognized and easy-to-use object detection model. This training is hands-on, and you will spend most of the course coding on Google Colab notebooks, so at least basic familiarity with Python and deep learning models (preferentially with PyTorch) is recommended. Also, please have your Gmail account set up and ready to use!

#### LEARNING OBJECTIVES

1) Define object detection deep learning models, their scope, and applications in medical imaging. 2) Introduce the object detection model "You Look Only Once (YOLO)" and explain its general underlying principles, different versions, and recent advancements. 3) Using a public dataset of brain CT scans including different hemorrhage types, Demonstrate how to train a PyTorch implementation of YOLO v5 on custom medical imaging datasets, apply it to unseen images, and interpret the inference results.\*Course Description  
In Person Session Only. On-demand beginning on December 5th. Deep learning is attracting more and more attention in all medical fields, especially medical imaging. Nowadays we have access to many valid and reliable deep learning models that can help radiologists in detecting pathologies, differentiating benign and malignant masses, segmenting organs, or even enhancing the quality of different imaging modalities. This course aims to further improve the toolbox diversity of those interested in applying deep learning to medical imaging by introducing an easy way to train and apply object detection deep learning models. These models are used to detect objects of interest in given images and put bounding boxes around them. We will start our course with a brief review of the field of object detection and then proceed to introduce You Look Only Once (YOLO), version 5, which is probably the most recognized and easy-to-use object detection model. This training is hands-on, and you will spend most of the course coding on Google Colab notebooks, so at least basic familiarity with Python and deep learning models (preferentially with PyTorch) is recommended. Also, please have your Gmail account set up and ready to use!

Printed on: 02/07/23



## Abstract Archives of the RSNA, 2022

DLL13

### Deep Learning Lab: Building Custom Deep Learning Models with PyTorch

Wednesday, Nov. 30 11:30AM - 12:30PM Room: NA

#### Participants

Felipe C. Kitamura, MD, PhD, Sao Paulo, SP (*Presenter*) Consultant, MD.ai, Inc;Speaker, General Electric Company  
Ian Pan, MD, Brookline, MA (*Presenter*) Consultant, MD.ai, Inc;Consultant, Centaur Labs Inc;Consultant, Diagnosticos da America SA;Consultant, CoRead AI

#### COURSE DESCRIPTION

In Person Session Only. On-demand beginning on December 5th. Building custom deep learning models with PyTorch. This session will focus on using the pytorch-image-models library ("timm") to train both standards and modified deep learning models for radiology. Intermediate audience. Experience with Python and a basic understanding of deep learning.

#### LEARNING OBJECTIVES

1) Explain the syntax of PyTorch model architecture  
2) Load pretrained architectures and modify them  
3) Define train and eval modes  
\*Course Description In Person Session Only. On-demand beginning on December 5th. Building custom deep learning models with PyTorch. This session will focus on using the pytorch-image-models library ("timm") to train both standards and modified deep learning models for radiology. Intermediate audience. Experience with Python and a basic understanding of deep learning.

Printed on: 02/07/23



## Abstract Archives of the RSNA, 2022

DLL14

### Deep Learning Lab: DICOM In, DICOM Out for Segmentation

Wednesday, Nov. 30 1:00PM - 2:00PM Room: NA

#### Participants

Thomas Loehfelm, MD, PhD, Sacramento, CA (*Presenter*) Nothing to Disclose

#### COURSE DESCRIPTION

In Person Session Only. On-demand beginning on December 5th. In this hands-on workshop participants will learn about DICOM standard segmentation objects, including their storage and retrieval from a DICOMweb-compliant PACS. We will also train an abdominal organ segmentation algorithm using native DICOM/DICOMSEG as the training inputs.

#### LEARNING OBJECTIVES

1) Review DICOM SEG and open-source DICOM SEG libraries 2) Create and store DICOM SEG using DICOMweb 3) Train an abdominal organ segmenter from native DICOM/DICOM SEG inputs\*Course Description In Person Session Only. On-demand beginning on December 5th. In this hands-on workshop participants will learn about DICOM standard segmentation objects, including their storage and retrieval from a DICOMweb-compliant PACS. We will also train an abdominal organ segmentation algorithm using native DICOM/DICOMSEG as the training inputs.

Printed on: 02/07/23



## Abstract Archives of the RSNA, 2022

DLL15

### Deep Learning Lab: Accelerate your AI-based Medical Imaging Research with MONAI Core on SageMaker

Thursday, Dec. 1 9:00AM - 10:00AM Room: NA

#### Participants

Steve Fu, East Palo Alto, CA (*Presenter*) Nothing to Disclose

Christoph Russ, CH-8002 Zurich, Switzerland (*Presenter*) Nothing to Disclose

Christopher Austin, MD,MSc, Sammamish, WA (*Moderator*) Nothing to Disclose

#### COURSE DESCRIPTION

In Person Session Only. On-demand beginning on December 5th. Artificial Intelligence has been proven to support radiologist clinical decision making and to help reduce doctor burnout. Amazon SageMaker is end-to-end data science platform to build, train, and run machine learning models. MONAI Core is a PyTorch-based, open-source library for deep learning training of medical imaging models. In this workshop, researchers and data scientists will learn how MONAI Core running on SageMaker lets them explore more deep neural network architectures, more hyperparameters, and more hypotheses compared to static on-prem infrastructure for medical imaging workloads. They will also learn how to use the open source ITKWidgets library as part of the data science preprocessing phase to create interactive 3D medical image visualizations directly in Jupyter notebooks.

#### LEARNING OBJECTIVES

1) Running managed training and hyperparameter tuning jobs on Amazon SageMaker in combination with MONAI Core. 2) Creating interactive visualizations of medical images using ITKWidgets in SageMaker Notebooks.\*Course Description In Person Session Only. On-demand beginning on December 5th. Artificial Intelligence has been proven to support radiologist clinical decision making and to help reduce doctor burnout. Amazon SageMaker is end-to-end data science platform to build, train, and run machine learning models. MONAI Core is a PyTorch-based, open-source library for deep learning training of medical imaging models. In this workshop, researchers and data scientists will learn how MONAI Core running on SageMaker lets them explore more deep neural network architectures, more hyperparameters, and more hypotheses compared to static on-prem infrastructure for medical imaging workloads. They will also learn how to use the open source ITKWidgets library as part of the data science preprocessing phase to create interactive 3D medical image visualizations directly in Jupyter notebooks.

Printed on: 02/07/23



## Abstract Archives of the RSNA, 2022

DLL16

### Deep Learning Lab: Multimodal Fusion for Pulmonary Embolism Detection Using CTs and Patient EMR

Thursday, Dec. 1 10:30AM - 11:30AM Room: NA

#### Participants

Matthew P. Lungren, MD, Palo Alto, CA (*Presenter*) Advisor, Segmed, Inc; Shareholder, Segmed, Inc; Advisor, Bunkerhill Health; Shareholder, Bunkerhill Health; Employee, Microsoft Corporation  
Mars Huang, PhD, Stanford, CA (*Presenter*) Nothing to Disclose

#### COURSE DESCRIPTION

In Person Session Only. On-demand beginning on December 5th. The practice of modern medicine relies heavily on the synthesis of information from multiple sources. Yet most deep learning models for medical imaging applications consider only pixel-value without data informing clinical context. As with human physicians, automated detection and classification systems that can successfully utilize both medical imaging data together with clinical data from the EHR (multimodal fusion), such as patient demographics, previous diagnoses, and laboratory values, may lead to better performing and more clinically relevant models. In this course, you will learn the fundamentals of different data fusion strategies and gain hands-on experience applying them for the task of pulmonary embolism detection.

#### LEARNING OBJECTIVES

1) Understand key terminologies and techniques for multimodal fusion (early, late, joint) and learn the pros and cons of each strategy. 2) Gain practical experiences applying different fusion strategies to a real-world dataset for the task of Pulmonary Embolism detection. \*Course Description In Person Session Only. On-demand beginning on December 5th. The practice of modern medicine relies heavily on the synthesis of information from multiple sources. Yet most deep learning models for medical imaging applications consider only pixel-value without data informing clinical context. As with human physicians, automated detection and classification systems that can successfully utilize both medical imaging data together with clinical data from the EHR (multimodal fusion), such as patient demographics, previous diagnoses, and laboratory values, may lead to better performing and more clinically relevant models. In this course, you will learn the fundamentals of different data fusion strategies and gain hands-on experience applying them for the task of pulmonary embolism detection.

Printed on: 02/07/23



## Abstract Archives of the RSNA, 2022

M1-CAS02

### Feeling Crispy? How To Stay Cool in The Burnout Climate (Sponsored by the Associated Sciences Consortium)

Monday, Nov. 28 8:00AM - 9:00AM Room: NA

#### Participants

Jennifer Clayton, MBA, RT, Albany, OR (*Presenter*) Nothing to Disclose

Susie Moseley, MS, RT, Albuquerque, NM (*Moderator*) Nothing to Disclose

#### COURSE DESCRIPTION

It's clear that burnout is creating a major impact on healthcare disciplines including imaging. Burnout affects personnel at all levels in every organization leading to historic staffing shortages, impacting patient outcomes, and is causing us to redefine our roles as healthcare professionals. During this lecture, we will discuss contributing factors and review practical solutions to help us create a more sustainable environment for personnel and patients.

#### LEARNING OBJECTIVES

1) Identify trends relating to fatigue in imaging 2) Discuss how burnout impacts personnel, patients, and organizations 3) Review practices to mitigate burnout 4) Consider approaches to restoring enthusiasm in our roles (e.g., leadership, technologists)\*Course Description It's clear that burnout is creating a major impact on healthcare disciplines including imaging. Burnout affects personnel at all levels in every organization leading to historic staffing shortages, impacting patient outcomes, and is causing us to redefine our roles as healthcare professionals. During this lecture, we will discuss contributing factors and review practical solutions to help us create a more sustainable environment for personnel and patients.

Printed on: 02/07/23



## Abstract Archives of the RSNA, 2022

M1-CBR11

### Challenging Breast Cases: A Game Show USA Versus Europe

Monday, Nov. 28 8:00AM - 9:00AM Room: NA

#### Participants

Stamatia Destounis, MD, Rochester, NY (*Presenter*) Medical Advisory Board, iCad, Inc  
Thiemo Van Nijnatten, Maastricht, Netherlands (*Presenter*) Nothing to Disclose  
Mary Sun, MD, New York, NY (*Presenter*) Nothing to Disclose  
John Lewin, MD, Denver, CO (*Presenter*) Officer, Novian Health Inc  
Michael H. Fuchsjager, MD, Graz, Austria (*Presenter*) Nothing to Disclose  
Nisha Sharma, MBChB, FRCR, Leeds, United Kingdom (*Presenter*) Nothing to Disclose  
Rudolf Pijnappel, MD, PhD, Huis ter Heide, Netherlands (*Presenter*) Nothing to Disclose

#### COURSE DESCRIPTION

This Game Show "USA Versus Europe" is a highly entertaining image interpretation quiz focused on breast imaging cases in an intriguing competitive format between two teams. A delegation of a junior and a senior breast imaging expert as well as the respective president, from the Society of Breast Imaging (SBI) and the European Society of Breast Imaging (EUSOBI), will "clash" in a friendly contention. Based on clinical information and images, intermediate and expert breast cases will be discussed and solved beyond BI-RADS and management recommendations. All of this will be happening in an highly interactive format involving the audience. In case of an official draw, a tiebreak will be considered. Don't miss out on this greatest of radiology shows!

#### LEARNING OBJECTIVES

1) To appreciate expert stepwise approach to solving breast imaging cases 2) To understand linking imaging features to potential histopathology diagnosis 3) To enjoy radiology beyond image interpretation\*Course Description This Game Show "USA Versus Europe" is a highly entertaining image interpretation quiz focused on breast imaging cases in an intriguing competitive format between two teams. A delegation of a junior and a senior breast imaging expert as well as the respective president, from the Society of Breast Imaging (SBI) and the European Society of Breast Imaging (EUSOBI), will "clash" in a friendly contention. Based on clinical information and images, intermediate and expert breast cases will be discussed and solved beyond BI-RADS and management recommendations. All of this will be happening in an highly interactive format involving the audience. In case of an official draw, a tiebreak will be considered. Don't miss out on this greatest of radiology shows!

Printed on: 02/07/23



## Abstract Archives of the RSNA, 2022

M1-CCA12

### Mentored Cardiac Case Review: Imaging the Heart: Imaging Techniques, Anatomy and Function

Monday, Nov. 28 8:00AM - 9:00AM Room: NA

#### Participants

Diana Litmanovich, MD, Boston, MA (*Presenter*) Nothing to Disclose  
Suhny Abbara, MD, Dallas, TX (*Presenter*) Royalties, RELX  
Carole A. Ridge, MD, London, (*Presenter*) Nothing to Disclose  
Kyle Spearman, MD, Seattle, WA (*Presenter*) Nothing to Disclose  
Jill Jacobs, MD, New York, NY (*Moderator*) Nothing to Disclose

Printed on: 02/07/23



## Abstract Archives of the RSNA, 2022

M1-CCH09

### Pulmonary Vascular Imaging: CTEPH/Pulmonary Hypertension

Monday, Nov. 28 8:00AM - 9:00AM Room: NA

#### Participants

Martine J. Remy-Jardin, MD, PhD, Lille, France (*Presenter*) Research Grant, Siemens AG; *Speaker*, Siemens AG

Seth J. Kligerman, MD, La Jolla, CA (*Presenter*) Speakers Bureau, Boehringer Ingelheim GmbH Consultant, Riverain Technologies, LLC Consultant, Bayer AG

Ann N. Leung, MD, Stanford, CA (*Presenter*) Nothing to Disclose

Deepa Gopalan, MRCP, FRCR, Stockholm, Sweden (*Presenter*) Speakers Bureau, Bayer AG; *Speakers Bureau*, Actelion Ltd

#### COURSE DESCRIPTION

Chronic thromboembolic pulmonary hypertension (CTEPH) is a potentially curable form of pulmonary hypertension that develops in approximately 3% of patients with pulmonary embolism. CTEPH is a dual vascular disorder characterized by obstruction of the pulmonary vasculature by organized thromboembolic material and a secondary arteriopathic process affecting small resistance vessels. Untreated, CTEPH can lead to right heart failure and death. Diagnosis of CTEPH is made on the basis of imaging. This course presented in lecture-style format will discuss the relative strengths and weaknesses of the different diagnostic modality options as well as the characteristic imaging features of CTEPH on each. The session will include a case-based review to reinforce the imaging appearance of CTEPH and allow its differentiation from mimics.

#### LEARNING OBJECTIVES

1) Recognize and diagnose CTEPH on imaging studies 2) Distinguish CTEPH from other conditions that affect the pulmonary vasculature\*  
Course Description Chronic thromboembolic pulmonary hypertension (CTEPH) is a potentially curable form of pulmonary hypertension that develops in approximately 3% of patients with pulmonary embolism. CTEPH is a dual vascular disorder characterized by obstruction of the pulmonary vasculature by organized thromboembolic material and a secondary arteriopathic process affecting small resistance vessels. Untreated, CTEPH can lead to right heart failure and death. Diagnosis of CTEPH is made on the basis of imaging. This course presented in lecture-style format will discuss the relative strengths and weaknesses of the different diagnostic modality options as well as the characteristic imaging features of CTEPH on each. The session will include a case-based review to reinforce the imaging appearance of CTEPH and allow its differentiation from mimics.

Printed on: 02/07/23



## Abstract Archives of the RSNA, 2022

M1-CGI12

### Artificial Intelligence in Abdominal Imaging

Monday, Nov. 28 8:00AM - 9:00AM Room: NA

#### Participants

Tessa S. Cook, MD, PhD, Philadelphia, PA (*Presenter*) Grant, Siemens AG; Grant, Independence Blue Cross; Speaker, Sectra AB  
Brett Marinelli, MD, MS, New York, NY (*Presenter*) Research Consultant, Cibiem Inc  
Imon Banerjee, Stanford, GA (*Presenter*) Nothing to Disclose  
Errol Colak, MD, Toronto, ON (*Presenter*) Nothing to Disclose  
George L. Shih, MD, New York, NY (*Presenter*) Consultant, MD.ai, Inc; Shareholder, MD.ai, Inc

Printed on: 02/07/23



## Abstract Archives of the RSNA, 2022

M1-CGU02

### Prostate MRI and Molecular Imaging: Core and Advanced Applications

Monday, Nov. 28 8:00AM - 9:00AM Room: NA

#### Participants

Aytekin Oto, MD, Crete, IL (*Presenter*) Research Grant, Koninklijke Philips NV; Medical Advisory Board, Profound Medical Inc; Consultant, IBM Corporation; Co-founder, Qmis LLC; Co-owner, Qmis LLC

Baris Turkbey, MD, Rockville, MD (*Presenter*) Nothing to Disclose

Delphine Chen, MD, Seattle, WA (*Presenter*) Grant, Telix Pharmaceuticals Limited; Speaker, Telix Pharmaceuticals Limited

Anwar Padhani, MD, FRCR, Northwood, United Kingdom (*Presenter*) Advisory Board, Siemens AG; Speakers Bureau, Siemens AG; Advisory Board, Lucida Medical Ltd; Stockholder, Lucida Medical Ltd

#### COURSE DESCRIPTION

This session aims to provide a comprehensive update on the latest developments on prostate imaging with a special focus on MR and PET imaging. The presentations cover a well-balanced, broad scope from practical, updated tips for optimized prostate MR acquisition and interpretation to new techniques such as PET MRI. PSMA PET imaging. Their role in the management of prostate cancer will be reviewed in addition to other hot topics in prostate MR including disparities in imaging access, quality control efforts and artificial intelligence.

#### LEARNING OBJECTIVES

1) Learn about the latest updates on prostate imaging with special emphasis on MRI and PET imaging 2) Review the quality control efforts for prostate MR and explain the current and future applications of artificial intelligence on prostate imaging 3) Understand the potential roles and added value of PSMA PET and PET MR in the management of patients with prostate cancer 4) Identify the basics of healthcare disparities in prostate imaging and review ways for mitigating them.\*Course Description This session aims to provide a comprehensive update on the latest developments on prostate imaging with a special focus on MR and PET imaging. The presentations cover a well-balanced, broad scope from practical, updated tips for optimized prostate MR acquisition and interpretation to new techniques such as PET MRI. PSMA PET imaging. Their role in the management of prostate cancer will be reviewed in addition to other hot topics in prostate MR including disparities in imaging access, quality control efforts and artificial intelligence.

Printed on: 02/07/23



## Abstract Archives of the RSNA, 2022

M1-CIN01

### Artificial Intelligence and Cybersecurity in Healthcare

Monday, Nov. 28 8:00AM - 9:00AM Room: NA

#### Participants

Benoit Desjardins, MD, PhD, Philadelphia, PA (*Presenter*) Nothing to Disclose  
Shandong Wu, PhD, Pittsburgh, PA (*Presenter*) Nothing to Disclose  
Richard Staynings, New York, NY (*Presenter*) Nothing to Disclose

#### COURSE DESCRIPTION

Cybercrime against healthcare institutions has exploded in recent years. In 2021, more than 1 in 3 healthcare organizations reported being hit by ransomware. The situation has been considerably worsened by the pandemic, which produced a triple threat for healthcare systems: a rapid expansion of internet-connected technologies and services causing an expanded attack surface, an increase in many types of cyberattacks, and fewer available resources to defend against cyberattacks. Cybersecurity has become an important part of healthcare, and every radiology practice can become a victim of a cyber-attack. Artificial Intelligence (AI) is now extensively used by both attackers ("Offensive AI") and defenders ("Defensive AI"). In this refresher course, we will explore three forms of interaction between AI and cybersecurity that affect healthcare: (1) Offensive AI: how cybercriminals are weaponizing artificial intelligence to improve their attacks against medical institutions. This will be discussed by Richard Staynings, a cybersecurity guru and consultant for multiple companies. He will provide a cutting-edge picture of how cyber-criminals are currently using AI to improve success of different types of attacks, such as phishing, scanning, and intrusions of medical centers. (2) Defensive AI: how cyber-defense teams at medical centers are using artificial intelligence to supplement the limited capabilities of humans to detect and defend against cyberattacks, especially now that many of those cyberattacks are controlled by artificial intelligence. This will be discussed by Benoit Desjardins, a radiologist and world leader in cybersecurity in healthcare, recently a Visiting Professor in artificial intelligence at Stanford. (3) AI model safety: how cyber-threats can disrupt the integrity of medical images, and how this affects diagnosis by AI and humans. This provides an overview of the multiple ways in which data can be modified to fool AI algorithms. This will be discussed by Shandong Wu, a top leader in artificial intelligence. This will be followed by a panel combining our three experts, to discuss the practical implications for radiology practices. This refresher course will bring the radiology community up to date on the latest interaction between artificial intelligence and cybersecurity affecting healthcare, including recent attacks, and techniques of defense. The course will be presented by radiologists and top cybersecurity and artificial intelligence experts. The information technology issues will be addressed at a technical level appropriate for the radiology community at large, to make the community aware of this growing era of digital warfare and its implications for radiology practices. Our refresher course will have practical, actionable suggestions that radiologists and IT administrators could act on now.

#### LEARNING OBJECTIVES

1) Identify how cybercriminals are using offensive artificial intelligence (AI) to attack medical centers 2) Explain how defensive AI can be used to protect healthcare systems from cyberattacks 3) Illustrate how cyber-manipulations of images can affect outcomes of AI algorithms\*Course Description Cybercrime against healthcare institutions has exploded in recent years. In 2021, more than 1 in 3 healthcare organizations reported being hit by ransomware. The situation has been considerably worsened by the pandemic, which produced a triple threat for healthcare systems: a rapid expansion of internet-connected technologies and services causing an expanded attack surface, an increase in many types of cyberattacks, and fewer available resources to defend against cyberattacks. Cybersecurity has become an important part of healthcare, and every radiology practice can become a victim of a cyber-attack. Artificial Intelligence (AI) is now extensively used by both attackers ("Offensive AI") and defenders ("Defensive AI"). In this refresher course, we will explore three forms of interaction between AI and cybersecurity that affect healthcare: (1) Offensive AI: how cybercriminals are weaponizing artificial intelligence to improve their attacks against medical institutions. This will be discussed by Richard Staynings, a cybersecurity guru and consultant for multiple companies. He will provide a cutting-edge picture of how cyber-criminals are currently using AI to improve success of different types of attacks, such as phishing, scanning, and intrusions of medical centers. (2) Defensive AI: how cyber-defense teams at medical centers are using artificial intelligence to supplement the limited capabilities of humans to detect and defend against cyberattacks, especially now that many of those cyberattacks are controlled by artificial intelligence. This will be discussed by Benoit Desjardins, a radiologist and world leader in cybersecurity in healthcare, recently a Visiting Professor in artificial intelligence at Stanford. (3) AI model safety: how cyber-threats can disrupt the integrity of medical images, and how this affects diagnosis by AI and humans. This provides an overview of the multiple ways in which data can be modified to fool AI algorithms. This will be discussed by Shandong Wu, a top leader in artificial intelligence. This will be followed by a panel combining our three experts, to discuss the practical implications for radiology practices. This refresher course will bring the radiology community up to date on the latest interaction between artificial intelligence and cybersecurity affecting healthcare, including recent attacks, and techniques of defense. The course will be presented by radiologists and top cybersecurity and artificial intelligence experts. The information technology issues will be addressed at a technical level appropriate for the radiology community at large, to make the community aware of this growing era of digital warfare and its implications for radiology practices. Our refresher course will have practical, actionable suggestions that radiologists and IT administrators could act on now.



## Abstract Archives of the RSNA, 2022

M1-CIR05

### IR Game Show - JeopIRdy

Monday, Nov. 28 8:00AM - 9:00AM Room: NA

#### Participants

Anne Marie Cahill, MBBCh, Philadelphia, PA (*Presenter*) Advisory Committee, Siemens AG;Speakers Bureau, Avanos Medical, Inc  
Ron C. Gaba, MD, Chicago, IL (*Presenter*) Research Grant, Guerbet SA;Research Grant, Johnson & Johnson;Research Grant, NeoTherma Oncology;Research Grant, TriSalus Life Sciences;;  
Anne Roberts, MD, La Jolla, CA (*Presenter*) Nothing to Disclose  
Brian Funaki, MD, Riverside, IL (*Presenter*) Consultant, Okami Medical;Advisory Board, Balt USA  
Saher S. Sabri, MD, Washington, DC (*Presenter*) Advisory Board, Medtronic plc;Advisory Board, Boston Scientific Corporation;Data Safety Monitoring Board, Alucent Biomedical, Inc  
Sarah White, MD, MS, Milwaukee, WI (*Presenter*) Consultant, Cook Group Incorporated;Consultant, Guerbet SA;Research support, Guerbet SA;Consultant, DB Medical Supplies, Inc;Consultant, Sirtex Medical Ltd;Research support, InSightec Ltd;Speakers Bureau, Penumbra, Inc  
Osmanuddin Ahmed, MD, Northbrook, IL (*Presenter*) Speaker, Canon Medical Systems Corporation;Research Grant, Canon Medical Systems Corporation;Speaker, Becton, Dickinson and Company;Speaker, Cook Group Incorporated;Advisory Board, Boston Scientific Corporation;Advisory Board, Argon Medical Devices, Inc;Speaker, Koninklijke Philips NV;Speaker, Argon Medical Devices, Inc;Advisory Board, Argon Medical Devices, Inc;Consultant, Asahi Kasei Medical Co, Ltd;Consultant, Medtronic plc;Speaker, Penumbra, Inc;Speaker, Inari Medical, Inc  
Robert L. Vogelzang, MD, Chicago, IL (*Presenter*) Nothing to Disclose  
Sean Tutton, MD, Milwaukee, WI (*Presenter*) Consultant, Boston Scientific Corporation;Consultant, Galil Medical Ltd;Consultant, Stryker Corporation;Consultant, Siemens AG;  
Ziv J. Haskal, MD, Charlottesville, VA (*Moderator*) Speakers Bureau, W. L. Gore & Associates, Inc;Consultant, Becton, Dickinson and Company;Stockholder, Sirtex Medical Ltd;Consultant, Sirtex Medical Ltd;Consultant, Boston Scientific Corporation  
Amy Taylor, MD, Charlottesville, VA (*Moderator*) Nothing to Disclose

#### COURSE DESCRIPTION

The JeopIRdy game show will provide a full educational quiz show experience using the familiar Jeopardy-style format. Renown panelists will answer IR-related questions in a team based approach. Expect a fast pace, facts, humor...and a bit of a roller-coaster experience

#### LEARNING OBJECTIVES

1) Explain the role of IR in treatment of peripheral arterial disease and critical limb ischemia 2) Explain the clinical applications of embolotherapy in benign and malignant disease\*Course Description The JeopIRdy game show will provide a full educational quiz show experience using the familiar Jeopardy-style format. Renown panelists will answer IR-related questions in a team based approach. Expect a fast pace, facts, humor...and a bit of a roller-coaster experience

Printed on: 02/07/23



## Abstract Archives of the RSNA, 2022

M1-CMK09

### MSK Interventions: How I Do It

Monday, Nov. 28 8:00AM - 9:00AM Room: NA

#### Participants

Connie Y. Chang, MD, Boston, MA (*Presenter*) Nothing to Disclose  
Matthew Bucknor, MD, San Francisco, CA (*Presenter*) Nothing to Disclose  
Ronald S. Adler, MD, PhD, New York, NY (*Presenter*) Nothing to Disclose  
Joel S. Newman, MD, Needham, MA (*Presenter*) Nothing to Disclose  
Kenneth Lee, MD, Madison, WI (*Presenter*) Grant, NFL; Research support, Hologic, Inc; Royalties, RELX

#### COURSE DESCRIPTION

This course reviews advanced techniques of image-guided musculoskeletal procedures. Come hear from experts who have honed their techniques. There will also be an opportunity for Q&A so bring your questions!

#### LEARNING OBJECTIVES

1) To review the indications for PRP of lower extremity tendons 2) To review technique of ultrasound-guided cyroneurolysis 3) To introduce tips for efficient fluoroscopy-guided foot injections 4) To discuss indications and technique for MR-guided focused ultrasound ablation 5) To introduce advanced tips and techniques for facet cyst ruptures\*Course Description This course reviews advanced techniques of image-guided musculoskeletal procedures. Come hear from experts who have honed their techniques. There will also be an opportunity for Q&A so bring your questions!

Printed on: 02/07/23



## Abstract Archives of the RSNA, 2022

M1-CNR11

### Imaging of Spinal CSF Leaks

Monday, Nov. 28 8:00AM - 9:00AM Room: NA

#### Participants

Wende Gibbs, MD, MA, Scottsdale, AZ (*Presenter*) Nothing to Disclose  
Wouter I. Schievink, MD, Los Angeles, CA (*Presenter*) Nothing to Disclose  
Timothy Amrhein, MD, Durham, NC (*Presenter*) Nothing to Disclose  
Joseph Chazen, MD, New York, NY (*Moderator*) Nothing to Disclose

#### COURSE DESCRIPTION

This diagnostic and interventional spine session will focus on current advances in the diagnosis and treatment of spinal CSF leaks. Diagnosis of SIH based on brain MRI findings will be reviewed along with noninvasive spinal MRI. Current advances in myelography including digital subtraction myelography and decubitus CT myelography will be reviewed. Treatment options including epidural blood patch, fibrin glue injections, and an overview of surgical management will be presented. This course will give Neuroradiologists an understanding of the latest advances in diagnostic and therapeutic options for this complex condition.

#### LEARNING OBJECTIVES

1) Identify the core diagnostic criteria for spinal CSF leak on MRI and myelography 2) Highlight the treatment options for spinal CSF leak including percutaneous and surgical strategies\*Course Description This diagnostic and interventional spine session will focus on current advances in the diagnosis and treatment of spinal CSF leaks. Diagnosis of SIH based on brain MRI findings will be reviewed along with noninvasive spinal MRI. Current advances in myelography including digital subtraction myelography and decubitus CT myelography will be reviewed. Treatment options including epidural blood patch, fibrin glue injections, and an overview of surgical management will be presented. This course will give Neuroradiologists an understanding of the latest advances in diagnostic and therapeutic options for this complex condition.

Printed on: 02/07/23



## Abstract Archives of the RSNA, 2022

M1-COB03

### The Leiomyosarcoma vs Leiomyoma: The Case for Multiparametric MRI

Monday, Nov. 28 8:00AM - 9:00AM Room: NA

#### Participants

Nicole M. Hindman, MD, New York, NY (*Presenter*) Nothing to Disclose  
Angela Tong, MD, New York, NY (*Presenter*) Equipment support, Siemens AG  
Annie Leung, MD, Montreal, QC (*Presenter*) Nothing to Disclose

#### COURSE DESCRIPTION

This session will review the current challenges in the MRI evaluation of uterine masses, with focus on assessing for risk of leiomyosarcoma. This is a current hot topic in gynecologic oncology since 2014 after a physician was treated for symptomatic leiomyomata and an unsuspected uterine leiomyosarcoma was disseminated throughout her pelvis. Since that time, new research has given insight into MR protocols for predicting these tumors with a sensitivity of at least 83% and a specificity of at least 88%. Through a combination of didactic lectures and case based review, this course will review the literature to date on this topic, cover the seminal papers, discuss an algorithmic approach to evaluation and show case-based review of these masses. Attendees will have improved understanding of using MRI to accurately predict leiomyosarcoma, and understand the ability of MRI to serve a key role in helping gynecology-oncologists manage risk with this patient population.

#### LEARNING OBJECTIVES

1) Learn about the increasing prevalence of unsuspected uterine leiomyosarcoma in the general population 2) Learn about the role of various modalities in screening for uterine leiomyosarcoma in a symptomatic population, with focus on MRI 3) Evaluate the literature to date on proposed screening algorithms to predict uterine leiomyosarcoma 4) Review cases of uterine leiomyosarcoma and its mimickers\*Course Description This session will review the current challenges in the MRI evaluation of uterine masses, with focus on assessing for risk of leiomyosarcoma. This is a current hot topic in gynecologic oncology since 2014 after a physician was treated for symptomatic leiomyomata and an unsuspected uterine leiomyosarcoma was disseminated throughout her pelvis. Since that time, new research has given insight into MR protocols for predicting these tumors with a sensitivity of at least 83% and a specificity of at least 88%. Through a combination of didactic lectures and case based review, this course will review the literature to date on this topic, cover the seminal papers, discuss an algorithmic approach to evaluation and show case-based review of these masses. Attendees will have improved understanding of using MRI to accurately predict leiomyosarcoma, and understand the ability of MRI to serve a key role in helping gynecology-oncologists manage risk with this patient population.

Printed on: 02/07/23



## Abstract Archives of the RSNA, 2022

M1-CPD11

### Contrast Use and Abuse in Pediatric Imaging

Monday, Nov. 28 8:00AM - 9:00AM Room: NA

#### Participants

Judy Squires, MD, Pittsburgh, PA (*Presenter*) Nothing to Disclose  
Helen Hye Ryong Kim, MD, Seattle, WA (*Presenter*) Nothing to Disclose  
Lindsay Griffin, MD, Chicago, IL (*Presenter*) Nothing to Disclose

#### COURSE DESCRIPTION

Many studies in diagnostic imaging require the use of IV and/or enteric contrast media for optimal quality. However, there are many different types of contrast media to be best utilized in certain clinical scenarios, and there are variable supply chain constraints. Additionally, there are many important short and long term safety considerations for use of certain types of contrast media, as well as many myths about effects of different contrast media. This course will review common contrast media available for use in ultrasound, CT, and MRI, including possible alternatives, safety considerations, and controversies.

#### LEARNING OBJECTIVES

1. Review available contrast media in ultrasound, CT, and MRI, as well as availability and possible substitutions.
2. Review safety considerations for different contrast media, including need for clinical and biochemical monitoring before, during, and after contrast administration.
3. Review appropriate dosing and re-dosing of contrast media.
4. Debunk common misperceptions about harmful effects of different contrast media.

\*Course Description Many studies in diagnostic imaging require the use of IV and/or enteric contrast media for optimal quality. However, there are many different types of contrast media to be best utilized in certain clinical scenarios, and there are variable supply chain constraints. Additionally, there are many important short and long term safety considerations for use of certain types of contrast media, as well as many myths about effects of different contrast media. This course will review common contrast media available for use in ultrasound, CT, and MRI, including possible alternatives, safety considerations, and controversies.

Printed on: 02/07/23



## Abstract Archives of the RSNA, 2022

M1-CPH08

### Digital PET in Current Radiology Practices

Monday, Nov. 28 8:00AM - 9:00AM Room: NA

#### Participants

Dustin Osborne, PhD, Knoxville, TN (*Presenter*) Consultant, Siemens AG  
Osama R. Mawlawi, PhD, Houston, TX (*Presenter*) Nothing to Disclose

#### COURSE DESCRIPTION

PET scanners with digital detectors are one of the latest innovations in PET scanner system designs. This course will cover the detector design and system performance of digital PET scanners from various manufacturers. The course will also cover the resultant image quality for these systems as well as the various capabilities of these commercial systems.

#### LEARNING OBJECTIVES

At the end of this session, the audience should have gained knowledge of: 1) The design characteristics of digital PET detectors and systems from various manufacturers 2) The performance characterizations of PET systems from various manufacturers 3) PET systems options and clinical examples from the various manufacturers\*Course Description PET scanners with digital detectors are one of the latest innovations in PET scanner system designs. This course will cover the detector design and system performance of digital PET scanners from various manufacturers. The course will also cover the resultant image quality for these systems as well as the various capabilities of these commercial systems.

Printed on: 02/07/23



## Abstract Archives of the RSNA, 2022

M1-CRO09

### Genitourinary Case-based Multidisciplinary Review

Monday, Nov. 28 8:00AM - 9:00AM Room: NA

#### Participants

Michael Leapman, New Haven, CT (*Presenter*) Nothing to Disclose

Andrei S. Puryško, MD, Westlake, OH (*Presenter*) Contract, Profound Medical Inc; Research support, Blue Earth Diagnostics Ltd; Consultant, KOELIS;

Sophia Kamran, MD, Boston, MA (*Presenter*) Nothing to Disclose

Tyler Seibert, MD, PhD, La Jolla, CA (*Presenter*) Research Consultant, Cortechs.ai; Scientific Advisory Board, Cortechs.ai; Stock options, Cortechs.ai; Travel support, Siemens AG; Speaker, Siemens AG; Institutional research agreement, General Electric Company

Tristan Barrett, MBBS, Cambridge, United Kingdom (*Presenter*) Nothing to Disclose

#### COURSE DESCRIPTION

This course uses a case-based approach to diagnostic and management decision making in the work-up of patients presenting with prostate cancer. The panel includes radiologists, urologists and radiation oncologists.

#### LEARNING OBJECTIVES

1) To understand the typical imaging findings of prostate cancer on mpMRI 2) To assess the impact of MRI on staging prostate cancer in a multidisciplinary setting 3) To assess the role of imaging in the diagnosis of prostate cancer through case examples\*Course Description This course uses a case-based approach to diagnostic and management decision making in the work-up of patients presenting with prostate cancer. The panel includes radiologists, urologists and radiation oncologists.

Printed on: 02/07/23



## Abstract Archives of the RSNA, 2022

M1-RCP06

### **MESH Core: Healthcare Innovation and Medical Technology Bootcamp (Part 1)**

Monday, Nov. 28 8:00AM - 12:00PM Room: NA

#### **Participants**

Chris Coburn, Boston, MA (*Presenter*) Nothing to Disclose

Carl Berke, PhD, Boston, MA (*Presenter*) Nothing to Disclose

Mike Freni, Boston, MA (*Presenter*) Nothing to Disclose

Marc Succi, MD, Boston, MA (*Presenter*) Inventor, Frequency Therapeutics

Raul N. Uppot, MD, Boston, MA (*Presenter*) Consultant, Boston Scientific Corporation; Consultant, Koninklijke Philips NV

#### **COURSE DESCRIPTION**

MESH Core addresses the lack of training in medical technological innovation in residency and faculty radiologists. In Core, We run short innovation bootcamps and train radiologists, residents, and other non-radiology physicians. After attending MESH Core, the participant will be able to understand the fundamentals of informatics, prototyping, corporate business structures, artificial intelligence, machine learning, research grants, research lab creation, and entrepreneurship. They will know how to progress an idea to prototype, and talk intelligently at conferences, network with innovators, and interact with vendors such as at RSNA.

#### **LEARNING OBJECTIVES**

Attendees will learn: 1) Fundamentals of artificial intelligence and machine learning, including real demos and algorithm development 2) Fundamentals of Digital Health 3) Fundamentals of Augmented and Mixed Reality 4) Intellectual Property and Patent basics with interactive case-based problems 5) Hands-on programming in C and C++ and prototyping -Importance of Equity in Technology 6) Fundamentals of startups, corporations, investing 7) How to start your own research lab (including the lesser known things no-one tells you! 8) How to excel at getting grants, federal, private, and industry\*Course Description MESH Core addresses the lack of training in medical technological innovation in residency and faculty radiologists. In Core, We run short innovation bootcamps and train radiologists, residents, and other non-radiology physicians. After attending MESH Core, the participant will be able to understand the fundamentals of informatics, prototyping, corporate business structures, artificial intelligence, machine learning, research grants, research lab creation, and entrepreneurship. They will know how to progress an idea to prototype, and talk intelligently at conferences, network with innovators, and interact with vendors such as at RSNA.

Printed on: 02/07/23



## Abstract Archives of the RSNA, 2022

M1-RCP16

### United Kingdom Presents: Building and Sustaining Imaging Services in the UK

Monday, Nov. 28 8:00AM - 9:30AM Room: NA

#### Participants

Kath Halliday, MD, London, United Kingdom (*Presenter*) Nothing to Disclose  
Julian Elford, FRCR, MBBS, Winchester, United Kingdom (*Presenter*) Nothing to Disclose  
Raman Uberoi, MBChB, FRCR, Oxford, United Kingdom (*Presenter*) Nothing to Disclose  
Priya Suresh, Plymouth, United Kingdom (*Presenter*) Nothing to Disclose  
William Ramsden, MD, London, United Kingdom (*Moderator*) Nothing to Disclose

#### COURSE DESCRIPTION

This course describes current U.K. initiatives to build the imaging workforce, improve service quality and ensure the optimal utilisation of radiological resources in the face of ever-increasing demands for complex imaging. Many of these issues were addressed in the Getting it Right First Time (GIRFT) programme and its recommendations and potential impact upon U.K. radiology will be discussed. Allied to this is the development of the Royal College of Radiologists' iRefer guidelines, designed to provide evidence-based recommendations to ensure referrers request the most appropriate imaging investigations for their patients' clinical presentation. Departmental delivery of imaging is covered by the Quality Standard for Imaging - an overarching quality framework which enables both hospital departments and imaging networks to develop their services to the highest standards. The provision of sufficient trained personnel is a critical part of delivering a quality service, and initiatives which have been used to increase and upskill the U.K. imaging workforce will also be described.

#### LEARNING OBJECTIVES

1) Explain methods being used in the UK to ensure that imaging is utilised efficiently and appropriately 2) Appreciate how the Quality Standard for Imaging is being used to drive service improvement 3) Understand current initiatives to expand and develop the UK imaging workforce\*Course Description This course describes current U.K. initiatives to build the imaging workforce, improve service quality and ensure the optimal utilisation of radiological resources in the face of ever-increasing demands for complex imaging. Many of these issues were addressed in the Getting it Right First Time (GIRFT) programme and its recommendations and potential impact upon U.K. radiology will be discussed. Allied to this is the development of the Royal College of Radiologists' iRefer guidelines, designed to provide evidence-based recommendations to ensure referrers request the most appropriate imaging investigations for their patients' clinical presentation. Departmental delivery of imaging is covered by the Quality Standard for Imaging - an overarching quality framework which enables both hospital departments and imaging networks to develop their services to the highest standards. The provision of sufficient trained personnel is a critical part of delivering a quality service, and initiatives which have been used to increase and upskill the U.K. imaging workforce will also be described.

Printed on: 02/07/23



## Abstract Archives of the RSNA, 2022

M1-RCP23

### Safety Net Hospitals, Health Disparities, and Unique Barriers to Care (Sponsored by the RSNA Committee on Diversity, Equity & Inclusion)

Monday, Nov. 28 8:00AM - 9:00AM Room: NA

#### Participants

Lucy Spalluto, MD,MPH, Nashville, TN (*Presenter*) Nothing to Disclose

Chrissy Hartsfield, Nashville, TN (*Presenter*) Nothing to Disclose

Ronda Henry-Tillman, Little Rock, AR (*Presenter*) Nothing to Disclose

Pearl McElfish, PhD, MBA, Little Rock, AR (*Presenter*) Nothing to Disclose

Jinel A. Scott, MD, Brooklyn, NY (*Presenter*) Nothing to Disclose

Jorge Soto, MD, Boston, MA (*Moderator*) Nothing to Disclose

Gwendolyn M. Bryant-Smith, MD, Little Rock, AR (*Moderator*) Nothing to Disclose

#### COURSE DESCRIPTION

This course will spotlight safety net hospitals, health disparities, and unique barriers to care. Many physicians and other members of the health care team are unaware of the unique barriers to care that marginalized, diverse, and rural populations endure and have limited understanding of how safety net hospitals and rural programs meet these challenges. This course will address many of these challenges and will provide strategies to mitigate some of these unique barriers to care.

#### LEARNING OBJECTIVES

1) Explain the history of safety net hospitals in the United States and the role of these hospitals in current day healthcare 2) Discuss the unique challenges to person centered care delivery in the rural setting 3) Identify strategies to access and reach rural and diverse populations\*Course Description This course will spotlight safety net hospitals, health disparities, and unique barriers to care. Many physicians and other members of the health care team are unaware of the unique barriers to care that marginalized, diverse, and rural populations endure and have limited understanding of how safety net hospitals and rural programs meet these challenges. This course will address many of these challenges and will provide strategies to mitigate some of these unique barriers to care.

Printed on: 02/07/23



## Abstract Archives of the RSNA, 2022

M1-RCP44

### Navigating the Job Market (Sponsored by the RSNA Resident and Fellow Committee)

Monday, Nov. 28 8:00AM - 9:00AM Room: NA

#### Participants

Jeremy Heit, MD, PhD, Los Altos, CA (*Presenter*) Consultant, Medtronic plc; Consultant, Terumo Corporation; Consultant, iSchemaView, Inc; Scientific Advisory Board, iSchemaView, Inc; Medical Advisory Board, iSchemaView, Inc; Committee Member, Vesalio

Timothy T. Klostermeier, MD, Lebanon, OH (*Presenter*) Nothing to Disclose

Kurt Schoppe, MD, Grapevine, TX (*Presenter*) Nothing to Disclose

Brandon K-K. Fields, MD, San Francisco, CA (*Moderator*) Nothing to Disclose

#### COURSE DESCRIPTION

The RSNA Resident & Fellow Committee will host a session of lectures on evaluating different practice settings, the current job market, and how the Radiology marketplace is changing, followed by a career panel Q&A with panelists from academics, private practice, hybrid models, and teleradiology practices. This session will provide participants, particularly trainees, with the knowledge needed to navigate the current job market.

#### LEARNING OBJECTIVES

1) Learn how to evaluate and compare different practice settings and jobs 2) Understand how the shifts in the Radiology marketplace are affecting the job market\*Course Description The RSNA Resident & Fellow Committee will host a session of lectures on evaluating different practice settings, the current job market, and how the Radiology marketplace is changing, followed by a career panel Q&A with panelists from academics, private practice, hybrid models, and teleradiology practices. This session will provide participants, particularly trainees, with the knowledge needed to navigate the current job market.

Printed on: 02/07/23



## Abstract Archives of the RSNA, 2022

M3-CAS07

### Design Insights Drive the Patient Experience (Sponsored by the Associated Sciences Consortium)

Monday, Nov. 28 9:30AM - 10:30AM Room: NA

#### Participants

Morris Stein, BArch, Phoenix, AZ (*Presenter*) Nothing to Disclose  
Carlos Amato, Los Angeles, CA (*Presenter*) Nothing to Disclose  
Susie Moseley, MS, RT, Albuquerque, NM (*Moderator*) Nothing to Disclose

#### COURSE DESCRIPTION

Learn how to use research insights to define and model the patient experience. The presentation will describe physical, social and digital design innovations that change the way we work.

#### LEARNING OBJECTIVES

1) Describe how digital and practice transformation will influence the patient experience 2) Recognize transformational design examples driving the future of healthcare environments 3) Explore the interface of personal technology and mobile devices to improve patient and staff satisfaction\*Course Description Learn how to use research insights to define and model the patient experience. The presentation will describe physical, social and digital design innovations that change the way we work.

Printed on: 02/07/23



## Abstract Archives of the RSNA, 2022

M3-CCA08

### Cardiac Imaging in Private Practice: Lessons Learned

Monday, Nov. 28 9:30AM - 10:30AM Room: NA

#### Participants

Richard L. Hallett II, MD, Carmel, IN (*Presenter*) Consultant, Bracco Group

Michael F. Morris, MD, Paradise Valley, AZ (*Moderator*) Educator, Medtronic plc

#### COURSE DESCRIPTION

The impact of cardiac imaging in optimizing patient care has never been greater. Although cardiac imaging techniques have matured and exam volumes have rapidly increased, development and implementation of cardiovascular imaging into radiology practices has been challenging. This session will present lectures highlighting the challenges, risks, and benefits involved in the private practice of cardiac imaging. Specifically, methods to start up and grow the practice will be discussed, as well as challenges related to equipment selection, referring clinician education, turf battles, group buy-in, and mentoring. Real-life examples from successful cardiac imagers' practices will be discussed. The importance of collaboration and sub-specialization will be emphasized. Ample opportunity for in-person and online questions will be provided.

#### LEARNING OBJECTIVES

1) Explain techniques and challenges to implement and expand a cardiac imaging program in private practice. 2) Explain methods to grow the cardiac imaging program to enhance patient care and clinician satisfaction. 3) Explain potential conflicts /barriers to progress in cardiac imaging and possible solutions. \*Course Description The impact of cardiac imaging in optimizing patient care has never been greater. Although cardiac imaging techniques have matured and exam volumes have rapidly increased, development and implementation of cardiovascular imaging into radiology practices has been challenging. This session will present lectures highlighting the challenges, risks, and benefits involved in the private practice of cardiac imaging. Specifically, methods to start up and grow the practice will be discussed, as well as challenges related to equipment selection, referring clinician education, turf battles, group buy-in, and mentoring. Real-life examples from successful cardiac imagers' practices will be discussed. The importance of collaboration and sub-specialization will be emphasized. Ample opportunity for in-person and online questions will be provided.

Printed on: 02/07/23



## Abstract Archives of the RSNA, 2022

M3-CCA13

### Mentored Cardiac Case Review: Imaging of Coronary Atherosclerotic Disease: From Straight Forward to Most Complicated

Monday, Nov. 28 9:30AM - 10:30AM Room: NA

#### Participants

Prachi P. Agarwal, MD, Ann Arbor, MI (*Presenter*) Nothing to Disclose

Brian B. Ghoshhajra, MD, Boston, MA (*Presenter*) Research Grant, Siemens AG; Consultant, Koninklijke Philips NV; Consultant, Siemens AG

Elsie Nguyen, MD, Toronto, ON (*Presenter*) Nothing to Disclose

U. Joseph Schoepf, MD, Charleston, SC (*Presenter*) Research Grant, Bayer AG; Research Grant, Bracco Group; Research Grant, Elucid BioImaging Inc; Consultant, Elucid BioImaging Inc; Research Grant: General Electric Company; Research Grant, Guerbet SA; Research Grant, Heartflow, Inc; Speakers Bureau, Heartflow Inc

Michelle Williams, MBChB, PhD, Kelso, United Kingdom (*Moderator*) Speakers Bureau, Canon Medical Systems Corporation; Speakers Bureau, Siemens AG

#### COURSE DESCRIPTION

This course will feature lectures and discussion around imaging cases of coronary artery disease, including a range of complexity from basic to advanced.

#### LEARNING OBJECTIVES

1) Understand how different imaging modalities can be used in risk stratification, diagnosis, and management optimisation of patients 2) Learn how current guidelines guide the assessment of individual patients with suspected or known coronary artery disease 3) Develop skills to identify and interpret coronary artery disease findings on cardiac imaging\*Course Description This course will feature lectures and discussion around imaging cases of coronary artery disease, including a range of complexity from basic to advanced.

Printed on: 02/07/23



## Abstract Archives of the RSNA, 2022

M3-CER14

### Musculoskeletal Trauma In the ER - Injuries You Don't Want To Miss! A Case-based Review of High Yield Do Not Miss Injury Patterns

Monday, Nov. 28 9:30AM - 10:30AM Room: NA

#### Participants

Manickam Kumaravel, MD, FRCR, Houston, TX (*Presenter*) Nothing to Disclose

Claire Sandstrom, MD, Seattle, WA (*Presenter*) Nothing to Disclose

Lee A. Myers, MD, Los Angeles, CA (*Presenter*) Nothing to Disclose

#### COURSE DESCRIPTION

Challenging musculoskeletal injuries that present in the ER will be reviewed in an interactive session. The session will discuss shoulder, ankle, and pelvic musculoskeletal cases.

#### LEARNING OBJECTIVES

1) Identify subtle musculoskeletal (MSK) injuries in the ER 2) Understand the underlying pathophysiology of musculoskeletal injury 3) Recognize the clinical implications of the MSK injuries\*Course Description Challenging musculoskeletal injuries that present in the ER will be reviewed in an interactive session. The session will discuss shoulder, ankle, and pelvic musculoskeletal cases.

Printed on: 02/07/23



## Abstract Archives of the RSNA, 2022

M3-CIN15

### Creating Links Between Radiology and Health Informatics Systems to Improve Quality

Monday, Nov. 28 9:30AM - 10:30AM Room: NA

#### Participants

Richard Kinh Gian Do, MD, PhD, New York, NY (*Presenter*) Author, RELX; Consultant, General Electric Company; Consultant, Bayer AG; Spouse, Author, Wolters Kluwer nv; Spouse, Committee Member, ALK-Abello A/S; Spouse, Consultant, JDP Therapeutics Inc; Spouse, Consultant, F. Hoffmann-La Roche Ltd

Thomas Loehfelm, MD, PhD, Sacramento, CA (*Presenter*) Nothing to Disclose

Marta Flory, MD, Redwood City, CA (*Presenter*) Nothing to Disclose

Rajan Gupta, MD, Durham, NC (*Presenter*) Consultant, Bayer AG; Speakers Bureau, Bayer AG; Consultant, Invivo Corporation; Consultant, C. R. Bard, Inc; Consultant, Quibim; Consultant, Bracco Group

Kirti Magudia, MD, PhD, Durham, NC (*Moderator*) Nothing to Disclose

#### COURSE DESCRIPTION

The session will include presentations reviewing real projects highlighting the challenges and successes of large scale radiology data collection and processing pipelines, followed by a moderated panel discussion and interactive conversation.

#### LEARNING OBJECTIVES

1) Review the rationale, techniques, and challenges to implementing large scale radiology data collection and processing pipelines 2) Identify IT resources and skillsets required to successfully implement robust, sustainable, comprehensive radiology data collection and processing pipelines 3) Review real-world projects built on comprehensive radiology data processing pipelines and explore the novel research, quality, and operational insights they enable\*Course Description The session will include presentations reviewing real projects highlighting the challenges and successes of large scale radiology data collection and processing pipelines, followed by a moderated panel discussion and interactive conversation.

Printed on: 02/07/23



## Abstract Archives of the RSNA, 2022

M3-CNPM09

### Medicolegal Issues and Managing Risk

Monday, Nov. 28 9:30AM - 10:30AM Room: NA

#### Participants

Jonathan Mezrich, MD, Guilford, CT (*Presenter*) Nothing to Disclose

Stephen D. Brown, MD, Boston, MA (*Presenter*) Stockholder, GSK plc ;Stockholder, Johnson & Johnson;Stockholder, AbbVie Inc;Stockholder, Merck & Co, Inc;Stockholder, CVS Health Corporation;Stockholder, Pfizer Inc

Kelly Yousem, JD, Owings Mills, MD (*Presenter*) Nothing to Disclose

#### COURSE DESCRIPTION

This course will explore timely medicolegal issues relevant to radiologic practice:1) Medicolegal issues in Emergency Radiology: Emergency Radiology is a subspecialty which is disproportionately impacted by liability risk given the pace, hours and patient acuity. The speaker is an Emergency Radiologist with a background as a practicing attorney, and who has published extensively on medicolegal topics.2) Error Disclosure – Systems Considerations: Responsibly discussing medical errors with patients and families requires the implementation of principled, coordinated, enterprise-wide processes that support both patients and providers. This presentation, by a pediatric radiologist with extensive experience speaking on ethics, communication, professionalism and error disclosure, will discuss systems processes that facilitate open communication with patients and families about medical errors.3) Error Disclosure - Reality Check: Lofty ideals about “doing the right thing” in communicating honestly and transparently with patients and families about preventable adverse events feel unattainable to many radiologists fearful of the legal consequences. This presentation, by an attorney with extensive malpractice expertise, will offer perspectives about the practical realities involved and consequences for physicians when considering whether and how to bring open communication about errors to patients and families.

#### LEARNING OBJECTIVES

1) Describe medicolegal issues in emergency radiology 2) Identify systems processes that facilitate open communication with patients and families about medical errors 3) Understand the laws, obligations, and risks and benefits regarding open communication with patients and families about medical errors\*Course Description This course will explore timely medicolegal issues relevant to radiologic practice:1) Medicolegal issues in Emergency Radiology: Emergency Radiology is a subspecialty which is disproportionately impacted by liability risk given the pace, hours and patient acuity. The speaker is an Emergency Radiologist with a background as a practicing attorney, and who has published extensively on medicolegal topics.2) Error Disclosure – Systems Considerations: Responsibly discussing medical errors with patients and families requires the implementation of principled, coordinated, enterprise-wide processes that support both patients and providers. This presentation, by a pediatric radiologist with extensive experience speaking on ethics, communication, professionalism and error disclosure, will discuss systems processes that facilitate open communication with patients and families about medical errors.3) Error Disclosure - Reality Check: Lofty ideals about “doing the right thing” in communicating honestly and transparently with patients and families about preventable adverse events feel unattainable to many radiologists fearful of the legal consequences. This presentation, by an attorney with extensive malpractice expertise, will offer perspectives about the practical realities involved and consequences for physicians when considering whether and how to bring open communication about errors to patients and families.

Printed on: 02/07/23



## Abstract Archives of the RSNA, 2022

M3-CNR10

### AI: Intelligent Clinical Neuroimaging On the Horizon

Monday, Nov. 28 9:30AM - 10:30AM Room: NA

#### Participants

Mai-Lan Ho, MD, Columbus, OH (*Presenter*) Research Grant, Siemens AG; Research Grant, Cardinal Health, Inc; Research Grant, Italfarmaco SpA

Christopher Filippi, MD, Boston, MA (*Presenter*) Research Consultant, Syntactx, LLC; Stockholder, Avicenna.ai;

Daniel S. Chow, MD, Irvine, CA (*Presenter*) Shareholder, Avicenna.ai; Consultant, Canon Medical Systems Corporation; Grant, Canon Medical Systems Corporation; Consultant, Cullen & Grandy; Grant, NovoCure Ltd

Yvonne Lui, MD, New York, NY (*Moderator*) Nothing to Disclose

#### COURSE DESCRIPTION

This course reviews the major neuroimaging applications of machine learning including CNS tumors, stroke and cerebrovascular disease, pediatric neurological disorders. We explore the research in machine learning that are altering the imaging field and the impact on clinical practice. We discuss some of the limitations and barriers to progress in this area and provide some potential solutions.

#### LEARNING OBJECTIVES

After attending this session, a participant will 1) Understand the breadth of areas in neuroimaging where machine learning is making an impact 2) Know how machine learning is used to augment traditional neuroimaging approaches, and 3) Know some of the limitations of using a machine learning approach with limited datasets\*Course Description This course reviews the major neuroimaging applications of machine learning including CNS tumors, stroke and cerebrovascular disease, pediatric neurological disorders. We explore the research in machine learning that are altering the imaging field and the impact on clinical practice. We discuss some of the limitations and barriers to progress in this area and provide some potential solutions.

Printed on: 02/07/23



## Abstract Archives of the RSNA, 2022

M3-CPD05

### Fetal Imaging

Monday, Nov. 28 9:30AM - 10:30AM Room: NA

#### Participants

Eva Rubio, MD, Washington, DC (*Presenter*) Nothing to Disclose

Usha D. Nagaraj, MD, Cincinnati, OH (*Presenter*) Author with royalties, Reed Elsevier;

Vijaya Vemulakonda, MD, Aurora, CO (*Presenter*) Author, Wolters Kluwer nv

#### COURSE DESCRIPTION

This 3-lecture session will review the imaging features and causes of urogenital malformations and obstructive pathology in the fetus. The focus will be on bladder outlet obstruction (BOO) and cloacal spectrum abnormalities. Postnatal imaging and therapy will be discussed.

#### LEARNING OBJECTIVES

1) Understand the embryologic origins of bladder outlet obstruction and cloacal malformation 2) Identify the imaging clues distinguishing among urogenital obstructive conditions 3) Anticipate postnatal imaging findings and therapeutic options\*Course Description This 3-lecture session will review the imaging features and causes of urogenital malformations and obstructive pathology in the fetus. The focus will be on bladder outlet obstruction (BOO) and cloacal spectrum abnormalities. Postnatal imaging and therapy will be discussed.

Printed on: 02/07/23



## Abstract Archives of the RSNA, 2022

M3-CPH09

### Data Curation for AI with Proper Medical Imaging Physics Context

Monday, Nov. 28 9:30AM - 10:30AM Room: NA

#### Participants

Zhihua Qi, PhD, Detroit, MI (*Presenter*) Nothing to Disclose  
John Garrett, PhD, Madison, WI (*Presenter*) Nothing to Disclose  
Ran Zhang, PhD, Madison, WI (*Presenter*) Nothing to Disclose  
Nicholas Bevins, PhD, Detroit, MI (*Presenter*) Nothing to Disclose

#### COURSE DESCRIPTION

Lecture course to review the selection, procurement, quality, and evaluation of data for AI tools in radiology.

#### LEARNING OBJECTIVES

1) To learn how data quality and data size affect the performance and generalizability of deep neural network models 2) To understand practical methods for series and study selection for clinically deployed AI models, common issues that arise in deployment, and several techniques for evaluating AI in an ongoing fashion 3) To review the process and to demonstrate methods and tools for used to collect and prepare clinical data for AI model development\*Course Description Lecture course to review the selection, procurement, quality, and evaluation of data for AI tools in radiology.

Printed on: 02/07/23



## Abstract Archives of the RSNA, 2022

M3-RCP29

### Bring on Your Game: Best of RSNA Case Collection Hot Seat Review (NUCS, NEURO, GI, OB, IR)

Monday, Nov. 28 9:30AM - 10:30AM Room: NA

#### Participants

Kush Desai, MD, Chicago, IL (*Presenter*) Speakers Bureau, Cook Group Incorporated Consultant, Cook Group Incorporated Consultant, Koninklijke Philips NV Speakers Bureau, Becton, Dickinson and Company Consultant, Becton, Dickinson and Company Speakers Bureau, Boston Scientific Corporation  
Douglas Katz, MD, Mineola, NY (*Presenter*) Nothing to Disclose  
Xin Wu, MD, Atlanta, GA (*Presenter*) Nothing to Disclose  
Catherine Phillips, MD, Nashville, TN (*Presenter*) Nothing to Disclose  
Osmanuddin Ahmed, MD, Northbrook, IL (*Presenter*) Speaker, Canon Medical Systems Corporation; Research Grant, Canon Medical Systems Corporation; Speaker, Becton, Dickinson and Company; Speaker, Cook Group Incorporated; Advisory Board, Boston Scientific Corporation; Advisory Board, Argon Medical Devices, Inc; Speaker, Koninklijke Philips NV; Speaker, Argon Medical Devices, Inc; Advisory Board, Argon Medical Devices, Inc; Consultant, Asahi Kasei Medical Co, Ltd; Consultant, Medtronic plc; Speaker, Penumbra, Inc; Speaker, Inari Medical, Inc  
Saeed Elojeimy, MD, PhD, Charleston, SC (*Presenter*) Nothing to Disclose  
Sarah Bastawrous, DO, Seattle, WA (*Moderator*) Nothing to Disclose  
Mariam Moshiri, MD, Brentwood, TN (*Moderator*) Nothing to Disclose

#### LEARNING OBJECTIVES

1) Develop differential diagnoses for the five radiology subspecialties presented in this course 2) Recognize imaging features that aid in differential diagnoses, allowing for a more specific diagnosis Learn evaluation of cases in a methodical and clinically applicable fashion\*Course Description

Printed on: 02/07/23



## Abstract Archives of the RSNA, 2022

M3-RCP36

### Professionalism and Ethics in Research (Sponsored by RSNA Professionalism Committee)

Monday, Nov. 28 9:30AM - 10:30AM Room: NA

#### Participants

David Bluemke, MD, PhD, Madison, WI (*Presenter*) Nothing to Disclose

Kate Hanneman, MD, FRCPC, Toronto, ON (*Presenter*) Speaker, Groupe Sanofi Speaker, Amicus Therapeutics, Inc

Aine Kelly, MD, Decatur, GA (*Presenter*) Nothing to Disclose

Refky Nicola, DO, Pittsford, NY (*Presenter*) Royalties, RELX

#### COURSE DESCRIPTION

A. Ethics of Human Research in Radiology This lecture will discuss the role of institutional research ethics boards and informed consent. B. Publication Ethics in Radiology Research This lecture will review key concepts related to authorship roles, plagiarism and duplicate publications. C. Peer Review in Radiology An editor of one of the Radiology journals will be invited to discuss the peer review and editorial process. D. Managing Conflicts of Interest in Radiology Research This lecture will discuss conflicts of interest related to research in radiology including relationships with vendors including device and pharmaceutical companies.

#### LEARNING OBJECTIVES

1) The purpose of this session is to discuss important ethical and professionalism issues regarding research including informed consent, data management, conflict of interest, authorship and peer-review\*Course Description A. Ethics of Human Research in Radiology This lecture will discuss the role of institutional research ethics boards and informed consent. B. Publication Ethics in Radiology Research This lecture will review key concepts related to authorship roles, plagiarism and duplicate publications. C. Peer Review in Radiology An editor of one of the Radiology journals will be invited to discuss the peer review and editorial process. D. Managing Conflicts of Interest in Radiology Research This lecture will discuss conflicts of interest related to research in radiology including relationships with vendors including device and pharmaceutical companies.

Printed on: 02/07/23



## Abstract Archives of the RSNA, 2022

M4-CAS03

### Wait!! What?! A MRI System is Going WHERE???? (Sponsored by the Associated Sciences Consortium)

Monday, Nov. 28 11:00AM - 12:00PM Room: NA

#### Participants

Christina Calvin, San Francisco, CA (*Presenter*) Shareholder, Siemens AG  
Craig Devinent, ARRT, BA, San Francisco, CA (*Presenter*) Nothing to Disclose  
Brandy Reed, MBA, RT, Houston, TX (*Moderator*) Nothing to Disclose  
Nancy McDonald, MS, Dallas, TX (*Moderator*) Nothing to Disclose

#### COURSE DESCRIPTION

Lecture format. Many places are creating hybrid working environments to incorporate new technology, merge modalities and departments, thus improving patient care. With the implementation of MRI in Radiation Oncology or PET into MRI, there are many safety issues that must be thought of and strategies that must be implemented.

#### LEARNING OBJECTIVES

1) Identify MRI Safety issues in Hybrid Environments 2) Learn how to implement best practices for MRI Safety within a Rapidly Expanding Medical Center\*Course Description Lecture format. Many places are creating hybrid working environments to incorporate new technology, merge modalities and departments, thus improving patient care. With the implementation of MRI in Radiation Oncology or PET into MRI, there are many safety issues that must be thought of and strategies that must be implemented.

Printed on: 02/07/23



## Abstract Archives of the RSNA, 2022

M4-CIN21

### New Modeling Approaches for Radiology AI

Monday, Nov. 28 11:00AM - 12:00PM Room: NA

#### Participants

Maciej Mazurowski, MS, PhD, Durham, NC (*Presenter*) Nothing to Disclose

Akshay Chaudhari, PhD, Stanford, CA (*Presenter*) Research support, General Electric Company; Research support, Koninklijke Philips NV; Research Consultant, Subtle Medical, Inc

Valentina Padoia, PhD, San Francisco, CA (*Presenter*) Nothing to Disclose

#### COURSE DESCRIPTION

Despite the rapid advances that artificial intelligence (AI) has the potential to make in radiology, several challenges still persist in building techniques that transition from research studies to clinical practice. Such challenges revolve around contending with the scale of data required to train robust models, especially in light of the heterogeneity of data distributions across healthcare practices. Moreover, while many AI techniques can provide insights at a group-level, can some of these methods be as efficacious at the individual level? In this lecture-based session, we will address these questions revolving around building robust AI models for implementing new personalized solutions to critical healthcare problems.

#### LEARNING OBJECTIVES

1) Identify methods to overcome the paucity and heterogeneity of data for training radiology AI models 2) Discover how to leverage large research repositories to uncover new disease mechanisms 3) Learn how AI can personalize healthcare delivery\*Course Description Despite the rapid advances that artificial intelligence (AI) has the potential to make in radiology, several challenges still persist in building techniques that transition from research studies to clinical practice. Such challenges revolve around contending with the scale of data required to train robust models, especially in light of the heterogeneity of data distributions across healthcare practices. Moreover, while many AI techniques can provide insights at a group-level, can some of these methods be as efficacious at the individual level? In this lecture-based session, we will address these questions revolving around building robust AI models for implementing new personalized solutions to critical healthcare problems.

Printed on: 02/07/23



## Abstract Archives of the RSNA, 2022

M4-CMS01

### Imaging Considerations in Challenging Populations

Monday, Nov. 28 11:00AM - 12:00PM Room: NA

#### Participants

Margarita Revzin, MD, Wilton, CT (*Presenter*) Nothing to Disclose  
Kalpana M. Kanal, PhD, Seattle, WA (*Presenter*) Nothing to Disclose  
Megan B. Marine, MD, Indianapolis, IN (*Presenter*) Nothing to Disclose  
Marcia C. Javitt, MD, Haifa, Israel (*Presenter*) Spouse, Consultant, NeuroRx, Inc

#### COURSE DESCRIPTION

This session will review imaging challenges and specific health related issues in obese, elderly, pediatric, and pregnant patients. Relevant problem-solving techniques, clinical information and multidisciplinary collaboration will be discussed. Imaging pearls and pitfalls will be provided. The format will be lectures and some discussion.

#### LEARNING OBJECTIVES

The learner will: 1) gain increased awareness about caring for vulnerable or marginalized patients in the Radiology Department 2) understand the imaging modalities best suited to safe and appropriate personalized care of these populations 3) recognize and respond quickly and effectively to urgent and emergent conditions requiring imaging triage to essential treatment and intervention\*Course Description This session will review imaging challenges and specific health related issues in obese, elderly, pediatric, and pregnant patients. Relevant problem-solving techniques, clinical information and multidisciplinary collaboration will be discussed. Imaging pearls and pitfalls will be provided. The format will be lectures and some discussion.

Printed on: 02/07/23



## Abstract Archives of the RSNA, 2022

M6-CAS04

### A Hefty Ransom: Facing the Ongoing and Increasing Threat of Ransomware (Sponsored by the Associated Sciences Consortium)

Monday, Nov. 28 1:30PM - 2:30PM Room: NA

#### Participants

David Miller, Charlotte, NC (*Presenter*) Shareholder, Technology Partners, LLC, dba ImagineSoftware

Barbara Rubel, MBA, Green Cove Springs, FL (*Presenter*) Shareholder, Management Services Network, LLC; Employee, Management Services Network, LLC

Nancy McDonald, MS, Dallas, TX (*Moderator*) Nothing to Disclose

Jennifer Kroken, MBA, Lewisville, TX (*Moderator*) Nothing to Disclose

#### COURSE DESCRIPTION

Ransomware attacks have increased in frequency and scope. Practices, hospitals and well-known companies have fallen victim to attacks worldwide. The session will discuss how these attacks occur and why medical records are especially valuable. What does it take for a company to recover after a breach?

#### LEARNING OBJECTIVES

1) Explain how ransomware is increasing as a global threat and how your practice may be at risk 2) Identify how to insulate your practice against attacks, how to respond to an attack and how to recover from an attack\*Course Description Ransomware attacks have increased in frequency and scope. Practices, hospitals and well-known companies have fallen victim to attacks worldwide. The session will discuss how these attacks occur and why medical records are especially valuable. What does it take for a company to recover after a breach?

Printed on: 02/07/23



## Abstract Archives of the RSNA, 2022

M6-CCA14

### Mentored Cardiac Case Review: Imaging of Post Coronary and Valvular Surgical and Trans Vascular Interventions

Monday, Nov. 28 1:30PM - 2:30PM Room: NA

#### Participants

Cristina Fuss, MD, Portland, OR (*Presenter*) Nothing to Disclose  
Harold I. Litt, MD, PhD, Philadelphia, PA (*Presenter*) Research Grant, Siemens AG; Research Grant, Koninklijke Philips NV  
Eric E. Williamson, MD, Rochester, MN (*Presenter*) Nothing to Disclose  
Amar B. Shah, MD, New York, NY (*Presenter*) Nothing to Disclose  
Kate Hanneman, MD, FRCPC, Toronto, ON (*Moderator*) Speaker, Groupe Sanofi Speaker, Amicus Therapeutics, Inc

#### COURSE DESCRIPTION

This case based session will review imaging of post coronary and valvular surgical and trans vascular interventions

#### LEARNING OBJECTIVES

1) Identify complications after coronary and valvular interventions on imaging and 2) discuss pre and post intervention imaging acquisition and analysis\*Course Description This case based session will review imaging of post coronary and valvular surgical and trans vascular interventions

Printed on: 02/07/23



## Abstract Archives of the RSNA, 2022

M6-CCH02

### HRCT Advanced Topics

Monday, Nov. 28 1:30PM - 2:30PM Room: NA

#### Participants

Chi Wan Koo, MD, Rochester, MN (*Presenter*) Nothing to Disclose

Min Jae Cha, Seoul, Korea, Republic Of (*Presenter*) Nothing to Disclose

Kimberly Kallianos, MD, San Rafael, CA (*Presenter*) Nothing to Disclose

David A. Lynch, MBBCh, Denver, CO (*Presenter*) Research Consultant, CALYX Inc; Research Consultant, Boehringer Ingelheim GmbH; Research Consultant, Veracyte, Inc; Research Consultant, DAIICHI SANKYO Group; Research Consultant, AstraZeneca PLC; Consultant, Polarean, Inc; Consultant, Bristol Myers Squibb Company

Edward Lee, MD, MPH, Boston, MA (*Presenter*) Nothing to Disclose

#### COURSE DESCRIPTION

Clinically relevant interpretation of HRCT requires knowledge of the clinical and imaging aspects of interstitial lung disease. This course aims to provide the practicing radiologist with greater understanding of the clinical role of high resolution CT. Discussion topics will include Post-COVID lung injury, clinical importance of early interstitial lung abnormality, features of interstitial lung disease in children, use of machine learning in ILD and evolving aspects of drug induced ILD.

#### LEARNING OBJECTIVES

1) Understand the clinical course of post-COVID lung injury and early interstitial lung abnormality 2) Recognize imaging findings in drug-induced lung disease 3) Review pearls and pitfalls of HRCT imaging in children 4) Understand benefits and limitations of machine learning in interstitial lung disease\*Course Description Clinically relevant interpretation of HRCT requires knowledge of the clinical and imaging aspects of interstitial lung disease. This course aims to provide the practicing radiologist with greater understanding of the clinical role of high resolution CT. Discussion topics will include Post-COVID lung injury, clinical importance of early interstitial lung abnormality, features of interstitial lung disease in children, use of machine learning in ILD and evolving aspects of drug induced ILD.

Printed on: 02/07/23



## Abstract Archives of the RSNA, 2022

M6-CGI11

### Essentials of GI Imaging

Monday, Nov. 28 1:30PM - 2:30PM Room: NA

#### Participants

Courtney Moreno, MD, Atlanta, GA (*Presenter*) Nothing to Disclose

Mark Sugi, MD, San Francisco, CA (*Presenter*) Consultant, Nextrast, Inc; Author with royalties, RELX

Silvia D. Chang, MD, FRCPC, Vancouver, BC (*Presenter*) Nothing to Disclose

Anil Dasyam, MD, Pittsburgh, PA (*Presenter*) Nothing to Disclose

David Disantis, MD, Jacksonville, FL (*Presenter*) Nothing to Disclose

#### COURSE DESCRIPTION

This Course will be a didactic refresher course covering a range of GI imaging essentials including difficult post-operative GI anatomy, essential techniques for GI fluoroscopy, imaging of patients with diverticulitis, and essentials of hepatobiliary imaging and diagnosis.

#### LEARNING OBJECTIVES

1) Describe expected and unexpected GI findings including difficult post-operative GI anatomy 2) Describe essential techniques for GI fluoroscopy and pertinent imaging findings in patients with diverticulitis 3) Identify and accurately diagnose common and uncommon hepatobiliary pathology\*Course Description This Course will be a didactic refresher course covering a range of GI imaging essentials including difficult post-operative GI anatomy, essential techniques for GI fluoroscopy, imaging of patients with diverticulitis, and essentials of hepatobiliary imaging and diagnosis.

Printed on: 02/07/23



## Abstract Archives of the RSNA, 2022

M6-CHN05

### Horse/Zebra Head and Neck Case Based Session

Monday, Nov. 28 1:30PM - 2:30PM Room: NA

#### Participants

Paul Bunch, MD, Winston Salem, NC (*Presenter*) Research Grant, General Electric Company

Elizabeth George, MD, San Francisco, MA (*Presenter*) Nothing to Disclose

Jennifer Gillespie, MBBS, Brisbane, (*Presenter*) Speakers Bureau, Philips Australia 2021 (past). Speakers Bureau, Radiopaedia 2021, 2022 (past).

Mark D. Mamlouk, MD, Santa Clara, CA (*Presenter*) Nothing to Disclose

Salman Qureshi, MBChB, Doha, (*Moderator*) Nothing to Disclose

#### COURSE DESCRIPTION

In this case-based head and neck imaging session, attendees will be presented with typical and atypical imaging examples of squamous cell carcinoma, parathyroid adenoma, invasive fungal sinusitis, and vascular malformations. Speakers will emphasize pearls for differentiating each entity from common mimics, pitfalls of interpretation to avoid, and relevant clinical management considerations with which radiologists should be familiar. This session offers attendees the opportunity to refine their interpretation of complex head and neck imaging studies by incorporating tips from world experts.

#### LEARNING OBJECTIVES

1) Recognize typical and atypical imaging features of squamous cell carcinoma, parathyroid adenoma, invasive fungal sinusitis, and vascular malformations 2) Differentiate squamous cell carcinoma, parathyroid adenoma, invasive fungal sinusitis, and vascular malformations from relevant mimics\*Course Description In this case-based head and neck imaging session, attendees will be presented with typical and atypical imaging examples of squamous cell carcinoma, parathyroid adenoma, invasive fungal sinusitis, and vascular malformations. Speakers will emphasize pearls for differentiating each entity from common mimics, pitfalls of interpretation to avoid, and relevant clinical management considerations with which radiologists should be familiar. This session offers attendees the opportunity to refine their interpretation of complex head and neck imaging studies by incorporating tips from world experts.

Printed on: 02/07/23



## Abstract Archives of the RSNA, 2022

M6-CIN10

### Breaking Through the Hype of AI: A Case-based Review of Benefits and Pitfalls

Monday, Nov. 28 1:30PM - 2:30PM Room: NA

#### Participants

Jayashree Kalpathy-Cramer, MS, PhD, Charlestown, MA (*Presenter*) Institutional Research Grant, General Electric Company; Institutional Research Grant, F. Hoffmann-La Roche Ltd; Institutional Research Grant, Bayer AG  
Paul Yi, MD, Baltimore, MD (*Presenter*) Consultant, FH Orthopedics SAS; Consultant, BunkerHill Health  
Paras Lakhani, MD, Media, PA (*Moderator*) Nothing to Disclose

#### COURSE DESCRIPTION

This is a refresher course that will cover the benefits and pitfalls of using artificial intelligence (AI) in radiology, showing real-world examples of AI successes and failures, current needs, and future directions.

#### LEARNING OBJECTIVES

1) Show the benefits of using artificial intelligence (AI) in radiology via a case-based review 2) Demonstrate pitfalls and current limitations of AI in radiology with real-world examples in clinical practice\*Course Description This is a refresher course that will cover the benefits and pitfalls of using artificial intelligence (AI) in radiology, showing real-world examples of AI successes and failures, current needs, and future directions.

Printed on: 02/07/23



## Abstract Archives of the RSNA, 2022

M6-CIR07

### Global IR and Practice Development

Monday, Nov. 28 1:30PM - 2:30PM Room: NA

#### Participants

Erik Mbuguje, MD, Dar es Salaam, Tanzania, United Republic Of (*Presenter*) Nothing to Disclose

Moritz Wildgruber, MD, PhD, Iffeldorf, Germany (*Presenter*) Consultant, Sirtex Medical Ltd; Consultant, iThera Medical GmbH; Consultant, Bayer AG

Maija Cheung, MD, New Haven, CT (*Presenter*) Consultant, Medtronic plc

Charles Sanyika, MD, Johannesburg, South Africa (*Presenter*) Speaker, Cook Group Incorporated; Speaker, Boston Scientific Corporation

Vijay Ramalingam, MD, Boston, MA (*Presenter*) Nothing to Disclose

Ofonime Ukwueh, MBCh, Calabar, Nigeria (*Presenter*) Nothing to Disclose

Fabian Laage Gaupp, MD, New Haven, CT (*Moderator*) Nothing to Disclose

#### COURSE DESCRIPTION

The evolution of Interventional Radiology over the past 50 years was based on international collaboration with exchange of techniques, ideas, and research. However, most of the global population did not benefit from the rapid advances made in high-income countries. Over the past five years, new strategies to address these disparities have been implemented and there is renewed understanding that Interventional Radiologists need to collaborate closely across borders to advance the specialty to the benefit of all patients, irrespective of location, gender, ethnicity, age, finances, politics, wars, and other factors. This session will feature lectures and discussions on global IR and practice development by international leaders from Africa, Europe, and North America.

#### LEARNING OBJECTIVES

1) Explain the status, availability, challenges, and evolution of Interventional Radiology globally 2) Discuss strategies to build an Interventional Radiology practice in a variety of settings 3) Identify strategies for a successful career as a clinician-scientist in Interventional Radiology\*Course Description The evolution of Interventional Radiology over the past 50 years was based on international collaboration with exchange of techniques, ideas, and research. However, most of the global population did not benefit from the rapid advances made in high-income countries. Over the past five years, new strategies to address these disparities have been implemented and there is renewed understanding that Interventional Radiologists need to collaborate closely across borders to advance the specialty to the benefit of all patients, irrespective of location, gender, ethnicity, age, finances, politics, wars, and other factors. This session will feature lectures and discussions on global IR and practice development by international leaders from Africa, Europe, and North America.

Printed on: 02/07/23

## Abstract Archives of the RSNA, 2022

M6-CMK14

### Musculoskeletal Ultrasound: Normal Appearances, Pathologic Conditions and Hands-on Demo

Monday, Nov. 28 1:30PM - 3:00PM Room: NA

#### Participants

Linda Probyn, MD, Toronto, ON (*Presenter*) Nothing to Disclose

Viviane Khoury, MD, Laval, QC (*Presenter*) Nothing to Disclose

Marnix Van Holsbeeck, MD, Northville, MI (*Presenter*) Stockholder, Koninklijke Philips NV; Stockholder, General Electric Company; Stockholder, MedEd3D

Jon Jacobson, MD, Ann Arbor, MI (*Presenter*) Research Consultant, BioClinica, Inc; Advisory Board, Koninklijke Philips NV; Royalties, RELX; Contactor, POCUS PRO

Rob Campbell, MBBCh, Liverpool, United Kingdom (*Presenter*) Nothing to Disclose

Luca Maria Sconfienza, MD, PhD, Milano, MI (*Presenter*) Travel support, Bracco Group; Travel support, Esaote SpA; Speakers Bureau, Esaote SpA; Travel support, ABIOGEN PHARMA SpA; Speakers Bureau, P&R Holding; Speakers Bureau, Pfizer Inc ; Speaker, Novartis AG; Speaker, Merck KGaA; Speaker, MSD

Mark Cresswell, MBBCh, Vancouver, BC (*Presenter*) Consultant, Koninklijke Philips NV

#### COURSE DESCRIPTION

This session will review US of normal anatomy, normal variants and appearances of the pathologic conditions that commonly affect the Wrist, Hip & Knee, with tips on how to optimize US imaging to best evaluate the most important MSK structures. The hands-on demonstration will illustrate the standard US protocols, with further guidance on techniques that are utilised for dynamic US assessment as problem-solving tools to enhance image interpretation and increase diagnostic confidence. At the end of the session, participants will improve their approach to US assessment of MSK structures and diagnosis of common musculoskeletal pathology.

#### LEARNING OBJECTIVES

1) Improve knowledge of the anatomy and US imaging techniques for evaluation of the Wrist, Hip, and Knee and recognise the normal appearances of MSK structures and common image artefacts relevant to those body areas 2) Become familiar with the standard US image planes and useful dynamic imaging techniques that can enhance diagnosis of musculoskeletal conditions 3) Improve competency of US imaging of the common MSK pathologies and compare the relative merits of utilisation of US vs MRI\*Course Description This session will review US of normal anatomy, normal variants and appearances of the pathologic conditions that commonly affect the Wrist, Hip & Knee, with tips on how to optimize US imaging to best evaluate the most important MSK structures. The hands-on demonstration will illustrate the standard US protocols, with further guidance on techniques that are utilised for dynamic US assessment as problem-solving tools to enhance image interpretation and increase diagnostic confidence. At the end of the session, participants will improve their approach to US assessment of MSK structures and diagnosis of common musculoskeletal pathology.

Printed on: 02/07/23



## Abstract Archives of the RSNA, 2022

M6-CMS02

### Acute Ultrasound Pearls and Pitfalls: Case-based Review

Monday, Nov. 28 1:30PM - 2:30PM Room: NA

#### Participants

Michael R. Aquino, MD, MS, Cleveland, OH (*Presenter*) Co-author with royalties, RELX

Shweta Bhatt, MD, Jacksonville, FL (*Presenter*) Nothing to Disclose

Akshya Gupta, MD, Pittsford, NY (*Presenter*) Nothing to Disclose

Luck J. Louis, MD, Vancouver, BC (*Presenter*) Nothing to Disclose

#### COURSE DESCRIPTION

This course is designed to highlight the vital role ultrasound plays in imaging and diagnosis throughout the body with a focus on challenging emergent cases. A wide range of applications will be covered including vascular, pelvic, pediatric, and musculoskeletal. Attendees will have the opportunity to test their knowledge in real time as interesting unknown cases are presented in a case based format with topic review by the speakers. Our goal is to provide a broad update in the field while addressing new opportunities and challenges for everyday practice

#### LEARNING OBJECTIVES

1) Identify the role of ultrasound in common and uncommon pediatric and musculoskeletal emergencies 2) Understand some common and uncommon causes of acute pelvic pain in women 3) Identify the Doppler findings of abdominal and pelvic vascular pathologies presenting in the acute setting\*Course Description This course is designed to highlight the vital role ultrasound plays in imaging and diagnosis throughout the body with a focus on challenging emergent cases. A wide range of applications will be covered including vascular, pelvic, pediatric, and musculoskeletal. Attendees will have the opportunity to test their knowledge in real time as interesting unknown cases are presented in a case based format with topic review by the speakers. Our goal is to provide a broad update in the field while addressing new opportunities and challenges for everyday practice

Printed on: 02/07/23



## Abstract Archives of the RSNA, 2022

M6-CNMMI04

### Pediatric Molecular Imaging: Read with the Experts

Monday, Nov. 28 1:30PM - 2:30PM Room: NA

#### Participants

Frederic H. Fahey, DSc, Boston, MA (*Presenter*) Nothing to Disclose

Neha Kwatra, MBBS, MD, Boston, MA (*Presenter*) Nothing to Disclose

Frederick Grant, MD, Philadelphia, PA (*Presenter*) Nothing to Disclose

Susan E. Sharp, MD, Cincinnati, OH (*Presenter*) Nothing to Disclose

#### COURSE DESCRIPTION

This course will provide an update on pediatric general nuclear medicine and PET. We will include an introduction including patient preparation, clinical indications for various studies, pearls and pitfalls and artifacts as well as a discussion of both oncologic and non-oncologic topics with illustrative cases. The course will include primarily core topics in pediatric nuclear medicine and PET with focus on the general radiologist, residents and fellows.

#### LEARNING OBJECTIVES

1) To discuss current practice and advances in pediatric general nuclear medicine and PET 2) To review patient preparation and clinical indications for nuclear medicine and PET studies in pediatrics 3) To illustrate pearls and pitfalls of imaging in the pediatric population\*Course Description This course will provide an update on pediatric general nuclear medicine and PET. We will include an introduction including patient preparation, clinical indications for various studies, pearls and pitfalls and artifacts as well as a discussion of both oncologic and non-oncologic topics with illustrative cases. The course will include primarily core topics in pediatric nuclear medicine and PET with focus on the general radiologist, residents and fellows.

Printed on: 02/07/23



## Abstract Archives of the RSNA, 2022

M6-CNPM02

### The Resonant Leader: Stories of Impactful Leaders

Monday, Nov. 28 1:30PM - 2:30PM Room: NA

#### Participants

Marta Heilbrun, MD,MS, Atlanta, GA (*Presenter*) Nothing to Disclose

Hernan Bello Velez, MD, Atlanta, GA (*Presenter*) Nothing to Disclose

Reed Omary, MD, Nashville, TN (*Presenter*) Nothing to Disclose

Christopher Hess, MD, PhD, San Francisco, CA (*Presenter*) Consultant, General Electric Company Consultant, Siemens AG DSMB, Focused Ultrasound Foundation DSMB, uniQure Biopharma DSMB, Asklepios BioPharmaceutical

Pari V. Pandharipande, MD, MPH, Chestnut Hill, MA (*Presenter*) I serve as a member of the Association of University Radiologists (AUR) General Electric (GE) Radiology Research Academic Fellowship (GERRAF) Board of Review (term: 7/1/22-2/28/23).

#### COURSE DESCRIPTION

Resonant leadership is described as a method of leading by designing and nurturing an environment where people work because they believe in the mission and feel united behind a common goal. Using a combination of vignettes and interactive conversation this session will explore challenges that exist and opportunities that arise to shape a department or practice when resonant leadership tools are leveraged.

#### LEARNING OBJECTIVES

1) Recognize pitfalls of leadership  
2) Develop insights to grow as a resonant leader  
3) Build skills in recognizing and addressing micro- and macroaggressions\*  
Course Description Resonant leadership is described as a method of leading by designing and nurturing an environment where people work because they believe in the mission and feel united behind a common goal. Using a combination of vignettes and interactive conversation this session will explore challenges that exist and opportunities that arise to shape a department or practice when resonant leadership tools are leveraged.

Printed on: 02/07/23



## Abstract Archives of the RSNA, 2022

M6-CPD03

### Pediatric GI/GU

Monday, Nov. 28 1:30PM - 2:30PM Room: NA

#### Participants

Shailee Lala, MD, New York, NY (*Presenter*) Editor, RELX

Rama Ayyala, MD, Cincinnati, OH (*Presenter*) Nothing to Disclose

Michael Callahan, MD, Boston, MA (*Presenter*) Nothing to Disclose

#### COURSE DESCRIPTION

Ultrasound is often the first line imaging modality for pediatric gastrointestinal (GI) and genitourinary (GU) indications. Although CT has historically served as an adjunctive and second line imaging modality, there is growing MRI utilization for common pediatric GI and GU pathologies due to increasing MRI availability and continual development of new and faster MRI pulse sequences. This session will highlight the imaging of pediatric inflammatory bowel disease, appendicitis and ovarian torsion with an emphasis on the after-hours approaches. This session will include a panel discussion of the different imaging approaches, with practical advice about implementation in pediatric and adult radiology departments.

#### LEARNING OBJECTIVES

1) Review the advantages and disadvantages of CT enterography and MR enterography and approaches to imaging and appropriate utilization in children with known or suspected inflammatory bowel disease 2) Understand the incidence and potential imaging approaches to suspected acute appendicitis in the pediatric population, and highlight evening/overnight imaging of suspected appendicitis at a large urban pediatric center 3) Summarize the incidence of ovarian torsion and review current approaches and highlight novel methods for imaging ovarian torsion, specifically after normal working hours, at a large academic pediatric center\*Course Description Ultrasound is often the first line imaging modality for pediatric gastrointestinal (GI) and genitourinary (GU) indications. Although CT has historically served as an adjunctive and second line imaging modality, there is growing MRI utilization for common pediatric GI and GU pathologies due to increasing MRI availability and continual development of new and faster MRI pulse sequences. This session will highlight the imaging of pediatric inflammatory bowel disease, appendicitis and ovarian torsion with an emphasis on the after-hours approaches. This session will include a panel discussion of the different imaging approaches, with practical advice about implementation in pediatric and adult radiology departments.

Printed on: 02/07/23



## Abstract Archives of the RSNA, 2022

M6-CPH17

### Basic Physics Lecture for the RT

Monday, Nov. 28 1:30PM - 2:30PM Room: NA

#### Participants

Clinton E. Jokerst, MD, Scottsdale, AZ (*Presenter*) Nothing to Disclose  
Frank Dong, PhD, Sugar Land, TX (*Presenter*) Nothing to Disclose  
Thaddeus Wilson, PhD, Memphis, TN (*Moderator*) Nothing to Disclose

#### LEARNING OBJECTIVES

1) To understand the technical aspects of cardiac CT. 2) To learn the basics of various cardiac CT acquisition modes and its radiation dose implication. 3) To be familiar with patient-related factors on the selection of cardiac CT acquisition mode.\*Course Description

Printed on: 02/07/23



## Abstract Archives of the RSNA, 2022

M6-CVA05

### Pulmonary Vascular Imaging

Monday, Nov. 28 1:30PM - 2:30PM Room: NA

#### Participants

Katherine Kaproth-Joslin, MD, PhD, Rochester, NY (*Presenter*) Nothing to Disclose

Shaunagh McDermott, FFR(RCSI), Boston, MA (*Presenter*) Nothing to Disclose

Fernando R. Gutierrez, MD, Saint Louis, MO (*Presenter*) Nothing to Disclose

Hamid R. Mojbibian, MD, New Haven, CT (*Moderator*) Nothing to Disclose

Printed on: 02/07/23



## Abstract Archives of the RSNA, 2022

M6-RCP07

### MESH Core: Healthcare Innovation and Medical Technology Bootcamp (Part 2)

Monday, Nov. 28 1:00PM - 4:30PM Room: NA

#### Participants

Efren J. Flores, MD, Boston, MA (*Presenter*) Speaker, WebMD LLC; Speaker, Consulting Medical Associates, Inc  
Katherine Andriole, PhD, Branford, CT (*Presenter*) Nothing to Disclose  
Marc Succi, MD, Boston, MA (*Presenter*) Inventor, Frequency Therapeutics  
James Brink, MD, Boston, MA (*Presenter*) Board of Directors, Accumen Inc  
Michael S. Gee, MD, PhD, Boston, MA (*Presenter*) Researcher, General Electric Company Researcher, Siemens AG Researcher, Motilent LLC

#### COURSE DESCRIPTION

MESH Core addresses the lack of training in medical technological innovation in residency and faculty radiologists. In Core, We run short innovation bootcamps and train radiologists, residents, and other non-radiology physicians. After attending MESH Core, the participant will be able to understand the fundamentals of informatics, prototyping, corporate business structures, artificial intelligence, machine learning, research grants, research lab creation, and entrepreneurship. They will know how to progress an idea to prototype, and talk intelligently at conferences, network with innovators, and interact with vendors such as at RSNA.

#### LEARNING OBJECTIVES

Attendees will learn: 1) Fundamentals of artificial intelligence and machine learning, including real demos and algorithm development 2) Fundamentals of Digital Health 3) Fundamentals of Augmented and Mixed Reality 4) Intellectual Property and Patent basics with interactive case-based problems. 5) Hands-on programming in C and C++ and prototyping -Importance of Equity in Technology 6) Fundamentals of startups, corporations, investing 7) How to start your own research lab (including the lesser known things no-one tells you!) 8) How to excel at getting grants, federal, private, and industry\*Course Description MESH Core addresses the lack of training in medical technological innovation in residency and faculty radiologists. In Core, We run short innovation bootcamps and train radiologists, residents, and other non-radiology physicians. After attending MESH Core, the participant will be able to understand the fundamentals of informatics, prototyping, corporate business structures, artificial intelligence, machine learning, research grants, research lab creation, and entrepreneurship. They will know how to progress an idea to prototype, and talk intelligently at conferences, network with innovators, and interact with vendors such as at RSNA.

Printed on: 02/07/23



## Abstract Archives of the RSNA, 2022

M7-CAS05

### Shielding: The Continued Discussion (Sponsored by the Associated Sciences Consortium)

Monday, Nov. 28 3:00PM - 4:00PM Room: NA

#### Participants

Melissa Pergola, RT, Albuquerque, NM (*Presenter*) Former Employee, Siemens AG  
Napapong Pongnapang, Salaya, Thailand (*Presenter*) Nothing to Disclose  
Susie Moseley, MS, RT, Albuquerque, NM (*Moderator*) Nothing to Disclose  
Sharon Wartenbee, RT, Sioux Falls, SD (*Moderator*) Nothing to Disclose  
Donna E. Newman, BA, Fargo, ND (*Moderator*) Nothing to Disclose

#### COURSE DESCRIPTION

For over 7 decades, radiographers have been taught that shielding patients is one of the core principles of radiation safety. This all came into question with the 2019 American Association of Physicists in Medicine (AAPM) Position Statement (PP 32-A) and the U.S. Food and Drug Administration's action to rescind its longstanding gonadal shielding recommendation (21 CFR part 1000.50). In 2020, the British Institute of Radiology published Guidance on using shielding on patients for diagnostic radiology applications and in 2021, recommendations from the National Council on Radiation Protection and Measurements supported an end to shielding specifically during abdominal and pelvic radiography. While science may have new conclusions, this debate continues as stopping a practice that is so ingrained leaves radiographers feeling confused. This session will discuss the latest guidance on using shielding, explain the pros and cons and most importantly, identify resources to help practitioners understand and communicate the change to their patients.

#### LEARNING OBJECTIVES

1) Discuss the latest guidance on using shielding on patients during diagnostic radiography examinations 2) Explain the pros and cons of shielding 3) Identify resources for practitioners\*Course Description For over 7 decades, radiographers have been taught that shielding patients is one of the core principles of radiation safety. This all came into question with the 2019 American Association of Physicists in Medicine (AAPM) Position Statement (PP 32-A) and the U.S. Food and Drug Administration's action to rescind its longstanding gonadal shielding recommendation (21 CFR part 1000.50). In 2020, the British Institute of Radiology published Guidance on using shielding on patients for diagnostic radiology applications and in 2021, recommendations from the National Council on Radiation Protection and Measurements supported an end to shielding specifically during abdominal and pelvic radiography. While science may have new conclusions, this debate continues as stopping a practice that is so ingrained leaves radiographers feeling confused. This session will discuss the latest guidance on using shielding, explain the pros and cons and most importantly, identify resources to help practitioners understand and communicate the change to their patients.

Printed on: 02/07/23



## Abstract Archives of the RSNA, 2022

M7-CBR04

### Challenging Cases in Breast Imaging

Monday, Nov. 28 3:00PM - 4:00PM Room: NA

#### Participants

Jean Seely, MD, Ottawa, ON (*Presenter*) Nothing to Disclose

Bonnie Joe, MD, PhD, San Francisco, CA (*Presenter*) Institutional Research Grant, Kheiron Medical Technologies Ltd; Institutional research agreement, General Electric Company; Institutional research agreement, Siemens AG

Sarah J. Vinnicombe, FRCR, MRCP, Cheltenham, (*Presenter*) Consultant, Bayer AG

#### LEARNING OBJECTIVES

1) Recognize challenging cases that occur in screening to avoid delayed diagnosis of breast cancer 2) Learn appropriate use of breast imaging in the diagnostic setting 3) Apply a skillful approach to radiologic- pathologic correlation in breast imaging\*Course Description

Printed on: 02/07/23



## Abstract Archives of the RSNA, 2022

M7-CCA15

### Mentored Cardiac Case Review: Imaging of Pulmonary Veins, Pericardium and Adult Congenital Heart Disease

Monday, Nov. 28 3:00PM - 4:00PM Room: NA

#### Participants

Phillip Young, MD, Rochester, MN (*Presenter*) Nothing to Disclose

Gregory Kicska, MD, PhD, Seattle, WA (*Presenter*) Nothing to Disclose

Dominique DaBreo, BMedSc, FRCPC, KINGSTON, ON (*Presenter*) Nothing to Disclose

Carole Dennie, MD, Ottawa, ON (*Presenter*) Research Consultant, AstraZeneca PLC

Susan Hobbs, MD, PhD, Rochester, NY (*Moderator*) Nothing to Disclose

Printed on: 02/07/23



## Abstract Archives of the RSNA, 2022

M7-CER16

### Multi-Energy CT in the Emergency Department

Monday, Nov. 28 3:00PM - 4:00PM Room: NA

#### Participants

Lakshmi Ananthakrishnan, MD, Dallas, TX (*Presenter*) Nothing to Disclose

Ismail Ali, MD,FRCP, Toronto, ON (*Presenter*) Nothing to Disclose

Myrna C. Godoy, MD, PhD, Houston, TX (*Presenter*) Siemens Healthineers Research Grant

#### COURSE DESCRIPTION

This course will provide an excellent educational opportunity to understand the role of Dual-energy/ spectral CT (DECT) in the acute setting, in the oncology arena and role in the assessment of the musculoskeletal systems The course will cover key findings – pearls and pitfalls in oncology, acute setting and musculoskeletal applications . It will provide comprehensive instruction on the appropriate indications and imaging protocols for DECT. This course will help participants understand various applications of DECT that lead to improving patient care and increasing diagnostic confidence in confirming diagnoses

#### LEARNING OBJECTIVES

1) Briefly review the basic principles of Dual Energy CT/Spectral imaging 2) Review organ perfusion and oncologic applications in the chest and abdomen 3) To outline novel applications of dual energy CT in assessing bone marrow edema, gout, ligament/tendon analysis and metal artifact reduction\*Course Description This course will provide an excellent educational opportunity to understand the role of Dual-energy/ spectral CT (DECT) in the acute setting, in the oncology arena and role in the assessment of the musculoskeletal systems The course will cover key findings – pearls and pitfalls in oncology, acute setting and musculoskeletal applications . It will provide comprehensive instruction on the appropriate indications and imaging protocols for DECT. This course will help participants understand various applications of DECT that lead to improving patient care and increasing diagnostic confidence in confirming diagnoses

Printed on: 02/07/23



## Abstract Archives of the RSNA, 2022

M7-CIN12

### Imaging Quality Control in the Era of Artificial Intelligence

Monday, Nov. 28 3:00PM - 4:00PM Room: NA

#### Participants

Giridhar Dasegowda, MBBS, Boston, MA (*Presenter*) Nothing to Disclose

Myron A. Pozniak, MD, Waunakee, WI (*Presenter*) Support, General Electric Company

David Larson, MD, MBA, Portola Valley, CA (*Moderator*) Research Grant, Siemens AG ;Advisor, Bunkerhill Health;Shareholder, Bunkerhill Health

#### COURSE DESCRIPTION

Despite decades of effort, excessive CT radiation dose remains a widespread challenge. Since the limiting factor for minimizing dose is image quality, the problem of consistently optimized CT radiation doses has two parts: 1) image quality optimization and 2) process control. While artificial intelligence technology holds promise for lowering dose, without protocol management and other process controls, radiation doses will continue to remain higher than what is reasonably achievable. This session will focus on how AI might be used to lower dose as well as key aspects of protocol management and process control that AI alone will not solve.

#### LEARNING OBJECTIVES

1) Identify key elements of process control that enable image quality and dose optimization, 2) learn how to comprehensively manage protocols for an entire fleet, and 3) understand opportunities and limitations of AI in managing CT dose.\*Course Description Despite decades of effort, excessive CT radiation dose remains a widespread challenge. Since the limiting factor for minimizing dose is image quality, the problem of consistently optimized CT radiation doses has two parts: 1) image quality optimization and 2) process control. While artificial intelligence technology holds promise for lowering dose, without protocol management and other process controls, radiation doses will continue to remain higher than what is reasonably achievable. This session will focus on how AI might be used to lower dose as well as key aspects of protocol management and process control that AI alone will not solve.

Printed on: 02/07/23



## Abstract Archives of the RSNA, 2022

M7-CIN19

### Pareto Principle and IT Projects: What Improves Throughput?

Monday, Nov. 28 3:00PM - 4:00PM Room: NA

#### Participants

Marta Heilbrun, MD,MS, Atlanta, GA (*Presenter*) Nothing to Disclose

Seth Berkowitz, MD, Boston, MA (*Presenter*) Research Grant, Change Healthcare; Research Grant, Koninklijke Philips NV

James Rawson, MD, Boston, MA (*Presenter*) Nothing to Disclose

Natasha Larocque, MD, Hamilton, ON (*Presenter*) Nothing to Disclose

#### COURSE DESCRIPTION

Over the next year, all of us will see IT projects implemented in our institutions. They range from essential upgrades of existing information systems (e.g. cybersecurity or regulatory requirements) to completely new systems (e.g. stand alone or integrated in our PACS workflow). This lecture will focus on identifying IT projects that can improve Radiologists workflow and patient throughput. Examples of projects and tools will be given in population health, incidental findings, artificial intelligence and radiology workflow.

#### LEARNING OBJECTIVES

1) Identify opportunities and tools for improving Radiologists workflow 2) Identify opportunities and tools for improving patient throughput 3) Identify metrics to track and demonstrate improvement\*Course Description Over the next year, all of us will see IT projects implemented in our institutions. They range from essential upgrades of existing information systems (e.g. cybersecurity or regulatory requirements) to completely new systems (e.g. stand alone or integrated in our PACS workflow). This lecture will focus on identifying IT projects that can improve Radiologists workflow and patient throughput. Examples of projects and tools will be given in population health, incidental findings, artificial intelligence and radiology workflow.

Printed on: 02/07/23



## Abstract Archives of the RSNA, 2022

M7-CMK13

### Fast 5 Presentations: How Your Life Will Change in the Next 5 Years

Monday, Nov. 28 3:00PM - 4:00PM Room: NA

#### Participants

William Morrison, MD, Philadelphia, PA (*Presenter*) Co-founder, Trace Orthopedics;Patent agreement, Trace Orthopedics;Consultant, AprioMed AB;Patent agreement, AprioMed AB;Consultant, Centinel Spine, LLC;Consultant, Medical Metrics, Inc

Michael Recht, MD, New York, NY (*Presenter*) Nothing to Disclose

Donald L. Resnick, MD, San Diego, CA (*Presenter*) Nothing to Disclose

Bruce Forster, MD, Vancouver, BC (*Presenter*) Stockholder, Canada Diagnostic Centres

Hollis G. Potter, MD, New York, NY (*Presenter*) Research support, General Electric Company;Institutional research agreement, General Electric Company;Stockholder, Imagen Technologies Inc;Consultant, Atria Academy of Science and Medicine

Mark Schweitzer, MD, Detroit, MI (*Presenter*) Board of Directors, CareMore ;Consultant, MMI Munich Medical International GmbH;

Timothy J. Mosher, MD, Hershey, PA (*Presenter*) Stockholder, Johnson & Johnson;

Leon Lenchik, MD, Winston-salem, NC (*Presenter*) Nothing to Disclose

Reed Omary, MD, Nashville, TN (*Presenter*) Nothing to Disclose

Bethany Casagrande, DO, Pittsburgh, PA (*Presenter*) Nothing to Disclose

#### COURSE DESCRIPTION

The session will feature 5-minute TED-style talks by musculoskeletal radiology leaders tasked with predicting the future of radiology practice. Each speaker will offer one prediction, discuss its reasons, and indicate how it would be a game-changer for radiology if it came true in 5 years.

#### LEARNING OBJECTIVES

1) Identify emerging trends in radiology that are promising to transform the field 2) Discuss the impact of these trends on clinical practice\*Course Description The session will feature 5-minute TED-style talks by musculoskeletal radiology leaders tasked with predicting the future of radiology practice. Each speaker will offer one prediction, discuss its reasons, and indicate how it would be a game-changer for radiology if it came true in 5 years.

Printed on: 02/07/23



## Abstract Archives of the RSNA, 2022

M7-CNPM07

### Translational Research Education Course (TREC) (Sponsored by the RSNA Research Development Committee)

Monday, Nov. 28 3:00PM - 4:00PM Room: NA

#### Participants

Maurizio Conti, PhD, Knoxville, TN (*Presenter*) Employee, Siemens AG  
Austin Pantel, MD, Philadelphia, PA (*Presenter*) Institutional research support, Lantheus Holdings; Consultant, Blue Earth Diagnostics Ltd; Consultant, General Electric Company; Consultant, Lantheus Holdings  
Joel Karp, Philadelphia, PA (*Presenter*) Research Grant, Siemens AG; Research Grant, Koninklijke Philips NV  
Shadi Abdar Esfahani, MD, MPH, Boston, MA (*Moderator*) Scientific Advisory Board, RefleXion Medical Inc; Scientific Advisory Board, ImaginAb, Inc; Scientific Advisory Board, General Electric Company; Scientific Advisory Board, Trevarx Biomedical, Inc; Consultant, General Electric Company; Spouse, CEO, Trevarx Biomedical, Inc; Spouse, Owner, Trevarx Biomedical, Inc  
David A. Mankoff, MD, PhD, Philadelphia, PA (*Moderator*) Speaker, Siemens AG Advisory Board, ImaginAb, Inc Advisory Board, RefleXion Medical Inc Consultant, Blue Earth Diagnostics Ltd Consultant, General Electric Company Research funded, Siemens AG Spouse, Owner, Trevarx Biomedical, Inc  
J. Brian Fowlkes, PhD, Ann Arbor, MI (*Moderator*) Research Grant, Koninklijke Philips NV; Equipment support, General Electric Company

#### COURSE DESCRIPTION

While there are current RSNA courses on grant writing and various aspects of academic radiology, there is not an educational course for guiding the researchers to successfully translate research into clinical practice. This 1-hour session is designed to address this knowledge gap on the steps that need to be taken from developing the idea, assessing the clinical need, pharmaceutical and industrial demand, securing funding, making a team of collaborators to translate and commercialize the product and finally make it part of daily clinical practice. These topics will be covered by speakers with expertise on different aspects of translational imaging research. This inaugural TREC education session will focus on Total-Body (long axial FOV) PET devices and their use in research and clinical practice.

#### LEARNING OBJECTIVES

1) Describe the approach to translating new basic science discoveries to clinical trials and clinical practice. 2) List hurdles that may hinder translation and approaches to overcome these hurdles. 3) Discuss the role of industry partners in the translation of new radiology methods and technologies\*Course Description While there are current RSNA courses on grant writing and various aspects of academic radiology, there is not an educational course for guiding the researchers to successfully translate research into clinical practice. This 1-hour session is designed to address this knowledge gap on the steps that need to be taken from developing the idea, assessing the clinical need, pharmaceutical and industrial demand, securing funding, making a team of collaborators to translate and commercialize the product and finally make it part of daily clinical practice. These topics will be covered by speakers with expertise on different aspects of translational imaging research. This inaugural TREC education session will focus on Total-Body (long axial FOV) PET devices and their use in research and clinical practice.

Printed on: 02/07/23



## Abstract Archives of the RSNA, 2022

M7-COB08

### Imaging Ovarian Cancer: Radiologists as Partners in Cancer Care

Monday, Nov. 28 3:00PM - 4:00PM Room: NA

#### Participants

Stephanie Nougaret, MD, PhD, Montpellier, (*Presenter*) Nothing to Disclose

Yuliya Lakhman, MD, New York, NY (*Presenter*) Stockholder, Y-mAbs Therapeutics Inc; Consultant, Perceptive Informatics, LLC

Annie Leung, MD, Montreal, QC (*Presenter*) Nothing to Disclose

Evis Sala, MD, PhD, Cambridge, United Kingdom (*Presenter*) Co-founder, Lucida Medical Ltd

#### COURSE DESCRIPTION

This course will give a comprehensive view of the current and state of the art therapy for ovarian cancer patients. It will review the role of multimodality imaging in treatment selection and planning focusing on the added value of various imaging modalities for detection of peritoneal implants that change management. It will also provide a glimpse into the future of personalized care by highlighting the role of artificial intelligence and radiogenomics in improving prediction of response to neoadjuvant chemotherapy and early detection of treatment resistance which determines patient outcome.

#### LEARNING OBJECTIVES

1) Learn the current treatment paradigms available to patients with ovarian cancer 2) Review the the role of multi-modality imaging in treatment selection and planning of ovarian cancer patients 3) Highlight the potential added value of radiogenomics/AI in prediction of treatment response and outcome in patients with ovarian cancer\*Course Description This course will give a comprehensive view of the current and state of the art therapy for ovarian cancer patients. It will review the role of multimodality imaging in treatment selection and planning focusing on the added value of various imaging modalities for detection of peritoneal implants that change management. It will also provide a glimpse into the future of personalized care by highlighting the role of artificial intelligence and radiogenomics in improving prediction of response to neoadjuvant chemotherapy and early detection of treatment resistance which determines patient outcome.

Printed on: 02/07/23



## Abstract Archives of the RSNA, 2022

M7-CPH07

### Recent Advances in PET/MRI and PET/CT Imaging

Monday, Nov. 28 3:00PM - 4:00PM Room: NA

#### Participants

Thomas Beyer, PhD, Vienna, Austria (*Presenter*) Co-founder, cmi-experts GmbH; Co-founder, Dedicaid GmbH  
Ciprian Catana, MD, PhD, Charlestown, MA (*Presenter*) Nothing to Disclose

#### COURSE DESCRIPTION

This session will provide an overview of the recent developments in hybrid PET/CT and PET/MRI instrumentation. It will also present the latest progress in the integration of the multimodality information for research and clinical applications. Finally, the use of artificial intelligence for addressing remaining challenges in hybrid imaging and for performing advanced analyses of the multimodal datasets will be discussed.

#### LEARNING OBJECTIVES

1) Describe the state-of-the-art hardware for hybrid imaging 2) Explain software innovations in combining the multimodality information 3) Identify current applications of artificial intelligence in hybrid imaging \*Course Description This session will provide an overview of the recent developments in hybrid PET/CT and PET/MRI instrumentation. It will also present the latest progress in the integration of the multimodality information for research and clinical applications. Finally, the use of artificial intelligence for addressing remaining challenges in hybrid imaging and for performing advanced analyses of the multimodal datasets will be discussed.

Printed on: 02/07/23



## Abstract Archives of the RSNA, 2022

M7-CPH18

### Physics Symposium: Highlights of Physics Summer School: Practical Medical Image Analysis

Monday, Nov. 28 3:00PM - 4:00PM Room: NA

#### Participants

Ingrid Reiser, PhD, Chicago, IL (*Presenter*) Family member, Employee, Clarix Imaging  
Samuel G. Armato III, PhD, Chicago, IL (*Presenter*) Nothing to Disclose  
William Sensakovic, PhD, Cave Creek, AZ (*Presenter*) Nothing to Disclose

#### COURSE DESCRIPTION

Computer processing and analysis of medical imaging data has seen a resurgence in recent years, fueled by rapidly improving hardware and advances in computational techniques. Major medical imaging and therapy vendors emphasize their post-processing and software packages when selling their systems, and start-ups are aiming to alter the medical establishment with advanced algorithms and data-intensive products. This session will highlight selected topics from the 2019 American Association of Physicists in Medicine (AAPM) Summer School. Lectures will review key messages and concepts related to assessment, quality control, data commons, responsible use, basic informatics, and related topics.

#### LEARNING OBJECTIVES

1) Identify data repository and grand challenge resources 2) Discuss responsible use and ethics of AI 3) Understand methods to assess algorithms 4) Explain basic informatics standards and image processing methods\*Course Description Computer processing and analysis of medical imaging data has seen a resurgence in recent years, fueled by rapidly improving hardware and advances in computational techniques. Major medical imaging and therapy vendors emphasize their post-processing and software packages when selling their systems, and start-ups are aiming to alter the medical establishment with advanced algorithms and data-intensive products. This session will highlight selected topics from the 2019 American Association of Physicists in Medicine (AAPM) Summer School. Lectures will review key messages and concepts related to assessment, quality control, data commons, responsible use, basic informatics, and related topics.

Printed on: 02/07/23



## Abstract Archives of the RSNA, 2022

M7-CRO05

### Gastrointestinal Case-based Multidisciplinary Review

Monday, Nov. 28 3:00PM - 4:00PM Room: NA

#### Participants

Noelle LoConte, MD, Madison, WI (*Presenter*) Advisory Board, AbbVie Inc; Advisory Board, Personal Genome Diagnostics Inc  
Jennifer Wo, MD, Boston, MA (*Presenter*) Research funded, F. Hoffmann-La Roche Ltd  
Vitaliy Poylin, MD, Chicago, IL (*Presenter*) Nothing to Disclose  
Ann Raldow, MD, MPH, Los Angeles, CA (*Presenter*) Consultant, ViewRay, Inc  
Spencer C. Behr, MD, San Francisco, CA (*Presenter*) Grant, Cancer Targeted Technology; Scientific Advisory Board, Novartis AG; Research Consultant, GenVivo

#### COURSE DESCRIPTION

This course will be a case-based multidisciplinary tumor board to explore emerging treatment paradigms, and the critical role of imaging in these discussions. Within patterns of care, there has been increasing focus on total neoadjuvant therapy and non-operative management as treatment paradigms. This course will further highlight important imaging characteristics that help guide these conversations.

#### LEARNING OBJECTIVES

1) Develop an understanding of evolving treatment paradigms of multimodality care for colorectal cancer 2) Identify key radiographic features which are critical for clinical decision making 3) Define imaging characteristics that are predictive for clinical complete response for rectal cancer in the setting non-operative management\*Course Description This course will be a case-based multidisciplinary tumor board to explore emerging treatment paradigms, and the critical role of imaging in these discussions. Within patterns of care, there has been increasing focus on total neoadjuvant therapy and non-operative management as treatment paradigms. This course will further highlight important imaging characteristics that help guide these conversations.

Printed on: 02/07/23



## Abstract Archives of the RSNA, 2022

M7-CVA01

### Multimodal Thoracic Aortic Imaging: What the Radiologist and Surgeon Need to Know

Monday, Nov. 28 3:00PM - 4:00PM Room: NA

#### Participants

Diana Litmanovich, MD, Boston, MA (*Presenter*) Nothing to Disclose  
Minhaj S. Khaja, MD, MBA, Charlottesville, VA (*Presenter*) Institutional Research Grant, Boston Scientific Corporation; Speaker, Boston Scientific Corporation; Speaker, Medtronic plc; Advisory Board, Medtronic plc; Institutional Grant, Penumbra, Inc  
Maral Ouzounian, Toronto, ON (*Presenter*) Consultant, Edwards Lifesciences Corporation; Consultant, Medtronic plc  
Kate Hanneman, MD, FRCPC, Toronto, ON (*Moderator*) Speaker, Groupe Sanofi Speaker, Amicus Therapeutics, Inc

#### COURSE DESCRIPTION

This didactic session will review multimodal imaging of the thoracic aorta with a focus on what the radiologist and surgeon needs to know

#### LEARNING OBJECTIVES

1) Identify thoracic aortic pathology requiring intervention on imaging 2) Explain imaging analysis and measurements that are needed to guide management and for risk stratification\*Course Description This didactic session will review multimodal imaging of the thoracic aorta with a focus on what the radiologist and surgeon needs to know

Printed on: 02/07/23



## Abstract Archives of the RSNA, 2022

M7-RCP13

### Humanism in Radiology - Combatting Burnout and Robots (Sponsored by the RSNA Public Information Committee)

Monday, Nov. 28 3:00PM - 4:00PM Room: NA

#### Participants

Nicole Restauri, MD, Denver, CO (*Presenter*) Nothing to Disclose

Bettina Siewert, MD, Brookline, MA (*Presenter*) Editor, Wolters Kluwer nv; Reviewer, Wolters Kluwer nv

Jennifer Kemp, MD, Denver, CO (*Moderator*) Stockholder, Scanslated, Inc

#### COURSE DESCRIPTION

Medical literature and lay news media have portrayed the growing challenges of burnout among physicians, including radiologists. Reports of impending displacement of radiologists by advanced computers and machine learning have added to stress in our specialty and may be discouraging medical students from pursuing diagnostic radiology as a career. Loss of autonomy, isolation, and dehumanization are important contributors to the burnout epidemic, and loss of professional identity and diminished engagement in patient care give credence to the rumors of radiology's demise. Creation of a more humanistic culture in radiology is one way to avert the crisis. Strategies to increase humanism in radiology involve finding ways to increase empathy, foster connectedness, and restore meaning in the workplace. This course will present methods that have been shown to improve radiologist engagement and joy in the work. Using narrative to share experiences, developing gratitude practices, and developing a focus on personal and organizational values and fulfilling work tasks will be presented as methods to mitigate burnout and demonstrate value in radiology. Facilitators will engage participants in the process of exploring self, the culture of the healthcare system, and the role of the imagination in creating change. Objectives for the session include fostering connection with self and community using expressive arts and reflective writing as access points that inspire joy, facilitate cognitive reframing, and bring forth the texture of our individual and collective identities so that we may feel and be seen as more than "cogs in a wheel."

#### LEARNING OBJECTIVES

1) Explore the healing power of narrative to combat burnout. 2) Understand connection as an integral element of meaningful work. 3) Foster connection with self and community using expressive arts and reflective writing.\*Course Description Medical literature and lay news media have portrayed the growing challenges of burnout among physicians, including radiologists. Reports of impending displacement of radiologists by advanced computers and machine learning have added to stress in our specialty and may be discouraging medical students from pursuing diagnostic radiology as a career. Loss of autonomy, isolation, and dehumanization are important contributors to the burnout epidemic, and loss of professional identity and diminished engagement in patient care give credence to the rumors of radiology's demise. Creation of a more humanistic culture in radiology is one way to avert the crisis. Strategies to increase humanism in radiology involve finding ways to increase empathy, foster connectedness, and restore meaning in the workplace. This course will present methods that have been shown to improve radiologist engagement and joy in the work. Using narrative to share experiences, developing gratitude practices, and developing a focus on personal and organizational values and fulfilling work tasks will be presented as methods to mitigate burnout and demonstrate value in radiology. Facilitators will engage participants in the process of exploring self, the culture of the healthcare system, and the role of the imagination in creating change. Objectives for the session include fostering connection with self and community using expressive arts and reflective writing as access points that inspire joy, facilitate cognitive reframing, and bring forth the texture of our individual and collective identities so that we may feel and be seen as more than "cogs in a wheel."

Printed on: 02/07/23



## Abstract Archives of the RSNA, 2022

M7-RCP19

### Building Evidence Through Observational Research in Radiology (BETORR): A Primer on Observational "Big" Data Analysis (Sponsored by the RSNA Research Development Committee)

Monday, Nov. 28 3:00PM - 4:00PM Room: NA

#### Participants

Ammar Sarwar, MD, Boston, MA (*Presenter*) Stockholder, Agile Devices, Inc;Scientific Advisory Board, Agile Devices, Inc;Grant, Sirtex Medical Ltd;Consultant, Sirtex Medical Ltd

Richard Duszak JR, MD, Jackson, MS (*Presenter*) Advisor, Ethos Medical, Inc;Shareholder, Ethos Medical, Inc

Alexandria Jensen, Aurora, CO (*Presenter*) Nothing to Disclose

Premal Trivedi, MD, Denver, CO (*Presenter*) Speakers Bureau, ForTec MedicalAdvisory Board, PneumoNIX Medical

Gelareh Sadigh, MD, Irvine, GA (*Moderator*) Research Grant, TailorMed Medical Ltd

#### COURSE DESCRIPTION

Observational "big data" research studying access, utilization, cost and outcomes are essential to providing evidence for, and improving the value of, imaging. Studies leveraging claims or registry data can advance the clinical sciences by offering real world, effectiveness data. This session serves as a primer on the use of large population data sets for high quality and clinically meaningful outcomes research. The objectives are to highlight methodologic best practices, to explore strengths and weaknesses of commonly used data sources and to provide attendees with a toolset to assess the quality of observational studies in the radiology literature.

#### LEARNING OBJECTIVES

1) Understand the strengths and weaknesses of big data observational research 2) Identify common data sources and understand their strengths and weaknesses 3) Understand common sources of bias in observational data research and how to deal with them\*Course Description Observational "big data" research studying access, utilization, cost and outcomes are essential to providing evidence for, and improving the value of, imaging. Studies leveraging claims or registry data can advance the clinical sciences by offering real world, effectiveness data. This session serves as a primer on the use of large population data sets for high quality and clinically meaningful outcomes research. The objectives are to highlight methodologic best practices, to explore strengths and weaknesses of commonly used data sources and to provide attendees with a toolset to assess the quality of observational studies in the radiology literature.

Printed on: 02/07/23



## Abstract Archives of the RSNA, 2022

M7-RCP46

### **Radiologia Centrada en el Paciente: Seguridad, Gestion y Tecnologia (CIR) / Patient-Centered Radiology: Quality, Safety, Management, and Technology (CIR)**

Monday, Nov. 28 3:00PM - 4:30PM Room: NA

#### **Participants**

Mariana Rovira Canellas, Barcelona, Spain (*Presenter*) Nothing to Disclose  
Alejandro Tempra, Mendoza, Argentina (*Presenter*) Nothing to Disclose  
Daniel Guerrero-Gavilanes, MD, Quito, Ecuador (*Presenter*) Nothing to Disclose  
Maria Francesca Castoldi, MD, Vitacura, Chile (*Presenter*) Nothing to Disclose  
Luis R. Campos, MD, Dominican Republic, Dominican Republic (*Presenter*) Nothing to Disclose  
Fatima Matute Teresa, MD, Madrid, Spain (*Moderator*) Nothing to Disclose  
Pablo Soffia, MD, Santiago, Chile (*Moderator*) Nothing to Disclose

#### **COURSE DESCRIPTION**

To learn some key elements in quality and safety management of a Radiology Department, with emphasis on the patient's journey with the support of new technologies.

#### **LEARNING OBJECTIVES**

1) Analyze the patient's bumpy journey in the Radiology Department 2) Identify the strategies to improve the patient's experience with the new technologies 3) Transform the role of the radiologist Keys for the radiologist empowerment 4) Be aware of the type and reasons of errors and adverse events in the radiological practice 5) Create a culture that promotes error reporting 6) Develop strategies to learn from errors 7) Encourage the radiologist-patient relationship to reduce errors and improve safety 8) Make the radiologist visible as a pillar in the diagnosis and guide for therapeutic management 9) Identify the best virtues of face-to-face radiology versus teleradiology from the medical and patient point of view 10) Analyze the options of both methodologies for the knowledge of our colleagues\*Course Description To learn some key elements in quality and safety management of a Radiology Department, with emphasis on the patient's journey with the support of new technologies.

Printed on: 02/07/23



## Abstract Archives of the RSNA, 2022

M7-RCP60

### The Academy's Imaging Shark Tank Session (Sponsored by the Academy for Radiology & Biomedical Imaging Research)

Monday, Nov. 28 3:00PM - 4:30PM Room: NA

#### Participants

Abhijeet Pradhan, MBA,MS, Austin, TX (*Presenter*) Stockholder, Galileo CDS, Inc;CEO, Galileo CDS, Inc  
Hersh Sagreiya, MD, Philadelphia, PA (*Presenter*) Nothing to Disclose  
Kelsey Tsai, Chicago, IL (*Presenter*) Employee, Blue Venture Fund  
Michael A. Jacobs, PhD, Houston, TX (*Presenter*) Nothing to Disclose  
Suyash Mohan, MD, Philadelphia, PA (*Presenter*) Research Grant, NovoCure Ltd;Research Grant, Galileo CDS, Inc;Consultant, Northwest Biotherapeutics, Inc;Consultant, AIRS Medical Inc;Consultant, Qynapse SAS  
Susan Harris, Wauwatosa, WI (*Presenter*) Employee, General Electric Company  
Emir Sandhu, MD, Stanford, CA (*Presenter*) Nothing to Disclose  
Alireza Akhbardeh, PhD, Stanford, CA (*Presenter*) Nothing to Disclose  
John Moon, MD, Atlanta, GA (*Presenter*) Founder, TissueGen, Inc  
Scott Penner, JD, San Diego, CA (*Presenter*) Spouse, Research Grant, General Electric Company;Spouse, Consultant, Human Longevity, Inc;Spouse, Stockholder, CureMetrix, Inc;Spouse, Stock options, Cortechs.ai  
Mitchell Schnall, MD, PhD, Philadelphia, PA (*Presenter*) Research Grant, Siemens AG

#### COURSE DESCRIPTION

An educational session, where 3 nominated Pitch Teams are chosen through a competitive process in advance. The chosen Pitch Teams, generally comprised of early-mid career investigators, then have a timed period during which the pitch their ideas to a panel consisting of representatives from industry, academia and venture capital, who in turn offer advice on each specific pitch. 2022 will mark the 7th session we've held at RSNA - this is a widely-attended event that becomes more and more popular each year, with a high level of engagement virtually in 2020 and a large hybrid audience both in-person and online in 2021.

#### LEARNING OBJECTIVES

1. Identifying strategies for bringing research to the competitive marketplace 2. Presenting a proposal in a way that elicits interest from potential investors 3. Taking steps to secure investor funding while developing and protecting their intellectual property 4. Identifying ways to generate business value through licensing and collaborations \*Course Description An educational session, where 3 nominated Pitch Teams are chosen through a competitive process in advance. The chosen Pitch Teams, generally comprised of early-mid career investigators, then have a timed period during which the pitch their ideas to a panel consisting of representatives from industry, academia and venture capital, who in turn offer advice on each specific pitch. 2022 will mark the 7th session we've held at RSNA - this is a widely-attended event that becomes more and more popular each year, with a high level of engagement virtually in 2020 and a large hybrid audience both in-person and online in 2021.

Printed on: 02/07/23



## Abstract Archives of the RSNA, 2022

M8-CAS01

### Developing a System-Wide Imaging Capital Plan: Strategies and Innovative Methodologies (Sponsored by the Associated Sciences Consortium)

Monday, Nov. 28 4:30PM - 5:30PM Room: NA

#### Participants

Peter St John, Boston, MA (*Presenter*) Nothing to Disclose  
Jason Newmark, BA,MBA, Boston, MA (*Presenter*) Nothing to Disclose  
Sandra Strycker, BS, Lake Oswego, OR (*Moderator*) Nothing to Disclose  
Michelle Wall, MS, RT, Cincinnati, OH (*Moderator*) Nothing to Disclose

#### COURSE DESCRIPTION

One of the best parts about a career in imaging is having the opportunity to work with ever changing and improving technology. Faster scans, reduced radiation, new sources of energy, enhanced image quality, more patient comfort, and more efficient workflows for staff. All combined to provide the diagnostic backbone to support and enhance the overall care continuum/coordination of patient care for our referrers and patients. True, it can be overwhelming at times to keep up with all of the new innovations, the nuances of service agreements with vendors, and the constant demand from staff and providers to have the latest and greatest tools --- however, it is exciting. For imaging leaders, the use of the right methodologies and tools to proactively manage and plan for their organization's imaging capital needs is essential. In this session we will present real life examples of the effectiveness and impact of proven tools and methodologies to develop a system-wide, multi-year, imaging capital plan. In addition, we will provide recommendations on building stronger and more innovative relationships with your vendor partners.

#### LEARNING OBJECTIVES

1) Learn about proven methodologies and tools to manage a highly visible and complex effort with multiple stakeholders and elements, proactive tracking and projecting and planning for imaging capital needs. 2) Understand key terms and considerations to incorporate into equipment and vendor assessments and negotiations. 3) How to develop, initiate, and complete a multi-year, system-wide imaging capital plan.\*Course Description One of the best parts about a career in imaging is having the opportunity to work with ever changing and improving technology. Faster scans, reduced radiation, new sources of energy, enhanced image quality, more patient comfort, and more efficient workflows for staff. All combined to provide the diagnostic backbone to support and enhance the overall care continuum/coordination of patient care for our referrers and patients. True, it can be overwhelming at times to keep up with all of the new innovations, the nuances of service agreements with vendors, and the constant demand from staff and providers to have the latest and greatest tools --- however, it is exciting. For imaging leaders, the use of the right methodologies and tools to proactively manage and plan for their organization's imaging capital needs is essential. In this session we will present real life examples of the effectiveness and impact of proven tools and methodologies to develop a system-wide, multi-year, imaging capital plan. In addition, we will provide recommendations on building stronger and more innovative relationships with your vendor partners.

Printed on: 02/07/23



## Abstract Archives of the RSNA, 2022

M8-CER02

### Hot Topics in Emergency Radiology

Monday, Nov. 28 4:30PM - 5:30PM Room: NA

#### Participants

Douglas Katz, MD, Mineola, NY (*Presenter*) Nothing to Disclose

Bharti Khurana, MD, Brookline, MA (*Presenter*) Consultant, General Electric Company; Editor, Wolters Kluwer nv; Author, Cambridge University Press; Consultant, ROKIT Healthcare, Inc

Armonde Baghdanian, MD, San Francisco, CA (*Presenter*) Nothing to Disclose

#### COURSE DESCRIPTION

Brief presentations of current topics in the literature from authorities in these specific subtopics in emergency radiology, including 'damage control' surgery, intimate partner violence, and imaging of trauma in pregnancy.

#### LEARNING OBJECTIVES

1) To understand the current algorithms and safety considerations for imaging suspected trauma to the abdomen and pelvis in pregnancy, with review of multi-modality imaging findings, and a brief review of the literature2) To overview the potential findings, the current literature, and the responsibility of the radiologist in the identification, characterization, and reporting of imaging findings on various types of imaging examinations in suspected intimate partner violence3) To demonstrate examples of, explain the current role of, and review the current literature on, imaging of the abdomen and pelvis after damage control surgery, with an emphasis on CT findings\*Course Description Brief presentations of current topics in the literature from authorities in these specific subtopics in emergency radiology, including 'damage control' surgery, intimate partner violence, and imaging of trauma in pregnancy.

Printed on: 02/07/23



## Abstract Archives of the RSNA, 2022

M8-CIN06

### 3D Printing for Cardiac and Musculoskeletal Applications with Interactive Clinical Perspectives

Monday, Nov. 28 4:30PM - 5:30PM Room: NA

#### Participants

Robert Buly, MD,MS, New York, NY (*Presenter*) Nothing to Disclose

Beth Ripley, MD, PhD, Seattle, WA (*Presenter*) Nothing to Disclose

John A. Carrino, MD, MPH, New York, NY (*Presenter*) Research Consultant, Pfizer Inc; Research Consultant, AstraZeneca PLC; Research Consultant, Regeneron Pharmaceuticals, Inc; Research Consultant, Globus Medical, Inc; Consultant, Covera Health, Inc; Advisory Board, Carestream Health, Inc; Advisory Board, Image Analysis Group (IAG)

Andrew Christensen, BS, Littleton, CO (*Presenter*) Consultant, Ricoh Co, Ltd; Stockholder, Somaden LLC; Stockholder, Unyq Design, Inc; Stockholder, Vizua, Inc; Stockholder, Dimension Inx; Stockholder, Integrum AB; Board of Directors, Integrum AB; Stockholder, Onkos Surgical; Stockholder, Precision ADM; Board of Directors, Precision ADM

Dmitry Levin, Seattle, WA (*Presenter*) Nothing to Disclose

Thomas A. Foley, MD, Rochester, MN (*Moderator*) Nothing to Disclose

Kenneth Wang, MD, PhD, Ellicott City, MD (*Moderator*) Co-founder, DexNote, LLC

#### COURSE DESCRIPTION

This course brings together physicians and innovators from Radiology, Orthopaedic Surgery and Cardiology to interactively discuss the role of image-based 3D printing in providing personalized healthcare solutions to patients. Based on key clinical scenarios in cardiac and musculoskeletal disease, the panelists will describe approaches to diagnostic imaging, the clinical motivations for 3D printing, and the impact of 3D printing on the quality of care. Course attendees will be active participants, using multiple technologies to provide audience responses and ask questions in real time. By participating in this course, attendees can expect to gain important real-world insights into the tangible benefits of 3D printing for patient care.

#### LEARNING OBJECTIVES

1) Describe the fundamental role of imaging in patient-specific 3D printing 2) Explain the importance of 3D printing for key cardiac and musculoskeletal diseases 3) Compare the physical properties of 3D printing materials\*Course Description This course brings together physicians and innovators from Radiology, Orthopaedic Surgery and Cardiology to interactively discuss the role of image-based 3D printing in providing personalized healthcare solutions to patients. Based on key clinical scenarios in cardiac and musculoskeletal disease, the panelists will describe approaches to diagnostic imaging, the clinical motivations for 3D printing, and the impact of 3D printing on the quality of care. Course attendees will be active participants, using multiple technologies to provide audience responses and ask questions in real time. By participating in this course, attendees can expect to gain important real-world insights into the tangible benefits of 3D printing for patient care.

Printed on: 02/07/23



## Abstract Archives of the RSNA, 2022

M8-CNPM04

### Mentorship, Sponsorship and Coaching: Not Just for Early Career

Monday, Nov. 28 4:30PM - 5:30PM Room: NA

#### Participants

Lucy Spalluto, MD,MPH, Nashville, TN (*Presenter*) Nothing to Disclose

Scott Cameron, MD, Auburndale, MA (*Presenter*) Stockholder, RadAI; Stockholder, Cognoptix Inc; Stockholder, Agile Devices, Inc; Consultant, Intrinsic Imaging, LLC; Consultant, Radiology Peer Review Panel, LLC; Consultant, Coverys, Inc

Jay R. Parikh, MD, West University Place, TX (*Presenter*) Nothing to Disclose

Cheri Canon, MD, Birmingham, AL (*Moderator*) Royalties, The McGraw-Hill Companies

#### COURSE DESCRIPTION

This session will explore the important roles of mentorship, sponsorship, and coaching for all professionals, not just early career. Both private practice and academic practice perspectives will be included. It will also highlight the value of each of these as we develop a more diverse profession.

#### LEARNING OBJECTIVES

1) Define and contrast the activities of mentoring, sponsoring, and coaching in both academic and private practice settings\*Course Description This session will explore the important roles of mentorship, sponsorship, and coaching for all professionals, not just early career. Both private practice and academic practice perspectives will be included. It will also highlight the value of each of these as we develop a more diverse profession.

Printed on: 02/07/23



## Abstract Archives of the RSNA, 2022

R1-CCA03

### Artificial Intelligence & Machine Learning in CV Imaging

Thursday, Dec. 1 8:00AM - 9:00AM Room: NA

#### Participants

Alex Bratt, MD, Rochester, MN (*Presenter*) Nothing to Disclose

Albert Hsiao, MD, PhD, La Jolla, CA (*Presenter*) Co-founder, Arterys Inc; Shareholder, Arterys Inc; Co-founder, Vektor.AI; Shareholder, Vektor.AI; Research Grant, Bayer AG; Research Grant, General Electric Company; Research Grant, KA Imaging

Carlo N. De Cecco, MD, Atlanta, GA (*Moderator*) Research Grant, Siemens AG; Consultant, Covanos, Inc

#### COURSE DESCRIPTION

The course will provide an overview of current and potential applications of artificial intelligence (AI) in cardiovascular imaging. The course will address the basic technological considerations and AI fundamentals, potentials and pitfalls, including current and future AI applications in CV imaging. At the end of the course participants will be able to understand and critically appraise existing AI applications.

#### LEARNING OBJECTIVES

1) Understand the basic technological considerations and fundamentals of AI 2) Illustrate current AI applications in cardiovascular imaging 3) Discuss the potentials and pitfalls of AI applied to CV imaging\*Course Description The course will provide an overview of current and potential applications of artificial intelligence (AI) in cardiovascular imaging. The course will address the basic technological considerations and AI fundamentals, potentials and pitfalls, including current and future AI applications in CV imaging. At the end of the course participants will be able to understand and critically appraise existing AI applications.

Printed on: 02/07/23



## Abstract Archives of the RSNA, 2022

R1-CER09

### Non-traumatic Thoracic Emergencies

Thursday, Dec. 1 8:00AM - 9:00AM Room: NA

#### Participants

Stephen Ledbetter, MD, Boston, MA (*Presenter*) Nothing to Disclose

Marianna Zagurovskaya, MD, Lexington, KY (*Presenter*) Nothing to Disclose

Diana Litmanovich, MD, Boston, MA (*Presenter*) Nothing to Disclose

#### COURSE DESCRIPTION

The series of lectures in this session will review the most common use cases for thoracic CT angiography in the non-traumatic setting. Speakers will specifically address pulmonary embolus, acute aortic syndromes, and acute coronary syndrome. Attendees can expect to strengthen their skills in the interpretation of thoracic CT angiography in the setting of non-traumatic chest pain.

#### LEARNING OBJECTIVES

1) Review CT-based diagnostic criteria for acute pulmonary embolism and right ventricular dysfunction 2) Consider causes and imaging features of nonthrombotic pulmonary embolism and mimickers 3) Understand common and differentiating features among the acute aortic syndromes 4) Review common cardiac and coronary causes of acute chest pain in the ED. 5) Review the modern approach to non-invasive cardiac/coronary imaging in the ED\*Course Description The series of lectures in this session will review the most common use cases for thoracic CT angiography in the non-traumatic setting. Speakers will specifically address pulmonary embolus, acute aortic syndromes, and acute coronary syndrome. Attendees can expect to strengthen their skills in the interpretation of thoracic CT angiography in the setting of non-traumatic chest pain.

Printed on: 02/07/23



## Abstract Archives of the RSNA, 2022

R1-CGU04

### Genitourinary Case-based Audience Participation Peer-Learning

Thursday, Dec. 1 8:00AM - 9:00AM Room: NA

#### Participants

Michael Ohliger, MD, PhD, Burlingame, CA (*Presenter*) Nothing to Disclose  
Anuradha Shenoy-Bhangle, MD, Boston, MA (*Presenter*) Nothing to Disclose  
Nelly Tan, MD, Scottsdale, AZ (*Presenter*) Nothing to Disclose  
Elizabeth Edney, MD, Omaha, NE (*Presenter*) Nothing to Disclose  
Gitanjali Bajaj, MD, Little Rock, AR (*Presenter*) Nothing to Disclose  
Joanie Garratt, MD, Wynnewood, PA (*Presenter*) Nothing to Disclose

#### COURSE DESCRIPTION

The course will briefly review peer learning, and its role in promoting a learning culture, and sharing minimum requirements to meet regulatory requirements. We will have audience participate in peer learning cases focused on the genitourinary system.

#### LEARNING OBJECTIVES

1) Learn differences between peer learning and peer review to review challenging/difficult cases and how to use peer learning to promote a learning culture 2) Review the peer review pathway now offered by ACR to meet regulatory purposes 3) Learn from peer learning cases focused on GU applications\*Course Description The course will briefly review peer learning, and its role in promoting a learning culture, and sharing minimum requirements to meet regulatory requirements. We will have audience participate in peer learning cases focused on the genitourinary system.

Printed on: 02/07/23



## Abstract Archives of the RSNA, 2022

R1-CIN24

### Regulations, Governance, AI, and You: How Policy Will Impact Radiology AI and What You Need To Know

Thursday, Dec. 1 8:00AM - 9:00AM Room: NA

#### Participants

Leon Doorn, Amsterdam, Netherlands (*Presenter*) Employee, RadNet, Inc

Kicky van Leeuwen, MSc, Nijmegen, Netherlands (*Presenter*) Technical Expert, Scarlet NB

Karandeep Badwal, , United Kingdom (*Presenter*) Nothing to Disclose

Hugh Harvey, MBBS, London, United Kingdom (*Moderator*) Advisor, Segmed.ai;Advisor, AlgoMedica, Inc;Advisor, Regulatory Agency;Consultant, Qure.ai;Managing Director, Hardian Health

#### COURSE DESCRIPTION

As AI gains traction, the underlying regulatory framework is also maturing. This course will give participants insider knowledge on the current state of regulations, with tips on best practice for quality management, regulatory success and post market surveillance, with a look to what the future holds.

#### LEARNING OBJECTIVES

1) Learn about the current regulatory state in both the US and EU 2) Understand the principles of quality management related to AI software as a medical device 3) Understand how to conduct post market surveillance and identify bias and drift in deployed AI\*Course Description As AI gains traction, the underlying regulatory framework is also maturing. This course will give participants insider knowledge on the current state of regulations, with tips on best practice for quality management, regulatory success and post market surveillance, with a look to what the future holds.

Printed on: 02/07/23



## Abstract Archives of the RSNA, 2022

R1-CIR12

### Thoracic Interventions

Thursday, Dec. 1 8:00AM - 9:00AM Room: NA

#### Participants

Maria Lucia Madariaga, Chicago, IL (*Presenter*) Nothing to Disclose

Michael Lanuti, MD, Boston, MA (*Presenter*) Consultant, Iovance Biotherapeutics, Inc; Consultant, AstraZeneca PLC; Consultant, Bristol-Myers Squibb Company

Robert Suh, MD, Los Angeles, CA (*Presenter*) Nothing to Disclose

Shaunagh McDermott, FFR(RCSI), Boston, MA (*Presenter*) Nothing to Disclose

Afshin Gangi, MD, PhD, Strasbourg, France (*Presenter*) Patent holder, AprioMed AB; Consultant, Boston Scientific Corporation; Consultant, Medtronic plc

Elsie Nguyen, MD, Toronto, ON (*Presenter*) Nothing to Disclose

Florian Fintelmann, MD, Boston, MA (*Moderator*) Nothing to Disclose

#### COURSE DESCRIPTION

This session will cover the current status of thoracic interventions including fiducial placement, needle biopsy, thermal ablation (percutaneous and transbronchial), as well as the management of associated complications.

#### LEARNING OBJECTIVES

1) Explain the role of transbronchial ablation, percutaneous ablation, percutaneous needle biopsy, and fiducial placement in the management of thoracic neoplasms 2) Review associated complications and their management\*Course Description This session will cover the current status of thoracic interventions including fiducial placement, needle biopsy, thermal ablation (percutaneous and transbronchial), as well as the management of associated complications.

Printed on: 02/07/23



## Abstract Archives of the RSNA, 2022

R1-CNPM20

### Maximizing Your Career Trajectory: Negotiating and Refocusing

Thursday, Dec. 1 8:00AM - 9:00AM Room: NA

#### Participants

Jessica Wen, MD, PhD, Nashville, TN (*Presenter*) Nothing to Disclose

David M. Yousem, MD, Evergreen, CO (*Presenter*) Royalties, RELX; Speaker, MRI Online; Board Member, MRI Online;

Soonmee Cha, MD, San Francisco, CA (*Presenter*) Nothing to Disclose

Jay R. Parikh, MD, West University Place, TX (*Moderator*) Nothing to Disclose

#### COURSE DESCRIPTION

The primary goal of this session is to underscore the importance of non-interpretive skills given the challenges facing radiologists today and going forward. Many radiologists currently experience job dissatisfaction and burnout in an environment dominated by the pandemic and demands for increased productivity. Because of current workforce shortages, radiologists are also being increasingly tasked with administrative duties and other non-clinical responsibilities. Radiologists are taking pause in their careers and considering different opportunities. As radiologists recalibrate their careers, non-interpretive skillsets may potentially assist with their next career step. In this didactic presentation followed by interactive panel discussion, three specific non-interpretive skills will be described to help attendees contemplating career options: additional formal education and training, negotiation, and fueling internal satisfaction.

#### LEARNING OBJECTIVES

1) Describe the benefits that formal business education and negotiation techniques may provide radiologists to help achieve their next career step 2) Identify strategies for radiologists to help self-fuel career satisfaction\*Course Description The primary goal of this session is to underscore the importance of non-interpretive skills given the challenges facing radiologists today and going forward. Many radiologists currently experience job dissatisfaction and burnout in an environment dominated by the pandemic and demands for increased productivity. Because of current workforce shortages, radiologists are also being increasingly tasked with administrative duties and other non-clinical responsibilities. Radiologists are taking pause in their careers and considering different opportunities. As radiologists recalibrate their careers, non-interpretive skillsets may potentially assist with their next career step. In this didactic presentation followed by interactive panel discussion, three specific non-interpretive skills will be described to help attendees contemplating career options: additional formal education and training, negotiation, and fueling internal satisfaction.

Printed on: 02/07/23



## Abstract Archives of the RSNA, 2022

R1-CNR04

### Don't Miss Subtle Emergency Neuroimaging Findings

Thursday, Dec. 1 8:00AM - 9:00AM Room: NA

#### Participants

Bruno P. Soares, MD, Burlington, VT (*Presenter*) Nothing to Disclose

Andrew Callen, MD, Aurora, CO (*Presenter*) Nothing to Disclose

Michele Johnson, MD, New Haven, CT (*Presenter*) Medical Advisory Board, iSchemaView, Inc

Jason F. Talbott, MD, PhD, Novato, CA (*Moderator*) Nothing to Disclose

#### COURSE DESCRIPTION

The radiologist plays a critical role in the evaluation of neuroradiology emergencies, both traumatic and nontraumatic. Often, subtle imaging findings on CT and MRI are important for accurate diagnosis, timely triage, and appropriate management of patients with neurological emergencies. The primary focus of this session is to familiarize the radiologist with the spectrum of subtle imaging findings that must be included in the search pattern for CT and MRI exams of the head and spine in the setting of neurologic emergency. A case-based approach will be utilized implementing up-to-date classification systems for a variety of neurological emergencies. Evidenced-based indications for obtaining follow-up and/or advanced imaging such as MRI for subtle CT findings will also be emphasized.

#### LEARNING OBJECTIVES

1) Gain familiarity with subtle CT findings which may suggest more significant soft tissue injury and need for MRI in the setting of known spinal trauma 2) Review appropriate indications for obtaining MRI and key MRI imaging findings in patients with traumatic brain injury 3) Review a systematic checklist for subtle spinal and cranial imaging findings in the setting of suspected non-traumatic spinal and cranial emergencies\*Course Description The radiologist plays a critical role in the evaluation of neuroradiology emergencies, both traumatic and nontraumatic. Often, subtle imaging findings on CT and MRI are important for accurate diagnosis, timely triage, and appropriate management of patients with neurological emergencies. The primary focus of this session is to familiarize the radiologist with the spectrum of subtle imaging findings that must be included in the search pattern for CT and MRI exams of the head and spine in the setting of neurologic emergency. A case-based approach will be utilized implementing up-to-date classification systems for a variety of neurological emergencies. Evidenced-based indications for obtaining follow-up and/or advanced imaging such as MRI for subtle CT findings will also be emphasized.

Printed on: 02/07/23



## Abstract Archives of the RSNA, 2022

R1-COB02

### Endometriosis: Hiding in Plain Site

Thursday, Dec. 1 8:00AM - 9:00AM Room: NA

#### Participants

Scott Young, MD, Phoenix, AZ (*Presenter*) Nothing to Disclose

Nancy Kim, MD, Washington, DC (*Presenter*) Nothing to Disclose

#### COURSE DESCRIPTION

Endometriosis is a painful condition affecting about 10% of women of child-bearing age, yet its diagnosis is often delayed for 7 or more years. Both ultrasound and MRI play an increasing role in the detection and preoperative management of endometriosis. Reliance on laparoscopy to make the diagnosis is no longer the gold standard. Learners will be exposed to new information on how to detect endometriosis on routine ultrasound beyond endometrioma. The importance of MRI and ultrasound for preoperative surgical planning will be emphasized.

#### LEARNING OBJECTIVES

1) Identify patterns of Deep Endometriosis on MRI 2) Identify common locations of Deep Endometriosis on routine ultrasound and implement an ultrasound imaging protocol to increase endometriosis detection 3) Review imaging measurements and observations important to surgical planning for minimally invasive resection of deep endometriosis\*Course Description Endometriosis is a painful condition affecting about 10% of women of child-bearing age, yet its diagnosis is often delayed for 7 or more years. Both ultrasound and MRI play an increasing role in the detection and preoperative management of endometriosis. Reliance on laparoscopy to make the diagnosis is no longer the gold standard. Learners will be exposed to new information on how to detect endometriosis on routine ultrasound beyond endometrioma. The importance of MRI and ultrasound for preoperative surgical planning will be emphasized.

Printed on: 02/07/23



## Abstract Archives of the RSNA, 2022

R1-CRO03

### Lung/Mediastinum Case-based Multidisciplinary Review

Thursday, Dec. 1 8:00AM - 9:00AM Room: NA

#### Participants

Michelle S. Ginsberg, MD, New York, NY (*Presenter*) Speaker, Ultimate Opinions In Medicine LLC

Rafael Santana-Davila, Seattle, WA (*Presenter*) Nothing to Disclose

David Johnstone, Milwaukee, WI (*Presenter*) Nothing to Disclose

Stephen Chun, MD, Houston, TX (*Presenter*) Consultant, AstraZeneca PLC

Simon Lo, MD, Seattle, WA (*Presenter*) Committee member, Elekta AB

#### COURSE DESCRIPTION

This course will include imaging and multidisciplinary management of a case of advanced non-small cell lung cancer, a case of extensive stage small cell lung cancer, and a case of thymic tumor.

#### LEARNING OBJECTIVES

After the course, attendees should be able: 1) To describe the appropriate imaging and multidisciplinary management of locally advanced non-small cell lung cancer 2) To describe the appropriate imaging and multidisciplinary management of extensive stage small cell lung cancer 3) To describe the appropriate imaging and multidisciplinary management of thymic tumors\*Course Description  
This course will include imaging and multidisciplinary management of a case of advanced non-small cell lung cancer, a case of extensive stage small cell lung cancer, and a case of thymic tumor.

Printed on: 02/07/23



## Abstract Archives of the RSNA, 2022

R1-RCP20

### An Introduction to the Learning Healthcare System & Tackling the Critical Data Hurdles (Sponsored by the RSNA Research Development Committee)

Thursday, Dec. 1 8:00AM - 9:00AM Room: NA

#### Participants

Joshua Yung, PhD, Houston, TX (*Presenter*) Nothing to Disclose

Safwan Halabi, MD, Chicago, IL (*Presenter*) Advisor, Change Healthcare

Jeremy Warner, MD,MS, Nashville, TN (*Presenter*) Consultant, Westat, Inc;Consultant, Melax Tech;Consultant, F. Hoffmann-La Roche Ltd;Consultant, Flatiron Health, Inc;Owner, HemOnc.org LLC

Caroline Chung, MD, FRCPC, Houston, TX (*Moderator*) Research support, RaySearch Laboratories AB;Research support, Siemens AG;Clinical Advisory Board, CRnR

#### COURSE DESCRIPTION

As we aspire to deliver personalized health care, we will face growing volumes of increasingly complex care delivery options and decisions. In this introduction to the Learning Healthcare System, we will bring forward the value of effective integration of medical imaging data into a learning healthcare system and bring forward the foundational data challenges that we face today in medicine. Through several lectures including highlighted examples of large systemic data management and collaboration efforts, the course should provide a framework for starting to build this environment and culture as well as provide helpful key topics for interdisciplinary dialogue your teams within the institution including but not limited to radiologists, clinicians and clinical team members, radiology techs, imaging physics, data scientists, imaging scientists, trainees, health administrators, bioinformatics researchers and IT.

#### LEARNING OBJECTIVES

1) Review approaches and challenges of aggregating structured data to support a Learning Healthcare System (LHS) 2) Describe the value of generating quantitative imaging to support an LHS 3) Describe specific examples of data management approaches around medical imaging and highlight lessons learned\*Course Description As we aspire to deliver personalized health care, we will face growing volumes of increasingly complex care delivery options and decisions. In this introduction to the Learning Healthcare System, we will bring forward the value of effective integration of medical imaging data into a learning healthcare system and bring forward the foundational data challenges that we face today in medicine. Through several lectures including highlighted examples of large systemic data management and collaboration efforts, the course should provide a framework for starting to build this environment and culture as well as provide helpful key topics for interdisciplinary dialogue your teams within the institution including but not limited to radiologists, clinicians and clinical team members, radiology techs, imaging physics, data scientists, imaging scientists, trainees, health administrators, bioinformatics researchers and IT.

Printed on: 02/07/23



## Abstract Archives of the RSNA, 2022

R1-RCP48

### Optimizing Your 3D printing Workflow to Ensure Accurate Medical Models (Sponsored by the RSNA 3D Printing Special Interest Group)

Thursday, Dec. 1 8:00AM - 9:00AM Room: NA

#### Participants

Anish Ghodadra, MD, Pittsburgh, PA (*Presenter*) Nothing to Disclose  
Peter Liacouras, PhD, North Potomac, MD (*Presenter*) Nothing to Disclose  
Shannon Walters, RT, MS, Stanford, CA (*Presenter*) Advisor, MedVizi; Consultant, TeraRecon, Inc  
Nicole Wake, PhD, Aurora, OH (*Presenter*) Employee, General Electric Company  
Lumarie Santiago, MD, Houston, TX (*Moderator*) Nothing to Disclose

#### COURSE DESCRIPTION

3D printed anatomic models must reliably represent the patient's anatomy to be useful to the clinician, but the workflow required to create these models from medical imaging data is complex and time consuming. The inherent complexity of image-based 3D printing allows the possibility of errors at any stage of the workflow. These stages include imaging acquisition, fusion of multiple exam types, segmentation, computer aided design, 3D printing, and post processing of the final 3D printed product. In this educational course, the stages where variances in the 3D printing workflow can occur will be reviewed. Tips on how to assess quality as well as improve efficiency and address variances will be presented.

#### LEARNING OBJECTIVES

1) Describe the various stages in the 3D printing process 2) Develop imaging protocols for source exams used in the creation of 3D printed anatomical models 3) Compare segmentation tools and their impact on time management and model accuracy 4) Recognize factors associated with print failures 5) Review quality assurance interventions at the various steps of the 3D printing process\*Course Description 3D printed anatomic models must reliably represent the patient's anatomy to be useful to the clinician, but the workflow required to create these models from medical imaging data is complex and time consuming. The inherent complexity of image-based 3D printing allows the possibility of errors at any stage of the workflow. These stages include imaging acquisition, fusion of multiple exam types, segmentation, computer aided design, 3D printing, and post processing of the final 3D printed product. In this educational course, the stages where variances in the 3D printing workflow can occur will be reviewed. Tips on how to assess quality as well as improve efficiency and address variances will be presented.

Printed on: 02/07/23



## Abstract Archives of the RSNA, 2022

R3-CBR02

### AI in Breast Imaging: Implementation in Routine Clinical Practice

Thursday, Dec. 1 9:30AM - 10:30AM Room: NA

#### Participants

Fredrik Strand, MD, PhD, Stockholm, Sweden (*Presenter*) Speaker, Lunit Inc

Maryellen Giger, PhD, Chicago, IL (*Presenter*) Stockholder, Hologic, Inc; Royalties, Hologic, Inc; Shareholder, Quantitative Insights, Inc; Co-founder, Quantitative Insights, Inc; Shareholder, QView Medical, Inc; Royalties, General Electric Company; Royalties, Median Technologies; Royalties, Riverain Technologies, LLC

Constance Lehman, MD, PhD, Boston, MA (*Presenter*) Institutional Grant, General Electric Company; Institutional Grant, Hologic, Inc; Co-founder, Clarity, Inc.

#### COURSE DESCRIPTION

Build your knowledge with top experts in evaluating, implementing and understanding the wider impact of AI systems in breast imaging. This 3-part lecture will include panel and audience discussion of most current challenges and opportunities in AI and imaging.

#### LEARNING OBJECTIVES

1) Understand science behind development and testing of breast AI models 2) Identify strengths and weaknesses of clinical research studies of breast AI models 3) Explain the current clinical applications of deep learning applied to mammography\*  
Course Description Build your knowledge with top experts in evaluating, implementing and understanding the wider impact of AI systems in breast imaging. This 3-part lecture will include panel and audience discussion of most current challenges and opportunities in AI and imaging.

Printed on: 02/07/23



## Abstract Archives of the RSNA, 2022

R3-CCH08

### Fundamentals of Diffuse Lung Disease

Thursday, Dec. 1 9:30AM - 10:30AM Room: NA

#### Participants

Joanna Escalon, MD, New York, NY (*Presenter*) Research Consultant, Vingroup

David M. Naeger, MD, Denver, CO (*Presenter*) Nothing to Disclose

Brett M. Elicker, MD, San Francisco, CA (*Presenter*) Nothing to Disclose

Laura Heyneman, MD, Durham, NC (*Presenter*) Author, RELX

#### COURSE DESCRIPTION

This course will review four important topics needed to evaluate diffuse lung disease. The course is intended for radiologists re-reviewing the fundamentals of this important aspect of chest radiology. We will use didactic and case-based material to review how to evaluate consolidations and ground-glass opacities, cystic lung disease, mosaic lung attenuation, and micronodular lung disease.

#### LEARNING OBJECTIVES

1) Evaluate chest CT images for the presence of diffuse lung disease 2) Define key imaging features used to characterize diffuse lung diseases 3) Formulate a differential diagnosis based on the presence or absence of key chest CT imaging features\*Course Description This course will review four important topics needed to evaluate diffuse lung disease. The course is intended for radiologists re-reviewing the fundamentals of this important aspect of chest radiology. We will use didactic and case-based material to review how to evaluate consolidations and ground-glass opacities, cystic lung disease, mosaic lung attenuation, and micronodular lung disease.

Printed on: 02/07/23



## Abstract Archives of the RSNA, 2022

R3-CER07

### Spine Trauma

Thursday, Dec. 1 9:30AM - 10:30AM Room: NA

#### Participants

Matthew Dattwyler, MD, Chevy Chase, MD (*Presenter*) Nothing to Disclose

Alexis Boscak, MD, Baltimore, MD (*Presenter*) Nothing to Disclose

Nicholas Beckmann, MD, Houston, TX (*Presenter*) Nothing to Disclose

#### COURSE DESCRIPTION

In this didactic session, blunt and penetrating trauma of the spine will be discussed. Discussion will include typical mechanisms of injury, injury patterns, and relevant classifications systems. Viewers of this session will have a better understanding of spine trauma to identify subtle injuries, but important injuries, and concisely convey pertinent imaging findings of spine trauma that impact management.

#### LEARNING OBJECTIVES

1) Recognize typical mechanisms of spine trauma  
2) Describe common injury patterns of spine trauma  
3) Apply relevant classification systems of spine trauma  
\*Course Description In this didactic session, blunt and penetrating trauma of the spine will be discussed. Discussion will include typical mechanisms of injury, injury patterns, and relevant classifications systems. Viewers of this session will have a better understanding of spine trauma to identify subtle injuries, but important injuries, and concisely convey pertinent imaging findings of spine trauma that impact management.

Printed on: 02/07/23



## Abstract Archives of the RSNA, 2022

R3-CGI05

### Focused/Fast Abdomino-pelvic MRI Protocols

Thursday, Dec. 1 9:30AM - 10:30AM Room: NA

#### Participants

Jonathan Mezrich, MD, Guilford, CT (*Presenter*) Nothing to Disclose

Laura Kulik, MD, Chicago, IL (*Presenter*) Speaker, Eisai Co, Ltd; Speaker, Peerview; Consultant, F. Hoffmann-La Roche Ltd; Consultant, Bayer AG; Consultant, Exelixis, Inc; Consultant, Eisai Co, Ltd; Researcher, HCC Target; Researcher, Glycotest  
Ivan Pedrosa, MD, Dallas, TX (*Presenter*) Scientific Advisor, Health Tech International; Scientific Advisor, Merck & Co, Inc  
Hersh Chandarana, MD, Scarsdale, NY (*Presenter*) Institutional research agreement, Siemens AG; Equipment support, Siemens AG; Software support, Siemens AG

Pari V. Pandharipande, MD, MPH, Chestnut Hill, MA (*Presenter*) I serve as a member of the Association of University Radiologists (AUR) General Electric (GE) Radiology Research Academic Fellowship (GERRAF) Board of Review (term: 7/1/22-2/28/23).

#### COURSE DESCRIPTION

Indications for fast/focused MRI in abdomino-pelvic conditions continue to increase. We review challenges and opportunities to maximize the efficiency in the implementation of such protocols in a busy clinical practice.

#### LEARNING OBJECTIVES

1) Explain developments in artificial intelligence that enable fast acquisitions and opportunities to maximize efficiency in the reporting of abbreviated MRI exams  
2) Recognize the importance of engaging referring physicians in the use of abbreviated/fast MRI scans for screening of hepatocellular cancer  
3) Identify the clinical, financial, and medico-legal implications of abbreviated MRI exams  
\*Course Description Indications for fast/focused MRI in abdomino-pelvic conditions continue to increase. We review challenges and opportunities to maximize the efficiency in the implementation of such protocols in a busy clinical practice.

Printed on: 02/07/23



## Abstract Archives of the RSNA, 2022

R3-CIN05

### The Analytics and Dashboarding of Value-Based Imaging Care

Thursday, Dec. 1 9:30AM - 10:30AM Room: NA

#### Participants

Christopher J. Roth, MD, Durham, NC (*Presenter*) Nothing to Disclose

Keith D. Hentel, MD, MS, Briarcliff, NY (*Presenter*) Nothing to Disclose

John Mongan, MD, PhD, San Francisco, CA (*Presenter*) Research Grant, General Electric Company; Research Grant, Siemens AG; Research Grant, Amazon Web Services, Inc; Royalties, General Electric Company; Spouse, Employee, Annexon, Inc; Spouse, Employee, AbbVie Inc

Pamela T. Johnson, MD, Baltimore, MD (*Presenter*) Institutional license agreement, AgileMD, Inc; Royalties, AgileMD, Inc

Hanna M. Zafar, MD, Philadelphia, PA (*Moderator*) Nothing to Disclose

#### COURSE DESCRIPTION

This interactive course will canvas how imaging clinical decision support is currently used to leverage utilization management and can be used to impact population health. Brief lectures will be followed by break out groups designed to explore facilitators and barriers to the implementation of clinical decision support analytics. Output from small groups will be shared at the conclusion of the session through virtual chat and open microphone.

#### LEARNING OBJECTIVES

- 1) Explain 3 ways that imaging CDS is currently used to improve utilization management and to potentially impact population health
- 2) Identify 3 facilitators and barriers to the implementation of CDS for utilization management and population health\*Course Description This interactive course will canvas how imaging clinical decision support is currently used to leverage utilization management and can be used to impact population health. Brief lectures will be followed by break out groups designed to explore facilitators and barriers to the implementation of clinical decision support analytics. Output from small groups will be shared at the conclusion of the session through virtual chat and open microphone.

Printed on: 02/07/23



## Abstract Archives of the RSNA, 2022

R3-CMK10

### MARS MRI and CT: Protocols, Pearls, Pitfalls

Thursday, Dec. 1 9:30AM - 10:30AM Room: NA

#### Participants

Benjamin Fritz, MD, Zurich, Switzerland (*Presenter*) Nothing to Disclose

Kenneth Buckwalter, MD, Ann Arbor, MI (*Presenter*) Nothing to Disclose

Hollis G. Potter, MD, New York, NY (*Presenter*) Research support, General Electric Company; Institutional research agreement, General Electric Company; Stockholder, Imagen Technologies Inc; Consultant, Atria Academy of Science and Medicine

Matthew A. Frick, MD, Rochester, MN (*Presenter*) Nothing to Disclose

Jan Fritz, MD, New York, NY (*Presenter*) Institutional research support, Siemens AG; Scientific Advisor, Siemens AG; Patent agreement, Siemens AG; Institutional research support, Johnson & Johnson; Institutional research support, Zimmer Biomet Holdings, Inc; Institutional research support, BTG International Ltd

#### COURSE DESCRIPTION

Metal artifact reduction MRI and CT are effective non-invasive imaging tests for evaluating pain and dysfunction of arthroplasty and orthopedic implants. This course includes lectures and live case reviews of basic and advanced metal artifact reduction techniques, complications after arthroplasty, and checklists for systematic image evaluations and reporting.

#### LEARNING OBJECTIVES

1) Define basic and advanced metal artifact reduction (MARS) techniques in MRI and CT 2) Apply basic and advanced techniques in clinical practice to optimize MRI and CT of arthroplasty implants 3) Develop a checklist for detecting MRI and CT abnormalities around common orthopedic implants\*Course Description Metal artifact reduction MRI and CT are effective non-invasive imaging tests for evaluating pain and dysfunction of arthroplasty and orthopedic implants. This course includes lectures and live case reviews of basic and advanced metal artifact reduction techniques, complications after arthroplasty, and checklists for systematic image evaluations and reporting.

Printed on: 02/07/23



## Abstract Archives of the RSNA, 2022

R3-CMS08

### Infection Induced Tumors and Tumorlike Conditions Multimodality Imaging and Complications

Thursday, Dec. 1 9:30AM - 10:30AM Room: NA

#### Participants

Meghan G. Lubner, MD, Madison, WI (*Presenter*) Spouse, Consultant, Elephas Bio  
Jonathan Revels, DO, Albuquerque, NM (*Presenter*) Nothing to Disclose  
Venkata Katabathina, MD, San Antonio, TX (*Presenter*) Nothing to Disclose  
Vincent M. Mellnick, MD, Saint Louis, MO (*Presenter*) Nothing to Disclose

#### COURSE DESCRIPTION

This session will include four lectures on infection-induced malignancy in the chest, abdomen, and pelvis, including both transplant and non-transplant patients. Complications of these conditions will be discussed. In addition, infections and inflammation that may mimic malignancy will be reviewed.

#### LEARNING OBJECTIVES

1) Identify infection-induced tumors in the chest, abdomen and pelvis 2) Understand specific malignancies associated with organ transplant 3) Recognize infectious and inflammatory conditions in the chest, abdomen, and pelvis that may mimic malignancy\*Course Description This session will include four lectures on infection-induced malignancy in the chest, abdomen, and pelvis, including both transplant and non-transplant patients. Complications of these conditions will be discussed. In addition, infections and inflammation that may mimic malignancy will be reviewed.

Printed on: 02/07/23



## Abstract Archives of the RSNA, 2022

R3-CNPM21

### Innovative Education for the Future of Radiology

Thursday, Dec. 1 9:30AM - 10:30AM Room: NA

#### Participants

Jessica Robbins, MD, Madison, WI (*Presenter*) Nothing to Disclose  
Petra Lewis, MBBS, Lebanon, NH (*Presenter*) Committee member, CairnSurgical IncEducator, MRI Online, LLC  
David Sarkany, MD, Staten Island, NY (*Presenter*) Nothing to Disclose  
Priscilla Slanetz, MD, MPH, Boston, MA (*Presenter*) Royalties, Wolters Kluwer nv  
Joseph Philip, MD, Dallas, TX (*Presenter*) Nothing to Disclose

#### COURSE DESCRIPTION

Over the past few decades, radiology education has transitioned from primarily passive didactic to more active learning. Although case-based teaching remains central to radiology, most educators have embraced newer techniques into their teaching, such as audience response, flipped classroom and design thinking. More recently, the COVID-19 pandemic acutely challenged educators to adapt their teaching to a virtual and now often hybrid environment. This session is designed to provide medical educators with the latest tips on how to effectively engage learners both in-person and virtually. Following a short introductory presentation and four brief presentations, the session will end with an open Q&A allowing attendees the opportunity to ask panelists about topics that may not have been covered and to share their own teaching tips.

#### LEARNING OBJECTIVES

By the end of this session, the attendee will be able to: 1) Envision how to interact with learners and educators across space and time 2) Incorporate effective evidence-based active learning techniques into workstation teaching and didactic hybrid presentations 3) Design creative sessions to teach non-interpretative skills\*Course Description Over the past few decades, radiology education has transitioned from primarily passive didactic to more active learning. Although case-based teaching remains central to radiology, most educators have embraced newer techniques into their teaching, such as audience response, flipped classroom and design thinking. More recently, the COVID-19 pandemic acutely challenged educators to adapt their teaching to a virtual and now often hybrid environment. This session is designed to provide medical educators with the latest tips on how to effectively engage learners both in-person and virtually. Following a short introductory presentation and four brief presentations, the session will end with an open Q&A allowing attendees the opportunity to ask panelists about topics that may not have been covered and to share their own teaching tips.

Printed on: 02/07/23



## Abstract Archives of the RSNA, 2022

R3-CPH04

### Deep Learning in CT Image Formation

Thursday, Dec. 1 9:30AM - 10:30AM Room: NA

#### Participants

Guang-Hong Chen, PhD, Madison, WI (*Presenter*) Nothing to Disclose  
Lifeng Yu, PhD, Rochester, MN (*Presenter*) Nothing to Disclose  
Marc Kachelriess, PhD, Heidelberg, Germany (*Presenter*) Nothing to Disclose

#### COURSE DESCRIPTION

This course will provide an overview of deep learning applications in CT image formation, including image reconstruction and artifact correction. It will also summarize current clinical implementations of deep learning methods on CT scanners and describe how to appropriately evaluate these methods. Potential pitfalls of deep learning methods in CT image formation will be described. There are three lectures in this course:(1) Deep learning in CT reconstruction(2) Deep learning in CT artifact correction(3) Clinical implementation and evaluation

#### LEARNING OBJECTIVES

1) Describe deep learning applications in CT image formation process, including image reconstruction and artifact reduction.  
2) Explain current clinical implementations of deep learning methods on CT scanners and how to evaluate these methods.\*Course Description This course will provide an overview of deep learning applications in CT image formation, including image reconstruction and artifact correction. It will also summarize current clinical implementations of deep learning methods on CT scanners and describe how to appropriately evaluate these methods. Potential pitfalls of deep learning methods in CT image formation will be described. There are three lectures in this course:(1) Deep learning in CT reconstruction(2) Deep learning in CT artifact correction(3) Clinical implementation and evaluation

Printed on: 02/07/23



## Abstract Archives of the RSNA, 2022

R3-RCP11

### Developing a Quality Improvement (QI) Pipeline to Ensure Sustained Success: Approaches to Engage Medical Students, Trainees, and Junior Radiologists (Sponsored by the RSNA Quality Improvement Committee)

Thursday, Dec. 1 9:30AM - 10:30AM Room: NA

#### Participants

Nelly Tan, MD, Scottsdale, AZ (*Presenter*) Nothing to Disclose  
Roman Shrestha, MD, Phoenix, AZ (*Presenter*) Nothing to Disclose  
Marc Willis, DO, MMM, Stanford, CA (*Presenter*) Stockholder, Resonea, Inc.  
Akriti Khanna, MD, Rochester, MN (*Presenter*) Nothing to Disclose  
Richard E. Sharpe JR, MD, MBA, Scottsdale, AZ (*Presenter*) Nothing to Disclose

#### COURSE DESCRIPTION

Quality improvement is a required component of radiology training, preparing learners for the professional practice and optimal patient care. Residents must complete a quality improvement project to demonstrate their competency. However, there is scant guidance and literature to prepare students or guide residents in their journey to complete this competency. This inherently provides many obstacles and may additionally impede development of future improvement leaders in both academic and private practice settings. This educational program will assist development of a pipeline to successfully attract improvement minded medical students, guide trainees on how to successfully complete a quality improvement project within the constraints of their program, and define a path for junior radiologists' professional development. This session will be helpful for those interested in pursuing quality along with those responsible to oversee a department, struggling to find ways to support junior faculty interested in a career in quality and safety.

#### LEARNING OBJECTIVES

1) Describe the educational elements of quality improvement and patient safety that are beneficial to trainees 2) Identify strategies to recruit and develop junior faculty interested in quality and safety 3) Describe a pathway to develop an academic career in quality and safety\*Course Description Quality improvement is a required component of radiology training, preparing learners for the professional practice and optimal patient care. Residents must complete a quality improvement project to demonstrate their competency. However, there is scant guidance and literature to prepare students or guide residents in their journey to complete this competency. This inherently provides many obstacles and may additionally impede development of future improvement leaders in both academic and private practice settings. This educational program will assist development of a pipeline to successfully attract improvement minded medical students, guide trainees on how to successfully complete a quality improvement project within the constraints of their program, and define a path for junior radiologists' professional development. This session will be helpful for those interested in pursuing quality along with those responsible to oversee a department, struggling to find ways to support junior faculty interested in a career in quality and safety.

Printed on: 02/07/23



## Abstract Archives of the RSNA, 2022

R3-RCP55

### Implementing AI in Practice: A Demonstration of Interoperability Standards

Thursday, Dec. 1 9:30AM - 10:30AM Room: NA

#### Participants

Ali Tejani, MD, Frisco, TX (*Presenter*) Nothing to Disclose  
Madhavi Duvvuri, MD, MPhil, San Francisco, CA (*Presenter*) Nothing to Disclose  
Mohannad Hussain, Waterloo, ON (*Presenter*) Consultant, Techie Maestro Inc  
Katherine Andriole, PhD, Branford, CT (*Moderator*) Nothing to Disclose  
Kirti Magudia, MD, PhD, Durham, NC (*Moderator*) Nothing to Disclose

#### COURSE DESCRIPTION

The Imaging AI in Practice demonstration project was started in 2020 to demonstrate the utility of AI applications throughout the radiology workflow to the benefit. Central to this mission are semantic and interoperability standards that allow different vendor products to seamlessly interact with each other for an optimal end user experience, namely for a clinical radiologist at his or her workstation. This session will share potential automation challenges.

#### LEARNING OBJECTIVES

1) Understand the future of AI applications throughout the entire radiology workflow  
2) Recognize practical implementation considerations, most importantly semantic and interoperability standards  
3) Consider model automation challenges  
4) Review the history of the Imaging AI in Practice demonstration project  
\*Course Description The Imaging AI in Practice demonstration project was started in 2020 to demonstrate the utility of AI applications throughout the radiology workflow to the benefit. Central to this mission are semantic and interoperability standards that allow different vendor products to seamlessly interact with each other for an optimal end user experience, namely for a clinical radiologist at his or her workstation. This session will share potential automation challenges.

Printed on: 02/07/23



## Abstract Archives of the RSNA, 2022

R4-CBR09

### Management of Elevated Risk (high-risk) Breast Lesions

Thursday, Dec. 1 11:00AM - 12:00PM Room: NA

#### Participants

Peter Eby, MD, Seattle, WA (*Presenter*) Nothing to Disclose

Nisha Sharma, MBChB, FRCR, Leeds, United Kingdom (*Presenter*) Nothing to Disclose

Husain Sattar, MD, Chicago, IL (*Presenter*) Nothing to Disclose

#### COURSE DESCRIPTION

3 talks are Management of elevated Risk (high-risk) Breast Lesions: European view. Management of elevated Risk (high-risk) Breast Lesions: Lessons learned from pathology. Management of elevated Risk (high-risk) Breast Lesions: USA view. This session will focus on high risk lesions which are diagnosed following a core biopsy and how these lesions are managed from a European and USA perspective. We will also highlight the challenges in diagnosing these high risk lesions and the lesions subtypes that are classified as high risk lesions

#### LEARNING OBJECTIVES

1) Gain a greater understanding of what high risk lesions are 2) Learn about the different strategies to manage to these high risk lesions from an international perspective\*Course Description 3 talks are Management of elevated Risk (high-risk) Breast Lesions: European view. Management of elevated Risk (high-risk) Breast Lesions: Lessons learned from pathology. Management of elevated Risk (high-risk) Breast Lesions: USA view. This session will focus on high risk lesions which are diagnosed following a core biopsy and how these lesions are managed from a European and USA perspective. We will also highlight the challenges in diagnosing these high risk lesions and the lesions subtypes that are classified as high risk lesions

Printed on: 02/07/23



## Abstract Archives of the RSNA, 2022

R4-CER05

### Abdominopelvic Trauma: The Essentials

Thursday, Dec. 1 11:00AM - 12:00PM Room: NA

#### Participants

Christina LeBedis, MD, Newton, MA (*Presenter*) Nothing to Disclose

Vincent M. Mellnick, MD, Saint Louis, MO (*Presenter*) Nothing to Disclose

Jennifer Uyeda, MD, Lexington, MA (*Presenter*) Nothing to Disclose

#### COURSE DESCRIPTION

In this didactic course on Abdominopelvic trauma, learn state-of-the-art imaging of hepatobiliary trauma, splenic trauma and blunt and penetrating bowel trauma from expert emergency radiologists. Radiologists at all levels of training will benefit from the material presented as it can be readily incorporated into their core knowledge base to care for acutely injured patients.

#### LEARNING OBJECTIVES

1) Explore the role of CT, including CT protocols, in the diagnosis of patients who have sustained abdominopelvic trauma specifically with respect to hepatobiliary trauma, splenic trauma and blunt and penetrating bowel trauma 2) Identify key CT imaging findings in these organ injury types through case examples 3) Discuss the imaging findings crucial to patient triage and management\*Course Description In this didactic course on Abdominopelvic trauma, learn state-of-the-art imaging of hepatobiliary trauma, splenic trauma and blunt and penetrating bowel trauma from expert emergency radiologists. Radiologists at all levels of training will benefit from the material presented as it can be readily incorporated into their core knowledge base to care for acutely injured patients.

Printed on: 02/07/23



## Abstract Archives of the RSNA, 2022

R4-CHN03

### All About the Temporal Bone

Thursday, Dec. 1 11:00AM - 12:00PM Room: NA

#### Participants

Amy Juliano, MD, Boston, MA (*Presenter*) Nothing to Disclose

David Zander, MD, Englewood, CO (*Presenter*) Nothing to Disclose

Mohit Agarwal, MD, Milwaukee, WI (*Presenter*) Nothing to Disclose

Mai-Lan Ho, MD, Columbus, OH (*Presenter*) Research Grant, Siemens AG; Research Grant, Cardinal Health, Inc; Research Grant, Italfarmaco SpA

#### COURSE DESCRIPTION

In this Head and Neck session devoted to the temporal bone, attendees will be review the imaging approach and be presented with clinical case examples of patients with conductive hearing loss, sensorineural hearing loss, a temporal bone mass and suspected cholesteatoma. Speakers will emphasize pearls for imaging evaluation and differentiating each entity from common mimics, pitfalls of interpretation to avoid, and relevant clinical management considerations with which radiologists should be familiar. This session offers attendees the opportunity to refine their interpretation of complex head and neck imaging studies by incorporating tips from world experts.

#### LEARNING OBJECTIVES

1) Understand the imaging algorithm and search patterns for patients presenting with conductive hearing loss, sensorineural hearing loss, a temporal bone mass and suspected cholesteatoma. 2) Differentiate between entities on the differential diagnosis that cause conductive hearing loss and sensorineural hearing loss 3) Distinguish cholesteatoma and temporal bone masses from common mimics. \*Course Description In this Head and Neck session devoted to the temporal bone, attendees will be review the imaging approach and be presented with clinical case examples of patients with conductive hearing loss, sensorineural hearing loss, a temporal bone mass and suspected cholesteatoma. Speakers will emphasize pearls for imaging evaluation and differentiating each entity from common mimics, pitfalls of interpretation to avoid, and relevant clinical management considerations with which radiologists should be familiar. This session offers attendees the opportunity to refine their interpretation of complex head and neck imaging studies by incorporating tips from world experts.

Printed on: 02/07/23



## Abstract Archives of the RSNA, 2022

R4-CIN18

### Enhancing Patient Journeys Through Imaging: Leveraging Informatics (Supported in part by an unrestricted educational grant from Bayer)

Thursday, Dec. 1 11:00AM - 12:00PM Room: NA

#### Participants

Arun Krishnaraj, MD, MPH, Charlottesville, VA (*Presenter*) Nothing to Disclose

Dania Daye, MD, PhD, Medford, MA (*Presenter*) Research Consultant, Sigilon Therapeutics, Inc; Research Consultant, Medtronic plc

Namita S. Gandhi, MD, Cleveland, OH (*Presenter*) Nothing to Disclose

Marc Kohli, MD, San Francisco, CA (*Presenter*) Founder, Alara Imaging; Stockholder, Alara Imaging

#### COURSE DESCRIPTION

Patient journey refers to patient's experience throughout an episode of care; for radiology this begins at the time when an imaging order is placed and carries through till the patients receive their imaging reports with guidance for further care and an ability to consult on the imaging results. Traditionally, strategies to improve patient experience in radiology are focused on enhancing only the radiology encounter. This course will focus on the entire episode of care ( pre and post radiology encounter) in a patient's imaging journey and discuss informatics strategies and initiatives which can enhance the entire journey. The session will be organized as short presentations by the speakers followed by a panel discussion at the end. There will be an opportunity of audience participation via interactive polling and in person questions.

#### LEARNING OBJECTIVES

1) Informatics strategy and initiatives to enhance the pre imaging exam journey 2 )Informatics strategy and challenges with patient friendly report 3) Informatics strategies for patient friendly image exchange 4) Informatics considerations for establishing a virtual imaging consult program\*Course Description Patient journey refers to patient's experience throughout an episode of care; for radiology this begins at the time when an imaging order is placed and carries through till the patients receive their imaging reports with guidance for further care and an ability to consult on the imaging results. Traditionally, strategies to improve patient experience in radiology are focused on enhancing only the radiology encounter. This course will focus on the entire episode of care ( pre and post radiology encounter) in a patient's imaging journey and discuss informatics strategies and initiatives which can enhance the entire journey. The session will be organized as short presentations by the speakers followed by a panel discussion at the end. There will be an opportunity of audience participation via interactive polling and in person questions.

Printed on: 02/07/23



## Abstract Archives of the RSNA, 2022

R4-CNMMI03

### Nuclear Cardiology Update 2022: Read with the Experts

Thursday, Dec. 1 11:00AM - 12:00PM Room: NA

#### Participants

E. Gordon Depuey, MD, New York, NY (*Presenter*) Nothing to Disclose

Richard Weinberg, MD, Chicago, IL (*Presenter*) Ionetix Corporation: educational consulting (paid)

#### COURSE DESCRIPTION

This course will cover updates in cardiac SPECT and PET including new generation SPECT scanners, novel applications of PET myocardial perfusion and flow quantification, novel Tc-99m-PYP amyloidosis imaging, imaging of inflammation and infection with F-18 FDG PET/CT and more. A case based format will be used to make the discussion more interactive.

#### LEARNING OBJECTIVES

1) Explain current clinical applications of cardiac PET  
2) Identify strategies to accurately interpret SPECT and PET cardiac images  
3) List strategies to overcome artifacts on cardiac SPECT and PET imaging  
\*Course Description This course will cover updates in cardiac SPECT and PET including new generation SPECT scanners, novel applications of PET myocardial perfusion and flow quantification, novel Tc-99m-PYP amyloidosis imaging, imaging of inflammation and infection with F-18 FDG PET/CT and more. A case based format will be used to make the discussion more interactive.

Printed on: 02/07/23



## Abstract Archives of the RSNA, 2022

R4-CNPM16

### Engaging Patients: Opportunities and Challenges

Thursday, Dec. 1 11:00AM - 12:00PM Room: NA

#### Participants

Katerina Dodelzon, MD, New York, NY (*Presenter*) Nothing to Disclose

Gautham P. Reddy, MD, Seattle, Usa (*Presenter*) Nothing to Disclose

Kerry L. Thomas, MD, Chapel Hill, NC (*Presenter*) Stockholder, Medtronic plc; Stockholder, UnitedHealth Group; Stockholder, Amgen Inc; Stockholder, AbbVie Inc

Guy Johnson, MD, Seattle, WA (*Presenter*) Consultant, Boston Scientific Corporation

Matthew Cham, MD, Kenmore, WA (*Moderator*) Nothing to Disclose

#### COURSE DESCRIPTION

This lecture session will explore actionable ways to increase Patient Engagement in Radiology through the lens of multiple subspecialties. As healthcare continues to evolve towards patient- and family-centered care, we will also discuss strategies for patient advocacy and the promotion of Equity, Diversity, and Inclusion.

#### LEARNING OBJECTIVES

1) Discuss areas of focus for patient engagement in the Radiology Department 2) Provide examples of strategies for increased patient engagement and feedback 3) Appreciate different approaches in engaging patients to form a therapeutic alliance 4) Recognize the role of communication in advocacy and enhancing access to care for diverse populations\*Course Description This lecture session will explore actionable ways to increase Patient Engagement in Radiology through the lens of multiple subspecialties. As healthcare continues to evolve towards patient- and family-centered care, we will also discuss strategies for patient advocacy and the promotion of Equity, Diversity, and Inclusion.

Printed on: 02/07/23



## Abstract Archives of the RSNA, 2022

R6-CER03

### Emergency Radiology Practice Management: Taking it to the Next Level

Thursday, Dec. 1 1:30PM - 2:30PM Room: NA

#### Participants

Suzanne Chong, MD, Superior Township, MI (*Presenter*) Nothing to Disclose

Tarek N. Hanna, MD, Atlanta, GA (*Presenter*) Nothing to Disclose

Aaron Sodickson, MD, PhD, Boston, MA (*Presenter*) Institutional research agreement, Siemens AG ;Speaker, Siemens AG;Consultant, Canon Medical Systems Corporation

#### COURSE DESCRIPTION

There are now more dedicated Emergency Radiology section and divisions than ever before. This session will focus on key elements for leaders to consider when designing or expanding these programs, including scope of practice, staffing and scheduling considerations, and impact of staffing models on quality and trainee education.

#### LEARNING OBJECTIVES

1) Recognize key considerations when building or expanding Emergency Radiology programs 2) Describe scope of practice variations in different models 3) Explore varied staffing and scheduling models 4) Consider the impact of staffing models on quality and trainee education\*Course Description There are now more dedicated Emergency Radiology section and divisions than ever before. This session will focus on key elements for leaders to consider when designing or expanding these programs, including scope of practice, staffing and scheduling considerations, and impact of staffing models on quality and trainee education.

Printed on: 02/07/23



## Abstract Archives of the RSNA, 2022

R6-CGI07

### Case-based Review of GI Imaging

Thursday, Dec. 1 1:30PM - 2:30PM Room: NA

#### Participants

Jessica Zarzour, MD, Vestavia, AL (*Presenter*) Nothing to Disclose  
Jorge Soto, MD, Boston, MA (*Presenter*) Nothing to Disclose  
Frank H. Miller, MD, Chicago, IL (*Presenter*) Advisory Board, Bayer AG; Advisory Board, Guerbet SA  
Aarti Sekhar, MD, Atlanta, GA (*Presenter*) Nothing to Disclose  
Khaled M. Elsayes, MD, Houston, TX (*Presenter*) Nothing to Disclose

#### COURSE DESCRIPTION

This course will use an interactive, case-based format where the attendees will be presented with cases that will highlight important practical tips for the differential diagnosis of diseases affecting various organs of the gastrointestinal tract and organs. After each case, the presenters will ask questions and offer potential answers that will be followed by a discussion. The faculty for this course are experienced gastrointestinal and abdominal radiologists and they will present cases with varying degrees of complexity and difficulty.

#### LEARNING OBJECTIVES

1) To highlight important findings that help in the differential diagnosis of diseases affecting the gastrointestinal tract 2) To emphasize the importance of a careful and systematic review of all imaging modalities when evaluating complex cases 3) To illustrate, with representative cases, the characteristic appearance of important diseases affecting the gastrointestinal tract and solid organs\*Course Description This course will use an interactive, case-based format where the attendees will be presented with cases that will highlight important practical tips for the differential diagnosis of diseases affecting various organs of the gastrointestinal tract and organs. After each case, the presenters will ask questions and offer potential answers that will be followed by a discussion. The faculty for this course are experienced gastrointestinal and abdominal radiologists and they will present cases with varying degrees of complexity and difficulty.

Printed on: 02/07/23



## Abstract Archives of the RSNA, 2022

R6-CGU03

### GU Essentials! A Case-Based Audience Participation Session

Thursday, Dec. 1 1:30PM - 2:30PM Room: NA

#### Participants

Lori Mankowski Gettle, MD, Madison, WI (*Presenter*) Stockholder, Elucent Medical; Research support, General Electric Company; Research support, HistoSonics, Inc; Royalties, RELX  
Aradhana Venkatesan, MD, Houston, TX (*Presenter*) Research Grant, Siemens; Honorarium, Elsevier  
Peter S. Liu, MD, Cleveland, OH (*Presenter*) Nothing to Disclose  
Tharakeswara Bathala, MD, Houston, TX (*Presenter*) Nothing to Disclose  
Tristan Barrett, MBBS, Cambridge, United Kingdom (*Presenter*) Nothing to Disclose

#### COURSE DESCRIPTION

GU Live! A Case-Based Audience Participation Session is an expert-moderated session featuring a series of interactive genitourinary case studies that will challenge radiologists' diagnostic skills and knowledge. In this session, participants will be automatically assigned to teams depending on the number of participants in the session. They will then use their mobile devices to test their knowledge of genitourinary radiology in a fast-paced session that will be both educational and entertaining.

#### LEARNING OBJECTIVES

1) To interpret interesting cases related to kidney, ureter, bladder, and gynecological pathologies to form a differential diagnosis and a definitive diagnosis via interactive audience participation. 2) To apply the teaching points from the individual challenging cases to future clinical cases seen in the practice of genitourinary radiology. \*Course Description GU Live! A Case-Based Audience Participation Session is an expert-moderated session featuring a series of interactive genitourinary case studies that will challenge radiologists' diagnostic skills and knowledge. In this session, participants will be automatically assigned to teams depending on the number of participants in the session. They will then use their mobile devices to test their knowledge of genitourinary radiology in a fast-paced session that will be both educational and entertaining.

Printed on: 02/07/23



## Abstract Archives of the RSNA, 2022

R6-CIN13

### The Basics of AI: An Interactive Session to Test your Knowledge

Thursday, Dec. 1 1:30PM - 2:30PM Room: NA

#### Participants

Luciano M. Prevedello, MD, MPH, Columbus, OH (*Presenter*) Nothing to Disclose

Tara Retson, MD, PhD, San Diego, CA (*Presenter*) Research Consultant, CureMetrix, Inc; Stock options, CureMetrix, Inc

Ian Pan, MD, Brookline, MA (*Presenter*) Consultant, MD.ai, Inc; Consultant, Centaur Labs Inc; Consultant, Diagnosticos da America SA; Consultant, CoRead AI

Felipe C. Kitamura, MD, PhD, Sao Paulo, SP (*Moderator*) Consultant, MD.ai, Inc; Speaker, General Electric Company

#### COURSE DESCRIPTION

This session will cover basic concepts of artificial intelligence in radiology. Participants should bring their mobile devices with an internet connection to participate. Presenters will ask questions and display alternatives on slides, and participants will answer questions on their mobile devices. After each question, presenters will discuss the main concepts pertaining to the topic.

#### LEARNING OBJECTIVES

1) Describe the main concepts in artificial intelligence as they apply to the implementation of AI programs in clinical practice. 2) Understand pitfalls during training and the limitations they impose on clinical use.\*Course Description This session will cover basic concepts of artificial intelligence in radiology. Participants should bring their mobile devices with an internet connection to participate. Presenters will ask questions and display alternatives on slides, and participants will answer questions on their mobile devices. After each question, presenters will discuss the main concepts pertaining to the topic.

Printed on: 02/07/23



## Abstract Archives of the RSNA, 2022

R6-CIR10

### Advanced MSK Interventions

Thursday, Dec. 1 1:30PM - 2:30PM Room: NA

#### Participants

Thierry J. De Baere, MD, Villejuif, France (*Presenter*) Research support, Terumo Corporation; Research support, General Electric Company; Research support, Boston Scientific Corporation; Research support, Quantum Medical Imaging, LLC; Consultant, Guerbet SA; Consultant, Terumo Corporation; Consultant, Johnson & Johnson; Consultant, General Electric Company; Consultant, AstraZeneca PLC; Consultant, H&D Technologies; Consultant, Quantum Medical Imaging, LLC

Steven Yevich, MD, MPH, Houston, TX (*Presenter*) Advisory Board, Medtronic plc; Editor, HMP Global, LLC

Frederic Deschamps, Villejuif, France (*Presenter*) Consultant, Medtronic plc; Consultant, General Electric Company; Consultant, Ablatech; Consultant, Boston Scientific Corporation; Consultant, Surgnova Healthcare Technologies; Consultant, InnoProd, Inc

Guillaume Koch, MD, MSc, Strasbourg, France (*Presenter*) Nothing to Disclose

Matthew Callstrom, MD, PhD, Rochester, MN (*Presenter*) Research Grant, EDDA Technology, Inc; Consultant, Johnson & Johnson; Consultant, Boston Scientific Corporation; Consultant, Pulse Biosciences, Inc

#### COURSE DESCRIPTION

Imaging-guided interventional procedures are becoming increasingly important in the management of cancer patients. Thanks to the development of new technologies, interventional radiologists have pushed the indications further and increased the procedures' safety. This session will focus on new technologies that have been developed recently for percutaneous bone procedures.

#### LEARNING OBJECTIVES

1) To describe new percutaneous techniques that have emerged during the past years for the treatment of bone metastases 2) To describe strategies that make the bone procedures safer\*Course Description Imaging-guided interventional procedures are becoming increasingly important in the management of cancer patients. Thanks to the development of new technologies, interventional radiologists have pushed the indications further and increased the procedures' safety. This session will focus on new technologies that have been developed recently for percutaneous bone procedures.

Printed on: 02/07/23



## Abstract Archives of the RSNA, 2022

R6-CMK06

### Muscle and Nerve Imaging: Case-based Review and Update

Thursday, Dec. 1 1:30PM - 2:30PM Room: NA

#### Participants

Jim S. Wu, MD, Lexington, MA (*Presenter*) Nothing to Disclose

Avneesh Chhabra, MD, Flowermound, TX (*Presenter*) Consultant, ICON plc; Consultant, Treace Medical Concepts, Inc; Author with royalties, Wolters Kluwer nv; Author with royalties, Jaypee Brothers Medical Publishers Ltd; Speaker, Siemens AG; Medical Advisor, ImageBiopsy Lab; Research Grant, ImageBiopsy Lab

Darryl Sneag, MD, Plainview, NY (*Presenter*) Researcher, General Electric Company; Researcher, Siemens AG; Research support, AMAG Pharmaceuticals, Inc

William E. Palmer, MD, Boston, MA (*Presenter*) Nothing to Disclose

Shivani Ahlawat, MD, Ellicott City, MD (*Presenter*) Nothing to Disclose

#### COURSE DESCRIPTION

Imaging plays a vital role in the diagnosis and treatment of a variety of conditions that affect muscles and nerves. This course will discuss several of these topics through a series of high-yield cases drawing on the most up-to-date concepts. By the end of the course, the listener will learn how to identify and optimally report these muscle and nerve imaging findings.

#### LEARNING OBJECTIVES

1) Become familiar with a variety of conditions that can affect muscle and nerve 2) Learn how to identify the key imaging findings and optimal reporting lexicon for certain muscle and nerve disorders\*Course Description Imaging plays a vital role in the diagnosis and treatment of a variety of conditions that affect muscles and nerves. This course will discuss several of these topics through a series of high-yield cases drawing on the most up-to-date concepts. By the end of the course, the listener will learn how to identify and optimally report these muscle and nerve imaging findings.

Printed on: 02/07/23



## Abstract Archives of the RSNA, 2022

R6-CNPM18

### Human Factors in Radiology (Sponsored by RSNA Professionalism Committee)

Thursday, Dec. 1 1:30PM - 2:30PM Room: NA

#### Participants

Michael K. Atalay, MD, PhD, Providence, RI (*Presenter*) Nothing to Disclose  
Kate Hanneman, MD, FRCPC, Toronto, ON (*Presenter*) Speaker, Groupe Sanofi Speaker, Amicus Therapeutics, Inc  
Grainne Murphy, MBBCh, MMedSc, Birmingham, United Kingdom (*Presenter*) Nothing to Disclose  
Niall Downey, Newry, United Kingdom (*Presenter*) Nothing to Disclose  
Bettina Siewert, MD, Brookline, MA (*Presenter*) Editor, Wolters Kluwer nv; Reviewer, Wolters Kluwer nv

#### COURSE DESCRIPTION

This course will take the form of lectures, with discussion. Human Factors are environmental, organisational and job factors, and human and individual characteristics which influence behaviour at work in a way which can affect health and safety. Human factors can encompass nature of the task, ergonomics, processes and procedures (e.g. interruptions), decision making and errors, as well as communication between team members and organisational culture, and are therefore crucial in healthcare in general, and very relevant to work in radiology. Aviation has been a leader in the topic of human factors, which has contributed to the excellent safety record, and there are many commonalities between the aviation industry and medicine, allowing us to learn from each other. The course will involve a talk from an airline captain who will discuss how we can learn from aviation, from an expert on perception, and from radiologists who will discuss the specific challenges in radiology, and what we can do to improve.

#### LEARNING OBJECTIVES

1) Identify human factors in radiology and learn how to recognise how they may impact clinical practice  
2) Develop strategies to minimize or prevent error in a variety of settings, and reduce risk of burnout. \*Course Description This course will take the form of lectures, with discussion. Human Factors are environmental, organisational and job factors, and human and individual characteristics which influence behaviour at work in a way which can affect health and safety. Human factors can encompass nature of the task, ergonomics, processes and procedures (e.g. interruptions), decision making and errors, as well as communication between team members and organisational culture, and are therefore crucial in healthcare in general, and very relevant to work in radiology. Aviation has been a leader in the topic of human factors, which has contributed to the excellent safety record, and there are many commonalities between the aviation industry and medicine, allowing us to learn from each other. The course will involve a talk from an airline captain who will discuss how we can learn from aviation, from an expert on perception, and from radiologists who will discuss the specific challenges in radiology, and what we can do to improve.

Printed on: 02/07/23



## Abstract Archives of the RSNA, 2022

R6-CNR01

### Stroke: Advances in Imaging for Stroke Prevention

Thursday, Dec. 1 1:30PM - 2:30PM Room: NA

#### Participants

Hediyeh Baradaran, MD, MS, Salt Lake City, UT (*Presenter*) Nothing to Disclose

Argye Hillis, MD, Baltimore, MD (*Presenter*) Nothing to Disclose

Ajay Gupta, MD, MS, New York, NY (*Presenter*) Nothing to Disclose

Mahmud Mossa-Basha, MD, Seattle, WA (*Moderator*) Nothing to Disclose

#### COURSE DESCRIPTION

This course will be comprised of didactic lectures, followed by a Q&A session, discussing imaging for stroke prevention. Specifically, we will cover the latest clinical and imaging approaches for stroke etiologic diagnosis, stroke risk stratification, and prognostic factors. This course will provide the latest evidence-based data on advanced neurovascular imaging techniques, and their role in current stroke assessment. We will also present updates on stroke prevention best practices. The contribution of burden of white matter hyperintensities to stroke outcomes and cognitive function will also be discussed.

#### LEARNING OBJECTIVES

1) Discuss updates in stroke prevention practices from the perspective of stroke neurology 2) Explain added value of vessel wall and plaque imaging to stroke etiology diagnosis and risk stratification, and best approaches to integrate these techniques into your practice 3) Explain the prognostic value of white matter hyperintensity burden on stroke on cognitive function outcomes\*Course Description This course will be comprised of didactic lectures, followed by a Q&A session, discussing imaging for stroke prevention. Specifically, we will cover the latest clinical and imaging approaches for stroke etiologic diagnosis, stroke risk stratification, and prognostic factors. This course will provide the latest evidence-based data on advanced neurovascular imaging techniques, and their role in current stroke assessment. We will also present updates on stroke prevention best practices. The contribution of burden of white matter hyperintensities to stroke outcomes and cognitive function will also be discussed.

Printed on: 02/07/23



## Abstract Archives of the RSNA, 2022

R6-CPD12

### Pediatric Ultrasound Session

Thursday, Dec. 1 1:30PM - 2:30PM Room: NA

#### Participants

Patricia Acharya, MD, Monrovia, CA (*Presenter*) Nothing to Disclose

Brian Coley, MD, Cincinnati, OH (*Presenter*) Royalties, RELX; Board of Directors, Eyas Medical Imaging, Inc

Jonathan D. Samet, MD, Chicago, IL (*Presenter*) Nothing to Disclose

#### COURSE DESCRIPTION

Ultrasound is invaluable in pediatric imaging, and new developments (sometimes by other specialties) continue to expand ultrasound's role. This interactive polling session will expand the utility of US and including talks on: 1. Point of care US- controversies- keeping ourselves relevant. 2. Contrast Enhanced Ultrasound (CEUS) Applications in Pediatric Abdominal Imaging. 3. Musculoskeletal US in pediatrics: How to make your referrers happy.

#### LEARNING OBJECTIVES

1) Understand the value of point of care ultrasound and Radiology's importance in it 2) Explain the value of contrast-enhanced ultrasound in pediatric abdominal imaging 3) Explain the ultrasound findings of pediatric musculoskeletal conditions\*Course Description Ultrasound is invaluable in pediatric imaging, and new developments (sometimes by other specialties) continue to expand ultrasound's role. This interactive polling session will expand the utility of US and including talks on: 1. Point of care US- controversies- keeping ourselves relevant. 2. Contrast Enhanced Ultrasound (CEUS) Applications in Pediatric Abdominal Imaging. 3. Musculoskeletal US in pediatrics: How to make your referrers happy.

Printed on: 02/07/23



## Abstract Archives of the RSNA, 2022

R6-RCP14

### Improving Patient Experience Through Human Design Thinking (Sponsored by the RSNA Public Information Committee)

Thursday, Dec. 1 1:30PM - 2:30PM Room: NA

#### Participants

Lucy Spalluto, MD, MPH, Nashville, TN (*Presenter*) Nothing to Disclose

Achala Vagal, MD, Cincinnati, OH (*Presenter*) Departmental Research Grant, Johnson & Johnson

Ruth C. Carlos, MD, MS, Ann Arbor, MI (*Presenter*) In-kind support, RELX; Editor, RELX; Travel support, General Electric Company

Jennifer Kemp, MD, Denver, CO (*Moderator*) Stockholder, Scanslated, Inc

#### LEARNING OBJECTIVES

1) Apply human design thinking processes to create practical solutions to improve patient experience 2) Use novel teaching methods to improve empathy and communication between physicians and patients 3) Develop a health equity curriculum through human design thinking\*Course Description

Printed on: 02/07/23



## Abstract Archives of the RSNA, 2022

R7-CBR01

### Contrast Enhanced Mammography: Technique and Indications

Thursday, Dec. 1 3:00PM - 4:00PM Room: NA

#### Participants

Janice S. Sung, MD, New York, NY (*Presenter*) Research Grant, General Electric Company

Vasiliki Papalouka, MD, Cambridge, United Kingdom (*Presenter*) Nothing to Disclose

Ulrich Bick, MD, Berlin, Germany (*Presenter*) License agreement, Hologic, Inc; Royalties, Hologic, Inc

#### COURSE DESCRIPTION

Contrast enhanced mammography (CEM) is an FDA approved technique that is emerging as an alternative vascular based technique to conventional breast imaging and MRI in both the screening and diagnostic settings. This session will review considerations in beginning a CEM program and review data supporting the use of CEM in both the screening and diagnostic settings.

#### LEARNING OBJECTIVES

1) Review how to perform contrast enhanced mammography (CEM) and considerations when starting a CEM program 2) Discuss the emerging roles of contrast enhanced mammography in both the screening and diagnostic settings\*Course Description Contrast enhanced mammography (CEM) is an FDA approved technique that is emerging as an alternative vascular based technique to conventional breast imaging and MRI in both the screening and diagnostic settings. This session will review considerations in beginning a CEM program and review data supporting the use of CEM in both the screening and diagnostic settings.

Printed on: 02/07/23



## Abstract Archives of the RSNA, 2022

R7-CCA11

### 24h Coronary CT Program: Unnecessary, Optional or Essential?

Thursday, Dec. 1 3:00PM - 4:00PM Room: NA

#### Participants

Phillip Young, MD, Rochester, MN (*Presenter*) Nothing to Disclose

Saurabh Jha, MD, Philadelphia, PA (*Presenter*) Nothing to Disclose

Kate Hanneman, MD, FRCPC, Toronto, ON (*Moderator*) Speaker, Groupe Sanofi Speaker, Amicus Therapeutics, Inc

#### COURSE DESCRIPTION

This session will discuss the pros and cons of 24 hour coronary CT programs in a debate format.

#### LEARNING OBJECTIVES

1) Identify pros and cons of 24 hour coronary CT programs and 2) Explain current landscape of 24 hour coronary CT programs\*Course Description This session will discuss the pros and cons of 24 hour coronary CT programs in a debate format.

Printed on: 02/07/23



## Abstract Archives of the RSNA, 2022

R7-CCH06

### Chest MRI, PET-CT and Photon Counting CT Updates

Thursday, Dec. 1 3:00PM - 4:00PM Room: NA

#### Participants

Shuai Leng, PHD, Rochester, MN (*Presenter*) License agreement, Siemens AG

Lea Azour, MD, Mamaroneck, NY (*Presenter*) Nothing to Disclose

Christopher Francois, MD, Rochester, MN (*Presenter*) Nothing to Disclose

Osama R. Mawlawi, PhD, Houston, TX (*Presenter*) Nothing to Disclose

#### COURSE DESCRIPTION

This course will deliver a fast-paced dive into advanced thoracic imaging techniques including photon counting CT, non-vascular and vascular MRI, and PET-CT.

#### LEARNING OBJECTIVES

1) Describe applications of photon counting CT in thoracic imaging 2) Explain implementation of MRI for evaluation of pulmonary embolism 3) Explore pearls and pitfalls of MRI for mediastinal mass imaging 4) Present innovations in PET-CT integral to chest imaging\*Course Description This course will deliver a fast-paced dive into advanced thoracic imaging techniques including photon counting CT, non-vascular and vascular MRI, and PET-CT.

Printed on: 02/07/23



## Abstract Archives of the RSNA, 2022

R7-CER13

### Emergency and Trauma Imaging: Translating Science to Practice

Thursday, Dec. 1 3:00PM - 4:00PM Room: NA

#### Participants

David Dreizin, MD, Baltimore, MD (*Presenter*) Nothing to Disclose  
Melissa Davis, MD, MBA, Atlanta, GA (*Presenter*) Nothing to Disclose  
Michael J. Thali, MD, Zurich, Switzerland (*Presenter*) Nothing to Disclose

#### COURSE DESCRIPTION

This course serves to acquaint radiologists with specific aspects of translating scientific research into Emergency Imaging techniques. This will span the breadth of automation and forensic analysis.

#### LEARNING OBJECTIVES

1) To understand the link between scientific analysis and translation into clinical practice 2) To explain current applications of scientific research in Emergency Imaging 3) To expose radiologists to novel uses of imaging in forensics\*Course Description This course serves to acquaint radiologists with specific aspects of translating scientific research into Emergency Imaging techniques. This will span the breadth of automation and forensic analysis.

Printed on: 02/07/23



## Abstract Archives of the RSNA, 2022

R7-CGI10

### Management of Cystic Pancreatic Lesions

Thursday, Dec. 1 3:00PM - 4:00PM Room: NA

#### Participants

Hanna M. Zafar, MD, Philadelphia, PA (*Presenter*) Nothing to Disclose

Chenchan Huang, MD, Manhasset, NY (*Presenter*) Nothing to Disclose

Anne Marie Lennon, MD, Baltimore, MD (*Presenter*) Patent holder, Exact Sciences Corporation;

William W. Mayo-Smith, MD, Weston, MA (*Presenter*) Nothing to Disclose

David M. Hough, MD, Rochester, MN (*Presenter*) Nothing to Disclose

Eric Tamm, MD, Houston, TX (*Presenter*) Institutional Research Grant, General Electric Company. This relationship ended 8/31/21 with end of the period of grant support.

Desiree Morgan, MD, Birmingham, AL (*Moderator*) Institutional Research Grant, General Electric Company

#### COURSE DESCRIPTION

The controversy over surveillance of pancreatic cysts remains heated, and care for patients heterogenous. In a course exploring evidence based data for pancreatic cyst risk assessment together with a discussion of the role of endoscopic ultrasound, the learners will be engaged in case discussion and debate among experts to help inform and develop strategies to meet the needs of patients in their individual practices.

#### LEARNING OBJECTIVES

1) Identify commonalities and differences in the spectrum of pancreatic cyst guidelines, capped by a debate on the pros and cons of following the ACR incidental pancreatic cyst surveillance recommendations 2) Explore the evidence for pancreatic cyst risk stratification and apply in conjunction with imaging features introduced in challenging case presentations 3) Explain the role of endoscopic ultrasound and cyst aspiration in surveillance and management\*Course Description The controversy over surveillance of pancreatic cysts remains heated, and care for patients heterogenous. In a course exploring evidence based data for pancreatic cyst risk assessment together with a discussion of the role of endoscopic ultrasound, the learners will be engaged in case discussion and debate among experts to help inform and develop strategies to meet the needs of patients in their individual practices.

Printed on: 02/07/23



## Abstract Archives of the RSNA, 2022

R7-CHN07

### Practical Tips to Fine Tune Your Head and Neck Imaging Techniques

Thursday, Dec. 1 3:00PM - 4:00PM Room: NA

#### Participants

Greg Avey, MD, Madison, WI (*Presenter*) Research Consultant, General Electric Company

Remy Lobo, MD, Ann Arbor, MI (*Presenter*) Nothing to Disclose

Xin Wu, MD, Atlanta, GA (*Presenter*) Nothing to Disclose

Ashley H. Aiken, MD, Atlanta, GA (*Presenter*) Nothing to Disclose

Katie S. Traylor, DO, Pittsburgh, PA (*Presenter*) Nothing to Disclose

Claudia Kirsch, MD, New York, NY (*Moderator*) Consultant, Informa PLC; Royalties, Informa PLC

#### COURSE DESCRIPTION

Session ID/Title: CHN07: Practical Tips to Fine Tune Your Head and Neck Imaging Techniques: Moderator C. F. Kirsch; New York, NY. Moderator/Presenter A. H. Aiken Atlanta, GA; "Keeping it Steady" Optimizing techniques in MRI CISS sequences to identify Cranial Nerves and Skull Base Foramina Presenter: R. R. Lobo; Ann Arbor, MI. "In Therapy" Post-Treatment Neck Advanced CT & MRI Imaging" Presenter X. Wu; Atlanta, GA. "Got a Lot of Nerve", Head and Neck MRI Neurography Presenter: G. D. Avey; Madison, WI. "Teacher's PET", PET Advances in Head and Neck Cancer Presenter: K. S. Traylor; Mars, PA. "Twist and Shout", Advanced Techniques for Evaluating Neurovascular Compression in the Head and Neck Course Description: Likely a beautifully played string quintet, these 5 phenomenal lectures on "Practical Tips to Fine Tune Your Head and Neck Imaging Techniques" given by outstanding head and neck radiologists, teachers, and speakers, all recently published in their topic, are music to the radiologists' ears. Each lecture provides tips to fine tune imaging instruments and enhance head and neck imaging techniques. Dr. Aiken starts the session reviewing how MRI heavily T2 weighted CISS techniques improves visualization of cranial nerve and skull base foramina. Dr. Lobo presenting on advanced CT and MRI imaging highlights how these improve post treatment neck evaluation. Dr. Wu elaborates on tips for MRI neurography in the head and neck soft tissues, followed by Dr. Avey providing the latest PET advances in head and neck cancer imaging. The last lecture by Dr. Traylor provides tips to evaluate vessels and enhance visualization of neurovascular compression. At the outcome of this session, radiologists will have heard a beautiful medley of expert CT, MRI, PET head and neck imaging tips that fine tune imaging and improve identification of head and neck pathology.

#### LEARNING OBJECTIVES

1) Optimize head and neck protocols including diffusion weighted imaging, fat saturation techniques, biopsies, dual energy and PET/MRI 2) Circumvent common artifacts/pitfalls of diffusion weighted imaging, fat saturation techniques, biopsies, dual energy and PET/MRI\*Course Description Session ID/Title: CHN07: Practical Tips to Fine Tune Your Head and Neck Imaging Techniques: Moderator C. F. Kirsch; New York, NY. Moderator/Presenter A. H. Aiken Atlanta, GA; "Keeping it Steady" Optimizing techniques in MRI CISS sequences to identify Cranial Nerves and Skull Base Foramina Presenter: R. R. Lobo; Ann Arbor, MI. "In Therapy" Post-Treatment Neck Advanced CT & MRI Imaging" Presenter X. Wu; Atlanta, GA. "Got a Lot of Nerve", Head and Neck MRI Neurography Presenter: G. D. Avey; Madison, WI. "Teacher's PET", PET Advances in Head and Neck Cancer Presenter: K. S. Traylor; Mars, PA. "Twist and Shout", Advanced Techniques for Evaluating Neurovascular Compression in the Head and Neck Course Description: Likely a beautifully played string quintet, these 5 phenomenal lectures on "Practical Tips to Fine Tune Your Head and Neck Imaging Techniques" given by outstanding head and neck radiologists, teachers, and speakers, all recently published in their topic, are music to the radiologists' ears. Each lecture provides tips to fine tune imaging instruments and enhance head and neck imaging techniques. Dr. Aiken starts the session reviewing how MRI heavily T2 weighted CISS techniques improves visualization of cranial nerve and skull base foramina. Dr. Lobo presenting on advanced CT and MRI imaging highlights how these improve post treatment neck evaluation. Dr. Wu elaborates on tips for MRI neurography in the head and neck soft tissues, followed by Dr. Avey providing the latest PET advances in head and neck cancer imaging. The last lecture by Dr. Traylor provides tips to evaluate vessels and enhance visualization of neurovascular compression. At the outcome of this session, radiologists will have heard a beautiful medley of expert CT, MRI, PET head and neck imaging tips that fine tune imaging and improve identification of head and neck pathology.

Printed on: 02/07/23



## Abstract Archives of the RSNA, 2022

R7-CIN25

### Opportunistic Screening and Superhuman AI for Radiology

Thursday, Dec. 1 3:00PM - 4:00PM Room: NA

#### Participants

Hari Trivedi, MD, Atlanta, GA (*Presenter*) Founder, Lightbox AI ; Consultant, Sirona Medical, Inc ; Consultant, Flatiron Health ; Consultant, PMX Inc ; Research support, Kheiron Medical Technologies ; Research support, Clarity, Inc ; Research support, Nightingale Open Science ;

Kirti Magudia, MD, PhD, Durham, NC (*Presenter*) Nothing to Disclose

Akshay Chaudhari, PhD, Stanford, CA (*Presenter*) Research support, General Electric Company; Research support, Koninklijke Philips NV; Research Consultant, Subtle Medical, Inc

#### COURSE DESCRIPTION

This course will introduce the potential and current applications of AI to allow opportunistic screening of disease and outcomes using radiology images.

#### LEARNING OBJECTIVES

1) Identify potential applications of AI for opportunistic screening 2) Explain the current clinical AI applications that allow opportunistic screening using radiologic images\*Course Description This course will introduce the potential and current applications of AI to allow opportunistic screening of disease and outcomes using radiology images.

Printed on: 02/07/23



## Abstract Archives of the RSNA, 2022

R7-CIR03

### Hepato-Bilio-Pancreatic Interventions

Thursday, Dec. 1 3:00PM - 4:00PM Room: NA

#### Participants

Ahsun Riaz, MD, Chicago, IL (*Presenter*) Consultant, Boston Scientific Corporation  
Juan Camacho, MD, Sarasota, FL (*Presenter*) Research Grant, Elesta Echolaser  
Eva Criado, MD, Sant Cugat del Valles, Spain (*Presenter*) Nothing to Disclose  
Peter Park, MD, Duluth, GA (*Presenter*) Nothing to Disclose  
Kevin W. Dickey, MD, Charleston, SC (*Presenter*) Nothing to Disclose  
Govindarajan Narayanan, MD, Miami, FL (*Presenter*) Consultant, AngioDynamics, Inc; Consultant, Boston Scientific Corporation; Consultant, Stryker Corporation; Consultant, Agilent Technologies, Inc  
Anne M. Covey, MD, New York, NY (*Moderator*) Stockholder, Amgen Inc

#### COURSE DESCRIPTION

Hepatobiliary and pancreatic procedures make up a large part of most busy interventional practices. Over the past decade there have been novel innovations (e.g. cholangioscopy, biodegradable stents) that improve our ability to treat these patients. Also utilization of standard equipment in new applications has also greatly improved patient care; as in total hepatic venous deprivation. In this session content experts will provide insight into the current and future treatment options to optimize the care of patients undergoing liver and pancreas interventions.

#### LEARNING OBJECTIVES

1) Learn advanced interventional techniques to manage patients with complex benign biliary disease 2) Understand the role of interventional radiology in patients with pancreatitis and pancreatic carcinoma 3) Discuss use of various hepatic venous deprivation techniques to optimize patients for major hepatic resection\*Course Description Hepatobiliary and pancreatic procedures make up a large part of most busy interventional practices. Over the past decade there have been novel innovations (e.g. cholangioscopy, biodegradable stents) that improve our ability to treat these patients. Also utilization of standard equipment in new applications has also greatly improved patient care; as in total hepatic venous deprivation. In this session content experts will provide insight into the current and future treatment options to optimize the care of patients undergoing liver and pancreas interventions.

Printed on: 02/07/23



## Abstract Archives of the RSNA, 2022

R7-CMK11

### Sports Imaging: Lessons Learned

Thursday, Dec. 1 3:00PM - 4:00PM Room: NA

#### Participants

Russell C. Fritz, MD, Mill Valley, CA (*Presenter*) Nothing to Disclose

Adam Zoga, MD, Philadelphia, PA (*Presenter*) Nothing to Disclose

Kirkland Davis, MD, Madison, WI (*Presenter*) Nothing to Disclose

Soterios Gyftopoulos, MD, MBA, Scarsdale, NY (*Presenter*) Nothing to Disclose

#### COURSE DESCRIPTION

This 60 minute course was designed to provide a practical update on MRI of sports-related conditions of the musculoskeletal system. The faculty consists of 5 experienced radiologists, all of whom are noted for their lecturing and teaching ability. There will be 5 separate 10 minute talks, with 10 additional minutes available for questions and discussion.

#### LEARNING OBJECTIVES

1) To provide the course registrants with a strategy to efficiently detect sports-related conditions of the musculoskeletal system with MRI 2) To provide the course registrants with the key points to evaluate and understand the most important sports-related orthopedic conditions in the spine, upper extremity, and lower extremity with MRI 3) To provide the course registrants with of up to date knowledge about diagnosing the most important sports-related orthopedic conditions\*Course Description This 60 minute course was designed to provide a practical update on MRI of sports-related conditions of the musculoskeletal system. The faculty consists of 5 experienced radiologists, all of whom are noted for their lecturing and teaching ability. There will be 5 separate 10 minute talks, with 10 additional minutes available for questions and discussion.

Printed on: 02/07/23



## Abstract Archives of the RSNA, 2022

R7-CNMMI09

### Musculoskeletal Imaging: When Molecular Imaging Helps

Thursday, Dec. 1 3:00PM - 4:00PM Room: NA

#### Participants

Kevin P. Banks, MD, San Antonio, TX (*Presenter*) Nothing to Disclose  
Olga G. James, MD, Chapel Hill, NC (*Presenter*) Nothing to Disclose  
Janis P. O'Malley, MD, Birmingham, AL (*Presenter*) Nothing to Disclose

#### COURSE DESCRIPTION

This course will provide a review of when molecular imaging (including PET/CT and SPECT/CT) is most helpful in the evaluation of musculoskeletal pathology.

#### LEARNING OBJECTIVES

1) To review cases with musculoskeletal pathology and correlative imaging 2) To discuss where/ when to use molecular imaging with an emphasis on malignancy, trauma and infection 3) To illustrate incidental findings and review what to do with them\*Course Description This course will provide a review of when molecular imaging (including PET/CT and SPECT/CT) is most helpful in the evaluation of musculoskeletal pathology.

Printed on: 02/07/23



## Abstract Archives of the RSNA, 2022

R7-CNPM05

### Shielding from Burnout with Financial Health: Fundamentals on Financial Literacy and Investments

Thursday, Dec. 1 3:00PM - 4:00PM Room: NA

#### Participants

Christopher M. Walker, MD, Fairway, KS (*Presenter*) Author, RELX;Speakers Bureau, Boehringer Ingelheim GmbH  
Sherwin Chan, MD, PhD, Kansas City, MO (*Presenter*) Consultant, Jazz Pharmaceuticals plc;Research Grant, Jazz Pharmaceuticals plc;Research Grant, Hyperfine, Inc;Research Grant, General Electric Company  
Grace S. Mitchell, MD, Fairway, KS (*Presenter*) Nothing to Disclose  
Jenny K. Hoang, MBBS, Baltimore, MD (*Moderator*) Spouse, Employee, Merck & Co, Inc

#### COURSE DESCRIPTION

Many radiologists are unable to translate their high income into a high net worth. This is due to high student debt, poor financial literacy and lifestyle creep. High debt drives choices in career path for trainees and practicing radiologists, and contributes to physician burnout and mental health issues. Despite the importance of personal financial health, education on finances is absent from the majority of radiology training programs. Some highly successful and intelligent radiologists who contribute enormously to research, radiology education, and clinical care have not spent the necessary time learning about finances and preparing for retirement. The gap in financial literacy for women is even greater.

#### LEARNING OBJECTIVES

1) Understand the basics of budgeting, debt reduction, and planning for retirement 2) Recognize the importance of wealth building and advantages of major asset classes for radiologists 3) Gain insight into asset protection, insurance and loan forgiveness programs\*Course Description Many radiologists are unable to translate their high income into a high net worth. This is due to high student debt, poor financial literacy and lifestyle creep. High debt drives choices in career path for trainees and practicing radiologists, and contributes to physician burnout and mental health issues. Despite the importance of personal financial health, education on finances is absent from the majority of radiology training programs. Some highly successful and intelligent radiologists who contribute enormously to research, radiology education, and clinical care have not spent the necessary time learning about finances and preparing for retirement. The gap in financial literacy for women is even greater.

Printed on: 02/07/23



## Abstract Archives of the RSNA, 2022

R7-CNR05

### Imaging of AD (MRI Protocols and ARIA, PET, Amyloid/Tau biomarkers, Glymphatics, What the Radiologist Needs to Know)

Thursday, Dec. 1 3:00PM - 4:00PM Room: NA

#### Participants

Tammie Benzinger, MD, PhD, Saint Louis, MO (*Presenter*) Research Grant, Eli Lilly and Company; Investigator, Eli Lilly and Company; Investigator, F. Hoffmann-La Roche Ltd; Consultant, Siemens AG; Research Grant, Siemens AG; Consultant, ADM Diagnostics, LLC; Speakers Bureau, Biogen Idec Inc; Advisory Board, Biogen Idec Inc

Val J. Lowe, MD, Rochester, MN (*Presenter*) Research Grant, General Electric Company; Research Grant, Siemens AG; Research Grant, Eli Lilly and Company; Research Consultant, Eli Lilly and Company

Geir Ringstad, MD, Oslo, Norway (*Presenter*) Shareholder, BrainWideSolutions

Gloria C. Chiang, MD, New York, NY (*Moderator*) Advisory Board, Biogen Idec Inc; Consultant, Life Molecular Imaging; Speaker, Horizon CME

#### COURSE DESCRIPTION

This course will provide a comprehensive update on imaging biomarkers of Alzheimer's disease, based on the "ATN" framework put forth by the National Institutes on Aging and Alzheimer's Association. Through lectures, leading experts in the field will discuss qualitative and quantitative MR metrics of atrophy, imaging of amyloid-related imaging abnormalities (ARIA), PET imaging biomarkers, and imaging of glymphatics. Attendees will come away with a standard reporting algorithm to provide the most relevant clinical imaging findings to referring neurologists, as well as understand the role of imaging in identifying the underlying biology of Alzheimer's disease.

#### LEARNING OBJECTIVES

1) Understand the role of the radiologist in evaluating a patient presenting with cognitive impairment 2) Identify the types of amyloid-related imaging abnormalities in the setting of aducanumab therapy 3) Provide updates on PET imaging biomarkers of Alzheimer's disease, including amyloid, tau, and FDG. 4) Understand the potential role of glymphatic imaging in characterizing Alzheimer's disease\*Course Description This course will provide a comprehensive update on imaging biomarkers of Alzheimer's disease, based on the "ATN" framework put forth by the National Institutes on Aging and Alzheimer's Association. Through lectures, leading experts in the field will discuss qualitative and quantitative MR metrics of atrophy, imaging of amyloid-related imaging abnormalities (ARIA), PET imaging biomarkers, and imaging of glymphatics. Attendees will come away with a standard reporting algorithm to provide the most relevant clinical imaging findings to referring neurologists, as well as understand the role of imaging in identifying the underlying biology of Alzheimer's disease.

Printed on: 02/07/23



## Abstract Archives of the RSNA, 2022

R7-COB01

### Adenomyosis Update 2022: Clinical, Diagnostic and Reporting Challenges

Thursday, Dec. 1 3:00PM - 4:00PM Room: NA

#### Participants

Mindy Horrow, MD, Philadelphia, PA (*Presenter*) Spouse, Employee, Bristol-Myers Squibb Company  
Susan M. Ascher, MD, Washington, DC (*Presenter*) Nothing to Disclose

#### COURSE DESCRIPTION

Adenomyosis is an often misunderstood and underdiagnosed uterine disorder that is frequently asymptomatic or unrelated to the symptoms experienced by the patient. Depending on the histological definition, the reported prevalence of adenomyosis has ranged from 8.85-61.5% underscoring the challenge in diagnosing and managing symptomatic patients. Dr. Malcolm Munro, Professor of Obstetrics and Gynecology at the David Geffen School of Medicine at UCLA and cofounder of FIGO's Committee on Menstrual Disorders and Related Health Impacts, will provide the latest information on the pathogenesis, clinical manifestations, and treatment options for patients with adenomyosis. He will highlight the imaging information needed by treating gynecologists to correlate symptoms with findings and, if necessary, craft a menu of treatment options for consideration by the patient. Dr. Mindy Horrow, Professor of Radiology and Vice Chair at Einstein-Jefferson Medical Center, and Dr. Susan Ascher, Professor of Radiology and Vice Chair (Research) at Georgetown University School of Medicine, will discuss current transvaginal and MR diagnostic criteria, respectively, to include pearls and pitfalls. Current reporting systems will also be provided. The course format is didactic, and at the conclusion, attendees will have enhanced knowledge of adenomyosis and be able to apply the latest TVS and MRI criteria to diagnose and report adenomyosis.

#### LEARNING OBJECTIVES

1) Describe our current understanding of the pathogenesis of adenomyosis and the varied clinical presentations - from symptomatic to asymptomatic 2) Diagnose adenomyosis on TVS and MRI using the latest criteria to include pearls and pitfalls/mimics 3) Report adenomyosis-related features useful for gynecologists for treatment planning and surveillance\*Course Description Adenomyosis is an often misunderstood and underdiagnosed uterine disorder that is frequently asymptomatic or unrelated to the symptoms experienced by the patient. Depending on the histological definition, the reported prevalence of adenomyosis has ranged from 8.85-61.5% underscoring the challenge in diagnosing and managing symptomatic patients. Dr. Malcolm Munro, Professor of Obstetrics and Gynecology at the David Geffen School of Medicine at UCLA and cofounder of FIGO's Committee on Menstrual Disorders and Related Health Impacts, will provide the latest information on the pathogenesis, clinical manifestations, and treatment options for patients with adenomyosis. He will highlight the imaging information needed by treating gynecologists to correlate symptoms with findings and, if necessary, craft a menu of treatment options for consideration by the patient. Dr. Mindy Horrow, Professor of Radiology and Vice Chair at Einstein-Jefferson Medical Center, and Dr. Susan Ascher, Professor of Radiology and Vice Chair (Research) at Georgetown University School of Medicine, will discuss current transvaginal and MR diagnostic criteria, respectively, to include pearls and pitfalls. Current reporting systems will also be provided. The course format is didactic, and at the conclusion, attendees will have enhanced knowledge of adenomyosis and be able to apply the latest TVS and MRI criteria to diagnose and report adenomyosis.

Printed on: 02/07/23



## Abstract Archives of the RSNA, 2022

R7-CPD10

### Pediatric Imaging Protocols

Thursday, Dec. 1 3:00PM - 4:00PM Room: NA

#### Participants

Ashishkumar Parikh, MD, Atlanta, GA (*Presenter*) Nothing to Disclose  
Cara Morin, PhD, Memphis, TN (*Presenter*) Nothing to Disclose  
Erica Riedesel, MD, Atlanta, GA (*Presenter*) Nothing to Disclose

#### COURSE DESCRIPTION

This course will focus on optimizing imaging protocols in CT, MRI, and Ultrasound for pediatric patients.

#### LEARNING OBJECTIVES

1) Identify practical tips to optimize pediatric US, CT and MRI imaging 2) Recognize role of imaging protocols in decreasing sedation needs in pediatric MRI 3) Understand role of DECT in pediatric CT dose reduction\*Course Description This course will focus on optimizing imaging protocols in CT, MRI, and Ultrasound for pediatric patients.

Printed on: 02/07/23



## Abstract Archives of the RSNA, 2022

R7-CPH06

### Innovations in MRI

Thursday, Dec. 1 3:00PM - 4:00PM Room: NA

#### Participants

Kawin Setsompop, Stanford, CA (*Presenter*) Research Grant, General Electric Company; Royalties, General Electric Company; Royalties, Koninklijke Philips NV; Scientific Advisory Board, KinetiCor, Inc; Scientific Advisory Board, Subtle Medical, Inc  
James Pipe, PhD, Rochester, MN (*Presenter*) Research Grant, Koninklijke Philips NV  
Matthew Bernstein, PhD, Rochester, MN (*Presenter*) Former Employee, General Electric Company  
Yunhong Shu, PhD, Rochester, MN (*Presenter*) Patent agreement, General Electric Company

#### COURSE DESCRIPTION

Three topics on Innovations in MR will be presented: Novel systems, Fast MR, and Value MR.

#### LEARNING OBJECTIVES

1) Review recent advances in novel MR scanners including: low-field, low-cryogen, dedicated, and compact systems 2) Review emerging techniques that can be used to accelerate MR-based methods including: simultaneous multislice (SMS), compressed sensing, and MR fingerprinting 3) Review advances in value MR including: dedicated protocols that can rapidly answer focused clinical questions, and emerging acquisition methods\*Course Description Three topics on Innovations in MR will be presented: Novel systems, Fast MR, and Value MR.

Printed on: 02/07/23



## Abstract Archives of the RSNA, 2022

R7-CRO01

### CNS Case-based Multidisciplinary Review

Thursday, Dec. 1 3:00PM - 4:00PM Room: NA

#### Participants

Clark Chen, MD, PhD, Minneapolis, MN (*Presenter*) Consultant, Medtronic plc; Consultant, MRI Interventions, Inc; Consultant, GT Medical Technologies, Inc  
Christina Tsien, MD, Washington, DC (*Presenter*) Advisory Board, Blue Earth Diagnostics Ltd; Speakers Bureau, Agilent Technologies, Inc; Consultant, Carl Zeiss AG  
Soonmee Cha, MD, San Francisco, CA (*Presenter*) Nothing to Disclose  
Roger Stupp, MD, Chicago, IL (*Presenter*) Research Consultant, Carthera; Research Grant, Carthera; Scientific Advisory Board, Alpheus Medical Inc; Scientific Advisory Board, Hemispherian AS; Consultant, GT Medical Technologies, Inc; Consultant, Triact Therapeutics Inc; Research Consultant, AstraZeneca PLC; Research Consultant, Boston Scientific Corporation

#### COURSE DESCRIPTION

In a rapid-fire CNS tumor board format, we will review recent CNS updates including the 5th edition WHO Classification of CNS tumors 2001. Significant progress has been made in the treatment of CNS tumors with an emphasis on molecular prognostic and predictive biomarkers that allow for appropriate treatment selection. The role of neuroimaging to help clinicians improve the diagnosis, treatment and response assessment for CNS tumors will be emphasized in the era of novel therapeutic approaches including immunotherapy. This session highlights the need for a multi-disciplinary treatment approach.

#### LEARNING OBJECTIVES

1. Review recent CNS updates including 5th edition WHO Classification of Tumors of the CNS 2021.2. Discuss key imaging modalities and features to differentiate recurrent tumor and treatment effect3. Explain the role of each modality including surgery, radiotherapy, and chemotherapy in the appropriate management of CNS tumors. \*Course Description In a rapid-fire CNS tumor board format, we will review recent CNS updates including the 5th edition WHO Classification of CNS tumors 2001. Significant progress has been made in the treatment of CNS tumors with an emphasis on molecular prognostic and predictive biomarkers that allow for appropriate treatment selection. The role of neuroimaging to help clinicians improve the diagnosis, treatment and response assessment for CNS tumors will be emphasized in the era of novel therapeutic approaches including immunotherapy. This session highlights the need for a multi-disciplinary treatment approach.

Printed on: 02/07/23



## Abstract Archives of the RSNA, 2022

R7-CVA03

### Imaging of Acute Coronary Syndrome

Thursday, Dec. 1 3:00PM - 4:00PM Room: NA

#### Participants

Brian B. Ghoshhajra, MD, Boston, MA (*Presenter*) Research Grant, Siemens AG; Consultant, Koninklijke Philips NV; Consultant, Siemens AG

Julian Luetkens, MD, Bonn, (*Presenter*) Speakers Bureau, Koninklijke Philips NV; Research Consultant, Bayer AG

Hamid R. Mojiabian, MD, New Haven, CT (*Presenter*) Nothing to Disclose

Printed on: 02/07/23



## Abstract Archives of the RSNA, 2022

R7-RCP25

### Robust AI Solutions: Essential Image Acquisition Requirements

Thursday, Dec. 1 3:00PM - 4:00PM Room: NA

#### Participants

Gudrun Zahlmann, PhD, Neumarkt, Germany (*Presenter*) Nothing to Disclose

Michael Boss, PhD, Philadelphia, PA (*Presenter*) Research Consultant, Psychology Software Tools, Inc; Research Consultant, CaliberMRI, Inc

Andrew J. Buckler, MS, PhD, Boston, MA (*Presenter*) Stockholder, Elucid Bioimaging Inc; President, Elucid Bioimaging Inc; Officer, Elucid Bioimaging Inc

Daniel Sullivan, MD, Chapel Hill, NC (*Presenter*) Nothing to Disclose

#### COURSE DESCRIPTION

Many AI solutions are currently developed but only a limited number are ultimately robust enough to receive FDA approval or achieve widespread clinical use. Too often there is a disconnect between the imaging and the AI communities on data quality, relevant imaging biomarkers, reliable data bases and clinical decision making. The data within medical images is highly complex. Specialized knowledge is needed not only to generate such images, but also to segment and analyze the quantifiable data that can be extracted from them. QIBA (Quantitative Imaging Biomarker Alliance) describes in its profiles ways in which to generate reliable, reproducible and repeatable biomarkers from medical images. This lecture-based course aims to build a bridge between imaging scientists and clinicians in order to facilitate quantitative imaging biomarkers for AI solutions.

#### LEARNING OBJECTIVES

1) Learn what a quantitative imaging biomarker (QIB) is, and how they are generated and validated 2) Understand the relationship between QIBs and AI solutions 3) Learn why so few AI algorithms have become commercialized\*Course Description Many AI solutions are currently developed but only a limited number are ultimately robust enough to receive FDA approval or achieve widespread clinical use. Too often there is a disconnect between the imaging and the AI communities on data quality, relevant imaging biomarkers, reliable data bases and clinical decision making. The data within medical images is highly complex. Specialized knowledge is needed not only to generate such images, but also to segment and analyze the quantifiable data that can be extracted from them. QIBA (Quantitative Imaging Biomarker Alliance) describes in its profiles ways in which to generate reliable, reproducible and repeatable biomarkers from medical images. This lecture-based course aims to build a bridge between imaging scientists and clinicians in order to facilitate quantitative imaging biomarkers for AI solutions.

Printed on: 02/07/23



## Abstract Archives of the RSNA, 2022

RCP59

### NIH Grantsmanship Workshop

Sunday, Nov. 27 12:00PM - 3:30PM Room: S102AB

#### Participants

Tina Gatlin, PhD, Bethesda, MD (*Presenter*) Nothing to Disclose

David A. Mankoff, MD, PhD, Philadelphia, PA (*Presenter*) Speaker, Siemens AG Advisory Board, ImaginAb, Inc Advisory Board, Reflexion Medical Inc Consultant, Blue Earth Diagnostics Ltd Consultant, General Electric Company Research funded, Siemens AG Spouse, Owner, Trevarx Biomedical, Inc

Maryellen Giger, PhD, Chicago, IL (*Presenter*) Stockholder, Hologic, Inc; Royalties, Hologic, Inc; Shareholder, Quantitative Insights, Inc; Co-founder, Quantitative Insights, Inc; Shareholder, QView Medical, Inc; Royalties, General Electric Company; Royalties, Median Technologies; Royalties, Riverain Technologies, LLC

Elizabeth A. Krupinski, PhD, Atlanta, GA (*Presenter*) Nothing to Disclose

Michael W. Vannier, MD, Crete, IL (*Presenter*) Nothing to Disclose

Ruth C. Carlos, MD, MS, Ann Arbor, MI (*Presenter*) In-kind support, RELX; Editor, RELX; Travel support, General Electric Company

Gayle Woloschak, PhD, Chicago, IL (*Moderator*) Nothing to Disclose

#### COURSE DESCRIPTION

Please note: This workshop is being held as an in-person event and will not be live-streamed or recorded. The goal of this course is to help participants understand the basic approach of how to write a grant (particularly for NIH) including all of the components of the grant itself and how to approach funding agencies within NIH for advice on process. The course includes didactic lectures, a question and answer session, and a "mock study section" that allows participants to learn about the process of review.

#### LEARNING OBJECTIVES

1) Identify the parts of an NIH grant application. 2) Explain the current structure of the NIH and its agencies particularly focusing on grant reviews. 3) Examine a study section through an example mock study section\*Course Description Please note: This workshop is being held as an in-person event and will not be live-streamed or recorded. The goal of this course is to help participants understand the basic approach of how to write a grant (particularly for NIH) including all of the components of the grant itself and how to approach funding agencies within NIH for advice on process. The course includes didactic lectures, a question and answer session, and a "mock study section" that allows participants to learn about the process of review.

Printed on: 02/07/23



## Abstract Archives of the RSNA, 2022

S1-CBR03

### Reducing Overtreatment of Breast Cancer: Leveraging Insights from Imaging, Population Data, and Radiomics (Supported by an unrestricted educational grant from Hologic)

Sunday, Nov. 27 9:00AM - 10:00AM Room: NA

#### Participants

Marc Ryser, PhD, Durham, NC (*Presenter*) Nothing to Disclose

Lars Grimm, MD, Durham, NC (*Presenter*) Advisor, Hologic, Inc; Consultant, Hologic, Inc; Editorial Advisory Board, WebMD Health Corp (WebMD, Inc)

Despina Kontos, PhD, Philadelphia, PA (*Presenter*) Institutional Research Grant, Hologic, Inc; Institutional Research Grant, iCAD, Inc

#### COURSE DESCRIPTION

In this course, we will review current evidence surrounding early breast cancer diagnosis with a focus on insights from imaging and population data to describe biology and magnitude of overdiagnosis. We will also examine potential ways to decrease overdiagnosis and overtreatment using a combination of active surveillance and radiomics informed by artificial intelligence and mathematical modeling.

#### LEARNING OBJECTIVES

1) Describe imaging features that are associated with DCIS biology and the feasibility of radiology-guided active surveillance approaches 2) Discuss how population data can provide valuable insights on the magnitude of the breast cancer overdiagnosis problem and identification of potential solutions 3) Describe the current data surrounding the potential of radiomics to decrease unnecessary treatment of early breast cancer, including DCIS\*Course Description In this course, we will review current evidence surrounding early breast cancer diagnosis with a focus on insights from imaging and population data to describe biology and magnitude of overdiagnosis. We will also examine potential ways to decrease overdiagnosis and overtreatment using a combination of active surveillance and radiomics informed by artificial intelligence and mathematical modeling.

Printed on: 02/07/23



## Abstract Archives of the RSNA, 2022

S1-CER08

### Pediatric Trauma: A Case-based Session

Sunday, Nov. 27 9:00AM - 10:00AM Room: NA

#### Participants

Summer Kaplan, MD, MS, Philadelphia, PA (*Presenter*) Nothing to Disclose  
Birgit Ertl-Wagner, MD, Toronto, ON (*Presenter*) Spouse, Employee, Siemens AG  
Arnold Merrow JR, MD, Cincinnati, OH (*Presenter*) Consultant, RELX; Author with royalties, RELX  
Sara E. Lay, MD, Fishers, IN (*Presenter*) Nothing to Disclose

#### COURSE DESCRIPTION

This case-based session will highlight important findings of blunt and abusive trauma to the pediatric chest, abdomen, pelvis, and spine. The focus will be on findings that affect patient management, morbidity and mortality. Discussion will cover appropriate imaging strategies and protocols for pediatric trauma patients. Differences in the imaging findings and management of pediatric patients compared to adult patients will also be reviewed.

#### LEARNING OBJECTIVES

1) Become familiar with appropriate imaging work-up and protocols used in pediatric trauma patients 2) Understand how pediatric anatomy and mechanism of injury relate to imaging findings 3) Explain how specific imaging findings impact patient outcome and management\*Course Description This case-based session will highlight important findings of blunt and abusive trauma to the pediatric chest, abdomen, pelvis, and spine. The focus will be on findings that affect patient management, morbidity and mortality. Discussion will cover appropriate imaging strategies and protocols for pediatric trauma patients. Differences in the imaging findings and management of pediatric patients compared to adult patients will also be reviewed.

Printed on: 02/07/23



## Abstract Archives of the RSNA, 2022

S1-CGI02

### Crohn's Disease Imaging

Sunday, Nov. 27 9:00AM - 10:00AM Room: NA

#### Participants

Jonathan Dillman, MD, MSc, Cincinnati, OH (*Presenter*) Research Grant, Perspectum Ltd; Research Grant, Siemens AG; Research Grant, Canon Medical Systems Corporation; Research support, Koninklijke Philips NV; Research support, General Electric Company; Research support, Motilent Ltd

Tracy A. Jaffe, MD, Durham, NC (*Presenter*) Nothing to Disclose

Bari Dane, MD, New York, NY (*Presenter*) Nothing to Disclose

Kristina Flicek, MD, Rochester, MN (*Presenter*) Nothing to Disclose

Sudha A. Anupindi, MD, Philadelphia, PA (*Presenter*) Nothing to Disclose

Mahmoud M. Al-Hawary, MD, Ann Arbor, MI (*Presenter*) Nothing to Disclose

#### COURSE DESCRIPTION

This course will deliver concise updates on specific facets of imaging in Crohn's disease. Speakers will review the clinical applications of multimodality imaging, including US, CT and MRI, and the role of the Radiologist in multidisciplinary care of this complex disease process.

#### LEARNING OBJECTIVES

1) Learn up-to-date imaging techniques and interpretation applications for imaging patients with Crohn's disease 2) Understand the application of these tools in clinical care with an emphasis on the role of the Radiologist in the multidisciplinary management of Crohn's disease\*Course Description This course will deliver concise updates on specific facets of imaging in Crohn's disease. Speakers will review the clinical applications of multimodality imaging, including US, CT and MRI, and the role of the Radiologist in multidisciplinary care of this complex disease process.

Printed on: 02/07/23



## Abstract Archives of the RSNA, 2022

S1-CIN03

### Imaging Interoperability: From Governance to the Nuts and Bolts

Sunday, Nov. 27 9:00AM - 10:00AM Room: NA

#### Participants

Joyce Sensmeier, MS, RN, Chicago, IL (*Presenter*) Nothing to Disclose

Didi Davis, Knoxville, TN (*Presenter*) Nothing to Disclose

David S. Mendelson, MD, Larchmont, NY (*Presenter*) Consultant, General Electric Company; Advisor, Maverick Medical AI Ltd; Spouse, Employee, Novartis AG

Christopher J. Roth, MD, Durham, NC (*Moderator*) Nothing to Disclose

#### LEARNING OBJECTIVES

1) To understand the importance of safe and secure interoperability for patient care 2) To understand the importance of the adoption of standards in establishing interoperable solutions 3) Learn about national and international organizations that foster healthcare interoperability by defining standards and offering testing environments to solution providers: - IHE International -IHE USA - The Sequoia Project, Carequality 4) Learn about Radiology specific interoperability solutions and how those are being adopted by the Radiology Community - The RSNA ImageShare\*Course Description

Printed on: 02/07/23



## Abstract Archives of the RSNA, 2022

S1-CMS04

### Contrast Enhanced Ultrasound (CEUS): A Problem-Solving Tool

Sunday, Nov. 27 9:00AM - 10:00AM Room: NA

#### Participants

David Fetzter, MD, Dallas, TX (*Presenter*) Research support, General Electric Company; Research support, Koninklijke Philips NV; Research support, Siemens AG; Consultant, Koninklijke Philips NV; Advisory Board, Koninklijke Philips NV; Consultant, General Electric Company; Advisory Board, General Electric Company

John Pellerito, MD, Syosset, NY (*Presenter*) Nothing to Disclose

Paul S. Sidhu, MRCP, FRCR, London, United Kingdom (*Presenter*) Consultant, Samsung Electronics Co, Ltd; Speaker, Samsung Electronics Co, Ltd; Speaker, Bracco Group; Consultant, Itreas Ltd; Speaker, Siemens AG

Andrej Lyshchik, MD, PhD, Philadelphia, PA (*Presenter*) Royalties, RELX; Speaker, General Electric Company; Consultant, General Electric Company; Research support, General Electric Company; Consultant, BioClinica, Inc; Consultant, WCC, Inc; Consultant, Bracco Group; Advisory Board, Bracco Group

#### COURSE DESCRIPTION

This case-based course will highlight the vital role of CEUS over a broad range of applications, including abdominal visceral organs, abdominal vessels including management of bleeds and endoleaks, advances in small parts imaging and pre procedural assessment, performance and evaluation of interventional procedures. Techniques of contrast administration will be emphasized as they vary with body part and dynamic imaging. Our goal is to provide a broad update in the field while addressing new opportunities and challenges for everyday practice.

#### LEARNING OBJECTIVES

1) Describe the current clinical applications of CEUS 2) Facilitate identification of strategies to fully integrate CEUS into clinical practice \*Course Description This case-based course will highlight the vital role of CEUS over a broad range of applications, including abdominal visceral organs, abdominal vessels including management of bleeds and endoleaks, advances in small parts imaging and pre procedural assessment, performance and evaluation of interventional procedures. Techniques of contrast administration will be emphasized as they vary with body part and dynamic imaging. Our goal is to provide a broad update in the field while addressing new opportunities and challenges for everyday practice.

Printed on: 02/07/23



## Abstract Archives of the RSNA, 2022

S1-CNMMI06

### Prostate Cancer Theranostics

Sunday, Nov. 27 9:00AM - 10:00AM Room: NA

#### Participants

Lilja Solnes, MD, Owings Mills, MD (*Presenter*) Consultant, Lantheus Holdings; Research funded, Novartis AG; Research funded, Precision Molecular Inc; Research funded, Celectar Biosciences, Inc; Royalties, RELX  
Katherine Zukotynski, MD, PhD, Hamilton, ON (*Presenter*) Research Consultant, Konica Minolta, Inc; Research Consultant, General Electric Company; Speakers Bureau, Jubilant DraxImage Inc  
Carina Mari Aparici, MD, San Francisco, CA (*Presenter*) Nothing to Disclose

#### COURSE DESCRIPTION

Please join our educational session on theranostics, where we will address the present, past and future of molecular targeted radioligand therapy in patients diagnosed with prostate cancer. Indications, patient preparation, toxicities and compliance with the therapy will be few of the aspects that will be reviewed by our two excellent presenters.

#### LEARNING OBJECTIVES

At the end of the session, the audience will be able to: 1) Identify when is the optimal time for referral of patients to the theranostics clinic for Lu177-PSMA therapy 2) Learn the toxicity rate observed with Lu177-PSMA 3) Assess when the right time is for dose reduction based on toxicities\*Course Description Please join our educational session on theranostics, where we will address the present, past and future of molecular targeted radioligand therapy in patients diagnosed with prostate cancer. Indications, patient preparation, toxicities and compliance with the therapy will be few of the aspects that will be reviewed by our two excellent presenters.

Printed on: 02/07/23



## Abstract Archives of the RSNA, 2022

S1-CNPM06

### Clinical Trials Methodology Workshop Spotlight (Sponsored by the RSNA Research Development Committee)

Sunday, Nov. 27 9:00AM - 10:00AM Room: NA

#### Participants

Efren J. Flores, MD, Boston, MA (*Presenter*) Speaker, WebMD LLC; Speaker, Consulting Medical Associates, Inc  
Miriam Peckham, MD, Salt Lake City, UT (*Presenter*) Nothing to Disclose  
Chaya Moskowitz, PhD, New York, NY (*Presenter*) Nothing to Disclose  
Jeffrey Jarvik, MD, MPH, Seattle, WA (*Presenter*) Royalties, Mannheim Media; Co-editor, Mannheim Media; Travel support, General Electric Company; Author with royalties, Wolters Kluwer nv  
Michael Soulen, MD, Lafayette Hill, PA (*Presenter*) Consultant, F. Hoffmann-La Roche Ltd; Consultant, Guerbet SA; Consultant, AstraZeneca PLC; Research support, Guerbet SA; Research support, Sirtex Medical Ltd; Research support, Pfizer Inc

#### COURSE DESCRIPTION

RSNA's Clinical Trials Methodology Workshop (CTMW) has provided first-class education in clinical trials methodology and has greatly expanded interest and successful efforts in radiology and radiation oncology clinical research. While previously available exclusively to those accepted to the in-person CTMW, this course will make accessible to all RSNA annual meeting attendees the rigor and expertise of the CTMW in a lecture course format. We will spotlight two important radiology clinical trials from alumni of the CTMW. Each clinical trialist will present an overview of their trial, followed by methodological lessons learned by a CTMW course director and biostatistician. The session will conclude with Q&A from the audience. The CTMW faculty have considerable expertise in study design, conduct, and analysis. As expert discussants, they will utilize content developed from the CTMW curriculum to present focused examples of the strengths and limitations of the clinical trials under our spotlight.

#### LEARNING OBJECTIVES

1) Review important aspects of clinical trial design and conduct through presentations by original principal investigators (PIs) of successful trials initially "workshopped" at the RSNA Clinical Trials Methodology Workshop (CTMW). 2) Learn key biostatistical lessons regarding trial design and data analysis directly from CTMW biostatisticians using the trials presented by the PIs\*  
Course Description RSNA's Clinical Trials Methodology Workshop (CTMW) has provided first-class education in clinical trials methodology and has greatly expanded interest and successful efforts in radiology and radiation oncology clinical research. While previously available exclusively to those accepted to the in-person CTMW, this course will make accessible to all RSNA annual meeting attendees the rigor and expertise of the CTMW in a lecture course format. We will spotlight two important radiology clinical trials from alumni of the CTMW. Each clinical trialist will present an overview of their trial, followed by methodological lessons learned by a CTMW course director and biostatistician. The session will conclude with Q&A from the audience. The CTMW faculty have considerable expertise in study design, conduct, and analysis. As expert discussants, they will utilize content developed from the CTMW curriculum to present focused examples of the strengths and limitations of the clinical trials under our spotlight.

Printed on: 02/07/23



## Abstract Archives of the RSNA, 2022

S1-CNR09

### Advanced (But Not So New) MRI Techniques (Perfusion, Spectroscopy, DTI, fMRI): What Is the Role in Clinical Practice in 2022?

Sunday, Nov. 27 9:00AM - 10:00AM Room: NA

#### Participants

Eva-Maria Ratai, Charlestown, MA (*Presenter*) Nothing to Disclose  
Jody L. Tanabe, MD, Aurora, CO (*Presenter*) Nothing to Disclose  
Haris Sair, MD, Baltimore, MD (*Presenter*) Research Grant, Siemens AG  
Pamela W. Schaefer, MD, Boston, MA (*Moderator*) Nothing to Disclose

#### COURSE DESCRIPTION

This course will address the basic physics behind and CNS clinical applications of perfusion imaging, diffusion tensor imaging, functional magnetic resonance imaging and spectroscopy. It is important that radiologists keep informed of new applications of these advanced imaging techniques. Attendees will have an improved understanding of the clinical utility of these four techniques and will be able to implement them in their individual practice settings. This course will include four lectures with time for questions.

#### LEARNING OBJECTIVES

1) Explain the current clinical applications of perfusion imaging in Neuroradiology, 2) Explain the current clinical applications of spectroscopy in Neuroradiology, 3) Explain the current clinical applications of fMRI in Neuroradiology, 4) Explain the current clinical applications of DTI in Neuroradiology\*Course Description This course will address the basic physics behind and CNS clinical applications of perfusion imaging, diffusion tensor imaging, functional magnetic resonance imaging and spectroscopy. It is important that radiologists keep informed of new applications of these advanced imaging techniques. Attendees will have an improved understanding of the clinical utility of these four techniques and will be able to implement them in their individual practice settings. This course will include four lectures with time for questions.

Printed on: 02/07/23



## Abstract Archives of the RSNA, 2022

S1-COB07

### Placenta Accreta Spectrum: Tips and Tricks for Best Diagnosis

Sunday, Nov. 27 9:00AM - 10:00AM Room: NA

#### Participants

Catherine Spong, MD, Dallas, TX (*Presenter*) Nothing to Disclose  
Diane M. Twickler, MD, Dallas, TX (*Presenter*) Nothing to Disclose

#### COURSE DESCRIPTION

Caring for the patient with placenta accreta spectrum necessitates an understanding on how prior ob/gyn procedures, gestational age at diagnosis, and ultrasound and MR imaging findings affect prognosis of the current pregnancy and future reproductive outcomes. Pre-partum diagnosis is key for appropriate management delivery and improves obstetric outcome. Specialists in obstetrics, MR placental diagnosis and ultrasound obstetric imaging will share their expertise in clinical care and imaging diagnosis to aid body imagers (as well as US and MR specialists) in their care of patients with placenta accreta spectrum.

#### LEARNING OBJECTIVES

1) Understand risk factors for placenta accreta spectrum 2) Incorporate information from a perinatologist specialist on placenta accreta spectrum -- what the clinician needs to know from our imaging reports 3) Illustrate findings of placenta accreta, increta, and percreta on ultrasound and MRI including evaluation of the bladder serosal interface and first trimester evaluation of the implantation as it relates to the cesarean scar with pearls and pitfalls of imaging diagnosis 4) Discuss how the integration of obstetric/gynecologic surgical history, imaging findings, and gestational age affect counseling of patients, need for follow-up imaging, and timing of delivery\*Course Description Caring for the patient with placenta accreta spectrum necessitates an understanding on how prior ob/gyn procedures, gestational age at diagnosis, and ultrasound and MR imaging findings affect prognosis of the current pregnancy and future reproductive outcomes. Pre-partum diagnosis is key for appropriate management delivery and improves obstetric outcome. Specialists in obstetrics, MR placental diagnosis and ultrasound obstetric imaging will share their expertise in clinical care and imaging diagnosis to aid body imagers (as well as US and MR specialists) in their care of patients with placenta accreta spectrum.

Printed on: 02/07/23



## Abstract Archives of the RSNA, 2022

S1-CPH14

### Photon Counting

Sunday, Nov. 27 9:00AM - 10:00AM Room: NA

#### Participants

Shuai Leng, PHD, Rochester, MN (*Presenter*) License agreement, Siemens AG  
Ke Li, PhD, Madison, WI (*Presenter*) Research Consultant, Pulmera Inc.

#### COURSE DESCRIPTION

Photon counting detector (PCD) has been an active research area in recent years. Commercial PCD-CT has been available for routine clinical use since FDA cleared the first PCD-CT in late 2021, which represents a major imaging device advancement for CT. In this lecture, we will discuss fundamental principles of PCD and explain major benefits of this technology relative to energy integrating detector which are used on most commercial CT scanners. History and current status of PCD-CT will also be discussed. Potential clinical applications will be demonstrated using sample phantom and patient images. Challenges and opportunities will also be discussed.

#### LEARNING OBJECTIVES

1. Understand principles of photon counting detector
2. Explain benefits of photon counting detector CT
3. Identify potential clinical applications of photon counting detector CT

\*Course Description Photon counting detector (PCD) has been an active research area in recent years. Commercial PCD-CT has been available for routine clinical use since FDA cleared the first PCD-CT in late 2021, which represents a major imaging device advancement for CT. In this lecture, we will discuss fundamental principles of PCD and explain major benefits of this technology relative to energy integrating detector which are used on most commercial CT scanners. History and current status of PCD-CT will also be discussed. Potential clinical applications will be demonstrated using sample phantom and patient images. Challenges and opportunities will also be discussed.

Printed on: 02/07/23



## Abstract Archives of the RSNA, 2022

S1-CVA04

### Vasculitides: Imaging Findings and Complications

Sunday, Nov. 27 9:00AM - 10:00AM Room: NA

#### Participants

Constantine Raptis, MD, Saint Louis, MO (*Presenter*) Nothing to Disclose

Linda C. Chu, MD, Lutherville, MD (*Presenter*) Nothing to Disclose

Anil Pillai, MD, Dallas, TX (*Presenter*) Nothing to Disclose

#### COURSE DESCRIPTION

Vasculitides are diseases that involve inflammation of the blood vessel walls. Broadly, these can be divided into infectious vasculitides, in which a pathogen directly invades vessel walls, and non-infectious vasculitides, which are not caused by an infectious pathogen. Non-infectious vasculitides are further subdivided by the vessel size most commonly affected and whether they are associated with another disease or etiology. Patients with vasculitides have a wide range of presenting symptoms and can be encountered in outpatient, inpatient, or emergency settings. Furthermore, because the clinical signs and symptoms overlap with other diseases, they are often difficult to diagnose. A multidisciplinary approach in which imaging findings play a critical role is needed for diagnosis, follow-up, and management. As such, radiologists must be familiar with these conditions, their imaging features, and the features of potential complications. In this case-based didactic review, important considerations related to vasculitides that are applicable to radiologists in any practice setting will be presented in order to improve the care of this important patient group.

#### LEARNING OBJECTIVES

1) Review the diagnostic imaging findings of vasculitides 2) Discuss how these findings can be useful in developing differential diagnoses 3) Identify imaging findings that have implications for patient management and prognosis\*Course Description Vasculitides are diseases that involve inflammation of the blood vessel walls. Broadly, these can be divided into infectious vasculitides, in which a pathogen directly invades vessel walls, and non-infectious vasculitides, which are not caused by an infectious pathogen. Non-infectious vasculitides are further subdivided by the vessel size most commonly affected and whether they are associated with another disease or etiology. Patients with vasculitides have a wide range of presenting symptoms and can be encountered in outpatient, inpatient, or emergency settings. Furthermore, because the clinical signs and symptoms overlap with other diseases, they are often difficult to diagnose. A multidisciplinary approach in which imaging findings play a critical role is needed for diagnosis, follow-up, and management. As such, radiologists must be familiar with these conditions, their imaging features, and the features of potential complications. In this case-based didactic review, important considerations related to vasculitides that are applicable to radiologists in any practice setting will be presented in order to improve the care of this important patient group.

Printed on: 02/07/23



## Abstract Archives of the RSNA, 2022

S1-RCP21

### 100th Anniversary of RADIOLOGY: Highlight of Landmark Articles from Our Flagship Journal

Sunday, Nov. 27 9:00AM - 10:00AM Room: NA

#### Participants

Linda Moy, MD, New York, NY (*Presenter*) Grant, Siemens AG ;Advisory Board, Lunit Inc;Advisory Board, iCad, Inc  
Philippe C. Douek, MD, PhD, Lyon, France (*Presenter*) Grant, Koninklijke Philips NV  
Elliot Fishman, MD, Owings Mills, MD (*Presenter*) Co-founder, HipGraphics, Inc;Stockholder, HipGraphics, Inc;Institutional Grant support, Siemens AG;Institutional Grant support, General Electric Company;Consultant, Exact Sciences Corporation;Consultant, Imaging Endpoints  
Christopher Hess, MD, PhD, San Francisco, CA (*Presenter*) Consultant, General Electric Company Consultant, Siemens AG DSMB, Focused Ultrasound Foundation DSMB, uniQure Biopharma DSMB, Asklepios BioPharmaceutical  
David Bluemke, MD, PhD, Madison, WI (*Moderator*) Nothing to Disclose

#### COURSE DESCRIPTION

The journal RADIOLOGY has been published for 100 years and is the leading scientific journal in imaging. As we celebrate this anniversary accomplishment, this session looks back at key publications published in the journal that have shaped the practice of radiology, with emphasis on CT and MRI. Looking forward, this session will review dramatic changes expected to occur with the development of photon counting CT and artificial intelligence. Recent and key publications that have set the stage for the century going forward will be reviewed.

#### LEARNING OBJECTIVES

Identify key studies published in the journal Radiology that have influenced the field and that have established the role of imaging studies throughout the field of medicine.\*Course Description The journal RADIOLOGY has been published for 100 years and is the leading scientific journal in imaging. As we celebrate this anniversary accomplishment, this session looks back at key publications published in the journal that have shaped the practice of radiology, with emphasis on CT and MRI. Looking forward, this session will review dramatic changes expected to occur with the development of photon counting CT and artificial intelligence. Recent and key publications that have set the stage for the century going forward will be reviewed.

Printed on: 02/07/23



## Abstract Archives of the RSNA, 2022

S1-RCP32

### Translational AI Science: Bringing Advances in Deep Learning into Clinical Practice

Sunday, Nov. 27 9:00AM - 10:00AM Room: NA

#### Participants

Mariam Aboian, MD, PhD, New Haven, CT (*Presenter*) Researcher, Blue Earth Diagnostics Ltd; Researcher, Fusion Pharmaceuticals; Research collaboration, Pro Medicus Limited  
Spyridon Bakas, PhD, Philadelphia, PA (*Presenter*) Nothing to Disclose  
Marius Linguraru, DPhil, MSc, Washington, DC (*Presenter*) Co-founder, PediaMetric Inc  
Charles Kahn JR, MD, MS, Philadelphia, PA (*Moderator*) Nothing to Disclose

#### COURSE DESCRIPTION

Researchers have developed medical imaging AI systems and evaluated AI systems in clinical practice. A gap exists in the translation of imaging AI's scientific advances to allow them to be realized in clinical practice. This course will address the ways that radiologists and radiation oncologists can work with AI researchers to accelerate and improve the translation of AI systems into clinical practice. The panel of expert physicians and AI scientists will give brief presentations and engage in interactive discussion on: (1) image-based AI applications such as segmentation, diagnosis, and treatment response prediction; (2) AI techniques to reduce imaging time, radiation dose, and noise; (3) Treatment planning; and (4) natural language processing.

#### LEARNING OBJECTIVES

1) Define the goals and specific challenges of translational research in imaging AI. 2) Describe the current state of translational imaging AI research and highlight recent advances. 3) Identify opportunities for radiologists to work with imaging AI scientists. 4) Describe learning resources to help radiologists contribute to translational AI research.\*Course Description Researchers have developed medical imaging AI systems and evaluated AI systems in clinical practice. A gap exists in the translation of imaging AI's scientific advances to allow them to be realized in clinical practice. This course will address the ways that radiologists and radiation oncologists can work with AI researchers to accelerate and improve the translation of AI systems into clinical practice. The panel of expert physicians and AI scientists will give brief presentations and engage in interactive discussion on: (1) image-based AI applications such as segmentation, diagnosis, and treatment response prediction; (2) AI techniques to reduce imaging time, radiation dose, and noise; (3) Treatment planning; and (4) natural language processing.

Printed on: 02/07/23



## Abstract Archives of the RSNA, 2022

S2-CCA07

### Efficient and Focused Cardiac MRI

Sunday, Nov. 27 10:30AM - 11:30AM Room: NA

#### Participants

Tim Leiner, MD, PhD, Rochester, MN (*Presenter*) Research support, Pie Medical Imaging BV; Advisory Board, Cart-Tech BV; Advisory Board, AI4MedImaging; Advisor, Quantib BV; Consultant, Guerbet SA

Jens Bremerich, MD, Basel, (*Presenter*) Nothing to Disclose

Jeremy D. Collins, MD, Rochester, MN (*Moderator*) Nothing to Disclose

Printed on: 02/07/23



## Abstract Archives of the RSNA, 2022

S2-CCH11

### Thoracic Malignancy II: Beyond Non-small Cell Lung Cancer

Sunday, Nov. 27 10:30AM - 11:30AM Room: NA

#### Participants

Kristopher W. Cummings, MD, Phoenix, AZ (*Presenter*) Nothing to Disclose

Edith Marom, MD, Tel Aviv, Israel (*Presenter*) Speaker, Boehringer Ingelheim GmbH; Speaker, Merck & Co, Inc; Speaker, AstraZeneca PLC

Chad D. Strange, MD, Seabrook, TX (*Presenter*) Nothing to Disclose

John Lichtenberger III, MD, Washington, DC (*Presenter*) Nothing to Disclose

Michelle S. Ginsberg, MD, New York, NY (*Moderator*) Speaker, Ultimate Opinions In Medicine LLC

#### COURSE DESCRIPTION

This didactic session will focus on the important diagnostic imaging findings of and management implications for neuroendocrine malignancies, mesothelioma, thymoma and other thoracic neoplasms less commonly encountered in clinical practice. After attending this session, the learner will be able to more accurately diagnosis these non-small cell thoracic malignancies and provide crucial imaging information which will impact patient care.

#### LEARNING OBJECTIVES

1) Describe and differentiate the typical imaging manifestations of the various neuroendocrine malignancies 2) List key imaging findings that affect management and staging of mesothelioma and thymoma\*Course Description This didactic session will focus on the important diagnostic imaging findings of and management implications for neuroendocrine malignancies, mesothelioma, thymoma and other thoracic neoplasms less commonly encountered in clinical practice. After attending this session, the learner will be able to more accurately diagnosis these non-small cell thoracic malignancies and provide crucial imaging information which will impact patient care.

Printed on: 02/07/23



## Abstract Archives of the RSNA, 2022

S2-CIN09

### The Business of Medical Imaging AI

Sunday, Nov. 27 10:30AM - 11:30AM Room: NA

#### Participants

Andrew Smith, MD, PhD, Birmingham, AL (*Presenter*) Owner, AI Metrics LLC; Chairman, AI Metrics LLC; Officer, AI Metrics LLC; Patent agreement, AI Metrics LLC; Owner, Radiostics LLC; CEO, Radiostics LLC; Speaker, Canon Medical Systems Corporation; Patent holder, AI and Image Processing Algorithms

Peter Chang, MD, Irvine, CA (*Presenter*) Co-founder, Avicenna.ai; Stockholder, Avicenna.ai; Research Grant, Canon Medical Systems Corporation; Speakers Bureau, Canon Medical Systems Corporation; Research Grant, General Electric Company

John V. Crues III, MD, Los Angeles, CA (*Presenter*) Board Member, Turner Imaging Systems ; Medical Director, RadNet, Inc ;

Hari Trivedi, MD, Atlanta, GA (*Moderator*) Founder, Lightbox AI ; Consultant, Sirona Medical, Inc ; Consultant, Flatiron Health ; Consultant, PMX Inc ; Research support, Kheiron Medical Technologies ; Research support, Clairity, Inc ; Research support, Nightingale Open Science ;

#### COURSE DESCRIPTION

This session will comprise of a short presentation followed by a panel discussion from academic, private, and industry thought leaders regarding the barriers and drivers of real-world radiology AI adoption. As radiology AI models mature, there is no shortage of commercial models that achieve human or super-human performance. However, overall adoption in clinical practice remains low. We will explore the business side of AI adoption and factors to consider whether you are an AI creator or consumer.

#### LEARNING OBJECTIVES

1) Identify dominant business use cases for radiology AI 2) Explore drivers and barriers to adoption of AI 3) Understand financial considerations that contribute to medical AI adoption \*Course Description This session will comprise of a short presentation followed by a panel discussion from academic, private, and industry thought leaders regarding the barriers and drivers of real-world radiology AI adoption. As radiology AI models mature, there is no shortage of commercial models that achieve human or super-human performance. However, overall adoption in clinical practice remains low. We will explore the business side of AI adoption and factors to consider whether you are an AI creator or consumer.

Printed on: 02/07/23



## Abstract Archives of the RSNA, 2022

S2-CIN14

### Patients and Providers Talk: Radiology Informaticists Listen

Sunday, Nov. 27 10:30AM - 11:30AM Room: NA

#### Participants

Tessa S. Cook, MD, PhD, Philadelphia, PA (*Presenter*) Grant, Siemens AG; Grant, Independence Blue Cross; Speaker, Sectra AB  
Gelareh Sadigh, MD, Irvine, GA (*Presenter*) Research Grant, TailorMed Medical Ltd  
Nina S. Vincoff, MD, New York, NY (*Presenter*) Nothing to Disclose  
Jennifer Kemp, MD, Denver, CO (*Presenter*) Stockholder, Scanslated, Inc

#### COURSE DESCRIPTION

This course will center on patient preferences regarding patient portals, radiology reports, price transparency, and quality in radiology. Each speaker will give a short talk that addresses patients comments with examples of implementation and success measurement. The 21st Century Cures Act unique challenges and opportunities will also be discussed.

#### LEARNING OBJECTIVES

1) Identify methods to continue to optimize patient portal usage and function while addressing new challenges brought on by 21st Century CURES Act 2) Understand patient desires when viewing their radiology report with methods to address report comprehension and patient engagement 3) Give examples of price transparency initiatives and describe implementation and outcome measurement 4) Describe unique role of radiologists in alleviating some of the unforeseen consequences of 21st Century Cures act on referring clinician workload while still embracing health record transparency\*Course Description This course will center on patient preferences regarding patient portals, radiology reports, price transparency, and quality in radiology. Each speaker will give a short talk that addresses patients comments with examples of implementation and success measurement. The 21st Century Cures Act unique challenges and opportunities will also be discussed.

Printed on: 02/07/23



## Abstract Archives of the RSNA, 2022

S2-CIR09

### Liver Cancer Interventions

Sunday, Nov. 27 10:30AM - 11:30AM Room: NA

#### Participants

Jens Ricke, MD, PhD, Berlin, Germany (*Presenter*) Research Grant, Sirtex Medical Ltd; Research Grant, Bayer AG; Research Grant, Terumo Corporation; Research Grant, Boston Scientific Corporation

Parissa Tabrizian, New York, NY (*Presenter*) Research Consultant, Boston Scientific Corporation; Research Consultant, Bayer AG; Research Consultant, AstraZeneca PLC

Riad Salem, MD, MBA, Chicago, IL (*Presenter*) Consultant, Boston Scientific Corporation; Consultant, Eisai Co, Ltd; Consultant, Sirtex Medical Ltd; Consultant, Cook Group Incorporated; Consultant, Siemens AG

Gregory J. Nadolski II, MD, Fort Washington, PA (*Presenter*) Research Grant, Sirtex Medical Ltd; Research Grant, Instylla, Inc

Irene Bargellini, MD, Viareggio, Italy (*Presenter*) Consulting fees from: AstraZeneca, Eisai, Ge Healthcare, Guerbet, Merck, Sirtex, Terumo Lecture fees from: AstraZeneca, Bayer, Boston Scientific, Eisai, Guerbet, Merck, Sirtex, Sobi, Terumo Institutional research grant from: Boston Scientific Serves on Independent Data Safety Monitoring Board for: AstraZeneca

#### COURSE DESCRIPTION

This is a course that reviews contemporary surgical, locoregional and systemic options for HCC.

#### LEARNING OBJECTIVES

1) To learn about indications for locoregional and surgical approaches for HCC, 2-to learn about systemic therapy for HCC\*Course Description This is a course that reviews contemporary surgical, locoregional and systemic options for HCC.

Printed on: 02/07/23



## Abstract Archives of the RSNA, 2022

S2-CMK08

### Hip Pre-op and Post-op: Impingements and Other Hot Topics

Sunday, Nov. 27 10:30AM - 11:30AM Room: NA

#### Participants

Philip Robinson, MBChB, Leeds, United Kingdom (*Presenter*) Advisory Board, Pfizer Inc; Advisory Board, General Electric Company;  
Donna Blankenbaker, MD, Fitchburg, WI (*Presenter*) Nothing to Disclose  
Reto Sutter, MD, Zurich, (*Presenter*) Nothing to Disclose  
Eric A. Bogner, MD, Boca Raton, FL (*Presenter*) Research Consultant, Globus Medical, Inc  
Guillaume Bierry, MD, PhD, Strasbourg, France (*Presenter*) Consultant, Koninklijke Philips NV; Consultant, Bracco Group

#### COURSE DESCRIPTION

This session covers several important topics in hip imaging: pathomechanisms and imaging features of femoroacetabular impingement, extraarticular impingement as well as groin pain are discussed. In addition, imaging pearls for pre- and postoperative imaging of hip preservation surgery and total hip arthroplasty are presented.

#### LEARNING OBJECTIVES

1) Explain the mechanism and imaging features of extraarticular impingement 2) Describe the current controversies concerning FAI and differentiate injury patterns in core muscle injury 3) Recognize imaging features in the post-operative hip\*Course Description  
This session covers several important topics in hip imaging: pathomechanisms and imaging features of femoroacetabular impingement, extraarticular impingement as well as groin pain are discussed. In addition, imaging pearls for pre- and postoperative imaging of hip preservation surgery and total hip arthroplasty are presented.

Printed on: 02/07/23



## Abstract Archives of the RSNA, 2022

S2-CMS07

### Pitfalls and Mimics in Oncologic Imaging

Sunday, Nov. 27 10:30AM - 11:30AM Room: NA

#### Participants

John Heymann, MD, Galveston, TX (*Presenter*) Nothing to Disclose  
Cristina Fuss, MD, Portland, OR (*Presenter*) Nothing to Disclose  
Maria Zulfiqar, MD, Saint Louis, MO (*Presenter*) Nothing to Disclose  
Khaled M. Elsayes, MD, Houston, TX (*Presenter*) Nothing to Disclose

#### COURSE DESCRIPTION

The purpose of this course is to illustrate the various pitfalls, mimics, and atypical features that can lead to inaccurate diagnosis in cancer patients. The content includes relevant pathogenesis and background as well as specific clues that can be used to reach an accurate diagnosis. It is important to avoid pitfalls and misdiagnoses that can alter the management plan. Helpful strategies for avoiding pitfalls include paying close attention to the clinical history of the patient, carefully evaluating all of the available imaging studies, and being aware of the various radiologic mimics.

#### LEARNING OBJECTIVES

1) Identify various pitfalls in Oncological imaging that can lead to erroneous diagnoses 2) Describe relevant technical background, pathophysiology and hemodynamics of these pitfall 3) Be familiar with various clues to reach a specific diagnosis\*Course Description  
The purpose of this course is to illustrate the various pitfalls, mimics, and atypical features that can lead to inaccurate diagnosis in cancer patients. The content includes relevant pathogenesis and background as well as specific clues that can be used to reach an accurate diagnosis. It is important to avoid pitfalls and misdiagnoses that can alter the management plan. Helpful strategies for avoiding pitfalls include paying close attention to the clinical history of the patient, carefully evaluating all of the available imaging studies, and being aware of the various radiologic mimics.

Printed on: 02/07/23



## Abstract Archives of the RSNA, 2022

S2-CNPM01

### Professional Disruptions in the Workplace

Sunday, Nov. 27 10:30AM - 11:30AM Room: NA

#### Participants

Jessica Leschied, MD, Detroit, MI (*Presenter*) Nothing to Disclose

Marika Pitot, MD, Rochester, MN (*Presenter*) Nothing to Disclose

Vikas Gulani, MD, PhD, Ann Arbor, MI (*Presenter*) Research support, Siemens AG; Consulting, Cook Group Incorporated

Jessica Robbins, MD, Madison, WI (*Moderator*) Nothing to Disclose

#### COURSE DESCRIPTION

Unprofessional and disruptive behavior in the radiology workplace can be on the spectrum of overt to insidious. In this course, we will explore microaggressions, sexual harassment, professionalism transgressions, and disruptive behaviors due to mental illness. We will discuss how these behaviors may manifest themselves and provide examples of mitigation strategies.

#### LEARNING OBJECTIVES

1) Recognize the manifestations of professional disruptions in the workplace 2. Identify mitigation strategies for professional disruptions in the workplace\*Course Description Unprofessional and disruptive behavior in the radiology workplace can be on the spectrum of overt to insidious. In this course, we will explore microaggressions, sexual harassment, professionalism transgressions, and disruptive behaviors due to mental illness. We will discuss how these behaviors may manifest themselves and provide examples of mitigation strategies.

Printed on: 02/07/23



## Abstract Archives of the RSNA, 2022

S2-CPD01

### Pediatric Neuroradiology

Sunday, Nov. 27 10:30AM - 11:30AM Room: NA

#### Participants

David M. Mirsky, MD, Aurora, CO (*Presenter*) Nothing to Disclose  
Carolina Guimaraes, MD, Woodside, CA (*Presenter*) Nothing to Disclose  
Suzanne Laughlin, MD, Etobicoke, ON (*Presenter*) Nothing to Disclose

#### COURSE DESCRIPTION

This action-packed overview of Pediatric Neuroradiology in the Emergency Department setting will breakdown the ABCs of demyelinating diseases (MS, NMO, and MOG, oh my!), shine a light on all of the hypo- and hyperdensities of emergent head CT imaging, and provide a 'who's who' of the 2021 pediatric brain tumor classification. The format will be didactic lectures and the expected outcome will be enlightenment!

#### LEARNING OBJECTIVES

1. Differentiate imaging features of MOG antibody-associated disease, AQP4 antibody NMOSD, and MS according to brain, optic nerve, and spinal cord MRI findings.
2. Become familiar with the common findings on emergency head CT in the pediatric population.
3. Understand some of the major updates within the 2021 WHO classification of pediatric brain tumors.

\*Course Description This action-packed overview of Pediatric Neuroradiology in the Emergency Department setting will breakdown the ABCs of demyelinating diseases (MS, NMO, and MOG, oh my!), shine a light on all of the hypo- and hyperdensities of emergent head CT imaging, and provide a 'who's who' of the 2021 pediatric brain tumor classification. The format will be didactic lectures and the expected outcome will be enlightenment!

Printed on: 02/07/23



## Abstract Archives of the RSNA, 2022

S2-RCP24

### The URM Trainee Experience - Resident, Fellow and Medical Student Perspective (Sponsored by the RSNA Committee on Diversity, Equity & Inclusion)

Sunday, Nov. 27 10:30AM - 11:30AM Room: NA

#### Participants

Lucy Spalluto, MD,MPH, Nashville, TN (*Presenter*) Nothing to Disclose  
Amy Garvey, MD, Atlanta, GA (*Presenter*) Nothing to Disclose  
Jordan Fenner, MD, Hurdle Mills, NC (*Presenter*) Nothing to Disclose  
Efren J. Flores, MD, Boston, MA (*Presenter*) Speaker, WebMD LLC; Speaker, Consulting Medical Associates, Inc  
Melissa Davis, MD, MBA, Atlanta, GA (*Presenter*) Nothing to Disclose  
Chidubem Ugwueze, MD, New York, NY (*Presenter*) Nothing to Disclose  
Farouk Dako, MD,MPH, Philadelphia, PA (*Presenter*) Nothing to Disclose  
Geraldine McGinty, MD, MBA, New York, NY (*Presenter*) Board Member, NextGen Healthcare ; Stockholder, NextGen Healthcare  
Daryl Goldman, MD, New York, NY (*Moderator*) Nothing to Disclose  
Maureen Kohi, MD, Chapel Hill, NC (*Moderator*) Nothing to Disclose

#### COURSE DESCRIPTION

The purpose of this educational session is to provide trainees an opportunity to discuss experiences of unconscious bias, microaggression, and harassment in training and learn strategies to manage these situations, and cope with and overcome such experiences. This session will begin with a brief review of the concepts of unconscious bias, microaggression, and harassment followed by an in-depth discussion on these topics including first-hand experiences from trainees. The second part of the session will include an overview of different toolkits and strategies to manage these situations, including specific scenario examples. After a brief introduction, the educational format will include trainees and faculty discussion of personal experiences and additional faculty and trainee panel discussion. The course will conclude with an opportunity for open audience discussion.

#### LEARNING OBJECTIVES

1) Learn strategies to manage situations of unconscious bias, microaggression, and harassment as a trainee 2) Learn strategies to cope with and overcome experiences of unconscious bias, microaggression, and harassment while in training 3) Identify ways to help support trainees who have experienced unconscious bias, microaggression, and harassment\*Course Description The purpose of this educational session is to provide trainees an opportunity to discuss experiences of unconscious bias, microaggression, and harassment in training and learn strategies to manage these situations, and cope with and overcome such experiences. This session will begin with a brief review of the concepts of unconscious bias, microaggression, and harassment followed by an in-depth discussion on these topics including first-hand experiences from trainees. The second part of the session will include an overview of different toolkits and strategies to manage these situations, including specific scenario examples. After a brief introduction, the educational format will include trainees and faculty discussion of personal experiences and additional faculty and trainee panel discussion. The course will conclude with an opportunity for open audience discussion.

Printed on: 02/07/23



## Abstract Archives of the RSNA, 2022

S4-CBR10

### Factors Influencing Breast Risk

Sunday, Nov. 27 1:00PM - 2:00PM Room: NA

#### Participants

Jennifer A. Harvey, MD, Rochester, NY (*Presenter*) Stockholder, Volpara Health Technologies Limited; Research Consultant, Besins Healthcare SA; Advisory Board, Sharepoint Medical  
Christiane Kuhl, MD, PhD, Bonn, Germany (*Presenter*) Advisory Board, Guerbet SA; Speaker, Bracco Group; Speaker, Bayer AG  
Wendie A. Berg, MD, PhD, Gibsonia, PA (*Presenter*) Institutional Research Grant, Koios Medical, Inc

#### COURSE DESCRIPTION

Mammographic screening is proven to reduce deaths due to breast cancer, but not all women benefit equally. This session will detail how to assess risk and which women may benefit from supplemental screening in addition to (or even instead of) mammography. The superior performance of MRI will be detailed, but not every woman can have screening MRI. Ultrasound is an alternative when MRI is indicated but cannot be performed. At the conclusion of this session, participants will be knowledgeable of tailored screening approaches and appropriate implementation in practice.

#### LEARNING OBJECTIVES

1) Understand the influence of breast density, family history, biopsy history, and genetic factors on personal risk assessment and interval cancer rate, and how the use of AI may impact our metrics 2) Describe indications for screening MRI and expected outcomes 3) Describe indications for screening US and expected outcomes\*Course Description Mammographic screening is proven to reduce deaths due to breast cancer, but not all women benefit equally. This session will detail how to assess risk and which women may benefit from supplemental screening in addition to (or even instead of) mammography. The superior performance of MRI will be detailed, but not every woman can have screening MRI. Ultrasound is an alternative when MRI is indicated but cannot be performed. At the conclusion of this session, participants will be knowledgeable of tailored screening approaches and appropriate implementation in practice.

Printed on: 02/07/23



## Abstract Archives of the RSNA, 2022

S4-CER15

### Non-traumatic Musculoskeletal Emergencies

Sunday, Nov. 27 1:00PM - 2:00PM Room: NA

#### Participants

Corrie M. Yablon, MD, Ann Arbor, MI (*Presenter*) Nothing to Disclose  
Behrang Amini, MD, PhD, Houston, TX (*Presenter*) Nothing to Disclose  
Susanna C. Spence, MD, Houston, TX (*Presenter*) Nothing to Disclose

#### COURSE DESCRIPTION

Challenging cases of nontraumatic musculoskeletal emergencies will be reviewed in this session, with emphasis on difficult diagnoses that change patient management, including whether osteomyelitis is present (or not), whether a fracture is truly concerning for a pathologic fracture or an impending fracture is present, as well as review of complications of arthroplasties in which imaging is key to directing patient management.

#### LEARNING OBJECTIVES

1) Identify key features that differentiate osteomyelitis from other conditions 2) Identify and classify findings suspicious for pathologic fracture 3) Identify key arthroplasty complications that present emergently\*Course Description Challenging cases of nontraumatic musculoskeletal emergencies will be reviewed in this session, with emphasis on difficult diagnoses that change patient management, including whether osteomyelitis is present (or not), whether a fracture is truly concerning for a pathologic fracture or an impending fracture is present, as well as review of complications of arthroplasties in which imaging is key to directing patient management.

Printed on: 02/07/23



## Abstract Archives of the RSNA, 2022

S4-CGI06

### Dual- and Multi-energy CT of the Abdomen and Pelvis

Sunday, Nov. 27 1:00PM - 2:00PM Room: NA

#### Participants

Joel Fletcher, MD, Rochester, MN (*Presenter*) Research Grant, Siemens AG; Research Grant, Pfizer Inc; Research Grant, Takeda Pharmaceutical Company Limited; Consultant, Takeda Pharmaceutical Company Limited; Research Grant, Nextrast, Inc; Consultant, Medtronic plc

Alvin C. Silva, MD, Scottsdale, AZ (*Presenter*) Scientific Advisory Committee, HealthMyne, Inc; Consultant, Exact Sciences Corporation; Research Grant, Ascelia Pharma AB

Bari Dane, MD, New York, NY (*Presenter*) Nothing to Disclose

Benjamin M. Yeh, MD, Hillsborough, CA (*Presenter*) Grant, Koninklijke Philips NV; Grant, General Electric Company; Consultant, Canon Medical Systems Corporation; Speaker, Canon Medical Systems Corporation; Royalties, Oxford University Press; Shareholder, Nextrast, Inc; Board Member, Nextrast, Inc

Cynthia McCollough, PhD, Byron, MN (*Presenter*) Research Grant, Siemens AG

#### COURSE DESCRIPTION

Multi-energy CT imaging continues to evolve rapidly and provides numerous benefits over conventional CT for the evaluation of common abdominopelvic disease. This course will review the basics of multi-energy CT, including an emphasis on photon counting CT and contrast agent usage. Practical tips on how to implement dual-energy and photon counting CT into daily practice as well as review of how to interpret such images will be discussed.

#### LEARNING OBJECTIVES

1) Explain the capabilities of dual energy and photon counting CT for daily abdominopelvic imaging 2) Describe strategies for effective implementation of multi-energy CT in daily practice\*Course Description Multi-energy CT imaging continues to evolve rapidly and provides numerous benefits over conventional CT for the evaluation of common abdominopelvic disease. This course will review the basics of multi-energy CT, including an emphasis on photon counting CT and contrast agent usage. Practical tips on how to implement dual-energy and photon counting CT into daily practice as well as review of how to interpret such images will be discussed.

Printed on: 02/07/23



## Abstract Archives of the RSNA, 2022

S4-CGU05

### GU Tumor Boards: How to Bring Value and Become Indispensable

Sunday, Nov. 27 1:00PM - 2:00PM Room: NA

#### Participants

Krupa Patel-Lippmann, MD, Nashville, TN (*Presenter*) Nothing to Disclose  
Antonio Westphalen, MD, Kirkland, WA (*Presenter*) Shareholder, ScanMed, LLC; Research funded, BotImage, Inc  
Atul Shinagare, MD, Boston, MA (*Presenter*) Consultant, VirtualScopics, Inc; Consultant, Imaging Endpoints  
Matthew Davenport, MD, Ann Arbor, MI (*Presenter*) Royalties, Wolters Kluwer nv

#### COURSE DESCRIPTION

With advances in oncology, the role of radiologist in management of GU cancers is rapidly evolving. At GU tumor boards, the radiologist plays a key role in diagnosis, staging, and clinical decision-making. This course guides the attendees through the various challenges and pitfalls faced by the radiologist at the GU tumor boards to successfully guide patient management.

#### LEARNING OBJECTIVES

1) Use case-based format to identify key imaging features that significantly impact management 2) Understand the common pitfalls in imaging assessment of GU tumors 3) Improve communication with referring providers to help improve outcomes\*Course Description With advances in oncology, the role of radiologist in management of GU cancers is rapidly evolving. At GU tumor boards, the radiologist plays a key role in diagnosis, staging, and clinical decision-making. This course guides the attendees through the various challenges and pitfalls faced by the radiologist at the GU tumor boards to successfully guide patient management.

Printed on: 02/07/23



## Abstract Archives of the RSNA, 2022

S4-CIN27

### Radiology AI Innovation: Academics vs Industry

Sunday, Nov. 27 1:00PM - 2:00PM Room: NA

#### Participants

Nickolas Papanikolaou, PhD, Lisbon, Portugal (*Presenter*) Stockholder, MRIcons Ltd; Stockholder, Advantis Medical Imaging  
Mona Flores, MD, MBA, Santa Clara, CA (*Presenter*) Employee, NVIDIA Corporation  
Rowland O. Illing, BMBCh, FRCR, Arlington, VA (*Presenter*) Officer, Amazon Web Services, Inc; Director, Amazon Web Services, Inc

#### COURSE DESCRIPTION

This panel discussion will include Dr Mona Flores, Global Head of Medical AI at NVIDIA, and Dr Nikos Papanikolaou, Computational Clinical Imaging Group Lead at the Champalimaud Foundation & Machine Learning Imaging Lead at the Royal Marsden Hospital, London. It will be chaired by Dr Rowland Illing, Director & Chief Medical Officer, International Public Sector Health at AWS & Hon Assoc Prof at UCL, London. The panel will describe how researchers and radiologists can best leverage tech industry partners to accelerate their research, providing real-world examples of how this has taken place internationally. They will describe the next generation of imaging AI capabilities that will be coming to market, and how the audience will be able to leverage these in the future.

#### LEARNING OBJECTIVES

1) Understand how engaging directly with industry can help you achieve your research objectives 2) Learn from real-world examples where Radiology Researchers and Industry have successfully collaborated around AI 3) Apply the next set of Industry capabilities that are being delivered to Researchers in 2023\*  
Course Description This panel discussion will include Dr Mona Flores, Global Head of Medical AI at NVIDIA, and Dr Nikos Papanikolaou, Computational Clinical Imaging Group Lead at the Champalimaud Foundation & Machine Learning Imaging Lead at the Royal Marsden Hospital, London. It will be chaired by Dr Rowland Illing, Director & Chief Medical Officer, International Public Sector Health at AWS & Hon Assoc Prof at UCL, London. The panel will describe how researchers and radiologists can best leverage tech industry partners to accelerate their research, providing real-world examples of how this has taken place internationally. They will describe the next generation of imaging AI capabilities that will be coming to market, and how the audience will be able to leverage these in the future.

Printed on: 02/07/23



## Abstract Archives of the RSNA, 2022

S4-CMS03

### Immunotherapy: New Paradigms for Interpretation and Imaging

Sunday, Nov. 27 1:00PM - 2:00PM Room: NA

#### Participants

Priya R. Bhosale, MD, Bellaire, TX (*Presenter*) Nothing to Disclose

Malak Itani, MD, Saint Louis, MO (*Presenter*) Nothing to Disclose

Mark Anderson, MD, Boston, MA (*Presenter*) Nothing to Disclose

Kevin Kim, MD, Loma Linda, CA (*Presenter*) Nothing to Disclose

#### COURSE DESCRIPTION

A review of how newer immunotherapy changes the paradigm for cancer treatment and image interpretation. This session will also review potential side effects and complications associated with immunotherapy in the chest and abdomen, and interventional radiology applications of immunotherapy

#### LEARNING OBJECTIVES

1) Understand basics of immunotherapy and image interpretation 2) Identify imaging features of side effects and complications associated with immunotherapy in the chest and abdomen 3) Learn about interventional radiology applications of immunotherapy\*Course Description A review of how newer immunotherapy changes the paradigm for cancer treatment and image interpretation. This session will also review potential side effects and complications associated with immunotherapy in the chest and abdomen, and interventional radiology applications of immunotherapy

Printed on: 02/07/23



## Abstract Archives of the RSNA, 2022

S4-CNPM12

### Innovations for Follow-up and Tracking Communications

Sunday, Nov. 27 1:00PM - 2:00PM Room: NA

#### Participants

Ella Kazerooni, MD, Ann Arbor, MI (*Presenter*) Nothing to Disclose

Christopher Gange JR, MD, MMedSc, New Haven, CT (*Presenter*) Stockholder, Pfizer Inc Stockholder, Bristol-Myers Squibb Company Research Consultant, Bayer AG Medical Advisory Board, AIXSCAN, Inc Shareholder, AIXSCAN, Inc

Dorothy Sippo, MD, Westport, CT (*Presenter*) Nothing to Disclose

Stacy D. O'Connor, MD, MPH, Wauwatosa, WI (*Presenter*) Nothing to Disclose

#### COURSE DESCRIPTION

This course will explore innovations in communicating significant findings and management of follow up recommendations. Topics will include: (1) creating a communications center to deliver critical results and track follow up recommendations within the Electronic Health Record (EHR), (2) a "how to" example of an EHR-based incidental lung nodule management program, (3) non-EHR-based follow-up recommendation informatics tools, and (4) measures of success for these types of programs. With a lecture format, followed by question-and-answer discussion, presenters will share innovative approaches and pearls learned from their experiences implementing and maintaining communication and follow up management systems.

#### LEARNING OBJECTIVES

1) Understand methods of communicating radiology findings with a focus on the pros and cons of using messaging within the EHR 2) Describe clinical and financial justifications for an EHR-based incidental lung nodule tracking and management tool 3) Describe non-EHR-based follow-up recommendation informatics tools 4) Review measures of success for follow up communication and tracking management systems\*Course Description This course will explore innovations in communicating significant findings and management of follow up recommendations. Topics will include: (1) creating a communications center to deliver critical results and track follow up recommendations within the Electronic Health Record (EHR), (2) a "how to" example of an EHR-based incidental lung nodule management program, (3) non-EHR-based follow-up recommendation informatics tools, and (4) measures of success for these types of programs. With a lecture format, followed by question-and-answer discussion, presenters will share innovative approaches and pearls learned from their experiences implementing and maintaining communication and follow up management systems.

Printed on: 02/07/23



## Abstract Archives of the RSNA, 2022

S4-CNR07

### Pediatric Neuroimaging (Practical Questions Faced in Clinical Practice)

Sunday, Nov. 27 1:00PM - 2:00PM Room: NA

#### Participants

Manohar Shroff, MD, Toronto, ON (*Presenter*) Nothing to Disclose  
Judith Gadde, DO, Chicago, IL (*Presenter*) Nothing to Disclose  
Tina Y. Poussaint, MD, Boston, MA (*Presenter*) Nothing to Disclose  
Rupa Radhakrishnan, MS, MBBS, Indianapolis, IN (*Moderator*) Nothing to Disclose

#### COURSE DESCRIPTION

Course Title: Pediatric CNS Tumors and cancer predisposition syndromes – The experts speak. This practical lecture session will provide information on how to approach pediatric tumors and tumor like conditions of the central nervous system. The speakers will focus on common pediatric CNS cancer predisposition syndromes, pediatric posterior fossa tumors, pediatric spine neoplasms, and recent WHO 2021 Tumor Classification updates with how these updates impact the radiologist's report. At the end of the course, the audience will gain insight into 1) imaging techniques and sequences that will help in appropriate work up of a child with suspected CNS tumor or tumor predisposition syndrome 2) common CNS tumor and non-tumor conditions in the pediatric population, and 3) understanding the updated classification of pediatric CNS tumors. Manohar Meghraj Shroff – Tumor or not? Pediatric posterior fossa tumors and non-tumor conditions Tina Young Poussaint – How does the WHO 2021 Tumor Classification Impact Radiological Practice? Rupa Radhakrishnan – Common CNS cancer predisposition syndromes – what should I be looking for? Judith A. Gadde – Pediatric spine tumors – how to arrive at a diagnosis

#### LEARNING OBJECTIVES

1) Provide strategies for imaging work up of common and challenging pediatric CNS tumors and tumor like conditions 2) Review the latest updates in pediatric CNS Tumor classification and how they impact radiological practice\*Course Description Course Title: Pediatric CNS Tumors and cancer predisposition syndromes – The experts speak. This practical lecture session will provide information on how to approach pediatric tumors and tumor like conditions of the central nervous system. The speakers will focus on common pediatric CNS cancer predisposition syndromes, pediatric posterior fossa tumors, pediatric spine neoplasms, and recent WHO 2021 Tumor Classification updates with how these updates impact the radiologist's report. At the end of the course, the audience will gain insight into 1) imaging techniques and sequences that will help in appropriate work up of a child with suspected CNS tumor or tumor predisposition syndrome 2) common CNS tumor and non-tumor conditions in the pediatric population, and 3) understanding the updated classification of pediatric CNS tumors. Manohar Meghraj Shroff – Tumor or not? Pediatric posterior fossa tumors and non-tumor conditions Tina Young Poussaint – How does the WHO 2021 Tumor Classification Impact Radiological Practice? Rupa Radhakrishnan – Common CNS cancer predisposition syndromes – what should I be looking for? Judith A. Gadde – Pediatric spine tumors – how to arrive at a diagnosis

Printed on: 02/07/23



## Abstract Archives of the RSNA, 2022

S4-COB05

### Interactive Case-based Review of Crazy OB/GYN Cases

Sunday, Nov. 27 1:00PM - 2:00PM Room: NA

#### Participants

Anne M. Kennedy, MD, Salt Lake City, UT (*Presenter*) Author with royalties, RELX

Roya Sohaey, MD, Portland, OR (*Presenter*) Nothing to Disclose

Paula J. Woodward, MD, Salt Lake City, UT (*Presenter*) Royalties, RELX

#### COURSE DESCRIPTION

This will be an interactive session reviewing complex OBGYN cases. We will demonstrate problem solving using "radiology rules" such as - You see what you look for and you look for what you know- Common things are commonest - The easiest way to miss a finding is to find a finding.

#### LEARNING OBJECTIVES

1) Develop a logical, systematic approach to complex cases 2) Identify strategies to reduce a broad differential to a specific diagnosis or a short list of likely options\*Course Description This will be an interactive session reviewing complex OBGYN cases. We will demonstrate problem solving using "radiology rules" such as - You see what you look for and you look for what you know- Common things are commonest - The easiest way to miss a finding is to find a finding.

Printed on: 02/07/23



## Abstract Archives of the RSNA, 2022

S4-CPD02

### Pediatric MSK

Sunday, Nov. 27 1:00PM - 2:00PM Room: NA

#### Participants

Delma Y. Jarrett, MD, New York, NY (*Presenter*) Nothing to Disclose  
Victor M. Ho-Fung, MD, Philadelphia, PA (*Presenter*) Nothing to Disclose  
Victor M. Ho-Fung, MD, Philadelphia, PA (*Presenter*) Nothing to Disclose  
Maria Bedoya-Velez, MD, Boston, ME (*Presenter*) Nothing to Disclose  
Victor M. Ho-Fung, MD, Philadelphia, PA (*Moderator*) Nothing to Disclose  
Victor M. Ho-Fung, MD, Philadelphia, PA (*Moderator*) Nothing to Disclose

#### COURSE DESCRIPTION

This course will focus on musculoskeletal imaging in pediatric patients focusing on imaging techniques, common pathology, pitfalls and differential diagnosis some of which are unique to children.

#### LEARNING OBJECTIVES

1- To discuss the imaging techniques used to evaluate the synovium in pediatric patients, the imaging appearance of normal synovium and different pathologies that can lead to synovitis and their differential diagnosis in the pediatric population  
2- To discuss the imaging techniques (mainly MRI) to evaluate articular cartilage in children, the imaging appearance of the developing articular surface and pathology that is commonly seen in the pediatric population.  
3- To recognize the normal pattern of bone marrow development from neonates to adulthood, the process of conversion from red to yellow marrow as well as to recognize pathologic bone marrow processes, including infiltrative disease and nutritional abnormalities.  
\*Course Description This course will focus on musculoskeletal imaging in pediatric patients focusing on imaging techniques, common pathology, pitfalls and differential diagnosis some of which are unique to children.

Printed on: 02/07/23



## Abstract Archives of the RSNA, 2022

S4-CPH15

### **AAPM/RSNA Physics Tutorial: Differences Between Pediatric and Adult Imaging from A Radiologists Perspective**

Sunday, Nov. 27 1:00PM - 2:00PM Room: NA

#### **Participants**

Vijetha Maller, DMRD, MBBS, Memphis, TN (*Presenter*) Nothing to Disclose  
Thaddeus Wilson, PhD, Memphis, TN (*Moderator*) Nothing to Disclose

#### **LEARNING OBJECTIVES**

1) Discuss the difference in approach to imaging, between adults and children with emphasis on radiation protection. 2) Understand the difference in anatomy and physiology of adults and children which affect imaging techniques. 3) Illustrate the spectrum of pathologies commonly encountered in pediatric imaging which differs from those in adults.\*Course Description

Printed on: 02/07/23



## Abstract Archives of the RSNA, 2022

S4-CRO02

### Head & Neck Case-based Multidisciplinary Review

Sunday, Nov. 27 1:00PM - 2:00PM Room: NA

#### Participants

Chad Zender, MD, Cincinnati, OH (*Presenter*) Nothing to Disclose

Sung Kim, MD, New Brunswick, NJ (*Presenter*) Consultant, Nanobiotix

Francis Worden, MD, Ann Arbor, MI (*Presenter*) Speaker, Merck & Co, Inc; Advisory Board, Merck & Co, Inc; Institutional research support, Merck & Co, Inc; Travel support, Merck & Co, Inc; Speaker, Eisai Co, Ltd; Advisory Board, Eisai Co, Ltd; Institutional research support, Eisai Co, Ltd; Speaker, Bristol-Myers Squibb Company; Advisory Board, Bristol-Myers Squibb Company; Research funded, Bristol-Myers Squibb Company; Speaker, Eli Lilly and Company; Advisory Board, Eli Lilly and Company; Research funded, Eli Lilly and Company; Speaker, Bayer AG; Advisory Board, Bayer AG; Travel support, Bayer AG; Speaker, Cue Biopharma, Inc; Advisory Board, Cue Biopharma, Inc; Advisory Board, Rakuten Group, Inc; Research funded, Oragenics, Inc; Institutional research support, Pfizer Inc

Suresh K. Mukherji, MD, Carmel, IN (*Presenter*) Nothing to Disclose

#### COURSE DESCRIPTION

This is a case-based review of head and neck cancer cases. The format replicates a multidisciplinary tumor board. The attendee will be exposed to how their image interpretation directly affects staging, treatment and management. The session will be interactive and focus on key elements that should be included in the radiologists when interpreting head and neck oncologic imaging.

#### LEARNING OBJECTIVES

1) Review various oncology case which show how imaging directly affects treatment and management 2) Discuss key elements that should be included in your report that directly affects staging, treatment and management\*Course Description This is a case-based review of head and neck cancer cases. The format replicates a multidisciplinary tumor board. The attendee will be exposed to how their image interpretation directly affects staging, treatment and management. The session will be interactive and focus on key elements that should be included in the radiologists when interpreting head and neck oncologic imaging.

Printed on: 02/07/23



## Abstract Archives of the RSNA, 2022

S5-CCA04

### State of the Art Coronary CT

Sunday, Nov. 27 2:30PM - 3:30PM Room: NA

#### Participants

Jonathan Weir-McCall, MBBCh, FRCR, Cambridge, (*Presenter*) Nothing to Disclose

Michelle Williams, MChB, PhD, Kelso, United Kingdom (*Presenter*) Speakers Bureau, Canon Medical Systems Corporation; Speakers Bureau, Siemens AG

Kristopher W. Cummings, MD, Phoenix, AZ (*Moderator*) Nothing to Disclose

#### COURSE DESCRIPTION

This didactic session on state of the art coronary CT imaging will focus on newer advanced applications, including incorporation of CT fractional flow reserve in the evaluation of coronary ischemia and methods of quantification of atherosclerotic plaque and epicardial fat. Emphasis will be placed on current literature, clinical application and prognostic benefits of newer techniques.

#### LEARNING OBJECTIVES

1) Explain the primary benefits of adding CT Fractional Flow Reserve (FFRCT) to CT Coronary imaging 2) Understand the methods for and prognostic importance of quantitative plaque assessment from CT Coronary imaging 3) Explain the prognostic significance of epicardial fat and how to quantitate from CT Coronary imaging\*Course Description This didactic session on state of the art coronary CT imaging will focus on newer advanced applications, including incorporation of CT fractional flow reserve in the evaluation of coronary ischemia and methods of quantification of atherosclerotic plaque and epicardial fat. Emphasis will be placed on current literature, clinical application and prognostic benefits of newer techniques.

Printed on: 02/07/23



## Abstract Archives of the RSNA, 2022

S5-CCH12

### Pearls and Pitfalls in Chest Radiography

Sunday, Nov. 27 2:30PM - 3:30PM Room: NA

#### Participants

Gerald F. Abbott, MD, Boston, MA (*Presenter*) Nothing to Disclose

H. Page McAdams, MD, Durham, NC (*Presenter*) Consultant, MedQIA; Author, RELX; Research Consultant, Novartis AG; Stockholder, Novartis AG; Stockholder, Abbott Laboratories; Stockholder, AbbVie Inc; Stockholder, Bristol-Myers Squibb Company; Stockholder, CVS Health Corporation

Andetta R. Hunsaker, MD, Boston, MA (*Presenter*) Nothing to Disclose

#### COURSE DESCRIPTION

The chest radiograph is one of the most, if not the most, commonly performed imaging examinations. Nevertheless, accurate interpretation of the chest radiograph remains one of the most challenging tasks for radiologists. This course is designed to improve the proficiency of all radiologists for accurate interpretation of chest radiographs. This course is also designed to improve understanding of the role of chest radiographs for diagnosis and management of common clinical scenarios.

#### LEARNING OBJECTIVES

1) Improve proficiency in interpretation of the lateral chest radiograph to improve diagnostic accuracy 2) Improve understanding of role of the chest radiograph in diagnosis and management of pulmonary infection 3) Be familiar with important signs on the chest radiograph that can indicate a specific diagnosis 4) Improve ability to recognize various manifestations of atelectasis on the chest radiograph\*Course Description The chest radiograph is one of the most, if not the most, commonly performed imaging examinations. Nevertheless, accurate interpretation of the chest radiograph remains one of the most challenging tasks for radiologists. This course is designed to improve the proficiency of all radiologists for accurate interpretation of chest radiographs. This course is also designed to improve understanding of the role of chest radiographs for diagnosis and management of common clinical scenarios.

Printed on: 02/07/23



## Abstract Archives of the RSNA, 2022

S5-CHN02

### Head and Neck Masses: Case-based Review

Sunday, Nov. 27 2:30PM - 3:30PM Room: NA

#### Participants

Tabassum A. Kennedy, MD, Madison, WI (*Presenter*) Nothing to Disclose

Asha Sarma, MD, Nashville, TN (*Presenter*) Nothing to Disclose

Marin McDonald, MD, PhD, San Diego, CA (*Presenter*) Speakers Bureau, Canon Medical Systems Corporation

Kathryn Dean, MD, Brooklyn, NY (*Presenter*) Nothing to Disclose

Mariah Bashir, MD, Oak Brook, IL (*Moderator*) Nothing to Disclose

#### COURSE DESCRIPTION

Course Description: In this case-based Head and Neck session, attendees will be presented with typical and atypical imaging examples of masses in the adult neck, sinuses, teeth/jaw and pediatric neck. Speakers will emphasize pearls for differentiating each entity from common mimics, pitfalls of interpretation to avoid, and relevant clinical management considerations with which radiologists should be familiar. This session offers attendees the opportunity to refine their interpretation of complex head and neck imaging studies by incorporating tips from world experts.

#### LEARNING OBJECTIVES

1) Recognize typical and atypical imaging features of masses in the adult neck, sinuses, teeth/jaw and pediatric neck2) Differentiate between entities on the differential diagnosis of masses in the neck, sinuses and teeth/jaw based on imaging features, location and age. \*Course Description Course Description: In this case-based Head and Neck session, attendees will be presented with typical and atypical imaging examples of masses in the adult neck, sinuses, teeth/jaw and pediatric neck. Speakers will emphasize pearls for differentiating each entity from common mimics, pitfalls of interpretation to avoid, and relevant clinical management considerations with which radiologists should be familiar. This session offers attendees the opportunity to refine their interpretation of complex head and neck imaging studies by incorporating tips from world experts.

Printed on: 02/07/23



## Abstract Archives of the RSNA, 2022

S5-CIN20

### Multimodal Data Model Development in Radiology: Beyond the Pixel Data

Sunday, Nov. 27 2:30PM - 3:30PM Room: NA

#### Participants

Yifan Peng, New York, NY (*Presenter*) Nothing to Disclose  
Christoph Lee, MD, Mercer Island, WA (*Presenter*) Royalites, The McGraw-Hill Companies; Royalties, Oxford University Press; Royalties, Wolters Kluwer nv; Research Consultant, GRAIL, LLC  
Jayashree Kalpathy-Cramer, MS, PhD, Charlestown, MA (*Presenter*) Institutional Research Grant, General Electric Company; Institutional Research Grant, F. Hoffmann-La Roche Ltd; Institutional Research Grant, Bayer AG  
Maciej Mazurowski, MS, PhD, Durham, NC (*Presenter*) Nothing to Disclose  
Imon Banerjee, Stanford, GA (*Moderator*) Nothing to Disclose

#### COURSE DESCRIPTION

One of the primary limitations of the state-of-the-art deep learning models for radiology applications is that they consider only pixel-value information without data informing clinical context. This session will focused on analyzing recent developments related to multimodal deep learning methodologies using radiology images. We will have an interactive session with extremely knowledgeable speakers to present the views from both clinical and technical sides - Dr. Christoph Lee (UW Radiology), Maciej Mazurowski (Duke Radiology), Jayashree Kalpathy-Cramer (University of Colorado) and Dr. Yifan Peng (Cornell Radiology). Dr. Imon Banerjee (Mayo Clinic) will moderate the session.

#### LEARNING OBJECTIVES

1) Identify learning strategy to process contextual data from electronic health records (EHR) in addition to pixel data from radiology images for developing deep learning model 2) Explain important results and provide implementation guidelines to serve as a reference for researchers interested in the application of multimodal fusion in medical imaging\*Course Description One of the primary limitations of the state-of-the-art deep learning models for radiology applications is that they consider only pixel-value information without data informing clinical context. This session will focused on analyzing recent developments related to multimodal deep learning methodologies using radiology images. We will have an interactive session with extremely knowledgeable speakers to present the views from both clinical and technical sides - Dr. Christoph Lee (UW Radiology), Maciej Mazurowski (Duke Radiology), Jayashree Kalpathy-Cramer (University of Colorado) and Dr. Yifan Peng (Cornell Radiology). Dr. Imon Banerjee (Mayo Clinic) will moderate the session.

Printed on: 02/07/23



## Abstract Archives of the RSNA, 2022

S5-CIR02

### IR Hot Topics and Career Development

Sunday, Nov. 27 2:30PM - 3:30PM Room: NA

#### Participants

Amy Deipolyi, MD, PhD, New York, NY (*Presenter*) Nothing to Disclose

Amanda Smolock, MD, PhD, Milwaukee, WI (*Presenter*) Consultant, HistoSonics, Inc;Shareholder, HistoSonics, Inc;Employee, NeuWave Medical, Inc;Grant, NeuWave Medical, Inc;Consultant, NeuWave Medical, Inc;;

Jeffrey Chick, MD, MPH, Ann Arbor, MI (*Presenter*) Consultant, Inari Medical, Inc;Speaker, Inari Medical, Inc;Consultant, Guerbet SA;Speaker, Guerbet SA;Consultant, Becton, Dickinson and Company;Speaker, Becton, Dickinson and Company;Consultant, Argon Medical Devices, Inc;Speaker, Argon Medical Devices, Inc;Consultant, Boston Scientific Corporation;Speaker, Boston Scientific Corporation

Mitchell Schnall, MD, PhD, Philadelphia, PA (*Presenter*) Research Grant, Siemens AG

Meridith J. Englander, MD, Albany, NY (*Presenter*) Medical Director, Capital District Physicians' Health Plan, Inc

Nadine Abi-Jaoudeh, MD, Orange, CA (*Moderator*) Institutional research collaboration, Koninklijke Philips NV;Institutional research collaboration, Teclison Limited;Intellectual property, Bruin Biosciences Inc;Owner, Bruin Biosciences Inc;Institutional research collaboration, Sirtex Medical Ltd

#### COURSE DESCRIPTION

This session consists of lecture series divided into two topics. The first part of the session will cover upcoming technologies, controversies, and novel development in the entire spectrum of interventional radiology including ablation, embolization, arterial and venous interventions as well as pain and musculoskeletal procedures. The second part of the session will discuss career growth with the help of mentors and advisors as well as tips and tricks on how to grow practice and diversity in interventional radiology particularly in the hiring process. Although different, both topics have a vital importance. There are several exciting ablative and embolic technologies and innovation in existing technologies that are quite transformative that will be reviewed in this session. Moreover, deep vein arterialization, endo-venous fistula creation have been developed in recent years just to name a few. This session will provide an overview and understanding of the changing landscape. The second portion is equally important as it provides very concrete tools for professional success.

#### LEARNING OBJECTIVES

1) Identify novel developments in IR specifically upcoming ablative technologies, new embolic materials, novel interventions in venous disease as well as newer techniques to treat peripheral arterial disease as well as MSK interventions 2) Explain the importance of diversity during recruitment and the role of mentor for career and practice growth\*Course Description This session consists of lecture series divided into two topics. The first part of the session will cover upcoming technologies, controversies, and novel development in the entire spectrum of interventional radiology including ablation, embolization, arterial and venous interventions as well as pain and musculoskeletal procedures. The second part of the session will discuss career growth with the help of mentors and advisors as well as tips and tricks on how to grow practice and diversity in interventional radiology particularly in the hiring process. Although different, both topics have a vital importance. There are several exciting ablative and embolic technologies and innovation in existing technologies that are quite transformative that will be reviewed in this session. Moreover, deep vein arterialization, endo-venous fistula creation have been developed in recent years just to name a few. This session will provide an overview and understanding of the changing landscape. The second portion is equally important as it provides very concrete tools for professional success.

Printed on: 02/07/23



## Abstract Archives of the RSNA, 2022

S5-CMK04

### MSK Infection and its Mimics: Pearls and Pitfalls

Sunday, Nov. 27 2:30PM - 3:30PM Room: NA

#### Participants

Mark J. Kransdorf, MD, Scottsdale, AZ (*Presenter*) Nothing to Disclose

Megan Mills, MD, Salt Lake City, UT (*Presenter*) Nothing to Disclose

Stacy E. Smith, MD, Weston, MA (*Presenter*) Nothing to Disclose

Donald Flemming, MD, Hershey, PA (*Presenter*) Nothing to Disclose

Mark D. Murphey, MD, Silver Spring, MD (*Presenter*) Nothing to Disclose

#### COURSE DESCRIPTION

The session will review the imaging features characteristic of MSK infection. It will also highlight those lesions and processes that may mimic infection, and features that will allow their identification.

#### LEARNING OBJECTIVES

1) Identify the imaging characteristic of MSK infection 2) Recognize features that can identify infection mimics\*Course Description  
The session will review the imaging features characteristic of MSK infection. It will also highlight those lesions and processes that may mimic infection, and features that will allow their identification.

Printed on: 02/07/23



## Abstract Archives of the RSNA, 2022

S5-CNMMI07

### Theranostics of NETS and Thyroid Cancer

Sunday, Nov. 27 2:30PM - 3:30PM Room: NA

#### Participants

Delphine Chen, MD, Seattle, WA (*Presenter*) Grant, Telix Pharmaceuticals Limited; Speaker, Telix Pharmaceuticals Limited  
Rathan M. Subramaniam, MD, PhD, Dunedin, (*Presenter*) Nothing to Disclose  
Terence Z. Wong, MD, PhD, Durham, NC (*Presenter*) Consultant, General Electric Company  
Don Yoo, MD, Lexington, MA (*Presenter*) Consultant, Konica Minolta, Inc

#### COURSE DESCRIPTION

The goal of this course is to describe and illustrate the clinical applications of imaging, including dotatate PET and radioactive iodine whole body imaging, and therapy with Lu-177 dotatate and I-131 through case-based presentations. These presentations will include the use of imaging for patient selection and management decisions related to therapy as well as practical strategies for reducing potential risks of therapy with Lu-177 dotatate and I-131.

#### LEARNING OBJECTIVES

1) Review clinical applications of Lu-177 dotatate and management strategies to reduce risk of potential treatment complications 2) Understand current practice for radioactive iodine therapy for thyroid cancer 3) Review imaging applications to guide radiopharmaceutical therapy decisions for neuroendocrine tumors and thyroid cancer\*Course Description The goal of this course is to describe and illustrate the clinical applications of imaging, including dotatate PET and radioactive iodine whole body imaging, and therapy with Lu-177 dotatate and I-131 through case-based presentations. These presentations will include the use of imaging for patient selection and management decisions related to therapy as well as practical strategies for reducing potential risks of therapy with Lu-177 dotatate and I-131.

Printed on: 02/07/23



## Abstract Archives of the RSNA, 2022

S5-CNPM17

### Cost Effectiveness Analysis: Principles and Update on Applications

Sunday, Nov. 27 2:30PM - 3:30PM Room: NA

#### Participants

Stella Kang, MD, MSc, New York, NY (*Presenter*) Nothing to Disclose

Bart Ferket, MD, PhD, New York, NY (*Presenter*) Nothing to Disclose

Pari V. Pandharipande, MD, MPH, Chestnut Hill, MA (*Presenter*) I serve as a member of the Association of University Radiologists (AUR) General Electric (GE) Radiology Research Academic Fellowship (GERRAF) Board of Review (term: 7/1/22-2/28/23).

#### COURSE DESCRIPTION

Economic evaluation serves a major purpose in health care policy, guiding the adoption and assessment of clinical interventions. An important form of economic evaluation is cost-effectiveness analysis, which compares alternative strategies in terms of both the cumulative costs as well as differences in health outcomes. To guide imaging-related policy, clinical practice, and research prioritization, this course will address principles and applications of cost-effectiveness analysis. Participants will learn about basic principles of cost-effectiveness analysis, review recent applications of economic evaluation in imaging research and policy, and explore the implications of cost-effectiveness analysis through a software demonstration.

#### LEARNING OBJECTIVES

1) Define how the long-term costs, effectiveness, and cost-effectiveness of imaging can be measured 2) Understand how policymakers utilize data from cost-effectiveness analyses, both within the U.S. and internationally 3) Gain insight into the strengths and drawbacks of cost-effectiveness analysis as a means for judging value 4) Understand current applications of cost-effectiveness analysis in imaging research and policy through clinical examples and a software demonstration\*Course Description  
Economic evaluation serves a major purpose in health care policy, guiding the adoption and assessment of clinical interventions. An important form of economic evaluation is cost-effectiveness analysis, which compares alternative strategies in terms of both the cumulative costs as well as differences in health outcomes. To guide imaging-related policy, clinical practice, and research prioritization, this course will address principles and applications of cost-effectiveness analysis. Participants will learn about basic principles of cost-effectiveness analysis, review recent applications of economic evaluation in imaging research and policy, and explore the implications of cost-effectiveness analysis through a software demonstration.

Printed on: 02/07/23



## Abstract Archives of the RSNA, 2022

S5-CNPM25

### Principles of Health Care Delivery & Safety

Sunday, Nov. 27 2:30PM - 3:30PM Room: NA

#### Participants

Lane F. Donnelly, MD, Chapel Hill, NC (*Presenter*) Nothing to Disclose

David Larson, MD, MBA, Portola Valley, CA (*Presenter*) Research Grant, Siemens AG ;Advisor, Bunkerhill Health;Shareholder, Bunkerhill Health

Arun Krishnaraj, MD, MPH, Charlottesville, VA (*Moderator*) Nothing to Disclose

#### COURSE DESCRIPTION

The organization and delivery of health care in the United States is haphazard at best. Costs for healthcare delivery in the US far out pace comparable industrialized nations yet health outcomes consistently fall well below peers. More recent efforts to curb costs and improve outcomes have focused on delivering greater value and improving margins of safety. In an era of big data and trends toward greater consumerism in health care, radiology has an opportunity to better define its value and grows its influence in the greater health care landscape.

#### LEARNING OBJECTIVES

1) Identify opportunities where radiology can add greater value and contribute to improved safety margins in the delivery of health care 2) Explore the role of radiology system leaders in impacting quality and safety in a health care organization 3) Evaluate the impact patients can have in contributing to a culture of safety\*Course Description The organization and delivery of health care in the United States is haphazard at best. Costs for healthcare delivery in the US far out pace comparable industrialized nations yet health outcomes consistently fall well below peers. More recent efforts to curb costs and improve outcomes have focused on delivering greater value and improving margins of safety. In an era of big data and trends toward greater consumerism in health care, radiology has an opportunity to better define its value and grows its influence in the greater health care landscape.

Printed on: 02/07/23



## Abstract Archives of the RSNA, 2022

S5-CPH01

### AI in Ultrasound Imaging

Sunday, Nov. 27 2:30PM - 3:30PM Room: NA

#### Participants

Karen Drukker, PhD, Chicago, IL (*Presenter*) Royalties, Hologic, Inc

Jeremy J. Dahl, PhD, Durham, NC (*Presenter*) Technical Advisory Board, MAUI Imaging, Inc; Technical Advisory Board, Cephasonics  
Ultrasound; Technical Advisor, Vortex Imaging

Jong Chul Ye, PhD, Daejeon, Korea, Republic Of (*Presenter*) Co-founder, Promedius

#### COURSE DESCRIPTION

This course will consist of 3 lectures that will update the audience on new developments in all aspects of AI for medical ultrasound from high-quality image generation, including beam formation and image reconstruction, to image analysis intended as a decision aid to radiologists in clinical practice.

#### LEARNING OBJECTIVES

1) To understand applications of AI/deep learning in 2) ultrasonic imaging modalities and devices, 3) methods for ultrasonic beamforming, image reconstruction, speckle reduction and image artifact removal, and 4) ultrasound image analysis for detection, diagnosis, and prognosis of disease\*Course Description This course will consist of 3 lectures that will update the audience on new developments in all aspects of AI for medical ultrasound from high-quality image generation, including beam formation and image reconstruction, to image analysis intended as a decision aid to radiologists in clinical practice.

Printed on: 02/07/23



## Abstract Archives of the RSNA, 2022

S5-CPH16

### AAPM/RSNA Physics Tutorial: Balancing Risks and Benefits in Pediatric Imaging

Sunday, Nov. 27 2:30PM - 3:30PM Room: NA

#### Participants

Christina Sammet, PhD, Manhattan, IL (*Presenter*) Nothing to Disclose  
Cynthia K. Rigsby, MD, Chicago, IL (*Presenter*) Nothing to Disclose  
Thaddeus Wilson, PhD, Memphis, TN (*Moderator*) Nothing to Disclose

#### LEARNING OBJECTIVES

1) The medical community has a heightened awareness of the risk associated with radiation exposure to children from medical imaging procedures. It is important for ordering providers to understand the full set of risks associated with each diagnostic modality. 2) X-ray, CT, fluoroscopy, ultrasound, nuclear medicine, and MRI have different levels of risk in not only radiation exposure, but also sedation/anesthesia exposure, contrast administration risks, and medical implant safety. 3) Ultimately, the ordering provider, radiologist, and medical physicist need to work together to balance all the risks associated with an imaging procedure with the clinical benefit to care management for optimal risk-benefit outcomes in pediatric imaging.\*Course Description

Printed on: 02/07/23



## Abstract Archives of the RSNA, 2022

S5-CVA06

### Imaging of Venous Congestion Syndromes

Sunday, Nov. 27 2:30PM - 3:30PM Room: NA

#### Participants

Candice Bookwalter, MD, PhD, Rochester, MN (*Presenter*) Nothing to Disclose

Gloria Salazar, MD, Boston, MA (*Presenter*) Consultant, Speakers Bureau, Medtronic plc; Consultant, Boston Scientific Corporation; Speakers Bureau, Boston Scientific Corporation; Speakers Bureau, Cook Group Incorporated; Consultant, Avail Medsystems, Inc; Consultant, Mentice AB

Rebecca Rakow-Penner, MD, PhD, San Diego, CA (*Presenter*) Research Grant, General Electric Company; Consultant, Human Longevity Inc; Stockholder, CureMetrix, Inc; Stock options, CorTechs Labs, Inc

#### COURSE DESCRIPTION

This course will discuss and illustrate abdominal and pelvic venous compression and congestive syndromes with multimodality imaging. An important aspect of this course will focus on interventional procedures used in alleviation of abdominal and pelvic congestion and compression syndromes.

#### LEARNING OBJECTIVES

1) Identify and discuss key imaging features of abdominal & pelvic venous congestive and compressive syndromes 2) Review multimodality imaging for diagnosis and treatment planning. Present non-invasive interventional radiology options for treatment and alleviation of symptoms\*Course Description This course will discuss and illustrate abdominal and pelvic venous compression and congestive syndromes with multimodality imaging. An important aspect of this course will focus on interventional procedures used in alleviation of abdominal and pelvic congestion and compression syndromes.

Printed on: 02/07/23



## Abstract Archives of the RSNA, 2022

S5-RCP35

### Artificial Intelligence in Radiology: Managing Professionalism Challenges (Sponsored by RSNA Professionalism Committee)

Sunday, Nov. 27 2:30PM - 3:30PM Room: NA

#### Participants

Tessa S. Cook, MD, PhD, Philadelphia, PA (*Presenter*) Grant, Siemens AG; Grant, Independence Blue Cross; Speaker, Sectra AB  
Geoffrey D. Rubin, MD, Tucson, AZ (*Presenter*) Consultant, Fovia, Inc; Advisor, HeartFlow, Inc; Advisor, Nano-X Imaging Ltd; Advisor, Bayer AG

Zi Zhang, MD, Fort Washington, PA (*Presenter*) Nothing to Disclose

Ryan K. Lee, MD, Philadelphia, PA (*Presenter*) Bayer, Speaker's Bureau; Philips, Speaker's Bureau; Bracco, Advisor

Kate Hanneman, MD, FRCPC, Toronto, ON (*Moderator*) Speaker, Groupe Sanofi; Speaker, Amicus Therapeutics, Inc

#### COURSE DESCRIPTION

This course includes 4 lectures: 1) A nutshell of radiology AI ethics: how to mitigate bias in radiology AI. This lecture will introduce the key concepts regarding radiology AI ethics. It will discuss a variety of bias in AI from clinically confounding attributes to technical factors, and how to minimize the bias from training data to over time use in clinical practice. 2) Managing patient privacy in radiology AI: informed consent and potential safeguards. This lecture will cover the key areas in acquiring, managing, and assessing data, as well as discussing the resources to manage large data sets. 3) Transparency in AI: balance between patient and provider trust and privacy. This lecture will discuss the development of interpretable AI systems for clinical radiology, and allow radiologists and patients to understand the elements of decision-making behind classification decisions. 4) Clinical application and reimbursement of radiology AI. This lecture will discuss clinical application of AI, and possible models and frameworks for AI reimbursement.

#### LEARNING OBJECTIVES

Artificial intelligence (AI) is rapidly advancing and may dramatically reshape modern radiology practice. AI has multiple applications, from image acquisition and processing, to aided reporting, follow-up planning, data storage, data mining, and others. The application of AI can potentially reduce human labor, lower costs, and improve diagnostic accuracy that will ultimately benefit patient care. However, these changes pose many new professionalism related challenges for radiologists. The goal of this course is to discuss how to manage new professionalism challenges related to AI, including ethics, bias, data ownership, privacy and data protection, regulation, transparency, and reimbursement related issues. \*Course Description This course includes 4 lectures: 1) A nutshell of radiology AI ethics: how to mitigate bias in radiology AI. This lecture will introduce the key concepts regarding radiology AI ethics. It will discuss a variety of bias in AI from clinically confounding attributes to technical factors, and how to minimize the bias from training data to over time use in clinical practice. 2) Managing patient privacy in radiology AI: informed consent and potential safeguards. This lecture will cover the key areas in acquiring, managing, and assessing data, as well as discussing the resources to manage large data sets. 3) Transparency in AI: balance between patient and provider trust and privacy. This lecture will discuss the development of interpretable AI systems for clinical radiology, and allow radiologists and patients to understand the elements of decision-making behind classification decisions. 4) Clinical application and reimbursement of radiology AI. This lecture will discuss clinical application of AI, and possible models and frameworks for AI reimbursement.

Printed on: 02/07/23



## Abstract Archives of the RSNA, 2022

S5-RCP43

### Building A Career in Academic Radiology: A Dialogue on the Trajectory from Residency Onward (Sponsored by the RSNA Resident and Fellow Committee)

Sunday, Nov. 27 2:30PM - 3:30PM Room: NA

#### Participants

Thomas M. Grist, MD, Madison, WI (*Presenter*) Nothing to Disclose  
Cheri Canon, MD, Birmingham, AL (*Presenter*) Royalties, The McGraw-Hill Companies  
Christine Chung, MD, Solana Beach, CA (*Presenter*) Nothing to Disclose  
MeNore Lake, MD, Cambridge, MA (*Moderator*) Nothing to Disclose

#### COURSE DESCRIPTION

This program will provide a framework for the approach to an academic career in radiology and will highlight the fundamental tools for successful advancement in the field. Through a brief presentation by the keynote speaker followed by a panel discussion with leading academic radiologists of various subspecialties, this session aims to empower trainees and early career radiologists interested in academic radiology with an awareness of the resources and processes that lead to a satisfying and fulfilling career.

#### LEARNING OBJECTIVES

1) Describe the framework for academic appointments in radiology 2) Identify pathways of careers in academic radiology, emphasizing the development of clinical, research and/or educational domain expertise 3) Describe strategies to advance in academic radiology and outcome measures of success\*Course Description This program will provide a framework for the approach to an academic career in radiology and will highlight the fundamental tools for successful advancement in the field. Through a brief presentation by the keynote speaker followed by a panel discussion with leading academic radiologists of various subspecialties, this session aims to empower trainees and early career radiologists interested in academic radiology with an awareness of the resources and processes that lead to a satisfying and fulfilling career.

Printed on: 02/07/23



## Abstract Archives of the RSNA, 2022

T1-CAS06

### Learning From the Pandemic Using Simulation Tools to Support Excellence in Training (Sponsored by the Associated Sciences Consortium)

Tuesday, Nov. 29 8:00AM - 9:00AM Room: NA

#### Participants

Caroline Khazei, Vancouver, BC (*Presenter*) Nothing to Disclose

Naomi Shiner, Derby, United Kingdom (*Presenter*) Nothing to Disclose

Charlotte Beardmore, MBA, London, United Kingdom (*Moderator*) Nothing to Disclose

Catherine Gunn, MBA, RT, Halifax, NS (*Moderator*) Nothing to Disclose

#### COURSE DESCRIPTION

This course aims to discuss the opportunities for the use of simulation in the education and training of radiological technologists/ radiographers and considers how programmes can be adapted to support deep learning from simulation. It will take learning from the pandemic. Two expert educators from the profession will share their experiences, and research, and will offer practical solutions to support robust and innovative education and training for professionals in the 21st Century.

#### LEARNING OBJECTIVES

1) The Role of Simulation in Radiography Education 2) Recognize the value of simulation in promoting deep learning within radiography education 3) Consider how to embed various simulation modalities into your curriculum 4) Adapt existing clinical/practical placement using simulation to expand radiography workforce\*Course Description This course aims to discuss the opportunities for the use of simulation in the education and training of radiological technologists/ radiographers and considers how programmes can be adapted to support deep learning from simulation. It will take learning from the pandemic. Two expert educators from the profession will share their experiences, and research, and will offer practical solutions to support robust and innovative education and training for professionals in the 21st Century.

Printed on: 02/07/23



## Abstract Archives of the RSNA, 2022

T1-CBR12

### Imaging Guided Localization Procedures

Tuesday, Nov. 29 8:00AM - 9:00AM Room: NA

#### Participants

Sarah M. Friedewald, MD, Marlborough, MA (*Presenter*) Consultant, Hologic, Inc; Research Grant, Alphabet Inc  
Laurie Margolies, MD, New York, NY (*Presenter*) Stock options, Nuevozen Corporation Medical Advisory Board, Screenpoint Medical

#### COURSE DESCRIPTION

In this course, the attendee will learn the basics of tomosynthesis guided biopsies and image guided localizations. The most recent literature supporting these techniques will be reviewed. Additionally, through imaging examples, different scenarios will be presented that the radiologist may encounter during these procedures. A practical guide on how to troubleshoot various issues that might arise will be presented.

#### LEARNING OBJECTIVES

1) Identify different ways to optimize tomosynthesis guided biopsies 2) Understand the advantages and disadvantages of upright versus prone biopsies 3) Appreciate different methods of image guided localizations, and understand their strengths and limitations\*Course Description In this course, the attendee will learn the basics of tomosynthesis guided biopsies and image guided localizations. The most recent literature supporting these techniques will be reviewed. Additionally, through imaging examples, different scenarios will be presented that the radiologist may encounter during these procedures. A practical guide on how to troubleshoot various issues that might arise will be presented.

Printed on: 02/07/23



## Abstract Archives of the RSNA, 2022

T1-CCA05

### Imaging of Transcatheter Intervention: Planning Novel Therapies Beyond the Aortic Valve

Tuesday, Nov. 29 8:00AM - 9:00AM Room: NA

#### Participants

Monika Radike, MMedSc, Barcelona, Spain (*Presenter*) Nothing to Disclose

Prabhakar Rajiah, MD, FRCR, Rochester, MN (*Presenter*) Nothing to Disclose

Jonathon Leipsic, MD, Vancouver, BC (*Moderator*) Consultant, Heartflow, Inc; Consultant, Circle Cardiovascular Imaging

Inc; Speakers Bureau, General Electric Company; Research Grant, Edwards Lifesciences Corporation; Research Grant, Medtronic plc; Research Grant, Abbott Laboratories; Research Grant, Boston Scientific Corporation; Research Grant, PI-Cardia Ltd

#### COURSE DESCRIPTION

Lecture based discussion where the audience will leave with a deeper understanding of the role of cross sectional imaging for planning transcatheter valve interventions

#### LEARNING OBJECTIVES

1) To describe the role of CT for the planning of transcatheter valve interventions 2) To review the evidence highlighting the use of CT to reduce complications related to transcatheter interventions 3) To discuss ongoing imaging advancements and novel modeling techniques to help further refine procedural planning and reduce complications\*Course Description Lecture based discussion where the audience will leave with a deeper understanding of the role of cross sectional imaging for planning transcatheter valve interventions

Printed on: 02/07/23



## Abstract Archives of the RSNA, 2022

T1-CCH04

### Thoracic Malignancy I: Imaging and Treatment in Non-small Cell Lung Cancer

Tuesday, Nov. 29 8:00AM - 9:00AM Room: NA

#### Participants

Brett W. Carter, MD, Houston, TX (*Presenter*) Nothing to Disclose

Girish S. Shroff, MD, Houston, TX (*Presenter*) Nothing to Disclose

Florian Fintelmann, MD, Boston, MA (*Presenter*) Nothing to Disclose

Jane P. Ko, MD, New York, NY (*Presenter*) Research collaboration, Siemens AG

Mizuki Nishino, MD, Boston, MA (*Presenter*) Institutional Research Grant, DAIICHI SANKYO Group; Institutional Research Grant,

AstraZeneca PLC; Institutional Research Grant, Canon Medical Systems Corporation; Consultant, AstraZeneca PLC

Mylene T. Truong, MD, Houston, TX (*Moderator*) Nothing to Disclose

#### COURSE DESCRIPTION

The lectures in this session will review current treatments for lung cancer including targeted therapy, immunotherapy and radiation therapy as well as discuss the imaging of various treatment complications. This session will address lung cancer in the setting of interstitial lung disease and provide an update on radiomics in lung cancer.

#### LEARNING OBJECTIVES

1) Discuss lung cancer in the setting of interstitial lung disease and update on use of radiomics 2) Review imaging of lung cancer treatment complications including targeted therapy, immunotherapy and radiation therapy\*Course Description The lectures in this session will review current treatments for lung cancer including targeted therapy, immunotherapy and radiation therapy as well as discuss the imaging of various treatment complications. This session will address lung cancer in the setting of interstitial lung disease and provide an update on radiomics in lung cancer.

Printed on: 02/07/23



## Abstract Archives of the RSNA, 2022

T1-CGU06

### Emerging Technologies in GU Imaging

Tuesday, Nov. 29 8:00AM - 9:00AM Room: NA

#### Participants

Masoom A. Haider, MD, Toronto, ON (*Presenter*) Nothing to Disclose

Sadhna Verma, MD, Cincinnati, OH (*Presenter*) Nothing to Disclose

Spencer C. Behr, MD, San Francisco, CA (*Presenter*) Grant, Cancer Targeted Technology; Scientific Advisory Board, Novartis AG; Research Consultant, GenVivo

#### COURSE DESCRIPTION

The overall healthcare industry is striving to make healthcare more effective. In medical imaging, this translates to improving diagnosis while keeping dose as low as possible; and increasing efficiencies to minimize costs. This course discusses the emerging techniques in GU imaging. Recent technical advances and novel discoveries make this an exciting but challenging time for GU imaging.

#### LEARNING OBJECTIVES

In emerging GU technologies course, we explore five significant technology innovations They are: 1) Faster acquisition enables improved image quality 2) Gains in optimal dose efficiency 3) Biomarkers for Imaging Development 4) Targeted Imaging, biopsy and treatment 5) AI for medical image acquisition and analysis\*Course Description The overall healthcare industry is striving to make healthcare more effective. In medical imaging, this translates to improving diagnosis while keeping dose as low as possible; and increasing efficiencies to minimize costs. This course discusses the emerging techniques in GU imaging. Recent technical advances and novel discoveries make this an exciting but challenging time for GU imaging.

Printed on: 02/07/23



## Abstract Archives of the RSNA, 2022

T1-CIN16

### Virtual Radiology: From Logistics to Impact on Radiology

Tuesday, Nov. 29 8:00AM - 9:00AM Room: NA

#### Participants

K. Elizabeth Hawk, MD, PhD, Studio City, CA (*Presenter*) Nothing to Disclose  
Mindy Yang, MD, Philadelphia, PA (*Presenter*) Clinical Advisory Board, Solutionreach, Inc  
Hannah L. Chung, MD, Houston, TX (*Presenter*) Nothing to Disclose  
Samir S. Shah, MD, Gibsonia, PA (*Presenter*) Nothing to Disclose

#### COURSE DESCRIPTION

Teleradiology has rapidly expanded over the past few years, with a plethora of remote reading models now being utilized by various practices, both academic and private alike. This course will focus on the logistics of teleradiology from technological set-up and maintenance of home workstations, the balance of teleradiology with on-site duties within a practice, a focus on telemammography including the challenges and benefits, and the potential impact of teleradiology on our profession as radiologists.

#### LEARNING OBJECTIVES

1) Identify technical requirements for deployment of remote reading solutions  
2) Discuss how to optimally balance remote reading with on-site duties and maintain an equitable culture  
3) Discuss challenges and benefits of telemammography  
4) Discuss potential impacts of teleradiology on our profession as radiologists

\*Course Description Teleradiology has rapidly expanded over the past few years, with a plethora of remote reading models now being utilized by various practices, both academic and private alike. This course will focus on the logistics of teleradiology from technological set-up and maintenance of home workstations, the balance of teleradiology with on-site duties within a practice, a focus on telemammography including the challenges and benefits, and the potential impact of teleradiology on our profession as radiologists.

Printed on: 02/07/23



## Abstract Archives of the RSNA, 2022

T1-CNMMI10

### Case-based Review of Brain, Head, Neck: PET/CT Workshop (In Conjunction with SNMMI)

Tuesday, Nov. 29 8:00AM - 9:00AM Room: NA

#### Participants

Lawrence E. Ginsberg, MD, Houston, TX (*Presenter*) Nothing to Disclose

Phillip Kuo, MD, PhD, Tucson, AZ (*Presenter*) Consultant, Invicro Consultant, Amgen Inc Consultant, Blue Earth Diagnostics Ltd Research Grant, Blue Earth Diagnostics Ltd Consultant, Novartis AG Speaker, Novartis AG Consultant, Chimerix, Inc Consultant, Fusion Pharmaceuticals Inc Consultant, Bayer AG Consultant, General Electric Healthcare Company Speaker, General Electric Healthcare Company Research Grant, General Electric Company Speaker, Digital Science Press, Inc Consultant, Radionetics Former Employee, Invicro, Inc (ended employment October 2022)

#### COURSE DESCRIPTION

The head/neck is as area of high anatomic and metabolic complexity. In this session, experts on dementia imaging and PET/CT for head/neck malignancy will use clinical cases to demonstrate fundamentals of interpretation, as well as pearls and pitfalls to help improve interpretation of these studies.

#### LEARNING OBJECTIVES

1) Understand best clinical practices for use and interpretation of dementia PET imaging 2) Understand best clinical practices for use and interpretation of PET/CT in patients with head/neck cancer\*Course Description The head/neck is as area of high anatomic and metabolic complexity. In this session, experts on dementia imaging and PET/CT for head/neck malignancy will use clinical cases to demonstrate fundamentals of interpretation, as well as pearls and pitfalls to help improve interpretation of these studies.

Printed on: 02/07/23



## Abstract Archives of the RSNA, 2022

T1-CNPM14

### Satisfaction All Around! Providing a Better Experience for Patients, Providers, and Radiology Staff (Sponsored by the RSNA Quality Improvement Committee)

Tuesday, Nov. 29 8:00AM - 9:00AM Room: NA

#### Participants

Rachel Smith, MS, Cincinnati, OH (*Presenter*) Nothing to Disclose

Gloria Hwang, MD, Hillsborough, CA (*Presenter*) Spouse, Stockholder, Thrombx Medical, Inc; Spouse, Consultant, Terumo Corporation; Spouse, Consultant, Johnson & Johnson; Spouse, Research Grant, Stryker Corporation; Spouse, Research Grant, Siemens AG; Spouse, Research Grant, Route 92 Medical, Inc

Xuan V. Nguyen, MD, PhD, Columbus, OH (*Presenter*) Stockholder, Apple Inc; Stockholder, Alphabet Inc; Stockholder, Amazon.com, Inc; Stockholder, Advanced Micro Devices, Inc; Stockholder, NVIDIA Corporation; Stockholder, Microsoft Corporation

Nadja Kadom, MD, Atlanta, GA (*Moderator*) Nothing to Disclose

#### COURSE DESCRIPTION

This session features successful approaches to patient, provider, and technologist satisfaction.

#### LEARNING OBJECTIVES

1) Outline possible improvement projects to increase internal and external customer satisfaction 2) Understand provider priorities for radiology services 3) Discuss the importance of communications with technologists for safety\*Course Description This session features successful approaches to patient, provider, and technologist satisfaction.

Printed on: 02/07/23



## Abstract Archives of the RSNA, 2022

T1-CNR12

### Post-op Spine: Tips and Tricks From the Experts

Tuesday, Nov. 29 8:00AM - 9:00AM Room: NA

#### Participants

Anousheh Sayah, MD, McLean, VA (*Presenter*) Nothing to Disclose

Marin McDonald, MD, PhD, San Diego, CA (*Presenter*) Speakers Bureau, Canon Medical Systems Corporation

Carlos H. Torres, MD, FRCPC, Ottawa, ON (*Presenter*) Nothing to Disclose

Lubdha Shah, MD, Salt Lake City, UT (*Moderator*) Nothing to Disclose

#### COURSE DESCRIPTION

Post-op Spine: Tips and Tricks From the Experts will be a comprehensive session on everything a radiologist needs to know about post-operative spine imaging. The number of spinal surgeries performed has been steadily increasing, and these procedures are being accompanied by a growing number of postoperative imaging studies to interpret. Accurate interpretation requires the identification of several critical points, including delineation of the location and integrity of surgical implants; evaluation of the success of decompression procedures; delineation of fusion status; and identification of complications. Knowledge of the numerous spinal surgery techniques and devices aids in differentiating expected postoperative findings from complications. The various types of spinal surgery instrumentation and commonly used spinal implants will be reviewed. It is important to be familiar with normal postoperative spine findings, signs of successful surgery, and the broad spectrum of postoperative complications. The key points to include in the radiology report that address issues that the surgeon needs to know for optimal patient management will be discussed.

#### LEARNING OBJECTIVES

1) Describe the different categories of spinal surgery and the various instrumentations and implants used in spinal procedures 2) Identify normal and abnormal imaging findings in the post-operative spine 3) Review the key points to include in the post-operative spine imaging report\*Course Description Post-op Spine: Tips and Tricks From the Experts will be a comprehensive session on everything a radiologist needs to know about post-operative spine imaging. The number of spinal surgeries performed has been steadily increasing, and these procedures are being accompanied by a growing number of postoperative imaging studies to interpret. Accurate interpretation requires the identification of several critical points, including delineation of the location and integrity of surgical implants; evaluation of the success of decompression procedures; delineation of fusion status; and identification of complications. Knowledge of the numerous spinal surgery techniques and devices aids in differentiating expected postoperative findings from complications. The various types of spinal surgery instrumentation and commonly used spinal implants will be reviewed. It is important to be familiar with normal postoperative spine findings, signs of successful surgery, and the broad spectrum of postoperative complications. The key points to include in the radiology report that address issues that the surgeon needs to know for optimal patient management will be discussed.

Printed on: 02/07/23



## Abstract Archives of the RSNA, 2022

T1-COB06

### Obstetric Emergencies: Pearls and Pitfalls

Tuesday, Nov. 29 8:00AM - 9:00AM Room: NA

#### Participants

Tara A. Morgan, MD, San Francisco, CA (*Presenter*) Nothing to Disclose  
Jill Langer, MD, Villanova, PA (*Presenter*) Nothing to Disclose  
Mary C. Frates, MD, Sharon, MA (*Presenter*) Nothing to Disclose

#### COURSE DESCRIPTION

This lecture style presentation will review urgent and emergent conditions during pregnancy, divided by trimester. Attendees will become familiar with variants and abnormalities seen with ultrasound that indicate pregnancy complications and learn how they may alter the course of fetal management and delivery.

#### LEARNING OBJECTIVES

At the conclusion of this live activity, learners will be able to: 1) Identify sonographic abnormalities seen in the first trimester that are associated with fetal non-viability 2) Differentiate and assess second trimester fetal anomalies that require emergent care including hydrops, hypoplastic left heart, thoracic masses 3) Understand the role of ultrasound in third trimester obstetrical emergencies including abruption, cervical insufficiency, placenta accreta spectrum\*Course Description This lecture style presentation will review urgent and emergent conditions during pregnancy, divided by trimester. Attendees will become familiar with variants and abnormalities seen with ultrasound that indicate pregnancy complications and learn how they may alter the course of fetal management and delivery.

Printed on: 02/07/23



## Abstract Archives of the RSNA, 2022

T1-CPH10

### Advanced Ultrasound Technology and Applications

Tuesday, Nov. 29 8:00AM - 9:00AM Room: NA

#### Participants

Carl Herickhoff, PhD, Memphis, TN (*Presenter*) Technical Advisory Board, Maui Imaging, Inc; Shareholder, Maui Imaging, Inc; Consultant, Bioventus LLC; Consultant, Open Water Internet, Inc; Shareholder, Open Water Internet, Inc; Consultant, Scitus Engineering

Thaddeus Wilson, PhD, Memphis, TN (*Presenter*) Nothing to Disclose

Stephen McAleavey, PhD, Rochester, NY (*Presenter*) Research collaboration, Siemens AG

#### COURSE DESCRIPTION

Provide an update in current ultrasound technologies in flow imaging, beamforming techniques and advanced transducers.

#### LEARNING OBJECTIVES

1) Explain the approach, capabilities, and limitations of conventional Doppler imaging techniques. 2) Present how new technologies are improving sensitivity and visualization of flow in smaller vessels (with high resolution and contrast) and how this could impact clinical practice. 3) Explain the principles that enable software beamforming, and the advantages over conventional sequential delay-and-sum beamforming. 4) Describe the benefits of advanced ultrasound transducer technologies and geometries, and their clinical impact.\*Course Description Provide an update in current ultrasound technologies in flow imaging, beamforming techniques and advanced transducers.

Printed on: 02/07/23



## Abstract Archives of the RSNA, 2022

T1-CRO10

### Pediatric Case-based Multidisciplinary Review

Tuesday, Nov. 29 8:00AM - 9:00AM Room: NA

#### Participants

Susan Sotardi, MD, Philadelphia, PA (*Presenter*) Nothing to Disclose

David Ebb, MD, Boston, MA (*Presenter*) Nothing to Disclose

Hesham Elhalawani, MD, MSc, Boston, MA (*Presenter*) Nothing to Disclose

Michael S. Gee, MD, PhD, Boston, MA (*Presenter*) Researcher, General Electric Company Researcher, Siemens AG Researcher, Motilent LLC

#### COURSE DESCRIPTION

The course will be a multidisciplinary review of pediatric oncology cases that will include radiation oncology, medical oncology, and radiology perspectives and considerations for clinical management of pediatric oncology patients. Issues related to relevant imaging anatomy, imaging modalities, radiation planning, and therapeutic options will be discussed. The format of the course will be a multidisciplinary case review and discussion mirroring that of a tumor board conference. This synopsis can be used as a marketing/promotional tool to gauge interest in the session. The expected outcome is that the audience will have familiarity with diagnostic imaging and treatment planning of pediatric cancer patients.

#### LEARNING OBJECTIVES

1) Identify important imaging anatomy relevant to pediatric tumors. 2) Explain the pros and cons of different imaging modalities in pediatric oncology staging. 3) Understand imaging and clinical considerations related to the treatment decisions in pediatric cancer.\*Course Description The course will be a multidisciplinary review of pediatric oncology cases that will include radiation oncology, medical oncology, and radiology perspectives and considerations for clinical management of pediatric oncology patients. Issues related to relevant imaging anatomy, imaging modalities, radiation planning, and therapeutic options will be discussed. The format of the course will be a multidisciplinary case review and discussion mirroring that of a tumor board conference. This synopsis can be used as a marketing/promotional tool to gauge interest in the session. The expected outcome is that the audience will have familiarity with diagnostic imaging and treatment planning of pediatric cancer patients.

Printed on: 02/07/23



## Abstract Archives of the RSNA, 2022

T1-CVA02

### Imaging of Vascular Trauma: Optimization of Imaging Techniques

Tuesday, Nov. 29 8:00AM - 9:00AM Room: NA

#### Participants

Sameer Raniga, FRCR, MD, Muscat, (*Presenter*) Nothing to Disclose

Patrick Sutphin, MD, PhD, Boston, MA (*Presenter*) Stockholder, Gilead Sciences, Inc; Stockholder, Editas Medicine; Stockholder, CRISPR Therapeutics AG; Stockholder, Intellia Therapeutics; Stockholder, Amwell; Stockholder, Teladoc Health Inc; Stockholder, Jazz Pharmaceuticals plc; Stockholder, ViewRay, Inc; Research funded, TriSalus Life Sciences

Jennifer Uyeda, MD, Lexington, MA (*Presenter*) Nothing to Disclose

Avneesh Gupta, MD, Boston, MA (*Moderator*) Speaker, Koninklijke Philips NV;;

#### COURSE DESCRIPTION

The course focuses on various aspects of optimizing imaging protocols in the setting of vascular trauma. At the end of the session, the participant will be able to apply different techniques to streamlining vascular imaging studies for trauma patients.

#### LEARNING OBJECTIVES

1) To understand various methods for optimizing imaging in the setting of vascular trauma 2) To apply image optimization techniques to timely imaging of vascular trauma patients\*Course Description The course focuses on various aspects of optimizing imaging protocols in the setting of vascular trauma. At the end of the session, the participant will be able to apply different techniques to streamlining vascular imaging studies for trauma patients.

Printed on: 02/07/23



## Abstract Archives of the RSNA, 2022

T1-RCP18

### Chile Presents: From the End of the World: Women Empowerment in Radiology, Imaging Transcendence Beyond Death, Overcoming Difficulties to Publish and Changing Paradigms over the Andes Mountains in Interventional Radiology

Tuesday, Nov. 29 8:00AM - 9:30AM Room: NA

#### Participants

Marcos Tapia II, MD, Temuco, Chile (*Presenter*) Nothing to Disclose  
Marcelo Galvez, MD, Santiago., Chile (*Presenter*) Nothing to Disclose  
Gian Paolo Zamboni, MD, Santiago, Chile (*Presenter*) Nothing to Disclose  
Cecilia Besa, MD, Santiago, Chile (*Presenter*) Nothing to Disclose  
Eleonora Horvath, MD, Santiago, Chile (*Presenter*) Nothing to Disclose  
Mario G. Santamarina, MD, Vina del Mar, Chile (*Presenter*) Nothing to Disclose  
Ximena Wortsman, MD, Santiago, Chile (*Presenter*) Speakers Bureau, AbbVie Inc;Royalties, Springer Nature  
Christian P. Perez, MD, Santiago, Chile (*Moderator*) Nothing to Disclose

#### COURSE DESCRIPTION

The Chile presents session is an educational program focused to radiologist all over the world interested in learning from the experience of colleagues developing local radiology in a small country far away from technological and professional centers, overcoming language and geographical barriers. In the course we highlight the role of women radiologist in achieving these goals, aiming to be a regional contribution on the radiological field. Course Description: An introductory module will give the attendants a background on cultural, geographical and radiological facts from Chile. In the main module attendants will receive from first-hand the experience, pitfalls, and barriers to overcome in developing a successful career, from recognized Chilean women radiologists with and outstanding contributions in their field of expertise, that have surpassed local geographical boundaries, reaching a global impact. The next module shows some of Chileans radiology contribution on direct and indirect fields dealing with the specialty. A final module will share with the assistant's new areas of development that are improving local radiological practice.

#### LEARNING OBJECTIVES

At the end of the course, you will be able to: 1) As radiologist ask yourself and reason about your daily clinical practice 2) Identify drivers of empowerment for women radiologist in your practice 3) By the shared experience avoid some of the problems in the process and deploy some of the solutions showed 4) Identify levers to implement and achieve local development in clinical practice and research as radiologist\* Course Description The Chile presents session is an educational program focused to radiologist all over the world interested in learning from the experience of colleagues developing local radiology in a small country far away from technological and professional centers, overcoming language and geographical barriers. In the course we highlight the role of women radiologist in achieving these goals, aiming to be a regional contribution on the radiological field. Course Description: An introductory module will give the attendants a background on cultural, geographical and radiological facts from Chile. In the main module attendants will receive from first-hand the experience, pitfalls, and barriers to overcome in developing a successful career, from recognized Chilean women radiologists with and outstanding contributions in their field of expertise, that have surpassed local geographical boundaries, reaching a global impact. The next module shows some of Chileans radiology contribution on direct and indirect fields dealing with the specialty. A final module will share with the assistant's new areas of development that are improving local radiological practice.

Printed on: 02/07/23



## Abstract Archives of the RSNA, 2022

T1-RCP39

### MR Safety: From Program Creation to Best Practices (Part 1) (Sponsored by the RSNA Quality Improvement Committee)

Tuesday, Nov. 29 8:00AM - 9:00AM Room: NA

#### Participants

Candice Bookwalter, MD, PhD, Rochester, MN (*Presenter*) Nothing to Disclose  
Maureen Hood, PhD, RN, Bethesda, MD (*Presenter*) In-kind support, General Electric Company  
Jonathan Flug, MD, Phoenix, AZ (*Presenter*) Nothing to Disclose  
Heidi Edmonson, PhD, Rochester, MN (*Presenter*) Nothing to Disclose  
Samuel Fahrenholtz, PhD, Scottsdale, AZ (*Presenter*) Stockholder, Nano X Imaging  
William Sensakovic, PhD, Cave Creek, AZ (*Presenter*) Nothing to Disclose  
Scott Reeder, MD, PhD, Madison, WI (*Presenter*) Owner, Calimetrix; Owner, Reveal Pharmaceuticals; Owner, Collectar Biosciences, Inc.; Owner, Elucent Medical; Owner, HeartVista, Inc.;

#### COURSE DESCRIPTION

MRI safety is a critical safety issue in radiology departments due to the inherent risks associated with the modality and the potential for harm to staff and patients in this environment. Many MRI safety courses focus only on the physics aspects of MRI safety. While critical, this only addresses one element of the many facets of an effective program. The purpose of this session is to describe how to build an effective MRI safety program from the ground up, including the motivation for a program, program structure overview, and review of each of the necessary staff members required to form a functioning program. This session will address the why and how to help your group develop or fine tune an effective MR safety program.

#### LEARNING OBJECTIVES

1) Review the importance and requirements of an MRI safety program 2) Describe strategies to effectively build a multidisciplinary MRI safety team and program 3) Identify the roles and responsibilities of MR Safety Program team members\*Course Description MRI safety is a critical safety issue in radiology departments due to the inherent risks associated with the modality and the potential for harm to staff and patients in this environment. Many MRI safety courses focus only on the physics aspects of MRI safety. While critical, this only addresses one element of the many facets of an effective program. The purpose of this session is to describe how to build an effective MRI safety program from the ground up, including the motivation for a program, program structure overview, and review of each of the necessary staff members required to form a functioning program. This session will address the why and how to help your group develop or fine tune an effective MR safety program.

Printed on: 02/07/23



## Abstract Archives of the RSNA, 2022

T2-CBR13

### RSNA Simulation Lab (Hands on): Breast US Biopsy 1

Tuesday, Nov. 29 9:00AM - 10:30AM Room: NA

#### Participants

Beatriz Adrada, MD, Houston, TX (*Presenter*) Nothing to Disclose  
Sarah Pittman, MD, Stanford, CA (*Presenter*) Nothing to Disclose  
Stamatia Destounis, MD, Rochester, NY (*Presenter*) Medical Advisory Board, iCad, Inc  
Jean Seely, MD, Ottawa, ON (*Presenter*) Nothing to Disclose  
Marcio Saito, Barretos, Brazil (*Presenter*) Speaker, General Electric Company  
Liane E. Philpotts, MD, Madison, CT (*Presenter*) Nothing to Disclose  
Cecilia L. Mercado, MD, New York, NY (*Presenter*) Nothing to Disclose  
Gary Whitman, MD, Houston, TX (*Presenter*) Consultant, Siemens AG; Editor, Wolters Kluwer nv  
Haydee Ojeda-Fournier, MD, San Diego, CA (*Presenter*) Research Consultant, View Point Medical, Inc; Stock options, CureMetrix, Inc  
Phan Huynh, MD, Bellaire, TX (*Presenter*) Nothing to Disclose  
Paula B. Gordon, MD, Vancouver, BC (*Presenter*) Stockholder, OncoGenex Pharmaceuticals, Inc; Stockholder, Volpara Health Technologies Limited; Scientific Advisor, Besins Healthcare SA  
Richard G. Barr, MD, PhD, Canfield, OH (*Presenter*) Consultant, Siemens AG; Speakers Bureau, Siemens AG; Research Grant, Siemens AG; Consultant, Koninklijke Philips NV; Speakers Bureau, Koninklijke Philips NV; Consultant, Canon Medical Systems Corporation; Advisor, Hologic, Inc; Research Grant, Hologic, Inc  
Michael Linver, MD, Alexandria, VA (*Presenter*) Medical Advisory Board, Three Palm Software LLC; Scientific Advisory Board, Seno Medical Instruments, Inc  
Linda J. Warren, MD, Vancouver, BC (*Presenter*) Shareholder, Hologic, Inc  
Tanya W. Moseley, MD, PhD, Houston, TX (*Presenter*) Consultant, Hologic, Inc; Consultant, Merit Medical Systems, Inc; Owner, TW Moseley, LLC; CEO, TW Moseley, LLC  
Norrin H. Said, MD, FRCR, Cairo, Egypt (*Presenter*) Nothing to Disclose  
Shadi Aminololama-Shakeri, MD, Sacramento, CA (*Presenter*) Consultant, Becton, Dickinson and Company; Consultant, Izotropic Corporation; Stock options, Izotropic Corporation  
Laurie Margolies, MD, New York, NY (*Presenter*) Stock options, Nuevozen Corporation Medical Advisory Board, Screenpoint Medical  
Maria Helena S. Mendonca, MD, PhD, Sao Paulo, Brazil (*Presenter*) Expert Advisory Committee, Guerbet SA  
Jessica Leung, MD, Houston, TX (*Presenter*) Scientific Advisory Board, Subtle Medical, Inc; Speaker, General Electric Company; Speaker, Hologic, Inc; Scientific Advisory Board, Seno Medical Instruments, Inc

#### COURSE DESCRIPTION

In Person Session Only. Tickets must be purchased in advance for this course. This course can be added through the registration portal or by stopping by the Registration Desk. Space is limited. A brief didactic lecture will be given on needle biopsy technique and the various equipment. The attendee at completion of course should have some familiarity of how to handle different biopsy devices under ultrasound guidance. Masses and cysts will be identified and biopsied or drained. Various wire localization equipment will also be available. Every attendee will have opportunity to use hands on biopsy equipment. Instruction will be given on how to perform procedure and before and after care. Various ultrasound equipment will be available for scanning and localizations of lesions.

#### LEARNING OBJECTIVES

1) Introduction of various tru cut and vacuum needle breast biopsy devices and their utilization within clinical practice 2) Utilization of different ultrasound technology to perform interventional procedures in the breast 3) Introduction of additional procedures in the breast such as cyst aspiration, fine needle aspiration, marker placement\*Course Description In Person Session Only. Tickets must be purchased in advance for this course. This course can be added through the registration portal or by stopping by the Registration Desk. Space is limited. A brief didactic lecture will be given on needle biopsy technique and the various equipment. The attendee at completion of course should have some familiarity of how to handle different biopsy devices under ultrasound guidance. Masses and cysts will be identified and biopsied or drained. Various wire localization equipment will also be available. Every attendee will have opportunity to use hands on biopsy equipment. Instruction will be given on how to perform procedure and before and after care. Various ultrasound equipment will be available for scanning and localizations of lesions.

Printed on: 02/07/23



## Abstract Archives of the RSNA, 2022

T3-CAS08

### Career Ladders: Navigating Your Way (Sponsored by the Associated Sciences Consortium)

Tuesday, Nov. 29 9:30AM - 10:30AM Room: NA

#### Participants

Denise Vander Werf, MS,BS, Tampa, FL (*Presenter*) Nothing to Disclose

Janice St. John-Matthews, BSC,MSc, Leeds, United Kingdom (*Presenter*) Nothing to Disclose

Charlotte Beardmore, MBA, London, United Kingdom (*Presenter*) Nothing to Disclose

Catherine Gunn, MBA,RT, Halifax, NS (*Moderator*) Nothing to Disclose

#### COURSE DESCRIPTION

If you're interested in progressing your career please do come along to this session which will discuss career opportunities for radiological technologists/ radiographers. Two expert speakers, one from the UK and one from the US will consider how career progression and career ladders are supported, and how these could be further be developed within the radiological technologist/radiographer profession. The lecturers will discuss the impact of the pandemic upon these opportunities and share real life experiences to support discussion.

#### LEARNING OBJECTIVES

1) Introduction to imaging career ladders, how, why, criteria and examples 2) Explain pros and cons of career ladders based on real life experiences 3) Discussion will career ladders be sustainable post covid- market changes?\*

Course Description If you're interested in progressing your career please do come along to this session which will discuss career opportunities for radiological technologists/ radiographers. Two expert speakers, one from the UK and one from the US will consider how career progression and career ladders are supported, and how these could be further be developed within the radiological technologist/radiographer profession. The lecturers will discuss the impact of the pandemic upon these opportunities and share real life experiences to support discussion.

Printed on: 02/07/23



## Abstract Archives of the RSNA, 2022

T3-CER06

### Head and Face Trauma

Tuesday, Nov. 29 9:30AM - 10:30AM Room: NA

#### Participants

Christopher T. Whitlow, MD, PhD, Winston Salem, NC (*Presenter*) Consultant, Biogen Idec Inc

Divya Gunda, MD, Oklahoma City, OK (*Presenter*) Nothing to Disclose

Clint W. Sliker, MD, Baltimore, MD (*Presenter*) Nothing to Disclose

Koenraad Nieboer, MD, Brussels, (*Presenter*) Speakers Bureau, General Electric Company

#### COURSE DESCRIPTION

This session offers 4 highly recommended lectures on the basic assessment of CT scan of the brain, facial bones and cerebrovascular lesions in the context of acute trauma for all experience levels. Clear identification and description of acute traumatic lesions are essential for rapid communication with referring physicians and trauma surgeons. And when do you recommend advanced imaging?

#### LEARNING OBJECTIVES

1) Identify and describe correctly acute traumatic lesions on CT scan of the head, facial bones and blunt cerebrovascular injury 2) When to use advanced neuroimaging techniques in the setting of traumatic brain injury\*Course Description This session offers 4 highly recommended lectures on the basic assessment of CT scan of the brain, facial bones and cerebrovascular lesions in the context of acute trauma for all experience levels. Clear identification and description of acute traumatic lesions are essential for rapid communication with referring physicians and trauma surgeons. And when do you recommend advanced imaging?

Printed on: 02/07/23



## Abstract Archives of the RSNA, 2022

T3-CGI03

### Colorectal Imaging

Tuesday, Nov. 29 9:30AM - 10:30AM Room: NA

#### Participants

Natally Horvat, MD, PhD, New York, NY (*Presenter*) Nothing to Disclose

Judy Yee, MD, New York, NY (*Presenter*) Research Grant, General Electric Company

Kartik S. Jhaveri, MD, Mississauga, ON (*Presenter*) Research Grant, General Electric Company; Research Grant, Bayer AG; Research Consultant, Perspectum Diagnostics Ltd;

Kevin Chang, MD, Sharon, MA (*Presenter*) Speaker, Anderson Publishing, Ltd; Speaker, Koninklijke Philips NV

#### COURSE DESCRIPTION

This session will provide best practices for obtaining optimal CT Colonography exams and will show how CTC can play a role in decreasing disparities in colorectal cancer screening and diagnosis. Core concepts of rectal cancer MRI will be discussed including staging and reporting and appearance after neoadjuvant treatment.

#### LEARNING OBJECTIVES

1) Identify best practices to obtain maximally diagnostic CT Colonography exams 2) Explain strategies as to how to implement and disseminate CTC to decrease disparities 3) Provide key concepts about MR for rectal cancer staging, reporting and treatment\*Course Description This session will provide best practices for obtaining optimal CT Colonography exams and will show how CTC can play a role in decreasing disparities in colorectal cancer screening and diagnosis. Core concepts of rectal cancer MRI will be discussed including staging and reporting and appearance after neoadjuvant treatment.

Printed on: 02/07/23



## Abstract Archives of the RSNA, 2022

T3-CHN04

### Focal Cranial Nerve Deficits - A Symptom Based Session

Tuesday, Nov. 29 9:30AM - 10:30AM Room: NA

#### Participants

Katherine Reinshagen, MD, Boston, MA (*Presenter*) Nothing to Disclose

Richard H. Wiggins III, MD, Salt Lake City, UT (*Presenter*) Nothing to Disclose

Hillary R. Kelly, MD, Cambridge, MA (*Presenter*) Investigator, Bayer AG; Institutional research agreement, Bayer AG

Karen K. Moeller, MD, Louisville, KY (*Moderator*) Nothing to Disclose

#### COURSE DESCRIPTION

In this clinical correlation didactic head and neck imaging session, speakers will review the imaging evaluation and common causes of diplopia, trigeminal neuralgia and facial weakness. Speakers will emphasize search patterns, pitfalls of interpretation to avoid, and relevant clinical management considerations with which radiologists should be familiar. This session offers attendees the opportunity to refine their interpretation of complex head and neck imaging studies by incorporating tips from world experts.

#### LEARNING OBJECTIVES

1) Select the appropriate imaging algorithm for patients presenting with diplopia, trigeminal neuralgia and facial weakness 2) Identify the common causes of diplopia, trigeminal neuralgia and facial weakness 3) Review the common diagnostic pitfalls in imaging evaluation of diplopia, trigeminal neuralgia and facial weakness\*Course Description In this clinical correlation didactic head and neck imaging session, speakers will review the imaging evaluation and common causes of diplopia, trigeminal neuralgia and facial weakness. Speakers will emphasize search patterns, pitfalls of interpretation to avoid, and relevant clinical management considerations with which radiologists should be familiar. This session offers attendees the opportunity to refine their interpretation of complex head and neck imaging studies by incorporating tips from world experts.

Printed on: 02/07/23



## Abstract Archives of the RSNA, 2022

T3-CMK02

### Shoulder Pre-op and Post-op: Pearls and Pitfalls

Tuesday, Nov. 29 9:30AM - 10:30AM Room: NA

#### Participants

Miriam A. Bredella, MD, Boston, MA (*Presenter*) Nothing to Disclose  
Erin F. Alaia, MD, New York, NY (*Presenter*) Biorez Inc, Consultant  
Donald L. Resnick, MD, San Diego, CA (*Presenter*) Nothing to Disclose  
David A. Rubin, MD, Saint Louis, MO (*Presenter*) Scientific Advisory Board, ImageBiopsy Lab  
Michael J. Tuite, MD, Verona, WI (*Presenter*) Nothing to Disclose

#### COURSE DESCRIPTION

Get Pearls and Pitfalls from five experts in shoulder MRI. These lectures will discuss MRI findings that surgeons want to know prior to arthroscopy about tendon delamination and the supraspinatus outlet, and atypical injuries after anterior dislocation. You will improve your accuracy in assessing patients with prior rotator cuff repair, as well as what to look for on imaging in the novel techniques performed for irreparable rotator cuff tears. You will be able to integrate these useful tips into your practice and read shoulder MRI like the experts.

#### LEARNING OBJECTIVES

1) Describe shoulder MRI features that will help the surgeon with pre-operative planning of the rotator cuff, supraspinatus outlet, and anterior labrocapsular complex 2) Explain the MRI findings of the intact and re-torn post-surgical rotator cuff, and the post-operative imaging of new techniques for irreparable cuff tears\*Course Description Get Pearls and Pitfalls from five experts in shoulder MRI. These lectures will discuss MRI findings that surgeons want to know prior to arthroscopy about tendon delamination and the supraspinatus outlet, and atypical injuries after anterior dislocation. You will improve your accuracy in assessing patients with prior rotator cuff repair, as well as what to look for on imaging in the novel techniques performed for irreparable rotator cuff tears. You will be able to integrate these useful tips into your practice and read shoulder MRI like the experts.

Printed on: 02/07/23



## Abstract Archives of the RSNA, 2022

T3-CNMMI11

### Case-based Review of Chest: PET/CT Workshop (In Conjunction with SNMMI)

Tuesday, Nov. 29 9:30AM - 10:30AM Room: NA

#### Participants

Gary Ulaner, MD, PhD, Irvine, CA (*Presenter*) Speaker, Siemens AG; Speaker, Lantheus Holdings; Research support, General Electric Company; Research support, F. Hoffmann-La Roche Ltd; Research support, Lantheus Holdings; Research support, Novartis AG  
Rathan M. Subramaniam, MD, PhD, Dunedin, (*Presenter*) Nothing to Disclose

#### COURSE DESCRIPTION

PET/CT has greatly impacted the imaging and therapy of chest malignancies, including longstanding value for staging of lung cancer, as well as novel Estrogen Receptor targeted imaging for breast cancer. In this session, experts on lung and breast cancers will use clinical cases to demonstrate fundamentals of interpretation, as well as pearls and pitfalls to help improve interpretation of FES (Cerianna) PET.

#### LEARNING OBJECTIVES

1) Understand best clinical practices for use and interpretation of PET imaging in patient with lung cancer 2) Understand best clinical practices for use and interpretation of FES PET/CT in patients with breast cancer\*Course Description PET/CT has greatly impacted the imaging and therapy of chest malignancies, including longstanding value for staging of lung cancer, as well as novel Estrogen Receptor targeted imaging for breast cancer. In this session, experts on lung and breast cancers will use clinical cases to demonstrate fundamentals of interpretation, as well as pearls and pitfalls to help improve interpretation of FES (Cerianna) PET.

Printed on: 02/07/23



## Abstract Archives of the RSNA, 2022

T3-CPD09

### Artificial Intelligence in Pediatric Radiology

Tuesday, Nov. 29 9:30AM - 10:30AM Room: NA

#### Participants

Marla Sammer, MD, Houston, TX (*Presenter*) Nothing to Disclose

Safwan Halabi, MD, Chicago, IL (*Presenter*) Advisor, Change Healthcare

Alex Towbin, MD, Cincinnati, OH (*Presenter*) Author, RELX; Consultant, Anderson Publishing, Ltd; Advisory Board, KLAS Enterprises LLC; Travel support, Merative LP

#### COURSE DESCRIPTION

Noninterpretive Artificial intelligence promises to change the way radiology departments work. The purpose of this session is to describe non-interpretive AI, describe a framework for its creation, and describe use cases needed in radiology departments.

#### LEARNING OBJECTIVES

1) Define non-interpretive AI 2) Describe a framework to consider non-interpretive AI 3) Provide examples of how non-interpretive AI could improve Radiology workflows\*Course Description Noninterpretive Artificial intelligence promises to change the way radiology departments work. The purpose of this session is to describe non-interpretive AI, describe a framework for its creation, and describe use cases needed in radiology departments.

Printed on: 02/07/23



## Abstract Archives of the RSNA, 2022

T3-RCP01

### Fast 5

Tuesday, Nov. 29 10:30AM - 11:00AM Room: Arie Crown

#### Participants

Sherry Wang, MBBS, Salt Lake City, UT (*Moderator*) Royalties, RELX

#### Sub-Events

##### **T3-RCP01 Bringing Patients to the AI Table**

Participants

Ali Tejani, MD, Frisco, TX (*Presenter*) Nothing to Disclose

##### **T3-RCP01 Compensate Radiologists for Tumor Board Participation!**

Participants

Sanna Herwald, MD, PhD, Menlo Park, CA (*Presenter*) Nothing to Disclose

##### **T3-RCP01 Palliative Care in Radiology: More Than Meets the Eye**

Participants

Samuel Galgano, MD, Birmingham, AL (*Presenter*) Research support, Blue Earth Diagnostics Ltd; Research support, Novartis AG; Research Support, Curium SAS

##### **T3-RCP01 Increase Patient Access to Radiologists**

Participants

Beth Vettiyil, MBBS, Farmville, VA (*Presenter*) Nothing to Disclose

##### **T3-RCP01 Achieving Health Equity and Healthcare Systems Transformation through Meaningful Community Engagement and Upstream Partnerships**

Participants

Peter Abraham, MD, San Diego, CA (*Presenter*) Nothing to Disclose

Printed on: 02/07/23



## Abstract Archives of the RSNA, 2022

T3-RCP01

### Bringing Patients to the AI Table

Tuesday, Nov. 29 10:30AM - 11:00AM Room: Arie Crown

#### Participants

Ali Tejani, MD, Frisco, TX (*Presenter*) Nothing to Disclose

Printed on: 02/07/23



## Abstract Archives of the RSNA, 2022

T3-RCP01

### Compensate Radiologists for Tumor Board Participation!

Tuesday, Nov. 29 10:30AM - 11:00AM Room: Arie Crown

#### Participants

Sanna Herwald, MD, PhD, Menlo Park, CA (*Presenter*) Nothing to Disclose

Printed on: 02/07/23



## Abstract Archives of the RSNA, 2022

T3-RCP01

### Palliative Care in Radiology: More Than Meets the Eye

Tuesday, Nov. 29 10:30AM - 11:00AM Room: Arie Crown

#### Participants

Samuel Galgano, MD, Birmingham, AL (*Presenter*) Research support, Blue Earth Diagnostics Ltd; Research support, Novartis AG; Research Support, Curium SAS

Printed on: 02/07/23



## Abstract Archives of the RSNA, 2022

T3-RCP01

### Increase Patient Access to Radiologists

Tuesday, Nov. 29 10:30AM - 11:00AM Room: Arie Crown

#### Participants

Beth Vettiyil, MBBS, Farmville, VA (*Presenter*) Nothing to Disclose

Printed on: 02/07/23



## Abstract Archives of the RSNA, 2022

T3-RCP01

### **Achieving Health Equity and Healthcare Systems Transformation through Meaningful Community Engagement and Upstream Partnerships**

Tuesday, Nov. 29 10:30AM - 11:00AM Room: Arie Crown

#### **Participants**

Peter Abraham, MD, San Diego, CA (*Presenter*) Nothing to Disclose

Printed on: 02/07/23



## Abstract Archives of the RSNA, 2022

T3-RCP40

### MR Safety: MR Safety: Case-based Approached (Part 2) (Sponsored by the RSNA Quality Improvement Committee)

Tuesday, Nov. 29 9:30AM - 10:30AM Room: NA

#### Participants

Yuxiang Zhou, PhD, Phoenix, AZ (*Presenter*) Nothing to Disclose  
Wende Gibbs, MD, MA, Scottsdale, AZ (*Presenter*) Nothing to Disclose  
R. Jason Stafford, PhD, Houston, TX (*Presenter*) Nothing to Disclose  
Andrew Bowman, MD, PhD, Jacksonville, FL (*Presenter*) Nothing to Disclose  
Jonathan Flug, MD, Phoenix, AZ (*Presenter*) Nothing to Disclose  
Anshuman Panda, PhD, Scottsdale, AZ (*Presenter*) Nothing to Disclose  
Samuel Fahrenholtz, PhD, Scottsdale, AZ (*Presenter*) Stockholder, Nano X Imaging  
William Sensakovic, PhD, Cave Creek, AZ (*Presenter*) Nothing to Disclose

#### COURSE DESCRIPTION

MRI safety is a multi-faceted issue that encompasses diverse issues ranging from acquisition parameter selection to off-label scanning decisions. Although guidance exists in multiple forms for each topic, real-world examples are not always available to ground abstract knowledge. This session will review several facets of MRI Safety and convey best practices through the lens of real-world situations encountered by the speakers.

#### LEARNING OBJECTIVES

1) Identify safety issues related to active implants 2) Describe strategies to meet implant scanning requirements 3) Review considerations when scanning off-label or during interventional procedures 4) Understand actions to take when a safety incident occurs\*Course Description MRI safety is a multi-faceted issue that encompasses diverse issues ranging from acquisition parameter selection to off-label scanning decisions. Although guidance exists in multiple forms for each topic, real-world examples are not always available to ground abstract knowledge. This session will review several facets of MRI Safety and convey best practices through the lens of real-world situations encountered by the speakers.

Printed on: 02/07/23



## Abstract Archives of the RSNA, 2022

T4-CMS05

### Multi-system Imaging Manifestations of COVID-19 and Related Complications

Tuesday, Nov. 29 11:00AM - 12:00PM Room: NA

#### Participants

Kate Hanneman, MD, FRCPC, Toronto, ON (*Presenter*) Speaker, Groupe Sanofi Speaker, Amicus Therapeutics, Inc  
Margarita Revzin, MD, Wilton, CT (*Presenter*) Nothing to Disclose  
Otto Rapalino, MD, Boston, MA (*Presenter*) Nothing to Disclose  
David A. Lynch, MBBCh, Denver, CO (*Presenter*) Research Consultant, CALYX Inc; Research Consultant, Boehringer Ingelheim GmbH; Research Consultant, Veracyte, Inc; Research Consultant, DAIICHI SANKYO Group; Research Consultant, AstraZeneca PLC; Consultant, Polarean, Inc; Consultant, Bristol Myers Squibb Company

#### COURSE DESCRIPTION

This session will provide a comprehensive review of the diagnostic imaging hallmarks of COVID-19 infection and related complications with emphasis on the organ-specific imaging features, complexity and multisystemic involvement of the disease, and evolution of imaging findings in patients post COVID-19. Pulmonary, cardiac, abdominopelvic and neurological systems will be discussed including neurological syndromes and cardiac imaging findings after vaccination.

#### LEARNING OBJECTIVES

The learner will: 1) gain awareness of the available imaging modalities and abbreviated protocols for multisystemic evaluation of the patients with COVID-19 infection 2) recognize organ-specific evolution of the imaging findings associated with COVID-19 infection from its initial presentation to long standing disease with special emphasis on the common and rare complications 3) discuss imaging findings associated with post-vaccination\*Course Description This session will provide a comprehensive review of the diagnostic imaging hallmarks of COVID-19 infection and related complications with emphasis on the organ-specific imaging features, complexity and multisystemic involvement of the disease, and evolution of imaging findings in patients post COVID-19. Pulmonary, cardiac, abdominopelvic and neurological systems will be discussed including neurological syndromes and cardiac imaging findings after vaccination.

Printed on: 02/07/23



## Abstract Archives of the RSNA, 2022

T4-CRT06

### ASRT@RSNA: Leading Medical Imaging Like a Start-Up

Tuesday, Nov. 29 11:00AM - 12:00PM Room: NA

#### Participants

Ryan Duggan, Halifax, NS (*Presenter*) Consultant, Densitas Inc; Stockholder, Densitas Inc

#### COURSE DESCRIPTION

(Lecture) Successful start-up businesses create significant value for customers, employees, and shareholders. Implementing management philosophies from effective start-ups could improve both the patient and employee experience in medical imaging.

#### LEARNING OBJECTIVES

1) Review the foundational elements of successful start-ups 2) Discuss practical examples of applying these elements to medical imaging environments 3) Recognize situations within medical imaging that could benefit from the application of successful start-up elements\*Course Description (Lecture) Successful start-up businesses create significant value for customers, employees, and shareholders. Implementing management philosophies from effective start-ups could improve both the patient and employee experience in medical imaging.

Printed on: 02/07/23



## Abstract Archives of the RSNA, 2022

T6-CBR07

### Breast MRI: Role of Abbreviated MRI

Tuesday, Nov. 29 1:30PM - 2:30PM Room: NA

#### Participants

Ritse M. Mann, MD, PhD, Nijmegen, (*Presenter*) Researcher, Siemens AG;Consultant, Siemens AG;Researcher, Bayer AG;Consultant, Bayer AG;Researcher, Medtronic plc;Consultant, Medtronic plc;Researcher, Becton, Dickinson and Company;Consultant, Becton, Dickinson and Company;Researcher, ScreenPoint Medical BV  
Christopher E. Comstock, MD, New York, NY (*Presenter*) Speakers Bureau, Bracco Group;Advisory Board, Guerbet SA;Consultant, Bayer AG;Speaker, Northwest Imaging Forums, Inc  
Pascal A. Baltzer, MD, Vienna, (*Presenter*) Nothing to Disclose

#### COURSE DESCRIPTION

This session will review Abbreviated Breast MRI (AB-MR) and its emerging role as a powerful supplemental breast cancer screening tool. Discussions will cover the different techniques of performing AB-MR, various aspects of its deployment, potential expanded applications and the current data on its performance.

#### LEARNING OBJECTIVES

1) Describe the concept of Abbreviated Breast MRI (AB-MR)2) Understand the role of AB-MR and potential expanded applications3) Review the current data on the performance of AB-MR\*Course Description This session will review Abbreviated Breast MRI (AB-MR) and its emerging role as a powerful supplemental breast cancer screening tool. Discussions will cover the different techniques of performing AB-MR, various aspects of its deployment, potential expanded applications and the current data on its performance.

Printed on: 02/07/23



## Abstract Archives of the RSNA, 2022

T6-CCH07

### Practice Updates in Chest Imaging: Guidelines and Research

Tuesday, Nov. 29 1:30PM - 2:30PM Room: NA

#### Participants

Micheal McInnis, MD, Toronto, ON (*Presenter*) Speakers Bureau, Boehringer Ingelheim GmbH;Speakers Bureau, Bayer AG  
Constantine Raptis, MD, Saint Louis, MO (*Presenter*) Nothing to Disclose  
Stephen Hobbs, MD, Lexington, KY (*Presenter*) Author with royalties, Wolters Kluwer nv;Author with royalties, RELX  
Pamela Woodard, MD, Saint Louis, MO (*Presenter*) Researcher, Siemens AG;Consulting, Medtronic plc;Researcher, Bayer AG;Patent, Washington University  
Carol C. Wu, MD, Houston, TX (*Presenter*) Nothing to Disclose

#### COURSE DESCRIPTION

Several entities, including the American College of Radiology and the Fleischner Society, provide best practice guidelines and recommendations for the imaging of various thoracic diseases. These recommendations are continually revised and updated, resulting in an evolving landscape that can be difficult for radiologists to follow. In this case-based review, guidelines for several important thoracic diseases will be presented. When available, important recent changes and ongoing research that serves as the basis for these recommendations will be highlighted. Furthermore, practical pearls that go beyond the recommendations will be identified. This information will be of value to radiologists in both specialized and general practice and improve attendees' confidence in managing patients with common thoracic conditions.

#### LEARNING OBJECTIVES

1) Review relevant practice guidelines for important conditions affecting the thorax 2) Discuss best practice suggestions for image interpretation and follow-up recommendations 3) Present relevant research related to the development of practice guidelines in the thorax\*Course Description Several entities, including the American College of Radiology and the Fleischner Society, provide best practice guidelines and recommendations for the imaging of various thoracic diseases. These recommendations are continually revised and updated, resulting in an evolving landscape that can be difficult for radiologists to follow. In this case-based review, guidelines for several important thoracic diseases will be presented. When available, important recent changes and ongoing research that serves as the basis for these recommendations will be highlighted. Furthermore, practical pearls that go beyond the recommendations will be identified. This information will be of value to radiologists in both specialized and general practice and improve attendees' confidence in managing patients with common thoracic conditions.

Printed on: 02/07/23



## Abstract Archives of the RSNA, 2022

T6-CHN01

### Can't Touch This: Distinguishing Between Actionable and Non-Actionable Lesions of the Brain, Spine, Skull Base and Neck (combined session with Neuroradiology Course)

Tuesday, Nov. 29 1:30PM - 2:30PM Room: NA

#### Participants

Luke Ledbetter, MD, Los Angeles, CA (*Presenter*) Royalties, RELX  
Girish Fatterpekar, MBBS, New York, NY (*Presenter*) Nothing to Disclose  
Wende Gibbs, MD, MA, Scottsdale, AZ (*Presenter*) Nothing to Disclose  
Alok A. Bhatt, MD, Jacksonville, FL (*Presenter*) Nothing to Disclose  
Judith Gadde, DO, Chicago, IL (*Moderator*) Nothing to Disclose

#### COURSE DESCRIPTION

In this case-based combined Neuroradiology and Head and Neck session, attendees will be presented with incidental lesions that occur in the brain, spine, skull base and neck. Speakers will emphasize imaging pearls that distinguish actionable from "don't touch" findings. This session offers attendees the opportunity to refine their interpretation of complex neuroradiology and head and neck imaging studies by incorporating tips from world experts.

#### LEARNING OBJECTIVES

1) Recognize typical and atypical imaging features of common incidental lesions of the brain, spine, skull base and neck 2) Differentiate between actionable and don't touch incidental lesions of the brain, spine, skull base and neck\*Course Description In this case-based combined Neuroradiology and Head and Neck session, attendees will be presented with incidental lesions that occur in the brain, spine, skull base and neck. Speakers will emphasize imaging pearls that distinguish actionable from "don't touch" findings. This session offers attendees the opportunity to refine their interpretation of complex neuroradiology and head and neck imaging studies by incorporating tips from world experts.

Printed on: 02/07/23



## Abstract Archives of the RSNA, 2022

T6-CIN02

### Understanding and Communicating Artificial Intelligence: Reading, Writing and Reviewing

Tuesday, Nov. 29 1:30PM - 2:30PM Room: NA

#### Participants

Linda Moy, MD, New York, NY (*Presenter*) Grant, Siemens AG ;Advisory Board, Lunit Inc;Advisory Board, iCad, Inc  
John Mongan, MD, PhD, San Francisco, CA (*Presenter*) Research Grant, General Electric Company;Research Grant, Siemens AG;Research Grant, Amazon Web Services, Inc;Royalties, General Electric Company;Spouse, Employee, Annexon, Inc;Spouse, Employee, AbbVie Inc  
Ross Filice, MD, Washington, DC (*Moderator*) Advisor, BunkerHill Health, Inc;Shareholder, BunkerHill Health, Inc;Speaker, General Electric Company;Speaker, Koios Medical;Researcher, Koios Medical

#### COURSE DESCRIPTION

Understanding how to characterize the performance of artificial intelligence applications is important for academic pursuits but critical for purchasing decisions and ongoing quality improvement. Join us to learn how to review artificial intelligence publications in the literature and to gain familiarity with key concepts in how performance of these tools is measured.

#### LEARNING OBJECTIVES

1) Understand the minimum requirements of a scientific publication: description sufficient to permit the work to be evaluated and reproduced 2) Gain familiarity with key concepts of machine learning and training data sets that should be described in a manuscript to meet minimum requirements 3) Learn how to use checklists like CLAIM to ensure completeness of manuscripts you write and evaluate manuscripts you read and review\*Course Description Understanding how to characterize the performance of artificial intelligence applications is important for academic pursuits but critical for purchasing decisions and ongoing quality improvement. Join us to learn how to review artificial intelligence publications in the literature and to gain familiarity with key concepts in how performance of these tools is measured.

Printed on: 02/07/23



## Abstract Archives of the RSNA, 2022

T6-CIR08

### Portal Hypertension

Tuesday, Nov. 29 1:30PM - 2:30PM Room: NA

#### Participants

Bartley Thornburg, MD, Chicago, IL (*Presenter*) Nothing to Disclose  
Victoria Chernyak, MD,MS, Bronx, NY (*Presenter*) Consultant, Bayer AG  
Brett Fortune, MD, New York, NY (*Presenter*) Speaker, W. L. Gore & Associates, Inc;Speaker, Cook Group Incorporated  
Pilar Bayona, Saint Louis, MO (*Presenter*) Nothing to Disclose  
Sirish Kishore, MD,BA, New York, NY (*Presenter*) Nothing to Disclose  
Eric Monroe, MD, Seattle, WA (*Presenter*) Advisory Board, Biogen Idec Inc  
David C. Madoff, MD, New Haven, CT (*Moderator*) Advisory Board, Zimmer Biomet Holdings, Inc;Consultant, General Electric Company;Consultant, Guerbet SA;Consultant, Merck & Co, Inc;Consultant, Sirtex Medical Ltd;Consultant, Boston Scientific Corporation;Consultant, Johnson & Johnson;Consultant, Siemens AG

#### COURSE DESCRIPTION

Interventional radiologists play an increasingly prominent role in the multidisciplinary management of portal hypertension, especially when vascular liver disease is present. This lecture-based course will review the pathophysiology, medical management, imaging workup, endovascular procedures, and periprocedural care required for adult and pediatric patients with thrombotic disorders of the portomesenteric system. The management of portal hypertension in the setting of malignancy will also be discussed.

#### LEARNING OBJECTIVES

1) Describe the pathophysiology, imaging features and medical management for patients with splanchnic thrombosis and portal hypertension 2) Review endovascular treatment options for splanchnic thrombosis and hepatic outflow vascular disease in the setting of portal hypertension 3) Define the role of IR in the management of extrahepatic portal vein obstruction and other causes of pediatric portal hypertension 4) Discuss how IR can provide impact in the management of portal hypertension in the setting of hepatic malignancy\*Course Description Interventional radiologists play an increasingly prominent role in the multidisciplinary management of portal hypertension, especially when vascular liver disease is present. This lecture-based course will review the pathophysiology, medical management, imaging workup, endovascular procedures, and periprocedural care required for adult and pediatric patients with thrombotic disorders of the portomesenteric system. The management of portal hypertension in the setting of malignancy will also be discussed.

Printed on: 02/07/23



## Abstract Archives of the RSNA, 2022

T6-CMS06

### Head to Toe Tumor Challenging Cases: Lessons Learned

Tuesday, Nov. 29 1:30PM - 2:30PM Room: NA

#### Participants

Alexander Kessler, MD, Pittsford, NY (*Presenter*) Nothing to Disclose

Jack A. Porrino JR, MD, New Haven, CT (*Presenter*) Nothing to Disclose

Rachna Madan, MD, Boston, MA (*Presenter*) Nothing to Disclose

Maria Manning, MD, Silver Spring, MD (*Presenter*) Nothing to Disclose

#### COURSE DESCRIPTION

This course will use a case-based format and highlight the role of imaging in the diagnosis of challenging oncology cases using a multimodality approach. The session will focus on a variety of head and neck, pediatric, chest, musculoskeletal, and abdominal malignancies. Clinical presentation and pathological correlations will be provided when possible. Differential diagnoses will include infection, inflammation, neoplasm, ischemia, hemorrhage. The session will provide a broad update in imaging advances that help to make the correct diagnosis.

#### LEARNING OBJECTIVES

1) Understand key principles in radiologic-pathologic correlation as applicable to a variety of head & neck, thoracic, abdominal and musculoskeletal malignancies 2) Formulate a focused differential diagnosis for head & neck, thoracic, abdominal and musculoskeletal malignancies based on these principles 3) The differential diagnoses would cover cases with infection, inflammation and hemorrhage\*Course Description This course will use a case-based format and highlight the role of imaging in the diagnosis of challenging oncology cases using a multimodality approach. The session will focus on a variety of head and neck, pediatric, chest, musculoskeletal, and abdominal malignancies. Clinical presentation and pathological correlations will be provided when possible. Differential diagnoses will include infection, inflammation, neoplasm, ischemia, hemorrhage. The session will provide a broad update in imaging advances that help to make the correct diagnosis.

Printed on: 02/07/23



## Abstract Archives of the RSNA, 2022

T6-CNMMI12

### Case-based Review of Genitourinary: PET/CT Workshop (In Conjunction with SNMMI)

Tuesday, Nov. 29 1:30PM - 2:30PM Room: NA

#### Participants

Gary Ulaner, MD, PhD, Irvine, CA (*Presenter*) Speaker, Siemens AG; Speaker, Lantheus Holdings; Research support, General Electric Company; Research support, F. Hoffmann-La Roche Ltd; Research support, Lantheus Holdings; Research support, Novartis AG  
Katherine Zukotynski, MD, PhD, Hamilton, ON (*Presenter*) Research Consultant, Konica Minolta, Inc; Research Consultant, General Electric Company; Speakers Bureau, Jubilant DraxImage Inc

#### LEARNING OBJECTIVES

1) Understand the limitations urinary excretion of PET tracers can cause for interpretation of images around the kidneys, ureters, and bladder. 2) Understand best clinical practices for use of PSMA-targeted PET/CT for patients with prostate cancer.\*Course Description

Printed on: 02/07/23



## Abstract Archives of the RSNA, 2022

T6-CNPM23

### Taking Stock of AI: The Value Proposition and Economic Evaluation

Tuesday, Nov. 29 1:30PM - 2:30PM Room: NA

#### Participants

Christoph Lee, MD, Mercer Island, WA (*Presenter*) Royalties, The McGraw-Hill Companies; Royalties, Oxford University Press; Royalties, Wolters Kluwer nv; Research Consultant, GRAIL, LLC  
Stella Kang, MD, MSc, New York, NY (*Presenter*) Nothing to Disclose  
Bibb Allen JR, MD, Mountain Brk, AL (*Presenter*) Nothing to Disclose  
Nina E. Kottler, MD, MS, San Diego, CA (*Presenter*) Partner, Radiology Partners; Stockholder, Radiology Partners; Employee, Radiology Partners; Consultant, ES3; Consultant, W.L. Gore & Associates, Inc; Consultant, Synapsica Healthcare Pvt Ltd

#### COURSE DESCRIPTION

Artificial intelligence (AI) developers and researchers work toward realizing the potential of AI-driven improvements in health care effectiveness and efficiency. As radiologists collaborate with data scientists on AI evaluation, understanding study design and data collection will drive progress. This course will facilitate familiarity with the value proposition of AI, study design, and state of the art in evaluating AI impact on quality and health outcomes.

#### LEARNING OBJECTIVES

1) Describe the value proposition of AI for imaging 2) Consider important aspects of data collection and a high-impact analytic plan 3) Consider strategies for evaluating imaging AI at scale and for outcomes monitoring over time\*Course Description Artificial intelligence (AI) developers and researchers work toward realizing the potential of AI-driven improvements in health care effectiveness and efficiency. As radiologists collaborate with data scientists on AI evaluation, understanding study design and data collection will drive progress. This course will facilitate familiarity with the value proposition of AI, study design, and state of the art in evaluating AI impact on quality and health outcomes.

Printed on: 02/07/23



## Abstract Archives of the RSNA, 2022

T6-CPD06

### Pediatric Emergencies

Tuesday, Nov. 29 1:30PM - 2:30PM Room: NA

#### Participants

Brooke Lampl, DO, Pepper Pike, OH (*Presenter*) Nothing to Disclose  
Cassandra Sams, MD, Providence, RI (*Presenter*) Nothing to Disclose  
Laura L. Hayes, MD, Orlando, FL (*Presenter*) Nothing to Disclose

#### COURSE DESCRIPTION

This case-based session will focus on imaging of non-traumatic pediatric emergencies involving the head, neck, chest, abdomen, and pelvis. Presenters will review appropriate imaging methods and salient imaging findings that allow prompt and accurate diagnoses in the emergency setting. Some of the topics that will be discussed include foreign bodies, infection, and stroke. After this session, learners should feel more comfortable choosing and interpreting imaging studies of children presenting with non-traumatic emergencies.

#### LEARNING OBJECTIVES

1) Know appropriate methods for imaging children with non-traumatic emergencies 2) Identify typical and atypical findings on imaging of children presenting with non-traumatic emergencies 3) Recognize potential pitfalls in the performance and interpretation of imaging studies for non-traumatic pediatric emergencies\*Course Description This case-based session will focus on imaging of non-traumatic pediatric emergencies involving the head, neck, chest, abdomen, and pelvis. Presenters will review appropriate imaging methods and salient imaging findings that allow prompt and accurate diagnoses in the emergency setting. Some of the topics that will be discussed include foreign bodies, infection, and stroke. After this session, learners should feel more comfortable choosing and interpreting imaging studies of children presenting with non-traumatic emergencies.

Printed on: 02/07/23



## Abstract Archives of the RSNA, 2022

T6-CPH05

### Deep Learning in MRI

Tuesday, Nov. 29 1:30PM - 2:30PM Room: NA

#### Participants

Greg Zaharchuk, MD, PhD, Stanford, CA (*Presenter*) Research Grant, General Electric Company; Research Grant, Bayer AG; Stockholder, Subtle Medical, Inc; Advisory Board, Biogen Idec Inc

Fang Liu, PhD, Boston, MA (*Presenter*) Nothing to Disclose

Li Feng, PhD, New York, NY (*Presenter*) Research support, Hyperfine Research, Inc; Research collaboration, Hyperfine Research, Inc

#### COURSE DESCRIPTION

This course offers an overview of present deep learning (DL) techniques for MRI, including an introduction to DL principles in image acquisition, reconstruction, post-processing, and analysis. Speakers will deliver a review of current DL utility and impact in clinical MRI, and an outlook on challenges and future directions of DL in MRI translational and clinical applications.

#### LEARNING OBJECTIVES

1) Explain the current clinical applications of deep learning in MRI 2) Understand the basic methods applied in MRI reconstruction, quantification, and image enhancement \*Course Description This course offers an overview of present deep learning (DL) techniques for MRI, including an introduction to DL principles in image acquisition, reconstruction, post-processing, and analysis. Speakers will deliver a review of current DL utility and impact in clinical MRI, and an outlook on challenges and future directions of DL in MRI translational and clinical applications.

Printed on: 02/07/23



## Abstract Archives of the RSNA, 2022

T6-CRO06

### Musculoskeletal Case-based Multidisciplinary Review

Tuesday, Nov. 29 1:30PM - 2:30PM Room: NA

#### Participants

F. Joseph Simeone, MD, Boston, MA (*Presenter*) Nothing to Disclose

Seth Pollack, MD, Chicago, IL (*Presenter*) Consultant, Bayer AG; Consultant, Deciphera Pharmaceuticals, LLC; Consultant, Apexigen Inc; Consultant, T-Knife, GmbH; Consultant, Aadi Bioscience, Inc; Consultant, Epizyme, Inc; Consultant, Obsidian; Consultant, Sensei; Consultant, SpringWorks Therapeutics, Inc

Kevin Raskin, MD, Boston, MA (*Presenter*) Nothing to Disclose

Edward Y. Kim, MD, Seattle, WA (*Presenter*) Nothing to Disclose

#### COURSE DESCRIPTION

This multidisciplinary panel will discuss a series of challenging soft tissue and bone sarcoma cases. The session will highlight the importance of imaging in the diagnosis and treatment of these rare tumors. Panelists will represent radiology, orthopedic oncology, medical oncology, and radiation oncology.

#### LEARNING OBJECTIVES

1) Identify ways to incorporate imaging data into the management of soft tissue and bone sarcomas 2) Explain optimal management strategies for rare soft tissue tumors\*Course Description This multidisciplinary panel will discuss a series of challenging soft tissue and bone sarcoma cases. The session will highlight the importance of imaging in the diagnosis and treatment of these rare tumors. Panelists will represent radiology, orthopedic oncology, medical oncology, and radiation oncology.

Printed on: 02/07/23



## Abstract Archives of the RSNA, 2022

T6-CRT02

### ASRT@RSNA: Imaging Transgender Patients: What the Radiologic Technologist Needs to Know

Tuesday, Nov. 29 1:30PM - 2:30PM Room: NA

#### Participants

Evelyn Carroll, MD, Rochester, NY (*Presenter*) Nothing to Disclose

#### COURSE DESCRIPTION

Transgender and gender diverse (TGD) patients are a growing patient population who often experience health inequities both in the radiology department and throughout the healthcare system. Healthcare disparities in this population are compounded by a lack of knowledge and understanding of TGD persons and their healthcare related needs by well-intentioned health care providers. In this session, Dr. Evelyn Carroll will break down the basic terminology and concepts of gender diversity, provide a high-level overview of gender affirming medical care, and share strategies to create an inclusive environment for our TGD patients and colleagues in the radiology department. Dr. Carroll draws on both her years of lived experience and her expertise in imaging transgender patients to deliver an authentic presentation on a topic relevant to all radiologic technologists. Following the presentation, there will be a question and answer session open to all attendees.

#### LEARNING OBJECTIVES

1) Understand basic terminology and concepts of gender diversity 2) Become familiar with the healthcare disparities facing the transgender and gender diverse (TGD) patient population 3) Learn how to create an inclusive clinical practice and work environment for our TGD patients and colleagues\*Course Description Transgender and gender diverse (TGD) patients are a growing patient population who often experience health inequities both in the radiology department and throughout the healthcare system. Healthcare disparities in this population are compounded by a lack of knowledge and understanding of TGD persons and their healthcare related needs by well-intentioned health care providers. In this session, Dr. Evelyn Carroll will break down the basic terminology and concepts of gender diversity, provide a high-level overview of gender affirming medical care, and share strategies to create an inclusive environment for our TGD patients and colleagues in the radiology department. Dr. Carroll draws on both her years of lived experience and her expertise in imaging transgender patients to deliver an authentic presentation on a topic relevant to all radiologic technologists. Following the presentation, there will be a question and answer session open to all attendees.

Printed on: 02/07/23



## Abstract Archives of the RSNA, 2022

T6-RCP04

### Medicare and U.S. Healthcare Policy: A National Conversation

Tuesday, Nov. 29 1:30PM - 2:30PM Room: NA

#### Participants

Kavita Patel, MD, Bethesda, MD (*Presenter*) Board Member, Radiology Partners; Board Member, Strive Health Care; Board Member, Everside Health Care

Mark McClellan, MD, Durham, NC (*Presenter*) Director, Alignment Healthcare USA, LLC; Advisor, Arsenal Capital Partners; Advisor, Blackstone Inc ; Director, Cigna Corporation; Advisor, Health Care Payment Learning & Action Network ; Chairman, PrognomIQ, Inc; Director, Johnson & Johnson; Advisor, MITRE

Richard Heller III, MD, Chicago, IL (*Moderator*) Consultant, Gerson Lehrman Group, Inc;

Amanda Starc, Evanston, IL (*Moderator*) Nothing to Disclose

#### COURSE DESCRIPTION

The economics of the United States health care system are under stress. Medicare, a central pillar of the US health care system, faces many challenges. This session features a discussion between two nationally respected authorities on Medicare policy. Moderated by a subject matter expert, the session will focus on US health care policy and the future of the Medicare system, paying special attention to diagnostic and interventional radiology and radiation oncology.

#### LEARNING OBJECTIVES

1) Distinguish between the different parts of Medicare, their roles in the US healthcare system, and the challenges facing them 2) Describe Medicare's approach to medical imaging and radiologist reimbursement and expected future changes 3) Describe Medicare's approach to radiation oncology reimbursement and expected future changes\*Course Description The economics of the United States health care system are under stress. Medicare, a central pillar of the US health care system, faces many challenges. This session features a discussion between two nationally respected authorities on Medicare policy. Moderated by a subject matter expert, the session will focus on US health care policy and the future of the Medicare system, paying special attention to diagnostic and interventional radiology and radiation oncology.

Printed on: 02/07/23



## Abstract Archives of the RSNA, 2022

T7-CBR14

### RSNA Simulation Lab (Hands on): Breast US Biopsy 2

Tuesday, Nov. 29 3:00PM - 4:30PM Room: NA

#### Participants

Sarah Pittman, MD, Stanford, CA (*Presenter*) Nothing to Disclose  
Stamatia Destounis, MD, Rochester, NY (*Presenter*) Medical Advisory Board, iCad, Inc  
Jean Seely, MD, Ottawa, ON (*Presenter*) Nothing to Disclose  
Marcio Saito, Barretos, Brazil (*Presenter*) Speaker, General Electric Company  
Gary Whitman, MD, Houston, TX (*Presenter*) Consultant, Siemens AG;Editor, Wolters Kluwer nv  
Haydee Ojeda-Fournier, MD, San Diego, CA (*Presenter*) Research Consultant, View Point Medical, Inc;Stock options, CureMetrix, Inc  
Georgia Spear, MD, Park Ridge, IL (*Presenter*) Research Grant, General Electric Company;Speakers Bureau, General Electric Company;Scientific Advisory Board, Hologic, Inc  
Paula B. Gordon, MD, Vancouver, BC (*Presenter*) Stockholder, OncoGenex Pharmaceuticals, Inc;Stockholder, Volpara Health Technologies Limited;Scientific Advisor, Besins Healthcare SA  
Michael Linver, MD, Alexandria, VA (*Presenter*) Medical Advisory Board, Three Palm Software LLC;Scientific Advisory Board, Seno Medical Instruments, Inc  
Tanya W. Moseley, MD, PhD, Houston, TX (*Presenter*) Consultant, Hologic, Inc;Consultant, Merit Medical Systems, Inc;Owner, TW Moseley, LLC;CEO, TW Moseley, LLC  
Shadi Aminololama-Shakeri, MD, Sacramento, CA (*Presenter*) Consultant, Becton, Dickinson and Company;Consultant, Izotropic Corporation;Stock options, Izotropic Corporation  
Maria Helena S. Mendonca, MD, PhD, Sao Paulo, Brazil (*Presenter*) Expert Advisory Committee, Guerbet SA  
Jessica Leung, MD, Houston, TX (*Presenter*) Scientific Advisory Board, Subtle Medical, Inc;Speaker, General Electric Company;Speaker, Hologic, Inc;Scientific Advisory Board, Seno Medical Instruments, Inc

#### COURSE DESCRIPTION

In Person Session Only. Tickets must be purchased in advance for this course. This course can be added through the registration portal or by stopping by the Registration Desk. Space is limited.A brief didactic lecture will be given at beginning of course to review types of needle biopsy equipment and technique. The attendee at completion of course should have some familiarity of how to handle different biopsy devices under ultrasound guidance. Masses and cysts will be identified and biopsied or drained. Various wire localization equipment will also be available. Every attendee will have opportunity to use hands on biopsy equipment. Instruction will be given on how to perform procedure and before and after care. Various ultrasound equipment will be available for scanning and localizations of lesions.

#### LEARNING OBJECTIVES

1) Introduction of various types and sizes of needle breast biopsy devices and their utilization within clinical practice 2) Utilization of different ultrasound technology to perform interventional procedures in the breast 3) Introduction of additional procedures in the breast such as cyst aspiration, fine needle aspiration, marker placement\*Course Description In Person Session Only. Tickets must be purchased in advance for this course. This course can be added through the registration portal or by stopping by the Registration Desk. Space is limited.A brief didactic lecture will be given at beginning of course to review types of needle biopsy equipment and technique. The attendee at completion of course should have some familiarity of how to handle different biopsy devices under ultrasound guidance. Masses and cysts will be identified and biopsied or drained. Various wire localization equipment will also be available. Every attendee will have opportunity to use hands on biopsy equipment. Instruction will be given on how to perform procedure and before and after care. Various ultrasound equipment will be available for scanning and localizations of lesions.

Printed on: 02/07/23



## Abstract Archives of the RSNA, 2022

T7-CER12

### On Call Primer for Residents - Don't Miss Diagnoses: Tricky Trauma That Keeps You Up at Night

Tuesday, Nov. 29 3:00PM - 4:00PM Room: NA

#### Participants

Uttam Bodanapally, MD, Owings Mills, MD (*Presenter*) Speakers Bureau, Siemens AG; Travel support, Siemens AG; Research support, Siemens AG

Ashwin V. Asrani, MD, Short Hills, NJ (*Presenter*) Nothing to Disclose

Polina Kanj, MD, Boston, MA (*Presenter*) Nothing to Disclose

Laura L. Avery, MD, Boston, MA (*Presenter*) Nothing to Disclose

#### COURSE DESCRIPTION

Are night shifts in the ED causing you stress and anxiety? Does the sight of trauma surgeons make you want to run and hide in a stairwell? This course is your Xanax. The course is targeted at improving the time to recognition and diagnosis of various traumatic injuries. The information will be presented in a case-based format emphasizing problem-solving rather than grading systems. The learner will improve their chances of achieving a Zen state during their next call shift.

#### LEARNING OBJECTIVES

1) Identify clinically important traumatic injuries with speed and grace\*Course Description Are night shifts in the ED causing you stress and anxiety? Does the sight of trauma surgeons make you want to run and hide in a stairwell? This course is your Xanax. The course is targeted at improving the time to recognition and diagnosis of various traumatic injuries. The information will be presented in a case-based format emphasizing problem-solving rather than grading systems. The learner will improve their chances of achieving a Zen state during their next call shift.

Printed on: 02/07/23



## Abstract Archives of the RSNA, 2022

T7-CGI01

### Jeopardy: GI/GU Cases

Tuesday, Nov. 29 3:00PM - 4:00PM Room: NA

#### Participants

Alessandro Furlan, MD, Pittsburgh, PA (*Presenter*) Royalties, RELX; Research support, Endra, Inc; Consultant, Bracco Group  
Douglas Katz, MD, Mineola, NY (*Presenter*) Nothing to Disclose  
Lakshmi Ananthakrishnan, MD, Dallas, TX (*Presenter*) Nothing to Disclose  
Elizabeth A. Sadowski, MD, Madison, WI (*Presenter*) Nothing to Disclose  
Sherry Wang, MBBS, Salt Lake City, UT (*Presenter*) Royalties, RELX  
Kartik S. Jhaveri, MD, Mississauga, ON (*Presenter*) Research Grant, General Electric Company; Research Grant, Bayer AG; Research Consultant, Perspectum Diagnostics Ltd;  
Cooky Menias, MD, Phoenix, AZ (*Moderator*) Royalties, RELX  
John R. Leyendecker, MD, Dallas, TX (*Moderator*) Nothing to Disclose  
Olga R. Brook, MD, Boston, MA (*Moderator*) Nothing to Disclose

#### COURSE DESCRIPTION

This course will use a Jeopardy-style format to present challenging unknown cases to a panel of expert abdominal imagers. Each case will be followed by a brief discussion highlighting the key imaging features that lead to the correct diagnosis.

#### LEARNING OBJECTIVES

1) Learn to diagnose difficult gastrointestinal and genitourinary cases on various imaging modalities 2) Learn from experts how to approach challenging abdominal and pelvic imaging cases\*Course Description This course will use a Jeopardy-style format to present challenging unknown cases to a panel of expert abdominal imagers. Each case will be followed by a brief discussion highlighting the key imaging features that lead to the correct diagnosis.

Printed on: 02/07/23



## Abstract Archives of the RSNA, 2022

T7-CIN11

### AI Isn't Just for Diagnosis: Example Applications Throughout the Radiological Imaging Chain

Tuesday, Nov. 29 3:00PM - 4:00PM Room: NA

#### Participants

Nabile Safdar, MD, MPH, Milton, GA (*Presenter*) Nothing to Disclose

Nina E. Kottler, MD, MS, San Diego, CA (*Presenter*) Partner, Radiology Partners; Stockholder, Radiology Partners; Employee, Radiology Partners; Consultant, ES3; Consultant, W.L. Gore & Associates, Inc; Consultant, Synapsica Healthcare Pvt Ltd

Katherine Andriole, PhD, Branford, CT (*Moderator*) Nothing to Disclose

#### COURSE DESCRIPTION

The goal of many AI tools is to provide clinical decision support for radiology examination interpretation. But AI and machine learning can be applied at various points in the radiological imaging chain, including at examination ordering, imaging modality protocoling, image creation and quality assessment, study diagnosis, reporting, and billing. Such applications may improve workflow efficiency and reduce errors and cost. Example applications throughout the radiology workflow will be described along with integration standards necessary to implement AI tools clinically. AI workflow for both academic and private practice settings will be discussed.

#### LEARNING OBJECTIVES

1) Identify the points throughout the radiology imaging chain at which AI tools may be implemented and how they may impact workflow 2) Become familiar with the integration standards required to clinically implement AI tools 3) Learn about AI radiology workflow tools useful for the academic and private practice settings\*Course Description The goal of many AI tools is to provide clinical decision support for radiology examination interpretation. But AI and machine learning can be applied at various points in the radiological imaging chain, including at examination ordering, imaging modality protocoling, image creation and quality assessment, study diagnosis, reporting, and billing. Such applications may improve workflow efficiency and reduce errors and cost. Example applications throughout the radiology workflow will be described along with integration standards necessary to implement AI tools clinically. AI workflow for both academic and private practice settings will be discussed.

Printed on: 02/07/23



## Abstract Archives of the RSNA, 2022

T7-CMK07

### MSK Tumors: Pearls and Pitfalls

Tuesday, Nov. 29 3:00PM - 4:00PM Room: NA

#### Participants

Laura M. Fayad, MD, Baltimore, MD (*Presenter*) Nothing to Disclose

Kambiz Motamedi, MD, Los Angeles, CA (*Presenter*) Royalties, RELX

Mark D. Murphey, MD, Silver Spring, MD (*Presenter*) Nothing to Disclose

Ty K. Subhawong, MD, Miami, FL (*Presenter*) Research Consultant, Arog Pharmaceuticals, Inc; Stockholder, AbbVie Inc; Stockholder, AstraZeneca PLC; Stockholder, Johnson & Johnson; Stockholder, Pfizer Inc ; Stockholder, F. Hoffmann-La Roche Ltd; Stockholder, Teva Pharmaceutical Industries Ltd

Doris E. Wenger, MD, Rochester, MN (*Presenter*) Nothing to Disclose

#### COURSE DESCRIPTION

In this educational course, we will review salient benign musculoskeletal lesions that are commonly encountered in clinical practice, in both pediatric and adult populations. In addition, what imaging features are associated with a potentially malignant lesion and what imaging modalities and techniques are important for radiologists to use to recognize clearly benign entities and avoid a referral for biopsy? Through five lectures from experienced musculoskeletal radiologists, examples and strategies will be presented that help the radiologist arrive at the decision "to touch" or "not to touch" a lesion.

#### LEARNING OBJECTIVES

1) To review the imaging appearance of common benign musculoskeletal lesions in children and adults 2) To identify imaging strategies for confidently diagnosing lesions that are benign or probably benign 3) To emphasize lesional features that suggest a potentially malignant nature\*Course Description In this educational course, we will review salient benign musculoskeletal lesions that are commonly encountered in clinical practice, in both pediatric and adult populations. In addition, what imaging features are associated with a potentially malignant lesion and what imaging modalities and techniques are important for radiologists to use to recognize clearly benign entities and avoid a referral for biopsy? Through five lectures from experienced musculoskeletal radiologists, examples and strategies will be presented that help the radiologist arrive at the decision "to touch" or "not to touch" a lesion.

Printed on: 02/07/23



## Abstract Archives of the RSNA, 2022

T7-CNMMI13

### Case-based Review of Neuroendocrine: PET/CT Workshop (In Conjunction with SNMMI)

Tuesday, Nov. 29 3:00PM - 4:00PM Room: NA

#### Participants

Nadine Mallak, MD, Portland, OR (*Presenter*) Nothing to Disclose

Lisa Bodei, MD, PhD, New York, NY (*Presenter*) Consultant, Novartis AG ;Speaker, Novartis AG;Research Grant, Novartis AG;Consultant, Ipsen SA;Consultant, ITM Isotopen Technologien Muenchen AG;Speaker, ITM Isotopen Technologien Muenchen AG;Consultant, Clovis Oncology, Inc;Consultant, Ion Beam Applications, SA

#### COURSE DESCRIPTION

Course Description:PET/CT has greatly impacted the imaging and therapy of neuroendocrine malignancies, including continuing improvements in somatostatin receptor-targeted PET. In this session, experts on neuroendocrine tumors will use clinical cases to demonstrate fundamentals of interpretation, as well as pearls and pitfalls to help improve interpretation of PET studies.

#### LEARNING OBJECTIVES

1) Understand best clinical practices for use and interpretation of PET/CT in patients with neuroendocrine tumors 2) Compared and contrast Ga68-Dotatate with 64Cu-Dotatate\*Course Description Course Description:PET/CT has greatly impacted the imaging and therapy of neuroendocrine malignancies, including continuing improvements in somatostatin receptor-targeted PET. In this session, experts on neuroendocrine tumors will use clinical cases to demonstrate fundamentals of interpretation, as well as pearls and pitfalls to help improve interpretation of PET studies.

Printed on: 02/07/23



## Abstract Archives of the RSNA, 2022

T7-CNPM15

### Radiology Extenders and Beyond: How to Alleviate the Radiology Workflow Crisis

Tuesday, Nov. 29 3:00PM - 4:00PM Room: NA

#### Participants

Saurabh Jha, MD, Philadelphia, PA (*Presenter*) Nothing to Disclose  
Jessica Fried, MD, Ann Arbor, MI (*Presenter*) Nothing to Disclose  
Howard Fleishon, MD, Phoenix, AZ (*Presenter*) Nothing to Disclose

#### COURSE DESCRIPTION

How do we alleviate the radiology workforce shortage? With AI? Should we train more radiologists? With extenders? This session will discuss the solutions and the trade-offs. Audience participation encouraged.

#### LEARNING OBJECTIVES

1) Identify mechanisms to reduce radiology workforce shortage 2) Understand the pros and cons with each solution 3) Appreciate that diverse perspectives on the solutions\*Course Description How do we alleviate the radiology workforce shortage? With AI? Should we train more radiologists? With extenders? This session will discuss the solutions and the trade-offs. Audience participation encouraged.

Printed on: 02/07/23



## Abstract Archives of the RSNA, 2022

T7-CNPM19

### Life After COVID: Enhancing Wellness and Growth in the "New Normal" (Sponsored by RSNA Professionalism Committee)

Tuesday, Nov. 29 3:00PM - 4:00PM Room: NA

#### Participants

Jeffrey Klein, MD, Williston, VT (*Presenter*) Editor with royalties, Wolters Kluwer nv

Michael Lanier, MD, PhD, Saint Louis, MO (*Presenter*) Nothing to Disclose

Kevin McGill, MD, MPH, San Francisco, CA (*Presenter*) Consultant, Teleflex Incorporated

Carl Flink, MD, Salt Lake City, UT (*Presenter*) Nothing to Disclose

Zi Zhang, MD, Fort Washington, PA (*Presenter*) Nothing to Disclose

Kate Hanneman, MD, FRCPC, Toronto, ON (*Moderator*) Speaker, Groupe Sanofi Speaker, Amicus Therapeutics, Inc

#### COURSE DESCRIPTION

This course includes three lectures and one interactive panel: 1. Overview of the shift of radiology practice environment during the pandemic and its impact. This lecture will review the myriad ways in which the radiology practice environment has changed during the pandemic. It will review both the intended effects and discuss some of the potential collateral damage for professional growth. 2. How to determine the balance between remote work and in-person work. This lecture will discuss the generational differences in the opportunities for remote work versus in-person work. It will also review the strategies for increasing efficiency of remote working and improving communication with the medical team. 3. Networking strategies to maximize social interactions in the "New Normal". This lecture will discuss methods that can be used to continue to seek out opportunities for networking while adjusting to the "New Normal". This lecture will also discuss how maximizing social interactions can serve as a tool for promoting professional growth. 4. Interactive panel to discuss the opportunities and challenges in the "New Normal". This panel will include radiologists at different stages of their career to discuss the opportunities and challenges they are facing in the "New Normal" and answer questions from the audience.

#### LEARNING OBJECTIVES

Unprecedented challenges brought on by the COVID-19 pandemic have changed the radiology practice environment. The way in which we practice and interact with our colleagues has never been more challenging 1) This program will discuss changes in the practice of radiology related to the pandemic, and generational differences in facing the opportunities and challenges of the "New Normal" at the workplace 2) We will also discuss strategies to promote professional growth in this new environment\*Course Description This course includes three lectures and one interactive panel: 1. Overview of the shift of radiology practice environment during the pandemic and its impact. This lecture will review the myriad ways in which the radiology practice environment has changed during the pandemic. It will review both the intended effects and discuss some of the potential collateral damage for professional growth. 2. How to determine the balance between remote work and in-person work. This lecture will discuss the generational differences in the opportunities for remote work versus in-person work. It will also review the strategies for increasing efficiency of remote working and improving communication with the medical team. 3. Networking strategies to maximize social interactions in the "New Normal". This lecture will discuss methods that can be used to continue to seek out opportunities for networking while adjusting to the "New Normal". This lecture will also discuss how maximizing social interactions can serve as a tool for promoting professional growth. 4. Interactive panel to discuss the opportunities and challenges in the "New Normal". This panel will include radiologists at different stages of their career to discuss the opportunities and challenges they are facing in the "New Normal" and answer questions from the audience.

Printed on: 02/07/23



## Abstract Archives of the RSNA, 2022

T7-CRT03

### ASRT@RSNA: Compassionate Communication - Keeping Patients at the Heart of Practice

Tuesday, Nov. 29 3:00PM - 4:00PM Room: NA

#### Participants

Amy Taylor, PhD, Exeter, United Kingdom (*Presenter*) Nothing to Disclose

#### COURSE DESCRIPTION

Back in 2013, how UK healthcare professionals gave care to their patients came under the spotlight with the release of the Francis report. The need to understand compassion and how radiographers can engage in compassionate practices became central in the drive to enhance patient-centred care and experience. This lecture integrates the findings of two UK radiography doctoral projects (one diagnostic and one therapeutic), undertaken independently over the period 2014-2020. The outcome of this will be to illustrate the complexity of a concept which, on the face of it appears straightforward and to emphasise the centrality of communication in giving individualised care to patients undergoing diagnostic imaging and therapy.

#### LEARNING OBJECTIVES

By the end of the lecture the delegates will: 1) Understand the importance of compassionate communication in radiography and appreciate its role in its clinical delivery 2) Be able to recognise and engage in practices which communicate compassion to patients\*Course Description Back in 2013, how UK healthcare professionals gave care to their patients came under the spotlight with the release of the Francis report. The need to understand compassion and how radiographers can engage in compassionate practices became central in the drive to enhance patient-centred care and experience. This lecture integrates the findings of two UK radiography doctoral projects (one diagnostic and one therapeutic), undertaken independently over the period 2014-2020. The outcome of this will be to illustrate the complexity of a concept which, on the face of it appears straightforward and to emphasise the centrality of communication in giving individualised care to patients undergoing diagnostic imaging and therapy.

Printed on: 02/07/23



## Abstract Archives of the RSNA, 2022

T7-CVA07

### Imaging After Endovascular Aortic Repair: What to Look for, How To Report

Tuesday, Nov. 29 3:00PM - 4:00PM Room: NA

#### Participants

Santiago Restrepo, MD, San Antonio, TX (*Presenter*) Nothing to Disclose

Constantino S. Pena, MD, Key Biscayne, FL (*Presenter*) Speakers Bureau, Cook Group Incorporated Speakers Bureau, Abbott

Laboratories Speakers Bureau, ShockWave Medical Speakers Bureau, Penumbra, Inc Speakers Bureau, Cardinal Health, Inc Speakers

Bureau, Becton, Dickinson and Company Advisory Board, Surmodics, Inc

Sandeep S. Hegdige, MD, Lexington, MA (*Presenter*) Nothing to Disclose

#### COURSE DESCRIPTION

Surveillance follow-up is critical after TEVAR procedure. Imaging plays a critical role in the identification and management of complications. During the course the lectures will discuss the current recommendations on follow-up of patients who have had endovascular aortic repair.

#### LEARNING OBJECTIVES

1) Discuss the role of imaging in the surveillance follow-up of patients after TEVAR, including optimal protocols 2) Discuss the most common complications after TEVAR 3) Briefly discuss recommended management guidelines\*Course Description Surveillance follow-up is critical after TEVAR procedure. Imaging plays a critical role in the identification and management of complications. During the course the lectures will discuss the current recommendations on follow-up of patients who have had endovascular aortic repair.

Printed on: 02/07/23



## Abstract Archives of the RSNA, 2022

T7-RCP02

### From the Editors of RADIOLOGY: New Research That Should Impact Your Practice

Tuesday, Nov. 29 3:00PM - 4:00PM Room: NA

#### Participants

David Bluemke, MD, PhD, Madison, WI (*Presenter*) Nothing to Disclose

Linda Moy, MD, New York, NY (*Presenter*) Grant, Siemens AG ;Advisory Board, Lunit Inc;Advisory Board, iCad, Inc

Birgit Ertl-Wagner, MD, Toronto, ON (*Presenter*) Spouse, Employee, Siemens AG

Kathryn Fowler, MD, San Diego, CA (*Presenter*) Consultant, Bayer AG;Research support, General Electric Company;Research Grant, Pfizer Inc;Institutional Grant, MEDIAN Technologies;Consultant, General Electric Company

#### COURSE DESCRIPTION

RADIOLOGY is the leading journal for publications leading to new, important and translatable discoveries in imaging research. In the past year, there continue to be new developments in radiology and in the application of imaging, as well as new guidelines and clinical trials in imaging that affect your practice. While COVID-19 remains critically important, overall trends for new scientific studies reflect an increasing number of clinical trials being submitted from around the world in addition to those of North America. Large numbers of study subjects in imaging trials are now common. This results in more robust demonstration of the efficacy of imaging interventions. Advanced artificial intelligence applications increasingly submitted in our publications, as are radiomics studies with large numbers of study subjects. This seminar will highlight the results of key publications in the past year that are most likely to affect your practice in the near future, as well as presenting novel topics that are likely to be important to the field over the next 5 years.

#### LEARNING OBJECTIVES

1) Identify key publications over the past year that may affect your clinical practice 2) Evaluate new research developments in the field of radiological imaging 3) Describe new developments in radiology that may affect the management of your patients\*Course Description RADIOLOGY is the leading journal for publications leading to new, important and translatable discoveries in imaging research. In the past year, there continue to be new developments in radiology and in the application of imaging, as well as new guidelines and clinical trials in imaging that affect your practice. While COVID-19 remains critically important, overall trends for new scientific studies reflect an increasing number of clinical trials being submitted from around the world in addition to those of North America. Large numbers of study subjects in imaging trials are now common. This results in more robust demonstration of the efficacy of imaging interventions. Advanced artificial intelligence applications increasingly submitted in our publications, as are radiomics studies with large numbers of study subjects. This seminar will highlight the results of key publications in the past year that are most likely to affect your practice in the near future, as well as presenting novel topics that are likely to be important to the field over the next 5 years.

Printed on: 02/07/23



## Abstract Archives of the RSNA, 2022

T7-RCP17

### Argentina Presents: Developments and Improvement in Diagnostic Imaging

Tuesday, Nov. 29 3:00PM - 4:30PM Room: NA

#### Participants

Sebastian Rossini SR, Mar del Plata, Argentina (*Presenter*) Speaker, Bayer AG; Speaker, Boehringer Ingelheim GmbH

Hernan Chaves, MD, Buenos Aires, Argentina (*Presenter*) Consultant, Entelai AENTI SRL

Daniela Stoisa, MD, Rosario, Argentina (*Presenter*) Nothing to Disclose

Patricia M. Carrascosa, MD, PhD, FSCCT, MSCCT, Buenos Aires City, Argentina (*Presenter*) Speakers Bureau, General Electric Company

Alberto A. Marangoni, MD, Cordoba, Argentina (*Moderator*) Nothing to Disclose

Eduardo P. Eyheremendy, MD, Buenos Aires, Argentina (*Moderator*) Nothing to Disclose

Shigeru Kozima, Buenos Aires City, Argentina (*Moderator*) Nothing to Disclose

#### LEARNING OBJECTIVES

1) Demonstrate the efficacy and low incidence of complications of percutaneous fine needle puncture in pulmonary nodules smaller than 1 cm 2) Show the efficacy of US and MRI in detecting specific signs of deep endometriosis and demonstrate the incidence and complications caused by the disease 3) Introduce the technique of virtual hysterosalpingography and the utility in the different causes of infertility 4) Describe the technical aspects and demonstrate the clinical utility of intracranial and extracranial magnetic resonance vessel wall imaging (VWI)\*Course Description

Printed on: 02/07/23



## Abstract Archives of the RSNA, 2022

T7-RCP45

### Practical Guide for Publishing Your Research: Data Analysis and Figure Making (Sponsored by the RSNA Resident and Fellow Committee)

Tuesday, Nov. 29 3:00PM - 4:00PM Room: NA

#### Participants

David Ballard, MD, Saint Louis, MO (*Presenter*) Nothing to Disclose

Ronnie Sebros, MD, PhD, Jacksonville Beach, FL (*Presenter*) Nothing to Disclose

Brian Burkett, MD, MPH, Rochester, MN (*Moderator*) Nothing to Disclose

#### COURSE DESCRIPTION

The RSNA Resident Fellow Committee will host a session of expert lectures on the practical aspects of publishing. The session will include a high-yield discussion of data analysis and statistical methods commonly used in imaging research, followed by a presentation on how to generate publication-quality figures with high resolution image files and annotations using common and proprietary software platforms. The lectures will provide participants and especially trainees with the fundamental knowledge and practical skills required to successfully publish academic work.

#### LEARNING OBJECTIVES

1) To understand the fundamentals of imaging research data analysis methods and learn to choose appropriately statistical analysis techniques 2) To successfully prepare medical imaging and simple illustrations for publication\*Course Description The RSNA Resident Fellow Committee will host a session of expert lectures on the practical aspects of publishing. The session will include a high-yield discussion of data analysis and statistical methods commonly used in imaging research, followed by a presentation on how to generate publication-quality figures with high resolution image files and annotations using common and proprietary software platforms. The lectures will provide participants and especially trainees with the fundamental knowledge and practical skills required to successfully publish academic work.

Printed on: 02/07/23



## Abstract Archives of the RSNA, 2022

T8-CCA01

### Rapid Fire: 60 Cardiac Cases in 60 Minutes

Tuesday, Nov. 29 4:30PM - 5:30PM Room: NA

#### Participants

Juan Batlle, MD, Boulder, CO (*Presenter*) Speakers Bureau, Boehringer Ingelheim GmbH  
Jordi Broncano, MD, Cordoba, (*Presenter*) Nothing to Disclose  
Jean Jeudy JR, MD, Baltimore, MD (*Moderator*) Nothing to Disclose

#### COURSE DESCRIPTION

Enjoy an exciting and fast-paced review of cardiac radiology! With a case review format, the speakers will discuss a diversity of cardiac pathology and imaging-based differential diagnosis. Topics include: coronary and myocardial disease, cardiac masses, pericardial disease, valvular and congenital heart disease.

#### LEARNING OBJECTIVES

1) Provide a review of interesting cardiac radiology cases, with classic focus on pericardial disease and disease of the coronary arteries and myocardium 2) Highlight and discuss imaging of other diverse myocardial pathological processes including structural heart disease, and cardiothoracic oncology\*Course Description Enjoy an exciting and fast-paced review of cardiac radiology! With a case review format, the speakers will discuss a diversity of cardiac pathology and imaging-based differential diagnosis. Topics include: coronary and myocardial disease, cardiac masses, pericardial disease, valvular and congenital heart disease.

Printed on: 02/07/23



## Abstract Archives of the RSNA, 2022

T8-CCH10

### Acute and Chronic Lung Injury

Tuesday, Nov. 29 4:30PM - 5:30PM Room: NA

#### Participants

Travis Henry, MD, Durham, NC (*Presenter*) Advisor, Aer Therapeutics, Inc; Stockholder, Aer Therapeutics, Inc  
Demetrios Raptis, MD, Frontenac, MO (*Presenter*) Nothing to Disclose  
Ryoko Egashira, MD, PhD, Saga, (*Presenter*) Speakers Bureau, Boehringer Ingelheim GmbH; Speakers Bureau, AstraZeneca PLC; Speakers Bureau, Shionogi & Co, Ltd; Speakers Bureau, KYORIN Holdings, Inc; Speakers Bureau, DAIICHI SANKYO Group; Speakers Bureau, Bayer AG; Speakers Bureau, Otsuka Holdings Co, Ltd;  
Anu Brixey, MD, Portland, OR (*Presenter*) Research support, 4D Medical

#### COURSE DESCRIPTION

This session will review multiple aspects of acute and chronic lung injury. This includes a radiologic and pathologic review of diffuse alveolar damage; imaging of specific causes of lung injury including EVALI, other exposures, and hypersensitivity pneumonitis. The management of patients with lung injury on ECMO will be covered. Finally, pleuroparenchymal fibroelastosis will be reviewed as a long term sequela of lung injury.

#### LEARNING OBJECTIVES

1) Recognize the common and uncommon imaging manifestations of acute and chronic lung injury 2) Understand the limitations of identifying specific causes of lung injury on imaging and provide a reasonable differential diagnosis\*Course Description This session will review multiple aspects of acute and chronic lung injury. This includes a radiologic and pathologic review of diffuse alveolar damage; imaging of specific causes of lung injury including EVALI, other exposures, and hypersensitivity pneumonitis. The management of patients with lung injury on ECMO will be covered. Finally, pleuroparenchymal fibroelastosis will be reviewed as a long term sequela of lung injury.

Printed on: 02/07/23



## Abstract Archives of the RSNA, 2022

T8-CER01

### Essentials of Disaster Preparedness

Tuesday, Nov. 29 4:30PM - 5:30PM Room: NA

#### Participants

Eric Roberge, MD, Fox Island, WA (*Presenter*) Nothing to Disclose  
Ferco H. Berger, MD, Toronto, ON (*Presenter*) Nothing to Disclose  
Krystal Archer-Arroyo, MD, Decatur, GA (*Presenter*) Nothing to Disclose

#### COURSE DESCRIPTION

Ready for anything: A series of lectures will guide the learner from theory to practice in Disaster Preparedness using a "how I did it" tutorial approach...because sometimes you must expect the unexpected.

#### LEARNING OBJECTIVES

1) Introduce a framework for approaching Disaster Preparedness 2) Give practical examples for creating a disaster response plan at your own institution 3) Provide a how-to guide for creating a simulation to test your own plan\*Course Description Ready for anything: A series of lectures will guide the learner from theory to practice in Disaster Preparedness using a "how I did it" tutorial approach...because sometimes you must expect the unexpected.

Printed on: 02/07/23



## Abstract Archives of the RSNA, 2022

T8-CGI08

### Non-invasive Assessment of Chronic Liver Disease

Tuesday, Nov. 29 4:30PM - 5:30PM Room: NA

#### Participants

Bachir Taouli, MD, New York, NY (*Presenter*) Research Grant, Bayer AG; Research Grant, Takeda Pharmaceutical Company Limited; Consultant, Bayer AG; Consultant, Guerbet SA; Research Grant, Regeneron Pharmaceuticals, Inc  
Paul S. Sidhu, MRCP, FRCR, London, United Kingdom (*Presenter*) Consultant, Samsung Electronics Co, Ltd; Speaker, Samsung Electronics Co, Ltd; Speaker, Bracco Group; Consultant, Itreas Ltd; Speaker, Siemens AG  
Claude Sirlin, MD, San Diego, CA (*Presenter*) Research Grant, General Electric Company; Research Grant, Siemens AG; Research Grant, Bayer AG; Research Grant, Gilead Sciences, Inc; Research collaboration, Gilead Sciences, Inc; Research Grant, Koninklijke Philips NV; Research Grant, Pfizer Inc; Equipment support, General Electric Company; Consultant, Pfizer Inc; Consultant, AMRA AB; Consultant, Guerbet SA; Officer, Livivos, Inc; Advisor, Quantix Bio LLC  
Scott Reeder, MD, PhD, Madison, WI (*Presenter*) Owner, Calimetrix; Owner, Reveal Pharmaceuticals; Owner, Collectar Biosciences, Inc; Owner, Elucent Medical; Owner, HeartVista, Inc;;

#### COURSE DESCRIPTION

This course will provide an overview on current ultrasound and MRI methods for noninvasive detection of liver fibrosis, and liver fat and iron quantification.

#### LEARNING OBJECTIVES

1) Provide an overview on elastography and T1 mapping methods for noninvasive characterization of liver disease 2) Provide an overview on noninvasive methods for liver iron and fat quantification\*Course Description This course will provide an overview on current ultrasound and MRI methods for noninvasive detection of liver fibrosis, and liver fat and iron quantification.

Printed on: 02/07/23



## Abstract Archives of the RSNA, 2022

T8-CIN22

### Who Is Watching The AI? MLOps for Radiology AI in Production

Tuesday, Nov. 29 4:30PM - 5:30PM Room: NA

#### Participants

Bernardo Bizzo, MD, PhD, Newton, MA (*Presenter*) Consultant, Diagnosticos da America (Dasa)

Walter Wiggins, MD, PhD, Durham, NC (*Presenter*) Advisor, Qure.ai;

Imon Banerjee, Stanford, GA (*Presenter*) Nothing to Disclose

Nina E. Kottler, MD, MS, San Diego, CA (*Presenter*) Partner, Radiology Partners; Stockholder, Radiology Partners; Employee, Radiology Partners; Consultant, ES3; Consultant, W.L. Gore & Associates, Inc; Consultant, Synapsica Healthcare Pvt Ltd

#### COURSE DESCRIPTION

This didactic session will provide an overview of the current state-of-the-art in evaluation and monitoring of clinically deployed medical imaging AI tools. The science around bias and performance drift is evolving, but we aim to convince attendees of the need and provide them with strategies for pre-deployment evaluation and post-deployment monitoring of imaging AI tools.

#### LEARNING OBJECTIVES

1) Identify potential sources of bias and performance drift in radiology AI tools 2) Enumerate strategies for pre-deployment evaluation and post-deployment monitoring of radiology AI tools\*Course Description This didactic session will provide an overview of the current state-of-the-art in evaluation and monitoring of clinically deployed medical imaging AI tools. The science around bias and performance drift is evolving, but we aim to convince attendees of the need and provide them with strategies for pre-deployment evaluation and post-deployment monitoring of imaging AI tools.

Printed on: 02/07/23



## Abstract Archives of the RSNA, 2022

T8-CIR04

### Basic Science and Technology Highlights in IR

Tuesday, Nov. 29 4:30PM - 5:30PM Room: NA

#### Participants

Federico Collettoni, MD, Berlin, Germany (*Presenter*) Research Grant, PharmaCept Research Grant, Philips Research Grant, Siemens Healthineers Speakers Bureau, Bayer AG Speakers Bureau, PharmaCept Speakers Bureau, Angiodynamics  
Terence Gade, MD, PhD, Philadelphia, PA (*Presenter*) Scientific Advisory Board, TriSalus Life Sciences; Research Consultant, Instylla, Inc; Research Grant, Instylla, Inc  
Alda Tam, MD, Houston, TX (*Presenter*) Consultant, Johnson & Johnson; Research Grant, Boston Scientific Corporation; Research Grant, Johnson & Johnson; Consultant, AstraZeneca PLC; Consultant, Endocare, Inc;  
Tim Greten, MD, Bethesda, MD (*Presenter*) Nothing to Disclose  
Paul F. Laeseke, MD, PhD, Madison, WI (*Presenter*) Consultant, Johnson & Johnson; Consultant, NeuWave Medical, Inc; Shareholder, HistoSonics, Inc; Consultant, HistoSonics, Inc; Research Grant, HistoSonics, Inc; Shareholder, Elucent Medical; Consultant, Elucent Medical; Shareholder, McGinley Orthopaedic Innovations, LLC  
S. Nahum Goldberg, MD, Efrat, Israel (*Presenter*) Consultant, Cosman Medical, Inc; Consultant, Sarasota Interventional Radiology  
Rony Avritscher, MD, Houston, TX (*Moderator*) Speakers Bureau, Boston Scientific Corporation; Research Consultant, Siemens AG

#### COURSE DESCRIPTION

The course includes the current and future state-of-the-art concepts in interventional oncology, including novel immunotherapy agents, changing paradigms in ablation and the future of embolization by the utmost leading experts in the field. The discussions will introduce the most up-to-date knowledge on these topics and enable attendees to prepare for and benefit from these upcoming changes in practice.

#### LEARNING OBJECTIVES

1) Identify novel therapeutic strategies to enhance image-guided interventions 2) Incorporate new concepts in ablation and embolization 3) Explain the current and future role of immunotherapy in interventional radiology\*  
Course Description The course includes the current and future state-of-the-art concepts in interventional oncology, including novel immunotherapy agents, changing paradigms in ablation and the future of embolization by the utmost leading experts in the field. The discussions will introduce the most up-to-date knowledge on these topics and enable attendees to prepare for and benefit from these upcoming changes in practice.

Printed on: 02/07/23



## Abstract Archives of the RSNA, 2022

T8-CMK05

### Spine Degeneration and Inflammation: Misses that Matter

Tuesday, Nov. 29 4:30PM - 5:30PM Room: NA

#### Participants

Jacob Mandell, MD, Waltham, MA (*Presenter*) Author with royalties, Cambridge University Press

Christian W. Pfirrmann, MD, MBA, Forch, Switzerland (*Presenter*) Nothing to Disclose

Anne Cotten, MD, Lille, France (*Presenter*) Nothing to Disclose

John A. Carrino, MD, MPH, New York, NY (*Presenter*) Research Consultant, Pfizer Inc; Research Consultant, AstraZeneca PLC; Research Consultant, Regeneron Pharmaceuticals, Inc; Research Consultant, Globus Medical, Inc; Consultant, Covera Health, Inc; Advisory Board, Carestream Health, Inc; Advisory Board, Image Analysis Group (IAG)

Patrick Omoumi, MD, Lausanne, Switzerland (*Presenter*) Nothing to Disclose

#### COURSE DESCRIPTION

Refine your approach to spine imaging in this one hour course with five global spine imaging experts, where we will discuss both commonly encountered and unusual clinical scenarios. By emphasizing potential pitfalls and near-misses, we hope to increase your confidence in spine imaging interpretation.

#### LEARNING OBJECTIVES

1) To become familiar with common diagnostic errors and pitfalls in imaging of the spine for degenerative, inflammatory, and infectious conditions 2) To learn about the spectrum of normal and asymptomatic findings in imaging of the spine 3) To broaden the differential diagnosis when interpreting imaging of the spine\*Course Description Refine your approach to spine imaging in this one hour course with five global spine imaging experts, where we will discuss both commonly encountered and unusual clinical scenarios. By emphasizing potential pitfalls and near-misses, we hope to increase your confidence in spine imaging interpretation.

Printed on: 02/07/23



## Abstract Archives of the RSNA, 2022

T8-CNMMI02

### Therapy Response Assessment: Read with the Experts

Tuesday, Nov. 29 4:30PM - 5:30PM Room: NA

#### Participants

Phillip Kuo, MD, PhD, Tucson, AZ (*Presenter*) Consultant, Invicro Consultant, Amgen Inc Consultant, Blue Earth Diagnostics Ltd Research Grant, Blue Earth Diagnostics Ltd Consultant, Novartis AG Speaker, Novartis AG Consultant, Chimerix, Inc Consultant, Fusion Pharmaceuticals Inc Consultant, Bayer AG Consultant, General Electric Healthcare Company Speaker, General Electric Healthcare Company Research Grant, General Electric Company Speaker, Digital Science Press, Inc Consultant, Radionetics Former Employee, Invicro, Inc (ended employment October 2022)

David A. Mankoff, MD, PhD, Philadelphia, PA (*Presenter*) Speaker, Siemens AG Advisory Board, ImaginAb, Inc Advisory Board, RefleXion Medical Inc Consultant, Blue Earth Diagnostics Ltd Consultant, General Electric Company Research funded, Siemens AG Spouse, Owner, Trevarx Biomedical, Inc

Esmā Akin, MD, Washington, DC (*Presenter*) Nothing to Disclose

Eric M. Rohren, M.D., Ph.D., Houston, TX (*Presenter*) Nothing to Disclose

#### COURSE DESCRIPTION

This session is part of a series on advanced PET interpretation. The session focuses on the application of PET to cancer response assessment and will include (1) a brief overview of the framework for considering cancer response assessment, (2) illustrative examples of PET response assessment (including PET-based response criteria), and (3) pitfalls in interpreting response assessment by PET.

#### LEARNING OBJECTIVES

1) Discuss approaches to using PET/Molecular imaging to assess cancer response to therapy 2) Describe disease-specific approaches to response assessment, including criteria for different categories of response 3) List pitfalls for imaging response assessment\*Course Description This session is part of a series on advanced PET interpretation. The session focuses on the application of PET to cancer response assessment and will include (1) a brief overview of the framework for considering cancer response assessment, (2) illustrative examples of PET response assessment (including PET-based response criteria), and (3) pitfalls in interpreting response assessment by PET.

Printed on: 02/07/23



## Abstract Archives of the RSNA, 2022

T8-CNPM13

### Personalized Imaging and Theranostics in 2022

Tuesday, Nov. 29 4:30PM - 5:30PM Room: NA

#### Participants

Nicole Seiberlich, PhD, Ann Arbor, MI (*Presenter*) Royalties, Siemens AG; Research support, Siemens AG  
Agata A. Exner, PhD, Cleveland, OH (*Presenter*) Research Consultant, Akrotome Imaging, Inc  
Joseph R. Osborne, MD, New York, NY (*Presenter*) Nothing to Disclose  
Vikas Gulani, MD, PhD, Ann Arbor, MI (*Moderator*) Research support, Siemens AG; Consulting, Cook Group Incorporated

#### COURSE DESCRIPTION

Medicine increasingly aims to provide highly accurate diagnosis, treatment, and treatment monitoring, ideally all personalized for the patient. Recent research has seen significant advancement in image acquisition, reconstruction, analysis, contrast agent development and drug delivery, all of which contribute to this goal of personalized imaging. Specific approaches include quantitative imaging (i.e. use of imaging to objectively measure a disease process or treatment), molecularly targeted imaging and treatment agents (including theranostic agents which serve both diagnostic and treatment purposes), and novel delivery mechanisms such as ultrasound nanobubbles. In this course, we will explore these advances across multiple modalities, and in context of the entire spectrum of diagnosis, treatment delivery, and treatment monitoring.

#### LEARNING OBJECTIVES

1) Identify imaging approaches to achieving personalized diagnosis and treatment across multiple modalities 2) Understand and describe the concept of theranostics, and some approaches to this goal 3) Identify barriers to translation of cutting edge personalized imaging approaches\*Course Description Medicine increasingly aims to provide highly accurate diagnosis, treatment, and treatment monitoring, ideally all personalized for the patient. Recent research has seen significant advancement in image acquisition, reconstruction, analysis, contrast agent development and drug delivery, all of which contribute to this goal of personalized imaging. Specific approaches include quantitative imaging (i.e. use of imaging to objectively measure a disease process or treatment), molecularly targeted imaging and treatment agents (including theranostic agents which serve both diagnostic and treatment purposes), and novel delivery mechanisms such as ultrasound nanobubbles. In this course, we will explore these advances across multiple modalities, and in context of the entire spectrum of diagnosis, treatment delivery, and treatment monitoring.

Printed on: 02/07/23



## Abstract Archives of the RSNA, 2022

T8-CNR06

### Neuro 911 Infections Brain/Spine/Head & Neck (Combined Session)

Tuesday, Nov. 29 4:30PM - 5:30PM Room: NA

#### Participants

Mari Hagiwara, MD, Brooklyn, NY (*Presenter*) Nothing to Disclose  
Nicholas A. Koontz, MD, Indianapolis, IN (*Presenter*) Nothing to Disclose  
Carlos H. Torres, MD, FRCPC, Ottawa, ON (*Presenter*) Nothing to Disclose  
Peter G. Kranz, MD, Durham, NC (*Moderator*) Nothing to Disclose

#### COURSE DESCRIPTION

This session will review the approach to urgent and emergent infections of the brain, skull base, neck, and spine, using a lecture-based didactic format to emphasize high-yield, practical tips.

#### LEARNING OBJECTIVES

1) Review optimal imaging strategies for intracranial infections, differences in appearance based on organism type, and variations in appearance based on patient age 2) Discuss clinicoradiological features of infectious processes involving the paranasal sinuses, temporal bones, and skull base, highlighting the multimodality imaging appearance and differential diagnostic considerations 3) Identify imaging findings of infectious emergencies involving the neck, including odontogenic infections, tonsillitis, sialadenitis and retropharyngeal infections 4) Discuss imaging of spinal infections, including differentiation from non-infectious causes and imaging clues that may suggest specific etiologies\*Course Description This session will review the approach to urgent and emergent infections of the brain, skull base, neck, and spine, using a lecture-based didactic format to emphasize high-yield, practical tips.

Printed on: 02/07/23



## Abstract Archives of the RSNA, 2022

T8-CPD07

### Pediatric Oncology

Tuesday, Nov. 29 4:30PM - 5:30PM Room: NA

#### Participants

Anne Gill, MD, Atlanta, GA (*Presenter*) Nothing to Disclose

Gary Schooler, MD, Dallas, TX (*Presenter*) Nothing to Disclose

Adam Goldman-Yassen, MD,MS, New York, NY (*Presenter*) Nothing to Disclose

#### COURSE DESCRIPTION

Pediatric oncologic care is rapidly progressing, and radiology has a prominent and ever-increasing role in diagnosis and treatment. This lecture-based course will provide an review of pediatric abdominal tumors, focusing on common differential diagnoses, advanced imaging techniques – including the incorporation of biomarker imaging, and the role of interventional oncology in treatment. Attendees will refresh fundamental imaging-based diagnostic knowledge and learn about advanced imaging and the role of interventional oncology in the care of pediatric patient with abdominal tumors.

#### LEARNING OBJECTIVES

1) Refresh imaging-based knowledge of pediatric abdominal tumors 2) Learn how imaging biomarkers can contribute to care in pediatric abdominal oncology 3) Identify the role of interventional radiology in treatment of pediatric patients with abdominal tumors\*Course Description Pediatric oncologic care is rapidly progressing, and radiology has a prominent and ever-increasing role in diagnosis and treatment. This lecture-based course will provide an review of pediatric abdominal tumors, focusing on common differential diagnoses, advanced imaging techniques – including the incorporation of biomarker imaging, and the role of interventional oncology in treatment. Attendees will refresh fundamental imaging-based diagnostic knowledge and learn about advanced imaging and the role of interventional oncology in the care of pediatric patient with abdominal tumors.

Printed on: 02/07/23



## Abstract Archives of the RSNA, 2022

T8-CPH11

### Protocol Optimization for Low Dose CT

Tuesday, Nov. 29 4:30PM - 5:30PM Room: NA

#### Participants

Timothy Szczykutowicz, PhD, Madison, WI (*Presenter*) Consultant, Aidoc Medical Ltd; Consultant, Flowhow.ai; Consultant, medInt Holdings, LLC; Consultant, Alara, Inc; Consultant, AstoCT, Inc; Research Grant, General Electric Company; Research Grant, Canon Medical Systems Corporation

Lakshmi Ananthakrishnan, MD, Dallas, TX (*Presenter*) Nothing to Disclose

Lawrence N. Tanenbaum, MD, Riverside, CT (*Presenter*) Speaker, General Electric Company; Speaker, Siemens AG; Speaker, Guerbet SA; Speaker, Koninklijke Philips NV; Consultant, icoMetrix NV; Consultant, Subtle Medical, Inc; Consultant, Columbo; Consultant, iMedis; Consultant, Agamon; Consultant, FUJIFILM Holdings Corporation

#### COURSE DESCRIPTION

This session will offer actionable advice for practices desiring lower dose CT scanning. We will offer perspectives and experiences from private practice, academic, and smaller imaging sites. We will discuss technology, practice culture, and dose optimization projects.

#### LEARNING OBJECTIVES

1) Provide actionable advice for how to set up a protocol optimization effort 2) Explain what technologies can be used to obtain lower dose CT 3) Explain what practice culture changes can be used to obtain lower dose CT\*Course Description This session will offer actionable advice for practices desiring lower dose CT scanning. We will offer perspectives and experiences from private practice, academic, and smaller imaging sites. We will discuss technology, practice culture, and dose optimization projects.

Printed on: 02/07/23



## Abstract Archives of the RSNA, 2022

T8-CRO04

### Breast Case-based Multidisciplinary Review

Tuesday, Nov. 29 4:30PM - 5:30PM Room: NA

#### Participants

Lorena Gonzalez, Torrance, CA (*Presenter*) Nothing to Disclose

Anna Shapiro, MD, Syracuse, NY (*Presenter*) Nothing to Disclose

Avan Armaghani, MD, Tampa, FL (*Presenter*) Nothing to Disclose

Bethany L. Niell, MD, PhD, Tampa, FL (*Presenter*) Equipment support, Hologic, Inc

#### COURSE DESCRIPTION

This course utilizes a case-based multi-disciplinary approach to discuss appropriate breast imaging examinations, available radiotherapy options, as well as medical and surgical oncologic treatment planning in the setting of breast cancer.

#### LEARNING OBJECTIVES

1) Describe the latest advances in breast cancer imaging before, during, and after treatment 2) Facilitate a multidisciplinary approach to the diagnosis, management, and treatment of breast cancer\*Course Description This course utilizes a case-based multi-disciplinary approach to discuss appropriate breast imaging examinations, available radiotherapy options, as well as medical and surgical oncologic treatment planning in the setting of breast cancer.

Printed on: 02/07/23



## Abstract Archives of the RSNA, 2022

T8-RCP03

### Young Investigators in Cancer Imaging

Tuesday, Nov. 29 4:30PM - 5:30PM Room: NA

#### Participants

Jocelyn A. Rapelyea, MD, Washington, DC (*Moderator*) Speakers Bureau, General Electric Company  
Erik Shapiro, PhD, East Lansing, MI (*Moderator*) Nothing to Disclose

#### Sub-Events

#### **T8-RCP03 Predicting DCIS Upgrade at Surgery with Ultrafast Imaging**

#### Participants

Rachel Miceli, MD, New York, NY (*Presenter*) Nothing to Disclose

#### COURSE DESCRIPTION

Young investigators session papers in Cancer Imaging: This session will focus on the importance of research and technological advances in the field of oncologic imaging. Attendees will be introduced to timely and relevant topics in imaging malignant tumors in a wide range of subspecialties. The session will highlight those achievements made by Young Investigators as defined by NIH Early Stage Investigator guidelines.

#### LEARNING OBJECTIVES

Paper presentations will: 1) Highlight the current status of original scientific research in multimodality imaging of malignant tumors 2) Emphasize advances in imaging technology and its implications on clinical care 3) Describe optimal practice-based strategies to improve diagnoses and patient management 4) Underscore the achievements and ingenuity of junior physician/scientists in cancer imaging 5) Encourage junior scientists to use their imaging skill sets to solve the most pressing and complex problems in cancer imaging\*Course Description Young investigators session papers in Cancer Imaging: This session will focus on the importance of research and technological advances in the field of oncologic imaging. Attendees will be introduced to timely and relevant topics in imaging malignant tumors in a wide range of subspecialties. The session will highlight those achievements made by Young Investigators as defined by NIH Early Stage Investigator guidelines.

#### **T8-RCP03 CT-Based Radiomics Signature for Differentiating Lymphoma/Leukemia versus Benign Splenomegaly**

#### Participants

Jih-An Cheng, MD, Taoyuan, Taiwan (*Presenter*) Nothing to Disclose

#### **T8-RCP03 Generalizable Learning of a CT Number Bias Correction Scheme in Low-Dose Photon Counting CT**

#### Participants

Dalton Griner, Madison, WI (*Presenter*) Nothing to Disclose

#### **T8-RCP03 Quantifying Enhancing Tumor Burden Without Contrast-Enhanced Imaging**

#### Participants

James Ruffle, FRCR, MSc, London, United Kingdom (*Presenter*) Nothing to Disclose

#### **T8-RCP03 Ga-68 FAPI Imaging Versus FDG-PET Imaging In Hepatocellular Carcinoma**

#### Participants

Sunanda Nimmalapudi, MBBS, Velangi, India (*Presenter*) Nothing to Disclose

#### **T8-RCP03 Cancer Detection Rate and Abnormal Interpretation Rate as Performance Metrics of Screening Prostate MRI Interpretation**

#### Participants

Hiroki Nagayama, Nagasaki, Japan (*Presenter*) Nothing to Disclose

Printed on: 02/07/23



## Abstract Archives of the RSNA, 2022

T8-RCP03

### Predicting DCIS Upgrade at Surgery with Ultrafast Imaging

#### Participants

Rachel Miceli, MD, New York, NY (*Presenter*) Nothing to Disclose

#### COURSE DESCRIPTION

Young investigators session papers in Cancer Imaging: This session will focus on the importance of research and technological advances in the field of oncologic imaging. Attendees will be introduced to timely and relevant topics in imaging malignant tumors in a wide range of subspecialties. The session will highlight those achievements made by Young Investigators as defined by NIH Early Stage Investigator guidelines.

#### LEARNING OBJECTIVES

Paper presentations will: 1) Highlight the current status of original scientific research in multimodality imaging of malignant tumors 2) Emphasize advances in imaging technology and its implications on clinical care 3) Describe optimal practice-based strategies to improve diagnoses and patient management 4) Underscore the achievements and ingenuity of junior physician/scientists in cancer imaging 5) Encourage junior scientists to use their imaging skill sets to solve the most pressing and complex problems in cancer imaging\*Course Description Young investigators session papers in Cancer Imaging: This session will focus on the importance of research and technological advances in the field of oncologic imaging. Attendees will be introduced to timely and relevant topics in imaging malignant tumors in a wide range of subspecialties. The session will highlight those achievements made by Young Investigators as defined by NIH Early Stage Investigator guidelines.

Printed on: 02/07/23



## Abstract Archives of the RSNA, 2022

T8-RCP03

### CT-Based Radiomics Signature for Differentiating Lymphoma/Leukemia versus Benign Splenomegaly

#### Participants

Jih-An Cheng, MD, Taoyuan, Taiwan (*Presenter*) Nothing to Disclose

Printed on: 02/07/23

## Abstract Archives of the RSNA, 2022

T8-RCP03

### Generalizable Learning of a CT Number Bias Correction Scheme in Low-Dose Photon Counting CT

**Participants**

Dalton Griner, Madison, WI (*Presenter*) Nothing to Disclose

Printed on: 02/07/23



## Abstract Archives of the RSNA, 2022

T8-RCP03

### Quantifying Enhancing Tumor Burden Without Contrast-Enhanced Imaging

#### Participants

James Ruffle, FRCR, MSc, London, United Kingdom (*Presenter*) Nothing to Disclose

Printed on: 02/07/23



## Abstract Archives of the RSNA, 2022

T8-RCP03

### Ga-68 FAPI Imaging Versus FDG-PET Imaging In Hepatocellular Carcinoma

#### Participants

Sunanda Nimmalapudi, MBBS, Velangi, India (*Presenter*) Nothing to Disclose

Printed on: 02/07/23

## Abstract Archives of the RSNA, 2022

T8-RCP03

### Cancer Detection Rate and Abnormal Interpretation Rate as Performance Metrics of Screening Prostate MRI Interpretation

**Participants**

Hiroki Nagayama, Nagasaki, Japan (*Presenter*) Nothing to Disclose

Printed on: 02/07/23



## Abstract Archives of the RSNA, 2022

T8-RCP22

### Cultivating Allyship: Building an All-inclusive Specialty (Sponsored by the RSNA Committee on Diversity, Equity & Inclusion)

Tuesday, Nov. 29 4:30PM - 5:30PM Room: NA

#### Participants

Yoshimi Anzai, MD, MPH, Salt Lake City, UT (*Presenter*) Nothing to Disclose  
Nicole M. Hindman, MD, New York, NY (*Presenter*) Nothing to Disclose  
Judy Yee, MD, New York, NY (*Presenter*) Research Grant, General Electric Company  
Florence Doo, MD, MA, Sunset Beach, NY (*Presenter*) Nothing to Disclose  
Iris Gibbs, MD, Stanford, CA (*Presenter*) Speaker, Accuray Incorporated  
Cindy Chew, FRCR, MSc, Glasgow, United Kingdom (*Presenter*) Nothing to Disclose  
Reed Omary, MD, Nashville, TN (*Presenter*) Nothing to Disclose

#### COURSE DESCRIPTION

Diversity and Inclusion have been discussed increasingly within academic organizations and communities in the past several years. As a result, many academic radiology departments, private practices, and professional societies have created a "diversity committee" to implement various initiatives. A diversity committee is often composed of women and minority backgrounds on race/ethnicity or sexual orientation. However, we must accelerate allyship to build an all-inclusive culture where every voice is heard, and people treat each other with respect. This educational lecture will discuss why allyship is critical to advance EDI missions and how to accelerate allyship from those considered the "majority."

#### LEARNING OBJECTIVES

1) Understand why diversity and Inclusion are critical for our profession and any organizations 2) Identify opportunities to activate allyship and embrace diversity and inclusive culture in the fabric of organizations 3) Learn how other institutions have done to create an inclusive culture\*Course Description Diversity and Inclusion have been discussed increasingly within academic organizations and communities in the past several years. As a result, many academic radiology departments, private practices, and professional societies have created a "diversity committee" to implement various initiatives. A diversity committee is often composed of women and minority backgrounds on race/ethnicity or sexual orientation. However, we must accelerate allyship to build an all-inclusive culture where every voice is heard, and people treat each other with respect. This educational lecture will discuss why allyship is critical to advance EDI missions and how to accelerate allyship from those considered the "majority."

Printed on: 02/07/23



## Abstract Archives of the RSNA, 2022

W1-CBR05

### BI-RADS Next Edition Update: Mammography, Breast Ultrasound and Breast MRI

Wednesday, Nov. 30 8:00AM - 9:00AM Room: NA

#### Participants

Stamatia Destounis, MD, Rochester, NY (*Presenter*) Medical Advisory Board, iCad, Inc  
Wendy B. Demartini, MD, Stanford, CA (*Presenter*) Advisory Board, Kheiron Medical Technologies Ltd  
Jessica Leung, MD, Houston, TX (*Presenter*) Scientific Advisory Board, Subtle Medical, Inc; Speaker, General Electric Company; Speaker, Hologic, Inc; Scientific Advisory Board, Seno Medical Instruments, Inc

#### COURSE DESCRIPTION

This lecture will present anticipated significant updates for mammography, breast ultrasound and breast MRI to the next edition of the Breast Imaging Reporting and Data System (BI-RADS).

#### LEARNING OBJECTIVES

1) Describe anticipated significant updates for mammography, breast ultrasound and breast MRI to the next edition of the Breast Imaging Reporting and Data System (BI-RADS)\*Course Description This lecture will present anticipated significant updates for mammography, breast ultrasound and breast MRI to the next edition of the Breast Imaging Reporting and Data System (BI-RADS).

Printed on: 02/07/23



## Abstract Archives of the RSNA, 2022

W1-CCH05

### Thoracic Imaging Practice - Polling Session

Wednesday, Nov. 30 8:00AM - 9:00AM Room: NA

#### Participants

Ella Kazerooni, MD, Ann Arbor, MI (*Presenter*) Nothing to Disclose  
Cristopher Meyer, MD, Middleton, WI (*Presenter*) Investor, Elucent Medical  
Ann N. Leung, MD, Stanford, CA (*Presenter*) Nothing to Disclose  
Jo-Anne O. Shepard, MD, Boston, MA (*Presenter*) Editor with royalties, RELX  
Brett M. Elicker, MD, San Francisco, CA (*Presenter*) Nothing to Disclose  
Loren H. Ketai, MD, Albuquerque, NM (*Presenter*) Nothing to Disclose  
Sanjeev Bhalla, MD, Saint Louis, MO (*Moderator*) Advisory Board, Precisa Gravimetrics AG  
Ioannis Vlahos, MRCP, FRCR, Houston, TX (*Moderator*) Director, Grayscale Ltd; Co-owner, Grayscale Ltd;

#### COURSE DESCRIPTION

Have you ever encountered a clinical situation where you wish you could just ask an expert? You try and find the answers in the literature, but you just can't? These are the situations for which this course is designed. This panel discussion will try and answer clinical conundrums pertinent to Cardiothoracic Imaging and will focus on aspects of lung cancer screening, high resolution chest CT and cardiac imaging. This enjoyable discussion will help the learner understand the similarities and differences in specialty practice

#### LEARNING OBJECTIVES

1) Identify techniques in performing and reporting HRCT 2) Understand the variations of lung cancer screening and reporting 3) Highlight variations and similarities of performing cardiac and thoracic vascular imaging\*Course Description Have you ever encountered a clinical situation where you wish you could just ask an expert? You try and find the answers in the literature, but you just can't? These are the situations for which this course is designed. This panel discussion will try and answer clinical conundrums pertinent to Cardiothoracic Imaging and will focus on aspects of lung cancer screening, high resolution chest CT and cardiac imaging. This enjoyable discussion will help the learner understand the similarities and differences in specialty practice

Printed on: 02/07/23



## Abstract Archives of the RSNA, 2022

W1-CER10

### GI Causes of Acute Abdominal Pain

Wednesday, Nov. 30 8:00AM - 9:00AM Room: NA

#### Participants

James Lee, MD, Lexington, KY (*Presenter*) Nothing to Disclose

Anjali Agrawal, MD, Delhi, PA (*Presenter*) Nothing to Disclose

Meghan G. Lubner, MD, Madison, WI (*Presenter*) Spouse, Consultant, Elephas Bio

Robin B. Levenson, MD, Newton, MA (*Presenter*) Nothing to Disclose

#### LEARNING OBJECTIVES

1) Review gastrointestinal causes of acute abdominal pain 2) Identify key imaging findings and pitfalls of acute GI related conditions, including imaging features of potential complications 3) Discuss current imaging protocol considerations\*Course Description

Printed on: 02/07/23



## Abstract Archives of the RSNA, 2022

W1-CGI09

### LI-RADS

Wednesday, Nov. 30 8:00AM - 9:00AM Room: NA

#### Participants

Victoria Chernyak, MD,MS, Bronx, NY (*Presenter*) Consultant, Bayer AG  
Mishal Mendiratta-Lala, MD, Ann Arbor, MI (*Presenter*) Nothing to Disclose  
Mustafa Bashir, MD, Cary, NC (*Presenter*) Research Grant, Siemens AG; Research Grant, NGM Biopharmaceuticals, Inc; Research Grant, Madrigal Pharmaceuticals, Inc; Research Grant, Metacrine, Inc; Research Grant, ProSciento, Inc; Research Grant, MedPace, LLC; Research Grant, Carmot Therapeutics Inc  
Claude Sirlin, MD, San Diego, CA (*Presenter*) Research Grant, General Electric Company; Research Grant, Siemens AG; Research Grant, Bayer AG; Research Grant, Gilead Sciences, Inc; Research collaboration, Gilead Sciences, Inc; Research Grant, Koninklijke Philips NV; Research Grant, Pfizer Inc; Equipment support, General Electric Company; Consultant, Pfizer Inc; Consultant, AMRA AB; Consultant, Guerbet SA; Officer, Livivos, Inc; Advisor, Quantix Bio LLC  
Jeong Min Lee, MD, PhD, Seoul, (*Moderator*) Grant, Bayer AG Grant, Canon Medical Systems Corporation Grant, Koninklijke Philips NV Grant, General Electric Healthcare Grant, Guerbet SA Grant, Samsung Electronics Co, Ltd Grant, Bracco Group Grant, Dongkuk Pharma Grant, Starmed Ltd Grant, RF medical Grant, Siemens AG Speakers, Bayer AG Speakers, Philips Healthcare Speakers, Samsung Medison Speakers, GE Healthcare

#### COURSE DESCRIPTION

This education session covers high-yield concepts in Liver Imaging Reporting and Data Systems (LI-RADS). The engaging and informative course, taught by internationally renowned experts in liver imaging, consists of didactic lectures that discuss the pathomolecular subtypes and prognostic imaging features of HCC, recent updates to LI-RADS treatment response algorithm, and the gaps in current knowledge and future directions. The course offers learning opportunities for both novice and experienced LI-RADS users, as the faculty will highlight practical tips along with an overview of the latest scientific evidence, current challenges, and future directions for CT/MR LI-RADS algorithms. In addition, the attendees will be introduced to the concept of the pathomolecular subtypes and prognostic imaging features of HCC

#### LEARNING OBJECTIVES

1) Overview of the latest scientific evidence supporting the use of CT/MRI diagnostic algorithms 2) Explain the current gaps in knowledge and future direction of all LI-RADS algorithms 3) Explain recent updates of LI-RADS Treatment Response Algorithm application when using different modalities and contrast agents\*Course Description This education session covers high-yield concepts in Liver Imaging Reporting and Data Systems (LI-RADS). The engaging and informative course, taught by internationally renowned experts in liver imaging, consists of didactic lectures that discuss the pathomolecular subtypes and prognostic imaging features of HCC, recent updates to LI-RADS treatment response algorithm, and the gaps in current knowledge and future directions. The course offers learning opportunities for both novice and experienced LI-RADS users, as the faculty will highlight practical tips along with an overview of the latest scientific evidence, current challenges, and future directions for CT/MR LI-RADS algorithms. In addition, the attendees will be introduced to the concept of the pathomolecular subtypes and prognostic imaging features of HCC

Printed on: 02/07/23



## Abstract Archives of the RSNA, 2022

W1-CHN06

### Best Head and Neck Cases of 2022 From the Experts

Wednesday, Nov. 30 8:00AM - 9:00AM Room: NA

#### Participants

Deborah Shatzkes, MD, New York, NY (*Presenter*) Nothing to Disclose  
William T. O'Brien Sr, DO, Cincinnati, OH (*Presenter*) Nothing to Disclose  
Philip Chapman, MD, Durham, NC (*Presenter*) Nothing to Disclose  
Tanya Rath, MD, Scottsdale, AZ (*Presenter*) Nothing to Disclose  
Erin N. McComb, MD, Chicago, IL (*Moderator*) Nothing to Disclose

#### COURSE DESCRIPTION

In this case-based head and neck imaging session, attendees will be presented with classic, unusual and diagnostic dilemma cases within the head and neck as selected by the experts. Speakers will emphasize pearls for differentiating each entity from common mimics, pitfalls of interpretation to avoid, and relevant clinical management considerations with which radiologists should be familiar. This session offers attendees the opportunity to refine their interpretation of complex head and neck imaging studies by incorporating tips from world experts.

#### LEARNING OBJECTIVES

1) Recognize typical and atypical entities that occur within the head and neck 2) Differentiate between common head and neck pathologies and relevant mimics\*Course Description In this case-based head and neck imaging session, attendees will be presented with classic, unusual and diagnostic dilemma cases within the head and neck as selected by the experts. Speakers will emphasize pearls for differentiating each entity from common mimics, pitfalls of interpretation to avoid, and relevant clinical management considerations with which radiologists should be familiar. This session offers attendees the opportunity to refine their interpretation of complex head and neck imaging studies by incorporating tips from world experts.

Printed on: 02/07/23



## Abstract Archives of the RSNA, 2022

W1-CIN07

### Demystifying Population Health: What Does It Mean for Radiologists in 2023

Wednesday, Nov. 30 8:00AM - 9:00AM Room: NA

#### Participants

Neville Irani, MD, Stilwell, KS (*Presenter*) Nothing to Disclose  
Arun Krishnaraj, MD, MPH, Charlottesville, VA (*Presenter*) Nothing to Disclose  
James Rawson, MD, Boston, MA (*Presenter*) Nothing to Disclose  
Syed Furqan Zaidi, MD, Washington, DC (*Presenter*) Nothing to Disclose  
Elizabeth Rula, PhD, Brentwood, TN (*Moderator*) Nothing to Disclose

#### COURSE DESCRIPTION

Improving population health – the health outcomes and distribution of those outcomes in a population – has gained heightened importance, as reflected in emerging value-based payment models. Radiologists have an opportunity to increase value to health systems looking to capture population health savings. This panel discussion with local and national leaders will discuss major initiatives and share opportunities to demonstrate value within these models and generate collaborative, high-value growth. Come prepared to ask questions and gain insights on how Radiology can both deliver greater value and capture that value tied to improving population health outcomes.

#### LEARNING OBJECTIVES

1) Understand population health models and supporting payment models in relation to radiology. 2) Recognize opportunities for radiologists to add measurable value in population health. 3) Review goals of the Population Health Blue Ribbon Panel and results of real-world population health initiatives.\*Course Description Improving population health – the health outcomes and distribution of those outcomes in a population – has gained heightened importance, as reflected in emerging value-based payment models. Radiologists have an opportunity to increase value to health systems looking to capture population health savings. This panel discussion with local and national leaders will discuss major initiatives and share opportunities to demonstrate value within these models and generate collaborative, high-value growth. Come prepared to ask questions and gain insights on how Radiology can both deliver greater value and capture that value tied to improving population health outcomes.

Printed on: 02/07/23



## Abstract Archives of the RSNA, 2022

W1-CIR01

### Vascular Interventions

Wednesday, Nov. 30 8:00AM - 9:00AM Room: NA

#### Participants

Anne Gill, MD, Atlanta, GA (*Presenter*) Nothing to Disclose

Raman Uberoi, MBChB, FRCR, Oxford, United Kingdom (*Presenter*) Nothing to Disclose

Joo-Young Chun, MBBS, FRCR, London, United Kingdom (*Presenter*) Nothing to Disclose

Gordon McLennan, MD, Aurora, CO (*Presenter*) Consulting, Becton, Dickinson and Company; Consulting, General Electric Company; Stock Options, TriSalus Life Sciences; Grant, TriSalus Life Sciences

Peter Goverde, Antwerp, Belgium (*Presenter*) Nothing to Disclose

#### COURSE DESCRIPTION

!) Drug-eluting Technology in Peripheral Vascular Disease Peripheral Vascular Disease- Role of CERAB2) Peripheral Vascular Disease- Venous Arterialisation 3) Use of Covered Stents in Vascular Emergencies 4) Managing Complications in Hemodialysis Access and AV Fistulas 5) Endovascular Treatment of Pediatric Venous Malformation

#### LEARNING OBJECTIVES

1) To learn techniques and outcomes of common and advanced peripheral arterial techniques 2) Latest endovascular options and outcomes in renal failure patient 3) Endovascular management of malformations in the pediatric population\*Course Description

!) Drug-eluting Technology in Peripheral Vascular Disease Peripheral Vascular Disease- Role of CERAB2) Peripheral Vascular Disease- Venous Arterialisation 3) Use of Covered Stents in Vascular Emergencies 4) Managing Complications in Hemodialysis Access and AV Fistulas 5) Endovascular Treatment of Pediatric Venous Malformation

Printed on: 02/07/23



## Abstract Archives of the RSNA, 2022

W1-CMK03

### Ankle and Foot: Pre-op and Post-op

Wednesday, Nov. 30 8:00AM - 9:00AM Room: NA

#### Participants

Zaid Jibri, MBChB, Ottawa, ON (*Presenter*) Nothing to Disclose

Tetyana A. Gorbachova, MD, Huntingdon Valley, PA (*Presenter*) Nothing to Disclose

Alice S. Ha, MD, Seattle, WA (*Presenter*) Nothing to Disclose

Kathryn Stevens, MBBS, FRCR, Stanford, CA (*Presenter*) Nothing to Disclose

Yulia Melenevsky, MD, Vestavia, AL (*Presenter*) Nothing to Disclose

#### COURSE DESCRIPTION

This course is composed of a series of lectures focused on preoperative and postoperative imaging of the ankle and foot, in a format of short didactic lectures and Q&A. Individual lectures will highlight the tips and pitfalls of imaging diagnosis of common conditions that occur in clinical practice including diagnostic interpretation of postoperative imaging.

#### LEARNING OBJECTIVES

1) To review imaging features and technical and interpretational pitfalls in the diagnosis of the abnormalities of the ankle and foot  
2) To analyze the biomechanics and clinical significance of injuries to the ankle and foot  
3) To become familiar with the expected findings and complications in imaging of the post-operative ankle and foot\*  
Course Description This course is composed of a series of lectures focused on preoperative and postoperative imaging of the ankle and foot, in a format of short didactic lectures and Q&A. Individual lectures will highlight the tips and pitfalls of imaging diagnosis of common conditions that occur in clinical practice including diagnostic interpretation of postoperative imaging.

Printed on: 02/07/23



## Abstract Archives of the RSNA, 2022

W1-CNMMIO1

### PET/MR: Read with the Experts (Clinical and Technology Update)

Wednesday, Nov. 30 8:00AM - 9:00AM Room: NA

#### Participants

Georges El Fakhri, PhD, Boston, MA (*Presenter*) Nothing to Disclose

Helen Nadel, MD, Menlo Park, CA (*Presenter*) Consultant, ICON plc;;

Jonathan E. McConathy, MD, PhD, Birmingham, AL (*Presenter*) Research Consultant, Eli Lilly and Company; Research Grant, Eli Lilly and Company; Research Consultant, Blue Earth Diagnostics Ltd; Research Grant, Blue Earth Diagnostics Ltd; Research Consultant, General Electric Company; Research support, General Electric Company; Research support, CytoSite Biopharma; Research Consultant, ImaginAb, Inc; Research support, ImaginAb, Inc; Spouse, Research Consultant, Baird Capital; Spouse, Research Grant, Navidea Biopharmaceuticals, Inc

Geoffrey Johnson, MD, PhD, Rochester, MN (*Presenter*) Research Grant, Novartis AG; Research Grant, Pfizer Inc; Research Grant, Bayer AG; Research Grant, MedTrace Pharma AS; Research Grant, Viewpoint Medical Ltd; Research Grant, Clarity Medical Systems, Inc; Research Grant, Clovis Oncology, Inc; Research Grant, Sofie Biosciences

#### LEARNING OBJECTIVES

1) To discuss advances in PET/MR technology 2) To review clinical applications where PET/MR adds value 3) To illustrate advances in PET/MR with images from the field.\*Course Description

Printed on: 02/07/23



## Abstract Archives of the RSNA, 2022

W1-COB04

### Integrating O-RADS MRI in Your Practice: Why, When and How?

Wednesday, Nov. 30 8:00AM - 9:00AM Room: NA

#### Participants

Elizabeth A. Sadowski, MD, Madison, WI (*Presenter*) Nothing to Disclose

Caroline Reinhold, MD, MSc, Westmount, QC (*Presenter*) Research Grant, Imagia Cybernetics Inc

Andrea Rockall, FRCR, MRCP, London, United Kingdom (*Presenter*) Nothing to Disclose

Priyanka Jha, MBBS, San Francisco, CA (*Presenter*) Nothing to Disclose

#### COURSE DESCRIPTION

This lecture and case-based course will allow the attendee to successfully implement the O-RADS MRI risk stratification system for characterizing ovarian lesions in daily clinical practice. The added value and role of MRI in the evaluation of adnexal masses will be emphasized. Tips on the MR imaging protocol, in particular, generation of the time intensity curves (TIC) as well as highlights of the O-RADS MRI lexicon and risk stratification system will be presented. A case-based review of classical and challenging ovarian lesions will consolidate the knowledge gained during the didactic sessions.

#### LEARNING OBJECTIVES

1) identify learning strategies to integrate O-RADS MRI into your clinical practice for characterizing ovarian lesions. 2) Explain salient aspects of the MR imaging protocol, O-RADS MRI lexicon and risk stratification system. 3) Assign risk categories using O-RADS MRI to common and challenging ovarian lesions. \*Course Description This lecture and case-based course will allow the attendee to successfully implement the O-RADS MRI risk stratification system for characterizing ovarian lesions in daily clinical practice. The added value and role of MRI in the evaluation of adnexal masses will be emphasized. Tips on the MR imaging protocol, in particular, generation of the time intensity curves (TIC) as well as highlights of the O-RADS MRI lexicon and risk stratification system will be presented. A case-based review of classical and challenging ovarian lesions will consolidate the knowledge gained during the didactic sessions.

Printed on: 02/07/23



## Abstract Archives of the RSNA, 2022

W1-CPH02

### Innovations in Dual and Multi-Energy CT

Wednesday, Nov. 30 8:00AM - 9:00AM Room: NA

#### Participants

Megan Jacobsen, PhD, Houston, TX (*Presenter*) Nothing to Disclose

Wei Zhou, PhD, Aurora, CO (*Presenter*) Nothing to Disclose

Daniele Marin, MD, Cary, NC (*Presenter*) Research support, General Electric Company; Research support, Siemens AG; Research support, Bracco Group; Research Consultant, Bracco Group; Research Consultant, Bayer AG

#### COURSE DESCRIPTION

This session will have three speakers to cover the latest innovations in Dual- and Multi-energy CT. The first talk will introduce the technical approaches of emerging Dual-energy CT technology and systems. The second talk will discuss the experience when implementing Dual- and Multi-energy CT in clinical practice. Finally, the third talk will focus on various clinical applications of Dual- and Multi-energy CT to improve patients' diagnosis.

#### LEARNING OBJECTIVES

1) Understand the basic principles of Dual and Multi-energy CT 2) Discuss the clinical implementation of Dual- and Multi-energy CT, from acquisitions to post-processing 3) Learn recent clinical applications of Dual- and Multi-energy CT to improve patient care\*Course Description This session will have three speakers to cover the latest innovations in Dual- and Multi-energy CT. The first talk will introduce the technical approaches of emerging Dual-energy CT technology and systems. The second talk will discuss the experience when implementing Dual- and Multi-energy CT in clinical practice. Finally, the third talk will focus on various clinical applications of Dual- and Multi-energy CT to improve patients' diagnosis.

Printed on: 02/07/23



## Abstract Archives of the RSNA, 2022

W1-CRT04

### ASRT@RSNA: Radiation Safety Culture and You

Wednesday, Nov. 30 8:00AM - 9:00AM Room: NA

#### Participants

Timothy J. Blackburn, PhD, Dallas, TX (*Presenter*) Nothing to Disclose

#### COURSE DESCRIPTION

Radiographers and associated ARRT certificate holders dispense much of the radiation to the public in medical treatment. This course will examine changes in gonadal shielding policy and methods to ensure best practices in reducing patient and staff radiation exposure. Radiation safety culture and ethics associated with radiation risk will be discussed. <https://tinyurl.com/mw43e4ue>

#### LEARNING OBJECTIVES

1) Discuss shielding policy changes with patients and their families 2) Identify practice behaviors which may lead to reduced patient and staff radiation exposure 3) Describe ways you can improve radiation safety culture in your practice\*Course Description  
Radiographers and associated ARRT certificate holders dispense much of the radiation to the public in medical treatment. This course will examine changes in gonadal shielding policy and methods to ensure best practices in reducing patient and staff radiation exposure. Radiation safety culture and ethics associated with radiation risk will be discussed. <https://tinyurl.com/mw43e4ue>

Printed on: 02/07/23



## Abstract Archives of the RSNA, 2022

W1-RCP12

### Women in Radiology: Retrospective, Introspective and Prospective Analysis (Sponsored by the American Association for Women in Radiology)

Wednesday, Nov. 30 8:00AM - 9:00AM Room: NA

#### Participants

Catherine Everett, MD, New Bern, NC (*Presenter*) Shareholder, Radiology Partners; Officer, Radiology Partners; President, Eidetico Radiology Solutions; Medical Director, MSN Healthcare Solutions

Amy Patel, MD, Liberty, MO (*Presenter*) Medical Advisor, Kheiron Medical Technologies Ltd; Consultant, Hologic, Inc

Carol Rumack, MD, Aurora, CO (*Presenter*) Nothing to Disclose

Barbara K. Pawley, MD, Louisville, KY (*Moderator*) Nothing to Disclose

#### COURSE DESCRIPTION

Three presenters will provide a look at the history of women in radiology and radiation oncology over the past 40 years as it is important to know where we have been to best direct our future. There will be presentation of ongoing contributions of women in radiology and radiation oncology and a vision for the future.

#### LEARNING OBJECTIVES

1) Provide overview of past achievements, highlight current contributions, and offer insights into the future trajectory of women in the fields of radiology\*Course Description Three presenters will provide a look at the history of women in radiology and radiation oncology over the past 40 years as it is important to know where we have been to best direct our future. There will be presentation of ongoing contributions of women in radiology and radiation oncology and a vision for the future.

Printed on: 02/07/23



## Abstract Archives of the RSNA, 2022

W1-RCP51

### RSNA/ESR Symposium: Imaging of Neurodegenerative Disorders - Basics of Neuroimaging in Neurodegeneration

Wednesday, Nov. 30 8:00AM - 9:00AM Room: NA

#### Participants

Yoshimi Anzai, MD, MPH, Salt Lake City, UT (*Presenter*) Nothing to Disclose

Meike W. Vernooij, MD, PhD, Rotterdam, Netherlands (*Presenter*) Nothing to Disclose

Javier Arbizu Lostao, Pamplona, Spain (*Presenter*) Speaker, F. Hoffmann-La Roche Ltd; Speaker, Novartis AG; Speaker, General Electric Company; Research Grant, Siemens AG; Speaker, Life Molecular Imaging GmbH; Speaker, Biogen Idec Inc

Alexander Drzezga, MD, Cologne, Germany (*Moderator*) Research support, Siemens AG ; Research support, Life Molecular Imaging; Research support, General Electric Company; Research support, Eli Lilly and Company; Research support, Eisai Co, Ltd; Consultant, Siemens AG ; Consultant, General Electric Company

#### COURSE DESCRIPTION

Structural and molecular imaging techniques are able to demonstrate the onset of neurodegenerative and dementing disorders years before the onset of symptoms. This educational course will discuss the structural MRI changes that occur with normal aging and how they relate to specific neurodegenerative disorders. Molecular imaging probes for PET imaging will be discussed that can dissect the molecular pathology associated with neurodegenerative diseases, including parkinsonian syndromes. At the end of the course, the participants will better understand the sequences of molecular and structural imaging findings that may herald the onset of dementia and other neurodegenerative disorders.

#### LEARNING OBJECTIVES

1) To understand the standard MR Imaging protocol, normal aging findings, as well as Alzheimer disease mimic on structural brain MR imaging 2) To become familiar with existing and new molecular imaging tracers for dementia and parkinsonian disorders 3) To comprehend how molecular imaging features may show the onset of neurodegenerative disease\*Course Description Structural and molecular imaging techniques are able to demonstrate the onset of neurodegenerative and dementing disorders years before the onset of symptoms. This educational course will discuss the structural MRI changes that occur with normal aging and how they relate to specific neurodegenerative disorders. Molecular imaging probes for PET imaging will be discussed that can dissect the molecular pathology associated with neurodegenerative diseases, including parkinsonian syndromes. At the end of the course, the participants will better understand the sequences of molecular and structural imaging findings that may herald the onset of dementia and other neurodegenerative disorders.

Printed on: 02/07/23



## Abstract Archives of the RSNA, 2022

W2-CPD13

### RSNA Simulation Lab (Hands on): Pediatric MSK US

Wednesday, Nov. 30 9:00AM - 10:30AM Room: NA

#### Participants

Andrew Zbojnowicz, MD, Grand Rapids, MI (*Presenter*) Nothing to Disclose  
Emilio Inarejos Clemente, MD, Barcelona, Spain (*Presenter*) Nothing to Disclose  
Anna Alexiev, Chicago, IL (*Presenter*) Nothing to Disclose  
Falguni Patel, RDMS,RVT,BS, Willowbrook, IL (*Presenter*) Nothing to Disclose  
Lauren W. Averill, MD, Wilmington, DE (*Presenter*) Nothing to Disclose  
Nikki Hilbert, RDMS,RVT,MS,RT, Chicago, IL (*Presenter*) Nothing to Disclose  
Matthew Hammer, MD, Dallas, TX (*Presenter*) Nothing to Disclose  
Julia Michalek, RDMS, Arlington Heights, IL (*Presenter*) Nothing to Disclose  
Andrea S. Doria, MD, PhD, Toronto, ON (*Presenter*) Baxalta-Shire (Research Grant), Novo Nordisk (Research Grant), Terry Fox Foundation (Research Grant), PSI Foundation (Research Grant), Society of Pediatric Radiology (Research Grant), Garron Family Cancer Centre (Research Grant)  
Jonathan D. Samet, MD, Chicago, IL (*Presenter*) Nothing to Disclose  
Rachel Pevsner Crum, DO, Hollywood, FL (*Presenter*) Nothing to Disclose

#### COURSE DESCRIPTION

In Person Session Only. Tickets must be purchased in advance for this course. This course can be added through the registration portal or by stopping by the Registration Desk. Space is limited. This 90-min pediatric musculoskeletal hands-on session is targeted to general radiologists who aim to get an overview of technical and clinical application perspectives on ultrasound scanning and interpreting pathology of elbows, hands and ankles of children and adolescents. The information provided in this session adds value to the diagnostic tools that can be used for assessment of musculoskeletal disorders that affect growing joints, particularly in young children who may require general anesthesia for MRI assessment of their joints. The session has two parts, a 60-min hands-on part where pre-assigned radiologists scan teenager models' joints in real time and a second 30-min knowledge application part where the audience has the opportunity to scan models' joints by themselves. In the first part of the session lecturers will demonstrate ultrasound protocols for scanning of pediatric elbows, hands and ankles in real-time and will discuss ultrasound findings of pathologies in these joints. In the second part of the session tutoring to scanning by the audience will be provided by assigned radiologists in a controlled educational environment where the audience will have the opportunity to apply the a priori discussed ultrasound protocols into scanning the models' joints.

#### LEARNING OBJECTIVES

1) Review the anatomy and common pediatric pathologic musculoskeletal conditions in three pediatric joints: the elbow, hand and ankle 2) Use dynamic scanning of the joints to better demonstrate the anatomy of soft tissue and osteochondral components of three pediatric joints and will point out the distinction of soft tissue structures by a compression technique 3) Discuss pathologies in the aforementioned joints as an overview of common pediatric pathologic musculoskeletal conditions\*Course Description In Person Session Only. Tickets must be purchased in advance for this course. This course can be added through the registration portal or by stopping by the Registration Desk. Space is limited. This 90-min pediatric musculoskeletal hands-on session is targeted to general radiologists who aim to get an overview of technical and clinical application perspectives on ultrasound scanning and interpreting pathology of elbows, hands and ankles of children and adolescents. The information provided in this session adds value to the diagnostic tools that can be used for assessment of musculoskeletal disorders that affect growing joints, particularly in young children who may require general anesthesia for MRI assessment of their joints. The session has two parts, a 60-min hands-on part where pre-assigned radiologists scan teenager models' joints in real time and a second 30-min knowledge application part where the audience has the opportunity to scan models' joints by themselves. In the first part of the session lecturers will demonstrate ultrasound protocols for scanning of pediatric elbows, hands and ankles in real-time and will discuss ultrasound findings of pathologies in these joints. In the second part of the session tutoring to scanning by the audience will be provided by assigned radiologists in a controlled educational environment where the audience will have the opportunity to apply the a priori discussed ultrasound protocols into scanning the models' joints.

Printed on: 02/07/23



## Abstract Archives of the RSNA, 2022

W3-CCA02

### MRI of Nonischemic Cardiomyopathies: Case Based Review

Wednesday, Nov. 30 9:30AM - 10:30AM Room: NA

#### Participants

Jadranka Stojanovska, MD, New York, NY (*Presenter*) Nothing to Disclose

Karen Ordovas, MD, Seattle, WA (*Presenter*) Nothing to Disclose

Bradley Allen, MD, MS, Evanston, IL (*Moderator*) Consultant, Circle Cardiovascular Imaging Inc; Speaker, WebMD LLC

#### COURSE DESCRIPTION

Cardiac MRI (CMR) is an important tool for providing accurate diagnosis and risk-stratification for non-ischemic cardiomyopathies. In this course, learners will be presented with a broad overview of the current state-of-the-art for CMR evaluation of multiple non-ischemic cardiomyopathies. Topics will be presented in a case-based lecture format highlighting relevant CMR acquisitions and interpretation approaches, with a data-driven focus on current best-practices for providing optimal patient care.

#### LEARNING OBJECTIVES

1) Review current best-practices for CMR evaluation of non-ischemic cardiomyopathy 2) Discuss CMR interpretation and reporting in non-ischemic cardiomyopathy to provide accurate diagnosis and risk-stratification 3) Highlight areas of uncertainty in the current diagnostic approach and when other tools and modalities can be helpful\*Course Description Cardiac MRI (CMR) is an important tool for providing accurate diagnosis and risk-stratification for non-ischemic cardiomyopathies. In this course, learners will be presented with a broad overview of the current state-of-the-art for CMR evaluation of multiple non-ischemic cardiomyopathies. Topics will be presented in a case-based lecture format highlighting relevant CMR acquisitions and interpretation approaches, with a data-driven focus on current best-practices for providing optimal patient care.

Printed on: 02/07/23



## Abstract Archives of the RSNA, 2022

W3-CGU07

### Best of Sessions in GU Oncology

Wednesday, Nov. 30 9:30AM - 10:30AM Room: NA

#### Participants

Felix Feng, MD, San Francisco, CA (*Presenter*) Consultant, Johnson & Johnson; Consultant, Bayer AG; Consultant, Exact Sciences Corporation; Consultant, Sumitovant Biopharma Ltd; Consultant, Roivant Sciences Holdings Limited; Consultant, Astellas Group; Consultant, SerImmune Inc; Scientific Advisory Board, Serimmune Inc; Stock options, Serimmune Inc; Consultant, F. Hoffmann-La Roche Ltd; Consultant, Siemens AG; Consultant, Bristol-Myers Squibb Company; Consultant, BlueStar Genomics, Inc; Consultant, Artera Services, LLC; Medical Advisor, Artera Services, LLC; Stock options, Artera Services, LLC; Consultant, Novartis AG; Consultant, Tempus Labs

Daniel Margolis, MD, New York, NY (*Presenter*) In-kind support, Siemens AG; Consultant, Promaxo, Inc

Yaw Nyame, MD, Seattle, WA (*Presenter*) Research Consultant, Ortho-Clinical Diagnostics, Inc

Kathryn Fowler, MD, San Diego, CA (*Presenter*) Consultant, Bayer AG; Research support, General Electric Company; Research Grant, Pfizer Inc; Institutional Grant, MEDIAN Technologies; Consultant, General Electric Company

Antonio Westphalen, MD, Kirkland, WA (*Moderator*) Shareholder, ScanMed, LLC; Research funded, BotImage, Inc

#### COURSE DESCRIPTION

In this session we will summarize the newest and best GU oncology research published and presented at the most recent meetings in and outside radiology. Speakers will present research in their area of practice, but that are relevant for practicing radiologists.

Printed on: 02/07/23



## Abstract Archives of the RSNA, 2022

W3-CIN23

### Failures, Biases, and more: When Good AI Goes Bad

Wednesday, Nov. 30 9:30AM - 10:30AM Room: NA

#### Participants

Paul Yi, MD, Baltimore, MD (*Presenter*) Consultant, FH Orthopedics SAS; Consultant, BunkerHill Health

Florence Doo, MD, MA, Sunset Beach, NY (*Presenter*) Nothing to Disclose

Hari Trivedi, MD, Atlanta, GA (*Moderator*) Founder, Lightbox AI ; Consultant, Sirona Medical, Inc ; Consultant, Flatiron Health ; Consultant, PMX Inc ; Research support, Kheiron Medical Technologies ; Research support, Clarity, Inc ; Research support, Nightingale Open Science ;

Printed on: 02/07/23



## Abstract Archives of the RSNA, 2022

W3-CMS09

### Postpartum Complications: Head to Toe

Wednesday, Nov. 30 9:30AM - 10:30AM Room: NA

#### Participants

Gayatri Joshi, MD, Atlanta, GA (*Presenter*) Nothing to Disclose

Aya Kamaya, MD, Mountain View, CA (*Presenter*) Royalties, RELX; Research Grant, Canon Medical Systems Corporation

Shuchi K. Rodgers, MD, Cherry Hill, NJ (*Presenter*) Royalties, RELX

Nicholas A. Koontz, MD, Indianapolis, IN (*Presenter*) Nothing to Disclose

#### COURSE DESCRIPTION

This session will provide a detailed review of postpartum complications using a multisystem multimodality approach including neurologic, chest, breast, vascular, and pelvic complications.

#### LEARNING OBJECTIVES

1) Differentiate vascular postpartum complications such as retained products of conception from enhanced myometrial vascularity, pseudoaneurysm, or subinvolution of the placental implantation site, as well as the over-diagnosed but exceedingly rare AVM of the uterus 2) Review breast and chest complications seen in the post-partum setting such as mastitis, breast abscess, breast cancer, PE, COVID, peripartum dilated cardiomyopathy, aortic rupture, aortic dissection 3) Learn the imaging appearance of post-Cesarian section complications such as uterine dehiscence/rupture, pyometra, abscesses, fistula formation, and bladder flap hematoma 4) Understand the myriad neurologic complications that may occur in the brain, spine, and head and neck\*Course Description This session will provide a detailed review of postpartum complications using a multisystem multimodality approach including neurologic, chest, breast, vascular, and pelvic complications.

Printed on: 02/07/23



## Abstract Archives of the RSNA, 2022

W3-CNPM11

### Interactive Course on Statistical Methods for Radiologists

Wednesday, Nov. 30 9:30AM - 10:30AM Room: NA

#### Participants

Nancy Obuchowski, PhD, Cleveland, OH (*Presenter*) Research Consultant, Siemens AG; Research Consultant, IBM Corporation; Research Consultant, Elucid Bioimaging Inc; Research Consultant, Takeda Pharmaceutical Company Limited  
Chaya Moskowitz, PhD, New York, NY (*Moderator*) Nothing to Disclose

#### COURSE DESCRIPTION

This course will cover several advanced topics related to statistical methods for evaluating the diagnostic accuracy of imaging tests as well as methods for evaluating quantitative imaging biomarkers. Focusing on methods researchers are likely to use or encounter in their studies, subject matter will include approaches for evaluating data from multi-reader studies, for identifying and validating optimal cut-points, for assessing repeatability and reproducibility, for analyzing multiparametric data, and for understanding bias in the design and analysis of quantitative imaging (radiomic) studies. The format will be interactive with educational questions posed to the audience interspersed with didactic teaching.

#### LEARNING OBJECTIVES

By the end of this course, the audience should have gained: 1) A better understanding of the appropriate use of statistical analytic methods for evaluating the diagnostic accuracy of imaging tests 2) An awareness of statistical methods necessary for analyzing quantitative imaging biomarkers 3) A deeper appreciation of the elements of study design and study procedures that may lead to bias in quantitative imaging research\*Course Description This course will cover several advanced topics related to statistical methods for evaluating the diagnostic accuracy of imaging tests as well as methods for evaluating quantitative imaging biomarkers. Focusing on methods researchers are likely to use or encounter in their studies, subject matter will include approaches for evaluating data from multi-reader studies, for identifying and validating optimal cut-points, for assessing repeatability and reproducibility, for analyzing multiparametric data, and for understanding bias in the design and analysis of quantitative imaging (radiomic) studies. The format will be interactive with educational questions posed to the audience interspersed with didactic teaching.

Printed on: 02/07/23



## Abstract Archives of the RSNA, 2022

W3-CNR08

### Clinical Demands on Neuroradiologists Outside the Reading Room

Wednesday, Nov. 30 9:30AM - 10:30AM Room: NA

#### Participants

Nancy J. Fischbein, MD, Stanford, CA (*Presenter*) Nothing to Disclose

Achala Vagal, MD, Cincinnati, OH (*Presenter*) Departmental Research Grant, Johnson & Johnson

Luca Saba, MD, Cagliari, (*Presenter*) Nothing to Disclose

Max Wintermark, MD, San Carlos, CA (*Moderator*) Consultant, Magnetic Insight, Inc; Consultant, icoMetrix NV; Consultant, Subtle Medical, Inc; Consultant, EMTensor Imaging

#### COURSE DESCRIPTION

The clinical workload for neuroradiologists has increased to reach record numbers of studies to be read, this is addition to growing non-RVU-generating activities. This conflicts with the education and research missions of academic neuroradiologists, challenges recruitment of trainees into neuroradiology and threatens the future of our profession. This sessions will discuss this issues and brainstorms solutions to address them.

#### LEARNING OBJECTIVES

1) To review the burden of Non RVU generating activities typically performed by neuroradiologists 2) To discuss how to balance clinical workload and education mission for neuroradiologists 3) To discuss how to balance clinical workload and academic endeavors for neuroradiologists\*Course Description The clinical workload for neuroradiologists has increased to reach record numbers of studies to be read, this is addition to growing non-RVU-generating activities. This conflicts with the education and research missions of academic neuroradiologists, challenges recruitment of trainees into neuroradiology and threatens the future of our profession. This sessions will discuss this issues and brainstorms solutions to address them.

Printed on: 02/07/23



## Abstract Archives of the RSNA, 2022

W3-CPH12

### Making Patients and Staff Safer in Interventional Procedures

Wednesday, Nov. 30 9:30AM - 10:30AM Room: NA

#### Participants

A. Kyle Jones, PhD, Houston, TX (*Presenter*) Nothing to Disclose

Stephen Balter, PhD, New York, NY (*Presenter*) Speakers Bureau, MAVIG, GmbH; Consultant, ControlRad Systems, Inc

David Borrego, PHD, Washington, DC (*Presenter*) Nothing to Disclose

#### COURSE DESCRIPTION

This course will review risks, including radiation-related risks and other risks, to patients undergoing and staff participating in fluoroscopically-guided interventional procedures. Perspective on the magnitude of these risks will be provided, and strategies for managing risk will be discussed. Understanding risks and their magnitude is important for data-driven clinical decision-making, informed consent, and optimization of patient and staff protection.

#### LEARNING OBJECTIVES

1) Identify risks to patients and staff from fluoroscopically-guided interventions 2) Where possible, quantify the relative magnitudes of these risks 3) Formulate strategies for managing identified risks\*Course Description This course will review risks, including radiation-related risks and other risks, to patients undergoing and staff participating in fluoroscopically-guided interventional procedures. Perspective on the magnitude of these risks will be provided, and strategies for managing risk will be discussed. Understanding risks and their magnitude is important for data-driven clinical decision-making, informed consent, and optimization of patient and staff protection.

Printed on: 02/07/23



## Abstract Archives of the RSNA, 2022

W3-CRT05

### ASRT@RSNA: Making the Invisible Visible: Bringing Intimate Partner Violence in Focus

Wednesday, Nov. 30 9:30AM - 10:30AM Room: NA

#### Participants

Bharti Khurana, MD, Brookline, MA (*Presenter*) Consultant, General Electric Company; Editor, Wolters Kluwer nv; Author, Cambridge University Press; Consultant, ROKIT Healthcare, Inc

#### LEARNING OBJECTIVES

1. Recognize IPV as a highly prevalent public health issue. 2. Understand the key role that radiology can play in facilitating early diagnosis and disrupting the cycle of abuse. \*Course Description

Printed on: 02/07/23



## Abstract Archives of the RSNA, 2022

W3-CVA08

### Multimodal Imaging of Vascular Anatomy and Vascular Variants

Wednesday, Nov. 30 9:30AM - 10:30AM Room: NA

#### Participants

Sandeep S. Hegdige, MD, Lexington, MA (*Presenter*) Nothing to Disclose

Filipe Caseiro Alves, MD, PhD, Coimbra, Portugal (*Presenter*) Nothing to Disclose

Kedar Sharbidre, MD, Birmingham, AL (*Presenter*) Nothing to Disclose

#### COURSE DESCRIPTION

This course in lecture format will focus on the vascular anatomy of the chest, abdomen, and pelvis as seen on various imaging modalities. Upon completion of the course, the audience will be able to identify conventional as well as clinically relevant vascular anatomy on imaging.

#### LEARNING OBJECTIVES

1) Describe the various anatomic variations of the chest, abdomen, and pelvic vasculature 2) Describe the roles of MRI, CT, and ultrasound in the assessment of these vascular variations 3) Discuss the clinical relevance of some of the common variants\*Course Description This course in lecture format will focus on the vascular anatomy of the chest, abdomen, and pelvis as seen on various imaging modalities. Upon completion of the course, the audience will be able to identify conventional as well as clinically relevant vascular anatomy on imaging.

Printed on: 02/07/23



## Abstract Archives of the RSNA, 2022

W3-RCP52

### RSNA/ESR Symposium: Imaging of Neurodegenerative Disorders - Dementia: Towards an Aetiologic Diagnosis

Wednesday, Nov. 30 9:30AM - 10:30AM Room: NA

#### Participants

Alexander Drzezga, MD, Cologne, Germany (*Presenter*) Research support, Siemens AG ;Research support, Life Molecular Imaging;Research support, General Electric Company;Research support, Eli Lilly and Company;Research support, Eisai Co, Ltd;Consultant, Siemens AG ;Consultant, General Electric Company  
Meike W. Vernooij, MD, PhD, Rotterdam, Netherlands (*Presenter*) Nothing to Disclose

#### COURSE DESCRIPTION

This educational session will discuss how in current clinical practice imaging modalities such as MRI and molecular imaging techniques can be used to support an etiologic diagnosis of dementia. This session will give general radiologists and those interested in neuroradiology and nuclear medicine/molecular imaging the knowledge needed for appropriate selection and structured assessment of imaging exams in diagnostic work-up of dementia. The session format consist of in part lectures, followed by an interactive case-based discussion.

#### LEARNING OBJECTIVES

1) Explain the current use of MRI for etiologic dementia diagnosis 2) Explain the current use of molecular imaging for etiologic dementia diagnosis 3) Demonstrate structured selection and assessment of imaging exams through cases\*Course Description This educational session will discuss how in current clinical practice imaging modalities such as MRI and molecular imaging techniques can be used to support an etiologic diagnosis of dementia. This session will give general radiologists and those interested in neuroradiology and nuclear medicine/molecular imaging the knowledge needed for appropriate selection and structured assessment of imaging exams in diagnostic work-up of dementia. The session format consist of in part lectures, followed by an interactive case-based discussion.

Printed on: 02/07/23



## Abstract Archives of the RSNA, 2022

W3-RCP57

### MIDRC: The Imaging Research Community's Response to the COVID-19 Pandemic

Wednesday, Nov. 30 9:30AM - 10:30AM Room: NA

#### Participants

Rui Carlos Sa, PhD, Bethesda, MD (*Presenter*) Nothing to Disclose

Maryellen Giger, PhD, Chicago, IL (*Presenter*) Stockholder, Hologic, Inc; Royalties, Hologic, Inc; Shareholder, Quantitative Insights, Inc; Co-founder, Quantitative Insights, Inc; Shareholder, QView Medical, Inc; Royalties, General Electric Company; Royalties, Median Technologies; Royalties, Riverain Technologies, LLC

Adam Flanders, MD, Philadelphia, PA (*Presenter*) Nothing to Disclose

Kyle Myers, PhD, Silver Spring, MD (*Presenter*) Consultant, InformAI, LLC; Consultant, American Heart Technologies LLC; Member, Puente Solutions, LLC

Printed on: 02/07/23



## Abstract Archives of the RSNA, 2022

W4-CIN17

### Big Data for QI

Wednesday, Nov. 30 11:00AM - 12:00PM Room: NA

#### Participants

Ronilda Lacson, MD, PhD, Lexington, MA (*Presenter*) Nothing to Disclose  
Patricia Balthazar, MD, Atlanta, GA (*Presenter*) Nothing to Disclose  
Neena Kapoor, MD, Wellesley, MA (*Presenter*) Nothing to Disclose

#### COURSE DESCRIPTION

Big data refers to the use of large data sets for artificial intelligence, advanced analytics, and various research and non-research related applications. Big data is increasingly being used by informatics and quality improvement teams to increase quality, safety, performance standards in radiology. The purpose of this course will be to illustrate how big data is used in various informatics tools to create measurable goals and drive impactful change in radiology departments. The course will consist of several lectures with a question-and-answer portion. At the end of this course, participants will have a greater understanding of informatics tools that can improve their radiology practice.

#### LEARNING OBJECTIVES

1) Illustrate informatics tools that enable quality, patient safety and performance improvement 2) Describe how informatics tools can be used to create specific metric, communicate performance, and monitor and sustain gains 3) Describe relevance and use of informatics tools to enable various components of a performance improvement initiative\*Course Description Big data refers to the use of large data sets for artificial intelligence, advanced analytics, and various research and non-research related applications. Big data is increasingly being used by informatics and quality improvement teams to increase quality, safety, performance standards in radiology. The purpose of this course will be to illustrate how big data is used in various informatics tools to create measurable goals and drive impactful change in radiology departments. The course will consist of several lectures with a question-and-answer portion. At the end of this course, participants will have a greater understanding of informatics tools that can improve their radiology practice.

Printed on: 02/07/23



## Abstract Archives of the RSNA, 2022

W4-CNPM24

### Is Co-signing With Private Equity Good for The Future of Radiology?

Wednesday, Nov. 30 11:00AM - 12:00PM Room: NA

#### Participants

Geraldine McGinty, MD, MBA, New York, NY (*Presenter*) Board Member, NextGen Healthcare ;Stockholder, NextGen Healthcare  
Kurt Schoppe, MD, Grapevine, TX (*Presenter*) Nothing to Disclose  
Gavin P. Slethaug, MD, Paradise Vly, AZ (*Presenter*) Shareholder, Radiology Partners;Shareholder, Southwest Medical Imaging;Shareholder, Arizona Physicians Advancing Cardiovascular Treatment LLC  
Saurabh Jha, MD, Philadelphia, PA (*Moderator*) Nothing to Disclose

#### COURSE DESCRIPTION

With increasing mergers of small and large radiology practices and of private practice and large academic medical centers, and the rise of private equity in radiology, the question arises: which is the best financial model for the sustainability of the field. This'll be a moderated panel discussion on the nuances of radiology models.

#### LEARNING OBJECTIVES

1) Understand the current financial models for radiology 2) Appreciate the role of private equity model in radiology 3) Understand the advantages and disadvantages of each model\*Course Description With increasing mergers of small and large radiology practices and of private practice and large academic medical centers, and the rise of private equity in radiology, the question arises: which is the best financial model for the sustainability of the field. This'll be a moderated panel discussion on the nuances of radiology models.

Printed on: 02/07/23



## Abstract Archives of the RSNA, 2022

W4-CRT01

### ASRT@RSNA: Delivering a Superior Patient Experience

Wednesday, Nov. 30 11:00AM - 12:00PM Room: NA

#### Participants

Laura Aaron, PhD, RT, Natchitoches, LA (*Presenter*) Nothing to Disclose

#### COURSE DESCRIPTION

The patient experience is a common theme in healthcare due to the link with reimbursement. All areas of healthcare must know the ways in which they can create a positive experience for the patient and radiology is no exception. The factors that impact the patient experience will be explored. Attendees at this presentation will learn strategies and techniques that can be used by technologists to create a superior patient experience.

#### LEARNING OBJECTIVES

1) Discuss the concepts of patient and family-centered care 2) Explain the relationship between the patient experience and the impact on radiology 3) Develop techniques to create a superior patient experience\*Course Description The patient experience is a common theme in healthcare due to the link with reimbursement. All areas of healthcare must know the ways in which they can create a positive experience for the patient and radiology is no exception. The factors that impact the patient experience will be explored. Attendees at this presentation will learn strategies and techniques that can be used by technologists to create a superior patient experience.

Printed on: 02/07/23



## Abstract Archives of the RSNA, 2022

W6-CBR06

### Essentials of Breast Imaging: Diagnostic Practice on Ultrasound, Tomosynthesis, and MRI

Wednesday, Nov. 30 1:30PM - 2:30PM Room: NA

#### Participants

Andrew Evans, MRCP, FRCR, Chesterfeild, United Kingdom (*Presenter*) Speaker, Samsung Electronics Co, Ltd  
Sophia Zackrisson, Malmo, Sweden (*Presenter*) Speaker, Siemens AG;Speaker, Bayer AG;Speaker,Pfizer Inc;Patent holder, PCT/EP2014/057372;  
Katja Pinker-Domenig, MD, PhD, New York, NY (*Presenter*) Speakers Bureau, European Society of Breast Imaging;Speakers Bureau, Siemens AG;Speakers Bureau, IDKD;Speakers Bureau, Canon Medical Systems Corporation;Consultant, F. Hoffmann-La Roche Ltd;Consultant, Merantix Healthcare;Consultant, AURA Health

#### COURSE DESCRIPTION

This educational course will explain the technique and indications of breast ultrasound, digital breast tomosynthesis and breast MRI and summarize its indications in clinical breast imaging. Upon completion of this course participants will understand the current clinical applications and limitations of the methods.

#### LEARNING OBJECTIVES

1) To have a basic knowledge of the advantages and limitations of x-ray-based breast imaging methods. 2) To understand when to do ultrasound in symptomatic breast practice and in what situations add-on US techniques are useful. 3) To have a basic understanding of breast MRI techniques, indications, reporting and consequent management recommendations.\*Course Description This educational course will explain the technique and indications of breast ultrasound, digital breast tomosynthesis and breast MRI and summarize its indications in clinical breast imaging. Upon completion of this course participants will understand the current clinical applications and limitations of the methods.

Printed on: 02/07/23



## Abstract Archives of the RSNA, 2022

W6-CCH01

### HRCT Interpretation Session

Wednesday, Nov. 30 1:30PM - 2:30PM Room: NA

#### Participants

David A. Lynch, MBBCh, Denver, CO (*Presenter*) Research Consultant, CALYX Inc; Research Consultant, Boehringer Ingelheim GmbH; Research Consultant, Veracyte, Inc; Research Consultant, DAIICHI SANKYO Group; Research Consultant, AstraZeneca PLC; Consultant, Polarean, Inc; Consultant, Bristol Myers Squibb Company  
Santiago Rossi, MD, Buenos Aires City, (*Presenter*) Speaker, Boehringer Ingelheim GmbH  
Teri Franks, MD, Silver Spring, MD (*Presenter*) Nothing to Disclose  
Marie-Pierre Revel, Paris, France (*Presenter*) Consultant, General Electric Company; Consultant, Gleamer; Speaker, Bracco Group; Speaker, Boehringer Ingelheim GmbH  
Jeffrey Galvin, MD, Silver Spring, MD (*Presenter*) Nothing to Disclose  
Cornelia Schaefer-Prokop, MD, Amersfoort, Netherlands (*Presenter*) Speakers Bureau, Canon Medical Systems Corporation; Speakers Bureau, Samsung Electronics Co, Ltd

#### COURSE DESCRIPTION

The assessment of fibrotic diffuse lung injury can be problematic for radiologists who are key members of multidisciplinary conferences (MDD). This session is designed to help the radiologist understand the strengths and weaknesses of the MDD. Eight cases of diffuse lung injury will be presented to 4 experienced chest radiologists. The complete DICOM set of images will be displayed to both the panelists and the participants. This will allow the 4 panelists to describe the key features that support a diagnosis. The design of the session will also allow the participants to gauge the degree of agreement between experienced chest radiologists. The chief of pulmonary pathology at the Joint Pathology Center in Silver Spring will also participate giving a more accurate picture of the MDD. The unknown cases can also be viewed on your internet enabled phone, tablet or computer.

#### LEARNING OBJECTIVES

After participating in the HRCT Interpretation session, the participants will acquire: 1) Capacity to identify key imaging features of multi-compartment lung injury that lead to an understanding of pathophysiology 2) Capacity to analyze the key imaging features of diffuse lung disease that lead to pulmonary fibrosis including: organizing pneumonia, idiopathic pulmonary fibrosis, acute interstitial pneumonia/ARDS, cigarette smoke related fibrosis and sarcoidosis 3) Capacity to better manage and contribute to a multi-disciplinary conference (MDD) that focuses on diffuse lung disease\*Course Description The assessment of fibrotic diffuse lung injury can be problematic for radiologists who are key members of multidisciplinary conferences (MDD). This session is designed to help the radiologist understand the strengths and weaknesses of the MDD. Eight cases of diffuse lung injury will be presented to 4 experienced chest radiologists. The complete DICOM set of images will be displayed to both the panelists and the participants. This will allow the 4 panelists to describe the key features that support a diagnosis. The design of the session will also allow the participants to gauge the degree of agreement between experienced chest radiologists. The chief of pulmonary pathology at the Joint Pathology Center in Silver Spring will also participate giving a more accurate picture of the MDD. The unknown cases can also be viewed on your internet enabled phone, tablet or computer.

Printed on: 02/07/23



## Abstract Archives of the RSNA, 2022

W6-CIN08

### AI Governance in Medical Imaging: How to Herd the Cats and Avoid Chaos

Wednesday, Nov. 30 1:30PM - 2:30PM Room: NA

#### Participants

Jeevesh Kapur, FRCR, MMed, Singapore, Singapore (*Presenter*) Co-founder, Medo.ai Inc; Stock Holder, Medo.ai Inc  
Marc Kohli, MD, San Francisco, CA (*Presenter*) Founder, Alara Imaging; Stockholder, Alara Imaging  
Paul J. Chang, MD, Chicago, IL (*Moderator*) Research Grant, Koninklijke Philips NV; Advisory Board, Bayer AG; Advisory Board, Aidoc Inc; Advisory Board, Inference Analytics, Inc; Advisory Board, Subtle Medical, Inc; Advisory Board, Gesund.ai

#### COURSE DESCRIPTION

While there has been significant initial hype and anxiety regarding the application of artificial intelligence approaches to help improve the radiology value proposition, radiologists now have a more realistic and practical perspective with respect to AI in radiology. Many are now beginning to make decisions regarding how best to leverage AI in their practices. This session will discuss the absolute necessity of developing and implementing an appropriate AI governance model as part of any successful AI implementation strategy.

#### LEARNING OBJECTIVES

1) The importance of AI governance as part of any successful AI implementation will be explained 2) Attendees will be introduced to best practice characteristics of effective and sustainable AI governance 3) Strategies on how to best develop and implement AI governance will be presented\*Course Description While there has been significant initial hype and anxiety regarding the application of artificial intelligence approaches to help improve the radiology value proposition, radiologists now have a more realistic and practical perspective with respect to AI in radiology. Many are now beginning to make decisions regarding how best to leverage AI in their practices. This session will discuss the absolute necessity of developing and implementing an appropriate AI governance model as part of any successful AI implementation strategy.

Printed on: 02/07/23



## Abstract Archives of the RSNA, 2022

W6-CIR06

### Metastatic Disease and Palliative Care Interventions

Wednesday, Nov. 30 1:30PM - 2:30PM Room: NA

#### Participants

John Kunstman, MD, New Haven, CT (*Presenter*) Nothing to Disclose

Paul Romesser, MD, New York, NY (*Presenter*) Research Consultant, Merck KGaA ;Research funded, Merck KGaA

Carin F. Gonsalves, MD, Penn Valley, PA (*Presenter*) Nothing to Disclose

Stephen Solomon, MD, New York, NY (*Presenter*) Consultant, Sarasota Interventional Radiology;Consultant, Siemens AG ;Consultant, Aperture Medical;Consultant, Olympus Corporation;Consultant, Microbot Medical Inc;Consultant, Advantagene, Inc;Research Grant, Johnson & Johnson ;Research Grant, General Electric Company;Research Grant, AngioDynamics, Inc;Research Grant, Elesta Srl;Shareholder, Johnson & Johnson;Shareholder, Lantheus Holdings;Shareholder, Motus, LLC;Shareholder, Impulse Dynamics Limited

William S. Rilling, MD, Milwaukee, WI (*Presenter*) Consultant, Boston Scientific Corporation;Consultant, Agilent Technologies, Inc;Consultant, Terumo Corporation;Consultant, Becton, Dickinson and Company;Consultant, Sirtex Medical Ltd;Consultant, AstraZeneca PLC

Michael Soulen, MD, Lafayette Hill, PA (*Presenter*) Consultant, F. Hoffmann-La Roche Ltd;Consultant, Guerbet SA;Consultant, AstraZeneca PLC;Research support, Guerbet SA;Research support, Sirtex Medical Ltd;Research support, Pfizer Inc

Constantinos T. Sofocleous, MD, PhD, New York, NY (*Moderator*) Consultant, Siemens AG;Consultant, Johnson & Johnson;Research support, Johnson & Johnson;Consultant, Terumo Corporation;Consultant, Sirtex Medical Ltd;Research support, Sirtex Medical Ltd;Research support, Boston Scientific Corporation

#### COURSE DESCRIPTION

Overview of the role of Interventional Oncology in the management of metastatic disease. The common concepts in the use of local curative therapies for hepatic and pulmonary metastases will be presented. Multidisciplinary discussion will be encouraged. The use of locoregional treatment in the setting of metastatic disease will also be presented and discussed.

#### LEARNING OBJECTIVES

1) Describe the role of interventional Oncology in the setting of metastatic disease 2) Indications and Expectations of locoregional therapies in oligometastatic disease 3) Liver directed therapies for common metastatic hepatic pathologies\*Course Description  
Overview of the role of Interventional Oncology in the management of metastatic disease. The common concepts in the use of local curative therapies for hepatic and pulmonary metastases will be presented. Multidisciplinary discussion will be encouraged. The use of locoregional treatment in the setting of metastatic disease will also be presented and discussed.

Printed on: 02/07/23



## Abstract Archives of the RSNA, 2022

W6-CMK01

### Knee MRI Pre-op and Post-op: Pearls and Pitfalls

Wednesday, Nov. 30 1:30PM - 2:30PM Room: NA

#### Participants

Theodore T. Miller, MD, New York, NY (*Presenter*) Nothing to Disclose

Carl S. Winalski, MD, Rocky River, OH (*Presenter*) Research Consultant, Siemens AG; Stockholder, Pfizer Inc

Emma Rowbotham, MBBChIR, FRCR, Leeds, United Kingdom (*Presenter*) Nothing to Disclose

Dana Lin, MD, New York, NY (*Presenter*) Research support, Siemens AG

Andrew J. Grainger, MD, Cambridge, (*Presenter*) Speakers Bureau, General Electric Company

#### COURSE DESCRIPTION

The course will comprise 5 short lectures offering tips and tricks for the interpretation of pre and post operative MRI of the knee. It will highlight light pitfalls that exist in the interpretation of knee MRI and ways to avoid them. The course will focus on the pre and post operative imaging of meniscal and ligament injury

#### LEARNING OBJECTIVES

1) Identify helpful features to aid the interpretation of pre and postoperative MRI of the knee 2) To recognise pitfalls that exist in the interpretation of pre and postoperative knee and MRI and understand how to avoid them\*Course Description The course will comprise 5 short lectures offering tips and tricks for the interpretation of pre and post operative MRI of the knee. It will highlight light pitfalls that exist in the interpretation of knee MRI and ways to avoid them. The course will focus on the pre and post operative imaging of meniscal and ligament injury

Printed on: 02/07/23



## Abstract Archives of the RSNA, 2022

W6-CNMMI05

### Chest Imaging: When Molecular Imaging Helps

Wednesday, Nov. 30 1:30PM - 2:30PM Room: NA

#### Participants

Robert K. Zeman, MD, Potomac, MD (*Presenter*) Nothing to Disclose

Pamela Woodard, MD, Saint Louis, MO (*Presenter*) Researcher, Siemens AG; Consulting, Medtronic plc; Researcher, Bayer AG; Patent, Washington University

Rachna Madan, MD, Boston, MA (*Presenter*) Nothing to Disclose

Ryan J. Avery, MD, Chicago, IL (*Presenter*) Research Consultant, Konica Minolta, Inc

#### COURSE DESCRIPTION

Molecular imaging has the distinct advantage of providing functional and physiologic data that can be interpreted in conjunction with the traditional anatomic imaging. While pulmonary nodules and mediastinal masses have traditionally been assessed with cross sectional imaging, the complementary approach of evaluating tumor characteristics, whether by metabolic activity or tumor marker expression, has fundamentally changed chest imaging. Further, the physiologic detection of functional loss of lung perfusion continues to exemplify the use of molecular imaging techniques for both pulmonary function evaluation and the assessment of pulmonary perfusion abnormalities. Finally, the increasing quantitative assessment of myocardial blood flow and perfusion utilizing nuclear cardiac scintigraphy, including cardiac PET/CT, has become increasingly useful to detect functional assessment of coronary artery disease that can be utilized for chest pain and myocardial injury assessment.

#### LEARNING OBJECTIVES

1) Identify the increasing availability and use of PET imaging techniques for detection and characterization of lung lesions. This will include a review of important incidental findings on chest CT with emphasis on pulmonary nodule management, discussion of potential clinical significance and appropriate work-up, and a review of guidelines for reporting and management 2) Discuss the persistent role of lung perfusion scintigraphy techniques for both qualitative and quantitative analysis of lung function in the setting of lung transplantation and surgical planning, including planning for resection planning and techniques for assessment and treatment of chronic thromboembolic pulmonary hypertension. 3) Discussion of the mechanism and techniques available for detection of obstructive coronary artery disease, small vessel disease, Covid-19, amyloidosis, and sarcoid related pathology using a multimodality approach in cardiothoracic imaging, to include Nuclear Medicine, PET/CT, CT and MRI.\*Course Description Molecular imaging has the distinct advantage of providing functional and physiologic data that can be interpreted in conjunction with the traditional anatomic imaging. While pulmonary nodules and mediastinal masses have traditionally been assessed with cross sectional imaging, the complementary approach of evaluating tumor characteristics, whether by metabolic activity or tumor marker expression, has fundamentally changed chest imaging. Further, the physiologic detection of functional loss of lung perfusion continues to exemplify the use of molecular imaging techniques for both pulmonary function evaluation and the assessment of pulmonary perfusion abnormalities. Finally, the increasing quantitative assessment of myocardial blood flow and perfusion utilizing nuclear cardiac scintigraphy, including cardiac PET/CT, has become increasingly useful to detect functional assessment of coronary artery disease that can be utilized for chest pain and myocardial injury assessment.

Printed on: 02/07/23



## Abstract Archives of the RSNA, 2022

W6-CNPM08

### What Every Radiologist Should Know about Current Payer Issues

Wednesday, Nov. 30 1:30PM - 2:30PM Room: NA

#### Participants

Melissa Chen, MD, Houston, TX (*Presenter*) Nothing to Disclose  
Richard Heller III, MD, Chicago, IL (*Presenter*) Consultant, Gerson Lehrman Group, Inc;  
Ed Gaines III, JD, Greensboro, NC (*Presenter*) Officer, Zotec Partners LLC

#### COURSE DESCRIPTION

To maintain operations, medical practices require reasonable reimbursement for their services. As the expression goes, "no money, no mission". With the United States outspending every other high-income nation on a per capita basis for healthcare, there is increasing pressure to reduce healthcare spending where feasible. Part of those efforts include attempts to reduce reimbursement for certain specialties, including radiology. This session explores these challenges to radiology, examining both private and public payer issues. In addition, artificial intelligence (AI) tools have the potential to re-shape the way radiologic care is delivered. The session will also examine the issue of reimbursement for AI and its impact on radiology.

#### LEARNING OBJECTIVES

1) Understand the current issues facing patients and medical practices related to the No Surprises Act and construct an approach to deal with these challenges 2) Understand the current issues facing patients and radiology practices related to Medicare reimbursement and construct an approach to deal with these challenges 3) Understand the various mechanisms that are utilized by payers to reimburse for artificial intelligence tools in medical care and distinguish their effects on tool adoption\*Course Description To maintain operations, medical practices require reasonable reimbursement for their services. As the expression goes, "no money, no mission". With the United States outspending every other high-income nation on a per capita basis for healthcare, there is increasing pressure to reduce healthcare spending where feasible. Part of those efforts include attempts to reduce reimbursement for certain specialties, including radiology. This session explores these challenges to radiology, examining both private and public payer issues. In addition, artificial intelligence (AI) tools have the potential to re-shape the way radiologic care is delivered. The session will also examine the issue of reimbursement for AI and its impact on radiology.

Printed on: 02/07/23



## Abstract Archives of the RSNA, 2022

W6-CPD04

### Pediatric Chest

Wednesday, Nov. 30 1:30PM - 2:30PM Room: NA

#### Participants

Meryle Eklund, MD, Charleston, SC (*Presenter*) Nothing to Disclose

David Saul, MD, Wilmington, DE (*Presenter*) Nothing to Disclose

Pallavi Sagar, MBBS, Boston, MA (*Presenter*) Nothing to Disclose

#### COURSE DESCRIPTION

Explore the world of pediatric chest imaging! From the bubbly lesions to solid masses, a wide breadth of abnormalities of the lung and chest wall will be discussed in this educational lecture to increase familiarity with disease processes and highlight key imaging features of diagnosis.

#### LEARNING OBJECTIVES

- 1) Understand the differential diagnosis of lucent chest lesions in pediatric patients based on clinical context and imaging features
- 2) Apply imaging features of single or multiple solid lung masses to guide management in children based on clinical context
- 3) Review the differential diagnosis and imaging manifestations of pediatric chest wall abnormalities\*Course Description Explore the world of pediatric chest imaging! From the bubbly lesions to solid masses, a wide breadth of abnormalities of the lung and chest wall will be discussed in this educational lecture to increase familiarity with disease processes and highlight key imaging features of diagnosis.

Printed on: 02/07/23



## Abstract Archives of the RSNA, 2022

W6-CPH13

### Virtual Clinical Trial

Wednesday, Nov. 30 1:30PM - 2:30PM Room: NA

#### Participants

Hilde Bosmans, PhD, Leuven, (*Presenter*) Stockholder, Qaelum NV; Research Grant, Siemens AG; Research Grant, General Electric Company

Aldo Badano, PhD, Silver Spring, MD (*Presenter*) Research Grant, Barco nv

Ehsan Samei, PhD, Durham, NC (*Presenter*) Research Grant, General Electric Company; Advisory Board, General Electric Company; Research Grant, Siemens AG; Advisory Board, Siemens AG; Advisory Board, medInt Holdings, LLC; Advisory Board, Metis Health Analytics; Research Consultant, Nanox Imaging Ltd; Royalties, General Electric Company; Royalties, medInt Holdings, LLC; Royalties, 12 Sigma Technologies; Royalties, Mirion Technologies, Inc; Royalties, Cambridge University Press; Royalties, John Wiley & Sons, Inc

#### COURSE DESCRIPTION

The complexity and diversity of medical imaging technologies have continued to accelerate, outpacing our ability to optimize their use. This has become a significant challenge across the spectra of scientific inquires, product designs, and clinical applications. New imaging technology has been traditionally evaluated through clinical trials. However, such trials are often not feasible or even definitive due to ethical limitations, expense, time requirements, difficulty in accruing enough subjects - especially with low prevalence conditions, or the fundamental lack of ground truth. Virtual Clinical Trials (VCT) provide a new paradigm to assess the impact of medical imaging innovations on patient care. VCTs offer a new disease-known approach to conduct medical trials that can be clinically relevant, timely, and accurate while reflecting the variabilities of human subjects and disease, as well as the complexities of technologies, providing answers that would otherwise be impractical to obtain or simply unattainable. A VCT consists of 1) realistic populations of computational patients spanning ages and a range of phenotypical characteristics including sex and race with realistic models of disease, 2) detailed models of clinical imaging systems, and 3) computational models of the image interpretation processes. This session offers a summary of VCT methods and processes in the field of radiology and highlights applications in clinical practice and in the regulatory assessment of imaging products.

#### LEARNING OBJECTIVES

1) Understand the role of virtual trials in medicine and in radiology 2) Understand the components of virtual imaging trials 3) Understand the research, clinical, and regulatory potentials of virtual trials\*Course Description The complexity and diversity of medical imaging technologies have continued to accelerate, outpacing our ability to optimize their use. This has become a significant challenge across the spectra of scientific inquires, product designs, and clinical applications. New imaging technology has been traditionally evaluated through clinical trials. However, such trials are often not feasible or even definitive due to ethical limitations, expense, time requirements, difficulty in accruing enough subjects - especially with low prevalence conditions, or the fundamental lack of ground truth. Virtual Clinical Trials (VCT) provide a new paradigm to assess the impact of medical imaging innovations on patient care. VCTs offer a new disease-known approach to conduct medical trials that can be clinically relevant, timely, and accurate while reflecting the variabilities of human subjects and disease, as well as the complexities of technologies, providing answers that would otherwise be impractical to obtain or simply unattainable. A VCT consists of 1) realistic populations of computational patients spanning ages and a range of phenotypical characteristics including sex and race with realistic models of disease, 2) detailed models of clinical imaging systems, and 3) computational models of the image interpretation processes. This session offers a summary of VCT methods and processes in the field of radiology and highlights applications in clinical practice and in the regulatory assessment of imaging products.

Printed on: 02/07/23



## Abstract Archives of the RSNA, 2022

W6-CRT07

### ASRT@RSNA: A Case for Fluoroscopy

Wednesday, Nov. 30 1:30PM - 2:30PM Room: NA

#### Participants

Travis Prowant, MS, RT, Mechanicsville, VA (*Presenter*) Nothing to Disclose

#### COURSE DESCRIPTION

This course will provide a broader understanding of the principles of fluoroscopy in radiology and a familiarity with the many diagnostic techniques available, their values and limitations, and how they may best be used in the management of the patient. With advancements in other imaging modalities such as CT and MR, many fluoroscopic examinations are no longer performed routinely. This course is designed to express the value of fluoroscopy, in both the dynamic nature whereby clinical questions can be answered, but also in the safety and cost-effectiveness realms.

#### LEARNING OBJECTIVES

1. Explain how fluoroscopy is used to enhance overall patient care and department efficiency. 2. Describe fluoroscopic operation to include the basic image production chain. 3. Explain radiation protection strategies for the patient, radiographer and radiologist during fluoroscopic examination. 4. Recite the patient preparation, various contrast materials used, basic patient positioning and patient education for gastrointestinal and genitourinary procedures. 5. Discuss normal anatomy, variants and pathological conditions. 6. Summarize the important role of the Registered Technologist (R.T.) and Registered Radiologist Assistant (R.R.A.) in day-to-day fluoroscopy schedules.\*Course Description This course will provide a broader understanding of the principles of fluoroscopy in radiology and a familiarity with the many diagnostic techniques available, their values and limitations, and how they may best be used in the management of the patient. With advancements in other imaging modalities such as CT and MR, many fluoroscopic examinations are no longer performed routinely. This course is designed to express the value of fluoroscopy, in both the dynamic nature whereby clinical questions can be answered, but also in the safety and cost-effectiveness realms.

Printed on: 02/07/23



## Abstract Archives of the RSNA, 2022

W6-RCP08

### Fakes, Forgeries, and Hidden Repairs in Art and Archaeology - The Role of Forensic Imaging

Wednesday, Nov. 30 1:30PM - 2:30PM Room: NA

#### Participants

Jonathan Brown, MS, Chicago, IL (*Presenter*) Nothing to Disclose  
Vahid Yaghmai, MD, Orange, CA (*Presenter*) Nothing to Disclose  
Barry Daly, MD, Baltimore, MD (*Presenter*) Nothing to Disclose

#### COURSE DESCRIPTION

A major challenge in the world of art is the prevalence of faux or stolen treasures or works with concealed repairs. One of the major applications of modern imaging technology in this setting is the ability to non-invasively investigate the 3D structure and hidden internal contents of ancient and fragile treasures, with detail not previously possible. Using a case-based approach, this course addresses the use of advanced imaging techniques to confirm or refute the authenticity of ancient artworks, from 3,000 year old Mezo-American statues to late Renaissance musical instruments and paintings. The implications of forgery, erroneous provenance, and concealed alterations or repairs to ancient artworks are discussed. The use of modern imaging technology in this setting has been shown to promote greater understanding of the cultural value of art treasures among the general public. This work has also helped to better inform the wider community of the very high resolution and 3D capabilities of modern CT machines and of the role of radiology professionals.

#### LEARNING OBJECTIVES

1) To introduce the use of high resolution CT technology for non-invasive investigation of ancient and fragile cultural treasures 2) To raise awareness of the prevalence of widespread fraud and fakery in the world of historic art and learn how radiology professionals may contribute to this work\*Course Description A major challenge in the world of art is the prevalence of faux or stolen treasures or works with concealed repairs. One of the major applications of modern imaging technology in this setting is the ability to non-invasively investigate the 3D structure and hidden internal contents of ancient and fragile treasures, with detail not previously possible. Using a case-based approach, this course addresses the use of advanced imaging techniques to confirm or refute the authenticity of ancient artworks, from 3,000 year old Mezo-American statues to late Renaissance musical instruments and paintings. The implications of forgery, erroneous provenance, and concealed alterations or repairs to ancient artworks are discussed. The use of modern imaging technology in this setting has been shown to promote greater understanding of the cultural value of art treasures among the general public. This work has also helped to better inform the wider community of the very high resolution and 3D capabilities of modern CT machines and of the role of radiology professionals.

Printed on: 02/07/23



## Abstract Archives of the RSNA, 2022

W6-RCP53

### RSNA/ESR Symposium: Imaging of Neurodegenerative Disorders - Movement Disorders

Wednesday, Nov. 30 1:30PM - 2:30PM Room: NA

#### Participants

Kejal Kantarci, MD, Rochester, MN (*Presenter*) Research support, Eli Lilly and Company; Consultant, Biogen Idec Inc  
Val J. Lowe, MD, Rochester, MN (*Presenter*) Research Grant, General Electric Company; Research Grant, Siemens AG; Research Grant, Eli Lilly and Company; Research Consultant, Eli Lilly and Company  
Stephane Lehericy, MD, PhD, Clichy, France (*Presenter*) Research Grant, Biogen Idec Inc; Consultant, F. Hoffmann-La Roche Ltd  
Meike W. Vernooij, MD, PhD, Rotterdam, Netherlands (*Moderator*) Nothing to Disclose

#### COURSE DESCRIPTION

This educational session will discuss how MRI and molecular imaging techniques can be used to understand the underlying pathology in patients with Lewy body disorders. This session will give general radiologists and those interested in neuroradiology and nuclear medicine/molecular imaging the knowledge needed for appropriate selection and structured assessment of imaging exams in diagnostic work-up of movement disorders. The session format consists of in part lectures, followed by an interactive case-based discussion.

#### LEARNING OBJECTIVES

1) Explain the current use of MRI in Lewy body disease and movement disorders. 2) Explain the current use of molecular imaging in Lewy body disease and movement disorders. 3) Demonstrate structured selection and assessment of imaging exams through cases.\*Course Description This educational session will discuss how MRI and molecular imaging techniques can be used to understand the underlying pathology in patients with Lewy body disorders. This session will give general radiologists and those interested in neuroradiology and nuclear medicine/molecular imaging the knowledge needed for appropriate selection and structured assessment of imaging exams in diagnostic work-up of movement disorders. The session format consists of in part lectures, followed by an interactive case-based discussion.

Printed on: 02/07/23



## Abstract Archives of the RSNA, 2022

W7-CCA06

### Challenges in Imaging the Very Sick Heart Failure Patient: Imaging in the Peri-transplant Period

Wednesday, Nov. 30 3:00PM - 4:00PM Room: NA

#### Participants

Daniel Vargas, MD, Denver, CO (*Presenter*) Nothing to Disclose

Carole Dennie, MD, Ottawa, ON (*Presenter*) Research Consultant, AstraZeneca PLC

#### COURSE DESCRIPTION

This lecture-based session will focus on CT imaging of the severe heart failure patient. We will cover practical tips and tricks to image the heart and coronary arteries in patients who have a low ejection fraction and/or arrhythmias with or without support devices. Imaging of complications of LVAD and RVAD will also be reviewed including pitfalls and technical aspects that help improve image quality. Lectures will be followed by a 20 minute question and answer period

#### LEARNING OBJECTIVES

- 1) Recall protocols to improve CT imaging of the heart and coronary arteries in patients with low ejection fraction and/or arrhythmia
- 2) Explain imaging pitfalls and complications of left and right ventricular assist devices\*Course Description This lecture-based session will focus on CT imaging of the severe heart failure patient. We will cover practical tips and tricks to image the heart and coronary arteries in patients who have a low ejection fraction and/or arrhythmias with or without support devices. Imaging of complications of LVAD and RVAD will also be reviewed including pitfalls and technical aspects that help improve image quality. Lectures will be followed by a 20 minute question and answer period

Printed on: 02/07/23



## Abstract Archives of the RSNA, 2022

W7-CER04

### Thoracic Trauma: The Essentials

Wednesday, Nov. 30 3:00PM - 4:00PM Room: NA

#### Participants

Demetrios Raptis, MD, Frontenac, MO (*Presenter*) Nothing to Disclose

Scott Hamlin, MD, Atlanta, GA (*Presenter*) Nothing to Disclose

Krystal Archer-Arroyo, MD, Decatur, GA (*Presenter*) Nothing to Disclose

#### COURSE DESCRIPTION

This series of lectures will give the learner tools to discern acute pathology seen in the setting of blunt and penetrating chest trauma.

#### LEARNING OBJECTIVES

1) Discuss the importance of traumatic chest wall injuries and how it affects patient outcomes and management 2) Illustrate findings of blunt and penetrating cardiac injury 3) Review acute injuries of the diaphragm\*Course Description This series of lectures will give the learner tools to discern acute pathology seen in the setting of blunt and penetrating chest trauma.

Printed on: 02/07/23



## Abstract Archives of the RSNA, 2022

W7-CIN04

### Image Exchange: How Do We Ditch the Disk by 2024?

Wednesday, Nov. 30 3:00PM - 4:00PM Room: NA

#### Participants

Gloria Hwang, MD, Hillsborough, CA (*Presenter*) Spouse, Stockholder, Thrombx Medical, Inc; Spouse, Consultant, Terumo Corporation; Spouse, Consultant, Johnson & Johnson; Spouse, Research Grant, Stryker Corporation; Spouse, Research Grant, Siemens AG; Spouse, Research Grant, Route 92 Medical, Inc

Amy Kotsenas, MD, Rochester, MN (*Presenter*) Nothing to Disclose

David Larson, MD, MBA, Portola Valley, CA (*Presenter*) Research Grant, Siemens AG ; Advisor, Bunkerhill Health; Shareholder, Bunkerhill Health

Audrey Verde, MD, PhD, Nashville, TN (*Moderator*) Nothing to Disclose

#### COURSE DESCRIPTION

When most home computers no longer have an external disc drive, why do we continue to provide our patients their images on discs? Join us in this didactic, and panel session to learn about the current state of image sharing, possible models for our field to transition with vendors to fully electronic image sharing, and how vendors can engage in this process.

#### LEARNING OBJECTIVES

1) Learn the current state of image sharing across the US 2) Learn models for moving forward to full electronic image sharing 3) How to engage with vendors to transition from disk to electronic imaging sharing\*Course Description When most home computers no longer have an external disc drive, why do we continue to provide our patients their images on discs? Join us in this didactic, and panel session to learn about the current state of image sharing, possible models for our field to transition with vendors to fully electronic image sharing, and how vendors can engage in this process.

Printed on: 02/07/23



## Abstract Archives of the RSNA, 2022

W7-CNPM10

### Shaping Your Online Brand through Social Media Use, Analytics, and Research

Wednesday, Nov. 30 3:00PM - 4:00PM Room: NA

#### Participants

Omer Awan, MD, MPH, Lutherville Timonium, MD (*Presenter*) Nothing to Disclose

Sherry Wang, MBBS, Salt Lake City, UT (*Presenter*) Royalties, RELX

Vinay Prabhu, MD, Brooklyn, NY (*Presenter*) Stockholder, AbbVie Inc; Stockholder, Alphabet Inc; Stockholder, Meta Platforms Inc; Stockholder, Moderna, Inc; Stockholder, Repligen Corporation; Stockholder, Groupe Sanofi

#### COURSE DESCRIPTION

This lecture will provide radiologists with a strong foundation from which to launch or improve their social media experience, avoid common and problematic errors, and take advantage of unique opportunities available on these platforms.

#### LEARNING OBJECTIVES

1) Define important facets of a professional social media profile 2) Evaluate social media impact by assessing objective performance metrics 3) Explain common errors in professionalism on social media platforms 4) Perform unbiased research studies utilizing publicly available social media data 5) Formulate ways to positively shape a professional brand on social media\*Course Description This lecture will provide radiologists with a strong foundation from which to launch or improve their social media experience, avoid common and problematic errors, and take advantage of unique opportunities available on these platforms.

Printed on: 02/07/23



## Abstract Archives of the RSNA, 2022

W7-CNR02

### New Frontiers in Stroke Imaging and Treatment

Wednesday, Nov. 30 3:00PM - 4:00PM Room: NA

#### Participants

Jeremy Heit, MD, PhD, Los Altos, CA (*Presenter*) Consultant, Medtronic plc; Consultant, Terumo Corporation; Consultant, iSchemaView, Inc; Scientific Advisory Board, iSchemaView, Inc; Medical Advisory Board, iSchemaView, Inc; Committee Member, Vesalio

Sameer A. Ansari, MD, PhD, Chicago, IL (*Presenter*) CEO, Clearvoya; Research Consultant, Boston Scientific Corporation; Research Consultant, Hyperfine Research, Inc; Research Consultant, Imperative Care Inc; Data Safety Monitoring Board, RaPID Medical Technologies, LLC; Data Safety Monitoring Board, Medtronic plc

Jennifer Soun, MD, Irvine, CA (*Presenter*) Research Grant, Canon Medical Systems Corporation

Lily L. Wang, MBBS, Cincinnati, OH (*Presenter*) Committee member, F. Hoffmann-La Roche Ltd

#### COURSE DESCRIPTION

Acute ischemic stroke is the leading cause of disability in the United States and results in significant mortality worldwide. Recent advances in ischemic stroke patient treatment using both intravenous thrombolysis and endovascular thrombectomy have resulted in improved outcomes and increased utilization of brain imaging. In this course, we will review existing and emerging artificial intelligence platforms to evaluate ischemic stroke patients, novel methods to assess collateral blood flow in ischemic stroke patients, and advances in endovascular thrombectomy treatment of ischemic stroke due to large vessel occlusions.

#### LEARNING OBJECTIVES

1) To understand how new artificial intelligence and computer assisted imaging platforms are used clinically for the evaluation and treatment triage of ischemic stroke patients 2) To describe how venous outflow and a more comprehensive analysis of collateral blood flow in ischemic stroke patients predicts patient outcomes after treatment 3) To understand how endovascular thrombectomy is used for ischemic stroke patient treatment 4) To describe new frontiers in endovascular thrombectomy and how they may impact ischemic stroke treatment in the near future\*Course Description Acute ischemic stroke is the leading cause of disability in the United States and results in significant mortality worldwide. Recent advances in ischemic stroke patient treatment using both intravenous thrombolysis and endovascular thrombectomy have resulted in improved outcomes and increased utilization of brain imaging. In this course, we will review existing and emerging artificial intelligence platforms to evaluate ischemic stroke patients, novel methods to assess collateral blood flow in ischemic stroke patients, and advances in endovascular thrombectomy treatment of ischemic stroke due to large vessel occlusions.

Printed on: 02/07/23



## Abstract Archives of the RSNA, 2022

W7-CRO07

### Gynecologic Case-based Multidisciplinary Review

Wednesday, Nov. 30 3:00PM - 4:00PM Room: NA

#### Participants

Aoife Kilcoyne, MBBCh, Boston, MA (*Presenter*) Royalties, Wolters Kluwer nv; Author, Wolters Kluwer nv  
Stephanie Markovina, MD, PhD, Saint Louis, MO (*Presenter*) Research Grant, GlaxoSmithKline plc  
Premal Thaker, Saint Louis, MO (*Presenter*) Advisory Board, Mersana Therapeutics, Inc; Advisory Board, ImmunoGen, Inc; Advisory Board, NovoCure Ltd; Advisory Board, Merck & Co, Inc; Advisory Board, AstraZeneca PLC; Advisory Board, GSK plc; Advisory Board, Clovis Oncology, Inc; Advisory Board, Zentalis Pharmaceuticals, Inc; Advisory Board, Eisai Co, Ltd; Advisory Board, Novartis AG; Data Safety Monitoring Board, Celsion Corporation; Data Safety Monitoring Board, Iovance Biotherapeutics, Inc; Research Grant, Merck & Co, Inc; Research Grant, GSK plc; Stockholder, Celsion Corporation  
Lilie Lin, MD, Houston, TX (*Presenter*) Investigator, AstraZeneca PLC; Research Grant, Pfizer Inc

#### COURSE DESCRIPTION

This is a case-based, multidisciplinary, session focused on gynecologic malignancies and the optimal use of imaging for diagnosis, staging, treatment and follow-up.

#### LEARNING OBJECTIVES

1) Evaluate the role of CT, MR and PET-CT in the diagnosis, staging and follow-up of gynecologic malignancy 2) Assess the role of imaging for radiation and surgical treatment planning in gynecologic malignancy\*Course Description This is a case-based, multidisciplinary, session focused on gynecologic malignancies and the optimal use of imaging for diagnosis, staging, treatment and follow-up.

Printed on: 02/07/23



## Abstract Archives of the RSNA, 2022

W7-CRT08

### ASRT@RSNA: R(AI)DIOLOGY: An Introduction to Artificial Intelligence, and its Radiologic Future

Wednesday, Nov. 30 3:00PM - 4:00PM Room: NA

#### Participants

Bradford Gildon, BS, RT, Oklahoma City, OK (*Presenter*) Nothing to Disclose

#### COURSE DESCRIPTION

Artificial intelligence (AI) is a futuristic technology only used in the plots of science-fiction movies—or is it? This presentation will review the historical context of AI, what it is, and the general concepts of how it works. Examples of AI in public use, its use in healthcare, and its use specifically in radiology will also be identified. For example, its role with detecting cases of COVID-19 based on radiographic image data will be discussed. The science and technology of AI continue to make increasing gains in functionality, but ethical/legal implications may quickly outpace these advancements. The implications of AI are profound, and it may change the landscape of not only radiology, but also of future healthcare delivery as a whole.

#### LEARNING OBJECTIVES

1) Define artificial intelligence (AI), and review a brief history of its development 2) Contrast various aspects of AI, machine learning, and deep learning processes 3) Identify current and emerging applications of AI in everyday life; in healthcare; and in radiology 4) Review ethical and legal implications of the use of AI in healthcare and radiology spaces\*Course Description Artificial intelligence (AI) is a futuristic technology only used in the plots of science-fiction movies—or is it? This presentation will review the historical context of AI, what it is, and the general concepts of how it works. Examples of AI in public use, its use in healthcare, and its use specifically in radiology will also be identified. For example, its role with detecting cases of COVID-19 based on radiographic image data will be discussed. The science and technology of AI continue to make increasing gains in functionality, but ethical/legal implications may quickly outpace these advancements. The implications of AI are profound, and it may change the landscape of not only radiology, but also of future healthcare delivery as a whole.

Printed on: 02/07/23



## Abstract Archives of the RSNA, 2022

W7-RCP30

### Bring on Your Game: Best of RSNA Case Collection Hot Seat Review (MSK, CHEST, BREAST, GU, PEDS)

Wednesday, Nov. 30 3:00PM - 4:00PM Room: NA

#### Participants

Manickam Kumaravel, MD, FRCR, Houston, TX (*Presenter*) Nothing to Disclose  
Christopher M. Walker, MD, Fairway, KS (*Presenter*) Author, RELX;Speakers Bureau, Boehringer Ingelheim GmbH  
Yiming Gao, MD, New York, NY (*Presenter*) Nothing to Disclose  
Keyanoosh Hosseinzadeh, MD, Winston Salem, NC (*Presenter*) Nothing to Disclose  
Apeksha Chaturvedi, MD, Rochester, NY (*Presenter*) Nothing to Disclose  
Edward Lee, MD, MPH, Boston, MA (*Presenter*) Nothing to Disclose  
Benjamin Vega, MD, Columbia, MO (*Moderator*) Nothing to Disclose  
Mariam Moshiri, MD, Brentwood, TN (*Moderator*) Nothing to Disclose

#### LEARNING OBJECTIVES

1) Develop differential diagnoses for the five radiology subspecialties presented in this course 2) Recognize imaging features that aid in differential diagnoses, allowing for a more specific diagnosis Learn evaluation of cases in a methodical and clinically applicable fashion\*Course Description

Printed on: 02/07/23



## Abstract Archives of the RSNA, 2022

W7-RCP54

### RSNA/ESR Symposium: Imaging of Neurodegenerative Disorders - Perspectives / Outlook

Wednesday, Nov. 30 3:00PM - 4:00PM Room: NA

#### Participants

Ciprian Catana, MD, PhD, Charlestown, MA (*Presenter*) Nothing to Disclose

Yoshimi Anzai, MD, MPH, Salt Lake City, UT (*Presenter*) Nothing to Disclose

Javier Arbizu Lostao, Pamplona, Spain (*Presenter*) Speaker, F. Hoffmann-La Roche Ltd; Speaker, Novartis AG; Speaker, General Electric Company; Research Grant, Siemens AG; Speaker, Life Molecular Imaging GmbH; Speaker, Biogen Idec Inc

Alexander Drzezga, MD, Cologne, Germany (*Moderator*) Research support, Siemens AG ; Research support, Life Molecular Imaging; Research support, General Electric Company; Research support, Eli Lilly and Company; Research support, Eisai Co, Ltd; Consultant, Siemens AG ; Consultant, General Electric Company

#### LEARNING OBJECTIVES

1) To describe the role of anatomical and molecular imaging for patients with neurodegenerative disorders 2) To identify MR and PET features of specific neurodegenerative disease 3) To explain the role of machine learning approaches in the diagnosis of neurodegenerative disease\*Course Description

Printed on: 02/07/23

## Abstract Archives of the RSNA, 2022

W7-RCP58

### Ukraine: Lessons from War and How to Help

Wednesday, Nov. 30 3:00PM - 4:00PM Room: NA

#### Participants

Kateryna Yushchenko, , Ukraine (*Presenter*) Nothing to Disclose  
Luke Tomycz, MD, Nashville, TN (*Presenter*) Nothing to Disclose  
Ruslan Zelinskyi, Kyiv City, Ukraine (*Presenter*) Nothing to Disclose  
Tetyana Yalynska, Kiev, Ukraine (*Presenter*) Nothing to Disclose  
Nataliya Kovalchuk, PhD, Palo Alto, CA (*Presenter*) Nothing to Disclose  
Ulana Suprun, MD, Rochester Hills, MI (*Presenter*) Nothing to Disclose  
Leo Wolansky, MD, Bloomfield, CT (*Presenter*) Scientific Advisory Committee, Guerbet SA

#### COURSE DESCRIPTION

The full-scale Russian invasion of Ukraine on February 24th, 2022 brought the largest humanitarian disaster since the World War II to the heart of Europe. Ukraine has lost tens of thousands of civilian lives, out of which many were innocent children. Many more have been wounded, with approximately a third of the population of Ukraine being displaced: 7 million as refugees and 7.1 million as internally displaced people. According to Ukraine's Minister of Health, Viktor Liashko, during the first 100 days of war more than 600 healthcare facilities sustained damage, 105 of which were rendered beyond repair. Even if the war stopped today, the damage to the healthcare infrastructure will remain for years to come without world's continuing support. Prior to the full-scale Russian invasion, according to unpublished Ukrainian NCI (Tumor Registry) data, in Ukraine with 44 million population, an estimated 139,000 people were living with newly diagnosed cancer, and between 1,000 and 1,200 children were receiving active cancer treatment. Regarding radiotherapy, Ukraine is classified by DIRAC IAEA as a Low Middle Income country with the level of availability being 2.6 External Beam Radiation Therapy (EBRT) machines per 1 million people. Per DIRAC data, until Russia annexed Crimea and parts of the Donbas region in 2014, Ukraine had 52 radiation therapy centers with 86 Co-60 machines (81%) and 20 linear accelerators (19%). Since 2014 Ukraine has lost control of 10 cancer centers and over 13 EBRT machines in occupied part of Donbas and 5 machines in Crimea (totally 17% of Ukrainian EBRT machines). To address the growing need for cancer treatment, 16 linear accelerators were installed by 2022, and the ratio of Co-60 to linear accelerators became 54% to 46% (without taking into account EBRT machines in the occupied territories since 2014). The Ministry of Health of Ukraine planned to purchase additional 20 linear accelerators, but this plan did not materialize because of the Russian full-scale invasion on February 24th. In the fourth month of the war, the situation in Ukraine is fluid, and as of August 29th, 2022, 3 additional cancer centers are under occupation, 3 cancer centers have suspended operation, and 2 cancer centers are under constant shelling. Some of the centers in the west of Ukraine operate with double the volume of patients. This session will convey the Ukrainian ministry of health perspective on the healthcare situation in Ukraine, provide direct evidence of situation in radiology and radiation oncology in Ukraine, discuss US-led initiatives of to support Ukraine from Ukrainian Medical Association of Northern America (UMANA), Help Ukraine Group (HUG) and offer the call for action on practical ways to help.

#### LEARNING OBJECTIVES

1. Improve general understanding of the general healthcare challenges facing Ukraine  
2. Learn about situation in diagnostic radiology and radiation oncology in Ukraine  
3. Learn about the initiatives to support Ukraine\*  
Course Description The full-scale Russian invasion of Ukraine on February 24th, 2022 brought the largest humanitarian disaster since the World War II to the heart of Europe. Ukraine has lost tens of thousands of civilian lives, out of which many were innocent children. Many more have been wounded, with approximately a third of the population of Ukraine being displaced: 7 million as refugees and 7.1 million as internally displaced people. According to Ukraine's Minister of Health, Viktor Liashko, during the first 100 days of war more than 600 healthcare facilities sustained damage, 105 of which were rendered beyond repair. Even if the war stopped today, the damage to the healthcare infrastructure will remain for years to come without world's continuing support. Prior to the full-scale Russian invasion, according to unpublished Ukrainian NCI (Tumor Registry) data, in Ukraine with 44 million population, an estimated 139,000 people were living with newly diagnosed cancer, and between 1,000 and 1,200 children were receiving active cancer treatment. Regarding radiotherapy, Ukraine is classified by DIRAC IAEA as a Low Middle Income country with the level of availability being 2.6 External Beam Radiation Therapy (EBRT) machines per 1 million people. Per DIRAC data, until Russia annexed Crimea and parts of the Donbas region in 2014, Ukraine had 52 radiation therapy centers with 86 Co-60 machines (81%) and 20 linear accelerators (19%). Since 2014 Ukraine has lost control of 10 cancer centers and over 13 EBRT machines in occupied part of Donbas and 5 machines in Crimea (totally 17% of Ukrainian EBRT machines). To address the growing need for cancer treatment, 16 linear accelerators were installed by 2022, and the ratio of Co-60 to linear accelerators became 54% to 46% (without taking into account EBRT machines in the occupied territories since 2014). The Ministry of Health of Ukraine planned to purchase additional 20 linear accelerators, but this plan did not materialize because of the Russian full-scale invasion on February 24th. In the fourth month of the war, the situation in Ukraine is fluid, and as of August 29th, 2022, 3 additional cancer centers are under occupation, 3 cancer centers have suspended operation, and 2 cancer centers are under constant shelling. Some of the centers in the west of Ukraine operate with double the volume of patients. This session will convey the Ukrainian ministry of health perspective on the healthcare situation in Ukraine, provide direct evidence of situation in radiology and radiation oncology in Ukraine, discuss US-led initiatives of to support Ukraine from Ukrainian Medical Association of Northern America (UMANA), Help Ukraine Group (HUG) and offer the call for action on practical ways to help.



## Abstract Archives of the RSNA, 2022

W8-CBR08

### Case Based Breast Review: Focus on CEM & Mammography including Tomosynthesis

Wednesday, Nov. 30 4:30PM - 5:30PM Room: NA

#### Participants

Maxine S. Jochelson, MD, New York, NY (*Presenter*) Speaker, General Electric Company  
Almir Bitencourt, MD, PhD, Sao Paulo, Brazil (*Presenter*) Nothing to Disclose  
Jonathan James, BMBS, Nottingham, United Kingdom (*Presenter*) Nothing to Disclose

#### COURSE DESCRIPTION

This will be a series of 3 lectures using actual cases to discuss the utility and indications of the relatively new Contrast Enhanced Mammography as it compares to mammography including tomosynthesis, ultrasound and MRI. We will discuss the advantages and disadvantages of this technique including potential complications and workflow issues so that the audience can assess its potential role for their practices.

#### LEARNING OBJECTIVES

1) Compare the added value of contrast enhanced mammography compared with mammography, ultrasound and MRI 2) Describe the limitations of contrast enhanced mammography compared with mammography, ultrasound and MRI\*Course Description This will be a series of 3 lectures using actual cases to discuss the utility and indications of the relatively new Contrast Enhanced Mammography as it compares to mammography including tomosynthesis, ultrasound and MRI. We will discuss the advantages and disadvantages of this technique including potential complications and workflow issues so that the audience can assess its potential role for their practices.

Printed on: 02/07/23



## Abstract Archives of the RSNA, 2022

W8-CCA10

### CTffr Versus Stress Imaging for Acute Chest Pain Patients

Wednesday, Nov. 30 4:30PM - 5:30PM Room: NA

#### Participants

Christopher Francois, MD, Rochester, MN (*Presenter*) Nothing to Disclose

U. Joseph Schoepf, MD, Charleston, SC (*Presenter*) Research Grant, Bayer AG; Research Grant, Bracco Group; Research Grant, Elucid BioImaging Inc; Consultant, Elucid BioImaging Inc; Research Grant: General Electric Company; Research Grant, Guerbet SA; Research Grant, Heartflow, Inc; Speakers Bureau, Heartflow Inc

Jill Jacobs, MD, New York, NY (*Moderator*) Nothing to Disclose

#### COURSE DESCRIPTION

The course will discuss application of CT FFR and stress imaging for evaluating acute chest pain patients

#### LEARNING OBJECTIVES

1) To identify some of the advantages of utilizing CTFFR and stress imaging for assessing patients with acute chest pain\*Course Description The course will discuss application of CT FFR and stress imaging for evaluating acute chest pain patients

Printed on: 02/07/23



## Abstract Archives of the RSNA, 2022

W8-CCH03

### Lung Cancer Screening

Wednesday, Nov. 30 4:30PM - 5:30PM Room: NA

#### Participants

Debra Dyer, MD, Greenwood Village, CO (*Presenter*) Consultant, AstraZeneca PLC;Clinical Advisory Board, IMIDEX Inc  
Denise R. Aberle, MD, Los Angeles, CA (*Presenter*) Investigator, Johnson & Johnson;Research Grant, Johnson & Johnson  
Terrance Healey, MD, North Scituate, RI (*Presenter*) Nothing to Disclose  
Jared D. Christensen, MD,MBA, Durham, NC (*Presenter*) Advisory Board, Riverain Technologies, LLC;Consultant, Coreline Soft, Co Ltd  
Reginald F. Munden, MD, DMD, Charleston, SC (*Moderator*) Investor, TheraBionic GmbH;Advisory Board, Optellum Ltd;Stock options, Optellum Ltd

#### COURSE DESCRIPTION

Lung Cancer Screening with CT is a life saving technique that continues to evolve since adaptation following the publication NLST results in 2011. This session will provide the attendee with the latest information regarding changes in lung cancer screening policies, management of findings and challenges encountered with lung cancer screening.

#### LEARNING OBJECTIVES

1) Understand the updated USPSTF lung cancer screening guidelines 2) Learn about tools available for tracking lung nodules 3) Explain the challenges and opportunities of Lung-RADS now and in the future 4) Describe the role of Radiologists in mitigating harms of Lung Cancer Screening\*Course Description Lung Cancer Screening with CT is a life saving technique that continues to evolve since adaptation following the publication NLST results in 2011. This session will provide the attendee with the latest information regarding changes in lung cancer screening policies, management of findings and challenges encountered with lung cancer screening.

Printed on: 02/07/23



## Abstract Archives of the RSNA, 2022

W8-CER11

### Genitourinary and Gynecological Causes of Acute Abdominal Pain

Wednesday, Nov. 30 4:30PM - 5:30PM Room: NA

#### Participants

Gayatri Joshi, MD, Atlanta, GA (*Presenter*) Nothing to Disclose

Raffaella Basilio, MD, Chieti, Italy (*Presenter*) Nothing to Disclose

Refky Nicola, DO, Pittsford, NY (*Presenter*) Royalties, RELX

#### COURSE DESCRIPTION

Illustrate the findings of CT and MRI findings of urinary tract emergencies which include obstructive uropathy, infection and renovascular abnormalities. Describe the common and uncommon gynecological emergencies in the non-pregnant patient. Discuss key terminology of early 1st trimester pregnancy and review basic relevant anatomy. Demonstrate common and uncommon types of ectopic pregnancy. Illustrate mimics of ectopic pregnancy with sonographic techniques to make the correct diagnosis.

#### LEARNING OBJECTIVES

1) To discuss the relevant genitourinary emergencies such as obstructive uropathy and infection 2) To discuss the gynecological emergencies in the non-pregnant and pregnant patient in the first trimester\*Course Description Illustrate the findings of CT and MRI findings of urinary tract emergencies which include obstructive uropathy, infection and renovascular abnormalities. Describe the common and uncommon gynecological emergencies in the non-pregnant patient. Discuss key terminology of early 1st trimester pregnancy and review basic relevant anatomy. Demonstrate common and uncommon types of ectopic pregnancy. Illustrate mimics of ectopic pregnancy with sonographic techniques to make the correct diagnosis.

Printed on: 02/07/23



## Abstract Archives of the RSNA, 2022

W8-CGI04

### Pancreatic Tumor Imaging

Wednesday, Nov. 30 4:30PM - 5:30PM Room: NA

#### Participants

Michael H. Rosenthal, MD, PhD, Boston, MA (*Presenter*) Nothing to Disclose

Zhen J. Wang, MD, San Francisco, CA (*Presenter*) Stockholder, Nextrast, Inc

Avinash Kambadakone, MD, FRCR, Boston, MA (*Presenter*) Advisory Board, Bayer AG Research Grant, General Electric Company Research Grant, Koninklijke Philips NV Research Grant, PanCAN Research Grant, Bayer

Motoyo Yano, MD, PhD, Scottsdale, AZ (*Presenter*) Nothing to Disclose

Olga R. Brook, MD, Boston, MA (*Presenter*) Nothing to Disclose

#### COURSE DESCRIPTION

This course will review the current and emerging technological advancements in imaging of pancreatic tumors including deep learning based methods. Attendees will also learn updates on screening and surveillance of pancreatic cancer and importance of structured reporting.

#### LEARNING OBJECTIVES

1) Describe salient imaging manifestations of pancreatic tumors for diagnosis, staging and response assessment 2) Discuss the role of screening and surveillance in early diagnosis of pancreatic cancer 3) Review current and emerging applications of deep learning in pancreatic tumors 4) Explain role of structured reporting in pancreatic tumors and review recent advances in functional imaging tools\*Course Description This course will review the current and emerging technological advancements in imaging of pancreatic tumors including deep learning based methods. Attendees will also learn updates on screening and surveillance of pancreatic cancer and importance of structured reporting.

Printed on: 02/07/23



## Abstract Archives of the RSNA, 2022

W8-CIN26

### Back to Basics: What Do Rads Need To Know About Radiology AI In 2022?

Wednesday, Nov. 30 4:30PM - 5:30PM Room: NA

#### Participants

Linda Moy, MD, New York, NY (*Presenter*) Grant, Siemens AG ;Advisory Board, Lunit Inc;Advisory Board, iCad, Inc  
Dania Daye, MD, PhD, Medford, MA (*Presenter*) Research Consultant, Sigilon Therapeutics, Inc;Research Consultant, Medtronic plc  
Katherine Andriole, PhD, Branford, CT (*Presenter*) Nothing to Disclose  
Walter Wiggins, MD, PhD, Durham, NC (*Presenter*) Advisor, Qure.ai;

#### COURSE DESCRIPTION

In this course, learners will review the basic principles of artificial intelligence in radiology and will gain exposure to the main considerations for implementing an AI algorithm into clinical practice. This course will consist of 4 short presentations where the speakers will provide an introduction to AI, will introduce a framework for evaluating AI algorithms and will discuss best practices for implementing AI algorithms clinically. The session will also provide an overview of the most commonly used AI algorithms in clinical practice today.

#### LEARNING OBJECTIVES

1) Provide an overview of the basic principles of artificial intelligence in radiology 2) Provide a framework for evaluating an AI algorithm for clinical implementation 3) Provide exposure to the most commonly used AI algorithms in clinical radiology\*Course Description In this course, learners will review the basic principles of artificial intelligence in radiology and will gain exposure to the main considerations for implementing an AI algorithm into clinical practice. This course will consist of 4 short presentations where the speakers will provide an introduction to AI, will introduce a framework for evaluating AI algorithms and will discuss best practices for implementing AI algorithms clinically. The session will also provide an overview of the most commonly used AI algorithms in clinical practice today.

Printed on: 02/07/23



## Abstract Archives of the RSNA, 2022

W8-CIR11

### GU Interventions - Women's Health / Men's Health

Wednesday, Nov. 30 4:30PM - 5:30PM Room: NA

#### Participants

Jafar Golzarian, MD, Minneapolis, MN (*Presenter*) Consultant, BSCI; Consultant, Guerbet SA; Consultant, Medtronic plc; Consultant, Penumbra, Inc; Consultant, Sirtex Medical Ltd; Consultant, Embolic Accelerations; Consultant, Obsidio; Consultant, Okami; Consultant, BlackSwan; Consultant, Terumo Corporation; Research Grant, Sirtex Medical Ltd; Stockholder, Qxmedical; Stockholder, Embolic Acceleration; Stockholder, Shape Memory; Stockholder, BlackSwan; Stockholder, Obsidio

Janice M. Newsome, MD, Atlanta, GA (*Presenter*) Scientific Advisory Board, IO Biotech ApS ; Scientific Advisory Board, Boston Scientific Corporation; Consultant, Cook Group Incorporated; Consultant, Hyperfine Research, Inc; Consultant, Carestream Health, Inc ; Co-editor, RELX

Gloria Salazar, MD, Boston, MA (*Presenter*) Consultant, Speakers Bureau, Medtronic plc; Consultant, Boston Scientific Corporation; Speakers Bureau, Boston Scientific Corporation; Speakers Bureau, Cook Group Incorporated; Consultant, Avail Medsystems, Inc; Consultant, Mentice AB

Amy Taylor, MD, Charlottesville, VA (*Presenter*) Nothing to Disclose

Lindsay S. Machan, MD, Vancouver, BC (*Presenter*) Stockholder, A4L, Inc; Stockholder, Auxetics Medical; Stockholder, Calgary Scientific, Inc; Stockholder, Harmonic Medical; Stockholder, IKOMED Technologies Inc; Stockholder, Innovere Medical Inc; Medical Advisory Board, Boston Scientific Corporation; Medical Advisory Board, Medtronic plc

Theresa Caridi, MD, Birmingham, AL (*Presenter*) Consultant, Boston Scientific Corporation; Speaker, Boston Scientific Corporation; Consultant, Cook Group Incorporated; Speaker, Cook Group Incorporated; Consultant, Terumo Corporation; Speaker, Terumo Corporation; Consultant, Siemens AG; Speaker, Siemens AG; Speaker, Penumbra, Inc; Research Grant, Siemens AG

Maureen Kohi, MD, Chapel Hill, NC (*Moderator*) Nothing to Disclose

#### COURSE DESCRIPTION

This course aims to educate the audience regarding minimally invasive image-guided interventions involving the genitourinary tract. Through didactic and case-based lectures, the audience will learn the clinical presentation, recommended diagnostic imaging, procedural steps, and post-procedural care of patients presenting with uterine, prostate, and pelvic diseases.

#### LEARNING OBJECTIVES

1) Identify strategies to diagnose and treat patients with uterine artery embolization 2) Become familiar with the latest data and procedural steps for prostate artery embolization 3) Recognize the clinical presentation and treatment options for pelvic venous disease\*Course Description This course aims to educate the audience regarding minimally invasive image-guided interventions involving the genitourinary tract. Through didactic and case-based lectures, the audience will learn the clinical presentation, recommended diagnostic imaging, procedural steps, and post-procedural care of patients presenting with uterine, prostate, and pelvic diseases.

Printed on: 02/07/23



## Abstract Archives of the RSNA, 2022

W8-CMK12

### The AI Revolution in MSK: Hot Topics

Wednesday, Nov. 30 4:30PM - 5:30PM Room: NA

#### Participants

Naveen Subhas, MD, Cleveland, OH (*Presenter*) Research support, Siemens AG  
John V. Crues III, MD, Los Angeles, CA (*Presenter*) Board Member, Turner Imaging Systems ;Medical Director, RadNet, Inc;  
Paul Yi, MD, Baltimore, MD (*Presenter*) Consultant, FH Orthopedics SAS;Consultant, BunkerHill Health  
Michael L. Richardson, MD, Seattle, WA (*Presenter*) Nothing to Disclose  
David Larson, MD, MBA, Portola Valley, CA (*Presenter*) Research Grant, Siemens AG ;Advisor, Bunkerhill Health;Shareholder, Bunkerhill Health

#### COURSE DESCRIPTION

Artificial intelligence (AI) is set to transform the practice of musculoskeletal radiology and is already making waves across research and clinical practice. In this course, you'll experience a 'Power Hour' of 5 rapid-fire talks presented by experts in the field. Topics will cover a range of aspects of AI in MSK radiology, ranging from corporate perspectives and regulatory frameworks for AI in radiology to the use of AI to accelerate MRI acquisition and potential pitfalls of AI to a "DIY" data science crash course to get hands-on experience developing AI models. The 'Power Hour' will conclude with a 10 minute Q&A with speakers and audience. Join us in this course to learn more about the AI revolution in MSK!

#### LEARNING OBJECTIVES

1) To summarize perspectives on AI in MSK radiology from multiple stakeholders' perspectives, including corporate radiology practices and regulatory officials 2) To describe potential uses and pitfalls of AI in MSK radiology 3) To be aware of hands-on "DIY" resources to learn how to develop AI models\*Course Description Artificial intelligence (AI) is set to transform the practice of musculoskeletal radiology and is already making waves across research and clinical practice. In this course, you'll experience a 'Power Hour' of 5 rapid-fire talks presented by experts in the field. Topics will cover a range of aspects of AI in MSK radiology, ranging from corporate perspectives and regulatory frameworks for AI in radiology to the use of AI to accelerate MRI acquisition and potential pitfalls of AI to a "DIY" data science crash course to get hands-on experience developing AI models. The 'Power Hour' will conclude with a 10 minute Q&A with speakers and audience. Join us in this course to learn more about the AI revolution in MSK!

Printed on: 02/07/23



## Abstract Archives of the RSNA, 2022

W8-CNMMI08

### Neurologic Molecular Imaging: Read with the Experts

Wednesday, Nov. 30 4:30PM - 5:30PM Room: NA

#### Participants

Kirk A. Frey, MD, PhD, Ann Arbor, MI (*Presenter*) Nothing to Disclose

Alexander Drzezga, MD, Cologne, Germany (*Presenter*) Research support, Siemens AG ;Research support, Life Molecular Imaging;Research support, General Electric Company;Research support, Eli Lilly and Company;Research support, Eisai Co, Ltd;Consultant, Siemens AG ;Consultant, General Electric Company

Satoshi Minoshima, MD, PhD, Salt Lake City, UT (*Presenter*) Consultant, Hamamatsu Photonics KK;Grant, Hamamatsu Photonics KK;Grant, Nihon Medi-Physics Co, Ltd;Grant, FUJIFILM Holdings Corporation

Peter Herscovitch, MD, Chevy Chase, MD (*Presenter*) Nothing to Disclose

#### COURSE DESCRIPTION

This course will provide case-based presentations of PET and SPECT findings that are often seen in patients with cognitive and movement disorders, discuss current (FDG, amyloid, tau, and dopamine) and emerging radiotracers for molecular brain imaging, and explain current coverage / reimbursement status in the USA. The attendees to this course will be able to gain knowledge of the current status of molecular brain imaging, its clinical applications, and frequent imaging findings.

#### LEARNING OBJECTIVES

1) Identify PET and SPECT findings that are often seen in patients with cognitive and movement disorders in the clinic 2) Discuss clinical applications of amyloid PET and tau PET imaging 3) Explain emerging tracers for molecular brain imaging and current coverage / reimbursement status in the USA\*Course Description This course will provide case-based presentations of PET and SPECT findings that are often seen in patients with cognitive and movement disorders, discuss current (FDG, amyloid, tau, and dopamine) and emerging radiotracers for molecular brain imaging, and explain current coverage / reimbursement status in the USA. The attendees to this course will be able to gain knowledge of the current status of molecular brain imaging, its clinical applications, and frequent imaging findings.

Printed on: 02/07/23



## Abstract Archives of the RSNA, 2022

W8-CNPM03

### Addressing Organizational Bias, Opportunity for Allyship, and Inclusive Leadership

Wednesday, Nov. 30 4:30PM - 5:30PM Room: NA

#### Participants

Carolyn Meltzer, MD, Los Angeles, CA (*Presenter*) Nothing to Disclose  
Nabile Safdar, MD, MPH, Milton, GA (*Presenter*) Nothing to Disclose  
Miriam A. Bredella, MD, Boston, MA (*Presenter*) Nothing to Disclose  
Cheri Canon, MD, Birmingham, AL (*Presenter*) Royalties, The McGraw-Hill Companies

#### COURSE DESCRIPTION

A diverse biomedical workforce is essential for excellence in patient care. The physician workforce in radiology is predominately male and white. This interactive "Hot Topic" session will address conscious and unconscious biases, identify strategies to create a culture of inclusion with the goal to increase diversity and belonging in radiology.

#### LEARNING OBJECTIVES

1) Understand bias and how to counter it in yourself and others 2) Develop a culture of inclusivity and belonging 3) Identify strategies to increase diversity in radiology\*Course Description A diverse biomedical workforce is essential for excellence in patient care. The physician workforce in radiology is predominately male and white. This interactive "Hot Topic" session will address conscious and unconscious biases, identify strategies to create a culture of inclusion with the goal to increase diversity and belonging in radiology.

Printed on: 02/07/23



## Abstract Archives of the RSNA, 2022

W8-CNR03

### Post-treatment Gliomas (Case-based)

Wednesday, Nov. 30 4:30PM - 5:30PM Room: NA

#### Participants

Mariam Aboian, MD, PhD, New Haven, CT (*Presenter*) Researcher, Blue Earth Diagnostics Ltd; Researcher, Fusion Pharmaceuticals; Research collaboration, Pro Medicus Limited

Javier R. Villanueva-Meyer, MD, Houston, TX (*Presenter*) Nothing to Disclose

Rivka R. Colen, MD, Pittsburgh, PA (*Presenter*) Nothing to Disclose

Vinodh A. Kumar, MD, Houston, TX (*Moderator*) Nothing to Disclose

#### COURSE DESCRIPTION

This case-based session will focus on the use of Perfusion Imaging, PET imaging, Radiomics, and Molecular imaging in the post-treatment evaluation of gliomas.

#### LEARNING OBJECTIVES

1) Learn how to use a diverse variety of advanced neuroimaging techniques to distinguish recurrent glioma from treatment effect\*Course Description This case-based session will focus on the use of Perfusion Imaging, PET imaging, Radiomics, and Molecular imaging in the post-treatment evaluation of gliomas.

Printed on: 02/07/23



## Abstract Archives of the RSNA, 2022

W8-CPD08

### Neonatal Imaging

Wednesday, Nov. 30 4:30PM - 5:30PM Room: NA

#### Participants

Emilio Inarejos Clemente, MD, Barcelona, Spain (*Presenter*) Nothing to Disclose

Tamara G. Kreindel, MD, Buenos Aires, Argentina (*Presenter*) Nothing to Disclose

Asef B. Khwaja, MD, Philadelphia, PA (*Presenter*) Nothing to Disclose

Andrea S. Doria, MD, PhD, Toronto, ON (*Moderator*) Baxalta-Shire (Research Grant), Novo Nordisk (Research Grant), Terry Fox Foundation (Research Grant), PSI Foundation (Research Grant), Society of Pediatric Radiology (Research Grant), Garron Family Cancer Centre (Research Grant)

#### COURSE DESCRIPTION

This course focuses in current and new ultrasound and Doppler techniques used in the neonatal period as well as the ultrasound imaging of common neonatal pathology

#### LEARNING OBJECTIVES

1) To discuss features helpful differentiating portosystemic shunts, arterioportal fistulas and hepatic hemangiomas from Doppler Ultrasound and their clinical implications and prognosis based on the Doppler ultrasound findings 2) To discuss the current uses of microvascular imaging in neonates and its advantages specially in the follow-up neonates with necrotizing enterocolitis 3) To discuss normal imaging findings in musculoskeletal ultrasound in newborns as well as to discuss hip ultrasound (mainly developmental hip dysplasia) and lumps and bumps commonly seen in this age group and their differential diagnosis\*Course Description This course focuses in current and new ultrasound and Doppler techniques used in the neonatal period as well as the ultrasound imaging of common neonatal pathology

Printed on: 02/07/23



## Abstract Archives of the RSNA, 2022

W8-CPH03

### Practical Aspects of MRI

Wednesday, Nov. 30 4:30PM - 5:30PM Room: NA

#### Participants

Adam Bush, Austin, TX (*Presenter*) Nothing to Disclose

Walter Witschey, PhD, Philadelphia, PA (*Presenter*) Nothing to Disclose

Nicole Seiberlich, PhD, Ann Arbor, MI (*Presenter*) Royalties, Siemens AG; Research support, Siemens AG

Catherine Moran, PhD, San Jose, CA (*Presenter*) Research support, General Electric Company

#### COURSE DESCRIPTION

In this course, basic concepts of Magnetic Resonance Imaging which are relevant to clinical practice will be explained. Common image contrasts including T1-weighting, T2-weighting, and diffusion weighting, and how they can be controlled using pulse sequence parameters, will be described. Trade-offs between imaging time and resolution will be considered. Finally, common artifacts, their causes, and mitigation strategies will be explored.

#### LEARNING OBJECTIVES

1) Describe how altering pulse sequence parameters can lead to T1-weighted images, T2-weighted images, and diffusion-weighted images 2) Assess in clinical practice optimal trade-offs between image resolution and scan time 3) Identify common image artifacts, and understand how to adjust MRI parameters to reduce these artifacts\*Course Description In this course, basic concepts of Magnetic Resonance Imaging which are relevant to clinical practice will be explained. Common image contrasts including T1-weighting, T2-weighting, and diffusion weighting, and how they can be controlled using pulse sequence parameters, will be described. Trade-offs between imaging time and resolution will be considered. Finally, common artifacts, their causes, and mitigation strategies will be explored.

Printed on: 02/07/23



## Abstract Archives of the RSNA, 2022

W8-CRO08

### Lymphoma Case-based Multidisciplinary Review

Wednesday, Nov. 30 4:30PM - 5:30PM Room: NA

#### Participants

Sarah A. Johnson, MD, Toronto, ON (*Presenter*) Nothing to Disclose

Eugene Yu, MD,FRCPC, Toronto, ON (*Presenter*) Nothing to Disclose

Chelsea Pinnix, MD,PhD, Houston, TX (*Presenter*) Research Grant, Merck & Co, Inc

#### COURSE DESCRIPTION

Lymphoma comprises a group of malignancies which will in some form be encountered by all radiologists in their practice. This course will review principles of lymphoma diagnosis, staging, and response assessment which will be relevant for diagnostic radiologists involved in these cases. The session is organized in lecture format based on interesting cases of lymphoma drawn from the neuroimaging and body imaging domains. Cases will be further informed by a radiation oncology perspective. Participants will glean an advanced understanding of interpreting CT and PET/CT for lymphoma diagnosis, staging, and response assessment.

#### LEARNING OBJECTIVES

1) To identify characteristic imaging features of central nervous system and head and neck lymphoma 2) To interpret imaging findings in the context of response assessment 3) To distinguish appropriate uses and benefits of advanced imaging methods in diagnosis of lymphoma 4) To interpret nuances of imaging that will influence or impact treatment approach\*Course Description Lymphoma comprises a group of malignancies which will in some form be encountered by all radiologists in their practice. This course will review principles of lymphoma diagnosis, staging, and response assessment which will be relevant for diagnostic radiologists involved in these cases. The session is organized in lecture format based on interesting cases of lymphoma drawn from the neuroimaging and body imaging domains. Cases will be further informed by a radiation oncology perspective. Participants will glean an advanced understanding of interpreting CT and PET/CT for lymphoma diagnosis, staging, and response assessment.

Printed on: 02/07/23



## Abstract Archives of the RSNA, 2022

W8-RCP05

### AOSR-RSNA Joint Symposium: Pediatric Imaging Session

Wednesday, Nov. 30 4:30PM - 5:30PM Room: NA

#### Participants

Judy Squires, MD, Pittsburgh, PA (*Presenter*) Nothing to Disclose

Timothy Cain, MBBS, FRANZCR, Melbourne, Australia (*Presenter*) Nothing to Disclose

Sanjay Prabhu, FRCR, MBBS, Boston, MA (*Presenter*) Nothing to Disclose

Young Hun Choi, MD, Seoul, Korea, Republic Of (*Presenter*) Nothing to Disclose

#### COURSE DESCRIPTION

The educational session is a series of short pediatric focussed lectures with contributors from North America and the Asia Oceanic region. The contribution from two geographic regions symbolises the common goal of the Radiological Society of North America and the Asian and Oceanic Society of Radiology to improve child health through appropriate medical imaging. Attendees will hear presentations with up to date information on a range of pediatric imaging topics.

#### LEARNING OBJECTIVES

1) Identify key aspects of MR safety that are particularly important when performing MR studies on paediatric patients 2) Recognise the important MR imaging characteristics of haemorrhagic lesions of the neonatal brain 3) Be aware of the common imaging features of contrast enhanced ultrasound when studying the neonatal brain 4) Understand the significance of metabolic imaging in the staging and treatment of neuroblastoma\*Course Description The educational session is a series of short pediatric focussed lectures with contributors from North America and the Asia Oceanic region. The contribution from two geographic regions symbolises the common goal of the Radiological Society of North America and the Asian and Oceanic Society of Radiology to improve child health through appropriate medical imaging. Attendees will hear presentations with up to date information on a range of pediatric imaging topics.

Printed on: 02/07/23



## Abstract Archives of the RSNA, 2022

W8-RCP26

### **Beyond the Binary: Imaging Findings, Screening Guidelines, and Radiology Practice Considerations for Transgender and Gender-Diverse Patients (Sponsored by the RSNA Committee on Diversity, Equity & Inclusion)**

Wednesday, Nov. 30 4:30PM - 5:30PM Room: NA

#### **Participants**

Nolan J. Kagetsu, MD, New York, NY (*Presenter*) Spouse, Employee, Pfizer Inc, NY, NY, USA Daughter, CEO, Saathi, Ahmedabad, India  
Micah Weir, MD, North Andover, MA (*Presenter*) Nothing to Disclose  
David Pryluck, MD, MBA, Danville, PA (*Presenter*) Nothing to Disclose  
Justin Stowell, MD, Jacksonville, FL (*Presenter*) Nothing to Disclose  
Timothy J. Blackburn, PhD, Dallas, TX (*Presenter*) Nothing to Disclose  
Evelyn Carroll, MD, Rochester, NY (*Presenter*) Nothing to Disclose  
Florence Doo, MD, MA, Sunset Beach, NY (*Presenter*) Nothing to Disclose  
Vaz Zavaletta, MD, PhD, Aurora, CO (*Presenter*) Nothing to Disclose

#### **COURSE DESCRIPTION**

There are imaging findings, screening recommendations, and barriers to care that uniquely impact transgender and gender-diverse patients. Through a series of lectures and open discussion, course participants will develop a working knowledge of this information to facilitate the correct interpretation of radiologic studies for transgender and gender-diverse patients across imaging modalities and help create and promote an inclusive diagnostic and interventional radiology department. <https://tinyurl.com/yckre8uz>

#### **LEARNING OBJECTIVES**

1) Recognize and discuss the spectrum of gender identity and define and utilize correct terminology and personal pronouns for transgender and gender-diverse individuals 2) Recognize and describe imaging findings in transgender and gender-diverse patients after gender-affirming surgeries and medical interventions 3) Discuss and apply radiology screening guidelines for transgender and gender-diverse patients after gender-affirming surgeries and medical interventions 4) Discuss and apply strategies and best practices to create an inclusive diagnostic and interventional radiology department\*Course Description There are imaging findings, screening recommendations, and barriers to care that uniquely impact transgender and gender-diverse patients. Through a series of lectures and open discussion, course participants will develop a working knowledge of this information to facilitate the correct interpretation of radiologic studies for transgender and gender-diverse patients across imaging modalities and help create and promote an inclusive diagnostic and interventional radiology department. <https://tinyurl.com/yckre8uz>

Printed on: 02/07/23



## Abstract Archives of the RSNA, 2022

W8-RCP38

### Climate Change and Radiology (Sponsored by RSNA Professionalism Committee)

Wednesday, Nov. 30 4:30PM - 5:30PM Room: NA

#### Participants

Julia Schoen, MD,MS, Winston Salem, NC (*Presenter*) Stockholder, Merck & Co, Inc;Stockholder, Moderna, Inc;Stockholder, Aurinia Pharmaceuticals Inc;Speaker, Koninklijke Philips NV

Kate Hanneman, MD, FRCPC, Toronto, ON (*Presenter*) Speaker, Groupe Sanofi Speaker, Amicus Therapeutics, Inc

Reed Omary, MD, Nashville, TN (*Presenter*) Nothing to Disclose

Jonathan Gross, MD, Houston, NY (*Presenter*) Nothing to Disclose

Maura Brown, MD, Vancouver, BC (*Presenter*) Synthesis Health Inc - research collaboration, no financial relationship at this time (Nov 2022).

#### COURSE DESCRIPTION

The purpose of this course is to discuss the impact of health care (including imaging) on climate change and propose actionable steps we can take.

#### LEARNING OBJECTIVES

1) Discuss climate change and the impact on our health2) Describe impact of medical imaging on climate change and highlight opportunities for change3) Provide actionable steps radiologists can take to address climate change at work and in our personal lives \*Course Description The purpose of this course is to discuss the impact of health care (including imaging) on climate change and propose actionable steps we can take.

Printed on: 02/07/23



## Abstract Archives of the RSNA, 2022

M4-PL02

### Plenary Session: Three Visions for the Future of Medicine

Monday, Nov. 28 11:00AM - 12:00PM Room: Arie Crown

#### Participants

Siddhartha Mukherjee, MD, Oak Brook, IL (*Presenter*) Stockholder, Apollo Global Management, Inc; Board of Directors, Apollo Global Management, Inc; Owner, ApotheCo; Owner, CuraPatient, Inc; Scientific Advisory Board, CuraPatient, Inc; Owner, Composite Apps; Scientific Advisory Board, Composite Apps; Owner, Faeth Therapeutics, Inc; Owner, Immuneel Therapeutics Private Limited; Owner, Myeloid Therapeutics, Inc; Scientific Advisory Board, Myeloid Therapeutics, Inc; Stockholder, Unilever Group; Owner, Scriptsee, Inc; Advisory Board, PureTech Health; Stockholder, TrialSpark, Inc; Owner, Vor Biopharma, Inc; Scientific Advisory Board, Vor Biopharma, Inc

Printed on: 02/07/23



## Abstract Archives of the RSNA, 2022

M8-PL03

### Image Interpretation Session

Monday, Nov. 28 4:30PM - 5:30PM Room: Arie Crown

#### Participants

Tetyana A. Gorbachova, MD, Huntingdon Valley, PA (*Presenter*) Nothing to Disclose

Alvaro Huete Garin, MD, Santiago, (*Presenter*) Nothing to Disclose

James M. Provenzale, MD, Durham, NC (*Presenter*) Nothing to Disclose

Nisha Sharma, MBChB, FRCR, Leeds, United Kingdom (*Presenter*) Nothing to Disclose

Brett M. Elicker, MD, San Francisco, CA (*Presenter*) Nothing to Disclose

Mini N. Pathria, MD, La Jolla, CA (*Moderator*) Nothing to Disclose

#### LEARNING OBJECTIVES

1) Identify key abnormal findings on radiologic studies that are critical to making a specific diagnosis. 2) Construct a logical list of differential diagnoses based on the radiologic findings, focusing on the most probable differential diagnoses. 3) Determine which, if any, additional radiologic studies or procedures are needed in order to make a specific final diagnosis. 4) Choose the most likely diagnosis based on the clinical and the radiologic information.\*Course Description This session will employ an expert panel to discuss unknown cases in the fields of neuroradiology, musculoskeletal radiology, breast imaging, genitourinary imaging and cardiothoracic radiology. The material will include plain radiography, CT and MRI imaging with an overall theme of cases with unusual appearances that can be solved by carefully analyzing the images and recognized ancillary findings that help establish the correct diagnosis. The five expert readers will provide insights into how they approach challenging clinical cases, pearls and pitfalls during the creation of a differential diagnosis, and keys to a final diagnosis in a light-hearted entertaining format.

Printed on: 02/07/23



## Abstract Archives of the RSNA, 2022

R4-PL07

### RSNA/AAPM Symposium: Together We Can Make A Difference

Thursday, Dec. 1 11:00AM - 12:00PM Room: NA

#### Participants

Gillian M. Newstead, MD, Winter Harbor, ME (*Presenter*) Research Consultant, Bayer AG

Maryellen Giger, PhD, Chicago, IL (*Presenter*) Stockholder, Hologic, Inc; Royalties, Hologic, Inc; Shareholder, Quantitative Insights, Inc; Co-founder, Quantitative Insights, Inc; Shareholder, QView Medical, Inc; Royalties, General Electric Company; Royalties, Median Technologies; Royalties, Riverain Technologies, LLC

Guang-Hong Chen, PhD, Madison, WI (*Moderator*) Nothing to Disclose

#### LEARNING OBJECTIVES

1. Learn the importance of partnership between radiologists and medical physicists; 2. Learn the experiences from leaders in the field how to work together to make a difference to advance medicine.\*Course Description Highlight successful collaboration between AAPM and RSNA for imaging technical development and clinical translations.

Printed on: 02/07/23



## Abstract Archives of the RSNA, 2022

S6-PL01

### President's Address and Opening Session

Sunday, Nov. 27 4:00PM - 5:30PM Room: Arie Crown

#### Sub-Events

#### **S6-PL01 Doctor as Patient: Imagining Cancer Survival for All**

##### Participants

Elizabeth Morris, MD, Sacramento, CA (*Presenter*) Scientific Advisory Board, Bracco Group;Speaker, Bayer AG;Scientific Advisory Board, Bayer AG;Speaker, Guerbet SA;Researcher, Guerbet SA;Stockholder, Revel Transit Inc;Stockholder, Kheiron Medical Technologies Ltd

#### **S6-PL01 Diagnostic Imaging: Value from the Lens of the Patient**

##### Participants

Bruce Haffty, MD, New Brunswick, NJ (*Presenter*) Nothing to Disclose

Printed on: 02/07/23



## Abstract Archives of the RSNA, 2022

S6-PL01

### Doctor as Patient: Imagining Cancer Survival for All

Sunday, Nov. 27 4:00PM - 5:30PM Room: Arie Crown

#### Participants

Elizabeth Morris, MD, Sacramento, CA (*Presenter*) Scientific Advisory Board, Bracco Group;Speaker, Bayer AG;Scientific Advisory Board, Bayer AG;Speaker, Guerbet SA;Researcher, Guerbet SA;Stockholder, Revel Transit Inc;Stockholder, Kheiron Medical Technologies Ltd

Printed on: 02/07/23



## Abstract Archives of the RSNA, 2022

S6-PL01

### Diagnostic Imaging: Value from the Lens of the Patient

Sunday, Nov. 27 4:00PM - 5:30PM Room: Arie Crown

#### Participants

Bruce Haffty, MD, New Brunswick, NJ (*Presenter*) Nothing to Disclose

Printed on: 02/07/23



## Abstract Archives of the RSNA, 2022

T4-PL04

### Plenary Session: Designing Radiology for Patients, Communities, & the Planet

Tuesday, Nov. 29 11:00AM - 12:00PM Room: Arie Crown

#### Participants

Reed Omary, MD, Nashville, TN (*Presenter*) Nothing to Disclose

Printed on: 02/07/23



## Abstract Archives of the RSNA, 2022

W4-PL05

### Plenary Session: Exciting Radiology Game Show: What's Your Emergency? Life in the STAT Lane

Wednesday, Nov. 30 11:00AM - 12:00PM Room: Arie Crown

#### Participants

Jamlik-Omari Johnson, MD, Atlanta, GA (*Presenter*) Nothing to Disclose  
Christopher Potter, MD, Boston, MA (*Presenter*) Nothing to Disclose  
Nicolas Murray, MD, FRCPC, Vancouver, BC (*Presenter*) Co-investigator, Siemens AG  
Melissa Davis, MD, MBA, Atlanta, GA (*Presenter*) Nothing to Disclose  
Marc Camacho, MD, Tampa, FL (*Presenter*) Nothing to Disclose  
Robin B. Levenson, MD, Newton, MA (*Presenter*) Nothing to Disclose  
Claire Sandstrom, MD, Seattle, WA (*Presenter*) Nothing to Disclose  
Vincent M. Mellnick, MD, Saint Louis, MO (*Presenter*) Nothing to Disclose  
Susanna C. Spence, MD, Houston, TX (*Presenter*) Nothing to Disclose  
Laura L. Avery, MD, Boston, MA (*Presenter*) Nothing to Disclose  
Krystal Archer-Arroyo, MD, Decatur, GA (*Presenter*) Nothing to Disclose  
Tarek N. Hanna, MD, Atlanta, GA (*Moderator*) Nothing to Disclose  
Jennifer Uyeda, MD, Lexington, MA (*Moderator*) Nothing to Disclose

#### LEARNING OBJECTIVES

1) Identify traumatic and nontraumatic emergencies 2) Prioritize workflow scenarios 3) Resolve practice management conflicts\*Course Description ER stands for Exciting Radiology! Using a game show format, two teams of emergency radiologists will tackle a spectrum of traumatic and non-traumatic cases, solve clinical workflow scenarios, and address practice management issues. All in a fast-paced, multi-tasking manner representative of life in the ER STAT lane. If you're a radiologist, emergency radiology is most likely part of your life, day and/or night, and increasing in volumes. Interested in ER? Love ER? This game is for you.

Printed on: 02/07/23



## Abstract Archives of the RSNA, 2022

W6-PL06

### Plenary Session: Machine Learning in Radiation Oncology Clinical Trials and Clinical Practice

Wednesday, Nov. 30 1:30PM - 2:30PM Room: NA

#### Participants

Felix Feng, MD, San Francisco, CA (*Presenter*) Consultant, Johnson & Johnson; Consultant, Bayer AG; Consultant, Exact Sciences Corporation; Consultant, Sumitovant Biopharma Ltd; Consultant, Roivant Sciences Holdings Limited; Consultant, Astellas Group; Consultant, SerImmune Inc; Scientific Advisory Board, Serimmune Inc; Stock options, Serimmune Inc; Consultant, F. Hoffmann-La Roche Ltd; Consultant, Siemens AG; Consultant, Bristol-Myers Squibb Company; Consultant, BlueStar Genomics, Inc; Consultant, Artera Services, LLC; Medical Advisor, Artera Services, LLC; Stock options, Artera Services, LLC; Consultant, Novartis AG; Consultant, Tempus Labs

Quynh-Thu X. Le, MD, San Carlos, CA (*Presenter*) Consultant, Merck & Co, Inc; Advisory Board, Coherus BioSciences, Inc; Advisory Board, F. Hoffmann-La Roche Ltd

Michael Gensheimer, MD, Stanford, CA (*Presenter*) Research Grant, Siemens AG; Research Grant, Koninklijke Philips NV; Research Grant, RefleXion Medical Inc; Spouse, Employee, F. Hoffmann-La Roche Ltd

Ruijiang Li, PHD, Palo Alto, CA (*Presenter*) Nothing to Disclose

Printed on: 02/07/23

## Abstract Archives of the RSNA, 2022

M2-QI

### Quality Improvement Reports Monday Poster Discussions

Sunday, Nov. 27 9:00AM - 9:30AM Room: Learning Center - QI DPS

#### Sub-Events

#### M2-QI-1 Accelerating Radiologist Workflow by Leveraging Hyponyms in Structured Reporting

Participants

Cyrillo R. Araujo, MD, Tampa, FL (*Presenter*) Nothing to Disclose

#### METHODS

Three radiologists applied available capabilities in the dictation software that ties hyponyms (words that trigger a sentence to a hyponym-hypernym matched field) to higher order hypernym (Fig 1). When predetermined hyponyms are included in a dictated sentence, they are matched to the appropriate hypernym field at the completion of the dictation by the command "apply findings". For example, when a dictated sentence includes "...pulmonary?", it is matched to the "Lung" hypernym field (Fig 2). Once the first set of hyponyms were created for computed tomography body exam templates, additional radiologists adopted hyponym reporting using the established database, while recommending additional hyponyms based on variable reporting styles. We share the time spent creating the hyponyms, training the radiologists and workflow efficiency average time to open, proofread and sign the final report. We applied eye tracking to objectively compare traditional (Fig 3) versus hyponym (Fig 4) reporting attention on images and dictation screens.

#### RESULTS

The creation of a hyponym database for body imaging took approximately two days. For at least two to four weeks, the database was updated during the workflow to reflect the dictating style of the radiologists. By the end of the first month, the first radiologist dictated 100% of CT reports utilizing hyponyms with > 95% accuracy of matched hyponyms to hypernym fields in final reports. The average time to dictate a body CT study was reduced by more than 30% with more time spent during image interpretation than looking at the dictation screen.\*Discussion We present the concept of free form dictating that applies a database of select trigger hyponym words resulting in a final structured report. Our preliminary data shows reduction in time that radiologists spend looking at the non-diagnostic screen with more time interpreting the imaging findings, potentially improving radiologist efficiency and accuracy. Our first several months of hyponym reporting appears to be more efficient with a steep learning curve with a trend toward adoption. We plan on making our hyponym word bank publicly available that may facilitate a more widespread approach, especially with increasing structure reporting demands. Limitations Potential disruption in established radiologist routine, e.g. some radiologists are template and/or macro driven and may use templates and fields as a checklist.

#### M2-QI-2 Impact of Online MRI Safety Screening Questionnaires on Patient Workflow

Participants

Sheena Chu, (*Presenter*) Nothing to Disclose

#### METHODS

Safety screening was made available via a patient web portal to all outpatient MRIs prior to appointment. At the check-in desk, all patients receive a pager to alert them when the technologist is ready to initiate their final safety screening and exam. Data were retrospectively collected for all adult outpatient MRIs for one year before and after implementation of online screening, using electronic health records and an analytics platform. Time between page and first MR image (time-to-image) was the primary endpoint. Time-to-image was compared among 3 groups: those who completed online screening, those who did not during the same 1-year period (synchronous control), and all patients from 1 year prior to implementation (historical control). Exams with missing data were excluded. Post-arrival cancellations (patients who checked in but did not undergo MRI) were noted. Student's t-test compared online-screening with each control group; Mood's median test compared medians and analysis of variance compared other values across all three groups; P<0.05 was considered significant.

#### RESULTS

Of 13,626 outpatient MRIs, 113 were excluded. Included were 6,199 and 7,314 MRIs, respectively pre- and post-online screening initiation; 1,931/7,314 completed online screening. Post-arrival cancellations were significantly lower in the online screening group than both controls (0.05% vs. 8.2% 9.4%, P<0.001). Online screening group demonstrated a lower median and standard deviation (std) time-to-image, and fewer outliers than both control groups (P< 0.05). There was no significant difference in median or std of time-to-image between two control groups (P=0.28, 0.24 respectively). There was no difference in age, gender distribution, or fraction of patients with more than one MRI among the three groups (all P>0.05).\*Discussion We demonstrated a correlation between using an online safety screening and a reduction in post-arrival cancellations as well as workflow delays, with a significant reduction in the number of extreme delays. Our study benefited from a large patient cohort, use of analytic platforms, and two control groups; limitations included its retrospective nature and possible selection bias. Given these promising results, we will address these limitations in future evaluations in larger cohorts and by increasing the use of the online screening tool.

#### M2-QI-3 Image Quality Improvement of Digital Mammography Using an Artificial Intelligent Real Time Manage System

## Awards

### Quality Improvement Reports Award

#### Participants

Ying Guo, (*Presenter*) Nothing to Disclose

#### METHODS

The AI system uses deep learning technology to detect nine types of abnormalities that will occur during breast X-ray examinations. The intelligent quality control system of mammography includes acquisition module, quality evaluation module and result display module. Image data of 200 cases of digital X-ray mammography before and after quality control were evaluated with the standards of Mammography Quality Standards Act (MQSA). If the image quality meets the diagnostic criteria, it is defined as grade A; if one of standards does not meet the diagnostic criteria, it is defined as grade B; if two, defined as grade C; if more than three, defined as invalid. The two groups were statistically compared before and after quality control for radiation dose, lesion detection rate, image quality and ratio of grade A, B and C.

#### RESULTS

After the implementation of quality control, rate of grade A increased from 78.5% to 91.4%. The rate of grade B decreased from 21.5% to 3.2%, and the rate of grade C decreased from 5.6% to 1.2%. The invalid rate remained unchanged at 0%. The lesion detection rate of micro calcification and structural distortion after quality control was higher than that before ( $P < 0.01$ ). The diagnostic sensitivity of breast lesions increased ( $P < 0.01$ ), and the specificity of breast lesions increased ( $P > 0.01$ ). \*Discussion Through quality control and management of breast X-ray imaging by using an artificial intelligent system, the image quality of digital mammography is significantly improved. The diagnostic accuracy of breast lesions increased, so as to provide high-quality image data for clinic. AI has great potential in evaluating breast position in digital mammography by reducing subjectivity. In the future, standardized and evidence-based criteria for definitions, understandings and assessment methods are needed to reach optimal image quality in mammography.

### M2-QI-4 Minimizing Phone Call Interruptions in the Emergency Department Reading Room

#### Participants

Hossam Elbelasi, MD, (*Presenter*) Nothing to Disclose

#### METHODS

Data was obtained from our campus network and infrastructure specialist. Initial pilot data showed a total of 1885 received phone calls in the emergency department reading room between 7/18/2021 and 8/17/2021. Root cause analysis was performed, and causes were grouped into 4 major categories. Teleradiology related communications was targeted for intervention. We aimed to decrease the total number of phone call interruptions by 30 % by November 2021. This was done through hiring a coordinator to handle Teleradiology related communications. We collected phone records over the course of 1 week before and after the coordinator was hired.

#### RESULTS

The total number of phone calls during the entire week decreased from 639 to 431 (32.5% decrease). The total time spent on the phone decreased from 853 to 724 minutes (15% decrease). During the coordinator shift (3pm-12am) the total number of phone calls has decreased by 27.5% (from 276 to 200) with average time spent on the phone during a single shift decreased from 52 mins to 36 mins (31%). \*Discussion Hiring a coordinator for the Teleradiology communication showed a significant reduction in phone call interruptions. We believe that hiring full time reading room assistant to handle communication to and from the reading room will lead to even significant decrease in interruption and increase radiologist's efficiency.

### M2-QI-5 Implementing a Quality Improvement Framework to Reduce Missed Care Opportunities in Screening Mammography

#### Participants

Adrian Jaramillo-Cardoso, MD, Boston, MA (*Presenter*) Nothing to Disclose

#### METHODS

Our initiative was guided by a modified health disparities research framework following four steps. Detecting: identifying the possible breakdown areas contributing to MCO by creating a process map with multiple stakeholders; and further organizing identified factors in a driver diagram. Understanding: Surveying our patient population to gain in-depth knowledge about the context of these factors and creating a pareto chart to see their individual contribution. Reducing: Employing an Impact/Effort Matrix we identified key interventions. Evaluating: Including tracking the data from our interventions and identifying challenges in the implementation of our equity efforts.

#### RESULTS

Key high priority and actionable intervention fronts identified included: 1. Culturally Sensitive Education: we developed educational multilingual (EN, SP, PT) videos and posters addressing SM concerns and providing information of what to expect of the process. 2. Reminder Process Improvement: Contact information was updated in our EMR but no significant statistical difference detected ( $p > 0.05$ ), we developed the infrastructure to set up a text messaging reminder process that will include our educational video. 3. Increased Scheduling Flexibility: Weekend appointments were started as a pilot at one of our imaging sites. Showing a significant decrease in MCOs (6% during 4 weekends vs. 43% during weekdays). 4. Transportation: A ride-share program will be implemented to decrease the impact of transportation issues for high risk patients. \*Discussion We have developed a multi prong intervention front that attempts to address the most actionable contributing factors found to contribute to MCOs in two high risk sites within our system. Some of our interventions have provided outcomes to help our team reassess our efforts to allocate resources. We have found a modified health disparities research framework as a helpful guide on the design and implementation process of these efforts. Furthermore, using an iterative process including PDSA cycles has strongly informed the implementation of these interventions and increased our focus on mitigating the effect of health disparities in our patient population. Extending this approach to other QI initiatives holds great potential to aid in assuring health equity as a priority.

### M2-QI-6 Improving Order to Completion Time for Urgent/STAT Inpatient and ED Pediatric MRI's Requiring Anesthesia/Sedation

## Awards

### Identified for RadioGraphics

#### Quality Improvement Reports Award

#### Participants

Jay K. Pahade, MD, Southport, CT (*Presenter*) Consultant, General Electric Company; Consultant, Clario Medical Imaging, Inc;

#### METHODS

Multidisciplinary team was created with radiology and pediatric quality and safety teams, MRI operations, pediatric anesthesia, MRI scheduling, and pediatric hospitalists. A3 and Model for Improvement methodology was used with flow map creations, fishbone analysis, 5 why problem solving and PDSA cycles. Interventions included revision of triage process, creating fixed add on MRI anesthesia appointment slots Monday-Friday, and linking pediatric anesthesia NPO orders to the MRI order in our electronic medical record (Epic, Verona WI)

#### RESULTS

Baseline (07/2020 to 10/2020) weekday mean O to B MRI time for urgent or stat inpatient/ED MRI requiring anesthesia/sedation was 1125 minutes with SD of 1198 minutes. Post intervention (09/2021-2/2022) mean O to B time decreased to 559 minutes (50% reduction) and SD decreased to 388 minutes (68% reduction). \*Discussion Delays in completing urgent/stat pediatric MRI with anesthesia are often secondary to disorganized triage process, lack of slot availability in MRI, non-compliance with NPO rules for anesthesia and unclear MRI start times. This QI project redesigned workflow with all relevant stakeholders, created new fixed slots for add-on pediatric MRI anesthesia cases, and integrated expected MRI start time and pediatric anesthesia NPO order set within the MRI order in our EHR. This resulted in 50% reduction in mean order to begin time and a more reproducible process with less variation (SD reduced by 68%). Our program has displayed good sustainment after last key driver implementation in 09/2021.

#### M2-QI-7 Implementation of Ferrous-Free Dress Code for MRI Personnel - An MRI Safety Initiative

#### Participants

Julie Johnson, BS, ARRT, Atlanta, GA (*Presenter*) Nothing to Disclose

#### METHODS

We are a free-standing academic children's hospital. Baseline alarm rate for FMDS was obtained to evaluate frequency of passage of ferromagnetic items through our two most frequently used MRI scanners zone 4 doors. A task force was formed to establish a ferrous-free MRI environment with a focus on MRI personnel (technologists and sedation team) attire. Sub-committees of this task force included: ferrous-free clothing committee to provide resources to staff for ferrous free attire, process committee to screen and identify non-compliant staff, and an engagement committee to gain employee engagement. The engagement committee was also charged with developing a ferrous free campaign logo and posters to remind staff of go-live date. Ferrous-free dress code was implemented on October 11th 2021. Weekly alarm rates from the FMDS were evaluated to determine the impact of the ferrous-free attire initiative on alarm frequency. Processes were developed and implemented that required staff to stop and investigate any alarms produced by the doorway FMDS. Alarm rate data was collected weekly and reported to the task force monthly to serve as our metric.

#### RESULTS

Baseline alarm rate for the two most frequently used scanners in our pediatric facility was 172 (+/- 37) /week and 253 (+/- 59)/week. Since the implementation of ferrous-free attire, the alarm rate has trended down over time (attached plots) and is currently at 98 (+/- 29)/week and 74 (+/- 17)/week, respectively. Compliance of MRI personnel with ferrous free attire has been excellent. Most alarms are now caused due to non-MRI personnel attire, and proximity of moving zone 3 ferrous objects to the FMDS. \*Discussion Implementation of a ferrous-free attire for MRI personnel is feasible with high compliance, and is essential to decrease FMDS alarm rate and resultant alarm fatigue. In the next phase of this project, ferrous-free dress requirement will be expanded to all staff, patients and guardians entering the MRI suites.

#### M2-QI-8 Improving the Quality of Rectal MRI for Patients With Rectal Cancer Through an Iterative, Multi-Disciplinary Process With MR Physicists, Radiographers, and Radiologists

#### Participants

Nikhil Shah, MEng, BSc, (*Presenter*) Nothing to Disclose

#### METHODS

We undertook 3 audits and 2 surveys to measure the image quality of our rectal MRI scans and radiographers' confidence in performing these scans. Each audit reviewed 1 month of rectal MRI scans for rectal adenocarcinoma. The first audit highlighted issues with bowel wall motion artefact and image resolution. The initial survey identified the training limitations of radiology personnel. To address these problems, we performed 4 interventions: 1) protocol development to optimise sequences, and testing involving MR physicists, radiographers and radiologists; 2) radiology personnel training to improve understanding of scanning technique and disease identification, measured by a second survey; 3) 2nd audit: image quality of rectal MRI scans measured against indicators, including (a) use of anterior saturation band, (b) appropriate coil positioning, (c) adequate tumour coverage, (d) imaging of mesorectum to L5/S1, and (e) use of antispasmodics; and 4) 3rd audit: a review of rectal MRI scans after introducing Buscopan and continued case review for radiographers.

#### RESULTS

Audit Audit results after interventions showed marked improvements in the quality of rectal MRI scans for diagnosis and management. Anterior saturation band used: 0% (1st audit), 100% (2nd audit) and 100% (3rd audit); appropriate coil positioning: 69% (1st audit), 92% (2nd audit) and 100% (3rd audit); adequate tumour coverage: 69% (1st audit), 83% (2nd audit) and 89% (3rd audit); mesorectum imaged to L5/S1: 38% (1st audit), 50% (2nd audit) and 78% (3rd audit); antispasmodic used: 0% (1st audit), 0% (2nd audit) and 67% (3rd audit). Survey Following training sessions, there was an increase in radiographers' confidence in identifying rectal cancer and orientating imaging to the axis of the tumour. \*Discussion A limitation of our project was that we considered only patients with adenocarcinoma. However, patients with squamous cell carcinoma also require this level of imaging, as well as additional sequences to study the nature of the inguinal nodes. Our project resulted in significant improvements to the quality of our rectal MRI scans and our team's technical performance. It has optimised the staging of rectal cancer in our department and led to increased confidence in multidisciplinary decision making.





## Abstract Archives of the RSNA, 2022

M2-QI-1

### Accelerating Radiologist Workflow by Leveraging Hyponyms in Structured Reporting

Sunday, Nov. 27 9:00AM - 9:30AM Room: Learning Center - QI DPS

#### Participants

Cyrillo R. Araujo, MD, Tampa, FL (*Presenter*) Nothing to Disclose

#### METHODS

Three radiologists applied available capabilities in the dictation software that ties hyponyms (words that trigger a sentence to a hyponym-hypernym matched field) to higher order hypernym (Fig 1). When predetermined hyponyms are included in a dictated sentence, they are matched to the appropriate hypernym field at the completion of the dictation by the command "apply findings". For example, when a dictated sentence includes "...pulmonary?", it is matched to the "Lung" hypernym field (Fig 2). Once the first set of hyponyms were created for computed tomography body exam templates, additional radiologists adopted hyponym reporting using the established database, while recommending additional hyponyms based on variable reporting styles. We share the time spent creating the hyponyms, training the radiologists and workflow efficiency average time to open, proofread and sign the final report. We applied eye tracking to objectively compare traditional (Fig 3) versus hyponym (Fig 4) reporting attention on images and dictation screens.

#### RESULTS

The creation of a hyponym database for body imaging took approximately two days. For at least two to four weeks, the database was updated during the workflow to reflect the dictating style of the radiologists. By the end of the first month, the first radiologist dictated 100% of CT reports utilizing hyponyms with > 95% accuracy of matched hyponyms to hypernym fields in final reports. The average time to dictate a body CT study was reduced by more than 30% with more time spent during image interpretation than looking at the dictation screen.\*Discussion We present the concept of free form dictating that applies a database of select trigger hyponym words resulting in a final structured report. Our preliminary data shows reduction in time that radiologists spend looking at the non-diagnostic screen with more time interpreting the imaging findings, potentially improving radiologist efficiency and accuracy. Our first several months of hyponym reporting appears to be more efficient with a steep learning curve with a trend toward adoption. We plan on making our hyponym word bank publicly available that may facilitate a more widespread approach, especially with increasing structure reporting demands. Limitations Potential disruption in established radiologist routine, e.g. some radiologists are template and/or macro driven and may use templates and fields as a checklist.

Printed on: 02/07/23



## Abstract Archives of the RSNA, 2022

M2-QI-2

### Impact of Online MRI Safety Screening Questionnaires on Patient Workflow

Sunday, Nov. 27 9:00AM - 9:30AM Room: Learning Center - QI DPS

#### Participants

Sheena Chu, (*Presenter*) Nothing to Disclose

#### METHODS

Safety screening was made available via a patient web portal to all outpatient MRIs prior to appointment. At the check-in desk, all patients receive a pager to alert them when the technologist is ready to initiate their final safety screening and exam. Data were retrospectively collected for all adult outpatient MRIs for one year before and after implementation of online screening, using electronic health records and an analytics platform. Time between page and first MR image (time-to-image) was the primary endpoint. Time-to-image was compared among 3 groups: those who completed online screening, those who did not during the same 1-year period (synchronous control), and all patients from 1 year prior to implementation (historical control). Exams with missing data were excluded. Post-arrival cancellations (patients who checked in but did not undergo MRI) were noted. Student's t-test compared online-screening with each control group; Mood's median test compared medians and analysis of variance compared other values across all three groups;  $P < 0.05$  was considered significant.

#### RESULTS

Of 13,626 outpatient MRIs, 113 were excluded. Included were 6,199 and 7,314 MRIs, respectively pre- and post-online screening initiation; 1,931/7,314 completed online screening. Post-arrival cancellations were significantly lower in the online screening group than both controls (0.05% vs. 8.2% 9.4%,  $P < 0.001$ ). Online screening group demonstrated a lower median and standard deviation (std) time-to-image, and fewer outliers than both control groups ( $P < 0.05$ ). There was no significant difference in median or std of time-to-image between two control groups ( $P = 0.28, 0.24$  respectively). There was no difference in age, gender distribution, or fraction of patients with more than one MRI among the three groups (all  $P > 0.05$ ). \*Discussion We demonstrated a correlation between using an online safety screening and a reduction in post-arrival cancellations as well as workflow delays, with a significant reduction in the number of extreme delays. Our study benefited from a large patient cohort, use of analytic platforms, and two control groups; limitations included its retrospective nature and possible selection bias. Given these promising results, we will address these limitations in future evaluations in larger cohorts and by increasing the use of the online screening tool.

Printed on: 02/07/23



## Abstract Archives of the RSNA, 2022

M2-QI-3

### Image Quality Improvement of Digital Mammography Using an Artificial Intelligent Real Time Manage System

Sunday, Nov. 27 9:00AM - 9:30AM Room: Learning Center - QI DPS

#### Awards

##### Quality Improvement Reports Award

#### Participants

Ying Guo, (*Presenter*) Nothing to Disclose

#### METHODS

The AI system uses deep learning technology to detect nine types of abnormalities that will occur during breast X-ray examinations. The intelligent quality control system of mammography includes acquisition module, quality evaluation module and result display module. Image data of 200 cases of digital X-ray mammography before and after quality control were evaluated with the standards of Mammography Quality Standards Act (MQSA). If the image quality meets the diagnostic criteria, it is defined as grade A; if one of standards does not meet the diagnostic criteria, it is defined as grade B; if two, defined as grade C; if more than three, defined as invalid. The two groups were statistically compared before and after quality control for radiation dose, lesion detection rate, image quality and ratio of grade A, B and C.

#### RESULTS

After the implementation of quality control, rate of grade A increased from 78.5% to 91.4%. The rate of grade B decreased from 21.5% to 3.2%, and the rate of grade C decreased from 5.6% to 1.2%. The invalid rate remained unchanged at 0%. The lesion detection rate of micro calcification and structural distortion after quality control was higher than that before ( $P < 0.01$ ). The diagnostic sensitivity of breast lesions increased ( $P < 0.01$ ), and the specificity of breast lesions increased ( $P > 0.01$ ).  
\*Discussion Through quality control and management of breast X-ray imaging by using an artificial intelligent system, the image quality of digital mammography is significantly improved. The diagnostic accuracy of breast lesions increased, so as to provide high-quality image data for clinic. AI has great potential in evaluating breast position in digital mammography by reducing subjectivity. In the future, standardized and evidence-based criteria for definitions, understandings and assessment methods are needed to reach optimal image quality in mammography.

Printed on: 02/07/23



## Abstract Archives of the RSNA, 2022

M2-QI-4

### Minimizing Phone Call Interruptions in the Emergency Department Reading Room

Sunday, Nov. 27 9:00AM - 9:30AM Room: Learning Center - QI DPS

#### Participants

Hossam Elbelasi, MD, (*Presenter*) Nothing to Disclose

#### METHODS

Data was obtained from our campus network and infrastructure specialist. Initial pilot data showed a total of 1885 received phone calls in the emergency department reading room between 7/18/2021 and 8/17/2021. Root cause analysis was performed, and causes were grouped into 4 major categories. Teleradiology related communications was targeted for intervention. We aimed to decrease the total number of phone call interruptions by 30 % by November 2021. This was done through hiring a coordinator to handle Teleradiology related communications. We collected phone records over the course of 1 week before and after the coordinator was hired.

#### RESULTS

The total number of phone calls during the entire week decreased from 639 to 431 (32.5% decrease). The total time spent on the phone decreased from 853 to 724 minutes (15% decrease). During the coordinator shift (3pm-12am) the total number of phone calls has decreased by 27.5% (from 276 to 200) with average time spent on the phone during a single shift decreased from 52 mins to 36 mins (31%).\*Discussion Hiring a coordinator for the Teleradiology communication showed a significant reduction in phone call interruptions. We believe that hiring full time reading room assistant to handle communication to and from the reading room will lead to even significant decrease in interruption and increase radiologist's efficiency.

Printed on: 02/07/23



## Abstract Archives of the RSNA, 2022

M2-QI-5

### Implementing a Quality Improvement Framework to Reduce Missed Care Opportunities in Screening Mammography

Sunday, Nov. 27 9:00AM - 9:30AM Room: Learning Center - QI DPS

#### Participants

Adrian Jaramillo-Cardoso, MD, Boston, MA (*Presenter*) Nothing to Disclose

#### METHODS

Our initiative was guided by a modified health disparities research framework following four steps. Detecting: identifying the possible breakdown areas contributing to MCO by creating a process map with multiple stakeholders; and further organizing identified factors in a driver diagram. Understanding: Surveying our patient population to gain in-depth knowledge about the context of these factors and creating a pareto chart to see their individual contribution. Reducing: Employing an Impact/Effort Matrix we identified key interventions. Evaluating: Including tracking the data from our interventions and identifying challenges in the implementation of our equity efforts.

#### RESULTS

Key high priority and actionable intervention fronts identified included: 1. Culturally Sensitive Education: we developed educational multilingual (EN, SP, PT) videos and posters addressing SM concerns and providing information of what to expect of the process. 2. Reminder Process Improvement: Contact information was updated in our EMR but no significant statistical difference detected ( $p>0.05$ ), we developed the infrastructure to set up a text messaging reminder process that will include our educational video. 3. Increased Scheduling Flexibility: Weekend appointments were started as a pilot at one of our imaging sites. Showing a significant decrease in MCOs (6% during 4 weekends vs. 43% during weekdays). 4. Transportation: A ride-share program will be implemented to decrease the impact of transportation issues for high risk patients.\*Discussion We have developed a multi prong intervention front that attempts to address the most actionable contributing factors found to contribute to MCOs in two high risk sites within our system. Some of our interventions have provided outcomes to help our team reassess our efforts to allocate resources. We have found a modified health disparities research framework as a helpful guide on the design and implementation process of these efforts. Furthermore, using an iterative process including PDSA cycles has strongly informed the implementation of these interventions and increased our focus on mitigating the effect of health disparities in our patient population. Extending this approach to other QI initiatives holds great potential to aid in assuring health equity as a priority.

Printed on: 02/07/23



## Abstract Archives of the RSNA, 2022

M2-QI-6

### Improving Order to Completion Time for Urgent/STAT Inpatient and ED Pediatric MRI's Requiring Anesthesia/Sedation

Sunday, Nov. 27 9:00AM - 9:30AM Room: Learning Center - QI DPS

#### Awards

**Identified for RadioGraphics  
Quality Improvement Reports Award**

#### Participants

Jay K. Pahade, MD, Southport, CT (*Presenter*) Consultant, General Electric Company; Consultant, Clario Medical Imaging, Inc;

#### METHODS

Multidisciplinary team was created with radiology and pediatric quality and safety teams, MRI operations, pediatric anesthesia, MRI scheduling, and pediatric hospitalists. A3 and Model for Improvement methodology was used with flow map creations, fishbone analysis, 5 why problem solving and PDSA cycles. Interventions included revision of triage process, creating fixed add on MRI anesthesia appointment slots Monday-Friday, and linking pediatric anesthesia NPO orders to the MRI order in our electronic medical record (Epic, Verona WI)

#### RESULTS

Baseline (07/2020 to 10/2020) weekday mean O to B MRI time for urgent or stat inpatient/ED MRI requiring anesthesia/sedation was 1125 minutes with SD of 1198 minutes. Post intervention (09/2021-2/2022) mean O to B time decreased to 559 minutes (50% reduction) and SD decreased to 388 minutes (68% reduction). \*Discussion Delays in completing urgent/stat pediatric MRI with anesthesia are often secondary to disorganized triage process, lack of slot availability in MRI, non-compliance with NPO rules for anesthesia and unclear MRI start times. This QI project redesigned workflow with all relevant stakeholders, created new fixed slots for add-on pediatric MRI anesthesia cases, and integrated expected MRI start time and pediatric anesthesia NPO order set within the MRI order in our EHR. This resulted in 50% reduction in mean order to begin time and a more reproducible process with less variation (SD reduced by 68%). Our program has displayed good sustainment after last key driver implementation in 09/2021.

Printed on: 02/07/23



## Abstract Archives of the RSNA, 2022

M2-QI-7

### Implementation of Ferrous-Free Dress Code for MRI Personnel - An MRI Safety Initiative

Sunday, Nov. 27 9:00AM - 9:30AM Room: Learning Center - QI DPS

#### Participants

Julie Johnson, BS, ARRT, Atlanta, GA (*Presenter*) Nothing to Disclose

#### METHODS

We are a free-standing academic children's hospital. Baseline alarm rate for FMDS was obtained to evaluate frequency of passage of ferromagnetic items through our two most frequently used MRI scanners zone 4 doors. A task force was formed to establish a ferrous-free MRI environment with a focus on MRI personnel (technologists and sedation team) attire. Sub-committees of this task force included: ferrous-free clothing committee to provide resources to staff for ferrous free attire, process committee to screen and identify non-compliant staff, and an engagement committee to gain employee engagement. The engagement committee was also charged with developing a ferrous free campaign logo and posters to remind staff of go-live date. Ferrous-free dress code was implemented on October 11th 2021. Weekly alarm rates from the FMDS were evaluated to determine the impact of the ferrous-free attire initiative on alarm frequency. Processes were developed and implemented that required staff to stop and investigate any alarms produced by the doorway FMDS. Alarm rate data was collected weekly and reported to the task force monthly to serve as our metric.

#### RESULTS

Baseline alarm rate for the two most frequently used scanners in our pediatric facility was 172 (+/- 37) /week and 253 (+/- 59)/week. Since the implementation of ferrous-free attire, the alarm rate has trended down over time (attached plots) and is currently at 98 (+/- 29)/week and 74 (+/- 17)/week, respectively. Compliance of MRI personnel with ferrous free attire has been excellent. Most alarms are now caused due to non-MRI personnel attire, and proximity of moving zone 3 ferrous objects to the FMDS.\*Discussion Implementation of a ferrous-free attire for MRI personnel is feasible with high compliance, and is essential to decrease FMDS alarm rate and resultant alarm fatigue. In the next phase of this project, ferrous-free dress requirement will be expanded to all staff, patients and guardians entering the MRI suites.

Printed on: 02/07/23

## Abstract Archives of the RSNA, 2022

M2-QI-8

### Improving the Quality of Rectal MRI for Patients With Rectal Cancer Through an Iterative, Multi-Disciplinary Process With MR Physicists, Radiographers, and Radiologists

Sunday, Nov. 27 9:00AM - 9:30AM Room: Learning Center - QI DPS

#### Participants

Nikhil Shah, MEng, BSc, (*Presenter*) Nothing to Disclose

#### METHODS

We undertook 3 audits and 2 surveys to measure the image quality of our rectal MRI scans and radiographers' confidence in performing these scans. Each audit reviewed 1 month of rectal MRI scans for rectal adenocarcinoma. The first audit highlighted issues with bowel wall motion artefact and image resolution. The initial survey identified the training limitations of radiology personnel. To address these problems, we performed 4 interventions: 1) protocol development to optimise sequences, and testing involving MR physicists, radiographers and radiologists; 2) radiology personnel training to improve understanding of scanning technique and disease identification, measured by a second survey; 3) 2nd audit: image quality of rectal MRI scans measured against indicators, including (a) use of anterior saturation band, (b) appropriate coil positioning, (c) adequate tumour coverage, (d) imaging of mesorectum to L5/S1, and (e) use of antispasmodics; and 4) 3rd audit: a review of rectal MRI scans after introducing Buscopan and continued case review for radiographers.

#### RESULTS

Audit Audit results after interventions showed marked improvements in the quality of rectal MRI scans for diagnosis and management. Anterior saturation band used: 0% (1st audit), 100% (2nd audit) and 100% (3rd audit); appropriate coil positioning: 69% (1st audit), 92% (2nd audit) and 100% (3rd audit); adequate tumour coverage: 69% (1st audit), 83% (2nd audit) and 89% (3rd audit); mesorectum imaged to L5/S1: 38% (1st audit), 50% (2nd audit) and 78% (3rd audit); antispasmodic used: 0% (1st audit), 0% (2nd audit) and 67% (3rd audit). Survey Following training sessions, there was an increase in radiographers' confidence in identifying rectal cancer and orientating imaging to the axis of the tumour.\*Discussion A limitation of our project was that we considered only patients with adenocarcinoma. However, patients with squamous cell carcinoma also require this level of imaging, as well as additional sequences to study the nature of the inguinal nodes. Our project resulted in significant improvements to the quality of our rectal MRI scans and our team's technical performance. It has optimised the staging of rectal cancer in our department and led to increased confidence in multidisciplinary decision making.

Printed on: 02/07/23



## Abstract Archives of the RSNA, 2022

M5A-QI

### Quality Improvement Reports Monday Poster Discussions - A

Monday, Nov. 28 12:15PM - 12:45PM Room: Learning Center - QI DPS

#### Sub-Events

#### **M5A-QI-1 Large Scale Implementation of an Artificial Intelligence Software to Improve Patient Experience and Enhance Productivity in Magnetic Resonance Departments**

##### Participants

Augusto B. Antunes, MD, MSc, Nova Lima, Brazil (*Presenter*) Nothing to Disclose

##### METHODS

The implemented software is fully automatized and compatible with any MRI suite, operating on a local server without outside traffic of patient data. It improves the image's signal-to-noise ratio by using a proprietary volumetric machine-learning assisted image enhancement algorithm. The software was implemented in 2021 in 18 MRI suites located in different clinics pertaining to our teleradiology group, in 4 states in Brazil. Adherence to the optimized protocols increased throughout the year in these machines, reaching in December up to 70% of the imaging protocols of each body region

##### RESULTS

We compared scan length reduction, patient recall percentages, and the number of newly created slots for patient scheduling in the periods during and after the implementation of the software. An average reduction of 24% in scan length was observed in all imaging protocols in which the software was being used (range 2% to 86%), meaning a reduction from an average of 16 minutes and 14 seconds per scan to 12 minutes and 17 seconds. In 2021, we performed a total of 724476 MRI studies (an average of 60373 studies per month). On average, 667 patients (1,1%) were recalled each month due to various reasons, but mainly to administer intravenous contrast or to repeat sequences that were spoiled by motion artifacts. After software implementation, the patient's recall number dropped to an average of 458 (0,7%). In addition, with scan length reduction we were able to offer more slots for patient scheduling, going from an average of 487 available machine/hours before software installation to 617 after its installation (an increase of 27%).\*Discussion This analysis was limited to a purely operational angle, regarding how improvements in MRI acquisition can lead to better patient experience and enhanced productivity. Patient satisfaction or increase in the total number of patients scanned per month, among other metrics, depends not only on these improvements in protocols but also on a myriad of factors such as confirmation procedures, bureaucratic processes, season, etc

#### **M5A-QI-2 A Novel Breast Imaging Intake Survey Inclusive of Transgender and Non-binary Populations to Foster Inclusion, Improve Breast Care and Better Understand Breast Cancer Risk and Outcomes**

##### Participants

David Ly, (*Presenter*) Nothing to Disclose

##### METHODS

At our institution, patients who present for breast imaging complete an iPad-administered breast imaging history and breast cancer risk assessment survey. Using the modified International Breast Cancer Intervention Study (IBIS) model, the lifetime risk of developing breast cancer is estimated and additional clinical and family history that may impact breast care and future breast imaging is collected. Under the original survey workflow, patients are identified as either "male" or "female" and complete a corresponding gender-specific survey. The previous existing survey does not capture information specific to TGNB patients. In conjunction with transgender health experts and the MagView survey software development team, we developed a more comprehensive survey to better capture the experiences of TGNB patients.

##### RESULTS

We revised the survey using gender-inclusive language and developed four different versions to allow patients to separately self-report their sex assigned at birth and gender identity. In addition, we added questions regarding relevant medical history such as exposure to certain hormones and prior pertinent surgical history such as gender-affirming chest/breast surgery that are concordant with six gender-identity groups.\*Discussion To our knowledge, this breast cancer risk assessment survey is the first among radiology departments to collect more accurate information among TGNB patients. Our survey may serve as a model for other institutions to develop gender-inclusive surveys. Moreover, long-term collection of this inclusive data by imaging centers will enhance the dataset available to improve breast care and better understand breast cancer risk and outcomes among TGNB populations.

#### **M5A-QI-3HC Are we overdoing it? Optimizing Utilization of Renal Ultrasound in Patients with Recent Cross-Sectional Imaging**

##### Awards

Identified for RadioGraphics

##### Participants

Selin Ocal, BS, Mineola, NY (*Presenter*) Nothing to Disclose

## **METHODS**

This study was identified as IRB-exempt. 4 trainees (1 medical student, 3 radiology residents) and 2 attending radiologists reviewed electronic medical record data of patients with RUS orders within identified pre- and post-intervention periods. Information documented included: recent CSI within 48 hours, study indication, ordering department, and clinical benefit. Study intervention involved ultrasound technologist (UST) identification of RUS orders in patients with CSI in the past 48 hours and subsequent discussion with ordering team on benefit of RUS given CSI, with cancellation of orders determined to be low-yield. Pre- and post-intervention data was compared via Chi-square test.

## **RESULTS**

Of the pre-intervention group N=210, 9.04% (19/210) of RUS orders were for patients who had undergone CT/MRI CSI in the previous 48 hours. 100% of these RUS orders were for clinical indications already answered on previous imaging. In the post-intervention group (N=714), 6.02% (43/714) of orders were for patients who had undergone recent CSI. For those with recent imaging in the post-intervention group, only 32.56% of US orders were deemed clinically beneficial, as the remaining 67.44% were for indications already answered on CSI studies. Of these post-intervention orders for patients with recent imaging, a majority of 62.79% (27/43) were ordered by internal medicine providers. The percentage of RUS orders for patients with recent CSI decreased from 9.05% to 6.02% with this intervention ( $p=0.12$ ). \*Discussion Intervention of UST review of RUS orders for patients who have undergone CSI within the past 48 hours provides some benefit in reducing redundant RUS studies, though not statistically significant. Following analysis of these findings, a best-practice advisory (BPA) tool was implemented for ordering clinicians that notifies of a recent CT or MRI, and confirms his/her decision to pursue the order. This tool also notifies the receiving UST of recent imaging and encourages communication with the clinician. In the first month of BPA use, 34.5% of RUS orders were canceled after BPA was triggered. Please visit the Learning Center to also view this presentation in hardcopy format.

### **M5A-QI-4 There's Waldo! Standardized Workflow for Optimizing Communication for Retained Surgical Instruments**

Participants

Sheila C. Berlin, MD, Cleveland, OH (*Presenter*) Nothing to Disclose

## **METHODS**

This project was performed at a large academic medical center where call-to-OR times (RSI TAT) for RSI radiographs were inconsistent and often exceeded our target limit of 15 minutes. Technologists (RT) and radiologists were surveyed to determine major factors contributing to delays. They identified that details about the type, expected appearance, and likely location of the potential RSI were frequently missing. This information was noted to be critical given intraoperative radiographs are frequently limited by overlying non-biological material in the surgical field, incomplete visualization of the relevant anatomy and suboptimal technique in a fully-draped patient. To address these problems, a multidisciplinary team of radiologists, surgeons and RT's designed a standardized workflow to optimize identification and minimize RSI TAT. Key workflow components included: 1) two alert notification, 2) a simple OR checklist, and 3) a sample radiograph of the missing RSI (if any) to accompany the intraoperative radiograph. An alert is sent to the radiologist approximately 10 minutes prior to ("RSI Radiograph in Progress") as well as upon image transfer to PACS. The checklist sent to PACS notes: 1) specific surgical procedure 2) anatomy for potential RSI discovery and 3) specific missing item (if any). RT records: 1) time of the final alert and 2) time of the radiologist call to the OR. The impact of these interventions was assessed by comparing 40 consecutive RSI TAT for cases prior to workflow implementation to 40 consecutive RSI TAT for cases following workflow implementation. RSI TAT was measured as the time in minutes from radiologist notification of exam completion to the time a result was called to the OR.

## **RESULTS**

Following implementation of the standardized workflow, the mean TAT for communication with the OR decreased from  $17.7 \pm 5.7$  minutes to  $4.3 \pm 1.9$  minutes. No RSI were reported prior to the workflow; one RSI (white towel with opaque ribbon) was identified using the standardized workflow. \*Discussion Our workflow expedited time to surgical site closure by improving TAT for RSI radiograph reporting. A limitation of this study is that we did not have a process (e.g. follow-up imaging) for determining accuracy of identification of RSI. Using the core process improvement tools of standardization and communication, we developed a clear and detailed workflow to expedite results reporting for RSI radiographs.

### **M5A-QI-5 Use of an Auto-Protocol" Workflow to Decrease Provider and Technologist Protocoling Burden in Radiology**

Participants

Daniella Asch, MD, New Haven, CT (*Presenter*) Nothing to Disclose

## **METHODS**

A team composed of subspecialty radiologists, CT technologists and quality improvement specialists formed consensus on CT studies for which manual protocol assignment provides little value. An auto-protocol workflow optimization was created in the EHR (Epic Systems Corp., Verona, WI) using human-centered design principles and iterative Plan-Do-Study-Act cycles. These selected orders were removed from radiologist protocol worklists with programming to automatically label the studies as auto-protocol eligible. A new column was created on CT technologist worklists with a designated icon mapped to the auto-protocol codes and language inserted into protocol instructions stating, "perform as ordered per protocol." This process was tested on four pilot codes and then expanded to include all eligible codes. Percent protocol reduction for all CTs and study order to begin (O-B) time for ED studies were analyzed before and after implementation. Time to protocol a case was measured by stopwatch via human observation.

## **RESULTS**

28% (53/192) of CT codes were selected as eligible for auto-protocol. Baseline data revealed 10,185/13,093 (78%) of all ordered CT scans were manually protocolled. Post intervention data revealed 5,548/10,259 (54%) of exams were manually protocolled (24% absolute, 30% relative reduction from baseline). Percentage of CT orders requiring a manual protocol is depicted in the run chart. Median O-B time for ED CTs decreased from 61 to 56 minutes (8% relative improvement) post intervention. Based on measured mean time to protocol a CT of 15 seconds, an estimated 170 work hours are saved annually. \*Discussion This QI project used an automated EHR driven algorithm to reduce protocoling burden and decrease ED CT order-begin time. A limitation is potential for incorrectly ordered exams to result in incorrect or suboptimal imaging. In recognition of this, CT codes were carefully selected for

inclusion and technologists were encouraged to discuss any discrepancies between the order and provided indication with the appropriate radiology service. Following success at our tertiary center, the initiative was expanded to include more CT codes and has been implemented throughout our health system delivery networks. Work is underway to adapt the new auto-protocol workflow to MRI.

#### **M5A-QI-6 The Effect of Radiologist-Patient Interaction: Are Patients Benefiting from Patient-Centered Communication Before Prostate Image-Guided Interventions?**

Participants

Zoe D'Costa, BA, Skillman, NJ (*Presenter*) Nothing to Disclose

#### **METHODS**

A single-arm pre- and post-intervention study involving 5-10 minute radiologist consultations was performed. Virtual and in-person consultations took place in the pre-procedure holding area while patients awaited image-guided prostate biopsy and entailed basic anatomy, identification of prostate lesions on MRI and their implications. We utilized 5-point rating scales to evaluate patients' understanding of prostate MRI, prostate cancer, and anxiety levels before and after consultations. We also evaluated patients' understanding of the role of radiologists, level of satisfaction with the consultation and preference for receiving MRI results. Responses with ratings (1-5 scale) were analyzed with generalized linear mixed models (GLMM) with cumulative-logit link function. Dichotomous responses were analyzed with GLMM with logit link function. Statistical models were adjusted for age and race/ethnicity.

#### **RESULTS**

25 patients were included in the analysis. All patients reported satisfaction with the radiologist consultation. 21 patients (88%) stated they were very likely to return to our department knowing the availability to speak to a radiologist about their MRI was an option. The intervention was associated with significantly higher levels of self-reported understanding of prostate cancer ( $p=.04$ ) and significantly decreased levels of anxiety prior to biopsy ( $p=.003$ ). A trend towards improved understanding of the role of the radiologist and MRI was observed post-consultation, though statistically insignificant ( $p=0.134$  and  $p=0.2$ , respectively). Most patients reported preference for discussing imaging results with a radiologist or both the radiologist and referrer ( $n=21$ , 88%), however the intervention did not have a statistically significant impact on patients' preference ( $p=0.1$ ).*\*Discussion* Our study seeking to understand the effects of radiology consultation showed the intervention improved quality of care by improving patient's understanding of their illness and by lowering patient anxiety prior to image-guided prostate biopsy. While our study had limited sample size, the findings are supportive of action in favor of implementation of this program, particularly given minimal time requirements and virtual capabilities.

#### **M5A-QI-7HC Optimization of Whole-Body CT Technique for Trauma Patients Presenting to a Level-One Trauma Center**

Participants

Nnamdi Udeh, MD, (*Presenter*) Nothing to Disclose

#### **METHODS**

The whole-body CT protocol consists of an unenhanced CT of the head and cervical spine, administration of a split contrast bolus with a 1-minute delay, and contrast-enhanced CT of the chest, abdomen, and pelvis. By comparison, organ-specific imaging combines 4 standard protocols with a single-phase contrast bolus. 100 patients, 50 with whole-body CTs and 50 with organ-specific scans, were included in a retrospective analysis. 4 attending radiologists rated image quality and indicated whether traumatic injury was present. Attenuation values of the liver, spleen and aorta were concurrently reported. Statistical analyses to assess for differences in image quality and injury detection included kappa statistics for observer agreement and the Kruskal Wallis test for attenuation measurements.

#### **RESULTS**

When compared to organ-specific imaging, there was no significant difference in image quality for the whole-body CT protocol (both protocols with median 3.25 on 4-point scale, Kruskal Wallis test,  $p = 0.70$ ). There was no significant difference between the two protocols in the rate of injury detection or the interobserver agreement on injury detection (median weighted kappa for protocol 1 = 0.50, 95% CI 0.16-0.85; protocol 2 = 0.47, 95% CI 0.20-0.75). Attenuation values were not significantly different between both protocols for the liver, spleen, or aorta (Kruskal Wallis test,  $p = 0.07$ ).*\*Discussion* The implementation of a whole-body CT protocol maintains image quality and allows for the acceleration of polytrauma imaging. Please visit the Learning Center to also view this presentation in hardcopy format.

Printed on: 02/07/23



## Abstract Archives of the RSNA, 2022

M5A-QI-1

### Large Scale Implementation of an Artificial Intelligence Software to Improve Patient Experience and Enhance Productivity in Magnetic Resonance Departments

Monday, Nov. 28 12:15PM - 12:45PM Room: Learning Center - QI DPS

#### Participants

Augusto B. Antunes, MD, MSc, Nova Lima, Brazil (*Presenter*) Nothing to Disclose

#### METHODS

The implemented software is fully automatized and compatible with any MRI suite, operating on a local server without outside traffic of patient data. It improves the image's signal-to-noise ratio by using a proprietary volumetric machine-learning assisted image enhancement algorithm. The software was implemented in 2021 in 18 MRI suites located in different clinics pertaining to our teleradiology group, in 4 states in Brazil. Adherence to the optimized protocols increased throughout the year in these machines, reaching in December up to 70% of the imaging protocols of each body region

#### RESULTS

We compared scan length reduction, patient recall percentages, and the number of newly created slots for patient scheduling in the periods during and after the implementation of the software. An average reduction of 24% in scan length was observed in all imaging protocols in which the software was being used (range 2% to 86%), meaning a reduction from an average of 16 minutes and 14 seconds per scan to 12 minutes and 17 seconds. In 2021, we performed a total of 724476 MRI studies (an average of 60373 studies per month). On average, 667 patients (1,1%) were recalled each month due to various reasons, but mainly to administer intravenous contrast or to repeat sequences that were spoiled by motion artifacts. After software implementation, the patient's recall number dropped to an average of 458 (0,7%). In addition, with scan length reduction we were able to offer more slots for patient scheduling, going from an average of 487 available machine/hours before software installation to 617 after its installation (an increase of 27%).\*Discussion This analysis was limited to a purely operational angle, regarding how improvements in MRI acquisition can lead to better patient experience and enhanced productivity. Patient satisfaction or increase in the total number of patients scanned per month, among other metrics, depends not only on these improvements in protocols but also on a myriad of factors such as confirmation procedures, bureaucratic processes, season, etc

Printed on: 02/07/23



## Abstract Archives of the RSNA, 2022

M5A-QI-2

### **A Novel Breast Imaging Intake Survey Inclusive of Transgender and Non-binary Populations to Foster Inclusion, Improve Breast Care and Better Understand Breast Cancer Risk and Outcomes**

Monday, Nov. 28 12:15PM - 12:45PM Room: Learning Center - QI DPS

#### **Participants**

David Ly, (*Presenter*) Nothing to Disclose

#### **METHODS**

At our institution, patients who present for breast imaging complete an iPad-administered breast imaging history and breast cancer risk assessment survey. Using the modified International Breast Cancer Intervention Study (IBIS) model, the lifetime risk of developing breast cancer is estimated and additional clinical and family history that may impact breast care and future breast imaging is collected. Under the original survey workflow, patients are identified as either "male" or "female" and complete a corresponding gender-specific survey. The previous existing survey does not capture information specific to TGNB patients. In conjunction with transgender health experts and the MagView survey software development team, we developed a more comprehensive survey to better capture the experiences of TGNB patients.

#### **RESULTS**

We revised the survey using gender-inclusive language and developed four different versions to allow patients to separately self-report their sex assigned at birth and gender identity. In addition, we added questions regarding relevant medical history such as exposure to certain hormones and prior pertinent surgical history such as gender-affirming chest/breast surgery that are concordant with six gender-identity groups.\*Discussion To our knowledge, this breast cancer risk assessment survey is the first among radiology departments to collect more accurate information among TGNB patients. Our survey may serve as a model for other institutions to develop gender-inclusive surveys. Moreover, long-term collection of this inclusive data by imaging centers will enhance the dataset available to improve breast care and better understand breast cancer risk and outcomes among TGNB populations.

Printed on: 02/07/23



## Abstract Archives of the RSNA, 2022

M5A-QI-3HC

### Are we overdoing it? Optimizing Utilization of Renal Ultrasound in Patients with Recent Cross-Sectional Imaging

Monday, Nov. 28 12:15PM - 12:45PM Room: Learning Center - QI DPS

#### Awards

Identified for RadioGraphics

#### Participants

Selin Ocal, BS, Mineola, NY (Presenter) Nothing to Disclose

#### METHODS

This study was identified as IRB-exempt. 4 trainees (1 medical student, 3 radiology residents) and 2 attending radiologists reviewed electronic medical record data of patients with RUS orders within identified pre- and post-intervention periods. Information documented included: recent CSI within 48 hours, study indication, ordering department, and clinical benefit. Study intervention involved ultrasound technologist (UST) identification of RUS orders in patients with CSI in the past 48 hours and subsequent discussion with ordering team on benefit of RUS given CSI, with cancellation of orders determined to be low-yield. Pre- and post-intervention data was compared via Chi-square test.

#### RESULTS

Of the pre-intervention group N=210, 9.04% (19/210) of RUS orders were for patients who had undergone CT/MRI CSI in the previous 48 hours. 100% of these RUS orders were for clinical indications already answered on previous imaging. In the post-intervention group (N=714), 6.02% (43/714) of orders were for patients who had undergone recent CSI. For those with recent imaging in the post-intervention group, only 32.56% of US orders were deemed clinically beneficial, as the remaining 67.44% were for indications already answered on CSI studies. Of these post-intervention orders for patients with recent imaging, a majority of 62.79% (27/43) were ordered by internal medicine providers. The percentage of RUS orders for patients with recent CSI decreased from 9.05% to 6.02% with this intervention ( $p=0.12$ ). \*Discussion Intervention of UST review of RUS orders for patients who have undergone CSI within the past 48 hours provides some benefit in reducing redundant RUS studies, though not statistically significant. Following analysis of these findings, a best-practice advisory (BPA) tool was implemented for ordering clinicians that notifies of a recent CT or MRI, and confirms his/her decision to pursue the order. This tool also notifies the receiving UST of recent imaging and encourages communication with the clinician. In the first month of BPA use, 34.5% of RUS orders were canceled after BPA was triggered. Please visit the Learning Center to also view this presentation in hardcopy format.

Printed on: 02/07/23

## Abstract Archives of the RSNA, 2022

M5A-QI-4

### There's Waldo! Standardized Workflow for Optimizing Communication for Retained Surgical Instruments

Monday, Nov. 28 12:15PM - 12:45PM Room: Learning Center - QI DPS

#### Participants

Sheila C. Berlin, MD, Cleveland, OH (*Presenter*) Nothing to Disclose

#### METHODS

This project was performed at a large academic medical center where call-to-OR times (RSI TAT) for RSI radiographs were inconsistent and often exceeded our target limit of 15 minutes. Technologists (RT) and radiologists were surveyed to determine major factors contributing to delays. They identified that details about the type, expected appearance, and likely location of the potential RSI were frequently missing. This information was noted to be critical given intraoperative radiographs are frequently limited by overlying non-biological material in the surgical field, incomplete visualization of the relevant anatomy and suboptimal technique in a fully-draped patient. To address these problems, a multidisciplinary team of radiologists, surgeons and RT's designed a standardized workflow to optimize identification and minimize RSI TAT. Key workflow components included: 1) two alert notification, 2) a simple OR checklist, and 3) a sample radiograph of the missing RSI (if any) to accompany the intraoperative radiograph. An alert is sent to the radiologist approximately 10 minutes prior to ("RSI Radiograph in Progress") as well as upon image transfer to PACS. The checklist sent to PACS notes: 1) specific surgical procedure 2) anatomy for potential RSI discovery and 3) specific missing item (if any). RT records: 1) time of the final alert and 2) time of the radiologist call to the OR. The impact of these interventions was assessed by comparing 40 consecutive RSI TAT for cases prior to workflow implementation to 40 consecutive RSI TAT for cases following workflow implementation. RSI TAT was measured as the time in minutes from radiologist notification of exam completion to the time a result was called to the OR.

#### RESULTS

Following implementation of the standardized workflow, the mean TAT for communication with the OR decreased from 17.7±5.7 minutes to 4.3±1.9 minutes. No RSI were reported prior to the workflow; one RSI (white towel with opaque ribbon) was identified using the standardized workflow.\*Discussion Our workflow expedited time to surgical site closure by improving TAT for RSI radiograph reporting. A limitation of this study is that we did not have a process (e.g. follow-up imaging) for determining accuracy of identification of RSI. Using the core process improvement tools of standardization and communication, we developed a clear and detailed workflow to expedite results reporting for RSI radiographs.

Printed on: 02/07/23



## Abstract Archives of the RSNA, 2022

M5A-QI-5

### Use of an Auto-Protocol Workflow to Decrease Provider and Technologist Protocols Burden in Radiology

Monday, Nov. 28 12:15PM - 12:45PM Room: Learning Center - QI DPS

#### Participants

Daniella Asch, MD, New Haven, CT (*Presenter*) Nothing to Disclose

#### METHODS

A team composed of subspecialty radiologists, CT technologists and quality improvement specialists formed consensus on CT studies for which manual protocol assignment provides little value. An auto-protocol workflow optimization was created in the EHR (Epic Systems Corp., Verona, WI) using human-centered design principles and iterative Plan-Do-Study-Act cycles. These selected orders were removed from radiologist protocol worklists with programming to automatically label the studies as auto-protocol eligible. A new column was created on CT technologist worklists with a designated icon mapped to the auto-protocol codes and language inserted into protocol instructions stating, "perform as ordered per protocol." This process was tested on four pilot codes and then expanded to include all eligible codes. Percent protocol reduction for all CTs and study order to begin (O-B) time for ED studies were analyzed before and after implementation. Time to protocol a case was measured by stopwatch via human observation.

#### RESULTS

28% (53/192) of CT codes were selected as eligible for auto-protocol. Baseline data revealed 10,185/13,093 (78%) of all ordered CT scans were manually protocolled. Post intervention data revealed 5,548/10,259 (54%) of exams were manually protocolled (24% absolute, 30% relative reduction from baseline). Percentage of CT orders requiring a manual protocol is depicted in the run chart. Median O-B time for ED CTs decreased from 61 to 56 minutes (8% relative improvement) post intervention. Based on measured mean time to protocol a CT of 15 seconds, an estimated 170 work hours are saved annually.\*Discussion This QI project used an automated EHR driven algorithm to reduce protocoling burden and decrease ED CT order-begin time. A limitation is potential for incorrectly ordered exams to result in incorrect or suboptimal imaging. In recognition of this, CT codes were carefully selected for inclusion and technologists were encouraged to discuss any discrepancies between the order and provided indication with the appropriate radiology service. Following success at our tertiary center, the initiative was expanded to include more CT codes and has been implemented throughout our health system delivery networks. Work is underway to adapt the new auto-protocol workflow to MRI.

Printed on: 02/07/23

## Abstract Archives of the RSNA, 2022

M5A-QI-6

### The Effect of Radiologist-Patient Interaction: Are Patients Benefiting from Patient-Centered Communication Before Prostate Image-Guided Interventions?

Monday, Nov. 28 12:15PM - 12:45PM Room: Learning Center - QI DPS

#### Participants

Zoe D'Costa, BA, Skillman, NJ (*Presenter*) Nothing to Disclose

#### METHODS

A single-arm pre- and post-intervention study involving 5-10 minute radiologist consultations was performed. Virtual and in-person consultations took place in the pre-procedure holding area while patients awaited image-guided prostate biopsy and entailed basic anatomy, identification of prostate lesions on MRI and their implications. We utilized 5-point rating scales to evaluate patients' understanding of prostate MRI, prostate cancer, and anxiety levels before and after consultations. We also evaluated patients' understanding of the role of radiologists, level of satisfaction with the consultation and preference for receiving MRI results. Responses with ratings (1-5 scale) were analyzed with generalized linear mixed models (GLMM) with cumulative-logit link function. Dichotomous responses were analyzed with GLMM with logit link function. Statistical models were adjusted for age and race/ethnicity.

#### RESULTS

25 patients were included in the analysis. All patients reported satisfaction with the radiologist consultation. 21 patients (88%) stated they were very likely to return to our department knowing the availability to speak to a radiologist about their MRI was an option. The intervention was associated with significantly higher levels of self-reported understanding of prostate cancer ( $p=.04$ ) and significantly decreased levels of anxiety prior to biopsy ( $p=.003$ ). A trend towards improved understanding of the role of the radiologist and MRI was observed post-consultation, though statistically insignificant ( $p=0.134$  and  $p=0.2$ , respectively). Most patients reported preference for discussing imaging results with a radiologist or both the radiologist and referrer ( $n=21$ , 88%), however the intervention did not have a statistically significant impact on patients' preference ( $p=0.1$ ).  
\*Discussion Our study seeking to understand the effects of radiology consultation showed the intervention improved quality of care by improving patient's understanding of their illness and by lowering patient anxiety prior to image-guided prostate biopsy. While our study had limited sample size, the findings are supportive of action in favor of implementation of this program, particularly given minimal time requirements and virtual capabilities.

Printed on: 02/07/23



## Abstract Archives of the RSNA, 2022

M5A-QI-7HC

### Optimization of Whole-Body CT Technique for Trauma Patients Presenting to a Level-One Trauma Center

Monday, Nov. 28 12:15PM - 12:45PM Room: Learning Center - QI DPS

#### Participants

Nnamdi Udeh, MD, (*Presenter*) Nothing to Disclose

#### METHODS

The whole-body CT protocol consists of an unenhanced CT of the head and cervical spine, administration of a split contrast bolus with a 1-minute delay, and contrast-enhanced CT of the chest, abdomen, and pelvis. By comparison, organ-specific imaging combines 4 standard protocols with a single-phase contrast bolus. 100 patients, 50 with whole-body CTs and 50 with organ-specific scans, were included in a retrospective analysis. 4 attending radiologists rated image quality and indicated whether traumatic injury was present. Attenuation values of the liver, spleen and aorta were concurrently reported. Statistical analyses to assess for differences in image quality and injury detection included kappa statistics for observer agreement and the Kruskal Wallis test for attenuation measurements.

#### RESULTS

When compared to organ-specific imaging, there was no significant difference in image quality for the whole-body CT protocol (both protocols with median 3.25 on 4-point scale, Kruskal Wallis test,  $p = 0.70$ ). There was no significant difference between the two protocols in the rate of injury detection or the interobserver agreement on injury detection (median weighted kappa for protocol 1 = 0.50, 95% CI 0.16-0.85; protocol 2 = 0.47, 95% CI 0.20-0.75). Attenuation values were not significantly different between both protocols for the liver, spleen, or aorta (Kruskal Wallis test,  $p = 0.07$ ). \*Discussion The implementation of a whole-body CT protocol maintains image quality and allows for the acceleration of polytrauma imaging. Please visit the Learning Center to also view this presentation in hardcopy format.

Printed on: 02/07/23

## Abstract Archives of the RSNA, 2022

M5B-QI

### Quality Improvement Reports Monday Poster Discussions - B

Monday, Nov. 28 12:45PM - 1:15PM Room: Learning Center - QI DPS

#### Sub-Events

#### **M5B-QI-2 To Investigate the Effect of Combined DLIR Reconstruction Algorithm With Different Concentrations of Contrast Agents on Coronary CTA Image Quality**

##### Participants

Lijuan Zhu, (*Presenter*) Nothing to Disclose

##### METHODS

Thirty patients who underwent low-voltage coronary CT angiography (CCTA) with a 256-row wide-body detector CT scanner (Revolution Apex CT; GE Healthcare) in our hospital from September 2021 to January 2022 were collected and divided into two groups with 15 cases in each group according to the concentration of contrast agent used. Contrast agent concentration in group 320mg/mL, contrast agent concentration in group B 370mg/mL (conventional), group A medium-grade (DLIR-M), high-grade (DLIR-H) deep learning algorithm for reconstruction, group B using clinical routine 40% weight Adaptive Statistical Iterative Reconstruction (ASIR-V). The image noise of the aortic root and proximal main coronary artery of each group of images was recorded, and the Signal-to-Noise Ratio (SNR) and Contrast-to-Noise Ratio (CNR) were calculated. Subjective image quality was rated on a 5-point scale by two diagnostic radiologists with more than 5 years of experience.

##### RESULTS

1) Compared with ASIR-V40%, both DLIR-M and DLIR-H performed better noise reduction effect (P value <0.05). The SNR and CNR of DLIR-M and DLIR-H groups were significantly improved by 69.91% %, 67.91% and 120.25%, 119.85%, compared to ASIR-40%, respectively. 2) The scoring results of two observers, physician A and physician B, showed that the noise reduction level increased with the increase of the deep learning image reconstruction technology (DLIR) (P value < 0.05), and both observers believed that the diagnosis effect was the best The one is DLIR-H, and its subjective image quality is significantly improved by 40% compared with ASIR-V, which is 28.52% higher.\*Discussion Compare to the CCTA scanning scheme of 370mg/mL contrast agent combined with ASIR-V40% algorithm, the results show that the SNR and CNR of using 320mg/mL contrast agent combined with DLIR-H algorithm group was higher than those of the high contrast agent concentration group, indicating that DLIR had better image correction ability, which has higher clinical application value.

#### **M5B-QI-3 Building Radiology Residents' Confidence in Managing Contrast Reactions: Our Institution's First Ever High-Fidelity Contrast Reaction Simulation**

##### Participants

Kara Demarco, MD, (*Presenter*) Nothing to Disclose

##### METHODS

In partnership with the Simulation center, we created our institution's first ever High-Fidelity Contrast Reaction Simulation, in which three scenario algorithms were created to simulate real-life adverse contrast reactions. Learners were first given a short brief on potential reactions, and how to identify and respond to such patient presentations. They were then separated into three groups, rotating through each simulation. The simulations ranged from mild to severe reactions, with the latter evolving into a full code. During the simulations, the residents were challenged to interpret vitals, perform physical examinations, and determine next steps and management. The addition of bronchospasm reaction deliberately extends beyond the ACLS algorithm to challenge learners to identify a reaction that is more specific to contrast reactions, and may occur with asthmatics, particularly children. Each scenario was followed by an immediate debrief emphasizing the salient points of the specific reaction and its safe management.

##### RESULTS

Using a 10-point scale, participants were asked 7 questions surveying their comfort and knowledge level regarding the identification and management of contrast reactions. Prior to the simulation, the average was 4.3 out of 10. After the simulation, the average was 8.3 out of 10.\*Discussion Reactions to contrast media are uncommon but do happen, and often the radiology resident is the first physician to assess the patient. Acting out the management of such reactions is more effective than reading how to do so, and this simulation proved to be a useful endeavor in building the residents' competency. Moreover, it encouraged teamwork within a group of residents that are more accustomed to operating alone. Our intention is to continue this simulation with future classes, and expand the participation to staff radiologists and technologists, all of whom may be the first provider in saving an anaphylactic patient's life.

#### **M5B-QI-4 Benefits of a Composite Report Incorporating Interactive Multimedia Reporting Principles**

##### Participants

David J. Vining, MD, (*Presenter*) Royalties, Bracco Group;CEO, VisionSR, Inc;Stockholder, VisionSR, Inc

##### METHODS

We developed an IMR solution that records medical events (e.g., radiological findings, surgical procedures) and voice descriptions of those events, tags the information with metadata using natural language processing, and assembles an IMR report with related data linked in timelines and presented as a "composite report." A composite report presents the most recent information for each anatomical site of disease, regardless of modality, to create a holistic view of a patient. When a user clicks on a finding, the history of that entity is presented with images, graphs, tables, and related information.

## RESULTS

To date the system has been used to generate 2505 composite reports from 1509 patients with a total of 12,943 findings comprising 37,769 items. In this composite reporting concept, a "finding" represents a timeline of connected "items" from individual exams and medical events. The average timeline length consists of 4 items with the longest comprising 24 items.\*Discussion Disparate information in an electronic health record (EHR) resides in silos related to the specialty that generated the source data (e.g., radiology, pathology, laboratory, surgery). The review of historical information by radiologists and clinicians in order to mentally construct a history of disease and treatment is often tedious and time-consuming. An IMR composite report can assimilate data from disparate sources and present the information in a logical fashion using visual displays to efficiently communicate information. Quantitative disease graphs assembled from the entire compendium of radiological data can reveal insights that may not be evident when a radiologist only compares a current exam to a limited number of prior exams. The use of metadata to tag related items enables data mining for the derivation of medical outcomes. Furthermore, a composite report has the potential to improve safety by mitigating discrepant results. For example, when a pathologist reports a left upper lung biopsy but that information is linked to a radiological exam indicating a right upper lung biopsy, the system immediately alerts the report author to make necessary corrections. A composite report represents a radical change from traditional independent medical reports, and as such it provides a means to connect data and cultivate knowledge.

### **M5B-QI-5 Wait, Where are the Apices? Improving Portable Chest Xray Techniques Through Image Review and Education of Radiology Technologists**

Participants  
Kevin Gilotra, Stony Brook, NY (*Presenter*) Nothing to Disclose

## METHODS

From July 12, 2021 to July 25, 2021 pCXRs were evaluated by radiology residents for failures in technical image quality affecting their use for diagnostic interpretation. Figure 1 highlights the criteria used to assess image quality. To address the baseline frequency of technical quality errors, three programs aiming to improve the quality of pCXRs were implemented. First, a curriculum led by experienced technicians didactic sessions were provided to radiology technologists. Second, nursing staff was recruited to assist radiology technologists with patient positioning when obtaining images for pCXRs. Finally, internal medicine residents verified that films were interpretable for pathology once images had been collected. Figure 1 was subsequently used by radiology residents to assess post-intervention films.

## RESULTS

Technical errors were present in 231 of the 500 pre-intervention radiographs and in 126 of the 287 post-intervention studies. Using a 0 to 3 scale for evaluating patient rotation (0 being no rotation and 3 being severe rotation), a 0.46-point reduction was observed post-intervention ( $p < 0.005$ ). There was also a 25% reduction in films with rotation in the post-intervention pCXRs, but no percentage change in pCXRs with mild rotation. The number of pCXRs with obscured anatomy declined by 20.9% post-intervention. A potential missed diagnosis was observed in 43.5% of studies pre-intervention in comparison to only 12.2% of studies post-intervention.\*Discussion In conclusion, our study suggests that the quality of the images post-intervention significantly impacted the ease of interpretation for radiologists. We observed that almost half of the pre-intervention pCXRs had technical issues that could impact diagnostic interpretation, with one-third of the studies having missed a diagnosis as a result of technical errors. The limitations of this study include inter-observer discrepancy in determining what is considered a missed diagnosis, short duration of follow-up after the intervention, and biases associated with a non-blinded study. Our study highlights the importance of educating and creating optimal work environments for technologists to capture high-quality pCXR images.

### **M5B-QI-6 Peer Learning Program Metrics: A Pediatric Neuroradiology Example**

Participants  
Nadja Kadom, MD, Atlanta, GA (*Presenter*) Nothing to Disclose

## METHODS

Context and Intervention: Transitioning from random score-based peer review to PL. Study of the Intervention: Pilot program designed and implemented. Measures/Metrics: Number of cases submitted per faculty per month; percentage of radiologists meeting PL program targets for case submissions; monthly faculty PL attendance; the number of cases reviewed during the PL session; number and nature of learning points; the number and nature of improvement actions; a faculty survey. Analysis: Descriptive statistics.

## RESULTS

Data on measures and outcome: 324 cases were submitted for the PL conference, averaging seven cases per faculty per month, and ranging from 0 to 26 cases for a single faculty member/month. There was no month when more than 80% of the faculty met the submission target of 5 cases. PL meeting attendance was 100%. A total of 179 cases were reviewed throughout the year, approximately 50% of all case submissions. On average, we reviewed 14 cases per PL conference (range 6-24). There were 22 learning points throughout the year. There were 30 documented improvement actions throughout the year. Faculty issued the highest star ratings for ease of meeting the 100% attendance requirement and for learning value. A slightly lower rating was given for feeling safe during case discussions, for the ease of submitting cases, and for the ability to gain CME credit for session participation. The lowest rating was given for effectiveness of improvements as a result of PL discussions.\*Discussion Limitations: This study does not provide proof that PL improves physician practice, but we have evidence that our faculty highly value PL. Conclusion: We demonstrate feasibility in PL program design and implementation. We noted considerable time commitment for running a PL program and for documenting program metrics. Survey feedback has been helpful in making changes to certain aspects of the program, such as improving trust in the PL program, including meaningful case submission types, and more thoughtful improvement actions. We are also making changes to decrease the PL faculty leads' time commitment, and are working towards simplifying the case submission system.

### **M5B-QI-7 The Structure and Support of Robust, System-wide Magnetic Resonance Safety Program**

Participants  
Randy Parker, ARRT, Grand Rapids, MI (*Presenter*) Nothing to Disclose

## **METHODS**

In a health-care system operating 22 MRI systems, MR exam orders flagged for safety review are tracked electronically. The tracking tool identifies the total number of safety reviews performed, the number of patients with contraindications for MR studies and patients requiring vendor or physician coordination. A lead MRSO is primarily responsible for review and follow-up action, but has support from additional, qualified MRSO recruited from staff. A designated MRMD and MRSE participate along with an MR Safety Expert Improvement Team (EIT). A radiology business support structure is in place to provide data collection and tools to demonstrate benefit achieved through improved use of available MR slots. The primary metrics are avoided last-moment cancellations and delays due to MRSO review.

## **RESULTS**

For 19,878 MR exams scheduled over a three-month period, 3,854 patients were screened by the six members of the MRSO team. 410 (10.6%) of these required review before proceeding with an MR appointment. 203 of 330 patients (61%) were determined to be eligible for an MR study, based on review and investigation by the team, using aligned resources of vendors and leveraging available teams to support MR technologists for pacemakers. 80 studies were completed for non-pacemaker implants/devices and 127 patients were identified with contraindications for MR and flagged in the EMR to avoid future orders. Daily referrals for MR studies range between 275 and 425 per day which results in approximately 50 to 80 daily MRSO reviews. Schedule utilization is consistently maintained at a high rate. Safety culture awareness is reinforced by department staff, radiologists, and administrators. Lessons learned from Zone IV infractions (preventable and non-preventable) and "good catches" are reviewed by the EIT and summarized in a monthly departmental MR operations newsletter.\*Discussion The benefits of a comprehensive MR safety program: maximized access to MR technology for patients within and outside our hospital system, standardized and rigorous MR safety screening and awareness, and patient and provider satisfaction. Cost savings based on efficient MR slot utilization defray the operation of a comprehensive institutional MR safety program.

## **M5B-QI-8 Encouraging the Assignment of LI-RADS Scores by Radiologists via Reporting Template Changes**

Participants  
Joon Oh, MD, New Brunswick, NJ (*Presenter*) Nothing to Disclose

## **METHODS**

The first template change occurred on 5/30/2018. A pick list at the impression field lets the radiologist select the LI-RADS score based on relevant features determined by the ACR consensus criteria. The second template change occurred on 10/1/2020 and involved an addition of a field that reminds the radiologist whether the patient qualifies for a LI-RADS score by asking whether the patient has a history of HBV, cirrhosis, or prior HCC (conditions that warrant a LI-RADS score). The LI-RADS criteria scoring guide is also attached within the PACS system as a visual aid for the radiologist. To calculate the compliance rate prior to any template changes, May 2018 was chosen as a representative month for data. Studies that met criteria for LI-RADS score or given a score were counted. The same time period (10/1/2020 to 12/22/2020) was used to compare the differences in compliance rates. Nominal and adjusted compliance rates are calculated. Nominal compliance refers to LI-RADS use on patients with history of HBV, cirrhosis, or prior HCC. Adjusted compliance excludes findings not felt to be clinically significant (benign findings, cirrhosis, interval follow up of a known lesion).

## **RESULTS**

Prior to any template changes, the nominal compliance was 3.23% while the adjusted compliance was 35.48%. After the first template change, the nominal compliance was 20.83% while the adjusted compliance was 93.75%. After the second template change, the nominal compliance was 40.91% while the adjusted compliance was 97.73%.\*Discussion The introduction of the LI-RADS score was meant to provide clearer management options for referring clinicians. At baseline before any template changes, the compliance rate for LI-RADS score reports was low, with an adjusted compliance rate of 35.48%. However, after two template changes, both the nominal and adjusted compliance rates have increased dramatically. After the second template change, the adjusted compliance rate is 97.7%. In other words, 97.7% of the time where there is a suspicious liver nodule, LI-RADS score was assigned. This shows that the right structured reporting template will increase compliance rates.

Printed on: 02/07/23

## Abstract Archives of the RSNA, 2022

M5B-QI-2

### To Investigate the Effect of Combined DLIR Reconstruction Algorithm With Different Concentrations of Contrast Agents on Coronary CTA Image Quality

Monday, Nov. 28 12:45PM - 1:15PM Room: Learning Center - QI DPS

#### Participants

Lijuan Zhu, (*Presenter*) Nothing to Disclose

#### METHODS

Thirty patients who underwent low-voltage coronary CT angiography (CCTA) with a 256-row wide-body detector CT scanner (Revolution Apex CT; GE Healthcare) in our hospital from September 2021 to January 2022 were collected and divided into two groups with 15 cases in each group according to the concentration of contrast agent used. Contrast agent concentration in group 320mg/mL, contrast agent concentration in group B 370mg/mL (conventional), group A medium-grade (DLIR-M), high-grade (DLIR-H) deep learning algorithm for reconstruction, group B using clinical routine 40% weight Adaptive Statistical Iterative Reconstruction (ASIR-V). The image noise of the aortic root and proximal main coronary artery of each group of images was recorded, and the Signal-to-Noise Ratio (SNR) and Contrast-to-Noise Ratio (CNR) were calculated. Subjective image quality was rated on a 5-point scale by two diagnostic radiologists with more than 5 years of experience.

#### RESULTS

1) Compared with ASIR-V40%, both DLIR-M and DLIR-H performed better noise reduction effect (P value <0.05). The SNR and CNR of DLIR-M and DLIR-H groups were significantly improved by 69.91%, 67.91% and 120.25%, 119.85%, compared to ASIR-40%, respectively. 2) The scoring results of two observers, physician A and physician B, showed that the noise reduction level increased with the increase of the deep learning image reconstruction technology (DLIR) (P value < 0.05), and both observers believed that the diagnosis effect was the best. The one is DLIR-H, and its subjective image quality is significantly improved by 40% compared with ASIR-V, which is 28.52% higher. \*Discussion Compare to the CCTA scanning scheme of 370mg/mL contrast agent combined with ASIR-V40% algorithm, the results show that the SNR and CNR of using 320mg/mL contrast agent combined with DLIR-H algorithm group was higher than those of the high contrast agent concentration group, indicating that DLIR had better image correction ability, which has higher clinical application value.

Printed on: 02/07/23



## Abstract Archives of the RSNA, 2022

M5B-QI-3

### Building Radiology Residents' Confidence in Managing Contrast Reactions: Our Institution's First Ever High-Fidelity Contrast Reaction Simulation

Monday, Nov. 28 12:45PM - 1:15PM Room: Learning Center - QI DPS

#### Participants

Kara Demarco, MD, (*Presenter*) Nothing to Disclose

#### METHODS

In partnership with the Simulation center, we created our institution's first ever High-Fidelity Contrast Reaction Simulation, in which three scenario algorithms were created to simulate real-life adverse contrast reactions. Learners were first given a short brief on potential reactions, and how to identify and respond to such patient presentations. They were then separated into three groups, rotating through each simulation. The simulations ranged from mild to severe reactions, with the latter evolving into a full code. During the simulations, the residents were challenged to interpret vitals, perform physical examinations, and determine next steps and management. The addition of bronchospasm reaction deliberately extends beyond the ACLS algorithm to challenge learners to identify a reaction that is more specific to contrast reactions, and may occur with asthmatics, particularly children. Each scenario was followed by an immediate debrief emphasizing the salient points of the specific reaction and its safe management.

#### RESULTS

Using a 10-point scale, participants were asked 7 questions surveying their comfort and knowledge level regarding the identification and management of contrast reactions. Prior to the simulation, the average was 4.3 out of 10. After the simulation, the average was 8.3 out of 10.\*Discussion Reactions to contrast media are uncommon but do happen, and often the radiology resident is the first physician to assess the patient. Acting out the management of such reactions is more effective than reading how to do so, and this simulation proved to be a useful endeavor in building the residents' competency. Moreover, it encouraged teamwork within a group of residents that are more accustomed to operating alone. Our intention is to continue this simulation with future classes, and expand the participation to staff radiologists and technologists, all of whom may be the first provider in saving an anaphylactic patient's life.

Printed on: 02/07/23



## Abstract Archives of the RSNA, 2022

M5B-QI-4

### Benefits of a Composite Report Incorporating Interactive Multimedia Reporting Principles

Monday, Nov. 28 12:45PM - 1:15PM Room: Learning Center - QI DPS

#### Participants

David J. Vining, MD, (*Presenter*) Royalties, Bracco Group;CEO, VisionSR, Inc;Stockholder, VisionSR, Inc

#### METHODS

We developed an IMR solution that records medical events (e.g., radiological findings, surgical procedures) and voice descriptions of those events, tags the information with metadata using natural language processing, and assembles an IMR report with related data linked in timelines and presented as a "composite report." A composite report presents the most recent information for each anatomical site of disease, regardless of modality, to create a holistic view of a patient. When a user clicks on a finding, the history of that entity is presented with images, graphs, tables, and related information.

#### RESULTS

To date the system has been used to generate 2505 composite reports from 1509 patients with a total of 12,943 findings comprising 37,769 items. In this composite reporting concept, a "finding" represents a timeline of connected "items" from individual exams and medical events. The average timeline length consists of 4 items with the longest comprising 24 items.\*Discussion Disparate information in an electronic health record (EHR) resides in silos related to the specialty that generated the source data (e.g., radiology, pathology, laboratory, surgery). The review of historical information by radiologists and clinicians in order to mentally construct a history of disease and treatment is often tedious and time-consuming. An IMR composite report can assimilate data from disparate sources and present the information in a logical fashion using visual displays to efficiently communicate information. Quantitative disease graphs assembled from the entire compendium of radiological data can reveal insights that may not be evident when a radiologist only compares a current exam to a limited number of prior exams. The use of metadata to tag related items enables data mining for the derivation of medical outcomes. Furthermore, a composite report has the potential to improve safety by mitigating discrepant results. For example, when a pathologist reports a left upper lung biopsy but that information is linked to a radiological exam indicating a right upper lung biopsy, the system immediately alerts the report author to make necessary corrections. A composite report represents a radical change from traditional independent medical reports, and as such it provides a means to connect data and cultivate knowledge.

Printed on: 02/07/23



## Abstract Archives of the RSNA, 2022

M5B-QI-5

### Wait, Where are the Apices? Improving Portable Chest Xray Techniques Through Image Review and Education of Radiology Technologists

Monday, Nov. 28 12:45PM - 1:15PM Room: Learning Center - QI DPS

#### Participants

Kevin Gilotra, Stony Brook, NY (*Presenter*) Nothing to Disclose

#### METHODS

From July 12, 2021 to July 25, 2021 pCXRs were evaluated by radiology residents for failures in technical image quality affecting their use for diagnostic interpretation. Figure 1 highlights the criteria used to assess image quality. To address the baseline frequency of technical quality errors, three programs aiming to improve the quality of pCXRs were implemented. First, a curriculum led by experienced technicians didactic sessions were provided to radiology technologists. Second, nursing staff was recruited to assist radiology technologists with patient positioning when obtaining images for pCXRs. Finally, internal medicine residents verified that films were interpretable for pathology once images had been collected. Figure 1 was subsequently used by radiology residents to assess post-intervention films.

#### RESULTS

Technical errors were present in 231 of the 500 pre-intervention radiographs and in 126 of the 287 post-intervention studies. Using a 0 to 3 scale for evaluating patient rotation (0 being no rotation and 3 being severe rotation), a 0.46-point reduction was observed post-intervention ( $p < 0.005$ ). There was also a 25% reduction in films with rotation in the post-intervention pCXRs, but no percentage change in pCXRs with mild rotation. The number of pCXRs with obscured anatomy declined by 20.9% post-intervention. A potential missed diagnosis was observed in 43.5% of studies pre-intervention in comparison to only 12.2% of studies post-intervention.\*Discussion In conclusion, our study suggests that the quality of the images post-intervention significantly impacted the ease of interpretation for radiologists. We observed that almost half of the pre-intervention pCXRs had technical issues that could impact diagnostic interpretation, with one-third of the studies having missed a diagnosis as a result of technical errors. The limitations of this study include inter-observer discrepancy in determining what is considered a missed diagnosis, short duration of follow-up after the intervention, and biases associated with a non-blinded study. Our study highlights the importance of educating and creating optimal work environments for technologists to capture high-quality pCXR images.

Printed on: 02/07/23



## Abstract Archives of the RSNA, 2022

M5B-QI-6

### Peer Learning Program Metrics: A Pediatric Neuroradiology Example

Monday, Nov. 28 12:45PM - 1:15PM Room: Learning Center - QI DPS

#### Participants

Nadja Kadom, MD, Atlanta, GA (*Presenter*) Nothing to Disclose

#### METHODS

Context and Intervention: Transitioning from random score-based peer review to PL. Study of the Intervention: Pilot program designed and implemented. Measures/Metrics: Number of cases submitted per faculty per month; percentage of radiologists meeting PL program targets for case submissions; monthly faculty PL attendance; the number of cases reviewed during the PL session; number and nature of learning points; the number and nature of improvement actions; a faculty survey. Analysis: Descriptive statistics.

#### RESULTS

Data on measures and outcome: 324 cases were submitted for the PL conference, averaging seven cases per faculty per month, and ranging from 0 to 26 cases for a single faculty member/month. There was no month when more than 80% of the faculty met the submission target of 5 cases. PL meeting attendance was 100%. A total of 179 cases were reviewed throughout the year, approximately 50% of all case submissions. On average, we reviewed 14 cases per PL conference (range 6-24). There were 22 learning points throughout the year. There were 30 documented improvement actions throughout the year. Faculty issued the highest star ratings for ease of meeting the 100% attendance requirement and for learning value. A slightly lower rating was given for feeling safe during case discussions, for the ease of submitting cases, and for the ability to gain CME credit for session participation. The lowest rating was given for effectiveness of improvements as a result of PL discussions.\*Discussion Limitations: This study does not provide proof that PL improves physician practice, but we have evidence that our faculty highly value PL. Conclusion: We demonstrate feasibility in PL program design and implementation. We noted considerable time commitment for running a PL program and for documenting program metrics. Survey feedback has been helpful in making changes to certain aspects of the program, such as improving trust in the PL program, including meaningful case submission types, and more thoughtful improvement actions. We are also making changes to decrease the PL faculty leads' time commitment, and are working towards simplifying the case submission system.

Printed on: 02/07/23



## Abstract Archives of the RSNA, 2022

M5B-QI-7

### The Structure and Support of Robust, System-wide Magnetic Resonance Safety Program

Monday, Nov. 28 12:45PM - 1:15PM Room: Learning Center - QI DPS

#### Participants

Randy Parker, ARRT, Grand Rapids, MI (*Presenter*) Nothing to Disclose

#### METHODS

In a health-care system operating 22 MRI systems, MR exam orders flagged for safety review are tracked electronically. The tracking tool identifies the total number of safety reviews performed, the number of patients with contraindications for MR studies and patients requiring vendor or physician coordination. A lead MRSO is primarily responsible for review and follow-up action, but has support from additional, qualified MRSO recruited from staff. A designated MRMD and MRSE participate along with an MR Safety Expert Improvement Team (EIT). A radiology business support structure is in place to provide data collection and tools to demonstrate benefit achieved through improved use of available MR slots. The primary metrics are avoided last-moment cancellations and delays due to MRSO review.

#### RESULTS

For 19,878 MR exams scheduled over a three-month period, 3,854 patients were screened by the six members of the MRSO team. 410 (10.6%) of these required review before proceeding with an MR appointment. 203 of 330 patients (61%) were determined to be eligible for an MR study, based on review and investigation by the team, using aligned resources of vendors and leveraging available teams to support MR technologists for pacemakers. 80 studies were completed for non-pacemaker implants/devices and 127 patients were identified with contraindications for MR and flagged in the EMR to avoid future orders. Daily referrals for MR studies range between 275 and 425 per day which results in approximately 50 to 80 daily MRSO reviews. Schedule utilization is consistently maintained at a high rate. Safety culture awareness is reinforced by department staff, radiologists, and administrators. Lessons learned from Zone IV infractions (preventable and non-preventable) and "good catches" are reviewed by the EIT and summarized in a monthly departmental MR operations newsletter.\*Discussion The benefits of a comprehensive MR safety program: maximized access to MR technology for patients within and outside our hospital system, standardized and rigorous MR safety screening and awareness, and patient and provider satisfaction. Cost savings based on efficient MR slot utilization defray the operation of a comprehensive institutional MR safety program.

Printed on: 02/07/23



## Abstract Archives of the RSNA, 2022

M5B-QI-8

### Encouraging the Assignment of LI-RADS Scores by Radiologists via Reporting Template Changes

Monday, Nov. 28 12:45PM - 1:15PM Room: Learning Center - QI DPS

#### Participants

Joon Oh, MD, New Brunswick, NJ (*Presenter*) Nothing to Disclose

#### METHODS

The first template change occurred on 5/30/2018. A pick list at the impression field lets the radiologist select the LI-RADS score based on relevant features determined by the ACR consensus criteria. The second template change occurred on 10/1/2020 and involved an addition of a field that reminds the radiologist whether the patient qualifies for a LI-RADS score by asking whether the patient has a history of HBV, cirrhosis, or prior HCC (conditions that warrant a LI-RADS score). The LI-RADS criteria scoring guide is also attached within the PACS system as a visual aid for the radiologist. To calculate the compliance rate prior to any template changes, May 2018 was chosen as a representative month for data. Studies that met criteria for LI-RADS score or given a score were counted. The same time period (10/1/2020 to 12/22/2020) was used to compare the differences in compliance rates. Nominal and adjusted compliance rates are calculated. Nominal compliance refers to LI-RADS use on patients with history of HBV, cirrhosis, or prior HCC. Adjusted compliance excludes findings not felt to be clinically significant (benign findings, cirrhosis, interval follow up of a known lesion).

#### RESULTS

Prior to any template changes, the nominal compliance was 3.23% while the adjusted compliance was 35.48%. After the first template change, the nominal compliance was 20.83% while the adjusted compliance was 93.75%. After the second template change, the nominal compliance was 40.91% while the adjusted compliance was 97.73%. \*Discussion The introduction of the LI-RADS score was meant to provide clearer management options for referring clinicians. At baseline before any template changes, the compliance rate for LI-RADS score reports was low, with an adjusted compliance rate of 35.48%. However, after two template changes, both the nominal and adjusted compliance rates have increased dramatically. After the second template change, the adjusted compliance rate is 97.7%. In other words, 97.7% of the time where there is a suspicious liver nodule, LI-RADS score was assigned. This shows that the right structured reporting template will increase compliance rates.

Printed on: 02/07/23

## Abstract Archives of the RSNA, 2022

R2-QI

### Quality Improvement Reports Thursday Poster Discussions

Thursday, Dec. 1 9:00AM - 9:30AM Room: Learning Center - QI DPS

#### Sub-Events

#### **R2-QI-1HC Underserved Women Understand the Importance of Screening Mammography Yet Exam Scheduling Still Remains a Barrier**

Participants  
Jean Mutambuze, MD, (*Presenter*) Nothing to Disclose

#### **METHODS**

Our study was a survey of screening mammography-eligible female patients from the federally qualified health centers that utilize the screening mammography services at at Eskanzi Health, a city-county hospital in Indianapolis, IN. This survey queried patients about possible barriers to getting a screening mammogram. Preliminary results are submitted here and statistical analysis of survey results are in progress.

#### **RESULTS**

While several hundred patients were invited to the survey, a total of 70 patients answered the survey. The racial and ethnic demographics of the surveyed patients was 44% Black, 48 %white, 4% Hispanic/Latina, 1.5 % Asian-American, 1.4 % multirace/other. Possible barriers that were queried included: scheduling the exam, transportation, need for childcare, lack of insurance, unable to take time off of work, fear of the exam results, absence of a recommendation from primary MD for the exam, or discomfort from the mammography exam. The more frequent barrier cited was scheduling the exam (21/70 patients, 30%). The majority of the surveyed patients: understood the importance of the exam (82.9%), understood that absence of a family history meant they were still at risk for developing breast cancer (72.9%), understood that they needed a mammogram even if they didn't have breast pain (71.4%), and thought that getting a mammogram would reduce their risk of dying from breast cancer (72.8%).\*Discussion Internal review surveys such as these allow hospitals to assess local barriers to preventive care, such as screening mammography, and thus allow interventions be performed to improve patient access to preventive health services in the local community. Please visit the Learning Center to also view this presentation in hardcopy format.

#### **R2-QI-2 Enhancement of Safety Barriers in a Magnetic Resonance Unit: A Brazilian Experience**

Participants  
Suzana Oliveira Latarula Sozza, MBBS, Sao Paulo, Brazil (*Presenter*) Nothing to Disclose

#### **METHODS**

In order to promote improvements for the safety of patients and healthcare professionals who are subjected to the magnetic field, this project was developed in the MRI unit of a Brazilian tertiary hospital (8 MRI machines) from September 2019 to September 2021. To this end, the following security barriers were implemented: • Barrier 1 - The exam scheduling sector asks a series of questions to ensure that the patient does not have any contraindications. • Barrier 2 - Application of the safety questionnaire and change of clothing removing expendable metallic belongings. • Barrier 3 - Checking the completed safety questionnaires. • Barrier 4 - The technologist confirms the identification data and the safety questionnaire, before entering the examination room with the patient. Upon entering the room, the locker key and belongings such as glasses are removed and stored in an appropriate place. After improving these safety barriers, training was carried out for employees in the area and other care professionals, who could have contact with the sector indirectly (such as the nursing team that sends and transports the hospitalized patient) or directly (employees who have probability of entering or staying in place). The impact of these interventions was evaluated by the number of occurrences of accidents related to undue exposure to the magnetic field. The analysis was performed through the occurrence notification records.

#### **RESULTS**

With the improvement of safety barriers, we managed to ensure that during the duration of the project (2 years) we had no accidents related to exposure to the magnetic field.\*Discussion Magnetic fields in MRI units can cause dangerous interactions in individual with metallic foreign bodies, including projectile effect, twisting, burning, artifacts, and device malfunction (interference with a pacemaker). Therefore, all patients need to thoroughly be screened individually for foreign bodies before undergoing an MRI scan. All healthcare professionals that work in MRI units must be aware of safety recommendations and educational actions related to MRI safety, such as the presented project, must be carried out periodically. Limitations of our study include the fact that omission of information regarding questions that contraindicate the MRI examination by patients could not be assessed.

#### **R2-QI-3 Setting up a Workflow: Optimizing the Wait Times in the MRI Anesthesia**

Participants  
Maria Vicente, (*Presenter*) Nothing to Disclose

#### **METHODS**

The RSNA Learning Center is a free, self-paced, interactive educational platform that provides a variety of educational resources, including courses, webinars, and on-demand content. For more information, visit <https://www.rsna.org/learning-center>.

The PDCA method (Plan-Do-Check-Act) was used to understand the main points of improvement and to help to create an MRI anesthesia workflow. In an initial investigation, many points were recognized such opportunities: errors related to call center scheduling, the non-optimized slot usage, health insurance authorization, communication failure between teams, delay in schedules, wrong choice of equipment according to the required magnetic field for specific examinations, incorrect anamnesis about the patient's background and delays associated to choose the appropriate MRI protocol and the choice of anesthetic procedure. According to the PDCA framework, in the next step, several action plans were implemented, such as schedule control sheets, checklist created to be applied during a telephone call for triage with guiding questions that allow filtering failures before the client arrives at the hospital and clarify the patient's doubts regarding anesthesia. The analysis was performed using the quantification of successful MRI performed with anesthesia (numerator) / Month of completion (denominator) and the quantification of optimized schedule times due to prior confirmation (numerator)/ Month of the procedure done (denominator).

## RESULTS

After the project implementation, from July 2020 to September 2020, 393 patients who underwent MRI anesthesia were analyzed. Through prior confirmation, we were able to optimize more than 30 hours, making available an average of 45 MRI exams for scheduling.\*Discussion This workflow proved to be effective in terms of guidance to the patient in advance, clarifying doubts, humanizing the patient experience focusing on their own individualities, increasing customer satisfaction and loyalty levels, exceeding their expectations. With the information and patient history prior obtained before the exam date, was possible to reduce errors related to exams scheduling, optimizing the wait times and improve throughput caused by absent patients in the MRI department.

### R2-QI-4 Increasing Bone Scan Capacity by Optimizing Appointments

Participants

Meedy Sharifpour, FRCR, MS, (*Presenter*) Nothing to Disclose

## METHODS

Retrospective review of 12 months bone scans performed for prostate cancer patients across two different hospitals to assess the frequency of SPECT CT performed. We also collected additional data on patients who had recent CT within four weeks prior to the bone scan, prior bone scan, prostate cancer risk group (PSA, Gleason score, and MRI radiological staging) in order to assess the frequency of SPECT CT imaging amongst patients needing a bone scan.

## RESULTS

Over the 12 months period, 53% of the patients required planar imaging and therefore only needed a 30-minute appointment slot. We also noted that 24% of the patients needed one body part SPECT CT (45-minute appointment) and 23% of the patients needed two body part SPECT CT (60 minutes appointment). We also identified that none of the patients who had CT scan performed within four weeks of the bone scan required any SPECT CT imaging unless a lesion was identified on the prior scan which needed characterisation.\*Discussion The need for optimisation of services is becoming a vital part of any healthcare service. The above retrospective review has resulted in criteria identified for shorter appointment times an example of which included a recent CT scan within four weeks prior to the bone scan. This has resulted in an increase of between 20% to 100% capacity in bone scan imaging within our department. Increasing capacity by 100% on some days was achieved by solely booking patients with recent prior CT imaging and therefore reduction of all appointment times from 60 minutes to 30 minutes. Radiologists do not commonly get involved in all aspects of the radiology department and how appointments are allocated to the patients however, we have demonstrated that the background clinical knowledge can help in risk stratifying patients and therefore optimising healthcare services accordingly.

### R2-QI-5HC Bringing Technology and the Human Experience Together: Radiology's Journey to a Digital Check-in Process

Participants

Christina Hertel, BA, (*Presenter*) Nothing to Disclose

## METHODS

A multidisciplinary team approached this issue using the Define-Measure-Analyze-Improve-Control (DMAIC) and A3 framework to advise a solution strategy using a series of Plan-Do-Study-Act (PDSA) cycles. Patients, technologists, and desk operations staff were surveyed throughout the process to guide adjustments or further interventions needed for the subsequent cycles. Department on-time starts were monitored as a counterbalance. The results of the surveys guided the team to evaluate four comprehensive areas of improvement. The lobby space, the role of the desk operations staff, the electronic environment, and patient experience. A root cause analysis was performed on each topic to determine possible solutions. Solutions were then put into an impact effort grid to determine the sequence of possible approaches. A detailed review of patient and staff feedback was carefully considered after each PDSA cycle to determine success.

## RESULTS

The outcome of this project revealed that it was not the actual digital check-in process patients struggled with but the feelings of losing the human connection. The identification of this core concern guided the team to transform the role of our desk operations staff to create a concierge-type service bringing the staff out from behind the barrier of a formal desk to assist with technology, wayfinding, and promotion of a welcoming environment. We were able to increase the use of digital patient check-in from 45% in December 2021 to 76% in March 2022. In addition, patient and staff satisfaction scores increased by an average of 10%, and the average check-in was reduced from 2.3 to 1.0 minutes without negatively impacting exam on-time starts.\*Discussion In the end, maintaining the human experience was key in instituting a successful digital check-in process. Representation from each role was instrumental in detecting any nuances that may arise. Limitations of the project include construction constraints and the timely availability of electronic devices during the PDSA cycles. Please visit the Learning Center to also view this presentation in hardcopy format.

### R2-QI-6 Faster CT Scan Protocol Authorization Based on Web Scraping Solutions Improves Patient Care

Participants

Eduardo Caminha Nunes, MD, Sao Paulo, Brazil (*Presenter*) Nothing to Disclose

## METHODS

We developed a web scraping tool using Selenium with Python and ChromeDriver to check the HIS and return a text via

WhatsApp® to the resident on call. We calculated the mean averages for the times required to authorize a new CT scan protocol with and without our tool and then performed the Mann-Whitney U test to assess statistical significance.

## **RESULTS**

The mean average for the authorization time without our tool was 52.28 minutes and 14.71 minutes using our solution. The estimated p-value calculated with the Mann-Whitney U test was 0.0075.\*Discussion We observed a decrease in time between exam order and authorization. This resource is able to shorten the time between exam authorization and execution, which facilitates the hospital workflow and improves patient care.

## **R2-QI-7 Streamlining an MRI Implant Clearance Process to Improve Radiology Workflow**

Participants

Stephanie Shieh, MSN,RN, Orange, CA (*Presenter*) Nothing to Disclose

## **METHODS**

This study was performed in the Department of Radiology at a quaternary academic medical center. A centralized HIPAA-compliant Excel tracker was created in May 2021 to document the following data for patients receiving an outpatient MRI: date requested, scheduler, reason for clearance, clearance status (cleared, in progress, or not cleared), date request completed, appointment scheduled date, and additional notes. A Radiology Quality Team consisting of MRI technologists (Supervisor, Lead Tech, and Senior Tech), Nursing (Quality Nurse and Radiology Nurse), and Scheduling (Lead Schedulers) were able to access and update this tracker to ensure proper implant clearance. Our metrics for quality improvement included average time from notification of an implant to implant clearance ("notification-to-clearance") and average time from implant clearance to scheduling time ("clearance-to-scheduling").

## **RESULTS**

From May 2021 to April 2022, there were 440 implant requests that needed clearance for MRI. The average number of days for "notification-to-clearance" was less than 6 days, with 291 requests completed in 3 days or less. The median "clearance-to-scheduling" time was 19 days for outpatients.\*Discussion The implementation of implant clearance process by a centralized database has streamlined the scheduling and completion of MRI studies. The shared tracker ensures that implant requests are cleared prior to patient arrival in the department. It has also facilitated collaboration among the Quality Team in addressing this patient safety issue. A limitation of this study is exclusion of other factors that affect MRI availability.

Printed on: 02/07/23



## Abstract Archives of the RSNA, 2022

R2-QI-1HC

### Underserved Women Understand the Importance of Screening Mammography Yet Exam Scheduling Still Remains a Barrier

Thursday, Dec. 1 9:00AM - 9:30AM Room: Learning Center - QI DPS

#### Participants

Jean Mutambuze, MD, (*Presenter*) Nothing to Disclose

#### METHODS

Our study was a survey of screening mammography-eligible female patients from the federally qualified health centers that utilize the screening mammography services at at Eskanzi Health, a city-county hospital in Indianapolis, IN. This survey queried patients about possible barriers to getting a screening mammogram. Preliminary results are submitted here and statistical analysis of survey results are in progress.

#### RESULTS

While several hundred patients were invited to the survey, a total of 70 patients answered the survey. The racial and ethnic demographics of the surveyed patients was 44% Black, 48 %white, 4% Hispanic/Latina, 1.5 % Asian-American, 1.4 % multirace/other. Possible barriers that were queried included: scheduling the exam, transportation, need for childcare, lack of insurance, unable to take time off of work, fear of the exam results, absence of a recommendation from primary MD for the exam, or discomfort from the mammography exam. The more frequent barrier cited was scheduling the exam (21/70 patients, 30%). The majority of the surveyed patients: understood the importance of the exam (82.9%), understood that absence of a family history meant they were still at risk for developing breast cancer (72.9%), understood that they needed a mammogram even if they didn't have breast pain (71.4%), and thought that getting a mammogram would reduce their risk of dying from breast cancer (72.8%).\*Discussion Internal review surveys such as these allow hospitals to assess local barriers to preventive care, such as screening mammography, and thus allow interventions be performed to improve patient access to preventive health services in the local community.Please visit the Learning Center to also view this presentation in hardcopy format.

Printed on: 02/07/23



## Abstract Archives of the RSNA, 2022

R2-QI-2

### Enhancement of Safety Barriers in a Magnetic Resonance Unit: A Brazilian Experience

Thursday, Dec. 1 9:00AM - 9:30AM Room: Learning Center - QI DPS

#### Participants

Suzana Oliveira Latarula Sozza, BMBS, Sao Paulo, Brazil (*Presenter*) Nothing to Disclose

#### METHODS

In order to promote improvements for the safety of patients and healthcare professionals who are subjected to the magnetic field, this project was developed in the MRI unit of a Brazilian tertiary hospital (8 MRI machines) from September 2019 to September 2021. To this end, the following security barriers were implemented: • Barrier 1 - The exam scheduling sector asks a series of questions to ensure that the patient does not have any contraindications. • Barrier 2 - Application of the safety questionnaire and change of clothing removing expendable metallic belongings. • Barrier 3 - Checking the completed safety questionnaires. • Barrier 4 - The technologist confirms the identification data and the safety questionnaire, before entering the examination room with the patient. Upon entering the room, the locker key and belongings such as glasses are removed and stored in an appropriate place. After improving these safety barriers, training was carried out for employees in the area and other care professionals, who could have contact with the sector indirectly (such as the nursing team that sends and transports the hospitalized patient) or directly (employees who have probability of entering or staying in place). The impact of these interventions was evaluated by the number of occurrences of accidents related to undue exposure to the magnetic field. The analysis was performed through the occurrence notification records.

#### RESULTS

With the improvement of safety barriers, we managed to ensure that during the duration of the project (2 years) we had no accidents related to exposure to the magnetic field.\*Discussion Magnetic fields in MRI units can cause dangerous interactions in individual with metallic foreign bodies, including projectile effect, twisting, burning, artifacts, and device malfunction (interference with a pacemaker). Therefore, all patients need to thoroughly be screened individually for foreign bodies before undergoing an MRI scan. All healthcare professionals that work in MRI units must be aware of safety recommendations and educational actions related to MRI safety, such as the presented project, must be carried out periodically. Limitations of our study include the fact that omission of information regarding questions that contraindicate the MRI examination by patients could not be assessed.

Printed on: 02/07/23



## Abstract Archives of the RSNA, 2022

R2-QI-3

### Setting up a Workflow: Optimizing the Wait Times in the MRI Anesthesia

Thursday, Dec. 1 9:00AM - 9:30AM Room: Learning Center - QI DPS

#### Participants

Maria Vicente, (*Presenter*) Nothing to Disclose

#### METHODS

The PDCA method (Plan-Do-Check-Act) was used to understand the main points of improvement and to help to create an MRI anesthesia workflow. In an initial investigation, many points were recognized such opportunities: errors related to call center scheduling, the non-optimized slot usage, health insurance authorization, communication failure between teams, delay in schedules, wrong choice of equipment according to the required magnetic field for specific examinations, incorrect anamnesis about the patient's background and delays associated to choose the appropriate MRI protocol and the choice of anesthetic procedure. According to the PDCA framework, in the next step, several action plans were implemented, such as schedule control sheets, checklist created to be applied during a telephone call for triage with guiding questions that allow filtering failures before the client arrives at the hospital and clarify the patient's doubts regarding anesthesia. The analysis was performed using the quantification of successful MRI performed with anesthesia (numerator) / Month of completion (denominator) and the quantification of optimized schedule times due to prior confirmation (numerator)/ Month of the procedure done (denominator).

#### RESULTS

After the project implementation, from July 2020 to September 2020, 393 patients who underwent MRI anesthesia were analyzed. Through prior confirmation, we were able to optimize more than 30 hours, making available an average of 45 MRI exams for scheduling.\*Discussion This workflow proved to be effective in terms of guidance to the patient in advance, clarifying doubts, humanizing the patient experience focusing on their own individualities, increasing customer satisfaction and loyalty levels, exceeding their expectations. With the information and patient history prior obtained before the exam date, was possible to reduce errors related to exams scheduling, optimizing the wait times and improve throughput caused by absent patients in the MRI department.

Printed on: 02/07/23

## Abstract Archives of the RSNA, 2022

R2-QI-4

### Increasing Bone Scan Capacity by Optimizing Appointments

Thursday, Dec. 1 9:00AM - 9:30AM Room: Learning Center - QI DPS

#### Participants

Meedy Sharifpour, FRCR, MS, (*Presenter*) Nothing to Disclose

#### METHODS

Retrospective review of 12 months bone scans performed for prostate cancer patients across two different hospitals to assess the frequency of SPECT CT performed. We also collected additional data on patients who had recent CT within four weeks prior to the bone scan, prior bone scan, prostate cancer risk group (PSA, Gleason score, and MRI radiological staging) in order to assess the frequency of SPECT CT imaging amongst patients needing a bone scan.

#### RESULTS

Over the 12 months period, 53% of the patients required planar imaging and therefore only needed a 30-minute appointment slot. We also noted that 24% of the patients needed one body part SPECT CT (45-minute appointment) and 23% of the patients needed two body part SPECT CT (60 minutes appointment). We also identified that none of the patients who had CT scan performed within four weeks of the bone scan required any SPECT CT imaging unless a lesion was identified on the prior scan which needed characterisation.\*Discussion The need for optimisation of services is becoming a vital part of any healthcare service. The above retrospective review has resulted in criteria identified for shorter appointment times an example of which included a recent CT scan within four weeks prior to the bone scan. This has resulted in an increase of between 20% to 100% capacity in bone scan imaging within our department. Increasing capacity by 100% on some days was achieved by solely booking patients with recent prior CT imaging and therefore reduction of all appointment times from 60 minutes to 30 minutes. Radiologists do not commonly get involved in all aspects of the radiology department and how appointments are allocated to the patients however, we have demonstrated that the background clinical knowledge can help in risk stratifying patients and therefore optimising healthcare services accordingly.

Printed on: 02/07/23



## Abstract Archives of the RSNA, 2022

R2-QI-5HC

### Bringing Technology and the Human Experience Together: Radiology's Journey to a Digital Check-in Process

Thursday, Dec. 1 9:00AM - 9:30AM Room: Learning Center - QI DPS

#### Participants

Christina Hertel, BA, (*Presenter*) Nothing to Disclose

#### METHODS

A multidisciplinary team approached this issue using the Define-Measure-Analyze-Improve-Control (DMAIC) and A3 framework to advise a solution strategy using a series of Plan-Do-Study-Act (PDSA) cycles. Patients, technologists, and desk operations staff were surveyed throughout the process to guide adjustments or further interventions needed for the subsequent cycles. Department on-time starts were monitored as a counterbalance. The results of the surveys guided the team to evaluate four comprehensive areas of improvement. The lobby space, the role of the desk operations staff, the electronic environment, and patient experience. A root cause analysis was performed on each topic to determine possible solutions. Solutions were then put into an impact effort grid to determine the sequence of possible approaches. A detailed review of patient and staff feedback was carefully considered after each PDSA cycle to determine success.

#### RESULTS

The outcome of this project revealed that it was not the actual digital check-in process patients struggled with but the feelings of losing the human connection. The identification of this core concern guided the team to transform the role of our desk operations staff to create a concierge-type service bringing the staff out from behind the barrier of a formal desk to assist with technology, wayfinding, and promotion of a welcoming environment. We were able to increase the use of digital patient check-in from 45% in December 2021 to 76% in March 2022. In addition, patient and staff satisfaction scores increased by an average of 10%, and the average check-in was reduced from 2.3 to 1.0 minutes without negatively impacting exam on-time starts.\*Discussion In the end, maintaining the human experience was key in instituting a successful digital check-in process. Representation from each role was instrumental in detecting any nuances that may arise. Limitations of the project include construction constraints and the timely availability of electronic devices during the PDSA cycles. Please visit the Learning Center to also view this presentation in hardcopy format.

Printed on: 02/07/23



## Abstract Archives of the RSNA, 2022

R2-QI-6

### Faster CT Scan Protocol Authorization Based on Web Scraping Solutions Improves Patient Care

Thursday, Dec. 1 9:00AM - 9:30AM Room: Learning Center - QI DPS

#### Participants

Eduardo Caminha Nunes, MD, Sao Paulo, Brazil (*Presenter*) Nothing to Disclose

#### METHODS

We developed a web scraping tool using Selenium with Python and ChromeDriver to check the HIS and return a text via WhatsApp® to the resident on call. We calculated the mean averages for the times required to authorize a new CT scan protocol with and without our tool and then performed the Mann-Whitney U test to assess statistical significance.

#### RESULTS

The mean average for the authorization time without our tool was 52.28 minutes and 14.71 minutes using our solution. The estimated p-value calculated with the Mann-Whitney U test was 0.0075.\*Discussion We observed a decrease in time between exam order and authorization. This resource is able to shorten the time between exam authorization and execution, which facilitates the hospital workflow and improves patient care.

Printed on: 02/07/23



## Abstract Archives of the RSNA, 2022

R2-QI-7

### Streamlining an MRI Implant Clearance Process to Improve Radiology Workflow

Thursday, Dec. 1 9:00AM - 9:30AM Room: Learning Center - QI DPS

#### Participants

Stephanie Shieh, MSN,RN, Orange, CA (*Presenter*) Nothing to Disclose

#### METHODS

This study was performed in the Department of Radiology at a quaternary academic medical center. A centralized HIPAA-compliant Excel tracker was created in May 2021 to document the following data for patients receiving an outpatient MRI: date requested, scheduler, reason for clearance, clearance status (cleared, in progress, or not cleared), date request completed, appointment scheduled date, and additional notes. A Radiology Quality Team consisting of MRI technologists (Supervisor, Lead Tech, and Senior Tech), Nursing (Quality Nurse and Radiology Nurse), and Scheduling (Lead Schedulers) were able to access and update this tracker to ensure proper implant clearance. Our metrics for quality improvement included average time from notification of an implant to implant clearance ("notification-to-clearance") and average time from implant clearance to scheduling time ("clearance-to-scheduling").

#### RESULTS

From May 2021 to April 2022, there were 440 implant requests that needed clearance for MRI. The average number of days for "notification-to-clearance" was less than 6 days, with 291 requests completed in 3 days or less. The median "clearance-to-scheduling" time was 19 days for outpatients.\*Discussion The implementation of implant clearance process by a centralized database has streamlined the scheduling and completion of MRI studies. The shared tracker ensures that implant requests are cleared prior to patient arrival in the department. It has also facilitated collaboration among the Quality Team in addressing this patient safety issue. A limitation of this study is exclusion of other factors that affect MRI availability.

Printed on: 02/07/23



## Abstract Archives of the RSNA, 2022

R5A-QI

### Quality Improvement Reports Thursday Poster Discussions - A

Thursday, Dec. 1 12:15PM - 12:45PM Room: Learning Center - QI DPS

#### Sub-Events

#### R5A-QI-1 The Importance of Imaging and Safety for Yttrium90-Microsphere Therapy

Participants

Ryan Misseldine, BS, MBA, (*Presenter*) Nothing to Disclose

#### METHODS

Treatment planning at our facility is performed using liver cross sectional imaging (CT/MRI) followed by intraarterial delivery of 5mCi Tc99m-MAA to the lesion(s) of interest. Treatment area volume calculation is then determined using the preprocedure CT/MRI. Nuclear medicine images are used to assess the lung-shunt fraction and any other extrahepatic shunting. After treatment with Y90, patients are imaged using PET/CT to verify site of dose delivery. Our facility decided to track cases after the vendor informed our team that outside facilities were discontinuing the use of pre-therapeutic imaging. These facilities would skip the Tc-99m-MAA SPECT/CT for treatment localization and treat the patient using an assumed lung shunt fraction. We felt it prudent to track cases to determine the validity of this practice. We followed patients where the additional nuclear medicine imaging showed elevated lung-shunting and nontarget extrahepatic activity to assess whether the patient's treatment plan was modified. Modifications included reduction in dose delivered, splitting the dose angiographically between different arteries (Case 1), or changes in treatment plan if patients were precluded from Y90 therapy due to unacceptably high levels of lung shunting (Case 2 3). Case 1: Modified/Split Dose. No Cystic Artery in Angio, visualized gallbladder on SPECT/CT resulted in modified interventional approach and split dose. See Case Image 1. Case 2: Elevated Lung-Shunt: See Case Image 2. Case 3: Elevated Lung-Shunt: - See Case Image 3.

#### RESULTS

Case evaluation confirmed utilizing advanced imaging techniques (preplanning angiography, Geometric lung-shunt evaluation, SPECT/CT, and PET/CT) lead to improved image quality, interventional approach, and patient safety. This is achieved via reduced dose, splitting the dose between different lobar arteries, and validation that dose was delivered without significant exposure to non-target organs.\*Discussion Our facility utilized advanced imaging techniques. It should be noted that all facilities performing Y90s may not have access to a hybridized SPECT/CT, PET/CT, etc.

#### R5A-QI-2 Improving Communication of Unexpected Findings: The Radiology Actionable Findings Tracking (RAFT) System

Participants

Surbhi Trivedi, MD, (*Presenter*) Nothing to Disclose

#### METHODS

The Radiology Actionable Findings Tracking (RAFT) program was developed at our institution to compile and track unexpected findings on imaging reports and their follow up. The first step of the pipeline occurs when the reading radiologist integrates a special macro in the report to flag an unexpected finding. The macro includes four fields including the acuity, status of communication, finding and clinical relevance, and recommended follow-up. These macros are then compiled by our EMR into a spreadsheet of findings which is monitored daily by a medically trained coordinator. The coordinator notifies the ordering provider with a message via the EMR. The patient is also contacted within three days of the radiology report via the EMR patient portal notification, traditional mail, or phone. If no action is taken by 8 days, the message is escalated to the ordering provider as well as the primary care provider. In cases when a follow up study was recommended, the task is automatically marked complete and the communication loop closed when the recommended study is ordered. When the coordinator messages the provider within our EMR, the provider can communicate with the staff and also immediately order a follow up study if one was recommended. Additionally, a pop-up notification occurs in the chart as an advisory for the provider to follow up with the recommended order similar to when critical vitals prompt an alert for sepsis work-up.

#### RESULTS

This program has been in use for 2 years and has been adopted among radiologists due to the ease of the macro within the dictation system. On average, 86 unexpected findings were acted on by the provider per month due to the RAFT program. Additionally, an average of 10 findings were escalated per month to an additional provider. Cases of improved patient outcomes include diagnosis of an early-stage pancreatic tumor as well as a suspicious lung nodule found to be early-stage lung cancer.\*Discussion The implementation of the RAFT tracking program for incidental and unexpected findings has likely reduced missed follow-ups with a focus on improving patient outcomes. Limitations include follow up beyond the best efforts to escalate findings. Overall, this is a promising program for tracking data from our high-volume department and ensuring that every unexpected finding is effectively handled to ensure optimal patient health and safety.

### **R5A-QI-3 Contrast Enhanced Mammography - A Potential Game Changer for Breast Conservation Surgery in Developing Nations**

#### Participants

Haleema Sherene, MBBS, Coimbatore, India (*Presenter*) Nothing to Disclose

#### **METHODS**

This project was undertaken by the Breast imaging division in a developing urban tertiary academic hospital. 161 women with breast cancer underwent CEM. The number of mastectomy and BCS and re-surgeries for patients in early and advanced stages were analysed.

#### **RESULTS**

153 patients (Stage 1: 18, Stage 2: 95, Stage 3: 28 and Stage 4: 11) completed their treatment at the same hospital, of which 72 underwent mastectomy and 78 underwent breast conservation surgery and 11 had metastasis. CEM detected additional lesions and converted to mastectomies in 10 and thereby avoided re-surgeries. CEM defined the extent of lesions better in 14 patients and resulted in negative surgical margins. CEM influenced patient management and avoided re-surgery in 24/153 (15.7%) patients. 3/78 had re-surgeries (3.9%) after CEM due to positive margins.\*Discussion The total procedure cost was 50dollars compared to 200dollars spent for patients who underwent mammography and MRI with contrast. The total time each of these patients spent in the department was less than 4 hours to give them a final decision on surgery. Contrast enhanced mammography may change the perception of breast conservation surgery in a developing country, especially for the lower-income groups.

### **R5A-QI-6 Implementation of a Protocol for Non-Conditional Cardiac Implantable Electronic Devices**

#### Participants

Cyndy Kao, BSN, Orange, CA (*Presenter*) Nothing to Disclose

#### **METHODS**

This was a pilot program performed from April 2021 until April 2022 at a quaternary academic hospital in both inpatient and outpatient settings. The radiology (Radiology Nurse, Quality Nurse) and electrophysiology (EP) (cardiologists, Nurse Practitioner) departments created a protocol to screen and scan patients with non-conditional CIEDs based off the MagnaSafe Registry multicentered study. For the workflow, the Radiology Nurse trained in CIED programming determined appropriate MR labeling and safety using CIED information obtained by schedulers. The appropriate radiologist, ordering provider and patient were notified, and EP evaluation was performed. An EP provider determined if a CIED was appropriate for scanning and documented program parameters in the consultation note. The patient was provided the appropriate educational materials explaining the risks of scanning a CIED off-label prior to the scan. Prior to the scan, the device was interrogated and programmed into the MRI safe mode as specified by the cardiologist. During the MRI, the patient was monitored by the Radiology Nurse while connected to physiologic monitoring equipment (Figure 1A and 1B), We evaluated the number of requests that were obtained in this workflow and how many were able to be scanned safely.

#### **RESULTS**

Out of 226 CIED requests, 43 (19%) were determined to be non-conditional, while the rest were MRI conditional. 15 of the non-conditional patients were successfully scanned under this new protocol. The remaining 28 patients were not scanned due to various factors including: alternate imaging recommended instead of MRI, insurance denials, permanent epicardial or abandoned/fractured leads, patient declination in participating in protocol due to safety concerns, patient opting to be scanned offsite, and provider cancellation of exam. No adverse events were noted intra or post MRI scan.\*Discussion The implementation of this protocol has increased access to MRI for patients with implanted CIED. We successfully expanded a key imaging modality to 7% of the sample population who previously would not have been considered for MR scan. Patient and staff education were key to the success of this program.

### **R5A-QI-7HC Quality of Communications; the Unintended Consequences of Decision Support in Advanced Abdominal Imaging**

#### Participants

Lillian Dominguez-Konicki, MD, Lebanon, NH (*Presenter*) Nothing to Disclose

#### **METHODS**

A retrospective review was conducted of all consecutive orders for Abdominal CT exams performed at our institution over a 30-day period following institution of DS, a new, mandatory field in CT imaging orders. Content assessed included the presence/absence of DS free text clinical history (FTCH), the ordering practitioner degree, ordering location, and ordering specialty. Concordance of the DS vs FTCH was assessed by two radiologists. The DS history provided was scored with regard to confidence in protocol selection by an abdominal radiologist with 20 years of experience.

#### **RESULTS**

450 individual abdominal CT orders were assessed, and in 20%, the FTCH was left blank; DS history was the only history provided. The DS history did not provide sufficient information to enable selection of the optimal CT protocol 24% of the time. When FTCH was provided, it was discordant with the DS history 15% of the time. Orders placed through the emergency department, surgical clinics, and internal medicine subspecialty clinics neglected to include FTCH the most often (23%, 22%, 17%). Inpatient orders failed to include FTCH only 8% of the time. Orders placed by MD/DO failed to provide FTCH 25% of the time compared with 13% for associate providers.\*Discussion This study quantified the unintended consequences to the implementation of DS at our institution, specifically showing a lack of adequate and accurate clinical histories in a substantial number of orders for Abdominal CT exams. We have identified subgroups of providers who could be targeted for initiatives to improve the quality of CI provided in imaging orders. This work is important because safe, high quality patient care in radiology relies on accurate and complete communications from the ordering providers, primarily obtained through the imaging orders. Inaccurate and incomplete clinical information may lead to inappropriate or suboptimal imaging techniques, exposure to ionizing radiation and contrast agents, and negatively impact work efficiency. Please visit the Learning Center to also view this presentation in hardcopy format.

**R5A-QI-8 Increasing Utilization of 3D Reconstructions in Pediatric Head CTs for Trauma through Order Set Modification: A Simple Way to Improve Fracture Detection**

Participants

Thomas Marini, MD, (*Presenter*) Nothing to Disclose

**METHODS**

A root cause analysis was performed to identify factors as to why reconstructions were not being ordered by providers. Based on the results, we implemented modifications to the order set for pediatric trauma. Modifications included automatic selection of the 3D reconstruction, explanation as to how the reconstruction assists in fracture detection, and specification that no additional radiation was needed. We performed an audit of pediatric head CTs from patients aged 0-5 for 3 months before and 3 months after our intervention to assess for the number with a reconstruction and compare the utilization rates.

**RESULTS**

In the 3 months prior to our intervention, of the 60 pediatric head CTs ordered for trauma in patients ages 0-5, 5 patients had a 3D reconstruction ordered (8% utilization rate). In the 3 months after our intervention, there were 41 pediatric head CTs ordered with 15 of them having reconstructions (37% utilization rate). The difference in utilization rates was statistically significant (chi-square statistic of 12.2 ( $p = <0.001$ )).\*Discussion Simple modifications to an order set for pediatric trauma can increase utilization of 3D reconstructions. As 3D reconstructions increase diagnostic accuracy for fracture in pediatric head CTs without increased scan time, increased radiation exposure, or increased cost, incorporating their usage into regular clinical practice is a simple way to increase quality of care. By making these simple changes in order sets, we can significantly improve the quality of patient care by aiding in accurate diagnosis of fractures.

Printed on: 02/07/23

## Abstract Archives of the RSNA, 2022

R5A-QI-1

### The Importance of Imaging and Safety for Yttrium90-Microsphere Therapy

Thursday, Dec. 1 12:15PM - 12:45PM Room: Learning Center - QI DPS

#### Participants

Ryan Misseldine, BS, MBA, (*Presenter*) Nothing to Disclose

#### METHODS

Treatment planning at our facility is performed using liver cross sectional imaging (CT/MRI) followed by intraarterial delivery of 5mCi Tc99m-MAA to the lesion(s) of interest. Treatment area volume calculation is then determined using the preprocedure CT/MRI. Nuclear medicine images are used to assess the lung-shunt fraction and any other extrahepatic shunting. After treatment with Y90, patients are imaged using PET/CT to verify site of dose delivery. Our facility decided to track cases after the vendor informed our team that outside facilities were discontinuing the use of pre-therapeutic imaging. These facilities would skip the Tc-99m-MAA SPECT/CT for treatment localization and treat the patient using an assumed lung shunt fraction. We felt it prudent to track cases to determine the validity of this practice. We followed patients where the additional nuclear medicine imaging showed elevated lung-shunting and nontarget extrahepatic activity to assess whether the patient's treatment plan was modified. Modifications included reduction in dose delivered, splitting the dose angiographically between different arteries (Case 1), or changes in treatment plan if patients were precluded from Y90 therapy due to unacceptably high levels of lung shunting (Case 2 3). Case 1: Modified/Split Dose. No Cystic Artery in Angio, visualized gallbladder on SPECT/CT resulted in modified interventional approach and split dose. See Case Image 1. Case 2: Elevated Lung-Shunt: See Case Image 2. Case 3: Elevated Lung-Shunt: - See Case Image 3.

#### RESULTS

Case evaluation confirmed utilizing advanced imaging techniques (preplanning angiography, Geometric lung-shunt evaluation, SPECT/CT, and PET/CT) lead to improved image quality, interventional approach, and patient safety. This is achieved via reduced dose, splitting the dose between different lobar arteries, and validation that dose was delivered without significant exposure to non-target organs.\*Discussion Our facility utilized advanced imaging techniques. It should be noted that all facilities performing Y90s may not have access to a hybridized SPECT/CT, PET/CT, etc.

Printed on: 02/07/23



## Abstract Archives of the RSNA, 2022

R5A-QI-2

### Improving Communication of Unexpected Findings: The Radiology Actionable Findings Tracking (RAFT) System

Thursday, Dec. 1 12:15PM - 12:45PM Room: Learning Center - QI DPS

#### Participants

Surbhi Trivedi, MD, (*Presenter*) Nothing to Disclose

#### METHODS

The Radiology Actionable Findings Tracking (RAFT) program was developed at our institution to compile and track unexpected findings on imaging reports and their follow up. The first step of the pipeline occurs when the reading radiologist integrates a special macro in the report to flag an unexpected finding. The macro includes four fields including the acuity, status of communication, finding and clinical relevance, and recommended follow-up. These macros are then compiled by our EMR into a spreadsheet of findings which is monitored daily by a medically trained coordinator. The coordinator notifies the ordering provider with a message via the EMR. The patient is also contacted within three days of the radiology report via the EMR patient portal notification, traditional mail, or phone. If no action is taken by 8 days, the message is escalated to the ordering provider as well as the primary care provider. In cases when a follow up study was recommended, the task is automatically marked complete and the communication loop closed when the recommended study is ordered. When the coordinator messages the provider within our EMR, the provider can communicate with the staff and also immediately order a follow up study if one was recommended. Additionally, a pop-up notification occurs in the chart as an advisory for the provider to follow up with the recommended order similar to when critical vitals prompt an alert for sepsis work-up.

#### RESULTS

This program has been in use for 2 years and has been adopted among radiologists due to the ease of the macro within the dictation system. On average, 86 unexpected findings were acted on by the provider per month due to the RAFT program. Additionally, an average of 10 findings were escalated per month to an additional provider. Cases of improved patient outcomes include diagnosis of an early-stage pancreatic tumor as well as a suspicious lung nodule found to be early-stage lung cancer.\*Discussion The implementation of the RAFT tracking program for incidental and unexpected findings has likely reduced missed follow-ups with a focus on improving patient outcomes. Limitations include follow up beyond the best efforts to escalate findings. Overall, this is a promising program for tracking data from our high-volume department and ensuring that every unexpected finding is effectively handled to ensure optimal patient health and safety.

Printed on: 02/07/23

## Abstract Archives of the RSNA, 2022

R5A-QI-3

### Contrast Enhanced Mammography - A Potential Game Changer for Breast Conservation Surgery in Developing Nations

Thursday, Dec. 1 12:15PM - 12:45PM Room: Learning Center - QI DPS

#### Participants

Haleema Sherene, MBBS, Coimbatore, India (*Presenter*) Nothing to Disclose

#### METHODS

This project was undertaken by the Breast imaging division in a developing urban tertiary academic hospital. 161 women with breast cancer underwent CEM. The number of mastectomy and BCS and re-surgeries for patients in early and advanced stages were analysed.

#### RESULTS

153 patients (Stage 1: 18, Stage 2: 95, Stage 3: 28 and Stage 4: 11) completed their treatment at the same hospital, of which 72 underwent mastectomy and 78 underwent breast conservation surgery and 11 had metastasis. CEM detected additional lesions and converted to mastectomies in 10 and thereby avoided re-surgeries. CEM defined the extent of lesions better in 14 patients and resulted in negative surgical margins. CEM influenced patient management and avoided re-surgery in 24/153 (15.7%) patients. 3/78 had re-surgeries (3.9%) after CEM due to positive margins. \*Discussion The total procedure cost was 50dollars compared to 200dollars spent for patients who underwent mammography and MRI with contrast. The total time each of these patients spent in the department was less than 4 hours to give them a final decision on surgery. Contrast enhanced mammography may change the perception of breast conservation surgery in a developing country, especially for the lower-income groups.

Printed on: 02/07/23



## Abstract Archives of the RSNA, 2022

R5A-QI-6

### Implementation of a Protocol for Non-Conditional Cardiac Implantable Electronic Devices

Thursday, Dec. 1 12:15PM - 12:45PM Room: Learning Center - QI DPS

#### Participants

Cyndy Kao, BSN, Orange, CA (*Presenter*) Nothing to Disclose

#### METHODS

This was a pilot program performed from April 2021 until April 2022 at a quaternary academic hospital in both inpatient and outpatient settings. The radiology (Radiology Nurse, Quality Nurse) and electrophysiology (EP) (cardiologists, Nurse Practitioner) departments created a protocol to screen and scan patients with non-conditional CIEDs based off the MagnaSafe Registry multicentered study. For the workflow, the Radiology Nurse trained in CIED programming determined appropriate MR labeling and safety using CIED information obtained by schedulers. The appropriate radiologist, ordering provider and patient were notified, and EP evaluation was performed. An EP provider determined if a CIED was appropriate for scanning and documented program parameters in the consultation note. The patient was provided the appropriate educational materials explaining the risks of scanning a CIED off-label prior to the scan. Prior to the scan, the device was interrogated and programmed into the MRI safe mode as specified by the cardiologist. During the MRI, the patient was monitored by the Radiology Nurse while connected to physiologic monitoring equipment (Figure 1A and 1B). We evaluated the number of requests that were obtained in this workflow and how many were able to be scanned safely.

#### RESULTS

Out of 226 CIED requests, 43 (19%) were determined to be non-conditional, while the rest were MRI conditional. 15 of the non-conditional patients were successfully scanned under this new protocol. The remaining 28 patients were not scanned due to various factors including: alternate imaging recommended instead of MRI, insurance denials, permanent epicardial or abandoned/fractured leads, patient declination in participating in protocol due to safety concerns, patient opting to be scanned offsite, and provider cancellation of exam. No adverse events were noted intra or post MRI scan.\*Discussion The implementation of this protocol has increased access to MRI for patients with implanted CIED. We successfully expanded a key imaging modality to 7% of the sample population who previously would not have been considered for MR scan. Patient and staff education were key to the success of this program.

Printed on: 02/07/23



## Abstract Archives of the RSNA, 2022

R5A-QI-7HC

### Quality of Communications; the Unintended Consequences of Decision Support in Advanced Abdominal Imaging

Thursday, Dec. 1 12:15PM - 12:45PM Room: Learning Center - QI DPS

#### Participants

Lillian Dominguez-Konicki, MD, Lebanon, NH (*Presenter*) Nothing to Disclose

#### METHODS

A retrospective review was conducted of all consecutive orders for Abdominal CT exams performed at our institution over a 30-day period following institution of DS, a new, mandatory field in CT imaging orders. Content assessed included the presence/absence of DS free text clinical history (FTCH), the ordering practitioner degree, ordering location, and ordering specialty. Concordance of the DS vs FTCH was assessed by two radiologists. The DS history provided was scored with regard to confidence in protocol selection by an abdominal radiologist with 20 years of experience.

#### RESULTS

450 individual abdominal CT orders were assessed, and in 20%, the FTCH was left blank; DS history was the only history provided. The DS history did not provide sufficient information to enable selection of the optimal CT protocol 24% of the time. When FTCH was provided, it was discordant with the DS history 15% of the time. Orders placed through the emergency department, surgical clinics, and internal medicine subspecialty clinics neglected to include FTCH the most often (23%, 22%, 17%). Inpatient orders failed to include FTCH only 8% of the time. Orders placed by MD/DO failed to provide FTCH 25% of the time compared with 13% for associate providers. \*Discussion This study quantified the unintended consequences to the implementation of DS at our institution, specifically showing a lack of adequate and accurate clinical histories in a substantial number of orders for Abdominal CT exams. We have identified subgroups of providers who could be targeted for initiatives to improve the quality of CI provided in imaging orders. This work is important because safe, high quality patient care in radiology relies on accurate and complete communications from the ordering providers, primarily obtained through the imaging orders. Inaccurate and incomplete clinical information may lead to inappropriate or suboptimal imaging techniques, exposure to ionizing radiation and contrast agents, and negatively impact work efficiency. Please visit the Learning Center to also view this presentation in hardcopy format.

Printed on: 02/07/23



## Abstract Archives of the RSNA, 2022

R5A-QI-8

### **Increasing Utilization of 3D Reconstructions in Pediatric Head CTs for Trauma through Order Set Modification: A Simple Way to Improve Fracture Detection**

Thursday, Dec. 1 12:15PM - 12:45PM Room: Learning Center - QI DPS

#### **Participants**

Thomas Marini, MD, (*Presenter*) Nothing to Disclose

#### **METHODS**

A root cause analysis was performed to identify factors as to why reconstructions were not being ordered by providers. Based on the results, we implemented modifications to the order set for pediatric trauma. Modifications included automatic selection of the 3D reconstruction, explanation as to how the reconstruction assists in fracture detection, and specification that no additional radiation was needed. We performed an audit of pediatric head CTs from patients aged 0-5 for 3 months before and 3 months after our intervention to assess for the number with a reconstruction and compare the utilization rates.

#### **RESULTS**

In the 3 months prior to our intervention, of the 60 pediatric head CTs ordered for trauma in patients ages 0-5, 5 patients had a 3D reconstruction ordered (8% utilization rate). In the 3 months after our intervention, there were 41 pediatric head CTs ordered with 15 of them having reconstructions (37% utilization rate). The difference in utilization rates was statistically significant (chi-square statistic of 12.2 ( $p = <0.001$ )).\*Discussion Simple modifications to an order set for pediatric trauma can increase utilization of 3D reconstructions. As 3D reconstructions increase diagnostic accuracy for fracture in pediatric head CTs without increased scan time, increased radiation exposure, or increased cost, incorporating their usage into regular clinical practice is a simple way to increase quality of care. By making these simple changes in order sets, we can significantly improve the quality of patient care by aiding in accurate diagnosis of fractures.

Printed on: 02/07/23



## Abstract Archives of the RSNA, 2022

R5B-QI

### Quality Improvement Reports Thursday Poster Discussions - B

Thursday, Dec. 1 12:45PM - 1:15PM Room: Learning Center - QI DPS

#### Sub-Events

#### R5B-QI-1 A Clear Picture: Leveraging Automated Technology to Gain Insight into Real-Time Workflows

##### Participants

Ayman Abunimer, MD, Atlanta, GA (*Presenter*) Nothing to Disclose

##### METHODS

The intervention was performed in two high volume interventional suites in a large academic center. IRB approval was waived. HIPPA compliant depth detection sensors installed in each room were trained to identify the following states: "patient in (I)", "patient on table (OT)", "patient off table (FT)", "patient out (O)". For ground truth, images were labeled by the study team. A ML algorithm was developed to generate timestamps for the states from the images. Timestamps from the RIS were accessed. We compared the ML and RIS data to ground truth. Deviation is measured as minutes in excess of the ground truth average. Z-testing was used to determine significance.

##### RESULTS

511 procedures were performed in the IR suites between May 11, 2021 and December 9, 2021. We found gaps in data 38% of the time with the ML data and 48% of the time with RIS data. Gaps in the ML data occurred due to unplugging and/or moving of the equipment and computer memory storage. Gaps in the RIS were due to missing data entries, e.g. human error. At ground truth patients transited the room at the following average times: room A I=0, OT=6, FT=105, O=110 minutes; room B [0, 3, 76, 78] minutes. Data from the ML algorithm was closer to ground truth than from the RIS data. Deviation from ground truth for each state was: ML: room A I=1, OT=3, FT=2, O=4 minutes, 5% average error; room B [2, 3, 4, 3, 8% error rate] minutes; RIS room A [1, 6, 21, 17, 28% error rate] and room B [1, 3, 14, 13, 24% error rate]. Z-test confirmed that the mean differential of the ML data is lower than the mean for the institutional data source beyond 3 standard deviations ( $P < 0.001$ ). \*Discussion ML algorithm data was more accurate than the manually entered RIS data in evaluating IR room utilization. Although gaps in data were found in the ML generated data, these are all easily solved by increased computing memory and device location redesign.

#### R5B-QI-2 A New Era of Quality Improvement: Creating a Digital Twin of the Radiology Department to Drive Efficiencies in Operations and Workflow

##### Participants

Robert MacDougall, PhD, (*Presenter*) Employee, Quantivly Inc

##### METHODS

We used a commercially available software platform, Quantivly, that harmonizes radiology metadata to provide a unified data layer describing MRI operations. The unified data layer is the basis of the digital twin which can be used to simulate intervention without the cost of real-world experimentation. We identified exams that would have the biggest impact, ordered exams by cumulative duration, i.e. the sum in hours for a given exam, over a 90 day period. The top exam in the "body" section was "MR PROSTATE WITH AND WITHOUT CONTRAST" by a wide margin - 123 hours vs. 50.4 hours for the second highest. We compared slot sizes ranging from 30 - 60 mins to quantify the benefit (additional patients per week) and risk (number of exams delayed and median delay time). We identified the top 10 longest instances to investigate methods to further reduce delays in the schedule.

##### RESULTS

We calculated results for each potential slot size over the analysis period of 90 days (197 exams total). At the current slot size (60 min), no patients that exceeded the slot. At 45 mins, the cumulative time saved was 49.3 hours, representing 5 additional patients per week, with 15 (9.6%) patients exceeding the slot size with a median delay of 4.3min. \*Discussion While there were no delays with our current slot, this does not represent the best trade-off in terms of patient access. Through simulation, we were able to predict the benefit and risks of changing a scheduled slot size for the top body exam from 60 min to 45 min, creating slots for 5 additional patients per week, reducing wait times, and increasing department revenue. In the future, by troubleshooting the longest instances, we plan to identify the clinical, technical, and demographic factors that lead to longer exam durations which can lead to additional improvements in MRI operations and workflow.

#### R5B-QI-3 Identification of Health Literacy Disparity - Delivering Patient-friendly Radiology Reports to Spanish-speaking Populations

##### Participants

Jennifer Kemp, MD, Denver, CO (*Presenter*) Stockholder, Scanslated, Inc

##### METHODS

At 10 outpatient imaging centers in a metropolitan city, patients receive a notification when their radiology report is available to be viewed on a web-based interactive patient portal with lay language definitions and diagrams. The interactive report has a toggle

switch that patients can use to display the content in Spanish (Figure 1). The population in this city is 31% Latino and 57% of those identify Spanish as their primary language. Based on local population data we would expect up to 17% of our patient population to prefer to view patient-friendly explanations in Spanish. We analyzed data to determine what percentage of our patients were using the Spanish translation feature, and compared this with demographics of the local population.

## RESULTS

95 patients utilized our Spanish language content over a 1.5 year period, which is 0.1% of all patients who viewed a patient-friendly report. These 95 patients viewed 1,670 plain language definitions in Spanish. During this same time period, 402,445 definitions were viewed in English. The Feedback from patients utilizing Spanish language content was favorable, with 96% indicating that the definitions and diagrams help them to understand their report.\*Discussion Health equity is a priority for RSNA and ACR, and the identification of specific healthcare disparities is the first step in addressing them. Our analysis found that only 0.1% of patients viewing a patient-friendly radiology report have utilized the available Spanish language content, despite Pew research data showing that 17% identify Spanish as their preferred language. This discrepancy has motivated efforts to improve accessibility for our Spanish speaking patients. Beyond providing a toggle switch for Spanish translation, efforts need to be made to educate patients that this tool is available. Educated and informed patients make better healthcare decisions and have improved health outcomes. Helping Spanish speaking patients to better understand imaging results through access to patient-friendly reports may help address current disparities in this patient population.

### **R5B-QI-4HC Investigating Optimal Protocol for Image-Guided Tissue Sampling in Cases of Suspected Lymphoid Neoplasm**

Participants  
Mathew Smith, MD, (*Presenter*) Nothing to Disclose

## METHODS

Context and Intervention: No institutional standardized process was in place for image-guided tissue sampling in cases of suspected or possible lymphoid neoplasm with significant variability in tissue sampling, tissue processing, and subsequent results between cases. To identify the significant factors which contributed to obtaining a diagnosis and WHO classification in these cases, the relevant cases from 2018 were identified using the Illuminate InSight search engine and the discoverable variables were collected. Study of the Intervention: We compare various features of specimen collection based on the classification outcome (diagnosis of LN with WHO classification, diagnosis of LN without WHO classification, and Indeterminate) Measures/Metrics: We provide descriptive statistics, including mean (standard deviation), median (interquartile range), range for continuous variables, and counts/percentages for categorical variables. We test for a significant difference between the three groups using univariate tests. For continuous variables, we use the Kruskal-Wallis test; for categorical variables, we use the Fisher's Exact Test. We consider a p-value of less than 0.05 to be significant.

## RESULTS

Table 1 compares the specimen collection characteristics between cases which resulted in LN diagnosis plus WHO classification (LN +WHO), LN diagnosis without WHO classification (LN - WHO), and indeterminate samples from the first 6 months of data collection. There is a significant difference in the type of analysis performed, core minimal length, core gauge, and flow.\*Discussion The preliminary results from the first 6 months of data collection suggest that specimen with a diagnosis and WHO classification have a larger core biopsy gauge and length, use both core biopsy and fine-needle aspiration, and provide adequate sampling for flow cytometry. Limitations to the study were mainly secondary to a lack of standardized reporting, limiting the number of factors that were able to be teased out retrospectively. Please visit the Learning Center to also view this presentation in hardcopy format.

### **R5B-QI-5 Improving Consistency in Physician Performance in Cardiac Fluoroscopic Procedures within Six Facilities Using Outlier Analyses**

Participants  
James Winslow, PhD, Glenwood, IL (*Presenter*) Nothing to Disclose

## METHODS

This project was performed for six different hospitals. Twelve months of fluoroscopic procedure data was collected for each facility using two dose monitoring software products, Landauer OPTIMIZE(Fluke Health Solution, Glenwood, IL) and Radimetrics(Bayer HealthCare, Leverkusen, Germany). The data fields collected/analyzed included facility, scanner model, performing physician, study description, and reference point dose(RPD). For each facility, the most frequently performed cardiac procedure and scanner model was identified. For these procedures, means and standard deviations for RPD were calculated for each facility. Outliers for each facility were defined as procedures having dose values more than three standard deviations greater than the mean value. The percentage of outliers of total procedures were calculated for each facility and for each individual physician. Calculated data from all facilities were combined and sorted by Performing Physician from greatest percentage of outliers to least. Cumulative percentage values for total exams and total outliers were then calculated.

## RESULTS

Facility outlier percentage ranged from 1.5-2.7%. From this, an achievable target for percentage of outliers at three percent was selected. For physicians with >10 procedures, individual physician outlier percentage values ranged from 0-16.7%(Figure 1). A subset of performing physicians who exceeded the achievable target for outlier percentage were identified at each facility for quality review (Table 1). For 5 of 6 facilities, more than 70% of outliers were performed by physicians marked for quality review even though those physicians performed fewer than 43% of the total procedures(Table 1). After sorting physicians from highest to lowest by individual percentage of outliers, cumulative percentages of exams and outliers were calculated. 17% of physicians were responsible for 100% of outliers (Figure 2).\*Discussion The data analyzed is sufficient to give valuable physician feedback to improve fluoroscopy patient doses. Use of this data in a quality improvement context would yield improved clinical outcomes This approach identifies physicians who may benefit from shared education from physicians identified as less prone to having high dose procedures. One limitation of our study is that it presumes physicians using the same study description and system are performing similar procedures.

### **R5B-QI-6 Development and Optimization of Multiparametric MRI for Bladder Cancer: Opportunities for Standardization and Quality Improvement**

Participants

## **METHODS**

Once an initial protocol was developed from the VI-RADS literature(2,3,5), more nuanced optimization of performance used (n =5) healthy volunteers. The image quality and scan time optimized protocol was run with an initial sample of patients by a niche technologist team trained and supervised by the radiologist and MR physics team. Image quality metrics, including SNR and CNR were calculated on acquired images using open source software MRQy(6). All scanning was performed on either 750w or Premier 3T MRIs (GE Healthcare Chicago, IL). Three iterations of the protocol are displayed in Table 1 and Figure 1. The initial protocol, an intermediate protocol optimized based upon an image quality review of the protocol performed in volunteers and the, final protocol.

## **RESULTS**

Protocol changes include improving DWI SNR by increasing slice thickness from 3 to 4 mm. Additionally, the synthetic b-value image was found to be of limited use and was not included in the final protocol. Small FOV T2 resolution was improved by reducing the FOV and increasing the frequency encode matrix. Due to scan time limitations no other offsets were made which resulted in a reduction of SNR, seen in Figure 2b. Optimization of resolution and SNR improved the quality of both T2 and DWI imaging of the bladder (Figure 2, 3).\*Discussion VI-RADS compliant multiparametric bladder MR imaging provides a standardized approach for imaging bladder lesions that improves the quality of care for patients with suspected bladder cancer. The development and optimization of this protocol necessitates an iterative approach incorporating phantom, volunteer and patient imaging for quantitative assessments of image quality and validation. This workflow illustrates key considerations pertinent to protocol development.

## **R5B-QI-7 Impact of PET/MR Imaging in Patients with Gynecologic Cancers Undergoing Same-Day PET/CT: A Patient-Centric Approach**

### Participants

Dhakshina Ganeshan, FRCR,MBBS, , (*Presenter*) Nothing to Disclose

## **METHODS**

In this traditional model, apart from the actual lengthy scanning time, the patients had to wait for a significant amount of time between the procedures, contributing to patient discomfort. In our project, combined PET/MR imaging was only performed in those patients who were undergoing same-day PET/CT, utilizing the same radioactivity as required for a stand-alone PET/CT study. We evaluated the time taken for performing the PET/CT, standard pelvic MRI, and the combined PET/MR. We also evaluated the diagnostic performance of the PET/CT and PET/MRI for TNM staging. The McNemar test was employed for statistical analysis.

## **RESULTS**

49 patients were included in the final analysis of this HIPAA-compliant, prospective quality improvement board approved, and IRB-approved retrospective study. The time spent in the imaging area for undergoing a diagnostic PET/CT was 143 minutes and that for a pelvic MRI was 134 minutes. The combined overall time spent in the imaging area for a PET/CT followed by pelvic MR was 277 minutes. In contrast, the patients spent only 170 minutes on the combined PET/MR procedure. Hence, performing a PET/MR reduced the time spent by the patient in the imaging department by 38.6%. PET/MRI was superior to the PET/CT in nodal staging, as PET/MRI detected adenopathy in 5 patients, which was missed on the PET/CT (P=0.031). Furthermore, PET/MRI detected pelvic metastases in 10 patients that were missed using PET/CT, and PET/CT also falsely upstaged pelvic metastasis in 4 patients. However, this was not statistically significant (P=0.12)..\*Discussion Our study indicates that in patients with gynecologic cancers who are scheduled to undergo both PET/CT and MRI, it may be feasible to consider performing combined PET/MR. Performing a PET MR will reduce the time spent by the patient in the hospital and may improve patient experience and satisfaction. Performing a PET/MR reduced the time spent by the patient in the department by 38.6%.

Printed on: 02/07/23



## Abstract Archives of the RSNA, 2022

R5B-QI-1

### A Clear Picture: Leveraging Automated Technology to Gain Insight into Real-Time Workflows

Thursday, Dec. 1 12:45PM - 1:15PM Room: Learning Center - QI DPS

#### Participants

Ayman Abunimer, MD, Atlanta, GA (*Presenter*) Nothing to Disclose

#### METHODS

The intervention was performed in two high volume interventional suites in a large academic center. IRB approval was waived. HIPPA compliant depth detection sensors installed in each room were trained to identify the following states: "patient in (I)", "patient on table (OT)", "patient off table (FT)", "patient out (O)". For ground truth, images were labeled by the study team. A ML algorithm was developed to generate timestamps for the states from the images. Timestamps from the RIS were accessed. We compared the ML and RIS data to ground truth. Deviation is measured as minutes in excess of the ground truth average. Z-testing was used to determine significance.

#### RESULTS

511 procedures were performed in the IR suites between May 11, 2021 and December 9, 2021. We found gaps in data 38% of the time with the ML data and 48% of the time with RIS data. Gaps in the ML data occurred due to unplugging and/or moving of the equipment and computer memory storage. Gaps in the RIS were due to missing data entries, e.g. human error. At ground truth patients transited the room at the following average times: room A I=0, OT=6, FT=105, O=110 minutes; room B [0, 3, 76, 78] minutes. Data from the ML algorithm was closer to ground truth than from the RIS data. Deviation from ground truth for each state was: ML: room A I=1, OT=3, FT=2, O=4 minutes, 5% average error; room B [2, 3, 4, 3, 8% error rate] minutes; RIS room A [1, 6, 21, 17, 28% error rate] and room B [1, 3, 14, 13, 24% error rate]. Z-test confirmed that the mean differential of the ML data is lower than the mean for the institutional data source beyond 3 standard deviations ( $P < 0.001$ ). \*Discussion ML algorithm data was more accurate than the manually entered RIS data in evaluating IR room utilization. Although gaps in data were found in the ML generated data, these are all easily solved by increased computing memory and device location redesign.

Printed on: 02/07/23



## Abstract Archives of the RSNA, 2022

R5B-QI-2

### A New Era of Quality Improvement: Creating a Digital Twin of the Radiology Department to Drive Efficiencies in Operations and Workflow

Thursday, Dec. 1 12:45PM - 1:15PM Room: Learning Center - QI DPS

#### Participants

Robert MacDougall, PhD, (*Presenter*) Employee, Quantivly Inc

#### METHODS

We used a commercially available software platform, Quantivly, that harmonizes radiology metadata to provide a unified data layer describing MRI operations. The unified data layer is the basis of the digital twin which can be used to simulate intervention without the cost of real-world experimentation. We identified exams that would have the biggest impact, ordered exams by cumulative duration, i.e. the sum in hours for a given exam, over a 90 day period. The top exam in the "body" section was "MR PROSTATE WITH AND WITHOUT CONTRAST" by a wide margin - 123 hours vs. 50.4 hours for the second highest. We compared slot sizes ranging from 30 - 60 mins to quantify the benefit (additional patients per week) and risk (number of exams delayed and median delay time). We identified the top 10 longest instances to investigate methods to further reduce delays in the schedule.

#### RESULTS

We calculated results for each potential slot size over the analysis period of 90 days (197 exams total). At the current slot size (60 min), no patients that exceeded the slot. At 45 mins, the cumulative time saved was 49.3 hours, representing 5 additional patients per week, with 15 (9.6%) patients exceeding the slot size with a median delay of 4.3min. \*Discussion While there were no delays with our current slot, this does not represent the best trade-off in terms of patient access. Through simulation, we were able to predict the benefit and risks of changing a scheduled slot size for the top body exam from 60 min to 45 min, creating slots for 5 additional patients per week, reducing wait times, and increasing department revenue. In the future, by troubleshooting the longest instances, we plan to identify the clinical, technical, and demographic factors that lead to longer exam durations which can lead to additional improvements in MRI operations and workflow.

Printed on: 02/07/23



## Abstract Archives of the RSNA, 2022

R5B-QI-3

### Identification of Health Literacy Disparity - Delivering Patient-friendly Radiology Reports to Spanish-speaking Populations

Thursday, Dec. 1 12:45PM - 1:15PM Room: Learning Center - QI DPS

#### Participants

Jennifer Kemp, MD, Denver, CO (*Presenter*) Stockholder, Scanslated, Inc

#### METHODS

At 10 outpatient imaging centers in a metropolitan city, patients receive a notification when their radiology report is available to be viewed on a web-based interactive patient portal with lay language definitions and diagrams. The interactive report has a toggle switch that patients can use to display the content in Spanish (Figure 1). The population in this city is 31% Latino and 57% of those identify Spanish as their primary language. Based on local population data we would expect up to 17% of our patient population to prefer to view patient-friendly explanations in Spanish. We analyzed data to determine what percentage of our patients were using the Spanish translation feature, and compared this with demographics of the local population.

#### RESULTS

95 patients utilized our Spanish language content over a 1.5 year period, which is 0.1% of all patients who viewed a patient-friendly report. These 95 patients viewed 1,670 plain language definitions in Spanish. During this same time period, 402,445 definitions were viewed in English. The Feedback from patients utilizing spanish language content was favorable, with 96% indicating that the definitions and diagrams help them to understand their report.\*Discussion Health equity is a priority for RSNA and ACR, and the identification of specific healthcare disparities is the first step in addressing them. Our analysis found that only 0.1% of patients viewing a patient-friendly radiology report have utilized the available Spanish language content, despite Pew research data showing that 17% identify Spanish as their preferred language. This discrepancy has motivated efforts to improve accessibility for our Spanish speaking patients. Beyond providing a toggle switch for Spanish translation, efforts need to be made to educate patients that this tool is available. Educated and informed patients make better healthcare decisions and have improved health outcomes. Helping Spanish speaking patients to better understand imaging results through access to patient-friendly reports may help address current disparities in this patient population.

Printed on: 02/07/23

## Abstract Archives of the RSNA, 2022

R5B-QI-4HC

### Investigating Optimal Protocol for Image-Guided Tissue Sampling in Cases of Suspected Lymphoid Neoplasm

Thursday, Dec. 1 12:45PM - 1:15PM Room: Learning Center - QI DPS

#### Participants

Mathew Smith, MD, (*Presenter*) Nothing to Disclose

#### METHODS

**Context and Intervention:** No institutional standardized process was in place for image-guided tissue sampling in cases of suspected or possible lymphoid neoplasm with significant variability in tissue sampling, tissue processing, and subsequent results between cases. To identify the significant factors which contributed to obtaining a diagnosis and WHO classification in these cases, the relevant cases from 2018 were identified using the Illuminate InSight search engine and the discoverable variables were collected. **Study of the Intervention:** We compare various features of specimen collection based on the classification outcome (diagnosis of LN with WHO classification, diagnosis of LN without WHO classification, and Indeterminate) **Measures/Metrics:** We provide descriptive statistics, including mean (standard deviation), median (interquartile range), range for continuous variables, and counts/percentages for categorical variables. We test for a significant difference between the three groups using univariate tests. For continuous variables, we use the Kruskal-Wallis test; for categorical variables, we use the Fisher's Exact Test. We consider a p-value of less than 0.05 to be significant.

#### RESULTS

Table 1 compares the specimen collection characteristics between cases which resulted in LN diagnosis plus WHO classification (LN +WHO), LN diagnosis without WHO classification (LN - WHO), and indeterminate samples from the first 6 months of data collection. There is a significant difference in the type of analysis performed, core minimal length, core gauge, and flow.\***Discussion** The preliminary results from the first 6 months of data collection suggest that specimen with a diagnosis and WHO classification have a larger core biopsy gauge and length, use both core biopsy and fine-needle aspiration, and provide adequate sampling for flow cytometry. Limitations to the study were mainly secondary to a lack of standardized reporting, limiting the number of factors that were able to be teased out retrospectively. Please visit the Learning Center to also view this presentation in hardcopy format.

Printed on: 02/07/23



## Abstract Archives of the RSNA, 2022

R5B-QI-5

### Improving Consistency in Physician Performance in Cardiac Fluoroscopic Procedures within Six Facilities Using Outlier Analyses

Thursday, Dec. 1 12:45PM - 1:15PM Room: Learning Center - QI DPS

#### Participants

James Winslow, PhD, Glenwood, IL (*Presenter*) Nothing to Disclose

#### METHODS

This project was performed for six different hospitals. Twelve months of fluoroscopic procedure data was collected for each facility using two dose monitoring software products, Landauer OPTIMIZE(Fluke Health Solution, Glenwood, IL) and Radimetrics(Bayer HealthCare, Leverkusen, Germany). The data fields collected/analyzed included facility, scanner model, performing physician, study description, and reference point dose(RPD). For each facility, the most frequently performed cardiac procedure and scanner model was identified. For these procedures, means and standard deviations for RPD were calculated for each facility. Outliers for each facility were defined as procedures having dose values more than three standard deviations greater than the mean value. The percentage of outliers of total procedures were calculated for each facility and for each individual physician. Calculated data from all facilities were combined and sorted by Performing Physician from greatest percentage of outliers to least. Cumulative percentage values for total exams and total outliers were then calculated.

#### RESULTS

Facility outlier percentage ranged from 1.5-2.7%. From this, an achievable target for percentage of outliers at three percent was selected. For physicians with >10 procedures, individual physician outlier percentage values ranged from 0-16.7%(Figure 1). A subset of performing physicians who exceeded the achievable target for outlier percentage were identified at each facility for quality review (Table 1). For 5 of 6 facilities, more than 70% of outliers were performed by physicians marked for quality review even though those physicians performed fewer than 43% of the total procedures(Table 1). After sorting physicians from highest to lowest by individual percentage of outliers, cumulative percentages of exams and outliers were calculated. 17% of physicians were responsible for 100% of outliers (Figure 2).\*Discussion The data analyzed is sufficient to give valuable physician feedback to improve fluoroscopy patient doses. Use of this data in a quality improvement context would yield improved clinical outcomes This approach identifies physicians who may benefit from shared education from physicians identified as less prone to having high dose procedures. One limitation of our study is that it presumes physicians using the same study description and system are performing similar procedures.

Printed on: 02/07/23

## Abstract Archives of the RSNA, 2022

R5B-QI-6

### Development and Optimization of Multiparametric MRI for Bladder Cancer: Opportunities for Standardization and Quality Improvement

Thursday, Dec. 1 12:45PM - 1:15PM Room: Learning Center - QI DPS

#### Participants

Chris Walker, PhD, Houston, TX (*Presenter*) Researcher, Siemens AG

#### METHODS

Once an initial protocol was developed from the VI-RADS literature(2,3,5), more nuanced optimization of performance used (n =5) healthy volunteers. The image quality and scan time optimized protocol was run with an initial sample of patients by a niche technologist team trained and supervised by the radiologist and MR physics team. Image quality metrics, including SNR and CNR were calculated on acquired images using open source software MRQy(6). All scanning was performed on either 750w or Premier 3T MRIs (GE Healthcare Chicago, IL). Three iterations of the protocol are displayed in Table 1 and Figure 1. The initial protocol, an intermediate protocol optimized based upon an image quality review of the protocol performed in volunteers and the, final protocol.

#### RESULTS

Protocol changes include improving DWI SNR by increasing slice thickness from 3 to 4 mm. Additionally, the synthetic b-value image was found to be of limited use and was not included in the final protocol. Small FOV T2 resolution was improved by reducing the FOV and increasing the frequency encode matrix. Due to scan time limitations no other offsets were made which resulted in a reduction of SNR, seen in Figure 2b. Optimization of resolution and SNR improved the quality of both T2 and DWI imaging of the bladder (Figure 2, 3).\*Discussion VI-RADS compliant multiparametric bladder MR imaging provides a standardized approach for imaging bladder lesions that improves the quality of care for patients with suspected bladder cancer. The development and optimization of this protocol necessitates an iterative approach incorporating phantom, volunteer and patient imaging for quantitative assessments of image quality and validation. This workflow illustrates key considerations pertinent to protocol development.

Printed on: 02/07/23

## Abstract Archives of the RSNA, 2022

R5B-QI-7

### Impact of PET/MR Imaging in Patients with Gynecologic Cancers Undergoing Same-Day PET/CT: A Patient-Centric Approach

Thursday, Dec. 1 12:45PM - 1:15PM Room: Learning Center - QI DPS

#### Participants

Dhakshina Ganeshan, FRCR, MBBS, , (Presenter) Nothing to Disclose

#### METHODS

In this traditional model, apart from the actual lengthy scanning time, the patients had to wait for a significant amount of time between the procedures, contributing to patient discomfort. In our project, combined PET/MR imaging was only performed in those patients who were undergoing same-day PET/CT, utilizing the same radioactivity as required for a stand-alone PET/CT study. We evaluated the time taken for performing the PET/CT, standard pelvic MRI, and the combined PET/MR. We also evaluated the diagnostic performance of the PET/CT and PET/MRI for TNM staging. The McNemar test was employed for statistical analysis.

#### RESULTS

49 patients were included in the final analysis of this HIPAA-compliant, prospective quality improvement board approved, and IRB-approved retrospective study. The time spent in the imaging area for undergoing a diagnostic PET/CT was 143 minutes and that for a pelvic MRI was 134 minutes. The combined overall time spent in the imaging area for a PET/CT followed by pelvic MR was 277 minutes. In contrast, the patients spent only 170 minutes on the combined PET/MR procedure. Hence, performing a PET/MR reduced the time spent by the patient in the imaging department by 38.6%. PET/MRI was superior to the PET/CT in nodal staging, as PET/MRI detected adenopathy in 5 patients, which was missed on the PET/CT ( $P=0.031$ ). Furthermore, PET/MRI detected pelvic metastases in 10 patients that were missed using PET/CT, and PET/CT also falsely upstaged pelvic metastasis in 4 patients. However, this was not statistically significant ( $P=0.12$ ). \*Discussion Our study indicates that in patients with gynecologic cancers who are scheduled to undergo both PET/CT and MRI, it may be feasible to consider performing combined PET/MR. Performing a PET MR will reduce the time spent by the patient in the hospital and may improve patient experience and satisfaction. Performing a PET/MR reduced the time spent by the patient in the department by 38.6%.

Printed on: 02/07/23

## Abstract Archives of the RSNA, 2022

S3A-QI

### Quality Improvement Reports Sunday Poster Discussions - A

Sunday, Nov. 27 11:45AM - 12:15PM Room: Learning Center - QI DPS

#### Sub-Events

#### S3A-QI-1 **Can an Artificial Intelligence System (AIS) help human readers in a Digital Mammography (DM) Breast Screening Program (BSP)? Our preliminary experience.**

##### Participants

Claudia M. Weiss, MD, Treviso, Italy (*Presenter*) Nothing to Disclose

##### METHODS

From November 2021 to March 2022, 19310 women attended BSP of Treviso (Italy) (range age 50-74yrs, mean age 60.6 yrs) using different DM units (Hologic, Fuji, Philips) and analyzed with AIS Lunit INSIGHT MMG. ExSs were grouped into four levels: normal/benign/probably benign (=10%) as group 1 (G1); moderate suspicion of malignancy (>10%- =50%) as group 2 (G2); high suspicion of malignancy (>50%- <95%) as group 3 (G3); highly suggestive of malignancy (=95%) as group 4 (G4). Except for ExS =10%, all suspicious lesions were marked and % reported. After being processed, all DMs were successively assessed by five Dedicated Breast Radiologists (DBRs) with at least two years of experience (median 10.8 yrs). Arbitration of discordant reports of HBDR was used in cases of disagreement. During AIS-aided HBDR, ExS was visible to DBRs. The positive predictive values (PPV), negative predictive values (NPV), sensitivity, and specificity of AIS were calculated using the ExS cutoff of >10% as positive.

##### RESULTS

The distribution of ExS among the different groups was: G1 79.5%(15359/19310), G2 17.3%(3350/19310), G3 2.7%(512/19310), G4 4%(80/19310). In a subgroup analysis, 12570/19310 (65%) were scored =5%. AIS classified 20.4%(3942/19310) of the DMs as positive (>10%), while AIS-aided HBDR recalled patients were 447/19.310(RR 2.3%). The detected biopsy-confirmed BCs were 127(DR 6.6‰): 80% (102/127; DR 5.3‰) detected by both readers, the remaining 20% (25/127) only by one reader; AIS correctly identified 98%(125/127; DR 6.5‰) BCs. The average ExS of the BCs was 84% (range 5.97%-99.89%) with following distribution: G1 1.6% (2/127), G2 10.2% (13/127), G3 36.2% (46/127), G4 52% (66/127). The AIS demonstrates a sensitivity of 98.43%, specificity of 80.10%, NPV of 99.99%, and PPV of 3.2% against AIS-aided HBDR PPV of 28.4%. No BC was detected in exams with ExS =5% (NPV 100%).\*Discussion The very low AIS PPV makes it challenging to propose a BSP with only AIS standalone reading. Human reading compensates for the very low PPV of AIS because DBRs also have access to previous mammograms. However, the exceptional AIS's NPV in the subgroup of exams with Exs =5% allows us to hypothesize their automatic preselection for DBRs single reading, thus significantly reducing the BSP workload while maintaining the overall sensitivity.

#### S3A-QI-2 **Improving Rates of Breast Cancer Risk Assessment Completion at Time of Screening Mammography**

##### Participants

Jocelyn Cheng, (*Presenter*) Nothing to Disclose

##### METHODS

This project was performed at a high volume quaternary breast imaging center in addition to two community imaging centers. The study sample was all women presenting for screening mammography. Beginning November 2, 2020, patients who presented for screening mammography began receiving breast cancer risk assessment (CRA), specifically, the Tyrer-Cuzick risk assessment model. the first month of administration, 9% of patients completed CRA screening. CRA administrators were surveyed to determine major factors contributing to low rates of CRA screening completion. Common responses included window of assessment availability during business hours, English-only administration, limited options for completing CRA screening tool at time of mammography, and insufficient training in explaining CRA screening to patients. To address these barriers to screening, multiple interventions were performed: CRA screening was emailed to participants prior to mammography visit, patients were actively encouraged to complete screening by staff at time of mammogram, forms with multiple languages were offered in both virtual (iPad) and paper format, and screening completion was double-checked by a technologist and administrator to ensure correct entry of data. The impact of these interventions was assessed by comparing the number of successfully completed CRA screening surveys at time of mammography visit to total number of mammograms using an interrupted time series model in MATLAB.

##### RESULTS

Analysis demonstrated that our interventions resulted in an immediate increase in CRA completion rates. The percent of patients with successful CRA completion increased from 8.8% to 50% in the first four months (p<0.01) and to 71% at 18 months (p<0.01).\*Discussion Limitations in our study include generalizability and difficulty in ascribing increase in CRA completion rates to a single intervention. Using classic process improvement tools and a multi-step intervention focused largely on removing patient barriers to CRA completion, we significantly increased the rate of CRA completion at our three breast imaging centers.

#### S3A-QI-3 **The FIND Program: Improving Follow-Up of Incidental Imaging Findings**

##### Participants

Kaitlin Zaki-Metias, MD, Pontiac, MI (*Presenter*) Nothing to Disclose

## **METHODS**

This study was approved by the institutional review board. A retrospective analysis of 2000 patients with computed tomographic cross-sectional imaging was performed; 1000 patients prior to implementation of the FIND Program and 1000 patients one year after establishment of the program. Data collected included the frequency of incidental findings, inclusion of follow-up recommendations in the radiology report, and adherence to suggested follow-up. These metrics were analyzed using the SPSS statistics software version 25.0.

## **RESULTS**

There was a higher rate of completion of recommended follow-up imaging in the post-implementation group (47/104, 45.2%) compared to the pre-implementation group (41/128, 32.0%) ( $p=0.043$ ), of which 88.2% (30/34) occurred within the recommended time frame, compared to 56.3% (18/32) in the pre-implementation group ( $p=0.005$ ). \*Discussion Implementation of an incidental findings tracking program resulted in improved follow-up of incidental imaging findings and adherence to follow-up within the recommended time frame. This has the potential to reduce the burden of clinically significant incidental findings on the healthcare system due to lack of follow-up possibly resulting in later presentation of advanced disease. Given its value, further studies should explore the utility of more sophisticated artificial intelligence softwares in incidental findings tracking programs.

### **S3A-QI-4 Untangling the Spaghetti: Improving Retrieval Time for CT Supplies Using 5S**

#### **Awards**

**Identified for RadioGraphics  
Quality Improvement Reports Award**

#### **Participants**

Theresa Pham, MD, BS, Salt Lake City, UT (*Presenter*) Nothing to Disclose

## **METHODS**

This project was performed in the Huntsman Cancer Hospital (HCH) CT room which stores supplies for two CT scanners, including a busy interventional procedure scanner. Images were taken of the supplies in the CT closet, workroom, and procedure room before and after storage reorganization. Storage reorganization was based off the Lean 5S Methodology (Sort, Set in order, Shine, Standardize, and Sustain). Analysis of the impact of supply reorganization and labeling was performed using three methods: 1) spaghetti diagrams of participants during a 10-item supply retrieval scavenger hunt before and after, 2) timed 10-item supply retrieval scavenger hunt before and after, 3) satisfaction surveys of medical providers/staff before and after. Items participants were asked to retrieve for the timed scavenger hunt included commonly used items such as: sterile gloves, sterile gauze, 50 mL syringe, sterile gown, 18G needle, biopsy tray, Christmas tree adapter, sterile saline/water, a mask, and a 3-way stopcock.

## **RESULTS**

Seven radiology residents voluntarily participated in the timed supply scavenger hunt before and after our intervention. Spaghetti diagrams demonstrated a reduction in redundant foot traffic with supply retrieval after storage reorganization. Additionally, there was a 61.7% decrease in the average amount of time it took to find the 10 items in the scavenger hunt with a p-value of 0.0013. Satisfaction surveys after the intervention had overall more positive responses. \*Discussion Using the 5S Methodology for storage reorganization, we were able to achieve our goal of reducing the time to find supplies and increasing satisfaction scores from both CT technicians and medical providers. We were also able to decrease redundant foot traffic throughout the storage areas. Future directions include extending the organization/labeling system to other CT storage areas within our academic institution, implementing a Kanban system, and working with management to maintain this current level of organization.

### **S3A-QI-5 Use of Bunker shifts alleviates Long List Anxiety Syndrome (LLAS)**

#### **Awards**

**Quality Improvement Reports Award**

#### **Participants**

Eric A. Brandser, MD, (*Presenter*) Owner, Shift Procurement Services, LLC

## **METHODS**

The group created several voluntary and additionally compensated Bunker shifts, including a shift based on a fixed number of wRVU, a short time-based shift, and a time and productivity hybrid shift. Bunkers were deployed sparingly at first, with increased usage in each subsequent year. In 2020 the group added "ad hoc" bunkers, with a group text system to anyone interested in helping if needed when the list of cases to read became long. Ad hoc bunkers would be called by a member of the scheduled team on a given day whose job included watching the workload for imbalances.

## **RESULTS**

The Bunker shifts have significantly improved practice scheduling on our busier days, allowing ad hoc recruitment of reading capacity when needed on a day by day and hour by hour basis. Use of Bunker shifts has increased every year since inception in 2018. Number of days where day shift stays longer than 30 minutes beyond expected end of day has been reduced dramatically. Group productivity increased every year. wRVU/FTE/year (total wRVU in a given year divided by FTE in the group) increased 12% in 2018, 21% in 2019, 13% in 2020 and 29% in 2021 when compared to 2017 values. Group bonus increased every year since 2017, with increases of 7% in 2018, 26% in 2019, 22% in 2020, and 37% in 2021 compared to baseline 2017. \*Discussion Implementation and expansion of the Bunker shifts has had several group benefits. The publishing of individual wRVU data has stopped, as the group abandoned the idea that slower readers can or should read faster. Morale of the group has improved, with significantly fewer tough and late days. Group productivity has increased by shifting more cases to readers in highly efficient shifts. The increased efficiency has translated to improved bonus compensation, which has increased every year comparing to 2017 (pre bunker).

### **S3A-QI-7 Clinical Implementation of an AI-driven Lung Nodule Algorithm QA Project in the ED Setting**

#### **Awards**

**Quality Improvement Reports Award**

#### **Participants**

Irene Dixe de Oliveira Santo, MD, New Haven, CT (*Presenter*) Nothing to Disclose

## METHODS

An innovative workflow tool previously developed by our team in collaboration with AIDOC, the proprietary company that created the lung nodule detection algorithm, was implemented in the emergency radiology division of our academic, tertiary center. Data was collected in accordance with the HIPAA Privacy Rule using our institution's EMR, and an IRB waiver was granted. Our project's process map can be found in figure 1.

## RESULTS

15750 CT scans were analyzed between October 1, 2021, to April 9, 2022. Aidoc identified pulmonary nodules not referenced by the radiologist in radiology reports of CT scans of 26 patients: 16 females and 10 males. Our group found an odds ratio of 2.65 for algorithm detection of missed lung nodules in patients in which the CT scan included the full chest in comparison to those in which only a portion of the chest was imaged. The average age at the time of CT was 64.3 years (range: 41-87 years). Addendums were issued for 16 patients (61.5%), and the time from the original report to the addendum was 1 day and 9 hours, or 1980 minutes, on average. The average size of the nodules in which an addendum was issued was 6 mm (range 3-10 mm).\*Discussion The intervention was non-intrusive, with only 0.17% of all CTs requiring additional review. Based on the prevalence of incidental pulmonary nodules, it can be estimated that thousands of ultimately irrelevant notifications were avoided, greatly reducing the time spent by the reading radiologist to adjudicate AI findings during interpretation. Relevant addendums were issued promptly, when necessary. The actual impact on patient outcomes is unclear at this point but can be further explored over time. Until such time as AI programs become sophisticated enough to incorporate comparison imaging and clinical history into their assessment in real-time, a QA program such as the one utilized by this department provides a nonobtrusive means for ensuring appropriate reporting and follow-up of incidental pulmonary nodules in the emergent setting with minimal disruption to radiologist workflow.

### S3A-QI-8 Creation and Implementation of a PACS-Integrated Vasari Feature Classification Tool

#### Participants

Irene Dixe de Oliveira Santo, MD, New Haven, CT (*Presenter*) Nothing to Disclose

## METHODS

The manual approach for VASARI feature extraction involved online consulting of the VASARI set, evaluation of the images on the PACS, and entering the information for each individual patient into an excel sheet prior to sharing with other users. For the creation of our tool, the VASARI feature set was integrated into the PACS application programming interface. After clicking the VASARI tool icon in the PACS, the features appear in a separate pop-up window, with options to be selected by the user. The answers can then be saved directly into the PACS and reviewed by other users.

## RESULTS

Our PACS-integrated tool allows for dramatically improved efficiency, resulting in a 50 minute decrease in the time needed to complete VASARI feature extraction, from the 1 hour required by the previously used multi-platform approach to approximately 10 minutes. Furthermore, our tool allows batch exporting of the VASARI features simultaneously for multiple patients prior to data analysis and processing.\*Discussion Integration of a VASARI features classification tool into PACS substantially improves workflow of both physicians and data scientists involved in the classification of brain tumors and the creation and validation of machine learning algorithms. This allows for much-needed time efficient radiomic feature extraction and has numerous potential applications in the clinical setting.

Printed on: 02/07/23

## Abstract Archives of the RSNA, 2022

S3A-QI-1

### Can an Artificial Intelligence System (AIS) help human readers in a Digital Mammography (DM) Breast Screening Program (BSP)? Our preliminary experience.

Sunday, Nov. 27 11:45AM - 12:15PM Room: Learning Center - QI DPS

#### Participants

Claudia M. Weiss, MD, Treviso, Italy (*Presenter*) Nothing to Disclose

#### METHODS

From November 2021 to March 2022, 19310 women attended BSP of Treviso (Italy) (range age 50-74yrs, mean age 60.6 yrs) using different DM units (Hologic, Fuji, Philips) and analyzed with AIS Lunit INSIGHT MMG. ExSs were grouped into four levels: normal/benign/probably benign (=10%) as group 1 (G1); moderate suspicion of malignancy (>10%-=50%) as group 2 (G2); high suspicion of malignancy (>50%-<95%) as group 3 (G3); highly suggestive of malignancy (=95%) as group 4 (G4). Except for ExS =10%, all suspicious lesions were marked and % reported. After being processed, all DMs were successively assessed by five Dedicated Breast Radiologists (DBRs) with at least two years of experience (median 10.8 yrs). Arbitration of discordant reports of HBDR was used in cases of disagreement. During AIS-aided HBDR, ExS was visible to DBRs. The positive predictive values (PPV), negative predictive values (NPV), sensitivity, and specificity of AIS were calculated using the ExS cutoff of >10% as positive.

#### RESULTS

The distribution of ExS among the different groups was: G1 79.5%(15359/19310), G2 17.3%(3350/19310), G3 2.7%(512/19310), G4 4%(80/19310). In a subgroup analysis, 12570/19310 (65%) were scored =5%. AIS classified 20.4%(3942/19310) of the DMs as positive (>10%), while AIS-aided HBDR recalled patients were 447/19.310(RR 2.3%). The detected biopsy-confirmed BCs were 127(DR 6.6‰): 80% (102/127; DR 5.3‰) detected by both readers, the remaining 20% (25/127) only by one reader; AIS correctly identified 98%(125/127; DR 6.5‰) BCs. The average ExS of the BCs was 84% (range 5.97%-99.89%) with following distribution: G1 1.6% (2/127), G2 10.2% (13/127), G3 36.2% (46/127), G4 52% (66/127). The AIS demonstrates a sensitivity of 98.43%, specificity of 80.10%, NPV of 99.99%, and PPV of 3.2% against AIS-aided HBDR PPV of 28.4%. No BC was detected in exams with ExS =5% (NPV 100%).\*Discussion The very low AIS PPV makes it challenging to propose a BSP with only AIS standalone reading. Human reading compensates for the very low PPV of AIS because DBRs also have access to previous mammograms. However, the exceptional AIS's NPV in the subgroup of exams with Exs =5% allows us to hypothesize their automatic preselection for DBRs single reading, thus significantly reducing the BSP workload while maintaining the overall sensitivity.

Printed on: 02/07/23



## Abstract Archives of the RSNA, 2022

S3A-QI-2

### Improving Rates of Breast Cancer Risk Assessment Completion at Time of Screening Mammography

Sunday, Nov. 27 11:45AM - 12:15PM Room: Learning Center - QI DPS

#### Participants

Jocelyn Cheng, (*Presenter*) Nothing to Disclose

#### METHODS

This project was performed at a high volume quaternary breast imaging center in addition to two community imaging centers. The study sample was all women presenting for screening mammography. Beginning November 2, 2020, patients who presented for screening mammography began receiving breast cancer risk assessment (CRA), specifically, the Tyrer-Cuzick risk assessment model. In the first month of administration, 9% of patients completed CRA screening. CRA administrators were surveyed to determine major factors contributing to low rates of CRA screening completion. Common responses included window of assessment availability during business hours, English-only administration, limited options for completing CRA screening tool at time of mammography, and insufficient training in explaining CRA screening to patients. To address these barriers to screening, multiple interventions were performed: CRA screening was emailed to participants prior to mammography visit, patients were actively encouraged to complete screening by staff at time of mammogram, forms with multiple languages were offered in both virtual (iPad) and paper format, and screening completion was double-checked by a technologist and administrator to ensure correct entry of data. The impact of these interventions was assessed by comparing the number of successfully completed CRA screening surveys at time of mammography visit to total number of mammograms using an interrupted time series model in MATLAB.

#### RESULTS

Analysis demonstrated that our interventions resulted in an immediate increase in CRA completion rates. The percent of patients with successful CRA completion increased from 8.8% to 50% in the first four months ( $p < 0.01$ ) and to 71% at 18 months ( $p < 0.01$ ). \*Discussion Limitations in our study include generalizability and difficulty in ascribing increase in CRA completion rates to a single intervention. Using classic process improvement tools and a multi-step intervention focused largely on removing patient barriers to CRA completion, we significantly increased the rate of CRA completion at our three breast imaging centers.

Printed on: 02/07/23



## Abstract Archives of the RSNA, 2022

S3A-QI-3

### The FIND Program: Improving Follow-Up of Incidental Imaging Findings

Sunday, Nov. 27 11:45AM - 12:15PM Room: Learning Center - QI DPS

#### Participants

Kaitlin Zaki-Metias, MD, Pontiac, MI (*Presenter*) Nothing to Disclose

#### METHODS

This study was approved by the institutional review board. A retrospective analysis of 2000 patients with computed tomographic cross-sectional imaging was performed; 1000 patients prior to implementation of the FIND Program and 1000 patients one year after establishment of the program. Data collected included the frequency of incidental findings, inclusion of follow-up recommendations in the radiology report, and adherence to suggested follow-up. These metrics were analyzed using the SPSS statistics software version 25.0.

#### RESULTS

There was a higher rate of completion of recommended follow-up imaging in the post-implementation group (47/104, 45.2%) compared to the pre-implementation group (41/128, 32.0%) ( $p=0.043$ ), of which 88.2% (30/34) occurred within the recommended time frame, compared to 56.3% (18/32) in the pre-implementation group ( $p=0.005$ ). \*Discussion Implementation of an incidental findings tracking program resulted in improved follow-up of incidental imaging findings and adherence to follow-up within the recommended time frame. This has the potential to reduce the burden of clinically significant incidental findings on the healthcare system due to lack of follow-up possibly resulting in later presentation of advanced disease. Given its value, further studies should explore the utility of more sophisticated artificial intelligence softwares in incidental findings tracking programs.

Printed on: 02/07/23



## Abstract Archives of the RSNA, 2022

S3A-QI-4

### Untangling the Spaghetti: Improving Retrieval Time for CT Supplies Using 5S

Sunday, Nov. 27 11:45AM - 12:15PM Room: Learning Center - QI DPS

#### Awards

Identified for RadioGraphics

Quality Improvement Reports Award

#### Participants

Theresa Pham, MD, BS, Salt Lake City, UT (*Presenter*) Nothing to Disclose

#### METHODS

This project was performed in the Huntsman Cancer Hospital (HCH) CT room which stores supplies for two CT scanners, including a busy interventional procedure scanner. Images were taken of the supplies in the CT closet, workroom, and procedure room before and after storage reorganization. Storage reorganization was based off the Lean 5S Methodology (Sort, Set in order, Shine, Standardize, and Sustain). Analysis of the impact of supply reorganization and labeling was performed using three methods: 1) spaghetti diagrams of participants during a 10-item supply retrieval scavenger hunt before and after, 2) timed 10-item supply retrieval scavenger hunt before and after, 3) satisfaction surveys of medical providers/staff before and after. Items participants were asked to retrieve for the timed scavenger hunt included commonly used items such as: sterile gloves, sterile gauze, 50 mL syringe, sterile gown, 18G needle, biopsy tray, Christmas tree adapter, sterile saline/water, a mask, and a 3-way stopcock.

#### RESULTS

Seven radiology residents voluntarily participated in the timed supply scavenger hunt before and after our intervention. Spaghetti diagrams demonstrated a reduction in redundant foot traffic with supply retrieval after storage reorganization. Additionally, there was a 61.7% decrease in the average amount of time it took to find the 10 items in the scavenger hunt with a p-value of 0.0013. Satisfaction surveys after the intervention had overall more positive responses.\*Discussion Using the 5S Methodology for storage reorganization, we were able to achieve our goal of reducing the time to find supplies and increasing satisfaction scores from both CT technicians and medical providers. We were also able to decrease redundant foot traffic throughout the storage areas. Future directions include extending the organization/labeling system to other CT storage areas within our academic institution, implementing a Kanban system, and working with management to maintain this current level of organization.

Printed on: 02/07/23



## Abstract Archives of the RSNA, 2022

S3A-QI-5

### Use of Bunker shifts alleviates Long List Anxiety Syndrome (LLAS)

Sunday, Nov. 27 11:45AM - 12:15PM Room: Learning Center - QI DPS

#### Awards

##### Quality Improvement Reports Award

#### Participants

Eric A. Brandser, MD, (*Presenter*) Owner, Shift Procurement Services, LLC

#### METHODS

The group created several voluntary and additionally compensated Bunker shifts, including a shift based on a fixed number of wRVU, a short time-based shift, and a time and productivity hybrid shift. Bunkers were deployed sparingly at first, with increased usage in each subsequent year. In 2020 the group added "ad hoc" bunkers, with a group text system to anyone interested in helping if needed when the list of cases to read became long. Ad hoc bunkers would be called by a member of the scheduled team on a given day whose job included watching the workload for imbalances.

#### RESULTS

The Bunker shifts have significantly improved practice scheduling on our busier days, allowing ad hoc recruitment of reading capacity when needed on a day by day and hour by hour basis. Use of Bunker shifts has increased every year since inception in 2018. Number of days where day shift stays longer than 30 minutes beyond expected end of day has been reduced dramatically. Group productivity increased every year. wRVU/FTE/year (total wRVU in a given year divided by FTE in the group) increased 12% in 2018, 21% in 2019, 13% in 2020 and 29 % in 2021 when compared to 2017 values. Group bonus increased every year since 2017, with increases of 7% in 2018, 26% in 2019, 22% in 2020, and 37% in 2021 compared to baseline 2017.\*Discussion Implementation and expansion of the Bunker shifts has had several group benefits. The publishing of individual wRVU data has stopped, as the group abandoned the idea that slower readers can or should read faster. Morale of the group has improved, with significantly fewer tough and late days. Group productivity has increased by shifting more cases to readers in highly efficient shifts. The increased efficiency has translated to improved bonus compensation, which has increased every year comparing to 2017 (pre bunker).

Printed on: 02/07/23



## Abstract Archives of the RSNA, 2022

S3A-QI-7

### Clinical Implementation of an AI-driven Lung Nodule Algorithm QA Project in the ED Setting

Sunday, Nov. 27 11:45AM - 12:15PM Room: Learning Center - QI DPS

#### Awards

Quality Improvement Reports Award

#### Participants

Irene Dixe de Oliveira Santo, MD, New Haven, CT (*Presenter*) Nothing to Disclose

#### METHODS

An innovative workflow tool previously developed by our team in collaboration with AIDOC, the proprietary company that created the lung nodule detection algorithm, was implemented in the emergency radiology division of our academic, tertiary center. Data was collected in accordance with the HIPAA Privacy Rule using our institution's EMR, and an IRB waiver was granted. Our project's process map can be found in figure 1.

#### RESULTS

15750 CT scans were analyzed between October 1, 2021, to April 9, 2022. Aidoc identified pulmonary nodules not referenced by the radiologist in radiology reports of CT scans of 26 patients: 16 females and 10 males. Our group found an odds ratio of 2.65 for algorithm detection of missed lung nodules in patients in which the CT scan included the full chest in comparison to those in which only a portion of the chest was imaged. The average age at the time of CT was 64.3 years (range: 41-87 years). Addendums were issued for 16 patients (61.5%), and the time from the original report to the addendum was 1 day and 9 hours, or 1980 minutes, on average. The average size of the nodules in which an addendum was issued was 6 mm (range 3-10 mm).\*Discussion The intervention was non-intrusive, with only 0.17% of all CTs requiring additional review. Based on the prevalence of incidental pulmonary nodules, it can be estimated that thousands of ultimately irrelevant notifications were avoided, greatly reducing the time spent by the reading radiologist to adjudicate AI findings during interpretation. Relevant addendums were issued promptly, when necessary. The actual impact on patient outcomes is unclear at this point but can be further explored over time. Until such time as AI programs become sophisticated enough to incorporate comparison imaging and clinical history into their assessment in real-time, a QA program such as the one utilized by this department provides a nonobtrusive means for ensuring appropriate reporting and follow-up of incidental pulmonary nodules in the emergent setting with minimal disruption to radiologist workflow.

Printed on: 02/07/23



## Abstract Archives of the RSNA, 2022

S3A-QI-8

### Creation and Implementation of a PACS-Integrated Vasari Feature Classification Tool

Sunday, Nov. 27 11:45AM - 12:15PM Room: Learning Center - QI DPS

#### Participants

Irene Dixe de Oliveira Santo, MD, New Haven, CT (*Presenter*) Nothing to Disclose

#### METHODS

The manual approach for VASARI feature extraction involved online consulting of the VASARI set, evaluation of the images on the PACS, and entering the information for each individual patient into an excel sheet prior to sharing with other users. For the creation of our tool, the VASARI feature set was integrated into the PACS application programming interface. After clicking the VASARI tool icon in the PACS, the features appear in a separate pop-up window, with options to be selected by the user. The answers can then be saved directly into the PACS and reviewed by other users.

#### RESULTS

Our PACS-integrated tool allows for dramatically improved efficiency, resulting in a 50 minute decrease in the time needed to complete VASARI feature extraction, from the 1 hour required by the previously used multi-platform approach to approximately 10 minutes. Furthermore, our tool allows batch exporting of the VASARI features simultaneously for multiple patients prior to data analysis and processing.\*Discussion Integration of a VASARI features classification tool into PACS substantially improves workflow of both physicians and data scientists involved in the classification of brain tumors and the creation and validation of machine learning algorithms. This allows for much-needed time efficient radiomic feature extraction and has numerous potential applications in the clinical setting.

Printed on: 02/07/23



## Abstract Archives of the RSNA, 2022

S3B-QI

### Quality Improvement Reports Sunday Poster Discussions - B

Sunday, Nov. 27 12:15PM - 12:45PM Room: Learning Center - QI DPS

#### Sub-Events

#### S3B-QI-2 Breast Interventions e-Consent

##### Participants

Haydee Ojeda-Fournier, MD, San Diego, CA (*Presenter*) Research Consultant, View Point Medical, Inc; Stock options, CureMetrix, Inc

##### METHODS

A gap analysis was performed as part of a lean sigma six green belt project to identify the root cause and guide improvement. We performed a "5 Whys" and completed a fishbone diagram. Why is there a problem (use of paper consent forms)? Not aware that EPIC has a solution and that we could do e-Consents. The target conditions identified were Zero paper, Zero scans. The countermeasures proposed were: using e-Consent and documenting brief procedure notes in Epic. Purchase of Topaz for ease of obtaining the patient's signature. No further purchasing of duplicate paper consent forms or paper progress notes. Not involving six team members to achieve one task and removing the courier service, shredding service, scanning, storage of paper forms. Investing in training in the use of e-Consent and Epic documenting. Creation of "standard work" documents for e-Consent and EPIC progress notes. The plan included: visiting divisions that were currently using e-Consent. Meet with information technology representative specializing in EPIC to learn how to use e-Consent and to make sure it is available to breast radiologists. Purchase and set up of Topaz. Made sure all radiologists were trained on e-Consent EPIC. Additional training of technologists and RNs in creating and bringing up e-Consent. Discussion with risk management to confirm the process for signature. Creation of template for brief procedure note in EPIC. Coordinate with EPIC topaz.

##### RESULTS

Safely changed to e-Consents. Cost of Topaz signature pad \$1,000/unit. Culture changed rather quickly as the radiologist saw the value once a completed swim lane and spaghetti diagram were presented to them. The target condition was achieved. No longer ordering paper consent forms or assembling packages for biopsy. No longer utilizing courier service.\*Discussion Breast imaging centers at institutions that utilize EPIC EMR can leverage the e-Consent features to reduce waste and streamline operations. Future steps include an audit to ensure that consent forms are being signed. Also, convening with other procedural divisions in radiology to share best practices and lessons learned and considering an alternative to Topaz signature capture device: tablet for e-Consent or utilizing iPhone to capture signatures.

#### S3B-QI-3 Strategies for Improving the Impact and Outcomes of the Peer Learning and Improvement Meeting

##### Participants

Jonathan Kruskal, MBChB, Boston, MA (*Presenter*) Nothing to Disclose

##### METHODS

In an ongoing IRB-approved project, we used standard data collection and analytical tools to identify hurdles to the effective introduction and function of peer learning across our enterprise. Tools included a steering think tank, direct observation of PLI meetings, surveys of meeting participants and leaders, and analysis of case review data submitted after each meeting. Data sources were from monthly section PLI forums (9 sections), modality operations meetings, and data submitted into a PLI platform (almost 18,000 cases). Once hurdles were identified, practice leaders and quality officers developed strategies for their mitigation.

##### RESULTS

We identified 10 hurdles to effective PLI practice. (1) The need to educate radiologists about the structural components of PLI, the specific criteria for meeting accreditation requirements, and differences between PLI and peer review. (2) Implement effective strategies to foster submissions and participation. (3) Identify and train PLI meeting leaders. A wide variation of PLI meeting moderating approaches was identified. We designed a PLI leader training curriculum. (4) Building enduring learning repositories. We implemented strategies for minimizing perceptual and interpretive biases, built enduring and expanding collections of recognized pearls and pitfalls, and engaged trainees in PLI practices. (5) Foster academic advancement in the teaching and education track for PLI leaders. (6) Structure personal case reviews. We developed programs on bias awareness, personal reflection and personal bias profiles. (7) Identification and management of PQI opportunities. We trained and tasked a group of radiologists in systems thinking to identify improvement opportunities. (8) Ensure workflow automation and minimal interruptions to work processes. (9) Sharing and communicating the benefits and outcomes of PLI case submission and review. (10) Address the fact that PLI requirements are perceived as yet another "moral insult".\*Discussion We identified 10 hurdles to implementation of effective PLI practices, then designed and implemented specific and novel strategies to mitigate their impact.

#### S3B-QI-4 Driving Mammography Image Quality Improvement Using A.I. In Guyana During the COVID-19 Pandemic

##### Participants

Mohamed Abdoell, MSc, Halifax, NS (*Presenter*) Founder and CEO, Densitas Inc

## METHODS

In-person MIT training by RAD-AID breast radiologists is restricted during the COVID-19 pandemic, impeding critical MG positioning feedback. An A.I. mammography quality platform (Densitas® IntelliMammo™), introduced at GPHC in August 2022, provides technologists (trained on software use 9/2021) with positioning feedback. Pre-adoption, positioning error rates on 897 mammograms (8/1/2020-10/31/2021) were retrospectively evaluated. Post-adoption error rates were assessed prospectively on 585 mammograms (11/1/2021-4/15/2022). Five common positioning errors (CC exaggeration, inadequate pectoralis muscle length, inframammary fold (IMF) missing, nipple not in profile and pectoralis muscle concave) were evaluated. A test of equal proportions was used to test the null hypothesis of equality of proportions for each positioning error prior to and following adoption; four MITs utilized the software and one did not. Two RAD-AID radiologists were interviewed to understand quality improvement experiences, workflows and challenges pre/post software adoption.

## RESULTS

MG positioning error rates were statistically significant ( $p < 0.05$ ) pre/post-software adoption for four MITs who used A.I. software compared to one that did not (Fig. 1a). MG positioning error rates were statistically significant ( $p < 0.05$ ) for 4 out of 5 positioning errors for four MITs utilizing AI compared to one that did not (Fig. 1b). Prior to A.I. adoption, MITs infrequently communicated challenges with positioning and radiologists' feedback was subjective. Post-adoption, MIT-radiologist communication improved and A.I. quantitative results sparked development of educational training videos to improve MG image quality. \*Discussion A.I. drives MG image quality improvements in Guyana by reducing MG positioning error rates and enhancing MIT-radiologist communications to guide effective, remote, MG positioning training. A study limitation is the low number of MITs (one in the control arm and four in the intervention arm).

### S3B-QI-8 Increasing Utilization and Improving Documentation in a Radiology Critical Alert System

#### Participants

Robert W. Morris, MD, (*Presenter*) Nothing to Disclose

## METHODS

**Context Intervention:** This project was performed at a 720-bed academic medical center. Our system utilizes 3 alert levels: Red (emergency), Orange (requires attention) and Yellow (follow-up needed). Prior to intervention, an average of 662 monthly critical alerts were submitted, with a time compliance rate of 99%, and with 89.8% of alerts to providers with current contact info in our system. Compliance with Red alert documentation requirements was 83.3%. Our intervention was as follows: We distributed a streamlined critical results policy to radiology faculty residents, with periodic policy reminders. Event reports were generated for inadequate documentation. To address the provider contact database, we engaged providers and leadership to increase submission of current contact info. **Study of the Intervention:** The intervention was studied by our Critical Results Coordinators using our critical results software. As there were no other interventions involving our critical alert system, we were able to attribute all changes to our interventions. **Measures/Metrics** Over 15 months, we tracked the numbers of critical alerts, radiologic exams, and alerts to providers without contact info. We also tracked compliance with Red alert documentation and communication times. **Analysis:** The data was plotted versus time, and trendlines were generated for each parameter. The trendline slopes were interpreted as the average monthly change. Change-point analysis was performed to assess statistical significance.

## RESULTS

There was an average increase of 23 alerts per month (95% CI: 13.2-33.2). Yellow alerts increased by 17 per month, which was statistically significant ( $p = 0.033$ ). Red alert documentation compliance increased 0.65% per month. Alerts to providers with current contact information increased 0.5% per month. Closed-loop communication time compliance remained =99%. \*Discussion Implementation of a quality project to increase usage of the critical alert system showed an increase in the number of alerts generated. In particular, alerts for follow-up recommendations increased, helping to ensure that patients receive follow-up care. The major limitation of our project was that it did not evaluate for findings that should have generated an alert but did not. Our intervention improved documentation for emergency alerts, and improved our provider contact database. Compliance with communication time goals was not sacrificed to achieve these results.

Printed on: 02/07/23



## Abstract Archives of the RSNA, 2022

S3B-QI-2

### Breast Interventions e-Consent

Sunday, Nov. 27 12:15PM - 12:45PM Room: Learning Center - QI DPS

#### Participants

Haydee Ojeda-Fournier, MD, San Diego, CA (*Presenter*) Research Consultant, View Point Medical, Inc; Stock options, CureMetrix, Inc

#### METHODS

A gap analysis was performed as part of a lean sigma six green belt project to identify the root cause and guide improvement. We performed a "5 Whys" and completed a fishbone diagram. Why is there a problem (use of paper consent forms)? Not aware that EPIC has a solution and that we could do e-Consents. The target conditions identified were Zero paper, Zero scans. The countermeasures proposed were: using e-Consent and documenting brief procedure notes in Epic. Purchase of Topaz for ease of obtaining the patient's signature. No further purchasing of duplicate paper consent forms or paper progress notes. Not involving six team members to achieve one task and removing the courier service, shredding service, scanning, storage of paper forms. Investing in training in the use of e-Consent and Epic documenting. Creation of "standard work" documents for e-Consent and EPIC progress notes. The plan included: visiting divisions that were currently using e-Consent. Meet with information technology representative specializing in EPIC to learn how to use e-Consent and to make sure it is available to breast radiologists. Purchase and set up of Topaz. Made sure all radiologists were trained on e-Consent EPIC. Additional training of technologists and RNs in creating and bringing up e-Consent. Discussion with risk management to confirm the process for signature. Creation of template for brief procedure note in EPIC. Coordinate with EPIC topaz.

#### RESULTS

Safely changed to e-Consents. Cost of Topaz signature pad \$1,000/unit. Culture changed rather quickly as the radiologist saw the value once a completed swim lane and spaghetti diagram were presented to them. The target condition was achieved. No longer ordering paper consent forms or assembling packages for biopsy. No longer utilizing courier service.\*Discussion Breast imaging centers at institutions that utilize EPIC EMR can leverage the e-Consent features to reduce waste and streamline operations. Future steps include an audit to ensure that consent forms are being signed. Also, convening with other procedural divisions in radiology to share best practices and lessons learned and considering an alternative to Topaz signature capture device: tablet for e-Consent or utilizing iPhone to capture signatures.

Printed on: 02/07/23



## Abstract Archives of the RSNA, 2022

S3B-QI-3

### Strategies for Improving the Impact and Outcomes of the Peer Learning and Improvement Meeting

Sunday, Nov. 27 12:15PM - 12:45PM Room: Learning Center - QI DPS

#### Participants

Jonathan Kruskal, MBChB, Boston, MA (*Presenter*) Nothing to Disclose

#### METHODS

In an ongoing IRB-approved project, we used standard data collection and analytical tools to identify hurdles to the effective introduction and function of peer learning across our enterprise. Tools included a steering think tank, direct observation of PLI meetings, surveys of meeting participants and leaders, and analysis of case review data submitted after each meeting. Data sources were from monthly section PLI forums (9 sections), modality operations meetings, and data submitted into a PLI platform (almost 18,000 cases). Once hurdles were identified, practice leaders and quality officers developed strategies for their mitigation.

#### RESULTS

We identified 10 hurdles to effective PLI practice. (1) The need to educate radiologists about the structural components of PLI, the specific criteria for meeting accreditation requirements, and differences between PLI and peer review. (2) Implement effective strategies to foster submissions and participation. (3) Identify and train PLI meeting leaders. A wide variation of PLI meeting moderating approaches was identified. We designed a PLI leader training curriculum. (4) Building enduring learning repositories. We implemented strategies for minimizing perceptual and interpretive biases, built enduring and expanding collections of recognized pearls and pitfalls, and engaged trainees in PLI practices. (5) Foster academic advancement in the teaching and education track for PLI leaders. (6) Structure personal case reviews. We developed programs on bias awareness, personal reflection and personal bias profiles. (7) Identification and management of PQI opportunities. We trained and tasked a group of radiologists in systems thinking to identify improvement opportunities. (8) Ensure workflow automation and minimal interruptions to work processes. (9) Sharing and communicating the benefits and outcomes of PLI case submission and review. (10) Address the fact that PLI requirements are perceived as yet another "moral insult".\*Discussion We identified 10 hurdles to implementation of effective PLI practices, then designed and implemented specific and novel strategies to mitigate their impact.

Printed on: 02/07/23



## Abstract Archives of the RSNA, 2022

S3B-QI-4

### Driving Mammography Image Quality Improvement Using A.I. In Guyana During the COVID-19 Pandemic

Sunday, Nov. 27 12:15PM - 12:45PM Room: Learning Center - QI DPS

#### Participants

Mohamed Abdoell, MSc, Halifax, NS (*Presenter*) Founder and CEO, Densitas Inc

#### METHODS

In-person MIT training by RAD-AID breast radiologists is restricted during the COVID-19 pandemic, impeding critical MG positioning feedback. An A.I. mammography quality platform (Densitas® intelliMammo™), introduced at GPHC in August 2022, provides technologists (trained on software use 9/2021) with positioning feedback. Pre-adoption, positioning error rates on 897 mammograms (8/1/2020-10/31/2021) were retrospectively evaluated. Post-adoption error rates were assessed prospectively on 585 mammograms (11/1/2021-4/15/2022). Five common positioning errors (CC exaggeration, inadequate pectoralis muscle length, inframammary fold (IMF) missing, nipple not in profile and pectoralis muscle concave) were evaluated. A test of equal proportions was used to test the null hypothesis of equality of proportions for each positioning error prior to and following adoption; four MITs utilized the software and one did not. Two RAD-AID radiologists were interviewed to understand quality improvement experiences, workflows and challenges pre/post software adoption.

#### RESULTS

MG positioning error rates were statistically significant ( $p < 0.05$ ) pre/post-software adoption for four MITs who used A.I. software compared to one that did not (Fig. 1a). MG positioning error rates were statistically significant ( $p < 0.05$ ) for 4 out of 5 positioning errors for four MITs utilizing AI compared to one that did not (Fig. 1b). Prior to A.I. adoption, MITs infrequently communicated challenges with positioning and radiologists' feedback was subjective. Post-adoption, MIT-radiologist communication improved and A.I. quantitative results sparked development of educational training videos to improve MG image quality. \*Discussion A.I. drives MG image quality improvements in Guyana by reducing MG positioning error rates and enhancing MIT-radiologist communications to guide effective, remote, MG positioning training. A study limitation is the low number of MITs (one in the control arm and four in the intervention arm).

Printed on: 02/07/23



## Abstract Archives of the RSNA, 2022

S3B-QI-8

### Increasing Utilization and Improving Documentation in a Radiology Critical Alert System

Sunday, Nov. 27 12:15PM - 12:45PM Room: Learning Center - QI DPS

#### Participants

Robert W. Morris, MD, (*Presenter*) Nothing to Disclose

#### METHODS

**Context Intervention:** This project was performed at a 720-bed academic medical center. Our system utilizes 3 alert levels: Red (emergency), Orange (requires attention) and Yellow (follow-up needed). Prior to intervention, an average of 662 monthly critical alerts were submitted, with a time compliance rate of 99%, and with 89.8% of alerts to providers with current contact info in our system. Compliance with Red alert documentation requirements was 83.3%. Our intervention was as follows: We distributed a streamlined critical results policy to radiology faculty residents, with periodic policy reminders. Event reports were generated for inadequate documentation. To address the provider contact database, we engaged providers and leadership to increase submission of current contact info. **Study of the Intervention:** The intervention was studied by our Critical Results Coordinators using our critical results software. As there were no other interventions involving our critical alert system, we were able to attribute all changes to our interventions. **Measures/Metrics** Over 15 months, we tracked the numbers of critical alerts, radiologic exams, and alerts to providers without contact info. We also tracked compliance with Red alert documentation and communication times. **Analysis:** The data was plotted versus time, and trendlines were generated for each parameter. The trendline slopes were interpreted as the average monthly change. Change-point analysis was performed to assess statistical significance.

#### RESULTS

There was an average increase of 23 alerts per month (95% CI: 13.2-33.2). Yellow alerts increased by 17 per month, which was statistically significant ( $p=0.033$ ). Red alert documentation compliance increased 0.65% per month. Alerts to providers with current contact information increased 0.5% per month. Closed-loop communication time compliance remained =99%. **Discussion** Implementation of a quality project to increase usage of the critical alert system showed an increase in the number of alerts generated. In particular, alerts for follow-up recommendations increased, helping to ensure that patients receive follow-up care. The major limitation of our project was that it did not evaluate for findings that should have generated an alert but did not. Our intervention improved documentation for emergency alerts, and improved our provider contact database. Compliance with communication time goals was not sacrificed to achieve these results.

Printed on: 02/07/23

## Abstract Archives of the RSNA, 2022

T2-QI

### Quality Improvement Reports Tuesday Poster Discussions

Tuesday, Nov. 29 9:00AM - 9:30AM Room: Learning Center - QI DPS

#### Sub-Events

#### T2-QI-1 Effectiveness of Palm Vein Recognition Biometric Technology to Prevent Patient Misidentification Errors

##### Participants

Rekha Mody, MD, Cleveland, OH (*Presenter*) Nothing to Disclose

##### METHODS

Palm vein recognition devices which integrated with the health system's electronic health record (EHR) were installed at an imaging center's front desk and at workstations on wheels (WOWs) throughout the department. We conducted a 4 week pilot to test the accuracy of a palm vein recognition device to: 1. Re-identify patients at the point of care when the imaging study was performed on the same date 2. Re-identify patients at the front desk who had a repeat appointment on a different date during the pilot time period. The pilot program was performed at a hospital with intermediate imaging exam volume and scope included outpatient imaging only. This site provided a small, controlled environment with quick throughput, a cross section of most imaging studies, and exams performed with IV contrast. The unique environment allowed for the patient to undergo initial enrollment with the device at the front desk and authentication when the patient's imaging exam was performed later in the same encounter. Patients were queried on desire to participate in the pilot with initial enrollment utilizing a palm vein biometric recognition device as the patient commenced the check-in process at the front desk. Subsequently, the patient was escorted to the imaging exam area and both the standard process, confirmation of the patient's name and date of birth via the EHR, and the test process, re-identification of the patient via the palm vein recognition device, were done prior to the imaging exam being performed.

##### RESULTS

During the 4 week pilot time period, approximately 570 unique patients were seen with a total of 596 patient visits (total of 3.5% enrolled patients had repeat encounters). Total exams performed (including 8 imaging modalities) was 759 with a total enrollment of 455 unique patients. The enrollment rate was 80% and authentication rate at the point of care was 75%. 88% of repeat patients were re-authenticated at the front desk and 50% of repeat patient were re-authenticated at the point of care. The pilot demonstrate 100% accurate identification of re-authenticated repeat patient (at the front desk registration and the point of care when imaging exam was performed).\*Discussion 100% of re-authenticated repeat patient (at the front desk registration and the point of care) were identified accurately using palm vein recognition biometric technology. Thus, this technology can serve as a safe, accurate and consistent method to prevent patient misidentification errors at imaging front desks and re-authentication of a patient's identity prior to imaging exam point of care and may help to decrease or eliminate wrong patient and wrong site, side or contrast administration type imaging safety events.

#### T2-QI-3 Optimizing the Abdominal CT Oral Contrast Service in the Covid-19 Pandemic

##### Participants

Mary Renton, MBBCh, (*Presenter*) Nothing to Disclose

##### METHODS

Leveraging a multidisciplinary stakeholder collaboration, we optimized the oral contrast service by 2 interventions:1) Creation of 'oral contrast policy' document and revision of standardized CT protocols with judicious use of oral contrast only when supported by literature evidence.2) Creation of a new shorter oral contrast regime (30 minutes vs 60 minutes previously).We conducted a multicentre retrospective service evaluation of our outpatient (OP) CT at baseline (pre-pandemic, pp), baseline pandemic prior to intervention(p), and post-intervention. Time-efficiency was assessed using patient waiting times. A blinded image quality review was conducted on the old and new oral contrast regimes by 2 abdominal radiologists. Cost evaluation was performed. Patient experience was evaluated with a voluntary survey. Statistical analysis was performed to compare the baseline and evaluation outcomes.

##### RESULTS

Over one-month periods, OP CT scans were assessed in baseline(pp) n = 302, baseline(p) n=228 and post-intervention n=270 groups. There was a significant reduction in oral contrast use, from 57.6% to 16.7%, p<0.001 (Intervention 1). The wait time was significantly reduced by 17 minutes per patient, p<0.001 (Interventions 12). The diagnostic quality did not statistically differ between the new shortened oral contrast regime and the baseline regime (Intervention 2). No repeat CTs were needed due to lack of oral contrast (Intervention 1) or poor opacification (Intervention 2). We made significant cost reductions, with an average monthly reduction of over \$5000 across the service, p<0.001. Patient's reported their overall experience was improved post-intervention, compared to baseline (Interventions 12).\*Discussion Optimising CT oral contrast use through judicious use of oral contrast and using a shorter regime, reduced patient wait times which helped decongesting the crowded waiting rooms and decreased the time the patient spent in the hospital for OP CT. In addition, these interventions also reduced costs and improved patient experience. A decreased proportion of patients required oral contrast and diagnostic quality was comparable with the shorter regime. The multifactorial success of our quality improvement project demonstrates how radiology pandemic response

initiatives can positively impact patient care.

## **T2-QI-4 The Clinical Factors Most Likely to Result in an Abnormal CT Head - A UK Trauma Centre Experience**

Participants

Abul Haque, (*Presenter*) Nothing to Disclose

### **METHODS**

Retrospective data collection looking at all CT Heads for acute head injury performed within the Emergency Department (ED) over the course of four months between 15th October 2021 - 15th January 2022. Reports were analysed for the presence of intracranial and/or extracranial injuries and commonly related clinical indicators identified to look for trends between these factors.

### **RESULTS**

1542 CT Heads were analysed in total of which 15.3% (n=236) were abnormal. Almost 82% of these patients had a Glasgow Coma Scale (GCS) score of 14 or more. Approximately 10% had GCS between 8-13 and less than 8% of patients had GCS <8. Within these groups, the proportion of CT scans with an intracranial abnormality (used as a marker of more severe injury - compared to extracranial injury alone) was 39%, 72% and 94% respectively. 44% of patients were on some form of anticoagulation and this was the most common indication for requesting a CT Head. Retrograde amnesia was second most common (20%). Most clinical indicators demonstrated intracranial abnormalities on 40-50% of scans. However, Bruising around the ears/eyes was found to be of least value as a clinical factor with a positivity rate of only 22%. In comparison, Post-traumatic seizure was the indicator most commonly associated with intracranial abnormality (present in 75% of CTs with this factor). \*Discussion For acute head injury CT scans, GCS has clear prognostic value as the lower it is, the greater the likelihood of an abnormal scan. Within our Trust, being on anticoagulation is the most common indication for a CT Head overall, followed by Retrograde amnesia. Together these factors constitute almost 2/3 of our study population. Post-traumatic seizure is the clinical indicator most likely to be associated with intracranial abnormalities (75% correlation). In contrast, Bruising around the ears or eyes is the least useful clinical indicator with just over 20% of these patients demonstrating intracranial findings. This study was limited to a single centre and data from other centres would be useful to ascertain if results are similar.

## **T2-QI-5 Long Term Follow-up of Patients With Indeterminate Breast (B3) Lesions: A 10 Year Prospective Review**

Participants

Nerys Forester, MBCh, PhD, (*Presenter*) Nothing to Disclose

### **METHODS**

Prospective review B3 lesions (with no previous or concurrent malignancy) identified between 01/12-12/16 for subsequent breast cancer diagnoses in comparison to control group of women with screen-detected benign lesions from 2012.

### **RESULTS**

514 B3 lesions identified (radial scar/complex sclerosing lesions (22.2%), atypical intraepithelial ductal proliferation (21.4%), papillomas (21.8%), lobular neoplasia (18.3%), flat epithelial atypia (8.4%), misc (5.3%)). 391 patients underwent VAE, with 36 (9.2%) upgraded to B5. 18 patients upgraded to B5 following diagnostic excision (overall upgrade 10.5%). Remaining 460 patients had surveillance mammography, yearly or 3 yearly. Patients had mean of 3.4 follow-up mammograms (range 0-8). 44 had no further follow up (age/personal choice). 14 deaths (1 breast cancer). 33 women (7.2%) subsequently developed breast cancer (24 invasive), with 23 identified on mammography. One developed lymphoma detected on mammography. Median time-to-diagnosis was 4 years (range 1-11 years). 10 cancers were at the site of the initial B3 lesion. No significant difference between cancer development in B3 lesion subgroups was observed. 147 women had benign lesions identified at screening during 2012 (B2/C2 pathology). 8 (5.5%) subsequently developed cancer. No significant difference between rate of subsequent cancer between B3 lesions or controls at 5 years was identified. \*Discussion 7.2% of women with prior B3 lesions subsequently develop breast cancer. Cancer occurred at original B3 site in less than one third and was screen detected in approximately two thirds of cases. Rate of cancer development was not significantly higher than that in screened controls. As such, enhanced surveillance strategies do not offer additional cancer detection over usual screening and may result in over diagnosis and increased patient anxiety. Therefore a safe follow-up strategy of indeterminate breast lesions could comprise a mammographic review at one year followed by return to routine breast screening.

## **T2-QI-6 Improving Non-targeted Native Renal Biopsy Specimen Adequacy: A Province-Wide, Multicenter and Interdepartmental Quality Initiative**

Participants

James Nugent, MD, Vancouver, BC (*Presenter*) Nothing to Disclose

### **METHODS**

In our province, the vast majority of non-targeted adult native renal biopsies are performed at 13 hospitals by radiologists, and samples are sent to a central lab for analysis, averaging 850 biopsies per year. Prior to this project, adequacy was subjectively assessed by a pathologist, which depended on tissue allocation and disease-specific histological features. Four adequacy categories were defined from the perspective of tissue collection rather than tissue allocation or disease specific guidelines, to help guide in real-time how many cores should be obtained: inadequate (< 15 glomeruli and no diagnosis), suboptimal (< 15 glomeruli but diagnosis possible), minimally adequate (15-24 glomeruli) and ideally adequate (> 25 glomeruli, allowing classification and prognostication). Intervention 1 was to display the specimen adequacy category on the formal pathology report. Specimen adequacy was defined retrospectively through the pathology database that tracked number of glomeruli. Subsequent interventions and QI cycles are in progress. Two targets were evaluated. Target 1 was combined inadequate and suboptimal rate < 10%, and Target 2 was ideally adequate rate > 80%. Inferential statistics included mean and standard deviation adequacy rates. Control charts were employed to determine if there was sustained variability in adequacy.

### **RESULTS**

Pre-intervention, Target 1 was nearly achieved with a rate of 10.5%. Control chart analysis revealed sustained process change in the ideally adequate rate following intervention 1. The ideally adequate rate improved from a baseline of 66% to 73%, nearing Target 2. \*Discussion Limitations included not being able to compare adequacy rates to other institutions because there was no standard definitions in the literature. In summary, by defining specimen adequacy objectively, adequacy rates were measured,

reported and performance relative to targets was assessed. This resulted in sustained improvement in the mean rate of ideally adequate biopsies following intervention 1.

## **T2-QI-7 Can AI Support Mammography Image Quality Improvement?**

Participants

Elle Spear, Park Ridge, IL (*Presenter*) Intern, Densitas Inc

### **METHODS**

At NorthShore University HealthSystem, population-level positioning error rates are unknown. MG positioning was assessed on 188,609 mammograms from September 1, 2021 to April 15, 2022, to establish reference positioning error benchmarks. Error rates were measured using automated MG quality A.I. software (densitas® intelliMammo™) to assess CC exaggeration, missing inframammary fold (IMF), inadequate pectoralis muscle, and concave pectoralis muscle. Error rates were measured and stratified by body habitus and acquisition parameters (compression pressure, laterality, patient age, and breast size). A test of equal (independent) proportions tested the null hypothesis of equality in proportions (error rates) to assess sensitivity of the software to detect expected relationships.

### **RESULTS**

CC exaggeration error rate was 0.22 and differed by laterality ( $p < 0.001$ ). IMF missing error rate was 0.46 and differed by breast density ( $p < 0.001$ ), breast volume ( $p < 0.001$ ) and compression pressure ( $p < 0.001$ ). Nipple not in profile error rate was 0.59 and differed by breast volume ( $p < 0.001$ ) and breast area ( $p < 0.001$ ). Sagging error rate was 0.07 and differed by compression pressure ( $p < 0.001$ ). Inadequate pectoralis muscle length error rate was 0.18 and differed by breast thickness ( $p < 0.001$ ). Concavity of pectoralis muscle error rate was 0.08 and differed by breast thickness ( $p < 0.001$ ). \*Discussion AI decision tools may help establish population-based reference benchmarks of positioning error rates on MG. Face-validity of the decision tool is demonstrated by its sensitivity to varying patient and acquisition parameters reflected in the expected differences in error rates. This supports evidence-based quality improvement with training and educational interventions to improve positioning technique. Standardized and comprehensive application of this tool supports equitable service delivery and quality of care. A limitation of this study is that it did not attribute positioning error rates to patient characteristics versus radiological technologist technique.

## **T2-QI-8 Development of a Patient Face Recognition System in the Radiology Department (Patient Recognition Accuracy of a Face Mask-Enabled Face Recognition System in a CT Examination Environment)**

Participants

Hiroyuki Ota, RT, Kashiwa, Japan (*Presenter*) Nothing to Disclose

### **METHODS**

The facial recognition system used was PFAS with mask (Canon Medtec Supply, Kawasaki, Japan). The subjects were 142 patients (mean age 59+/-11 years, male/female ratio 59:41) who gave written consent between March and April 2022. Cameras were installed to capture the patients when they entered the CT room (walking) and when they were positioned (supine), and recognition was possible in both situations. The recognition task was performed with the face mask worn, and the success rate was calculated from the recognition score. In addition, a significant difference test was conducted using Welch's t test for the recognition scores obtained in the two situations. In this system, an authentication score of 550 or higher is considered as a successful authentication.

### **RESULTS**

Of 142 patients, 136 were successfully recognized, for a success rate of 96%. The reasons for the unsuccessful cases were that the patients were wearing hats too deeply, 3 cases of overlapping with staff members, and 2 cases of unknown cause. Of the 136 patients, 113 (83%) were recognized when entering the room (walking) and 23 (17%) when positioning (supine). The mean recognition scores (mean +/- standard deviation) at entry and positioning were 648+/-66 and 643+/-64, with no significant difference ( $p > 0.05$ ) between the two. \*Discussion We conducted an authentication test of a newly developed face mask-enabled face recognition system under actual CT examination environments, and found that the accuracy of face recognition was ensured even when the patient wore a face mask. In addition, by enabling recognition in both walking and supine positions, the practical application of patient recognition using a face recognition system has been realized.

Printed on: 02/07/23



## Abstract Archives of the RSNA, 2022

T2-QI-1

### Effectiveness of Palm Vein Recognition Biometric Technology to Prevent Patient Misidentification Errors

Tuesday, Nov. 29 9:00AM - 9:30AM Room: Learning Center - QI DPS

#### Participants

Rekha Mody, MD, Cleveland, OH (*Presenter*) Nothing to Disclose

#### METHODS

Palm vein recognition devices which integrated with the health system's electronic health record (EHR) were installed at an imaging center's front desk and at workstations on wheels (WOWs) throughout the department. We conducted a 4 week pilot to test the accuracy of a palm vein recognition device to: 1. Re-identify patients at the point of care when the imaging study was performed on the same date 2. Re-identify patients at the front desk who had a repeat appointment on a different date during the pilot time period. The pilot program was performed at a hospital with intermediate imaging exam volume and scope included outpatient imaging only. This site provided a small, controlled environment with quick throughput, a cross section of most imaging studies, and exams performed with IV contrast. The unique environment allowed for the patient to undergo initial enrollment with the device at the front desk and authentication when the patient's imaging exam was performed later in the same encounter. Patients were queried on desire to participate in the pilot with initial enrollment utilizing a palm vein biometric recognition device as the patient commenced the check-in process at the front desk. Subsequently, the patient was escorted to the imaging exam area and both the standard process, confirmation of the patient's name and date of birth via the EHR, and the test process, re-identification of the patient via the palm vein recognition device, were done prior to the imaging exam being performed.

#### RESULTS

During the 4 week pilot time period, approximately 570 unique patients were seen with a total of 596 patient visits (total of 3.5% enrolled patients had repeat encounters). Total exams performed (including 8 imaging modalities) was 759 with a total enrollment of 455 unique patients. The enrollment rate was 80% and authentication rate at the point of care was 75%. 88% of repeat patients were re-authenticated at the front desk and 50% of repeat patient were re-authenticated at the point of care. The pilot demonstrate 100% accurate identification of re-authenticated repeat patient (at the front desk registration and the point of care when imaging exam was performed). \*Discussion 100% of re-authenticated repeat patient (at the front desk registration and the point of care) were identified accurately using palm vein recognition biometric technology. Thus, this technology can serve as a safe, accurate and consistent method to prevent patient misidentification errors at imaging front desks and re-authentication of a patient's identity prior to imaging exam point of care and may help to decrease or eliminate wrong patient and wrong site, side or contrast administration type imaging safety events.

Printed on: 02/07/23

## Abstract Archives of the RSNA, 2022

T2-QI-3

### Optimizing the Abdominal CT Oral Contrast Service in the Covid-19 Pandemic

Tuesday, Nov. 29 9:00AM - 9:30AM Room: Learning Center - QI DPS

#### Participants

Mary Renton, MBBCh, (*Presenter*) Nothing to Disclose

#### METHODS

Leveraging a multidisciplinary stakeholder collaboration, we optimized the oral contrast service by 2 interventions: 1) Creation of 'oral contrast policy' document and revision of standardized CT protocols with judicious use of oral contrast only when supported by literature evidence. 2) Creation of a new shorter oral contrast regime (30 minutes vs 60 minutes previously). We conducted a multicentre retrospective service evaluation of our outpatient (OP) CT at baseline (pre-pandemic, pp), baseline pandemic prior to intervention(p), and post-intervention. Time-efficiency was assessed using patient waiting times. A blinded image quality review was conducted on the old and new oral contrast regimes by 2 abdominal radiologists. Cost evaluation was performed. Patient experience was evaluated with a voluntary survey. Statistical analysis was performed to compare the baseline and evaluation outcomes.

#### RESULTS

Over one-month periods, OP CT scans were assessed in baseline(pp) n = 302, baseline(p) n=228 and post-intervention n=270 groups. There was a significant reduction in oral contrast use, from 57.6% to 16.7%,  $p < 0.001$  (Intervention 1). The wait time was significantly reduced by 17 minutes per patient,  $p < 0.001$  (Interventions 1&2). The diagnostic quality did not statistically differ between the new shortened oral contrast regime and the baseline regime (Intervention 2). No repeat CTs were needed due to lack of oral contrast (Intervention 1) or poor opacification (Intervention 2). We made significant cost reductions, with an average monthly reduction of over \$5000 across the service,  $p < 0.001$ . Patient's reported their overall experience was improved post-intervention, compared to baseline (Interventions 1&2). \*Discussion Optimising CT oral contrast use through judicious use of oral contrast and using a shorter regime, reduced patient wait times which helped decongesting the crowded waiting rooms and decreased the time the patient spent in the hospital for OP CT. In addition, these interventions also reduced costs and improved patient experience. A decreased proportion of patients required oral contrast and diagnostic quality was comparable with the shorter regime. The multifactorial success of our quality improvement project demonstrates how radiology pandemic response initiatives can positively impact patient care.

Printed on: 02/07/23



## Abstract Archives of the RSNA, 2022

T2-QI-4

### The Clinical Factors Most Likely to Result in an Abnormal CT Head - A UK Trauma Centre Experience

Tuesday, Nov. 29 9:00AM - 9:30AM Room: Learning Center - QI DPS

#### Participants

Abul Haque, (*Presenter*) Nothing to Disclose

#### METHODS

Retrospective data collection looking at all CT Heads for acute head injury performed within the Emergency Department (ED) over the course of four months between 15th October 2021 - 15th January 2022. Reports were analysed for the presence of intracranial and/or extracranial injuries and commonly related clinical indicators identified to look for trends between these factors.

#### RESULTS

1542 CT Heads were analysed in total of which 15.3% (n=236) were abnormal. Almost 82% of these patients had a Glasgow Coma Scale (GCS) score of 14 or more. Approximately 10% had GCS between 8-13 and less than 8% of patients had GCS <8. Within these groups, the proportion of CT scans with an intracranial abnormality (used as a marker of more severe injury - compared to extracranial injury alone) was 39%, 72% and 94% respectively. 44% of patients were on some form of anticoagulation and this was the most common indication for requesting a CT Head. Retrograde amnesia was second most common (20%). Most clinical indicators demonstrated intracranial abnormalities on 40-50% of scans. However, Bruising around the ears/eyes was found to be of least value as a clinical factor with a positivity rate of only 22%. In comparison, Post-traumatic seizure was the indicator most commonly associated with intracranial abnormality (present in 75% of CTs with this factor). \*Discussion For acute head injury CT scans, GCS has clear prognostic value as the lower it is, the greater the likelihood of an abnormal scan. Within our Trust, being on anticoagulation is the most common indication for a CT Head overall, followed by Retrograde amnesia. Together these factors constitute almost 2/3 of our study population. Post-traumatic seizure is the clinical indicator most likely to be associated with intracranial abnormalities (75% correlation). In contrast, Bruising around the ears or eyes is the least useful clinical indicator with just over 20% of these patients demonstrating intracranial findings. This study was limited to a single centre and data from other centres would be useful to ascertain if results are similar.

Printed on: 02/07/23

## Abstract Archives of the RSNA, 2022

T2-QI-5

### Long Term Follow-up of Patients With Indeterminate Breast (B3) Lesions: A 10 Year Prospective Review

Tuesday, Nov. 29 9:00AM - 9:30AM Room: Learning Center - QI DPS

#### Participants

Nerys Forester, MBCh, PhD, (*Presenter*) Nothing to Disclose

#### METHODS

Prospective review B3 lesions (with no previous or concurrent malignancy) identified between 01/12-12/16 for subsequent breast cancer diagnoses in comparison to control group of women with screen-detected benign lesions from 2012.

#### RESULTS

514 B3 lesions identified (radial scar/complex sclerosing lesions (22.2%), atypical intraepithelial ductal proliferation (21.4%), papillomas (21.8%), lobular neoplasia (18.3%), flat epithelial atypia (8.4%), misc (5.3%)). 391 patients underwent VAE, with 36 (9.2%) upgraded to B5. 18 patients upgraded to B5 following diagnostic excision (overall upgrade 10.5%). Remaining 460 patients had surveillance mammography, yearly or 3 yearly. Patients had mean of 3.4 follow-up mammograms (range 0-8). 44 had no further follow up (age/personal choice). 14 deaths (1 breast cancer). 33 women (7.2%) subsequently developed breast cancer (24 invasive), with 23 identified on mammography. One developed lymphoma detected on mammography. Median time-to-diagnosis was 4 years (range 1-11 years). 10 cancers were at the site of the initial B3 lesion. No significant difference between cancer development in B3 lesion subgroups was observed. 147 women had benign lesions identified at screening during 2012 (B2/C2 pathology). 8 (5.5%) subsequently developed cancer. No significant difference between rate of subsequent cancer between B3 lesions or controls at 5 years was identified. \*Discussion 7.2% of women with prior B3 lesions subsequently develop breast cancer. Cancer occurred at original B3 site in less than one third and was screen detected in approximately two thirds of cases. Rate of cancer development was not significantly higher than that in screened controls. As such, enhanced surveillance strategies do not offer additional cancer detection over usual screening and may result in over diagnosis and increased patient anxiety. Therefore a safe follow-up strategy of indeterminate breast lesions could comprise a mammographic review at one year followed by return to routine breast screening.

Printed on: 02/07/23



## Abstract Archives of the RSNA, 2022

T2-QI-6

### Improving Non-targeted Native Renal Biopsy Specimen Adequacy: A Province-Wide, Multicenter and Interdepartmental Quality Initiative

Tuesday, Nov. 29 9:00AM - 9:30AM Room: Learning Center - QI DPS

#### Participants

James Nugent, MD, Vancouver, BC (*Presenter*) Nothing to Disclose

#### METHODS

In our province, the vast majority of non-targeted adult native renal biopsies are performed at 13 hospitals by radiologists, and samples are sent to a central lab for analysis, averaging 850 biopsies per year. Prior to this project, adequacy was subjectively assessed by a pathologist, which depended on tissue allocation and disease-specific histological features. Four adequacy categories were defined from the perspective of tissue collection rather than tissue allocation or disease specific guidelines, to help guide in real-time how many cores should be obtained: inadequate (< 15 glomeruli and no diagnosis), suboptimal (< 15 glomeruli but diagnosis possible), minimally adequate (15-24 glomeruli) and ideally adequate (> 25 glomeruli, allowing classification and prognostication). Intervention 1 was to display the specimen adequacy category on the formal pathology report. Specimen adequacy was defined retrospectively through the pathology database that tracked number of glomeruli. Subsequent interventions and QI cycles are in progress. Two targets were evaluated. Target 1 was combined inadequate and suboptimal rate < 10%, and Target 2 was ideally adequate rate > 80%. Inferential statistics included mean and standard deviation adequacy rates. Control charts were employed to determine if there was sustained variability in adequacy.

#### RESULTS

Pre-intervention, Target 1 was nearly achieved with a rate of 10.5%. Control chart analysis revealed sustained process change in the ideally adequate rate following intervention 1. The ideally adequate rate improved from a baseline of 66% to 73%, nearing Target 2.\*Discussion Limitations included not being able to compare adequacy rates to other institutions because there was no standard definitions in the literature. In summary, by defining specimen adequacy objectively, adequacy rates were measured, reported and performance relative to targets was assessed. This resulted in sustained improvement in the mean rate of ideally adequate biopsies following intervention 1.

Printed on: 02/07/23



## Abstract Archives of the RSNA, 2022

T2-QI-7

### Can AI Support Mammography Image Quality Improvement?

Tuesday, Nov. 29 9:00AM - 9:30AM Room: Learning Center - QI DPS

#### Participants

Elle Spear, Park Ridge, IL (*Presenter*) Intern, Densitas Inc

#### METHODS

At NorthShore University HealthSystem, population-level positioning error rates are unknown. MG positioning was assessed on 188,609 mammograms from September 1, 2021 to April 15, 2022, to establish reference positioning error benchmarks. Error rates were measured using automated MG quality A.I. software (densitas® intelliMammo™) to assess CC exaggeration, missing inframammary fold (IMF), inadequate pectoralis muscle, and concave pectoralis muscle. Error rates were measured and stratified by body habitus and acquisition parameters (compression pressure, laterality, patient age, and breast size). A test of equal (independent) proportions tested the null hypothesis of equality in proportions (error rates) to assess sensitivity of the software to detect expected relationships.

#### RESULTS

CC exaggeration error rate was 0.22 and differed by laterality ( $p < 0.001$ ). IMF missing error rate was 0.46 and differed by breast density ( $p < 0.001$ ), breast volume ( $p < 0.001$ ) and compression pressure ( $p < 0.001$ ). Nipple not in profile error rate was 0.59 and differed by breast volume ( $p < 0.001$ ) and breast area ( $p < 0.001$ ). Sagging error rate was 0.07 and differed by compression pressure ( $p < 0.001$ ). Inadequate pectoralis muscle length error rate was 0.18 and differed by breast thickness ( $p < 0.001$ ). Concavity of pectoralis muscle error rate was 0.08 and differed by breast thickness ( $p < 0.001$ ). \*Discussion AI decision tools may help establish population-based reference benchmarks of positioning error rates on MG. Face-validity of the decision tool is demonstrated by its sensitivity to varying patient and acquisition parameters reflected in the expected differences in error rates. This supports evidence-based quality improvement with training and educational interventions to improve positioning technique. Standardized and comprehensive application of this tool supports equitable service delivery and quality of care. A limitation of this study is that it did not attribute positioning error rates to patient characteristics versus radiological technologist technique.

Printed on: 02/07/23

## Abstract Archives of the RSNA, 2022

T2-QI-8

### Development of a Patient Face Recognition System in the Radiology Department (Patient Recognition Accuracy of a Face Mask-Enabled Face Recognition System in a CT Examination Environment)

Tuesday, Nov. 29 9:00AM - 9:30AM Room: Learning Center - QI DPS

#### Participants

Hiroyuki Ota, RT, Kashiwa, Japan (*Presenter*) Nothing to Disclose

#### METHODS

The facial recognition system used was PFAS with mask (Canon Medtec Supply, Kawasaki, Japan). The subjects were 142 patients (mean age 59+/-11 years, male/female ratio 59:41) who gave written consent between March and April 2022. Cameras were installed to capture the patients when they entered the CT room (walking) and when they were positioned (supine), and recognition was possible in both situations. The recognition task was performed with the face mask worn, and the success rate was calculated from the recognition score. In addition, a significant difference test was conducted using Welch's t test for the recognition scores obtained in the two situations. In this system, an authentication score of 550 or higher is considered as a successful authentication.

#### RESULTS

Of 142 patients, 136 were successfully recognized, for a success rate of 96%. The reasons for the unsuccessful cases were that the patients were wearing hats too deeply, 3 cases of overlapping with staff members, and 2 cases of unknown cause. Of the 136 patients, 113 (83%) were recognized when entering the room (walking) and 23 (17%) when positioning (supine). The mean recognition scores (mean +/- standard deviation) at entry and positioning were 648+/-66 and 643+/- 64, with no significant difference ( $p>0.05$ ) between the two. \*Discussion We conducted an authentication test of a newly developed face mask-enabled face recognition system under actual CT examination environments, and found that the accuracy of face recognition was ensured even when the patient wore a face mask. In addition, by enabling recognition in both walking and supine positions, the practical application of patient recognition using a face recognition system has been realized.

Printed on: 02/07/23



## Abstract Archives of the RSNA, 2022

T5A-QI

### Quality Improvement Reports Tuesday Poster Discussions - A

Tuesday, Nov. 29 12:15PM - 12:45PM Room: Learning Center - QI DPS

#### Sub-Events

#### T5A-QI-1 The RQM(R): Redefining Value in Peer Review

Participants

Emilie Albee, St Louis Park, MN (*Presenter*) Nothing to Disclose

#### METHODS

In RQM®, review cases are randomly selected throughout the network, manually vetted for appropriateness, and assigned via an algorithm of ~3% interpretation volume per subspecialty on a rotating monthly schedule. After assignment, the radiologist selects from: Agree, Agree w/comment, Disagree 1, Disagree 2 or Cannot review. If Agree, case is closed. If Agree w/comment, case is discussed amongst reviewer and interpreter. If Disagree 1 or 2, feedback can be accepted or disputed; if the latter, a 3rd-party reviewer provides input. This reviewer is an elected subspecialty section leader or an experienced exam interpreter. Data is compiled via an in-house reporting system and can be accessed at any time. Formalized reporting occurs on a scheduled cycle, with metrics including quantity of reviews per modality and subspecialty, conclusions tracking, and participation rate (number of reviews submitted/ total reviews assigned per radiologist). Individual participation rates make up total participation rates for a radiology group, and an aggregate rate for all RQM® participants is also calculated. In general, reports blind the names of individual radiologists and radiology groups, preserving peer review protection and the purpose of a non-punitive learning environment. In 2021, an RQM® Accuracy Assessment was launched. This assessment utilizes data from the conclusions tracking report by comparing the quantity of Disagree 1 and 2 review conclusions to the number of total reviews.

#### RESULTS

In 2021, a total of 240 reviewers from 32 independent rad groups completed 14,501 reviews, with an overall participation rate of 95%. This included 7,148 MRI, 3,250 CT, and 2,018 mammography cases, distributed by subspecialty (MSK=3,547; spine=3,227; body=2,931; breast=2,216; neuro=1,788; other=792). The 2021 Accuracy Assessment error rate was 1.42%; lower than the industry average (3-5% in the peer-reviewed literature).\*Discussion Unlike other systems, the RQM® provides discussion among physicians and selects only current cases, organized by subspecialty for more meaningful mentorship. The program also blinds names, removing partiality from the process to encourage candid responses, and gives radiologists the opportunity to review cases from outside of their own practice. The RQM® Accuracy Assessment also revealed a below industry average error rate for participants, leading to more critical findings at earlier stages.

#### T5A-QI-2 Simplifying the AI Consumption Process Through the Implementation of a Standard-Based AI Platform

Participants

Alberto F. Goldszal, PhD, MBA, (*Presenter*) Nothing to Disclose

#### METHODS

As healthcare organizations interface with different AI solutions, it becomes imperative to streamline and control the transfer of images to multiple AI engines as well as standardize the returning AI results. The AI engines, in turn, may be hosted within the institutional LAN, may be cloud-based or hybrid. Regardless of the architecture, the AI platform provides data flow orchestration to the AI engines: it automates the export of cases, it creates queues based on study priority and improves hardware scalability through load balancing. The AI platform also supports flexible integration profiles for the incoming AI results, including an open API, HL7 and DICOM profiles like GSPS, DICOM SC, DICOM SEG, CAD SR. Through these standards, AI results display directly into the PACS viewer as overlays which can be toggle on or off. Notifications in the worklist indicate AI processing status, AI algorithm utilized and any triage assignment based on AI findings.

#### RESULTS

We have used an AI platform to orchestrate the exporting of imaging data and incorporation of results from two distinct AI engines processing breast tomography and CTA studies, respectively. In the 1st quarter of 2022, we successfully processed 15,200 breast exams and 4,500 CTA's. Returning AI results consisted of an imaging overlay and associated AI score. It is interesting to note that for diagnostic breast exams where the interpretation occurs in near real-time, the entire processing pipeline takes an average of 3 minutes from study acquisition to AI results reported. This is critical in order to provide the AI results prior to the radiologist's start of interpretation.\*Discussion We have implemented an AI platform to orchestrate the exchange of imaging data and AI results in a standardized and simplified manner. This standard-based platform provides AI-vendor independence, therefore, facilitating the consumption of best-of-breed AI solutions. It is tightly integrated with our PACS, delivering AI overlays into the imaging viewer and notifications into the worklist. The AI platform is highly scalable to any number of downstream, commercially-available AI solutions, including algorithms developed within our own organization.

#### T5A-QI-3 Increasing Utilization of Contrast-Enhanced Ultrasound During Abdominal Biopsies: Impact of an Educational Training Program

Participants  
Lisa Ho, MD, Durham, NC (*Presenter*) Nothing to Disclose

#### **METHODS**

Two educational training interventions were performed to increase use of UCA. First, radiologists and sonographers attended an educational event which included didactic teaching and case presentations on the use of UCA. Second, direct hands-on teaching on how to use UCA during procedures was provided to the same group. To determine the efficacy of these two interventions, the percentage of UCA assisted biopsies (number of UCA assisted targeted liver and renal biopsies divided by total number of liver and renal biopsies) was compared for the 6 months before and 6 months after the educational training. In addition, radiologists completed anonymous surveys to determine the level of understanding and acceptability of using UCA before and 6 months after initiating UCA educational training.

#### **RESULTS**

UCA-assisted targeted liver and renal biopsies increased from 5.8% (10/172) to 10.0% (16/160) ( $p=0.09$ , 1-sided Boschloo test) after educational intervention. Before training, 3/14 attending radiologists reported using UCA versus 8/14 attending radiologists after training ( $p=0.03$ ). After training, 5/8 were new UCA users (never used or infrequent use). Pre-training survey was completed by 11 abdominal radiology attendings (63.6% > 10 years interventional experience) and 7 abdominal radiology fellows (1 year fellowship). Unfamiliarity on how to use it was the main reason (70.6%) for not using UCA, followed by doubt of its utility (17.7%). Before educational training, only 10.5% of survey responders use UCA routinely whereas 47.4% never used it, and 42.1% used it rarely. Post-intervention survey was completed by 9 attendings (66.6% > 10 years of experience) and 4 fellows. Educational training increased radiologists understanding (40.0%) and acceptability (30.0%) of UCA and decreased concern about risks (15.0%). After training, 53.8% of respondents were new users of UCA. For those respondents who did not use UCA after the training program, only 25.0% reported unfamiliarity as the reason for not using UCA, whereas 25.0% reported no cases needed it and 37.5% reported they planned to use it in the future if needed.\*Discussion An educational training program increased utilization of UCA during targeted US-guided liver and renal biopsies. Increasing use of UCA improves patient care by increasing target visibility and biopsy success rates when performing ultrasound-guided targeted liver and renal biopsies.

#### **T5A-QI-4 Moving Beyond Alphabet Soup - Using Root Cause Analysis (RCA) and Failure Mode and Effect Analysis (FMEA) to Learn from Errors in the Breast Imaging Clinic**

Participants  
Tanya W. Moseley, MD, PhD, Houston, TX (*Presenter*) Consultant, Hologic, Inc; Consultant, Merit Medical Systems, Inc; Owner, TW Moseley, LLC; CEO, TW Moseley, LLC

#### **METHODS**

Root Cause Analysis (RCA) is a technique used to deduce the cause of unfavorable occurrences that have already occurred. The Joint Commission now requires that all sentinel occurrences occurring in a clinical department undergo an RCA within 45 days. Failure Mode and Effect Analysis (FMEA) is a proactive risk assessment technique used to identify areas of vulnerability. FMEA establishes strategies for preventing and mitigating errors. FMEA is less commonly used in medicine despite its military and industrial origins dating back to WWII.

#### **RESULTS**

FMEAs and RCAs are effective tools for enhancing patient safety. When the names are repeated in court alongside evidence demonstrating that the operations they represent were performed, they may protect individuals and institutions from lawsuit expenses and damages by demonstrating that appropriate steps were taken to avoid a patient's avoidable injury.\*Discussion The objective of using comprehensive systemic analyses such as RCA and FMEA is to analyze medical errors, find the root causes or reasons for such failures, learn from them and try to prevent their recurrence. Even though they're quite different, FMEA and RCA cannot be separated. FMEA seeks to know the effects of each of all possible causal sets. RCA seeks to know the causal set of each of all possible effect FMEA is the temporal mirror of RCA reflected in the "now" moment.

#### **T5A-QI-5 Adding Friction to the Electronic Health Record to Improve Adherence With Best Practices for Diagnostic Testing Across Multiple Hospital System Intensive Care Units**

Participants  
Sherry Knott, BS, Aurora, CO (*Presenter*) Nothing to Disclose

#### **METHODS**

This project was performed at an urban quaternary academic hospital. We hypothesized that modification of the electronic health record, wherein we added friction by eliminating Daily as a frequency option when ordering CXRs would reduce the frequency of daily CXRs. The impact of this intervention was tracked by recording the number of repeat ICU CXR that were ordered simultaneously for 3 months both before and after making EHR change intervention. We also surveyed radiology technologists' level of stress and burnout after EHR changes were made.

#### **RESULTS**

Between Sept 1, 2021 and Dec 30, 2021 there were 9307 ICU CXR orders, of which 3923 (42%) were ordered as standing daily orders. Since the process change there were 4832 CXR orders from Jan 13, 2021, to Mar 31, 2021, of which 2 (4%) were ordered as a standing daily order. This is a reduction in standing orders of 93%. As a result, ICU CXR volume decreased from 76 CXR per day to 62 CXR per day, for a decrease of 18.5% in total daily ICU CXR. Surveys were sent to radiology technologists who participate in ICU morning CXRs after the change was made asking about their job satisfaction and burnout since the change was made. Of technologist respondents 87% stated they were more satisfied or much more satisfied with their jobs since the change, and 75% described much less or less burnout than before the change was made.\*Discussion Limitations of our study include that we did not test if there were other factors that may have affected ordering habits of ICU physicians during this time. In addition, we surveyed technologists about their job satisfaction burnout only after the change was made. Adding friction to the electronic health record, by eliminating daily as a frequency option when ordering CXRs, effectively significantly reduced low-value care, to the benefit of patients healthcare professionals.

#### **T5A-QI-6 How to Transition From Transrectal to Transperineal Prostate Biopsy - Experience After 1000 TP Biopsies**

Participants  
Jack Power, MBBCh, MRCP, DUBLIN, Ireland (*Presenter*) Nothing to Disclose

## **METHODS**

In 2019 our hospital had a post TRUS sepsis rate of 3.9%, including two prolonged HDU admissions. Following review of these data, and cognisant of the arguments being made for a move away from TRUS, a decision was made to introduce TP biopsy under local anaesthetic in our radiology department. Two radiologists with experience in guiding transperineal brachytherapy for radiation oncologists assisted in the training of other radiologists in the procedure. Funding for equipment was obtained on the basis of savings predicted by a reduction in post procedure admissions for sepsis and haemorrhage. A centre experienced in outpatient TP biopsy was visited by radiologists and nursing staff and protocols were established locally. Initially, TP biopsy was offered to a small number of patients and TRUS continued to be the main biopsy method. With the onset of the COVID-19 pandemic, the decision to transition completely to TP biopsy was made in an effort to avoid the risk of post biopsy admission with the resultant demand on hospital services.

## **RESULTS**

Radiologists experienced in TP procedures worked with other GU radiologists to train them in the technique of TP biopsy under local anaesthetic. Initially 2 cases per morning were performed taking up to 90 minutes per case. After 6 months, 4-6 cases per morning are performed taking 30 minutes per case. All radiologists previously performing TRUS now perform TP biopsy exclusively. Radiology residents are now being trained in the technique. 13.5% of men require sedation. The sepsis rate has been less than 1% in 1000 cases (0.17%). No cases of significant haemorrhage have occurred.\*Discussion Our department successfully transitioned completely from TRUS biopsy to TP biopsy with a marked reduction in post procedure sepsis and no cases of severe sepsis seen. We outline the barriers to making the switch and address these in turn (set-up cost, increased time required, reimbursement issues, perceived difficulty of procedure, perceived increased invasiveness of procedure, additional personnel required). The elimination of severe sepsis makes continued use of TRUS medico-legally untenable and transition to TP biopsy is inevitable even if it is taking a long time.

### **T5A-QI-7 Oxford Tertiary Hospital Referral Pathway for Urgent Radiological Investigations for Paediatric Septic Arthritis: Are We Sensitive and Specific Enough?**

Participants  
Anuja Joshi, MBBS, BSc, (*Presenter*) Nothing to Disclose

## **METHODS**

A retrospective search of the radiology reporting system identified patients under 16 years who had US examinations of hips, knees, ankles, shoulders, or elbows between 01/01/19 to 30/11/21. The key word 'septic' pinpointed requests for possible SA. The electronic patient record was used to obtain data about presenting signs and symptoms. Patients who presented with at least two red flags of; Fever >38.5degC in the last week, non-weight bearing/reduced range of joint movement, CRP >20mg/L / ESR >40mm/h or WCC >12k/mm<sup>3</sup> as per Kocher's criteria were deemed as an appropriate referral for urgent US +/- percutaneous aspiration. Microbiology results confirmed positive SA cases. Kocher's criteria were assigned a number for data entry and recorded on the database according to the patient's presentation. Entries were assigned "Yes" if presented with at least 2 red flags and "No" otherwise. The "No" entries were counted, signifying cases which did not meet the pathway standard for urgent US.

## **RESULTS**

Over the time period, 76 urgent US examinations were performed. 22% of scans were confirmed SA cases, all presenting with more than two red flags. Despite presenting less than 2 red flags, 9% of cases underwent urgent US. All but 1 of these cases were reviewed by senior specialists and deemed high risk. There were no missed cases of SA. In the first review in 2016 prior to the current guideline, 142 US were performed in 12 months, with only 4% positive for SA.\*Discussion Children can present with unusual symptoms which do not follow criteria and high clinical suspicion of senior clinicians may result in urgent US. Awareness to accommodate exceptions to the pathway is necessary. Our trust has demonstrated good pathway adherence. This retrospective review shows the pathway accurately identifies those with SA and correctly refers them for urgent US without missed cases. The proportion of positive cases scanned has significantly increased compared to before our guideline implementation, indicating this has streamlined the workload without compromising patient care.

### **T5A-QI-8 Improving Compliance of Post-Procedural Documentation in the Electronic Health Record at a Medium-Sized Community Hospital**

Participants  
David Berezovsky, DO, (*Presenter*) Nothing to Disclose

## **METHODS**

Thirteen IR providers (10 physicians and 3 PAs) performed all IR procedures at this medium-sized community teaching hospital which uses Paragon as its EHR. A standardized EHR post-procedural note template containing all necessary elements, some of which auto-populated, was created and could not be signed unless all required elements were filled. A new workflow was created to nudge providers to write their note in the EHR immediately after the procedure. Buy-in from providers, technologists, nurses, and administrators was obtained at a pre-implementation meeting. Laminated directions were attached to every workstation to remind providers to write the note and help them navigate the EHR. Baseline data from one year prior and during the eight weeks leading to implementation were obtained. Weekly analyses were conducted after implementation. Feedback and progress were sent weekly to all stakeholders. Individual scorecards were sent to select providers to highlight their compliance or non-compliance for encouragement.

## **RESULTS**

Baseline compliance was 27% one year prior to implementation and 72% during the eight weeks prior to implementation. Mean weekly procedures excluding PICCs was 47. After implementation, compliance was nearly consistently above 85%.\*Discussion The keys to success in this project were obtaining buy-in from the entire team, designing a simple workflow with nudges, and delivering prompt feedback on progress. A barrier to compliance was provider perception of redundancy of routine post-procedural notes in addition to the radiology dictation. This was addressed with education about its importance for patient safety and regulatory compliance. An additional barrier was the lack of standardization of the post-procedural note in the EHR. The newly designed note template made it easy to quickly write notes that captured required information. Weekly team feedback with select individual

scorecards encouraged everyone to be an active participant. Limitations included not verifying the accuracy of the notes and verifying that the note was written prior to the patient leaving the IR suite. Assessment for continued compliance is planned at 3 months and every 6 months thereafter.

Printed on: 02/07/23



## Abstract Archives of the RSNA, 2022

T5A-QI-1

### The RQM(R): Redefining Value in Peer Review

Tuesday, Nov. 29 12:15PM - 12:45PM Room: Learning Center - QI DPS

#### Participants

Emilie Albee, St Louis Park, MN (*Presenter*) Nothing to Disclose

#### METHODS

In RQM®, review cases are randomly selected throughout the network, manually vetted for appropriateness, and assigned via an algorithm of ~3% interpretation volume per subspecialty on a rotating monthly schedule. After assignment, the radiologist selects from: Agree, Agree w/comment, Disagree 1, Disagree 2 or Cannot review. If Agree, case is closed. If Agree w/comment, case is discussed amongst reviewer and interpreter. If Disagree 1 or 2, feedback can be accepted or disputed; if the latter, a 3rd-party reviewer provides input. This reviewer is an elected subspecialty section leader or an experienced exam interpreter. Data is compiled via an in-house reporting system and can be accessed at any time. Formalized reporting occurs on a scheduled cycle, with metrics including quantity of reviews per modality and subspecialty, conclusions tracking, and participation rate (number of reviews submitted/ total reviews assigned per radiologist). Individual participation rates make up total participation rates for a radiology group, and an aggregate rate for all RQM® participants is also calculated. In general, reports blind the names of individual radiologists and radiology groups, preserving peer review protection and the purpose of a non-punitive learning environment. In 2021, an RQM® Accuracy Assessment was launched. This assessment utilizes data from the conclusions tracking report by comparing the quantity of Disagree 1 and 2 review conclusions to the number of total reviews.

#### RESULTS

In 2021, a total of 240 reviewers from 32 independent rad groups completed 14,501 reviews, with an overall participation rate of 95%. This included 7,148 MRI, 3,250 CT, and 2,018 mammography cases, distributed by subspecialty (MSK=3,547; spine=3,227; body=2,931; breast=2,216; neuro=1,788; other=792). The 2021 Accuracy Assessment error rate was 1.42%; lower than the industry average (3-5% in the peer-reviewed literature). \*Discussion Unlike other systems, the RQM® provides discussion among physicians and selects only current cases, organized by subspecialty for more meaningful mentorship. The program also blinds names, removing partiality from the process to encourage candid responses, and gives radiologists the opportunity to review cases from outside of their own practice. The RQM® Accuracy Assessment also revealed a below industry average error rate for participants, leading to more critical findings at earlier stages.

Printed on: 02/07/23



## Abstract Archives of the RSNA, 2022

T5A-QI-2

### Simplifying the AI Consumption Process Through the Implementation of a Standard-Based AI Platform

Tuesday, Nov. 29 12:15PM - 12:45PM Room: Learning Center - QI DPS

#### Participants

Alberto F. Goldszal, PhD, MBA, (*Presenter*) Nothing to Disclose

#### METHODS

As healthcare organizations interface with different AI solutions, it becomes imperative to streamline and control the transfer of images to multiple AI engines as well as standardize the returning AI results. The AI engines, in turn, may be hosted within the institutional LAN, may be cloud-based or hybrid. Regardless of the architecture, the AI platform provides data flow orchestration to the AI engines: it automates the export of cases, it creates queues based on study priority and improves hardware scalability through load balancing. The AI platform also supports flexible integration profiles for the incoming AI results, including an open API, HL7 and DICOM profiles like GSPS, DICOM SC, DICOM SEG, CAD SR. Through these standards, AI results display directly into the PACS viewer as overlays which can be toggle on or off. Notifications in the worklist indicate AI processing status, AI algorithm utilized and any triage assignment based on AI findings.

#### RESULTS

We have used an AI platform to orchestrate the exporting of imaging data and incorporation of results from two distinct AI engines processing breast tomography and CTA studies, respectively. In the 1st quarter of 2022, we successfully processed 15,200 breast exams and 4,500 CTA's. Returning AI results consisted of an imaging overlay and associated AI score. It is interesting to note that for diagnostic breast exams where the interpretation occurs in near real-time, the entire processing pipeline takes an average of 3 minutes from study acquisition to AI results reported. This is critical in order to provide the AI results prior to the radiologist's start of interpretation.\*Discussion We have implemented an AI platform to orchestrate the exchange of imaging data and AI results in a standardized and simplified manner. This standard-based platform provides AI-vendor independence, therefore, facilitating the consumption of best-of-breed AI solutions. It is tightly integrated with our PACS, delivering AI overlays into the imaging viewer and notifications into the worklist. The AI platform is highly scalable to any number of downstream, commercially-available AI solutions, including algorithms developed within our own organization.

Printed on: 02/07/23

## Abstract Archives of the RSNA, 2022

T5A-QI-3

### **Increasing Utilization of Contrast-Enhanced Ultrasound During Abdominal Biopsies: Impact of an Educational Training Program**

Tuesday, Nov. 29 12:15PM - 12:45PM Room: Learning Center - QI DPS

#### **Participants**

Lisa Ho, MD, Durham, NC (*Presenter*) Nothing to Disclose

#### **METHODS**

Two educational training interventions were performed to increase use of UCA. First, radiologists and sonographers attended an educational event which included didactic teaching and case presentations on the use of UCA. Second, direct hands-on teaching on how to use UCA during procedures was provided to the same group. To determine the efficacy of these two interventions, the percentage of UCA assisted biopsies (number of UCA assisted targeted liver and renal biopsies divided by total number of liver and renal biopsies) was compared for the 6 months before and 6 months after the educational training. In addition, radiologists completed anonymous surveys to determine the level of understanding and acceptability of using UCA before and 6 months after initiating UCA educational training.

#### **RESULTS**

UCA-assisted targeted liver and renal biopsies increased from 5.8% (10/172) to 10.0% (16/160) ( $p=0.09$ , 1-sided Boschloo test) after educational intervention. Before training, 3/14 attending radiologists reported using UCA versus 8/14 attending radiologists after training ( $p=0.03$ ). After training, 5/8 were new UCA users (never used or infrequent use). Pre-training survey was completed by 11 abdominal radiology attendings (63.6% > 10 years interventional experience) and 7 abdominal radiology fellows (1 year fellowship). Unfamiliarity on how to use it was the main reason (70.6%) for not using UCA, followed by doubt of its utility (17.7%). Before educational training, only 10.5% of survey responders use UCA routinely whereas 47.4% never used it, and 42.1% used it rarely. Post-intervention survey was completed by 9 attendings (66.6% > 10 years of experience) and 4 fellows. Educational training increased radiologists understanding (40.0%) and acceptability (30.0%) of UCA and decreased concern about risks (15.0%). After training, 53.8% of respondents were new users of UCA. For those respondents who did not use UCA after the training program, only 25.0% reported unfamiliarity as the reason for not using UCA, whereas 25.0% reported no cases needed it and 37.5% reported they planned to use it in the future if needed.\*Discussion An educational training program increased utilization of UCA during targeted US-guided liver and renal biopsies. Increasing use of UCA improves patient care by increasing target visibility and biopsy success rates when performing ultrasound-guided targeted liver and renal biopsies.

Printed on: 02/07/23



## Abstract Archives of the RSNA, 2022

T5A-QI-4

### Moving Beyond Alphabet Soup - Using Root Cause Analysis (RCA) and Failure Mode and Effect Analysis (FMEA) to Learn from Errors in the Breast Imaging Clinic

Tuesday, Nov. 29 12:15PM - 12:45PM Room: Learning Center - QI DPS

#### Participants

Tanya W. Moseley, MD, PhD, Houston, TX (*Presenter*) Consultant, Hologic, Inc; Consultant, Merit Medical Systems, Inc; Owner, TW Moseley, LLC; CEO, TW Moseley, LLC

#### METHODS

Root Cause Analysis (RCA) is a technique used to deduce the cause of unfavorable occurrences that have already occurred. The Joint Commission now requires that all sentinel occurrences occurring in a clinical department undergo an RCA within 45 days. Failure Mode and Effect Analysis (FMEA) is a proactive risk assessment technique used to identify areas of vulnerability. FMEA establishes strategies for preventing and mitigating errors. FMEA is less commonly used in medicine despite its military and industrial origins dating back to WWII.

#### RESULTS

FMEAs and RCAs are effective tools for enhancing patient safety. When the names are repeated in court alongside evidence demonstrating that the operations they represent were performed, they may protect individuals and institutions from lawsuit expenses and damages by demonstrating that appropriate steps were taken to avoid a patient's avoidable injury.\*Discussion The objective of using comprehensive systemic analyses such as RCA and FMEA is to analyze medical errors, find the root causes or reasons for such failures, learn from them and try to prevent their recurrence. Even though they're quite different, FMEA and RCA cannot be separated. FMEA seeks to know the effects of each of all possible causal sets. RCA seeks to know the causal set of each of all possible effect FMEA is the temporal mirror of RCA reflected in the "now" moment.

Printed on: 02/07/23



## Abstract Archives of the RSNA, 2022

T5A-QI-5

### Adding Friction to the Electronic Health Record to Improve Adherence With Best Practices for Diagnostic Testing Across Multiple Hospital System Intensive Care Units

Tuesday, Nov. 29 12:15PM - 12:45PM Room: Learning Center - QI DPS

#### Participants

Sherry Knott, BS, Aurora, CO (*Presenter*) Nothing to Disclose

#### METHODS

This project was performed at an urban quaternary academic hospital. We hypothesized that modification of the electronic health record, wherein we added friction by eliminating Daily as a frequency option when ordering CXRs would reduce the frequency of daily CXRs. The impact of this intervention was tracked by recording the number of repeat ICU CXR that were ordered simultaneously for 3 months both before and after making EHR change intervention. We also surveyed radiology technologists' level of stress and burnout after EHR changes were made.

#### RESULTS

Between Sept 1, 2021 and Dec 30, 2021 there were 9307 ICU CXR orders, of which 3923 (42%) were ordered as standing daily orders. Since the process change there were 4832 CXR orders from Jan 13, 2021, to Mar 31, 2021, of which 2 (4%) were ordered as a standing daily order. This is a reduction in standing orders of 93%. As a result, ICU CXR volume decreased from 76 CXR per day to 62 CXR per day, for a decrease of 18.5% in total daily ICU CXR. Surveys were sent to radiology technologists who participate in ICU morning CXRs after the change was made asking about their job satisfaction and burnout since the change was made. Of technologist respondents 87% stated they were more satisfied or much more satisfied with their jobs since the change, and 75% described much less or less burnout than before the change was made.\*Discussion Limitations of our study include that we did not test if there were other factors that may have affected ordering habits of ICU physicians during this time. In addition, we surveyed technologists about their job satisfaction burnout only after the change was made. Adding friction to the electronic health record, by eliminating daily as a frequency option when ordering CXRs, effectively significantly reduced low-value care, to the benefit of patients healthcare professionals.

Printed on: 02/07/23

## Abstract Archives of the RSNA, 2022

T5A-QI-6

### How to Transition From Transrectal to Transperineal Prostate Biopsy - Experience After 1000 TP Biopsies

Tuesday, Nov. 29 12:15PM - 12:45PM Room: Learning Center - QI DPS

#### Participants

Jack Power, MBBCh, MRCPI, DUBLIN, Ireland (*Presenter*) Nothing to Disclose

#### METHODS

In 2019 our hospital had a post TRUS sepsis rate of 3.9%, including two prolonged HDU admissions. Following review of these data, and cognisant of the arguments being made for a move away from TRUS, a decision was made to introduce TP biopsy under local anaesthetic in our radiology department. Two radiologists with experience in guiding transperineal brachytherapy for radiation oncologists assisted in the training of other radiologists in the procedure. Funding for equipment was obtained on the basis of savings predicted by a reduction in post procedure admissions for sepsis and haemorrhage. A centre experienced in outpatient TP biopsy was visited by radiologists and nursing staff and protocols were established locally. Initially, TP biopsy was offered to a small number of patients and TRUS continued to be the main biopsy method. With the onset of the COVID-19 pandemic, the decision to transition completely to TP biopsy was made in an effort to avoid the risk of post biopsy admission with the resultant demand on hospital services.

#### RESULTS

Radiologists experienced in TP procedures worked with other GU radiologists to train them in the technique of TP biopsy under local anaesthetic. Initially 2 cases per morning were performed taking up to 90 minutes per case. After 6 months, 4-6 cases per morning are performed taking 30 minutes per case. All radiologists previously performing TRUS now perform TP biopsy exclusively. Radiology residents are now being trained in the technique. 13.5% of men require sedation. The sepsis rate has been less than 1% in 1000 cases (0.17%). No cases of significant haemorrhage have occurred.\*Discussion Our department successfully transitioned completely from TRUS biopsy to TP biopsy with a marked reduction in post procedure sepsis and no cases of severe sepsis seen. We outline the barriers to making the switch and address these in turn (set-up cost, increased time required, reimbursement issues, perceived difficulty of procedure, perceived increased invasiveness of procedure, additional personnel required). The elimination of severe sepsis makes continued use of TRUS medico-legally untenable and transition to TP biopsy is inevitable even if it is taking a long time.

Printed on: 02/07/23

## Abstract Archives of the RSNA, 2022

T5A-QI-7

### Oxford Tertiary Hospital Referral Pathway for Urgent Radiological Investigations for Paediatric Septic Arthritis: Are We Sensitive and Specific Enough?

Tuesday, Nov. 29 12:15PM - 12:45PM Room: Learning Center - QI DPS

#### Participants

Anuja Joshi, MBBS, BSc, (*Presenter*) Nothing to Disclose

#### METHODS

A retrospective search of the radiology reporting system identified patients under 16 years who had US examinations of hips, knees, ankles, shoulders, or elbows between 01/01/19 to 30/11/21. The key word 'septic' pinpointed requests for possible SA. The electronic patient record was used to obtain data about presenting signs and symptoms. Patients who presented with at least two red flags of; Fever >38.5degC in the last week, non-weight bearing/reduced range of joint movement, CRP >20mg/L / ESR >40mm/h or WCC >12k/mm<sup>3</sup> as per Kocher's criteria were deemed as an appropriate referral for urgent US +/- percutaneous aspiration. Microbiology results confirmed positive SA cases. Kocher's criteria were assigned a number for data entry and recorded on the database according to the patient's presentation. Entries were assigned "Yes" if presented with at least 2 red flags and "No" otherwise. The "No" entries were counted, signifying cases which did not meet the pathway standard for urgent US.

#### RESULTS

Over the time period, 76 urgent US examinations were performed. 22% of scans were confirmed SA cases, all presenting with more than two red flags. Despite presenting less than 2 red flags, 9% of cases underwent urgent US. All but 1 of these cases were reviewed by senior specialists and deemed high risk. There were no missed cases of SA. In the first review in 2016 prior to the current guideline, 142 US were performed in 12 months, with only 4% positive for SA. \*Discussion Children can present with unusual symptoms which do not follow criteria and high clinical suspicion of senior clinicians may result in urgent US. Awareness to accommodate exceptions to the pathway is necessary. Our trust has demonstrated good pathway adherence. This retrospective review shows the pathway accurately identifies those with SA and correctly refers them for urgent US without missed cases. The proportion of positive cases scanned has significantly increased compared to before our guideline implementation, indicating this has streamlined the workload without compromising patient care.

Printed on: 02/07/23



## Abstract Archives of the RSNA, 2022

T5A-QI-8

### Improving Compliance of Post-Procedural Documentation in the Electronic Health Record at a Medium-Sized Community Hospital

Tuesday, Nov. 29 12:15PM - 12:45PM Room: Learning Center - QI DPS

#### Participants

David Berezovsky, DO, (Presenter) Nothing to Disclose

#### METHODS

Thirteen IR providers (10 physicians and 3 PAs) performed all IR procedures at this medium-sized community teaching hospital which uses Paragon as its EHR. A standardized EHR post-procedural note template containing all necessary elements, some of which auto-populated, was created and could not be signed unless all required elements were filled. A new workflow was created to nudge providers to write their note in the EHR immediately after the procedure. Buy-in from providers, technologists, nurses, and administrators was obtained at a pre-implementation meeting. Laminated directions were attached to every workstation to remind providers to write the note and help them navigate the EHR. Baseline data from one year prior and during the eight weeks leading to implementation were obtained. Weekly analyses were conducted after implementation. Feedback and progress were sent weekly to all stakeholders. Individual scorecards were sent to select providers to highlight their compliance or non-compliance for encouragement.

#### RESULTS

Baseline compliance was 27% one year prior to implementation and 72% during the eight weeks prior to implementation. Mean weekly procedures excluding PICCs was 47. After implementation, compliance was nearly consistently above 85%.\*Discussion The keys to success in this project were obtaining buy-in from the entire team, designing a simple workflow with nudges, and delivering prompt feedback on progress. A barrier to compliance was provider perception of redundancy of routine post-procedural notes in addition to the radiology dictation. This was addressed with education about its importance for patient safety and regulatory compliance. An additional barrier was the lack of standardization of the post-procedural note in the EHR. The newly designed note template made it easy to quickly write notes that captured required information. Weekly team feedback with select individual scorecards encouraged everyone to be an active participant. Limitations included not verifying the accuracy of the notes and verifying that the note was written prior to the patient leaving the IR suite. Assessment for continued compliance is planned at 3 months and every 6 months thereafter.

Printed on: 02/07/23

## Abstract Archives of the RSNA, 2022

T5B-QI

### Quality Improvement Reports Tuesday Poster Discussions - B

Tuesday, Nov. 29 12:45PM - 1:15PM Room: Learning Center - QI DPS

#### Sub-Events

#### **T5B-QI-1 An Educational Intervention with a Radiology-Based Ordering Checklist Can Expedite the Evaluation of Acute Pulmonary Embolism**

##### Participants

Christopher Husson, MD, (*Presenter*) Nothing to Disclose

##### METHODS

The project took place throughout the hospital and satellite clinics. Our institution is a tertiary, academic, military treatment facility with undergraduate/graduate medical trainees. We included CT pulmonary angiograms (CTPA) and deep venous thrombosis ultrasounds (DVTUS) in our project. At baseline, 68% of CTPA's and 61% of DVTUS's were ordered STAT. CTPA's took over an hour to complete (67 minutes) from when the order was placed, defined as OST. Extreme instances for CTPA's and DVTUS's were also documented with some OST's exceeding 8 hours. A panel of 2 staff radiologists, 3 radiology residents, and 3 technologists determined the most common reasons for delayed exams. The main issues identified were: "non-STAT" order, improper IV access, inadequate communication, incorrect order, and patient transportation. To address these problems, we created a streamlined "ordering checklist" as a reference tool for our providers. A QR code was also provided with a link to the ACR appropriateness criteria for PE imaging. The checklist was electronically disseminated throughout the hospital system. Subsequently, our team presented educational sessions to several departments that frequently order PE imaging.

##### RESULTS

We collected anonymized data for CTPA's and DVTUS's from our hospital PACS in five-week time periods, both pre and post intervention. In the five weeks after intervention, STAT orders for CTPA demonstrated a statistically significant increase from 68% to 90% ( $p=0.02$ ). The median OST decreased by 21 minutes, from 67 minutes to 46 minutes. DVTUS's demonstrated no significant change in the percentage of STAT orders (61% to 63%) nor in median OST (31 vs 42 minutes). \*Discussion Through a radiology-based ordering checklist and educational intervention, we expedited the performance of CTPA's and evaluation for patients with acute PE. Our intervention also demonstrates key qualitative benefits, such as inter-departmental communication and improved patient safety. Important limitations of our project include lack of generalizability, small sample size, and lack of patient outcome data.

#### **T5B-QI-2 Improving the Quality of Ultrasound Reporting for Pediatric Breast Masses through Implementation of an Investigation and Management Algorithm.**

##### Participants

Tracee Wee, MD, BSc, Vancouver, BC (*Presenter*) Nothing to Disclose

##### METHODS

A retrospective audit of breast ultrasound reports was performed of female patients aged 8-20 years at initial presentation, at a single tertiary pediatric hospital between April 1, 2011 and March 31, 2021. Reports were excluded if no lesion was identified. Reports were evaluated for the presence of lesion descriptors, diagnosis/differential diagnoses, and management recommendations. Pathology reports of patients who underwent breast mass biopsy/excision were also reviewed. Electronic medical records were reviewed for the presence of breast cancer risk factors. An evidence-based algorithm for pediatric breast mass investigation management was developed in collaboration with the pediatric general surgeons/pediatric oncologists at our institution. The audit data algorithm was presented at the Radiology department's quality improvement rounds in July 2021. The project targets were 80% of reports having adequate lesion descriptors, and 90% of reports containing diagnosis/differential diagnosis and recommendations concordant with the algorithm. The second cycle audit of breast mass ultrasound reports between July 2021 and March 2022 was undertaken to evaluate quality of ultrasound reports concordance with management recommendations.

##### RESULTS

At initial audit cycle, 87 breast ultrasound reports identified a breast lesion. 47 were solid or mixed solid-cystic (complex) masses, which is the most common presentation of malignancy in this population. Size is the most consistent descriptor reported (94%). 67% of reports for solid/complex masses included diagnosis/differential diagnosis, while 35% provided management recommendations. At the second cycle review, 6 of 31 breast ultrasound exams reported solid/complex masses. There was significant improvement of reporting lesion descriptors (Fig. 1). All 6 reports provided a diagnosis/differential diagnosis, but only 3 offered recommendations, all concordant with the algorithm (Fig. 1). \*Discussion This project shows, with education an algorithm, pediatric breast mass ultrasound reports can be improved by consistent inclusion of diagnosis/differential diagnosis management recommendations. Limitations of our study include the small number of subjects, due to the low incidence of pediatric breast masses.

#### **T5B-QI-3 Saving Time Without Compromising Quality: Using an Abbreviated MR Brain Protocol in Melanoma Surveillance**

Participants  
Isabel Cornell, MD, MSc, (*Presenter*) Nothing to Disclose

## **METHODS**

The Plan Do Study Act method was used within a single tertiary referral cancer centre. An abbreviated MRI head protocol was constructed (volumetric T1 post contrast, axial FLAIR post contrast and diffusion weighted MRI; omitting standard axial T2 and pre contrast T1 volumetric sequences) and inclusion criteria agreed (high risk asymptomatic melanoma patients with previous normal standard MRI head). The abbreviated MRI head protocol was used for 3 months. Data recorded included number of abbreviated protocols conducted, scan findings, recalls, follow up findings. Reviews were conducted bimonthly. Following data review this was selected as standard practice. A sustainability/follow on review was conducted at 2 years.

## **RESULTS**

In 2019, 144 patients were scanned over 3 months with the abbreviated MR head protocol: 0 recalls, 2% positive for intracranial metastases and 36 scanning hours were saved compared to standard MRI. In 2021, 127 patients were scanned over 3 months with the abbreviated protocol: 0 recalls, 1% were positive for intracranial metastases and 32 scanning hours were saved.\*Discussion The use of an abbreviated MRI Brain protocol in the surveillance of asymptomatic high risk melanoma patients is effective and efficient saving on average, 34 hours of MRI scanning time over 3 months in a tertiary referral cancer centre.

### **T5B-QI-5 Reduction in Technical Repeat and Recall Rate After Implementation of Artificial Intelligence Driven Quality Improvement Software**

Participants  
Peter Eby, MD, Seattle, WA (*Presenter*) Nothing to Disclose

## **METHODS**

In 2019, Analytics™ AI software (Volpara Health) was rolled out across 9 clinics at our institution. Techs could review dashboards and reports that provided metric-, image-, and study-level IQ feedback alongside vendor-neutral display images, to identify areas for improvement and monitor performance against institution/global benchmarks. IQ metrics and aggregated patient demographics were extracted per Tech (i.e. quality score (QS), percentage of images scored as Perfect or Good (%PG) or in the target compression pressure (%TCP) range of 7-15 kPa (pressure=force/contact area), median age, breast volumes (BV) and volumetric breast densities (VBD)). Between April 2019 to March 2022, TR data was extracted for 40 Techs (>198K images) (Centricity, GE Healthcare) and AI IQ metrics were available for 42 Techs (>205K images). Diagnostic and digital breast tomosynthesis (DBT) images and implant cases were excluded. Using Chi2 and paired t-tests, AI IQ metrics and TR rates were compared for the initial to most recent 12-month periods following AI software implementation (i.e. "baseline" April 2019-March 2020 vs "current" April 2021-March 2022). To evaluate if IQ improvement was associated with reduced TR, 22 Techs were identified who acquired images in both baseline and current periods. Current TR was compared for Techs with >3% of Inadequate scored images in baseline to <3% in current (improvers) against those whose rate stayed at >3% (non-improvers).

## **RESULTS**

Comparing baseline to current, TR reduced from 0.77% to 0.17% ( $p<0.001$ ) and overall mean QS improved by 6% (2.28 vs 2.42;  $p=0.001$ ). The %PG (56% vs 60%,  $p<0.001$ ) and %TCP (59% vs 64%,  $p<0.001$ ) also increased significantly. Current TR was significantly lower for improvers vs non-improvers (0.12% vs 0.47%,  $p<0.001$ ). Although patient demographics differed between baseline and current ( $p<0.001$ ), median age (63/62 y), BV (804/791 cm<sup>3</sup>) and VBD (5.6/5.3%) were similar.\*Discussion AI software facilitated mammographic IQ evaluation and feedback on a massive scale not previously feasible with conventional manual assessment, and produced significant, objectively measured improvements in IQ. Limitations included the exclusion of DBT and inability to match TR and IQ data exactly.

### **T5B-QI-6 Systematic Analysis of Chest Radiographs and Their Dose Exceedances - How Can We Get Better?**

Participants  
Andrea Steuwe, PhD, Dusseldorf, Germany (*Presenter*) Nothing to Disclose

## **METHODS**

In this IRB approved, retrospective study planar radiographs of the chest acquired between October and November 2021 on a single x-ray modality were evaluated. X-ray examinations with dose exceedance were filtered and the reason of dose exceedance was documented. As a basis for dose alerts national diagnostic reference levels for p.a. and planar chest radiographs served as the standard of reference. The following data were documented: patient height and weight to calculate body-mass-index, type of projection (lateral or p.a.), tube potential and tube-current-time product, dose area product (cGycm<sup>2</sup>), as well as the reason for dose exceedance.

## **RESULTS**

A total of 677 adult patients (427 male, 250 female, range 18-95 years) were included, resulting in a total of 1354 radiographs. BMI was as follows: not available (26%), BMI <18kg/m<sup>2</sup>: 1%, BMI 18.5-24.9 kg/m<sup>2</sup>: 26%, BMI 25-29.9 kg/m<sup>2</sup>: 29%, and BMI >30kg/m<sup>2</sup>: 18%. 24% of all examinations (lateral and p.a.) resulted in dose exceedances. 85% of these dose exceedances were documented in lateral projections, whereas only 15% of the p.a. projections resulted in dose exceedances. For lateral projections, the major reasons for dose exceedance were collimation (52%), obesity (25%), their combination (8%), and low arm positioning (6%). For p.a. projections, the major reasons were obesity (50%) and collimation (28%).\*Discussion Diagnostic reference levels are applicable for patients with a weight of 70 ± 3kg. Thus, a relevant number of overweight and obese patients in every-day patient populations explains dose exceedances to some degree in order to maintain proper image quality. Despite patient weight, collimation is a strong influencing factor on radiation exposure. Collimation and patient arm positioning need to be improved by regular supportive feedback of technicians, training, and mentoring of new team members. Repetitive training must be considered mandatory, especially in a larger department with rotating staff.

### **T5B-QI-7HC Optimizing Radiology Ablation Access Through Utilization of a Predictive Scheduling Matrix**

Participants  
Molly Boelter, MBA, (*Presenter*) Nothing to Disclose

## METHODS

A team of radiology nurses, schedulers, physicians, and quality improvement personnel utilized the DMAIC (Define, Measure, Analyze, Improve, Control) and A3 problem-solving methodologies. The current condition of the practice was studied through data analysis with measures such as: patient lead time, procedure duration, and on-time starts. A Fishbone Diagram was utilized to better understand root causes. Analysis of procedure durations showed significant differences between how long the procedure was predicted to take and how long it actually took. Patient report times were based on radiologists' prediction of when the preceding case would end, as there was not an available data-driven tool to anticipate procedure length.

## RESULTS

From root cause analysis, the team identified two issues: longer than necessary procedure slots and report times (resulting in an average lead time of 113 minutes) and white space between procedures. These issues precluded the addition of a third procedure to the schedule. The team devised several PDSA cycles to streamline these processes. Report times were modified from 90 minutes prior to appointment to 60 minutes. A predictive scheduling matrix was created using previous case data. The scheduling matrix was tested over several months for accuracy showing that 66% of cases were accurately predicted within 30 minutes, 80% within 45 minutes, and 92% within 60 minutes. The average end-of-day time decreased also, allowing for a third procedure to be scheduled, reducing the backlog of procedure requests. The team selected safety events as a counterbalance measure, there was not an increase in safety events related to ablation procedures from the pre-intervention to post-intervention time periods.\*Discussion Radiology ablation procedures have highly variable procedure times, however utilizing a predictive scheduling matrix positively impacted patient lead times, resulting in a decrease of almost 33%, allowing for a third procedure to be scheduled most days, thereby reducing the backlog of body ablation requests. This project is limited by sample size, the predictive scheduling matrix has been tested with 333 patients over seven months. Data analysis was also manual, which limited the depth of analysis and could inhibit future study. Protracted lead times along with non-standardized scheduling practices led to a backlog of ablation procedure requests. The practice was hesitant to believe that procedure durations could be predicted, but this team has proven that it's possible. Please visit the Learning Center to also view this presentation in hardcopy format.

### T5B-QI-8 Data Driven Optimization and Monitoring of MR Scheduling

#### Participants

Leo Tsai, MD, PhD, Boston, MA (*Presenter*) Stockholder, Agile Devices Inc; Consultant, Agile Devices Inc

## METHODS

Outpatient MR exam durations, defined as the time between the first and last image of an exam, were extracted using Quantivly, a software application that harmonizes DICOM header data across all MR scanners and platforms. The timeliness of exams was classified as one of the following: "ideal"- duration 10-25 minutes less than the nominal time slot; "acceptable"- duration within 10 minutes of the nominal time slot; "too long" - duration longer than the nominal time slot; and "too short" - duration more than 25 minutes less than the nominal time slot. The distinction between ideal and acceptable prioritizes leaving some buffer to turn the room over between patients. Prostate w/wo contrast was identified as a candidate to move from a 60 to 45 min. slot provided that exams could be preferentially scheduled on our more efficient 3T scanner. MRCP w/wo contrast was found to have a relatively high percentage of exams considered too long and was a candidate for a time slot increase from 30 to 45 min. Preferential scheduling of prostate exams was monitored for 23 weeks after which the schedule changes were made. The effectiveness of the schedule changes was evaluated by analyzing the change in the timeliness of exams and the net amount of time made available on the outpatient schedule over a 6-week period.

## RESULTS

Preferential scheduling of prostate exams was successful with over 95% of exams scheduled on the more efficient scanner. (Figure 1a) The percentage of ideally timed prostate exams increased from 11.0% to 86.1% while the percentage of exams considered too short decreased from 87.7% to 0.8%. (Figure 1a-b) The percentage of ideally timed MRCP exams increased from 9.3% to 79.1% while reducing the number of exams considered too long from 25.4% to 2.5%. (Figure 1c-d) The difference in volumes and time slot changes resulted in a net gain of 3.2 hours/week for scheduling other exams\*Discussion Retrospective analysis of exam durations is a useful tool for optimizing MR scheduling. A disparity in efficiency between our two 3-Tesla scanners was known previously but the feasibility and benefits of reducing the time slot was difficult to quantify. The initial performance of MRCP exams was likely caused by an underestimation of the time required to perform breath holds and respiratory triggered sequences which is challenging to estimate without true exam duration data.

Printed on: 02/07/23



## Abstract Archives of the RSNA, 2022

T5B-QI-1

### An Educational Intervention with a Radiology-Based Ordering Checklist Can Expedite the Evaluation of Acute Pulmonary Embolism

Tuesday, Nov. 29 12:45PM - 1:15PM Room: Learning Center - QI DPS

#### Participants

Christopher Husson, MD, (*Presenter*) Nothing to Disclose

#### METHODS

The project took place throughout the hospital and satellite clinics. Our institution is a tertiary, academic, military treatment facility with undergraduate/graduate medical trainees. We included CT pulmonary angiograms (CTPA) and deep venous thrombosis ultrasounds (DVTUS) in our project. At baseline, 68% of CTPA's and 61% of DVTUS's were ordered STAT. CTPA's took over an hour to complete (67 minutes) from when the order was placed, defined as OST. Extreme instances for CTPA's and DVTUS's were also documented with some OST's exceeding 8 hours. A panel of 2 staff radiologists, 3 radiology residents, and 3 technologists determined the most common reasons for delayed exams. The main issues identified were: "non-STAT" order, improper IV access, inadequate communication, incorrect order, and patient transportation. To address these problems, we created a streamlined "ordering checklist" as a reference tool for our providers. A QR code was also provided with a link to the ACR appropriateness criteria for PE imaging. The checklist was electronically disseminated throughout the hospital system. Subsequently, our team presented educational sessions to several departments that frequently order PE imaging.

#### RESULTS

We collected anonymized data for CTPA's and DVTUS's from our hospital PACS in five-week time periods, both pre and post intervention. In the five weeks after intervention, STAT orders for CTPA demonstrated a statistically significant increase from 68% to 90% ( $p=0.02$ ). The median OST decreased by 21 minutes, from 67 minutes to 46 minutes. DVTUS's demonstrated no significant change in the percentage of STAT orders (61% to 63%) nor in median OST (31 vs 42 minutes). \*Discussion Through a radiology-based ordering checklist and educational intervention, we expedited the performance of CTPA's and evaluation for patients with acute PE. Our intervention also demonstrates key qualitative benefits, such as inter-departmental communication and improved patient safety. Important limitations of our project include lack of generalizability, small sample size, and lack of patient outcome data.

Printed on: 02/07/23



## Abstract Archives of the RSNA, 2022

T5B-QI-2

### Improving the Quality of Ultrasound Reporting for Pediatric Breast Masses through Implementation of an Investigation and Management Algorithm.

Tuesday, Nov. 29 12:45PM - 1:15PM Room: Learning Center - QI DPS

#### Participants

Tracee Wee, MD, BSc, Vancouver, BC (*Presenter*) Nothing to Disclose

#### METHODS

A retrospective audit of breast ultrasound reports was performed of female patients aged 8-20 years at initial presentation, at a single tertiary pediatric hospital between April 1, 2011 and March 31, 2021. Reports were excluded if no lesion was identified. Reports were evaluated for the presence of lesion descriptors, diagnosis/differential diagnoses, and management recommendations. Pathology reports of patients who underwent breast mass biopsy/excision were also reviewed. Electronic medical records were reviewed for the presence of breast cancer risk factors. An evidence-based algorithm for pediatric breast mass investigation management was developed in collaboration with the pediatric general surgeons pediatric oncologists at our institution. The audit data algorithm were presented at the Radiology department's quality improvement rounds in July 2021. The project targets were 80% of reports having adequate lesion descriptors, and 90% of reports containing diagnosis/differential diagnosis and recommendations concordant with the algorithm. The second cycle audit of breast mass ultrasound reports between July 2021 and March 2022 was undertaken to evaluate quality of ultrasound reports concordance with management recommendations.

#### RESULTS

At initial audit cycle, 87 breast ultrasound reports identified a breast lesion. 47 were solid or mixed solid-cystic (complex) masses, which is the most common presentation of malignancy in this population. Size is the most consistent descriptor reported (94%). 67% of reports for solid/complex masses included diagnosis/differential diagnosis, while 35% provided management recommendations. At the second cycle review, 6 of 31 breast ultrasound exams reported solid/complex masses. There was significant improvement of reporting lesion descriptors (Fig. 1). All 6 reports provided a diagnosis/differential diagnosis, but only 3 offered recommendations, all concordant with the algorithm (Fig. 1).\*Discussion This project shows, with education an algorithm, pediatric breast mass ultrasound reports can be improved by consistent inclusion of diagnosis/differential diagnosis management recommendations. Limitations of our study include the small number of subjects, due to the low incidence of pediatric breast masses.

Printed on: 02/07/23



## Abstract Archives of the RSNA, 2022

T5B-QI-3

### Saving Time Without Compromising Quality: Using an Abbreviated MR Brain Protocol in Melanoma Surveillance

Tuesday, Nov. 29 12:45PM - 1:15PM Room: Learning Center - QI DPS

#### Participants

Isabel Cornell, MD, MSc, (*Presenter*) Nothing to Disclose

#### METHODS

The Plan Do Study Act method was used within a single tertiary referral cancer centre. An abbreviated MRI head protocol was constructed (volumetric T1 post contrast, axial FLAIR post contrast and diffusion weighted MRI; omitting standard axial T2 and pre contrast T1 volumetric sequences) and inclusion criteria agreed (high risk asymptomatic melanoma patients with previous normal standard MRI head). The abbreviated MRI head protocol was used for 3 months. Data recorded included number of abbreviated protocols conducted, scan findings, recalls, follow up findings. Reviews were conducted bimonthly. Following data review this was selected as standard practice. A sustainability/follow on review was conducted at 2 years.

#### RESULTS

In 2019, 144 patients were scanned over 3 months with the abbreviated MR head protocol: 0 recalls, 2% positive for intracranial metastases and 36 scanning hours were saved compared to standard MRI. In 2021, 127 patients were scanned over 3 months with the abbreviated protocol: 0 recalls, 1% were positive for intracranial metastases and 32 scanning hours were saved.\*Discussion The use of an abbreviated MRI Brain protocol in the surveillance of asymptomatic high risk melanoma patients is effective and efficient saving on average, 34 hours of MRI scanning time over 3 months in a tertiary referral cancer centre.

Printed on: 02/07/23

## Abstract Archives of the RSNA, 2022

T5B-QI-5

### Reduction in Technical Repeat and Recall Rate After Implementation of Artificial Intelligence Driven Quality Improvement Software

Tuesday, Nov. 29 12:45PM - 1:15PM Room: Learning Center - QI DPS

#### Participants

Peter Eby, MD, Seattle, WA (*Presenter*) Nothing to Disclose

#### METHODS

In 2019, Analytics™ AI software (Volpara Health) was rolled out across 9 clinics at our institution. Techs could review dashboards and reports that provided metric-, image-, and study-level IQ feedback alongside vendor-neutral display images, to identify areas for improvement and monitor performance against institution/global benchmarks. IQ metrics and aggregated patient demographics were extracted per Tech (i.e. quality score (QS), percentage of images scored as Perfect or Good (%PG) or in the target compression pressure (%TCP) range of 7-15 kPa (pressure=force/contact area), median age, breast volumes (BV) and volumetric breast densities (VBD)). Between April 2019 to March 2022, TR data was extracted for 40 Techs (>198K images) (Centricity, GE Healthcare) and AI IQ metrics were available for 42 Techs (>205K images). Diagnostic and digital breast tomosynthesis (DBT) images and implant cases were excluded. Using Chi2 and paired t-tests, AI IQ metrics and TR rates were compared for the initial to most recent 12-month periods following AI software implementation (i.e. "baseline" April 2019-March 2020 vs "current" April 2021-March 2022). To evaluate if IQ improvement was associated with reduced TR, 22 Techs were identified who acquired images in both baseline and current periods. Current TR was compared for Techs with >3% of Inadequate scored images in baseline to <3% in current (improvers) against those whose rate stayed at >3% (non-improvers).

#### RESULTS

Comparing baseline to current, TR reduced from 0.77% to 0.17% ( $p<0.001$ ) and overall mean QS improved by 6% (2.28 vs 2.42;  $p=0.001$ ). The %PG (56% vs 60%,  $p<0.001$ ) and %TCP (59% vs 64%,  $p<0.001$ ) also increased significantly. Current TR was significantly lower for improvers vs non-improvers (0.12% vs 0.47%,  $p<0.001$ ). Although patient demographics differed between baseline and current ( $p<0.001$ ), median age (63/62 y), BV (804/791 cm<sup>3</sup>) and VBD (5.6/5.3%) were similar. \*Discussion AI software facilitated mammographic IQ evaluation and feedback on a massive scale not previously feasible with conventional manual assessment, and produced significant, objectively measured improvements in IQ. Limitations included the exclusion of DBT and inability to match TR and IQ data exactly.

Printed on: 02/07/23

## Abstract Archives of the RSNA, 2022

T5B-QI-6

### Systematic Analysis of Chest Radiographs and Their Dose Exceedances - How Can We Get Better?

Tuesday, Nov. 29 12:45PM - 1:15PM Room: Learning Center - QI DPS

#### Participants

Andrea Steuwe, PhD, Dusseldorf, Germany (*Presenter*) Nothing to Disclose

#### METHODS

In this IRB approved, retrospective study planar radiographs of the chest acquired between October and November 2021 on a single x-ray modality were evaluated. X-ray examinations with dose exceedance were filtered and the reason of dose exceedance was documented. As a basis for dose alerts national diagnostic reference levels for p.a. and planar chest radiographs served as the standard of reference. The following data were documented: patient height and weight to calculate body-mass-index, type of projection (lateral or p.a.), tube potential and tube-current-time product, dose area product (cGycm<sup>2</sup>), as well as the reason for dose exceedance.

#### RESULTS

A total of 677 adult patients (427 male, 250 female, range 18-95 years) were included, resulting in a total of 1354 radiographs. BMI was as follows: not available (26%), BMI <18kg/m<sup>2</sup>: 1%, BMI 18.5-24.9 kg/m<sup>2</sup>: 26%, BMI 25-29.9 kg/m<sup>2</sup>: 29%, and BMI >30kg/m<sup>2</sup>: 18%. 24% of all examinations (lateral and p.a.) resulted in dose exceedances. 85% of these dose exceedances were documented in lateral projections, whereas only 15% of the p.a. projections resulted in dose exceedances. For lateral projections, the major reasons for dose exceedance were collimation (52%), obesity (25%), their combination (8%), and low arm positioning (6%). For p.a. projections, the major reasons were obesity (50%) and collimation (28%).\*Discussion Diagnostic reference levels are applicable for patients with a weight of 70 ± 3kg. Thus, a relevant number of overweight and obese patients in every-day patient populations explains dose exceedances to some degree in order to maintain proper image quality. Despite patient weight, collimation is a strong influencing factor on radiation exposure. Collimation and patient arm positioning need to be improved by regular supportive feedback of technicians, training, and mentoring of new team members. Repetitive training must be considered mandatory, especially in a larger department with rotating staff.

Printed on: 02/07/23



## Abstract Archives of the RSNA, 2022

T5B-QI-7HC

### Optimizing Radiology Ablation Access Through Utilization of a Predictive Scheduling Matrix

Tuesday, Nov. 29 12:45PM - 1:15PM Room: Learning Center - QI DPS

#### Participants

Molly Boelter, MBA, (*Presenter*) Nothing to Disclose

#### METHODS

A team of radiology nurses, schedulers, physicians, and quality improvement personnel utilized the DMAIC (Define, Measure, Analyze, Improve, Control) and A3 problem-solving methodologies. The current condition of the practice was studied through data analysis with measures such as: patient lead time, procedure duration, and on-time starts. A Fishbone Diagram was utilized to better understand root causes. Analysis of procedure durations showed significant differences between how long the procedure was predicted to take and how long it actually took. Patient report times were based on radiologists' prediction of when the preceding case would end, as there was not an available data-driven tool to anticipate procedure length.

#### RESULTS

From root cause analysis, the team identified two issues: longer than necessary procedure slots and report times (resulting in an average lead time of 113 minutes) and white space between procedures. These issues precluded the addition of a third procedure to the schedule. The team devised several PDSA cycles to streamline these processes. Report times were modified from 90 minutes prior to appointment to 60 minutes. A predictive scheduling matrix was created using previous case data. The scheduling matrix was tested over several months for accuracy showing that 66% of cases were accurately predicted within 30 minutes, 80% within 45 minutes, and 92% within 60 minutes. The average end-of-day time decreased also, allowing for a third procedure to be scheduled, reducing the backlog of procedure requests. The team selected safety events as a counterbalance measure, there was not an increase in safety events related to ablation procedures from the pre-intervention to post-intervention time periods.\*Discussion Radiology ablation procedures have highly variable procedure times, however utilizing a predictive scheduling matrix positively impacted patient lead times, resulting in a decrease of almost 33%, allowing for a third procedure to be scheduled most days, thereby reducing the backlog of body ablation requests. This project is limited by sample size, the predictive scheduling matrix has been tested with 333 patients over seven months. Data analysis was also manual, which limited the depth of analysis and could inhibit future study. Protracted lead times along with non-standardized scheduling practices led to a backlog of ablation procedure requests. The practice was hesitant to believe that procedure durations could be predicted, but this team has proven that it's possible. Please visit the Learning Center to also view this presentation in hardcopy format.

Printed on: 02/07/23



## Abstract Archives of the RSNA, 2022

T5B-QI-8

### Data Driven Optimization and Monitoring of MR Scheduling

Tuesday, Nov. 29 12:45PM - 1:15PM Room: Learning Center - QI DPS

#### Participants

Leo Tsai, MD, PhD, Boston, MA (*Presenter*) Stockholder, Agile Devices Inc; Consultant, Agile Devices Inc

#### METHODS

Outpatient MR exam durations, defined as the time between the first and last image of an exam, were extracted using Quantivly, a software application that harmonizes DICOM header data across all MR scanners and platforms. The timeliness of exams was classified as one of the following: "ideal"- duration 10-25 minutes less than the nominal time slot; "acceptable"- duration within 10 minutes of the nominal time slot; "too long" - duration longer than the nominal time slot; and "too short" - duration more than 25 minutes less than the nominal time slot. The distinction between ideal and acceptable prioritizes leaving some buffer to turn the room over between patients. Prostate w/wo contrast was identified as a candidate to move from a 60 to 45 min. slot provided that exams could be preferentially scheduled on our more efficient 3T scanner. MRCP w/wo contrast was found to have a relatively high percentage of exams considered too long and was a candidate for a time slot increase from 30 to 45 min. Preferential scheduling of prostate exams was monitored for 23 weeks after which the schedule changes were made. The effectiveness of the schedule changes was evaluated by analyzing the change in the timeliness of exams and the net amount of time made available on the outpatient schedule over a 6-week period.

#### RESULTS

Preferential scheduling of prostate exams was successful with over 95% of exams scheduled on the more efficient scanner. (Figure 1a) The percentage of ideally timed prostate exams increased from 11.0% to 86.1% while the percentage of exams considered too short decreased from 87.7% to 0.8%. (Figure 1a-b) The percentage of ideally timed MRCP exams increased from 9.3% to 79.1% while reducing the number of exams considered too long from 25.4% to 2.5%. (Figure 1c-d) The difference in volumes and time slot changes resulted in a net gain of 3.2 hours/week for scheduling other exams\* Discussion Retrospective analysis of exam durations is a useful tool for optimizing MR scheduling. A disparity in efficiency between our two 3-Tesla scanners was known previously but the feasibility and benefits of reducing the time slot was difficult to quantify. The initial performance of MRCP exams was likely caused by an underestimation of the time required to perform breath holds and respiratory triggered sequences which is challenging to estimate without true exam duration data.

Printed on: 02/07/23



## Abstract Archives of the RSNA, 2022

W2-QI

### Quality Improvement Reports Wednesday Poster Discussions

Wednesday, Nov. 30 9:00AM - 9:30AM Room: Learning Center - QI DPS

#### Sub-Events

#### W2-QI-1 Augmented Reality and On-Site Projections: Taking Pediatric CT Examinations to the Next Level

##### Participants

Adriano Tachibana, PhD, MBA, Sao Paulo, Brazil (*Presenter*) Research Grant, Guerbet SA

##### METHODS

First, a field research was carried out to choose the characters that would most please children in a group of n=25 outpatient individuals ranging from 2 to 12 years old. Second, a field survey was carried out with the leadership of the TC department to understand the main problems that the CT sector had in relation to processes. And finally, the development of designs, scenes and script by the 3D animation team, in addition to the physical structuring, and installation of equipment. (Figure 1) To measure patient satisfaction with the new technology, a survey was carried out with five questions.

##### RESULTS

The project began in February 2022, 14 patients aged between 2 and 12 years have used the new setting. Through the satisfaction survey "Ambiance and digital personalization in examination rooms and preparation of computed tomography for pediatric care" we could observe that the exams performed had an average duration of 10 minutes, and the results showed that 92.8% (13) of the respondents considered the environment "pleasant", 7.2% (1) considered it "indifferent", 71.4% (10) reported a feeling of "tranquility", 14.2% (2), "no interference" and 14.2% (2) reported feelings of "happiness". On the satisfaction scale, the average was 9.4. In addition, 100% of respondents reported that they prefer the personalized environment "with ambience". (Table 1)\*Discussion Although we did not perform comparisons before and after the new concept of digital personalized ambience of the CT room, we can already perceive a very positive reaction from the patient and parents perspective. We see as a potential confounder the differences of care in the setting by the tech and nursery staff. We expect, as the number of examinations increase over time, to be able to measure other important indicators such as anesthesia rates, total time in the CT room and CT image quality.

#### W2-QI-2 Official Radiology Policies for Residents in a Hurry: Increasing the Confidence of Radiology Residents Answering Policy-Based Questions on Call and Injection Coverage Shifts

##### Participants

Sanna Herwald, MD, PhD, Menlo Park, CA (*Presenter*) Nothing to Disclose

##### METHODS

The 54 Radiology residents in our quaternary academic hospital routinely answer after-hours policy-based questions. The anonymous baseline survey of our Radiology residents demonstrated that junior residents were less confident answering after-hours policy-based questions than senior residents. Reported on a 1-5 Likert scale, the baseline mean confidence was 1.6, 2.8, 3.5, and 4.0 for the R1, R2, R3, and R4 respondents, respectively. Root cause analysis with frontline team members revealed that the challenges facing residents answering policy-based questions included the lack of a central policy resource, the need to answer these questions quickly during busy shifts, and the unclear mechanism for residents to ask questions about an official policy. During a structured quality improvement course, these challenges were addressed with three interventions: 1) Establishing a central online repository of Radiology-relevant policies, 2) Sharing a brief FAQ document about imaging potentially-pregnant patients, and 3) Creating an official policy feedback page on the online repository. The impact of these interventions was assessed through anonymously-reported resident confidence answering after-hours policy-based questions on a 1-5 Likert scale. No other improvement projects focused on Radiology policies or resident after-hours experience occurred during this project, and the changes in reported confidence were attributed to our specific interventions.

##### RESULTS

Our run chart shows that our interventions significantly increased resident confidence answering after-hours policy-based questions, from an average of 2.9 at baseline to 4.0 post-intervention on a 1-5 Likert scale ( $p = 0.009$ , with a similar distribution of residency years in both respondent groups). Confidence also increased in each residency class except the R4 class (baseline vs. post-intervention confidence of 1.6 vs. 3.0 for R1, 2.8 vs. 4.0 for R2, 3.5 vs. 4.7 for R3, and 4.0 vs. 4.0 for R4).\*Discussion Limitations of our study include generalizability, and limited ability to track which repository resources are most frequently used by residents. With interventions focused on policy centralization and ease-of-access, we increased resident confidence answering after-hours policy-based questions within every residency class except the fourth-year residents.

#### W2-QI-3 An Audit of Nasogastric Tube Check Chest Radiographs to Assess Safe and Timely Reporting

##### Participants

Abhinav Jha, MBBS, BSc, London, United Kingdom (*Presenter*) Nothing to Disclose

##### METHODS

The audit standards are as follows; all CXRs for NGT tube check should be flagged on Soliton Radiology Information System (RIS) to be prioritised for urgent reporting; 90% of NGT check CXRs should be reported within 3 hours; and all reports should give a definitive statement on the position of the NGT. Retrospective data analysis of chest radiographs (excluding paediatrics and neonates) was carried out, using RIS. Data sets were collected over 8 day periods in 2020 (cycles 1, 2 and 3) and 2021 (cycle 4). Following cycle 1, radiographers were encouraged to flag CXRs for NGT check on RIS at the time of image acquisition (manual process). Following cycle 2, departmental and trust wide interventions included: implementation of a standardised NGT check reporting template; inclusion of the entire NGT on the CXR if the study is flagged for NGT check; and mandatory NGT check tick box on the electronic request form for CXRs.

## RESULTS

The average number of NGT check CXRs increased from 4 per day in 2018, to 19 in cycle 1, and to 29 in cycle 4, coinciding with the COVID-19 peaks. All examinations for NGT check were flagged on RIS following the introduction of mandatory NGT tick box on electronic requests. The median time to report NGT check CXRs has decreased from 12 hours in cycle 1, to 4 hours in cycle 4 due to automated flagging. In total, the standardised template was used to report 67.0% and 76.5% of all radiographs flagged for NGT check in cycles 3 and 4 respectively. The percentage of NGT check CXRs reported within 3 hours ranged between 20-35%.\*Discussion There has been excellent uptake of the standardised template for NGT CXR reporting amongst reporters. CXRs in a series, or with other findings commonly limited usage of the template. The mandatory tick box has resulted in 100% flagging of NGT check CXRs, which may contribute to the reduction in time taken to report these studies. The 3-hour turnaround target for NGT check CXRs has not been met. This is likely secondary to a 625% percentage increase in radiographs conducted for NGT check since 2018, coinciding with the increase in number of critically unwell admissions during the COVID-19 pandemic.

## W2-QI-4HC Improving Compliance of Barcode Medication Administration of Contrast in CT

Participants

Molly Boelter, MBA, (*Presenter*) Nothing to Disclose

## METHODS

A team of CT technologists, nurses, and quality improvement personnel approached this issue with the DMAIC (Define, Measure, Analyze, Improve, Control) and A3 problem-solving methodologies. The current condition of the practice was reviewed and studied via observational audits. Relevant policies, procedures, and standards were reviewed. Analysis of baseline audits was completed along with a Fishbone Diagram to assist in understanding the root causes of issues and barriers. The team devised several PDSAs (Plan, Do, Study, Act) to find the most effective and efficient way to improve compliance. Compliance with the barcode medication administration policy related audit, as well as exam durations, were monitored throughout.

## RESULTS

A root cause analysis yielded several themes. The practice was utilizing a standard laminated sheet containing barcodes for contrast media as opposed to scanning the contrast bottles. This workaround was being utilized due to a change in EHR with insufficient time and resources to devise a compliant workflow without extending exam durations. There was a lack of understanding among team members as to what is and is not compliant when it comes to barcode medication administration. Scanning equipment was not accessible to the staff in the exam room where contrast was being administered. There was variation in the workflow between the different CT locations related to who administered and documented contrast. Four different PDSA cycles were completed with variation in the location and type of technology used for barcode medication administration of contrast. PDSAs one through three all yielded compliance rates of 100%, and exam durations ranging from 11 to 24.5 minutes. PDSA #4 is still ongoing.\*Discussion Barcode scanning allows frontline staff an opportunity to catch medication errors before they reach the patient. This team came together with the goal of improving the workflow and compliance for barcode medication administration of contrast in the CT practice. Currently the scope of this project limited, it is taking place in only one of the four CT locations due to variations in roles and responsibilities across the different locations. Introducing appropriate technology at the site where work is being done resulted in barcode compliance improvement from 9% to 100% without extending exam durations. Utilizing a team-based cooperative method for addressing non-compliance was highly effective in this project. Please visit the Learning Center to also view this presentation in hardcopy format.

## W2-QI-5HC Assessment of an Artificial Intelligence (AI) System in Indicating Breast Laterality for Breast Cancer Detection Within a Service Evaluation

Participants

Jonathan Nash, San Francisco, CA (*Presenter*) Medical Director, Kheiron Medical Technologies Ltd; Stockholder, Kheiron Medical Technologies Ltd

## METHODS

A commercially available AI system (Mia; Kheiron Medical Technologies) was employed at a BCS provider in the NHS within a service evaluation. The first phase was a retrospective local validation. The AI's standalone laterality performance was assessed on 25,547 examinations, randomly sampled from 2014-2018, from two device vendors (GE, Hologic). All screen-detected cancers were pathology-confirmed.

## RESULTS

The dataset included 205 screen-detected cancers (cancer prevalence 0.8%), of which the AI correctly recalled 187 (91.2% sensitivity, 7.2% positive predictive value). Among the correctly recalled, the AI: A) indicated laterality agreed with pathology in 85.6% (1.6% bilateral, 84.0% unilateral), B) recalled unilateral cases as bilateral in 11.2%, C) recalled one side in bilateral cancer cases in 2.1%, and D) indicated the opposite side not assessed in 1.1%. For category D, it is unknown if an early abnormality could be present as the AI-indicated side was not assessed by biopsy nor by additional diagnostic imaging.\*Discussion The AI demonstrated accurate laterality performance in the majority of its correct recalls (85.6%) as evidenced in scenario A, making the AI's laterality indication relevant for screening and diagnostic use at this centre. While the AI provided uncertain laterality in scenario B, it covered the side of concern. In scenario C, the AI indicated one of two sides of concern, which is sufficient for women to be correctly recalled. Scenarios A-C comprise 98.9% of the AI's correct recalls for which it provides screening utility. This evaluation goes beyond binary recall suggestions, typical of aggregate level AI validations, to show that, in this BCS service, AI can support the clinical workflow with laterality information for follow-up assessments. Please visit the Learning Center to also view this presentation in hardcopy format.

## W2-QI-6 Design, Implementation, and Evaluation of an Education Program for Medical and Undergraduate

## Students to Advocate Diversity, Equity, and Inclusion in Radiology

Participants

Divya Surabhi, MPH, (*Presenter*) Nothing to Disclose

### METHODS

A series of virtual and in-person events were conducted at an urban, academic medical school and affiliated university. Events for medical students included one faculty-led career advising event, two M4-led post-MATCH panels, three radiology skills workshops, and one procedure workshop; one introduction to radiology event was for undergraduate students. Students were invited to participate in a survey, consisting of a demographics questionnaire and a knowledge questionnaire, at the end of each event. The demographics questionnaire gathered information regarding gender, race/ethnicity, training level, and radiology exposure; the knowledge questionnaire gathered thoughts on how effective the event was at addressing misconceptions and work-life balance along with event satisfaction and future interests in radiology. Responses were obtained using a Likert scale to gauge agreement with questions. Completed surveys were analyzed for trends based upon survey type, question type, race/ethnicity, and gender. Across all events, there were 97 attendees with a 52% survey completion rate (50 responses). 50 responses consisted of 39 individual students. One-tailed test assessed statistical significance for race/ethnicity and gender trends.

### RESULTS

Events demonstrate a statistically significant positive impact in elucidating misconceptions and increasing URM's interest in radiology. Although not statistically significant, trends demonstrate a positive impact in combating women's misconceptions of radiology.\*Discussion Limitations include limited emphasis on coaching and collaborating factors of the 5C's. Future programming will identify mentors, host a women and minorities in radiology panel, and schedule more in-person procedure workshops. Events will be repeated in the upcoming academic year to increase participation. Future data analysis includes identifying which modality is most effective at increasing women's and URM's interest.

## W2-QI-7HC The Automated Inline Delivery to PACS of Abdominal and Hepatic Fat Imaging-Derived Phenotypes using Cloud-based Machine Learning Software

Participants

Ameena Elahi, MA, ARRT, Philadelphia, PA (*Presenter*) Nothing to Disclose

### METHODS

Figure 1a. Shows the AI end-to-end pipeline workflow that begins after the CT technologist completes the study and sends the images from the scanner to PACS. After verifying that the images have arrived in PACS, the CT technologist ends the study in the Electronic Medical Record (EMR). After the study is ended, the EMR sends an order final HL7 message to the Vendor Neutral Archive (VNA). The order final message then triggers the VNA to send a command to PACS to move the study to the AI server. The AI system processes the images and outputs the AI images to PACS.

### RESULTS

Three tests were conducted during two-hour periods of peak work hours of a tertiary care radiology practice. All CT studies conforming to two current procedural terminology (CPT) codes were transferred. There were 11 studies transferred with 1029±674 instances per study (896±1018 MB per study) in 7.3±8.8 min. The transfer rate was 123 MB/min. The minimum study had 553 instances (284 MB) transferred in <2 min, and the maximum study had 1518 instances (3.4 GB) in 31 minutes. In subsequent two two-hour periods, CT studies with 10 CPT codes were transferred. During that period, we received a total of 86 studies.\*Discussion One limitation is how dependent the workflow is on the technologist ending the study in the EHR after all images arrive in PACS. If the technologist ends the study before all images arrive in PACS, the AI output will not be fully processed and would require a manual push from the VNA to trigger the illustrated workflow. Conclusion We developed a high performance cloud-based software for inline annotation and quantification of imaging derived phenotypes. It was feasible to receive and analyze studies inline during high traffic periods. This work shows the potential to automatically obtain quantitative data using machine learning from multiple heterogeneous CT scanners with radiologists "in-the-loop". Please visit the Learning Center to also view this presentation in hardcopy format.

Printed on: 02/07/23



## Abstract Archives of the RSNA, 2022

W2-QI-1

### Augmented Reality and On-Site Projections: Taking Pediatric CT Examinations to the Next Level

Wednesday, Nov. 30 9:00AM - 9:30AM Room: Learning Center - QI DPS

#### Participants

Adriano Tachibana, PhD, MBA, Sao Paulo, Brazil (*Presenter*) Research Grant, Guerbet SA

#### METHODS

First, a field research was carried out to choose the characters that would most please children in a group of n=25 outpatient individuals ranging from 2 to 12 years old. Second, a field survey was carried out with the leadership of the TC department to understand the main problems that the CT sector had in relation to processes. And finally, the development of designs, scenes and script by the 3D animation team, in addition to the physical structuring, and installation of equipment. (Figure 1) To measure patient satisfaction with the new technology, a survey was carried out with five questions.

#### RESULTS

The projet began in February 2022, 14 patients aged between 2 and 12 years have used the new setting. Through the satisfaction survey "Ambiance and digital personalization in examination rooms and preparation of computed tomography for pediatric care" we could observe that the exams performed had an average duration of 10 minutes, and the results showed that 92.8% (13) of the respondents considered the environment "pleasant", 7.2% (1) considered it "indifferent", 71.4% (10) reported a feeling of "tranquility", 14.2% (2), "no interference" and 14.2% (2) reported feelings of "happiness". On the satisfaction scale, the average was 9.4. In addition, 100% of respondents reported that they prefer the personalized environment "with ambience".(Table 1)\*Discussion Although we did not perform comparisons before and after the new concept of digital personalized ambience of the CT room, we can already perceive a very positive reaction from the patient and parents perspective. We see as a potential confounder the differences of care in the setting by the tech and nursery staff. We expect, as the number of examinations increase over time, to be able to measure other important indicators such as anesthesia rates, total time in the CT room and CT image quality.

Printed on: 02/07/23



## Abstract Archives of the RSNA, 2022

W2-QI-2

### Official Radiology Policies for Residents in a Hurry: Increasing the Confidence of Radiology Residents Answering Policy-Based Questions on Call and Injection Coverage Shifts

Wednesday, Nov. 30 9:00AM - 9:30AM Room: Learning Center - QI DPS

#### Participants

Sanna Herwald, MD, PhD, Menlo Park, CA (*Presenter*) Nothing to Disclose

#### METHODS

The 54 Radiology residents in our quaternary academic hospital routinely answer after-hours policy-based questions. The anonymous baseline survey of our Radiology residents demonstrated that junior residents were less confident answering after-hours policy-based questions than senior residents. Reported on a 1-5 Likert scale, the baseline mean confidence was 1.6, 2.8, 3.5, and 4.0 for the R1, R2, R3, and R4 respondents, respectively. Root cause analysis with frontline team members revealed that the challenges facing residents answering policy-based questions included the lack of a central policy resource, the need to answer these questions quickly during busy shifts, and the unclear mechanism for residents to ask questions about an official policy. During a structured quality improvement course, these challenges were addressed with three interventions: 1) Establishing a central online repository of Radiology-relevant policies, 2) Sharing a brief FAQ document about imaging potentially-pregnant patients, and 3) Creating an official policy feedback page on the online repository. The impact of these interventions was assessed through anonymously-reported resident confidence answering after-hours policy-based questions on a 1-5 Likert scale. No other improvement projects focused on Radiology policies or resident after-hours experience occurred during this project, and the changes in reported confidence were attributed to our specific interventions.

#### RESULTS

Our run chart shows that our interventions significantly increased resident confidence answering after-hours policy-based questions, from an average of 2.9 at baseline to 4.0 post-intervention on a 1-5 Likert scale ( $p = 0.009$ , with a similar distribution of residency years in both respondent groups). Confidence also increased in each residency class except the R4 class (baseline vs. post-intervention confidence of 1.6 vs. 3.0 for R1, 2.8 vs. 4.0 for R2, 3.5 vs. 4.7 for R3, and 4.0 vs. 4.0 for R4).\*Discussion Limitations of our study include generalizability, and limited ability to track which repository resources are most frequently used by residents. With interventions focused on policy centralization and ease-of-access, we increased resident confidence answering after-hours policy-based questions within every residency class except the fourth-year residents.

Printed on: 02/07/23

## Abstract Archives of the RSNA, 2022

W2-QI-3

### An Audit of Nasogastric Tube Check Chest Radiographs to Assess Safe and Timely Reporting

Wednesday, Nov. 30 9:00AM - 9:30AM Room: Learning Center - QI DPS

#### Participants

Abhinav Jha, MBBS, BSc, London, United Kingdom (*Presenter*) Nothing to Disclose

#### METHODS

The audit standards are as follows; all CXRs for NGT tube check should be flagged on Soliton Radiology Information System (RIS) to be prioritised for urgent reporting; 90% of NGT check CXRs should be reported within 3 hours; and all reports should give a definitive statement on the position of the NGT. Retrospective data analysis of chest radiographs (excluding paediatrics and neonates) was carried out, using RIS. Data sets were collected over 8 day periods in 2020 (cycles 1, 2 and 3) and 2021 (cycle 4). Following cycle 1, radiographers were encouraged to flag CXRs for NGT check on RIS at the time of image acquisition (manual process). Following cycle 2, departmental and trust wide interventions included: implementation of a standardised NGT check reporting template; inclusion of the entire NGT on the CXR if the study is flagged for NGT check; and mandatory NGT check tick box on the electronic request form for CXRs.

#### RESULTS

The average number of NGT check CXRs increased from 4 per day in 2018, to 19 in cycle 1, and to 29 in cycle 4, coinciding with the COVID-19 peaks. All examinations for NGT check were flagged on RIS following the introduction of mandatory NGT tick box on electronic requests. The median time to report NGT check CXRs has decreased from 12 hours in cycle 1, to 4 hours in cycle 4 due to automated flagging. In total, the standardised template was used to report 67.0% and 76.5% of all radiographs flagged for NGT check in cycles 3 and 4 respectively. The percentage of NGT check CXRs reported within 3 hours ranged between 20-35%.\*Discussion There has been excellent uptake of the standardised template for NGT CXR reporting amongst reporters. CXRs in a series, or with other findings commonly limited usage of the template. The mandatory tick box has resulted in 100% flagging of NGT check CXRs, which may contribute to the reduction in time taken to report these studies. The 3-hour turnaround target for NGT check CXRs has not been met. This is likely secondary to a 625% percentage increase in radiographs conducted for NGT check since 2018, coinciding with the increase in number of critically unwell admissions during the COVID-19 pandemic.

Printed on: 02/07/23



## Abstract Archives of the RSNA, 2022

W2-QI-4HC

### Improving Compliance of Barcode Medication Administration of Contrast in CT

Wednesday, Nov. 30 9:00AM - 9:30AM Room: Learning Center - QI DPS

#### Participants

Molly Boelter, MBA, (*Presenter*) Nothing to Disclose

#### METHODS

A team of CT technologists, nurses, and quality improvement personnel approached this issue with the DMAIC (Define, Measure, Analyze, Improve, Control) and A3 problem-solving methodologies. The current condition of the practice was reviewed and studied via observational audits. Relevant policies, procedures, and standards were reviewed. Analysis of baseline audits was completed along with a Fishbone Diagram to assist in understanding the root causes of issues and barriers. The team devised several PDSAs (Plan, Do, Study, Act) to find the most effective and efficient way to improve compliance. Compliance with the barcode medication administration policy related audit, as well as exam durations, were monitored throughout.

#### RESULTS

A root cause analysis yielded several themes. The practice was utilizing a standard laminated sheet containing barcodes for contrast media as opposed to scanning the contrast bottles. This workaround was being utilized due to a change in EHR with insufficient time and resources to devise a compliant workflow without extending exam durations. There was a lack of understanding among team members as to what is and is not compliant when it comes to barcode medication administration. Scanning equipment was not accessible to the staff in the exam room where contrast was being administered. There was variation in the workflow between the different CT locations related to who administered and documented contrast. Four different PDSA cycles were completed with variation in the location and type of technology used for barcode medication administration of contrast. PDSAs one through three all yielded compliance rates of 100%, and exam durations ranging from 11 to 24.5 minutes. PDSA #4 is still ongoing.\*Discussion Barcode scanning allows frontline staff an opportunity to catch medication errors before they reach the patient. This team came together with the goal of improving the workflow and compliance for barcode medication administration of contrast in the CT practice. Currently the scope of this project limited, it is taking place in only one of the four CT locations due to variations in roles and responsibilities across the different locations. Introducing appropriate technology at the site where work is being done resulted in barcode compliance improvement from 9% to 100% without extending exam durations. Utilizing a team-based cooperative method for addressing non-compliance was highly effective in this project. Please visit the Learning Center to also view this presentation in hardcopy format.

Printed on: 02/07/23



## Abstract Archives of the RSNA, 2022

W2-QI-5HC

### Assessment of an Artificial Intelligence (AI) System in Indicating Breast Laterality for Breast Cancer Detection Within a Service Evaluation

Wednesday, Nov. 30 9:00AM - 9:30AM Room: Learning Center - QI DPS

#### Participants

Jonathan Nash, San Francisco, CA (*Presenter*) Medical Director, Kheiron Medical Technologies Ltd; Stockholder, Kheiron Medical Technologies Ltd

#### METHODS

A commercially available AI system (Mia; Kheiron Medical Technologies) was employed at a BCS provider in the NHS within a service evaluation. The first phase was a retrospective local validation. The AI's standalone laterality performance was assessed on 25,547 examinations, randomly sampled from 2014-2018, from two device vendors (GE, Hologic). All screen-detected cancers were pathology-confirmed.

#### RESULTS

The dataset included 205 screen-detected cancers (cancer prevalence 0.8%), of which the AI correctly recalled 187 (91.2% sensitivity, 7.2% positive predictive value). Among the correctly recalled, the AI: A) indicated laterality agreed with pathology in 85.6% (1.6% bilateral, 84.0% unilateral), B) recalled unilateral cases as bilateral in 11.2%, C) recalled one side in bilateral cancer cases in 2.1%, and D) indicated the opposite side not assessed in 1.1%. For category D, it is unknown if an early abnormality could be present as the AI-indicated side was not assessed by biopsy nor by additional diagnostic imaging.\*Discussion The AI demonstrated accurate laterality performance in the majority of its correct recalls (85.6%) as evidenced in scenario A, making the AI's laterality indication relevant for screening and diagnostic use at this centre. While the AI provided uncertain laterality in scenario B, it covered the side of concern. In scenario C, the AI indicated one of two sides of concern, which is sufficient for women to be correctly recalled. Scenarios A-C comprise 98.9% of the AI's correct recalls for which it provides screening utility. This evaluation goes beyond binary recall suggestions, typical of aggregate level AI validations, to show that, in this BCS service, AI can support the clinical workflow with laterality information for follow-up assessments. Please visit the Learning Center to also view this presentation in hardcopy format.

Printed on: 02/07/23



## Abstract Archives of the RSNA, 2022

W2-QI-6

### Design, Implementation, and Evaluation of an Education Program for Medical and Undergraduate Students to Advocate Diversity, Equity, and Inclusion in Radiology

Wednesday, Nov. 30 9:00AM - 9:30AM Room: Learning Center - QI DPS

#### Participants

Divya Surabhi, MPH, (*Presenter*) Nothing to Disclose

#### METHODS

A series of virtual and in-person events were conducted at an urban, academic medical school and affiliated university. Events for medical students included one faculty-led career advising event, two M4-led post-MATCH panels, three radiology skills workshops, and one procedure workshop; one introduction to radiology event was for undergraduate students. Students were invited to participate in a survey, consisting of a demographics questionnaire and a knowledge questionnaire, at the end of each event. The demographics questionnaire gathered information regarding gender, race/ethnicity, training level, and radiology exposure; the knowledge questionnaire gathered thoughts on how effective the event was at addressing misconceptions and work-life balance along with event satisfaction and future interests in radiology. Responses were obtained using a Likert scale to gauge agreement with questions. Completed surveys were analyzed for trends based upon survey type, question type, race/ethnicity, and gender. Across all events, there were 97 attendees with a 52% survey completion rate (50 responses). 50 responses consisted of 39 individual students. One-tailed test assessed statistical significance for race/ethnicity and gender trends.

#### RESULTS

Events demonstrate a statistically significant positive impact in elucidating misconceptions and increasing URM's interest in radiology. Although not statistically significant, trends demonstrate a positive impact in combating women's misconceptions of radiology. \*Discussion Limitations include limited emphasis on coaching and collaborating factors of the 5C's. Future programming will identify mentors, host a women and minorities in radiology panel, and schedule more in-person procedure workshops. Events will be repeated in the upcoming academic year to increase participation. Future data analysis includes identifying which modality is most effective at increasing women's and URM's interest.

Printed on: 02/07/23

## Abstract Archives of the RSNA, 2022

W2-QI-7HC

### The Automated Inline Delivery to PACS of Abdominal and Hepatic Fat Imaging-Derived Phenotypes using Cloud-based Machine Learning Software

Wednesday, Nov. 30 9:00AM - 9:30AM Room: Learning Center - QI DPS

#### Participants

Ameena Elahi, MA, ARRT, Philadelphia, PA (*Presenter*) Nothing to Disclose

#### METHODS

Figure 1a. Shows the AI end-to-end pipeline workflow that begins after the CT technologist completes the study and sends the images from the scanner to PACS. After verifying that the images have arrived in PACS, the CT technologist ends the study in the Electronic Medical Record (EMR). After the study is ended, the EMR sends an order final HL7 message to the Vendor Neutral Archive (VNA). The order final message then triggers the VNA to send a command to PACS to move the study to the AI server. The AI system processes the images and outputs the AI images to PACS.

#### RESULTS

Three tests were conducted during two-hour periods of peak work hours of a tertiary care radiology practice. All CT studies conforming to two current procedural terminology (CPT) codes were transferred. There were 11 studies transferred with  $1029 \pm 674$  instances per study ( $896 \pm 1018$  MB per study) in  $7.3 \pm 8.8$  min. The transfer rate was 123 MB/min. The minimum study had 553 instances (284 MB) transferred in <2 min, and the maximum study had 1518 instances (3.4 GB) in 31 minutes. In subsequent two two-hour periods, CT studies with 10 CPT codes were transferred. During that period, we received a total of 86 studies.\*Discussion One limitation is how dependent the workflow is on the technologist ending the study in the EHR after all images arrive in PACS. If the technologist ends the study before all images arrive in PACS, the AI output will not be fully processed and would require a manual push from the VNA to trigger the illustrated workflow. Conclusion We developed a high performance cloud-based software for inline annotation and quantification of imaging derived phenotypes. It was feasible to receive and analyze studies inline during high traffic periods. This work shows the potential to automatically obtain quantitative data using machine learning from multiple heterogeneous CT scanners with radiologists "in-the-loop". Please visit the Learning Center to also view this presentation in hardcopy format.

Printed on: 02/07/23



## Abstract Archives of the RSNA, 2022

W5A-QI

### Quality Improvement Reports Wednesday Poster Discussions - A

Wednesday, Nov. 30 12:15PM - 12:45PM Room: Learning Center - QI DPS

#### Sub-Events

#### **W5A-QI-1 Leveraging Process Redesign Techniques to Improve Workflow, Patient Care and Reimbursement of Second Opinions in Radiology**

##### Participants

Zarine K. Shah, MD, (*Presenter*) Nothing to Disclose

##### METHODS

The original process was evaluated and several opportunities for improvement were identified. The redesigned process started with automating the importation outside imaging studies leveraging a patient reconciliation tool that harmonizes patient identifiers and links studies to the appropriate patient's chart. Details of the process provided in the schematic. A second opinion order is then placed. Support staff (reading room assistants) monitor a worklist for second opinions first ensuring that the second opinion request meets departmental criteria (report availability and study performed within a specific time-frame - 30 days initially and 3 months more recently). Once these initial steps are completed, the study automatically populates a specialty-specific radiologist worklist, beyond which the reporting process is exactly like a study performed in-house. Standardized reporting templates are used, similar to studies performed at our institution, and billing second opinion uses the original CPT code of outside study performed.

##### RESULTS

The second opinion process has integrated well into our routine radiology workflow allowing radiologists to use the same worklists, PACS, and dictation software as used for all internal studies. As a part of this model we have been able to implement effective coding, billing and successful collections supporting and sustaining this effort. Prior to our process improvement we performed an average of 10 second opinion interpretations per month and were not able to bill for these. Our process improvement initiative has led to an average of 22 second opinions per month and successful reimbursement from payers with a low denial rate of 6% for the 178 studies successfully interpreted to date.\*Discussion Our new second opinion workflow has led directly to increases in efficiency, quality and sustainability by standardizing and automating workflows, using structured reporting to enhance clinical quality and support successful reimbursement.

#### **W5A-QI-2 Management of Clinical Trial Imaging Data with Structured Voice Recognition Reports and Cloud Processing: A Novel Clinical Approach**

##### Participants

Levi Sokol, MD, (*Presenter*) Nothing to Disclose

##### METHODS

An anonymous survey was sent out to the oncologist and research coordinators who have experience using the software. The survey was designed to gauge the effectiveness of the software. Questions asked included the decrease in turnaround time between initiation of scan and completion of research protocol calculations, and regarding the decrease in time the oncologists personally need to make calculations. Additionally, respondents were inquired regarding the accuracy of the data, and how much time they had to spend verifying the integrity of the data. Finally, users were also asked if there were any changes regarding the number of audit requests.

##### RESULTS

The survey was sent to approximately 170 recipients, with 46 respondents. 82.3% of respondents said they strongly agreed or agreed that there was a decreased turnaround time between scan initiation, and completion of research protocol calculations, and 17.8% were neutral. 81.2% strongly agreed or agreed that there was a decreased time they personally performed the calculations, and 18.2% were neutral. 23.8% said they saved less than 5 minutes per time point personally performing the calculations, 35.7% said 5-15 minutes, 21.43% 15 to 30 minutes, 14.3% 30-60 minutes, and 4.8% of people responded that they saved greater than 60 minutes per time point. Users were also asked regarding their time spend verifying the data. 68.9% of people spent less than 5 minutes per time point verifying the integrity and quality of the data. 17.8% spent 5-15 minutes, 11.1% spent 15-30 minutes, and 2.2% 30-60 minutes. No one spent greater than 60 minutes verifying the data. 67.4% of people strongly agreed that they were confident in the accuracy of the data, 23.4% agreed, and 8.7% neither agreed or disagreed.\*Discussion We have piloted an approach to provide clinical trials imaging metrics to oncologists using non-proprietary technology that runs from any standard radiology voice recognition system and PACS. The majority of respondents agreed that they would recommend this system for its time-saving, automated calculation and ease of use, user features.

#### **W5A-QI-3 3D Printed Vascular Model to Improve Resident Exposure and Time to Perform Coil Embolization in a Community Hospital**

##### Participants

Cristina Olivas Chacon, MD, (*Presenter*) Nothing to Disclose

## METHODS

A model of an abdominal aorta with its branches extending to the common femoral arteries with a splenic artery aneurysm was manufactured using fused deposition modelling (FDM) 3D printing technology. The 3D printer used to produce our model was an Artillery Sidewinder X1. A non-flexible thermoplastic PVB filament. The model was printed in parts given its complex configuration to allow for shorter printing times. The separate parts were put together and fused using a cautery. Each radiology resident for a total of 10 residents was given an introducer sheath, a cobra catheter, a magic torque wire, a 10mL saline push, and a 3mm coil. The residents were given the task to use the 3D printed vascular model with the goal of deploying an embolization coil on the splenic aneurysm in 3 attempts. None of the residents had previously observed or assisted an embolization procedure in the past. The resident's timings were recorded in minutes including time to cannulate the celiac trunk, time to cannulate the splenic artery and time to successfully deploy a coil within the aneurysm. The time in minutes was converted to decimal points. Data was presented using summary statistics of mean time to attain target cannulation for each of the attempts. Comparison of their mean times to success was performed using the paired t-test. Only two tail p-values were reported using a predetermined statistically significant level of  $p < 0.05$  for all our comparisons. All analysis was performed in STATA version 11.2 (StataCorp College Station, Texas).

## RESULTS

There was a significant improvement in the times to success after the first attempt as evidenced by reduction in the total time taken for each of those participants to deploy the coil within the targeted splenic aneurysm. The mean time taken for them to success after one attempt decreased from 11.5 min to 5.97 minutes with a significant P value of 0.004. \*Discussion Thanks to the advancement in the technology with subsequent decreased costs, entry-level 3D printing can now be within the reach of community hospitals. 3D printing presents an opportunity to community hospitals to increase resident exposure to complex vascular procedures that otherwise are rare in the community setting and more common in large academic institutions. 3D printing also offers an opportunity to improve the manual skills of radiology trainees by increasing their exposure to manipulation of IR equipment such as catheters and wires.

### W5A-QI-4HC Decreasing Time From Pediatric MRI/CT Order Placement to Protocol Completion

Participants

Evan Zucker, MD, Palo Alto, CA (*Presenter*) Research Consultant, F. Hoffmann-La Roche Ltd

## METHODS

This project was performed in the radiology department of an academic children's hospital. Based on staff discussions, Gemba walks, and root cause analysis, the following key drivers of protocolling delays were identified: (1) mismatch between official protocols and selectable protocol options in the electronic health record (EHR); (2) frequent radiologist reliance on custom, free text protocols; (3) numerous manual technologist selection steps (4) inefficient routing order; and (5) heterogeneous radiologist (often trainee) protocol knowledge. To address these issues, the EHR protocolling interface was overhauled with a more intuitive appearance and updated to achieve as close as possible a 1:1 correspondence between selectable protocol options and official protocols. Hard stops were implemented to minimize free text protocolling without an actual protocol selection. Moreover, the protocol routing order was automated based on exam/protocol type and the order changed from radiologist first to nurse (rather than technologist) second, as nurses were key in determining sedation needs. Prior tasks of the technologist (e.g., choosing magnet type and exam length) were now auto-selected based on the protocol. In addition, senior experienced technologists were enlisted to pre-protocol exams prior to radiologist signoff, leading to more accurate selections. Training/coaching was provided to all involved staff regarding process changes with feedback and iterative updates. The time from MRI/CT order placement to protocol completion by all parties was tracked monthly via a run chart and shared at regular huddles to maintain vigilance.

## RESULTS

From the pre-intervention 5-month baseline mean of 4.2 days from MRI/CT order placement to protocol completion, the post-intervention mean decreased to 1.9 days within 6 months, exceeding the project goal. The mean has been sustained at 1.5-2.2 days in the recent 9 months after project completion. \*Discussion By streamlining inefficiencies, automating manual workflows, encouraging standardized rather than customized processes where possible, and leveraging personnel expertise through a team approach, this project was successful in substantially decreasing protocolling time, leading to likely downstream gains in departmental throughput, patient access, and overall satisfaction. Please visit the Learning Center to also view this presentation in hardcopy format.

### W5A-QI-6HC Improve Reject Rate for Portable Chest Imaging Exams

Participants

Ben C. Wandtke, MD, MS, Rochester, NY (*Presenter*) Clinical Advisory Board, CAK Tech, Inc

## METHODS

This project was performed in the diagnostic radiology division of an urban academic center, level one trauma hospital with over 800 beds and was exclusive to adult portable chest imaging. Over the past year, 11.4% of portable chest x-rays per month were rejected and repeated to ensure diagnostic quality. An average of 4,500 bedside portable chest x-rays were performed per month, resulting in an average of 513 additional radiation exposures to patients each month to obtain diagnostic images. The goal of our project was to decrease the monthly portable chest x-ray reject rate from 11.4% to 8% by March 2022. Using several performance improvement methodologies including, rapid PDSA cycles, Gemba walks, surveys, fishbone diagram, and pareto and run charts, we identified multiple opportunities for improvement.

## RESULTS

Figure 1. Pareto chart validates clipped anatomy and patient positioning as responsible for 85% of PCXR rejections. Figure 2. Fishbone diagram demonstrates several key drivers. These included clear and consistent portable assignments, education and orientation processes, standardization of key components of diagnostic images, and routinely sharing reject data. Figure 3. Over 5 months, reject rates reduced from 11.4% to 8.2% (38% decrease). We updated our orientation process, developed education that was shared with technologist staff, and modified existing workflows to reduce technologist travel time between inpatient units. To ensure non-diagnostic images were not accepted, cardiothoracic radiologists defined a diagnostic portable chest x-ray and used this standard to develop education materials. To ensure sustainability, PCXR reject rate is now shared with staff on a monthly basis. \*Discussion The sustainable reduction in PCXR reject rate achieved required a multi-faceted approach. We defined a diagnostic study, technologists were trained and educated on key components of diagnostic portable chest imaging exams, and

staffing schedules were modified. Additionally, the results of the monthly reject data were shared with staff. A limitation of the project included the inability to directly measure the impact on labor efficiency and turnaround times. Staff did not have access to the electronic medical record on inpatient units to log start and end times, which would have allowed us to directly measure these additional outcomes. Please visit the Learning Center to also view this presentation in hardcopy format.

#### **W5A-QI-7HC      Reduce Patient No Show Rate and Improperly Prepared Patients for DaTscan Exams**

Participants

Ben C. Wandtke, MD,MS, Rochester, NY (*Presenter*) Clinical Advisory Board, CAK Tech, Inc

#### **METHODS**

This project was performed in the Nuclear Medicine Division of an urban, academic hospital. Utilizing A3 process improvement methodology, a review of the current problem and processes revealed several key drivers and interventions. We created a standard workflow for pre-calls for patients or caregiver to discuss the need to withhold interfering medications prior to the appointment. We added an interfering medication list to appear in the EMR when DaTscans exams are ordered. A list of interfering medications was provided as a reference for referring providers. Additionally, radiology residents were educated on interfering medications and required to review medications prior to DaTscan exam protocolling.

#### **RESULTS**

From June to December 2020 (Figure 1), 5.6 % of DaTscan patients did not show for their appointment, and 32% were inadequately prepared on the day of their exam (interfering medication not held). From January to June 2021, (Figure 2) inadequately prepared patients for DaTscans decreased from 32% to 3.8% (89% decrease) after implementing stated interventions. The number of no shows dropped from 5.6% to 1.9% (66% decrease). Patient scans were more confidently interpreted due to new consistency with which interfering medications were held prior to the exam. Patients were no longer regularly rescheduled after arriving for their appointments improving patient experience and reducing radiopharmaceutical waste.\*Discussion With an average radiotracer expense for one exam of \$2,570, no show/unprepared patients prior to interventions resulted in \$102,800 in wasted pharmaceutical costs annually. The 84% waste reduction created through this project yielded an \$86,350 annual cost savings. Additionally, the Imaging Department benefits by utilizing time slots more efficiently and effectively. By ensuring standardized patient preparation and communication, optimal and timely diagnosis for the patient was obtained more consistently while reducing waste, and improving scheduling efficiency and the patient experience. We believe similar interventions could be replicated at other sites performing DaTscan examinations. Please visit the Learning Center to also view this presentation in hardcopy format.

#### **W5A-QI-8HC      Fast-Track protocol: a patient-centered approach to improved radioactive iodine therapy for Graves' Disease patients**

Participants

Kyle Stevens, DO, JBSA Ft Sam Houston, TX (*Presenter*) Nothing to Disclose

#### **METHODS**

In the FT protocol, suspected GD patients discuss treatment options with Endocrinology. Endocrinologists place a dual order for RAIU and RAIA for patients desiring RAIA. The patient receives an appointment for RAIU and potential RAIA on the same day as the RAIU scan. If the patient's RAIU scan is consistent with GD, the NM physician counsels and consents the patient for RAIA and then administers the RAIA treatment dose. We collected basic demographic data and outcome measures for 19 patients before (6/2019 - 9/2020) and 10 patients after implementation of the FT protocol (12/2020 - 1/2022). We obtained patient experience survey results by oral interview. The primary study outcome measure was the median time from RAIU to RAIA. A secondary study outcome measure was patient experience survey results on the GD therapy process. Another secondary study outcome measure was the median number of total clinic visits before RAIA. There were four patients (two before and two after FT intervention) that were not reachable for the patient surveys. Wilcoxon/Kruskal-Wallis non-parametric tests of significance were performed on the median outcome measures before and after initiation of the FT protocol.

#### **RESULTS**

Before FT protocol implementation, GD patients waited a median 36 days between their RAIU and RAIA, which significantly decreased to 0 days post implementation (Figure 1A, p-value < 0.001). The number of total visits decreased from a median 4 to 3 visits (Figure 1B, p-value < 0.05). Importantly, on a three-point satisfaction scale, more patients reported increased satisfaction with their wait time after (100%), compared to before the FT protocol intervention (76.5%). There were no reported patient safety concerns during the FT protocol implementation.\*Discussion We successfully implemented a FT protocol to treat GD patients with RAIA on the same day as their RAIU scan. The process significantly reduced the time between RAIU and RAIA, decreased patient visits, and improved patient satisfaction, without an observed reduction in patient safety. Limitations include a small sample size and the inability to obtain survey results on four patients. Please visit the Learning Center to also view this presentation in hardcopy format.

Printed on: 02/07/23



## Abstract Archives of the RSNA, 2022

W5A-QI-1

### Leveraging Process Redesign Techniques to Improve Workflow, Patient Care and Reimbursement of Second Opinions in Radiology

Wednesday, Nov. 30 12:15PM - 12:45PM Room: Learning Center - QI DPS

#### Participants

Zarine K. Shah, MD, (*Presenter*) Nothing to Disclose

#### METHODS

The original process was evaluated and several opportunities for improvement were identified. The redesigned process started with automating the importation outside imaging studies leveraging a patient reconciliation tool that harmonizes patient identifiers and links studies to the appropriate patient's chart. Details of the process provided in the schematic. A second opinion order is then placed. Support staff (reading room assistants) monitor a worklist for second opinions first ensuring that the second opinion request meets departmental criteria (report availability and study performed within a specific time-frame - 30 days initially and 3 months more recently). Once these initial steps are completed, the study automatically populates a specialty-specific radiologist worklist, beyond which the reporting process is exactly like a study performed in-house. Standardized reporting templates are used, similar to studies performed at our institution, and billing second opinion uses the original CPT code of outside study performed.

#### RESULTS

The second opinion process has integrated well into our routine radiology workflow allowing radiologists to use the same worklists, PACS, and dictation software as used for all internal studies. As a part of this model we have been able to implement effective coding, billing and successful collections supporting and sustaining this effort. Prior to our process improvement we performed an average of 10 second opinion interpretations per month and were not able to bill for these. Our process improvement initiative has led to an average of 22 second opinions per month and successful reimbursement from payers with a low denial rate of 6% for the 178 studies successfully interpreted to date.\*Discussion Our new second opinion workflow has led directly to increases in efficiency, quality and sustainability by standardizing and automating workflows, using structured reporting to enhance clinical quality and support successful reimbursement.

Printed on: 02/07/23



## Abstract Archives of the RSNA, 2022

W5A-QI-2

### Management of Clinical Trial Imaging Data with Structured Voice Recognition Reports and Cloud Processing: A Novel Clinical Approach

Wednesday, Nov. 30 12:15PM - 12:45PM Room: Learning Center - QI DPS

#### Participants

Levi Sokol, MD, (*Presenter*) Nothing to Disclose

#### METHODS

An anonymous survey was sent out to the oncologist and research coordinators who have experience using the software. The survey was designed to gauge the effectiveness of the software. Questions asked included the decrease in turnaround time between initiation of scan and completion of research protocol calculations, and regarding the decrease in time the oncologists personally need to make calculations. Additionally, respondents were inquired regarding the accuracy of the data, and how much time they had to spend verifying the integrity of the data. Finally, users were also asked if there were any changes regarding the number of audit requests.

#### RESULTS

The survey was sent to approximately 170 recipients, with 46 respondents. 82.3% of respondents said they strongly agreed or agreed that there was a decreased turnaround time between scan initiation, and completion of research protocol calculations, and 17.8% were neutral. 81.2% strongly agreed or agreed that there was a decreased time they personally performed the calculations, and 18.2% were neutral. 23.8% said they saved less than 5 minutes per time point personally performing the calculations, 35.7% said 5-15 minutes, 21.43% 15 to 30 minutes, 14.3% 30-60 minutes, and 4.8% of people responded that they saved greater than 60 minutes per time point. Users were also asked regarding their time spend verifying the data. 68.9% of people spent less than 5 minutes per time point verifying the integrity and quality of the data. 17.8% spent 5-15 minutes, 11.1% spent 15-30 minutes, and 2.2% 30-60 minutes. No one spent greater than 60 minutes verifying the data. 67.4% of people strongly agreed that they were confident in the accuracy of the data, 23.4% agreed, and 8.7% neither agreed or disagreed.\*Discussion We have piloted an approach to provide clinical trials imaging metrics to oncologists using non-proprietary technology that runs from any standard radiology voice recognition system and PACS. The majority of respondents agreed that they would recommend this system for its time-saving, automated calculation and ease of use, user features.

Printed on: 02/07/23

## Abstract Archives of the RSNA, 2022

W5A-QI-3

### 3D Printed Vascular Model to Improve Resident Exposure and Time to Perform Coil Embolization in a Community Hospital

Wednesday, Nov. 30 12:15PM - 12:45PM Room: Learning Center - QI DPS

#### Participants

Cristina Olivas Chacon, MD, (*Presenter*) Nothing to Disclose

#### METHODS

A model of an abdominal aorta with its branches extending to the common femoral arteries with a splenic artery aneurysm was manufactured using fused deposition modelling (FDM) 3D printing technology. The 3D printer used to produce our model was an Artillery Sidewinder X1. A non-flexible thermoplastic PVB filament. The model was printed in parts given its complex configuration to allow for shorter printing times. The separate parts were put together and fused using a cautery. Each radiology resident for a total of 10 residents was given an introducer sheath, a cobra catheter, a magic torque wire, a 10mL saline push, and a 3mm coil. The residents were given the task to use the 3D printed vascular model with the goal of deploying an embolization coil on the splenic aneurysm in 3 attempts. None of the residents had previously observed or assisted an embolization procedure in the past. The resident's timings were recorded in minutes including time to cannulate the celiac trunk, time to cannulate the splenic artery and time to successfully deploy a coil within the aneurysm. The time in minutes was converted to decimal points. Data was presented using summary statistics of mean time to attain target cannulation for each of the attempts. Comparison of their mean times to success was performed using the paired t-test. Only two tail p-values were reported using a predetermined statistically significant level of  $p < 0.05$  for all our comparisons. All analysis was performed in STATA version 11.2 (StataCorp College Station, Texas).

#### RESULTS

There was a significant improvement in the times to success after the first attempt as evidenced by reduction in the total time taken for each of those participants to deploy the coil within the targeted splenic aneurysm. The mean time taken for them to success after one attempt decreased from 11.5 min to 5.97 minutes with a significant P value of 0.004. \*Discussion Thanks to the advancement in the technology with subsequent decreased costs, entry-level 3D printing can now be within the reach of community hospitals. 3D printing presents an opportunity to community hospitals to increase resident exposure to complex vascular procedures that otherwise are rare in the community setting and more common in large academic institutions. 3D printing also offers an opportunity to improve the manual skills of radiology trainees by increasing their exposure to manipulation of IR equipment such as catheters and wires.

Printed on: 02/07/23



## Abstract Archives of the RSNA, 2022

W5A-QI-4HC

### Decreasing Time From Pediatric MRI/CT Order Placement to Protocol Completion

Wednesday, Nov. 30 12:15PM - 12:45PM Room: Learning Center - QI DPS

#### Participants

Evan Zucker, MD, Palo Alto, CA (*Presenter*) Research Consultant, F. Hoffmann-La Roche Ltd

#### METHODS

This project was performed in the radiology department of an academic children's hospital. Based on staff discussions, Gemba walks, and root cause analysis, the following key drivers of protocolling delays were identified: (1) mismatch between official protocols and selectable protocol options in the electronic health record (EHR); (2) frequent radiologist reliance on custom, free text protocols; (3) numerous manual technologist selection steps (4) inefficient routing order; and (5) heterogeneous radiologist (often trainee) protocol knowledge. To address these issues, the EHR protocolling interface was overhauled with a more intuitive appearance and updated to achieve as close as possible a 1:1 correspondence between selectable protocol options and official protocols. Hard stops were implemented to minimize free text protocolling without an actual protocol selection. Moreover, the protocol routing order was automated based on exam/protocol type and the order changed from radiologist first to nurse (rather than technologist) second, as nurses were key in determining sedation needs. Prior tasks of the technologist (e.g., choosing magnet type and exam length) were now auto-selected based on the protocol. In addition, senior experienced technologists were enlisted to pre-protocol exams prior to radiologist signoff, leading to more accurate selections. Training/coaching was provided to all involved staff regarding process changes with feedback and iterative updates. The time from MRI/CT order placement to protocol completion by all parties was tracked monthly via a run chart and shared at regular huddles to maintain vigilance.

#### RESULTS

From the pre-intervention 5-month baseline mean of 4.2 days from MRI/CT order placement to protocol completion, the post-intervention mean decreased to 1.9 days within 6 months, exceeding the project goal. The mean has been sustained at 1.5-2.2 days in the recent 9 months after project completion.\*Discussion By streamlining inefficiencies, automating manual workflows, encouraging standardized rather than customized processes where possible, and leveraging personnel expertise through a team approach, this project was successful in substantially decreasing protocolling time, leading to likely downstream gains in departmental throughput, patient access, and overall satisfaction. Please visit the Learning Center to also view this presentation in hardcopy format.

Printed on: 02/07/23

## Abstract Archives of the RSNA, 2022

W5A-QI-6HC

### Improve Reject Rate for Portable Chest Imaging Exams

Wednesday, Nov. 30 12:15PM - 12:45PM Room: Learning Center - QI DPS

#### Participants

Ben C. Wandtke, MD,MS, Rochester, NY (*Presenter*) Clinical Advisory Board, CAK Tech, Inc

#### METHODS

This project was performed in the diagnostic radiology division of an urban academic center, level one trauma hospital with over 800 beds and was exclusive to adult portable chest imaging. Over the past year, 11.4% of portable chest x-rays per month were rejected and repeated to ensure diagnostic quality. An average of 4,500 bedside portable chest x-rays were performed per month, resulting in an average of 513 additional radiation exposures to patients each month to obtain diagnostic images. The goal of our project was to decrease the monthly portable chest x-ray reject rate from 11.4% to 8% by March 2022. Using several performance improvement methodologies including, rapid PDSA cycles, Gemba walks, surveys, fishbone diagram, and pareto and run charts, we identified multiple opportunities for improvement.

#### RESULTS

Figure 1. Pareto chart validates clipped anatomy and patient positioning as responsible for 85% of PCXR rejections. Figure 2. Fishbone diagram demonstrates several key drivers. These included clear and consistent portable assignments, education and orientation processes, standardization of key components of diagnostic images, and routinely sharing reject data. Figure 3. Over 5 months, reject rates reduced from 11.4% to 8.2% (38% decrease). We updated our orientation process, developed education that was shared with technologist staff, and modified existing workflows to reduce technologist travel time between inpatient units. To ensure non-diagnostic images were not accepted, cardiothoracic radiologists defined a diagnostic portable chest x-ray and used this standard to develop education materials. To ensure sustainability, PCXR reject rate is now shared with staff on a monthly basis. \*Discussion The sustainable reduction in PCXR reject rate achieved required a multi-faceted approach. We defined a diagnostic study, technologists were trained and educated on key components of diagnostic portable chest imaging exams, and staffing schedules were modified. Additionally, the results of the monthly reject data were shared with staff. A limitation of the project included the inability to directly measure the impact on labor efficiency and turnaround times. Staff did not have access to the electronic medical record on inpatient units to log start and end times, which would have allowed us to directly measure these additional outcomes. Please visit the Learning Center to also view this presentation in hardcopy format.

Printed on: 02/07/23



## Abstract Archives of the RSNA, 2022

W5A-QI-7HC

### Reduce Patient No Show Rate and Improperly Prepared Patients for DaTscan Exams

Wednesday, Nov. 30 12:15PM - 12:45PM Room: Learning Center - QI DPS

#### Participants

Ben C. Wandtke, MD,MS, Rochester, NY (*Presenter*) Clinical Advisory Board, CAK Tech, Inc

#### METHODS

This project was performed in the Nuclear Medicine Division of an urban, academic hospital. Utilizing A3 process improvement methodology, a review of the current problem and processes revealed several key drivers and interventions. We created a standard workflow for pre-calls for patients or caregiver to discuss the need to withhold interfering medications prior to the appointment. We added an interfering medication list to appear in the EMR when DaTscans exams are ordered. A list of interfering medications was provided as a reference for referring providers. Additionally, radiology residents were educated on interfering medications and required to review medications prior to DaTscan exam protocolling.

#### RESULTS

From June to December 2020 (Figure 1), 5.6 % of DaTscan patients did not show for their appointment, and 32% were inadequately prepared on the day of their exam (interfering medication not held). From January to June 2021, (Figure 2) inadequately prepared patients for DaTscans decreased from 32% to 3.8% (89% decrease) after implementing stated interventions. The number of no shows dropped from 5.6% to 1.9% (66% decrease). Patient scans were more confidently interpreted due to new consistency with which interfering medications were held prior to the exam. Patients were no longer regularly rescheduled after arriving for their appointments improving patient experience and reducing radiopharmaceutical waste. \*Discussion With an average radiotracer expense for one exam of \$2,570, no show/unprepared patients prior to interventions resulted in \$102,800 in wasted pharmaceutical costs annually. The 84% waste reduction created through this project yielded an \$86,350 annual cost savings. Additionally, the Imaging Department benefits by utilizing time slots more efficiently and effectively. By ensuring standardized patient preparation and communication, optimal and timely diagnosis for the patient was obtained more consistently while reducing waste, and improving scheduling efficiency and the patient experience. We believe similar interventions could be replicated at other sites performing DaTscan examinations. Please visit the Learning Center to also view this presentation in hardcopy format.

Printed on: 02/07/23

## Abstract Archives of the RSNA, 2022

W5A-QI-8HC

### Fast-Track protocol: a patient-centered approach to improved radioactive iodine therapy for Graves' Disease patients

Wednesday, Nov. 30 12:15PM - 12:45PM Room: Learning Center - QI DPS

#### Participants

Kyle Stevens, DO, JBSA Ft Sam Houston, TX (*Presenter*) Nothing to Disclose

#### METHODS

In the FT protocol, suspected GD patients discuss treatment options with Endocrinology. Endocrinologists place a dual order for RAIU and RAIA for patients desiring RAIA. The patient receives an appointment for RAIU and potential RAIA on the same day as the RAIU scan. If the patient's RAIU scan is consistent with GD, the NM physician counsels and consents the patient for RAIA and then administers the RAIA treatment dose. We collected basic demographic data and outcome measures for 19 patients before (6/2019 - 9/2020) and 10 patients after implementation of the FT protocol (12/2020 - 1/2022). We obtained patient experience survey results by oral interview. The primary study outcome measure was the median time from RAIU to RAIA. A secondary study outcome measure was patient experience survey results on the GD therapy process. Another secondary study outcome measure was the median number of total clinic visits before RAIA. There were four patients (two before and two after FT intervention) that were not reachable for the patient surveys. Wilcoxon/Kruskal-Wallis non-parametric tests of significance were performed on the median outcome measures before and after initiation of the FT protocol.

#### RESULTS

Before FT protocol implementation, GD patients waited a median 36 days between their RAIU and RAIA, which significantly decreased to 0 days post implementation (Figure 1A, p-value < 0.001). The number of total visits decreased from a median 4 to 3 visits (Figure 1B, p-value < 0.05). Importantly, on a three-point satisfaction scale, more patients reported increased satisfaction with their wait time after (100%), compared to before the FT protocol intervention (76.5%). There were no reported patient safety concerns during the FT protocol implementation. \*Discussion We successfully implemented a FT protocol to treat GD patients with RAIA on the same day as their RAIU scan. The process significantly reduced the time between RAIU and RAIA, decreased patient visits, and improved patient satisfaction, without an observed reduction in patient safety. Limitations include a small sample size and the inability to obtain survey results on four patients. Please visit the Learning Center to also view this presentation in hardcopy format.

Printed on: 02/07/23



## Abstract Archives of the RSNA, 2022

W5B-QI

### Quality Improvement Reports Wednesday Poster Discussions - B

Wednesday, Nov. 30 12:45PM - 1:15PM Room: Learning Center - QI DPS

#### Sub-Events

#### **W5B-QI-1 Clinician's Ability to Accurately Determine Patient Angulation in Portable Chest Radiography With a More Quantitative Marker**

##### Participants

Kurt Lee, MD, (*Presenter*) Nothing to Disclose

##### METHODS

As part of a quality improvement initiative, the X-clometer was used to obtain patient positioning in portable chest X-rays for one week at a level 1 trauma center in a metropolitan academic institution. Images were retrospectively reviewed to identify those with CT exams within one day of chest radiograph. A physician-directed survey encompassing five such cases was administered to radiologist and non-radiologist volunteers. A total of 27 responses were collected, including eight radiology residents, thirteen non-radiology residents, four fellowship trained cardiothoracic radiologists, and two non-cardiothoracic radiologists. Respondents were tasked with estimating each patient's angle of inclination based on conventional markers alone. Additionally, they were asked to identify findings in each case twice: first with the X-clometer reading withheld, and again with a visible X-clometer reading. Responses were compared to each case's corresponding CT report. Nonparametric and descriptive statistics were used for evaluation of collected data.

##### RESULTS

Estimation of the patient's position based on BB markers and technician labels alone was highly inaccurate: respondents estimated correctly only 23% of the time (defined as being within 15 degrees of the true angle per X-clometer). In one case, an image labeled "upright" drew 90° as the most frequent estimate, while in fact the true angle was 50°. Respondents accurately identified the correct findings 66% of the time on average across all five cases when the X-clometer angulation reading was withheld. After being shown the angle of inclination for each case, this figure was 59% on second evaluation. Attending radiologists scored 73% at first, and 70% on the second attempt.\*Discussion Traditional labels were highly unreliable and in some cases misleading in conveying accurate information about patient position. It is clear that subjective markers are inadequate and a more precise method of communicating patient angulation, such as the X-clometer, is needed. Respondents, especially radiologists, were relatively successful at identifying findings even before being given angle information.

#### **W5B-QI-2 Improving Protocol Turnaround Time in Nuclear Medicine Division at a Tertiary Referral Medical Center**

##### Participants

Hong Song, MD, PhD, Stanford, CA (*Presenter*) Nothing to Disclose

##### METHODS

Our team established pre-intervention baseline of protocol turnaround time for the month of August, 2021. We then employed a LEAN A3 problem solving approach to analyze the problem of inefficient protocolling. We performed process observations, root cause analysis and stakeholder interviews for the current workflow. Using Key Driver Diagram, we identified several key drivers to the protocol process and interventions that could impact the most key drivers.

##### RESULTS

The key drivers of the protocol process include Radiologist/Technologist workflow, communication to community referral physician, division policy clearly defining roles of trainees, Radiologist, technologists and reading room assistance in the protocol process, limitation of electronic medical record system to identify wrong study order or indication. So far, we implemented interventions in technologist workflow and division policy. More specifically, for technologist workflow, we created a two-tiered protocol review system where new protocols that require immediate review is put into one folder while the protocols that were reviewed but not completed including wrong orders to be cancelled, research protocol, treatment protocols requiring special review will be put into a second folder. This new workflow will enable the technologists to review and complete the protocols more efficiently. We also revised our division policy to clarify roles of trainees in the protocol process. We analyzed more than three thousand studies and found that the protocol turnaround time improved from 2.7 days/study in August 2021 to 1.6 days/study in December 2021 after we implemented these initial changes in September 2021.\*Discussion We employed a LEAN A3 problem solving approach to identify root causes and key drivers that caused delays in outpatient protocol turnaround time. We showed that a simple task of protocol for imaging studies can be the ramification of multiple complex factors in the modern healthcare system. Additional interventions include improving communication to community referral provides, establishing built-in feedback for orders on electronic medical record system are necessary to further improve protocol efficiency.

#### **W5B-QI-4 Improving MRI Order-to-Scan" Times in an Inpatient Quaternary Academic Hospital Setting: Our Revitalization Project.**

##### **Participants**

Ritesh Patel, MD, Manhasset, NY (*Presenter*) Nothing to Disclose

##### **METHODS**

This project was performed in an inpatient, quaternary, academic hospital setting. At the start of 2022, >20% of all inpatient (IP) MRIs had an OTS time of >48 hours, some exceeding over 100 hours. Scanner utilization data was acquired and used to identify cases contributing to extended OTS times. Identified problems included a single radiologist managing all complex clinical conversations with ordering providers, inappropriate use of standing orders by ordering providers, and incomplete MRI screening forms. To target these problems, the following pilot interventions were implemented at the start of March 2022. An MRI scanning supervisor was transitioned to a non-scanning manager role with expert level fund of knowledge and the ability to manage the workflow directly. The MRI manager reviewed all cases with >36 hours pending time as well as identified "problem" cases and actively addressed ongoing concerns, only escalating to the radiologist when necessary. In addition, the radiology service line collaborated with ED/IP service line and the EMR team to design MRI screening questions that were required to be completed at the time of an order. Sample questions include the presence of a pacemaker, history of claustrophobia, and the patient's ability to communicate. The impact of these interventions was assessed by tracking OTS time.

##### **RESULTS**

Prior to the enactment of these interventions, the average OTS times were 28.7 and 29.1 hours, with 25% and 23% of IP MRIs having an OTS time >48 hours, in January and February 2022, respectively. After the implementation of our interventions in March 2022, our analysis demonstrated a significant reduction in cases >48 hours, down to 5% of all IP MRIs, previously 23%. Even with a stable IP MRI case volume between February and March 2022, there was a significant decrease in OTS time from 29 to 18 hours. This decrease in OTS times was maintained for the month of April 2022 despite a 10% increase in IP MRI case volume.\*Discussion This study demonstrates a significant reduction in IP MRI OTS times after the implementation of an MRI manager with increased privileges to manage the workflow in conjunction with a detailed MRI screening questionnaire at the time of ordering has led to a significant decrease in OTS times despite increasing IP MRI case volumes. This data is limited to 2 months; however, data collection and re-evaluation is ongoing.

#### **W5B-QI-5 Investigating the Feasibility of Using A.I. For Population-Level Mammography Image Quality Improvement Initiatives at Leeds Teaching Hospitals NHS Trust**

##### **Participants**

Nisha Sharma, MBChB, FRCR, Leeds, United Kingdom (*Presenter*) Nothing to Disclose

##### **METHODS**

An AI IQ tool (densitas® intelliMammo™) was used to assess mammography positioning errors aligning with the NHS criteria on all mammograms acquired at our institution from December 2021 to March 2022. Population-based error rates were assessed using means and time plots. Agreement between radiographers and the AI IQ tool was assessed using the Kappa statistic on a set of 50 exams (100 CC and 100 MLO images).

##### **RESULTS**

There were 59264 studies (29964 CC and 29300 MLO images) acquired during the study period. The agreement between radiographers and the AI tool ranged from Kappa=0.70 (95%CI: 0.502, 0.898) to 0.95 (95%CI: 0.756, 1.00) (Table 1). Positioning error rate means over the study period were stable (fig 1) and ranged from 11% to 51% (Table 1)\*Discussion A study limitation was that results were not stratified by screening and diagnostic exams. With the differences in imaging requirements, there may be variation in the error rates. This project establishes that A.I. can provide reliable and reproducible quantitative mammography IQ assessments that make it feasible to evaluate population-wide IQ improvement initiatives. Future work will focus on radiographer-tailored quality improvement initiatives to enhance mammography quality at LTHT.

#### **W5B-QI-6 Automatic Assessment of the Quality of Patient Positioning in Mammography Using an Artificial Intelligent System**

##### **Participants**

Huizhi Cao, PhD, (*Presenter*) Nothing to Disclose

##### **METHODS**

The system uses deep learning technology to find nine types of abnormalities that will occur during breast X-ray examinations. The intelligent quality control system of mammography includes acquisition module, quality evaluation module and result display module. The automatic detection of landmarks in medio-lateral oblique (MLO) and cranio-caudal (CC) mammograms, named incomplete gland, incomplete pectoralis major muscle, and over or insufficient exposure for overall evaluation and skin fold, nipple not in the contour line, shoulder overlap shadow, abdominal skin, contralateral breast and foreign body for partial evaluation in the image. Finally, the relations between the detected landmarks are investigated to assess the positioning quality and results of the assessment are compared to ground truth collected from expert readers. External validation was performed by four radiographers on 1223 examinations of women to evaluate the performance of AI system and determine the agreement between AI system and radiographers.

##### **RESULTS**

The AUC of poor imaging quality prediction by AI system according to incomplete gland, incomplete pectoralis muscle, over or insufficient exposure was 0.903 vs 0.937 vs 982. The intraclass correlation for the pectoral nipple line between the radiographers and AI was >0.80. A substantial to almost perfect agreement (? > 0.85) was observed between the radiographers and AI on the nipple in profile criterion. We observed a slight to moderate agreement for the other criteria (? = 0.40-0.65) and generally a higher agreement between the two pairs of radiographers (mean ? = 0.70) than between the radiographers and AI (mean ? = 0.61).\*Discussion Breast position with AI system has great importance for quality control of mammography and are great value to reach optimal image quality in mammography.AI system has great potential in evaluating breast position criteria in mammography by reducing subjectivity. However, varying agreement between radiographers and AI was observed. Future research should focus on the clinical impact of the automatized quality ratings and investigate to what extent the low quality mammograms lead to more

interval detected cancers.

## **W5B-QI-8 Implementation of Radiology E-Consults at an Academic Medical Center**

### **Awards**

#### **Identified for RadioGraphics**

#### Participants

Kulpana Suresh, MD, Philadelphia, PA (*Presenter*) Nothing to Disclose

### **METHODS**

Beginning in October 2020 we piloted the utilization of radiology e-consults with a subset of primary care providers at our institution. An order was built into our Electronic Medical Record (EMR) to deliver a message for review by one of two body radiologists - responses were returned via EMR. The e-consult order asked the ordering provider how much they spent preparing the request and if a specialist referral would have been used had the e-consult been unavailable.

### **RESULTS**

Between October 2020 and March 2022, 294 e-consults were placed, of which 285 were completed and 9 were cancelled. In 62 consults (21%), the providers indicated they would have referred the patient to a subspecialist had the service been unavailable. Placing an e-consult took less than 15 minutes in 94% of cases. 76% of consults were placed by physicians, the remainder by advanced practice providers. Questions most often pertained to body imaging (36.5%), neuro (20.7%), chest (17.5%) and MSK imaging (7%). Common themes included guidance for follow-up imaging and which study to order. Provider feedback has been overall positive.\*Discussion Our study shows that there is clear demand for radiology e-consults from primary care providers. It also shows that such a service can reduce specialist referrals and likely improve patient and provider experience. Further work is needed to confirm these savings and to identify a sustainable reimbursement model. Based on the experience, our institution plans to expand this service to additional radiologists and primary care practices.

Printed on: 02/07/23

## Abstract Archives of the RSNA, 2022

W5B-QI-1

### Clinician's Ability to Accurately Determine Patient Angulation in Portable Chest Radiography With a More Quantitative Marker

Wednesday, Nov. 30 12:45PM - 1:15PM Room: Learning Center - QI DPS

#### Participants

Kurt Lee, MD, (*Presenter*) Nothing to Disclose

#### METHODS

As part of a quality improvement initiative, the X-clometer was used to obtain patient positioning in portable chest X-rays for one week at a level 1 trauma center in a metropolitan academic institution. Images were retrospectively reviewed to identify those with CT exams within one day of chest radiograph. A physician-directed survey encompassing five such cases was administered to radiologist and non-radiologist volunteers. A total of 27 responses were collected, including eight radiology residents, thirteen non-radiology residents, four fellowship trained cardiothoracic radiologists, and two non-cardiothoracic radiologists. Respondents were tasked with estimating each patient's angle of inclination based on conventional markers alone. Additionally, they were asked to identify findings in each case twice: first with the X-clometer reading withheld, and again with a visible X-clometer reading. Responses were compared to each case's corresponding CT report. Nonparametric and descriptive statistics were used for evaluation of collected data.

#### RESULTS

Estimation of the patient's position based on BB markers and technician labels alone was highly inaccurate: respondents estimated correctly only 23% of the time (defined as being within 15 degrees of the true angle per X-clometer). In one case, an image labeled "upright" drew 90° as the most frequent estimate, while in fact the true angle was 50°. Respondents accurately identified the correct findings 66% of the time on average across all five cases when the X-clometer angulation reading was withheld. After being shown the angle of inclination for each case, this figure was 59% on second evaluation. Attending radiologists scored 73% at first, and 70% on the second attempt.\*Discussion Traditional labels were highly unreliable and in some cases misleading in conveying accurate information about patient position. It is clear that subjective markers are inadequate and a more precise method of communicating patient angulation, such as the X-clometer, is needed. Respondents, especially radiologists, were relatively successful at identifying findings even before being given angle information.

Printed on: 02/07/23



## Abstract Archives of the RSNA, 2022

W5B-QI-2

### Improving Protocol Turnaround Time in Nuclear Medicine Division at a Tertiary Referral Medical Center

Wednesday, Nov. 30 12:45PM - 1:15PM Room: Learning Center - QI DPS

#### Participants

Hong Song, MD, PhD, Stanford, CA (*Presenter*) Nothing to Disclose

#### METHODS

Our team established pre-intervention baseline of protocol turnaround time for the month of August, 2021. We then employed a LEAN A3 problem solving approach to analyze the problem of inefficient protocolling. We performed process observations, root cause analysis and stakeholder interviews for the current workflow. Using Key Driver Diagram, we identified several key drivers to the protocol process and interventions that could impact the most key drivers.

#### RESULTS

The key drivers of the protocol process include Radiologist/Technologist workflow, communication to community referral physician, division policy clearly defining roles of trainees, Radiologist, technologists and reading room assistance in the protocol process, limitation of electronic medical record system to identify wrong study order or indication. So far, we implemented interventions in technologist workflow and division policy. More specifically, for technologist workflow, we created a two-tiered protocol review system where new protocols that require immediate review is put into one folder while the protocols that were reviewed but not completed including wrong orders to be cancelled, research protocol, treatment protocols requiring special review will be put into a second folder. This new workflow will enable the technologists to review and complete the protocols more efficiently. We also revised our division policy to clarify roles of trainees in the protocol process. We analyzed more than three thousand studies and found that the protocol turnaround time improved from 2.7 days/study in August 2021 to 1.6 days/study in December 2021 after we implemented these initial changes in September 2021.\*Discussion We employed a LEAN A3 problem solving approach to identify root causes and key drivers that caused delays in outpatient protocol turnaround time. We showed that a simple task of protocol for imaging studies can be the ramification of multiple complex factors in the modern healthcare system. Additional interventions include improving communication to community referral provides, establishing built-in feedback for orders on electronic medical record system are necessary to further improve protocol efficiency.

Printed on: 02/07/23



## Abstract Archives of the RSNA, 2022

W5B-QI-4

### Improving MRI Order-to-Scan Times in an Inpatient Quaternary Academic Hospital Setting: Our Revitalization Project.

Wednesday, Nov. 30 12:45PM - 1:15PM Room: Learning Center - QI DPS

#### Participants

Ritesh Patel, MD, Manhasset, NY (*Presenter*) Nothing to Disclose

#### METHODS

This project was performed in an inpatient, quaternary, academic hospital setting. At the start of 2022, >20% of all inpatient (IP) MRIs had an OTS time of >48 hours, some exceeding over 100 hours. Scanner utilization data was acquired and used to identify cases contributing to extended OTS times. Identified problems included a single radiologist managing all complex clinical conversations with ordering providers, inappropriate use of standing orders by ordering providers, and incomplete MRI screening forms. To target these problems, the following pilot interventions were implemented at the start of March 2022. An MRI scanning supervisor was transitioned to a non-scanning manager role with expert level fund of knowledge and the ability to manage the workflow directly. The MRI manager reviewed all cases with >36 hours pending time as well as identified "problem" cases and actively addressed ongoing concerns, only escalating to the radiologist when necessary. In addition, the radiology service line collaborated with ED/IP service line and the EMR team to design MRI screening questions that were required to be completed at the time of an order. Sample questions include the presence of a pacemaker, history of claustrophobia, and the patient's ability to communicate. The impact of these interventions was assessed by tracking OTS time.

#### RESULTS

Prior to the enactment of these interventions, the average OTS times were 28.7 and 29.1 hours, with 25% and 23% of IP MRIs having an OTS time >48 hours, in January and February 2022, respectively. After the implementation of our interventions in March 2022, our analysis demonstrated a significant reduction in cases >48 hours, down to 5% of all IP MRIs, previously 23%. Even with a stable IP MRI case volume between February and March 2022, there was a significant decrease in OTS time from 29 to 18 hours. This decrease in OTS times was maintained for the month of April 2022 despite a 10% increase in IP MRI case volume.\*Discussion This study demonstrates a significant reduction in IP MRI OTS times after the implementation of an MRI manager with increased privileges to manage the workflow in conjunction with a detailed MRI screening questionnaire at the time of ordering has led to a significant decrease in OTS times despite increasing IP MRI case volumes. This data is limited to 2 months; however, data collection and re-evaluation is ongoing.

Printed on: 02/07/23



## Abstract Archives of the RSNA, 2022

W5B-QI-5

### Investigating the Feasibility of Using A.I. For Population-Level Mammography Image Quality Improvement Initiatives at Leeds Teaching Hospitals NHS Trust

Wednesday, Nov. 30 12:45PM - 1:15PM Room: Learning Center - QI DPS

#### Participants

Nisha Sharma, MBChB, FRCR, Leeds, United Kingdom (*Presenter*) Nothing to Disclose

#### METHODS

An AI IQ tool (densitas® intelliMammo™) was used to assess mammography positioning errors aligning with the NHS criteria on all mammograms acquired at our institution from December 2021 to March 2022. Population-based error rates were assessed using means and time plots. Agreement between radiographers and the AI IQ tool was assessed using the Kappa statistic on a set of 50 exams (100 CC and 100 MLO images).

#### RESULTS

There were 59264 studies (29964 CC and 29300 MLO images) acquired during the study period. The agreement between radiographers and the AI tool ranged from  $\text{Kappa}=0.70$  (95%CI: 0.502, 0.898) to 0.95 (95%CI: 0.756, 1.00) (Table 1). Positioning error rate means over the study period were stable (fig 1) and ranged from 11% to 51% (Table 1)\*Discussion A study limitation was that results were not stratified by screening and diagnostic exams. With the differences in imaging requirements, there may be variation in the error rates. This project establishes that A.I. can provide reliable and reproducible quantitative mammography IQ assessments that make it feasible to evaluate population-wide IQ improvement initiatives. Future work will focus on radiographer-tailored quality improvement initiatives to enhance mammography quality at LTHT.

Printed on: 02/07/23



## Abstract Archives of the RSNA, 2022

W5B-QI-6

### Automatic Assessment of the Quality of Patient Positioning in Mammography Using an Artificial Intelligent System

Wednesday, Nov. 30 12:45PM - 1:15PM Room: Learning Center - QI DPS

#### Participants

Huizhi Cao, PhD, (Presenter) Nothing to Disclose

#### METHODS

The system uses deep learning technology to find nine types of abnormalities that will occur during breast X-ray examinations. The intelligent quality control system of mammography includes acquisition module, quality evaluation module and result display module. The automatic detection of landmarks in medio-lateral oblique (MLO) and cranio-caudal (CC) mammograms, named incomplete gland, incomplete pectoralis major muscle, and over or insufficient exposure for overall evaluation and skin fold, nipple not in the contour line, shoulder overlap shadow, abdominal skin, contralateral breast and foreign body for partial evaluation in the image. Finally, the relations between the detected landmarks are investigated to assess the positioning quality and results of the assessment are compared to ground truth collected from expert readers. External validation was performed by four radiographers on 1223 examinations of women to evaluate the performance of AI system and determine the agreement between AI system and radiographers.

#### RESULTS

The AUC of poor imaging quality prediction by AI system according to incomplete gland, incomplete pectoralis muscle, over or insufficient exposure was 0.903 vs 0.937 vs 982. The intraclass correlation for the pectoral nipple line between the radiographers and AI was  $>0.80$ . A substantial to almost perfect agreement ( $\kappa > 0.85$ ) was observed between the radiographers and AI on the nipple in profile criterion. We observed a slight to moderate agreement for the other criteria ( $\kappa = 0.40-0.65$ ) and generally a higher agreement between the two pairs of radiographers (mean  $\kappa = 0.70$ ) than between the radiographers and AI (mean  $\kappa = 0.61$ ). \*Discussion Breast position with AI system has great importance for quality control of mammography and are great value to reach optimal image quality in mammography. AI system has great potential in evaluating breast position criteria in mammography by reducing subjectivity. However, varying agreement between radiographers and AI was observed. Future research should focus on the clinical impact of the automatized quality ratings and investigate to what extent the low quality mammograms lead to more interval detected cancers.

Printed on: 02/07/23



## Abstract Archives of the RSNA, 2022

W5B-QI-8

### Implementation of Radiology E-Consults at an Academic Medical Center

Wednesday, Nov. 30 12:45PM - 1:15PM Room: Learning Center - QI DPS

#### Awards

Identified for RadioGraphics

#### Participants

Kulpana Suresh, MD, Philadelphia, PA (*Presenter*) Nothing to Disclose

#### METHODS

Beginning in October 2020 we piloted the utilization of radiology e-consults with a subset of primary care providers at our institution. An order was built into our Electronic Medical Record (EMR) to deliver a message for review by one of two body radiologists - responses were returned via EMR. The e-consult order asked the ordering provider how much they spent preparing the request and if a specialist referral would have been used had the e-consult been unavailable.

#### RESULTS

Between October 2020 and March 2022, 294 e-consults were placed, of which 285 were completed and 9 were cancelled. In 62 consults (21%), the providers indicated they would have referred the patient to a subspecialist had the service been unavailable. Placing an e-consult took less than 15 minutes in 94% of cases. 76% of consults were placed by physicians, the remainder by advanced practice providers. Questions most often pertained to body imaging (36.5%), neuro (20.7%), chest (17.5%) and MSK imaging (7%). Common themes included guidance for follow-up imaging and which study to order. Provider feedback has been overall positive.\*Discussion Our study shows that there is clear demand for radiology e-consults from primary care providers. It also shows that such a service can reduce specialist referrals and likely improve patient and provider experience. Further work is needed to confirm these savings and to identify a sustainable reimbursement model. Based on the experience, our institution plans to expand this service to additional radiologists and primary care practices.

Printed on: 02/07/23